

SYMPOSIUM BI01

Energy Justice in Materials Science and Engineering
November 28 - November 29, 2023

Symposium Organizers

Ahmet Alatas, Argonne National Laboratory
Katherine Anderson, National Renewable Energy Laboratory
Lauren Marbella, Columbia University
Michael Toney, University of Colorado Boulder

* Invited Paper
+ JMR Distinguished Invited Speaker

SESSION BI01.01: Materials Research and Energy Justice
Session Chairs: Lauren Marbella and Michael Toney
Tuesday Morning, November 28, 2023
Hynes, Level 2, Room 209

8:30 AM *BI01.01.01

Environmental and Social Justice Considerations in a Circular Economy Taylor Uekert, Hope Wikoff, Julien Walzberg, Meredith Doyle and Alberta Carpenter; National Renewable Energy Laboratory, United States

A consideration of environmental justice (EJ) and social justice (SJ) is critical to minimize the impacts of technology deployment on local communities. SJ and EJ impacts occur in specific geographic locations but can cover a wide range of effects (e.g., air pollution, access to clean water, jobs, wages, and education), making it challenging to determine which metrics are appropriate to evaluate and which data are required for qualitative or quantitative analysis. This issue is only exacerbated when the technology in question is at an early technology readiness level (TRL) without community specific data. Here, we present a framework for evaluating the human health, local environment, and job implications of processes that are at early to middle TRLs. Using a case study on enzymatic polyethylene terephthalate (PET) recycling (middle TRL), we demonstrate how to qualitatively and quantitatively assess these EJ and SJ metrics for a circular economy context and how to communicate the results in a manner beneficial to both researchers and local communities.

9:00 AM *BI01.01.02

Developing & Evaluating Energy Justice Metrics for Early-Stage Materials Research Nikita S. Dutta, Bettina K. Arkhurst, Clara Houghteling, Katherine Anderson and Elizabeth Gill; National Renewable Energy Laboratory, United States

Materials science is a central component of early-stage research and development of virtually all clean energy technologies. But as much as material breakthroughs often hold the key to high efficiencies, long lifetimes, and high stability in eventual devices, early-stage choices about material types, structures, and processing can also serve to lock in long-term social and equity impacts of deployed energy technologies. Thus, to achieve a just and sustainable energy transition, tools to assess the energy justice impacts of early-stage materials research are critical. Here, we discuss development of the Justice Underpinning Science and Technology Research (JUST-R) metrics framework—a suite of metrics targeted at early-stage researchers to assess energy justice considerations in their work. The framework is evaluated for its appeal to researchers and effectiveness at promoting integration of energy justice into research through case studies, which reveal its ability to broaden researcher perspectives and key avenues for future improvement.

9:30 AM BI01.01.03

Pathways for Incorporating Justice into Materials Science Research Casey M. Davis¹, Sasha Neefe¹, Lacey Roberts¹, Ronan Kennedy^{1,2} and Michael F. Toney¹; ¹University of Colorado Boulder, United States; ²University College Dublin, Ireland

As the climate crisis worsens, it becomes increasingly clear that solutions will be found at the intersection of science, policy, and community. Attracting and retaining graduate students who work to integrate energy justice into materials science will create a workforce with the tools to address climate change. It is important to consider energy justice when developing materials for a clean energy transition as marginalized communities that have been affected most by climate change tend to benefit least from new energy technology.

Scientists often exclusively receive scientific training, their research motivated by advancement of the field with little regard to societal needs. Graduate students who may take interest in supplementing their work with justice considerations frequently face resistance from advisors and delayed graduation. Energy justice in materials science at the academic level has only recently been garnering attention, so there are few studies in how to engage, retain, and train graduate students in this interdisciplinary field to employ just technologies. We propose a set of solutions at various levels aimed at enabling graduate students with existing interest in justice and engaging students who have not yet considered bringing this aspect into their graduate degrees.

In a doctorate degree, students are regularly discouraged from pursuing interests that do not directly relate to their PhD projects. If research students follow pursuits outside of conventional STEM research, they likely will face extra time in graduate school, which can be a significant deterrent. To address this, interdisciplinary PhD tracks can be created for the purpose of combining energy justice and materials science will explicitly train graduate students in this area. Additionally, adjusting departmental culture to encourage inclusion of justice in current materials science, chemistry, and engineering programs is a significant component. This shift can be partially accomplished by preferentially admitting students and hiring faculty who are committed to intersectionality, as well as encouraging students to include justice results in their dissertation alongside scientific development.

The participation of current graduate students who may not have previously considered societal implications in their degree is crucial. Education is a proven effective path to inspire interest. This exposure is possible through amending required course syllabi to include justice concepts, hosting speakers knowledgeable in these areas, and encouraging students to openly discuss ideas during prescribed meetings. Attracting and retaining researchers in this field will rely on conveying the benefits of environmental and justice work, which is often believed to be draining or even hopeless. Portraying the excitement of working in a cutting-edge field and seeing tangible positive impacts on communities will garner more interest.

Scientific journals are another important factor, as they shape the material that researchers are exposed to. Many journals consider pieces that discuss justice as less scientific and will even instruct authors to remove these components. However, by openly accepting papers which include a justice component related to the materials research, journals will not only educate readers about the societal context of researched technologies, but also encourage potential authors to include justice in their own work while acting as an example of how to do so. This prioritization can have a large impact on how academics view materials science.

In this work we put forth a set of solutions to be used as guidelines for academic departments and journals to teach students to be well-rounded scientists who develop technologies to equitably benefit all communities. Implementing these solutions will ultimately help create a workforce that has the tools to address the climate crisis in an effective and thoughtful manner.

9:45 AM BI01.01.04

Team Based Sustainable Nanotechnology Research for Energy Justice in Materials Science and Engineering Christine C. Broadbridge^{1,2}, Thomas Sadowski^{1,2}, Suzanne E. Huminski² and Justin Lipse³; ¹Southern Connecticut State University, United States; ²SCSU Center for Nanotechnology, United States; ³Quantum Biopower, Inc., United States

Sustainable nanotechnology is an interdisciplinary field with potential to catalyze innovative solutions to global issues such as climate change and biodiversity loss in areas ranging from science, technology and environment to economics, education, and society. By introducing sustainable nanotechnology to students at many different levels, potential also exists to engage and educate a diverse STEM literate workforce better equipped to tackle society's most challenging problems. In this talk, a range of activities will be briefly described with focus on methods employing industry-motivated research with important implications for energy justice through technological advancement of sustainable products, and as an educational pathway prioritizing recruitment and training for groups traditionally underrepresented in STEM careers, including women and racial minorities. These activities leverage strong intra- and cross-institutional partnerships to beneficially impact participants at all levels with diverse backgrounds. In particular, the Werth Industry Academic Fellowship (IAF) program at Southern Connecticut State University (SCSU) will be discussed in detail to demonstrate how a tiered approach to mentorship with industry participation can be applied to optimize societal impact, including deployment of clean energy solutions that improve energy justice for groups disproportionately burdened with pollution or climate risk, and, strong minority recruitment and retention in a rigorous undergraduate and Masters level research training program. The core focus of the Werth IAF is team-based interdisciplinary and industry-motivated research through rigorous research experiences, as well as professional development in business and entrepreneurship topics. A fellowship team is composed of individuals with diverse but complementary interests and typically includes a STEM faculty researcher, a School of Business faculty and industry mentor, as well as undergraduate and graduate students (often pre-service teachers in a 7-12 STEM discipline). To date, 38 students have completed the IAF (31 undergraduate students and 7 graduate students), and the 2023 cohort is the largest to date. Half of all IAF fellows are minorities and 37% are female. Program cohorts are small, providing individualized attention, instruction, mentorship and support to IAF fellows to encourage them with sound preparation for their research journeys. SCSU has a Title III designation because of the large number of low-income students who attend. Current fellowship teams are addressing important sustainability questions from a variety of different avenues including renewable or low carbon energy generation, energy storage, carbon remediation. The primary focus of this presentation will be a well-developed multi-tiered SCSU collaborative partnership with Quantum Biopower – a local Connecticut company that is the first in the state and one of a few in the region to specialize in commercial scale anaerobic digestion of food scrap for producing biogas and sustainable landscape products. In addition to processing SCSU's food scrap from dining services, Quantum Biopower has partnered in a variety of sustainable nanotechnology research projects with SCSU since 2016. Using biochar as a through line, the collaborative team prioritizes research on a material that has been identified for its flexible application in many industries, and as one of only a small number of technologies with scalable global carbon sink potential necessary for avoiding the worst impacts of climate change. IAF research at SCSU is exploring biochar in applications ranging from water and nutrient retention in soil to supercapacitors, which has strong potential for Quantum Biopower's future growth as a company.

10:00 AM BREAK

10:30 AM *BI01.01.05

Sustainable Battery Chemistries and Materials for Next-Generation Battery Technologies Arumugam Manthiram; The University of Texas at Austin, United States

The ever-increasing demand for energy and the rapidly escalating environmental concerns have created enormous interest in the development of affordable clean energy technologies. Renewable energies, such as solar and wind, offer an appealing solution, but they are intermittent. A widespread adoption and utilization of renewable energy sources will need an economic and efficient storage of electricity produced from them; storage is currently the bottleneck to utilize renewable energies. Rechargeable batteries are the most viable option to store and utilize the electricity produced from renewable energies. However, a widespread adoption of battery technologies for grid electricity storage as well as for electric vehicles requires optimization of several parameters, such as cost, energy density, power density, cycle life, safety, and environmental impact, all of which are directly linked to severe materials challenges. Among them, cost, sustainability, supply chain issues will be the single dominant factor as we move forward to establish energy justice. This presentation will focus on the development of sustainable next-generation battery chemistries and materials.

The lithium-ion battery technology is currently dominated by layered oxide cathodes with expensive cobalt and nickel and graphite anode, which have supply chain challenges. In essence, cobalt is a problem today, nickel is a problem tomorrow, and lithium could become a problem day after tomorrow. This presentation will center on a path forward to eliminate cobalt first, followed by progressively eliminating mined transition metals, lithium, and finally any mined metal altogether. However, the task is met with fundamental materials science and engineering challenges. This presentation will focus on delineating the intricacies involved with them and the progress made in the following battery chemistries: cobalt-free lithium-ion, cobalt- and nickel-free lithium-ion, lithium-sulfur, sodium-sulfur, and sodium-organic batteries as an illustration to realize a sustainable battery technology future. For example, sodium is plenty in the ocean and sulfur is a byproduct in petrochemical industry, and both of them are mining-free. Specifically, innovative materials design, novel chemical synthesis, advanced materials characterization, prototype device assembly, and an establishment of the structure-property performance relationships will be presented to illustrate the progress.

11:00 AM *BI01.01.06

Advancing Energy Equity Through Distributed Energy Resources (DERs) Bethel Tarekegne; Pacific Northwest National Laboratory, United States

Energy justice and equity examinations uncover the reality that not all customers have the same needs of the energy system. For example: Elderly and disabled populations use energy in different ways and have different vulnerability profiles. Low-income households spend a higher percentage of their income on energy bills, relatively three times higher than affluent households (i.e., 6% of income on energy bills is a high energy burden and 10% is a severe energy burden). There is a clear demand for explicit work on energy equity and stakeholder engagement. More analysis can be done around: differentiating needs & interactions by demographics (age, race, health, rural, deep poverty) and compound, cumulative effects; understanding the relationships between policies and grid futures and the impact on people; designing technologies to be safer, to support well-being, and to include life-cycle implications; and recognizing the procedural limitations of energy system decision-making.

11:30 AM BI01.01.07

Community-Engagement in Clean Energy: 15 Years of Tribal Partnerships in the Pacific Northwest Daniel T. Schwartz; University of Washington, United States

The U.S. Inflation Reduction Act (IRA) and Bipartisan Infrastructure Law (BIL) will mobilize unprecedented capital investments in clean energy technologies that can demonstrate tangible benefits to underserved and overburdened communities. In this era of clean energy development, the most successful scientists and engineers will need the ability to formulate scholarly questions and develop practical strategies that are informed by an understanding that clean energy is a socio-techno-economic grand challenge. Consequently, early in any scientific or technical advance, questions of material supply chains, life-cycle impacts, and the need for authentic community-engagement will be deemed an essential preliminary step toward scaling. Trainees able to balance the social, technical, and economic dimensions of clean energy will be ideally prepared to succeed in the Professional, Scientific, and Technical Services (PSTS) sector of the economy, where materials science and engineering job growth is projected to be more than double the rate of manufacturing employment over the next decade.[1-2]

The Northwest U.S. has a hundred-year legacy of major federal investment in clean energy infrastructure, but is widely acknowledged as a cautionary tale for the consequences of inequitable and unjust energy development.[3] With this as place-based context, the author will discuss lessons learned from 15 years of community-engaged clean energy research and educational activities with Northwest tribal nations supported through NSF IGERT, USDA CAP, and State of Washington funding that has involved students (undergraduate and graduate) and professional staff. Using a variety of bioenergy, wind, and solar-related education, research, and demonstration projects as tangible examples, we will describe a common trajectory our community-engaged clean energy projects have taken, typically starting as "technical assistance" questions that community decision-makers and influencers (such as elders) want addressed by an arms-length third party, and evolving to more scholarly questions. The training elements of community-engaged projects are ideal for PSTS careers, and participation in year-long tribal partnership projects was cited as a primary reason 9 Native American students chose to return to graduate school as part of a NSF IGERT training program led by the speaker. Other research and student outcomes will be documented, as well as professional challenges associated with community-engaged research and education given that this scholarly model remains fairly uncommon in the physical sciences and engineering.

[1] BLS employment projection for materials engineers (2021-2031) <https://data.bls.gov/projections/nationalMatrix?queryParams=17-2131&ioType=o>

[2] BLS employment projection for materials scientists (2021-2031)

<https://data.bls.gov/projections/nationalMatrix?queryParams=19-2032&ioType=o>

[3] L. Ortolano and K.K. Cushing, Grand Coulee Dam 70 years later: What can we learn, *Intl J. Water Res. Dev.*, **18**(3), 373-390 (2002).

SESSION BI01.02: Justice Considerations in Sustainable Energy
Session Chairs: Casey Davis and Michael Toney
Wednesday Morning, November 29, 2023
Hynes, Level 1, Room 111

8:30 AM *BI01.02.01

A Molecular View of Social and Environmental Justice Jeffrey A. Reimer^{1,2}; ¹University of California, Berkeley, United States; ²Lawrence Berkeley National Laboratory, United States

The deposition of human waste carbon into the atmosphere, oceans, and lands is changing the planet. Indeed, the practice of extracting hydrocarbons from the earth and then littering it with artificially produced polymers and plastics not only fails to economically uplift local communities (an environmental justice issue) but also disproportionately impacts communities that are not equipped to handle these consequences (a climate justice issue). The absence of environmental and climate justice represents a legal and governance issue, and is an ethical lapse that affects all of humanity. Additionally, the inability to support underprivileged communities, and the creation of conditions that worsen their disadvantage, is a moral failure. Consequently, there's an increasing demand for the materials research community to conduct comprehensive research that addresses these justice concerns. Specifically, those in influential research roles are urged to ensure their work meaningfully connects to these ethical dilemmas.

Herein I will discuss two research agendas my group is undertaking that aim to link the molecular level to the macroscopic, and the macroscopic to process scale systems that reduce our carbon waste. The first involves a mechanistic exploration of carbon capture by porous materials, such as MOFs and porous polymers. This research is driven by the need to understand carbon capture processes from various carbon dioxide sources and sinks. The second is about designing polymers for systemic circularity, such as polydiketoenamines, which requires an examination of reaction and diffusion processes at molecular, nano-, and meso-scales. In both these cases, we use magnetic resonance spectroscopy and imaging methods. As the author, I consider it my responsibility to ensure such studies are framed within the context of systems and processes capable of delivering meaningful technological solutions.

9:00 AM *BI01.02.02

Electrified Ammonia Synthesis at Ambient Conditions Karthish Manthiram; California Institute of Technology, United States

Chemical synthesis is responsible for significant emissions of carbon dioxide worldwide. These emissions arise not only due to the energy requirements of chemical synthesis, but since hydrocarbon feedstocks can be overoxidized or used as hydrogen sources. Using renewable electricity to drive chemical synthesis may provide a route to overcoming these challenges, enabling synthetic routes which operate at benign conditions and utilize sustainable inputs. We are developing an electrochemical toolkit in which distributed feedstocks, including carbon dioxide, dinitrogen, water, and renewable electricity, can be converted into diverse fuels, chemicals, and materials.

In this presentation, we will share recent advances made in our laboratory on nitrogen fixation to synthesize ammonia at ambient conditions. Specifically, our lab has investigated a continuous lithium-mediated approach to ammonia synthesis and understood the reaction network that controls selectivity. We have developed non-aqueous gas-diffusion electrodes which lead to high rates of ammonia synthesis at ambient conditions. The solid electrolyte interphase is found to be controlling of lithium-mediated nitrogen reduction rates and selectivities, as understood through cryogenic transmission electron microscopy.

9:30 AM BI01.02.03

The Energy Justice of Soft Materials for Photoelectrochemical Hydrogen Generation Casey M. Davis¹, Michael F. Toney¹ and Ann L. Greenaway²; ¹University of Colorado Boulder, United States; ²National Renewable Energy Laboratory, United States

Hydrogen generation has been gaining traction as a form of relatively cheap, safe, and flexible renewable energy as it becomes increasingly important to transition away from fossil fuels. However, the majority of hydrogen is generated using fossil fuels, hindering progress towards a sustainable energy future. To address this challenge, it will be necessary to use renewable energy with economic and non-toxic materials to generate hydrogen. Soft materials such as π -conjugated polymers have shown promise for photoelectrochemical (PEC) hydrogen generation. Although inorganic PEC systems are more developed, organic systems have advantages such as tunability, narrow bandgap, and cost-effective synthesis.

In addition to scientific viability, the implementation of PEC technology requires careful analysis of the relevant social and environmental landscapes. Therefore, this work illustrates the energy justice aspects associated with soft materials for PEC to maximize the technology's success and societal benefits. In the scientific process, end-product impacts are generally not considered during early stages. It is crucial to analyze soft PEC systems at an early technology readiness level to create equitable outcomes as well as develop materials and chemical processes with minimal negative impact. Producing a fossil-free technology does not guarantee positive social and environmental outcomes, and marginalized communities may still experience disproportionate burdens. While it may appear counterintuitive to long-term plan for a technology that is still in the developmental stage, the scientific community has historically been driven by advancing to the next step in the scientific process rather than thoroughly assessing societal needs.

Before the development of technology, it will be crucial to identify key sectors where hydrogen deployment can make a difference, whether that be grid supplementation, cement manufacturing, or shipping. To implement soft PEC systems in the selected sector three tenets of justice must be considered: distributional justice, recognition justice, and procedural justice. Distributional justice involves planning the PEC infrastructure in a way to benefit marginalized communities. Soft materials have an advantage due to the lower impact of resource extraction compared to inorganic systems. Recognition justice requires respecting and valuing all sections of society. Oil and gas workers could be retrained for PEC plants in communities that are economically reliant on fossil fuel generation. Lastly, procedural justice ensures equal consideration of all stakeholders without discrimination. Large-scale transparency and education on incoming infrastructure will address this issue. A series of metrics are applied to understand how soft PEC hydrogen generation will meet these three tenets of justice.

Hydrogen infrastructure is a controversial topic in the renewable energy community, partly because of the grey hydrogen dominating the market. Understanding and thoroughly assessing the implementation of green hydrogen will have significant benefits. Effectively implementing these equity considerations may delay time to full implementation of these technologies but is a necessary step. We argue that having a solid plan ensures that technology aligns with actual needs, promoting long-term social and environmental justice.

SESSION BI01.03: Batteries and Energy Justice
Session Chairs: Emma Kendrick and Nicholas Weadock
Wednesday Afternoon, November 29, 2023
Hynes, Level 1, Room 111

1:30 PM BI01.03.01

Sustainability for Materials Research: A Quebec Strategy and Approach Laura Cacot; University of Montreal, Canada

How can sustainability be integrated into the research culture?

In September 2015, UN member states adopted the Sustainable Development Program known as Agenda 2030. This program defines targets to be reached by 2030 to meet the challenges of the current and future environmental crisis.

The UN's Sustainable Development Goals (SDGs) provide a reference framework for operationalizing sustainable development, including adaptation to climate change, improving global health and reducing social and environmental inequalities. This framework proposes 17 SDGs divided into a number of targets which, taken together, will ensure a more viable future for generations to come.

Universities have a role to play in building a more sustainable future, through knowledge development, education and knowledge transfer on major societal issues. Furthermore, universities can contribute by adopting sustainable approaches throughout the entire research process, from conceptualization to execution.

Our work builds on these concepts by developing tools for more sustainable scientific research, both in terms of the research object and the way research is carried out in the laboratory.

Additionally, our objective is to identify barriers and overlooked areas in research when adopting a sustainable development approach. This works aims to bring researchers together to explore and discuss innovative strategies and best practices for incorporating sustainability into research practices. By recognizing the intrinsic connection between research and sustainability, we can foster interdisciplinary collaboration, enhance knowledge transfer, and accelerate the adoption of sustainable principles across various academic disciplines.

1:45 PM *BI01.03.02

Implementing Societal Considerations and Energy Justice into FECM's Carbon Management R&D Kelli Roemer¹ and Lisa Grogan-McCulloch²; ¹Department of Energy, Office of Fossil

To reach U.S. climate goals of net-zero emissions economy-wide by 2050, the United States will likely have to capture, transport, and permanently sequester significant quantities of carbon dioxide (Larson et al., 2020). In addition, there is growing scientific consensus that carbon capture, utilization, and sequestration (CCUS) and carbon dioxide removal (CDR) will likely play an important role in decarbonization efforts globally (IPCC, 2018). The Department of Energy's (DOE) Office of Fossil Energy and Carbon Management (FECM) envisions enabling the demonstration and ultimately deployment of technologies for carbon management and mitigating challenges of fossil fuel use in a just and sustainable way, with the goal of achieving net-zero greenhouse gas emissions by mid-century (FECM, 2022). Building the clean energy economy will create new infrastructure that holds the potential to drive new regional economic development, technological innovation, and high-wage employment for communities across the United States as we work to make progress on the nation's climate goals. At the same time, it is critical to understand and address the societal considerations and impacts of these projects at local, regional, and global levels. This presentation will share how FECM is implementing the principles of energy and environmental justice throughout the planning, processes, and outcomes of its work in alignment with Executive Orders 14008 and 13985 (Federal Register 2021a, 2021b); share lessons learned from early, two-way community and regional engagement efforts discussing carbon management; and discuss requirements for Community Benefit Plans necessary for FECM funded projects R&D.

References:

Federal Register, 2021a. Tackling the Climate Crisis at Home and Abroad. Retrieved from Federal Register: <https://www.federalregister.gov/documents/2021/02/01/2021-02177/tackling-the-climate-crisis-at-home->

Federal Register, 2021b. Advancing Racial Equity and Support for Underserved Communities Through the Federal Government. Retrieved from Federal Register: <https://www.federalregister.gov/documents/2021/01/25/2021-01753/advancing-racial-equity-and-support->

Fossil Energy and Carbon Management (FECM), 2022. Strategic Vision: The Role of Fossil Energy and Carbon Management in Achieving Net-Zero Greenhouse Gas Emissions. 2022-Strategic-Vision-The-Role-of-Fossil-Energy-and-Carbon-Management-in-Achieving-Net-Zero-Greenhouse-Gas-Emissions_Updated-4.28.22.pdf

Intergovernmental Panel on Climate Change (IPCC), 2018: Summary for Policymakers. In: Global Warming of 1.5°C. An IPCC Special Report on the impacts of global warming of 1.5°C above pre-industrial levels and related global greenhouse gas emission pathways, in the context of strengthening the global response to the threat of climate change, sustainable development, and efforts to eradicate poverty [Masson-Delmotte, V., P. Zhai, H.-O. Pörtner, D. Roberts, J. Skea, P.R. Shukla, A. Pirani, W. Moufouma-Okia, C. Péan, R. Pidcock, S. Connors, J.B.R. Matthews, Y. Chen, X. Zhou, M.I. Gomis, E. Lonnoy, T. Maycock, M. Tignor, and T. Waterfield (eds.)]. Cambridge University Press, Cambridge, UK and New York, NY, USA, pp. 3-24. <https://doi.org/10.1017/9781009157940.001>

Larson, E., Greig, C., Jenkins, J., Mayfield, E., Pascale, A., Zhang, C., Drossman, J., Williams, R., Pacala, S., Socolow, R., Baik, E., Birdsey, R., Duke, R., Jones, R., Haley, B., Leslie, E., Pautstian, K., & Swan, A. (2020, December 15). Net-Zero America: Potential Pathways, Infrastructure, and Impacts, interim report. Princeton, NJ: Princeton University. [https://netzeroamerica.princeton.edu/the-report-National-Academies-of-Sciences,-Engineering,-and-Medicine-\(NASEM\)-2021-Accelerating-Decarbonization-of-the-U.S.-Energy-System](https://netzeroamerica.princeton.edu/the-report-National-Academies-of-Sciences,-Engineering,-and-Medicine-(NASEM)-2021-Accelerating-Decarbonization-of-the-U.S.-Energy-System). Washington, DC: The National Academies Press. <https://doi.org/10.17226/25932>

2:15 PMBREAK

3:15 PM BI01.03.03

Global PV Supply Chains: Costs and Energy Savings, GHG Emission Reductions[Jiel Liu](#) and XiaoShen; Bo-Zhi Digital Labs, China

In the battle against climate change, accelerating clean energy development is crucial. A global supply chain and cooperation in renewable energy technologies are vital for success. However, the increasing trend towards domestic protectionism in the clean energy sector may result in significant cost increases and hinder efforts to tackle climate change. Our study examined the cost savings, energy savings, and greenhouse gas emissions reduction achieved through a globalised solar PV module supply chain compared to a hypothetical scenario where domestic manufacturers supplied an increasing proportion of installed capacities over ten years from 2004 to 2021. We focused on five representative countries: China, the United States, Germany, Japan, and India. Our analysis revealed substantial cumulative savings in these countries, with cost savings totalling US\$181 billion (165-179 billion), energy savings reaching 2.26 EJ-eq (1.99-2.56 EJ-eq), and greenhouse gas emissions avoidance amounting to 105 Mt CO₂-eq (73-145 Mt CO₂-eq). Future projections from 2022 to 2050 under two IEA scenarios indicate continued savings. This analysis highlights a globalised supply chain's significant cost, energy, and emissions benefits. Coordinated policy reforms are needed to facilitate clean energy trade and technology transfer to achieve global environmental goals.

3:30 PM *BI01.03.04

Sustainability in New Battery Technology Developments[Emma Kendrick](#); University of Birmingham, United Kingdom

The definition of sustainability is such that it can mean many things to different people. In this work we discuss the aspects of sustainability which relate to new battery technologies and developments. We examine the impact of materials, energy, and the environment in achieving a comprehensive circular supply chain for battery materials. This includes considering the importance and scarcity of materials, the manufacturing process for both materials and batteries, their lifespan, and the potential for recycling and reusing materials at the end of their life cycle.

Circular Materials choices and supply are influenced mainly currently by cost, however with different minerals and materials being on different global critical materials lists, alternatives may be needed. Lithium, graphite, phosphate, silicon and cobalt are all on the EU and the UK critical materials lists, indicating that there is a supply chain risk and that the materials are of high economic importance. Using the 4 R's of sustainability, reduce, reuse, recover and recycling we can start to reduce our reliance on these materials. In this way sodium-ion batteries are being considered as an alternative, where substitution for lithium, cobalt and graphite for sodium, iron and hard carbon can be achieved. This leads to significantly lower cost materials, however when initial LCA's are performed on these batteries (per kWh) the embedded carbon is significantly higher. Other factors of sustainability must be taken into consideration; recyclability and time in use.

In this work we discuss some of the design for disassembly aspects for sodium-ion and lithium-ion batteries. Recycling routes are discussed and the materials recovery and the reuse cases for these materials. Often the recovery rates are influenced by the design of the cells and the electrodes, and we propose routes for electrode manufacturing, compositions and design considerations to maximise the performance and the recovery rates of those materials.

4:00 PM *BI01.03.05

This Isn't a Simulation: A View from the Common Tangent of Social Justice and Computational Materials Science[Gerald J. Wang](#); Carnegie Mellon University, United States

The fields of *computational materials science* and *social justice* are not -- to use a term more popular in the latter -- heavily intersectional. Nevertheless, in this talk, we will argue that there are numerous opportunities for -- to use a term more popular in the former -- common-tangent constructions between the two. Faced with accelerating global crises that both partially stem from and can be partially solved through materials science, it is clear today that the scientists and engineers of tomorrow must have fluency with both technical and social considerations, including their interrelationships. We highlight two opportunities to engineer a virtuous cycle that simultaneously elevates technical rigor and social-justice awareness, specifically in the context of computational materials science education: (1) identifying physical and mathematical concepts that are value-neutral in the abstract yet have significant justice-related implications in practice (especially in the context of thermodynamics, entropy, and optimization); and (2) deeply integrating the history of science and mathematics to highlight technical contributions from diverse individuals (especially in the context of the history of condensed-matter simulation). We emphasize throughout that technical rigor is a *sine qua non* for social justice, and that both are mutually enriching for the other.

4:30 PM *BI01.03.06

Lithium-Ion Batteries for Electric Vehicles—Impacts Across the Entire Life Cycle[Linda L. Gaines](#); Argonne National Laboratory, United States

Materials for lithium-ion batteries (LIBs) come from across the globe to the United States, leaving a variety of impacts along the way, both positive and negative, ranging from opportunities for economic growth to possible habitat destruction to disruption of sacred ground to emissions that must be mitigated. This presentation will track the batteries through their entire lifecycle from materials in the ground through transportation, manufacture, and use, via possible repurposing, all the way to recycling to characterize energy use and emissions, and to identify the inequities that unavoidably arise in any supply chain.

5:00 PM BI01.03.07

Metal Hydride Reclamation from Ni-MH batteries for Small-Scale Power Generation Nicholas J. Weadock; University of Colorado at Boulder, United States

Electrification of rural communities and technologically- or economically-developing countries can be limited by the pace of infrastructure installation. Point-of-use power generation from hydrogen fuel cells offers a scalable solution provided the design is low-cost, safe, and robust. A major source of cost and reliability issues is the hydrogen storage technology itself, with the current state-of-the-art being high-pressure gas storage in composite tanks [1,2]. The balance-of-plant components for compression, filling, temperature and pressure regulation, and safety only add to the cost and complexity. Hydrogen storage in intermetallic metal hydrides (MH), a class of materials which store hydrogen interstitially in a metal alloy, circumvents the issues related to high pressures by targeting a hydrogen release pressure equivalent to fuel-cell operational requirements. MH storage for fuel cell generation has been explored and initial reports suggest a reduction in cost and safety is possible with the correct selection of the MH alloy [1–3]. Leading candidates for MH storage are LaNi₅-based AB₅ alloys which have favorable kinetics, cycle life, and hydrogen release pressures [4,5]. However, the monetary and environmental costs of rare-earth mining, and competition for other applications of rare-earth metals were not considered in previous analyses.

Here, I present an alternative source for AB₅ MH alloys – discarded hybrid electric vehicle (HEV) batteries. HEV like the Toyota Prius utilize the Ni-MH battery chemistry with AB₅ alloys in a cathode-limited design. Prius batteries alone contain up to 8 million kg of AB₅ MH, representing 3850 MWh of power generation from fuel cells [6]. I will demonstrate that AB₅ MH recovered from end-of-life Toyota Prius battery modules readily absorb and desorb hydrogen and retain the AB₅ crystal structure with limited La(OH)₃ corrosion product. Furthermore, I will present structural, spectroscopic, and hydrogen capacity and release characterization of these AB₅ MHs and assess the feasibility for re-use as gas-phase hydrogen storage materials. Finally, I will contextualize the approach proposed here within the established field of rare-earth recovery from e-waste.

[1] K. Kubo, Y. Kawaharazaki, and H. Itoh, *International Journal of Hydrogen Energy* **42**, 22475 (2017).

[2] G. Han, Y. Kwon, J. B. Kim, S. Lee, J. Bae, E. Cho, B. J. Lee, S. Cho, and J. Park, *Applied Energy* **259**, 114175 (2020).

[3] E. MacA. Gray, C. J. Webb, J. Andrews, B. Shabani, P. J. Tsai, and S. L. I. Chan, *International Journal of Hydrogen Energy* **36**, 654 (2011).

[4] K. Beard, *Linden's Handbook of Batteries*, 5th ed., Vol. Section D: Nickel-Metal Hydride (McGraw-Hill Education, 2019).

[5] K. Young and J. Nei, *Materials* **6**, 4574 (2013).

[6] E. L. Schneider, W. Kindlein, S. Souza, and C. F. Malfatti, *Journal of Power Sources* **189**, 1264 (2009).

SESSION BI01.04: Poster Session

Session Chairs: Ahmet Alatas, Katherine Anderson, Lauren Marbella and Michael Toney

Wednesday Afternoon, November 29, 2023

Hynes, Level 1, Hall A

8:00 PM BI01.04.01

Approaches of Centering Indigenous Concerns in The Context of Material Science and The Environment Gregor Kos¹, Cole Delisle², Wassim Nijaoui¹, Yan Liu¹, Julie Delisle², Patrick Ragaz², Ingo Salzmänn¹ and Tanja Tajmel¹; ¹Concordia University, Canada; ²Kahnawà:ke Environment Protection Office (KEPO), Canada

Indigenous communities are often disproportionately affected by environmental pollution, either because of nearby resource extraction in remote areas or due to industrial and transport emissions in urban areas, amongst other reasons. The latter is the case for the Mohawk community of Kahnawà:ke, located on the South Shore of Tiohtiá:ke/Montreal, where major sources of air pollution such as car/ship/train traffic arteries converge towards a bridge across the St. Lawrence River and the St. Lawrence Seaway passes very close to the centre of daily activities. Furthermore, major industrial installations are located just across the limits of the community with little information about local emissions. While the community has long identified these sources of pollution and potential impact on health, little data has been collected so far due to a lack of suitable monitoring systems. Together with community members, we as scholars working in fields as different as Material Science, First Peoples Studies, Science Education, Decolonizing Curriculum and Pedagogy, Environmental Science, and Science and Technology Studies, came together to explore how these issues which the community of Kahnawà:ke is experiencing, can be addressed and how science and technologies can be employed to support the community's concerns.

The establishment of a Community Science Low-Cost Air Quality Monitoring Network (AQMN Kahnawà:ke) - (together with a small number of commercial sensors -) addresses several goals formulated by the Kahnawà:ke Environment Protection Office (KEPO) and Concordia University in the framework of the "Decolonizing Light" project. Funded by the New Frontiers in Research Fund (NFRF) of the Government of Canada, the Decolonizing Light project explores different ways to contribute to anti-colonial scientific practices and to center Indigenous issues and concerns. The theme of the project exemplarily focuses on light (rather than optics) because light is ubiquitous in every society, language, and culture. In everyday life, light is a key element that defines familiar aspects like color and warmth. In physics, light is exploited as the primary carrier of information about nature (e.g., in astronomy), used as the primary probe for the fundamental properties of matter (e.g., in spectroscopy). Therefore, "decolonizing light" can be seen as a metaphor for anti-colonial science and technological development that reflects on the broader social impact as well as on the politics of science and technology.

The goals of AQMN Kahnawà:ke include (i) making the monitoring of hyper-local pollutant concentrations available to the community, (ii) installing a representation of regional air quality due to a dense network of stations (much denser than government or municipality operated networks) to represent regional air quality, (iii) studying the potential to study the impact of specific installations and infrastructure, and, (iv) democratizing scientific expertise by raising awareness and scientific knowledge about air quality and its measurement within the community at large, rather than among experts alone.

To date, fourteen air quality monitors have been built by community members during workshops held in Kahnawà:ke in 2022 and 2023. Locations are chosen across the community following local knowledge available across the community. This project provides tools for data management, processing, and visualisation to make concentrations and pollution maps available for the benefit of all community members and the particular air quality studies conducted by KEPO. Preliminary results, lessons learned, and conclusions for the broader material science community will be presented.

SYMPOSIUM CH01

Advanced Characterization Methods of Energy Material Applications
November 27 - December 6, 2023

Symposium Organizers

Liam Collins, Oak Ridge National Laboratory
Rajiv Giridharagopal, University of Washington
Philippe Leclere, University of Mons
Thuc-Quyen Nguyen, University of California, Santa Barbara

Symposium Support

Silver
Digital Surf

* Invited Paper
+ JMR Distinguished Invited Speaker

SESSION CH01.01: Photovoltaics I
Session Chairs: Rajiv Giridharagopal and Philippe Leclere
Monday Morning, November 27, 2023
Sheraton, Third Floor, Commonwealth

10:30 AM *CH01.01.01

Multimodal Probes Nanoscale Structure-Function Relationships—From Halide Perovskite Photovoltaics to Organic Neuromorphic Materials David S. Ginger; University of Washington, United States

Establishing structure-function relationships is a key challenge for new semiconductor materials ranging from the halide perovskites being commercialized for thin film photovoltaics to organic semiconductors being explored for applications ranging from energy storage to neuromorphic computing. For example, in both families of materials, mixed ionic/electronic conduction takes place. This mixed conduction is often desirable in organic semiconductor films in the case of bioelectronics or neuromorphic computing. However, ionic motion is often deleterious to the performance and stability of materials like halide perovskite semiconductors. We describe applications of multimodal microscopy -- with a particular emphasis on combining scanning probes with optical and electron microscopy -- to understand the correlations between local microstructure, defect densities, conductivity, and ionic motion in these materials. The results point the way to reduced halide vacancy concentrations and improved the stability of halide perovskites, while suggesting new ways for increasing the performance of organic mixed ionic/electronic conductors such as redox active conjugated polymers.

11:00 AM *CH01.01.02

Time-Resolved KPFM in UHV Benjamin Grevin; CNRS, France

Kelvin Probe Microscopy (KPFM) is a well-known variant of AFM that allows probing the electrostatic landscape on the surface of a sample at the nanoscale by measuring the contact potential difference. Since the early 1990s, various approaches have been implemented to improve the performance of KPFM in terms of spatial, potentiometric and temporal resolution. Several research teams continue to work in this direction, and KPFM is still an evolving technique in many respects. In particular, the development of KPFM-based approaches specifically designed to study photogeneration mechanisms and nanoscale charge dynamics in photovoltaic and optoelectronic materials is a very active research area. Over the past decade, several powerful approaches for time-resolved surface photovoltage measurements have been developed, thanks to the efforts of an ever-growing community of researchers working with AFM setups operated under ambient (or neutral gas) conditions. In contrast, time-resolved KPFM implementations on UHV non-contact AFMs remain confidential. In this communication we will show that the "nc-AFM under UHV community" can learn a lot from the experiences of the "ambient AFM community". First, we will show how a data-cube spectroscopic variant of the pump-probe KPFM (pp-KPFM) scheme originally proposed by Murawski et al. [1] can be implemented on an nc-AFM. This implementation allows mapping 2D - truly quantitative - time-resolved images of the SPV. An interesting alternative for time-resolved SPV measurements is the analysis of the intermodulation products between the mechanical oscillation of the cantilever and the photogenerated surface potential [2]. The translation of this promising technique from ambient conditions, where it has been well established, to ultra-high vacuum poses significant challenges due to the enhanced quality factors [3]. We will show how this issue can be overcome and that time-resolved SPV images - consistent with the output of pp-KPFM data - can be obtained by intermodulation spectroscopy with an nc-AFM. Pros and cons of both approaches are discussed through a series of examples on organic, inorganic and hybrid photoactive materials. In particular, it will be shown that beyond the ability to probe the SPV dynamics, these new approaches allow revealing phenomena that would remain hidden to conventional SPV imaging. Finally, we will also show how these developments offer real prospects for ultimate resolution photo-potential imaging.

[1] Murawski J et al. Pump-probe Kelvin-probe force microscopy: Principle of operation and resolution limits, *J. Appl. Phys.* **118** 154302, **2015**.

[2] Borgani R and Haviland D B Intermodulation spectroscopy as an alternative to pump-probe for the measurement of fast dynamics at the nanometer scale *Rev. Sci. Instr.* **90** 013705, **2019**.

[3] A. Mascaro et al. Review of time-resolved non-contact electrostatic force microscopy techniques with applications to ionic transport measurements *Beilstein J. Nanotechnol.* **10** 617, **2019**.

11:30 AM CH01.01.03

Probing The Interfacial Energetics in Organic Semiconductor Blends for Photovoltaics Anirudh Sharma¹, Jules Bertrand¹, Jianhua Han², Julien Gorenflot¹, Frederic Laquai¹ and Derya Baran¹; ¹King Abdullah University of Science & Technology, Saudi Arabia; ²University of Wuerzburg, Saudi Arabia

The energetics of materials play a critical role in charge transfer at the donor (D) - acceptor (A) interface in organic photovoltaics (OPVs),^[1] yet a clear correlation between material energetics and key device parameters is missing. This is primarily because of a lack of criteria for choosing the most suitable method to determine the ionization energy (IE) and electron affinity (EA) of solar cell materials that could precisely predict the energy level alignment at the D/A interfaces. Consequently, the development of new high-performing donor and non-fullerene acceptor materials has led to contradictory claims about the role of energetic offsets at the D-A interface. This makes it difficult to establish design rules for the development of future materials. In this work, we systematically investigate the frontier molecular orbital energies of a library of organic semiconductors and their molecularly mixed blends via different methods; in particular, low-energy inverse photoelectron spectroscopy (LE-IPES), which is a relatively novel and non-destructive technique that enables the direct determination of EA of organic semiconductors with high precision. By characterizing and fabricating thin films and devices based on over 12 different D/A blends, we demonstrate the significant differences which have been an ongoing debate in the field for energetic losses and device performances.^[2] We show that the IE and EA values measured using ultraviolet photoelectron spectroscopy (UPS) and LE-IPES are the most relevant in understanding the charge generation mechanism in solar cells. We further demonstrate how the energy levels of organic semiconductors evolve when blended with energetically dissimilar materials,^[3] and the impact of morphology and phase segregation on the resultant energetics. Probing a range of small molecule - small molecule and polymer: small molecule D/A blends, we show that the photovoltaic gap E_{pv} ($IE_{donor} - EA_{acceptor}$)

measured from neat materials can be insufficient in some cases, for establishing material-property relationships in solar cells. By controlling the D/A ratio in molecular blend films, we probe the changes induced in E_{pv} of D/A blends as a result of intermixing, intermolecular and electrostatic interactions between the D/A materials. We rationalize these findings to the resultant photovoltaic parameters and voltage losses in OPVs.

Lastly, from OPVs based on six different D-A blends having systematically varying IE -offsets (ΔIE), we convincingly demonstrate that ΔIE plays a crucial role in charge generation. In contrast to earlier works, we show that a vanishing ΔIE is detrimental to device performance.

Overall, these findings establish a solid base for reliably evaluating material energetics and interpreting property-performance relationships in solution-processed organic solar cells.

- [1] S. Karuthedath, J. Gorenflot, Y. Firdaus, N. Chaturvedi, C. S. P. De Castro, G. T. Harrison, J. I. Khan, A. Markina, A. H. Balawi, T. A. D. Peña, W. Liu, R.-Z. Liang, A. Sharma, S. H. K. Paleti, W. Zhang, Y. Lin, E. Alarousu, D. H. Anjum, P. M. Beaujuge, S. De Wolf, I. McCulloch, T. D. Anthopoulos, D. Baran, D. Andrienko, F. Laquai, *Nature Materials* **2021**, 20, 378.
[2] J. Bertrandie, J. Han, C. De Castro, E. Yengel, J. Gorenflot, T. Anthopoulos, F. Laquai, A. Sharma, D. Baran, *Advanced Materials* **2022**, 2202575.
[3] X.e. Li, Q. Zhang, J. Yu, Y. Xu, R. Zhang, C. Wang, H. Zhang, S. Fabiano, X. Liu, J. Hou, F. Gao, M. Fahlman, *Nature Communications*, **2022**, 13, 2046.

11:45 AM CH01.01.04

Cascading Exciton Management for Efficient Organic Photovoltaic Cells YuanLi, ZhaoyunJin and GuodanWei; Tsinghua-Berkeley Shenzhen Institute, China

Compared with non-fullerene acceptor (NFA), which has the advantages of high crystallinity and exciton diffusion coefficient, the polymer donors are limited by large Stokes shift and energy disorder, showing a lower exciton diffusion distance and higher non-radiative energy loss which limit their application in organic solar cells (OSCs). Herein, we reported a simple reverse-sensitization strategy and an organic small molecule thermally activated delayed fluorescence (TADF) material (BPhA-QAO) was designed and synthesized, which as solid additives was introduced into the widely studied PM6:BTP-4F based OSCs to enable a significant efficiency increase from 16.3% to 18.2%. Ultrafast optic and spectroscopic studies reveal that BPhA-QAO can transfer its long-lifetime singlet excitons to the polymer donor through energy transfer to ensure adequate exciton lifetime to expand its diffusion distance, and achieve better exciton dissociation efficiency. Morphological studies show that BPhA-QAO promotes the formation of more J-type aggregation for PM6, while inhibiting the stacking behavior of BTP-4F, regulating the degree of phase separation, and forming smaller domain sizes. Conductive AFM (C-AFM) shows that more thorough mixing of donor/acceptor improves the efficiency of exciton dissociation and charge transfer. This work demonstrates that the introduction of small molecule TADF materials based on the reverse-sensitization strategy is an effective method to achieve highly efficient organic solar cells.

SESSION CH01.02: Electrodes I

Session Chairs: Rajiv Giridharagopal and Michael Toney

Monday Afternoon, November 27, 2023

Sheraton, Third Floor, Commonwealth

1:30 PM CH01.02.01

Interfacial Water and Ionic Liquids on Electrode Surfaces with Angstrom Resolution DianaMendez Arvelo and RicardoGarcia; ICMM-CSIC, Spain

Solid-liquid interfaces play a key role in several disciplines and applications, including electrochemical conversion and storage. The understanding at the molecular scale of the electrical double layer is critical in many applications¹. Three dimensional AFM (3D AFM) is an advanced Atomic Force Microscopy technique that allows imaging in the angstrom range the structuring of liquids next to a solid surface^{2,3}. Here, 3D AFM was applied to study the interaction of liquid water and some ionic liquids on graphite surfaces. We have imaged in real-time the evolution of graphite-water interfaces. We show a transition from hydration layers separated by 0.3 nm (similar to van der Waals diameter of a water molecule) to hydrocarbon layers characterized by distances of 0.45 nm. A molecular dynamics simulations model explains the process³. The 3D AFM was also applied to study the structure of the electrical double layer of ionic liquids on graphite when applying an external voltage to the surface, which changes the organization of the liquid molecules.

- [1] Simon, P.; Gogotsi, Y. *Nat. Mater.* **19**, 1151–1163 (2020)
[2] T. Fukuma, R. Garcia, *ACS Nano* **12**, 11785–11797(2018)
[2] M. R. Uhlig, D. Martin-Jimenez, R. Garcia, *Nat. Commun.* **10**, 2606 (2019)
[3] Arvelo, D. M.; Uhlig, M. R.; Comer, J.; Garcia, R. *Nanoscale* **14**, 14178–14184 (2022)

1:45 PM CH01.02.02

Electrochemical Performance of Mo Doped LiNiO₂ Cathodes for Next Generation LIBs MisbahMumtaz, Narayan SimritKaur and SerenaCussen; The University of Sheffield, United Kingdom

At present the choice for cathodes in electric vehicles (EVs) due to high power and energy density are $\text{LiNi}_x\text{Co}_y\text{Al}_{1-x-y}\text{O}_2$ (NCA, $x > 0.8$) and $\text{LiNi}_x\text{Mn}_y\text{Co}_{1-x-y}\text{O}_2$ (NMC, $x \geq 0.5$). Cobalt poses problems to these cathode chemistries with regards to its high price, environmental damage during its mining, and ethical concerns during its acquisition. To overcome this, research has led to nickel-rich cathodes to maximise theoretical capacity while decreasing the reliance on cobalt. However, Ni-rich cathodes have problems practically achieving this increased capacity of (200–220) mAh g^{-1} due to the occurrence of degradation mechanisms that hinder cycling stability, for example the formation and propagation of microcracks in the secondary particles during galvanostatic cycling. One method of combatting the electrochemical cycling instability in the cathodes is doping, which tailors the elemental composition of the transition metal material to stabilise the layered structure. Molybdenum is reported to effectively enhance the cycling stability of the lithium nickel oxide (LiNiO_2 , LNO) structure. A solid-state approach was used to synthesise Mo-doped LiNiO_2 compositions by milling lithium hydroxide monohydrate, nickel hydroxide and molybdenum oxide and calcining the material in an oxygen-rich atmosphere. The $\text{Ni}(\text{OH})_2$ precursor was synthesized using CSTR via co-precipitation method. The X-ray diffraction pattern collected between (10° to 90°) revealed that all powders are well crystallised and single phase with no additional peaks. All the powders belong to R3m space group. At 003 hkl, peak broadening phenomenon is observed, which shows increased Mo content causes broadening. This feature can be correlated to the presence of micro strain due to Li/Ni cation mixing. The X-Ray analysis of the powders revealed a degree of off stoichiometry due to variation of (I_{003}/I_{104}) peak intensity. As a result of doping the lattice parameters underwent changes (expansion/contraction) as depicted by XRD and confirmed by Topas refinement. Scanning electron microscopic (SEM) images depicted that growth of the primary particles is affected by the Mo doping. As there is a massive difference in particles size of LNO and Mo-1% doped LNO. Mo cause increased anisotropy by modifying the surface energy leading to a superior growth direction. The SEM images verify the doping process and show a change in microstructure by forming smaller primary particles. SEM images revealed the formation of pore free particles with central equiaxed in shape particles where quasi-spherical secondary construction is maintained. The electrochemical performance of the LNO and Mo doped LNO (1 and 2%) was characterized at (3.0 - 4.3) V using a 2032 coin-type half-cell with a Li metal anode. The electrochemical data revealed 251.7 mAh g^{-1} first charge capacity compared to 207.6 mAh g^{-1} for LNO. Mo doped cathodes revealed 90% better retention capacity after the first 50 cycles. Mo-doped cathodes have cycled noticeably better than LNO. The kinetic hindrance peak below 3.6 V is an additional redox couple that is only present in LNO. This variation in the lattice due to doping is beneficial for the electrochemical performance helping stabilise the lattice. It is observed that Mo doped compositions exhibited less polarization as compared to LNO in dQ/dV vs. Voltage plots. This feature assisted in smooth transition of H2 to H3 phase during the electrochemical cycling process. The proposed Mo (1 and 2%) doped compositions have delivered superior energy density and stable cycling ability unlike conventional cathodes. The long cycling of Mo doped 1% for 500 cycles shows improved performance against microcracks in the cathode.

References

C. Geng, D. Rathore, D. Heino, N. Zhang, I. Hamam, N. Zaker, G.A. Botton, R. Omessi, N. Phattharasupakun, T. Bond, C. Yang, J. R. Dahn, *Adv. Energy Mater.* 2022, 12, 2103067.

2:00 PM CH01.02.03

Structure-Performance Relationships in Energy Conversion Applications: Multi-Stage Data Quantification Method for Comprehensive Surface Analysis of Large-Scale Anode Electrodes VineethaVinayakumar^{1,2}, AdarshJain¹ and DorisSegets^{1,2}; ¹Institute for Energy and Materials Processes-Particle Science and Technology (EMPI-PST), University of Duisburg-Essen (UDE), Germany; ²Center for Nanointegration Duisburg-Essen (CENIDE), University of Duisburg-Essen (UDE), Germany

Efficient operation of energy conversion applications relies on the optimization of anode electrodes. Improving anode performance and efficiency involves optimizing their fabrication process (1). The surface microstructure of anodes plays a crucial role in their functionality, necessitating precise characterization (2). Atomic force microscopy (AFM) has proven to be a powerful technique for examining the nanoscale microstructure of anodes. However, AFM has limitations when investigating large electrode areas, posing challenges in evaluating the surface microstructure of large-scale electrodes.

In this study, we developed a multi-stage data quantification method to overcome AFM's limitations and measure large electrode areas. We validated our approach by testing anodes fabricated under various spray coating process conditions. Our method effectively provides valuable information on homogeneity, surface smoothness, and the presence of cracks or defects, enabling an overall assessment of electrode quality. Additionally, the combination of statistical analysis and matrix-based analysis in our approach demonstrates its potential to benefit material scientists and extend its application to analyze the micro/nanostructure of other materials in various applications, providing new insights for optimization. Integrating surface analysis measurements with electrochemical analysis is a crucial step in determining overall anode quality. The findings obtained through our multi-stage data quantification method using AFM can be directly correlated with electrochemical analysis to gain a comprehensive understanding of the anode's performance and establish structure-performance relationships. By combining these techniques, we can understand the relationship between surface morphology and the anode's electrochemical properties, activity, and cycling stability. This connection between surface analysis and electrochemical analysis yields crucial insights into anode performance and ultimately advances the development of energy conversion technologies.

References

- (1) David, M., C. Ocampo-Martínez, and R. Sánchez-Peña, *Advances in alkaline water electrolyzers: A review*. Journal of Energy Storage, 2019. **23**: p. 392-403.
- (2) Siegmund, D., et al., *Crossing the valley of death: from fundamental to applied research in electrolysis*. JACS Au, 2021. **1**(5): p. 527-535.

2:15 PMBREAK

2:45 PM CH01.02.04

Revealing the Bonding Nature and Electronic Structure of Early Transition Metal Dihydrides Anna Regoutz¹, Curran Kalha¹, Laura Ratcliff², Gorgio Colombi³, Christoph Schlueter⁴, Bernard Dam³, Andrei Gloskovskii⁴, Tien-Lin Lee⁵, Pardeep Thakur⁵, Prajna Bhatt¹, Yujiang Zhu¹, Juerg Osterwalder⁶, Francesco Offi⁷ and Giancarlo Panaccione⁸; ¹University College London, United Kingdom; ²University of Bristol, United Kingdom; ³Delft University of Technology, Netherlands; ⁴DESY, Germany; ⁵Diamond Light Source, United Kingdom; ⁶Universitaet Zuerich, Switzerland; ⁷Universita di Roma, Italy; ⁸IOM-CNR, Italy

Hydrogen as a fuel plays a crucial role in driving the transition to net zero greenhouse gas emissions. To realize its potential, obtaining a means of efficient storage is paramount. One solution is using metal hydrides, owing to their good thermodynamical absorption properties and effective hydrogen storage. Although metal hydrides appear simple compared to many other energy materials, understanding the electronic structure and chemical environment of hydrogen within them remains a key challenge.

This work presents a new analytical pathway to explore these aspects in technologically relevant systems using Hard X-ray Photoelectron Spectroscopy (HAXPES) on thin films of two prototypical metal dihydrides: $\text{YH}_{2-\delta}$ and $\text{TiH}_{2-\delta}$. By taking advantage of the tunability of synchrotron radiation, a non-destructive depth profile of the chemical states is obtained using core level spectra. Combining experimental valence band spectra collected at varying photon energies with theoretical insights from density functional theory (DFT) calculations, a description of the bonding nature and the role of d versus sp contributions to states near the Fermi energy are provided. Moreover, a reliable determination of the enthalpy of formation is proposed by using experimental values of the energy position of metal s band features close to the Fermi energy in the HAXPES valence band spectra.

3:00 PM CH01.02.05

Troubleshooting CNT Bundling using the Electrospray Method to Achieve Thick Electrodes Ilgyu Kim and Ji-Won Jung; University of Ulsan, Korea (the Republic of)

CNT, a nanomaterial with a 1D structure providing efficient electron transport, is well known as an excellent electron-conducting material and a key element for realizing thick electrodes. However, due to its high aspect ratio, there is significant Van der Waals force present; therefore, when used at a certain level or higher, it aggregates, which causes performance degradation, limiting its use.

In this work, we solve the bundling problem by applying a feasible electrospray method. This approach achieves a $\text{LiFePO}_4/\text{CNT}$ composite with uniform morphology, even with high CNT content, and is confirmed with Scanning Electron Microscopy (SEM) and Transmission Electron Microscopy (TEM) analysis. In addition, we found out that it shows enhanced capacity retention and longer battery life compared to the conventional mixing-only method.

SESSION CH01.03: Energy Harvesting I
Session Chairs: Liam Collins and Georg Gramse
Monday Afternoon, November 27, 2023
Sheraton, Third Floor, Commonwealth

3:30 PM *CH01.03.01

Improved Sensitivity of Printed Piezoelectric Sensor Arrays for Large Area Ballistocardiography Peter Zalar, Marieke Burghoorn, Joost Fijn, Lars Rikken, Peter Rensing, Jeroen van den Brand, Dagode Leeuw and Edsger Smits; Holst Centre / TNO, Netherlands

Holst Centre is an applied research institute specializing in the development of flexible and thin electronics through industrially relevant fabrication methods. Our mission over the past two decades has been to drive technological advancements that enable the industrialization of printed electronics systems, transforming future concepts into tangible realities.

Ballistocardiography (BCG) is a non-invasive technique that examines the heart's activity by measuring the ballistic forces generated during each heartbeat, eliminating the need for on-skin sensors, unlike electrocardiography (ECG). This unique characteristic makes it an unobtrusive measurement method.

To achieve sensors with optimal sensitivity, we have successfully demonstrated a universal method for enhancing effective transverse charge constants. Our methodology has been validated using a printable piezoelectric polymer called poly(vinylidene fluoride-co-trifluoroethylene) (P(VDF-TrFE)). Through our research, we have shown that discrete sensors can accurately detect displacements of less than 1 μm , dynamic forces of approximately mN, and accelerations of around 1 mm/s^2 , precisely meeting the requirements for high-quality BCG measurements.

By employing printable sensors, we have scaled up our demonstration to a "human-sized" prototype measuring 60 x 90 cm, equipped with 255 piezoelectric sensors. This enabled us to measure spatially resolved BCG measurements of an individual with exceptional quality. The heart rate obtained from our measurements has been corroborated optically using photoplethysmography (PPG). The universality of our approach allows for the creation of increasingly sensitive piezoelectric sensor architectures, crucial not only in healthcare but also in various sensing and actuating applications.

4:00 PM *CH01.03.02

Diffuse Scattering as a Probe of Static and Dynamic Local Structure Michael F. Toney; University of Colorado Boulder, United States

Local atomic structure often differs from the global average structure as measured with diffraction and yet the local structure has a profound impact on properties. This structure-function relationship applies in many materials classes, ranging from organics to Li-ion battery cathodes to perovskites. Accurately characterizing this local structure has proven challenging but recent advances in diffuse scattering ("between" Bragg peaks) has enabled local structure determination.

In this talk, I will discuss the importance of local structure and how this can be quantified and will demonstrate this for organic-inorganic hybrid halide perovskites [1,2]. These materials are a recently re-invigorated class of semiconductor that have demonstrated very high efficiencies for solar cells after just over a decade of research. While the importance of lattice dynamics and dynamical (dis)order has been recognized in these materials, their nature is only poorly known and understood. We used X-ray and neutron diffuse scattering coupled with molecular dynamics to quantify the nature, size, and time scale associated with dynamical local order in $\text{CH}_3\text{NH}_3\text{PbI}_3$ and $\text{CH}_3\text{NH}_3\text{PbBr}_3$ perovskites. We observe that the nominally cubic perovskite consists of dynamical, two-dimensional sheets of lower symmetry tetragonal regions of about 3 nm diameter with several picosecond lifetimes. The implications on halide perovskite properties will be discussed.

[1] NJ Weadock et al., *Joule* **7**, 5, 1051-1066 (2023)

[2] DM Ladd, unpublished.

4:30 PM CH01.03.03

Energy Harvesting at Solid/Solid and Solid/Liquid Interfaces: Decoupling Charge Ronald Leon¹, Shuaijia Chen¹, Peter C. Sherrell^{2,1}, Joseph J. Berry¹ and Amanda Ellis¹; ¹The University of

Smart wearable energy harvesting devices can convert friction or mechanical energy (i.e., applied stress) into electric energy and are hence, highly sought after for a variety of applications such as: smart watches, smart gloves, smart shoes, and other electronic devices. However, reported piezoelectric outputs in literature are often convoluted with friction induced contact electrification. In this talk we use a simple signal processing method to analyse different contact and motion induced voltage signals, probing the origin of charge from piezoelectric fluoropolymers and various triboelectric polymers. We have developed a method to identify the source of generated charge by taking time domain data, traditionally used by researchers in the field of contact electrification and processed this data for the first time into the frequency domain (via a Fast Fourier Transform (FFT)). The bandwidth (Hz) of the signal varies based on the motion of charge within solid | solid interfaces. The differences in bandwidth of the FFT signal is intrinsically linked to the type of charge being measured. This type of detail cannot be observed in the time domain data, and we have used this to decouple piezoelectric responses from contact electrification and electrostatic charge induction. We propose simple steps to analyze piezoelectric measurements by placing more emphasis on data extraction and data analysis with a clear set of parameters, that will promote sustainable electrical characterization practices of future piezoelectric and hybrid triboelectric energy harvesters.

We also apply this method to liquid | solid interfaces to determine the mechanisms of charge generation at liquid and solid interfaces and apply this knowledge to control and precisely utilize charge. Data collection was performed using a combination of dynamic contact angle measurements with correlated voltage and charge measurements. Correlated electrical measurements to contact angle enabled effects such as contact-line pinning on charge and voltage outputs to be elucidated.

4:45 PM CH01.03.04

High-Efficiency a Transpiration-Driven Electrokinetic Power Generator based on Two-Faced Hydrophilic/Hydrophobic Carbon Nanofibers Utilizing Water TranspirationHo-JinLee¹, Tae GwangYun² and Ji-WonJung¹; ¹University of Ulsan, Korea (the Republic of); ²Ajou University, Korea (the Republic of)

Hydro-electric technology, which uses minimal amounts of water to generate electricity, is receiving substantial attention due to its simplicity and environmental friendliness. However, the low energy density of such technology constrains its practical applications. In this study, we present the application of a transpiration-driven electrokinetic power generator (TEPG) based on nitric acid-treated carbon nanofibers (N-CNFs). These N-CNFs possess both hydrophilic and hydrophobic properties, which enables high energy efficiency. A polyacrylonitrile (PAN) solution was electrospun and underwent a carbonization process to create carbon nanofibers (CNFs). Half of the hydrophobic CNFs were then treated with nitric acid to convert them into hydrophilic, while the other half retained their hydrophobic properties. The TEPG system, equipped with these dual-featured CNFs, utilizes the capillary action of water on the hydrophilic carbon surfaces. This interaction facilitates the absorption of water, and the resulting electrical double layer at the solid (CNF)/liquid (water) interface provokes the accumulation of protons (H⁺). The existence of these two distinct regions – the proton-driven electrical double layer and hydrophobic CNFs – creates a potential difference between the wet and dry regions, thereby producing the driving force for energy generation. Consequently, the N-CNF-TEPG is a self-sufficient energy generator that does not require continuous work input due to its inherent transpiration action.

SESSION CH01.04: Electrochemistry
Session Chairs: Liam Collins and Peter Zalar
Tuesday Morning, November 28, 2023
Sheraton, Third Floor, Commonwealth

8:00 AM *CH01.04.01

Atto-Ampere NanoelectrochemistryGeorgGramse; Johannes Kepler University, Austria

We recently introduced a new technique for versatile nano-electrochemical measurements at the atto-Ampere level (3 orders of magnitude below the previous state of the art) based on an up-conversion of the electrochemical current to GHz frequencies.¹ For example, this allowed us to image the electrochemical current of non-moving redox molecules at the nanoscale for the first time.

We also showed that the potential of this approach is even more prosperous, since it can be employed for quantitative mapping of the nanoscale impedance spectra as a function of electrochemical potential (CV) and frequency (EIS). We developed a closed framework that allows for a rigorous analysis and quantification of the measured complex impedance signal covering a wide frequency domain (DC to GHz).² A global understanding of the nano-electrochemistry at the nanoscale on these systems is now possible, including the diffusive double layer effects.

Interestingly, we stress that an important feature is that DC and GHz excitations have a different impact on the ions at the solid electrolyte interface (SEI), which provides additional degrees of freedom to understand the nano electrochemical processes. Our work was demonstrated on a model system (ferrocene undecane thiol) that has greatly interested electrochemists and molecular electronics communities^{1,2}. Finally we will show exciting new applications on more complex 2-dimensional material systems for energy applications.

¹ S. Grall et al, Atto-Ampere Nanoelectrochemistry, *Small* 17, 2101253 (2021) [Cover]

² M. Awadein, et al. 2022, *Nanoscale Adv.*, 2023,5, 659-667

8:30 AM CH01.04.02

In Situ Raman-Electrochemistry for Routinely Characterizing Electronic Properties of Doped SWCNTsNaimishSardesai; Metrohm, United States

Electrical conductivity of single wall nanotubes (SWCNTs) plays a critical role in high-performance flexible batteries. Doping SWCNT is a well-known technique to modify their electronic properties and improve electrical conductivity. In this presentation, we demonstrate *in situ* Raman-electrochemistry as a unique technique for both predicting electronic properties and understanding the charging mechanism of SWCNTs. We demonstrate this by electrochemically doping SWCNT with both chloride and tetraethylammonium tetrafluoroborate to study simultaneous changes in Raman intensity and/or shifts with respect to applied potential. Our study shows hysteresis of the cyclic voltammogram and Raman spectra during doping cycles. We demonstrate the impact of doping on D, G, 2D and RBM bands of the nanotubes at different voltage states.

8:45 AM CH01.04.03

Investigation of the Mechanism of Polydiacetylene Mechanochromism in the Aqueous SolutionJianluZheng and KaoriSugihara; The University of Tokyo, Japan

1. Introduction

Polydiacetylene (PDA) is a special kind of pi-conjugated material widely used in sensing applications¹ due to its facile polymerization and dual signals (blue-to-red color change and turn-on fluorescence) upon exposure to external stimuli. The chromatic transition has been explained as a shortening in effective conjugation caused by the torsion of polydiacetylene backbone². Despite pH-dependent or ion strength-dependent thermochromism having been extensively studied before, the related mechanochromism at the nanoscale is left unstudied. In 2021, Sugihara Group³ demonstrated the first quantitative and anisotropic force-fluorescence correlation of polydiacetylene in air by friction force microscopy (FFM) combined with fluorescence microscopy. In this work, we expanded this technique towards a biological buffer solution to study the mechano-responses fluorescence of PDA.

2. Method

10, 12-Tricosadiynoic acid was assembled onto an oxygen-plasma-activated glass coverslip by the Langmuir-Blodgett (LB) method, followed by UV exposure to fabricate the PDA multilayer films. FFM combined with fluorescence microscopy was an appropriate technique to investigate the quantitative relationship between the applied force and the readout signal, fluorescence.

3. Result and discussion

As the standard atomic force microscopy (AFM) could only apply vertical force which is perpendicular to the substrate at the nanoscale, it usually fails to activate the PDA due to its anisotropic properties. FFM being one mode of AFM can detect the lateral force (friction force)⁴. FFM combined with fluorescence microscopy was an appropriate technique to investigate the quantitative relationship between the applied force and the readout signal, fluorescence. PDA film was scanned by FFM at different setpoints under HEPES buffer solution (pH 7.4, NaCl 150 mM). At the same time, the responses of PDA against the nano-forces were recorded by fluorescence microscopy. The force-fluorescence correlation in buffer solution is different from that in the air due to the water molecule may break the hydrogen bonding between the headgroup. After then we varied the pH and the ionic strength to modulate the hydrogen bonding, and the electrostatic interaction, and investigated how they affect the force sensitivity. Consequently, PDA film became more force-sensitive in the basic environment due to the deprotonation at the carboxyl headgroups. In addition, the force sensitivity slightly rose as the NaCl concentration became higher which can be explained by the reduction of the interfacial pKa.

4. Conclusion

We proved the quantitative mechanochromism of PDA under an aqueous environment by integrating FFM and fluorescence microscopy. pH change or NaCl was used to pre-treat the PDAs, whereas lateral forces were subsequently applied to measure the force sensitivity. In other words, non-mechanical stimuli can be used to pre-stimulate PDAs to improve their force sensitivity.

Both pH change and the addition of NaCl elevated the blue state energy, which made it easier for the system to go over the potential wall when the force was applied, enhancing the force sensitivity. This strategy to pre-stimulate by pH or NaCl is convenient for improving the force sensitivity of PDA, which will open a new pathway for developing easy-to-use (naked-eye detection) point-of-care diagnostic tools.

References

1. Qian, X.; Städler, B. *Chem. Mater.* 2019, 31, (4), 1196-1222.
2. Carpick, R. W.; Sasaki, D. Y.; Marcus, M. S.; Eriksson, M. A.; Burns, A. R. *J. Phys. Condens. Matter.* 2004, 16, (23), R679-R697.
3. Juhasz, L.; Ortuso, R. D.; Sugihara, K. *Nano Lett* 2021, 21, (1), 543-549.
4. Ortuso, R. D.; Sugihara, K. *J. Phys. Chem. C* 2018, 122, (21), 11464-11474.

9:00 AM CH01.04.04

Operando X-Ray Absorption Spectroscopy of Solid Electrolyte Interphase Formation on Silicon Anodes Jack Swallow and Robert Weatherup; University of Oxford, United Kingdom

The development of improved lithium-ion batteries (LiBs) is critical to societies transition towards net-zero. However, more widespread deployment requires improvements in energy density, economic cost and cycle-lifetime. Various cathode and anode materials are under consideration for next-generation LIBs, and the interfacial stability of these materials in contact with the electrolyte is a critical consideration. The formation of a stable solid electrolyte interphase (SEI) is critical to long term LiB performance, however a detailed mechanistic understanding of SEI formation remains elusive, in-part due to the complex electrolyte decomposition reactions that occur. Whilst X-ray spectroscopy, and in particular X-ray absorption spectroscopy, has become a staple characterisation technique to obtain electronic structure and chemical information from battery materials interfaces, it is nearly always performed post-mortem (with cells disassembled in a glovebox, washed, and transferred into the measurement chamber) which can result in unwanted side reactions and removal of labile SEI species.

Here, we demonstrate a novel operando methodology to explore the formation and evolution of the SEI on amorphous silicon (a-Si) anodes during the formation cycle. a-Si is of particular interest in the Li-ion battery community as a result of its extremely high specific capacity¹. A specially designed cell that incorporates a silicon nitride membrane as an X-ray transmissive window allows the electrode surface to be probed in real time whilst performing electrochemical cycling^{1,2,3}. This synchrotron-based approach uses a modulating beam chopper and lock-in amplifier, to perform total electron yield mode X-ray absorption spectroscopy, providing unique nm-scale sensitivity to buried-interfaces. The methodology allows spectroscopic tracking of the onset potentials for the formation of different SEI species, and for identification of O- and F-containing species in the SEI. Cross-referencing to cycling data, complementary bulk sensitive fluorescent yield (FY) XAS measurements, and density function theory (DFT) calculated core-hole spectra enables identification of the electrolyte and SEI species, and the dominant mechanisms of SEI formation. Without FEC present, LiF formation is detected at 0.6 V vs. Li/Li⁺ prior to significant lithiation of the a-Si, whilst at lower potentials the SEI grows in thickness with an increased contribution from organic components containing -C(=O)O- species. The observed sequential formation of inorganic and organic components is implicated in layering of the SEI. With FEC as an additive we see the onset of SEI formation at much higher potentials (1.0 V vs. Li/Li⁺), and attribute the improved cycle life seen with this additive to the rapid healing of SEI defects formed during delithiation. This work demonstrates a new X-ray measurement approach that can provide surface sensitive chemical information of buried electrode interfaces, which has the potential to allow us to better understand the complex degradation and formation processes occurring at battery electrode interfaces during cycling. This work was performed in collaboration with two internationally-leading user facilities (Diamond Light Source, UK and ALBA, Spain) and involved collaboration between researchers at the Universities of Oxford and Cambridge.

References

1. Swallow et al. *Nature Commun.* 2022, 13, 6070.
2. Wu et al. *Phys. Chem. Chem. Phys.* 2015, 17, 30229.
3. Weatherup et al. *Top. Catal.* 2018, 61, 2085.

9:15 AM CH01.04.05

High Speed Mapping of Surface Charge Dynamics via Sparse Scanning Kelvin Probe Force Microscopy Marti Checa, Addis S. Fuhr, Rama K. Vasudevan, Maxim Ziatdinov, Ilia Ivanov, Kyle P. Kelley, Neus Domingo Marimon, Stephen Jesse and Liam Collins; Oak Ridge National Laboratory, United States

Unraveling local dynamic charge processes is vital for progress in diverse fields, from microelectronics to energy storage. This relies on the ability to map charge carrier motion across multiple length- and timescales and understanding how these processes interact with the inherent material heterogeneities. Towards addressing this challenge, we introduce high-speed Sparse Scanning Kelvin Probe Force Microscopy (SS-KPFM), which combines sparse spiral scanning and image reconstruction via Gaussian process optimization. SS-KPFM enables sub-second imaging rates (3.3 fps) of nanoscale charge dynamics, representing several orders of magnitude improvement over traditional KPFM methods. Bridging this improved spatiotemporal resolution with macroscale device measurements, we demonstrate the applicability of this approach by visualizing electrochemically mediated diffusion of mobile surface ions on a LaAlO₃/SrTiO₃ planar device, processes which are known to impact band-alignment and charge-transfer dynamics at such heterointerfaces. Additionally, we track oxygen vacancy diffusion generated under a biased tip, at the single grain level in polycrystalline TiO₂. Temperature-dependent measurements reveal a charge diffusion activation energy of 0.18 eV, in good agreement with previously reported values and backed up here by further modelling. Together, these findings highlight the effectiveness and versatility of our method in understanding ionic charge carrier motion in microelectronics or nanoscale material systems.

9:30 AM *CH01.04.06

Following and Controlling Formation and Function of Bottom-Up Assembled Nanomaterials Christian Tanner¹, Vivian R. Wall¹, Matthew Hurley², Joshua Portner³, Ahhyun Jeong³, Muntaz Gababa¹, Nicholas Leonard², Bryan Sanchez-Monserrate⁴, James Utterback¹, Leo M. Hamerlynck¹, Jonathan Raybin¹, Igor Coropceanu³, Avishek Das¹, Yanwen Sun⁵, Andrei Fluerașu⁶, Christopher Tassone⁵, Karena Chapman⁴, David Limmer¹, Dmitri V. Talapin³, Samuel Teitelbaum² and Naomi S. Ginsberg¹; ¹University of California, Berkeley, United States; ²Arizona State University, United States; ³The University of Chicago, United States; ⁴Stony Brook University, The State University of New York, United States; ⁵SLAC National Accelerator Laboratory, United States; ⁶Brookhaven National Laboratory, United States

Design advances for the bottom-up assembly of highly ordered functional nanomaterials have generated a wide range of fundamental questions that must be answered to continue to advance material properties, recently including strong electronic and mechanical coupling. We focus on colloidal nanocrystal advances that incorporate electrostatics to promote the formation of ordered superlattice structures from nanocrystals with high dielectric constants. Through a multiscale suite of hard X-ray scattering experiments ranging from small- to wide-angle, incoherent to coherent, and storage ring to free electron laser over a wide dynamic range of time scales, we characterize the phases, their fluctuations, and the dynamic interconversion between phases of this enigmatic system, non-invasively and in real-time, identifying the helpful role of a liquid-like intermediate phase that admits an unusually high degree of control over product yield, size, and order. We find that controlled, ordered assembly requires a balance of nanocrystal screening and surface charge that is facilitated by moderate to high dielectric ratios between the nanocrystals and their surroundings. We also find that laser absorption reversibly alters the surface charge and growth of the ordered superlattice phase and intend to leverage these findings to infer strategies to self-assemble more common low-dielectric nanocrystals into ordered structures by driving them far from equilibrium with optical excitation.

10:00 AM BREAK

SESSION CH01.05: Electrodes II
Session Chairs: Rajiv Giridharagopal and Erin Ratcliff
Tuesday Morning, November 28, 2023
Sheraton, Third Floor, Commonwealth

10:30 AM CH01.05.01

Surface Studies to Understand Formation and Lithiation of New Silicon-Based Anodes via Neutron Depth Profiling Ralph Gilles¹, Lukas Grossmann¹, Jiri Vacik², Antonino Cannavo² and Giovanni Ceccio²; ¹TU München, Germany; ²Nuclear Physics Institute, Czechia

Analytical methods for characterizing surfaces that have been under electrochemical influence are in great demand, as many electrochemical processes originate here and are therefore important for cell performance. Electrode surfaces are a good example of how neutron techniques contribute to the understanding of lithiation processes [1,2]. Currently, attempts are being made to replace graphite anodes with silicon-based anodes with a significantly higher specific capacity. Since pure silicon anodes have a short lifetime due to the large volume expansion,

microscale silicon particles with partial lithiation are investigated [3]. This type of anode combines high capacity, rate stability, and low cost. Besides an overview of how neutrons with their unique properties solve specific electrochemical problems on different length and time scales, this contribution shows how neutron depth profiling determines the Li distribution across the whole depth of the electrode coating in the pristine state, after the formation cycles and after 15%, 25% and 30% of the lithiation process. Taking into account SEI formation, electrode swelling and phase transformation from crystalline to amorphous Si, conclusions are drawn on how the surface lithiation process occurs under electrochemical changes.

- [1] R. Gilles, How neutrons facilitate research into gas turbines and batteries from development to engineering applications, *Journal of Surface Investigations: X-Ray, Synchrotron and Neutron Techniques* (2020), 14, Suppl. 1, S69.
- [2] J. Hattendorff, S. Seidlmayer, H.A. Gaseiger, R. Gilles, Li-ion half cells studied operando during cycling by small-angle neutron scattering, *Journal of Applied Crystallography* (2020), 53, 210.
- [3] M. Graf, C. Berg, R. Bernhard, S. Haufe, J. Pfeiffer, H.A. Gasteiger, Effect and Progress of the Amorphization Process for Microscale Silicon Particles under Partial Lithiation as Active Material in Lithium-Ion Batteries, *Journal of the Electrochemical Society* (2022), 169, 020536.

10:45 AM CH01.05.02

Tracking Charge of Disordered Carbon Electrodes with Raman Spectroscopy - Mapping Insights from Electron Doped Activated, Hard and Black Carbons, Hector J. Lancaster, Thomas S. Miller and Christopher A. Howard; University College London, United Kingdom

Disordered carbon is an essential ingredient in batteries, fuel cells, supercapacitors and electrolysers. The types typically used are chars (commonly referred to as hard carbons), carbon blacks and activated carbons. For a given application, these often-overlooked materials provide several key functions, such as tuning conductivity, porosity or surface area. They are all cheap, widespread and integral to their parent devices.

Raman spectroscopy is a powerful, non-destructive, inexpensive and relatively facile surface-sensitive technique. That being said, in the electrochemical literature the vast majority of Raman characterization on carbon materials is limited to often tenuous claims, derived from poor statistical inferences, about an electrode's defectiveness. These are based on an oversimplified understanding of the ratios of D (disordered) and G (graphitic) Raman peaks. Promisingly, recent studies have begun to explore the potential power of using operando Raman spectroscopy as an effective tool for determining things such as the sodiation mechanism in hard carbon electrodes. [1] The relative power of Raman analysis in electrochemical systems is highlighted by comparison with a contemporary study, which employed far more complex and expensive techniques to reach similar findings. [2]

In this presentation, I will share new and fundamental insights into the Raman effects of heavy electron doping disordered carbons, revealed by controllably tuning the concentration of electrons in an isolated system. The work serves as an analogue for surface and interfacial charge transfer phenomena present in electrochemical devices. I will discuss how D peak trends can be used as a sensitive and simple fingerprint of electrode charge and explain why conventional D:G ratio rules may not apply to these systems. Ultimately, this technique can be widely implemented to measure and optimise the next generation of disordered carbon containing electrodes.

- [1] J. S. Weaving, A. Lim, J. Millichamp, T. P. Neville, D. Ledwoch, E. Kendrick, P. F. McMillan, P. R. Shearing, C. J. Howard, D. J. L. Brett, *ACS Applied Energy Materials*, **3**, 7474–7484 (2020).
- [2] H. Au, H. Alptekin, A. A. Jensen, E. Olsson, C. A. O'Keefe, T. J. Smith, M. Crespo-Ribadeneyra, T. F. Headen, C. P. Grey, Q. Cai, A. J. Drew, M.-M. Titirici, *Energy and Environmental Science*, **13**, 3469–3479 (2020).

11:00 AM CH01.05.03

Modulating the Voltage Decay and Cationic Redox Kinetics of Li-Rich Cathodes via Controlling the Local Electronic Structure Heng-Liang Wu and Hung-Ling Yu; National Taiwan University, Taiwan

Li-rich layered oxide cathodes with conventional transition metal cation and unique oxygen anion redox reactions deliver high capacities in Li-ion batteries. However, the oxygen redox process causes the oxygen release, voltage fading/hysteresis, and sluggish electrochemical kinetics, which undermine the performance of these materials¹⁻⁴. In this talk, the effect of the local electronic structure is elucidated on the reaction mechanism and electrochemical kinetics of Li-rich cathodes by using operando quick-scanning X-ray absorption spectroscopy with online gas chromatography⁵. The local electronic structure of Li-rich cathodes varies with the excess Li (i.e., Li₂MnO₃ phase) and Ni contents. Compared to the Li-rich cathodes with higher amounts of Li₂MnO₃ phase (high excess lithium content (HLC) cathode), those with lower Li₂MnO₃ contents (low excess lithium content (LLC) cathode) exhibit reversible anion redox reactions and suppressed voltage hysteresis. Interestingly, the kinetics of the TM redox process in the LLC cathode is slower than that in the HLC cathode. Thus, the amount of Li₂MnO₃ phase affects both the reaction mechanism and kinetics of Li-rich cathodes. The evolution of the dynamic structure needs to be taken into account when addressing the cation and anion redox chemistry in Li-rich cathode. Our findings provide new insights into the reaction mechanism and kinetics of the TM redox reactions, showing that the electrochemical stability and kinetics of TM redox can be tuned by modifying the Li₂MnO₃ phase content.

References:

1. Nat. Energy, **2020**, 5, 777.
2. Nat. Chem., **2016**, 8, 684.
3. Adv. Energy Mater., **2016**, 6, 1502398.
4. J. Am. Chem. Soc., **2020**, 142, 8522
5. Adv. Funct. Mater., **2022**, 32, 2112394.

11:15 AM CH01.05.04

Temperature-Dependent Dynamic Spin Disproportionation in the Battery Cathode LiNiO₂, Andrey Poletayev¹, Jack Swallow¹, Robert Green², Rob House¹, Benjamin J. Morgan³, Robert Weatherup¹ and M. Saifullah^{1,3}; ¹University of Oxford, United Kingdom; ²University of Saskatchewan, Canada; ³University of Bath, United Kingdom

Layered lithium nickel oxide LiNiO₂ represents the end-member of industry-leading lithium-ion battery cathodes, Li(NiMnCo)O₂. The properties of LiNiO₂ (LNO) are responsible for much of the degradation of such cathodes, especially during high-voltage operation above 4.2 V, presenting an opportunity to improve their energy density by extending the operating voltage window. Here we focus on the computational and experimental understanding of LNO and its presumed delithiated state, layered NiO₂. LNO possesses several unusual properties: (1) gradual lattice distortions rather than abrupt phase transitions upon cooling, (2) gradual changes to vibrational spectra upon cooling, (3) heat-activated electronic conductivity with a variable activation energy, (4) temperature-dependent NiO₆ distortions, and (5) ubiquitous antisite defects.

We reconcile all of these observations with a dynamic spin disproportionation model where nickels exist in three interconverting spin states ($S = 1, \frac{1}{2},$ and 0), reminiscent of formal charges +2, +3, and +4. This model explains the gradual variation of the physical properties of LNO across temperatures [1]. Since small variations in the level of theory lead to substantial changes in the predicted behavior and its temperature dependence, we verify computational predictions experimentally. Resonant inelastic x-ray scattering (RIXS), temperature-resolved bulk-sensitive x-ray absorption spectra, and x-ray magnetic circular dichroism (XMCD), all at the nickel L-edge, confirm first-principles predictions.

- [1] Poletayev *et al.*, pre-print arXiv:2211.09047

11:30 AM CH01.05.05

Covalent-Assisted Seeding Silicon Nanoparticles into Sn/SiOC Dual Active Matrix as a High-Performance Anode Material for Lithium-Ion Batteries Kwanghyun Do, Changyong Park, Jeonguk Hwang, Suchoel Kim, Yeju Jung and Heejoon Ahn; Hanyang University, Korea (the Republic of)

Research for high-capacity electrode materials is being actively conducted to realize high-energy-density batteries for electric vehicles. This direction of research necessarily requires silicon-based anodes. Si shows the highest theoretical capacity among anode materials and low working voltage but has a critical drawback of mechanical instability from which all electrode degradation begins. Various materials have been introduced to accommodate the volume expansion of silicon and protect the surface of pulverized silicon from penetration of electrolyte. Among them, silicon oxycarbide (SiOC) is an attractive active matrix for silicon. SiOC active matrix has a higher specific capacity than graphite and a very low theoretical volume change (~22%). In addition to capacity and volume change, the tetrahedral C-doped silica network and free carbon domain of SiOC give higher connectivity of glass network than SiO₂ and act as a chemical and/or physical barrier to alkaline or HF solution, resulting in superior electro-chemo-mechanical stability.

Several approaches, such as pyrolysis with silicone oil or crosslinking with polysiloxanes, have been tried to combine Si nanoparticles (Si NPs) and SiOC matrix. However, the particle size cannot be controlled, forming a bulky SiOC monolith, which causes sluggish Li⁺ diffusion. In addition, there is a problem in that the surface of Si NPs is exposed during lithiation/delithiation

because the previous methods simply engage Si NPs without chemical bonding or interaction. Therefore, a method of controlling the size of SiOC and inducing chemical bonds between Si NPs and SiOC is desired.

In this study, the silicon alkoxide-based sol-gel method was introduced to design Si NPs-seeded preceramic SiOC based on covalent bonds. Additionally, to further enhance several electrochemical performances of the Si@SiOC composite, we incorporated Sn nanocrystals into the SiOC matrix via carbothermal reduction. We expected that the formation of SnO(OH), a precursor of metallic Sn, would change the morphology of composite particles into secondary particles by hindering the growth of spherical SiOC particles and creating nanovoids between the primary particles. This morphological change can be anticipated to improve cyclability by providing voids that can additionally accommodate the volume change of the entire particles. Moreover, the Sn/SiOC dual active matrix can enhance the (de)lithiation kinetics of the Si@Sn/SiOC electrode due to improved electrical and ionic conductivity. Firstly, we confirmed that the composite was successfully synthesized through various material analyses. We successfully controlled the size of particles by setting the reaction time and unveiled the mechanism of Si@Sn/SiOC complexation. Secondly, the coin cell-type battery test was performed to figure out the effect of covalent-assisted seeding (CAS) of Si NPs on the electrochemical behavior of Si@SiOC electrode and the effect of Sn/SiOC dual active matrix on the electrochemical behavior of Si@Sn/SiOC electrode. After cycling, we conducted ex-situ cross-sectional SEM analysis and electrochemical impedance spectroscopy of the electrodes and demonstrated the beneficial effects of Sn/SiOC dual active matrix in which the propagation of charge transfer resistance and mechanical fracture were much suppressed than that of Si@SiOC. We also revealed that incorporating Sn nanocrystals improved the specific capacity of the electrode by reducing the polarization of the electrode and increasing the lithiation kinetics of Si. Finally, through this study, we proposed an approach that takes advantages while complementing the disadvantages of each Si and SiOC and clarified the role of each Si, Sn, and SiOC component in the Si@Sn/SiOC electrode during (de)lithiation.

11:45 AM CH01.05.06

NaCuO₂ as Cathode Materials Studied Through Resonant Inelastic Soft X-Ray Spectroscopy (RIXS) Zengqing Zhuo, Wanli Yang and Jinghua Guo; Lawrence Berkeley National Laboratory, United States

Anionic redox reactions have been proposed for a decade to provide higher capacity and higher power compared with conventional transition metal redox. However, the fundamental mechanism remains elusive and highly debated. Here, we are working on a model electrode system, NaCuO₂, to reveal the both cation and anion evolution upon the electrochemical cycling through high efficiency mapping of resonant inelastic X-ray scattering (mRIXS). Through the characterization of the oxygen state and copper state, we finally provide a comprehensive understanding of the electrochemical cycling mechanism of the NaCuO₂. We clarify that lattice oxygen redox dominates the reversible bulk redox, while the surface reactions with carbonation decomposition and Cu reaction also contribute the cycling capacity. This work suggests the important role of transition metals and their coupling and hybridization effect to oxygen for maintaining reversible oxygen redox activities.

SESSION CH01.06: Photovoltaics II
Session Chairs: Ilka Hermes and Philippe Leclere
Tuesday Afternoon, November 28, 2023
Sheraton, Third Floor, Commonwealth

1:30 PM *CH01.06.01

The Nanoscale Photovoltaics Laboratory on a Tip Stefan A. Weber^{1,2}, Yenal Yalcinkaya¹, Pascal N. Rohrbeck¹, Konstantinos Bidinakis¹, Rüdiger Berger¹ and Ilka Hermes³; ¹Max Planck Institute for Polymer Research, Germany; ²University of Stuttgart, Germany; ³Leibniz Institute for Polymer Research, Germany

Solar cells based on metal halide perovskite (MHP) materials will enable cheaper and more energy-efficient photovoltaic and optoelectronic devices compared to current silicon-based technologies. To advance MHP technology further, however, will require a better understanding of the fundamental processes leading to energy losses, unstable operation conditions and premature aging. The macroscopically observed properties of optoelectronic MHP materials and devices are the result of the complicated interplay between nanoscale structure and function. Thus, the key to understanding MHP materials is the micro- and nanoscale characterization of the many nano- and microscale structures; from sub-granular twin domains, over grain boundaries and interfaces to lateral variations in crystal grains orientations and facets. For such nanoscale photovoltaic measurements, scanning force microscopy methods are ideal, as they allow correlated measurements of structure and function.

In this presentation, I will present some of our recent activities in the development of specialized scanning probe microscopy methods to study hybrid perovskite materials. Based on static and time-resolved Kelvin probe force microscopy (KPFM), we have developed unique techniques for mapping the surface potential and photovoltage. Using cross sectional measurements, we map and record the potential distribution across different layers of solar cell devices under operating conditions [1–4]. Here, the key to a reliable cross-sectional KPFM measurement is the connection of a high-resolution quantitative KPFM operation mode [5] and the preparation of a smooth surface through the solar cell. We use a combination of mechanical fracturing of the cells with a complex polishing process using ion beams. Using a pointwise spectroscopy technique, we can record and map the surface photovoltage (SPV) dynamics with 10–20 nm lateral resolution. With this Nano-SPV technique, we revealed local SPV overshoots in the vicinity of grain boundaries following an illumination pulse. The overall aim of our research is to address some of the key challenges of MHP research, such as phase segregation, degradation and interface heterogeneity, to enable a deeper understanding of the different loss mechanisms and intrinsic instabilities that currently limit the application of MHP solar cells.

- [1] V. W. Bergmann, S. A. L. Weber, F. Javier Ramos, M. K. Nazeeruddin, M. Grätzel, D. Li, A. L. Domanski, I. Lieberwirth, S. Ahmad, and R. Berger, *Real-Space Observation of Unbalanced Charge Distribution inside a Perovskite-Sensitized Solar Cell*, Nat Commun **5**, 6001 (2014).
- [2] V. W. Bergmann, Y. Guo, H. Tanaka, I. M. Hermes, D. Li, A. Klasen, S. A. Bretschneider, E. Nakamura, R. Berger, and S. A. L. Weber, *Local Time-Dependent Charging in a Perovskite Solar Cell*, ACS Appl. Mater. Interfaces **8**, 19402 (2016).
- [3] S. A. L. Weber, I. M. Hermes, S.-H. Turren-Cruz, C. Gort, V. W. Bergmann, L. Gilson, A. Hagfeldt, M. Graetzel, W. Tress, and R. Berger, *How the Formation of Interfacial Charge Causes Hysteresis in Perovskite Solar Cells*, Energy Environ. Sci. **11**, 2404 (2018).
- [4] I. M. Hermes, Y. Hou, V. W. Bergmann, C. J. Brabec, and S. A. L. Weber, *The Interplay of Contact Layers: How the Electron Transport Layer Influences Interfacial Recombination and Hole Extraction in Perovskite Solar Cells*, J. Phys. Chem. Lett. **9**, 6249–6256 (2018).
- [5] A. Axt, I. M. Hermes, V. W. Bergmann, N. Tausendpfund, and S. A. L. Weber, *Know Your Full Potential: Quantitative Kelvin Probe Force Microscopy on Nanoscale Electrical Devices*, Beilstein J. Nanotechnol. **9**, 1809 (2018).

2:00 PM CH01.06.02

TEM and XPS Investigations of Multi-Layer Solar Selective Absorber: Thermal Stability Florian Chabanais¹, Mireille Richard-Plouet¹, Jonathan Hamon¹, Nicolas Gautier¹, Aissatou Diop², Babacar Diallo³, Béatrice Plujat², Thierry Sauvage³, Éric Tomasella⁴, Laurent Thomas², Audrey Soum-Glaude² and Antoine Gouillet¹; ¹Nantes Université, CNRS, Institut des Matériaux de Nantes Jean Rouxel, IMN, France; ²Université de Perpignan Via Domitia - PROMES-CNRS UPR 8521, France; ³CEMHTI-CNRS UPR 3079 (Conditions Extrêmes et Matériaux : Haute Température et Irradiation), Université d'Orléans, France; ⁴Université Clermont Auvergne, CNRS, SIGMA Clermont, ICCF, France

The solar energy resource is still relatively under-exploited although it could cover most of our energy needs. Beyond the development of photovoltaics, there is a worldwide challenge to deploy large-scale concentrated solar thermal power plants. To address this issue, materials with high absorption in the visible range, low emissivity and good temperature resistance are required. To this end, multi-layered optical thin films produced by plasma processes are developed in the NANOPLAST project (nanoplast-project.cnrs.fr, ANR-19-CE08-0019).

This study is focussed on the investigation of the absorbing active layer with or without air annealing at 500°C.

First, composite monolayers W-SiC:H are obtained by reactive magnetron sputtering from a W target combined with tetramethylsilane (TMS-Si(CH₃)₄) diluted in Ar plasma. TEM and XPS characterisations were carried out to get insight into the nature of the absorber and the anti-reflective top films. Depending on the TMS fraction in the discharge, the quantity of Si introduced in the W-SiC:H material can be tuned.

In dedicated conditions (5 and 8% TMS), W nano-crystallites could be identified by coupling STEM-HAADF (Scanning Transmission Electron Microscopy - High-Angle Annular Dark Field) images, EDS mapping and High Resolution imaging. In other conditions (20 and 28% TMS), amorphous layers are observed. In XPS, we were able to analyse the different surface chemical environments of the samples. Under low TMS content, we observed a significant occurrence of W-C bonding whereas no Si is incorporated in the layer. By decomposing the obtained survey spectra and identifying the related components, we were able to achieve quantification of the species as a function of the TMS concentration.

Second, multi-layers of SiC:H/metallic W/SiC:H were also prepared. Upon annealing at 500°C in air for duration up to 48h, XPS profiles indicate that excepting a diffusion of oxygen from

the surface in the upper SiC:H layer, the W interlayer acts as a blocking layer for oxidation. However after annealing for 96h, the triple layer is severely modified with segregation of the different species involved.

TEM images confirmed these major modifications.

2:15 PM CH01.06.03

Direct Measurements of Donor HOMO – Acceptor LUMO Offset at The Interface of C60/Pentacene Model Organic Solar Cells using Photoemission and Inverse Photoemission Spectroscopy GyuhyeonLee, Min-JaeMaeng, Kyu-MyungLee, Jong-AmHong and [YongsupPark](#); Kyung Hee University, Korea (the Republic of)

In organic light-emitting diodes (OLEDs) and heterojunction organic solar cells (OSCs), the energy offset between HOMO and LUMO, also called the transport gap (E_{tr}) is substantially different from optical gaps due to the relatively large exciton binding energies. However, the difficulty to independently measure the LUMO levels makes it hard to elucidate important things like electron injection barrier at the cathode in OLEDs and the voltage loss mechanisms in Voc of OSCs.

We have recently developed highly sensitive inverse photoemission spectroscopy (IPES) instrument specifically for the LUMO level measurement of organic semiconductors. In combination with the existing ultraviolet photoemission spectroscopy (UPS) we could determine all the relevant transport energy levels (HOMO, LUMO, Fermi level and vacuum level) in any organic semiconductor surface and interface. In addition, combination of the electron source for IPES and the electron energy analyzer for UPS allowed us to utilize reflection electron energy loss spectroscopy (REELS) to determine optical gaps. We first demonstrate that all these measurements can be performed for an identical sample as a function of thickness. We also determine the energy levels at C60/pentacene interface so that the factors affecting the voltage losses that led to observed Voc value of this model planar heterojunction organic solar cells can be evaluated.

2:30 PM BREAK

3:00 PM CH01.06.04

Multimodal Operando Microscopy Reveals that Nanoscale Performance Disorder Dictates Efficiency and Stability of Perovskite Solar Cells KyleFrohna¹, CullenChosy¹, AmranAl-Ashouri², Yu-HsienChiang¹, MilosDubajic¹, JuliaE. Parker³, JessicaM. Walker³, BartRoose¹, SteveAlbrecht², MiguelAnaya¹ and SamuelD. Stranks¹; ¹University of Cambridge, United Kingdom; ²Helmholtz-Zentrum Berlin für Materialien und Energie, Germany; ³Diamond Light Source, United Kingdom

The optoelectronic properties of next generation semiconductors such as halide perovskites are dominated by nanoscale variations in structure^{1,2}, composition^{3,4} and photophysics^{5,6}. While microscopy provides a proxy for ultimate device function, past works have typically focused on neat films fabricated on insulating substrates – therefore missing additional recombination losses from transport layers and charge extraction losses entirely⁷⁻⁹.

In this presentation, I will discuss a multimodal, *operando*, microscopy toolkit designed to measure nanoscale current-voltage curves, recombination losses and chemical composition in a wide array of state-of-the-art perovskite solar cells before and after extended operational stress. By imaging the same scan areas before and after operation, we determine point by point changes in recombination and transport losses on length scales from entire device down to sub-micron.

We apply this toolkit to reveal that perovskite solar cells with the highest performance and stability have the lowest initial performance spatial heterogeneity. We show that perovskite solar cells can tolerate considerable chemical and photophysical heterogeneity in the absorber itself, but cannot tolerate heterogeneous charge extraction, a finding missed by conventional microscopy. If the interfaces are not stabilised appropriately, the contacts dominate degradation pathways, introducing spatially varying transport, recombination, and hysteresis losses. With well-tuned contact layers, perovskite absorbers dominate degradation and minor modulations of the composition can induce or prevent extreme halide segregation and precipitate formation which are both detrimental to performance. These *operando* measurements uniquely unveil the underpinnings of perovskite solar cell performance and stability. The microscopy toolbox can be readily tuned for alternative device structures and semiconductors.

References

1. Doherty, T. A. S. *et al.* Performance-limiting nanoscale trap clusters at grain junctions in halide perovskites. *Nature* vol. 580 360–366 (2020).
2. Doherty, T. A. S. *et al.* Stabilized tilted-octahedra halide perovskites inhibit local formation of performance-limiting phases. *Science* vol. 374 1598–1605 (2021).
3. Frohna, K. *et al.* Nanoscale chemical heterogeneity dominates the optoelectronic response of alloyed perovskite solar cells. *Nature Nanotechnology* vol. 17 190–196 (2022).
4. Correa-Baena, J.-P. *et al.* Homogenized halides and alkali cation segregation in alloyed organic-inorganic perovskites. *Science* vol. 363 627–631 (2019).
5. de Quillettes, D. W. *et al.* Impact of microstructure on local carrier lifetime in perovskite solar cells. *Science* vol. 348 683–686 (2015).
6. Macpherson, S. *et al.* Local nanoscale phase impurities are degradation sites in halide perovskites. *Nature* vol. 607 294–300 (2022).
7. Stolterfoht, M. *et al.* Visualization and suppression of interfacial recombination for high-efficiency large-area pin perovskite solar cells. *Nature Energy* vol. 3 847–854 (2018).
8. Stolterfoht, M. *et al.* The impact of energy alignment and interfacial recombination on the internal and external open-circuit voltage of perovskite solar cells. *Energy & Environmental Science* vol. 12 2778–2788 (2019).
9. Cacovich, S. *et al.* Imaging and quantifying non-radiative losses at 23% efficient inverted perovskite solar cells interfaces. *Nat. Commun.* **13**, 2868 (2022).

3:15 PM CH01.06.05

Uncovering the Individual JV Curves of Fully Evaporated Perovskite-Silicon Tandem Solar Cells FedericoVentosinos^{1,2}, SofiaChozas Barrientos¹ and HenkJ. Bolink¹; ¹University of Valencia, Spain; ²IFIS Litoral, Argentina

Tandem devices combining perovskite and silicon solar cells are promising candidates to achieve high power conversion efficiencies at low cost, with already proven devices exceeding 33%. Despite the ever-increasing performance and the improved stability of perovskite solar cells, there is need for characterization techniques for these complex structures to fully understand and optimize them. This becomes a challenge in 2 terminal (2T) tandem devices given the nature of the series connection between them. Due to this junction, the density current in the JV curve corresponds to the minimum of both subcells, while the total voltage is the sum of each subcell. This implies that knowing the short circuit current density (J_{sc}), the open circuit voltage (V_{oc}) and the fill factor (FF) of the full device does not translate into knowing the individual behavior of each subcell. In the case of J_{sc} , quantum efficiency measurements with light and voltage biasing can be used to reveal the behavior of each subcell. Suns-Voc with selective illumination can also give approximate values of individual V_{oc} in the case of very good selectivity.

However, it is difficult to obtain information about the FF for each subcell. In this communication we show how a technique developed for studying tandem devices based on thin film silicon materials can be applied to our fully evaporated perovskite on textured silicon 2T tandem devices. To accomplish this, an extra source of illumination (a laser for each subcell in our case) is used to keep one of the subcells at its V_{oc} while changing the working point at 1 sun illumination of the full stack, hence, revealing the behavior of the other subcell. This allows us to reconstruct each subcell individual JV curve of each subcell at 1 sun illumination, giving direct access to all the relevant parameters.

We will explain how the technique works and what are the underlying assumptions and limitations. Particularly, I will discuss the relevance of having good selectivity (meaning, generating voltage in only one of the subcells) and how to solve this issue in the case of poor selectivity. Secondly, we will point out how an extra procedure is needed, since perovskite based solar cells suffer from known issues, such as ion migration and scan rate dependency, from which silicon based tandem devices did not suffer. To overcome these problems, we will propose a methodology that ensures the reliability of the constructed individual JV curves.

Finally, we show this method for our vacuum deposited perovskite tandem solar cells, highlighting the evolution of the main parameters (V_{oc} , J_{sc} and FF) as a function of light soaking time.

3:30 PM CH01.06.06

The Critical Morphological Structures for Solvents Insensitive Processed Organic Solar Cells RuiZhang and FengGao; Linköping University, Sweden

The power conversion efficiencies (PCEs) of lab-sized organic solar cells (OSCs), usually processed from low-boiling-point and toxic solvents, have reached high values over 19%. However, the key limiting factor for green-processed OSCs is imperfect micro-morphology, which dominating a significant drop of the efficiency. Importantly, the final device parameters are always super sensitive to the solvents selected during solution-processed procedures. Herein, we obtain uniform PCEs over 18% in OSCs processed from a series of different solvents involving chloroform, chlorobenzene, toluene, (p-, o-, m-) Xylene by carefully designing of the OEG side chains in non-fullerene small molecules. The specific intermolecular interactions formed in solution states dominate those uniform device parameters. Our inspiring strategy provides a broader land view to develop large-area and high-efficiency OSCs from green solvents, figuring out the way towards industrial development of OSCs.

3:45 PM CH01.07.01

EXAFS Analysis of Mn-Alloyed TiO₂ Coatings Grown by Atomic Layer Deposition: Probing the Crystallization Behavior [DevanSolanki](#)^{1,2}, [DeyuLu](#)³ and [ShuHu](#)^{1,2}; ¹Yale University, United States; ²Energy Sciences Institute, United States; ³Brookhaven National Laboratory, United States

Introduction

TiO₂ is a nontoxic, wide bandgap semiconductor with many excellent physical properties such as high chemical stability in acids and bases and good optical transparency to visible light, making it an excellent candidate for photoelectrocatalysis. Atomic Layer Deposition (ALD) enables synthesis of conformal coatings on various substrates by its layer-by-layer, surface-growth mechanism. However, controlling the crystal structure, which can modulate properties such as the band gap and band edge positions, remains a challenge as TiO₂ is often amorphous as deposited but can be annealed into multiple polymorphs such as anatase, rutile, and brookite. Despite progress in understanding the reaction mechanisms and intermediates associated with the deposition of binary materials via ALD, there are still many questions surrounding the structure-processing relationship of ternary materials. For example, the role that dopants or alloying agents play in determining key properties such as oxidation state and crystal structure remain open questions.

Methods:

The X-Ray Absorption Spectroscopy (XAS) and X-ray Absorption Near Edge Structure (XANES) measurements were conducted at the Inner Shell Spectroscopy beamline of the National Synchrotron Light Source II (NSLS-II) at Brookhaven National Lab. The data was collected at room temperature with the energy calibrated using a Ti foil. The Athena software package was used to calibrate the energy and normalize the data using the recommended parameters. XAS was collected in fluorescence mode with $\mu(E) = I_f/I_0$ where I_f is the fluorescence intensity and I_0 the incident intensity. Each spectrum is flattened so that the overall spectrum has an asymptotic behavior approaching 1.

Results:

The primary pre-edge feature in the TiO₂ sample, centered at 4968 eV is due to the oxygen vacancies and resultant undercoordinated Ti. The absorption maximum of that pre-edge feature is unchanged after the incorporation of Mn. However, there is a narrowing of the peak in TiMnO_x samples relative to the TiO₂ and an enhancement of the shoulder peak that appears at 4972 eV. The separation between the apex of the first and second pre-edge feature corresponds to the crystal field splitting energy of the Ti 3d states. This indicates that the incorporation of Mn, while not having an effect in the oxidation state of the Ti, does perturb the local steric coordination environment. Quantitative analysis of this feature was not possible due to the background variation between the different samples and the low absolute intensity of the peak.

Analysis of the Mn K-edge reveals that the oxidation state of Mn in the as-grown TiMnO_x is independent of Mn concentration. One explanation for this fractional oxidation state could be the incorporation of Mn into multiple different sites. The pre-edge feature is comparable to experimental and computational Mn₃O₄ spectra. The position of the white line can be explained either by the electrostatic model or as continuum resonances. In the electrostatic model, as the oxidation state increases, the electrons are more tightly bound to the nucleus, requiring higher energy to be excited. The continuum model considers both the excited atom and the surrounding ones, and as the absorber-scatterer distance gets shorter, the energy of the continuum state increases with $1/r^2$. As higher oxidation states result in shorter bond lengths, the energy increases as oxidation state increases. In addition, the intensity of the white line intensity is proportional to the filling of 3d orbitals. As the 3d orbitals gets more occupied, the intensity of the white line goes down due to the reduction in possible population states. As the position of the white line remains constant between the as grown TiMnO_x samples, the increase in sharpness of the K-edge in the 16:1 sample relative to the 2:1 sample could be explained by the combination of a slightly increased oxidation state and longer Mn-O bond.

4:00 PM CH01.07.02

Microwave Resonator-Based Characterization of Surface-Adsorbate Interactions and Carrier Dynamics in the Photocatalytic Production of Solar Fuels [KarthikShankar](#), [NavneetKumar](#), [AminMoradkhani](#), [JohnGarcia](#), [Md MasudRana](#) and [MasoudBaghelani](#); University of Alberta, Canada

Solar fuels such as hydrogen (generated through water-splitting) and short chain hydrocarbons - methanol, methane & formate (generated through the photoreduction of CO₂) capture the energy of photons in the chemical bonds of portable gaseous and/or liquid fuels. Solar fuels solve the intermittency and energy storage density problems associated with photovoltaic and solid-state battery technologies respectively. Furthermore, solar fuels are highly compatible with the existing energy production and distribution infrastructure and therefore constitute an economically feasible method to make the transition to more renewable energy sources. However, such positive outcomes first require a several fold increase in the photoconversion efficiency (PCE) of photocatalytic solar fuel production processes from values of 2-5% to at least 10-15%. The principal bottlenecks limiting higher PCEs in photocatalytic water-splitting and CO₂ photoreduction relate to large electron-hole recombination losses and inefficient charge transfer processes involving adsorbed reactants and/or reaction intermediates. Conventional methods used to measure carrier dynamics in photocatalytic systems such as femtosecond transient absorption spectroscopy, DC photoconductivity, DLTS, EPR, etc only provide information on either free or trapped carriers but not both simultaneously and are frequently difficult to use for *operando* characterization. Microwave resonators integrated with photoreactors offer a novel characterization methodology to obtain deeper insights into the underlying chemical & electronic processes and also perform *operando* monitoring of the reaction. A key advantage of this methodology is that both mobile and trapped photogenerated carriers interact strongly with microwaves through the photodielectric effect and photoconductive effect respectively. Thus microwave resonators are able to provide information on the number of free and trapped carriers and the time-scales of trapping & recombination processes through monitoring the real and imaginary portions of the complex permittivity of photocatalysts placed in the coupling gap of high-Q microwave resonators. In addition, the high frequency spectra also provide information on the nature of the adsorbates and their interaction with the surface of the photocatalyst. Microwave characterization has enabled us to measure & monitor the interactions of a single monolayer of organic adsorbate with free and trapped carriers generated using light illumination in a TiO₂ photocatalyst. We recently extended the microwave resonator-based characterization to other semiconductor systems of interest for energy applications. Regenerative feedback techniques are used to achieve very high quality factors since the sensitivity of the complex permittivity detection is directly related to the value of Q. The selectivity of this characterization methodology has been expanded by monitoring multiple resonance frequencies in the GHz range on a single microwave resonator. This work will discuss the design, fabrication and testing of high-Q microwave resonators consisting of photocatalysts in their active region.

4:15 PM CH01.07.03

Thermal Characterization of an Epitaxial Gallium Nitride Film via Spatial-Temporal-Resolved X-Ray Diffraction [ThanhNguyen](#)¹, [TyraEspedal](#)¹, [BuxuanLi](#)¹, [ZhantaoChen](#)², [HaidanWen](#)³ and [MingdaLi](#)¹; ¹Massachusetts Institute of Technology, United States; ²SLAC National Accelerator Laboratory, United States; ³Argonne National Laboratory, United States

The characterization of the thermal properties of thin films, in simultaneous cross-plane and in-plane measurements, remains nontrivial and challenging despite the development of advanced techniques. Non-contact methods such as time-domain and frequency-domain thermoreflectance are typically the measurement of choice for different films, but tends to suffer from a relatively large error and a lack of sensitivity to the in-plane thermal transport; thus, new novel approaches continue to be investigated especially in the context of thermal management in prospective electronic devices. In this work, we report preliminary measurements of thermal properties of an epitaxial thin film of gallium nitride (GaN) transferred onto a silicon wafer using synchrotron-based pump-probe x-ray diffraction. We observe a decaying signal of the (002) Bragg peak position of GaN as a function of delay time as well as by the spatial distance set between the pump laser and x-ray probe. These measurements provide simultaneous time- and spatial-resolved information about the phonon thermal transport in the system allowing us to characterize both cross-plane and in-plane thermal properties of the film. In addition, we support the analysis with frequency-domain thermoreflectance and Raman measurements. The measurements provided by this novel x-ray based approach enables detailed characterization of the thermal properties of an epitaxial gallium nitride film -- with important implications for epitaxial thin film characterizations and enhancing thermal management in power electronics.

4:30 PM CH01.07.05

Direct Measurement of Solid-Liquid Interfacial Energy Using a Meniscus [shratZarin](#)¹, [JingchengMa](#)^{1,2} and [NenadMiljkovic](#)^{1,3,1}; ¹University of Illinois at Urbana-Champaign, United States; ²The University of Chicago, United States; ³Kyushu University, Japan

Solid-liquid interactions are central to diverse processes. Human wellness benefits from understanding cellular behavior in complex biofluids. The soil and crops in our environment respond to the absorption of rain and agricultural sprays. In energy systems, the affinity of a solid to the working fluid determines the efficiency of boiling and condensation. Within fuel cells and batteries, the electric double layer, made up of water molecules near a metal electrode, plays a key role in electrochemistry. To quantitatively describe these solid-liquid interfaces and interactions, the solid-liquid interfacial free energy is used. This free energy arises from the imbalanced force on the liquid surface molecules that are attracted by the solid atoms on one side, and by the bulk liquid on the other side. Although vital to many processes, the direct and accurate measurements of solid-liquid interfacial energy remain a challenge. The most widely used approach to determine solid-liquid interfacial energy is the liquid droplet contact angle technique, which was first introduced in the 1960s. When a liquid droplet is in contact with a chemically homogenous and smooth solid surface, it shows partial wetting and forms a spherical liquid cap, enabling the estimation of solid-liquid interfacial energy from the measured droplet contact angle. Although this method works well for soft and low-surface-energy materials such as polymers, it is not applicable for high-energy surfaces like metals, ceramics, or semiconductors, because the droplet spreads and eliminates the ability to measure a finite contact angle. Here, in contrast with the classical approach of probing a droplet, we instead probe a liquid meniscus to directly measure the solid-liquid interfacial energy of a solid surface. We develop the solid-liquid interface by using the following steps: we first let a vertically suspended plate touch a liquid surface and allow a liquid meniscus to form. We then attach a thin and smooth solid film on this liquid meniscus, thus creating a solid-liquid interface that replaces the original liquid-air interface. The curvature of the solid-liquid-meniscus changes when compared to a free water meniscus, which is caused by the solid-liquid interfacial interaction, and which enables the measurement of solid-liquid interfacial energy from analysis of the meniscus profile.

8:00 PM CH01.08.01

First-Principles ELNES Simulation of P-O Based Materials Kosuke Kawabata and Tomoyuki Tamura; Nagoya Institute of Technology, Japan

Phosphate materials have been attracted attention for as energy materials and used for cathode materials in rechargeable batteries. In particular, the phosphate materials are expected to be used as storage electrodes storing sodium because they have many voids [1]. The physical properties of phosphate materials are greatly affected by the Q^n value (the number of bridging oxygens coordinated to phosphorus). We found that the difference in $P-Q^n$ values greatly affects the diffusion of Na^+ ions and protons in phosphate glasses using first-principles molecular dynamic simulations [2]. This suggests that ionic conductivity can be designed by controlling the $P-Q^n$ distribution of phosphate materials. In the experiment, Q^n values are usually measured using magic angle spinning nuclear magnetic resonance (MAS-NMR) techniques. But they are average information, and spatial information cannot be obtained. In recent years, electron energy-loss spectroscopy (EELS) in transmission electron microscopy (TEM) has become increasingly important for the structural characterization of materials in high spatial resolution. In particular, the near-edge structure (ELNES) can provide detail and local information on chemical bonding, valence states, and coordination. In this study, the spatial distribution of $P-Q^n$ value in phosphate materials will be observed in the combination of TEM-EELS observation and first-principles calculations.

We performed a series of first-principles PAW calculations of P L -edge ELNES spectra with QMAS code [3] for phosphate crystal models with different $P-Q^n$ values. These crystal models were taken from Materials project [4]. In the calculated spectra, the first peak shifted to the lower energy side as the $P-Q^n$ value decreased. This trend agrees with experimental results. This suggests that the $P-Q^n$ value can be determined using first peaks of ELNES spectra. To investigate the origin of each peak, we compared the partial density of states (PDOS) to the ELNES spectra. It was found that peak positions of ELNES spectra clearly coincided with the PDOS peak. This suggests that the first peak $p1$ originates from excitation from the core $2p$ state to the $4s$ state, while the second peak originates from excitation from the core $2p$ state to the $3d$ state.

In conclusion, TEM-EELS will play an important role in the practical application of high-performance phosphate-based materials.

1) A. Sanaa et al., Mater. Sci. Technol. 6, 493-501 (2023)

2) K. Takada et al., Phys. Chem. Chem. Phys. 23, 14580-14586 (2021).

3) T. Tamura et al., Phys. Rev B 85, 205210 (2012).

4) A. Jain et al., APL Materials, 1, 011002 (2013).

8:00 PM CH01.08.02

Ion Insertion and Transport in Between the MXene Layers: Control the Charging Mechanism Yuan Zhang, Danzhen Zhang and Yury Gogotsi; A.J. Drexel Nanomaterials Institute, United States

Owing to an expanding economy and growing population, there is increasing consumer demand for freshwater. Electrochemical water desalination technologies such as capacitive deionization (CDI) can achieve energy-efficient water desalination. MXene is a cation-selective material that can intrinsically suppress the ion-swapping effect in the desalination process. However, to explore MXene application in electrochemical water treatment, a deeper understanding of the charge transfer mechanism is required. In this work, the ion transport in between MXene layers under in-situ-UV-vis spectroscopy has been monitored. Compared with unconstrained spray-coated $Ti_3C_2T_x$ MXene films, physically confined MXene with fixed interlayer spacing has shown an unextraordinary ability to suppress redox reactions.

8:00 PM CH01.08.03

Dynamic Glycol Additive Adsorption for Durable Aqueous Zn-Ion Batteries and Rationalized the Performance Through Machine Learning Yuan Shang and Dipan Kundu; University of New South Wales, Australia

The benefits of aqueous zinc battery (AZB) chemistry are primarily derived from the energy-rich zinc metal anode and mild aqueous electrolytes. However, the incompatibility between these two, evident in zinc's corrosion and consequent dendrite problem, presents a significant challenge in enhancing the battery's cycle life under practical conditions. Although electrolyte additives are an effective solution, finding additives that operate at low volume concentrations remains challenging. In this study, we screened alkanol and alkanediol chemistries and discovered highly efficient additives that function at a feasible concentration of 1 volume%, thereby preserving the electrolyte's aqueous nature. These additives generate a dynamic solid-electrolyte interphase through electrode interfacial film, successfully mitigating zinc corrosion and dendrite formation, and enhancing cyclability under strenuous conditions in both half-cell and full-cell configurations. We also offer a machine learning-based analysis of the additive's performance, emphasizing the relative significance of key physicochemical descriptors. This analysis provides a logical approach to future additive discoveries.

8:00 PM CH01.08.04

High-Performance Oxide Thin-Film Transistors based on Indium with Nano-Laminate Structure using Plasma-Enhanced Atomic Layer Deposition Cheol Hee Choi¹ and Taikyung Kim²; ¹Hanyang University, Korea (the Republic of); ²Korea Institute of Science and Technology, Korea (the Republic of)

Since the discovery of amorphous indium-gallium-zinc oxide (a-IGZO) by the Hosono group in 2004, oxide semiconductors have been intensively studied. a-IGZO, with desirable electrical characteristics such as moderate mobility (~ 10 cm²/Vs), very low leakage current ($< 10^{-12}$ A), and reasonable bias stability, gained significant attention in the display industry as a backplane technology due to its low processing temperature ($\sim 400^\circ\text{C}$) and relatively low manufacturing cost. Consequently, a-IGZO became the standard backplane technology for active-matrix organic light-emitting diode (AMOLED) television displays. However, a-IGZO faced challenges in high-end mobile AMOLED displays requiring short switching times due to the high pixel density (ppi). As a result, low-temperature polysilicon (LTPS), which offers high mobility (> 80 cm²/Vs) and excellent bias stability, has been predominantly used as the backplane technology for mobile AMOLED displays. Currently, high-end mobile AMOLED displays employ LTPS and oxide (LTPO) technologies for the backplane, consisting of LTPS and IGZO TFTs for driving and switching transistors, respectively. The hybrid concept of LTPO technology can provide high resolution, fast frame rates, and low power consumption simultaneously. However, the challenging manufacturing process of LTPO technology remains a drawback, resulting in high manufacturing costs and low yield rates. Developing oxide TFTs with high mobility and reliability to compete with LTPS TFTs is a demanding engineering task.

In this study, a single diode with a 2 nm confinement layer (CL) thickness of either indium-gallium-oxide ($In_{0.84}Ga_{0.16}O$) or indium-zinc-oxide ($In_{0.75}Zn_{0.25}O$) and a barrier layer (BL) of gallium oxide (Ga_2O_3) was designed to achieve excellent electrical performance in thin-film transistors (TFTs). The formation of multiple channels within the oxide nano-laminate (NL) structure was proven to occur near the CL/BL hetero-interface in the form of a quasi-2D electron gas (q2DEG), where free charge carriers accumulate, leading to superior carrier mobility. The q2DEG near the oxide interface, designed for Fermi level (EF) engineering, was utilized to implement the NL structure in oxide semiconductors by adopting different oxide materials. The engineered q2DEG structure ensures excellent stability by reducing the trap density of the oxide NL compared to single-layer oxide TFTs. The optimized device with $In_{0.75}Zn_{0.25}O/Ga_2O_3$ NL TFT exhibited remarkable electrical performance: a mobility (μ_{FE}) of 77.1 ± 0.67 cm²/Vs, a threshold voltage (V_{TH}) of 0.70 ± 0.25 V, a steep subthreshold swing (SS) of 100 ± 10 mV/decade, an $I_{ON/OFF}$ ratio of 8.9×10^9 , a low operating voltage range of ≤ 2 V, and excellent stability (ΔV_{TH} of +0.27, -0.55, and +0.04 V for positive bias temperature stress, negative bias illumination stress, and constant current stress, respectively). The improved electrical performance, based on in-depth analysis, is attributed to the existence of q2DEG formed near the carefully designed CL/BL hetero-interface. TCAD simulations were performed theoretically to validate the formation of multiple channels in the oxide NL structure, with the formation of q2DEG near the CL/BL hetero-interface. These results clearly demonstrate that introducing heterojunction or NL structure concepts into this ALD-induced oxide semiconductor system is a highly effective strategy to enhance carrier transport characteristics and improve the bias stability in TFTs.

8:00 PM CH01.08.05

Nanographenes with Fully-Substituted Group 7A Elements: The Chemistry in Lithium-ion Battery Anodes Hui Qi Wong^{1,2}, Febri Baskoro¹ and Hung-Ju Yen¹; ¹Academia Sinica, Taiwan; ²National Taiwan University, Taiwan

Graphene has received intensive scientific attentions as an electrode material for lithium-ion batteries because of its extraordinary physical and electrical properties. However, the lacking of structural control and restacking issues have hindered its application as carbon-based anode materials for next generation lithium-ion batteries. To tackle these problems and improve its performance, several modification approaches such as edge-functionalization and electron-donating/withdrawing substitution have been considered as promising strategies. In addition, group 7A elements have been known as critical elements due to their electronegativity and electron withdrawing character, which can regulate the electronic and structural properties of materials. Herein we elucidated the chemistry of nanographenes with fully-substituted group 7A elements as lithium-ion battery anodes. The nanographenes have been synthesized via bottom-up organic synthesis to ensure the structural control. Our study reveals that the present of halogen atoms on the edge not only tuned their structural and electronic properties, but also impacted material stability and reactivity as well as Li^+ storage capability. Further systematically spectroscopic study indicates that the charge polarization caused by halogen atoms could also regulate the

Li⁺ transport, charge transfer energy, and charge storage behavior of nanographenes. This study provides a deep understanding on the molecular design of nanographene anodes for next-generation lithium-ion batteries.

8:00 PM CH01.08.06

0.01 to 0.5 Sun is a Realistic and Alternative Irradiance Window to Analyze Urban Outdoor Photovoltaic Cells Ka Lai Wong, Chujun Zhang, Zhuoqiong Zhang, Mingwei Hao, Yuanyuan Zhou and Shu Kong So; Hong Kong Baptist University, Hong Kong

Solar cells have penetrated many cities as Building Integrated Photovoltaic (BIPV) or the energy source for standalone Internet of Things (IoT) devices. Traditionally, photovoltaic (PV) cells are evaluated using 1 sun irradiance. However, in a city, factors such as air pollution, cloudiness and cell installation orientation may attenuate the receivable solar energy. Also, the power conversion efficiency (PCE) of a PV cell is highly irradiance-dependent. Evaluating urban outdoor PV cells using 1 sun irradiance could lead to inaccurate prediction of PCE and overestimated output power in actual usage. Herein, we analyzed daytime irradiances of 11 cities located across the globe. Our results show that realistic irradiances (RI) in most cities are between 0.01 and 0.5 sun, reflecting the irradiance under a cloudy to mostly sunny sky. Under such an RI window, the PCEs of 9 different PV technologies were compared. 7 PV technologies have compromised performance. 2 PV technologies, organic and perovskite PVs, show enhanced PCE under the RI window and are favorable for urban outdoor applications. The tested perovskite PV reached 21% PCE while the non-fullerene-based organic solar cell has improved to 18% PCE under a cloudy sky. The potential of powering IoT devices with these PV technologies under sub-optimal irradiance conditions in cities is also highlighted.

8:00 PM CH01.08.07

Functional Separator Enabling Improved Cycling Performance of Lithium Metal Batteries Dahee Song¹, JunHyeokSeo¹, MinjaeKim¹, Kuk YoungCho² and JuyeonIm¹; ¹Hanyang University, Korea (the Republic of); ²Hanyang University(ERICA campus), Korea (the Republic of)

Battery research worldwide is focused on developing next-generation batteries, and the lithium metal battery has emerged as a promising candidate. This advanced battery design replaces the conventional graphite anode with a lightweight lithium metal anode, offering high capacity and a low oxidation-reduction potential. A high-nickel cathode with increased nickel content and a lithium metal anode are required to achieve high-energy-density lithium batteries.

However, rapid capacity degradation caused by dendrite formation due to the deposition of transition metals from the cathode onto the lithium metal and the formation of an unstable solid electrolyte interface (SEI) layer during battery operation is challenging. A well-designed functional separator approach can effectively mitigate these issues and improves the performance of the lithium metal battery by minimizing the byproducts of side reactions. This study demonstrates the crucial importance of restricting the movement of transition metal ions to the lithium metal anode, contributing to enhanced operational performance and stability of the lithium metal battery.

8:00 PM CH01.08.08

Understanding the Relationship between Separator Parameters and Characteristics of Practical Lithium Metal Batteries JunHyeokSeo, MinjaeKim, DaheeSong and Kuk YoungCho; Hanyang University(ERICA campus), Korea (the Republic of)

The demand for low-cost, high-energy-density lithium-ion batteries (LIBs) has risen due to the entry of grid-level energy storage systems (ESSs) and electric vehicles (EVs) into the market. Lithium metal batteries (LMBs) promise improved energy density, but safety issues related to Li dendrite growth and reactivity persist. The separator, which prevents short circuits, plays a vital role in the performance and safety of LIBs.

Selecting an appropriate separator thickness is crucial because reducing the separator thickness significantly enhances the volumetric energy density and electrochemical performance of LMBs. In addition, the results of the study identify pore closure within the separator as a critical issue affecting cell failure. Effective prevention of pore closure involves maintaining robust mechanical properties, achieving the appropriate solid electrolyte interface composition, and suppressing lithium dendrite growth during cycling. Balancing mechanical strength and low resistance in the separator, along with developing materials to inhibit pore closure, advances the commercialization of high-energy-density LMBs with improved performance and longevity. This study investigates the relationship between separator parameters and practical lithium metal batteries (LMBs) characteristics to achieve stable and long-term cycling performance for successful commercialization.

8:00 PM CH01.08.09

On the Electro-Mechanical Property Characterization of Piezoelectric Inorganic and Hybrid Materials for Energy Harvesting Systems PierreNickmilder¹, EmelineSchmidt^{1,2}, MartinLefebvre¹, Marie-HélèneChambrier², AntonioDa Costa², AnthonyFerri², RachelDesfeux² and PhilippeE. Leclere¹; ¹University of Mons, Belgium; ²Universite d'Artois, France

The energy crisis presents one of the most significant challenges of our century, necessitating the urgent exploration of new methods for electricity generation. A promising approach involves the development of systems made of materials with piezoelectric properties for charge generation and transport. While certain materials such as PZT exhibit excellent piezoelectric properties, the presence of toxic lead hinders their applicability. Consequently, alternative materials such as innovative lanthanide-based tungsten oxide (Ln₂WO₆), which demonstrate piezoelectric behavior, need to be explored in detail [1-3]. Furthermore, organic materials such as poly(vinyl difluoro ethylene) (PVDF) – based materials possess inherent piezoelectric properties, albeit with weaker coefficients than their inorganic counterparts. However, the addition of piezoelectric nanoparticles like BiFeO₃ (BFO) nanoparticles can enhance their piezoelectric response. This study aims to characterize two distinct types of materials, the inorganic Gd₂WO₆ oxide in thin film and the hybrid system made of PVDF-b-trifluoro ethylene (PVDF-trFE) block copolymer containing BFO nanoparticles, and subsequently develop a hybrid material that combines the flexibility of the organic component with the structural resistance of the inorganic counterpart, while ensuring piezoelectric sensitivity. To achieve this, we utilized Piezoresponse Force Microscopy (PFM), an Atomic Force Microscopy (AFM) mode based on the inverse piezoelectric effect. Even though the PFM is still universally used to quantify piezo and ferroelectric properties, recent studies have revealed that a significant contribution of the electromechanical response captured by PFM is unfortunately due to artifacts, mostly by electrostatic interactions between the surface and the tip being the most dominant of them [4]. In addition to conventional PFM, another mode has been developed, such as switching spectroscopy PFM (ssPFM). This mode uses a script where the electromechanical response is continuously monitored while alternating between the polarization step and the non-polarization step. The contribution of electrostatic interaction can be minimized by identifying the electrostatic blind spot (ESBS) [5], the laser position on the cantilever that minimizes the electrostatic contribution. This limitation of long-distance electrostatic interaction can be verified through an “almond nut” test. [6] From those data, the ferroelectric hysteresis from the studied material can be extracted.

Through our research, we aim to contribute to the development of piezoelectric hybrid materials with enhanced electromechanical properties. These materials hold significant potential for addressing the energy crisis and driving advancements in electricity generation and utilization.

[1] Carlier, T., et al. ACS Applied Materials & Interfaces (2015) 7(44) 24409-24418

[2] Carlier, T., et al. Materials Chemistry 32(17) (2020) 7188-7200

[3] Lheureux, M., et al. “ACS Applied Electronic Materials (2022) 4(11) 5234-5245

[4] Seol, D.; et al. Current Applied Physics (2017), 17 (5), 661-674.

[5] Killgore, J. P.; et al. Nanoscale Adv. (2022), 4 (8), 2036–2045.

[6] Collins, Let al. ACS Nano (2019), 13 (7), 8055–8066.

8:00 PM CH01.08.10

Understanding the Role of Lithium Borate as the Surface Coating on High Voltage Single Crystal LiNi_{0.5}Mn_{1.5}O₄Na RiPark¹, WeikangLi¹ and Y. ShirleyMeng²; ¹University of California, San Diego, United States; ²The University of Chicago, United States

Researchers investigated the potential of using lithium borate (LBO) to enhance the performance of high-voltage spinel lithium nickel manganese oxide (LNMO) cathode material in lithium-ion batteries (LIBs). LNMO/graphite (LNMO/Gr) full cells commonly suffer from capacity fading, limiting their practical applications. To address this issue, a dry mixing method was employed to apply an LBO coating on the LNMO surface. The LBO-coated LNMO exhibited improved cycling stability compared to uncoated LNMO in full cells, achieving a practical 3 mAh/cm² areal capacity. Various characterizations were conducted to understand the coating's effect on the cathode, electrolyte, and anode. The LBO-coated LNMO demonstrated a 5 nm cathode electrolyte interphase (CEI) with reduced phase change after long-term cycling, while the uncoated LNMO showed negligible CEI with noticeable phase change. Surprisingly, no boron was detected on the surface of the coated sample. Electrolyte and anode analyses revealed that the coating acted as a reservoir, gradually dissolving into the electrolyte and generating BF₄⁻ species. Consequently, the coating mitigated the dissolution of nickel and manganese from LNMO, as well as the extensive formation of a solid electrolyte interphase (SEI) on the anode side, leading to significant improvements in the cycling stability of the full cells. The insights gained from this study may serve as a guide for surface modification techniques applied to other high-voltage cathode materials with related electrolyte additive designs.

8:00 PM CH01.08.11

Structural-Plasmonic Relationship of Crystalline Copper Oxide Microcubes Decorated with Plasmonic Gold Nanoparticles EsterV. De Almeida^{1,2}, Diericd. Abreu³, Douglasd. Lopes^{1,2}, BrunoG. Fonseca², EduardoR. Nascimento², MichelleL. de Souza², LuisH. de Lima⁴, PaolaCorio¹ and AlexandreBrolto²; ¹University of Sao Paulo, Brazil; ²University of Victoria, Canada; ³Universidade Federal do Ceara, Brazil; ⁴Universiade Federal do ABC, Brazil

Copper oxide semiconductors are the most prominent catalyst for CO₂ electrochemical reduction. In recent years, a myriad of properties has been arising from new combinations between distinct nanomaterials. The superficial decoration of copper oxide with noble metal nanoparticles presents plasmonic synergistic effects resulting from local crystalline structure perturbation. In this way, different characterization methods of materials can be used to elucidate the structural, electronic, and optic properties of nanomaterials. In this work, we combined these three approaches to understand the role of the addition of plasmonic gold nanostructures to semiconductive copper oxide microcubes. The green synthesis of nanomaterials is an important factor. This way, we used a CuCl₂ salt in basic medium and later a soft reductant addition. To add the Au nanoparticles, we added a Au³⁺ solution and due to the reduction potential of Cu₂O being lower than gold, nanoparticles are naturally formed. On our SEM images of synthesized nanoparticles, we observed that Cu₂O nanoparticles have a well-defined cubic shape and flat surface and mean size of 536.40 nm ± 179.41 nm. Also, the gold addition to the Cu₂O nanoparticles does not change its shape but creates a rugous surface with size distribution of rough structures of about 35.47 nm ± 9.38 nm. EDS analysis of Au-Cu₂O confirms that this roughness can be attributed to gold nanostructures. A XPS analysis shows that on Cu₂O the surface is composed of Cu⁰ (931.1 eV), CuO (934.2 eV) and Cu₂O (932.5 eV) while Au-Cu₂O surface is composed by CuO (932.0 eV) and Cu₂O (932.4 eV) due to copper oxidation on gold presence. To understand about the crystalline structure of our materials, we used a XRD analysis which shows very sharp peaks for both materials, indicating a monocrystalline behavior. The peaks present in Cu₂O sample can be attributed to Cu₂O cubic (ICSD: 98-062-8621) with the main facet (111). The addition of gold to the Cu₂O does not change the crystallinity but we observed the arising of peaks attribute to gold structures (ICSD: 98-016-3723). These results are consistent with the SEM images and show the success of the proposal synthesis. Cyclic voltammetry was performed to understand the electrochemical behavior of materials and shows a reduction event occurring at -0.40 V on Cu₂O sample, which can be associated with the reduction of Cu⁺ to Cu⁰ (-0.36 V). On Au-Cu₂O, the voltammogram does not show the -0.40 V event, but a new event is observed at -0.90 V. The presence of gold on the surface could protect the Cu⁺ on the surface by the spillover effect. When oxygen atoms are adsorbed on the catalyst surface, the gold structure act as an electron source reducing O₂ to active species. Electronic properties were analyzed by UV-vis-NIR showing two bands of Cu₂O in 506 and 651 nm and 624 nm for Au-Cu₂O, there were no observed gold plasmonic bands for Au-Cu₂O but a broad shoulder on the infrared region. Dark field microscopy data shows the optical properties. Two bands with a maximum at 488 and 583 nm are attributed to Mie resonance of copper oxide. When gold is added to the Cu₂O bands positions change to 476 and 623 nm, respectively. According to the literature, gold nanoparticles around 40 nm have a λ_{scattering} at 500 nm. Applying potential from 0.00 V to -0.80 V (vs. Ag/AgCl), we observed that Cu₂O sample does not present changes in the spectral pattern, however on Au-Cu₂O, as more cathodic the applied potential, the higher the intensity of 476 nm band. To apply a negative potential to a metallic structure means to inject electrons on its Fermi level, dislocating it to a different energy. Combining these results with Raman spectroscopy in different potentials, we observed changes in position and intensity for Cu₂O bands. Thus, our hypothesis is that gold nanoparticles cause distortion on Cu₂O crystalline lattice, favoring electronic density on gold nanostructures rather than a distribution over the surface.

8:00 PM CH01.08.12

Imaging of Photoinduced Electrochemiluminescence at Hematite (α-Fe₂O₃) Photoanodes TaeyoonKim, JooheonKim, SungeunHan and MisolHwang; Department of Chemistry, Kyung Hee University, Korea (the Republic of)

We study intuitive observation of electrochemical reactions through images obtained from photoinduced electrochemiluminescence (PECL), which combines light-addressable electrochemistry (LAE) and electrochemiluminescence (ECL). LAE provides information about electrochemical reactions through photogenerated carriers. In this study, we used stable hematite (α-Fe₂O₃) as a photoanode in an aqueous solution. Hematite has the advantage of obtaining a high spatial resolution due to the short diffusion distance of the minority carrier. By comparing the images of ECL and PECL, it was confirmed that the onset potential in PECL was lower. Using this method, we were able to observe that photogenerated carrier induces additional ECL reactions. Additionally, we used a digital mirror device (DMD) that allows for the flexible controllability of the light illumination shape of and confirmed the matching of the illuminated area and the ECL emission area. Furthermore, we propose the potential application of PECL imaging for characterizing the properties of single nanorods.

8:00 PM CH01.08.13

Operando Diffraction Technique to Investigate the Electrochemically Deposited Mg Interface ShengqiFan¹ and NiyaSa^{2,1,3}; ¹Indiana University Bloomington, United States; ²Argonne National Laboratory, United States; ³University of Massachusetts Boston, United States

Shengqi Fan¹, Niya Sa¹
University of Massachusetts Boston¹

Magnesium (Mg) has gained significant attention as a potential candidate for high-performance energy storage systems due to its high volumetric capacity and abundance. However, the practical implementation of Mg-based batteries faces challenges stemming from a limited fundamental understanding of the Mg electrodeposition/dissolution process. The complex crystallographic structure evolution at the deposited Mg interface during electrochemical cycling plays a crucial role in the performance and durability of Mg batteries. In this study, we present an in-situ X-ray diffraction technique that enables real-time monitoring and characterization of the electrochemically deposited Mg interface. By analyzing the diffraction patterns obtained under various applied voltages, we have obtained valuable insights into the dynamic changes in peak positions and the lattice parameters at the electrode surface during Mg deposition and dissolution. Our findings could potentially contribute to the development of optimized electrolyte formulations and improved electrochemical cell designs for Mg-based batteries.

8:00 PM CH01.08.14

Importance of Interface Engineering Between the Hole Transport Layer and the Indium-Tin-Oxide Electrode for Highly Efficient Polymer Solar Cells SujungPark¹, FebrianT. Wibowo², NarraV. Krishna², JihoRyu¹, HeunjeongLee¹, JinheeLee³, Yung JinYoon², Jin YoungKim², Jung HwaSeo³, Seung-HwanOh⁴, Sung-YeonJang² and ShinukCho¹; ¹University of Ulsan, Korea (the Republic of); ²Ulsan National Institute of Science and Technology, Korea (the Republic of); ³University of Seoul, Korea (the Republic of); ⁴Korea Atomic Energy Research Institute, Korea (the Republic of)

In early studies on organic solar cells with high conductivity PEDOT:PSS, the contact between ITO and PEDOT:PSS was considered ohmic. However, because low-conductivity PEDOT:PSS (such as AI4083) is mainly utilized in contemporary solar cells, the contact between ITO and PEDOT:PSS is not ohmic anymore. Despite the high possibility that there are serious interface problems, little attention has been paid to the interface between PEDOT:PSS and ITO. Most of the previous studies of interfaces in organic solar cells have focused on the interface between the active and charge transport layers. In this work, we have employed a conjugated polyelectrolyte that uses potassium poly[9,9-bis(3'-sulfonatopropyl)fluorene-alt-(9-(2,7-diethylheptyl)-carbazole)] (WPFSCz-) between ITO and low-conductivity PEDOT:PSS to overcome complicated organic-inorganic interfacial problems. The insertion of the WPFSCz- layer provides substantial advantages in the operation of polymer solar cells. First, the inserted WPFSCz- layer modifies the work-function of ITO, thereby forming an effective cascading energy alignment, which is favorable for good hole transport. Second, the introduction of the WPFSCz- layer eliminates interfacial trap sites. The reduction in traps reduces recombination losses at the interface, resulting in an improvement in the fill factor. These effects result in a significant increase in the efficiency of non-fullerene solar cells based on PM6 and Y6, from 15.86 to 17.34%. In addition, we have found that the problem of the interface in contact with ITO occurs not only in PEDOT:PSS, but also in oxide-based charge transport layers. We have confirmed that the insertion of the WPFSCz- layer between ITO and a MoO₃ (or ZnO) charge transport layer shows the same positive results.

8:00 PM CH01.08.15

Impact of Morphology Change on Hole Transfer Dynamic During Charge Separation Process DongchanLee^{1,1}, JihoRyu¹, SebinKim¹, Chang-MokOh², In-WookHwang² and ShinukCho^{1,1}; ¹University of Ulsan, Korea (the Republic of); ²Gwangju Institute of Science and Technology, Korea (the Republic of)

Although it was clearly elucidated that the change in the overall bulk-heterojunction (BHJ) morphology of PM6:Y6 induced by the difference in solvents results in a performance variation in the entire solar cell. The charge dynamics during the charge separation process induced by morphological changes have not yet been deeply studied. Based on mobility and photocurrent related studies, it was inferred that holes were deeply involved in these charge generation and separation processes. The decrease in exciton dissociation probability observed in the PM6:Y6 solar cell fabricated using CB (PM6:Y6-CB) was found to be due to the change in hole transfer state caused by morphological changes. For the PM6:Y6 solar cell fabricated using CF (PM6:Y6-CF), it was determined that the density of state (DOS) of effective hole transfer state (^hE_{CT}) was small, as ^hE_{CT} and Y6 HOMO were almost degenerate, and the lower ^hE_{CT}, which can interfere with hole transfer, was also formed minimally. However, for PM6:Y6-CB, the overlapping region of ^hE_{CT} and highest occupied molecular orbital (HOMO) of Y6 shifted towards the lower energy side (upper ^hE_{CT}) and a lower effective ^hE_{CT} that can act as a defect was significantly formed. These facts obtained by EL deconvolution were clearly confirmed in time-resolved photoinduced absorption spectroscopy. As a result, it is concluded that the decrease in fill factor (FF) and current density (J_{SC}) in PM6:Y6-CB is due to the degradation of hole transfer from Y6 HOMO to PM6 HOMO, which is analyzed as the morphological changes in non-fullerene acceptor (NFA) solar cells affect the formation of hole transfer levels, which in turn affects the charge separation efficiency.

8:00 PM CH01.08.16

Characterization of Ag₃BiI₆ Rudorffite Absorber for Ambient-Air-Stable, Lead-Free and Efficiency Solar Cells Through Scanning Kelvin Probe Analyzer Ming-ChungWu^{1,2}, Kai-ChiHsiao¹, Yin-HsuanChang¹, Jia-MaoChang¹ and Ting-HanLin¹; ¹Chang Gung University, Taiwan; ²Chang Gung Memorial Hospital at Linkou, Taiwan

Perovskite solar cells, renowned for their exceptional power conversion efficiency (PCE), hold promise as a sustainable and renewable energy solution. However, the utilization of lead-based absorbers in these cells raises significant concerns due to the toxic nature of lead. Their stability in ambient conditions is also a challenge should be overcome for their further development. To

address these issues, we investigated the feasibility of adopting a novel lead-free material, Ag_3BiI_6 ruderffite absorber, as an alternative active layer to replace the conventional lead-based perovskite absorber. [1,2] Ag_3BiI_6 ruderffite absorber layer is prepared by using a large scalable thermal-assisted doctor blade coating method. As a novel light absorber layer, realizing the localized work function of Ag_3BiI_6 helps to optimize the energy level in its device. In this study, we employed a scanning Kelvin probe analyzer (KP Technology, SKP 5050), equipped with red, green, and blue LED light sources with a total power of 300 mW, to measure the constant potential difference (CPD) and investigate the local work function of the Ag_3BiI_6 ruderffite absorber. The scanning Kelvin probe analyzer, a highly sensitive and non-contact scanning probe technique, allows us to assess the light response of the absorber layer by measuring the light-induced CPD under different wavelengths. The CPD of the absorber layer serves as an indicator of the light response of Ag_3BiI_6 ruderffite, providing insights into its performance when exposed to various incident light. With assistance of Kelvin probe analyzer, we optimized the energy level alignment between the carrier transporting layers and the Ag_3BiI_6 ruderffite absorber layer, resulting in an improved PCE of doctor-bladed devices from 2.06% to 2.77%. Taking advantages of band alignment, these devices retain 90% of their initial PCE over 3,000 hours in ambient without any unencapsulation. Moreover, the scalability of our approach is also demonstrated and the device with an active area of 1.00 cm^2 achieves a PCE of 2.03%. [3] In summary, our study highlights the potential of Ag_3BiI_6 ruderffite as a viable substitute for lead-based perovskite absorbers in solar cells. Its superior environmental safety, stability, and scalability make it an attractive candidate for the development of sustainable energy technologies.

References

- [1] Kai-Chi Hsiao, Yen-Fu Yu, Ching-Mei Ho, Meng-Huan Jao, Yu-Hsiang Chang, Shih-Hsuan Chen, Yin-Hsuan Chang, Wei-Fang Su, Kun-Mu Lee*, and Ming-Chung Wu*, "Doping Engineering of Carrier Transporting Layers for Ambient-Air-Stable Lead-Free Rudorffite Solar Cells Prepared by Thermal-Assisted Doctor Blade Coating", 2023, *Chemical Engineering Journal*, 451, 138807.
- [2] Ming-Chung Wu*, Qian-Han Wang, Kai-Chi Hsiao, Shih-Hsuan Chen, Ching-Mei Ho, Meng-Huan Jao, Yin-Hsuan Chang, and Wei-Fang Su, "Composition Engineering to Enhance the Photovoltaic Performance and to Prolong the Lifetime for Silver Bismuth Iodide Solar Cell", 2022, *Chemical Engineering Journal Advances*, 10, 100275.
- [3] Ming-Chung Wu*, Rwei-Yu Kuo, Yin-Hsuan Chang, Shih-Hsuan Chen, Ching-Mei Ho, and Wei-Feng Su, "Alkali Metal Cation Incorporated Ag_3BiI_6 Absorbers for Efficient and Stable Rudorffite Solar Cells", 2021, *Oxford Open Materials Science*, 1, itab017.

8:00 PM CH01.08.17

Tracing Electrochemical Charge-Carrier Insertion into Vanadium Oxide Cathode in Aqueous Zinc-Ion Batteries Changmin Lee, [Dongho Kim](#), Youngjae Hong, Younghwan Lim and Sung-Yoon Chung; Korea Advanced Institute of Science and Technology, Korea (the Republic of)

With growing concerns regarding the safety and cost issues of Li-ion batteries, extensive research is focusing on suitable alternatives. Among the candidates, aqueous electrolyte-based batteries have recently gained significant attention due to their non-flammable nature compared to organic electrolytes. As a water-based solution is utilized as the electrolyte, the role of protons, in addition to the primary redox charge carriers inserted in cathode materials, has become a crucial scientific issue in the field of aqueous battery research. Especially, under low-pH conditions, i.e., highly acidic electrolyte, the presence of protons becomes significant, potentially affecting the overall capacity and redox potential. Despite numerous studies investigating proton insertion into oxide cathodes, there is a lack of clear interpretations regarding the intercalation behavior. Therefore, to comprehensively understand the ambiguous role of protons in cathode materials within aqueous rechargeable batteries, it is essential to conduct systematic investigations covering a wide range of proton concentrations. Herein, we investigate the behavior of inserted charge carriers in V_2O_5 cathode oxide in two different cell types. In the presence of sufficient proton supply, such as beaker-cell configuration, the pH of the electrolyte influences the insertion process. Under low-pH conditions, we found that protons are inserted into the cathode before Zn ions. Otherwise, under high-pH conditions, Zn-ion serves as a major charge carrier, while the impact of protons on discharge voltage or capacity becomes less significant. To validate the generality of our hypothesis, we also demonstrate similar pH-dependent behavior in Na-, Mg- and Al-ion electrolytes. We established this mechanism through the integration of various analytical techniques. X-ray photoemission spectroscopy (XPS) spectra reveal valence state change of cathode materials and energy dispersive X-ray spectroscopy (EDS) elemental mapping directly visualizes and quantifies the Zn-ion and proton insertion. By employing a combination of X-ray absorption near-edge structure (XANES) and extended X-ray absorption fine structure (EXAFS) spectra, we gain insights into the overall oxidation state changes and bonding length alternations as a result of carrier-ion insertion. Furthermore, we examined the influence of electrolyte volume by adopting a coin-cell configuration. In this type of cell with a relatively small volume of acidic electrolyte, a substantial influence of protons observed in the low-pH beaker-cell test was not identified. Based on the aforementioned results, we conclude the proton contribution to discharge capacity is only significant when a sufficient amount of highly acidic electrolyte is utilized.

8:00 PM CH01.08.18

Zinc-Bridged Lithium on Carbon Nanofibers for Enhancing Anode-Free Li-Metal Battery Performance [Ilgyu Kim](#)¹, HoJin Lee¹, Suhyeon Lee², Sangjoon Kim² and Ji-Won Jung¹; ¹University of Ulsan, Korea (the Republic of); ²Korea Research Institute of Chemical Technology, Korea (the Republic of)

With the introduction of the "Anode-Free" concept in Li-metal batteries, various studies have been conducted to address the chronic issue of irreversible cycle performance caused by Li dendrite growth. To this end, here we synthesized a Zn-deposited carbon nanofiber (Zn-CNF) composite using thermal shock synthesis to employ as the Li-Metal battery anode. By incorporating Zn as an electrodeposition catalyst, we achieved a remarkably low Li nucleation overpotential, promoting homogeneous Li growth on the CNF substrate and limiting Li dendrite formation. This was confirmed through half-cell and symmetric cell plating-stripping tests and full-cell galvanostatic tests. Furthermore, morphological and chemical analyses, including Scanning Electron Microscopy (SEM) and Transmission Electron Microscopy (TEM), were conducted to elucidate the structural and compositional properties of the synthesized materials.

8:00 PM CH01.08.19

Non-Destructive Steady-State and Time-Resolved Photoluminescence (TRPL) Characterization of Photovoltaic Devices [Christian Oelsner](#), Volker Buschmann, Eugeny Ermilov, Bitara Rezania, Felix Koberling and Rainer Erdmann; PicoQuant GmbH, Germany

Over years, (time-resolved) photoluminescence spectroscopy (TR)PL has been established as one of the fundamental methods for analyzing the photophysical properties of a wide variety of samples, ranging from organic molecules to semiconductor materials and photovoltaic (PV) devices. The combination of luminescence spectral and lifetime information provides a better understanding of photophysical processes and their dynamics in PV materials. This understanding can be further enhanced by including spatial information.

Herein, we will demonstrate that the combination of time-resolved laser scanning microscopy and PL spectroscopy provides a powerful characterization tool. This combination allows mapping of a broad range of phenomena including TRPL, carrier diffusion, SHG/2PE, wavelength and power dependent emission with high spatial resolution, for various sample geometries e.g., thin films. Therefore, one can infer structural-to-photophysical relationships in new classes of PV materials which ultimately leads to the optimization of the PV device performance.

8:00 PM CH01.08.20

Time-Resolved Concentration Profiling of LiPF_6 in EC:EMC Electrolytes in Lithium Ion Batteries [Conor Phelan](#), Gregory J. Rees and Robert Weatherup; Department of Materials, University of Oxford, United Kingdom

Liquid phase electrolyte lithium-ion batteries (LIBs) typically consist of a lithium salt dissolved in a mixture of cyclic and linear alkyl carbonates. Continuum models typically treat the electrolyte co-solvents as a single variable, dubbed the "single-solvent approximation". However, recent work in the area has called the validity of this assumption into question [1]. Herein, we develop a new continuum model to describe the dynamics of multicomponent electrolyte solutions and directly compare model predictions with experimentally measured concentration profiles which can be obtained using potentiometric magnetic resonance imaging (MRI) [2] and Raman spectroscopy [3] to investigate the validity of this significant assumption. The developed model is applied to a 1M LiPF_6 in EC:EMC v%:v% 3:7 to better understand the salt and solvent dynamics in commercial LIB electrolytes. This demonstrates that EC and EMC show distinct concentration gradients, challenging the validity of the "single-solvent approximation" which has been widely used to this point in LIB modelling. The developed model was parameterized solely using classical MD simulations for a 1M LiPF_6 type electrolyte. The effects of electrolyte solvation structures are manifested on the continuum scale. Most notably effects arising from Li^+ ion solvation by EC and EMC molecules are observed. A dragging effect is observed on solvent molecules due to the motion of the Li^+ ions they solvate, which influences the concentration gradient of the solvent molecules under an applied current. The concentration gradients of both the solvent molecules and salt ions influence the composition of the solid-electrolyte interphases that form in LIBs, making the understanding of how these gradients change under applied currents of crucial importance. These results have provided fundamental insight into how the solvation structure of commercial LiPF_6 electrolytes affects the transport properties and concentration gradients of the electrolyte components, which will inform the development of improved electrolytes for LIB applications.

[1] Andrew A. Wang, Samuel Greenbank, Guanchen Li, David A. Howey, Charles W. Monroe, Current-driven solvent segregation in lithium-ion electrolytes, *Cell Reports Physical Science*, Volume 3, Issue 9, 2022, 101047, ISSN 2666-3864.

[2] *ACS Energy Lett.* 2021, 6, 9, 3086–3095 Publication Date: August 15, 2021

[3] Fawdon, J., Ihli, J., Mantia, F.L. et al. Characterising lithium-ion electrolytes via operando Raman microspectroscopy. *Nat Commun* 12, 4053 (2021). <https://doi.org/10.1038/s41467-021-24297-0>

8:00 PM CH01.08.21

Enhancing Next-Gen Photovoltaic Cells: Unveiling Optoelectronic Properties through Hyperspectral Imaging Laura-Isabelle Dion-Bertrand¹, Felix Thouin¹, Christof Schultz², Bert Stegemann² and César Omar Ramírez Quiroz³; ¹Photon etc., Canada; ²University of Applied Sciences – HTW Berlin, Germany; ³FOM Technologies, Denmark

In recent years, the photovoltaics scene has undergone significant transformations, resulting in an unprecedented diversity of solar materials. Despite recent advancements, the widespread commercialization of most emerging technologies remains challenging. This can be partly attributed to material inhomogeneities and the difficulties associated with up-scaling. One specific aspect that requires attention to bridge the cell-to-module gap while maintaining high efficiencies in both CIGS and perovskite-based solar cells, is the laser patterning process for series interconnections of cells. It is crucial to establish control over the underlying process of P1, P2, and P3 laser ablation lines and identify any associated power losses.

The optimization of a solar cell fabrication process, including the laser ablation process, requires high-performance and specialized measurement systems. To address this demand, Photon etc. in collaboration with IRDEP (Institute of Research and Development on Photovoltaic Energy), has developed a global hyperspectral imaging platform (IMA™) for solar cell analysis. This platform provides rapid acquisition of photoluminescence (PL), electroluminescence (EL), and absorbance maps. Most luminescence imaging characterization techniques provide data in arbitrary units, which limits their interpretation because of the lack of information. With this challenge in mind, researchers at IRDEP have designed a method for spectral and photometric calibration [1]. This technique has been implemented in Photon etc.'s platform and allows obtaining the absolute number of photons emitted at a specific energy from every point on the sample's surface. By performing this calibration, researchers can further investigate Planck's law to access the quasi-fermi level splitting (QFLS) [2].

In this framework, we combined global hyperspectral imaging with absolute calibrated photoluminescence to extract spatial distribution of several optoelectronic of triple cation perovskite ($\text{Cs}_{0.05}(\text{FA}_{0.79}\text{MA}_{0.16})_{0.95}\text{PbI}_{2.49}\text{Br}_{0.51}$), CIGS ($\text{Cu}(\text{In}_x\text{Ga}_{1-x})\text{Se}_2$) [3] and CIGS/perovskite tandem solar cells patterned with ns and ps laser pulses. Maps of the PL quantum yield (PLQY), effective QFLS, open circuit voltage (V_{oc}), Urbach energy (E_u), optical diode factor (ODF), and shunt resistance (R_{sh}) were obtained. These mappings provide insights that help determine the optimum process window for patterning. Moreover, this hyperspectral imaging system enables selective excitation and characterization of the bottom cell (CIGS) and the top cell (perovskite). This capability allows a spatially resolved detection and analysis of the laser-induced defects at each individual patterning step, thereby enabling conclusions to be drawn regarding the specific effects on each sub-cell.

[1] Delamarre, A., Paire, M., Guillemoles, J.-F., & Lombez, L. (2014). Quantitative luminescence mapping of Cu(In, Ga)Se₂ thin-film solar cells. In *Progress in Photovoltaics: Research and Applications* (Vol. 23, Issue 10, pp. 1305–1312). Wiley. <https://doi.org/10.1002/pip.2555>

[2] Rau, U. (2007). Reciprocity relation between photovoltaic quantum efficiency and electroluminescent emission of solar cells. In *Physical Review B* (Vol. 76, Issue 8). American Physical Society (APS). <https://doi.org/10.1103/physrevb.76.085303>

[3] Ramírez Quiroz, C. O., Dion-Bertrand, L.-I., Brabec, C. J., Müller, J., & Orgassa, K. (2020). Deciphering the Origins of P1-Induced Power Losses in Cu(In Ga)Se₂ (CIGS) Modules Through Hyperspectral Luminescence. In *Engineering* (Vol. 6, Issue 12, pp. 1395–1402). Elsevier BV. <https://doi.org/10.1016/j.eng.2019.12.019>

8:00 PM CH01.08.22

Fabrication of ZnV₂O₄ Nanoparticles Embedded in Carbon Nanofibers as a Cathode Material for High-Performance Aqueous Zn-Ion Batteries Jeong-Ho Park, Ilgyu Kim, Na yeong Kim, Subin Lee and Ji-Won Jung; University of Ulsan, Korea (the Republic of)

Recently, lithium-ion batteries have led the related market. However, the price of Li is expected to increase continuously, leading to unbalance of demand and supply for LIBs used for electric vehicles (EVs) and energy storage systems (ESS). For replacing LIBs, electrically rechargeable aqueous zinc-ion batteries (ZIBs) have been spotlighted due to Zn's attractive properties, such as being environmentally friendly, low price, and high stability. Nevertheless, the low capacity of ZIBs is attributed to low-capacity cathode material, restricting their practical utilization. To increase the capacity of ZIBs, ZnV₂O₄ containing the Zn element has recently been considered. However, the ZnV₂O₄ cathode developed so far shows various problems of low electronic conductivity and low surface area limiting reaction sites. Here, we suggest ZnV₂O₄ nanoparticles embedded in carbon nanofibers (ZVO@CNFs) as a promising cathode material for ZIBs. The ZVO@CNFs were synthesized using the electrospinning process and heat treatments, including stabilization and carbonization. The fabricated ZVO@CNFs were investigated by SEM, TEM, XRD and XPS to confirm how can the ZVO nanoparticles form inside. In addition, Raman analysis was conducted to know the composition of ZVO@CNFs and crystal lattice information and EA analysis was carried out to obtain wt% of ZVO in the CNFs. The ZIB cell with the ZVO@CNFs was evaluated for its feasibility. Charge and discharge tests and rate tests were conducted and CV (Cyclic Voltammetry) test was conducted to determine the voltage window, reversibility, and impurities in the system where the redox reaction occurs.

8:00 PM CH01.08.23

X-Ray Elemental and Crystalline Phase Distribution Analysis of the Process to Produce Hydrogen and Ammonia from Iron and Carbonated Water Hiromi Eba¹, Yagi Hayao¹, Tian Liu¹, Norika Nakazawa¹, Keiichi Fukami¹ and Kenji Sakurai²; ¹Tokyo City University, Japan; ²Imaging Physics Laboratory, Japan

Currently, hydrogen energy is attracting much attention as a clean and sustainable energy alternative to fossil fuels, and the demand for hydrogen fuel used in fuel cell vehicles is expected to increase. We focused on the hydrogen (H₂) production through the reaction of Fe metal obtained from scrap iron with carbonate water (CO₂ and H₂O) [1]. Ammonia (NH₃) is also an important raw material for nitrogen fertilizers used in agriculture, and it has been identified as a potential hydrogen carrier in recent years. However, NH₃ is mainly synthesized by the Haber–Bosch process, which requires high temperature and pressure. To lower the environmental burden, it is necessary to achieve NH₃ synthesis under milder conditions. Therefore, we investigated the production of NH₃ ammonia from iron nitride (Fe₄N) and carbonated water at ambient temperature and pressure [2].

The reaction mechanism was understood to be a redox reaction of hydrogen (H) derived from water molecules carried by carbonic acid (H₂CO₃ and HCO₃⁻) with Fe to ionize Fe and produce H₂. When iron nitride was used as the raw material, NH₃ was formed by reaction with N. CO₂ promoted the reactions, allowing them to proceed at lower temperatures, and was absorbed and immobilized as iron carbonate (FeCO₃). Since the reaction involved solid, liquid, and vapor phases, analysis of each phase was conducted. In particular, we analyzed the distribution of elements and crystal structures, considering that it is important to observe the electrochemical reaction on the solid phase surface, i.e., the corrosion phenomenon of iron material.

We have developed a non-scanning X-ray fluorescence (XRF) imaging setup that enables rapid observation of elemental distribution using a projection-type configuration and a two-dimensional detector [3]. 2D spatial XRF image is acquired in a single shot, and temporal changes in the distribution can be obtained by repeating the imaging step.

For the analysis of specific mini-regions, a confocal X-ray setup was constructed [4]. The first polycapillary focusing optic was used as the X-ray incident channel and the second polycapillary focusing optic was used as the X-ray detection channel. The focal points of both overlap, and the X-ray signal from the confocal can be observed. Using this confocal X-ray optics, the measurement was repeated while scanning the sample on the XYZ stage. A 3D scan of the sample through the confocal provides a spatial distribution of the components that make up the sample. Both the projection and confocal setups are not limited to the XRF analysis, but can be applied to other X-ray analyses as well: by detecting X-ray diffraction (XRD) signals, distribution images of crystalline phases can be obtained. In the presentation, we will report the results of the observation of the reaction processes as changes in XRF and XRD distributions using these setups.

[1] Hiromi Eba et al., *Int. J. Hydrogen Energy* 45(2020)13832-13840.

[2] Hiromi Eba et al., *Int. J. Hydrogen Energy* 46(2021)10642-10652.

[3] Hiromi Eba et al., *J. Anal. At. Spectrom.* 31(2016)1105-1111.

[4] Hiromi Eba et al., *Chem. Lett.* 47(2018)1545-1548.

8:00 PM CH01.08.24

Polarization-Induced Inversion of Singlet and Triplet Excited States: Towards New Photocatalytic and Optoelectronic Materials Jaeyune Ryu^{1,2}; ¹Seoul National University, Korea (the Republic of); ²Harvard University, United States

The phenomenon of inversion between singlet and triplet excited states (INVEST), which runs counter to Hund's rule, holds great potential for revolutionizing the mechanisms underlying photocatalysis and optoelectronics. Despite the recent theoretical advancements in understanding this phenomenon, there is a dearth of experimentally feasible approaches for implementing INVEST, which impedes its systematic integration in future applications. This work presents a compelling instance of INVEST that is prompted by environmental polarization effects. By utilizing a simple heptazine molecule as a model chromophore, we demonstrate the switching of the delayed fluorescence mechanism from the conventional thermal activation to one that involves INVEST upon phase transition of solvents. The freezing medium alters the local electrostatics surrounding the chromophore, as evidenced by the observed luminescence rigidochromic shift, which leads to the reversal of the relative spin energetics as measured by temperature-dependent time-resolved PL kinetics. Our preliminary computation suggests that there may exist a differential polarization effects on singlet and triplet excited states as they possess disparate polarity. Ultimately, this work lays a new mechanistic foundation for utilizing local polarization to achieve INVEST. The phenomenon of singlet-triplet inversion, which defies Hund's rule, holds tremendous potential for revolutionizing the mechanisms underlying photocatalysis and optoelectronics.

8:00 PM CH01.08.25

Characterization and Identification of Precipitates Formed on the Cathode Surface in Static Zn-Br Battery Dongrun Ju and DanSteingart; Columbia University, United States

Static zinc-bromine batteries (ZBBs) are a promising and low-cost grid electrochemical energy storage device for energy generation shifting to the use of renewable energy. The sacrifice of an externally forced flow source and membranes in the cell design lowers the battery manufacturing cost but leads to long-term cycling fading. Specifically, an unknown precipitation reaction at the cathode surface during charging forms a thin solid film raising the charge transfer resistance and lowering cycling efficiency and capacity. For the first time, the precipitate was characterized and identified as an insoluble polycrystalline zinc hydroxide bromide hydrate (ZHB) with a layered structure. By investigating the influence of different compositions and concentrations of electrolytes and charging conditions, we proposed that pH variation of electrolytes caused by electrolyte concentration polarization during charging are the immediate factors contributing to ZHB precipitates. In addition, in the long-term cycling, hydrogen and bromine loss also indirectly contributes to irreversible precipitation. In turn, optimization cycling protocols and control of pH are key to suppressing the formation of the precipitate. Overall, understanding and addressing long-term cycling fading is crucial for the advancement of rechargeable battery technologies, allowing for improved performance, extended cycle life, and enhanced reliability in grid energy storage systems.

<quillbot-extension-portal></quillbot-extension-portal>

8:00 PM CH01.08.26

T-SEM EDS and TKD Combined for Elemental and Crystallographic Analysis Meiken Falke, Purvesh Soni and Robert Brandom; Bruker, Germany

To understand the behavior of any nanostructure, analysis of the chemical composition and its arrangement on the nanoscale is vital. We demonstrate the combination of energy-dispersive X-ray spectroscopy (EDS) and transmission Kikuchi diffraction (TKD) in SEM for studying the elemental composition and crystallographic properties of solar cell materials prepared as FIB lamellae. We show that achieving useful results at nanometer scale in a suitable amount of time in SEM, not STEM, is possible by combining on-axis TKD [1] with an annular EDS detector [2] and specimen preparation by FIB. The results are quantitative element maps and line profiles combined with crystal phase and orientation distribution in the absorber and buffer layers of CIGS solar cells investigated in SEM.

The annular EDS detector is placed horizontally between the specimen and the pole piece achieving a solid angle for X-ray collection of about 1 steradian enabling high count rates also in case of low X-ray yield, for example from thin lamellae, light elements and during fast scanning of beam sensitive and/or large specimens. The annular arrangement of the active SDD quadrants parallel to the specimen surface around a central aperture to pass the electron beam enables a high take-off angle as well, minimizes absorption effects and allows the analysis of rough topography or bent specimens. This geometry is easily combined with diffraction pattern acquisition using a detector directly underneath the specimen.

Quantitative EDS of electron transparent lamellae can deliver element distribution and even the specimen thickness, the latter if applying the EDS Zeta-factor method [3]. Crystallographic grain phase, size and orientation are accessible via TKD. The combination of crystallographic and chemical information on the nanoscale via TKD and EDS is particularly promising for correct quantitative analysis. Small grains can lie in front of each other and produce mixed diffraction patterns. Therefore, to interpret grain size and orientation from TKD correctly, the lamella thickness must be known. Lamella thickness can be determined using sample tilt in the FIB which also enables calibrating the Zeta-factors for successful quantitative chemical analysis.

[1] Brodu E, Bouzy E and Funderberger: *J 2017 Microsc. Microanal.* **23** (Suppl. 1) 530-531.

[2] Terborg R and Rohde M: *EMC 2008 14th European Microscopy Congress.* (Luysberg M, Tillmann K and Weirich T; Eds.) 1-5 September 2008, Aachen, Germany. (Berlin, Heidelberg: Springer). https://doi.org/10.1007/978-3-540-85156-1_317.

[3] Watanabe M and Williams D B: 2006 *J. Microscopy* **221** 89-109.

8:00 PM CH01.08.27

Testing Microscopic Theories of Electric Field Fluctuations Over Metal Films Virginia E. McGhee, Christopher Petroff, Konrad Hedderick, Lara A. Estroff, Roger F. Loring and John A. Marohn; Cornell University, United States

Stochastic electric and magnetic fields are present near metal surfaces. These fluctuations can have a number of experimental consequences. They can lead to extraneous friction and frequency noise in scanning probe experiments, limiting the achievable force sensitivity. They can furthermore result in decoherence in nitrogen vacancy center and ion trap quantum computing experiments. The theoretical description of these fluctuations is a topic of active research.¹⁻³ To test these theories we are carrying out measurements of electric field fluctuations over thin metal films at room temperature in high vacuum. In these experiments we infer the height dependence of stochastic electric fields and electric field gradients, from measurements of non-contact friction and frequency noise, respectively. This data can be used to decide among competing theories – are the stochastic electric fields caused by dielectric fluctuations of surface adsorbates or thermal fluctuations of electrons in the underlying metal? The study of electric field fluctuations could be a powerful tool for probing the electronic structure of quantum materials.

(1) Brownnutt, M.; Kumph, M.; Rabl, P.; Blatt, R. Ion-Trap Measurements of Electric-Field Noise near Surfaces. *Rev. Mod. Phys.* **2015**, *87* (4), 1419–1482.

<https://doi.org/10.1103/RevModPhys.87.1419>.

(2) Loring, R. F. Noncontact Friction in Electric Force Microscopy over a Conductor with Nonlocal Dielectric Response. *J. Phys. Chem. A* **2022**, *126* (36), 6309–6313.

<https://doi.org/10.1021/acs.jpca.2c04428>.

(3) Hite, D. A.; Colombe, Y.; Wilson, A. C.; Allcock, D. T. C.; Leibfried, D.; Wineland, D. J.; Pappas, D. P. Surface Science for Improved Ion Traps. *MRS Bull.* **2013**, *38* (10), 826–833.

<https://doi.org/10.1557/mrs.2013.207>.

8:00 PM CH01.08.28

Methodology for Measuring 1/f Noise in Thin Film Piezoelectric Devices for Energy Harvesting and Sensor Applications Kevin Kam, Christine McGinn, Oliver A. Durnan, Qingyuan Zeng and Ioannis Kyriassis; Columbia University, United States

Polyvinylidene difluoride-trifluoroethylene (PVDF-TrFE) thin films have been utilized as a flexible sensing and energy harvesting material due to their piezoelectric capabilities [1]. A common use of PVDF-TrFE is in the development of acoustic sensors. Previous literature has reported applications as a microphone for cochlear implants [2] and as piezoelectric energy harvesters [3]. For these applications, it is important to understand the electrical noise generated by the device to accurately determine its noise floor, as it is the primary factor in determining critical sensor metrics like limit of detection and signal to noise ratio (SNR).

The primary challenge in measuring noise in an acoustic MEMS system is the normalization of the noise floor. PVDF thin films are constantly vibrating, even without external input, due to its flexible and deformable nature. Small fluctuations in the acoustic and electronic environment can then make drastic changes in the noise floor, impacting the accuracy of the overall sensor or system.

In this work, we are interested in characterizing the noise current generated by the sensor due to the underlying properties of the material in the absence of external interference. This measurement is useful in providing a more accurate noise budget and electrical model to aid in the design of interfacing circuitry. Proper characterization of noise allows for the rigorous quantification of SNR and minimum detectable signal amplitude which are important metrics for any sensor.

The metrology system has three main components, 1) an insulated, anechoic chamber made with thick metal walls to reduce acoustic and electromagnetic interference 2) an SRS low-noise pre-amplifier to amplify the generated noise current 3) a spectrum analyzer, to measure the noise spectral density of signals in the range 40 Hz to 25 kHz. Together, these components provide a low-noise measurement environment suitable to study intrinsic noise generation.

To test the efficacy of the system described above, a printed PVDF-TrFE device described in [4] was measured. Before any noise measurements were taken, the test device's capacitance was measured. Likewise, its output voltage over time when exposed to acoustic stimulation was recorded using an ADMET Universal Testing System with readout electronics designed in [4].

These measurements affirm that the device acts as a capacitive piezoelectric acoustic sensor. Finally, once the devices were characterized, they were placed in the chamber and the current noise measurements were taken in the 40 Hz - 25 kHz band.

[1] B. Stadlober, M. Zirkel, and M. Irimia-Vladu, "Route towards sustainable smart sensors: Ferroelectric polyvinylidene fluoride-based materials and their integration in flexible electronics," *Chemical Society Reviews*, vol. 48, no. 6, pp. 1787–1825, 2019.

[2] S. Park, X. Guan, Y. Kim, F. (P. Creighton, E. Wei, I. J. Kyriassis, H. H. Nakajima, and E. S. Olson, "PVDF-based piezoelectric microphone for sound detection inside the cochlea: Toward totally implantable cochlear implants," *Trends in Hearing*, vol. 22, 2018.

[3] D. Vatansver, R. L. Hadimani, T. Shah, and E. Siores, "An investigation of energy harvesting from renewable sources with PVDF and PZT," *Smart Materials and Structures*, vol. 20, no. 5, p. 055019, 2011.

[4] C. K. McGinn, K. A. Kam, M.-M. Laurila, K. Lozano Montero, M. Mäntysalo, D. Lupo, and I. Kyriassis, "Formulation, printing, and Poling method for piezoelectric films based on PVDF-TrFE," *Journal of Applied Physics*, vol. 128, no. 22, p. 225304, 2020.

8:00 PM CH01.08.29

CaFe₂O₄-Type Post-Spinel Host Compounds as Mg Battery Cathodes Patrick P. Ding¹, John T. Vaughey², G. J. Snyder¹ and Kenneth R. Poeppelmeier¹; ¹Northwestern University, United

The development of an Mg battery promises a high energy density at a low material cost. A primary roadblock for Mg batteries is the identification of a cathode material with sufficient kinetics and stability. Previous first-principles calculations have suggested a low migration barrier for Mg^{2+} in host compounds with the $CaFe_2O_4$ (CF) structure. In this work we experimentally investigate the electrochemical properties against Mg metal of several lithium post-spinel compounds with the CF structure including $LiVTiO_4$, $LiCrTiO_4$, $LiMnSnO_4$, and $LiFe_{0.5}Ti_{1.5}O_4$. To open the tunnels for Mg intercalation, the lithium post-spinels are chemically delithiated with Br_2 /acetonitrile prior to electrochemical characterization. Structural characterization of the delithiated cathode materials is carried out including powder x-ray diffraction, scanning electron microscopy, and solid-state nuclear magnetic resonance spectroscopy. The capacity, potential, and stability of the cathode materials are detailed along with a consideration of the interactions of the Mg anode/cathode with the $Mg(TFSI)_2$ -based electrolyte. From these results and a comparison of the Mg cathode performance with the performance of the lithium post-spinels as lithium battery cathodes, we further our understanding of the CF structure as a monovalent and multivalent intercalation host.

8:00 PM CH01.08.31

SNDM Study on Cubic and Hexagonal Epitaxially Stacked SiC MOS Interfaces Yasuo Cho¹, Hiroyuki Nagasawa², Masao Sakuraba¹ and Shigeo Sato¹; ¹Tohoku University, Japan; ²CUSIC Inc., Japan

The layer structure of 3C-SiC(111) stacked on 4H-SiC(0001) is expected to be effective in reducing the specific on-resistance (R_{on}) of power MOSFETs operating at high voltages. This is because the channel is formed in the 3C-SiC layer, which shows low interface density of state (D_{it}) at interface with SiO_2 , and the depletion region extends toward the 4H-SiC layer with high breakdown electric field.

Recently, the simultaneous lateral epitaxy (SLE) method, in which 3C-SiC and 4H-SiC are grown transversely at the same time, has been proposed as a technique for fabricating this structure and has attracted much attention [1].

However, there was no specific study that experimentally evaluated D_{it} at the MOS (SiO_2/SiC) interface on the SiC layer grown by SLE and verified the effect of 3C-SiC (111)/4H-SiC (0001) structure with simultaneously formed SiO_2 oxide film on the MOSFET performance.

On the other hand, we have studied the evaluation of the SiO_2/SiC interface using scanning nonlinear dielectric constant microscopy (SNDM) and reported that the relative standard deviation (RSD), which is the signal fluctuation (standard deviation) in the SNDM image (dC/dV image) normalized by its mean value, can be used to evaluate D_{it} [2] and that the local deep level transient spectroscopy (DLTS) method using the time-resolved SNDM (tr-SNDM) method can quantitatively evaluate the two-dimensional distribution of D_{it} itself [3].

In this paper, by using these two techniques, we characterize MOS interfaces on epitaxially stacked 3C-SiC(111)/4H-SiC(0001) grown by SLE.

References:

[1] H. Nagasawa, European Patent No. EP 4 135 047 A1 (27 April 2021).

[2] Norimichi Chinone, Alpna Nayak, Ryoji Kosugi, Yasunori Tanaka, Shinsuke Harada,

Hajime Okumura, and Yasuo Cho, "Evaluation of silicon- and carbon-face SiO_2/SiC MOS interface quality based on scanning nonlinear dielectric microscopy", Appl. Phys. Lett. Vol.111, 061602 (2017).

[3] Yuji Yamagishi, and Yasuo Cho, "Nanosecond microscopy of capacitance at $SiO_2/4H-SiC$ interfaces by time-resolved scanning nonlinear dielectric microscopy", Appl. Phys. Lett. Vol.111, 163103 (2017).

8:00 PM CH01.08.32

Nanoscale Fluctuation Analysis on Capacitance-Voltage Profiles of Semiconductors by Time-Resolved Scanning Nonlinear Dielectric Microscopy Kohei Yamasue and Yasuo Cho; Tohoku University, Japan

Wide-bandgap semiconductors such as SiC, GaN, and diamond are promising materials for next-generation power devices. However, the performance of MOS devices using wide-bandgap semiconductors has not yet reached the level expected from their excellent material properties. For example, the on-resistance of 2-3 kV-class SiC MOSFETs is limited by low MOS channel mobility. Channel mobility is dominated by the quality of the dielectric-semiconductor interface such as SiO_2/SiC . To investigate the cause of low channel mobility from a microscopic perspective, we have proposed the application of scanning nonlinear dielectric microscopy (SNDM) to study dielectric-semiconductor interfaces. SNDM is a near-field microwave scanning probe microscopy method that is exceptionally sensitive to the change in capacitance between the conductive tip and the sample [1]. SNDM can detect the change in microscopic MOS capacitance when measuring a semiconductor wafer with gate dielectric top layer. In particular, time-resolved SNDM (tr-SNDM), an extension method of SNDM, has recently permitted the detection of rapid changes in local capacitance more accurately than conventional SNDM [2]. Tr-SNDM has therefore enabled local DLTS (deep level transient spectroscopy) and local CV (capacitance-voltage) profiling, which give nanoscale spatial resolution to DLTS and CV profiling [3].

Here we present a local CV profiling method based on tr-SNDM and application to the SiO_2/SiC interface [3]. We show how microscopic CV profiles are obtained by tr-SNDM and their nanoscale spatial fluctuations are analyzed in a real-space. Spatial fluctuations of local CV profiles reflect the potential fluctuations at the interface, or surface potential fluctuations. We apply our method to a SiO_2/SiC interface treated by NO-POA (post-oxidation-annealing). We extract feature values from the local CV profiles and their derivative (dC/dV-V) profiles to quantitatively investigate the fluctuations of local CV profiles. By extracting the voltages at the inflection points of local CV and dC/dV-V profiles, we can characterize the fluctuations of local CV profiles in depletion, accumulation, and intermediate regions. We found that the spatial fluctuations of local CV profiles are reduced by NO-POA (post-oxidation-annealing) treatment, as expected, but still larger than the thermal energy at room temperature (~26 meV) even in deep depletion region. This indicates the density fluctuations of fixed charges including the carriers trapped at the deep levels are high enough to create significant potential fluctuations at the interface. In addition, we found that fluctuations become higher as the interface are accumulated by the dominant carriers. This suggests that dominant carriers trapped to acceptor-type interface defects further increase the spatial non-uniformity of the interface. It is known that surface potential fluctuations are strongly related to the carrier transport properties of the channel. Therefore, our results suggest that high surface potential fluctuations may be the cause of low channel mobility in SiC MOSFETs. Our method can also be applied to other dielectric-semiconductor interfaces such as $Al_2O_3/diamond$ and Al_2O_3/GaN and will give microscopic insights on these interfaces.

References:

[1] Y. Cho, Scanning Nonlinear Dielectric Microscopy: Investigation of Ferroelectric, Dielectric, and Semiconductor Materials and Devices. Elsevier, ISBN 978-0-08-102803-2 (2020).

[2] Y. Yamagishi and Y. Cho, Appl. Phys. Lett. 111, 163103 (2017).

[3] K. Yamasue and Y. Cho, Microelectron. Reliab. 135, 114588 (2022).

8:00 PM CH01.08.33

The New Strategy of the Gas Sensor Platform through Triboelectric Nanogenerator Yujang Cho, Jaehyun Ko and Il-Doo Kim; KAIST, Korea (the Republic of)

In the age of the Internet of Things (IoT), the significance of sensor devices that can operate independently through self-power sources has taken center stage. In this regard, the triboelectric nanogenerator (TENG), which is gaining attention as a renewable energy source, has been applied as a self-powered gas sensor by coupling it with a gas sensor. However, the existing TENG only serves as a power supplier for the gas sensor's minimal power requirements, making it challenging to apply it as a practical gas sensor while ensuring its continuity. Herein, we report on a self-powered multifunctional hydrogen gas sensor (SPMH-gas sensor) that utilizes a palladium-deposited polytetrafluoroethylene (PTFE) nanofiber-based membrane as the TENG friction surface, enabling sensing of hydrogen gas. The SPMH-gas sensor detects changes in voltage resulting from the movement of electrons during the conversion of mechanical energy into electrical energy, enabling effective sensing. The highly durable PTFE nanofiber substrate ensures stable sensor detection performance even under mechanical deformation. Moreover, it operates at room temperature and provides feedback on gas leakage through the spontaneously generated electrical energy. The change in output performance of the TENG according to the electron movement variation in the presence of gas exposure brings about expandability to various gases.

8:00 PM CH01.08.34

Explaining Concepts and Applications of Second-Order X-Ray Diffuse Scattering in Materials Characterization Mauricio B. Estradiote, Rafaela F. Penacchio and Sergio L. Morelhaio; University of Sao Paulo, Brazil

X-ray diffuse scattering (DS) generally arises from any departure that structures have from a perfectly regular atomic lattice. In crystals, thermal DS is caused by scattering from lattice vibrations and provides valuable information about the lattice dynamics of materials. Historically, DS was the first tool to determine phonon dispersion relations experimentally [1]. With the advent of synchrotron radiation technology, it has reemerged as a feasible method for studying phonons in contrast with inelastic X-ray and neutron scattering that require complex experimental equipment, long acquisition times, and, in the case of neutron scattering, large single crystals [2]. However, high-flux synchrotron X-rays, approaching 10^{15} ph/s/mm², in addition to zero noise area detectors, have also revealed a relatively unknown 2nd-order DS process, first called diffuse multiple scattering (DMS) [3], which appears as a kind of Kikuchi lines [4] for monochromatic X-rays. In recent years, accidental observation of DMS lines has become increasingly frequent for high-flux synchrotron beamline users working with monocrystalline materials such as epitaxy-based nanostructured devices. Although DMS lines carry intrinsic 3D information on structural and vibrational properties of the crystal lattice, their predictability and

practical applications have been open to investigation for about a decade. In this work, we introduce the concept of bright and dark Bragg cones required to understand and describe DMS lines. The intensity distribution along DMS lines depends on the actual primary source of DS in the material, as demonstrated for isotropic DS plus truncation rod of a perfect semiconductor surface and a particular case of thermal DS in skutterudites [5,6] as obtained by first principle calculation. A survey is given on computer codes for 3D reciprocal space maps [7], thermal DS simulation, and prediction of the most visible and susceptible DMS lines.

Acknowledgments: FAPESP (2022/09531-8; 2021/01004-6) and CNPq (310432/2020-0).

[1] B. E. Warren. X-ray Diffraction. Dove, New York, 1990.

[2] A. B. Mei et al. Reflection thermal diffuse x-ray scattering for quantitative determination of phonon dispersion relations. Phys. Rev. B 92, 174301 (2015). 10.1103/PhysRevB.92.174301

[3] A. G. A. Nisbet, G. Beutier, F. Fabrizi, B. Moser, S. P. Collins. Diffuse Multiple Scattering. Acta Cryst. A 71, 20-25 (2015). 10.1107/S2053273314026515

[4] D. A. Muller et al. Simulation of thermal diffuse scattering including a detailed phonon dispersion curve. Ultramicroscopy 86, 371-380 (2001). 10.1016/S0304-3991(00)00128-5

[5] S. El Oualid et al. High Power Density Thermoelectric Generators with Skutterudites. Advanced Energy Materials 11, 2100580 (2021). 10.1002/aenm.202100580

[6] A. Valério et al. Phonon scattering mechanism in thermoelectric materials revised via resonant x-ray dynamical diffraction. MRS Commun. 10, 265-271 (2020). 10.1557/mrc.2020.37

[7] R. F. S. Penacchio et al. A simple recipe to create three-dimensional reciprocal space maps. ArXiv 2210.05427 (2022). 10.48550/arXiv.2210.05427 (<https://github.com/rafaela-felix/rsm>)

8:00 PM CH01.08.35

Quantifying the Interface Delamination between Polymer Binder and Active Materials for High Energy Density Electrode Materials AkshayPakhare, MartinaBorges, AbdulrahmanAlfadhli, IgorBezsonov, AmitChanda and SivaNadimpalli; Michigan State University, United States

High capacity and durable Li-ion batteries is important for the advancement of electric vehicle and renewable energy technologies. Group IV elements such as Si, Ge, and Sn are promising alternatives as anodes in lithium ion batteries compared to the conventional graphite and these elements offer significantly higher theoretical capacities as compared to traditional graphite anode. However, these high capacity materials suffer from poor cyclic performance due to volume expansion (e.g. Si expands $\approx 300\%$) induced stresses and the associated electrode fracture. In a commercial composite electrode, such volume expansion also induces significant stresses at the interface between active (e.g. Si) particle and polymer binder; the binder holds the active particles together and enables successful operation of battery. The volume expansion of particles during cycling causes interface failure, leading to electrical isolation of active particle. This mechanism results in significant capacity fade in composite electrode batteries during cycling. In spite of the importance, no systematic study on the interface failure behavior exists at present. In this talk, we will focus on quantifying the interface fracture between the PVdF (a polymer binder) and Si. We have also measured the effect of thermal oxide (SiO₂) on the interface failure and quantified the interface degradation due to electrochemical cycling.

8:00 PM CH01.08.36

Hysteresis and Transient Behaviour in Current Voltage Measurements of Antimony Selenide Solar Cells Panchirala Arachchige Udari Imalka Wijesinghe and OliverHutter; Northumbria University, United Kingdom

Antimony selenide (Sb₂Se₃) is an attractive light-absorber used in low-cost, non-toxic, earth-abundant thin-film solar cells with rapidly rising efficiency values. Currently, many n-type metal oxides have been investigated as buffer layers in Sb₂Se₃ solar cell architectures. Among them, titanium oxide (TiO₂) is commonly used as the buffer layer because of its significant optoelectrical properties. The current density-voltage measurement of Sb₂Se₃ solar cells in FTO/TiO₂/Sb₂Se₃/P3HT/Au configuration shows a hysteresis-like distortion that depends on the voltage scan direction, scan rate, scan range, and voltage bias conditions prior to measurement. The presence of hysteresis can significantly influence the photovoltaic properties of devices, which can overestimate or underestimate the accurate power conversion efficiency of solar cells. The fabricated solar cells showed a normal hysteresis where the forward scan result exhibits lower performance than the reverse scan under certain circumstances. We identify this phenomenon is caused due to charge carrier accumulation which may be because the capacitive charge is quickly discharged through charge separation. In addition, the accumulation of oxygen vacancies at the TiO₂/Sb₂Se₃ interface can reduce charge extraction, and at the same time, significantly accelerate the charge recombination at the interface, which also leads to unfavorable hysteresis. However, the hysteretic effects are not observed in devices utilizing alternative buffer layers like ZnO and SnO₂, suggesting that the buffer absorber interfaces have a significant effect on transients in Sb₂Se₃ absorber devices. Therefore, further improvements of Sb₂Se₃ solar cells are essential through careful surface engineering of existing TiO₂ or through a judicious choice of alternative interfacial layers.

8:00 PM CH01.08.37

Minimizing the Perturbation of the Applied Magnetic Field by Optimizing Solid-State NMR Probe Structures JasminSchoenartz^{1,2}, JohnStringer² and ThomasGennett¹; ¹Colorado School of Mines, United States; ²PhoenixNMR, LLC, United States

The NMR probe is likely the most specialized part of the NMR spectrometer with respect to the sample and is often the only component that needs to be exchanged when switching between different NMR samples (e.g. liquid, solids, gels) and experiments (e.g. static, spinning). It is essential that the probe locates the sample in the most homogeneous part of the magnetic field within the magnet, to allow for the best recorded spectra possible. In an ideal case, the probe itself would not perturb the applied magnetic field, yet effects of perturbation can be observed, which is why shimming of the probe is essential before every NMR experiment. In this work we want to present ways to minimize the perturbation of the applied magnetic field by optimizing solid-state NMR probe structures. This is achieved by a combination of simulations and experiments, which take susceptibilities of all parts in the NMR probe into account to then study the net effect upon the sample. Based on those results, modifications to NMR probes can be made, to minimize unwanted contributions. The smaller the perturbation of the applied magnetic field, the narrower the observed possible linewidth and the higher the resolution of the experiment.

8:00 PM CH01.08.38

Characterization of Beam Sensitive Samples Through Dose Fractionated Spectrum Imaging AndrewThron¹, LiamSpillane¹, RayD. Twesten¹ and RobertColby²; ¹Gatan Inc., United States; ²ExxonMobil Technology and Engineering Company, United States

Acquisition of EELS spectrum images (SI) from dose-sensitive samples has proved technically challenging due to the relatively low critical dose thresholds above which Radiolysis occurs. Multipass SI continuously sums multiple, rapidly acquired passes together until the desired accumulated dwell time is achieved, rather than acquiring a single pass with a long pixel dwell time. This fractionates the dose over several passes, gives rapid feedback on sample integrity, and the ability to correct sample drift between frames. If passes continue to be summed above a critical dose, spectra analysis will be compromised. Due to read noise, optically coupled CCD and CMOS cameras require longer dwell times to achieve a sufficient signal-to-noise ratio. This requires the dose to spread over a larger sample area, limiting the measurement's spatial resolution [1].

Here we show how multi-pass, *in-situ* SI enables the application of EELS to dose-sensitive samples. Multi-pass *in-situ* SI saves each pass individually while fractionating the dose over multiple passes. If the acquisition of a SI continues above the critical dose, compromised spectra are removed post-acquisition, and only the pristine passes are summed together. This is particularly advantageous since the critical dose for a sample may be unknown. Combining the sensitivity of a direct electron counting detector with multi-pass *in-situ* SI decreases the pixel dwell time. This fractionates the dose over more passes and enables the SI to be acquired at a higher spatial resolution.

Calcium carbonate (CaCO₃) was used as a model system since the critical dose thresholds for reduction and mass loss are well characterized [2]. We observe mass loss through the reduction of O and C concentrations. The formations of voids are observed to occur heterogeneously, likely at defects. Due to the increased sensitivity of direct detection, we can track the evolution of the Ca L_{2,3} near-edge fine structure (ELNES) to pinpoint when the onset of radiolysis starts. Furthermore, by monitoring the ELNES, we confirm that reducing the dose rate increases the critical dose at which voids form, from $4.4 \times 10^4 \text{ e}^-/\text{\AA}^2$ to greater than $1.3 \times 10^5 \text{ e}^-/\text{\AA}^2$.

We then apply EELS Multi-pass *in-situ* spectrum imaging to a more challenging blended polymer film of polycarbonate (PC) and poly(styrene-acrylonitrile) (SAN). The PC/SAN film has a significantly lower dose threshold of $10 \text{ e}^-/\text{\AA}^2$, compared with the calcium carbonate films. By fractionating the dose over several passes, we can map the distribution of the PC and SAN phases using references from the C K-edge ELNES. Due to the direct electron detector sensitivity, we acquired phases maps with a spatial resolution of 20-30nm, which was previously impossible with optically coupled cameras [1].

[1] Colby R. et al., Ultramicroscopy 246 (2023) 113688

[2] R. Hooley, A. Brown, R. Brydson Micron 120 (2019)

8:00 AM *CH01.09.01

Recent Progress in Cryogenic Electron Microscopy and Spectroscopy for Energy Materials Y. ShirleyMeng^{1,2}; ¹The University of Chicago, United States; ²Argonne National Laboratory, United States

The applications of cooling holders into energy materials started from the very beginning of the commercialization of side entry holders. Its primary applications were focused on minimizing electron beam induced damage in beam sensitive materials. These materials include for example reactive materials for energy storage and conversion (lithium, sodium metal anodes, lithiated graphite and silicon, etc.), soft materials for membrane technologies, interphase materials after wet-electrochemical cycling, catalysts that are extremely small (<3-5nm), or those containing ligands and molecules. A more profound application of Cryo-EM perhaps is the enabling of tomographic S/TEM imaging, which requires an extended acquisition time, of beam sensitive materials. The biggest challenge in cryo-EM experiments, particular for high resolution imaging and chemical analysis, lies in the limited stability, which is affected by multiple factors, such as the temperature variation on the specimen tip, the mechanical instability induced by the heavy liquid dewar, the bubbling and the constant evaporation of liquid nitrogen/helium. In this talk, I will discuss a few recent endeavours to overcome these barriers, using the energy storage materials studies as the example.

8:30 AM CH01.09.02

Exploring Surface Properties: A Multi-Frequency AFM Approach Lamiaa S. Elsherbiny¹, Sergio Santos², Matteo Chiesa¹ and Amal AlGhaferi¹; ¹Khalifa University, United Arab Emirates; ²UiT-The Arctic University of Norway, Norway

In the field of atomic force microscopy (AFM), a comprehensive understanding of surfaces is of the utmost importance, particularly in the energy industry. The quest for cost-effective and sustainable GaAs production is addressed in this study through the novel use of graphene as a key component. This approach hinges on the understanding of the van der Waals interactions between graphene and semiconductors, with the goal of reducing production costs for GaAs-based devices, primarily solar cells. To decipher the complex dynamics governing tip-surface interactions, a thorough investigation was conducted by combining multimodal AFM techniques with advanced machine learning algorithms, thereby facilitating a systematic and data-driven investigation. The significance of surface comprehension within the AFM field formed the basis of this study. The surface forces are analyzed through Atomic Force Microscopy (AFM), providing high-resolution topographical data and valuable insights into the surface energy of materials. By using a combination of bimodal and trimodal AFM techniques, they were able to increase sensitivity and resolution, allowing for the collection of multiple datasets that accurately reflected the complex interaction of forces. Having established the critical role surfaces play, it is essential to dive into a complex examination of tip-surface interactions. Through meticulous analysis, we were able to identify specific analytical properties that provided valuable insights into the essence underlying these interactions. These properties were crucial in deciphering the governing power law, thereby shedding light on the optimal parameters that define the system. Machine learning was used to correlate the different parameters with the governing power law. Through extensive training on diverse datasets containing known power laws, the model acquired the remarkable ability to classify and identify the power corresponding to the given properties. This development sped up the analysis process, improving efficiency and guaranteeing precision. Beyond the domain of GaAs substrates, the refined capabilities of the machine learning model represented a significant step forward. Automatic identification and classification of the power law became possible, resulting in enhanced accuracy and a streamlined process for determining optimal parameters. This methodology has repercussions outside of the energy industry, enabling insights into diversified tip-surface interactions in a variety of applications. The developed method can accelerate the understanding of surfaces for the purpose of photoelectric devices. By digging deep into the vast domain of van der Waals forces, analytical properties, and machine learning techniques, we can gain unmatched understanding of the interactions within GaAs substrates. Thus, enhancing the fabrication process of thin film solar cells.

8:45 AM CH01.09.03

Local Capacitance-Voltage Profiling of Al₂O₃/OH-Diamond (111) by Scanning Nonlinear Dielectric Microscopy Kohei Yamasue¹, Yu Ogata¹, Tsubasa Matsumoto², Norio Tokuda² and Yasuo Cho¹; ¹Tohoku University, Japan; ²Kanazawa University, Japan

Diamond is one of a wide bandgap semiconductor materials and receiving considerable attention because of its high potential to power device applications. It has recently been shown that inversion type p-channel metal-oxide-semiconductor field-effect transistors (MOSFETs) with normally-off operation have been fabricated using a P-doped and OH-terminated diamond body on a diamond (111) substrate with an atomic layer deposited Al₂O₃ gate dielectric [1]. However, there still remains an issue of lower channel mobility towards the practical applications of diamond based power MOSFETs [2].

To give a microscopic insight on the physical origins of the low channel mobility, here we investigate an Al₂O₃/OH-diamond (111) interface by time-resolved scanning nonlinear dielectric microscopy (tr-SNDM). Tr-SNDM is a near-field microwave based scanning probe microscopy that has high sensitivity to the variation of microscopic MOS capacitance formed by the metallic tip, insulating gate dielectric layer in contact with it, and underlying semiconductor layer [3]. By using tr-SNDM, here we performed local (microscopic) capacitance-voltage (CV) profiling of Al₂O₃/OH-diamond (111). Unlike typical macroscopic CV profiling, we can obtain local CV profiles at different measurement points and visualize their nanoscale spatial fluctuations in a real-space. Spatial fluctuations of the local CV profiles reflect potential fluctuations at the interface, or surface potential fluctuations, that should be suppressed to increase the channel mobility of MOSFETs.

The sample was fabricated from a highly B-doped p⁺ CVD diamond layer (200 nm) grown on a high-temperature high-pressure synthesized p-doped (111) substrate (300 μm) for ohmic contact formation with an underlying gold electrode layer. The sample had atomically flat surfaces by etching the bare surfaces by anisotropic diamond etching process based on carbon solid solution reaction into Ni. Subsequently, hydrogen plasma etching treatment was applied to form (111)-oriented terrace and step structures on the p-type diamond surfaces. The sample was further treated by the OH-termination process of the diamond surface. A 50 nm thick Al₂O₃ top dielectric layer was formed by atomic layer deposition. For comparison, we also measured a hydrogen-annealed thermally oxidized Si (H-annealed SiO₂/Si) wafer with very high interface quality.

By using our local CV profiling method, we were able to visualize spatial fluctuations of the local CV profiles on the Al₂O₃/OH-diamond (111) sample. In addition, we found that the Al₂O₃/OH-diamond (111) has much higher spatial fluctuations than hydrogen-annealed SiO₂/Si. The standard deviation of the observed fluctuations was as high as 0.9 V, while that of hydrogen-annealed SiO₂/Si was 0.08 V. Basically, the high fluctuations are attributable to the high density and non-uniform spatial distributions of interface charges such as interface defects and fixed charges. A more detailed analysis suggests that the high fluctuations at the Al₂O₃/OH-diamond(111) interface are dominated by voltage-independent charge states such as fixed charges and interface defects with deep energy levels. An additional measurement called local DLTS using tr-SNDM also indicates that interface defects at shallower energy levels also contribute to the fluctuations. These results suggest that the reduction of interface defects, fixed charges, and their density fluctuations is necessary to improve the quality of the Al₂O₃/OH-diamond(111) interface.

References:

[1] T. Matsumoto, H. Kato, K. Oyama, T. Makino, M. Ogura, D. Takeuchi, T. Inokuma, N. Tokuda, and S. Yamasaki, *Sci. Rep.* 6, 31585 (2016).

[2] T. Matsumoto, H. Kato, T. Makino, M. Ogura, D. Takeuchi, S. Yamasaki, T. Inokuma, and N. Tokuda, *Appl. Phys. Lett.* 114, 242101 (2019).

[3] Y. Cho, *Scanning Nonlinear Dielectric Microscopy: Investigation of Ferroelectric, Dielectric, and Semiconductor Materials and Devices*. Elsevier, ISBN 978-0-08-102803-2 (2020).

9:00 AM CH01.09.04

Automated Band Gap Characterization Matches the Rate of High-Throughput Materials Synthesis Alexander E. Siemenn¹, Basita Das¹, Hamide Kavak^{1,2}, Eunice Aissi¹, Fang Sheng¹ and Tonio Buonassisi¹; ¹Massachusetts Institute of Technology, United States; ²Cukurova University, Turkey

Significant progress has been made in recent years to accelerate the rate of materials synthesis using high-throughput methods. For example, we use combinatorial solution-based synthesis methods to produce and anneal 100 unique FA_xMA_{1-x}PbI₃ perovskite samples in only 20 minutes. However, traditional characterization techniques are not designed to match this accelerated rate of synthesis. Depending on the number of samples processed, the characterization of materials often requires hours or days for a domain expert to complete using conventional techniques, in turn, bottlenecking the process of high-throughput experimentation. We record that it takes a domain expert approximately 4.3 hours to characterize the band gaps of 100 unique FA_xMA_{1-x}PbI₃ perovskite samples. To accelerate the rate of characterization, we design an automated method to measure and extract the direct band gap of perovskite materials using computer vision segmentation of spatially resolved hyperspectral reflectance data. This vision-driven band gap extractor uses the Tauc-transformed reflectance data of each sample to recursively segment and iteratively minimize the RMSE of regression fit lines to those curves, enabling the autonomous computation of band gap across arbitrarily many samples captured and segmented in a single hyperspectral image. We demonstrate the processing throughput of the band gap extractor to be 100 samples in 180 seconds (and the potential for further acceleration using more powerful computational resources), with the spatial hyperspectral measurement only taking 10 seconds. Hence, our proposed method of automated band gap characterization is approximately 6x faster than our high-throughput sample synthesis and annealing process, circumventing a characterization bottleneck during the high-throughput experimentation of materials. We validate the proposed method on over 1,200 unique FA_xMA_{1-x}PbI₃ perovskite samples and demonstrate an accuracy of over 90% relative to ground truth acquired by a domain expert while achieving a throughput 85x faster than the domain expert.

Code is publicly available: <https://github.com/PV-Lab/Vision-Automatic-Band-Gap-Extractor>

9:15 AM CH01.09.05

Implications of Dispersivity and Crystallinity on X-Ray Scattering of Nanoparticles Adriana Valerio¹, Rafaela F. Penacchio¹, Fabiane Trindade², Mauricio B. Estradiote¹, Andre Santarosa

Control of shape and size dispersivity and crystallinity of nanoparticles (NPs) has been a challenge in identifying these parameters' role in the physical and chemical properties of NPs. There are many examples, such as improved catalytic performance of CeO₂ NPs by adjusting size, morphology, and lattice perfection [1,2], tuned nonlinear optical response in BiFeO₃ nanocrystals for biomedical imaging applications by narrowing phase and size dispersivity [3,4], and self-stabilized catalysts based on NPs with crystalline core and amorphous shell [5]. The need for reliable quantitative tools for analyzing the dispersivity and crystallinity of NPs is a considerable problem in optimizing scalable synthesis routes capable of controlling NP properties. The most common tools are electron microscopy and X-ray scattering techniques. However, each technique has different susceptibility to these parameters, implying that more than one technique is necessary to characterize NP systems with minimum reliability. Wide-angle X-ray scattering (WAXS) is mandatory to access information on crystallinity. In contrast, electron microscopy (EM) or small-angle X-ray scattering (SAXS) is required to access information on the whole NP sizes. EM provides average values on relatively small ensembles compared to bulk values accessed by X-ray techniques. Besides the fact of SAXS and WAXS weight size distribution differently [6], SAXS is easily affected by NP-NP interaction distances. Because of all the variables involved, there have yet to be proposed methodologies for cross-analyzing data from two techniques that can provide reliable quantitative results of dispersivity and crystallinity. In this work, we propose a SAXS/WAXS-based methodology for simultaneously quantifying size distribution and degree of crystallinity of NPs. We demonstrate the most reliable and easy-to-access size result for each technique, how to compare them, and how to identify NP-NP interaction effects underneath the SAXS intensity curve. Experimental results are shown for cubic-like CeO₂ NPs. WAXS size results from two analytical procedures are compared, line profile fitting of individual diffraction peaks in opposition to Rietveld analysis via GSAS software. The impact of shape dispersivity is also evaluated for both techniques. A possible extension of the proposed methodology for cross-analyzing EM and WAXS data is suggested.

[1] A. Trovarelli, J. Llorca. Ceria Catalysts at Nanoscale: How Do Crystal Shapes Shape Catalysis? ACS Catal. 2017, 7, 4716–4735. 10.1021/acscatal.7b01246

[2] F. J. Trindade et al. Tuning of Shape, Defects, and Disorder in Lanthanum-Doped Ceria Nanoparticles: Implications for High-Temperature Catalysis. ACS Appl. Nano Mater. 5, 8859–8867, 2022. 10.1021/acsnm.2c00942

[3] G. Clarke et al. Preparation From a Revisited Wet Chemical Route of Phase-Pure, Monocrystalline and SHG-Efficient BiFeO₃ Nanoparticles for Harmonic Bio-Imaging. Sci. Rep. 2018, 8, 10473. 10.1038/s41598-018-28557-w

[4] A. J. Freitas Cabral et al. Controlled Formation and Growth Kinetics of Phase-Pure, Crystalline BiFeO₃ Nanoparticles. Cryst. Growth Des. 2020, 20, 600–607. 10.1021/acs.cgd.9b00896

[5] Y. Wu, M. Zhao, J.-P. Cao, J. Xu, T. Jin, N. Asao. Amorphous/low-crystalline core/shell-type nanoparticles as highly efficient and self-stabilizing catalysts for alkaline hydrogen evolution. Chem. Commun. 56, 8984–8987 (2020). 10.1039/D0CC03016C

[6] S. L. Morelhão, S. W. Kycia. A simple formula for determining nanoparticle size distribution by combining small-angle X-ray scattering and diffraction results. Acta Cryst. A 78, 459–462 (2022). 10.1107/S2053273322007215

9:30 AMBREAK

10:00 AM CH01.09.06

Analysis of Dynamics of Sodium Electrolyte with Aluminum Additives with Nuclear Magnetic Resonance Spectroscopy [AllenZheng](#)¹, StevenG. Greenbaum¹ and MicheleVittadello²; ¹Hunter College, United States; ²Medgar Evers College, United States

As part of the development of beyond-lithium batteries, research on sodium electrolyte chemistries have shown many promising systems. Though more challenging, there is also great interest in developing electrolytes for aluminum-based batteries. Mixed Na/Al-catenated ionic liquid electrolytes were developed utilizing an atomically disordered form of sodium chloride salt, denoted as δ -NaCl, of various concentrations which was mixed with 1-ethyl-3-methylimidazolium chloride and aluminum chloride (EmImCl/AlCl₃)_{1.5}/(δ -NaCl)_x. Pulsed-field-gradient nuclear magnetic resonance spectroscopy was utilized to determine transport mechanics of ions at various concentrations. The results reveal improved aluminum transport mobility with higher sodium salt concentration despite increased viscosity, indicating significant changes in the Al coordination shell with increasing δ -NaCl concentration.

10:15 AM CH01.09.08

Quantitative Analysis of Tomographic Images for Understanding Discharge Phenomena in Alkaline Zn-MnO₂ Batteries [DominickGuida](#), AlyssaStavola and JoshuaW. Gallaway; Northeastern University, United States

In situ synchrotron CT was used to obtain volumetric reconstructions of sealed commercial Zn-MnO₂ batteries. The voxel resolution was 2.93 μm /voxel with sufficient field of view (FOV) that a volume of approximately 200 mm³ encompassing the entire battery diameter could be probed in a reasonable time frame. The reconstructions show the internals of partially discharged anodes, which visualizes the morphology and distribution of the active phases. A novel segmentation algorithm converted the tomographic images to the discrete phases present, allowing quantitative analyses to be performed. In particular, one dimensional (1D) radial profiles of ZnO and undischarged Zn were calculated, for direct comparison to the output of a computational battery model. Within these batteries, the Zn anode includes a current collecting pin that is frequently off centered. A pseudo-cylindrical coordinate system was designed to characterize the competing ionic and electronic effects in these batteries. This allows cylindrical symmetry to be maintained, despite the off centered current collecting pin. This is an imperative step in directly comparing quantitative experimental results to 1D model predictions.

The discharge of an alkaline Zn-MnO₂ battery involves a dissolution-precipitation mechanism at the Zn anode, where Zn dissolves into the electrolyte and precipitates out as ZnO. The zincate ion is highly mobile in alkaline media, leading to active material redistribution and complex morphologies of ZnO discharge products. Throughout the discharge, a Zn particle must be connected to the electronically conducting Zn network, while also maintaining contact with the electrolyte to sustain further discharge.¹ Localized precipitation of ZnO will impede hydroxide transport through that region and degrade cell performance.² Modeling has been used to simulate the performance of these commercial batteries, though model predictions do not match experimental results under numerous discharge conditions that are typical in real-world use cases.³ By characterizing commercial Zn-MnO₂ batteries under various discharge conditions, this work seeks to improve modeling capabilities through a better understanding of the discharge behavior of Zn anodes.⁴

These quantitative analyses showed Zn and ZnO distribution was highly dependent on the discharge protocol. A pulsed discharge allows more microporous and spatially distributed ZnO to form off of the active Zn surface, reducing the passivating effects of ZnO formation.^{4,5} Furthermore, the rate at which the cell is discharged dictates where the bulk of the reaction occurs in the anode. At high rates, a conventional reaction zone near the separator can be seen and is verified by model predictions. However, at lower rates this reaction zone inverts and has the majority of Zn dissolution and ZnO precipitation near the current collecting pin, which is not predicted by current models.³ By analyzing the discharge of Zn anodes using segmented tomography in pseudo-cylindrical coordinates, the factors that dictate ZnO distribution and morphology can be more thoroughly understood and used to guide the development of battery models.

Acknowledgements

This research was supported by funding from Energizer Holdings, Inc. We acknowledge collaborators Xiaotong Chadderdon, Matthew Wendling, Andrew Chihpin Chuang, and John Okasinski. This research also used resources of the Advanced Photon Source beamline 6-BM, a U.S. Department of Energy (DOE) Office of Science User Facility operated for the DOE Office of Science by Argonne National Laboratory under Contract No. DE-AC02-06CH11357.

References

[1] I. Arise et al 2013 J. Electrochem. Soc. 160 D66

[2] Q. C. Horn and Y. Shao-Horn 2003 J. Electrochem. Soc. 150 A652

[3] E. J. Podlaha and H. Y. Cheh 1994 J. Electrochem. Soc. 141 15

[4] D. P. Guida et al 2023 J. Power Sources 556 232460

[5] C.G. Smith 1978 Lawrence Berkeley National Laboratory

10:45 AM CH01.10.01

The Influence of Ammonia Concentration on the Precipitation of Ni(OH)₂ Precursor in the Synthesis of LiNiO₂ Cathode Materials for Lithium-Ion Batteries Narayan Simrit Kaur^{1,2}, Serena Cussen^{1,2} and Bethany L. Johnston^{1,2}; ¹University of Sheffield, United Kingdom; ²Faraday Institution, United Kingdom

Lithium-ion batteries have been implemented in the energy storage market for many decades, used as rechargeable batteries in portable devices, electric vehicles and a wide range of other applications. Ni-rich layered oxides as cathode materials in Li-ion batteries are of great interest due to the high energy density and theoretical capacity of 274 mAh/g of LiNiO₂. [1] To improve fast lithium-ion diffusion in lithium-ion battery cathodes, enhance the limited capacity due to oxygen release and phase changes, reduce cost and toxicity and most importantly, inhibit unethical mining of cobalt, alternative compounds to replace cobalt in LiCoO₂ are investigated by substituting different transition metals, such as Ni, Mn, or Al on the Co site in the structure. The increase of the Ni content and decrease of the Co content increases the capacity and lowers the costs in \$/kWh, as Ni provides higher performance and a high energy-density. To cope with the higher demand of volume constrained applications, the volumetric energy-density is to be considered and is achieved by a high tap density of the active material, which is related to particle size, particle size distribution and morphology. [2] However, for high-nickel content cathodes, degradation processes like Li/Ni mixing [3], surface layer deconstruction [4], particle cracking [5], decomposition reactions with the electrolyte [6] and slow Li⁺ diffusion kinetics [7] occur, leading to lower capacity retention, a loss of capacity in the first cycle and thus an overall insufficient cycling stability.

There are many research publications about optimising the calcination process of the Ni(OH)₂ precursor and LiOH·H₂O, [8][9][10], but currently, very little focus on the precursor material itself, its particle size and morphology, which affects the structural and electrochemical behaviour. The accumulation of mechanical strain due to repeated c-axis contraction and relaxation during charge/discharge processes lead to particle cracking, electrolyte infiltration, structural decay and results in a reduced electrochemical performance. To counter this, a large study regarding the morphology, particle size, and electrochemical behaviour of Ni(OH)₂ precursor material produced in a highly controlled environment (*batch stirred tank reactor* BSTR) has been undertaken and the first results are presented here. A higher transition metal to ammonia ratio during synthesis leads to larger and more spherical secondary particles, a narrow particle size distribution, a higher tap density and also improved electrochemical cycling. We are able to tune the particle size and morphology by adjusting the ammonia ratio, leading to initial discharge capacities up to 254 mAh/g (3-4.3V, C/2) while the 1st cycle capacity loss increases with increasing Ni:ammonia ratio.

[1] T. Ohzuku, A. Ueda and M. Nagayama, *J. Electrochem. Soc.*, 1993, **140**, 1862.

[2] S. Yang, X. Wang, X. Yang, Z. Liu, Q. Wei, and H. Shu, *Int. J. Electrochem.*, 2012, **9**.

[3] R. V. Chebiam, F. Prado and A. Manthiram, *J. Electrochem. Soc.*, 2001, **148**, A46-A53.

[4] A. Gosh, J. M. Foster, G. Offer and M. Marinescu, *J. Electrochem. Soc.*, 2021, **168**, 020509.

[5] R. Ruess, S. Schweidker, H. Hemmelmann, G. Conforto, A. Bielefeld, D. A. Weber, M. T. Elm and J. Janek, *J. Electrochem. Soc.*, 2020, **167**, 100532.

[6] H. Rong, M. Xu, L. Xing and W. Li, *J. Power Sources*, 2014, **261**, 148-155.

[7] M. D. Radin, S. Hy, M. Sina, C. Fang, H. Liu, J. Vinkeviciute, N. Zhang, M. S. Wittingham, Y. S. Meng and A. Van der Ven, *Adv. Energy Mater.*, 2017, **7**, 1602888.

[8] M. Bianchini, F. Fauth, P. Hartmann, T. Brezesinski and J. Janek, *J. Mater. Chem. A*, 2020, **8**, 1808.

[9] J. Välikangas, P. Laine, M. Hietaniemi, T. Hu, P. Tynjälä and U. Lassi, *Appl. Sci.*, 2020, **10**, 8988.

[10] C. S. Yoon, M. H. Choi, B-B. Lim, E-J. Lee and Y-K. Sun, *J. Electrochem. Soc.*, 2015, **162**, A2483.

11:00 AM CH01.10.02

Rapid *In-Situ* Electrochemical Formation of Partially Disordered Spinel from Mn-Rich Disordered Rocksalt Cathodes Tucker M. Holston^{1,2}, Tara Mishra², Liliang Huang², Xiaochen Yang^{1,2} and Gerbrand Ceder^{1,2}; ¹University of California, Berkeley, United States; ²Lawrence Berkeley National Laboratory, United States

We present the development of an electrochemical formation method that enables rapid and *in-situ* formation of a partially disordered spinel phase from an initially disordered rocksalt (DRX) cathode. Recent studies on Mn-rich DRX materials have demonstrated the emergence of a spinel-like phase during cycling, resulting in improved capacity retention, energy density, and rate capability compared to materials which do not transform^{1,2}. However, this transformation process typically requires weeks of cycling at relatively low rates, posing significant challenges for the commercialization of such materials.

To gain a deeper understanding of this transformation process, we carry-out a systematic study to determine whether the formation process of these spinel-like materials can be accelerated through a precycling formation process. By employing a novel electrochemical approach to purposefully stimulate the transformation, we successfully reduce the time required from several weeks to as little as one day for Mn-rich DRX. Extended cycling and synchrotron X-ray diffraction confirm that these materials exhibit both equivalent performance and resulting structure to those obtained through conventional cycling over a much longer duration. Further characterization of this material using HAADF and 4-D STEM reveals the complex local structure of the spinel-like partial ordering. It is hoped that such a practical electrochemical formation method will allow for an acceleration of research on these earth-abundant and energy-dense materials.

References:

[1] Li, L.; Chen, D.; Yue, Y.; Tong, W.; Chen, G.; Ceder, G.; Wang, C. Fluorination-Enhanced Surface Stability of Cation-Disordered Rocksalt Cathodes for Li-Ion Batteries. *Adv. Funct. Mater.* 2021, 31 (25), 2101888. <https://doi.org/10.1002/adfm.202101888>.

[2] Ahn, J.; Giovine, R.; Wu, V. C.; Koirala, K. P.; Wang, C.; Clément, R. J.; Chen, G. Ultrahigh-Capacity Rocksalt Cathodes Enabled by Cycling-Activated Structural Changes. *Adv. Energy Mater.* 2023. <https://doi.org/10.1002/aenm.202300221>.

11:15 AM CH01.10.03

Thin-Film SiO_x Coated Carbon Nanofibers as Stable Anodes for Lithium-Ion Batteries Na Yeong Kim and Ji-Won Jung; University of Ulsan, Korea (the Republic of)

With the increase in the capacity of cathode materials in lithium-ion batteries (LIBs), the demand for novel anode materials with high theoretical energy density is following. Up to now, many candidates have been reported; silicon-based composites are considered a prospective alternative due to their abundant reserves and high energy density. However, The primary disadvantage of Si, electrochemical irreversibility during the charge/discharge process, hinder widespread use.

In this study, we adapted SiO_x-coated carbon nanofibers (SiO_x-CNFs) composite to the binder-free anode current collector for lithium-ion batteries. The composite has a structure where a thin amorphous SiO_x (thickness ~100nm) is coated on the CNFs surface and is successfully synthesized by electrospinning and sputtering. This structure, surface SiO_x-coated porous CNF, breaks through the significant drawback of Si-based composites, pulverization of Si element during the charge/discharge cycle. In addition to this, due to the structure of porous CNF, we achieved the curtail of electrode weight.

Scanning Electron Microscopy (SEM) and X-ray diffraction (XRD) analyses are carried out to confirm the morphology and crystallinity. Furthermore, with cyclic voltammetry analysis, fast reaction kinetics and excellent electrochemical reversibility are verified. The cycle test is also conducted to prove excellent capacity and cyclic stability.

11:30 AM CH01.10.04

Realization of Highly Stable O-Redox Cathodes via Real-Time Analysis on the Solid-State Synthesis for High-Energy-Density Batteries Seungmin Lee, Sang Hyuk Gong and Hyung-Seok Kim; Korea Institute of Science and Technology (KIST), Korea (the Republic of)

Layered sodium manganese oxides (NMO) have been proposed as promising cathode materials for large-scale batteries owing to their cost-effectiveness [1]. However, their low capacities have hindered the increase in energy density, necessitating the development of high-capacity NMO cathodes. One approach to increasing the theoretical capacities of NMO cathodes is by utilizing the oxygen (O)-redox reaction, which is enabled by the electrochemically-active lattice oxygens through the introduction of substitutes or vacancies in the transition metal (TM) layer [1]. The stability of the O-redox reaction depends on the in-plane distribution of substitutes or vacancies in the TM layer, influencing the distance between the participating O atoms and the energy barrier for TM migration [1-2]. However, the realization of in-plane structure during synthesis and its correlation with the O-redox stability, has not been studied.

In this context, we aim to explore the structural changes of NMO during solid-state synthesis and assess the effect of synthetic parameters on its in-plane structure and O-redox stability. To monitor the changing structure during synthesis, we employ time-resolved X-ray diffraction (TR-XRD) analysis throughout the synthesis process. In addition, electrochemical tests are conducted to evaluate the O-redox stability. By analyzing these results and conducting further structural characterization (e.g., high-resolution electron microscopy (HR-TEM) and X-ray absorption spectroscopy (XAS)), the correlation between synthetic parameter and O-redox stability is suggested.

[1] C. Wu et al., *Adv. Mater.* 34, 2106171 (2022)

[2] P. G. Bruce et al., *Nature* 577, 502–508 (2020)

11:45 AM CH01.10.05

Cryo-TEM for Atomic Imaging of Solid Electrolytes in Li-Ion Batteries Hongkui Zheng and Kai He; University of California, Irvine, United States

Transmission electron microscopy (TEM) is an indispensable method to characterize materials structure and composition at the atomic scale, which is particularly important for battery research to investigate crystal lattices, defects, as well as microstructural and chemical heterogeneities within materials used in battery electrodes, electrolytes, and other components. Despite the rapid advancement of in situ TEM that has enabled the real-time observation of various dynamical phenomena and chemical processes during battery cycling and phase transformations, there are still pressing challenges that need to be addressed in order to obtain accurate and reliable findings relevant to real-world applications. For example, the radiation damage by the high-energy electron beam, as well as the side reactions between lithium compounds and moisture and oxygen in the air, are required to be avoided or mitigated. Therefore, it is desired to develop reliable electron microscopy and microanalysis strategies for the characterization, analysis, and diagnosis of real-world battery materials, for which cryo-TEM is of unique powerfulness.

Here, we report the technical development of effective methodologies and instrumentation to tackle the critical issues described above. Specifically, we developed a seamless workflow to integrate the cryo-TEM techniques with low-kV and low-dose settings to minimize the impact of electron beam radiation and sustain the original material structures from radiolysis and knock-on damage. We also built a dedicated air-free transfer system to prevent unwanted by-products of sensitive Li-containing species caused by side reactions with oxygen and moisture during sample preparation and transfer. With careful control of imaging conditions through a series of control experiments, we provided benchmarks for damage-free atomic-scale microscopy and microanalysis using cryo-TEM. These results were demonstrated in the atomic imaging of garnet-type solid electrolyte $\text{Li}_7\text{La}_3\text{Zr}_2\text{O}_{12}$ (LLZO), a promising superionic conductor for next-generation solid-state Li-ion batteries. It is expected that this approach can be generalizable to implement in the reliable characterization of a large variety of sensitive materials for energy storage relevant to real-world technologies.

SESSION CH01.11: Functional Thermal Materials
Session Chairs: Amanda Ellis and Philippe Leclere
Wednesday Afternoon, November 29, 2023
Sheraton, Third Floor, Commonwealth

1:30 PM CH01.11.01

The Barocaloric and Structural Properties of Choline-Based Plastic Crystals Joshua Levinsky¹, Philippa Partridge¹, Dominik Daisenberger² and Claire Hobday¹; ¹University of Edinburgh, United Kingdom; ²Diamond Light Source, United Kingdom

The currently ubiquitous vapor-compression method of refrigeration has a significant downside, namely its reliance on volatile refrigerants with large global warming potentials. In order to overcome this challenge, alternative solid-state refrigerants which exhibit similarly large entropy and temperature changes by the application of external stimuli have to be identified. A promising approach to this problem is found in the utilization of the hydrostatic pressure-induced entropy and temperature change, the so-called barocaloric effect, which accompanies structural phase transitions. This approach avoids the need for volatile refrigerants with large global warming potentials and promises a higher thermodynamic efficiency [1]. Thus far only the class of molecular plastic crystals, compounds which exhibit solid phases characterized by large degrees of orientational disorder and plastic-like mechanical properties, have been shown to exhibit colossal barocaloric effects on par with commercial hydrofluorocarbon refrigerants [2]. The exceptionally large barocaloric response found in plastic crystals originates from structural phase transitions from an ordered state to an orientationally disordered state, characterised by a large isothermal entropy change, dS , and large barocaloric coefficient dT/dP . Plastic phases can also be obtained in ionic systems built from weakly interacting highly symmetric globular ions. Additionally, the introduction of transition-metals into this type of system provides an avenue towards designing multifunctional or multicaloric materials [3]. In this work, we explore the expansive chemical parameter space of hybrid ionic plastic crystals and study the effect of anion substitution on the structural phase transitions and barocaloric properties of plastic crystals based on the choline cation. By employing pressure- and temperature-dependent single crystal/powder diffraction and differential scanning calorimetry experiments, this structure-property relationship is studied in detail. Demonstrating the ability to tune the transition temperature, dS and dT/dP via chemical exchange, the results of this work can then be used to inform the design of future solid-state refrigerants.

References:

- [1] C. Aprea, A. Greco, A. Maiorino, and C. Masselli, *The Use of Barocaloric Effect for Energy Saving in a Domestic Refrigerator with Ethylene-Glycol Based Nanofluids: A Numerical Analysis and a Comparison with a Vapor Compression Cooler*, *Energy* **190**, 116404 (2020).
- [2] B. Li et al., *Colossal Barocaloric Effects in Plastic Crystals*, *Nature* **567**, 506 (2019).
- [3] J. Salgado-Beceiro, J. M. Bermúdez-García, A. L. Llamas-Saiz, S. Castro-García, M. A. Señarís-Rodríguez, F. Rivadulla, and M. Sánchez-Andújar, *Multifunctional Properties and Multi-Energy Storage in the $[(\text{CH}_3)_3\text{S}][\text{FeCl}_4]$ Plastic Crystal*, *J Mater Chem C Mater* **8**, 13686 (2020).

1:45 PM *CH01.11.02

Measuring Chemical Composition, Optical and Thermal Properties at the Nanoscale with AFM Probes—Applications to Energy Materials. Andrea Centrone; National Institute of Standards and Technology, United States

Measuring and controlling chemical composition and optical properties (i.e., stoichiometry, defects, bandgap) at the nanoscale is critical for engineering materials in photovoltaics and other optoelectronics applications. Measuring nanoscale thermal properties such as thermal conductivity (η) and interfacial thermal conductance (G) is crucial for engineering thermoelectric devices. While conventional Fourier-transform IR (FTIR) spectroscopy and time-domain thermoreflectance (TDTR) reliably measure, chemical composition and thermal properties, respectively; unluckily they have insufficient spatial resolutions (few μm). Furthermore, TDTR typically requires long measurement times (≈ 120 s/pixel) and suffers from high uncertainties (i.e., $\Delta G > 35\%$) when measuring materials with low η .

Photothermal induced resonance (PTIR) [1,2,3] is a scanning probe technique that employs an AFM tip as a local detector to transduce proportionally the photothermal expansion of the sample induced by light absorption into AFM cantilever oscillation amplitudes. By leveraging lasers tunable from 400 nm to 16000 nm the PTIR set up in my lab yields absorption spectra (electronic or vibrational) and maps with a wavelength-independent resolution as high as 5 nm. This way, PTIR can map the sample composition, molecular conformation, and bandgap at the nanoscale.

After introducing the PTIR working principle, I will discuss its application in measuring ion migration,[4] bandgap,[5] and ferroelastic domains[6] in trihalide perovskites that are of great interest in photovoltaics as they combine high efficiency with ease of fabrication and low materials cost.

While PTIR has found broad applications in measuring materials compositions, conventional AFM probes lack the sensitivity and bandwidth required to measure the fast, time-domain, sample thermalization which is linked to the local thermal properties (η and G) of the sample. In contrast, the PTIR setup developed at NIST leverages new optomechanical AFM probes [7,8,9] that achieve low detection-noise (≈ 1 fm/Hz^{1/2}) over a wide (>100 MHz) bandwidth. This way, the entire, time-domain, thermal expansion of the sample is measured at once with high spatial (≈ 10 nm) and temporal (≈ 4 ns) resolutions, yielding composition (IR absorption), η and G maps, concurrently. Compared to conventional TDTR, these measurements achieve $\approx 6000\times$ higher throughput (20 ms/pixel), $>140\times$ higher spatial resolution and record-low uncertainty ($\Delta G \approx 2\%$). Compared to conventional PTIR (ringdown, AFM-IR), they achieve higher sensitivity ($\approx 700\times$) and throughput (≈ 500000). Furthermore, the high resonance frequency of these custom probes (10 MHz) is ideal to achieve high spatial resolution.[10] We believe that this novel setup will be critical for measuring thermal properties at the nanoscale and for improving the performance of thermoelectric devices.

- [1] *Annu. Rev. Anal. Chem.* 2015, 8, 101-126.
- [2] *Chem. Soc. Rev.*, 2020, 49, 3315-3347.
- [3] *Chem. Soc. Rev.*, 2022, 51, 5248-5267.
- [4] *Adv. Energy Mater.*, 2015, 5, 1500615.
- [5] *Nano Lett.*, 2015, 15, 8114-8121.
- [6] *Science Adv.*, 2017, 3, e1602165.
- [7] *Nano Lett.* 2017, 17, 5587-5594.
- [8] *Nano Lett.* 2022, 22, 11, 4325-4332
- [9] *Science Adv.* 2023, 9, ead759.
- [10] *Anal. Chem.* 2022, 94, 13126-13135

2:15 PM CH01.11.03

Owing to their relatively low thermal conductivity, heat is trapped in most organic semiconducting devices resulting in operational instability and shortened device lifetime. To overcome these issues, it is important to understand and enhance device heat-dissipation. However, related studies on organic semiconductors are rare. Here, we present a self-developed scanning photothermal deflection (SPD) technique to study the thermal transport of common organic photovoltaic (OPV) polymers and bulk-heterojunctions (BHJs). In SPD, heat diffusion in an organic film is probed by photothermal deflection method utilizing the mirage effect. In general, the thermal diffusivities for conjugated polymers increase in the order of amorphous $< 1D < 2D$ polymers in the range of 0.1 to $2 \text{ mm}^2 \text{ s}^{-1}$ (Nano Select, 2(4), 768-778). High-performance 2D polymers such as PM6 has high thermal diffusivity values comparable to stainless steel. In contrast, fullerene- and ITIC-based BHJs have significantly lower thermal diffusivities, as the heterogeneous blend may disrupt the polycrystalline structure of the polymer and slow down the intramolecular phonon transport. On the other hand, reduction due to heterogeneous blend is less noticeable in all-polymer BHJs, indicating that a polymer-rich topology benefits dominated intramolecular phonon transport. Also, SPD technique can be applied to study γ acceptors and their BHJs (Advanced Functional Materials, 31(32), 2101627).

2:30 PM BREAK

3:30 PM CH01.11.04

Entropy-Engineered Thermoelectrics: The Role of Symmetry-Driven Structure and Transport Property Evolution Yukun Liu, Hongyao Xie, Zhi Li, Christopher Wolverton, Mercurio G. Kanatzidis and Vinayak David; Northwestern University, United States

High-entropy thermoelectrics are garnering considerable attention owing to their exceptional energy conversion efficiency, improved stability, and expanded composition space. Nevertheless, understanding the impact of entropy engineering on thermoelectrics remains a challenge. The presence of diverse atomic species can give rise to a variety of mixing reactions, potentially leading to structural and chemical inhomogeneity at multiple length scales. This heterogeneity can profoundly affect transport properties, whereas a comprehensive exploration of these effects is lacking.

IV–VI group semiconductors, including PbQ, SnQ (Q = S, Se, Te), and GeTe, are among the most promising thermoelectric materials. In light of their potential, we choose PbGeSnTe₃ as the model system for further research. Through alloying CdTe to PbGeSnTe₃, we progressively increase the configurational entropy and study the resulting evolution in structure and transport properties in PbGeSnCd_xTe_{3+x}. Our findings reveal that PbGeSnTe₃ adopts a rhombohedral structure (*R3m*) at room temperature and undergoes a phase transformation to a cubic structure (*Fm-3m*) above 373 K. Through transmission electron microscopy (TEM) analysis, we observe densely distributed polar domains mediated by inversion and twin boundaries, leading to structural inhomogeneity. *In situ* heating TEM results reveal the disappearance of domains during phase transformation at high temperatures, followed by reversible formation upon cooling. These observations indicate that the loss of inversion symmetry induces the formation of domains with different polarities. The polarity switching between each domain results in significant strain fluctuations that suppress phonon propagation. Variable temperature 4D-STEM (scanning transmission electron microscopy) analysis demonstrates the strain distribution evolves upon heating due to domain evolution, contributing to an abnormal temperature-dependent thermal conductivity in the low-temperature range.

We further demonstrate the effectiveness of entropy engineering in tailoring the microstructure and transport properties through controlling crystal symmetry. By alloying CdTe, the increase in configurational entropy of PbGeSnCd_xTe_{3+x} results in a progressive reduction of the phase transition temperature and stabilizes PbGeSnCd_{0.2}Te_{3.2} in a cubic structure (*Fm-3m*) at room temperature. The increase in crystal symmetry eliminates the symmetry-breaking process during synthesis, preventing the formation of domains and consequently eliminating abnormal thermal conductivity behavior. Additionally, the Seebeck coefficient exhibits significant improvement, attributed to an increased density-of-states effective mass from $1.36 m_0$ (free electron mass) to $2.63 m_0$. This enhancement compensates for the degradation in charge carrier mobility, resulting in an improved thermoelectric performance with a maximum figure-of-merit (*ZT*) of 1.63 achieved at 875 K.

This study reveals the presence of structural inhomogeneity in high-entropy thermoelectrics, emphasizing the need for a comprehensive investigation at nanoscale to establish a robust structure-property relationship. Furthermore, we demonstrate that entropy engineering offers a promising avenue for tailoring microstructures and transport properties by modifying crystal structures. This finding opens new possibilities for the development of next-generation thermoelectric materials.

3:45 PM CH01.11.05

Barocaloric Cooling: A Combined Experimental and Computational Study Phillippa Partridge¹, Jenny Pringle², Charles J. McMonagle³, Anthony E. Phillips⁴, Richard J. Dixey⁴, Joshua Levinsky¹ and Claire Hobday¹; ¹University of Edinburgh, United Kingdom; ²Deakin University, Australia; ³SNBL at ESRF, France; ⁴Queen Mary University of London, United Kingdom

Refrigeration accounts for 17% of the global electricity usage. The current vapour-compression technology releases greenhouse gases which has led to the demand for solid-state replacements.¹ Refrigerant effects can be induced in materials named barocaloric solids through the application of hydrostatic pressure which causes a change in isothermal entropy and adiabatic temperature of the system.

Organic ionic plastic crystals (OIPCs) are a class of materials which exhibit at least one solid-solid phase transition upon varying the temperature of the system. Upon cooling these structures, the mobility of the ions becomes limited, increasing the order within the structures. It is thought that OIPCs have the ability to undergo disorder-order phase transitions which would result in large entropy changes.² In this work we investigate the phase behaviour of the OIPC (cyanomethyl)trimethylammonium hexafluorophosphate, via experiment and simulation. Variable temperature and high-pressure crystallography and thermoanalytical methods were performed to understand if it has the desired characteristics of a barocaloric material. At room temperature, (cyanomethyl)trimethylammonium hexafluorophosphate is in a high symmetry, disordered, trigonal phase, upon cooling to 253 K the structure transitions to an ordered, monoclinic phase. The isothermal entropy change associated with this solid-solid phase transition has been experimentally determined to be $138 \text{ J K}^{-1} \text{ kg}^{-1}$ and molecular dynamic simulations will be used in order to understand the configurational, rotational and vibrational contributions towards this value.

[1] X. Moya and N. D. Mathur, *Science*, **2020**, 370, 797–803. [2] J. M. Pringle, P. C. Howlett, D. R. MacFarlane and M. Forsyth, *Journal of Materials Chemistry*, **2010**, 20, 2056.

4:00 PM CH01.11.06

Heat Transfer across Van der Waals Atomic Interaction at Solid Interface Seunghoe Koo¹, Jaehee Park¹, Junki Jung¹, Hyo Jae Yoon², Seungha Shin³, Minsub Han¹ and Kyeongtae Kim¹; ¹Incheon National University, Korea (the Republic of); ²Korea University, Korea (the Republic of); ³The University of Tennessee, Knoxville, United States

Thermal energy transfer at the interface by the atomic interactions is the most fundamental energy transport mechanism for transferring thermal energy between materials. Recent advances in nano and atomic technology have made the size of device structures reach from several nanometers to several angstroms. As a result, heat transfer through the interface is more important than heat transfer within the material. Because of this importance, various studies on heat transfer through the interface have been conducted, but since the development of a device that can precisely control atomic interaction and measure heat transfer is very challenging, accurate verification of interfacial heat transfer through atomic interaction has not been achieved. Here, we developed and utilized scanning thermal probes to measure interfacial heat transfer while controlling van der Waals (vdW) energy at nanometer contacts. In particular, the atomic-milling method was used to fabricate the tip of the probe with an atomically flat surface and the relationship between vdW interaction and interfacial heat transfer was investigated proceeding the milling. Based on the experimental results obtained from the four samples, it was confirmed that high-frequency phonon modes were suppressed according to the binding energy inside each material and the vdW interaction energy. We also use the lattice-dynamical calculation and Molecular Dynamics (MD) simulation to validate the approach of suppression effects due to vdW interactions. Finally, we present the advanced approach that applies the vdW interaction energy of the interface to the DMM. This study provides insight into the theory of heat transfer through interface made of vdW interactions, and presents a milestone for considering interactions between materials for the development of various devices such as 2D materials and self-assembled monolayers.

Highly scalable, durable π -conjugated polymer materials provide control over local environments afforded through synthesis, long-lived charge carrier lifetimes, and flexible, low-cost, and scalable thin film formats which circumvent the shortcomings of inorganic materials (surface states, grain boundaries, challenges in processing, and mechanically unstable platforms). The Center for Soft PhotoElectroChemical Systems (SPECS) is an Energy Frontier Research Center focused on the basic science questions that underpin the development of low-cost, robust energy conversion and energy storage technologies based on new organic polymer (plastic) electronic materials. These materials are predicted to fill a critical position in the U.S. energy portfolio, providing for next-generation fuel-forming platforms (energy conversion) and batteries (energy storage) that cannot currently be achieved with conventional (hard) inorganic materials.

The realization of all-organic semiconductor systems that capture light energy and convert it into chemical energy requires a detailed understanding of structure-property relationships governing the interconnected dynamics of photo-generation, transport, and electron transfer across multiple interfaces. Dark electrochemical processes must be understood before increasing the complexity via light-matter interactions. This talk will focus on increasing complex, multiple interface platforms, towards the goal of photons-to-electrons-to-molecules energy conversion processes. A number of emerging *in situ/operando* spectroelectrochemical and scanning electrochemical cell microscopy approaches will be discussed for this exciting new area of energy conversion. Examples of *operando* x-ray photoelectron spectroscopy will also be discussed for chemically-resolved electrochemical measurements (CREM).

4:45 PM CH01.12.02

Ultra-High Resolution Electrocapillarity Correlates Interfacial Structure and Battery Performance Jianwei S. Lai and Feifei Shi; The Pennsylvania State University, United States

The electrode-electrolyte interface governs the kinetics and reversibility of all electrochemical processes. However, its structure and key properties often remain in theoretical models and simulations, due to the long-standing absence of direct experimental techniques. Electrocapillarity is a classical technique that directly probes the interfacial structure via interfacial tension measurement. In this work, we modernized this technique with ultra-high resolution and sampling rate. Its application on Zn-battery electrolytes reveals a unique local Zn^{2+} concentration distribution and interfacial structure constructed by Cl^- specific adsorption, which favors fast Zn deposition/stripping kinetics. The renaissance of electrocapillarity allows us to directly correlate the electron transfer kinetics and zinc battery performance with interfacial structure, which will serve as a universal tool to guide the design of better electrolytes.

SESSION CH01.13: Poster Session II
Session Chairs: Liam Collins, Rajiv Giridharagopal and Philippe Leclere
Wednesday Afternoon, November 29, 2023
Hynes, Level 1, Hall A

8:00 PM CH01.13.01

In Situ Formed Inorganic Conductive Network Enables High Stability and Rate Capability of Single-Crystalline Nickel-Rich Cathodes Xi Chen; City University of Hong Kong, Hong Kong

Single-crystalline Ni-rich cathodes are promising for the next generation of high-energy-density Li-ion batteries due to their better capacity retention than their polycrystalline counterparts. However, there is still much room for improving the electrochemical performances when considering their surface degradation and severe kinetic hindrance during cycling. Herein, we report a strategy to construct an *in situ* formed robust Li-conductive Li_3PO_4 layer on the surface of the single crystalline $LiNi_{0.83}Co_{0.12}Mn_{0.05}O_2$ cathode particles. This Li-conductive layer significantly increases the Li-ion diffusion coefficients and suppresses detrimental surface phase transformation. *In situ* XRD reveals that the improved kinetics alleviate the local stress at high voltage. The as-prepared single-crystalline $LiNi_{0.83}Co_{0.12}Mn_{0.05}O_2$ delivers good durability (96.8 % after 100 cycles at 1 C) and excellent rate capability (177.08 mAh g^{-1} at 5 C). This work provides a facile and efficient strategy to improve the cyclic performance and boost the rate capability of single-crystalline Ni-rich cathodes.

8:00 PM CH01.13.02

Platinum Selenide Nanoparticles Synthesis and Their Reaction with Butyllithium Breaking the Long-Range Ordering Structure Victor S. Lemos, Danielde Moraes, Iara Pataca, Olavo F. Verruma, Carolina Torres, Naga Vishnu Mogili, Angela Albuquerque, Flavio L. Souza, Edson R. Leite, Ingrid Gutiérrez, Danilo B. Janes and João B. Souza Junior; National Center for Research in Energy and Materials, Brazil

$PtSe_2$ is a Transition Metal Dichalcogenide (TMDC) material with potential applications in fields such as sensors, electronics, and catalysis¹. Despite significant progress in the production of 2D monolayers of $PtSe_2$, the synthesis of controlled $PtSe_2$ nanoparticles (NPs) remains unexplored². Here, we present a novel procedure for selenizing previously synthesized Pt NPs, resulting in high-quality crystalline $PtSe_2$ NPs. Pt NPs were initially synthesized using platinum acetylacetonate (II) as precursor and oleic acid and oleylamine as ligands. The reaction was performed using standard colloidal wet chemical synthesis in air-free system. These Pt NPs were then combined with excess of selenium and sealed in a custom stainless-steel reactor with an interior composed of high-purity alumina (Al_2O_3) ceramic TGA pan, under an inert N_2 atmosphere inside a glovebox. Then, the reactor was heated at 400°C for two hours. After cooling, excess selenium was solubilized with trioctylphosphine (TOP) and separated via centrifugation under inert conditions. The material was further purified by adding acetone, followed by centrifugation and supernatant removal. $PtSe_2$ reaction with n-butyllithium was also studied. The mixture was stirred at room temperature in an ultrasonic bath. Afterward, the mixture was washed sequentially with hexane, acetone, and deionized water to eliminate the LiOH byproduct. This reaction with butyllithium led to cleavage of the covalent bond along the ab-plane of the 2D material (intralayer) and disrupted the $PtSe_2$ long-range structure. The result was a $PtSe_x$ nanomaterial with a minor deselenization process, retaining short-range ordering while altering the local structure, as confirmed by Raman and ePDF analyses. XPS analysis also revealed a decrease in the concentration of selenium at the surface compared to $PtSe_2$. Both types of nanoparticles exhibited improved performance in the hydrogen evolution reaction (HER) compared to bulk $PtSe_2$. TEM analyses indicated that $PtSe_x$ kept the morphology of previously $PtSe_2$ samples, however the crystallite volume are much smaller. Unusual crystallographic facets could appear in the $PtSe_x$ sample potentially serving as additional active sites for hydrogen adsorption, in contrast to the standard catalytic performance on the basal plane (001) and its defects reported in the literature. The disruption of Long-Range Ordering (LRO) in $PtSe_x$, compared to $PtSe_2$ NPs, appears to enhance charge carrier mobility, further contributing to the improved catalytic performance as studied by electrochemical impedance spectroscopy (EIS). Consequently, the results presented here suggest that $PtSe_2$ NPs can be produced using a rapid and straightforward method compared to the conventional selenization process, making them valuable as catalysts³. Future advancements in $PtSe_2$ NPs, including doping, defect control, and nano-heterojunction studies, have the potential to enhance their performance.

[1] MANZELI, S.; *et al.*, *Nature Reviews Materials*. 2(8), 1–15, 2017.

[2] GONG, Y.; *et al.*, *Nano-Micro Letters*. 12(1), 1-34, 2020.

[3] ZHU, Y.; *et al.*, *Advanced Materials*. 30(15), 2018.

8:00 PM CH01.13.03

Effect of Pore Size on Surface Properties of Porous Solids: Determining the Hydrophilicity of Carbon Supports using the Hansen Solubility Parameters and Dielectric Spectroscopy Abdullah AlShu'aibi^{1,2} and Emmanuel P. Giannelis¹; ¹Cornell University, United States; ²King Faisal University, Saudi Arabia

Hydrophilicity is a crucial property in determining the performance and applications of porous materials. In this study, we investigate the correlation between the hydrophilicity and pore size of porous carbons, focusing on microporous carbon (Vulcan XC72) and mesoporous Hierarchical Porous Carbons (HPCs). We evaluate the stability of the suspension and relate it to the Hansen Solubility or Affinity Parameters (HSP). In addition to the above, we correlate the properties of the solids with dielectric spectroscopy in order to provide insights into the surface characteristics of the materials.

Using the HSP method, we calculate affinity parameters for different porous carbon samples. The method provides a quantitative way to evaluate their affinity behavior and compatibility in various solvents. The results show a correlation between pore size and hydrophilicity. Microporous carbon exhibits higher hydrophilicity due to enhanced water interaction with the surface within smaller pores. In contrast, mesoporous carbons show relatively lower hydrophilicity. These findings agree with the observed trends in dielectric response, reflecting smaller water clusters for microporous carbon and larger clusters for mesoporous carbon as calculated from their anomalous low-frequency dispersion (ALFD) behavior. The work provides further insights into the surface behavior of porous carbons (and porous solids in general) and be used to design materials for specific applications such as water treatment and energy storage enabling opportunities for efficient and sustainable technologies in the future.

8:00 PM CH01.13.04

Insights on The Disordered Nature in Amorphous-Based Anode Materials from Electron Pair Distribution Function AnujPokle¹, MarteSkare², ShihuiFeng³, CheukW. Tai³, AsbjørnUlvestad², XiaodongZou³ and ØysteinPrytz¹; ¹University of Oslo, Norway; ²Institute for Energy Technology, Norway; ³Stockholm University, Sweden

In material science, the ability of structural determination at high spatial resolution is critical for understanding their properties. Over the years, traditional X-ray and electron diffraction techniques have successfully determined crystalline structures. Nevertheless, new techniques are necessary as conventional methods cannot provide detailed structural information to probe the disordered structures, such as nanostructured and amorphous materials.

The pair distribution function (PDF) method based on X-ray and neutron diffraction is widely employed for providing quantitative information in amorphous materials¹. Nonetheless, understanding medium-range structural order in amorphous materials is non-trivial, where the position of atoms cannot be assigned by any equation based on translation vectors. Electron Diffraction (ED) related PDF (ePDF) in Transmission Electron Microscope has the advantage of investigating ordering locally. However, ePDF-based analyses may be affected by dynamical effects, altering the scattering intensities.

This work aims to expand the developed methodology to battery materials, by employing electron diffraction data to obtain PDF coupled with electron energy loss spectroscopy². This will enable us to investigate the role of volume expansion during lithiation in silicon-carbon-based anode materials which is crucial for the functioning of the electrode.

References:

1. Zeng, L., Tran, D. T., Tai, C.-W., Svensson, G. & Olsson, E. Atomic structure and oxygen deficiency of the ultrathin aluminium oxide barrier in Al/AlO_x/Al Josephson junctions. *Sci Rep* **6**, 29679 (2016).
2. Tran, D. T., Svensson, G. & Tai, C.-W. SUEPDF: a program to obtain quantitative pair distribution functions from electron diffraction data. *J Appl Cryst* **50**, 304–312 (2017).

8:00 PM CH01.13.05

Thickness Dependence and In Situ Studies of Nanomechanical Properties of Polymer Thin Films Upon Gas-Polymer Interaction using Amplitude Modulation Frequency Modulation (AMFM) Atomic Force Microscopy (AFM) SuwarnaDatar, BishakhaRay and PramodBankar; Defence Institute of Advanced Technology (DIAT), India

Polymer thin films are used for several applications and their thickness reduction is most important in future generation storage devices when they are used as dielectrics. Thickness reduction inevitably affects the quality of the polymer films. Furthermore, for environment safety these polymers are also used for the adsorption of the Volatile organic compounds (VOCs). Understanding the nanomechanical properties of thin polymer films and the effect of their interactions with VOCs on these properties is important in several applications like environment monitoring systems in closed spaces, sensors, electronics and packaging systems. In the present work we try to study the effect of thickness on the nanomechanical properties of polymer thin films in two different forms; deposited on the substrate and free standing films using Amplitude Modulation Frequency Modulation (AMFM) Atomic Force Microscopy (AFM). The study has been done for polymer films of polystyrene and polymethacrylate deposited on the substrate and as free standing films. Changes in the measurement of Young's modulus of the polymer when it is free standing and deposited on the substrates were observed with respect to the thickness of the film. It has been observed that as the thickness of the film is reduced the young's modulus measured for the two forms of the films do not match. The causes of changes have been discussed based on the interaction of tip with the free-standing and substrate deposited films. Furthermore, it is observed that the interaction of VOCs is quite different in both cases which is analyzed based on the changes observed in young's modulus by AMFM measurement. AMFM is a unique technique to study nanoscale viscoelastic properties of polymers. It can map the elastic properties of materials with unprecedented spatial resolution. In AMFM, conventional amplitude modulation and frequency modulation modes are combined to measure viscoelastic properties of materials with sub-10 nm resolution. The results have been discussed highlighting the importance and uniqueness of AMFM techniques in such measurements.

8:00 PM CH01.13.06

Cathode Electrolyte Interphase on the Surface of High-Nickel Cathode Materials based on Different Residual Lithium Species SangbeomKim¹, InhyeKim¹, Hyun-seungKim² and YoungjinKim¹; ¹Kangwon National University, Korea (the Republic of); ²Korea Electronics Technology Institute, Korea (the Republic of)

The development of residual lithium compounds (LiOH and Li₂CO₃) on the surface of high-Ni cathodes pose severe practical challenges that are extremely important to battery performance, despite the fact that such high Ni content in layered oxide cathodes might deliver desired energy density enhancement [1]. Residual lithium compounds may undergo spontaneous formation on cathode materials with high nickel content when subjected to H₂O and CO₂ in the surrounding atmosphere during storage. The presence of residual lithium on the surface enables the electrochemical oxidation of Li₂CO₃, leading to the evolution of gases such as O₂ and CO₂ at a high voltage. The release of gas during the cycling process leads to the expansion of the battery, hence substantially elevating the likelihood of cell rupture while in operation. In addition, the highly alkaline hydroxide ion derived from remaining lithium content induces the gelation and flocculation phenomena during the slurry coating procedure, mostly through the defluorination process of the polyvinylidene fluoride (PVdF) binder present in the slurry. The occurrence of gelation and flocculation during the slurry casting process gives rise to the formation of uneven surfaces, which represents a significant challenge in the commercial mass manufacturing of high-nickel layered oxide cathodes. This suggests that the practical application of the high-nickel layered oxide, which exhibits superior performance, is challenging unless there is meticulous control over the remaining lithium content. Extensive research has been performed in recent times to address the challenges associated with the dry coating process of high-Ni multilayer oxides. The careful management of residual lithium contents in high-nickel cathodes is imperative due to the safety and slurry gelation problems associated with their impact. However, research on cathode electrolyte interphase (CEI) components and electrolyte decomposition according to residual lithium components (LiOH and Li₂CO₃) is insufficient to date because experimental design and advanced analysis are challenging.

In this study, we present for the first time a comprehensive analysis of the formation of CEI with regard to residual lithium components from LiNi_{0.9}Co_{0.05}Mn_{0.05}O₂ (NCM90) with little difference in bulk structure. The NCM90 was obtained with different lithium hydroxide sources to form different residual lithium compounds and their content. It was shown that an increase in Li₂CO₃ content in NCM90 results in the significant formation of CEI as well as the presence of distinct CEI species. This finding was obtained by advanced analytical techniques such as Time-of-Flight secondary ion mass spectrometry (TOF-SIMS) and X-ray photoelectron spectroscopy (XPS). Furthermore, the LiOH concentration present on the surface of NCM90 electrode materials was analyzed using the titration method, wherein methanol was utilized as the solvent for the preparation of the analyte [2]. It is anticipated that this study will make a valuable contribution to the comprehension of methods for lowering residual lithium as well as developing new electrolyte additives in high-nickel layered oxide cathodes, benefiting both the academic and industrial sectors.

[1] W. M. Seong et al., *Chem. Mater.* 2020, 32, 22, 9479–9489

[2] Y. Kim et al., *ACS Energy Lett.* 2021, 6, 3, 941–948

8:00 PM CH01.13.07

Subnanometer-Scale Mobile Structures Localized at an Interface Between One-Dimensionally Aligned Sulfonate Groups and Water Investigated by Three-Dimensional Scanning AFM MasayukiMorimoto and HitoshiAsakawa; Kanazawa University, Japan

The sulfonate groups play critical roles in various interfacial phenomena, such as proton conduction and ion exchange. In proton-conductive materials such as Nafion, control of the network structure formed by the coexistence of hydrophobic chains and sulfonate groups leads to efficient proton conduction. Understanding the spatial distribution of water molecules and ions around sulfonate groups at the single functional group scale is required to elucidate the proton conduction mechanism. For this purpose, a technique for directly measuring the interface between sulfonate groups and water at the nanoscale is required. Although direct measurements of local interfacial waters and ions are difficult even with well-established methods, a three-dimensional scanning atomic force microscope (3D-AFM) can visualize the local interfacial structures at subnanometer resolution by combining frequency modulation AFM (FM-AFM).

In this study, we directly measured the interfacial structure formed on one-dimensionally arranged sulfonate groups in a self-assembled monolayer (SAM) with the coexistence of hydrophobic alkyl chains by 3D-AFM. Prepared sulfonate-terminated alkanethiols SAMs (SO₃-SAM) showed stripe-like structures. Owing to the lying-down orientations of sulfonate-terminated alkanethiol molecules in the stripe-like structures, one-dimensionally aligned structures of the sulfonate groups were formed. As a result, the 1D-aligned sulfonate groups were surrounded by hydrophobic alkyl chains. The lying-down SO₃-SAM structures can be considered a structural model for a controlled nano-environment where hydrophobic groups and sulfonate groups coexist. Our results suggested that the growth and collapse of mobile interfacial structures exist at the SO₃-SAM surfaces based on analysis of the successive AFM images. In addition, the mobile interfacial structures were localized in the hydrophilic region with the 1D-aligned sulfonate groups. The 3D-AFM measurements were performed to understand the spatial distribution of the mobile interfacial structures. By analyzing the 3D-AFM images obtained at the interfacial nanospace, the mobile interfacial structures were visualized as localized regions with higher repulsive forces than the surrounding areas. In the presentation, we will discuss the detailed analysis of FM-AFM and 3D-AFM images and the origin of mobile interfacial structures.

8:00 PM CH01.13.08

Ferroelectric SrTiO₃ Induced by Energetic Ion Irradiation FuxiangZhang; Songshan Lake Materials Laboratory, China

SrTiO₃(STO) is a very important electric material and bulk STO has a centrosymmetric cubic structure at room temperature, and there is a cubic to tetragonal structural transition at 105 K [1].

The dielectric constant of SrTiO₃ deviates from the classical Curie–Weiss law at low temperature, and it increases rapidly (up to 1.8×10^4 at 1.4 K) as the temperature is reduced [2]. The low temperature electric behavior of STO approaches a ferroelectric phase transition; however, bulk STO is still paraelectric to the lowest temperature as a result of quantum fluctuations [3]. The ‘quantum paraelectrics’ or ‘incipient ferroelectrics’ of STO and other perovskite oxides have been a topic of considerable interest during the past few decades [3]. The ferroelectric transition of STO at low temperature can be induced by strains from lattice mismatch for thin films, chemical or isotopic substitution, electric field, pressure and controlled grain size. Due to important applications in electronic devices, the coupling between strain and ferroelectricity in STO has been intensively studied, and the relevant work is well illustrated in a recent review article [4]. By controlling the in-plane lattice strain, the critical temperature T_c of ferroelectric transition in thin film SrTiO₃ or superlattice can be profoundly enhanced [5,7,8], even to room temperature [6]. However, the biaxial strains in thin films depend on the choice of substrate and film thickness, which turns out to be challenging for the synthesis of uniformly strained films because of the undesirable relaxation that occur when the thickness of a sample exceeds the critical values. In this work [9,10], with energetic ion irradiation, bulk STO turns from paraelectric to ferroelectric at room temperature due to the irradiation-induced strain. The strain profile in bulk STO is determined by symmetric X-ray diffraction and simulation. The irradiation induced atomic-level defects are characterized with high resolution TEM. The ferroelectric properties of the damaged zone is measured directly with microelectronic techniques. All the results suggest that the out-of-plane strains induced by ion bombardment make a local phase transformation of bulk STO from cubic to tetragonal and result in ferroelectricity at room temperature.

References

- [1] Rimai L and Demars G A 1962 Electron paramagnetic resonance of trivalent gadolinium ions in strontium and barium titanates *Phys. Rev.* 127 702–10
- [2] Weaver H E 1959 Dielectric properties of single crystals of SrTiO₃ at low temperatures *J. Phys. Chem. Solids* 11 274–77
- [3] Müller K A and Burkard H 1979 SrTiO₃: an intrinsic quantum paraelectric below 4 K *Phys. Rev. B* 19 3593–602
- [4] Pai Y, Tylan-Tyler A, Irvin P and Levy J 2018 Physics of SrTiO₃-based heterostructures and nanostructures: a review *Rep. Prog. Phys.* 81 036503
- [5] Uwe H and Sakudo T 1976 Stress-induced ferroelectricity and soft phonon mode in SrTiO₃ *Phys. Rev. B* 13 271
- [6] Haeni J H *et al* 2004 Room-temperature ferroelectricity in strained SrTiO₃ *Nature* 430 758–61
- [7] Jang H W *et al* 2010 Ferroelectricity in strain-free SrTiO₃ thin films *Phys. Rev. Lett.* 104 197601
- [8] Sirenko A A, Bernhard C, Golnik A, Clark A M, Hao J, Si W and Xi X X 2000 Soft-mode hardening in SrTiO₃ thin films *Nature* 404 373–6
- [9] Zhang FX, Xue H, Keum JK, Boule A, Zhang Y and Weber WJ 2020, *J. Phys.: Condens Matter* 32
- [10] S. Nan, F.X. Zhang *et al* 2023, (not published)

8:00 PM CH01.13.09

Resistive Switching Behaviors of TiO₂ Protection Layers via Electrochemical Forming Process for Robust Photoelectrochemical Water Splitting Dong SuKim, Hak HyeonLee, Kun WoongLee and Hyung KounCho; Sungkyunkwan University, Korea (the Republic of)

In typical photoelectrochemical (PEC) cells using cuprous oxide (Cu₂O), semiconductor photoabsorbers have passivated by protection layers, such as TiO₂, where the trade-off between high photocurrent and durable stability is inevitably involved with their thickness in the typical energy band transport along the conduction band. Herein, as a strategically advanced charge transport mechanism, an outstanding conducting filament transport mechanism for vigorous and robust PEC operation is innovatively suggested, which is motivated from the concept of nano-filaments showing non-volatile metallic-like current flow characteristics in resistance-change memory devices. The breakdown-like electrochemical forming behavior effectively occurs with rapid current increase in voltage sweep over ~ 2 V vs. RHE and the fundamental properties of filaments, such as diameter, density, and conductivity, have been controlled by varying artificially compliance currents. Especially, it should be noticed that this process requires i) no top electrodes obstructing the light harvesting and the injection of photo-charges into electrolytes and ii) no individual forming process sweeping point-by-point bias, and provides iii) electrochemical forming sites with homogeneous and dense distribution. Additionally, some photocorrosive sites inducing photocurrent degradation are perfectly bypassed by preferential photoelectrodeposition of co-catalysts. In consequence, from the electrochemical filament forming process and selective Pt-photoelectrodeposition on filaments, the Cu₂O/AZO/TiO₂ photocathodes exhibit unprecedented photocurrent density of about 11.9 mA/cm² and open circuit potential of 0.73 V and produces vigorous hydrogen and oxygen evolutions for over 100 h, even though the TiO₂ passivation film has exceeding 100 nm thickness.

8:00 PM CH01.13.10

Revealing of Photocatalytic Performance Variations of ZnIn₂S₄ Nanoparticles using In-Situ XPS HangilLee; Sookmyung Women's University, Korea (the Republic of)

ZnIn₂S₄ nanoparticle (NP) photocatalysts were successfully synthesized to investigate the wavelength-dependent photocatalytic activity owing to the concentration of Zn vacancies at the surface of the ZnIn₂S₄ NPs. In situ X-ray photoelectron spectroscopy were performed to investigate the effect of Zn vacancies on the photocatalytic activity of the ZnIn₂S₄ NPs. Furthermore, the wavelength-dependent photocatalytic degradation (PCD) activity of the ZnIn₂S₄ NPs using 2,5-hydroxymethylfurfural (HMF) was investigated over a wide range. The selective oxidation of HMF using ZnIn₂S₄ NPs resulted in the formation of 2,5-furandicarboxylic acid via 2,5-diformylfuran with an efficiency of over 40% over a wide wavelength range. Thus, the irradiation wavelength for PCD depended on the number of defect structures introduced into the ZnIn₂S₄ NPs by the sulfur source.

8:00 PM CH01.13.11

Highly Reversible Zinc Metal Anode Enabled by Zinc Fluoroborate Salt-Based Hydrated Organic Electrolyte ShuyunWang; City University of Hong Kong, Hong Kong

Although Zn(BF₄)₂ contains favorable ingredients of fluorine for the formation of ZnF₂ rich- Zn²⁺ ion conducting SEI, the aqueous electrolyte based on inorganic Zn salt of Zn(BF₄)₂ xH₂O shows high Hammett acidity with pH value <1, which gives rise to severe corrosion of metallic Zn electrode and thermodynamically spontaneous HER. Here, we employ a hydrophilic organic solvent of VC and Zn(BF₄)₂ 4H₂O for a hydrated organic electrolyte, denoted as ZnBF-VC. With the ZnBF-VC electrolyte used, the VC molecules preferably adsorb on the Zn surface to block H₂O molecules and Zn metals, which formed the structure of Zn(VC)_{2,80}(H₂O)_{1,28}(BF₄)_{1,83}. The distinct SEI enables favorable Zn²⁺ ion transport and can protect metallic Zn electrode from corrosion, side reactions and dendrite formation. Consequently, the Zn-Zn cells cycled over 2200 h and the Zn-Cu asymmetric cells maintained a CE of $\sim 99.7\%$ over 550 cycles at 1 mA cm⁻². Whereas, the Zn-Zn cells broke after only 74 cycles in aqueous electrolyte. Additionally, the Zn-MnHCF full cell with ZnBF-VC demonstrates excellent cycling stability, achieving a high specific capacity of 146.2 mAh g⁻¹, and a high retention rate of 85.3% over 1300 cycles at 0.4 A g⁻¹, while the cell using the referred ZnBF- H₂O electrolyte survived only ~ 6 cycles.

8:00 PM CH01.13.12

Characterization and Testing of Porous Boron Nitride Towards Application in Adsorption-Based Processes AnoukL'Hermite^{1,2}, DanielM. Dawson³, PilarFerrer⁴, KanakRoy⁵, GeorgHeld⁴, MarcusH. Yio², TakuyaHiroSawa⁶, ToshihiroIso⁶, SharonAshbrook³ and CamillePetit²; ¹University of Cambridge, United Kingdom; ²Imperial College London, United Kingdom; ³University of St Andrews, United Kingdom; ⁴Diamond Light Source, United Kingdom; ⁵Banaras Hindu University, India; ⁶Tokyo Institute of Technology, Japan

Industrial separation processes account for 10-15% of the global energy consumption.¹ The energy cost of large-scale gas and liquid separations like distillation can be significantly reduced by moving towards adsorption processes. An example of an inorganic adsorbent is porous boron nitride (BN): this material exhibits high surface area and porosity, and benefits from greater oxidative and thermal stability than common carbonaceous adsorbents.² Our group previously developed a new method to produce porous BN with enhanced surface area, tunable porosity³ and promising liquid and gas separations performance. In more recent work, we explored the potential of porous BN as an efficient and moisture-resistant adsorbent for molecular separations at industrial scale. To do so and foster scaling-up, two questions have been addressed: 1) “How does porous BN form and what are the controlling synthesis parameters?” and 2) “How can one enhance the water stability of this adsorbent?”

To address point 1, we investigated the formation mechanism of porous BN using a range of analytical and spectroscopic techniques including, among others, solid-state NMR and synchrotron-based X-ray absorption spectroscopy.⁴ This in-depth characterization exercise of porous BN and its intermediates obtained at different temperatures allowed us to propose a detailed formation mechanism that involves carbon nitride as intermediate. We showed how the porosity develops in the material, what synthesis factors can influence it and what gases are responsible for its generation. Overall, our study allowed to support with more certainty the hypotheses formulated in previous reports in the field.

To address point 2, we developed two functionalization routes to modify the surface of porous BN and enhance its hydrophobicity and resistance to moisture.⁵ The first route involved direct silylation of porous BN powder followed by pelletization, whereas the second route used chemical vapor deposition on porous BN pellets. In parallel, we developed a method relying on saturated salt solutions⁶ to mimic two different levels of humidity exposure relevant to storage and sorption testing conditions. Using FTIR, XRD, XPS, μ XRF, TGA, N₂ sorption and mercury intrusion porosimetry, we analyzed the samples before and after functionalization, as well as before and after exposure to humidity. Our results pointed to the efficiency of the functionalization approach to produce moisture-resistant BN-based adsorbents. Therefore, thanks to the extensive use of characterization techniques, this research paved the way for scaling up the synthesis of porous BN towards lower carbon emissions in industrial applications.⁷

References:

1. D. S. Sholl and R. P. Lively, *Nature* **532** (2016) 435-437
2. X.-F. Jiang *et al.*, *J. Mater. Sci. Technol.* **31** (2015) 589-598
3. S. Marchesini *et al.*, *ACS Nano* **11** (2017) 10003-10011
4. A. L'Hermite *et al.*, *J. Phys. Chem. C* **125** (2021) 27429–27439

5. A. L'Hermitte et al., *Microporous Mesoporous Mater.*, **352** (2023) 112478
6. L. Greenspan, *J. Res. Natl. Bur. Stand. A Phys. Chem.* (1977) 89-96
7. I. Itskou et al., *Acc. Mater. Res.* **4** (2023) 143-155

8:00 PM CH01.13.13

Correlating Electrical, Catalytic Properties with Pair Distribution Functions of Nano-Cu-Ceria Siu-Wai Chan, Yanhe Li, Syed Saam Rassol, Haotian Chen and Haolan Sun; Columbia University, United States

This study delves into the influence of copper doping on the electrical conductivity of cerium oxide nanoparticles. We employ a combination of Pair Distribution Function (PDF) analysis and Impedance Spectroscopy (EIS) to investigate the structural and electrical characteristics of Cu-doped CeO₂ nanoparticles synthesized via a coprecipitation method. Previously, such prepared nano-Cu-ceria has shown exceptional catalytic activity better than other nano Cu-ceria's.

To conduct our investigation, we pressed and sintered nanoparticles of 2-8% Cu-doped CeO₂ into bulk pellets, enabling AC impedance measurements. Synchrotron PDF results reveal correlations between doping concentration, particle size, and the equilibrium lattice parameter, providing insights into the structural modifications induced by Cu incorporation. Additionally, we find Cu doping to have a significant impact on the electrical properties of CeO₂ nanoparticles, seeing a correlation between doping concentration, conductivity, and charge carrier density, which also correlate catalytic activities.

In summary, this research advances our understanding of the structural changes induced by Cu doping in cerium oxide nanoparticles and underscores the direct influence of doping concentration on electrical characteristics as well as catalytic properties. These findings hold promise for tailoring materials with enhanced electrical and catalytic performance for a wide range of applications and reactions.

8:00 PM CH01.13.14

Generating Electrical Power from Low-Grade Waste Heat through Thermoelectrochemical Cells Utilizing Titanium Carbide Electrodes Byung-Jo Lee, Sang-Mun Jung and Yong-Tae Kim; POSTECH, Korea (the Republic of)

In response to growing environmental concerns and the limitations of traditional carbon-based fuels, there has been significant research into sustainable energy resources, particularly those that harness ambient energy sources such as thermal, wind, kinetic, and solar energy. However, efficiently harvesting low-grade waste heat, produced by sources like power plants and environmental body heat, has remained a challenge due to the cost and inefficiency of large-scale thermal energy conversion devices. Thermoelectrochemical cells (TECs) are highly effective devices for converting low-grade waste heat into electricity. However, TECs that rely on hexacyanoferrate (Fe(CN)₆⁴⁻/Fe(CN)₆³⁻, HCF) electrodes often use expensive metals like platinum (Pt), which hinders their practical use. In this study, we propose an alternative to Pt electrodes for TECs in the form of titanium carbide (TiC) electrodes, synthesized through the thermal decomposition of CH₄. While titanium itself is challenging to use in TECs, TiC emerges as a promising non-noble metal electrode due to its exceptional stability and reaction kinetics, suitable for various electrochemical systems. Our experiments revealed that TiC-based TECs achieved a power output of 397.20 mW m⁻², nearly matching that of Pt electrodes. Additionally, TiC demonstrated long-term stability in the electrolyte during operation, suggesting its potential to replace Pt electrodes and facilitate the commercialization of TECs.

8:00 PM CH01.13.15

Bias-Free Copper-Nickel Alloy/Graphene/Si Heterojunction as Catalytic Photocathode for Photovoltaic-Assisted Ammonia Production Hsing-Wen Wu¹, Lu Yang-Sheng¹, Li Shao-Sian¹ and Chen Chun-Wei²; ¹National Taipei University of Technology, Taiwan; ²National Taiwan University, Taiwan

With the rise of world's population, the demand of energy is also getting higher, which further accelerates the consumption of fossil fuels and the destruction of natural ecosystems. Solar energy is an alternative to fossil fuels because it has the highest energy content. However, the development of solar energy is limited by its intermittency and volatility, therefore storing solar energy becomes an important issue. Since ammonia is a suitable compound for storing solar energy, and it is a carbon-free chemical with high energy density, the production of ammonia becomes an important goal in our research.

The mainstream production of ammonia in the industry relies on the Haber-Bosch process, which requires harsh operating conditions at high temperatures and pressure. An alternative technique based on the green synthesis route of ammonia by catalytic reactions has recently attracted tremendous interest.

With efficient catalyst materials, ammonia is produced from nitrogen or nitrate by sequential reactions at ambient conditions. However, nitrogen is an inert molecule and has strong triple bond, causing a lower faradaic efficiency under nitrogen (N₂) reduction reaction (NRR). Furthermore, the potential barrier to triggering ammonia reduction is still high; thus, external energy, such as electric potential, is always required to drive the reaction. Here we report an improved ammonia reduction system of Cu-Ni coated graphene/HJT photocathode promoted by the photovoltaic effect. A commercial Si solar cell was attached with a monolayer of graphene where Cu-Ni catalyst was then directly grown on it by electrochemical deposition.

We attempted to electrochemically electrodeposit Cu-Ni nanostructures on graphene/HJT as an electrocatalyst for NRR. Cu and Ni have the same crystal structure (FCC), similar valence, close values of atomic radii, and electronegativity, allowing the formation of homogeneous solutions over the entire composition range. Next, we test the catalytic performance of Cu-Ni/Gr/HJT in the electrochemical nitrate reduction reaction. Our results show that graphene is an excellent supporting material for Cu-Ni catalysts and an efficient medium for transferring photogenerated electrons from Si solar cell to Cu-Ni nanostructure.

As a result, the additional solar energy boosted the reaction kinetic of Cu-Ni catalysts for ammonia reduction. Under AM 1.5G solar simulator illumination, the overpotential required for ammonia reduction is suppressed at least by 100mV, leading to improved Faraday efficiency from 80% to over 90% and yield rate from 525 μg h⁻¹cm⁻² to 750 μg h⁻¹cm⁻².

To achieve bias-free reaction, we intend to replace batteries with solar cell. Additionally, we replace Pt (anode material) with Ni-Fe LDH since it possesses better performance for oxygen evolution reaction (OER).

8:00 PM CH01.13.16

Micro Four-Point Probe for Anisotropic Thermal Diffusivity Mapping Neetu Lamba¹, Braulio Beltrán Pitarch^{1,2}, Muhamed Dawod³, Alex Berner³, Benny Guralnik², Yaron Amoyal³, Ole Hansen¹, Nini Pryds¹ and Dirch Hjorth Petersen¹; ¹Technical University of Denmark, Denmark; ²KLA, Denmark; ³Technion-Israel Institute of Technology, Israel

High-resolution microscale thermal diffusivity characterization is vital for a deeper understanding of materials used in thermoelectric energy harvesters, nano/microelectronic, and thermal management. Analyzing the thermal properties of individual grains can advance the development of these materials, however, only a few techniques currently exist for microscale characterization of the thermal properties.

Micro four-point probe (M4PP) has been widely used by the semiconductor industry to characterize thin films for sheet resistance, carrier mobility, and magnetoresistance. Currently, we are exploring the use of M4PP for estimating the thermal properties of materials including the Seebeck coefficient, thermal diffusivity, and the temperature coefficient of resistance.

Here, I will present a novel method for measuring the thermal diffusivity of individual grains with varying orientations using the M4PP. The local thermal diffusivity measurements were performed on a prototypical bulk thermoelectric Bi₂Te₃ sample at room temperature. The thermal diffusivity was then correlated with the orientation of the grains measured with electron-backscattered diffraction (EBSD). The method for measuring thermal diffusivity proposed in this study provides rapid and accurate thermal characterization, thereby opening up opportunities for a detailed understanding of microstructures.

8:00 PM CH01.13.17

Ester Side Chain Functionalization Enhances Mechanical Properties of Poly(3-hexylthiophene) while Maintaining High Hole Mobility Lexi R. Knight¹, Quynh Tran¹, Guanchun Rui¹, Gage Mason², Piumi Kulatunga², Alexander Bushnell¹, Sonia Hou¹, Lei Zhu¹, Simon Rondeau-Gagne² and Genevieve Sauve¹; ¹Case Western Reserve University, United States; ²University of Windsor, Canada

Poly(3-alkylthiophene)s represent a class of polymers known for their easy synthesis and tendency to crystallize which makes them promising candidates for facilitating charge transport in organic electronics. Organic electronics, including organic photovoltaics (OPVs) and organic thin-film transistors (OTFTs), have several advantages including their lightweight nature, cost-effectiveness, ease of fabrication, and flexibility. For a polymer to be a good candidate in organic electronics, it must have high charge transport and high flexibility, two properties that are often mutually exclusive. To increase both electrical and mechanical properties, we introduced ester groups in the side chains into poly(3-alkylthiophene). Esters are known for their plasticizing effect. Here, we synthesized and characterized two sets of random copolymers: poly(3-alkylthiophene-2,5-diyl)-ran-(3-(6-pentanoatehexyl)thiophene-2,5-diyl) in which the alkyl side chain is either hexyl (P3HT series) or dodecyl (P3DDT series) with varying ester content. The optical, thermal, structural, mechanical, and electrical properties of the copolymer series were investigated. Both electrical and mechanical properties were optimized at 10% ester content in the P3HT series: high fracture strain of 29%, high tensile strength at 3.9 MPa, and large toughness of 90 J/m³ all while maintaining the same charge carrier mobility as P3HT at 0.12 cm²V⁻¹s⁻¹. The mechanical and electrical properties of the P3DDT series did not fluctuate much with varying ester content between 0-25%, potentially due to the crystallization of the longer side chains altering the microphase separation. Differential Scanning Calorimetry (DSC) and Grazing Incidence Wide-Angle X-ray Diffraction (GIWAXD) suggest microphase separation between the dodecyl side chain and main chain of the P3DDT series which was not observed in

the P3HT series. Therefore, the ester functionalization did not plasticize the P3DDT series as well as in the P3HT series. These results show that a small ester functionalization can significantly increase the flexibility of the polymer while maintaining high charge transport.

8:00 PM CH01.13.18

Thin Films of Fluorescent Pigments acting as a Wavelength-Shifters to Improve The Efficiency of Solar Cells Otávio J. de Oliveira¹, Natália D. Coutinho¹, Thais Crestani², Gabriel Thomas D. de Freitas¹, Ana Paulad. Modesto¹, Wesley C. Muscelli¹, Marcelo G. Villalva¹ and Francisco C. Marques¹; ¹State University of Campinas, Brazil; ²BYD, Brazil

Although silicon and perovskite solar cells have achieved efficiency as high as 26% [1], their efficiency is still limited by several factors, such as reduced efficiency in the ultraviolet region of the solar spectrum [2]. One of the proposed mechanisms to overcome this problem is to use wavelength-shifting materials. Here we investigate the properties of low-cost photoluminescent pigment thin films currently used in coatings, graphic arts, cosmetics, and adhesives. The objective was to evaluate the ability to shift ultraviolet light to the wavelength where silicon solar cells are most efficient (around 600 nm). Precursor solutions were prepared by dissolving the pigment in ethanol. The deposition of the thin film was carried out using the spin-coating technique. After each deposition, the substrates were placed on a heating plate (100°C) for 10 minutes to evaporate the solvent. The pigments (powder and thin films) were characterized by X-ray diffraction, AFM, UV-Vis transmittance, and photoluminescence. The XRD diffractogram is compatible with the expected structure of organic pigments, presenting an amorphous characteristic. Photoluminescence measurements show that PL emission covers a range of 500 – 650 nm, which is in the region of highest efficiency of silicon solar cells. Thin films deposited by spin-coating have good uniformity. Absorption occurs in the wavelength range of 300 to 700 nm, being more intense in the UV range. PL emission, on the other hand, is shifted to the range 550 to 700 nm. The optical and structural properties of the films demonstrated the potential use of low-cost fluorescent pigments as wavelength shifters for application in solar cells. Further investigations are needed to evaluate the effect of these films on solar cells.

Acknowledgements:

BYD Energy Brazil, FAPESP and CNPq.

References:

[1] Best Research-Cell Efficiency Chart, available at <https://www.nrel.gov/pv/cell-efficiency.html>. Accessed on 09/11/2023.

[2] T. Trupke, M. A. Green and P. Würfel, Journal of Applied Physics 94 (3) (2002) 1668-1674.

8:00 PM CH01.13.19

Temperature-Dependent Transport Properties of High-Performance Metal Halide Perovskites Chaeyoung Kim¹, Oki Gunawan², Minjin Kim³, Dong Suk Kim⁴ and Byungha Shin¹; ¹Korea Advanced Institute of Science and Technology (KAIST), Korea (the Republic of); ²IBM T. J. Watson Research Center, United States; ³Korea Institute of Energy Research (KIER), Korea (the Republic of); ⁴Ulsan National Institute of Science and Technology (UNIST), Korea (the Republic of)

We have recently developed a “temperature-dependent carrier-resolved photo-Hall” technique that enables measurements of various transport properties in temperature ranges from 20K to 340K. In the field of optoelectronics applications, the transport characteristics of minority carriers as well as majority carriers are crucial. However, Hall measurement, which is one of the fundamental characterization methods in the semiconductor field, has a limitation in that only information on the majority carrier can be obtained. We have previously developed a “carrier-resolved photo-Hall” technique that enables the extraction of critical parameters for both majority and minority carriers in electronic materials, such as carrier density, mobility, recombination lifetime, and diffusion length. This technology is enabled by a new photo-Hall equation and a highly sensitive AC Hall system based on parallel dipole line magnets. Furthermore, since the temperature can significantly affect the carrier transport and recombination processes in solar cells, understanding the temperature-dependent behavior of charge carrier transport is important for comprehending solar cell performance and operation. Here we report our recent advancements in the “carrier-resolved photo-Hall” technique that allows photo-Hall measurements in the temperature range of 20-340K. A temperature-dependent photo-Hall analysis was successfully performed on a reference single crystalline p-type silicon and on a metal halide perovskite exhibiting a solar cell efficiency of 25.7%. We investigated important information such as temperature-dependent photoconductivity, mobility scattering mechanisms, and dopant energy levels. In the high-performance perovskite thin film samples, the mobility of electrons and holes increased with temperature up to room temperature and then decreased with the further increase of temperature, indicating impurity scattering and phonon scattering are dominant below and above room temperature, respectively. Also, we investigated the influence of temperature and light intensity on transport characteristics, such as carrier density of photo-generated charges, lifetime, and diffusion length. The lifetime and carrier density of photo-generated charges increased with temperature, and this increase can be advantageous in situations where solar cells heat up during operation. This advance in transport characterization technologies will provide a more detailed understanding of carrier transport properties of electronic materials and contribute to the further development in many applications including solar cells.

8:00 PM CH01.13.20

Title: Structural, Magnetic, and Magnetocaloric Properties of Erbium and Aluminum Co-Doped HoCrO₃ Compound Jolaikha Sultana; The University of Memphis, United States

This study describes the synthesis and magnetocaloric properties of rare-earth chromite's, viz., HoCrO₃, Ho_{0.67}Er_{0.33}CrO₃ and Ho_{0.67}Er_{0.33}Cr_{0.5}Al_{0.5}O₃ orthochromites. These materials are considered functional materials with interesting magnetic and magnetocaloric properties, making them suitable for potential applications in magnetic refrigeration. The samples were synthesized using facile sol-gel auto combustion method. As confirmed by X-ray diffraction analysis, the resulting compounds have a pure orthorhombic crystal structure with the space group Pbnm. The lattice parameters and volume of the samples were observed to decrease with the substitution of Al³⁺ ions. This decrease can be attributed to the smaller ionic radius of Al³⁺ compared to Cr³⁺. The bond angle and bond-length of Cr-O-Cr of studied compounds were observed to vary with the substitution, which observed to have influence on their magnetic and magnetocaloric properties. The magnetic measurements were performed using PPMS in the temperature range 5K -300K and field up to 5T. The temperature dependent magnetization curve shows magnetic transition at 141 K for HoCrO₃, 135 K for Ho_{0.67}Er_{0.33}CrO₃, and 35 K for Ho_{0.67}Er_{0.33}Cr_{0.5}Al_{0.5}O₃, respectively. The magnetization and magnetic entropy change (ΔS_m), determined from magnetic isotherms, were found to increase with the introduction of Er and Al doping. The maximum magnetic entropy change observed was 6.46 Jkg⁻¹K⁻¹ for HoCrO₃, 8.04 Jkg⁻¹K⁻¹ for Ho_{0.67}Er_{0.33}CrO₃, and further increased to 9.70 Jkg⁻¹K⁻¹ for Ho_{0.67}Er_{0.33}Cr_{0.5}Al_{0.5}O₃ under an applied field of up to 5T. This enhancement in magnetization and magnetic entropy change is attributed to the Al³⁺ substitution, which affects the Cr³⁺-Cr³⁺ exchange coupling due to changes in the Cr1-O1-Cr1 bond angle and Cr1-O1 bond lengths. The study concludes that the co-doped chromite's, particularly Er³⁺ and Al³⁺ co-doped HoCrO₃, have not been previously reported in the literature. The observed magnetocaloric properties, especially in the Al³⁺ doped samples, suggest their potential for low-temperature magnetic refrigeration applications.

Authors: Jolaikha Sultana, Christopher Hanley, Dr. Arjun K Pathak, and Dr. Sanjay R Mishra

8:00 PM CH01.13.21

Aluminum Doped GdCr_{0.5}Al_{0.5}O₃ and TbCr_{0.5}Al_{0.5}O₃ Chromate Compounds: A Comparative Magnetocaloric Effect Study Jolaikha Sultana¹, Asraf Sawon², Grace Brzykcyk², Arjun Pathak² and Sanjay Mishra¹; ¹The University of Memphis, United States; ²University at Buffalo, The State University of New York, United States

Magnetocaloric materials are substances that exhibit a change in temperature in response to an applied magnetic field. They have the potential to be more efficient and environmentally friendly than conventional refrigeration systems that rely on vapor compression. Lanthanides orthochromites are materials that include both lanthanides and transition metals, making them suitable candidates for magnetocaloric research because of their unique magnetic properties. Earlier studies showed that doping with Lanthanide ion (A-site) or, transition metal ion (B-site) or both sites can bring about desirable structural and electronic changes in the material, enhancing its magnetic properties. This study examines the effect of substituting Al³⁺ ions at the B-site of GdCrO₃ and TbCrO₃ orthochromites on their structural, magnetic, and magnetocaloric properties.

The samples were synthesized using the sol-gel auto combustion method. X-ray diffraction study confirms the presence of a pure orthorhombic phase with the *Pbnm* space group. The lattice parameters and volume of the samples decreased with Al³⁺ substitution due to the smaller ionic radius of Al³⁺ (0.535 Å) compared to Cr³⁺ (0.615 Å). Magnetic measurements were conducted between 5K and 300K under magnetic fields up to 0.2 T. The magnetization measurements revealed the antiferromagnetic ordering of Cr³⁺ spins with a Neel temperature (T_N) of approximately 169K for GdCrO₃ and 157K for TbCrO₃. The substitution of Al³⁺ at the Cr³⁺ site led to a decrease in Neel temperature, T_N, indicating a modification of the magnetic behavior in the doped samples. The temperature dependence of the magnetic entropy change (ΔS_m) for different applied magnetic fields (ΔH) demonstrated that the values of $-\Delta S_m$ decreased with increasing Al³⁺ substitution. The maximum values of $-\Delta S_m$ were found to be 27.30 Jkg⁻¹K⁻¹ at 7K with a 5T applied field for GdCrO₃ and 16.60 Jkg⁻¹K⁻¹ at 7K with a 5T applied field for GdCr_{0.5}Al_{0.5}O₃. Similarly, for TbCrO₃, the maximum value was 11.53 Jkg⁻¹K⁻¹ at 7K with a 5T applied field, while for TbCr_{0.5}Al_{0.5}O₃, it was 4.20 Jkg⁻¹K⁻¹ at 11K with a 5T applied field. The observed variation in maximum entropy changes is attributed to the Al³⁺ substitution in the studied chromite's, which influences the Cr³⁺-O²⁻-Cr³⁺ exchange coupling by altering the Cr1-O1-Cr1 bond angle and Cr1-O1 bond lengths. It is noted that Al³⁺ doped GdCrO₃ and ErCrO₃ have not been previously reported in the literature. The magnetic entropy values obtained are comparable to those of other studied chromite's, suggesting that these compounds hold promise for low-temperature magnetic refrigeration applications.

8:00 PM CH01.13.22

Leveraging Image and Data Processing Techniques to Investigate Ionomer Distribution within Catalyst Layers of PEMFCs and PEMWEs Mariah Batool¹, Maryam Ahmadi¹, Carlos Baez-Cotto², Linda Ney³, Jeronimo Horstmann³, Jayson Foster⁴, Nada Zamel³, Scott Mauger², Svitlana Pylypenko⁴ and Jasna Jankovic¹; ¹University of Connecticut, United States; ²National

Advanced materials characterization tools such as scanning transmission electron microscopy and energy dispersive spectroscopy (STEM/EDS) offer a surfeit of information, only a fraction of which is comprehensible and evident to the human eye. This is especially true for complex, multi-component electrochemical systems such as polymer electrolyte membrane fuel cells (PEMFC) and water electrolyzers (PEMWE) where understanding component interactions within membrane electrode assembly (MEA) is a challenging task [1]. This understanding is crucial to optimize the electrodes in MEAs and achieve a high performance and durability of these devices. Therefore, to aid deeper analysis ranging from better visualization to quantification of such microstructural features, the utilization of advanced data science algorithms and image processing tools and techniques, in conjunction with advanced imaging and spectroscopy techniques, become categorically essential [2].

In this study, an in-house developed framework built on Python is utilized to study ionomer distribution and its interaction with the catalyst within the catalyst layer for PEMFCs and PEMWEs synthesized/fabricated via different manufacturing processes. Ionomer-catalyst interaction affects the protonic conduction, mass transport, and catalyst utilization but is often difficult to visualize and quantify without optimized imaging and specialized data processing which is made possible via the developed framework [3]. Sensitivity analysis was carried out to optimize the framework's performance to accurately reflect the changes in microstructure due to variations in synthesis/fabrication parameters. Not only did the framework help explore ionomer connectivity but also measured the degree of ionomer-catalyst coverage through rapid analysis requiring minimal user interaction. Furthermore, the applicability and implications of using the developed framework to form structure-performance correlations were evaluated yielding valuable insights about ionomer behavior in inks and electrodes. The introduced framework exhibits great potential which allows it to extend its utility to other clean energy applications with minimal adjustments.

References

- [1] Y. Guo *et al.*, "The Controllable Design of Catalyst Inks to Enhance PEMFC Performance: A Review," *Electrochem. Energy Rev.*, vol. 4, no. 1, pp. 67–100, 2021, doi: 10.1007/s41918-020-00083-2.
- [2] J. I. Goldstein, "Quantitative microanalysis with high spatial resolution," *Met. Soc.*, vol. 5, 1981.
- [3] A. Suzuki *et al.*, "Ionomer content in the catalyst layer of polymer electrolyte membrane fuel cell (PEMFC): Effects on diffusion and performance," *Int. J. Hydrogen Energy*, vol. 36, no. 3, pp. 2221–2229, 2011, doi: <https://doi.org/10.1016/j.ijhydene.2010.11.076>.

8:00 PM CH01.13.23

Non-Destructive Performance Comparison of Li-Ion 2032 Coin Cells for Non-Ambient Temperature Applications Shintaro Inaba¹, Simon Ji² and Hillary Smith¹; ¹Swarthmore College, United States; ²Princeton University, United States

Coin cell batteries have long found diverse applications in small consumer products. Rechargeable lithium-based coin cells are now commercially available offering an eco-friendly alternative, but their use is not as widespread. Performance of these batteries under non-ambient temperature conditions is important for many applications, but not widely investigated. We report on a non-destructive, temperature-dependent performance comparison of three different commercially available, rechargeable 2032 coin cell models. Batteries were cycled galvanostatically over at least 100 cycles at three different temperatures: 60°C, 24°C, and 0°C. In-situ data collection was performed using temperature-controlled test chambers. We observed highest initial capacity in higher temperature cycling, but faster capacity fade. During room temperature cycling we also observe an increase in initial capacity over the first ~40 cycles that may be consistent with a similar phenomenon observed in Li-ion pouch cells with graphite anodes. Differential capacity analysis was performed to determine the mechanism of cell deterioration and investigate the rise in capacity. Detailed results from temperature-dependent electrochemical cycling, along with X-ray diffraction and scanning electron microscopy analysis, will be presented to explain differences in cell performance across battery models and temperatures.

8:00 PM CH01.13.24

Laser-Based Measurements Meet or Exceed Electron Microscopy in The Detection of Surface Damage Thomas W. Pfeifer¹, Eric R. Hoglund^{2,1} and Patrick E. Hopkins¹; ¹University of Virginia, United States; ²Oak Ridge National Laboratory, United States

The detection of surface or near-surface abnormalities, whether in the form of contamination, oxide growth or crystalline defects, is of interest across a wide variety of research areas. Similarly, common tools for sample preparation may create surface defects without the user realizing. For example, we found that Focused Ion Beam (FIB) milling, used for Transmission Electron Microscopy (TEM) sample preparation or for the generation of fiducial markers, may create a large ion-affected region surrounding the milled hole.

To investigate the detectability and spatial extent of these defects, we mill a series of holes in a silicon wafer (Using a Helios UC G4 FIB-SEM with gallium ions. holes are 10µm square, created under a variety of beam current / energy / exposure time conditions). We then use two pump-probe laser metrology tools (Time Domain (TDTR) and Steady State Thermoreflectance (SSTR)) with samples mounted on motorized stages to explore detection of the spatial extent of damage. We also use atomic-resolution Scanning Transmission Electron Microscopy (STEM) and Energy-dispersive X-ray spectroscopy (EDX) (using a Thermo Fisher Scientific Themis system at 200 kV) on samples prepared at varying distances from the FIB hole.

As the pump-probe experiments typically require a metal film to be deposited on all samples, we first use TDTR and SSSTR to measure the thermal boundary resistance (TBR) between a metal film (80 nm aluminum, e-beam evaporated) and silicon, observing changes measurable up to 300 µm from the edge of the hole in the most severe case. Comparing this to the STEM results, an unusually high gallium concentration can be found between the aluminum and silicon at 200 µm away (more than seen in a reference TEM sample prepared in an identical manner). Similarly, a slightly disordered region is seen within the first ~ 10 nm of silicon, suggesting low-energy errant gallium ions may be responsible.

When the aluminum capping layer is excluded however, SSSTR was capable of measuring a difference out to > 600 µm. This signal is less easily interpreted as a change in thermal properties, but a notable change is visible nonetheless. By comparison, the only visible changes to the sample occur no more than 50 µm beyond the edge of the hole. Two more TEM samples were made at 500 µm and 1 mm away from the hole, and no substantial differences were found.

These findings suggest that laser-based pump-probe experiments are equally if not more capable at detecting surface damage as compared to EDX or atomic-resolution STEM. These laser based experiments are also substantially cheaper and faster to operate, not requiring the use of electron microscopy or extensive sample preparation. Furthermore, this is the first observation of extreme spatial effects due to FIB milling to our knowledge, and the precise nature of this damage warrants further study.

8:00 PM CH01.13.25

Investigating The Effect of Manufacturing Processes on The Ionomer Network in PEMWE and PEMFC Catalyst Layers using Microscopy and Python-Based Data Processing Maryam Ahmadi¹, Mariah Batool¹, Carlos Baez-Cotto², Linda Ney³, Jeronimo Horstmann³, Jayson Foster⁴, Nada Zamel³, Scott Mauger², Svitlana Pylypenko⁴ and Jasna Jankovic¹; ¹University of Connecticut, United States; ²National Renewable Energy Laboratory, United States; ³Fraunhofer Institute for Solar Energy Systems ISE, Germany; ⁴Colorado School of Mines, United States

With the increasing demand for hydrogen production as a source of clean energy, proton exchange membrane water electrolyzers (PEMWEs) and proton exchange membrane fuel cells (PEMFCs) are crucial components of the clean energy field, offering sustainable alternatives for energy conversion and storage. With the need to significantly increase the production of these devices, scale up manufacturing of their catalyst layers using different methods, such as slot die, gravure, screen printing or rod coating, is becoming a focus of industry and researchers. The aim is to speed up the fabrication, but also enhance the efficiency, durability, and cost-effectiveness of these systems [2].

Quality assessment in terms of electrochemical performance, but also in terms of visualization and quantification of the catalyst layer parameters are essential. Advanced characterization techniques, including microscopy and spectroscopy, are powerful tools to elucidate microstructure, morphology and spatial distribution of elements in these layers [3]. Of special interest is the ionomer network within the catalyst layers, influencing proton conductivity and electrochemical reactions, and playing a vital role in the efficiency and performance of both PEMWEs and PEMFCs [1]. Elucidating and quantifying its distribution is a challenging task.

This work presents our recently developed framework to visualize and quantify ionomer distribution, together with other structural and compositional parameters, for the catalyst layers fabricated using different manufacturing processes. The framework utilizes advanced image processing algorithms to process acquired STEM EDS maps from inks and electrodes [4]. It aims to automatically identify phases, particles, and elemental distributions within the microstructure, to see the ionomer connectivity in inks and their corresponding electrodes via different manufacturing processes such as slot die with different flow rates and gravure with different rod sizes, as well as different mixing times in ink preparations [5]. Moreover, in order to establish correlations between inks and electrodes for different materials systems and microstructural arrangements, the developed data processing protocols are applied in both fuel cells and electrolyzers.

References

- [1] Y. V. Yakovlev *et al.*, "Ionomer content effect on charge and gas transport in the cathode catalyst layer of proton-exchange membrane fuel cells," *J. Power Sources*, vol. 490, p. 229531, Apr. 2021, doi: 10.1016/J.JPOWSOUR.2021.229531.
- [2] X. Lyu *et al.*, "Aging gracefully? Investigating iridium oxide ink's impact on microstructure, catalyst/ionomer interface, and PEMWE performance," *J. Power Sources*, vol. 581, p. 233503, Oct. 2023, doi: 10.1016/J.JPOWSOUR.2023.233503.
- [3] A. Peyman Soleymani, M. Reid, J. Jankovic, A. P. Soleymani, J. Jankovic, and M. Reid, "An Epoxy-Free Sample Preparation Approach to Enable Imaging of Ionomer and Carbon in Polymer Electrolyte Membrane Fuel Cells," *Adv. Funct. Mater.*, vol. 33, no. 6, p. 2209733, Feb. 2023, doi: 10.1002/ADFM.202209733.
- [4] M. Batool, A. O. Godoy, M. Birnbach, D. R. Dekel, and J. Jankovic, "Evaluation of Automatic Microstructural Analysis of Energy Dispersive Spectroscopy (EDS) Maps via a Python-Based Data Processing Framework," *ECS Trans.*, vol. 104, no. 8, pp. 137–153, Oct. 2021, doi: 10.1149/10408.0137ecst.
- [5] C. M. Baez-Cotto *et al.*, "The effect of ink ball milling time on interparticle interactions and ink microstructure and their influence on crack formation in rod-coated catalyst layers," *J. Power Sources*, vol. 583, p. 233567, Nov. 2023, doi: 10.1016/J.JPOWSOUR.2023.233567.

8:00 PM CH01.13.26

Study of Growth and Structural Phase Transition in CrN/MgO(001) Thin Films Studied by Variable Temperature X-Ray Diffraction KhanAlam^{1,1}, RodrigoPonce-Perez^{2,3}, KaiSun⁴, AndrewFoley², NoboruTakeuchi^{2,3} and ArthurR. Smith²; ¹King Fahd University of Petroleum and Minerals, Saudi Arabia; ²Ohio University, United States; ³Universidad Nacional Autonoma de Mexico, Mexico; ⁴University of Michigan–Ann Arbor, United States

Abstract

Interest in studying CrN thin films has been increasing due to their interesting structural[1,2], electronic[3], and magnetic[4] properties. We have investigated the structural phase transition in high-quality CrN thin films grown on MgO(001) substrates using molecular beam epitaxy. Our analysis, which combines cross-sectional transmission electron microscopy and X-ray diffraction, has revealed that the CrN film exhibits an epitaxial relationship with the MgO substrate along three orientations: $[100]_{\text{CrN}}/[100]_{\text{MgO}}$, $[110]_{\text{CrN}}/[110]_{\text{MgO}}$, and $[001]_{\text{CrN}}/[001]_{\text{MgO}}$. These films display tensile strain or compression at the CrN/MgO(001) interface, which gradually relaxes during film growth. Furthermore, our temperature-dependent X-ray diffraction measurements have provided evidence of a first-order structural phase transition. Complementing our experimental findings, we conducted first-principles theoretical calculations to identify a stable model for the CrN/MgO interface. These calculations yielded two possible models for the interface, both of which feature a monolayer of chromium oxide positioned between the CrN and MgO layers.

Acknowledgements

This work was supported by the Interdisciplinary Research Center for Renewable Energy and Power Systems of King Fahd University of Petroleum and Minerals, Dhahran, Saudi Arabia under grant No. INRE2216.

References

1. K. Alam, S. M. Disseler, W. D. Ratcliff, J. A. Borchers, R. Ponce-Pérez, G. H. Cocoletzi, N. Takeuchi, A. Foley, A. Richard, and D. C. Ingram, *Phys. Rev. B* **96**, 104433 (2017).
2. K. Alam, R. Ponce-Pérez, K. Sun, A. Foley, N. Takeuchi, and A. R. Smith, *J. Vac. Sci. Technol. A* **41**, 053411 (2023).
3. K. Alam, M. B. Haider, M. F. Al-Kuhaili, K. A. Ziq, and B. U. Haq, *Ceram. Int.* **48**, 17352 (2022).
4. K. Alam, R. Ponce-Pérez, K. Sun, A. Foley, N. Takeuchi, and A. R. Smith, *J. Vac. Sci. Technol. Vac. Surf. Films* **39**, 063209 (2021).

8:00 PM CH01.13.27

All-Electronic and Flow-Through Differentiation of Microparticles based on Permittivity UzayTefek¹, BurakSari², HashimAlhmod¹ and SelimHanay¹; ¹Bilkent University, Turkey; ²Sabancı University, Turkey

There is an increasing need for the identification of microparticles in environmental and material science applications. Microplastic pollution in water resources has especially attracted the attention of the scientific community in recent years. Currently, Raman Spectroscopy and Fourier Transform Infrared Spectroscopy are used for the identification of microplastics: however, these techniques are expensive, non-portable, and extremely time-consuming. On the other hand, portable microplastic analysis systems can increase the localization accuracy while decreasing the cost and response time of pollution in water resources.

For microparticle analysis, impedance cytometry may serve as an ideal platform. Indeed, the differentiation of microplastics (e.g. polystyrene microparticles) *versus* cells has been demonstrated long time ago and repeatedly reported in different applications. However, these demonstrations are facilitated by the fact that cells have a large water content which induces a sharp contrast in impedance signal compared to non-biological particles. In other words, the high permittivity of water found in biological particles (such as cells and seeds) render them readily distinguishable from any other non-biological particle with no water content. Therefore, the real challenge in environmental screening is the differentiation of **non-biological microparticles amongst themselves** (e.g., plastics *versus* glass particles) since the impedance difference they generate is very similar due to the shielding effect of water. This capability can also be applied to the screening of engineered microparticles.

Here we demonstrate an all-electronic way to differentiate two important class of non-biological microparticles based on their permittivity differences: polystyrene (a typical microplastic) and soda lime glass (the most common household glass). To do so, we integrated a low frequency impedance cytometry sensor with a high frequency microwave sensor on the same microfluidic channel. The low frequency sensor detects the geometrical volume of the particle, whereas the microwave sensor yields a value proportional to the multiplication of the geometrical volume and the Clausius-Mossotti factor of the particle, a factor which depends on particle permittivity.

The analysis results indicate that with high classification accuracy (>94%), microparticles of these two material class can be differentiated from each other. In this case the experimentally extracted values of the Clausius-Mossotti factors of the two species closely follow the theoretically expected value. We further demonstrate the capability to monitor the changes in the permittivity values of single cell as they are fixed with glutaraldehyde.

The classification capability for microparticles of different composition at high throughputs opens the way for important applications in environmental, materials and biological sciences.

8:00 PM CH01.13.28

Nanomechanical Testing of Printed Nanolayers for Application on Flexible Organic Electronics Devices SpyridonKassavetis¹, TheodoraKalampaliki¹, ArgirisLaskarakis¹, ChristosKapnopoulos¹, VolhaHeben¹, VasiliosKyriazopoulos², EvangelosMekeridis² and StergiosLogothetidis¹; ¹Aristotle University of Thessaloniki, Greece; ²Organic Electronic Technologies P.C. (OET), Greece

Flexible organic printed electronics devices (FOPEs) such as Organic Photovoltaics (OPVs) and Organic Light Emitting Diodes are paving the way to new advanced low-cost and large area products for solar energy harvesting and lighting, respectively. FOPE devices are comprised by sequential functional nanolayers with a thickness ranging from 30 nm to 500 nm, which are printed the one on top of the other using different solution, printing and curing conditions. The mechanical properties of the individual layers, the adhesion among these nanolayers and their interfaces play critical role to the FOPEs performance and service life.

In this work, we focus on the OPVs devices and we extensively test the mechanical properties of the OPV nanolayers such as the Transparent Conductive Oxide (TCO), the Electron transport layer (ETL), and the active nanolayer with the target to enable understanding on the nanomechanical testing of soft and flexible materials and hybrid (inorganic / organic) interfaces a, and contribute to the performance and durability optimization of new next generation FOPEs. Therefore, we have developed a protocol for the nanomechanical testing of the OPVs' nanolayers based on the nanoindentation (NI) to probe the mechanical properties of the individual layers as well as the OPV device as a whole and to provides quantitative results at the nanoscale level. The Continuous Stiffness Measurements NI set-up was used to study the mechanical behavior of the nanolayers and their interfaces in the OPV stack in relation to the thickness and the surface roughness of the nanolayers, with the aim of accurately extracting the Elastic Modulus (E) and the Hardness (H) of the nanolayers. Atomic Force Microscopy and Spectroscopic Ellipsometry (SE) was also used to gain information about the surface and the optical properties, respectively, while SE was also used measure the thickness of the printed nanolayers layers. Two different TCOs were tested, ITO and IML, grown on top of flexible PET substrate. Both samples showed elastic / plastic deformation. For ITO/PET the E and H values were calculated to 26 GPa and 4.5 GPa, while for the IMI/PET the E=15 GPa and H=3.2 GPa. In both cases, the E and H values were affected by the compliant PET substrate. Both TCO did not de-adhere from the substrate after NI testing. Tin Oxide (SnO) nanolayer was used as the ETL functional nanolayer and it was printed by slot die coating on top of TCO. The NI testing showed that the printed SnO nanolayers did not de-adhere from the flexible TCO/PET substrate, while their E and H values were 9.2 GPa and 0.58 GPa, respectively.

8:00 PM CH01.13.29

Advanced Fluorescence Microscope and Smart Cloud Algorithm in Real-Time Quantitative Processing and Analysis of ElectroconvectionDuhanZhang; Massachusetts Institute of Technology, United States

In an electrochemical cell at high current densities, electroconvection plays a critical role in determining the morphology of electrodeposited metals. The resultant dendrite formation leads to risky battery performance failure. Over the past decades, though intensive theoretical analysis and experimental effort have been done, the detailed structure and dynamics of electroconvection remain unknown, because experimental observations lacked the resolution to expose the fundamental, hierarchical spatial structure of these flows, while the data processing algorithms were not fully established for large sample size. To address this shortcoming, we built an advanced optical electrochemical cell that fits in situ imaging with a superresolution fluorescence microscope. By observing and recording real-time motions of electrolytes, electroconvection flows have been interrogated at unprecedented, high temporal and spatial resolution. As a complement to the visualization studies, a cloud computing analysis algorithm was developed by combining a higher resolution Particle Image Velocimetry algorithm and a machine learning model to enable velocity distribution data over the entire optical field of view at nanoscale or microscale spatial resolution. Consequently, detailed velocity maps are obtained across the optical electrochemical cell, allowing us to quantitatively measure and analyze the initiation and evolution of the hierarchical microstructures inside the electroconvection in a unidirectional electric field. With these powerful tools, we further studied the effect of polymer viscoelasticity on electroconvection and electrodeposition. The addition of an ultrahigh molar mass polyethylene oxide to the electrolytes transforms the materials to a viscoelastic fluid state that changes the electroconvection dependence on time and voltage and induces a smooth electrodeposition on the metal anode by unique polymer rheological properties. Especially, the relaxation of long polymer chains in the electrolyte provides a promising manner to prevent dendrite growth. We further analyzed these observations using direct numerical simulations for Newtonian and viscoelastic fluid models, and the quantitative analysis of experimental results indicates good consistency with simulation predictions.

8:00 PM CH01.13.30

Advanced Hydrovoltaic Energy Generation using a Hierarchical NiFe LDH-Decorated CuO Nanowire Mesh DeviceJi YoungPark, Jun YoungKim, Gwang-MyeongGo and Yong-HoChoa; Hanyang University, Korea (the Republic of)

The contemporary energy landscape is undergoing a transformative shift, driven by the dual imperatives of environmental sustainability and technological advancement. As traditional energy sources deplete and global concerns over carbon emissions and environmental degradation mount, there's a pronounced urgency to find viable renewable energy solutions. Central to this quest is the principle of energy harvesting—capturing ambient energy from the environment and converting it into usable electrical power. Traditional methods such as solar and wind, while revolutionary, come with their own sets of challenges including intermittency and geographical limitations. In such a scenario, the prospect of harvesting energy from more omnipresent and less variable sources has gained significant scientific attention. Hydrovoltaic energy, which leverages the potential energy in water, presents one such avenue. The structural foundation of this advanced hydrovoltaic device is a meticulous assembly of nickel-iron layered double hydroxides (NiFe LDHs) deposited on copper oxide nanowires (CuO NWs). These NWs are firmly anchored to Cu meshes, creating a stable yet intricately detailed hierarchical nanostructure. Such a configuration has been optimized for the rapid diffusion of ion-rich water infiltration. Central to this capability is the LDH layer, which acts as a mediator, enhancing the device's inherent hydrophilic attributes and subsequent energy-harvesting efficiency. When subjected to a 3.3 M CaCl₂ solution droplet of 200 μL, the device consistently registers a power output in the vicinity of 250 nW/cm³. Remarkably, the energy generation capability of this configuration remains robust over prolonged durations, with a life cycle exceeding one month without noticeable degradation. The underlying mechanisms propelling this efficiency were thoroughly investigated. We identified that the NiFe LDH layer plays a pivotal role in augmenting the potential difference across the device, resulting in enhanced electricity generation. The electricity stemming from ionic infiltration and diffusion was elucidated, and strategies for device renewability were explored. Anticipating industrial applications, we also evaluated the device's scalability. Emphasis was placed on serial allocation strategies, demonstrating the potential for modular expansion and integration into larger systems. Collectively, this research signifies a substantial stride in hydrovoltaic energy generation, utilizing sophisticated nanostructures to effectively capitalize on readily available hygroscopic salts and seawater, paving the way for future green energy applications.

SESSION CH01.14: Batteries II

Session Chairs: Liam Collins and Michael Toney

Thursday Morning, November 30, 2023

Sheraton, Third Floor, Commonwealth

8:00 AM CH01.14.01

In Situ Monitoring Redox Processes in Energy Storage Materials using UV-Vis SpectroscopyDanzhenZhang¹, Ruocun (John)Wang¹, XuehangWang² and YuryGogotsi¹; ¹Drexel University, United States; ²Delft University of Technology, Netherlands

Understanding energy storage mechanisms in electrochemical energy storage devices lays the foundations for improving their energy and power density. Herein, we introduce a simple and easily accessible *in situ* ultraviolet-visible (UV-Vis) spectroscopy method to distinguish battery-type, pseudocapacitive, and electrical double-layer charge storage processes. Ti₃C₂T_x MXene in aqueous acidic and neutral electrolytes, and lithium titanium oxide (LTO) in an organic electrolyte will be used to demonstrate the technique. We found a correlation between the evolution of UV-Vis spectra and the charge storage mechanism. The electron transfer number for Ti₃C₂T_x in an acidic electrolyte was calculated using quantitative analysis, which was close to previous measurements using X-ray absorption spectroscopy. Further, we tested the methodology to distinguish the non-Faradaic process in Ti₃C₂T_x MXene in a water-in-salt electrolyte, despite well-defined peaks in cyclic voltammograms. *In situ* UV-Vis spectroscopy is a fast and cost-effective technique that effectively supplements electrochemical characterization to track changes in oxidation state and materials chemistry and determine the charge storage mechanism.

8:15 AM CH01.14.02

In-Situ TEM Probing of Charge Transport Behavior Across Solid Electrolyte Interphase in Rechargeable BatteriesChongminN. Wang; Pacific Northwest National Laboratory, United States

Solid electrolyte interphase (SEI), a thin layer that forms between active electrode and electrolyte, critically governs the performance of rechargeable batteries. An ideal SEI is expected to be electrically insulative to prevent a persistently parasitic reaction between the electrode and the electrolyte, while ionically conductive to facilitate Faradaic reactions of the electrode. However, the true nature of these two characteristics of SEI layer remains hitherto unclear due to the lack of a direct characterization method, leaving a range of behaviors of rechargeable batteries unelucidated. Here, we use *in-situ* bias transmission electron microscopy to directly measure the electrical properties of SEIs formed on Cu and Li. We discover that the current-voltage characteristics of SEIs resemble certain electrical conductance, rather than electrical insulation as conventionally assumed. The SEI with a higher electrical conductance tends to exhibit a greater thickness and more complex topographic features, consequently leading to an inferior electrochemical performance. The work solves the long-standing mystery as how SEI function electrically during electrochemical operation, providing unprecedented insight towards achieving better battery performance by rationally designing SEI properties.

8:30 AM CH01.14.03

Treatment of Polyethylene Terephthalate Glycol Sheet using Liquid-Liquid Treated PEDOT:PSS using Ethylene Glycol and Dimethyl Sulphide for Supercapacitor ApplicationMelkieG. Tadesse^{1,2} and Jörn FelixLübben¹; ¹Albstadt-Sigmaringen University, Germany; ²EiTEX-Bahir Dar University, Ethiopia

Flexible electronics are the growing demand for wearable electronics. Intrinsically conductive polymers such as poly(3,4-ethylene dioxythiophene) polystyrene sulfonate (PEDOT: PSS) is the most widely studied polymers with two mixtures of monomers. Many breakthroughs have been made in enhancing the conductivity of PEDOT: PSS using various ionic liquids treatments. However, getting high conductivity remains the challenge for these types of treatment. Herein, the production of highly conductive PEDOT: PSS polymer is obtained through a density-based liquid-liquid contact method which realizes the separation of highly conductive PEDOT with the hydrophilic PSS. This was confirmed by measuring the conductivity and observing through FTIR and Ramana spectroscopy. Polyethylene terephthalate glycol (PETG) sheet was surface modified using oxygen-plasma and the liquid-liquid was treated using ethylene glycol and dimethyl sulfoxide PEDOT: PSS was drop cast on the PETG and dried for several hours. The treated PETG was surface analysed using SEM and the potential application of the sample for supercapacitor was confirmed using cyclic voltammetry and impedance measurements. Both confirmed the use of these films for supercapacitor fabrication was possible.

8:45 AM CH01.14.04

Non-Depletable Electrolyte Design for High Energy Li-S BatteriesXiaoweiWang¹, SaurabhParab¹ and Y. ShirleyMeng²; ¹University of California, San Diego, United States; ²The University of Chicago, United States

The cycling stability of high-energy lithium-sulfur batteries is severely hampered by the consumption of electrolytes and lithium metal. The bottleneck urges the development of new electrolyte systems. Herein, we developed a toolbox of characterization to identify the limiting factors in Li-S batteries under practical lean Li and electrolyte conditions like Cryo-FIB 3D reconstruction, Cryo-TEM, and Plasma FIB EBSD. As guided by the root reasons specified, we strategically synthesized a stable aromatic lithium salt as a LiNO_3 alternative that is mostly used in current Li-S batteries. This lithium salt has a similar redox mediation property to LiNO_3 that inhibits the overcharging issue causing polysulfide shuttle. Uniquely, the newly developed aromatic lithium salt forms stable intramolecular bonding that avoids decomposition like LiNO_3 . Besides, the salt can coordinate with polysulfide to alleviate the reaction with lithium. The non-depletable electrolyte design is evaluated by the conventional C-S cathode with a high loading under lean electrolyte and lithium conditions. The Li-S cells using the new electrolyte deliver over 370 cycles with 75% retention in sharp contrast to 75 cycles of the cells in baseline electrolyte (1 M LiTFSI, DOL/DME=1:1). This work sheds light on the pivotal role of Li-S electrolytes and paves the way for extending the cycle life of practical high energy Li-S batteries.

9:00 AM CH01.14.05

Understanding Formation Processes in Anode-Free Lithium Metal Batteries GunnarThorsteinsson¹, WesChang², ZoeHerman¹ and DanSteingart¹; ¹Columbia University, United States; ²Drexel University, United States

Cell formation is a critical step in the manufacturing of secondary batteries. The mechanisms governing formation in next-generation lithium metal batteries, where lithium is plated a copper substrate, differ from conventional lithium ion batteries, where lithium intercalates into graphite. Understanding how rate of formation relates to subsequent cell cycling performance is critical to unlock the potential of high energy-density anode-free cells. However, the effect of formation rate in anode-free lithium metal batteries on capacity retention is not well understood. Here we show that a faster C/3 formation protocol results in markedly altered chemomechanical signature as compared to a standard C/10 formation step. Operando acoustic transmission is used to measure physical changes during the first formation cycle and its effects on long-term cycling of anode-free lithium metal pouch cells. Variations in amplitude and time-of-flight across different electrolytes tested are attributed to differences in gas formation, cell swelling and lithium deposition morphology. NMC532 cathodes paired with a high concentration ether electrolyte is shown to be particularly prone to gas formation, which is mitigated by the use of a localized high concentration ether electrolyte and single-crystal NMC532. The results highlight differences in formation behavior between anode-free lithium metal cells and lithium-ion cells.

9:15 AM CH01.14.06

Low Melting Alkali-Based Molten Salt Electrolytes for Lithium Metal BatteriesCanhM. Vu and ChibuezeAmanchukwu; The University of Chicago, United States

Liquid electrolytes for lithium metal batteries (LMBs) raise safety concerns because the highly volatile and flammable organic solvents hinder their practical deployment. In contrast, solid-state electrolytes promise improved safety but suffer from poor electrode/electrolyte interfaces. In this work, we develop nonvolatile and nonflammable low melting alkali-based molten salts as electrolytes for LMBs. A ternary mixture of bis(fluorosulfonyl)imide salts shows a eutectic temperature at 45 °C and exhibits higher current densities and improved cycling compared to nonvolatile ionic liquids, polymer composites, and inorganic solid-state conductors. The molten salt electrolyte exhibits excellent compatibility with both Li metal anodes (Coulombic efficiency ~99.8% and fast activation within five cycles) and high-voltage cathodes (~6 V stability). Li||NMC batteries retain 80% capacity after 100 cycles with an average Coulombic efficiency of 99.98%. Our low-melting molten salts provide a new class of electrolytes for the development of high-energy, long-cycling Li metal batteries.

9:30 AM CH01.14.07

Surface Analysis of Engineered Particles for Improved Battery Performance and StabilitySarahZaccarine¹, IsaiahOladeji², KoukouSuu², JenniferMann¹ and KaterynaArtyushkova¹; ¹Physical Electronics (PHI USA), United States; ²ULVAC Technologies, United States

Next-generation battery materials are needed to achieve high energy density, fast charging times, and long device lifetimes while remaining reliable and low-cost. Lithium metal batteries are a promising alternative to lithium-ion batteries but face stability concerns such as unstable solid-electrolyte interphase (SEI) growth and Li dendrite formation. Similarly, high-energy-density cathode materials like nickel manganese cobalt (NMC) and nickel manganese oxide (LNMO) have stable performance at high potentials but are susceptible to cathode dissolution in the electrolyte as well as unstable SEIs. Engineered particles (Ep) can stabilize electrode interactions, improving battery safety, SEI formation, and performance. However, batteries are multi-layered, complex systems with many components and interfaces that are difficult to handle and characterize. Understanding the chemical composition, distribution, and morphology of Ep-treated anodes/cathodes is necessary to prepare uniform, well-dispersed, high-capacity electrodes for optimized performance.

Developments in X-ray photoelectron spectrometers open up new capabilities to address these challenges. X-ray photoelectron spectroscopy (XPS) is ideal for analyzing thin layers and interfaces of battery materials due to its surface (~10nm) and chemical state sensitivity. Multi-technique XPS instruments offer additional operating modes and analytical options to enable the thorough characterization of battery materials. In this talk, a fully automated, multi-technique scanning XPS/HAXPES microprobe was used to address many challenges of analyzing battery materials, including an inert environment transfer vessel for air-free handling; microprobe X-ray source with <5µm spatial resolution for 100% certainty of area selection for small-area spectroscopic analysis and chemical mapping; and the hard X-ray source and cluster ion gun source for analyzing buried interfaces without damaging the chemistry. Combined, these powerful capabilities enable thorough characterization of macro- and microscopic battery materials for a direct link between the chemistry and performance of Ep-treated battery electrodes.

9:45 AMBREAK

SESSION CH01.15: Novel Characterization Techniques IV
Session Chairs: Philippe Leclere and Stefan Weber
Thursday Morning, November30, 2023
Sheraton, Third Floor, Commonwealth

10:15 AM +CH01.15.01

Resolving the Impact of Structural Defects on the Charge Carrier Transport in (Opto)electronicsIkaHermes¹, StefanA. Weber², YenalYalcinkaya² and LiamCollins³; ¹Leibniz Institute for Polymer Research Dresden e.V., Germany; ²Max Planck Institute for Polymer Research, Germany; ³Oak Ridge National Laboratory, United States

Extended structural defects, like grain or domain boundaries in polycrystalline semiconductors, can introduce mid-bandgap trap states, host dopants or lead to electrostatic barriers. The implications of these local defects for charge carriers in materials used for (opto)electronic applications can be manifold: They can act as non-radiative recombination centers, delay or restrict the charge transport or, in some cases, improve the transport properties though a change in doping.

Here, we will discuss how electrical and electromechanical atomic force microscopy (AFM) in combination with complimentary techniques can not only resolve extended defects, but also capture their electronic or (electro)mechanical properties and relate these defects to local changes in charge carrier transport. For instance, using electromechanical AFM, we visualized subcrystalline twin domains present in hybrid organic inorganic perovskites that are applied in photovoltaic devices. With the data analysis exacerbated by the mixed ionic and electronic conductivity of hybrid perovskites, we conducted advanced electromechanical AFM to decouple mechanical and electrostatic crosstalk, which finally revealed the ferroelastic nature of the domains. Correlating to spatial- and time-resolved photoluminescence suggest that the domain walls as extended structural defects delay the charge carrier diffusion by acting as electrostatic barriers. However, the possibility to tailor the arrangement and density of these ferroelastic domains allows engineering a directional charge transport and improved device performance.

10:45 AM CH01.15.02

Oxygen Redox Activity Characterization of Li-Stoichiometric Layered Oxides Through the Resonant Inelastic X-Ray Scattering (RIXS)Gi-HyeokLee and WanliYang; Lawrence Berkeley National Lab, Korea (the Republic of)

As the development of analytical technology has helped to identify ambiguous phenomena, applying the state-of-art resonant inelastic X-ray scattering (RIXS) technique to cathode materials closely identifies various phenomena in batteries. One of the most important discoveries through RIXS is oxygen redox, which can experimentally show the redox activity of oxygen, which was impossible to analyze with classical X-ray absorption or emission spectra. In highly charged electrodes, the discovery of features distinguishable from those of TM hybridized O further elucidates the redox mechanism oversimplified with the concept of the formal charge. The redox mechanism of Li-rich anode materials, which cannot be solely explained by TM oxidation, has been explained with a focus on their characteristic oxygen redox feature.

However, the discovery of oxygen redox features is not limited to cathode materials with Li-rich chemical composition. Oxygen redox features through RIXS were found in commercial anode materials such as LiCoO_2 and $\text{LiNi}_x\text{Co}_y\text{Mn}_{1-x-y}\text{O}_2$ as well as trendy cathode materials such as $\text{LiNi}_{0.85}\text{Co}_{0.10}\text{Al}_{0.05}\text{O}_2$ and LiNiO_2 . This means that the understanding of oxygen in the existing

redox process was inaccurate and suggests a lot about the strategy for coping with material degradation in the high state of charge established based on the incorrect understanding. Here, we look back at the generation of oxygen redox in “non-Li-rich” commercial cathode materials and revisit their redox mechanism. In addition, we intend to interpret based on a new redox mechanism along with the observed results of material degradation at high SOC, such as X-ray diffraction and differential electrochemical mass spectroscopy.

11:00 AM CH01.15.03

Three-Dimensional Imaging of Surface and Interface of Catalyst Nanoparticles by Electron Ptychography [Zixiao Shi](#)¹, Yu-Tsun Shao^{1,2}, Harikrishnan K. P.¹, Dasol Yoon¹, Hector D. Abruna¹ and David A. Muller¹; ¹Cornell University, United States; ²University of South Carolina, United States

Atomic-level understanding of nanoparticle structure is a central goal of modern heterogeneous catalysis. Many nanoparticles transform their surface structure during catalytic processes and generate a different phase on the surface to form a heterostructure, also known as “core-shell” structure. The influence of the core structure can result in modification of surface termination, strain effect, and polarization of shell catalyst, which will have a huge impact on catalyst performance. However, the shell structure can be discontinuous and relax its strain at the surface as it grows thicker. These details would be hidden by projection artifacts and the limited spatial resolution via conventional STEM imaging, and thus resolving these details requires a method that can reveal the 3D information with high spatial resolution.

Here we investigate MnN nanoparticles that serve as cathode electrode catalysts for anion-exchange membrane fuel cells (AEMFCs). We use multi-slice electron ptychography to characterize the catalyst surface layers in 3D, imaging with both heavy (Mn) and light elements (N, O) at lateral resolution which is limited by the thermal vibration of atoms themselves.¹ For 3D information, a single ptychographic reconstruction shows details of different MnN/Mn₃O₄ surfaces and interfaces at different depths of view. We separate the structural information from two different spinel nanoislands at different depths of view even when overlapped with sufficient details to allow us to study lattice displacements and strain separately from each grain. At the MnN/Mn₃O₄ interface, the Mn₃O₄ monolayer shows up to 3.0 % in-plane strain compared to Mn₃O₄, and leads to superior catalytic activity than Mn₃O₄ nanoparticles. This tensile strain of Mn₃O₄ shell decreases monolayer by monolayer when the Mn₃O₄ shell is growing thicker and starts to form nanoislands, and will relax to 1.2 % at the surface. This strain relaxation from the interface to surface of Mn₃O₄ provides quantitative insights into the relationship between the catalytic activity and in-plane tensile strain of Mn₃O₄ on MnN core.

1. Chen, Z. *et al.* Electron ptychography achieves atomic-resolution limits set by lattice vibrations. *Science* **372**, 826–831 (2021).

11:15 AM CH01.15.04

Measuring Lithium Loss during Synthesis and Densification of Li₇La₃Zr₂O₁₂ by Synchrotron Diffraction and Tomography [Tim Fister](#)¹, Tiffany Kinnibrugh¹, Jessica D. Macholz¹, Albert Lipson¹, Alexandra Moy², Jeff Sakamoto², Joanne Stubbs³, Peter Eng³, Yanbin Wang³ and Tony Yu³; ¹Argonne National Laboratory, United States; ²University of Michigan, United States; ³The University of Chicago, United States

The conductivity and, especially, the voltage stability of cubic Li₇La₃Zr₂O₁₂ (LLZO) make it one of the most attractive solid electrolytes for solid state batteries. However, the high temperatures required to synthesize and densify the ceramic electrolyte can lengthen its calcination and eventually lead to lithium loss. Here, we explore the interplay between cubic and tetragonal LLZO with the La₂Zr₂O₇ pyrochlore phase at high temperature as a function of precursor composition and size. Using *operando* synchrotron powder diffraction we show that nanoscale hydroxide precursors dramatically lower the formation temperature of LLZO compared to traditional, micron-sized oxide precursors. However, the nanoscale LLZO is prone to rapid lithium loss at high T, which can complicate further sintering and densification. To better understand the lithium loss mechanisms at both high temperature *and* pressure, we also study the densification of calcined LLZO pellets using computed tomography at pressures ranging from 0-5 GPa and temperatures up to 1400C using a novel large-volume press developed at the Advanced Photon Source. Using this setup, we demonstrate the ability to directly image lithium loss using computed tomography and show that high pressure lowers the temperature onset for surface decomposition to La₂Zr₂O₇.

11:30 AM CH01.15.05

Correlative SEM / AFM Microscopy - Combining Two High-Performance Methods for Nanoscale Measurements [Hajo Frerichs](#), Sebastian Seibert, Lukas Stuehn, Marion Wolff, Darshit Jangid and Christian H. Schwalb; Quantum Design Microscopy GmbH, Germany

The combination of different analytical methods for the qualitative and quantitative evaluation of material properties has become an essential part of today's characterization methods. In this context, the field of correlative microscopy represents an important technique for the simultaneous acquisition of complementary information. In particular, the combination of two of the most powerful microscopy techniques – scanning electron microscopy (SEM) and atomic force microscopy (AFM) – provides completely new insights into the micro- and nano-world to investigate even the smallest features of a sample with the highest resolution.[1-2] However, combining these two methods is not easy and remains challenging in terms of the instrumentation required. In most cases, both methods are used separately, and the obtained results cannot be truly spatially correlated. In this work, we present a unique inspection device that seamlessly combines SEM and AFM for characterization and process control of micro- and nanostructures. Due to the self-sensing piezoresistive cantilever technology used for the AFM scanner, the cantilever deflection signal can be measured completely electrically,[3] and a joint coordinate system between SEM and AFM allows the simultaneous acquisition of data directly at the region of interest. We will present a series of novel case studies to illustrate the advantages of this new tool for the interactive, correlative *in-situ* characterization of various materials and nanostructures at the nanoscale.

The first results focus on semiconducting ceramics based on BaTiO₃ with a positive temperature coefficient of resistance (PTCR). These materials, widely used in the field of self-regulating heating elements or temperature sensors, offer a wide range of applications in the energy sector. In this context, electrostatic force microscopy (EFM) combined with SEM shows that an accurate colocalized analysis of the grain boundary potential barriers of various BaTiO₃-based samples can be performed within nanometer resolution. The grain boundaries were localized using backscattered electron (BSE) detection and subsequently measured using the *in-situ* EFM technique demonstrating the influence of SiO₂ as a sintering agent on the barriers. Moreover, these results can be directly correlated with electron backscatter diffraction (EBSD) measurements to link the AFM and SEM data to the crystallographic microstructure of the samples.[4]

We will also present results for the *in-situ* characterization of nanowires, 2-D thin film materials, and multilayer samples to characterize their electrical, magnetic, topographic, and mechanical properties. The SEM allows the easy localization of single or multiple surface features, while the *in-situ* AFM allows the characterization of various “visible” and “hidden” surface and bulk properties. In this context, some aspects of advanced tip fabrication techniques such as focused electron beam induced deposition (FEBID) will also be briefly outlined to give an impression of how the fine-tuning of tip properties can be beneficial for correlated measurements.[5]

Due to the wide range of applications in inspection and process control of various materials and components, we expect this new inspection device to be one of the future key characterization tools for correlative SEM and AFM analysis.

- [1] D. Yablon, et al., *Microscopy and Analysis – EMEA*, **29**, 14-18 (2017).
- [2] S. H. Andany, et al., *Beilstein Journal of Nanotechnology*, **11**, 1272-1279 (2020).
- [3] M. Dukic, et al., *Scientific Reports*, **5** (1), 16393 (2015).
- [4] J. M. Prohinig, et al., *Scripta Materialia*, **214**, 114646 (2022).
- [5] L. M. Seewald, et al., *Nanomaterials*, **12** (24), 4477 (2022).

11:45 AM CH01.15.06

Nanometer-Scale Viscoelastic Measurements of Polymers by Peak-Tracking Scanning Thermal Noise Microscopy [Kei Kobayashi](#); Kyoto University, Japan

We recently developed (classical) scanning thermal noise microscopy (STNM), where the thermal noise spectra of the cantilever were measured at every pixels during the raster scan, from which the resonance frequency (f_c) and Q images are reconstructed by the off-line analysis [1]. We demonstrated visualization of buried Au nanoparticles in a polymer matrix, since the surface viscoelastic property was modulated by the buried Au nanoparticles. STNM is a viscoelastic measurement technique based on the contact-mode AFM but without excitation of the sample stage or the cantilever unlike the conventional viscoelastic measurement techniques. However, collection of the thermal noise spectra typically requires more than 1 h, which has not been practical for wide applications.

In this presentation, we demonstrate the local viscoelastic property measurements of polymeric samples by peak-tracking (PT) STNM, which utilizes two lock-in amplifiers and a feedback loop to enable tracking of the resonance frequency peak in a real-time manner as well as frequency-modulation AFM, but based on the detection of the thermal noise of the cantilever. It allows us to simultaneously measure f_c and Q , which correspond to elasticity and viscosity in the frequency range of typically 100 kHz. The technique is compatible with force curve measurement, which is a low-frequency viscoelastic measurement technique. Therefore, we can obtain quantitative viscoelastic properties in different frequency ranges at the same time, which is useful to study viscoelastic properties of polymeric samples and their composites that are often frequency dependent.

- [1] A. Yao et al. *Sci. Rep.* **7**, 42718 (2017).

1:30 PM *CH01.16.01

Observation of Structural Changes in Organometallic Perovskite Thin Film using Synchrotron X-Rays Sung Hun Lee, Seungyeon Hong, In Hwa Cho and Hyo Jung Kim; Pusan National University, Korea (the Republic of)

Organometallic perovskite solar cells (PSCs) have been considered as one of the most attractive and promising next-generation solar cells due to their excellent photoelectric properties, including potential for low-cost fabrication based on solution processing. After Miyasaka's report of 3.9% power conversion efficiency (PCE) in 2009, PSCs have been developed rapidly, of which performance reached a highest PCE of 26.02% by Seok in 2023. The meticulous control of crystalline properties has played a pivotal role in significantly enhancing the PCE of PSCs. By manipulating and fine-tuning the crystalline characteristics, such as identifying specific crystalline phases and clarifying the domain orientations within organometallic perovskite thin films, substantial advancements in PCE have been achieved. Especially, *in situ* observation of structural changes during the film formation gives insights how to effectively control the crystalline properties of the perovskite thin films. In this presentation, we would like to show the structural studies on perovskite thin films under various fabrication conditions such as post-annealing and spin-coating using synchrotron X-rays. We will present recent results of *in situ* Grazing Incidence Wide Angle X-ray Scattering (GIWAXS) of samples to observe their crystalline properties during film formation, especially in the anti-solvent free system.

2:00 PM CH01.16.02

Charge Distribution in Perovskites Spatially Resolved by Scanning Microwave Impedance Microscopy Verena Werf, Jiashang Zhao, Jim Koning, Jasmeen Nespoli, Jos Thieme, Marcel Bus and Tom J. Savenije; Delft University of Technology, Netherlands

Metal halide perovskites (MHPs) have demonstrated great potential for various electronic applications including solar cells, LEDs and X-Ray detectors. Most remarkably, high quality layers can be deposited by simple, wet chemical deposition techniques, yielding solar cells with a reported power conversion efficiency above 25%. Despite this simple and versatile processing method, the concentrations of trap states are very modest, which is attributed to the fact that most defects do not form a state within the optical band-gap. However, detailed analyses of photovoltaic devices based on these materials show that still the maximum attainable voltage is not yet reached. Part of the voltage deficit is often associated with loss mechanisms, which is a result of undesired non-radiative recombination of light induced charge carriers mediated by e.g. surface defect states. Hence to reduce the voltage deficit more information regarding these defects is necessary, e.g. what's the origin and how are these distributed over the MHP surface? It is important to realize that a locally high concentration of defect states leads to a locally smaller Fermi level splitting, reducing the PCE of the entire solar cell substantially.

Over the last few years a number of nanoscale techniques have been used to study the opto-electronic properties in MHP layers, including confocal photoluminescence measurements, Scanning Kelvin probe force microscopy and photoconductive atomic force microscopy. From these studies it was concluded that defect states are not homogeneously distributed over the surface. Despite these insights it is unclear to what extent excess charge carriers still get evenly spread over the MHP surface. To address this question, we use in this work scanning microwave impedance microscopy (sMIM) to reveal the local conductivity induced by optical illumination. sMIM is a rather new non-contact method able to locally probe the dielectric properties, i.e. the local permittivity and conductivity. This method has only been scarcely used to study MHPs and in particular effects of degradation on the local scale have been studied. Here we examined the charge concentration in two MHPs i.e. $\text{Cs}_{0.17}\text{FA}_{0.83}\text{PbI}_3$ (hereafter denoted as CsFAPbI₃) and MAPbI₃. We study these materials by comparing the MIM-Re and MIM-Im images recorded in the dark and under optical excitation using a green power LED. While in the dark the MIM-Re images show no contrast, with increasing the light intensities the contrast increases. By analyzing the images in detail we conclude that, in particular for MAPbI₃, the charge distribution is rather homogeneous. In contrast for the CsFAPbI₃ illumination leads to additional contrast even over a single grain, which we associate with the fact that CsFAPbI₃ shows a non-preferential orientation growth. Various facets with different surface termination will have an effect on the defect density and thus on the excess charge concentration. Hence for a CsFAPbI₃ layer featuring various planes, possibly even within a grain, a variation in excess charge concentration and hence more contrast over a single grain. This insight highlights the need for a homogeneous, preferential growth of the MHP absorber layer to generate a homogeneous charge distribution over the surface. For solar cells, a non-homogeneous distribution in carrier concentration leads to variation in the local Fermi level splitting, which should be suppressed to reduce the voltage deficit.

2:15 PM CH01.16.03

Structural Characterisation of BaZrS_(3-y)Se_y Perovskite Thin Films via Scanning Transmission Electron Microscopy Tigran Simonian^{1,2}, Michael Xu², Ida Sadeghi², Jack Van Sambeek², Kevin Ye², Rafael Jaramillo², James M. LeBeau² and Valeria Nicolosi¹; ¹Trinity College Dublin, Ireland; ²Massachusetts Institute of Technology, United States

Chalcogenide perovskites show great potential for becoming solar cell materials due to their tuneable and direct bandgaps in the visible range, great physical properties compared to oxide perovskites, and use of nontoxic and abundant elements [1]. However, difficulties in growing thin films using chalcogen sources has hindered their progress until recently. Expanding on previous work on one-step synthesis of BaZrS₃ (BZS) thin films via molecular beam epitaxy [2], here we demonstrate the synthesis of a BaZrS_(3-y)Se_y (BZSSe) alloy system using a BZS template layer on LaAlO₃ (LAO).

These BZSSe films are analysed via high resolution scanning transmission electron microscopy (STEM), energy dispersive X-ray spectroscopy (EDX) and electron energy loss spectroscopy (EELS). Both the template and the alloy are noted to be of a perovskite structure, with both growth modes as previously seen in pure BZS films, present. While the film is relaxed overall, there is a large concentration of out-of-plane antiphase boundaries (APBs) in the template region; conversely, there is a large concentration of in-plane APBs in the alloy region. EDX and EELS indicate the presence of diffused Se even down to the substrate interface, which correlates with the presence of APBs as a strain relaxation mode.

References:

- [1] Jaramillo, R. & Ravichandran, J. In praise and in search of highly-polarizable semiconductors: Technological promise and discovery strategies. *APL Mater.* 7, 100902 (2019).
- [2] Sadeghi, I. *et al.* Making BaZrS₃ Chalcogenide Perovskite Thin Films by Molecular Beam Epitaxy. *Adv. Funct. Mater.* 31, 2105563 (2021).

2:30 PM BREAK

3:00 PM CH01.16.04

Microstructural Evolution of Perovskite Solar Cells during Thermal Annealing Holger Roehm, Alexander Schulz, Tobias Leonhard and Alexander Colmann; Karlsruhe Institute of Technology, Germany

MAPbI₃ amongst other OMH perovskites is undergoing tetragonal-to-cubic phase transitions within the operational temperature range of solar cells. Many properties of these hybrid perovskite materials, such as piezoelectricity, pyroelectricity, ferroelectricity and ionic conductivity are directly linked to the crystal phase and temperature of the sample. Notably, polar domains that form in MAPbI₃ thin-films during the solar cell fabrication have been observed.[1,2,3] We have previously shown that poling of these domains can be achieved in an external E-field that is similar to built-in fields in solar cells during operation.[4]

In this work, we use Piezoresponse Force Microscopy to monitor an evolution of these domains that is triggered by common thermal treatment of perovskite solar cell at 100°C.[5] Our findings suggest that control over the domain structure in these light absorbing, semiconducting compounds may be essential in order to maximize performance and stability of hybrid perovskite solar cells. In particular, microstructural changes due to stress and strain when the thin-films undergo a tetragonal/cubic phase transition are an often overlooked factor responsible for degradation of perovskite solar cells. We show that local crystal defects can form and vanish both at ferroic domain walls and crystal grains and in turn modulate ionic conductivity and diffusion.

Finally, we extend our investigations towards triple-cation perovskites and investigate the dependence of the ferroelectric properties on the stoichiometric composition.[6]

- [1] H. Röhm, *et al.*, Energy Environ. Sci. 10, 950-955 (2017) [2] T. Leonhard *et al.*, Energy Technol. 7, 1800989 (2019) [3] H. Röhm *et al.*, Adv. Mater., 31, 1806661 (2019) [4] H. Röhm *et al.*, Adv. Funct. Mater., 30, 1908657, (2019) [5] T. Leonhard *et al.*, J. Mater. Chem. A., 9(38), pp. 21845-21858 (2021) [6] A.D. Schulz *et al.*, Solar RRL 2200808 (2022).

3:15 PM CH01.16.05

Surface Structure of Lecithin-Capped Cesium Lead Chloride Nanocrystals using Solid-State and DNP NMR Spectroscopy Diganta Sarkar¹, Abhoy Karmakar¹, Andriy Stelmakh^{2,3}, Marcel Aebli^{2,3}, Franziska Krieg^{2,3}, Amit Bhattacharya¹, Shane Pawsey⁴, Maksym V. Kovalenko^{2,3} and Vladimir Michaelis¹; ¹University of Alberta, Canada; ²ETH Zürich, Switzerland; ³Empa-Swiss Federal Laboratories for Materials Science and Technology, Switzerland; ⁴Bruker BioSpin Corporation, United States

Colloidal nanocrystals (NCs) of all-inorganic cesium lead halide perovskites (CsPbX_3 ; X = Cl, Br, I) have garnered significant attention due to their superior optoelectronic properties for LCD and LED displays, lasers, photovoltaic and photodetector applications compared to their bulk perovskite counterparts [1]. The choice of capping ligand, which controls the growth and dispersion of these nano-sized perovskites in organic solvents, can profoundly affect their surface structure by disrupting the atomic periodicity, consequently influencing their tailorable optical and electronic features [2]. Although there have been numerous theoretical and experimental investigations into CsPbX_3 NCs, only a limited number of studies provide a comprehensive, atomic-level description of the termination and ligand binding sites on the surface of CsPbX_3 NCs.

Solid-state nuclear magnetic resonance (NMR) spectroscopy is a powerful and robust spectroscopic method that offers an unprecedented understanding of atomic-scale structures of various classes of nanomaterials [3]. Here, we discuss a multinuclear (^1H , ^{13}C , ^{31}P , ^{133}Cs , and ^{207}Pb) solid-state and dynamic nuclear polarization (DNP) NMR spectroscopic approach to explore the structure of CsPbCl_3 , ranging from bulk material to NCs capped with an inexpensive, natural, and mass-produced zwitterionic ligand, soy lecithin with trimethylammonium and phosphate head groups [4]; further complemented by diffraction-based techniques.

The solid-state ^{133}Cs and ^{207}Pb NMR experiments, employing both direct and indirect detection methods (such as cross-polarization, CP) on CsPbCl_3 NCs demonstrate high sensitivity towards the large differences in surface-to-core ratios between bulk and NCs as the crystal size decreases from microns to nanometres. We exploit the unique heteronuclear dipolar couplings between the lecithin ligand (^1H , ^{13}C , and ^{31}P) and the surface (^{133}Cs and ^{207}Pb) of the CsPbCl_3 NCs that allows us to directly determine the surface structure. For instance, the ^1H - ^{133}Cs heteronuclear correlation (HETCOR) DNP NMR method investigates the proximity of the trimethylammonium group of lecithin to the surface ^{133}Cs atoms. Additionally, a combination of $^1\text{H}\{^{133}\text{Cs}\}$, ^1H - $^{31}\text{P}\{^{133}\text{Cs}\}$ CP, and ^1H - $^{31}\text{P}\{^{207}\text{Pb}\}$ CP rotational-echo double-resonance (REDOR) NMR techniques provides a comprehensive understanding of how the phosphate group of lecithin binds to the surface of CsPbCl_3 NCs. These results were further substantiated by a series of classical molecular dynamics simulations to find the most thermodynamically stable binding mode of the lecithin ligand onto the CsPbCl_3 NCs surface. These findings have the potential to significantly advance the future spectroscopic investigation of ligand binding and surface structures in nanomaterials.

References:

- [1] Zhang, Q., & Yin, Y. *ACS Cent. Sci.* **2018**, *4*, 668.
- [2] Haydous, F., Gardner, J. M., & Cappel, U. B. *J. Mater. Chem. A* **2021**, *9*, 23419.
- [3] Marchetti, A., Chen, J., Pang, Z., Li, S., Ling, D., Deng, F., & Kong, X. *Adv. Mater.* **2017**, *29*, 1605895.
- [4] Krieg, F., Ong, Q. K., Burian, M., Rainoo, G., Naumenko, D., Amenitsch, H., Suess, A., Grotevent, M. J., Krumeich, F., Bodnarchuk, M. I., Shorubalko, I., Stellacci, F., & Kovalenko, M. *V. J. Am. Chem. Soc.* **2019**, *141*, 19839.

3:30 PM CH01.16.06

Tomographic AFM for Nanoscale Volumetric Mapping of Photovoltaics Luis A. Ortiz-Flores¹, Yuanyuan Zhou² and Bryan D. Huey¹; ¹University of Connecticut, United States; ²Hong Kong Baptist University, Hong Kong

A range of characterization methods have been developed to investigate materials for energy systems, including their microstructure, chemical composition, and functionality—even in situ or in operando. However, the performance of many practical energy systems depends on, or succeeds despite, mesoscale features. Grain boundaries are unavoidable for most commercially viable devices, electrode interfaces are often critical, and property gradients naturally result from or indeed are engineered during fabrication. Truly nanoscale volumetric studies are therefore crucial, albeit challenging. Accordingly, we have advanced Tomographic Atomic Force Microscopy (TAFM) for studies of polycrystalline photovoltaics such as MAPbI_3 and related halide perovskites. Clear enhancements in photocurrents are observed for grain boundaries, which are investigated individually and networked. The effects of incorporating selective carrier transport layers such as SnO_2 , NiO, and SPIRO are also discussed. Wider applications of this TAFM approach for piezoelectric energy harvesters, supercapacitors, fuel cells, batteries, and thermoelectrics will also be presented, all in the context of improving future device performance by better understanding 3-dimensionally heterogeneous structure-property correlations.

3:45 PM CH01.16.08

Electrical Scanning Probe Microscope Measurements Reveal Surprisingly High Dark Conductivity of Y6 and PM6:Y6 Rachael Cohn, Christopher Petroff, Virginia E. McGhee and John A. Marohn; Cornell University, United States

Polymer:nonfullerene acceptor (NFA) solar cells have recently achieved record power conversion efficiency (PCE) of 19% [1], but the operation of NFA based solar cells is poorly understood and irreproducibility remains an issue. Charge injection from the substrate is proposed to lead to irreproducibility [2]. We use an electric force microscopy (EFM) technique, broadband local dielectric spectroscopy (BLDS) [3], to determine the film's conductivity. Here we report BLDS studies of the conductivity of PM6:Y6, PM6, and Y6 films in the dark and under illumination.

The Y6 conductivity is high and light-independent, dominated by background carriers even at 20 suns. The PM6:Y6 conductivity is linearly dependent on light intensity with an exponent of 0.58 ± 0.10 , consistent with photoconductivity dominated by a single carrier (with the other carrier trapped). PM6 data indicate that the conductivity is out of range of our microscope's capability. This means that the conductivity is either lower or higher than we are able to detect. Based on the observed moderate conductivity of the PM6:Y6 blend, it is unphysical that the PM6 control would have higher conductivity than the blend.

It is generally assumed that a "good" solar cell material has a low dark conductivity, which gives a high V_{oc} [4]. Here we show that that is not necessarily the case, as we find PM6:Y6, a solar cell with high PCE, and Y6 to have a high dark conductivity. It is a challenge to understand how Y6 could have a high dark conductivity, yet form an excellent solar-cell junction with PM6. We adapt Gouy-Chapman theory from electrochemistry to estimate the charge injected from a metal into an intrinsic, undoped organic semiconductor. We conclude that the dark carriers are not being injected from the metallic substrate; they more likely come from impurities or chemical oxidation/reduction of the Y6.

BLDS is used to determine the film's charge response times. The charge response time is inversely proportional to conductivity; conductivity is calculated and plotted versus light intensity. We find that the ratio of the sample to tip capacitance, C_s/C_{tip} , is independent of light intensity. We know that C_{tip} is constant, so C_s/C_{tip} being independent of light intensity indicates that C_s is also constant; this means that the sample resistance, R_s , must be decreasing with increasing light intensity. From this we conclude that light changes R_s , not C_s , as is universally assumed in EFM experiments. We can thus resolve the change in conductivity and capacitance in a single measurement using BLDS.

References:

- [1] Zhu, L. *et al. Nat. Mater.* **2022**, *21* (6), 656–663. DOI: 10.1038/s41563-022-01244-y
- [2] Luria, J. L.; Hoepker, N.; Bruce, R.; Jacobs, A. R.; Groves, C.; Marohn, J. A. *ACS Nano* **2012**, *6* (11), 9392–9401. DOI: 10.1021/nm300941f
- [3] Tirmzi, A. M.; Dwyer, R. P.; Hanrath, T.; Marohn, J. A. *ACS Energy Lett.* **2017**, *2* (2), 488–496. DOI: 10.1021/acsenerylett.6b00722
- [4] Nelson, J. *The Physics of Solar Cells*; Imperial College Press, 2003.

4:00 PM CH01.16.09

Oxygen Incorporation in Close Space Sublimed ZnTe Thin Films for Photovoltaic Cells Tamara Potlog; Moldova State University, Moldova (the Republic of)

From 0.5% to 5% oxygen is incorporated into ZnTe through close space sublimated CdS/ZnTe thin film solar cells. The structural and optical properties of the oxygenated ZnTe thin films and CdS/ZnTe devices are investigated using field emission scanning electron microscopy, X-ray diffraction, optical spectroscopy and current-voltage characterization. The 5% oxygen content slightly increase the grain size while the crystallinity does not change. XRD analysis revealed a single-phase crystallinity of zincblende for all grown films. The bandgap of the as-deposited cells ZnTe thin films was bigger than the oxygenated ones. The values of the optical band gaps (E_g) vary in interval from 2.24 eV to 2.14 eV with increasing oxygen content from 0.5% to 5%. The values of the open circuit voltage (V_{oc}) and short circuit current density (J_{sc}) increase when the O_2 content increases in ZnTe. The current-voltage characteristics curve of the 5% oxygenated CdS/ZnTe solar cell at different illuminations show that decrease in illumination from 100 mW/cm^2 to 20 mW/cm^2 decreases the open circuit voltage from 0.76 V to 0.67 V. The fill factor and open circuit voltage are influenced by both the series and shunt resistances. The open circuit voltage V_{oc} and the efficiency increase logarithmically. Also, in this paper is discussed how illumination intensity affect the capacitance of the CdS/ZnTe solar cells.

8:00 AM CH01.17.01

Investigating Oxygen-Rich Alternative Calcination Approaches for NMC-811 Cathodes Thomas Entwistle, Enrique Sanchez-Perez and Serena Cussen; University of Sheffield, United Kingdom

The calcination of nickel-manganese-cobalt 8:1:1 hydroxide precursor to produce the $\text{LiNi}_{0.8}\text{Mn}_{0.1}\text{Co}_{0.1}\text{O}_2$ (NMC-811) is critical to maximise the practical capacity yielded from the cathode active material. This conventionally occurs in a high temperature furnace under a flow of oxygen gas for up to 15 hours at 750-850 °C, which promotes the formation of trivalent and tetravalent nickel ions which facilitate the electrochemical storage of energy in the desired $\alpha\text{-NaFeO}_2$ layered $\text{LiNi}_{0.8}\text{Mn}_{0.1}\text{Co}_{0.1}\text{O}_2$ phase [1-3]. Here, we present an alternative calcination approach which utilises microwave heating to reduce the reaction time to 4 hours. Lithium peroxide (Li_2O_2) is also used as an alternative lithium precursor to act as an oxygen source during thermal decomposition. This removes the need for a separate oxygen gas source which, as well as being safer, could improve the processing conditions when moving to high-throughput syntheses.

This work investigates the impact of this microwave calcination procedure on the heat treatment of $\text{Ni}_{0.8}\text{Mn}_{0.1}\text{Co}_{0.1}(\text{OH})_2$ with Li_2O_2 and a control lithium salt, lithium hydroxide (LiOH). The reaction conditions, and the material and electrochemical properties of the NMC-811 products are assessed to detail the difference between the conventional oxygen-fed calcination procedure and the alternative microwave calcination procedure. The microwave calcined approach using the Li_2O_2 salt yields initial discharge capacities of 160.5 mAh g^{-1} ; whereas the conventional, oxygen-fed calcination approach with LiOH produces 204.4 mAh g^{-1} , when cycled between 3.0-4.3 V at C/20.

The cause of the disparity between the specific capacities was investigated, with high temperature in-situ X-ray diffractometry of $\text{Ni}_{0.8}\text{Mn}_{0.1}\text{Co}_{0.1}(\text{OH})_2$ revealing the different mechanisms for the lithium integration and structural evolution during calcination with Li_2O_2 or LiOH. This, alongside morphological differences, provides insight into the challenges associated with the current microwave calcination procedures and highlights the requirements for further control over the particle morphology to minimise inter-granular resistance and capacity loss compared to conventionally heated furnaces.

References:

- [1] A. Habibi, M. Jalaly, R. Rahmanifard, New J. Chem. 42 (2018) 19026-19033
- [2] H-J. Noh, S. Youn, C. S. Yoon, J. Power Sources. 233 (2013) 121-130
- [3] D.-J. Vu, J.-Y. Choi, W.-B. Kim, J. Electrochem. Soc. 164 (2017) A2670

8:15 AM CH01.17.02

Characterization of CeO_x -decorated Pd/C Catalysts Synthesized by Controlled Surface Reactions for Hydrogen Oxidation in Anion Exchange Membrane Fuel Cells Richard Andres Ortiz Godoy¹, Ramesh K. Singh², Dario Dekel² and Jasna Jankovic¹; ¹University of Connecticut, United States; ²Technion - Israel Institute of Technology, Israel

The high cost and difficult task of eliminating platinum (Pt) catalyst in a Proton Exchange Membrane Fuel Cells (PEM-FCs) are some of the main obstacles that thwart the wide adoption of fuel cells. For this reason, Anion Exchange Membrane Fuel Cell (AEM-FC) has been suggested as an alternative to the PEM-FC technology in which non-Pt metals may be employed. However, the common slow kinetics at the anode experienced during Hydrogen Oxidation Reaction (HOR) has been one of the challenges preventing the achievement of high-power density in the Pt-free AEM-FC. Here, our objective is to improve the efficiency of HOR catalysts by depositing various ratios of CeO_x/Pd catalysts onto carbon support using the Controlled Surface Reactions (CSR) process. It is expected that a homogenous distribution of CeO_x preferentially attached to Pd nanoparticles (NPs) can produce highly active $\text{CeO}_x\text{-Pd/C}$ catalysts for HOR. In the present study, we offer a comprehensive characterization approach for the synthesized highly active catalyst and correlate the obtained structural/compositional parameters to its performance. The characterization of the catalysts was carried out using Inductively Coupled Plasma-Atomic Emission Spectroscopy (ICP-AES), X-ray Diffraction (XRD), High-Resolution Transmission Electron Microscopy (HR-TEM), Scanning Transmission Electron Microscopy (STEM) - Energy Dispersive Spectroscopy (EDS), Electron Energy Loss Spectroscopy (EELS), and X-ray Photoelectron Spectroscopy (XPS) to confirm the bulk composition, phases present, morphology, elemental mapping, local oxidation state and surface chemical states, respectively. The HRTEM micrographs indicated that Pd NPs were uniformly distributed on the carbon support with only some minor agglomeration. Additionally, the achieved high interfacial contact between CeO_x and Pd acquired on single Pd NPs was, for the first time, segmented and calculated using High-resolution STEM-EDS maps and Image J processing program by measuring the overlap intensities between Pd and Ce in the NPs. The intimate contact between CeO_x and Pd and the increase in their interfacial contact area with the addition of CeO_x in these NPs was observed. This interfacial contact area is higher than other previously reported Pd- CeO_x catalyst systems synthesized by other methods, suggesting that the CSR method can provide a more selective deposition of CeO_x on Pd. EELS was used to determine that the primary oxidation state of our oxide was in the form of CeO_2 and Ce^{4+} was predominantly present in CeO_x . However, the presence of Ce^{3+} cannot be ruled out, especially near the surface of the particles. The study also found that the already mentioned interfacial contact area was directly correlated to the electrochemical performance reflected on the HOR activity of the $\text{CeO}_x\text{-Pd/C}$ catalysts. Additionally, to track the morphological, compositional, and structural changes at the nanoscale we used postmortem Identical location transmission electron microscopy (IL-TEM), to reveal the degradation mechanisms governing this new $\text{CeO}_x\text{-Pd/C}$ catalyst material following Accelerated Stress Tests in a three-electrode electrochemical cell. The preliminary results have shown that CeO_x can act as a promising anchoring mechanism that prevents the mobility, agglomeration, and detachment of Pd at a considerably high degree when compared to samples without CeO_x .

8:30 AM CH01.17.03

Investigating Reversible Electrochemical Calcination in Tin (Sn) Alloy Anode for Calcium Ion Batteries Saida Cora¹, Vincent Briselli¹, Mingyuan Ge² and Niyasa¹; ¹University of Massachusetts, United States; ²Brookhaven National Laboratory, United States

Calcium (Ca) ion batteries have recently gained recognition as a viable, safe, and cost-effective solution to increase energy density capabilities of next-generation battery technology. However, their practical application has been hindered by the lack of suitable anode materials. Alloy anodes present an attractive avenue for the development of practical calcium-ion batteries, as they can overcome the surface passivation issues associated with Ca metal anodes. Recent studies have highlighted the electrochemical alloying capability of tin (Sn) anodes with calcium, making Sn a promising candidate for beyond lithium-ion battery technologies. In this study, we delve into the calcination and decalcination processes within Sn anodes for next-generation Ca-ion batteries. Utilizing Synchrotron X-ray nanotomography, we track the three-dimensional structural and chemical evolution of tin anodes in calcium electrolyte. Our investigation focuses on understanding the voltage-dependent distribution and homogeneity of Sn-Ca phases, as well as the morphological and structural changes of calcinated Sn. The findings from this study open up exciting possibilities for the design and optimization of calcium-ion batteries, bringing us closer to achieving high-performance energy storage solutions.

8:45 AM CH01.17.04

Revealing Charge Compensation Mechanisms in Battery Cathode Materials with X-ray Raman and Valence-to-Core X-Ray Emission Spectroscopy Lijin An; University of Oxford, United Kingdom

Ni-rich lithium nickel manganese cobalt oxides ($\text{LiNi}_x\text{Mn}_y\text{Co}_z\text{O}_2$ ($x+y+z=1$), NMCs) materials are amongst the most promising cathodes to achieve higher energy density and lower cost batteries for electric vehicles. When reaching high charge states, an abrupt lattice contraction along the c-axis is observed giving rise to a large anisotropic volume change. This contraction has long been considered a consequence of oxygen participation in charge compensation arising from strong transition metal-oxygen (TM-O) covalency. Understanding how the structural change is related to electronic properties in the state of charge is essential to design NMCs with enhanced properties. However only limited information is available on the changes of cathode electronic structure upon cycling.

Although soft X-ray techniques such as X-ray photoemission spectroscopy (XPS) and soft X-ray absorption spectroscopy (sXAS) of O K-edge and metal L-edges can provide such information, the very short inelastic mean free paths of photoelectrons and short attenuation length of soft X-rays usually limit these techniques to vacuum condition. This changes the electrode working environment between operation and measurement, losing valuable information in the process. X-ray Raman spectroscopy (XRS) provides a viable alternative to sXAS where hard incident X-rays are used which become inelastically scattered by the sample. By selecting appropriate incident and analyser energies, light element K-edges (e.g. O K-edge) and TM L-edges become accessible without any modification to the battery set-up. Thus XRS combines the depth resolution of hard X-ray techniques with the electronic structure sensitivity of sXAS [1]. Furthermore, X-ray emission spectroscopy (XES) in the valence-to-core (VtC) region provides a more sensitive probe of bonding coordination and hybridisation for both metals and ligands [2]. This spectral region has proven to be particularly important in establishing a probe of metal-ligand interactions. It is uniquely suited to probe changes in TM-oxygen covalency in cathodes, that cannot be obtained through purely structural or other electronic structure measurements alone.

In this study, XRS and XES were employed to probe the electronic structures of conventional cathode materials ($\text{LiNi}_{0.8}\text{Mn}_{0.1}\text{Co}_{0.1}\text{O}_2$ and LiNiO_2) at different state of charge. Using the benefits of XRS and VtC-XES discussed above, we can obtain unambiguous results that are not limited by the short penetration depths or unrealistic sample environments. We aim to answer long standing questions such as: how the oxidation state of the TM centres changes during (de)lithiation, and its excess capacity at high potentials mostly linked with the TM cationic redox or anionic (oxygen) redox. Whilst XRS and XES-VtC spectra can be complex to analyse, we have experience in computational calculation of K-edges using density functional theory, which will help elucidate their nature. Modelling the spectra will provide complementary information to interpret the charge compensation mechanism and structural phase changes that are still not well understood in cathode materials. The combination of experimental and theoretical approaches provides a new perspective for future studies toward the fundamental understanding of the mechanism governing the TM-O redox reactions in cathode materials. Such insight can inform future materials design, paving the way for the next-generation higher capacity batteries.

[1] C. Sternemann, et al. *High Pressure Research*, 2016, 36, 3, 275–292

[2] C. J. Pollock and S. DeBeer, *J. Am. Chem. Soc.*, vol. 133, p. 5594–5601, 2011.

9:00 AM CH01.17.05

Microsized Hollow Silicon-Graphene Composite Anode for High-Performance Lithium-Ion Batteries Subin Lee, Na yeong Kim and Ji-Won Jung; University of Ulsan, Korea (the Republic of)

The silicon-based anode has been studied as a potential replacement for the traditional graphite anode due to its abundance, low price, and high theoretical capacity (3,579 mAh/g@room temperature) for lithium storage, which is approximately ten times greater than that of graphite (372 mAh/g). Despite these advantages of silicon-based anodes, there are still several remaining vexing problems, such as structural instability induced by huge volume changes, low electrical conductivity, and an excessive, irregular formation of the solid electrolyte interphase (SEI) layers.

In this work, highly durable graphene-silicon composite materials were fabricated by using porogen to generate void space between graphene and silicon. We elaborately controlled the relative composition of active silicon and graphene. The composite properties were analyzed by scanning Electron Microscopy (SEM), transmission EM (TEM), X-ray photoelectron spectroscopy (XPS), and X-ray diffraction (XRD) analysis, which provide an insight into how the composite properties correlate with the lithium-ion battery performance.

9:15 AM CH01.17.06

Tracking the First-Cycle Evolution of Fe-Li, Mn-Rich (Fe:LMR) Cathode Material by Advanced Hard X-Ray Spectroscopic Methods Chun Yuen Kwok¹, Subhadip Mallick², Christopher Pollock³, Arturo Gutierrez², Marm Dixit¹, Jason Croy² and Mahalingam Balasubramanian¹; ¹Oak Ridge National Laboratory, United States; ²Argonne National Laboratory, United States; ³Cornell High Energy Synchrotron Source, United States

As we strive for the decarbonization of our society, electrochemical energy storage technology emerges as a key player for enabling renewable energy sources. In this context, the development of battery cathode materials using earth abundant materials that can be ethically sourced is of utmost importance. However, our current understanding of the intricate causal relationships and correlations between redox mechanisms and structural changes in some of these materials remains severely limited. One of many of these examples is the Fe:LMR material.

A prominent challenge in designing functional Fe:LMR materials lies in the comprehension of the complex $\text{Fe}^{3+/4+}$ redox couple. Conventional X-ray absorption and Mössbauer spectroscopies have not been able to provide a definitive answer on the relationship between the state of charge/discharge of the battery and the status of the transitional metal species. In particular, the charge-compensation mechanism during and after the LiMn_6 activation process is a subject of ongoing debate, with conflicting results and theories proposed. These include reversible iron redox, iron oxidation followed by charge disproportionation, reductive coupling accompanied by metal migration, transient oxidized iron species followed by oxygen oxidation via ligand-to-metal charge transfer (LMCT), and peroxide formation, etc. This knowledge gap poses a significant challenge in developing the next-generation efficient and sustainable cathode materials.

To address the issue at hand, we exploit the important traits of hard x-ray spectroscopic methods to track the oxidation state and local structural environment of transition metals and correlate the structural evolution to the electrochemical profile. Through this work, we elucidate the intricate mechanisms occurring in these materials, which will contribute to the development of improved earth-abundant cathode materials and to develop Li-ion batteries that exhibit enhanced performance and longevity.

9:30 AMBREAK

10:00 AM CH01.17.07

Development and Characterization of Novel Cation-Disordered Battery Electrode Materials Dongchang Chen, You Wang, Basirat Raji-Adefila and Alexandra Outka; University of New Mexico, United States

The emergence of cation-disordered battery electrode materials represents a major progress in solid-state materials for electrochemical energy storage applications. The disordered distribution of cations allows rich opportunities in designing diverse cation-disordered structures/compositions but also bring challenges in understanding their nature and energy storage mechanism. In this presentation, we will demonstrate our effort in developing all-new cation-disordered battery electrode materials and investigating their electrochemical properties. Moreover, we will present our approach in characterizing the unique structural features and working mechanisms of these novel electrode materials via a comprehensive array of spectroscopic techniques, ranging from X-ray absorption, solid-state UV-Vis absorption, vibrational spectroscopy, etc. Results of the work will bring transformative insights for various subfields of energy storage materials and investigation of hidden yet critical materials properties via in-depth spectroscopic characterizations.

10:15 AM CH01.17.08

Characterisation of Local Environments in Strongly Paramagnetic Battery Cathodes: A Combined Experimental and Theoretical Approach Euan Bassey^{1,2} and Clare P. Grey²; ¹Materials Science Laboratory, United States; ²University of Cambridge, United Kingdom

Non-invasive techniques which probe the local environment around the paramagnetic redox-active transition metal (TM) centres in lithium- and sodium-ion battery (LIB and NIB, respectively) cathode materials are critical in developing a clear understanding of the phase transformations, redox processes and degradation mechanisms which take place at the cathode during operation of the battery.¹ Where NMR is increasingly used as a characterization technique for studying, for example, Li, Na and O local environments in paramagnetic battery materials, direct observation of the redox-active paramagnetic (TM) centres using NMR is not possible owing to rapid nuclear relaxation times.^{2–4} EPR, however, enables investigation of these centres and is far less reported. Further, an understanding and assignment of these EPR spectra—made all the more challenging by strong electron-electron dipolar and magnetic exchange interactions—does not yet exist. In this work, we present a combined high-frequency EPR and density functional theory (DFT) study of the local paramagnetic environments in Li_2MnO_3 , a model compound for the family of commercially successful, layered lithium-ion battery cathodes. By collecting EPR spectra at a range of frequencies (9 – 383 GHz) and temperatures (5 – 300 K) and comparing to DFT-calculated g -tensors, we clearly observe several unique local environments and assign these observed resonances to Mn^{4+} centres with different local environments [Figure 1]. We also examine the effect of magnetic exchange interactions on the spectra to explain the temperature evolution of these complex EPR spectra. The methodology presented in this work will be invaluable for studying paramagnetic centres in paramagnetic solids not only for LIBs and NIBs, but also in a range of TM-based materials for devices.

References:

- (1) Nguyen, H.; Clément, R. J. Rechargeable Batteries from the Perspective of the Electron Spin. *ACS Energy Lett.* **2020**, 5 (12), 3848–3859. <https://doi.org/10.1021/acsenerylett.0c02074>.
- (2) Grey, C. P.; Dupré, N. NMR Studies of Cathode Materials for Lithium-Ion Rechargeable Batteries. *Chem. Rev.* **2004**, 104 (10), 4493–4512. <https://doi.org/10.1021/cr020734p>.
- (3) Carlier, D.; Ménétrier, M.; Grey, C. P.; Delmas, C.; Ceder, G. Understanding the NMR Shifts in Paramagnetic Transition Metal Oxides Using Density Functional Theory Calculations. *Phys. Rev. B* **2003**, 67 (17), 174103. <https://doi.org/10.1103/PhysRevB.67.174103>.
- (4) Bassey, E. N.; Reeves, P. J.; Seymour, I. D.; Grey, C. P. 17O NMR Spectroscopy in Lithium-Ion Battery Cathode Materials: Challenges and Interpretation. *J. Am. Chem. Soc.* **2022**, 144 (41), 18714–18729. <https://doi.org/10.1021/jacs.2c02927>.

10:45 AM *CH01.18.01

A Spin on Redox Processes in Battery Electrodes[Raphaële Clément](#); University of California, United States

Rechargeable batteries generate current through the transfer of electrons between paramagnetic and/or metallic electrodes. The interrelation between a material's magnetic and electronic properties, and its performance as a battery electrode, motivates the use of magnetometry and magnetic resonance tools to investigate redox processes during electrochemical cycling.¹ Moreover, interactions between magnetic moments or spins strongly depend on bond lengths and angles (orbital overlap), making such tools ideal probes of the local structure in crystalline, disordered, or even amorphous electrode materials.

In this talk, I will present our recent work combining *operando* magnetometry, high resolution *ex situ* solid-state NMR, and first principles calculations, to better understand the working principles and sources of irreversibility of magnetic and metallic conversion and intercalation electrodes. We show, for example, that the first cycle irreversibility of LiNiO₂ is partly caused by planar defects in the as-synthesized material, preventing Li intercalation at standard cycling rates.² NMR, magnetometry and ⁵⁷Fe Mössbauer spectroscopy allow us to identify and quantify conversion of the cryolite-like Na₃FeF₆ electrode,³ and to monitor polymorphism and an electrochemically-induced phase transformation in the weberite Na₂Fe₂F₇ intercalation cathode.⁴

References

1. Nguyen, H., Clément, R., "Rechargeable batteries from the perspective of the electron spin", *ACS Energy Lett.*, 5(12), 3848-3859 (2020).
2. Nguyen, H., Zaveri, A., Cui, W., Silverstein, R., Kurzhals, P., Sicolo, S., Bianchini, M., Seidel, K., Clément, R., "Twin boundaries contribute to the first cycle irreversibility of LiNiO₂", *submitted*.
3. Foley, E., Wong, A., Vincent, R., Manche, A., Zaveri, A., Gonzalez-Correa, E., Ménard, G., Clément, R., "Probing reaction processes and reversibility in Earth-abundant Na₃FeF₆ for Na-ion batteries", *Phys. Chem. Chem. Phys.*, 23(36), 20052-20064 (2020).
4. Foley, E. E., Wu, V., Jin, W., Cui, W., Yoshida, E., Manche, A., Clément, R., "Polymorphism in Weberite Na₂Fe₂F₇ and its Effects on Electrochemical Properties as a Na-Ion Cathode", *Chem. Mater.*, 35(9), 3614-3627 (2023).

11:15 AM CH01.18.02

A Novel Light Scattering Technique for the Study Of Li-Ion Dynamics and Characterisation of Battery Electrode Materials[Christoph Schnedermann](#)^{1,2}, [Alice Merryweather](#)^{1,2}, [Cathryn Langley](#)², [Clare P. Grey](#)¹ and [Akshay Rao](#)^{1,2}; ¹University of Cambridge, United Kingdom; ²Illumion Ltd., United Kingdom

We introduce a recently developed *operando* optical microscopy technique and provide examples of how it can be applied to mechanistic studies of lithium-ion battery electrodes and active material characterisation. Our technique probes state-of-charge changes in the active particles within the electrode during battery operation, based on the intensity variation of scattered light across each active particle. This enables detailed spatially-resolved data on an individual particle level to be built up for mechanistic studies but can also allow global statistics to be established at the electrode level.

The ability to quantify ion transport during battery operation within active particles and across the electrode helps to provide insights into how lithium-ion dynamics affect the (de)lithiation mechanisms and degradation mechanisms of battery electrodes, which is crucial to improving their electrochemical performance. Here, we present highlights demonstrating how our technique can be used to (1) track and quantify phase transitions in lithium cobalt oxide (LCO), (2) reveal kinetic phase separation in high-rate niobium tungsten oxide (NWO) anode materials, and (3) determine mechanistic origins of first-cycle capacity losses in Ni-rich nickel manganese cobalt oxides (NMC).

Finally, we showcase how the performance of the electrode can be quantified by monitoring the heterogeneous rate of (de)lithiation across hundreds of active particles in the electrode during normal battery operation. Using NMC and NWO as examples, we demonstrate how our technique can be used to determine both the proportions of active particles in the electrode exhibiting irregular, slower, faster and normal (de)lithiation rates, and the proportions of cracked and intact particles after successive cycles to monitor degradation and electrode cycling performance.

The generality of our technique means that it is agnostic to the underlying battery chemistry, and can be applied to study any battery electrode, such as Na-ion and multivalent-ion batteries.

References

- (1) A. J. Merryweather et al., *Nature* **594**, 522 (2021)
- (2) A. J. Merryweather et al., *Nat. Mater.* **21**, 1306 (2022)
- (3) C. Xu et al., *Joule* **6**, 2535 (2022)

11:30 AM CH01.18.03

Operando Study of Thermal and Chemical Events in Lithium Metal Batteries using Optical Fiber Bragg Grating Sensor[Charlotte Gervillie](#)¹, [Wurigumula Bao](#)² and [Y. Shirley Meng](#)^{2,1}; ¹University of California San Diego, United States; ²The University of Chicago, United States

In the era of rapid energy transition, energy storage technologies offer a unique opportunity to facilitate a sustainable, low-carbon transition, thereby paving the way towards a cleaner and more resilient future. Lithium metal batteries have attracted significant research attention due to their groundbreaking high theoretical capacities, exceeding conventional graphite anodes in lithium-ion batteries by a factor of ten (3,860 milliampere hours per gram). However, the commercialization of lithium metal batteries is hindered by substantial challenges, including the growth of dendrites at the negative electrode as a result of uneven lithium plating and stripping. Additionally, the reactivity between lithium metal and the electrolyte leads to the formation of unstable solid-electrolyte interphase (SEI) layers, further compromising battery performance and cycle life.

To address these issues, researchers have extensively developed destructive characterization techniques to observe the lithium metal anode and quantify irreversible lithium metal formation. However, these studies lack real-time *operando* information, crucial for understanding the dynamic behavior of these systems. Recently, the emergence of optical fiber-based techniques has enabled the tracking of battery properties under realistic conditions, providing chemical, thermal, and mechanical data for lithium-ion and sodium-ion cells.

In this study, we demonstrate the utilization of optical fiber Bragg grating (FBG) sensors to monitor thermal and chemical events in anode-free commercial cells during real cycling conditions. By confirming the *operando* results with destructive characterization methods such as titration gas chromatography (TGC) and focused ion beam (FIB) imaging, we highlight the capability of this method to monitor the parasitic reactions (as solid electrolyte interface formation) happening in lithium metal cells under diverse conditions, including varying pressure, electrolyte formulation, and rate performances. Overall, the utilization of FBG sensors offers valuable insights into the reactivity, stability, and safety aspects of lithium metal batteries, thereby contributing to the ongoing development and optimization of these energy storage systems.

11:45 AM CH01.18.04

Freestanding LiPON: From Fundamental Study to Uniformly Dense Li Metal Deposition Under Zero External Pressure[Diyi Cheng](#), [Minghao Zhang](#) and [Y. Shirley Meng](#); University of California, San Diego, United States

Lithium phosphorus oxynitride (LiPON) is a well-known amorphous thin film solid electrolyte that has been extensively studied in the last three decades. Despite the promises to pair with various electrode materials, the presence of rigid substrate and LiPON's unique amorphous, air-sensitive nature set limitations to comprehensively understand its intrinsic properties for future development and applications. This work demonstrates a methodology to synthesize LiPON in a freestanding form that manifests remarkable flexibility and a Young's modulus of ~33 GPa. Solid-state nuclear magnetic resonance and differential scanning calorimetry results with high signal-to-noise ratio reveal the Li/LiPON interface bonding environments quantitatively and a well-defined glass transition temperature for LiPON. Combining interfacial stress and a seeding layer, FS-LiPON demonstrates a uniform and fully dense Li metal deposition without the aid of external pressure. Such a FS-LiPON film offers more opportunities for the fundamental study of LiPON material and associated interfaces, and provides perspectives for interface engineering in bulk solid-state battery.

1:30 PM *CH01.19.01

Scanning Probe IR Microscopy and Soft X-Ray Spectroscopy Reveal Local Composition and Molecular Orientation in Solution Processed Films for Organic Photovoltaics Ellen Moons, Leticia P. Christopholi, Ishita Jalan, Cleber Marchiori, Leif K. Ericsson, Stela Andrea Muntean and Jan van Stam; Karlstad University, Sweden

Solution-processed organic solar cells (OSC), a low-cost renewable energy technology, have shown record power conversion efficiencies approaching 20%. The recent leap in performance of OSC can be ascribed to the development of new electron acceptors, such as the Y-series of small molecules, that efficiently contribute to photogeneration of charges in the visible range. These molecules provide, however, new challenges for film processing due to their limited solubility and tendency to aggregate. The presentation will cover two examples where morphological analysis by means of advanced characterization techniques have provided in new insights in the molecular organization in spin-coated films. First, we present a study of the influence of the processing solvent on the orientation and packing of Y-series acceptor molecules in pure acceptor films by angle-resolved Near-Edge X-ray Absorption Fine Structure (NEXAFS) spectroscopy. Secondly, we demonstrate the use of AFM-IR spectromicroscopy to map the nano-scale composition of spin-coated donor-acceptor bulk heterojunction films. AFM-IR spectromicroscopy combines the high resolution of scanning probe microscopy with the precise chemical fingerprint of infrared spectroscopy. Using a pulsed, tuneable MIRcat laser, resonant enhanced tapping mode AFM-IR yields compositional maps of donor and acceptor molecules with low beam damage. This chemical mapping yields new insights in the nanostructure formation in molecular semiconductor films for emerging photovoltaic materials.

2:00 PM CH01.19.02

New Era of Material Characterisation: Resolving Electron and Hole Charge Carriers Properties by Constant Light Induced Magneto Transport Artem Musiienko¹ and Fengjiu Yang²; ¹Helmholtz-Zentrum Berlin für Materialien und Energie, Germany; ²National Renewable Energy Laboratory, United States

The development of novel and improvement of existing semiconductor and semi-insulating materials relies on the knowledge of free-charge transport properties. In particular, knowledge of minority and majority charge carrier diffusion lengths, lifetimes, mobilities, and concentrations allows tailoring the design of semiconductor devices and control effectiveness of solar cells, transistors, detectors, sensors, and LEDs. At the moment, the detection of minority and majority charge (electrons or holes) properties is challenging due to the natural limitation of the experimental methods. The broadly spread methods such as time-resolved photoluminescence (trPL), terahertz conductivity, and photoconductivity decay can detect lifetime for only a minority or only the majority of carriers, which control the fast decay component of the signal [1]. The additional drawback of the commonly used methods is that they probe charge carriers' properties in a transient regime which is not matched with device or material operation conditions in a steady state.

Recently, several studies used the Hall effect in a single carrier regime assuming an equal concentration of holes and electrons to assess the properties of photocarriers [2–5]. In most cases, the concentrations, lifetimes, and diffusion length of electrons and holes are not equal in semiconductors due to the presence of traps. Thus, the equality of hole and electron concentrations leads to an incomplete or sometimes incorrect description of charge transport. This study introduces the Constant Light Induced Magneto Transport (CLIMAT) method [6], which combines light and magnetic fields to assess the transport properties of holes and electrons separately. CLIMAT provides access to fourteen material parameters compared to only two in the classical approach. We demonstrate that having direct knowledge of electron and hole properties enables us to determine quasi-Fermi level splitting and ideality factor, and predict the material's performance in a photovoltaic (PV) device configuration without constructing the full device.

We illustrate the implications of CLIMAT in two different systems: silicon and halide perovskite solar cells. For the first time, we differentiate electron and hole transport in these material systems using CLIMAT. We identify dominant recombination mechanisms in materials that hinder lifetime and diffusion length. Additionally, we reveal the differences in electron and hole lifetimes due to trap states. The experimental data are supported by charge transport drift-diffusion simulations.

The use of CLIMAT with AC magnetic fields can revolutionize the field by providing unique feedback on magnetic fields and light. This enables the study of carrier concentration, lifetime, diffusion length, and mobility as a function of light intensity. Furthermore, it allows for predicting the material's performance in a PV device configuration without constructing the full device. We anticipate that our approach will have applications in optoelectronic systems where device efficiency strongly depends on electron and hole transport. Specifically, CLIMAT can be utilized to characterize and optimize diffusion length and lifetimes in solar cells, sensors, LEDs, and transistors.

[1] H. Hempel *et al.*, *Adv. Energy Mater.* 12, 2102776 (2022).

[2] O. Gunawan, *Nature* 575, 151–155 (2019).

[3] Y. Chen, *Nat. Commun.* 7, 12253 (2016).

[4] A. Musiienko, *Phys. Rev. Appl.* 10, 014019 (2018).

[5] A. Musiienko, *Adv. Funct. Mater.* 2104467 (2021).

[6] A. Musiienko, EP23173681.0 and DE102023112934.1, A. Method, computer program, and system for determining respective transport properties of majority as well as minority charge carriers in a sample. (2023).

2:15 PM CH01.19.03

Quantifying Local Conductivity and Complex Dielectric Constant of Solar Cell Films Using Electrical Scanning Probe Microscope Measurements and Microscopic Theory John A. Marohn, Christopher Petroff, Virginia E. McGhee, Rachael Cohn and Roger F. Loring; Cornell University, United States

Electrical scanning probe measurements, such as scanning Kelvin probe force microscopy (KPFM) and electric force microscopy (EFM), have been widely used to study inorganic, organic, and hybrid semiconductors. Frustratingly, the established theoretical description of electrical scanning probe measurements calculates cantilever forces and frequency shifts as a function of sample capacitance, essentially ignoring sample resistance. We have developed a new Lagrangian-mechanics theory of electrical scanning probe measurements that fixes this shortcoming [1]. In the new theory, the cantilever signal depends on sample resistance, sample capacitance, and tip capacitance.

A central feature of the new theory is a complex-valued transfer function, written in terms of tip capacitance and sample impedance, that relates the cantilever charge to the applied oscillating tip voltage. We show that cantilever frequency shift and dissipation (i.e., non-contact friction) depend, respectively, on the real and imaginary part of this transfer function evaluated at the cantilever frequency. The entire transfer function can be measured in a broadband local dielectric spectroscopy (BLDS) measurement [2] in which the mean cantilever force is observed as a function of the tip voltage's oscillation frequency [3]. BLDS measurements carried out on a wide range of organic and lead-halide perovskite semiconductors as a function of light intensity show that light primarily changes sample resistance, not capacitance (as assumed nearly universally in electrical scanning probe measurements).

From the measured sample resistance and capacitance, we wish to infer the sample's intrinsic resistivity and dielectric constant. The starting point for this task is the continuum electrostatic theory describing the forces, force gradients, and friction experienced by a charged cantilever over a semiconductor on a dielectric substrate developed by Lekkala, Marohn, and Loring [4]. Work is underway to apply this theory to a semiconductor on a metal substrate by taking the dielectric constant of the substrate to infinity in Lekkala's equations. The output of these computations will be semi-analytic theory for the cantilever frequency shift and dissipation versus voltage, and the BLDS signal versus frequency, written in terms of tip capacitance, sample thickness, sample resistivity, and sample dielectric constant.

Our theory covers both electronic and ionic conductivity. Having a quantitative scanning probe method to measure thin-film ionic and electronic properties is important because many new ionic/electronic materials for battery and solar-cell applications are, as synthesized, highly heterogeneous. Bulk measurements such as Hall effect, dielectric spectroscopy, and current-voltage measurements are dominated by the average behavior. Scanning probe measurements, in contrast, have high spatial resolution and can be used to demonstrate that some region of the heterogeneous material has favorable properties and is thus worth a further investment of capital to improve synthesis and/or processing.

[1] R. P. Dwyer, L. E. Harrell, and J. A. Marohn. *Phys. Rev. Appl.* (2019) 11(6): 064020, DOI:10.1103/PhysRevApplied.11.064020.

[2] M. Labardi, M. Lucchesi, D. Prevosto, and S. Capaccioli. *Appl. Phys. Lett.* (2016) 108(18): 182906, DOI:10.1063/1.4948767.

[3] (a) A. M. Tirmzi, R. P. Dwyer, T. Hanrath, and J. A. Marohn. *ACS Energy Letters* (2017) 2(2): 488, DOI:10.1021/acsenenergylett.6b00722; (b) A. M. Tirmzi, J. A. Christians, R. P. Dwyer, D. T. Moore, and J. A. Marohn. *J. Phys. Chem. C* (2019) 123(6): 3402, DOI:10.1021/acs.jpcc.8b11783.

[4] S. Lekkala, J. A. Marohn, and R. F. Loring, *J. Chem. Phys.* (2013) 139: 184702, DOI:10.1063/1.4828862

2:30 PM CH01.19.04

Optimisation of a Polymerised Fullerene-Based Transport Layer for Organic Photovoltaics - Effect on Energetics, Active Layer Formation, and Device Performance Nicky Evans¹, Philipp Weitkamp², Olivia Gough¹, Benjamin Putland¹, Raghunath R. Dasari³, Seth R. Marder⁴, Klaus Meerholz², Selina Olthof², Moritz Riede¹ and Henry Snaith¹; ¹University of Oxford, United Kingdom; ²University of Cologne, Germany; ³Georgia Institute of Technology, United States; ⁴University of Colorado Boulder, United States

Investigations into the charge transport layers used within organic photovoltaics (OPV) can help us in finding ways to improve device efficiency and stability. In particular, dedicated charge transport layers have the purpose of aiding in selective charge transport to the respective electrodes. Care has to be taken to ensure advantageous energy level alignment, resulting in minimised losses in solar cell device performance. Though the more commonly used electron transport layer materials in OPV, such as metal oxides, exhibit satisfactory optical and electronic properties, there is limited control over their energy-level matching within a device. Additionally, the stability of many of these materials, particularly under ultraviolet irradiation, is a limiting factor. This study investigates the use of an electronically and energetically tuneable, fullerene-derived electron transport layer for OPV, namely PCBCB. These films exhibit a reduction in solubility once they are treated by specific annealing conditions, which intriguingly allows for non-orthogonal-solvent based films to be processed on top of these layers. We investigated these films with respect to their conductivity as well as energetic properties and were able to tune these properties via the use of an electron-donating additive. It was observed that with an increased additive concentration, the conductivity increased while at the same time the physical film quality improved. Furthermore, the use of the additive led to a shift in the position of the Fermi level toward the lowest unoccupied molecular orbital, ultimately improving the energy level matching of the layer within the device stack.

Device stacks comprised of a PM6:Y6 donor-acceptor blend active layer were fabricated atop a series of such electron transport layers in an n-i-p architecture. Intriguingly, this resulted in variations in active layer morphology. The changes were explored using GIWAXS and significant differences in the crystalline stacking were found for the active layer deposited on top of doped fullerene-derivative ETL, in contrast to a metal-oxide transport layer. This is thought to be a product of different levels of phase segregation throughout the active layer, relating to differences in contact angle between the active layer and ETL when deposited. These morphological changes appear to result in significant differences in device performance characteristics, particularly in J_{SC} and consequently fill factor and power conversion efficiency. Thus, understanding the impact of prior layers on active layer formation could be integral to further understanding and optimising device performance characteristics.

Furthermore, a series of stability studies are currently being conducted to test the lifetime of OPV devices comprised of a fullerene-derivative ETL, in comparison to those using a typical zinc oxide (ZnO) electron transport layer. From initial results, we see that a highly 'doped' organic ETL and a bilayer of doped and nominally intrinsic transport layers, both lead to device performance that is close to competing with ZnO based devices, and an increased lifetime as compared to devices comprising of the metal oxide.

2:45 PM BREAK

SESSION CH01.20: Novel Characterization Techniques V
Session Chairs: Rajiv Giridharagopal and Benjamin Grevin
Friday Afternoon, December 1, 2023
Hynes, Level 2, Room 208

3:15 PM CH01.20.01

Determining the Depth Profile of the Active Ce³⁺ Species at Reduced Surfaces of Ceria Patrick M. Donahue¹, Qing Ma^{1,2}, Paul Chery¹ and Sossina M. Haile¹; ¹Northwestern University, United States; ²Argonne National Laboratory, United States

Rapid and reversible surface reduction is central to the functionality of ceria (CeO₂ and doped derivatives) in catalysis and sustainable energy technologies, yet unanswered questions remain regarding its fundamental surface redox properties. This work supplies novel in-situ characterization of ceria surfaces, namely the termination dependence of surface reduction and the complete depth profile of the reduced Ce³⁺ species. This work is based on in-situ depth-resolved X-ray absorption near-edge spectroscopy (XANES) of CeO₂ thin films, for which we have developed a robust analysis method. As of the abstract submission date, the Ce³⁺ depth profile at the CeO₂ (111) termination has been determined at 800°C under an H₂/H₂O atmosphere ($p_{O_2} = 1.0 \times 10^{-19}$ atm); planned experiments in the coming months will characterize the CeO₂ (100) and (110) terminations and investigate an additional high-temperature reducing environment (~1000°C in medium vacuum). Previous studies suggest environment-dependent variations in both the form and magnitude of the Ce³⁺ profile [1], and surface reducibility is predicted to vary by termination [2]. This study directly addresses those areas of inquiry and considerably expands current knowledge of ceria surface properties under technologically relevant conditions. In turn, a deeper understanding of the exceptional redox properties of ceria can inform advanced design of catalysts and oxygen storage materials.

References:

1. W. Yuan, Q. Ma, Y. Liang, C. Sun, K. V. L. V. Narayanachari, M. J. Bedzyk, I. Takeuchi, S. M. Haile, Unexpected trends in the enhanced Ce³⁺ surface concentration in ceria-zirconia catalyst materials. *J Mater Chem A*, 8, 9850–9858 (2020).
2. M. Nolan, S. C. Parker, G. W. Watson, The electronic structure of oxygen vacancy defects at the low index surfaces of ceria. *Surf Sci*, 595, 223–232 (2005).

3:30 PM CH01.20.02

In Situ and Operando Characterization of Photocatalytically Active Faceted Semiconducting Nanoparticles Frieder Mugele¹, Igor Siretanu¹, Shaoqiang Su¹, Bastian Mei^{1,2} and Guido Mul¹; ¹University of Twente, Netherlands; ²Ruhr-Universität Bochum, Germany

Photo- and electrocatalytically active materials are expected to play an essential role in the transition towards sustainable processes for energy storage and chemical conversion. Performance and stability of the materials still need to be improved. Yet, the microscopic origin of their current limitations are often poorly understood. One key limitation is the lack of suitable techniques that allow for a detailed characterization of the structural and electrical properties of the interfaces on the nanometer scale. In this lecture, I describe our recent progress in establishing in situ and operando AFM spectroscopy for characterizing the surface charge and its response to illumination on photocatalytically active faceted nanoparticles of SrTiO₃ and BiVO₄ in ambient electrolytes of variable composition. Our measurements demonstrate the existence and pH-dependence of differences in surface potential between adjacent crystal facets, which are believed to drive the separation of photo-generated electron-hole pairs in photocatalysis. For visible light-driven BiVO₄, we monitor the variations of the local surface charge upon illumination, from which we extract the local surface photovoltage and thus the accumulation of charge carriers at the interfaces. The measurements suggest a strong influence of surface defects such as steps and disordered regions between adjacent facets for the accumulation of photo-excited charge carriers.

I will conclude the lecture with an outlook on upcoming challenges in AFM-based characterization of catalytic materials for the energy transition.

3:45 PM *CH01.20.03

Structure, Thermodynamic and Thermomechanical Characteristics of Semiconducting Polymers: Nomenclature and Property Conundrums Harald Ade; North Carolina State University, United States

Organic semi-conducting polymer thin films are used in many organic electronic devices and have shown promising results in applications ranging from organic light emitting diodes to solar cells and biosensors. The molecular packing of the polymers controls a number of optical and electronic properties and the thermal and thermomechanical properties are critical for device stability in blends, processing strategies, and mechanical failure modes. Due to the molecular design, semi-conducting polymers exhibit a continuing range of paracrystalline disorder, yet at the same time, they do not behave like classic paracrystalline materials. In fact, the classic structure and property paradigms and associated nomenclature don't seem to apply. Classic material design labels such as random coil, rigid rod, hairy rod and bottlebrush seem to be delimiting structural characteristics, with semi-conducting polymers occupying the concept and parameter space in-between these limits, yet with characteristics that appear to be not just linear combination of the characteristics found in the classical limits. We review the current understanding and the various conundrums. For example, paracrystallites in a semi-conducting thin film are usually assumed to have a certain size and shape in three dimensions, which then can have a preferred edge-on or face-on orientation relative to the substrate with a random orientation in-plane. X-ray analysis indicates though that most materials exhibit only two-dimensional paracrystalline platelet ordering and might often resemble a layered glass. Thermomechanical characterization frequently indicate multiple relaxation transitions without the presence of a clear glass transition, yet a high temperature liquid-crystalline-like phase. Furthermore, the phase diagrams of semi-conducting polymers with 'small molecule' acceptors such as fullerenes or modern non-fullerene acceptors frequently exhibit reentrant phase boundaries that reflect upper and lower-critical solution temperature characteristics. The totality of information suggests that a new reference frame if not new paradigm and associated nomenclature is required to facilitate understanding and communication about the order, molecular packing, texture, thermomechanical properties, and structure-properties relations in semi-conducting polymers.

8:30 AM +CH01.21.01

Examining Indoor and Outdoor Stability of Non-Fullerene Acceptor Organic Solar Cells using a Bottom-Up and Top-Down Hybrid Approach Manjunatha Reddy G.N.; University of Lille, France

Efforts on molecular design, material processing and device engineering enabled new looms in the small molecule acceptor-based organic photovoltaics (OPVs) with power conversion efficiency (PCE) of over 19%, enticing further developments toward scalability and commercial viability. In doing so, it is paramount to resolve structure-stability-property interrelationships.[1-3] Here, we present a hybrid bottom-up and top-down NMR crystallography approach to correlate between morphology deterioration and performance degradation.[4] and provide an example of structure-stability-property relationship in PM6:Y6 bulk heterojunction (BHJ) solar cells.[5] The bottom-up strategy combines time-resolved magnetic resonance spectroscopy and crystallography modelling to disentangle the impact of the environment on the bulk and interfacial BHJ morphology, in order to gain insight into the molecular origins of photochemical, thermal and moisture-induced degradation reactions in PM6 and Y6 moieties.[5] A complementary top-down model examines macroscopic device properties including short circuit current density (J_{sc}), open-circuit voltage (V_{oc}), fill factor (FF), external quantum efficiency (EQE) and PCE values as a function of environmental parameters. The nanoscale PM6:Y6 BHJ morphology is resistant to an indoor operational condition at 22 °C, 700 lx and 45% relative humidity (RH) for over 4 years. In contrast to this, morphological degradation occurs upon photoirradiation (AM 1.5G), exposure to moisture at 85% RH and thermal annealing at 100-200 °C, leading to performance deterioration. The PM6:Y6 blend, PM6 and Y6 films exhibit different instability and degradation mechanisms, whereby the Y6 is more vulnerable to photoirradiation and (hydro)thermal treatment. Our results corroborate that PM6:Y6 morphology is acquirescent to indoor applications, calling for the design of environmentally stable molecular entities in order to formulate stable and efficient BHJ morphology for outdoor photovoltaics.

[1] Advanced Materials, 2019, 31, 1903868

[2] Energy & Environmental Science, 2020, 13, 3679-3692

[3] Advanced Materials, 2022, 34, 2105943

[4] Nature Reviews Materials, 2020, 5, 910-930

[5] Advanced Energy Materials, 2023, in revision

9:00 AM CH01.21.02

Charge Density in Nanorings from Scanning Force Microscopy Moshe Gordon, Benjamin Goykadosh, Yonathan Magendzo and Fredy R. Zypman; Yeshiva University, United States

Several systems of nanometer or sub-nanometer dimensions are electrically charged rings. For example, molecular pumps use electrically charged rings to link amino acids into growing peptides, the efficiency depending on charge magnitude and location. Knowledge of charge content is necessary to apply these pumps to assemble other architectures. More generally, charge plays a key role in the structure attained by large molecules when they self-assemble. Also, charged rings are current candidates as physical support of information storage for qubits for quantum computing. In addition, for applications in biosensing and nano-optoelectronics, micrometer and nanometer rings of charge have been synthesized from a variety of materials. For example, carbon nanorings with radii of a few have been obtained by self-assembly of carbonized pluronic P123. The most common gold nanoring has been synthesized by a variety of methods, while whole silver nanorings of diameter have been produced by solvothermal methods.

These examples underscore the relevance of understanding electrostatic measurements at the nanoscale with the SFM (scanning force microscope), and in particular, to understand those measurements on charged ring structures. While the SFM sensor mechanically responds to electrostatic inputs, it is not straightforward to connect this response to the electrostatic content of the sample under study. Specifically, SFM records a force trace which varies as the sensor explores different regions of the sample. In this study, we propose a method to convert this force curve into charge density content in the sample. We first solve the direct problem, whereby the SFM force is computed from the assumed know charge density. Afterward, we move to the realistic practical situation in microscopy and address the inverse problem. In the inverse problem, forces are measured in each voxel of a volume region above the sample and, using that information as input, the charge on the ring is produced.

9:15 AM CH01.21.03

Potassium Ions Pre-Intercalated Vanadium Oxide Cathodes for Aqueous Zn-Ion Batteries Yinan Lu; University College London, United Kingdom

Aqueous rechargeable zinc-ion batteries (ZIBs) have garnered considerable attention due to their safety, cost-effectiveness, and eco-friendliness. There is a growing interest in finding suitable cathode materials for ZIBs. Layered vanadium oxide has emerged as a promising candidate due to its high storage capacity for zinc ions. However, the development of high-performance zinc-ion batteries faces challenges such as irreversible phase transformation, sluggish diffusion of zinc ions caused by the high energy barrier between V_2O_5 layers, and hence low capacity than the theoretical value. In this study, we synthesized nanofibers of V_2O_5 intercalated with potassium ions (KVO) through a straightforward hydrothermal process. The introduction of potassium ions not only increased the interlayer distance ($d_{001} = 9.35 \text{ \AA}$) but also reduced the V^{5+}/V^{4+} redox couple (from 7.18 to 1.01) thereby improving the electrochemical performance. The resulting KVO cathode exhibited a high specific discharge capacity ($274.18 \text{ mAh g}^{-1}$ at 0.1 A g^{-1} , second cycle), enhanced cycling stability, and significantly reduced charge transfer resistance (8.92 \Omega) compared to pristine V_2O_5 (98.67 mAh g^{-1} at 0.1 A g^{-1} and 67.31 \Omega charge transfer resistance). This study contributes to the understanding and advancement of KVO cathode materials, providing valuable insights for the design and optimization of cathode materials to enhance the electrochemical performance of ZIBs.

<quillbot-extension-portal></quillbot-extension-portal>

9:30 AM CH01.21.04

X-Ray Micro-Computed Tomography (XMCT) for Quantitative Morphometry of Topological Graphene-Based Aerogels and Carbon Foams Sanju Gupta; Penn State University, United States

We report quantitative morphometry of freeze-dried graphene-based aerogels (GA, NGA, Gr-MWCNTs) and carbon foam (CF, CF-GA) monoliths, prepared by hydrothermal and organic sol-gel, respectively. X-ray micro-computed tomography (XMCT), in combination with SEM, allowed to visualize of internal microstructure in 3D space and the reconstructed volume renderings from 2D sliced images revealed hierarchical structures (interlaced thin sheets, honeycomb organization) and topological (interconnected pores background) domains. The influence of multi-walled carbon nanotubes (MWCNT) additions to graphene-like sheets and integration with carbon foam (CF) are assessed through volume-weighted pore size, wall thickness, and porosity levels, in compliance with physical properties. Composite porous solids elucidated crosslinking reinforced by a homogeneous distribution of CNTs into graphene aerogel (GA) and CF matrices. A consistent trend of $NGA > CF > Gr-MWCNT_{2,1} > CF-GA > Gr-MWCNT_{3,1} > Gr-MWCNT_{5,1}$ was found from XMCT image processing and analyses significantly corroborate stability. These results provided insights and guide the design of porous carbonaceous materials for energy sciences and environmental engineering.

9:35 AM *CH01.21.05

Commercializing Materials for Solution-Processable Near-Infrared and Short-Wave Infrared Photodiodes: Challenges and Solutions in Performance, Process and Production Hidenori Nakayama, Yasuo Miyata, Kazuhiro Mouri, Kazuhiro Nakabayashi and Shigeru Nakane; Mitsubishi Chemical Corporation, Japan

Solution-processed near-infrared (NIR) and short-wave infrared (SWIR) organic photodiodes (OPDs) hold great promise as they can offer higher external quantum efficiency (EQE) for infrared light detection compared to silicon-based photodiodes, at a lower cost than InGaAs-based alternatives. However, commercialization of these OPDs faces hurdles in materials development and device engineering. In this presentation, we discuss the challenges encountered during our decade-long research as a chemical company, dedicated to providing reliable organic semiconductor materials to the market. These challenges can be classified into three categories: lab-scale device performance, fabrication process, and industrial-scale production.

To meet demands for higher sensing performance, particularly higher EQE with suppressed dark current, we have developed novel materials for the photo-active layer (PAL) and the hole transport layer (HTL) positioned beneath it. The PAL consists of a blend of donor polymers and non-fullerene acceptors (NFAs) which absorb lights in the NIR and SWIR regions. An OPD designed for sensing NIR exhibited an EQE of 80% at 940 nm with $5 \times 10^{-6} \text{ mA/cm}^2$, while another OPD designed for sensing SWIR exhibited an EQE of 45% at 1100 nm with a dark current of $4 \times 10^{-5} \text{ mA/cm}^2$. We will present updates on the device performances. The achieved low dark current in these devices can be partly attributed to the material design of the HTL. The HTL comprises a polymer with thermal-crosslinking moiety, enabling a wider range of solvent choice for PAL deposition, eliminating the need for "orthogonal" solvents. The HTL contains no additives or catalysts for cross-linking, which ensures minimal contamination in both the HTL and PAL, preserving the desired hole mobility. This HTL design is also successfully applied to our organic light emitting diodes and organic/perovskite photovoltaics technologies.

Addressing the process-related requirements in the electronics industry, we optimized the ink formulations for the PAL and HTL without the use of halogenated solvents. These inks maintain

consistent device performance for over three months. When fabricating OPDs on CMOS readout circuits on a silicon wafer, spin-coating emerges as the preferred choice due to its widespread utilization in the semiconductor industry's patterning process. We have achieved successful spin coating of our HTL on an 8-inch silicon wafer with a thickness variation of less than 3 nm across the entire layer. The PAL inks have been optimized to prevent dewetting on the HTL and ensure a smooth coating on top. To withstand subsequent reflow soldering and encapsulation processes, the OPD-CMOS stacks are heated to at least 200°C. We will present various technologies implemented to avoid thermal degradation and crystallization of NFAs during the heating process.

As for manufacturing, stringent quality control measures are imperative for reliable commercial production. The organic semiconductor community widely recognizes the batch-to-batch variations in semiconductor performance using commercially-available or laboratory-made organic semiconductors. We will discuss our approach to address this critical issue.

10:05 AM CH01.21.06

Effect of Polymer Coating on Magnetocaloric Properties of Garnet¹JolaikhaSultana¹, Santosh KarkiChhetri², JinHu² and SanjayMishra¹; ¹The University of Memphis, United States; ²University of Arkansas, United States

Magnetocaloric materials can be applicable in magnetic cooling technologies, thermomagnetic motors, or medical treatments. For any practical applications, magnetocaloric materials are formed into various geometries, e.g., cylinders, plates, spheres, etc. Oxide-based MCE materials can be formed using high-temperature sintering or via mixing with polymers to increase the material's formability. Further, coating these particles with polymers is a practical and effective method for inhibiting their agglomeration. However, the effect of polymer coating on MCE oxide material is not well explored. Given the above, this study focuses on understanding the influence of polyvinylpyrrolidone (PVP) on Gd₃Fe₅O₁₂ garnet's structural, magnetic, and magnetocaloric properties.

The garnet Gd₃Fe₅O₁₂ samples were synthesized using the sol-gel auto combustion method. PVP coating of powder proceeds by adding 5% PVP (M_w -31000-50000) to a solution of 150 mg of Gd₃Fe₅O₁₂ nanoparticles suspended in distilled water. The presence of PVP was recorded via FTIR and TGA. The XRD studies showed that the PVP coating did not affect the crystal structure of Gd₃Fe₅O₁₂. However, the XRD peaks became slightly broadened and decreased in intensity after coating. The BET-specific surface area of nanostructured uncoated and PVP-coated Gd₃Fe₅O₁₂ oxides was determined to be 54.41 (m²/g) and 109.1 (m²/g), respectively. A marked increase in BET surface area is observed for the PVP-Gd₃Fe₅O₁₂ sample.

Magnetic measurements revealed that both coated and uncoated particles exhibited superparamagnetic behavior at 300K and 5K, respectively. The PVP-coated particles showed lower magnetization than the uncoated particles, attributed to reduced effective mass and degradation of particle dipole-dipole interactions caused by the non-magnetic PVP coating. Further pinning of surface spins via bonding with PVP molecules may extend deeper into the particle, reducing the effective magnetization of the compound. Magnetic entropy (-ΔSm) and the samples' relative cooling power (RCP) were determined from the isothermal magnetization M vs. H data at different temperatures. The results showed a considerable increase in the peak temperature (57.5K) for PVP-coated Gd₃Fe₅O₁₂ compared to the uncoated sample. The peak temperature of 57.5K corresponds to a significant alteration in the material's magnetic properties. The maximum value of magnetic entropy change (-ΔSm) for uncoated Gd₃Fe₅O₁₂ was determined to be 3.80 Jkg⁻¹K⁻¹ at 37.5K with a 5T applied field, accompanied by a relative cooling power (RCP) of 380 Jkg⁻¹. On the other hand, for PVP-coated Gd₃Fe₅O₁₂, the maximum -ΔSm was found to be 3.38 Jkg⁻¹K⁻¹ at 47.5K with a 5T applied field, and the RCP was 308 Jkg⁻¹. Indeed, the observed maximum magnetic entropy changes at higher temperatures for the PVP-coated Gd₃Fe₅O₁₂ sample are noteworthy. Further, there is an unnoticeable change in -ΔSm value with PVP coating. This characteristic indicates that the PVP-coated garnet may have an advantage in terms of usability over a wider temperature range compared to the uncoated counterpart, which can potentially be a promising material for applications in cryogenic temperature magnetic refrigeration.

SESSION CH01/CH02: Joint Virtual Session

Session Chairs: Liam Collins, Madeline Dukes, Rajiv Giridharagopal, Djamel Kaoumi, Philippe Leclere, Dongsheng Li and Yujun Xie
Wednesday Morning, December6, 2023
CH01-virtual

8:00 AM CH01/CH02.01

The Effect of Deposition Temperature and Oxygen Concentration on The Properties of NiO_x Films obtained by Sputtering: The Potential Use of NiO as Hole Transport Layers in Large-Area Perovskite Solar CellsWesleyC. Muscelli, Ana Paulad. Modesto, OtavioJ. de Oliveira, RafaelMerlo and FranciscoC. Marques; University of Campinas, Brazil

Perovskite solar cells are currently the most promising photovoltaic devices and have lately experienced extraordinary progress in efficiency and manufacturing technologies. The organic-inorganic perovskite with structure ABX₃ where A is typically methyl ammonium (MA), Formamidinium (FA) or Cesium (Cs); B is Pb or Sn; and X is Cl, Br or I, have recently emerged as an excellent class of semiconductors [1-3]. There are huge efforts to increase large-scale production of perovskite solar cells. One strategy is to develop the structure of the devices using physical techniques such as sputtering, thermal evaporation and atomic layer deposition. The sputtering technique has some advantages, as it is a well-known technique and already used to produce various materials in large areas. Among the materials used in the structure of perovskite solar cells, NiO has been proposed as a good option to replace Spiro-OMeTAD as a p-type layer for hole transport [2,3]. Here, we study the effect of O₂ partial pressure and temperature on the preparation of NiO_x films by reactive sputtering. The films were deposited on glass and silicon substrates, with a polarization voltage of 200 V, base pressure of 6.5 x 10⁻⁶ torr and deposition pressure in an argon plus oxygen atmosphere of 5.0 x 10⁻³ torr, using nickel target. The films were characterized by XRD, FTIR and Raman in order to investigate the structure of the NiO_x films. AFM and SEM were obtained to verify the morphology and surface roughness of the deposited films. The sheet resistance was obtained from the films deposited on glass substrate through the I x V curve using parallel coplanar contacts. EDS measurements were performed to estimate the composition of Ni and O atoms in the films. To evaluate the electrical properties, Hall Effect measurements were carried out on films. The sputtered NiO_x layers exhibit amorphous structure, high transmittance and uniform surface at low deposition temperature. The Tauc s band gap estimated for the film with the highest oxygen concentration is in agreement with the value for NiO reported in the literature [2,3]. The results indicate sputtered-deposited NiO as a promising candidate for hole transport layer in the production of large-area perovskite solar cells.

[1] Wang, R. et al. *Advanced Functional Materials*. v. 29, p. 1-25, 2019.

[2] Sun, H. et al. *A. Journal of the European Ceramic Society*. v. 39, p. 5285-5291, 2019.

[3] Awais, M. et al. *Surface & Coatings Technology*. v. 204, p. 2729-2736, 2010.

8:05 AM CH01/CH02.02

Properties of AZO Films Grown by ALD as a TCO for Perovskite Solar CellsAna Paulad. Modesto^{1,2}, DiegoG. Guzmán¹, RafaelMerlo¹, OtávioJ. de Oliveira¹, Thebano EmilioA. Santos² and FranciscoC. Marques¹; ¹Institute of Physics Gleb Wataghin, Unicamp, Brazil; ²Centro de Tecnologia da Informação CTI Renato Archer, Brazil

In recent years, aluminum-doped zinc oxide (AZO) has attracted much attention as a transparent conductive oxide (TCO) layer due to its high transmittance and low resistivity, which makes it an excellent candidate for various applications in optoelectronics, transparent photoelectric electronic devices, and in perovskite solar cells [1]. However, producing an AZO film with desirable electronic properties is still a challenge. Furthermore, the manufacture of perovskite solar cells in large areas still requires a lot of research, since all advances in the development of this type of cells have been obtained through the spin coating technique. As this technique does not allow the production of cells in large areas, it is necessary to develop cells with techniques compatible with production in large areas. Atomic Layer Deposition (ALD) is a relatively new technique that has been increasingly used in the study of perovskite solar cells, as it allows the production of films of high quality, homogeneity and conformal distribution on the substrate [2]. Therefore, in this work we studied the influence of aluminum concentration in zinc oxide on the optical and electronic properties of films deposited by ALD. Here, AZO thin film was deposited at 150°C employing trimethylaluminum (TMA), diethyl zinc (DEZ), and deionized water (DI) as precursors. DEZ and TMA were used as a source of metals (Zn and Al), while DI water was used as an oxidizing source to form AlZnO. The deposition consisted of 100 cycles, with each cycle having a pulse of the TMA precursor, a purge, a pulse of H₂O, a purge, following the same conditions as the DEZn precursor; and a purge. The films were characterized by UV-VIS to verify the optical properties of the films, profilometry to obtain the film thickness, and SEM to observe the morphology. From the optical data and film thickness, the refractive index (n) and band gap were calculated [3,4]. Electrical measurements were carried out using the Hall Effect measurement system, where resistivity, mobility and charge carriers' concentration were obtained. The ratio of Al:Zn pulses, which changes the aluminum concentration in zinc oxide, affected the measured optical and electrical properties. The results showed transmittance above 80%, optical gap between 3.3 to 3.8 eV, thickness of 153 to 196 nm. AZO films, deposited at relatively low temperature, have shown good electrical properties, making them promising TCOs in perovskite solar cells.

Acknowledgements:

BYD Energy Brazil, PADIS, FAPESP and CNPq.

References:

- [1] Van Toan, N., Tuoi, T.T.K., Inomata, N. *et al. Sci Rep* 11, 1204 (2021).
- [2] Hossain, Md. Anower, Khoo, Kean Thong, Cui, Xin, *et al. Nano Materials Science* 2 (3) 204-226 (2020).
- [3] Kunene, T. J., Tartibu, L. K., Ukoba, K., Jen, T-C. *Materials Today: Proceedings*. 62 S95-S109 (2022).
- [4] Zhao, K., Xie, J., Zhao, Y., Han, D., Wang, Y., Liu, B., Dong, J. *Nanomaterials*. 12 172 (2022).

8:10 AM CH01/CH02.03

Constructing High-Performance Solar Cells and Photodetectors with A Doping-free Polythiophene Hole Transport Material Junjiang Wu, Junwei Liu and Long Ye; Tianjin University, China

Over the past decades, there has been a growing interest in solution-based solar cells and photodetectors. Hole transport materials (HTMs) have played a critical role in advancing these electronics. However, the development of low-cost and efficient HTMs has not been satisfactory. In this study, we propose the use of poly(3-pentylthiophene) (P3PT) as a dopant-free polymeric HTM for quantum dot (QD) and perovskite electronic devices. P3PT offers a simple, low-cost and versatile solution. Compared to the commonly used poly(3-hexylthiophene), P3PT exhibits reduced molecular aggregation and preferential face-on orientation. These properties greatly enhance hole transport in optoelectronic devices. As a result, the photovoltaic performance of QD/polythiophene solar cells improves from about 8.6% to 9.5%, while that of perovskite/polythiophene solar cells increases from about 16% to 18.8%. These values are the highest reported in their respective fields. In addition, the use of P3PT HTMs significantly improves the photodetection performance of QD and perovskite photodetectors by a factor of about 3. This indicates the great potential of P3PT in various emerging optoelectronic applications.

8:25 AM CH01/CH02.04

Achieving Record-High Stretchability and Mechanical Stability in Organic Photovoltaic Blends with A Dilute-Absorber Strategy Saimeng Li and Long Ye; Tianjin University, China

Organic solar cells (OSCs) offer a unique advantage over other photovoltaic technologies in terms of flexibility. To realize high-performance stretchable and wearable OSCs, apart from high power conversion efficiency (PCE), they must also have excellent tensile properties and mechanical stability, whereas the present metrics of photovoltaic films can hardly meet the application requirements. The stretchability and mechanical stability of active layer blend films are crucial for intrinsically stretchable devices that can work effectively under stress. Herein, we put forward a facile yet low-cost strategy to construct intrinsically stretchable OSC active layers by introducing a readily accessible polymer elastomer as a diluent to the organic photovoltaic blends. Remarkably, record-high stretchability with fracture strain up to 1000% and mechanical stability with elastic recovery >90% under cyclic tensile tests are realized in OSC active layers for the first time. Specifically, the tensile properties of best-performance all-polymer photovoltaic blends can be increased by up to 250 times after blending. Previously unattainable performance metrics (fracture strain >50%, PCE >10%) are simultaneously achieved in the resulting photovoltaic films. Furthermore, an overall evaluation parameter γ is proposed for the efficiency-cost-stretchability balance of organic photovoltaic blend films. The γ value of our dilute-absorber photovoltaic system is two orders of magnitude greater than the prior state-of-the-art. With the help of advanced neutron scattering and X-ray scattering techniques, the microstructure-mechanical performance/stability relationships of intrinsically stretchable OSCs are established.

8:40 AM CH01/CH02.05

Deuterated Solvents Yield Organic Solar Cells with Enhanced Efficiency and Thermal Stability Kai Zhang; Tianjin University, China

The utilization of deuterium plays a crucial role in advancing the fundamental understanding of aggregate materials and their emerging functionalities. Specifically, resolving the solution structure of conjugated polymers becomes challenging in the absence of deuteration, particularly when employing solvents with high X-ray absorption coefficients such as chloroform. Nevertheless, there is a dearth of studies investigating the isotopic effects of casting solvents on the aggregated structures of photovoltaic polymers and their bulk-heterojunction blends. In this study, we presented a feasible and widely applicable approach of using deuterated organic solvents to establish the structure-performance relationships of organic solar cells (OSCs). We also unraveled the isotope effect of casting solvents on photovoltaic polymer systems from the aspects of thermal properties, molecular stacking, morphology, and device performance. This is the first-ever report to showcase the potential of deuterated solvent in OSCs. Our findings highlight the pronounced impact of relatively poor miscibility between deuterated solvents and photovoltaic polymers, which leads to an enhanced π - π stacking order. Furthermore, the utilization of deuterated solvents in film processing facilitates higher crystallinity and optimized morphology, resulting in improved device efficiency and notable enhancement in thermal stability. These results underscore the significance of solvent isotopic effects on the aggregated structure of conjugated polymer systems and unveil the potential of innovative approaches for fabricating high-efficiency solar cells with enhanced thermal stability.

8:55 AM CH01/CH02.06

Thermal Dynamics of Graphene-Seals Hjalte Ambjørner; Technical University of Denmark, Denmark

Hjalte R. Ambjørner¹, Anton S. Bjørnlund¹, Tobias G. Bonczyk², Edwin Dollekamp², Lau M. Kaas¹, Sofie Colding-Fagerholt¹, Kristian S. Mølhav³, Christian D. Damsgaard³, Stig Helveg¹, Peter C. K. Vesborg^{1,2*}

¹Center for Visualizing Catalytic Processes (VISION), Department of Physics, Technical University of Denmark, DK-2800 Kgs. Lyngby, Denmark

²Surface Physics and Catalysis (SURFCAT), Department of Physics, Technical University of Denmark, DK-2800 Kgs. Lyngby, Denmark

³National Centre for Nano Fabrication and Characterization (Nanolab), Technical University of Denmark, DK-2800 Kgs. Lyngby, Denmark

Electron microscopy studies of dynamic processes in technological relevant gas environments have advanced considerably. Such *in situ* and *operando* observations can nowadays be obtained with atomic-scale resolution by confining the reactive environments between thin, electron-transparent membranes (1-2). While Si-based membranes are widely used, their several-nanometer-thicknesses impact the electron microscopy data and hamper quantitative image interpretations at the atomic-scale. To suppress this footprint of the membranes, it would be desirable to employ two-dimensional materials, such as graphene, that represent the thinnest imaginable membrane with nearly ideal molecular impermeability (3). In practise, however, graphene must be supported by solid substrates which establish graphene-substrate interfaces that compromise the impermeability of the graphene-seal (3-6).

Here, we provide a kinetic study of the gas leakage from SiO₂-based cavities sealed by few-layer-graphene (5-6). Specifically, we focus on electron energy loss spectroscopy (EELS) measurements to unambiguously probe the Ar content of sealed cavities as a function of time and temperature. The EELS data show that the gas content decreased exponentially with time and that the temporal decay constant followed an Arrhenius-like temperature dependency with an apparent activation energy on the order of 0.4 eV. Thus, these findings indicate that gas diffusion along the graphene-SiO₂ interface is a thermally activated process. Surprisingly, successive heating cycles of the cavities modified the Arrhenius dependency and reduced the Ar leakage at room temperature considerably, with up to six orders of magnitude as compared to leak-rates equivalent to those reported in literature. Thus, the thermal dynamics of the graphene-seals can be used to engineer the interface leakage and perfect two-dimensional materials as electron-transparent windows in miniaturized reactors for *in-situ* electron microscopy (6).

J.F. Creemer *et al.*, *Ultramicroscopy* **108**, 993 (2008).

S.B. Vendelbo *et al.*, *Nat. Mater.* **13**, 884 (2014).

J.S. Bunch *et al.*, *Nano Lett.* **13**, 2458 (2008).

P.Z. Sun *et al.*, *Nature* **579**, 229 (2020).

Y.X. Liu *et al.*, *J. Phys. Chem.* **157**, 191101 (2022).

H.R. Ambjørner *et al.*, submitted (2023).

9:10 AM CH01/CH02.07

In Situ Ion Irradiation Study of Hollandite Ceramics Waste Forms Yuhang Li¹, Lumin Wang¹, Tao Ma¹, Kai Sun¹, Kyle S. Brinkman² and Jake Amoroso³; ¹University of Michigan, United States; ²Clemson University, United States; ³Savannah River National Laboratory, United States

The ceramic materials with the structure of hollandite mineral have been proposed to serve as the nuclear waste form to host radionuclides (e.g., Cs) in the high-level nuclear waste (HLW) due to high waste loading capacity and excellent chemical durability. Radiation effects of a series of Ba_{1.33-x}Cs_xFe_{2.66-x}Ti_{5.34+x}O₁₆ hollandite (x = 0, 0.1, 0.667, and 1.33) were evaluated for their potential application as waste forms for both fission products (e.g., Cs) and transuranic elements (e.g., Pu and Am).

200-300 keV electrons were used to simulate the effects of ionizing radiation by beta- and gamma-decay of Cs, and 1.2 MeV Kr ions were used to simulate the effects of displacement damage caused by alpha-decay of the transuranic elements. Atomic resolution transmission electron microscopy (TEM) with elemental mapping was used to characterize the material before irradiation. *In situ* TEM was conducted during both electron and ion beam irradiations. *Ex situ* ion irradiation experiment with 8 MeV Fe³⁺ ion was conducted on bulk Ba- and Cs-hollandite samples and cross-section TEM images were captured with depth dependence.

The results are analyzed and evaluated comparing to the radiation tolerance of other potential ceramic waste forms, and to the doses that might be received in the required service times of waste forms with various level of loadings of different radionuclides.

SYMPOSIUM CH02

Advances in In Situ TEM Characterization of Dynamic Processes in Materials
November 27 - November 29, 2023

Symposium Organizers

Madeline Dukes, Protochips, Inc.
Djamel Kaoumi, North Carolina State University
Dongsheng Li, Pacific Northwest National Laboratory
Yujun Xie, Shanghai Jiao Tong University

Symposium Support

Silver

Bestron (Beijing) Science and Technology Co., LTD.

Bronze

Bruker
Protochips

* Invited Paper

+ JMR Distinguished Invited Speaker

SESSION CH02.01: Electrochemical Reactions
Session Chairs: Qian Chen and Jungwon Park
Monday Morning, November 27, 2023
Sheraton, Third Floor, Berkeley

10:30 AM *CH02.01.01

Operando Electrochemical Liquid-Cell STEM at Energy Materials Interfaces Yao Yang¹, David A. Muller², Hector D. Abruna² and Peidong Yang¹; ¹UC Berkeley, United States; ²Cornell University, United States

One of the outstanding grand challenges facing energy materials is to directly resolve the complex nature of active structures and capture real-time “movies” of reaction dynamics under operating conditions. The need for such fundamental understanding has stimulated the development of *operando/in situ* methods, which have greatly enhanced our ability to establish *operando* (operating) structure-property relationships of energy materials.

In this presentation, I will introduce our recent progress on developing *operando* electrochemical liquid-cell scanning transmission electron microscopy (EC-STEM), which simultaneously enables quantitative electrochemistry on microelectrodes and quantitative STEM based imaging, diffraction and spectroscopy. *Operando* electrochemical 4D-STEM in liquid has shown great potentials to interrogate complex structures of active sites of energy materials at solid-liquid interfaces. In particular, I will introduce two examples on dynamic Cu underpotential deposition at nanocrystal surfaces and counterintuitive cathodic (reductive) corrosion processes. I will present my latest work on multimodal *operando* studies of combining EC-STEM and correlative synchrotron based X-ray methods to elucidate the longstanding enigmatic nature of Cu active sites as Cu nanograins for selective CO₂ electroreduction.

References:

1. Yang, Y., Muller, D., Abruna, H. Yang, P. et al. *Operando* Studies Reveal Active Cu Nanograins for CO₂ Electroreduction. *Nature* 2023, 614, 262.
2. Yang, Y., Muller, D., Abruna, H. Elucidating Cathodic Corrosion Mechanisms with *Operando* Electrochemical Transmission Electron Microscopy. *J. Am. Chem. Soc.* 2022, 144, 15698.
3. Yang, Y., Muller, D., Abruna, H. et al. Metal Monolayers on Command: Underpotential Deposition at Nanocrystal Surfaces: A Quantitative *Operando* Electrochemical Transmission Electron Microscopy Study. *ACS Energy Lett.* 2022, 7, 1292.
4. Yang, Y., Yang, P. et al. *Operando* Resonant Soft X-ray Scattering Studies of Chemical Environment and Interparticle Dynamics of Cu Nanocatalysts for CO₂ Electroreduction. *J. Am. Chem. Soc.* 2022, 144, 8927.

11:00 AM *CH02.01.02

Advanced Liquid Phase TEM for Nanoscale Investigation of Electrochemical Interfaces Jungwon Park; Seoul National University, Korea (the Republic of)

Solid-solid and solid-liquid interfaces are key components for diverse systems of electrocatalytic chemical conversion and rechargeable battery. Critical electrochemical reactions at the diverse interfaces in those systems occur at the nanometer length scale. Despite the importance of the interfacial reactions, a lack of analytical tools that can characterize structural changes at the nanoscale level has hindered fundamental mechanistic understanding of them. The recent development of liquid phase transmission electron microscopy (LPTEM) is gaining attention as a new tool to directly observe electrochemical reactions that occur in solid-solid and solid-liquid interfaces with high resolution. Here, we introduce a few examples where liquid phase TEM, in conjunction with other in situ characterization techniques, directly reveals important reactions at the interfaces of electrocatalysts and the electrolyte. Special efforts have been made to improve LPTEM as a reliable method for monitoring electrochemical process of supported metal catalysts in a condition of minimized electron beam perturbation. With this approach, LPTEM can successfully reveal how supported catalysts respond to electrochemical cycles in nanoscale spatial resolution. In situ observation based on LPTEM is also extended to investigation of important processes occurring at the electrode surfaces of diverse battery systems. Direct in situ TEM observation discloses the gradual growth of toroidal Li₂O₂ discharge product in the electrolyte with the redox mediator upon discharge in Li-air battery. The liquid phase TEM with electrochemical biasing capability is also applied to the studies of direct Li deposition on the metal electrode in Li metal battery system. Combined with cryo-TEM, it is found that the kinetics of Li deposition is determined by the mechanical and chemical properties of SEI, formed differently depending on the electrolyte.

11:30 AM CH02.01.03

In Situ TEM Characterization of Dislocation Dynamics in ZnS Under an Electric Field Yu Zhou; University of Toronto, Canada

Dislocation motion, an important mechanism underlying crystal plasticity, is critical for the hardening, processing, and application of a wide range of structural and functional materials. For decades, the movement of dislocations has been widely observed in crystalline solids under mechanical loading. However, the goal of manipulating dislocation motion via a non-mechanical

field alone remains elusive. Here we present real-time observations of dislocation motion controlled *solely* by using an external electric field in single-crystalline zinc sulfide (ZnS) – the dislocations can move back and forth depending on the direction of the electric field. We reveal the nonstoichiometric nature of dislocation cores and determine their charge characteristics. Both negatively and positively charged dislocations are directly resolved, and their glide barriers decrease under an electric field, explaining the experimental observations. This study provides direct evidence of dislocation dynamics controlled by a non-mechanical stimulus and opens up the possibility of modulating dislocation-related properties.

[1] Li M. et al. Nature Materials (2023) <https://www.nature.com/articles/s41563-023-01572-7>

11:45 AM CH02.01.04

Electrochemical Liquid Phase TEM for CO₂ reduction: The Role of Liquid Flow Configuration Cecilia Irene Gho^{1,2}, Katarzyna Bejtka^{1,2}, Marco Fontana^{1,2}, Stefan Merckens³, Andrey Chuvilin³ and Angelica M. Chiodoni¹; ¹Istituto Italiano di Tecnologia, Italy; ²Politecnico di Torino, Italy; ³CIC nanoGUNE, Spain

Recently energy transition, together with climate change issue, is raising a lot of interest in research due to the need to reduce the fossil fuels dependence in favor of more clean technologies. In this context are involved particular chemical reactions, allowing to convert abundant and waste gases into valuable products, as fuels or chemicals. These are mainly thermochemical or electrochemical processes and take place in the presence of a catalyst, which is a material containing active sites that weakly bind the reactants to provide them into the correct orientation to form the desired products. Among these reactions, CO₂ electro-reduction reaction in aqueous electrolyte is of particular interest because it allows the exploitation of a pollutant gas using green solvents.

In order to study the catalytic activity, including the identification of active sites, the reaction intermediates and the chemical path of reactions, *in situ* approaches have been developed for different characterization techniques. *In-situ* liquid-phase TEM (LP-TEM) is gaining more and more attention, as it allows to observe the evolution of the morphology and crystalline structure of materials in liquid environment, under electrical or thermal stimulus¹.

In particular, the miniaturized electrochemical cell used to perform the LP-TEM has some drawbacks especially when the applied potential of the experiments is strongly negative. Unfortunately, the potentials required to perform the majority of the electrochemical reactions, in particular CO₂RR, requires potential lower than -0.8 V vs RHE. At these voltages, the platinum forming the electrodes catalyzes the water splitting reaction, causing the production of gaseous hydrogen and oxygen, which aggregates forming bubbles. As the cell is miniaturized, the formation of these bubbles tends to fill the cell and de-wet the electrodes, thus blocking the electrochemical activity. The flow of electrolyte inside the cell is supposed to bring away these side products but it is too weak to force bubbles away, due to the non-optimal geometry of the today available commercial chips.

In this paper we present a novel chip configuration, a prototype optimized to provide better liquid exchange inside the cell and expected to bring faster the gaseous products away. This chip has been validated first under the optical microscope observation with the aid of ad-hoc top glass chips, to confirm that the optimized microfluidic pattern can favor the gas bubbles removal from the electrode surface. With the validated configuration, LP-TEM measurements have been positively performed, also with increased flow rates, where a preferential path for bubbles has been assessed. This ensures that electrodes are continuously wetted by electrolyte during experiments, being able to perform electroreduction reactions for longer time, even when opening the potential window and going to more negative voltages. As a proof of concept, the electrodeposition of Zn has been performed, which was reported not being feasible with standard commercial chips². This experiment confirms the good performance of the modified chips, with conditions similar to those used in literature², (e.g. 500 nA) and points out that the new geometry could be effective also for different electrochemical applications.

[1] Hwang, S. et al., **2020**, *Adv. Energy Mater.*, 10, 1902105

[2] Sasaki, Y. et al., **2021**, *J. Electrochem. Soc.*, 168, 112511

ACKNOWLEDGMENT

The authors would like to sincerely thank Protochips for providing the prototype chips for experimental flow tests. This work has received funding partly from the European Union's Horizon 2020 Research and Innovation Action programme under the Project SunCoChem (Grant Agreement No 862192) and partly by the European Union – NextGenerationEU under the Project iENTRANCE (Project code: IR0000027, Concession Decree No. 128 of 21/06/2022 adopted by the Italian Ministry of Research, CUP: B33C22000710006).

SESSION CH02.02: Crystal Growth, Assembly, and Transformation

Session Chairs: Qian Chen and Jungwon Park

Monday Afternoon, November 27, 2023

Sheraton, Third Floor, Berkeley

1:30 PM +CH02.02.01

Study of Nanoparticle Reaction Dynamics Through Integration of Liquid-Phase EM with 4D-STEM and Electron Tomography Qian Chen; University of Illinois at Urbana-Champaign, United States

Nanoscale spatial heterogeneity (e.g., in composition, solution structure, temperature) and reaction kinetics are interdependent in various systems. For nanocrystals, on one hand, they are the prevalent functional materials for diverse applications in bioimaging, photoemission, catalysis, energy storage, and mechanical and optical metamaterials. On the other hand, the reactions related to the synthesis and functions of nanocrystals, such as growth, corrosion, and catalysis, can all be affected by nanostructural heterogeneity. In this talk, we will discuss our recent efforts on the study of nanoparticle reaction dynamics. While liquid-phase TEM provides direct imaging of solution phase nanoparticle reactions (growth or etching) in real-space and real time at nanometer resolution, four-dimensional scanning transmission electron microscopy (4D-STEM) discerns spatial heterogeneities in the phase, crystal orientation, and molecular species. Electron tomography, on the other hand, reveals the three-dimensional (3D) morphology of nanocrystals. Its coupling with liquid-phase TEM allows us to track the complete reaction coordinate instead of only two-dimensional projections of reaction trajectories. Our work new opportunities to study nanoscale solution-phase reactions where structural heterogeneity is a crucial integrand, such as the synthesis and application of heterostructured nanocrystals (e.g., Janus, core-shell), understanding nanocrystal reactivity which is empirically found to be related to nanostructure and strain, and mapping of orientational dynamics of nanocrystals in bioimaging and self-assembly.

2:00 PM CH02.02.02

Assembly and Phonon Vibrations of Nanoparticle-Based Maxwell Lattice Chang Qian¹, Ethan Stanifer², Zhan Ma³, Binbin Luo¹, Lehan Yao¹, Chang Liu¹, Wenxiao Pan³, Xiaoming Mao² and Qian Chen¹; ¹University of Illinois at Urbana-Champaign, United States; ²University of Michigan–Ann Arbor, United States; ³University of Wisconsin–Madison, United States

Maxwell lattice is idealized frames with marginally constrained degrees of freedom. The interesting properties such as isoenergetic structural degeneracy and topological soft modes are of growing research interest. However, both experimental materialization and theoretical modeling in the nanoscale remained unexplored. Here, we report the realization of Maxwell lattice in the nanoscale for the first time. A mass-spring model considering interaction beyond nearest neighbors is purposed to capture the relaxation modes in different experimental conditions. We expect this work to provide a guideline for the materialization of Maxwell lattice.

2:15 PM CH02.02.03

***In-Situ* Observation of Nucleation and Growth of Nanocrystals In and Out of Equilibrium** Zuo Chen Wang, Chang Liu, Chang Qian and Qian Chen; University of Illinois Urbana-Champaign, United States

Crystallization, the emergence of order from disorder, is a ubiquitous process underpinning different fields across the length scales over four orders of magnitude, with ramifications of epitaxial growth for metallurgy and semiconductor industry, mineralization, protein crystallization, geometric packing in colloidal physics. These fields investigate the formation kinetics and thermodynamics of crystal nucleation and growth with an emphasis on the length scale that the building blocks follow. However, the building blocks at different length scale may sample distinct energy landscape, owing to the increased importance of external fluctuations for smaller sized units. Here, using liquid-phase transmission electron microscope (TEM), we observe nucleation and growth process of both gold nanoparticle superlattices driven by electric fields and atomic crystals utilizing CaCO₃ as a model system. With the aid of machine learning, we realize single nanoparticle tracking, through which a series of dynamic processes are unveiled, including formation, annealing and reconfiguration of such assembly using gold nanospheres. Further scaling down to atomic level, we combine liquid-phase TEM imaging with four-dimensional scanning transmission electron microscopy (4D-STEM) to decipher and quantify the morphology change from real space and phase evolution from reciprocal space during crystallization process. We discuss the differences and similarities of nucleation and growth behaviors in nanoparticle superlattice and atomic crystals, providing opportunities and guidance to engineering of crystallization pathways and thus allowing quality control of crystalline materials for next-generation applications.

2:30 PM BREAK

3:00 PM *CH02.02.04

Unveiling Atomic Pathways of Nanomaterials Transformations Using Liquid Cell Electron Microscopy HaimeiZheng^{1,2}; ¹Lawrence Berkeley National Laboratory, United States; ²University of California, Berkeley, United States

With our development of advanced high-resolution liquid cell transmission electron microscopy (TEM), we study the transformation pathways of nanomaterials at the atomic level. Nanoscale materials growth and transformations are often directed by defects, thus the transformation pathways may deviate from the thermodynamic predictions. For example, we found ripening of Cd-CdCl₂ core-shell nanoparticles is mediated by defects. Our observations revealed that the ripening was initiated by dissolution of the nanoparticle with an incomplete CdCl₂ shell. And, the growth of a nanoparticle was achieved by generating dislocations followed by crack defects in the shell, and ion diffusion through the cracks. The formation and annihilation of crack defects in the CdCl₂ shell, accompanied by disordering and ordering of the shell crystal lattice, allow for the core-shell nanoparticle ripening in the solution. In this talk, I present our most recent results on the unseen atomic pathways of nanomaterials transformations in liquid media.

3:30 PM CH02.02.05

Uncovering the Size-Dependent Thermal Solid Transformation of Akaganéite to Maghemite and Hematite XiangWang¹, XinZhang¹, YangHe^{1,2}, LiliLiu¹, LiborKovarik¹, MarkBowden¹, MarkEngelhard¹, YinggeDu¹, QuinMiller¹, ChongminN. Wang¹, JamesJ. De Yoreo^{1,3} and KevinM. Rosso¹; ¹Pacific Northwest National Laboratory, United States; ²University of Science and Technology Beijing, China; ³University of Washington, United States

Investigating the structural evolution and phase transformation of iron oxides is crucial for gaining a deeper understanding of geological changes on diverse planets and identifying oxide materials suitable for industrial applications. In this study, we employed in-situ heating techniques in conjunction with transmission electron microscopy (TEM) observations and ex-situ characterization to thoroughly analyze Akaganéite nanowires of varying sizes. Our findings offer compelling evidence for a size-dependent morphology evolution in Akaganéite nanowires, which can be attributed to the transformation from Akaganéite to Maghemite and subsequent crystal growth. Specifically, we observed that 50 nm Akaganéite nanorods transformed into hollow polycrystalline Maghemite nanorods, which demonstrated remarkable stability without arresting crystal growth under continuous heating. In contrast, smaller Akaganéite nanowires ranging from 20 to 8 nm displayed a propensity for forming single-crystal nanowires through phase transformation and densifying. Furthermore, we successfully captured the solid transformation of Maghemite to Hematite under vacuum heating conditions, suggesting a potential influence of orientation-dependent behavior on this transformation process. These significant findings provide new insights into the size-dependent structural evolution and phase transformation of iron oxides at the nanoscale, specifically in relation to diffusion-controlled crystal growth.

3:45 PM CH02.02.06

In Situ TEM Observation of Atomic Ordering in MnAl: Insights into Structural Transformation and Phase Evolution ChaoyaHan¹, BrianLejeune², XiaoyuZhang², ChaoyingNi¹ and LauraH. Lewis^{2,2}; ¹University of Delaware, United States; ²Northeastern University, United States

Rare-earth-free magnets, MnAl in particular, have gained increasing interest due to concerns related to critical mineral supply chains. MnAl orders into the distinctive atomically ordered tetragonal L1₀ structure, referred to as the τ -phase, that exhibits high magnetocrystalline anisotropy and other desirable magnetic characteristics. In this work, the technique of *in situ* heating transmission electron microscopy (TEM) is employed to understand L1₀ ordering in MnAl and associated formation of lattice defects. Additionally, effects of applied magnetic field on ordering, as supplied by the built-in magnetic field of the objective lens of the TEM, are also investigated.

MnAl samples were synthesized by rapid solidification under an argon atmosphere, resulting in polycrystalline thin ribbons comprising the precursor disordered ϵ -phase that possesses a hexagonal close-packed structure. Specimens for TEM investigation were prepared using a focused ion beam (FIB). The lift-off samples were mounted on a heating chip with temperature control provided by an *in situ* heating specimen holder. The *in situ* heating experiment was performed with a TalosTM F200C TEM operating at 200 kV, with additional post-heating observations conducted with TEM and with a spherical-aberration-corrected (S)TEM. To induce atomic order, the specimen was first heated from room temperature to 390 °C at 20 °C/min, held isothermally at 390 °C for 15 minutes, and then slowly cooled to room temperature.

Results indicate that atomic ordering initiates at grain boundaries at 365 °C and is completed in 8 minutes and 15 seconds after reaching at the isothermal treatment temperature of 390 °C in the magnetic field environment provided by the TEM pole-piece. The rate of ordering significantly decreases after the first 60 seconds since the start of the isothermal treatment at 390 °C. It is hypothesized that preexisting strain arising from the rapid solidification process promotes formation of the ordered phase from the disordered matrix phase. Atomic ordering is found to occur via a martensitic mechanism; strain introduced by this process may slow down the ϵ to τ phase transformation. The effect of magnetic field provided by the TEM objective lens on the phase transformation is still under investigation.

This work was supported by the U.S. Department of Energy, Office of Basic Energy Sciences under Award Number DE SC0022168. Technical support from Dr. Yong Zhao and Dr. Yuying Zhang, and the instrument use at the W. M. Keck Center for Advanced Microscopy and Microanalysis of the University of Delaware are greatly appreciated.

SESSION CH02.03: Electro-thermal Processes

Session Chairs: Yujun Xie and Yao Yang

Tuesday Morning, November 28, 2023

Sheraton, Third Floor, Berkeley

8:00 AM *CH02.03.01

Optimized Focused Ion Beam (FIB) Sample Preparation for High-Quality MEMS-Based In-Situ Electrical and Electro-Thermal (S)TEM Experiments VesnaSrot¹, RainerStraubinger², FelicitasPredel¹ and PeterA. Van Aken¹; ¹Max Planck Institute for Solid State Research, Germany; ²Protochips Inc., United States

We present a novel and optimized FIB-based methodology for preparing samples on micro-electro-mechanical-system (MEMS) chips, enabling in-situ electrical and electro-thermal experiments within a scanning transmission electron microscope ((S)TEM). The fabrication of clean, contamination- and damage-free, electron-transparent lamellae is crucial for successful transmission electron microscopy (TEM) experiments. While FIB instruments are commonly used for preparing standard TEM samples, they often introduce damage and contamination, affecting the measured electrical properties.

Our newly developed FIB sample-preparation routine minimizes attachment/detachment steps and reduces the use of Pt fixation, enhancing the reliability of in-situ electrical and electro-thermal measurements. We extensively characterized the impact of different sample preparation parameters and lamella geometries on electrical measurements. Single-crystalline silicon (Si) wafers were utilized for our experiments. Our approach involves directly fixing the extracted lamella to the E-chip without intermediate attachment steps to the grid, resulting in superior sample quality. We demonstrate this through high-resolution STEM imaging and analytical methods [1].

We investigated the influence of various parameters on the current-voltage characteristics. Firstly, we studied the effect of Pt contact size and position on the electrical characteristics. Samples with Pt contacts deposited over the lamella surface exhibited superior stability and reproducibility. Secondly, different incident Ga-beam energies were employed for Pt contact deposition. Lamellae fixed with Pt contacts at 30 kV showed cleaner surfaces and sharper edges, leading to distinct differences in electrical responses compared to those fixed at 8 kV. Lastly, we examined the effect of lamella thickness on electrical characteristics, revealing distinct resistance variations attributed to different volume and area cross-sections.

Our optimized FIB sample-preparation methodology, based on an alternative geometry for the lift-out procedure, enables the production of high-quality and mechanically stable FIB samples on MEMS-based chips for in-situ electrical and electro-thermal (S)TEM experiments. This approach is applicable to various materials amenable to regular FIB preparation [2].

[1] Srot V *et al.*, Microscopy and Microanalysis 29 (2023) 596-605. doi.org/10.1093/micmic/ozad004

[2] This project has received funding from the European Union's Horizon 2020 research and innovation programme under Grant Agreement No. 823717 – ESTEM3.

8:30 AM CH02.03.02

In Situ Heating and Biasing TEM Investigation of the Microstructural Evolution Occurring in Gold Nanogranular Films Showing Neuromorphic Behavior AndreaFalqui¹, AlbertoCasu¹, YuriIvanov², GiorgioDivitini², AngelicaM. Chiodoni³ and PaoloMilani¹; ¹University of Milan, Italy; ²Italian Institute of Technology, Italy; ³Italian Institute of Technology - CSFT@PoliTo, Italy

Nanogranular gold films prepared by supersonic cluster beam deposition, with thickness above the electrical percolation threshold, are well-known to show an overall neuromorphic behavior.

Indeed, they exhibit electrical features like those of biological neural networks, such as spiking and adaptation, and this makes them promising candidates for neuromorphic computing applications [1]. The current understanding for the phenomena underpinning such behavior is based on electrical measurements and speculative modelling. Thus, *in situ* heating and biasing transmission electron microscopy (TEM) imaging was performed, both in high resolution mode and at low magnification with high temporal resolution, to directly investigate what gives rise to the films' neuromorphic properties. Nanogranular gold films were deposited just above the percolation threshold, in order to ensure their electrical conductivity while keeping them sufficiently thin for TEM imaging. Upon overall *in situ* heating, the films de-percolated, i.e., they retracted their branched structure with no apparent mass loss. As a consequence, quite thick, well separated gold polycrystalline islands were formed over the whole heating substrate, a behavior resembling what previously reported for atom assembled films [2]. However, when subjected to sole *in situ* biasing in a two-electrode configuration, the thin, percolating films show electrical behavior quite similar to the thicker ones. Aiming at understanding what happened to the films morphology globally and locally, the whole area comprised between the biasing electrodes was imaged with high temporal resolution by a CMOS direct detection camera (Gatan K3) working with a limited dose rate, while the films were electrically stimulated first over a voltage ramp and then at constant voltage. Again, the main effect of the biasing is branches retraction, but in this case so spatially confined that the films undergo a very local de-percolation, thus with spatially limited rearrangement of their microstructure and concomitant formation of few, small and thick gold islands in the close, little areas involved. These results overall indicate a likely occurrence of extremely intense and local hot spots. Their temperature and extension are shown to increase with the applied voltage and can finally bring to local melting-dictated breaks of the amorphous silicon nitride constituting the deposition substrate of the films. Besides, further aspects still need to be investigated, such as, for instance, the possible determination of the temperature in the very local hot spots, and the chance of a not trivial concomitance of local heating by Joule effect and electromigration of gold atoms, which in previous studies have been indicated as possible physical mechanisms giving origin to the neuromorphic behavior of metal films. In any case, the *in situ* TEM imaging demonstrates its capability in providing new insights on the underlying physical phenomena giving rise to the unique electrical behavior of metal nanogranular films, with several implications for further developing of advanced materials with neuromorphic properties.

[1] M. Mirigliano, *et al.* Binary classifier based on a reconfigurable dense network of metallic nanojunctions. *Neuromorph. Comput. Eng.* **2021**, *1*, 024007A. DOI: 10.1088/2634-4386/ac29c9

[2] F. Niekiel, *et al.* The process of solid-state dewetting of Au thin films studied by *in situ* scanning transmission electron microscopy. *Acta Mater.* **2015**, *90*, 118. DOI: 10.1016/j.actamat.2015.01.072

8:45 AM CH02.03.03

***In-Situ* TEM Study of Breakdown and Thermal Annealing Effects on Silver Nanowire for Memristive Applications** Katarzyna Bejtko^{1,2}, Marco Allione¹, Gianluca Milano³ and Fabrizio Pirri^{1,2}; ¹Politecnico di Torino, Italy; ²Istituto Italiano di Tecnologia, Italy; ³INRiM Istituto Nazionale di Ricerca Metrologica, Italy

Ag nanowires (NWs) are of interest among others, for memristive applications, including neuromorphic architecture based on self-assembled nanowire networks [1]. In the device the nanowire undergoes breakdown and then the switching behavior is based on creation and rupture of the filament lying across a gap. The experimental *in situ* observation of the breakdown behavior and reconfiguration of the filament is of high interest as it could provide better understanding of the switching mechanisms in these nanoobjects. In this work, we investigate breakdown in single memristive Ag NWs, during voltage sweep stimulation, by *in-situ* TEM. Joule heating and electromigration are the two possible causes of fracture for metal wires during operation and *in-situ* observation sheds some more light on its mechanisms [2].

It is also of interest to investigate the temperature influence on the morphology and structure of the single NWs and of small networks of NWs. It was observed that the morphology of single Ag NWs starts changing at around 550 °C with observable creation of humps and valleys, which indicate surface roughening. Eventually the NWs break at even higher temperatures. Once the NW undergoes breakdown the change in morphology proceeds following the crystalline orientations of preference. We report on the investigation of local structural and morphological evolution over time as a function of the temperature both for the NWs themselves and within the nanogap appearing after the wire breakdown. We also shed some light on the temperature influence on the morphology of the AgNW junctions within nanowire networks.

ACKNOWLEDGMENT

Part of this work was supported by the European project MEMQuD, code 20FUN06. This project (EMPIR 20FUN06 MEMQuD) has received funding from the EMPIR programme co-financed by the Participating States and from the European Union's Horizon 2020 research and innovation programme.

REFERENCES

G. Milano *et al.* *Adv. Intell. Syst.* **2**, 2000096, 2020.
M. Batra *et al.* *Nanoscale* **11**, 3606, 2019.

9:00 AM *CH02.03.04

Atomic Resolved Mechanical Testing System and Approach of Synergy of High Strength yet Ductile Alloys Xiaodong Han; Beijing University of Technology, China

How to characterize and measure the interface phenomena on the microscopic level is one of the most fundamental questions [1]. We report here the development of mechanical-thermal-electrical functional instruments to accommodate characterizing and measuring of plasticity properties of intra-grain and inter-grain dislocation activities at microscopic level, particularly at nano and atomic scale with the sub-Å spatial resolution with time-resolved abilities [2]. By monitoring and measuring intra-grain and inter-grain plasticity at atomic level, it is discovered that: large angle unsymmetrical tilt grain boundaries slide by intrinsic dislocations climb and extrinsic disconnection slide [4]. The interactions of sliding extrinsic disconnections with intrinsic GB dislocations creates dislocation locks. The unlock and re-lock processes of the interacted GB dislocation-disconnection pairs accommodate GB sliding by GB atom transfers. For the TB, dislocations pin, pile up and cross-slip are directly revealed and uncovered. From these, new routes are proposed to develop advanced structural materials with synergy of high strength and ductility.

References:

[1] Exploration and Discovery (125 questions: How can we measure interface phenomena on the microscopic level?), SHJT-SCIENCE, 2021.
[2] JF Zhang, YR Li, XC Li, YD Zhai, Q Zhang, DF Ma *et al.*, *Nat. Commun.* **12**, 2218, 2021.
[3] LH Wang, Y Zhang, Z Zeng, H Zhou, J He, P Liu *et al.*, *Science*, **375**, 6586, 2022
[4] ZP Li *et al.*, *Materials Res. Lett.* **10**, 539-546, 2022.
[5] LH Wang, P Liu, PF Guan, MJ Yang, JL Sun *et al.*, *Nat. Commun.* **4**, 2413, 2013.
[6] Zibing An *et al.*, *Mater. Horizon* **8**, 948955, 2021

9:30 AM CH02.03.05

Single Nanocrystal Etching by 4D Graphene Liquid Cell Electron Microscopy Sungsu Kang^{1,2} and Jungwon Park^{1,2}; ¹Seoul National University, Korea (the Republic of); ²Institute for Basic Science, Korea (the Republic of)

Etching of nanocrystals is a process in which surface-exposed atoms on nanocrystals are detached in specific chemical environments, predominating the structures and properties of nanocrystals, and occurs ubiquitously when nanocrystals are applied in applications such as thermal catalysis, electrochemical energy conversion, and drug delivery. However, surface structures of chemically-etched nanocrystals can differ from those of the bulk due to the high population of less-coordinated surface atoms and their preferential detachment during the etching. Structural transformations such as surface strains and phase transitions are predominant in crystals as small as a few nanometers and may further affect the structures of nanocrystals during etching. Thus, the structural changes in nanocrystal surfaces during etching should be understood beyond the scope established for bulk crystals. Here, we introduce a new method for investigating the atomic structure changes of single nanocrystals in liquid, namely "4D Brownian one-particle reconstruction" method, using graphene liquid cell (GLC) electron microscopy. We applied this method to track the atomic structures of Pt nanocrystals during their etching in an oxidative liquid medium. The reconstructed time-resolved three-dimensional (3D) atomic maps reveal that the Pt nanocrystals undergo a transformation from the ordered face-centered cubic (fcc) to a disordered structure. The transformation initiates on the surface via emerging hexagonal closed packed (hcp)-like disordered states, stabilizing less-coordinated surface-exposed atoms during the etching.

9:45 AM BREAK

10:15 AM +CH02.04.01

Near Surface Solution Structure Controls the Oriented Attachment of Metal Nanoparticles—Reactive Molecular Dynamics[Kristen A. Fichthorn](#); The Pennsylvania State University, United States

Oriented attachment (OA) of nanoparticles has been recognized as a common mechanism for crystal growth, affecting the micro- and macroscale morphologies for a large variety of materials. However, the role of environmental constraints such as pH, temperature, and ionic concentration in controlling the pathways and kinetics of OA remains unaddressed, which makes it difficult to control and exploit OA syntheses to create unique materials. Experimental studies with *in situ* liquid-cell and *ex situ* transmission electron microscopy indicated that the solution pH affects the OA of Pt nanoparticles. With pH varying from ~3 -1.5, the attachment facet of Pt nanospheres switches from {001} to {111}. The initial {001} attachment of ~2-5 nm nanoparticles leads to the formation of nanocubes (~50-200 nm), and the subsequent {111} attachment results in the extrusion of Pt nanorods from the surface of the nanocubes. Using molecular dynamics simulations based on a ReaxFF reactive force field fit to results from quantum density-functional theory, we simulated the approach of two Pt nanocrystals in HCl and C₁₂ solution under conditions of relatively low and high pH. Our studies confirm the experimental findings and reveal the key role of solution environment in controlling OA.

10:45 AM CH02.04.02

How Do Nanofillers Influence the Glass Transition Temperature of Polymer Nanocomposites?: Insights from Local Characterizations of Interfacial Adsorption[Katelyn Randazzo](#)¹, [Sneha Srinivasan](#)¹, [Abraham Joshua](#)¹, [Daniele Cangialosi](#)², [Biao Zuo](#)³ and [Rodney Priestley](#)¹; ¹Princeton University, United States; ²Consejo Superior de Investigaciones Científicas - Universidad del País Vasco, Spain; ³Zhejiang Sci-Tech University, China

Polymers play a foundational role in shaping the modern world, with critical applications in healthcare, energy, and the environment. Their remarkable tunability affords avenues towards enhanced properties via the incorporation of a second phase. However, the consequences of introducing a second phase remain inadequately understood in several key aspects. Particularly, the effect of nanofillers on the glass transition temperature (T_g) of polymer nanocomposites remains unclear, with conflicting reports observing T_g enhancement, depression, or no perturbation. The underlying cause of these inconsistencies is unclear because conventional characterization techniques lack spatial resolution, preventing a comprehensive understanding of how nanofillers influence local polymer properties and, consequently, the overall system behavior.

One route towards understanding the phenomenon of perturbed T_g in nanocomposites is glassy physics. It has been reported in the framework of glassy physics that polymers annealed at elevated temperatures can irreversibly adhere to adjacent substrates, thereby forming adsorbed polymer layers. Once considered "dead" due to restricted chain conformations, adsorbed layers are now recognized as regions of active dynamics, as revealed by the occurrence of a glass transition in adsorbed 2D nanofilms. Conventional investigations of 2D adsorbed nanofilms are limited in their ability to distinguish perturbations between the substrate interface and the free interface, but these studies highlight the important implications of irreversible adsorption in polymer nanocomposites. Polymer nanocomposites are routinely prepared via high-temperature annealing and feature a large interfacial area. Accordingly, it can be expected that they feature a significant degree of overall chain adsorption at the polymer-nanofiller interface. Nevertheless, conventional techniques pose technical obstacles to understanding the evolution and impact of irreversibly adsorbed layers in nanocomposites, as approaches such as bulk differential scanning calorimetry provide data averaged across the entire system.

In this study, we present a novel and comprehensive approach that overcomes the limitations of conventional techniques, thereby allowing us to characterize the structural evolution and glassy properties of nanocomposites' adsorbed layers. Our approach leverages a stepwise assembly of nanocomposites: Nanoparticles are well dispersed within a polymer matrix, then annealed for various durations to induce interfacial adsorption from the matrix. Subsequent isolation of these nanoparticles allows for direct investigation of the adsorbed polymer structure through low-dose cryo-TEM imaging. Furthermore, by incorporating covalently attached fluorescent and dielectric labels into the adsorbed polymer, we can reintegrate them into an analogous unlabeled polymer matrix. This integration enables targeted in-situ measurements of the adsorbed layer properties within the nanocomposite. Importantly, our approach unravels the intricate relationships between local structure and properties in nanocomposites, elucidating the role of processing conditions that give rise to interfacial adsorption—an often overlooked factor with significant explanatory power for resolving discrepancies in the literature and for advancing material design strategies.

11:00 AM CH02.04.03

Direct Observation of Atomic Step-Assisted Stabilization of Polar Oxide Surface[Zhipeng Wang](#)¹, [Jinho Byun](#)², [Jaekwang Lee](#)³ and [Sang Ho Oh](#)²; ¹Sungkyunkwan University, Korea (the Republic of); ²Korea Institute of Energy Technology, Korea (the Republic of); ³Pusan National University, Korea (the Republic of)

Polar surface is intrinsically unstable and thus highly reactive due to the uncompensated surface charges. The charge compensation is accompanied by various surface reconstructions, establishing novel functionality for its applications. Our in-situ atomic-scale electron microscopy study directly shows that the atomic step and step-assisted reconstruction play central roles in the charge compensation of polar oxide surface. The flat (LaO)⁺-terminated LaAlO₃ (001) polar surface, when annealed at high temperature in vacuum, transits to the (015) vicinal surface via the dynamic motion and interaction of atomic steps. While the (015) vicinal surface possesses zero polarization along the surface normal, the thermodynamic ground state is achieved when the in-plane polarization is fully compensated via the reconstruction of step edge atoms; the step edge La atoms are displaced from their ordinary atomic sites toward the adjacent Al step edge site, resulting in the formation of negatively charged La vacancy at the corresponding step edges. As confirmed by first-principles calculations, the observed step reconstruction of (015) vicinal surface can completely cancel both out-of-plane and in-plane electric fields. This hitherto unknown mechanism reveals the central role of step reconstruction in stabilizing polar surfaces, providing valuable insights for understanding the novel charge compensation mechanism accompanied by the step reconstruction.

11:15 AM CH02.04.04

Surface Dynamics of Hf- and Zr- based Thin Films During Oxidation Studied with *In Situ* STEM and SEM to Guide the Design of Innovative Electronic Devices[Alexandre Foucher](#), [Wouter Mortelmans](#), [Rafael Jaramillo](#) and [Francesca M. Ross](#); Massachusetts Institute of Technology, United States

Transition metal dichalcogenides (TMDs) are increasingly under scrutiny for their implementation in novel nanodevices. More specifically, Hf- and Zr-based TMDs (HfS₂, ZrS₂, HfSe₂, and ZrSe₂) are promising materials for field-effect transistors. To that end, it is advantageous to oxidize the surface of the thin films to form an HfO_x or ZrO_x layer and ultimately obtain an oxide/TMD interface that will be crucial for next-generation nanodevices. However, the exposed surface's oxidation mechanism and structural changes have not been described in sufficient details for controlling the interface in these applications. In this work, *in situ* scanning transmission electron microscopy (STEM) analysis was simultaneously performed with *in situ* scanning electron microscopy (SEM) imaging. We show the impact of oxidation treatment parameters (temperature and pressure) on the ability to obtain a smooth and uniform oxide layer. We find that the surface of the oxide layer is smooth and homogeneous after a harsh oxidative treatment at low pressure. We also demonstrate that HfS₂ and ZrS₂ surface de-sulfurization occurs when the samples are oxidized. In contrast, segregation of Se in HfSe₂ and ZrSe₂ was observed upon oxidation, which explains the high compositional heterogeneities and leads to challenges in the control of the surface morphology. These structural changes provide valuable insights for designing a controlled oxide/TMD interface with high surface smoothness and will guide the improvement of efficient and stable nanostructures for electronic devices.

11:30 AM CH02.04.05

Insights into Nanoscale Adhesion via *In Situ* Transmission Electron Microscopy[Andrew Baker](#), [Sai Vishnuhotta](#), [Sanjana Karpe](#), [Yahui Yang](#), [Götz Veser](#) and [Tevis Jacobs](#); University of Pittsburgh, United States

Adhesion governs the performance of material interfaces, from large-scale applications such as the energy loss in an automobile engine to small-scale applications such as the stability of nanoparticles. An emerging technique for investigating nanoscale adhesion is performing nanoscale contact-and-separation tests via *in situ* transmission electron microscopy. In this work, we used this technique to reveal fundamental principles of nanoscale adhesion. First, we showed that nanoscale adhesion is governed primarily by strength-limited separation, rather than by fracture as previously believed. Here our adhesion tests of nanoscale contacts demonstrated the need for a different paradigm in interpreting nanoscale adhesion data. Next, we measured the nanoscale adhesion of noble-metal nanoparticles to their oxide supports, a critical parameter related to the efficiency and lifetime of nanoparticle technologies. In addition to validating our measurements with reported trends in adhesion energy, the flexibility of our technique enabled the characterization of new combinations of nanoparticles and supports. Finally, we demonstrated that the adhesive strength between a nanoparticle and its support is highly sensitive to the properties of the nanoparticles such as composition and size. Together, these results enable new fundamental insight into nanoscale adhesion that will inform the design of emerging technologies.

1:30 PM *CH02.05.01

Grain Boundary Migration, Triple Junction Dynamics, and Atomic-Scale Grain Rotation Mechanisms in Polycrystalline Materials: Insights from Novel TEM Studies [Xiaoqing Pan](#); University of California, United States

Grain boundary migration, triple junction dynamics, and grain rotation are fundamental phenomena that profoundly influence the properties and behavior of polycrystalline materials. Understanding the mechanisms driving these processes is crucial for advancing materials science and engineering. This abstract presents two significant studies, shedding light on the intricate dynamics of grain boundary and triple junction migration, as well as the atomic-scale mechanisms underlying grain rotation.

The first study focuses on disconnection-mediated twin/twin-junction migration. By employing a combination of in situ high-resolution transmission electron microscopy (HRTEM) observations, molecular dynamics (MD) simulations, and disconnection theory, we investigate the coupling effect of grain boundary motion through disconnection motion and reactions at and adjacent to triple junctions. Specifically, we analyze twin/twin-junctions composed of coherent twin boundaries (CTBs) and a $\Sigma 9$ grain boundary in copper. Experimental and simulated results reveal multiple modes and local mechanisms for CTB migration, including motion through pure steps driven by a chemical potential jump and stress-driven migration involving disconnections with non-zero Burgers vectors. Furthermore, we observe distinct migratory behaviors of different triple junction types, providing valuable insights into the coupling dynamics at these interfaces.

The second study focuses on the direct observation of atomic-scale grain rotation mechanisms. Utilizing in situ and four-dimensional scanning transmission electron microscopy with atomic resolution, we uncover compelling evidence of grain rotation taking place through the propagation of disconnections along grain boundaries in polycrystalline materials. The propagation of disconnections induces shear displacement across the grain boundary, correlating with grain boundary migration and grain rotation. These findings highlight the critical role of disconnections, analogous to dislocations in crystals, in determining the behavior of polycrystals. The observed mechanisms offer new quantitative insights into polycrystal dynamics, impacting grain growth kinetics, deformation mechanisms in nanocrystalline solids, and texture evolution.

Collectively, these studies provide significant advancements in our understanding of grain boundary migration, triple junction dynamics, and atomic-scale grain rotation mechanisms in polycrystalline materials. The insights gained from these investigations have broad implications for materials science, enabling the design and development of advanced materials with tailored properties for various applications.

2:00 PM CH02.05.02

Dynamic Changes in Intermetallic CuPt Catalysts Studied with *In Situ* Gas-Heating STEM-EELS Analysis at 1 Bar [Alexandre Foucher](#)¹, Daniel J. Rosen², Shengsong Yang², Christopher B. Murray², Anatoly Frenkel³ and Eric A. Stach²; ¹Massachusetts Institute of Technology, United States; ²University of Pennsylvania, United States; ³Stony Brook University, The State University of New York, United States

It is crucial to develop and understand innovative nanocatalysts to improve the efficiency of major catalytic processes and reduce their cost. Intermetallic CuPt has been reported as a promising material as a catalyst for CO oxidation, but changes in structure in a reactive environment at high pressure and temperature are not well described. In this work, we performed an atomic scale *in situ* scanning transmission electron microscopy (STEM) analysis at 1 bar to track changes in the intermetallic CuPt phase upon oxidation and reduction. These conditions mimic the reactive environment when the CuPt particles are used for catalyzing CO molecules. The atomic structure of the intermetallic phase remained primarily unchanged in 1 bar of O₂ or H₂ at 800 °C, which explains the remarkable stability of the sample. *In situ* STEM-EELS showed some light oxidation of Cu on the edges of particles upon exposure to O₂ at 800 °C, which can be entirely re-reduced after treatment in H₂ at 800 °C. Thus, partial segregation and oxidation of Cu occur in an oxidative environment but remain limited and can be reversed through annealing. *In situ* XAS confirms the STEM-EELS results observed and shows that segregation and oxidation of Cu is a generalized trend not limited to the small number of particles studied with in situ STEM. Determining dynamic restructuring effects in CuPt catalysts is valuable information for the improvement and rational design of novel bimetallic catalysts.

2:15 PM BREAK

2:45 PM CH02.05.03

***In-Situ* Liquid TEM Studies of Cu₂O-SnO₂ Catalysts during Carbon Dioxide Reduction Reaction** [Katarzyna Bejtka](#)^{1,2}, [Marco Fontana](#)^{1,2}, [Cecilia Irene Gho](#)^{1,2}, [Alberto Lopera López](#)³, [Maria José López Tintero](#)³, [Simelys Hernández](#)², [Hilmar Guzmán](#)² and [Angelica M. Chiodoni](#)¹; ¹Istituto Italiano di Tecnologia, Italy; ²Politecnico di Torino, Italy; ³Laurentia Technologies, Spain

The production of carbon-based chemicals and fuels by exploiting anthropogenic CO₂ is nowadays a topic of huge attention within the scientific community. Recently, CO₂ concentration in the atmosphere have exceeded 410 ppm, and its growth has remained constant since the 50s [1]. An advantageous method to reduce its concentration is to consider it as a valuable raw material for electrochemical reduction. Its reduction can result in value-added products and among many products that can be obtained, which depend on the catalyst characteristics, reaction conditions and electrolyte, the CO₂ reduction reaction (CO₂RR) to carbon monoxide (CO) or formic acid (HCOOH) are up to now the economically most viable processes and can challenge conventional production routes [2]. Renewable and green approaches to CO₂ valorisation are aimed to minimize the worrying impact of its emission to the environment, and to drive the transition to a new circular economy approach in chemistry and energy production.

In this framework, efficient but abundant and inexpensive catalysts for the electroreduction of CO₂ are required. Among them, non-precious metal oxides like Cu₂O and SnO₂ can catalyze both CO or HCOOH. In addition, copper-based catalysts enable CO₂-to-multicarbon product (C₂+) conversion.

Here, we present an in-situ liquid phase transmission electron microscopy (LP-TEM) investigation of the morphological and structural dynamics during the life cycle of Cu₂O-SnO₂ catalysts for the CO₂ electroreduction to syngas, exploiting a Protochips Poseidon TEM electrochemical holder. The catalysts are prepared by wet precipitation, and the oxides formed have the shape of nanocubes and nanoparticles. For the LP-TEM, a dispersion of the catalyst in ethanol is drop casted on a Glassy Carbon working electrode in a microchip-based electrochemical set-up. This chip, together with an optimized prototype second chip, provided by Protochips, are used to compose the electrochemical cell. The catalyst was studied in 0.1M KHCO₃ saturated with CO₂. The electrochemical activity for the CO₂ reduction reaction was tested by means of Linear Sweep Voltammetry (LSV) and Chrono Amperometry (CA) analyses. In-situ LP-TEM helped to shed light on the changes the material undergoes during electrocatalytic activity, and thanks to improved cell we have been able to study this catalyst in relatively wide range of potentials, which are close to those of interest for the applications, even as low as -2.0V vs. Pt. The obtained results on the catalysts are of huge interest from the fundamental point of view, and, in addition, the optimised design of the LP flow TEM cell allowed to perform stability tests, which are of huge interest for the future application of these catalysts in real devices.

ACKNOWLEDGMENTS

The authors would like to sincerely thank Protochips for providing the prototype chips for the catalysts testing.

This work has received funding from the European Union's Horizon 2020 Research and Innovation Action programme under the Project SunCoChem (Grant Agreement No 862192).

[1] X. Lan et al., (2020). Atmospheric composition in: State of the Climate in 2018, Chapter 2: Global Climate.

[2] M. Jouny et al., General Techno-Economic Analysis of CO₂ Electrolysis Systems. Ind. Eng. Chem. Res. 2018, 57, 2165–2177.

3:00 PM CH02.05.04

Atomic-Scale Understanding of Cu-Ni Alloy Oxidation using *In-Situ* ETEM with Advanced Data Quantification [Meng Li](#)¹, [Jack G. McEver](#)^{1,2}, [Wissam A. Saidi](#)^{1,3} and [Judith C. Yang](#)^{1,2}; ¹University of Pittsburgh, United States; ²Brookhaven National Laboratory, United States; ³U.S. Department of Energy National Energy Technology Laboratory, United States

Understanding the complex interplay between multiple oxidizing alloy elements during oxidation is critical for fundamental understanding of alloy oxidation. Cu-Ni binary alloys, despite their wide industrial applications of Cu-Ni alloy, also serve as valuable model materials for studying binary alloy oxidation due to the mutual solubility of Cu and Ni and the non-mutual solubility of the formed oxides. In this study, we used in situ Environmental Transmission Electron Microscopy (ETEM) with advanced data quantification to investigate the initial oxidation processes of CuNi alloys and compared it with that of pure Cu [1-2].

Using a state-of-the-art in situ ETEM setup (Hitachi H9500), we examine the oxidation behavior of single-crystalline CuNi(100) alloy thin films at 300 C, under controlled O₂ gas pressure ranging from 0.1 to 1 mTorr. At atomic resolution, we observed the competing oxidation process of CuNi alloy. Specifically, we observed the nucleation and growth of NiO nano islands, followed by secondary nucleation and growth of Cu₂O nano islands are observed. Compared with the oxidation of pure Cu, the addition of Ni not only leads to the formation of NiO islands, but also altered the growth dynamics of Cu₂O islands. These observations highlight the complex dynamics during alloy oxidation. To elucidate the underlying mechanisms, correlated DFT simulations are performed, providing further insights into the role of Ni in the oxidation process.[3]

To further quantify the experimentally observed data, machine-learning enhanced advanced data analysis tools are developed. Currently, we are training neural networks to segregate and

quantify the Cu₂O and NiO islands, enabling more precise interoperation of the oxidation process. These innovative data analysis methods not only enhance our understanding of alloy oxidation but also hold potential for broader applications in *in situ* TEM studies.

In summary, our *in situ* ETEM study provides insights into the competing oxidation mechanisms in CuNi alloys and the impact of Ni on the oxidation behavior. The advanced data analysis tools developed in this work allow for a quantitative analysis of the experimental results, further deepening our understanding of alloy oxidation processes. These findings contribute to the fundamental knowledge of alloy oxidation and pave the way for future research in related fields.[4]

References

1. Li, M. *et al. Nano Lett.* **22**, 1075–1082 (2022).
2. Li, M. *et al. Nat. Commun.* **12**, 2781 (2021).
3. Garza, R. B. *et al. J. Chem. Theory Comput.* **18**, 4447–4455 (2022).
4. The authors acknowledge the funding support from NSF-CMMI-1905647.

3:15 PM CH02.05.05

Oxide Reduction Continuously Quantified in Real Time by EELS and EDS Mapping Benjamin Miller and Liam Spillane; Gatan, Inc., United States

In-situ (scanning) transmission electron microscopy (S)TEM or *in-situ* TEM imaging are powerful techniques for observing the dynamics of oxidation and reduction reactions at the smallest scales. Many researchers combine these imaging techniques with spectroscopic characterization using electron energy-loss spectroscopy (EELS) or energy dispersive x-ray spectroscopy (EDS/EDX) to add complimentary information on the oxidation states or other compositional changes. Some have even performed continuous acquisition of EELS or EDS data [1], but continuous acquisition of spectrum images has been challenging and only possible using custom scripts [2]. Now, in the 3.6.0 version of the Gatan DigitalMicrograph software it is much easier to collect continuous spectroscopic data, including *in-situ* time series of spectrum images with live drift correction and real-time elemental quantification.

We will show data and screen capture videos of the acquisition of high-speed continuous spectrum imaging of the reduction of FeOOH to FeO with simultaneously acquired EELS and EDS data during *in-situ* heating to just over 850°C with a DENSolutions Wildfire holder. Temperature data from the holder was also automatically captured and synchronized with the *in-situ* spectrum image data. While EDS would normally be impossible at such high temperatures, in this case an IR filter was used enabling the simultaneous collection of EDS spectrum image data all the way through the *in-situ* experiment. Live drift correction was also essential, since the sample moves during *in-situ* acquisition. Further precise drift correction can also be easily applied in post-processing. We will also discuss the live EELS quantification used as well as the format of the generated data, which can be easily processed further with built-in tools in the software, or analyzed via infinitely customizable Python scripting.

[1] Shen, T.-H., Spillane, L., Peng, J., Shao-Horn, Y. & Tielei, V. Switchable wetting of oxygen-evolving oxide catalysts. *Nat Catal* **5**, 30–36 (2021).

[2] Spillane, L. & Schaffer, B. Automated Spectrum Imaging Using Hybridized DMScript and Python Code in DigitalMicrograph. *Microscopy and Microanalysis* **28**, 2922–2923 (2022).

3:30 PM CH02.05.06

Liquid-Electron Microscopy: Making Waves in SARS-CoV-2 Research Samantha M. Berry, Liza-Anastasia DiCecco, Jennifer L. Gray and Deborah Kelly; The Pennsylvania State University, United States

In 2019, the emergence of the SARS-CoV-2 virus quickly spread across the global community. The resulting pandemic devastated health fields and economies throughout the world. In turn, viral research exploded as scientists rose to the occasion to develop novel therapeutics against SARS-CoV-2. Cryo-electron microscopy (EM) allowed researchers to characterize its viral structure, aiding in vaccine design. One limitation of this technique, however, is that the proteins must be vitrified and therefore are confined to static imaging. Protein regions can be highly flexible, and valuable data on protein-protein interactions and conformational changes could be lost through this technique. An emerging field known as liquid-electron microscopy solves this issue by enabling imaging in a fluid, near-native environment. By using liquid-EM, dynamic protein mechanisms can be captured in real-time at sub-angstrom resolution. In addition to capturing dynamic data, liquid-EM provides *in situ* experimental capabilities such as ramp heating and flow experiments to better characterize materials. In a biological sense, this technique can create hydrated, more biologically relevant imaging conditions in which to investigate protein structure.

In this work, we reveal a novel look into protein structure and dynamics of SARS-CoV-2 virions extracted from COVID-19 patient serum. Using liquid-EM, we deployed our innovative microchip sandwich technique to capture and image extracted SARS-CoV-2 virions. With this method, a thin liquid sample is sandwiched between a SiN chip and a carbon-coated gold grid and sealed using an autoloader clip. Samples can either be imaged instantaneously or stored for months without drying out, impressively. Another advantage to this technique is that a traditional single-tilt holder can be used, making it both accessible and affordable. When imaging our COVID-19 patient serum sample using this assembly, we discovered interesting protein behaviors in liquid. Over the course of a few days, SARS-CoV-2 virions appeared to begin self-assembling in round, heterogenous aggregates (~80 nm). Micrographs were obtained to render a 3D model of this behavior at 8.25 Å resolution. By imaging in a hydrated native environment, liquid-EM can provide us glimpses as to how SARS-CoV-2 interacts in the human body. In addition to observing the large aggregates, we also captured and modeled the spike (S) protein that is responsible for infection at 4.3 Å resolution using single particle analysis. Models revealed the presence of partial S protein trimers, suggesting how the body possibly fights off infection and degrades foreign virions. This work helps to elucidate structural features and functionality of authentic SARS-CoV-2 in a dynamic, near-native environment using liquid-electron microscopy.

3:45 PM CH02.05.07

Degradation of Quantum-Sized Semiconductor Nanocrystals Induced by Moisture Exposure through The Involvement of Amorphous Intermediates Hyeonjong Ma¹, Sungsu Kang², Jungwon Park² and Jiwoong Yang¹; ¹Daegu Gyeongbuk Institute of Science and Technology, Korea (the Republic of); ²Seoul National University, Korea (the Republic of)

Comprehending the mechanism underlying the degradation initiated by water in quantum-sized semiconductor nanocrystals holds significant importance for their practical utilizations, given their higher sensitivity to moisture compared to their bulk counterparts. *In-situ* liquid-phase transmission electron microscopy has emerged as a desirable method for investigating nanocrystal decomposition, and recent notable advancements have further enhanced its technological capabilities. This presentation will describe the degradation process of moisture-induced semiconductor nanocrystals, using graphene double-liquid-layer cells that provide precise control over reaction initiation. During the quantum-sized CdS nanorod decomposition, these advanced liquid cells enable clear differentiation between crystalline and non-crystalline domains due to their high-resolution imaging capability. Our observations enhance fundamental understanding on the degradation pathway, involving the formation of an amorphous phase, which stands apart from the traditional trajectories of nanocrystal etching. Notably, the decomposition process persists even in the absence of electron beam irradiation, indicating that the reaction is triggered by water exposure. This work unveils the remarkable pathways by which semiconductor nanocrystals degrade upon moisture exposure, a phenomenon elucidated through the involvement of amorphous intermediates.

4:00 PM CH02.05.08

Young's Modulus of Multiwalled Boron Nitride Nanotubes measured by In-Situ Nanoelectromechanical Resonance Jae-Won Bryan Seo¹, Won-IL Lee¹, Kushal Kumar Iyyapareddy², Sooyeon Hwang³, Eunkwang Park⁴, Jaewoo Kim⁴, David Hwang² and Chang-Yong Nam^{1,3}; ¹Stony Brook University, The State University of New York, United States; ²Stony Brook University, United States; ³Brookhaven National Laboratory, United States; ⁴NAiEEL Technology, Korea (the Republic of)

Boron nitride nanotubes (BNNTs) with alternating boron and nitrogen atoms arranged in hexagonal lattice in a tubular structural form factor are known to have excellent thermal and mechanical properties. However, in general it remains challenging to characterize mechanical properties of individual nanomaterials, such as BNNTs. In this study, we have characterized the nanomechanical properties of individual, multiwalled BNNTs using an *in-situ* nanoelectromechanical resonance method in transmission electron microscopy. BNNTs dispersed in isopropyl alcohol were first drop-cast and dried on a Si substrate. The BNNTs on the substrate were then transferred and fixed to the tip of an electrochemically sharpened tungsten needle using silver paste, which was baked on a hot plate at 100 °C. Scanning electron microscopy (SEM) confirmed a successful sample preparation by visualizing individual BNNTs with one free end and the other firmly rooted on the tip. The tungsten tip was then loaded to an *in-situ* TEM holder with electrical feedthroughs. During TEM, while observing individual BNNTs, the tungsten tip was biased with respect to a counter electrode separated by vacuum using oscillating voltage wave input with peak-to-peak voltage of 10 V and frequency varied from 0 to 20 MHz. When the external frequency matched the natural mechanical resonant frequency of a given BNNT, the tube started to vibrate. A series of images taken at various frequencies around the resonance were analyzed to yield the vibration amplitude vs. frequency plot that enabled the determination of the resonance frequency and quality factor of the BNNT. By applying the Euler-Bernoulli beam theory, the measured resonance frequency then determined the Young's modulus of the given BNNT. We found that the measured Young's modulus of BNNTs was in the 1.6 – 224 GPa range. It was observed that the determined Young's modulus was increasing with increasing BNNT's outer diameter but also rendered lower when a BNNT had a larger hollow core. We also identified a reduced Young's modulus also had correlation with atomic structural defects, such as missing atoms and buckled tube surfaces. The study represents one of the first reports of the nanomechanical properties of individual BNNTs measured by the *in-situ* nanoelectromechanical resonance method. The results also highlight the importance of atomic structures on the resulting mechanical properties of BNNTs.

8:00 AM *CH02.06.01

***In-Situ* and Cryogenic Electron Microscopy of Electrochemical Energy Material** YiCui; Stanford University, United States

Electrochemical energy materials often involve in dynamic movement of atoms and electrons simultaneously. To understand these materials down to the atomic scale resolution under intrinsic environment is a challenge. Here I report my lab's nearly two-decade long effort in developing electron microscopy methods to image battery electrode materials and electrocatalysts. I will show in-situ electron microscopy of electrochemical biasing during charging/discharging of battery materials and gas reaction of reactive materials. I will also share the breakthrough development of cryogenic electron microscopy for fragile energy materials and reveal novel knowledge not available previously.

8:30 AM CH02.06.02

Investigation of the Resistivity Switching Mechanisms of Different Types of Oxide Memristor Devices via *In Situ* STEM and EELS DiZhang¹, RohanDhall², ChengyuSong², JimCiston², MattSchneider¹, SundarKunwar¹, MichaelT. Pettes¹, RodneyMcCabe² and AipingChen¹; ¹Los Alamos National Laboratory, United States; ²Lawrence Berkeley National Laboratory, United States

The resistive-switching (RS) phenomenon observed in a variety of transitional metal oxides (TMO) is of great research interest since it opens enormous opportunities for the next-generation electronic devices such as nonvolatile memory and neuromorphic computing units, etc. However, the RS mechanism for many TMO memristor devices are still unclear, not alone the distinction between filament-type and interface-type devices. In this project, we use *in situ* transmission electron microscopy (TEM) and Electron Energy Loss Spectroscopy (EELS) to investigate the RS mechanisms of different types of memristor devices. The high resolution STEM images captured during the *in situ* biasing experiment revealed the potential phase transition processes and polarized cations displacements, and the core EELS spectra confirmed the cations valence states change and the oxygen stoichiometry modulation during the RS processes. This study has shined great light on clarifying the RS mechanisms of different types memristor devices, which can be applied to the development of next-generation nanoelectronic devices towards advanced memory and neuromorphic computing units etc.

8:45 AM CH02.06.03

***In-Situ* Observation of Polarization Switching in Novel Ferroelectrics.** SebastianCalderon¹, JohnHayden², StevenM. Baksa², SamanthaJaszewski³, JonF. Ihlefeld³, IsmailaDabo², Jon-PaulMaria² and ElizabethC. Dickey¹; ¹Carnegie Mellon University, United States; ²The Pennsylvania State University, United States; ³University of Virginia, United States

The discovery of ferroelectricity in HfO₂ [1] and wurtzite-based ternary materials such as AlScN [2] and AlBN [3] has attracted tremendous attention due to their compatibility with CMOS processes and their potential to be integrated in non-volatile memory devices. The origin of the ferroelectricity and the fundamental switching mechanisms in these materials is still under intensive investigation. Understanding the mechanisms that control and induce switchable states in these materials is an important goal to find solutions to the high coercive fields and avoid breakdown failures. We employ scanning transmission electron microscopy to observe the polarization of the films at atomic scale, by differential phase contrast, which allows simultaneous observation of light and heavy atomic columns. An internal electric field capable of switching these materials is attained by exposing them to long periods to the electron beam, provoking a positive charge accumulation due to the emission of secondary and auger electrons that are not compensated due to the insulating properties of these materials. STEM-DPC experimental images are acquired in a probe-corrected ThermoFisher Titan-Themis at 200kV, using a four-segment annular detector (DF4), a probe convergence angle of 18 mrad and a camera length that results in acceptance angles between 11 and 43 mrad. The experimental data are complemented with STEM simulations using Dr. Probe V1.9 software package [4]. Simulations are carried out using the frozen-phonon configuration method at 200 keV and 1 μm of spherical aberration. Our results show conclusively the pathway for the polarization inversion at the atomic scale in both wurtzite [5] and fluorite ferroelectrics, offering unprecedented insights into the mechanisms for ferroelectric switching. DFT calculations also support our finding, demonstrating the pathways for the polarization inversion.

Acknowledgements

This material is based upon work supported by the Center for 3D Ferroelectric Microelectronics (3DFeM), an Energy Frontier Research Center funded by the U.S. Department of Energy, Office of Science, Office of Basic Energy Sciences Energy Frontier Research Centers program under Award Number DE-SC0021118. The authors acknowledge use of the Materials Characterization Facility at Carnegie Mellon University supported by grant MCF-677785.

[1] T. Böschke, J. Müller, D. Bräuhäus, U. Schröder, U. Böttger, Ferroelectricity in hafnium oxide thin films. Appl. Phys. Lett. 99, 102903 (2011).

[2] S. Fichtner, N. Wolff, F. Lofink, L. Kienle, B. Wagner, AlScN: A III-V semiconductor based ferroelectric. J. Appl. Phys. 125, 114103 (2019).

[3] J. Hayden, M.D. Hossain, Y. Xiong, K. Ferri, W. Zhu, M.V. Imperatore, N. Giebink, S. Trolier-McKinstry, I. Dabo, J.-P. Maria, Ferroelectricity in boron-substituted aluminum nitride thin films, Phys Rev Mater. 5 (2021) 044412. <https://doi.org/10.1103/PhysRevMaterials.5.044412>.

[4] J. Barthel, Dr. Probe: A software for high-resolution STEM image simulation, Ultramicroscopy. 193 (2018) 1–11. <https://doi.org/https://doi.org/10.1016/j.ultramic.2018.06.003>.

[5] Sebastian Calderon V, John Hayden, Steven M. Baksa, William Tzou, Susan Trolier-McKinstry, Ismaila Dabo, Jon-Paul Maria, Elizabeth C. Dickey, Atomic-scale polarization switching in wurtzite ferroelectrics, Science 380, 1034–1038 (2023)

9:00 AM *CH02.06.04

4D-STEM & *In Situ* ec-TEM to Study the Lithiation Dynamics in Battery Cathode Materials ArnaudDemortiere, NicolasFolastre, JunhaoCao, KevynGallegos Moncayo and GozdeOney; CNRS, LRCS Laboratory & RS2E Battery Network, France

This 4D-STEM method using ASTAR-ACOM system allows to build maps of crystalline phase and orientation, using scanning nano-diffraction with precession with nanometer resolution. The recent use of high-speed cameras, pixelated detectors such as CMOS cameras and hybrid-pixel detectors enabled larger areas to be scanned, and a higher resolution close to 1 nm with high SNR. The goal of our data preparation methods (ePattern suite) proposed here is to improve the quality of ASTAR pattern-matching using a dataset of diffraction patterns acquired with a CMOS Oneview camera. The high sensitivity of the CMOS camera and the data filtering developed here modify the diffraction images leading to a compromise between image quality and template matching result quality. In this work, we show that the mapping of crystal structures and orientations provides essential information for the determination of individual particle lithiation mechanisms of cathode materials for Li-ion and Na-ion batteries, as NaMnV(PO₄)₃ and LiFe_{0.3}Mn_{0.7}PO₄ was used in this study. In addition, this image processing method gives more confidence in phase determinations in such polycrystalline materials as well as local maps of strains and order parameters.

9:30 AM CH02.06.05

Deciphering Nanoscale Corrosion Mechanisms from 2D to 3D using Liquid-Phase TEM ZhihengLyu, LehanYao, SamyuktaShrivastav, DanielV. Krogstad, JessicaA. Krogstad and QianChen; University of Illinois at Urbana-Champaign, United States

As a ubiquitous phenomenon, corrosion has raised vital concerns globally as one of the major causes of infrastructure failure, leading to substantial financial losses and environmental damage. On the other hand, with careful control of reaction rate and selectivity, corrosion can also be utilized as a top-down method in material sculpting, tuning its size, shape, and component adapting to applications ranging from plasmonics, electronics, catalysis to biomedicine. Either prevention or utilization of corrosion requires fundamental understanding of reaction mechanisms, where in situ, high-resolution characterization techniques are necessitated for uncovering the localized, nanoscale processes. Recent advances in liquid-phase transmission electron microscopy (TEM) have shown its great promise in tracking the morphological and compositional change of materials during reactions with nanometer or even atomic resolution. With corrosion of carbon steel as an example, cavity generation and its anisotropic expansion were observed in real time using liquid-phase TEM, the process of which can be further correlated to strain distribution, crystal orientation, and component variation inside the steel. Advancing from two-dimensional projections to three-dimensional reconstructions, we also highlight our efforts in combining liquid cell with electron tomography to achieve a more comprehensive understanding of nanocrystal etching process. The intermediate shapes of core-shell or hollow nanocrystals at different stages into etching were captured and reconstructed, from which particle volume, surface curvature, and local etching depth were derived, unveiling the anisotropy in etching caused by structural and environmental heterogeneity. We hope these works could inspire more efforts devoted to in situ characterization of material shape transformation, enabling nanoscale observation and understanding of corrosion processes.

9:45 AM CH02.06.06

Probing Nanoscale Creep in Confined Dimensions Mehrdad T. Kiani¹, Quynh Sam¹, Yeon Sik Jung², Hyeuk Jin Han³ and Judy Cha¹; ¹Cornell University, United States; ²Korea Advanced Institute of Science and Technology, Korea (the Republic of); ³Sungshin Women's University, Korea (the Republic of)

The thermomechanical behavior of nanostructures can greatly diverge from their bulk counterparts due to their high surface area to volume ratio. In particular, diffusion-dominated creep at free surfaces and interfaces is greatly enhanced, enabling rapid deformation in short time scales. While traditionally considered a deleterious behavior in structural materials, enhanced creep at the nanoscale has been used to drive thermomechanical nanomolding (TMNM), where a bulk feedstock of a desired material is pressed through a nanoporous mold to form high aspect single crystal nanowires of metals, alloys, and intermetallics. For 1D nanowires, TMNM is thought to be driven by interfacial diffusion along the mold wall; however, there have been no *in situ* studies of TMNM confirming this mechanism. Furthermore, it is unknown whether interfacial diffusion still governs kinetics of TMNM for nanostructures other than 1D nanowires where other mechanisms may begin to dominate.

Here, we probe nanoscale creep during TMNM, focusing on fabrication of 2D nanostructures. Using a Si mold with 40 nm wide trenches, we successfully observe nanomolding of both nanoribbons and nanofins over wafer-length scales at back end of line compatible temperatures. In contrast to 1D TMNM, the final grain size of the nanostructure matches the grain size in the bulk, up to and including single crystal nanostructures. From nanoscale grain orientation mapping via 4D-STEM, we observe random grain orientations in the nanomolded samples. From the final microstructure and *in situ* TEM compression studies of nanomolding, we discuss possible diffusion-driven creep mechanisms at play and the importance of grain boundary diffusion in 2D TMNM.

10:00 AM BREAK

SESSION CH02.07: Advances in In-Situ TEM
Session Chairs: Madeline Dukes and Djamel Kaoumi
Wednesday Morning, November 29, 2023
Sheraton, Third Floor, Berkeley

10:30 AM *CH02.07.01

Imaging Ghosts with 4D-STEM: Diffuse Scattering, Vacancies and Vanishing Dislocations Sean Mills¹, Jenn Donohue¹, Yang Yang² and Andrew M. Minor^{1,3}; ¹University of California, Berkeley, United States; ²Penn State University, United States; ³Lawrence Berkeley National Laboratory, United States

In situ transmission electron microscopy (TEM) experiments are typically recorded either in real space or diffraction space [1]. However, it would be ideal to have both real and diffraction space for when transient events occur that cannot be repeated exactly (ie- defect generation or irreversible phase transformations). Real space imaging provides context for these transient events by spatially-resolving microstructural features to one another while diffraction space provides better structural clarity about phase identification and lattice parameters. Four-dimensional scanning transmission electron microscopy (4D-STEM) [2], can come close to providing both simultaneous real-space imaging and diffraction analysis during *in situ* testing. Here, we use 4D-STEM with high precision bullseye apertures [3] to map the nanoscale strain landscape during *in situ* cooling of a NiTi through the phase transformation from the high temperature B2 cubic austenite phase to the low temperature B19' monoclinic martensite phase. Using this method, we can map both the phase distributions and the strain as the sample approaches and then proceeds through the phase transformation, including the diffuse scattering ahead of the phase transformation. 4D-STEM also provides an opportunity to map vacancy distributions with nanoscale resolution. Our experiment using a model Au film demonstrates the 4D-STEM method for measuring vacancy concentration by closely following the differential thermal expansion method [4] of measuring concentrations of point defects [5]. In a more complicated scenario, we have used vacancy mapping with 4D-STEM to also help explain the mechanism behind a new type of one-dimensional corrosion in metals [6]. Lastly, this talk will also describe our recent results utilizing in situ 4D-STEM during nanomechanical testing to provide insight into multiscale deformation phenomena in the CrCoNi medium entropy alloy (MEA). 4D-STEM can provide both real-space imaging and diffraction analysis during *in situ* testing, making it possible to classify defects during in situ deformation before they disappear. These vanishing dislocations help to explain the correlation between SRO and planar defects during deformation of the CrCoNi MEA.

References:

- [1] F. Ross and A. M. Minor, "In situ Transmission Electron Microscopy", in *Springer Handbook of Microscopy*, edited by Peter Hawkes and John Spence, Springer Nature Switzerland AG, 2019
- [2] C. Ophus, "Four-dimensional scanning transmission electron microscopy (4D-STEM): From scanning nanodiffraction to ptychography and beyond," *Microsc. Microanal.*, vol. 25, no. 3, pp. 563–582, (2019).
- [3] Zeltmann, S. E., Müller, A., Bustillo, K. C., Savitzky, B., Hughes, L., Minor, A. M., & Ophus, C. (2020). Patterned probes for high precision 4D-STEM bragg measurements. *Ultramicroscopy*, 209, 112890.
- [4] R. O. Simmons and R. W. Balluffi, "Measurement of equilibrium concentrations of lattice vacancies in gold," *Phys. Rev.*, vol. 125, no. 3, p. 862, (1962).
- [5] S. Mills, et al, "Nanoscale mapping of point defects with 4D-STEM", *Acta Materialia*, vol. 246, pp. 118721, (2023)
- [6] Y. Yang, et al., "One-dimensional wormhole corrosion in metals", *Nature Communications*, (2023)

11:00 AM *CH02.07.02

Machine Learning in Operando TEM—Let Me Count the Ways Mitra L. Taheri^{1,2}; ¹Johns Hopkins University, United States; ²Pacific Northwest National Laboratory, United States

In recent years, applications of artificial intelligence (AI) and machine learning (ML) methods in microscopy have enabled utility of noisy data, monitoring of rare events, and even elucidation of metastable phenomena. Unfortunately, there is no one methodology that suits the wide variety of operando techniques, due in large part to the multiple data types and dimensions present in such experiments. This talk reviews the application of AI/ML to various data types, ranging from images to spectra, concentrating on the opportunities and challenges associated with their use. Also discussed is the possibility of generalizing such methods toward a more uniform approach to in situ and operando acquisition toward closed loop, intelligent or autonomous microscopy.

11:30 AM CH02.07.03

Novel Liquid Transmission Electron Microscopy Tools to Study Viral Pathogens Liza-Anastasia DiCecco, Liam Kaylor, Jennifer L. Gray and Deborah Kelly; The Pennsylvania State University, United States

Interest in the study of viruses has dramatically increased since the emergence of the deadly SARS-CoV-2 virus and its devastating impact in the United States and beyond. Globally, research has pivoted towards understanding such pandemic pathogens to identify new vaccines and drug therapies to save lives and curb viral transmission. To this end, traditional and cryo-transmission electron microscopy (TEM) methods have been primarily used to study virions and elicit key details of their structure; However, these methods lack the capacity to visualize necessary dynamic interactions that occur within these virions and their impact on treatment efficacy. Liquid-TEM tools are needed to visualize high-resolution viral interactions in real-time, giving researchers the capability to capture *in situ* dynamics and perform structural characterization of these important assemblies in native hydrated conditions.

Here in this presentation, we describe newly developed liquid-TEM methods for imaging human viruses that can be used in both liquid and cryo-TEM conditions using novel silicon nitride microchip sandwich assemblies. The hybrid liquid-TEM enclosures, composed of a SiN wafer clipped together with a carbon-coated gold TEM grid, are highly affordable and repeatable to use – providing accessible means for others to perform liquid-TEM. Bright-field TEM and high-angle annular dark-field imaging (HAADF) scanning TEM (STEM) are deployed in correlation in this proof-of-concept study to provide unparalleled insight into these structures, highlighting exciting new possibilities that liquid-TEM offers for the field of structural biology. Paired with automated workflows and low-dose imaging using direct electron acquisition, we highlight this method can effectively characterize the structures of viruses like Rotavirus and sub-viral SARS-CoV-2 assemblies with nanometer resolution. These efficient new toolsets offer a versatile way to study biological materials that could lead to meaningful contributions in the fight against future pandemic pathogens and may someday provide capabilities to visualize molecular dynamics *live*.

11:45 AM CH02.07.04

Pushing the Limits of Tunable Laser-Free Ultrafast Electron Microscopy Spencer Reisbick¹, Chuhang Liu¹, Alex Pofelski¹, Myung-Geun Han¹, Eric Montgomery², Chunguang Jing² and Yimei Zhu¹; ¹Brookhaven National Lab, United States; ²Euclid Techlabs, United States

Typically, ultrafast electron microscopy (UEM) has been performed by photoexciting short electron packets from a TEM cathode with sub-picosecond laser pulses that are synchronized to an excitation on the sample. Adjusting the relative delay between the electron packets and the sample excitations allows time-resolved measurements that elucidate dynamics with picosecond resolution. Examples include the elucidation of dynamics relating to phonon propagation, electromechanical breathing, or magnetic domains. Here, I discuss a novel technique that removes lasers from the experimental setup by replacing them with RF compatible strip-line technology (referred to as the pulser). By doing so, we can expand the excitation space up to tens of gigahertz while retaining picosecond resolution. Additionally, the development of the pulser enables the entire setup to be contained within the TEM in a user-friendly environment. Unfortunately, covering a massively tunable domain in frequency, power, excitation type and applications cannot be contained in a simple solution, so I will discuss the necessary hardware, software and control that enables us to access such a wide variety of applications.

I will also discuss a few emerging applications that are becoming realized due to our laser-free UEM system. One such example is the excitation of spin-waves in rectangular permalloy stripes at frequencies near 5 GHz. We find transmitting RF near magnetic cross-tie domains induces a modulation along the domain boundary which propagates into the magnetic domains. Further, we have fully characterized the wavelength and velocity as they propagate through the material. Another example is controlling phase transitions using electrical excitation in materials such as VO₂ or TaS₂. Both materials exhibit structural phase transitions near room-temperature that have been shown to occur with at least some effect due to an electrical excitation. In both instances, there is some controversy regarding whether the transition is purely electrically driven or if the current flow causes a temperature increase that induces the change. The tunability of our system enables us to conduct experiments at extraordinarily high frequencies the laser-driven UEM is incapable of. Therefore, we can lock the experimental systems into a resonance state and explore these systems knowing that the thermal excitation is long lived and reaches a steady state which can be ignored.

SESSION CH02.08: Poster Session: In Situ Characterization of Materials Synthesis and Processing
Session Chairs: Yujun Xie and Yao Yang
Wednesday Afternoon, November 29, 2023
Hynes, Level 1, Hall A

8:00 PM CH02.08.01

Understanding Heterogeneous Electrocatalytic CO₂ Reduction over Zn-Ag Bimetallic Electrocatalysts via *In-Situ* Liquid Phase Transmission Electron Microscopy [Kholoud E. Abousalem](#) and [Ahmed Shehab](#); McMaster University, Canada

The electrocatalytic reduction of carbon dioxide (CO₂R) into valuable fuels is of urgent scientific importance to satisfy the sustainable carbon cycle, which remains a grand challenge. Due to the large energy barrier of CO₂R, the development of efficient catalysts is urgently required. On the other hand, understanding the mechanistic pathways of CO₂R will definitely introduce more opportunities to develop highly active catalysts. In this regard, several approaches have been used including *in-situ* characterization methods in order to get a deep insight into this kind of reaction. Herein, *in-situ* liquid phase TEM measurements have been systematically conducted to realize the electrocatalytic CO₂ reaction mechanism and track all dynamic changes concerning the electrocatalysts' composition and reconstruction under investigated experimental conditions, which could affect the reaction pathway. Amongst the investigated electrocatalysts, Zn-based alloys have proved an outstanding selective CO production with high activity and enhanced stability. For this purpose, we have investigated the influence of Ag metal incorporation into porous Zn nanostructured electrodes on the product selectivity and stability of CO₂R. Bimetallic Ag-Zn alloys with different Ag ratios synthesized by the scalable electrodeposition approach have significantly promoted the electrode porosity and surface area, revealing high CO adsorption characteristics with improved selectivity over several electrocatalytic cycles; compared to bare Zinc electrocatalysts. Moreover, to investigate the mechanistic pathways of these reactions, TEM measurements including imaging and diffraction have been collected under CO₂ electrochemical reaction conditions "*in-situ*". Afterward, in order to investigate the activity and selectivity of these catalysts, the same CO₂ electro-reaction has been conducted without TEM measurements to quantify the formed products using the gas chromatography (GC) technique. Accordingly, the Ag-supported Zn electrocatalyst exhibits high faradic efficiency and improved current density at low overpotential, which suggests that Ag metal incorporation plays a crucial role in favoring the production of CO during the long-term operation over those reported by purely Zn metal catalysts. By combining both measurements with/without TEM, this study will produce some performance descriptors of the CO₂R, which will positively influence the catalyst development orientation in this field. Those findings could open further future suggestions on monitoring the *in-situ* catalyst performance during the CO₂ reduction process.

<quillbot-extension-portal></quillbot-extension-portal>

8:00 PM CH02.08.02

Surface Diffusion and Sintering of Single Metal Atoms on Graphene. [Kenji Yamazaki](#), [Makoto Moriya](#) and [Yunosuke Ikeda](#); Hokkaido University, Japan

Single-atom catalysts consisting of single metal atoms dispersed on a supporting substrate are considered to be very advantageous in terms of both cost and catalytic activity due to their extremely large surface areas and quantum size effects and thus have attracted much attention. In particular, researchers have focused on the miniaturization of platinum (Pt) nanoparticles, which are used in many important chemical processes and solid-state fuel cells. We have achieved single Pt atoms adsorbed on graphene by plasma sputtering. We have shown that Pt atoms are dominantly adsorbed near the step edges of nanoscale graphene stacked on monolayer pristine graphene, which is called nanographene, and hardly adsorbed on the terraces. In addition, we found that the Pt 5d_{xy}-orbital forms a bond to the step edge. However, Pt atoms may cause aggregation from single atoms into 2D clusters or 3D nanoparticles at high concentrations. We analyzed the atomic structure and electronic states of single Pt atoms dispersed on N-doped graphene by plasma sputtering. We showed that the N atoms were dominantly adsorbed on nanographene. We achieved the atomic arrangement of Pt, N, and C at the step edge of nanographene and clarified that the N atom increases the population of the Pt 5d_{xy}-orbital and enhances the stability of single Pt atoms. Exhaustive calculations have been performed to elucidate the major adsorbed structures of single Pt atoms bound to step edge. Similarly, it is important to perform exhaustive calculations on N-doped step edges. Moreover, we have revealed the components of the Pt 5d orbitals that contribute to binding. Both structural stability and high catalytic activity are important for monatomic catalysts. It is important to investigate the thermal stability of the structure and its activity in chemical reactions for application to catalysts. Thus far, the amount of single Pt atoms formed in graphene on a TEM grid has not been sufficient to test a catalytic reaction such as hydrogen evolution reaction (HER) or oxygen reduction reaction (ORR). In the near future, it will be necessary to experimentally clarify the relationship between the monatomic catalyst having these structures and catalytic performance. Detailed information about the highly reactive Pt 5d orbitals will be essential in studying these properties. We also showed that Pt and gold (Au) single atoms dispersed on free-standing monolayer graphene were continuously observed via aberration-corrected scanning transmission microscopy (STEM), and the difference in the dynamic behavior of the single atoms on graphene under electron beam irradiation was observed. Analysis was performed after the drift corrections to track the movement of the metal atoms from their binding sites with angstrom order accuracy. Approximately 70% of Pt single atoms traveled less than the nearest carbon atom distance of graphene (1.4 Å) during the observation interval (10 s). Thus, Pt was confirmed to be stably dispersed on graphene as single atoms. Au atoms could be dispersed on graphene by the same method as that used with Pt, and they were present at the nanographene edge, like Pt. However, the Au single atom mobility was larger than that of Pt. More than 40% of the particles traveled a distance exceeding the size of the six-membered ring of graphene (2.8 Å) during the minimum observation interval (4 s), and the variation in moving distance during the observation time was large. Upon analyzing the three-dimensional structure of nanographene, we found that these single metal atoms were mainly present on more than three-layer nanographene, and almost no atoms were found on the terrace of first-layer graphene. One reason for this result is that the higher layer nanographene has many binding sites for metal atoms because it is structurally unstable and has many defects and edges compared with lower-layered nanographene.

8:00 PM CH02.08.03

***In-Situ* TEM Deformation of CrCoNi Medium Entropy Alloys** [Madelyn L. Payne](#)^{1,2}, [Lilian Vogl](#)¹, [Peter Schweizer](#)², [Mingwei Zhang](#)³, [Punit Kumar](#)^{2,1}, [Mark Asta](#)^{1,2}, [Robert Ritchie](#)^{1,2} and [Andrew M. Minor](#)^{1,2}; ¹University of California, Berkeley, United States; ²Lawrence Berkeley National Laboratory, United States; ³University of California, Davis, United States

The CrCoNi medium entropy alloy (MEA) is known for having exceptional properties at cryogenic temperatures, including the highest fracture toughness recorded in history. Even at room temperature these alloys are known to display microstructures including nanotwins and stacking faults that contribute to strain hardening. Defect structures such as, stacking fault tetrahedra and Lomer-Cottrell locks, introduced by sample processing temperatures and techniques can influence deformation processes. For example, studies have shown that cryogenic rolling of these alloys produce Lomer-Cottrell locks that enhance strain hardening at room temperature. In this study, we use advanced *in-situ* TEM techniques, to observe dislocation motion and interactions with existing microstructural features in differently processed CrCoNi bars pulled in tension. We perform *in-situ* TEM tensile deformation at room temperature and use image correlation to identify changes in structural features and local strain values.

8:00 PM CH02.08.04

Atomic Mechanisms Underlying The Phase Transformation in 2D CdSe Quantum Nanosheets Induced by Off-Stoichiometry [Hyeonjong Ma](#)¹, [Dongjun Kim](#)², [Jungwon Park](#)² and

The phase transformation in semiconductor crystals have great potential for various applications, because intrinsic characteristics of materials primarily determined by their atomic arrangements. Nevertheless, the atomic-scale mechanisms governing phase transformations in quantum-sized semiconductors requires further understanding, particularly in smaller crystals where structural changes are more probable. This presentation will elucidate the phase transformation of two-dimensional (2D) CdSe quantum nanosheets triggered by changes in stoichiometric characteristics. *In-situ* transmission electron microscopy is used for observing the dynamic pathways of this transformation. Initially characterized by a wurtzite phase and atomically flat morphology, the CdSe nanosheets undergo a transformation into zincblende-CdSe nanosheets due to changes in stoichiometry. This transformation is investigated in detail using a combination of experimental and theoretical methods. The phase transformation is initiated within the reconstruction of (11-20) basal planes of the wurtzite-CdSe nanocrystals induced by the loss of Se atoms, resulting in the construction of zincblende-like basal planes. Moreover, we directly captured unconventional phenomena, including dynamic fluctuations in atomic arrangements, such as domain coalescence and separation, during the structural evolution. We envision that this study can enhance our fundamental understanding of phase transformation mechanisms in semiconductor nanocrystals, offering an intuitive perspective for various applications.

SYMPOSIUM CH03

Nanoscale Materials Characterization Through Atom Probe Tomography
November 27 - November 28, 2023

Symposium Organizers

David Diercks, Colorado School of Mines
Baishakhi Mazumder, University at Buffalo, The State University of New York
Frederick Meisenkothen, National Institute of Standards and Technology
Pritesh Parikh, Eurofins Nanolab Technologies

Symposium Support

Bronze
CAMECA

* Invited Paper
+ JMR Distinguished Invited Speaker

SESSION CH03.01: Atom Probe Tomography—Metals and Alloys I
Session Chairs: Baishakhi Mazumder and Frederick Meisenkothen
Monday Morning, November 27, 2023
Sheraton, Third Floor, Dalton

10:30 AM *CH03.01.01

Structural Materials Characterisation for Hydrogen Systems [Peter Felfel](#); Friedrich-Alexander-Universität, Germany

Due to increased demand for decarburization, the transport of hydrogen from low energy cost production locations to high energy cost locations of demand is rapidly moving into focus. Here, the costs are heavily influenced by the material costs for the required infrastructure. As a result, full utilisation of currently available structural materials under hydrogen and the development of new, cost effective materials is becoming increasingly important. Since all parts dealing with hydrogen under pressure or in cryogenic form are safety relevant, a deep understanding of the underlying mechanisms is highly desired. This demands the ability to recreate hydrogen loading and accelerated testing in the lab, characterisation of the effects of hydrogen on the material from the macro to the atomic scale and new theories on the failure mechanisms exhibited by hydrogen resistant materials.

In this talk, we will present the testing environment built up at the Friedrich-Alexander University Erlangen-Nuremberg (FAU) as well as a new development in the area of low-cost hydrogen resistant steels. In order to create a full materials development cycle for hydrogen resistant materials, we combine materials synthesis, materials testing and materials characterisation. At FAU, we are able to create new alloys through various powder and melt metallurgical means with associated hot deformation and heat treatment schedules. Materials testing under hydrogen is provided through electrochemical charging (in-situ and ex-situ) and through a high pressure autoclave station up to 1000 bar and 300°C. The latter is especially important for hydrogen resistant materials such as austenitic steels and Ni based superalloys due to their relatively low diffusion coefficients for hydrogen. Mechanical testing is then done ex-situ from the macro (tensile, fatigue) to the micro (pillars, cantilevers SEM-in-situ) scale. In order to understand the mechanical behaviour, characterisation is especially important. Here, hydrogen is especially challenging due to its relatively mobile nature.

At FAU, we have therefore built a special set of equipment to gain a deeper understanding of the microstructural response of structural materials under hydrogen. Besides standard materials characterisation equipment (SEM/EBSD, TEM, ...) this includes specialized equipment including a hydrogen capable titanium atom probe and a very high sensitivity titanium thermal desorption spectrometry (TDS) unit. Both of these instruments are UHV characterisation instruments built from titanium, in order to remove the usual hydrogen background found in UHV systems. For the atom probe, this enables the direct analysis of hydrogen at crystal defects without the use of tracers, as well as the analysis of hydrogen in materials using laser assisted atom probe tomography where typically even deuterium/tritium tracers are not suitable. The latter is especially important since analysis yields of hydrogen exposed materials are relatively low in voltage pulsed atom probe tomography. In the case of TDS, the drastically lower hydrogen background potentially allows for much smaller specimen sizes, increasing analysis dynamics and locality. The latter system is currently in the testing phase. Both systems are connected to a cryo-FIB system through a transfer suitcase in order to preserve hydrogen distributions.

In this talk we will also present the development of a novel, low cost class of hydrogen resistant steels. In these materials, we use high amounts of carbon to stabilise the austenitic phase. This has a major cost advantage over the use of Ni, Mn or N. These steels show no change of mechanical properties after exposure to hydrogen and provide good strength levels at a yield strength of 700 MPa and above. In the future, we hope to be able to develop these steels to mechanical properties under hydrogen of the highly cold worked Cr-Ni-Mo austenitic stainless steels currently used, at a fraction of the cost.

11:00 AM *CH03.01.02

Atomic Scale Analysis Reveals the Interplay between Grain Boundary Structure and Composition [Xuyang Zhou](#)¹, [Ali Ahmadian](#)¹, [Sourabh Kumar](#)², [Tilman Hicke](#)^{1,2}, [Baptiste Gault](#)^{1,3}, [Colin Ophus](#)⁴, [Christian Liebscher](#)¹, [Gerhard Dehm](#)¹ and [Dierk R. Raabe](#)¹; ¹Max-Planck-Institut fuer Eisenforschung GmbH, Germany; ²Federal Institute for Materials Research and Testing (BAM), Germany; ³Imperial College London, United Kingdom; ⁴Lawrence Berkeley National Laboratory, United States

Boron and carbon preferentially segregate at grain boundaries, i.e., two-dimensional defects between crystals with different orientations, to reduce the Gibbs energy of the system. The adsorption of these two elements can improve the cohesion of grain boundaries, making them important alloying elements for improving the mechanical properties of steels.

However, even for the simplest $\Sigma 5$ -grain boundaries, the atomic structure and composition of the grain boundaries are poorly understood. Several factors contribute to this difficulty: 1) representing the structure of grain boundaries requires more than five degrees of kinematic freedom; 2) the interplay between grain boundary structure and composition remains elusive, especially when it comes to imaging and quantifying light interstitial solutes, e.g. boron and carbon.

To address these challenges, we have designed special sample geometries that restrict the kinematic freedom of the grain boundary, allowing for a systematic investigation of the relationship between structure and composition. Additionally, we have developed custom software to quantify the solute composition and distribution along the grain boundary planes using atom probe tomography (APT). This information is then correlated with the atomic structure obtained by state-of-the-art differential phase contrast (DPC)–four-dimensional scanning transmission electron microscopy (4DSTEM), which allows direct imaging of both the light solute atoms and the heavier iron atoms at the grain boundaries.

Our combined results demonstrate that even a change in the inclination of the grain boundary plane with identical misorientation impacts grain boundary composition and atomic arrangement. It is the smallest structural hierarchical level, the atomic motifs, that controls the most important chemical properties of the grain boundaries.

Furthermore, when alloyed with boron, a grain boundary with the same crystallographic configuration can exhibit a nanoscale morphology transition from wavy to serrated. In-situ transmission electron microscopy (TEM) heating experiments demonstrate that at elevated temperatures, wavy or serrated grain boundaries tend to flatten. Interestingly, the presence of boron increases the temperature at which flattening occurs by at least 200 K. We attribute this difference to local grain boundary phase transformations triggered by boron atoms, as well as the pinning effect of boron-enriched nano-particles. Density functional theory calculations support the underlying mechanism of boron-induced local grain boundary phase transformation. This work not only closes a missing link between the structure and chemical composition of such defects but also enables the targeted design and passivation of the chemical state of grain boundaries to free them from their role as entry gates for corrosion, hydrogen embrittlement, or mechanical failure.

11:30 AM CH03.01.03

Studying the Mechanisms of Hydrogen-Based Iron Oxide Reduction for Green Steel Making at the Atomic-And Nanoscale Using Atomprobe TomographyDierk R. Raabe, Ayman El-Zoka, Baptiste Gault, Isnaldi Souza Filho and Yan Ma; Max Planck Institute for Iron Research, Germany

1.9 billion tons of steel have been produced last year, making it the most important material in terms of volume and environmental impact. Steel is a sustainability enabler, in lightweight vehicles, wind mills and magnets. However, its primary production is the opposite. Iron is today reduced from oxide ores using fossil reductants, translating to about 2t CO₂ per ton of steel produced [1,2]. This stands for more than 30% of the global CO₂ emissions in manufacturing. These emissions can be reduced when replacing carbon by hydrogen or ammonia as reductants [1-4].

The lecture discusses some key mechanisms of hydrogen- and ammonia-based solid-state direct reduction and hydrogen-based plasma-based liquid state reduction from a near-atomistic perspective using atom probe tomography [3-5].

Our perception of such reactions has not only been limited so far by the availability of state-of-the-art techniques which can delve into the structure and near-atomic scale chemistry of the reacted solids, but we continue to miss an important reaction partner that defines the thermodynamics and kinetics of gas phase reactions: the gas molecules. We present here results from cryogenic-atom probe tomography to study the quasi in-situ evolution of iron oxide in the solid and gas phases of the direct reduction of iron oxide by deuterium gas at 700°C [6]. We observed several so far unknown atomic-scale characteristics, including, D₂ accumulation at the reaction interface; formation of a core (wüstite)-shell (iron) structure; inbound diffusion of D through the iron layer and partitioning of D among phases and defects; outbound diffusion of oxygen through the wüstite and/or through the iron to the next free available inner/outer surface; and the internal formation of heavy nano-water droplets at nano-pores.

References

- [1] Raabe D, Tasan CC, Olivetti EA. Strategies for improving the sustainability of structural metals. *Nature*. 2019 Nov; 575 (7781): 64-74.
- [2] Raabe, D. The Materials Science behind Sustainable Metals and Alloys. *Chem. Rev.* 2023, 123, 2436–2608.
- [3] Kim, S. H.; Zhang, X.; Ma, Y.; Souza Filho, I. R.; Schweinar, K.; Angenendt, K.; Vogel, D.; Stephenson, L. T.; El-Zoka, A. A.; Mianroodi, J. R.; Rohwerder, M.; Gault, B.; Raabe, D. Influence of Microstructure and Atomic-Scale Chemistry on the Direct Reduction of Iron Ore with Hydrogen at 700°C. *Acta Mater.* 2021, 212, 116933.
- [4] Ma, Y.; Bae, J. W.; Kim, S.; Jovi, M.; Li, K.; Vogel, D.; Ponge, D.; Rohwerder, M.; Gault, B.; Raabe, D. Reducing Iron Oxide with Ammonia: A Sustainable Path to Green Steel. *Adv. Sci.* 2023, 2300111, 1–7.
- [5] Souza Filho, I. R.; Ma, Y.; Kulse, M.; Ponge, D.; Gault, B.; Springer, H.; Raabe, D. Sustainable Steel through Hydrogen Plasma Reduction of Iron Ore: Process, Kinetics, Microstructure, Chemistry. *Acta Mater.* 2021, 213, 116971.
- [6] El-Zokaa, A.A., L.T. Stephenson, S.–H. Kim, B. Gault, D. Raabe, The fate of water in hydrogen-based iron oxide reduction. *Adv. Sci.* 2023, in press.

11:45 AM CH03.01.04

Ultra-Fine-Scale Observation of Trapped Hydrogen using Atom Probe TomographyPang-YuLiu¹, RanmingNiu¹, Hung-WeiYen², JulieCairney¹ and EasonChen^{1,2}; ¹The University of Sydney, Australia; ²National Taiwan University, Taiwan

Hydrogen embrittlement poses a significant challenge to the durability of structural steels, a crucial factor in the advancement of the hydrogen economy. A potential remedy involves integrating hydrogen traps into the microstructure of steel. The efficacy of this approach is greatly influenced by the capacity of these hydrogen traps.

Theoretical models suggest carbon vacancies within metal carbide precipitates exhibit notable effectiveness as hydrogen traps in ferritic steels. In contrast, conventional structural defect traps such as dislocations and iron lattice vacancies have limited trapping energies and uncertain impact on countering hydrogen embrittlement. Therefore, enhancing the population of carbon vacancies within metal carbides holds significance. By introducing abundant metal carbides into steels, which can be feasibly achieved, the overall hydrogen trapping capacity can be substantially increased.

In order to validate this concept of material design, we produced two variants of titanium-microalloyed ferrite steels. The first variant contained stoichiometric titanium carbides (TiC) lacking carbon vacancies, serving as a reference. The second variant was an experimental steel infused with a small quantity of molybdenum (Mo). This addition led to the formation of Ti-Mo carbides, characterized by substitutional Mo atoms alongside carbon vacancies within the same TiC lattice.

We then used atom probe tomography to experimentally observe the hydrogen trapping behaviors of both the reference and Ti-Mo carbides. The outcomes demonstrate a shift in the hydrogen trapping mechanism within the metal carbide precipitates upon Mo addition. This alteration allows hydrogen to access the carbon vacancy traps within the carbide structure, causing a substantial escalation of trapping capacity. The identification of the influence of carbon vacancies on hydrogen trapping, achieved through a straightforward Mo addition, holds valuable implications for the development of carbide-strengthened steels with enhanced compatibility for hydrogen applications.

SESSION CH03.02: Atom Probe Tomography—Metals and Alloys II

Session Chairs: Baishakhi Mazumder and Frederick Meisenkothen

Monday Afternoon, November 27, 2023

Sheraton, Third Floor, Dalton

1:30 PM *CH03.02.01

Atom Probe Tomography Analysis of Nano-Scale Precipitate Evolution in Ni alloyed Fe-Mn-SteelPradeepKonda Gokuldoss; Indian Institute of Technology Madras, India

The presence of Al in Fe-Mn-C based multi-component steels induces ordered precipitate formation and depending on the thermomechanical processing, the size of the precipitates can be varied from micrometer down to nanometer. Ni addition further promotes the formation of Ni-Al type B2 precipitates localized within the BCC matrix depending on the Mn content. This work therefore attempts to analyze correlatively the crystal structure of the nano-scale precipitates formed in a duplex (i.e. FCC matrix and embedded BCC phase) steel along with their precise local chemical composition in a high statistical manner.

To achieve the above, correlative SEM based microscopic techniques such as TKD and STEM is utilized while the precise local chemical composition at near atomic-resolution is obtained from the investigated volume using APT. This correlative methodology applied to as hot rolled and annealed conditions, provides deeper insights into the role of starting microstructures on the precipitation kinetics and hence to the final mechanical properties of the steel.

2:00 PM *CH03.02.02

Forensics at the Nanoscale: Mapping Elemental and Isotopic Distributions in Metallic Nuclear Fuels via Atom Probe TomographyElizabethKautz^{1,2}, Sten V. Lambeets², DanielPerea²,

Atom probe tomography (APT) provides a unique, 3D map of element and isotope distributions with near-atomic scale resolution that can enable improved understanding of nuclear material origin and process history, central to forensic investigations. The identification of material origin is a critical step needed to improve safety and security measures to prevent proliferation. Traditional forensic investigations rely on a variety of analytical techniques, including mass spectrometry methods, gamma spectroscopy, and electron microscopy. Recently, the application of APT in nuclear fuel processing and irradiation response has provided key insights into the role of impurity elements and fission products in phase transformations and material performance. APT has also been a critical tool in geochemical studies on age-dating. These related studies have paved the way for APT to be developed and utilized in forensic investigations. Here, two case studies will be presented and discussed, focused on understanding the origin of non-metallic inclusions and oxidation behavior of a uranium-molybdenum (U-Mo) alloy. In cast U-Mo fuels, the mapping of both U enrichment and composition in nanoscale inclusions and the surrounding metallic matrix are critical to identifying origin of non-metallic inclusions. Nanoscale elemental and isotopic mapping via APT has identified several possible sources of impurity elements (e.g., oxygen, carbon) that can lead to formation of oxides and carbides during solidification. Several pathways are possible for the production or retention of CO, CO₂, or O₂ including: (1) reaction of the U alloy with the crucible or the crucible coating, (2) exposure of the melt to trace CO₂, O₂ or H₂O from the atmosphere, and (3) small defects in the mold coating that can lead to the direct contact of the molten U with the graphite crucible. U enrichment measured via APT in all inclusions and the U-Mo matrix phases was approximately 20 at. % (consistent with nominal enrichment for LEU fuels), indicating that nonmetallic inclusions were formed in the casting process and not retained from raw materials.

In addition to mapping U enrichment, elemental distributions accompanying oxidation or corrosion of nuclear fuels are important to track to understand how fuels degrade in waste storage containers, or how U-bearing post-detonation debris ages in different environments of interest. U oxidation and corrosion can occur when U metal is exposed to environments such as those typical of material processing, storage, and waste disposal. The corrosion of U has been proposed to proceed through the advancement of two reaction fronts between: (1) a (pyrophoric) UH₃ and UO₂, and (2) the U metal and hydride. This corrosion mechanism is supported by prior atom probe tomography (APT) characterization that demonstrated a thin subsurface hydride layer is present between the U oxide and metal when U metal is exposed to water vapor environments. Recent work employing an in situ APT approach revealed that alloying and impurity elements also play an important role in the formation of an oxide film.

Overall, we find that the use of APT can enable signature discovery and insight into material origin and behavior in corrosive environments. Lastly, we highlight ongoing challenges and opportunities for APT in forensic investigations.

2:30 PM CH03.02.03

Atomic Scale Understanding of the Role of Alloying Elements in the Hydrogen Embrittlement of Austenitic Steels [HeenaKhanchandani](#); FAU, Germany

High strength twinning induced plasticity (TWIP) steels are prone to oxidation and hydrogen embrittlement. They are austenitic and have high manganese (above 20 wt%) content. We studied the segregation of oxygen and hydrogen at the grain boundaries of a Fe 27Mn 0.3C (wt%) TWIP steel by atom probe tomography which also appears to be associated to the depletion of manganese. We observed that oxygen and hydrogen do not tend to segregate at the grain boundaries decorated with carbon. Motivated by this atomic scale study, we developed an austenitic steel with high carbon content and propose the stabilization of austenitic microstructure in steels by using carbon. The newly developed carbon austenitic steel did not show any embrittlement when it was exposed to the cathodic hydrogen charging. The role of alloying elements in the hydrogen embrittlement susceptibility of the austenitic steels will hence be discussed in the talk along with the novel concept of carbon austenitic steels resistant to hydrogen embrittlement.

2:45 PMBREAK

SESSION CH03.03: Atom Probe Tomography—Instrumentation and Data Analysis

Session Chairs: Baishakhi Mazumder and Frederick Meisenkothen

Monday Afternoon, November 27, 2023

Sheraton, Third Floor, Dalton

3:15 PM *CH03.03.01

Atom Probe Tomography for Semiconducting Materials for Microelectronics and Optoelectronics Applications [KatherineRice](#), YimengChen, IsabelleMartin, TyProsa, RobertUlfig, DavidReinhard and DavidLarson; CAMECA, United States

Atom probe tomography is one of the highest resolution techniques for elemental analysis at the nanoscale. The 3D data also provides a more complete picture of typical semiconductor structures which is challenging to obtain with other nanoscale characterization techniques. The semiconductor manufacturing industry has largely adopted the atom probe tomography technique, but this hasn't come without challenges. Typically problems include yield or survivability of the sample through key regions of interest, sample throughput and speed of data acquisition, results matching between instruments, certainty in low-concentration measurements, and time-to-knowledge of critical data in the analysis process.

In this talk, technological and methodological innovations that CAMECA has adopted to support the semiconductor manufacturing industry specific to microelectronics and optoelectronics and tackle some of these challenges will be presented. Examples include automation, instrument matching, simultaneous voltage and laser pulsing, adoption of shorter wavelength lasers, and new reconstruction methods for closer feature fidelity. CAMECA has also initiated a large-scale collaboration effort with Interuniversity Microelectronics Centre (imec) as an independent semiconductor research institution to support the goals of applying atom probe to semiconductor manufacturing by creating test structures for semiconductor research.

Atom probe applications for semiconductors, power electronics, and optoelectronics are growing and driven by advances in instrument technology. Higher yield, automated reconstruction and analysis, and the ability to conduct design of experiments studies have all been recently enabled by technology development at CAMECA. In this presentation, we will discuss these developments and how we can enable the atom probe technology community in analysis of semiconductor materials.

3:45 PM CH03.03.02

Full-Dynamics Field Evaporation Simulation: Overcoming Limitations of Transition State Theory for Atom Probe Tomography [JiayuwenQi](#)¹, [EmmanuelleMarquis](#)² and [WolfgangWindl](#)¹; ¹The Ohio State University, United States; ²University of Michigan, United States

In atom probe tomography (APT), individual atoms or molecules are field-evaporated by an intense electric field from the surface of a needle-shape specimen. Following a linear projection law, APT allows for the reconstruction of a three-dimensional distribution of atoms within the specimen using recorded impact positions and the chemical identity information obtained from a mass spectrometer. However, due to the destructive nature of the field evaporation process, the verification of reconstruction results and quantification of their uncertainty necessitate atomic-scale forward modeling, where each atom can be traced.

Previous atomic-scale models in APT have implicitly relied on harmonic transition state theory (TST) [1]. However, TST is limited to predicting the rate of transition between states and fails to describe the underlying dynamics. Consequently, these models introduce ad-hoc assumptions, typically assigning a zero-launch velocity to evaporating atoms, which introduces biases in the calculation of atom trajectories and impact positions on the detector. As a result, many distinct features observed in field evaporation maps and reconstruction, arising from the full dynamics of atoms, cannot be faithfully reproduced or explained.

To overcome the limitations of TST in describing field evaporation, we employ molecular dynamics (MD) simulations with appropriate acceleration algorithms as an alternative. Our "ab-initio" field evaporation simulation method "TAPSim-MD" [2] integrates evaporation events as part of the MD simulation. This approach combines the classical finite-element field evaporation modeling from the TAPSim code [3] with the MD code LAMMPS [4]. In the resulting full-dynamics approach, atoms in the specimen are evaporated in an "ab-initio" way during the competition between the interatomic forces and the electrostatic forces. This eliminates the need for ad-hoc assumptions regarding activation energy or launch velocity.

By employing full-dynamics simulations, we successfully reproduce and explain the emergence of enhanced zone lines in field evaporation maps, which are dynamic features beyond the capabilities of TST-based models [5]. In a recent study, we revisited field evaporation in an [001] oriented γ -TiAl intermetallic compound, where experimental observations often exhibit mixed-layer reconstruction results due to the alternating Ti/Al layers. While traditional simulation approaches explained this artifact by assuming a higher evaporation field for Al compared to Ti [6], they failed to account for the distinct field evaporation maps obtained for Ti and Al, which should be inherently related to the dynamics. Through our full-dynamics approach, we accurately predicted the correct evaporation sequence in an [001] oriented γ -TiAl virtual tip and reproduced the mixed-layer artifact in reconstruction without any ad-hoc assumptions regarding the evaporation field of Ti or Al. Furthermore, we identified two distinct paths of bond breaking during the evaporation process: Ti initially breaks 4 Ti-Al bonds before breaking 2 Ti-Ti bonds (a two-step process), while Al-Al simultaneously breaks 4 Ti-Al and 2 Al-Al bonds (a one-step process). These two distinct bond-breaking paths elucidate the distinct evaporation

maps of Ti and Al, which also rationalizes the counter-intuitive higher evaporation field of Al, considering its generally weaker bonding ability.

References:

- [1] M Marcelin, *Ann. Phys.* 9 (3) (1915), p. 120–231.
- [2] J Qi et al., *Phys. Rev. Mater.* 6, 093602 (2022), p. 11.
- [3] C Oberdorfer et al., *Mater. Charact.* 146 (2018), p. 324.
- [4] S Plimpton, *J. Comput. Phys.* 117 (1995), p. 19.
- [5] J Qi et al., *Scr. Mater.* 230, 115406 (2023)
- [6] T Boll and T Al-Kassab, *Ultramicroscopy* 124 (2013), p. 1–5.
- [7] Funding for this work was provided by Dr. Ali Sayir's portfolio within the Air Force Office of Scientific Research under grant number FA9550-14-1-0249 and FA9550-19-1-0378.

SESSION CH03.04: Poster Session: Atom Probe Tomography
Session Chairs: David Diercks and Baishakhi Mazumder
Monday Afternoon, November 27, 2023
Hynes, Level 1, Hall A

8:00 PM CH03.04.01

Analysis of the Effect of Milling Temperature on the Antioxidation Behavior of Oxide-Dispersion-Strengthened Steel Won Sang Shin and Yoon-Jun Kim; Inha University, Korea (the Republic of)

Oxide-dispersion-strengthened (ODS) steel exhibits remarkable creep and oxidation resistance and therefore has potential for use in severe environments such as the core components of advanced nuclear reactors. The combination of appropriate factors and parameters such as nanometer-sized oxide features, milling methods, temperature and time enable the steels to withstand high-temperature degradation. Y-Ti-O nanometer-sized particles with a diameter of less than 5 nm play a key role in the properties of these materials. Therefore the oxidation resistance characteristics of ODS steel manufactured by ball milling at two temperatures were analyzed through various techniques via Atom-Probe tomography.

In this study, a comparative analysis was performed on the difference in the oxidation behavior of ODS steel according to the milling temperature. ODS steel were produced by mechanical alloying with milled Y_2O_3 powder in a ball mill at room temperature and cryotemperature (≈ -150 °C). Both samples were exposed to air for 6000 h at 800 °C for examining their long-term oxidation resistance at a high temperature. After long-term exposure both samples showed subsurface degradation occurred concurrently such as internal precipitation, phase formation, and phase dissolution.

The resulting oxide scaling kinetics were more sluggish for room cryotemperature compared to room temperature condition. On the basis of the reduction of the interfacial energies calculated by using the Gibbsian interfacial excess and the partial radial distribution functions of major alloying elements, Y atoms in room temperature condition were found to show a strong tendency to form Y-Ti-O nanoparticles (NPs), while N atoms did not form NPs on the surface. Analysis results showed that Y-Ti-O NPs were present at the grain boundaries at room temperature and that cryotemperature condition contained Y-Ti-O(N) NPs and sub-micrometer-sized TiN precipitates. Due to differences in the formed NPs, more Y atoms segregated at the matrix/oxide interface of room temperature compared to cryotemperature condition inhibited oxide growth. Therefore, the Y atom can be considered as a controlling factor for the oxidation rate at high temperature, and that the difference in oxidation resistance between the two samples is also related to this.

SESSION CH03.05: Atom Probe Tomography—Advanced Materials and Correlative Analysis
Session Chairs: David Diercks and Pritesh Parikh
Tuesday Morning, November 28, 2023
Sheraton, Third Floor, Dalton

8:30 AM *CH03.05.01

Field Emission Physics and Correlative Microscopy within a Photonic Atom Probe Lorenzo Rigutti¹, Abraham Diaz Damian¹, Jonathan Houard¹, Georges Beainy¹, Pradip Dalapati^{1,2}, Angela Vella¹, François Vurpillot¹, Jean-Michel Chauveau³, Maxime Hugues⁴, Denis Lefebvre⁴, Grzegorz Muziol⁵ and Henryk Turski⁵; ¹University of Rouen Normandie, France; ²Technological University, Singapore; ³Université Paris Saclay, Université Versailles Saint Quentin en Yvelines, CNRS, France; ⁴Université Côte d'Azur, CNRS, France; ⁵Polish Academy of Sciences, Poland

The Photonic Atom Probe (PAP) allows for the measurement of Photoluminescence (PL) of a sample tip while it is being analyzed by Laser-Assisted Atom Probe. The femtosecond Laser pulse required for the La-APT measurement also serves to excite the free charge carriers, whose recombination provide the PL signal. As a consequence, it becomes possible to correlate the optical signature of the different parts of a complex structure with the 3D distribution of the contained chemical species [1].

We present an application of the PAP on III-nitride p-i-n junctions, namely a thick ($> 1\mu\text{m}$ thickness) multi-layer structure containing InGaN quantum wells and a buried tunnel junction [2]. Plasma-assisted molecular beam epitaxy-grown structures, which were used in the study, are characterized by diverse doping concentrations in both p- and n-type regions. The PL spectra can be correlated with the 3D chemical information from APT [3]. The PL signals exhibit indeed a donor-acceptor pair (DAP) emission, whose spectral features can be related to the 3D distribution of the Mg dopants and of the InGaN heterostructures. These results open interesting perspectives for studies of light-emitting defects at the nanoscale.

Besides the interest of this instrument as a microscope [3], the particular conditions in which the optical signatures of localized light emitters are collected open intriguing possibilities for the study of field ion emission under high field and under laser illumination [4]. As an example, the PL spectral shift allows measuring the stress induced by the application of a strong electric field at the tip apex and its propagation through the tip. This has been evidenced both through the study of the stress-induced splitting of the zero-phonon line of the NV⁰ center in diamond [5] and of the quantum well (QW) emission in a ZnO/(Mg,Zn)O system [6], allowing measuring stress levels ranging from 9 GPa to ~ 1 GPa.

- [1] J. Houard *et al.*, “A photonic atom probe coupling 3D atomic scale analysis with in situ photoluminescence spectroscopy,” *Review of Scientific Instruments*, vol. 91, no. 8, p. 083704, Aug. 2020, doi: 10.1063/5.0012359.
- [2] H. Turski *et al.*, “Nitride LEDs and Lasers with Buried Tunnel Junctions,” *ECS J. Solid State Sci. Technol.*, vol. 9, no. 1, p. 015018, Dec. 2019, doi: 10.1149/2.0412001JSS.
- [3] E. Di Russo *et al.*, “Super-resolution Optical Spectroscopy of Nanoscale Emitters within a Photonic Atom Probe,” *Nano Lett.*, vol. 20, no. 12, pp. 8733–8738, Dec. 2020, doi: 10.1021/acs.nanolett.0c03584.
- [4] E. Di Russo and L. Rigutti, “Correlative atom probe tomography and optical spectroscopy: An original gateway to materials science and nanoscale physics,” *MRS Bulletin*, vol. 47, no. 7, pp. 727–735, Jul. 2022, doi: 10.1557/s43577-022-00367-6.
- [5] L. Rigutti *et al.*, “Optical Contactless Measurement of Electric Field-Induced Tensile Stress in Diamond Nanoscale Needles,” *Nano Lett.*, vol. 17, no. 12, pp. 7401–7409, Dec. 2017, doi: 10.1021/acs.nanolett.7b03222.
- [6] P. Dalapati *et al.*, “In Situ Spectroscopic Study of the Optomechanical Properties of Evaporating Field Ion Emitters,” *Phys. Rev. Applied*, vol. 15, no. 2, p. 024014, Feb. 2021, doi: 10.1103/PhysRevApplied.15.024014.

9:00 AM CH03.05.02

Correlative In-Situ Liquid Cell Electrochemistry TEM and Cryogenic APT of Liquid-Solid Interfaces Shelly Michele Conroy, Neil Mulcahy, James Douglas, Lukas Wolch, Mary Ryan and Baptiste Gault; Imperial College London, United Kingdom

Liquid cell transmission electron microscopy (LCTEM) allows for solution phase dynamic processes to be visualised and probed at the nanoscale at unprecedented temporal and spatial resolutions in comparison to other liquid microscopy techniques such as light and physical probe microscopes. Additionally, MEMS based biasing sample holder chip design has provided a platform to perform electrochemical experiments to replicate battery cycling experiments within the electron microscope.

While these experiments have been useful for gaining a micro and nanoscale in-situ understanding of electrochemical processes that occur at solid-liquid interfaces of battery materials, the current spatial resolution of liquid processes within the TEM is still not capable of resolving and quantifying complex dynamic nanoscale structures at atomic resolutions. As a result, the performance of electrochemical systems is currently limited due to a lack of understanding of complex interactions that occur between mobile species and electrode materials. Finding a

correlative high-resolution characterisation method which is compatible with both the liquid and solid component of the interface is of great importance to gain a fundamental understanding of these processes at an atomic level.

Cryogenic focused ion beam (FIB) preparation and atom probe tomography (APT) has allowed researchers to investigate the native liquid-solid interfaces of samples by vitrifying the liquid phase at the near to atomic scale. In this presentation we will present how one can combine in-situ electrochemistry LCTEM with site specific cryogenic atom probe tomography. We investigate Li based solid electrode interfaces and dendrites formed during the lithiation cycling.

While there have been numerous examples in recent years of room temperature correlative TEM and APT, there has been no such examples of correlative LCTEM-APT or correlative cryogenic TEM-APT. The primary reason for this is the difficulty in transferring, preparing, and maintaining specimens in **cryogenic conditions**. In this study, the liquid in the LCTEM chips are cryogenically vitrified following in-situ electrochemical LCTEM experiments, in order to allow APT needle samples to be created from the liquid-solid interface of interest. Recent advances in vacuum cryo transfer module technology, and cryogenic FIB site specific sample preparation workflows, have allowed for this type of correlative cryogenic multi-microscopy approach to be realised.

9:15 AM CH03.05.03

Design and Observation of Multiscale Defect Structures in Bulk Thermoelectric Materials Employing Atomic Resolution Scanning TEM and Atom Probe TomographyInChung; Seoul National University, Korea (the Republic of)

Nearly ~70% of total energy input is being lost as waste heat, and electrical energy is mostly generated by consuming fossil fuels such as coal and natural gas. Thermoelectric technology can simultaneously contribute to addressing these urgent energy and environmental crises that humanity faces. Thermoelectric materials can directly convert thermal and electrical energy reversibly without releasing undesirable chemical residues. Thermoelectric figure of merit, ZT, is a complex combination of charge and thermal transport properties. Because they are closely interrelated by the fundamental physics laws, it is extremely difficult to increase ZT by adjusting one of the constituents in the ZT formula. Very recently, designing and stabilizing defect structures have emerged as a new powerful strategy to increase ZT because they can decouple otherwise tightly bound physical quantities in ZT, thereby providing innovative and unconventional pathways for higher ZT materials. Until recently, formation mechanisms of defect structures and their effects on thermoelectric properties have not well understood mainly because of the technical difficulties. In this talk, I will present our recent works on designing multiscale defect structures in bulk inorganic crystal matrices by chemical composition controls to develop high performance thermoelectric materials. We directly observe the induced defect structures using atom probe tomography (APT) and atomic resolution spherical aberration-corrected scanning TEM (Cs-STEM). The achievements help understand how they affect bulk thermoelectric properties, thereby developing highly predictable defect design principles. This talk will highlight the importance of the combined utilization of ATP and Cs-STEM for a highly productive search for high performance thermoelectric materials.

9:30 AMBREAK

10:00 AM *CH03.05.04

Understanding the Atomic Scale Mechanisms of Oxidation and Hydrogen Embrittlement of Nuclear Structural Materials using *In Situ* and Cryogenic Transfer Atom Probe TomographyArunDevaraj, DallinBarton, StenV. Lambeets, TingkunLiu, MarkWirth and DanielPerea; Pacific Northwest National Lab, United States

When nuclear structural materials, specifically stainless steel is subjected simultaneously to applied tensile stress and a corrosive, high-temperature water, interplay of hydrogen and oxygen interactions with the alloy microstructure are thought to lead to intergranular stress corrosion cracking (SCC). Despite decades of research on SCC mechanisms of stainless steel, crucial knowledge gaps remain about the atomic scale mechanisms responsible for intergranular oxidation and hydrogen embrittlement. To overcome these knowledge gaps, we used the novel in situ atom probe tomography (APT) experiments and cryogenic transfer workflow of steel samples after electrochemical hydrogen charging. These APT experiments were complemented by insights from atomic force microscopy, nanomechanical testing, synchrotron high-energy x-ray diffraction, ex-situ transmission electron microscopy, and computational simulations. Through this multimodal approach, we developed an atomic scale understanding of the mechanochemical coupling during SCC of Fe-Cr-Ni model alloys. This effort leveraged the Ferrovac Ultrahigh vacuum cryogenic transfer module, environmental transfer hub, and cryogenically cooled sample transfer carousel and the cryogenic transfer workflow developed in PNNL for a CAMECA LEAP 4000 XHR and a CAMECA LEAP 6000 XR. This talk will highlight the new scientific understanding of oxidation and hydrogen embrittlement mechanisms enabled by these unique experimental capabilities and expertise in PNNL.

10:30 AM CH03.05.05

Quantification of Dopants in Silicon using Atom Probe TomographyKarenDeRocher, MarkMcLean and FrederickMeisenkothen; National Institute of Standards and Technology, United States

The ever-increasing demand for semiconductor devices to shrink into the 3 nm regime without compromising computing power has made characterizing these materials incredibly challenging. In order to maintain device performance, there is a growing need to characterize these materials at device dimensions and accurately quantify and localize dopant atoms [1].

Atom probe tomography (APT) is currently the lone characterization technique with the ability to provide dopant distributions in semiconductor devices at device dimensions and in 3-dimensions. While APT can measure chemical information down to concentrations of 10¹'s of μg/g (ppm_{at}), it has also been shown that, for some materials, analysis conditions can result in biased quantitative results [2, 3]. While the use of reference materials to calibrate data analysis is common in many characterization techniques, it is not generally used in APT. However, it has been shown that a standards-based approach to APT analysis can dramatically improve the accuracy of composition measurements [4, 5]. More recently, our work with phosphorous-doped silicon showed similar improvement in the accuracy of dopant quantification in the atom probe. In this work, we used a reference material with a known dose of phosphorous (NIST SRM 2133 [6]). We collected data from this material under a variety of analysis conditions and used that data to construct a calibration curve. We then performed similar analysis on a sample doped with a known concentration of phosphorous. After correcting our measurements using the calibration curve, reduced the relative error from 26% to less than 4% [7].

The reference material used for this work (NIST SRM 2133) was originally developed for use in secondary ion mass spectrometry (SIMS) and has a phosphorous concentration that varies with depth, with the total retained dose being the certified value. This required us to capture the entire doped profile in an atom probe experiment in order to use the results for our calibration curve. However, this introduces complexity both in sample preparation, and in the collection and analysis of the atom probe data. Therefore, we are also working to develop a research grade test material (RGTM) that is better suited for use with atom probe tomography. This material has a blanket film of P-doped Si at a constant composition, eliminating the need to preserve the precise sample surface during FIB sample preparation and speeding up acquisition times, as an entire doped profile no longer needs to be captured [8].

References:

1. Fuechsle, M., et al., Nature Nanotechnology, 2012. 7(4): p. 242-246.
2. Morris, R.J.H., et al., Journal of Vacuum Science & Technology B, 2018. 36(3): p. 03F130.
3. Meisenkothen, F., et al., Ultramicroscopy, 2015. 159: p. 101-111.
4. Gopon, P., et al., Microscopy and Microanalysis, 2022. 28(4): p. 1127-1140.
5. Meisenkothen, F., et al., Microscopy and Microanalysis, 2020. 26(S2): p. 176-177.
6. Simons, D.S., et al., Journal of Vacuum Science & Technology B: Microelectronics and Nanometer Structures Processing, Measurement, and Phenomena, 2007. 25(4): p. 1365-1375.
7. DeRocher, K., M. McLean, and F. Meisenkothen, Microscopy and Microanalysis, 2022. 28(S1): p. 728-729.
8. Certain commercial equipment, instruments, or materials are identified in this paper in order to specify the experimental procedure adequately. Such identification is not intended to imply recommendation or endorsement by the National Institute of Standards and Technology, nor is it intended to imply that the materials or equipment identified are necessarily the best available for the purpose.

10:45 AM CH03.05.06

Successes and Challenges for Atom Probe Tomography of Small-Molecule Organic MaterialsJeremyD. Zimmerman, RolandBennett, PaulNiyonkuru and JaehyunSuh; Colorado School of Mines, United States

We will highlight several successes using atom probe tomography (APT) to analyze small-molecule organic materials and discuss challenges and opportunities for APT of these materials. Organic small molecule materials are used in a variety of applications, such as organic light emitting diodes (OLEDs); OLEDs are widely used in displays, yet there are many open questions about how molecular design ultimately impacts device properties. The light-emitting layer of an OLED is comprised of a co-deposited layer of two or more molecules, but little is known about how well these dissimilar molecules mix. A primary challenge with APT of organic molecules is that they are very sensitive to both electron-beam and ion-beam damage during conventional FIB-based tip preparation. We will review techniques to prepare and analyze these organic molecular materials,¹ including the development of large-radius APT tip coupons that enable fast sample preparation through thermal evaporation of materials onto the tips, entirely avoiding damage associated with FIB preparation and a quantitative model for understanding and predicting fragmentation of small molecules during APT measurement.² We will also address challenges associated with these materials, including low detector efficiencies, which can limit the

sensitivity of APT measurements. This research expands the capabilities of APT, enabling additional materials science of organic small molecule materials research.

¹ A. P. Proudian, M. B. Jaskot, D. R. Diercks, B. P. Gorman, and J. D. Zimmerman, “*Atom Probe Tomography of Molecular Organic Materials: Sub-Dalton Nanometer-Scale Quantification*” *Chem. Mater.* **31** (7), 2241 (2019).

² Jacob T. Bingham, Andrew P. Proudian, Shubham Vyas, and Jeremy D. Zimmerman, “*Understanding Fragmentation of Organic Small Molecules in Atom Probe Tomography*” *The Journal of Physical Chemistry Letters* **12** (42), 10437 (2021).

11:00 AM CH03.05.07

Atomic-Level Investigation of Oxygen Distribution in Grain Boundaries in Yttria-Stabilized Zirconia using Graph-Order Parameter Parth Desai, Prachi Garg, Baishakhi Mazumder and Olga Wodo; State University of New York at Buffalo, United States

Yttria-stabilized zirconia (YSZ) is a widely utilized ceramic material renowned for its remarkable mechanical and thermal properties. However, it is susceptible to low-temperature degradation (LTD), adversely affecting its long-term performance. This degradation process is hypothesized to be closely linked to the occurrence of oxygen vacancies within the crystal lattice. To understand the origins of LTD, Atom Probe Tomography (APT) is employed as a characterization technique to investigate the microstructure of YSZ. To analyze the sample and understand oxygen distribution, we translate the local atomistic environment characterization method from molecular dynamics into the APT field. The method is based on the graph representation of point cloud data coupled with the information theory entropy measures to capture the local environment's chaos/order and density. In this study, we learned that this method is highly sensitive to small changes in the number and connectivity of the oxygen ions. We unravel that grain boundaries are lean in the less connected oxygen ions compared to the grains, offering direct atomistic evidence of noticeable differences between grain and grain boundaries of zirconia. This knowledge contributes to developing strategies for enhancing the material's resistance to low-temperature degradation and optimizing its performance in diverse applications.

11:15 AM CH03.05.08

Li₀ FeNi Tetraenaite in Iron Meteorites: An Atom Probe Tomography Investigation Frederic Danoix¹, Raphael Danoix¹, Fabien Cuvilly¹, Jerome Gattacceca², Clara Maurel², Mathieu Roskosz² and Matthieu Gounelle³; ¹CNRS Normandy University, France; ²CEREGE, France; ³MNHN, France

Metal matrix in siderites are iron based alloys containing up to 35at%Ni as well as other minor elements such as Co and P, at levels lower than 1at%, the microstructure of which keeps records of their thermal and mechanical history. The initial metal alloy was melted in the heart of planetesimals in the early days of the solar system. After formation, the planetesimal slowly cooled down, leading to the solidification of the metal alloy as FCC austenite. Due to the extremely slow cooling rate (between 1 and 100K/10⁶ years), austenite grains could reach sizes up to several meters. During cooling, austenite experienced several solid-state transformations, starting with the precipitation of Widmanstätten ferrite, resulting in the development of the iconic microstructures of iron meteorites [1]. As it grows, ferrite rejects nickel, creating a Ni composition gradient in austenite, that extends over several hundred microns. This gradient, starts at more than 50% Ni at the interface with the ferrite, down to the initial Ni content, usually close to 7at%Ni. This naturally graded material makes it possible to explore the Fe rich part of the low temperature FeNi phase diagram [2]. In addition, due to the small cooling rate it possible to explore the reach full equilibrium conditions, at least for temperatures higher than approx. 300°C. In this work, we used atom probe tomography (APT), combined with electron backscattered diffraction (EBSD) and transmission Kikuchi diffraction (TKD) on focused ion beam (FIB) lift outs for site specific specimen preparation, allowing investigation of the compositional and nanostructural features of this gradient material. The fine scale complexity of the final microstructures revealed in octaedites and ataxites, two types of Ni rich iron meteorites, is discussed in the framework of the FeNi phase diagram. Of particular technological interest is Fe-36Ni alloy, also known as INVAR®, for which equilibrium phases can be described, providing an alternative investigation route to electron irradiation. Another technologically important phase present in iron meteorites is tetraenaite, an equiatomic FeNi Li₀ ordered variant of austenite. This phase, only present in meteoritic irons, is an extremely promising substitute to rare earth element (REE) based permanent magnet, as it exhibits very similar magnetic properties. Being REE free, and based on low cost and widely available elements, it would reduce dependence on toxic, environmentally harmful rare earth mines, and on China's multi-billion rare earth element monopoly. Understanding the formation path of tetraenaite is becoming a global geo-strategic issue of the next decade. Complex nanostructures containing tetraenaite are analysed by atom probe tomography, and some will be shown, in particular in the Santa Catharina meteorite.

References:

[1] Buchwald V.F., Handbook of Iron Meteorites - Vol. 1 (1975) Univ. of California Press.

[2] Goldstein J.I., Short J.M., *Geochim. Cosmochim. Acta* **31** (1967) 1733-1770

SESSION CH03.06: Atom Probe Tomography—Minerals, Biominerals, and Oxides

Session Chairs: David Diercks and Pritesh Parikh

Tuesday Afternoon, November 28, 2023

Sheraton, Third Floor, Dalton

1:30 PM *CH03.06.01

Atom Probe Tomography (APT) Analysis of Minerals Alberto Perez-Huerta; University of Alabama, United States

The use of atom probe tomography (APT) in the analysis of minerals is becoming a powerful tool for geoscience applications. Most of the work has been focused on the study of isotropic minerals, mainly for geochronology and elucidating mineral formation under different temperature and pressure conditions. Thus, for the last ten years, we have been studying the different variables that control the quality of APT data for these minerals. The first part of the talk will be a summary of what we have learned so far about the influence of the crystallo-chemistry and physical properties of minerals (i.e., thermal conductivity) for the best outcomes of APT analyses. The second part will be centered around our most recent efforts in the analysis of layered, anisotropic minerals. We will be discussing challenges in sample preparation and 3D reconstructions of datasets, as well as potential applications of APT to the study of these ubiquitous minerals on Earth's crust and other planets. Finally, we will be talking about new directions in the use of APT for the characterization of geomaterials.

2:00 PM CH03.06.02

Ranging Atom Probe Spectra for Multi-Element Analyses Frederick Meisenkothen, David Newton, Karen DeRocher and Mark McLean; National Institute of Standards and Technology, United States

Atom probe tomography (APT) is becoming an essential nano-characterization tool in a wide variety of fields. In principle, APT can deliver 3-dimensional chemically resolved images of nano-scale analysis volumes, thereby making the technique uniquely suited for applications requiring composition measurements at dimensions approaching atomic-scale (e.g., semiconductors) and nano-scale analysis in fields such as nano-geology. In practice, APT analyses can be hindered by two broad types of limitations – ion trajectory aberrations and composition measurement bias – leading to image distortions and erroneous chemical analysis results. However, these limitations are not constrained by physics, and thus should be possible to overcome through measurement science, technological advances, and application of standards. Ion ranging – i.e., how to properly attribute regions of interest in the spectrum to specific ion species – and associated measurement bias have long been topics of discussion within the APT community. APT spectra are complex, with peak forms often varying significantly between ion species and between data sets. No single model peak form can be applied universally to range spectra and there is no community-wide consensus on how best to range spectra, which can lead to erroneous analysis results and lack of reproducibility.

We have previously achieved accurate and repeatable single-element isotopic analysis results by employing a three-step analysis approach that relies on data filtering (artifact removal), adaptive peak fitting (assumes all isotopic variants within a given ion species have the same peak shape), and standards-based calibration (using known reference materials) [1-3]. However, this three-step approach cannot be used for complex multi-element analyses. In multi-element analyses, the peak forms often cannot be assumed to be identical, as required for adaptive peak fitting, and filtering the data to remove artifacts can introduce additional composition measurement bias. An alternative methodology must be developed.

We present the results of a systematic ion ranging study for multi-element analyses that compares about ten different APT peak sampling methodologies. A natural mineral specimen was chosen for the study since the material was characterized by multiple complementary methods and produced complex multi-element APT spectra with a high fraction of multi-hit detection events. Clear trends in the analysis results were observed for the measured element ratios of interest. The trends could be demonstrably associated with peak sampling bias and data interpretation artifacts. By applying a custom correction method to account for peak sampling bias, the analysis results improved significantly, with up to a 10-fold reduction in bias for the relevant peak ratios measured. Surprisingly, all APT ion ranging methodologies explored yielded similar analysis results, once peak sampling bias was accounted for. Further, the APT results largely agreed with the other complementary analysis methods employed for validation.

References

[1] P. Gopon, J.O. Douglas, F. Meisenkothen, J. Singh, A.J. London, M.P. Moody, Atom Probe Tomography for Isotopic Analysis: Development of the 34S/32S System in Sulfides, *Microsc. Microanal.*, (2021) 1-14.

[2] F. Meisenkothen, M. McLean, I. Kalish, D.V. Samarov, E.B. Steel, Atom Probe Mass Spectrometry of Uranium Isotopic Reference Materials, *Analytical Chemistry*, 92 (2020) 11388-11395.

[3] F. Meisenkothen, D.V. Samarov, I. Kalish, E.B. Steel, Exploring the accuracy of isotopic analyses in atom probe mass spectrometry, *Ultramicroscopy*, 216 (2020).

2:15 PMBREAK

2:45 PM +CH03.06.03

Imaging Interfaces and Interphases in Mineralized TissuesDerkJoester; Northwestern University, United States

Mineralized tissues are sophisticated materials with properties that include high toughness at low weight, outstanding fatigue life, self-repair capabilities, and sustainable synthesis. Often hierarchically structured, grain and interphase boundaries play an important role in the biosynthesis and final functional properties of mineralized tissues. However, the complex structure and phase composition, often with characteristic features at the nanoscale, the low atomic number of many physiologically relevant elements, and sensitivity to electron and X-ray beams creates significant challenges to the characterization of these biological materials.

I will discuss how UV-laser pulsed atom probe tomography (APT) has provided us with deep insights into compositional gradients at organic-organic interfaces in invertebrate teeth and bone-type tissues, helped us identify the role of an amorphous intergranular phase that acts as a cement in rodent enamel, and discover nanoscale gradients in hydroxylapatite crystallites in vertebrate tooth enamel.[1-5] I will further report on development of correlative elemental imaging using X-ray diffraction at the mesoscale (here: 0.25-20 μm) that allows us to extend the field of view beyond what APT can deliver.[6] Finally, I will provide a progress report on our characterization of a highly unusual biomineral, celestine (SrSO_4), that is found in single crystalline endoskeletal spicules in Acantharea, a class of marine zooplankton. This investigation is motivated by the high level of biological control over single-crystal growth evident in different Acantharea species, and because understanding how Acantharea selectively sequester Sr^{2+} over chemically similar ions present in seawater, is of interest for example for removal of ^{90}Sr from nuclear waste.

[1] Gordon and Joester, *Nature* **2011**, 469, 194-197. [2] Gordon, Tran, and Joester, *ACS nano* **2012**, 6, 10667-10675. [3] Gordon, Cohen, MacRenaris, Pasteris, Seda, and Joester, *Science* **2015**, 347, 746-750. [4] Gordon, Joester, *Front Physiol* **2015**, 6. [5] DeRoche, Smeets, Goodge, Zachman, Balachandran, Stegbauer, Cohen, Gordon, Rondinelli, Kourkoutis, Joester, D. *Nature* **2020**, 583, 66-71. [6] Free, DeRoche, Cooley, Xu, Stock, and Joester, *Proc Natl Acad Sci USA* **2022**, 119, e2211285119.

3:15 PM CH03.06.04

High Diffusivity Pathways in Human Dental EnamelXingchenZhao, DieterIsheim, XinqiChen and DerkJoester; Northwestern University, United States

Tooth enamel is an acellular, mineralized tissue with limited regenerative potential. Loss of enamel integrity and function, whether congenital, acquired, or environmental in origin, is irreversible, ubiquitous, and imposes great burdens on society [1]. Ions such as F^- , CO_3^{2-} , Na^+ , Ag^+ , Sr^{2+} , Fe^{3+} , and Mg^{2+} , are important determinants of enamel solubility; some are widely used in the prevention or treatment of defects. However, their mechanism of action and mode of transport in enamel remain poorly understood. This is at least in part due to the fact that the complex, hierarchical architecture of enamel was not taken into account in prior work studying diffusion in enamel under physiological conditions [2].

At the microscale, human enamel consists of rods that run from the dentino-enamel junction towards the external enamel surface and interrod enamel. Both are comprised of crystallites of hydroxylapatite (OHAp) that are highly elongated along the c-axis direction but display typical cross-sectional edge lengths of only 25-50 nm. Atom probe tomography (APT) and synchrotron X-ray microdiffraction revealed that crystallites are cemented together by an amorphous intergranular phase (AIGP) [3], are compositionally graded with a core enriched in minority components and a depleted shell [4], and that their average composition differs between rod and interrod enamel [5]. In the context of these recent insights, our long-term goal is to improve the understanding of transport processes in healthy enamel and enamel lesions as an integral step towards understanding the mechanisms by which lesions form and therapeutics act.

Herein, we describe a multi-scale correlative approach using depth profiling time-of-flight secondary ion mass spectrometry (ToF-SIMS) and X-ray photo-electron spectroscopy (XPS) to determine average concentration profiles for multiple rods and interrod enamel ($\sim 2500 \mu\text{m}^2$) and APT to systematically determine effective diffusivities of F^- , Na^+ , Ag^+ , Sr^{2+} , Fe^{3+} , Zn^{2+} , and Mg^{2+} in the intergranular phase and, by extension, in rod and interrod enamel. For this purpose, ground and polished sections roughly parallel to the external surface of human premolars were treated with aqueous solutions of selected ions (0-1000 ppm, pH 7, 25 C, 24h). Concentration depth profiles (normal to the surface) were determined using ToF-SIMS and/or XPS. Chemical diffusivities were determined by fitting concentration profiles. Preliminary analysis suggest that diffusivities in rod and interrod enamel may differ by a factor of up to 30. Effective bulk diffusivities for both rods and interrods fell into the range between 10^{-16} to $10^{-19} \text{cm}^2/\text{s}$ and decreased in the following order: $\text{Sr}^{2+} = \text{F}^- > \text{Mg}^{2+} = \text{Na}^+ > \text{Cl}^- \gg \text{Ba}^{2+} \gg \text{K}^+$. Effective and absolute diffusivities at nanoscale level were acquired by fitting the APT reconstruction along with ion profiles from TOF-SIMS or XPS. APT analysis has been conducted on enamel treated with Na^+ , Mg^{2+} , Ag^+ , F^- , and Sr^{2+} compared with the original untreated enamel. Na^+ and F^- uptake by the AIGP can differ from crystallites by a factor of up to 100; Mg^{2+} and Sr^{2+} uptake by the AIGP was less than 10 times than from crystallites; Ag^+ barely infiltrates both crystallites and AIGP.

[1] N. Kassebaum, E. Bernabé, M. Dahiya, B. Bhandari, C. Murray, W. Marcenes, *Journal of dental research*, 94 (2015) 650-658.

[2] V.K. Kis, A. Sulyok, M. Hegedus, I. Kovács, N. Rózsa, Z. Kovács, *Acta Biomaterialia*, 120 (2021) 104-115.

[3] L.M. Gordon, M.J. Cohen, K.W. MacRenaris, J.D. Pasteris, T. Seda, D. Joester, *Science*, 347 (2015) 746-750.

[4] K.A. DeRoche, P.J. Smeets, B.H. Goodge, M.J. Zachman, P.V. Balachandran, L. Stegbauer, M.J. Cohen, L.M. Gordon, J.M. Rondinelli, L.F. Kourkoutis, *Nature*, 583 (2020) 66-71.

[5] R. Free, K. DeRoche, V. Cooley, R. Xu, S.R. Stock, D. Joester, *Proc Natl Acad Sci U S A*, 119 (2022) e2211285119.

3:30 PM CH03.06.05

Multiscale Microscopic Insights into Low-Temperature Degradation in Zirconia: Enhancing Ceramic StabilityPrachiGarg, PrathimaNalam and BaishakhiMazumder; University at Buffalo, The State University of New York, United States

Zirconia, a ceramic material known for its high fracture toughness, strength, and stability at elevated temperatures and pressures, is utilized in various applications such as solid oxide fuel cells, thermal barrier coatings, and sensors. Tetragonal zirconia, in particular, is highly desirable due to its unique properties, such as high fracture toughness, low thermal conductivity, and high melting temperature. Zirconia doped with 3-mol% Yttria helps stabilize the tetragonal phase and prevents its transformation to the monoclinic (t-m) phase at room temperature. However, extended exposure to extreme conditions, a process known as aging, has been observed to induce spontaneous phase transformations, leading to the development of microcracks and mechanical failure, referred to as low-temperature degradation (LTD). Our study hypothesizes that aging results in the preferential segregation of elements near the grain boundaries, initiating local phase transformations and altering the grain environment.

To investigate this hypothesis, a multi-scale microscopy approach, specifically employing Atomic Force Microscopy (AFM) and Atom Probe Tomography (APT) was utilized to examine the yttria-stabilized zirconia (YSZ) to provide fundamental insights into the degradation mechanisms. The investigation includes a comprehensive study of the material's response to artificial aging, including structural, crystallographic, and chemical analyses. Firstly, the Design of Experiments approach was employed to predict the process parameters necessary for artificially aging samples, relying on information collected from existing literature. AFM allowed us to examine surface topography and changes in grain size, providing detailed morphological changes that occur at the material's surface with aging. APT assisted in acquiring elemental distribution and segregation, offering 3-D compositional mapping with sub-nanometer resolution. The initial results show variation in grain size distribution and grain curvature at all stages of aging, i.e., among unaged, partially aged, and fully aged samples. We also observed preferential segregation of Aluminum and Silicon at certain grain boundaries. Additionally, a difference in Yttria concentration at the grain boundaries between the aged and unaged samples was observed, leading to a possible initiation of local phase transformation. These fundamental investigations enabled to generate novel insights for LTD mechanisms, which is a critical need for designing robust and durable ceramics for practical applications.

This work is supported by NSF award number DMR2114595. APT research was supported by the Center for Nanophase Materials Sciences (CNMS), which is a US Department of Energy, Office of Science User Facility at Oak Ridge National Laboratory. The authors thank Dr. Jonathan Poplawsky and Mr. James Burns for APT specimen preparations and conducting the APT experiments.

SYMPOSIUM CH04

Emerging Electron Microscopy Techniques to Understand Structure-Property Relationships in Quantum Materials
November 29 - December 1, 2023

Symposium Organizers

Juan Carlos Idrobo, University of Washington
Yu-Tsun Shao, University of Southern California
Sandhya Susarla, Arizona State University
Luiz Tizei, Université Paris-Saclay

Symposium Support

Bronze
Attolight AG

* Invited Paper
+ JMR Distinguished Invited Speaker

SESSION CH04.01: High Resolution Imaging of Quantum Materials
Session Chairs: Yu-Tsun Shao and Sandhya Susarla
Wednesday Morning, November 29, 2023
Sheraton, Third Floor, Gardner

8:15 AM *CH04.01.01

The Synthescope—An Approach for Synthesis at the Atomic Scale Ondrej Dyck¹, Andrew Lupini and Stephen Jesse; Oak Ridge National Laboratory, United States

The scanning transmission electron microscope (STEM) is evolving from a workhorse instrument for materials characterization to an atomic-scale material manipulation platform. With its capability to image and characterize atomic-scale structural formation as it occurs, the STEM is being reconceptualized as a powerful instrument for fabrication and synthesis. By incorporating synthesis processes into the STEM, new transformations can be discovered and the atomic scale evolution of material growth can be better understood.

Within the STEM, there is a controlled environment with a focused beam of electrons that creates a highly localized perturbation of the sample. This perturbation can be considered a chamberless synthesis environment (CSE). Within this perturbed region of space, the sample environment is drastically different from regions outside the perturbation. The CSE can be moved around with great spatial precision and encounter a variety of different physical systems in a non-uniform sample. A reaction process can be prepared by adjusting global parameters without the intended process occurring until the CSE is created through e-beam exposure. When described in these terms, it can be seen that electron beam induced deposition (EBID) functions on the same principle. The e-beam dissociates molecular precursor gas molecules which become chemically reactive and bond with the substrate. This dissociative environment is created by e-beam exposure and can be considered to form a CSE within which the dissociation and growth of a new material occurs. The CSE concept, however, does not specify what reaction should occur, merely that the beam-sample interaction volume is a significantly different environment from that of the surrounding material.

With this idea in hand, we can begin to ask what environmental parameters could be varied such that *some* material transformation occurs within the CSE. A number of experimental results have shown that the positioning of single atoms in graphene is possible and that this could be extended to atomic scale patterning and writing if the sample environment could be better controlled, specifically the supply of various materials as is done in a synthesis chamber. To enable this capability, a prototype *in situ* evaporative delivery platform has been built. The basic functionality is demonstrated and test runs confirm the delivery of material down to the level of single atoms. With separate control over evaporation and substrate temperature, conditions were found where Sn atoms could be directly 'written' atom-by-atom into graphene.

The incorporation of synthesis processes in the STEM is opening up new possibilities for atomic-scale material manipulation and the discovery of new transformations. The concept of a chamberless synthesis environment (CSE) can lead to precise and controlled atomic-scale patterning and writing. With a prototype *in situ* evaporative delivery platform that can deliver material down to the level of single atoms, the future realization of the synthescope—a platform for synthesis and fabrication at the scale of an atom—shows great promise.¹

(1) This work was supported by the U.S. Department of Energy, Office of Science, Basic Energy Sciences, Materials Sciences and Engineering Division (O.D. A.R.L., S.J.), and was performed at the Center for Nanophase Materials Sciences (CNMS), a U.S. Department of Energy, Office of Science User Facility.

8:45 AM CH04.01.02

Atomic Lattice Resolved Electron Tomography of a 3D Self Assembled Mesocrystal Xiaolei Chu¹, Alex Abelson², Caroline Qian², Ethan M. Field¹, Oleg Igouchkine¹, Kwan-Liu Ma¹, Matt Law² and Adam J. Moule¹; ¹University of California, Davis, United States; ²University of California, Irvine, United States

Complex 3D architectures of nanoscale building blocks can be created by self-assembly, but characterization of the atomic to mesoscale structure of such materials is limited by the difficulty of visualizing atoms across multiple length scales. Here, scanning transmission electron microscopy (STEM) and full-tilt tomographic reconstruction are used to image a single-crystalline region of a 3D epitaxially-fused PbSe quantum dot (QD) superlattice containing 633 QDs at a spatial resolution of 2.16 Å. The combined real-space and reciprocal-space analysis enables 3D mesoscale correlations of atomic lattice and superlattice order across hundreds of nanocrystals in 3D for the first time. Inhomogeneity in QD positional and orientational order reveals that the QD surface layers template the superlattice and that orientational entropy is higher in the interior layers than the surface layers. The measurement and analysis techniques presented here are applicable to a broad range of 3D nanostructured materials.

9:00 AM *CH04.01.03

Domain Configuration and Interface Characterization in Ferroelectric Oxides Wanbing Ge¹, Dorin Rusu^{1,2}, Marin Alexe¹, Richard Beanland¹ and Ana M. Sanchez¹; ¹University of Warwick, United Kingdom; ²University College London, United Kingdom

The rapid improvement in materials growth and processing techniques has produced novel structures with unique functionalities. Electron microscopy plays a key role in understanding the structure of these novel materials and controlling them at an atomic level. The development of spherical aberration correctors for electromagnetic lenses established a major improvement in the new generation of electron microscopes.

Using aberration-corrected scanning transmission electron microscopy (STEM), we analysed in detail the domain structure in bulk and thin film ferroelectric oxide materials. Two different cases of studies will be presented:

(i) A dense domain structure alternating sawtooth and flat domains walls in flux-grown single crystal BiFeO₃ has been previously reported [1,2]. This intriguing ferroelectric structure of

domain walls has been controversial and the nature of these domains has remained ambiguous over the years. We demonstrated that although both type of domains are 180° their domain walls are different. (i) Flat walls, lying on (112) planes, have that head-to-head polarity. These flat domain walls are coincident with a 1/2[110] stacking fault, with a clear reconstruction visible in atomic resolution images [3]. (ii) Sawtooth walls are tail-to-tail with peaks elongated along the polar [111] axis. The formation and geometry of these sawtooth domain walls have been analysed in detail. These tail-to-tail domain walls form a crinkled 3D structure with three-faceted teeth consisting of a (11-2) facet allowing charge-free reversal of polarisation, and two facets close to (3-21) and (-321). Vortex structures are found at these domain walls. The neutral DW facets are Ising type and very abrupt, while the charged DW facets have mixed Néel/Bloch/Ising character with a chiral nature and a width of about 2 nm [4].

(ii) Ferroics can form vortices and skyrmions under particular boundary conditions. The formation of modulated ferroelectric vortices in PbTiO₃ sandwiched between two SrRuO₃ electrodes on SrTiO₃-buffered DyScO₃ (110) has been demonstrated. The local structure is resolved using a combination of STEM and conventional TEM. Two orthogonal modulations were revealed. This incommensurate polar crystal may be an equivalent to the incommensurate spin crystals found in ferromagnetic materials.

[1] Berger et al. 2012, Phys. Rev. B 85 064104

[2] Jia et al. 2015, Acta Mat. 82 156

[3] Ge et al. Microstructures 2023;3:2023026

[4] Ge et al, 2023 Adv. Funct. Mater. 2301171

[5] Peters et al. 2016 Nat. Commun. 7, 13484 (2016)

[6] Rusu et al. Nature 602, 240–244 (2022)

9:30 AMBREAK

10:00 AM CH04.01.04

Understanding Inherent Structural Defects and Chemical Distribution at Topological Superconductor-Semiconductor Interfaces and Heterostructures using Advanced Electron Microscopy Rosa E. Diaz¹, Roy Peña², Tian Wang³ and Michael Manfra¹; ¹Purdue University, United States; ²Universidad Nacional San Antonio Abad del Cusco, Peru; ³Beijing Academy of Quantum Information Sciences, China

In the zoo of quantum systems that might disrupt the storage and manipulation of information, topological superconductors have received significant interest for their potential application in quantum computing, mainly due to their capacity to harbor non-Abelian states and provide fault-tolerant computation. One of the platforms proposed to host topological superconductivity is the interface between a superconducting metal and a semiconductor (SS)¹ with strong spin-orbit scattering [1] – where topological qubits are manifested. However, epitaxially interfacing two dissimilar materials, such as a superconductor metal and a semiconductor heterostructure, inherent challenges emerge in the form of grain boundaries (black arrow in Fig. 1), grain misorientations (grains G1/G2 in Fig. 1), atomic distortions across the SS interface (white circle in Fig. 1), which might be detrimental to the device performance. Additionally, precise control of the semiconductor heterostructure interfaces and their chemical distribution across the interface is also needed to improve electron mobility and device performance. Thus, identifying and understanding these inherent structural defects at the multiple interfaces of this hybrid devices, and connecting our findings with growth process, might contribute to the performance improvement of topological qubits. Here we explore a combination of electron and ion microscopy together with advance image processing and mathematical modeling using Python libraries to understand structural properties at the SS interface, and quantify roughness and chemical distribution across the heterostructure interfaces. Our findings deliver metrology parameters to assess the quality of semiconductor heterostructure and highlight the relationship between such parameters and growth conditions.

10:15 AM *CH04.01.05

Atomic Structure Analysis of Metal Chlorides and Alkali Metals Intercalated in Bilayer Graphene Yung-Chang Lin^{1,2}, Matsumoto Rika³, Qiunan Liu², Pablo Solís-Fernández⁴, Po-Wen Chiu⁵, Hiroki Ago⁴ and Kazu Suenaga²; ¹National Institute of Advanced Industrial Science and Technology, Japan; ²Osaka University, Japan; ³Tokyo Polytechnic University, Japan; ⁴Kyushu University, Japan; ⁵National Tsing Hua University, Taiwan

Intercalation of metal species within graphene layers has attracted significant attention due to its potential for tailoring the electronic, magnetic, and optical properties of graphene-based materials. The precise characterization of the intercalation process and resulting atomic arrangements is crucial for understanding the fundamental interactions and the impact on material properties. In this study, we employ scanning transmission electron microscopy (STEM) to investigate the atomic structure of metal chlorides (AlCl₃, CuCl₂, MoCl₅, FeCl₃) and alkali metals (K, Rb, Cs) intercalated in bilayer graphene (BLG). Through STEM imaging, we have achieved high-resolution visualization and analysis of the atomic structure within the intercalated BLG samples. Our results reveal distinct patterns and arrangements of metal chloride and alkali metal atoms within the graphene lattice. We observe variations in interlayer spacing, local bonding configurations, and atomic ordering depending on the specific metal chloride and alkali metal employed. Additionally, we investigate the influence of intercalation on the electronic structure of the bilayer graphene using spectroscopic techniques.

SESSION CH04.02: Cryogenic Electron Microscopy

Session Chairs: Ondrej Dyck and Sandhya Susarla

Wednesday Morning, November 29, 2023

Sheraton, Third Floor, Gardner

10:45 AM *CH04.02.01

Probing the Atomic-Scale Internal Phases of Multiferroic and Hyperferroelectric Domain Walls During Dynamics with *In-Situ* Biasing and Cryogenic STEM Shelly Michele Conroy; Imperial College London, United Kingdom

Dynamic multiferroic domain wall topologies overturn the classical idea that our nanoelectronics need to consist of fixed components of hardware. To harness the true potential of domain wall-based electronics, we must take a step back from the device design level, and instead re-look at the subatomic internal properties. With recent advances in experimental characterization and theoretical calculation approaches, in the last 5 years reports of non-classic internal structures and functionalities within domain walls have become a common occurrence. As the region of interest is at the nanoscale and dynamic, it is essential for the physical characterization to be at this scale spatially and time resolved.

This presentation focuses on using the applied electric field of aberration corrected scanning transmission electron microscopy (STEM) probes to move domain walls, and thus investigate their dynamics while imaging at the subatomic scale. As the STEM probe can be controlled in terms of dose, probe size, direction and speed, a diverse set of experiments is possible without complicated sample preparation. Using a segmented STEM detector (or 4DSTEM CoM experimental set-up) any changes in deflection and thus the changes in polarisation for each domain, can also be investigated with controlled variants in applied field conditions. By controlling the incoming STEM probe direction, parallel domain walls could be moved around to form stable vertex junctions, thus switching from a neutral to charged state. Then in each frame by quantifying the atomic displacement per unit cell using our open-source python based TopoTEM software package, [1] the local polarisation at these charged topologies can also be monitored. Finally, we will show how changes in band structure can be monitored via ultrahigh energy resolution electron energy loss spectroscopy (EELS) as the domain walls switch from neutral to charge states. By combining the local atomic resolution structure, strain, charge density and band structure measurements we can resolve all the measurable parameters of interest within domain walls and thus start unravelling the fundamental physics governing their formation, dynamics and resulting functionality. We will show that this technique can be used for several different types of multiferroic oxide and oxy halide material systems, such as improper ferroelectric boracites and hyper-ferroelectric lead germanate. Additionally we will utilise new MEMS based cryogenic holder design to probe the low temperature phases of such materials and their topological features.

11:15 AM CH04.02.02

Exploring the Effects of Structural Defects on the Charge Density Wave Behavior of Rare-Earth Tritellurides Saif Siddique¹, James L. Hart¹, Ratnadwip Singh², Myung-Geun Han³, Michael Colletta¹, Noah Schnitzer¹, Lena F. Kourkoutis¹, Yimei Zhu³, Leslie Schoop² and Judy Cha¹; ¹Cornell University, United States; ²Princeton University, United States; ³Brookhaven National Laboratory, United States

Rare-earth tritellurides (RTe₃; R = rare-earth elements) are a family of layered compounds exhibiting charge density wave (CDW) order. They have rich phase diagrams involving other quantum phases, such as superconductivity and magnetism, providing an opportunity to understand the interplay between these phases by studying the mechanisms influencing the phase transitions. RTe₃ with lighter rare-earth elements (La-Gd) has a unidirectional CDW, while the ground state for the heavier rare-earths (Tb-Tm) has a second CDW at a lower temperature, and is orthogonal to the first with a slightly larger wavevector, creating a bidirectional CDW. The direction of the charge and lattice modulations in the CDW state is governed by the orthorhombicity

of the crystal structure. The in-plane axes in these materials are nearly equal, but the presence of a glide plane only along one of the axes makes the unit cell orthorhombic, and the higher temperature CDW (for lighter RTE_3 , the only CDW) emerges along this direction. In this study, we use *in-situ* cryogenic scanning transmission electron microscopy (STEM) techniques to understand the influence of structural defects on the orthorhombicity and the CDW order in exfoliated flakes of LaTe_3 , GdTe_3 and ErTe_3 : two unidirectional and one bidirectional CDW system. Atomic-resolution STEM images in cross-section reveal the layer stacking in these materials to be disordered, with the disorder density increasing for heavier rare-earths in RTE_3 . These layer stacking defects lead to the presence of glide planes along both in-plane directions rather than along only one in-plane direction, and hence the material loses orthorhombicity. Temperature dependent electron diffraction and 4D-STEM, down to 15 K and 120 K, respectively, are used to study the CDW phase transition behavior of these flakes that reveal the existence of in-plane domain walls. We observe that the loss of orthorhombicity and the presence of domain walls significantly affect the CDW order in these exfoliated flakes of RTE_3 . Our results demonstrate the correlation of stacking defects and domain boundaries with the properties and dynamics of CDW phase transition.

11:30 AM *CH04.02.03

Emerging Electron Microscopy Techniques for Probing Quantum Materials [YimeiZhu](#); Brookhaven National Laboratory, United States

In this presentation I will give an overview of the recent work at BNL on advancements in electron microscopy characterization of quantum materials. I will focus on sample holder development, including holders designed for previously inaccessible microwave frequency range in TEM for in-situ RF excitation/ultrafast-dynamics and for liquid helium temperature cooling with temperature control and stability better than a few mK. I will also show our preliminary results on the evaluation of three direct electron detectors: Dectris Quadro, Quantum Directors Merlin (Medipix 3), and Gatan K3. The performance, especially at extremely electron low-dose and high acquisition speed, of these detectors installed on our aberration corrected JEOL ARM200FC and Laser-Free Ultrafast Electron Pulser will be compared. Applications on strongly correlated quantum materials and test results using these holders and detectors will be presented. The ability to probe materials dynamic responses under RF and microwave excitations at extremely low temperatures has promising applications for qubit devices and quantum information science.

Collaborations with S. Reisbick, X. He, C. Liu, MG Han, and L. Wu at BNL and C. Jing and R. Kostin at Euclid are acknowledged. Work at BNL was supported by the DOE-BES-MSE under contract No. DE-SC0012704.

SESSION CH04.03: Imaging Magnetic Materials
Session Chairs: Juan Carlos Idrobo and Yu-Tsun Shao
Wednesday Afternoon, November 29, 2023
Sheraton, Third Floor, Gardner

1:30 PM *CH04.03.01

Real-Space Observation of Spontaneous Vortex-Antivortex Pairs and Their Topological Transitions Through Transmission Electron Microscopy [Xiuzhen Yu](#)¹, Naoya Kanazawa², Xiaocao Zhang³, Konstantin Iakubovskii¹, Kiyomi Nakajima¹, Masahito Mochizuki³ and Yoshinori Tokura¹; ¹RIKEN, Japan; ²The University of Tokyo, Japan; ³Waseda University, Japan

The spontaneous formation of vortex-antivortex pairs and their topological transitions have been extensively studied in various branches of physics, demonstrating their crucial role in phenomena such as superconductivity and quantum computing¹. Unlike conventional magnets that typically exhibit collinear spin textures, helimagnets with non-centrosymmetric crystal structures offer additional degrees of freedom essential for manipulating noncollinear spin textures, such as a proper screw structure at zero field². This unique characteristic makes helimagnets promising candidates for exploring and engineering topological states, such as a skyrmion lattice state, under specific conditions of temperature and external magnetic field³. However, achieving multiple topological magnetic states and their transitions within a single helimagnet presents a significant challenge due to the inherent topological protection associated with each state.

In this talk, I will present real-space observations of a spontaneous vortex pair composed of a meron and an antimeron, possessing topological charges of $N = \pm 1/2$, respectively, in a helimagnet $\text{Fe}_{0.5}\text{Co}_{0.5}\text{Ge}$ through advanced transmission electron microscopy. In addition, a meron pair, referred to as a bimeron (i.e., a vortex-antivortex pair), carrying a topological charge of $N = -1$, will also be presented. We successfully achieved the mutual transition between skyrmions and bimerons and the transformation of individual bimerons into a skyrmion lattice by carefully controlling the external magnetic field and electric current⁴.

Overall, this research piece offers valuable insights into the manipulation of topological states, paving the way for potential future applications in fields such as spintronics and quantum technologies.

*This work was supported in part by Grants-In-Aid for Scientific Research (A) (Grant No. 19H00660, 23H05431) from the Japan Society for the Promotion of Science (JSPS) and the Japan Science and Technology Agency (JST) CREST program (Grant No. JPMJCR1874, JPMJCR20T1), Japan.

[1] L. Chibotaru, *et al. Nature* 408, 833 (2000).

[2] Y. Tokura, and N. Kanazawa, *Chem. Rev.* 121, 2857 (2021).

[3] N. Nagaosa, and Y. Tokura, *Nat. Nanotechnol.* 8, 899 (2013).

[4] X. Z. Yu, et al. to be submitted.

2:00 PM *CH04.03.02

Multiscale Insights to the Origins and Dynamics of Chiral Magnetic Textures in Intercalated TMDs [Berit H. Goodge](#)^{1,2}, Oscar Gonzalez¹, Lilia Xie¹ and Daniel K. Bediako^{1,3}; ¹University of California, Berkeley, United States; ²Max Planck Institute for Chemical Physics of Solids, Germany; ³Lawrence Berkeley National Laboratory, United States

Dynamically tunable properties such as magnetic textures have many potential applications for next-generation information and communication technologies ranging from spintronics to broadband resonators. One promising class of materials are intercalated transition metal dichalcogenides (TMDs), in which a wide range of electronic and magnetic phases which can be tuned by varying the host lattice or the species, amount, and ordering of intercalants. Chromium-intercalated TMDs, for example, stabilize low-temperature helical magnetic order with chiral winding along the *c*-axis of the crystal where the helical pitch is tunable by both spin-orbit coupling of the host TMD compound and by external in-plane magnetic fields. The extensive phase space of stoichiometry- and field-dependence of these textures provides a rich playground for real-space visualization of the interplay between atomic lattice and mesoscale magnetic order. Here, we leverage a combination of high-resolution and cryogenic imaging techniques in the (scanning) transmission electron microscope (S/TEM) to directly probe both atomic and magnetic (dis)order across multiple length scales. We reveal the dramatic impact of subtle changes in the atomic lattice on mesoscale magnetic textures and their dynamic evolution, and offer suggestions for more precisely-controlled synthesis of these compounds for future applications [1].

[1] Goodge*, Gonzalez*, et al. arXiv:2305.06656 (2023).

*This work supported by University of California President's Postdoctoral Fellowship Program, Schmidt Science Fellows in partnership with the Rhodes Trust, the National Science Foundation (DMR-2039380, DMR-1719875, MRI-1429155, DMR-1539918), and the Air Force Office of Scientific Research (FA9550-20-1-0007).

2:30 PM BREAK

3:30 PM CH04.03.03

Three-Dimensional Inverse Scattering Problems Using Electron Ptychography: Atomic-Scale Imaging of Magnetization and Thermal Diffuse Scattering [Georgios Varnavides](#)^{1,2}, Stephanie Ribet², Reed Yaliso^{1,2}, Joel Moore^{1,2}, Colin Ophus² and Mary Scott^{2,1}; ¹University of California, Berkeley, United States; ²Lawrence Berkeley National Laboratory, United States

Accelerated electrons passing through a thin sample acquire Aharonov-Bohm phase shifts due to sample interactions which scatter the incident electron wavefunction. These include coherent sources such as electrostatic scattering off atomic columns and scattering against a magnetic vector potential [1], as well as incoherent sources such as thermal diffuse scattering and plasmon excitations [2,3]. Despite the large mechanistic differences between these scattering sources the fact that they are simultaneously collected as far-field diffraction intensities, as well as the large order of magnitude difference in the acquired phase shifts, suggests the signals are hard to deconvolve. Reconstructing these various scattering sources from diffraction intensities is thus a high-dimensional non-convex inverse problem.

Electron ptychography is a recently rekindled phase-retrieval technique which attempts to solve this inverse problem using the redundant information in a set of converged-beam diffraction intensities with sufficient real-space illumination overlap [4], e.g., using a defocused 4DSTEM experiment [5]. Here, we introduce a general framework, implemented in the open-source analysis toolkit py4DSTEM [6], to reconstruct common coherent and incoherent scattering sources in materials using physically inspired forward and adjoint operators. We illustrate the utility of the framework by jointly reconstructing the coherent electrostatic potential and magnetic vector potential of an anti-ferromagnetically ordered NiO sphere with atomic resolution, as well as elucidating the real-space character of incoherent thermal diffuse scattering.

We demonstrate how the usual projection-limitation of electron microscopy can be overcome by solving a joint inverse problem for two orthogonal tilt-series directly to obtain the three-dimensional nature of scalar and vector scattering sources such as electrostatic and magnetic vector potentials, respectively. Finally, we investigate the role of optimizing common experimental parameters such as convergence angle, scan step-size, and illuminating probe defocus on the reconstruction quality.

- [1] C Phatak, M Beleggia, M De Graef, *Ultramicroscopy*, 108, (2008), doi: 10.1016/j.ultramic.2007.08.002
- [2] D Van Dyck, *Ultramicroscopy*, 109, (2009), doi: 10.1016/j.ultramic.2009.01.001
- [3] BG Mendis, *Microscopy*, 69, (2020), doi: 10.1093/jmicro/dfaa003
- [4] J Rodenburg, A Maiden, *Springer Handbook of Microscopy*, (2019), doi: 10.1007/978-3-030-00069-1_17
- [5] C Ophus, *Microscopy and Microanalysis*, 25 (2019), doi: 10.1017/S1431927619000497
- [6] B Savitzky et al., *Microscopy and Microanalysis*, 207, (2021), doi: 10.1017/S1431927621000477

3:45 PM CH04.03.04

Tracking Antiskyrmion Dynamics Induced by Nanosecond-Current Pulses Through Transmission Electron Microscopy YaoGuang¹, XichaoZhang², YizhouLiu¹, LicongPeng¹, FehmiS. Yasin¹, KosukeKarube¹, DaisukeNakamura¹, NaotoNagaosa¹, YasujiroTaguchi¹, MasahitoMochizuki², YoshinoriTokura^{1,3,3} and XiuzhenYu¹; ¹RIKEN Center for Emergent Matter Science (CEMS), Japan; ²Waseda University, Japan; ³The University of Tokyo, Japan

The collective behaviors of strongly correlated systems, such as the interaction of electronic states, demonstrate emergent phenomena and novel functionalities that are essential for developing quantum technologies and advanced materials.¹ Meanwhile, topological spin textures, which combine real-space topology and collective spins, have garnered significant attention in the field of electronic materials due to their emergent electromagnetic properties.² To understand the nature of topological spin textures, advanced transmission electron microscopy (TEM) serves as a privileged and efficient platform for direct observations and study with various stimuli, including heat, mechanical forces, external fields, and electricity. Recently, antiskyrmions, a type of spin texture in non-centrosymmetric magnets with D_{2d} and S_4 symmetries, showcase the abundant topological transition physics because of anisotropic Dzyaloshinskii-Moriya interaction.³ However, the dynamics of antiskyrmions driven by electric current flows remain elusive and largely overlooked. Therefore, the purpose of this study is to investigate the dynamic behaviors and underlying physics of antiskyrmions with pulsed current stimulations.

In this work, we employ in-situ Lorentz TEM observations to reveal the dynamic behaviors of antiskyrmions under electric current flows in the presence of a helical texture background. Since helical stripes along [1-10] and [110] are energetically equitable due to the S_4 symmetry in $\text{Fe}_{1.9}\text{Ni}_{0.9}\text{Pd}_{0.2}\text{P}$, we can demonstrate the ability to control the directional motion of antiskyrmions along the stripes, regardless of whether they are confined by [1-10] or [110] stripes. The results show that the moving direction of antiskyrmions is parallel to the stripe direction, and the corresponding speed of antiskyrmions is linearly proportional to the current density. Notably, an enhancement of the antiskyrmion speed has been observed when the current flows vertically to the stripe, which is six times higher compared to the case when the current flows along the stripe. Our findings offer valuable insights into the development and advancement of quantum technologies and materials science.

*This work was supported in part by Grants-In-Aid for Scientific Research (A) (Grant No. 19H00660, 23H05431, 23H01841) from the Japan Society for the Promotion of Science (JSPS) and the Japan Science and Technology Agency (JST) CREST program (Grant No. JPMJCR1874, JPMJCR20T1), Japan.

References

- 1. Y. Tokura, et al., *Nat. Phys.* 13, 1056 (2017).
- 2. N. Nagaosa & Y. Tokura., *Nat. Nanotechnol.* 8, 899 (2013).
- 3. A.K. Nayak, et al., *Nature* 548, 561 (2017).
- 4. L. Peng, et al., *Nat. Nanotechnol.* 15, 181 (2020).
- 5. K. Karube, et al., *Nat. Mater.* 20, 335 (2021).

SESSION CH04.04: Poster Session
Session Chairs: Juan Carlos Idrobo and Yu-Tsun Shao
Wednesday Afternoon, November 29, 2023
Hynes, Level 1, Hall A

8:00 PM CH04.04.01

Limits of Quantitativeness In DPC-STEM Studies of Charge Density Matthew J. Coupin; University of Texas at Austin, United States

Differential phase contrast (DPC) based methods are increasingly popular for the characterization of electrostatic fields and charge densities in materials [1]. Unlike conventional diffraction-based techniques STEM-DPC methods can be used to probe the local environment surrounding defects [2, 3, 4, 5] which are very difficult to measure without the precise spatial resolution of microscopy techniques. 2D materials have been popular candidates for DPC-STEM due to their thinness and suitability for study in TEM; however, these methods can, with sufficient skill in sample preparation, be extended to bulk materials [6].

However, as the interest in these methods expands beyond the microscopy-focused community, it becomes increasingly important to acknowledge that there exist a wide range of deleterious experimental factors that degrade the magnitude of the measured properties, causing deviations from theoretically-predicted values. These include sample contamination, optical aberrations, partial coherence of the electron beam, stage-induced motion, and thermal and electron beam induced sample motion. Each of these factors can introduce uncertainty into the measurements and can lead to incorrect interpretation of experimental observations, especially because they may depend on spatial frequency, acting differently upon differently sized features within a given dataset. Under the influence of these deleterious experimental conditions it becomes challenging to perform quantitative DPC-STEM studies without relying on first principles physics to generate relaxed structural models for TEM simulation and to calibrate the magnitudes of the observed signal using the resulting DFT-derived potentials. Inevitably there will be situations where experiment and first-principles simulation cannot be brought into agreement, and this relationship between experiment and theory will break down. When novel physics is observed in TEM without complementary simulation, which should be believed?

This serves to motivate the development of new methods towards 'blind' quantitative STEM methods that do not rely upon existing frameworks for physics simulation. Although newer methods, such as those based off of iterative ptychography, can reduce the influence of lens aberrations, scan position uncertainty, and even dynamical scattering, there remain many possibilities for incorrect analysis of STEM data. The present work is a review of the challenges and common pitfalls associated with DPC-STEM based studies of electrostatic fields and charge densities, with a target audience beyond the core community of advanced TEM users.

- [1] Müller-Caspary, K., *et al.* Atomic-scale quantification of charge densities in two-dimensional materials. *Physical Review B* 2018, 90, 121408.
- [2] Fang, S., *et al.* Atomic electrostatic maps of 1D channels in 2D semiconductors using 4D scanning transmission electron microscopy. *Nature Communications* 2019, 10, 1127.
- [3] Wen, Y., *et al.* Mapping 1D Confined Electromagnetic Edge States in 2D Monolayer Semiconducting MoS_2 using 4D-STEM. *ACS Nano*. 2022, 16, 6657-6665.
- [4] Cretu, O., *et al.* Atomic-Scale Electrical Field Mapping of Hexagonal Boron Nitride Defects. *ACS Nano*. 2021, 15, 5316-5321.
- [5] Calderon, S., *et al.* Atomic Electrostatic Maps of Point Defects in MoS_2 . *Nano Letters*. 2021, 21, 10157-10164.

8:00 PM CH04.04.02

Electron Beam Modification with an Electrostatic Phase Plate for Characterization of Quantum Materials Stephanie Ribet¹, Steven Zeltmann² and Colin Ophus¹; ¹Lawrence Berkeley National Laboratory, United States; ²Cornell University, United States

For Scanning Transmission Electron Microscopy (STEM) imaging, producing a high-resolution image generally requires focusing the beam to a fine point by eliminating aberrations and making a more uniform phase profile. However, further electron beam modification creates a myriad of opportunities to characterize material properties that are inaccessible through traditional methods. Existing phase modification devices often lack the necessary physical or phase stability to enable routine implementation of such experiments. In this presentation, I will share our design for an electrostatic phase plate that can be used for electron beam modification. Our phase plate is composed of many smaller apertures, each of which has a two terminal device that can be adjusted independently to impart a linear ramping or constant phase shift on the probe. The support bars for the electrostatic apertures ensure structural integrity, while the dynamic nature of the design enables spatial and temporal control over the electron beam. The electrostatic phase plate has implications for the characterization of quantum materials, such as through the creation of vortex beams that can be used to characterize chirality and magnetic ordering.

8:00 PM CH04.04.03

Multi-Modal Spectroscopic Characterization and Defect Identification in SnO₂/Ga₂O₃ Nanostructures Praveena Manimunda¹, João-Lucas Rangel¹, Didier Hocrelle¹, Francis Ndi¹, Emilio Nogales² and Bianchi Mendez²; ¹Horiba, United States; ²Universidad Complutense, Spain

Semiconducting oxide nanostructures with a wide range of morphologies are emerging as a viable candidate for applications such as optical and mechanical resonators and solar cells. However, attaining effectively doped oxide nanowires with controllable conductivity is still a challenge. Designing semiconducting oxide nanostructures requires extensive understanding of their morphology and demands efficient multimodal characterization methods. Multimodal spectroscopy is the concept of combining several different spectroscopies onto one platform, thereby expanding the range of analytical capabilities available on that single platform. Besides the obvious benefit of cost reduction, having multiple analytical spectroscopies offers the added benefit of sample colocalization so that multiple complementary measurements can be made at the same location of the sample. The benefit of colocalization is particularly important as feature sizes get smaller, from a few microns to nanometers in size. In this study, Scanning Electron Microscope was integrated with cathodoluminescence (F-CLUE) and as a complementary information an external optical microscope coupled with photoluminescence (PL) and Raman spectroscopy were used to achieve co-localized high-resolution imaging and chemical mapping. Further shape engineered SnO₂ nanostructures grown on Ga₂O₃ nanowires were characterized in detail to understand the optical properties and defect characteristics. Panchromatic CL images identified the region of illumination on connected nanowires. The CL emission from Ga₂O₃ is composed of two components (3.3 and ~ 3.0 eV). However, the Ga₂O₃ nanowire tested had covered SnO₂ nanostructures and hence a weaker 3.3 eV emission, a stronger orange band (~ 1.94 eV) corresponding to the SnO₂ nanostructure was observed. The orange band was attributed to the oxygen vacancies in SnO₂. Photoluminescence and Raman mapping of the nanowires are carried out to understand the chemical nature of the local defects on SnO₂/Ga₂O₃ nanostructures.

SESSION CH04.05: Four-dimensional Scanning Transmission Electron Microscopy I

Session Chairs: Juan Carlos Idrobo and Yu-Tsun Shao

Thursday Morning, November 30, 2023

Sheraton, Third Floor, Gardner

8:30 AM *CH04.05.01

Imaging the Properties of Atoms and Fields at the Picometer Scale inside Quantum Materials David A. Muller; Cornell University, United States

Electron microscopes use electrons with wavelengths of a few picometers, and are potentially capable of imaging individual atoms in solids at a resolution ultimately set by the intrinsic size of an atom. Until very recently, the best resolution was more than an order magnitude worse than this limit. This was caused by two things – first the intrinsic aberrations in electron lenses are much worse than for optical lenses – comparable to using a beer bottle as a magnifying glass. Second, electrons are multiply-scattered inside the sample – a process described by Hans Bethe over 90 years ago. It's been a headache for electron microscopists ever since, but with recent advances in detector technology [1] and reconstruction algorithms, the resolution of the electron microscope is now limited only by the dose to the sample, and thermal vibrations of the atoms themselves [2], giving greater insight into the lattice contribution to exotic phases. These approaches have also allowed us to image the internal structures of both magnetic and ferroelectric vortices, skyrmions and merons, including their singular points that are critical for accurately describing the topological properties of these field textures [3,4]. [5]

[1] H. Philipp *et al.*, *Microscopy and Microanalysis* **28** (2022), p. 425-440.

[2] Z. Chen *et al.*, *Science* **372** (2021), p. 826-831.

[3] Y.-T. Shao *et al.*, *Nature Communications*, (2023) **14**:1355

[4] Z. Chen *et al.* *Nature Nanotechnology*, (2022) **17**:1165–1170.

[5] In collaboration with Harikrishnan K. P., Yu-Tsun Shao, Zhen Chen and Yi Jiang. Funding from the U.S. Army Research Office under the MURI ETHOS (W911NF-21-2-0162). Facility support from the Cornell Center for Materials Research (National Science Foundation grants MRI-1429155, DMR-1719875, DMR-1539918).

9:00 AM *CH04.05.02

Large-Scale 3D Phase-Contrast Imaging from 4D-STEM Measurements Philipp M. Pelz¹, Sinead M. Griffin², Alex Zetti³, Peter Ercius², Mary Scott^{3,2}, Colin Ophus², Daniel G. Stroppa⁴ and Mingjian Wu¹; ¹Friedrich-Alexander-Universität Erlangen-Nürnberg, Germany; ²The National Center for Electron Microscopy (NCEM), United States; ³University of California, Berkeley, United States; ⁴DECTRIS AG, Switzerland

Spurred by the development and widespread availability of fast pixelated direct electron detectors (DEDs), scanning transmission electron microscopy (STEM) is undergoing a computational imaging renaissance. Experiments envisaged more than ten years ago can finally be realized with modern detector technology and reconstruction algorithms for 4D-STEM datasets.

We show the experimental demonstration of one such experiment relying on fast DEDs: ptychographic electron tomography at atomic resolution. Using ptychographic electron tomography, we have reconstructed an atomic-resolution 3D volume of a double-wall carbon nanotube encapsulating a complex core-shell Zr₁₁Te₅₀ structure from 34 million diffraction patterns [5]. From this volume, the atomic structure was determined using atom tracing methods known from annular dark-field atomic electron tomography [3]. Ptychographic electron tomography relies on the projection approximation, such that samples have to be ~10nm or less in thickness. Multi-slice ptychographic tomography [6] alleviates this constraint by modeling multiple scattering and allowing 3D atomic resolution phase-contrast imaging beyond the depth of focus limit. I will show first results using multi-slice ptychographic electron tomography to reconstruct samples with thickness beyond the depth of focus limit. With further technical developments, this method will be able to solve the 3D atomic structure of general TEM samples like FIB lamellas or needle specimens at atomic resolution in 3D. The datasets for these reconstructions were recorded with the 4DCamera, a direct electron detector capable of 87kHz frame rate. I will also present 3D imaging results using the DECTRIS ARINA DED, capable of 120kHz data acquisition and online data compression, alleviating large-scale 4D-STEM experiments. Finally, the limitations of current algorithms will be discussed, and developments towards imaging much larger volumes with 4D-STEM will be detailed.

9:30 AMBREAK

10:00 AM *CH04.05.03

Optimizing the Analytical System to be Flexible yet Capable for Advanced Experimentation Jan Ringnalda and Lee Casalena; Thermo Fisher Scientific, United States

Navigating the decision-making process for high-value instrumentation purchases has become increasingly complex and treacherous. While performance specifications play a crucial role in this process, it's important to avoid considering any single specification in a vacuum. Frequently, these specifications are tailored to highlight the superior performance of the advertised hardware, omitting key aspects/limitations that should be carefully considered in the decision-making process.

A new generation of ultra-high-brightness cold field emission guns (CFEGs) can deliver a current of more than 1 nanoamp into a sub-Ångström sized beam. This level of coherent current performance is critical to meeting the demands of emerging camera and detector technologies, where short dwell times are needed for atomic resolution diffraction-based and analytical experiments.

Current detector technology poses challenges in meeting all requirements simultaneously. A trade-off must be made between selecting a fast detector or one capable of handling large currents.

Fast detectors tend to saturate quickly due to their limited current-handling capacity, while detectors capable of handling high currents tend to be slower. Rapid detectors that saturate at low currents fail to collect sufficient electrons for generating complete, low-noise images, often resulting in frames with negligible electron counts. This compromises the quality of the image or diffraction pattern obtained, making data processing more challenging. To address this, the concept of maximum usable imaging speed (MUIS¹) has emerged, representing the fastest achievable detector speed that still produces the desired signal-to-noise ratio.

In this presentation, we will illustrate a few essential factors that should not be overlooked when deciding on instrumentation for conducting the widest range of experiments possible within the shortest timeframe. We will also illustrate the significance of selecting the appropriate electron source and sensors for specific experiments. Data will be presented using a microscope that can produce a coherent current exceeding 600 pA, coupled with a sensor capable of accommodating 1,000,000 electrons within a single pixel without saturation. Additionally, this sensor can handle ~20 nanoamps of current for a single frame readout. This combination provides the flexibility required for accurate quantification even at high beam currents, avoiding non-linear behavior and the challenges associated with frames containing only one or no electrons. The Maximum Usable Imaging Speed for such a complete system will be discussed, rather than just beam current, resolution or camera speed. New results of a flexible 30-300kV multimodal microscope system will be shown.

References:

1) Hugh T Phillip et al, *Microscopy and Microanalysis* (2022), 28, 425–440.

10:30 AM *CH04.05.04

Using Phase Contrast 4D-STEM to Solve 2D and 3D NanostructuresColin Ophus; Lawrence Berkeley National Laboratory, United States

Scanning transmission electron microscopy (STEM) has been successfully employed to image many materials at atomic resolution with techniques such as annular dark field (ADF), high angle ADF (HAADF), and annular bright field (ABF) imaging. Recently developed atomic electron tomography (AET) methods have been used to solve atomic resolution structures in 3D. However, these AET studies have relied on ADF imaging, which provides approximately linear and incoherent contrast. This makes the 3D tomographic reconstruction procedure robust and easy to apply, but it can only be used for materials with medium or high atomic numbers which can tolerate a high electron dose without damage, and can struggle to distinguish atoms with similar scattering profiles. Moving beyond these limitations will require more dose-efficient phase contrast imaging methods such as differential phase contrast (DPC) or ptychography, where computational imaging methods are used to solve for the complex probe in order to fully deconvolve it from the object. Ptychographic reconstruction algorithms can also correct for multiple scattering of the electron beam in order to reconstruct thicker samples which produce multiple scattering of the electron beam. In this talk, I will demonstrate the promise of ptychographic AET by solving the structure of a complex ZrTe nanowire embedded in a double walled carbon nanotube, and discuss how we can develop a general reconstruction framework incorporating any number of simultaneous measurement channels and performing joint reconstructions.

11:00 AM CH04.05.05

Unraveling Strain and Deformation in Two-Dimensional Materials: Insights from Nanobeam 4D-STEMYimo Han and Chunqiao Shi; Rice University, United States

Two-dimensional (2D) materials and their heterostructures have emerged as key components for innovative applications and exhibit unique properties distinct from bulk materials. Understanding the behavior of strain and deformation in 2D materials is crucial for their potential device applications and offers valuable insights into precisely engineering nano-scale strain in these layered materials. In this study, utilizing nanobeam four-dimensional scanning transmission electron microscopy (4D-STEM), we introduce novel approaches to investigate both in-plane and out-of-plane strain and deformation in 2D materials. Our findings reveal a new mechanism of strain relaxation in 2D materials through the formation of out-of-plane ripples. Additionally, we uncover how 2D materials employ long-range lattice rotation and confined nanoscale uniaxial strain to compensate for lattice mismatch, and we elucidate different stacking orders in van der Waals heterostructures mediated by interlayer strain effects.

11:15 AM *CH04.05.06

Optimized Detectors and Acquisition Modes for EELS, EFTEM and 4D-STEM Data AnalysisRay D. Twetten and Liam Spillane; Gatan, United States

The number of electrons in a beam can be parsed in many ways, but the total flux of the beam is fixed. The finer you slice the time domain to increase acquisition speed, the fewer electrons you have at each data slice leaving you starved for counts. The same can be said for other data acquisition modes that parse the electrons into finer bins, such as increasing the energy dispersion to achieve better EELS resolution or reducing the energy selecting slit size to get sharper energy filtered images. The final limit of your experiment may not be the sensitivity or resolution of the hardware, but the Poisson or “shot” noise associated with counting discrete electron events. For a signal with N electrons in each bin, you can never have better noise than square root of N, which sets a limit to your data quality. Even for a perfect detector, if you want to double the signal to noise ratio of your data, you need to quadruple the number of electrons detected.

The advent of counting detectors for electrons has revolutionized electron microscopy in many ways, but they too cannot get around the Poisson limit. However, due to the fast readout rate, sharp point spread function and near zero added noise of these cameras, the traditional methods of acquiring electron microscopy data have been turned on their heads. In this presentation, we will discuss and illustrate the strategies for acquiring EELS, EFTEM and 4D STEM data using electron counting detectors to optimally use the fixed number of electrons available in the system. We will draw on examples from high-speed multimodal data acquisition and extreme low dose EELS fine structure analysis to demonstrate these strategies.

SESSION CH04.06: Four-dimensional Scanning Transmission Electron Microscopy II

Session Chairs: Colin Ophus and Yu-Tsun Shao

Thursday Afternoon, November 30, 2023

Sheraton, Third Floor, Gardner

1:30 PM *CH04.06.01

Exploiting Dynamical Scattering to Characterise Functional MaterialsJoanne Etheridge¹, WeiChao¹, WeilunLi¹, BryanEsser¹, EspenDrath Bojesen² and Timothy Petersen¹; ¹Monash University, Australia; ²Aarhus University, Denmark

Fast electrons interact strongly with the electrostatic potential of matter and are scattered “dynamically”. Put colloquially, this means that electrons scatter multiply within and between different scattering paths as they are transmitted within the specimen. Dynamical scattering can deliver a wealth of specimen information, such as the phase of a crystal structure factor, that is absent from experiments that are limited to single scattering.

Despite the complexity of dynamical scattering, under relevant conditions some properties of the specimen, such as electrostatic potential and symmetry, can be revealed in the distribution of scattered intensity as stable features, independent of experimental parameters, such as thickness or accelerating voltage. This is a consequence of mathematical structures, such as eigenvalue confluences, that are stable and embedded within the mathematics of dynamical scattering.

In this talk, we will explore how to exploit these features in the intensity distribution to measure different types of specimen information efficiently from various electron-optical configurations, including convergent beam electron diffraction (CBED) and four-dimensional scanning transmission electron microscopy (4D-STEM). We consider how to do this in different detection planes, providing access to coordinate, momentum and energy space and discuss the pros and cons in terms of information content, speed, and electron dose. We illustrate these approaches with applications to the measurement of structure, electronic structure and structural dynamics of functional materials, including photoactive and ferroic perovskites and plasmonic and semiconducting nanoparticle systems.

Acknowledgements: This work was supported by Australian Research Council (ARC) grants DP200103070, DP220103800, FL220100202. The authors acknowledge the use of the instruments and scientific and technical assistance at the Monash Centre for Electron Microscopy and used a Titan3 80-300 FEG-TEM (ARC LE0454166) and the Spectra Phi FEG-TEM (ARC LE170100118).

2:00 PM CH04.06.02

Fast 4D STEM with ARINA Hybrid-Pixel DetectorDaniel G. Stroppa; DECTRIS, Switzerland

characterization in both Materials Sciences and Life Sciences, particularly when beam-sensitive samples are involved [1]. The hybrid-pixel detector (HPD) concept [2] has the distinctive advantage of a flexible design with respect to the sensor material and electronics, allowing the direct electron detection and counting optimization for a range of TEM experimental parameters

(such as electron energy) and different applications.

Building on its successful HPD technology for X-ray detectors, DECTRIS fine-tuned its design to enable the precise detection of electrons. Its most recent development is an application-specific integrated circuit (ASIC) designed to allow read-out rates above 100 kHz and to perform electron counting up to 10 pA beam current per detector pixel with zero read-out noise [3]. ARINA detector combines this newly-designed ASIC with a flexible choice of sensor materials, an easy-to-use application programming interface (API), and a detector retraction mechanism, making it fit to most TEMs with electron energies from 30 to 300 keV and 4D STEM experiments requirements. Initial tests show that ARINA is suitable for flexible virtual STEM imaging with dwell time below 10 μ s, allowing for flexible differential phase contrast (DPC) with atomic resolution, and electron diffraction experiments with high dynamic range for crystal phase/orientation mapping.

[1] A. R. Faruqi et al., Nucl. Inst. Meth. Phys. Res. A **878** 180-190 (2018)

[2] M. Bochenek et al. IEEE Trans Nucl Sci **65** (6), 1285-1291 (2018).

[3] P Zambon et al., Nucl. Inst. Meth. Phys. Res. A **1048** (2023).

[4] C. Ophus et al., Microsc. Microanal. **28**, 390-403 (2022).

2:15 PM *CH04.06.03

Atomic Resolution Inline Holography of Quantum Materials Jian-Min Zuo¹, Hsu-Chih Ni¹ and Jiong Zhang²; ¹University of Illinois-Urbana-Champ, United States; ²Intel Corporation, United States

Characterization plays a critical role in the discovery of quantum materials, which is still challenging despite tremendous progress being made during past decades. Extending the study of point defects from 2D materials to crystals and thin films, probing novel charge states and complex structures, for example, are all difficult problems that require novel characterization approaches. Here we explore inline holography for quantitative defect imaging and defect analysis based on the collection and analysis of coherent convergent beam electron diffraction (CBED) patterns using an aberration corrected electron probe. At large convergence angles, the CBED patterns can be considered as Gabor's inline hologram formed by a spherical wave, while at smaller convergence interference between CBED disks provide phase information that forms the basis for electron ptychography [1,2]. With fast electron detectors, four-dimensional (4D, two-dimensional scan and diffraction pattern) diffraction data as in 4D-STEM can be collected efficiently with high signal/noise ratio [3]. All of these provide fertile ground for revisiting Gabor's original idea of inline holography. This talk will highlight our recent progress in developing atomic resolution inline holography using the combination of an aberration corrected STEM and EMPAD detector. Examples will be provided related to point defect detection in heavily doped semiconductors. The experimental study will be compared to dynamical diffraction simulations. The reconstruction algorithms will be proposed and discussed, as well as prospects [4].

References

[1] J. M. Rodenburg, in *Advances in Imaging and Electron Physics*, Vol 150 Vol. 150, 87-184 (2008).

[2] J.C.H. Spence, *High resolution electron microscopy*, 4th Edition ed., Oxford University Press, Oxford, UK, 2013.

[3] J.-M. Zuo, R. Yuan, Y.-T. Shao, H.-W. Hsiao, S. Pidaparthy, Y. Hu, Q. Yang, J. Zhang, *Data-driven electron microscopy: electron diffraction imaging of materials structural properties*, *Microscopy*, (2022) In print.

[4] This work is funded by Intel and DOE BES.

2:45 PM CH04.06.04

4D-STEM Characterization of MBE-Grown Barium Titanate for Electro-Optic and Ferroelectric Devices Ashley Cavanagh, Larissa Little, Charles Brooks, Jules Gardener, Julia Mundy and Robert Westervelt; Harvard University, United States

Synthesis and characterization of thin film barium titanate is of great interest due to its promise for use in electro-optic modulators [1]. These devices require a thin film with a high electro-optic coefficient that can operate at low voltages and integrate into photonic circuits, so barium titanate's strong nonlinearity makes it an attractive candidate material. Barium titanate's ferroelectricity means that it is also of interest for applications in nonvolatile ferroelectric memories. To pursue these applications, we must understand how variations in film stoichiometry affect the electro-optic properties, local atomic structure, and ferroelectric structure of thin film barium titanate. In this work, we use four dimensional scanning transmission electron microscopy (4D-STEM) and high-resolution imaging techniques to analyze the crystal structure thin films of barium titanate grown via molecular beam epitaxy. 4D-STEM can detect small movements of an electron beam due to local electric fields and therefore image the ferroelectric domains in barium titanate. High-resolution electron microscopy imaging allows us to evaluate atomic-level variations in crystal structure, local defects, and polarization in thin films of barium titanate.

Acknowledgements

This work has been supported in part by the NSF STC for Integrated Quantum Materials DMR-1231319, and the NSF Nanotechnology Nanotechnology Coordinated Infrastructure ECCS-1541959.

References

[1] C Wang, M Zhang, B Stern, M Lipson, M Loncar, "Nanophotonic lithium niobate electro-optic modulators," *Optics Express* **26**, 1547 (2018).

3:00 PM BREAK

3:30 PM *CH04.06.05

Understanding Antiferroelectric Thin Film Structure-Property Relationships with Emerging Scanning Transmission Electron Microscopy Techniques James M. LeBeau; Massachusetts Institute of Technology, United States

Although antiferroelectric materials have been studied for decades, they have gained renewed interest for potential applications in energy storage, actuation, and non-volatile memory. This is enabled by the polar behavior of AFEs, where the antiparallel alternation can be switched to lie in the same direction with a sufficiently strong electric field — i.e. an AFE to ferroelectric transition. Moreover, thin film growth of antiferroelectrics, including PbZrO₃ (PZO) and Pb₂MgWO₆ (PMW), has been pursued to modify the properties of this transition and offers many new tantalizing opportunities to engineer the behavior of these materials. To further gain insights, direct investigations of the transformation mechanisms responsible will be key.

In this talk, we will highlight our results from ex and in situ aberration-corrected scanning transmission electron microscopy (STEM) studies of PZO and PMW thin films. In particular, we will focus on insights into the AFE-FE phase transformations during biasing of thin film PbZrO₃. We will discuss the details of polarization switching and the evolution of domain structure, shedding light on the underlying mechanisms and defects governing the behavior. The role of strain, measured with cepstral analysis, and thin film growth orientation will also be explored to determine their impacts on the antiferroelectric/ferroelectric transition.

We will also highlight results from multislice electron ptychography to characterize chemical order and disorder in PMW, specifically at antiphase boundaries. By characterizing and mapping these boundaries, we gain a deeper understanding of their influence on local polarization and implications for polarization switching. Overall, STEM analysis provides critical insights into the defect/structure relationships and the impact of intrinsic and extrinsic factors on the behavior of antiferroelectric materials.

4:00 PM CH04.06.06

Joint Ptychographic-Tomographic 3D Reconstruction of Perovskite Nanowires in Carbon Nanotubes Hannah Devyldere¹, Georgios Varnavides^{1,2}, Stephanie Ribet², Yuxin Jiang^{1,2}, Colin Ophus², Peidong Yang^{1,2} and Mary Scott^{1,2}; ¹University of California, Berkeley, United States; ²Lawrence Berkeley National Laboratory, United States

Atomic-resolution electron tomography (AET) can be used to recover the 3D locations of atoms within nanomaterials without crystal priors from a set of 2D projections. However, AET requires precise subpixel alignments as well as exact tilt angles for each tomogram, limiting its applicability since these parameters are often not obtainable experimentally and must instead be solved for during the reconstruction process [1]. Additionally, experimentally-demonstrated atomic resolution tomographic reconstructions have thus far utilized high angle annular dark field projections - a dose inefficient imaging technique which limits the resolution for low scattering elements. Electron ptychography is a phase-retrieval technique capable of providing high resolution imaging of light elements at comparatively low dose [2]. Importantly, multislice electron ptychography has recently been shown to use the redundant information in overlapping illuminated regions to recover nonlinear information along the axis of projection [3]. The resolution along this "depth-sectioning" direction however, is limited by the lack of diverse angular information in a typical converged probe experiment, and thus not suitable for atomic resolution 3D reconstructions [4].

More recently, these two techniques have been combined in a serial fashion, whereby 2D ptychographic reconstructions are then utilized in 3D tomographic algorithms, enabling a unit cell averaged atomic resolution reconstruction of both low-z and high-z elements [5]. While this enables the efficient transfer of nonlinear information through the multislice propagator, it makes limited use of information redundancy across the tilt-series.

Conversely, the ptychography and tomography inverse problems can be solved jointly - reconstructing the volume directly from the tilt-series of 4D diffraction datasets. Here, we report on experimental results for a joint ptychographic-tomographic 3D reconstruction of perovskite nanowires encapsulated by carbon nanotubes [6]. We discuss the sensitivity of the technique in reconstructing the light carbon atoms of the nanotube and show how efficient regularization of the volume helps recover information in the missing wedge direction.

- [1] Xu, R. et al. *Nature Materials*, 14(11), 1099–1103 (2015). DOI: 10.1038/nmat4426
- [2] Pelz, P.M., et al. *Sci Rep* 7, 9883 (2017). DOI: 10.1038/s41598-017-07488-y
- [3] Gao, S., et al. *Nat Commun* 8, 163 (2017). DOI: 10.1038/s41467-017-00150-1
- [4] Zhen Chen et al. *Science* 372, 826-831(2021). DOI: 10.1126/science.abg2533
- [5] Pelz, P. et al. *arXiv* (2022). DOI: 10.48550/arXiv.2206.08958
- [6] Mengyu Gao et al. *J. Am. Chem. Soc.* 145 (8), 4800-4807 (2023). DOI: 10.1021/jacs.2c13711

4:15 PM *CH04.06.07

Development of Fast Direct Detectors for 4D STEM, *In Situ* TEM, and Other Applications Barnaby D. Levin; Direct Electron LP, United States

Advanced transmission electron microscopy (TEM) techniques such as four-dimensional scanning TEM (4D STEM), and *in situ* TEM, require detectors with fast imaging speeds and single-electron sensitivity. Direct Electron has recently developed new fast direct detectors to meet the needs of these advanced applications.

Celeritas and Celeritas XS are 1024 x 1024 pixel detectors that are designed for extremely high frame-rate readout. The Celeritas XS detector can generate images at speeds of up to 87,000 frames per second, when reading out a small central region. For applications such as 4D STEM, this allows high-throughput data collection at speeds approaching conventional 2D STEM. Celeritas XS has recently applied to study the local ordering in amorphous materials such as molecular glasses [1], and metallic glasses [2]. When coupled with a programmable DE FreeScan scan generator, these detectors can be used to explore novel scanning techniques to collect data more efficiently.

The Apollo detector is a 4096 x 4096 pixel detector that has, to date, primarily been used for biological TEM imaging applications [3,4]. Apollo may also be promising for TEM imaging of beam sensitive materials such as polymers. Apollo uses a unique event-based readout method [5] to generate electron counting images with greater data efficiency than previous frame-based detectors, which helps to minimize coincidence loss, maximize detective quantum efficiency, and reduces the detector's cost.

Here, we will discuss the development of these detectors and a variety of potential applications, including 4D STEM and *in situ* TEM.

References:

- [1] Chatterjee et al. *Nano Lett.*, **23**, 5, 2009–2015 (2023)
- [2] Huang et al. *Ultramicroscopy*, **241**, 113612 (2022)
- [3] Peng et al. *J. Struct Bio X*, **7**, 100080 (2023)
- [4] Bhella et al. Data DOI: 10.6019/EMPIAR-11404
- [5] Levin et al. *Microscopy & Analysis*, January Issue, 15-17 (2023)

4:45 PM CH04.06.08

Multimodal Electron Microscopy for Unravelling Structure-Coherence Relationships in Superconducting Quantum Materials and Systems ThangPham^{1,2}, MatthewCheng^{1,2}, DominicGoronzy^{1,2}, CameronKopas³, HilalCansizoglu³, JoshMutus³, Robertodos Reis^{1,4}, MarkC. Hersam^{1,1,1} and VinayakDravid^{1,4,2}; ¹Northwestern University, United States; ²Superconducting Quantum Materials and Systems (SQMS), United States; ³Rigetti Computing, United States; ⁴NUANCE-Northwestern University, United States

The quest to build quantum computers requires coordinated advances in materials science, device fabrication, and quantum architecture. Recently, superconducting qubits based on transmons have achieved coherence times on the order of hundreds of microseconds, but additional improvements are needed to achieve reliable and high-fidelity quantum computing that can outcompete conventional digital computing. The difficulties in understanding the structure-coherence relationships in transmons stem from the complex nature of different interfaces in the device, such as the metal-air, metal-dielectric, and metal substrate interfaces in Josephson junctions (JJs), which are believed to host two-level-system loss channels. This talk will present our recent efforts to elucidate structure-coherence relationships using multimodal electron microscopy in two interfaces in JJs – namely the Al-AIOx and Al-Si substrate interfaces. We combine core-loss electron energy loss spectroscopy (EELS) and four-dimensional scanning transmission electron microscopy (4D-STEM) at cryogenic temperatures to investigate the chemical composition, bonding environment, and nanoscale structure of Al-AIOx and Al-Si interfaces. These electron microscopy findings are correlated with electrical characterization and theoretical calculations to provide a comprehensive understanding of the influences of atomic-scale quantum disorder on coherence time, which can help inform efforts to mitigate decoherence sources in superconducting qubit devices.

SESSION CH04.07: Electron Energy Loss Spectroscopy I
Session Chairs: Maureen Joel Lagos and Sandhya Susarla
Friday Morning, December 1, 2023
Hynes, Level 3, Room 301

8:00 AM *CH04.07.01

Demystifying Quantum Phenomena at Functional Oxide Interfaces Y. ErenSuyolcu^{1,2}, Yu-MiWu¹, NicolasBonmassar¹, GennadyLogvenov¹ and PeterA. Van Aken¹; ¹Max Planck Institute for Solid State Research, Germany; ²Cornell University, United States

Quantum materials possess extraordinary properties making them highly promising for next-generation electronic devices and quantum information processing. Among these materials, transition metal oxide heterostructures provide a versatile playground for quantum phenomena, including high-temperature superconductivity, magnetism, and metal-to-insulator transition. The origin of these phenomena is the competition between different degrees of freedom, such as charge, orbital, and spin, which are interrelated with the crystal structure, the oxygen stoichiometry, and the doping dependence. Therefore, understanding the intricate structure-property relationship in these materials is crucial for harnessing their full potential.

The unique combination of aberration-corrected scanning transmission electron microscopy (STEM) and oxide molecular beam epitaxy (MBE) techniques allows the engineering of novel interface properties with precise control at the atomic scale^[1]. Combining different oxide layers through heterostructural design opens access to interface physics and leads to engineering interface properties, where the degrees of freedom can be artificially modified. In this talk, I will focus on complex oxide interfaces with extraordinary structural quality and properties. We designed cuprate-manganite interfaces using oxide MBE and focused on interface superconductivity compared to cuprate-cuprate interfaces^[2-4] and tuning interfacial magnetism^[5]. The interfaces are extensively probed with STEM techniques, including high-angle annular dark-field (HAADF) and annular bright-field (ABF) imaging, electron energy-loss spectroscopy (EELS), and energy-dispersive X-ray spectroscopy (EDXS). High-resolution STEM investigations provide crucial feedback to improve structural quality and a detailed understanding of the properties.

Through different epitaxial designs, we demonstrate that (i) charge transfer and local magnetism can be tuned by epitaxial strain^[5], (ii) sharper interfaces can be realized by pushing the interface superconductivity down to one monolayer thickness but with a cost of filamentary superconducting behavior^[6] and, (iii) how superconductivity can be tuned via epitaxial integration of ultra-thin 214-manganate slabs^[7]. Notably, our investigations further underline that the sharpness of interfaces requires a meticulous definition: Structurally perfect and coherent interfaces may exhibit dissimilar chemical sharpness, ascribed to the elemental intermixing that dominates the physical properties. In summary, our research showcases the remarkable potential of quantum materials and highlights the crucial role of STEM techniques in unraveling their properties and designing interfaces for next-generation electronic devices and quantum information processing systems^[8,9].

References

- [1] Y. E. Suyolcu, G. Christiani, P. A. van Aken, G. Logvenov, *J. Supercond. Nov. Magn.* **2020**, *33*, 107.
- [2] Y. E. Suyolcu, Y. Wang, W. Sigle, F. Baiutti, G. Christiani, G. Logvenov, J. Maier, P. A. van Aken, *Adv. Mater. Interfaces* **2017**, *4*, 1700737.
- [3] Y. E. Suyolcu, J. Sun, B. H. Goodge, J. Park, J. Schubert, L. F. Kourkoutis, D. G. Schlom, *APL Mater.* **2021**, *9*, 021117.
- [4] N. Bonmassar, G. Christiani, U. Salzberger, Y. Wang, G. Logvenov, Y. E. Suyolcu, P. A. van Aken, *ACS Nano* **2023**.
- [5] Y.-M. Wu, Y. E. Suyolcu, G. Kim, G. Christiani, Y. Wang, B. Keimer, G. Logvenov, P. A. van Aken, *ACS Nano* **2021**, *15*, 16228.

- [6] Y. E. Suyolcu, Y.-M. Wu, G. Kim, G. Christiani, G. Logvenov, P. A. van Aken, **2023**, *submitted*.
[7] N. Bonmassar, G. Christiani, T. Heil, G. Logvenov, Y. E. Suyolcu, P. A. van Aken, *Adv. Sci.* **2023**, 2301495.
[8] I kindly acknowledge all precious scientists for their significant contributions to the work presented, especially Prof. D. G. Schlom, Prof. B. Keimer, Dr. G. Kim, and G. Christiani.
[9] This project has received funding from the European Union's Horizon 2020 research and innovation programme under grant agreement 823717 – ESTEEM3.

8:30 AM CH04.07.02

Harnessing the Power of Defect Engineering: Unveiling Oxygen Vacancies in 2D Indium Oxide for Advanced Memory Regions and Pioneering 2D Materials Discovery Kuan-HungChen¹, Chang HsunHuang¹, Chen-ChihHsiang¹, Chia-YiWu², Yi-HsiangYen¹ and Yi-ChiaChou¹; ¹National Taiwan University, Taiwan; ²National Yang Ming Chiao Tung University, Taiwan

The rapid progress in the field of two-dimensional (2D) materials has revolutionized various industries and paved the way for exciting advancements in technology. These materials, with their unique properties and atomic-level thickness, hold immense potential for applications in electronics, optoelectronics, and beyond. To harness the full capabilities of 2D materials, it is crucial to develop effective fabrication techniques that enable their synthesis and manipulation. Among the range of techniques available for the fabrication of 2D materials, liquid metal printing (LMP) has emerged as an innovative approach. This method allows for fast, low-temperature, low-cost, and high-quality exfoliation of metal oxides with atomic-level precision. One particular 2D material that has attracted significant attention is indium oxide (InO_x). InO_x is a wide bandgap material with remarkable structural stability and tunable electronic properties, making it highly desirable for applications in metal oxide semiconductors. However, the exploration of InO_x in 2D forms remains uncharted territory, presenting a compelling avenue for further development. In the realm of nanoscale memristive devices, the engineering of defects plays a critical role in tailoring the electronic performance. Conducting filaments in insulating oxides, which are essential for memristive behavior, rely on the field-induced migration of oxygen vacancies within the material[1]. Recent studies by Huang et al. shed light on the influence of printing temperatures on the electrical properties of 2D-InO_x. By altering the printing temperatures, they observed variations in the concentration of oxygen vacancies, leading to the presence or disappearance of memristive switching[2].

Building upon this prior research, the present study aims to investigate the defect characteristics of 2D-InO_x in more detail. To achieve this, X-ray photoelectron spectroscopy (XPS) and photoluminescence (PL) were employed. The results revealed that higher printing temperatures led to an increase in the concentration of oxygen vacancies, suggesting that the defect characteristics can be tailored through precise control of the fabrication process. Additionally, the microstructure and crystallinity of 2D-InO_x were analyzed using transmission electron microscopy (TEM) and selected area diffraction patterns (SADP). To gain further insight into the atomic arrangement and defect structures of 2D-InO_x, spherical aberration corrected scanning transmission electron microscopy (Cs-corrected STEM) and electron energy loss spectroscopy (EELS) were employed. STEM provides high-resolution images with atomic-level details, enabling the visualization and analysis of crystallographic features, grain boundaries, and defect structures. EELS measurements, on the other hand, offer information about the electronic properties and local chemical environment of the material. Notably, an observable shift in the In-M_{4,5} and O-K peaks indicated a preferential segregation of oxygen vacancies at grain boundaries. Peak ratio calculations based on the EELS spectra also provided quantitative information about the defect concentration in 2D-InO_x. Surprisingly, the results suggested a higher defect concentration in 2D-InO_x printed at lower temperatures. The deeper insights gained from this study into the exact nature of oxygen defects and the ability to modify the concentration of oxygen vacancies in atomically-thin oxide films are of great significance. By tailoring defects, researchers can unlock the full potential of 2D-InO_x and pave the way for next-generation memory devices with enhanced performance, energy efficiency, and functional capabilities.

References:

1. Waser, R. and M. Aono, *Nanoionics-based resistive switching memories*. Nature materials, 2007. **6**(11): p. 833-840.
2. Huang, C.-H., et al., *Multiple-State Nonvolatile Memory Based on Ultrathin Indium Oxide Film via Liquid Metal Printing*. ACS Applied Materials & Interfaces, 2023.

8:45 AM *CH04.07.03

Lanthanide-Transition Metal Intermetallics Studied by Electron Energy Loss Spectroscopy EllisKennedy¹, TrentKyrk², SelinCetin¹, MoisesBravo², GregoryMcCandless², ColinOphus³, JuliaChan² and MaryScott^{1,3}; ¹University of California, Berkeley, United States; ²Baylor University, United States; ³Lawrence Berkeley National Laboratory, United States

The valence states of *f*-block elements strongly influence their magnetic quantum states. Lanthanide (Ln) transition metal (M) intermetallics in particular have been shown to host a variety of quantum properties, such as charge density waves, Kondo lattice behavior, fluctuating valency, and unconventional superconductivity¹. These distinctive characteristics result from interplay between itinerant *d*-electrons and more localized *f*-electrons. While the basic model of Ln+M intermetallics consists of delocalized *3d* electrons interacting with localized *4f* orbitals, recent work shows that the tight binding description of *f*-electron materials is not accurate in some cases². The ability to alter valency and *f*-electron itinerancy presents an opportunity to study magnetism in quantum materials as well as tune the degree of correlation. Furthermore, the breakdown of the tight binding model implies that crystal field interactions may play an important role in directing the properties of Lanthanide compounds³. The ability to modify the Ln valency through adjustments in composition, local coordination, or crystal phase therefore provides an excellent platform for the exploration and development of new materials with tunable and coexisting quantum properties.

Here, we probe the relationship between valency and crystal structure by coupling electron energy loss spectroscopy (EELS) with detailed structural characterization. We apply these methods to intermetallics with composition Ln₂Co₃Ge₅. Using *in-situ* monochromated EELS, we detect a strong dependence of the Pr valency in Pr₂Co₃Ge₅ as it undergoes a subtle structural transition from a monoclinic (m) to orthorhombic (o) phase. This alteration of the Pr environment from o-Pr₂Co₃Ge₅ to m-Pr₂Co₃Ge₅ is expected to influence the crystal electric field splitting of the Pr *4f* orbital, and therefore likely plays a role in the observed complex magnetic transitions in this material⁴. The density of unoccupied states of Co are redistributed during the phase transition as well, suggesting compensating behavior between the Co *3d* and Pr *4f* electrons. Similarly, we combine high resolution transmission electron microscopy and spatially resolved EELS measurements to determine the influence of twin boundaries in monoclinic Sm₂Co₃Ge₅. Although the deviation of the twins from the bulk crystal structure is not large, these local distortions of the crystal periodicity are shown to increase the hybridization of the delocalized Co *3d* electrons. As the magnetic moment of this material cannot be accounted for by Co alone, we expect that changes in Co hybridization at the twin boundaries will influence the bulk magnetic properties.

Our observations directly relate the electronic states of the Ln and Co ions in Ln₂Co₃Ge₅ compounds to their local crystal environment. These results directly show the relationship between the valency of the lanthanides and their local environment in the crystal structure, which are ultimately factors that direct their role in the material's quantum properties. Both of the observations illustrate the tunability of properties that is introduced by the complex behavior of *f*-electrons in the Ln₂Co₃Ge₅ of intermetallics, and point to the rich landscape of quantum phenomena available for exploration in these materials.

References

1. Kyrk, T. M. et al. Anisotropic magnetic and transport properties of orthorhombic o-Pr₂Co₃Ge₅. *J. Phys. Mater.* **5**, 044007 (2022).
2. Li, Y., Ma, Q., Huang, S. X. & Chien, C. L. Thin films of topological Kondo insulator candidate SmB₆: Strong spin-orbit torque without exclusive surface conduction. *Sci Adv* **4**, eaap8294 (2018).
3. Ramanathan, A. et al. Chemical design of electronic and magnetic energy scales of tetravalent praseodymium materials. *Nat. Commun.* **14**, 3134 (2023).
4. Layek, S., Anand, V. K. & Hossain, Z. Valence fluctuation in Ce₂Co₃Ge₅ and crystal field effect in Pr₂Co₃Ge₅. *J. Magn. Magn. Mater.* **321**, 3447–3452 (2009).

9:15 AM CH04.07.04

Backscattered Electron Energy Loss Spectroscopy with an Analytical High-Resolution Ultra-Low-Voltage SEM DanielRyklin¹, JochenKammerer² and RasmusSchroeder¹; ¹Heidelberg University, Germany; ²Queensland University of Technology, Australia

In scanning transmission electron microscopy (STEM) electron energy loss spectroscopy (EELS) is a well-established high resolution analytical characterization technique for a large range of materials and applications. However, the required sample dimension (i.e. < 100 nm thickness) is a limiting factor and often makes sample preparation rather challenging. Furthermore, beam-induced sample degradation at typical TEM electron energies is hampering the observation of beam-sensitive materials. The realization of EELS at very low electron landing energies on bulk materials, however, would definitely provide a completely new characterization tool – from simple materials identification to dynamic in-situ studies, such as plasmon excitations by electrons or light.

Using a prototype of an aberration corrected, ultra-low-energy SEM (Zeiss Delta-SEM [1]) modified with an electrostatic energy-selective detector, we show for the first time that it is possible to identify the excitation of states (e.g., plasmon and fluorescence excitations) in a SEM by their typical excitation energy loss signature in the energy spectrum of the backscattered electrons. We call this new analytical signal backscattered electron energy loss spectroscopy (bsEELS).

As initial model system we analyze the spectral data obtained from graphene on silicon wafer, materials where TEM-EELS measurements can serve as a reference [2,3]. The measured bsEEL spectra can be simulated in the framework of a naïve model which convolves TEM-EELS data with the energy response of the energy-selective detector. Although the energy resolution of our current experimental setup is limited (about 5 eV), we find good agreement of the experimental SEM-bsEELS spectral data to, e.g., the known characteristic surface plasmon signal of

graphene. This is the first experimental evidence that backscattered electrons carry specific material information resulting from their elastic and inelastic interaction with the sample. Applying this to an organic PBDB-T:ITIC blend for solar cells we can use the plasmon loss signals in the bsEEL spectra to identify and distinguish the two materials inside the blend to create a surface map of the material distribution.

Using bsEELS relaxes constraints on the sample preparation (thickness, size) while aberration correction allows to use ultra-low electron landing energies, comparable to energies usually used for high-resolution EELS. We show that contrast and imaging quality are significantly improved for electron energies below 500 eV (as far down as 20 eV) – while retaining high spatial resolution (< 1 nm at 100 eV).

To prove the high sensitivity of this novel imaging modality we study organic samples such as DNA and DNA labelled with fluorophores. The results show that at ultra-low electron energies beam damage is minimized and that contrast is strongly increased for organic, low atomic number materials. First results of bsEELS on DNA origamis with 12 covalently bound fluorophore molecules reveal a pronounced signal for the DNA's UV absorption as well as the excitation signal of the fluorophores.

Acknowledgements: The authors thank Yannick Dreher and Kerstin Göpfrich (MPI Heidelberg, Germany), and Wolfgang Köntges (Heidelberg University) for samples. Research funded by DFG (German Research Foundation) via the Excellence Cluster "3D Matter Made to Order" (EXC-2082/1-390761711).

[1] RR Schröder et al., *Microsc. Microanal.* 24 (Suppl 1), 2018

[2] Wachsmuth et al, *Physical Review B* 90, 235434, 2014

[3] Park et al, *Ultramicroscopy* 109, 9, 2009

9:30 AM CH04.07.05

HAADF-STEM and EELS Characterization of Stoichiometry and Defects in the Pyrochlore Quantum Magnet $Tb_2Ti_2O_7$ Margaret A. Anderson, Johanna Nordlander, Ismail El Baggari, Charles Brooks and Julia Mundy; Harvard University, United States

Quantum spin liquids, highly entangled magnetic materials which lack a long-range symmetry-breaking ordering transition down to absolute zero, host anyonic quasiparticles that are promising platforms for quantum computing. The quantum spin liquid state results from magnetic frustration, which relies on a careful balance of magnetic interactions. Defects in the crystal structure disrupt this balance and may obscure the intrinsic spin liquid behavior in candidate materials. Using reactive-oxide molecular beam epitaxy, we synthesize a series of thin films of the pyrochlore quantum spin liquid candidate $Tb_2Ti_2O_7$ with varying composition on YSZ (111) substrates. We use scanning transmission electron microscopy (STEM) and electron energy loss spectroscopy (EELS) to observe and characterize point and extended defects in this composition series. We present the first atomic-resolution EELS maps that directly show excess titanium incorporated via 'antistuffing' on the terbium site as both Ti^{3+} and Ti^{4+} along $\{1\ 1\ 1\}$ antiphase boundaries. Using multivariate curve resolution (MCR), we map out changes in valence and in the titanium L -edge structure across these defects. In contrast, we find that terbium-rich films exhibit mainly $\{2\ -1\ -1\}$ antiphase boundaries. Using phase lock-in analysis, we reveal quasi-periodic dislocations along the film-substrate interface that act to relieve strain in nominally stoichiometric films. Finally, we characterize the films' magnetic behavior with SQUID magnetometry. While none of the films exhibit a magnetic transition down to 1.8 K, the magnetization is impacted by the presence of defect spins in the off-composition films.

This work was supported by the Air Force Office of Scientific Research (MURI Grant No. FA9550-21-1-0429).

9:45 AMBREAK

10:15 AM *CH04.07.06

Wavefront Shaping in the TEM: What Promise Does it Hold for Materials Characterisation? Johan Verbeeck and Chu-Ping Yu; EMAT, University of Antwerp, Belgium

Wavefront shaping or the ability to freely change the phase of a coherent wave is a powerful concept in diverse areas of science ranging e.g. from light optics, telecommunication, radar, acoustics and seismology. The ability to freely shape the wavefront of a coherent electron wave in transmission electron microscopy has become a recent possibility with our 48 pixel array of electrostatic phase shifters that can be placed in an aperture position of a modern electron microscope. This changes the paradigm from attempting to make ever smaller probe sizes for spatial resolution to create a large basis set of orthogonal quantum states to interact with a sample. We discuss several potential applications of this new tool with proof of concept implementation and simulations. Such applications can include increased selectivity in probing EELS excitations based on symmetry selection, adaptive optics providing high contrast images while dynamically correcting aberrations and bringing out relevant (eg phase) contrast. It also helps for inverse problems in ptychography and diffraction problems where the phase control over the incoming beam can break point symmetry and make it easier for inverse algorithms to converge to a single solution.

10:45 AM *CH04.07.07

Advances in High Energy and Spatial Resolution STEM EELS Demie Kepaptsoglou^{1,2}, Khalil El Hajraoui^{1,2}, Matthieu Bugnet^{1,3}, Guillaume Radtke⁴, Michele Lazzeri⁴, Vlado Lazarov², Jan Rusz⁵ and Quentin Ramasse^{1,6}; ¹SuperSTEM, United Kingdom; ²University of York, United Kingdom; ³Institut National des Sciences Appliquées de Lyon, France; ⁴Sorbonne Université, France; ⁵Uppsala University, Sweden; ⁶University of Leeds, United Kingdom

Engineering the structural or chemical architecture of functional materials at the nano or even atomic level enables emergent properties that rely on the interplay between fundamental properties of matter such as charge, spin and local atomic-scale chemistry. Thanks to advances in monochromators, state-of-the-art electron energy loss spectroscopy (EELS) in the scanning transmission electron microscope (STEM), offers nowadays the ability to map materials and atomic structures with an angstrom size electron beam and an energy resolution for EELS under 5meV. (Krivanek *et al.*, 2014) These capabilities have allowed to probe the spectroscopic signature of phonons down to the single atom level. (Hage *et al.*, 2020) Here, we present strategies for high spatial and energy resolution STEM-EELS experiments to interrogate proximity effects of heterostructure materials at the atomic scale and present opportunities for new experiments using monochromated electron probes.

Bi_2Se_3 is a topological insulator (TI) with topologically protected helical two-dimensional surface states and one-dimensional bulk states associated with crystal defects, in proximity with graphene. The strong spin-orbit interaction and proximity effects result in subtle and controllable electronic band structure changes at and near the interface, with exciting potential for spintronic applications. Here we probe at high energy resolution the interfaces in a system consisting of Bi_2Se_3 films grown by chemical vapor deposition on epitaxial graphene/SiC(0001), where the number of carbon layers can be carefully controlled to tune possible proximity effects between the film and the substrate. In addition to a direct interrogation of the chemical bonds (Bugnet *et al.*, 2022) between the layers via their vibrational response, these observations are linked to the interplay between the various phonon modes and the Dirac plasmons in the TI layers, whose dispersion is mapped in momentum space with nm spatial sensitivity using a recently developed methodology for nanoscale momentum-resolved spectroscopy. Magnonics is an emergent field within spintronics utilizing the ability to generate and propagate controllably a spin-wave in nm-sized magnetic structures, with a view to build a new generation of devices for data processing and storage. It was also recently demonstrated that magnons can be utilized to convert spin to charge (or charge to spin) currents, a critical step for integration of spin and charge devices. STEM EELS is proposed to be a leading candidate technique to attempt the detection of magnons at the nanoscale, perhaps down to at the atomic scale, thanks to a recently developed theoretical calculation framework and preliminary experimental investigations (Lyon *et al.*, 2021). Here, we report on progress in designing experiments building on these initial steps using in-situ STEM-EELS. The prototypical spin-to-charge conversion system considered for this proof of principle attempt consists of Yttrium Iron Garnet (YIG)/platinum (Pt) bilayer, a widely used materials combination where a magnon created by a thermal gradient creates spin accumulation at the YIG/Pt interface, which subsequently diffuses into the nonmagnetic Pt, and via inverse spin Hall effect (ISHE) creates a voltage signal in the Pt layer.

References

[1] O. L. Krivanek *et- al*, *J. Phys. Conf. Ser.* **522**, 012023 (2014).

[2] F. S. Hage *et- al*, *Science* **367**, 1124 LP (2020).

[3] M. Bugnet *et- al*, *Phys. Rev. Lett.* **128**, 116401 (2022).

[4] K. Lyon, *et- al*, *Phys. Rev. B* **104**, 214418 (2021).

11:15 AM *CH04.07.08

Vibrational and Electronic Structure of Superlattices using Monochromated Electron Energy-Loss spectroscopy Eric R. Hoglund¹, De-Liang Bao², Harrison Walker², Mahmut Sami Kavrik^{3,4}, Geemin Kim⁵, Matt Law^{5,5,5}, Patrick E. Hopkins^{6,6}, Sokrates T. Pantelides^{2,2} and Jordan A. Hachtel¹; ¹Oak Ridge National Laboratory, United States; ²Vanderbilt University, United States; ³Lawrence Berkeley National Laboratory, United States; ⁴University of California, San Diego, United States; ⁵University of California, Irvine, United States; ⁶University of Virginia, United States

Many quantum phenomena emerge from reducing the size of materials and therefore increasing the discretization of quantum states. When multiple materials of reduced size are combined into heterostructures, their interaction results in new emergent states at the interface between the materials that can be as prevalent as bulk-like state that are intrinsic to the lattice of the parent materials. These interface states can result in new optical, thermal, or electronic properties. Herein, we demonstrate structure-vibration and structure-electronic relations resulting from the formation of superlattices using scanning transmission electron microscopy (STEM) imaging combined with monochromated electron energy-loss spectroscopy (EELS) and density-

functional-theory calculations.

To design properties dictated by atomic vibrations at interfaces in an informed manner, we need to probe vibrations with lateral spatial resolution to resolve the local vibrations. We connect the localized vibrational response of interfaces in SrTiO₃-CaTiO₃ superlattices observed with EELS to the structurally diffuse interfaces observed with integrated differential-phase contrast. As the layer thickness of the superlattices decrease, the interface structure extends further into the layers and the related vibrations. The progression of the local atomic structure and interface vibrations come to determine the vibrational response of an entire superlattice, which explains new infrared activity and crossovers from incoherent to coherent thermal transport observed in the superlattices.

In ferroelectric superlattices phonon modes linked with static atomic displacements can spatially vary, in particular at the interfaces. Here we will show that the structurally non-equivalent interfaces in a period are also vibrationally non-equivalent as a result of different coupling between the lattice and electronic structure at the different interfaces.

Lastly, we will concentrate on the emergence of new electronic states in self-assembled quantum dot superlattices. Quantum dots can exhibit unique excitonic behavior and quantized electronic states that result from the limited number of atoms in the material. Recently, epitaxially fused superlattice of PbSe QD film show delocalized states, which are not derivative of bulk materials. However, this “confined” but “connected” structure results in new electronic behavior that is sensitive to defects in different length scale lattices, such as missing or undercoordinated QDs (superlattice) and point defects in the necks between fused QDs (atomic). We will show the connection between the electronic and structural properties across both length-scales and the impact of defects using cryogenic high-spatial and spectral resolution STEM-EELS.

SESSION CH04.08: Electron Energy Loss Spectroscopy II
Session Chairs: Demie Kepaptsoglou and Sandhya Susarla
Friday Afternoon, December 1, 2023
Hynes, Level 3, Room 301

1:30 PM *CH04.08.01

Probing Excitations and Structures by Ultrafast Electron Microscopy Claus Ropers^{1,2} and Jan-Wilke Henke¹; ¹Max Planck Institute for Multidisciplinary Sciences, Germany; ²University of Göttingen, Germany

Providing the most detailed views of atomic-scale structure and composition, transmission electron microscopy serves as an indispensable tool for structural biology and materials science. The combination of electron microscopy with pulsed electrical or optical stimuli allows for the study of transient phenomena, involving magnetization dynamics, strain evolution and structural phase transformations. Ultrafast transmission electron microscopy (UTEM) is a pump-probe technique, in which non-equilibrium processes can be tracked with simultaneous femtosecond temporal and nanometer to atomic-scale spatial resolutions.

This talk will cover recent methodical developments and applications in UTEM based on laser-triggered field emitters, including real-space imaging [1] and ultrafast nanobeam diffraction [2] of structural phase transitions. Moreover, the mechanisms involved in free-electron beams interacting with optical fields at photonic structures will be discussed, emphasizing quantum effects. In particular, recent progress in the coupling of electron beams to whispering gallery modes [3] and integrated photonic resonators [4] will be presented. Finally, using event-based electron spectroscopy, the preparation and characterization of electron-photon pair states [5] and Coulomb-correlated electron number states [6] will be discussed.

References:

- [1] “Ultrafast nanoimaging of the order parameter in a structural phase transition”, T. Danz, T. Domröse, C. Ropers, *Science* **371**, 6527 (2021).
- [2] “Light-induced hexatic state in a layered quantum material”, T. Domröse, Th. Danz, and C. Ropers, *Nature Materials* (in press, 2023), arXiv:2207.05571 (2022), URL: <https://www.nature.com/articles/s41563-023-01600-6>
- [3] “Controlling free electrons with optical whispering-gallery modes”, O. Kfir *et al.*, *Nature* **582**, 46 (2020).
- [4] “Integrated photonics enables continuous-beam electron phase modulation”, J.-W. Henke *et al.*, *Nature* **600**, 653 (2021).
- [5] “Cavity-mediated electron-photon pairs”, A. Feist *et al.*, *Science* **377**, 777 (2022).
- [6] “Coulomb-correlated electron number states in a transmission electron microscope beam”, R. Haindl *et al.*, *Nat. Phys.* (appeared online, 2023). <https://doi.org/10.1038/s41567-023-02067-7>

2:00 PM *CH04.08.02

STEM Developments: Atomic-Resolution SE Imaging, Fast 4D STEM, Ultrahigh Energy Resolution Tracy C. Lovejoy¹, Nikalas Delby¹, Chris Meyer¹, Michael Holtz¹, Joel Martis¹, Andreas Mittelberger¹, Ben Plotkin-Swing¹, Steven Quillin¹ and Ondrej Krivanek^{1,2}; ¹Nion R&D, United States; ²Arizona State University, United States

A modern STEM can achieve atomic-scale spatial resolution (1.1 Å) and phonon-scale energy resolution (2.6 meV) at 20 keV primary energy [1], and improved spatial but worsened energy resolutions at higher keV. These capabilities come from advanced electron-optical instrumentation, such as monochromators, correctors, and spectrometers. In parallel developments, many researchers are turning attention to combining advanced electron-optical capabilities with new developments in, detectors, software, and operating modes.

A new type of secondary electron (SE) detector designed by Nion for a modern STEM combines SE detection with an atom-sized probe in the operating range 20-200 kV, clean (metal-sealed and bakable) UHV vacuum conditions, and state-of-the-art electron energy loss spectroscopy (EELS) and 4D-STEM capabilities [2,3]. Running experience reveals that common S/TEM samples (e.g. MoS₂ or metal nanoparticles on a carbon film) that give atomic-resolution annual dark field (ADF) images initially show only surface contamination in the SE signal. We use multiple methods for UHV surface cleaning, including resistive heating of the whole sample in a side entry holder (e.g. Protochips) and direct laser illumination of a small spot (20 μm x 40 μm). Direct laser illumination is particularly interesting because the laser light modulates the SE signal in some samples by changing the local charge distribution on the surface [4].

After cleaning, atomic-resolution SE signals are readily visible. Expanding on previous work with atomic-resolution SE imaging [5], lower operation voltage in a modern STEM avoids knock-on damage and enables atomic-resolution SE studies of 2D materials. We will show an example combining atomic resolution ADF, SE, and 4D-STEM to study monolayer MoS₂ with intentional Vanadium dopants at 60 keV primary energy.

4D-STEM and especially EELS experiments on 2D materials have traditionally been complicated by slow detectors and readout noise. The latest direct detectors avoid readout noise and achieve high DQE and dynamic range with speed approaching that of traditional single-channel detectors (>10,000 frames/second). Combining these detectors with powerful open-source software for smart acquisition/compression and live processing makes multi-frame (time series) 4D-STEM or EELS imaging possible, bringing significant advantages when changing the sample environment (e.g. heating, cooling, light-, or gas-injection) causes sample drift that makes longer exposures impractical.

Doing these experiments in an instrument capable of <5 meV energy resolution opens the door for synergistic experiments such as mapping the absolute temperature of the sample in and around the spot illuminated by a laser using electron energy gain spectroscopy [6], and measuring the presence and local bonding configuration of hydrogen in the sample by detecting the “infrared absorption” signal of the H bonds with vibrational EELS [7]. Phonon spectroscopy of surface dopants visible in the SE signal is also very promising.

References [1] N. Dellby *et al.*, *Microsc. Microanal.* (2023) to be published [2] M.T. Hotz *et al.*, *Microsc. Microanal.* (2023) to be published [3] J. Martis, B. Plotkin-Swing *et al.*, *Proceedings 20th IMC (Busan, 2023)* to be published [4] J. Martis, N. Dellby *et al.*, *Proceedings 20th IMC (Busan, 2023)* to be published [5] Y. Zhu *et al.*, *Nature Materials* **8** (2009) 808-812. [6] J.C. Idrobo *et al.*, *Phys. Rev. Lett.* **120** (2018) 095901 [7] P. Rez *et al.*, *Nature Comm.* **7** (2016) 10945

2:30 PM BREAK

3:00 PM *CH04.08.03

Momentum-Resolved Electron Spectroscopy of Kagome Crystal YCr₆Ge₆ Babafemi S. Agboola, Jonah Gautreau, Graeme Luke and Maureen Joel Lagos; McMaster University, Canada

The YCr₆Ge₆ Kagome crystal exhibits unique electronic band structure like flat bands¹ which drive quantum properties (e.g. flat band ferromagnetism, superconductivity). YCr₆Ge₆ can also sustain plasmons and their behavior is driven by the complex electronic structure of the Kagome crystal. Material synthesis and characterization of structural and plasmonic properties are challenging and in progress. Here we report on the synthesis of YCr₆Ge₆ Kagome crystals and on the dispersion behavior of anisotropic bulk plasmons using momentum-resolved EELS.

We grew single crystals of YCr_6Ge_6 with the flux method and TEM/STEM methodologies (e.g., diffraction and imaging) were used to obtain structural information. The electron diffraction patterns obtained from different micrometer-sized regions revealed a single crystalline phase. Furthermore, atomic-resolution imaging was performed in STEM mode to spatially identify the hexagonal close pack crystal structure and the Kagome lattice structural profile. We also conducted spatially resolved core-loss EELS experiments to identify the chemical composition of the crystal and valence states of the Kagome crystal. EELS spectrum images were collected at different ionization edge energies (e.g. Cr $L_{2,3}$), revealing different degrees of scattering delocalization.

We studied the dispersion of bulk plasmons along the orthogonal ΓA and ΓM dispersion directions, accessing plasmon behavior beyond the first Brillouin zone. We found anisotropic response of bulk plasmons, dispersing with different velocities along the high symmetry directions. Anomalous non-linear dispersion is also visualized suggesting a complex behavior of valence electrons. Our work represents progress towards understanding the complex electronic behavior of anisotropic plasmons sustained in quantum materials.

References

- [1] Y. Ishii, et al. *Jour. Phys. Soc. Jap.* 82 (2013) 023705.
- [2] We acknowledge NSERC under a Discovery Grant and CCEM for access to microscopy facilities.

SESSION CH04.09: Cathodoluminescence Spectroscopy
Session Chairs: Juan Carlos Idrobo and Sandhya Susarla
Friday Afternoon, December 1, 2023
Hynes, Level 3, Room 301

3:30 PM *CH04.09.01

Recent Advances in Cathodoluminescence Spectroscopy and in-TEM Light Injection Christian Monachon: Attolight AG, Switzerland

Cathodoluminescence spectroscopy is a technique consisting in the analysis of the light emitted in the UV-IR range by a material upon its excitation with an electron beam. This technique is particularly useful in semiconductors, where it allows local probing of the material properties such as quantum well properties, dopant concentration, or alloy composition. Another of its exciting prospects is plasmonics, where it allows direct modal probing of nanostructures.

Several new developments and technical improvements make it more flexible than ever, and open the way for unparalleled light injection densities. This contribution will treat the technological choices made at Attolight in order to foster ever better and more consistent results, in particular in terms of mirror architecture vs collection efficiency, as well as field of view. Necessary constraints on the electron microscope will also be reviewed and explained in order to outline the capabilities as well as limits of light injection and collection in a STEM.

4:00 PM *CH04.09.02

Time Resolved Cathodoluminescence of InGaN/GaN Quantum Well in an Ultrafast Transmission Electron Microscope Cléo Santini¹, Luiz Tizei², Delphine Lagarde³, Robin Cours¹, Sebastien Weber¹, Alexei V. Sakharov⁴, Andrey F. Tsatsulnikov⁴, Andrey E. Nikolaev⁴, Arnaud Arbouet¹, Mathieu Kociak², Andrea Balocchi³, Nikolay Cherkashin¹ and Sophie Meuret¹; ¹CEMES/CNRS, Netherlands; ²Université Paris-Saclay, France; ³LPCNO, France; ⁴Ioffe Institute, Russian Federation

Cathodoluminescence is the emission of visible light when an electron interacts with matter. It is a powerful technique to study the luminescence properties of semiconductors below the diffraction limit of visible light. The development of time-resolved Cathodoluminescence (TR-CL) in a scanning electron microscope enabled the measurement of the lifetime of excited states in semiconductors with a sub-wavelength spatial resolution. It was used for example to measure the influence of stacking faults on the GaN exciton [1], to probe the role of a silver layer on the dynamics of a YAG crystal [2] or to show the influence of stress on the optical properties of ZnO nanowires [3]. These results demonstrate that TR-CL is essential to study the correlation between semiconductor optical and structural properties (composition, defects, strain...). While all these pioneering studies were done using a scanning electron microscope, the improvement of the spatial resolution and the combination with other electron-based spectroscopies offered by transmission electron microscopes has been a step forward for TR-CL. Indeed, we recently succeed to do the first time-resolved cathodoluminescence experiments within an ultrafast transmission electron microscope [4], followed soon after by Ye-Jin Kim et al [5]. Our TRCL experiment are performed in a unique electron microscope, based on a cold-FEG electron gun [6]. This technology allows among other things to reach a spatial resolution of a few nanometers, essential for the study of III-V heterostructures.

In this presentation we will discuss the advantage and inconvenient of TRCL in a UTEM and present our results on the study of charge carrier dynamics in a 4 nm $\text{In}_{0.3}\text{Ga}_{0.7}\text{N}/\text{GaN}$ quantum well with a resolution below 10 nm. We studied the QW emission dynamic both along and across the quantum well and correlate the results with strain map and high resolution HADF images.

References

- [1] P. Corfdir *et al.*, "Exciton localization on basal stacking faults in a-plane epitaxial lateral overgrown GaN grown by hydride vapor phase epitaxy," *J. Appl. Phys.*, vol. 105, no. 4, p. 043102, 2009.
- [2] R. J. Moerland, I. G. C. Weppelman, M. W. H. Garming, P. Kruit, and J. P. Hoogenboom, "Time-resolved cathodoluminescence microscopy with sub-nanosecond beam blanking for direct evaluation of the local density of states," *Opt. Express*, vol. 24, no. 21, p. 24760, 2016.
- [3] X. Fu *et al.*, "Exciton Drift in Semiconductors under Uniform Strain Gradients: Application to Bent ZnO Microwires," *ACS Nano*, vol. 8, no. 4, pp. 3412–3420, 2014.
- [4] S. Meuret *et al.*, "Time-resolved cathodoluminescence in an ultrafast transmission electron microscope," *Appl. Phys. Lett.*, vol. 119, no. 6, p. 6, 2021.
- [5] Y. J. Kim and O. H. Kwon, "Cathodoluminescence in Ultrafast Electron Microscopy," *ACS Nano*, vol. 15, no. 12, pp. 19480–19489, 2021.
- [6] F. Houdellier, G. M. Caruso, S. Weber, M. Kociak, and A. Arbouet, "Development of a high brightness ultrafast Transmission Electron Microscope based on a laser-driven cold field emission source," *Ultramicroscopy*, vol. 186, pp. 128–138, 2018.

4:30 PM *CH04.09.03

Effects of Coupling in Atomically-Thin Transition Metal Dichalcogenides Revealed by Electron Spectroscopies Steffi Y. Woo¹, Fuhui Shao¹, Ashish Arora^{2,3}, Robert Schneider², Benjamin J. Carey², Johann A. Preuß², Steffen Michaelis de Vasconcellos², F. Javier Garcia de Abajo⁴, Rudolf Bratschkitsch², Andrea Konečná⁵ and Luiz Tizei¹; ¹Université Paris-Saclay, France; ²University of Münster, Germany; ³Indian Institute of Science Education and Research, India; ⁴ICFO-Institut de Ciències Fotoniques, Spain; ⁵Brno University of Technology, Czechia

Understanding and controlling the interlayer coupling in van der Waals homo- and heterostructure devices containing transition metal dichalcogenides (TMDs) has been an ongoing effort in the two-dimensional material community. Due to the reduced Coulomb screening at atomic thicknesses, TMD optical properties are extremely sensitive to their local dielectric environment. This contributes detrimentally to the exciton linewidth due to inhomogeneous broadening [1], but also provides opportunities for tuning of the electronic gap and exciton binding energy [2] or neutralization of charged exciton emission [3] as demonstrated previously with graphene. Obtaining exciton linewidths towards the homogeneous limit for TMD monolayers in both optical absorption and emission (by photoluminescence) has been made possible by encapsulation in hexagonal boron nitride (*h*-BN).

A monochromated electron microscope is the ideal platform with capabilities for analogous measurement on such 2D materials at the nanoscale, including cathodoluminescence and electron energy-loss spectroscopy (EELS). Until recently [4-6], freely suspended TMD layers have long suffered broad EELS exciton linewidths and have easily succumbed to electron-beam damage. Incorporating *h*-BN encapsulation has put electron spectroscopies on a level playing field as well-known optical measurements, with supplementary structural and chemical information down to the atomic-scale [4,6].

In the first part of this presentation, the influence of two dielectric materials (Si_3N_4 and *h*-BN) in various TMD monolayer configurations (suspended, supported, and encapsulated) is explored using EELS coupled with electron diffraction to measure the layer roughness [5]. Surprisingly, interfacial cleanliness and substrate-induced charge inhomogeneity/trapping predominate the influence on absorption linewidth more than monolayer flatness, which is significantly improved by the atomically flat *h*-BN. In the second part, complementary EELS (absorption) and CL (emission) measurements offer valuable insight into the coupling behavior in monolayer $\text{WSe}_2/\text{graphene}$ heterostructures (encapsulated in *h*-BN). This includes evidence for Coulomb interactions modified by the graphene, namely a redshifted neutral exciton emission energy and reduced exciton binding energy from absorption [7]. Spectral differences with mixed *h*-BN and/or graphene encapsulation with increasing graphene layer thickness will also be discussed.

- [1] Raja, A. *et al.*, *Nat. Nanotechnol.* 14, 832 (2019).
- [2] Raja, A. *et al.*, *Nat. Commun.* 8, 15251 (2017).
- [3] Lorchat *et al.*, *Nat. Nanotechnol.* 15, 283 (2020).

- [4] Bonnet, N. *et al.*, *Nano Lett.* **21**, 10178–10185 (2021).
[5] Shao, F. *et al.*, *Phys. Rev. Mater.* **6**(7), 074005 (2022)
[6] Woo, S.Y. *et al.* *Phys. Rev. B.* **107**(15), 155429 (2023).
[7] Woo, S.Y., Shao, F. *et al.* in preparation.

SYMPOSIUM DS01

Accelerating Materials Research with AI-Assisted Experimentation
November 27 - December 6, 2023

Symposium Organizers

Milad Abolhasani, North Carolina State University
Keith Brown, Boston University
B. Reeja Jayan, Carnegie Mellon University
Xiaonan Wang, Tsinghua University

* Invited Paper
+ JMR Distinguished Invited Speaker

SESSION DS01.01: Innovations in Autonomous Experimentation I
Session Chairs: Peter Beaucage and Michael Thompson
Monday Morning, November 27, 2023
Sheraton, Third Floor, Fairfax B

10:30 AM *DS01.01.01

Flexible Automation Accelerates Materials Discovery[Curtis P. Berlinguette](#); The University of British Columbia, Canada

Automated systems perform repetitive tasks quickly and consistently with minimal human intervention. These characteristics are particularly effective in manufacturing, where speed and reproducibility drive down cost and increase quality. In materials science laboratories, however, automation is rarely used. The diverse experimental workflows used in materials science often require highly customized automation that is not commercially available. Even when automated tools for materials synthesis or characterization are available, they are often linked together by manual steps. “Flexible automation” is changing this situation because of the recent emergence of safer, cheaper, and more user-friendly robotics. I define flexible automation as the concept of using robotics to create reconfigurable automated experiments. A powerful feature of flexible automation is the ability to program multiple experimental procedures together into fully automated workflows. These experimental procedures can be performed by commercially-available or customized hardware modules that operate on samples either serially or in parallel. Flexible automation platforms can be readily reconfigured to the changing needs of the experiment. It is for these reasons that flexible automation can accelerate the unique experiments characteristic to materials science. As a proof-of-principle set of experiments, I will show how Ada, our self-driving laboratory for thin-film materials, discovers and optimizes high-performance, low-cost hole-transport materials for use in advanced solar cells. I will also showcase how Ada’s modular design (see below) can enable the automated and autonomous discovery of materials for other clean energy technologies.

11:00 AM DS01.01.02

Autonomous Chemical Reactions in High Resolution Scanning Probe Microscopy[Nian Wu](#)¹, [Markus Aapro](#)¹, [Alexander Ilin](#)¹, [Drost Robert](#)¹, [Peter Lijeroth](#)^{1,2} and [Adam Foster](#)^{1,2}; ¹Aalto University, Finland; ²WPI Nano Life Science Institute, Kanazawa University, Japan

High resolution Scanning Probe Microscopy (SPM) not only enables visualizing material structures at atomic resolution, but also provides an opportunity to manipulate individual atoms or molecules [1]. More recent studies have even harnessed the capability of SPM to selectively form and break bonds as a method for controlling chemical reactions in on-surface molecular synthesis [2]. In general, the SPM manipulations are predominantly controlled via parameters of the tip position, bias voltages and tunneling conductance. However, the selection of proper parameters requires extensive domain knowledge, which is not necessarily transferable to new systems. Improper parameters could lead to manipulation failure and even damage to the tip through a crash. Therefore, it is of great value to develop efficient and autonomous SPM techniques with an excellent control system for manipulation to both optimize experiments and explore non-intuitive manipulation pathways. Recent research combining machine learning algorithms with SPM has allowed the automation of a wide range of challenges, including image quality assessment, tip conditioning, tip functionalization, lateral manipulation and vertical manipulation, and nanofabrication [3].

In this work, we build on our deep reinforcement learning atomic manipulation approach [4] to automate a chemical reaction by the controlled removal of an atom from a molecule and selectively reattaching it. To achieve the objective, we split the challenging task into three major parts as follows: 1) selection of manipulation regions, detection of atoms and identification of elements toward SPM scanning images at atomic resolution; 2) learning manipulation parameters to dissociate chemical bonds; 3) learning lateral manipulation parameters to separate atoms or molecules and perform selective recombination.

[1] N. Pavliček and L. Gross, *Nature Reviews Chemistry* **1**, 1–11 (2017)

[2] Albrecht, F. *et al.* *Science* **377**, 298–301 (2022)

[3] O.M. Gordon and P.J. Moriarty, *Mach. Learn. Sci. Technol.* **1**, 023001 (2020)

[4] I-Ju Chen, Markus Aapro, Abraham Kipnis, Alexander Ilin, Peter Lijeroth and Adam S. Foster, *Nat. Commun.* **13**, 7499 (2022)

11:15 AM DS01.01.03

Towards AI-Controlled Continuous Flow Chemistry and Polymerizations[Rigoberto C. Advincula](#); The University of Tennessee/Oak Ridge National Laboratory, United States

The study of structure-composition-property (SCP) relationships in soft matter is of high interest since advances in simulation and the use of statistical optimization methods have been widely used. The macroscopic properties can also be defined by the processing methods and therefore more finite element analysis (FEA) methods have found wide utilization. The use of artificial intelligence and machine learning (AI/ML) in polymer materials has appended the ability to rapidly optimize synthetic routes and manufacturing. The use of Bayesian and statistical methods enables the application of logic-derived design and regression analysis into an otherwise trial-and-error approach in polymer synthesis, fabrication, and characterization. We demonstrate in this talk the use of continuous flow reaction chemistry and polymerizations to enable unit operation optimization and the possibility of autonomous design and synthesis with a hierarchical approach and learning. There is a high possibility that a combination of P, V, T, and flow rate control enables new methods of copolymerization and the ability to use kinetics as a handle for optimized macromolecular properties and design for controlled yield. The automation for online monitoring is a possibility with improved instrumentation and the development of a feedback loop learning for possible deep learning (DL) development.

11:30 AM DS01.01.04

AI-Guided Discovery of the Hidden Life of Oxides in Extreme Environments Steven R. Spurgeon^{1,2}, Bethany Matthews¹, Jenna Bilbrey¹, Arman Ter-Petrosyan¹, Christina Doty¹, Christopher Barr³, Khalid Hattar⁴, Le Wang¹, Yingge Du¹, Rajendra Paudel⁵, Ryan Comes⁵ and Sarah Akers¹; ¹Pacific Northwest National Laboratory, United States; ²University of Washington, United States; ³Sandia National Laboratories, United States; ⁴The University of Tennessee, Knoxville, United States; ⁵Auburn University, United States

Directing the evolution of functional oxides in extreme environments is a longstanding challenge that requires new approaches to precision synthesis, characterization, and analytics. Our present inability to acquire, interpret, and act on multi-modal signatures limits our control of oxide-based devices, such as fuel cells and neuromorphic computing architectures, particularly in high-radiation environments. Here I will show how we are operationalizing machine reasoning to induce, probe, and model oxide degradation pathways more richly than ever before. I will describe a bespoke instrument and analytics workflow that combines on-machine sparse data-guided control with cloud-based analytics, which together yield better out of distribution model performance, improved capacity for discovery, and more interpretable analysis of fast-evolving phenomena. I will show how this new approach can accelerate the discovery and design of oxide-based devices for extreme environments.

11:45 AM DS01.01.05

Bayesian Optimization of Wet-Impregnated Co-Mo/Al₂O₃ Catalyst for High-Yield Carbon Nanotubes Sang Su Shin and Jaegeun Lee; Pusan National University, Korea (the Republic of)

Carbon nanotubes (CNTs) have become a significant component for various fields because of their outstanding electronic and mechanical properties. To meet the requirement of specific applications, CNTs synthesis with controlled properties is significantly required. Chemical vapor deposition (CVD) using solid supported catalysts is considered an attractive approach for controllability of the nanostructure and large scale production. Since the early 2000s, many researchers have used mono-metallic catalysts to control CNT properties, but it was hard. To overcome these limitations, bi- and tri-metallic catalysts are being studied. However, there are a variety of possible combinations of multi-metallic catalyst systems. In addition, the development of multi-metallic catalysts requires a more complicated optimization than that of mono-metallic catalysts. In this presentation, we introduce our research efforts to implement Bayesian optimization (BO) in optimizing a bimetallic catalyst for the CVD growth of CNTs. BO, one of a machine learning processes based on Bayes' theorem that finds the optimum value of a black-box function, could quickly optimize parameters of less than 20 dimensions. BO consists of two main components: surrogate model and acquisition function. The surrogate model is a model that performs probabilistic estimation of the shape of a black-box function based on the investigated input-output values ($(x_1, f(x_1)), \dots, (x_n, f(x_n))$). The acquisition function is a function that recommends input values for the next experiment based on the probabilistic estimation of the surrogate. Specifically, we attempted to optimize the wet impregnation of Co-Mo/Al₂O₃ catalyst. Co-Mo is one of the famous bimetallic system because of their ability to synthesize chirality-specific single-walled CNTs. Here, we optimized the experimental variables to maximize the CNT yield. Four input parameters were chosen: total wt% of catalyst, ratio of Co and Mo of catalyst, drying temperature, and calcination temperature. To compare the performance of two types of acquisition functions: Expected improvement (noise-free) and One-shot knowledge gradient (with noise), we parallelly performed two BO processes. As a result, both the acquisition functions successfully optimized the CNT yield with similar performance. The contour plot established by the surrogate model that predicts black-box function show that addition of Mo has negative effect on CNT yield. This study demonstrates the potential of BO in the material synthesis.

SESSION DS01.02: Innovations in Autonomous Experimentation II
Session Chairs: Milad Abolhasani and Keith Brown
Monday Afternoon, November 27, 2023
Sheraton, Third Floor, Fairfax B

1:30 PM *DS01.02.01

SARA—Autonomous Agents for High-Throughput Exploration of Composition/Time/Temperature Processing Space by Lateral Gradient Laser Spike Annealing Michael O. Thompson; Cornell University, United States

The coupling of fast, high-throughput, automated experiments with autonomously directed protocols, based on active learning (AL) agents, promises to dramatically accelerate both the exploration and exploitation of new material systems. SARA, a Scientific Autonomous Reasoning Agent, was developed to manage efficient exploration of the complex composition, time, and temperature phase processing space enabled by non-equilibrium laser spike annealing. Integrating robotic materials synthesis and characterization with a hierarchy of AI methods, SARA has demonstrated efficient exploration of processing phase maps in unary, binary and ternary oxide systems. Lateral gradient laser spike annealing (lgLSA), coupled with focused X-ray synchrotron sources, generates and characterizes over a thousand unique processing conditions per minute, with upwards of 100,000 conditions on a single ternary compositional library plate. To autonomously manage the search at a commensurate rate, SARA utilizes a hierarchical set of characterization and decision algorithms based on nested active learning cycles and machine learning models incorporating the underlying physics and end-to-end uncertainty quantification. To enable specific phase exploitation as well as exploration, a probabilistically quantitative, multi-phase labeling algorithm has been incorporated to provide full in-loop structural information to the AI agents, including quantitative lattice distortions from composition or strains, peak broadening and grain size, and probability estimates of likely multi-phase combinations. We demonstrate the efficacy of SARA by autonomously mapping processing/synthesis phase boundaries in several unary and binary oxide composition spread systems, with orders-of-magnitude acceleration over exhaustive searches previously used.^{1,2} With this search acceleration, we also demonstrate the ability of SARA to implement a two-stage objective function, switching between exploration and exploitation modes based on uncertainty of the material processing space with structurally labeled phase fields. Finally, I will discuss future directions enabled by the autonomous search, including the potential to track also kinetic parameters through time-resolved characterization directed by SARA. While demonstrated for mapping of processing phase maps, SARA has the potential to be incorporated into numerous high-throughput workflows, and can be equally used to provide physical knowledge to train machine learning models for accelerated materials discovery.

¹Ament, S., Amsler, M., Sutherland, D.R., Chang, M.C., Guevarra, D., Connolly, A.B., Gregoire, J.M., Thompson, M.O., Gomes, C.P. and van Dover, R.B., 2021. Autonomous materials synthesis via hierarchical active learning of nonequilibrium phase diagrams. *Science Advances*, 7 (2021).

²Sutherland, D.R., Connolly, A.B., Amsler, M., Chang, M.C., Gann, K.R., Gupta, V., Ament, S., Guevarra, D., Gregoire, J.M., Gomes, C.P. and Bruce van Dover, R., 2020. Optical identification of materials transformations in oxide thin films. *ACS Combinatorial Science*, 22, 887-894 (2020).

2:00 PM DS01.02.02

Automated Microscopy for Physics Discovery—From High-Throughput to Hypothesis Learning-Driven Experimentation Yongtao Liu¹, Rama K. Vasudevan¹, Maxim Ziatdinov¹ and Sergei V. Kalinin²; ¹Oak Ridge National Laboratory, United States; ²The University of Tennessee, Knoxville, United States

In this work, we explore the ferroelectric polarization switching in relation to the applied pulse bias (i.e., bias voltage and time) in an automated manner in scanning probe microscopy (SPM). We perform (1) high-throughput experimentation for a comprehensive understanding of the relationship between pulse biases and ferroelectric domain growth, (2) autonomous experimentation driven by machine learning (ML) algorithm to optimize experimental conditions based on real-time experiment results.

SPM has been a powerful tool for manipulating and visualizing ferroelectric domains at the nanoscale. Investigations of ferroelectric domain size and stability can advance understandings of ferroelectrics application in memory devices, such as operating time, retention time, bit size, and so on. However, these SPM measurements have traditionally been time-intensive and dependent on experienced researchers for monotonous operations and real-time decision-making of measurement parameters, e.g. researchers determine and manually tune the parameters for next iteration of experiment according to the previous results. Here, we perform automated experiments in SPM to explore the mechanism of ferroelectric polarization. First is a high-throughput experiment of writing ferroelectric domains by applying various bias pulse conditions and subsequently conducting piezoresponse force microscopy to image the written domain structure. The high-throughput experimentation enables systematically varying the bias pulse parameters, therefore comprehensively understanding the relationship between the bias parameters and the resulting domain structures. In this experiment, we discovered different polarization states that show up upon different bias conditions. Second, we implement a hypothesis active learning (HypoAL) algorithm to control the SPM for ferroelectric domain writing. The HypoAL is based on structured Gaussian process (sGP), which analyzes the relationship between the bias pulse parameters and the written domain size during operating experiments, and subsequently determines the bias pulse parameters for the next experiment. The HypoAL aims to establish the best physical model from a hypothesis list for the material's behaviour within the smallest number of experiment step. The HypoAL indicates that the domain growth in a BaTiO₃ film is ruled by kinetic control. We anticipate the established approaches here can be extended to microscopy methods other than SPM in the future to accelerate materials and physics discovery.

Acknowledgement: This work (high-throughput experimentation) is supported by the Center for Nanophase Materials Sciences, a US Department of Energy Office of Science User Facility. This work (HypoAL experimentation) is partially supported by the U.S. Department of Energy, Office of Science, Office of Basic Energy Sciences Energy Frontier Research Centers program

under Award Number DE-SC0021118.

2:15 PM DS01.02.03

Active Learning for Efficient Parameter Space Mapping—A Case Study with using Quantum Dots[Jeff Xu¹](#), Katherine Young², Logan Keating¹, Ajit Vikram³, Moonsub Shim¹ and Paul Kenis¹; ¹University of Illinois at Urbana-Champaign, United States; ²Purdue University, United States; ³Merck & Co Inc, United States

Autonomous workflows have increasingly been implemented across disparate facets of materials research to accelerate materials discovery or materials optimization. One application of autonomous workflows is the generation of accurate parameter space maps of synthesis spaces. These accurate parameter space can then be probed by subject matter experts to generate deeper insight and propose new hypotheses for further research.

Building an accurate parameter space map requires efficient sampling of the parameter space, which can be done effectively with active learning. Active learning algorithms involve both a surrogate model to fit existing data and an acquisition function to decide the next experiment(s) based on some pre-defined heuristic. Presently the selection of surrogate models and acquisition functions relies on human intuition and requires both an understanding of statistical learning fundamentals and the nature of the material systems studied. Increased adoption of active learning, however, requires a set of heuristics regarding the selection of surrogate models and acquisition functions that is beginner friendly: scientists should be able to build effective active-learning algorithms without prior machine learning experience.

This talk will report on a generalized modular active learning approach to combine various surrogate models and acquisition functions for mapping the synthesis parameter space of quantum dot (QD) synthesis. We tested different surrogate models, acquisition functions, and batch sizes using simulated data and digital twins of real experiment data and compared their relative performances in terms of accuracy and computational resources required. We then experimentally applied these active learning algorithms on an automated QD synthesis platform on different synthesis chemistries to test the generalizability of our approach. Results from this endeavor generated useful heuristics for building active learning algorithms that will help future scientists who wish to use machine learning to accelerate their automated online or manual offline workflows. The modular approach for implementing active learning also provides a useful framework for analyzing and assessing new active learning approaches.

2:30 PM BREAK

3:00 PM DS01.02.04

Modeling and Design of Heterogeneous Hierarchical Bioinspired Spider Web Structures using Deep Learning and Additive Manufacturing[Wei Lu](#), Nic Lee and Markus J. Buehler; Massachusetts Institute of Technology, United States

Spider webs are incredible biological structures, comprising thin but strong silk filament and arranged into complex hierarchical architectures with striking mechanical properties (e.g., lightweight but high strength, achieving diverse mechanical responses). While simple 2D orb webs can easily be mimicked, the modeling and synthesis of 3D-based web structures remain challenging, partly due to the rich set of design features. Here we provide a detailed analysis of the heterogeneous graph structures of spider webs, and use deep learning as a way to model and then synthesize artificial, bio-inspired 3D web structures. The generative models are conditioned based on key geometric parameters (including average edge length, number of nodes, average node degree, and others). To identify graph construction principles, we use inductive representation sampling of large experimentally determined spider web graphs, to yield a dataset that is used to train three conditional generative models: 1) An analog diffusion model inspired by nonequilibrium thermodynamics, with sparse neighbor representation, 2) a discrete diffusion model with full neighbor representation, and 3) an autoregressive transformer architecture with full neighbor representation. All three models are scalable, produce complex, *de novo* bio-inspired spider web mimics, and successfully construct graphs that meet the design objectives. We further propose algorithm that assembles web samples produced by the generative models into larger-scale structures based on a series of geometric design targets, including helical and parametric shapes, mimicking, and extending natural design principles towards integration with diverging engineering objectives. Several webs are manufactured using 3D printing and tested to assess mechanical properties.

3:15 PM DS01.02.05

Autonomous Thin-Film Materials Synthesis by Machine Learning and Robotics[Kazunori Nishio¹](#), Akira Aiba¹, Shigeru Kobayashi², Ryo Nakayama², Ryota Shimizu² and Taro Hitosugi^{2,1}; ¹Tokyo Institute of Technology, Japan; ²The University of Tokyo, Japan

Accelerating the development of new materials is indispensable for a sustainable society. However, new materials development in laboratories involves repeated cycles of conception, synthesis, and characterization, manually performed by researchers. Under such circumstances, the inclusion of machine learning, robotics, and big data into these cycles promises to revolutionize materials research.

Recently, we have designed and built a closed-loop system that combines Bayesian optimization, automatic synthesis, and automatic physical property evaluation for inorganic thin-film materials. This system implements a concept; lab equipment and instruments should be Connected, Autonomous, Shared, and operate in a High-throughput manner. With this approach, we have already achieved a proof-of-concept of autonomous material synthesis, which was demonstrated by autonomously optimizing the synthesis conditions specified by Bayesian optimization to minimize the electrical resistance for Nb-doped TiO₂ thin films fabricated via the sputtering method [1]. We present an expanded system to evaluate various physical properties: X-ray diffraction, scanning electron microscope/energy dispersive X-ray spectroscopy, Raman spectroscopy, and UV-Vis spectroscopy. Coevolution with such technologies, researchers work on more creative research, accelerating materials science research.

[1] R. Shimizu, and T. Hitosugi *et al.*, APL Mater. 8, 11110 (2020).

3:30 PM DS01.02.06

Machine Learning-Guided Precision Synthesis of Colloidal Nanocrystals[Yugang Zhang¹](#), Hyeong Jin Kim¹, Fang Lu¹, Matthew Carbone¹ and Kristofer G. Reyes²; ¹Brookhaven National Laboratory, United States; ²University at Buffalo, The State University of New York, United States

Colloidal nanocrystals, also known as 'artificial atoms', offer a new avenue for packing atoms and interfaces, which are essential for catalysis, photonics, and energy storage. Over the past several decades, tremendous advancements have been made in the synthesis of colloidal nanocrystals with controlled size, shape and composition. However, conventional synthesis methods largely depend on Edisonian (trial-and-error) approaches, which are both labor-intensive and time-consuming. In this talk, we will showcase our experimental work on machine-learning-assisted synthesis of nanocrystals. This machine learning strategy allows for rapid and efficient exploration of the synthetic space, leading to the successful synthesis of targeted nanocrystals with a high degree of control over size and size distribution.

3:45 PM *DS01.02.07

The NIST Autonomous Formulation Laboratory—Accelerating Liquid Formulation and Reaction Landscape Exploration with AI and X-Ray/Neutron Scattering[Peter Beaucage](#), Duncan Sutherland and Tyler Martin; National Institute of Standards and Technology, United States

Liquid formulations are ubiquitous in products ranging from deicing liquids and fuels/lubricants to biologic drugs, shampoo, and food/beverage ingredients. All these products require precise tuning of 10s-100s of components to produce a desired product: viscosity modifiers, surfactants, dyes, fragrances, flammability inhibitors, etc. This large number of components often precludes rational mapping between component fractions, structure, and product stability. Multimodal characterization and machine learning (ML) tools promise to greatly reduce the expense of exploring the stability boundaries of a particular, desirable phase in highly multicomponent products. This talk will describe the development of the Autonomous Formulation Laboratory, a highly adaptable platform capable of autonomously synthesizing and characterizing liquid mixtures with varying composition and chemistry using x-ray and neutron scattering. Highlights will include closed-loop AI-guided exploration of composite nanoparticle synthesis for coatings development and bioformulation exploration incorporating neural networks into scattering pattern classification. I will further discuss our ongoing efforts to incorporate a multimodal suite of secondary measurements such as optical imaging, UV-vis-NIR and capillary rheometry to provide greater-than-sum-of-parts materials characterization.

4:15 PM DS01.02.08

Autonomous Synthesis of Sputtered Nitride Thin Films with Controlled Cation Composition[Davi M. Febba](#), Kevin R. Talley, Kendal Johnson, Stephen Schaefer, Sage Bauers, John S. Mangum, Rebecca Smaha and Andriy Zakutayev; National Renewable Energy Laboratory, United States

Autonomous experimentation has emerged as an efficient approach to accelerate the pace of materials discovery. Although instruments for autonomous synthesis have become popular in molecule and polymer science, solution processing of hybrid materials and nanoparticles, examples of autonomous tools for physical vapor deposition (PVD) are scarce yet important for the semiconductor industry.

Although some of the few existing reports of autonomous PVD focused on the optimization of material properties such as resistivity and crystallinity, precise control of cation and anion

composition in inorganic thin films is of paramount importance. For example, it has been theoretically predicted and experimentally demonstrated that short-range ordering tunes the optical absorption edge in the long-range disordered alloy $(\text{ZnSnN})_{1-x}(\text{ZnO})_{2x}$ at a very specific composition of $x = 0.25$. Also, the resistivity and bandgap of ternary nitrides and their alloys depend mostly on cation composition.

In this presentation, we will discuss the design and implementation of a closed-loop autonomous workflow for sputter deposition of thin films with controlled composition, leveraging a highly automated sputtering reactor custom-controlled by Python, optical emission spectroscopy (OES), and Bayesian optimization. By fabricating $\text{Zn}_x\text{Ti}_{1-x}\text{N}_y$ thin films with simultaneous monitoring of optical emission lines from the co-sputtering of elemental targets, we will show that cation composition, spanning a wide range, can be expressed as a linear function of emission lines.

Informed by OES, a control algorithm with Bayesian optimization as its decision-making agent can effectively optimize the power on each sputtering source, achieving deviations from the targeted cation composition within relative 3.5 %, even for 15 nm-thick films, which demonstrates that the methods described in this work can reliably synthesize thin films with specific composition and minimal human interference.

Moreover, we will show that our approach can enhance reproducibility in the synthesized films by assuring that the desired composition will be achieved regardless of the N_2/Ar mixture and total power applied on elemental targets. Finally, we will also discuss how substrate effects and chamber pressure affect the calibration of the current approach and suggest future improvements of its accuracy.

This presentation will be based on the following preprint: <https://arxiv.org/abs/2305.11122>

4:30 PM DS01.02.09

ML-Assisted Fully Autonomous Robotics for High-Throughput Performance Optimization of Organic Mixed Ionic–Electronic Conductors Yuhao Dai¹, Henry Chan², Aikaterini Vriza², Fredrick Kim², Sihong Wang¹ and Jie Xu²; ¹University of Chicago, United States; ²Argonne National Laboratory, United States

Machine learning (ML) has revolutionized the way materials research is performed nowadays by intelligently navigating to vast experimental design space and identifying promising material candidates with desired properties, thereby reducing the time and cost associated with traditional trial-and-error approaches. Recently, a novel category of materials: organic mixed ionic–electronic conductors (OMIECs) attract considerable attention for simultaneously facilitating highly efficient electron/hole and ion transport, and thereby are widely adopted in signal processing, sensing, and energy storage devices. Among these, the organic electrochemical transistor (OECT) is of particular interest due to its high transconductance (G_m), which is essential for enabling biosensing with high sensitivity. To gain the high G_m , high $[\mu C^*]$ needs to be achieved, which is determined by the intrinsic morphology and energy profile of OMIECs that can be tuned by vast processing conditions and molecular design strategies, resulting in a large searching space. Therefore, ML can play an important role in not only accelerating the OMIEC exploration but also uncovering the underlying knowledge. However, to realize this, it requires built-in fully autonomous robotics for acquiring high-fidelity source data, and a well-designed ML algorithm and workflow for enhancing exploration efficiency. Herein, we build the fully autonomous Polybot system to carry out the closed-loop workflow for screening out the best processing conditions of OMIECs. The entire system is monitored in real-time by a built-in live streaming platform providing imaging and data analytics tools. During the ML-guided experimentation, we identify the optimal processing conditions of our model OMIEC with improved $[\mu C^*]$ by over 2 folds. Interpretability techniques were also employed during the process to facilitate a deeper understanding of the materials' mixed conducting behaviors and unveil fundamental relationships between $[\mu C^*]$ and processing conditions.

4:45 PM DS01.02.10

Autonomous Synthesis of Thin Films with Pulsed Laser Deposition Enabled by *In Situ* Diagnostics and Characterization Sumner B. Harris, Arpan Biswas, Christopher M. Rouleau, Alexander A. Puzetzy, Seok Joon Yun, Gyula Eres, Mina Yoon, Rama K. Vasudevan, David B. Geohegan and Kai Xiao; Oak Ridge National Laboratory, United States

Synthesis of thin films has traditionally relied upon slow, sequential processes conducted with substantial human intervention, often using a mix of experience and serendipity to optimize material structure or discover properties. With recent advances in autonomous systems which combine automated synthesis, characterization, and artificial intelligence (AI), large parameter spaces can be explored autonomously at rates beyond what is possible by human experimentalists, promising to greatly accelerate our understanding of synthesis science. In this talk, I will discuss the infrastructure development of two highly versatile, autonomy-capable pulsed laser deposition (PLD) platforms: one based on real-time and *in situ* gas-phase and optical diagnostics and the other based around *in vacuo* robotic transfer for characterization. I will then show how we incorporated *in situ* and real-time diagnostics and characterization, a high-throughput methodology, and cloud connectivity to enable an autonomous synthesis experiment with PLD. We grew ultrathin WSe_2 films using co-ablation of two targets with real-time laser reflectivity for thickness control and showed a 10x increase in throughput over traditional PLD workflows. Bayesian optimization with Gaussian process regression was used with *in situ* Raman spectroscopy to drive synthesis and autonomously discover the growth window with a sparse sampling of only 0.25% of a broad 4D parameter space. Moreover, the process-property relationship predicted by the Gaussian process surrogate model suggests two different growth regimes and offers a more global understanding of the synthesis space than a human experimenter could gain without machine learning, information that is crucial for simultaneous, cooperative refinement of both synthesis experiments and theory. Any material that can be grown with PLD can be autonomously synthesized with our platforms and workflows, enabling AI-driven synthesis and accelerated discovery of a vast number of materials. This work was supported by the U.S. DOE, Office of Science, Materials Sciences and Engineering Division and was performed at the Center for Nanophase Materials Sciences, which is a DOE Office of Science User Facility.

SESSION DS01.03: From Self-Driving Labs to an Accelerated Research Ecosystem

Session Chairs: Milad Abolhasani and Keith Brown

Tuesday Morning, November 28, 2023

Sheraton, Third Floor, Fairfax B

8:00 AM *DS01.03.01

Exploiting Diverse Knowledge Sources for Autonomous Materials Research A. Gilad Kusne^{1,2}, Ichiro Takeuchi^{1,2}, Haotong Liang², Felix Adams², Austin McDannald¹, Brian L. DeCost¹ and Mikko Lippmaa³; ¹National Institute of Standards and Technology, United States; ²University of Maryland, United States; ³The University of Tokyo, Japan

Autonomous research systems seek to accelerate materials exploration and discovery by placing materials synthesis and characterization under control of machine learning. For such systems, machine learning controls experiment design, execution, and analysis, thus accelerating knowledge capture while also reducing the burden on experts. The system-driving machine learning algorithms can be dramatically enhanced by integrating knowledge from varied sources including theory, computation, and human intuition. In this talk I will discuss NIST's diverse set of autonomous systems, including autonomous control over user facility measurement systems, and their improved capabilities by drawing on new sources of knowledge.

8:30 AM *DS01.03.02

A-Lab—An Autonomous Laboratory for the Accelerated Synthesis of Novel Inorganic Materials Gerbrand Ceder; University of California, Berkeley/Lawrence Berkeley National Laboratory, United States

We will present the development and initial successes of A-lab: an autonomous facility for the closed-loop synthesis of inorganic materials from powder precursors. All synthesis and characterization actions in A-lab, including powder mixing and grinding, firing, characterization by XRD and SEM, and all sample transfers between them are fully automated, leading to a lab that can synthesize and structurally characterize novel compounds within 10–20 hrs of initiation. The A-lab leverages ab-initio computations through an API with the Materials Project, historical data sets that are text-mined from the literature, machine learning for optimization of synthesis routes and interpretation of characterization data, and active learning to plan and interpret the outcomes of experiments performed using robotics. Over 17 days of continuous operation, the A-Lab successfully developed synthesis routes for 41 novel compounds from a set of 58 targets that were identified using large-scale ab-initio phase stability data from the Materials Project and Google Brain. Synthesis recipes were proposed by natural language models trained on the literature and optimized using an active learning approach grounded in thermodynamics. Analysis of failed syntheses provide direct and actionable suggestions to improve current techniques for materials screening and synthesis design. The high success rate exemplifies the new paradigm of autonomous materials discovery and motivates further integration of computations, historical knowledge, and robotics into AI-driven, closed-loop platforms.

9:00 AM DS01.03.03

Object-Oriented Software Architecture (control-lab-ly) to Control Automated Workflows—A Case Study of Quantum Dot Ligand Cocktails Chang Jie Leong¹, Jayce J. Cheng¹ and Kedar Hippalgaonkar^{1,2}; ¹Institute of Materials Research and Engineering, Singapore; ²Nanyang Technological University, Singapore

Given the multitude of ways to produce new materials, such as altering composition and processing parameters, the state space in materials research is vast, and AI algorithms are vital in

exploring the space and reducing discovery time. To accelerate the collection of copious amounts of experimental data required for these algorithms, many research groups are increasingly turning to automated and autonomous workflows.

Within the community, significant strides have been made in creating flexible and reconfigurable setups by using modular hardware. However, less thought is put into the software that controls these workflows, which are usually custom setups. Bespoke software is typically written to orchestrate actions and communicate between components in the setup. Once working, code is commonly left untouched, which does not leverage on the flexibility and reconfigurability afforded by having modular hardware. This has two complications. First, code is not easily reusable. For a group setting up a new workflow, it is difficult to adapt code from a previous project or from another group. Second, changing a component in the workflow requires substantial rework of the code, since abstractions of how different components interact have not been established. These serve as barriers to teams that intend to set up a new automated workflow or update its components during the course of a campaign.

In this work, we propose a modular software architecture that controls automated experimentation setups, and we use it in our study to improve the charge mobility of quantum dot (QD) thin films by investigating the combinatorial space of multi-ligand passivation of QDs. Effective passivation of QDs can be achieved by matching the appropriate ligand type with each QD facet and we examine combinations of up to five different ligands. Fabricating spin-coated thin films was the major bottleneck in our workflow, as making just one sample already takes multiple spin steps, each having considerable wait times. Evolution of our thin-film fabrication tools was enabled by the proposed software architecture, implemented as a Python package. The package (*control-lab-ly*) exposes available actions for each tool in a standard manner for its particular category. For example, tools with the same function of moving items around a workspace are given identical methods, regardless of form (e.g. gantry vs articulated robots). The modular nature of the package also allows for extension via user plugins, so drivers for new equipment can easily be written and integrated.

9:15 AM DS01.03.04

Machine Learning-Assisted High-Throughput Robot for Electrocatalytic Seawater Splitting Masanori Koderu and Kazuhiro Sayama; National Institute of Advanced Industrial Science and Technology, Japan

The expected shift from fossil fuels to H₂ as the main renewable energy carrier inspires the search for inexpensive, reliable, and green H₂ production methods such as seawater electrolysis. However, the noble metal-based catalysts used for electrolytic H₂ production are costly and should be replaced by cheaper non-noble metal-based ones. Effects of the composition of electrocatalysts have been widely investigated while the search space is too large to investigate manually. For example, reports on electrocatalysts that contain more than three cations are still very limited.

Here, a high-throughput automatic robot was used to prepare Co-Mn-Fe-Ni-based composite-oxide anodic electrocatalysts and characterize their ability to promote the selective and stable production of O₂/HClO at the anode during the electrolysis of model seawater (aqueous NaCl). This robot can deal with 88 samples in a single run from preparing to measuring.

First, the pipetting arm dispenses and mixes up to 10 different metal ion-containing solutions. Then, mixed solutions were deposited onto conductive substrates with a size of 5 mm × 30 mm and dried on a hotplate. The samples are transported to an electric furnace using the transfer arm and calcined to obtain electrodes with different compositions. Subsequently, the measuring sequence starts with the following procedures. The pick-up arm, which has two pins connected to a potentiostat and functions as a working electrode, transfers each electrode to an H-type cell for electrochemical measurements. Finally, the pipetting arm dispenses a small amount of the solution from the cell, mixes it with a coloring reagent, and measures the absorption using a plate reader to quantitate the generated HClO. After each measurement, the solution is automatically replenished from the tank behind the robot.

This robot can perform several electrochemical measurements such as cyclic voltammograms, chronoamperometry, and chronopotentiometry. Therefore, current density at 2.0 V vs. the Ag|AgCl reference electrode, reaction selectivity (faradaic efficiency of HClO formation (FE_{HClO}) for a charge of 0.2 C (1 mA for 200 s)), and the ratio of current densities at 2.0 V vs. Ag|AgCl after 1000 and 100 s (stability) were calculated from these results. It was revealed that a wide range of FE_{HClO} values could be controlled by composition tuning. Co-Fe-Ni-based catalysts such as Co_{0.6}Fe_{0.3}Ni_{0.1}O_x exhibited high current densities for HClO production and good stability, whereas Co-Mn-based catalysts such as Co_{0.2}Mn_{0.5}Ni_{0.3}O_x showed superior O₂ evolution performance and relatively high stability.

Moreover, machine learning-assisted composition optimization was performed using a Bayesian optimization framework. The dataset of the four-element Co-Mn-Fe-Ni system with 286 samples was used. The explanatory and target variables were composition and current density at 2.0 V vs. Ag|AgCl, respectively. The initial 10 points were selected using a D-optimal design, and 10 candidates were suggested after Bayesian optimization. Then, 10 measured samples were added to the initial points. Gaussian process regression was performed to suggest another 10 points, and this cycle was repeated until all samples with top-ten current density were searched. As a result, compositions with high current densities were successfully found after examining 40 out of 286 data points. Furthermore, the best composition was found after examining 30 samples. Thus, Bayesian optimization-based composition optimization worked well in our system and could be applied to a larger feature space.

In summary, we developed a high-throughput robot for electrocatalyst screening that performs from preparing to measuring samples. Bayesian optimization-assisted screening further improved the effective optimization of electrocatalysts composition. The adopted approach is not limited to electrocatalysts and thus accelerates research and development in the field of materials chemistry.

9:30 AMBREAK

10:00 AM *DS01.03.05

Delocalized Close-Loop Discovery to Rapidly Access Functional Organic Molecules—Process Scale-Up to Support the Campaign Jason Hein; University of British Columbia, Canada

Delocalized closed-loop discovery represents a ground-breaking approach that revolutionizes the exploration of synthesis, optimization, property testing, and scale-up synthesis of functional organic molecules. This step-by-step process distinguishes itself by employing geographically isolated labs, each with unique hardware architectures and capabilities. Together, these labs cover the entire life cycle of design, synthesis, testing, and scale-up required to advance a molecule from inception to tested material. By integrating iterative cycles of synthesis, analysis, and property evaluation, this approach enables rapid exploration of the chemical space, leading to the discovery of novel molecules with desired properties. Additionally, delocalized closed-loop discovery connects geographically isolated research groups, leveraging their specialized skills, equipment, and capabilities to achieve collective objectives.

This presentation aims to highlight the advantages and benefits of delocalized closed-loop discovery, providing insights into how the process was executed to develop novel organic laser candidates. The delocalized exploration process expedites synthesis optimization by offering real-time feedback and adjustment based on property evaluation, enabling specialized members to contribute asynchronously, following the canonical design-make-build strategy. This iterative approach significantly reduces the time and resources required for optimization, facilitating the discovery of high-performance organic laser molecules. Moreover, the delocalized closed-loop approach plays a critical role in improving scalability by considering scale-up synthesis considerations early in the discovery process, ensuring the feasibility of large-scale production of synthesized molecules.

This presentation emphasizes the value of delocalized closed-loop discovery as a comprehensive approach for the exploration of synthesis, optimization, testing, and scale-up of organic laser molecules. Its step-by-step process facilitates the discovery of functional organic molecules by iteratively refining their properties. The advantages of employing this approach include accelerated synthesis optimization, enhanced property control, and improved scalability. Furthermore, the inclusion of case studies serves to exemplify the effectiveness of delocalized closed-loop discovery in advancing the field of organic laser molecule development.

10:30 AM DS01.03.06

Making an Accessible Automation Tool Autonomous Robert W. Epps¹, Ross Kerner¹ and Joseph J. Berry^{1,2,2}; ¹National Renewable Energy Laboratory, United States; ²University of Colorado Boulder, United States

Automated and autonomous experimentation is most effective when it can be easily adopted by a diverse range of researchers. In this light, the company Opentrons has developed a library of low-cost, user-friendly robotic tools that have recently been leveraged in material science and chemistry. The OT-2 offers an extremely low barrier of entry in robotics accelerated research through facile liquid handling and simple job automation software. However, this platform lacks two critical features necessary for closed-loop studies. First, there are no simple metrology tools for process characterization. The number of compatible metrology techniques in literature are limited on biological applications, and Opentrons does not officially support any developed methods. In the typical workflow, human users are required to transfer prepared samples to an ex-situ monitoring system before data can be collected. This inhibits the rate of data generation, produces imprecise reaction time features, and prevents efficient algorithm driven research. Second, the OT-2 system does not have a simple machine facing API. The instrument is controlled through individual jobs that are uploaded onto the machine itself then executed. This can be done easily by a human using the instrument software or SSH commands; however, for a computer to identify and select experiments, additional steps are necessary. Accessing the API indirectly would enable the OT-2 to be paired with offline computational power and to be more easily integrated into larger closed-loop and automated systems and algorithms.

In this work, we present an open-access and user-friendly strategy for adapting the OT-2 robot for closed-loop, autonomous research. The system features a generalizable sample aliquoting tool which has been combined with absorption spectroscopy, machine-facing control of the OT-2 API, and a single user interface for sampling, liquid handling, and experiment selection algorithm specification. We applied the tool toward the exploration of perovskite solar cell ink compositions in order to gain insight into material combination dynamics through active learning and algorithm-based feature prediction.

The aliquot system operates by collecting samples from the OT-2 through a low volume funnel connected to microfluidic tubing. Samples are pulled from the funnel using a positive displacement pump and sent through an optical flow cell where absorption spectra are collected. While this work leverages absorption spectroscopy, alternative techniques, including destructive and non-destructive characterization methods may be easily included. This tool can be used outside of closed-loop systems to facilitate precise time resolved data collection and more efficient experimentation.

The OT-2 is algorithmically controlled through automated experiment scripting, upload, and execution. With each new set of experimental conditions, the algorithm arranges a set of instructions along with the system features in the language specified by the OT-2 Python API and saves them to a new Python script. This submission is then pushed to the OT-2 server along with the command to execute the script. This method automates a process that otherwise requires a human to manually program the experiment script, upload it to the OT-2, and send the execution command. By algorithmically interacting with the OT-2 through the OpenTrons supported API, users can easily leverage the actively developed library of modules without manually implementing updates.

The software and techniques presented in this work will enable users without extensive programming or robotics experience to implement their own closed-loop reaction explorations and optimization. Further development of the modules available for sampling and similar user friendly and low-cost autonomous tools will improve the rate of adoption of autonomous technologies by the broader scientific community.

10:45 AM *DS01.03.07

Discovery of New Materials using Chemputation[Lee Cronin](#); University of Glasgow, United Kingdom

Chemputation' is a universal approach to explore chemical reactivity, discovery of new reactions, and molecules / materials, as well as program chemical synthesis that allows us to translate all procedures, manual or automatic, into a executable chemical programming language that can run the processes on a chemputer. This code is written in the world's first universal programming language for chemistry and materials: χ DL (pronounced Chi-DL). This new approach maps into a universal programming language for chemistry that is accessible to ALL synthetic chemists and will work on ALL robotic systems (subject to suitable specification). We demonstrate that the process is universal, and by analogy with computation, we call systems capable of universally turning code into reliable chemistry and materials processes *Chemputation*.

11:15 AM DS01.03.08

A Distributed and High-Performance Compute Cluster and Data Science Framework for Handling Materials Data—CRADLE TM 3.2[Arafath Nihar](#), Rounak Chawla, Pawan K. Tripathi, Yinghui Wu, Vipin Chaudhary and Roger H. French; Case Western Reserve University, United States

The foundation of materials data science capabilities is well curated datasets, often of disparate types such as tabular data, images, movies and unique data formats from distinct instruments combined with data science models and their metadata. We present the Common Research Analytics and Data Lifecycle Environment (CRADLE™), a groundbreaking research computing infrastructure that seamlessly integrates Hadoop Distributed Computing with High-Performance Computing (HPC) capabilities to store, query, and process FAIRified, structured and semi-structured materials data including XCT, XRD, Pyrometry, spectroscopy and high-speed camera images at terabyte scales. We outline a structured data pipeline used to transform large volumes of tabular data into the efficient Apache Parquet file format and store it in the Hadoop Distributed File System (HDFS). For non-tabular, semi-structured data such as images, we leverage Apache Ozone for highly scalable, distributed storage for analytics. Additionally, we utilize Apache Spark for Data Ingestion (the distributed version of traditional Extract, Transform, Load (ETL)) jobs and Apache Impala for distributed analytical queries, ensuring comprehensive data processing capabilities within the CRADLE™ distributed computing environment. This data lifecycle environment is integrated in a large-scale multi-node HPC environment with thousands of CPU and GPU cores for parallel data processing. Finally, to simplify the dependency management of our numerous materials data science modeling tools and their associated scientific investigations, we use containerized Singularity environments. We utilize Continuous Integration/Continuous Deployment (CI/CD) principles to automatically build Singularity containers in our container registry and deploy them in our HPC compute environment. We securely integrate the Hadoop cluster with the Singularity containers in the HPC cluster via the HDFS client, Spark client, and ODBC (Open Database Connectivity) for Impala with full Kerberos authentication compatible with NIST 800-171 cybersecurity requirements. The result is a massive yet flexible research computing infrastructure with petabyte-scale storage and thousands of CPU and GPU cores, allowing researchers to process billions of data points in seconds, and train hundreds of thousands of models in minutes. This innovative approach to computing infrastructure development has the potential to transform research across various domains, opening up new possibilities for scientific exploration and discovery. This material is based upon research in the Materials Data Science for Stockpile Stewardship Center of Excellence (MDS3-COE), and supported by the Department of Energy's National Nuclear Security Administration under Award Number(s) DE-NA0004104.

11:30 AM *DS01.03.09

ARES™ Autonomous Experimentation for Accelerated Research[Benji Maruyama](#), Rahul Rao and Robert Waelder; Air Force Research Laboratory, United States

The current materials research process is slow and expensive; taking decades from invention to commercialization. The Air Force Research Laboratory pioneered ARES™, the first autonomous experimentation system for materials development. A rapidly growing number of researchers are now exploiting advances in artificial intelligence (AI), autonomy & robotics, along with modeling and simulation to create research robots capable of making research progress orders of magnitude faster than today. We will discuss concepts and advances in autonomous experimentation in general, and associated hardware, software and autonomous methods.

We will distinguish between non-iterative AI/ML approaches that use large data sets (e.g., CNN, LLM) and small data, iterative approaches that strive to identify & confirm scientific hypotheses using AI reasoning.

We consider the impact of autonomous experimentation on human scientists and the scientific enterprise: Changing roles for humans and robots, expectations. In the future, we expect autonomous experimentation to revolutionize the research process, and propose a "Moore's Law for the Speed of Research," where the rate of advancement increases exponentially, and the cost of research drops exponentially. We also consider a renaissance in "Citizen Science" where access to online research robots makes science widely available.

SESSION DS01.04: Machine Learning Innovations in the Loop

Session Chairs: Milad Abolhasani and Keith Brown

Tuesday Afternoon, November 28, 2023

Sheraton, Third Floor, Fairfax B

1:30 PM *DS01.04.01

Analyzing Machine Learning Models to Forecast Hybrid Perovskites' Dynamic Response to Environmental Stressors[Marina S. Leite](#); University of California, Davis, United States

Machine learning (ML) can significantly accelerate the discovery of materials for clean energy. Hybrid perovskites (an emerging class of materials for photovoltaics and light-emitting diodes) encompass an enormous chemical composition space, resulting in a hyperparameter space that is nearly impossible to be interrogated via traditional trial-and-error methods. Thus, there has been a pressing need within the materials research community to identify ML models that can be implemented to inform the physical and chemical behavior of the perovskites. Here, we apply distinct ML models (mostly based on recurrent neural networks) to classify and forecast physical properties encompassing electrical conductivity, photoluminescence response, the power conversion efficiency of photovoltaic devices, etc. Specifically, we use automated, *in situ* optical measurements to predict the optical response of a series of perovskites for 50+ hours, upon materials' exposure to moisture. We quantitatively compare linear regression, echo state network, and seasonal auto-regressive integrated moving average with eXogenous regressor algorithms and achieve accuracy of >90% for the latter. Demonstrating the ability of this model to capture non-linear features. Our high-throughput measurements and ML-assisted data analysis exemplifies the potential of ML to diagnose and forecast hybrid perovskites' response with a variety of chemical compositions.

2:00 PM DS01.04.02

Machine-Learning Assisted Global Optimization of Equivalent Circuit Parameters in the Field of Electrochemical Impedance Spectroscopy[Carl P. Klemm](#)^{1,2}; ¹TU-Darmstadt, Germany; ²Rhd-Instruments GmbH, Germany

In this paper, we introduce a machine-learning regression system for initial-parameter guessing for optimization of Electrochemical impedance spectroscopy equivalent circuit parameters. In Electrochemical impedance spectroscopy, the fitting of equivalent circuits models to experimental data is the standard technique for data interpretation. The currently used techniques and tools for solving this global optimization problem require the user to guess starting parameters, which degenerates the problem into a local optimization problem, or apply an expensive stochastic optimization algorithm with performance characteristics that are incompatible with large scale automated data analysis. To help alleviate this deficiency, a Machine-learning

regression stage for initial-parameter guessing is proposed and implemented.

2:15 PM DS01.04.03

Exploration of Machine Learning (ML) Methods for Determining Unit Cell Parameters from Powder XRD Patterns Elyssa Hofgard¹, Vanessa Oklejas², David Mittan-Moreau², Aria Mansouri Tehrani¹, Daniel Paley², Aaron Brewster² and Tess Smidt¹; ¹Massachusetts Institute of Technology, United States; ²Lawrence Berkeley National Laboratory, United States

We investigate different machine learning (ML) methods to determine unit cell parameters and classify Bravais lattices from powder X-ray diffraction (XRD) data. Traditional powder indexing algorithms encounter errors when dealing with noisy experimental data and overlapped regions from multiple phases. The dominant zone problem also causes errors, arising when certain crystal planes significantly overshadow other planes in the diffraction pattern due to differences in the magnitudes of unit cell axes. This causes complications in accuracy of peak identification, peak intensity measurements, and subsequent crystal structure determination [1-3]. ML methods offer the potential to surpass time-consuming conventional techniques through their ability to learn complex patterns from diverse datasets and provide fast inference speeds.

Previous research has primarily addressed lattice type classification using ML models with decreased accuracy for lower symmetry crystal structures [4-7]. A recent publication on unit cell parameter regression showed that 1-D convolutional neural networks (CNNs) could predict unit cell lengths across all crystal systems but struggled to predict unit cell angles for monoclinic or triclinic systems [8]. However, CNNs assume translational invariance in the input data, which is absent in powder XRD data.

Therefore, we explore the effectiveness of ML models specifically designed for identifying 1D patterns in sequential data. We train and test these models on established crystallographic databases and assess their performance on Bravais lattice classification and unit cell parameter regression. We also consider other essential factors such as regression targets, spectrum complexity, data augmentation techniques to improve performance with large unit cells or dominant zones, and the use of physically meaningful loss functions. Ultimately, our goal is to integrate these models with powder XRD analysis software such as GSAS-II or TOPAS to accelerate crystal structure determination for complex or challenging systems.

[1] Esmaili et al. *J. Appl. Cryst.* (2017) 50, 651–659

[2] Lutterotti et al. *J. Appl. Cryst.* (2019) 52, 587-598

[3] Coelho J. *J. Appl. Cryst.* (2017) 50, 1323-1330

[4] Oviedo, et al. *npj Comput Mater* (2019) 5, 60

[5] Corriero et al., *J. Appl. Cryst.* (2023) 56, 409-419

[6] Lolla et al., *J. Appl. Cryst.* (2022) 55, 882-889

[7] Suzuki, et al. *Sci Rep* (2020) 10, 21790

[8] Chitturi et al., *J. Appl. Cryst.* (2021) 54, 1799-1810.

2:30 PM BREAK

3:00 PM DS01.04.04

Interpreting *In Situ* 4D-STEM Data for Accurate Measurement of Ferroelectric Polarization using Machine Learning Technique Inho Byun, Lee Keeyong, Geun Ho Gu and Sang Ho Oh; Korea Institute of Energy Technology, Korea (the Republic of)

Ferroelectric materials, such as barium strontium titanate ($\text{Ba}_{0.5}\text{Sr}_{0.5}\text{TiO}_3$, BST), exhibit tiny amounts of ionic displacement under an electric field, which is challenging for reliable detection by STEM based imaging techniques due to the limited precision (typically ~4 pm). Recent progress in 4D-STEM have made it possible to measure these small polarizations with a high degree of accuracy in the reciprocal space as the diffraction intensity varies very sensitively with ionic displacement. However, the quantitative interpretation of the diffraction intensity in 4D-STEM data is challenging due to the unavoidable dynamical diffraction effects included in most 4D-STEM data. In this study, we present a practical machine learning technique to interpret the *in situ* 4D-STEM data obtained from 20 nm-thick BST thin film capacitors under electric fields, which allows accurate measurement of the tiny ionic displacements induced by the applied electric field. Our results demonstrate the effectiveness of this approach in accurately detecting and measuring the field-induced ionic polarization in high- κ oxide thin film devices. This breakthrough opens up new avenues for studying not only ferroelectric materials but also piezoelectric and flexoelectric materials. The methodology presented in this study has the potential to revolutionize the field of ferroelectric materials research, enabling researchers to detect and measure tiny amounts of polarization with greater accuracy and efficiency.

3:15 PM *DS01.04.05

Co-Development of Experiment Automation and Data Science for Accelerated Materials Discovery John M. Gregoire¹, Joel A. Haber¹, Dan Guevarra¹, Lan Zhou¹, Di Chen², Shufeng Kong², Francesco Ricci³, Jeffrey B. Neaton³ and Carla P. Gomes²; ¹California Institute of Technology, United States; ²Cornell University, United States; ³Lawrence Berkeley National Laboratory, United States

As materials discovery efforts increasingly expand in high-order composition spaces and/or far-from-equilibrium syntheses, efficient exploration requires both automation of experiments and advancement of data science to interpret and plan experiments. We will discuss the automation of experiments for research modalities including exploratory experimentation, validation of theory predictions, and incorporation of artificial intelligence for accelerating both experiment design and data interpretation. In the area of solar fuels materials discovery, these modalities have been prolific for discovery of (photo)electrocatalysts. Furthermore, the interplay of experiment, theory, and data science has inspired the development of new artificial intelligence methods for materials research, including prediction of electronic structure to accelerate computational screening (Mat2Spec) as well as the integration of physical constraints in deep learning models, which enables super-human analytic capabilities for inference of phases in x-ray diffraction patterns via Deep Reasoning Networks (DRNs).

3:45 PM DS01.04.06

Neural Networks Trained on Synthetically Generated Crystals can Extract Structural Information from ICSD Powder X-Ray Diffractograms Henrik Schopmans, Patrick Reiser and Pascal Friederich; Karlsruhe Institute of Technology, Germany

Machine learning techniques have successfully been used to extract structural information such as the crystal space group from powder X-ray diffractograms, especially in self-driving lab settings [1,2]. However, training directly on simulated diffractograms from databases such as the ICSD is challenging due to its limited size, class-inhomogeneity, and bias toward certain structure types. We propose an alternative approach of generating synthetic crystals with random coordinates by using the symmetry operations of each space group [3]. Based on this approach, we demonstrate online training of deep ResNet-like models on up to a few million unique on-the-fly generated synthetic diffractograms per hour. For our chosen task of space group classification, we achieved a test accuracy of 79.9% on unseen ICSD structure types from most space groups. This surpasses the 56.1% accuracy of the current state-of-the-art approach of training on ICSD crystals directly. Our results demonstrate that synthetically generated crystals can be used to extract structural information from ICSD powder diffractograms, which makes it possible to apply very large state-of-the-art machine learning models in the area of powder X-ray diffraction. We further show first steps toward applying our methodology to experimental data, where automated XRD data analysis is crucial, especially in high-throughput settings. While we focused on the prediction of the space group, our approach has the potential to be extended to related tasks in the future.

[1] Velasco, L., Castillo, J.S., Kante, M.V., Olaya, J.J., Friederich, P. and Hahn, H., 2021. Phase–property diagrams for multicomponent oxide systems toward materials libraries. *Advanced Materials*, 33(43), p.2102301.

[2] Schweidler, S., Schopmans, H., Reiser, P., Boltynjuk, E., Olaya, J.J., Singaraju, S.A., Fischer, F., Hahn, H., Friederich, P. and Velasco, L., 2023. Synthesis and Characterization of High-Entropy CrMoNbTaVW Thin Films Using High-Throughput Methods. *Advanced Engineering Materials*, 25(2), p.2200870.

[3] Schopmans et al., 2023, <https://arxiv.org/abs/2303.11699>

4:00 PM DS01.04.07

Metrology and Characterization of Defects in Transition Metal Dichalcogenides using Scanning Tunneling Microscopy with Machine Learning Darian Smalley^{1,1}, Stephanie D. Lough^{1,1}, Luke Holtzman², Madisen Holbrook², James Hone², Katayun Barmak² and Masahiro Ishigami^{1,1}; ¹University of Central Florida, United States; ²Columbia University, United States

The electronic and optical properties of transition metal dichalcogenides (TMDs) are influenced by the presence of atomic point defects within the crystal lattice. Identifying the quantity and nature of these point defects is important for engineering TMD synthesis, ensuring TMD device consistency, and verifying single photon emission sources. Scanning tunneling microscopy (STM) can determine the nature of such point defects by correlating their electronic structure with atomic-scale spatial properties, which is typically done manually. However, manual identification, counting and measurement of point defects in STM images is painstakingly slow and unreliable, causing reported point defect densities to have large experimental uncertainty, preventing directed refinements of synthesis and controlled reduction in TMD point defect density. We address this problem by processing our STM data with a machine learning algorithm and show atomic-scale defect metrology in scanning tunneling microscopy images of tungsten diselenide using an ensemble of U-Net-like convolutional neural networks. Using this technique, we determined the coordinates, densities, and real space properties of over 3000 defects with statistical significance. Our results demonstrate that STM data analysis aided by machine learning can be used to rapidly determine the quality of TMDs and provide much needed quantitative input to systematically improve the synthesis process. As such our machine learning enhanced

STM can impact many two-dimensional materials researchers.

4:15 PM DS01.04.08

Assisting the Design of Chiral Metal Halide Semiconductors with Machine Learning Ruilong Wang, Haofeng Zheng and Shaocong Hou; Wuhan University, China

Chiral metal halide semiconductor (CMHS) can directly resolve circularly polarized light and has high carrier mobility and strong defect tolerance, which is highly promising for applications in quantum communication, asymmetric catalysis, medical diagnosis, and so on. However, the tortuous and costly experimental process of designing high-performance CMHS is detrimental to the application of CMHS. Therefore, there is a need to find efficient methods for the design of CMHS.

Here, we built the map between the structure, composition, and chiral intensity of CMHS efficiently using machine learning. Then, we performed SHAP analysis on the established model and calculate the chirality intensity of 1080 potential chiral CMHSs through high-throughput screening. By combining the result of SHAP analysis and prediction, we infer that 1NEA^+ in A-site, Cu^{2+} in B-site, and Cl in X-site are positively related to the chirality intensity of CMHSs. Furthermore, we successfully synthesized unreported material, such as $1\text{NEA}_2\text{PbCl}_4$ with a g_{CD} of 0.00805, which further validates the credibility of our predictive model. Our work provides an in-depth understanding of combining machine learning and experimentation and helps accelerate the development of CMHS.

4:30 PM DS01.04.09

Autonomous Robotic Experiments Accelerate Discovery of Multi-Components Electrolyte for Rechargeable Lithium-Metal Batteries Shoichi Matsuda; National Institute for Materials Science, Japan

Artificial intelligence (AI) driven approach for materials discovery, has attracted significant recent attention even in the field of rechargeable batteries. Instead of relying on the experience and intuition of researchers for exploring new materials, the approach employs data scientific techniques that can, in principle, reduce the time and cost of the discovery of new materials with superior battery performance and predict cycle life. Actually, an automated robotic experimental system was recently developed by our group for discovering new multi-component electrolytes for lithium-metal based rechargeable batteries, which exhibited superior energy density compared with conventional lithium-ion batteries (ref.1). Although superior searching throughput analyzing more than 1000 samples per day was achieved, adequate experimental design is essential to realize high-throughput exploration of electrolyte composition from large searching space. For example, when considering a combination of selecting 5 types from 20 types of chemicals, the candidates are over 10^7 . Thus, it is not realistic to comprehensively evaluate all the possible combination even through such robotic experiments. Therefore, a specific electrolyte composition that realizes a superior battery performance must be determined with only a limited number of experimental trials.

In the present study, the effectiveness of a data-driven automated robotic experiments was investigated to discover multi-component electrolyte additives for lithium-metal based rechargeable batteries. Established machine-learning methodologies using Bayesian optimization were employed to solve optimization problems for analyzing datasets obtained from the automated robotic experiments, thereby minimizing the number of trials required to identify the ideal electrolyte composition. As results, we identified the specific electrolyte composition (1.5 M LiNO_3 , 0.1 M LiTFSI , 0.1 M LiBr , 0.5 mM LiCl , and 10 mM LiBOB in dimethylamide, with 5 vol.% 1,3-dioxolane) that enhanced the cycle life of the lithium-oxygen rechargeable batteries (ref.2). In additions, we also put our attention for the development of the orchestration system to realize a closed loop between AI searching algorithms and robotic experiments. Generally, different searching algorithms are utilized depending on the motivation of a materials exploration task and the procedure for controlling the devices largely depends on the characteristics of the robotic systems. Thus, the control software has far been developed on a case-by-case manner, limiting the widespread use of searching algorithms for robotic experiments. Based on these considerations, we recently developed the NIMS-OS to implement a closed loop of AI and robotic experiments for automated materials exploration (ref.3). Notably, NIMS-OS treats each AI algorithm and each robotic system as separate modules, resulting in the implementation of a closed loop with any combination of these modules. When modules for new AI algorithms or robotic systems are prepared, new closed-loop systems can be easily controlled via NIMS-OS. We believe that the such generic control software is the advantageous for NIMS-OS as standard platform for autonomous materials exploration with robotic experiments.

References

- [1] S. Matsuda et al. Scientific Reports, 2019, 9, 6211
- [2] S. Matsuda et al. Cell Reports Physical Science, 2022, 3, 100832
- [3] R. Tamura, S. Matsuda et al. Science and Technology of Advanced Materials: Methods, doi.org/10.1080/27660400.2023.2232297

SESSION DS01.05: Poster Session: Accelerating Materials Research
Session Chairs: Milad Abolhasani and Keith Brown
Tuesday Afternoon, November 28, 2023
Hynes, Level 1, Hall A

8:00 PM DS01.05.01

Deep Learning-Based Terahertz Inspection Technique for Internal Defect Detection in Ceramic, Polymer and Metal Composites Tae Wan Kim, Sang-I Kim, You-Gwon Kim, Heon-Su Kim and Hak-Sung Kim; Hanyang University, Korea (the Republic of)

Abstract

In this study, internal defects in composites composed of ceramics, polymers, and metals were inspected using terahertz technology in combination with a convolutional neural network (CNN) model and anomaly detection employing a generative adversarial neural network (AnoGAN) model. The defective specimens were intentionally fabricated in the hole and edge regions of the polymer layer, which are vulnerable regions in the composites. The defect region in the polymer layer of the composite was detected in the THz scanning image due to the scattering of THz waves.

The THz scanning image dataset was constructed based on the presence or absence of defects in different regions using a terahertz time-domain spectroscopy (THz-TDS) system. The CNN model was trained to determine the scanning regions (hole, edge) of the composites, while the AnoGAN model was trained to detect defects in the THz images. The CNN model demonstrated a 95% accuracy in classifying the THz scanning regions, and the AnoGAN model achieved a 95% accuracy in detecting defects in the composites. This technique enables automated, real-time inspection for detecting internal defects in semiconductor composite products.

Acknowledgment

This work was supported by Korea Institute of Energy Technology Evaluation and Planning (KETEP) grant funded by the Korea government (MOTIE) (20212020800090, Development and Demonstration of Energy-Efficiency Enhanced Technology for Temperature-Controlled Transportation and Logistics Center) and this work was supported by This research was also supported by a National Research Foundation of Korea (NRF) grant funded by the Korean Government (MEST) (2021M2E6A1084690)

8:00 PM DS01.05.02

Rapid Analysis of Secondary Phases and Prediction of Photovoltaic Performance in Multinary Chalcogenides Christian Utama¹, Leo Choubrac² and Thomas Unold³; ¹Freie Universität Berlin, Germany; ²Université de Nantes, France; ³Helmholtz-Zentrum Berlin, Germany

Multinary chalcogenide thin film technologies are interesting for various energy conversion related applications, such as photovoltaics, photocatalysis or thermoelectrics. Due to the large degrees compositional and structural degrees of freedom of this multicomponent materials class, the establishment and control of single-phase deposition routes and material homogeneity is a challenging task, while the detection of secondary phases with X-ray diffraction, electron microscopy and Raman spectroscopy can be tedious and time-consuming. Using the model system of combinatorially-deposited $\text{Cu}_2\text{ZnSnSe}_4$ thin film libraries we demonstrate how rapid hyperspectral optical reflection measurements in conjunction with machine-learning can be used to predict the presence of secondary phases in these material libraries covering a large region of the $\text{Cu}_2\text{Se-ZnSe-SnSe}_2$ ternary phase diagram with high accuracy. The advantages and limitations of different machine-learning algorithms for secondary phase prediction will be discussed. Extending this approach to include hyperspectral photoluminescence measurements, we show how photovoltaic performance can be predicted on a 575 sample library within a 2-hour measurement/analysis cycle.

8:00 PM DS01.05.03

Bayesian Inference in High-Dimensions for Root Cause Analysis of Underperformance Basita Das¹, Zekun Ren², Alexander E. Siemenn¹, Thomas Kirchartz³ and Tonio Buonassisi¹; ¹Massachusetts Institute of Technology, United States; ²National University of Singapore, Singapore; ³Forschungszentrum Jülich GmbH, Germany

In any solar cell, the root cause for underperformance could be manifolds, arising from recombination in different layers and interfaces, low mobility of the transport layers etc. Traditionally different characterization and data fitting techniques are used to analyze underperforming devices and are often slow as well as destructive to the device. Also, most often the data is fitted to simple rate equations which does not give enough information about the system. Ideally one can try to fit more complex device models to the characterization data, but the sheer number of parameters that usually goes into a device simulator, and the correlation between the parameters make the problem intractable. To infer unknown parameters from higher dimensional spaces, we make use of Bayesian inference.

Bayesian inference methods have been previously used in the field of solar cells for well-studied solar cell technologies like Si solar cells, which are already well studied such that a lot of material parameters are well known. It has also been used for material systems like SnS solar cells where the number of unknown parameters is small [1-3]. However, in previous implementations there were the following challenges: (1) not easily scalable to higher dimensions, (2) solution depending on the initialization condition of the sampler, and (3) the speed of operation was also limited by the device model.

In this presentation we will address these challenges and discuss the strategies we have implemented to overcome them. We take the following strategies to solve the challenges.:

- (1) We solve the problem of scalability by using the state-of-the-art Markov chain Monte Carlo (MCMC) sampling technique.
- (2) However, even though MCMC makes Bayesian inference scalable to higher dimensions, the solution is highly sensitive to the initialization condition of the samplers. To solve this problem, we introduce a hybrid MCMC method coupled with optimization algorithms such that our solution is reproducible from one run to another. This method of initialization is also robust at finding multiple minima/maxima in case of multi modal solution space.
- (3) To achieve performance beyond that limited by the speed of the device model we also incorporated a neural network based surrogate model[4] to replace the device model.

Overall, as an effect of the three improvements, we achieve improvement in scalability, reproducibility, and speed. We show

(1) scalability and reproducibility of our algorithm to up to 10 dimensions,

(2) 15 times faster convergence of MCMC in 10 dimensions, and

(3) 10-100x [4] performance boost from introduction of NN surrogate model.

We also show that the improvements discussed have a overarching impact on high dimensional parameter estimation in both multimodal space as well as needle-in-haystack like situations.

1. Brandt, R. E., Kurchin, R. C., Steinmann, V., Kitchaev, D., Roat, C., Levenco, S., Ceder, G., Unold, T., & Buonassisi, T. (2017). Rapid Photovoltaic Device Characterization through Bayesian Parameter Estimation. *Joule*, 1(4), 843–856. doi: 10.1016/j.joule.2017.10.001

2. Kurchin, R. C., Poindexter, J. R., Vähänissi, V., Savin, H., Carlos Del Cañizo, J., & Buonassisi, T. (2019). *How much physics is in a current-voltage curve? Inferring defect properties from photovoltaic device measurements.*

3. Kurchin, R., Romano, G., & Buonassisi, T. (2019). Bayesim: A tool for adaptive grid model fitting with Bayesian inference. *Computer Physics Communications*, 239, 161–165. doi: 10.1016/j.cpc.2019.01.022

4. Ren, Z., Oviedo, F., Thway, M., Tian, S. I. P., Wang, Y., Xue, H., Perea, J. D., Layurova, M., Heumueller, T., Birgersson, E., Aberle, A., Brabec, C. J., Stangl, R., Sun, S., Lin, F., Peters, I. M., Buonassisi, T., Ren, Z., Oviedo, F., & Buonassisi, T. (2020). Embedding physics domain knowledge into a Bayesian network enables layer-by-layer process innovation for photovoltaics. *Npj Computational Materials* 2020, 6.

8:00 PM DS01.05.04

Artificial Neural Networks for Predicting Springback of aa6061 Sheet Based on Environmental and Forming Data Obtained from Smart Sensors Chanhee Won and Hyejin Lee; Korea Institute of Industrial Technology, Korea (the Republic of)

This research mainly proposes the artificial neural network (ANN) model for predicting the springback of AA6061-T6 sheet using manufacturing process and environmental data, which are collected by temperature, vibration, and force smart sensors. Heat-treated high-strength aluminum alloys, such as AA6061-T6 and AA7075-T6, exhibit low formability and high springback at room temperature, and they are typically formed at elevated temperatures. It is highly necessary to control the elevated temperature of the aluminum sheet before the forming process, as its strength degrades due to the annealing effect at specific temperatures above 250°C. The influencing factors contributing to temperature reduction include ambient temperature, wind speed, and transportation time, among others. Additionally, forming conditions such as forming speed, holding force, and dwell time interact in a complex manner with the environmental conditions to determine the amount of springback in the final product.

To obtain a large dataset for training the ANN model, we newly developed an empirical testing system to simulate the actual warm forming process. This feasibility testing system allows for the systematic application of various combinations of process parameters, such as heating temperatures, transportation time, external wind speed, ambient temperature, and forming conditions. It also enables the attachment of smart sensors to monitor the process status and interconnection. We suggest specific variables from the environmental sensing data as input parameters, along with the forming load-depth curves and vibration data. Various environmental data, including the target temperature, transportation time, wind speed, and duration of exposure to external wind, are used to analyze the characteristics of temperature reduction in the elevated temperature of AA6061-T6 before the forming process. The material properties, maximum forming force, duration time of the maximum force, slope of the load-displacement curve, and FFT analysis of vibration data are used to determine the main influencing factors on the amount of springback in terms of the springback angle of U-channel.

To examine the effect of each input parameter, the performance of each input parameter was evaluated in terms of mean squared error. To confirm the prediction accuracy of the proposed ANN model, the obtained dataset was divided into two subsets: a training dataset and a test dataset, with 30% of the data utilized for the test dataset. Additionally, the proposed ANN model was compared with other conventional machine learning algorithms such as linear regression, decision trees, lasso regression, and ridge regression. Various error statistics, including mean absolute error (MAE), root mean squared error (RMSE), and R-square, were analyzed. The proposed ANN model exhibited remarkable performance in the prediction of the springback angle, which makes it possible to apply in feedback control in the manufacturing process to obtain quick dimensional accuracy when the manufacturing environment undergoes rapid changes.

ACKNOWLEDGEMENT

This research was supported by Korea Evaluation Institute of Industrial Technology (KEIT) grant funded by Ministry of Trade, Industry and Energy (MOTIE, Korea) (No. 20016357, Demonstration platform development of smart sensing unit).

8:00 PM DS01.05.05

Function Space Representations for Complex Material Workflows Kiran Vaddi, Kacper Lachowski, Huat Thart Chiang, Karen Li and Lilo D. Pozzo; University of Washington, United States

Self-driving laboratories (SDL) are primed to improve the pace of material discovery and provide tangible solutions to emergent energy, health care, and sustainability applications using a combination of robotic agents and machine learning tools. They replace the traditional, time-consuming experimental-based ideate-synthesize-characterize loop with a more efficient set of agents that accelerate them in all aspects by being able to autonomously make decisions consistent with the physics and chemistry of the underlying system. Data-driven methods are the primary workhorse for developing autonomous agents and have been successfully applied in various applications ranging from closed-loop mapping of synthesis-property relationships to material retrosynthesis of semiconductors, nanoparticles, and 3D printed structures. However, unlike other autonomous agents developed elsewhere, SDL generates a data set of different modalities ranging from scalar outputs (e.g.: efficiency) to a function (e.g.: spectroscopy measurement). I will describe the challenges associated with building models for knowledge extraction and autonomous decision-making using functional data generated to study the nanoscale structure of colloidal and polymer materials and provide a tractable mathematical framework using the differential geometry of function spaces.

8:00 PM DS01.05.06

Optimization of Silicon Particle Milling Process for Lithium Secondary Battery Anode Using Deep Learning and Bayesian Optimization Jong Ho Kim; Research Institute of Industrial Science and Technology, Korea (the Republic of)

Lithium rechargeable batteries are developing rapidly in response to the rapid growth of electric vehicles. Electric vehicle batteries require high energy density to increase performance and ensure the ability to drive long distances. Conventional lithium-ion batteries use graphite as the anode material, and recent results have shown that silicon can increase the energy density. However, silicon has been shown to deteriorate due to volume expansion during charge and discharge, and nanoscale particles have been proposed to overcome this problem. In this study, we optimized the milling process to produce silicon particles through deep learning and Bayesian optimization. It was found that the size of silicon particles varies depending on the type of milling process and variables, which in turn changes the characteristics of the battery. Image analysis using deep learning and Bayesian optimization using a Gaussian process have the effect of shortening the analysis and reaching the target size in the silicon particle manufacturing process.

8:00 PM DS01.05.07

Machine Learning-Based Prediction of Crystal Structure Proportions in Ag-TiO₂ Nanofibers for Enhanced Photocatalytic Activity Yin-Hsuan Chang¹, Rei-Yang Li¹, Ying-Han Liao¹, Ting-Han Lin¹ and Ming-Chung Wu^{1,2}; ¹Chang Gung University, Taiwan; ²Chang Gung Memorial Hospital at Linkou, Taiwan

In the past decade, mechanism learning has surged a revolution in the field of materials science and bringing about advancements in predicting materials properties, materials discovery, and materials characterization. Due to the remarkable activity, stability, and non-toxic nature, TiO₂ has emerged as a highly promising photocatalyst for pollutant removal and self-cleaning paints. The diverse crystal structures inherent in TiO₂ play a crucial role in modulating its energy band structure, thereby enhancing its photocatalytic activity. However, the precise determination of

optimal conditions for multi-phase TiO₂ poses a challenge, as it necessitates a thorough and time-consuming analysis of the quantitative crystal structure. To overcome this difficulty, we embarked on developing a robust model for predicting the proportion of crystal structures in multi-phase TiO₂. Prior to build a reliable model, we assembled a collection of Raman spectra encompassing various proportions of anatase and rutile phases for serving as database of machine learning. Over the past decade, our research team has focused on investigating metal-doped TiO₂ nanofibers (NFs). Among the studied compositions, silver doped TiO₂ NFs (Ag-TiO₂ NFs) exhibits the highest photocatalytic performance. Except for the interaction between incident light and self-precipitated silver nanoparticles, the phase composition of TiO₂ photocatalysts is also an influential factor for their photocatalytic activity. Although the anatase-to-rutile phase transition occurs at 900 to 1,100 °C in pristine TiO₂ NFs, the scenario is totally different as a dopant induced into TiO₂ NFs. How to precisely control metal dopant and anatase-to-rutile phase transition in TiO₂ NFs still remains an ongoing challenge. Herein, we employed the "Variational Autoencoder" machine learning model to perform unsupervised learning and extract meaningful characteristics from the Raman spectra. After thorough inspection and verification, we successfully applied the model to predict the proportion of crystal structures in Ag-TiO₂ nanofibers with different calcination temperatures. By employing innovative and efficient methods, our research offers valuable insights into the correlation between quantitative crystal structure and photocatalytic activity. Notably, our model achieved a mean absolute error of 2.33% and a root mean square error of 0.0291, demonstrating its high predictive accuracy. By leveraging machine learning techniques, our study provides a powerful tool for predicting crystal structure proportions in multi-phase TiO₂, specifically focusing on Ag-TiO₂ NFs. This enables researchers and practitioners to efficiently analyze the relationship between crystal structure and photocatalytic activity, paving the way for the design and optimization of advanced TiO₂-based materials with enhanced performance in pollutant removal and self-cleaning applications.

8:00 PM DS01.05.08

Automated EXAFS and Nanoindentation Analysis using Artificial Intelligence in Addressing Reproducibility ChallengesMinLong¹, Miu LunLau¹ and JeffreyTerry²; ¹Boise State University, United States; ²Illinois Institute of Technology, United States

We have developed a novel, artificial intelligence-based methodology that can be utilized to reliably analyze experimental results from Extended X-ray Absorption Fine Structure (EXAFS) measurements and other spectral analyses. This development will help to address (1) the reproducibility problems that slow research progress and inhibit effective technology transfer and manufacturing innovation in these scientific disciplines and (2) ultimately a challenge in obtaining the best model fitting parameters from the large and growing quantities of real-time materials characterization data produced by modern instruments, with minimal human intervention. The existing EXAFS analysis approach relies on a human analyst to suggest a potential set of chemical compounds in the form of feff.inp input files that may be present, which can cause reproducibility issues. The situation is made even worse with advances in instrumentation that have been enabled to produce data 2-3 orders of magnitude more rapidly than it can be analyzed. Instead, we applied a machine learning approach to the analysis of EXAFS spectroscopy measurements collected using a synchrotron radiation facility. Specifically, for the first time, we developed a genetic algorithm (GA) for fitting the measured spectra to extract the relevant structural parameters. The algorithm attempts to determine the best structural paths from these compounds that are present in the experimental measurement. It starts with a population consisting of a number of temporary fittings and looks for the primary EXAFS path contributors from the potential compounds. It calculates goodness of fit value that can be used to identify the chemical moieties present. To improve the accuracy and efficiency of finding an optimized final solution, evolutionary-inspired operators (e.g., crossover, mutator) are applied to each solution throughout subsequent generations. The advantage of using GA is that it can explore large and complex parameter spaces for model solutions and does not require computation of the derivatives of the functional objectives, nor assumptions of continuity and convexity for the objective functions and constraints. The analysis package is called EXAFS Neo and is open-source and written in Python. It requires using Larch and Feff to calculate the initial EXAFS paths. We have recently extended the code to make use of Feff8.5lite so it can calculate the paths needed for populating the analysis from within the EXAFS Neo package. We have also expanded the Neo to fitting Nanoindentation, the analysis of core-level photoemission, and spectral fitting in other fields like X-ray astronomical data and published the analysis results.

8:00 PM DS01.05.09

Rapid Mechanical Property Prediction and De Novo Design of Three-Dimensional Spider Webs Through Graph and GraphPerceiver Neural NetworksWeiLu, ZhenzeYang and MarkusJ. Buehler; Massachusetts Institute of Technology, United States

Spider webs feature advanced structural performance due to the evolutionary success of over hundreds of millions years, including lightweight design, and exceptional mechanical properties. Spider webs are appealing for bio-inspired design since web designs serve multiple functions including mechanical protection and prey catching. However, high computational cost and limited quantified web properties render extensive spider web studies challenging, in part due to the high structural complexity and randomness of fiber arrangements in 3D webs. Here we report a computational method to relate spider web graph microstructures to effective mechanical properties, focusing on strength and toughness, upscaling from the microscopic to the mesoscale level. The dataset is developed based on experimentally determined spider web graphs, through sheet laser tomography. The new computational framework uses deep neural networks, trained on graph-structured *Cyrtophora citricola* spider web mechanical data, in order to capture complex cross-scale structural relationships. Three different models are developed and compared. First two Graph Neural Network (GNN) models, a Graph Convolutional Network (GCN) and a Principal Neighborhood Aggregation (PNA) method. Second, a GraphPerceiver transformer model that is fed similar input data as provided to the GNN approach, but within a natural language modeling context using self-attention mechanisms. The GraphPerceiver model can achieve similar performance as the GNN model, offering added flexibility for building deep learning models of diverse hierarchical biological materials. As an application of the model, we propose a computational optimization tool for synthetic web design that is used to generate synthetic, *de novo* spider web architectures. Finally, multi-objective optimization enables us to discover web structures that meet specific mechanical properties as design objectives.

8:00 PM DS01.05.10

Machine Learning Analysis and Predictions of PAMBE III-Nitride GrowthAndrewS. Messecar, RobertMakin and SteveDurbin; Western Michigan University, United States

There is considerable interest in applying machine learning techniques to aid in rapidly identifying optimal process parameters for materials growth. For example, Bayesian optimization has been employed to optimize the molecular beam epitaxy synthesis of SrRuO₃ and TiN thin films, and random forest classifiers have been applied to predict monolayer coverage for MoS₂ thin films. Here, we explore how supervised machine learning (ML) techniques can be applied to understand and predict the relationship between the plasma-assisted molecular beam epitaxy (PAMBE) growth parameter space and both the crystalline quality and structural properties of thin-film binary compounds of GaN and InN by utilizing over a decade's worth of detailed film growth records for the same system.

Data from over one hundred PAMBE growth runs of GaN and InN (each) have been organized into material-specific data sets, and includes substrate temperature, metal source effusion cell temperature, plasma source gas pressure, and plasma source RF power. These variables were selected for model training as they are the direct system parameters an ML model would control. Each film growth experiment was performed using a Perkin Elmer model 430 MBE system equipped with an Oxford Applied Research HD-25 RF plasma source, and custom effusion cells and substrate heater from E-Science. Reflection high-energy electron diffraction (RHEED) was used as the primary quality metric, with crystallinity represented for the initial study by a binary numerical value (1 for monocrystalline and 0 for polycrystalline). Images were acquired using a k-Space Associates model 400 system. The values of the growth variables were then mapped to RHEED data and other structural properties measured ex-situ to perform both inference and prediction using a range of supervised learning algorithms, in order to determine which techniques performed the best on the datasets. The methods applied include classical machine learning methods of state vector machines, k-nearest neighbors, quadratic discriminant analysis, linear discriminant analysis and naive Bayes classifiers, as well as the deep learning techniques of neural networks.

Prior to training each model, K-fold cross-validation was performed for each model in order to determine optimal parameter to be used during training. All of the supervised learning algorithms were subsequently trained on the synthesis data and used to predict the crystallinity and other metrics including the Bragg-Williams order parameter across a broad range of possible process variables. Across most models, the resulting machine learning predicted growth spaces, when adjusted to machine agnostic parameters such as flux using calibration data from specific growth runs in the machine, agreed with conventional experimental wisdom for PAMBE growth of nitride semiconductors, while also providing new insight on the processing space for these materials. This the work re first step towards developing a more general model for rapid optimization of PAMBE growth parameters for new materials-based discovery applications. Ultimately such generalized models can be combined with models for similar techniques to further enhance the material discovery process. This work was supported in part by NSF grant DMR-203581.

8:00 PM DS01.05.11

An Adaptive Method Based on Machine Learning for the State-of-Charge and State-of-Health Estimation of Lithium-Ion BatteriesBenWenig and BabakKasmaei; American University, United States

The accurate estimation of the state-of-charge (SOC) and the state-of-health (SOH) of lithium-ion batteries is crucial for reliability assurance and maintenance of the energy systems in various applications including electric vehicles, cell phones, and aerospace satellite missions. Due to the complicated and nonlinear nature of the physical mechanisms involved in these batteries and their dependence on several variables, in the past few years, various algorithms based on machine learning have been used for the SOC/SOH estimation. One of the challenges is that the estimator models need to be adaptive for different batteries, application scenarios, and environmental parameters. We present a novel adaptive method for SOC/SOH estimation of lithium-ion batteries based on techniques in machine learning. We apply the proposed method on real datasets of battery operation, and we compare the performance of various algorithms used in this

context. Our findings contribute to the growing field of efficient battery management systems and facilitate creating effective maintenance schedules and enhancing the reliability and safety of battery-powered applications.

8:00 PM DS01.05.12

Enzeptional: Enzyme Optimization via a Generative Language Modeling-Based Evolutionary Algorithm Yves Gaetan Nana Teukam^{1,2}, Federico Zipoli¹, Teodoro Laino¹, Matteo Manica¹ and Francesca Grisoni²; ¹IBM Research Europe, Switzerland; ²Technische Universiteit Eindhoven, Netherlands

Enzymes are molecular machines optimized by nature to allow otherwise impossible chemical processes to occur. Besides the increased reaction rates, they present remarkable characteristics to enable more sustainable reactions: mild conditions, less toxic solvents, and reduced waste. Billion years of evolution have made enzymes extremely efficient. However wide adoption in industrial processes requires faster design using in-silico methodologies, a daunting task far from being solved. The majority of methods operate by introducing mutations in an existing amino acid (AA) sequence using a variety of assumptions and strategies to introduce variants in the original sequence. More recently, machine learning and deep generative networks have gained popularity in the field of protein engineering by leveraging prior knowledge on protein binders, their physicochemical properties, or the 3D structure. Here, we cast the problem of enzyme optimization as an evolutionary algorithm where mutations are modeled via a generalized autoregressive language model trained on fragments of AA sequences from UniProtKB. Relying on a pre-trained language model, we apply transfer learning and train a Random Forest as the scoring model on a dataset of biocatalysed chemical reactions to drive the optimization process. With our approach, using the least amount of assumptions, we can adapt active sites to perform new reactions. Our methodology allows designing enzymes with higher predicted biocatalytic activity, emulating the evolutionary process occurring in nature by sampling optimal sequences modeling the underlying proteomic language.

SESSION DS01.06: Novel Learning Strategies for Materials Discovery
Session Chairs: John Gregoire and Kedar Hippalgaonkar
Wednesday Morning, November 29, 2023
Sheraton, Third Floor, Fairfax B

8:30 AM *DS01.06.01

Revamping Robotic Minds—Unleashing Bias-Free Machines Jason R. Hattrick-Simpers; University of Toronto, Canada

Over the past five years, the emergence of materials science self-driving labs (SDL) has witnessed a remarkable surge. Although their implementation is not yet widespread, recent substantial federal investments aim to establish dedicated SDL user facilities, aimed at eliminating obstacles around access to equipment and data across various subdomains. Key among the shared challenges faced by SDLs is the influence of human bias, which permeates activities such as building predictive models, extracting knowledge from data, and planning experiments or calculations. The reliance on data selected by risk-averse topical experts, generation of ground truth labels made through heuristic decisions, and the influence of years of choice made through “solid physical intuition” raise important questions: How can we ensure that SDLs do not repeat our mistakes and have the potential to discover truly novel insights? In this talk, I will present compelling examples from our recent work, where we have encountered biases and developed innovative methods to overcome them. Specifically, I will delve into (1) the identification and mitigation of bias in large materials datasets, (2) the development of bias-free tools for analysis in electrochemical impedance spectroscopy, and (3) bridging the trust gap between AI and experimental experts when the model suggests unconventional paths that challenge intuition. As an example I will show how for specific regression tasks as much as 95% of data available in large data sets can be dropped without degradation of their predictive power.

9:00 AM DS01.06.02

Efficient Bayesian Reaction Optimization Guided by Graph Neural Networks for Quantifying Difficulty of Chemical Synthesis Youngchun Kwon, Jin Woo Kim, Joonhyuk Choi, Seungmin Baek and Youn-Suk Choi; Samsung Advanced Institute of Technology, Korea (the Republic of)

Synthetic reaction planning is an inevitable tool for expediting the exploration of groundbreaking drugs and materials. In order to achieve the synthesis of a newly conceived molecular structure that meets the desired properties, it becomes imperative to optimize a multitude of experimental condition parameters such as catalyst, solvent, ligand, etc. To rapidly find the optimal reaction conditions is one of the key factors that can reduce the long cycle of new drug and material discovery. Because synthetic experiments are required very high financial costs, time, and domain experts. Therefore, the many different types of methods such as design of experiments (DOE) and Bayesian optimization (BO) have been employed to solve this optimization tasks. However, BO has a cold-start problem, which necessitates conducting crucial initial experiments to train the surrogate model. Moreover, assessing the feasibility or difficulty of synthesis encounters a challenge where the search space inefficiently expands due to variations arising from individual human’s knowledge and experience. In this study, we propose to solve the trade-off problem of chemical reaction optimization by combining machine learning approaches and Bayesian optimization techniques using accumulated experimental data to efficiently define the search space using by a generative model. We also quantify the difficulty of experiments with our uncertainty-aware yield prediction model and construct an optimization strategy, and dynamically reflect the results of repeated experiments into the strategy. In first research focus is to effectively reduce the wide range of parameters using by our generative model to predict the best combination of conditions, not just a classification model. Second research aims to predict yield of a chemical synthesis reaction along with the uncertainty of the prediction results. The utilization of uncertainty models enables us to estimate the likelihood and challenges associated with the process of synthesis. By considering the constrained search space, the difficulty of synthesis, and a chemical reaction yield prediction model, we devised an approach to tackle the optimization trade-off problem effectively, facilitating efficient execution of optimization experiments. We verified the effects of our proposed framework-based optimization algorithm with various existing approaches. In this study, we successfully found condition combinations that achieved the target yield with the least number of experimental trials compared to other optimization algorithm. To further validate the performance of proposed study in comparison to synthesis experts, we conducted additional verification using a high throughput experimentation.

9:15 AM DS01.06.03

Improved Carbon Nanotube Growth via Autonomous Active Learning of Catalyst Metal Oxide Phase Transition by Jump Regression Robert Waelder^{1,2}, Chiwoo S. Park³, Jennifer Carpena-Núñez^{1,2}, Josh Yoho^{1,2}, Rahul Rao¹ and Benji Maruyama¹; ¹Air Force Research Laboratory, United States; ²UES, Inc, United States; ³Florida State University, United States

Nanoparticle catalyst control is critical to carbon nanotube (CNT) growth and scaling their production. In supported catalyst CNT growth, the reduction of an oxidized metal catalyst enables growth, but its reduction also leads to catalyst deactivation via Ostwald ripening, agglomeration, and other effects. Here, we conducted autonomous experiments guided by a hypothesis-driven machine learning planner based on a novel jump regression. This planning algorithm iteratively builds a model to identify discontinuities in the experimental response surface, such as those created by a material phase change, and selects further experiments to better identify those discontinuities. This approach led us to identify input conditions that resulted in the greatest CNT yields as a function of the driving forces of catalyst reduction in a fraction of the time and cost of conventional experimental approaches. Specifically, by varying temperature and the reducing potential of the growth atmosphere, we identified a discontinuous jump in CNT growth resulting in the largest observed yields at a critical thermodynamic equilibrium between metallic iron and iron oxide for two different thicknesses of thin film iron catalysts. In addition to the greatest overall yields, we observed the longest growth lifetimes and a greater degree of diameter control at the jump, compared to other regions in the search space. We believe that conducting CNT growth at the jump identified in thermodynamic space optimizes catalyst activity, since the presence of oxidized species inhibits Ostwald ripening-induced deactivation, thereby keeping catalyst nanoparticles smaller and more numerous. This work identifies optimal thermodynamic conditions for the production of small diameter single-walled CNTs using a supported iron catalyst, establishes a thermodynamic framework for a generalized understanding of other metal catalysts in CNT growth, and demonstrates the capability of iterative, hypothesis-driven autonomous experimentation to greatly accelerate materials science.

9:30 AM BREAK

10:00 AM *DS01.06.04

Accelerating Materials Discovery via Bayesian Optimization—“A Case Study in High-Performance Polymers” and its Possible Future Improvement Jay H. Lee¹ and Mujin Cheon²; ¹University of South Carolina, United States; ²Korea Advanced Institute of Science and Technology, Korea (the Republic of)

Bayesian optimization (BO) has emerged as a powerful technique for accelerating materials research, both in academic and industrial settings, due to its exceptional data efficiency in black-box optimization problems. This presentation will give a comprehensive overview of BO, its underlying principles, and its application in the pursuit of high-performance materials. Furthermore, we highlight the limitations of conventional BO approaches, specifically their myopic nature and vulnerability to local minima, and propose one possible novel solution using reinforcement learning (RL)-based BO.

Bayesian optimization (BO) combines statistical modeling and sequential design to efficiently explore and optimize objective functions with limited evaluations. Unlike traditional Design of

Experiments (DoE) methods, which require a pre-defined grid or set of samples, BO adaptively selects new candidate points based on previous observations, dynamically refining its search towards promising regions of the design space. This adaptive nature of BO allows it to allocate experimental resources more efficiently, resulting in significant time and cost savings compared to DoE approaches. Furthermore, BO incorporates uncertainty estimation, enabling effective decision-making in the face of noisy or scarce data. These key principles make BO particularly well-suited for accelerating materials research, where data collection can be noisy and time-consuming, and the design space is often high-dimensional.

In collaboration with Kolon, Inc., we conducted a case study aimed at discovering a high-performing polymer with minimal experimentation. The problem had 15 dimensional search space, and 4 measured output properties. Our objective we chose was to maximize the values of output properties 2 and 3, while adhering to specific constraints associated with each output property. Initially, the company provided us with 32 initial data points to kick-off BO iterations.

Remarkably, after just the first iteration of the Bayesian optimization, we discovered a polymer that satisfied all the imposed constraints and aligned with the company's specific requirements. This accelerated discovery showcased the efficiency and effectiveness of BO in navigating the high-dimensional design space while optimizing for multiple objectives and constraints. The successful outcome of this case study illustrates the potential of BO for expedited material discovery, significantly reducing the number of required experiments.

However, traditional heuristic Bayesian optimization algorithms do not provide a universally good solution for every system. Conventional BO approaches, such as PI, EI, and UCB, tend to prioritize short-term gains within a single step, often resulting in being trapped in local minima and failing to explore the wider landscape of undiscovered possibilities. To overcome this limitation, we propose RL-based BO, which offers a non-myopic perspective. By integrating RL algorithms into the BO framework, we enable more intelligent exploration and exploitation strategies. By considering the future utility of exploration in current decision-making, RL-based BO actively seeks out unexplored regions, facilitating the discovery of high-performing materials.

In this abstract, we present a narrative that highlights the potential of various BO techniques in expediting materials discovery. Our case study exemplifies the power of BO-assisted experimentation in accelerating materials research. Additionally, we introduce RL-based BO as a promising approach to overcome the limitations of conventional BO. This presentation aims to inspire researchers, and industry professionals to leverage the synergistic relationship between AI and materials science.

10:30 AM DS01.06.05

Physics Inspired Batch Bayesian Optimization for Autonomous Polymer Electrolyte DiscoveryJurgisRuza¹, MichaelStolberg¹, JeffreyLopez², SawyerCawthern³, AbrahamHerzog-Arbeitman³, Ha-KyungKwon⁴, DanielSchweigert⁴, RafaelGómez-Bombarelli¹, YangShao-Horn¹ and Jeremiah A.Johnson³; ¹DMSE, MIT, United States; ²Northwestern University, United States; ³Massachusetts Institute of Technology, United States; ⁴Toyota Research Institute, United States

Polymer electrolytes have been identified as a promising alternative to liquid electrolytes in Li-ion batteries due to their potential for improved stability and enhanced mechanical properties. At the core of a successful candidate is the selection of a symbiotic pair of a salt, polymer, and the salt concentration in the polymer. However, the vast number of possible salt and polymer combinations hinders the discovery of new polymer candidates. Machine learning has proven essential in the search for new polymer electrolytes. Prior research on polymer electrolytes in existing literature can be used as a resource for discovering new and interesting polymer-salt combinations. Machine learning methods can be trained on this data as a starting point for suggesting new experiments and guiding them until best composition is found.

In this work, we propose a physics-inspired batch Bayesian Optimization (BO) model to guide the discovery of new and optimal salt-polymer combinations. To achieve this, we used a previously developed model for predicting the ionic conductivity Arrhenius parameters, which was trained with ionic conductivity data from literature, as a surrogate model for BO with ensemble uncertainty estimation. The latent embedding space of the polymer-salt candidates constructed by the machine learning model was used as the sampling space for batch BO. This approach ensured chemical diversity for each experimental run. Our results show that this model efficiently explores the search space by reducing model uncertainty in unexplored regions while quickly reaching the optimal ionic conductivity limit.

10:45 AM DS01.06.06

Towards Better Guided Experiments and Adaptive Learning with Human-AI Collaborated Bayesian Optimized Active Recommender SystemArpanBiswas¹, YongtaoLiu¹, Yu-ChenLiu², Jan-ChiYang², SergeiV. Kalinin³, MaximZiatdinov¹ and RamaK. Vasudevan¹; ¹Oak Ridge National Laboratory, United States; ²National Cheng Kung University, Taiwan; ³The University of Tennessee, Knoxville, United States

Optimization for different tasks like material characterization, synthesis, and functional properties for desired applications over multi-dimensional control parameter and function spaces need a rapid strategic search through active learning. However, in all cases prior to optimization, the target structure-material property relationship to be explored are assumed known, with the ability to shift the trajectory of the optimization based on human-identified findings during the experiment is lacking. This can be critical for running expensive experiments on new materials, when the experimental results are fuzzy for any scientific outcomes due to improper target setting, ultimately wasting time and cost. The failure rate and cost are even higher over exploring on multi-target space, where we want to learn the pareto among multiple properties, to jointly optimize during material synthesis for desired applications. To address the challenge and highlight the best of both machine learning and domain experts with appropriate balance between accelerated and meaningful scientific discoveries, here we introduce the human-AI collaborated active recommender system which aims to design and shape the target property to explore "on the fly" with real time visual assessment during the course of Bayesian optimized sequential experiments, ultimately bypassing the need to define any target scalarizer prior to the optimization process. The proposed approach allows to seamlessly combine the human input at the policy of the ML agent during the early explorations (when prior knowledge is minimal) to refine the target to explore, and with future adaptive explorations, the preferences shifts completely towards artificial intelligence to accelerate the learning with human assessed goal. The approach has been demonstrated to peizoresponse force spectroscopy of a ferroelectric thin film, exploring (finding symmetric hysteresis loops) with different kernels and acquisition functions, and finally extended the proposed tool to explore over human assessed multi-target (jointly exploration of symmetric loops and higher left loop) spaces (Pareto frontier). This work shows an advancement towards human-AI collaborated automated experiments, simultaneously steering optimization trajectories and accelerating the path to optimal learning with human guidance and AI-driven experimentation.

Acknowledgements:

The experiments, autonomous workflows and deep kernel learning was supported by the Center for Nanophase Materials Sciences (CNMS), which is a US Department of Energy, Office of Science User Facility at Oak Ridge National Laboratory. Algorithmic development was supported by the US Department of Energy, Office of Science, Office of Basic Energy Sciences, MLEExchange Project, award number 107514.

11:00 AM *DS01.06.07

Advanced Gaussian Process Function Approximation for Uncertainty Quantification and Autonomous ExperimentationMarcusM. Noack; Lawrence Berkeley National Laboratory, United States

The fields of machine learning (ML) and artificial intelligence (AI) have transformed almost every aspect of science and engineering. The excitement for AI/ML methods is in large part due to their perceived novelty, as compared to traditional methods of statistics, computation, and applied mathematics. But clearly, all methods in ML have their foundations in mathematical theories, such as function approximation, uncertainty quantification, and function optimization. Autonomous experimentation is no exception; it is often formulated as a chain of off-the-shelf tools, organized in a closed loop, without emphasis on the intricacies of each algorithm involved. The uncomfortable truth is that the success of any ML endeavor, and this includes autonomous experimentation, strongly depends on the sophistication of the underlying mathematical methods and software that have to allow for enough flexibility to consider functions that are in agreement with particular physical theories, knowledge, and intuition. We have observed that standard off-the-shelf tools, used by many in the applied ML community, often hide the underlying complexities and therefore perform poorly. In this talk, I want to give a perspective on the intricate connections between mathematics and ML, with a focus on Gaussian processes for uncertainty quantification and autonomous experimentation. Although the Gaussian process is a powerful mathematical concept, it has to be implemented and customized correctly for optimal performance; it is often criticized for unrealistic uncertainty quantification and poor scaling when used in its standard setup. The reason, however, is often not the method itself but missing flexibility and domain awareness of the underlying prior probability distribution. I will start this talk by discussing some recent examples in which GPs were applied to various approximation and decision-making problems; we will discover, by example, where the challenges, intricacies, and complexities of this methodology lie, and subsequently, how they can be addressed to yield improved performance. We will continue this thought process by focusing on how the right customizations can improve autonomous experimentation. I will present several simple toy problems to explore these nuances and highlight the importance of mathematical and statistical rigor in autonomous experimentation, uncertainty quantification, and ML.

11:30 AM DS01.06.08

Inverse Design for Printable Photovoltaics—Improving Efficiencies through Single Experiment Optimisation Enabled by High-Throughput Experimentation and Machine LearningLeonardNg Wei Tat¹, Na GyeongAn², JeungeunKim², LukeSutherland², Yinhuazhou³, LiuYang³, Dong WookChang⁴, TawfiqueHasan³, MeiGao² and DoojinVak²; ¹Nanyang Technological University, Singapore; ²Commonwealth Scientific and Industrial Research Organisation, Australia; ³Huazhong University of Science and Technology, China; ⁴Pukyong National University, Korea (the Republic of); ⁵University of Cambridge, United Kingdom

Roll-to-roll (R2R) printed photovoltaics (PVs) can reduce solar energy costs with their flexible form factors and manufacturing footprint. Machine-learning techniques and high-throughput experimentation have enabled multiple opportunities to accelerate materials discovery to break previous power conversion efficiency (PCE) records. Here, we demonstrate a 'MicroFactory', a high-throughput, autonomous and modular research platform for R2R printed PVs that enables inverse design. Consisting of an R2R fabricator, characteriser, and a cloud database, we use the MicroFactory to fabricate, characterise and record manufacturing parameters of an unprecedented 11,800 non-fullerene acceptor (NFA) organic photovoltaic devices (OPV) devices in a single

24-hour experiment. We further demonstrate how a rich dataset of 649,055 data points across 54 features collected in a single experiment can be used for inverse design to generate new input parameters that can produce enhanced devices. This is done firstly by solving an optimisation problem, making predictions on simulated data whose results can be measured to real-world performance, and then taking the generated inputs from the simulated data to produce printed PVs with enhanced PCEs. Using this process, we make a set of 1,200 enhanced devices that outperformed our initial experiments and achieved a PCE of 9.35%, an 87% improvement from a previous record efficiency of 5% for printed R2R PVs. This established heuristic presents an opportunity to accelerate materials discovery with the assistance of AI that is transferrable to other research platforms and material classes.

11:45 AM DS01.06.09

Enhancing Active Learning Framework for Material Discovery and Optimization Through Incorporation of Physical Insights and Multimodal Data Ming-Chiang Chang¹, Sebastian Ament¹, Maximilian Amsler^{1,2}, Duncan Sutherland¹, Hongrui Zhang¹, Lan Zhou^{3,3}, John M. Gregoire^{3,3}, Carla P. Gomes¹, Louisa Smieska¹, Arthur R. Woll¹, R.B. Van Dover¹ and Michael O. Thompson¹; ¹Cornell University, United States; ²University of Bern, Switzerland; ³California Institute of Technology, United States

Recently, artificial intelligence (AI) and active learning (AL) have been adapted by the experimental material science community for on-the-fly decision making and experiment planning, enabling autonomous research. Although researchers have demonstrated the ability of AL to efficiently explore materials spaces and identify compositions with extraordinary properties, existing methods mostly "learn" from the experimental data without significant physical insight. Additionally, inputs to the AI are typically based on single characterization data (unimodal). These constraints limit the physical reasoning ability of current AL agents. The incorporation of specific physical characteristics from the experiments as inputs to the AI models, and including data not directly related to the objective properties, has the potential to significantly improve the overall exploration and exploitation efficacy.

In this work, we demonstrate these improvements through two case studies. In the first, we incorporate concurrent probabilistic labeling of complex XRD patterns generated during laser spike annealing of composition gradients. A new phase labeling algorithm provides quantitative identification of potential multiphase structures with probabilistic assessment that is used by the AL agents to develop full temperature/time/composition phase processing maps. This has enabled us to readily expand the active learning AI from simple phase space exploration tasks to the more complex task of searching for specific targeted phase(s). We demonstrate the utility of this approach in the Bi-Ti-O system where phase maps for multiple structures were autonomously generated during an X-ray synchrotron run, with the AI transitioning from exploration mode to exploitation mode mid-experiment to optimize the anatase structure.

Second, we have incorporated additional "low-cost" measurements (e.g. optical microscopy) as indirect indicators of the objective property into the data analytic workflow, further accelerating the property optimization process. Using these additional data sources, the AI efficiency is shown to be significantly enhanced with minimal experimental overhead. In the first demonstration, this additional data was used to more efficiently utilize limited X-ray synchrotron time to maximize the AI learning. In second work, these data enable optimal use of more complex experimental protocols such as contact-mode electrical measurements. For both examples, we carefully examine the efficacy of the data processing and active learning methods, and demonstrate that the inclusion of these elements indeed improves the overall autonomous workflow.

SESSION DS01.07: Frontiers of AI-Accelerated Materials Research

Session Chairs: Milad Abolhasani and Keith Brown

Wednesday Afternoon, November 29, 2023

Sheraton, Third Floor, Fairfax B

1:30 PM *DS01.07.01

Battery Charge Curve Prediction via Feature Extraction and Supervised Machine Learning Laisuo Su¹, Shuyan Zhang², Alan McGaughey², B. Reejajayan² and Arumugam Manthiram¹; ¹The University of Texas at Dallas, United States; ²Carnegie Mellon University, United States

Real-time onboard state monitoring and estimation of a battery over its lifetime is indispensable for the safe and durable operation of battery-powered devices. In this study, a methodology to predict the entire constant-current cycling curve with limited input information that can be collected in a short period of time is developed. A total of 10,066 charge curves of LiNiO₂-based batteries at a constant C-rate are collected. With the combination of a feature extraction step and a multiple linear regression step, the method can accurately predict an entire battery charge curve with an error of < 2% using only 10% of the charge curve as the input information. The method is further validated across other battery chemistries (LiCoO₂-based) using open-access datasets. The prediction error of the charge curves for the LiCoO₂-based battery is around 2% with only 5% of the charge curve as the input information, indicating the generalization of the developed methodology for predicting battery cycling curves. The developed method paves the way for fast onboard health status monitoring and estimation for batteries during practical applications.

2:00 PM DS01.07.02

Autonomous Multimodal Optimization of Surfactant Solutions Utilizing The AFL Platform Duncan Sutherland, Peter Beaucage and Tyler Martin; National Institute of Standards and Technology, United States

Biological formulations such as protein therapies, vaccines, insulin solutions are complex mixtures of a variety of carefully balanced components, for example surfactant stabilizers, anti-microbial agents, buffer salts, and the active biological component. Such solutions are optimized for shelf life, potency, and efficacy of the biologic. Neutron scattering techniques are a critical but costly tool for understanding the solution structure and interplay between the insipient and excipient components. A naïve grid search over each independent component results in an increasingly intractable space due to a span of resource limitations. (experiment and analysis time, cost of reagents, beamline availability, etc.) The autonomous formulation lab (AFL) was developed to conduct an optimized and iterative search of such spaces utilizing neutron scattering. While sensitive to the underlying structure, the neutron scattering is not capable of measuring all the desired properties of the end formulation. Previous work indicates successful exploration through large dimensional spaces but operates only on identifying solution morphology boundaries in the scattering data. A solution that becomes turbid indicates aggregation, a non-starter in biomedical formulations, and can be detected by simple image processing techniques. The combination of both structure information and turbidity can reduce the number of experiments in exploring *useful* solution composition space, lowering the overall resource cost. Here we present the recent results of combining two sources of information, Gaussian process classification of the neutron scattering patterns and gaussian process regression over the optical turbidity, in active learning campaigns trialing different acquisition functions and search strategies. We benchmark independent source learning with a joint optimization scheme that explore the space via the uncertainty in the classification model while exploiting the expected turbidity of the regression model. This accelerated the exploration and optimization of solutions containing a PS188 surfactant, and two preservative and antimicrobial components benzyl alcohol and phenol in a sodium phosphate buffer.

2:15 PM DS01.07.03

Demonstration of Iron-Based Superconducting Magnet through Complemental Researcher- & Bayesian-Driven Process Design and Twinning Network Graph Analysis Akiyasu Yamamoto^{1,2}, Shotalshiwata¹, Shinjiro Kikuchi¹, Yuta Hasegawa¹, Shinnosuke Tokuta^{1,2}, Akimitsu Ishii^{3,2}, Akinori Yamanaka^{1,2}, Yusuke Shimada^{4,2}, Zimeng Guo^{5,2}, Satoshi Hata^{5,2}, Takuto Kojima^{6,2}, Kentaro Kutsukake^{7,2}, Hiroaki Kudo^{6,2} and Noritaka Usami^{6,2}; ¹Tokyo University of Agriculture and Technology, Japan; ²JST-CREST, Japan; ³NIMS, Japan; ⁴Tohoku University, Japan; ⁵Kyushu University, Japan; ⁶Nagoya University, Japan; ⁷RIKEN, Japan

122 phase iron-based high temperature superconductors show high upper critical field with small electromagnetic anisotropy¹ and large critical grain boundary angle², and therefore is a promising material for applications in polycrystalline form. Foreseeing magnet applications, Weiss et al. have reported demonstration of trapped field of 1 T for K-doped BaFe₂As₂ (Ba122) polycrystalline bulks synthesized by hot isostatic pressing³. In this study, K-doped Ba122 bulks were synthesized from mechanochemically synthesized precursor which was prepared by high-energy ball-milling of elemental metals with the molar ratios of Ba:K:Fe:As = 0.6:0.4:2:2 in a Ar glove box^{4,5}. The precursor powder was then spark plasma sintered. Two approaches to optimizing the processing conditions were considered: optimization by researchers' experience and intuition and by data driven process based on machine learning⁶. Bayesian optimization was applied to find the best input parameters that maximize the target output property, critical current density (J_c) under magnetic field of 3 Tesla, on the experimentally available range of processing conditions with pre-optimization data by researchers using a software BOXVIA⁶. High J_c value exceeding 10⁵ A/cm² was developed by both experiments guided by researchers and Bayesian optimization process. Doubled trapped magnetic field exceeding the previous record by Weiss et al.³ was measured. Detailed trapped magnetic field properties of Ba122 bulk magnets and the key microstructural features revealed by 3-dimensional multiscale analysis⁷, precession electron diffraction (PED) nano-orientation STEM analysis and the twinning network graph analysis⁸ will be discussed.

Acknowledgement:

This work was supported by JST CREST (JPMJCR18J4 & JPMJCR17J1).

References:

- 1) H. Hosono et al., *Materials Today* 21, 278 (2018).
- 2) T. Katase et al., *Nat. Commun.* 2, 409 (2011); J. Durrell et al., *Rep. Prog. Phys.* 74, 124511 (2011).
- 3) J. D. Weiss et al., *Supercond. Sci. Technol. Letter* 28, 112001 (2015).
- 4) S. Tokuta and A. Yamamoto, *APL Materials* 7, 111107 (2019).
- 5) S. Tokuta, Y. Shimada, and A. Yamamoto, *iScience* 25, 103992 (2022).
- 6) A. Ishii et al., *SoftwareX* 18, 101019 (2022); *J. Alloy Compd.* 966, 2239133 (2023).
- 7) Y. Shimada et al., *SuST* 32, 084003 (2019); *J. Alloy Compd.* 923, 166358 (2022).
- 8) T. Kojima et al., 2021 MRS Fall Meeting & Exhibit, CH04.09.01 (2021).

2:30 PMBREAK

3:30 PM *DS01.07.04

Generative Design and Validation of Inorganic Crystals Kedar Hippalgaonkar^{1,2}; ¹Nanyang Technological University, Singapore; ²Institute of Materials Research and Engineering, Singapore

We present a generative model framework for rapidly discovering inorganic materials. By leveraging deep generative models and a property prediction target learning branch, the model efficiently explores the chemical space and identifies materials with desirable properties (in this case, formation energy and synthesizability[1]). The generative model consists of constructed latent space representation from known materials and generating new materials by sampling from this space. The main ingredient is our newly designed reconstructable Wyckoff site based crystal representation that includes symmetry considerations.

Beyond reducing reconstruction loss, to validate the generated materials, Density Functional Theory has been performed in addition to high-throughput synthesis and validation of the generated compounds.

In summary, our generative model framework offers a promising approach for accelerated inorganic materials discovery. Its integration with robotic, high-throughput workflows and self-driving labs ensures efficient validation of the generated materials, facilitating their successful translation into real-world applications.

[1] R. Zhu et al. 2023 ACS omega 8 (9), 8210-8218

4:00 PM DS01.07.05

Continuous Flow Synthesis of Pyridinium Salts Accelerated by Multi-Objective Bayesian Optimization with Active Learning John H. Dunlap^{1,2}, Jeffrey G. Ethier^{1,2}, Amelia A. Putnam-Neeb^{1,3}, Abigail G. Doyle⁴, Timothy M. Swager⁵, Christopher A. Crouse¹ and Luke A. Baldwin¹; ¹Air Force Research Laboratory, United States; ²UES, Inc., United States; ³National Research Council, United States; ⁴University of California, Los Angeles, United States; ⁵Massachusetts Institute of Technology, United States

We report a human-in-the-loop implementation of the multi-objective experimental design via Bayesian Optimization platform (EDBO+) towards the optimization of butylpyridinium bromide synthesis under continuous flow conditions. The algorithm simultaneously optimized reaction yield and production rate (or space-time yield) and generated a well defined Pareto front. The versatility of EDBO+ was demonstrated by expanding the reaction space mid-campaign by increasing the upper temperature limit. Incorporation of continuous flow techniques enabled improved control over reaction parameters compared to common batch chemistry processes, while providing a route towards future automated syntheses and improved scalability. To that end, we applied the open-source Python module, nmrglue, for semi-automated NMR analysis, and compared the acquired outputs against those obtained through manual processing methods from spectra collected on both low-field (60 MHz) and high-field (400 MHz) NMR spectrometers. The EDBO+ based model was retrained with these four different datasets and the resulting Pareto front predictions provided insight into the effect of data analysis on model predictions. Finally, quaternization of poly(4-vinylpyridine) with bromobutane illustrated the extension of continuous flow chemistry to synthesize functional materials.

4:15 PM DS01.07.06

Improvement of Extrapolative Prediction Performance by Quantum Chemical Calculations for Machine Learning Predictions of Flow-Synthesized Binary Copolymers Shogo Takasuka¹, Shunto Oikawa¹, Takayoshi Yoshimura², Sho Ito¹, Yosuke Harashima¹, Tomoaki Takayama¹, Shigehito Asano³, Akira Kurosawa³, Tetsunori Sugawara³, Miho Hatanaka², Tomoyuki Miyao¹, Takamitsu Matsubara¹, Yu-ya Oonishi³, Hiroharu Ajiro¹ and Mikiya Fujii¹; ¹Nara Institute of Science and Technology, Japan; ²Keio University, Japan; ³JSR Corporation, Japan

The properties of polymers are highly dependent on the combination and composition ratio of the monomers used to prepare them; however, the large number of available monomers makes an exhaustive investigation of all the possible combinations difficult. In the present study, five binary copolymers were prepared by radical polymerization using a flow reactor, and the prediction performance of a machine learning model was evaluated in the interpolation and extrapolation regions for the estimation of the monomer conversion and monomer composition ratio in the polymer, which were used as objective variables. The prediction model was constructed using the process variables during polymerization and additional molecular descriptors (i.e., molecular flags (one-hot encoding), fingerprints or quantum chemical calculation values) related to the monomer type as explanatory variables. In the interpolated regions where all monomer types used were included in the training data, the prediction accuracy was high irrespective of the molecular descriptors. In the extrapolation region, the model that included explanatory variables corresponding to quantum chemical calculation values representing the energy related to the radical reactions such as energies of transition states and radicals, showed a high prediction accuracy for each objective variable. We found that quantum chemical calculation are important factors in the search for new binary copolymers. Besides, we will make a presentation about Bayesian optimization to synthesize a desired copolymer by optimizing the process variables.

SESSION DS01.08: Virtual Session I
Session Chairs: Milad Abolhasani and Keith Brown
Wednesday Morning, December 6, 2023
DS01-virtual

8:45 AM *DS01.08.01

Chemist-Intuited Atomic Robotic Probe for Intelligent Synthesis of Magnetic Nanographenes Jie Su¹, Jiali Li¹, Xiaonan Wang² and Jiong Lu¹; ¹National University of Singapore, Singapore; ²Tsinghua University, China

Atomic-scale manufacturing of carbon-based quantum materials with single-bond precision holds immense potential in advancing tailor-made quantum materials with unconventional properties, which are crucial in developing next-generation spintronic devices and quantum information technologies. To date, on-surface chemistry approaches, including surface-assisted synthesis and probe-assisted manipulation, while demonstrating huge potential in fabricating these materials, are impeded by the challenges of reaction selectivity control, or restricted by scalability and production efficiency, severely hindering their practical deployment. Herein, we demonstrate the concept of the chemist-intuited atomic robotic probe (CARP) by integrating probe chemistry and artificial intelligence, allowing for conducting precise molecular surgery, aiming for the on-demand synthesis and comprehension of the elusive carbon-based quantum matters with single-bond precision. Such a concept is validated by a novel multi-bond molecular surgery to fabricate open-shell magnetic nanographenes, known as single-molecule quantum π -magnets (SMQMs), with tunable topology and spin multiplicity triggered by site-selective probe chemistry. Our deep neural networks not only transform such a complex probe-chemistry issue into machine-understandable tasks but also provide valuable chemist-intuition into elusive reaction mechanisms by extracting the critical chemical information within the data. A joint experimental and theoretical investigation demonstrates that a voltage-controlled two-electron-assisted electronic excitation enables synchronous six-bond transformations to extend the zigzag topology of SMQMs, triggered from the phenyl sp^2 -CH bond activation, aligning with initial conjectures given by the deep neural models. Our work represents a significant leap from autonomous fabrication to intelligent synthesis with unparalleled levels of selectivity and precision beyond the current synthetic tools, thus creating a major paradigm shift in the on-demand manufacturing of novel organic quantum materials for on-chip integration

9:15 AM DS01.08.02

Bayesian Optimization with Experimental Failure for High-Throughput Materials Growth Yuki K. Wakabayashi¹, Takuma Otsuka², Yoshiharu Krockenberger¹, Hiroshi Sawada²,

Recent developments in materials informatics leveraging machine learning methods, including Bayesian optimization (BO) and artificial neural networks, have been accelerating materials research [1,2]. However, appropriate handling of missing data caused by experimental failures has been a common but significant challenge for the application of machine learning and automation technologies, such as BO and robotic experimentation, toward efficient high-throughput materials synthesis.

BO is a sample-efficient approach for global optimization. In this presentation, we will introduce a novel BO algorithm that effectively handles missing data. Missing data instances arise when the target material is evasive due to inadequate synthesis parameters [3]. Our algorithm aims to complement and address this issue, enabling more robust and efficient optimization even in the presence of missing data. Though one may restrict the parameter search space to avoid experimental failures, this approach can exclude good parameters for the target material. In contrast, our algorithm can fully search complex parameter spaces by substituting the evaluation value for the missing data to the worst evaluation value available at that time. First, we show the efficacy of the BO method in handling experimental failures by utilizing simulated data. Subsequently, we validate its performance by implementing real materials growth data, namely machine-learning-assisted molecular beam epitaxy (ML-MBE) [4,5] of itinerant ferromagnetic perovskite SrRuO₃ thin films. We used the residual resistivity ratio (RRR) as the evaluation metric. The growth conditions, specifically the Ru/Sr flux ratio, growth temperature, and ozone flux rate, of SrRuO₃ thin films on DyScO₃ substrates were optimized for achieving high RRR values. The optimization process uses five random initial growth parameters and measured experimental RRR values for the updated Gaussian process regression model that predicted RRR values at unseen growth parameters using the past observations. We achieved the RRR of 80.1, the highest ever reported among tensile-strained SrRuO₃ films. We explored a wide three-dimensional parameter space, while complementing missing data within only 35 MBE growth runs. Our tensile-strained SrRuO₃ thin films stabilized by epitaxial strain show higher Curie temperature than bulk or compressive-strained films [6]. The proposed BO method is capable to properly handle experimental failure and will play an essential role in the growth/synthesis of various materials.

References [1] Mueller *et al.*, *Reviews in Computational Chemistry* **29** (Wiley, Hoboken, 2015). [2] F. Ren *et al.*, *Sci. Adv.* **4**, eaaq1556 (2018). [3] Y. K. Wakabayashi*, T. Otsuka* *et al.*, *npj Comput. Mater.* **8**, 180 (2022) [4] Y. K. Wakabayashi*, *et al.*, *APL Mater.* **7**, 101114 (2019). [5] K. Takiguchi, Y. K. Wakabayashi*, *et al.*, *Nat. Commun.* **11**, 4969 (2020). [6] G. Koster *et al.*, *Rev. Mod. Phys.* **84**, 253 (2012).

9:30 AM DS01.08.03

Towards Self-Driving Laboratory for Perovskite Ceramics: An Automated Rapid-Sintering and Dielectric-Analysis Platform (ASAP) MojanOmidvar¹, AchinthaA. Ihalage¹, HangfengZhang¹, TheoG. Saunders¹, HenryGiddens¹, MichaelForrester², SajadHaque² and YangHao¹; ¹Queen Mary University of London, United Kingdom; ²QinetiQ, United Kingdom

The convergence of machine learning (ML) and automated experimentation offers promising avenues for advancements in materials and manufacturing. As a result, an entirely integrated automated process facilitates the creation of the autonomous "self-driving laboratory" (SDL) for material discovery.^[1] Yet, challenges remain in creating comprehensive maps connecting the Process-Structure Properties (PSPs) of materials, largely due to the intricate relationship between a material's microstructure and its manufacturing process, as well as associated costs and energy consumption of trial-and-error experimentation. One exemplar is the Solid-State Reaction (SSR), a standard method for producing 3D bulk ferroelectrics. This method requires significant energy, driving up both costs and environmental impact, particularly with the need for prolonged high-temperature sintering and subsequent reheating for dielectric characterization of ML-predicted compositions.^[2] Addressing these challenges, we introduce the Automated Rapid Sintering and Dielectric Analysis Platform (ASAP), designed to streamline the dielectric characterization process of 3D tunable perovskites and the discovery of new disordered layered materials. This platform adopts a holistic approach to sample production, sidestepping potential bottlenecks, particularly in operations carried out by robotic arms connected to off-the-shelf lab equipment. Validated successfully with previously known samples, ASAP drastically reduces processing times to minutes compared to traditional methods that can span hours or days. Moreover, ASAP's capabilities extend to the efficient validation of innovative perovskite solutions, as demonstrated with samples from the barium family, particularly (Ba_xSr_{1-x})CeO₃ identified using ML-based combinatorial chemical space screening presented in our previous publication.^[3] We used ASAP to create relation between sintering condition and Phase structure of these particular unknown samples. In addition, the ASAP characterisation tool monitored the dielectric performance of number of ferroelectric (such as: BST and BTS samples) rapidly sintered samples over the frequency range of 0.2 to 3GHz with no sample surface modification required. Using this probe, the robot recorded resonance frequency, permittivity and temperature tunability for each sample. Looking ahead, we anticipate a growing trend towards user-friendly automation, open sourcing, and the use of collaborative robots (cobots) in laboratories. These advancements will undoubtedly accelerate the adoption of automation, enabling more efficient exploration in materials science.

References.

[1] S. T. S. Bukkapatnam, *IJSE Trans* **2023**, 55, 75.
[2] H. Zhang, H. Giddens, Y. Yue, X. Xu, V. Araullo-Peters, V. Koval, M. Palma, I. Abrahams, H. Yan, Y. Hao, *J Eur Ceram Soc* **2020**, 40, 3996.
[3] A. Ihalage, Y. Hao, *NPJ Comput Mater* **2021**, 7, 75.

9:45 AM DS01.08.04

Machine Learning Models for Predicting the Morphology of Chalcogenide Thin Films IsaijahA. Moses and WesleyReinhart; The Pennsylvania State University, United States

2D materials are growing in popularity due to their unique and intriguing properties that make them promising for technological applications in areas including electric and optoelectronic, energy, and sensing. The synthesis of these materials involves careful tuning of a number of independent design variables which determine the success of the growth and/or the properties of the synthesized materials. The optimization of the growth recipe usually entails intuition-based experimentation with different process variables, which requires a large investment of time, effort, and resources before high quality materials are obtained. Developing machine learning models to predict suitable conditions for materials growth is therefore essential for more timely design of these technologically relevant materials. We study synthesis recipe optimization including dimensionality reduction, latent feature representation using transfer learning, and the evaluation of various machine learning model architectures as applied to a dataset produced in-house at the 2D Crystal Consortium, a Materials Innovation Platform housed at Penn State. Given that a limited volume of experimental data will be typical of the 2D materials design process, different data augmentation and training schemes are evaluated to build robust models. As a case study, we predict MoS₂ thin film morphology based on the growth temperature. High validation accuracy shows that our models and training protocols are suitable for this and similar predictive tasks for accelerated 2D materials discovery.

SESSION DS01.09: Virtual Session II
Session Chairs: Milad Abolhasani and Keith Brown
Wednesday Morning, December6, 2023
DS01-virtual

10:30 AM *DS01.09.01

Autonomous In-Silico Accelerated Design of Novel Energy Materials Ivano EligioCastelli; Technical University of Denmark, Denmark

The development of automated computational tools is required to accelerate the discovery of new functional materials to speed up the transition to a sustainable future. Here, I address this topic by designing new electrodes with controlled interfaces for different applications which accelerate the transition to a sustainable future. These workflows are implemented in the framework of Density Functional Theory, using MyQueue and the Atomistic Simulation Environment (ASE). In the first part, I describe a fully autonomous workflow, which identifies materials to be used as intercalation electrodes in batteries based on thermodynamic and kinetic descriptors like adsorption energies and diffusion barriers [1]. A substantial acceleration for the calculations of the kinetic properties has been obtained due to a recent implementation of the Nudged Elastic Bands (NEB) method, which considers the system's symmetries to reduce the number of images to calculate. Moreover, we have established a surrogate model to identify the transition states, which can further reduce the computational cost to at least one order of magnitude [2, 3]. We have applied this workflow to discover new cathode materials for Mg batteries as well as solid-state electrolytes for Li, Na, and Mg all-solid-state batteries [1, 3]. In the second part of my talk, I discuss how engineering the interface can positively impact surface properties. I show this concept using two examples. In the first one, I nanostructure materials to increase the Li-storage capacity in C-anodes or to adjust the change in volume during charge/discharge in Si-anodes for Li-ion batteries [4]. In the second example, I apply strain engineering and external stimuli to switch the material's polarization to decrease the reaction overpotential in oxynitride materials for the oxygen evolution reaction [5, 6].

References

[1] F. T. Bölle, N. R. Mathiesen, A. J. Nielsen, T. Vegge, J. M. García-Lastra, and I. E. Castelli, *Batteries & Supercaps* **3**, 488 (2020).
[2] F. T. Bölle, A. Bhowmik, T. Vegge, J. M. García-Lastra, and I. E. Castelli, *Batteries & Supercaps* **4**, 1516 (2021).
[3] B. H. Sjølin, P. B. Jørgensen, A. Fedrigucci, T. Vegge, A. Bhowmik, and I. E. Castelli, *Batteries & Supercaps* **2023**, e202300041 (2023).
[4] S. B. Oliva, F. T. Bölle, A. T. Las, X. Xia, and I. E. Castelli, *under review* (2022).

[5] Z. Lan, D. R. Småbråten, C. Xiao, T. Vegge, U. Aschauer, and I. E. Castelli, *ACS Catal* **11**, 12692 (2021).

[6] C. Spezzati, Z. Lan, and I. E. Castelli, *Journal of Catalysis* **413**, 720 (2022).

11:00 AM *DS01.09.02

A Tutorial on Functional Data Analysis for High-Throughput ExperimentsKiranVaddi^{1,2}; ¹University of Washington, United States; ²Science Institute, United States

In this tutorial, I will describe a novel mathematical framework called 'Function Data Analysis' that combines tools from Statistics and Riemannian differential geometry to analyze data of a functional form. Functional data are ubiquitous in material science such as Spectroscopy, X-ray scattering, and Diffraction to list a few examples. Analyzing functions using traditional 'vector-based' methods is challenging as information is encoded in both the x-axis (warping or phase) and y-axis (intensity or amplitude). Intuitively, we analyze functional data such as those listed above using a notion of 'shape' that is hard to capture and analyze in a statistical sense. This tutorial will cover a basic introduction to performing statistics on Riemannian manifolds, relations between multi-variate and functional data analysis, and a few example applications to high-throughput polymeric material design and discovery problems. We will also include some code walkthroughs using synthetic datasets. Attendees will learn about performing tasks such as dimensionality reduction and clustering and have the opportunity to try them on a dataset of their own choice.

SYMPOSIUM DS02

Automated Experimentation with Synchrotrons, Neutrons and Microscopes
November29 - December1, 2023

Symposium Organizers

Yunseok Kim, Sungkyunkwan University
Yongtao Liu, Oak Ridge National Laboratory
Steven Spurgeon, Pacific Northwest National Laboratory
Daniela Uschizima, Lawrence Berkeley National Laboratory

* Invited Paper

+ JMR Distinguished Invited Speaker

SESSION DS02.01: Cutting-Edge Automation and Machine Learning Approaches in Microscopy I
Session Chairs: Yunseok Kim and Rama Vasudevan
Wednesday Morning, November29, 2023
Sheraton, Third Floor, Dalton

10:30 AM *DS02.01.01

Machine Learning Analysis and Automation in High-Resolution Scanning Probe MicroscopyAdamFoster^{1,2}; ¹Aalto University, Finland; ²Kanazawa University, Japan

Scanning Probe Microscopy (SPM) has been the engine of characterization in nanoscale systems in general, and the evolution of functionalized tips as a reliable tool for high-resolution imaging without material restrictions has been a breakthrough in studies of molecular systems. In parallel, machine learning (ML) methods are increasingly being applied to data challenges in SPM. In particular, the success of deep learning in image recognition tasks has led to their application to the analysis of SPM images, especially in the context of surface feature characterisation and techniques for autonomously-driven SPM [1].

In this work, we explore the potential for using ML approaches to aid in the analysis of high resolution Atomic Force Microscopy (AFM) and Scanning Tunnelling Microscopy images. Building upon a deep learning infrastructure that matches a set of AFM images with a unique descriptor characterizing the molecular configuration [2-4], we further develop a workflow that takes experimental images of complex molecular systems and revises initial ML structure predictions with neural network potential simulations. In this context, we discuss the challenges of handling experimental data and possible data augmentation strategies. Alongside this, we show how ML approaches can be used actively during SPM experiments to aid in both tip functionalization [5] and in the construction of nanostructures through atomic manipulation [6], while also highlighting approaches towards automated construction of complex systems.

[1] O.M. Gordon and P.J. Moriarty, *Mach. Learn.: Sci. Technol.* **1** (2020) 023001

[2] B. Alldritt, P. Hapala, N. Oinonen, F. Urtev, O. Krejci, F. F. Canova, J. Kannala, F. Schulz, P. Liljeroth, and A. S. Foster, *Sci. Adv.* **6** (2020) eaay6913

[3] Niko Oinonen, Chen Xu, Benjamin Alldritt, Filippo Canova, Fedor Urtev, Ondrej Krejci, Juho Kannala, Peter Liljeroth and Adam S. Foster, *ACS Nano* **16** (2022) 89

[4] Niko Oinonen, Lauri Kurki, Alexander Ilin and Adam S. Foster, *MRS Bulletin* **47** (2022)

[5] Benjamin Alldritt, Fedor Urtev, Niko Oinonen, Markus Aapro, Juho Kannala, Peter Liljeroth and Adam S. Foster, *Comp. Phys. Comm.* **273** (2022) 108258

[6] I-Ju Chen, Markus Aapro, Abraham Kipnis, Alexander Ilin, Peter Liljeroth and Adam S. Foster, *Nat. Commun.* **13** (2022) 7499

11:00 AM *DS02.01.02

Automated Nano-Metrology with AI-Assisted AFM for High-Resolution Material ResearchSang-JoonCho; Park Systems Corp., Korea (the Republic of)

The Atomic Force Microscope (AFM) has been a powerful instrument in nanoscale imaging, manipulation, and material property characterization. The capability of AFM allows repeated and reliable surface topography measurements in three dimensions with subnanometer resolution. Additional information, such as nanomechanical, electrical, magnetic, or even chemical information, can be obtained simultaneously, yielding a vast array of data from a single instrument with minor hardware and electronic system variations and adding software features.

However, AFM is also known to be complex in operation and analysis. There are too many parameters to control and variables to influence the data. Tip-sample interactions are affected by the tip's material and shape and the environmental conditions such as vibration, temperature, humidity, noise, vibration, and system leveling. However, the importance of AFM analysis is growing due to the vital necessity to investigate and characterize innovative nanomaterials. Finding new materials with innovative characteristics at the nanoscale has helped guide many industries to grow. The newly found materials have contributed to breakthroughs in energy, the semiconductor industry, and life science, to name a few. Recently introduced artificial intelligence and robotics solutions could greatly simplify the complex operation of AFM and help upgrade the quality of AFM data. AFM must be robust and easy to use in many areas to expand its use. To do that, AFM operation and data management should be automated and categorized by AI to expand its usability further. We introduced the various AFM automation technologies, including probe exchange, probe identification, beam alignment, sample location, tip approach, and possible AI applications. In addition, the new optomechanical design increases data quality and measurement precision. The automation of AFM could open the door to new ways to control the development of the material's facets, dramatically boost its productivity, and drive innovation across the field of nanometrology.

11:30 AM DS02.01.03

Image Interpretation Methods for High-Resolution SPM[Lauri Kurki](#)¹, [Niko Oinonen](#)¹, [Ondrej Krejci](#)¹, [Shigeki Kawai](#)^{2,3} and [Adam Foster](#)^{1,4}; ¹Aalto-Yliopisto, Finland; ²University of Tsukuba, Japan; ³National Institute for Materials Science, Japan; ⁴Kanazawa University, Japan

Scanning tunnelling microscopy (STM) and atomic force microscopy (AFM) functionalized with a CO molecule on the probe apex are methods capable of capturing sub-molecular level detail of the electronic and physical structures of a sample [1]. While high-resolution STM is a widely adopted method in materials science, the produced images are often difficult to interpret due to the convoluted nature of the signal. In this work, we propose image interpretation tools to extract physical information directly from STM images using machine learning.

In recent years, there has been rapid development in image analysis methods using machine learning, with particular impact in medical imaging. These concepts have been proven effective also in scanning probe microscopy (SPM) in general and in particular for extracting sample properties from AFM images [2,3,4]. Leveraging these developments, we extend these models to demonstrate the extraction of atomic positions directly from STM images. We also further explore how the accuracy of these predictions varies with the use of a simultaneous AFM signal and finally establish the limits of the approach in an experimental context by predicting atomic structures from STM images of silico-organic compounds [5].

[1] Cai, S., Kurki, L., Xu, C., Foster, A. S., Liljeroth, P. Water Dimer-Driven DNA Base Superstructure with Mismatched Hydrogen Bonding. *J. Am. Chem. Soc.* 2022, 144, 44, 20227–20231

[2] Alldritt, B., Hapala, P., Oinonen, N., Urtev, F., Krejci, O., Canova, F. F., Kannala, J., Schulz, F., Liljeroth, P., Foster, A. S. Automated structure discovery in atomic force microscopy. *Sci. Adv.* 2020; 6 : eaay6913

[3] Carracedo-Cosme, J., Romero-Muñiz, C., Pérez, R. A Deep Learning Approach for Molecular Classification Based on AFM Images. *Nanomaterials* 2021, 11, 1658.

[4] Oinonen, N., Kurki, L., Ilin, A., Foster, A. S. Molecule graph reconstruction from atomic force microscope images with machine learning. *MRS Bulletin* 2022, 47, 895-905

[5] Sun, K., Silveira, O. J., Ma, Y., Hasegawa, Y., Matsumoto, M., Kera, S., Krejci, O., Foster, A. S., Kawai, S. On-surface synthesis of disilabenzene-bridged covalent organic frameworks. *Nature Chemistry* 2022. 15, 136-142

SESSION DS02.02: Cutting-Edge Automation and Machine Learning Approaches in Microscopy II

Session Chairs: Adam Foster, Yongtao Liu and Steven Spurgeon

Wednesday Afternoon, November 29, 2023

Sheraton, Third Floor, Dalton

1:30 PM *DS02.02.01

Programmatic and Deep Learning Analysis Pipelines for 4D-STEM Materials Science Experiments[Colin Ophus](#); Lawrence Berkeley National Laboratory, United States

Many materials science studies use scanning transmission electron microscopy (STEM) to characterize atomic-scale structure. Conventional STEM imaging experiments produce only a few intensity values at each probe position. However, modern high-speed detectors allow us to measure a full 2D diffraction pattern, over a grid of 2D probe positions, forming a four dimensional (4D)-STEM dataset. These 4D-STEM datasets record information about the local phase, orientation, deformation, and other parameters, for both crystalline and amorphous materials. However, 4D-STEM datasets can contain millions of images and therefore require highly automated and robust software codes to extract the target properties. In this talk, I will introduce our open source py4DSTEM analysis toolkit, and show how we use these codes to perform data-intensive studies of materials over functional length scales. This includes measurements of macroscopic properties such as crystal phase, orientation, and local deformation maps, and microscopic properties such as atomic structures in 2D and 3D measured with ptychography and other phase contrast imaging mode. I will also demonstrate some applications of modern machine learning tools, to perform measurements on electron diffraction patterns where property signals have been scrambled by multiple scattering of the electron beam. All our analysis, simulation, and machine learning codes and datasets are freely available for download, as we try to adhere to FAIR data principles.

2:00 PM *DS02.02.02

AI/ML Analytics Suite for the Automated Interpretation of Scanning Transmission Electron Microscopy Data[Jenna Bilbrey](#), [Sarah Akers](#), [Arman Ter-Petrosyan](#), [Christina Doty](#), [Bethany Matthews](#) and [Steven R. Spurgeon](#); Pacific Northwest National Laboratory, United States

With the rise of automated experimentation, the topic of few-shot and semi-supervised learning techniques are increasingly relevant in the context of creating adaptable AI designed for flexibility in both analytics and data acquisition. We have developed a platform with a custom central controller that automatically utilizes these techniques for both quantitative characterization and adaptive sampling in scanning transmission electron microscopes (STEM). We previously developed a flexible, semi-supervised few-shot machine learning approach for segmentation of STEM images that uses a small support set of canonical examples across a material system to detect and quantify discrete regions. We expand our previously developed few-shot approach to include multiple modalities by incorporating energy dispersive X-ray spectroscopy (EDS) data, which allows both lattice structure and elemental composition to be taken into account during segmentation. We also demonstrate methods for unsupervised clustering using similarity graphs and semi-supervised clustering to automate support set generation. High-throughput characterization through rapid and accurate image classification and unsupervised microstructural feature mapping take us one step closer to truly autonomous microscope platforms.

2:30 PM BREAK

3:30 PM *DS02.02.03

Towards Femtogram-Scale Materials Discovery using Scanning Probes as a Self-Driving Lab[Keith A. Brown](#); Boston University, United States

This work explores recent progress in transforming scanning probe systems into platforms for materials discovery studying samples approaching the femtogram scale. There is a need to discover advanced materials to address the pressing challenges facing humanity, however there are far too many combinations of material composition and processing conditions to explore using conventional experimentation. One powerful approach for accelerating the rate at which materials are explored is by miniaturizing the scale at which experiments take place. Scanning probe lithography has the dual benefits of being capable of patterning nanoscale features and providing a system for measuring their properties at a commensurate scale. However, before this potential can be realized, methods must be developed for controllably patterning and mixing samples at the nanoscale. Thus, the focus of this talk is recent progress in developing new methods for ultra-miniaturized combinatorial materials research using scanning probes. To begin, we describe the use of inertial sensing as a path to quantifying the amount of fluid on the probe and thus the amount of fluid transferred when patterning. This method allows us to study the fluid transport between a tipless scanning probe and a surface to develop relationships that allow for predictable control over feature size. This process is used to realize closed-loop patterning of fluids with better than 1% mass accuracy. This level of control also allows us to attach metal-organic framework (MOF) crystallites to probes and study MOF-polymer interactions with high throughput. Following these innovations, we explore the use of ultrafast probes together with spherical tips that allow for patterning of fluids down to the femtogram scale. Finally, we show that these methods allow one to mix fluids on a surface to realize compositional gradients of materials. We close with a demonstration of a combinatorial experiment in which a scanning probe is used to prepare a gradient of polymer composition and then perform mechanical testing to functionally read out these materials. Taken together, these advances set the stage for scanning probes to function as a single system for materials discovery.

4:00 PM *DS02.02.04

Reinforcement Learning for Electron Microscopy Automation[James M. LeBeau](#); Massachusetts Institute of Technology, United States

Theory, synthesis, and characterization are essential components of the materials informatics cycle. While significant emphasis has been placed on theory and synthesis, comparatively limited progress has been made in materials characterization. Initial efforts to apply machine learning to characterization have mainly focused on the backend data analysis, but capturing reproducible data in a statistically significant way remains a major challenge. Although electron microscopy can provide atomic-level structural measurements of materials to unravel structure-property relationships, some critical limitations to the current workflow severely limit the current usage and future potential for materials informatics. The largely manual nature of the technique requires a significant amount of time to characterize an extremely small volume of material. This makes it challenging to collect extensive enough datasets that truly represent the material, especially when the material is inhomogeneous or contains various defects. Moreover, the human input in collecting images and spectroscopic data inherently has bias and random error that is undesirable for any comprehensive and systematic study.

In this talk, we will highlight the application of reinforcement learning (RL) techniques in automating and optimizing operations within electron microscopy. RL has proven its capabilities in surpassing human performance in complex systems, including high-skill games. In the context of electron microscopy, RL offers a reliable approach to enhance and automate materials characterization through instrument control. While significant progress has been made in theory and synthesis within the materials informatics cycle, materials characterization remains

challenging with comparatively fewer advancements. Current workflows suffer from limitations such as manual data collection, time-consuming processes, and inherent biases and errors. We present machine learning-assisted electron microscopy to address these challenges. By creating a virtual RL environment, we develop a network capable of autonomously aligning the electron beam without prior knowledge. Through extensive simulation and experimental validation, we showcase the robustness and effectiveness of our approach, emphasizing the significance of appropriate virtual environments. The results highlight the potential of RL in streamlining electron microscopy workflows, reducing algorithm design complexities, and facilitating the integration of machine learning techniques for accelerated discovery.

4:30 PM *DS02.02.05

Autonomous Elucidation of Structure-Property Relationships in Ferroelectrics via Human in the Loop Bayesian Optimization, Reinforcement Learning and Scanning Probe Microscopy RamaK. Vasudevan¹, SaiM. Valleti^{1,2}, YongtaoLiu¹, ArpanBiswas¹, BenjaminSmith², StephenJesse¹, BharatPant³, YeCao³, SergeiV. Kalinin² and MaximZiatdinov¹; ¹Oak Ridge National Laboratory, United States; ²The University of Tennessee, Knoxville, United States; ³The University of Texas at Arlington, United States

Recent progress in the areas of autonomous experiments, particularly at major user facilities, has ushered in a new paradigm over traditional human-based operations, thereby enabling new experiments that were hitherto impossible via traditional operations. To date, however, most autonomous systems in materials characterization and synthesis facilities rely on straightforward Bayesian optimization where targets are pre-defined by the user, and no subsequent interactions between the operator and the instrument are expected.

Here, we will discuss autonomous experiments performed on scanning probe microscopes (SPM) at the Center for Nanophase Materials Sciences. We first show that using human in the loop models, where the operator is presented with a subset of the experimental results that can be voted on, is an effective strategy for leveraging the best features of human-based curiosity along with machine learning -based optimization. This is implemented in the form of a Bayesian optimization active recommender system model, on a functioning scanning probe microscope to investigate relationships between the local domains structure and the characteristic features of ferroelectric hysteresis.

Next, we explore the use of automated and autonomous SPM platforms for (a) developing surrogate models of domain wall dynamics, and (b) training and deploying reinforcement learning (RL) agents to automatically manipulate domain wall structures towards desired morphologies. Of note, these surrogate models are validated via phase-field simulations and reveal peculiar features including effects of local wall stresses on functional responses. The RL agents are implemented on the working instrument, and challenges and future directions of this strategy towards autonomous manipulation of materials is discussed. Overall, this work shows that utility of automated and autonomous SPM platforms, that enable qualitatively new types of experiments and additional physical insights that are difficult to capture through non-autonomous means. This work was supported by Center for Nanophase Materials Sciences (CNMS), which is a US Department of Energy, Office of Science User Facility at Oak Ridge National Laboratory.

5:00 PM DS02.02.06

Autonomous Defect Analysis of 3D Atom Probe Microscopy Data using Machine Learning PrachiGarg¹, KristoferG. Reyes^{2,1} and BaishakhiMazumder¹; ¹University at Buffalo, The State University of New York, United States; ²Brookhaven National Laboratory, United States

Tetragonal yttria stabilized zirconia (t-YSZ) is a ceramic material that exhibits excellent mechanical strength, fracture toughness, thermal shock resistance, and high ionic conductivity. Its unique combination of properties has led to its widespread use in oxygen sensors, dental restorations, solid oxide fuel cells, and other applications that require exceptional performance and reliability. To increase the tetragonal phase stability of the material, a critical vacancy concentration is desired. Annihilated vacancies, or the presence of excessive vacancies in oxide materials, can result in material degradation and reduced performance. Vacancy serves as a diffusion pathway for atomic species resulting in unwanted atomic arrangements and phase transformation. To mitigate these issues, vacancy mapping and detection are significant. While conventional microscopy tools have limitations in detecting vacancies, advanced characterization techniques such as Atom Probe Tomography (APT) can provide valuable information for predicting local structure including vacancies. APT is a powerful 3D nano-analytical tool that provides atomic positions, structural information, and chemical composition with exceptional spatial resolution. It works by field-evaporating atoms from the surface of a sample and detecting them individually, allowing for precise atom-by-atom reconstruction of the material. While APT can provide valuable insights into the atomic-scale structure, its capability for directly detecting vacancies is limited. This motivates us to complement APT data analysis with an advanced machine learning model to detect vacancy concentration and reconstruction. To detect vacancies in the microscopic 3D positional data, we build, train, and deploy a deep learning (DL) model, using architectures common in computer vision and image processing tasks. The DL model detects structural features in 3D voxelated images. To train this model on large data, synthetic dataset with known vacancy positions and associated structural and chemical information is simulated using an empirical ball-and-spring model. The learnt DL model is applied on the real APT data for automated vacancy mapping and detection in t-YSZ. By predicting the local structure, including vacancies, the model can provide insights into the defects in the material. This information can help optimize the phase structure and stability of t-YSZ and guide the design of improved oxygen sensors and solid oxide fuel cells. This approach of combining deep learning with APT data analysis holds great potential for advancing our understanding of vacancy detection and its impact on the mechanical stability of oxide materials like t-YSZ.

5:15 PM DS02.02.07

Automating Convergence of STM Controls using Bayesian Optimization GaneshNarasimha, SabanHus, ArpanBiswas, RamaK. Vasudevan and MaximZiatdinov; Oak Ridge National Laboratory (ORNL), United States

Scanning Tunneling Microscopy (STM) is a widely used tool for atomic-scale imaging of novel materials. However, the tip optimization is a tedious process due to the extremely complex nature of the tip-surface interaction, and thus limits the throughput efficiency. Here we demonstrate a Machine Learning (ML) based framework to realize the automated optimization of the scan controls for high quality STM imaging of graphene. We deploy a Bayesian Optimization (BO) method on the STM controls in real-time to enhance the imaging quality, given by the peak intensity in the Fourier space. The BO prediction is dynamically incorporated into the microscopy controls, i.e., the current setpoint and the tip bias, to rapidly optimize the imaging conditions. We present strategies to either selectively explore or exploit across the parameter space. As a result, suitable policies are developed for autonomous convergence of the control-parameters. The ML-based framework serves as a general workflow methodology across a wide range of materials.

SESSION DS02.03: Poster Session: Leveraging Machine Learning for Materials Design and Characterization II

Session Chairs: Yongtao Liu and Steven Spurgeon

Wednesday Afternoon, November 29, 2023

Hynes, Level 1, Hall A

8:00 PM DS02.03.01

Real-Time and Absolute Quantification of Infectious Pathogens using Wide-Field Imaging-Based Droplet Analysis System SunghyunKi¹ and Dong-KuKang^{1,2,3}; ¹Incheon National University, Korea (the Republic of); ²Research Institute of Basic Sciences, Korea (the Republic of); ³Bioplastic Research Center, Korea (the Republic of)

Droplet-based microfluidic (DMF) system has been widely used as molecular diagnostic tool for digital analysis with absolute quantification and high-resolution. Especially, droplet digital analysis is useful and powerful diagnostic tool because droplets are worked as chemical and biological containers to partition biomarkers, such as virus, bacteria and nucleic acid, in single molecule manner. Due to coronavirus disease 2019 (COVID-19) pandemic, digital analysis is becoming more important as a next-generation diagnostic platform to monitor infectious pathogens affecting human health. For example, droplet digital PCR (ddPCR), the third-generation PCR, has been used because it can provide more accurate and sensitive results for monitoring infectious pathogens at a single-molecule manner comparing real-time PCR, the second-generation PCR. However, commercialized-digital analytical systems (ddPCR, digital ELISA and digital Cell Analyzer) require expensive and complex optical systems to detect droplets containing target molecule such as DNA, RNA, protein and bacteria. Even commercialized imaging systems also have a small field of view because of high-magnification lens. Examples include high-performance optical, fluorescence and confocal microscopes. To address these issues, we have developed an analytical system that combines a wide-field imaging system with DMF system to capture and quantify target droplets (we called the DropVIST, Droplet analysis system with Vast Imaging and Statistical Tools). In this approach, first of all, droplets are encapsulated with microfluidic devices and incubate for chemical reaction. Then, reacted droplets are imaged and quantified with the DropVIST for absolute quantification and high-throughput assay. In this work, droplets were encapsulated within flow-focusing structure of microfluidic devices made of polydimethylsiloxane (PDMS) material using soft-lithography technology. To setup the DropVIST, this system was composed of a simple optical system using a 50.2-megapixel CMOS image sensor-based DSLR camera and a 100mm macro lens to obtain wide-field images with high-resolution. A MATLAB-based software, called the dFinder software, was also made for absolute quantification of target droplets. In this study, the DropVIST was identified with the dFinder software that simultaneously analyzes eight individual colors for multiplexed and absolute quantification from a single image. Then, a size of detectable droplet was characterized to be over 30 μm in diameter. Also, it can be analyzed using the dFinder software that a droplet image with a minimum size of 32 pixels in a field of view of 201.8 cm^2 (The focal length of camera was 65 cm). The DropVIST allowed a field of view from a

minimum of 11.48 cm² to a maximum of 201.8 cm² and theoretical total sample volume of droplets were calculated from 69.65 μL to 1224 μL when droplets are encapsulated at 91 μm in a diameter. We demonstrated with the DropVIST that digital proliferation assay and digital colony forming unit (CFU) assay were performed to identify more rapid and accurate analysis than conventional assays (microbroth dilution and CFU assays). In these cases, bacterial cells were used at concentrations ranging from 10⁶ cells/μL to 0.1 cells/μL and a limit of detection (LOD) was 0.1 cells/μL when used the DropVIST. In the future, this system will be utilized as a diagnostic tool for rapid and accurate droplet digital analysis such as digital antimicrobial susceptibility test and real-time digital nucleic acid amplification test.

8:00 PM DS02.03.02

3D Reconstruction of Polycrystalline Microstructure of Iron-Based Superconductors using Deep LearningYoshikiNishiyama¹, TakahiroHosokawa¹, YuHirabayashi¹, HarukaIga¹, ShinnosukeTokuta¹, YusukeShimada² and AkiyasuYamamoto¹; ¹Tokyo University of Agriculture and Technology, Japan; ²Tohoku University, Japan

Image analysis to identify the constituent phases from microstructural images is an important topic in understanding the mechanism of functional materials and in applying to informatics techniques. Classic automatic thresholding methods are well known as a phase segmentation tool of functional polycrystalline materials and quantification of microstructural factors. On the other hand, polycrystalline materials often contain characteristic microstructural defects and secondary phases, and those electron microscopy images are affected by artifacts that occur during sample preparation and observation, making it challenging to achieve high phase segmentation accuracy. In this study, we focused on semantic segmentation by deep learning, which is successfully applied to medical images [1] and automatic driving [2]. Secondary electron images from the iron-based polycrystalline superconductor Ba122[3] were acquired in three dimensions by 3D FIB-SEM [4] and segmented by a deep learning model. A high IoU value over 90% was obtained [5, 6] for the images captured from the same sample and observation condition. Moreover, by tuning the learning conditions and adopting data augmentation, we have succeeded in significantly improving the segmentation accuracy of electron microscopy images of samples with different chemical compositions and observed under different conditions than the learned images.

References

- [1] O. Ronneberger *et al.*, *Proc. MICCAI* (2015).
- [2] M. Cordts *et al.*, *In IEEE Conference on CVPR* (2016).
- [3] S. Tokuta and A. Yamamoto, *APL Mat.* 7, 111107 (2019)
- [4] Y. Shimada *et al.*, *J. Alloys Compd.*, **923**, 166358(2022)
- [5] Y. Hirabayashi *et al.*, *Materials research Meeting*. A4-PR15-04 (2021)
- [6] A. Yamamoto., *European Conference on Applied Superconductivity*. 4-MO-FM2-011 (2023)

SESSION DS02.04: Exploring Physics and Simulation with Machine Learning
Session Chairs: Sijia Dong, Ayana Ghosh, Yunseok Kim and Daniela Uschizima
Thursday Morning, November 30, 2023
Sheraton, Third Floor, Dalton

8:15 AM *DS02.04.01

Physics-Informed Machine Learning Workflows Connecting Electron Microscope to Atomistic SimulationsAyanaGhosh; Oak Ridge National Laboratory, United States

In recent years, artificial intelligence, and machine learning (AI/ML) methods are being rapidly adapted in physical sciences to gain comprehensive understandings of material structures, properties, system evolutions over spatial-temporal resolution, processes involving phase transitions across various time- and length scales. With the emergence of efficient algorithms and advancement in electron microscopes, there is a scope to utilize theoretical models to guide, perform experiments while refining the parameters in both spaces, to establish a continuous feedback-loop. Instrument specificity, implementation complexity, information transferability by addressing fundamentally different latencies of imaging and simulations, remain the primary challenges. This presentation will focus on how deep learning (DL) frameworks are employed to extract atomic level information from 2D systems such as graphene followed by first-principles based studies to develop comprehensive understanding of the materials physics. These enable seamless deployment of several DL algorithms on-the-fly for appropriate feature finding, property predictions in combination with atomistic simulations to explore underpinning causal mechanisms, suited for guiding next set of experiments. A discussion on extending such workflows for other functional materials with targeted properties on-the-fly will also be included.

This effort (machine learning) is based upon work supported by the U.S. Department of Energy (DOE), Office of Science, Office of Basic Energy Sciences Data, Artificial Intelligence and Machine Learning at DOE Scientific User Facilities, INTERSECT Initiative as part of the LDRD Program of Oak Ridge National Laboratory.

8:45 AM *DS02.04.02

The Multi-Tiered Iterative Projection Framework for Solving Complex Inverse Problems from Experimental DataJeffreyDonatelli; Lawrence Berkeley National Laboratory, United States

Recent upgrades at experimental facilities throughout the world are enabling several new experiments to capture the properties and behavior of important biological objects and materials that were not previously possible to study. However, a major barrier in enabling new scientific breakthroughs from these experiments is the capability to accurately, efficiently, and robustly solve the inverse problem of reconstructing information about the sample from increasingly complex, fast, large, and sensitive detector measurements. There is a critical need to develop new math and algorithms that can accurately solve these inverse problems from new and challenging data.

I will present a new general mathematical and algorithmic framework capable of overcoming many of these challenges in inversion. This framework, called Multi-Tiered Iterative Projections (M-TIP), is based on exploiting the multi-tiered structure inherent in many inverse problems, by breaking them up into several tiers of underdetermined subproblems, each of which can be solved efficiently via mathematical projection operations that are applied iteratively. This property allows M-TIP to leverage optimal mathematical solutions for the subproblems to improve speed, robustness, convergence, and accuracy of the overall inversion. I will demonstrate the application of this M-TIP framework in solving several important open problems in inversion from challenging data for experiments including fluctuation X-ray scattering, coherent surface scattering imaging, and more.

9:15 AM DS02.04.03

Embedding Theory, Classification and Decision in Variational Autoencoders for the Transmission Electron MicroscopeJonathanHollenbach and MitraL. Taheri; Johns Hopkins University, United States

In-situ Electron Energy Loss Spectroscopy (EELS) is an instrumental technique in understanding how processing materials changes local structure and composition, but acting on the transient changes occurring at high temporal resolutions requires new artificial intelligence frameworks for characterization and analysis to match the data rate of the detector. We demonstrate a machine learning framework for rapid assessment and characterization of operando EELS data, informing decision frameworks and updating process changes. Variational Autoencoders (VAEs) have been proven ideal for encoding the complex relations of chemical changes to latent representations. By incorporating both experimental data and a sparse library of simulated data linked to theory-based structures into a single, cohesive latent embedding, this framework seeks to not only classify spectroscopy but also update input controls on edge. Pairing on edge decision with operando control of the electron beam, laser processing, and other instrument controls enables a feedback loop capable of autonomous materials processing within the Transmission Electron Microscope (TEM).

9:30 AM *DS02.04.04

Human-In-The Loop Automated Experiment (hAE)—Explainable ML for Physics Discovery in MicroscopySergeiV. Kalinin¹, YongtaoLiu², KevinRoccapriore², ArpanBiswas², RamaK. Vasudevan² and MaximZiatdinov²; ¹University of Tennessee, Knoxville, United States; ²Oak Ridge National Laboratory, United States

Rapid advancements in machine learning over the last decade have attracted broad attention of scientific community towards the possibility of automated and autonomous experimentation (AE) in areas spanning synthesis, characterization, and microscopy. For microscopy, this interest is driven both by the opportunity to automate the often repetitive and tedious process of operation and data collection, and also capitalize on the fact that for many imaging modalities the intrinsic limits for microscope operation are considerably faster than human decision making and response times. Even for imaging, the achievable sampling sizes can exceed the depth of human perception by orders of magnitude, whereas addition of microscopy optimization and spectroscopy measurements opens infinite vistas for ML-driven workflow developments. In AE, the machine learning agent is interacting with the instrument driving the sequence of the

operations, either autonomously (no human in the loop) or with human oversight. However, the incorporation of the AE requires significant changes in the human-machine interaction and in particular requires introduction or adoption of fundamentally new concepts describing the experiment planning and execution. In this presentation, I introduce the description of the AE workflows in microscopy and the fundamental concepts necessary for their development including rewards, policies, explainability, and strategies for human in the loop monitoring and intervention. I will illustrate several scenarios for automated microscopy for characterization of ferroelectric and electrochemically active materials including supervised learning, identification of microstructures responsible for desired responses, and autonomous physical discovery. I further pose that the emergence of the user facilities and cloud labs necessitate development of universal frameworks for workflow design, including universal hyper-languages describing laboratory operation, reward functions and their integration between domains, and policy development for workflow optimization. These tools will enable knowledge-based workflow optimization, enable lateral instrumental networks, sequential and parallel orchestration of characterization between dissimilar facilities, and empower distributed research.

10:00 AMBREAK

10:30 AM *DS02.04.05

Accelerating Simulations of the Excited States of Molecules and Materials Through Machine Learning and AutomationSijiaDong; Northeastern University, United States

Automated experimentation can be informed and directed by on-the-fly first-principles simulations. However, accurate first-principles simulations of the electronic excited states of molecules and materials are usually computationally expensive, especially those that involve strong correlation or excitons. In this talk, we will discuss 1) a strategy to accelerate many-body perturbation theory through machine learning for efficient simulation of the excited states of macromolecules and extended systems, and 2) a strategy to automate multireference methods for the simulation of molecules with strong correlation.

11:00 AM DS02.04.06

Comparison and Investigation of Mobility in BDT Trimers by DFT Simulating of Inelastic Neutron Scattering—The Impact of FluorinationFarahnazMaleki¹, MakennaDettmann¹, DanielVong¹, LukeDaemen², JohnAnthony³ and AdamJ. Moule¹; ¹University of California, Davis, United States; ²Oak Ridge National Laboratory, United States; ³University of Kentucky, United States

Fluorination of conjugated organic molecules is known as a way of enhancing charge mobilities in organic semiconducting materials. The tri(n-hexyl)silylethynyl benzodithiophene (BDT) trimer is an example of a molecule that has shown significant high mobility. Although the mobility in both non-fluorinated and fluorinated structures is high, the fluorinated one exhibits significantly larger mobility. To better understand the impact of fluorination on mobility, we used our DFT-based open-source Davis Computational Spectroscopy (DCS) workflow to analyze phonon spectra of anti and syn isomers of these materials. These results were also verified using inelastic neutron scattering (INS) measurements. We employed a novel method to analyze the INS spectra for each atom in the structure. By comparing the INS spectra of similar atoms in different isomers of both non-fluorinated and fluorinated structures, first we can gain insights into the reflection of isomerism in INS spectra and second influence of fluorine atoms on the INS spectra of other atoms.

11:15 AM *DS02.04.07

Pushing the Boundaries of Waste Heat Recovery—Novel Approaches at the Intersection of Phonon Theory and ExperimentsMingdaLi; Massachusetts Institute of Technology, United States

Every year, over 2/3 of the global generated energy end up as waste heat. Phonons are major carriers of heat in semiconductors and insulators, and play an indispensable role in global decarbonization. However, phonon calculations experience high computational cost, while phonon measurements with momentum resolution often have high technical barrier and limited resources. The broadband nature of phonons further impedes the acquisition of phonon mode-resolved information from experiments.

In this lecture, we introduce three of our recent efforts aiming to acquire phonon properties with the aid of machine learning that integrates with experiments. Besides introducing the immediate topic, we highlight why the research challenges naturally lead to the solutions.

Phonon Density-of-states: First, we introduce a predictor that takes in crystal structures as input and phonon density-of-states – a key property to determine specific heat – as output [1]. With very limited training data, symmetry argumentation in a graph neural network plays a key role reaching high-quality density-of-states prediction but with much reduced computational cost. This enables a search for alloys for superior thermal transport.

Phonon Transport: Second, we introduce an integrated experimental-computational framework that can extract frequency-resolve phonon relaxation and transmittance and relaxation time. Ultrafast diffraction offers high-dimensional data in time-momentum space where phonon thermal transport is reflected on the atomic vibrations and thereby diffraction intensities, and data-free scientific machine learning is used to solve an inverse thermal transport problem and extract those frequency-resolved phonon transport information [2].

Full Phonon Bandstructure: Finally, we introduce our latest work on predicting phonon spectra at arbitrary k-points, by designing a generically applicable approach that can augment graph neural networks, termed virtual node graph networks [3]. It overturns the conventional wisdom that graph nodes represent real-space atoms but instead build the needed reciprocal space. The method enables rapid and high-precision calculation of full phonon bandstructure calculations in nearly arbitrarily complex materials, such as alloys, interfaces, amorphous materials, or materials with very large unit cells. We conclude with a number of applications in thermal energy storage, thermoelectric energy harvesting, and alloy designs.

[1] <https://onlinelibrary.wiley.com/doi/10.1002/advs.202004214>

[2] <https://onlinelibrary.wiley.com/doi/10.1002/adma.202206997>

[3] <https://arxiv.org/abs/2301.02197>

SESSION DS02.05: Leveraging Machine Learning for Materials Design and Characterization I

Session Chairs: Jeffrey Donatelli, Farahnaz Maleki, Steven Spurgeon and Daniela Uschizima

Thursday Afternoon, November 30, 2023

Sheraton, Third Floor, Dalton

2:00 PM *DS02.05.01

Autonomous Laboratory for Bespoke Synthesis of NanoparticlesSang SooHan, Hyuk JunYoo, NayeonKim and DonghunKim; Korea Institute of Science and Technology, Korea (the Republic of)

The demand for bespoke synthesis of nanoparticles (NPs) has significantly increased in various applications due to their tunable properties depending on the synthesis process conditions. And, an autonomous laboratory based on AI and robotics has been rapidly employed for the time-consuming and labor-intensive NP synthesis. This approach accelerates the NP synthesis with the target properties and readily helps to understand the synthesis process-property relationship through experimental data. In this talk, we will introduce our homemade autonomous laboratory for the bespoke synthesis of commercial Ag NPs, focusing on optical properties. Bayesian optimization with an earlystopping process greatly improves the efficiency for the bespoke synthesis, in which five experimental variables are considered. Also, the data analysis and visualization help us to understand the AI-based synthetic route without human intuition. Furthermore, we can readily discover a new chemical knowledge regarding the synthesis of Ag NPs. This study shows that autonomous laboratories can accelerate materials discovery and readily help to find new knowledge.

2:30 PM DS02.05.02

Towards an Artificial Intelligence-Driven Automated Workflow for Battery Material SynthesisMargaretLund, SarahAkers, DerekHopkins, PedroRodriguez Fernandez, HeatherJob, YangangLiang and StevenR. Spurgeon; Pacific Northwest National Laboratory, United States

The realization of breakthrough energy storage technologies depends on design of new battery materials, informed by high-throughput synthesis and characterization pipelines. Here we present an artificial intelligence (AI)-driven workflow that harnesses the predictive capabilities of machine learning to optimize electrolyte solutions for improved battery materials design. In this closed-loop automated workflow, a robotic synthesis platform is integrated with two diagnostics systems (UV-vis / electrochemical impedance [EIS]) using an analysis and experimental

design feedback loop. An analysis program, written specifically for this work, reads diagnostic spectroscopy data for a plate of samples and studies absorbance or impedance spectra. Standards are used to fit an absorbance vs. concentration curve, to identify the range where the model has high confidence in its predictive capability, and this is used to predict concentrations for all samples. These predicted concentrations are fed into a machine learning optimizer that automatically determines dilution amounts for the next plate of samples. The automated workflow continues, with the robot initiating the next round of sample preparation, synthesis, and diagnostics. Using AI-driven analysis platforms such as this, we can guide synthesis and characterization of electrolytes to improve design and performance and streamline our path to game-changing research breakthroughs. PNNL-SA-185959

2:45 PM DS02.05.07

Missing Wedge Correction Without Ground Truth—Unsupervised Sinogram Inpainting for Nanoparticle Electron Tomography (UsiNet) [Lehan Yao](#), [Zhiheng Lyu](#), [Jiahui Li](#) and [Qian Chen](#); University of Illinois at Urbana-Champaign, United States

Complex natural and synthetic materials, such as subcellular organelles, device architectures in integrated circuits, and alloys with microstructural domains, require characterization methods that can investigate the morphology and physical properties of these materials in three dimensions (3D). Electron tomography has unparalleled (sub-)nm resolution in imaging 3D morphology of a material, critical for charting a relationship among synthesis, morphology, and performance. However, electron tomography has long suffered from an experimentally unavoidable missing wedge effect, which leads to undesirable and sometimes extensive distortion in the final reconstruction. Here we develop and demonstrate for the first time Unsupervised Sinogram Inpainting for Nanoparticle Electron Tomography (UsiNet) to correct missing wedges. UsiNet is the first sinogram inpainting method that can be realistically used for experimental electron tomography by circumventing the need for ground truth. We quantify its high performance using simulated electron tomography of nanoparticles (NPs). We then apply UsiNet to experimental tomographs, where more than 100 decahedral NPs and vastly different byproduct NPs are simultaneously reconstructed without missing wedge distortion. The reconstructed NPs are sorted based on their 3D shapes to understand the growth mechanism. Our work presents UsiNet as a potent tool to advance electron tomography, especially for heterogeneous samples and tomography datasets with large missing wedges, e.g. collected for beam sensitive materials or during temporally-resolved in-situ imaging.

3:00 PM BREAK

3:30 PM *DS02.05.03

Deep Learning Sub-nm Resolution Crystallographic Mapping of Polycrystalline Doped Hafnium Oxide Thin Films [Young-Min Kim](#); Sungkyunkwan University, Korea (the Republic of)

Deep learning (DL)-assisted analysis of electron microscopy datasets has revealed promising prospects for automated interpretation and signal enhancement with high fidelity, offering an unparalleled ability to address complex challenges in electron microscopy. Four-dimensional scanning transmission electron microscopy (4D-STEM)-based diffraction has been proposed as a potential approach for correlating crystal symmetries and orientations with nanograin distribution when integrated with DL. This DL-assisted crystallographic analysis is expected to demonstrate significant potential for resolving structural issues in the polycrystalline thin film domain, as it can provide crucial information for the advancement of nanoelectronics at reduced dimensions down to 1 or 2 nm.

In this study, we present a deep learning-based method for mapping crystal phases and orientations in polycrystalline oxide thin films composed of similar polymorphs. As a representative system, polycrystalline hafnium zirconium oxide ($\text{Hf}_{0.5}\text{Zr}_{0.5}\text{O}_2$, HZO) thin films with a thickness of approximately 10 nm were investigated, which are expected to play a critical role as a ferroelectric switching component in future ultrathin field effect transistors.

Incorporating 4D-STEM (position-averaged) convergent beam electron diffraction ((PA)CBED) with a hybrid deep neural network for automated feature clustering and classification enables efficient management of extensive CBED datasets acquired from polymorphic nanograins oriented arbitrarily in polycrystalline HZO thin films. This facilitates expeditious mapping of crystallographic characteristics and their geometric configuration throughout the films. The precision of this method is commensurate with zone-axis STEM imaging on an atomic scale, and its effective spatial resolution for symmetry determination can reach below 0.5 nm^2 , surpassing existing diffraction-based phase mapping techniques in terms of efficiency, accuracy, and spatial resolution.

4:00 PM DS02.05.04

Automated Determination of Electron Affinity from Low-Energy Inverse Photoelectron Spectra using Machine Learning [Yuki Kusano](#) and [Hiroyuki Yoshida](#); Chiba University, Japan

Introduction

The edges of the valence and conduction bands are essential for the operation of semiconductor devices. The energy of the conduction band edge with respect to the vacuum level is the electron affinity (EA). The precise measurement of EA became possible by the development of low-energy inverse photoelectron spectroscopy (LEIPS) in 2012 [1]. In LEIPS spectra analysis, the spectral onset is usually determined from the intersection of fitted lines to the baseline and the rising edge of the spectra. However, this method requires expertise and is time-consuming. As the LEIPS instruments are commercialized and widely used, quick and reliable analysis by non-experts is highly demanded. This study demonstrates an automated analysis method for LEIPS spectra based on machine learning.

Method

So far, machine learning analysis of photoemission yield spectroscopy (PYS) spectra has been reported [2]; to determine the ionization energy, the spectral onset is determined using Random Forest (RF) and Gradient Boosting (GB) models. We also use these models in this work. Many machine learning studies on spectral analysis use simulated data because large numbers of data are required. However, there is no theoretical model for the spectral shape of LEIPS. Moreover, the simulations do not include the variations in spectral line shape owing to different film preparation methods or material-specific variations. Therefore, we utilized a dataset of 253 experimental LEIPS spectra of 28 organic semiconductors measured in our laboratory. The intensity for each energy was used as the explanatory variable, and the EA values determined by a skilled analyst (referred to as the analysis values) as the objective variable. The data set was divided into 80% training data set and 20% test data set. The model was trained on the training data and then validated on the test data. The predicted EA was output by inputting the LEIPS spectra into the trained model. The EA values predicted by each trained model were compared to the analytical values as a validation method.

Results and Discussion

The results show that both RF and GB satisfactorily predict EA. For example, the differences between the analytical and the predicted values were only 0.04 eV and 0.00 eV for the C60 spectra, respectively. The differences between the analytical values and the predicted values (residuals) of the two models are summarized for all the test data: for RF and GB, 61% and 51% of the test data were predicted within $\pm 0.1 \text{ eV}$, and 78% and 73% when the predicted values were extended to $\pm 0.2 \text{ eV}$. The R^2 values were 0.915 and 0.856 for RF and GB, respectively. For some spectra, machine learning shows large deviation from the analytical values. We analyze the reason and propose the preprocess method to improve the precision.

References

- [1] H. Yoshida, *Chem. Phys. Lett.*, **539-540**, 180 (2012)
- [2] S. Yagyu, *Hyomen to Kagaku (Surface and Science)* **62**, 504 (2019) in Japanese

4:15 PM DS02.05.05

A Deep Learning Framework for the Spatiotemporal Feature Extraction and Statistical Characterization of Terabyte-Scale XCT Datasets [Thomas Ciardi](#), [Pawan K. Tripathi](#), [Benjamin Palmer](#), [John Lewandowski](#) and [Roger H. French](#); Case Western Reserve University, United States

Materials science faces a bottleneck in the ability to analyze large-scale image data. Datasets produced by modern imaging modalities such as X-Ray Computed Tomography (XCT) at synchrotrons output Terabytes of data per sample. Traditional approaches that use commercial software fail to effectively scale, while classical machine learning requires labeled data which can be impossible to obtain depending on the expertise required and volume of features present. As a result, analysis is reduced to hand-crafted features and small subsets of data which introduce human bias and only captures region-specific defect interactions as opposed to sample-wide behavior. To solve this, we have developed a framework that leverages distributed and high performance computing and machine learning (ML) to build an automated pipeline for the translation of 2D XCT images into 3D spatiotemporal graph representations of all microstructural features of interest. This graph-based representation provides a full statistical characterization of all defects within a given sample volume and enables additional downstream analyses.

We apply this spatiotemporal graph (st-graph) framework to XCT scans characterizing stress corrosion cracking (SCC) in Al-Mg alloys during a slow-strain tension test. The tests were conducted with collaborators at the Diamond Light Source on field-retrieved Al-Mg plate material. Samples had experienced 42-years of real world exposure to determine the effects of long-term service on stress corrosion cracking. Our st-graph pipeline 1) segments all fractures, precipitates, and pores on Terabytes of scans 2) provides a complete statistical characterization of all features of interest 3) constructs a spatiotemporal graph representation of the microstructural defect profile. We demonstrate the ability to extract over 150,000 features in a single scan, build a complete microstructural feature profile, and derive novel insights into degradation patterns from the interactions of features across a sample.

4:30 PM DS02.05.06

Semantic Segmentation and Feature Extraction from X-Ray Computed Tomography of Aluminum Bond Wires Using Deep Learning and Image Processing Pawan K. Tripathi^{1,2}, Maliesha Sumudumalie², Thomas Ciardi^{2,2}, Philip J. Noell³, James Griego³, Laura Bruckman^{1,2}, Roger H. French^{1,2,2} and Alp Sehirlioglu^{1,2}; ¹Case Western Reserve University, Cleveland, Ohio, USA, United States; ²Case Western Reserve University, United States; ³Sandia National Laboratories, United States

Advancements in X-Ray Computed Tomography (XCT) techniques have reached a stage where high-resolution data can be rapidly acquired. However, analysis of XCT scans, particularly in the context of semantic segmentation and feature extraction, remains a challenging task. The traditional segmentation methods are no longer practical due to their time-consuming nature and the substantial volume of data generated, necessitating the development of automated data pipelines capable of handling complex 3D images. In this study, we present an automated characterization pipeline that can efficiently process a batch of XCT scans of Aluminum wires exposed to a saline environment over an extended period resulting in pitting corrosion, to perform semantic segmentation and feature extraction. The developed pipeline leverages deep learning and image processing to accurately identify and segment different regions within the XCT scans, such as the wire, pitting corrosion sites, and droplets. The dataset is used to train a UNet model, specially designed for segmentation tasks, to accurately classify and segment features of interest. The automated analysis provided by this pipeline offers valuable insights into the statistical feature extraction at the voxel level, and corrosion evolution, including information on the location, size, and severity of pitting corrosion sites.

SESSION DS02.06: Automated Experiments and Machine Learning Approaches in Synchrotron and Neutron Sources-I
Session Chairs: Yijin Liu, Yongtao Liu and Daniela Ushizima
Friday Morning, December 1, 2023
Hynes, Level 2, Room 205

8:30 AM *DS02.06.01

Understanding Lithium Metal Plating and Stripping using High-Resolution X-Ray Tomography and Semantic Segmentation Iryna Zenyuk^{1,1,1}, Ying Huang¹, Jermone Quenum^{2,3} and Daniela Ushizima^{2,3,4}; ¹University of California, Irvine, United States; ²Lawrence Berkeley National Laboratory, United States; ³University of California, Berkeley, United States; ⁴University of California, San Francisco, United States

This scientific study presents a novel computational approach to inspecting and quantifying the durability of batteries using high-resolution X-ray data obtained from the Argonne National Laboratory Advanced Photon Source (ANL APS) and Lawrence Berkeley National Laboratory Advanced Light Source (LBNL ALS). The focus of the investigation was on lithium metal batteries (LMB), which are prone to lithium dendrite formation, impacting battery efficiency and posing safety hazards. The study employed in-situ and operando imaging techniques, including 3D microtomography, to detect battery defects and monitor the dynamics of lithium plating during cycling experiments. A multiclass semantic segmentation method based on the Iterative Residual U-net architecture was proposed for accurately identifying lithium plating dynamics. The computations were performed using the NERSC Perlmutter high-performance systems, exploiting both CPU, GPU, and large memory nodes. The results demonstrated the successful application of the proposed computational tool, batteryNET, for semantic segmentation and classification of different phases in the battery after cycles of charge and discharge. The analysis included volume quantification of different phases, spatial correlation among different components at different points during the cycling and renderings of the semantic segmentation results, showcasing the effectiveness of the approach. Ongoing and future work includes exploring larger datasets and new semantic segmentation algorithms based on vision transformers and other transformer-based deep learning architectures for the detection of battery defects using semantic segmentation techniques.

References

- [1] Ushizima, Huang, Quenum, Perlmutter, Parkinson, Zenyuk, "Lithium Metal Battery Characterization using X-ray Imaging and Machine Learning", American Physical Society Meeting, USA 2022.
- [2] Huang, Perlmutter, Su, Quenum, Shevchenko, Parkinson, Zenyuk, Ushizima, "Detecting lithium plating dynamics in a solid-state battery with operando X-ray computed tomography using machine learning". Nature Partner Journal Computational Materials 2023.
- [3] Quenum, Perlmutter, Huang, Zenyuk, Ushizima, "Lithium Metal Battery Diffraction Contrast Tomography via Transformer-CNN Segmentation", Journal of Imaging 2023.

9:00 AM DS02.06.02

Acceleration of Time Resolved X-Ray Imaging using Deep Learning Techniques Eshan Ganju and Nikhilesh Chawla; Purdue University, United States

Quantifying the three-dimensional (3D) microstructure of materials is vital across various domains, including materials science, condensed matter physics, and semiconductor research. Despite the efficacy of traditional characterization methods such as optical microscopy, electron microscopy, and serial sectioning, these techniques tend to be dimensionally limited, destructive, and require a significant time investment. Over the past few decades, advancements in synchrotron and lab-scale 3D x-ray tomography (XCT) have drastically enhanced researchers' capacity to uncover complex 3D microstructures across numerous materials and fields of research. Specifically, lab-scale XCT systems have facilitated the broader utilization of 3D characterization methods among diverse researchers. Despite their advantages, 3D XCT techniques also present substantial challenges, including but not limited to extended experimentation time, substantially large datasets compared to 2D methods, and high computational demands associated with analyses of the 3D tomography data. These limitations are exacerbated in lab-scale systems, which have flux limitations compared to their synchrotron-scale counterparts. The challenges are further intensified when working with time-resolved 3D tomography or 4D datasets. Applying deep learning, which excels at handling large datasets, offers a potential solution to these challenges. Deep learning can significantly optimize the most time-consuming aspects of lab-scale 4D experimentation—data collection and data analysis or segmentation. In this study, we have utilized Generative Adversarial Networks (GANs) to filter, enhance, and segment low-dose Absorption Contrast Tomography (ACT) and Diffraction Contrast Tomography (DCT) datasets captured using a lab-scale x-ray microscope (XRM). In our GAN-based approach, we adopted the U-Net++ network architecture to improve the quality of the 3D datasets captured at the lab scale. Our study encompassed two model samples: hyper-spherical Aluminum (Al) particles dispersed in a resin matrix and micro-scale Silicon (Si) cubes dispersed within a resin matrix. The Al particles were scanned under low and high x-ray doses (controlled by the exposure time and the number of X-ray projections) and resolutions. The Al particle datasets were used to train our GAN network to filter and enhance the low-dose and low-resolution scans, respectively. The results from this approach demonstrated clear improvements in image quality and significant savings in scan time. Our approach was also carried out on Diffraction contrast tomography (DCT) scans of single-crystal Si cubes to obtain diffraction spots with varying noise levels. The high-dose diffraction spots were manually segmented, a process that is both time-consuming and labor-intensive, and this segmented data was used to train our GAN network to segment the diffraction spots from the low-dose DCT scans directly. The manual and GAN-based segmentation results were used to reconstruct the 3D grain structure of the Si cubes using a forward modeling approach. The reconstructions from the GAN-based and manually segmented datasets were compared to assess the accuracy of the GAN segmentation and quantify the time savings achieved with this approach. The deep learning-based approach outlined in this study helps advance our ability to perform 4D material characterization and analysis at the lab scale. Integrating deep convolutional neural networks into lab-scale 4D material characterization can accelerate data collection and analysis, automate the characterization of materials and open up new avenues for analyses of diverse material classes at an expedited rate.

9:15 AM DS02.06.03

Pair-Variational Autoencoders (PairVAE) for Linking and Cross-Reconstruction of Characterization Data from Complementary Structural Characterization Techniques Shizhao Lu and Arthi Jayaraman; University of Delaware, United States

In materials research, structural characterization often requires multiple complementary techniques to obtain a holistic morphological view of the synthesized material. Depending on the availability and accessibility of the different characterization techniques (e.g., scattering, microscopy, spectroscopy), each research facility or academic research lab may have access to high-throughput capability in one technique but face limitations (sample preparation, resolution, access time) with other technique(s). Furthermore, one type of structural characterization data may be easier to interpret than another (e.g., microscopy images are easier to interpret than small angle scattering profiles). Thus, it is useful to have machine learning models that can be trained on paired structural characterization data from multiple techniques (easy and difficult to interpret, fast and slow in data collection or sample preparation), so that the model can generate one set of characterization data from the other. In this talk, we demonstrate one such machine learning workflow, PairVAE, that works with data from Small Angle X-Ray Scattering (SAXS) that presents information about bulk morphology and images from Scanning Electron Microscopy (SEM) that presents two-dimensional local structural information of the sample. Using paired SAXS and SEM data of newly observed block copolymer assembled morphologies [open access data from Doerk G.S., et al. Science Advances. 2023 Jan 13;9(2): eadd3687], we have trained our PairVAE. After successful training, we have demonstrated that the PairVAE can generate SEM images of the block copolymer morphology when it takes as input that sample's corresponding SAXS 2D pattern, and vice versa. This method can be extended to other soft materials morphologies as well and serves as a valuable tool for easy interpretation of 2D SAXS patterns as well as an engine for generating ensembles of similar microscopy images to create a database for other downstream calculations of structure-property relationships.

9:30 AM DS02.06.04

Machine Learning-Based Interpretation of Spectroscopy and Diffraction Data for Materials Characterization[Daniel E. Vizoso](#) and [Remi Dingreville](#); Sandia National Laboratories, United States

A wide variety of spectroscopic and diffraction techniques are commonly used for the identification and characterization of materials in many fields of study. Traditional interpretation of diffractograms or spectral profiles relies on the practitioner's ability to accurately and systematically featureize these profiles and make comparisons to reference profiles or correlate changes in these measurements to some material characteristic of interest. However, several studies have shown that traditional human-identifiable features such as peak positions and widths can be unreliable metrics depending on the methods used to identify them, particularly when the material deviates significantly from pristine, defect-free states or when the feature of interest is similar in magnitude to experimental noise. To address these challenges, machine learning methods have been used for the classification or featureization of simulated and experimental profiles for the purposes of rapid materials characterization and identification. In this presentation, we propose a reliable protocol based on supervised manifold learning meant for the extraction of meaningful features from simulated vibrational density of states as well as simulated X-ray diffraction data as exemplar data captured via spectroscopic or diffraction techniques, respectively. Using the extracted features (both separately as well as a combined feature set from the simulated vibrational density of states and simulated X-ray diffraction), we present accurate and robust regression models that are able to disentangle complex overlapping material states from individual profiles, demonstrating comprehensive decoding of profiles beyond classical peak analysis. Sandia National Laboratories is a multi-mission laboratory managed and operated by National Technology and Engineering Solutions of Sandia, LLC., a wholly owned subsidiary of Honeywell International, Inc., for the U.S. Department of Energy National Nuclear Security Administration under contract DE-NA0003525.

9:45 AM DS02.06.05

Predicting the Number of Grains Contributing to 2-D XRD Patterns of Ti-6Al-4V Using Deep Neural Networks Trained by Ab-Initio XRD Simulations[Mohammad Redad Mehdi](#)^{1,2}, [Weiqi Yue](#)^{1,2}, [Ethan Fang](#)^{1,2}, [Pawan K. Tripathi](#)^{1,2}, [Matthew A. Willard](#)^{1,2}, [Vipin Chaudhary](#)^{1,2}, [Daniel J. Savage](#)³, [Donald W. Brown](#)³, [Roger H. French](#)^{1,2} and [Frank Ernst](#)^{1,2}; ¹Case Western Reserve University, United States; ²Materials Data Science for Stockpile Stewardship: Center of Excellence, United States; ³Los Alamos National Laboratory, United States

Beamline X-ray diffractometry, where a high-energy X-ray beam is transmitted through a material and sequences of 2D diffractograms (diffraction patterns) are obtained on X-ray detectors, provides a wealth of data, including crystal structure, phase composition, and microstructure. While containing information similar to that in 2D (e.g. light-optical) images, comprehensive quantitative evaluation of information from diffractograms is less intuitive. One example is the number of grains in the field of view, which is straight-forward to determine in an image, but less obvious in a diffractogram.

Using this example, we present a novel approach to determine the number of grains contributing to sequences of diffractograms recorded during in-situ experiments. Our approach uses deep learning, based on neural networks that are trained by ab-initio simulations of 2D diffractograms. The simulations incorporate the relevant material and diffractometry parameters, allowing us granular control over the features in the simulated diffractograms. Using large numbers of simulated diffractograms, we train several DNNs (deep neural networks), designed using various architectures and appropriate hyperparameters. These DNNs are capable of learning significant features from the simulated diffractograms, which allows them to predict the number of grains in the irradiated volume with good accuracy. The effectiveness of our approach will be validated by applying it to real-time evaluation of experimental beamline 2D diffractograms obtained during additive manufacturing of Ti-6Al-4V.

10:00 AM BREAK

10:30 AM *DS02.06.06

Streamlined Curation and Mining for Synchrotron Multi-Modal Microscopic Study of Battery Materials[Yijin Liu](#); The University of Texas at Austin, United States

As modern material science moves beyond the homogeneous model system and towards research into real-world materials under realistic conditions, it usually requires using high spatial resolution probes to survey a relatively large sample, preferably in 3D and within an acceptable time frame. The research of lithium-ion batteries is a typical example. The prolonged operation of a lithium-ion battery could lead to redox heterogeneity, local phase transformation, surface passivation, particle cracking, and local domain deactivation. All these processes critically affect the electrochemical behavior and cell performance. The characterization of these processes is an important research area and synchrotron analytic methods stand out as a suite of effective approaches. The technical challenge is further amplified by the desire to integrate X-ray probes in different modalities that offer different sensitivities to various material properties. In this talk, I will discuss our efforts to utilize high-resolution, high-throughput diffractive imaging and spectro-imaging methods to investigate a few different types of battery cathode materials. I will present a few case studies that highlight the leverage of computational developments to streamline the data curation and mining. Finally, I will briefly discuss our perspective on the future developments that could be applicable to the application of X-ray inspection for industrial manufacturing of battery components and cells.

11:00 AM DS02.06.07

Leveraging Deep Neural Networks for Feature Extraction from 2D XRD Diffractogram Movies Acquired at the NSF CHESS Synchrotron Beamline[Pawan K. Tripathi](#)^{1,2}, [Weiqi Yue](#)^{2,2}, [Ethan Fang](#)^{2,2}, [Hoang HaMy Le](#)^{2,2}, [Donald W. Brown](#)³, [Matthew A. Willard](#)^{1,2}, [Vipin Chaudhary](#)^{2,2}, [Frank Ernst](#)^{1,2} and [Roger H. French](#)^{1,2,2}; ¹Case Western Reserve University, Cleveland, Ohio, USA, United States; ²Case Western Reserve University, United States; ³Los Alamos National Laboratory, United States

Analysis of 2-D X-ray diffraction (XRD) diffractogram movies acquired at synchrotron beamlines such as the Cornell High Energy Synchrotron Source (CHESS) beamline plays a crucial role in understanding the temporal changes in the atomic-scale structure and crystallographic properties of polycrystalline materials such as the Ti-6Al-4V (Ti-64) as they undergo heat treatment and related grain growth. By combining automated image preprocessing pipelines to standardize the diffractogram image sequences, we can then use pre-trained deep neural networks (DNNs) to harness the temporal coherence present in image sequences obtained during in-situ XRD experiment of heat treatment. DNNs have demonstrated their importance in learning complex patterns and extracting insights from sequential image data. The temporal coherence present in image sequences contains information about evolving features of the material's microstructure, such as the Ti-64 α to β phase transition and grain growth.

These 2D XRD diffractogram image sequences are massive and rich with information, yet could be overwhelming, becoming a bottleneck for extracting research insights due to their terabyte sizes. Therefore, we use automated analysis pipelines on FAIRified datasets, implemented in our CRADLETM Distributed and High-Performance Computing Cluster, where we can ingest, and perform image pre-processing to remove bias in the XRD patterns and perform DNN model training. The 2-D XRD patterns were directly used for DNN learning, instead of the typical down-sampled, dimension-reduced 1-D XRD peak patterns typically analyzed using GSASII. To identify the role of neural network architecture in learning from 2-D XRD movies, we trained 168 DNNs with different architecture and hyper-parameters using an experimental dataset acquired over multiple samples and beamline runs that contains 3,012 2048x2048 pixel Ti-64 XRD images and we evaluated their performance on an image test set of 1,102 Ti-64 XRD images, achieving a mean square error (MSE) of 0.076%. Using the trained DNN models, we can predict the titanium beta phase volume percentage during the thermal heat treatment.

This material is based upon research in the Materials Data Science for Stockpile Stewardship Center of Excellence (MDS3-COE), and supported by the Department of Energy's National Nuclear Security Administration under Award Number(s) DE-NA0004104.

11:15 AM DS02.06.08

Computational Reverse Engineering of Scattering Experiments (CREASE) Method for Interpreting Structure in Soft Materials[Zijie Wu](#), [Christian Heil](#) and [Arthi Jayaraman](#); University of Delaware, United States

In this talk, we will describe 'Computational Reverse Engineering of Scattering Experiments (CREASE)', a computational method that we have developed for analysis of small angle scattering profiles and interpretation of the structure in soft materials. CREASE is useful to interpret structural detail at a range of length scales for soft materials without relying on fitting small angle scattering profiles with off-the-shelf analytical models that may be too approximate for novel polymers and/or unconventional assembled structures. We will share multiple examples of how we have applied CREASE to experimental small angle X-ray scattering (SAXS) and neutron scattering (SANS) profiles obtained from different classes of soft materials [e.g., methylcellulose fibrillar structures (*Macromolecules* 2022, 55, 24, 11076–11091), micelles in amphiphilic polymer solutions (*ACS Polymers Au*, 2021, 1, 3, 153–164), and segregation in binary nanoparticle mixtures (*JACS Au*, 2023, 3, 3, 889–904 and *ACS Central Science*, 2022, 8, 7, 996–1007)]. Through these examples we will show how CREASE can be used to test various hypotheses regarding the assembled domain shapes and sizes within the materials' structure and identify the relevant structural dimensions. Besides identifying relevant structural dimensions, the structures' representative 3D configurations that CREASE outputs can also serve as an input for other computational methods that predict macroscopic properties (e.g., color, reflectance profiles) thus serving as a valuable tool for predicting structure-property relationships [e.g., *Science Advances* 2023, 9, 21, eadf2859; *ACS Materials Letters* 2022, 4, 9, 1848–1854] Machine

learning enhanced CREASE also enables fast automated analyses of high throughput SAXS or SANS data facilitating future automation in soft materials structural characterization. Interested readers can find more information about CREASE on these two links:

<https://crease-ga.readthedocs.io/en/latest/> and https://github.com/arthijayaraman-lab/crease_ga.

11:30 AM DS02.06.09

Combining Synchrotron Imaging with Artificial Intelligence—The Key for Elucidating Bone Multi-Scale Fracture Origin Federica Buccino¹, Zhao Qin², Milad Masrouri², Giuliana Tromba³, Giuseppe Banfi⁴ and Laura Maria Vergani¹; ¹Polytechnic University of Milan, Italy; ²Syracuse University, United States; ³Elettra Synchrotron, Italy; ⁴IRCCS Galeazzi Orthopaedic Institute, Italy

The detection and diagnosis of early fractures pose a challenging goal due to the complex and intertwined nature of bone structures. In this context, the field of healthcare is embracing deep learning and artificial intelligence as a means to overcome the subjectivity associated with clinicians' analysis of medical images. However, the current utilization of neural networks is primarily focused on the macro-scale of bone structures, limiting their ability to comprehend the initial stages of crack formation. To gain a better understanding of crack occurrence, it is crucial to adopt a multi-scale perspective and investigate the micro-scale, where the presence of a dense network of lacunae could indicate the initiation or deviation site of a crack. Unfortunately, speculations at this scale can only be made with the assistance of high-resolution imaging techniques, which are time-consuming when it comes to analyzing output images. In this research, we aim to combine an understanding of the mechanisms behind micro-crack propagation with the promising application of convolutional neural networks (CNNs) and coarse-grained simulation for mechanics prediction.

Trabecular samples obtained from healthy and osteoporotic human femoral heads are considered for this study. These samples are subjected to image-guided failure assessment inside a synchrotron, which emits a monochromatic beam at an energy of 25.6 keV, with a resolution of 1.6 μm . For the detection of cracks and lacunae, a CNN is implemented based on the Keras VGG16 built-in model. During the training and validation stages of the CNN, a total of 648 images are utilized, with a split of 20% for validation and 80% for training. In terms of lacunae identification, the input set consists of three different samples, each containing three images.

The designed CNN demonstrates a high level of accuracy in automatically detecting lacunae and micro-cracks at different compression levels. With the baseline setup, the networks achieve accuracy levels exceeding 0.99 for both cracks and lacunae, with a meanIoU validation metric of over 0.87. This result is particularly encouraging, considering the complexity of the scanning procedure and the challenges encountered when micro-cracks coalesce into larger meso-cracks.

The CNN proves successful in identifying cracks at their initial stages. These cracks become visible and progress further as the applied displacement increases. However, in the final compression stages, cracks are difficult to highlight using the implemented algorithm due to the complete collapse of the bone structure. From a diagnostic standpoint, the higher accuracy in detecting the initial stages of cracks is of great interest, as meso- and macro-scale cracks already represent a critical stage for the subject. Regarding lacunae detection, the CNN achieves optimal results, reducing the computational cost associated with manually segmenting these micrometric elliptical features.

Additionally, experimental images are converted into CG models and then LAMMPS is exploited to run fracture test of the trabecular biological material, which architecture is particularly complex and needs for repeating tests for extrapolating the deviation range. Here, we combined this tool with the up-to-date generative imaging methods to massively generate reasonable artificial phase images and test their fracture, so to get a reliable range of the mechanical properties without actually scanning or testing all of them.

The adopted approaches and methodologies hold promise for developing powerful classifiers and recognition systems to study the microdamage initiation and progression and the mechanical response prediction of bone tissue. Ultimately, this paves the way for the application of machine learning in the study of bone micromechanics.

SYMPOSIUM DS03

Emerging Challenges and Opportunities in Materials by Design
November 27 - December 5, 2023

Symposium Organizers

James Chapman, Boston University
Victor Fung, Georgia Institute of Technology
Prashun Gorai, National Renewable Energy Laboratory
Qian Yang, University of Connecticut

* Invited Paper

+ JMR Distinguished Invited Speaker

SESSION DS03.01: Machine Learning and Simulation I
Session Chairs: James Chapman and Qian Yang
Monday Morning, November 27, 2023
Sheraton, Second Floor, Liberty B/C

10:30 AM *DS03.01.01

Synthesis Predictions in AI-Based Materials Design Yousung Jung; Seoul National University, Korea (the Republic of)

Chemical research is primarily focused on discovering new molecules and materials that possess desired properties. To improve this process, an effective strategy involves utilizing all accessible knowledge and data to strategically design future materials using computers. However, a notable hurdle in digital discovery is that many molecules and materials designed computationally are often impractical to synthesize in the laboratory. In this presentation, I will delve into the synthesizability of molecules and materials, including the prediction of synthesis pathways (retrosynthesis) and chemical reactivity. Additionally, I will explore several challenges and opportunities that await further advancements in accelerated chemical platforms.

11:00 AM DS03.01.02

A Three-Dimensional Generative Framework for Designing High Performance Complex Material Structures Zhengyang Zhang, HanFang and Yanming Wang; Shanghai Jiao Tong University, China

Generative design for materials has recently gained significant attention due to the rapid evolution of generative deep learning models. There have been successful demonstrations of molecular-level generative design, including conditional generation based on specific criteria¹. In the realm of macroscopic structures, voxel representations of two-dimensional^{2,3} and three-dimensional⁴ structures have been extensively studied. However, the challenge lies in the insufficient resolution of these models, hindering their ability to accurately represent real structures. Various other approaches based on point cloud^{5,6}, mesh⁷, and neural radiance fields (NeRF)⁸⁻¹⁰ have been explored but have yet to be introduced in the fields of material science. In this study, we aim to address these issues with a novel framework consisting of a mesh-based 3D structure generator and physics-informed functions. We utilize non-linear mapping networks as soft constraints to capture the complex nature of 3D material structures. The incorporated physics-based methods are capable of evaluating the performances of generated structures in real-time. The composition of the loss function considers these evaluation results to drive active structure optimization. Our framework endeavors to achieve high-resolution 3D structures generation

guided by desired material properties, expected as a significant step forward toward the inverse design of novel functional materials.

References

1. Luo, S., Guan, J., Ma, J. & Peng, J. A 3D generative model for structure-based drug design. *Adv. Neural Inf. Process. Syst.* **8**, 6229–6239 (2021).
2. Mao, Y., He, Q. & Zhao, X. Designing complex architected materials with generative adversarial networks. *Sci. Adv.* **6**, (2020).
3. Qian, C., Tan, R. K. & Ye, W. Design of architected composite materials with an efficient, adaptive artificial neural network-based generative design method. *Acta Mater.* **225**, 117548 (2022).
4. Nguyen, P. C. H. *et al.* Synthesizing controlled microstructures of porous media using generative adversarial networks and reinforcement learning. *Sci. Rep.* **12**, 1–16 (2022).
5. Luo, S. & Hu, W. Diffusion probabilistic models for 3D point cloud generation. in *2021 IEEE/CVF Conference on Computer Vision and Pattern Recognition (CVPR)* (2021).
6. Wu, W., Qi, Z. & Fuxin, L. PointConv: Deep Convolutional Networks on 3D Point Clouds. in *2019 IEEE/CVF Conference on Computer Vision and Pattern Recognition (CVPR)* (2019).
7. Gao, J. *et al.* GET3D: A generative model of high quality 3D textured shapes learned from images. in *Advances in Neural Information Processing Systems 35 (NeurIPS)* 1–14 (2022).
8. Shen, J., Agudo, A., Moreno-Noguer, F. & Ruiz, A. Conditional-Flow NeRF: accurate 3D modelling with reliable uncertainty quantification. in *ECCV 2022: 17th European Conference 540–557* (2022).
9. Jun, H. & Nichol, A. Shap-E: Generating conditional 3D implicit functions. *arXiv* (2023).
10. Mildenhall, B. *et al.* NeRF: Representing scenes as neural radiance fields for view synthesis. *European Conference on Computer Vision (ECCV)* (2020).

11:15 AM DS03.01.03

CrystalGAN—Crystal Generative Adversarial Network for Periodic Materials Discovery Divya Sharma¹, Charlie Guan², Margaret Quinn³ and Paulette Clancy¹; ¹Johns Hopkins University, United States; ²Northwestern University, United States; ³DC Energy, United States

There are several online databases available that make available the periodic structure of a wide variety of crystal structures. These can play a crucial role in generative tasks to produce new, previously undiscovered periodic materials. Such a generative task can be achieved by using a Generative Adversarial Network (GAN) on ‘crystal images’, a representation built from other various voxel-based data that comprises of the 3D-fractional coordinates of each element in the crystal structure, that are stored in a separate ‘channel’, similar to the RGB representation of conventional images. We use a Wasserstein GAN to generate new materials, learning from Materials Project data. To take advantage of a larger subset of the MP dataset, we learn on all ternary materials and predict the lattice vector and the elemental identity of each channel of a given structure. We also preserve periodic, rotational, and translational invariance by also performing data augmentation. The trained GAN will allow us to reconstruct new materials from the different generative and prediction heads of the network.

11:30 AM DS03.01.04

Bispectral Analysis of Local Atomic Environments in Metal-Organic Chalcogenide Assemblies and Related Material Classes Tuong Phung, Aria Mansouri Tehrani and Tess Smidt; Massachusetts Institute of Technology, United States

In this talk, we explore the use of bispectra as a tool to analyze and cluster local atomic environments, enabling the identification of geometric trends across different material classes. The local environments in a material play a significant role in determining its overall properties. Understanding the complex interplay between local environment geometries and material properties is crucial to designing next-generation materials with desired properties. Bispectra are well-suited to characterizing local environments due to being a rotationally invariant, smooth, invertible (modulo a global rotation), and fixed-length descriptor. We define the bispectrum in this context as the scalars and pseudoscalars resulting from the triple tensor product of a local environment's spherical harmonic expansion with itself.

We apply the bispectra to compare the local environments of a new class of hybrid inorganic-organic materials called MOChAs with those found in other transition-metal and chalcogen-containing materials from the Materials Project and Cambridge Structural Database. MOChAs, or Metal-Organic Chalcogenides Assemblies, are self-assembled hybrid crystals in which low-dimensional transition metal chalcogenide structures are scaffolded by organic ligands. The structural diversity of organic ligands leads to a wide range of possible local environments in MOChAs, which are effectively captured by bispectra. These bispectra can be visualized and clustered, ultimately guiding the design and discovery of new MOChAs.

11:45 AM DS03.01.05

Strategies for Assessing and Improving the Diversity and Utility for Generative Models for Material Structure Alexander New¹, Michael Pekala¹, Elizabeth Pogue¹, Nam Q. Le¹, Janna Domenico¹, Christine Piatko¹ and Christopher Stiles^{1,2}; ¹Johns Hopkins University Applied Physics Laboratory, United States; ²Johns Hopkins University, United States

Generative machine learning (ML) models can use computational and experimental materials databases to create large quantities of novel material structures. Via additional property-prediction models, generated materials can be assessed for suitability in design tasks. Identified materials can be studied in detail, synthesized, and characterized. Here, we assess how one state-of-the-art generative model, the physics-guided crystal generation model (PGCGM), can be used as part of the inverse design process. We show that the PGCGM's learned latent space is not smooth with respect to variation in model inputs and output material properties, making material optimization difficult and limited. We also demonstrate that most of its generated structures are predicted to be thermodynamically unstable by a separate property-prediction model, partially due to out-of-domain data challenges in stability-prediction. Our findings suggest strategies and mechanisms for improving the effectiveness of generative models for inverse design. In particular, we implement and evaluate some of these suggested strategies, such as developing smoother latent spaces and more generalizable property-prediction models.

SESSION DS03.02: Machine Learning and Simulation II

Session Chairs: Peter Schindler and Qian Yang

Monday Afternoon, November 27, 2023

Sheraton, Second Floor, Liberty B/C

1:30 PM *DS03.02.01

Inverse Crystal Structure Prediction Aron Walsh; Imperial College London, United Kingdom

What set of chemical elements can adopt a given three-dimensional crystal structure? This question is challenging to answer, especially for multi-component solids where the compositional search space across the periodic table is vast. I will discuss routes by which we are attempting to tackle this, including rules-based chemical filters and data-driven statistical measures, implemented in the SMACT package [1]. Recent advances will be presented including the use of chemical similarity metrics to match compositions to prototype crystal structures, and symmetry descent down the crystallographic Bärnighausen tree to explore both metastable and ground-state configurations [2]. Finally, metrics to assess the stability and synthesizability [3,4] of the resulting materials will be covered.

[1] D. Davies, K. Butler, A. Jackson, A. Morris, J. Frost, J. Skelton, A. Walsh, *Chem* **1**, 617–627 (2016)

[2] W. Rahim, J. Skelton, C. Savory, I. Evans, J. Evans, A. Walsh, D. Scanlon, *Chemical Science* **11**, 7904–7909 (2020)

[3] G. Gu, J. Jang, J. Noh, A. Walsh, Y. Jung, *npj. Computational Materials* **8**, 71 (2022)

[4] K. Tolborg, J. Klarbring, A. Ganose, A. Walsh, *Digital Discovery* **1**, 586–595 (2022)

2:00 PM DS03.02.02

High-Throughput Screening of Symmetry-Breaking Reconstructions at Vacancies in Oxides Seán R. Kavanagh^{1,2}, Irea Mosquera-Lois¹, David O. Scanlon², Aron Walsh¹ and Yu Kumagai³; ¹Imperial College London, United Kingdom; ²University of Birmingham, United Kingdom; ³Tohoku University, Japan

Point defects are a universal feature of crystalline materials, whose identification is often addressed by combining experimental measurements with theoretical models. The standard approach of simulating defects is, however, prone to miss the ground state atomic configurations of defects, due to energy-lowering reconstructions from the idealised crystallographic environment.^{1–4} Missed ground states severely compromise the accuracy of calculated properties.

To address this issue, we report an approach to efficiently navigate the defect configurational landscape using targeted bond distortions and rattling.⁵ In this study, we apply our defect structure-searching method (implemented in ShakeNBreak⁶) in a high-throughput methodology to oxygen vacancies in over 200 metal oxides, building on the work of Kumagai *et al.*⁷

Our results reveal energy-lowering reconstructions missed by the standard modelling approach in ~50% of cases, demonstrating the widespread prevalence of this phenomenon. Analysis of this large defect dataset allows us to correlate the host material properties with the likelihood of defect symmetry-breaking and the motifs observed. Finally, we extend this analysis by re-training a graph neural network force-field on this large dataset of defect relaxations and applying it to a much wider oxide dataset (~1000 oxides), demonstrating the future potential of machine learning methods to accelerate defect calculation workflows.

1 M. Arrigoni and G. K. H. Madsen, *npj Comput Mater*, 2021, **7**, 1–13.

2 I. Mosquera-Lois and S. R. Kavanagh, *Matter*, 2021, **4**, 2602–2605.

3 S. Lany and A. Zunger, *Phys. Rev. Lett.*, 2004, **93**, 156404.

4 S. R. Kavanagh, A. Walsh and D. O. Scanlon, *ACS Energy Lett.*, 2021, **6**, 1392–1398.

5 I. Mosquera-Lois, S. R. Kavanagh, A. Walsh and D. O. Scanlon, *npj Comput Mater*, 2023, **9**, 1–11.

6 I. Mosquera-Lois, S. R. Kavanagh, A. Walsh and D. O. Scanlon, *Journal of Open Source Software*, 2022, **7**, 4817.

7 Y. Kumagai, N. Tsunoda, A. Takahashi and F. Oba, *Phys. Rev. Materials*, 2021, **5**, 123803.

2:15 PM DS03.02.03

Towards Atomistic Phase Diagrams for Surface Reconstructions and Nanoparticle Responses to Adsorbates using Machine-Learned Dynamics Cameron J. Owen¹, Nicholas Marcella², Gengnan Li³, Christopher O'Connor^{1,4}, Yu Xie¹, Clare Y. Xie¹, Anders Johansson¹, Jin Soo Lim¹, Lixin Sun¹, Christian Reece^{1,4}, Anibal Boscoboinik³, Anatoly Frenkel^{5,3}, Ralph Nuzzo² and Boris Kozinsky^{1,6}; ¹Harvard University, United States; ²University of Illinois at Urbana-Champaign, United States; ³Brookhaven National Laboratory, United States; ⁴Rowland Institute, United States; ⁵Stony Brook University, The State University of New York, United States; ⁶Robert Bosch LLC Research and Technology Center, United States

Metal surfaces have long been known to reconstruct in both facile and activated fashions, exhibiting substantial influence in their resulting catalytic and mechanical performance. We provide an unbiased simulation method by which surface reconstructions can be studied with atomistic resolution under the effects of temperature and chemisorption of adsorbates. A machine-learned force field (MLFF) is trained from *ab initio* (first principles) calculations that can capture each of the low-index mesoscopic surface reconstructions of Au (e.g., the Au(111)-'Herringbone,' Au(110)-(1x2)-'Missing-Row,' and Au(100)-'Quasi-Hexagonal' reconstructions) using large scale molecular dynamics (MD) simulations. Additionally, we present another independent MLFF that can provide proper description of the Pt(100)-(1x1) to 'hex' reconstruction, as well as subsequent lifting via exposure to CO.

Analysis of these MD trajectories yields direct atomistic understanding of the dynamic evolution of these surfaces from their initial facets, providing previously inaccessible information such as nucleation timescales under the effects of strain, local deviations from the original stoichiometry, and adsorbate exposure. Both MLFFs can also be used to study surface reconstructions and responses to adsorbates on Au or Pt nanoparticles (NPs) under similar environmental stimuli. These methodological advancements set a new standard for determining surface reconstructions along the axes of surface stoichiometry, mechanical strain, and adsorbate exposure without bias and with atomic resolution, thus providing a comprehensive picture of the nucleation environments and time-scales for such phenomena and moving the surface science community towards surface phase diagrams for these complicated mesoscopic systems.

2:30 PM *DS03.02.04

Code, Data and Infrastructure Gaps in Machine Learning for Materials Science Shyue Ping Ong; University of California, San Diego, United States

Machine learning has emerged in recent years as a powerful new tool in the study and design of materials. Nevertheless, significant challenges remain to the application and dissemination of machine learning models and architectures. In this talk, I will share my perspectives on the gaps in code, data and infrastructure for machine learning in materials science. I will highlight the Materials Virtual Lab's efforts toward addressing some of these gaps in collaboration with the broader computational materials science community.

3:00 PM BREAK

3:30 PM *DS03.02.05

Overcoming the Limits of Approximate Electronic Structure Models in Machine Learning Accelerated Materials Discovery Heather J. Kulik; Massachusetts Institute of Technology, United States

Machine learning (ML)-accelerated discovery of transition metal containing materials such as light-harvesting chromophores, phosphors, and other photoactive complexes holds great promise. Nevertheless, the open shell d electrons that impart many of the desirable properties to these systems also make them notoriously challenging to study with conventional electronic structure techniques such as density functional theory (DFT). Thus, when ML is used to accelerate computational screening, it often inherits the biases of the underlying method used to generate training data. I will describe our recent efforts to overcome these limits through three complementary approaches. First, I will describe how we have developed machine learning models trained directly on experimental reports of iridium phosphors, leading to the development of ML models that can predict experimental emission energies and lifetimes with superior or equivalent performance to conventional methods such as time-dependent DFT but in a fraction of the computational time. Next, I will describe how we overcome limits of DFT uncertainty in screening for light harvesting chromophores with earth abundant 3d metals by incorporating method insensitivity into a multi-objective optimization workflow, requiring a consensus of functionals to agree on a property in order for a material to be selected as optimal. These workflows accelerate materials discovery by at least 1000-fold. Finally, I will describe our development of a density functional "recommender" that can identify which DFT functional is most predictive to obtain accurate vertical spin excitation energies in transition metal complexes.

4:00 PM DS03.02.06

Finding Stable Zintl Phases using an Upper-Bound Energy Minimization Approach Manish Kumar Kothakonda¹, Cheng-Wei Lee¹, Jeff Law², Qian Yang³ and Prashun Gorai^{1,2}; ¹Colorado School of Mines, United States; ²National Renewable Energy Laboratory, United States; ³University of Connecticut, United States

Thermodynamic phase stability is a prerequisite in the search for novel functional materials. Density functional theory (DFT) has been the workhorse for phase stability predictions but is computationally expensive for large search spaces. In this context, machine learning models have become powerful in predicting phase stability and material properties. In particular, graph neural networks (GNNs) have outperformed more traditional ML models in phase stability predictions. In GNNs, the periodic crystal structures are converted into graphs with atom positions represented by nodes and bonds with edges connecting the nodes. In materials searches, often, hypothetical structures are created either by chemical substitutions in prototype structures or other strategies. The resulting hypothetical structure needs to be relaxed before it can be used as an input to a GNN for predicting stability. Such relaxation requires expensive DFT calculations or is achieved with machine-learned interatomic potentials. To address this challenge, we have recently proposed an upper-bound energy minimization approach (UBEM) that finds very stable structures that lie deep in the convex hull, without having to perform structural relaxations [1]. We demonstrate the efficacy of this approach by discovering novel Zintl phases that possess complex structures, and are located between saltlike compounds and intermetallic phases with a combination of ionic and covalent bonding. Although Zintl phases represent a chemically and structurally diverse family of materials, only a limited number of such phases are currently known. The potential for discovering new Zintl phases remains largely untapped and traditional experimental approaches are resource-intensive and slow. We performed a search over ~100,000 hypothetical Zintl phases using UBEM and discovered 2,140 stable Zintl phases. We have validated these predictions with DFT. Furthermore, we compared our predictions with M3GNet, which utilizes machine-learned interatomic potentials to explicitly perform structural relaxations and predict phase stability [2]. Further investigation of the thermoelectric performance of the predicted stable phases and experimental validation are currently underway.

[1] Law et al., *JACS Au* **3**, 113 (2023). [2] Chen et al., *Nature Comp. Sci.* **2**, 718 (2022).

4:15 PM DS03.02.07

Estimating and Correcting DFT Error of Metal-Organic Frameworks Through Molecular Derivatives Yeongsu Cho and Heather J. Kulik; Massachusetts Institute of Technology, United States

Metal-organic frameworks (MOFs) are composed of metal clusters linked by organic molecules, forming a porous structure that is suitable for a range of applications, including catalysis, hydrogen storage, and CO₂ capture. While an accurate theoretical analysis is crucial for characterizing and designing functional MOFs, the presence of transition metals makes MOFs exhibit strong static correlation and considerable errors in their density functional theory (DFT) calculations. Additionally, post-DFT methods are computationally prohibitive for MOFs due to the large number of atoms per unit cell. We estimate the magnitude of static correlation of MOFs using low-cost multireference diagnostics based on finite-temperature DFT, which is the first time they are applied to solid-state systems. By comparing the behavior of the diagnostics on MOFs and their molecular derivatives, we demonstrate that the DFT-based multireference diagnostics are equally applicable to solids as to their molecular derivatives. Moreover, we show that estimates provided by multireference diagnostics of a MOF have a good correlation with those of its molecular derivatives, which can be calculated much more affordably in comparison to those of the full MOF. The additivity of the multireference character discussed here suggests the set of molecular derivatives to be a good representation of a MOF, allowing it to be utilized to extract empirical parameters. Therefore, we propose to determine the Hubbard U

parameter by fitting DFT results of molecular derivatives to their theoretical benchmark, and apply the same parameter to DFT+U calculations of MOFs to effectively correct the multireference error. The quality of fitted U parameters was evaluated on the adsorption energy of N₂, O₂, and CO₂ gas molecules. The ability to perform high-level calculations for molecular systems and the low cost of DFT+U make this procedure a practical strategy for designing MOFs with improved accuracy and efficiency.

4:30 PM DS03.02.08

High-Throughput Identification of Quantum Defects in Semiconductors [Yihuang Xiong](#)¹, [Natalya Sheremetyeva](#)¹, [Wei Chen](#)², [Weiru Chen](#)¹, [Diana Dahliah](#)², [Céline Bourgois](#)², [Sinead M. Griffin](#)^{3,4}, [Alp Sipahigil](#)^{5,4,3} and [Geoffroy Hautier](#)¹; ¹Dartmouth College, United States; ²Université Catholique de Louvain, Belgium; ³Lawrence Berkeley National Laboratory, United States; ⁴Lawrence Berkeley National Laboratory, United States; ⁵University of California, Berkeley, United States

Color centers, or quantum defects, in semiconductors are emerging as promising candidates for the spin-photon interface—an indispensable building block that combines the memory capability of a spin with the information transfer capabilities of photons. This interface holds significant potential for the realization of various quantum technologies. However, the challenge remains in building a database documenting tens of thousands of quantum defects due to the complexities of accurately describing their electronic structures in an efficient manner. In this talk, we will present our work on a high-throughput search for promising spin-photon interfaces using first-principles computations. We will discuss our approach for addressing the prescribed issue by employing single-shot hybrid computations, as well as our strategies for designing defects that emit at technologically relevant wavelengths. Our results suggest promising candidates and shed light on strategies for designing novel spin-photon interfaces.

4:45 PM DS03.02.09

Machine Learning of Density Functionals for Accurate, Large-Scale Materials Simulations [Kyle W. Byström](#), [Stefano Falletta](#) and [Boris Kozinsky](#); Harvard University, United States

We have recently developed the CIDER formalism for machine learning exchange-correlation functionals, with a particular emphasis on using nonlocal features to achieve hybrid density functional theory (DFT) accuracy at semilocal DFT cost for large solid-state simulations. In this talk, we will cover current directions being pursued to further improve CIDER functionals, including training full exchange-correlation functionals for applications to heterogeneous systems and improving the accuracy of CIDER functionals for band gap and charge transfer-related problems. We will also discuss how CIDER can be used to overcome cost-accuracy trade-offs for materials science applications where both large system sizes and hybrid DFT accuracy are required, such as the calculation of charged point defect properties in semiconductors.

SESSION DS03.03: Machine Learning and Simulation III

Session Chairs: [James Chapman](#) and [Prashun Gorai](#)

Tuesday Morning, November 28, 2023

Sheraton, Second Floor, Liberty B/C

8:30 AM *DS03.03.01

Predictive Materials Design and Discovery with Causal Machine Learning [Ayana Ghosh](#); Oak Ridge National Laboratory, United States

Applications of machine learning/deep learning (ML/DL) methods have become common in a variety of scientific disciplines. However, capabilities of such techniques are yet to be fully realized in fundamental physical disciplines due to limited access to labeled data, lack of extensibility, and robustness of traditional ML models. More importantly, the intrinsically in-built correlative nature of ML models does not capture the causal hypothesis-driven nature of physical sciences. The interpretability and explainability of large parameter-dependent deep networks also pose significant challenges for fashioning more informative and physically intuitive data-driven approaches. As a result, current ML approaches for materials design fail to provide quantitative and reliable predictions about structure/property relationships, useful for theory-based design workflows for targeted synthesis/characterization to accelerate time-to-solution and reduce expensive laboratory costs. This talk will focus on how causal ML models can be exploited in combination with generalized materials representation to solidify our understanding of governing fundamental atomistic mechanisms with direct ties to experimental observables. While the family of perovskite oxides remain at the center of this exploration, discussion on extending such frameworks to other material classes with real-life applications in energy, catalysis, photovoltaics, drug design, reaction mechanisms mapping, will also be incorporated in the presentation.

This research is sponsored by the Laboratory Directed Research and Development Program of Oak Ridge National Laboratory, managed by UT-Battelle, LLC, for the U. S. Department of Energy.

9:00 AM DS03.03.02

Efficacy of Materials Representations on Prediction of Superconductor Properties [Victor Leon](#)¹, [Alexander New](#)¹, [Michael Pekala](#)¹, [Elizabeth Pogue](#)¹ and [Christopher Stiles](#)^{1,2}; ¹Johns Hopkins University Applied Physics Laboratory, United States; ²Johns Hopkins University, United States

The search for high temperature superconductors with mechanical flexibility is motivated by critical applications in healthcare (magnetic resonance imaging), MAGLEV vehicles, and reduction in power line transmission energy waste. The discovery of novel superconductors is hindered experimentally and computationally by the huge numbers of combinations of possible elements and crystal structures. In recent years, significant interest has been directed towards using machine learning and materials informatics for inverse design of materials. However, there is no standard way to represent materials for inverse design problems. An ideal material representation would keep the most predictive power for the design application relevant materials properties. In this study, we conduct a systematic evaluation of the predictive power of various materials representations (e.g. Roost, Magpie descriptors, element-fraction) with a variety of distance measures (e.g. Euclidean, earth movers distance). We compare their performance as inputs to a variety of machine learning algorithms (e.g. k-nearest neighbors regression, neural networks) to predict relevant superconductor materials properties (e.g. critical temperature, elastic modulus). We present a systematic comparison between these representation methods and algorithms for the application of superconductor property prediction.

9:15 AM DS03.03.03

Physics-Informed Deep Learning Framework for Material Discovery [Maitreyee Sharma Priyadarshini](#), [Oluwaseun Romiluyi](#), [Yiran Wang](#), [Kumar P. Miskin](#) and [Paulette Clancy](#); Johns Hopkins University, United States

The lack of efficient discovery tools for advanced functional materials is a major bottleneck to enabling future-generation energy, health, and sustainability technologies. One main factor contributing to this inefficiency is the large combinatorial space of materials which is very sparsely observed. Searches of this large combinatorial space are often biased by expert knowledge and clustered close to material configurations that are known to perform well. Moreover, experimental characterization or first principles quantum mechanical calculations of all possible materials are extremely expensive leading to small available data sets. As a result, there is a need for the development of computational algorithms that can efficiently search this large space for a given material application. Here, we introduce, PAL 2.0, a method that combines a physics-informed belief model with Bayesian optimization. Every material is characterized by physical and chemical properties of components of the material in a complex manner but *a priori* knowledge of the identity of the important properties is often lacking. The key contributing factor of our proposed framework is the creation of a physics-based hypothesis using XGBoost and Neural Networks. The generated hypothesis provides a physics-based prior to the Gaussian process model which is then used to perform a search of the material space. Our method is unique since it picks out the physical descriptors that are most representative of the material domain making the search unbiased toward expert knowledge, which in many cases is unknown. The model also provides valuable chemical insight into the domain that can be used to develop new materials that were outside the domain that was initially searched. Some materials that we have tested our approach on include metal halide perovskites and thermoelectric semiconductors. More recently our approach is being used in a closed-loop setup with experimentalists to discover high-temperature shape memory alloys.

Funding acknowledgment: MSP, OVR and PC acknowledge support from the U.S. Department of Energy (DOE), Basic Energy Sciences (BES), under award DE-SC0022305. Kumar Miskin thanks Johns Hopkins University for his support. The authors acknowledge the support afforded by access to the computing 376 facilities at the petascale Advanced Research Computing at 377 Hopkins (ARCH) facility (rockfish.jhu.edu), supported by the 378 National Science Foundation (NSF), Grant Number OAC 379 1920103, for providing the extensive computational resources needed here. Partial funding for the infrastructure for ARCH was originally provided by the State of Maryland.

9:30 AM *DS03.03.04

Machine-Learning-Driven Advances in Modeling Inorganic Materials [Volker L. Deringer](#); University of Oxford, United Kingdom

Understanding the connections between atomic-scale structures and macroscopic properties is among the most important research challenges in solid-state and materials chemistry. Computer simulations based on the laws of quantum mechanics have played a key role in this – but they are computationally demanding, and therefore they will inevitably reach their limits when materials with highly complex structures are to be studied. Machine learning (ML) based interatomic potentials are a rapidly emerging approach that helps to overcome this limitation: being “trained” on a suitably chosen set of quantum-mechanical data, they achieve comparable accuracy whilst giving access to much larger-scale simulations – with thousands or even millions of atoms.

In this presentation, I will showcase some recent advances in the modeling and understanding of inorganic materials that have been enabled by ML-driven molecular dynamics (MD) simulations. I will argue that ML potentials are particularly useful for modeling structurally complex inorganic solids, such as non-crystalline (amorphous) phases that are difficult to characterize experimentally. I will survey recent work that ranges from structural studies of amorphous elements at ambient and high pressure to the modeling of materials for practical applications – for example, of disordered carbon phases for lithium- and sodium-ion battery anodes, or phase-change memories for digital data storage. I will discuss perspectives for combining these increasingly popular ML-driven simulation tools with first-principles electronic-structure computations and chemical-bonding studies, as well as possible new synergies with experimental approaches – with a vision to more fully understand, and ultimately to design, complex inorganic materials on the atomic scale.

10:00 AMBREAK

10:30 AM *DS03.03.05

ChIMES—Enabling Accurate Modeling of Complex Reacting Systems on Large Spatiotemporal Scales [Rebecca K. Lindsey](#); University of Michigan, United States

For decades, atomistic modelers interested in studying condensed phase reacting systems have been forced to choose between highly predictive yet computationally expensive first principles methods, and parametric “force field” approaches affording greater computational efficiency at the expense of accuracy and predictive power. But now, modelers have a third option in machine-learned interatomic potentials (ML-IAP), which can yield models approximating quantum-based potential energy surfaces with computational expense that scales linearly with system size. These ML-IAPs have had a transformative effect by enabling “quantum accurate” simulations on previously inaccessible scales; however (1) their development for systems of more than a few atom types (especially those for which molecular chemistry is involved) necessitates large volumes of high expense (e.g., quantum) training data, and (2) they remain significantly more computationally intensive than classical “force field” models. In this presentation, we discuss ChIMES, a ML-IAM and artificial intelligence-driven generation framework designed to overcome these challenges. Recent advances and applications to complex reacting systems are overviewed.

11:00 AM DS03.03.06

GPU-Accelerated Simulations of Thermal Transport using Machine Learning Force Fields [Anders Johansson](#), [Jennifer Coulter](#), [Andrea Cepellotti](#) and [Boris Kozinsky](#); Harvard University, United States

Controlling thermal conductivities of materials is important for a wide range of applications, from thermoelectrics for clean energy generation to electronic devices and thermal barrier coatings. The thermal conductivity is commonly estimated using molecular dynamics simulations within the Green-Kubo formulation. This requires a force field that is both 1) an accurate estimate of the interatomic interactions and 2) fast enough to allow simulations with sufficiently large length and time scales. An accurate force field can also be used to accelerate the calculation of force constants for transport simulations via the Boltzmann transport equation.

In this work, we employ the Gaussian Process-based FLARE force field, which automatically learns the interactions of more complex materials than empirical force fields. The resulting model can then be mapped to a low-dimensional, computationally efficient model. Through GPU-acceleration with LAMMPS and the Kokkos library, we achieve excellent performance and obtain well-converged estimates for the thermal conductivity with Green-Kubo molecular dynamics. Our newly developed transport code, Phoebe, computes the thermal conductivity with force constants calculated by FLARE. The data efficiency of FLARE reduces the total number of DFT calculations required, and Phoebe has been highly optimized to solve the Boltzmann transport equation efficiently on GPUs using the Kokkos and cuSOLVER libraries.

11:15 AM DS03.03.07

Exploring Self-Assembly Models and Transformation Pathways of Complex Crystal Structures [Julia Dshemuchadse](#)¹, [Hillary Pan](#)¹, [Maya Martirosyan](#)¹ and [Matthew Spellings](#)²; ¹Cornell University, United States; ²Vector Institute for Artificial Intelligence, Canada

The emergence of ordered structures from simple building blocks is as ubiquitous as it is mysterious. The process of how long-range ordered structures—whether complex or simple, universal or unique—emerge from short-range interactions, remains poorly understood and an area ready for exploration with computational approaches. We model crystallization with molecular dynamics simulations of particles that interact via isotropic pair potentials: by exhibiting multiple features that represent competing length scales, these simple models have been shown to enable the self-assembly of a large variety of crystal structures. On the basis of these systems, we study which crystal structures can be self-assembled from isotropic interactions alone and how such phase transitions proceed on the particle-by-particle level. We employ rational forward design to target the assembly of varied structures, and we classify different local environments in the observed phases via high-dimensional, machine-learning-enabled order parameters (using principal component analysis and Gaussian mixture models). Through these investigations, we gain insights into processes that occur on time and length scales typically inaccessible to direct observation, and we hope to develop models for different types of interactions that enable the assembly of a wide variety of structures. Ultimately, we envision a framework within which the driving forces and mechanisms of crystal growth and self-assembly are causally linked to the types of phase transitions and emergent ordered phases that will enable the design of new materials.

11:30 AM DS03.03.08

Meta-Learning—Efficient Force-Field Parameterization for Accurate Molecular Simulations [Aditya Koneru](#)^{1,2}, [Henry Chan](#)² and [Subramanian Sankaranarayanan](#)^{2,1}; ¹University of Illinois at Chicago, United States; ²Argonne National Laboratory, United States

Accurate interatomic potentials in molecular dynamics are crucial for predicting the behavior of materials, enabling exploration of the vast materials landscape. This study focuses on the application of meta-learning techniques for force-field parameterization. Traditional approaches to force-field parameterization rely on global or local optimization strategies, often requiring extensive sampling to achieve satisfactory results when the parameter space is large. However, by leveraging meta-learning techniques, we can minimize the need for extensive sampling by acquiring knowledge about the specific regions in the parametric space that align with the desired properties. Meta-learning involves capturing the experience of navigating the parametric space automatically. For example, to capture multiple material properties like local and global structural features, energetics, mechanical and thermal properties, it is important to understand their mapping to the force-field parameter space. In this research, we have successfully applied meta-learning to various force-fields, enabling accurate descriptions of multiple polymorphs and diverse material properties. The results highlight the effectiveness of meta-learning in improving force-field parameterization for enhanced modeling and simulation of molecular systems.

11:45 AM DS03.03.09

Learning the Interatomic Potential of Ionic Liquids and Salt-In-Ionic Liquids with Machine Learning [Zachary A. Goodwin](#), [Nicola Molinari](#), [Albert Musaelian](#), [Simon Batzner](#) and [Boris Kozinsky](#); Harvard University, United States

Ionic liquids are a promising class of electrolytes for battery and supercapacitor applications, as well as universal solvents for chemical reactions. In their pure form, these two-component liquids have complex molecular environments and their disordered structures can have large length scales. Moreover, how these electrolytes behave at interfaces, how they transport ions and how additives, such as Li-based salts or/and water, affect their properties is challenging to study using empirical interatomic potentials due to their limited accuracy. Here we develop machine learning interatomic potentials, based on the equivariant graph neural networks with NequIP [1], for representative ionic liquid and salt-in-ionic liquid [2]. As capturing the complex intermolecular interactions is subtle, training a potential for this system is not as straightforward as a simple solid-electrolyte, for example, and we highlight some of the challenges encountered with this process. In addition, we study the question of model transferability across the composition space of salt-in-ionic liquids, the effect of long-range interactions and uncertainty of the model.

[1] Batzner, S., Musaelian, A., Sun, L., Geiger, M., Mailoa, J.P., Kornbluth, M., Molinari, N., Smidt, T.E. and Kozinsky, B. E(3)-equivariant graph neural networks for data-efficient and accurate interatomic potentials. Nat. Commun., 13, 1-11 (2022)

[2] Molinari, N., Mailoa, J.P. and Kozinsky, B. General trend of a negative Li effective charge in ionic liquid electrolytes. J Phys. Chem. Lett., 10, 2313-2319 (2019)

1:30 PM *DS03.04.01

The Second Decade of the Materials Genome Initiative James A. Warren; National Institute of Standards and Technology, United States

Two years ago, the US Materials Genome Initiative (MGI) released an updated strategic plan that outlined the priorities and tactics for this multi-agency effort to accelerate the discovery, design, development, and deployment of new materials into manufactured products. The means to achieve this overarching goal is the Materials Innovation Infrastructure, a federated, yet tightly knit, interplay of computational, experimental and data resources. In this presentation I will briefly review the MGI's progress to date and explore the new strategic plan, especially its focus on data and artificial intelligence. I will then focus the remainder of the talk exploring the variety of social, technical, and intellectual challenges that have both made the MGI an ambitious and exciting undertaking as well as providing a number of sobering lessons in the reluctance of the R&D community to adopt paradigm shifts.

2:00 PM DS03.04.02

Machine Learning-Guided Materials Discovery—How Fast and How Novel? Michael Pekala¹, Elizabeth Pogue¹, Alexander New¹, Brandon Wilfong², Gregory Bassen², Kyle McElroy¹, Tyrel M. McQueen² and Christopher Stiles^{1,2}; ¹Johns Hopkins University Applied Physics Laboratory, United States; ²Johns Hopkins University, United States

Discovery is central to the advancement of science but the rate of discovery and the novelty of discovery associated with individual methods is rarely quantified. While machine learning (ML) approaches have accelerated experimental materials research, the ability of different sampling and ML approaches to discover fundamentally new classes of materials with desired properties has not been fully evaluated. Ultimately, ML is limited by existing data even in a closed-loop framework. Questions remain regarding how effectively these methods can truly generalize beyond the limited training data. In existing materials datasets, high-performance families of materials tend to be over-represented and "negative data" is often missing or sparse. When designing ML for material discovery, these effects are likely to be magnified because the goal is often to discover promising novel families of materials far from the training dataset. This requires generalization of the ML model to regions where optimal sampling strategies are less straightforward. Adaptive sampling strategies add data to databases in ways that enable tradeoffs between model fidelity and training set breadth but this has not been widely explored systematically or quantified in the materials discovery context. Here, we use a combination of the Supercon Database and Materials Project to simulate the needle-in-a-haystack material discovery problem to compare the ability of several adaptive sampling strategies to rediscover promising superconductor families like the cuprates and iron-based superconductors when those are excluded from the training data. This framework allows for quantification of the rate of discovery and the novelty of predictions associated with individual ML and adaptive sampling approaches, which extends beyond the superconductor discovery to any discovery problem.

2:15 PM DS03.04.03

polyBERT—A Large Language Model to Make Ultrafast Predictions of Polymers Christopher Kuenneth^{1,2} and Rampi Ramprasad²; ¹University of Bayreuth, Germany; ²Georgia Institute of Technology, United States

Polymers play a crucial role in our daily lives, offering a wide range of applications. The vast polymer cosmos possesses both exciting opportunities and significant challenges when it comes to identifying suitable candidates for specific applications. Here, we show an end-to-end polymer informatics pipeline that searches this vast space for suitable candidates at unprecedented speed and accuracy. The pipeline includes a large language model-based fingerprinting capability called polyBERT. polyBERT acts as a "chemical linguist", treating the chemical structure of polymers as chemical language. A multitask learning approach maps the polyBERT fingerprints to a variety of polymer properties. In comparison to manually designed fingerprinting schemes, our polyBERT pipeline achieves a remarkable speed improvement of two orders of magnitude while maintaining accuracy, making it a highly promising candidate for deployment in scalable architectures, including cloud infrastructures.

2:30 PM DS03.04.04

Non-Centrosymmetric Materials Discovery for Nonlinear Optic and Ferroelectric Applications Using Phonon Database Louis Alaerts¹, Jingyang He², Yu Wang^{2,2}, Victor Trinquet³, Victor Sanni¹, Romain Claes³, Rowan Katzbaer², Evan Krysko², Raymond Schaak^{2,2,2}, Gian-Marco Rignanese³, Geoffroy Hautier¹, Zhiqiang Mao^{2,2} and Venkatraman Gopalan^{2,2}; ¹Dartmouth College, United States; ²The Pennsylvania State University, United States; ³UCLouvain, Belgium

Materials belonging to non-centrosymmetric point groups, i.e. lacking an inversion center, can exhibit a series of important physical properties such as ferroelectricity (FE) or nonlinear optical (NLO) response. This leads to potential applications in low-power electronic devices, transducers or beyond von-Neumann computers for FE and in lithography and spectroscopy for NLO materials. Discovering new classes of non-centrosymmetric materials is therefore of great interest. Over the last couple of decades, density functional theory (DFT) has become a method of choice for the high-throughput search of new materials thanks to the considerable increase in computational power. Notable early successes of DFT for materials discovery include cathode for electrochemical storage, electrocatalysts or thermoelectrics. Nowadays, properties that used to be computationally-intensive are routinely calculated and in particular, phonons. Starting from a phonon database, materials with polar imaginary phonon modes are identified as being dynamically unstable. Following the eigenmodes associated with these phonon instabilities, we can assess the energy stability of all the distortions (limited to 2x2x2 supercell) to find out whether the true structural ground-state is polar or not. This method was already applied to the discovery of new ferroelectric materials. Here, I will present some results about the discovery of new classes of non-centrosymmetric material with a focus on a new family with general chemical formula MBa₃(B₃O₆)₃ (M=Sc, In, Y, Lu, Eu). Previously reported as belonging to the centrosymmetric space group P6₃/m, our calculations show that the structural ground-state is actually P3 or P6₃. The compound EuBa₃(B₃O₆)₃ (EBBO) was subsequently synthesized and characterized using XRD and SHG, demonstrating that indeed, it forms into the non-centrosymmetric space group P3. This work shows that new class of NLO and possibly FE materials can be identified through the use of phonon databases.

2:45 PM DS03.04.05

Scientific Understanding of Materials using Multi-Explanation Graph Attention Network Jonas Teufel, Luca Torresi, Patrick Reiser and Pascal Friederich; Karlsruhe Institute of Technology, Germany

Explainable artificial intelligence (XAI) methods are expected to improve trust during human-AI interactions, provide tools for model analysis and extend human understanding of complex scientific problems [1]. Explanation-supervised training allows to improve explanation quality by training self-explaining XAI models on ground truth or human-generated explanations. However, existing explanation methods have limited expressiveness and interoperability due to the fact that only single explanations in form of node and edge importance are generated. To that end we propose the novel multi-explanation graph attention network (MEGAN) [2]. Our fully differentiable, attention-based model features multiple explanation channels, which can be chosen independently of the task specifications. We first validate our model on a synthetic graph regression dataset. We show that for the special single explanation case, our model significantly outperforms existing post-hoc and explanation-supervised baseline methods. Furthermore, we demonstrate significant advantages when using two explanations, both in quantitative explanation measures as well as in human interpretability. Finally, we demonstrate our model's capabilities on multiple real-world datasets [3,4]. We find that our model produces sparse high-fidelity explanations consistent with human intuition about those tasks and at the same time matches state-of-the-art graph neural networks in predictive performance, indicating that explanations and accuracy are not necessarily a trade-off.

A interactive version of the trained model is available on <https://megan.aimat.science>

[1] Teufel, J., Torresi, L., Reiser, P. and Friederich, P., 2022. MEGAN: Multi-Explanation Graph Attention Network. arXiv preprint arXiv:2211.13236.

[2] Krenn, M., Pollice, R., Guo, S.Y., Aldeghi, M., Cervera-Lierta, A., Friederich, P., dos Passos Gomes, G., Häse, F., Jinich, A., Nigam, A. and Yao, Z., 2022. On scientific understanding with artificial intelligence. Nature Reviews Physics, 4(12), pp.761-769.

[3] Teufel, J., Torresi, L. and Friederich, P., 2023. Quantifying the Intrinsic Usefulness of Attributional Explanations for Graph Neural Networks with Artificial Simulatability Studies. arXiv preprint arXiv:2305.15961.

[4] Sturm, H., Teufel, J., Isfeld, K.A., Friederich, P. and Davis, R.L., 2023. Mitigating Molecular Aggregation in Drug Discovery with Predictive Insights from Explainable AI. arXiv preprint arXiv:2306.02206.

3:00 PM BREAK

3:30 PM *DS03.04.06

Revisiting the "I" in FAIR: Opportunities and Challenges Claudia Draxl; Humboldt-Universität zu Berlin, Germany

Advanced machine learning (ML) and, more generally, artificial intelligence (AI) algorithms have entered many fields of research, also successfully predicting new materials with improved

properties. However, one drawback remains that almost all of these investigations are based on data sets that have been created or adapted for the specific purpose. Therefore, ML results are mainly interpolations rather than out-of-the-box predictions. To change this situation, data from different sources must be brought together. Leveraging the knowledge created by the entire community promises major breakthroughs in AI for materials research. This raises the issues of veracity and variety, two of the 4V challenges of big data. Both have a strong impact on the FAIRness of materials science results, especially the "I" - interoperability. One challenge here is to introduce metrics to assess the conditions under which data can be shared. Of course, this also depends on the specific research question. Again, AI can help speed up the process. In this talk, I will first focus on how to compare data, how to "define" data quality, and how to select data suitable for a given purpose. I will illustrate of how seemingly the "same" data can behave differently when used in a given context. I will discuss challenges related to data from the computational materials side as well as from experimental characterization techniques. For the theoretical side, I will also present ML approaches that are able to extrapolate results from computations with computational settings used in daily practice to highly converged results. The availability of such tools is a big step towards the interoperability of computational data.

4:00 PM DS03.04.07

High-Throughput Computational Search for New Solar Absorbers Taking into Account Defect ToleranceZhenkun Yuan¹, Diana Dahliah^{2,3}, Muhammad R. Hasan^{4,5}, Gideon Kassa¹, Andrew Pike¹, Romain Claes², Cierra Chandler⁶, Sita Dugu⁷, Shaham Quadir⁷, Yihuang Xiong¹, Victoria Kyveryga^{4,5}, Philip Yox^{4,5}, Gian-Marco Rignanese², Sage Bauers⁷, Andriy Zakutayev⁷, Ismaila Dabo⁶, David P. Fenning⁸, Jifeng Liu¹, Kirill Kovnir^{4,5} and Geoffroy Hautier¹; ¹Dartmouth College, United States; ²UCLouvain, Belgium; ³An-Najah National University, Palestine, State of; ⁴Iowa State University, United States; ⁵Ames Laboratory, United States; ⁶The Pennsylvania State University, United States; ⁷National Renewable Energy Laboratory, United States; ⁸University of California, San Diego, United States

With the rapid rising of halide perovskites for photovoltaic applications, defect tolerance has emerged as a critical factor in assessing the efficiency potential of photovoltaic materials. Indeed, one of the most detrimental processes in solar cells is the recombination of photogenerated carriers mediated by deep defect levels. The question remains how to discover defect-tolerant materials? Here, we present a high-throughput computational workflow to search for new solar absorbers taking into account defect tolerance as a screening parameter. We apply this high-throughput workflow to a very large data set of materials in the Materials Project across various chemistries. We identify a few interesting candidates and especially a new family of ternary phosphides with extremely promising properties. We show that these phosphides show very attractive defect tolerance highlighted by extensive defect computations including nonradiative recombination. We will discuss the origin of these favorable defects and report on promising experimental results on the synthesis and characterization of this new family of solar absorbers.

4:15 PM DS03.04.08

A Universal Language for Experimental Protocol Reporting and Community Driven Platform for Enforcement of Field StandardsRobert W. Epps¹, Robert R. White¹ and Joseph J. Berry^{1,2,2}; ¹National Renewable Energy Laboratory, United States; ²University of Colorado Boulder, United States

Many scientific disciplines are undergoing a crisis of reproducibility, and chemistry and materials science are no exception. Despite widespread adoption of the FAIR (Findable, Accessible, Interoperable, Reusable) guidelines in 2016, there is no indication of the issue lessening, and countless hours and resources continue to be wasted on failed protocol replication. Research communication is simply not being carried out in a way that facilitates complete knowledge transfer. With the rapid growth of new and innovative automated experimental platforms, the scientific community is under the threat of even more diverse and incompatible data reporting formats that conflict with FAIR principles and are neither machine-to-machine nor machine-to-human readable. With no clear system for the communication of research procedures between and among machines and researchers, there is a critical need for a robust and flexible universal protocol standard.

In this work, we present the Universal Workflow Language (UWL). UWL is a directed graph-based data entry language that enables the reporting of any arbitrary procedure in a machine-readable format. The system replicates the sequence of physical actions taken in a protocol and translates them into a data rich workflow architecture. Counter to the more traditional tabular data entry format, UWL enables flexibility to match the diverse and unique methods in which protocols are carried out in the real world. Instead of attempting to compress a full complex protocol into a series of tabulated parameters, UWL retains the initial complexity of a process.

Complementary to UWL, we have developed a user interface for management and recording of protocols in the UWL format with an emphasis on minimal user inputs and maximum data density. The entry management tool allows users to create and edit UWL entries with a drag and drop block-based interface. The software allows users to import, visualize, and modify shared workflows in a more accessible format. It also includes automated error checking and validation, and it enables experimentalists to create a framework for data entry through automated/robotic experiment conduction. Additionally, the tool transcribes the workflows into both plain text and interactive tabulated formats. The plain text system reads the UWL protocol and transcribes it into a natural language protocol with corresponding material and tool details and specifications. Through the language feature, users may validate their modifications to workflows in real-time and display protocols in a variety of spoken languages.

Finally, the user interface is linked to a field reporting standards system, driven by the research community. The standard system enables researchers to create and implement clear guidelines on protocol reporting standards so that procedures meet minimum detail requirements and adhere to FAIR principles. Standard creators can specify a library of workflow segments and designate error messages for missing or incomplete parameter reporting for their field of research. Every submitted standard undergoes a forum-based peer-reviewed certification process, where it is given a rating to designate comprehensiveness and field approval. This system allows researchers and manuscript reviewers to quickly evaluate whether a protocol is reported with sufficient detail without setting arbitrary constraints on the type of protocols that can be reported.

UWL and the accompanying software offers comprehensive, standardized, and machine-readable data entry for both human and robotic researchers, enabling greater detail and precision in communal database generation efforts. Application of these tools would likely reduce the impact of reproducibility challenges in human led research, improve universal communication of protocols, and facilitate more effective autonomous materials research.

4:30 PM DS03.04.09

Chemistry-Informed Machine Learning for Predictive Design of Fluorescent DNA-Stabilized Silver NanoclustersPeter M. Mastracco¹, Anna Gonzalez Rosell¹, Josh Evans¹, Crystal Murillo¹, Carlos Melchor¹, Stacy Copp¹ and Petko Bogdanov²; ¹University of California, Irvine, United States; ²University at Albany, State University of New York, United States

DNA-stabilized silver nanoclusters (Ag_N-DNAs) are promising emissive nanomaterials for applications in biosensing, bioimaging, and nanophonics. These nanoclusters of just 10-30 Ag atoms are stabilized by DNA oligomers whose sequence selects the size, shape, and photophysical properties of the nanocluster¹. DNA ligand sequence provides a unique way to select Ag_N-DNA emission wavelengths from 400 nm to 1,200 nm and achieve favorable properties such as high quantum yields and controlled chiralities. However, it is a major challenge to predictively design DNA ligand sequence for Ag_N-DNAs because there is a large sequence space of possible DNA oligomers and limited understanding of how DNA stabilizes Ag_N. Moreover, the nascency of first-principles models for Ag_N-DNAs currently prohibits their use in Ag_N-DNA design.

Here, we present a novel approach for machine learning-guided discovery of Ag_N-DNAs. A large data set of ~3,000 10-base DNA sequences and the emission spectra of the Ag_N-DNAs they stabilize was generated by high-throughput experiments. A machine learning classifier ensemble was then trained to classify DNA sequences by emission spectral ranges defined based on their known magic number properties. The model was designed to perform well for the scarce, imbalanced experimental training data set. Model performance was enabled by chemistry-inspired feature representation, informed by the first crystal structures of Ag_N-DNAs², to accurately capture how DNA sequence selects for Ag_N-DNA structure and emission spectrum. Moreover, feature analysis enabled model interpretability, providing insights into the sequence-to-color relationships of Ag_N-DNAs learned by the model. Sequences were designed by the model to select for green, far red, and near-infrared Ag_N-DNA emission were successfully designed, increasing prevalence of the target color range by 536%, 390%, and 1230%, respectively³. Our current work is focused on expanding the predictive power of these models for NIR-emissive Ag_N-DNAs for specific applications in deep tissue bioimaging. We are employing active learning methods to efficiently train models for prediction of DNA sequences that select NIR emission, which are more scarce in the training data, using a best vs second best approach. We are also expanding our models to design Ag_N-DNAs that are stable in biologically relevant solutions and have suitable photostabilities. This work demonstrates the power of machine learning for nanomaterials discovery and applications design, particularly for systems that cannot currently be modeled by traditional computational methods.

1. González-Rosell, A., Cerretani, C., Mastracco, P., Vosch, T., & Copp, S. M. *Nanoscale Adv.* **3**(5), 1230-1260, (2021).

2. Cerretani, C., Kanazawa H., Vosch, T., Kondo J., *Angew. Chem. Int. Ed.* **58**, 17153–17157 (2019)

3. Mastracco, P., González-Rosell, Evans J., Bogdanov, P., Copp, S., *ACS Nano.* **16** (10), 16322–16331 (2022).

4:45 PM DS03.04.10

KAMEL-LOBE—A Tool for Data Standardization of Radial Distribution FunctionsS. Arman Ghaffarizadeh and Gerald J. Wang; Carnegie Mellon University, United States

Radial distribution functions (RDFs) are widely used in materials simulation. Most approaches to computing RDFs require assembling a histogram over inter-particle separation distances, which in turn depends upon an arbitrary choice of discretization for bins. In this talk, we show that this arbitrary choice can lead to spurious phenomena in several commonplace computational materials science techniques that make use of RDFs. We demonstrate a data-standardization strategy ("KAMEL-LOBE"), which eliminates these issues. This approach is based on systematic and mass-conserving mollification of RDFs using a Gaussian kernel. We discuss several advantages of this technique, including in scenarios where original simulation data are unavailable and the only available data are the RDFs themselves. We present results from several molecular-simulation analyses, including detection of phase boundaries and prediction of transport properties, which benefit significantly from the use of KAMEL-LOBE.

8:30 AM *DS03.05.01

Self Supervised Learning and Language Models for Material Property Prediction Amir Barati Farimani; Carnegie Mellon University, United States

Machine learning (ML) models have been widely successful in the prediction of material properties. However, large labeled datasets required for training accurate ML models are elusive and computationally expensive to generate. Recent advances in Self-Supervised Learning (SSL) frameworks capable of training ML models on unlabeled data mitigate this problem and demonstrate superior performance in computer vision and natural language processing. Drawing inspiration from the developments in SSL, we introduce multiple recent models that incorporate language models, SSL, and multimodal training to enhance the performance of material property prediction tasks. For example, we will show that by sharing the pre-trained weights when fine-tuning the GNN for downstream tasks, we can significantly improve the performance of GNN on 14 challenging material property prediction benchmarks.

9:00 AM DS03.05.02

Data-Driven, Physics-Informed Descriptors of Cation Ordering in Multicomponent Perovskite Oxides Jiayu Peng, James K. Damewood and Rafael Gómez-Bombarelli; Massachusetts Institute of Technology, United States

The chemical flexibility and versatility of multicomponent perovskite oxides have enabled their various key properties, including ion conductivity for batteries and surface reactivity for heterogeneous catalysis and electrocatalysis. Notably, the ordering and distribution of different cations in multicomponent perovskite oxides have a profound influence on their optical absorption, magnetic behaviors, ion mobility, catalytic activity, and electromechanical properties for diverse applications.

Unfortunately, the design and optimization of multicomponent perovskite oxides have been severely hampered by the lack of physical rules that universally rationalize and accurately predict their cation ordering. Essentially, experimentalists have only established empirical principles correlating the cation ordering in such oxides with the atomic parameters of their constituent ions, which often fail at accurately classifying perovskite oxides into cation-ordered and disordered structures.

High-throughput first-principles calculations could provide new, accurate design principles of cation ordering, but this exploration is constrained by the lack of a systematic benchmark between ab initio calculations and experimentally quantified ordering across a broad oxide space. This lack of co-validation between simulations and experiments can further impede the data-driven discovery of multicomponent perovskite oxides by high-throughput virtual screening, machine learning, and experimental validation.

To address these knowledge gaps, we established new data-driven, physically interpretable descriptors that can accurately classify ~90% multicomponent perovskite oxides as cation-ordered or disordered for an experimental dataset of 190 multicomponent perovskites (<https://arxiv.org/abs/2305.01806>). Notably, these descriptors can be obtained from the low-cost density functional theory (DFT) calculations of a few simple prototype structures and rationalized as physics-informed material parameters, such as thermodynamic probability and configurational entropy. Such new cation-ordering design principles outperform their conventional counterparts, accelerating high-throughput virtual screening by balancing the breadth and cost in the DFT sampling of multicomponent oxides with different cation configurations. Overall, this work offers a rigorous benchmark between theory and experiments and demonstrates an effective paradigm for understanding and predicting chemical ordering in multicomponent materials across a vast chemical space.

9:15 AM DS03.05.03

Interpretable Machine Learning-Aided Discovery of Multicomponent Catalysts for Propane Dehydrogenation Jisu Park¹, Jungmok Oh¹, Jin-soo Kim², Jungho Shin², Namgi Jeon¹, Hyunju Chang² and Yongju Yun¹; ¹Pohang University of Science and Technology, Korea (the Republic of); ²Korea Research Institute of Chemical Technology, Korea (the Republic of)

Propylene serves as a crucial primary feedstock in the production of a wide range of chemical derivatives, including polypropylene, propylene oxide, and acrylonitrile. With the increasing demand for propylene, there is a growing interest in propane dehydrogenation (PDH), a selective reaction that produces propylene. In this study, we trained sparse independence screening and sparsifying operator (SISSO) regression models to discover new catalysts exhibiting high performance for the PDH reaction. A database was established by compiling the performance of alumina-supported catalysts in PDH, obtained from our own experimental investigations. The SISSO model was trained using input variables that included the type, loading, and elemental properties of up to four active components, as well as reaction conditions, to predict propylene yield. The performance of the trained SISSO models was evaluated in order to select the optimal model, by comparing the predictive accuracy and simplicity of the resulting formulas. The formula derived from the optimal model was employed to predict the propylene yields of a total of 4,080 candidate catalysts, each consisting of three active components. Based on the predicted PDH performance, the catalysts were classified into categories of high-, moderate-, and low-performance. To experimentally validate these predictions, the actual performance of carefully chosen representative catalysts from each category was measured and compared with the predicted propylene yield. The superior performance of the catalysts categorized in the high-performance group, compared to those in the other groups, demonstrated the reliability of the developed SISSO model. Most importantly, the model identified highly efficient PDH catalysts that outperformed the catalysts tested during the construction of the database. The successful discovery of new and high-performing catalysts demonstrates the benefits of utilizing interpretable machine learning models in the development of multicomponent catalysts for heterogeneous catalysis.

9:30 AM *DS03.05.04

Scaling Up Materials Discovery using Deep Learning Ekin Dogus Cubuk; Google, United States

Materials science data and computational resources are growing rapidly. While machine learning offers a promising set of tools for learning models for large volumes of data (IID), these tools are not inherently good at generalizing to new (OOD) data. For this reason, the impact of deep learning on the computational discovery of stable inorganic materials has been limited. There are two observations from deep learning that encourage optimism: 1) scaling up neural networks with more data and compute can monotonically improve their IID generalization and 2) while OOD performance is almost always worse than IID performance, better IID performance is correlated with better OOD performance.

We explored these two directions to investigate if stable material discovery can be made more efficient via deep learning. I will introduce our pipelines for scaling up DFT calculations and graph neural networks, which allow us to discover a large number of inorganic crystals that are stable. Due to the diversity of candidate generation algorithms that has been employed, we discovered thousands of novel crystal prototypes. By screening these crystals for electronic and energy applications, we find that our dataset improves the number of promising candidates for certain applications by more than an order of magnitude. Finally, I will present the scaling behavior of our networks for robustness and zero-shot predictions on tasks they were not trained on.

10:00 AM BREAK

10:30 AM *DS03.05.05

Design and Understanding of Photovoltaic and Battery Materials Maria K. Chan; Argonne National Laboratory, United States

We will discuss the use of high throughput computation combined with AI/ML to understand and design battery and photovoltaic materials. For example, we will discuss the understanding of materials nanoscale structure and local environments in NMC battery materials and CdTe solar cell materials through ML-guided microscopy/spectroscopy.

11:00 AM DS03.05.06

Computational Approach for Structure Generation of Anisotropic Particles (CASGAP) for Data Driven Methods to Establish Structure-Property Relationships Nitant Gupta and Arthi Jayaraman; University of Delaware, United States

The presence of anisotropic building blocks in synthetic or biological soft materials can have a direct influence on their physical properties. Characterization of structural anisotropy is critical in understanding their impact on structure-property relationships and for designing materials with target properties. Computational generation of three-dimensional real space structures with desired structural features will aid in the analysis of experimental characterization results like small angle scattering (SAS) profiles and will also serve to model initial configurations for

physics-based simulation techniques that relate structure to properties (e.g., structural color [2], mechanical properties). Moreover, generation of structures with anisotropic particles/domains presents unique challenges as compared to their spherical counterpart and in this talk, we will highlight these challenges and as a solution present the Computational Approach for Structure Generation of Anisotropic Particles (CASGAP) method [1]. This method generates structures with anisotropic particles/domains that have a target distribution of shapes, sizes, and orientational order. We will demonstrate the use of structures generated by CASGAP in preparing large datasets that connect a structure to their scattering profile and to their calculated property such as color. Such datasets can be used to train machine learning models linking design of materials, the 3D structure, and properties, enabling forward and inverse design.

[1] Nitant Gupta, Arthi Jayaraman, "Computational Approach for Structure Generation of Anisotropic Particles (CASGAP) with Targeted Distributions of Particle Design and Orientational Order" *submitted for peer review in May 2023*

11:15 AM DS03.05.07

Closed-Loop Multi-Property Materials Discovery, Progress and Opportunities Christopher Stiles^{1,2}, Elizabeth Pogue¹, Alexander New¹, Nam Q. Le¹, Brandon Wilfong², Gregory Bassen², Izze Hendrick², Eddie Gienger¹, Christine Piatko¹, Janna Domenico¹, Kyle McElroy¹, Michael Pekala¹, Victor Leon¹, Christopher Ratto¹, Andrew Lennon¹ and Tyrel M. McQueen²; ¹Johns Hopkins University Applied Physics Laboratory, United States; ²Johns Hopkins University, United States

Machine learning (ML) techniques present tremendous opportunities to accelerate materials design and discovery, but significant developments are required to build on approaches from other domains. For example, ML models for materials must generally contend with sparser and more inhomogeneous data, these challenges compound in practical tasks that require simultaneous optimization of multiple properties. We present results from a "closed-loop" approach that integrates ML model predictions with experimental synthesis and characterization to provide new data and update the models. We first demonstrated success in the discovery of superconducting compounds by utilizing information from several public databases with in-house synthesis and characterization of crystal structure and critical temperature to train our ML models. Building on that framework, we expanded the task to include prediction of mechanical properties, as characterized experimentally using high-throughput nanoindentation. Finally, we explore the promise of ML techniques applied toward practical materials discovery; targeting multiple properties simultaneously, and outlining some of the near term opportunities.

11:30 AM *DS03.05.08

Machine Learning for Electron Microscopy—Large Scale Imaging Studies for Nanomaterial Synthesis Katherine Sytwu¹, Min Gee Cho², Luis Rangel Da Costa^{1,2} and Mary Scott^{1,2}; ¹University of California, Berkeley, United States; ²Lawrence Berkeley National Laboratory, United States

Electron microscopy (EM) is the characterization method of choice to observe the atomic-scale and microstructural local features within materials that play a critical role in material performance. Current TEM capabilities include a wide variety of imaging modalities to probe a material's local structure and composition. With resolution that can be deeply sub-Angstrom, a single image from a high-resolution electron microscope can measure atomic positions, defects, and strain. Coupled with advances in detector speed, automated imaging, and robotic sample preparation, EM imaging is becoming increasingly high throughput. Directly incorporating these EM methods for structural validation into high throughput materials prediction, design and synthesis routines would profoundly speed up the materials discovery process. However, image analysis and interpretation remains a bottleneck.

Machine learning offers an attractive solution to this problem. Recent advances in machine learning tools for computer vision, specifically convolutional neural nets (CNNs), make them promising options for high throughput analysis of EM data. However, CNNs are often designed for application to natural images, and optimizing performance and reducing bias when they are applied to scientific imaging data requires careful consideration. For example, data curation, CNN architecture, and performance metric choice can all play a role in the accuracy and usefulness of CNN predictions on EM data. Customizing CNNs for scientific data can therefore be challenging, especially when dataset sizes are small.

Here, we present a systematic study of application of CNNs to EM data. We consider how architecture influences image classification and segmentation, and illustrate the role that data curation can play in the tradeoff between flexibility and accuracy of CNNs. We then show application of these methods to a large-scale synthesis study of Cobalt oxide nanoparticles. By varying experimental parameters during synthesis, we produce cubic-shaped metal oxide nanoparticles with varying sizes, degrees of corner truncation, and face convexity. We illustrate successful strategies for application of CNNs to the hundreds of thousands of nanoparticles imaged in this study, and discuss error metrics and interpretation of the CNN results. The resulting statistical distributions of the nanoparticle enable us to understand the role of synthetic parameters on nanoparticle structure and shape, which ultimately will influence the catalytic behavior of these particles. These results provide intuition as to how neural network workflow design choices affect TEM image analysis, and provide guidance for researchers using CNNs for analysis of scientific images. Ultimately, this work is an example of large-scale EM analysis of hundreds of thousands or nanoparticles synthesized under a variety of conditions enabled by machine learning, and represents an important step towards incorporating high throughput EM analysis into automated and autonomous nanomaterial synthesis workflows.

SESSION DS03.06: Machine Learning and Experiment II

Session Chairs: Victor Fung and Prashun Gorai

Wednesday Afternoon, November 29, 2023

Sheraton, Second Floor, Liberty B/C

1:30 PM *DS03.06.01

Informatics-Driven Design and Optimization of Materials for Industrial Applications Ghanshyam Pilania; GE Research, United States

After providing a bird's-eye view of probabilistic design and materials informatics capabilities at GE Global Research, this talk will focus on specific examples where machine learning is synergistically combined with simulations, experimental synthesis, characterization, testing and domain knowledge to expedite materials screening and development for certain applications of industrial relevance. I will conclude with a brief discussion of challenges and opportunities that lie ahead in this exciting field.

2:00 PM DS03.06.02

Voxelized Atomic Structure Framework for Atomistic Modeling of Multifunctional Materials Matthew C. Barry¹, Michael Chandross², Surya R. Kalidindi¹ and Satish Kumar¹; ¹Georgia Institute of Technology, United States; ²Sandia National Laboratories, United States

The behavior of material systems is governed by complex physical phenomena taking place over a hierarchy of length scales, making it computationally infeasible to model the full material response with physics-driven simulation methods alone. Machine learning (ML) approaches offer new opportunities to efficiently learn the multiscale, multiphysics process-structure-property relationships necessary to design, discover, develop, and understand the physics of complex material systems. However, the development of a single integrated, comprehensive ML framework that is capable of both bridging multiple length scales and accurately extrapolating over arbitrarily large material design spaces remains a significant challenge. The recently developed Voxelized Atomic Structure (VAsT) framework establishes a protocol for developing structure-property relationships with atomic systems that can also serve as the foundation of a fully integrated hierarchical multiscale materials modeling framework. In this talk, we demonstrate that the VAsT framework can be utilized to efficiently and accurately model complex material properties over a large material design space. We develop a VAsT structure-property relationship to predict thermo-mechanical properties of a 7-component high entropy alloy as a function of chemical composition and show that high accuracy can be achieved over the complete chemical composition space with a limited set of training samples. The results of this study are then used to demonstrate the practical usefulness of the VAsT framework for inverse design of materials by showing how it can directly correlate one or more properties of interest with controllable design parameters.

2:15 PM DS03.06.03

Introduction and Operation of Specialized Machine Learning Web Applications for Material Design in a Chemical Corporation Yoshishige Okuno and Shimpei Takemoto; Resonac Corporation, Japan

Utilizing past experimental data is advantageous in material design. Recently, many scientists have applied machine learning methods to predict material properties. However, for successful machine learning, choosing an appropriate method, selecting attributes, and adjusting various hyperparameters are crucial. These settings can cause differences in machine learning results. Although constructing machine learning models has become easier with the advent of valuable libraries or software packages, it remains a challenge for materials scientists unfamiliar with machine learning. While materials scientists are exceptionally skilled at setting up the materials design space considering various constraints, coding for machine learning is difficult. Although data scientists can build appropriate machine learning models with their expertise in statistics, machine learning, and computer science, many need more domain knowledge, especially tacit expertise in materials design. As a result, data scientists' machine learning model predictions may seem unnatural to materials scientists.

To overcome the difficulties arising from the difference in expertise between materials scientists and data scientists, we have developed web applications with a user-friendly Graphical User

Interface for materials scientists. Data scientists specialize in building machine learning models and deploying them on cloud-based web applications. Even if some of the recommendations proposed by machine learning models are not reasonable to materials scientists, they can choose their favorites based on their experience and domain knowledge. This approach also helps reduce communication costs between materials and data scientists.

A large chemical corporation must deal with over a hundred types of chemical products. In most cases, we must prepare a separate machine learning model for each chemical, which requires us to handle and maintain numerous machine learning models deployed on web applications. This situation has motivated us to introduce Machine Learning Operations (MLOps) to manage both the machine learning models and the web applications. MLOps is a set of methods and philosophies for integrating the development and operation of machine learning models. MLOps include tools and operations for continuous training of machine learning models, continuous integration, continuous delivery, managing the lifecycle of machine learning models, and collaborative development between data scientists and web application developers.

We have already deployed over 100 machine learning web applications to business units within our corporation, and many materials scientists have used them. This deployment demonstrates our successful digital transformation in the field of materials.

2:30 PMBREAK

3:30 PM *DS03.06.04

Prospects for Autonomous Materials Discovery Guided by *In Situ* Diffraction Simon J. Billinge; Columbia University, United States

Although theory has been quite successful at using AI and machine learning for predicting stable materials with potentially interesting properties, experimental science is playing catch-up. In this talk I will discuss some of the challenges and emerging opportunities for using AI and machine learning to guide experiments. I will focus on the use of advanced scattering sources coupled with *in situ* experiments that can be used together for materials discovery. I will discuss the challenges of extracting quantitative information from the data in real-time but the opportunities that emerge when this is possible, including the ability to carry out adaptive, no human in the loop, autonomous experiments. I will discuss challenges of data reduction in the presence of uncertainty, real time analysis approaches, and the development of autonomous *in situ* and *operando* experiments at synchrotrons and neutron sources. The talk will introduce the concepts and present preliminary results to illustrate them, with a goal of guiding the audience to think about how they might use these approaches in their own work.

4:00 PM DS03.06.05

Spectroscopy-To-Structure Prediction via Conditional Diffusion Model and its Application to Disordered Materials Yu-Ting Hsu, [Hyuna Kwon](#), Wenyu Sun and Tuan Anh Pham; Lawrence Livermore National Laboratory, United States

We approach the problem of property-to-structure inverse prediction for disordered materials by combining forward prediction and generative diffusion models. Such a combination is naturally implemented as the conditional score function in the theory of diffusion models. As a case study, we apply this conditional generation framework to sample the spatial coordinates of amorphous carbons conditioned on given or desirable spectroscopic signatures. Several important aspects of this framework will be highlighted and discussed: (1) the generation is not limited to the scale of the training sets (e.g., <1000s of atoms) and can be easily scaled up to any arbitrary size (e.g., 100,000 atoms); (2) the generative model (the prior) and the forward model (the likelihood) are completely decoupled and can be trained separately, thereby allowing a plug-and-play flexibility where the generative prior can work with different forward models for inverse prediction with respect to various output properties; (3) the generation outcome can be fine-tuned to better adhere to the generative prior or the specified output property. Finally, besides inverse prediction, we summarize the potential impact of our work in the broader context, such as out-of-distribution sampling for active learning.

This work was performed under the auspices of the U.S. Department of Energy by Lawrence Livermore National Laboratory under Contract DE-AC52-07NA27344. Funding was provided by LLNL Laboratory Directed Research and Development (LDRD) Program Tracking No. 22-ERD-014.

4:15 PM DS03.06.06

Digital Materials Discovery in Organic Electronics Alessandro Troisi; University of Liverpool, United Kingdom

We describe a general high-throughput virtual screening procedure to discover new molecular materials for organic electronics. The procedure is employed for a range of distinct application (i) low energy emitters (ii) dual emitters (iii) singlet fission molecules (iv) non-fullerene acceptors and (v) molecules with inverted single-triplet gap. Experimental verification is presented for some of the examples shown. The approach led to the construction of a software platform for the discovery of new organic electronics materials (DIADeM) where the search and refinement of computed property is linked with the chemical supply chain and predictions can be immediately verified experimentally.

[1] D. Padula, O.H. Omer, T. Nematiam, A. Troisi, *Energ. Environ. Sci.* 12, 2412 (2019)

[2] T. Nematiam, D. Padula, A. Landi, A. Troisi, *Adv. Funct. Mater.* 30, 2001906 (2020)

[3] D. Padula, J.D. Simpson, A. Troisi, *Mater. Horiz.* 6, 343-349, (2019)

[4] T. Nematiam, A. Troisi, *Mater. Horiz.* 7 (11), 2922-2928 (2020)

[5] T. Nematiam, D. Padula, A. Troisi, *Chem. Mater.* 33, 3368-3378 (2021)

[6] T. Nematiam, A. Troisi, *Chem. Mater.* 34, 4050 (2022)

[7] O.H. Omer, D. Padula, T. Nematiam, A. Troisi, *Scientific Data* 9, 54 (2022)

4:30 PM *DS03.06.07

Automated Classification of Big X-Ray Diffraction Data Using Deep Learning Models Jerardo Salgado, Zhaotong Du, Samuel Lerman, Ayoub Shahnazari, Zeliang Zhang, Chenliang Xu and [Niaz Abdollahim](#); University of Rochester, United States

The development of new technologies such as superconductors, fusion energy, and superfast quantum computers heavily relies on a deep understanding of material properties. X-ray diffraction (XRD) is a powerful technique used for material characterization, providing valuable information about the atomic symmetry of materials. However, despite recent advancements in dynamic *in-situ* XRD experiments, fully characterizing these materials remains challenging due to the large amounts of data generated. This data contains crucial insights into material structure, behavior, and transformation pathways that could otherwise be overlooked.

To address this challenge, we have developed deep learning models integrated with physics-based reasoning, enabling automatic classification of the crystal system and space group of 1D XRD data. Our models were trained using a comprehensive dataset consisting of hundreds of thousands of diffraction images. These images were generated using our Python-based pipeline, which incorporates fundamental principles such as Bragg's Law and atomic scattering factors.

By leveraging high-quality training and evaluation data, we achieved accurate classification based on Bragg's Law and improved performance when applied to experimental data. Our models provide instantaneous feedback and can classify data without requiring human intervention, making them highly efficient for extracting valuable material insights from large XRD datasets.

Moreover, the versatility of our models extends beyond XRD data. They can be applied to other spectral data, such as Raman spectroscopy or nuclear magnetic resonance spectroscopy, broadening their applicability to diverse material characterization techniques.

By combining the power of deep learning with physics-based justification, our approach enables efficient and accurate analysis of material properties, paving the way for accelerated advancements in various technological fields that rely on a deep understanding of materials.

SESSION DS03.07: Poster Session
Session Chairs: Prashun Gorai and Qian Yang
Wednesday Afternoon, November 29, 2023
Hynes, Level 1, Hall A

8:00 PM DS03.07.01

Tuning Elinvar Effect in Severely Distorted Single Phase High Entropy Alloys Hang Wang; City University of Hong Kong, China

Elinvar alloys are well known for their elastic moduli being almost a constant over a certain temperature range, which can find many useful engineering applications, such as high precision mechanical equipment (e.g., reeds, reed relays, delay lines and chronometers). Fundamentally, the Elinvar effect in conventional ferromagnetic Fe-Ni and Fe-Co-based alloys originates from the loss of magnetic ordering with increasing temperature, which leads to elastic stiffening and counterbalances thermal softening over a temperature range of ~300 K. However, this

magnetism induced Elinvar effect has its limitation, which cannot function properly in a magnetic environment if there is a residual magnetic field.

In this work, we fabricated a series of severely distorted high-entropy Elinvar alloys through micro-alloying of $(\text{CoNi})_{50-x}(\text{TiZrHf})_{50}\text{Fe}_x$ (in atomic percentage). Through carefully designed experiments, we demonstrate a tunable Elinvar effect that is positively correlated with the overall lattice distortion in the single phase B2 high entropy alloys. Finally, we propose a simple physical model that captures the general trend of our experimental findings.

8:00 PM DS03.07.02

The Interplay of Quantum Capacitance with Van Der Waals Forces, Intercalation, Co-Intercalation and the Number of MoS₂ Layers [Nageh K. Allam](#); American University in Cairo, Egypt

Polymorph MoS₂ attracts great attention for supercapacitor and Li-ion battery applications. Although the capacitance origin is usually attributed to the intercalation process, MoS₂ exhibits a well-defined electrical double layer (EDL) behavior. Nonetheless, the nature of the EDL behavior of MoS₂ is yet to be revealed. Herein, we investigate the quantum capacitance (C_Q) of the three main phases of MoS₂ (the semiconductor 2H and 3R phases and the metallic 1T phase). Interestingly, the number of MoS₂ layers greatly affects the C_Q of the material. In addition, the absence of Van der Waals (VdW) interactions overestimates the bandgap and C_Q , emphasizing the importance of the VdW correction in the C_Q calculations. As MoS₂ usually stores charges *via* the intercalation of cations, the effect of H⁺, Na⁺, Li⁺, and K⁺ intercalation on the C_Q of the three phases of MoS₂ is thoroughly investigated. The intercalation of all studied alkali metal cations leads to the transformation of the 2H and 3R phases into the metallic 1T phase and increases its stability. Importantly, the K⁺ and Na⁺ intercalations show the greatest impact in enhancing the C_Q of the studied phases. However, the charging process of K⁺ and Na⁺ ions is not as reversible as that of Li⁺ as revealed from the estimated binding energies. To this end, herein, we demonstrate the co-intercalation of Li⁺/Na⁺ ions as a strategy to enhance the overall capacitance performance. The Li⁺/Na⁺ co-intercalation shows a C_Q of 3163 F/g with a more thermodynamically stable adsorption process. Finally, the study recommends the use of 2H–MoS₂ only as a positive electrode and 1T–MoS₂ as a negative and/or positive electrode in energy storage devices. Also, K⁺ intercalation is recommended to achieve the highest C_Q and the Li⁺/Na⁺ co-intercalation for the best overall performance.

8:00 PM DS03.07.03

TADF-Based X-Ray Screens with Simultaneously Efficient Singlet and Triplet Energy Transfer for High Spatial Imaging Resolution [Shorooq A. Alomar](#); Kaust, Saudi Arabia

In recent years, X-ray imaging scintillators have garnered significant attention for their potential in real-world applications such as medical radiography, food industry, and security inspection. However, high-performance scintillators have been limited to inorganic ceramic and perovskite materials, which are known to require harsh preparation conditions, high environmental toxicity, low stability, and very high fabrication costs. Alternatively, organic scintillators, particularly thermally-activated delayed fluorescent (TADF) systems, offer efficient utilization (nearly 100%) of both singlet and triplet excitons, making them a strong contender in the scintillation market. Their stability, low toxicity, scalability, and diverse radioluminescence mechanisms also make them an excellent alternative choice to compete, even not replace ceramic and perovskite scintillators.

In this contribution, we successfully introduce, for the first time, a novel approach for X-ray imaging scintillators that utilizes very efficient and ultrafast energy transfer at the interface of TADF chromophores for X-ray imaging scintillators with exceptional spatial resolution. More specifically, our study showcases the successful use of efficient singlet-singlet (S-S) and triplet-triplet (T-T) energy transfer mechanisms between the TADF donor (sensitizer) and the TADF acceptor (scintillator) to achieve high-resolution imaging of up to 20 lp/mm, representing the highest resolution reported thus far for organic scintillators, and is at least two times higher than that achieved by commonly used commercial inorganic scintillators. Our results highlight a new path to improve the resolution and sensitivity of imaging by leveraging the advantages of simultaneous S-S and T-T energy transfer mechanisms that nearly completely use the absorbed X-ray energy. Our experimental findings also demonstrated the enormous potential of this energy transfer strategy in yielding high-performance organic X-ray imaging scintillators, providing a robust and cost-effective alternative for X-ray imaging applications that are free from harsh preparation conditions and significant fabrication costs.

We believe that these innovative TADF-based X-ray screens, with their efficient interfacial energy transfer, will not only serve as a benchmark for the fabrication of efficient organic scintillators with a simple molecular engineering strategy, but also garner significant interest from the scientific community and expand the current understanding of X-ray imaging scintillators.

8:00 PM DS03.07.04

Terahertz Time Domain Transmission Characterization of Magnetic Nanoparticles for Frequency Selective Surface Application [Kousik Pradhan](#); Indian Institute of Technology Bombay, India

Terahertz Time Domain Transmission Characterization of Magnetic Nanoparticles for Frequency Selective Surface Application

[Kousik Pradhan](#)¹, Shobha Shukla², Shri Ganesh Prabhu³, Sumit Saxena²

¹Centre for Research in Nanotechnology and Science, Indian Institute of Technology Bombay, Mumbai, MH, India – 400076

²Nanostructures Engineering and Modeling Laboratory, Department of Metallurgical Engineering and Materials Science, Indian Institute of Technology Bombay, Mumbai, MH, India – 400076

³Department of Condensed Matter Physics & Materials Science, Tata Institute of Fundamental Research, Mumbai, MH, India – 400005

Corresponding author email: *kousik.pradhan@iitb.ac.in

Abstract

Terahertz time-domain transmission spectroscopy (THz-TDS), is an effective method for characterizing materials and monitoring processes. Metals, semiconductors, 2D materials, and superconductors have all been tested with this technique, which does not require physical touch to obtain accurate results. Terahertz (THz) spectroscopy has developed as a method for investigating dielectric and transient photoconductive characteristics of materials over the past few decades. Since it can measure electrical resistance without touching the sample and has a temporal precision of a few picoseconds. Due to the low energy of THz radiation and the narrow pulse width, THz-TDS technology is non-destructive when used for extracting visual data from materials (picosecond range). This paper reveals optical parameters extraction methods by using THz transmission spectroscopy technology. In summation, materials with a low absorption of terahertz radiation can benefit from the adaptability of transmission methods, while materials with a high absorption capacity can take advantage of the advantages of reflection methods. To measure the magnetic material's optical properties like refractive index and absorption coefficient, we employ a transmission-type terahertz time domain spectroscopic instrument. The observations and analysis are performed in both the time domain and frequency domain, and we examine the transmission of terahertz radiation through magnetic nanoparticles at frequencies from 0.1 to 3 terahertz (THz). In the past few years, magnetic materials based on frequency selective surfaces (FSS) have become indispensable in the design of gigahertz (GHz) and terahertz (THz) millimeter-wave filters, polarizers, absorbers, EMI shielding, antenna reflectors, and radar applications. Here we also propose frequency selective surface structure theoretically by using CST-MW studio software.

Keywords: Magnetic material, THz, FSS, CST-MW

References :

- Ji, Y., Fan, F., Xu, S., Yu, J. & Chang, S. Manipulation enhancement of terahertz liquid crystal phase shifter magnetically induced by ferromagnetic nanoparticles. *Nanoscale* **11**, 4933–4941 (2019).
- Fan, F., Zhong, C., Zhang, Z., Li, S. & Chang, S. Terahertz chiral sensing and magneto-optical enhancement for ferromagnetic nanofluids in the chiral metasurface. *Nanoscale Adv* **3**, 4790–4798 (2021).
- Hlaing, M. Z. *et al.* 3D Microstructured Frequency Selective Surface Based on Carbonized Polyimide Films for Terahertz Applications. *Adv Opt Mater* **10**, (2022).

<quillbot-extension-portal></quillbot-extension-portal>

8:00 PM DS03.07.05

Optimizing 2.8 Micron Emission in Er:YLF Q-Switched Lasers [Ryan Bulharowski](#)¹, Carlos Gutierrez¹, Wesley Kinney¹ and Makhin Thitsa^{1,2}; ¹Mercer University, United States; ²Laboratory of Information and Decision Systems, MIT, United States

We aim to develop advanced control strategies to be utilized in modulating and stabilizing the laser output characteristics in optical and photonic devices which face increasingly high demands on precision and level of performance. Especially, when these devices are used in medical applications or when high-energy ultra short pulses are involved, there is virtually no room for error. Open loop control is inept to handle issues arising from unexpected disturbances or when these devices need to perform well in harsh environment, which is the case for many defense applications. Built-in feedback control capabilities in these devices will regulate the desired output characteristics rendering the device reliable and robust. Pulsed 3-micron diode-pumped lasers find vast applications in a variety of fields ranging from medical instrumentation, environmental applications, and material processing to spectroscopy. For 2.6-3-micron emissions, Er:YLF has generated a lot of research interest recently as a laser gain medium due to its adequate radiation life time at key energy levels to support Q-switching. We studied the laser dynamics of Q-switching at 2.8 micron in Er:YLF laser with cascade lasing at 1.6 and 1.7 micron by control theoretic approach. We investigate the effect of pump power on population density at key energy levels as well as the average output power and various parameters of the laser dynamics such as heat generated in the material. We also propose pumping schemes which produce desired output pulse characteristics. Both mathematical analysis of the feedback control strategy and the numerical simulation results will be presented.

8:00 PM DS03.07.06

Sulfur-Containing High Refractive Index, Low Birefringence Thermoplastic Polymers SoohyePark and JeewooLim; Kyung Hee University, Korea (the Republic of)

High refractive index polymers (HRIPs) play a crucial role in various optoelectronic devices, such as display substrates, microlenses for image sensors, and optical adhesives. The conventional method for producing HRIPs involves incorporating aromatic units into polymer structures. However, this approach can result in excessively high glass transition temperatures and, more importantly, increased chromatic aberration and birefringence. To address these issues, we have introduced a sulfur-containing functional groups with high molar refraction into fluorene-based cardo monomer structure. The placement of high molar refraction, sulfur-containing aromatic functional groups at the 9-position of fluorene allowed for the preparation of a new class of functional monomers which was used as monomers for thermoplastic polyesters, poly(aryl ether)s, and poly(aryl thioether)s with refractive indexes exceeding 1.65. These polymers exhibit birefringence below 0.003, achieving a desirable combination of high refractive index and low birefringence. Furthermore, by varying the nature of the linking groups between monomers, the glass transition temperatures of the high refractive index thermoplastic polymers could be varied over a wide range of 90°C to 250°C.

8:00 PM DS03.07.07

Molecular Design of Hydroquinone-Based Compounds for High Energy Proton Batteries BiaoLiu; University of Puerto Rico at Río Piedras, Puerto Rico

Proton batteries offer higher energy storage capacity, enhanced safety, and a better environmental profile than traditional lithium-ion batteries. However, developing electrode materials remains a critical challenge for their widespread adoption as a viable energy storage solution. In this study, we used density functional theory computations to investigate the impact of hydroquinone-based compounds on the electrochemical performance of organic electrode materials in proton batteries. Our findings indicate that hydroquinone-based compounds hold significant potential as high-energy organic electrode materials for proton batteries, and we established a quantitative relationship between their structural properties and electrochemical performance. This research provides a valuable guideline for designing more efficient and sustainable proton batteries in the future, and contributes to the ongoing effort to develop better energy storage solutions to meet the growing demand for renewable energy sources.

8:00 PM DS03.07.08

Hybridization of Magnetic Fe₃O₄ with Mn-MOFs for High Performance Supercapacitor SaumayaKirti, ShobhaShukla and SumitSaxena; Indian Institute of Technology Bombay, India

Encapsulating guest compounds in metal-organic frameworks (MOFs) architectures is one of the most promising paths to achieve properties beyond those of the pristine MOFs and/or guest species. Contrary to the conventional host/guest composites encapsulating guest species inside MOF cavities, core-shell architectures exhibit a better accessibility to the pores ensuring an optimal diffusion of the substrate while presenting a unique structure that prevents the aggregation and the runoff of the active guests and ensures a tight interaction between core and shell, leading to synergistic effects. Herein, the integration of Fe₃O₄ with manganese-based MOF i.e., Fe₃O₄@Mn-MOF-NH₂ with varying shell thickness and hierarchical pore structure is synthesized. As a proof of concept, the obtained Fe₃O₄@Mn-MOF-NH₂ composite is used as an active material for supercapacitor applications which showed an enhancement of ~ 80% in specific capacitance with respect to pristine compounds.

8:00 PM DS03.07.09

A Paramagnetic NMR Cluster Expansion Toolkit for Spectral Assignment EuanBassey¹, AntonVan der Ven² and RaphaëleClement^{1,2}; ¹Materials Science Laboratory, United States; ²University of California, Santa Barbara, United States

Solid-state nuclear magnetic resonance (NMR) spectroscopy is an invaluable characterisation method for investigating local structural phenomena. Recently, NMR has been increasingly applied to paramagnetic systems, most notably in the field of Li- and Na-ion battery cathode materials, where unpaired electrons on redox-active transition metal (*TM*) ions result in severely broadened lines and large-magnitude shifts.¹⁻⁵ Invariably, these materials contain many different paramagnetic *TM* species, each contributing differently to the observed shift. These shifts can be computed using high-cost hybrid DFT methods and qualitatively rationalised using the Anderson-Goodenough-Kanamori rules.^{6,7} Applying these methods to all local environments, however, becomes impractical and computationally demanding when the *TM* sublattice comprises more than one species—e.g., Ni²⁺ and Mn⁴⁺, as in Li[Ni_xMn_yCo_{1-x-y}]O₂ cathodes used in electric vehicles. Here, we perform a cluster expansion of the NMR chemical shift of Li⁺ and O²⁻ ions in the family of layered cathode materials Li_{1+x}[Ni_{1/2-3x/2}Mn_{1/2-x/2}]O₂ in terms of both local composition (i.e., coordination environments of Li⁺ and O²⁻) and magnetic configurations. We compare our results against experimental ⁷Li NMR spectra and extend the theory to perform Monte Carlo simulations at variable field strengths and temperatures. This new methodology will have benefits not only in battery fields, but for a large range of materials science problems.

References:

- (1) Seymour, I. D.; Middlemiss, D. S.; Halat, D. M.; Trease, N. M.; Pell, A. J.; Grey, C. P. Characterizing Oxygen Local Environments in Paramagnetic Battery Materials via 17O NMR and DFT Calculations. *J. Am. Chem. Soc.* **2016**, *138* (30), 9405–9408. <https://doi.org/10.1021/jacs.6b05747>.
- (2) Clément, R. J.; Pell, A. J.; Middlemiss, D. S.; Strobridge, F. C.; Miller, J. K.; Whittingham, M. S.; Emsley, L.; Grey, C. P.; Pintacuda, G. Spin-Transfer Pathways in Paramagnetic Lithium Transition-Metal Phosphates from Combined Broadband Isotropic Solid-State MAS NMR Spectroscopy and DFT Calculations. *J. Am. Chem. Soc.* **2012**, *134* (41), 17178–17185. <https://doi.org/10.1021/ja306876u>.
- (3) Bassey, E. N.; Reeves, P. J.; Seymour, I. D.; Grey, C. P. 17O NMR Spectroscopy in Lithium-Ion Battery Cathode Materials: Challenges and Interpretation. *J. Am. Chem. Soc.* **2022**, *144* (41), 18714–18729. <https://doi.org/10.1021/jacs.2c02927>.
- (4) Bassey, E.; Reeves, P.; Jones, M.; Lee, J.; Seymour, I.; Cibin, G.; Grey, C. Structural Origins of Voltage Hysteresis in the Na-Ion Cathode P2–Na_{0.67}[Mg_{0.28}Mn_{0.72}]O₂: A Combined Spectroscopic and Density Functional Theory Study. *Chem. Mater.* **2021**, *33* (13), 4890–4906. <https://doi.org/10.1021/acs.chemmater.1c00248>.
- (5) Märker, K.; Reeves, P. J.; Xu, C.; Griffith, K. J.; Grey, C. P. Evolution of Structure and Lithium Dynamics in LiNi_{0.8}Mn_{0.1}Co_{0.1}O₂ (NMC811) Cathodes during Electrochemical Cycling. *Chem. Mater.* **2019**, *31* (7), 2545–2554. <https://doi.org/10.1021/acs.chemmater.9b00140>.
- (6) Kim, J.; Middlemiss, D. S.; Chernova, N. A.; Zhu, B. Y. X.; Masquelier, C.; Grey, C. P. Linking Local Environments and Hyperfine Shifts: A Combined Experimental and Theoretical 31 P and 7 Li Solid-State NMR Study of Paramagnetic Fe(III) Phosphates. *J. Am. Chem. Soc.* **2010**, *132* (47), 16825–16840. <https://doi.org/10.1021/ja102678r>.
- (7) Middlemiss, D. S.; Ilott, A. J.; Clément, R. J.; Strobridge, F. C.; Grey, C. P. Density Functional Theory-Based Bond Pathway Decompositions of Hyperfine Shifts: Equipping Solid-State NMR to Characterize Atomic Environments in Paramagnetic Materials. *Chem. Mater.* **2013**, *25* (9), 1723–1734. <https://doi.org/10.1021/cm400201t>.

8:00 PM DS03.07.10

Self-Assembly of Atomically Aligned Nanoparticle Superlattices from Pt–Fe₃O₄Heterodimer Nanoparticles ShengsongYang¹, R.A. LaCour², Yi-YuCai¹, YugangZhang³, CherieR. Kagan¹, SharonGlotzer² and Christopher B.Murray¹; ¹University of Pennsylvania, United States; ²University of Michigan–Ann Arbor, United States; ³Brookhaven National Laboratory, United States

Multicomponent nanoparticle superlattices (SLs) promise the integration of nanoparticles (NPs) with remarkable electronic, magnetic, and optical properties into a single structure. Here, we demonstrate that heterodimers consisting of two conjoined NPs can self-assemble into novel multicomponent SLs with a high degree of alignment between the atomic lattices of individual NPs, which has been theorized to lead to a wide variety of remarkable properties. Specifically, by using simulations and experiments, we show that heterodimers composed of larger Fe₃O₄ domains decorated with a Pt domain at one vertex can self-assemble into an SL with long-range atomic alignment between the Fe₃O₄ domains of different NPs across the SL. The SLs show an unanticipated decreased coercivity relative to nonassembled NPs. In situ scattering of the self-assembly reveals a two-stage mechanism of self-assembly: translational ordering between NPs develops before atomic alignment. Our experiments and simulation indicate that atomic alignment requires selective epitaxial growth of the smaller domain during heterodimer synthesis and specific size ratios of the heterodimer domains as opposed to specific chemical composition. This composition independence makes the self-assembly principles elucidated here applicable to the future preparation of multicomponent materials with fine structural control.

8:00 PM DS03.07.11

Composition Search in Multi-Component Alloys through Diffusion Generative Models Amirhossein Naghdi Dorabati^{1,2}, Grzegorz Kaszuba², Stefanos Papanikolaou¹ and Piotr Sankowski²; ¹Nomaten CoE, Poland; ²Ideas NCBR, Poland

Exploring the vast composition space of multi-component alloys present a challenging task for both ab initio (first principles) and experimental methods due to the multitude of possible compositions and the time-consuming procedures involved. These limitations ultimately impede the discovery of new stable materials with exceptional properties. Here, we utilize the Crystal Diffusion Variational Autoencoder (CDVAE) to characterize the stable compositions of NiFeCr alloys, including well-established compositions such as NiFe and CrNi₂ from binaries, and then optimize the bulk elastic modulus across the entire compositional space. To this end, a computationally efficient framework is proposed which employs Molecular Dynamics (MD) simulations, equipped with high-quality interatomic potentials for inverse design of multi-component alloys in general. We also propose modifications to CDVAE that enhance its robustness when dealing with data characterized by large supercells and low variety of elements as well different material phases. The resulting workflow is valuable for the inverse design of other systems of interest involving various element types and varieties.

8:00 PM DS03.07.12

Advancing 2D Materials Research: A Unified Platform for Data Management, Visualization and Machine Learning Jin Hoon Yang¹, Yea-Lee Lee¹, Jonghwan Kim^{2,3}, Young Jun Chang⁴ and Hyunju Chang¹; ¹Korea Research Institute of Chemical Technology, Korea (the Republic of); ²Pohang University of Science and Technology, Korea (the Republic of); ³Institute for Basic Science, Korea (the Republic of); ⁴University of Seoul, Korea (the Republic of)

We present a comprehensive and user-friendly data platform tailored for 2D materials research, 2DMat.chemDX.org. This platform integrates efficient data management, specialized visualization, and machine learning toolkits, significantly enhancing research productivity. At this point, the platform supports primary research data obtained from Reflection High Energy Electron Diffraction (RHEED), Photoluminescence (PL), and Raman measurements, providing a robust foundation for uploading, managing, and sharing research data through a web-based platform. Data templates and parsing systems specialized for handling these data aid researchers in managing large datasets, reducing manual efforts, and enhancing data consistency. The platform features powerful visualization and analysis tools for RHEED, PL, and Raman spectra, facilitating easy data comprehension and enabling valuable insights with just a few clicks. Additionally, the platform incorporates machine learning toolkits for investigating 2D film growth mechanisms and super-resolution techniques for analyzing PL/Raman mapping data, promising a significant increase in efficiency. Our platform's modular design allows for seamless expansion and adaptation, ensuring it remains a valuable resource for the evolving field of 2D materials.

8:00 PM DS03.07.13

Using Text Descriptions to Predict Physical and Electronic Properties of Crystalline Solids Andre Niyongabo Rubungo, Craig Arnold, Barry P. Rand and Adji BousoDieng; Princeton University, United States

Developing methods capable of crystal property prediction is an important task that plays a crucial role in material design for advanced applications. Surprisingly, predicting crystal properties from its text description is understudied, despite the rich information and expressiveness that textual data have. In this work, we leverage the general-purpose learning capabilities of large language models (LLMs) to predict the crystal discrete and continuous properties from text descriptions. We propose an efficiently fine-tuned LLM on crystal text descriptions to predict physical and electronic properties such as band gap, direct vs indirect band gaps, and volume. The proposed approach outperforms three previously reported structure-based baselines, offering improvements of approximately 4%, 3%, and 66% with respect to predictions of band gap, direct vs indirect band gaps, and volume, respectively.

8:00 PM DS03.07.15

Application-Driven Design of Materials: Advancements in Composite Materials and Coatings Abul Faza M. Arif, Syed Sohail Akhtar, Khaled Al-Athel and Abba Abubakar; King Fahd University of Petroleum and Minerals, Saudi Arabia

In recent years, materials science and engineering have evolved significantly, emphasizing application-driven design—a strategy that customizes materials to meet precise performance criteria, resulting in notable innovations in composite materials and coatings. Composite materials, exemplified by carbon-fiber-reinforced composites in aerospace, have revolutionized aircraft design, offering outstanding strength-to-weight ratios and enhanced fuel efficiency. The automotive industry has similarly shifted towards high-strength, lightweight composites, as seen in Tesla's use of carbon fiber composites, improving structural integrity and reducing fuel consumption and emissions. Coatings have gained pivotal importance, adapting materials to specific environmental demands, with anti-corrosion coatings extending the service life of steel structures and smart coatings with embedded sensors monitoring structural health in real-time. Aerospace employs thermal barrier coatings to protect components from extreme temperatures, extending operational lifespan and enabling high-performance aviation and space exploration. These achievements highlight the transformative potential of application-driven design in materials development, offering tailored solutions to complex challenges across industries. As technology advances, application-driven design will play an increasingly vital role in creating innovative materials that meet modern demands. Our presentation will highlight extensive research conducted at KFUPM in the field of computational materials design, spanning various applications. Over the years, our dedicated team has developed advanced computational methods for precise heterogeneous materials design, incorporating homogenization techniques that consider crucial material design parameters, including phase volume fractions, material properties, inclusion characteristics, dispersion, and interface conditions. This comprehensive approach enables highly accurate predictions of thermo-mechanical responses in complex materials. Furthermore, we've introduced an innovative multi-scale modeling methodology capable of simulating the thermo-mechanical behavior of heterogeneous materials across various length scales. These computational tools have practical applications in diverse fields, from composite materials to membranes and coatings. Additionally, we've introduced the concept of functionally graded (FG) materials to create SiAlON-based ceramic composites optimized for cutting tool applications, incorporating hybrid reinforcements like TiCN, Co, and hBN. To validate our predictions and optimize these composites, we've diligently applied effective medium theories and mean-field homogenization schemes, considering variables such as volume fractions, interfacial thermal resistance, reinforcement particle sizes, and porosity. This rigorous approach extends to the comprehensive characterization and analysis of fabricated ceramic samples, aligning computational predictions with real-world measurements. Additionally, we've explored the cold spray deposition process for tailored composite coatings, utilizing a physics-based hybrid computational approach that models the deposition of Ni-Ti/Al₂O₃ composite coatings for wear applications. This approach efficiently simulates critical aspects, including particle impact, deformation, and temperature variations, by combining point cloud and finite element techniques, providing valuable insights for optimizing wear-resistant coatings. Our presentation will comprehensively showcase the groundbreaking progress achieved in the field of application-driven materials design. The group is currently working on the application of machine learning methods and the development of digital twins for the design and development of coatings and composites. We look forward to sharing these insights and contributing to the exciting possibilities in this ever-evolving domain.

8:00 PM DS03.07.16

Computational Investigation of Ordered Framework Materials for Photocatalysis Beatriz Mourino^{1,2}, Kevin Jablonka¹, Sauradeep Majumdar¹, Andres Ortega-Guerrero¹, Jeffrey B. Neaton² and Berend Smit¹; ¹EPFL, Switzerland; ²Lawrence Berkeley National Laboratory, United States

Metal (MOFs) and covalent (COFs) organic frameworks comprise a class of countless porous crystalline materials with building block construction[1]. In particular, the interest in investigating this class of materials for photocatalytic applications lies in the tunability of their optoelectronic properties with different building blocks, which ideally could be assessed computationally in an efficient way to redirect experimental efforts. However, the computational exploration of MOFs and COFs for photocatalysis can be challenging due to their large unit cells that can have hundreds of atoms. Therefore, investigating the optoelectronic properties of those materials with first principles requires cost-effective alternatives. To tackle this challenge, we have adopted strategies at different levels of theory to first explore large datasets, and then focus on investigating a few materials in depth. The first approach leverages cost-effective alternatives to compute DFT-based photocatalytic descriptors at a low level of theory to assess the fundamental steps of photocatalysis, that is, light absorption, thermodynamic feasibility of the photoredox reactions, charge carrier mobility and charge separation[2]. Such an approach allowed us to shortlist promising materials, and gain insights into structure-property relationship such as the use of β -ketoenamine linkages in COFs for right band edge alignment to the hydrogen evolution reaction and enhanced charge-carrier mobility[2]. Going further, ongoing work aims to investigate the electronic band gap and related properties of our best candidates with a higher level of theory. For that purpose, we make use of non-empirical screened range separated hybrids (SRSH) in density functional theory as it enables electronic band gap calculations in close agreement with more expensive state of the art GW methods[3]. The so far promising results of using wannier localization-based optimally tuned SRSH for MOFs suggest a potential cost-effective pathway to more accurately evaluate complex physical phenomena encompassing the electronic band gap.

References

- [1] O. M. Yaghi, M. O'Keeffe, N. W. Ockwig, H. K. Chae, M. Eddaoudi, and J. Kim, "Reticular synthesis and the design of new materials," *Nature*, vol. 423, pp. 705–714, June 2003.
- [2] B. Mourino, K. M. Jablonka, A. Ortega-Guerrero, and B. Smit, "In search of covalent organic framework photocatalysts: A dft-based screening approach," *Advanced Functional Materials*, p. 2301594, 2023.
- [3] D. Wing, G. Ohad, J. B. Haber, M. R. Filip, S. E. Gant, J. B. Neaton, and L. Kronik, "Band gaps of crystalline solids from wannier-localization-based optimal tuning of a screened range-

SESSION DS03.08: Machine Learning and Experiment III
Session Chairs: James Chapman and Victor Fung
Thursday Morning, November 30, 2023
Sheraton, Second Floor, Liberty B/C

8:30 AM *DS03.08.01

Addressing Challenges of Multi-Property Optimization and Synthesizability in Inverse Design Evan Antoniuk, Bhavya Kailkhura, Nathan Keilbart, Stephen Weitzner and Anna M. Hiszpanski; Lawrence Livermore National Laboratory, United States

Inverse or generative models that can suggest novel molecules with optimized properties have promise to decrease materials discovery timelines for pharmaceuticals, energetics, organic semiconductors, and polymers. However, the utility and promised time-savings of these models have yet to be fully realized due to challenges associated with co-optimizing multiple material properties, reducing model uncertainty when extrapolating beyond a known and trained chemical space to identify new molecules with extreme desired properties, and accounting for molecular synthesizability in a robust manner for suggested molecules. In our work, we have evaluated two state-of-the-art generative models – JTVAE and JANUS – for multi-property optimization of small molecules and have developed strategies for addressing the extrapolation and synthesizability challenges. We specifically focus on identifying novel and synthesizable molecules that have high density and high solid heat of formation – two important qualities for energetic molecules. Between the two models considered, we found that JANUS generally yielded more molecules with both higher density and heat of formation. To address the first challenge of accurately extrapolating to a chemical space beyond the known chemical space used for training, we employ two strategies. First, we created a high-throughput density functional theory pipeline capable of computing the density and heat of formation of ~1,000 molecules/day. We utilize the results from this pipeline to iteratively retrain our model, thereby increasing the data we have available in the chemical space we are extrapolating to and the accuracy of our predictions in this space. Second, we found that incorporating uncertainty quantification (where the uncertainty is the variance from an ensemble of models) in our property predictions also aided in filtering for suggested molecules that are more likely to have the predicted targeted properties. To address the second challenge of synthesizability, we found that the inclusion of a synthesizability score in our objective function is necessary for steering the generative model away from a completely unrealistic chemical space. However, the synthesizability score by itself does not directly correlate to true synthesizability. Thus, we utilize SciFinder’s retrosynthesis planning tool to specifically screen for likely synthesis routes of the top candidate molecules. Using these tools in aggregate, we are identifying novel molecules that are most likely to have the desired properties we aim for and also a means of synthesizing them. Now, synthesizing our best candidates and experimentally validating their properties is the final necessary step towards realizing generative models’ full utility.

This work was performed under the auspices of the U.S. Department of Energy by Lawrence Livermore National Laboratory under Contract DE-AC52-07NA27344.

9:00 AM DS03.08.02

AI-Enabled Active Exploration of Small Molecules for n-Charge Generation Layer in Tandem Organic Light-Emitting Diodes Jisu Kim¹, Jaesun Kim¹, Jinmu You¹ and Seungwu Han^{1,2}; ¹Seoul National University, Korea (the Republic of); ²Korea Institute for Advanced Study, Korea (the Republic of)

The rapid evolution of organic light-emitting diodes (OLEDs) has profoundly transformed display technology, facilitating the development of flexible and thin solid-state lighting devices. Tandem OLEDs, composed of multiple stacked electroluminescent units connected by a charge generation unit, have emerged as an innovative solution for achieving high current efficiency and intense luminance. However, they confront the challenge of increased operational voltages due to the additional layers within the device structure. Hence, the development of an intermediate charge generation unit with efficient charge generation and transportation properties is crucial to mitigate the voltage drop.

In this study, we propose a two-step process involving unsupervised and supervised learning to investigate small molecule organic semiconductors suitable for the n-charge generation layer (n-CGL), a key component of the charge generation unit. Specifically, we focus on Li-doped phenanthroline derivatives, which have been extensively studied as n-CGL. Initially, we utilize unsupervised learning, demonstrated by k-means clustering, to generate a set of molecules that can represent the vast chemical space of phenanthroline derivatives. This condensed set of molecules serves as a manageable starting point for further exploration of the broader n-CGL chemical space.

Subsequently, we employ a relational graph neural network as a means of supervised learning, in conjunction with the Monte Carlo dropout method to quantify prediction uncertainty. We calculate multiple molecular properties including reorganization energy and electron affinity by density functional theory (DFT) calculation to formulate a scoring function for evaluating the suitability of molecular properties as n-CGL. We then design a novel active exploration algorithm by integrating query strategy and data augmentation. This algorithm not only enhances the prediction accuracy but also generates new promising molecules that were not initially sampled by unsupervised learning.

Our approach led to the discovery of molecules that surpass known phenanthroline derivatives, such as bathophenanthroline (BPhen), according to our scoring system. Furthermore, we gain insights into the common characteristics of promising molecules, including the substituted carbon position in the phenanthroline. This comprehensive approach presents a systematic and efficient strategy for exploring the vast and challenging chemical space of n-CGL.

9:15 AM DS03.08.03

Data-Driven Electrospinning Process Surrogate Modeling with Guided Experiments Chandrachur Bhattacharya, Jungkuk Lee, Joshua Christopher, Ashley Simmons, Bethany Lusch, Yuepeng Zhang and Debolina Dasgupta; Argonne National Laboratory, United States

Electrospinning is a manufacturing process used to fabricate fibers of various chemical composition with fiber diameters in the nanometer range. These fibers find a variety of applications including fuel cells, batteries, and medical membranes such as masks. The manufacturing process itself is governed by highly non-linear physics. The working material is fed as a solution into the electrospinning system through a needle. An applied electric field attracts the material from the needle tip to a depositor drum. This draws out the fibers and if the conditions are amenable, leads the formation of uniform fibers. Conversely, certain combinations of input parameters may cause unwanted phenomenon such as bead formation in the fibers, webbing, or even wet deposition and dripping from the needle tip with no fiber formation at all. The electric field, governed by the voltage difference and distance across which it is applied, i.e., between the needle and the drum, plays an important role in controlling the outcome. Additionally, the concentration of the solution and the flowrate of the solution into the system are the two other principal governing parameters. Thus, it is important to know which operating conditions can produce good fibers. A step further is being able to select operating conditions required to produce fibers of a desired morphology. In this research, the goal is to develop a surrogate model of an electrospinning process using polyethylene oxide (PEO) material. To learn good models using limited experiments, advanced machine learning based surrogate modeling methods are leveraged from the very onset of this study. A few initial experiments are used to develop a preliminary surrogate which invokes active learning to select conditions for subsequent experimentation. This allows developing good models using limited data, saving on experimental costs by making informed decisions. During the experiments, near-needle videos are taken to capture the flow features of the jet formed between the needle and drum via image processing. The experiments that successfully produce fibers then have Scanning Electron Microscope (SEM) imaging done on the samples produced. Fiber morphology information is extracted by another image processing algorithm along with an outcome label as specified by the user requirement. A custom-designed multi-modal machine learning framework combines findings from the various observations into a singular model that can now predict the experimental outcome given the operating conditions. The experimental data was collected in phases, with the machine learning model informing the choices of subsequent experiments by choosing informative samples. This research also demonstrates how the machine learning models are flexible and can be adapted in various phases of such studies to accommodate for additional experimental considerations learnt along the way to make the surrogate model more robust. In this research, the surrogate model framework is built using GPU-accelerated open-source libraries.

9:30 AM *DS03.08.04

Data-Driven Chemical Understanding with Bonding Analysis Janine George^{1,2}; ¹Federal Institute for Materials Research and Testing (BAM), Germany; ²Friedrich-Schiller-Universität Jena, Germany

Bonds and local atomic environments are crucial descriptors of material properties. They have been used to create design rules and heuristics for materials.^[1] More and more frequently, they are used as features in machine learning.^[2,3] Implementations and algorithms (e.g., *ChemEnv* and *LobsterEnv*) for identifying these local atomic environments based on geometrical characteristics and quantum-chemical bonding analysis are nowadays available.^[4,5] Fully automatic workflows and analysis tools have been developed to use quantum-chemical bonding analysis on a large scale and for machine-learning approaches.^[5,6] The latter relates to a general trend toward automation in density functional-based materials science.^[7] The lecture will demonstrate how our tools, that assess local atomic environments, helped to test and develop heuristics and design rules and an intuitive understanding of materials.^[5,8-11]

References

[1] J. George, G. Hautier, *Trends Chem.* **2021**, 3, 86–95.

- [2] A. M. Ganose, A. Jain, *MRS Commun.* **2019**, *9*, 874–881.
- [3] J. George, G. Hautier, A. P. Bartók, G. Csányi, V. L. Deringer, *J. Chem. Phys.* **2020**, *153*, 044104.
- [4] D. Waroquiers, J. George, M. Horton, S. Schenk, K. A. Persson, G.-M. Rignanese, X. Gonze, G. Hautier, *Acta Cryst B* **2020**, *76*, 683–695.
- [5] J. George, G. Petretto, A. Naik, M. Esters, A. J. Jackson, R. Nelson, R. Dronskowski, G.-M. Rignanese, G. Hautier, *ChemPlusChem* **2022**, e202200123, DOI: 10.1002/cplu.202200123.
- [6] “LobsterPy.” can be found under <https://github.com/JaGeo/LobsterPy>, **2022**.
- [7] J. George, *Trends Chem.* **2021**, *3*, 697–699.
- [8] W. Chen, J. George, J. B. Varley, G.-M. Rignanese, G. Hautier, *Npj Comput. Mater.* **2019**, *5*, 72.
- [9] D. Dahliah, G. Brunin, J. George, V.-A. Ha, G.-M. Rignanese, G. Hautier, *Energy Environ. Sci.* **2021**, *14*, 5057–5073.
- [10] A. A. Naik, C. Ertural, N. Dhamrait, P. Benner, J. George, **2023**, DOI 10.48550/arxiv.2304.02726.
- [11] P. Benner, J. George, *In Preparation* **2023**.

10:00 AMBREAK

10:30 AM *DS03.08.05

Machine Learning Enabled Inorganic Synthesis Planning and Materials Design Elsa Olivetti, Elton Pan and Christopher Karpovich; Massachusetts Institute of Technology, United States

Data-driven synthesis planning with machine learning is a key step in the design of novel inorganic compounds with desirable properties. Inorganic materials synthesis is often guided by heuristics and chemists’ prior knowledge and experience, built upon experimental trial-and-error that can be both time and resource consuming. Recent developments in natural language processing (NLP) have enabled large-scale text mining of scientific literature, providing open source databases of synthesis information of realized compounds, material precursors, and reaction conditions (temperatures, times). An obstacle to the realization of novel inorganic materials with desirable properties is efficient optimization over both the materials property and synthesis spaces. We will present two novel reinforcement learning (RL) approaches to inverse inorganic materials design which can efficiently identify promising compounds with specified properties and synthesizability constraints. These approaches learn chemical guidelines such as thermodynamic stability, charge neutrality, and electronegativity neutrality while maintaining high chemical diversity and uniqueness. We demonstrate a multi-objective reinforcement learning approach which can generate novel compounds with both desirable materials properties (formation energy, bulk modulus, shear modulus) and synthesis objectives (low sintering temperatures). Using this approach, the model can predict promising compounds of interest, while suggesting an optimized chemical design space for inorganic materials discovery.

11:00 AM DS03.08.06

ZeoSyn: A Comprehensive Zeolite Synthesis Dataset Enabling Machine-Learning Rationalization of Hydrothermal Parameters Elton Pan, Soonhyoung Kwon, Zachary Jensen, Yuriy Roman and Elsa Olivetti; Massachusetts Institute of Technology, United States

Zeolites, crystalline aluminosilicate materials with well-defined porous structures, have emerged as versatile materials with applications in various fields, including catalysis, gas separation, and ion exchange. Hydrothermal synthesis is the most widely used method for zeolite production, offering control over composition, crystallinity, and pore size. However, the intricate interplay of synthesis parameters and their impact on zeolite properties necessitates a comprehensive understanding to optimize the synthesis process. Hitherto, publicly available zeolite synthesis databases only contain a subset of key parameters. Furthermore, they are small in scale, with the largest consisting of only a few thousand unique synthesis routes. In this paper, we present ZeoSyn, a comprehensive dataset of 23,925 unique zeolite hydrothermal synthesis routes, encompassing over 200 zeolite topologies and 900 organic structure-directing agents (OSDAs). Each unique synthesis route consists of a comprehensive set of key synthesis variables: 1) gel compositions (molar ratios between heteroatoms, mineralizing agents, and water) 2) reaction conditions (crystallization/aging temperature and time), 3) OSDA, and 4) resultant zeolite product. Extracted from over 50 years of zeolite scientific literature using a semi-automatic approach leveraging a natural language processing pipeline, the dataset enables a holistic analysis of zeolite synthesis parameters and their influence on the final zeolite product. Analysis of the dataset reveals clear, physical relationships between synthesis parameters and the resultant frameworks. To showcase the utility of this dataset, we train a supervised classification machine learning model on ZeoSyn to predict the zeolite framework product given a synthesis route. The model exhibits strong performance on the challenging 220-way classification task with an overall accuracy of >70% and macro-averaged F1 of >0.6. In addition, we show that Shapley Additive Explanations (SHAP) can serve as a powerful tool to reveal the most important synthesis parameters driving the formation of over 200 known zeolite frameworks. Furthermore, we introduce an aggregation approach to extend SHAP analysis for explaining the formation of all known composite building units reported. Lastly, we show potential applications of such analysis on the rational design of parameters for phase-selective and intergrowth synthesis. Analysis at this unprecedented scale sheds light on key synthesis parameters driving zeolite crystallization and has the potential to guide zeolite synthesis.

11:15 AM DS03.08.07

Extracting Information from TEM—Battling Noise with Machine Learning Matthew Helmi Leth Larsen, William B. Lomholdt, Cuauhtémoc N. Valencia, Thomas W. Hansen and Jakob Schiotz; Technical University of Denmark, Denmark

High-Resolution Transmission Electron Microscopy (HRTEM) will always be a compromise between signal-to-noise ratio (S/N) and beam damage, as the energetic electrons passing through the sample inevitably heats and damages the sample on their way to the detector. In conventional HRTEM, the entire sample is illuminated simultaneously by the electron beam, and while this lowers the electron dose rate (and often also the total dose), it comes at the price of the image being phase contrast, and thus not always easy to interpret.

Machine learning has been shown to be a powerful way to interpret HRTEM images [1-3]. We here investigate the minimal required frame dose (in electrons per area) for object detection and segmentation with neural networks. We show that the Multi-Scale Dense (MSD) network architecture proposed by Pelt et al. [4] is particularly promising in the low S/N regime, where it outperforms the industry standard U-Net architecture both for simulated and experimental images. The MSD-net displays mild visibility of an Au nanoparticle at 20-30 e⁻/Å² and converges at 200 e⁻/Å² where a full segmentation of the nanoparticle is achieved. Between 30 and 200 e⁻/Å² object detection applications are still possible.

We also highlight the importance of modelling the modulation transfer function (MTF) of the detector when training with simulated images for applications on images acquired with scintillator-based detectors such as the Gatan OneView camera.

For further information, see also Leth Larsen et al. [5].

REFERENCES:

- [1] J. Madsen, *et al.* A Deep Learning Approach to Identify Local Structures in Atomic-Resolution Transmission Electron Microscopy Images, *Adv. Theory Simul.* **1**, 1 (2018). doi:10.1002/adts.201800037.
- [2] M. H. Leth Larsen, *et al.* Reconstructing the exit wave of 2D materials in high-resolution transmission electron microscopy using machine learning, *Ultramicroscopy* **243**, 113641 (2022). doi:10.1016/j.ultramic.2022.113641.
- [3] J. M. Ede. Deep Learning in Electron Microscopy, *Mach. Learn.: Sci. Technol.* **2**, 011004 (2021). doi:10.1088/2632-2153/abd614.
- [4] D. M. Pelt and J. A. Sethian. A mixed-scale dense convolutional neural network for image analysis, *PNAS* **115**, 254 (2017). doi:10.1073/pnas.1715832114.
- [5] M. H. Leth Larsen, *et al.* Quantifying Noise Limitations of Neural Network Segmentations in High-Resolution Transmission Electron Microscopy, arXiv:2302.12629.

11:30 AM *DS03.08.08

The Vendi Score: A Diversity Metric For Science And Machine Learning Adji BousoDieng; Princeton University, United States

Measuring diversity correctly is important for science and machine learning. In this talk, I'll describe the Vendi Score, a diversity metric that connects and extends ideas from ecology and quantum mechanics. The Vendi Score is applicable in any domain where similarity can be defined. I'll showcase the usefulness of the Vendi Score in efficiently exploring molecular conformation spaces and in enabling the discovery of novel MOFs and organic photoredox catalysts.

1:30 PM *DS03.09.01

Entropic Sampling and its use in Automatic Materials Design [Koji Tsuda](#); The University of Tokyo, Japan

In automatic materials design, samples obtained from black-box optimization offer an attractive opportunity for scientists to gain new knowledge. Statistical analyses of the samples are often conducted, e.g., to discover key descriptors. Since most black-box optimization algorithms are biased samplers, post hoc analyses may result in misleading conclusions. To cope with the problem, we propose a new method called self-learning entropic population annealing (SLEPA) that combines entropic sampling and a surrogate machine learning model. Samples of SLEPA come with weights to estimate the joint distribution of the target property and a descriptor of interest correctly. In short peptide design, SLEPA was compared with pure black-box optimization in estimating the residue distributions at multiple thresholds of the target property. While black-box optimization was better at the tail of the target property, SLEPA was better for a wide range of thresholds. Our result shows how to reconcile statistical consistency with efficient optimization in materials discovery. We also present an application of entropic sampling to chemical processes.

2:00 PM DS03.09.02

Bayesian Active Machine Learning for Cluster Expansion Construction [Hantong Chen](#)¹, [Sayan Samantha](#)¹, [Siya Zhu](#)¹, [Jan Schroers](#)², [Stefano Curtarolo](#)³ and [Axel van de Walle](#)¹; ¹Brown University, United States; ²Yale University, United States; ³Duke University, United States

The Cluster expansion (CE) is a powerful method for representing the energetics of alloys from a fit to first principles energies. However, many common fitting methods are computationally demanding and do not provide the guarantee that the system's ground states are preserved. Thus, we have developed an efficient implementation of a Bayesian algorithm for cluster expansion built upon the method proposed by Cockayne and van de Walle (2010), which ensures all the input structural energies are fitted perfectly while reducing computational cost. This method also enjoys favorable convergence properties as it allows user to incorporate physics-based priors on the magnitude of the interactions. We have also made multiple improvements over this approach. First, we propose a procedure based on optimizing the hyper-parameters of the prior to improve the predictive power of the CE. Secondly, we devise an efficient algorithm to calculate the cross-validation (CV) score in linear time. Third, we use an active machine learning scheme that autonomously searches for new ground state structures to incorporate in the CE training set. Finally, all mechanisms described above have been integrated into the Alloy Theoretic Automated Toolkit (ATAT), thus allowing users to seamlessly adopt the new method. As performance tests, we calculate the phase diagram of the Fe-Fe system and study the short range order (SRO) in an equimolar MoNbTaVW system. We find that we typically need about 1/5 of the structures to reach the same precision of the CE constructed via traditional methods.

2:15 PM *DS03.09.03

Overcoming Challenges in Real-World Materials Science Optimization—A "Choose Your Own Adventure" Approach with Ax [Taylor D. Sparks](#)^{1,2}, [Sterling Baird](#)¹, [Jason Hall](#)^{1,3} and [Ramsey Issa](#)¹; ¹University of Utah, United States; ²University of Liverpool, United Kingdom; ³Northrop Grumman Corporation, United States

Real-world materials science optimization tasks are often noisy, heteroskedastic, multi-fidelity, multi-objective, high-dimensional, constrained, and mixed numerical/categorical optimization problems. While each of these have state-of-the-art implementations in computer science, the application of these to materials science tasks have been limited. One of the few optimization platforms that can support all of the use-cases mentioned above without oversimplification and therefore poor efficiency is Meta's Adaptive Experimentation (Ax) platform. While Ax and its backbone, BoTorch, have seen increasing usage in chemistry and materials science, project-specific implementations and adaptations of advanced Bayesian optimization topics are non-trivial, even for veteran materials informatics practitioners. Inspired by the PyTorch installation docs (<https://pytorch.org/get-started/locally/>), we implement a "choose your own adventure" template generator for Ax scripts tailored towards materials science applications. We demonstrate its usage and performance in three case studies: composition-based optimization, physics-based simulations, and a self-driving lab demo. We envision that this tool will dramatically reduce the barrier-to-entry for utilizing advanced Bayesian optimization for real-world materials science tasks.

2:45 PM BREAK

3:15 PM *DS03.09.04

Decreasing the Environmental Impact of Cement with Data-Driven Design [Kristen Severson](#); Microsoft, United States

Concrete is the most widely used building material in the world with an estimated global annual production of 30 billion metric tons. Largely because of this scale, the concrete industry is estimated to produce approximately 8% of all global CO₂ emissions, therefore decreasing the carbon footprint of the concrete industry is an important consideration for the global decarbonization effort. In this talk, I will present a method to design concretes with decreased global warming potential using an optimization framework which relies upon quality attributes estimated from an amortized Gaussian process model. Using industrial data, our approach proposed novel concrete formulations with 60% reductions in climate impact. I will also demonstrate how the model can be used to accelerate experimentation.

3:45 PM DS03.09.05

Computational Prediction of Stacking Mode in Conductive Two-Dimensional Metal-Organic Frameworks—An Exploration of Chemical and Electrical Property Changes [Mingyu Leon](#) and [Jihan Kim](#); KAIST, Korea (the Republic of)

Conductive two-dimensional metal-organic frameworks (2D MOFs) have attracted interest as they induce strong charge delocalization and improve charge carrier mobility and concentration. However, characterizing their stacking mode depends on expensive and time-consuming experimental measurements. Here, we construct a potential energy surface (PES) map database for 36 2D MOFs using density functional theory (DFT) for the experimentally synthesized and non-synthesized 2D MOFs to predict their stacking mode. The DFT PES results successfully predict the experimentally synthesized stacking mode with an accuracy of 92.9% and explain the coexistence mechanism of dual stacking modes in a single compound. Furthermore, we analyze the chemical (i.e. host-guest interaction) and electrical (i.e. electronic structure) property changes affected by stacking mode. The DFT results show that the host-guest interaction can be enhanced by the transition from AA to AB stacking, taking H₂S gas as a case study. The electronic band structure calculation confirms that as AB stacking displacement increases, in-plane charge transport pathway is reduced while the out-of-plane charge transport pathway is maintained or even increased. These results indicate that there is a trade-off between chemical and electrical properties in accordance with the stacking mode.

4:00 PM DS03.09.06

Towards Oxygen Ion Conductor Designs Based on Lattice Dynamics [Daniele Vivona](#)¹, [Kiarash Gordiz](#)¹, [Lambert Hu](#)¹, [Sumathy Raman](#)², [Randall Meyer](#)² and [Yang Shao-Horn](#)¹; ¹Massachusetts Institute of Technology, United States; ²ExxonMobil Research and Engineering, United States

The existing oxygen ion conductors exhibit insufficient conductivity for practical applications in solid oxide electrochemical cells. To design oxygen ion conductors with higher conductivities at lower temperatures, a deeper understanding of the processes governing ionic conductivity is needed. This understanding is crucial to identify new chemistries with superior conductivities. In pursuit of this goal, the Arrhenius law emphasizes the importance of decreasing activation energy and increasing the pre-exponential factor for enhancing oxygen ion conductivity. However, a major obstacle lies in the lack of understanding surrounding the compensation law, where reducing activation energy is typically associated with decreasing the pre-exponential factor. This limitation hampers progress in designing improved oxygen ion conductors. In this presentation, we discuss designs of oxygen ion conductors with low activation energies and high pre-exponential factors. Specifically, we establish a correlation between pre-exponential factors and changes in lattice dynamics that occur during oxygen migration from equilibrium to the transition state. Variations in the order of magnitude of pre-exponential factor values across oxides with the perovskite and fluorite structures are attributed to changes in vibrational properties, such as the vibrational entropy of migration. By utilizing density functional theory simulations, we gain atomic-scale insights into these vibrational property changes and investigate their coupling with the electronic structure and activation energy. Our new findings and proposed descriptors hold great potential for accelerating the discovery of new oxygen ion conductors through machine learning and high-throughput virtual screening (HTVS). By leveraging the growing approaches of computation-aided designs, the next generation of oxygen ion conductors can be developed to catalyze the clean energy transition.

4:15 PM *DS03.09.07

Traversing Scales for the Design of Catalyst Materials for Energy Conversion [Sneha A. Akhade](#); Lawrence Livermore National Laboratory, United States

With growing emphasis on decarbonization and increasing energy demand, materials that can efficiently capture, store, and utilize energy can potentially pave the path for sustainable decentralized energy networks that are powered using renewable electricity while simultaneously abating carbon emissions. Inherent in the future energy system will be greater operational uncertainty, regional and temporal variability, and larger price fluctuations in the renewable electricity available for the energy infrastructure. Material design for the infrastructure elements that can catalytically move, store, and use carbon and hydrogen needs to consider the variability and dynamics of the larger system into which it is integrated. Consequently, the optimal catalyst material may differ greatly depending on its mode of usage and what sector it supports. While existing material design efforts place significant emphasis on improving the activity and selectivity of catalysts for energy conversion, they often fail to address the critical durability of the material under real-time operating conditions. The structure, composition, and electronic properties of the material are all key factors that impact the performance and extent of degradation. Moreover, material evolution often is a multiscale problem; necessitating the need to develop multi-physics modeling frameworks for realistic operational understanding of materials for energy conversion and eventual design of more durable systems. In this talk, I will provide an overview of some of our multi-scale and cross-scale efforts to examine various factors contributing to selection, performance, and process integration of catalyst materials. I will discuss how atomistic, mesoscale, continuum and system level modeling can be leveraged towards realizing the complexities of catalyst material design for energy conversion. To this end, our efforts at LLNL in traversing multiple length and time scales in developing these models for sustainable carbon and hydrogen energy conversion will be showcased. This work was performed under the auspices of the U.S. DOE by Lawrence Livermore National Laboratory under contract DE-AC52-07NA27344.

SESSION DS03.10: Machine Learning and Modeling

Session Chairs: James Chapman and Qian Yang

Friday Morning, December 1, 2023

Hynes, Level 2, Room 206

8:45 AM *DS03.10.01

The Structure Dynamics Dyad in Concentrated Aqueous Electrolytes Aurora E. Clark; University of Utah, United States

Concentrated aqueous electrolytes, so called water-in-salt solutions, are emerging new materials for high-voltage batteries. Although long-studied, concentrated electrolytes exhibit multiple lengthscale organizational behavior in their neutron and X-ray scattering pair distribution functions, the origin of which can be challenging to interpret. At the same time, recent work studying the dynamic behavior of ions and water (using quasi elastic neutron scattering, NMR, and optical Kerr effect spectroscopy) are revealing distinctive multiscale dynamic behavior. The connection between solution structure and dynamics is essential toward the rational design of electrolyte compositions designed to optimize transport and energy density characteristics. This work will describe our combined efforts to understand this “structure dynamics dyad” using atomistic simulations, predictive characterization and applied mathematics.

9:15 AM DS03.10.02

Nature of the Superionic Transition of Lithium Nitride Gabriel Krenzer¹, Johan Klarbring^{1,2}, Kasper Tolborg¹, Chang-Eun Kim³, Hugo Rossignol⁴, Andrew McCluskey⁵, Benjamin J. Morgan⁶ and Aron Walsh^{1,7}; ¹Imperial College London, United Kingdom; ²Linköping University, Sweden; ³Lawrence Livermore National Laboratory, United States; ⁴Trinity College Dublin, The University of Dublin, Ireland; ⁵European Spallation Source ERIC, Denmark; ⁶University of Bath, United Kingdom; ⁷Ewha Womans University, Korea (the Republic of)

Understanding ion transport in the superionic regime and the underlying physics of the superionic phase transition remains a long-standing challenge for computational chemistry and materials science. This presents a barrier to the development and optimisation of superionic solid electrolytes.

There has also been much attention given recently to material descriptors that explore the connection between lattice dynamics and ion diffusion. Moreover, in some materials the superionic transition is accompanied by significant changes in vibrational spectra.

We use *ab initio* lattice dynamics calculations to demonstrate that harmonic and quasi-harmonic descriptions of the phonons in lithium nitride show no change in features across the superionic transition. The anharmonic model, however, exhibits a breakdown for all modes. The implications for developing anharmonic lattice-dynamics-based descriptors to accelerate the discovery of superionic conductors are discussed.

To further explore the superionic phase transition of lithium nitride and accurately simulate diffusion above and below the superionic transition temperature, T_s , we take advantage of the recent developments in the field of Machine Learning Force Fields (MLFF). We train a Gaussian Approximation (GAP)-style MLFF using on-the-fly sampling of reference configurations. We demonstrate that our MLFF trained for lithium nitride ($T_s=678\text{K}$) offers near-*ab initio* accuracy at a significantly reduced computational cost compared to direct *ab initio* molecular dynamics simulations. Crucially, the MLFF allows us to accurately simulate the long-timescale diffusive behaviour of lithium nitride for temperatures as low as 400K, where ion transport is slow. Using our trained MLFF, we characterise lithium nitride above and below the superionic transition temperature by calculating the heat capacity, Li^+ ion self-diffusion coefficient, and Li defect concentrations as functions of temperature. We show that both the Li^+ self-diffusion coefficient and Li vacancy concentration follow distinct Arrhenius relationships in the normal and superionic regimes. The activation energies for self-diffusion and Li vacancy formation decrease by a similar proportion across the superionic phase transition. This result suggests that the superionic transition may be driven by a change in defect formation behaviour, rather than changes in Li transport mechanism. This insight may hold implications for other superionic materials.

We address a question at the heart of materials chemistry for over a century – why do some materials exhibit a superionic phase transition? This is linked to the design of solid-state batteries to address some of society’s biggest problems around energy storage. The application of machine learning methods and the resulting novel understanding of the superionic phase transition in terms of both lattice dynamics descriptors and defect formation behaviour are of interest to experimental and theoretical researchers within materials chemistry, from both academic and industrial backgrounds. This research is deeply relevant to the wide audience of the symposium on emerging challenges and opportunities in materials by design.

9:30 AM DS03.10.03

Directing Assembly Through Variation of the Inter-Particle Attractive Interactions Jessica Niblo, Jacob Swartley, Zhongmin Zhang and Kateri H. DuBay; University of Virginia, United States

The self-assembly of complex structures typically occurs within a narrow window of interaction strength due to large kinetic barriers that emerge as attractive interactions become too strong. At moderate interaction strengths, thermodynamic products form as the system relaxes to thermodynamic equilibrium. However, as interaction strength increases, there is a switch from thermodynamic to kinetic products, which emerge as high energetic barriers develop. By dynamically changing the free energy landscape through modification of the inter-particle interactions, certain kinetic traps may be overcome or the system may assemble into novel non-equilibrium structures. In this work, we model the assembly of rigid, 2D triangular particles into capsid-like hexamers to investigate the relationship between assembly and dynamic changes in the inter-particle potential. Specifically, we examine how oscillations of the attractive interactions in time and spatially variant attractions can allow for differences within the assembly process. Variation of the attractive interactions enables particles to diffuse out of original configurations and readily reorganize. We find that oscillation periods that are equivalent to the timescales needed for particles to diffuse from one another shifts the window of capsid formation. The distance particles diffuse from one another to shift the window of assembly is comparable to the lengthscales of the inter-particle interactions and particle size. Our results provide insights on how dynamic inter-particle interactions can alter self-assembly, and predicts how different systems can respond to attractive interaction variation.

9:45 AM DS03.10.04

Adaptive Kinetic Monte Carlo Simulation on Platinum Oxidation at Electrochemical Conditions using Machine-Learned Potentials Jisu Jung¹, Hyungmin An¹, Deokgi Hong¹ and Seungwu Han^{1,2}; ¹Seoul National University, Korea (the Republic of); ²Korea Institute for Advanced Study, Korea (the Republic of)

Platinum is the most commonly used electrochemical catalyst. However, platinum suffers from oxidation in the operation conditions, which gradually degrades activity and lifetime of catalysts in applications like fuel cells and CO oxidation. Although many experiments have investigated oxidation kinetics of Pt, a comprehensive understanding has not yet been achieved. For instance, it is known that platinum oxidation occurs through a place-exchange mechanism, but the detailed atomic pathway remains elusive. While computational study could supplement the experiment, the spatial and temporal scales of platinum oxidation reactions are beyond the capabilities of computational approaches such as density functional theory (DFT) and classical molecular dynamics (MD) simulations. Kinetic Monte Carlo (kMC) simulations, which use an event table to transition between local minima, can investigate long-term evolution but require an efficient algorithm for identifying saddle points on-the-fly, in the open-ended style.

In this presentation, we will discuss our adaptive kMC simulation for platinum oxidation behavior on a 2 nm × 2 nm Pt(111) surface. This is achieved by combining two computational advancements. Firstly, we employ Behler-Parinello type machine-learned potentials (MLPs) as surrogate models of DFT for increased computational speed. The present MLP achieved energy and force root-mean-square errors of 7 meV/atom and 0.22 eV/Å, respectively, on the DFT validation set consisting of platinum oxide crystal and platinum surface with randomly distributed oxygen atoms at various coverages. Secondly, we found that the state-of-the-art algorithm for identifying saddle points, such as ARTn, is inefficient in the presence of soft modes prevalent on the surface. To address this, we developed the SHERPA (Saddle point Hunting based on Energy surface for Reaction Pathways) package, incorporating two key features: constrained-orthogonal relaxation within ARTn and dynamic-active volume. These improvements resulted in a 50% higher success ratio and halved computational time compared to the conventional

ARTn approach.

To emulate oxygen flux from the electrolytes, we combine KMC simulation with a grand-canonical Monte Carlo (GCMC) simulation, controlling the oxygen chemical potential based on voltage and pH. Our simulation provides detailed pathways for the platinum surface oxidation via a place exchange mechanism, with oxygen atoms penetrating the platinum subsurface and displacing platinum atoms. For comparison, we also perform a hybrid GCMC-MD simulation at elevated temperatures. We believe this study deepens the understanding of platinum oxidation and paves the way to long-term atomistic simulation.

10:00 AMBREAK

10:30 AM DS03.10.05

Computational Studies to Understand the Effect of Polysulfamide Designs on Structure and Properties Jay A. Shah, Zijie Wu and Arthi Jayaraman; University of Delaware, United States

Plastic waste is currently generated at a rate of 400 million tons per year. The amount of plastics accumulating in the environment is growing rapidly since the degradation time for the plastics on the surface is in order of micrometres per year. Due to rising environmental concerns, there is a need for environmentally friendly and sustainable alternatives to these common commodity plastics. One such commonly used commodity plastic is polyurea which is used in many applications such as concrete coating, waterproofing and anti-corrosion on ships and a protective material. The wide range of applications for polyurea is due to the flexibility of changing the backbone chemistries. This leads to the formation of different morphologies, which are driven by the hydrogen bonding between the urea groups. However, polyurea takes a long time to degrade. Thus, there is a quest for alternate polymers that have similar structural features as polyurea but can be degraded easily, making them sustainable and environmentally more friendly. Michaudel and coworkers have recently introduced one such alternate for polyurea called polysulfamide, where the carbonyl group in polyurea is replaced with a sulfamide group in polysulfamide. They have shown that polysulfamides exhibit high thermal stability, tunable glass transition temperature and are degradable in green aqueous conditions. These attractive properties and sulfamide's chemical structure being analogous to urea, make polysulfamides a potential replacement for polyurea. To facilitate such replacement, we need a fundamental understanding of how varying polysulfamide design impacts its structure (chain-level and self-assembled domains) and physical properties, which require synergistic molecular modeling, simulations, and experiments are needed. To complement experiments from Michaudel and coworkers, we have developed a coarse-grained (CG) model for polysulfamide to use in molecular dynamics simulations to investigate how polysulfamide design impacts the hydrogen bonding induced self-assembly of polysulfamides. This computational approach is validated by comparing simulated structures' positional and orientational order for varying polysulfamide designs to that observed in experiments using X-ray diffraction (XRD) and infrared (IR) spectroscopy. Ongoing work is focused on extending this computational approach to a larger set of design parameters, including polydispersity in molar masses. Using the simulated and experimental data, we will train machine learning models to establish a design-structure-property relationship and accelerate the understanding of polysulfamides.

10:45 AM DS03.10.06

Unified Design Flow for Facilitating Fast Li-Kinetics in Layered Oxide Cathodes Juncheol Hwang¹ and Duho Kim^{1,2}; ¹Kyunghee University, Korea (the Republic of); ²Kyung Hee University, Korea (the Republic of)

Non-parallel flow of electric vehicles (EVs) and the rechargeable battery market motivates energy materials researchers to study advanced batteries. Although, it is possible to produce a 90 kWh battery pack with a 300-mile cruise range, unfortunately, their charging rate still lags significantly behind that of internal combustion engine vehicles (ICEVs). This shortfall in power density causes a 'range anxiety' for existing EV owners and poses a barrier for potential owners. Li-layered oxides (LLOs), typically with an O3-type stacking sequence, have been the most mainstream cathode material since their commercialization by Sony in 1991. For O3-type LLOs, Li-ion occupies thermodynamically stable octahedral sites, which are the phases that have edge sharing with neighboring transition metals at the initial state of the hopping mechanism. And the environment at the intermediate tetrahedral site significantly influences the Li-kinetics, affecting the power density of a battery. And the activation barrier for Li-kinetics is determined by the size of the intermediate site, and the valence state of the transition metal surrounding the Li-ion at the tetrahedral site. Despite attempts to induce fast mass transport using traces of various dopants, the fundamental limitations of the O3-type stacking sequence have prevented breakthroughs. Therefore, a study aiming to break the originated limitations of the O3-type LLOs and uncover novel Li-ion transport mechanisms is indispensable. By performing computational calculations, we propose a two-design perspective to enhance the rate of (de)lithiation by intentionally arranging Li-ion sites for O3-type LiCoO₂ (O3-LCO), the most conventional cathode material. For the first step, we introduce a new framework to overcome the fundamental limitations of the existing O3-type LLOs. We manipulated the stacking sequence of O3-LCO from O3- to O2-type, which induces a stable intermediate tetrahedral site. The O2-type LCO has edge-sharing relationships between the LiO₄ tetrahedral site, serving as an intermediate step in the hopping mechanism, and the adjacent MO₆ (M refers to transition metal) octahedron in the transition metal layer. This configuration makes the intermediate site energetically more stable than the O3-type and allows for fast Li hopping from the relatively unstable intermediate site to the final site in the O2-type framework due to the lower activation barrier than the O3-type. Additionally, the anionic electrostatic repulsion between facing O-O in the LiO₂ layer results in a larger Li slab thickness, creating wider pathways for Li-ion movement. The second step involves screening the optimal material candidates for fast Li-kinetics by inducing even more stable intermediate sites through a change in material content by trace amounts of substitutional dopants. We design a strategy to lower the activation barrier by substituting contents (y) in O2-type Li_{1-x}(Co_{1-y}M_y)O₂ with 3d transition metals that have a large ionic radius, aiming for volumetric expansion of the tetrahedral site through in-plane direction broadening. While the nine candidates showed similar values of Li-slab thickness, the ionic radius, and ab-plane area showed overwhelmingly high values when Ti was substituted. The larger ionic radius causes a wider ab-plane and thus increases the volume of the LiO₄ tetrahedral site. We demonstrated through density functional theory (DFT) calculations that an expansion in the volume of the tetrahedral site lowers the activation barrier for Li-ion, resulting in high-rate performance that can be implemented. Furthermore, we figure out that materials designed according to our proposed concept induce fast Li-kinetics. Our unified design flow for facilitating fast Li-kinetics can serve as a cornerstone for the design of fast-charging LLOs cathode materials.

11:00 AM DS03.10.07

Shape Dependence of Two-Body Interatomic Potential Functions on Phase Stability of Close-Packed Polytype Structures Shinya Ogane¹, Koji Moriguchi¹ and Kazumasa Tsutsui²; ¹Tohoku University, Japan; ²Nippon Steel, Japan

Many crystalline compounds are composed of one or more structural units. When these units can be "stacked" in various ways to form stable or metastable phases, the resulting phases are known as polytypes [1]. Among these polytypes, the crystal systems composed of close-packed (CP) layers have received particular attention over the years due to their fundamental and technological significance. While the demand for material engineering in controlling polytype structures is spanning across various fields such as wide-gap semiconductors [2], catalytic science [3], lightweight structural materials [4], and more, the scientific control of the polytype phase is still incomplete in the realm of industrial practical materials. Despite the fact that there are mathematically countless stacking arrangements with equal packing densities, most observed CP crystal structures exhibit short repeating sequences such as face-centered cubic (fcc) or hexagonal CP (hcp). There is, however, currently no general theory explaining why these structures can take the robust ground state.

Since the descriptors for the energetics of crystal structures are typically discrete physical quantities such as atomic configurations, we are forced to search their energetic stability in a discontinuous descriptor space, which makes it challenging to completely predict the most stable structure. For polytype structures, the convergent series lattice theories, such as the axial next-nearest neighbor Ising (ANNNI) model [5] and the model recently submitted by Loach and Ackland [6], are useful for representing the infinite continuous energetic space spanned by the expansion parameters. The computational analyses based on these models have suggested that it is necessary to consider at least the interactions involving the third-nearest-neighbor distance or longer-range interlayer interactions to accurately estimate the total energetics of metallic CP polytypes [6, 7]. Furthermore, molecular dynamics (MD) simulations have shown that the ground state structures based on the finite-range Lennard-Jonesium can encompass not only fcc and hcp arrangements, but also a wide range of more complex stacking sequences, depending on the interatomic interaction distance and cutoff function [8].

In the previous work, in order to investigate the bifurcation of polytype energetics as a function of interaction distance, we have presented the interlayer partial energy model where the total energy constructed from the two-body interactions is projected onto the interlayer interactions in CP polytype structures [9]. While the polytype structural energies tend to degenerate with respect to hexagonality in the systems with the short interaction distance, the energetic degeneracy manifested by the short-range interactions has been found to split in the systems with the third neighbor interlayer interactions based on this analytical model [9]. To confirm the theoretical results, this work has systematically investigated the shape dependence of the interatomic potentials on the phase stability of the CP polytype structures by constructing specific two-body potential functions, referring to [10]. In the presentation on the day, we will discuss the variations in the phase diagram of the polytype ground state in the space defined by the potential variables associated.

[1] A. L. Ortiz, et al., J. Appl. Cryst. 46, 242 (2013).

[2] E. M. T. Fadaly et al., Nature. 580, 205 (2020).

[3] Z. Fan et al., Nat. Commun. 6, 7684 (2015).

[4] E. Abe et al. Philos. Mag. Lett. 91, 690 (2011).

[5] W. Selke, Phys. Repo. 170, 213 (1988).

[6] C. H. Loach, and G. J. Ackland, Phys. Rev. Let. 119, 205701 (2017).

[7] K. Moriguchi et al., MRS Advances 6, 163 (2021).

[8] L. B. Pártay et al., Phys. Chem. Chem. Phys. 19, 19369 (2017).

[9] S. Ogane and K. Moriguchi, MRS Advances 6, 170 (2021).

11:15 AM DS03.10.08

Particle Self-Organization Under Oscillatory Interaction Potentials[Kateri H. DuBay](#) and Jessica Niblo; University of Virginia, United States

Multiple simulations on colloidal self-assembly have demonstrated that an oscillatory inter-particle potential can alter the self-assembly process, potentially expanding the interaction space that leads to orderly assembly or establishing non-equilibrium steady-state structures that may be inaccessible to equilibrium assembly processes. Previous theoretical work in this area has shown that the assembly dynamics at the limit of fast inter-particle potential oscillations should proceed in the same way as those under the constant interaction potential that is equal to the interaction potential averaged over a single oscillation. In this work, we first use a 2D model of the assembly of a viral-capsid-like structure to confirm this result in our model system. We then work through the implications of that earlier finding for designing novel self-organizing materials via physically realizable interaction potentials.

11:30 AM DS03.10.09

Harnessing Structural Stochasticity in Designing Architected Materials: Deep Generative Design and Curvature Functional-Based Design[Hongyi Xu](#), [Leidong Xu](#) and [Kiarash Naghavi Khanghah](#); University of Connecticut, United States

Bridging the gaps among various categories of microstructures, which include the periodic microstructures and various types of stochastic microstructure, remains a challenge in architected material design. Traditionally, different microstructure categories require significantly different mathematical methods to define the design space. The purpose of this work is to establish a computational framework that provides a unified design space that embodies various categories of structural patterns for the design automation of mixed-category microstructures. The structural patterns include various stochastic patterns such as random particles, random fibers, random cells, spinodal structures, random amorphous structures, etc., as well as periodic structural patterns collected from metamaterial research works.

First, we established a property-aware Variational Autoencoder-based deep generative design framework that embodies both stochastic and periodic 2D microstructure patterns. The proposed framework is demonstrated on two sets of design case studies: (i) searching a periodic metamaterial pattern with desired properties with a stochastic pattern as the starting point, and (ii) searching a stochastic microstructure with desired properties with a periodic pattern as the starting point.

Second, we present an in-depth investigation on designing 3D mixed-category stochastic microstructures for desired properties. We establish and compare two methods, a data-driven method based on deep generative models and a mathematical method based on curvature functionals. The metrics of comparison include design performance, computational cost, scalability, interpretability of the statistical equivalency, and convenience of generating functional graded structure designs. This work is concluded with a summary of the pros and cons of each method.

11:45 AM DS03.10.10

Inverse Design of Low-Carbon Concrete Materials by Machine Learning[Mathieu Bauchy](#); University of California, Los Angeles, United States

Concrete—which is by far the most manufactured material in the world—is responsible for 5-to-10% of human CO₂ emissions. Here, we present an uncertainty-aware, machine-learning-enabled optimization scheme that aims to accelerate the discovery of new optimized concrete mixes featuring minimum embodied CO₂ while meeting target performance and manufacturing constraints. We curate an unprecedented dataset comprising more than 1 million concrete mixtures with varying mixture proportions, together with their measured properties (compressive strength, slump, shrinkage, setting time, etc.). The dataset is used to train a series of Gaussian Process regression (GPR) forward models that accurately map concretes' mixture proportions to their properties, and uncertainty thereof. We then introduce a new inverse design approach that simultaneously leverages (i) multi-property predictions from the GPR model, (ii) uncertainty thereof, and (iii) physical knowledge to guide the discovery of new concrete mixtures featuring minimum embodied CO₂ while presenting required performance metrics (e.g., with a strength meeting or exceeding a given target) and obeying manufacturing constraints (e.g., with compliant slump, pumpability, finishability, etc.). This pipeline leads to the discovery of several new concrete mixtures presenting a >50% decrease in embodied CO₂, with no cost increase.

SESSION DS02/DS03/DS05: Joint Virtual Session

Session Chairs: Lihua Chen, Prashun Gorai, Deepak Kamal, Christopher Kuenneth, Yongtao Liu, Steven Spurgeon and Qian Yang

Tuesday Morning, December 5, 2023

DS03-virtual

8:00 AM DS02/DS03/DS05.01

An Inverse Design Scheme of Creation of Crystal Structure Reproducing X-Ray Diffraction Pattern Without Relying on Database[Joo-hwi Lee](#), Junpei Oba, Nobuko Ohba and Seiji Kajita; Toyota Central R&D Lab. Inc., Japan

An X-ray Diffraction (XRD) analysis is widely used for determination of crystal structure. A measured XRD of the synthesized sample is identified by comparing it with the XRD patterns of the candidate crystal structures searched in database (DB). In addition, a Rietveld refinement is used to slightly modify the structure to reduce the gap the XRD patterns of the measured sample and the candidate structure. However, such a method strongly depends on the DB. If the measured XRD pattern is from an unknown structure, it is difficult to identify the correct crystal structure of the measured sample. Therefore, it is needed to develop an inverse design method to automatically create a crystal structure which reproduces the given XRD pattern.

In this study, we propose an inverse design scheme, named Evolv&Morph, to generate a crystal structure reproducing the target XRD pattern. It consists of Evolutionary algorithm [1] and crystal morphing [2]. This scheme tries to create enormous crystal structures with maximizing the similarity score between the XRD pattern of the created structure and the target.

Evolutionary algorithm is an optimization method with generating various structures based on genetic operators such as random selection, crossover, and mutation. Crystal morphing is an interpolation method to generate intermediate structures between the input structures. It can also optimize the similarity score of XRD pattern with the support of Bayesian optimization. For sixteen different material systems, Evolv&Morph successfully created crystal structures with the XRD pattern almost the same as the given target XRD pattern.

This scheme is an automated crystal structure creation scheme, not relying on a database. Therefore, the suggested algorithm is applicable to other material design application for specific properties. More detailed descriptions for Evolv&Morph can be found in Ref. [3].

References

- 1) A. R. Oganov, C. W. Glass, J. Chem. Phys. 124, 244704 (2006).
- 2) J. Oba, S. Kajita, Phys. Rev. Mater. 6, 023801 (2022).
- 3) J. Lee, J. Oba, N. Ohba, S. Kajita, submitted., preprint arXiv 2302.10464 (2023).

8:15 AM DS02/DS03/DS05.02

Macromechanical Modeling of hBN Aided by Molecular Dynamics Simulations Provides Key Insights on Novel Toughening and Strengthening Mechanism[Simanta Lahkar](#); Indian Institute of Technology Gandhinagar, India

The practical exploitation of novel properties of the diverse range of 2D materials known today relies crucially on the availability of effective computational techniques for their efficient design and modeling in emerging material applications like nanodevices and nanocomposites. Hexagonal boron nitride is one such promising 2D material whose unique and significantly-anisotropic failure behavior makes its comprehensive mechanical characterization particularly challenging. The issues of reliably predicting material failure under varied stresses also extend to other 2D materials and macro-scale anisotropic layered structures, such as layered composites, further restricting their computational as well as experimental design applications. While macro-mechanical strength theories and failure criteria, which can potentially help determine a material's maximum stress tolerance in a structure, have been typically employed with variations depending on the unique failure characteristics of a given class of materials, there remains a significant gap in adapting them for layered materials with one of the key challenges being to assess the accuracy of the failure as they require the operation in full 6D tensor stress space. In this study, we carried out comprehensive MD failure simulations of hBN and obtained a methodology for optimization of the general Tsai-Wu strength criterion by proposing an equivalent-stress-based quantification technique that can be used to determine the error between the failure surface prediction and the simulation data objectively. The final optimized criterion was tested with over 99% accuracy against multiaxial stress simulations in two arbitrary orientations, which also indicated significant strengthening behavior in hBN on ripple formation in the layers. Detailed analysis of crack nucleation toughness and bond strength revealed an intrinsic distortion-mediated mechanism of simultaneous toughening and strengthening in hBN, which is also expected in other asymmetric 2D materials. Furthermore, our study can act as an important reference for future work on multiscale failure modeling of highly anisotropic materials.

8:30 AM DS02/DS03/DS05.03

Effect of Naturally Generated Microstructure of a Ceramic on Ion Transport—Lithiation of Titania SergeiManzhos¹, TakumaOkamoto¹, AnastasiaSorkin², KeisukeKameda¹, Manabulhara² and HaoWang²; ¹Tokyo Institute of Technology, Japan; ²National University of Singapore, Singapore

Microstructural features of ceramics can have a significant effect on ion transport in different renewable energy generation and storage technologies, most notably fuel cells and metal-ion batteries. Microstructural features such as grain boundaries also affect electronic properties relevant for optoelectronic application (e.g. creating band gap states). Experimental insight is difficult into bulk (as opposed to surface) structure. Atomistic modeling is usually done on *postulated* grain boundaries, while real microstructures have distributions of different grain boundaries.

Microstructural features can be generated 'naturally' with molecular dynamics (MD) by simulating a heat treatment. While this has been successfully done for several monoatomic systems (e.g. Fe, Si), achieving microstructure of ceramics by MD is more difficult. We show the generation of titania grains with MD which required a finer control of the computational heat treatment than in monoelemental systems. We demonstrate that a distribution of grain sizes and grain boundaries obtains, and is dependent on the heat treatment. We compute the lithiation of the obtained structures and compare them to ideal crystal titania, and also compare mechanical properties including plasticity and fracture.

8:45 AM DS02/DS03/DS05.04

Comprehensive Multimodal Deep Learning for Designing Materials with Diverse Properties ShunMuroga, YasuakiMiki and KenjiHata; National Institute of Advanced Industrial Science and Technology, Japan

In response to the increasing need for rapid advances in materials and manufacturing processes, the field of computational materials science, particularly data-centric methodology, has gained significant traction. Traditional data-centric methods have primarily focused on molecular descriptors such as elemental composition, chemical bond types, neighborhood associations, and electronic interactions to facilitate the discovery of molecules, inorganic compounds, and crystals. However, these techniques fall short when applied to complex materials with indeterminate structures, as molecular descriptors require accurate elemental coordinate information. As a result, a variety of everyday materials, such as plastics, metal alloys, rubber, and wood, with indeterminate structures face significant challenges in the context of a data-centric approach.

This study introduces an innovative technique for materials design, called multimodal deep learning, to overcome the limitations of traditional methods. This approach mimics human cognition by integrating information from multiple sensory modalities (e.g., vision, hearing) to achieve a holistic understanding. Due to its superior performance, multimodal deep learning has attracted considerable interest, especially in the field of human activities, such as emotion analysis and psychological testing. Despite these advances and growing interest, the application of this methodology to materials design has remained largely unexplored.

Our primary strategy in applying multimodal deep learning is to incorporate rich information about the physical and chemical structures of materials. The proposed advanced multimodal deep learning methodology consists of several modules: (1) multiple generative deep learning models that represent physical or chemical structure characterization data, (2) an integrated deep learning model that fuses a wide range of information from different sources to predict various properties of materials. The effectiveness of the proposed multimodal deep learning method was clearly demonstrated on polymer composites consisting of ten compositions (matrices, additives, fillers) and encompassing eight mechanical, thermal, and electrical properties. By merging optical microscope images, infrared spectra, Raman spectra, and compositional data, the trained multimodal deep learning model successfully predicts the eight physical properties. This trained multimodal deep learning model was then used to virtually screen materials over 114,210 compositional conditions. Pareto frontiers under conflicting multiple physical properties and optimal compositional changes in materials were clearly identified from the predictions of the trained multimodal deep learning model. We are confident that the proposed multimodal deep learning has the flexibility and adaptability required for a wide range of materials, paving the way for profound insights into materials and inspiring future research in advanced materials design.

References:

- [1] Shun Muroga, Yasuaki Miki, Kenji Hata, *Advanced Science* (2023), in printing.
- [2] Shun Muroga, Yasuaki Miki, Kenji Hata, arXiv:2303.16412 (2023).
- [3] Shun Muroga, figshare (2023), available at <https://doi.org/10.6084/m9.figshare.23358398>.

Acknowledgements: This work was supported by a project (JPNP16010) commissioned by the New Energy and Industrial Technology Development Organization (NEDO). Computational resource of AI Bridging Cloud Infrastructure (ABCI) provided by National Institute of Advanced Industrial Science and Technology (AIST) was used.

9:00 AM *DS02/DS03/DS05.05

The BIGMAP Approach Towards Holistic Battery Characterization SandrineLyonnard¹ and CinthyaK. Trujillo Herrera²; ¹University of Grenoble Alpes, France; ²Institute Laue Langevin, France

Energy storage devices such as Li-ion batteries are key towards a fossil-fuel free society. The characterization of material evolutions during battery cycling is critical in understanding the reaction mechanisms and finding the origin of capacity fading, which limits the cycle life of the system. Operando techniques are widely used to probe the structural and chemical changes that occur in the bulk and at interfaces in electrodes and electrolytes while the battery is charged and discharged. In this quest to visualize and quantify the various processes in real-time and at all relevant scales, neutron and synchrotron techniques are instrumental thanks to their capacity to deeply penetrate dense systems, therefore enabling to probe battery cells working in close-to-real or real conditions. Moreover, unprecedented time and space resolutions are achievable in some cases, leading to ultimate views of particle evolutions and electrode-scale heterogeneities. In this talk, we will present examples of correlative experiments performed using 2D scanning techniques and 3D imaging techniques. We will focus on the benefits of multimodal approaches [1] where isotopic-contrasted neutron experiments are combined, for instance, to high resolution scanning microXRD experiments. We will also present the complex experimental workflow developed in the frame of the BIGMAP project, where a central AI orchestrates advanced characterization, multiscale modelling, machine learning methods, high throughput synthesis and robotics to accelerate materials discovery. Taking the graphite/LNO battery as a use case, we will show how we combine a variety of experiments ranging from spectroscopies to advanced tomography and 2D/3D mapping techniques in order to gain a more holistic understanding of the ageing mechanisms in the electrodes, as well as to evaluate the impact of electrolyte additives onto the Solid Electrolyte Interphase (SEI) formation and growth.

- [1] *Advanced Energy Materials*, 2022, 2102694. D. Atkins, E. Capria, K. Edström, T. Famprakis, A. Grimaud, Q. Jacquet, M. Johnson, A. Matic, P. Norby, H. Reichert, J-P. Rueff, C. Villeveille, M. Wagemaker*, S. Lyonnard*. Accelerating Battery Characterization Using Neutron and Synchrotron Techniques: Toward a Multi-Modal and Multi-Scale Standardized Experimental Workflow. DOI:10.1002/aenm.2021026944

9:30 AM DS02/DS03/DS05.06

Deep Learning for Improving Piezoresponse Force Microscopy Sensitivity for Weak Ferroelectrics PanithanSriboriboon¹, HuiminQiao^{1,2}, OwoongKwon^{1,2}, RamaK. Vasudevan³, StephenJesse³ and YunseokKim^{1,2}; ¹Sungkyunkwan University, Korea (the Republic of); ²Sungkyunkwan University (SKKU), Korea (the Republic of); ³Oak Ridge National Laboratory, United States

Hafnium oxide-based ferroelectrics have been extensively studied because of their existence of ferroelectricity, even in ultra-thin film form. However, studying the weak response of the ultra-thin film requires high-sensitivity piezoresponse measurements. In general, resonance-enhanced piezoresponse force microscopy (PFM) has been used to characterize ferroelectricity by fitting between the acquired piezoresponse spectrum and a simple harmonic oscillation model. However, an iterative approach, such as traditional least square (LS) fitting, is highly sensitive to noise and can result in the misinterpretation of weak responses. In this study, we introduce a deep denoising autoencoder (DDA) and principal component analysis (PCA) to hybridize with a deep neural network (DNN) for the extraction of piezoresponse information. The DDA/PCA-DNN improves the PFM sensitivity down to 0.3 pm, allowing measurement of weak piezoresponse with low excitation voltage in 10-nm-thick Hf_{0.5}Zr_{0.5}O₂ thin films. Our hybrid approaches could provide more chances to explore the low piezoresponse of the ultra-thin ferroelectrics and could be applied to other resonance-based microscopic techniques.

9:45 AM DS02/DS03/DS05.07

Simplifying the Identification of Differential Scanning Calorimetry (DSC) Curves YanxiZhang; Netzsch Instruments North America, United States

Currently DSC is a very common instrument in material characterization lab. Interpretation of DSC curve requires a lot of experience and time by looking up in application note and literature or consulting with experts. Thanks to "Identify" software, interpretation of DSC curve is not a tough job anymore, can with a single mouse click.

"Identify" is a unique database system in thermal analysis for the recognition and comparison of measurement curves of DSC, TGA, DIL/TMA as well as data on the specific heat capacity, Cp. "Identify" is the first database search software in thermal analysis. The database includes more than 2000 entries from the fields of ceramics and inorganics, metals and alloys, polymers, organics, food and pharmaceuticals, as well as chemical elements. "Identify" software offers an automatic DSC curve recognition of unknown measurements and thus interpretation via

database search, which is in general be very helpful for material identification, failure analysis and quality control. "Identify" serves as archiving system, too, for data mining since evaluated curves can restore in database easily. The database can expand by users' own libraries shared with several users in the computer network.

Limitation of database search is that curve recognition is not automatically material recognition. Sometimes multiple interpretation is possible. "Identify" software develops to use with combined TGA and DSC, TGA-c-DTA® and STA measurements. Not only the best hit with one signal considers, but also several signals (DSC, TGA etc), which allows for material identification with greater certainty.

SYMPOSIUM DS04

Accelerating Data-Driven Materials Research for Energy Applications
November 27 - December 6, 2023

Symposium Organizers

Andrew Detor, GE Research
Jason Hattrick-Simpers, University of Toronto
Yangang Liang, Pacific Northwest National Laboratory
Doris Segets, University of Duisburg-Essen

Symposium Support

Bronze
Cohere

* Invited Paper

+ JMR Distinguished Invited Speaker

SESSION DS04.01: Autonomous Experimental Methods I
Session Chairs: Jason Hattrick-Simpers and Benji Maruyama
Monday Morning, November 27, 2023
Sheraton, Second Floor, Back Bay B

10:30 AM *DS04.01.01

ARES™ Autonomous Experimentation Systems for Clean Energy Materials Benji Maruyama¹, Rahul Rao¹ and Robert Waelder^{2,1}; ¹Air Force Research Laboratory, United States; ²UES, Inc., United States

The current materials research process is so slow and expensive, taking decades from invention to commercialization, that it may not impact 2050 CO₂ emission goals to mitigate disastrous impacts from human-driven climate change. The Air Force Research Laboratory pioneered ARES™, the first autonomous research system for materials development. A rapidly growing number of researchers are now exploiting advances in artificial intelligence (AI), autonomy & robotics, along with modeling and simulation to create research robots capable of doing iterative experimentation orders of magnitude faster than today. We will discuss concepts and advances in autonomous experimentation in general, and associated hardware, software and autonomous decision methods.

We will focus on the simultaneous generation of clean hydrogen plus sequestered carbon to lightweight transportation and construction materials through natural gas pyrolysis to hydrogen plus carbon nanotubes. For Carbon Nanotubes (CNTs), we show progress in autonomous and data science methods to understand and control the fundamental mechanisms that drive CNT synthesis via CVD.

In the future, we expect autonomous research to revolutionize the research process, and propose a "Moore's Law for the Speed of Research," where the rate of advancement increases exponentially, and the cost of research drops exponentially. We also consider a renaissance in "Citizen Science" where access to online research robots makes science widely available.

11:00 AM DS04.01.02

Direct Materials Printing Makes Autonomous Energy-Materials Research Accessible for Smaller Labs Eunice Aissi, Alexander E. Siemenn, James Serdy, Fang Sheng, Basita Das, Hamide Kavak and Tonio Buonassisi; Massachusetts Institute of Technology, United States

While autonomous research presents a promising approach to accelerate the development of new energy materials, acquiring the human and capital resources to establish and maintain these advanced tools can be daunting. For smaller labs investigating a wide range of energy materials, there is demand for flexible, high-throughput, and high-quality materials synthesis and characterization tools. For such an approach, an additional constraint is demonstrating equivalence with, and translatability to, standard synthesis techniques — a task complicated by the fact that optoelectronic properties of energy materials are often sensitive to dilute concentrations of defects.

We address the material synthesis and characterization bottleneck by presenting a framework that we believe is suitable for smaller labs: Self-built, low-cost automation for energy applications. The design philosophy is to de-risk the lab automation process by keeping costs low, failing fast, and leveraging common resources in electronic systems and additive manufacturing. We present the example of a home-built Direct Multi-Material Printer (DMMP) adapted to operation in the glovebox, hood, and benchtop environments. The DMMP takes two or more fluid precursors and prints a materials gradient within a set of droplets, line segments, or another user-specified shape. The tool is self-built, leveraging a low-cost 3D printer chassis, and is affordable at about \$500. Our build cycle takes one day and utilizes open-source platforms for its firmware. The DMMP can deposit up to 1,000 different energy material compositions from liquid precursors in under one minute, requiring only three steps: creating a print pattern, loading the precursors, and printing the materials. We evaluate the fluid mixing dynamics of the system through imaging.

We validate the material synthesis capacity of the DMMP on a perovskite alloy series of interest to photovoltaic engineers, from methylammonium lead iodide (MAPbI₃) to formamidinium lead iodide (FAPbI₃), by showing equivalence to traditional spin-coated samples through X-ray diffraction measurements and other microstructural, compositional, and optoelectronic characterization methods. To screen for materials durability (an early step toward long-lasting perovskite-based solar PV modules), we demonstrate high-throughput characterization of the perovskite materials through an automated image segmentation algorithm that quantifies color changes in each material as a proxy for material degradation. To close the loop in a data-driven fashion (toward autonomy), we can use "stability" as a response variable for an active learning loop.

In summary, we present and validate a framework of customized automation for energy materials, focused on improving reproducibility, speed, adaptivity, and accessibility for smaller labs.

11:15 AM DS04.01.03

An Automated Multi-Scale NMR Framework Helps Understand Solvent Exchange Dynamics in Multivalent BatteriesRashaAtwi¹, YingChen², Dan ThienNguyen², Kee SungHan², KarlMueller², VijayakumarMurugesan² and Nav NidhiRajput¹; ¹Stony Brook University, The State University of New York, United States; ²Joint Center for Energy Storage Research (JCESR), Pacific Northwest National Laboratory, United States

Liquid electrolytes are integral parts of numerous materials science applications, including energy storage devices and solar panels. Optimizing these technologies requires designing optimal electrolytes, which calls for an exhaustive, unbiased exploration of wide chemical and parameter spaces. This process involves detailed investigations of the structural, dynamical, and thermodynamical properties of the chemical species that comprise complex, multi-component liquid electrolytes. To accelerate these investigations, we developed a fully automated, high-throughput multi-scale computational framework^{1,2} that predicts solvation structures. The framework automatically processes hundreds of thousands of atomic clusters from MD simulations, identifies stable species, and performs their NMR chemical shift calculations via DFT. The output is an extensive database of chemical shifts from a broad range of electrolyte solutions, generated with minimal user intervention and free from any trial-and-error process. By coupling the framework with experimental NMR measurements, we investigate solvation structure and solvent exchange rates of magnesium electrolytes in a wide range of solvent classes. We uncovered a correlation between solvent exchange dynamics and charge transfer efficiency at the electrolyte/electrode interface, suggesting the desolvation process as the rate-determining step.

References

1. Atwi, R., Chen, Y., Han, K.S., Mueller, K.T., Murugesan, V., and Rajput, N.N. (2022). An automated framework for high-throughput predictions of NMR chemical shifts within liquid solutions. *Nature Computational Science*. 10.1038/s43588-022-00200-9.
2. Atwi, R., Bliss, M., Makeev, M., and Rajput, N.N. (2022). MISPR: an open-source package for high-throughput multiscale molecular simulations. *Scientific Reports* 12, 15760. 10.1038/s41598-022-20009-w.

11:30 AM DS04.01.04

Automated Computation and Machine Learning of Electron Scattering and Charge Transport of SemiconductorsTianqiDeng¹, MichaelB. Sullivan², GangWu², Shuo-WangYang² and KedarHippalgaonkar^{3,4}; ¹Zhejiang University, China; ²Institute of High Performance and Computing, Singapore; ³Nanyang Technological University, Singapore; ⁴Institute of Materials Research and Engineering, Singapore

Charge carrier scattering and transport processes are fundamental to semiconductors for electronics, thermoelectrics, and many other applications. However, detailed scattering and transport characterizations are limited to a small number of materials. In this work, we profile the charge transport properties of about 1800 experimentally known semiconductors by incorporating electron-phonon and electron-impurity scatterings from density functional theory calculations. We demonstrate that electron-optical-phonon interaction is unambiguously the dominant scattering mechanism for the majority of these semiconductors, while many of them exhibited trend which was conventionally associated with acoustic phonon scatterings. Combining the knowledge with machine learning models, we further predicted the carrier mobilities of over 19000 semiconductors with substantially reduced cost. High-performance semiconductors and their key structural and electronic features are also identified to assist materials discovery and optimization.

SESSION DS04.02: Autonomous Experimental Methods II

Session Chairs: Yangang Liang and Shijing Sun

Monday Afternoon, November 27, 2023

Sheraton, Second Floor, Back Bay B

1:30 PM *DS04.02.01

How AI and Automation Can Help in Experimental Materials ResearchShijingSun^{1,2}; ¹Toyota Research Institute, United States; ²University of Washington, United States

Innovation in energy storage and conversion is essential for addressing global challenges such as climate change. Artificial intelligence (AI) has emerged as a powerful tool to accelerate materials discovery, but there are still challenges in realizing the potential of computational designs in the laboratory. One question increasingly get asked on self-driving labs is that 'will robots replace scientists?' In this talk, I will discuss, rather than replacing researchers, how emerging technologies can augment and amplify human expertise, leading to unprecedented breakthroughs in energy materials, device and systems. I will present examples of data-driven approaches that can address atomic-to-device level challenges in materials science. I will focus on how to predict experimental outcomes, explain results with interpretable machine learning, and design new experiments that incorporate physical knowledge into an automated framework, thereby guiding the discovery of new materials.

2:00 PM DS04.02.02

Materials Acceleration Platforms—Toward the Laboratory of the Future for Perovskite and Organic PV ResearchTobiasStubhan¹, AndrejClassen¹, MoritzScholl¹, PeterFendt¹, MatthiasKoegele¹, JerritWagner^{2,3}, ChristianBerger^{2,3}, JensHauch^{2,3} and ChristophJ. Brabec^{2,3}; ¹SCIPRIOS GmbH, Germany; ²Friedrich-Alexander-Universität Erlangen-Nürnberg, Germany; ³Helmholtz Institute Erlangen-Nuremberg, Germany

The development of complex functional materials poses a multi-objective optimization problem in a large multi-dimensional parameter space. Solving it requires reproducible, user-independent laboratory work and intelligent preselection of experiments. However, experimental materials science is a field where manual routines are still predominant, although other domains like medicine, biotechnology or pharmacy have long used robotics and automation. As the number of publications on Materials Acceleration Platforms (MAPs) increases steadily, we review selected systems [1,2] and fit them into the stages of a general material development process to examine the evolution of MAPs up to the AMANDA (Autonomous Materials and Device Application) platform [3]. Subsequently, we present our newest approach to lab automation for perovskite and organic PV research with the example of precise time-controlled quenching processes for perovskite film formation with solvent, gas and vacuum and autonomous perovskite film deposition optimization using automated optical characterization (Abs, photoluminescence) and machine learning for planning of the next generation of experiments.

References:

- [2] Discovery of temperature-induced stability reversal in perovskites using high-throughput robotic learning, Yicheng Zhao, Jiyun Zhang, Zhengwei Xu, Shijing Sun, Stefan Langner, Noor Titan Putri Hartono, Thomas Heumueller, Yi Hou, Jack Elia, Ning Li, Gebhard J Matt, Xiaoyan Du, Wei Meng, Andres Osvet, Kaicheng Zhang, Tobias Stubhan, Yexin Feng, Jens Hauch, Edward H Sargent, Tonio Buonassisi, Christoph J Brabec, *Nature communications* 12 (1), 2191
- [2] Stefan Langner, Florian Häse, José Darío Perea, Tobias Stubhan, Jens Hauch, Loïc M Roch, Thomas Heumueller, Alán Aspuru Guzik, Christoph J Brabec, *Journal of Materials Science* 56, 16422-16446
- [3] The evolution of Materials Acceleration Platforms: toward the laboratory of the future with AMANDA, J Wagner, CG Berger, X Du, T Stubhan, JA Hauch, CJ Brabec *Journal of Materials Science* 56, 16422-16446.

2:15 PM DS04.02.03

Automated Phase Identification in Large Material Spaces Using Neural NetworksNamQ. Le¹, MichaelPekala¹, AlexanderNew¹, EddieGienger¹, JannaDomenico¹, ChristinePiatko¹, ElizabethPogue¹, TyrelM. McQueen² and ChristopherStiles^{1,2}; ¹Johns Hopkins University Applied Physics Laboratory, United States; ²Johns Hopkins University, United States

High-throughput materials discovery systems require the ability to rapidly screen promising candidates. X-ray diffraction (XRD) provides a useful modality in settings where properties are strongly tied to particular crystalline phases. For example, many A15 phases are Type-II superconductors at relatively high temperatures among metallic alloys; identifying novel A15 phases could therefore lead to a high proportion of novel superconductors. Machine learning (ML) models have been shown effective for automating similar phase identification tasks from XRD patterns. However, previous work has generally been limited to material systems of up to five elements. We report the results of convolutional neural networks trained to classify A15-like phases from XRD patterns from a broad space of binary and ternary material systems spanning 23 elements. High performance can be achieved whether using crystal structures measured experimentally (Inorganic Crystal Structure Database, ICSD) or computed theoretically using density functional theory (Materials Project, MP). Performance decreased significantly when trained and tested on different sources, but can be recovered by augmenting datasets with both experimentally- and theoretically-derived structures. High classification performance can even be maintained on held-out XRD patterns measured experimentally in-house. This work suggests that ML models for XRD screening can be effective for phase identification not only within

material systems with already experimentally-measured patterns, but also in novel material systems through careful augmentation with theoretically-computed structures.

2:30 PM *DS04.02.04

Rules and Goals to Replace Clockwork Automation Jason Hein, University of British Columbia, Canada

Automation and real-time reaction monitoring have revolutionized synthetic chemistry by enabling data-rich experimentation, leading to a comprehensive understanding of chemical processes. This talk emphasizes the significance of data-rich experimentation (DRE) in reaction process optimization and discovery and explores the potential of artificial intelligence (AI) and machine learning (ML) tools in enhancing automated real-time reaction monitoring.

DRE focuses on extracting real-time reaction progress data to gain insights into reaction kinetics, intermediates, rate constants, and by-product reaction pathways. Automation plays a crucial role in enabling DRE by accurately capturing and analyzing reaction aliquots, processing complex analytical data, and executing precise reaction manipulations. This approach enhances decision-making capabilities, reduces optimization time and resource requirements, and facilitates the exploration of reaction mechanisms and dynamics.

This presentation highlights the current paradigm of data-driven reaction investigation, which often relies on human interpretation. However, the integration of real-time monitoring data with AI and ML tools presents an opportunity to accelerate process optimization and reaction discovery. Real-time monitoring telemetry allows automated systems to receive critical feedback and adapt to variable circumstances, enabling error-free autonomous synthesis. ML-based predictive models and autonomous optimization platforms reduce the number of experiments needed and consider a broader range of reaction parameters beyond simple yield measurements.

Real-time reaction monitoring provides comprehensive kinetic data that addresses issues of data integrity, bias, and oversimplification. It captures variations in reaction performance, identifies intermediates and by-products, and facilitates the classification of underlying reaction mechanisms. By combining automated data-gathering methods with AI and ML tools, synthetic chemistry can predict optimal conditions and discover new synthetic routes more efficiently.

3:00 PMBREAK

SESSION DS04.03: High-Throughput Experimentation and Data-Driven Methods I

Session Chairs: Alfred Ludwig and Doris Segets

Monday Afternoon, November 27, 2023

Sheraton, Second Floor, Back Bay B

3:30 PM *DS04.03.01

Mastering Compositional Complexity in High Entropy Materials for Energy Applications - Towards Accelerated Materials Discovery by Integration of High-Throughput Experimentation, Simulation, and Materials Informatics Alfred Ludwig, Ruhr University Bochum, Germany

Discovery of new materials is a key challenge in materials science. New materials for sustainable production/storage/conversion of energy carriers are necessary to improve existing and to enable future energy systems. Compositionally complex materials, frequently called high entropy materials, offer a vast multidimensional search space, which provides opportunities for discovering new materials. However, efficient methods for the exploration and exploitation of this search space are necessary. Here, the integration of high-throughput thin-film combinatorial materials science methods with simulation and materials informatics (1) is presented as an effective means to produce large datasets on new materials, which enables mastering of the search space. The approach combines theoretical predictions from high-throughput computations with production of large, consistent and complete experimental datasets, which are used for materials informatics. Thin-film materials libraries are fabricated by combinatorial sputter deposition and optional post-deposition treatments, followed by high-throughput characterization, and finally the organization of the acquired multi-dimensional data in adequate databases as well their effective computational analysis and visualization, e.g., of quinary systems in the form of composition-processing-structure-function diagrams, interlinking compositional data with structural and functional properties. The talk will discuss examples of combinatorial discoveries (2, 3) and the targeted development of new compositionally complex materials for electrocatalysis (4) where compositional complexity offers a new design principle (5). Furthermore, a new approach (6) to accelerate atomic-scale measurements for complex alloys is presented as well as applications of materials informatics to accelerate and improve the materials discovery process (7, 8).

(1) A. Ludwig (2019) *Discovery of new materials using combinatorial synthesis and high-throughput characterization of thin-film materials libraries combined with computational methods*, npj computational materials 5, 70

(2) T. Löffler, H. Meyer, A. Savan, P. Wilde, A. Garzón Manjón, Y. T. Chen, E. Ventosa, C. Scheu, A. Ludwig, W. Schuhmann (2018) *Discovery of a multinary noble metal free oxygen reduction catalyst*, Adv. Energy Mater. 8, 1802269

(3) V. Strotkötter, O. A. Krysiak, J. Zhang, X. Wang, E. Suhr, W. Schuhmann, A. Ludwig (2022) *Discovery of High-Entropy Oxide Electrocatalysts – From Thin-Film Materials Libraries to Particles*, Chemistry of Materials, 34, 10291-10303

(4) T. A. A. Batchelor, T. Löffler, B. Xiao, O. A. Krysiak, V. Strotkötter, J. K. Pedersen, C. M. Clausen, A. Savan, Y. Li, W. Schuhmann, J. Rossmeisl, A. Ludwig (2021) *Complex solid solution electrocatalyst discovery by prediction and high-throughput experimentation*, Angewandte Chemie 60, 6932–6937

(5) T. Löffler, A. Ludwig, J. Rossmeisl, W. Schuhmann (2021) *What makes high-entropy alloys exceptional electrocatalysts?*, Angew. Chem. Int. Ed., 60, 26894–26903

(6) Y. J. Li, A. Savan, A. Kostka, H. S. Stein, A. Ludwig (2018) *Accelerated atomic-scale exploration of phase evolution in compositionally complex materials*, Materials Horizons 5, 86 - 92

(7) P. M. Maffettone, L. Banko, P. Cui, Y. Lysogorskiy, M. Little, D. Olds, A. Ludwig, A. I. Cooper (2021) *Crystallography companion agent for high-throughput materials discovery*, Nature Computational Science 1, 290 – 297.

(8) L. Banko, O. A. Krysiak, J. K. Pedersen, B. Xiao, A. Savan, T. Löffler, S. Baha, J. Rossmeisl, W. Schuhmann, A. Ludwig (2022) *Unravelling composition-activity-stability trends in high entropy alloy electrocatalysts by using a data-guided combinatorial synthesis strategy and computational modelling*, Adv. Energy Mater., 2103312

4:00 PM DS04.03.02

High-Throughput Mechanical and Elastic Properties of Two-Dimensional Materials from First Principles Changpeng Lin¹, Samuel Ponce², Francesco Macheda³, Davide Campi⁴, Francesco Mauri⁵ and Nicola Marzari^{1,6}; ¹École Polytechnique Fédérale de Lausanne, Switzerland; ²Université Catholique de Louvain, Belgium; ³Istituto Italiano di Tecnologia, Italy; ⁴Università degli Studi di Milano-Bicocca, Italy; ⁵Università di Roma La Sapienza, Italy; ⁶Paul Scherrer Institute, Switzerland

Mechanical and elastic properties of materials are among the most fundamental quantities for many engineering and industrial applications. Here, we present an efficient and accurate approach for calculating the elastic and bending rigidity tensor of crystalline solids based on interatomic force constants and Born perturbation theory, valid equivalently for any dimension. We implement the theory in the first-principles Quantum ESPRESSO software suite, and perform an extensive validation against conventional finite-difference calculations and experimental measurements for Si, NaCl, graphene and monolayer MoS₂. The developed computational approach is then applied to the high-throughput screening of around one-thousand two-dimensional materials from the MC2D database, where we identify various candidates with outstanding or unique mechanical properties. The methodology developed and elastic database of two-dimensional materials produced in this work will benefit the discovery and design of novel functional materials.

4:15 PM DS04.03.03

A Comprehensive Inert-Gas Workflow for High-Throughput Combinatorial Aging Studies of Vapor-Deposited Metal Halide Perovskite Thin-Films Alexander Wiczorek¹, Austin G. Kuba², Jan Sommerhäuser¹, Luis Caceres¹, Siarhei Zhuk¹, Christian Wolff² and Sebastian Sio¹; ¹Empa – Swiss Federal Laboratories for Materials Science and Technology, Switzerland; ²EPFL – École Polytechnique Fédérale de Lausanne, Switzerland

High-throughput experimentation (HTE) is increasingly being employed to accelerate metal halide perovskite (MHP) thin-film development.^[1] As of now, most approaches focus on solution-based deposition methods.^[2–4] To address the need for scalable fabrication approaches, vapor-based deposition methods are gaining popularity. However, durability concerns remain a major obstacle for large-scale deployment.^[5] This motivates high-throughput stability studies of vapor-deposited MHP thin films.

Combinatorial materials science is perfectly suited to address this challenge, specifically for time-consuming degradation studies where parallelization of experiments is key.^[6] Using vapor deposition techniques, large parameter spaces can be covered on single substrates, whereas automated characterization and data analysis facilitate rapid properties screening.^[7]

In this work, we present a comprehensive workflow for the aging behavior of thin-film MHPs which includes structural, optical and chemical characterization. To mitigate ambient degradation of pristine thin films during characterization or transfers, we employ a complete inert-gas workflow. Furthermore, we perform a rapid *in situ* screening of the transmission and reflectance in a broad wavelength range under accelerated aging conditions. Specifically, the samples are exposed to 85 °C and 1 kW m⁻² white light bias, probing intrinsic material degradation in an accelerated fashion. With a temperature variation of ±1 °C and light intensity variation of <2% across combinatorial libraries, meaningful combinatorial stability screening is enabled. Automated characterizations of the structural properties as well as optoelectronic properties relevant to device applications yield deep insights into the aging process, extending and validating insights from changes in the optical transmission. Furthermore, the workflow can be combined with high-throughput surface characterization techniques that our group previously demonstrated as a novel tool for accelerated materials discovery.^[8-10] Consequently, the investigation of surfaces and interfaces relevant for device applications is enabled.

We investigate the effect of residual precursors on the stability of two-step deposited MHP thin films grown on vapor-deposited templates for multiple chemical spaces. As a result, we discuss strategies to derive guidelines for the two-step synthesis of stable MHP thin films.

References:

- [1] M. Ahmadi, M. Ziatdinov, Y. Zhou, E. A. Lass, S. V. Kalinin, *Joule* **2021**, *5*, 2797.
- [2] S. Sun, N. T. P. Hartono, Z. D. Ren, F. Oviedo, A. M. Buscemi, M. Layurova, D. X. Chen, T. Ogunfunmi, J. Thapa, S. Ramasamy, C. Settens, B. L. DeCost, A. G. Kusne, Z. Liu, S. I. P. Tian, I. M. Peters, J. P. Correa-Baena, T. Buonassisi, *Joule* **2019**, *3*, 1437.
- [3] Y. Zhao, J. Zhang, Z. Xu, S. Sun, S. Langner, N. T. P. Hartono, T. Heumueller, Y. Hou, J. Elia, N. Li, G. J. Matt, X. Du, W. Meng, A. Osvet, K. Zhang, T. Stubhan, Y. Feng, J. Hauch, E. H. Sargent, T. Buonassisi, C. J. Brabec, *Nat. Commun.* **2021**, *12*, 2191.
- [4] R. E. Kumar, A. Tiihonen, S. Sun, D. P. Fenning, Z. Liu, T. Buonassisi, *Matter* **2022**, *5*, 1353.
- [5] T. D. Siegler, A. Dawson, P. Lobaccaro, D. Ung, M. E. Beck, G. Nilsen, L. L. Tinker, *ACS Energy Lett.* **2022**, *7*, 1728.
- [6] S. Sun, A. Tiihonen, F. Oviedo, Z. Liu, J. Thapa, Y. Zhao, N. T. P. Hartono, A. Goyal, T. Heumueller, C. Batali, A. Encinas, J. J. Yoo, R. Li, Z. Ren, I. M. Peters, C. J. Brabec, M. G. Bawendi, V. Stevanovic, J. Fisher, T. Buonassisi, *Matter* **2021**, *4*, 1305.
- [7] J. M. Gregoire, L. Zhou, J. A. Haber, *Nat. Synth.* **2023**, DOI 10.1038/s44160-023-00251-4.
- [8] A. Wiczorek, H. Lai, J. Pious, F. Fu, S. Siol, *Adv. Mater. Interfaces* **2023**, *10*, 2201828.
- [9] S. Zhuk, S. Siol, *Appl. Surf. Sci.* **2022**, *601*, 154172.
- [10] S. Zhuk, A. Wiczorek, A. Sharma, J. Patidar, K. Thorwarth, J. Michler, S. Siol, arXiv:2305.19875 [cond-mat.mtrl-sci], **2023**.

4:30 PM DS04.03.04

MISPR: A High-Throughput Multi-Scale Infrastructure for Automating Materials Science Computations Nav Nidhi Rajput, Rasha Atwi and Matthew Bliss; Stony Brook University, United States

Developing the capability to accurately predict the macroscopic properties of complex multicomponent solutions from microscopic features of molecular species is a grand challenge spanning chemistry, materials science, and engineering. Despite significant efforts undertaken in the past, the existing studies fall short of predicting the properties of multicomponent solutions due to multiple length and time scales of functional properties and a vast chemical and parameter space, which cannot be efficiently explored using trial and error based experimental approaches, brute-force computational approaches, and/or high-throughput computational approach that typically focus on just a single scale.

Driven by these needs, we developed a high-throughput computational framework coined **MISPR (Materials Informatics for Structure-Property Relationships)** - <https://github.com/molmd/mispr> that seamlessly integrates density functional theory (DFT) calculations with classical molecular dynamics (MD) simulations to robustly predict molecular and ensemble properties in complex multi-component liquid solutions. Functionalities of MISPR include (i) full automation of DFT and MD simulations, (ii) creation of computational databases for establishing structure-property relationships and maintaining data provenance and reproducibility, (iii) automatic error detection and handling, (iv) support for flexible and well-tested DFT workflows for computing properties such as bond dissociation energy, binding energy, and redox potentials, and (v) derivation of ensemble properties such radial distribution functions, ionic conductivity, and residence time. The infrastructure allows running 100-1000s of calculations in parallel by minimizing manual interference and generates high-fidelity databases of computational properties and force field parameters.

In this talk, I will demonstrate the unique features of MISPR by highlighting its different automated workflows and their application in designing optimal electrolytes for next-generation energy storage devices.¹ I will then show (1) a novel “*DFT-CMD-DFT*” approach to accurately predict various stable species present in a multi-component solution by analyzing experimental nuclear magnetic resonance (NMR) spectra³ and (2) how MISPR can help screen thousands of potential solvents and salts to identify optimal electrolyte systems.

References

1. Atwi, R.; Bliss, M.; Makeev, M.; Rajput, N. N., MISPR: an open-source package for high-throughput multiscale molecular simulations. *Scientific Reports* **2022**, *12* (1), 15760.
2. Atwi, R.; Chen, Y.; Han, K. S.; Mueller, K. T.; Murugesan, V.; Rajput, N. N., An automated framework for high-throughput predictions of NMR chemical shifts within liquid solutions. *Nature Computational Science* **2022**.

<!--[endif]---->

4:45 PM DS04.03.05

Investigating Combinatorial Thin Films and Scanning Electrochemical Techniques for High Throughput Data Generation Natalie Page¹, Naohiro Fujinuma², Jeffrey Hettinger¹ and Samuel E. Lofland¹; ¹Rowan University, United States; ²Sekisui Chemical Co., Ltd, Japan

Heterogeneous catalysts demonstrate promise for generating sustainable carbon neutral fuels and recycling carbon resources, but high cost has made implementation economically unfeasible, and a lack of understanding of catalytic reaction mechanisms has hampered new developments needed for scalability and production. High throughput experimentation (HTE) has had success in novel material discovery, but there are limited HTE techniques for electrochemical catalysts. Here we discuss HTE on precious metal quaternary alloys for electrocatalysis. Combinatorial thin films synthesized via magnetron sputtering were investigated with a custom scanning electrochemical cell made by additive manufacturing. The scanning system allows for a variety of measurements including cyclic voltammetry, chronoamperometry, electrochemical impedance spectroscopy, and electrolyte analysis. Using robust machine learning algorithms, we correlate these results with the physical properties investigated by traditional techniques such as scanning electron microscopy, energy dispersive spectroscopy, x-ray diffraction, and atomic force microscopy in order to identify candidate alloys that satisfy key metrics such as selectivity, productivity, durability, and efficiency.

SESSION DS04.04: High-Throughput Experimentation and Data-Driven Methods II

Session Chairs: Jason Hattrick-Simpers, Del Jackson and Yangang Liang

Tuesday Morning, November 28, 2023

Sheraton, Second Floor, Back Bay B

8:30 AM *DS04.04.01

Designing High Throughput Workflows: From Experiment Automation to Data Management John M. Gregoire¹, Joel A. Haber¹, Dan Guevarra¹, Lan Zhou¹, Kevin Kan¹, Ryan Jones¹, Yungchieh Lai¹, Ja'Nya Breedon¹, Michael Statt², Brian Rohr² and Santosh Suram³; ¹California Institute of Technology, United States; ²Modelyst LLC, United States; ³Toyota Research Institute, United States

In the quest to accelerate materials discovery via experiment automation and artificial intelligence, we recognize the challenges in emulating human capabilities with respect to contextualizing data and rapidly adapting experiments based on real-time data streams. In the development of infrastructure for next-generation workflows, these aspects of traditional research are most tightly connected to instrument control software and the management of experimental data. We will describe the evolution of these capabilities at Caltech, from automated workflows focused on throughput and consistency to workflows that embrace modularity and responsiveness to new knowledge, where techniques for this latter approach are being developed collaboratively with Modelyst, Inc. and Toyota Research Institute. The lessons learned with respect to data management may be the most generalizable to the materials chemistry community, especially our development of Event-Sourced Architecture for Materials Provenance Management (ESAMP) and the Materials Experiment Knowledge Graph (MekG), which addresses the hierarchical nature of materials data. Regarding representation of materials data, high-level descriptors can be provided by the chemical elements, crystal structure motifs, and types of materials properties,

and ultimately a given piece of data must be considered in the context of its acquisition. Detailed descriptors of a piece of experimental data include not only the metadata for the experiment that generated it, but also the prior history of synthesis and metrology experiments. Graph databases offer an opportunity to represent such hierarchical relationships among data, organizing semantic relationships into a knowledge graph. Initial reports of knowledge graphs in materials science highlight the breadth of approaches for their development. We describe a knowledge graph of materials experiments whose construction encodes the complete provenance of each material sample and its associated experimental data and metadata. Additional relationships among materials and experiments further encode knowledge and facilitate data exploration. MekG is sufficiently large and complex to demonstrate a path toward a global materials knowledge graph. We characterize the scalability of this approach, especially with respect to executing queries, illustrating the value that modern graph databases can provide to the enterprise of data-driven materials science.

9:00 AM DS04.04.02

Predicting Synthesizability using Positive-Unlabeled LearningGeun HoGu; Korea Institute of Energy Technology, Korea (the Republic of)

The high-throughput screening of the crystal databases has accelerated the discovery of new materials. To expand the screening scope, density functional theory (DFT) optimization is combined with generative models, evolutionary algorithms, and element substitution to create “virtual” crystals that have not been synthesized previously but are predicted to be stable *in silico*. However, the synthesizability of the virtual candidates remains a critical concern as their actual synthesis methods are unknown. To address the synthesizability of virtual candidates, DFT calculated energy such as formation energy, and energy above the hull is often used as intuitive screening criteria. While some of the thermodynamically stable virtual crystals are indeed synthesizable and functional, many virtual candidates are unsynthesizable, deeming the virtual crystal search impractical. These results are, however, not unexpected as the density functional theory-based energy metrics do not account for chemical potentials at the synthesis condition, as well as the kinetics of the complex synthesis. Quantifying the synthesizability is crucial to improving the reliability and practicality of virtual crystal exploration and advancing materials discovery.

Here, we present a probabilistic approach called positive-unlabeled learning to predict the synthesizability of the virtual crystals to improve the quality of the virtual crystal screening. The model framework implicitly considers the structural similarities between the virtual candidates and the previously synthesized candidates by training an ensemble of binary classification models with previously synthesized data as positive and randomly selected unlabeled data as negative. The average of the ensemble of the model predicts the synthesizability score that we call the crystal-likeness score. We train our model with Materials Project data, demonstrating the 87.4% true positive rate (TPR) for the test set of experimentally reported cases (9356 materials). We further validate the model by predicting the synthesizability of newly reported experimental materials in the last 5 years (2015–2019) with an 86.2% true positive rate using the model trained with the database as of the end of the year 2014. Our analysis shows that our model captures the structural motif for synthesizability beyond what is possible by Ehull. We find that 71 materials among the top 100 high-scoring virtual materials have indeed been previously synthesized in the literature.

We further explore the applications by performing transfer learning to inorganic perovskite crystals. We find that the model shows a 95.7% TPR. Further validation is established by demonstrating that 179 virtual crystals that are predicted to be synthesizable have already been synthesized in literature, and those with the lowest synthesizability scores have not been reported. These numbers are comparable to 943 perovskite crystals in OQMD, MP, and AFLOW that are registered as previously synthesized. While previous methods focused on metal oxides, our model applies to other classes of perovskites, including chalcogenide, halide, and hydride perovskites, as well as anti-perovskites. For comparison, Goldschmidt factor-based screening is applied which was only applicable to 388 perovskites out of 943 registered perovskites, and a TPR of 0.863 was obtained for the 388 crystals. We apply the method to identify synthesizable perovskite candidates for metal halide optical materials. With the proposed data-driven metric of the crystal-likeness score, high-throughput virtual screenings can benefit significantly by reducing and prioritizing the candidate for experimental testing.

9:15 AM DS04.04.03

Predict Thermodynamic, Thermal and Mechanical Properties of High Entropy Alloys using Physics-Informed Machine LearningMichaelGao, WilliamTrehern, YiWang and SaroSan; National Energy Technology Laboratory, United States

High entropy alloys represent a new paradigm shift in materials design. The main challenges in high entropy alloys development are the lack of efficient and reliable tools to predict the composition-processing-microstructure-properties relationships of vastly unexplored compositional space as well as their dependence on temperature, pressure, and other environmental/operating conditions. In this talk we will present our ongoing research effort in predicting thermodynamic, thermal and mechanical properties of HEAs by integrating multi-scale computational modeling with machine learning. Modeling techniques include high throughput CALPHAD calculations, density functional theory methods (DFT), and continuum models. CALPHAD method allows us to predict phase diagram information including phases and their mole fractions and phase transformations. Single crystal elastic constants and average elastic properties, defect energetics (such as surface energy and stable and unstable stacking fault energies), and intrinsic ductility are predicted using DFT methods. To predict coefficient of thermal expansion (CTE) and temperature-dependent elastic constants, we adopt an optimized Debye model by calibrating the Debye temperature and its volume dependence of pure elements by comparing the predicted heat capacity and CTE to the experimental results. Based on these predicted properties from physics-based models and reported experimental results, machine learning modeling are performed to predict thermal and mechanical properties of HEAs. The integration of high-fidelity multiscale modeling with machine learning not only helps decipher complex materials challenges such as high temperature strength and creep behavior but also accelerates the design of cost-competitive high-performance alloys for extreme environment applications.

9:30 AM DS04.04.04

Convex Hull Aware Active Search for Phase Stability in High-Dimensional Composition SpacesAndrewNovick¹, DianaCai², QuanNguyen³, VladanStevanovic¹, RomanGarnett³, RyanAdams² and EricS. Toberer¹; ¹Colorado School of Mines, United States; ²Princeton University, United States; ³Washington University in St. Louis, United States

High-entropy ceramics have a variety of clean-energy applications including catalysis, thermoelectrics, and batteries. Building a library of stable, high-entropy ceramics is a critical first step for eventually discovering exceptional compositions. As such, considerable efforts have been made in producing high-throughput screening methods for identifying single-phase compositions. A convex hull is required for assessing the stability of a composition; despite ongoing efforts, it remains incredibly costly—and often infeasible—to produce an accurate free energy convex hull in many dimensions.

For this purpose, we have developed convex-hull aware active search to efficiently produce the free energy convex hull. In each iteration of the active search algorithm, we choose the composition that is expected to give the most information about the hull. As such, we do not waste calculations trying to accurately model irrelevant compositions that are clearly above the hull. Often, large swaths of composition space are far above the hull, and by ignoring them, our algorithm allows for efficient exploration. Since Bayesian methods are employed, the uncertainty in the hull is naturally resolved as a function of composition, allowing for intelligent decisions based on the produced predictions. We offer this method as a tool for effectively building a library of stable, high-entropy ceramics. As a proof of concept, we calculate the free energy convex hull for the ternary (Pb,Sn,Ge)(S,Se,Te), a relevant composition space for thermoelectrics.

9:45 AM DS04.04.05

Data-Driven Bayesian Optimization of P-Type Polymer Dopant Complexes for Next-Generation ThermoelectricsConnorGanley¹, TushitaMukhopadhyaya^{1,2}, HowardE. Katz¹ and PauletteClancy¹; Johns Hopkins University, United States; ²Georgia Institute of Technology, United States

Semiconducting polymers have shown remarkable performance in applications such as organic light-emitting diodes (OLEDs), organic solar cells (OSCs), and thermoelectric materials, establishing their status as formidable candidates for “greener” next-generation materials. These materials are solution-processable, hence their manufacture is low-cost and highly scalable. Doping suitable polymers with small molecules has a demonstrably positive impact on the electronic properties of the final polymeric thin film by increasing the charge carrier concentration and electrical conductivity. We have previously published several studies exploring different *p*- and *n*-type polymers, dopants, and their respective properties, showing, in some select cases, record-breaking thermoelectric performance. Unfortunately, the search for optimal polymer-dopant pairs thus far has been largely Edisonian and based on ill-quantified means like expert knowledge and chemical intuition. This work seeks to leverage the power of *ab initio* electronic structure calculations in conjunction with a machine-learning-based optimization for high-performing *p*-type doped semiconducting polymers.

The goal of this work is to identify a novel high-performing *p*-type polymer-dopant combination from a combinatorially expansive pool of candidates, which will consequently demonstrate the utility of a data-based approach toward polymer engineering. Such an identification will be conducted using the Physical Analytics pipeline (PAL), a Bayesian Optimization (BO) code written in Python and developed by the Clancy group. PAL has been shown previously to incorporate physical domain knowledge (*e.g.* DFT results) into an efficient optimization over a large compositional space. The input data will consist of electronic properties obtained from density functional theory (DFT) calculations, such as sigma profiles, HOMO-LUMO gaps, and ionization potentials/electron affinities. For reference, sigma profiles are unnormalized histograms of the screened surface charge of a molecule that provide important information about charge distribution in a molecule. This important information provides information on the degree of localization of charges, which impacts electron transfer. A large amount of model training data already exists from our previous papers about doped *p*-type polymers. The BO algorithm will attempt to maximize electron transport properties such as the Seebeck coefficient, power factor, and conductivity, in separate single-objective experiments. These properties will be calculated for candidate complexes using BoltzTrap2, a Python code that quantifies electron transport behavior.

10:00 AM BREAK

10:30 AM *DS04.04.06

High-Throughput Automation and AI Accelerate New Material Development Grant Gavranovic, Rick Sidler and DeJ Jackson; Unchained Labs, United States

High-throughput lab automation systems are well established for dramatically accelerating the development of novel pharmaceutical treatments and other functional chemicals. More recently, this technology has been directed to energy storage applications, including synthesis and characterization of electrode materials, electrolytes, catalyst inks, and more. These advances have involved the evolution of existing technologies and creation of new capabilities specific to material development applications.

By combining the inherent characteristics of lab automation, including high accuracy and precision, and capture of structured data with advances in software interoperability, such as open APIs and widespread use of Python, researchers are now able to develop and train ML/AI models more easily for their specific research goals. These models have also been used to direct automated systems to perform the desired experiments, including in fully autonomous systems.

This presentation will include examples of key hardware and software capabilities that have been applied to high-throughput material development workflows. It will also address challenges and important factors to consider when implementing new automated systems, such as self-driving labs.

11:00 AM DS04.04.07

Pre-Treatment Methods for Machine Learning in Finer UV Spectrum Inference Hajime Shinohara, Indra Priyadarsini S, Daiju Nakano, Akihiro Kishimoto and Seiji Takeda; IBM Research - Tokyo, Japan

Spectroscopy is a crucial modality for evaluating the properties of materials. In particular, UltraViolet (UV) spectra enable the measurement of important energy gap structures that provide information about the electronic structure. Spectral features encompass not only direct properties such as peak positions and bandwidths but also quantitative evaluations of features like graph curvature, which can be challenging. This highlights the potential effectiveness of spectroscopy as a modality for machine learning.

Previous studies utilizing Long Short-Term Memory (LSTM) have achieved partial success in predicting the shape of spectra for certain substances, while struggling with others. Meanwhile, Transformers have gained significant attention in machine learning in recent years due to their ability to combine structures and exhibit various variations.

In this study, we constructed a Transformer architecture to train on UV spectra. The input consisted of Simplified Molecular Input Line Entry System (SMILES) representations tokenized using a tokenizer, allowing us to infer spectra from chemical structures. The training data included both existing data from prior studies. Furthermore, several techniques were implemented to enhance the model's performance, and the results were compared and examined. Additionally, a comparison was made with other models such as LSTM and Gated Recurrent Unit (GRU) to further assess the model's performance.

In this presentation, we will provide an explanation of the results, discussions, and considerations derived from this comparative analysis.

11:15 AM DS04.04.08

High-Throughput Calculation Workflows for Solid State Systems Alp E. Samli¹, Rachel N. Kerber², Misbah Sarwar² and David O. Scanlon^{1,3}; ¹University College London, United Kingdom; ²Johnson Matthey Technology Centre, United Kingdom; ³University of Birmingham, United Kingdom

The automation of calculations is key for high-throughput computational screening which can accelerate materials discovery and characterisation for a myriad of applications. These include Johnson Matthey's areas of expertise such as the catalysis of green hydrogen production via electrolysis and NO_x reduction for clean air using rutile oxides (e.g. IrO₂ and RuO₂). AiiDA^{1,2} is one of several platforms that can be used to automate calculations with a focus on preserving data provenance using a database backend.

In this work, we have used AiiDA^{1,2} to create material-agnostic workflows for high-throughput CASTEP³ density functional theory calculations of materials' properties. These workflows can automate various calculations including convergence testing, density of states, band structure, phonon, and core electron loss calculations. In addition to running these calculations, our workflows use several packages such as Sumo⁴ and Galore⁵ to produce publication ready plots of the density of states, band structure, phonon dispersion, and simulated spectra of materials. The simulated spectra cover both electronic (UPS, XPS, HAXPES, EELS) and vibrational (IR, Raman) spectroscopy techniques, and can be compared to experimental spectra to aid the characterisation of new materials. We have tested these workflows with rutile TiO₂, a widely studied photocatalyst, and found that our results are in good agreement with the literature. We will now extend our workflows for cluster expansion and surface slab calculations in order to study rutile oxides and their alloys for green hydrogen catalysis.

References:

1 S. P. Huber, S. Zoupanos, M. Uhrin, L. Talirz, L. Kahle, R. Häuselmann, D. Gresch, T. Müller, A. V. Yakutovich, C. W. Andersen, F. F. Ramirez, C. S. Adorf, F. Gargiulo, S. Kumbhar, E. Passaro, C. Johnston, A. Merkys, A. Cepellotti, N. Mounet, N. Marzari, B. Kozinsky and G. Pizzi, *Sci Data*, 2020, **7**, 300.

2 M. Uhrin, S. P. Huber, J. Yu, N. Marzari and G. Pizzi, *Computational Materials Science*, 2021, **187**, 110086.

3 S. J. Clark, M. D. Segall, C. J. Pickard, P. J. Hasnip, M. I. J. Probert, K. Refson and M. C. Payne, *Zeitschrift für Kristallographie - Crystalline Materials*, 2005, **220**, 567–570.

4 A. M. Ganose, A. J. Jackson and D. O. Scanlon, *Journal of Open Source Software*, 2018, **3**, 717.

5 A. J. Jackson, A. M. Ganose, A. Regoutz, R. G. Egdell and D. O. Scanlon, *Journal of Open Source Software*, 2018, **3**, 773.

11:30 AM *DS04.04.09

Functional High Entropy Alloys Discovered by Active Learning Dierk R. Raabe and Ziyuan Rao; Max Planck Institute for Iron Research, Germany

High-entropy alloys are solid solutions of multiple principal elements, capable of reaching composition and feature regimes inaccessible for dilute materials. Discovering those with valuable properties, however, often relies on serendipity, as thermodynamic alloy design rules alone often fail in high-dimensional composition spaces. In this talk we present an active-learning strategy to accelerate the design of novel high-entropy Invar alloys in a practically infinite compositional space, based on very sparse data. Our approach works as a closed-loop, integrating machine learning with density-functional theory, thermodynamic calculations, and experiments. After processing and characterizing 17 new alloys (out of millions of possible compositions), we identified 2 high-entropy Invar alloys with extremely low thermal expansion coefficients around $2 \times 10^{-6} \text{ K}^{-1}$ at 300 K. Our study thus opens a new pathway for the fast and automated discovery of high-entropy alloys with optimal thermal, magnetic and electrical properties [1].

1. Rao, Z. et al. Machine learning-enabled high-entropy alloy discovery. *Science* (80). 85, 78–85 (2022).

SESSION DS04.05: High-Throughput Experimentation and Data-Driven Methods III

Session Chairs: Doris Segets and Yizhou Zhu

Tuesday Afternoon, November 28, 2023

Sheraton, Second Floor, Back Bay B

1:30 PM *DS04.05.01

Automated Phase Mapping of High Throughput X-Ray Diffraction Data Encoded with Domain-Specific Knowledge Yizhou Zhu; Westlake University, China

Combinatorial synthesis and high-throughput characterization have emerged as powerful tools for expediting the discovery and design of novel materials. A crucial step in establishing the structure-properties relationship is the accurate extraction of constituent phase information and gaining insights from high-throughput X-ray diffraction data obtained from combinatorial libraries. Essential information includes the identification, abundance, and distribution of phases across all samples, while advanced details encompass lattice changes, texture information, defects, and solid solutions. Integrating domain-specific knowledge, such as crystallography, X-ray diffraction, thermodynamics, kinetics, and solid-state chemistry, into automated algorithms is imperative for the development of automatic phase mapping algorithms. In this presentation, we show that how we combine first-principles calculations, machine learning techniques, and physics-encoded constraints within an automated workflow to solve multiple combinatorial library datasets. We show that by implementing domain-specific-knowledge-based constraints, our model successfully solved these datasets and gain important materials insights. Furthermore, we explore future directions, offering recommendations and ideas for data-driven combinatorial approaches in dataset generation and collection.

2:00 PM DS04.05.02

Machine Learning of Magnetoelectric Multipoles[Aria Mansouri Tehrani](#) and Tess Smidt; Massachusetts Institute of Technology, United States

In this work, we have developed and implemented equivariant neural networks to help understand and discover new magnetoelectric multiferroics, a class of energy materials with application in energy-efficient memory devices. Magnetoelectric multiferroics are materials exhibiting simultaneous spontaneous switchable electric polarization (ferroelectricity) and magnetization (ferromagnetism or other types of magnetic ordering). A bottleneck in the design of these materials is evaluating their linear magnetoelectricity, which we addressed by using the irreducible representations of their magnetoelectric multipole tensor. We achieved this by constructing efficient symmetry-preserving neural networks (leveraging the e3nn library) that can learn scalar, vector, and tensorial quantities. Next, we employed our methodology to predict new crystal structures and magnetic orientations that maximize linear magnetoelectricity in the BiFeO₃ phase space. Not only our work provide a framework to discover new multiferroics, but it will also provide new data-driven frameworks for materials design by enabling the efficient prediction of materials properties with complex forms.

2:15 PM *DS04.05.03

The Era of Data-Driven Innovation and Design of Energy Materials[Kristina A. Persson](#)^{1,2}; ¹UC Berkeley, United States; ²Lawrence Berkeley National Laboratory, United States

Entering the era of the fourth paradigm of materials science, we recognize that highly curated, tested, and provenanced data is the fuel for machine learning. As part of the Materials Genome Initiative, the Materials Project (www.materialsproject.org) was founded in 2010 at Lawrence Berkeley National Laboratory to accelerate materials design using supercomputing and software infrastructure together with state-of-the-art quantum mechanical theory. Today, the Project has over 400,000 registered users and supplies millions of data records every day to an increasingly data-hungry community. As one example, early attention to the importance of data, the Project saved and curated millions of relaxation trajectories, which since 2017 has provided the basis of training highly accurate interatomic machine learning potentials. In this talk we will give an update on recent work in the realm of data-driven materials design for energy applications, showcase successes and comment on remaining bottlenecks in accelerating materials innovation.

2:45 PM BREAK

SESSION DS04.06: Accelerated Catalysis Discovery I
Session Chairs: Jason Hatrick-Simpers and Yangang Liang
Tuesday Afternoon, November 28, 2023
Sheraton, Second Floor, Back Bay B

3:15 PM *DS04.06.01

AI Guided Workflows for Efficiently Screening the Materials Space: Examples for Thermal Insulators and Heterogeneous Catalysis[Matthias Scheffler](#), Thomas A. Purcell and Lucas Foppa; The NOMAD Laboratory at the FHI of the Max Planck Gesellschaft, Germany

Reliable artificial-intelligence models are key to accelerate the discovery of new functional materials with optimal properties for the applications of interest. In this talk, we present a general, data-driven framework for steering data creation via a combination of symbolic regression, compressed sensing, and sensitivity analysis. Our SISO approach (sure-independence screening and sparsifying operator) provides *quantitative rules* in terms of *analytical functions* that depend on the governing materials-characteristics parameters (also called “*materials genes*” for the function of interest).[1, 2]

We demonstrate the power of the framework for the lattice thermal conductivity using only 75 experimentally measured values. By extracting the most influential material properties from this model, we are then able to hierarchically screen 732 materials and find 20 materials with an ultra-low thermal conductivity of < 1 W/mK.[3] Further examples include the performance of heterogeneous catalysts.[4]

1) R. Ouyang, E. Ahmetcik, C. Carbogno, M. Scheffler, and L. M. Ghiringhelli, *Simultaneous Learning of Several Materials Properties from Incomplete Databases with Multi-Task SISO*. J. Phys. Mater. 2, 024002 (2019). <https://doi.org/10.1088/2515-7639/ab077b>

2) T. A. R. Purcell, M. Scheffler, and L. M. Ghiringhelli, *Recent advances in the SISO method and their implementation in the SISO++ code*, submitted to The Journal of Chemical Physics (2023). <https://arxiv.org/abs/2305.01242>

3) T. A. R. Purcell, M. Scheffler, L. M. Ghiringhelli, C. Carbogno, *Accelerating Materials-Space Exploration for Thermal Insulators by Mapping Materials Properties via Artificial Intelligence Conductivity*. npj Computational Materials, in print (2023). <https://arxiv.org/abs/2204.12968>

4) L. Foppa, et al., *Data-Centric Heterogeneous Catalysis: Identifying Rules and Materials Genes of Alkane Selective Oxidation*, J. Am. Chem. Soc. 145 (6), 3427 (2023). <https://pubs.acs.org/doi/pdf/10.1021/jacs.2c11117>

3:45 PM DS04.06.02

Unraveling the Catalytic Effect of Hydrogen Adsorption on Pt Nanoparticle Shape-Change[Cameron J. Owen](#)¹, Nicholas Marcella², Yu Xie¹, Jonathan Vandermause¹, Anatoly Frenkel^{3,4}, Ralph Nuzzo² and Boris Kozinsky^{1,5}; ¹Harvard University, United States; ²University of Illinois at Urbana-Champaign, United States; ³Stony Brook University, The State University of New York, United States; ⁴Brookhaven National Laboratory, United States; ⁵Robert Bosch LLC Research and Technology Center, United States

Understanding atomic-level processes in surface science and heterogeneous catalysis is complicated by the wide range of time- and length-scales needed for realistic simulations for comparison to experiments. To accelerate molecular dynamics simulations, we rely on machine-learning methods to capture interatomic interactions with quantum-mechanical accuracy. Our method (FLARE) enables autonomous selection of training sets for reactive systems, based on an adaptive closed-loop algorithm that constructs accurate and uncertainty-aware Bayesian force fields on-the-fly from molecular dynamics simulations. From this accelerated sampling routine, a machine-learned force field (MLFF) is built that can access long time- and length-scale simulations of catalytic reaction dynamics. We use ML-accelerated MD simulations to study heterogeneous reactions and nanoparticle shape-changes that are catalyzed under exposure to reactive atmospheres. These observations allow for improved opportunities in material design, where material exposure to temperature or adsorbates can yield shape-changes or reconstruction, and consequently different catalytic behavior under operating conditions.

To illustrate these phenomena, we present the catalytic effect of hydrogen adsorption on small Pt nanoparticle shape-change [1]. The MLFF provides an accurate description of these systems under the effects of temperature and reactive adsorbates, which are corroborated by experimental observations, establishing confidence in the ability of the MLFF to provide atomic resolution regarding the underlying mechanisms driving these processes.

[1] Owen, C.J., Marcella, N., Xie, Y., Vandermause, J., Nuzzo, R.G., Frenkel, A.I., Kozinsky, B. “Unraveling the Catalytic Effect of Hydrogen Adsorption on Pt Nanoparticle Shape-Change.” arXiv preprint: arXiv:2306.00901 (2023).

4:00 PM DS04.06.03

Exploring Optimal Candidates for Water-Splitting Reactions in ZnTe-Based Alloys: A Machine Learning Approach using Small Dataset[Seunghyun V. Oh](#)¹, Su-Hyun Yoo² and Aloysius Soon¹; ¹Yonsei University, Korea (the Republic of); ²Korea Research Institute of Chemical Technology, Korea (the Republic of)

Aiming towards a sustainable-and-clean-energy era, designing efficient photocatalysts for water splitting has been an active area of research, especially pertaining to deliberate band engineering and its related properties. To discover potential candidate materials, synthesizing solid-solutions and alloys are some of the promising approaches to meet the criteria. However, the enormous possible configurations of solid-solutions and alloys hinder the experimental screening within this multidimensional materials space, and thus machine-learning (ML) approaches may accelerate the discovery of new and novel mixed material systems. A conventional prerequisite for ML approaches is a large database containing accurate properties/data of materials that will essentially require a huge amount of computing resources. In this work, we demonstrate that the screening of mixed binary alloys (up to hexanary systems) can be performed accurately and successfully by utilizing a small database. This approach allows us to minimize the number of high-level theoretical calculations with ZnTe-based alloys as a prototypical example, based on the Sure Independent Screening and Sparsifying Operator (SISO) and the *agreement* method (-method) [1]. With this, we propose ML-designed ZnTe-based alloys as optimal candidates for water-splitting reactions.

4:15 PM *DS04.06.04

Automated Catalyst Layer Fabrication and Characterization for Faster Electrocatalyst Screening Dominik Dworschak¹, Thomas Ackstaller^{1,2}, Gün D. Akkoç^{1,2}, Simon Thiele^{1,2} and Karl J. Mayrhofer^{1,2}; ¹Forschungszentrum Juelich, Helmholtz Institute Erlangen-Nuremberg, Germany; ²Friedrich-Alexander-Universität Erlangen-Nürnberg, Germany

Facing the consequences of climate change, the demand for highly efficient energy solutions is increasing rapidly. Still, before large-scale use of the existing technical devices like fuel cells and electrolyzers, they still require the implementation of new materials and components making them more efficient and less expensive. However, the pace of the innovation chain is a huge technical barrier for the commercial implementation of innovative materials and components in technical devices. While related research fields as batteries^[1] and printable photovoltaics^[2] are already using fully automated laboratories for accelerated materials screening, a comprehensive infrastructure for electrocatalysis is still missing.

Here we show how we apply the concept of an automated research platform on electrocatalysis research. In a high-throughput manner we can fabricate and characterize catalyst layers. Starting with catalyst powder, solvents and ionomers, the setup is capable to produce and characterize catalyst inks and subsequently fabricate catalyst layers on substrates. Those get electrochemically characterized with a robot-mounted flow cell. Besides activity from electrochemistry we as well track stability by downstream degradation analysis with ICP-MS. Application of robots not only increases the amount of tested samples but also repeatability. A structured data acquisition along the workflow further enables the later use of machine learning algorithms.

Showcased on acidic oxygen evolution reaction (OER) the system can be widely applied for other ink-based electrocatalytic reactions. Our automated, high-throughput approach is an important step towards self-driving laboratories for accelerated electrocatalysis research.

[1] Benayad, A.; Diddens, D.; Heuer, A.; Krishnamoorthy, A. N.; Maiti, M.; Le Cras, F.; Legallais, M.; Rahmanian, F.; Shin, Y.; Stein, H.; *et al.* High-Throughput Experimentation and Computational Freeway Lanes for Accelerated Battery Electrolyte and Interface Development Research. *Adv. Energy Mater.* **2022**, *12*, 2102678. DOI: 10.1002/aenm.202102678.

[2] Wagner, J.; Berger, C. G.; Du, X.; Stubhan, T.; Hauch, J. A.; Brabec, C. J. The evolution of Materials Acceleration Platforms: toward the laboratory of the future with AMANDA. *J Mater Sci* **2021**, *56*, 16422–16446. DOI: 10.1007/s10853-021-06281-7.

4:45 PM DS04.06.05

The "Materials Genes" of Catalysis Identified via AI Lucas Foppa^{1,2} and Matthias Scheffler^{1,2}; ¹Fritz-Haber-Institut der Max-Planck-Gesellschaft, Germany; ²Humboldt-Universität zu Berlin, Germany

The performance in heterogeneous catalysis is an example of a materials function governed by an intricate interplay of multiple underlying processes, such as the surface reaction networks, the material restructuring under the reaction, and the transport of reactants and products. In this talk, the combination of experimental and theoretical data with artificial intelligence (AI) is presented as an approach to model catalysis and determine the key physicochemical descriptive parameters ("materials genes") reflecting the processes that trigger, facilitate, or hinder the materials performance.[1] The symbolic regression and subgroup discovery AI approaches leverage the small number of materials that can be accessed experimentally and identify nonlinear correlations that can be exploited for the design of materials with statistically exceptional performance.

[1] L. Foppa, L. M. Ghiringhelli, F. Girgsdies, M. Hashagen, P. Kube, M. Hävecker, S. Carey, A. Tarasov, P. Kraus, F. Rosowski, R. Schlögl, A. Trunschke, and M. Scheffler, *MRS Bull.* **46**, 1016-1026 (2021).

SESSION DS04.07: Poster Session I: Accelerated Discovery of Materials for Energy I

Session Chairs: Jason Hatrick-Simpers, Yangang Liang and Michael Thuis

Tuesday Afternoon, November 28, 2023

Hynes, Level 1, Hall A

8:00 PM DS04.07.01

Unraveling the Mechanisms of Stability in $\text{Co}_x\text{Mo}_{70-x}\text{Fe}_{10}\text{Ni}_{10}\text{Cu}_{10}$ High Entropy Alloys via Physically Interpretable Graph Neural Networks Miguel Tenorio and James Chapman; Boston University, United States

In recent years high entropy alloys (HEA) have become a topic of significant interest due to their combinatorial nature, showing promise for hypersonics and catalysts. In particular, the HEA system $\text{Co}_x\text{Mo}_{70-x}\text{Fe}_{10}\text{Ni}_{10}\text{Cu}_{10}$ has been studied experimentally and computationally due to its reported superiority as a catalyst for ammonia decomposition. However, such catalytic reactions take place at elevated temperatures, leading to potential HEA instability and eventual phase separation at catalytically active temperatures. To this end, we combine density functional theory (DFT) calculations of mixing free energies, that include mixing and vibrational entropy terms, with physics-inspired graph neural networks (GNN) and consider binary ($A \leftrightarrow B + C$), ternary and quaternary decomposition routes. We show that by learning the mixing free energy with our GNN framework we can rank geometric and chemical HEA features to better understand which features are more important than others at stabilizing HEA stability at catalytically active temperatures.

8:00 PM DS04.07.02

Autoencoder Based on Graph and Recurrent Neural Networks and Application to Property Prediction Akihiro Kishimoto, Hiroshi Kajino, Indra Priyadarsini S, Hajime Shinohara, Daiju Nakano and Seiji Takeda; IBM Research - Tokyo, Japan

Machine learning has been applied to various subjects in material science, including property prediction and molecular structure generation. Successful machine learning models can lead to discovering promising materials more quickly. However, a challenge remains on automatically acquiring features that can effectively represent materials.

An autoencoder attempts to learn an effective representation in a so-called latent space and has been applied to learn for molecular structures. Given a molecular structure as input, the encoder of the autoencoder encodes its input into a vector in the latent space called a latent vector. The decoder of the autoencoder decodes that latent vector back to the original molecular structure. The autoencoder has a potential to be able to learn features as latent vectors even without labeled training data.

Molecular Hypergraph Grammar Variational Auto-Encoder (MHG-VAE) consists of an encoder and a decoder based on recurrent neural networks combined with molecular hypergraph grammar. While MHG-VAE can additionally ensure structural validity of decoded molecules, it suffers from a drawback that new molecular structures cannot always be encoded. MHG-VAE, therefore, has a limited applicability to address downstream tasks on new molecules, when their features need to be represented as the latent vectors of MHG-VAE.

We introduce a new autoencoder that can always encode any molecular structure. Our autoencoder achieves this advantage by replacing the encoder of MHG-VAE with a graph neural network. Our autoencoder inherits all the other advantages of MHG-VAE including the structural validity of the decoder.

We have trained an autoencoder model with a large set of molecules available at the PubChem database. We have also trained a prediction model that receives the latent space of the autoencoder model as input to perform a prediction of a material property. We show that such a downstream task can have molecules that cannot be encoded by MHG-VAE. Additionally, our prediction model outperforms MHG-VAE even if the training and test datasets are restricted to the molecules encoded by MHG-VAE.

8:00 PM DS04.07.03

Chemical State Analysis Assisted Combinatorial Exploration of New Phase Spaces: Application to Ternary Zn-M-N Nitrides and Synthesis of Wurtzite Zn_2TaN_3 Siarhei Zhuk¹, Alexander Wiczorek¹, Amit Sharma², Jyotish Patidar¹, Kerstin Thorwarth¹, Johann Michler² and Sebastian Siol¹; ¹Empa-Swiss Federal Institute of Materials Science and Technology, Switzerland; ²Empa-Swiss Federal Laboratories for Materials Science and Technology, Switzerland

The experimental realization of predicted functional materials is a key challenge in the development of new technologies.[1,2] Combinatorial high-throughput approaches using reactive sputtering and automated analysis are commonly employed to screen unexplored phase spaces.[1,2] Especially, when synthesizing new materials in complex phase spaces results from a conventional structural phase screening can be ambiguous.

In this presentation, we show how chemical state analysis based on X-ray photoelectron spectroscopy can complement conventional high-throughput workflows. Specifically, we highlight how studies based on the Auger parameter are ideally suited to probe the local chemical state and coordination in insulating or semiconducting materials. Firstly, the Auger parameter is insensitive to charging and erroneous calibration of the instrument.[3,4] Secondly, the analysis typically does not require multi-component peak fitting, which facilitates high-throughput

As a proof of concept, we perform a combinatorial screening of the Zn-Ta-N phase space with the aim to synthesize the novel semiconductor Zn_2TaN_3 . While the results of the XRD phase screening are inconclusive, including chemical state analysis mapping in our workflow allows us to see a very clear discontinuity in the evolution of the Ta Auger parameter. This is indicative of a change in the Ta oxidation state and coordination and consequently confirms the formation of the phase of interest. In additional experiments, we then isolate the material and perform a detailed characterization confirming the formation of single phase WZ- Zn_2TaN_3 . [5] Besides the formation of the new ternary nitride, we map the functional properties of $Zn_xTa_{1-x}N$ and report previously unreported clean chemical state analysis for Zn_3N_2 , TaN and Zn_2TaN_3 .

Overall, the results of this study showcase common challenges in high-throughput materials screening and highlight the merit of employing characterization techniques sensitive towards changes in the materials' short-range order and chemical state. The workflows and concepts described in this presentation are applicable to many different energy materials and can be applied using standard XPS equipment.

[1] W. Sun *et al.*, *Nature Materials*, **2019**, 18, 732–739

[2] S. Zhuk, A. Kistanov, S. Boehme, N. Ott, F. La Mattina, M. Stiefel, M. V. Kovalenko, S. Siol, *Chem. Mater.* **2021**, 33, 23, 9306–9316

[3] A. Wieczorek, H. Lai, J. Pious, F. Fu, S. Siol, *Adv. Mater. Interfaces* **2023**, 10, 2201828.

[4] S. Zhuk, S. Siol, *Appl. Surf. Sci.* **2022**, 601, 154172.

[5] S. Zhuk, A. Wieczorek, A. Sharma, J. Patidar, K. Thorwarth, J. Michler, S. Siol, *under review*, **2023**. (arXiv:2305.19875)

8:00 PM DS04.07.04

Data-Driven Doping for Semiconductors: Identifying Top Dopant Candidates for Complex Crystals [JiwooLee](#)¹, [AnthonyOnwuli](#)², [KeithT. Butler](#)² and [AronWalsh](#)²; ¹Yonsei University, Korea (the Republic of); ²Imperial College London, United Kingdom

Stoichiometric crystals, while often insulators, pose a challenge for technological applications that require excess electrons (n-type) or holes (p-type) through p-n junctions. Complex crystals, such as ternary and quaternary systems, offer numerous dopant possibilities, making it difficult to determine the optimal substituting element. This research utilizes a data-driven approach to identify the top 10 potential dopants for multicomponent materials.

Our "doper" code utilizes chemical similarity metrics based on structure analysis and machine-learned representations. It generates n-type p-type cation and anion potential dopants based on the input species of multicomponent materials. We validate our approach using density functional theory (DFT) calculations, considering solubility energy and defect levels. Our methodology is implemented within the Semiconducting Materials from Analogy and Chemical Theory (SMACT) framework, which offers rapid screening tools based on chemical element data.

Our results demonstrate a strong correlation between the data-driven top dopant candidates generated by "doper" and DFT calculations. This validates the efficacy of our approach in identifying promising dopant elements for semiconductors. By leveraging machine learning and structure analysis, our data-driven technique accelerates materials discovery and optimization, significantly reducing time and cost in dopant selection.

8:00 PM DS04.07.05

Optimizing Active Learning in Materials Discovery Through a Holistic Pruning Strategy for NN-based Agents [WeikeYe](#), [XiangyunLei](#) and [AmalieTrewartha](#); Toyota Research Institute, United States

During a closed-loop materials discovery process, a surrogate model is often used to form hypotheses about which new regions of parameter space to explore, and then more expensive experiments or higher-fidelity computations are performed to confirm or deny these hypotheses. The relatively high cost of re-training/fine-tuning surrogate models as high-fidelity data is acquired leads to a trade-off between accuracy and computational cost, which can in practice limit the ability to deploy state-of-the-art neural networks as surrogate models. In this work, we first propose a holistic pruning technique based on the Lottery Ticket Hypothesis that allows for structure optimization of neural networks (NN). We demonstrate that, for both fully connected NNs and graph-based convolutional NNs, we can find sparse sub-nets of the original models that can be trained faster to achieve commensurate or better accuracy and better generalizability with ~ 70 % or fewer weights. Subsequently, we combine the pruning technique with active learning frameworks for materials discovery to show that the additional pruning step reduces the total iterations required to locate all desired samples by up to 20% and decreases the retraining time of the NN-based agent by up to 40% in each iteration. We believe this acceleration allows for more rapid exploration of the parameter space, leading to faster identification and validation of new materials.

8:00 PM DS04.07.06

Hydrogen Absorption and Diffusion in High Entropy Alloys: Insights from DFT and Machine Learning [VladislavKorostelev](#) and [KonstantinKlyukin](#); Auburn University, United States

The emergence of hydrogen as a promising clean energy source has underscored the critical need for the development of advanced alloys that can efficiently store this valuable resource. However, the presence of hydrogen also poses challenges, particularly in the form of hydrogen embrittlement, which can compromise the structural integrity of alloys. As a result, there is a pressing demand for the exploration and design of new alloys that not only enable efficient hydrogen storage but also exhibit enhanced resistance to the detrimental effects of hydrogen. In order to simultaneously address the challenges of efficient hydrogen storage and resistance to hydrogen embrittlement, we have embarked on the development of a comprehensive model with the capability to predict hydrogen solubility and diffusivity.

The focus of our research lies in unraveling the atomistic factors that dictate hydrogen's interactions in high entropy alloys (HEAs) and investigating the underlying descriptors that influence its absorption and diffusion processes. Our ultimate objective is to construct an interpretable machine learning model that can accurately predict hydrogen absorption energy and diffusion rates, utilizing local physical descriptors associated with each interstitial site.

To achieve this, we used Density Functional Theory (DFT) to calculate hydrogen absorption energies for over 1000 unique octahedral, tetrahedral and triangular interstitial sites within 12 HEAs. Subsequently, we performed calculations to determine the relevant local environment descriptors, which encompassed a comprehensive analysis of electronic structure features such as the d-band center. Additionally, we investigated structural descriptors, including interstitial pore volume, and examined the dynamical structure of the lattice atoms through an analysis of the phonon structure.

To build an actual model, we used the sure-independence-screening-and-sparsifying-operator (SISSO) machine learning algorithm. This allowed us to develop physics-based model that accurately predict hydrogen absorption energy across various metallic systems. By identifying the key descriptors governing hydrogen absorption in HEAs, our models enable accelerated screening of potential compositions with optimal hydrogen solubility and diffusivity properties.

During the presentation, we will discuss the key descriptors, which have a profound impact on hydrogen absorption and diffusion. Additionally, we will present the performance of our model on previously unseen HEAs and other metallic systems, including intermetallic compounds.

8:00 PM DS04.07.07

A Convergence of Fast Sintering, Grain Growth Analysis, High Throughput Measurements, and Data Driven Computer Models to Develop New Solid-State Sodium-Ion Battery Materials [MichaelThuis](#)¹, [SeyedAreifpour](#)², [BrysonClifford](#)², [SufendLiu](#)², [RamanujaSaravanan](#)², [ShuoWang](#)², [AliciaKoenig](#)³, [ChrisMarvel](#)², [MartinHarmer](#)³, [LiangbingHu](#)², [YifeiMo](#)² and [SossinaM. Haile](#)¹; ¹Northwestern University, United States; ²University of Maryland, United States; ³Lehigh University, United States

Rapidly increasing demand for electric vehicles is straining the supply of battery materials. This need could be met with improved batteries using solid-state electrolytes and alternative battery chemistries. The ADD-Ions collaborative project is working to combine high throughput electrochemical measurements and data analysis with computational models to predict and develop new sodium-ion solid-state battery materials, in particular electrolytes. These methods are paired with an ultra-fast high-temperature synthesis (UHS) method allowing access to previously theoretical structures with simplified manufacturing steps. Scanning transmission electron microscopy (STEM) analysis is used to understand the unique grain growth and microstructure of these materials under fast sintering conditions. Bulk pellets are made using traditional and UHS methods to compare processing effects on the properties of solid-state electrolytes. Thin film samples are used to probe the chemical compositional and structure effects on the ionic conductivity of these materials.

8:00 PM DS04.07.08

A Unified Theory Quantifying How Lattice Dynamics Facilitate Proton Transport in Various Ternary-Oxide Phases [HeejungW. Chung](#), [PjotrZguns](#), [JuLi](#) and [BilgeYildiz](#); Massachusetts Institute of Technology, United States

Understanding the lattice dynamics of proton-conducting metal oxides is important for many applications, from optimizing hydrogen production to designing low-power neuromorphic-computing devices. Transport mechanisms in metal oxides are well-studied [1], so we know that protons stay localized to oxygens and hop between neighboring O...O pairs; the energy barrier of hopping is lower for pairs separated by shorter distances.

However, studies considering lattice dynamics are usually limited to simple perovskites, and phonons are only used to estimate attempt frequencies [2]. Others only treat phonons implicitly by correlating energy barrier with coarse quantities like unit-cell volume [3]. Recent work from our research groups has found phonon-based descriptors for proton-conduction in solid acids, which contain hydrogen in their nominal structures [4]. However, studying metal oxides requires a different approach, since the conduction pathways and proton sites within the lattice differ from those in solid acids.

Here, we developed a more general theory describing how lattice dynamics affect proton-transport energy-barriers in a variety of ternary oxides. In particular, we focused on phonon modes which bring neighboring O...O pairs closer together, thereby lowering the associated energy barrier. Lower-frequency modes, which are more accessible at lower temperatures, are more suitable for assisting proton transport. Following this principle, we formulated descriptors like thermal relative displacement between O...O pairs. We interpreted these descriptors by extracting the dominant phonon modes, and we found that they align well with the literature for systems like the perovskite, BaZrO₃. In order to validate this principle more broadly, we aim to correlate phonon-based descriptors with calculated energy barriers for emerging phases like brownmillerite and Ruddlesden-Popper. Although energy barriers are most commonly estimated using nudged-elastic-band, we are evaluating whether these static calculations sufficiently capture lattice flexibility, or whether dynamic simulations are required.

Developing these descriptors and analyzing the dominant modes will enhance our understanding of proton transport. This will enable various downstream applications, such as physically interpretable, high-throughput virtual screening and data generation. Building on prior high-throughput studies [4, 5], we can first pull oxides from a database, then expand the pool of candidates using elemental substitution and doping. Phonon-based descriptors can then be included in a suite of filters which help identify the most promising proton conductors. Given a large enough design space, active learning can also be employed to intelligently select candidates for more thorough calculations.

- [1] Kreuer K-D. *Chemistry of Materials*. 8 (1996) 610-641
- [2] Bork N., Bonanos N., Rossmeisl J., Vegge T. *Physical Review B*. 82 (2010) 014103
- [3] Wakamura K. *Solid State Ionics*. 180 (2009) 1343-1349
- [4] Klyukin K., Zguns P., Li J., Yildiz B. *In Preparation* (2023)
- [5] Islam M. S., Wang S., Hall A. T., Mo Y. *Chemistry of Materials*. 34 (2022) 5938-5948

This material is based upon work supported by the National Science Foundation Graduate Research Fellowship under Grant No. INC0546071. Any opinion, findings, and conclusions or recommendations expressed in this material are those of the authors(s) and do not necessarily reflect the views of the National Science Foundation.

8:00 PM DS04.07.09

Machine Learning Prediction of Heat Capacity for Solid Mixtures of Pseudo-Binary Oxides Julián Barra¹, Simone Audesse¹, Rajni Chahal² and Stephen Lam¹; ¹University of Massachusetts Lowell, United States; ²Oak Ridge National Laboratory, United States

Direct resistance-heated thermal energy storage in firebricks has been proposed as a low-cost energy storage alternative that could improve the economics of carbon-free electricity generation through both renewable and nuclear energy sources. The bricks used in these energy storage systems must be composed of oxide mixtures with specific material properties, amongst them a high heat capacity. While there are many methods available for the prediction of heat capacity in oxide mixtures, they all face different problems, with the Neumann-Kopp rule underperforming at higher temperatures and computational methods such as CALPHAD and Density Functional Theory being computationally expensive. Machine Learning algorithms have already shown promise in applications to predict the heat capacity of pure solid inorganics and could be used as a less computationally-demanding tool for the prediction of this property in pseudo-binary oxide mixtures, with the main impediment to its use being the unavailability of a heat capacity database for oxide mixtures. For this work, we use the CALPHAD software Thermo-Calc and its TCOX11 database of oxide Gibbs Free Energy functions obtained by approximation of empirical data in order to generate a molar heat capacity dataset for pseudo-binary oxide mixtures at different temperatures and percentage compositions, and then use this dataset to train and test Machine Learning algorithms to predict molar heat capacity, using descriptors obtained from publically available DFT result repositories. By this process, we obtain algorithms capable of predicting heat capacity, some of them with an r^2 over 0.98, a MAE under 0.2 J/(molK) and a MAPE under 0.7%.

8:00 PM DS04.07.10

An Artificial Intelligence's Interpretation of Complex High-Resolution In Situ Transmission Electron Microscopy Data Xingzhi Wang^{1,2}, Chang Yan^{1,2,3}, Justin Ondry^{1,4,5}, Peter Ercius² and Paul Alivisatos^{1,2,5}; ¹University of California, Berkeley, United States; ²Lawrence Berkeley National Laboratory, United States; ³Shanghai Jiao Tong University, China; ⁴Kavli Energy NanoScience Institute, United States; ⁵The University of Chicago, United States

In situ transmission electron microscopy (TEM) has enabled researchers to visualize complicated nano- and atomic-scale processes with sub-Angstrom spatial resolution and millisecond time resolution. These processes are often highly dynamical and can be time-consuming to analyze and interpret. Here, we report how variational autoencoders (VAEs), a deep learning algorithm, can provide an artificial intelligence's interpretation of high-resolution *in situ* TEM data by condensing and deconvoluting complicated atomic-scale dynamics into a latent space with reduced dimensionality. In this work, we designed a VAEs model with high latent dimensions capable of deconvoluting information from complex high-resolution TEM data. We demonstrate how this model with high latent dimensions trained on atomically resolved TEM images of lead sulfide (PbS) nanocrystals is able to capture movements and perturbations of periodic lattices in both simulated and real *in situ* TEM data. The VAEs model shows capability of detecting and deconvoluting dynamical nanoscale physical processes, such as the rotation of crystal lattices and intraparticle ripening during the annealing of semiconductor nanocrystals. With the help of the VAEs model, we can identify an *in situ* observation that can serve as a direct experimental evidence of the existence of intraparticle ripening. The VAEs model provides a potent tool for facilitating the analysis and interpretation of complex *in situ* TEM data as a part of an autonomous experimental workflow.

8:00 PM DS04.07.11

A Transformer Based Large-Scale Molecular Representation Model Indra Priyadarsini S., Seiji Takeda, Akihiro Kishimoto, Hajime Shinohara and Daiju Nakano; IBM Research - Tokyo, Japan

Large scale molecular representation methods have shown to be useful in several applications and areas of material science including virtual screening, drug discovery, chemical modeling, material design and molecular dynamics simulation. These representations prove to provide both effective and efficient analysis of molecular data. With the advancements in deep learning, several models have been developed to learn the representations directly from the molecular structures. Recently, transformer based molecular representations have gained significant importance in the field of material informatics. The importance of transformer-based molecular representation continues to grow as researchers explore their potential in advancing drug discovery, materials science, and other areas of molecular research.

In this study, we develop one such transformer-based model that is capable of capturing complex relationships and interactions within molecules. While most of the existing works focus on only capturing the representations through encoder-only models, we present an encoder-decoder model based on BART (Bidirectional and Auto-Regressive Transformers) that is not only capable of efficiently learning the molecular representations but also auto-regressively generate molecules from the representations. This can prove to be highly impactful especially in cases of new molecule design and generation, enabling efficient and effective analysis and manipulation of the molecular data.

The model is trained on a dataset of 10 billion molecules from the publicly available ZINC-22 database, rendering it the most extensive training dataset employed to date. The dataset is encoded to SELFIES (SELF-referencing Embedded Strings) representation as SELFIES provides a more concise and interpretable representation, making it suitable for machine learning applications where compactness and generalization are important. The encoded SELFIES are then tokenized using an efficient tokenization scheme with masking in order to improve generalizability. We show that the learned molecular representation outperforms existing baselines on downstream tasks, thus validating the efficacy of the large pre-trained model.

8:00 PM DS04.07.12

Statistical and Machine-Learning-Based Durability-Testing Strategies for Energy Storage Maher Alghalayini, Marcus M. Noack and Stephen J. Harris; Lawrence Berkeley National Lab, United States

As the global climate is heating up at accelerated rates, human civilization is turning away from fossil fuels to renewable energy sources. While abundant, wind, solar, and water power are intermittent, motivating investment in long-duration energy storage technology research. The grand vision is to predict circa 20 years of energy-storage cycling behavior with less than one year of new testing data. On the other hand, machine learning and artificial intelligence are revolutionizing most aspects of science and engineering, but adopting those advancements has been slow in the energy-storage community. The reasons are the expense of battery testing and the associated sparsity of datasets, the need to extrapolate instead of interpolating, the inherent stochasticity of the problem, and the deep connection between failure mechanisms and physical and chemical processes. All of this causes a purely data-driven approach to be suboptimal. Herein we propose a new customization of a Gaussian Process for stochastic, domain-knowledge-informed energy storage-failure-distribution prediction. For that, we equip the Gaussian

Process with tailored prior mean and kernel functions to give it the ability to use experts' domain knowledge of candidate failure mechanisms to extrapolate into the future while minimizing the amount of required data. Our results show that our method can, in fact, approximate failure distributions early in the testing process. In short, this work provides the basis for revolutionizing energy storage testing and discovering new technologies for energy storage systems.

8:00 PM DS04.07.13

Achieving Low-Thermal Conductivity with Inverse-Designed Nanostructures [Giuseppe Romano](#); Massachusetts Institute of Technology, United States

Tuning thermal transport in nanostructures is currently done with try-and-error; while established concepts, such as phonon bottlenecks [1], may help identify promising structures, the majority of the configuration space is often left unexplored. To fill this gap, we recently introduced a framework [2] based on the adjoint gray phonon Boltzmann transport equation (BTE) to perform systematic topology optimization for nanoscale heat transport applications. In this talk, we will describe our recent efforts in extending our framework to the mode-resolved BTE, enabling a direct comparison with experiments. Our approach is based on the adjoint method and differentiable programming, which enables a fast experimentation with various objective functions. The code is implemented in the open-source code OpenBTE [3]. Length scale constraints are also included in the optimization framework, thus the optimized structures adhere to the specification of a given foundry. Several examples will be showcased, including tuning the anisotropic thermal conductivity tensor and maximizing phonon size effects. The talk will conclude with current efforts in fabricating the optimized structures.

[1] G. Romano and J. C. Grossman. Phonon bottleneck identification in disordered nanoporous materials *Physical Review B* 96 (11), 115425

[2] G. Romano and S. G. Johnson, Inverse Design in Nanoscale Heat Transport via Interpolating Interfacial Phonon Transmission. *Structural and Multidisciplinary Optimization* 65, 297

[3] G. Romano, OpenBTE: a solver for ab-initio phonon transport in multidimensional structures arXiv preprint arXiv:2106.02764

SESSION DS04.08: Accelerated Discovery and Optimization of Batteries I

Session Chairs: Yangang Liang, Doris Segets and Wei Wang

Wednesday Morning, November 29, 2023

Sheraton, Second Floor, Back Bay B

8:30 AM *DS04.08.01

Self-Driving Laboratories for Organic Flow Batteries [Alan Aspuru-Guzik](#)^{1,2}; ¹University of Toronto, Canada; ²Vector Institute, Canada

In this talk, I will discuss the progress of my research group at the University of Toronto in developing technology for the accelerated discovery of molecules for organic flow batteries. This work includes efforts towards automating the synthesis and characterization of these compounds, as well as AI-driven molecular design.

9:00 AM DS04.08.02

An Integrated High-Throughput Robotic Platform and Active Learning Approach to Accelerate Electrolytes Discovery [Yangang Liang](#)¹, Juran Noh¹, Hieu A. Doan², Heather Job¹, Lily A. Robertson², Lu Zhang², Rajeev Surendran Assary², Karl Mueller¹ and Vijayakumar Murugesan¹; ¹Pacific Northwest National Laboratory, United States; ²Argonne National Laboratory, United States

Solubility is an essential physicochemical property of redox-active molecules and closely associated with the energy density of redox flow batteries. However, the lack of large-scale and high-fidelity experimental solubility databases limits the potential application of data-driven approaches to accelerate electrolyte materials discovery. Here, we describe a highly efficient and robust automated workflow that combines a high-throughput experimentation platform with active learning to optimize the solubility of redox active molecules in organic solvent systems. We successfully demonstrate this platform by identifying several solvents that yield high solubility (> 6 M) of a model redox active molecule, 2,1,3-benzothiadiazole, among 2,101 solvent candidates. More significantly, our combined approach only requires solubility measurement of less than 10% (~200) of the solvent candidates. Our findings indicate that binary solvent mixtures based on 1,4-dioxane significantly enhance the solubility of 2,1,3-benzothiadiazole, providing promising prospects for high-energy density redox flow battery applications. While this work focuses on flow battery solvent formulation, our AI-guided high-throughput robotic platform can be used as a versatile tool for discovering energy materials with desired properties in a cost-effective and efficient manner.

9:15 AM DS04.08.03

Predictive Supremacy of Chemical Foundational Model for Battery Electrolytes [Vidushi Sharma](#), Eduardo A. Soares, Emilio V. Brazil, Young H. Na and Renato Cerqueira; IBM, United States

Electrolytes are a critical design black-box for batteries that aspects all major performance metrics. Electrolyte discovery and optimization can accelerate decarbonization and has drawn major focus from across all economic sectors. Consequently, electrolyte formulations are now guarded trade secrets of battery companies that are rarely shared publicly, making electrolyte data landscape scarce for AI-driven discovery. The most challenging aspect of development of battery electrolytes is their non-generalizability. There exist several major battery chemistries in research stages that require unique concoction of solvent-salt systems with special attention to underlying phenomena such as lithium solvation, surface reactions and self-discharge. These challenges of limited data and non-generalizability can be overcome with large transformers-based foundation models that have mastered extraction of molecular information in a self-supervised manner of learning from extensive unlabeled corpora. MolFormer, a chemical large language model, has learned chemical and physical panorama of over 1 billion molecules from simple extractable chemical representations such as SMILES strings. As the result, MolFormer's reliance on labeled data for downstream task is significantly reduced. In present work, we demonstrate the predictive capabilities of a customized MolFormer model for battery electrolytes with a mere 140 electrolyte formulations datapoints. Gathering electrolyte formulations vs battery performance data from experimental process is a challenging endeavor. The proposed model predicts battery performance metrics such as coulombic efficiency and specific capacity based on 2 separate electrolyte formulation datasets with best accuracies among all the known machine learning models that simultaneously map structure and composition of formulation constituents. The potential of foundation models in designing mixed material systems such as liquid battery electrolytes present a groundbreaking opportunity to accelerate the discovery and optimization of new formulations across various industries.

9:30 AM DS04.08.04

Accelerating Battery Organic Materials Discovery [Dong Young Kim](#), Seulwoo Kim, Seung Bum Suh, Soojin Kim, Jiten Singh, Sunmin Lee, Dong-Hee Yeon, Seok Joon Yoon and Gi-Heon Kim; Samsung SDI, Korea (the Republic of)

The increasing energy storage capacity of next-generation materials for Li-ion batteries underscores the crucial role of organic electrolyte materials in suppressing degradation and enhancing performance of the systems, highlighting the criticality of electrolyte material development. Recently, the material development paradigm has been changing into employing automation, data, and deep learning. However, in the case of organic electrolyte materials, it is arduous to define and model multifaceted behaviors, let alone computational automation to extract features, due to complex interplay of various physicochemical properties of electrolyte materials such as ion transport in a solvation state, interaction between electrode and electrolyte components, and formation and evolution of interfaces. Organic molecules have inherently enormous chemical diversity, making it more difficult to develop hypotheses related to the function of electrolyte materials. While there have been attempts to apply data-driven methodologies for developing organic electrolyte materials in batteries, most previous studies have described models for the complex behavior of electrolytes with simple chemical properties in a single molecular state, and there have been no reports of building intermolecular relational databases.

This presentation provides a pioneering framework for accelerating the discovery of battery organic materials by establishing the first-ever intermolecular relational database. For organic electrolyte materials that are difficult to understand due to their multifaceted behavior, more than 10 material design factors based on systematic operating mechanisms were quantified using density functional theory (DFT) modeling. These design factors define crucial functions of electrolyte materials such as behavior at the interface and electrolyte stabilization, and were verified using representative electrolyte materials with known functionalities, including commercially used electrolyte materials. We have developed python-based automation program AUTOMOL that encompasses the entire process from SMILES (Simplified Molecular Input Line Entry System) input to database construction, including molecular modeling of intermolecular interactions. The AUTOMOL-DB of thousands of organic material has been established by high-performance computing whereby conducting practical material development. This study is worthwhile due to the scarcity of automated modeling processes for intermolecular interactions, and thus, the exclusive database that includes molecular interactions with hydrogen, proton, cation, anion, radical, and small molecule, is invaluable as a source that can be extended to applications in chemical, biological, medical, functional molecular and nanomaterial research. It also developed a web-based system that integrates all design factors of the database so that material data can be searched, selected, and analyzed. The AUTOMOL-DB web system provides all researchers at our R&D center with a new approach to enhancing research horizons with insight into development while understanding the location of electrolyte materials in the big data space of organic matter. This system serves as a navigator for electrolyte material excavation as well as accelerate material discovery. In addition, in order to overcome the inherent disadvantage in computational cost and minimize the intervention of human intuition, state-of-the-art machine learning technology that predicts design factors and generates target materials in

real time is being applied to our workflow.

9:45 AM DS04.08.05

Beyond Words and Numbers: Pioneering Sodium-Ion Battery Advancements with NLP and Cost Modeling Synergy Mrigi Munjal¹, Thorben Prein², Mahmoud Ramadan¹, Hugh Smith¹, Vineeth Venugopal¹, Jennifer L. Rupp², Iwnetimf. Abate¹, Kevin Huang¹ and Elsa Olivetti¹; ¹Massachusetts Institute of Technology, United States; ²Technische Universität München, Germany

Sodium-ion batteries (SIBs) have been increasingly gaining attention for applications like grid-scale energy storage, largely owing to the abundance of sodium and an expected favorable \$/kWh figure. Consequently, the published literature in this field has been increasing exponentially, making it difficult for researchers to keep up with the latest developments and challenges. Improving the performance of SIB electrode materials will enable these batteries to compete with mature technologies like lithium-ion batteries (LIBs) at scale. SIBs can leverage the well-established manufacturing infrastructure knowledge of LIBs, but several materials and synthesis-based challenges for electrode materials need to be addressed for SIBs to mature from lab to market scale. This work aims to extract challenges in the performance and synthesis of SIB Cathode Active Materials (CAMs) and systematically review corresponding mitigation strategies from a combination of SIB and related LIB literature employing custom Natural Language Processing (NLP) tools. Finally, selected mitigation strategies are evaluated using a process-based cost model. This approach facilitates the generation of quantitative insights and enables a unique comparison among a broad set of existing lab-proposed mitigation strategies. These derived insights enable researchers and industry to navigate a large number of proposed strategies and focus on impactful mitigation strategies to accelerate the transition between laboratory-scale research and market-scale implementation.

10:00 AM BREAK

10:30 AM *DS04.08.06

Data-Driven Research for Aqueous Organic Redox Flow Batteries Wei Wang, Yangang Liang, Emily Saldanha, Vijayakumar Murugesan, Aaron Hollas, Heather Job and Will Dean; Pacific Northwest National Laboratory, United States

Aqueous organic redox active materials have recently shown great promise as alternatives to transition metal ions as energy-bearing active materials in redox flow batteries for large-scale energy storage due to their structural tunability, cost-effectiveness, availability, and safety features. However, development to date has been limited to a small palette of aqueous soluble organics. This presentation will provide an overview of a data-driven approach to accelerate the discovery and development of aqueous organic redox-active molecules for flow batteries, including database curation, structure-property correlation, and automated property characterization and performance testing.

Reference: P. Gao, etc. "SOMAS: a platform for data-driven material discovery in redox flow battery development", *Scientific Data*, **9**, 740, 2022

11:00 AM DS04.08.07

Data-Driven Understanding of Battery Formation and Lifetime Prediction Xiao Cui¹, Shijing Sun² and William C. Chueh¹; ¹Stanford University, United States; ²Toyota Research Institute, United States

Formation plays a critical role in battery manufacturing as it significantly impacts the quality of the solid electrolyte interface (SEI) formed, which in turn affects battery performance. However, formation can be time-consuming, costly, and difficult to optimize. In this study, a dataset comprising 150 cells, 50 different formation protocols, and 6 formation parameters was generated. The results reveal a wide range of battery lifetime based on different formation conditions. Interpretable machine learning is used to systematically study the contribution of formation parameters to battery performance. Furthermore, since cycling aging is kept the same for all the cells, the value of using this dataset for feature testing is discussed, along with an investigation into the predictive origin of the dominant features. We highlight the multi-purpose of this dataset for both Bayesian optimization and feature testing.

11:15 AM DS04.08.08

Battery Lifetime Predictions: Information Leakage from Biased Training Alexis Geslin^{1,2}, Bruisvan Vlijmen^{1,2}, Xiao Cui^{1,2}, Arjun Bhargava³, Patrick Asinger⁴, Richard Braatz⁴ and William C. Chueh^{1,2}; ¹Stanford University, United States; ²SLAC National Accelerator Laboratory, United States; ³Toyota Research Institute, United States; ⁴Massachusetts Institute of Technology, United States

Data-driven models are being developed to predict battery lifetime because of their ability to capture complex aging phenomena. In this work, we demonstrate that it is critical to consider the use cases when developing prediction models. Specifically, model features need to be classified to differentiate whether or not they encode cycling conditions, which are sometimes used to artificially increase the diversity in battery lifetime. Many use cases require the prediction of cell-to-cell variability between identically cycled cells, such as production quality control. Developing models for such prediction tasks thus requires features that are blind to cycling conditions. Using the dataset published by Severson et al. in 2019 as an example, we show that features encoding cycling conditions boost model accuracy because they predict the protocol-to-protocol variability. However, models based on these features are less transferable when deployed on identically cycled cells. Our analysis underscores the concept of using the right features for the right prediction task. We encourage researchers to consider the usage scenarios they are developing models for, and whether or not to include features encoding cycling conditions in order to avoid data leakage. Equally important, benchmarking model performance should be carried out between models developed for the same use case

11:30 AM DS04.08.09

Data-Driven Optimization of Polymer Electrolytes for High-Performance Solid-State Li-Ion Batteries Chuhong Wang, Siwen Wang and Ling Chen; Toyota Research Institute of North America, United States

High-performance polymer electrolytes are of paramount importance for advancing solid-state batteries due to the advantages such as high chemical stability and enhanced safety. In addition, the desirable flexural strength of polymer electrolyte offers the effective strategy to mitigate the effect of vast volume variation of Si anodes during electrochemical operations. However, the ionic conductivity of most polymer electrolytes is at the level of 10^{-4} S/cm, about one to two orders magnitudes lower than that of typical liquid electrolytes and even ceramic solid electrolytes. The discovery of novel polymer electrolytes with improved conductivities is crucial for their implementation in battery applications. In this talk, we present a data-driven optimization approach to enable the fast screening and identification of polymer electrolytes with desirable electrochemical properties. Our method combines the molecular dynamics (MD) workflow and multi-objective Bayesian optimization to streamline the candidate selection and property evaluation process. Through the screening in the vastly large chemical space of potential polymer electrolytes, the data-driven approach discovers a series of promising candidates with the ionic conductivity reaching to the level of 10^{-3} S/cm and above. The discovery of novel polymer electrolytes through data-driven optimization paves the road for enabling the realization of high-performance solid-state Li-ion batteries and propelling the clean energy revolution forward.

11:45 AM DS04.08.10

Machine Learning Aided Screening of MXenes as Sulfur Host Cathodes for Al-S Batteries Souvik Manna and Biswarup Pathak; Indian Institute of Technology Indore, India

The dissolution of polysulfide intermediates into electrolytes has been a major bottleneck in the development of Al-Sulfur battery. To address this, the introduction of promising anchoring materials is highly necessary. The anchoring agents must be able to adsorb the polysulfides optimally as strong adsorption can lead to irreversible electron flow process whereas weak adsorption will result in the dissolution of polysulfides into the electrolyte. MXenes have garnered considerable interest as electrode materials in energy storage devices for their exceptional metal-like conductivity, rapid charge transfer capabilities, and remarkable surface charge accumulation. These unique properties make MXenes highly promising for applications in metal-sulfur batteries, where they can facilitate rapid charge transfer and ensure excellent electrode conductivity. Notably, properties of MXenes can be tuned according to requirements by varying the terminal groups which is quite easy during the synthesis process. In this regard, MXenes are expected to show good anchoring effect for Al-S batteries. However, identifying potential sulfur host cathode material from a large space of MXenes materials through traditional experiments or density functional theory (DFT) methods will be a very tedious job. Machine Learning (ML) tools have emerged as an efficient tool known for their ultra-fast high throughput screening potential in recent years. In this regard we propose a novel approach combining DFT and ML to monitor the anchoring capability of a large number of MXenes for possible Al-S polysulfide intermediates. Accurate DFT generated data can be utilized for the training and testing purpose of various ML models to acquire knowledge regarding the adsorption phenomena of possible polysulfides. Suitable and easily available descriptors are chosen to accurately distinguish each of the systems to ensure efficient training of ML models. An optimized ML model along with a set of suitable descriptors will enable us to explore unknown material space to identify novel and potential MXene materials for the enhancement of Al-S battery performance. Further the suitable MXenes showing optimum anchoring will be analyzed in detail to identify the role played by various components of the MXenes and factors influencing the adsorption processes. Thus, the present work paves the way forward for accelerated screening of MXenes as host cathodes for Al-S batteries as well as providing crucial insights for rational designing of materials for next-generation energy storage technologies.

1:30 PM *DS04.09.01

Leaning Governing Relations in Battery Electrodes: Hybridizing Physics- and Data-Driven Approaches William C. Chueh; Stanford University, United States

The vast design space and long lifetime of batteries have limited the speed of innovations at the materials, cell, and systems level. In this talk, I will overview efforts at Stanford to dramatically accelerate the pace of research and development for lithium-ion batteries by hybridizing physics-based and data-driven approaches. Specifically, I will present our recent work on predicting not only battery lifetime but also aging mechanisms, which lays the foundation for transferable learnings between multiple battery chemistries. I will also showcase new methods for learning heterogeneities at the particle and electrode levels by combining multi-fidelity characterizations, physics-based modeling, and machine learning.

2:00 PM DS04.09.02

Discharge Capacity Prediction from Unstructured Cathode Material Data in Li-Ion Batteries Changyoung Park, Jaewan Lee, Hongjun Yang, Sehui Han and Woohyung Lim; LG AI Research, Korea (the Republic of)

In the process of material development such as battery materials, structured tabular data such as Excel is widely utilized to integrate data such as material information, process information, and analysis information. Recently, various machine learning techniques have been applied to analyze such structured data. 1) In particular, tree-based machine learning models and deep learning models are mainly used to analyze structured data. 2) Among the models, deep learning models can (1) directly process unstructured data such as cathode materials and (2) consider the relationships between interrelated features such as composition and crystal information - LiNi_{0.6}Mn_{0.2}Co_{0.2}O₂ and lattice constants from X-ray diffraction. In this study, we developed a deep learning model to predict the discharge capacity from data collected during the development of cathode materials, which is originally unstructured data. The features were grouped by name to consider the relationship between the features. Each group, for example composition, were embedded into a representation, and used to predict the discharge capacity.

References

- 1) Guanyu Wang, et al. ACS Cent. Sci. (2021) 7, 9, 1551-1560
- 2) L. Grinsztajn, E. Oyallon, and G. Varoquaux. (2022) arXiv:2207.08815

2:15 PM DS04.09.03

Reaction and Ionic Migration at the Electrode-Electrolyte Interface in Solid State Batteries from Machine Learning Molecular Dynamics Jingxuan Ding, Yu Xie, Albert Musaelian, Menghang Wang, Anders Johansson, Simon Batzner and Boris Kozinsky; Harvard University, United States

Atomistic-level understanding of the chemical reactions forming the solid-electrolyte interphase (SEI) in solid-state lithium batteries has remained challenging, primarily due to the limited resolution in experimental techniques and the insufficient accuracy in large-scale simulations. In this work, we combine on-the-fly active learning based on Gaussian Process regression (FLARE) with local equivariant neural network interatomic potentials (Allegro) to construct a machine-learning force field (MLFF) to perform large-scale long-time explicit reactive simulation of a complete symmetric battery with ab initio accuracy. The MLFF is validated with experimental values of mechanical properties of bulk lithium and diffusion coefficient of solid electrolyte. For the symmetric battery, atomic descriptors are used to identify the reaction products and estimate the evolution of the SEI. We observe prominent fast reactions at the interface and characterize the dominant reaction products along with their evolution time scales. The methods in this study exhibit great potential in revealing atomistic mechanisms in complicated systems and provide insights for the development of solid-state lithium batteries.

2:30 PM BREAK

3:30 PM DS04.09.04

Artificial Intelligence Aided In-Silico-Design of Organic Cathode Materials for Li-Ion Battery Devices Rodrigo Carvalho¹, Cleber Marchiori², Daniel Brandell¹ and Moyses Araujo^{2,1}; ¹Uppsala University, Sweden; ²Karlstad University, Sweden

The organic electrode materials (OEM) are emerging as a promising alternative to develop greener and sustainable battery technologies. However, significant improvements are still required in their cycling stability, rate capability and energy density. This can only be achieved through a fundamental understanding of the electrochemistry at molecular level establishing the structure-properties relationships. To contribute to this end, we are developing methodologies based on evolutionary algorithms (EA) and artificial neural networks (ANN) at interplay with density functional theory (DFT) based calculations. The EA has initially been employed to predict the structure and electrochemistry of a set of dicarboxylates. In a second stage, we have developed a wider database of organic materials for energy applications that contains information about molecular geometries and high-level features extracted from DFT calculations. Based on this database, we have developed a machine learning approach to predict the redox potentials by giving only chemical species and molecular structures, completely by-passing the computer-demanding DFT calculations. A number of learning algorithms based on ANN have been investigated along with different molecular representations. Here we have also included a layer to predict redox-stable compounds. This machinery has been employed to screen a large organic materials library (45 million molecules) leading to the discovery of novel cathode materials¹, which is actually one of the bottlenecks on the development of organic batteries. The computational materials design platform developed here has the potential of significantly contribute to accelerate the discovery of organic electrode materials with superior properties.

[1] Rodrigo P. Carvalho, Cleber F. N. Marchiori, Daniel Brandell and C. Moyses Araujo "Artificial intelligence driven in-silico discovery of novel organic lithium-ion battery cathodes" *Energy Storage Materials* **44**, 313-325 (2022).

3:45 PM DS04.09.05

Investigation of Li-Ion Diffusion in Argyrodite Solid-State Electrolytes using Machine-Learned Potentials Suyeon Ju¹, Jiho Lee¹, Jinmu You¹, Jisu Jung¹ and Seungwu Han^{1,2}; ¹Seoul National University, Korea (the Republic of); ²Korea Institute for Advanced Study, Korea (the Republic of)

Solid-state batteries incorporating solid Li-ion conductors have gained significant attention due to their advantages in safety and higher energy density compared to conventional liquid electrolyte batteries. However, these solid-state conductors inherently suffer from low ionic conductivities at room temperature, spurring investigation into diverse materials. Among them, argyrodite sulfide systems such as Li₆PS₅Cl have shown promising outcomes, achieving ionic conductivity higher than 10 mS/cm at room temperature. The high conductivities in argyrodites have been attributed to the presence of substitutional anion disorders. Yet, the precise mechanisms governing Li-ion diffusion remain unclear due to limitations in experimental analysis resolution. Theoretical investigations based on density functional theory (DFT) calculations are illuminating in this regard. However, recent DFT studies have encountered challenges in accurately quantifying diffusivities or ionic conductivities across various disorder levels, leading to substantial discrepancies with experimental results. These discrepancies mainly stem from two factors: i) the selection of semilocal exchange-correlation functionals based on the generalized-gradient approximation, which tends to overestimate lattice parameters and consequently increase conductivity, and ii) small simulation cells, which are susceptible to correlated Li-ion diffusions between periodic images and do not adequately account for the disorder of S/Cl ions. Furthermore, Li-ion jumps are rare at room temperatures, requiring simulations over an extended timescale, which is beyond the scope of current DFT calculations. In this presentation, to overcome the aforementioned computational issues, we employ Behler-Parrinello type neural network potentials (NNPs) to obtain Li-ion conductivities in argyrodite Li₆PS₅Cl with 0–100% Cl disorder at 4c sites. Leveraging the speed and accuracy of NNPs, we estimate the Li-ion conductivity directly at room temperatures, fully considering the S/Cl disorder and ergodicity of Li distributions. Using the SIMPLE-NN package, we train the NNP with strained bulk crystals and *ab initio* MD data at 600 and 1200 K. For the exchange-correlation energy among electrons, we select the SCAN functional, which reproduces the lattice parameter within 0.2% from the experimental value. We carry out NNP MD simulations with 4×4×4 supercells, encompassing more than 3,000 atoms, up to 15 ns simulation time at 300 K. Through parameter tests on the simulation timescale and ensemble averages of initial Li distributions, we were able to minimize the statistical fluctuations in the conductivity within 0.5 mS/cm. The estimated activation energies and ionic conductivities in the presence of disorders align well with experimental data. Interestingly, Li-ion conductivity peaks at 25% Cl at 4c sites. Free energy analysis confirms that these structures are thermodynamically accessible, suggesting a method to enhance the intrinsic Li-ion conductivity in Li₆PS₅Cl by tuning the site disorder. Furthermore, we analyze the diffusion mechanisms of ordered and disordered structures, focusing on the jumps between Li-ion cages. This work paves the way for predicting and analyzing properties of disordered complex solid-state electrolyte materials using accurate and cost-effective NNPs.

4:00 PM DS04.09.06

Extracting Physics from Database with Systematic DFT Calculations: Intercalation Energies of Layered Intercalation Compounds with Various Ions Naoto Kawaguchi,

Layered intercalation compounds, which have a structure in which atoms or molecules (intercalants) are inserted into the interlayer of a layered compound (host), have been extensively studied due to their characteristic physical properties and the variety of synthetic methods^[1]. Their applications in energy storage have been investigated due to their ability to intercalate/de-intercalate ions, and various properties resulting from their two-dimensional nature, such as superconductivity and topological electronic states, have also been studied. In this context, we have recently reported the possibility of new graphite intercalation compounds with superconductivity and charge density states.^[2] There are various combinations of intercalants and hosts in layered intercalation compounds, and it is important to control the combinations to achieve some functional development. However, a comprehensive understanding of which combinations of hosts and intercalants are stable has not been achieved.

To achieve this, we performed systematic DFT calculations for 9,024 layered intercalation compounds with a structure in which a single atom is inserted into the host changing the intercalant atom, and constructed database of their optimized crystal structures, electronic states, and intercalation energies, which is the reaction energy between the host and the intercalant.

Consequently, we revealed that the intercalation energy can be linearly regressed, using only two experimental values. The obtained equation was found to be similar to reported ones in crystalline solids with divalent metal ion^[3] and metal-ligand complex.^[4]

This result develops material design criteria for layered intercalation compounds and has the potential to be applied to other inorganic compounds with different structures. The details will be shown in my presentation.

This study was supported by the Ministry of Education, Culture, Sports, Science and Technology (MEXT) (Grant no. 19H00818 and 19H05787), and the special fund (Tenkai) by the Institute of Industrial Science, the University of Tokyo.

References

- [1] M. Lapijan *et al.*, *Prog. Mater. Sci.* **109** (2020) 100631.
- [2] N. Kawaguchi *et al.*, *J. Phys. Chem. C* **127** (2023) 9833-9843.
- [3] D. A. Sverjensky *et al.*, *Nature* **356** (1992) 231-234.
- [4] H. Xu *et al.*, *ACS Omega* **2** (2017) 7185-7193.

4:15 PM DS04.09.07

Characterizing Grain Boundary Effects on Mg²⁺ Conduction in Metal–Organic Frameworks [Tongtong Luo](#), Yang Wang, Dunwei Wang, Udayan Mohanty and Junwei L. Bao; Boston College, United States

Next generation solid-state materials for fast ion conduction have the potential to revolutionize battery technology. Metal-organic frameworks (MOF) are a promising material for achieving this goal. Given their structural diversity and complexity, design of efficient MOF-based ion conductors can be accelerated by detailed understanding and quantitative prediction of ion conductivity. To this end, the chemical behavior and transport properties of an Mg(TFSI)₂/DME electrolyte system inside Mg-MOF-74 were studied by a combination of computational and experimental methods. The dominant minimum energy pathway (MEP) for Mg²⁺ conduction inside Mg-MOF-74 was found to be “solvent hopping” mechanism, with an energy barrier of 4.4 kcal/mol.

However, due to the polycrystalline nature of solid-state materials, specifically MOF-74 in our case, grain boundary effects need to be taken into consideration, which is complicated by challenges in grain boundary characterization, as well as modeling of ensemble transport properties. To address these issues, we developed an approach for modeling ion transport at grain boundaries and predicting their contribution to conductivity. In particular, Mg²⁺ conduction in Mg-MOF-74 thin film was studied as a representative system. Using computational techniques and guided by experimental data, we investigated the structural details of MOF grain boundary interfaces to determine accessible Mg²⁺ transport pathways. Computed transport kinetics were input into a simplified model of the MOF nanocrystal, which combined ion transport in bulk structure and at grain boundaries. The model was able to predict Mg²⁺ conductivity in MOF-74 thin film within chemical accuracy (<1 kcal/mol difference for apparent activation energy), validating our approach. The results indicate that Mg²⁺ conduction in MOF-74 is inhibited due to strong Mg²⁺ binding at grain boundaries. Only favorable alignments of the grain boundary interface allow for fast Mg²⁺ transport through MOF and contribute notably to ion conductivity. The relative scarcity (~0.1% frequency) of these favorable alignments results in a reduction of conductivity by 2-3 orders of magnitude, illustrating the large impact of the grain boundary contribution. Grain boundary structure and its interaction with ions are critical for a molecular-level understanding of solid-state ion transport and quantitative prediction of conductivity.

Our work provides a computation-aided synergistic platform for quantifying the role of grain boundaries in mediating ion transport, which can serve as a complementary characterization tool for the solid-state ion conductor community and providing insights for MOFs' application in Mg battery area.

4:30 PM *DS04.09.08

Leveraging Community Knowledge in Machine Learning Models to Accelerate the Discovery of New MOF Catalysts and Materials [Heather J. Kulik](#); Massachusetts Institute of Technology, United States

I will discuss our efforts to use machine learning (ML) to accelerate the computational tailoring and design of metal-organic framework (MOF) materials for catalysis as well as gas separations and storage. One limitation in a challenging materials space such as open shell transition metal chemistry present in the open metal sites of most catalytically active MOFs is that ML models and ML-accelerated high-throughput screening traditionally rely on density functional theory (DFT) for data generation, but DFT is both computationally demanding and prone to errors that limit its accuracy in predicting new MOFs. I will describe how we have curated a dataset of thousands of MOFs that have been experimentally synthesized and used this data to train ML models to predict experimentally reported measures of stability. These models are able to predict experimental thermal stability and activation stability, which would be extremely difficult to predict using computational modeling. I will describe how we have leveraged these models to then screen for mechanically stable materials as well as stable catalysts in the direct conversion of methane to methanol. I will also describe how we have used these models to accelerate the discovery of novel stable MOFs, creating a dataset of transition metal complexes enriched with stability and diversity 1-2 orders of magnitude beyond what is typically included in most hypothetical MOF datasets.

SESSION DS04.10: Poster Session II: Accelerated Discovery of Materials for Energy II

Session Chairs: Jason Hattrick-Simpers, Steven King and Yangang Liang

Wednesday Afternoon, November 29, 2023

Hynes, Level 1, Hall A

8:00 PM DS04.10.01

Machine-Learning-Based Solvent-Antisolvent Screening for Tin-Based Perovskite Solar Cells [Noor Titan Putri Hartono](#), Mahmoud Hussein, Shengnan Zuo, Chiara Frasca, Guixiang Li, Zafar Iqbal and Antonio Abate; Helmholtz-Zentrum Berlin, Germany

All perovskite solar cells (PSCs) with an efficiency beyond 20% contain lead, which is bioavailable and toxic, posing a high risk for health and safety and becoming a highly-debatable issue within PSCs research field, industry, and regulator. The alternative to lead-based PSCs, tin-based PSCs, have several advantages: (1) they are less bioavailable, which lower the risk for environment in the case of leakage, and (2) they have a more optimum bandgap, which increase the theoretical maximum power conversion efficiency. However, the progress of tin-based PSCs efficiency is still lagging behind lead-based PSCs, mainly because it is challenging to minimize Sn²⁺ oxidation and control the crystallization dynamics during fabrication. On top of that, DMSO, the commonly used solvent for tin-based PSC precursors is known to oxidize the Sn²⁺, causing defects, which hamper performance (<https://doi.org/10.1002/chem.202103919>). Finding an alternative solvent-antisolvent pair to improve crystallization dynamics and reduce Sn²⁺ oxidation is important but challenging because of the large number of possible solvents, and understanding which properties of solvent-antisolvent pairs lead to formation of thin film is not straightforward. In this study, we screen 14 solvents and 73 antisolvents, totaling to 1,022 pairs of solvent-antisolvent in the vials screening of formamminium tin iodide perovskite solution, and select 6 solvents and 73 antisolvents for the thin-films screening. We automate the data processing using the solution and thin film color, and develop a machine learning algorithm for the thin-film color prediction. We also use feature importance rank, namely Shapley value (<https://doi.org/10.1038/s42256-019-0138-9>), to find solvent-antisolvent properties which affect dark film formation the most. We discover several alternatives for solvent-antisolvent pairs which can replace DMSO as a solvent and hence, reduce the risk of Sn²⁺ oxidation and improve the efficiency of tin-based PSCs.

8:00 PM DS04.10.02

Optimization of Silver Nanowire Spin Coating for Flexible Transparent Conducting Electrodes Guided by Machine Learning [Julia W. Hsu](#), Mark Lee, Robert Piper and Bishal Bhandari; The University of Texas at Dallas, United States

Transparent conducting electrodes (TCEs) play a crucial role in various energy applications, including light-emitting diodes (LEDs), photovoltaics, and thin-film transistors. Achieving both

high transparency and high conductivity in TCEs poses a significant challenge. When using metal grids, a higher filling factor produces a layer with a higher conductivity but lower transmittance. Similarly, indium tin oxide (ITO), the most commonly used transparent conducting oxide, exhibits reduced transmittance with increasing film thickness, even though its conductivity improves. To fabricate TCEs on polyethylene terephthalate (PET) substrates, we combine silver nanowires (AgNWs) with sol-gel indium zinc oxide (IZO). Doing so can enhance the conductivity of solution-processed IZO films to meet the sheet resistance requirements for TCEs used in LEDs and photovoltaics. [1]

Our study primarily focuses on optimizing the spin-coating process of AgNWs, as they significantly influence the transmittance and sheet resistance of TCEs. Our goal is to achieve high transmittance and low sheet resistance simultaneously. The optimization problem involves mapping a three-dimensional input (AgNW solution concentration, spin speed, and dispense volume) to a two-objective output (transmittance and sheet resistance). Using data obtained by Latin hypercube sampling (LHS) of the input space, we construct two independent Gaussian process (GP) regression models: one for transmittance and one for sheet resistance, using cross-validation to tune their hyperparameters. These models have distinct kernel parameters due to the differing nature of the objectives. Having two models also enables us to conduct multi-objective analysis. We analyze the data and GP models in two ways. Firstly, we utilize a well-established criterion [2] to define a scalar figure-of-merit (FOM) and utilize the GP models to predict the maximum FOM and associated uncertainty. Secondly, we construct a Pareto frontier based on the GP models, which helps identify processing conditions that strike the best trade-off between higher transmittance and lower sheet resistance. It is important to note the difference between the two approaches. Using FOM cannot individually specify the objective values, so it proves useful when separate requirements for transmittance and sheet resistance are desired when optimizing FOM. Finally, we compare the predictions of models with tuned hyperparameters using different cross-validation methods. Subsequently, we conduct experiments using the identified input parameters, from both the predicted maximum FOM and the Pareto frontier, and compare the results with the model predictions.

This work is supported by NSF CMMI-2109554.

References:

- [1] R. T. Piper, W. Xu, and J. W. P. Hsu, "Silver Nanowire-Indium Zinc Oxide Composite Flexible Transparent Conducting Electrodes Made by Spin-coating and Photonic Curing," *MRS Adv.* 8, 177-182 (2023)
- [2] M. Dressel and G. Gruner, "Electrodynamics of Solid", Cambridge University Press, 2002

8:00 PM DS04.10.03

A Statistical Understanding of the Growth and Etching of Anisotropic Colloidal Gold Nanoparticles Assisted by Machine Learning Xingzhi Wang^{1,2} and Paul Alivisatos^{1,2,3}; ¹University of California, Berkeley, United States; ²Lawrence Berkeley National Laboratory, United States; ³The University of Chicago, United States

Colloidal gold nanoparticles (AuNPs) have been widely studied due to their various chemical and biomedical applications. Recently, anisotropic AuNPs, such as Au nanorods, nanodisks, and triangular nanoprisms, have received much attention, due to their shape-specific, tunable plasmonic properties ideal for a variety of potential applications. While reliable colloidal pathways to the synthesis of many anisotropic AuNPs have been developed, the mechanisms leading to the formation of these shapes remain a matter of debate. To better elucidate the mechanism of the formation of anisotropic Au nanoparticles, statistical level information on the evolution of the shapes of AuNPs during their growth is necessary. Previously, shapes of AuNPs and their evolution during colloidal growth and etching have been studied by transmission electron microscopy (TEM). However, few previous studies were able to analyze the shapes of AuNPs at a population level (>1000 nanoparticles), due to the inefficiency of manual analysis of TEM data. We have previously developed AutoDetect-mNP, an algorithm that can automatically extract and classify the shapes of nanoparticles from TEM data with minimum human intervention, enabling the analysis of the shapes of thousands of nanoparticles in a matter of minutes. In this work, applying AutoDetect-mNP, we will demonstrate the mechanism and thermodynamics governing the formation of anisotropic Au NPs based on statistical analysis, using Au triangular nanoprisms as a model system. By analyzing the shapes of Au triangular nanoprisms at different stages of their growth and etching, on a statistically significant level, we will attempt to elucidate the formation of anisotropic AuNPs as a function of the relative reactivities and stability of different crystal facets. In this way, we hope to provide a systematic and quantitative understanding of how anisotropic shapes form during the growth of AuNPs. Further, we believe that this method of statistical analysis of nanoparticles shapes can be generalized to nanoparticle systems beyond AuNPs, including, for example, semiconductor quantum dots, and hence provides a potential solution to a range of fundamental questions in nanosciences.

8:00 PM DS04.10.04

Confocal Raman Microscopy and Machine Learning Analysis for Spatiochemical Characterization of Battery Electrodes Steven T. King¹, Lei Wang^{2,1}, Esther S. Takeuchi^{1,2}, David Bock^{2,1}, Shan Yan^{2,1}, Amy Marschilok^{1,2} and Kenneth J. Takeuchi^{1,2}; ¹Stony Brook University, United States; ²Brookhaven National Laboratory, United States

Battery electrodes are extremely complex and dynamic chemical environments, typically comprised of a broad range of different materials, often representing more than one chemical or physical phase, in a heterogeneous spatial configuration. Comprehensive study of such devices necessitates the use of a probe which can capture and resolve information arising from each of these physicochemical components in a way which permits consideration of the electrode as being greater than the sum of its parts. Confocal Raman microscopy provides just such a probe; it is chemically sensitive to nearly all materials regardless of their phase or crystallinity, permits spatially-constrained measurements with 3-dimensional resolution on the order of single microns, and is intrinsically capable of measuring all chemical components present in a sample in a single measurement. Moreover, the large datasets which result from such analyses are well-suited for processing using SVD-like machine learning techniques, especially non-negative matrix factorization, for rapid signal deconvolution and accurate measurement and mapping of individual chemical components. In this presentation, studies will be presented which highlight the capabilities and utility of confocal Raman microscopy combined with machine learning-assisted analysis for the study of electrodes for electrochemical energy storage devices.

References

- (1) Lutz, D. M.; Dunkin, M. R.; King, S. T.; Stackhouse, C. A.; Kuang, J.; Du, Y.; Bak, S. M.; Bock, D. C.; Tong, X.; Ma, L.; Ehrlich, S. N.; Takeuchi, E. S.; Takeuchi, K. J.; Marschilok, A. C.; Wang, L. Hybrid MoS₂+ XNanosheet/Nanocarbon Heterostructures for Lithium-Ion Batteries. *ACS Appl. Nano Mater.* **2022**, *5* (4), 5103–5118. <https://doi.org/10.1021/acsnm.2c00141>.
- (2) Zhang, X.; Hui, Z.; King, S. T.; Wu, J.; Ju, Z.; Takeuchi, K. J.; Marschilok, A. C.; West, A. C.; Takeuchi, E. S.; Wang, L.; Yu, G. Gradient Architecture Design in Scalable Porous Battery Electrodes. *Nano Lett.* **2022**, *22* (6), 2521–2528. <https://doi.org/10.1021/acs.nanolett.2c00385>.
- (3) Luo, J.; Arnot, D. J.; King, S. T.; Kingan, A.; Nicoll, A.; Tong, X.; Bock, D. C.; Takeuchi, E. S.; Marschilok, A. C.; Yan, S.; Wang, L.; Takeuchi, K. J. Two-Dimensional Siloxene Nanosheets: Impact of Morphology and Purity on Electrochemistry. *ACS Appl. Mater. Interfaces* **2023**, *15* (20), 24306–24318. <https://doi.org/10.1021/acsmi.3c00355>.
- (4) Ju, Z.; King, S. T.; Xu, X.; Zhang, X.; Raigama, K. U.; Takeuchi, K. J.; Marschilok, A. C.; Wang, L.; Takeuchi, E. S.; Yu, G. Vertically Assembled Nanosheet Networks for High-Density Thick Battery Electrodes. *Proc. Natl. Acad. Sci. U. S. A.* **2022**, *119* (40), 1–9. <https://doi.org/10.1073/pnas.2212777119>.
- (5) Dunkin, M. R.; King, S. T.; Takeuchi, K. J.; Takeuchi, E. S.; Wang, L.; Marschilok, A. C. Improved Ionic Conductivity and Battery Function in a Lithium Iodide Solid Electrolyte via Particle Size Modification. *Electrochem. Acta* **2021**, *388*, 138569. <https://doi.org/10.1016/j.electacta.2021.138569>.

8:00 PM DS04.10.05

Revisit Bi₂Te₃ Thermoelectric Material: From Existing Literature to Machine Learning Model Sarthak Roy and Sukanti Behera; Maulana Azad National Institute of Technology Bhopal, India

Thermoelectric materials are hot topic in materials research, mainly due to renewed focus to tackle climate change and global warming from renewable sources of energy. Bismuth Telluride (Bi₂Te₃) based materials are one of the most researched materials with regards to their thermoelectric properties primarily, their relative ease of preparation and impressive thermoelectric properties at room temperature. Recently, there are methods/tools in addition to experiments by which the properties of a material can be known or predicted accurately to a certain degree. Here, in this project, we intend to utilize machine learning principles on literature, databases and other information sources containing thermoelectric data to find the optimum doped stoichiometry required for the bismuth telluride-based materials under different conditions which yield the maximum figure of merit. This is utilized by the proper use of material informatics to gather data, data science to curate and clean the data, and finally machine learning to create models via different regression algorithms such as Decision Tree, Random Forest and SVM, etc. Such models will yield information that can then be investigated by the use of DFT studies with different exchange correlations and further experimental work, thus trying to bridge the gap between computational studies and experiments. By doing so, we reach a synergy that is established between ML-aided materials informatics, computational materials science through DFT, and experimental work.

8:00 PM DS04.10.06

Doped: A Python Package for Solid-State Defect and Dopant Calculations Sean R. Kavanagh^{1,2}, Aron Walsh¹ and David O. Scanlon³; ¹Imperial College London, United Kingdom; ²University College London, United Kingdom; ³University of Birmingham, United Kingdom

Point defects are a universal feature of crystalline materials, dictating the functionality of most semiconductor materials, such as microelectronics, solar cells and batteries.¹ The major impact, despite minute concentrations, of defects in solids, renders their identification and characterisation by experiment extremely challenging. Thus, computational methods (typically Density Functional Theory (DFT) but also quantum embedding, *GW* and empirical potentials approaches) are widely used to predict defect behavior in solids, before combining and comparing theoretical predictions with experimental measurements. However, there are many critical stages in the computational workflow for defects in solids, which, when performed manually, not only leave room for human error but also consume significant time and effort of the researcher.

Here we report *doped*, our python package for the full generation, calculation setup, post-processing and analysis of defect supercell calculations.²⁻⁵ The generation and thermodynamic analysis (i.e. defect formation energy diagrams, chemical potentials & stability region, doping analysis etc.) are agnostic to the underlying first-principles software, while input file generation is supported for several of the most widely-used DFT codes, including VASP, FHI-aims, CP2k, Quantum Espresso and CASTEP. Moreover, *doped* is built to be compatible with other computational toolkits for advanced defect characterisation, including *ShakeNBreak*⁶ for defect structure-searching, *py-sc-fermi*⁷ for in-depth concentration and Fermi level analysis, and *CarrierCapture.jl⁸/nonrad*⁹ for non-radiative recombination calculations. Its object-oriented python framework make it readily-usable in high-throughput architectures such as *atomate(2)* or *AiiDA*, with examples included in the documentation.

We will discuss the key features of *doped* for computational defect workflows, exemplified with relevant systems (CdTe, *t*-Se, Y₂Ti₂O₅S₂). We anticipate that *doped* will serve as a highly useful tool for computational defect researchers, being an efficient platform for conducting reproducible calculations of solid-state defect properties.

1 D. Broberg, B. Medasani, N. E. R. Zimmermann, G. Yu, A. Canning, M. Haranczyk, M. Asta and G. Hautier, *Computer Physics Communications*, 2018, **226**, 165–179.

2 S. R. Kavanagh, A. Walsh and D. O. Scanlon, *ACS Energy Lett.*, 2021, **6**, 1392–1398.

3 Y.-T. Huang, S. R. Kavanagh, M. Righetto, M. Rusu, I. Levine, T. Unold, S. J. Zelewski, A. J. Sneyd, K. Zhang, L. Dai, A. J. Britton, J. Ye, J. Julin, M. Napari, Z. Zhang, J. Xiao, M. Laitinen, L. Torrente-Murciano, S. D. Stranks, A. Rao, L. M. Herz, D. O. Scanlon, A. Walsh and R. L. Z. Hoyer, *Nat Commun*, 2022, **13**, 4960.

4 S. R. Kavanagh, D. O. Scanlon, A. Walsh and C. Freysoldt, *Faraday Discuss.*, 2022, **239**, 339–356.

5 A. Nicolson, S. R. Kavanagh, C. N. Savory, G. W. Watson and D. O. Scanlon, 2023.

6 I. Mosquera-Lois, S. R. Kavanagh, A. Walsh and D. O. Scanlon, *Journal of Open Source Software*, 2022, **7**, 4817.

7 A. G. Squires, D. O. Scanlon and B. J. Morgan, *Journal of Open Source Software*, 2023, **8**, 4962.

8 S. Kim, S. N. Hood, P. van Gerwen, L. D. Whalley and A. Walsh, *Journal of Open Source Software*, 2020, **5**, 2102.

9 M. E. Turiansky, A. Alkauskas, M. Engel, G. Kresse, D. Wickramaratne, J.-X. Shen, C. E. Dreyer and C. G. Van de Walle, *Computer Physics Communications*, 2021, **267**, 108056.

8:00 PM DS04.10.07

Machine Learning-Assisted Design of Vapor-Deposited Perovskite Solar CellsRuilongWang, HaofengZheng and ShaocongHou; Wuhan University, China

In recent years, the power conversion efficiency (PCE) of perovskite solar cells (PSCs) has been significantly improved by the lab-scale solution fabrication process. Compared with solution method, the vapor deposition method is beneficial for the large-scale preparation of PSCs, however, its development lags behind that of the solution method.

Here, we used machine learning to analyze the device compositions and the preparation conditions of more than 200 PSCs data collected from the literature. Combining random forest and genetic algorithm, we constructed a prediction model of PCE with a Pearson coefficient of 0.67. Furthermore, we applied SHAP analysis to the model, the ratio of cations to anions in the perovskite layer and the annealing temperature are the two factors that most influence PCE. After thoroughly examining the available variable spaces, we proposed an ideal device architecture and its manufacturing parameters, predicting the greatest PCE of 26.1%, which surpasses the previous record for the most advanced efficiency. Our work advances the industrial production of vapor-deposited PSCs and speeds up their development.

8:00 PM DS04.10.08

Discovery of Stable Surfaces with Extreme Work Functions by Machine LearningPeterSchindler; Northeastern University, United States

The discovery of thermally stable materials with surfaces that exhibit an ultra-low work function would allow thermionic energy conversion of heat directly to electricity with high efficiencies and enable next-generation electron emission devices such as THz sources and fluorescent light bulbs. In contrast, surfaces with ultra-high work functions are crucial for devices where large contact barriers are required to suppress electron leakage such as in dynamic RAM and modern transistor architectures. Further, the work function is crucial for band alignment in heterostructures and interfaces. Recently, data-driven approaches based on high-throughput first principles computation have emerged as a new paradigm to facilitate the search through vast chemical spaces for new materials with tuned properties. Most material databases largely lack to report surface properties like the work function and surface energy, as each bulk material typically has dozens of distinct low-index crystalline surfaces and terminations.

Here, we report on recent progress in our high-throughput workflow using density functional theory (DFT) to calculate both the work functions and the cleavage energies of over 55,000 surfaces that we created from ~3,700 bulk materials (with a zero bandgap and including up to ternary compounds). Moreover, we developed a physics-based approach to design surface descriptors and established a surrogate machine learning model to predict the work function. Our machine learning model achieves a mean absolute test error 4 times lower than the baseline, comparable to the accuracy of DFT. This surrogate model enables rapid predictions of the work function (~10⁵ faster than DFT) across a vast chemical space. This facilitates the discovery of metallic surfaces that have an extreme work function but also a low surface energy paving the way for new materials solutions in thermionic energy conversion, electron emission devices, and contact electronics.

8:00 PM DS04.10.09

Informing Precursor Choices for Sol-Gel Synthesis of BiFeO₃ Thin Films using Text-Mining and Chemical Reaction NetworksViktorijaBaibakova¹, KevinCruise¹, CarolinM. Sutter-Fella², AnubhavJain² and SamuelM. Blau²; ¹University of California, Berkeley, United States; ²Lawrence Berkeley National Laboratory, United States

This research proposes a novel approach to streamline the choice of precursors for the sol-gel synthesis of BiFeO₃ (BFO) thin films [1], leveraging text-mining and chemical reaction networks. An initial dataset of 340 recipes from 178 scientific papers was manually compiled, providing insight into typical experiment steps. However, the reasonings behind material choices and their interplay remain largely obscure [2]. To clarify these aspects, the study categorizes precursor materials by roles (e.g., metal source, solvent, chelating agent) and analyzes their interactions and influence on the synthesis process. A major challenge is the gelation step, influenced by material selection, which can introduce impurities in the final film [2]. We also highlight the crucial roles of solvent in forming a dense, stable precursor molecule and the chelating agent in enhancing the film's homogeneity. We propose to integrate chemical reaction networks [3] representing all plausible reactions within the materials system, allowing for a more profound understanding of the processes in the precursor. In our study, we employed an integrated automated computational pipeline including a semi-empirical xTB package [4] for high-throughput calculations. This setup facilitated ab-initio calculations revealing that Bi prefers a coordination number of 8 and stabilizes when bidentately coordinated with solvent ligands. To generate a comprehensive chemical reaction network, we utilized Molecular Graphs to represent molecules, creating an exhaustive set of intermediate species for each reaction step. For the reaction between Bi nitrate and 2-methoxyethanol solvent, we identified 634 unique molecular graphs, and fed their 3D representations into the chemical reaction network pipeline. Recovering reactions with chemical reaction networks for various systems (e.g., metal source + solvent, metal source + solvent + chelating agent) is an effective strategy to track final film formation and study the role of chelating agent. This method enhances our understanding of sol-gel precursor processes and promises to facilitate the design and optimization of synthesis methods for high-quality BFO thin films.

References:

[1] JBNJ Wang, JB Neaton, H Zheng, V Nagarajan, SB Ogale, B Liu, D Viehland, V Vaithyanathan, DG Schlom, UV Waghmare, et al. Epitaxial bifeo₃ multiferroic thin film heterostructures. *science*, 299(5613):1719–1722, 2003.

[2] Qi Zhang, Nagarajan Valanoor, and Owen Standard. Epitaxial (001) bifeo₃ thin-films with excellent ferroelectric properties by chemical solution deposition-the role of gelation. *Journal of Materials Chemistry C*, 3(3):582–595, 2015.

[3] Daniel Barter, Evan Walter Clark Spotte-Smith, Nikita S Redkar, Aniruddh Khanwale, Shyam Dwaraknath, Kristin A Persson, and Samuel M Blau. Predictive stochastic analysis of massive filter-based electrochemical reaction networks. *Digital Discovery*, 2023.

[4] Christoph Bannwarth, Sebastian Ehlert, and Stefan Grimme. Gfn2-xtb—an accurate and broadly parametrized self-consistent tight-binding quantum chemical method with multipole electrostatics and density-dependent dispersion contributions. *Journal of chemical theory and computation*, 15(3):1652–1671, 2019.

8:00 PM DS04.10.10

High-Throughput Identification of Materials for Silicon Tandem Solar CellsYanzenZhao¹, ZhikunYao¹, ChangLiu¹, WeiRen¹ and LeeA. Burton²; ¹Shanghai University, China; ²Tel Aviv University, Israel

Today, more than 90% of the market share of solar energy uses silicon (Si) as an absorber material. However, it is well established that Si is not an optimal light absorber because it has a band gap that is both indirect and lower than ideal according to the Shockley–Queisser efficiency limit. While some researchers seek alternate technologies to supplant silicon solar cells, building on the existing success of Si is the most efficient way to increase PV deployment. Therefore, a dual-junction device is desirable, which uses two materials to absorb different portions of the

solar spectrum in the same cell rather than one in so-called “tandem” cells.

High-throughput calculations are employed to identify the most promising materials for silicon tandem solar cells. Starting with the Materials Project database of more than 131 000 materials, we evaluate the relevant properties of thermodynamic stability, lattice mismatch with silicon, band gap, effective mass, optical absorption coefficient and dynamic stability. The identified 11 optimal candidates represent a variety of material chemistries with oxides, pnictogenides, and chalcogenides included. Among them, perhaps the most promising is Cu₂ZnSiSe₄, which has almost ideal properties for all physical criteria and is composed of relatively earth-abundant constituents.

8:00 PM DS04.10.11

High-Throughput Synthesis and Screening of Mn²⁺ Doped Perovskite Nanoparticle Megalibraries for Customized Single-Component White Light Emitters TongCai and ChadA. Mirkin; Northwestern University, United States

Materials that efficiently convert energy into white light would mitigate the consumption of energy in optoelectronic applications, such as lighting and displays. Yet commercial white light generation currently relies on devices that incorporate multiple materials, including color conversion layers, which suffer from issues like long-term instability. One solution to this challenge is to explore materials capable of single-component white light emission while simultaneously accommodating different emission channels to achieve polychromatic light. In this pursuit, here we explore metal halide perovskite materials using high throughput synthesis of Mn²⁺ doped PEA₂PbX₄ (PEA: Phenethylammonium, X: halide anions) nanoparticle (NP) megalibraries. Megalibraries are centimeter scale chips that contain millions of individually addressable NPs prepared by scanning probe lithography techniques. In this work, we combine evaporation-crystallization polymer pen lithography, thermal annealing assisted doping and solvent vapor assisted recrystallization processes to yield Mn²⁺ doped NP megalibraries. Single particle optical studies revealed that dual-wavelength photoluminescence (PL) profiles of the obtained Mn²⁺ doped perovskite NPs originated from both exciton recombination and energy transfer processes. Combinatorial synthesis and high throughput PL screening of NP megalibraries were also pursued and analysis of the composition-PL-chromaticity coordinate relationships resulted in a “chromaticity triangle” tuning diagram. The ideal perovskite composition for white light emission was identified within a megalibrary containing a compositional gradient (i.e., PEA₂Pb_{1-x}Mn_xBr_{4-4y}I_y (0 ≤ x ≤ 1, 0 ≤ y ≤ 1)). This study advances our understanding of composition-structure-function relationships of doped perovskite NPs and exemplifies how NP megalibraries can be used to accelerate materials discovery for next-generation optoelectronic materials for solar energy conversion applications.

8:00 PM DS04.10.12

Modeling Complex Materials with Chemical Accuracy using the Constrained and Smoothed Empirical (CASE) Framework for Next-Generation Density Functionals ZacharyM. Sparrow, BrianErnst, TrineQuady and RobertA. DiStasio Jr.; Cornell University, United States

Density functional theory (DFT) has become the *de facto* standard when performing electronic structure calculations—a critical need in both simulation-based and data-driven thrusts in materials screening and discovery. While DFT is an exact theory, its accuracy depends on the underlying density functional approximation (DFA) used to describe the non-trivial and many-body exchange-correlation interactions between electrons in molecules and complex materials. To date, DFAs have been primarily designed using either non-empirical strategies (*via* satisfaction of physical constraints and appropriate norms) or empirical strategies (*via* data-driven optimization). In this work, we present a general framework that unites these two seemingly contrasting strategies. The proposed method employs B-splines, bell-shaped spline functions with compact support, to construct the inhomogeneity correction factors (ICF) in a given DFA. This choice offers several distinct advantages over traditional polynomial expansions, including: (1) the ability to explicitly enforce both linear and non-linear constraints as well as ICF smoothness using Tikhonov and penalized B-splines (P-splines) regularization, and (2) the flexibility to leverage high-quality quantum-mechanical and/or experimental data during the optimization process. As proof-of-concept, we use the resulting Constrained and Smoothed Empirical (CASE) framework to construct a constraint-satisfying and data-driven global hybrid DFA that exhibits enhanced performance across a wide and diverse set of chemical properties. By maintaining the physical rigor and transferability of non-empirical DFAs and simultaneously leveraging high-quality quantum-mechanical and/or experimental data to remove the arbitrariness of ansatz selection and improve performance, we argue that the CASE approach can be used to develop next-generation DFAs able to model complex materials with chemical accuracy.

SESSION DS04.11: Materials Computation and Artificial Intelligence I
Session Chairs: Jason Hattrick-Simpers, Doris Segets, Taylor Sparks and Daniel Tabor
Thursday Morning, November 30, 2023
Sheraton, Second Floor, Back Bay B

8:30 AM *DS04.11.01

Quantum Chemistry-Enabled Machine Learning for Designing Improved Molecular Materials for Energy and Conversion RajeevSurendran Assary; Argonne National Laboratory, United States

A priori and reliable simulations can enable timely and cost-efficient design and discovery of materials for energy. Therefore, ‘*Let’s Start from Computing*’ is an optimal approach to initialize modern day R&D processes. In energy storage, *beyond lithium-ion (BLI) research* has the potential to revolutionize consumer electronics including portable and stationary power, transportation, and grid energy storage sectors. Multi-valent (Mg, Ca, Zn) energy storage or economically viable monovalent (Na, K) batteries, high-density metal-air, metal-sulfur batteries, or grid-storage systems are considered in the beyond lithium-ion research and development. *All these R&D efforts require significant fundamental knowledge via a priori computations for materials discovery, property prediction, and optimization.* Atomistic modeling when coupled with reliable Artificial Intelligence (AI) approaches can provide *accurate* insights to *accelerate* discovery of *optimal* electrolytes, electrodes, and membranes for BLI systems to *reduce the cost*. Thus, coupled with AI and multi-scale simulations techniques, atomistic modeling can address prediction of molecular level properties of materials (redox potentials, solvation, spectroscopic, and reactivity) to down-select *optimal materials or material combinations*. In this presentation, I will describe some of our recent efforts (2018-2022) in active learning coupled with large scale first principles simulations to down select/optimize desired molecules for *flow battery* technology. This concept can be utilized for design of experiments using autonomous experimentation. Additionally, I will describe some of our quantum chemistry-informed molecular property predictions redoxmers and liquid organic hydrogen carriers. In addition to molecules, I will present. A data driven approach to study longer time scale diffusion of ions for multivalent battery concepts. Finally, I will describe our computational catalysis program development timeline with details of a recent data-driven approach for catalytic property prediction using high performance periodic density functional computing and deep learning .

9:00 AM DS04.11.02

Coupling Reinforcement Learning Approaches with Efficient Quantum Chemical Models for Organic Electronic Materials Discovery and Design DanielTabor; Texas A&M University, United States

In this talk, we will focus on two angles for accelerating organic materials design, with our application spaces focusing on optoelectronic and redox-active organic materials. The first angle focuses on developing discriminative machine learning models that can predict non-extensive organic material properties (e.g., redox potential, reorganization energy) from a low number of training points. In this area, our main areas of focus are on developing appropriate features for the model, quantifying uncertainty in prediction, and developing active learning strategies for developing robust models with as few training points as possible. The second angle focuses on developing methods that pick the right materials to simulate and ensuring that algorithms avoid the numerous local minima that exist in chemical space. We will discuss our work on leveraging reinforcement learning schemes for the inverse design of conjugated and non-conjugated materials and if time permits, our work on integrating these reinforcement learning methods with other representations for molecular materials.

9:15 AM DS04.11.03

Rotation Assisted Proton Conduction Mechanism in Solid Acid Compounds using Machine Learning Molecular Dynamics MenghangWang¹, CameronJ. Owen¹, GraceXiong², JingxuanDing¹, YuXie¹, SimonBatzner³, AlbertMusaelian¹, AndersJohansson¹, NicolaMolinari¹, NiZhan⁴, SossinaM. Haile² and BorisKozinsky¹; ¹Harvard University, United States; ²Northwestern University, United States; ³Google DeepMind, United States; ⁴Princeton University, United States

Rotation-assisted diffusion has emerged as a prevalent mechanism in various superionic conductors, offering wide-ranging applications from highly efficient solid-state electrolytes to hydrogen electrooxidation catalysts. However, a comprehensive understanding of the specific contribution of anion dynamics to the superionic behavior across different compound types has remained elusive. In the superprotonic phase, solid acid proton conductors exhibit intriguing behaviors characterized by local proton hop within the O-H···O bond and anion reorientation, both of which presumably contribute to long-range proton motion. Therefore, gaining insight into the intricate interplay between protons and anions in the superprotonic phase is essential for further advancing our understanding of the mechanisms underlying superprotonic behavior.

Previous experimental endeavors have successfully characterized the timescales of proton oscillation and anion rotation using techniques such as NMR. However, to fully interpret these

timescales, computational studies are necessary to provide atomistic level mechanistic insight into the transport process. Existing computational studies, while shedding light on some aspects of the transport, are constrained by their limited scale, typically involving simulations with a few hundred atoms over a timescale of a few hundred picoseconds.

In this study, we employ machine learning molecular dynamics (MLMD) to investigate the dynamics of anion reorientation and its interaction with proton motion in solid acid proton conductors, specifically focusing on CsH_2PO_4 and CsHSO_4 . Our approach leverages machine learning interatomic force fields (MLFFs) developed through uncertainty-aware active learning and equivariant neural networks. By combining the accuracy of ab-initio methods with the scale required to simulate thousands of atoms over nanosecond timescales, our MLFFs enable us to explore the correlation between anion dynamics and proton transfer with more sufficient statistics. Using this approach, we find that polyanion group reorientation can occur without contributing to long-range proton motion, a feature not observed in prior simulations.

9:30 AM DS04.11.04

De Novo Design of Molecules with Low Viscosity (1): MD Calculations and the Design by Applying the REINVENT Method Nobuyuki N. Matsuzawa¹, Hiroyuki Maeshima¹, Tatsuhito Ando¹, Atif Afzal², Kyle Marshall², Benjamin Coscia², Andrea Browning², Alex Goldberg², Mathew D. Halls², Karl Leswing², Mayank Misra², Farhad Ramezanghorbani² and Tsuguo Morisato³; ¹Panasonic Industry Co., Ltd., Japan; ²Schrödinger Inc., United States; ³Schrödinger K.K., Japan

Molecules exhibiting lower viscosities than conventional organic solvents are in high demand for applications of electrochemical devices such as lithium-ion batteries and various capacitors, as such molecules improve the electric resistance of the devices, thus improve the efficiency of the devices, especially at low temperatures. In order to find such molecules, intensive molecular dynamics (MD) calculations were performed to predict viscosities of 10,000 molecules that were randomly selected from the GDB-17 [1] chemical structural database with a restriction of the selection to be the number of heavy atoms being less than 11. The prediction of viscosities was done based on the Nernst-Einstein and Green-Kubo equations. In addition to the MD calculations for the viscosities, DFT calculations were also performed to predict energies of highest occupied molecular orbital (HOMO) of the 10,000 molecules. By using the 10,000 values each of the viscosity and HOMO level as training datasets, machine-learned models were built to predict the two quantities. With the models built, de novo design of molecules was subsequently performed by applying the REINVENT method [2], which is a method based on reinforcement learning of SMILES strings. The method explored molecules that minimize viscosity while having a sufficiently low HOMO level to ensure the stability of the designed molecules, and succeeded in obtaining chemical structures whose viscosity is lower than 2 mPa s while exhibiting a sufficiently low HOMO energy level. Further details will be presented on the de novo design of molecules with low viscosity for electrochemical applications.

[1] L. Ruddigkeit *et al.*, J. Chem. Inf. Modeling 53 (2013) 56.

[2] M. Olivecrona *et al.*, J. Cheminf. 9 (2017) 48.

9:45 AM DS04.11.05

De Novo Design of Molecules with Low Viscosity (2): Multi-Property Optimization using the REINVENT Method Atif Afzal¹, Benjamin Coscia¹, Andrea Browning¹, Alex Goldberg¹, Karl Leswing¹, Mathew D. Halls¹, Tsuguo Morisato¹, Nobuyuki N. Matsuzawa², Hiroyuki Maeshima² and Tatsuhito Ando²; ¹Schrödinger Inc., United States; ²Panasonic Industry Co., Ltd., Japan

Molecular modeling and machine learning are becoming essential tools in designing new materials. However, optimizing for a specific property often results in a compromise on other critical properties. Thus, it is crucial to develop a method that considers multiple targeted properties for efficient material design in specific applications. For instance, electrochemical devices such as liquid electrolyte lithium-ion batteries and various capacitors require molecules with lower viscosities, specific electronic properties, and boiling points above the maximum operating temperature. This study demonstrates the use of physics-based modeling and advanced machine learning techniques to design molecules with such target properties. We use molecular dynamics (MD) to compute the viscosity and boiling point; and density functional theory (DFT) to compute the HOMO energy of molecules. We validate the results by comparing them with experimental values. We generate ML models for all these properties and subsequently use the models for the de novo design of molecules. For the de novo design, we implement the REINVENT method [1], based on reinforcement learning of SMILES strings. We create targeted molecules based on two criteria: minimizing viscosity while keeping the boiling point above 82°C and minimizing viscosity while attempting to minimize HOMO under a constraint of the boiling point being higher than 82°C. Based on these criteria, we selected the best 200 candidates from the REINVENT method and validated the molecules using MD and DFT characterization. We demonstrate that de novo design approaches are effective in designing molecules with various desired characteristics.

[1] M. Olivecrona *et al.*, J. Cheminf. 9 (2017) 48.

10:00 AM BREAK

10:30 AM *DS04.11.06

Improving Crystal Structure Prediction: Accelerating Flexible Unit Structure Engine (FUSE) with Machine Learning Predictions Taylor D. Sparks^{1,2}, Hasan Sayeed¹, Christopher Collins² and Matthew Rosseinsky²; ¹University of Utah, United States; ²University of Liverpool, United Kingdom

To enable efficient exploration of vast composition spaces and enhance crystal structure prediction, we have extended the capabilities of the Flexible Unit Structure Engine (FUSE) by integrating machine learning (ML) techniques. FUSE is a widely used computational tool for materials discovery across diverse compositions. Our approach consists of two key components. Firstly, we employ classical ML models to accurately predict volume/atom ratios, facilitating the estimation of unit cell sizes for various compositions. Secondly, we integrate a well-established ML-driven crystal structure prediction technique, utilizing advanced methods such as graph networks to establish correlations between crystal structures and formation enthalpies. To expedite the search for crystal structures with the lowest formation enthalpy, this technique incorporates an optimization algorithm. Through the integration of ML-based volume/atom prediction and crystal structure prediction within FUSE, our approach significantly accelerates the discovery of experimentally realizable compounds. This integration offers a promising pathway for efficient materials discovery, pushing the boundaries of knowledge in complex composition spaces.

11:00 AM DS04.11.07

Proton Transfer in Nanoporous TiO₂ Films: Insights from Deep Potential Molecular Dynamics Simulations Hyuna Kwon, Marcos Calegari, Tadashi Ogitsu and Tuan Anh Pham; Lawrence Livermore National Laboratory, United States

Understanding proton transfer and water splitting reactions in nano-porous materials is critical for a wide range of emerging technologies, including hydrogen production through photoelectrochemical water splitting. However, elucidating mechanism and energetics of these processes remains a significant challenge for experimental probes. In this work, we combine large-scale molecular dynamics simulations with machine learning potential derived from first-principles calculations to investigate kinetics of proton transfer in nano-porous TiO₂ as a representative photocatalyst material. We developed and applied a deep neural network potential to reconstruct the free energy surface of water dissociation and proton transport for a wide range of pore sizes to elucidate confinement effects. We show that reactivity of porous TiO₂ with water recovers its behavior at the interface with the bulk liquid for a pore diameter larger than 10 Å. On the other hand, confinement below 5 Å diameter significantly affects the water reactivity and proton transport near the interface with the pores. Specifically, we show that a limited hydrogen bond network in these narrow pores facilitates redox reactions and enhances proton transfer. Our study highlights the critical competition between kinetic and thermodynamic factors introduced by nano-confinement, suggesting potential strategies for optimization of photocatalytic systems for efficient water splitting reactions.

This work was supported as part of the Center for Enhanced Nanofluidic Transport (CENT), an Energy Frontier Research Center funded by the U.S. Department of Energy, Office of Science, Basic Energy Sciences under award DE-SC0019112. T.O. acknowledges support from Ensembles of Photosynthetic Nanoreactors (EPN) funded by the U.S. Department of Energy, Office of Science, Basic Energy Sciences. The work at the Lawrence Livermore National Laboratory was performed under the auspices of the U.S. Department of Energy under contract DE-AC52-07NA27344.

11:15 AM DS04.11.08

Multi-Modal Foundation Model for Material Discovery with Conversational User Interface Seiji Takeda, Akihiro Kishimoto, Indra Priyadarsini S, Hajime Shinohara and Daiju Nakano; IBM Research Tokyo, Japan

Background

The advent of AI-driven models has revolutionized material discovery process through predictive as well as generative modeling. However, a majority of these models remain constrained in their utility due to their isolation in three aspects: (i) data modality used for training, (ii) specificity to certain material domains, and (iii) focus on independent application tasks. This approach curtails the sharing of knowledge across models, restricts access to diverse datasets, and fosters redundancy through the parallel development of analogous models globally. These constraints delineate the inefficiencies in recent AI development within the materials and chemistry sector.

Objective

We introduce Foundation Model (FM) tailored for material discovery, seeking to surmount the aforementioned limitations. This FM employs a pre-training phase leveraging massive datasets

across multiple modalities such as SMILES, property tables, and spectra, spanning diverse material domains (e.g., electronics, polymers, pharmaceuticals). By encoding generalized knowledge and representations onto its latent space, the FM serves as a versatile foundation for numerous downstream applications including predictive analysis and material generation.

Methodology

To adeptly capture multi-modal representations, our FM utilizes a late-fusion scheme, which aligns representation vectors from distinct modalities into a shared latent space. This is achieved by pre-training modality-specific autoencoders (e.g., for SMILES) and subsequently aligning each modality's individual latent spaces through contrastive learning on the shared latent space. We constructed three modality-specific models trained with SELFIES, DFT properties tables, and UV/Vis optical absorption spectra using self-supervised learning. Data was curated from public database such as PubChem and ZINC, in conjunction with DFT-simulated datasets, over 10 billion samples in total. The models were then integrated into a fusion model that projects the representations into a shared latent space.

Results and Demonstration

Our FM exhibited exceeding performance across diverse downstream tasks, including material property predictions and generative applications utilizing pre-trained datasets. We will also showcase the FM's efficacy in predicting properties on distinct datasets through fine-tuning external predictive models connected to the FM's shared latent space. Additionally, we will unveil an multi-modal conversational Graphical User Interface (GUI) for human interaction. The GUI integrates text-based interaction with a multi-modal input panel featuring a molecular editor, property table editor, and spectrum drawer. This innovative interface heralds new possibilities for human-model synergy within materials science and chemistry.

Conclusion

This research introduces a transformative Foundation Model for material discovery, bridging modalities and domains. Through its versatile architecture and intuitive human-interface, it paves the way for more efficient and interactive material and chemistry research.

11:30 AM DS04.11.09

Methods for Feature and Image Selection for Machine Learning Potentials: A Comparative Study ChengZeng, ZacheryHindley, NathanPost and JackLesko; Roux Institute at Northeastern University, United States

Machine learning interatomic potentials (MLIPs) have revolutionized atomistic simulations, enabling predictions of materials properties with first-principles precision while only taking a small fraction of DFT time cost. The reliability and transferability of MLIPs strongly depend on the quality of features and structures used to represent the underlying *ab initio* potential energy surfaces. To reduce the computational overload of expensive first-principles calculations, there is an urgent need to select informative image and features, in particular for complex materials such as high-entropy materials. Current methods for image and feature selection use linear correlations in the feature space (and output space) spanned by the training data. However, the relationship between features and properties can be highly non-linear, rendering it questionable for linear methods. Here, we propose an alternative method for image and feature selections. This approach uses auto-encoder to perform non-linear dimensional reduction. Images selection will then be conducted in the low-dimensional latent space, and the following feature selection will be realized through sensitivity analysis. We benchmark the method on first-principles data of AlCrFeNiCo high-entropy alloys. This class of high-entropy alloys is crucial in many applications as it is an emerging material with superior mechanical properties and corrosion resistance. We compare the new feature and image selection method with existing ones using atom-centered neural network potentials as models and Gaussian symmetry functions as local chemical environment descriptors.

SESSION DS04.12: Materials Computation and Artificial Intelligence II
Session Chairs: Jason Hattrick-Simpers, Anubhav Jain, Doris Segets and Olga Wodo
Thursday Afternoon, November 30, 2023
Sheraton, Second Floor, Back Bay B

1:30 PM *DS04.12.01

Data-Driven Microstructure-Property Mapping: The Importance of Microstructure Representation, Size of Data and Implications for Model Generalization OlgaWodo; State University of New York at Buffalo, United States

Mapping microstructure-sensitive properties with microstructure representation is invariably challenging due to the mismatch between the high dimensionality of microstructural information (e.g., via microscopy or simulations) and the principal degrees of freedom (or salient features) governing the properties. This is because microstructural imaging aims to provide detailed, high-resolution maps. Hence, imaging techniques inevitably produce high-dimensional representations of microstructure, while the goal of establishing practically useful structure-property models is to identify the smallest set of features that can successfully predict the effective properties exhibited by the material. Often, this set is not known a priori, especially for complex multi-physics phenomena governing the material properties.

Data-driven approaches become the integral approach to establishing reliable microstructure-property mappings. However, materials science datasets are typically small, or the property evaluations are computationally or experimentally demanding, and this requires approaches that integrate the small datasets or seek smart sampling strategies. One critical aspect of data-driven approaches is the ability to represent materials microstructure in machine-friendly formats. This talk presents three methods: statistical descriptors (e.g., 2-point correlations), vector of physically meaningful descriptors, and latent space learned using autoencoder. Using the combination of different representations, we explore three questions: Given a few datasets with distinct microstructure annotated with the property of interest: 1) Can a small subset of features be selected to train a robust microstructure-property predictive model? And is this subset agnostic to the choice of feature selection algorithm? 2) Can the addition of expert-identified features improve model performance? 3) Can the generalizable model be trained for independent microstructure datasets (different microstructure types)? The questions are essential for any microstructure-sensitive properties. Still, in this talk, we will utilize the problem of constructing structure-property models for organic photovoltaics applications (OPV) to understand data-driven SP models.

2:00 PM DS04.12.02

Understanding Green Solvents for Metals Recycling using Machine-Learned Molecular Dynamics JuliaYang¹, Amanda Whai ShinOoi², Ah-Hyung AlissaPark^{2,2} and BorisKozinsky^{1,1}; ¹Harvard University, United States; ²Columbia University, United States

A projected two million tons of lithium-ion battery waste in the next decade requires development of novel, low-energy, minimally wasteful metals recycling processes to enable a sustainable and environmentally just energy transition. Recently, type III deep eutectic solvents have been gaining great interest as they can supposedly address all of these practical constraints. In particular, ethaline, a 2:1 molar ratio of ethylene glycol and choline chloride, leaches and electrodeposits critical minerals efficiently [1], albeit at the cost of thermal decomposition into toxic products [2]. Computationally-driven efforts to assess neat solvent and its phase stability over temperature cannot be achieved using refined classical molecular dynamics which do not include bond breaking, nor with accurate *ab initio* simulations due to prohibitive costs. However, machine-learning assisted molecular simulations can bridge the gap between accurate simulations and thermodynamic sampling of these fully explicit models.

Herein, we systematically benchmark density functional and quantum chemistry calculations and use them to construct a machine-learned force field (MLFF) for ethaline. We verify the fidelity of the MLFF against its existing thermodynamic properties and use large-scale molecular dynamics simulations to evaluate the onset of thermal decomposition, after which, at higher temperatures, we find that toxic byproducts such as chloromethane and dimethylaminoethanol are formed irreversibly. Our molecular-level assessment suggests a temperature upper operating limit of ethaline, and is the first to computationally examine the utility and stability of ethaline as a stable solvent for metals recovery applications. The results of our analysis can rationalize the selection of other solvents which span a vast underexplored, combinatorial design space.

[1] M. K. Tran, M.-T. F. Rodrigues, K. Kato, G. Babu, P. M. Ajayan, Nat. Energy 4, 339-345 (2019). doi.org/10.1038/s41560-019-0368-4

[2] P. G. Schiavi, P. Altamari, E. Sturabotti, A. G. Marrani, G. Simonetti, F. Pagnanelli, ChemSusChem 15, 18, (2022). doi.org/10.1002/cssc.202200966

2:15 PM DS04.12.03

Accelerating the Construction of ANN Interatomic Potentials using Surrogate Models In WonYeou¹, AnnikaStuke¹, JonLópez-Zorrilla², JamesStevenson³, DavidR. Reichman¹, RichardA. Friesner^{1,3}, AlexanderUrban¹ and NongnuchArtrith⁴; ¹Columbia University, United States; ²University of the Basque Country, Spain; ³Schrödinger, Inc., United States; ⁴Utrecht University, Netherlands

Artificial neural network (ANN) potentials trained on data from first-principles calculations enable large-scale atomistic simulations with thousands to millions of atoms with an accuracy comparable to the reference method used to train them. However, applying ANN potentials to complex materials may require huge first-principles energy databases to sample the potential

energy surface (PES) with sufficient precision. Including atomic force information in ANN potential training greatly reduces the data requirements, improves PES prediction accuracy, and increases transferability, but it is computationally demanding. We previously showed that force training can be accelerated through energy extrapolation via Taylor expansion [1] or parallelization on graphics processing units (GPUs) [2]. Here, we discuss an extension of the extrapolation methodology that allows us to further improve ANN potentials without increasing the training databases. We demonstrate how a surrogate model based on Gaussian process regression (GPR) can be used to translate atomic forces into approximate energies, augmenting ANN training data with more accurate and robust energy information than the Taylor expansion method. We benchmarked this synthetic data approach for diverse and complex materials, including ethylene carbonate (EC) molecules and Li metal-EC interfaces which are technologically relevant for solid-electrolyte interphases in Li metal batteries. We also thoroughly compared ANN potentials trained with the GPR-augmented data set against conventionally trained ANN potentials regarding accuracy and training cost.

References

- [1] A.M. Cooper, J. Kästner, A. Urban, and N. Artrith, *npj Comput. Mater.* **6**, 54, (2020).
- [2] J. López-Zorrilla, X.M. Aretxabala, I. W. Yeu, I. Etxebarria, H. Manzano, and N. Artrith, *Journal of Chemical Physics* **158**, 164105 (2023)

2:30 PM DS04.12.04

An Intrusive, Bayesian Paradigm for Scientific Machine Learning Outperforms Neural Networks in Typical Scientific Modeling Contexts David S. Mebane^{1,2}; ¹West Virginia University, United States; ²KBR Wyle Services, United States

Neural networks (NNs) are powerful tools for machine learning, with stunning results in computer vision and large language models dominating the news. However NNs are often misapplied in scientific modeling contexts, in which the input-output space dimensionalities are small to moderate. There are numerous examples of other methods such as decision trees and Gaussian processes (GPs) outperforming NNs in both accuracy and inference speed for tabular estimation. A shift away from NNs in scientific modeling contexts promises faster and more accurate performance. A framework for scientific machine learning in which fast, decomposed GPs represent well-defined scientific functions has shown considerable promise, outperforming recurrent neural networks (such as LSTM) on multiple benchmark dynamic modeling tasks. These well-defined functions also present opportunities for multi-scale modeling, linking electronic and atomistic scales to device scales. Multiple applications in materials modeling for energy applications -- including in solid-state batteries and high-temperature CO₂ electrolyzers -- will be presented.

2:45 PM DS04.12.05

Alternative Machine-Readable Representation of Molecules for More Efficient Use of Computational Resources in Machine Learning Applications Emilio Alexis de la Cruz Nuñez Andrade¹, Isaac Vidal-Daza^{2,1}, Rafael Gómez-Bombarelli³ and Francisco Martín-Martínez¹; ¹Swansea University, United Kingdom; ²Universidad de Granada, Spain; ³Massachusetts Institute of Technology, United States

The rapid increase in computational resources demand is unprecedented because of the surge in artificial intelligence (AI), big data, and high-throughput computing. In chemistry, machine learning (ML) is revolutionizing molecular discovery, materials design, and property predictions in areas ranging from biomedicine to energy harvesting and storage, among many others. In practice, the implementation of ML methods relies on the codification of chemical structures into a suitable format for practical implementation in computational tools. To this end, the chemistry community adopted the Simplified Molecular Input Line Entry System (SMILES)[1] for initial structure codification, and the subsequent DeepSMILES[2] and SELFIES[3] (SELF-referencing Embedded Strings) as more sophisticated approaches. These representations are further encoded into a machine-readable format that captures the structural and chemical characteristics of molecules, such as One Hot Encoding (OHE), Molecular Graphs (MG) or Descriptors (Molecular Fingerprints), whose selection depends on the application, the data set, and the ML model to train. In this study, we propose an alternative representation to traditional OHE of SMILES, DeepSMILES and SELFIES, which allows for comparable results in model accuracy and robustness but improves the efficiency in the use of computational resources compared with the traditional alternatives. To evaluate the effectiveness of this alternative representation, we conducted a set of benchmarks and comparative analysis with a Variational Autoencoder and a Recurrent Neural Network. We also explored the impact of this alternative representation in the required size of the training dataset, the molecular diversity, novelty, and validity, as well as in the model complexity for different number of hyperparameters. This alternative representation provides a new avenue for more efficient computing with less use of computational resources and faster performance, which impacts ML methods for chemistry, but also for any other fields that uses OHE as data representation.

- [1] Weininger, D. (1988). SMILES, a chemical language and information system. 1. Introduction to methodology and encoding rules. *Journal of chemical information and computer sciences*, 28(1), 31-36.
- [2] O'Boyle, N., & Dalke, A. (2018). DeepSMILES: an adaptation of SMILES for use in machine-learning of chemical structures.
- [3] Krenn, M., Häse, F., Nigam, A., Friederich, P., & Aspuru-Guzik, A. (2020). Self-referencing embedded strings (SELFIES): A 100% robust molecular string representation. *Machine Learning: Science and Technology*, 1(4), 045024.

3:00 PM BREAK

3:30 PM *DS04.12.06

Informing Energy Technology Scalability Elsa Olivetti; Massachusetts Institute of Technology, United States

This presentation will provide updates around our groups efforts to inform manufacturing scalability in clean energy technologies

4:00 PM DS04.12.07

Applications of Large Language Models in Materials Discovery and Design Anubhav Jain; Lawrence Berkeley National Laboratory, United States

In the past year, natural language processing has quickly evolved from a relatively niche field used by a small community of materials researchers to a commonplace and wide-ranging tool used worldwide. In particular, large language models such as GPT-3, ChatGPT, and GPT-4 have demonstrated that many natural language processing tasks that have conventionally been challenging are now within reach - but with important limitations. In this presentation, I will review our group's recent work in using large language models to extract structured data sets from the literature, including techniques to make such extractions effective. Applications include parsing nanoparticle and solid state synthesis recipes, creating data sets of doping data for subsequent machine learning, and understanding known materials and their properties. I will also demonstrate how we are deploying this information through platforms such as the Materials Project to make the results from these models publicly accessible and usable in real-world materials design applications. Finally, I will conclude with an outlook on future use cases and potential pitfalls of using large language models in the materials domain.

4:15 PM DS04.12.08

Robustness of Local Predictions in Machine Learning Models for Materials Sanggyu Chong¹, Federico Grasselli¹, Chihab Ben Mahmoud¹, Joe D. Morrow², Volker L. Deringer² and Michele Ceriotti¹; ¹EPFL, Switzerland; ²University of Oxford, United Kingdom

Many machine learning (ML) models for the prediction of material properties rely on a decomposition of the global target quantity (e.g. total energy, magnetic dipole, electronic density of states, etc.) into local contributions associated with individual atoms, or clusters of atoms. By interpreting and learning the global quantities as a sum of local contributions, the models are essentially trained to make predictions on the locally decomposed environments of a given structure. This approach is computationally convenient, significantly improves the transferability and scalability of the resulting ML models, and allows one to discover useful structure-property relationships as they associate simple atomic motifs with complicated macroscopic properties. While the practical benefits of the local decomposition is clear, one must recognize that only the global quantity is rigorously defined, and the decomposition can arbitrarily take place in numerous different ways. It hence remains largely unclear to what extent the local predictions of the ML model can be trusted.

In this contribution, we introduce the local prediction rigidity (LPR)[1] a generally applicable metric that quantifies how "rigid", or robust, the ML model is in the local predictions that it makes. Through our investigation on a range of models and materials datasets, we reveal that the LPR can vary drastically between different local predictions, and it largely depends on the degeneracies associated with locally decomposing the global target quantity. We then investigate strategies to systematically increase the LPR by the careful curation of the training dataset, and demonstrate these strategies in linear, kernel, and neural network models for silicon, carbon and GaAs. The LPR has great potential for proposing effective active learning schemes, where the assessment and improvement of the ML model performance can all take place at the local level. We also note that, as the derivation of LPR is not limited to an atomic decomposition, it can be extended to other decomposition schemes: multiple body-order decomposition, short-range vs. long-range decomposition, etc. This allows one to scrutinize the model and precisely identify where it lacks robustness, and propose effective ways to improve the ML model.

[1] Sanggyu Chong, Federico Grasselli, Chiheb Ben Mahmoud, Joe D. Morrow, Volker L. Deringer, Michele Ceriotti, "Robustness of Local Predictions in Atomistic Machine Learning Models", *In preparation*.

4:30 PM DS04.12.09

Uncertainty Quantification in the Atomistic Modelling of Grain Boundaries Anqi Qiu¹ and Elizabeth Holm²; ¹Carnegie Mellon University, United States; ²University of Michigan–Ann Arbor, United States

Atomistic simulations have been successful in the prediction of materials properties in many applications. Commonly used atomistic simulation methods such as density functional theory (DFT) and molecular dynamics (MD) possess inherent uncertainties that may greatly impact simulation results. However, the uncertainties are rarely quantified, mostly due to the limitations in computational resources and the complexity of the methods for uncertainty quantification.

Grain boundaries are interfaces between grains in polycrystalline materials, being in an intermediate state in between crystalline and amorphous materials, has many unique properties, such as the ability to provide fast transport paths for atoms and ions. Grain boundary motion is a key process that governs the microstructural evolution in materials. In energy materials such as batteries, grain boundaries are crucial to ionic transport. Due to the limitations of current experimental methods in understanding the mechanisms of grain boundary motion at the atomic level, atomistic simulations have become an essential tool for mechanistic studies.

In our study, we adopt elemental metallic materials as model materials, and investigate the migration and diffusion of grain boundaries using MD simulations. We demonstrate that some sources of uncertainty can significantly impact simulation results, but were usually ignored in prior works. In the simulations, atomic velocities are randomly assigned according to the Maxwell-Boltzmann distribution. The different assignments of initial velocities can significantly impact the simulation results of grain boundary migration rate and diffusion coefficient, but the effects are rarely quantified. This work highlights the impact of different assignments of initial velocities and the quantification of the uncertainty in the measurement of grain boundary migration rate and diffusion. We also show that the simulation box sizes at which similar types of simulations are usually performed may cause unphysical artifacts that can be resolved by using larger simulation box sizes.

SESSION DS04.13: Accelerated Catalysis Discovery II
Session Chairs: Anders Johansson and Yangang Liang
Friday Morning, December 1, 2023
Hynes, Level 2, Room 207

8:30 AM DS04.13.01

Extracting Catalytic Reaction Mechanisms from Large-Scale Simulations Accelerated by Machine Learning Interatomic Potentials Anders Johansson, Yu Xie, Cameron J. Owen, Jin Soo Lim, Lixin Sun, Jonathan Vandermause and Boris Kozinsky; Harvard University, United States

Machine learning interatomic potentials (MLIPs) have become a prevalent approach to bridging the gap between slow-but-accurate ab initio calculations and fast-but-inaccurate empirical potentials for molecular dynamics. Among MLIPs, there is a Pareto front of models with different tradeoffs between accuracy and speed. The FLARE interatomic potential aims to push the boundary of scalability and performance, while maintaining sufficient accuracy to study complex, reactive systems.

In our recent work [1], we demonstrated the ability of FLARE to simulate catalytic systems of up to 0.5 trillion atoms using 27336 GPUs, with an accurate MLIP efficiently trained using active learning. With the exceptional speed of FLARE on modern HPC architectures, we can combine the atomistic resolution of molecular dynamics simulations with the large length and time scales required for realistic simulations and sufficient sampling of rare catalytic events, while providing the near-quantum level of accuracy provided by the MLIP. In this talk, we will showcase how this combination of scales and accuracy enables new insights into chemically complex processes such as heterogeneous catalysis.

[1] arXiv:2204.12573

8:45 AM DS04.13.02

Multi-Code Benchmark on Simulated Ti K-Edge X-Ray Absorption Spectra of Ti-O Compounds Fanchen Meng¹, Benedikt Maurer², Fabian Peschel², Sencer Selcuk¹, Mark Hybertsen¹, Xiaohui Qu¹, Christian Vorwerk³, Claudia Draxl², John Vinson⁴ and Deyu Lu¹; ¹Brookhaven National Laboratory, United States; ²Humboldt University of Berlin, Germany; ³The University of Chicago, United States; ⁴National Institute of Standards and Technology, United States

X-ray absorption spectroscopy (XAS) is an element-specific materials characterization technique that is sensitive to structural and electronic properties. First-principles simulated XAS has been widely used as a powerful tool to interpret experimental spectra and draw physical insights. Recently, there has also been growing interest in building computational XAS databases to enable data analytics and machine learning applications. However, there are non-trivial differences among commonly used XAS simulation codes, both in underlying theoretical formalism and in technical implementation. Reliable and reproducible computational XAS databases require systematic benchmark studies. In this work, we benchmarked Ti K-edge XAS simulations of ten representative Ti-O binary compounds, which we refer to as the Ti-O-10 dataset, using three state-of-the-art codes: XSPECTRA, OCEAN and exciting. We systematically studied the convergence behavior with respect to the input parameters and developed a workflow to automate and standardize the calculations to ensure converged spectra. Our benchmark comparison shows: (1) the two Bethe-Salpeter equation (BSE) codes (OCEAN and exciting) have excellent agreement in the energy range studied (up to 35 eV above the onset) with an average Spearman's rank correlation score of 0.998; (2) good agreement is obtained between the core-hole potential code (XSPECTRA) and BSE codes (OCEAN and exciting) with an average Spearman's rank correlation score of 0.990. Our benchmark study provides important standards for first-principles XAS simulations with broad impact in data-driven XAS analysis.

9:00 AM DS04.13.03

Exploring the Family of AM₂Pn₂ Materials and Their Alloys for Use as Solar Absorbers Andrew Pike¹, Zhenkun Yuan¹, Muhammad R. Hasan², Gideon Kassa¹, Kirill Kovnir², Jifeng Liu¹ and Geoffroy Hautier¹; ¹Dartmouth College, United States; ²Iowa State University of Science and Technology, United States

Some compositions of the formula AM₂Pn₂ have recently been observed as promising solar absorbers through high-throughput computing. In this talk, I will explore how isovalent substitutions on this crystal structure can tune the band structure and defects (A = Ba, Sr, Ca, Yb, Eu, Mg, M = Mn, Mg, Cd, Zn, Pn = Bi, Sb, As, P). In order to increase the design space for an optimal material, the alloys between the endmember AM₂Pn₂ compounds will be considered for their effect on stability and optical properties. Our results show that many members of this class of materials are stable and have a range of bandgaps from metallic behavior to well above what is optimal for solar applications.

9:15 AM DS04.13.04

Unbiased Graph Embedding Prediction of Graphene Nanoflake Properties Amanda J. Parker; The Australian National University, Australia

In order to apply machine learning to the study of structure-property relationships domain knowledge is typically required for feature extraction. However, this process may introduce bias if there is a focus on known aspects of structure, thereby impeding the discovery of new science. Here, we develop an approach that uses only atomic Cartesian coordinates to predict the electronic properties of simulated graphene nanoflakes (from a publicly available data set). Our approach addresses the limits of current methods by greatly extending the degree of material complexity, asymmetry, surface details and size differences that can be encoded by a graph embedding.

The workflow developed describes graphene nanoflakes with graphs that are more representative than the ball-stick atom-bond representation that is intuitive to researchers. We generate fixed-size embeddings of these graphs using a neural embedding framework. Pairing the graph embeddings with a convolutional neural network produces a highly accurate predictive model for electron affinities, band gap energies, Fermi energies and ionization potentials. The hold out test set model performance fit has R² from 0.9-0.96 for nanoflakes with a very challenging variation in size from tens to thousands of atoms. These predictions were benchmarked against results for optimized predictive models with geometric domain-driven features and exceeded their model accuracy for predictions of Fermi energy, electron affinity and ionisation potential and met their model accuracy for band gap energy. We also introduce and optimize a model hyperparameter that gives insight into the relevant lengthscales of interactions for the material modelled.

\end{abstract}

9:30 AM DS04.13.05

From Cells to Batteries: Semantic Segmentation's Evolution in Quality Control Daniela Ushizima^{1,2}; ¹Lawrence Berkeley National Laboratory, United States; ²University of California, Berkeley, United States

In an unexpected leap forward for the world of battery technology, an investigation that was first introduced at the Materials Research Society (MRS) conference in 2019 has evolved into a cutting-edge computational tool with potential application to the quality and reliability of batteries. This remarkable innovation leverages the power of semantic segmentation, a sophisticated image analysis technique, to detect and monitor crucial morphological structures such as dendrites during the cycling of batteries.

The journey of semantic segmentation in the realm of science and technology has been nothing short of remarkable. It all began with pioneering efforts to apply this technique to understanding and detecting abnormal cells in the early 2000s [1]. Researchers ventured into the intricate world of "hairy cells" in leukemia, demonstrating the potential of semantic segmentation to dissect and analyze complex biological structures with unprecedented precision.

For over a decade, scientists delved into the mysteries of brain cells, harnessing semantic segmentation to unravel the intricate shapes of brain cells and neuroproteins that power our minds. Their tireless efforts culminated in a groundbreaking paper published in the esteemed NeuroImage journal, earning them the prestigious Precision Medicine World Conference Pioneer Award in 2023 [2]. This recognition marked a turning point in the field, solidifying the importance of semantic segmentation in advancing our understanding of radioactive tags to be used in the human brain.

Now, this transformative technology has taken another leap into the world of energy storage. Researchers have successfully adapted semantic segmentation to scrutinize the inner workings of batteries, specifically targeting dendrites, which have long been a challenge in the realm of battery research. The results of this innovative work were published in the prestigious Nature Partner Journal Computational Materials journal in 2023 [3]*, showcasing the immense potential of semantic segmentation to revolutionize battery quality control. The implications of this breakthrough are immense. Imagine batteries that are not only more powerful but also safer, thanks to the ability to detect and mitigate dendrite-related issues before they become problematic. This advancement promises to usher in a new era of protocols for testing energy storage devices.

As the research community eagerly awaits further details on the practical applications of this technology, one thing is clear: the future of batteries is brighter than ever, thanks to the extraordinary journey of semantic segmentation from leukemia cells to brain cells and now to the heart of our energy solutions. Stay tuned for more updates on this development that promises to reshape how we understand morphologies within batteries.

*This work was funded by the Office of Science, of the U.S. Department of Energy under Contract No. DE-AC02-05CH11231.

[1] Ushizima Sabino D M, Costa LF, Zago MA (2003), Automatic leukemia diagnostic, Acta Microscopica (12)1:1-6

[2] Ushizima, Chen, Alegro, Ovando, Eser, Lee, Poon, Shankar, Kantamneni, Satrawada, Amaro Jr, Heinsen, Tosun, Grinberg, "Deep learning for Alzheimer's disease: Mapping large-scale histological tau protein for neuroimaging biomarker validation", NeuroImage 2022

[3] Huang, Perlmutter, Su, Quenum, Shevchenko, Parkinson, Zenyuk, Ushizima, "Detecting lithium plating dynamics in a solid-state battery with operando X-ray computed tomography using machine learning". Nature Computational Materials (2023)

9:45 AM DS04.13.06

Creating Materials Databases Autonomously using Open Large Language Models Vineeth Venugopal and Elsa Olivetti; Massachusetts Institute of Technology, United States

It is estimated that there are around 150 million scientific papers altogether, of which at least 10 million deal with materials and their structure-property-processing relationships exclusively. Despite this enormous abundance of scientific information, there are very few machine readable databases of materials and their experimentally determined processing, property relations. This has in turn severely limited our ability to extend artificial intelligence models to materials discovery and development which have proved revolutionary in some tasks such as image and text recognition and generation. Efforts to develop databases autonomously have usually relied on rule based string extraction from text, training of BERT based models using manually annotated data or recently through large GPT based models. The last one in particular has attracted the attention of the wider community given the success that ChatGPT has enjoyed. However, GPT 3.5 and 4 are unsuitable for large scale text mining given the proprietary API restrictions placed by the developers.

We show that open large language models such as Llama 1 and 2, Flan T-5, Alpaca, Dolly etc can perform on par with much larger GPT models when fine tuned on specific tasks. This is demonstrated on a range of entity recognition, relationship extraction, text classification, and text generation tasks. By combining large language models with large embedding vector stores, we show that a single prompt or extraction task can lead to the generation of a complete database of materials and their required property fields. Strategies are discussed to mitigate and remove factually incorrect data points that arise as a natural consequence of language model generations. The fine points of training models using bit quantization approaches, and the challenges in model performance are discussed.

In addition to the significant strides made in harnessing open large language models for materials science tasks, it's important to highlight the broader implications of this breakthrough. The ability to effectively extract, process, and organize information from scientific literature using these models extends beyond materials science alone. This approach has the potential to revolutionize the way we access and utilize scientific knowledge across various domains. The success in entity recognition, relationship extraction, text classification, and text generation tasks not only paves the way for comprehensive materials databases but also opens doors to more efficient knowledge discovery and innovation in fields ranging from medicine to environmental science. As we continue to refine and expand these methods, the impact on scientific research and technological advancement is poised to be profound.

SESSION DS04.14: Virtual Session

Session Chairs: Andrew Detor, Jason Hattrick-Simpers, Yangang Liang and Doris Segets

Wednesday Morning, December 6, 2023

DS04-virtual

10:30 AM DS04.14.01

High-Throughput Screening and Experimental Validation of Aqueous Organic Redox Flow Battery Electrolytes Ayush Narsaria¹, Murat C. Sorkun², Kaustubh Kaluskar¹, Xuan Zhou², Nicola Menegazzo¹, Peter Klusener¹, Sharan Shetty¹ and Süleyman Er²; ¹Shell, India; ²Dutch Institute for Fundamental Energy Research, Netherlands

Increasing renewables share in power mix has necessitated improvement and further research on various battery technologies. Aqueous organic redox flow batteries (AORFBs) exhibit many advantages, such as high ionic conductivity, safety, cost-effectiveness, and well-developed technology to compensate for the narrow voltage window that is limited by the electrolysis of water. For this purpose, discovery of novel organic electroactive molecules is highly warranted. Herein, we have developed a computational workflow that can screen millions of organic molecules in a modular fashion using similarity metrics with known electroactive molecules, machine learning based prediction of redox potential and solubility, and finally on the ease of availability and cost. Through this workflow we were able to narrow down to almost 60 molecules, among which some are already reported to have high performance in AORFBs, while some are completely new molecules for the redox flow battery application that are also experimentally validated through cyclic voltammetry experiments.

10:45 AM DS04.14.02

Systematic Modification of Functionality in Disordered Elastic Networks Through Free Energy Surface Tailoring Dan Mendels¹, Fabian Bylehn², Tim Sirk³ and Juan J. de Pablo²; ¹Technion-Israel Institute of Technology, Israel; ²The University of Chicago, United States; ³U.S. Army Research Laboratory, United States

Advances in manufacturing and characterization of complex molecular systems have created a need for new methods for design at molecular length scales. Emerging approaches are increasingly relying on the use of Artificial Intelligence (AI), and the training of AI models on large data libraries. This paradigm shift has led to successful applications, but shortcomings related to interpretability and generalizability continue to pose challenges. Here, we explore an alternative paradigm in which AI is combined with physics-based considerations for molecular and materials engineering. Specifically, collective variables, akin to those used in enhanced sampled simulations, are constructed using a machine learning (ML) model trained on data gathered from a single system. Through the ML-constructed collective variables, it becomes possible to identify critical interactions in the system of interest, the modulation of which enables a systematic tailoring of the system's free energy landscape [1]. To explore the efficacy of the proposed approach we have applied it to numerous case studies, a few of which will be discussed

and illustrated within this talk.

[1] Dan Mendels, Fabian Bylén, Timothy W. Sirk, Juan J. de Pablo, *Sci. Adv.* **9**, eadf7541 (2023)

11:00 AM DS04.14.03

Autonomous Discovery of Triple-Conducting high-Entropy Oxides for Protonic Ceramic Fuel Cells Ivano Eligio Castelli and Benjamin H. Sjølin; Technical University of Denmark, Denmark

We develop and implement an autonomous multi-fidelity computational workflow to explore the chemical space of high-entropy perovskite oxide materials with general formula ABO_3 , screening for stable, high-performance cathodes for low-temperature protonic ceramic fuel cells. The workflow, implemented in the framework of Density Functional Theory (DFT), is based on the calculation of thermodynamic, electric and kinetic properties, which include phase and electrochemical stability, electronic conductivity, and ionic diffusivity. To accelerate the calculation of the kinetic properties, we employ accelerated methods that leverage recent advances in machine learning for materials science to predict transition barriers for ionic diffusion. The computational cost of the workflow is additionally decreased while retaining the quality of results through a thorough examination of the required level of theory for all descriptive properties. Moreover, the aim is a general and chemistry-neutral approach that can be applied to other crystal prototypes and materials screenings.

11:15 AM DS04.14.04

Deep Reinforcement Learning for Dopants Design in Crystalline Materials Xiangyu Yin¹, Xiangyun Lei², Weike Ye² and Joseph Montoya²; ¹Carnegie Mellon University, United States; ²Toyota Research Institute, United States

Deciphering the atomic or crystal structure of doped materials is a crucial endeavor in materials science, serving the dual purpose of controlling material properties and enhancing device performance. However, this task is compounded by the minuscule scale of the materials, complexity from dopant disruption, and intricate dopant-host material interactions, along with other quantum mechanical effects. Given the intricate nature of this task, it is often compared to solving a perpetually evolving puzzle, situating it at the heart of materials science and condensed matter physics research. Despite the importance of this task, existing computational dopant design methods grapple with challenges such as imbalanced exploration-exploitation, scalability limitations, and a lack of generalizability. To address these persistent issues, we propose a novel use of reinforcement learning (RL) to manage the complexity of dopant design. This approach encompasses a framework that effectively casts generic dopant design problems as RL games, facilitating an interactive and iterative design process. Concurrently, we construct an invariant, explainable policy network employing a policy gradient method, allowing us to derive an optimal doping strategy that is both effective and interpretable. To illustrate the practicality and unique advantages of our RL-based design approach, we applied the method to an oxygen storage material ($CeZrO_4$) and a garnet phosphor host material ($Y_3Al_5O_{12}$). These applications highlight the impressive search efficiency of this approach, its potential to generalize to larger systems, and its robustness in handling systems with varied dopant concentrations. Overall, this research provides a promising, efficient, and adaptable pathway for designing doped materials.

11:30 AM *DS04.14.05

Active Search for Efficient Discovery of Visible Light-Activated Azoarene Photoswitches with Long Half-Lives Fatemah Mukadam¹, Quan Nguyen², Daniel M. Adrion³, Gabriel Appleby⁴, Rui Chen⁴, Haley Dang³, Remco Chang⁴, Roman Garnett² and Steven A. Lopez³; ¹New York University, United States; ²Washington University in St. Louis, United States; ³Northeastern University, United States; ⁴Tufts University, United States

We will discuss a twist on Bayesian optimization called "active search," where we seek to discover as many members of a rare, valuable class as possible. Active search is a simple model of scientific discovery settings such as drug or materials discovery. We'll establish the surprising difficulty of this problem and introduce nonmyopic-yet-efficient policies for solving it. Finally, we will outline a successful application of active search to the discovery of photoswitches with desirable properties.

SYMPOSIUM DS05

Polymer Informatics—Polymer Research with Classical and Data-Driven Informatics
November 27 - November 28, 2023

Symposium Organizers

Debra Audus, National Institute of Standards and Technology
Lihua Chen, Schrödinger, Inc.
Deepak Kamal, Solvay Inc
Christopher Kuenneth, University of Bayreuth

Symposium Support

Gold
Solvay

* Invited Paper

+ JMR Distinguished Invited Speaker

SESSION DS05.01: Polymer Informatics I
Session Chairs: Christopher Kuenneth and Janhavi Nistane
Monday Morning, November 27, 2023
Sheraton, Third Floor, Gardner

10:30 AM *DS05.01.04

Designing Formulations of Bio-Based, Multi-Component Epoxy Resin Systems via Machine Learning Rodrigo Albuquerque, Florian Rothenhäusler and Holger Ruckdäschel; University of Bayreuth, Germany

Petroleum-based epoxy resins are commonly used as matrix in fiber reinforced polymer composites. Bio-based epoxy resin systems might be a more environmentally friendly alternative to conventional epoxy resins. In this work, novel formulations of multi-component, amino acid-based resin systems exhibiting high or low glass transition temperatures (T_g) were designed via Bayesian optimization and active learning techniques. After only five high- T_g experiments, thermosets with T_g already higher than those of the individual components were obtained, suggesting the existence of synergistic effects among the amino acids used and confirming the efficiency of the theoretical design. Linear and non-linear Machine Learning (ML) models successfully predicted T_g with a mean absolute error of 3.98 °C and R^2 score of 0.91. A price reduction of up to 13.7 % was achieved while maintaining the T_g of 130 °C by using an optimized formulation. The LASSO model provided information about the dependence of T_g on the number of active hydrogen atoms and aromaticity. This study highlights the importance of

Bayesian optimization and ML to achieve a more sustainable development of epoxy resin materials.

11:00 AM DS05.01.02

Machine Learning Strategies for Improved Polyolefin Sorting Based on Near-Infrared Spectroscopy [Bradley P. Sutliff](#), Shailja Goyal, Tyler Martin, Peter Beaucage, Debra Audus and Sara Orski; National Institute of Standards & Technology, United States

Polyolefins are cost-effective and exhibit a myriad of desirable characteristics such as chemical, shock, and impact resistance. While practical for consumer and industrial applications, the stability of polyolefins enables long-term environmental persistence. Recycling and reuse of waste materials would mitigate their long-term environmental impact, but incompatible molecular architectures often result in downgraded material properties for the recyclates. To prevent degradation of the polymers during recycling, the various subclasses of low-density (LD-), high-density (HD-), and linear low-density (LLD-) polyethylene (PE) must be separated from one another as well as from polypropylenes (PP) and other polymers. Unfortunately, the chemical similarities between these polyolefins present a large hurdle to facile separation using common high throughput techniques such as near-visible infrared spectroscopy (NIR). In this work, we explore using machine learning (ML) techniques, coupled with NIR measurements, to enable enhanced sorting of polyolefin species beyond what is possible using current NIR databases. NIR spectra of polyolefins were collected for polyolefins spanning a range of branch content, processing conditions, and additives. Common scattering corrections and preprocessing steps such as multiplicative scatter correction, linear detrending, and Savitzky-Golay filtering were evaluated for their effects on classifier outcomes. Data reduction techniques such as functional principal component analysis (FPCA) and uniform manifold approximation and projection (UMAP) were also investigated for data visualization and classification enhancements. This survey of preprocessing steps and ML algorithm combinations identified multiple data pipelines capable of successfully sorting polyolefin materials. Multiple combinations properly distinguished PP from PE, and separated subclasses of these polyolefins. This work discusses the effects of each data analysis step on the final classification results.

11:15 AM DS05.01.03

Unbiased In-Silico Design of pH-Sensitive Tetrapeptides. [Yue Hu](#)¹, Federica Rigoldi¹, Alfonso Gautieri² and Benedetto Marelli¹; ¹MIT, United States; ²Politecnico di Milano, Italy

Oligopeptides are short peptides consisting of two to twenty amino acids (AA) that can spontaneously fold and assemble through a combination of hydrogen bonds and π - π interactions to form functional nanostructures. From an engineering perspective, oligopeptides folding and assembly can be designed to fabricate fibers, tubes, nanosheets, pellets, gels, vesicles, and nanoparticles, with applications in biomedicine, food science, regenerative medicine, and biosensing. Peptide-based biomaterials offer in fact the opportunity to combine the simplicity of small biomolecules with the functionality of proteins. The design of oligopeptides that assemble in nanostructured materials often follows principles of bioinspiration and rational design. Most of the short (i.e. <5 AA) oligopeptides-based biomaterials found in literature are directly derived from AA motifs with biological relevance (e.g. DFNKF, KLVFF) and are composed of hydrophobic AA (e.g. FFF, VYV) to drive self-assembly in water. The combination of bioinspiration with rational design, despite successful, has limited the design of oligopeptides to few sequences tested experimentally, when compared to the x^n (where $x=20$ AA and n =number of AA in the oligopeptide) theoretical possibilities, and biased the AA choice to impart low solubility. Such restrictions have strongly limited the discovery of new AA sequences.

As an alternative route, in silico tools can be used to predict oligopeptides' properties, accelerating their design into biomaterials. Machine learning (ML) algorithms such as TorchMD, Convolutional neural networks, and Deep neural networks have been successfully used to quickly model and predict peptides' folding, energies, and reaction pathways, but the limited accuracy and completeness of high-quality training data still limit the resolution of predictive results of ML when compared to molecular dynamics (MD) simulations, which in turn are extremely intensive. To combine the benefits and limit the individual weaknesses of MD and ML, hybrid ML-MD approaches are now pursued to accelerate simulations and improve the understanding of complex biomolecular systems (e.g. flexible molecular force fields, where ML tools are used to accelerate the simulation process). However, these tools are still in their infancy and their applications to decrease the intensity of MD simulations have to be fully explored.

Here, we developed a new computational design protocol to discover oligopeptides that self-assemble in nanostructured biomaterials by combining an unbiased AA selection (i.e. agnostic to chemical features) with coarse grain (CG) MARTINI forcefield (highly parameterized for natural amino acids), which yields a speed-up of 2-3 orders of magnitude compared to atomistic forcefield. We focused on tetrapeptides as $n=4$ represents a wide but approachable sequences space (20^4 possible unique sequences) to screen and test computational unbiased methods while possessing an amphiphilic form and the proven ability to self-assemble into nanofibrillar structures. This method allowed us to simulate the assembly of all the possible tetrapeptides without bias, resulting in the screening of appropriate side chain combinations to embed responsiveness to environmental stimuli, such as pH. This pH-triggered assembly of tetrapeptides can be used to engineer new biomaterials for drug delivery that assemble/disassemble in response to pH changes, nanofibrillar matrices for separation of large biomolecules like proteins, antimicrobial surfaces, and scaffolds to support for cell growth.

11:30 AM DS05.01.05

Virtual Forward Synthesis: Designing Novel Polymers from Commercially Available Chemistries [Joseph D. Kern](#), Shivank S. Shukla, Madhubanti Mukherjee and Rampi Ramprasad; Georgia Institute of Technology, United States

Every year, humanity churns out a staggering 380 million tons of plastic, with millions of these tons escaping into the environment. The modern plastics we rely on possess such remarkable thermodynamic stability that recycling them remains a daunting task, with only a meager 9% successfully recycled, while they persist for decades, if not centuries, in our ecosystems. This dire situation has ignited an ecological crisis as these plastics seep into the environment, fragment into minuscule particles, and accumulate within the bodies of humans, plants, and animals.

In response to this critical issue, we've developed a computational method known as 'Virtual Forward Synthesis' (VFS) to explore the creation of hypothetical polymers using readily available chemicals. This approach involves the automated retrieval of chemical data and pricing from vendors, followed by systematic cataloging of the substructures of these chemicals. Viable chemicals are then subjected to virtual reaction templates, yielding hypothetical polymers, with machine learning being used to predict the polymers' properties.

The most promising polymers, along with comprehensive information on their chemical composition, pricing, vendors, and the reaction procedure used to create them, are then shared with our collaborating chemists who attempt to synthesize these novel polymers. We evaluate a polymer's potential by assessing how well it matches the required properties for common plastic applications like packaging. We assign scores based on how closely its predicted properties align with the desired values. Additionally, this presentation provides an overview of our carefully designed, performance-optimized relational database schema.

SESSION DS05.02: Polymer Informatics II
Session Chairs: Rodrigo Albuquerque and Deepak Kamal
Monday Afternoon, November 27, 2023
Sheraton, Third Floor, Gardner

1:30 PM *DS05.02.01

Playing with Entanglements to Structure Polymer Materials [Kurt Kremer](#); Max Planck Institute for Polymer Research, Germany

Entanglements are known to dominate the rheological properties of long chain polymer melts and dense solutions. Their properties and consequences lead to the generally accepted and well established reptation/tube model, which is at the basis of our understanding of many properties and processes. However, beyond analysing their effects and understanding the very nature of entanglements, one also can take the approach to use them to manipulate and structure materials. The talk will give a few such examples ranging from melts of non-entangled to very long, highly entangled polymer systems. By appropriately mapping chemical chain lengths onto idealized bead spring models one can (semi-) quantitatively compare simulation and experiment and predict new materials. Based on predictions from simulations we recently prepared stable nanoporous polymer films just by mechanical deformation. Furthermore, we applied a new data driven approach to determine the glass transition temperature of polymer melts and (ultra) thin films.

Free Standing Dry and Stable Nanoporous Polymer Films Made through Mechanical Deformation
HP Hsu, MK Singh, Y Cang, H Thérien-Aubin, M Mezger, R Berger, I Lieberwirth, G Fytas, K Kremer
Adv. Sci. 2023, 2207472

Data-driven identification and analysis of the glass transition in polymer melts
A Banerjee, HP Hsu, K Kremer, O Kukharenko
ACS Macro Lett. 2023, 12, 679-684

Glass transition of disentangled and entangled polymer melts: Single-chain-nanoparticles approach
MK Singh, M Hu, Y Cang, HP Hsu, H Thérien-Aubin, K Koynov, G Fytas, K Landfester, K Kremer

2:00 PM DS05.02.02

Morphology, Structure and Dynamics of Ionic Polydimethylsiloxane-Silica Nanocomposites [Argyrios Karatrantos](#)¹, [Clement Mugemana](#)¹, [Ahmad Moghimikheirabadi](#)² and [Martin Kroger](#)²; ¹Luxembourg Institute of Science and Technology, Luxembourg; ²ETH Zürich, Switzerland

We designed ionic polydimethylsiloxane (PDMS)-silica nanocomposites from (cationic) ammonium-functionalized PDMS and (anionic) sulfonate-functionalized nanosilicas, with the aim of influencing the distribution and dispersion of the nanoparticles. The impact of the PDMS molecular weight, charge density and charge location on the distribution, dispersion of ionic nanosilicas and on the mechanical reinforcement of the nanocomposites is explored. Self-healing property arises from reversible ionic interactions located at the interface between PDMS matrix and nanosilicas. We use coarse grained equilibrium molecular dynamics to model ionic nanocomposites and to investigate their behavior, in particular, polymer conformations, entanglements and dynamics for different loadings, for two types of charge-sequenced polymers at two different Bjerrum lengths. We calculate the lifetimes of temporary ionic crosslinks that are created between ionic nanoparticles and polymers. Non equilibrium molecular dynamics is used to investigate the stress - stress behavior, ionic crosslinks and entanglements under deformation.

2:15 PM DS05.02.03

Breaking Down the Building Blocks: Multi-Scale Model of Diels-Alder Reactions for Future Self-Healing and Recyclable Polymer Networks [Lise Vermeersch](#)¹, [Freija De Vleeschouwer](#)¹, [Adri Van Duin](#)² and [Niko Van Den Brande](#)¹; ¹Vrije Universiteit Brussel, Belgium; ²The Pennsylvania State University, United States

Self-healing network materials (SHNs) have the potential to entirely change the way we view and use materials. By using SHNs, damage prevention will no longer be the key factor dictating the properties of a material, which makes that overdesigning will no longer be the strategy at hand to increase the lifetime of a material. SHNs based on Diels-Alder reversible crosslinks are a proven technology - furan-maleimide systems, for example, have been used to create self-healing soft robotic grippers. These materials have yet to be valorised, as the current materials still face some issues. Synthesis and healing times are too long, which pose a barrier for application in industry. Besides this, the large number of diene-dienophile combinations allow for a range of material properties, which can open doors towards other applications in construction materials, coatings and renewable energy. Exploring this chemical space using experiments, however, would be a tedious process. By creating a multi-scale model, ranging from the quantum-chemical level to molecular dynamics, we can predict suitable candidates depending on the desired material properties. In this study, density functional theory (DFT) is used to relate the structure of the diene and dienophile to the resulting kinetics and thermodynamics of 100 Diels-Alder reactions, for which both *endo* and *exo* cycloaddition have been considered. For seemingly interesting combinations, this data will be used to train a force field in the ReaxFF molecular dynamics software, which will in turn allow to predict macroscopic material properties, such as the glass transition temperature and Young's modulus of the resulting polymer. Each step in the multi-scale model will be benchmarked to available experimental data.

2:30 PM DS05.02.04

Predicting Polymer Properties via Quantitative Disorder Metrics [Robert Makin](#)¹, [Steve Durbin](#)¹, [Samerender Nagam Hanumantharao](#)² and [Smitha Rao](#)²; ¹Western Michigan University, United States; ²Michigan Technological University, United States

The Bragg-Williams approach to quantifying disorder through x-ray diffraction measurements is routinely applied to a range of crystalline materials including metallic alloys. In this formulation, which dates to the early 1930s, a numeric value (represented by S) is assigned to represent the degree of ordering, where $S = 1$ corresponds to fully ordered and $S = 0$ corresponds to fully randomized. Recently, the methodology has been extended to enable the use of additional measurement techniques, including Raman spectroscopy and scanning electron microscopy, both of which are straightforward to apply to organic polymer materials; typically, two decimal place agreement or better is obtained from any of these methods, as validated by measuring samples with multiple techniques. Whereas S in the context of metallic alloys represents the number and type of antisite defects within the atomic lattice, for polymers the value of S is associated with tacticity ($S = 0$ corresponds to atactic whereas $S = 1$ corresponds to syndiotactic).

We have shown that certain electronic as well as mechanical properties exhibit a linear dependence on the squared value of S , specifically that $P(x, S) = [P(x, S = 1) - P(x, S = 0)]S^2 - P(x, S = 0)$, where P is the property dominated by pair-wise interaction between methyl groups, and x relates to the ratio of methyl groups on either side of the polymer chain. Example properties which exhibit this dependence include bandgap, specific capacitance, and Young's modulus, and creating an experimental plot of the property under consideration as a function of S^2 enables a determination of the full accessible range of values for that property. Further, identifying the relationship between S and synthesis parameters provides a direct pathway to achieving the full range of property values, which is valuable given that a typical process may naturally confine itself to a narrow range of S in the absence of explicit modification. For example, we have shown that when electrospinning PANI-PCL increasing the applied voltage from 20 kV to 23kV can cause the S value the PANI-PCL to double from 0.31 to 0.63.

Here, we present results of our disorder based predictive property analysis--specifically highlighting the potential for accessing property values outside the ranges commonly reported in the literature -- for four types of polymers: polyvinyl fluoride (PVDF), polycaprolactone (PCL), polyaniline (PANI) and polyaniline-polycaprolactone (PANI-PCL) fibers. For PANI, our experimentally derived results predict an $S=1$ band gap of 0.7 eV and specific capacitance of 643 F/g. Similarly, for the Young's modulus of PVDF, PCL, and PANI-PCL our analysis predicts values for the $S=1$ value of: 33 MPa, -1.25 MPa and -1.13 MPa, respectively. We will also examine how, in some instances, certain macroscopic sample properties can also exhibit a linear dependence on S^2 , which provides an alternative route to engineering final properties for specific applications from the synthesis stage.

2:45 PM DS05.02.05

A Computational Approach to Insights into Aggregate Formation between Cellulose Acetate and Xylan Acetate [Md Imrul Reza Shishir](#), [Melissa Pasquinelli](#) and [Sunkyu Park](#); North Carolina State University, United States

The production of insoluble gel particles (IGP) during cellulose acetylation is a persistent issue in the industry, adversely affecting both processability and final product quality. The formation of IGP has been attributed to factors such as uneven cellulose acetylation and the presence of hemicellulose acetates, yet there is still debate surrounding the underlying mechanisms. Cellulose acetate (CA) and xylan acetate (XA), both derived from cellulose, exhibit intricate aggregation phenomena, further complicating the understanding of IGP formation. These cellulose-derived polymers possess unique structural and chemical characteristics, which influence their aggregation behavior. The interplay between molecular interactions, such as hydrogen bonding and hydrophobic interactions, plays a crucial role in the formation and stability of aggregates in CA and XA systems. This study adopts a comprehensive computational approach to unravel the complex processes underlying aggregate formation and stability in cellulose acetate and xylan acetate systems. In this comprehensive study, we adopt a synergistic approach by combining molecular dynamics (MD), dissipative particle dynamics (DPD), and density functional theory (DFT) to gain a multifaceted understanding of the systems under investigation. Our primary focus is on the behavior of XA and CA in various solvents, which we explore through MD simulations. By closely examining their interactions and dynamics, we obtain valuable insights into these cellulose-derived polymers' solubility characteristics and behavior. Additionally, DPD simulations are employed to investigate the formation of aggregates, allowing us to explore the dynamic behavior, intermolecular interactions, and aggregation kinetics. Our investigation extends to the formation of aggregates, a phenomenon of great significance in the field. Through these simulations, we delve into the driving forces and underlying mechanisms that govern the formation of IGP, a common challenge encountered during cellulose acetylation processes. This integrated computational framework offers valuable information on the underlying driving forces and mechanisms that govern the formation of IGP.

3:00 PM BREAK**3:30 PM *DS05.02.06**

Sequence Dependent Phase Separation and Aggregation of Macromolecules: What Can We Learn from Simulations and Machine Learning? [Antonia Statt](#)¹, [Debjyoti Bhattacharya](#)², [Helena Casademunt](#)³, [Devon Kleebblatt](#)² and [Wesley Reinhart](#)²; ¹University of Illinois, United States; ²The Pennsylvania State University, United States; ³Harvard University, United States

In this talk, I will present the phase separation behavior of different sequences of a coarse-grained model for intrinsically disordered proteins or sequence defined block copolymers. They exhibit a surprisingly rich phase behavior, and not only conventional liquid-liquid phase separation is observed, but also reentrant phase behavior, in which the liquid phase density decreases at lower temperatures. Most sequences form open phases consisting of aggregates, rather than a normal liquid. These aggregates had overall lower densities than the conventional liquid phases and complex geometries with large interconnected string-like or membrane-like clusters. Minor alterations in the sequence may lead to large changes in the overall phase behavior, a fact of significant potential relevance for biology and for designing self-assembled structures using block copolymers. I will also discuss recent results from unsupervised manifold learning (UMAP) to classify the different aggregate types and what we can learn from machine learning. Using a bidirectional-gated recurrent units-based Neural Network (RNN), we can now predict which sequence will self-assemble into what aggregate structure.

4:00 PM DS05.02.07

Machine Learning to Bridge Scales in the Multiscale Modeling of Radical-Containing Polymers [Riccardo Alessandri](#) and [Juan J. de Pablo](#); The University of Chicago, United States

Polymers with electronic properties offer unique solutions for stretchable electronics, biomedical sensors, and all-organic batteries. Due to their multiscale nature, the rational design of polymers with tailored electronic properties is obscured by the interplay of electronic and structural degrees of freedoms over a wide range of spatiotemporal scales. This interplay renders quantum mechanical descriptions at mesoscopic spatiotemporal scales critical to accurately predict electronic functionalities in these polymers. Hence, efficient computational approaches incorporating both mesoscale morphological features and electronic properties are required.

We present an efficient computational approach, combining physics-based and machine learning techniques, to incorporate electronic structure information at coarse-grained scales. As an example, we focus on radical-containing, redox-active polymers, an emerging class of materials for all-organic energy storage. Coarse-grained modeling allows to probe relevant polymeric material length- and timescales. At the same time, electronic structure information is retained, enabling trained machine learning models to rapidly predict electronic properties from coarse-grained polymer morphologies. In this way, the approach allows to obtain relationships between electronic properties and the material morphology and processing conditions. We compare our results to the standard methodology which involves backmapping the coarse-grained morphology to atomistic resolution followed by quantum chemical calculations, and find that our approach retains good accuracy while achieving orders of magnitude speedups. As such, the proposed approach holds promise in greatly expediting multiscale computational workflows aimed at bridging the quantum and mesoscopic scales in polymer modeling.

4:15 PM DS05.02.08

AI-Assisted Discovery of High-Temperature Record-Breaker Dielectrics for Energy Storage[RishiGurmani](#)¹, [StutiShukla](#)², [DeepakKamal](#)¹, [ChaoWu](#)², [JingHao](#)², [ChristopherKuenneth](#)¹, [YangCao](#)², [GregorySotzing](#)² and [RampiRamprasad](#)¹; ¹Georgia Institute of Technology, United States; ²University of Connecticut, United States

Electrostatic capacitors serve as critical energy storage units in advanced electrical and electronic systems used in the energy, defense, aerospace, and transportation sectors. Energy density, the figure of merit for electrostatic capacitors, is primarily determined by the choice of dielectric material. Most industry-grade polymer dielectrics are flexible polyolefins or rigid aromatics. These polymers possess high energy density or high thermal stability, but not both. Here, we use advanced artificial intelligence (AI) techniques, established polymer chemistry, and molecular engineering to discover a handful of dielectrics in the polynorborene and polyimide families. One exhibits a record-setting energy density of 8.3 J/cc at 200 °C, 11× that of any commercially available polymer dielectric. We find that each of the discovered dielectrics has high thermal stability but varying energy density. By incorporating oxygen into the polymer backbone, we observed the greatest impact on energy density, with an increase of over 5.5 J/cc at °C. Additionally, position and identity of the phenyl substituents modulate the energy density by nearly 1 J/cc. Our findings broaden the range of potential applications for electrostatic capacitors within the 85–200 °C range, such as wind pitch control, hybrid vehicles, and pulsed power systems. We also evaluate available pathways to further enhance the polynorborene and polyimide families so that these capacitors may perform in even more demanding applications (e.g., aerospace) while being environmentally sustainable. More broadly, this research demonstrates the impact of AI on chemical structure generation and property prediction, highlighting the potential for materials design advancement beyond electrostatic capacitors.

4:30 PM DS05.02.09

High-Throughput Exploration of Amorphous Multicomponent Phase Diagram Space for the Accelerated Design of Organic Thin Films[HaoLiu](#) and [OlgaWodo](#); State University of New York at Buffalo, United States

During solvent-based fabrication of organic blends, the blend composition changes significantly as solvent is removed from the blend triggering phase transformations and structure formation. The choice of the solvent in conjunction with the processing pathways (i.e. quench profile) affects this process. Using a combination of solvents as well as solvent additives has produced favorable structures for organic electronic applications. For example, in the context of organic solar cells, changing solvents, utilizing solvent blends, including solvent additives, and adding thermal annealing as a post-processing step, have all produced significant jumps in photovoltaic efficiency. With the number of possible solvents potentially in the hundreds, choosing solvent blends, solvent additives and similar strategies represent a combinatorially large set of possibilities. Most processing variants reported have invariably been chosen through a trial-and-error approach, suggesting that only a small subset of the selection set has been explored. The selection of solvents has a rich history of empirical and theoretical design rules. The solubility sphere (HSP sphere) technique is an often used approach that allows the down selection of solvents when dealing with blends of materials. However, this becomes impractical with an increasing number of components and has no straightforward way to consider quench depths, crystalline phases or processing pathways as no additional thermodynamics (let alone kinetics) is considered. Consequently, it has remained challenging to establish reliable design rules that can be used for solvent blend selection, as well as selecting (and expanding) the processing space. In this work, we consider using the full phase diagram as a signature for solvent selection. The phase diagram is a comprehensive representation of the thermodynamic characteristics of the multi-component material system. Using high throughput exploration and clustering method, we learn simple and interpretable rules of phase diagram type and its sensitivity to the changes in the interaction parameter. This work has implications for the solvent selection but also solvent replacement for the efficient devices.

4:45 PM DS05.02.10

Forming Long-Range Order in Solution-Processed Semiconducting Polymers[Minh NhatPham](#)¹, [Yu-ChingHuang](#)², [Chun-JenSu](#)³, [Yu-YingLai](#)¹, [Ting-HanLin](#)¹, [Yong-KangLiaw](#)¹, [Kun-TaLin](#)¹, [Ting YuHuang](#)¹, [Yun ShuanChu](#)¹, [U-SerJeng](#)³, [Jr-jengRuan](#)¹ and [BenB. Hsu](#)¹; ¹National Cheng Kung University, Taiwan; ²Ming Chi University of Technology, Taiwan; ³National Synchrotron Radiation Research Center, Taiwan

Intermolecular interactions control molecular dissolving and stacking through directional solution processes, which determine the thin-film morphologies. While directional solution processes have been widely used, their resulting morphologies are often disordered or ordered in small scale, making their electronic characterizations unreliable. To overcome this issue, ordered structures created by regulating complex intermolecular interactions is required. This study aims to quantitatively identify and control the intermolecular interactions between semiconducting polymers and self-assembled monolayers (SAMs) in solutions to achieve long-range order. The proposed methodology of intermolecular guidance involves optimizing the processing temperature for dissolving aggregates into shorter bundles, finding their guidable intermolecular scale, and then guiding them along 1D nano-templated SAMs to form unidirectional fibers. The validity of this methodology is confirmed by various spectroscopic and morphologic techniques, demonstrating highly-ordered molecular stacking in unidirectional fabric structures. Based on Flory-Huggins theory and our experiments, the critical intermolecular scale and energy of the guidance and ordering are confirmed to be about 3 Å and 40 meV. In this range, small and random aggregates can be aligned to form macroscopically-ordered fibers, showing an increase in anisotropic Raman scattering intensity from around 1 to 10. Overall, this work provides a quantitative guideline to control complex intermolecular interactions of dissolving, stacking, and ordering between semiconducting polymers and self-assembled monolayers, showing the angstrom-scale controllability in molecular assembly.

SESSION DS05.03: Poster Session: Polymer Informatics
Session Chairs: Deepak Kamal and Christopher Kuenneth
Monday Afternoon, November 27, 2023
Hynes, Level 1, Hall A

8:00 PM DS05.03.01

Templating Effects by Pre-Formed Seed Oligomers in Irreversible Step-Growth Copolymerization[WenxinXu](#), [NhuQ. Nguyen](#) and [KateriH. DuBay](#); University of Virginia, United States

The synthesis of sequence-controlled polymers is believed to be an effective way to produce materials with desirable properties. However, the complexity of polymerization processes makes precise control of sequences difficult to achieve for synthetic polymers. In previous studies from our group, unexpected kinetics and self-assembly have been observed to arise from relatively weak non-bonded interactions between like monomers and be controlled by solvent selectivity, chain geometry, and activation energy. This influence is attributed to the phase separation of growing oligomers following Flory-Huggins Theory. Additionally, the appearance of non-monotonic growth of dispersity and a characteristic block length at sufficient stiffness and non-bonded interactions suggests the presence of self-templating effects. Self-templating effects are common in the synthesis of biopolymers and may provide an interesting opportunity to control the sequence of synthetic copolymers and supramolecules. Therefore, in this work, we seek to investigate templating effects for reaction kinetics and polymer sequences arising from the addition of seed oligomers to an irreversible step-growth copolymerization through coarse-grained simulations. We found that the rate of polymerization and resultant chain sequences depend on the sequence and length of seed chains. Moreover, the addition of seeds can yield combined effects with other reaction conditions, such as the viscosity and non-bonded attraction, on the block-length distribution and the characteristic block length.

8:00 PM DS05.03.02

Investigating Pathways to Solid-State Refrigeration: Simulating the Barocaloric Effect in Polymers[SaabirPetker](#), [ClaireHobday](#) and [AntoniaMey](#); The University of Edinburgh, United Kingdom

New refrigeration technologies are in demand with global targets to reduce the use of hydrofluorocarbons in refrigeration due to their environmental harm.¹ Materials that exhibit a barocaloric effect (BCE) are solid state alternatives, changing temperature as a hydrostatic force is applied.² We focus on BCE exhibiting polymers (BCEPs), specifically vulcanised natural rubber (VNR). A complete theoretical framework of the mechanism behind the BCE in BCEPs is yet to be produced, with hypotheses the BCE arises from either reversible re-aligning of polymer chains or stress induced crystallisation.^{3,4}

In this work, we will show that by using molecular dynamics simulations, we can generate a pressure-temperature phase diagram of VNR. These simulations uncover atomistic information about the BCE in VNR, e.g. we will demonstrate where the colossal entropy changes ($137 \text{ J kg}^{-1} \text{ kg}^{-1}$) originate on an atomistic level, as well as determine the barocaloric coefficient of VNR to be $\sim 60 \text{ K GPa}^{-1}$.

References:

- [1] UN Treaty Collection, Kigali, 2016. <https://treaties.un.org/doc/Publication/MTDSG/Volume%20II/Chapter%20XXVII/XXVII-2-f.en.pdf>
- [2] L. Cirillo et al. *TSEP*, 2022, **33**, 101380. <https://doi.org/10.1016/j.tsep.2022.101380>
- [3] E.O. Usoda et al. *European Polymer Journal*, 2017, **92**, 287-293. <https://doi.org/10.1016/j.eurpolymj.2017.05.017>
- [4] J. Che et al. *ACS*, 2013, **46**, 24, 9712-9721. <https://doi.org/10.1021/ma401812s>

8:00 PM DS05.03.04

Conformation Transition of Polyelectrolytes Induced by Temperatures, Salt Concentrations and Electric Fields via Atomistic Molecular Dynamics Simulations [Tianyi Wang](#) and Yaxin An; Louisiana State University, United States

Polyelectrolytes are a class of polymers that contain repeated units with electrolyte groups categorized roughly as polycations, polyanions, and polyampholytes. They exhibit strong interaction with ionic solutes, polar solvents and surface and electrons under electric fields, making them crucial to energy storage, drug delivery, adhesives, and other applications. However, the atomistic understanding of the interplay between polyelectrolytes and ions/solvents/electrons is still limited, impeding the precise control of their conformation and properties. To gain atomistic insights into the local ion/solvent structure and its impact on the conformation of polyelectrolytes, we performed atomistic simulations of two representative polyelectrolytes, poly(vinylbenzyl trimethylammonium chloride) (PVBTA) and polystyrene sulfonate (PSS) at varying salt concentrations. The behaviors of PVBTA and PSS differed as the salt concentration increases. Specifically, the radius of gyration of PVBTA increased while that of PSS decreased at 310 K. As the temperature increased to 350 K, the PVBTA chain exhibited slight changes, whereas the PSS chain became significantly stretched. Furthermore, we investigated the effects of the electric field on the conformations of PVBTA and PSS. To elucidate the mechanism driving the conformation changes induced by salt concentrations, temperatures, and electric fields, we analyzed the local solvent and ion structures, as well as hydrogen bonds. This study provides atomistic insight into the interplay between polyelectrolytes and ions/solvents, offering guidelines for precise control over the conformation and properties of polyelectrolytes by adjusting salt concentrations, temperatures, and electric fields.

8:00 PM DS05.03.05

Enhanced Thermal Performance Properties of EPDM Carbon Black Composites via Crossover Curing Agents [Arshad Rahman Parathodika](#) and Kinsuk Naskar; Indian Institute of Technology Kharagpur, India

Elastomeric products in the automotive and industrial sectors often have to meet conflicting performance requirements, such as both high flexibility and higher thermal resistance. However the feasibility of using ultra-high-performance elastomers like FKM is often restricted by financial constraints. The practical solution involves modifying the crosslinking system and developing a synergistic hybrid system to achieve contradictory properties. This work discusses the possibility of developing a hybrid crosslinking system in the ethylene propylene rubber (EPDM) matrix. Sulfur-cured EPDM is more flexible due to its carbon sulfur and sulfur sulfur crosslinks, while peroxide-cured EPDM has carbon-carbon crosslinking and higher thermal stability, making it less flexible. This study focuses on the development of systems creates co-existence of both forms of crosslinks, in order to meet the conflicting property requirements. EPDM is chosen for this study due to its viability and established industrial applications with both curing systems. This study also examines the multifunctional role of 1,3-bis(citraconimidomethyl)benzene (BCIMB) in two different curing systems, acting as a reversion-resistant agent in sulfur curing and as a coagent in peroxide curing. The study investigates the potential of a hybrid curing system that containing BCIMB to maintain the stability of networks and temperature-stable compounds while preserving their flexibility. The results of the study indicate that optimized hybrid systems containing BCIMB can retain performance properties after 504 hours of thermal aging at 125°C with only a 13% change in initial values.

8:00 PM DS05.03.06

Designing High Glass Transition Temperature Fluoropolymers using Transfer Learning [Jin Hoon Yang](#), Ji Young Lee, Eun Ho Sohn, Hyunju Chang and Seunghun Jang; Korea Research Institute of Chemical Technology, Korea (the Republic of)

In this study, we propose a novel machine learning approach to accurately predict fluoropolymers' glass transition temperature (T_g) and demonstrate its potential in guiding the design of high T_g copolymers. Firstly, we utilize the QM9 dataset for model pre-training, providing robust molecular representations for subsequent transfer learning on a specialized copolymer dataset. Our pre-trained model expertly encodes complicated molecular structures and general molecular properties using atom-level (graph) and global molecular-level (global state) features. This extensive feature set is processed via a dual network system, with the outputs merged to form a comprehensive molecular descriptor. Dealing with a small copolymer dataset, we encounter significant discrepancies between individual models, a common issue in limited data. We address this problem by adopting an ensemble approach and providing more reliable and robust predictions. Finally, we can navigate a vast chemical space comprising 61 monomers and identify promising candidates for developing high T_g fluoropolymers. Our work shows the potential of machine learning in materials design and discovery and the effectiveness of ensemble models in addressing the challenges associated with small datasets.

8:00 PM DS05.03.07

Accelerating Discovery of Liquid Crystal Polymeric Materials with Extreme Properties using Machine Learning [Haichao Wu](#); Harvard University, United States

Liquid crystal polymeric materials are polymers combining the ordering properties of liquid crystals and rubbery elasticity from the polymer network. Liquid crystal polymers have demonstrated great potential as implants and medical devices due to the versatile stimuli responsiveness and programmable actuation. Here, we are interested in identifying new liquid crystal polymeric materials with extreme properties, such as body-temperature phase transition temperature, high fatigue resistance, and high actuation strain. The traditional way to identify materials with desired properties is intuition-driven, based on trial-and-test strategies, which is not only time-consuming but highly likely to miss the optimal candidates, especially under the scenarios that multiple "conflicting" properties need to meet at the same time. To address this issue, we inverse design of polymer with desired properties using machine learning methods. In particular, we use generative models to explore potential chemical space and use transfer learning to find the quantitative structure-property relationship (QSPR) based on a limited dataset. The methods developed here are highly generalizable to solve other polymer design problems from the molecular scale.

SESSION DS05.04: Polymer Informatics III
Session Chairs: Christopher Kuenneth and Janhavi Nistane
Tuesday Morning, November 28, 2023
Sheraton, Third Floor, Gardner

10:00 AM *DS05.04.01

Polymer Informatics—Algorithmic Advances for Materials Design [Rampi Ramprasad](#); Georgia Institute of Technology, United States

Polymers display extraordinary diversity in their chemistry, structure, and applications. However, finding the ideal polymer possessing the right combination of properties for a given application is non-trivial as the chemical space of polymers is practically infinite. This daunting search problem can be mitigated by surrogate models, trained using machine learning algorithms on available property data, that can make instantaneous predictions of polymer properties. I will present a versatile, interpretable, and scalable scheme to build such predictive models. Our "multi-task learning" approach is used for the first time within materials informatics and efficiently, effectively, and simultaneously learns and predicts multiple polymer properties. It is thus a powerful tool to solve "forward materials problems", i.e., property predictions. I will also discuss new approaches to solve "inverse materials problems", i.e., identifying materials that satisfy target property criteria. These forward and inverse method developments are expected to have a significant impact on data-driven materials discovery.

- [1] Rohit Batra, Le Song and Rampi Ramprasad, "Emerging materials intelligence ecosystems propelled by machine learning", *Nature Reviews Materials* (2020).
- [2] Christopher Kuenneth, Arunkumar Chitteth Rajan, Huan Tran, Lihua Chen, Chiho Kim, and Rampi Ramprasad, "Polymer informatics with multi-task learning", *Patterns* (2021)
- [3] Rishi Gurnani, Deepak Kamal, Huan Tran, Harikrishna Sahu, Kenny Scharm, Usman Ashraf and Rampi Ramprasad, "polyG2G: A Novel Machine Learning Algorithm Applied to the

Generative Design of Polymer Dielectrics”, *Chemistry of Materials* (2021).

[4] Christopher Kuenneth and Rampi Ramprasad, “polyBERT: A chemical language model to enable fully machine-driven ultrafast polymer informatics”, *Nature Communications* (2023).

[5] Rishi Gurnani, Christopher Kuenneth, Aubrey Toland and Rampi Ramprasad, “Polymer informatics at-scale with multitask graph neural networks”, *Chemistry of Materials* (2023).

10:30 AM DS05.04.02

Extensive Evaluation and Advancement of Extrapolation Performance in Polymer Property Prediction Hajime Shimakawa, Akiko Kumada and Masahiro Sato; The University of Tokyo, Japan

Polymer Informatics (PI), an emerging field which integrates computational science and data science, has gained significant attention as a powerful approach for accurately predicting intricate polymer properties. The prevalent approach in PI heavily depends on structure-based models, specifically deep learning and nonlinear regression models, which excel at capturing complex relationships within polymer molecular structures. However, these structure-based models face challenges when dealing with small data predictions, particularly in PI where the available database is still insufficient. Despite their effectiveness with interpolation of large datasets, the generalization performance of these models can be compromised in limited data [1]. Moreover, the highly expressive nature of these black-box models poses difficulties in interpreting and explaining their predictions, especially when extrapolating beyond the range of available data [2]. It is crucial to explore the potential of PI in identifying highly functional polymers that surpass the limits of existing data.

In this study, we evaluate the extrapolation performance of baseline ML models used in polymer property prediction. Our evaluation employs experimental and computational datasets encompassing a wide range of data scales, including mechanical, thermal, and electrical properties. Additionally, we propose a novel ML model that effectively extrapolates polymer properties by leveraging a framework previously demonstrated in extrapolating the properties of small organic molecules. In contrast to conventional approaches relying on black-box ML techniques, our constructed ML model incorporates microscopic physical features derived from molecular computations. This integration allows for the explicit extraction of correlations between microscopic physical quantities and macroscopic polymer properties, resulting in an explainable ML model with enhanced extrapolation capabilities. Through extensive evaluations of the extrapolation performance, we demonstrate the limitations of conventional models in extrapolation tasks while highlighting the effectiveness of our proposed approach.

[1] Xu, P., Ji, X., Li, M. et al. Small data machine learning in materials science. *npj Comput Mater* 9, 42 (2023). <https://doi.org/10.1038/s41524-023-01000-z>

[2] Li, K., DeCost, B., Choudhary, K. et al. A critical examination of robustness and generalizability of machine learning prediction of materials properties. *npj Comput Mater* 9, 55 (2023). <https://doi.org/10.1038/s41524-023-01012-9>

10:45 AM DS05.04.03

Designing Novel Polymer Dielectrics using polyVERSE Shivank S. Shukla, Madhubanti Mukherjee, Rishi Gurnani, Kuan-Hsuan Shen and Rampi Ramprasad; Georgia Institute of Technology, United States

As the demand for polymers with improved properties and performance in dielectric applications continues to grow, researchers are exploring alternative polymer chemistries that differ from the conventional polymers commonly used in the industry. The traditional polymer compositions present a compromise between high energy density and high thermal stability, preventing the simultaneous achievement of both attributes. To overcome this challenge, we employ a high-throughput virtual screening approach, exploring an extensive and diverse chemical space of monomers and polymerization templates that can lead to synthetically accessible high-performance polymers. We call this approach polyVERSE: polymers created using Virtually-Executed Rule-Based Synthesis Experiments. Subsequently, the limitless number of virtually produced polymers undergo screening using machine learning (ML) model predictions of the relevant properties, namely, dielectric constant, band gap and glass transition temperature. These ML models leverage advanced learning techniques, including multi-task learning, and incorporate Molecular Dynamics simulation-generated data specifically for the glass transition temperature, enabling precise property predictions for a broad range of polymer chemistries. Data generation respecting synthetic feasibility, physics-driven computations, measured property databases, multi-task machine learning algorithms, virtual screening, and synthetic validation are integrated. By leveraging this approach, we present novel dielectrics predicted to simultaneously achieve both high energy density and high thermal stability, thereby surpassing conventional polymers.

11:00 AM DS05.04.04

Improving the Performance of Polymer Property Predictions Through Polymer Graph Development and Literature Data Extraction Evan Antoniuk, Peggy Li, Bhavya Kailkhura, David Buttlar and Anna M. Hiszpanski; Lawrence Livermore National Laboratory, United States

Across the physical sciences, machine learning models have been demonstrated as powerful tools for capturing the complex relationships between chemical systems and their properties with remarkable accuracy. However, the pursuit of such structure-property relationships in the domain of polymer chemistry has been hindered by two significant challenges: i) the lack of representations that can capture the periodic, ensemble that comprise polymeric structure, and ii) the lack of sufficiently diverse polymer property datasets.

In this talk, we will show how we address this first challenge through the creation of a periodic polymer graph representation. This periodic polymer graph representation improves over fingerprint-based descriptors on monomers by directly accounting for the periodicity of the polymer, as well as utilizing learned atomic descriptors. We benchmark this periodic polymer graph representation across 10 unique homopolymer property datasets and find that our periodic polymer graph representation achieves state-of-the-art predictive performance on 8 of the 10 properties. Ablation studies on our graph representation highlight that this improvement in predictive performance is the direct result of the use of both learned descriptors as well as including periodicity. In this way, our results highlight how accurate polymer property predictions can be achieved through the development of representations that better account for the unique and complex chemical structure of polymers.

Beyond predicting the properties of only homopolymers, there is considerable interest in expanding the scope of polymer property prediction models to encompass a broad range of polymer types including copolymers, crosslinked-polymers or network polymers. However, the development of such generalizable models is currently hindered by the lack of polymer property datasets that are accessible and sufficiently descriptive of the polymer structure. To combat this challenge, we have developed an automated pipeline for extracting polymer property data from the scientific literature. With this pipeline, we extract polymer property data from a diverse range of polymer types to augment existing homopolymer property datasets. By retraining the above periodic polymer graph on this augmented polymer dataset, we show that this approach is an effective strategy towards enabling polymer machine learning models to generalize well across all types of polymers.

This work was performed under the auspices of the U.S. Department of Energy by Lawrence Livermore National Laboratory under Contract DE-AC52-07NA27344.

11:15 AM DS05.04.05

Large Language Model-Based Pipeline for Extraction of Polymer Property Records Pranav Shetty, Sonakshi Gupta, Aishat Adeboye and Rampi Ramprasad; Georgia Institute of Technology, United States

Polymer informatics has made great strides in recent years in predicting polymer properties and designing new materials. These data-driven models are powered by curated data and require painstaking manual curation often from the rapidly growing corpus of journal articles. Data curators and materials scientists who search for material property information from this growing body of literature face an uphill task.

In this work, we present a pipeline that leverages large language models to extract material property information from the text of journal articles. We frame the problem as a text-completion problem by inputting the text containing material property data and a prompt with the relevant instructions to the GPT3.5 model accessed through the OpenAI API. An example prompt looks like ‘Extract all bandgap values from the following text in json format: ...’. The output produced by the language model for this prompt is the tuple of material and property value as a dictionary. We use the paradigm of few-shot prompting wherein a few representative examples are selected and input output pairs are provided as a prompt to the model. This specifies a format for the data to be extracted and increases extraction performance. We benchmarked our method on two datasets of abstracts containing polymer glass transition temperature and bandgap respectively and show that this method outperforms information extraction using fully supervised methods using named entity recognition and heuristic rules for relation extraction. The resulting method was then applied to a corpus of 2.6 million materials science articles to extract all polymer glass transition temperature and bandgap values recorded therein.

11:30 AM DS05.04.06

De Novo Design of Polymer Electrolyte with High Ionic Conductivity using GPT-Based and Diffusion-Based Generative Models Zhenze Yang^{1,2}, Weike Ye¹, Xiangyun Lei¹, Daniel Schweigert¹, Ha-Kyung Kwon¹ and Arash Khajeh¹; ¹Toyota Research Institute, United States; ²Massachusetts Institute of Technology, United States

Solid polymer electrolytes hold significant promise as materials for next-generation batteries due to their superior safety performance, enhanced specific energy, and extended lifespans compared to liquid electrolytes. However, the vast polymer space poses considerable challenges to their screening and design. In this study, we harness the capabilities of generative AI for the de novo design of polymer electrolytes. This approach not only augments the existing polymer data but also facilitates the generation of polymers towards tailored, desirable properties. To optimize the generation, we compare different deep learning architectures, including both GPT-based and diffusion-based models. We further employ full-atom molecular dynamics

simulations to validate the top candidates produced by each model and discover one polymer with superior ionic conductivity compared to any other polymers in our database. In addition, by adopting a pretraining and fine-tuning methodology, we significantly improved the efficacy of our generative models, achieving quicker convergence, enhanced performance with limited data, and greater diversity. Using the proposed method, we can easily generate hundreds of thousands of novel, diverse, valid, and synthesizable polymers, enabling us to identify promising candidates with markedly improved efficiency.

11:45 AM DS05.04.07

Machine Learning Strategies for The Structure-Property Relationship of Copolymers YingLi; University of Wisconsin–Madison, United States

Establishing the structure-property relationship is extremely valuable for the molecular design of copolymers. However, machine learning (ML) models can incorporate both chemical composition and sequence distribution of monomers, and have the generalization ability to process various copolymer types (e.g., alternating, random, block, and gradient copolymers) with a unified approach are missing. To address this challenge, we formulate four different ML models for investigation, including a feedforward neural network (FFNN) model, a convolutional neural network (CNN) model, a recurrent neural network (RNN) model, and a combined FFNN/RNN (Fusion) model. We use various copolymer types to systematically validate the performance and generalizability of different models. We find that the RNN architecture that processes the monomer sequence information both forward and backward is a more suitable ML model for copolymers with better generalizability. As a supplement to polymer informatics, our proposed approach provides an efficient way for the evaluation of copolymers.

SESSION DS05.05: Polymer Informatics IV
Session Chairs: Lihua Chen and Rishi Gurnani
Tuesday Afternoon, November 28, 2023
Sheraton, Third Floor, Gardner

1:30 PM *DS05.05.01

The NIST Autonomous Formulation Laboratory: Virtual Scattering Instruments for Active Learning Agent Development TylerMartin, Duncan Sutherland and Peter Beaucage; National Institute of Standards and Technology, United States

Machine-learning (ML) is revolutionizing the way we do material science with ML models that are discovering new polymer chemistries, designing syntheses, guiding measurements, and analyzing data, all with unprecedented accuracy and speed. Despite these advances, many challenges remain in creating the next generation of polymer ML models. A key limitation for polymer science focused models is the lack of high-quality, well-tagged measurement data in sufficient amounts for supervised training. The generation of measurement data for soft materials is hampered by limited polymer availability, tedious sample preparation, slow instruments, and involved data processing. While synthetic data can help alleviate this data scarcity, it is challenging to produce data that correctly accounts for instrument artifacts and resolution effects. Beyond the instrumental effects, mimicking the behavior of real soft-material samples requires accounting for impurities, processing effects, and other non-idealities that go beyond simple analytical models. In this talk we will describe our attempts to overcome these challenges with the development of a virtual small-angle scattering (SAS) instrument. This goal of our framework is to produce high-quality SAS data as a function of input parameters (e.g., sample composition, processing parameters, instrument configuration) that can be used for model training or ML agent development. We will specifically highlight the design of the virtual instrument and how it can be used to tune active learning agents. Finally, we will demonstrate how these tuned agents are performing in guiding real small-angle scattering experiments.

2:00 PM DS05.05.02

Chemometrics Approach Based on Wavelet Transforms for the Estimation of Monomer Concentrations from FTIR Spectra ArakiWakiuchi^{1,2}, Swarit Jasial^{1,1}, Shigehito Asano², Ryo Hashizume², Miho Hatanaka³, Yu-ya Oonishi², Takamitsu Matsubara^{1,1}, Hiroharu Ajiro^{1,1}, Tetsunori Sugawara², Mikiya Fujii^{1,1} and Tomoyuki Miyao^{1,1}; ¹Nara Institute of Science and Technology, Japan; ²JSR Corporation, Japan; ³Keio University, Japan

Traditionally, monitoring of chemical reactions has been performed by calculation of reactant concentrations through spectroscopies like NMR, IR, NIR, and UV-vis. But these methods often require complex isolation techniques before analysis, making concentration identification a slow process. Fourier-transform infrared (FTIR) spectroscopy holds potential for quick estimation of concentration, as it uses Beer-Lambert law to acquire concentration information from specific absorbance of substance. However, practical applications such as copolymerization reactions have difficulty in obtaining concentration due to multiple overlapping peaks from different components.

To address this problem, we are proposing a chemometric method that uses wavelet transforms (WT) for decomposing overlapped peaks into features which are then input to a sparse linear regression model built by the elastic net (EN) for predicting concentration of reactant. This new method, validated through careful comparison with other methods, shows superior predictive performance and is interpretable by humans. Visualization of regression coefficients with Gaussian distributions help in understanding the model by showing how broad regions in spectra are related to the model prediction.

We have used our method for predicting monomer concentrations in copolymerization reactions involving methyl methacrylate and five different monomers; styrene, glycidyl methacrylate, cyclohexyl methacrylate, p-acetoxystyrene and tetrahydrofurfuryl methacrylate, showing its practical use for complex chemical analysis. In addition, we have made our method, data sets, and implementation available to public (<https://github.com/Wa-Araki/WT-ENCV>) for promoting future progress in the field of chemometrics.

Our study introduces a powerful, interpretable, and an efficient tool for quantitative analysis of copolymerization reactions using FTIR spectra. By avoiding the need for complicated isolation techniques and careful handling of overlapping peaks, our WT-based method holds significant potential for a wide application in monitoring of chemical reaction and beyond.

Reference:

Wakiuchi et al. ACS Omega 2023, 8, 22, 19781-19788 DOI: 10.1021/acsomega.3c01515

2:15 PM DS05.05.03

Mechano-Spectroscopy of Soft Materials with Nanometer Spatial Resolution: When Atomic Force Microscopy is Combined with Machine Learning Mikhail Petrov¹, Nikita Kulachenkov¹, Daniel Canena¹, Pierre Nickmilder², Philippe Leclere² and Igor Sokolov¹; ¹Tufts University, United States; ²University of Mons, Belgium

Here we present a method to identify the material composition over a sample surface with the spatial resolution down to single nanometers. The method is based on the use of atomic force microscopy (AFM) working in imaging sub-resonance tapping Ringing mode, which allows collecting multiple physical/mechanical maps of the sample with subnanometer lateral resolution. Using a database of these properties collected on known materials, the presented method allows identification of the location of these materials on samples made of the known materials. The materials are identified at each pixel of the image with the help of machine learning algorithms, such as neural networks and decision trees. We demonstrate this approach on various blends made of three different polymers, namely polystyrene (PS), polyvinyl pyrrolidone (PVP), and polyethylene oxide (PEO). The advantages and limitations of the presented method compared to other spectroscopy methods will be discussed.

2:30 PM DS05.05.04

Graph-Based Machine Learning to Predict Particle Dispersion Evolution from Training Image Sequences Sameera Nalin Venkat¹, Thomas Ciardi¹, Mingjian Lu¹, Jube Augustino¹, Adam Goodman¹, Preston DeLeo¹, Pawan K. Tripathi¹, Anirban Mondal¹, Frank Ernst¹, Christine A. Orme², Yinghui Wu¹, Roger H. French¹ and Laura Bruckman¹; ¹Case Western Reserve University, United States; ²Lawrence Livermore National Laboratory, United States

We develop a spatiotemporal particle-based graph neural network (st-PGNN), an image-based graph machine learning framework to predict the shape and size evolution of growing particles as part of particle ensembles. Using crystallization of amorphous fluoroelastomer layers as a model system from atomic force microscopy image sequences. The new method involves implementing a spatiotemporal particle graph neural network. This will enable us to study the impact of neighboring crystallites on the growth kinetics and to obtain quantitative spatiotemporal correlations. The insights from this approach will enable quantification of radial particle growth rates and improve nucleation density statistics. In the long term, our approach is expected to provide data for detailed comparisons to existing particle-growth theories.

Work performed by CO was under the auspices of the U.S. Department of Energy by Lawrence Livermore National Laboratory under Contract DE-AC52-07NA27344.

2:45 PMBREAK

3:15 PM *DS05.05.05

Polymer Design Across Industries: Intersection of Physics-Based Simulation and Machine Learning [Andrea Browning](#), Atif Afzal, Benjamin Coscia, Anand Chandrasekaran and Mathew D. Halls; Schrodinger, INC, United States

Adoption of digital design in polymers has gained in both visibility and impact as more industries see the value in computer based analysis of materials. A key to continuing this adoption is to expand digital analysis capabilities to more and more complex systems to match the reality of polymer use in products from cosmetics to pharmaceuticals to aerospace composites. Understanding the role of the polymer chemistry and microstructure in these complex systems requires advances in physics-based calculations and the leveraging of machine learning techniques. In this presentation a series of three examples will be provided showing advancement of physics-based simulation for polymers in complex formulations, the application of physics-based calculations to the degradation of polymers, and the improvement of predictive capability of physics-based calculations through the combination of machine learning. The continued development of physics-based tools and leveraging of machine learning will be highlighted as critical to the successful digital design of polymers in important product applications.

3:45 PM DS05.05.06

AI-Driven Polymeric Membrane Design for Efficient Binary-Component Solvent Separation [Janhavi Nistane](#), Lihua Chen, Youngjoo Lee, Kuan-Hsuan Shen, Ryan Lively and Rampi Ramprasad; Georgia Institute of Technology, United States

Manufacturing polymers, plastics, fibers, solvents, and fuel additives in numerous industries rely extensively on starting materials like benzene and its derivatives, including toluene, ethylbenzene, and the xylene isomers. To use petroleum-based products effectively, they often require separation into different components. This separation is achieved through energy-intensive thermal distillation processes, accounting for 10-15% of global energy usage. However, emerging membrane-based technologies have the potential to achieve these separations with about one-tenth of the current energy consumption¹. A polymer membrane essentially acts as a selective filter for solvents based on their diffusion behavior. Solvents with low diffusivity are retained by the polymer membrane, while those with higher diffusivity permeate through. For a successful separation, observing a minimum two-order difference in diffusivity between the solvents as it diffuses through the polymer membrane is necessary. The main challenge associated with membrane-based separations is identifying a tailored membrane material suitable for a specific solvent-solvent separation. Given the unimaginably vast chemical polymer space, conventional experimental methods to design new polymers are slow. Hence, we employ AI-aided material design that can efficiently explore the vast chemical polymer space in a very time and cost-effective manner, as has been achieved in the design of dielectric polymers in the past.^{2,3} Around 10,000 potential polymer membrane candidates will be generated using our virtual forward synthesis, as an initial step to AI-aided material design. These hypothetical candidates will be screened using our best-in-class ML polymer-solvent diffusivity predictor, which has been trained on available experimental data, and our computationally generated data via molecular dynamics simulations. The ML polymer-solvent diffusivity predictor is trained on around 1200 data points (experimental and simulated) for 91 polymers and 50 solvents. This scheme to generate computational data is highly scalable, and we continue to keep augmenting new data to explore more polymer chemistries. Upon identifying promising candidates that meet the proposed screening criteria, experimental validation will follow. This approach will provide insights into the power, as well as the limitations of AI-driven materials design.

1.D. Sholl et al., Nature, vol. 532, pp. 435-437, 2016. DOI: 10.1038/532435a.

2.C. Wu et al., ACS Appl. Mater. Interfaces, vol. 13, no. 45, pp. 53416-53424, 2021. DOI: 10.1021/acsami.1c11885.

3.C. Wu et al., Matter, vol. 5, no. 9, pp. 2615-2623, 2023. DOI: 10.1016/j.matt.2022.06.064.

4:00 PM DS05.05.07

Multi-Fidelity Machine Learning Predictors for Gas Permeability Through Polymers: An Example of Experimental and Simulation Data Fusion [Brandon K. Phan](#), Kuan-Hsuan Shen, Rishi Gurmani and Rampi Ramprasad; Georgia Institute of Technology, United States

Polymer based gas separation membranes have a wide variety of applications ranging from carbon capture, drug delivery, and food packaging. Such technology, when extended to biodegradable or chemically recyclable polymers has the potential to advance green sustainable energy and applications. Polymer membrane discovery and design has been accelerated using machine learning (ML) prediction models trained on experimental gas transport property data. Predictions in the known scope of experimental chemical spaces are reputable; however, they are less reliable when extrapolating to new spaces. In this work, we use a high-throughput molecular dynamics (MD) simulation pipeline to explore new chemical spaces. This pipeline we built produces simulation data for gas diffusivity, solubility, and permeability. Subsequently, we create multi-task deep learning models trained on both "high-fidelity" experimental and "low-fidelity" simulation data. The new multi-task model shows a significantly improved performance over models trained with only experimental data, particularly in data-scarce situations. The algorithm ascertains the correlation between low- and high-fidelity data, and this basis allows for a more informed decision when making predictions in new chemical spaces. This approach demonstrates the benefit of high-throughput classical MD simulations with data fusion to produce best-in-class property predictors especially when experimental data is not as accessible for properties of interest.

4:15 PM DS05.05.08

In-Silico Polymer Generation using Fine-Tuned Regression Transformers with Open Reference Data [Ronaldo Giro](#)¹, Hsianghan Hsu², Matteo Manica³ and Mathias B. Steiner¹; ¹IBM Research - Brazil, Brazil; ²IBM Research - Albany, United States; ³IBM Research - Zurich, Switzerland

In-silico design for homopolymers accelerated by machine learning and high throughput screening has garnered widespread attention and recognition in recent years. However, applications to specific domains are still challenging because data scarcity (typically structure-property pairs) not only limits model generalization but increases uncertainty in model inference. QSPR (Quantitative Structure-Property Relationship), a method widely used to aid data augmentation, is suitable for exploring unaddressed feature spaces. The method performs satisfactorily for intrinsic materials properties such as density, molar weight, and cohesive energy. However, for properties reflecting a material's interaction with the chemical environment, such as refractive index or gas permeability, the QSPR method is less suited. In this contribution, we start materials discovery from tabulated information available in open-access literature. Furthermore, instead of training models from scratch, we rely on publicly available regression transformer models pretrained on large chemical datasets that we fine-tune on a small number of data points we extracted from literature. The models are tailored for finding new polymer membrane candidates with expected CO₂ and N₂ permeability.

We have evaluated published reference data beyond their initial scope of application. To that end, we have focused on tabulated data with clear experimental condition stated. The semi-automated extraction processes include an OCR (Optical Character Recognition) step, the validation with ground truth, and the merge into a data table. Some of the documents include either rich tables [1] or XML raw format data [2] which greatly accelerates the process. To obtain pSMILES (SMILES for specified homopolymers), we have fetched information from online database and documents. In total, we have collected 160 pSMILES with CO₂ and N₂ permeability values under comparable experimental condition. The molecular weights of the collected species range from 40 to 1000 and the pSMILES string length ranges from 5 to 148.

A regression transformer (RT) handles regression as a generative task by modeling continuous properties with a group of tokens representing digits and their orders of magnitude [3]. The RT algorithm used here exploits a custom pSMILES tokenizer and is available through GT4SD (Generative Toolkit 4 Scientific Discovery) [4]. Before fine tuning the model, both permeability values are converted to log scale for stabilizing model variance and minimizing skewed data distribution. 25 % of the dataset is used for model testing. Training the RT yields a dichotomous model that seamlessly transits between property prediction and conditional molecule design. As an example, a structure-property pair has the input format "<pc2log>2.255[*C(Cl)=C(*)CCCC". We have evaluated the pretrained models with both single and multiple properties. Some generated polymer candidates such as *C(F)SC(*)[Si](C)(C)C and *c1c(Cl)cc(c2cc(C)c(N3C(=O)c4cc5c(cc4C3=O)C3(C)CCC5(C)c4cc5c(cc43)C(=O)N(*)C5=O)c3ccccc23)c2ccccc12 show high permeability values for CO₂ and are currently under investigation in automated molecular dynamics simulation.

In this contribution, we have reported the generation of new homo-polymer candidates for gas separation applications which are currently being validated with gas filtration simulations. The advancement of natural language processing and machine learning has accelerated the automated scientific discovery process. The publicly available dataset and open-source algorithms will help researchers to reproduce our discovery results with minimum effort, and to expand the scope to other polymer applications.

[1] M. Songolzadeh et al., <https://doi.org/10.1155/2014/828131>

[2] Benjamin Dhuiège et al., <https://doi.org/10.3390/app10010414>

[3] J. Born and M. Manica, <https://www.nature.com/articles/s42256-023-00639-z>

[4] Manica, M., Born, J., Cadow, J. et al. <https://doi.org/10.1038/s41524-023-01028-1>

4:30 PM DS05.05.09

Utilizing Machine Learning to Model and Predict Interdependency of Bulk Molecular Weight, Solute Concentration and Thickness of Spin Coated Polystyrene Thin Films [Alexander C. Wang](#)¹, [Samuel Chen](#)², Evan Xie³, Matthew Chang⁴, Anthony Zhu⁵, Adam Hansen⁶, John Jerome⁷ and Miriam Rafailovich⁸; ¹Sewickley Academy Senior School, United

Spin coating is a widely used, quick, and inexpensive method to deposit nanometer-thick thin films of various polymers on top of solid substrates through the centrifugal force produced by a rapidly spinning platform [1]. Polystyrene (PS) is an amorphous polymer that is often spin-coated to create thin films for a variety of industrial and research applications [2]. Since the thickness of a film affects a number of mechanical, optical, and degradation properties, it is essential to develop a simple method to predict thickness based on other manipulatable factors, such as bulk polymer molecular weight and initial solution concentration. Previous works have attempted to model these spin coating relationships through complex mathematical models informed by theoretical physics and limited experimental data [3]. Therefore, advancements can be made in predicting spin coated film thickness. In this study, we implement a machine learning model to learn the relationship between initial solution concentration, thin film coverage thickness, and monodisperse bulk molecular weight

To model this relationship, we collected data points by creating PS solutions of molecular weight 30,000 amu, 50,000 amu, 123,000 amu, 200,000 amu, 311,000 amu, 650,000 amu, 1,080,000 amu, and 2,000,000 amu at concentrations of 10 mg/mL, 15 mg/mL, 20 mg/mL, 25 mg/mL, and 30 mg/mL. After spin coating these PS solutions onto silicon wafers at 2500 rpm velocity and 1000 rpm/s acceleration for 30 seconds, we then measured the thickness of these films via light-refraction ellipsometry (Auto El II Ellipsometer).

With the aforementioned ellipsometry thickness data, we trained 42 machine learning models to relate the three spin coating parameters: concentration, thickness, and molecular weight. The models accept molecular weight and thickness as inputs and predict the critical concentration, the solution concentration required to spin coat a sample of a specific molecular weight into the desired thickness. Compared to the 41 other models, the curve-fit model exhibited the best performance. It achieved the second lowest root-mean-square error (RMSE) and mean average percent error metric (MAPE) scores for its predictions on the training data set, at 2.39 and 6.46%, respectively. At the same time, it correctly modeled a continuous and monotonically increasing relationship between thickness and both molecular weight and solution concentration, aligning with previously formulated spin coating theories. Thus, it outperformed the lowest RMSE and MAPE scoring model, XGBoost, which failed to learn these general trends and instead overfitted to the training data.

To confirm the accuracy of the machine learning model beyond the training data set, we subsequently spin coated PS samples of previously unused molecular weights at several random concentrations to act as test data for the model. When predicting the critical concentration of these new molecular weights and thicknesses, the model achieved an RMSE of 2.51 and MAPE of 10.54%, which indicates that the model accurately learns and generalizes the relationship between concentration, thickness, and molecular weight, rather than overfitting to the training samples and data points. Further work will be completed on how polydisperse bulk molecular weight polystyrene samples fit on this machine learning model.

[1] Dangelad-Flores, José, et al. "Deposition of Polymer Films by Spin Casting: A Quantitative Analysis." *Chemical Engineering Science*, vol. 179, Apr. 2018, pp. 257-64, <https://doi.org/10.1016/j.ces.2018.01.012>

[2] Budkowski, Andrzej, et al. "Polymer Blends Spin-cast into Films with Complementary Elements for Electronics and Biotechnology." *Journal of Applied Polymer Science*, vol. 125, no. 6, 1 Mar. 2012, pp. 4275-84, <https://doi.org/10.1002/app.36574>

[3] Hall, David B., et al. "Spin Coating of Thin and Ultrathin Polymer Films." *Polymer Engineering & Science*, vol. 38, no. 12, Dec. 1998, pp. 2039-45, <https://doi.org/10.1002/pen.10373>

SYMPOSIUM DS06

Integrating Machine Learning with Simulations for Accelerated Materials Modeling
November 27 - December 7, 2023

Symposium Organizers

Mathieu Bauchy, University of California, Los Angeles
Ekin Dogus Cubuk, Google
Grace Gu, University of California, Berkeley
N M Anoop Krishnan, Indian Institute of Technology Delhi

Symposium Support

Bronze

Patterns and Matter | Cell Press

* Invited Paper

+ JMR Distinguished Invited Speaker

SESSION DS06.01: Material Informatics
Session Chairs: Mathieu Bauchy and Ekin Dogus Cubuk
Monday Morning, November 27, 2023
Sheraton, Second Floor, Back Bay A

10:30 AM *DS06.01.01

The Materials Galaxy: A Social Network Analysis Approach to Uncovering Materials Properties Mehrdad Jalali, Dinga Wonanke and Christof Wöll; Karlsruhe Institute of Technology, Germany

This study explores the application of social network analysis SNA in the field of materials science specifically focusing on analyzing metalorganic frameworks MOFs SNA a graph theory approach is employed to create a galaxy of MOFs and conduct community detection to predict MOF properties more accurately than conventional machine learning methods The study highlights the utility of SNA in predicting gas storage properties a popular application of MOFs

In the field of materials science where researchers deal with vast amounts of data it is crucial to streamline experimental and computational processes and improve result quality Developing a materials focused social network provides a valuable approach to analyzing data anticipating material properties identifying novel materials and investigating the factors influencing material behavior Previous research has employed SNA methods to study the properties of MOFs and high entropy alloys HEAs This study focuses on enhancing the gas adsorption properties of MOFs a typical application of porous materials

SNA utilizes graph theory and methods to examine network social relationships and communication patterns In materials science SNA can be used to understand the structure of materials networks analyze social relationships between them and predict properties or behaviors based on their connections Machine learning in social networks involves learning from graph representations of data In this study MOFs are represented as nodes and their connections are represented as edges in the developed social network The MOF social network is akin to a galaxy of materials from which communities of MOFs are extracted and utilized to predict gas adsorption properties by considering the behavior of other MOFs within the community The proposed research has the potential to lead to novel applications in various materials data problems and improve the prediction of material properties and materials discovery It can also extend the applicability of machine learning methods to materials that are currently not adequately addressed by conventional artificial intelligence techniques However the effectiveness of the proposed method should be validated through experimental evaluation in the laboratory

A subset of curated MOFs from the CSD dataset is used to construct the MOF social network The network is undirected and weighted resembling galaxies of MOFs Community detection algorithms such as Girvan Newman are employed to predict gas adsorption by iteratively removing edges with the highest number of shortest paths between nodes

The data preparation involves extracting and standardizing relevant features according to expert specifications Similarities between MOFs are calculated and the resulting adjacency matrix

represents the links between them. The adjacency matrix is transformed into a graph to visualize the MOF galaxy. SNA methods such as community detection are then applied to predict gas adsorption.

Gas adsorption analysis using the MOF social network involves establishing the network, identifying distinct communities, and predicting gas adsorption levels for each community. The mean absolute error (MAE) is used to evaluate the prediction performance of each community, and the overall MAE results are compared to three established machine learning algorithms. The results demonstrate that the constructed social network significantly improves prediction accuracy compared to traditional machine learning methods.

This study showcases the suitability of SNA for analyzing MOF databases in materials science. By leveraging SNA, the research demonstrates the ability to predict MOF properties by training communities extracted from the MOF galaxy social network. The method has the potential to uncover fundamental characteristics of materials and find applications in other areas of material science.

11:00 AM DS06.01.02

Large Language Models for Materials Science with Attribution and Physics-Based Simulations GowoonCheon, AmilMerchant, Ekin DogusCubuk, EmrahKostem, MuratahanAykol, SamuelYang, ShutongLi, SubhashiniVenugopalan and VaheTshitoyan; Google, United States

Recent advances in large language models (LLMs) have generated much excitement across our society, including applications for science. In materials science, LLMs are starting to perform complex scientific tasks such as synthesis planning. While LLMs show great promise for accelerating materials science research, concerns around hallucination and the reliability of LLM-generated content persist. This is especially problematic for science, where factual accuracy is critical and literature training data for cutting-edge research is sparse. We build LLM-assisted workflows for materials science that is grounded in scientific knowledge and simulations, and demonstrate how LLMs can accelerate materials science research using examples from real world materials discovery problems.

11:15 AM DS06.01.03

Inverse Design of Next-Generation Superconductors using Data-Driven Deep Generative Models DanielWines¹, KevinF. Garrity¹, TianXie² and KamalChoudhary¹; ¹National Institute of Standards and Technology, United States; ²Microsoft Research, United Kingdom

Over the past few decades, finding new superconductors with a high critical temperature (T_c) has been a challenging task due to computational and experimental costs. In this work, we present a diffusion model inspired by the computer vision community to generate new superconductors with unique structures and chemical compositions. Specifically, we used a crystal diffusion variational autoencoder (CDVAE) along with atomistic line graph neural network (ALIGNN) pretrained models and the Joint Automated Repository for Various Integrated Simulations (JARVIS) superconducting database of density functional theory (DFT) calculations to generate new superconductors with a high success rate. We started with a DFT dataset of ~1000 superconducting materials to train the diffusion model. We used the model to generate 3000 new structures, which along with pre-trained ALIGNN screening results in 62 candidates. For the top candidate structures, we carried out further DFT calculations to validate our findings. We extended this approach to high-pressure hydride superconductors, utilizing our deep learning and DFT workflows to discover new high- T_c hydride-based structures outside of the initial training. Our approaches go beyond the typical funnel-like materials design approaches and allow for the inverse design of next-generation materials.

[1] <https://arxiv.org/abs/2304.08446>

[2] <https://jarvis.nist.gov/>

[3] <https://github.com/usnistgov/alignn>

[4] <https://github.com/txie-93/cdvae>

11:30 AM DS06.01.04

Large Language Models for Materials Science Education and Research MohdZaki, N M AnoopKrishnan and MausamMausam; Indian Institute of Technology Delhi, India

Scientific theories and facts are available in books, research papers, and websites. The advancement of computing power enabled researchers to train language models that can understand scientific text and explain it in natural language when prompted. These models have more than ~100 billion parameters and are trained on programming codes and text data. This training paradigm imparts these models the capability to solve mathematical equations, write computer programs, analyse a given text and answer the associated questions. Recently, these models became available for public use and can be equally used by students and teachers. In this work, we analyse the capability of two generative large language models, GPT-3.5 and GPT-4, to solve and understand undergraduate-level materials science questions. Specifically, we take questions which require reasoning, logical thinking, and numerical solving abilities. This analysis will help the teachers to engage with students to enable an in-depth understanding of materials science. We have also classified questions from a materials science perspective. The performance of both the LLMs from the domain point of view will enable the decision-making of researchers on how to use them for different materials science tasks.

11:45 AM DS06.01.05

Leveraging Large Language Models for Crystal Structure Prediction: Text2Struc ViktoriiaBaibakova^{1,2}, WeikeYe² and StevenTorrisi²; ¹University of California, Berkeley, United States; ²Toyota Research Institute, United States

The process of experimental and theoretical materials discovery has witnessed remarkable acceleration through the integration of computational materials science workflows into the discovery process. However, recent advancements in Large Language Models (LLMs) (OpenAI, 2023) offer an alternative avenue for automation of key workflow steps. This study focuses on crystal structure prediction, the initial step in materials science, and explores the feasibility of employing LLMs for this task. Our contribution, Text2Struc, is a novel tool designed to transform natural language descriptions of crystals into valid crystal structures. The training protocol encompasses three key elements: the methodology, the training dataset, and the performance metrics. Inspired by Toolformer (Schick et al., 2023), our approach involves instructing LLMs to use an API interface through its calls which are then executed. We sourced structures from open-access databases and curated a dataset of question-answer pairs enriched with API calls. Text2Struc was also configured to execute the generated API calls. Fine-tuning of this model was shown to reduce test set prediction error, as measured by perplexity. To assess model performance, we compared sourced true crystal structures, structure predictions with post-text completion by LLMs, and structures generated after calling the API. Our primary findings demonstrate that API execution effectively mitigates hallucinations, as evidenced by a 10% reduction in invalid structure predictions. Furthermore, our metrics indicate that structure executions closely align with true structures compared to structure predictions. Additionally, we have developed and will demonstrate a graphical user interface (GUI) for Text2Struc, enhancing its accessibility and usability. This work demonstrates the potential of LLMs in automating crystal structure prediction, advancing materials discovery to be more efficient and user-friendly.

SESSION DS06.02: Machine Learning for Battery Materials

Session Chairs: Ekin Dogus Cubuk and Mehrdad Jalali

Monday Afternoon, November 27, 2023

Sheraton, Second Floor, Back Bay A

1:30 PM DS06.02.01

Development of Reactive Force Field (ReaxFF) for BaTiO₃ Electrode Interface YasuakiOkada, MizukiAnan, YayoiKatsu, NoriakiOzaki, HideyukiKamisaka, HiroyukiHarano and NobuhikoTanaka; Murata Manufacturing Co., Ltd., Japan

Barium titanate (BaTiO₃) based multi-layer ceramics capacitors (MLCCs) have been extensively used in various electrical devices such as home appliances, automobiles, and smartphones. Among several factors that affects its performance and reliability against insulation resistance degradation under functioning applied voltage, oxygen vacancy concentration at the grain-boundary and the BaTiO₃-electrode boundary are considered the crucial factors for the reliability of MLCCs. Density functional theory (DFT) is often used to investigate electronic structures and thermodynamic stabilities of such interfaces. However, feasible number of atoms in DFT calculations is limited up to a few hundred due to its high computational cost, which hinders its application to realistic interfacial models consist of more than several thousand atoms. For this reason, we developed an accurate machine learning assisted interatomic potential for systems containing BaTiO₃ and a few electrode materials. The ReaxFF [1] was adapted for its applicability to complicated interfacial systems consist of different types of materials. The accuracy of ReaxFF molecular dynamics (MD) simulations strongly depends on the quality of parameterization for target systems. In this study, we employed our in-house code based on multi-objective genetic algorithm optimization methods, by extending functionality of EZFF code developed by A. Krishnamoorthy *et al.* [2]. In 2019, D. Akbarian *et al.* reported a ReaxFF parameter set for BaTiO₃ that reproduce the crystal structures of Ba-Ti-O compounds and phase transition between tetragonal and cubic phases of BaTiO₃ [3]. However, their predicted phase transition temperature does not coincide with experimental data and their study does not take into account of the orthorhombic phase, which dominates the low temperature dynamics of BaTiO₃ occurring in the operating temperature of MLCCs. Besides, to the best of our knowledge, there has been no ReaxFF parameter set published so far for the BaTiO₃-electrode interfacial

systems. Therefore, we developed new ReaxFF parameters that can describe the successive phase transition including orthorhombic phase, and the interfacial structures of BaTiO₃ with base (Ni) and noble (Pt) metals, respectively. First, we performed several hundred DFT calculations to prepare training data for compounds consist of Ba, Ti, O, Ni, and Pt atoms and developed new ReaxFF parameters using the in-house code. Second, we confirmed its reproducibility of the successive phase transition among orthorhombic-tetragonal-cubic phases by conducting heating/cooling ReaxFF-MD simulations with 6 × 6 × 6 periodic BaTiO₃ supercell. Finally, we performed ReaxFF-MD simulations for realistic interfacial structure models, involving S 3 type symmetrically-tilt grain boundaries of BaTiO₃ and interface against the electrode materials. NPT-MD simulations were performed as preparation to optimize the lattice constants along the gradually increasing temperatures from 300 K to 1500 K. Then, NVT-MD simulations are carried out at each temperature to investigate sintering behavior of MLCC devices. Our simulations successfully reproduced the thermal expansion of electrode materials and revealed the difference in interfacial atomic structures among the electrode materials. Namely, the Ni-electrode, the base metal, has higher affinity toward oxygen atoms in BaTiO₃, thus forming Ni-O atomic layer at the interface. On contrary, the noble metal (Pt) has much lower affinity to the oxygen and preferred to form Pt-Ti atomic layer at the interface. We anticipate these findings and further MD simulations using this newly developed ReaxFF may play a key role in elucidation of the degradation mechanisms of MLCCs in future.

[1] A. C. T. van Duin *et al.*, *J. Phys. Chem. A* **105**, 9396–9409 (2001).

[2] A. Krishnamoorthy *et al.*, *SoftwareX* **13** 100663 (2021).

[3] D. Akbarian *et al.*, *Phys. Chem. Chem. Phys.* **21**, 18240-18249 (2019).

1:45 PM DS06.02.02

Rate Determining Step of Anhydrous Proton Transport in Phosphonic Acid Electrolytes Revealed by Machine-Learned PotentialSaoriMinami and RyosukeJinnouchi; Toyota Central R&D Labs., Inc., Japan

Phosphonic acid-based electrolyte is a key material for anhydrous proton transport in fuel cells that are operatable at medium temperature. These materials, however, suffer from a severe trade-off relation between proton conductivity and stability; immobilizing phosphonic anion groups prevents leaching out of anions while it suppresses proton transport [1]. To reveal the origin of the relation, we simulate proton transport in phosphoric and phosphonic acids with different alkyl chain length. MLFFs that precisely reproduce first principles interatomic potentials [2, 3] are generated by an efficient active learning scheme implemented in Vienna Ab initio Simulation Package (VASP) [4] on the fly during first-principles calculations. The generated MLFFs are used to simulate proton transports involving Grothuss mechanism. The simulations indicate that proton diffusivity is strongly corrected with the reorientation speed of anions; as the alkyl chain length increases, both the proton diffusivity and reorientation frequency decrease. Detailed analyses show that in all materials, proton shuttles between a pair of anions with a high frequency of ~10 ps⁻¹. However, the proton transport is limited by 3 order of magnitude slower reorientations of anions, and only 0.1% of shuttling protons can transport to the adjacent anion. As the alkyl chain length increases, the reorientation frequency decreases, and the proton diffusivity decreases. These results indicate that retaining rotational freedoms of anions is essential to enhance the anhydrous proton conductivity. This work was partially supported by NEDO (New Energy and Industrial Technology Development Organization) financially.

[1] Steininger, H., *et al.*, *Physical Chemistry Chemical Physics*, 2007, 9(15): p. 1764-1773.

[2] Jinnouchi, R., *Phys Chem Chem Phys*, 2022, 24(25): p. 15522-15531.

[3] Jinnouchi, R., *et al.*, *J Phys Chem Lett*, 2023, 14(14): p. 3581-3588.

[4] Jinnouchi, R., F. Karsai, and G. Kresse, *Physical Review B*, 2019, 100(1): p. 014105.

2:00 PM DS06.02.03

Information Extraction from Materials Science Research PapersMohdZaki, KausikHira, DevanshiKhatsuriya, N M AnoopKrishnan and MausamMausam; Indian Institute of Technology Delhi, India

Predicting properties of materials for inverse design requires the development of suitable machine learning models. These models require a large dataset of materials compositions and their respective properties. The preparation of such datasets through manual compilation is a tedious task. The required information is reported in tables, text, and figures, of which the tables contain about 85 % of glass compositions. Further, a given glass composition can be found in different research papers discussing its various properties. In this work, we use DiSCoMaT, a pipeline solution for composition extraction of materials, based on graph neural networks, rule-based parsers, and a materials domain language model – MatSciBERT, materials domain language model to extract materials compositions and its modified version to extract material properties. We then extract the properties of these compositions from respective research papers using a modified version of DiSCoMaT architecture and compile them into machine-readable databases, which can be used for discovering glass compositions for tailored applications.

2:15 PM DS06.02.04

De Novo Design Methods Benchmark of GAN and Flow Models for Minimizing Hole Reorganization EnergyKarlLeswing¹, AndreaBrowning¹, AlexGoldberg¹, MathewD. Halls¹, TsuguoMorisato¹, NobuyukiN. Matsuzawa², HiroyukiMaeshima² and TatsuhitoAndo²; ¹Schrodinger, United States; ²Panasonic Corporation, Japan

In recent years, generative design methods have gained significant attention in the field of molecular ideation, offering new possibilities for the discovery and optimization of novel molecules. These methods employ algorithms and machine learning techniques to explore vast chemical spaces, generating diverse molecular structures with desired properties. As these approaches rapidly evolve, it becomes crucial to benchmark and evaluate their performance to ensure their reliability and effectiveness in real-world applications.

In this work we study two classes of generative algorithms from literature, generative adversarial networks and normalizing flow models. Generative Adversarial Networks (GANs) have emerged as a powerful framework for generating ideas in various domains, offering unique advantages over traditional generative models. GANs offer remarkable capabilities for generating ideas by capturing complex data distributions, promoting creativity and exploration, facilitating the generation of diverse ideas, and adapting to specific requirements. For this study we benchmark MolGAN: An implicit generative model for small molecular graphs [1] and A de novo molecular generation method using latent vector based generative adversarial network [2]. The other architecture studied in this benchmark are normalizing flow algorithms, a family of algorithms which promise easy training and fast sampling. For normalizing flows we benchmark GraphAF: a Flow-based Autoregressive Model for Molecular Graph Generation [3], and GraphNVP: An Invertible Flow Model for Generating Molecular Graphs [4].

In this benchmark we build molecular distributions over 250,000 OLED like molecules using these four methods and attempt to minimize hole reorganization energy using three different quality machine learning models. We then analyze the performance characteristics of the methods, the ideas they create, the idea diversity, and the compute cost.

[1] Nicola De Cao, presented at ICM 2018 workshop on Theoretical Foundations and Applications of Deep Generative Models (unpublished)

[2] O. Prykhodko *et al.*, *J. Cheminf.* **11** (2019) 74.

[3] C. Shi, M. Xu, Z. Zhu, W. Zhang, M. Zhang, J. Tang, *arXiv* (2020), doi:10.48550/ARXIV.2001.09382.

[4] K. Madhawa, K. Ishiguro, K. Nakago, M. Abe, *GraphNVP: An Invertible Flow Model for Generating Molecular Graphs* (2019), doi:10.48550/ARXIV.1905.11600.

2:30 PM DS06.02.05

Multi-Physical Factor in Enabling Homogeneous Dendrite Growth for Alkali Metal BatteriesGwanghyeonChoi¹, YoungohKim^{2,3}, JoonmyungChoi^{2,3} and DuhoKim^{1,1}; ¹Kyung Hee University, Korea (the Republic of); ²Hanyang University, Korea (the Republic of); ³BK21 Four ERICA-ACE Center, Hanyang University, Korea (the Republic of)

Homogeneous dendritic growth in lithium-metal anode has been acknowledged as of paramount importance in achieving safe high-energy-density performance for lithium-metal batteries. However, its intrinsic origin during electrochemical growth is unclear, and it still continues to pose a serious challenge to enabling homogeneity. Therefore, a thermodynamic factor in controlling (in)homogeneous electrochemical growth is suggested here based on an in-depth understanding of three alkali metal (AM: Li, Na, and K) models using unified-multiscale atomistic calculations. First, the importance of alkali metal disordered phases as a transition state is covered with thermodynamic energy big dataset using density functional theory (DFT) calculations, which provides the intriguing concept that disordered-phase energy level (DPEL) plays a decisive role in controlling the degree of (in)homogeneity during electrochemical deposition. Second, the two-type physical parameters are derived by the DFT-assisted machine learning method, and DPEL-related cohesive energy (E_c) is investigated. Third, reliable molecular dynamics simulations systematically compare (in)homogeneous alkali metal growths upon charging, and their results show severe fluctuating-morphology including sharp tips in Li metal and smooth surfaces in Na and K metals. Finally, correlating the transition-state thermodynamics and (in)homogeneous growth is understood by molecular dynamics cross-sectional models. The metallic Li prefers to be adsorbed on its crystalline phase rather than the disordered phase containing grain boundaries, which leads to severe dendritic Li growth. Whereas, these characteristics are rarely observed in K metal over the entire deposition process. From our comprehensive understanding of the growth mechanisms of three-type alkali metal models, DPEL is expected to be a universal design strategy for evaluating the alkali metal anode's homogeneous growth. Based on this thermodynamic understanding, this study additionally suggested a mechanical factor that enables controlling (in)homogeneous electrochemical growth. A large dataset of thermodynamic energies for Li disordered phase decoupled the dual-body effective cluster interactions (ECI) into three components: i) crystal-like, ii) long, and iii) short bonds of Li–Li based on machine learning assisted by DFT calculations. Their dual-body contributions provided a mechanical factor for regulating a disordered-ordered phase transition upon electrochemical deposition, and the compressive effect, which was proposed to enable the homogeneity, was confirmed. In addition, to determine the correlation between the mechanical and thermodynamic factors, DFT calculations were performed to generate a large formation energy data set based on two disordered models: i) compression and ii) over-compression. The thermodynamic energy level under the compression mode is lower than that under the unstrained condition but the over-compression mode demonstrates higher DPEL than both the reference and the compression values owing to the evolution of strong Li–Li repulsion. Interestingly, the ECI values in the crystal-like bond group are closer to 0.0 eV/bond than those under the compression-free dataset but the ECI values in the short bond group are higher relative to those with the compression-free mode,

and the variation is induced by the over-compression dataset. These re-calculated ECI values more concretely depict the mechanical factor for stabilizing the disordered phase for giving rise to homogeneous Li metal growth upon charging. Finally, the proposed multi-physical factors are expected to be a critical design factor for harnessing the full potential of alkali metal-based batteries and provide fundamental insights into enabling homogeneous lithium-metal dendrite growth.

2:45 PM DS06.02.06

Physics-Informed Neural Networks for Radiative Transfer and Boltzmann Transport Problems of Optoelectronic Device Modeling Roberto Riganti and Luca Dal Negro; Boston University, United States

There is a growing interest in developing deep learning (DL) and artificial intelligence (AI) algorithms for electromagnetic wave engineering and materials design. Rapidly emerging approaches include training artificial neural networks (ANNs) to solve inverse problems and parameter estimation in complex photonic environments. Although successfully demonstrated at solving several inverse design problems, traditional DL methods are essentially data-driven techniques requiring time-consuming training steps that use massive datasets. Moreover, in order to improve on purely data-driven methods, it is important to constrain and regularize them by leveraging the underlying physics of the investigated problems. Here we discuss our advances in building a robust framework for the design of photonic materials and devices based on auxiliary physics-informed neural networks (APINNs) for the accurate solution of complex forward and inverse problems in electromagnetic scattering and radiative transfer theory. In particular, we introduce and discuss APINNs architectures for the inverse solution of high-dimensional integro-differential Boltzmann-type transport problems of relevance to optoelectronic devices and optical materials design and we demonstrate efficient parameter estimation in coupled conductive-radiative systems with applications to heat transfer in semiconductor devices. Specifically, we employ APINNs to solve the phonon Boltzmann transport equation (BTE) for AlGaN alloys in different geometries. Our work shows that APINNs possess the flexibility, accuracy, and noise robustness required to become a powerful design approach for inverse scattering and the non-local thermal modeling of optoelectronic devices beyond the Fourier thermal transport limit. The presented work expands upon the current capabilities and range of applications of physics-informed neural networks and paves the way to the study of complex transport problems and light-matter interactions in strongly scattering media with applications to nanophotonics, biomedical imaging, and semiconductor device modeling.

3:00 PM BREAK

3:30 PM DS06.02.07

Study of The Boson Peak in Phase-Change Materials using Machine-Learning Potential Simulations Pyunjin Park, Sungmin Song, Jesun Jang and Seung-Hoon Jhi; Pohang University of Science and Technology, Korea (the Republic of)

The boson peak is a peculiar feature in the vibrational density of states, mostly observed in disordered materials. Its origin has been attributed to various factors such as defects, atomic disorder, or mass density fluctuations [1,2], while a consensus is not reached yet. We investigate the boson peak in amorphous and metastable cubic Ge-Sb-Te phase-change materials to determine primary driving mechanism behind the boson peak. Utilizing the Gaussian approximation potentials [3] and a machine-learning scheme named the randomized atomic-system generator [4], we conduct large-scale simulations inaccessible from first-principles calculations to investigate this phenomenon. We employ an analytical approach involving the elastic theory, Voronoi cell analysis, atomic scale stress and strain to demonstrate the correlation between atomic disorder, density variation, shear elastic heterogeneity and the boson peak in the phase change materials.

References

1. Hu, Y.-C. & Tanaka, H. Nat. Phys. 18, 669–677 (2022).
2. Chumakov, A. I. et al. Phys. Rev. Lett. 112, 025502 (2014).
3. Bartók, A. P., Payne, M. C., Kondor, R. & Csányi, G. Phys. Rev. Lett. 104, 136403 (2010).
4. Choi, Y.-J. & Jhi, S.-H. J. Phys. Chem. B 124, 8704–8710 (2020).

3:45 PM DS06.02.08

Paddle-Wheel Effect Mediates Polymorph Transitions but not Li Transport in the Ionic Conductor Li₃PS₄ Andrey Poletayev¹, James A. Dawson², Benjamin J. Morgan³ and M. Saiful Islam¹; ¹University of Oxford, United Kingdom; ²Newcastle University, United Kingdom; ³University of Bath, United Kingdom

Ionic transport is a key determinant of performance in energy technology devices, and simultaneously a convenient testing ground for machine-learned neural-network interatomic potentials. Of particular interest is the influence of slow degrees of freedom on ion conduction. Here we investigate the influence of large-amplitude polyhedral-anion flips on Li transport in the modern solid-state ion conductor Li₃PS₄, where a paddle-wheel effect has been proposed to benefit transport, using ensembles of local equivariant graph neural network potentials.

We find that at elevated temperature a large variety of models yield consistent predictions for the rate of polyhedral flips, approximately one per nanosecond at 800 K, and variance within a factor of 2 between models trained with distinct hyperparameters and across different sizes of training data (32-128 atom cells) despite the large increase in out-of-dataset testing errors versus larger-scale ab initio frames.

Importantly, we find that the large-amplitude paddlewheel flips are orders of magnitude too slow to facilitate Li transport. Further, using well-tempered metadynamics enhanced sampling, we estimate the free-energy kinetic barriers for the polyhedral flips to be ≥ 0.7 eV, which is approximately double the activation of ion conduction. Instead, the lowest-activation polyhedral-anion flip is collective and mediates the phase transition between room-temperature and elevated-temperature polymorphs in a one-dimensional mechanism.

Overall, our simulations are consistent with the orientational disorder observed experimentally, and suggest that such disorder rather than a purely dynamic paddle-wheel effect is beneficial to ion conduction. Owing to its rich dynamical landscape and polymorphism coupled to it, Li₃PS₄ can serve as a benchmarking material for testing machine-learning interatomic potentials and enhanced sampling methods.

4:00 PM DS06.02.09

Deep Operator Machine Learning Framework for Modeling All-Solid-State Batteries Wei Li and Juner Zhu; Northeastern University, United States

All-solid-state batteries (ASSBs) have generated significant interest in recent years due to their high energy density and safety features, making them a promising candidate for next-generation storage systems that can support the societal goal of decarbonization. However, ASSBs continue to suffer from significant chemo-mechanical failures, such as lithium dendrite growth, penetration, various interfacial aging phenomena, and mechanical damage. As a result, most research efforts are currently focused on experimenting with materials and structures to overcome these challenges. Except for the experimental efforts, developing an accurate model that can reveal the underlying physics and predict the chemo-mechanical behaviors of ASSBs is also crucial. A model at the electrode level would be especially beneficial to practical implementations. However, traditional physics-based models often require relatively large computation costs, making them impractical for real-time applications.

To address this challenge, we propose a machine learning framework based on deep operator neural networks (DeepONets) to accurately and efficiently model ASSBs at the electrode level. The framework incorporates important physics, such as mass and charge conservation, as well as several mechanical and interfacial aging mechanisms. To successfully model the whole complex system, we first separately train the DeepONets for each governing equation or physics and then couple them together. For example, a DeepONet is trained to map the source term to the potential field for the charge conservation equation (Poisson's equation); and a separate DeepONet is trained to learn the mapping from the current concentration field to the next state for the diffusion equation. These two DeepONets are then coupled through the kinetics (Butler-Volmer) equation. The trained DeepONets can enable fast predictions for real-time control and optimization.

4:15 PM DS06.02.10

Predicting Kinetic Reactivity of Solid-State Battery Interfaces Eder G. Lomeli, Brandi Ransom, Akash Ramdas, Thomas Devereaux, Evan Reed and Austin Sendek; Stanford University, United States

In this work, we combine ab initio simulation with machine learning to build the first model for predicting the kinetics of interfacial reactivity in solid-state Li metal batteries. We first use density functional theory molecular dynamics (DFT-MD) to simulate the time evolution of several solid-state electrolyte (SSE) candidate materials interfaced with Li metal. Unlike state-of-the-art grand potential convex hull calculations for predicting interfacial stability, simulation with DFT-MD explicitly considers kinetic reaction barriers between two phases. We use the resulting data from these simulations to build a data-driven model that uses computationally inexpensive structural and thermodynamic features to predict the DFT-MD kinetic reactivity of these interfaces. This first-of-its-kind model enables more targeted and effective selection of solid electrolytes for solid-state Li metal batteries. Solid-state batteries offer safer and more energy-dense alternatives for energy storage systems. Like current liquid electrolyte batteries, the stability of interfaces between different battery components remains a critical requirement for longevity and device performance. With over 20,000 Li containing inorganic solids in the Materials Project database, the current high throughput technique to assess the chemical compatibility of candidate interfaces between SSEs and battery electrodes consists of a thermodynamic static parameter, the driving force for chemical mixing, with an arbitrary global assumption of a kinetic stabilization barrier. The current version of this kinetic reactivity model outperforms the purely thermodynamic parameter with a significantly lower misclassification of reactive/unreactive interfaces and predicts over 1,000 additional stable candidate interfaces that could be used for metric-specific material searches.

4:30 PM DS06.02.11

Machine Learning Design of More Accurate, Efficient, Stable and Transferable Coarse Grained Free Energy Models Blake Duschatko¹, XiangFu², YuXie¹, Albert Musaelian¹, Simon Batzner¹, Tommi Jaakkola² and Boris Kozinsky¹; ¹Harvard University, United States; ²Massachusetts Institute of Technology, United States

In complex material systems with long time- and length-scale dynamics, standard all-atom simulation techniques often become too expensive. In these settings, state of the art approaches to coarse graining are able to examine system properties at lower resolution with high fidelity. However, a number of practical barriers remain to be overcome in making bottom-up coarse graining approaches viable for addressing realistic problems. In this work, we introduce our recently developed on-the-fly active learning framework for coarse grained free energy models that directly addresses an outstanding challenge in the community of efficient data collection [1]. We demonstrate how this approach allows for optimal selection of training sets, and further examine how uncertainty based active learning opens the door to designing transferable models across structural and chemical spaces. Lastly, we proceed to demonstrate novel techniques for learning the PMF with greater fidelity, efficiency and simulation stability than was previously achievable.

1. Blake R. Duschatko, Jonathan Vandermause, Nicola Molinari, and Boris Kozinsky. *Uncertainty Driven Active Learning of Coarse Grained Free Energy Models*, arXiv preprint arXiv:2210.16364 (2022).

4:45 PM DS06.02.12

Short Range Order Clustering Leveraging New Technologies for Better Mechanical Properties Predictability Axel E. Poisvert¹, Stefanos Papanikolaou¹ and Marinica M. Cosmin²; ¹NCBJ-Nomaten, Poland; ²Commissariat à l'Énergie Atomique et Aux Énergies Alternatives, France

Chemical short-range order (C-SRO), meaning a sort of clustering depending on the nature of atoms present in the system, influences thermo-mechanical properties in a large variety of complex concentrated alloys (CCA), and in particular, high entropy alloys (HEA). However, short-range order (SRO) characterization and classification approaches, both experimentally and theoretically, have been a challenge, especially due to the fact that this order takes place locally in a range of few neighbors (typically less than 10).

SRO and C-SRO are commonly characterized by Warren-Cawley parameters representing a comparison between local and global element concentration. This method seems a bit archaic in light of all advances made in materials science thanks to.

In this work we hypothesize that new ways of discriminating SRO, using advances in machine learning and informatics for the characterization of local, chemically induced, distortions, may uncover new properties of ordered systems, and in particular CCAs and HEAs.

We use Molecular Dynamics (MD) and Machine Learning (ML) to implement an innovative method to discriminate C-SRO during MD runs. For this purpose, we leverage a SO(4) bispectrum descriptor in order to link the descriptors with mechanical and physical effects, using the MiLaDy [1] and LAMMPS [2] packages. This study leans on two specific systems, equiatomic NiCoCr and equiatomic CuCoFeNiPd.

We set up the systems using variance constrained semi grand canonical Monte Carlo simulations (VCSGC-MC) at low temperature, allowing reordering in both alloys. Then, the samples are mechanically loaded.

The determination of descriptors after the MD process leads to a distortion score that is determined with both swapped system and random equivalent system in order to compute a statistical distance matrix.

We find that the distortion score can allow the definition of SRO clusters with finer definition than other methods widely available, and then, individual clusters may be extracted and specially investigated. We further find a strong interplay between initial clustering and subsequent stress loading effects, while the local per atom volume representing the strongest predictor of C-SRO.

[1] Goryaeva, A. M., Lapointe, C., Dai, C., Dérés, J., Maillet, J. B., & Marinica, M. C. (2020). Reinforcing materials modelling by encoding the structures of defects in crystalline solids into distortion scores. *Nature communications*, 11(1), 4691.

[2] Thompson, A. P., Aktulga, H. M., Berger, R., Bolintineanu, D. S., Brown, W. M., Crozier, P. S., ... & Plimpton, S. J. (2022). LAMMPS—a flexible simulation tool for particle-based materials modeling at the atomic, meso, and continuum scales. *Computer Physics Communications*, 271, 108171.

SESSION DS06.03: Poster Session I: Machine Learning for Materials Modelling I

Session Chairs: Mathieu Bauchy and Ekin Dogus Cubuk

Monday Afternoon, November 27, 2023

Hynes, Level 1, Hall A

8:00 PM DS06.03.01

Highly Efficient Crystal Structure Prediction with Universal Neural Network Empirical Potential Payden Brown¹, Takuya Shibayama², So Takamoto², Daisuke Okanohara² and JuLi¹; ¹Massachusetts Institute of Technology, United States; ²Preferred Networks, Inc, Japan

Crystal structure prediction (CSP) has played a vital role in computational materials discovery for its ability to explore unknown energy landscapes of chemical systems. Crystal structure predictors that utilize ab initio techniques such as density functional theory (DFT) are limited by their computationally expensive and time-consuming calculations. The advent of neural network potentials (NNPs) has opened the door for more efficient CSP and, with recently developed models, can reach the same level of accuracy as DFT. One such NNP is the PreFerred Potential (PFP), a universal NNP that can be applied to any combination of 72 elements. In this work, we develop an evolutionary crystal structure predictor that exploits the computational advantages of PFP.

PFP was paired with our variable-composition CSP algorithm to explore diverse inorganic binary and ternary chemical systems. Numerous crystal structures were discovered that break the known ab initio convex hull for their chemical systems with remarkable efficiency. The average algorithm run-time for binary systems was under 4 hours, resulting in ~800 crystal structures. Random subsets of generated structures were verified with DFT, finding that PFP correctly predicts that a structure's energy is above or below the convex hull with ~80% accuracy. The successful and efficient discovery of new stable crystal structures with the technique developed in this work proves its potential to accelerate the discovery of new theoretical crystal structures.

8:00 PM DS06.03.02

Applicability of Universal Neural Network Potential to Organic Polymer Materials Hiroki Iriguchi, Akihiro Nagoya, Yusuke Asano and Taku Watanabe; Preferred Computational Chemistry Inc., Japan

With the recent development of materials exploration aided by machine learning (so-called materials informatics), atomistic simulations have been playing an increasingly important role. Density functional theory (DFT) calculations are widely used for accurate atomistic simulations, which usually take a few months due to high computational costs. Molecular dynamics (MD) simulations using classical force fields are much faster than DFT simulations and have been applied for atomistic simulations on nano- to micro-scale. However, the accuracy depends on the parameters of the force field. Therefore, there is a trade-off between computational cost and accuracy between these conventional methods. There are some approaches to calculate materials speedily with accuracy like first-principles calculations, such as density functional tight binding method (DFTB) or reactive force field (ReaxFF), but they have strong parameter dependence and poor versatility because they aim to reproduce specific systems with high accuracy in many cases.

Neural Network Potential (NNP) is a machine learning model that uses the results of first-principles calculations as a data set to infer the energy and force of molecular and crystal structures. While conventional NNPs can only be used in a limited number of material systems for each model because the corresponding structure depends on the training datasets, PreFerred Potential (PFP) was developed with the aim of becoming a universal NNP by efficiently collecting training data and constructing an architecture that reproduces the smooth interatomic potential energy surface. This enables fast calculation of any 72-element combination structure with accuracy equivalent to first-principles calculations, and has already been shown to be effective in material exploration in some areas such as batteries and catalysts. On the other hand, large condensed systems composed of organic molecules, such as liquid solutions and polymers, are conventionally analyzed by MD simulations using classical force fields. Due to its accuracy and universality, PFP can extend the application of atomistic simulation to inorganic/organic interfaces, chemical reactions, and degradation of these systems.

In this presentation, we will show examples of calculations to demonstrate that PFP can be useful not only for inorganic materials but also for organic materials. As a benchmark of the organic systems, we have calculated the density of various organic liquids obtained using PFP. The results are in good agreement with those obtained by DFT. For more practical examples, the thermal decomposition of epoxy resin was analyzed by PFP-based MD simulations. The results were similar to those calculated by ReaxFF, showing that epoxy resins initially produce small hydrocarbon compounds upon fragment decomposition, and that as the reaction temperature increases, the amount of water and hydrogen produced increases through radical reactions. Other examples of calculations made possible by PFP will be discussed.

8:00 PM DS06.03.03

Special Glass Structures for High-Throughput First Principles Studies of Bulk Metallic GlassesSiyaZhu¹, Axelvan de Walle¹, JanSchroers², StefanoCurtarolo³ and HagenEckert³; ¹Brown University, United States; ²Yale University, United States; ³Duke University, United States

The atomic-level structure of bulk metallic glasses (BMGs) is a key determinant of their properties. A large training dataset is required to construct a machine-learning modeling for the structure and properties of BMGs. However, an accurate representation of amorphous systems in computational studies has traditionally required large supercells that are unfortunately computationally demanding to handle using the most accurate *ab initio* calculations. To address this, we propose to specifically design small-cell structures that best reproduce the local geometric descriptors (e.g., pairwise distances or bond angle distributions) of a large-cell simulation. We rely on molecular dynamics (MD) driven by empirical potentials to generate the target descriptors, while we use reverse Monte Carlo (RMC) methods to optimize the small-cell structure. The latter can then be used to determine mechanical and electronic properties using more accurate electronic structure calculations. With high efficiency and accuracy of modeling and calculating properties of BMGs, a large and reliable dataset for ML of BMGs can be generated using our method. The method is implemented in the Metallic Amorphous Structures Toolkit (MAST) software package.

8:00 PM DS06.03.04

Quantifying the Lennard–Jones Potential between Two Hard Ellipsoids using Coarse-Grained Deep Learning TechniquesErinWong^{1,2}, DylanFei^{1,2}, GeorgiosKementzidis², YufengDeng² and MiriamRafailovich²; ¹William A. Shine Great Neck South High School, United States; ²Stony Brook University, The State University of New York, United States; ³Jericho Senior High School, United States

Equations: Eq. (1) is presented as the 12–6 Lennard–Jones potential: $V_{LJ} = 4\epsilon_{LJ}[(\sigma/r)^{12} - (\sigma/r)^6]$. Eq. (2) is presented as the Gay–Berne potential: $U_{AB} = 4\epsilon_{AB}\{[\sigma_0/(R_{AB} - \sigma_{AB} + \sigma_0)]^{12} - [\sigma_0/(R_{AB} + \sigma_{AB} + \sigma_0)]^6\}$. Eq. (3) is presented as the double summation of the 12–6 Lennard–Jones potential, V_{LJ} , over the individual points that subsume the pairwise rigid bodies.

Classical molecular dynamics (MD) is a highly intensive, $O(n^2)$, computational method for simulating the kinetics, thermodynamics, and structural properties of a many-body system over time. The initialization of such a method requires the use of multiple energy functions, which, in turn, describe the trajectory and momenta of the particles being simulated. We focus on the Lennard–Jones potential (LJP), which governs the van der Waals (vdW) energetics between, specifically, two interacting particles. We seek to modify the potential's conventional form, eq. (1), which fails to accurately model the vdW forces between large and anisotropic particles (ellipsoids). Eq. (3), however, overcomes those shortcomings by treating the ellipsoids as a collection of uniformly distributed points and, in turn, applying a double summation over those points to generate the LJP.

We learn the variables of eq. (2) using a physics-informed neural network (PINN), which, unlike our previously proposed feedforward neural network, assumes a physics-principled training process that, in our case, entails the parametrization of eq. (2). Our goal is to replicate the accuracy of eq. (3) by training our PINN to recognize the relationship between the variables of eq. (2) and the imputed parameters—relative orientation, semi-major/-minor axes, and center—of the two ellipsoids. Our PINN then uses those imputed parameters to generate the corresponding ϵ_{AB} and σ_{AB} values, thereby streamlining the complexity involved in the computation of eq. (3).

Our ground truth, serving as the basis of our training data, stemmed from the Monte Carlo approximation of eq. (3) and consisted of 2,080,000 potentials. The parameters of our two ellipsoids—relative orientation, semi-major/-minor axes, and center—were uniquely permuted such that no two potentials were generated using the same parameters.

One of the primary concerns about our data's accuracy was the extent to which an ellipsoid could be classified as a rigid body. Therefore, we ran three mini-experiments to verify the equations and code used to generate the ground truth. We referenced the three cases shown by Paramonov & Yaliraki and demonstrated (a) that the number of points per ellipsoid, upon exceeding 15,000, minimally impacted the generated potential and (b) that ground truth generation code proved scientifically sound, emulating the well depth and curvature in all three cases shown by Paramonov and Yaliraki. Moreover, in addressing part (a), we randomly sampled a subset of our ground truth (generated using 30,000 points per ellipsoid) and regenerated those LJP values using 5,000, 15,000, 25,000, and 30,000 points. The mean absolute percentage error (MAPE) started at 2.42% for 5,000 points, indicating, on average, a 2.42% error between a value from the dataset to a newly generated value using our code, but upon exceeding 15,000 points, gradually decreased to 0.96% (MAPE_{30,000}), thus confirming the accuracy of our ground truth.

We implemented two models using this ground truth. The first was a black box model, which used the parameters of two ellipsoids to predict the LJP. The second was a PINN that used the same parameters of the two ellipsoids to find the coefficients of ϵ_{AB} and σ_{AB} through two separate neural networks and tune σ_0 for eq. (2). By employing a combination of Adam and L-BFGS optimization, the PINN was able to achieve a minimum training loss of 0.0004 over 250 epochs. We plan to validate this PINN using a separate testing dataset and further improve upon it by investigating the use of other activation and loss functions.

8:00 PM DS06.03.05

In-Silico Studies on Fibrinogen Domain Adsorption on Polylactic AcidErinWong¹, MatthewSun² and RichardZhang³; ¹Great Neck South High School, United States; ²North Carolina School of Science and Mathematics, United States; ³Conestoga High School, United States

*All authors contributed equally

Fibrinogen, a vital blood clotting protein, transforms into active fibrin via thrombin activation, creating a scaffold for clots. It is key in interactions with medical device materials, especially those prone to adverse clotting. Investigating material-blood protein interactions, like those with polylactic acid (PLA), which is used for its biocompatibility, can aid in preventing device-induced clots and enhancing safety.

Prior research demonstrates the impact of surface chemistry on adsorbed fibrinogen's conformation, orientation, fiber formation, and platelet adhesion. This is attributed to distinct surface properties of fibrinogen domains: D and central E (C_e) domains are hydrophobic, while the α C domain is hydrophilic. On hydrophobic surfaces like PLA, D and C_e domains strongly adhere (with C_e showing weaker adherence) while the α C domain remains detached, promoting lateral aggregation via α C domain linkage. Conversely, on hydrophilic surfaces, α C domains bind to the C_e domain, reducing lateral aggregation. Additionally, P12, a proven stent coating, reduces fibrinogen fiber count on hydrophobic surfaces and supports endothelial cell growth without adverse effects. P12 obstructs the D domain's hole, impeding fiber formation; it potentially affects α C domains by surface binding as well.

To study this critical interaction between P12 and fibrinogen, we conducted molecular dynamics simulations. In order to lessen the computational cost, the problem was divided into parts for the three fibrinogen domains. For the D and C_e domains, the simulations were identical: run each domain alone in water, each domain face down on PLA, and each domain face up on PLA. By accounting for the different orientations of the domains on PLA, the actual binding configuration for each domain could be deduced as it is currently unknown. For the central complex (α C and C_e domain), umbrella sampling and steered molecular dynamics (SMD) were done to gain insight into the free energy landscape of the complex when the α C domains are separated and to determine the force necessary to pull the α C domain segments apart.

After 4.45 ns of D domain simulation, the total energy of the system was -2.99795e+06. After 6.01 ns of C_e domain simulation, the total energy of the system was -1.38023e+06. Both domains of the fibrinogen protein were shown to have stably folded, with reasonably invariant radii of gyration. Our next steps include running simulations with the D and C_e domains face down and face up on PLA, to examine the lowest energy conformations and chemical behaviors of these surface interactions. Moreover, we will use data from the SMD and umbrella sampling to train a machine learning model to predict whether the α C domain segments will be pulled apart, given various factors such as thermodynamics values and relative orientation.

8:00 PM DS06.03.06

Atomistic Simulation Incorporated with Science Pedagogy to Advance Machine Learning-Assisted Materials ResearchLexiHwang¹, MarlenTrigueros¹, PriyanshuLuhar² and SungwookHong²; ¹California State University, Los Angeles, United States; ²California State University, Bakersfield, United States

The current study aims to use a guided inquiry-based instruction framework and other evidence-based science strategies to advance materials research in coordination with computational modeling and machine learning approach. For the delivery of our program, guided inquiry-based instruction was used where students generate inquiry from their own experiences into authentic questions and are given opportunities to explore and discover materials processes such as computational synthesis of functional metal nanoparticles and 2D materials. Dynamic representations and manipulation of abstract and unobservable phenomena (e.g., chemical reactions at molecular and atomic levels) will be made available to student scholars where they build molecular structures, run atomistic simulations, and visualize and analyze simulation results via machine learning assisted characterization. We measure students' perception and motivation toward learning materials science and engineering; and machine learning assisted computational design skills using the existing tools and researcher-developed evaluation criteria. Results indicated positive impacts of our pedagogical approached simulation training. Implications and future directions will be discussed. We believe our approach will strengthen a diversity in the community of machine learning-based materials research.

8:00 PM DS06.03.07

Advancing Semiempirical Quantum Chemistry with Extended Lagrangian and Machine LearningMaksimKulichenko; Los Alamos National Laboratory, United States

Although semiempirical quantum chemistry provides better scalability and speed compared to sophisticated *ab initio* methods, Born-Oppenheimer Molecular Dynamics (BOMD) simulations

within semiempirical formalism still suffer from the computational bottleneck of iterative self-consistent field (SCF) optimization at each time step, limiting their applicability to large-scale simulations. An advanced formulation of Extended Lagrangian Born–Oppenheimer Molecular Dynamics (XL-BOMD), implemented in the PyTorch-based semiempirical quantum chemistry code PySeQM software, eliminates the need for SCF optimization by simultaneously propagating the electronic degrees of freedom along with the nuclear motion. The implementation incorporates several key features, including consideration of finite electronic temperatures, the use of canonical density matrix perturbation theory, and an adaptive Krylov subspace approximation for density matrix propagation. With the new XL-BOMD formulated for the Neglect of Differential Diatomic Overlap (NDDO) semiempirical model, we can now simulate large and challenging chemical systems characterized by charge instabilities and low HOMO-LUMO gaps. Applied to molecular dynamics, simulation of 840 carbon atoms, one molecular dynamics time step executes in 4 s on a single GPU.

The PyTorch implementation enables dynamic re-parameterization of semiempirical parameters by interfacing them with machine learning models, thereby enabling training to high-quality ab initio data, including reactive events. This approach leads to enhanced accuracy when compared to using static, pre-optimized semiempirical parameters.

[1] M. Kulichenko, K. Barros, N. Lubbers, N. Fedik, G. Zhou, S. Tretiak, B. Nebgen, A. M. N. Niklasson. “Semi-Empirical Shadow Molecular Dynamics: A PyTorch Implementation.” *J. Chem. Theory Comput.* (2023), 19, 11, 3209

[2] A. M. N. Niklasson. “Density-Matrix Based Extended Lagrangian Born–Oppenheimer Molecular Dynamics.” *J. Chem. Theory Comput.* (2020) 6, 6, 3628.

[3] G. Zhou, N. Lubbers, K. Barros, S. Tretiak, B. Nebgen. “Deep learning of dynamically responsive chemical Hamiltonians with semiempirical quantum mechanics.” *PNAS* (2022) 119, 27, e2120333119.

[4] <https://github.com/lanl/PYSEQM/tree/develop>

8:00 PM DS06.03.08

Using TD-DFT to Understand The Photochemistry of Functionalized Organic Systems [Moumita Banerjee](#) and Anakuthilanoop; Indian Institute Of Technology, India

Our research focuses on the investigation of carboxylic acid photorelease from functionalized systems acting as photocages, utilizing β -carboline and phenothiazine moieties. Specifically, the varying release rates of carboxylic acids from different benzylic positions in the β -carboline moiety and the impact of oxygen on phenothiazine photochemistry are being studied.

Advanced computational methods, such as Density Functional Theory (DFT) and Time-Dependent DFT (TD-DFT), are being employed to analyze electron excitation dynamics through hole-electron distribution and charge density difference visualization.

These insights are not only contributing to the advancement of fundamental understanding but are also holding promise for applications in functional materials, particularly in drug delivery.

By these moieties, innovative drug delivery systems are being developed, enabling precise control over drug release for enhanced therapeutic efficacy.

SESSION DS06.04: Machine Learning for Simulation of Materials I

Session Chairs: Grace Gu and Rama Vasudevan

Tuesday Morning, November 28, 2023

Sheraton, Second Floor, Back Bay A

8:30 AM DS06.04.01

Autonomous Learning of Atomistic Structural Transitions via Physics-Inspired Graph Neural Networks [Bamidele Aroboto](#)¹, [Shaohua Chen](#)², [Yu-Ting Hsu](#)³, [Brandon Wood](#)³, [Yang Jiao](#)² and [James Chapman](#)¹; ¹Boston University, United States; ²Arizona State University, United States; ³Lawrence Livermore National Laboratory, United States

Materials processing often occurs under extreme dynamic conditions leading to a multitude of unique structural environments. These structural environments generally occur at high temperatures and/or high pressures, often under non-equilibrium conditions, which results in drastic changes in the material's structure over time. Computational techniques such as molecular dynamics simulations can probe the atomic regime under these extreme conditions. However, characterizing the resulting atomistic structures has proved challenging due to the intrinsic levels of disorder present. Here, we introduce SODAS++, a universal and interpretable graph neural network framework that can accurately and intuitively quantify the transition between any two arbitrary phases. The SODAS++ framework also quantifies local atomic environments, providing one with the power to encode global state information at the atomic level. We showcase SODAS++ for both solid-solid and solid-liquid transitions for systems of increasing geometric and chemical complexity such as elemental metals, oxides, and ternary alloys.

8:45 AM DS06.04.02

Prediction of Forces and Energy Based on Rotational Invariant Spherical Representations [Kento Nishio](#)¹, [Kiyoshi Shibata](#)² and [Teruyasu Mizoguchi](#)²; ¹The University of Tokyo, Japan; ²Institute of Industrial Science, The University of Tokyo, Japan

Although hand-crafted descriptor-based methods have traditionally been used to construct accurate machine learning interatomic potentials, graph neural networks (GNNs), which can be trained end-to-end, have recently attracted attention due to their generality.

GNNs use rotational-invariant geometric features of materials, such as interatomic distances, and bond angles, to model interactions with neighboring atoms [1]. Recently, many efforts have been made to improve the prediction accuracy of equivariant quantities such as interatomic forces by imposing not only invariance but also equivariance on the model [2].

However, imposing equivariance imposes restrictions on the operations in the model and prevents the use of nonlinear transformations, which are particularly important for improving expressiveness. In addition, to express equivariance, higher-order tensor features may be required, and equivariant operations are expensive in terms of computational cost.

In response to these problems, previous studies have taken steps to loosen the restriction on nonlinearity by sampling points on a sphere or to lower the dimensionality of features by approximating equivariant operations [3], and efforts to develop equivariant models with excellent expressive power and computational cost [4].

In this study, we developed a GNN architecture for equivariant prediction with excellent expressiveness and computational cost by using a different method from these studies. We improved the efficiency by converting the rotational equivariant inter-atomic directional information into a rotational invariant representation, eliminating the limitations of nonlinearity, and incorporating efficient geometric message passing [5].

First, to make the directional information between atoms invariant, the coordinates of the neighborhood atoms were transformed using an orthonormal basis defined between two different neighborhood atoms and the central atom. This allows us to obtain directional information between atoms that is invariant to global rotations.

Next, the invariants created by the transformation and the geometric message passing proposed in previous studies were used to update the graph embedding vectors. Note that since only invariant features are used, the embedding itself is an invariant and there are no nonlinearity restrictions when updating it. The geometric message passing proposed in the previous study involves a very expensive operation, as it requires the calculation of the dihedral angles for a quartet of atoms in the material. In this study, the coordinate transformation allows us to efficiently consider higher-order geometric features, thus constituting geometrical message passing with excellent computational cost.

Finally, the predictions were made by extending the embedding vector, which is an invariant, to an equivariant in a manner similar to previous studies. Previous studies have already proven the extension from invariants to equivariants to be general [5].

This presentation will provide an overview of the developed model and the results of validating its accuracy and throughput on several data sets and comparing it to existing models.

[1] C. Chen and S. P. Ong, *Nature Computational Science*, 2, 718–728 (2022).

[2] K. T. Schütt et al., arXiv 2102.03150 (2021).

[3] C. Lawrence Zitnick et al., arXiv 2206.14331 (2022).

[4] S. Passaro and C. Lawrence Zitnick, arXiv 2302.0365 (2023).

[5] J. Gastegger et al., arXiv 2106.08903 (2021).

9:00 AM DS06.04.03

Investigation of Phase Stability and Ionic Conductivity of Solid Electrolytes $\text{Li}_{10}\text{MP}_2\text{S}_{12-x}\text{O}_x$ ($M = \text{Ge}, \text{Si}, \text{or Sn}$) with Universal Neural Network Potential [Chikashi Shinagawa](#), [Ryota Sawada](#), [Kosuke Nakago](#) and [So Takamoto](#); Preferred Networks, Inc., Japan

$\text{Li}_{10}\text{GeP}_2\text{S}_{12}$ (LGPS)-type structures are promising materials for solid electrolytes for all-solid-state lithium-ion batteries with high lithium-ion conductivity. One of the main challenges of these structures is stability. It has been reported that stability can be improved by substituting oxygen for sulfur, but there is a trade-off, as it reduces lithium-ion conductivity. Therefore, it is worth revealing the effects of oxygen substitution on stability and lithium-ion conductivity, and finding the optimal substitution ratio of the oxygen species that balances both properties.

Density functional theory (DFT) calculations have been widely applied to battery materials. However, because of the computational cost of DFT calculations, it is hard to apply for partially substituted structures that require considering various configurations of substituted elements. In contrast, empirical interatomic potentials are much faster than DFT calculations, but it is difficult to construct an empirical interatomic potential which can handle complex structures composed of as much as five elements with enough accuracy.

In this work, we investigated phase stabilities and lithium-ion diffusion barriers of $\text{Li}_{10}\text{MP}_2\text{S}_{12-x}\text{O}_x$ ($M=\text{Ge}, \text{Si}, \text{or Sn}$) with PFP, a neural network interatomic potential which supports any combination of 72 elements. Phase stabilities are calculated considering various configurations of substituted structures, and lithium-ion diffusion barriers are calculated with molecular dynamics (MD) simulations with finite temperatures. The accuracy of PFP was validated by comparing forces with DFT calculations for structures randomly selected from the MD trajectories, and it exhibited good agreement with a mean absolute error of 0.027 eV/\AA without fine-tuning for the target system. Our results reproduced that oxygen substitution increases phase stability and increases the lithium-ion diffusion barrier, i.e., decreases lithium-ion conductivity. Analysis of lithium-ion diffusion paths reveals that the disappearance of diffusion channels that are not adjacent to the oxygen atoms increases the lithium-ion diffusion barrier. It suggests that there is a critical mass for oxygen which will close all diffusion paths, and $\text{Li}_{10}\text{SnP}_2\text{S}_{11.5}\text{O}_{0.5}$ would be a promising solid electrolyte material, as it balances both stability and lithium-ion conductivity.

9:15 AM DS06.04.04

Benchmarking Optimization of Atomic Structures on Rough Landscapes[VaibhavBihani](#)¹, [SahilManchanda](#)¹, [SrikanthSastry](#)², [SayanRanu](#)^{1,3} and [N M AnoopKrishnan](#)^{1,3}; ¹Indian Institute of Technology Delhi, India; ²Jawaharlal Nehru Centre for Advanced Scientific Research, India; ³Indian Institute of Technology Delhi, India

Efficient optimization of atomic structures is crucial for accurately simulating and understanding the behavior of materials and molecules. Here, we present a comprehensive benchmarking study that evaluates the performance of various optimization methods on atomic structures, encompassing a wide range of atomic interactions. We study gradient-based methods such as Adam, SGD, second-order optimization methods including BFGS and conjugate gradient, molecular dynamic-based techniques like FIRE, Basin Hopping, and simulated annealing, as well as neural methods such as learned optimizers and reinforcement learning-based optimizers. Chosen systems represent diverse atomic interactions, covering various types of potentials, including pairwise potentials such as Lennard-Jones (LJ), three-body angular interactions represented by the Stillinger-Weber potential, Coulombic interactions in the Buckingham potential, and multi-body interactions in the embedded atom potential. We evaluate the performance of each optimization method on different systems, measuring factors such as final energy, computational efficiency, and scalability. Neural techniques leverage the power of neural networks to adaptively optimize the structures and capture complex relationships between atomic interactions. Initial findings suggest that neural methods hold great potential for enhancing the optimization process and achieving higher accuracy in complex atomic systems.

9:30 AMBREAK

10:00 AM *DS06.04.05

Harnessing the Properties of Equivariant Neural Networks to Understand and Design Materials[TessSmidt](#); Massachusetts Institute of Technology, United States

Atomic systems (molecules, crystals, proteins, etc.) are naturally represented by a set of coordinates in 3D space labeled by atom type. This poses a challenge for machine learning due to the sensitivity of coordinates to 3D rotations, translations, and inversions (the symmetries of 3D Euclidean space). Euclidean symmetry-equivariant Neural Networks (E(3)NNs) are specifically designed to address this issue. They faithfully capture the symmetries of physical systems, handle 3D geometry, and operate on the scalar, vector, and tensor fields that characterize these systems.

E(3)NNs have demonstrated state-of-the-art performance on diverse atomistic benchmarks, such as small molecule properties, protein-ligand binding, and force prediction for heterogeneous catalysis. These networks combine neural network operations with insights from group representation theory. Their success stems from a rigorous foundation, making them more robust, data-efficient, and capable of generalization compared to invariant or non-equivariant neural networks.

In this talk, I will provide an overview of recent applications of E(3)NNs in understanding and designing materials. I will also discuss the expansion of these methods' applicability to new domains and data modalities. Finally, I will explore open questions regarding the expressivity, data-efficiency, and trainability of methods that leverage invariance and equivariance.

10:30 AM DS06.04.06

Predicting Dynamics in Sodium Silicate Glasses using Graph Neural Networks[RasmusChristensen](#), [LisbethFajstrup](#) and [MortenM. Smedskjaer](#); Aalborg University, Denmark

Understanding the dynamics of atoms in glasses is crucial for unraveling their transport and dynamical properties, but it is challenging to identify the underlying structural features controlling atom dynamics. Recent studies have used machine learning models such as graph neural networks (GNNs) to predict long-term dynamics, but the focus has so far been on model systems like Kob-Andersen-type Lennard-Jones mixtures. This study extends this approach by using GNNs and molecular dynamics simulations to investigate the dynamics across varying timescales in a realistic system that forms the basis for most industrial glasses, namely sodium silicate glasses. By harnessing the capabilities of graph neural networks, our method provides an effective means for predicting the long-term dynamics of ions in glassy systems based solely on initial atom positions, without relying on handcrafted features. We compare our predictions with those of previously proposed methods. Our findings pave the way for designing glass formulations with tailored dynamical properties.

10:45 AM DS06.04.07

Modeling Phase Transformation in Complex Oxides with Charge-Informed Interatomic Potential[PeichenZhong](#), [BowenDeng](#) and [GerbrandCeder](#); University of California Berkeley, United States

Disordered rocksalt materials represent the most promising earth-abundant cathode materials for Li-ion batteries, potentially enabling the scaling of Li-ion energy storage to numerous TWh/year production. These advanced battery materials often comprise multiple elements and exhibit significant site disorder and structure complexity. Mn-rich DRX cathodes have observed a phase transformation from disorder to partial spinel-like order during charge/discharge cycling. To understand this phenomenon and reveal the underlying physics, we employed atomistic modeling with charge information derived from ab-initio calculations.

CHGNet is a novel machine-learning interatomic potential (MLIP) with atomic charge inference from magnetic moments. The explicit incorporation of magnetic moments allows CHGNet to learn and accurately represent the orbital occupancy of electrons, thereby enhancing its ability to describe both atomic and electronic degrees of freedom. We fine-tuned the pre-trained universal CHGNet within the Li-Mn-Ti-O-F chemical space using high-fidelity DFT calculations. The fine-tuned CHGNet was then applied to $\text{Li}_{1-x}\text{Mn}_{0.8}\text{Ti}_{0.1}\text{O}_{1.9}\text{F}_{0.1}$ DRX system, using charge-informed molecular dynamics to investigate the structural ordering change, charge distribution, and electrochemical properties of the transformed DRX compounds.

11:00 AM DS06.04.08

Scaling Up Equivariant Potentials: From Fragments Towards Exascale Simulations[AlbertMusaelian](#)¹, [AndersJohansson](#)¹, [SimonBatznner](#)¹ and [BorisKozinsky](#)^{1,2}; ¹Harvard University, United States; ²Robert Bosch Research and Technology Center, United States

Great progress in accuracy and data efficiency has been made in machine learning interatomic potentials (MLIPs) thanks to equivariant models, which leverage the symmetries of the underlying physics to learn rich geometric representations. But while MLIPs have long promised to bring ab-initio accuracy to calculations that could not possibly be conducted with methods like DFT, the need for representative training data from quantum methods has often restricted MLIPs' application too far from the regimes in which DFT is practical. Further, architectural limitations in the most accurate models have impeded their scaling and speed.

In this talk, we present recent developments on how Allegro—a machine learning architecture we recently developed to retain the benefits of equivariance while omitting previous schemes, like message passing, that limit computational performance—can scale to larger length-scales, longer time-scales, larger datasets, and scale up from fragments to complex systems. In particular, I will discuss techniques to improve simulation stability and thus the ability to run long timescale simulations; speed optimizations including variable cutoffs and a simplified multi-path tensor product; and how the Allegro architecture facilitates scaling model capacity for diverse, large data. Indications of its ability to scale up from large databases of fragments to complex systems never seen in the training data will be demonstrated using an example in biochemistry.

11:15 AM DS06.04.09

Machine Learned Interatomic Potential for Atomic Simulation of Dislocation in Ceramics[ShihaoZhang](#) and [ShigenobuOgata](#); Osaka University, Japan

Dislocations in ceramics are rapidly catching interest owing to their exciting application potential for dislocation toughening of intrinsically brittle ceramics and functional property tailoring, and thus are now perceived as promising atomic-scale entities for next generation device applications [1-3]. However, understanding at the atomic scale of the dislocation behaviors in ceramics is still lacking. The traditional empirical interatomic potential of ceramics usually suffers the bad transferability and low accuracy. In this work, we reported the development of machine learned interatomic potential for the atomic simulation of dislocation in ceramics, i.e., zinc oxide (ZnO), gallium nitride (GaN), and strontium titanate (SrTiO_3), yielding ab initial accuracy and large-scale atomic simulation (millions of atoms). The machine learned interatomic potentials describe well the core structure and slip barrier of dislocation in these ceramics comparing with the results of first-principles calculation and experiment. Finally, the indentation-induced dislocation nucleation and propagation in ceramics were studied using the developed

interatomic potential, in good agreement with the nanoindentation experimental results. This study not only demonstrates the effectiveness of machine learned interatomic potentials in the analysis of plastic deformation of ceramic materials, but also provides new insights into the dislocation-dominated deformation behavior of ceramics. Authors acknowledge the JSPS Postdoctoral Fellowships for Research in Japan (Standard) and the Grant-in-Aid for JSPS Research Fellow Grant No. 22F22056.

References

- [1] M. Höfling, et al. Control of polarization in bulk ferroelectrics by mechanical dislocation imprint. *Science*, 2021, 372(6545): 961-964.
- [2] M. Kissel, et al. Enhanced Photoconductivity at Dislocations in SrTiO₃. *Advanced Materials*, 2022, 34(32): 2203032.
- [3] L. Porz, et al. Dislocation-toughened ceramics. *Materials Horizons*, 2021, 8(5): 1528-1537.

11:30 AM DS06.04.10

Vibrations for Free: Fast Calculations of Vibrational Free Energies in Solid Solutions with Machine Learned Force Fields Kasper Tolborg and Aron Walsh; Imperial College London, United Kingdom

Alloys and solid solutions form an integral part of modern-day technology ranging from structural materials to semiconductors and catalysts. Recent years have seen a renewed interest in compositionally complex materials with the advent of high entropy alloys and compounds [1]. First principles calculations of their compositional phase diagrams can significantly aid the design and understanding of these complex materials.

Compositional phase diagrams are typically calculated from first principles using cluster expansion methods, in which effective cluster interactions are fitted to internal energies of a set of representative configurations calculated from density functional theory (DFT). Configurational entropy is then incorporated through Monte Carlo simulations at longer length scales. Despite calculations showing that vibrational entropic contributions are important [2], these effects are largely neglected due to their computational cost, and when included they are typically based on approximate bond-length-bond-strength relations [3].

Here, we introduce a method for fast calculations of vibrational free energies from machine learned force fields (MLFF). For cluster expansion construction, a large series of structural relaxations are performed, but only the final energies are used. Here, we use the energies, forces and stresses already available from these geometry relaxations to train an MLFF for a given solid solution, which is benchmarked against DFT lattice dynamics simulations. With this force field in hand, we perform lattice dynamics calculations and extract vibrational free energies for each configuration from which we construct a temperature dependent cluster expansion model.

We apply our method for simple solid solutions and demonstrate predictions of phase diagrams in significantly improved agreement with experiments. This paves the way for easy calculations of vibrational free energies of solid solutions allowing for more realistic predictions of materials thermodynamics from first principles [4].

- [1] A. Ferrari, F. Körmann, M. Asta, J. Neugebauer, *Nat. Comput. Sci.*, 2023, **3**, 221-229
- [2] A. van de Walle, G. Ceder, *Rev. Mod. Phys.*, 2002, **74**, 11-45
- [3] W. Shao, S. Liu, J. Llorca, *Comput. Mater. Sci.*, 2023, **217**, 111898
- [4] K. Tolborg, J. Klarbring, A. Ganose, A. Walsh, *Digital Discovery*, 2022, **1**, 586-595

11:45 AM DS06.04.11

Defect Density Minimization in ALD Passivation Layers by Bayesian Optimization Sinan OzgunDemir^{1,2}, GülDogan^{1,3}, UtkuCulha^{1,4}, KahramanKeskinbora¹ and MetinSitti^{1,5,6}; ¹Max Planck Institute for Intelligent Systems, Germany; ²University of Stuttgart, Germany; ³Robert Bosch GmbH, Germany; ⁴Technical University of Munich, Germany; ⁵ETH Zürich, Switzerland; ⁶Koc University, Turkey

Atomic layer deposition (ALD) is a highly efficient and effective method for providing conformal coating to sensitive materials and related surfaces, such as integrated circuits. While ALD has demonstrated its applicability across a wide range of materials and geometries, it is also crucial to achieve defect-free layers for better corrosion protection. This objective is heavily influenced by a multitude of fabrication parameters, resulting in a high-dimensional and cross-correlated parameter space that renders conventional optimization techniques impractical. To address this challenge and optimize the process parameters, we propose a probabilistic machine learning approach utilizing Bayesian Optimization (BO) with Gaussian Processes (GPs). Our approach leverages BO's data-efficient learning scheme to identify the optimal deposition parameters in just three iterations, leading to defect minimization in an ALD-Al₂O₃ passivation layer. Furthermore, our methodology enables the analysis of the impact of each process parameter on defect density, thereby providing insights into which parameters should be tuned for improved performance under varying conditions.

The presented study showcases the time and cost efficiency of optimizing ALD layers using our proposed approach. Our findings highlight the effectiveness of Bayesian Optimization in material science and fabrication technologies, offering a valuable tool for optimizing diverse materials and processes.

SESSION DS06.05: Machine Learning for Simulation of Materials II

Session Chairs: Mathieu Bauchy and Tess Smidt

Tuesday Afternoon, November 28, 2023

Sheraton, Second Floor, Back Bay A

1:45 PM *DS06.05.01

Using Reinforcement Learning for Manipulating and Synthesizing Thin Films Benjamin Smith¹, Anahita Khojandi¹, Ayana Ghosh², Sergei V. Kalinin¹, Eva Zarkadoulou², Panchapakesan Ganesh² and Rama K. Vasudevan²; ¹The University of Tennessee, Knoxville, United States; ²Oak Ridge National Laboratory, United States

Recent progress in reinforcement learning (RL), and in particular the combination of traditional RL methods with deep neural networks for function approximation, has resulted in tremendous advances in gameplay and sequential decision-making tasks. However, the applications of RL to materials simulation has been limited and best, largely due to difficulties stemming from the very large data requirements for traditional RL.

Here, we explore the application of RL within simulations and experiments, focused on the manipulation of structures within ferroelectric materials. We show that utilizing RL agents, it is possible to learn optimal defect positioning within a lattice-based ferroelectrics simulation environment modeled with nearest neighbor interactions. Investigation of the agent's policy reveals underlying information about the length scales of interactions between defects in the simulation. We then proceed to a more complex molecular dynamics environment of the synthesis of Tellurene, and proceed to run thousands of simulations of deposition of Te to assemble into Tellurene, and then employ off-policy RL to learn appropriate actions to maximize the crystallinity and target phase of the resultant structure. Finally, results on manipulation of materials experimentally with RL implemented on a microscope are discussed, with a view towards the need for better integrating simulations in such design and characterization workflows. This work was supported by Center for Nanophase Materials Sciences (CNMS), which is a US Department of Energy, Office of Science User Facility at Oak Ridge National Laboratory.

2:15 PM DS06.05.02

BroGNet: A Graph Neural SDE for Learning Brownian Dynamics Suresh Bishnoi, Jayadeva Jayadeva, Sayan Ranu and N M Anoop Krishnan; Indian Institute of Technology Delhi, India

Neural networks (NNs) that exploit strong inductive biases based on physical laws and symmetries have shown remarkable success in learning the dynamics of physical systems directly from their trajectory. However, these works focus only on the systems that follow deterministic dynamics, for instance, Newtonian or Hamiltonian dynamics. Here, we propose a framework, namely Brownian graph neural networks (BroGNet), combining stochastic differential equations (SDEs) and GNNs to learn Brownian dynamics directly from the trajectory. We theoretically show that BroGNet conserves the linear momentum of the system, which in turn, provides superior performance on learning dynamics as revealed empirically. We demonstrate this approach on several systems, namely, linear spring, linear spring with binary particle types, and non-linear spring systems, all following Brownian dynamics at finite temperatures. We show that BroGNet significantly outperforms proposed baselines across all the benchmarked Brownian systems. In addition, we demonstrate zero-shot generalizability of BroGNet to simulate unseen system sizes that are two orders of magnitude larger and to different temperatures than those used during training. Altogether, our study contributes to advancing the understanding of the intricate dynamics of Brownian motion and demonstrates the effectiveness of graph neural networks in modeling such complex systems.

2:30 PMBREAK

3:00 PM DS06.05.03

Neural Network Potential for Arbitrary Combination of 72 Elements Trained Against Large Scale Dataset SoTakamoto and ChikashiShinagawa; Preferred Networks, Inc., Japan

The development of neural network-based interatomic potentials has garnered growing interest in recent years. The field is rapidly progressing due to the availability of large datasets and aims to address challenging issues, including predicting complex phenomena such as chemical reactions and multi-component systems.

We have developed a neural network potential called PFP (Preferred Potential) Version 0, which can be applied to arbitrary combinations of 45 elements. Our in-house developed NNP architecture and datasets allow PFP to be applied to a wide range of substances with a single model, without the need for separate training for each specific system. In our previous publication, we demonstrated PFP's capabilities by applying it to a diverse range of materials systems, including a Li-ion battery cathode material, metal-organic frameworks, phase transition of Cu-Au alloys, and catalyst search for the Fischer-Tropsch reaction.

Continuing to develop the PFP architecture and dataset, we have spent 1,650 GPU years creating a dataset composed of 33 million DFT-calculated atomic structures. The latest PFP version, v4.0.0, supports 72 elements, which make up over 99.9969% of all materials on Earth and covers a majority of the periodic table. We have confirmed that the new version of PFP reproduces energy surfaces with better accuracy when compared to its previous version. In particular, we have demonstrated significantly improved reproducibility of the energy ordering of bulk crystal structures. This gives us accurate composition phase diagrams of multi-element mixtures.

We believe that our work in developing a universal potential applicable to a broad range of phenomena will greatly accelerate computer-based materials discovery.

3:15 PM DS06.05.04

Absorption and Dynamics of Gas Molecules in Metal-Organic Frameworks: Application of a Universal Neural Network Potential TakuWatanabe, HirokiIriguchi and AkihiroNagoya; Preferred Computational Chemistry Inc., Japan

Metal-organic frameworks are a class of nanoporous materials with extensive chemical and structural diversity deemed to hold promise in a variety of applications. One of the critical challenges of MOFs is their stability against chemical species present in the environment. Many of the MOFs are known to be unstable even to the humidity in the air. There have been extensive theoretical and experimental studies on the investigation on water-stable MOFs.

The development of machine learning potentials is rapid and becoming increasingly popular in the field of molecular simulations. They are becoming applicable to a wide range of materials including alloys, oxides, sulfides, surfaces, and molecules. However, the tremendous diversity of chemical and physical diversity of MOFs presents challenges to be modeled accurately. Preferred Potential (PFP) implemented on MatlantisTM is a recently developed neural network potential with its unique feature of universality even compared to other existing machine learning potentials.

In this paper, we present our study on the detailed examination of the chemical reactions leading to the degradation of selected MOFs using PFP. Some of the MOFs do indicate clear degradation pathways upon exposure to humidity under specified conditions. IRMOF-1 (a.k.a MOF-5) is well-known for its sensitivity to humidity at room temperature. Molecule dynamics simulations showed that IRMOF-1 remains stable under a mildly high temperature of 400 K with an external strain. Even under the highly humid condition of 8 wt.% water, the structure remains stable at room temperature for the simulation of 2 ns. Clear degradation was observed at high temperatures and strained conditions under high humidity. Other selected MOFs were also tested under the same simulation condition but some of them did not exhibit any degradations. The observed trend of stability is consistent with the known trend in the literature.

We also examine the trends in the preferred adsorption sites of gas species using grand canonical Monte Carlo simulations. Since PFP can treat both chemisorption and physisorption in a unified fashion, the adsorption behavior can be correctly captured regardless of the type of molecular interactions. For instance, MOF-74 contains open metal sites when properly dehydrated, and they play important roles in the interactions with guest molecules. Such hydration/dehydration behavior can be correctly captured without employing a highly tailored reactive potential. With this capability, the impact of the presence of defects in the MOF is examined and elucidated. Finally, we will discuss the implications of these characteristics to practical applications.

3:30 PM DS06.05.05

Equivariant Neural Network Potentials for Modelling Dynamics and Structure of Oxide Supported Metal Nanoparticles CuauhtémocN. Valencia, MathiasS. Nissen, WilliamB. Lomholdt, Matthew HelmiLeth Larsen, ThomasW. Hansen and JakobSchiotz; Technical University of Denmark, Denmark

Molecular Dynamics (MD) simulations require a model for the interatomic interactions that is both accurate and computationally inexpensive. Density Functional Theory (DFT) offers good accuracy and decent computational performance for small systems, and *ab-initio* molecular dynamics (AIMD) is now possible based on DFT. However, many simulations require system sizes and/or simulation times that makes AIMD impossible.

Machine learning potentials can be used to generate inter-atomic potentials for specific systems, with accuracy close to that of DFT and computational efficiency close to that of classical interatomic potentials [1]. While such machine learning potentials have been used to extend the size and time scale of MD simulations to obtain adequate sampling of structures and thermodynamical properties, they suffer from the need of very large training sets and are dependent on the quality of the rotationally invariant descriptors used as input to the neural networks [2]. Some of these problems can be relieved with Equivariant Neural Networks, where vector quantities can be used directly as input to the network, and then processed in a rotationally equivariant way by the network.

We use equivariant neural networks to simulate catalytic metal nanoparticles supported by metal oxides, focusing on two independent scientific problems. First, we studied the heat transport between gold nanoparticles and TiO₂ support and show that the interface acts as a barrier for heat transport. This barrier determines the amount of heating that a nanoparticle undergoes when irradiated by the beam of an electron microscope and is therefore of paramount importance for understanding and limiting beam damage and beam influence in high-resolution electron microscopy.

Secondly, we investigated how the lattice mismatch between platinum nanoparticles and the substrate relaxes in the interface, and how this influences the stress on the surface of the nanoparticle. Platinum is the main catalyst for the oxygen reduction reaction in fuel cells, and the catalytic activity is very sensitive to the strain of the platinum surface [3], which may be manipulated by using the right substrate.

We tested both the NequIP [4], a message-passing equivariant graph neural network, and Allegro [5], a strictly local equivariant graph neural network by the same group of authors. We found that NequIP produced slightly superior performance, and as we did not need the strict locality for parallel large-scale MD we chose to proceed with NequIP. We initially trained the networks with data from small AIMD simulations of similar systems. We then use a committee of five neural network potentials to evaluate the uncertainty of MD simulations and augment the training set with structures that are poorly described. In this way we obtain neural network potentials that are both transferable and reliable, and with the possibility of gauging their accuracy using query by committee.

REFERENCES:

- [1] S. K. Natarajan and J. Behler. Neural network molecular dynamics simulations of solid-liquid interfaces: Water at low-index copper surfaces, *Phys. Chem. Chem. Phys.* **18**, 28704 (2016).
- [2] A. E. G. Mikkelsen, *et al.* Is the water/Pt(111) interface ordered at room temperature? *J Chem Phys* **155**, 224701 (2021).
- [3] M. Escudero-Escribano, *et al.* Tuning the activity of Pt alloy electrocatalysts by means of the lanthanide contraction. *Science* **352**, 73–76 (2016).
- [4] S. Batzner *et al.* E(3)-equivariant graph neural networks for data-efficient and accurate interatomic potentials. *Nat. Commun.* **13**, 2453 (2022).
- [5] A. Musaelian *et al.* Learning Local Equivariant Representations for Large-Scale Atomistic Dynamics, arXiv:2204.05249

3:45 PM DS06.05.06

Strategic Optimization of Deep Learning Potentials to Model Catalyst Dynamics SumanBhasker Ranganath and JohannesVoss; SLAC National Accelerator Laboratory, United States

Machine learning interatomic potentials (MLIPs) trained on quantum mechanical simulation datasets are promising to study the evolution of catalytic processes at extended time and length scales, rendering accuracies comparable to the reference method at a reduced cost.¹ MLIPs approximate the underlying potential energy surface (PES) by learning solely on the correlation between the atomic coordinates and energies, forces in the training dataset. The potentials optimized via appropriate active learning schemes could be applied to identify unexplored regions of the PES, for example to predict novel catalyst morphologies, binding configurations, reaction pathways, and to further model their evolution at specific thermodynamic conditions.² However, strategies to optimize MLIPs through incremental dataset expansion guided by relevant uncertainty metrics in an active learning framework are not well recognized.

In this work, a minimal structured dataset is compiled by accounting for the factors commonly encountered in catalysis to train a base artificial neural network (ANN) potential. The atomic positions and energies from single point calculations using density functional theory, of the smallest model metal surface-adsorbate interface is transformed to training set using Chebyshev

descriptor implemented in aenet.³ We propose a strategy to educate the models on forces based on displacements of selective atoms. The trained base potential predicts energies, forces, and binding strengths of both relaxed and unrelaxed larger unit cells with average RMS errors of 4 meV/atom, 0.15 eV/Å, and 0.1 eV/atom respectively.

It gets challenging to apply the model, for example to predict catalyst dynamics at reaction conditions, as its ability to extrapolate to regions beyond the trained (near) equilibrium datapoints of the PES is very limited. We employ deep ensembles⁴ to investigate possible uncertainty driven active learning protocols to upgrade the base model. The spread in predicted energies, forces between the ensemble members correlates with the errors with respect to reference values⁵ when a reliable data splitting strategy is used to train the ensemble, and hence is used as a metric to ascertain uncertainty bounds. An apt solution is offered to generate effective ensemble members trained on extended datasets. Strapping an ANN ensemble with tools such as molecular dynamics allows for effective sampling of the configuration space.⁶ A better approximation of the PES is attained by iterative retraining of the ensemble on highly uncertain datapoints of the explored configuration space. Influence of the choice of uncertainty drivers on the evolution of deep ensemble potentials will be discussed. Approaches to further equip the ensemble, on the levels of both data as well as ANN model will be presented.

1. J. Behler, *Angew. Chemie - Int. Ed.* 56 (2017) 12828.
2. J.R. Kitchin, *Nat. Catal.* 1 (2018) 230.
3. N. Artrith, A. Urban, G. Ceder, *Phys. Rev. B* 96 (2017) 1.
4. K. Tran, W. Neiswanger, J. Yoon, Q. Zhang, E. Xing, Z.W. Ulissi, *Mach. Learn. Sci. Technol.* 1 (2020) 025006.
5. A.A. Peterson, R. Christensen, A. Khorshidi, *Phys. Chem. Chem. Phys.* 19 (2017) 10978.
6. M. Kulichenko, K. Barros, N. Lubbers, Y.W. Li, R. Messerly, S. Tretiak, J.S. Smith, B. Nebgen, *Nat. Comput. Sci.* 3 (2023) 230.

4:00 PM DS06.05.07

Modelling Phase Transformations and Diffusion in Doped Na-Ion Conductors using Machine Learned Interatomic PotentialsJohanKlarbring^{1,2} and AronWalsh¹; ¹Imperial College London, United Kingdom; ²Linköping University, Sweden

Machine learned interatomic potentials (MLIP) have become an indispensable tool in computational materials science, promising to extend the accessible length and timescales of *ab initio* molecular dynamics (AIMD), while retaining an accurate description of the relevant interactions. The last decade has seen a tremendous increase in the accuracy, data efficiency and scalability of the MLIPs. Consequently, their applications are being pushed towards increasingly complex materials and phenomena.

Here, we present an application of the Allegro [1] MLIP, a recently developed local E(3)-equivariant graph neural network potential, to a set of promising Na-ion conductors based on sodium thiophosphate, Na₃PS₄ [2]. Specifically, we study the Na_{3-x}Sb_{1-x}W_xS₄ system, where aliovalent W-dopants are introduced along with charge-compensating Na-vacancies in order to facilitate Na-ion diffusion. Describing this system and the relevant physical phenomena using an MLIP will require it to describe (1) the diverse local chemical environments of an alloy, (2) ionic diffusion and (3) structural phase-transformations.

In the talk, we showcase how the trained Allegro MLIP performs on this demanding set of tasks. In particular, we use large scale MD simulations to accurately reproduce the known tetragonal-to-cubic phase transformations, including the decrease of the critical temperature, T_c, with increasing W-concentration. We discuss the origin of this decrease in T_c, and the experimentally proposed differences between the local and average structure of the cubic phase [3]. We further show results on properties related to Na-ion diffusion and compare them to experimental and AIMD based results from the literature.

- [1] *Nature Communications*, 14, 579 (2023)
- [2] *J. Mater. Chem. A*, 9, 5134–5148. (2021)
- [3] *JACS* 145 (13), 7147-7158 (2023)

4:15 PM DS06.05.08

Using Symmetry-Equivariant Neural Networks (ENNs) to Uncover Symmetry-Implied Missing InformationElyssaHofgard¹, RayWang^{2,1} and TessSmidt¹; ¹Massachusetts Institute of Technology, United States; ²University of California, San Diego, United States

In this talk, we demonstrate how Symmetry-Equivariant Neural Networks (ENNs) can identify sources of symmetry breaking in diverse physical data and uncover symmetry-implied missing information unbeknownst to the researcher. Symmetry and symmetry-breaking is crucial for understanding complex physical systems (e.g. phase transitions in materials and the discovery of the neutrino). Physical systems adhere to Curie's Principle—stating that when effects show certain asymmetry, this asymmetry must be found in the causes that give rise to them. ENNs are built to preserve symmetry and thus obey the same principles [3].

Recorded data can appear to deviate from strict symmetry constraints, so recent studies emphasize the importance of relaxing equivariance to balance model bias with capturing complex patterns [4-6]. Here, we present a complementary approach showing that fully equivariant models can be used for real-world problems where symmetry may be broken due to some noise, external forces, or other asymmetries in the environment. We benchmark our against state-of-the-art approximately equivariant networks in [4]. These methods can be applied to materials science, where approximate symmetry commonly arises due to structural defects, strain, or phase transitions. Understanding and characterizing these deviations from perfect symmetry are crucial for investigating material properties and behavior.

- [1] T. E. Smidt, "Euclidean Symmetry and Equivariance in Machine Learning," *Trends in Chemistry* 3, 82 (2021).
- [2] M. Geiger and T. Smidt, "e3nn: Euclidean Neural Networks," <http://arxiv.org/abs/2207.09453>.
- [3] T. E. Smidt, M. Geiger, and B. K. Miller, Finding Symmetry Breaking Order Parameters with Euclidean Neural Networks, *Phys. Rev. Research* 3, L012002 (2021).
- [4] R. Wang, R. Walters, and R. Yu, "Approximately Equivariant Networks for Imperfectly Symmetric Dynamics," <https://arxiv.org/abs/2201.11969> (2022).
- [5] M. Finzi, G. Benton, and A.G. Wilson, "Residual Pathway Priors for Soft Equivariance Constraints," doi: 10.48550/arXiv.2112.01388 (2021).
- [6] S. d'Ascoli, H. Touvron, M. Leavitt, A. Morcos, G. Biroli, and L. Sagun, "ConViT: Improving Vision Transformers with Soft Convolutional Inductive Biases," doi: 10.48550/arXiv.2103.10697 (2021).

4:30 PM DS06.05.09

Scalable Parallel Algorithm for Graph Neural Network Potentials in Molecular Dynamics SimulationsYutackPark, JaesunKim and SeungwuHan; Seoul National University, Korea (the Republic of)

Machine-learned potentials have emerged as a preferred method for addressing the scale limitations inherent in *ab initio* molecular dynamics (MD) simulations. Early-stage machine-learned potentials utilized invariant, atom-centered descriptors to encode the atomic environment. Recently, however, attention has been drawn to graph-based neural network interatomic potentials (GNNs), especially those of the equivariant type. These GNNs generally surpass descriptor-based models in accuracy and can efficiently manage multi-component systems. However, the message propagation in GNNs inherently makes them challenging to integrate with spatial decomposition, a conventional parallel algorithm used in MD. To the best of our knowledge, no GNN package currently supports distributed-memory parallelism in MD. Consequently, the length scale that GNNs can study is restricted by the memory size of a single processor. In implementing spatial decomposition of GNNs, two problems arise when two atoms connected by a graph edge belong to different processors. The first problem occurs when inferring the atomic energy using the GNN. The message-passing layers in the GNN require atomic features of connected atoms, which become inaccessible due to spatial decomposition. The second problem arises when calculating the atomic forces by automatic differentiation derivatives of the energy (for instance, Autograd module in PyTorch). Force calculation requires gradient information of neighbor atoms, necessitating non-trivial evaluation and communication of partial derivatives of disconnected edges. To address these issues, we present SEVENN (Scalable EquiVariance-Enabled Neural Network), an implementation of a parallel algorithm that integrates GNNs with spatial decomposition. The baseline GNN model is the same as NequIP, and we employed the LAMMPS package for spatial decomposition. To optimize the parallel implementation, we have included a communication routine for GNNs with multiple GPUs, leveraging NVIDIA GPU Direct[®] technology for fast inter-GPU communication.

To assess the parallelization efficiency of our algorithm, we conducted MD simulations for SiO₂ up to 100,000 atoms on A100 GPU clusters. We tested up to 5 message passing layers and 32 GPUs, where intensive communication of atomic features and gradient information between processors occurs in each message passing layer. SEVENN demonstrated over 80%-90% parallel efficiency when scaling the number of atoms proportionally with the number of GPUs. This result indicates that the simulation using SEVENN can be linearly scaled up to accommodate a large number of atoms. We believe that this study paves the way for the application of GNNs in large-scale simulations.

8:00 PM DS06.06.01

Optimization of Aluminum Frame Design for Commercialization of Perovskite Tandem Solar Modules: A Deep Learning Surrogate Model Approach Dong-woon Han and Seongtak Kim; Korea Institute of Industrial Technology, Korea (the Republic of)

Perovskite cells have a lower manufacturing cost and higher efficiency compared to conventional silicon cells. However, perovskite materials are vulnerable to heat and moisture. Using only perovskites leads to a short lifespan, making commercialization challenging. Therefore, development of perovskite-silicon tandem cells, as an intermediate stage, is ongoing for commercialization purposes. On the other hand, in the silicon solar cell market, the size of wafers used in solar cell manufacturing is increasing, leading to larger module sizes. However, when applying the conventional aluminum frame, sagging can occur due to its own weight and external pressure. If the cells deform under the load, it can lead to an increase in dead cells due to internal cracks and damage, resulting in a decrease in charging rate and efficiency. Therefore, in this study, we conducted frame design optimization for large-area modules to facilitate the commercialization of perovskite tandem solar modules. We established five factors to determine the configuration of the commercial aluminum frame. We generated a total of 243 cases with 5 factors at 3 levels each using experimental design methodology. The module was assumed to use M10 cells with a power rating of 585W. We applied a wind pressure of 2,400Pa to the front area of the module and performed finite element analysis taking into account the self-weight. The stress and amount of deflection shown in the cell and frame were confirmed. Subsequently, we utilized artificial intelligence to train on the results of the finite element analysis, generating a surrogate model capable of mimicking the interpretation outcomes. As a result, we designed an aluminum frame for the module that minimizes deflection and weight under the applied load.

8:00 PM DS06.06.02

Data-Driven & Multiscale Approaches to Characterize & Optimize the Manufacturing Process of Powder Compaction Sangil Hyun, Jinhwa Park, Ga-Ae Ryu and Yoonsoo Han; Korea Institute of Ceramic Engineering and Technology, Korea (the Republic of)

For computer simulations to characterize the powder compaction, a continuum approximation approach based on the Drucker-Prager Cap model has been widely used for manufacturing various shapes of ceramic powder-based devices. The model can effectively describe the effective physical properties required for various individual materials and complex manufacturing processes. However, some realistic parameters required in this empirical model are limited to obtain by experimental methods due to inaccurate and highly-costed measurements on various specific conditions. To minimize these limitations, we developed a virtual data-generating scheme based on the multiscale analysis of the powder compaction. The homogenization method is introduced to determine the effective properties of the powder from a theoretical model of particle size distributions, and applied to a macroscopic continuum limit. In addition, we developed a digitized and automatic workflow accompanying these multi-scale simulation techniques to characterize and optimize the powder compaction process. This virtual data-driven design method can automatically generate the required data by adjusting process variables to provide optimal shapes or conditions for the desired requirements.

In this work, we introduce an automatic generation platform of virtual data for the press forming process under various manufacturing conditions for optimal design. In the wide range of manufacturing technology based on powder materials, this multiscale and data-driven approach can accelerate the optimal process for complex geometry and operating conditions. The ceramic manufacturing platform (called *VECTOR*) is developed to provide the optimization digital tools customized for fundamental study as well as industrial needs.

8:00 PM DS06.06.03

Exploration of New Materials for Nonlinear Optical Crystals using Materials Informatics Kosuke Shirai¹, Tomoyuki Tamura¹ and Ming-Hsien Lee²; ¹Nagoya Institute of Technology, Japan; ²Tamkang University, Taiwan

Recently, materials design approaches that introduce materials informatics have become extremely important in materials science. MI methods can accelerate the design of new materials by using machine learning to predict physical properties with accuracy comparable to density-functional-based first-principles calculations and with computational speeds an order of magnitude faster.

Among them, the Atomistic Line Graph Neural Network (ALIGNN) [1], which considers distance and angle information, has been shown to significantly improve feature representation between atoms and prediction accuracy. However, there is a tradeoff between prediction accuracy using deep learning such as ALIGNN and the number of training data. For many practical materials, it is difficult to obtain sufficient prediction accuracy because of the small amount of property data that is available, due to computational costs. In this study, we introduce transfer learning into ALIGNN to construct a sufficiently accurate property prediction model on a small data set by pre-training on a large amount of property data already obtained from databases and other sources.

Nonlinear optical materials are promising materials that have an important role in expanding the wavelength range of lasers.

Among them, there is an urgent need to develop ideal materials that simultaneously satisfy a wide band gap, a large second harmonic generation (SHG) susceptibility, and an appropriate birefringence. Nonlinear optical susceptibility and birefringence can be obtained by electric field calculations using density functional perturbation theory, but they remain computationally expensive.

Therefore, in this study, we predict nonlinear optical susceptibility and birefringence from a small data set by using ALIGNN and transfer learning.

ALIGNN and transfer learning were implemented in PYTORCH [2], a Python library. First, nonlinear optical properties were calculated with the CASTEP code [3] for about 500 structures obtained from the Inorganic Crystal Structure Database (ICSD) [4] including B and Ge. Then, thousands to tens of thousands of structural data and properties (band gap, refractive index, DOS) data that are close to the composition of the 500 structures were obtained from the Materials Project Database (MPD) [5] as pre-training data and prediction models were constructed for each of them. We predicted the nonlinear optical susceptibility and birefringence by training only the final layer of the optimized ALIGNN model. Finally we screened from various compositions and structures by using the predictive models of nonlinear optical properties constructed.

[1] Choudhary, K., DeCost, B. Atomistic Line Graph Neural Network for improved materials property predictions. *Npj Comput Mater* 7,185(2021).

[2] Paszke, A., Gross, S., Massa, F., Lerer, A., Bradbury, J., Chanan, G., ... Chintala, S. (2019). PyTorch: An Imperative Style, High-Performance Deep Learning Library. In *Advances in Neural Information Processing Systems* 32 (pp. 8024–8035).

[3] "First principles methods using CASTEP", *Zeitschrift fuer Kristallographie* 220(5-6) pp. 567-570 (2005) S. J. Clark, M. D. Segall, C. J. Pickard, P. J. Hasnip, M. J. Probert, K. Refson, M. C. Payne

[4] NIST Inorganic Crystal Structure Database, NIST Standard Reference Database Number 3, National Institute of Standards and Technology, Gaithersburg MD, 20899

[5] Anubhav Jain, Shyue Ping Ong, Geoffroy Hautier, Wei Chen, William Davidson Richards, Stephen Dacek, Shreyas Cholia, Dan Gunter, David Skinner, Gerbrand Ceder, Kristin A. Persson; Commentary: The Materials Project: A materials genome approach to accelerating materials innovation. *APL Mater* 1 July 2013; 1 (1): 011002.

8:00 PM DS06.06.04

Physics-Controlled Data Perturbation for One-Shot High-Fidelity Data Reconstruction Hadi Mansourifar, Ling Chen, Jaydeep Thik, Yuqing Zhou, Paul Schmalenberg, Ercan M. Dede and Debasish Banerjee; Toyota Research Institute of North America, United States

High-fidelity design is essential to capture intricate details, optimize performance, and understand local phenomena within many scientific disciplines, including materials simulation. Nevertheless, obtaining such data experimentally is often challenging and time-consuming. To address this issue, low-fidelity data are calculated as a computationally efficient alternative. Afterward, high-fidelity reconstruction is performed using the deep learning approaches. However, due to the limitations in obtaining a large number of low/high fidelity pairs for training generative models, one-shot learning is inevitable in this context. This paper introduces a novel idea for high-fidelity one-shot reconstruction based on physics-controlled data perturbation. The proposed approach leverages well-known partial differential equations (PDEs) with 2D solutions, like the heat equation and Burgers equation, to perturb low/high fidelity paired simulations for augmenting new data pairs. In fact, the proposed PDE-based perturbation technique reduces the need for a vast collection of paired data to efficiently train a generalizable generative model via synthesizing data variations from single, high/low fidelity paired inputs.

Our experimental results show that physics-controlled data perturbation can easily outperform traditional data augmentation in a one-shot high-fidelity reconstruction task. By leveraging the knowledge embedded in different PDEs and their solutions, we enable the generation of out-of-boundary augmented data for training a more generalizable generative model. The experimental results demonstrate the efficacy of our approach, showcasing its potential for enhancing high-fidelity reconstruction in various material research applications.

8:00 PM DS06.06.05

Evaluate Deep Learning Discrepancies Between High Fidelity and Low Fidelity Simulations PrachiGarg¹, ShaonDas¹, KristoferG. Reyes^{2,1} and BaishakhiMazumder¹; ¹University at Buffalo, The State University of New York, United States; ²Brookhaven National Laboratory, United States

Utilization of deep learning (DL) models has shown promising results in extraction of structural information from complex, three-dimensional atomistic data obtained from Atom Probe Tomography (APT). The primary requirement for DL models is a substantial amount of training data. To overcome this limitation, we propose the use of simulated training data. However, an open question arises regarding the level of accuracy (fidelity) that the synthetic training data should possess.

The objective of this research is to investigate the relationship between the fidelity of synthetic training data and the performance of the DL model when applied to real APT data. By varying the fidelity of the synthetic data, we assess the impact on the accuracy and reliability of the DL model's structural predictions. Through our findings, we aim to provide insights into the optimal fidelity requirements for synthetic training data to achieve accurate and robust results when analyzing real APT data. This research contributes to the advancement of DL-based approaches for extracting valuable structural information from atomistic data, enhancing our understanding of complex materials, and enabling more precise analysis in various scientific fields.

8:00 PM DS06.06.06

Machine Learning Approach to Time-Series Analysis of SARS-CoV-2 Spike Glycoproteins under Varying pH and Temperature Conditions ParthJain^{1,2}, MelvinThu^{3,2}, ZiyuanNiu², MiriamRafailovich² and YuefanDeng²; ¹Bergen County Academics, United States; ²Stony Brook University, The State University of New York, United States; ³Great Neck North High School, United States

As the SARS-CoV-2 pandemic persists, it's vital to evaluate how environmental factors such as temperature and pH affect the virus's molecular structure. Molecular dynamics (MD) simulations are commonly used to study nanoscale interactions. However, their computational complexity limits their suitability for larger-scale, longer-term modeling. Our research focuses on developing a machine learning (ML) approach that leverages supervised training on SASA (solvent accessible surface area) MD simulation data to predict properties of SARS-CoV-2 spike glycoproteins (S-proteins). SASA quantifies the accessible surface area around a protein, which plays a crucial role. Changes in these values over time provide insights into protein stability, folding behavior, and the virus's pathogenicity under specific conditions.[1]

We performed MD simulations of the S-protein using GROMACS. The protein structure (PDB: 6VXX) was modeled with the CHARMM27 force field. The explicit solvent was represented by a 20x20x20 nm³ box (SPC/E water model) at 1.02 g/cm³ density. The simulation was conducted at 37°C, with energy minimization via steepest descent. We employed canonical (NVT) and Parrinello-Rahman pressure coupling (NPT) methods with a 2 fs time step.

We denoised and processed data using Fast Fourier Transforms (FFT) to convert time-series SASA data into a frequency domain, enabling the identification of cyclic patterns. ML models, including k-Nearest Neighbors (k-NN), Long Short-Term Memory Neural Networks (LSTMs), and Convolutional Neural Networks (CNNs), are subsequently trained on 1,500 ns of MD SASA data to predict changes as a function of time. This large dataset allowed us to thoroughly test each model's performance across varying sample sizes. Prior research has indicated that larger datasets enhance the accuracy of the k-NN model.[2] LSTMs were also chosen to provide a contrasting approach to the k-NN and CNN models, which are known for their higher sensitivity in extracting categorical features and capturing patterns in data.[3] We ran the ML models on SASA data of the S-protein at temperatures of 3°C, 20°C, and 37°C and pH values of 1, 2, 3, 4, and 5, and used an 80-20 train-test split. The k-NN model demonstrated the greatest accuracy in forecasting simulation data out of three models, whereas the LSTM model performed poorly, likely requiring more training data to make accurate predictions. In the future, in vitro experiment results will be able to validate the accuracy of the ML models for long-term predictions and their efficacy as a replacement for computationally expensive MD simulations.

[1] Ali, S., et al. "A review of methods available to estimate solvent-accessible surface areas of soluble proteins in the folded and unfolded states." *Current protein & peptide science* vol. 15,5 (2014): 456-76. doi:10.2174/1389203715666140327114232

[2] Liang, D., Song, M., Niu, Z. et al. Supervised machine learning approach to molecular dynamics forecast of SARS-CoV-2 spike glycoproteins at varying temperatures. *MRS Advances* 6, 362–367 (2021). <https://doi.org/10.1557/s43580-021-00021-4>

[3] Liew, S., et al. (2016). Gender Classification: A Convolutional Neural Network Approach. *Turkish Journal of Electrical Engineering and Computer Sciences*. 24. 1248-1264. 10.3906/elk-1311-58.

SESSION DS06.07: Machine Learning for Simulation of Materials III

Session Chairs: Mathieu Bauchy and Binqun Luan

Wednesday Morning, November 29, 2023

Sheraton, Second Floor, Back Bay A

8:00 AM DS06.07.01

Efficient Crystal Structure Prediction using Universal Neural Network Potential and Genetic Algorithm TakuyaShibayama, HideakiImamura, KatsuhikoNishimura, ChikashiShinagawa and SoTakamoto; Preferred Networks, Inc., Japan

Crystal Structure Prediction (CSP) based on quantum chemistry calculations is used to discover new materials in various materials fields. However, its applicability is limited by its massive computational cost. An accurate and universal machine learning potential would greatly reduce the computational cost and enable CSP to investigate a wide range of realistic materials. We have developed a CSP system using the versatile and efficient NNP named Preferred Potential (PPF). The latest version, PPF v4.0.0, has been released with improved accuracy, enabling more precise CSP studies.

Our CSP system uses PPF and genetic algorithms (GA) to perform local optimization and evaluation of 10,000 samples within an hour using 100 GPUs (equivalent to 10,000 GPU hours). We modified the GA implemented in the Atomic Simulation Environment (ASE) library by extending the sampling algorithms, as well as mutation and crossover. We improved the GA sampler by considering the similarities between CSP and multi-objective optimization problems, and expanded the non-dominated sorting genetic algorithm II (NSGA-II) for crystal structure search, which is specifically designed for multi-objective optimization. To manage trials effectively and in parallel, we employed Optuna, an open-source software framework for hyperparameter optimization.

We performed CSP search for several binary systems and evaluated new crystal candidates using density functional theory (DFT) calculations. More than 10 structures are confirmed as newly found inorganic crystals, which break known convex hulls of the Materials Project database. The new crystals are discovered in systems such as Ti-O, Li-In, Ca-P, and Mg-Pd. More than 50% of the candidate structures suggested by the CSP system using PPF were confirmed by DFT calculations. These results demonstrate the effectiveness of PPF and GA-based CSP in accelerating materials discovery and design. We have also tested our CSP system on a high-performance computing environment using the MN-Core deep learning accelerator, which provided comparable performance to the NVIDIA V100 GPU.

8:15 AM DS06.07.02

Property-Structure-Process Relationship Trees and Contextual Understanding of Scientific Manuscripts using Large Language Models of Artificial Intelligence MaciejTomczak¹, DanielCieslinski¹, PaydenBrown², YangJ. Park², JuLi² and StefanosPapanikolaou¹; ¹National Centre for Nuclear Research, Poland; ²Massachusetts Institute of Technology, United States

The ever expanding corpus of scientific manuscripts contains vast amount of knowledge and descriptions of various experimental settings. As new articles are published daily, it is impractical for any single individual to grasp all that information. However, for each manuscript, the scientific human mind further trains a tree of connections between Properties (eg. hardness, strength, conductivity of materials), Structures (eg. crystalline type, defect content, composition) and Processes (eg. annealing, cold work). This tree of PSPs represents the human strategy for dimensional reduction in processing scientific manuscripts, and requires to quickly and efficiently find required information in the published works and compare it with similar texts or other sources.

Recent advancements in natural language processing (NLP) have given rise to high-performing foundation models, in particular large language models (LLM) such as OpenAI's GPT-4. These powerful models are capable of complex tasks such as text summarization and creative content generation. However, utilization of these models comes at a significant computational cost and contextual understanding is commonly limited. In this work, we develop small and efficient fine-tunable models for capturing PSPs in scientific manuscripts, using Elsevier's database. We

also propose to incorporate the Retrieval Augmented Generation (RAG) approach alongside our fine-tuning methods for ensuring a more robust and reliable model for capturing PSPs in scientific manuscripts.

We investigate the statistics of various ways of fine-tuning LLMs, and also extract PSPs in pre-defined sets. Using texts focused only on nuclear materials research from Journal of Nuclear Materials, we evaluate LLMs of different sizes and different strategies to determine their suitability as knowledge bases for scientists.

8:30 AM DS06.07.03

Atomistic Insights into CO Oxidation on Pt Single Crystals with Machine-Learned Force Fields and Spectroscopy [Clare Y. Xie](#)¹, [Cameron J. Owen](#)¹, [Gengnan Li](#)², [Anibal Boscoboinik](#)² and [Boris Kozinsky](#)¹; ¹Harvard University, United States; ²Brookhaven National Laboratory, United States

Dynamic mechanistic insights into CO oxidation are crucial for optimizing catalyst design and controlling chemical conversion processes, especially for reactions like water-gas-shift (WGS). Several experimental investigations have demonstrated oscillatory behavior in this reaction, wherein the local coverage of chemisorbed O or CO can lead to markedly different reactivity. However, atomistic insight to confirm this hypothesis is inaccessible given the spatial and temporal resolutions of experimental techniques. Coupling this with the poor scaling of ab initio methods means that the mechanisms governing this disparate behavior cannot be determined with (1) atomic resolution, and (2) under proper time- and length scales for comparison to experiment. Understanding CO oxidation in this context is essential for gaining fundamental insights into the mechanisms governing chemical conversion at surfaces, and ultimately providing guidance for effective catalyst design and operating procedures. Therefore, accelerated computational methods that retain high accuracy are necessary to resolve the structure-performance relationship of these catalytic systems.

In this work, we investigate the mechanisms of CO oxidation on Pt(111) and Pt(100) surfaces using reactive molecular dynamics (MD) simulations powered by machine-learned force fields coupled with spectroscopic experiments. We employ the FLARE code, which accelerates sampling of expensive ab initio training data via its active-learning module, which can then be used to train a MLFF for use in production MD. The model is first validated against theoretical benchmarks on the coverage effects and site dependency of CO adsorption on Pt(111) and Pt(100), and subsequently used to study the transient kinetics of CO oxidation reactions as a function of temperature and relative coverage of CO and O. In addition to revealing the timescales of these processes, our simulations provide direct insight into the dominating mechanisms when either CO or oxygen is covering the surface. Moreover, we show that our MLFF is capable of capturing mesoscopic reconstruction of the Pt(100) surface, which is also modulated via exposure to these adsorbates.

We compare our findings with experimental results from operando spectroscopy and spectrometry, where the oscillatory behavior in CO oxidation is observed through pulsing CO on Pt(111) and Pt(100) with O₂ in the background. Our work thus provides atomistic understanding of the structure-performance relationship of the Pt(111) and Pt(100) surfaces in CO oxidation, which is crucial for optimizing the design of catalysts and developing better control strategies for optimal reaction conditions.

8:45 AM DS06.07.04

Applying Virtual Reality Technology and Neural Network Potentials for Molecular Dynamics Simulations in Industrial R&D [Katsuhisa Yoshida](#), [Teruo Hirakawa](#) and [Yoshihige Okuno](#); Research Center for Computational Science and Informatics, Resonac Corporation, Japan

Neural Network Potentials (NNP) is a cutting-edge technique in computational materials science. This method employs atomic-level potentials learned from the ab-initio method to efficiently perform reactive molecular dynamics (MD) simulations with many atoms. As a result, NNP-MD can consider complex chemical systems such as organic-inorganic interfaces with water solvents.

However, analyzing the results of calculations with the software on a simple computer display, as in classical MD simulations, is difficult due to the large number of atoms involved in NNP-MD simulations. This difficulty has limited the analysis of MD calculations to the statistical level, even though atomistic-level observations are essential for understanding the origin of phenomena. Overcoming this limitation is essential for efficient academic research and industrial research and development (R&D).

To address this problem, we have employed virtual reality (VR) technology with a head-mounted display to analyze classical MD trajectories at an atomic scale, such as the motion of molecules at the interface of an inorganic substrate. VR technology not only assists computational science experts in analyzing calculation results but also dramatically supports phenomenological understanding by non-experts. Additionally, we found that VR technology is an effective communication tool between experts and non-experts, which is crucial for accelerating material R&D.

In this study, we apply VR technology to analyze complex catalytic reactions calculated by NNP-MD simulations and study the impact of the combination of VR and NNP-MD on industrial R&D. We employ Suzuki-Miyaura Cross-Coupling in water solvent with an atomically rough Pd substrate surface as an example of a complex chemical system.

By replaying the NNP-MD trajectory in VR, we could identify sites on the Pd substrate where chemical surface reactions occur, approach those reaction points, and observe the reaction step-by-step. As a result, VR proved to be a powerful tool for understanding the multi-step interfacial reactions obtained with NNP-MD. However, we realized that while NNP-MD has the advantage of observing the atomic behavior of chemical reactions, it is difficult to understand the physical origin of the reactions. Therefore, it is necessary to employ ab-initio calculations to gain a deeper understanding of physics.

From an industrial perspective, the combination of NNP-MD and VR should effectively share intuitive images of chemical reactions and accelerate materials R&D, as we have found in the case of classical MD.

9:00 AM DS06.07.05

Analysis of Monolayer to Bilayer Silicene Transformation in CaSi₂F_x (x<1) using Universal Neural Network Potential [Akihiro Nagoya](#), [Taku Watanabe](#) and [Hiroki Iriguchi](#); Preferred Computational Chemistry, Inc., Japan

Silicene is a silicone (Si) counterpart of graphene, a typical two-dimensional (2D) material which consists of a honeycomb structure of carbon. Silicene is predicted to have a Dirac cone-type electronic structure similar to that of graphene, and has been extensively studied as a promising material for ultra-energy-saving, high-mobility devices. In addition, silicene, graphene, and other 2D materials in the form of nanoribbons and nanodots have been investigated for applications in batteries and biological imaging. For practical applications, further development of fabrication techniques for silicene-derived structures is necessary because the monolayer structure is unstable under air due to the lack of vertical sp³ bonds.

Synthesis of 2D materials by chemical exfoliation of three-dimensional (3D) crystals with layered structures is a convenient top-down method. Calcium disilicide (CaSi₂) consists of alternating monolayers of silicene (MLSi) and calcium, where wet-chemical exfoliation can be applied to produce MLSi derivatives. A solid state reaction due to fluorine (F) diffusion into CaSi₂ leads to a phase transformation from MLSi to bi- or tri-layered silicene (BLSi and TLSi) sandwiched between non-conducting CaF₂ layers. This structure prevents exposure to the atmosphere and improves the stability of the materials. The thermodynamic mechanism of the phase transformation was investigated in the previous study using density functional theory (DFT) calculations and cluster expansion for MLSi and BLSi of CaSi₂F_x (0<x<1). However, the analysis of the reaction dynamics, which is important for nano-structure fabrications and battery development, was not feasible due to the high computational cost.

Machine learning potentials have been increasingly applied to various atomistic simulations. The Preferred Potential (PPF) implemented on Matlantis™ is a recently developed graph neural network potential with its unique feature of universality. PPF is trained on large DFT datasets, including not only stable crystals and molecules, but also surfaces and disordered structures. As a result, it is applicable to reaction analysis and molecular dynamics of various materials without compromising accuracy.

In this study, we have applied PPF to analyze the mechanism of the phase transformation of CaSi₂ due to fluorine diffusion. Firstly, the phase stability of CaSi₂F_x in ML and BL structures is studied as a function of the fluorine ratio x. A few hundred of CaSiF_x structures were generated using the *icet* package and the convex hull of the formation energy is evaluated using PPF. The results show that PPF reproduces the previous study using DFT: ML structure becomes unstable with increasing fluorine ratio, and BL structure becomes more stable for x > 0.6. This phase transformation is due to the charge imbalance of the ionic CaSi₂. With increasing electronegative fluorine atoms, strong ionic bonds are formed between F⁻ and Ca²⁺, while the formal charge of Si⁺ becomes neutral. This result indicates that PPF is applicable to our system with DFT accuracy, although the stability depends on both ionic and covalent sp³ electronic nature. Following this result, we have performed molecular dynamics simulations of stable structures on the convex hull. During the MD simulations at 800 K for more than 1 ns, interlayer diffusion of Si atoms are observed at the defects in the layered structure associated with the formation of CaF₂. These results reveal the dynamics of phase transformation of CaSi₂F_x, and demonstrate the accuracy and universality of PPF for materials with variable compositions, such as battery materials, alloys and solid solutions.

9:15 AM DS06.07.06

Accelerating the Discovery of Two-Dimensional Interfaces with Graph Neural Network and Evolutionary Search [Jianan Zhang](#)¹, [Aditya Koneru](#)^{1,2}, [Subramanian Sankaranarayanan](#)^{1,2} and [Carmen M. Lilley](#)¹; ¹University of Illinois at Chicago, United States; ²Argonne National Laboratory, United States

Machine learning (ML) methods have attracted considerable attention in the field of materials science due to their flexibility, accuracy, and efficiency compared to traditional simulation approaches for material discovery. Among the various ML methods available, graph neural networks (GNNs) have emerged as a prominent technique for predicting material properties. This is attributed not only to recent advancements in GNNs but also to the inherent correlation between atomic structures and graphs.

One significant challenge in harnessing the remarkable properties of two-dimensional (2D) materials is the occurrence of defects during synthesis, such as grain boundaries (GBs). Predicting the realistic atomic structure of GBs and their impact on material properties is a complex task that surpasses the capabilities of conventional trial-and-error methods, owing to the vast design space involved.

In this abstract, we propose a combination of GNN and evolutionary search methods to address this challenge. We originally developed a search workflow based on genetic algorithms (GA) for exploring 2D GBs applied to graphene and silicene. The workflow involves transforming GBs into graphs and utilizing graph isomorphism checks to identify multiple material states during the GA searches, and multiple novel silicene GBs were predicted. Separately, we developed a GNN architecture capable of predicting the energy of 2D GB structures, which serves as an efficient and accurate surrogate for computationally expensive quantum mechanical simulations. We utilized datasets generated from quantum mechanical simulations for training and testing the GNN model. The high accuracy of the GNN model on the test set demonstrates its ability to provide reliable estimations of quantum mechanical calculations.

In the work presented here, the research combines the GA search with this GNN surrogate, to fully leverage an automated design search. Using this method, we successfully uncovered previously unreported GBs in blue phosphorene. Additionally, the flexibility of the GNN approach allowed us to generalize the method to other 2D materials, thus expediting the process of discovering novel materials.

9:30 AMBREAK

10:00 AM *DS06.07.07

JARVIS-Leaderboard—A Comprehensive Benchmark of Materials Design Methods[KamalChoudhary](#); National Institute of Standards and Technology, United States

Reproducibility and validation are major hurdles for scientific development across many fields. Materials science in particular encompasses a variety of experimental and theoretical approaches that require careful benchmarking. Leaderboard efforts have been developed previously to mitigate these issues, however, a comprehensive comparison and benchmarking on an integrated platform with multiple data-modalities with both perfect and defect materials data is still lacking. This talk introduces the JARVIS-Leaderboard, an open-source and community-driven platform that facilitates benchmarking and enhances reproducibility. The platform allows users to set up benchmarks with custom tasks and enables contributions in the form of dataset, code, and meta-data submissions. We cover the following materials design categories: Artificial Intelligence (AI), Electronic Structure (ES), Force-fields (FF), Quantum Computation (QC), and Experiments (EXP). For AI, we cover several types of input data, including atomic structures, atomistic images, spectra, and texts. For ES, we consider multiple ES approaches, software packages, pseudopotentials, materials, and properties, comparing results to experiment. For FF, we compare multiple approaches for material property predictions. For QC, we benchmark Hamiltonian simulation using various quantum algorithms and circuits. Finally, for experiments, we use the round-robin approach to establish benchmarks. Currently, there are 1008 contributions to 225 benchmarks using over 100 different methods, and the leaderboard is continuously expanding. The JARVIS-Leaderboard is available at the website: https://pages.nist.gov/jarvis_leaderboard.

10:30 AM DS06.07.08

Probing Structural Heterogeneity of Disordered Materials with Machine Learning Interatomic Potentials and X-Ray Absorption Spectroscopy[WonseokJeong](#), [WenyuSun](#), [LiwenWan](#), [TrevorM. Willey](#), [MichaelH. Nielsen](#) and [Tuan AnhPham](#); Lawrence Livermore National Laboratory, United States

The precise determination of atomic structural information in functional materials holds transformative potential and broad implications for emerging technologies. Spectroscopic techniques, such as X-ray Absorption Near-Edge Structure (XANES), have been widely used for material characterization. However, extracting chemical information from experimental probes often intractable in disordered or heterogeneous systems. We present an integrated approach that combines atomic simulation, machine learning interatomic potentials, data-driven approaches and XANES calculations to investigate the chemical speciation of amorphous carbon nitride systems as a case study. We discuss the development of machine learning potentials that can efficiently explore the vast configurational space of amorphous carbon nitrides. By employing statistical methods, this structural database enables the elucidation of the most representative local structures, including carbon and nitrogen hybridization, and how they evolve with chemical compositions and density. Our simulations indicate that structure of amorphous carbon nitrides is highly complex, exhibiting non-linear and unexpected behavior at medium density and nitrogen concentration. Density functional theory (DFT)-based XANES simulations were carried out to establish a correlation between local structure and spectroscopic signatures. This serves as the basis for both forward and inverse models; the former predicts XANES spectroscopy when provided with macroscopic properties of density and chemical composition, while the latter enables a high-fidelity interpretation of local chemical motifs from experimental measurements. Although our framework is specifically applied to XANES and carbon nitrides, the approach described herein is readily adaptable to other experimental probes and materials classes.

This work was performed under the auspices of the U.S. Department of Energy by Lawrence Livermore National Laboratory under Contract DE-AC52-07NA27344. Funding was provided by LLNL Laboratory Directed Research and Development (LDRD) Program Tracking No. 22-ERD-014.

10:45 AM DS06.07.09

Thermomechanical Properties of SiC Ceramics using Convolutional Neural Network Potentials: An MD Study[MayurP. Singh](#) and [SatishKumar](#); Georgia Institute of Technology, United States

The excellent thermomechanical properties of SiC have made it an attractive material for applications at extreme environment such as space entry vehicles subjected to high temperatures. There has been extensive study and modelling of phases of SiC phases, most popular of which includes the 3C-SiC and 6H-SiC phases. These studies have led to the development of empirical potentials for the SiC phases. MD studies have been performed for studying SiC's properties using these empirical potentials but failed to capture the phase transformations of SiC at various temperatures. Machine Learning potentials are very promising to address this challenge. Neural network potentials (NNPs) have shown great promise at capturing complex physics of interatomic forces with ab-initio accuracy. In this work, we use Convolutional Neural Network potentials trained on DFT computed structures for the various phases of SiC and investigate the variation in thermal expansion coefficients of SiC at various temperatures. Our CNN potentials constructs 3D images of the atomic neighborhood for 3D convolution to predict the forces and energy. We implement this potential into the JAX-MD software package to perform MD simulations to take advantage of the Just-in-Time compilation and native GPU support of JAX-MD.

11:00 AM DS06.07.10

Training Protocol and Applications of Data-Driven Interatomic Potentials Based On Random Structure Searching[WilliamC. Witt](#); University of Cambridge, United Kingdom

Data-driven (or machine-learned) interatomic potentials have become an increasingly vital tool for the computational materials scientist. Created from the results of small quantum-mechanical calculations, such potentials enable first-principles-accurate simulations on unprecedented length- and time-scales. This talk will summarize recent work towards automated production of Atomic-Cluster-Expansion-type potentials, where the training protocol is adapted from the random structure searching approach to atomistic structure prediction.

11:15 AM DS06.07.11

Learning an Ab Initio-Based Bond Order Potential to Investigate Mechanical and Thermal Properties of Bismuthene[Partha SarathiDutta](#)^{1,2}, [AdityaKoneru](#)^{1,2}, [SukritiManna](#)^{1,2}, [AdilMuhammed](#)^{1,2}, [KarthikBalasubramanian](#)^{1,2}, [Troy DavidLoeffler](#)^{1,2}, [HenryChan](#)² and [SubramanianSankaranarayanan](#)^{1,2}; ¹University of Illinois at Chicago, United States; ²Argonne National Laboratory, United States

Bismuthene is a two-dimensional layer of bismuth arranged in a honeycomb lattice configuration. It possesses some unique properties – for example, it is a topological insulator which means it is conductive or allows electrons to flow on the edges but acts as an insulator in its bulk. Also, bismuthene has a direct bandgap, strong light-matter interaction, and its optical properties can be tailored by varying its layer thickness which makes it an exciting candidate for optoelectronics applications. Despite its technological significance, there is a scarcity of models that can accurately describe the structure and energetics of bismuthene. Using a Tersoff formalism and leveraging the recent advances in reinforcement learning, we introduce a potential model that captures the structures and energetics of several different bismuthene polymorphs. The training data consisted of ab-initio calculations of the crystal lattice structure, cohesive energy, equation of state, elastic constants of five polymorphs, and phonon dispersion curve of the most stable low-buckled structure of bismuthene. We deploy our in-house reinforcement learning-based continuous-Monte Carlo Tree Search Algorithm (c-MCTS) because of its suitability to model complex non-linear interatomic interactions and proven performance in solving high-dimensional parameter space optimization problems. The RL-optimized bond order potential model performs well in capturing the crystal lattice structure and energetics of all the polymorphs. It especially gives an excellent prediction of the elastic constants of the low-buckled polymorph and a reasonable agreement between the phonon dispersion predicted by the model relative to the DFT reference training data. The optimal parameters are used to study the mechanical behavior, mechanical performance in electronic or optoelectronic applications, and thermal properties of

bismuthene for applications in microelectronics.

11:30 AM DS06.07.12

Accurate Prediction of Melting Temperatures with Deep-Neural Network Atomistic Potentials [Wissam A. Saidi](#), Christopher M. Andolina and Pandu Wisesa; University of Pittsburgh, United States

Understanding melting behavior is essential for applying and developing a given material under various environmental conditions. Further, elucidating the nature of these materials at extreme states is essential for creating accurate analytical models, from predicting seismological activities to designing high-performance functional materials. While replicating intense temperatures and pressures is known to be experimentally challenging, less is known about the accuracy of first-principles modeling due to the intrinsically low scalability of first-principles methods. Herein, we assess the melting temperature accuracy of first-principle methods accelerated with deep neural network atomistic potentials (DNPs) in various systems, including single-element materials and magnesium oxide. We contrast the DNP results with existing density functional theory and experimental studies. We show that the temperature predictions have significant fluctuations, particularly at higher pressures and similarly for smaller system sizes typically employed by first-principles calculations. We suggest that our flexible approach to developing DNPs can be readily adapted to create specialized DNPs capable of creating robust, versatile potentials that describe solid, liquid, and phase transition from solid to liquid under various extreme conditions.

11:45 AM DS06.07.13

Connectivity Optimized Nested Graph Networks for Crystal Structures Robin Ruff, Patrick Reiser and [Pascal Friederich](#); Karlsruhe Institute of Technology, Germany

Graph neural networks (GNNs) have been applied to a large variety of applications in materials science and chemistry [1]. Here, we recapitulate the graph construction for crystalline (periodic) materials and investigate its impact on the GNNs model performance. We suggest the asymmetric unit cell as a representation to reduce the number of atoms by using all symmetries of the system. This substantially reduced the computational cost and thus time needed to train large graph neural networks without any loss in accuracy. Furthermore, with a simple but systematically built GNN architecture based on message passing and line graph templates, we introduce a general architecture (Nested Graph Network, NGN) that is applicable to a wide range of tasks [2]. We show that our suggested models systematically improve state-of-the-art results across all tasks within the MatBench benchmark [3]. Further analysis shows that optimized connectivity and deeper message functions are responsible for the improvement. Asymmetric unit cells and connectivity optimization can be generally applied to (crystal) graph networks, while our suggested nested graph framework will open new ways of systematic comparison of GNN architectures.

[1] Reiser, P., Neubert, M., Eberhard, A., Torresi, L., Zhou, C., Shao, C., Metni, H., van Hoesel, C., Schopmans, H., Sommer, T. and Friederich, P., 2022. Graph neural networks for materials science and chemistry. *Communications Materials*, 3(1), p.93.

[2] Ruff, R., Reiser, P., Stühmer, J. and Friederich, P., 2023. Connectivity Optimized Nested Graph Networks for Crystal Structures. arXiv preprint arXiv:2302.14102.

[3] Dunn, A., Wang, Q., Ganose, A., Dopp, D. and Jain, A., 2020. Benchmarking materials property prediction methods: the Matbench test set and Automattminer reference algorithm. *npj Computational Materials*, 6(1), p.138.

SESSION DS06.08: Machine Learning for Simulation of Materials IV

Session Chairs: Kamal Choudhary and Grace Gu

Wednesday Afternoon, November 29, 2023

Sheraton, Second Floor, Back Bay A

1:45 PM DS06.08.01

Using Machine-Learning Assisted Design for Reduction of the Quantum Decoherence in Room-Temperature Integrated Quantum Photonics [Pablo A. Postigo](#); University of Rochester, United States

The development of on-chip, CMOS-compatible quantum photonics is critical for future scalable quantum communications, quantum computing, and quantum sensing. Integrated photonic waveguides, photonic resonators, and single-photon emitters are essential building blocks for such a purpose. In this talk, I will present how machine learning (ML) can enhance the quantum properties of these building blocks, specifically the indistinguishability (I) of the generated single photons, with a further decrease in quantum decoherence. The model has been numerically evaluated through finite-difference time-domain (FDTD) simulations, showing consistent results. Also, we explored a hybrid slot-Bragg nanophotonic cavity to generate indistinguishable photons at RT from various quantum emitters through a combination of numerical methods. To relax the fabrication requirements (slot width) for near-unity I , we used an ML algorithm that provides the optimal geometry of the cavity. [1] Finally, we have developed a theory for estimating I in a two-emitter system with strong dephasing coupled to a single-mode cavity. We have derived an analytical expression of I as a function of the distance between the emitters, cavity decay rate, and pure dephasing rate. The results show how the requirements of the cavity for high I change with the strength of the dipolar interaction. We propose a new interpretation of the I value, which allows us to estimate its behavior with larger systems (i.e., systems with more than two emitters). We performed numerical simulations of five dipole-coupled emitters to find the optimal configuration for maximum I . For the optimization process, we developed a novel ML scheme based on a hybrid neural network (NN)-genetic algorithm (GA) to find the position of each emitter to maximize I . [2] The optimization procedure provides perfect I (i.e., $I = 1$) in arbitrary low Q cavities, offering relaxation of the cavity parameters and favoring emission from quantum emitters at room T.

References:

[1] J. Guimbao et al. *ACS Photonics* (2022), 9, 6, 1926-1935.

[2] J. Guimbao et al. *Nanomaterials* 2022, 12(16), 2800

2:00 PM DS06.08.02

Lattice Thermal Conductivity of Pb-Te Alloy System with Neural Network Potential [Wen Jay Lee](#)¹, Nan Yow Chen^{1,2}, Kuan Peng Chen¹, Wei Chun Tang², You Yi Lin², Kuo Ping Liao², Wei Chieh Zeng Chien², Yu Chieh Lo², Nien Ti Tsou² and An Cheng Yang^{1,2}; ¹National Center for High-Performance Computing, Taiwan; ²National Yang Ming Chiao Tung University, Taiwan

Thermoelectric materials are a category of substances capable of producing electrical power through temperature gradients. The efficiency of these materials is often assessed using the dimensionless thermoelectric figure of merit, $Z = S^2 \sigma \kappa^{-1}$, is calculated from the Seebeck coefficient (S), Electrical conductivity (σ), and thermal conductivity (κ). Improving the electrical transport properties has proven successful by manipulating carrier concentration and employing dopants, while reducing lattice thermal conductivity can be achieved through the introduction of defect and the creation of nanostructures. This study employs molecular dynamics simulations to calculate the lattice thermal conductivity. To enhance the reliability of these simulations, we have developed an innovative Pb-Te force field utilizing machine learning techniques. The forthcoming presentation will show the results of the lattice thermal conductivity across various temperature.

2:15 PM DS06.08.03

Dissociation of CO₂ and CO on MgO (001) Surface as Described by Machine Learning Based Atomistic Potentials [Christopher M. Andolina](#)¹ and [Wissam A. Saidi](#)^{1,2}; ¹University of Pittsburgh, United States; ²National Energy Technology Laboratory, United States

The use of heterogeneous catalysis for dissociating carbon dioxide (CO₂) is a research endeavor of substantial interest in energy conversion and environmental protection. In particular, the dissociation of CO₂ on metal oxide surfaces has received considerable attention due to their potential for mitigating greenhouse gas emissions by converting CO₂ into value-added chemicals (e.g., carbon monoxide). Magnesium oxide (MgO) is a promising candidate for CO₂ dissociation due to its high basicity and stability under high-temperature and high-pressure environments. However, the detailed mechanism of CO₂ dissociation on MgO surfaces remains poorly understood. We aim to elucidate CO₂ dissociation on MgO surfaces using DeepPMD-kit with DeepPot-SE approach atomistic potentials. We leverage the high fidelity of these potentials with the much lower computational costs to density functional theory to accurately describe adsorption energies, chemical energy barriers, and extensive supercell molecular dynamics simulations at various temperatures and monolayer compositions. Further, expanding machine learning atomistic potentials to model catalytic processes on the atomic scale will improve chemical insight into these abundant materials' (MgO or other oxides) role in critical industrial and environmental applications.

2:30 PM BREAK

3:30 PM DS06.08.04

Capturing Short-Range Order in High-Entropy Alloys with Machine-Learning Potentials[YifanCao](#), KillianSheriff and RodrigoFreitas; Massachusetts Institute of Technology, United States

Chemical short-range order (cSRO) is recently reported to strongly influence the mechanical properties of various high-entropy alloys (HEA). However, the intricate nature of cSRO has made it challenging for current machine-learning potentials (MLP) to capture this feature, and many proposed approaches lack quantitative analysis of MLP performance on this task. In this work, we propose a generalized strategy to construct first-principles training databases and effectively train MLPs capable of characterizing cSRO in HEAs. We demonstrate this strategy by quantitatively analyzing the MLP performances in reproducing cSRO effects in various properties of CrCoNi HEA, including defect properties and phase stability.

3:45 PM DS06.08.05

Autonomous Molecular Diffusion Agent using Deep Reinforcement Learning[TianSang](#), Ken-ichiNomura, RajivK. Kalia, AiichiroNakano and PriyaVashishta; University of Southern California, United States

Diffusion in solids is known to be a slow process and often becomes a rate limiting process in key chemical reactions. Unlike crystalline solids where dislocations and grain boundaries offer well-defined "diffusion highway," the lack of similar structural motifs in amorphous or glassy materials poses a great scientific challenge. Transition State Theory is widely used approach to explore the complex energy landscape and reaction kinetics, however obtaining an accurate reaction coordinate depends on the system of interest and often requires domain expert knowledge. To tackle this problem, we have developed Molecular Autonomous Pathfinder (MAP) framework based on Deep Reinforcement Learning (RL) technique. Our framework employs Deep Q-Network architecture and distributed online learning to asynchronously collect experiences sampled by multiple RL agents. After training MAP agents, they provide atomistic configurations and the energy profile of efficient diffusion pathways. Subsequently, we apply time-parallel nudged elastic band method to refine the corresponding diffusion time. In this talk, I will discuss recent applications of MAP framework on molecular diffusion in silicates and polymeric materials.

4:00 PM DS06.08.06

Comparison of an RL-Trained Model for Silicene with State-Of-The-Art Physics-Based and ML Models[Partha SarathiDutta](#)^{1,2}, AdityaKoneru^{1,2}, AdilMuhammed^{1,2}, SukritiManna^{1,2}, KarthikBalasubramanian^{1,2}, HenryChan², Troy DavidLoeffler^{2,1} and SubramanianSankaranarayanan^{1,2}; ¹University of Illinois at Chicago, United States; ²Argonne National Laboratory, United States

Silicene is a promising two-dimensional material consisting of a single layer of silicon, has a honeycomb lattice configuration, and has many similarities with graphene. Silicene has potential applications in transistors, flexible optoelectronic applications, energy storage, catalysis, sensors, quantum computing, spintronics, etc. There exist many potential models to perform dynamical simulations of Silicene. However, most of these models have been trained to a limited number of ab-initio data and therefore do not capture all the properties of all the Silicene polymorphs. Using a computationally cheap Tersoff formalism, we demonstrate that one can significantly improve upon the existing parameterizations using the advances in ML approaches. The training data for five different polymorphs of Silicene were computed using ab-initio calculations and our objective was to fit the crystal lattice structure, cohesive energy, equation of state, and elastic constants of all the polymorphs as well as the phonon dispersion of the most stable polymorph. We choose an in-house reinforcement learning (RL) based continuous-Monte Carlo Tree Search (c-MCTS) to solve this complex, non-linear, high-dimensional, multi-objective problem and get the optimum tersoff potential parameters. The optimization problem involves a trade-off between exploitation (navigating local search space of parameters for better fitting) and exploration (searching unexplored search space with the hope of getting better parameters). We use a reward mechanism wherein the reward was decided based on the agreement between the target property and the predicted property for a given set of potential model parameters. Our RL-trained potential parameters improve upon the performance of several existing models and adequately describe many of the properties of Silicene. We will discuss and compare the performance of our model with state-of-the-art physics-based and ML models for Silicene. We demonstrate that the RL-trained model performs very well in describing the thermal and mechanical properties of Silicene polymorphs. This opens a plethora of opportunities for studying the mechanical flexibility (for flexible electronics), thermal management, thermoelectric applications, strain engineering (for strain-tailored devices), and nanoelectromechanical systems (NEMS) of Silicene.

4:15 PM DS06.08.07

Exploring Zeolite Interatomic Potentials Through Multi-Reward Reinforcement Learning[AdityaKoneru](#)^{1,2}, HenryChan², SukritiManna^{2,1}, Troy DavidLoeffler¹, DebdasDhabal³, ValeriaMolinero³ and SubramanianSankaranarayanan^{2,1}; ¹University of Illinois at Chicago, United States; ²Argonne National Laboratory, United States; ³The University of Utah, United States

Zeolites belong to a versatile class of materials often used in applications such as catalysis and separations. Despite the advancements in experimental characterization techniques, our understanding of the possible metastable phases and growth mechanisms of zeolites has remained elusive. Molecular dynamics is a useful tool for exploring this vast and diverse materials landscape, but its usefulness relies on accurate interatomic potentials capable of predicting the time evolution and dynamics of zeolite polymorphs. Recently, state-of-the-art machine-learned models like GAP and NNPScan are developed with the use of large datasets (both feasible and hypothetical zeolite polymorphs), which provide an accurate description of structural features and energetics. However, the lack of explicit encoding of physics and limited computational efficiency due to increased model complexity makes them difficult to use in large-scale simulations. On the contrary, there are simple classical models like BKS, CHIK, Soules, Tersoff, ReaxFF that can model a small subset of the diverse zeolite dataset but with more emphasis on experimentally realized structures. In this talk, we present our Multi-Reward Reinforcement Learning (RL) framework and demonstrate its success in building a simple empirical model of silica suitable for long length and time scales simulations. Our framework has navigated the high dimensional potential energy surface of BKS, Soules, Tersoff and achieved accuracy without sacrificing model efficiency.

4:30 PM DS06.08.08

StriderNET: A Graph Reinforcement Learning Approach to Optimize Atomic Structures on Rough Energy Landscapes[VaibhavBihani](#)¹, SahilManchanda¹, SrikanthSastry², SayanRanu^{1,3} and N M AnoopKrishnan^{1,3}; ¹Indian Institute of Technology Delhi, India; ²Jawaharlal Nehru Centre for Advanced Scientific Research, India; ³Indian Institute of Technology Delhi, India

Optimization of atomic structures presents a challenging problem, due to their highly rough and non-convex energy landscape, with wide applications in the fields of drug design, materials discovery, and mechanics. Here, we present a graph reinforcement learning approach, StriderNET, that learns a policy to displace the atoms towards low energy configurations. We evaluate the performance of StriderNET on three complex atomic systems, namely, binary Lennard-Jones particles, calcium silicate hydrates gel, and disordered silicon. We show that StriderNET outperforms classical optimization algorithms and enables the discovery of a lower energy minimum. In addition, StriderNET exhibits a higher rate of reaching minima with energies, as confirmed by the average over multiple realizations. Finally, we show that StriderNET exhibits inductivity to unseen system sizes that are an order of magnitude different from the training system.

4:45 PM DS06.08.09

Predicting the Dynamics of Atoms by a Surrogate Machine-Learned Simulator[MathieuBauchy](#); University of California, Los Angeles, United States

Molecular dynamics (MD) is a workhorse of computational material science. However, the inner-loop algorithm of MD (i.e., numerically solving the Newton's law of motion) is computationally expensive. Here, we introduce a surrogate machine learning simulator that is able to predict the dynamics of liquid systems with no prior knowledge of the interatomic potential or nature of the Newton's law of motion. The surrogate model consists of a graph neural network (GNN) engine that is trained by observing existing MD-generated trajectories. We demonstrate that the surrogate simulator properly predicts the dynamics of a variety of systems featuring very different interatomic interactions, namely, model binary Lennard-Jones system, silica (which features long-term coulombic interactions), silicon (which comprises three-body interactions), and copper-zirconium alloy (which is governed by many-body interactions). The development of machine-learned surrogate simulators that can effectively replace costly MD simulations could expand the range of space and time scales that are typically accessible to MD simulations.

SESSION DS06.09: Machine Learning for Simulation of Materials V
Session Chairs: N M Anoop Krishnan and Kiran Sasikumar
Thursday Morning, November 30, 2023
Sheraton, Second Floor, Back Bay A

8:30 AM DS06.09.01

Graph Neural Networks to Predict Ordering-Dependent Properties from Multicomponent Crystal Structures[JiayuPeng](#), JessicaKaraguesian, JamesK. Damewood, DanielSchwalbe

Multicomponent perovskite oxides are an essential class of inorganic materials with diverse applications, where the ordering of cations can profoundly influence their physical and chemical properties. Unfortunately, the discovery and optimization of such oxides have been significantly hindered by their compositional and structural complexity. State-of-the-art brute-force experimental or computational methods can hardly resolve such complexity efficiently. Even one multicomponent oxide composition can have tens to hundreds of cation orderings, which are too expensive for brute-force high-throughput screening.

To boost the high-throughput screening of multicomponent perovskite oxides, graph neural network models can be used to effectively predict material properties from the connections of atoms in crystal structures, allowing efficient computational discovery over a vast search space. However, while these models have been demonstrated to capture the compositional dependence of material properties across a broad chemical space, it is unclear whether such models can also effectively learn the ordering dependence of similar properties for a given composition. In addition, structures after costly density functional theory (DFT) relaxations have been dominantly used for training and leveraging such graph neural network models, which cannot truly eliminate the prohibitive cost of DFT in high-throughput screening.

In this work, we developed graph neural network models to accurately predict key cation ordering-dependent properties of multicomponent perovskite oxides from DFT-unrelaxed cubic perovskite structures. Essentially, models that infer material properties by indirectly learning the thermodynamics of mixing lead to lower errors than those that predict these properties directly. Moreover, equivariant neural networks better capture the ordering dependence of such properties than their symmetry-invariant counterparts due to their higher expressivity in distinguishing the difference between the coordination environments and symmetries of various orderings. Lastly, using contrastive losses in the training of these models further increases the prediction accuracy by facilitating an optimal balance between capturing both the compositional and structural dependence of material properties. Overall, this work highlights an effective strategy for designing machine learning models with optimized robustness and generalizability for discovering multicomponent materials.

8:45 AM DS06.09.02

Screening for the Effect of Material Stability and Flexibility in Metal-Organic Frameworks for Gas Adsorption PropertiesChanghwanOh, ShuwenYue, AdityaNandy and GianmarcoTerrones; Massachusetts Institute of Technology, United States

Metal-organic frameworks (MOFs) are promising materials with diverse applications, including gas separation and storage. Their reticular nature consisting of inorganic secondary building units and organic linkers allow vast combinatorial design space. There exist many hypothetical MOF databases, but their stability in real-world applications is often unknown. Therefore, we use virtual high-throughput screening of hypothetical MOF database to search vast combinatorial space and find optimal MOFs that are stable and have optimal gas adsorption properties. This study consists of two parts: 1) training machine learning (ML) models for MOF stability and 2) investigating the effect of MOF flexibility in gas adsorption. We use bulk modulus as an indicator of mechanical stability and utilize molecular mechanics to calculate bulk moduli of hypothetical MOFs. We train and test ML models for predicting bulk moduli of MOFs and identify the key features governing high mechanical stability for MOFs. We also investigate the effect of flexibility of MOFs in gas adsorption, since the behavior of guest molecules within MOFs is significantly influenced by the flexible degrees of freedom, such as breathing, swelling, and linker rotation. Additionally, the adsorbed guest molecules have been observed to impact framework motion and pore size. However, in many molecular simulation studies of MOFs, the framework is assumed to be rigid to reduce computational costs. To understand how framework motion influences guest molecule behavior, we present a quantitative assessment focusing specifically on the linker rotation while keeping all other modes of framework motion constant. Through this study, we provide a range of property values, such as diffusivity and gas working capacity, that indicate the uncertainty of guest molecule behavior associated with linker rotation.

9:00 AM DS06.09.03

Multi-Scale Modeling of Plasticity with Machine Learning AlgorithmsArmandJ. Barbot^{1,2}, HisashiKashima¹ and RiccardoGatti²; ¹Kyoto University, Japan; ²Universite Paris-Saclay, ONERA, CNRS, Laboratoire d'étude des Microstructures, France

In crystals, plasticity is governed by dislocations, extended linear defects unavoidably present in the atomic structure. While in most crystalline systems, plasticity is governed by the multiplication of pre-existing dislocation, nucleation of dislocations is the leading mechanism in the plastic deformation of small crystalline systems (below 100-200 nm, such as metallic and semiconductor nanopillars, nanowires, nanofilms and nanoparticles). In addition, nucleation can play an important role in hindering cracks propagation by blunting the crack tip. To model and to predict nucleation of dislocation, Molecular Dynamics (MD) is a suitable tool, but it has the drawback of being limited to size of few dozens of nanometers. To simulate plasticity in larger systems, mesoscale simulations, such as the Discrete Dislocation Dynamics method (DDD) [1], are also developed. This method focuses on the evolution and interactions of the dislocation lines without considering each individual atom. This allows to simulate systems from up to 10-20 μ m. However, there is yet no reliable model able to implement the nucleation of heterogeneous dislocations, i.e. occurring at the surface of the material, for systems larger than a few dozens of nanometers, inaccessible by MD simulations. Implementing this phenomenon at mesoscopic scale would allow a better understanding of sub-micrometer crystal plasticity and crack propagation.

Here, we propose a multi-scale approach to implement the nucleation of heterogeneous dislocations at the mesoscopic scale from MD simulations data. We focused here on developing a nucleation criterion, obtained by training a machine learning (ML) algorithm with MD data, to nucleate a dislocation in mesoscopic simulations.

We built our database deforming with MD for Nickel (Ni) crystals of different sizes and shapes (from 1000 to 100000 atoms and with cubic and Wulf-like shapes) imposing a uniaxial compression along (001), tracking dislocation nucleation events in each simulation (nucleation occurs when a drop in potential energy-strain curve is observed). The choice of Ni was motivated by the reliability of its potential, however the proposed method is compatible with any potential. From this, we train a machine learning model to predict dislocation nucleation from: (i) the strain (ii) the potential energy (iii) the system size (i.e., the number of atoms) and (iv) the image of the initial shape of the system.

As the system is deformed, the model performs, at every applied strain interval of $\Delta\gamma=0.0004$, predictions of whether or not a nucleation will occur during the next strain interval. Our model attains a total accuracy of 74% and is able to predict 75% of nucleation events. In practice, 82% of the nucleation predictions are estimated earlier than the ground truth. It means that on average, the model begins to predict the following nucleation of dislocation at an applied strain of $\gamma=0.005$ before it actually occurs.

While we are working to improve the predictions by using a PINN approach, our model reliably predicts most of the nucleation events and can be already used as a nucleation criterion for mesoscopic simulations.

In conclusion, we developed a machine learning-based criteria which will allow from MD simulation data to know when to implement a nucleation of dislocation in mesoscopic simulation. This project is supported by a JSPS Grant-in-Aid for JSPS fellow (Grant No. 22F22708).

References :

1) B. Devincere et al., (Paris: Presses de l'Ecole des Mines de Paris) (2011)

9:15 AM DS06.09.04

Forward and Inverse Fuzzy Analysis for the Nonlinear Transient Heat Transfer ProblemsRuifeiPeng and YiyangLiu; Shenyang Institute of Automation, Chinese Academy of Sciences, China

Driven by the insufficiency investigation of nonlinear transient heat transfer problems with fuzzy uncertain parameters, this paper attempts to present efficient numerical approaches for the forward and inverse fuzzy analysis of nonlinear transient heat transfer problems. The inverse fuzzy problem is formulated as a series of α -level strategy-based inverse interval problems, which are described by optimization problems and are solved utilizing particle swarm method. Forward interval analysis required in inverse interval analysis is conducted by solving two optimization problems via modified coordinate search algorithm. To alleviate heavy computational burden, dimension-adaptive sparse grid (DSG) surrogate is embedded in optimization process. The surrogate is constructed on a solid platform of high fidelity deterministic solutions, which is provided by finite element method and temporally piecewise adaptive algorithm. Eventually, membership functions of fuzzy parameters can be obtained by fuzzy decomposition theorem with interval bounds acquired at each of α -sublevels. Parallelization is realized for the construction of DSG and implementation of particle swarm method for a further computation reduction. Various numerical tests are provided to verify the effectiveness of proposed approaches, and the proposed results agree well with reference.

9:30 AM DS06.09.05

Transfer Learning in Machine Learning for Materials Science: Enhancing Predictions and DiscoverySatadeepBhattacharjee¹, KishalayDas², PritamDas³, PawanGoyal², Seung-CheolLee⁴ and NiloyGanguly²; ¹Indo Korea Science and Technology Center, India; ²Indian Institute of Technology Kharagpur, India; ³Kookmin University, Korea (the Republic of); ⁴Korea Institute of Science and Technology, Korea (the Republic of)

Transfer learning, a powerful machine learning technique, has revolutionized materials science research by enabling the development of accurate predictive models for various material properties [1,2]. In this presentation, two different transfer learning-based works [3,4] will be presented, focusing on addressing the specific challenges in materials science applications.

The first part is a semi-supervised machine learning approach to predict hydrogen storage capacity in metal hydrides. To overcome data scarcity and high feature dimensionality, transfer learning is achieved through an autoencoder. By using elementary features, the autoencoder effectively learns a compact and informative latent space, thus capturing essential features of the data. A multi-layer perceptron (MLP) is then employed to predict the hydrogen storage capacity based on the learned representations. Physically significant features and Pearson correlation functions are included to identify materials with improved storage capacity. The predictions made by the combined autoencoder-MLP model are validated by density functional theory-based calculations and show the potential of transfer learning in accelerating the development of new and efficient materials for hydrogen storage.

In the second study, we showcase transfer learning in conjunction with a graph neural network where we introduce CrysXPP [4], a deep-learning framework designed to rapidly and accurately predict electronic, magnetic, and elastic properties of diverse materials. Addressing the challenge of limited property-tagged datasets, transfer learning is harnessed through an intelligently designed autoencoder named CrysAE. By effectively capturing crucial structural and chemical properties from a large collection of crystal graph data, CrysAE significantly reduces prediction errors. Additionally, a feature selector is incorporated to enhance the interpretability of the model's predictions. Notably, CrysXPP consistently outperforms conventional density functional theory (DFT) methods when provided with limited experimental data. Extensive experiments are used to determine the importance of various design steps in the model. In addition, we make available to the research community the large pre-trained model CrysAE, which allows researchers to refine it with small, property-annotated data sets and achieve superior performance in various applications with limited data sources.

References

- [1] Yamada H, Liu C, Wu S, Koyama Y, Ju S, Shiomi J, Morikawa J, Yoshida R. Predicting materials properties with little data using shotgun transfer learning. ACS central science. 2019 Sep 30;5(10):1717-30.
- [2] Feng S, Fu H, Zhou H, Wu Y, Lu Z, Dong H. A general and transferable deep learning framework for predicting phase formation in materials. Npj Computational Materials. 2021 Jan 25;7(1):10.
- [3] Das P, Lee Y.-S, Lee S.-C, Bhattacharjee S, A semisupervised approach for predicting the hydrogen storage capacity for the metal hydrides, (Manuscript under preparation)
- [4] Das K, Samanta B, Goyal P, Lee SC, Bhattacharjee S, Ganguly N., CrysXPP: An explainable property predictor for crystalline materials. npj Computational Materials. 2022 Mar 18;8(1):43

9:45 AMBREAK

10:15 AM DS06.09.06

Predicting Solvent-Dependent Optical Properties of Organic Molecules using Machine Learning with Physics-Based Descriptors Eric M. Collins, Hadi Abroshan, Mathew D. Halls and Anand Chandrasekaran; Schrödinger, United States

The development of optoelectronic materials has garnered substantial interest due to its wide range of potential applications, including organic light-emitting diodes (OLEDs), bioimaging, and fluorescent dyes. Thus, understanding and controlling the optical and photophysical properties of chromophores and fluorophores are important in both industrial and academic research across various disciplines. By leveraging physics-based simulations, researchers have made significant strides in the rational design of organic materials with specific photophysical characteristics, such as high photoluminescence quantum yields (PLQY) and control over the absorption and/or emission wavelengths. However, the computational methods employed to compute these excited-state properties, such as time-dependent density functional theory (TD-DFT), face challenges due to their high computational cost and scaling limitations, rendering them inadequate for large-scale screening of organic materials. Additionally, many of these properties are solvent-dependent, introducing further complexity to accurately model these compounds in solution. To overcome these challenges, this work aims to develop accurate quantitative structure-property relationship (QSPR) models to efficiently predict the photophysical behavior of organic compounds. We utilize an extensive collection of optical properties of over 20,000 organic chromophore-solvent pairs derived from scientific literature and databases to train our models. We evaluated both traditional and deep-learning QSPR models and identified models which can make accurate predictions by considering molecular descriptors of both the chromophore and the solvent. To further enhance the generalizability and predictive power of our models, we incorporated physically relevant descriptors derived from density functional theory (DFT) calculations. By developing machine learning models that are both accurate and informed by fundamental physical principles, we enable efficient screening of optical and photophysical properties for the design of novel materials.

10:30 AM DS06.09.07

High-Throughput Electronic Structure Prediction of Materials using Machine-Learned Extended Hückel Tight-Binding Models Suvo Banik^{1,2}, Qunfei Zhou³, Sri Lok Srinivasan², Subramanian Sankaranarayanan² and Pierre T. Darancet²; ¹University of Illinois at Chicago, United States; ²Argonne National Laboratory, United States; ³Northwestern University, United States

Accurate knowledge of electronic structures is crucial for high-throughput materials screening and inverse design of materials for many applications, including thermal transport, tunable electronics, and sensing. Electronic structures play a crucial role in determining the magnetic, electrical, and optical responses across different classes of materials, such as transition metals, low-dimensional materials, and especially materials with defects. While first-principles calculations based on Density Functional Theory (DFT) have demonstrated the numerical accuracy required for predicting the electronic structure, the principal challenge lies in their scalability, particularly in systems with heterogeneity and sizes that expand much beyond their unit cell representation, which makes them intractable for high-throughput applications. The Extended Hückel (eH) tight-binding method is a semiempirical quantum chemistry method that can predict a qualitatively correct electronic picture of materials with computational ease and clarity. While earlier studies have demonstrated the efficacy of the eH model in predicting electronic structures (e.g., phases of the Sr-Ti-O family), there is currently no generalized parameterization workflow to accurately parameterize eH tight-binding models across a broad class of materials. In this work, we leverage machine learning to develop a workflow that parametrizes the eH tight-binding model by mapping complex atomic configurations to tight-binding Hamiltonians and comparing them with the DFT-predicted electronic structure from material databases. We demonstrate the efficacy of our workflow in predicting electronic structures across different elemental systems such as C, Ge, Si, and P of different phases and dimensionalities. The predicted Hamiltonian by the parameterized eH model allows us to evaluate the electronic structures of two-dimensional B in the presence of defects and large-scale phase change materials (GexSbyTez) in both crystalline, amorphous, and mixed phases.

10:45 AM DS06.09.08

Understanding Ionomer Membrane Morphology Through Computational Analysis of Small Angle Scattering Experiments and Coarse-Grained Molecular Dynamics Simulations Jason Madinya, Nitant Gupta, Stephen Kronenberger and Arthi Jayaraman; University of Delaware, United States

Ionomer membranes are widely used in fuel cells and water electrolyzers due to their superior mechanical properties and ion transport capabilities. The ion transport within these membranes is dictated by the morphology of the ionomer hydrophilic domains. While it is known that the nanophase structure of these ionomer hydrophilic domains changes with the extent of hydration and other processing techniques, the structural evolution of these domains during processing is not well understood. Small-angle scattering (SAS) measurements are often used to characterize the structure of the membrane at various length scales and provide insights into the structural evolution of the ionomer domains at various conditions. In this talk, I will present ongoing work from the Jayaraman lab that seeks to elucidate the structural evolution of ionomer domains using a physics-based bottom-up (i.e., analysis of simulated structures using molecular models), and a data-driven top-down (i.e., analysis of scattering data) computational approaches.

First, we will describe the top-down approach which involves computational analysis of one-dimensional and two-dimensional small angle scattering profiles to interpret the structure of ionomer hydrophilic domains. Then we will describe the bottom-up computational approach using the Martini 2 coarse-grained model and molecular dynamics simulations to study self-assembly of ionomer chains at varying extents of hydration. These simulations link the ionomer chain design (sidechain placement, dispersity in spacing, backbone length, etc.) to the ionomer hydrophilic domain morphology as well as the distributions of domain sizes and shapes at varying hydration levels. Towards the end of the talk, we will show how we are connecting these bottom-up and top-down approaches to produce a convergent understanding of shapes and sizes of ionomer hydrophilic domains and the molecular packing within these domains.

11:00 AM DS06.09.09

PYSEQM2.0: GPU-Based Fast Semiempirical Mechanics for Ground and Excited States Nikita Fedik, Maksim Kulichenko, Nicholas Lubbers, Kipton Barros, Benjamin Nebgen and Sergei Tretiak; Los Alamos National Laboratory, United States

Recent advancements in atomistic machine learning model have showcased significant progress in chemistry and material science. However, these approaches often face challenges when applied to unexplored regions of chemical space. Interatomic potential models, for instance, lack crucial electronic structure information, often leading to limited transferability. To address these limitations, our research group has been dedicated to developing PYSEQM (Pytorch-based Semiempirical Quantum Mechanics), a differentiable physics model that combines domain knowledge of semiempirical quantum mechanics with machine learning as a corrective tool. Paired with atomistic neural network backend, PYSEQM allows backpropagation through Hamiltonian, replacing atom-type dependent constants with structure-aware parameters generated on-the-fly. This presentation will span the release of PYSEQM2.0 which expands capabilities to excited states through iterative solutions in Krylov subspace and dynamics beyond the ground state. GPU-based batched Davidson algorithm extends simulations to large organic molecules relevant to photovoltaics, organic solar cells and photoinduced processes.

11:15 AM DS06.09.10

Machine Learning Accelerated Computational Design of Materials and Processes[FedorGoumans](#), MattiHellstrom, PaulSpiering, MariaJ. Aliaga and NicolasOnofrio; Software for Chemistry & Materials, Netherlands

Machine learning (ML) can accelerate computational materials research & discovery in several ways, often in complimentary approaches. We will discuss a few directions where we can leverage ML to design new materials and their integrated use in devices and chemical reactors.

The central framework in the Amsterdam Modeling Suite (AMS) enables the exploration of potential energy surfaces (PESs), mechanical, and electronic properties at several levels of theory. The central AMS driver supports advanced PES explorations, molecular dynamics (MD) and Grand Canonical Monte Carlo (GCMC), based on energies and forces from engines. With this driver-engine set up, on-the-fly machine learned potentials such as NeQUIP [1], general purpose and universal graph neural network potentials such as ANI-1ccx [2], M3GNet [3] and CHGNet [4], and can be immediately used to calculate many useful processes and properties such as reaction pathways, viscosity, shear stress, or chemical vapor deposition.

The ParAMS module in AMS provides a comprehensive framework to build training data from DFT engines and optimize ReaxFF and DFTB parameters, with machine learning potentials to follow soon.

With different levels of electronic structure methods available in AMS, we are exploring ML methods to predict properties more efficiently for molecular materials. Examples for OLED applications include training DFTB transfer integrals on DFT data, TDDFT(B) luminescence and excitonic properties on accurate qsGW+BSE calculations, and predicting novel molecules that have the desired optical and electronic properties yielding the best OLED device performance in multiscale simulations.[5]

For catalysis, we can accelerate the multiscale workflow [6] through employing ML for reaction exploration, and by building surrogate models for a faster integration between kinetic Monte Carlo and Computational Fluid Dynamics.

We will briefly discuss where we envision future ML developments to accelerate materials discovery, including battery and polymer applications.

[1] S. Batzner et al. Nature Comm. 13:2453 (2022)

[2] J. S. Smith et al. Nature Comm. 10:2903 (2019)

[3] C. Chen, S. Ong, Nature Comp. Sci. 2, 718-728 (2022)

[4] B. Deng et al. arXiv:2302.14231 (2023)

[5] <https://www.scm.com/oled-workflow>

[6] <https://www.scm.com/reaxpro>

11:30 AM DS06.09.11

A Physics Domain of ML's Applications for Accelerating Large Scale Simulations: Microstructure and Property Evolution in Nuclear Fuels[ShenyangHu](#)¹ and BenjaminBeeler²; ¹Pacific Northwest National Laboratory, United States; ²North Carolina State University, United States

Monolithic UMo fuel is under development for converting highly enriched ²³⁵U fuels currently used in high-power research reactors in the United States to low enriched ²³⁵U fuels. The UMo fuel due to the radiation damage of high energy neutrons and fission fragments undergoes a large microstructure change such as grain refinement and gas bubble volumetric swelling, which dramatically impacts the thermomechanical properties and fuel performance. The microstructure change evolves strongly coupled multiphysics which have different length and time scales. In this work, a microstructure dependent rate theory is used to describe the evolution of radiation defects and their clusters. A random walk model is used to describe the fast diffusion of defects and species on grain boundaries. A phase-field model is used to describe the evolution of non-equilibrium gas bubbles. And the crystal plasticity model is used to describe the elastic-plastic deformation in polycrystalline structures. We developed an integrated model to capture these multiphysics coupling for predicting the kinetics of gas bubble swelling and creep. Simulation results demonstrate that swelling kinetics and creep rate depend on a broad space of model parameters and a large scale simulation is needed to capture the important length and time scales in the representative physics domain. We will discuss and explore the potential application of ML for accelerating the large scale simulation.

11:45 AM DS06.09.12

Active Learning of Continuum-Scale Mechanics by Guiding Discrete Dislocation Dynamics Simulations[NicholasJulian](#), NithinMathew and DannyPerez; Los Alamos National Laboratory, United States

Extracting a model of continuum-scale material dynamics from lower-scale simulations of the underlying deformation process has the potential to improve the accuracy of crystal-plasticity simulations and uncover new causal relationships between features and behavior. However, the cost of adequately exploring the underlying parameter space can be prohibitive and difficult to predict a priori. By representing the continuum-scale model as a Gaussian process, a measure of uncertainty may be embedded which can be used to guide parameter space exploration through a method known as Bayesian optimization. In this talk, we demonstrate our adaptation of Bayesian optimization to extract a continuum-scale crystal plasticity flow rule from meso-scale discrete dislocation dynamics in terms of microstructural feature parameterizations.

SESSION DS06.10: Machine Learning for Simulation of Materials VI

Session Chairs: Grace Gu and N M Anoop Krishnan

Thursday Afternoon, November30, 2023

Sheraton, Second Floor, Back Bay A

1:30 PM *DS06.10.01

Elements of Modern Industry-Grade Crystal Structure Prediction[KiranSasikumar](#), HannoDietrich, DzmitryFiraha and MarcusNeumann; Avant-Garde Materials Simulation GmbH, Germany

"Do not be afraid to launch a product without machine learning. Machine learning is cool, but it requires data, and if not absolutely required for your product, do not use it until you have data." -- paraphrasing Google's rules of machine learning [1].

Commercially relevant scientific applications requiring high-quality predictions at a reasonable computational cost often also suffer from the lack of a diverse database of experimental or high-fidelity simulation results. This necessarily stifles the development of machine learning focused solutions. The commercial product would then inevitably involve integrated machine learning and physics-based simulation workflows, where high-fidelity training data generation is done on-the-fly based on the requirements of the application.

In this presentation, we discuss the application-driven development of a scientific workflow for organic crystal structure prediction (CSP) and pharmaceutical solid form risk assessment, where machine learning is simply one cog in a larger machinery that is primarily driven by physics-based models [2]. Historically, the development of this scientific workflow was driven by the industry need to foresee cases of disappearing polymorphs, which are occasions when a crystal structure that has been prepared and marketed for years is unexpectedly superseded by a thermodynamically more stable polymorph, rendering the initial crystal structure almost impossible to obtain [3]. Despite the relative rarity of such events, famous cases such as the drug compounds ritonavir and rotigotine, where costly reformulations were required to manufacture the product again, underlined the commercial need for extensive screening of solid-state forms.

We introduce the key elements of modern industry-grade organic CSP, focusing on a) reference data generation and fragment-based force field parameterization, b) a comparison of parametric and machine learnt force fields, c) multi-fidelity statistics and machine learning (ML) for structure selection in the CSP funnel, d) accurate free energy predictions, and e) high- throughput optimization for solving the structures of what are often poor experimental powder diffraction imaging data. Overall, we argue that ML and ML-adjacent concepts, including high quality data generation and high-throughput optimization, form just a few cogs in a larger machinery for the prediction of free energies of organic crystal structures, and in general for accelerated materials modeling. Physics-based multi-fidelity models are not going out of fashion anytime soon.

References

[1] <https://developers.google.com/machine-learning/guides/rules-of-ml/>

[2] A. Mattei et al. (2022), "Efficient Crystal Structure Prediction for Structurally Related Molecules with Accurate and Transferable Tailor-Made Force Fields", *Journal of Chemical Theory and Computation* 18 (9), 5725-5738.

[3] D.-K. Bucar, R. W. Lancaster & J. Bernstein (2015), "Disappearing Polymorphs Revisited" *Angew. Chem., Int. Ed.* 54, 6972-6993.

2:00 PM DS06.10.02

Quantifying Chemical Short-Range Order in Metallic Alloys [Rodrigo Freitas](#); Massachusetts Institute of Technology, United States

Metallic alloys often form phases - known as solid solutions - in which chemical elements are spread out on the same crystal lattice in an almost random manner. The tendency of certain chemical motifs to be more common than others is known as chemical short-range order (SRO) and it plays a prominent role in alloys with multiple chemical elements present in large concentrations due to their extreme configurational complexity (e.g., high-entropy alloys). Short-range order renders solid solutions "slightly less random than completely random", which is a physically intuitive picture, but not easily quantifiable due to the sheer number of possible chemical motifs and their subtle spatial distribution on the lattice. In this talk I'll present a multiscale method to predict and quantify the SRO state of an alloy with atomic resolution, incorporating machine learning techniques to bridge the gap between electronic-structure calculations and the characteristic length scales of SRO. The result is an approach capable of predicting SRO domain sizes in agreement with experimental measurements, and to comprehensively correlate SRO with fundamental quantities such as local lattice distortions.

2:15 PM DS06.10.03

Accelerating Simulations of Nanoalloy Catalysts using Machine Learning [Sergey Kozlov](#), Arravind Subramanian and Yifan Li; National University of Singapore, Singapore

Heterogeneous catalysts are used to drive the majority of the chemical reactions in the industry. Almost always the surface area of such catalysts needs to be increased using nanostructuring to make them more exposed to the reactants. However, nanostructuring is also known to profoundly affect the properties of the catalysts through nanoconfinement effects and the generation of low-coordinated active sites. Since the atomic-scale characterization of heterogeneous catalysts remains challenging using modern experimental techniques, simulations have been playing an increasingly important role in the understanding of the nanostructuring effects on the catalytic activity. However, such simulations face three main challenges: 1) significant model size, 2) complex design of catalyst models to mimic the experimental materials, and 3) the necessity to analyze numerous active sites with diverse properties. For example, surfaces of alloy nanoparticles (nanoalloy) catalysts expose active sites with different catalytic activities and compositions, which are hard to deduce from the experimental data. Moreover, the structure of the alloys and the composition of the active sites on their surface is known to change depending on the reaction conditions.

In this work, we show how machine learning can help tackle the two last challenges in the simulations of nanoalloys on the example of Pd-Pt catalysts for hydrogen evolution reaction. Namely, we optimized the machine learning method based on local environment fingerprints for precise prediction of binding energies of H atoms on 100+ diverse sites exposed on the surface of 1.5 nm Pd-Pt alloy nanoparticles composed of 140 atoms. Thus, the fingerprint method enabled evaluation of the catalytic activity of the entire surface of Pd-Pt particles in hydrogen evolution reaction in fractions of a second. Moreover, the developed method also allowed us to investigate the effects of the reaction environment and the electrode potential on the surface composition of Pd-Pt nanoalloys. We achieved this by incorporating the contribution of H binding energies calculated using the fingerprint technique into previously developed lattice Hamiltonian [1] used to determine the most thermodynamically stable chemical orderings in (Pd-Pt)₁₄₀ nanocrystallites. Our simulations combining density functional theory, machine learning, and lattice Hamiltonian approach reveal how Pd segregates on the surface of Pd-Pt particles under high H coverage and electrode potentials below reversible hydrogen electrode potential. Thus, the developed machine-learning methods are demonstrated to greatly facilitate computational studies of the structure and catalytic activity of nanoalloys, which will increase the reliability of the computational rational design of such catalysts.

References:

[1] Kozlov, Kovács, Ferrando, Neyman, *How to Determine Accurate Chemical Ordering in Several Nanometer Large Bimetallic Crystallites from Electronic Structure Calculations*, *Chem. Sci.* 2015, 6, 3868

2:30 PM DS06.10.04

Quantitatively Accurate Modeling of the Phase Spaces of Alkali Metals and Their Alloys using Machine Learning [Mgcini K. Phuthi](#) and Venkatasubramanian Viswanathan; University of Michigan, United States

Alkali metals are important materials in batteries and other applications. Their alloys have interesting eutectic properties with applications as functional materials hence the importance in modeling them accurately. Machine Learning Interatomic Potentials (MLIPs) have significantly improved over other methods of modeling materials by being scalable, accurate and computationally efficient. Their accuracy however is limited by the data used to train them, typically Density Functional Theory (DFT) data generated using active learning which can fail to accurately model some systems. In this work we argue first that DFT can accurately model alkali metals due to their simple electronic structure, include complex electronegative phases at extreme pressure. Continuing off of our previous work on calculating properties of lithium with exceptional accuracy, we show that compact datasets can be transferred between chemically similar systems using simple transformations, eliminating the need for weeks of active learning to develop potentials for sodium. Finally, we calculate the properties of Na-Li alloys to investigate how MLIPs model phase separation and entropy calculations.

2:45 PM BREAK

3:15 PM DS06.10.05

Block Sparsity Promoting Algorithm for Efficient Construction of Cluster Expansion Models for Multicomponent Alloys [Krishnamohan Thekkepat](#)^{1,2,3} and Seung-Cheol Lee^{1,2,3}; ¹Korea Institute of Science and Technology, Korea (the Republic of); ²KIST School, Korea University of Science and Technology, Korea (the Republic of); ³Indo-Korea Science and Technology Centre, India

First-principles based electronic structure methods like density functional theory (DFT) with remarkable accuracy and sophistication have played an important role in the discovery and development of high-performing materials that drive technological breakthroughs. However, most recent breakthroughs, especially in materials for storage, conversion and transport of energy were reported in alloys, often with more than 1 additive element. Modelling multicomponent alloys becomes prohibitively expensive with DFT due to the exponential explosion in the configurational space (10^{10} - 10^{25}) of these alloys. Combining DFT calculation data with machine learning methods can overcome this issue. One of the most successful combinations of both is the development of cluster expansion method.¹ Cluster expansion Hamiltonians can be used to sample the vast configuration space of alloys at reduced costs and extract finite temperature thermodynamic properties via Monte Carlo Simulations.² Over the years, several algorithms ranging from simple regression to sophisticated Bayesian compressive sensing have been applied to train cluster expansion models for binary and ternary alloys from DFT energies.¹ However, modelling larger and complicated multicomponent alloys is still expensive due to requirements of large training sets ($\sim 10^4$).

We present a new compressive sensing-based algorithm for efficient construction of cluster expansion Hamiltonians of multicomponent alloys. The proposed algorithm constructs highly sparse and physically reasonable models from a carefully selected small training set of alloy structures. When compared with conventional fitting algorithms, the proposed algorithm achieves similar accuracy with a significantly smaller training set. We demonstrate this on 4 different alloy systems, namely Ag-Au, Ag-Au-Cu, Ag-Au-Cu-Pd, and (Ge,Sn)(S,Se,Te). For the ternary and quaternary alloys, the reduction in training set size is shown to be at least 50%. The resultant sparse models from training can sample the configuration space at least 3x faster and also reproduce known ground state orderings and order-disorder transitions. The new algorithm has been implemented in the Lattice Atomic Configuration Simulation (LACOS) package developed in-house. We have implemented special workflows to construct cluster expansion Hamiltonians starting from generating training structures for DFT calculations to validation of fitted models. Finite temperature Monte Carlo simulations can also be carried out to extract thermodynamic properties. Our code is designed to truly enable high-throughput multicomponent alloy thermodynamics by reducing the cost associated with model construction and configurational sampling.

References

1. Hart, G. L. W., Mueller, T., Toher, C., & Curtarolo, S. (2021). Machine learning for alloys. *Nature Reviews Materials*, 6(8), 730-755.

2. Van der Ven, A., Thomas, J. C., Puchala, B., & Natarajan, A. R. (2018). First-Principles Statistical Mechanics of Multicomponent Crystals. *Annual Review of Materials Research*, 48(1), 10.

3:30 PM DS06.10.06

Quantitative Assessment of Local Chemical Ordering in Atomistic Simulations of High-Entropy Alloys [Killian Sheriff](#), Yifan Cao and Rodrigo Freitas; Massachusetts Institute of Technology, United States

High-entropy alloys (HEAs) exhibit exceptionally good combinations of properties recently reported to correlate with chemical short-range ordering (cSRO). However, in atomistic

simulations, their state of cSRO has only been so far characterized using the Warren-Cowley parameters. Yet, this approach is incomplete as distinct local atomic configurations sharing the same chemical concentration are indistinguishable. Here, we propose a generalized framework, based on graph-convolution neural networks equivariant to E(3) symmetry operations, statistical mechanics, and information theory, capable of completely identifying the set of distinct local atomic binding environments and their associated population densities in HEAs. This approach leads to a quantitative characterization of the cSRO state and provides a predictive framework for evaluation of cSRO domain sizes, thus offering novel avenues to explore the relationships between processing, structure, and properties in HEAs.

3:45 PM DS06.10.07

Accelerated Training of Cluster Expansion Models for Simulating Complex Oxides in High-Temperature Energy Conversion ApplicationsJonasKaufman, Yu-TingHsu, KyoungE. Kweon and BrandonWood; Lawrence Livermore National Laboratory, United States

The cluster expansion is a reduced order model widely used to approximate the energetics of crystalline materials in large-scale thermodynamic and kinetic simulations. These models are typically trained on data from first-principles calculations, which act as the primary bottleneck in this method. Efficient generation of training data becomes increasingly challenging for complex, many-component oxide systems, which are often relevant in energy applications. In addition, the combinatorial explosion of cluster expansion basis functions necessitates a careful approach to model construction and fitting. Here, we navigate these issues in modeling lanthanum strontium cobalt ferrite (LSCF), a key material of interest for electrodes of high-temperature solid oxide fuel cells and electrolysis cells for hydrogen technology. Cluster expansions are constructed for LSCF and secondary oxide phases that appear as degradation products in device applications. High-throughput density functional theory calculations are performed within an active learning scheme, where Gaussian process regression is applied to identify optimal regions of configuration space to sample. Using a common set of training data, we benchmark various approaches to fitting the cluster expansion as well as alternative, nonlinear lattice models such as neural network alloy Hamiltonians. We also discuss the application of our models in kinetic Monte Carlo simulations as part of a broader multiscale modeling effort.

4:00 PM DS06.10.08

Short-Range Order in Group IV Alloys: Insights from First-principles Calculations and Machine Learning Based Atomistic SimulationsShundaChen, XiaochenJin and TianshuLi; George Washington University, United States

Group IV alloys are promising silicon-compatible versatile materials for electronic, photonic, and topological quantum applications. However, the determination of their structural properties remains elusive and challenging. By combining statistical sampling from extensive first-principles density functional theory (DFT) calculations, we show that group IV alloys exhibit a wide range of complex short-range order (SRO) behaviors within its entire investigated composition range¹⁻³. SRO is further predicted to substantially affect the electronic properties of group IV alloys¹⁻³ and its presence in group IV alloys is recently experimentally confirmed by different characterization techniques. To extend the spatiotemporal scale of atomistic modeling to enable a side-by-side comparison with advanced characterization methods such as atom probe tomography, we further develop machine-learning interatomic potentials for the alloys. We show that the machine-learning interatomic potentials not only can accurately reproduce the results based on DFT calculations, but also enable a discovery of new, interesting SRO structural properties that are not easily accessible by DFT calculations. Our results shed more light on the mysterious SRO structural properties of group IV alloys.

1. B. Cao, S. Chen, X. Jin, J. Liu, and T. Li, ACS Applied Materials & Interfaces 12, 57245 (2020)

2. X. Jin, S. Chen, and T. Li, Physical Review Materials 5, 104606 (2021)

3. X. Jin, S. Chen, and T. Li, Communications Materials 3, 66 (2022)

*This work is supported by Department of Energy, Office of Basic Energy of Sciences under Award No. DE-SC0023412.

4:15 PM DS06.10.09

Deep Material Network for Thermal Conductivity HomogenizationDongilShin, PeterJ. Creveling, ScottA. Roberts and RemiDingreville; Sandia National Laboratories, United States

The agile and accurate material simulation model is in demand for rapid material analysis and design. Especially a computational analysis model for multiphysics and multiscale applications is of major interest. Recently, Deep Material Network (DMN) has shown itself to be a powerful approach for the material's reduced-order modeling because of its ability to extrapolate the constitutive equations and its orders of lower computational cost. DMN learns the homogeneous pathway from the linear constitutive relation data and can be used as a reduced-order model for predicting the non-linear constitutive equations. However, currently, all the DMN work has been done only on the elastic mechanical problems. In this study, DMN has been explored to handle thermal conductivity analysis. By building the DMN architecture corresponding to the thermal conductivity homogenization, we have shown that the DMN can be expanded to different physics, which is essential to dealing with multiphysics problems. We had predicted the two-scale problem's homogenized response, corresponding to the thermal conductivity of the woven structure. To consider the woven structures' orthotropic properties, micromechanics-based DMN network parameters have also been updated to reflect the material's orientation. The trade-off of increasing the DMN network parameters, corresponding to the complexity of the homogenization process, has also been studied. We believe our material model will open new chances for multiphysics-multiscale design and analysis for composite materials and, furthermore, to explore the material design space with sufficient agility and accuracy. Sandia National Laboratories is managed and operated by NTESS under DOE NNSA contract DE-NA0003525.

4:30 PM DS06.10.10

Atomistic Insights into The High Temperature Dislocation Dynamics of Cu using a Bayesian Force Field from First PrinciplesCameronJ. Owen¹, AmirhosseinNaghdi Dorabati^{2,3}, AndersJohansson¹, DarioMassa^{2,3}, StefanosPapanikolaou² and BorisKozinsky¹; ¹Harvard University, United States; ²Nomaten CoE, Poland; ³Ideas NCBR, Poland

High temperature dislocation dynamics present a difficult simulation task for existing classical and ab initio methods due to the required accuracies and length-scales. These limitations ultimately prohibit advanced understanding of plastic deformation of materials under relevant stimuli. Here, we develop a Bayesian machine-learned force field (MLFF) from ab initio (first principles) training data that extends quantum-mechanical accuracy to large length-scale molecular dynamics simulations which permit reliable description of high-temperature dislocation dynamics in Cu and direct comparison to experimental observations. In concert, a general and intuitive training protocol is defined for construction of MLFFs for the description of dislocations, which can be employed for other systems of interest. The resulting MLFF provides excellent predictions of both static bulk properties (e.g. bulk modulus and elastic tensor), stacking fault energies, and the dynamic evolution of edge and screw dislocations, as well as cross-slip mechanisms and activation energy across a broad range of temperatures and applied shears. Such simulations allow for the unbiased, atomistic insight into plastic deformation under various stimuli, helping to ultimately explain experimental observations through an atomic-lense.

4:45 PM DS06.10.11

Convolutional Autoencoder and Koopman Operator-Based Markov Chaining for Time Series Forecasting of a Large-Scale Dissipative Particle Dynamics System for Thrombosis ModellingAkhilSamavedam¹, YicongZhu² and YuefanDeng²; ¹Westlake High School, United States; ²Stony Brook University, The State University of New York, United States

Background: Cardiovascular disease (CVD) is the world's leading cause of death, responsible for over 17.9 million deaths annually. The majority of CVD-related deaths are caused by thrombosis, the formation of a blood clot in a vein or artery that impedes the circulatory system. Therefore, it is necessary to create accurate platelet and flow dynamics models to simulate the thrombosis process effectively. Multiscale modeling (MSM) combines various spatiotemporal resolutions in order to achieve high accuracy while simultaneously reducing the computational cost. Preceding works defined MSM models involving Dissipative Particle Dynamics (DPD) for the Poiseuille flow of blood in the vessel and Coarse-Grained Molecular Dynamics (CGMD) for the fluid-platelet interface. However, these simulations are highly computationally intensive due to the large amount of DPD calculations performed on fluid particles at high resolutions with negligible benefits. It is necessary to find an accelerated solution to the fluid modeling aspect of the simulation.

Methods: We define the DPD system as a 3D velocity field on a defined particle plane 391.2 μm long x 21.3 μm wide. The velocity field is represented by a tensor of size (4200, 244, 3) for a total of 3074400 elements. The simulation is discretized in timestep increments of 250 μs with a corresponding state tensor at each timestep. In order to utilize a Koopman Operator to model time series evolution, we derived a series of observable functions that accurately reflect the state of the system in a lower dimensional space than the state tensor. We derived these functions by implementing a Convolutional Autoencoder (CAE) to learn a 256-element latent representation of the state tensor and consider spatial relationships in the velocity field; this latent vector acts as the observable function. We used Extended Dynamic Mode Decomposition (EDMD) to derive an approximated Koopman Operator (aKO). EDMD is performed by taking the product of a matrix of latent vectors for each state tensor time step joined as columns with the Moore-Penrose pseudoinverse of a time-shifted variant of this matrix. In order to model the time series evolution, the observable function at a discrete time is multiplied by the Koopman operator to predict the next observable function. This process forms a Markov chain where the model's

current state is the only consideration in predicting the future state.

Results: CAE-aKO resulted in a speed increase of 390x for single-step prediction, a value that increased linearly to 3570x for nine steps. CAE-aKO also achieved high accuracy with an average RMSE value of 0.1372 across 3 million elements and an average MAE of 0.1065. These averages were calculated across predictions ranging from 1-9 timesteps (250 μ s - 2.25 ms) into the future. We attribute the majority of the prediction error to flaws in the CAE's learned latent vectors, as the aKO presented low errors in latent vector time series prediction when the latent vectors are not converted back to state tensors.

Discussion and Future Work: We assessed the viability of a non-physics-guided approach to time series forecasting of a large-scale system with complex spatiotemporal relationships. CAE-aKO learned an accurate underlying representation of the state tensor and was able to accurately model the evolution of the system with minimal drops in accuracy as multiple steps of prediction were performed. Future work will focus on refining the CAE architecture to minimize reconstruction loss and then use CAE-aKO to produce new data upon which to calculate aKOs for larger time steps, allowing for greater speedups in modeling methodology that allow for simulations to move from predicting on time scales of milliseconds to larger scales of seconds and minutes.

Acknowledgments: This project was supported by Stony Brook University's Garcia Center for Polymer Research and the Garcia Scholars Program.

SESSION DS06.11: Machine Learning for Simulation of Materials VII
Session Chairs: Grace Gu and N M Anoop Krishnan
Friday Morning, December 1, 2023
Hynes, Level 2, Room 203

8:15 AM DS06.11.01

Artificial Intelligence Guided Materials Discovery of Two-Dimensional Magnets Trevor D. Rhone¹, Romakanta Bhattarai¹, Haralambos Gavras¹, Bethany Lusch², Misha Salim², Marios Mattheakis³, Daniel Larson³, Yoshiharu Krockenberger⁴ and Efthimios Kaxiras³; ¹Rensselaer Polytechnic Institute, United States; ²Argonne National Laboratory, United States; ³Harvard University, United States; ⁴NTT Basic Research Laboratory, Japan

The discovery of van der Waals (vdW) materials with intrinsic magnetic order in 2017 has given rise to new avenues for the study of emergent phenomena in two dimensions. In particular, monolayer CrI₃ was found to be ferromagnetic. Other vdW transition metal halides were later found to have different magnetic properties. How many vdW magnetic materials exist in nature? What are their properties? How do these properties change with the number of layers? A conservative estimate for the number of candidate vdW materials (including monolayers, bilayers and trilayers) exceeds $\sim 10^6$. Recent studies show that artificial intelligence (AI) can be harnessed to discover new vdW Heisenberg ferromagnets based on Cr₂Ge₂Te₆ [1, 2]. In this talk, we will harness AI to efficiently explore the large chemical space of vdW transition metal halides and to guide the discovery of magnetic vdW materials with desirable spin properties [3]. That is, we investigate crystal structures based on monolayer Cr₂I₆ of the form A₂X₆, which are studied using density functional theory (DFT) calculations and AI. Magnetic properties, such as the magnetic moment are determined. The formation energy is also calculated and used as a proxy for the chemical stability. We show that AI, combined with DFT, can provide a computationally efficient means to predict the thermodynamic and magnetic properties of vdW materials. We use semi-supervised learning to mitigate the challenge of data scarcity in AI-guided materials discovery. This study paves the way for the rapid discovery of chemically stable magnetic vdW materials with applications in spintronics, data storage and quantum computing.

[1] T. D. Rhone, et al., *Sci. Rep.* 10, 15795 (2020).

[2] Y. Xie, et al., *J. Phys. Chem. Lett.*, 12, 50, 12048–12054 (2021).

[3] T. D. Rhone *et al.*, "Artificial Intelligence Guided Studies of van der Waals Magnets," *Adv. Theory Simulations*, p. 2300019 (2023).

This research was primarily supported by the NSF CAREER, under award number DMR-2044842.

8:30 AM DS06.11.02

Accelerated Continuum Crystal Plasticity and Phase Field Microstructure Modeling using U-Net Dierk R. Raabe; Max Planck Institute for Iron Research, Germany

An overview of various continuum-level machine learning based models for microstructure evolution is presented, focussing on crystal plasticity and phase field methods [1, 2]. For accelerating mechanical boundary condition treatment for heterogeneous solids we propose a deep neural network as a fast surrogate model for local stress calculations in inhomogeneous linear or non-linear elasto-viscoplastic materials, using U-Net. We show that the surrogate model predicts the local stresses with <4% mean absolute percentage error for the case of heterogeneous elastic media and a mechanical contrast of up to factor of 1.5 among neighboring domains, while performing 100-500 times faster than spectral solvers. The model proves suited for reproducing the stress distribution in geometries different from those used for training. In the case of elasto-plastic materials with up to 4 times mechanical contrast in yield stress among adjacent regions, the trained model simulates the micromechanics with a MAPE of 6.4% in one single forward evaluation of the network, without any iteration. The results reveal an efficient approach to solve non-linear mechanical problems, with an acceleration up to a factor of 8300 for elastic-plastic materials compared to typical finite element solvers. A similar approach was chosen for phase-field models: these are costly when applied to large, complex systems [3,4]. To reduce the computational costs, a U-Net surrogate model has been developed. Training input is obtained from the results of the numerical solution of initial-boundary-value problems based on the Fan-Chen model for grain microstructure evolution. The trained network is applied recursively on initial order parameters to calculate the time evolution of the phase fields. The results are compared to the ones obtained from the conventional numerical solution in terms of the errors in order parameters and the system's free energy. The resulting order parameter error averaged over all points and all simulation cases is 0.005 and the relative error in the total free energy in all simulation boxes does not exceed 1%.

1. J.R. Mianroodi, et al., *npj Computational Materials* 7 (2021)

2. M.S. Khorrami, et al. *npj Computational Materials* 9 (2023)

3. D. Raabe et al. *Nature Comput. Sci.* 3 (2023)

4. I. Peivaste et al. *Comput. Mater. Sci.* 214 (2022)

8:45 AM DS06.11.03

Machine Learning-Aided First Principles Calculations of Free Energies Ryosuke Jinnouchi¹, Ferenc Karsai² and Georg Kresse^{3,2}; ¹Toyota Central R&D Labs., Inc., Japan; ²VASP Software GmbH, Austria; ³University of Vienna, Austria

The free energy of atoms and molecules in condensed matter is an extremely important property. Knowledge of free energy allows quantitative evaluation of a wide variety of physical properties, such as coexistence points of different phases, concentration of minority species, redox levels of atoms and molecules in condensed matter, and thermodynamic stability of reaction intermediates. However, accurate first-principles calculations of free energies are extremely challenging. Since free energies are not observable, the free energy difference between a known system and a real system of interest must be calculated in large-scale molecular dynamics simulations using thermodynamic perturbation theory (TPT) or thermodynamic integration theory (TI). Recently, machine-learned force fields (MLFFs) have enabled efficient computation of free energies [1-3]. By using MLFFs as surrogate models, computationally difficult TI from a known system to a real system becomes feasible. Errors in MLFF can also be corrected by TPT and TI. Machine-learned models can be also used to correct inexpensive low-level first-principles results, such as results by semi-local exchange-correlation functionals, to obtain accurate but expensive theoretical results [4]. Here, we show three applications of the MLFF framework to the free energies in aqueous solutions and interfacial systems: hydration free energies of ions in water, redox potentials of transition metal ions in water, and hydration free energies of adsorbates on the surface of platinum catalysts. All examples demonstrate that MLFFs enable efficient statistical sampling necessary for accurate computations of free energies.

[1] R. Jinnouchi, F. Karsai, and G. Kresse, *Phys. Rev. B* **100** 014105 (2019).

[2] R. Jinnouchi, F. Karsai, and G. Kresse, *Phys. Rev. B* **101** 060201(R) (2020).

[3] R. Jinnouchi, F. Karsai, C. Verdi, and G. Kresse, *J. Chem. Phys.* **154** 094107 (2021).

[4] P. Liu, C. Verdi, F. Karsai, and Georg Kresse, *Phys. Rev. B* **105**, L060102 (2022).

9:00 AM DS06.11.04

Understanding and Designing the Frustration in Super-Ionic Conductors aided by Machine Learning Shuo Wang^{1,2}, Yunsheng Liu¹ and Yifei Mo¹; ¹University of Maryland, United States; ²Massachusetts Institute of Technology, United States

Frustration is a physical phenomenon in which plenty competing states exist with similar energy levels. The frustration in super-ionic conductors enables their exceptionally high ionic

conductivities. Although atomistic modeling reveals a wide range of specific mechanisms in causing the frustration, a long-standing challenge is that analyzing many disordered configurations of the atomistic systems and their energies using first principles computation is computationally expensive. With the aid of machine learning interatomic potential to provide atomistic energies of individual atoms, we proposed density of atomistic states (DOAS) as quantitative analytics to elucidating, characterizing, and understanding the frustration mechanisms involving a diverse range of locally disordered atomic configurations. Using Li-ion conductors as model systems, the DOAS quantitatively characterizes the onset and degree of disordering, reveals the local configurational disorder and energetics in causing the frustration, and reveal how the frustration of atomistic states enhances ion diffusion. Furthermore, materials design strategies aided by the DOAS are devised and demonstrated for new super-ionic conductors. As demonstrated, the combination of atomistic modeling and machine learning can extend and empower conventional physics analytics for unraveling fundamental mechanisms and for guiding material design.

9:15 AM DS06.11.05

A Machine Learning Based Computational Approach for Prediction of Cation Distribution in Spinel Crystal YingFang and GuofengWang; University of Pittsburgh, United States

Spinel ferrites with a general chemical formula of AB_2O_4 ($A, B = Fe, Mg, Co, Ni, Cu, \text{ or } Al$) have interesting and technologically relevant magnetic and electrical properties. The crystal structure of spinel AB_2O_4 can be viewed as a superlattice consisting of eight ($2 \times 2 \times 2$) face-centered cubic unit cells with the lattice sites occupied by oxygen ions. In addition, one eighth of the tetrahedral and one half of the octahedral sites of the lattice are occupied by the A and B cations. In a normal spinel structure, all A ions will lie at the tetrahedral sites whereas all B ions at the octahedral sites. By contrast, half of the B ions will lie at the tetrahedral sites, whereas the octahedral sites are occupied by both A and B ions in an inverse spinel structure. Varying from the normal to inverse structures, the cation distribution in spinel AB_2O_4 could be quantified using degree of inversion which is the fraction of the tetrahedral sites occupied by B ions.

It has been found that both cation chemistry and degree of inversion play an important role in technically relevant properties of spinel oxides. In this study, we have developed and applied a machine learning based computational approach to predict the equilibrium cation distribution in multi-cation spinel oxides at high temperature. The computational approach integrates the construction of datasets consisting of the energies calculated from the density functional theory of the spinel oxides with various cation distributions, the training of the support vector machine model to derive relationship between system energy and structural features, and atomistic Monte Carlo simulations to sample the thermodynamic equilibrium structures of spinel crystal as a function of temperature. We have applied our computational approach to predict the cation distributions for material systems of single spinel $CoFe_2O_4$, $NiFe_2O_4$, $MgAl_2O_4$, $MgFe_2O_4$, and double spinel $MgAl_{2-x}Fe_xO_4$. Our predictions are found to agree well with available experimental results. Therefore, this study presents a reliable computational approach that can be extended to study the variation of cation distribution with processing temperature and chemical composition in complex multi-cation spinel oxides.

9:30 AM DS06.11.06

Coupling Between Moiré Patterns in Twisted Bilayer Graphene and Nanofluidics: A Deep Neural Network Approach ChenxingLiang and NarayanaAluru; The University of Texas at Austin, United States

Twisted bilayer graphene at the magic angle has garnered attention due to its intriguing superconductivity and correlated insulator behavior resulting from strong electronic correlations. However, the impact of the electronic properties due to Moiré Patterns in twist bilayer graphene on the structural and dynamic properties of water remains largely unexplored. This knowledge gap stems from computational challenges associated with simulating large unit cells using density functional theory. In this study, we present an approach utilizing a deep neural network potential (DP) model. The DP model is trained using a dataset obtained from ab initio molecular dynamics simulations of water on various large twist angle bilayer graphene. Our DP model accurately characterizes key water properties, such as OH bond length, HOH bond angle, and power spectra, on top of magic angle twisted bilayer graphene. Leveraging this model, we investigate the structural and dynamical properties of water on bilayer graphene with various twist angles, ranging from 1.08° to 9.43° . By analyzing the effects of these twist angles and their corresponding electronic properties, we gain insights into the nanofluidic behavior of water. This exploration opens avenues for future research, focusing on harnessing the unique properties of twisted bilayer graphene to control and optimize nanofluidic behavior.

9:45 AM BREAK

10:15 AM *DS06.11.07

Efficient Generation of Materials Data for Machine Learning Shyue PingOng, JiQi and Tsz WaiKo; University of California, San Diego, United States

The biggest bottleneck to machine learning (ML) for materials science is the generation of training data. In this talk, I will discuss various approaches to efficiently generate and use materials data to develop ML models. For instance, I will demonstrate the use of universal interatomic potentials to pre-generate a large configuration space of structures, as well as a Dimensionality Reduced Encoded Clusters with sTratified (DIRECT) sampling approach to create a robust training set for an ML interatomic potential (MLIP). I will also discuss the application of multi-fidelity techniques to maximize the return on scarce, high quality data. While a major focus of this talk will be on MLIP development, I will also highlight the applicability of these techniques to other ML-enabled applications.

10:45 AM DS06.11.08

Combining DFTB and Structure-Mapping for the Prediction of Transition Paths in Deactivation of ZnO@Cu Catalysts ArtemSamtsevych, ChiaraPanosetti, ChristophScheurer and KarstenReuter; Fritz Haber Institute der MPG, Germany

Solid-solid transformations are common in nature and in the aging of functional materials. Understanding the origin of these complex phenomena at the atomistic level is a pre-requisite for the design of long-living active materials. For example, catalysts undergo structural and compositional changes during aging, leading to a decline of their catalytic activity and selectivity. Understanding such transformations is necessary to rationally develop mitigation strategies.

From the energetical point of view, the involved activated processes can be modeled as transitions between basins on a complex, high-dimensional free energy surface (FES). Chain-of-states methods optimize presumed pathways between two structural endpoints on FES towards the minimum energy pathway (MEP), yielding transition state estimates. Using the harmonic approximation to transition state theory (HTST), one can estimate reaction rate constants from the location of saddle points on the FES. However, there are two pitfalls that exist in this scheme that typically limit the extent of accessible spatial and time scales. First, the number of possible transition pathways that must be evaluated grows exponentially with system size and, second, ab initio methods, like density functional theory (DFT), are still too computationally expensive to cover the enormously large region of interest in the configurational space.

The first problem can be solved using advanced techniques for the generation of the initial pathway(s) or, in other words, the mapping of atomic structures onto each other. This can be achieved either by purely geometrical methods (mapping of atomic positions and cells) or by topology-based methods, which map the graphs of interatomic bonds. Both approaches are complementary to each other and generate a diverse set of mappings. The combination of mapping algorithms with the chain-of-states method has recently been merged into a generalized workflow.

To tackle the second problem, we harness the power of machine learning (ML) and incorporate it into an approximate, semi-empirical electronic structure model resulting from Density Functional Tight Binding (DFTB) theory [1]. By doing so, we are able to achieve energetics and electronic properties with an accuracy comparable to DFT at a fraction of the cost. Such an approach is realized by means of DFTB parametrization with a Gaussian Process Regression repulsive potential (GPrep-DFTB) [2].

Previous theoretical and experimental studies have shown that ZnO tends to form a graphitic-like overstructure on a Cu surface (catalytically active system) if it is deposited in thin layers. However, the thicker the ZnO phase grows, the more wurtzitic ZnO structure, which is catalytically less active, becomes favored [3-5]. We will present the combination of mapping algorithms along with GPrep-DFTB to investigate the phase transformations involved in the aging process in ZnO@Cu catalysts.

11:00 AM DS06.11.09

Accelerating Crystal Structure Prediction of Properties of Organic Salts via Machine Learning EthanP. Shapera¹, Dejan-KresimirBucar², RohitPrasankumar³ and ChristophHeil¹; ¹Graz University of Technology, Austria; ²University College London, United Kingdom; ³Intellectual Ventures, United States

We demonstrate a machine learning-based approach to accelerating crystal structure prediction of organic salts. Use of crystal graph singular values reduces the number of features required to describe a crystal by more than an order of magnitude compared to the full crystal graph representation. We construct machine learning models using the crystal graph singular value representations in order to predict the volume, enthalpy per atom, and metal versus semiconducting phase of DFT-relaxed organic salt crystals based on randomly generated unrelaxed crystal structures. Initial base models are trained to relate 89,949 randomly generated structures of salts formed by varying ratios of 1,3,5-triazine and HCl with the corresponding volumes, enthalpies per atom, and phase of the DFT-relaxed structures. We further demonstrate that the base model is able to extrapolate to new chemical systems with the inclusion of as few as 2,000 crystal structures from the new system. After training a single model with a large number of data points, extrapolation can be done at significantly lower cost. The constructed machine learning models can be used to rapidly screen large sets of randomly generated organic salt crystal structures and efficiently downselect the structures most likely to be experimentally realizable.

11:15 AM DS06.11.10

Symphony: Symmetry-Equivariant Point-Centered Spherical Harmonics for Generating Molecules Song EunKim, Ameya Daigavane, Mario Geiger and Tess Smidt; Massachusetts Institute of Technology, United States

In-silico generation of diverse molecular structures has emerged as a promising method to navigate the complex chemical landscape, with direct applications to inverse material design and drug discovery. However, 3D molecular structure generation comes with several unique challenges; generated structures must be invariant under rotations and translations in 3D space, and must satisfy basic chemical bonding rules. Inspired by the success of machine learning models for generating coherent text and audio, there is much interest in building similar 'generative models' for 3D molecular structures.

One of the first successful attempts was G-SchNet, an autoregressive model that uses message-passing with rotationally invariant features to generate 3D structures of small molecules. At each iteration, a focus node is selected as the center of a 3D grid, then all pre-existing atoms collectively decide on the next atom's position within this grid. In this manner, G-SchNet generates molecules one atom at a time, completing molecular fragments into entire molecules. This construction raises several interesting questions; first, can we more accurately capture complex geometric motifs, and second, can we simplify the process of placing each atom without breaking symmetry via auxiliary tokens?

Here, we present our work on Symphony, an E(3)-equivariant autoregressive generative model. E(3)-equivariant neural networks that utilize higher-order rotationally-equivariant features have recently shown improved performance on a wide range of atomistic tasks. Motivated by these results, Symphony builds on G-SchNet by using message-passing with higher-order equivariant features. This allows a novel representation of probability distributions via spherical harmonic signals.

We will discuss the state of molecular generation models today and where Symphony sits amongst this rapidly changing landscape. We highlight several challenges we observed when developing Symphony, closely related to error accumulation and out-of-distribution generalization issues of machine learning methods. We present several applications of Symphony in generating small molecules and transition metal complexes, identifying key components of our model as well as areas of improvement. In particular, we demonstrate how higher-order equivariant features can model complex geometrical motifs which were unable to be captured by preceding methods such as G-SchNet. Finally, we discuss how hierarchical generation and building richer datasets beyond QM9 are important avenues to benchmark and improve generative models for molecules.

11:30 AM DS06.11.11

Accelerating Excited-States Calculations using Active Learning Configuration Interaction for Cyclic Organic Molecules WooSeokJeong; Korea Institute of Energy Research (KIER), Korea (the Republic of)

Understanding the electronic excited states of organic materials is key to the design of optoelectronic, photocatalytic and photovoltaic devices. For molecular systems, multiconfigurational methods can be used to compute the excitation states of such molecules as electronic correlations are included. A conceptually simple and robust approach among the multiconfigurational methods is the selected configuration interaction (SCI) theory, which utilizes only the energetically important electronic configurations for Configuration Interaction (CI) calculations. Compared to the Full Configuration Interaction (FCI) theory, SCI calculations can save a significant amount of computational cost, allowing to tackle much larger systems of interest. However, the success of the SCI calculations depends on how important configurations are selected, so different approaches have been introduced. To address this challenge, we developed the Active Space Configuration Interaction (ALCI) method [1] to predict the lowest singlet-singlet vertical excitation of several polycyclic aromatic hydrocarbons (i.e., acenes and pyrene), inspired by the Machine Learning Configuration Interaction (MLCI) approach [2] used for ground state calculations of small molecules. In the ALCI approach, a binary classification machine learning model is employed to identify candidate important configurations for subsequent SCI calculation during iterative CI calculations. It has been shown that our approach can accurately predict the excitation energies compared to CASCI results for relatively small- and medium-sized systems (i.e., active spaces up to (16e, 16o)), and capture the general trend of excitation energies of the systems up to (26e, 26o), for which a complete active space CI (CASCI) calculation is not yet affordable. In this talk, we present an updated scheme of the ALCI approach to predict excited states of various cyclic organic molecules in the QUEST database [3]. The updates include several features: First, unimportant configurations identified near the importance metric in previous cycles are recycled to obtain more accurate results. Second, any transition, not just for the lowest singlet-singlet transition, can be selected for calculation. Third, GPU-supported ML algorithms (i.e., LightGBM, XGBoost, Gaussian Process, ANNs) are implemented to speed up the ML training/prediction steps. We will also analyze the identified important/unimportant configurations to discuss what importance metric would be appropriate.

References

[1] W. Jeong, C. A. Gaggioli, L. Gagliardi. *J. Chem. Theory Comput.*, **2021**, *17*, 7518–7530.

[2] J. P. Coe. *J. Chem. Theory Comput.* **2018**, *14*, 5739–5749.

[3] M. V ril, A. Scemama, M. Caffarel, F. Lipparini, M. Boggio-Pasqua, D. Jacquemin, P.-F. Loos. *WIREs Comput. Mol. Sci.* **2021**; e1517

11:45 AM DS06.11.12

Search Trees in Large Continuous Action Spaces for Multiscale Modeling and Design of Materials SuvoBanik¹, Troy David Loeffler², Sukriti Manna², Henry Chan² and Subramanian Sankaranarayanan²; ¹University of Illinois at Chicago, United States; ²Argonne National Laboratory, United States

Modeling materials at various scales is of utmost importance in a diverse array of practical applications, allowing us to predict and gain insights into the favorable properties of novel materials, including super-hardness, electronic behaviors, and catalytic potential, among others. The understanding of material properties is intricately linked to the underlying structure and the potential energy landscape. Any approach to material modeling encompasses two key aspects: (a) the use of high-dimensional potential energy models to accurately predict material properties and (b) the navigation of the energy landscape to identify atomistic configurations that possess these desired traits. While first-principles-based approaches have demonstrated accurate property predictions, scalability remains a significant challenge, particularly in systems with heterogeneity and sizes that extend to scales with significant practical implications. Traditional potential energy models provide a cost-effective alternative, but their parameterization becomes challenging due to the dimensionality and continuous nature of search space. Additionally, the complexity of the energy landscape, exhibited by these potential models, makes it difficult to navigate toward local minima corresponding to metastable phases or locate global minima for inverse design problems. The high dimensionality of these problems necessitates the implementation of efficient approaches that can effectively explore the search space, capture the diversity of polymorphs, and converge toward desired properties. Drawing inspiration from the remarkable success of tree search algorithms in policy-driven reinforcement learning for games like Chess, Shogi, and Go, we have developed a continuous search space adaptation of Monte Carlo Tree Search to address these challenging material design problems. Our contribution to this continuous space adaptation includes modifying the rewards scheme to enhance exploration, implementing a "funneling" scheme for improved exploitation, and incorporating adaptive sampling during playouts to achieve efficient and scalable search. Using standardized high-dimensional artificial landscapes, we have successfully benchmarked our approach against popular metaheuristics-based global optimization techniques and state-of-the-art policy gradient methods. Our applications include exploring high-dimensional potential energy models of representative systems, such as nanoclusters of elements like Al, C, and Cu. Additionally, we have demonstrated the ability of our method to predict global minima crystal structures in systems with different dimensionalities and compositions, ranging from 0D (Au nanoclusters) to 2D (MoS₂) and oxides like TiO₂. Furthermore, we have extended our approach to addressing representative continuum-scale modeling problems, such as minimizing fabrication costs in welded joints or optimizing the weight of tension/compression springs. Additionally, we have applied our method to playing high-dimensional video games, showcasing its versatility. Future applications include implementing these algorithms to facilitate the discovery, exploration, and learning of synthesis pathways driven by protocols to enhance the understanding of phase transformations in material systems.

SESSION DS06.12: Machine Learning for Simulation of Materials VIII

Session Chairs: Ekin Dogus Cubuk and Shyue Ping Ong

Friday Afternoon, December 1, 2023

Hynes, Level 2, Room 203

1:30 PM *DS06.12.01

Data-Oriented Constitutive Models for Polycrystalline Metals Alexander Hartmaier, Ronak Shoghi and Jan Schmidt; Ruhr-Universit t Bochum, Germany

In classical constitutive modeling, the response of a material to mechanical loads is described by explicit mathematical expressions for the relations between stress and strain or strain-rates. Such mathematical formulations can become rather intricate, e.g., when describing history-dependent plasticity on the level of single-crystalline regions, as it is done in crystal plasticity. Yet, typically, such closed-form constitutive models do not take into account microstructural features, as grain size and shape or the crystallographic texture. This situation is rather unsatisfactory from a materials science point-of-view, as it is known that such microstructural features do not only control the mechanical behavior of a material but, moreover, they can be subject to change during plastic deformation. In this work, two approaches are highlighted how microstructure-sensitive data on plastic deformation of polycrystals are used to train numerically efficient machine learning models as constitutive relations that can directly be applied in finite-element models of engineering structures.

2:00 PM DS06.12.02

Subdiffusive Vacancy Dynamics in Complex Concentrated Alloys: Insights from Kinetic Monte Carlo Simulations and Machine LearningKamran Karimi and Stefanos Papanikolaou; Nomaten CoE, Poland

Chemically complex alloys (CCAs) have attracted significant attention due to their remarkable thermo-mechanical properties, often attributed to “core” effects such as sluggish diffusion, entropic contributions, and lattice distortions. In this study, we probe the microstructural kinetics of two exemplary equiatomic, single-phase, face-centered-cubic (FCC) alloys, NiCoCr and NiCoCrFeMn and perform a comparative study with the behavior observed in pure-Ni FCC metal. Employing long-time kinetic Monte Carlo (kMC) simulations, we examine the dynamics of atomic vacancies within these alloys driven by thermal fluctuations. Our findings reveal a significant deviation from the standard diffusive behavior observed in pure Ni, as vacancies in both concentrated alloys exhibit subdiffusive dynamics. This subdiffusive phenomenon is a signature of dynamical sluggishness in CCAs and can be characterized by long power-law-distributed rest periods. We demonstrate that these long wait times directly result from the broad distribution of energy barriers owing to the underlying lattice distortions in these complex alloys.

Building upon the results from our kMC framework, we train neural networks to classify defects based on machine-learning-based atomic descriptors. The surrogate model is further utilized to predict associated diffusion paths and energy barriers under thermal activation. We implement a customized kMC code that systematically incorporates the neural network's outcomes, allowing us to efficiently evolve dynamics of defects in atomistic configurations.

2:15 PM DS06.12.03

Characterizing Cu-Ni Surface Segregation and Oxidation with Machine-Learning Accelerated First-Principles Simulations and *In Situ* ExperimentsPandu Wisesa¹, Meng Li¹, Matthew Curran^{2,1}, Jeong Woo Han², Judith C. Yang¹ and Wissam A. Saidi¹; ¹University of Pittsburgh, United States; ²Pohang University of Science and Technology, Korea (the Republic of)

Comprehensively understanding oxidation mechanisms including surface reconstruction, interfacial segregation, and oxide growth on metallic and alloyed interfaces is crucial for preventing corrosion, manufacturing interfaces via layer-by-layer deposition, and elucidating catalytic reactions. However, the multiple competing simultaneous reactions constituting oxidation processes, in tandem with the heterogeneous binding affinities of different atom composition combinations, preclude facile kinetics and dynamics characterization via simple oxidation models such as Cabrera-Mott. Varying the partial pressure of oxygen and temperature on Cu-Ni alloyed surfaces can generally control prevalence of oxidized phases, such as c(2x2) and missing row reconstructions (MRRs). However, complete knowledge of such phase evolutions, how to control phase stability in applications, and the multidisciplinary methodology required to comprehensively characterize related energetics and kinetics are not currently available.

Pursuant to modeling such oxidation processes on Cu and Cu-Ni surfaces, this research resolves first-principles density functional theory (DFT) results, which are then leveraged to optimize deep neural-network potentials (DNPs). DNPs are subsequently implemented to complete molecular dynamics (MD), Monte Carlo (MC), and hybridized Grand Canonical Monte Carlo (MD/GCMC) simulations. These techniques model the relative energetic favorability of differently oxidized Cu and Cu-Ni surfaces, while developing kinetically relevant concentration profiles for Ni and O segregation across their layers. Interfacial oxidation dynamics are comprehensively described through stochastic time series analyses, identifying phase transformations as discrete breaks in structural features and cross-correlating different diffusion mechanisms with phenomenological observations. Experimental *in situ* environmental transmission electron microscopy (ETEM) visualizes and corroborates simulated surface oxidation and segregation modelling outcomes.

2:30 PM DS06.12.04

Assessing Al Ordering in CHA Zeolites with Organic Structure-Directing AgentsAlexander J. Hoffman¹, Mingrou Xie¹, Cecilia Paris², Manuel Moliner² and Rafael Gómez-Bombarelli¹; ¹Massachusetts Institute of Technology, United States; ²Instituto de Tecnología Química, Spain

Zeolites are microporous aluminosilicates within which molecules can diffuse and react. Frequently, these reactions occur at Brønsted acid sites, which form when Al³⁺ is substituted for Si⁴⁺ in framework tetrahedral sites (T-sites). The net anionic charge from Al substitution is balanced by a proton (H⁺) on an O atom adjacent to the Al substitution to form the Brønsted acid site. The positions of Al within the framework dictate the properties of zeolites; for example, CHA zeolites with the same composition (Si/Al ≈ 15) but with different fractions of Al sharing 6-membered rings (6-MR) have different turnover rates (per H⁺) for methanol dehydration [1, 2]. Therefore, controlling the distribution of Al within zeolites is a crucial step to controlling the properties of these zeolites.

Zeolite crystals are synthesized using structure-directing agents (SDAs), which are typically cationic and are either organic (OSDA; e.g., tetramethyl ammonium, TMA⁺) or inorganic (e.g., Na⁺). The size of these SDAs directs the formation of the void spaces of zeolites to produce different frameworks [3], while the locations of cationic centers in the SDAs guide the placement of anionic Al in the framework [4, 5]. Here, we use several computational tools to assess the stabilities of Al distributions as guided by OSDAs in CHA zeolites. The CHA framework has only one symmetrically unique T-site at which Al can be substituted (in a unit cell with 36 T-atoms); however, the addition of one Al breaks the symmetry of the unit cell. As such, the addition of more Al leads to growing numbers of distinct Al arrangements, with up to 13294 unique arrangements with Si/Al = 5 (6 Al substitutions in the unit cell). We use density functional theory (DFT) to optimize CHA structures substituted with different amounts of Al with and without charge-balancing OSDAs. These DFT data are used to train an equivariant graph neural network forcefield (NNFF) with the PaiNN architecture [6] to compute energies and perform optimization calculations on OSDA configurations for all the Al arrangements at low Si/Al ratios where combinatorics render rigorous DFT studies infeasible.

DFT calculations on Al distributions without any cationic SDAs in the framework favor Al distributions that maximize the average Al-Al distance, which indicates that Coulombic repulsion between anionic Al substitutions encourage Al separation. Similarly, DFT calculations of a sample of zeolites with cationic OSDAs show that the most favorable arrangements of Al involve those with short distances between the cation in the OSDA and nearby Al. The NNFF accurately captures the Coulombic interactions between charge centers in these structures to map the most likely Al distributions for a zeolite produced with a given OSDA. Such a workflow should enable a more rapid assessment of Al distributions in zeolites to tailor synthesis approaches and optimize Al distributions for different applications.

References

- [1] *ACS Catal.* **2017**, 7 (10), 6663–6674.
- [2] *Angew. Chem. Int. Ed* **2020**, 59 (42), 18686–18694.
- [3] *Angew. Chem. Int. Ed* **2013**, 52 (52), 13880–13889.
- [4] *Science* **2021**, 374 (6565), 308–315.
- [5] *Chem. Mater.* **2020**, 32 (21), 9277–9298.
- [6] In *Proceedings of the 38th International Conference on Machine Learning*; PMLR, 2021; Vol. 139, pp 9377–9388.

2:45 PM DS06.12.05

Deep Learning-Based Multimodal Analysis for Intelligent Characterization of Chemical Vapor Deposition-Grown Transition Metal DichalcogenidesShivani Bhawsar, Abdus Salam Sarkar and Eui-Hyeok Yang; Stevens Institute of Technology, United States

Deep learning (DL) offers a large set of tools and algorithms to analyze and extract features from the data. These can expedite the identification of nanomaterial optical and physical properties for efficient characterization. DL techniques have been used to address two-dimensional (2D) materials discovery [1], characterization [2], and determination of properties [3]. However, insufficient data generally cause overfitting, affecting accuracy [4,5].

Here, we present a generative deep learning-based solution that generates an arbitrary amount of 2D material samples when trained on only a limited amount of data. We used the resulting dataset to identify and segment MoS₂, WS₂, WSe₂, Fe:MoS₂, and Fe:WSe₂. We utilized a deep learning model along with optical and spectroscopic tools to determine the thickness and uniformity of the materials. The trained network extracted graphical features such as contrast, color, shapes, flake sizes, and their distributions from a dataset consisting of optical data and the Raman and photoluminescence (PL) spectra from chemical vapor deposition (CVD)-grown MoS₂, WS₂, WSe₂, Fe:MoS₂, and Fe:WSe₂ and mechanical exfoliated MoS₂, WS₂, and WSe₂. We also utilized an atomic force microscope (AFM) to collect thickness data, which provided information of the number of layers.

The image preprocessing on the dataset resized images to a standardized format, and normalized pixel intensities to ensure consistency, and implemented noise reduction algorithms to enhance image quality. We used deep generative models, *i.e.*, variation autoencoder (VAE), and generative adversarial network (GAN), to generate data for expanding small amounts of experimental datasets. The filtering algorithms were applied to the experimentally collected 2D images to identify graphical features including the area, location, color, coverage distributions, and optical features including contrast variation.

We plan to use convolutional neural networks and attention mechanisms in the convolutional neural networks to enhance the model's performance. This research will enable effective, high-throughput scanning of CVD-grown 2D materials.

References

- [1] *Nanophotonics* Volume 9 Issue 13
- [2] *Advanced Materials* Volume 32, Issue 29 2000953
- [3] *Computational Materials Science* Volume 150, July 2018, Pages 212-221

3:00 PMBREAK**3:30 PM DS06.12.06**

A Machine Learning Based Approach to Solve the Aerosol Dynamics Coagulation Model [Onochie C. Okonkwo](#)^{1,2}, [Rahul Patel](#)³, [Ravindra Gudi](#)³ and [Pratim Biswas](#)²; ¹Washington University in St. Louis, United States; ²University of Miami, United States; ³Indian Institute of Technology Bombay, India

Solving aerosol dynamic models accurately to obtain the size distribution function is often computationally expensive. Conventional artificial neural network (ANN) models offer an alternative procedure to solve the aerosol dynamic equations. However, conventional ANN models can result in violation of aerosol mass conservation. To further enhance accuracy and reduce computational time, a hybrid ANN approach to solve the aerosol coagulation equation is developed, validated, and demonstrated. The methodology and assumptions for the development of the hybrid ANN model which provides an analytical closed form solution for aerosol coagulation is described. The ANN model is trained and validated using a dataset from an accurate sectional model. Following this, the hybrid ANN aerosol model is used to describe the evolution of aerosol in a furnace aerosol reactor. The hybrid ANN model results are compared to the accurate sectional and moment coagulation models. The hybrid ANN coagulation model prediction was found to accurately describe the evolution of aerosol size distribution at a computational cost which is slightly more than the moment model but orders of magnitude less than the sectional model.

3:45 PM DS06.12.07

Leveraging Active Learning in Restricted, Discretized and Predefined Design Spaces for NMR Peak Prediction [Ramsey Issa](#) and [Taylor D. Sparks](#); University of Utah, Salt Lake City, United States

Active learning provides a strategy that allows us to intelligently select data points in our design space, that will provide machine learning models with maximum information. Since Density functional theory and Quantum simulations typically require costly computational resources and are very time consuming, active learning allows us to drastically reduce computational time and cost by selecting key points in the design space that reduce global uncertainty. This strategy leads to the development of a model that can quickly and adequately predict desired outputs from DFT using the fewest number of simulations. Typically, the use of acquisition functions to select informative points, leads to arbitrary solutions in the design space that we might not be interested in simulating. Here, we restrict our search to distinct, discretized and a predefined list of pyrochlore $\text{La}_2(\text{Sn}_x\text{Zr}_{1-x})_2\text{O}_7$ candidates avoiding arbitrary solutions. The predefined list of candidates results in 531 possible configurations upon the addition of Sn atoms into the 16-position crystal structure where we predict NMR peak position. We utilize a gaussian process as our surrogate model and compare three iterative point selection methods on this dataset. The three active learning strategies compared are random selection as a baseline, maximum predicted model uncertainty, and maximum-value entropy search acquisition function selected sampling.

4:00 PM DS06.12.08

Benchmarking Equivariant Graph Neural Network Potentials for Atomistic Simulations [Utkarsh Pratiush](#), [Suresh Bishnoi](#), [Jayadeva Jayadeva](#), [Sayan Ranu](#) and [N M Anoop Krishnan](#); Indian Institute of Technology Delhi, India

Graph neural networks (GNNs) have revolutionized the representation learning of graph-structured data in diverse domains. In atomic simulations, GNNs exhibit immense potential for capturing intricate interatomic interactions and predicting potential energy surfaces. Equivariant graph neural networks (EGNNs) excel in modeling the symmetries inherent in atomic systems, making them ideal for atomistic simulations. However, the lack of comprehensive benchmarking studies hampers their evaluation against other state-of-the-art potentials. To bridge this gap, we present a systematic benchmarking framework for EGNN potentials in atomic simulations. Our contributions include a standardized dataset encompassing diverse atomic systems, evaluation of six EGNN potentials, and a comprehensive benchmarking framework with various metrics. We assess energy predictions, forces, and structural properties, enabling an objective analysis of EGNN potential capabilities and limitations. Our research facilitates informed selection and development of accurate and efficient potential energy models. The results and insights presented herein will greatly benefit researchers and practitioners in the atomistic simulation field.

4:15 PM DS06.12.09

Inverse Design of Upconverting Nanoparticles via Deep Learning on Physics-Infused Heterogeneous Graphs [Eric Sivonxay](#)¹, [Lucas Attia](#)^{1,2}, [Xiaojing Xia](#)¹, [Brett A. Helms](#)¹, [Emory Chan](#)¹ and [Samuel M. Blau](#)¹; ¹Lawrence Berkeley National Laboratory, United States; ²Massachusetts Institute of Technology, United States

Heterostructured core-shell lanthanide-doped upconverting nanoparticles (UCNPs) have unique optical properties, capable of near-infrared excitation to yield visible and ultraviolet emissions. UCNPs have broad applications ranging from biosensing and super-resolution microscopy to 3D printing. Factors affecting the nonlinear photophysical properties of UCNPs include number of shells, shell thicknesses, dopant concentrations, and surface ligands, defining a vast chemical design space. While kinetic Monte Carlo (kMC) simulations allow for reasonably accurate in silico prediction of optical properties, calculations scale poorly with particle size and dopant loading, constraining the search for UCNPs with desirable properties to be fundamentally Edisonian. Despite the potential to use deep learning (DL) to navigate this space more efficiently, UCNPs previously had neither a viable structural representation for DL (they are unlike molecules, crystals, proteins, text, or images) nor sufficient data for DL (individual photophysical kMC simulations can take weeks). Here, we report efforts to overcome these challenges by combining high-throughput data generation with nanoparticle representation learning. We construct the first large dataset of over 10,000 simulated UCNP spectra with bespoke high-performance lanthanide energy transfer kMC driven by automated workflows on HPC resources. We investigate random forest, MLP, CNN, and GNN ML architectures, eventually converging on a physics-infused heterogeneous GNN as our best-performing model. We then use the trained GNN to perform inverse design of UCNP heterostructure via gradient-based optimization - maximizing UV emission under 800 nm illumination as a function of number of shells and maximum nanoparticle size, identifying novel structures with far higher predicted emission than any in our training data. To the best of our knowledge, this is the first time that data generation, representation development, and DL-enabled optimization have been performed in a novel space end-to-end.

4:30 PM DS06.12.10

A Machine Learning-Based Constitutive Modeling of Plastic Behavior in Polycrystalline Materials using Crystal Plasticity Simulations Including Strain Hardening [Ronak Shoghi](#) and [Alexander Hartmaier](#); Ruhr-Universität Bochum, Germany, Germany

Machine learning (ML) algorithms can provide an effective way of modeling complex material behavior, including plasticity. With their ability to analyze vast amounts of data and identify patterns, these advanced computational techniques can capture relationships between microstructure and mechanical properties and enable an accurate yet flexible description of material behavior. The importance of high-quality training data in machine learning cannot be overstated, as it directly impacts the performance and reliability of the resulting models. Therefore, finding an optimal data generation strategy for the training of ML yield functions and strain-hardening models is essential to ensure their accuracy and reliability. Our work revealed that Support Vector Machines (SVM) can be used as machine learning yield functions and can be successfully trained for materials with significant plastic anisotropy, like polycrystals with a Goss texture, using only 300 data points. The training data was carefully selected to cover a wide range of loading conditions in full 6-dimensional space. The accuracy and reliability of the trained ML yield functions were assessed using a variety of statistical measures, including mean squared error and confusion matrix. As the next step, the optimal training data strategy was employed for generating training data using micromechanical modeling. This allowed for further consideration of microstructural parameters like crystallographic texture or grain size in the input data for the training of the ML yield function. Moreover, this data also contains information of the strain-hardening behavior of the material. A database containing simulation data and metadata was developed, making it easier to train and refine the ML model. From this database, a proper data-oriented formulation for strain hardening was developed, which complements the previously established yield function. This study demonstrated the potential of ML algorithms as powerful tools for modeling complex material behavior. The careful selection and generation of training data, as well as the inclusion of microstructural parameters and work-hardening effects, were crucial for achieving reliable and accurate ML yield functions and strain-hardening models.

4:45 PM DS06.12.11

Data-Driven Failure Assessment Diagram Approach for Tubing and Casing Steel Grades [Mohamed Elkhodbia](#) and [Imad Barsoum](#); Khalifa University, United Arab Emirates

The objective of this study is to propose a data-driven approach to obtain an accurate J-based fracture assessment diagram (FAD) by creating a large database of J-based FAD curves for various cracks and materials in tubing and casing that are widely used in downhole applications, and then utilizing artificial neural networks (ANNs) to obtain the appropriate FAD curve shape. Methods, Procedures, Process: The proposed steps include selecting the crack shapes and materials of interest, creating an FEA model with geometry, boundary conditions, mesh, and loading conditions, and finding the critical limit load for plastic collapse. Next, elastic (Je) and elastic-plastic (Jep) FEA analyses are conducted for each crack shape as a function of applied load, and a J-based FAD is developed for all crack shapes, materials, and limit loads. Lastly, data-driven techniques such as artificial neural networks (ANNs) are used to predict the FAD shape. Results, Observations, Conclusions: The study highlighted the effectiveness of a data-driven FAD model by comparing it with the empirical FAD, emphasizing the advantages of the data-driven approach. ANNs accurately captured the FAD shape from the validation set, demonstrating their potential in understanding material behaviour. The comprehensive dataset offered

valuable insights for better decision-making in material selection, design, and safety considerations. Streamlined and automated structural analysis processes led to more efficient decisions concerning inspections, repairs, and infrastructure development. This work sets itself apart from previous studies by employing machine learning techniques to generate FADs, providing an extensive dataset and practical applications in refineries and plants for managing and maintaining critical infrastructure. The data-driven FAD model aids engineers and maintenance professionals in predicting structural integrity under various conditions, which is crucial for mitigating potential failures, reducing risks of leaks, and optimizing inspection schedules and repair strategies. The model also supports the design of safer and more reliable pipeline systems. Novel/Additive Information: The significance of the subject matter is evident through the key technical contributions to the downstream industry, enhancing structural integrity assessment accuracy and preventing failures while reducing environmental risks. This paper presents a novel approach by employing machine learning techniques, specifically ANNs, to generate data-driven FADs, providing an extensive dataset and practical applications in refineries and plants for managing and maintaining critical infrastructure. The data-driven FAD model improves structural integrity assessment accuracy, reduces environmental risks, and optimizes maintenance schedules, adding to the state of knowledge in the petroleum industry

SESSION DS06.13: Virtual Session
Session Chairs: Grace Gu and N M Anoop Krishnan
Thursday Morning, December 7, 2023
DS06-virtual

10:30 AM *DS06.13.01

Materials Informatics for Computational and Machine Learning (ML)-Assisted Design: An Overview for Polycrystalline Metals and Mechanical Metamaterials Pinar Acar, Sheng Liu, Ender Eger, Mohamed Elieithy, Hengduo Zhao and Matthew Long; Virginia Tech, United States

In this talk, we will present an overview of the computational methods developed by our group to design metals and metamaterials for enhanced mechanical performance by modeling them in terms of micro-scale ($\sim 10^{-6}$ m) features. First, we present numerical approaches to quantify the crystallographic texture and grain topology of polycrystalline metals. Similarly, a shape descriptor approach is developed to model the topology of mechanical metamaterials. Following the development and integration of such computational characterization approaches into numerical homogenization schemes to obtain mechanical properties, design optimization problems are developed and solved to design underlying microstructures of polycrystalline metals and mechanical metamaterials for improved mechanical performance.

Next, the talk will focus on the impact of manufacturing-related uncertainty arising from the imperfections and defects during the processing and fabrication of materials on reliability and mechanical performance. We will discuss how to develop design under uncertainty formulations to address forward and inverse design problems in order to improve the elasto-plastic properties of polycrystalline metals and mechanical metamaterials. Additional topics will cover the integration of Artificial Intelligence (AI)/Machine Learning (ML) techniques into physics-informed material models to accelerate the design of material systems processed with conventional and additive manufacturing techniques. We will demonstrate applications of forward and inverse design problems for polycrystalline metals using ML-driven design approaches. The AI/ML methods will also be used for mechanical metamaterials to identify their mechanical property spaces showing all possible values of the selected properties.

11:00 AM DS06.13.02

Improved Prediction of Adsorption Energies and Vibrational Frequencies of Molecules Adsorbed on Monometal Catalyst Surfaces by Machine Learning using Structural Descriptors Keigo Nakamura and Masakuni Okamoto; Hitachi Ltd., Japan

Designing surfaces of metallic catalyst is essential to improve the efficiency of reaction. Recently prediction of intermediate states of adsorbates by using both first-principles calculation and machine learning has been attracted much attention. First-principles calculations for adsorbates on surfaces have been performed, and various databases of adsorption energies have been reported [1]. In order to improve the accuracy of the prediction by machine learning, various descriptors have been developed [2]. Structures of both metal surfaces and adsorbates could affect the adsorption energies. We thus focus on the structural descriptors for machine learning to predict the adsorption energies and vibration properties of adsorbates on metals. We used a surface slab model which has (3 or 5)-layer mono metal (Ti, V, Cu, etc) fcc surface and evaluated the adsorption energies and vibrational frequencies of adsorbates (C, H, N, CO, etc) by first-principles calculation.

We calculated from first-principles more than 7000 surface structures which were employed for prediction of adsorption energies and vibrational frequencies. We evaluated the accuracy of prediction based on several machine learning techniques and found that structural descriptors such as bulk lattice parameter, d -band center and width of the surface model are effective to improve the accuracy compared to the prediction using only composition descriptors. The prediction accuracies of the mean squared error were improved from 0.161 to 0.136. The importance of structural descriptors was examined using the "permutational importance". The lattice parameter and d -band center were turned out to contribute highly to the prediction of adsorption energy.

[1] <https://www.catalysis-hub.org>

[2] H.-J. Peng, *et. al.*, Nature Communications **13**, 1 (2022).

11:05 AM DS06.13.03

Prediction of Toughness in Heterogeneous Materials using Machine Learning A. N.S. Sadi and Zubaer M. Hossain; University of Delaware, United States

Composites or heterogeneous materials have a wide range of applications in the fields of aerospace, structural materials, biomedical, energy conversion devices, high-temperature materials, etc. But the effective properties of composites, in particular, toughness and strength are hard to predict as a function of their constituent properties. By definition, heterogeneous materials contain different shapes, sizes, compositions, and material or phase distributions at different length scales, making iterative experiments inefficient, time-consuming, and expensive to use for this purpose. In this work, the toughness of heterogeneous brittle material is investigated using a combination of continuum scale simulations and machine learning techniques. Our goal is to predict the configurations (or different structural and material parameters) of the composite that optimize its effective toughness. The continuum simulations are based on the variational phase-field modeling of fracture, and we applied the novel surfing boundary condition, which allows adequate time for the crack to propagate, enabling evaluation of the critical energy release rate or toughness. In particular, we focus on understanding the criteria for deflection vs. penetration for a number of composite configurations and identify the structural or material descriptors that define the criteria. Using the descriptors, we develop supervised machine learning models for predicting the toughness of the composite. The models are trained using data sets, collected from continuum simulations and are used to ascertain the toughness-structure correlation for a number of unexplored variants of the configurations. This talk will discuss the findings and highlight the need for applying machine learning tools to predict the toughness of a composite, for an arbitrary choice of structural and material parameters.

11:20 AM DS06.13.04

Neural Networks with Optimized Neuron Activation Functions and Without Nonlinear Optimization or How to Prevent Overfitting, Cut CPU Cost and Get Physical Insight All at Once Sergei Manzhos and Manabulhara; Tokyo Institute of Technology, Japan

In machine learning (ML) applications in the fields of materials science, computational chemistry, and elsewhere, neural networks (NN) play a prominent role. For applications ranging from machine-learned interatomic potentials to DFT functionals to structure-property relations, they offer a high expressive power and generality (black-box character). However, they require optimization of a large number of nonlinear parameters, leading to a high CPU cost and the dangers of overfitting. These disadvantages become more severe as the dimensionality of the feature space increases and the data density necessarily becomes low. As many ML techniques, NNs also do not provide physical insight.

We will present a method to construct NNs with rule-based definitions of parameters which permits dispensing with non-linear parameter optimization altogether. We also construct optimal neuron activation functions for the problem at hand that are different for different neurons, thereby increasing the expressive power of the NN. It is the absence of the need to deal with nonlinear optimization that makes this meaningful (contrary to backpropagation that works best with the same neuron activation function for all neurons). The neuron activation functions are easily obtained from an additive Gaussian process regression [1] in redundant coordinates that are neuron arguments.

As a result, we obtain a method that combines the expressive power of an NN with the robustness of a linear regression: we will demonstrate on the examples of the fitting of interatomic potentials that the NN does not suffer from overfitting as the number of neurons is increased beyond optimal [2]. We will also show that by modifying the rules with which the NN parameters are defined, one can easily obtain an orders of coupling representation (often used in physics and computational chemistry under the names many-body and N-mode representation, respectively) [3] which also helps generate elements of insight [4] while maintaining the generality of the method.

[1] Mach. Learn.: Sci. Technol., 3, 01LT02 (2022)

[2] arXiv:2301.05567, <https://doi.org/10.48550/arXiv.2301.05567>

[3] arXiv:2302.12013, <https://doi.org/10.48550/arXiv.2302.12013>

[4] Comput. Phys. Commun., 271, 108220 (2022)

11:35 AM DS06.13.05

Employing Deep Neural Networks and High-Throughput Computing for The Identification and Prediction of Vein-Like Structures Junbo Niu, Xinxin Ma, Bin Miao, Zhiyu Chi and Feilong Wang; Harbin Institute of Technology, China

In this investigation, we leverage Convolutional Neural Networks (CNNs) to engineer a simple segmentation and recognition algorithm specialized for the delineation of complex, network-like morphologies—often termed "vein-like structures (VLSs)"—in Scanning Electron Microscopy (SEM) imagery. These intricate formations frequently appear during the nitriding treatment of medium- to high-carbon alloy steels. To navigate the multifaceted characteristics of such architectures, we synergize CNN-based methodologies with high-throughput thermodynamic computations via Thermo-Calc. This integration aims to quantify both the theoretical upper bounds and the empirical values of the VLSs. By establishing neural network models for both theoretical upper bounds and empirical measurements, we bridge the gap between thermodynamics and thermo-kinetics in the nitriding process. Applying this amalgamated predictive schema to 8Cr4Mo4V steel, we effectuate a groundbreaking departure from conventional paradigms that exclusively depend on thermodynamic calculation-based diffusion models. The emergent model yields transformative implications for the metallurgical sector, paving the way for the refinement of future nitriding algorithms and enhancements in nitriding methodologies.

11:40 AM DS06.13.06

Prediction of Li-Dendrite Growth with Physics-Informed Neural Network and Transformer Model Yi-Chia Han¹, Chun-Wei Pao¹ and Chih-Hung Chen²; ¹Academia Sinica, Taiwan; ²National Taiwan University, Taiwan

The growth of lithium-dendrite at anodes has long been a well-known hindrance limiting the development of lithium-ion batteries. Gaining a deeper understanding of the mechanism behind dendrite growth is a challenging yet pivotal task. Although phase-field models (PFM) have proven to be an effective numerical approach for modeling Li dendrite growth behaviors compatible with experiments in time and length scales, seeking for a computationally efficient surrogate model still remains imperative due to the computationally demanding fine meshes required for PFM. Recently, deep learning (DL) has demonstrated promising potential in learning dynamical systems. Herein, we introduce two DL models to capture the spatial and temporal evolution of Li dendrite growth, ion concentrations, and electrostatic potential of Li metal anode upon charging. The first model integrates the physics-informed neural networks (PINNs) with PFM. In the learning phase, we train our PINNs model to learn PFM with imposed governing equations and boundary conditions so as to retain consistency with physics laws. In the second model, we develop a transformer, originated from Natural Language Processing (NLP), for the prediction of dynamic evolution of lithium dendrite growth. We utilize embedded dynamical systems as input sequences and predict Li deposition based on past time steps with stochastic initial conditions. The results obtained from both models yield notable consistency with those from numerical models. While further efforts are required to delve deeper into the application of deep learning in PFM, our findings propose an alternative platform for exploring phase-field of Li-dendritic morphology.

SYMPOSIUM EL01

Defects and Strain in Two-Dimensional Materials
November 27 - November 30, 2023

Symposium Organizers

Sung Woo Nam, University of California, Irvine
Kayla Nguyen, University of Oregon
Michael Pettes, Los Alamos National Laboratory
Matthew Rosenberger, University of Notre Dame

* Invited Paper

+ JMR Distinguished Invited Speaker

SESSION EL01.01: Quantum Defects in 2D Materials
Session Chairs: Sung Woo Nam and Matthew Rosenberger
Monday Morning, November 27, 2023
Hynes, Level 2, Room 204

10:30 AM EL01.01.01

Building a Point Defect Genome in WS₂, Applications in the Search of Quantum Defects Geoffroy Hautier¹, John C. Thomas^{2,3}, Wei Chen⁴, Yihuang Xiong¹, Bradford A. Barker⁵, Junze Zhou², Weiru Chen¹, Antonio Rossi^{2,3,3}, Nolan Kelly⁵, Zhuohang Yu^{6,6}, Da Zhou^{6,6}, Shalini Kumari^{6,6}, Joshua A. Robinson^{6,6,6}, Mauricio Terrones^{6,6,6}, Adam Schwartzberg², D. Frank Oglethorpe³, Eli Rotenberg³, Marcus M. Noack³, Sinead M. Griffin^{2,3}, Archana Raja^{2,3}, David A. Strubbe⁵ and Alexander Weber-Bargioni^{2,3}; ¹Dartmouth College, United States; ²Lawrence Berkeley National Laboratory, United States; ³Lawrence Berkeley National Laboratory, United States; ⁴Université catholique de Louvain, Belgium; ⁵University of California, Merced, United States; ⁶The Pennsylvania State University, United States

Point defects in 2D materials are driving their opto-electronic performance. Color centers in 2D materials have been for instance, of interest for quantum sensing and networking applications. Most of the possible defects in 2D materials are however uncharacterized making defect design towards a specific application very challenging. On the other hand, first principles computations have made tremendous progresses in modeling the opto-electronic properties of point defects. Here, we report on a large computational database of point defects in WS₂. The database contains electronic structure data for more than 700 charged defects in WS₂ made by tungsten and sulfur substitutions from elements across the periodic table. We will show how to use this unique data set to search for new quantum defects presenting bright emission in the telecom and spin multiplicity. Importantly, we will report on the synthesis and scanning tunneling microscopy and spectroscopy of one of our quantum defect candidates; demonstrating good agreement with the theoretical high-throughput prediction and confirming the *in silico* discovery of an entirely new quantum defect with high potential for applications in WS₂.

10:45 AM EL01.01.02

Quantum Defects in 2D Transition Metal Dichalcogenides for THz-Technologies Jingda Zhang, Goki Eda and Su Ying Quek; National University of Singapore, Singapore

Two-dimensional (2D) transition metal dichalcogenides (TMDs) offer significant advantages for optically addressable defect systems, making them a promising host platform for spin-triplet transition metal impurities with remarkably large zero-field splitting (ZFS) ranging from sub-THz to THz. These defects can serve as the building blocks for quantum information systems and can potentially function as single-photon THz emitters if controlled population inversion is achieved. We employ first-principles materials discovery based on Density Functional Theory

(DFT) to identify the most suitable spin-triplet defects in 2D TMDs, followed by constrained DFT combined with group theory analysis to demonstrate the excited-state dynamics and its ability to perform THz qubit operations. Additionally, we propose a novel theoretical design for THz quantum emitters driven by near-infrared excitation. Our research broadens the scope of advancements in quantum information science and lays a robust foundation for their integration with THz technologies.

11:00 AM EL01.01.03

Probing Te Vacancies as a Source of the Chiral Anomaly in Layered Dirac Materials ZrTe₅ and HfTe₅[Elizabeth Peterson](#), Christopher Lane and Jian-Xin Zhu; Los Alamos National Laboratory, United States

The layered Dirac materials ZrTe₅ and HfTe₅ have been the subject of vigorous investigation in recent years to experimentally observe signatures of quantum anomalies in their transport. These materials exhibit negative longitudinal magnetoresistance (NLMR)—a reduction in the resistivity when parallel electric and magnetic fields are applied to a sample—that is speculated to be direct evidence of an asymmetry in the number of left- and right-handed carriers, or a *chiral anomaly*. If this is indeed the case, these materials would serve as a tractable tabletop testbed to probe cosmological theories of quantum anomalies and symmetry breaking that arises when moving from classical to quantum field theories.

Despite a wealth of experimental evidence of NLMR in ZrTe₅ and HfTe₅, in addition to a temperature-induced change in the sign of the Hall coefficient, the microscopic mechanism driving this anomalous transport behavior remains an open question. Prior first-principles calculations have demonstrated that strain drives a series of transitions between topological states, from a strong topological insulating, to a Dirac semimetallic, to a weak topological insulating state, which explains the diversity of experimental reports of different topological states in these materials. Further, it has been experimentally observed that off-stoichiometric, Te-deficient ZrTe₅ exhibits a stronger NLMR than pristine stoichiometric ZrTe₅. To determine if these materials truly exhibit a chiral anomaly, a rigorous modeling of the transport properties of ZrTe₅ and HfTe₅ in the presence of Te vacancies is necessary.

In this work we determine the effect of Te vacancies on the electronic and transport properties of ZrTe₅ and HfTe₅. From a systematic series of first-principles density functional theory calculations we demonstrate the effect of Te vacancies both as a source of defect states and as an effective intrinsic source of strain. We further perform ab initio-based transport calculations in the strong magnetic field regime with an eye towards unravelling the origin of their anomalous transport properties and to probe their utility as testbeds for the observation of quantum anomalies.

LA-UR-23-26340

11:15 AM *EL01.01.04

Atomic Defects in 2D Materials for Quantum Technologies[Pankaj K. Jha](#); Syracuse University, United States

Novel materials are the backbone of any technology. In this talk, I will discuss 2D materials that can be exfoliated down to a monolayer as well as grown layer by layer, with applications ranging from the generation of quantum light to the detection of single photons at visible and near-infrared wavelengths. In the first part of the talk, atomic defects (also known as color centers) in boron nitride as a promising candidate for single photon sources at room temperature will be discussed [1,2]. Experimental results ranging from the nanometric localization of hBN color centers [3] and sub-poissonian photon distribution to observing near-transformed limited lines will be presented [4]. I will conclude by sharing our near-term and long-term vision for hBN color centers interfaced with other 2D semi- and superconductors for sensing and photon detection applications.

References:

- [1] A. D. Franklin, in Point Defects in Solids, J. H. Crawford, L. M. Slifkin, Eds. (Plenum Press, New York, 1972), vol. 1, chap. 1.)
- [1] T. T. Tran, K. Bray, M. J. Ford, M. Toth, I. Aharonovich, Quantum Emission from Hexagonal Boron Nitride Monolayers. Nat. Nanotechnol. 11, 37-41 (2016)
- [3] P. K. Jha, H. Akbari, Y. Kim, S. Biswas, and H. A. Atwater, Nanoscale Axial Position and Orientation Measurement of Hexagonal Boron Nitride Quantum Emitters Using a Tunable Nanophotonic Environment, Nanotechnology 33, (2022)
- [4] H. Akbari, S. Biswas, P. K. Jha, J. Wong, B. Vest, and H. A. Atwater, Lifetime-Limited and Tunable Quantum Light Emission in h-BN via Electric Field Modulation, Nano Lett. 22, 7798 (2022).

SESSION EL01.02: Optical Properties of 2D Materials
Session Chairs: Michael Pettes and Matthew Rosenberger
Monday Afternoon, November 27, 2023
Hynes, Level 2, Room 204

1:30 PM *EL01.02.01

Macroscopic-Monolayers Excitons and Polaritons[Hui Deng](#); University of Michigan, United States

Transitional metal dichalcogenides (TMD) monolayers of composition MX₂ (M = Mo, W and X = S, Se) form a class of semiconductor with unique optical properties and unprecedented flexibility for engineering and integration. They exhibit many novel phenomena and promise new device concepts. However, TMD monolayers of high optical qualities have been limited to micron-sized flakes produced by low-throughput and labor-intensive processes, whereas large-area films are often affected by surface defects and large inhomogeneity. We show a rapid and reliable method to synthesize multi-millimeter-sized TMD monolayers of uniform, high optical quality using 1-dodecanol encapsulation combined with gold-tape-assisted exfoliation [1]. We demonstrate the utility of our encapsulated monolayers by scalable integration with arrays of photonic crystal cavities with varying parameters, all forming polaritons with the same monolayer. We furthermore show the dependence of stimulated relaxation and long-range transport of the polaritons on the photonic crystal parameters.

- [1] Q. Li, et al., "Macroscopic transition metal dichalcogenides monolayers with uniformly high optical quality." *Nat Commun* 14, 1837 (2023). doi:10.1038/s41467-023-37500-1

2:00 PM EL01.02.02

Near-Field Imaging of Interlayer Exciton in Strained Van Der Waals Heterostructure[Soyeong Kwon](#), Jin Myung Kim, Peiwen J. Ma, Weilin Guan and Sungwoo Nam; University of California, Irvine, United States

Recent discoveries on atomically thin Van der Waals materials have suggested new strategies for optoelectronic devices with reduced dimensionality and high elastic modulus. In particular, transition metal dichalcogenides (TMDs) and their vertical heterostructures host in-plane and out-of-plane interlayer excitons which can be tailored through strain engineering. In this talk, we investigated the interface phenomena in uniaxially strained TMD heterostructure. We prepared MoSe₂/WSe₂ heterostructure on an elastomeric substrate with near zero twist angle and performed photoluminescence and reflectance measurements. We found the signature of interlayer excitons and compared their behaviors in unstrained and strained regions in far-field optical characterizations. Furthermore, near-field mapping and spectroscopic methods of photo-induced force microscopy enabled nanoscale analysis of interlayer exciton coupling controllable with the strain magnitude. These results suggest that strain-modulated electronic and optical properties of twisted TMD/TMD heterostructures will be utilized for modifying interlayer exciton trapping and diffusion behaviors.

2:15 PM EL01.02.03

How to Improve the Luminescence and Valley Polarization Properties of Large-Area Monolayer MoS₂ Films Grown by Chemical Vapor Deposition?[Poulab Chakrabarti](#)¹, Faiha Mujeeb² and Subhabrata Dhar²; ¹University of Maryland, United States; ²Indian Institute of Technology Bombay, India

The development of future valley-based electronics or valleytronics requires a high degree of valley polarization (VP) in large area monolayer (1L)-MoS₂. Though it is possible to synthesize 1L-MoS₂ films with large area coverage, VP property of as-grown films is found to be very poor. Here, using temperature dependent photoluminescence (PL), polarization resolved PL and Raman spectroscopy, we investigate the effect of in situ vacuum annealing as well as the relaxation of strain on the luminescence and the VP properties of large area single layer MoS₂ films grown on *c*-sapphire and SiO₂/Si substrates by a microcavity based chemical vapor deposition (CVD) technique. The study shows that the strain as well as the physisorption of air molecules at the sulfur vacancy (V_S) sites play key roles in governing the optical quality of CVD grown 1L-MoS₂. Removal of air molecules from the V_S sites enhances the relative strength of the A-exciton/trion transition as compared to the broad defect luminescence (DL) band arising from those defects at low temperatures. It has also been found that such removal helps in improving the VP property of the film. Relaxation of biaxial tensile strain, which has been achieved by post growth transferring of 1L-MoS₂ film from the sapphire to a SiO₂/Si substrate by a polystyrene

assisted transfer process, is also found to be helpful to get back the high polarization character (~80%) of the K-valleys. The study further shows that the transfer process not only facilitates the removal of physisorbed air molecules from the V_S sites but also puts in place a long-lasting capping layer on 1L-MoS₂ that shields the film from reacting with air and hence enhances the relative yield of A-exciton/trion transition by suppressing the sub-bandgap DL transition. The study thus creates an opportunity to use CVD grown large area 1L-MoS₂ for the development of optoelectronic as well as valleytronic devices for practical applications for the future.

2:30 PM *EL01.02.04

Light Scattering and Emission from Hetero-Structures Andrea C. Ferrari; University of Cambridge, United Kingdom

Heterostructures based on layers of atomic crystals have a number of properties often unique and very different from those of their individual constituents and of their three dimensional counterparts. The combinations of such crystals in stacks can be used to design the functionalities of such heterostructures. I will show how Raman spectroscopy can be used to fingerprint such heterostructures, and how these can be exploited in novel light emitting devices, such as single photon emitters, and tuneable light emitting diodes

3:00 PM BREAK

SESSION EL01.03: Quantum Emission in 2D Materials

Session Chairs: SungWoo Nam and Kayla Nguyen

Monday Afternoon, November 27, 2023

Hynes, Level 2, Room 204

3:30 PM *EL01.03.01

Single Photon Emitters in 2D Materials Berend T. Jonker and Hsun Jen J. Chuang; Naval Research Laboratory, United States

Single photon emitters (SPEs), or quantum emitters, are key components in a wide range of nascent quantum-based technologies. A solid state host offers many advantages for realization of a functional system, but creation and placement of SPEs are difficult to control. We describe here a novel paradigm for encoding strain into 2D materials to create and deterministically place SPEs in arbitrary locations with nanometer-scale precision [1]. We demonstrate the direct writing of SPEs in monolayer WSe₂ using an atomic force microscope nano-indentation process. This quantum calligraphy allows deterministic placement and real time design of arbitrary patterns of SPEs for facile coupling with photonic waveguides, cavities and plasmonic structures. Because monolayer WSe₂ is a direct gap semiconductor, SPE emission at a given wavelength is often intermixed with classical light resulting from conventional excitonic recombination, reducing the purity of the quantum emission as quantified by the second order autocorrelation function $g(2)(t=0)$. We show that this undesirable classical emission, arising primarily from defect bound excitonic processes, can be significantly suppressed by electrostatic gating [2] or incorporating the WSe₂ layer in a simple van der Waals heterostructure [3]. Suppression of this classical emission allows a more accurate assessment of the quantum emission character, and results in values of $g(2)$ as low as 0.07 at low temperature. In addition, the SPE intensity at a given wavelength can be strongly modulated by changing the polarity of the gate bias, a feature of technological importance for practical applications. Initial results for SPEs in hBN will also be summarized, time permitting.

[1] M.R. Rosenberger et al, ACS Nano 13, 904 (2019). <https://doi.org/10.1021/acs.nano.8b08730>

[2] C.E Stevens et al, ACS Nano 16, 20956 (2022). <https://doi.org/10.1021/acs.nano.2c08553>

[3] H.-J. Chuang et al, under review (2023).

*Work done in collaboration with Matthew R. Rosenberger (Notre Dame), Hsun-Jen Chuang, Sungjoon Lee and Kathleen M. McCreary (Naval Research Laboratory), and Christopher Stevens and Joshua R. Hendrickson (Air Force Research Laboratory, Wright-Patterson AFB).

† This work was supported by core programs at NRL.

4:00 PM EL01.03.02

Defect Formation in Two-Dimensional Carbon-Doped Hexagonal Boron Nitride Tsz Wing Tang, Hongwei Liu, Yuyin Li, Jun Wang and Zhengtang Luo; Hong Kong University of Science and Technology, China

Tsz Wing Tang, Hongwei Liu, Yuyin Li, Jun Wang, and Zhengtang Luo

¹Department of Chemical and Biological Engineering, the Hong Kong University of Science and Technology, Clear Water Bay, Kowloon, Hong Kong, 999077, P.R. China

Visible-range single photon emitters (SPEs) from monolayer hexagonal boron nitride has demonstrated exceptional optical performance as a candidate for quantum optical technology application. However, the controllability of the carbon defect engineering in hBN has remained elusive, including the unadjustable SPE density, unconfined wavelength, and low uniform yield. Thus, the integration into on-chip quantum devices has suffered. Here, by precisely controlling the carbon incorporation via diffusion from molten copper during chemical vapor deposition (CVD) growth, we demonstrate a strategy to engineer the defect density in hBN, and achieve high uniform SPEs with confined emission wavelengths in hBN. By controlling the carbon diffusion rate, we observed an increase in carbon doping level and provided evidence for achieving high-yield uniform single photon emitters in hBN down to monolayer limit. Our method enables the density of SPE creation to become adjustable, from hBN monolayer samples, with high uniformity and confined wavelength. This method stimulates a significant step forward to integrating advanced two-dimensional (2D) material engineering into on-chip quantum devices.

The authors acknowledge the support from RGC (16304421).

4:15 PM EL01.03.03

Quantum Defect Candidates at Modified Substitution Sites within WS₂ John C. Thomas¹, Wei Chen², Yihuang Xiong³, Bradford A. Barker⁴, Junze Zhou¹, Weiru Chen³, Antonio Rossi¹, Nolan Kelly⁴, Zhuohang Yu⁵, Da Zhou⁵, Shalini Kumari⁵, Joshua A. Robinson⁵, Mauricio Terrones⁵, Adam Schwartzberg¹, D. Frank Ogletree¹, Eli Rotenberg¹, Marcus M. Noack¹, Sinead M. Griffin¹, Archana Raja¹, David A. Strubbe⁴, Alexander Weber-Bargioni¹ and Geoffroy Hautier³; ¹Lawrence Berkeley National Laboratory, United States; ²Université Catholique de Louvain, Belgium; ³Dartmouth College, United States; ⁴University of California, Merced, United States; ⁵The Pennsylvania State University, United States

Defect systems with in-gap electronic states are of high interest in atomic-scale photon emission applications with use in, e.g., quantum sensing and quantum networks. We investigate a two-dimensional material system that is treated within an ultrahigh vacuum environment to produce dense regions of chalcogen defectivity [1], and subsequently dope the system with a transition metal of interest that has been selected for its theoretically predicted optical transition and strong transition dipole moment. The chalcogen-substituted defect is formed at the atomic scale via tip-induced diffusion and subsequently visualized with scanning tunnelling microscopy. Scanning tunnelling spectroscopy, collected in an autonomous fashion using Gaussian process regression techniques [2], reveals anticipated in-gap states that are further verified with differential conductance maps paired with simulations obtained by density functional theory. High-throughput defect screening enables the selection of a handful of promising candidates, where the fabrication and investigation of one of these systems is shown to be experimentally obtainable.

References:

[1] Rossi, A., Thomas, J. C. et al. arXiv:2301.02721 (2023)

[2] Thomas, J. C., Rossi, A. et al. npj Comput. Mater. 8, 99 (2022)

4:30 PM *EL01.03.04

Integrated Quantum Photonics with 2D Materials Galan Moody, Kamyar Parto, Michael Choquer and Sahil Patel; University of California, Santa Barbara, United States

Optically active defects in 2D materials, such as hexagonal boron nitride and transition metal dichalcogenides, are an attractive class of quantum light emitters with high brightness, room-temperature operation, and tunability with external strain and electric fields. In this presentation, I'll introduce this field and discuss recent progress and challenges in engineering 2D quantum emitter properties through photonic, optoelectronic, and optomechanical device integration. I'll present exciting results from my group in which we have engineered arrays of 2D emitters, integrated them with dielectric metasurfaces and silicon nitride photonic resonators for bright emission, and achieved high-speed modulation using optomechanical resonators based on surface acoustic waves. I'll conclude with an outlook on the future of 2D materials for quantum information science and technologies, including challenges and opportunities for the community.

8:30 AM EL01.04.01

Using Four-Dimensional Scanning Transmission Electron Microscopy to Determine the Strain Profiles and Thermal Expansion Coefficient of Polycrystalline Epitaxial WSe₂ Theresa M. Kucinski and Michael T. Pettes; Los Alamos National Laboratory, United States

Thermal transport properties can be greatly impacted by the presence of grain boundaries and interfaces in two-dimensional (2D) materials. Previous techniques for determining the thermal expansion coefficient of 2D materials lacked the necessary spatial resolution in temperature measurements. We present a nanoscale approach to overcome this obstacle using Four-Dimensional Scanning Transmission Electron Microscopy (4D-STEM) and analysis by local statistical quantification of crystallographic parameters to determine the thermal expansion coefficient for epitaxial WSe₂ (2D material). From this approach, we determined the localized structural parameters as a function of temperature with high precision by analyzing the histogram of peak positions in a virtual peak profile. Experimentally, WSe₂ was heated through a temperature range (18°C to 564°C) using 4D-STEM to observe temperature-induced structural changes to WSe₂ which can be performed without additional alterations or destruction to the sample. From this analysis methodology, we determined lattice parameters with sub-picometer accuracy, microstrain, and coherent crystalline domains, (related to the sample thickness). The robustness of combining 4D-STEM measurements with quantitative structural analysis for 2D materials is illustrated by the direct determination of thermal expansion coefficients for epitaxial WSe₂.

8:45 AM *EL01.04.02

Probing Spatiotemporal Modulation of Strain in Van Der Waals Materials Yichao Zhang; University of Illinois Urbana-Champaign, United States

Transmission electron microscopy presents a unique opportunity to investigate the modulation of strain in both space and time. In this talk, I will discuss our electron-microscopy based methods for studying the impact of atomic- to nanoscale strain and defects on the properties of van der Waals materials. We utilize ultrafast electron microscopy to spatially map the nanoscale softening of vibrational modes near crystal step edges in response to strain induced by in situ laser excitation. This effective bond-stiffness reduction arises from both the modified force field at the step edge and the ultrafast anisotropic expansion in the layer stacking direction, as verified by our finite-element model. Additionally, we report a novel, simple technique for strain patterning in 2D materials using amorphous, holey silicon nitride substrates with periodic surface topography. The formation of regularly undulating tessellation patterns manifests as diffraction-contrast patterns. We measure up to 2% isotropic, tensile strain in the freestanding regions in the 2D flakes. Atomistic simulations reveal that the 3D elastic deformation is driven by interactions between the 2D crystal and the underlying substrate. Our results highlight the remarkable sensitivity of electron-imaging methods in probing the effects of atomic- to nanoscale heterogeneous strain and defects that influence the overall material properties and functionalities.

9:15 AM EL01.04.03

Atomic Defect Measurement by Lateral Force Microscopy Yucheng Yang¹, Kaikui Xu¹, Luke Holtzman², Kristyna Yang¹, James Hone², Katayun Barmak² and Matthew R. Rosenberger¹; ¹University of Notre Dame, United States; ²Columbia University, United States

Defects in two-dimensional (2D) materials impact important material properties, such as doping in semiconductor and localized quantum emission in semiconductors and insulators. A routine defect measurement technique is critical for understanding defect-property relationships and therefore essential for optimizing material performance. However, progress in understanding these critical relationships is hindered by the limitation of the existing defect characterization techniques. The existing techniques, such as conductive atomic force microscopy (CAFM) and scanning tunneling microscopy, cannot distinguish the out-of-plane defect location and require an electrically conductive sample for defect measurement in 2D materials without introducing additional defects. Here, for the first time, we demonstrate that lateral force microscopy (LFM) in ambient conditions can observe atomic defects in 2D materials. We improve the sensitivity of LFM through the consideration of cantilever mechanics and demonstrate the importance of minimizing tip-sample contact area for defect measurements. The defects observed with LFM are confirmed to be atomic defects based on a direct comparison of LFM with CAFM. Based on the Prandtl-Tomlinson model, LFM only interacts with the material surface. Thus, by comparing directly with CAFM defect measurement at the same region on MoSe₂, we found that the surface selenide site defects are conductive defects. We also show defect measurements on other transition metal dichalcogenides, WSe₂ and MoS₂. Due to the purely mechanical nature of LFM, LFM does not require a conductive pathway for defect measurement. Thus, LFM can also observe atomic defects on insulating 2D materials, such as hexagonal boron nitride (hBN). We show that LFM can differentiate high-quality hBN and low-quality hBN by measuring the intrinsic defect density in the hBN. To further establish the utility of LFM defect measurements, we introduced post-growth defects by annealing hBN in air and showed that increasing annealing temperature increases surface defect density in hBN exponentially, consistent with the Arrhenius equation. Our demonstration of a purely mechanical defect characterization technique not only provides new insight into the defects in electrically conductive materials but also enables routine defect-property determination for insulating materials. This new defect characterization technique will accelerate materials research in defect engineering.

9:30 AM *EL01.04.04

Imaging 2D Moirés at Deep Sub-Angstrom Resolution Kayla X. Nguyen^{1,2}, Chia-Hao Lee¹, Yi Jiang³, Yichao Zhang¹, Priti Kharel¹, Yue Zhang¹, Arend M. van der Zande¹ and Pinshane Y. Huang¹; ¹University of Illinois at Urbana-Champaign, United States; ²University of Oregon, United States; ³Argonne National Laboratory, United States

A challenge in the study of 2D moirés is that they are highly inhomogeneous across length scales, containing defects and strains that vary from site-to-site. In addition, solving the atomic structure is challenging because atoms in the moiré are separated by sub-angstrom distances in projection images, thus requiring deep sub-angstrom spatial resolution. While electron ptychography has demonstrated access to the deep sub-angstrom regime, this technique has required expensive, delicate aberration-corrected electron microscopes. Here, we demonstrate sub-angstrom resolution electron ptychography of 2D materials in an uncorrected scanning transmission electron microscopy (STEM). We demonstrate the power and flexibility of electron ptychography by showing that it can achieve sub-angstrom resolution across a broad range of microscope conditions to uncover details of the moiré structure. Counterintuitively, we find that geometric aberrations actually benefit electron ptychography because they produce structured beams that are more dose-efficient for ptychography than focused, aberration-free probes. This work should dramatically expand the ability to study 2D moirés with atomic precision.

10:00 AM BREAK

10:30 AM *EL01.04.05

Unraveling the Impact of Adventitious Carbon on Pit Formation in Monolayer MoS₂ Xiaolin Zheng; Stanford University, United States

Forming pits on molybdenum disulfide (MoS₂) monolayers is desirable for (opto)electrical, catalytic, and biological applications. Thermal oxidation is a potentially scalable method to generate pits on monolayer MoS₂, and pits are assumed to preferentially form around undercoordinated sites, such as sulfur vacancies. However, studies on the thermal oxidation of MoS₂ monolayers have not considered the effect of adventitious carbon (C) which is ubiquitous and interacts with oxygen at elevated temperatures. Herein, the effect of adventitious C on the pit formation of MoS₂ monolayers during thermal oxidation is studied. The in situ environmental transmission electron microscopy measurements herein show that pit formation is preferentially initiated at the interface between adventitious C nanoparticles and MoS₂, rather than only sulfur vacancies. Density functional theory (DFT) calculations reveal that the C/MoS₂ interface favors the sequential adsorption of oxygen atoms with facile kinetics. These results illustrate the important role of adventitious C on pit formation on monolayer MoS₂.

11:00 AM EL01.04.06

Conductive Atomic Force Microscopy as a Routine, Fast and Reliable Method for 2D Material Atomic Defect Characterization Kaikui Xu¹, Matthew R. Rosenberger¹, Madisen Holbrook², James Hone², Katayun Barmak², Luke Holtzman² and Abhay Narayan Pasupathy²; ¹University of Notre Dame, United States; ²Columbia University, United States

Defects are very influential on material behavior in terms of mechanical, electrical, optical and chemical properties. In two-dimensional materials, defects are inevitable because of impurities[1], thermodynamic equilibrium, or non-optimized growth conditions. Previous research has revealed that defects could act as carrier donors, recombination centers, or electrochemical reaction sites, thus inducing n-type doping, trap states, or increasing the material chemical activity[2]. However, the quantitative effect of defects on material behavior remains insufficiently studied, largely because we lack a simple and routine method to characterize the defect densities. The common defect detection methods, such as Transmission Electron Microscopy (TEM), Scanning Tunneling Microscopy (STM), and Raman Spectroscopy, have practical disadvantages rendering them not ideal for routine defect quantification. Specifically,

TEM requires complicated sample preparation, and frequently induces additional defects during the detection process itself, causing complex interpretation of experimental results. STM relies on strict environmental conditions and time-consuming experiments, making it difficult to operate quickly on different samples. Raman spectroscopy does not locate atomic defects accurately at the nanoscale, and is not sensitive to defects at low density levels.

Here, we show that conductive atomic force microscopy (CAFM) is a swift, simple, reliable and routine technique to characterize atomic defects. CAFM operates with ease under ambient environment, and does not require complicated sample preparation. We conduct CAFM measurement on MoSe₂ and WSe₂ bulk samples, finding that the sample electrical bias significantly influences defect appearance. Optimizing the sample bias enables CAFM to differentiate multiple types of atomic defects by their distinct appearance. We also show that CAFM can locate defects with true atomic resolution. To show the reliability of CAFM, we conduct both STM and CAFM defect measurement on MoSe₂ and WSe₂ crystals from the same growth batch, i.e., crystals with the same growth conditions, and compare the results to each other. We show that both CAFM and STM consistently reveal similar atomic defects. Also, both techniques reveal an additional kind of 10-nm-scale “large” defect. Such consistency between CAFM and STM indicates that the two techniques reveal defects in a similar fashion. Quantitatively, to determine the precision of our density results, we use a statistic model applying Poisson distribution to defect locations because the defect locations are random, which is confirmed by Moran’s Index based on the locations of more than 2000 defects measured by CAFM in a 250nm×240nm area. As a result, the density results of atomic defects and 10-nm-scale “large” defects obtained by CAFM and STM match with each other closely. Therefore, the qualitative (defect type differentiation) and quantitative (density results) consistency between CAFM and STM on TMD crystals from the same growth batch shows that CAFM is a reliable, accurate and precise technique for detecting defects in two-dimensional materials. Realization of a routine defect detection method opens many opportunities for exploring the influence of defects. The related fields can range from material science to electronics, chemical engineering and beyond.

References

1. Jiang J, Xu T, Lu J, Sun L, Ni Z. Defect Engineering in 2D Materials: Precise Manipulation and Improved Functionalities. Research. 2019;2019:2019/4641739. doi:10.34133/2019/4641739
2. Qiu H, Xu T, Wang Z, et al. Hopping transport through defect-induced localized states in molybdenum disulfide. Nat Commun. 2013;4(1):2642. doi:10.1038/ncomms3642

11:15 AM EL01.04.07

Imaging and Probing Point Defects in Gate-Tunable Two-Dimensional Semiconductors via Scanning Tunneling Microscopy [Tianhui Zhu](#), Carlos Gonzalez, Kejun Li, Qirong Yao, Zhehao Ge, Yuanping, Aiming Yan and Jairo Velasco Jr.; University of California, Santa Cruz, United States

With the recent advances in two-dimensional (2D) materials, semiconducting 2D transition metal dichalcogenides (TMDs) have shown potential as the next generation nanoelectronics to keep up with Moore’s law. Since the performance of semiconductor devices can be greatly affected by defects and gating, the ability to control defects in these 2D materials in a gate tunable device becomes vital. The species and density of defects depend on the growth method as well as the postgrowth device fabrication processes. In this talk, I will present atomically resolved images of the defects and show how their local electronic properties are modulated by the application of a gate electric field. Chemical vapor deposition (CVD) is used in this study to reliably produce 2D TMD monolayers while allowing for defect engineering. We use a low-temperature scanning tunneling microscope (STM) to study the point defects in a CVD-grown 2D TMD monolayer that is implemented in a heterostructure with gate tunability. First, the identification of the defects is realized by combining scanning probe microscopy with density functional theory (DFT) calculations. Next, the effect of a gate electric field is explored and compared to DFT modeling. Our results will provide guidance on future defect engineering in gate-tunable 2D TMD based devices.

This research is supported by the Gordon and Betty Moore Foundation award #10.37807/GBMF11569.

11:30 AM EL01.04.08

Ambient Atom to Bond Spectroscopy of Twinned Graphite Grain Boundary via STM [Nirjhar Sarkar](#)^{1,2}, Prabhakar Bandaru¹ and Robert Dynes¹; ¹University of California, San Diego, United States; ²University of California, Riverside, United States

Practical devices in semiconductor industry operate under ambient conditions and are progressing towards low-dimensional Dirac materials like graphene and carbon nanotubes (CNTs). The dimensional reduction from bulk to 1D introduces amplified quantum effects from edges and defects affecting device performance. In this work, we achieve finest resolution under ambient conditions to probe the mechanical strength and the electronic local density of states (LDOS) of individual atoms and bonds of the most common grain boundary (GB) favorably grown in graphene/graphite using scanning tunneling microscopy (STM). We show how the role of bias dependent flat band states contributes toward resolving the typical STM imaging clarity issues with defects. Surface elastic deformation due to tip-proximity reveals the comparable inter-layer van der Waals (VDW) strength of GB and grains.

11:45 AM EL01.04.09

Dopant Identification of Nitrogen-Doped Graphene on Pt (111) via Simultaneous Atomic Force Microscopy and Scanning Tunneling Microscopy [Taegeun Yoon](#)¹, Hyunmin Kang¹, Jeong Ah Seo², Andreas Heinrich², Hyo Won Kim³, Jungseok Chae³ and Young Jae Song¹; ¹Sungkyunkwan University Advanced Institute of NanoTechnology, Korea (the Republic of); ²Ewha Womans University, Korea (the Republic of); ³Samsung Advanced Institute of Technology, Korea (the Republic of)

Nitrogen (N) doped graphene has been gained prominence as a candidate for catalysis, electronic devices or sensors by keeping the advantages of significant properties of graphene along with additional physical or chemical features. The atomic configurations of the dopant, however, show numerous variations with each doping type manifesting distinct properties and features. Hence, identifying and controlling the bonding arrangements is highly crucial for further applications. In this work, we present a schematic distinction on two specific nitrogen defects; Graphitic-N and pyridinic-N. N doped graphene was grown on a Pt (111) surface using pyridine precursors, followed by low-energy electron diffraction (LEED) and X-ray photoelectron spectroscopy (XPS) for confirmation on graphene growth in a larger scale. Atomically resolved simultaneous scanning tunneling microscopy (STM) and atomic force microscopy (AFM) *via* qPlus sensor depicted complementary distinctions on the atomic and electronic structures between both defects. Electronic structure near graphitic-N site showed noticeable bulge with a vacancy-like morphology or a more distinctive protrusion in the center, while Δf image showed little difference from pristine graphene. Pyridinic-N, despite of its carbon-vacancy-based structure, did not show typical vacancy-like electronic topography, with a characteristic protrusive configuration in Δf image. Corresponding theoretical calculations *via* density functional theory (DFT) further verified the experimental data. In addition to the discernment on the two defects, effects of Pt substrate and a plausible growth mechanism are suggested, through which the numerical proportions of the defects and dissociated pyridine precursors can be explained. This study will provide further in-depth understanding for application-driven research for graphene devices with controlled defects.

SESSION EL01.05: Strain Engineering the Quantum Behavior of 2D Materials

Session Chairs: SungWoo Nam and Michael Pettes

Tuesday Afternoon, November 28, 2023

Hynes, Level 2, Room 204

1:30 PM *EL01.05.01

Investigating Quantum Materials with *In-Situ* Strain [Johanna Palmstrom](#); Los Alamos National Laboratory, United States

Electronic material properties are closely linked to the properties of the underlying crystal lattice. For instance, ferroelectric materials break spatial inversion symmetry and ferromagnetic materials break time reversal symmetry. With strain, i.e., deformations of the crystal structure, we can deform the lattice and have large effects on the electronic behavior of materials. This coupling between the electronic behavior and strain can be probed with measurements of the elastoresistivity, i.e., the relation between strain a material experiences and the induced resistivity change. Recently it has been shown that *in-situ* tunable strain is an effective knob to drive a topological phase transition by tuning the band gap and forcing a band crossing in the transition metal pentatellurides, ZrTe₅ and HfTe₅. In this talk, I will show how strain can be used as a conjugate field for electronic order in the prototypical electron doped iron pnictide superconductor, Ba(Fe_{1-x}Co_x)₂As₂ and as a tuning parameter for the topologically driven anomalous Hall effect in the Weyl semimetal Mn₃Sn. I will also discuss applications to 2D systems and preliminary *in-situ* strain measurements paired with large magnetic fields in the transition metal pentatellurides.

2:00 PM EL01.05.02

Curvature-Enhanced Localised Emission from Dark States in Wrinkled Monolayer WSe₂ at Room Temperature [Sebastian Wood](#), Filipe Richheimer, Tom Vincent, Vivian Tong, Alessandro Catanzaro, Yameng Cao, Olga Kazakova and Fernando A. Castro; National Physical Laboratory, United Kingdom

Localised emission from defect states in monolayer transition metal dichalcogenides is of great interest for optoelectronic and quantum device applications. Recent progress towards high

temperature localised emission relies on the application of strain to induce highly confined excitonic states. In this study we consider freestanding wrinkles of monolayer tungsten diselenide (WSe₂), which exhibit room temperature emission from states up to 150 meV below the main A-exciton emission of flat material. Using tip-enhanced optical spectroscopy we are able to probe this emission with nanoscale resolution revealing that it arises from the wrinkle apex and has an out-of-plane transition dipole. The Raman scattering and photoluminescence spectra show no evidence of substantial in-plane strain associated with the localised emission, this is supported by strain calculations based on simple materials engineering considerations. Our results cannot be accommodated within the dominant paradigm in published literature based on strain-localised emission and/or exciton funnelling. Rather, we propose that curvature, instead of in-plane strain, of the 1L WSe₂ offers a more appropriate means of understanding these results.

Whilst it has been shown elsewhere that in-plane tensile strain results in narrowing of the WSe₂ bandgap and is associated with highly localised emission, the distinction between in-plane strain and bending strain has not been adequately explored. The case of free-standing wrinkles is an instructive example since such buckling delaminations form under compressive strain, where the out-of-plane deflection acts to minimise the in-plane strain. This is supported by a simple evaluation of the local strain based on nanoscale surface topography measurements. Our tip-enhanced spectroscopy instrument uses side-illumination to probe the sample using out-of-plane optical polarisation so to explain our observations we propose the existence of a manifold of spin-forbidden excitonic states that we are able to access as a result of local symmetry breaking due to geometric curvature.

The results of this study suggest curvature engineering of 1L WSe₂ as an effective route towards localised emission at high temperature, and an alternative strategy to the pursuit of increasing in-plane stretching strain to confine excitons. The spectral features we report at room temperature show energetic confinement comparable with reports of single photon emission in 1L WSe₂ so photon antibunching experiments are an interesting area for future study. It is also significant that the emission we report here originates from optical coupling to spin-forbidden dark states, which are typically long-lived and therefore of potential interest for quantum information technologies. The out-of-plane transition dipoles for this emission are also relevant for many proposed applications of TMDs for plasmonic circuits and on-chip photonic devices, which require the coupling of light into 'horizontal' waveguides. This is in contrast to the typically observed free bright excitons in TMDs, which have in-plane dipoles that efficiently couple light in/out of thin film devices structures in a 'vertical' direction. Furthermore, the localised emission we observe exhibits semi-continuous spatial variation in the spectral positions of the peaks so we speculate that it may be possible to tune the emission through the local curvature of the 1L WSe₂.

2:15 PM EL01.05.03

Localized Excitons in Monolayer WSe₂ on Nano-Roughness Glass Substrates Yara Galvão Gobato¹, Caique Serati de Brito¹, Cesar Ribahi¹, D.F. Franco², M. Nalin², B. Rosa³, Stephan Reitzenstein³, Andrey Chaves⁴ and Ingrid Barcelos⁵; ¹Universidade Federal de São Carlos, Brazil; ²Institute of Chemistry, São Paulo State University—UNESP, Brazil; ³Technische Universität Berlin, Germany; ⁴Universidade Federal do Ceará, Brazil; ⁵Brazilian Center for Research in Energy and Materials (CNPEM), Brazil

Two-dimensional (2D) transition metal dichalcogenides (TMDs) materials are attractive systems with strong spin-valley coupling and excitonic effects. Nano-strain and defects engineering in TMDs play an important role in controlling their optical properties, particularly for generating atomic defect-based single-photon emitters, which are the platform to develop on-chip integrated single-photon sources for quantum information technology¹.

Here, we have investigated optical and magneto-optical properties of a monolayer WSe₂ on Tb³⁺-borogermanate glasses with different Tb³⁺ concentrations. Our results show that by using a simple method of a lithography-free approach, it is possible to generate nano-roughness glasses to localize excitons by local strain in a monolayer WSe₂. Remarkably, the photoluminescence (PL) reveal several stable sharp doublet emissions with small line jittering effects and with typical fine-structure splittings of $\approx 760 \mu\text{eV}$ from the same quantum dot (QD)-like emitters which are associated with an anisotropic electron-hole exchange interaction. In addition, the correlation function was measured for some emission lines and displayed a clearly effect of photon antibunching. In order to investigate in more detail the nature of these emission peaks, we have also measured circularly polarization-resolved PL under magnetic field (Faraday and Voigt configurations). Under perpendicular magnetic field, the extracted g-factor values for these PL peaks are $\sim 8.4\text{--}9.8$. Under parallel magnetic field, a clear red-shift for several emission peaks was observed for both circularly polarized PL detections. In general, our results suggest that nano-rough engineering on glass substrates is a promising tool for exploring single emitters for possible integration with photonics systems in quantum information technology¹.

References:

1-Caique Serati de Brito et al, Applied Physics Letters 121, 070601 (2022).

2:30 PM *EL01.05.04

Strain Engineering of Proximity Interaction for Controlling Polarization of Quantum Light Emitters Han Htoon; Los Alamos National Laboratory, United States

An ability to control the polarization of the single photons generated by the quantum light emitters holds the key to the realization of non-reciprocal single-photon devices, deterministic spin-photon interfaces, and complex quantum networks. To date, such control is usually achieved via coupling of the quantum emitters to the complex photonic/meta-structures. Achieving circularly polarized light emission is significantly more difficult than achieving linearly polarized light emission as it often requires more sophisticated structures, injection of spin-polarized carriers/excitons, or application of high magnetic fields. "Proximity effects" – the class of phenomena by which an atomically-thin material borrows properties of an adjacent material (such as magnetism) via quantum mechanical interactions – has recently been explored to achieve this highly desired polarization control. By coupling transition metal dichalcogenides with various bulk and 2D magnetic materials, exciting effects such as strong enhancement of valley Zeeman splitting and spin-dependent charge transfer have been demonstrated. However, chiral light emission without spin-polarized carrier/exciton injection at zero magnetic field remains elusive to date. Here in this talk, we will first demonstrate that chiral quantum light sources with a high degree of circular polarization (>0.9) and 80% single-photon purity can be realized by strain-engineering the WSe₂/NiPS₃ heterostructures with nanoscale indentations. Through state of art scanning diamond NV microscopy experiments and temperature-dependent magneto-photoluminescence studies, we show that the chiral quantum light emission arises from magnetic proximity interactions between localized excitons in the WSe₂ monolayer and out-of-plane magnetization of AFM defects in NiPS₃, both of which are co-localized by the strain field arising from the nanoscale indentations. Interestingly, a similar chiral localized excitonic emission is also observed in our more recent experiment performed on WSe₂/MnPS₃ and WSe₂/FePS₃ heterostructure with nano-indentations. Furthermore, we demonstrated that the application of the same strain engineering approach (i.e nanoindentation) to WSe₂/CrPS₄ heterostructure lead to the emission of linearly polarized quantum light reflecting the magnetic order of CrPS₄. These observations reveal that local strain engineering can be utilized not only to create quantum emitters but also to manipulate local proximity interaction for control of their PL polarization.

3:00 PM BREAK

SESSION EL01.06: Interlayer Interactions in 2D Materials
Session Chairs: Kayla Nguyen and Matthew Rosenberger
Tuesday Afternoon, November 28, 2023
Hynes, Level 2, Room 204

3:30 PM *EL01.06.01

The Interlayer Interaction of Rotated Graphene Breaks the Barrier for Intense Lithium Intercalation Resulting in Li₂C₂ Formation. Tereza M. Paronyan; Hexalayer LLC, United States

The demand for Li-ion rechargeable batteries exponentially grows due to their ability to restore the charge and provide consistency in the voltage in long-term cycling. Graphitic Carbon materials are successfully used as an active anode material in Li-ion Batteries (LIB) due to the sp² electronic configuration of hexagonal Carbon. They remain the safest, most cost-efficient, and environmentally stable anode material providing high-power density and energy in long-term cycling compared to any other active materials. Besides many advances, graphitic carbon faces the challenge of intercalating larger amounts of Lithium due to prohibited Van-der Waals interlayer forces that limit the capacity of those batteries.

HeXalayer develops a new type of incommensurate layered graphene consisting of over a 5° angle of closely packed rotated layers that serves as an advanced active anode for LIBs. The unique structural and binding features of pristine layered graphene will be discussed as beneficial for extreme Lithium diffusion.

The advanced anodes perform up to 2,100 mAh/g reversible capacity as evidence of Li₂C₂ formation once initial graphene layers are freely stacked with an average interspace distance of 3.32-3.45Å. The study battery evaluation shows the feasibility of this graphene use as an advanced anode for the next generation of lightweight, fast charging powerful batteries.

4:00 PM EL01.06.02

Exploring Moire Lattice Reconstruction using a Tight Binding Derived Force Model Daniel Palmer, Naheed Ferdous, Gabriel Brown, Tawfiqur Rakib, Kittithat Krongchon, Lucas Wagner and Harley Johnson; University of Illinois at Urbana-Champaign, United States

Lattice reconstruction in moire materials has proven to be difficult to study from first principles given the relatively large system sizes and strong electron correlation. While classical potentials are computationally tractable, these models lack an explicit dependence on electronic degrees of freedom. To overcome these obstacles, we present one orbital and four orbital semi-empirical total energy tight-binding parameterizations for twisted Bilayer Graphene (tBLG). To approximately account for strong electron correlation, we fit the interlayer pairwise correction energy to diffusion Quantum Monte Carlo (QMC) total energy data for a range of disregistry and interlayer separations. Our method of parameterization is generally transferable to other 2D heterostructures. The resulting parameterization enables large scale calculations, incorporating both electronic and lattice degrees of freedom with total energies that are more accurate than DFT-fit models. The models are used to relax structures of tBLG with twist angles as low as 0.88 degrees and systems containing as many as 16,876 atoms. At this scale, the calculation is orders of magnitude faster than recent density functional theory results. We find significant differences in the resulting relaxed structures relative to structures relaxed using empirical potentials. The differences in the relaxed geometries result in a broadened and shifted flat band magic angle regime. We also show that the magic angle regime size and location depend on the method of relaxation.

4:15 PM EL01.06.03

Deep Elastic Strain Engineering of Free-Standing 2D Materials and Twisted Van Der Waals Heterostructures YingHan^{1,2}, KeCao³, ShizheFeng⁴, ZhipingXu⁴ and YangLu^{1,5}; ¹City University of Hong Kong, China; ²Pennsylvania State University, United States; ³Xidian University, China; ⁴Tsinghua University, China; ⁵The University of Hong Kong, China

Due to the outstanding physical and chemical properties, two-dimensional (2D) materials, such as graphene and hexagonal boron nitride (hBN) hold great promise for a variety of mechanical, electrical, optical and many other functional applications. Van der Waals (vdW) heterostructures make 2D flexible electronics device possible with unique properties, especially twisted vdW heterostructures. Furthermore, applying mechanical strain to 2D material could lead to unusual and tunable physical properties for unprecedented strain engineering applications. However, due to the experimental limitation, introducing large uniform strain into 2D materials remains a great challenge. Recently, by developing a protocol for sample transfer, shaping and straining, we report the elastic properties and stretchability of free-standing single-crystalline monolayer graphene grown by chemical vapor deposition [1], with sample-wide elastic strain up to ~6% and Young's modulus close to theoretical value ~1TPa. Similarly, we demonstrate that large elastic deformation can be also achieved in free-standing h-BN monolayers [2], twisted bilayer graphene[3] and other emerging twisted vdW structures, allowing for unprecedented functional 2D material applications. Our results show that graphene, h-BN, twisted bilayer graphene and other emerging twisted vdW structures have outstanding mechanical properties. The near ideal mechanical strength and resilience of 2D materials and van der Waals heterostructures reported here, as well as our uniform, reversible, dynamic strain controlling mechanism, would facilitate the practical elastic strain engineering (ESE) applications, as well as piezoelectric electronics and flexible electronic.

1. Cao, K., et al., Elastic straining of free-standing monolayer graphene. Nature Communications, 2020. 11(1): p. 284.
2. Han, Y., et al., Large Elastic Deformation and Defect Tolerance of Hexagonal Boron Nitride Monolayers. Cell Reports Physical Science 1.8 (2020): 100172.
3. Han, Y., et al. Deep elastic strain engineering of 2D materials and their twisted bilayers. ACS Applied Materials & Interfaces 14.7 (2022): 8655-8663.

4:30 PM EL01.06.04

Electric Field Control of Interfacial Ferroelectric Switching in Twisted 2D Semiconductors Hung-ChangHsu¹, Hao-YuChen¹, Yi-HanLee¹, HsiangLee¹, Bo-HongWu¹, Yi-FengChen¹, Ming-YangLi² and Ya-PingChiu^{1,1}; ¹National Taiwan University, Taiwan; ²Taiwan Semiconductor Manufacturing Company, Taiwan

The stacking configuration of twisted 2D material plays a crucial role in determining their moiré electronic properties, such as strong correlation, quantum confinement, and ferroelectric behavior. Transitioning from one stacking configuration to another involves energy conversion, typically influenced by external interactions such as electric fields. In the case of a twisted-stacking transition metal dichalcogenide bilayer, there exist two commensurate domains with opposite interfacial ferroelectric polarizations. The atomic structure of the domain wall between these domains exhibits a strain gradient, which can respond to a vertical electric field through flexoelectric effects, thereby inducing a change in the stacking configuration. In this study, we demonstrate the ability to manipulate this domain wall by applying a local electric field using a scanning tunneling microscopy tip, thereby controlling the interfacial ferroelectric switching. This ability to control the stacking configuration of twisted 2D materials opens up possibilities for novel twist-stacked 2D devices that incorporate both structural and electronic moiré superlattices.

4:45 PM EL01.06.05

Reversibly Modifying The Structure of Graphite Moiré Domain Walls via STM-Tip Induced Deformations NirjharSarkar, PrabhakarBandaru and RobertDynes; University of California, San Diego, United States

Highly oriented pyrolytic graphite may be the only known monatomic crystal with the ability to host naturally formed moiré patterns on its cleaved surfaces, which are coherent over micrometer scales and with discrete sets of twist angles of fixed periodicity. Such an aspect is in marked contrast to twisted bilayer graphene and other multilayered systems, where the long-range coherence of the moiré is not easily maintained due to twist angle disorder. We investigate the electronic and mechanical response of coherent graphite moiré patterns through inducing external strain from scanning tunneling microscopy tip-induced deformation. Consequently, unique anisotropic mechanical characteristics are revealed. For example, a lateral widening of one-dimensional domain walls (DWs) bridging Bernal (ABA) and rhombohedral (ABC) stacking domains (A, B, and C refer to the atomic layer positioning), was indicated. Further, in situ tunneling spectroscopy as a function of the deformation indicated a tendency towards increased electrical conductance, which may be associated with a higher density of electronic states, and the consequent flattening of the electronic energy band dispersion. Such features were probed across the DWs, with implications for strain-induced electronic modulation of the moiré characteristics.

Ref: Sarkar N, Bandaru PR, Dynes RC. Characteristic nanoscale deformation on a large-area coherent graphite moiré pattern. Physical Review B. 2023 Apr 5;107(16):L161402.

SESSION EL01.07: Impact of Defects and Strain on Electronic Properties of 2D Materials
Session Chairs: SungWoo Nam, Kayla Nguyen, Michael Pettes and Matthew Rosenberger
Wednesday Morning, November 29, 2023
Hynes, Level 2, Room 204

8:30 AM EL01.07.01

Mechanically Gated Transistor via Flexoelectric Engineering of Two-Dimensional Materials BoyuanHuang and JiangyuLi; Southern University of Science and Technology, China

Silicon-based field effect transistors (FETs) have underpinned the information revolution in the last 70 years, and there is a strong desire for new materials, devices and architectures that can help sustain the computing power in the age of big data and artificial intelligence. Inspired by the Piezo channels, we develop a mechanical gated transistor (MGT) abandoning electric gating altogether, achieving ON/OFF ratio over three orders of magnitude under a mechanical force of hundreds nN. The two-terminal device utilizes flexoelectric polarization induced by strain gradient, which modulates the carrier concentration in a Van der Waals (vdW) structure significantly, and it mimics Piezo channels for artificial tactile perception. This simple device concept can be easily adapted in a wide range of semiconducting materials, helping promoting the fusion between mechanics and electronics in a similar way as mechanobiology.

8:45 AM EL01.07.02

The Tensile Strain Effect of In₂Se₃ Ferroelectric-Semiconductor Field-Effect Transistor Fabricated on a PI Substrate TaebinLim, JunmiLee and JinJang; Kyung Hee University, Korea (the Republic of)

Recently, the ferroelectric-semiconductor field-effect transistor (FS-FET) has been attracting a lot of attention for its application as an artificial synapse in neuromorphic systems and next-generation memory chips. The presence of polarization states in the ferroelectric-semiconductor (FS) allows for the implementation of hysteresis without the need for functional materials for the gate insulator, such as electrolyte ion migration, charge trapping, or ferroelectric materials. This advantage makes it suitable for highly integrated chips, as high-quality amorphous gate insulators such as SiO₂ and Al₂O₃ can be used.

In₂Se₃ is a representative ferroelectric 2-dimensional material for semiconductors. It has a small electron effective mass (e*), resulting in high electron mobility. The α and γ phases of In₂Se₃ have been reported to have a non-symmetric structure and exhibit out-of-plane (OOP) and in-plane (IP) ferroelectricity, making them excellent candidates for FS-FET applications. In₂Se₃ exhibits great potential as a candidate for next-generation neuromorphic or memory chips.

However, in order to apply it to flexible and wearable devices, there is a need to study the effect of strain of two-dimensional In₂Se₃ layer with the FS-FET structure. Therefore, it is necessary

to develop techniques that allow for controllable application of strain to FS-FET and accurately measure its electrical characteristics. In this work, we present an In_2Se_3 FS-FET fabricated on PI substrate. The In_2Se_3 layer consists of the γ phase, which exhibits ferroelectric characteristics. As a result, the fabricated In_2Se_3 FS-FET, even with a conventional SiO_2 gate insulator, shows a hysteresis window of 36.8 V (with ± 40 V of gate voltage sweep range) in the transfer curve. In_2Se_3 FS-FET exhibits an on/off ratio of 10^5 in the transfer curve at $V_{\text{DS}} = 1.0$ V, demonstrating excellent electrical performance. Because it was fabricated on a flexible PI substrate, we can precisely apply tensile strain and measure its electrical characteristics. We applied tensile strain using cylindrical structures with radius of 1, 2, and 3 mm, and analyzed the variation in the transfer curve. Our strategy for applying strain to the In_2Se_3 FS-FET can be a promising approach for studying the effect of strain on two-dimensional ferroelectric materials.

9:00 AM EL01.07.03

Anisotropic Electronic Transport in Strain Superlattices in Graphene Preetha Sarkar¹, Yingjie Zhang¹, Onur Tosun², Pinshane Y. Huang¹, Narayana Aluru¹, Matthew Gilbert¹ and Nadya Mason¹; ¹University of Illinois Urbana Champaign, United States; ²Rice University, United States

Strain superlattices in two-dimensional van der Waals materials can modify the electronic band structure via valley-polarized pseudomagnetic fields. In this talk, we report low temperature charge transport measurements on a graphene strain superlattice (SL) generated by stacking graphene on a self-assembly of dielectric nanospheres (NS). Previously [1], strain-tunable dips were observed in the two-probe conductance of these graphene SLs, as a consequence of SL miniband effects. We now report observations of anisotropies in the Hall and non-local transport characteristics of these graphene-NS systems. This anisotropic transport behavior might indicate an underlying symmetry breaking and lifting of the valley degeneracy in these systems.

[1] Y. Zhang et al, npj 2D Materials and Applications 2, 31 (2018)

The authors acknowledge the support of NSF-MRSEC under award no. DMR-1720633.

9:15 AM EL01.07.04

Enhanced Resistive Switching and Record Dielectric Breakdown of Defect Engineered hBN via Ammonia Incorporation Ankit S. Rao¹, Sumank. Mandal¹, Majid Ahmadi², Bart Kooi², Pavan Nukala¹ and Srinivasan Raghavan¹; ¹Indian Institute of Science, India; ²University of Groningen, Netherlands

Multilayer hexagonal boron nitride (hBN) has been touted as a versatile material for electronic devices as it can be used as a capacitive layer for resistive random-access memory (RRAM) devices and as a dielectric substrate for two-dimensional (2D) semiconductor devices. The performance of these devices based on multilayer hBN are impacted by the defects incorporated when grown via chemical vapor deposition (CVD). Insights into the effect of defects on resistive switching characteristics and dielectric breakdown is essential in enhancing the performance. This work focuses on improving the switching properties of multilayer hBN by incorporating ammonia (NH_3) during the CVD process to regulate the nucleation density and grain size of hBN. By varying the partial pressure of NH_3 , low nucleation density and high edge growth of hBN grain is achieved resulting in 4-order reduction in nucleation density and ($\times 70$) larger grain sizes for same growth times. The multilayer hBN obtained at these conditions by increasing the growth time is used to fabricate MIM (Ti/hBN/Cu) devices. When compared with hBN grown without NH_3 at same conditions, the devices exhibit upto 4 orders reduction in read currents, 3 orders improvement in variability of current during endurance measurements, 2 orders of improvement in retention, switching energies in the range of fW, lower leakage paths and high current on/off ratios of 10^8 . Also, the dielectric breakdown of multilayer hBN is impacted by the defects as they provide pathways for leakage. A post growth annealing (PGA) process at various NH_3 partial pressures (p_{NH_3}) is employed to modify the defect configurations and control the defect densities. The structural improvement of hBN results in drastic improvement in the breakdown field strength (V_{BD}) to a record high value of 13.1 MV/cm for a 2nm thick CVD hBN. The nature of this defect healing process is found to be thermodynamic in nature and reversible by reversal in the partial pressures of NH_3 .

9:30 AM *EL01.07.05

Bulging and Poking of 2D Materials Nanshu Lu; The University of Texas at Austin, United States

Bulging and poking of suspended thin films are widely used mechanical tests. They became particularly popular for characterizing atomically thin 2D materials, together with spontaneously formed nano-bubbles and nano-tents. The atomic thinness and smoothness of 2D materials pose new challenges to the bulging and indentation tests as well as models. Through scaling analysis and accurately solving the Föppl-von Kármán (FvK) theory, we unveil what sets the in-plane strains and work of adhesion in terms of their shape characteristics. Through a parent-satellite bubble system, we are able to uncover the transition from membrane theory to plate theory and from Griffith-type interface to cohesive-zone-type interface formed with the supporting substrate. With coarse-grained molecular dynamics (CGMD) simulations, we can reveal when continuum mechanics ultimately breaks down. Moreover, we find that recent indentation results on suspended 2D materials do not follow the well-known load-cubic-deflection relation that is widely accepted for linear elastic sheets. We identify a single dimensionless governing parameter—the sliding number—defined by comparing the sheet tension (that drives the slippage) with the interfacial traction (that resists the slippage). We also propose a more accurate load-deflection model for the extraction of 2D material modulus and its interfacial shear strength.

10:00 AM BREAK

10:30 AM *EL01.07.06

Study of Contact Metals to Transition Metal Dichalcogenides Alexander L. Mazzoni¹, Wendy Sarney¹, Patrick Taylor¹, Maria G. Sales², Peter Litwin², Yangchen He³, Joshua Eickhoff³, Robert Boyd³, Daniel A. Rhodes³, Stephen McDonnell², Sina Najmaei¹ and Madan Dubey¹; ¹U.S. Army Research Laboratory, United States; ²University of Virginia, United States; ³University of Wisconsin–Madison, United States

Confinement in two-dimensional materials leads to unique properties, including near-room temperature quantum material characteristics and excitonic condensation in transition metal dichalcogenide (TMD) van der Waals layers. Exciting new materials-by-design strategies for the novel structural properties of TMDs allow for highly tunable stacks and twisted configurations. One challenge standing in the way of developing these materials into useful devices is the lack of low resistance ohmic contacts.

In metal-TMD contacts the Fermi level is usually pinned, resulting in a Schottky barrier that impedes the movement of electrons and limits device performance. A recent report discusses using the semimetal bismuth deposited by e-beam evaporation as a contact to MoS_2 [1]. The use of a semimetal contact changed the character of the metal induced gap states, raising the Fermi level into the conduction band for MoS_2 beneath the Bi contact. While they made a significant advancement toward the quantum limit in contact resistance to TMDs, using ultra high vacuum deposition techniques to deposit the metal, such as molecular beam epitaxy, could allow further control over the metal-TMD interface properties.

Our current research is working toward exceeding the state-of-the-art for 2D material contacts, focusing initially on WSe_2 with Bi contact layers deposited via molecular beam epitaxy. We will show this technique leads to a uniform Bi layer on silicon dioxide and WSe_2 , in contrast to Bi deposited via a standard cleanroom high vacuum evaporator. We investigate the Bi- WSe_2 interface electrically via field-effect transistor structures and report on the wide-ranging electronic properties of the devices when using WSe_2 synthesized by different growth methods.

[1] P-C Shen, et al., Nature 593, 211 (2021).

11:00 AM EL01.07.07

Mobility Enhancement of Monolayer WS_2 from Biaxial Tensile Strain Jerry A. Yang, Robert K. Bennett, Lauren A. Hoang, Zhepeng Zhang, Kamila J. Thompson, Andrew J. Mannix and Eric Pop; Stanford University, United States

Two-dimensional (2D) semiconductors have attracted significant interest due to their unique electronic and mechanical properties, based on their atomically thin structure. Among these, monolayer tungsten disulfide, WS_2 , is a promising channel for 2D field-effect transistors due to its favorable combination of wide band gap for low leakage current, good electron and hole mobilities, controllable synthesis, and ambipolar conduction [1], [2]. However, how strain affects its electronic properties remains largely unknown.

Mechanical strain modulates the energy band structure of 2D semiconductors, and previous computational studies have predicted that strain can increase the electron mobility due to reduced transport effective masses and reduced intervalley electron-phonon scattering [3]. Experimentally, a recent study has found that even 0.7% uniaxial tensile strain can double the mobility of monolayer MoS_2 [4]. However, mobility improvements in WS_2 due to strain have not yet been experimentally demonstrated.

Here, for the first time, we study the effect of externally applied biaxial strain on the electrical characteristics of WS_2 field-effect transistors on flexible substrates. We first pattern a Ti/Au (5 nm/40 nm) back-gate stack onto 125- μm thick polyethylene naphthalate (PEN) substrates, then deposit ~ 16 nm Al_2O_3 gate dielectric. We grow WS_2 by chemical vapor deposition on a c-plane sapphire substrate and transfer the material onto the samples with an approach similar to Ref. [5]. We define the channel using an O_2 plasma etch and pattern Ni/Au (5 nm/40 nm) source and drain contacts. Lastly, we encapsulate the transistors with an AlO_x (10 nm) layer similar to Ref. [6], which serves as a final anneal and passivation layer.

We apply strain to our samples using a custom-designed five-point crossbeam biaxial tensile strain tool similar to Ref. [7]. The PEN sample is attached to an acrylic cruciform which is biaxially strained while the electrical and optical characteristics of the fabricated devices are measured *in situ* from 0.1% to 0.4% strain. We confirm strain transfer with Raman and

photoluminescence spectroscopy, showing that Raman 2LA(M) and A⁰ exciton peaks shift by 13 ± 5 cm⁻¹/‰ strain and 120 ± 61 meV/‰ strain, respectively, which is consistent with previous experimental literature on biaxially strained WS₂ [7]. We also show that the AlO_x encapsulation layer significantly alters the strain rates of the first-order Raman E' and A₁' modes in WS₂.

We demonstrate a ~1.5x improvement of electron mobility and transistor current at 0.3% biaxial tensile strain, and a ~0.3 V negative threshold voltage shift averaged over 60 devices. This improvement occurs at about half the strain magnitude compared to earlier reports of uniaxial strain for MoS₂ [4]. Through DFT simulations of the strained WS₂ band structure, we attribute this improvement to increased energy separation between K and Q conduction band valleys, which reduces intervalley electron-phonon scattering.

This work represents the first report of biaxial strain effects on the electronic properties of a monolayer TMD, showcasing the utility of strain engineering 2D materials for improved electrical performance. Future work will include exploring the effects of biaxial tensile strain on flexible WS₂-based circuit performance. This work was in part supported by the NSF Graduate Research Fellowship program (J.A.Y.), by the Stanford Graduate Fellowship (R.K.A.B.) and by the Stanford SystemX Alliance (other authors).

- [1] F. Lan *et al.*, *Vac.*, **201**, 111091 (2022).
- [2] W. Sik Hwang *et al.*, *Appl. Phys. Lett.*, **101**, 013107 (2012).
- [3] M. Hosseini *et al.*, *J. Phys. Appl. Phys.*, **48**, 375104 (2015).
- [4] I. M. Datye *et al.*, *Nano Lett.*, **22**, 8052 (2022).
- [5] S. Vaziri *et al.*, *Sci. Adv.*, **5**, eaax1325 (2019).
- [6] C. J. McClellan *et al.*, *ACS Nano*, **15**, 1587 (2021).
- [7] A. Michail *et al.*, *J. Phys. Chem. C*, **127**, 3506 (2023).

11:15 AM EL01.07.08

Strain-Induced Performance Enhancement in 2D Material Transistors Yue Zhang, Kelly Hwang, Mohammad A. Hossain and Arend M. van der Zande; University of Illinois Urbana Champaign, United States

Strain is a powerful technique for engineering the quantum properties of materials, which is important to both science and technology. For example, in CMOS manufacturing, a common approach for enhancing mobility in silicon transistors is through process-induced thin-film stress [1]. A recent idea is to apply the process-induced strain technique to engineer strain in 2D materials through the deposition of thin film stressors [2]. However, there are still knowledge gaps in understanding how the films interact to modify the strain and doping in 2D materials, the ultimate limits of applicable strain, and their impact on the material properties and transport in 2D transistors. Understanding these interactions are important for the heterogeneous integration with two-dimensional semiconductors into CMOS technologies.

Here, we present a device-compatible method to pattern and engineer strain in 2D monolayers using process-induced strain and propose a traction-separation model to understand and design the mechanics. Moreover, we demonstrate the process-induced enhancement of current density and field effect mobility of monolayer MoS₂ transistors. First, we investigate the strain transfer mechanism in stressor-capped 2D materials. We evaporate magnesium oxide stressor onto large, continuous monolayer MoS₂, and use lithography to pattern structures. We use Raman spectroscopy to quantify the local strain and doping [3] while systematically varying the stressor thickness and size. After stressor deposition, there is a constant doping concentration change of 5×10^{12} cm⁻² and a linearly increasing strain with stressor thickness, up to a value of 0.65%. The doping is uniform under the stressor, but the strain profile depends strongly on the shape and size of the stressor. We show that the strain profile is well described by a traction-separation model of strain transfer across the MoS₂-substrate interface [4]. We implement this model in finite element simulation and demonstrate the ability to predict the strain profile and extract the effective traction at the 2D interface to be 1.3 MPa/μm. Finally, we demonstrate the utility of process induced strains and the modeling to predict and design arbitrarily complex strain profiles in 2D monolayers.

Next, we investigate how process-induced strain affects carrier transport in monolayer MoS₂ transistor. We measured the electrical transfer curve onto the same 2D channel while sequentially depositing stressors of increasing thickness. Before stressor deposition, the devices showed mobility of 20 cm²/Vs, and current density of 30 μA/μm. With increasing strain, the carrier mobility and the current density continuously increased. At 0.5% strain, the current density is enhanced by 60%, due to the enhanced carrier mobility of 40% and the decreased threshold voltage. This enhancement is comparable with theoretical prediction [5] and bending 2D transistors on soft elastomer substrates [6].

These results demonstrate a powerful device compatible approach to strain engineering 2D materials, and a generalizable method to unravel the interaction of CMOS processes with the material properties and device performance of 2D materials. These approaches are important in both the heterogeneous integration of 2D materials into More than Moore technologies. Moreover, these techniques open up new opportunities for leveraging patternable and anisotropic strain for quantum phenomena in 2D materials like exciton funneling, single quantum emitters, spintronics and moiré engineering.

Reference

- [1] Thompson, E., *et al.*, *IEEE Trans Electron Dev* 51.11 (2004): 1790-1797.
- [2] Peña, T., *et al.*, *2D Materials* 8.4 (2021): 045001.
- [3] Michail, A. *et al.*, *Appl Phys Lett* 108.17 (2016): 173102.
- [4] Guo, G. *et al.*, *Journal of Applied Mechanics* 82.3 (2015): 031005.
- [5] Hosseini, M. *et al.*, *IEEE Trans Electron Dev* 62.10 (2015): 3192-3198.
- [6] Datye, M., *et al.*, *Nano Letters* 22.20 (2022): 8052-8059.

11:30 AM *EL01.07.09

Identifying and Engineering Defects in 2D Semiconductors James Hone; Columbia University, United States

This talk will describe ongoing efforts to identify the types and locations of point defects in transition metal dichalcogenide single crystals grown by self-flux and chemical vapor transport techniques. These efforts combine STM imaging, multi-mode AFM imaging (conductive AFM, lateral force microscopy), and elemental analysis of bulk crystals. Imaging is performed on cleaved bulk crystals and exfoliated flakes from one to a few layers thick. In order to unambiguously determine defect locations, we introduce intentional substitutional defects at the metal and chalcogen sites. These studies guide efforts to further purify these materials, leading to improved optical and electronic performance.

SESSION EL01.08: Mechanics of 2D Materials

Session Chairs: SungWoo Nam, Kayla Nguyen, Michael Pettes and Matthew Rosenberger

Wednesday Afternoon, November 29, 2023

Hynes, Level 2, Room 204

1:30 PM *EL01.08.01

Designing Slip and Strain into 2D Material Heterostructure Devices Arend M. van der Zande; University of Illinois at Urbana Champaign, United States

Mechanical strain and deformation offer an unprecedented ability to tailor the symmetry and structure of 2D materials and resulting electronic properties, making it important to diverse technologies like heterogeneous integration with CMOS, stretchable electronics, and engineering quantum systems. Across applications, understanding the nanoscale mechanics will enable the prediction and design of strain dependent properties and integration into devices. Here, we utilize atomic to micro scale imaging to unravel the breakdown of continuum mechanics and new scaling laws in the atomic limit, and their influence on the electronic properties of 2D materials. We will cover examples including: (1) Demonstrating designable strain using thin film stressors, which can be used to spatially pattern the electronic structure of 2D materials or interfacial heterostrain tuning of the moiré superlattice. (2) Imaging the nanoscale shape of bends in 2D heterostructures and discovering the scaling laws that define interlayer slip at van der Waals interfaces, enabling membranes orders of magnitude more deformable than conventional thin films, (3) Leveraging these insights to demonstrate the feasibility of strain and deformation engineering for applications such as mobility enhancement in 2D transistors, deformable transistors, and reconfigurable nanoelectromechanical systems.

2:00 PM EL01.08.02

2D materials are being intensively researched and used industrially worldwide due to their excellent transmittance, thermal conductivity, and electron mobility. The future applications include high-speed transistors, flexible display touch panels, solar cells, etc. Understanding the unique physical properties of 2D materials is essential for their industrial utilization. On the other hand, the evaluation method of the mechanical properties of 2D materials is performed by depositing them on a specific substrate due to the specificity of their shape. However, this measurement method is influenced by the interaction with the substrate, resulting in the measurement results being affected. The techniques that can be used to measure under conditions where substrate effects are excluded are atomic force microscopy (AFM), nanoindentation, bulge testing, etc. Also, these measurement methods are ex-situ techniques, which means they cannot monitor the actual testing process, so the disadvantages of these measurement methods are that various factors that may occur during nanoscale measurement can be reflected in the measurement results. Additionally, the load-displacement data measured by AFM nanoindentation may have a large error in the measured load due to the uncertainty in the AFM cantilever spring constant, which is a disadvantage. These reasons make it difficult to trust the results obtained from the measurement techniques listed above. On the other hand, in-situ measurement technology is a technology that uses MEMS devices to compensate for the limitations of the previous ex-situ measurement technology. The in-situ measurement technology performs tests within an electron microscope, observes the testing process, and analyzes the test results through post-processing of images after the measurement. For example, at the University of Hong Kong, CVD graphene was transferred to a push-to-pull (PTP) device using a wet transfer method with PMMA. Then, the measurement area was cut out from the rest of the area using a focused ion beam (FIB), and the PMMA that was covered was removed to produce the CVD graphene tensile test piece. The produced CVD graphene tensile test piece was used to measure the Young's modulus and tensile strength by inducing deformation through in-situ tensile testing based on SEM. However, the previously described method of producing the specimen also involves cutting it artificially using FIB, leading to physical damage. Therefore, it is necessary to improve the production of the specimen so that physical damage does not occur. This study improved the previously mentioned physical damage to 2D materials by using a dry transfer method instead of the physical transfer method. The pristine 2D material was mechanically transferred and then transferred to a substrate using the self-made transfer system with the PTP (Push-to-Pull) method, avoiding physical damage to the substrate. To increase the yield of substrate production, E-beam lithography was used to create PMMA clamping areas 3.5 μ m away from suspended areas. The remaining PMMA was then removed by exposing it to acetone for 2 hours. The 2D material on the suspended area was prevented from collapsing by going through a critical point dryer process. The samples were tested for Young's modulus of 2L and 3L graphene using low-voltage SEM, and the results showed Young's modulus of approximately 1 TPa for both. The reliability of the test was determined by comparing the obtained force-displacement curves with the actual SEM images.

2:15 PM EL01.08.03

Advancing Nanoindentation Analysis for Characterizing the Mechanical, Elastic and Interfacial Properties of Two-Dimensional MaterialsYifanRao¹, KaiLiu² and NanshuLu¹; ¹The University of Texas at Austin, United States; ²Tsinghua University, China

2D materials, such as graphene and Molybdenum disulfide (MoS₂), offer tremendous potential for future devices due to their atomic-level thinness, intrinsic flexibility, and strain-engineered properties. A thorough understanding of their mechanical, elastic, and interfacial properties is crucial for the successful design of functional 2D devices. However, this task presents challenges, as the ultra-thin nature and relatively large surface areas of 2D materials render them highly sensitive to elasto-capillarity, particularly at small sizes. The nanoindentation technique has demonstrated significant advantages, especially in simultaneously measuring the mechanical, elastic, and interfacial properties of 2D materials, as well as controlling local strain distribution. Nonetheless, the accurate interpretation of the measured indenting-force-to-deflection curves is hindered by the lack of suitable theoretical models. In this study, we have developed a comprehensive model for the nanoindentation of suspended 2D materials, taking into account various factors such as pretension, probe size, probe-suspended-membrane interaction, and interfacial sliding between the 2D materials and substrates in the supported region. Additionally, we have creatively proposed a minimum force method to select the zero points of the indenting-force-to-deflection curves in practical applications. By applying our model to analyze these curves, we have successfully determined the Young's modulus of the 2D materials, the interfacial shear strength against the supporting substrate, as well as the fracture strength of the 2D materials simultaneously. Our theoretical model for nanoindentation tests has provided accurate insights into the deformation and failure behaviors of 2D materials.

2:30 PM BREAK

3:30 PM *EL01.08.04

Novel Ferroelectric and Optoelectronic Responses in 2D Semiconducting Transition Metal Dichalcogenides by Defect and Strain EngineeringNai-ChangYeh^{1,2}, DuxingHao¹, Wei-HaoChang², Chen-HsuanLu¹, Yann-WenLan² and Ting-HuaLu²; ¹California Institute of Technology, United States; ²National Taiwan Normal University, Taiwan

Ferroelectric materials are important components for modern electronic applications, particularly in high-density data storage, microwave devices, pyroelectric sensors, non-volatile memories. Recently, ferroelectricity has been observed in a two-layer van der Waals (vdW) interfaces using marginally twisted two-dimensional (2D) materials that lack polar point groups in their parent lattices, such as hexagonal boron nitride (h-BN) and transition metal dichalcogenides (TMDs). For 2H-TMDs in the monolayer limit, the D_{3h} point group preserves the centrosymmetry so that there is no out-of-plane polarization nor ferroelectricity. On the other hand, if mirror symmetry breaking is introduced, such as in the distorted-1T phase, emergence of ferroelectricity may occur. However, due to domains of randomly orientated spontaneous polarization, a tip-induced flexoelectric training field would be needed to achieve polarization alignment before ferroelectricity could be detected by scanning probe microscopy. To date, robust ferroelectric responses of monolayer 2H-TMDs on device scales have not been reported.

Here we present our new discovery of giant magnetic field-induced ferroelectric responses and novel optoelectronic responses in monolayer MoS₂-based field effect transistors (FETs). We attribute the physical origin for the giant field-induced ferroelectric responses to combined effects of sulfur vacancies-induced centrosymmetric breaking and excess electric/magnetic dipole moments as well as asymmetric thermal relaxations between the top and bottom sulfur layers on a substrate at low temperatures (< 20 K). We further demonstrate that nanoscale strain-engineering of monolayer MoS₂ can induce significant centrosymmetric breaking regardless of the presence of sulfur vacancies, which can enhance the ferroelectric responses. We also observe sensitive responses of the ferroelectric signals from the monolayer MoS₂-FETs to light excitations as a function of the photon frequency, polarization, and orbital angular momentum, suggesting strong interactions of excitonic polaritons with carriers in the 2D-TMDs. The physical mechanisms for these novel findings and potential ferroelectric and optoelectronic applications based on monolayer TMD-FETs will be discussed.

This work was jointly supported by the National Science Foundation in the US, and the National Science and Technology Council and the Ministry of Education in Taiwan.

4:00 PM EL01.08.05

Bendable Membranes Based on Silicene and Silicene-Stanene HeterostructuresChristianMartella¹, ChiaraMassetti^{1,2}, Daya SagarDhungana¹, EmilianoBonera², CarloGrazianetti¹ and AlessandroMolle¹; ¹CNR Institute for Microelectronics and Microsystems, Italy; ²Università degli Studi di Milano-Bicocca, Italy

Two-dimensional (2D) materials exhibit a variety of physical properties with potential exploitation in nanotechnology [1]. In particular, when reduced in the form of 2D bendable membranes, they hold promises in the framework of flexible electronics, photonics and related applications including wearable and strain-responsive devices. Here, we demonstrate the realization of bendable membranes based on Xenes, [2] the monoelemental class of 2D materials, and Xene heterostructures. Starting from silicene and silicene-stanene heterostructure grown by molecular beam epitaxy [3], we show that it is possible to transfer them onto arbitrary flexible substrates [4], thus making feasible the realization of bendable membranes. The application of macroscopic mechanical deformations induces a strain-responsive behavior in the Raman spectrum of silicene. Under tensile strain, the bendable membrane shows Raman frequency shift comparable to other promising flexible systems, like those based on transition metal dichalcogenides, and high stability up to one thousand bending cycles. We also show that the membranes under elastic tension relaxation are prone to form microscale wrinkles displaying a local generation of strain in the silicene layer consistent with that observed under macroscopic mechanical deformation. Moreover, optothermal Raman spectroscopy measurements on wrinkled silicene reveal a curvature-dependent heat dispersion larger than that observed in the unstrained case [5]. Finally, as compelling evidence of the technological potential of the silicene membranes, we demonstrate that they can be readily introduced into a lithographic process flow resulting in the definition of flexible device-ready architectures, e.g. piezoresistor, and thus paving the way to a viable advance in a fully silicon-compatible technology framework. The work is within the ERC-COG 2017 Grant N0. 772261 "XFab" and ERC-PoC 2022 Grant N. 101069262 "XMem".

References

- [1] A. Molle and C. Grazianetti, "Xenes: 2D Synthetic Materials Beyond Graphene", Elsevier.
- [2] C. Martella, C. Massetti, D.S. Dhungana, E. Bonera, C. Grazianetti, and A. Molle, Adv. Mater. Accepted Author Manuscript 2211419 (2023) <https://doi.org/10.1002/adma.202211419>
- [3] D. S. Dhungana, C. Grazianetti, C. Martella, S. Achilli, G. Fratesi, A. Molle, Adv. Funct. Mater. 31, 2102797 (2021).
- [4] C. Martella, G. Faraone, M. H. Alam, D. Taneja, L. Tao, G. Scavia, E. Bonera, C. Grazianetti, D. Akinwande, A. Molle, Adv. Funct. Mater. 30, 2004546 (2020).
- [5] E. Bonaventura, D. S. Dhungana, C. Martella, C. Grazianetti, S. Macis, S. Lupi, E. Bonera, and A. Molle, Nanoscale Horiz. 7, 924 (2022).

4:15 PM EL01.08.06

Study of Internal and Interfacial Properties of 2D Nanomaterials for Understanding Toughening Mechanisms in Ceramic NanocompositesCristinaLopez Pernia¹, XingLiu², ChristosE. Athanasiou², JunLou³, HuajianGao^{1,4,5}, NitinP. Padture¹ and BrianW. Sheldon¹; ¹Brown University, United States; ²Georgia Institute of Technology, United States; ³Rice University, United

Despite his exceptional properties, such as high hardness, chemical and thermal stability, ceramics have long been recognized by their inherent brittleness. To overcome this challenge, ceramic nanocomposites reinforced with nanotubes or nanoplatelets have emerged as promising materials with enhanced mechanical properties, including improved toughness and strength. Designing and engineering advanced ceramic-based materials with tailored toughness, enable their application in a wide range of industries, including aerospace, energy, and electronics. The main challenge for these materials is still controlling and optimization of the toughening mechanisms. Most of the reported efforts are primarily associated with tailoring the microstructure and dispersion of the filler and studying the influence of processing parameters (powder processing methods, sintering conditions...) and nanoplatelet nature (loading content, aspect ratio, orientation throughout the ceramic matrix...) on the resulting microstructure and mechanical properties. However, microstructural features like the nanostructure-matrix interface properties, residual stresses, etc are still key aspects that has not been deeply explored.

Studying the role of interfacial bonding between nanoplatelets and ceramic matrices, interlayer spacing in the 2D nanomaterials and even surface functionalization techniques can provide essential knowledge for enhancing the interfacial strength and stress transfer across the composite. However, in this sense there is still a lack of studies on the impact of interfacial properties on the overall mechanical performance of these materials. This work seeks shedding light on the role of the nanoscale interaction for toughening the composites.

Through a simple experimental approach involving a lap shear configuration the interplay between the 2D nanostructures and the ceramic matrix is evaluated. Reduced graphene oxide (rGO) films are attached to Al₂O₃ ceramic substrates using polymer-derived ceramic as an intermediate layer. The lap shear tests are conducted under varying compressive loads to evaluate the influence of mechanical stress on the interfacial performance, friction, and toughening behavior. rGO films of different thicknesses are also considered in order to assess the influence of interlayer sliding on the mechanical behavior of these composites.

4:30 PM EL01.08.07

The Interplay of Intra- and Inter-Layer Interactions in Bending Rigidity of Ultrathin 2D Van Der Waals Crystals YingchunJiang¹, SrividhyaSridhar², ZihanLiu¹, DingliWang¹, JiaDeng¹, Huck BengChew² and ChanghongKe¹; ¹Binghamton University, The State University of New York, United States; ²University of Illinois at Urbana-Champaign, United States

Bending/flexural rigidity is one of the fundamental mechanical properties of mono- and few-layered two-dimensional (2D) van der Waals crystals (e.g., graphene, molybdenum disulfide (MoS₂) and hexagonal boron nitride (hBN)) that are of great importance to the pursuit of a variety of their applications. Continuum mechanics break down in bending stiffness calculations of these 2D crystals because their layered atomistic structures are uniquely characterized by strong intralayer bonding coupled with weak interlayer interactions. The lack of experimental measurements and the wide scattering of reported values in the literature pose additional challenges to scientific understanding and practical applications of these 2D materials. In this talk, we will present our recent research on quantitative measurements of bending stiffness of pristine monolayer or few-layer graphene, hBN, and MoS₂ flakes and elucidate how the bending rigidities of these 2D crystals are governed by their structural geometry, and intra- and inter-layer bonding interactions. Atomic force microscopy (AFM) experiments on the self-folded conformations of these 2D materials on flat substrates show that the bending rigidity of MoS₂ significantly exceeds those of graphene or hBN of comparable layers, despite its much lower tensile modulus. Even on a per-thickness basis, MoS₂ possesses similar bending stiffness to hBN and is much stiffer than graphene. Density functional theory (DFT) calculations reveal that this high bending rigidity of MoS₂ is due to its large interlayer thickness and strong interlayer shear, which prevail over its weak in-plane bonding. The high bending rigidity of ultrathin MoS₂ is of particular significance for its electronic applications, as it is less prone to out-of-plane structural instabilities, such as wrinkles and ripples, which can impact the material's electrical properties. The superior bending rigidity of MoS₂ makes it a promising building block for robust nanoelectronics and sensors.

4:45 PM EL01.08.08

Piezoelectric Electrostatic Superlattices in Monolayer MoS₂ AshwinRamasubramaniam¹ and DoronNaveh²; ¹University of Massachusetts-Amherst, United States; ²Bar Ilan University, Israel

Modulation of electronic properties of materials by electric fields is central to the operation of modern semiconductor devices, providing access to complex electronic behaviors and greater freedom in tuning the energy bands of materials. Here, we explore one-dimensional superlattices induced by a confining electrostatic potential in monolayer MoS₂, a prototypical two-dimensional semiconductor. Using first-principles calculations, we show that periodic potentials applied to monolayer MoS₂ induce electrostatic superlattices in which the response is dominated by structural distortions relative to purely electronic effects. These structural distortions reduce the intrinsic band gap of the monolayer substantially while also polarizing the monolayer through piezoelectric coupling, resulting in spatial separation of charge carriers as well as Stark shifts that produce dispersive minibands. Importantly, these minibands inherit the valley-selective magnetic properties of monolayer MoS₂, enabling fine control over spin-valley coupling in MoS₂ and similar transition-metal dichalcogenides.

SESSION EL01.09: Poster Session: Defects and Strain in 2D Materials

Session Chairs: Michael Pettes and Matthew Rosenberger

Wednesday Afternoon, November 29, 2023

Hynes, Level 1, Hall A

8:00 PM EL01.09.01

First-Principles Investigations of Quantum Defects in Two-Dimensional Transition Metal Dichalcogenides WeiruChen¹, YihuangXiong¹, JohnC. Thomas², ArchanaRaja², AlexanderWeber-Bargioni² and GeoffroyHautier¹; ¹Dartmouth College, United States; ²Lawrence Berkeley National Laboratory, United States

Quantum defects, considered as artificial atoms embedded within host materials, are key components in realizing applications in quantum information science. Low-dimensional materials, such as transition metal dichalcogenides (TMDs), are particularly promising hosts due to their inherent quantum confinement nature, long projected spin coherence time, and strong spin-orbit coupling (SOC). In this study, we focus on two common point defects in monolayer tungsten disulfide (WS₂): vacancies and carbon substitutions. We used computational modeling techniques along with hybrid functionals and SOC, factoring in the nonunique exact exchange fraction characteristic [1] of low-dimensional materials, to analyze the thermodynamic stability and electronic structures of these defects. Our results, combined with experimental characterizations, provide new insights into the properties of these defects, encouraging further research into the understanding and design of quantum defects in TMDs.

[1]. Chen, Wei, et al. "Nonunique fraction of Fock exchange for defects in two-dimensional materials." *Physical Review B* 106.16 (2022): L161107.

8:00 PM EL01.09.02

In Situ Observation of Wrinkle Evolution in Suspended 2D Materials JingzhuoZhou¹, YuanHou¹, JuzhengChen¹, MengyaZhu¹ and YangLu²; ¹City University of Hong Kong, Hong Kong; ²The University of Hong Kong, Hong Kong

Mechanical properties of atomically thin materials play a crucial role in the fabrication and stability of atomic-scale devices. As the thinnest materials in nature, two-dimensional (2D) materials can hardly tolerate compressions, so they are vulnerable to instability in response to geometrical restrictions such as shifting from planar structure to out-of-plane wrinkling. The complex instability pattern is determined by the intrinsic bending properties and external boundary conditions. However, because the dynamic instability process of 2D materials is elusive, their crucial instability conditions and morphological evolution remain enigmatic. Here, we develop an in-situ shearing experiment for suspended 2D materials include graphene and MoS₂ by employing the push-to-shear strategy. We comprehensively examine the reversible wrinkling-smoothing process and demonstrate that 2D materials under shearing have a dual instability that includes continuous wavelength decrease and snap-through period-halving bifurcation, respectively. This dual instability, governed by the materials' geometry and the elastic nonlinearity, makes it possible to measure the bending stiffness of single-layer 2D materials. Furthermore, we investigate the changes in optical properties of 2D materials within instability using shear straining. These findings not only provide direct evidence of dual instability of 2D materials, also raise new opportunities for shear-strain engineering of 2D devices.

8:00 PM EL01.09.03

TEM Dark Field Analysis on the Atomic Scale Reconstruction in Twisted Trilayer Graphene DaesungPark, Sang HwaPark, Jae HeonLee, Sang MoYang and HyobinYoo; Sogang University, Korea (the Democratic People's Republic of)

Interfaces formed by joining two van der Waals (vdW) crystals has offered a new route to access exotic electronic behaviors. The interplay between twist-tunable length scale of moire superlattice and underlying atomic scale reconstruction has been key to understand such unconventional electronic behaviors. In the twisted bilayer graphene, for instance, periodic rearrangement of atoms with the moire length scale was reported to be responsible for many exotic phenomena including anomalous electronic transport in small twist angle ($\theta < 1^\circ$) and the strongly correlated behavior in magic angle ($\theta \sim 1.1^\circ$). On the other hand, atomic configuration in twisted trilayer graphene and its correlation with the recently reported unconventional

superconductivity has yet to be investigated. Although robust superconductivity in the twisted trilayer graphene has been reported by multiple groups, their insight onto the atomic and moire structure remains elusive due to the complicated nature of the interlayer interaction in trilayer system. The reconstruction between the top and bottom layers through the middle layer in addition to that between the two adjacent layers should be considered to understand the atomistic details of twisted trilayer graphene.

In this study, we utilized the transmission electron microscopy (TEM) dark field (DF) imaging technique to investigate the reconstructed moiré lattice in twisted trilayer graphene. Assuming only a single event of electron scattering with the thin specimen, the intensity of TEM DF image can be interpreted as kinematical diffraction intensity variation in real space. Moreover, by obtaining the tilt-series DF images, one can monitor the change in such diffraction intensity as a function of the deviation from the exact Laue condition. We found that the atomic rearrangement occurs in all three layers, resulting in an array of commensurate domains of Bernal and rhombohedral stacking orders competing with each other.

8:00 PM EL01.09.04

Defect-Induced Bound States in the Continuum Band of Nanoribbons [Vicenta Sanchez](#) and Chumin Wang; Universidad Nacional Autonoma de Mexico, Mexico

Bound states in the continuum (BICs) can be induced by structural defects or impurities [1]. These bound states have numerous applications in devices as solid-state lasers [2], sensors [3], and narrowband filters [4]. In this work, we report a detailed study of BICs in a finite nanoribbon with defects. This study was carried out by means of the Kubo-Greenwood formula and tight-binding Hamiltonian, as well as a real-space renormalization plus convolution method [5]. The calculated density of states reveals the presence of a BIC, whose localization degree was quantified by the participation ratio [6]. In addition, significant changes in the electronic transport and localization are found when a small second-neighbor hopping integral between the impurities and neighboring atoms is considered. Moreover, this study shows the sensibility of such BICs to short-range hopping integrals. Finally, BICs in finite second-neighbor square lattices have also been analyzed by using a new convolution theorem [7].

This work has been partially supported by projects UNAM-IN12522, UNAM-IN110823 and CF-2023-I-830. Computations were performed at Miztli of DGTIC-UNAM.

[1] I. Piquero-Zulaica, *et. al, Rev. Mod. Phys.* **94** (4), 045008 (2022).

[2] A. Kodigala, T. Lepetit, Q. Gu, B. Bahari, Y. Fainman, and B. Kanté, *Nature* **541**, 196 (2017).

[3] A. A. Yanik, *et. al, Proc. Natl. Acad. Sci. USA* **108**, 11784 (2011).

[4] J. M. Foley, S. M. Young, and J. D. Phillips, *Phys. Rev. B* **89**, 165111 (2014).

[5] V. Sánchez and C. Wang, *Phys. Rev. B* **70**, 144807 (2004).

[6] V. Sanchez, F. Sanchez and C. Wang, *Phys. Status Solidi B* **256**, 1800369 (2019).

[7] F. Sanchez, V. Sanchez and C. Wang, *Eur. Phys. J. B* **91**, 132 (2018).

8:00 PM EL01.09.05

Exploring Local Doping in CVD-Grown Graphene on Sapphire Through Correlative Kelvin Probe Force Microscopy and Raman Spectroscopy Techniques [Ilka Hermes](#)¹ and Simonas Krotkus²; ¹Leibniz Institute for Polymer Research Dresden e.V., Germany; ²Aixtron SE, Germany

Graphene, transition metal dichalcogenides and synthetic 2D materials offer a vast potential for novel (opto-) electronic devices, membranes and energy storage among others. In particular, industrial application of 2D materials in high-performance nanoelectronics require homogeneous distributions of electrical properties on the nanoscale. Advanced atomic force microscopy (AFM) techniques like Kelvin probe force microscopy (KPFM) and conductive AFM (cAFM) resolve local surface potential and conductivity with a nanometer resolution and directly relate this information to the materials surface structure [1, 2]. Here, I present a correlative KPFM and μ Raman study on wafer-scale monolayer graphene on an insulating sapphire substrate prepared via chemical vapor deposition. The use of high temperature H₂-annealed sapphire instead of pristine sapphire improves the resulting graphene film by reducing the overall density of strain-induced wrinkles and increasing the crystal quality [3]. We found the annealing-induced sapphire steps introduce a heterogeneous surface potential distribution on the graphene monolayers caused by spatially variant p-doping concentrations. The decreased p-doping concentration at the position of underlying step edges suggest that a change in substrate-film interaction leads to the highly heterogeneous surface potential distribution.

[1] U. Zerweck et al., *Phys. Rev. B* **71** (2005) 125424

[2] J. Ludwig et al., *Nanotechnology* **30** (2019), 285705

[3] N. Mishra et al., *Small* **15** (2019), 1904906

8:00 PM EL01.09.06

Vanadium-Vacancy Defect Complexes in Monolayer Tungsten Diselenide [Jingda Zhang](#), Leyi Loh, Michel Bosman, Goki Eda and Su Ying Quek; National University of Singapore, Singapore

We present a comprehensive study of the formation of defect complexes of vanadium substitutional dopants and selenium vacancies in monolayer tungsten diselenide. Different defect complexes were identified and analyzed by the statistical treatment of scanning transmission electron microscope (STEM) datasets. Using density functional theory (DFT) calculations, we studied the thermodynamic stability of these defect complexes under experimental growth conditions. Both theory and experiment reveal that vanadium substitutional defects lower the formation energy of surrounding selenium vacancies. Increasing the vanadium concentration results in a larger density and average size of the vanadium-vacancy complexes. Nevertheless, the formation of larger complexes requires higher energy costs, and the most commonly observed defect complex configuration consists of a single vacancy adjacent to a vanadium defect. Our results pave the way for exploration of engineering impurity-vacancy complexes by substitutional doping in 2D TMDs.

8:00 PM EL01.09.07

Investigating the Influence of Grain Boundaries on Thermal and Electrical Conductivity in Two-Dimensional Molybdenum Disulfide [Ayu Irie](#)¹, Anikeya Aditya², Shogo Fukushima³, Ken-ichi Nomura², Fuyuki Shimojo¹, Aiichiro Nakano², Rajiv K. Kalita² and Priya Vashishtha²; ¹Kumamoto University, Japan; ²University of Southern California, United States; ³Tohoku University, Japan

Transition metal dichalcogenides (TMDCs) have emerged as key semiconductors with tremendous potential for future semiconductor devices. Understanding the impact of defects, such as grain boundaries (GBs), on the thermal and electrical transport properties of two-dimensional (2D) TMDC materials is crucial for their application in energy-harvesting devices based on the thermoelectric effect. In this study, we employed nonequilibrium molecular dynamics simulations and first-principles quantum-mechanical calculations to investigate the thermal and electrical transport properties across and along GBs in a monolayer of the prototypical TMDC material, MoS₂. The results reveal the presence of an interfacial phase (or interphase) located within ~3.5 nm around a GB, exhibiting distinct anisotropic transport properties compared to the perfect crystal. Specifically, the interphase exhibits an 80% reduction in thermal conductivity across the GB, while 17% enhancement along the GB, relative to the perfect crystal. On the other hand, the electrical conductivity appears to be enhanced in both directions. These unique thermal and electrical transport properties exhibited by GB interphases hold key to thermoelectric applications of 2D TMDCs. By manipulating the arrangement of GBs, it is possible to achieve reduced thermal conductivity and enhanced electrical conductivity in these materials. Consequently, atomically thin van der Waals materials, such as MoS₂, show great promise as candidates for thermoelectric devices.

8:00 PM EL01.09.08

Manipulating Thermal Transport of Atomically Thin Crystals via Multiscale Defects [Mingyu Jang](#)¹, Jeongin Yeol¹, Seonguk Yang¹, Sungkyu Kim² and Joonki Suh^{1,†}; ¹Ulsan National Institute of Science and Technology, Korea (the Republic of); ²Sejong University, Korea (the Republic of)

Semiconducting two-dimensional (2D) materials such as transition-metal dichalcogenides (TMDs) have attracted tremendous interest toward near-future applications in nanoelectronics, optoelectronics and thermoelectrics. For those applications, both deeply understanding and actively tuning their thermal transport is of crucial importance in that it intimately impacts the thermal management and energy consumption of devices. Given with the ultra-thin nature of 2D materials, defect engineering becomes much more powerful, so it can be a strategic approach to manipulate their thermal conduction on demand where defect generally acts as a phonon scattering center. In this presentation, we report highly tunable thermal conductivity of monolayer molybdenum disulfide (MoS₂) via multiscale defects, *i.e.*, mesoscale grain boundaries and atomic-scale point defects. Experimentally, thermal conductivity of defect engineered MoS₂ is measured by opto-thermal Raman thermometry by monitoring the temperature and power dependences of corresponding Raman peak shift. We found that the thermal conductivity of single- and poly-crystalline monolayer MoS₂ can be manipulated by additionally introducing point defects which is highly controllable by helium ion beam irradiation. Furthermore, we can decouple the effects of point defects and grain boundaries by analysing single- and poly-crystalline specimen. Our work can provide important insight for controlling thermal properties of 2D materials and the use of monolayer TMDs in the thermal management in modern electronics and energy harvesting devices.

8:00 PM EL01.09.09

Ultrahigh Photoresponse in Double-Strained Monolayer MoS₂ Films with Domain Adjustments Ye Seul Jung¹, Ji Yeon Kim¹, Jae Woo Park^{1,2}, Wenhui Shen¹ and Yong Soo Cho¹; ¹Department of Materials Science and Engineering, Yonsei University, Korea (the Republic of); ²Samsung Electronics Co. Ltd., Korea (the Republic of)

Strain engineering of two-dimensional (2D) transition metal chalcogenides, which aims primarily to tune the bandgap of a semiconductor with modulations of lattice strain, has emerged as a practical way to enhance their electrical and optical properties. Herein, we propose a flexible optoelectronic device based on large-scale monolayer MoS₂ film optimized with maximum tensile strain (via double strain engineering) and domain orientation (relative to the parallel electrodes). Controllable in situ strain spanning a compressive-to-tensile strain range of $\pm 1.27\%$ was applied to the domain-aligned MoS₂ monolayer as the 2D layer were transferred onto a polymer substrate bent concavely or convexly. To extend the benefit by the in situ tensile strain, we applied second strain by post-bending the resulting photodetectors to produce the final tensile strain of $+1.80\%$. Another key achievement is the adjustment of electrode positions depending on the domain orientation to produce maximum polarization field with minimum energy bandgap. As an optimal light-sensing performance, the maximum photoresponsivity of 1142 A W^{-1} was attained for the double-strained sample, representing a ~ 130 -fold increase relative to that for the unstrained one. This value corresponds to the highest value compared to those for any reported 2D-material-based visible photodetectors.

8:00 PM EL01.09.10

Boundaries; Kink Versus Ripplcation in Graphite, MAX phases and Other Layered Solids KaustubhSudhakar¹, GabrielPlummer², GarrittJ. Tucker² and MichelW. Barsoum¹; ¹Drexel University, United States; ²Colorado School of Mines, United States

Kink boundaries, KBs, in metals are well defined entities that at low disregistry angles are identical to low angle grain boundaries, LAGBs. The latter are comprised of basal dislocations aligned normal to the basal planes in such a way that their strain fields cancel. A ripplcation is best defined as an atomic scale ripple. When ripplcations on adjacent planes nest, they define a ripplcation boundary, RB. Two oppositely signed adjacent RBs define a ripplcation band. Until recently, most RBs have been classified as KBs. In layered crystalline solids, LCSs, when deformation is confined in two independent directions, with no possibility of twinning, most KBs should be classified as RBs. Herein, we show that in LCSs, RBs: i) are not atomically sharp; their strain fields are considerably delocalized, especially in comparison to KBs, ii) delaminate at high curvatures; iii) form nanobridges, and iv) are highly strained and, if not trapped, fully reversible. At extreme curvatures, the bonds are sundered and the RBs are no longer reversible and are reminiscent of KBs at the macroscopic scale. The distinction is important because whether delaminations nucleate and/or a material is highly strained has important and crucial ramifications on its deformation and ultimate failure.

8:00 PM EL01.09.11

New Intercalant Order in TaS₂ Achieved by Pulsed Laser Heating YangZhang¹, JoshuaLee², ThomasSutter², MarinPrecner³, GoranKarapetrov³, AnshulKogar² and IsmailEl Baggari¹; ¹Harvard University, United States; ²University of California, Los Angeles, United States; ³Drexel University, United States

Transition metal dichalcogenides (TMDs) have attracted significant interest due to their rich electronic states and intriguing properties. Among TMDs, tantalum disulfide (TaS₂) stands out as an archetypical system, showcasing multiple superstructures contributed by charge density waves (CDW), such as $\sqrt{13 \times 13}$ superstructures in 1T-TaS₂ and 3×3 in 2H-TaS₂ [1, 2]. In addition to the CDW, recent works have demonstrated another avenue for exotic superstructural harvest: the intentional doping through chemical intercalation within the van der Waals (vdW) gap, a process that also entails stoichiometric modification [3, 4].

Here, we discover a new 2×2 superstructure distinct from well-known chemically intercalated phases of TaS₂ with the assistance of pulsed laser heating. Employing *in situ* selected area electron diffraction (SAED) and atomic-resolution scanning transmission electron microscopy (STEM), we reveal the reversible order-disorder transition occurring at around $\sim 483 \text{ K}$. Furthermore, we unveil a robust modulation of atomic density in real space, explicitly elucidating the origin of the 2×2 superstructure. Additionally, the local fluctuations in the chemical order at the nanoscale is observed. These results could pave the way to further refine the phase diagram of intercalated TaS₂ and provide insights into the atomic origin of the chemical ordering.

References:

1. J. A. Wilson, et al. *Advances in Physics* 24, 117 (1975)
2. K. Rossnagel. *Journal of Physics: Condensed Matter* 23, 213001 (2021)
3. X. Zhao, et al. *Nature* 581, 171-177 (2020)
4. N. Agarwal, et al. *Microscopy and Microanalysis* 29, 1583-1584 (2023)

8:00 PM EL01.09.12

Defect State Characterization for p-Si-WS₂+₆ Devices using Frequency-Scanned Deep Level Transient Spectroscopy Mohd SamimReza, AnannyaMathur and MadhusudanSingh; Indian Institute of Technology Delhi, India

Transition metal dichalcogenides (TMDs), such as tungsten disulfide (WS₂), exhibit interesting and technologically relevant optoelectronic characteristics owing to the strong dependence of the bandgap on the dimensionality of the growth[1]. Previous scientific investigations have tended to focus on samples grown using chemical vapor deposition (CVD), with well-known limitations such as poor surface coverage, uncontrolled stacking, and device demonstrations have tended to employ electron-beam lithography for patterning, even for reasonably large flake sizes[2]. In practical two-terminal devices with a vertical transport geometry, nearly 100% surface coverage is essential. Usual methods employed for this purpose involve the use of reactively sputtered thin films, or using composite targets, which often results in sulfur-deficient film growth[3], followed by sulfurization. In this work, we have carried out growth of WS₂ using a simplified two-step growth process involving sulfurizing a DC-sputtered (Angstrom Engineering Evovac, 10^{-3} Torr) tungsten film (200Å with a growth rate $\sim 0.5 \text{ Å/s}$,) over a SiO₂ substrate (University Wafers). Sulfurization (500 mg, Sigma Aldrich) was carried out in a custom-designed twelve-zone horizontal split furnace (Quazar Technologies, 750–950 °C) under Ar flow (0–400 sccm). X-ray diffraction (Rigaku Ultima IV, Copper K α = 1.54Å) scans revealed hexagonal WS₂ growth. Raman spectra (Renishaw inVia) revealed an in-plane (E'_{2g}) and out-of-plane (A'_g) vibrational modes at $\sim 344.20/\text{cm}$ and $\sim 414.92/\text{cm}$, confirming the multilayer WS₂ growth[4]. Field-emission scanning electron microscope (FESEM, JEOL JSM-7800F Prime) scans indicate the growth of a pin-hole-free film. Energy dispersive X-ray (EDX, Oxford) analysis revealed a stoichiometry of W:S close to 1:2. Devices were fabricated in an analogous manner by directly sulfurizing pre-deposited tungsten on p-Si (B-doped, 1-10 Ohm-cm, Sievert Wafer), followed by silver contact metallization. A pulsed voltage source (33600A, Agilent) was synchronized with charge measurements (6514 System Electrometer, Keithley) in frequency-scan deep-level transient spectroscopy (DLTS) measurements at various temperatures, 25, 40, and 60 °C. A defect cross-section of $\sim 2.37 \times 10^{-13} \text{ cm}^2$ and a defect level of $\sim 0.43 \text{ eV}$ below the conduction band was inferred from constant capacitance analysis[5,6]. This trap state may be attributed to the sulfur excess or diffusive migration of boron during sulfurization process. We are currently carrying out higher resolution DLTS measurements to resolve the nature of the trap states.

- [1] Park et al., *Scientific Reports*, 7, 16121 (2017)
- [2] Shi et al., *Nano Lett.* 2022, 22,7667–7673
- [3] Villamayor et al., *Vacuum* 188 (2021) 110205
- [4] Berkdemir et al., *Scientific Reports*, 3, 1755 (2013)
- [5] Johnson et al., *J. Appl. Phys.*, 50, 4828-4833 (1979).
- [6] Henry et al., *J. Appl. Phys.*, 57, 628-630 (1985).

8:00 PM EL01.09.13

Two-Dimensional Monolayer Monochalcogenide Lateral Superlattices JingrongJi¹, Zi-AngGao², Shiva PrasadPoudel³, SalvadorBarraza-Lopez³, KaiChang² and StuartS. Parkin¹; ¹Max Planck Institute, Germany; ²Beijing Academy of Quantum Information Sciences, China; ³University of Arkansas, Fayetteville, United States

Two-dimensional heterostructures show the unconventional physical properties and have the huge potential applications in the electronics devices. Compared to the vertical heterostructures, lateral heterostructures are less explored due to the limitation of the fabrication methods and the difficulties in obtaining the high-quality heterostructures. Moreover, the existing work of the lateral heterostructures mostly only focus on the structures consisted by graphene family and transition metal dichalcogenides and the growth mechanism are even less discussed. Therefore, the exploring of the growth mechanism of the lateral heterostructures and superlattices are essential for fabricating the high-quality heterostructures. Here we report the molecular beam epitaxial growth and scanning tunneling microscope characterization of monolayer lateral heterostructures and superlattices consisted by two kinds of materials belonging to group IV monochalcogenide- SnTe and PbTe. We put forwards a surficial molecular diffusion mechanism to explain the defects in two dimensional lateral superlattices and present the achievements on the well-suppressed defects interdiffusion interface and controllable width of the superlattices. Based on the ferroelectricity in monolayer SnTe and paraelectricity in monolayer PbTe, our work provides the foundation of the future researches on the electronic properties and the potential applications in the ferroelectric devices in this two-dimensional monolayer SnTe/PbTe lateral superlattices.

8:00 PM EL01.09.14

Modulation of The Electronic and Transport Properties of MoS₂ Nanoribbons and Flakes via Strain and Vacancy NammeekKim, HeesangKim and SujeongYou; Soongsil University, Korea (the Republic of)

The strain effects on the edge-state transport of a MoS₂ zigzag nanoribbon, and the vacancy effect on the electronic and transport properties of MoS₂ nanoflakes are investigated numerically using a six-band tight-binding model with KWANT, where the strain effect was absorbed into the modified hopping coefficients. For metallic edge-states in the zigzag nanoribbon, introducing both an intrinsic spin-orbit coupling and local exchange field effects breaks the spin degeneracy and spin inversion symmetry to enable spin selective transport. Changes in the energy dispersion of the metallic edge-states due to uniaxial strain are asymmetric with respect to the strain direction. Transitions from metallic to insulating edge modes occur for a tensile strain of approximately 5% along the x-direction, but no such transition has been observed up to a tensile strain of 10% along the y-direction. The edge-current transmission and spin-polarized edge-currents are determined primarily by details of the energy dispersion of edge-states and are strongly affected by the incident energy of carriers for a given strain. The fully spin-polarized edge-currents can be obtained by modulating both the Fermi energy and gate potential. The energy band structures are modified by changing the shape, size, vacancy rate, and vacancy distribution of the flakes, resulting in additional energy states in the energy bandgap region. For large flakes, the effects of their geometric shape are found to be negligible, because shape effects on the density of states (DOS) decrease with increasing flake size. The positions and DOS of these additional in-gap states are strongly related to the vacancy rate as well as to the distribution of vacancies. The number of in-gap states and the magnitude of the density of these states are both proportional to the vacancy rate. However, if the rate is high enough for vacancy clusters to form, the transmission is somewhat degraded at certain incident energies, owing to backscattering and capture of carriers by the clusters. Since the current transmission is determined primarily by the detailed energy band structure, the in-gap states due to vacancies enable the realization of low-energy currents in devices based on low-dimensional materials. The results provide useful information to implement a spin-polarized current as a potential solution for wearable spin devices

8:00 PM EL01.09.15

Ab-Initio Calculations on Thermal Strain-Induced Dimerized Phase in Monolayer IrTe₂ [Sungmin Song](#), [Pyungjin Park](#), [Jesun Jang](#) and [Seung-Hoon Jhi](#); Pohang University of Science and Technology, Korea (the Republic of)

Two-dimensional materials are sensitive to external strain and may undergo strain-induced phase transitions depending on thickness. In particular, IrTe₂ has been shown to exhibit superconducting properties at nanometer-scale thickness [1]. However, as the thickness of IrTe₂ decreases further, it becomes susceptible to thermal strain from the substrate. Studies on monolayer IrTe₂ have shown that various phases appear depending on the types of substrates with respective thermal strain properties [2,3]. To see the intrinsic strain properties of monolayer IrTe₂ induced by thermal effect, firstly we study the stability of the phase transitions from electronic and phononic perspectives. In addition, we calculate the thermal expansion coefficient of monolayer IrTe₂. Our calculations show that pristine monolayer IrTe₂ tends to take on a dimerized phase at temperature ~ 630 K and strain, which is not observed in bulk IrTe₂. This finding suggests a possibility of engineering the phase transition of two-dimensional materials using the thermal strain with suitable substrates and of designing desired functionality of two-dimensional materials.

References

- [1] S. Park et al., Nat Commun 12, 3157 (2021).
- [2] J. Hwang et al., Nat Commun 13, 906 (2022).
- [3] H. K. Kim et al., Phys. Rev. B 107, 045112 (2023).

8:00 PM EL01.09.16

Thermal Effusion of Water and Carbon Oxides from Multilayered Graphene Oxide Thin Films [Douglas S. da Silva](#), [Gustavo A. Viana](#), [Rafael Merlo](#), [José M. da Silva Filho](#) and [Francisco C. Marques](#); UNICAMP, Brazil

Over the last years, several techniques have been developed for the production of graphene, such as direct physical exfoliation of graphite and epitaxial growth from SiC surfaces [1, 2, 3]. Regardless of the adopted producing protocol, the resulting GO is an insulating material of both physical and chemical characteristics very different from those of pristine graphene. Due to this, the implementation of processes able to efficiently remove the presence of oxygen-containing functional groups is imperative to convert the GO properties as close as possible into those of pristine graphene. Generally, these cleaning processes are called "reduction", and the resulting sample "reduced GO" (rGO). Here we report on water (H₂O) and carbon oxides (CO and CO₂) effusion from multilayered graphene oxide (GO) films during thermal reduction. The effusion of molecules as a function of temperature was monitored through the thermal desorption spectroscopy (TDS) technique in GO thin films prepared by evaporating a colloidal solution of GO at 70 °C. This method of preparation of GO films ensures a homogeneous GO deposition on different substrates and reduces the presence of adsorbed/trapped H₂O molecules between adjacent GO planes. That allows the observation of additional effusion mechanisms, which would be otherwise masked by a strong signal due to effusion of adsorbed/trapped H₂O molecules. Thermal reduction process, ranging from room temperature to ~1000 °C, was performed in a high-vacuum system with a mass spectrometer to monitor the outgassed species in real time. A collective outgassing of H₂O, CO₂, CO species is observed and centered at approximately 230°C. Above 400°C, CO₂ and CO are the only observed outgassed species. Multiple origins for water outgassing were inferred from the TDS spectrum asymmetry, revealing an intricate superposition of mechanisms. The thermal treatment also reduces both the GO interlayer separation and the film surface roughness.

Acknowledgements:

BYD Energy Brazil, FAPESP and CNPq.

References:

- [1] K.S. Novoselov, A.K. Geim, S. V Morozov, D. Jiang, Y. Zhang, S. V Dubonos, I. V Grigorieva, A.A. Firsov, Science 306 (2004) 666–669.
- [2] C. Virojanadara, M. Syväjärvi, R. Yakimova, L.I. Johansson, A.A. Zakharov, T. Balasubramanian, Phys. Rev. B 78 (2008) 1–6.
- [3] M. Sprinkle, M. Ruan, Y. Hu, J. Hankinson, M. Rubio-Roy, B. Zhang, X. Wu, C. Berger, W.A. de Heer, Nat. Nanotechnol. 5 (2010) 727–31.

SESSION EL01.10: Defect Formation in 2D Materials
Session Chairs: [SungWoo Nam](#) and [Michael Pettes](#)
Thursday Morning, November 30, 2023
Hynes, Level 2, Room 204

8:30 AM EL01.10.01

Controlling Morphology and Excitonic Disorder in Monolayer WSe₂ Grown by Salt-Assisted CVD Methods [Reynolds Dziobek-Garrett](#) and [Thomas J. Kempa](#); Johns Hopkins University, United States

Chemical synthesis is a compelling alternative to top-down fabrication for controlling the size, shape, and composition of two-dimensional (2D) crystals. Precision tuning of 2D crystal structure has broad implications for the discovery of new phenomena and the reliable implementation of these materials in optoelectronic, photovoltaic, and quantum devices. However, precise and predictable manipulation of the edge structure in 2D crystals through gas-phase synthesis is still a formidable challenge. Here we demonstrate a salt-assisted low-pressure chemical vapor deposition method that enables tuning W metal flux during growth of 2D WSe₂ monolayers and, thereby, direct control of their edge structure and optical properties. The degree of structural disorder in 2D WSe₂ is a direct function of the W metal flux, which is controlled by adjusting the mass ratio of WO₃ to NaCl. This edge disorder then couples to excitonic disorder which manifests as broadened and spatially varying emission profiles. Our work links synthetic parameters with analyses of material morphology and optical properties to provide a unified understanding of intrinsic limits and opportunities in synthetic 2D materials.

8:45 AM EL01.10.02

Unveiling the Dynamics of Defect Activation and Migration in Monolayer MoS₂ under Strain [Divya Nechiyil](#), [Gokul M. A](#) and [Atikur Rahman](#); IISER Pune, India

The remarkable capacity of two-dimensional (2D) materials to endure substantial strains and their ability to tune optoelectronic properties under strain positions them as highly promising contenders for flexible device applications requiring exceptional performance. The impact of defects within 2D materials on their optoelectronic response to strain is a significant factor to consider. In this context, we present an experimental study that sheds light on the role of intrinsic defects in monolayer MoS₂ regarding the properties of strain-induced photoresponse. We observed an enhancement in photocurrent, electron mobility and the emergence of persistent photoconductivity in the presence of strain. Our findings suggest that the activation of defects at

distinct strain values plays a pivotal role in augmenting the photoresponse of the material. The results also suggest defect migration in the presence of prolonged exposure to strain, which indicates a lowering of defect migration energy under strain. Our study unveils the significant role played by intrinsic defects in monolayer MoS₂ in shaping the properties induced by strain. These findings not only deepen our understanding of the material but also open up exciting new possibilities for the development of multifunctional ultra-thin flexible devices in the next generation of applications.

9:00 AM EL01.10.03

Ultra-Stable Plasmon-Enhanced Optical Nanospectroscopy for Defect Analysis of 2D Materials Ryo Kato^{1,2}, Toki Moriyama³, Takayuki Umakoshi³, Taka-aki Yano^{1,2}, Takuo Tanaka^{2,1} and Prabhat Verma³; ¹Institute of Post-LED Photonics, Japan; ²RIKEN, Japan; ³Osaka University, Japan

Plasmon-enhanced Raman and optical nanospectroscopy, which achieves true nanometric spatial resolution in optical microscopy, has been employed for chemical characterization of materials in various research fields, such as biology and 2D materials. While plasmon-enhanced optical nanospectroscopy has found its innovative multidimensional nanoscale applications in the recent past, it has a vital glitch in imaging large-sized samples, even for samples with the size of a few micrometers. This is because it is challenging to maintain stable optical signal of a sample during long-time measurement, especially when using an atomic force microscopy (AFM)-based plasmon-enhanced optical nanospectroscopy system. The instability of the scattered signal originates from thermal and vibrational drift of the metallic nanotip with respect to the focus spot of the incident light as well as the focus position in the optical axis. Because of these uncontrollable drifts, conventional plasmon-enhanced optical nano-imaging must be completed typically within 30 min; otherwise, optical signal deteriorates beyond the acceptable level. The restriction of measurement time indeed limits the use of plasmon-enhanced optical nanospectroscopy for advanced analysis, such as quality evaluation of optoelectronic devices, high-resolution imaging of biological cells, which requires large field of view.

In this work, we present ultrastable plasmon-enhanced optical nanospectroscopy setup that has a home-built feedback system to compensate possible drift in all three dimensions [R. Kato et al., *Science Advances* (2022)]. This technical development we achieved overcomes the long-standing issue of the system drift, and thus the imaging time is no longer limited by the mechanical drift. Our ultrastable optical nanoimaging system enables characterization of nanoscale defects in micrometer-sized WS₂ layers at a high pixel resolution down to 10 nm without losing substantial optical signal. Owing to the ultrastable nanospectroscopy system, we could reveal that the defect density on the surface of WS₂ layers in large area equivalent to the device scale was indeed higher than the previously reported defect density of the smaller area. Furthermore, such long-duration plasmon-enhanced optical imaging led us to find rare properties of the materials, such as unique defects of WS₂, which one can easily miss with conventional systems. The present work paves the way for nanoscale optical spectroscopy and imaging of large-sized samples not only for optoelectronic devices but also biological cells, heterogeneous catalysis.

9:15 AM EL01.10.04

Resonance Raman Spectroscopy of Plasma-Treated Monolayer MoS₂ Rodrigo G. Costa, André D. Barbosa, Fernando L. Freire and Marcelo E. da Costa; PUC-Rio, Brazil

Molybdenum disulfide (MoS₂) is a highly promising two-dimensional (2D) material, with applications in diverse fields such as optoelectronics and high-performance Li-S batteries. Defect engineering plays a pivotal role in fine-tuning the optical and electrical properties of 2D materials. This study investigates the controlled introduction of defects into MoS₂ monolayers through plasma treatments utilizing nitrogen and helium gases, enabling tailored properties for specific applications. We utilize resonance Raman spectroscopy, photoluminescence spectroscopy, and atomic force microscopy to investigate and characterize these defects. The samples are grown via Chemical Vapor Deposition (CVD).

Photoluminescence spectroscopy is utilized to investigate the optical properties of the MoS₂ monolayers. The main excitons change their intensity ratio for different treatment times, which is another defect-related phenomenon. Furthermore, atomic force microscopy enables detailed morphological analysis, contributing to the comprehensive characterization of the samples.

Resonance Raman spectroscopy reveals gradual changes in the MoS₂ monolayer's Raman spectra as the nitrogen plasma treatment time increases. We employ longitudinal acoustic LA(M) intensity, second-order 2LA(M) and 2LA(K) intensity, and full-width at half-maximum variations as quantitative figures of merit to assess defect density. This is particularly useful in heavily doped samples where photoluminescence is not present.

Additionally, we conducted plasma treatment with helium ions to further expand our understanding of defect engineering in MoS₂. Comparing the effects of different plasma sources provides valuable insights into defect formation and properties tuning.

9:30 AM *EL01.10.05

Laser Induced Oxidation and Defect Formation in 2D Materials Nicholas Glavin; Air Force Research Laboratory, United States

High throughput characterization and processing techniques are becoming increasingly necessary to navigate multivariable, data-driven design challenges for sensors and electronic devices. In this talk, a high-throughput approach for designing and customizing 2D materials that enable novel, multifunctional properties is presented. This technique involves the use of laser-processing to locally-induce crystallization, oxidation, and defect formation in 2D materials such as transition metal dichalcogenides, modifying local electronic and optical properties. Coupled with high-throughput characterization, this allows for the rapid evaluation of structure-property relationships and subsequent device design. This same process can be implemented in a roll-to-roll configuration to allow for manufacturing of ultralow cost 2D sensor devices for a host of different sensing environments, including the detection of pathogens.

10:00 AM BREAK

SESSION EL01.11: Impact of Strain and Defects on Properties of 2D Materials I

Session Chairs: Kayla Nguyen and Matthew Rosenberger

Thursday Morning, November 30, 2023

Hynes, Level 2, Room 204

10:30 AM *EL01.11.01

Numerical Simulation of Strain Variations in Graphene Aron Cummings¹, Zahra Khatibi², Jose Garcia¹ and Stephan Roche^{1,3}; ¹ICN2, Spain; ²Trinity College Dublin, Ireland; ³ICREA, Spain

Graphene is a highly promising material for a variety of applications, and in many of those, defects, strain, and strain variations can play a fundamental role in the material properties and resulting device performance. Here we present our group's use of numerical simulations to examine the role of defects and strain variations in a few different scenarios, related to the spintronic and photothermoelectric properties of graphene. We make use of linear-scaling numerical simulation techniques to study systems containing many millions of atoms, thus reaching the experimental scale.

Owing to its small spin-orbit coupling and high carrier mobility, graphene has proven to be a highly efficient transporter of spin, with measured spin diffusion lengths in the tens or hundreds of microns. It is predicted that phonon scattering or local strain variations will serve as the ultimate limiting factor in spin transport. Here we present our use of numerical simulations to explore the upper limit of spin transport in graphene arising from thermally- and substrate-induced corrugations and strain variations.

Graphene is also extremely promising for its use as a high-speed, low-power photodetector in next-generation optical communications technologies. The performance of such photodetectors is ultimately limited by the interaction between hot electrons and dynamic strain variations, i.e., phonons. Defect-mediated electron-phonon interactions can also play a crucial role in the photodetector performance. Here we employ a time-dependent version of our numerical simulation tool to study the relaxation of hot carriers in graphene, mediated by the presence of both phonons and defects, and we explore avenues for optimizing the resulting photodetector performance.

Finally, we discuss a positive aspect of local strain variations in graphene – the electrical generation of pure spin currents via the spin Hall effect. By combining tailored local strain with spin-orbit coupling, we aim to significantly enhance the spin Hall effect in graphene. Here we will present our numerical simulations of this effect, and discuss its potential applicability for future low-power memories based on spin-orbit torque.

11:00 AM EL01.11.03

Strain Tunable Quantum Thermoelectrics in Semi-Dirac Silicene Kalpana Panneerselvam and Bhaskaran Muralidharan; Indian Institute of Technology, Mumbai, India

The merging of K and K' points into a common M point through the synergic application of covalent addition and strain engineering becomes evident in a semi-Dirac semimetal that hosts the massless and massive fermions at the same point in the momentum space due to the existence of linear band dispersion along Γ -X direction and a parabolic band dispersion along Γ -Y direction (Zhong et al., 2017). Bringing the scenario of $t_2 = 2t_1$ (the relative strength of the hopping parameters) by oxygenating the silicene leads to the shifting of the Dirac points towards the Γ -point and the remaining deviation from the semi-Dirac point can be fine-tuned with the application of small compressive strain ($\delta = 0.1\%$) along armchair direction. The bandgap opening at M point by achieving $t_2 > 2t_1$ with the increase of compressive strain ($\delta = 3\%$) manifests itself by enhancing the power factor and the thermoelectric figure of merit (Mawrie et al., 2019). Theoretical analysis in the present work based on Landauer - Büttiker formalism offers the perspectives of how to modulate the thermal properties of a two-dimensional materials via functionalization and strain engineering which paves the way for designing a thermoelectric nano device based on semi-Dirac silicene that can be operated to yield the maximum power with the best thermoelectric efficiency.

References

- [1] C. Zhong, Y. Chen, Y. Xie, Y.-Y. Sun, and S. Zhang, *Phys. Chem. Chem. Phys.* 19, 3820, (2017).
[2] A. Mawrie, and B. Muralidharan, *Phys. Rev. B*, 100, 081403(R), (2019).

11:15 AM *EL01.11.04

Unusual Classical and Quantum Aspects of Defects and Strain in 2D Materials JuLi; Massachusetts Institute of Technology, United States

In this talk, I will address the classical mechanics of materials of extended defects in two-dimensional materials, and contrast the differences with traditional 3D materials ["Phase transitions in 2D materials," *Nature Reviews Materials* 6 (2021) 829; "Ripplocations in van der Waals Layers," *Nano Letters* 15 (2015) 1302]. I will also discuss the impact of defects and strain on functional properties, with applications such as quantum emitters and transducers ["First-Principles Calculation of the Temperature-Dependent Transition Energies in Spin Defects," *J. Phys. Chem. Lett.* 14 (2023) 3266], as well as optomechanical actuation ["Optomechanical control of stacking patterns of h-BN bilayer," *Nano Research* 12 (2019) 2634] and sliding ferroelectricity ["Sliding ferroelectricity in 2D van der Waals materials: Related physics and future opportunities," *PNAS* 118 (2021) e2115703118].

SESSION EL01.12: Impact of Strain and Defects on Properties of 2D Materials II

Session Chairs: SungWoo Nam and Matthew Rosenberger

Thursday Afternoon, November 30, 2023

Hynes, Level 2, Room 204

1:30 PM EL01.12.01

Strain Effects on Thermal Conductivity of 2D Materials using the Optothermal Raman Technique MicahVallin^{1,2}, MichaelT. Pettes¹ and RichardZhang²; ¹Los Alamos National Lab, United States; ²University of North Texas, United States

2D materials have gained more focus in the studies of materials science, often due to their properties compared to their bulk material counterparts, including a change in thermal conductivity. These changes in thermal conductivity from bulk materials to 2D materials has prompted investigations into the thermal properties of 2D materials in order to determine their suitability for applications such as energy sustainability. Because of this interest in 2D materials, there have been efforts to tune the properties of 2D materials in order to achieve a desired effect for a device; such tuning efforts methods include doping, adding layers to the 2D material, and strain. In studying the thermal conductivity of 2D materials, very little work has been done on the relationship between applied strain and thermal conductivity. This discussion aims to provide a comprehensive review on the effects of strain on the thermal conductivity of 2D materials using tin diselenide (SnSe₂) and graphene on a copper (Cu) substrate. The experiments were performed using a Razorbill UC200 cryogenic stress-strain instrument in order to induce strain given a voltage input and the thermal conductivity was measured using the optothermal Raman technique while also taking conduction, radiation, and substrate resistance effects into account. Raman dependence measurements due to power are measured for every strain voltage input in order to determine the overall shift in thermal conductivity due to induced strain. The preliminary results for SnSe₂ indicate that there is a shift of the Raman power dependence term (χ_P) from 0.004 18 cm⁻¹ / μ W at no strain induced to 0.003 48 cm⁻¹ / μ W at 0.5% strain induced, while preliminary theoretical results for graphene indicate a shift in the phonon dispersion when a 1% strain is induced to the unit cell; these indicate that shifts in the thermal conductivity due to strain is likely large enough to be observable experimentally.

1:45 PM EL01.12.02

Anomalous Size Effect and Strain Enhanced Thermal Transport in Dislocated vdW Nanowires YinLiu¹, LeiJin², TribhuwanPandey³, HaoyeSun², DarylChrzan², LucasLindsay⁴, JieYao² and JunqiaoWu²; ¹North Carolina State University, United States; ²Department of Materials Science and Engineering, University of California Berkeley, United States; ³Department of Physics, University of Antwerp, Belgium; ⁴Advanced Materials Science and Technology division, Oak Ridge National Laboratory, United States

Dislocations are crystallographic defects which can significantly thermal property of materials. The engineering and control of dislocations is important for thermal management in optoelectronic devices as well as improving thermoelectric properties. Here, we explore the effect of dislocations on thermal conduction using van der Waal (vdW) germanium sulfide nanowires with an Eshelby twist as a model system. Contrary to the expectation that dislocations decrease thermal conduction, we reveal the thermal conduction enhancement resulting from dislocations through the anomalous dependence of the thermal conductivity on the diameters of the dislocated nanowires. Our TEM imaging and 4D STEM strain analysis, in combination with theoretical modeling and DFT calculations suggest that dislocations possess a disassociated structure with mixed screw and edge characteristics and the enhancement results from the dislocation induced compressive strain. Our findings expand the fundamental understanding about dislocation-phonon interactions and provide key insight into the implementation of dislocation and strain engineering to tune thermal conduction in materials.

2:00 PM EL01.12.03

Sensing Disturbance in Magnetic Order of NiPS₃ with Spin-Correlated Ultra-Sharp Exciton Emission TaiC. Trinh¹, RabindraBasnet², VigneshChandrasekaran¹, XiangzhiLi¹, AndrewC. Jones¹, JinHu² and HanHtoon¹; ¹Los Alamos National Laboratory, United States; ²University of Arkansas, Fayetteville, United States

A van der Waals correlated antiferromagnet, metal phosphorus trichalcogenides (MPX₃, M = Mn, Fe, Ni; X = S, Se), have emerged as promising candidates for next-generation spintronics and quantum information technologies. Nickel phosphorus trisulfide (NiPS₃) is a notable member of this family and has been extensively studied for its unique properties, including the emergence of an ultra-sharp photoluminescence (PL) peak at ~1.476 eV below the Néel temperature of 150 Kelvin. While the highly anisotropic, linearly polarized emission of this PL peak has been shown to be directly correlated to the long-range spin order of NiPS₃, its ultra-narrow linewidth of a few hundred μ eV has led to the speculation that it originates from a coherent many-body exciton state. Observations of multiple phonon-bound states and the formation of exciton-polaritons also create more excitement as they present new possibilities for the design and control of correlated electron systems.

Aiming to understand how disturbances in the magnetic order of NiPS₃ could influence the characteristics of this spin-correlated exciton emission, we conducted temperature-dependent

polarization-resolved PL studies on alloyed $\text{Ni}_{1-x}\text{Mn}_x\text{PS}_3$ compounds, with Mn doping percentage x varying from 0 to 0.22. As the Mn content increases, we observe a reduction in the intensity of the ultra-sharp PL emissions, accompanied by a broadening of the PL linewidth from 0.57 meV (spectrometer resolution limit) to 4.2 meV. Notably, at $x = 0.22$, the previously sharp peak becomes negligible. Moreover, the degree of polarization also decreases as the Mn doping percentage increases. Temperature-dependent PL measurements reveal that the sharp emissions vanish at lower temperatures with higher Mn doping. These findings are consistent with prior studies of $\text{Ni}_{1-x}\text{Mn}_x\text{PS}_3$ alloy, revealing a highly sensitive dependence of the spin-flop transition on the inclusion of Mn impurities. We are currently conducting Magneto-PL and Raman spectroscopy experiments to gain further insights into this material system. Our studies clearly show that the spin-correlated exciton emission of NiPS_3 can serve as a sensitive sensor for the disturbance of the long-range spin order.

2:15 PM EL01.12.04

Pseudomagnetic Gauge Field-Based Waveguides using Graphene Shrushti K. Tapar and Bhaskaran Muralidharan; Indian Institute of Technology Bombay, Bombay, India

The Scaling on-chip interconnects pose unprecedented challenges as node technology advances. Interconnect materials such as copper, when used at smaller sizes, have greater effective resistivity, so they dissipate more heat. Graphene, a quantum material with high thermal conductivity, mobility, and elasticity, is an ideal material for interconnects. The zero-band gap and zero backscattering for normal incidence in graphene limit its ability to exhibit strong confinement for waveguide operationality. Here, we are proposing a way for localizing carriers in graphene by generating a powerful on-chip magnetic field. In graphene, applied non-uniform strain produces strong pseudo potential and pseudo magnetic gauge fields attributed to the change in bond length. The strain profiles in which the curl of the pseudo vector potential is non-zero produce a Pseudo magnetic field (PMF). The PMF forms the pseudo-Landau Levels and increases the local density of states in the deformed region [1]. A wave-guided medium is created according to the strain profile by localizing the carriers within the deformed region [2]. We showed the confinement of carriers (in a nm scale) and the effect gets stronger with increasing strain value. The maximum value of strain considered is under the elastic limit. The waveguide shape can be tuned by varying strain profiles. The proposed graphene waveguide is robust against defects and impurities. The numerical simulation of graphene waveguides was based on the Tight binding method and scattering matrix approach.

References

References

1. Guinea, et al. *Nature Physics* 6.1 (2010): 30-33
2. Wu, Yong, et al. *Nano letters* 18.1 (2018): 64-69.

2:30 PM EL01.12.05

Strain Engineering of Metal Thio(Seleno)phosphates for Nonlinear Photonics and Photodetection Abhishek Mukherjee¹, Morgan Blevins¹, Michael Susner², Mark Polking³ and Svetlana V. Boriskina¹; ¹Massachusetts Institute of Technology, United States; ²Air Force Research Laboratory, United States; ³Lincoln Laboratory, Massachusetts Institute of Technology (MIT), United States

We present an experimental and computational study of engineering in-situ strain in two-dimensional metal thio(seleno)phosphate materials aiming to unlock and enhance their fundamental magnetic, electronic, ferroelectric, and flexoelectric properties. The material families under study include MPX_3 ($X = \text{S}, \text{Se}$) materials and materials with P_2X_6 ($X = \text{S}, \text{Se}$) structural sublattice. The single-crystalline thio(seleno)phosphates exhibiting layered structure have been synthesized by vapor transport techniques reported in previous literature [1] and exhibit a wealth of promising nonlinear optoelectronic and magnetic properties, including bulk photovoltaic effect, second harmonic generation, and (anti)ferromagnetic response [1]. We will describe the process of fabricating optoelectronic cells from these materials via mechanical exfoliation as well as the process of engineering the in-situ strain fields with large, localized strain gradients in these cells by material bending, wrinkling, and nano-lithography [2]. Strain gradient mapping with Raman spectroscopy reveals the limits and advantages of different strain-engineering strategies, while the strain-induced linear and nonlinear optical responses and the surface polarization effects can be characterized by atomic force microscopy, second harmonic generation experiments, and spatially-resolved electrical current measurements.

This research has been supported by the Army Research Office (W911NF-13-D-0001, for the strain-engineering fundamentals development), Lincoln Laboratory, Massachusetts Institute of Technology Advanced Concepts Committee (ACC-777, for the cell design and fabrication process development), and the US Department of Energy (DE-FG02-02ER45977, for the development of a custom-designed optoelectronic microscopic measurement setup), and a Draper Fellowship to Morgan Blevins.

*Abhishek Mukherjee and Morgan Blevins contributed equally to this work.

References:

- [1] Susner, Michael A., et al. "Metal thio- and selenophosphates as multifunctional van der Waals layered materials." *Advanced Materials* 29.38 (2017): 1602852.
- [2] Lorenzi, Bruno, et al. "Self-powered broadband photo-detection and persistent energy generation with junction-free strained Bi_2Te_3 thin films." *Optics Express* 28.19 (2020): 27644-27656.

SYMPOSIUM EL02

Emerging Ultrafast Optical and Structural Probes in Materials Science
November 27 - November 30, 2023

Symposium Organizers

Peijun Guo, Yale University
Burak GuzelTURK, Argonne National Laboratory
Hannah Joyce, University of Cambridge
Ajay Ram Srimath Kandada, Wake Forest University

Symposium Support

Gold
LEUKOS

Silver
Light Conversion

* Invited Paper
+ JMR Distinguished Invited Speaker

SESSION EL02.01: Perovskites I
Session Chairs: Burak GuzelTURK and Ajay Ram Srimath Kandada
Monday Morning, November 27, 2023
Hynes, Level 3, Room 303

10:30 AM *EL02.01.01

Ultrafast Self-Localisation and Exciton Formation in Next-Generation Metal Halide Semiconductors [Laura Herz](#); University of Oxford, United Kingdom

Metal halide semiconductors have emerged as attractive materials for solar cells with power-conversion efficiencies now exceeding 25%. Ultrafast optical probes of photoconductivity dynamics have played a pivotal role in uncovering the mechanisms underpinning the superior light-harvesting performance of this materials class. Here, we further report on ultrafast charge-carrier self-trapping in lead-free silver-bismuth semiconductors^[1-4] which promise lower toxicity and potentially higher barriers against ion migration than their more prominent lead-halide counterparts. We examined the evolution of photoexcited charge carriers in the double perovskite Cs₂AgBiBr₆ using a combination of temperature-dependent photoluminescence, absorption and optical pump-terahertz probe spectroscopy.^[1] We observe rapid decays in terahertz photoconductivity transients that reveal an ultrafast, barrier-free localization of free carriers on the time scale of 1.0 ps to an intrinsic self-trapped small polaronic state. We further demonstrate the novel lead-free semiconductor Cu₂AgBiI₆ which exhibits a low exciton binding energy of ~29 meV and a lower and direct band gap near 2.1 eV,^[2,3] making it a significantly more attractive lead-free material for photovoltaic applications. However, charge carriers in Cu₂AgBiI₆ are found to exhibit similarly strong charge-lattice interactions^[3,4] suggesting a link with the presence of AgBi. Further work examining five compositions along the AgBiI₄-CuI solid solution line (stoichiometry Cu_{4x}(AgBi)_{1-x}I₄) shows that increased Cu⁺ content enhances the band curvature around the valence band maximum, resulting in lower charge-carrier effective masses, reduced exciton binding energies, and higher mobilities, as well as partly mitigating the extent of such ultrafast self-localisation.^[4] Self-trapping therefore emerges as a clear challenge for this class of materials.

We also discuss the charge-carrier photoconductivity dynamics in layered, 2D perovskites that have been found to improve the stability of metal halide perovskite thin films and devices.^[5] We show that the 2D perovskite PEA₂PbI₄ exhibits an excellent long-range mobility of 8.0 cm² (V s)⁻¹, ten times greater than the long-range mobility determined for a comparable 3D material FA_{0.9}CS_{0.1}PbI₃. These values show that the polycrystalline 2D thin films already have single-crystal-like qualities. We further demonstrate that PEA₂PbI₄ and BA₂PbI₄ exhibit unexpectedly high densities of sustained populations of free charge carriers, surpassing the Saha equation predictions even at low temperature.^[6] These findings provide new insights into the temperature-dependent interplay of exciton and free-carrier populations in 2D MHPs. Furthermore, such sustained free charge-carrier population and high mobilities demonstrate the potential of these semiconductors for applications such as solar cells, transistors, and electrically driven light sources.

[1] A. D. Wright, L. R. V. Buizza, K. J. Savill, G. Longo, H. J. Snaith, M. B. Johnston, and L. M. Herz, *J. Phys. Chem. Lett.*, 12 (2021), 3352–3360.

[2] H. C. Sansom, G. Longo, A. D. Wright, L. R. V. Buizza, S. Mahesh, B. Wenger, M. Zanella, M. Abdi-Jalebi, M. J. Pitcher, M. S. Dyer, T. D. Manning, R. H. Friend, L. M. Herz, H. J. Snaith, J. B. Claridge, and M. J. Rosseinsky, *JACS*, 143 (2021), 3983–3992.

[3] L. R. V. Buizza, A. D. Wright, G. Longo, H. C. Sansom, C. Q. Xia, M. J. Rosseinsky, M. B. Johnston, H. J. Snaith, and L. M. Herz, *ACS Energy Letters*, 6 (2021), 1729–1739.

[4] L. R. V. Buizza, H. C. Sansom, A. D. Wright, A. M. Ulatowski, M. B. Johnston, H. J. Snaith, L. M. Herz, *Advanced Functional Materials* 32, 2108392 (2022).

[5] *M. Kober-Czerny, S. G. Motti, P. Holzhey, B. Wenger, J. Lim, L. M. Herz, and H. J. Snaith, Adv. Func. Mater.* 32, 2203064 (2022).

[6] S. G. Motti, M. Kober-Czerny, M. Righetto, P. Holzhey, J. Smith, H. Kraus, H. J. Snaith, M. B. Johnston, and L. M. Herz *Adv. Func. Mater.* 33, 2300363 (2023).

11:00 AM EL02.01.02

Extracting Higher-Order Effects and the Related Multi-Particle Dynamics in Perovskites from Pump-Probe Spectroscopy [Shabnum Maqbool](#)^{1,2}, Pratyush Ghosh¹, Satyawan D. Nagane², Neil Greenham¹, Richard Friend¹, Samuel D. Stranks² and Akshay Rao¹; ¹Cavendish Laboratory, University of Cambridge, United Kingdom; ²University of Cambridge, United Kingdom

Lead halide perovskites are in the limelight due to their excellent semiconductor properties, making them ideal for photovoltaic and optoelectronic applications. The emergence of perovskites as a sought-after semiconductor owes to their unique electronic band structure, inherent defect tolerance, increased conversion efficiencies, synthetic flexibility, and easy and cost-effective processibility. Lead halide perovskites show near-unity PL quantum yield, narrow emission bandwidth, high solar cell efficiencies, etc. All these properties are due to the nature and dynamics of the excited states. For an exclusive understanding of a one-to-one correlation between excited state dynamics and the material properties, different time-resolved pump-probe spectroscopic techniques are used wherein a probe pulse interacts with the charge carriers, and subsequently, information can be extracted about the charge carrier transport, recombination dynamics, and carrier phonon interactions, nature of quasiparticles, etc. Various pump-probe techniques, such as transient absorption [1], time-resolved Terahertz [2] spectroscopies, etc., have been utilized to explore the excited state properties. However, these techniques do not provide a distinction of higher-order effects due to multi-particle excitations from the single-particle signatures present in the material of interest. To infer multi-particle dynamics, fluence dependent measurements are usually performed, while a very low pump intensity measurement is considered to have the information regarding single-particle dynamics predominantly. The presence of multi-particle dynamics can be inferred from a fluence-dependent material response. We employ an analysis methodology, by following Pavel et al. [3], to decouple the single- and multi-particle dynamics in transient absorption data by employing the perturbative description of light-matter interaction

[4]. To arrive at this, we performed fluence-dependent TA measurements on thin films of the perovskite system $\text{FA}_{0.79}\text{MA}_{0.16}\text{Cs}_{0.05}\text{Pb}(\text{I}_{0.83}\text{Br}_{0.17})_3$ (bandgap~770 nm, where FA is formamidinium and MA is methylammonium), which have a high degree of polycrystallinity [5]. We observe a dominant contribution from the single-particle dynamics (Chi3) to the raw TA data, with contributions from multi-particle (Chi5 and Chi7) dynamics. We aim to ascribe these higher-order responses (Chi5 and Chi7) to different physical processes to probe quasiparticle interactions such as Auger recombination, carrier multiplication, multiphonon scattering, polaron formation, and bandgap renormalization in perovskites.

11:15 AM EL02.01.03

Addressing the Charge Carrier Trapping Mechanism in CsPbBr₃ NCs Brener Rodrigo De Carvalho Vale, Claudevan A. Sousa, Diego S. da Silva, Andre Felipe Vale Fonseca, Luiz Gustavo Bonato, Diogo B. de Almeida, Jefferson Bettini, Ana F. Nogueira and Lazaro A. Padilha; Universidade Estadual de Campinas, Brazil

Perovskite nanocrystals (PNC) have been studied in recent years because of their interesting optical properties, which include high photoluminescence quantum yield (PLQY). However, despite the large number of reports on the effects of quantum confinement on the optical and electronic properties in PNCs, the literature still lacks information regarding the size dependence of the charge carrier trapping rate. To solve this puzzle, we investigate exciton dynamics for PNCs, with sizes ranging from 5 to 12 nm, using transient absorption spectroscopy (fs-TAS) and time-resolved photoluminescence (TR-PL) measurements. By combining both techniques, we were able to cover the dynamics with six orders of magnitude in time. Charge carrier trapping was observed to occur only on the nanosecond timescale. By considering the charge carrier trapping, and radiative recombination rates, we were able to quantify PLQY for these PNCs. The results show that PLQY increases with PNC size, which can be due to the reduction of the surface-volume ratio. We also observed that after carrier trapping and excitonic recombination, the PL decay is dominated by a very slow decay emission channel, which is related to detrapping. Our findings open new routes to take charge-carrier trapping mechanisms into account and precisely measure the PLQY of nano-structured materials and evaluate the effectiveness of surface passivation methods as well as investigate the basic phenomena in such materials.

Acknowledgments:

The authors gratefully acknowledge the financial support from the São Paulo Research Foundation (FAPESP).

11:30 AM *EL02.01.04

Exciton Transport in CsPbBr₃ Nanocrystal Solids William Tisdale; Massachusetts Institute of Technology, United States

In semiconductors, exciton or charge carrier diffusivity is typically described as an inherent material property. Here, we show that the transport of excitons (i.e., bound electron-hole pairs) in CsPbBr₃ perovskite nanocrystals (NCs) depends markedly on how recently those NCs were occupied by a previous exciton. Using fluence- and repetition-rate-dependent transient photoluminescence microscopy, we visualize the effect of excitation frequency on exciton transport in CsPbBr₃ NC solids. Surprisingly, we observe a striking dependence of the apparent exciton diffusivity on excitation laser power that does not arise from nonlinear exciton-exciton interactions nor from thermal heating of the sample. We interpret our observations with a model in which excitons cause NCs to undergo a transition to a metastable configuration that admits faster exciton transport by roughly an order of magnitude. This metastable configuration persists for ~microseconds at room temperature, and does not depend on the identity of surface ligands or presence of an oxide shell, suggesting that it is an intrinsic response of the perovskite lattice to electronic excitation. The exciton diffusivity observed here (>0.15 cm²/s) is considerably higher than that observed in other NC systems on similar timescales, revealing unusually strong excitonic coupling in a NC material. The finding of a persistent enhancement in excitonic coupling between NCs may help explain other extraordinary photophysical behaviors observed in CsPbBr₃ NC arrays, such as superfluorescence. Additionally, faster exciton diffusivity under higher photoexcitation intensity is likely to provide practical insights for optoelectronic device engineering.

SESSION EL02.02: Perovskites II
Session Chairs: Peijun Guo and Hannah Joyce
Monday Afternoon, November 27, 2023
Hynes, Level 3, Room 303

1:30 PM *EL02.02.01

Ultrafast Charge Carrier Dynamics in Solar Cell Materials Omar F. Mohammed; King Abdullah University of Science and Technology (KAUST), Saudi Arabia

The separation and collection of photo-generated charge carriers in light-harvesting devices are limited by the losses and ambiguous dynamical events at the surfaces and interfaces of the absorber layers. 1-3 These events occur in ultrafast time scales and can only be visualized selectively in space and time by scanning ultrafast electron microscopy (the sole technique capable of surface-selective visualization of light-triggered carrier dynamics at nanometer and femtosecond scales). In this method, the surface of the photoactive materials is excited by a clocking optical pulse and the photo-induced changes will be directly imaged using a pulsed electron beam that generate secondary electrons with a couple of electron volts energy, which are emitted from the very top surface of the material in a manner that is extremely sensitive to the localization of the electron and hole on the photoactive material surfaces. This powerful technique along with ultrafast laser spectroscopy allow us to directly and precisely investigate and decipher the trajectory of charge carriers on materials surfaces and interfaces in real space and real time. Through this work, we have optimized the properties of photoactive materials for applications in light-harvesting devices that led to the world-record solar cell devices based on perovskite crystals. Moreover, we have clearly demonstrated in space and time how the surface orientations, surface oxidation and passivation can significantly impact the overall dynamical processes of photo-generated charge carriers in optoelectronic materials. 4-5 Finally, I will talk about our recent ground-breaking work in X-ray imaging technology that include cutting-edge materials discovery, heavy-atom engineering, state-of-the-art characterization and efficient (nearly 100%) interfacial energy transfer between sensitizers and scintillators that has led to the development of novel X-ray imaging screens with outstanding sensitivity, ultralow detection limit, unprecedented spatial image resolution and low-cost fabrication, with potential applications in medical imaging, industrial monitoring and security screenings. 6-9

References 1- O. M. Bakr, O. F. Mohammed., Science 355, 1260 (2017). 2- R. Begum, M. R. Parida, A. L. Abdelhady, B. Murali, N. Alyami, G. H. Ahmed, M. N. Hedhili, O. M. Bakr, and O. F. Mohammed., J. Am. Chem. Soc. 139, 731 (2017). 3- O. F. Mohammed, D.-S. Yang, S. Pal, A. H. Zewail, J. Am. Chem. Soc. 133, 7708 (2011). 4- R. Bose, A. Bera, M. R. Parida, A. Adhikari, B. S. Shaheen, E. Alarousu, J. Sun, T. Wu, O. M. Bakr, O. F. Mohammed, Nano Lett. 16, 4417 (2016). 5- A. M. El-Zohry, B. S. Shaheen, V. M. Burlakov, J. Yin, M. N. Hedhili, S. Shikin, B. S. Ooi, O. M. Bakr, O. F. Mohammed, Chem, 5, 706-718 (2019). 6- P. Maity, N. A. Merdad, J. Yin, K. J. Lee, L. Sinatra, O. M. Bakr, O. F. Mohammed, ACS Energy Lett., 6, 2602 (2021). 7- Y. Zhang, R. Sun, X. Ou, K. Fu, Q. Chen, Y. Ding, L.-J. Xu, L. Liu, Y. Han, A. V. Malko, X. Liu, H. Yang, O. M. Bakr, H. Liu, O. F. Mohammed, ACS Nano, 13, 2520 (2019). 8- J.-X. Wang, L. Gutierrez-Arzaluz, X. Wang, M. Almalki, J. Yin, J. Czaban-Jozwiak, O. Shekhah, Y. Zhang, O. B. Bakr, M. Eddaoudi, O. F. Mohammed, Matter, 5, 253-265 (2022). 9- J.-X. Wang, Chen, L. Gutierrez-Arzaluz, X. Wang, T. He, Y. Zhang, M. Eddaoudi, O. M. Bakr, O. F. Mohammed, Nature Photonics, 16, 869-875 (2022).

2:00 PM EL02.02.02

Enhanced Lattice Dynamics in a Single-Layered Hybrid Perovskite Zhuquan Zhang¹, Jiahao Zhang², Zi-Jie Liu¹, Nabeel Dahod¹, Watcharaphol Paritmongkol¹, Niamh Brown¹, Alexia Stollmann¹, Woo Seok Lee¹, Yu-Che Chien¹, Zhenbang Dai², Keith A. Nelson¹, William Tisdale¹, Andrew Rappe² and Edoardo Baldini³; ¹MIT, United States; ²University of Pennsylvania, United States; ³The University of Texas at Austin, United States

Layered hybrid perovskites have attracted much attention in recent years due to their emergent physical properties and exceptional functional performances, but the coexistence of lattice order and structural disorder severely hinders our understanding of these materials. One unsolved problem regards how the lattice dynamics are affected by the dimensional engineering of the inorganic frameworks and the interaction with the molecular moieties. Here, we address this question by using a combination of high-resolution spontaneous Raman scattering, high-field terahertz spectroscopy, and molecular dynamics simulations. This approach enables us to reveal the structural vibrations and disorder in and out of equilibrium and provides surprising observables that differentiate single- and double-layered perovskites. While no distinct vibrational coherence is observed in double-layer perovskites, we discover that an off-resonant terahertz pulse can selectively drive a long-lived coherent phonon mode through a two-photon process in the single-layered system. This difference highlights the dramatic change in the lattice environment as the dimension is reduced. The present findings pave the way for the ultrafast structural engineering of hybrid lattices as well as for developing high-speed optical modulators based on layered perovskites.

2:15 PM EL02.02.03

Nonlinear Optical Properties of Colloidal Perovskite Nanocrystals Claudevan A. Sousa¹, Luiz Gustavo Bonato¹, Eduardo Gonçalves¹, Brener Rodrigo De Carvalho Vale¹, Arthur Alo¹, Diogo Almeida², Luiz F. Zagonel¹, Ana F. Nogueira¹ and Lazaro Padilha¹; ¹Universidade Estadual de Campinas, Brazil; ²Universidade Federal do ABC, Brazil

Colloidal perovskite nanocrystals (PNCs) have been explored in the last years because of their remarkable linear optical properties, such as high photoluminescence quantum yield, narrow emission spectra, and high tunability in the visible range. Most recently, several reports have claimed that this class of nanomaterials also possesses outstanding third-order nonlinear optical

properties, such as high two-photon absorption cross-section and high nonlinear refractive index. In this work, we investigate the size dependence of the nonlinear optical response in a series of cubic-shaped CsPbBr₃ PNCs and show that their nonlinear optical response is not particularly high. Different from what it has been claimed in the literature, we show that no experimental evidence that supports the claim that the nonlinear refractive index for these PNCs is larger than those observed for other semiconductors. When all possible sources of artifacts are eliminated from the results, we observe that the measured magnitude of the intrinsic nonlinear refractive index varies between 10⁻¹⁴ and 10⁻¹³ cm²/W, the same order of magnitude obtained for bulk semiconductors with similar bandgap energy. Differently from isolated PNCs, we show that, when grouped in superlattices, these nanomaterials can present unique nonlinear optical response due to collective effects.

Acknowledgements: FAPESP and CAPES.

2:30 PMBREAK

3:00 PM *EL02.02.04

Ultrafast Nano-Imaging Resolving Structure, Coupling and Dynamics of Matter on its Natural Length and Time Scales Markus Raschke; University of Colorado Boulder, United States

Understanding and ultimately controlling the properties of matter, from molecular to quantum systems, requires imaging the elementary excitations on their natural time and length scales. To achieve this goal, we developed scanning probe microscopy with ultrafast and shaped laser pulse excitation for multiscale spatio-temporal optical nano-imaging. In corresponding ultrafast movies we resolve the fundamental quantum dynamics from the few-femtosecond coherent to the thermal transport regime. I will discuss specific examples visualizing in space and time the nanoscale heterogeneity in competing structural and electronic dynamic processes that define the performance in perovskite photovoltaics or energy dissipation in 2D heterostructures. I will then extend the discussion to new forms of photon-matter hybrid states that emerge from confining light on the nano-scale to new regimes of nonlocal and quantum nonlinear nano-optics. As a perspective I will show that we are at the cusp of the ultimate goal of functional imaging and control, to link macroscopic properties to microscopic interactions in materials at their fundamental spatio-temporal levels using light.

3:30 PM *EL02.02.05

Unraveling Ultrafast Dynamics in Mixed-Phase Hybrid Metal Halide Perovskites Rebecca L. Milot; University of Warwick, United Kingdom

Metal halide perovskites are promising materials for many optoelectronic applications, particularly solar cells. However, the standard materials used in many high efficiency devices (e.g. 3D materials such as methylammonium lead triiodide, MAPbI₃) are unstable under ambient conditions due to their sensitivity to a number of environmental factors including humidity and light. To address stability issues, layered or quasi-2D materials are incorporated into 3D perovskite thin films as either a mixture or a capping layer. However, these materials can greatly alter the optoelectronic properties since the exciton binding energies in 2D perovskites can be as high as 100s of meV, meaning that a large population of excitons can be present at ambient temperatures.¹

Since the beginning of the perovskite field about a decade ago, ultrafast spectroscopy techniques including optical pump/THz probe spectroscopy (OPTP) have provided vital information about the charge transport and charge-carrier dynamics in metal halide perovskites.² For these newly-developed mixed 2D/3D materials, however, understanding charge transport can be challenging using just one spectroscopic technique due to the presence of multiple materials and photoexcited species. To untangle the contributions from all of these different species, we have used a combination of visible transient absorption spectroscopy (TAS) and OPTP. While TAS can easily distinguish the excited states of various phases of 2D and 3D perovskites, OPTP is sensitive only to mobile free charge carriers and can be used to evaluate the charge-carrier mobility and separate excitonic effects when compared to TAS data. With this combination of techniques, we have evaluated various lead-based 3D perovskite thin films which have been treated with phenylethylammonium salts in order to preferentially form Ruddlesden-Popper phases at the surface of the films. In addition to finding that the charge-carrier dynamics are sensitive to the film preparation method, we distinguish between bulk and surface passivation effects and query charge transfer between 2D and 3D species.

1. Sirbu, D., Balogun, F. H., Milot, R. L. & Docampo, P. Layered Perovskites in Solar Cells: Structure, Optoelectronic Properties, and Device Design. *Adv. Energy Mater.* **11**, 2003877 (2021).
2. Pereira dos Santos, T. *et al.* The 2021 Roadmap on Ultrafast Spectroscopic Probes of Condensed Matter. *J. Phys. - Condens. Mat.* **33**, 353001 (2021).

4:00 PM EL02.02.06

Probing Polaronic Effects via Optical Pump – Terahertz Range Raman Probe Guy Reuveni¹, Selina Nöcker^{2,1} and Omer Yaffe¹; ¹Weizmann Institute of Science, Israel; ²Friedrich-Alexander-Universität Erlangen-Nürnberg, Germany

Understanding the impact of excited electrons on structural dynamics is essential for comprehending various macroscopic phenomena, for example, carrier mobility. The investigation of polarons has predominantly relied on indirect probing techniques such as temperature-dependent photoluminescence and carrier mobility measurements. Alternatively, time-dependent X-ray diffraction methods have been employed, but they often involve complex instrumentation.

In this study, we present a cutting-edge optical setup that directly probes lattice distortions induced by excited electrons. Our state-of-the-art approach involves a visible pulsed pump and continuous off-resonance Raman probe, enabling a direct detection and differentiation of polaronic effects. I will demonstrate the effectiveness of this table-top optical setup mainly on BiVO₄ single crystal, showing clear signatures of small polarons.

4:15 PM EL02.02.07

Visualizing Polaron Formation in Lead Halide Perovskite Quantum Dots by Time-Resolved Serial Crystallography Kartik Avyer; Max Planck Institute for the Structure and Dynamics of Matter, Germany

Excitonic polaronic fields in metal halide perovskites (MHPs) are of intense research interest as a possible mechanism to explain their unique light harvesting and light emission properties. Quantum dots (QDs) of such materials exhibit additional size-dependent variations in their optoelectronic properties like the Stokes shift. We report the observation of signatures of polaronic deformation fields in CsPbBr₃ QDs upon single resonant excitation by adapting the technique of time-resolved serial femtosecond crystallography at X-ray free electron lasers (XFELs). This method allows one to observe changes to the three dimensional shape of diffracted Bragg peaks from these quantum dots upon optical excitation which are, in turn, exquisitely sensitive to inhomogeneous lattice deformations in the particle.

Due to this sensitivity we were able to observe statistically significant changes in the average deformation field after resonant excitation with, on average, one photon per particle. Initial modelling shows evidence for optical-phonon-like deformations and indicates a larger extent of the electron polaron compared to the hole polaron, as well as an anisotropic spatial distribution of the deformation field due to confinement effects.

4:30 PM *EL02.02.08

Spatiotemporally Following Charge, Heat and Their Coupling at the Nanoscale in Energy Conversion Materials Stephanie Hart¹, Leo M. Hamerlynck¹, Erin Moloney¹, Rongfeng Yuan¹, Hannah Weaver¹, Aidan O'Beirne², Henrique Bucker Ribiero², Finn Babbe³, James Utterback¹, Livia Belman-Wells¹, Alex King¹, Adam Weber³, Masakazu Iwai³, Scott K. Cushing⁴, Tony Heinz² and Naomi S. Ginsberg¹; ¹University of California, Berkeley, United States; ²Stanford University, United States; ³Lawrence Berkeley National Laboratory, United States; ⁴California Institute of Technology, United States

Ultrafast optical stroboscopic scattering microscopy (stroboSCAT) is emerging as an incisive technique to probe not only photogenerated electronic excitations and their transport as a function of nanoscale material structure, but also to simultaneously and distinctly probe the thermal energy generated and its transport, with temperature change sensitivity down to 100 mK. This ability opens opportunities to not only properly characterize each form of coexisting energy, but also to investigate the coupling and interconversion of charge to heat and heat to charge. After illustrating the mechanistic information accessible via carrier density-dependent transport in silicon, I will show a range of examples to support these abilities of interest for thermoelectric and photoelectrochemical applications. I will show how structural armchair anisotropy in black phosphorus generates energy transport anisotropies useful for thermoelectrics and describe how these processes are altered in the 2D limit. I will also show a series of structure-transport relationships in candidate photoelectrode transition metal oxides for photocatalysis and in natural photosynthesis. Finally, I will show how a related approach also enables investigation of solution phase reaction products and their transport.

8:00 AM *EL02.03.01

Ultrafast Quasiparticle Dynamics at Complex Interfaces from Different Angles: Opportunities and Challenge Julia Stähler^{1,2}; ¹Humboldt-Universität zu Berlin, Germany; ²Fritz Haber Institute, Germany

Our group investigates elementary processes in materials and at their interfaces by several different types of ultrafast techniques. In this presentation, I will highlight the strengths and weaknesses of ultrafast optical transient absorption and angle-resolved photoelectron spectroscopy as well as introduce our new approach to time-resolved scanning near field optical microscopy (SNOM):

Dynamic screening of quasiparticles in WS₂ monolayers: We unravel the influence of quasiparticle screening in the non-equilibrium exciton dynamics of monolayer WS₂ by femtosecond time-resolved reflectance contrast measurements and a simple, comprehensive model that provides a complete picture of the competing phenomena governing the exciton dynamics in WS₂ upon photoexcitation. Particularly, we unveil the specific impact of excitons and carriers on the renormalization of the quasi-free particle band gap through screening, the exciton binding energy, and the linewidth broadening [1,2].

Real photodoping: ultrafast surface metallization of ZnO: The advent of photoinduced phase transitions (PIPT) and the investigation of their non-equilibrium dynamics on ultrafast timescales coined various fashionable terms like hidden phases, new phases of matter, or photodoping. I will discuss these terms using the example of ZnO that undergoes a semiconductor-to-metal transition upon real photodoping at very low excitation densities [3]. Notably, the hidden, metallic phase has no equivalent in the equilibrium phase diagram and shows decay dynamics on ultrafast timescales, but can also be retained and metastable [4].

Time-resolved SNOM in the visible at kHz repetition rates: The compatibility of SNOM with pulsed sources is hampered by the requirement of a high-repetition rate imposed by lock-in detection. We developed a sampling method, called quadrature-assisted discrete (quad) demodulation [5], which releases this constraint. It will be shown how this enables the usage of tuneable kHz sources not only for near-field imaging in pseudoheterodyne mode, but also for ultrafast pump-probe studies.

[1] S. Calati et al., *Phys. Chem. Chem. Phys.* **23** 22640 (2021)

[2] S. Calati et al., *Phys. Rev. B*, submitted (2023)

[3] L. Gierster et al., *Nat. Commun.* **12** 978 (2021)

[4] L. Gierster et al., *Faraday Disc.* **237** 58 (2022)

[5] S. Palato et al., *Appl. Phys. Lett.* **120** 131601 (2022)

8:30 AM *EL02.03.02

New Ultrafast Optical and Structural Probes in Material Science Keith A. Nelson; Massachusetts Institute of Technology, United States

New methods for optical control and observation of electronic, spin, and lattice degrees of freedom have enabled previously inaccessible study of light-induced phase transitions and other transformations. Several such methods will be discussed.

Strong terahertz-frequency light fields have recently been used to drive far-from-equilibrium excursions and material transformations. Detailed understanding of the underlying mode-mode interactions involved can be obtained through 2-dimensional THz spectroscopy. Off-diagonal peaks in 2D THz spectra, as in other 2D spectra, directly reveal mode-mode couplings that are invisible to linear spectroscopy. Until recently, a single 2D spectrum typically required several days of data acquisition time because two time variables, the (interpulse) time between two THz pulses and the temporal profile of the nonlinear THz signal field induced by the incident pulses, needed to be scanned point-by-point on the two time axes. Instead, the entire time-dependent THz signal profile can be measured in a single laser shot using several hundred optical "readout" pulses with different time delays that are all overlapped spatially with the THz signal field in an electro-optic crystal and then directed to different regions of a multi-pixel detector. In recent work, systematically incremented THz magnetic field polarizations relative to the crystallographic axes of canted antiferromagnets were used to record 144 2D spectra in less than 24 hours, introducing *2D THz polarimetry* which revealed a previously unknown but likely ubiquitous mechanism for coupling between different magnon modes in this material class (*arXiv:2207.07103*; *arXiv:2301.12555*). Similar methodology has been used for true single-shot THz and optical measurements of a photoinduced transition into a metastable phase of TaS₂ at low temperatures (*Sci. Adv.* **8**, eabp9076).

New advances and results in x-ray diffraction and spectroscopy at x-ray free-electron lasers (XFELs) will be discussed very briefly. A THz-induced transient ferroelectric (FE) structure in low-temperature SrTiO₃ has been studied using two inverted THz generation crystals to drive the crystal with single-cycle THz fields of inverted polarity. The resulting inverted x-ray scattering signals recorded at wavevectors near but not on Bragg diffraction peaks revealed that the THz-induced FE rearrangements occur predominantly in pre-existing polar nanoregions, a key mechanistic insight not accessible through earlier optical measurements (*Science* **364**, 1079). In separate measurements in the extreme UV (EUV) transient grating facility at the FERMI beamline (*Sci. Adv.* **5**, eaaw5805), crossed EUV pulses generated coherent magnons with 50-100-nm wavelengths whose time-dependent oscillations revealed magnon dispersion in this often inaccessible wavevector range. Coherent driving of high-wavevector phonons, magnons, and other excitations with spatial periods <10 nm is anticipated.

Finally, very recent development (*arXiv:2209.13897*) of a method for *laser generation of shock waves without damage to the optically irradiated region of the sample* permits significant structural control to be incorporated into ultrafast measurements conducted at high repetition rates. A shock wave can be generated nondestructively and propagated into a pristine sample region where THz, optical, and/or x-ray pulses are used for ultrafast measurements. The shock-induced strain duration is ~1 ns, so ultrafast measurements can be conducted with quasi-DC strains whose magnitudes (up to 3%, ~10 GPa pressure) can be specified. Multimodal control using strain plus THz and/or optical excitation pulses can be used to guide materials into new phases or other states of interest. Repeated shock delivery to the same sample region also permits detailed study of fatigue, where macroscopic material failure occurs only after many shocks. X-ray imaging may permit characterization of the nanoscale defects that accumulate prior to failure.

9:00 AM EL02.03.03

Extreme Ultraviolet Transient Grating Spectroscopy of High-Wavevector Coherent Magnons Peter R. Mieder¹, Nadia Berndt¹, Jude Deschamps¹, Riccardo Comin¹, Filippo Bencivenga², Laura Foglia², Riccardo Mancigrucci², Danny Fainozzi², Ettore Paltanin², Sergei Urazhdin³, Nupur N. Khata^{4,5}, Stefano Bonetti⁴, Dmitriy Ksenzov⁶, Christian Gutt⁶, Riccardo Cucini⁷, Marta Brioschi^{8,7}, Pietro Carrara^{8,7}, Steffen Wittrock⁹, Dieter Engel⁹, Daniel Schick⁹, Keith A. Nelson¹ and Alexei Maznev¹; ¹Massachusetts Institute of Technology, United States; ²FERMI-Elettra, Italy; ³Emory University, United States; ⁴Stockholm University, Sweden; ⁵Università Ca' Foscari, Italy; ⁶University of Siegen, Germany; ⁷CNR-IOM Trieste, Italy; ⁸Università degli Studi di Milano, Italy; ⁹Max-Born-Institute, Germany

Magnons, or spin waves, are a subject of intense research aimed at both uncovering fundamental physics and paving the way towards applications such as spintronics [1]. Traditionally, magnons have been studied using scattering spectroscopy techniques such as Brillouin light scattering (BLS), inelastic neutron scattering (INS), and resonant inelastic x-ray scattering (RIXS). Combined, these techniques cover wavevector ranges from <0.03 nm⁻¹ (BLS) and >0.5 nm⁻¹ (INS/RIXS), thereby leaving the wavevector gap from 0.03 to 0.5 nm⁻¹ inaccessible. Furthermore, these techniques typically rely on scattering of thermal magnons, limiting the study of coherent magnons to microwave or femtosecond laser techniques. The wavevector of coherent magnons is limited by the need to fabricate nanostructures in the former case and by the optical wavelength in the latter case. We present an ultrafast coherent magnon spectroscopy technique based on the extreme ultraviolet transient grating (EUV-TG) approach developed at the free-electron laser facility FERMI [2], that bridges the wavevector gap between BLS and INS/RIXS while providing a way to excite coherent magnons with wavelengths in the nanometer range without resorting to extensive fabrication. Furthermore, as a time-resolved method, it is not limited by spectrometer resolution, and allows for the direct measure of damping parameters. Upon excitation, transient magnetic gratings [3] were excited in Fe-Gd ferrimagnetic multilayer samples by crossed femtosecond EUV pulses, and detected by diffraction of a time-delayed EUV probe pulse whose wavelength was tuned to the N-edge of Gd. The rapid change in the magnetic anisotropy following the excitation drove spin precession and launched coherent magnons at the wavelength dictated by the transient grating period. By varying the pump wavelength from 25 – 42 nm, the magnon wavevector was varied from 0.07 – 0.12 nm⁻¹. In combination with optical measurements at zero wavevector, magnon dispersion curves were constructed. We also report a drastic change in the magnon response between samples with compensated and perpendicular magnetic anisotropy, arising from slight changes in the Fe-Gd ratio. In addition, we have produced transient magnetization gratings with a period as small as 17 nm, which opens the prospect for ultrafast control of magnetism on the sub-10 nm spatial scale, which is necessary for applications such as magnetic memory.

[1] Anjan Barman et al., The 2021 Magnonics Roadmap, *J. Phys.: Condens. Matter* **33**, 413001 (2021); [2] F. Bencivenga et al., Nanoscale transient gratings excited and probed by extreme ultraviolet femtosecond pulses, *Sci. Adv.* **5**, eaaw5805 (2019); [3] D. Ksenzov et al., Nanoscale Transient Magnetization Gratings Excited and Probed by Femtosecond Extreme Ultraviolet Pulses, *Nano Lett.* **21**, 2905 (2021).

9:15 AM EL02.03.04

Transient Nanoscopy of Exciton Dynamics in Two-Dimensional Transition Metal Dichalcogenides Jingang Li and Costas P. Grigopoulos; University of California, Berkeley, United

The electronic and optical properties of 2D transition metal dichalcogenides (TMDCs) are dominated by strong excitonic resonances. Exciton dynamics plays a critical role in the functionality and performance of many miniaturized 2D optoelectronic devices. While time-resolved photoluminescence and transient absorption spectroscopies are widely used to characterize the exciton lifetime and transient behaviors of TMDC layers, the measurement of local excitonic responses at the nanoscale remains challenging.

Here, we report a near-field transient nanoscopy to probe exciton dynamics beyond the diffraction limit. Exciton recombination and exciton-exciton annihilation processes in monolayer and bilayer MoS₂ are studied as the proof-of-concept demonstration. Moreover, with the capability to access the local exciton dynamics, we directly observe the strain-induced suppression of exciton-exciton annihilation in a nano-wrinkled MoS₂ flake. Such nanoscale resolution highlights the potential of our optical nanoscopy for fundamental investigation of exciton physics and further optimization of functional devices. Our results further demonstrated the capability to probe carrier behaviors in other nanoscale materials and devices, which is of great significance to understanding the optoelectronic properties and practical functionality of semiconductor nanostructures.

9:30 AM *EL02.03.05

Floquet Engineering of Two-Dimensional Materials by Time-Periodic Light Field [Shuyun Zhou](#); Tsinghua University, China

Time-periodic light-field can dress the electronic states of quantum materials, providing fascinating opportunities for transient modification of the electronic band structure with light-induced emergent phenomena [1]. In this talk, I will present our recent experimental progress on the Floquet engineering of two-dimensional materials by time-periodic light field using time- and angle-resolved photoemission spectroscopy. Using black phosphorus as an example, I will present the light-induced engineering of the transient electronic structure upon near-resonance pumping with intriguing light polarization dependence, which reflects the pseudospin selectivity [2]. By further pushing the specifications of the pump pulses, the light-induced electronic structure renormalization can be further enhanced, and insights for extending Floquet engineering to more materials will be discussed.

[1] Changhua Bao *et al.*, "Light-induced emergent phenomena in two-dimensional materials and topological materials", *Nat. Rev. Phys.* 4, 33 (2022)

[2] Shaohua Zhou *et al.*, "Pseudospin-selective Floquet band engineering in black phosphorus", *Nature* 614, 75 (2023)

10:00 AM BREAK

10:30 AM *EL02.03.06

Out-of-Equilibrium Insights into Condensed Matter - Experimental Opportunities at Bernina/SwissFEL [Henrik Lemke](#); Paul Scherrer Institute, Switzerland

Functional transitions in materials can be effectively probed by ultrafast X-ray probes. Their structural sensitivity for electronic or magnetic structure in condensed matter systems gives insight into complex processes. Dedicated instrumentation and examples for experiments at Bernina/SwissFEL will be presented.

11:00 AM *EL02.03.07

A Time Domain View of 2D Van Der Waals Interfaces [Xiaoyang Zhu](#); Columbia University, United States

Interfaces of two dimensional (2D) van der Waals (vdW) crystals, formed from mechanical transfer stacking or chemical vapor deposition, constitute the most versatile material platforms for the exploration of new physical phenomena, particularly emergent quantum phases. Here we apply femtosecond pump-probe spectroscopy/microscopy to develop a time-domain view of quantum phases at 2D vdW interfaces. Using transitional metal dichalcogenide (TMDC) heterobilayers and 2D layered magnetic semiconductors (e.g., CrSBr), we probe the nature of the quantum phases and their coupling to different degrees of freedom. For TMDC moiré interfaces, we show the robustness of correlated electron phases and their coupling to excitons and phonons. In the layers magnetic semiconductors, we discover the coupling between interlayer electronic hybridization to magnetic order and, as a result, the strong coupling of excitons to coherent magnons. These time-domain views reveal not only the nature of the quantum phases, but also prospects of controlling these quantum phases by light.

11:30 AM EL02.03.08

Ultrafast Many-Body Interactions in Two-Dimensional Transition-Metal Dichalcogenides [Suman Kalyan Pal](#) and Ashish Soni; IIT Mandi, India

Two-dimensional (2D) transition-metal dichalcogenides (TMDCs) have sparked tremendous interest because of their versatile application possibilities owing to exceptional optical, electrical, and mechanical properties. [1, 2] Strong Coulomb interaction and reduced screening make them suitable candidates for investigating many-body interactions at room temperature. [3] In recent years, ultrafast optical techniques have been used to directly access many-body processes occurring in 2D TMDCs. [4] We investigated the charge carrier dynamics in chemical vapor deposition (CVD)-grown TMDC flakes using femtosecond transient absorption spectroscopy. In this talk, I will shed light on the interplay between exciton formation, relaxation, and trapping processes, providing insights into the dynamics of exciton annihilation in 2D TMDCs.

The first part of my talk is about the study of ultrafast carrier dynamics in monolayer WS₂. By monitoring the transient optical responses, we identified exciton trapping by defects, elucidating the impact of defect states on excitation-density dependent carrier decay dynamics. [5] Our findings shed light on the influence of defect states in CVD-grown TMDCs, thus paving the way for utilizing such TMDCs in optoelectronic devices. Next, I will demonstrate efficient multiple exciton generation (MEG) in monolayer MoS₂ by monitoring excitation photon-energy dependent carrier dynamics. We not only observed low threshold energy for MEG, but also high (86%) MEG efficiency. [6] The experimental findings obtained from this work will have greater implications in developing mechanically flexible and highly efficient next-generation solar cells and photodetectors.

References

[1] Busch R T, Torsi R, Drees A, et al. Effective Optical Properties of Laterally Coalescing Monolayer MoS₂ *"The Journal of Physical Chemistry Letters"* **13** 5808-14 (2022).

[2] Mondal K G, Jana P C and Saha S Optical and structural properties of 2D transition metal dichalcogenides semiconductor MoS₂ *"Bulletin of Materials Science"* **46** 15 (2023).

[3] Lin Y, Ling X, Yu L, et al. Dielectric Screening of Excitons and Trions in Single-Layer MoS₂ *"Nano Letters"* **14** 5569-76 (2014).

[4] Sun D, Rao Y, Reider G A, et al. Observation of Rapid Exciton-Exciton Annihilation in Monolayer Molybdenum Disulfide *"Nano Letters"* **14** 5625-9 (2014).

[5] Soni A, Kushavah D, Lu L-S, et al. Ultrafast Exciton Trapping and Exciton-Exciton Annihilation in Large-Area CVD-Grown Monolayer WS₂ *"The Journal of Physical Chemistry C"* **125** 23880-8 (2021).

[6] Soni A, Kushavah D, Lu L-S, et al. Efficient Multiple Exciton Generation in Monolayer MoS₂ *"The Journal of Physical Chemistry Letters"* **14** 2965-72 (2023).

11:45 AM EL02.03.09

Topological Resonance in Graphen-Like Materials [Krishna Rana Magar](#) and Vadym Apalkov; Georgia State University, United States

In topological materials, interacting with short and strong optical pulses, electrons can accumulate a topological phase during the pulse. Such phase can compensate the dynamic phase resulting in topological resonance, which is visible as a large inter-band transfer of electron population. We study theoretically the topological resonance in materials of the gapped multilayer graphene type. We show that the resonance can be observed only in the systems with finite bandgap. For monolayer graphene, the topological resonance can occur only in the field of an elliptically polarized pulse while for multilayer graphene, the resonance can also be realized in a linearly polarized pulse.

SESSION EL02.04/QT02.06: Joint Session: Time-Resolved Spectroscopies for Emergent Quantum Materials

Session Chairs: Burak Guzel Turk and Yao Wang

Tuesday Afternoon, November 28, 2023

Hynes, Level 3, Room 303

1:30 PM *EL02.04/QT02.06.01

New Physics in Driven Quantum Materials [Andrea Cavalleri](#)^{1,2}; ¹Max Planck Institute for the Structure and Dynamics of Matter, Germany; ²University of Oxford, United Kingdom

I will discuss how coherent electromagnetic radiation at Tera-Hertz and mid-infrared frequencies can be used to manipulate complex solids. As collective excitations are driven coherently and nonlinearly, virtually uncoupled normal modes of the material are made to interact. Hence, these drives give rise to non-thermal states with unconventional properties, and sometimes with emergent order under a drive. Interesting examples involve the nonlinear control of the crystal lattice, used to induce magnetic order, ferroelectricity and non-equilibrium superconductivity at

high temperatures.

2:00 PM *EL02.04/QT02.06.02

Unraveling Electron-Phonon and Phonon-Phonon Coupling in Momentum and Time with Ultrafast Electron Diffuse Scattering (UEDS)[Bradley Siwick](#); McGill University, Canada

The nature of the couplings within and between lattice and charge carrier degrees of freedom is central to condensed matter and materials physics. These interactions are essential to phenomena as diverse as superconductivity, charge density waves and carrier mobility in semiconductors and metals. Despite their fundamental importance, detailed momentum-dependent information on the strength of electron-phonon coupling (EPC) and phonon-phonon coupling (PPC) across the entire Brillouin zone has proved to be very difficult to obtain.

In this talk I will describe an emerging pump-probe technique, ultrafast electron diffuse scattering (UEDS), that provides such information from the perspective of the phonon system directly. Two recent examples of the application of UEDS to layered (2D) materials will be the focus. First, in the thermoelectric material SnSe – a strongly polar semiconductor – we directly observe the phonon dressing processes that yield carrier localization and polaron formation with UEDS. In SnSe these phonon dressing dynamics are profoundly bimodal, with the fast (300 fs) process associated with the formation of a quasi-1D lattice distortion and a relatively large polaron and the slower (4 ps, an order of magnitude slower timescale) process associated with small polaron formation. The observations in SnSe are consistent with electron and hole polarons being different sizes, or the process of polaron formation being intrinsically bimodal for both carriers in a manner reminiscent of Lars Onsager's inverse snowball effect. Second, the extension of UEDS to a MoS₂ monolayer heterostructure will be demonstrated. These results reveal substrate dielectric screening of the electron-phonon interaction within the monolayer as well as the momentum-dependent carrier-phonon equilibration. These results are compared directly against ab-initio simulations of these processes.

2:30 PM *EL02.04/QT02.06.03

Visualizing the Ultrafast Dynamics of Domain Walls via Non-Equilibrium X-Ray Photon Correlation Spectroscopy[Aaron Lindenberg](#); Stanford University, United States

We describe the application of ultrafast atomic-scale coherent imaging techniques based on single-shot x-ray photon correlation spectroscopy (XPCS) to resolve the nucleation and growth of a new phase during a prototypical light-induced solid-solid phase transition. We show that a two-time correlation approach provides enhanced sensitivity to the diffuse x-ray scattering which encodes the heterogeneous mesoscopic response of the material, in contrast to a standard crystallographic measurement which probes only the ensemble-averaged structure. Through this approach, we demonstrate a new way of visualizing the nucleation and growth of domains and probe selectively the dynamics occurring at domain wall boundaries and the annihilation of these defect states. We find unexpectedly that this non-equilibrium response spans approximately ten orders of magnitude in time scales (from 100 femtoseconds to 1 millisecond), extending a thousand times longer than expected from crystallographic studies. This work defines new possibilities for visualizing the non-equilibrium dynamics of disordered and heterogeneous materials and the atomic-scale dynamic processes underlying the synthesis of new phases of matter.

3:00 PM BREAK

3:30 PM EL02.04/QT02.06.04

Ultrafast Nano-Imaging of Dark Excitons[Marcel Reutz](#)¹, [David Schmitt](#)¹, [Jan Philipp Bange](#)¹, [Wiebke Bennecke](#)¹, [Giuseppe Meneghini](#)², [Abdulaziz Almutairi](#)³, [Marco Merboldt](#)¹, [Jonas Pöhls](#)¹, [Sabine Steil](#)¹, [Daniel Steil](#)¹, [Thomas Weitz](#)¹, [Stephan Hofmann](#)³, [Samuel Brem](#)², [G. S. Matthijs Jansen](#)¹, [Ermin Malic](#)² and [Stefan Mathias](#)¹; ¹Georg-August-Universität Göttingen, Germany; ²Philipps-Universität Marburg, Germany; ³University of Cambridge, United Kingdom

Dynamical processes in the condensed matter occur on the femtosecond time- and the nanometer length-scale. This very general statement holds true for fundamental processes such as the dissipation of energy after an optical excitation or the creation of light-matter coupled phases. At the same time, it showcases that any nanoscale inhomogeneity that affects the quasiparticle dynamics can, in the end, limit the performance of a real-world device. In consequence, there are a multitude of research efforts that work towards the development of new experimental techniques that can provide a holistic picture of dynamical processes on ultrashort time- and length-scales.

In this contribution, we discuss our recent efforts to extend the full capabilities of time- and angle-resolved photoemission spectroscopy (trARPES) to the nanoscale. In short, we will show how we can monitor the femtosecond evolution of spectral weight at a specific in-plane momentum k and kinetic energy E with 50 fs time- and 500 nm spatial-resolution [1]. Experimentally, this is achieved by the development of ultrafast dark-field photoelectron microscopy: We employ our table-top high-repetition rate high-harmonic generation beamline and time-of-flight momentum microscope [2] and combine it with the full capabilities of dark-field imaging techniques [1].

In the presentation, we then present the capabilities of ultrafast dark-field photoelectron microscopy in three steps: First, in a spatially integrated mode of the experiment, we will discuss momentum-resolved photoemission signatures of intralayer, interlayer and hybrid excitons and identify distinct hallmarks of the moiré superlattice [3]. Second, we will show that interlayer excitons are effectively formed via exciton-phonon scattering, and subsequent interlayer tunneling at the interlayer hybridized Σ_W valleys on the sub-100 fs timescale [3,4]. And third, we will report on the spatio-temporal and spatio-spectral dynamics of bright and dark excitons in a laterally inhomogeneous TMD heterostructure. Most interestingly, we find that the rate of charge transfer across the type-II band aligned WSe₂/MoS₂ interface can vary by more than a factor 2. We explain this discrepancy with a locally varying energy landscape of excitons, as directly accessible with ultrafast dark-field photoelectron microscopy [1].

[1] Schmitt *et al.*, arXiv:2305.18908 (2023).

[2] Keunecke *et al.*, Rev. Sci. Ins. **91**, 063905 (2020).

[3] Schmitt *et al.*, Nature **608**, 499 (2022).

[4] Bange *et al.*, 2D Materials **10**, 035039 (2023).

3:45 PM EL02.04/QT02.06.05

Ultrafast Optical Probing of Temperature-Induced Antiferrodistortive Phase Transition in SrTiO₃[Saqeeb Adnan](#)¹, [Amey Khanolkar](#)², [David Hurley](#)² and [Marat Khafizov](#)¹; ¹The Ohio State University, United States; ²Idaho National Laboratory, United States

SrTiO₃ (STO) is a highly versatile perovskite renowned for its wide array of ionic transport, dielectric and ferroelectric properties, making it a subject of great technological interest, particularly in energy, information processing, and data storage. In this study, we monitor the ultrafast dynamics of the antiferrodistortive (AFD) phase transition in STO via time-domain Brillouin scattering (TDBS). Monitoring the depth-resolved Brillouin oscillation (BO) frequency (associated with longitudinal coherent acoustic phonons), we demonstrate the presence of fingerprint frequencies of cubic and tetragonal phases across the high and low temperature regions of the sample, respectively. Coupled with a time-resolved heat diffusion model, the BO frequency profiles provide evidence of a ultrafast transformation of the low temperature tetragonal phase into cubic phase driven by thermal energy deposition^[1]. The initial rapid phase change is followed by a slower reverse cubic-to-tetragonal phase transformation occurring on a time scale of hundreds of picoseconds. The observed phase transformation can be attributed to a structural resemblance between atomic displacements of the R-point soft optic mode of the cubic phase and the tetragonal phase of the perovskites, both exhibiting an anti-phase rotation of oxygen octahedra. The evidence of such a fast structural transition in STO offers opportunities for developing novel ultrafast switching and phase-changing devices.

1. <https://doi.org/10.48550/arXiv.2309.03172>

4:00 PM *EL02.04/QT02.06.06

Battery Cathode Electrochemistry via X-Ray Spectroscopy[Thomas Devereaux](#); Stanford University, United States

In this talk I will present some thoughts on the mechanisms for cathode electrochemistry from the viewpoint of x-ray spectroscopy. A focus is placed on charge transfer energetics and how they can be connected to high battery capacity and cyclability. Efforts towards understanding high valent redox using time-domain x-ray spectroscopy will be reviewed.

4:30 PM *EL02.04/QT02.06.07

Time-Resolved Resonant Inelastic X-Ray Scattering Studies at the SCS Instrument of EuXFEL[Andreas Scherz](#); European XFEL, Germany

Femtosecond lasers are important tools to modify and control the properties of quantum materials on ultrashort time scales. Resonant inelastic X-ray scattering (RIXS) spectroscopy has emerged over the last decades as a powerful method to explore low-energy orbital, spin, lattice and charge excitations in quantum materials. The main limiting factor to attain RIXS at high energy- and time-resolution is the low repetition rate and photon flux of the first-generation X-ray free-electron lasers (XFEL). Taking advantage of the Megahertz repetition rate of the European X-ray free electron laser (EuXFEL), the high-resolution spectrometer of the Heisenberg User consortium (hRIXS) enables users to perform RIXS spectroscopy of material dynamics in nonequilibrium with unprecedented time- and energy-resolution.

We report from the user-assisted commissioning program in 2022 addressing charge transfer (CT) excitations in NiO and La₂CuO₄ transition metal oxides. The paradigmatic charge transfer insulator and antiferromagnet NiO was excited across the CT gap by a 50 fs laser pulse at 266 nm. Using time-resolved RIXS at the Ni L₃ edge with an energy resolution of 80 meV and a time-resolution of ~120 fs, we observe prominent localized CT excitons that decay and delocalize in a few picoseconds. The CT excitation is accompanied by a broadening and shift of the dd excitations indicative of ligand field effects in the excited state, seen over tens of picoseconds. The first results demonstrate the potential of time-resolved RIXS at MHz-repetition rate XFELs to explore nonequilibrium dynamics of quantum materials.

SESSION EL02.05: Poster Session
Session Chairs: Burak Guzelturk and Hannah Joyce
Tuesday Afternoon, November 28, 2023
Hynes, Level 1, Hall A

8:00 PM EL02.05.01

Using Time-Resolved Microscopy to Probe Exciton Diffusion in CsPbBr₃ Superlattices Thomas Sheehan¹, Wenbi Shcherbakov-Wu¹, Taras Sekh^{2,3}, Ihor Cherniukh^{2,3}, Maksym V. Kovalenko^{2,3} and William Tisdale¹; ¹Massachusetts Institute of Technology, United States; ²ETH Zürich, Switzerland; ³Empa-Swiss Federal Laboratories for Materials Science and Technology, Switzerland

Exciton transport is critical to the performance of semiconductor nanocrystals in optoelectronic devices. Within most nanocrystal assemblies, exciton transport is a diffusive process mediated by Förster resonant energy transfer (FRET). Both structural and dynamic disorder can affect FRET-mediated exciton diffusion through their impact on factors such as nanocrystal spacing, transition dipole alignment, exciton radiative lifetimes, and excitonic coherence. The combined impact of these factors on exciton transport is complex and not well-understood in emerging semiconductor materials like lead halide perovskites. Here, we use time-resolved photoluminescence microscopy to investigate the effects of different types of disorder on exciton transport in CsPbBr₃ nanocube assemblies. This technique allows us to directly visualize the movement of excitons within the nanocrystal assembly. We determine the effect of structural disorder across different nanocrystal sizes by comparing exciton transport in highly ordered superlattices and in disordered assemblies, and we determine the effect of dynamic disorder by varying the temperature from 5K to room temperature. These investigations shed light on exciton transport mechanisms and could inform future design strategies for nanocrystals in optoelectronic devices.

8:00 PM EL02.05.02

Electroluminescence and Photoluminescence Characterization of LEDs / OLEDs using a Single Micro-Photoluminescence Spectroscopy Setup Christian Oelsner; PicoQuant GmbH, Germany

Opto-electrical characterization of LEDs/OLEDs is of essential importance for thorough understanding of light generation and emission properties of light emitting materials as a response to an applied electric current. The combination of photoluminescence (PL) and electroluminescence spectroscopy techniques can reveal the relationship of structure-lighting properties of novel LED/OLED materials and whole devices. Without doubts, this can help to optimize the composition and as a result the performance (brightness, lifetime, color) of these devices.

Herein we demonstrate a cost-effective way to get the electroluminescence properties, namely steady-state emission spectra and luminescence decays of different species within LED devices by applying an electric current without requiring an additional external bias source and/or external arbitrary function generator. Our solution allows a unique control over pulse rate, intensity, and pattern. It enables steady-state as well as time-resolved electroluminescence together with PL characterization of LEDs/OLEDs utilizing a single setup consisting of a microscope coupled to a PL spectrometer. All the measurements can be performed with high spatial, spectral, and timing resolution for better device optimization.

8:00 PM EL02.05.03

Ultrafast Transient Absorption Anisotropy to Monitor Relaxation in Carbon Dots Sukanya Saha; Western Michigan University, United States

In recent years, carbon dots (CDs) have emerged as a new class of carbonaceous materials that are easy to synthesize and characterize and show promising optical properties. One of the interesting aspects is their excitation wavelength dependent photoluminescence (PL). Although several CDs with different precursors are synthesized and characterized. Corresponding excited state optical properties on these materials are sparse. In this study, ultrafast excited state relaxation dynamics of CDs based on Pyrene are presented. Steady state, femtosecond transient absorption, and anisotropy data measurements are carried out to understand the relaxation pathways in these CDs. Pyrene-based aminated CDs are synthesized by hydrothermal method. The CDs were transferred to organic solvents (e.g., toluene, THF, and ACN) using surfactants via the phase transfer method. It is interesting that the CDs in different solvents exhibit both solvent dependent and excitation wavelength dependent PL. Excited state absorption decay of these CDs has shown ultrafast excited state decay that can be assigned to inter chromophore or chromophore solvent bath interactions. Transient absorption anisotropy measurements have shown faster picosecond time scale relaxation that cannot be assigned to the rotational reorientation of the CDs as the volume is greater. Transient absorption measurements have also shown differences in relaxation for bare CDs in water and CDs passivated with surfactants as in the case of CDs in non-aqueous solvents. The decay of anisotropy was assigned to energy transfer between the chromophores of different conjugation lengths in the CD. This is ascribed to HOMO fluorescence resonance energy transfer (HOMO-FRET) with time constants ranging from 50 to 90 ps. In THF, long-lived anisotropy decay is observed which is assigned to the rotational relaxation of the entire CD. Interesting ultrafast growth of anisotropy was observed in non-aqueous solvents, which is assigned to faster localization of the excitation from the core to a chromophore.

8:00 PM EL02.05.04

Quantum Enhanced Nonlinear Spectroscopy of Strongly Coupled Microcavities Evan J. Kumar¹, Lorenzo Uboldi^{2,1}, Esteban Rojas-Gatjens^{3,1}, Luca Moretti^{2,1}, Cristian Manzoni², Giulio Cerullo² and Ajay Ram Srimath Kandada¹; ¹Wake Forest University, United States; ²Politecnico di Milano, Italy; ³Georgia Institute of Technology, United States

The use of quantum entangled photons is suggested as a way to improve upon limitations in measurement sensitivity in conventional nonlinear optical spectroscopy. In addition, time-frequency entangled photon probes can potentially enable isolation of specific many-body interactions in condensed matter. Here, we discuss an experimental implementation of a nonlinear spectroscopy system based on spectrally entangled biphoton states. Using modified Mach-Zehnder interferometry, we present a methodology to estimate spectral correlations between entangled photons, which are generated through spontaneous parametric down-conversion of ultrashort optical pulses. We observe that the correlations in the biphoton state, characterized by the two-dimensional joint spectral amplitude (JSA), are transformed due to matter interactions. Specifically, we explore estimation of many-body interactions of polaritons in a strongly coupled semiconductor microcavity through an in-depth analysis of the experimentally obtained JSA of the biphoton state transmitted through the microcavity.

Reference:

Moretti et al. (2023). "Measurement principles for quantum spectroscopy of molecular materials with entangled photons". arXiv:2304.07828

8:00 PM EL02.05.05

Excited State Dynamics of Metal Halide Perovskite Nanocrystals - Role of Surface States and Inter-Particle Interactions Katherine A. Koch¹, David O. Tiede² and Esteban Rojas-Gatjens³; ¹Wake Forest, United States; ²Institute of Materials Science of Seville, Spain; ³Georgia Institute of Technology, United States

Ultrafast spectroscopy has been successfully employed in the investigation of carrier dynamics in metal halide perovskite nanocrystals (NCs). While most of these studies have been performed primarily on perovskite NCs that are mostly fabricated as colloidal suspensions, recently a new synthesis route has emerged in which the NCs are grown within silica scaffolds. This method enables fabrication of formamidinium lead bromide (FAPbBr₃) NCs directly in a device compatible solid-state architecture, while keeping the effects of quantum confinement intact. Here we provide a comprehensive photo-physical characterization of these material architectures of FAPbBr₃ ranging from a bulk system to strongly quantum confined dot like structures. We employ two-photon excitation spectroscopy and temperature dependent ultrafast transient absorption spectroscopy to probe the effect of quantum confinement and surface states on the excited-state energy landscape, carrier thermalization and recombination. We also probe the nature of coherent nonlinear interactions, inter-particle and electron-phonon coupling through two-dimensional coherent electronic spectroscopy. We demonstrate that the NCs grown within the scaffold are subject to a large size distribution with substantial contribution from optically dark surface states in the carrier dynamics. However, we provide evidence for greater inter-particle coupling and optimal interconnectivity between the NCs, thus offering an effective strategy to control energy and charge transport.

8:00 PM EL02.05.06

Light-Driven Ultrafast Phenomena in Ferroelectric Complex Oxides Heterostructure Hyeon Jun Lee¹, Youngjun Ahn², Haidan Wen³, Ji Young Jo⁴ and Paul Evans²; ¹Kangwon National University, Korea (the Republic of); ²University of Wisconsin–Madison, United States; ³Argonne National Laboratory, United States; ⁴Gwangju Institute of Science and Technology, Korea (the Republic of)

Above bandgap excitation in ferroelectric oxides can lead to a series of changes in the energy landscape of polarization and domain configuration, ultimately resulting in lattice distortion. A key consequent result is the photoinduced lattice distortion on the picosecond timescale set by the acoustic wave propagation. Probing the time-dependent dynamics is crucial to understanding mechanisms of the transitions and discovering new physical phenomena that can exist at an ultrafast time scale.

The picosecond dynamics of structural distortion following photoexcitation were probed at the Pohang Accelerator Laboratory X-ray Free-electron Laser (PAL-XFEL). Acoustic pulses resulting from the above bandgap absorption leads to changes in the x-ray diffraction pattern over the picosecond time scales. The detailed analysis reveals that ultrafast changes in polarization and nanodomain configuration involve complex mechanisms. The mechanisms discussed in this presentation include enhanced polarization by depolarization field screening, polarization rotation, externally imposed mechanical strain, and sub-picosecond-timescale polarization change.

We report that complex strain pulses produced by the photoexcitation drive a time-dependent distortion of nanodomains in PbTiO₃/SrTiO₃ superlattice film on SrRuO₃/SrTiO₃ substrate. Acoustic pulses resulting from the absorption of the incident optical beam lead to changes in the x-ray diffraction pattern of the SL over the picosecond time scales. The picosecond scale variation of the nanodomain diffuse scattering intensity is consistent with a larger polarization change than would be expected due to the polarization-tetragonality coupling of uniformly polarized ferroelectrics. The strong coupling is consistent with polarization rotation facilitated by the reorientation of the in-plane component of the polarization at the domain boundaries of the striped polarization structure.

The fundamental timescale of the optically induced stress generation has been studied by comparing the measurement and simulation. Optical excitation leads to ultrafast stress generation in the multiterrier BiFeO₃ thin film. High-dynamic range femtosecond time-resolved x-ray diffraction to probe the initial stages of the impulsive stress generated by an optical pulse and find that fast components of the stress generation extend to characteristic 1/e times at least as short as 300 fs. The experiments reported here reveal that there are contributions to the stress generated by the absorption of a femtosecond-duration above-bandgap optical pulse that extend over a range of timescales spanning an immediate stress at a scale of far less than 1 ps to timescale of on the order of a few ps.

8:00 PM EL02.05.07

Impact of Different Ligands on Nanocrystal Structural Disorder and Quantum Yield Landon Rice¹, Eliza Wieman¹, Burak Guzeltek² and Benjamin Cotts¹; ¹Middlebury College, United States; ²Argonne National Laboratory, United States

The goal of our lab is to understand the influence of surface states and transient disorder on the photoluminescence efficiency of semiconductor nanocrystals for use in device applications. A few NC systems (e.g. CdSe:CdS and PbS) have been optimized to reach near-unity quantum yield under weak excitation, but have been shown to achieve lower quantum yield under intense excitation required for certain applications such as lasers or LEDs. We use correlative measurements to understand the role of structural disorder in increased nonradiative decay under high intensity excitation.

We first quantify the power-dependent photoluminescence quantum yield of semiconductor nanocrystals (NCs) as a function of surface ligand chemistry, using a homebuilt quantum yield spectrometer, calibrated by primary standards. Nanocrystals with differing ligand passivation are measured with time-resolved photoluminescence and photoluminescence quantum yield to understand their radiative and nonradiative decay pathways. Finally, time-resolved X-ray diffraction (XRD) is used to measure the influence of differing ligands on electron-photon coupling and transient disorder in NC systems.

8:00 PM EL02.05.08

Electron dynamics of modified p-InP surfaces Jonathan Diederich¹, Jennifer Velasquez-Rojas¹, Amin Zare Pour Mohammed², Agnieszka Paszuk^{2,3}, Azahel Ruiz⁴, Christian Höhn¹, David Ostheimer², Klaus Schwarzbarg¹, Rainer Eichberger^{1,2}, Gero Schmidt⁴, Thomas Hannappel², Roelvan de Krol¹ and Dennis Friedrich¹; ¹Helmholtz-Zentrum Berlin für Materialien und Energie, Germany; ²TU Ilmenau, Germany; ³Helmholtz Centre for Energy and Materials Berlin, Germany; ⁴Universität Paderborn, Germany

Within the transition towards renewable energies, green hydrogen is expected to play a prominent role due to its high gravimetric energy density and the complete absence of CO₂ emissions. A promising way of producing green hydrogen is photo-assisted electrochemical water splitting, using semiconductor absorbers with band gaps near the optimum for solar energy conversion. The highest solar-to-hydrogen efficiencies to date of up to 19% have been achieved using InP based absorbers protected by a TiO₂ layer through atomic layer deposition (ALD), both for voltage bias-assisted (p-InP)¹ and unassisted water splitting (AlInP window layer, GaInP top cell)².

However, understanding of electron dynamics both at the pure p-InP surface as well as at the p-InP / TiO₂ interface remains limited, in part due to the difficulty in experimentally probing surface conduction band states. We chose to study the (2×1/2×2)-reconstructed P-rich, p-type InP (100) surface prepared through metalorganic chemical vapor deposition (MOCVD), which is commonly utilized in record-breaking cells. Measurements using XPS, UPS, LEED, AFM and time-resolved two-photon photoemission spectroscopy (tr-2PPE) were performed, the latter accessing unoccupied states with a time resolution of 30fs.

We for the first time report detailed dynamics in sub-surface and surface conduction band states up to 2 eV above the p-InP conduction band minimum (CBM), tracking electron lifetimes and average decay paths. Moreover, we explore the impact of TiO₂ layers with varying thickness deposited via ALD on the formation of TiO₂ features, unveiling distinct TiO₂ conduction band states in thin layers, deviating from the conventional TiO₂ density of states reported in the literature. Dynamics and lifetimes of electrons photoexcited in the p-InP bulk are again for the first time tracked across the interface and through the observed TiO₂ states.

A surface treatment protocol using water- and heat exposure in ALD is described, which allows for TiO₂ conduction band states with favourable band alignment to be observed at considerably reduced layer thicknesses. Our measurements indicate enhanced interfacial charge transfer as well as a thinner interlayer region. These improvements are linked to changes in P-dimer surface domains of the p-InP surface during water- and heat exposure, leading to more homogenous P-oxide layer formation and TiO₂ nucleation. Such pre-treatment of the p-InP surface holds the potential to substantially enhance interfacial quality, allowing for thinner TiO₂ layers and reduced defect-mediated recombination, opening exciting opportunities for optimizing cell performance.

(1) Yin, X.; Battaglia, C.; Lin, Y.; Chen, K.; Hettick, M.; Zheng, M.; Chen, C.-Y.; Kiriya, D.; Javey, A. 19.2% Efficient InP Heterojunction Solar Cell with Electron-Selective TiO₂ Contact. *ACS Photonics* **2014**, *1* (12), 1245–1250. <https://doi.org/10.1021/ph500153c>.

(2) Cheng, W.-H.; Richter, M. H.; May, M. M.; Ohlmann, J.; Lackner, D.; Dimroth, F.; Hannappel, T.; Atwater, H. A.; Lewerenz, H.-J. Monolithic Photoelectrochemical Device for Direct Water Splitting with 19% Efficiency. *ACS Energy Lett.* **2018**, *3* (8), 1795–1800. <https://doi.org/10.1021/acsenylett.8b00920>.

SESSION EL02.06: 2D and Nanomaterials
Session Chairs: Hannah Joyce and Ajay Ram Srimath Kandada
Wednesday Morning, November 29, 2023
Hynes, Level 3, Room 303

8:30 AM *EL02.06.01

Many-Body Exciton-Polariton Quantum Dynamics in Ruddlesden-Popper Metal-Halide Optical Microcavities Esteban Rojas-Gatjens^{1,1}, Victoria Quiros Cordero¹, Martin Gomez-Dominguez¹, Carlo Perini¹, Arturo Camacho Guardian², Giuseppe Pirruccio², Hugo A. Lara-Garcia², Hao Li³, Eric Bittner³, Juan-Pablo Correa-Baena¹ and Carlos Silva^{1,1,1}; ¹Georgia Institute of Technology, United States; ²Universidad Nacional Autónoma de México, Mexico; ³University of Houston, United States

We probe the quantum dynamics of exciton-polaritons in the prototypical Ruddlesden-Popper metal halide (PEA)₂PbI₄ (PEA = phenylethylamine) by means of two-dimensional coherent electronic spectroscopy (2DES), over the temperature range 5–300 K, and as a function of excitation density. We analyze the coherent optical lineshape to extract the homogeneous linewidth, which is governed by optical dephasing of the third-order mesoscopic polarization generated by a time-ordered, phase-matched femtosecond pulse sequence. We quantify excitation-induced

dephasing (EID), which is the contribution to the dephasing due to multi-particle correlations that lead to elastic Coulomb scattering, by analysis of the homogeneous linewidth as a function of polariton density, and by the density dependence of the real and imaginary parts of the complex lineshape. Excitons in (PEA)₂PbI₄ films exhibit clear signatures of EID, with a homogeneous linewidth that increases linearly with excitation density, and by evidence of phase shifts of the real and imaginary spectra with respect to the low-density pure dephasing limit [1]. However, comparison of EID parameters with respect to covalent 2D semiconductors such as single-layer transition-metal dichalcogenides reveals that polaronic effects due to the ionic nature of the lattice screen the multi-particle correlations by orders of magnitude with respect to non-ionic semiconductors. In the optical microcavity, such signatures of polariton EID are amplified with respect to the bare excitons, and the spectral structure becomes more intricate, with cross-peak structure that differs with respect to that of the bare exciton. We model the optical lineshapes via quantum-dynamical simulations [2], and find that while the polariton dispersion relation reflects the exciton spectral fine structure, which we ascribe to polaronic effects that lead to distinct exciton polarons with binding energies that differ by ~35 meV [3] due to specific lattice dressing [4], which modulates the permittivity, the strength of multi-particle interactions is substantially higher in the microcavity. We hypothesize that this arises from diminished polaronic screening of polaritons with respect to excitons due to long-range interactions mediated by the photon component. We discuss these findings in the context of mechanisms for polariton condensation in this class of materials.

[1] A.R. Srimath Kandada *et al.*, *J. Chem. Phys.* **153**, 164706 (2000).

[2] S.A. Shah *et al.*, arXiv:2210.16355 [quant-ph].

[3] S. Neutzner *et al.*, *Phys. Rev. Materials* **2**, 064605 (2018).

[4] F. Thouin *et al.*, *Nature Materials* **18**, 349-356 (2019).

9:00 AM EL02.06.02

Alternative Referencing Scheme Suppresses Large Noise Contributions for Pump-Probe Spectroscopy with Visible to Near Infrared Detection Kaila M. Yallum, Natalie Banerji and Julien Réhault; Universität Bern, Switzerland

Femtosecond transient absorption (TA) allows us to observe photophysical processes on the pico-, nano-, and micro-second timescales with femtosecond time resolution. Broadband white-light generation and detection determine the scope and limits of a TA setup. With the goals of 1) extending the white light into the NIR, and 2) removing the gap in the 750-850 nm range, a different white light generation scheme was employed consisting of a 800 nm-pumped optical parametric amplifier (OPA) to generate an idler around 2000 nm. The 2000 nm idler is used as the driving beam in a Yttrium Aluminum Garnet (YAG) crystal to generate a white light supercontinuum that spans a range starting at 600 nm up to 1700 nm. Because the white light generation relies on the OPA, additional shot-to-shot noise is introduced yielding shot to shot noise of up to 15%. Such significant noise contributions prevent this generation mechanism from being useful for TA experiments with a classic ratiometric referencing scheme. Therefore, an improved referencing scheme was employed in the signal processing to recover the signal to noise ratio¹.

In short, the proposed B-matrix referencing scheme relies on a cross covariance matrix, **B**, to predict the change in intensity between two pumped shots, I_r^* , for each wavelength. The difference between the measured change in intensity, I_m^* , and the reconstructed I_r^* , is taken to isolate the sample response, $S = I_m^* - I_r^*$. Calculations to determine **B** can be carried out by a series of unpumped shots measured before the experiment, therefore removing the need for a chopper, or it can be simply calculated by the unpumped shots measured when the chopper is in the closed position. In practice, the B-matrix referencing method reduced the root mean square error in detection by a factor of 40 when compared to the ratiometric referencing scheme.

The case study presented herein focuses on the benefits of the white-light generation and noise reduction methods employed on a spectroscopic study of the organic photovoltaic (OPV) blend PM6:Y6. Newer generation organic semiconducting materials for photovoltaic applications have been chemically modified to absorb closer to the red edge of the visible light spectrum². Because of this, the spectra of triplet and charged states of these materials are often observable in the NIR. Furthermore, the ground-state bleach (GSB) associated with these materials falls into the detection gap brought about by the optical filters needed to remove the 800 light. Furthermore, the overlapping GSB and excited-state absorption result in a differential absorption of the exciton in the linear regime of often less than 1 mOD, sometimes as low as 50 mOD. The referencing scheme employed in this unique TA setup successfully represses the noise in order to recover such small signals.

1. Y. Feng, I. Vinogradov, and N-H. Ge, *Optics Express* (2017) Vol. 25, No. 21, 26263

2. J. Hou, O. Inganäs, R. H. Friend, F. Gao, *Nature Materials* (2018) Vol. 17, 119-128.

9:15 AM EL02.06.03

Hot Multiexciton Dynamics in CdTe Nanocrystals: Effect of Spin Blockade Apurba De¹, Jayanta Dana¹, Adar Levy¹, Efra Lifshitz², Uri Banin¹ and Sandy Ruhman¹; ¹The Hebrew University of Jerusalem, Israel; ²Technion Israel Institute of Technology, Israel

The relaxation dynamics of hot multiexcitons can be influenced by the presence of another charge carrier in the band edge level (cold carrier). This phenomenon can be understood by considering Pauli spin blockade where the same spin orientation of both the hot and the cold carrier can inhibit the relaxation of the former. This we first demonstrated in CdSe/CdS nanocrystals (NCs) in one of our earlier studies (*J. Phys. Chem. Lett.* **2019**, *10*, 2341-2348). The idea of 'spin blockade' of the hot multiexciton in semiconductor materials is of great interest since it can open up multiple opportunities like in hot-carrier solar cells, photo catalysis etc. To test the generality of such behavior in II-VI quantum dots family members, we extend our study to CdTe. Experimentally this is performed by adopting a unique approach, 'spectator exciton' approach where the multiexciton relaxation dynamics is compared with and without a singly deposited cold exciton (we call it 'spectator exciton'). This spectator exciton actually impose the spin conflict for the cooling of hot multiexcitons. A major observation is that the bleach associated to the state filling of 1s^e-1h^e level becomes half in amplitude in presence of spectator exciton. The comparison of carrier cooling time in the absence and presence of spectator reveal a prolonged time scale in case of later which is indicative of effective spin blockade. While in case of CdSe/CdS, there is clear separation between the cooling (~2 ps) and spin flip time (~25 ps), which made it easy for the determination of spin flipping time, for CdTe situation become a little complex. Mixed-up situation of the time scales in CdTe further influence the Auger process afterward. In this situation, the Auger process appeared to be slower than expected. We thus suggest that hot multiexciton dynamics should be investigated with extra caution since spin blockade can influence the decay dynamics of such. Further we validate this generality with varying sizes of CdS shell thickness for CdSe/CdS NCs. Overall, our findings prove the generic behavior of spin blockade and provides a unique visualization to the multiexciton dynamics of this II-VI family.

9:30 AM EL02.06.04

Determining Structural Response of CdSe:CdS Nanocrystals to High Energy Excitation Eliza Wieman¹, Nejc Nagelj², Landon Rice¹, Mia Tarantola¹, Jacob Olshansky², Burak Guzelurturk³ and Benjamin Cotts¹; ¹Middlebury College, United States; ²Amherst College, United States; ³Advanced Photon Source, Argonne National Laboratory, United States

Colloidal semiconductor nanocrystals (NCs) are used in optoelectronic applications due to their tunable size, shape, composition, and surface chemistry. NCs reach near-unity radiative efficiencies when excited under weak conditions. However, less is known about nonradiative events under high excitation conditions. In applications such as lasers, photodetectors, and electrically pumped LEDs, NCs are exposed to much higher excitation conditions, causing a rapid increase in nonradiative relaxations. Elucidating the structural origins of thermalization pathways is essential for engineering NCs that can suppress nonradiative processes to improve device efficiency.

Our past work examined the effect of different energy excitation levels on localized lattice disordering in CdSe:CdS core/shell particles using femtosecond electron diffraction. At lower excitation energy (510 nm), the lattice response was dominated by the Debye-Waller effect. However, at higher excitation energy (340 nm), which is significantly higher than the band gap, a deviation from the expected Debye-Waller response was observed, suggesting additional short-range localized disordering. Transient differential atomic pair distribution function analysis corroborated that the localized disorder was likely associated with hot hole trapping on the NC surface.

This work implies that the observed localized structural disorder may be associated with certain lattice planes. However, lower Q-resolution and lack of long delay time capabilities at the facilities used in earlier experiments prevented clear distinguishing of peaks, for determination of the structural geometry of the small polarons, and to measure their recovery dynamics. Additional time-resolved X-ray diffraction (TR-XRD) experiments were conducted on CdSe:CdS core-shell particles in order to resolve the observed structural disorder to specific lattice planes. Both liquid jet and solid-state experimental setups were used, and current work involves analyzing this TR-XRD data in order to both determine the relationship between localized disorder and non-radiative cooling and compare the efficacy of these two methods for resolving the structural response of NCs to photoexcitation.

Molecular dynamics (MD) simulations and X-ray pair distribution function (PDF) experiments were performed to examine the response of CdSe:CdS NCs to heating. Combining these three methods will help to decouple the purely thermal response in the MD simulations and X-ray PDF experiments from the additional photoinduced structural disorder observed in the TR-XRD data. Results of this work will allow for a more thorough understanding of the localized disorder caused by hot hole trapping processes and improve NC engineering methods to create more efficient optoelectronic devices.

9:45 AM EL02.06.05

Decoupling Two-Photon Absorption and Photoluminescence in Nanomaterials with Heterostructure Engineering Arthur Alo¹, Leonardo W. Barros¹, Gabriel Nagamine¹, Jonathan C. Lemus¹, Josep Planelles², José L. Movilla², Juan I. Clemente², Hak June Lee^{3,4}, Wan Ki Bae⁴ and Lazaro Padilha¹; ¹Universidade Estadual de Campinas (UNICAMP), Brazil; ²Universitat Jaume I, Spain; ³Seoul National University, Korea (the Republic of); ⁴Sungkyunkwan University (SKKU), Korea (the Republic of)

Quantum dots (QDs) were expected to offer enhanced nonlinear optical properties due to quantum confinement. However, it has been observed that QDs exhibit two-photon absorption (2PA) cross-sections that scale linearly with their volume. Consequently, the only way to increase the 2PA in QDs is by increasing their volume. Considering that the emission spectra of QDs are also coupled to their size, this can become a limiting factor if one wishes for QDs with large 2PA cross-sections that emit light in a specific wavelength range. Successful strategies to decouple emission wavelength and nanocrystal (NC) size involve doping, to create red-shifted trap-mediated emission, and heterostructuring, by growing core/shell NCs. On the other hand, little is known about how these heterostructures affect the nonlinear response.

Thus, in this work, we explore how heterostructures affect the 2PA volume scaling and how efficiently they can decouple 2PA cross-section and emission spectra. For this, we measured the 2PA cross-section of three types of samples: CdSe core-only QDs, CdSe/ZnCdS type-I, and CdSe/CdS quasi-type-II core/shell NCs. Type-I and quasi-type-II core/shells are differentiated by their band alignment and how their electron and hole are spatially confined, with type-I having electron and hole confined to the core of the heterostructure, while quasi-type-II have the electronic wavefunction spread through the entire heterostructure while the hole is confined to the core. These core/shell samples have fixed core sizes, and their total volume is increased by thickening their shells. This way, we found that type-I and quasi-type-II heterostructures present sublinear 2PA volume scaling, in contrast to the linear scaling observed in core-only QDs. Furthermore, type-I NCs exhibit a lower 2PA volume scaling than quasi-type-II.

To understand this difference in 2PA cross-section volume scaling, we performed theoretical calculations using the k.p method. As it has been previously reported in the literature, we verify that the linear volume scaling of the 2PA in core-only QDs is due to the reduced density of states for smaller QDs, which counteracts the increase in the oscillator strength for individual two-photon transitions. Similarly, the 2PA volume scaling in core/shell NCs is also dictated by their reduced density of states. Type-I NCs were seen to have the lowest volume scaling for their density of states, while quasi-type-II present an intermediate volume scaling for the density of states. Furthermore, these calculations along with experimental data suggest that, for the quasi-type-II NCs, the higher the shell-to-core volume ratio, the higher the density of states for the two-photon transitions. We verified this with another series of quasi-type-II samples with smaller core volumes, which we observed to have a 2PA volume scaling similar to the core-only samples. This way, as these core/shell samples offer minimum shift in their emission spectra with increasing shell thickness, they offer the possibility of obtaining NCs with larger 2PA cross-sections at a specific emission wavelength.

10:00 AMBREAK

10:30 AM *EL02.06.06

Transient Microscopy of Mobile Excitons in 2D Semiconductors Alexey Chernikov; TU Dresden, Germany

Transport of optical excitations in semiconducting solids plays a central role from both fundamental and technological perspectives. In systems with strong Coulomb interaction the propagation of optically injected carriers is dominated by excitons instead of free electrons or holes. These correlations can affect both the overall energy landscape and the interactions with vibrational modes, with a strong impact on the mobility of the excitations.

In this talk I will discuss recent studies employing the technique of transient microscopy to monitor propagation of mobile exciton quasiparticles in two-dimensional van der Waals semiconductors. In these systems, the electron-hole correlations present a particularly interesting case combining the properties of Wannier-Mott excitations in inorganic quantum well systems with high exciton binding energies that are more characteristic for Frenkel-like states in molecular crystals. I will discuss linear and non-linear phenomena, influence of environmental screening and disorder, and present strategies to externally manipulate exciton propagation. I will outline the limits of semi-classical and hopping transport in monolayer semiconductors and illustrate the impact of free charge carriers on the exciton diffusion.

11:00 AM EL02.06.07

Dynamics of Photoexcitations in SnS₂ Single Crystals Kateryna Kushnir, Sepideh Khanmohammadi, Erin Morissette, Erika Colin-Ulloa, Curtis Dorian, Julia Martin, Ronald L. Grimm and Lyubov V. Titova; Worcester Polytechnic Institute, United States

Tin disulfide (SnS₂) is a layered material that is environmentally stable, composed of earth-abundant materials, has a moderate bandgap of ~2.3 eV and high absorption in the blue-green spectral range, making it attractive for optoelectronic and solar energy applications. We have previously shown that photoexcited carriers in single crystalline SnS₂ and in vertical nanoflakes have a high mobility of ~300 cm²/Vs and lifetimes in excess of 1 ns [1,2]. Additionally, above band gap excitation of single crystalline SnS₂ at normal incidence results in emission of THz radiation, a hallmark of a second order nonlinearity. This observation is surprising due to inversion symmetry being present in unexcited SnS₂ even in a monolayer limit, and we hypothesize that photoexcitation dynamically breaks the inversion symmetry by excitation of an in-plane phonon mode. Here, we use time-resolved THz spectroscopy, THz emission spectroscopy and transient optical absorption to uncover the complete picture of the ultrafast electronic responses following photoexcitation. Our experimental results provide important checkpoints for theory of nonlinear effects in SnS₂ and other 2D dichalcogenide materials.

[1] Binod Giri, Maryam Masroor, Tao Yan, Kateryna Kushnir, Alexander D Carl, Curtis Doiron, Haochuan Zhang, Yanyan Zhao, Arthur McClelland, Geoffrey A Tompsett, Dunwei Wang, Ronald L Grimm, Lyubov V Titova, Pratap M Rao, Balancing Light Absorption and Charge Transport in Vertical SnS₂ Nanoflake Photoanodes with Stepped Layers and Large Intrinsic Mobility, Adv. Energy Materials 9, 1901236 (2019)

[2] K. Kushnir, E. Morissette, B. Giri, C.W. Doiron, R.L. Grimm, P.M. Rao and L.V. Titova, "Carrier Dynamics in SnS₂ Single Crystals and Vertical Nanostructures: Role of Edges," 2018 43rd International Conference on Infrared, Millimeter, and Terahertz Waves (IRMMW-THz), Nagoya, Japan, 2018, pp. 1-2, doi: 10.1109/IRMMW-THz.2018.8509909.

11:15 AM EL02.06.08

Probing The Carrier Dynamics around The Band Gap of Amorphous Silicon Telluride Md. Rafiqul Islam¹, Kiumars Aryana¹, Derek Stewart², Michael Grobis², Joyeeta Nag² and Patrick E. Hopkins¹; ¹University of Virginia, United States; ²Western Digital Corporation, United States

Amorphous chalcogenide alloys are key materials for data storage and energy scavenging applications due to their large non-linearities in optical and electrical properties. Silicon telluride (SiTe) is an example of these amorphous alloys because it undergoes a solid-state phase transformation upon the application of a sufficiently large electric field, commonly referred to as threshold switching. Here, we investigate the impact of this phase transformation on electrical properties by monitoring carrier lifetimes at and around the transformation. We implement an ultrafast near-infrared pump-probe spectroscopy technique that allows for direct monitoring of electronic and vibrational energy carrier lifetimes in amorphous silicon telluride. We confirm the ultrafast findings with the help of density functional theory calculations and ellipsometry. From the DFT calculation we find the optical bandgap of the film is 0.695 +/- 0.15 eV and the mobility gap is 1.12 +/- 0.05 eV. We probe the reflectivity response of this alloy after pump heating in the energy range of 0.5 to 2.07 eV. From ultrafast technique we find that SiTe demonstrates the direct valence mobility edge to conduction mobility edge transition at 1.24 eV. It is slightly larger than the reported optical band gaps. Besides, we identify a hole trap state at 1.08eV which is near the valence band edge, indicating that the flow of electrons in SiTe is possible under the threshold voltage. The electrons of the low energies relaxes faster than the free electrons of bandgap energy, confirming the presence of trap states in SiTe and its conductive nature under its threshold voltage. The presence of localized states at the band edge is expected in the electronic structure of amorphous materials and is consistent with previous studies of Si-Te materials. These findings open the way of tuning the property of this chalcogenide alloy, which will lead to building new electronic devices with higher efficiency and better performance.

11:30 AM *EL02.06.09

The High-Frequency Limit of Schottky Rectification Maria T. Schlecht¹, Tobias Weitz¹, Christian Heide², Sebastian Lotter^{1,2}, Stefan Malzer¹, Peter Hommelhoff¹ and Heiko B. Weber¹; ¹Friedrich-Alexander-Universität Erlangen-Nürnberg, Germany; ²Stanford University, United States

A Schottky diode, i.e. a metal-semiconductor junction, is among the simplest yet fastest electronic components. The underlying general theory has been developed by Schottky for the stationary, i.e. DC case. When operating it at high frequency, the RC timescale sets an extrinsic limit.

Using graphene as a metal and Silicon carbide (SiC) as semiconductor, epitaxial graphene on SiC provides a monolithic and extremely robust Schottky diode. Its current-voltage characteristics can accurately be described by Schottky's model. When driving the diode at high frequency, an RC damping at around 400 GHz could be determined [1]. We recently studied this diode replacing the voltage drop by the electric field of ultrashort light pulses in the mid-infrared regime. It turns out that the Schottky physics remains predictive up to 82 THz, even with the parameters determined at DC. One only has to make a correction that describes an incoherent and easily understood recapture mechanism [2].

We have now adapted the same experimental strategy to visible pulses, with a center frequency of 300 THz. Simultaneously, we have chosen a slightly lower Schottky barrier. The result is again a field driven current, as identified by a carrier-envelope phase dependent contribution. It increases with an effective power law. In order to understand this behavior, the Schottky model is inappropriate. Rather, a time-dependent Schrödinger equation is the correct description. This crossover of the physical description can be understood by a Keldysh-Parameter close to unity. We conclude that the Schottky description, being accurately predictive over many magnitudes from 1Hz-82 THz, fails at only slightly higher frequencies.

- [1] M.T. Schlecht, S. Preu, S. Malzer, H.B. Weber, An efficient Terahertz rectifier on the graphene/SiC materials platform, *Scientific Reports*, 9 (2019) 11205.
[2] T. Schlecht Maria, M. Knorr, P. Schmid Christoph, S. Malzer, R. Huber, B. Weber Heiko, Light-field-driven electronics in the mid-infrared regime: Schottky rectification, *Science Advances*, 8 (2022) eabj5014.

SESSION EL02.07: Ultrafast Microscopy and Near-Field Probes
Session Chairs: Peijun Guo and Ajay Ram Srimath Kandada
Wednesday Afternoon, November 29, 2023
Hynes, Level 3, Room 303

2:00 PM EL02.07.01

Predicting Dielectric Function from Scattering-Type Scanning-Near-Field Optical Microscopy (s-SNOM) Tom Vincent¹, Xinyun Liu¹, Daniel Johnson^{1,2}, Lars Mester³, Nathaniel Huang², Olga Kazakova² and Jessica L. Boland^{1,2}; ¹Photon Science Institute, University of Manchester, United Kingdom; ²National Physical Laboratory, United Kingdom; ³Attocube Systems AG, Germany

Scattering-type scanning near-field optical microscopy (s-SNOM) is a powerful tool that enables optical microscopy and spectroscopy with extreme sub-wavelength spatial resolution [1]. It is used heavily to characterise optical metamaterials, low-dimensional materials, and surface states in topological insulators, which may have nanoscale dimensions that can't be detected by traditional optical microscopy. But relating material dielectric function to the observed optical contrast requires modelling the interaction between a SNOM tip and the sample, which can be both conceptually and computationally challenging.

The finite dipole model (FDM) has shown excellent agreement between experimental and modelled data based on known dielectric functions [2]–[4]. However to date there are only a few works that fit the FDM to experimental SNOM data to retrieve *unknown* dielectric functions [5]–[7].

In this work, we investigate in-detail how the FDM relates the dielectric function to the observed optical contrast. We demonstrate its application on real SNOM spectra from topological insulator thin films and InN nanoparticles, with reference to measurements simulated by our soon-to-be-released modelling package, *pysnom*. We identify the key challenges involved in fitting to the FDM, including non-unique solutions and finite size effects, and we present the strategies we've developed to overcome them. By following the steps outlined in this presentation, and taking advantage of our optimised code library, we hope that extracting quantitative measurements of dielectric function from SNOM experiments will become more achievable for the wider scientific community.

- [1] F. Keilmann and R. Hillenbrand, "Near-field microscopy by elastic light scattering from a tip," *Philos. Trans. R. Soc. London. Ser. A Math. Phys. Eng. Sci.*, vol. 362, no. 1817, pp. 787–805, Apr. 2004, doi: 10.1098/rsta.2003.1347.
[2] A. Cvitkovic, N. Ocelic, and R. Hillenbrand, "Analytical model for quantitative prediction of material contrasts in scattering-type near-field optical microscopy," *Opt. Express*, vol. 15, no. 14, p. 8550, 2007, doi: 10.1364/oe.15.008550.
[3] B. Hauer, A. P. Engelhardt, and T. Taubner, "Quasi-analytical model for scattering infrared near-field microscopy on layered systems," *Opt. Express*, vol. 20, no. 12, p. 13173, Jun. 2012, doi: 10.1364/OE.20.013173.
[4] L. Mester, A. A. Govyadinov, S. Chen, M. Goikoetxea, and R. Hillenbrand, "Subsurface chemical nanoidentification by nano-FTIR spectroscopy," *Nat. Commun.*, vol. 11, no. 1, p. 3359, Dec. 2020, doi: 10.1038/s41467-020-17034-6.
[5] F. Mooshammer *et al.*, "Nanoscale Near-Field Tomography of Surface States on (Bi 0.5 Sb 0.5) 2 Te 3," *Nano Lett.*, vol. 18, no. 12, pp. 7515–7523, Dec. 2018, doi: 10.1021/acs.nanolett.8b03008.
[6] C. Lupo *et al.*, "Quantitative infrared near-field imaging of suspended topological insulator nanostructures," pp. 1–23, Dec. 2021, [Online]. Available: <http://arxiv.org/abs/2112.10104>
[7] A. A. Govyadinov, S. Mastel, F. Golmar, A. Chuvilin, P. S. Carney, and R. Hillenbrand, "Recovery of Permittivity and Depth from Near-Field Data as a Step toward Infrared Nanotomography," *ACS Nano*, vol. 8, no. 7, pp. 6911–6921, Jul. 2014, doi: 10.1021/nn5016314.

2:15 PM EL02.07.02

Terahertz Radiation of Hot Carriers: A Far-Field Probe for Near-Field Spatiotemporal Dynamics Mohammad Taghinejad¹, Chenyi Xia¹, Martin Hrtan¹, Kyutae Lee², Andrew Kim², Qitong Li¹, Burak Guzelturk¹, Fenghao Xu¹, Wenshan Cai², Aaron Lindenberg¹ and Mark L. Brongersma¹; ¹Stanford University, United States; ²Georgia Institute of Technology, United States

From the birth of plasmonics, the hot-carrier generation in nanostructured metals was considered as an innate roadblock towards the efficient usage of the light energy stored in sub-diffraction plasmon modes. The observation of the hot-carrier transport at metal/dielectric Schottky junctions, however, transformed this limitation into a unique opportunity for enabling a light-field control over photochemical and photophysical processes in a spectrally selective and spatially fashionable manner. Despite successful prototype device demonstrations, the scarcity of experimental knowledge about the spatiotemporal dynamics of the transport has impeded the expansion of hot-carrier applications, particularly in activating photocarrier-driven coherent processes. Here, we employ the electric-field of terahertz bursts radiated by transport-induced current pulses as a coherent electromagnetic probe to monitor the photoemission dynamics of hot carriers at a plasmonic Schottky junction. The time-domain analysis of the terahertz field indicates that the charge ejection process is dominated by nonthermal hot carriers and occurs within an ultrashort timeframe (~10 fs) controlled by the plasmon lifetime, electron-electron scattering rate, and the charge transport with a narrow interfacial boundary layer. By employing the polarization and phase attributes of the radiated THz field we are able to probe the in-plane ballistic transport trajectory of electron via a far-field detection scheme.

2:30 PM BREAK

3:30 PM *EL02.07.03

Ultrafast and Nanoscale Raman Approaches for Materials Science Renee Frontiera; University of Minnesota, United States

Our lab focuses on the development and application of Raman spectroscopies with high temporal and spatial resolution, with the goal of understanding local environmental impacts on chemical reaction dynamics. This talk will focus on the use of these spectroscopic and microscopic approaches in order to understand two coupled light-matter systems: plasmon-molecule interactions and excitonic polariton dynamics. In the quest to understand how plasmonic nanomaterials can serve as photocatalysts, we have developed ultrafast surface-enhanced Raman approaches to understand molecule responses following photoexcitation. This talk will focus on our quantitation of plasmon-to-molecule charge transfer, which enables us to determine the yield and energy of hot carriers relevant for driving chemical reactions. Secondly, we have used femtosecond stimulated Raman spectroscopy and resonance Raman intensity analyses in order to understand the similarly strong coupled light-matter system of excitonic polaritons. Here we map out multiple dimensions of the coupled potential energy landscape to determine how coupling to a photonic cavity can change molecular reaction coordinates. Taken together, these works demonstrate how probing multiple molecular degrees of freedom can lead to new insights into the rational design of coupled systems.

4:00 PM EL02.07.04

Imaging Nanosecond Charge Recombination Dynamics via Scanning Probe Microscopy Racheal Cohn, Christopher Petroff, Virginia E. McGhee and John A. Marohn; Cornell University, United States

Bulk heterojunction organic photovoltaics (OPVs) exhibit charge recombination times that are 10s to 1000s of times longer than predicted by Langevin theory. Understanding the mechanism of charge generation and recombination is critical to furthering the development of photoactive materials used in OPVs. We use electric force microscopy (EFM) to better understand the temporal dynamics and spatial distribution of charge generation and recombination in OPVs. Achieving nanosecond time resolution is required to observe photogenerated charges before they recombine.

We find that charge recombination in the OPV films that we study is too fast to observe in a real-time time resolved EFM (tr-EFM) experiment. We measure temporal changes in the film's photo-induced capacitance and resistance on the nanosecond timescale using an electrical scanned-probe microscope experiment. Time resolved microwave conductivity is typically used to measure photoinduced changes in the film charge density on the nanosecond time scale, but the technique lacks spatial resolution and devices with contacts pose difficulties. Scanning probe microscopy has nanometer spatial resolution, but has previously lacked nanosecond time resolution. A time resolution of 10 ns is claimed for the fast-free tr-EFM experiment [1], but this time is shorter than one cantilever oscillation cycle and is, therefore, unphysical [2,3].

The phase-kick EFM (pk-EFM) experiment, introduced by Dwyer *et al.* [2], measures the photocapacitance and photoresistance charging time, τ_R , by measuring the change in cantilever frequency and phase as a function of the delay times, t_p , between light and voltage pulses. After performing the experiment at various delay times, we plot the total phase shift $\Delta\phi$ vs. t_p to obtain the sample's charge recombination transient and the recombination time, τ_R . The pk-EFM method has a well-defined theory for both the signal [4] and the signal to noise ratio (SNR) [2] and is capable of achieving sub-cycle, nanosecond time resolution [2]. We describe our efforts to push pk-EFM's temporal resolution from microseconds to nanoseconds in an OPV film.

References:

- [1] Karatay, D. U.; Harrison, J. S.; Glaz, M. S.; Giridharagopal, R.; Ginger, D. S. *Rev. Sci. Instrum.* **2016**, *87* (5), 053702. DOI: 10.1063/1.4948396
- [2] Dwyer, R. P.; Nathan, S. R.; Marohn, J. A. *Sci. Adv.* **2017**, *3* (6), e1602951. DOI: 10.1126/sciadv.1602951.
- [3] (a) Rihaczek, A. W.; Bedrosian, E. *Proc. IEEE* **1966**, *54* (3), 434–435. DOI: 10.1109/PROC.1966.4742. (b) Boashash, B. *Proc. of the IEEE* **1992**, *80* (4), 520–538. DOI: 10.1109/5.135376. (c) Boashash, B. *Proc. of the IEEE* **1992**, *80* (4), 540–568. DOI: 10.1109/5.135378.
- [4] Dwyer, R. P.; Harrell, L. E.; Marohn, J. A. *Phys. Rev. Applied* **2019**, *11* (6), 064020. DOI: 10.1103/PhysRevApplied.11.064020.

4:15 PM *EL02.07.05

3D Ultrafast Optical Microscopy of Semiconductors and Quantum Materials AkshayRao; University of Cambridge, United Kingdom

Elucidating the three-dimensional transport of excitations in condensed matter systems is key to advancing in our understanding and utilisation of functional materials ranging from novel quantum systems to next-generation optoelectronic materials. Of particular interest are quantum coherent processes in heterogeneous, disordered systems which require both ultrafast time resolution and local measurements to study and understand their transport characteristics. In this talk, I will discuss our recent work using interferometrically enhanced femtosecond pump-probe microscopy, that now enable us to track carrier and quasi-particle motion in three dimensions with sub-10 nm spatial precision and sub-10 fs temporal resolution. I will highlight recent results looking at charge carrier and spin motion in hybrid perovskites [1-2], excitons and polaritons in organic semiconductors [3-4], quantum dot films [5] and exciton condensates [6]. This new methodology [7] unlocks new regimes of spatially resolved ultrafast dynamics for investigation across a range of solid-state systems.

- [1] Jooyoung *et al.*, *Nature Physics*, 2020, DOI:10.1038/s41567-019-0730-2
- [2] Ashoka *et al.*, *Nature Materials*, 2023, DOI: 10.1038/s41563-023-01550-z
- [3] Sneyd *et al.*, *Science Advances*, 2021, DOI: 10.1126/sciadv.abh4232.
- [4] Pandya *et al.*, *Nature Communications*, 2021, DOI: 10.1038/s41467-021-26617-w
- [5] Zhang *et al.*, *Nature Materials*, 2022, DOI: 10.1038/s41563-022-01204-6
- [6] Bretscher *et al.*, *Science Advances*, 2021, DOI: 10.1126/sciadv.abd6147
- [7] Ashoka *et al.*, *Nature Communications*, 2022, DOI: 10.1038/s41467-022-33647-5

SESSION EL02.08: Unconventional Probes
Session Chairs: Peijun Guo and Ajay Ram Srimath Kandada
Thursday Morning, November 30, 2023
Hynes, Level 3, Room 303

8:30 AM *EL02.08.01

Imaging Phonon and Phase Dynamics with Ultrafast Electron Microscopy David J. Flannigan^{1,2}, Jialiang Chen^{1,2} and Yichao Zhang^{1,2}; ¹University of Minnesota, United States; ²Minnesota Institute for Ultrafast Science, United States

Transmission electron microscopy (TEM) capabilities can be extended to the femtosecond (fs) timescale via coupling of a fs pulsed laser with an otherwise conventional TEM [1,2]. Here, I will begin by briefly describing the hardware components and the basics of operation of such an instrument, dubbed an ultrafast electron microscope (UEM). I will then share some brief vignettes of the types of measurements that can be done with UEM, focused specifically on the direct nanometer-picosecond imaging of coherent phonon dynamics in semiconductors and 2D materials [3-6]. I will then spend the remainder of the talk describing our experiments and results on the ultrafast imaging of nanoscale phase dynamics in superlattice structures. Interwoven with this will be descriptions of the UEM instrument advances we have made that have enabled low repetition rate, high-resolution UEM imaging [7-10].

- [1] A. H. Zewail, *Science* **328**, 187 (2010).
- [2] D. J. Flannigan, A. H. Zewail, *Acc. Chem. Res.* **45**, 1828 (2012).
- [3] D. R. Cremons, D. A. Plemmons, D. J. Flannigan, *Nat. Commun.* **7**, 11230 (2016).
- [4] D. R. Cremons, D. X. Du, D. J. Flannigan, *Phys. Rev. Mater.* **1**, 073801 (2017).
- [5] Y. Zhang, D. J. Flannigan, *Nano Lett.* **19**, 8216 (2019).
- [6] Y. Zhang, D. J. Flannigan, *Nano Lett.* **21**, 7332 (2021).
- [7] W. A. Curtis, D. J. Flannigan, *Phys. Chem. Chem. Phys.* **23**, 23544 (2021).
- [8] W. A. Curtis, S. A. Willis, D. J. Flannigan, *Phys. Chem. Chem. Phys.* **24**, 14044 (2022).
- [9] D. J. Flannigan, W. A. Curtis, E. J. VandenBussche, Y. Zhang, *J. Chem. Phys.* **157**, 180903 (2022).
- [10] This material is based on work supported by the U.S. Department of Energy, Office of Energy Science, Office of Basic Energy Sciences under Award No. DE-SC0023708. This material is based upon work supported by the National Science Foundation under Grant No. DMR-1654318.

9:00 AM EL02.08.02

THz Bandwidth Activation of Anharmonic Coupling in CdWO₄ Megan Nielson, Brittany Knighton, Lauren Davis, Aldair Alejandro, Claire Rader and Jeremy A. Johnson; Brigham Young University, United States

Terahertz (THz) frequency light is uniquely suited to resonantly probe collective electronic, phonon, magnon, and electromagnon modes, and we are showing that intense THz pulses enable coherent control and the direct measurements of coupling between these excitations.

When intense electromagnetic pulses are used in any kind of pump-probe spectroscopy, several nonlinear excitation pathways can result, leading to scenarios that required the development of multi-dimensional spectroscopies to illuminate the observed dynamics. New developments in 2D THz spectroscopy in our lab and others are enabling the direct measurement of nonlinear excitation of phonon, magnon, and electronic modes, and preliminary measurements are directly showing couplings between them. We have demonstrated clear examples where two-dimensional (2D) THz vibrational spectroscopy is needed to distinguish between nonlinear-excitation pathways, and it enables the selection of one pathway over another.

With intense THz pulses, Raman-active vibrational modes can be nonlinearly excited in centrosymmetric crystalline CdWO₄. However, in single-pulse measurements, it's unclear whether the nonlinear pathway is a photonic process (THz Raman excitation) or a phononic process (anharmonic coupling). In previous work, we showed that Raman excitation is the dominant nonlinear pathway at moderate THz field strengths. With an improved 2D THz experimental setup, we can minimize the Raman excitation and clearly isolate the anharmonic coupling signals.

Interestingly, our analysis shows that coupling between IR-active modes at 2.94 THz and 3.65 THz and the Raman-active mode at 2.33 THz clearly occurs. At first glance, the coupling between three modes should only be efficient when the frequencies of the IR-active modes add up to or subtract down to the frequency of the Raman-active mode, which is not the case here. But when we consider the IR-active mode motion after resonant excitation with a broadband THz pulse, we recognize that the spectrum of the initial motion contains the resonant frequency of the mode itself, as well as a broad range of frequencies that essentially matches the spectrum of the driving THz pulse. Therefore, although the anharmonic coupling between these modes is predicted to be inefficient based on the resonant frequencies of the IR-active modes, we show that the initial THz pulse itself drives motion with more than just the resonant frequency, activating efficient coupling between vibrational modes in CdWO₄.

9:15 AM EL02.08.03

In optical spectroscopy, the harmonic approximation is commonly used to assign peaks and lineshapes to eigenstates, providing valuable information about the system's internal structure. However, understanding explicit anharmonic effects, such as eigenstate coupling and phase transformations, typically necessitates advanced techniques like 2D spectroscopy or calorimetric measurements, which may not provide detailed mechanistic insights.

Nevertheless, the intensity of peaks in THz-range Raman spectroscopy measures the population of vibrational states and contains valuable information about anharmonic interactions. In this talk, I will illustrate how analyzing the temperature dependence of Raman peak intensities can provide valuable mechanistic insights into the coupling between eigenstates and phase transformations.

The first example is in Bismuth Vanadate, where the soft mode loses intensity and depopulates towards its first-order phase transition, evident in the discontinuity of integrated intensity for all lattice modes. The second example is in alpha-glycine, where we discover a local phase transformation manifested by a change in the hydrogen bond free energy surface and accompanied by highly anharmonic lattice behavior. These findings represent an important initial step towards utilizing THz-range Raman spectroscopy as a direct probe for studying equilibrium and non-equilibrium dynamics.

9:30 AMBREAK

10:00 AM *EL02.08.04

Charge Transport Mechanism in Photoconductive Metal Organic Frameworks [Jier Huang](#)¹, James Nyakuchena², Denan Wang¹, Daniel Streater², Jens Neu³ and Gary Brudvig⁴; ¹Boston College, United States; ²Marquette University, United States; ³University of North Texas, United States; ⁴Yale University, United States

Metal organic frameworks (MOFs), built from inorganic and organic linkers, represent an emerging class of porous crystalline materials that have demonstrated many potential applications encompassing energy conversion and storage, gas separation and storage, chemical sensor, and drug delivery. Recent reports of electrical conduction in MOFs expand their applications in devices such as supercapacitors, electrocatalysts, chemiresistive sensors, and batteries. However, the charge transport mechanism that guides the rational design of highly conductive MOFs remains underexplored; yet it is essential to further promote these materials for the above-mentioned applications.

In this talk, I will present our recent progress in fundamental understanding of charge transport mechanism in a series of MOFs and the correlation of the metal nodes and organic linkers with their photophysical property and photoconductivity. We found that structural preference in M-THQ MOFs (M = Fe, Ni, Cu and Zn; THQ = tetra-hydroxybenzoquinone) is controlled by metal node identity where Cu prefers a square planar coordination which leads to a 2D Kagome type structure. Fe, Ni and Zn prefer an octahedral sphere which leads to a 3D structure. Fe-THQ has the smallest band gap and highest photoconduction as well as a long-lived ligand to metal charge transfer state due to the mixed valence state revealed by time resolved optical and X-ray absorption and terahertz spectroscopy. On the other hand, charge transport mechanism is controlled by the size of the organic linker, where some MOFs prefer through space transport while others undergo through bond charge transport mechanism. These results demonstrate the importance of the building blocks in tuning the photophysical and photoconductive properties of MOFs.

10:30 AM *EL02.08.05

High Pressure Tuning of the Excited State Dynamics in Fe Complexes Toward Solar Energy Conversion [Yingqi Wang](#)¹, [Wenge Yang](#)¹, [Cumming Liu](#)² and [Xiaoyi Zhang](#)²; ¹Center for High Pressure Science & Technology Advanced Research, China; ²Argonne National Laboratory, United States

Earth-abundant-metal-based photosensitizers as substitutes for their noble metal analogues have attracted increasing interests in recent years owing to their environmental and economic benefits. However, the rapid deactivation of their charge transfer (CT) excited state hinders their practical applications in solar cells and photocatalysis. Here we demonstrate a novel approach to stabilize the metal to ligand CT (MLCT) state in iron polypyridyl complexes by tuning the potential surface of its main deactivation channel: the metal core spin state, using high pressure. The MLCT state lifetime increased by 5 orders of magnitude from sub-50 femtosecond at ambient condition, to 9 nanoseconds under high pressure. Applying ultra-fast optical transient absorption spectroscopy (OTA) technique, we witness the ligand field splitting increases significantly with applied pressure, which moves the energy of the metal centered T_{2g} state up while leaves the MLCT state relatively unchanged. From 0 to 5 GPa, the ground state bleaching lifetime decreases due to the increased energy gap between high spin (HS) and low spin (LS) transition. Beyond 5 GPa, the energy of T_{2g} state surpasses that of the MLCT state, resulting in prolonged photoactive MLCT state, which is further confirmed by the appearance of solvated electron peak in OTA spectra. Our results show that the excited state energy and lifetime of iron complexes can be tuned by reducing bond length and increasing ligand field strength, enabling the harvesting of photoexcited electrons and photoenergy with $3d$ metal complexes.

11:00 AM EL02.08.06

Artificial Neural Network-Aided Fast Determination of Electrical Conductivity From Contact-Free Terahertz Time-Domain Spectroscopy [Patrick Kung](#), [M.Zeki Güngördü](#) and [Seongsin M. Kim](#); University of Alabama, United States

Terahertz time-domain spectroscopy (THz-TDS) is a contact-free characterization method that is commonly used to yield conductivity, carrier density, and mobility in semiconductor materials. However, when doing so, these material characteristics are not immediately accessible. Instead, many extensive steps are involved in the analysis of the acquired terahertz signal data prior to being able to extract relevant material information. These typically include first carrying out a Fast Fourier Transform of the measured time-domain data, followed by fitting the resulting spectra to determine the conductivity spectra.

In this work, we demonstrate an effective, swift, and stable method for obtaining the conductivity of nanowire-based films by leveraging the power of artificial intelligence to streamline the process. Specifically, we show that both shallow neural networks (SNN) and deep neural networks (DNN) are capable of yielding the THz frequency-dependent conductivity directly from THz time-domain waveform data as input without data processing steps. As experimental validation, we used THz-TDS data measured from four independent datasets: Al-doped and undoped ZnO nanowires on sapphire substrates, and silver nanowires on polyethylene terephthalate and polyimide substrates. After training and testing the SNN and DNN to obtain the optimum model, the frequency-dependent conductivity predicted by our models successfully matched the conductivity calculated using the conventional multi-step method. Mean Squared Error and R-values are used as the main performance criteria of our systems analysis. This study revealed that one can determine a sample's conductivity within seconds without having to carry out Fast Fourier Transform and the conventional conductivity calculation steps from experimental THz-TDS waveform. This AI-based method of training and predicting conductivity will significantly facilitate the subsequent process of fitting the conductivity data to the Drude model in order to extract other physical parameters underlying ultrafast carrier dynamics.

11:15 AM EL02.08.07

Resonant Self-Diffraction of Femtosecond Extreme Ultraviolet Pulses at the M-Edge of Cobalt [Alexei Maznev](#)¹, [Filippo Bencivenga](#)², [Riccardo Mincigrucci](#)², [Ettore Paltanin](#)², [Wonseok Lee](#)³, [Scott K. Cushing](#)³, [Nicolas Jaouen](#)⁴, [Fabian Kammerbauer](#)⁵, [Vincent Polewczyk](#)⁶, [Cyril Léveillé](#)⁴, [Laura Foglia](#)², [Danny Fainozzi](#)², [Nupur N. Khatu](#)^{2,7}, [Dario De Angelis](#)², [Christian Gutt](#)⁸ and [Dmitriy Ksenzov](#)⁸; ¹Massachusetts Institute of Technology, United States; ²Elettra Sincrotrone Trieste, Italy; ³California Institute of Technology, United States; ⁴Synchrotron SOLEIL, France; ⁵University of Mainz, Germany; ⁶Istituto Officina dei Materiali, Italy; ⁷University of Venice, Italy; ⁸University of Siegen, Germany

The advent of free electron lasers (FELs) enabled the expansion of nonlinear optical spectroscopy methods into extreme ultraviolet (EUV) and x-ray ranges. In particular, four-wave mixing techniques with EUV and EUV/optical fields are being actively developed [1-4]. Self-diffraction is the simplest non-collinear four-wave mixing process, in which the interference of two beams crossed in the sample results in a spatially periodic excitation acting as a diffraction grating for the same beams. Self-diffraction is being widely used in optics but has not hitherto been observed in the EUV or x-ray ranges. Generally, the self-diffraction signal from femtosecond EUV FEL pulses is expected to be low, as the polarizability in the EUV range is mainly determined by the average electron density, which does not have time to change significantly within the femtosecond pulse duration. In this report, we show that the EUV self-diffraction efficiency is greatly enhanced and very bright signals are observed when the EUV photon energy is tuned to an absorption edge of the sample. In an experiment conducted at the TIMER beamline at the FERMI FEL, we crossed two 70 fs EUV pulses in a 20 nm-thick cobalt film and scanned the photon energy between 52 – 74 eV. At the $M_{2,3}$ -edge of Co (59 eV) we observed a sharp peak in the self-diffraction efficiency, with the signal level reaching ~4000 photons/shot. DFT/Bethe-Salpeter equation based simulations involving a model assumption that the excitation is equivalent to an increase of the electronic temperature are found to reproduce the peak at the M-edge but not the fine structure observed above the edge. We believe that the results open the prospect for a new element-specific nonlinear EUV spectroscopy technique.

[1] F. Bencivenga et al., Nature 520, 205 (2015), [2] L. Foglia et al., Phys. Rev. Lett. 120, 263901 (2018), [3] F. Bencivenga et al., Sci Adv. 5, eaaw5805 (2019), [3] H. Rottker et al., Sci Adv. 8, eabn5127 (2022).

11:30 AM *EL02.08.08

An Experimental Technique for Directly Measuring Ultrafast Ion Hopping and Its Inherent Many-Body Correlations [Scott K. Cushing](#) and [Kim Pham](#); Caltech, United States

In superionic conductors, ion hopping involves a complex interplay of ion-phonon, ion-electron, and ion-ion correlations that is challenging to measure experimentally. In this presentation, we present a new experimental technique that can directly measure ultrafast ion hopping on its inherent picosecond and longer timescale. The technique works by measuring the time-resolved

perturbation to a GHz impedance signal when potential ion-coupling interactions are driven with UV to THz irradiation. The use of high-bandwidth, real-time electronics allows synchronization of the impedance measurement to the ultrafast laser pulses for varying carrier frequencies. The result of the measurement is the relative strength of different correlations in the many-body ion hopping Hamiltonian. We demonstrate the technique on $\text{Li}_{0.5}\text{La}_{0.5}\text{TiO}_3$ (LLTO), a solid-state Li^+ conductor. The ultrafast laser-driven impedance measurements reveals that the dominant ion hopping mechanism in LLTO is through a coupled phonon-ion THz rocking mode. Although this higher frequency mode is less than one quarter of the overall phonon density of states, it leads to the majority of ion hops as compared to other optical and acoustic phonon modes. Metastable states lasting tens of minutes were also measured for ion-electron perturbations. Further work on extending the technique to measure ion-ion correlations is currently underway, but the technique is already generally applicable to any complex ion conducting system such as polymers, fuel cells, and membranes.

SYMPOSIUM EL03

Ferroc Materials and Heterostructures
November 27 - December 5, 2023

Symposium Organizers

John Heron, University of Michigan
Johanna Nordlander, Harvard University
Bhagwati Prasad, Indian Institute of Science
Morgan Trassin, ETH Zurich

Symposium Support

Bronze
Kepler Computing
SONERA

* Invited Paper
+ JMR Distinguished Invited Speaker

SESSION EL03.01: Antiferroelectrics and Relaxors I
Session Chairs: Johanna Nordlander and Morgan Trassin
Monday Morning, November 27, 2023
Hynes, Level 1, Room 107

10:30 AM *EL03.01.01

Emerging Ferroelectricity in Lead-Free Antiferroelectric Membranes Ruijuan Xu¹, Kevin Crust², Varun Harbola³, Remi Arras⁴, Kinnary Patel⁵, Sergey Prosandeev⁵, Yu-Tsun Shao⁶, Piush Behera⁷, Lucas Caretta⁸, Woo Jin Kim², Aarushi Khandelwal², Megha Acharya⁷, Yin Liu¹, Archana Raja⁹, Lane W. Martin⁷, Hua Zhou¹⁰, Ramamoorthy Ramesh¹¹, David A. Muller¹², Laurent Bellaiche⁵ and Harold Y. Hwang²; ¹North Carolina State University, United States; ²Stanford University, United States; ³Max Planck Institute for Solid State Research, Germany; ⁴Universite de Toulouse, France; ⁵University of Arkansas, Fayetteville, United States; ⁶University of Southern California, United States; ⁷University of California, Berkeley, United States; ⁸Brown University, United States; ⁹Lawrence Berkeley National Laboratory, United States; ¹⁰Argonne National Laboratory, United States; ¹¹Rice University, United States; ¹²Cornell University, United States

Despite extensive studies on size effects in ferroelectrics, how structures and properties evolve in antiferroelectrics with reduced dimensions still remains elusive. Given the enormous potential of utilizing antiferroelectrics for high energy-density storage applications, understanding their size effects would provide key information for optimizing device performances at small scales. In this presentation, I will introduce our recent study about the fundamental intrinsic size dependence of antiferroelectricity in lead-free NaNbO_3 freestanding membranes [1]. Via a wide range of experimental and theoretical approaches, we probe an intriguing antiferroelectric-to-ferroelectric transition upon reducing membrane thickness. This size effect leads to a ferroelectric single-phase below 40 nm as well as a mixed-phase state with ferroelectric and antiferroelectric orders coexisting above this critical thickness. Furthermore, we show that the antiferroelectric and ferroelectric orders are electrically switchable. Such a structural evolution also drives a non-monotonic thickness dependence of Young's modulus. We further reveal the observed transition is driven by the structural distortion arising from the membrane surface. Our work provides direct experimental evidence for intrinsic size-driven scaling in antiferroelectrics and demonstrates enormous potential of utilizing size effects to drive emergent properties in environmentally benign lead-free oxides with the membrane platform.

[1] R. Xu et al. *Advanced Materials* 35, 2370121 (2023)

11:00 AM EL03.01.02

Ultrahigh Electromechanical Response in Antiferroelectric Thin Films: Unconventional Coupling of Phase Transitions and Mechanical Clamping Hao Pan¹, Menglin Zhu², Ella Banyas³, Louis Alaerts⁴, Megha Acharya¹, Jiyeob Kim¹, Hongrui Zhang¹, Isaac Harris¹, James M. LeBeau², Jeffery Neaton³ and Lane W. Martin^{1,5,5}; ¹University of California, Berkeley, United States; ²Massachusetts Institute of Technology, United States; ³Lawrence Berkeley National Laboratory, United States; ⁴Dartmouth College, United States; ⁵Rice University, United States

Electromechanical transduction has been a fundamental enabler for various modern technologies such as actuation, ultrasound imaging, and resonators. Electrostrain (*i.e.*, the strain induced by an electric field) is one of the key parameters for electromechanical applications. Currently mainstream electromechanical materials are ferroelectric ceramics/crystals, in which the best cases have realized electrostrain values of $\sim 1.0\%$ due to their high piezoelectricity. When ferroelectrics are scaled down sub-micrometer thick films, however, the electrostrain performance is generally degraded significantly because of size effects and the mechanical constraint from the substrate (so-called clamping). Needless to say, such observations have been a critical obstacle to developing high-performance, micro-/nano-electromechanical systems. On the other hand, antiferroelectrics, which exhibit antipolar order and a reversible field-induced transition to polar (ferroelectric) order, also exhibit large electrostrains (0.4-1.0%) and have been considered as potential candidates for electromechanical devices since the 1960s. More intriguingly, in antiferroelectric films at the micrometer scale, electrostrain values comparable to those in bulk materials have been observed; this is distinctly different to the scaling behaviors of ferroelectrics. A clear understanding of the mechanism of electrostrain and the "absence" of size effects in antiferroelectrics is absent but would be of significance for their further optimization and application.

Combining macroscopic epitaxial thin-film growth, electromechanical measurements, first-principles calculations, and *in situ* transmission electron microscopy, we have systematically studied the antiferroelectric-to-ferroelectric phase transition and demonstrated an unconventional interaction of the phase transition and mechanical clamping that leads to high electrostrain properties in antiferroelectric films. Focusing on model systems such as PbZrO_3 , we find that detiling of oxygen octahedra happens along with a field-induced phase transition from antiferroelectric (orthorhombic, *Pbam*) to ferroelectric (rhombohedral, *R3m*), which causes an abrupt lattice-volume expansion and thus large electrostrain. We note that the lattice expands in all dimensions, that is, not only along the direction of the applied electric field. In this case, the substrate constraint actually enhances, instead of degrades, the electrostrain in the

antiferroelectric films (contrary to that in ferroelectric films) since the in-plane lattice expansion is hindered by the substrate constraint during the antiferroelectric-to-ferroelectric transition thus adding to the out-of-plane expansion. By thoughtfully designing antiferroelectric thin films to take best advantage of the phase transition and substrate constraint, we realize ultrahigh electrostrain as large as $\sim 1.7\%$ in the canonical antiferroelectric PbZrO_3 films in films just 100 nm thick. Such responses also exhibit robust frequency stability and fatigue resistance. The high performance and new understanding of the mechanism for response in antiferroelectric thin films provide a promising pathway to overcome general scaling obstacles for electromechanical materials for high-performance micro-/nano-electromechanical systems.

11:15 AM EL03.01.03

High-Throughput Screening Search for Antiferroelectricity and Experimental Validations Tomoki Murata¹, Hirofumi Akamatsu², Daisuke Hirai¹, Akira Takahashi³, Fumiyasu Oba³ and Sakyu Hirose¹; ¹Murata Manufacturing Co., Ltd., Japan; ²Kyushu University, Japan; ³Tokyo Institute of Technology, Japan

Ferroelectric materials have been widely used for many applications such as multilayer ceramic capacitors (MLCC), piezoelectric actuator, and random-access memory, and much effort has been made to explore new ferroelectric materials and improve their properties. Recently, antiferroelectric materials have attracted much attention due to their unique and useful responses to an electric field. An antiferroelectric material has a phase transition from an antipolar state to a polar state in an external electric field. This phase transition accompanies a drastic change in dielectric polarization. Consequently, the large dielectric responses (e. g. large permittivity and discharge capacity) are observed around the critical field. However, the known antiferroelectric materials are almost limited to the perovskite materials containing Pb^{2+} or Bi^{3+} ions on A-site, which strongly limits the designer's perspective.

Unlike ferroelectric materials, which can be identified from a space group symmetry, searching for antiferroelectric materials is not so simple because an antipolar structure could not be distinguished only by looking at the space group. Antipolar structures have no net polarization and are classified into nonpolar space groups. The symmetrical definition of antipolar structure is not apparent and had lacked for decades. In 2016, Tolédano *et al.* proposed a new symmetrical definition of antipolar structure based on a local symmetry on crystallographic sites [1]. When a crystallographic site undergoes a symmetry lowering and acquires a polar site symmetry on the phase transition, the low-symmetry structure can be antipolar.

In this study, we performed high-throughput screening of ICSD database in search for antiferroelectric materials. We adopted the symmetry criteria for antipolar structures in the initial screening, and the formula-based screening of chemical compositions to narrow down the candidates. Then, we picked up some candidate materials and performed a stable structure search via first-principles phonon calculations. In some materials, we successfully find polar and antipolar structures which are energetically comparable, possibly indicating antiferroelectricity. Finally, we experimentally synthesized the obtained candidate materials and fabricated MLCCs to characterize their dielectric and antiferroelectric properties. Though most of them are paraelectric, $\text{Bi}_2\text{Ti}_4\text{O}_{11}$ and $\text{Na}_2\text{Nb}_4\text{O}_{11}$ showed clear antiferroelectricity, evidenced by double-hysteresis polarization-field loops and positive DC-field dependences in dielectric permittivity. These experimental results clearly demonstrates that our screening search is effective. Our work provides an effective computational design strategy to explore antiferroelectricity, and moreover, this strategy could be applicable to other functionalities originating from structural phase transitions.

[1] P. Tolédano and M. Guennou, Phys. Rev. B 94, 014107 (2016)

SESSION EL03.02: Antiferroelectrics and Relaxors II

Session Chairs: John Heron and Morgan Trassin

Monday Afternoon, November 27, 2023

Hynes, Level 1, Room 107

1:30 PM *EL03.02.01

Understanding, Controlling and using Antiferroelectric Thin Films Lane W. Martin^{1,2,3}; ¹Rice University, United States; ²Lawrence Berkeley National Laboratory, United States; ³University of California, Berkeley, United States

Antiferroelectrics are experiencing a renaissance of interest. These materials possess antipolar order (*i.e.*, antiparallel alignment of polarization at zero field) that can be switched to polar (parallel) order by an external electric field thus producing a reversible antiferroelectric-to-ferroelectric phase transition and a characteristic double polarization-electric-field hysteresis loop. Such a unique field-induced antipolar-to-polar transition endows antiferroelectrics with properties that are of great interest for a range of applications including nonlinear dielectrics, capacitive-energy storage, electrothermal-energy conversion, and electromechanical actuation. While these materials have been known for many decades, they remain relatively less studied and well understood as compared to their ferroelectric brethren. To better understand the nature of such phase transitions in antiferroelectrics and to finely engineer the polarization properties for targeted applications requires that one can fabricate high-quality versions of antiferroelectric materials. In this spirit, recent years have seen a growth in efforts to study these materials, particularly as thin films. Epitaxial films offer researchers the opportunity to finely control and manipulate the structure, orientation, strain, and much more. In turn, we are offered unprecedented insights into the nature and evolution of these complex and, at times, poorly understood physical phenomena.

Here, we apply the lessons of thin-film epitaxy to the study of antiferroelectrics. This talk will provide an overview of our recent efforts to synthesize, control, and study antiferroelectric perovskite oxides. Our attention will focus on classic, prototypical antiferroelectric materials such as PbZrO_3 and PbHfO_3 and solid solutions derived from these parent materials. In turn, we will demonstrate how epitaxy, strain, and buffer layers can allow us to finely control the orientation of the resulting orthorhombic films and, in turn, how this orientation control affects the manifestation of properties. Furthermore, we will explore how the growth process – and namely the introduction of defects during growth – can dramatically impact the properties of these materials. For example, it is possible to induce ferroelectric-like response in PbZrO_3 despite the material remaining in the antiferroelectric phase. How defects can pin the antiferroelectric-to-ferroelectric phase boundary thus producing such effects will be developed and the effective pinning energies extracted (0.11-0.2 eV). This also allows us to reversibly adjust the nature of dielectric tunability from “positive” to “negative” tunability near zero field. From here, we will explore interesting applications of antiferroelectrics, including looking at their microwave dielectric response, potential for use in capacitive-energy storage, and for electromechanical actuation. For example, we will explore the use of materials such as $\text{Pb}_{1-x}\text{Sr}_x\text{HfO}_3$ and designer relaxor-antiferroelectrics to improve breakdown strengths, reduce loss, and extend energy-storage density. Finally, we will explore the large electromechanical responses reported in antiferroelectric thin films including developing a mechanistic understanding of the effects and showing routes to improve those responses (*e.g.*, through orientation control and multilayer structuring). Ultimately, antiferroelectrics represent a relatively understudied realm of ferroic materials, ripe for the application of thin-film epitaxy to accelerate our understanding and use of these interesting materials.

2:00 PM EL03.02.02

High-Throughput Combinatorial Approach to the Synthesis of a Lead-Free Ferroelectric Relaxor System Di Zhang¹, Katherine Harmon², Michael Zachman³, Ping Lu⁴, Doyun Kim⁵, Ken William Ssenyimba¹, Zhan Zhang², Reid Markland¹, Yogesh Sharma¹, Binod Paudel¹, Zach Hughes¹, Yue Cao², Hao Zheng², Chase Somodi¹, Ben Freiman¹, Matt Schneider¹, Alessandro Mazz¹, Nick Cucciniello¹, Sundar Kunwar¹, Pinku Roy¹, Qing Tu⁵, Rodney McCabe¹ and Aiping Chen¹; ¹Los Alamos National Laboratory, United States; ²Argonne National Laboratory, United States; ³Oak Ridge National Laboratory, United States; ⁴Sandia National Laboratories, United States; ⁵Texas A&M University, United States

Materials discovery and optimization have usually been a frustrating slow process due to the limited materials combination options in traditional synthesis methods. Here, a high-throughput combinatorial approach which can fabricate nanocomposite materials with compositional gradients at nanoscale has been demonstrated. In this work, the lead-free (BCT-BZT) nanocomposite system was chosen owing to their large piezoelectric coefficient, high dielectric permittivity and robust thermal stability, making it a promising candidate to replace Pb-based energy storage devices. A series of BCT-BZT superlattice structures with continuous compositional gradient were fabricated through a combinatorial pulsed laser technique (cPLD). Ferroelectric property measurements demonstrate the tunable ferroelectricity and relaxor behaviors at different locations on the specimens by changing the BCT: BZT composition ratio as well as the alternating layers number and thicknesses. Detailed microstructural characterization including high resolution X-ray, transmission electron microscopy, and spectroscopy analyses were conducted to clarify the superlattice epitaxy quality, interface structural coupling, and the structure-property correlation of the $\{x\text{BCT}/(1-x)\text{BZT}\}$ superlattice films. The high-throughput synthesis approach demonstrate in this work can be applied to various materials systems to expedite the synthesis and property optimization processes of novel materials systems.

2:15 PM EL03.02.03

Designing “Artificial Relaxor” Behavior in $[\text{BaTiO}_3]_m/[\text{BaZrO}_3]_n$ Superlattices Zishen Tian^{1,2}, Michael Xu³, Jieun Kim¹, Hao Pan¹, Djamilou Lou¹, Xiaoxi Huang¹, James M. LeBeau³ and Lane W. Martin^{1,2,4}; ¹University of California, Berkeley, United States; ²Lawrence Berkeley National Laboratory, United States; ³Massachusetts Institute of Technology, United States; ⁴Rice University, United States

Relaxor ferroelectrics, the disordered cousins of long-range ordered ferroelectrics, have sparked interest among both physicists and materials scientists, due to their exotic physics and immense potential for applications. Relaxor-like behavior is observed in complex solid solutions such as $(1-x)\text{PbMg}_{1/3}\text{Nb}_{2/3}\text{O}_3$ - $(x)\text{PbTiO}_3$ and $\text{BaZr}_x\text{Ti}_{1-x}\text{O}_3$ where the chemical disorder generates random fields in the lattice and breaks the long-range polar order into characteristic nanoscale polar order. Manipulation of the chemical order opens a pathway to control the

nanoscale polar order, which is useful tool for exploring the physics and tailoring material properties. In these *natural* relaxors based on solid solutions, however, deterministic control of the chemical order is challenging due to the inherent randomness, which calls for a new platform for manipulation of the chemical and polar order.

We will discuss the design and synthesis of *artificial* relaxors based on superlattices. Such an approach has been proposed as a novel pathway to control the chemical-order with unit-cell precision [1]. In this regard, $[\text{BaTiO}_3]_m/[\text{BaZrO}_3]_n$ superlattices were proposed and tested as a model system to explore the effect of chemical-order control, wherein the nanoscale-polar structures are confined to the ferroelectric BaTiO_3 layers, and the spacing between neighboring layers of nanoscale-polar structures is controlled by the dielectric BaZrO_3 layers. Superlattices with $m, n = 4-12$ unit cells were fabricated via reflection, high-energy electron diffraction-assisted pulsed-laser deposition and then characterized by X-ray diffraction and atomic-resolution microscopy. These studies confirm the production of high-quality heterostructures, wherein the BaTiO_3 and BaZrO_3 layers are coherently strained to each other with relatively sharp interfaces in between. Measurement of dielectric permittivity along the in-plane [100] revealed significantly enhanced dielectric-maximum temperature T_m in superlattices compared with the corresponding solid solution (from 173 K to ≥ 433 K), and further enhanced T_m in superlattices as the polar-layer thickness increases from $m = 4$ to 12 (from 433 K to ≥ 573 K). Subsequent measurements of polarization-electric field hysteresis and third-harmonic nonlinearity along the in-plane [100] revealed relaxor-like behavior in the superlattices with the thinnest polar layers $m = 4$ and ferroelectric-like behavior in the superlattices with thicker polar layers $m = 8-12$. Finally, the third-harmonic nonlinearity was fitted to the spherical-random-bond-random-field model. It was observed that the random-field strength sharply increased as the polar-layer thickness reduced from $m = 8$ to 4, which hints at the importance of random fields in the formation of the relaxor state.

Altogether, the chemical order in the $[\text{BaTiO}_3]_m/[\text{BaZrO}_3]_n$ superlattices can be deterministically controlled, and the polar order can be tuned between that with ferroelectric-like, long-range order and that with relaxor-like, nanoscale order. This allows the fabrication of an artificial relaxor, and provides a novel platform for exploring the complex physics and tailoring the useful properties of relaxor ferroelectrics.

REFERENCES

[1] Z. Tian, M. Xu, J. Kim, H. Pan, D. Lou, X. Huang, J. M. LeBeau, and L. W. Martin. Tunable Artificial Relaxor Behavior in $[\text{BaTiO}_3]_m/[\text{BaZrO}_3]_n$ Superlattices. *Phys. Rev. Lett.*, Accepted.

2:30 PM EL03.02.04

Oxygen-Displacement-Induced Polarization and Incommensurate Tilt Patterns in Strained Sodium Niobate Thin Films Harikrishnan K. P.¹, Kevin Crust², Aarushi Khandelwal², Kinnary Pate³, Sukriti Mantri³, Sergey Prosdandeev³, Ruijuan Xu⁴, Yu-Tsun Shao^{5,1}, Laurent Bellaiche³, Harold Y. Hwang² and David A. Muller¹; ¹Cornell University, United States; ²Stanford University, United States; ³University of Arkansas, Fayetteville, United States; ⁴North Carolina State University, United States; ⁵University of Southern California, United States

Sodium niobate (NaNbO_3) and other alkali metal niobates are seen as promising alternatives to replace the commonly used lead-based ferroic materials. NaNbO_3 has a rich phase diagram with multiple competing ground states and temperature-driven phase transitions, primarily governed by oxygen octahedral rotations¹. The characterization of NaNbO_3 phases is challenging due to the weak scattering cross-section of the light oxygen atoms. Here we study epitaxial thin films of NaNbO_3 grown using pulsed laser deposition on dysprosium scandate (DyScO_3) substrate using recent advances in electron ptychography that have enabled both robust imaging of the lighter atoms and provided depth-sectioning capabilities².

The epitaxial tensile strain transmutes NaNbO_3 from being a room-temperature antiferroelectric to a ferroelectric with a predominantly in-plane polarization along the (110) pseudo-cubic axis and a small out-of-plane polarization. Measurement of the atomic positions from ptychographic images reveal large displacements of the oxygen atoms, in contrast with the prototypical ferroelectric perovskites where cation displacements drive the polarization. The distorted octahedra also show an in-phase tilt pattern along both in-plane pseudo-cubic axes, a tilt pattern which has not been reported before for NaNbO_3 in literature. Using density functional theory (DFT) calculations, we confirm the existence of monoclinic phases of NaNbO_3 that match our observations from ptychographic images. Further, we also obtain direct visual evidence of the theoretically predicted nanotwin phase^{3,4} with an incommensurate tilt pattern of the oxygen octahedra along the growth direction.

REFERENCES

¹ Megaw H.D., *Ferroelectrics* 7, 87 (1974)

² Chen Z., et al., *Science* 372, 826-831 (2021)

³ Prosdandeev, S., et al., *Adv. Funct. Mater.*, 23, 234-240 (2013)

⁴ Yang Y., et al., *Phys. Rev. B* 97, 174106 (2018)

2:45 PM BREAK

SESSION EL03.03: Ferroelectrics I
Session Chairs: John Heron and Morgan Trassin
Monday Afternoon, November 27, 2023
Hynes, Level 1, Room 107

3:15 PM *EL03.03.01

Epitaxial Si-Integrated Defective BaTiO_3 as Giant Electrostrictors at >1kHz Pavan Nukala; Indian Institute of Science, India

Defect-engineering to induce giant electrostriction has been gaining popularity in CeO_2 and Bi_2O_3 based systems [1]. However, the enhancement is well pronounced only below 100 Hz. Here we show that 10% A-site deficient BTO, grown epitaxially on Si with TiN as a buffer layer, shows record electrostrictive strain coefficients ($M_{31} = 10^{-14} \text{ m}^2/\text{V}^2$) even upto 5 kHz frequencies. Our samples are replete with PNRs and twin boundaries. I'll show how Joule heating and ferroelectricity don't play any significant role in the observed electrostrain values, and it is indeed defect-induced electrostriction that contributes to it. Our impedance spectroscopy data clearly shows that the dielectric relaxation behavior of BTO layer correlates very closely with the observed electromechanical data (in both amplitude and phase). I'll end by suggesting guidelines to design Pb-free materials with large M at higher frequencies for MEMS based applications [2].

References

J. Yu, P.-E. Janolin, Defining Giant Electrostriction, *Journal of Applied Physics*, 131, pp:170701, 2023

S. Vura, S. Parathe, P. Nukala et al., Giant electromechanical response from defective non-ferroelectric epitaxial BaTiO_3 integrated on Si (100), doi: 10.21203/rs.3.rs-2661707/v1 [Pre-print]

3:45 PM EL03.03.02

Transient and Remanent Optical Control of the Domain Configuration in Ferroelectric Epitaxial Oxide Thin Films Martin F. Sarott¹, Marvin J. Müller¹, Jannis Lehmann², Benjamin J. Jacot¹, Manfred Fiebig¹ and Morgan Trassin¹; ¹ETH Zürich, Switzerland; ²RIKEN, Japan

Light-matter interaction in ferroelectric materials forms the basis for light to be used as a non-invasive probe for the spontaneous polarization. In recent years, a shift in perspective has given rise to the question whether light could also be used to actively manipulate domain configurations or even switch the ferroelectric polarization. Realizing such an electric-field-less remote handle of the polarization holds the potential to drastically simplify state-of-the-art ferroelectric device architectures and coin entirely new ferroelectrics-based optoelectronic applications.

In this work, we demonstrate optical control of the ferroelectric polarization in epitaxial PZT-based heterostructures. In this prototypical ferroelectric model system, we track the dynamic response of the polarization under above-bandgap excitation by UV light in real time using optical second harmonic generation. In films with a single-domain configuration, we find that UV-light exposure induces a transient change of the spontaneous polarization that depends on its out-of-plane direction. We attribute this behavior to a modification of the charge-screening environment driven by the separation of photoexcited charge carriers in the built-in electric field of the Schottky junction formed with the bottom electrode. Taking advantage of this phenomenon in films with a pristine depolarized multi-domain configuration, we accomplish remanent optical poling into a single-domain configuration at room temperature. We further demonstrate the reversibility of this optical poling by subsequent thermal annealing. Hence, our work paves the way for the all-optical control of the spontaneous polarization in ferroelectric thin films.

4:00 PM EL03.03.04

Ferroelectric Domain Observations with Helium Ion Microscopy Dong-Jik Kim¹, Valentin V. Hevelke^{1,2}, Jürgen Albert¹, Adnan Hammud³, Sebastian Schmitt¹, Young Jai Choi⁴, Veeresh Deshpande¹ and Catherine Dubourdieu^{1,2}; ¹Helmholtz-Zentrum Berlin fuer Materialien und Energie, Germany; ²Freie Universitaet Berlin, Germany; ³Fritz-Haber Institute of the Max-Planck Society, Germany; ⁴Yonsei University, Korea (the Republic of)

We present a systematic demonstration of the capability of helium ion microscopy (HIM) to visualize the polar and nonpolar domains in ferroelectric LiNbO_3 and ErMnO_3 single crystals. Through a wide range of acceleration voltages and beam currents of He^+ ions, HIM reproduces domain and domain wall maps with significant spatial resolution, consistent with the observations by piezoresponse force microscopy and conductive atomic force microscopy at the same locations. In the HIM domain images, the contrast of the polar domains with out-of-plane polarization can be attributed to the differences in the surface potential or the work function between oppositely poled domains. Intriguingly, HIM also exhibits contrast for nonpolar domains with in-plane polarization. During initial HIM scanning on the nonpolar surface of an ErMnO_3 single crystal, only domain walls are visible, but consecutive scanning leads to the growth of domain contrast along its polar axis, implying a complex interaction between He^+ ion implantation and the bulk photovoltaic effect of the ferroelectric materials. Our observations make HIM included in the list of the characterization tools for ferroelectric domains.

4:15 PM EL03.03.05

Polar Instability in Ferroelastic Bismuth Vanadate BiVO_4 [MaelGuennou](#)¹, [ChristinaHill](#)^{2,1}, [DavidVincent](#)³, [XavierRocquefelte](#)³, [CosmeMilesi-Brault](#)⁴, [ElenaBuixaderas](#)⁴ and [TorstenGranzow](#)²; ¹University of Luxembourg, Luxembourg; ²Luxembourg Institute of Science and Technology, Luxembourg; ³Université de Rennes, France; ⁴The Czech Academy of Sciences, Czechia

Bismuth vanadate BiVO_4 is known as a model ferroelastic crystal displaying a second-order transition where shear strain is the primary order parameter. More recently, it has attracted attention for its optical properties, but also for its potential antiferroelectric character, a property that might in fact be common to all proper or pseudo-proper ferroelastics. In this work, we report a combined theoretical and experimental study of the low frequency polar modes in BiVO_4 . Infrared spectroscopy and inelastic neutron scattering are used to measure the polar mode at the Brillouin zone center and follow its dispersion as a function of temperature. We demonstrate the existence of a strong coupling between the polar mode and the primary order parameter that causes the crystal to display a dielectric anomaly typical of antiferroelectric systems. We also discuss how the polar instability is reflected from first-principles calculations, and how polar displacements of Bismuth produce unusual phonon-phonon coupling in the inelastic neutron spectra.

SESSION EL03.04: Ferroelectrics II

Session Chairs: John Heron, Johanna Nordlander and Morgan Trassin

Tuesday Morning, November 28, 2023

Hynes, Level 1, Room 107

8:30 AM *EL03.04.01

Evidence of High Remanent Polarization in Epitaxial Thin Film Ferroelectric BaTiO_3 Integrated onto Silicon [ArbabSen Gupta](#), [RachelSteinhardt](#), [PratyushBuragohain](#), [JohnPlombon](#), [I-ChengTung](#), [PunyashlokaDebashish](#), [RaseongKim](#), [KevinP. O'Brien](#), [CarlyRogan](#), [MarkoRadosavljevic](#), [UygarE. Avci](#), [ErnisseS. Putna](#), [ShaneM. Harlson](#), [IanYoung](#), [TristanTronic](#) and [MatthewV. Metz](#); Intel Corporation, United States

The computing world is approaching a global energy crisis due to the exponential growth of energy requirement as CMOS transistors scale to smaller dimensions. One path forward is to lower the device supply voltages. In this regard, low power beyond-CMOS technologies such as devices based on ferroelectric materials are receiving renewed interest from both the scientific and technological communities. Perovskite BaTiO_3 (BTO) ferroelectric thin films are highly promising due to their low coercivity, large remanent polarization and environmental friendliness. Copious progress has been made towards optimizing ferroelectric BTO on oxide substrates including recent reports on BTO-based devices for ultra-low-voltage operation.¹ However, to be compatible with high volume manufacturing, integration of high quality BTO onto Silicon is key. Thus far, quantitative reports on the ferroelectric properties of BTO on Si substrates have been sparse. Properties tend to be degraded including higher leakage and low remanent polarization (Pr) of 5-12 $\mu\text{C}/\text{cm}^2$.¹⁻⁵ Additionally, films tend to be in the range of 50-200nm thick.¹⁻⁵ Ideally for scaled devices, films of BTO on Si would be as thin as possible, with low coercivity, low leakage, high endurance, and Pr close to the bulk value of 30 $\mu\text{C}/\text{cm}^2$. In this work, we report remanent polarization up to $\sim 20 \mu\text{C}/\text{cm}^2$ in Pulse laser deposition (PLD) grown ultrathin 30-nm-thick BTO films grown on Molecular Beam Epitaxial SrTiO_3 (STO)-buffered Si (Si:STO) substrates, with leakage in the order of $\sim 1\text{A}/\text{cm}^2$. The Si:STO/SRO/BTO/Ti/Pd devices did not undergo dielectric breakdown up to 10^9 cycles, with only a 5% reduction in Pr observed after cycling. Structural characterizations revealed epitaxial growth of BTO films with relaxed lattice parameters. The quality of the STO buffer on Si was found to be critical for optimizing the ferroelectricity in BTO. This improved remanent polarization in ultrathin BTO with low leakage paves the way towards integrating a semiconducting channel with this device to create the next generation transistor. Nevertheless, a pursuit towards a 300 mm compatible perovskite process entails a concerted effort among academia, semiconductor manufacturers and tool manufacturers.

Reference:

1. Jiang, Y., et al. Enabling ultra-low-voltage switching in BaTiO_3 . *Nat. Mater.* 21, 779–785 (2022)
2. Scigaj M. et al., Ultra-flat BaTiO_3 epitaxial films on Si(001) with large out-of-plane polarization. *Appl. Phys. Lett.* 102 (11): 112905 (2013)
3. Scigaj M. et al., High ferroelectric polarization in c-oriented BaTiO_3 epitaxial thin films on SrTiO_3/Si (001). *Appl. Phys. Lett.* 109, 122903 (2016)
4. Lyu J. et al., Tailoring Lattice Strain and Ferroelectric Polarization of Epitaxial BaTiO_3 Thin Films on Si(001). *Scientific Reports.* 8, 495 (2018)
5. Singamaneni S.R. et al., Ferroelectric and ferromagnetic properties in BaTiO_3 thin films on Si (100). *J. Appl. Phys.* 116, 094103 (2014)

9:00 AM EL03.04.02

Photo-Induced Transport Properties in Ferroelectric Domains and Domain Walls in Lithium Niobate Single Crystals [LiliDing](#)^{1,2}, [BeyreutherElke](#)¹, [KonradKempfl](#)¹, [MichaelRüsing](#)¹ and [LukasEngl](#)¹; ¹Technische Universität Dresden, Germany; ²School of Physics, Sun Yat-sen University, China

Ferroelectric materials exhibit a spontaneous and stable dielectric polarization, resulting in a rich and variable assembly of domain and domain wall structures that is receiving continued attention [1, 2]. Furthermore, the multifield-controlled (electrical, mechanical, optical) electrical transport across these crystals offers many prospects for the vivid application of ferroelectrics into electronic devices, such as ferroelectric sensors, memories, and even ferroelectric synaptic circuits [3-5]. Notably, (external) control of the electronic transport by means of photons is very desirable since being non-invasive and ultrafast, but has been studied only sparsely so far. In particular, polarization switching of domains and domain walls, band gap modulation, or domain wall dynamics, all are susceptible to the photon-electron interaction, and thus need fundamental and profound investigations as basis for further application.

In this work, we combine local-scale scanning probe techniques with analyzing the impact of light irradiation onto lithium niobate domains and domain walls, and vary both intensity and wavelength to probe the (local) electronic conductivity. On this basis, we can also realize the configuration of high density domain pattern array and modulate the domain wall conductivity through scanning probe microscopy and the assistance of UV light. Then, we demonstrate that the enhancement of transport properties and the switching behavior of lithium niobate domain walls can be regulated by illumination adjacent to the band gap. This multi-method approach thus will improve our in-depth knowledge on the local band structure and energy level distribution within domain walls, and will lay the foundation to design integrated electro-optical components thereof.

- [1] D. Meier, et al., *Nat. Rev. Mater.* 7, 157 (2022)
- [2] D. M. Evans, et al., *Phys. Sci. Rev.* 5, 9 (2020)
- [3] C. Godau, et al., *ACS Nano* 11, 5 (2017)
- [4] E. Singh, et al., *Phys. Rev. B* 106, 144103 (2022)
- [5] Z. D. Luo, et al., *ACS Nano* 14, 746 (2020)

9:15 AM EL03.04.03

Pushing the Limits of Retention, Endurance and Leakage in Ultra-Thin BaTiO_3 Films [HarishKumarasubramanian](#)¹, [PrasannaV. Ravindran](#)², [MythiliSurendran](#)¹, [AsifI. Khan](#)² and [JayakanthRavichandran](#)^{1,1}; ¹University of Southern California, United States; ²Georgia Institute of Technology, United States

Over the last fifty years, miniaturization has been the primary driver in improving efficiency, facilitating higher speed and reduced cost in MOSFETs while enabling an exponential increase in computational and storage capabilities. Progress in ferroelectric based memory and logic systems with the conventional perovskite systems have stagnated since the early 2000s on account of their high critical thickness and are therefore challenging to scale down. The thinner versions of these perovskite films have also been plagued by high leakage currents and depolarizing fields. Simultaneously, the discovery of ferroelectricity in CMOS-compatible gate dielectrics such as Hafnia and Zirconia at a few unit cells of thickness has facilitated their usage as high K dielectrics. This has provided an additional impetus in lowering the threshold voltage and the power dissipation in FETs [1]. However, despite the scaling down in physical dimensions of the gate oxide, the power supply voltage or the physical voltage has been stuck around 1 V or above for the last 15 years [2]. The extremely high coercive fields ($>1 \text{ MV}/\text{cm}$) of fluorite oxides has

impeded the reduction in switching voltage. It has thus become imperative to develop and investigate leakage free, low voltage technological platforms especially for low power applications. The more conventional ferroelectric systems like perovskite oxides have recently shown much lower switching voltages (<0.1 V) [3].

In this work, we have achieved robust retention ($>10^4$ s) and stable endurance ($> 10^9$ cycles) with low ultra-low switching voltages (<50 mV) [4] in sub 20 nm ferroelectric thin films based on epitaxial oxide perovskites in the Metal-Insulator-Metal geometry. More specifically we have deposited epitaxial BaTiO₃ (BTO) thin films on GdScO₃ (110) substrates using Pulsed Laser Deposition (PLD). We have minimized depolarization effects in our thin films by sandwiching the BTO with an epitaxial conductive oxide perovskite (SrRuO₃) on either side. Our BTO films have also shown leakage currents at least 3 orders of magnitude lower than HfO₂ and SiO₂ at sub 1 nm equivalent oxide thicknesses. Strategies to achieve low defect density and subsequently, robust ferroelectricity in ultra-thin BTO films would be discussed.

To satisfy a broader set of applications, it is essential to achieve a similar or better set of ferroelectric/leakage properties on Metal-Insulator-Semiconductor (MOS) structures. Even though Si has been the workhorse of the semiconductor industry for at least half a century, the scaling requirements have increasingly eaten into its primary advantages, namely its thermally grown dielectric native oxide. There is an urgent need to replace SiO₂ with other other high K oxides and hence there is an impetus towards replacing Si with other commercially viable semiconductors. Ge, in particular, has many advantages as the replacement channel material. Additionally, Ge provides an excellent epitaxial template for BTO (<0.5 % strain). Integration and performance of epitaxial BTO thin films on Ge would be elaborated upon. The effect of thin blocking layers of high band gap, epitaxially compatible perovskite dielectric oxides with large enough valence and conduction band offsets with Ge will also be discussed.

REFERENCES :

1. Böscke, T. S., J. Müller, D. Bräuhäus, U. Schröder, and U. Böttger. "Ferroelectricity in hafnium oxide thin films." *Applied Physics Letters* 99, no. 10 (2011): 102903.
2. Andrew Danowitz et al. "CPU DB: recording microprocessor history". In: *Communications of the ACM* 55.4 (2012), pp. 55–63.
3. Jiang, Y., E. Parsonnet, A. Qualls, W. Zhao, S. Susarla, D. Pesquera, A. Dasgupta et al. "Enabling ultra-low-voltage switching in BaTiO₃." *Nature Materials* (2022): 1-7

9:30 AM EL03.04.04

Exchange-Interaction-Like Behavior in Ferroelectric Bilayers Pravin Kavle^{1,2}, Aiden M. Ross³, Jacob A. Zorn³, Prish Behara^{1,2}, Eric Parsonnet¹, Xiaoxi Huang^{1,2}, Ching-Che Lin^{1,2}, Lucas Caretta^{1,2,4}, Long-Qing Chen³ and Lane W. Martin^{1,2,5}; ¹University of California, Berkeley, United States; ²Lawrence Berkeley National Laboratory, United States; ³The Pennsylvania State University, United States; ⁴Brown University, United States; ⁵Rice University, United States

Coupling across interfaces is vital for many fields from composite materials with different mechanical properties, to magnetoelectric coupling across magnetic and piezoelectric materials, to exchange interactions between ferromagnets and antiferromagnets. Among these, the exchange bias (or exchange anisotropy) between a ferromagnet and an adjacent ferromagnetic or antiferromagnetic layer has been widely studied and utilized in magnetic read-write heads and random-access memory. In exchange bias, the magnetic response of a ferromagnet is shifted away from zero magnetic field. Other related phenomena include exchange-spring magnets which are achieved by coupling hard and soft ferromagnets such that the hard magnet provides high anisotropy and coercive fields, while the soft magnet enhances the magnetic moment. The soft magnet rotates back into alignment with the hard magnet when the applied field is removed, hence the analogy to a spring. Likewise, analogous coupling across the interface between different ferroelectric materials via dipolar (electrostatic and potentially elastic) interactions could possibly lead to anisotropic dipole interactions. Effects akin to exchange bias have been observed in ferroelectrics as shifted hysteresis loops due to the internal bias field arising from aligned defect dipoles and compositional (or strain) gradients. Such observations, however, fall short of effects that are truly analogous to exchange interactions.

In-plane polarized ferroelectric films, where polarization lies parallel to the substrate surface, could provide an opportunity to tune interface-controlled effects. Here, we demonstrate the formation of such in-plane domains in Pb_{1-x}Sr_xTiO₃ ($0.4 \leq x \leq 0.8$) films grown on DyScO₃ (110) substrates. Strontium content in the Pb_{1-x}Sr_xTiO₃ impacts the domain size and coercivity to form "hard" and "soft" coercivity versions. Next, the switching mechanisms of these domains have been analyzed via piezoresponse force microscopy after applying an electric field at 0° and 45° with in-plane devices. Phase-field studies revealed low-energy, stepwise-90° switching steps as the most effective switching pathway instead of single 180° switching. To analyze the interface-controlled switching properties, bilayers of 50-nm-thick $x = 0.6$ layers on top of $x = 0.4$ layers were explored where two-step switching was observed. Phase-field studies provide details about the equilibrium domain structure where the difference in domain periodicity of two layers leads to the formation of needle-shaped domain-dislocations in the $x = 0.4$ layer along with continuous domains across the interface. The minor switching loop indicating the switching of the $x = 0.6$ layer showed a horizontal shift of 14 kV cm⁻¹ due to the formation of 90° domain walls at the interface, leading to the exchange-bias-like behavior. Further increase in the electric field led to domain reshuffling in the bottom $x = 0.4$ layer to realign domains across the interface in an elastically compatible way before switching, resulting in coercivity hardening. This two-step switching is then analyzed for multistate functions, where robust retention and fatigue performance was recorded. Inserting SrTiO₃ dielectric layers between the two layers led to a decoupling of layers and the disappearance of observed shifts, further strengthening the interlayer coupling claim. Switching of a bilayer of 50-nm-thick $x = 0.8$ top layer on a $x = 0.4$ bottom layer was analyzed where strong back switching minor loops for the $x = 0.8$ layer were observed, indicating exchange-spring-like behavior. Bilayers with 40-nm-thick $x = 0.6$ top layers on $x = 0.4$ bottom layers reveal single switching with reduced coercivity due to the absence of any domain dislocations and continuous propagation of switched domains observed via phase-field studies, like the exchange-spring. Such phenomena extend the parallels between ferromagnets and ferroelectrics beyond the structural analogs like skyrmions.

9:45 AMBREAK

10:15 AM EL03.04.05

Enhanced Hard and Soft Piezoelectric Properties of (Pb_{0.94}Sr_{0.06})(Zr_{1-x}Ti_x)-(Zn_{1/3}Nb_{2/3}) Multilayer Ceramics Sintered at Low-Temperature Geunsoo Lee, Jung-Soo Kim, SanKwak and SahnNahm; Korea University, Korea (the Republic of)

High-power piezoceramics have been utilized in different piezoelectric devices, such as piezoelectric transformers, motors, and ultrasonic transducers. As a large amount of heat is usually generated from high-power devices, the piezoceramics used in these devices need to have a Q_m . Moreover, these high-power piezoceramics should have a large d_{33} value and a high T_C . In this study, the (Pb_{0.94}Sr_{0.06})(Zr_{1-x}Ti_x)_{0.75}(Zn_{1/3}Nb_{2/3})_{0.25}O₃ (PS-ZT-ZN) piezoceramics were produced at a low temperature of 950°C and their structural and piezoelectric properties were investigated. In particular, the piezoceramic ($x = 0.50$) exhibited the excellent hard and soft piezoelectric properties ($d_{33} = 357$, $k_p = 0.53$, and $Q_m = 1511$) along with a high T_C of approximately 250°C. Hence, this piezoceramic is a promising material for the high-power devices. Moreover, the PS-ZT-ZN multilayers were fabricated using piezoceramic ($x = 0.5$) at 950°C with the 80Ag/20Pd inner electrodes and their structural and piezoelectric properties were also investigated to assess their suitability for use in high-power multilayer devices.

10:30 AM EL03.04.06

Preparation of {100}-Oriented Epitaxial (1-x)(Bi,K)TiO₃-xCaTiO₃ Solid Solution Films by Hydrothermal Method and Their Ferroelectric Property Taichi Murashita, Hu Yuxian, Yuma Takahashi, Reika Ota, Kazuki Okamoto; and Hiroshi Funakubo; Tokyo Institute of Technology, Japan

(Bi,K)TiO₃ is a well-known traditional tetragonal ferroelectric material discovered in the 1950s by Smolenskii *et al.* [1] However, the preparation of high-quality (Bi,K)TiO₃ is still challenging due to the preparation difficulty. The fundamental ferroelectric properties have not been well understood so far. In 2022, our group succeeded to grow the polar-axis-oriented epitaxial (Bi,K)TiO₃ films at the low deposition temperature of 240 °C by hydrothermal method. [2] Their tetragonality (c/a ratio) and remnant polarization (P_r) values are 1.046, and 84 $\mu\text{C}/\text{cm}^2$, respectively. These values are larger than previously reported ones for (Bi,K)TiO₃ ceramics. [3] The enhanced tetragonality of the (Bi,K)TiO₃ films is possibly attributed to the unique displacement of the Bi and K in A-site cations ascertained by TEM observation. These (Bi,K)TiO₃ films showed high Curie temperature, T_C , above 800 °C. Based on this research, solid solution epitaxial films of (Bi,K)TiO₃ with ferroelectric rhombohedral (Bi,Na)TiO₃ were successfully obtained by hydrothermal method. [4] X-ray diffraction analysis showed a continuous decrease of the c/a ratio with increasing K/(K+Na) ratio and the c/a ratio become unity near the K/(K+Na) ratio = 0.15. This suggests the existence of tetragonal-rhombohedral morphotropic phase boundary near $c/a = 1$. This research demonstrated the preparation of solid solution film by hydrothermal method. As the next challenge, we should decrease the extremely high T_C above 800 °C of (Bi,K)TiO₃ films for the application of pyroelectric devices.

In this study, we tried to hydrothermally grow epitaxial solid solution films of (Bi,K)TiO₃ with paraelectric CaTiO₃, (1-x)(Bi,K)TiO₃-xCaTiO₃ films to increase the pyroelectric coefficient by decreasing T_C . The film composition region can be divided into three from the viewpoint of the crystal structure. Films in the range of $x = 0 - 0.12$ (Region 1) and 0.60 - 1.0 (Region 3) consisted of single phases and their lattice parameters continuously changed with the x value. The phases are tetragonal and pseudo-cubic symmetry in Region 1 and Region 3, respectively. This suggests a formation of a solid solution in these two regions. On the other hand, these two phases (tetragonal and pseudo-cubic symmetry) coexisted in the intermediated range of $x = 0.18 - 0.43$ (Region 2). In this coexistence composition region, the volume fraction of these two phases changed with the x value, while their lattice parameters were almost independent of the x value. This suggests the solubility limit of this system. In Region 1 and Region 2, P - E hysteresis loops originating from the ferroelectricity were clearly observed. The P_r values continuously decreased with increasing x in Region 1, mainly due to the decrease in the c/a ratio of the ferroelectric phase. This decrease of P_r with x was also observed in Region 2 mainly due to the decrease in the volume fraction of the ferroelectric phase. In the next step, these films were annealed at 950 °C by face-to-face annealing to decrease T_C . After annealing the film with $x = 0.12$, the film showed lowered T_C of 450 °C and a higher pyroelectric coefficient than that of the film with $x = 0$ ((Bi,K)TiO₃). These data show that the properties of (Bi,K)TiO₃ films can be controlled by the synthesis of a solid solution.

[1] G. A. Smolenskii, *Sov. Phys. Solid State*, **1**, 1562 (1959).

[2] Y. Ito *et al.* *Appl. Phys. Lett.* **120**, 022903 (2022).

[3] Y. Hiruma *et al.* *Jpn. J. Appl. Phys.* **44**, 5040 (2005).

10:45 AM EL03.04.07

Dielectric and Electro-Mechanical Properties Controlled by Polarization Switching in PbZr_{0.2}Ti_{0.8}O₃-ZnO Thin-Film HeterostructureAlexeiGrigoriev, RuohanyangLeng and JuanWang; University of Tulsa, United States

Development and characterization of new heterostructure materials and interfaces is critical for a sustained progress of the performance and functionality of electronic, electro-mechanical, and electro-optical devices. We report experimental studies of ferroelectric-semiconductor PbZr_{0.2}Ti_{0.8}O₃-ZnO heterostructure that enables ferroelectric polarization control of ZnO electronic and dielectric properties. The time-resolved x-ray microdiffraction measurements have revealed the piezoelectric coefficient d₃₃ of about 2.8 pm/V for pure high-quality epitaxial ZnO thin films. This linear piezoelectric response becomes more complex in the ferroelectric-ZnO heterostructure revealing different regimes of the electro-mechanical response. Polarization switching of PbZr_{0.2}Ti_{0.8}O₃ controls the interface electronic properties leading to switchable capacitance of at least 35% and over an order of magnitude difference in the interface charge carrier densities for two different polarization states of the ferroelectric layer. These results are important for understanding ferroelectric-semiconductor interactions and engineering new ZnO-based ferroelectric-semiconductor heterostructures such as BiFeO₃-ZnO or HfO₂-ZnO with new switchable electronic and dielectric properties.

11:00 AM EL03.04.08

Determination of Nonlinear Dielectric and Electrostrictive Constants of Lithium Tantalate Single CrystalYasuoCho¹, RyoNakagawa², ToshimaroYoneda², TakeshiNakao² and MamoruIkura²; ¹Tohoku University, Japan; ²Murata Manufacturing Co., Ltd., Japan

To increase telecommunications capacity, surface acoustic wave (SAW) devices have become smaller and have more channels and higher power. However, the intermodulation caused by material nonlinearity has become increasingly apparent. To effectively utilize SAW devices in sixth-generation communication systems, it is necessary to mitigate this nonlinearity. However, a full set of nonlinear constants (nonlinear elastic, piezoelectric, electrostrictive, and dielectric constants) for piezoelectric single crystals has been measured for only lithium niobate (LiNbO₃) single crystals[1]. The nonlinearity of a single crystal of lithium tantalate (LiTaO₃), the most widely used ferroelectric crystal in SAW devices for communications, has not been quantitatively evaluated.

Against this background, we started research on the measurement of all nonlinear constants of LiTaO₃ single crystals as part of basic research for the realization of next-generation ultra-low-nonlinearity SAW devices.

This paper describes a measurement methods and reports the obtained nonlinear dielectric constants and electrostrictive constants for LiTaO₃. In the experiment, a dynamic measurement method based on capacitance variation with an alternating electric field was employed for the nonlinear dielectric constants [2] and capacitance variation under applied stress was also measured for electrostrictive constants.

We show the measured relative capacitance variation in LiTaO₃ single crystal plate as a functions of an applied electric field and stress, respectively. Using measured five data (for nonlinear dielectric constants) and twenty data (for electrostrictive constants) with different crystal orientation, we have determined three independent nonlinear dielectric constants and eight electrostrictive constants in the stress-free state (d-form) ϵ_{ijk}^T and d_{ijk}^2 . The corresponding nonlinear constants in the strain-free state (e-form) ϵ_{ijk}^S and e_{ijk}^2 were also calculated using the d-form constants and will be presented at the meeting.

References:

- [1] Y.Cho and K.Yamanouchi:"Nonlinear,Elastic, Piezoelectric, Electrostrictive, and Dielectric Constants of Lithium Niobate ", J. Appl. Phys.,Vol.61 (1987) pp.875-887.
- [2] Y.Cho and F.Matsuno:"Dynamic Measuring Method of Capacitance Variation of Piezoelectric Ceramics with Alternating Electric Field", Jpn. J. Appl. Phys., Vol.31 (1992) pp.3627-3631.

11:15 AM EL03.04.09

Strain Fluctuations Unlock Ferroelectricity in ZnO:MgOStevenM. Baksa¹, SimonGelin¹, RuiZu¹, SedaOturak¹, SusanE. Trolier-McKinstry¹, VenkatramanGopalan¹, Jon-PaulMaria¹, AndrewRappe² and IsmailaDabo¹; ¹The Pennsylvania State University, United States; ²University of Pennsylvania, United States

Abstract

The palette of ferroelectric materials for thin-film microelectronics is currently restricted to select families of non-centrosymmetric structures, including perovskite oxides (*e.g.*, PbZr_xTi_{1-x}O₃) and fluorite oxides (*e.g.*, Hf_{1-x}Zr_xO₂). While some of these ferroelectrics have been successfully integrated into electronic devices such as random-access memories, the fabrication of ultrathin microelectronics is challenging due to film-thickness scaling limitations, which impede ferroelectric switching. Non-centrosymmetric wurtzite materials, including Al_{1-x}B_xN [1] and Zn_{1-x}Mg_xO [2], have recently been found to exhibit ferroelectricity. Although applied epitaxial strains above 5% may induce a ferroelectric response in wurtzites [3,4], Zn_{1-x}Mg_xO shows strain magnitudes of less than 1%. Here, we demonstrate that atomic-scale strain fluctuations of up to 5% can emerge near Zn and Mg cations leading to a reduction of more than 40% in the local switching barriers. This observation strongly suggests that strain fluctuations from dopant cations can promote polarization reversal in wurtzite materials, opening up a general design strategy to discover and optimize ferroelectrics for use in thin-film devices.

References

- [1] Calderon, Hayden, Baksa, Tzou, Trolier-McKinstry, Dabo, Maria, Dickey, *Science* **380**, 1034-1038 (2023).
- [2] Ferri, Bachu, Zhu, Imperatore, Hayden, Alem, Giebink, Trolier-McKinstry, Maria, *J. of Appl. Phys.* **130**, 044101 (2021).
- [3] Konishi, Ogawa, Fisher, Kuwabara, Shimizu, Yasui, Itoh, Moriwake, *Appl. Phys. Lett.* **109**, 102903 (2016).
- [4] Moriwake, Konishi, Ogawa, Fujimura, Fisher, Kuwabara, Shimizu, Yasui, Itoh, *Appl. Phys. Lett.* **104**, 242909 (2014).

SESSION EL03.05: Ferroelectrics III
Session Chairs: John Heron and Morgan Trassin
Tuesday Afternoon, November 28, 2023
Hynes, Level 1, Room 107

1:30 PM EL03.05.01

Emerging Materials and Design Principles for Wurtzite-type FerroelectricsCheng-WeiLee¹, NaseemUd Din¹, KeisukeYazawa^{1,2}, GeoffL. Brennecke¹, AndriyZakutayev^{2,1} and PrashunGorai^{1,2}; ¹Colorado School of Mines, United States; ²National Renewable Energy Laboratory, United States

The semiconductor industry has been enabled by tetrahedral semiconductors such as Si, GaN etc. Historically, complex oxides with octahedral bonding have been the focus of ferroelectrics research. Unfortunately, such oxides are prone to oxygen-related defects, which along with a mismatch to tetrahedral symmetry, makes integration with conventional semiconductors challenging. Discovery of tetrahedral ferroelectrics will enable device integration and alleviate the need for aggressive defect engineering. At present, there are only a handful of modified wurtzite structures that exhibit robust polarization switching. These include wurtzite-type (Al,Sc)N, (Al,B)N, and (Zn,Mg)O alloys, but none are single-phase compounds. Furthermore, the coercive fields needed to switch these wurtzite-type alloys are on the order of few MV/cm, which is 1-2 orders of magnitude larger compared to oxide perovskites (<100 kV/cm). Instead of further engineering AlN-based alloys, we explore the possibility of identifying new ternary and multinary compounds with switching energy densities lower than AlN and ZnO while still possessing high enough dielectric breakdown fields. In this work, we use DFT calculations to search for new ternary and multinary wurtzite-type tetrahedral ferroelectric materials. We identify several promising nitrides and oxides as candidates for future experimental verification and engineering. Our results also show that small wurtzite c/a lattice parameter ratio is not a good descriptor of lower coercive fields, in agreement with recent studies [1]. We also derive design principles based on metal-anion bond ionicity and lattice softness for lower switching barriers. Finally, we offer new insights into the polarization switching mechanism in ternary compounds and wurtzite-type alloys.

- [1] Yazawa, K., *et al.*, *J. Mater. Chem. C* **10**, 17557 (2022)

1:45 PM EL03.05.02

Switching Kinetics and Wakeup Behavior of Wurtzite FerroelectricsKeisukeYazawa^{1,2}, DanielDrury², JohnHayden³, Jon-PaulMaria³, SusanE. Trolier-McKinstry³, AndriyZakutayev¹ and GeoffL. Brennecke²; ¹National Renewable Energy Laboratory, United States; ²Colorado School of Mines, United States; ³The Pennsylvania State University, United States

Ferroelectricity enables key integrated technologies from non-volatile memory to precision ultrasound. Wurtzite nitride ferroelectric materials such as (Al,Sc)N and (Al,B)N have recently received significant attention because of robust ferroelectricity [1,2] and the compatibility of the existing Si and III-V semiconductor processes. The mechanism and origin of the wurtzite ferroelectrics have been rigorously investigated [1,3] to control the ferroelectric properties and discover novel ferroelectric materials, but many questions remain, including in switching dynamics and the origin of wakeup behavior. Those questions are directly relevant to ferroelectric applications such as FeRAM.

In this presentation, we demonstrate and interpret anomalous switching dynamics in the wurtzite nitride thin film ferroelectrics $Al_{0.7}Sc_{0.3}N$ and $Al_{0.94}B_{0.06}N$, which is explained with neither the conventional KAI nor NLS models [4]. When substantial growth and impingement occur while nucleation rate is increasing, such as in these wurtzite ferroelectrics under high electric fields, abrupt polarization reversal leads to very large Avrami coefficients ($n = 11$), inspiring an extension of the KAI model that distinctly describes the nucleation rate and domain growth. This extended model explains the abrupt transition arising from significant growth prior to peak nucleation rate.

We also demonstrate that polarization switching to the polarity opposite of the growth polarity is critical to the observed wakeup behavior of thin film $Al_{0.94}B_{0.06}N$ [5]. The polarization switching curve, is orders of magnitude slower for the transition from the growth polarity to the antiparallel polarization state than going from antiparallel state back to the growth polarity. The domain wall density and/or domain wall mobility for switching from the antiparallel state to the growth polarity gradually increases with the number of cycles, causing the measured remanent polarization to increase for electric fields just above the coercive field, resulting in the observed wakeup behavior. Reversible and irreversible Rayleigh coefficients, piezoelectric coefficients, and chemical etching results reveal the domain structure and its evolution with the number of electric field cycles. These are consistent with the domain states predicted by the nucleation time and domain wall velocity from switching kinetics studies on the same films.

[1] S. Fichtner, N. Wolff, F. Lofink, L. Kienle and B. Wagner, *J. Appl. Phys.*, 2019, **125**, 114103.

[2] J. Hayden, M. D. Hossain, Y. Xiong, K. Ferri, W. Zhu, M. V. Imperatore, N. Giebink, S. Trolrier-Mckinstry, I. Dabo and J. P. Maria, *Phys. Rev. Mater.*, 2021, **5**, 044412.

[3] K. Yazawa, J. Mangum, P. Gorai, G.L. Brennecke, A. Zakutayev, *J. Mater. Chem. C*, 2022, **10**, 17557.

[4] K. Yazawa, J. Hayden, J.-P. Maria, W. Zhu, S. Trolrier-McKinstry, A. Zakutayev, and G. L. Brennecke, *Mater. Horiz.*, 2023, Advanced Article.

[5] K. Yazawa, D. Drury, J. Hayden, J.-P. Maria, S. Trolrier-McKinstry, A. Zakutayev, and G. L. Brennecke, *J. Am. Ceram. Soc.*, 2023, under review.

2:00 PM EL03.05.03

Ferroelectric Property Improvement of $(Al_{1-x-y}Ga_xSc_y)N$ Ternary Thin Films Reika Ota¹, Shinnosuke Yasuoka¹, Kazuki Okamoto¹, Yoshihiro Ueoka², Yoshiro Kusue², Masami Mesuda² and Hiroshi Funakubo¹; ¹Tokyo Institute of Technology, Japan; ²Tosoh Corporation, Japan

After the first demonstration of ferroelectricity of $(Al_{1-x}Sc_x)N$ films by Fichtner *et al* [1], wurtzite-based ferroelectric films have been one of an important family due to their large remanent polarization and high Curie temperature. However, a large coercive field (E_c) is one of the drawbacks to the real applications of ferroelectric memories with low-voltage operation even if the large ferroelectricity over $100 \mu C/cm^2$ is ascertained to be observed down to 9 nm in thickness.

Our research teams demonstrate the ferroelectricity of not only Sc-doped AlN films but also Sc-doped GaN [2-8]. Especially, Sc-doped GaN films show a lower coercive field than that of Sc-doped AlN films. However, Sc-doped GaN films show a relatively large leakage current density. In the present study, we investigate the Sc-(Al,Ga)N films to satisfy low coercive field with keeping large remanent polarization.

By adding Ga into Sc-doped AlN, $(Al_{1-x-y}Ga_xSc_y)N$, Sc content to keep wurtzite structure increased compared with widely investigated Sc-AlN films. Coercive field of the films monotonously decreased with increasing Sc content of the films. Resultantly E_c decreased down to 2 MV/cm comparable to HfO_2 -based ferroelectrics. Present results show that E_c of wurtzite ferroelectrics can decrease by designing the film composition and the possibility to use $(Al_{1-x-y}Ga_xSc_y)N$ films for ferroelectric memories with the low-voltage operation.

This work was partly supported by MEXT Initiative to Establish Next-generation Novel Integrated Circuits Centers (X-NICS) and MEXT Program: Data Creation and Utilization Type Material Research and Development Project Grant Number JPMXP1122683430. This work was supported by JSPS KAKENHI (Grant Numbers 22K18307 and 21H01617).

[1] Fichtner, *et al.*, *J. Appl. Phys.*, **125**, 114103 (2019).

[2] Yasuoka *et al.*, *J. Appl. Phys.*, **128**, 114103 (2020).

[3] Yasuoka *et al.*, *Phys. Status Solidi A*, **218**, 2170049 (2021).

[4] Uehara *et al.*, *Appl. Phys. Lett.*, **119**, 172901 (2021).

[5] Mizutani, *et al.*, *Appl. Phys. Exp.*, **14**, 105501 (2021).

[6] Yasuoka *et al.*, *J. Ceram. Soc. Jpn.*, **130**, 436 (2022).

[7] Uehara *et al.*, *Appl. Phys. Exp.*, **15**, 081003 (2022).

[8] Yasuoka *et al.*, *ACS Appl. Electron. Mater.*, **4**, 5165 (2022).

2:15 PM EL03.05.04

A Novel, High Temperature, Ferroelectric Non-Volatile Memory Device Dhiren K. Pradhan¹, David Moore², Gwangwoo Kim¹, Yunfei He¹, Nicholas Glavin², Joshua Kennedy², Roy H. Olsson III¹ and Deep M. Jariwala¹; ¹University of Pennsylvania, United States; ²Air Force Research Laboratory, United States

Non-volatile memory (NVM) technology that reliably operates at temperatures above 300 °C is not available commercially. There are numerous emerging harsh environment applications such as aerospace/defense, space exploration, and oil and gas exploration, that require complex computing and sensing capabilities in-situ. Such a vision is impossible without a NVM device which can reliably operate at temperatures exceeding 500 °C. Ferroelectric $Al_xSc_{1-x}N$ has strong potential to be utilized in NVM devices as it exhibits stable and high remanent polarization (P_r) above $100 \mu C/cm^2$ when operated at very high temperature (> 500 °C) and has a ferroelectric transition temperature (T_c) > 1000 °C. In the present study, we demonstrate a $Al_{0.68}Sc_{0.32}N$ ferroelectric diode based NVM memory that can operate up to 600 °C. Our devices are metal insulator metal (MIM) capacitors with a structure of the Ni/ $Al_{0.68}Sc_{0.32}N$ /Pt (111). $Al_{0.68}Sc_{0.32}N$ thin film of thickness of ~45 nm were grown on a 4" Pt (111)/Ti/SiO₂/Si substrate by pulsed-DC co-sputtering from separate Al (1000W) and Sc (655W) targets. The deposition was carried out at 350 °C, with a flow of N₂ gas (20 sccm) under a vacuum of 8×10^{-4} torr. Photolithographically defined 100-nm thick top Ni circular electrodes were sputtered to form MIM structures. The coercive field (E_c) from the I-V curves acquired by the dynamic hysteresis measurements is found to be -5.48 (E_c^-) and +6.26 (E_c^+) (+/- 0.2) MV/cm at room temperature. PUND current densities at RT show ferroelectric switching in both positive and negative voltage pulses. The temperature dependent DC I-V curves exhibit ferroelectric diode behavior with clear ferroelectric switching up to 600 °C with distinguishable ON and OFF states. The coercive field (E_c) and ON/OFF ratio decreases with increasing temperature. At 500 °C, these devices show ~1 million read cycles with a stable ON/OFF ratio above 1 for > 6 hours. The operating voltages of our devices are < 15 V even at 600 °C which is well matched and compatible with Silicon Carbide (SiC) based high temperature logic technology. Detailed temperature dependence studies and other memory device characterizations of these NVM devices will be presented in the meeting.

^aDhiren K. Pradhan and David Moore contributed equally to this work.

^{*}Authors to whom correspondence should be addressed: rolsson@seas.upenn.edu, dmj@seas.upenn.edu.

2:30 PM EL03.05.05

Combinatorial Synthesis of Highly-Oriented Ferroelectric AlScN Thin Films using Metal-Ion Synchronized High-Power Impulse Magnetron Sputtering. Jyotish Patidar¹, Sjarhei Zhuk¹, Amit Sharma², Monalisa Ghosh¹, Alexander Wiecek¹, Kerstin Thorwarth¹ and Sebastian Siol¹; ¹Empa - Swiss Federal Institute of Materials Science and Technology, Switzerland; ²Empa - Swiss Federal Laboratories for Materials Science and Technology, Switzerland

Piezoelectric micro-electro-mechanical systems (MEMS) are one of the building blocks of modern electronics and are used in many applications such as RF filters, resonators, and sensors. AlScN in wurtzite structure is one of the most promising materials for such applications due to its high-temperature stability and linear frequency response compatibility with CMOS processing.[1] Since the demonstration of ferroelectric switching in AlScN the material has gained a renewed interest for a number of alternative applications.[2]

The functional properties of AlScN, such as the piezoelectric response or the switching behavior are generally improved by high Sc contents. However, under those conditions the heterostructural nature of the alloy system and low Sc miscibility lead to a high degree of structural frustration. Hence, the synthesis of Sc-rich AlScN with high crystallinity and uniform texture remains an important challenge, especially at moderate substrate temperatures.

In this work, we present the utilization of metal-ion synchronized high-power impulse magnetron sputtering (MIS-HiPIMS) along with a combinatorial screening approach to deposit highly oriented AlScN films. A substrate bias potential is used to accelerate the ions onto the growing film. By synchronizing this potential to the metal-rich part of each HiPIMS-pulse we can tailor the ion kinetic energy of the film-forming species, while simultaneously avoiding process-gas incorporation and point-defect formation.[3]

Combinatorial libraries of AlScN are deposited with different biasing conditions as well as substrate temperatures leading to a set of roughly 300 distinct synthesis conditions. The

combinatorial libraries are then fully characterized with respect to their phase constitution, structure and composition using state-of-the-art techniques. Residual stress, piezoelectric coefficients and ferroelectric switching behavior are studied for selected samples.

We find, that applying synchronized substrate-bias potentials significantly improves the crystallinity as well as the texture of the AlScN thin films, especially at low deposition temperatures. Depending on the kinetic energy of the constituent metal-ions (i.e. Al and Sc) the residual stress in the films can be varied over a large range from 1.5 GPa (tensile) to -3.0 GPa (compressive). This is strongly correlated with a change in Sc solubility from 42 at.% to 22 at.%, respectively. In addition, we demonstrate that accelerating the ions with potentials as low as -30 V promotes growth along the substrate normal and virtually eliminates misoriented grains.

The synthesis approach demonstrated here can be transferred to many different piezoelectric and ferroelectric thin film materials. Furthermore, the ability to precisely tailor the residual stress and the potential to deposit highly-textured thin films on structured as well as temperature-sensitive substrates might open up exciting applications, e.g. for flexible electronics, in the future.

[1] M. Akiyama *et al. Advanced Materials* **2009**, 21 (5), 593-596.

[2] S. Fichtner *et al. Journal of Applied Physics* **2019**, 125, 114103.

[3] J. Patidar *et al. Surface and Coating Technology*, **2023** in press. (arXiv:2301.11183)

2:45 PM EL03.05.06

Single Crystal Epitaxial Ferroelectric Aluminum Scandium Nitride NanowiresXiaomanZhang¹, WangwangXu¹, WenJ. Meng¹ and AndrewC. Meng²; ¹Louisiana State University, United States; ²University of Missouri–Columbia, United States

Wurtzitic aluminum nitride based ferroelectrics such as aluminum scandium nitride hold significant promise for wide memory window, high on/off ratio, non-volatile memory devices for neuromorphic computing applications. However, both polycrystalline and single crystal wurtzitic aluminum nitride-based alloy thin films on a variety of substrates commonly exhibit crystallographic defects arising from mosaic disorder related to Volmer-Weber growth. We demonstrate that ultra-high vacuum reactive sputtering in a high substrate bias, low atomic flux regime results in a combination of growth and etching to achieve vertical nanowire arrays. Characterization of the nanowire arrays using X-ray diffraction and transmission electron microscopy show that the wires are epitaxial single crystals with significantly reduced mosaic spread. Using differential phase contrast scanning transmission electron microscope images, we observe nanowires consisting of single ferroelectric domains. Ferroelectric properties of the nanowires were characterized using piezoresponse force microscopy.

3:00 PM BREAK

3:30 PM EL03.05.07

Novel Ferroelectric CMOS Compatible Binary OxideZhuotongSun¹, NivesStrkalj¹, MingXiao², ZiyiYuan¹, AtifJan¹, SunilTaper¹, W.ChuckWitt¹, GiulianaDi Martino¹ and JudithL. Driscoll¹; ¹University of Cambridge, United Kingdom; ²Sun Yat-sen University, China

Interest in ferroelectric materials for processing, memory and sensing devices has been spurred by the discovery of nanoscale ferroelectricity in insulating binary oxides based on HfO₂ and ZrO₂. However, stabilizing the ferroelectric phase and achieving good ferroelectric performance in these materials is challenging because several non-ferroelectric phases have similar formation energy to the ferroelectric phase. The search for other binary oxide ferroelectrics which can be achieved by industry-friendly processes is therefore still ongoing. Here, we report the stabilization of epitaxial films of a binary oxide at temperatures below 400°C using atmospheric pressure chemical vapor deposition. In these films, strain imposed by the substrate gives rise to the spontaneous polarization evidenced by piezo-response force microscopy. Furthermore, conductive AFM shows different conductance in up and down polarized domains with a ratio over 500. Exploring ferroelectricity in binary oxide films could provide a new platform for polarization-controlled memory applications and allow combining ferroelectric and photosensitive properties for photoferroelectrics applications.

3:45 PM EL03.05.08

Experimental Observation of Polarization Screening via Free-Oxygen in Ultrathin Epitaxial Doped-HafniaMeganO. Hill¹, NivesStrkalj¹, MoritzMuller¹, Ji SooKim¹, MaximilianT. Becker¹, DibyaPhuyal^{2,1} and JudithL. Driscoll¹; ¹University of Cambridge, United Kingdom; ²KTH Royal Institute of Technology, Sweden

Ferroelectric (FE) HfO₂ is posed to overcome many of the scaling challenges that have limited the use of perovskites in ferroelectric random access memory, FE tunnel junctions, and FE field effect transistors. HfO₂ is CMOS-compatible, highly scalable, and over the past decade significant research has contributed to an improved understanding of the ferroelectric nature of this material. However, many open questions remain, particularly around the interfacial electrochemistry and effect of oxygen on ferroelectric polarization and screening. For instance, oxygen vacancies are predicted to stabilize multiple metastable ferroelectric phases in HfO₂ [1] and there is experimental evidence of field-driven oxygen migration between metal contact layers sandwiching FE HfO₂ films [2]. Despite recent advancements, understanding of the interfacial chemistry in such HfO₂-based metal-FE-metal devices is still largely unexplored. This is particularly true for ultrathin epitaxially grown HfO₂ films which offer advantages over more established amorphous/polycrystalline HfO₂ structures (ex: minimal wake up effects and better control of microstructure) [3].

In this work, hard X-ray photoelectron spectroscopy (HAXPES) studies of polarization-defined epitaxial Y-doped HfO₂ ultrathin films were conducted in order to investigate the relationship between interfacial chemistry and polarization in real device stacks. YHO devices were set to down and up polarized states and HAXPES was used to access the band position shifts and oxidation state changes in buried layers. A comparison was done on films poled using piezo-response force microscopy (PFM) and poled using sandwiched metal contact layers (LSMO and Ti/Au). By combining HAXPES analysis on sandwiched and bare films, we observe both polarization-driven oxidation occurring in the Ti/Au contact and changes in the electronic energy-level alignment at the interface. Further, X-ray energies of 1, 5.9, and 9.2 keV were utilized to probe multiple depths within the device stack, decoupling the performance at the YHO/metal and the YHO/LSMO interfaces.

HAXPES reveals a significant increase in non-lattice oxygen at the metal-ferroelectric interface in the polarization upwards condition. This reorganization of oxygen moving counter to the direction of the applied field suggests a polarization screening via free oxygen at the metal interface. Such screening effects using free oxygen species have not been experimentally reported. These results represent an important step towards understanding the role of oxygen motion and redox processes on the polarization and transport mechanisms in junctions based on ultrathin ferroelectric films.

References:

[1] K. Z. Rushchanskii, et al. "Ab initio phase diagrams of Hf–O, Zr–O and Y–O: a comparative study." *Faraday discussions* 213 (2019): 321-337.

[2] P. Nukala, et al. "Reversible oxygen migration and phase transitions in hafnia-based ferroelectric devices." *Science* 372.6542 (2021): 630-635.

[3] I. Fina and F. Sanchez. "Epitaxial ferroelectric HfO₂ films: growth, properties, and devices." *ACS Applied Electronic Materials* 3.4 (2021): 1530-1549.

SESSION EL03.06: Freestanding and 2D Materials

Session Chairs: John Heron and Morgan Trassin

Wednesday Morning, November 29, 2023

Hynes, Level 1, Room 107

8:30 AM *EL03.06.01

Free-Standing Epitaxial Oxide Nanomembranes—Opportunities and ChallengesBharatJalan; University of Minnesota, United States

With a rapidly growing family of vdW materials, the role of dielectric and metals have become more important than ever. In this talk, I will present challenges associated with the synthesis of atomically-precise three-dimensional (3D) perovskite nanomembranes followed by our group's effort to address them. Using hybrid molecular beam epitaxy that employs a metal-organic precursor, titanium isopropoxide (TTIP), to supply both Ti and oxygen (without the need for additional oxygen), epitaxial SrTiO₃ (STO) films were grown directly on a graphene layer transferred on to bulk STO substrate. Films were then successfully exfoliated and transferred onto other substrates. Using Raman spectroscopy and high-resolution X-ray diffraction, we show that the transferred STO membrane is single-crystalline and can be integrated with other vdW materials. I will also present sacrificial layer route to create oxide membranes resulting in room temperature dielectric constant of ~ 300. Finally, I will present several opportunities for materials physics and devices engineering using 3D nanomembranes.

9:00 AM EL03.06.02

High-Mobility Ferroelectric Two-Dimensional Electron Gases Based on Strain-Engineered SrTiO₃ Thin Films Ruchi Tomar¹, Tatiana Kuznetsova², Srijani Mallik¹, Luis M. Vicente-Arche¹, Maximilien Cazayous³, Roman Engel-Herbert^{2,4} and Manuel Bibes¹; ¹Unité Mixte de Physique, CNRS, Thales, Université Paris-Saclay, 91767 Palaiseau, France, France; ²Pennsylvania State University, University Park, PA 16802, USA, United States; ³Laboratoire Matériaux et Phénomènes Quantiques (UMR 7162 CNRS), Université de Paris, 75205 Paris Cedex 13, France, France; ⁴Paul Drude Institute, Berlin, Germany, Germany

Two-dimensional electron gases (2DEGs) based on the quantum paraelectric SrTiO₃ display fascinating properties such as large electron mobilities, superconductivity and efficient spin-charge interconversion owing to their Rashba spin-orbit coupling.¹⁻³ However, such 2DEGs have almost exclusively been generated in SrTiO₃ single crystals, with the few attempts to replace crystals by heteroepitaxial SrTiO₃ thin films leading to low carrier mobilities. This is limiting the potential to integrate SrTiO₃ 2DEGs in future devices as well as the possibility to introduce additional functionalities specific to SrTiO₃ thin films, such as strain-induced ferroelectricity. Here, we use oxide molecular beam epitaxy to grow high quality strain-engineered SrTiO₃ films that are ferroelectric up to 170 K. We then generate a 2DEG by sputtering a thin Al layer and demonstrate an increase in both the low and room temperature mobilities by up to factor of four compared to earlier literature. Furthermore, through Raman spectroscopy and magneto-transport measurements, we show that the ferroelectric character is retained after 2DEG formation. These results thus qualify our samples as ferroelectric 2DEGs up to temperatures well above previous results based on Ca-SrTiO₃ substrates (~30 K)⁴, opening the way towards ferroelectric 2DEGs operating at room temperature.

Références :

M. Bibes, J. E. Villegas, and A. Barthelemy, Adv. Phys. 60, 5 (2011).

H. Y. Hwang, Y. Iwasa, M. Kawasaki, B. Keimer, N. Nagaosa, and Y. Tokura, Nat. Mater. 11, 103 (2012).

S. Varotto, A. Johansson, B. Göbel, L. M. Vicente-Arche, S. Mallik, J. Bréhin, R. Salazar, F. Bertran, P. Le Fèvre, N. Bergeal, J. Rault, I. Mertig & M. Bibes, Nat. Commun., 13, 6165 (2022)

C. W. Rischau, X. Lin, C. P. Grams, D. Finck, S. Harms, J. Engelmayer, T. Lorenz, Y. Gallais, B. Fauqué, J. Hemberger, and K. Behnia, Nat Phys, 13, 643 (2017).

9:15 AM EL03.06.03

Buffer-Free Production of Single-Crystalline Complex-Oxide Membranes and Their Applications Xinyuan Zhang, Min-Kyu Song, Celesta S. Chang, Sangho Lee and Jeehwan Kim; Massachusetts Institute of Technology, United States

There have been serious efforts to develop a universal method for producing freestanding epitaxial membranes, which would allow for the creation of artificial heterostructures with interfacing structurally and chemically incompatible materials. In particular, a combination and match of complex-oxide membranes that exhibit unique electronic, photonic, and magnetic properties is expected to enable a wide range of innovative applications. Recent developments in graphene-based remote epitaxy and mechanical lift-off techniques have allowed for the generation of a variety of freestanding complex-oxide membranes, including perovskite SrTiO₃, spinel CoFe₂O₄, and garnet Y₃Fe₅O₁₂. However, it is particularly difficult to form an atomically clean graphene surface on growth substrates of complex-oxides in a scalable and controlled manner, which significantly limits the manufacturing of large-area oxide membranes of high quality. In addition, typical 2D materials, including graphene, are easily damaged during plasma processing in an oxygen environment, which is commonly required for complex-oxide film growth.

Here, alternative lift-off methods are introduced to expand the material spectrum of complex-oxide thin films that can be released from substrates and integrated onto platforms of interest. Firstly, chemical lift-off is used to obtain a single-crystalline BaTiO₃ (BTO) membrane by dissolving the water-soluble interlayer of Sr₃Al₂O₆, which is otherwise hard to be produced by remote epitaxy due to requirement of high growth temperature. It is then transferred onto a complementary metal-oxide-semiconductor (CMOS) platform. This provides an efficient route to fabricate capacitive memory devices with superior device performance, such as a noticeably large memory window and low energy consumption due to outstanding properties of single-crystalline BTO. Also, such BTO-based memory components integrated onto a silicon wafer ensure their great CMOS compatibility. Next, buffer-free mechanical lift-off is demonstrated to exfoliate a Pb(Mg_{1/3}Nb_{2/3})O₃-PbTiO₃ membrane with atomic precision and to develop pyroelectric devices with ultra-broad band response and significantly improved detectivity compared to the clamped counterparts.

9:30 AM BREAK

SESSION EL03.07: Multiferroics I
Session Chairs: John Heron and Morgan Trassin
Wednesday Morning, November 29, 2023
Hynes, Level 1, Room 107

10:00 AM *EL03.07.01

Domain Walls in Multiferroics and Multiferroic Domain Walls Manfred Fiebig; ETH Zurich, Switzerland

A reason for the interest in multiferroics is that magnetic and electric orders do not simply exist side by side, but exhibit "added value" in the form of magnetoelectric interactions and functionalities between the ordered states. Likewise, in a ferroic material, regions with different orientation of the order parameter, the domains, do not simply exist side by side, but they exhibit new phases and properties in the domain walls. Because of their discontinuous, confined, and topological nature, domain walls exhibit functional states that are not possible in the bulk. Continuing this line of thought, one should expect domain walls in multiferroics to be a particularly rich source of novel phenomena. Here one must distinguish between (i) "domain walls in multiferroics", where only the ferroelectric (or magnetic) order is considered so that little is learned about the multiferroic state, and (ii) "multiferroic domain walls" where the ferroic phase coexistence of the wall itself is of interest. The latter are rarely studied, and I will discuss some of their intriguing features in my talk. Specifically, I will report on the continuous transfer of a multiferroic order between a bulk and a wall state, novel types of domain walls in multiferroic thin films, and various examples of multiferroic domain walls in a non-multiferroic environment.

10:30 AM EL03.07.02

Vertically Aligned Nanocomposites and Interfacial Coupling of Multiferroic LuFeO₃ and Magnetic Co_xFe_{3-x}O₄ Thin Films Eunsoo Cho and Caroline A. Ross; Massachusetts Institute of Technology, United States

Nanocomposite thin films composed of two or more ferroic materials are particularly attractive for the development of energy-efficient, high-speed memory and logic devices. This is because such heterostructures provide a platform to incorporate multiple functionalities and utilize the interaction at the interface between different phases to enable magnetoelectric switching. For example, we showed voltage-controlled magnetic properties of a Sr(Co,Fe)O_{3-δ}-Co₃O₄ nanocomposite by ionic liquid gating [1].

Here, we investigated vertically aligned nanocomposite thin films grown using pulsed laser deposition, consisting of pillars of spinel Co_xFe_{3-x}O₄ and/or rocksalt CoO phases embedded in a matrix phase of perovskite LuFeO₃. LuFeO₃ is a rare earth orthoferrite with an orthorhombically distorted perovskite structure, and is a canted antiferromagnet with concurrent ferroelectricity (thus multiferroicity) depending on cation stoichiometry [2]. Spinel Co_xFe_{3-x}O₄ has a strong antiferromagnetic superexchange interaction between cations on the tetrahedral and octahedral sites, with Fe-rich compositions showing high temperature ferrimagnetic behavior and notable magnetoelastic properties. Lastly, rocksalt CoO is a G-type antiferromagnet.

Pulsed laser deposition yielded two-phase (perovskite and spinel) or three-phase (perovskite, spinel, and rocksalt) epitaxial nanocomposites on SrTiO₃ substrates, depending on which combination of targets was used and on the deposition temperature and oxygen pressure. For example, alternating ablation from Lu_{0.8}FeO_{3-δ} and Co₃O₄ targets produced CoO and Fe₃O₄ pillars embedded in Fe-rich LuFeO₃, whereas alternating ablation from Lu_{1.4}FeO_{3+δ} and CoFe₂O₄ targets resulted in pillars of Co_{1.3}Fe_{1.7}O₄ in a matrix of Fe-rich LuFeO₃. The structure and chemistry of the films are characterized in detail via x-ray diffraction and atomically resolved scanning transmission electron microscopy techniques. The perovskite phase preferentially contains Fe whereas the Co segregates to the spinel or rocksalt phase, especially when a Co₃O₄ target is used.

Magnetization-magnetic field hysteresis measurements revealed the correlation between magnetic properties and growth conditions. For instance, Lu_{0.8}FeO_{3-δ}-Co_{1.3}Fe_{1.7}O₄ films with about 37% Co_{1.3}Fe_{1.7}O₄ pillars with ~15 nm diameter had a saturation magnetization of 100 kA/m and coercivity of 450 Oe. By cooling the composites from 360 °C in a field of 10 kOe, an exchange coupling between antiferromagnetic Lu_{0.8}FeO_{3-δ} and ferrimagnetic Co_{1.3}Fe_{1.7}O₄ was established with an exchange bias of 110 Oe at room temperature. The magnetoelectric coupling in these two- and three-phase epitaxial nanocomposite thin films of LuFeO₃, Co_xFe_{3-x}O₄ and CoO will be described.

[1] Cho et al., ACS Appl. Nano Mater. 5 14646 (2022)

[2] Cho et al., Adv. Electron. Mater. 2300059 (2023)

10:45 AM EL03.07.03

Low-Temperature Epitaxial BiFeO₃ Thin Films on Bismuth Substituted Metal Perovskite Sajid Husain¹, Isaac Harris², Peter Meisenheimer², Piush Behera^{1,2}, Tae Y. Kim², Didier Perrodin¹, Lane W. Martin^{1,2}, Zhi Yao¹ and Ramamoorthy Ramesh^{1,2,3}; ¹Lawrence Berkeley National Laboratory, United States; ²University of California, Berkeley, United States

Bismuth Ferrite (BiFeO₃, BFO) has attracted considerable attention as a promising candidate for magnetoelectric spin-orbit coupled logic-in-memory compute elements. As a model system, epitaxial BFO thin films have been deposited typically at relatively high temperatures, (~650-800°C); somewhat higher than the maximum temperatures desired for direct integration of materials with silicon-CMOS platforms. Here, we circumvent this problem by growing La-substituted BiFeO₃ (La_{1-x}BiFeO₃, LBFO) thin films at 450°C (which is compatible with silicon-CMOS integration) on epitaxial bismuth-substituted a metallic perovskite BaPbO₃ (BaPb_{1-x}Bi_xO₃, BPBO) electrode. BPBO is recently reported to exhibit large spin Hall effect for spintronic applications. Using symmetric and asymmetric X-ray diffraction, LBFO is found to be fully relaxed on the BPBO electrode. Notwithstanding the large lattice mismatch between the LBFO, BPBO, and SrTiO₃ substrates, all the deposited layers in the heterostructure are well ordered. Piezoresponse force microscopy reveals a 180° phase reversal and suggests robust piezoelectric behavior for the LBFO. The ferroelectric nature of the LBFO is further evident from polarization-electric field hysteresis loops measurements. Current-voltage, pulsed switching, fatigue, and retention measurements follow the characteristic behavior of high-temperature grown LBFO, where SrRuO₃ typically serves as the metallic electrode. These results provide a possible route for realizing epitaxial multiferroics on complex oxides buffer layers at low temperatures and open the door for potential silicon-CMOS integration.

11:00 AM *EL03.07.04

Spin-Induced Multiferroicity in 2d Transition-Metal-Halides Silvia Picozzi; Consiglio Nazionale delle Ricerche, Italy

Two-dimensional multiferroics with large magnetoelectric coupling may open interesting avenues in the context of multifunctional systems. Here, we study a class of spin-chirality-driven van der Waals multiferroic monolayers, such as transition metal halides, by combining first-principles calculations with the generalized spin-current model. The recent reports of multiferroicity in NiI₂ layers [Q. Song et al, Nature **602**, 601 (2022)], obtained via a joint theory-experiments approach down to the single-layer limit, show the potentiality of cross-coupling phenomena in van der Waals magnets. Another example is represented by vanadium dihalide-monolayers, featuring 120-degree frustrated magnetic structures which develop on the underlying triangular lattice and show competing spin-spiral planes spanning the (001) and (100) crystalline planes. The non-collinear spin configurations induce a ferroelectric polarization which is perpendicular to the spin-spiral plane, switched by the spin-chirality change and whose magnitude is not only determined by the strength of the atomic spin-orbit coupling of the halogen anion, but also affected by structural properties.

11:30 AM EL03.07.05

Subnanosecond Reconfiguration of Ferroelectric Domains in Bismuth Ferrite Burak Guzelurk; Argonne National Laboratory, United States

Domain switching is crucial for achieving desired functions in ferroic materials that are used in various applications. Fast control of domains at subnanosecond timescales remains a challenge despite its potential for high-speed operation in random access memories, photonic, and nanoelectronic devices. In our recent work [1], we show that ultrafast laser excitation can transiently melt and reconfigure ferroelectric stripe domains in multiferroic bismuth ferrite on a timescale faster than 100 ps. This dynamic behavior is visualized by a novel approach of picosecond and nanometer-resolved X-ray diffraction. In addition, we developed and used time-resolved X-ray diffuse scattering to track the transient response of the domain walls. The disordering of stripe domains arises from the screening of depolarization fields by photogenerated carriers resulting in the formation of charged domain walls which is further supported by phase field simulations. Furthermore, the recovery of disordered domains exhibits subdiffusive growth on nanosecond timescales, with a nonequilibrium domain velocity reaching up to 10 m/s. These findings present a new approach to image and manipulate ferroelectric domains on subnanosecond timescales, which can be further extended into other photoferroic systems to modulate their electronic, optical, and magnetic properties beyond GHz frequencies. This approach could pave the way for high-speed ferroelectric data storage, computing and photonic applications in a range of photoferroics, and, more broadly, defines new approaches for visualizing the non-equilibrium dynamics of heterogeneous and disordered materials.

[1] B. Guzelurk et al. Advanced Materials (2023) - DOI: 10.1002/adma.202306029

SESSION EL03.08: Multiferroics II
Session Chairs: Johanna Nordlander and Bhagwati Prasad
Wednesday Afternoon, November 29, 2023
Hynes, Level 1, Room 107

1:30 PM *EL03.08.01

Ultra-Low-Voltage, Beyond CMOS Microelectronics Ramamoorthy Ramesh; Rice University, United States

Despite ever-improving computing efficiency, information technology (IT) represents the fastest growing energy consumer and will have significant implications for U.S. energy consumption. This impending cliff threatens the nation's ability to solve important problems across science, technology, national security, and energy. Without improvements in computing efficiency, the explosion of the Internet of Things (IoT) and artificial intelligence (AI) applications will exponentially increase energy consumption. A complete rethinking of how computing is performed today is needed to develop the next-generation of beyond-CMOS microelectronics. Our scientific mission is built on a core guiding principle that a significant opportunity exists for use-inspired basic science to enable highly energy efficient computing by exploiting correlated phenomena and consequently lowering the operating voltage. Orders of magnitude improvement in energy efficiency are possible by exploiting correlations (electronic charge/spin and dipolar). We aim to design and manipulate this energy barrier to specifically reduce the operating voltage substantially below what is achievable by today's CMOS technology. This fundamental physics approach to solving systems-level techno-economic problems can lead to dramatically lower energy consumption, in addition to a completely new hierarchy of logic-in-memory information technology building blocks.

2:00 PM EL03.08.02

Understanding and Optimizing Magnetoelectric Switching in BiFeO₃ Natalya Fedorova¹, Dmitri Nikonov², John Mangeri¹, Hai Li², Ian Young² and Jorge Iniguez^{1,3}; ¹Luxembourg Institute of Science and Technology, Luxembourg; ²Intel Corporation, United States; ³University of Luxembourg, Luxembourg

Magnetoelectric multiferroics are materials that simultaneously show magnetic and electric orders. Interest in them largely originates from the possibility of affecting one order using the stimulus that usually controls the other, offering great potential for development of multifunctional devices. BiFeO₃ is among the most exciting representatives of this family because it displays both orders at room temperature. Moreover, a deterministic reversal of magnetization by an electric field was experimentally observed in BiFeO₃ films by J. T. Heron et al. [1]. It has been proposed that this magnetoelectric switching is the result of a peculiar polarization switching process that occurs in two steps: a 109° out-of-plane polarization rotation followed by a 71° in-plane rotation. However, the origin of such two-step polarization reversal is still not well understood, which hampers its optimization (faster switching at a smaller coercive field).

In this work we combine density functional theory (DFT), a phenomenological Landau model and the Landau-Khalatnikov time-evolution equation (LKE) [2] to elucidate the origin of the two-step polarization switching process in BiFeO₃. First, we introduce the simplest Landau-like potential for BiFeO₃ and ensure that it accurately reproduces the DFT energies and distortion amplitudes for a set of relevant structural polymorphs of BiFeO₃ [3]. Then, we extend our model by introducing additional constraints which account for the presence of the substrate and multidomain configuration observed experimentally in BiFeO₃ films. We then solve this model using the LKE to investigate the role of the introduced constraints on ferroelectric switching. We are able to reproduce the two-step polarization switching in multidomain system, reveal its physical underpinnings, and identify potential strategies to optimize the switching characteristics.

Work funded by the Semiconductor Research Corporation and Intel via Contract No. 2018-IN-2865. We also acknowledge the support of the Luxembourg National Research Fund through Grant No. C21/MS/15799044/FERRODYNAMICS and the European Union's Horizon 2020 research and innovation programme under the Marie Skłodowska-Curie grant agreement SCALES-897614.

References:

[1] J. T. Heron, J. L. Bosse, Q. He, Y. Gao, M. Trassin, L. Ye, J. D. Clarkson, C. Wang, Jian Liu, S. Salahuddin, D. C. Ralph, D. G. Schlom, J. Iniguez, B. D. Huey and R. Ramesh, Deterministic switching of ferromagnetism at room temperature using an electric field. Nature 516, 370 (2014).

[2] A. Umantsev, Field theoretic method in phase transformations. Springer, New York (2012).

2:15 PM EL03.08.03

Nanoscale Multiferroic Properties for Neuromorphic Computing Applications Danilo G. Barrionuevo Diestra, Patricia Gierbolini-Santos, Edward Hickey-Figueroa, Eric Sanchez-Ayala and Cynthia Rodriguez-Cruz; University of Puerto Rico at Cayey, United States

Significant advancements in intelligent tasks, such as artificial intelligence, big data analytics, autonomous vehicles, and voice recognition, have presented increasingly demanding requirements for computing speed and power consumption. Addressing these demands, a neuromorphic computing system emerges as a viable solution. Moreover, a neuromorphic computing system possesses the ability to autonomously learn and execute tasks by engaging in its environment. Harnessing the potential applications of tunneling in the assembly of neuromorphic computation, the integration of multiferroic tunnel junctions offers a promising opportunity to combine the respective advantages of swift, low-power electrical write operations and non-destructive magnetic read operations. This amalgamation leads to the realization of four-state logic, thereby propelling the field forward. A single-phase multiferroic material, Pb(Zr_{0.53}Ti_{0.47})_{0.60}(Fe_{0.5}Ta_{0.5})_{0.40}O₃ (PZTFT), shows promise as a tunnel barrier in multiferroic tunnel junctions. To investigate the impact of thickness on electrical and magnetic properties across a spectrum ranging from thicker to ultrathin films, we conducted film growth experiments employing pulsed laser deposition (PLD) techniques, depositing PZTFT films with thicknesses ranging from 7 to 80 nm on (001) LSMO/(LaAlO₃)_{0.3}(Sr₂AlTaO₆)_{0.7} (LSMO/LSAT) substrates. Remarkably, we observed well-saturated ferroelectric loops in PZTFT films, exhibiting a remanent polarization of 32, 25, and 10 mC/cm² for films with thicknesses of 80, 50, and 20 nm, respectively. Additionally, an enhanced saturated magnetization (M_s) was observed with increasing PZTFT layer thickness in PZTFT/LSMO structures. At 300 K, the average M_s values for PZTFT/LSMO heterostructures were 33, 25, and 15 emu/cm³ for thicknesses of 80, 50, and 20 nm, respectively. This increase in magnetization can be attributed to the interface effect between the PZTFT and LSMO layers. Piezo force microscopy measurements conducted on ultrathin 7 nm PZTFT films displayed clear and reversible out-of-plane phase contrast above ± 3 V, indicating the ferroelectric nature of these ultra-thin films. Furthermore, magnetic force microscopy revealed magnetic stripe domains in the 7 nm ultrathin PZTFT films. The impact of PZTFT film thickness on temperature-dependent dielectric and transport properties will be addressed. Notably, our most significant finding is the retention of multiferroic properties in 7 nm ultrathin PZTFT films at room temperature, highlighting their potential as single-phase barriers in multiferroic tunnel junction devices. These devices demonstrate four resistance states: two electroresistance states and two magnetoresistance states, enabling the achievement of multilevel resistance states. This discovery underscores the possibility of fine-tuning their properties at the nanometer scale, thereby opening new avenues for technological applications in nanoelectronics, particularly in the realm of multiferroic tunnel junctions for next-generation nonvolatile memory devices.

2:30 PM BREAK

SESSION EL03.09: Oxide Electronics I
Session Chairs: Johanna Nordlander and Bhagwati Prasad
Wednesday Afternoon, November 29, 2023
Hynes, Level 1, Room 107

3:30 PM *EL03.09.01

KTaO₃ Two-Dimensional Electron Gases: Spin-Orbit Coupling, Superconductivity and the Introduction of Ferroic Orders Manuel Bibes; CNRS/Thales, France

Two-dimensional electron gases based on KTaO₃ (KTO) have recently emerged as an exciting new platform for oxide electronics and spintronics since they possess a large low-temperature mobility, a large Rashba spin-orbit coupling and are superconducting with a critical temperature of about 2 K for (111) oriented samples. The 2DEGs can be defined from KTO single crystals substrates by growing on top a perovskite film or a reactive metal such as Eu or Al (which oxidizes and creates oxygen vacancies in the KTO, doping it with electrons). We will shed light on the physics of this system through a combination of advanced measurements including ARPES, resonant microwave transport, harmonic transport and electron tunneling. We will finally discuss the role of the magnetic vs nonmagnetic overlayer materials and how to introduce ferroelectricity in the system.

4:00 PM EL03.09.02

Disentangling the Roles and Length Scales of the Crystal Lattice, Electronic and Magnetic Degrees of Freedom in Correlated Electron Materials Alexandru Georgescu; Indiana University Bloomington, United States

We present new phenomenological descriptions of electronic phase transitions in correlated electron materials, with a focus on metal-insulator transition (MIT) materials. First, we show how to build and understand a computational energy landscape, disentangling the role of electronic and crystal lattice symmetry breaking in the MIT of rare earth nickelates RNiO₃, with R a rare-earth metal, using dynamical mean field theory [1]. We find that the electron-lattice coupling is key to stabilizing the insulating state. This theory is general, and may be applied to other materials displaying a simultaneous electronic and crystal lattice phase transition. Then, by studying multiple superlattices including rare-earth nickelates (NdNiO₃/NdAlO₃ [1], NdNiO₃/SmNiO₃ [2,3] and NdNiO₃/LaAlO₃/SmNiO₃ [4]) we clarify the interplay of the crystal lattice, electronic symmetry breaking, and magnetic degrees of freedom and the length scales of the order parameter propagation throughout the transition. We find that the electronic order parameter characterizing the transition has a dominant role in its propagation. While the magnetic order parameter is subsidiary to the electronic order parameter in the bulk, the second order nature of the magnetic transition leads to longer length scales for the magnetic degrees of freedom than that of the MIT.

[1] A. B. Georgescu, Andrew J. Millis, 'Quantifying the role of the Lattice in Metal-Insulator Phase Transitions', Communications Physics, 5, 135 (2022)

[2] Claribel Dominguez Ordonez, A. B. Georgescu, Bernat Mundet, Yajun Zhang, Jennifer Fowlie, Alain Mercy, Sara Catalano, Duncan Alexander, Philippe Ghosez, Antoine Georges, Andrew J. Millis, Marta Gibert, and Jean-Marc Triscone 'Length-scales of interfacial coupling between metal-insulator phases in oxides', Nature Materials, 19, 1182-1187, August 2020

[3] C. Dominguez, J. Fowlie, A. B. Georgescu, B. Mundet, N. Jaouen, M. Viret, A. Suter, A. J. Millis, M. Gibert, J. M. Triscone, 'Coupling of Magnetic Phases at Nickelate Interfaces', In Press at Physical Review Materials, 2023, arXiv:2211.06811

[4] L. Varbaro, B. Mundet, C. Dominguez, J. Fowlie, A. B. Georgescu, L. Korosec, D. Alexander, J.M. Triscone, 'Electronic coupling of metal-insulator transitions in nickelate based heterostructures', Advanced Electronic Materials, 2201291, (2023)

4:15 PM *EL03.09.03

Structure-Property Relations at Charged Interfaces in Ferroic Oxides Dennis Meier; Norwegian University of Science and Technology (NTNU), Norway

Oxide materials exhibit a broad range of tunable phenomena, including magnetism, multiferroicity, and superconductivity. Oxide interfaces are particularly intriguing, giving a new dimension to property engineering of functional materials^[1]. The low local symmetry at the interfaces, combined with their sensitivity to electrostatics and strain, leads to unusual physical effects, offering amazing opportunities for fundamental and applied research.

In my talk, I will discuss the unique electronic properties that arise at natural and artificially designed charged interfaces in ferroelectric and multiferroic oxides. To give an overview and demonstrate how structural, electric, and compositional degrees of freedom at such interfaces control the material's behavior, I will present three examples: (i) ferroelectric domain walls in hexagonal manganite single crystals^[2], (ii) grain boundaries in ferroelectric ErMnO₃ polycrystals^[3,4], and (iii) epitaxial heterointerfaces in multiferroic (LuFeO₃)₉/(LuFe₂O₄)₁ superlattices. To characterize the different types of interfaces, we perform correlated microscopy measurements, combining scanning probe microscopy, electron microscopy, and atom probe tomography. The imaging experiments provide new insight into the atomic-scale structure and chemical composition at charged oxide interfaces, clarifying the key role polar discontinuities and point defects play for their emergent physical properties.

References

[1] D. Meier and S. M. Selbach, Nature Rev. Mater. 7, 15 (2022)

[2] K. A. Hunnestad, et al., Nature Commun. 13, 4783 (2022)

[3] J. Schultheiss, et al., Adv. Mater. 34, 2203449 (2022)

[4] K. A. Hunnestad, et al., arXiv:2212.07924 (2023)

8:00 PM EL03.10.01

High-Pressure Synthesis of Ferroelectric Y-Doped HfO₂ Takanori Mimura, Ayaka Shimazu, Naoki Noda and Yoshiyuki Inaguma; Gakushuin University, Japan

The discovery of ferroelectric HfO₂-based films by Börscke et al. was a great surprise since these materials were used as high-k gate dielectrics in Si-based complementary metal-oxide-semiconductor (CMOS) devices. Only the paraelectric monoclinic (*P2₁/c*), tetragonal (*P4₂/nmc*), cubic (*Fm-3m*), orthorhombic I (*Pbca*), and orthorhombic II (*Pnma*) phases exist in the equilibrium pressure-temperature phase diagram of HfO₂. On the other hand, the origin of the ferroelectric phase is the metastable orthorhombic *Pca2₁* phase which is usually stabilized by the film thickness effect due to surface energy. Therefore, the ferroelectricity was observed in thin HfO₂ films with a thickness below ~30 nm. This implies that the material properties include thin film-specific effects such as surface energy and strain effects, and the fundamental characteristics are unknown. To understand essential properties, the synthesis of ferroelectric bulk HfO₂ is indispensable. Recently, Mimura *et al.*, fabricated 1 μm-thick ferroelectric 7% YO_{1.5}-93% HfO₂ films, which suggests that ferroelectric bulk HfO₂ could be synthesized using Y doping. After that, Xu *et al.*, synthesized a 12% YO_{1.5}-HfO₂ single crystal with a *Pca2₁* structure using a laser-diode-heated floating zone technique. In this study, we demonstrate the high-pressure synthesis of ferroelectric bulk YO_{1.5}-HfO₂ using high-pressure synthesis.

Starting materials, Y₂O₃ and HfO₂ powders with compositions of *x*% YO_{1.5}-(1-*x*)% HfO₂ (*x* = 0, 3, 5, 7, 12) were mixed using an agate mortar. High-pressure synthesis was carried out by the following two routes. 1.) The mixed powders were pressed into pellets and calcined at 1500°C for 10 h in air. Then, the calcined pellets were ground into powder. The powders were allowed to treat in a TRY cubic multi-anvil-type high-pressure apparatus (NAMO 2001) and then quenched to room temperature. 2.) The mixed powders from starting materials were directly allowed to treat in a high-pressure apparatus. The pressure, temperature, and holding time were at 3-7.7 GPa, 800-1400°C, and for 30 min, respectively for each route. To identify the crystal phases, XRD *2θ-θ* scanning (X'Pert³ Powder, PANalytical, λ = 0.154 nm) was performed.

For route 1, the calcined samples before high-pressure synthesis showed the monoclinic and cubic phases in *x* = 3-12, suggesting consistency with the phase diagram of the Y₂O₃:HfO₂ system. After high-pressure synthesis, the orthorhombic phase *Pca2₁* or *Pbca* was obtained. With an increase in the pressure and temperature, the yield of the phase increased, but the maximum was 28.9 wt% in 5% YO_{1.5}-95% HfO₂ treated at 7.7 GPa, 1300°C. The yield of the cubic phase did not change much before and after the high-pressure synthesis, suggesting that only the lower-density monoclinic phase transforms into the higher-density phase while the highest-density cubic phase does not at high pressure. For route 2, the orthorhombic phase was obtained with > 70 wt%. These results suggest that the high-pressure synthesis method is one of the methods to stabilize bulk HfO₂-based ferroelectrics. The results of second harmonic generation (SHG) measurements to confirm the non-centrosymmetric ferroelectric phase will be discussed at the conference.

8:00 PM EL03.10.02

Correlation Between Reduced Dielectric Loss and Charge Migration Kinetics in NdFeO₃- Modified Ba_{0.7}Sr_{0.3}TiO₃ Ceramics Lakhwant Singh, Surinder Singh and Anumeet Kaur; Guru Nanak Dev University, India

We report here a significant reduction in the dielectric loss at room temperature from 0.149 to 0.027 in the composite of (NdFeO₃)_{0.1}-(Ba_{0.7}Sr_{0.3}TiO₃)_{0.9} as compared to the undoped Ba_{0.7}Sr_{0.3}TiO₃ and correlates with the charge compensation due to the ionic substitutions for both A site (Nd_{Ba}) and B (Fe_{Ti}) site generated excess electrons, localized hole states and robust oxygen vacancies (V_O) along with different cationic oxidation states. The V_O mediated F center charge transfer mechanism i.e., bound magnetic polaron behaviour and defect complex generated between acceptors and ionized V_O reduce electrical conductivity and loss factor. The presence of weak ferromagnetism in the M-H loop reconfirms the F center exchange mechanism in mixed phase symmetry. The activation energy calculated from impedance spectroscopy, electrical modulus and electrical conductivity analysis supports the presence of doubly ionized V_O. Further, density functional theory based first principle calculation manifests that the impurity induced depopulation of valence band edge electrons into a single spin up channel which distorts TiO₆ octahedra with fluctuating bond length and Ti 3d_g orbital splitting observed in decomposed density of states for accommodating excess electrons. These trapped and accommodated electrons reduce the effective electron concentration which in turn decreases the electrical conductivity and loss factor.

8:00 PM EL03.10.03

Characterization of Ferroelectric Switching Properties for (Al,Sc)N Films with Various Composition Shinnosuke Yasuoka¹, Kazuki Okamoto¹, Takao Shimizu^{2,3} and Hiroshi Funakubo¹; ¹Tokyo Institute of Technology, Japan; ²National Institute for Materials Science, Japan; ³Precursory Research for Embryonic Science and Technology, Japan

Ferroelectric wurtzite-(Al,Sc)N is promising for future ferroelectric devices because of its superior properties, including large remanent polarization that is almost 5 times larger than that of HfO₂-based ferroelectrics. Therefore, (Al,Sc)N film has been investigated by many researchers after the experimental demonstration of its ferroelectricity in 2019 [1-3]. Nevertheless, the investigation of switching kinetics of ferroelectric to elucidate the physical properties of this material has been still limited, although it is essential not only to understand the fundamental properties, but also to promote the development of next-generation ferroelectric devices.

In this study, we investigated the polarization switching kinetics of (Al,Sc)N thin films with different Sc/(Al+Sc)N. The pulse-width dependent polarization switching was conducted and analyzed in term of a phenomenological and macroscopic approach for the (Al_{0.9}Sc_{0.1})N, (Al_{0.8}Sc_{0.2})N, and (Al_{0.7}Sc_{0.3})N films. The switching characteristics obtained by switching test with various pulse width were in good agreement with the KAI model [4]. The fitting parameter, the Avrami index *n*, were approximately 2, indicating the bidimensional in-plane propagation of the switched domains as reported for typical oriented ferroelectric thin films [5,6]. The activation field, *E_a*, which is evaluated from the time dependent current (*I-t*) curve through the switching time, *t_{sw}* based on Merz's law, which is obtained from the current-dependent on the film composition. That of (Al_{0.8}Sc_{0.2})N was slightly smaller than those of the films with other composition [7]. This may be due to differences in fundamental switching characteristics, which is significantly affected by composition and/or crystal quality.

This work was partly supported by the project of MEXT Initiative to Establish Next-generation Novel Integrated Circuits Centers (X-NICS) (JPJ01438) and MEXT Program: Data Creation and Utilization Type Material Research and Development Project (JPMXP1122683430). This work was also partly supported by the Japan Society for the Promotion of Science (JSPS) KAKENHI Grant No. 21H01617, 22K18307, and 22K20427; and by JST PRESTO Grant Number JPMJPR20B3, Japan.

[1] Fichtner, *et al.*, J. Appl. Phys., **125**, 114103 (2019).

[2] Yasuoka *et al.*, J. Appl. Phys., **128**, 114103 (2020).

[3] Yasuoka *et al.*, ACS Appl. Electron. Mater., **4**, 5165 (2022).

[4] Ishibashi, J. Phys. Soc. Japan **31**, 506 (1971).

[5] Li *et al.*, Appl. Phys. Lett. **86**, 1 (2007)

[6] Fichtner *et al.*, Jt. Conf. IEEE (IFCS-ISAF), Proc., **5** (2020)

[7] Merz, Phys. Rev. **95**, 3 (1954)

8:00 PM EL03.10.04

Temperature-Composition Phase Diagram and Strain-Driven Domain Decomposition in the Ba_{1-x}Ca_xTiO₃ Thin Film System Aiden M. Ross, Jacob A. Zorn, Bo Wang and Long-Qing Chen; The Pennsylvania State University, United States

The macroscale properties of a ferroelectric crystal can be manipulated by controlling its mesoscale domain structure. Here, we performed a systematic theoretical analysis of Ba_{1-x}Ca_xTiO₃ (0 ≤ *x* ≤ 0.25) ferroelectric thin films on SmScO₃ substrates using thermodynamics and phase-field simulations to computationally establish the multi-phase/multi-domain composition-temperature phase diagrams. We identified a strain-driven decomposition of the *a₁a₂ - c/a* ferroelectric domains at room temperature similar to those reported recently in Pb_{0.8}Sr_{0.2}TiO₃ thin films. The strain-driven domain decomposition is shown to extend into the low temperature regime, wherein a distinct decomposition phenomenon between orthorhombic and rhombohedral phases is observed. Our results provide the theoretical guideline for experimentalists to compositionally and mechanically manipulate phase transitions and domain formation and optimize electromechanical responses in ferroelectric thin films of perovskite oxide solid solutions.

8:00 PM EL03.10.05

Exploring the Impact of Sr(Zr,Ti)O₃ Buffer Layers for Controlling Domain Structure of Ferroelectric Thin Films. Keisuke Ishihama¹, Kazuki Okamoto¹, Masanori Kodera^{1,2}, Tomohide Morikawa¹, Takao Shimizu^{1,3,4} and Hiroshi Funakubo¹; ¹Tokyo Institute of Technology, Japan; ²National Institute of Advanced Industrial Science and Technology, Japan; ³National Institute for Materials Science, Japan; ⁴Precursory Research for Embryonic Science and Technology, Japan

In recent years, ferroelectrics have been used as important components in many devices such as nonvolatile memory, sensors, and energy harvesters. This study focuses on ferroelectric thin films with domain structures affected by the strain induced from the substrate. It is known that the misfit strain caused by the difference in lattice constants between the substrate and ferroelectric thin film is important in controlling the stress in epitaxial thin films. However, there are limits to the range of lattice constants that can be achieved with single-crystal substrates. In this study, Sr(Zr,Ti)O₃ solid solution (SZTO), which has cubic-like structure and a wide lattice parameter selection range of 0.39–0.41 nm, was employed as a new buffer layer to overcome this problem.^[1] It can be expected to change the lattice constant continuously and control the amount of strain precisely by using SZTO with various compositions as a buffer layer. We prepared SZTO buffer layers on (100) LSAT substrates and Pb(Zr,Ti)O₃ (PZT) films on them by pulsed laser deposition (PLD). XRD 2θ - θ measurement results indicated that buffer layer lattice parameters could be effectively manipulated by altering Zr content of SZTO. This study reveals a strong dependence of crystal structure and thickness in SZTO films with different composition, and the domain structure of PZT films is found to be significantly influenced by the lattice constant of the buffer layer. These findings underline the potential of SZTO in controlling lattice constants and strain in ferroelectric thin films.

8:00 PM EL03.10.06

Electric Control of Spin Supercurrents in Hybrid Rashba Structures Qiaodong Sun¹, Adrian Ionescu¹, Nadia Stelmashenko¹, Leyla C. Arslan^{1,2} and Jason W. Robinson¹; ¹University of Cambridge, United Kingdom; ²Gebze Technical University, Turkey

The digital economy ever-increasingly requires denser, faster and more energy-efficient data processing, but heat-dissipating ohmic losses limit further performance improvements. Superconducting electronics offers the potential to enhance magnetic memory and logic performance because readout can be achieved with record-low heat dissipation. Furthermore, intrinsic or interfacial spin-orbit coupling (SOC) can enable a thin-film superconductor to exceed the paramagnetic limit. For Rashba-type SOC, theory indicates that the superconducting thermodynamic properties of a finite-size thin film are strongly sample-size dependent due to the creation of edge states: for example, for a geometrically anisotropic thin film superconductor, the critical field can be tunable through the direction of an externally applied in-plane magnetic field. These findings open perspectives for the development of superconducting spin-orbitronic devices as well as superconducting structures in which the superconducting state can be controlled with an electric field. In this poster, we discuss our experimental results towards the development of a hybrid superconducting device in which Rashba-SOC and charge accumulation within a thin-film heavy metal (HM) can be tuned via an electric field and so control the superconducting transition of a proximity-coupled thin film superconductor. The electric field is applied to the HM via a ferroelectric lead magnesium niobate-lead titanate (PMN-PT) substrate.

8:00 PM EL03.10.07

Impact of Phase Composition on Bipolar Resistive Switching Performance in Polycrystalline ErMnO₃ Based Devices Rong Wu^{1,2}, Florian Maudet¹, Thanh Luan Phan¹, Sebastian Schmitt¹, Veeresh Deshpande¹ and Catherine Dubourdieu^{1,2}; ¹Helmholtz-Zentrum Berlin, Germany; ²Freie Universität Berlin, Germany

Rare-earth hexagonal manganites, h-RMnO₃ (R=Y, Er, Ho to Lu) have been widely studied for their multiferroic properties. Polycrystalline hexagonal YMnO₃ thin films with promising resistive switching performance were reported recently [1], which gained interest for neuromorphic applications owing to the peculiar ferroelectric domain pattern and vortex lines in hexagonal RMnO₃ [2].

In this work, we report the demonstration of bipolar resistive switching behavior in polycrystalline ErMnO₃-based capacitors. The ErMnO₃ films (~60 nm) were prepared by room temperature RF sputtering on Pt/Ti/SiO₂/Si substrates, followed by post-deposition annealing. The Al/Ti top electrodes were patterned by photolithography. The post-deposition annealing resulted in the formation of polycrystalline ErMnO₃ thin films with orthorhombic and hexagonal phases as shown by X-ray diffraction. We investigated the influence of these different crystalline phases on the switching performance and, for this purpose, developed a way to quantify the relative amount of both phases by scanning electron microscopy, Raman spectroscopy and conductive atomic force microscopy. Through a detailed structural evaluation combined with electrical characterization we developed an understanding of the physical origin of resistive switching in polycrystalline ErMnO₃ and the role of the different phases. The Au/Ti/ErMnO₃/Pt devices exhibit a bipolar resistive switching with a R_{OFF}/R_{ON} ratio larger than 10⁴ and an ultra-low resistance of only 10 Ω in the low resistance state, which can be of interest for CMOS circuitry with low power consumption [3] and for RF power switches [4]. We attribute the switching performance to the formation and rupture of conductive oxygen vacancy-based filaments. We find that a higher fraction of orthorhombic phase reduces the operation voltage but leads to a decrease of the memory window, which can be ascribed to higher Mn⁴⁺ concentration and more oxygen vacancies in the orthorhombic phase. These findings emphasize the potential of polycrystalline ErMnO₃ films as promising candidates for neuromorphic applications and provide valuable insights for enhancing the device performances by engineering the ErMnO₃ switching layer.

References

- [1] V. R. Rayapati *et al.*, J. Appl. Phys. 126 (2019), doi:10.1063/1.5094748.
- [2] H. Schmidt, Appl. Phys. Lett. 118, 140502 (2021), doi: 10.1063/5.0032988.
- [3] H. Cao, *et al.*, Appl. Phys. Lett. 120, 133502 (2022), doi: 10.1063/5.0085045.
- [4] N. Wainstein, *et al.*, Proc. IEEE. 109, 77–95 (2021), doi:10.1109/JPROC.2020.3011953.

8:00 PM EL03.10.08

Improving the Activity and Selectivity of the CO₂ Reduction Reaction with 2D Ferroelectric Materials Mo Li and Joshua Young; New Jersey Institute of Technology, United States

With the great concern of global warming, removing CO₂ from the atmosphere and converting it into useful commercial chemical products through the electrochemical CO₂ reduction reaction has attracted intense interest. Two-dimensional (2D) materials such as Ti₂CO₂ and transition metal (TM)-doped graphene have been shown to be effective catalysts for the CO₂ reduction reaction (CO₂RR). However, due to the complexity of the CO₂RR, various species can be produced as products, indicating a poor selectivity of the reaction. Furthermore, ways to overcome limiting scaling relationships and break the Sabatier principle are also desired. To solve these problems, we investigated using 2D ferroelectric (FE) materials, which show a spontaneous electric polarization that is switchable by an electric field, as substrates for CO₂RR active catalysts. By switching the polarization, the activity of the surface can be changed, leading to a way to alter the adsorption strength or stability dynamically and overcoming the limiting Sabatier principle. Using density functional theory calculations, we first studied the 2D MXene Y₂CO₂ and found that switching the polarization results in different pathways for the reduction of CO₂ to methanol. Second, we studied heterostructures of the 2D ferroelectric In₂Se₃ and TM-doped graphene, with the TM coordinated in different ways. We found that (1) having the In₂Se₃ enhances the CO₂RR activity of the TM-doped graphene and (2) switching the polarization of the In₂Se₃ layer alters the adsorption properties of the intermediates. The beneficial nature of the switchability of the ferroelectric materials provides us with a promising way to control the surface properties, which leads to further control of the desired products in this challenging reaction.

8:00 PM EL03.10.09

Behaviour of Ferroelastic and Ferroelectric Domains in AgNbO₃ Under Temperature and Stress Influence Xi Shi¹, Neamul Khansur¹ and Hana Uršič²; ¹University of Erlangen Nuremberg, Germany; ²Jozef Stefan Institute, Slovenia

By deploying different modes of atomic force microscopy, both ferroelectric and ferroelastic domains with distinct morphology and orientations are observed in the well-known antiferroelectric AgNbO₃, consistent with the theoretical studies. With temperature, ferroelectric domains disappear across its M₁-M₂ phase boundary when it becomes antiferroelectric. In contrast, ferroelastic domains remain stable at 100 °C, consistent with the fact that the ferroelasticity persists till high-temperature antiferroelectric phase regions. In addition, it is found that the number of ferroelectric domains inside the sample is related to the level of Ag deficiency. With applying compressive stress, the ferroelectric surface domains would gradually respond to the stress, which either grows, shrinks or changes shape. In comparison, the ferroelastic surface domains seem to show better mechanical resistance and did not respond as much as the ferroelectric domains.

8:00 PM EL03.10.10

Increase of Faraday Rotation Angle of Cerium-Substituted Yttrium Iron Garnet Film using Vacuum Annealing Hibiki Miyashita¹, Yuki Yoshihara^{1,2}, Takumi Koguchi^{1,2}, Kanta Mori¹, Mitsuteru Inoue¹, Kazushi Ishiyama¹ and Taichi Goto¹; ¹Tohoku University, Japan; ²Toyohashi University of Technology, Japan

Magneto-optical materials have been applied in various devices, such as optical isolators, spatial light modulators, and Q-switches. A magnetic garnet was used in these devices because of its large Faraday rotation angle and low optical loss. In particular, cerium-substituted yttrium iron garnet (Ce:YIG) shows good magneto-optical characteristics in the near-infrared region, used in optical isolators [1]. In Ref [2], the polycrystalline Ce:YIG was deposited onto silica substrates, showing the Faraday rotation (FR) angle of 1.64 degree/micron at a wavelength of 532 nm and

the optical absorption α of 4.17 dB/micron. The figure of merit (FOM) defined as FR/α was 0.39 degree/dB. This study changed the annealing condition to increase this FOM, and magneto-optical properties were characterized.

A 338 nm thick $Ce_1Y_2Fe_5O_{12}$ film was deposited on a 1-inch synthetic fused silica substrate using a radio-frequency ion beam sputtering (RF-IBS). The substrate temperature was held at 200°C during deposition. The sample was cut into 5×5 mm² and annealed using a heater in a vacuum glass chamber. The pressure was less than 2 Pa during the annealing. The annealing procedure comprised three parts: heating up, keeping, and cooling down. We changed the heating-up speed, the temperature of the keeping step, and the cooling-down speed. The heating-up speed was varied from 0.11 to 16 °C/s, and the temperature of the keeping step was varied from 600 to 900°C. The temperature was kept for 10 minutes. The FR loops and absorption of all samples prepared by the various annealing conditions were measured at the wavelength of 532 nm. The largest FR of 1.55 degree/micron, the smallest absorption of 3.24 dB/micron, and the largest FOM of 0.48 degree/dB were obtained with a heating-up speed of 1.33°C/s and a temperature of 800°C. The cooling-down rate varied from -0.097 to -0.39 °C/s, unaffected the FR and absorption. Thus the fastest speed was used.

The obtained FOM of 0.48 degree/dB was 1.23 times larger than the prior study's. The microscopic image of the sample surface became uniform as the heating-up speed decreased. Such a behavior may indicate the consistent growth of nanocrystalline grains. In the symposium, crystalline, electronic structures, and magnetic and optical properties will also be discussed.

[1] T. Goto, M. C. Onbasli, D. H. Kim, V. Singh, M. Inoue, L. C. Kimerling, and C. A. Ross, "A nonreciprocal racetrack resonator based on vacuum-annealed magneto-optical cerium-substituted yttrium iron garnet," *Opt. Express* 22, 19047-19054 (2014).

[2] Y. Yoshihara, T. Sugita, P. B. Lim, Y. Tamba, H. Inoue, C. Ishiyama, M. Inoue, C. A. Ross, and T. Goto, "Thickness-dependent magneto-optical properties of ion beam sputtered polycrystalline $Ce_1Y_2Fe_5O_{12}$ films," *Opt. Mater.* 133, 112967 (2022).

8:00 PM EL03.10.11

Influence of Thickness and Composition Dependence on Dielectric Tunability in $Ba(Zr_xTi_{1-x})O_3$ Films Grown on MgO Substrate Ryo Takahashi¹, Yoshitaka Ehara¹, Yosuke Hamasaki¹, Shinya Sawai¹, Shintaro Yasui², Shinnosuke Yasuoka², Hiroshi Funakubo² and Ken Nishida¹; ¹National Defense Academy, Japan; ²Tokyo Institute of Technology, Japan

Microwave tunable devices are necessary components for next-generation communication applications. Semiconductors, ferrite and ferroelectrics are typical tunable materials. Ferroelectric films have been studied because of their high dielectric tunability and low power consumption. Moreover, for microwave dielectric materials, they show advantages in terms of simple device structure, low loss, good temperature stability and low cost in producing communication devices. To date, $(Ba_{1-x}, Sr_x)TiO_3$ [BST] is one of the most popular ferroelectric materials for tunable microwave devices. However, its dielectric loss is large and the temperature dependence of the dielectric constant is also insufficient for applications. $Ba(Zr_xTi_{1-x})O_3$ [BZT] solid solutions are tunable materials with potential use in elements of phased array antenna, just above their Curie temperature in a paraelectric state. BZT is a possible alternative to BST in tunable microwave applications. Zr^{4+} is chemically more stable than Ti^{4+} and maintains a low dielectric loss. BZT in the paraelectric phase also has higher temperature stability than BST. Therefore, we focused on BZT films as a tunable ferroelectric material.

To evaluate electric properties with microwave region, BZT films are deposited on MgO substrate, which has low dielectric constant compare to films. The lattice mismatch strain between substrate and film, induces remarkable change in crystal structure. This is important parameter to use BZT film into microwave application but not to be reported about influence of thickness and composition dependence of BZT film grown on MgO substrate. Thus, we will discuss these dependence and their impact on microwave applications.

(100)-oriented BZT ($x = 0 \sim 1.0$) thin films with various thickness by pulse laser deposition [PLD] technique on MgO substrates. The structural properties of the films were characterized by x-ray diffraction [XRD] (MRD, PANalytical). Wavelength-dispersive x-ray fluorescence spectrometry [WDX] (ZSX Primus4, Rigaku) was carried out to investigate the composition and thickness of BZT thin films. All the XRD patterns showed only (001)/(100) diffraction peaks and no secondary phase. Reciprocal space mappings (RSMs) of BZT thin films showed that BZT thin films epitaxially grew on MgO(100) substrates. The composition dependence of tetragonality, remanent polarization, and dielectric constant suggested that there may be a phase boundary between $x = 0.2$ and 0.3, and this tendency is similar to BZT ceramics. Therefore, our results suggest that BZT ($x = 0 \sim 0.5$) can be one of the significant candidates for microwave application which requires high tunability and low loss.

8:00 PM EL03.10.12

Free-Standing Functional Oxide Membrane Through CVD Graphene and MoS₂ Asraf ul Haque, Sumank Mandal, Ravi K. Mishra, Shubham K. Parate, Shankar K. Selvaraja, Pavan Nukala and Srinivasan Raghavan; Indian Institute of Science, India

The integration of complex oxides with myriad functionalities onto Si and flexible substrates is in high demand. One way to integrate functional oxides onto Si is to scavenge the inherent native oxide using TiN, MgO, and STO buffer layers on Si. Alternatively, it can be done by growing them on an oxide substrate and then transferring it onto Si. To enable the transfer process the interfacial bond between the film and substrate is weakened by incorporating 2D materials like graphene. Here, we have demonstrated the growth of BTO via remote/pin-hole epitaxy and then transferred it onto Si using a combination of Ni stressor layer and thermal release tape. We have employed pulsed laser deposition which is an easier and cheaper way to grow these functional oxides, unlike molecular beam epitaxy. Finally, we have shown PFM results to demonstrate the ferroelectricity of our free-standing membrane.

Integrating complex oxides with various functionalities onto Si and flexible substrates is in high demand. The traditional way includes growing TiN, MgO, SrTiO₃ (STO), etc. buffer templates for complex oxides integration¹. Alternatively, the complex oxides can be grown on a single crystalline substrate via a two-dimensional material at the interface, then transferred onto Si².

Here, we have demonstrated the growth of BaTiO₃ (BTO) via remote/pin-hole epitaxy on a graphene-coated STO substrate. We have employed pulsed laser deposition (PLD), a more accessible and cheaper way to grow these functional oxides, unlike molecular beam epitaxy. After that, the BTO layer has been successfully transferred from its parent STO substrate. Our piezo-force microscopy (PFM) results confirm the ferroelectricity of the BTO membrane. In this conference, I will discuss the underlying strategy to optimize the growth of functional oxide without damaging the graphene layer, followed by its transfer.

8:00 PM EL03.10.13

Effect of Epitaxial Strain and Strain-Mediated Defects on Crystal Structure and Ferroelectricity in Epitaxial SrMnO₃ Film Grown on Piezoelectric PMN-PT Substrate Seong Min Park¹, Jaegyung Kim², Gopinathan Anoop¹, Woo Jun Seol¹, Su Yong Lee³, Hyunjin Joh¹, Tae Yeon Kim¹, Je Oh Choi¹, Seungbum Hong², Chan-Ho Yang², Hyeon Jun Lee⁴ and Ji Young Jo¹; ¹GIST, Korea (the Republic of); ²Korea Advanced Institute of Science and Technology, Korea (the Republic of); ³Pohang Accelerator Laboratory, Korea (the Republic of); ⁴Kangwon National University, Korea (the Republic of)

Strain-engineering of perovskite SrMnO₃ (SMO) film has attracted research interest due to the theoretical prediction that the application of epitaxial strain (ϵ , < -1.4% and > 1%) can induce phase transition from paraelectric phase to ferroelectric phase [1]. The strain-induced ferroelectricity so far has been observed in SMO films grown on $(La_{0.5}Sr_{0.7})(Al_{0.65}Ta_{0.35})O_3$ ($\epsilon = 1.79\%$) and $DsScO_3$ ($\epsilon = 3.68\%$) substrates [2,3]; however, the film grown on SrTiO₃ ($\epsilon = 2.76\%$) substrate does not exhibit ferroelectric phase transition. This discontinuity in strain-induced ferroelectricity of SMO film can be attributed to distinct morphology and composition of the surface of the perovskite substrate [4]. Furthermore, the tensile strain promotes the formation of oxygen vacancy, which contributes to structural deformation, resulting in the modification of polar orders [5]. Research on deposition and characterization of SMO film using previously unused substrates provides a pathway to understand the effect of misfit strain with crystallographic orientation, crystal structure, and defects chemistry on ferroelectric properties.

Piezoelectric materials have been utilized as functional substrates that can change the biaxial strain of thin film in the real time through the piezoelectric distortion under the electric field [6]. $(1-x)Pb(Mg_{1/3}Nb_{2/3})O_3-xPbTiO_3$ (PMN-PT), which exhibits the outstanding piezoelectricity, is widely used for the growth of epitaxial oxide film [7]. However, the growth of single crystal SMO film on the PMN-PT substrate has not been studied yet. The significant lattice mismatch against SMO (larger than 5.79%) makes the growth of epitaxial film on PMN-PT substrate challenging. Growth of single crystal SMO film on PMN-PT substrate requires the buffer layer to reduce elastic energy of the SMO film and optimization of growth condition for maintaining the perovskite structure.

In this study, we demonstrate the structural and ferroelectric properties that arise from the interplay of strain and oxygen vacancy in the single crystal SMO film epitaxially grown on (110)-oriented $(La_{0.7}Sr_{0.3})MnO_3$ buffered PMN-PT substrate. We found that the 85 nm thick SMO film exhibits tetragonal structure simultaneously showing expansion in unit cell lattice than bulk structure derived by the strain-mediated oxygen vacancy. Unlike the previously reported tensile strained SMO film, piezoelectric response in both lateral and vertical direction with out-of-plane 180° phase reversal is observed, indicating the existence of ferroelectric polarization rotated toward the out-of-plane direction. Moreover, the use of piezoelectric PMN-PT substrate allows to control the epitaxial strain of SMO film through the converse piezoelectric effect exhibiting 90% of strain transferring efficiency.

References

1. J. H. Lee and K. M. Rabe, *Phys. Rev. Lett.* **104**, 2 (2010).
2. J. W. Guo, P. S. Wang, Y. Yuan, Q. He, J. L. Lu, T. Z. Chen, S. Z. Yang, Y. J. Wang, R. Ermi, M. D. Russell, V. Gopalan, H. J. Xiang, Y. Tokura, and P. Yu, *Phys. Rev. B* **97**, 1 (2018).
3. H. An, Y. Choi, Y. Jo, H. Hong, J. Kim, O. Kwon, S. Kim, M. Son, J. Yang, J. Park, H. Choi, J. Lee, J. Song, M. Ham, S. Ryu, Y. Kim, C. Bark, K. Ko, B. Kim, and S. Lee, *NPG Asia Materials* **13**, 69 (2021)
4. F. Sanchez, C. Ocal, and J. Fontcuberta, *Chem. Soc. Rev.* **43**, 2272 (2014)
5. J. Hwang, Z. Feng, N. Charles, X. Wang, D. Lee, K. Stoerzinger, S. Muy, R. Rao, D. Lee, R. Jacobs, D. Morgan, and Y. Horn, *Mater. Today* **31**, 100-118 (2019)
6. R. Liu and X. Wang, *Phosphor Handbook: Novel Phosphors, Synthesis, and Application*, 3rd ed. Routledge, 720 p. (2022)
7. S. Zhang, Y. Zhao, P. Li, J. Yang, S. Rizwan, J. Zhang, J. Seidel, T. Qu, Y. Yang, Z. Luo, Q. He, T. Zou, Q. Chen, J. Wang, L. Yang, Y. Sun, Y. Wu, X. Xiao, X. Jin, J. Huang, C. Gao, X. Han, and R. Ramesh, *Phys. Rev. Lett.* **108**, 137203 (2012)

8:00 PM EL03.10.14

Tunable Electronic Structure by In-Situ Ferroelectric Domain Writing in Graphene/BiFeO₃ Heterostructures Monika L. Eggenberger and Yoshinori Okada; Okinawa Institute of Science and Technology, Japan

Integration of functional ferroic domain structures in 2D systems with existing layered electronic architectures represents a major opportunity for advancement of tunable nanoelectronics. Here, we demonstrate nanoscale writable electronic structure of graphene by in-situ ferroelectric domain manipulation in high-quality graphene/BiFeO₃ heterostructures. Crystalline BiFeO₃ thin films are grown by pulsed laser deposition, and the ferroelectric domain structure and domain wall properties are characterized by piezoresponse force microscopy (PFM). Few- and monolayer graphene flakes are transferred in ultrahigh vacuum by direct bonding for a pristine interface. The ferroelectric polarization domains in BiFeO₃ determine the local charge landscape at the heterointerface, which modulates the band structure of the adjacent graphene layer and results in large switchable resistivity. We characterize the effect of the domain polarization on the electronic structure of the graphene layer by STM, with particular focus given to the domain wall region. Additionally, we show that the electronic structure of graphene can be locally patterned by in-situ manipulation of the ferroelectric domains by external field. Finally, we discuss the stability of written domains and suitability for device application.

8:00 PM EL03.10.15

Direct Probing of Dielectric Property of BaTiO₃ Nanoparticle on Conducting Substrate Wonhyung Kim^{1,2}, Eunjin Koh¹, Choongseop Jeon², Seungyong Lee², Junghyun An², Dongchan Seo², Jeongryeol Kim², Jungwon Lee² and Yunseok Kim¹; ¹Sungkyunkwan University, Korea (the Republic of); ²Samsung Electro-Mechanics Co. Ltd, Korea (the Republic of)

With the development of technology, the performance of electronic devices is improving, increasing the number of components need to be used, so the size of the passive components, including multi-layer ceramic capacitors (MLCCs), should be downsized. Therefore, the size of BaTiO₃, the raw dielectric material of MLCC, needs to be reduced. It is known that the dielectric properties of BaTiO₃ nanoparticles are dependent on size and synthesis method. In previous studies, the dielectric properties of BaTiO₃ nanoparticles were mainly studied using the slurry method, which is dielectric measurement of slurry consisted of solvent and nanoparticles. But this method has limitations in that the dielectric properties of the nanoparticles and solvent are measured together, so the information about the nanoparticles cannot be directly obtained. On the other hand, many researchers study dielectric properties in thin films or particles using scanning dielectric microscopy (SDM) measurement, which is an atomic force microscope (AFM)-based measurement method. In this study, the dielectric properties of BaTiO₃ according to size and the synthesis method were measured using SDM to directly observe BaTiO₃ nanoparticles. The capacitance gradient (dC/dz) was obtained using SDM measurement and the dielectric constant was studied. Through this study, we learned about the dielectric characteristics of BaTiO₃ at the particle level, and it is expected that this will help select the appropriate type of dielectric powder in the development of next-generation MLCCs.

8:00 PM EL03.10.16

Crystallization of Amorphous Hf_{1-x}Zr_xO₂ Thin Films by Electric Field Cycling Ahyoung Jeong, Deokjoon Eom, Hyoungsub Kim and Yunseok Kim; Sungkyunkwan University, Korea (the Republic of)

Hafnium oxide (HfO₂)-based ferroelectrics exhibit robust ferroelectricity even at extremely thin thicknesses, in contrast to conventional perovskite-based ferroelectrics. Numerous research efforts are underway to enhance the ferroelectric properties of HfO₂ and, recently, the crystallization of amorphous hafnium zirconium oxide (HZO) through electric field cycling has been reported. Electric-field-induced crystallization might enable the crystallization process to occur at lower temperatures compared to traditional methods. To investigate the mechanism of electric-field-induced crystallization, it is necessary to study nanoscale ferroelectricity analysis. However, the conventional approach of studying ferroelectricity using polarization-electric field hysteresis loop measurement is limited in its ability to discern the underlying nanoscale mechanisms due to the presence of leakage currents. In this study, we investigated the electric-field-induced crystallization of HZO thin film at the nanoscale level using piezoresponse force microscopy. This research can provide opportunities for understanding the electric-field-induced crystallization and origin of ferroelectricity of HfO₂-based thin films.

References

- [1] Lee, H. Choe, D.-H. Jo, S. Kim, J.-H. Lee, H. H. Shin, H.-J. Park, Y. Kang, S. Cho, Y. Park, S. Unveiling the Origin of Robust Ferroelectricity in Sub-2 Nm Hafnium Zirconium Oxide Films. ACS Appl. Mater. Interfaces 2021, 13, 36499–36506
- [2] S. Kang, W.-S. Jang, A. N. Morozovska, O. Kwon, Y. Jin, Y.-H. Kim, H. Bae, C. Wang, S.-H. Yang, A. Belianinov, S. Randolph, E. A. Eliseev, L. Collins, Y. Park, S. Jo, M.-H. Jung, K.-J. Go, H. W. Cho, S.-Y. Choi, J. H. Jang, S. Kim, H. Y. Jeong, J. Lee, O. S. Ovchinnikova, J. Heo, S. V. Kalinin, Y.-M. Kim, Y. Kim, Highly enhanced ferroelectricity in HfO₂-based ferroelectric thin film by light ion bombardment. Science 2022, 376, 731–738

8:00 PM EL03.10.17

Growth Orientation Dependence on the Stabilization of the Polar Orthorhombic Phase of Hf_{1/2}Zr_{1/2}O₂ Thin Films Arnab De¹, Seung Gyo Jeong¹, Jinyoung Oh¹, Seong Bin Bae², Young Hoon Kim¹, Young Min Kim¹, Sang Mo Yang² and Woo Seok Choi¹; ¹Sungkyunkwan University, Korea (the Republic of); ²Sogang University, Korea (the Republic of)

Ultrathin ferroelectrics possess enormous potential for the implementation of next-generation nonvolatile memories, actuators, sensors, and opto-electronic devices [1]. Since the discovery of the unexpected ferroelectricity in HfO₂ (hafnium-dioxide) thin films in 2011 [2], intensive research has been conducted for the realization of the silicon-compatible nanoscale devices. However, to fully exploit the potential of ferroelectric HfO₂-based thin films, we must address fundamental questions regarding the origin of ferroelectricity and develop strategies for controlled implementation at the nanoscale. The stability of the polar orthorhombic phase responsible for the robust polarization is believed to be influenced by various extrinsic factors, including finite-size effects, surface/interface effects of small grains, compressive stress, dopants, and oxygen vacancies [3,4]. However, a deeper understanding of the extrinsic and intrinsic parameters that control the phase transitions among different polymorphs (i.e., orthorhombic, tetragonal, and monoclinic) of HfO₂ is still needed. In this study, we investigate the influence of substrate orientations on the relative stability of different phases of Hf_{0.5}Zr_{0.5}O₂ grown epitaxially on (001) and (011) oriented La_{0.7}Sr_{0.3}MnO₃/SrTiO₃ using pulsed laser epitaxy (PLE). Ferroelectric measurement reveals remanent polarization as high as 40 μC/cm² with negligible wake-up effect. A systematic variation on the growth conditions show that the fraction of polar orthorhombic and non-polar monoclinic phases can be controlled by manipulating the epitaxial strain arising from the different substrate orientations. This study provides a promising direction for enhancing the stability of the ferroelectric phase in HfO₂ based thin films through substrate orientation engineering.

References

1. H. Qiao et al., Mater. Sci. Eng. R Rep. **145**, 100622 (2021)
2. T. S. Boscke et al. Appl. Phys. Letters **99**, 102903 (2011).
3. M. H. Park et al., Adv. Mater. **27**, 1811–1831, (2015).
4. Yu Yun et al., Nature Materials, **21**, 903–909 (2022).

SESSION EL03.11: Oxide Electronics II
Session Chairs: John Heron and Bhagwati Prasad
Thursday Morning, November 30, 2023
Hynes, Level 1, Room 107

8:30 AM *EL03.11.01

Giant Voltage Amplification Under Scrutiny Arkady P. Levanyuk¹, Ibrahim B. Misirlioglu², Mahmut B. Okatan³ and Andres Cano⁴; ¹University of Washington, United States; ²Sabancı University, Turkey; ³Izmir Institute of Technology, Turkey; ⁴University Grenoble Alpes, France

If a capacitor contains both ferroelectric and dielectric layers then, under certain conditions, the drop in the electrical potential across the dielectric can be higher than the external voltage applied to the capacitor. This is recently of practical interest in relation to field-effect transistors (FET) for example. Such a “voltage amplification”, which can be seen as arising due to a “negative-capacitance effect” associated with the ferroelectric, has been mostly discussed in relation to multidomain ferroelectricity (A. M. Bratkovsky and A. P. Levanyuk, Appl. Phys. Lett. **89**, 253108 (2006)). However, it can also be realized when the ferroelectric is in its paraelectric phase but such that it would be in the ferroelectric state had it been in a short-circuited capacitor without a dielectric and with ideal electrodes (A. Cano and D. Jimenez, Appl. Phys. Lett. **97**, 133509 (2010)). In a recent paper by Graf et al. (Nature Materials **21**, 1252 (2022)), a “giant voltage amplification” with a factor ~12 is reported for a special case of an infinite PbTiO₃/SrTiO₃ multilayer in the paraelectric state. In this presentation, drawing from the results of our earlier work (A. P. Levanyuk and I. B. Misirlioglu, J. Appl. Phys. **110**, 114109 (2011)), we report on our theoretical investigation so as to how this result transforms when applied to finite systems that are closer to those of interest for applications. Using the Landau-Ginzburg-Devonshire (LGD) theory we consider a uniaxial ferroelectric with different dielectric surroundings.

We find that the voltage amplification depends strongly on the configuration of the system and the characteristics of the electrodes of the capacitor. In a special case of symmetrical configuration of the dielectric layers and ideal electrodes our results reproduce the giant voltage amplification reported by Graf et. al. In asymmetric configurations, however, we find that the voltage amplification decreases substantially.

9:00 AM EL03.11.02

Local Investigations of the Electrocaloric Effect using Scanning Thermal Microscopy [Olivia Baxter](#), Amit Kumar, J. Marty Gregg and Raymond McQuaid; Queen's University Belfast, United Kingdom

The electrocaloric effect is a well-known phenomenon where adiabatic application of an external electric field to a material results in a reversible temperature change. Interest in using these materials for environmentally friendly solid-state refrigeration applications has been rejuvenated by the discovery of giant electrocaloric effects in thin films. While the electrocaloric effect can be well described macroscopically through a thermodynamic approach and is understood to arise from changes in dipolar configurational entropy, the effect at the microscopic scale is not as well characterised. To date, infrared cameras represent the best spatial resolution available for in-situ imaging of temperature fields associated with electrocaloric effects, but features are limited in detail to the level of a few microns.

Scanning Thermal Microscopy is emerging as a powerful Atomic Force Microscope based platform for mapping dynamic temperature distributions on the nanoscale. To date, however, spatial imaging of temperature changes in electrocaloric materials using this technique has been very limited. We build on the work of previous studies to show that Scanning Thermal Microscopy can be used to spatially map electrocaloric temperature changes on microscopic length scales, here demonstrated in a commercially obtained multilayer ceramic capacitor. In our approach, the electrocaloric response is measured at discrete locations with point-to-point separation as small as 150nm, allowing for reconstruction of spatial maps of heating and cooling as well as their temporal evolution. This technique offers a means to investigate electrocaloric responses at sub-micron length scales, which cannot easily be accessed by the more commonly used infra-red thermal imaging approaches. We intend to use this technique to elucidate the behaviour of other electrocaloric materials and to examine the influence of microstructural inhomogeneity on electrocaloric response.

9:15 AM EL03.11.03

Heat Assisted Ferroelectric Reading for High Speed Ferroelectric Probe Data Storage [Yasuo Cho](#); Tohoku University, Japan

We previously proposed ferroelectric data storage that uses scanning nonlinear dielectric microscopy (SNDM), called SNDM probe memory, as a next-generation ultrahigh-density information recording method. We confirmed an extremely high recording density and high-speed writing using LiTaO₃ single crystal media [1][2]. However, since reading is based on the detection of very small nonlinear dielectric constants of ferroelectric materials using SNDM technique, slow playback speed (actually 2Mbps) hinders the practical use of SNDM probe memory [3].

To solve this problem, a material with a large nonlinear dielectric constant is required. Our basic experiments revealed that a nonlinear dielectric constant has an extremely large temperature dependence and is proportional to $(T_0 - T)^{-3.5}$, where T is the medium temperature and T₀ is the Curie temperature[4]. This means that an increase in the nonlinear dielectric constant, which would enable ultrahigh-speed reading (Gbps or faster), can be easily obtained even in LiTaO₃ crystal by making T close to T₀. However, simply increasing the medium temperature closer to the Curie temperature under thermal equilibrium degrades the polarization retention characteristics.

Therefore, we propose a heat-assisted ferroelectric reading (HAFer) method that increases the reading speed while maintaining the polarization retention characteristics. This is achieved by locally heating the medium for a very short time at the data reading position using laser pulse irradiation. We conducted a basic experiment and confirmed that laser pulse irradiation increased the SNDM signal strength much more.

We also discuss the relationship between the maximum number of laser irradiation pulses and the optical pulse width for a medium heated to 550 °C (equivalent to a reading speed of 5 Gbps). The proposed method overcomes the fundamental problems of next-generation ultrahigh-density ferroelectric data storage.

References:

- [1] Kenkou Tanaka and Yasuo Cho, "Actual information storage with a recording density of 4 Tbit/in.² in a ferroelectric recording medium", Appl. Phys. Lett, Vol.97, 092901 (2010) .
- [2] Kenkou TANAKA, Yuichi KURIHASHI, Tomoya UDA, Yasuhiro DAIMON, Nozomi ODAGAWA, Ryusuke HIROSE, Yoshiomi HIRANAGA, and Yasuo CHO: "Scanning Nonlinear Dielectric Microscopy Nano-Science and Technology for Next Generation High Density Ferroelectric Data Storage", Jpn. J. Appl. Phys, Vol.47, 3311 (2008).
- [3] Yoshiomi Hiranaga, Tomoya Uda, Y. Kurihashi, H. Tochishita, M. Kadota and Y. Cho, "Nanodomain Formation on Ferroelectrics and Development of Hard-Disk-Drive-Type Ferroelectric Data Storage Devices", Jpn.J. Appl. Phys. Vol.48, 09KA18 (2009).
- [4] Yoshiomi Hiranaga and Yasuo Cho, "Material Design Strategy for Enhancement of Readback Signal Intensity in Ferroelectric Probe Data Storage", IEEE Trans. Ultrason. Ferroelectr. Freq. Control, Vol.68, 859 (2021).

9:30 AM EL03.11.04

In Situ Characterisation of Ephemeral p-n Junctions inside Ferroelectric Domain Walls [Kristina Holsgrove](#), Jesi Maguire, Conor J. McCluskey, Ahmet Suna, Raymond McQuaid, Amit Kumar and J. Marty Gregg; Queen's University, United Kingdom

Ferroelectric materials are renowned for their distinctive microstructure, characterised by a patchwork of domains where local electrical dipoles align, separated by domain walls that act as interfaces between these domains. When subjected to applied fields, certain domain orientations become stabilised and tend to grow, while unstable ones diminish. Consequently, the movement of domain walls becomes an inherent necessity. The creation of new domains necessitates the formation of domain walls, while the disappearance of domains leads to the disappearance of walls. Therefore, domain walls exhibit both mobility and transience in response to varying field conditions. What's particularly noteworthy is that while most ferroelectrics possess inherent electrical insulation properties, domain walls can exhibit conductivity [1]. In such cases, domain walls serve as quasi-2D electrical pathways within an otherwise insulating ferroelectric matrix. This intriguing characteristic paves the way for envisioning dynamically reconfigurable domain walls capable of creating, erasing, and rewriting entire nanoscale circuits in different configurations.

Our team has devoted several years to the study of conducting domain walls in thin film heterostructures of lithium niobate (LNO) [2-4]. It is now recognised that when a modest positive bias is applied, the domain walls exhibit a remarkable behaviour, tilting away from the polar axis and forming what are known as charged head-to-head (n-type) domain walls, which exhibit strong conductivity. In this study, we perform *in situ* cross-sectional transmission electron microscopy (TEM) imaging of bias-induced domain wall dynamics, allowing us to "live" image the domain wall tilting under applied electric fields.

This investigation has yielded a remarkable finding: certain sections of conducting domain walls transition from n-type to p-type as the direction of the applied bias changes - a result that has never been observed before and is incredibly exciting. It seems that we are creating a new kind of dynamically formed domain wall p-n junction. Although p-n junctions are commonly found in improper ferroelectric systems like boracites and rare-earth manganites, what we have observed in focused ion beam (FIB) slices of LNO represents a unique phenomenon. The in-wall p-n junctions (which could be described as 'zero-dimensional' entities due to the one-dimensional nature of the domain walls) only exist within a finite bias range, and hence are truly ephemeral in nature.

Through monitoring the current-voltage response, we observe striking diode-like characteristics. Moreover, thanks to the dynamic nature of these *in situ* TEM studies, we have been able to evaluate the switching mechanisms involved in the formation of these conductive pathways and transient p-n junctions. This work is expected to provide valuable insights into in-wall p-n junctions and contribute significantly to the advancement of domain wall nanoelectronics.

- [1] J. Seidel *et al. Nat. Mater.* 8, 229 (2009)
- [2] J. P. V. McConville *et al. Adv. Funct. Mater.* 30, 202000109 (2020)
- [3] C.J. McCluskey *et al. Adv. Mater.* 34 2204298 (2022)
- [4] A Suna *et al. Advanced Physics Research*, 2200095 (2023)

9:45 AM EL03.11.05

Ultrashort Electric Pulse-Driven Polar State in Paraelectric SrTiO₃ Thin Film at Room Temperature [Hyeon Jun Lee](#); Kangwon National University, Korea (the Republic of)

Access to hidden metastable phases of matter is a crucial early stage to explore exotic properties. Strontium titanate (SrTiO₃) is a quantum paraelectric in which quantum fluctuations of ionic positions prevent the long-range polar order even at zero kelvin. Application of external bias overcoming the fluctuations has dynamically induced metastable polar states at the cryogenic temperature. However, the existence of these polar states above room temperature has not been proved and explored yet because the magnitude of the electric field required to drive the polar state in SrTiO₃ can be larger than the low-frequency dielectric breakdown field in principle. Using nanosecond electric pulse for which the high field can be applied without the breakdown, we found an ultrafast phase transition into the polar state.

We measured the electromechanical response of a 50 nm-thick paraelectric SrTiO₃ epitaxial film grown on the (001) oriented SrRuO₃ electrode and SrTiO₃ substrate as a function of the

magnitude of electric field up to 1.5 MV/cm using advanced time-resolved x-ray microdiffraction. At a low field regime, the out-of-plane lattice constant of the film increased quadratically due to the electrostrictive response of the dielectric component. At above 1 MV/cm, SrTiO₃ film exhibited the linear lattice expansion with increasing the electric field, which is consistent with piezoelectric distortion, indicating that the high field induced the transition into polar states. We found that the electrostrictive coefficient (g_{11}) linking the applied electric field to the measured piezoelectric strain is 3 times larger than previously reported value for SrTiO₃ at 1985. Due to this large electrostrictive coefficient, ferroelectric phase of SrTiO₃ thin film can be stable even under -1 % compressive strain at room temperature. We will discuss the new phase diagram based on the electrostrictive coefficient measured in this study.

10:00 AMBREAK

SESSION EL03.12: Spintronics I
Session Chairs: John Heron and Bhagwati Prasad
Thursday Morning, November 30, 2023
Hynes, Level 1, Room 107

10:30 AM EL03.12.01

Simultaneous Growth of Lateral Heterostructures of Epitaxial Garnet and Polycrystalline Perovskite Phases Pete E. Lauer, Kensuke Hayashi, Yuichiro Kunai and Caroline A. Ross; Massachusetts Institute of Technology, United States

Iron garnets based on Y₃Fe₅O₁₂ (YIG) are ferrimagnetic insulators and form essential components of optical communications and microwave devices. To enhance their functionality and allow device scaling, it is of great interest to interface them with other functional oxides such as ferroelectric perovskites, which could enable electrical control of the magnetic properties. Here we describe a fabrication pathway capable of creating a lateral heterostructure that includes both a garnet and a perovskite phase with feature sizes as low as 50 nm during a single deposition step. The methodology first uses electron beam lithography to create a resist pattern on a Gd₃Ga₅O₁₂ (GGG) substrate. Pulsed laser deposition (PLD) is used to grow a 25 nm thick layer of amorphous SrTiO₃ (STO) at room temperature over the resist. After liftoff, the patterned STO is crystallized by a rapid thermal anneal at 700 °C. A 200 nm thick layer of YIG is then grown on the STO-patterned GGG substrate at elevated temperature (650 °C) to form the lateral heterostructure: in regions with exposed GGG, epitaxial growth of YIG occurs, but in regions seeded with STO, a polycrystalline Fe-rich YFeO₃ (YFO) perovskite forms. Electron-beam backscatter diffraction reveals the phase distribution of both YFO and YIG, the single-crystal growth of the YIG and the polycrystallinity of the YFO. This phase formation is consistent with prior work in which epitaxy stabilizes YIG or YFO phases even when the composition differs from the ideal bulk composition [1,2]. Furthermore, off-stoichiometric YFO can exhibit a ferroelectric response [2]. The YIG/YFO interfaces are vertical leading to YIG features separated by YFO walls or fins. We demonstrate the process conditions that yield vertical phase separation by changing the Y:Fe ratio of the deposited material and the deposition temperature and oxygen pressure. The thermodynamic and kinetic considerations of the competition between the two-phase growth will also be discussed. Extension to other materials systems will be described, in particular the growth of a ferroelectric/magneto-optical BiFeO₃/Bi₃Fe₅O₁₂ heterostructure.

[1] Su et al., Phys. Rev. Materials 5, 094403 (2021)

[2] Ning et al., Nature Com. 12, 4298 (2021)

10:45 AM EL03.12.02

Magnetic Proximity Effect in Oxide Heterostructures Bhagwati Prasad, Suryakanta Mondal and Naveen Negi; Indian Institute of Science, India

The fabrication of spintronics devices, encompassing spin transistors and spin valves, requires complex multi-layer structures composed of varying magnetic materials. This complexity opens the possibility of myriad interface effects, one of which is the proximity effect. This fascinating effect is the phenomenon where one layer's physical characteristics influence the properties of another layer within the same structure. Manganite thin film heterostructures could be a suitable candidate for the in-depth investigation of these proximity effects as manganites are known to display emergent phenomena stemming from the dynamic interplay between charge, spin, orbital, and lattice degrees of freedom [1]. Its intriguing properties include colossal magnetoresistance and metal-insulator transitions, among others. These unique features result from the complicated interplay between charge carriers, spin ordering, and lattice distortions, with modulating influences from external stimuli, such as magnetic fields or electric fields.

The physical properties of manganites, such as Sm_{1-x}Sr_xMnO₃ (SSMO), can be significantly changed by varying the percentage of Sr doping. Depending on the doping ratio, SSMO can manifest as a ferromagnetic or antiferromagnetic magnetic phase or even a mixture of both magnetic phases [2]. The vast range of tunable phenomena owing to Sr concentration in SSMO underscores its scientific significance and makes it an interesting candidate for the study of various properties [3, 4]. In this study, we explored the magnetic proximity effect in SSMO bilayer and tri-layer heterostructures. First, we deposited a single layer of ferromagnetic metal (FMM) and an anti-ferromagnetic insulator (AFI) using the pulsed laser deposition (PLD) method on a SrTiO₃ (STO) substrate. Their magnetic properties were analyzed using a SQUID magnetometer, with the results aligning well with the previously reported data. Next, we deposited a bi-layer stack of FMM/AFI and a corresponding tri-layer structure of AFI/FMM/AFI on the STO substrate. We discovered a significant increase in magnetic moment across these structures, suggesting the magnetic proximity effect in the heterostructures as the primary cause. In a nutshell, the manganite heterostructures provide a promising platform for delving deeper into new electronic and magnetic phenomena at the interfaces.

[1] Y. Tokura, Reports Prog. Phys. **69**, 797 (2006).

[2] Kurbakov et al., Journal of Physics: Condensed Matter. **20**, 104233 (2008).

[3] Bhagwati Prasad, et al., Advanced Materials **27**, 3079 (2015).

[4] Bhagwati Prasad and M. G. Blamire, Appl. Phys. Lett. **109**, 132407 (2016).

11:00 AM *EL03.12.03

Ferrimagnetic Garnets: Nanocomposites, Superlattices and Defect Engineering Caroline A. Ross; Massachusetts Institute of Technology, United States

Iron garnets (IGs) are exciting materials for spintronics, with TmIG and TbIG/Pt bilayers exhibiting interfacial DMI and field-free spin orbit torque switching, [1] and BiYIG exhibiting relativistic domain wall velocities of 4.3 km/s [2] and spin wave-driven domain wall motion [3]. In this presentation we will focus on the synthesis and behavior of garnet superlattices and garnet/perovskite nanocomposites and the effect of cation site-occupancy on the magnetic properties of garnet films.

Manipulating site-occupancy, for example by epitaxial growth of off-stoichiometric garnets, yields properties not seen in bulk. For example, in Tb-rich TbIG, excess Tb occupies octahedral sites making the compensation temperature 90K higher and the Curie temperature 40K lower than bulk [4]. Mixed REIGs such as EuTmIG exhibit ordering of the RE cations on non-equivalent dodecahedral sites during film deposition, leading to a strong growth-induced anisotropy that yields an out-of-plane easy axis even in unstrained films. Layered garnets provide another avenue for properties engineering. IG superlattices are unexplored, despite the emergent phenomena seen in other oxide superlattices such as interfacial conductivity, magnetism and anisotropy in perovskites. We show using transmission electron microscopy and atom probe measurements that pulsed laser deposition can produce epitaxial coherent TbIG/TmIG and BiYIG/LuIG superlattices with well defined nm layers. TbIG/TmIG superlattices exhibit perpendicular magnetic anisotropy in contrast to the in-plane easy axis of intermixed TbTmIG films, and BiYIG/LuIG superlattices exhibit lower damping than intermixed BiYLuIG films. Finally, garnet-perovskite nanocomposite thin films offer the possibility of magnetoelectric control of the garnet via coupling to a ferroelectric perovskite. We demonstrate a process to produce patterned YIG/YFeO₃ and BiIG/BiFeO₃ two-phase thin films on garnet substrates in which the perovskite orthoferrite forms selectively on regions of the substrate coated with a thin seed layer of SrTiO₃, and describe the nanocomposite structure and properties. The formation of complex heterogeneous garnet-based films and structures expands the range of properties and applications of this important class of materials.

[1] Caretta et al., Nature Commun., 11 1090 (2020)

[2] Caretta et al., Science 18 1438 (2020)

[3] Fan et al., Nat. Nanotechnol. (2023)

[4] Rosenberg et al., Small 2023, 2300824

11:30 AM *EL03.12.04

Incoherent Magnon Transport in Magnetic Insulators Tianxiang Nan; Tsinghua University, China

Magnon spin transport, with its low energy dissipation, has become a promising candidate for applications in information transmission. In this talk, I will present room-temperature measurements of magnon spin diffusion in ultra-thin epitaxial ferrimagnetic insulator MgAl_{0.5}Fe_{1.5}O₄ (MAFO) thin films. I will first show the observation of spin diffusion lengths > 0.8 μm at

room temperature in 6 nm films, with anisotropic spin diffusion lengths along different crystal axes, which can be attributed to the anisotropy in exchange stiffness. I will also show the magnon spin transport at near zero applied magnetic field where the sample forms a multi-domain state with 180° domain walls. We find, surprisingly, that the presence of the domain walls has very little effect on the spin diffusion – nonlocal spin transport signals in the multi-domain state retain at least 95% of the maximum signal strength measured for the spatially-uniform magnetic state, over distances at least five times the typical domain size. These findings provide additional approaches for controlling magnon transport via strain and magnetic domain walls, which opens new opportunities for designing magnonic devices.

SESSION EL03.13: Spintronics II
Session Chairs: Bhagwati Prasad and Caroline Ross
Thursday Afternoon, November 30, 2023
Hynes, Level 1, Room 107

1:30 PM *EL03.13.01

Structural Magnetic Properties Correlation in $(\text{Gd}_{1-y}\text{Ho}_y)_2\text{Ti}_2\text{O}_7$ and $\text{Ho}_2(\text{Ti}_{1-x}\text{Ge}_x)_2\text{O}_7$ Frustrated Pyrochlores Vinod Singh¹ and Kailash Chandra^{1,2}; ¹Delhi Technological University, India; ²Motilal Nehru College, University of Delhi, India

The effects of Ho substitution at A site on the structural and magnetic properties of $(\text{Gd}_{1-y}\text{Ho}_y)_2\text{Ti}_2\text{O}_7$ ($y = 0, 0.2, 0.4$ and 0.6) single phasic pyrochlore oxides have been investigated. Magnetic Ho substitution reduces the size of crystallites as calculated from the WH graph, validating the reduction in structural ordering of the produced samples. The compounds show a tendency towards a heightened ferromagnetic interaction on Ho substitution owing to the ferromagnetic connections between the Gd and Ho cations. The fight between ferromagnetic (FM) and antiferromagnetic (AFM) interaction, which is linked to magnetic frustration and local structural disorder, is speculated to be influenced by this property. The θ_{CW} can be regulated by doping at the A site, as demonstrated by a substantial rise in the θ_{CW} for $\text{Gd}_2\text{Ti}_2\text{O}_7$ doped with Ho. This might be due to the larger spin angles of the Gd-O-Ho spin, which encourage FM interactions. Further, by partially substituting Ti with Ge (B site doping), the magnetic and structural characteristics of $\text{Ho}_2(\text{Ti}_{1-x}\text{Ge}_x)_2\text{O}_7$ ($x = 0, 0.2,$ and 0.4) pyrochlore have also been investigated. Structural assessment has verified that impurity-free cubic type pyrochlore crystals form with a lattice constant that continuously lowers and follows Vegard's law. Further evidence for the pyrochlore phase's hardening of the phonon mode due to phonon anharmonic interaction came from Raman spectroscopy research. Magnetic investigations have revealed that $\text{Ho}_2\text{Ti}_2\text{O}_7$ elevated chemical pressure causes the ferromagnetic interaction to diminish. Furthermore, even when the temperature in both the (A and B site doping) series was reduced by up to 2K, the glassy pattern remained undetectable. It can be declared that doping at the B site controls magnetic characteristics more effectively than doping at the A site when comparing both of them. It would be stimulating to conduct further research on these system crystallographic modifications at temperatures where spin ices are known to freeze and lose their equilibrium.

2:00 PM *EL03.13.02

Novel Control of Magnetic Anisotropy in Ultrathin Ferromagnets by Interfacial Reconstruction Di Yi; Tsinghua University, China

The manipulation of spin in magnetic systems has been of great interest as it has given rise to a rich spectrum of magnetic ground states and has enabled high performance magnetic memory and logic devices. Magnetic anisotropy (MA), which describes the tendency of magnetic moment vectors to prefer directions, plays an important role in determining these ground states. Here, we present two recent advances in controlling MA in ultrathin ferromagnets by interfacial reconstruction. In the first case, we show that the interface reconstruction in heterostructures comprised of monolayers of 3d and 5d transition metal oxides induces a strong perpendicular magnetic anisotropy. Due to the suppression of thermal fluctuations, we stabilize ferromagnetic order in monolayer manganite with superior performances, which is otherwise challenging in single-phase oxides. In the second case, we show that a tilted magnetic easy axis is induced and can be tuned from nearly in-plane to out-of-plane in ultrathin Co layer, by controlling the crystal symmetry at the interface. This enables the field-free spin-orbit torque switching of perpendicular magnetization components at room temperature with a relatively low current density and excellent stability.

2:30 PM EL03.13.03

Room-Temperature Magnetic Glassiness in Zinc Ferrite Julia Lumetzberger¹, Verena Ney¹, Anna Zakharova², Nieli Daffe², Daniel Primetzhofer³, Fabrice Wilhelm⁴, Andrei Rogalev⁴ and Andreas Ney¹; ¹Johannes Kepler Universitat Linz, Austria; ²SLS, Switzerland; ³Uppsala University, Sweden; ⁴ESRF, France

Zinc ferrite in thin-film form possesses a range of possible applications such as gas sensors, photocatalytic applications or as an interesting semiconducting material in spintronics with tunable magnetic properties including unconventional magnetic order due to intrinsic or extrinsic frustration. Zinc ferrite (ZnFe_2O_4) belongs to the family of normal spinels of the form AB_2O_4 . In bulk form zinc ferrite is known to be antiferromagnetic with a low Néel-temperature [1]. The magnetic properties significantly change as a thin film, especially for a finite degree of inversion and/or off-stoichiometry where ferro(i)magnetic order up to room temperature can be found, e.g. [2]. In contrast, other studies report the existence of a spin-glass or cluster-glass behavior under various conditions in bulk [3] or in thin films [4] exhibiting a wide range of spin freezing temperatures. Here we present a systematic study of epitaxial, stoichiometric zinc ferrite thin films prepared using reactive magnetron sputtering over a wide range of preparation conditions which exhibit signatures of magnetic glassiness up to room temperature [5]. Using element-selective characterization with soft x-ray magnetic circular dichroism we can provide evidence for a finite degree of inversion accompanied by the formation of Zn on octahedral lattice sites as well as a finite magnetic polarization of Zn. In addition, hard x-ray linear dichroism allows a correlation of magnetic glassiness with disorder in the Zn cationic sublattice, which can be induced by increasing the sputtering power, thus further elucidating the microscopic origin for magnetic glassiness at unusually high temperatures exceeding room temperature.

[1] J. M. Hastings and L. M. Corliss, *Rev. Mod. Phys.* **25**, 114 (1953)

[2] V. Zviagin, M. Grundmann, and R. Schmidt-Grund, *Phys. Status Solidi B* **257**, 1900630 (2020)

[3] M. A. Hakim, M. Manjurul Haque, M. Huc, and P. Nordblad, *Phys. B: Condens. Matter* **406**, 48 (2011)

[4] Y. Yamamoto, H. Tanaka, and T. Kawai, *Jpn. J. Appl. Phys.* **40**, L545 (2001)

[5] J. Lumetzberger, V. Ney, A. Zakharova, N. Daffe, D. Primetzhofer, F. Wilhelm, A. Rogalev, and A. Ney, *Phys. Rev. B* **107**, 144416 (2023)

2:45 PM EL03.13.04

Molecular Field Coefficient Modeling of Temperature-Dependent Ferrimagnetism in a Complex Oxide Miela Gross, Tingyu Su, Jackson Bauer and Caroline A. Ross; MIT, United States

The temperature-dependence of the magnetic moment of a magnetically ordered material is fundamental to all aspects of its technological applications. In ferrimagnetic materials with multiple sublattices of magnetic ions coupled by exchange interactions with different strengths and signs, the magnetization can vary nonmonotonically with temperature and can pass through zero at a magnetization compensation temperature T_{comp} . The net angular momentum can also reach zero at the angular momentum compensation temperature T_A , which differs from T_{comp} if the sublattices have different Landé g-factors. Recent studies reveal fast magnetization dynamics near T_A , emphasizing its importance [1]. It is therefore useful to predict the temperature-dependent magnetic moment and angular momentum of a material with known site occupancy, or conversely to use the magnetization vs. temperature to identify the cation site occupancy.

In this work we designed and developed a Python computer code that models the magnetism of rare-earth iron garnets ($\text{RE}_3\text{Fe}_5\text{O}_{12}$, REIG) using a molecular field coefficient (MFC) approach. REIGs contain 8 formula units (160 atoms) per unit cell and the cations occupy three sublattices: tetrahedral Fe^{3+} , octahedral Fe^{3+} , and dodecahedral RE^{3+} . Following Dionne [2], the program calculates both the exchange interactions and the magnetic moment of each sublattice to determine the magnetization and angular momentum as a function of temperature. The model accounts for site occupancy on each sublattice including the effects of non-magnetic and magnetic substitutions, vacancies, Fe^{2+} , and deviations from the ideal RE:Fe stoichiometry by considering their effects on the net magnetization and the sublattice exchange coupling. Unlike previous iterative methods, our program recursively solves for the moment at each temperature which provides more accurate results with excellent match to magnetization vs temperature data for a range of bulk garnets. Using data of Tb-rich terbium iron garnet thin films with Tb:Fe = 0.86 from Rosenberg et al. [3], we show that the model is consistent with the excess Tb accommodated in octahedral sites (which contain $\text{Fe}_{1.52}\text{Tb}_{0.48}$) and vacancies (V) in the tetrahedral sites (which contain $\text{Fe}_{2.53}\text{V}_{0.47}$), giving an excellent match to the measured magnetization, T_{comp} , and Curie temperature, as well as to XPS, XMCD, and elementally resolved TEM data. This work provides accurate magnetic modeling of REIGs of a variety of compositions allowing for design and analysis of ferrimagnets with useful properties.

[1] Liang et al., *Phys Rev B*, 104 174421 (2021); Weissenhofer and Nowak, *Phys Rev B*, 107 064423 (2023). [2] Dionne, *J Appl Phys.* 41, 4874 (1970); *Lincoln Laboratory Technical Report*, 534 (1979). [3] Rosenberg et al., *Small*, doi: 10.1002/smll.202300824 (2023)

3:00 PM BREAK

3:30 PM *EL03.14.01

Polar Textures in Epitaxial BaTiO₃-Based Heterostructures on Silicon Valentin V. Hevelke^{1,2}, Olaniyan I. Ibukun^{1,2}, Ines Hauesler³, Adnan Hammud⁴, Christoph T. Koch³, Dong-Jik Kim¹ and Catherine Dubourdieu^{1,2}; ¹Helmholtz-Zentrum Berlin für Materialien und Energie, Germany; ²Freie Universität Berlin, Germany; ³Humboldt-Universität zu Berlin, Germany; ⁴Fritz Haber Institute of the Max Planck Society, Germany

In recent years, polar textures featuring curled polarization patterns (vortices, skyrmions, merons...) have been unraveled in ultrathin films, superlattices and nanostructures. The development of topological nanoelectronics on chips that would take advantage of such polar textures requires their integration on silicon.

I will discuss in this talk the growth and the resulting polarization patterns of (BaTiO₃/SrTiO₃)_n superlattices epitaxially grown on silicon substrates. The heterostructures were synthesized by molecular beam epitaxy on 4 nm SrTiO₃-buffered Si (001). Various BaTiO₃ and SrTiO₃ thicknesses in the range of 2-5 nm were investigated. The superlattices were characterized by X-ray diffraction, scanning transmission electron microscopy (STEM) and piezoresponse force microscopy. We will show that the biaxial in-plane tensile strain imparted by the silicon substrate upon cooling has a strong impact on the crystalline structure and strain distribution as shown by the in-plane and out-of-plane lattice parameter profiles throughout the stacks (calculated from high angle annular dark field STEM images and geometrical phase analysis). The in-plane lattice parameter of both SrTiO₃ and BaTiO₃ layers increases continuously from bottom to top, and dislocations are present throughout the stacks. The out-of-plane lattice parameter of BaTiO₃ indicates an overall tensile strain (tetragonal *c*-axis BaTiO₃). The atomic displacements of Ti atoms relative to the center of the unit cell (as defined by the Ba or Sr atoms) were determined. From the resulting electrical dipole maps, periodic polar domains are observed in the BaTiO₃ layers as well as nanodomains of curled polarization. The textures observed at different layers of the superlattices will be discussed. Finally, we will show how polar bubbles can also be generated in BaTiO₃ thin films on SrTiO₃-buffered Si. The evidence of curled polarization nanodomains in BaTiO₃-based heterostructures gives promises for a future integration of topological polar nanodomains into nanoscale devices.

4:00 PM EL03.14.02

Polar Vortices in Microwave Electronics Florian Bergmann^{1,2}, Bryan Bosworth¹, Nick Jungwirth¹, Eric Marks¹, Aaron Hagerstrom¹ and Nate Orloff¹; ¹National Institute of Standards and Technology, United States; ²University of Colorado Boulder, United States

Under the right lattice periodicity conditions, internal stress in PbTiO₃-SrTiO₃ superlattice thin films forces the polarization in the PbTiO₃ into a vortex structure. Often called Polar Vortices, theorists expect collective dynamics of Polar Vortices in the gigahertz range. Our group at NIST has experience characterizing thin films up to 1 THz with metallic transmission line structures deposited onto the thin film, producing dielectric and magnetic properties versus frequency. We designed an experiment on Polar Vortex thin films to quantify the electrical properties with devices both parallel and perpendicular to the vortex core. Our measurements show features that we have not observed in any other films, such as negative imaginary parts of the impedance or extremely large resistances per unit length. At this point, we are seeking engagement from the materials community to help understand our observations and how they might be coupled into new microwave electronics.

4:15 PM *EL03.14.03

3D-Atomic-Scale Analysis of Magnetoelectric Multiferroic Topologies via Scanning Transmission Electron Microscopy and Spectroscopy Complemented by Atom Probe Tomography Shelly Michele Conroy; Imperial College London, United Kingdom

Magnetoelectric multiferroic higher order topologies are an emerging solution for future low-power spintronic and quantum devices, due to a combination of their atomic-scale tunable multifunctionality and mobility. In addition to their potential for next-generation interactive technology, topologies with spin to charge coupling are a fertile ground for the exploration and engineering of new states of matter. In our recent report we have shown the presence of vortex topologies present in room temperature magnetoelectric multiferroic Bi₆Ti₂Fe₂Mn₂O₁₈ thin films by atomic-scale scanning transmission electron microscopy (STEM) polarization mapping. We find these chiral polar textures at antiphase boundaries within the thin films. Such topologies related to crystalline defects should be analyzed three-dimensionally to truly understand their formation. In this presentation, will discuss the use of atom probe tomography (APT) combined with STEM and spectroscopies to analyze the Fe and Mn elemental segregation at topological defects.

For Bi₆Ti₂Fe₂Mn₂O₁₈ the magnetic cation partitioning increases the probability of nearest-neighbor magnetic interactions in the central unit cell layer by up to 90% compared to random distributions over the other available B-sites. Using atomic resolution STEM with corresponding energy dispersive X-ray (EDX) and electron energy loss spectroscopy (EELS) elemental mapping we can determine the location of Fe and Mn within the unit cell. Monochromated STEM EELS is used to probe the atomic scale crystal field splitting at the different topologies and within the unit cell. As the topologies themselves are the active regions within such material systems, it is vital that we explore the higher order elemental segregation in full real space. We hence used APT's unique 3D characterization capability to move beyond the 2D projection of the elemental segregation knowledge, with an aim to unravel the magnetic cation partitioning of complex 3D vortices and associated crystallographic defect topologies. Theoretical calculations confirm the subunit cell cation site preference and charged topology energetics. We will discuss the opportunities APT characterization methods can bring to the field multiferroic higher order topology physics. Finally we will discuss recent advancements in MEMS based cryogenic microscopy stage and transfer design to investigate the low temperature phases.

4:45 PM EL03.14.04

Ferroelectric and Chiral Domains in the Polar Vortex System Piush Behera¹, Fernando Ortiz², Peter Meisenheimer¹, Pravin Kavle^{1,3}, Ching-Che Lin^{1,3}, Javier Junquera² and Ramamoorthy Ramesh^{1,4}; ¹UC Berkeley, United States; ²Universidad de Cantabria, Spain; ³Lawrence Berkeley National Laboratory, United States; ⁴Rice University, United States

Polar surface textures are a recent class of topological materials that host numerous unique physical properties such as chirality and collective sub-terahertz dynamics. These properties are directly linked to the fundamental structure of the vortices and their self-organization into a two-dimensional lattice. Here, we focus on how the fundamental structure of the polar vortices influences their mesoscale properties by first examining the intrinsic organization of the vortices at the atomic scale using planar transmission electron microscopy (TEM). By utilizing TEM, we observe three distinct domain wall variations, two of which separate domains with different chirality. Additional cross-sectional TEM measurements enhance our understanding of how the organization of the vortex lattice leads to a measurable net polarization both parallel and perpendicular to the vortex tube axis. Upon examining the vortex system at broader length scales, the vortices exhibit behavior similar to classical ferroelectrics, forming multiple domain variants. Through the usage of piezoresponse force microscopy and second harmonic generation (SHG) linear dichroism, we can clearly distinguish these ferroelectric domain variants and demonstrate that, on the mesoscale, the overall polarization aligns along the [110]_{pc} axis. Furthermore, by comparing SHG linear dichroism with SHG circular dichroism, we can differentiate how these different ferroelectric domain variants are connected to the chirality of the vortex system, providing a pathway to control the chirality of the vortices using an electric field.

8:30 AM *EL03.15.01

Fluctuating Domain Walls and Morphological Configurations in Chiral Magnetic Systems Jeffrey Brock, Ruben Saatjian and Eric Fullerton; University of California-San Diego, United States

The fluctuating nature of magnetic domain morphology transitions has been the subject of intense study, given that such behavior may offer a directly observable means of understanding the physics of underlying magnetic phase transitions. At the same time, stochastic processes in condensed-matter systems have attracted significant interest for neuromorphic computing applications. Recently, we have reported on a domain morphology transition that occurs in the limit of low ferromagnetic exchange stiffness in thin-films with substantial perpendicular magnetic anisotropy and a moderate interfacial Dzyaloshinskii-Moriya interaction [1]. The observed morphological transition was attributed to a severe reduction in the domain wall energy density. Building off these results, we discuss recent work in which we have employed temperature-dependent magneto-optic and AC susceptibility measurements to better understand the

dynamics of this morphological phase transition. Besides temperature-induced changes in the domain periodicity, these measurements have indicated that these systems exhibit two distinct types of temperature-dependent fluctuations – faster-scale fluctuations in the domain wall positions and slower-scale fluctuations in the configuration of the overall domain morphology. While the domain wall fluctuations demonstrate properties of Brownian motion modified by a sporadic pinning potential, the slower-scale morphological fluctuations exhibit characteristics typically ascribed to more solid-like, collective dynamics.

[1] J. A. Brock and E. E. Fullerton, *Advanced Materials Interfaces* **9**, 2101708 (2022)

9:00 AM *EL03.15.02

Manipulating Chiral-Spin Transport with Ferroelectric PolarizationXianzheChen¹, XiaoxiHuang¹, Zhi Yao² and RamamoorthyRamesh¹; ¹University of California, Berkeley, United States; ²Lawrence Berkeley National Laboratory, United States

A collective excitation of the spin structure in a magnetic insulator can transmit spin-angular momentum with negligible dissipation. This quantum of a spin wave, introduced more than nine decades ago, has always been manipulated through magnetic dipoles, (i.e., time-reversal symmetry). Here, we report the experimental observation of chiral-spin transport in multiferroic BiFeO₃, where the spin transport is controlled by reversing the ferroelectric polarization (i.e., spatial inversion symmetry). The ferroelectrically controlled magnons produce an unprecedented ratio of up to 18% rectification at room temperature. The spin torque that the magnons in BiFeO₃ carry can be used to efficiently switch the magnetization of adjacent magnets, with a spin-torque efficiency being comparable to the spin Hall effect in heavy metals. Utilizing such a controllable magnon generation and transmission in BiFeO₃, an all-oxide, energy-scalable logic is demonstrated composed of spin-orbit injection, detection, and magnetoelectric control. This observation opens a new chapter of multiferroic magnons and paves an alternative pathway towards low-dissipation nanoelectronics.

9:30 AM EL03.15.03

Novel Magnetic Topological Phases in BFO: A Computational ApproachTizianaMusso¹, BinXu², YousraNahas³, SergeiProkhorenko³, DanielSando^{4,1}, NagarajanValanoor¹ and LaurentBellaiche³; ¹University of New South Wales, Australia; ²Soochow University, China; ³University of Arkansas, Fayetteville, United States; ⁴University of Canterbury, New Zealand

As one of the most studied room-temperature multiferroics¹, the perovskite compound bismuth ferrite (BiFeO₃ - BFO) has intriguing magnetic structures, where a Dzyaloshinskii-Moriya interaction results in complex spin cycloids. BFO's appealing properties are not only photovoltaic, piezoelectric and optoelectronic, as different topological states have been recently found². These particular phases provide a topological protection necessary for information storage technology³.

In this work, a first-principles-based effective Hamiltonian approach⁴ is used, in conjunction with Monte Carlo simulations, to investigate the magnetic properties of BFO under certain constraints.

First, fast quenching simulations of BFO under strain reveal the presence of magnetic antiferromagnetic (AFM) skyrmions, quasiparticles topologically protected that form stable spin textures⁵. The Pontryagin density has been computed to unambiguously identify the topological nature of the obtained swirling field structures⁶. These novel AFM skyrmion patterns have different morphologies and are preferentially located at the ferroelectric domain walls.

Subsequently, the topological structures obtained from cycloids with different initial propagation directions have been investigated, highlighting the interplay between polarization, cycloids and topological magnetic configurations.

REFERENCES

1. Xu, B. *et al.* Revisiting spin cycloids in multiferroic BFO. *Phys. Rev. B* **98** 1–6 (2018)
2. Govinden, V. *et al.* Spherical ferroelectric solitons. 1–9 (2023)
3. Cortes-Ortuno, D. *et al.* Thermal stability and topological protection of skyrmions in nanotracks. *Sci. Rep.* 1–13 (2017)
4. Rahmedov, D. *et al.* Magnetic Cycloid of BiFeO₃ from Atomistic Simulations. *Phys. Rev. Lett.* **109**, 37207 (2012)
5. Nagaosa, N. & Tokura, Y. Topological properties and dynamics of magnetic skyrmions. *Nature Nanotech* **8**, 899–911 (2013)
6. Nahas, Y. *et al.* Discovery of stable skyrmionic state in ferroelectric nanocomposites. *Nat Comms* 1–6 (2019)

9:45 AM EL03.15.04

Atomistic Polar Topological Structures in Quasi-1D BaTiX₃ (X = S, Se)BoyangZhao¹, Gwan-YeongJung², HuandongChen¹, GuodongRen², ShantanuSingh¹, TiejianChang³, NickSettineri⁴, SimonJ. Teat⁴, Yu-ShengChen³, RohanMishra² and JayakanthRavichandran¹; ¹University of Southern California, United States; ²Washington University in St. Louis, United States; ³Argonne National Laboratory, United States; ⁴Lawrence Berkeley National Laboratory, United States

Polarization vortices¹ and skyrmions in epitaxial heterostructures² arise from boundary condition engineering of ferroelectric materials. Currently, there are no other physical origin for such polar topological structures. In this work, we report the observation of high order ferroic phase transitions in hexagonal quasi-1D chalcogenides, BaTiX₃ (X = S or Se) *via* single crystal synchrotron X-ray diffraction. By refining the crystal structure of BaTiX₃ at different temperatures, we observe large displacements of Ti in the TiX₆ octahedral of BaTiX₃ along and across the quasi-1D chains of TiX₃. BaTiS₃ undergoes a series of symmetry defined TiS₆ dipole ordering from a room temperature *P6₃cm* ferroelectric phase to a charge-density-wave *P3c1* vortex-anti-vortex phase below ~ 250 K and then transforms into a chiral *P2₁* phase below ~180 K. While BaTiSe₃ shows distinctive ferroic order than BaTiS₃, the breaking of the room temperature *P3c1* symmetry is accompanied by emergent correlated disorder ~200K, revealing a longer-range coupling of the ferroic chains in BaTiSe₃.

The observation of complex ferroic dipolar ordering in BaTiX₃ shows complex high order polar textures can be symmetry driven unlike the ferroelectric heterostructures. We presume the role of multipole interactions as the origin of these emergent polarization textures and note the accessibility of similar structural and electrical characteristics in charge density wave materials such as 1T-TiSe₂³ and Ta₂NiSe₅⁴. Our work sets up complex charge density waves with *d⁰* filling as a playground for realizing and understanding quantum polar topologies.

1. Yadav, A. K. *et al.* Spatially resolved steady-state negative capacitance. *Nature* **565**, 468–471 (2019).
2. Das, S. *et al.* Observation of room-temperature polar skyrmions. *Nature* **568**, 368–372 (2019).
3. Kitou, S. *et al.* Effect of Cu intercalation and pressure on excitonic interaction in 1T - TiS₂. *Phys. Rev. B* **99**, 104109 (2019).
4. Nakano, A. *et al.* Antiferroelectric distortion with anomalous phonon softening in the excitonic insulator Ta₂NiSe₅. *Phys. Rev. B* **98**, 045139 (2018).

10:00 AM EL03.15.05

Symmetry of Charge Density Waves and Response Tensors in AV₃Sb₅ Kagome MetalsTuranBiroli¹, EthanT. Ritz^{1,2} and RafaelFernandes¹; ¹University of Minnesota, United States; ²Harvey Mudd College, United States

Space group symmetries and multipole moments allowed by them can be used to predict the macroscopic response of ferroic materials, including ferroelectrics, (anti-)ferromagnets, and multiferroics. In this talk, we apply similar ideas to charge density wave materials with time-reversal symmetry breaking imaginary charge density wave phases. The AV₃Sb₅ (A=K, Rb, Cs) Kagome metals undergo multiple charge density wave transitions in addition to hosting superconducting and topological phases. This charge ordering behavior may involve both bond distortions ("real" charge density waves) and time-reversal symmetry breaking loop currents. In this talk, we classify different charge density wave phases using magnetic space groups and their representations. By studying the allowed elements of various macroscopic response tensors, including piezomagnetic and magneto-optical tensors, we lay out experimental pathways to pin down the symmetry of the charge density wave phases in these systems and possibly observe novel nonreciprocal optical effects. We also comment on the implications of the possible Kerr rotation in Kagome metals.

SESSION EL03.16: Virtual Session
Session Chairs: John Heron and Morgan Trassin
Tuesday Afternoon, December 5, 2023
EL03-virtual

6:30 PM *EL03.16.01

Crafting Novel Low-Symmetry and Topological Structures in Complex Oxide Thin Films Through Anisotropic Epitaxy and Superlattice EngineeringNagarajanValanoor¹, DanielSando² and LaurentBellaiche³; ¹UNSW Sydney, Australia; ²University of Canterbury, New Zealand; ³University of Arkansas, Fayetteville, United States

Complex oxide thin films and superlattices provide an exciting playground for exploring and fine-tuning structure-property relationships. By playing with the electrical and mechanical boundary conditions through epitaxial strain, substrate orientation, and superlattice design, completely new phases of these materials – with enhanced or new functionality – are possible. In piezoelectric oxides, for instance, tuning the morphotropic phase boundary by strain offers a route to generating improved electromechanical responses. At the same time, there has been increasing interest in ferroelectric solitons – topologically protected particle-like polarization textures with great promise for beyond-CMOS technologies – which can form in ferroelectric oxide thin films through the competition among various degrees of freedom. However, while polar skyrmions have been extensively studied (e.g., in the $\text{PbTiO}_3\text{-SrTiO}_3$ (STO) system), such polarization textures have scarcely been demonstrated in multiferroics.

In this talk we show that epitaxial strain and orientation engineering, as well as careful control of mechanical and electrical boundary conditions through superlattice design, can be used to craft new phases and topological textures in the popular multiferroic BiFeO_3 (BFO). First, using “anisotropic epitaxy” (i.e., growing epitaxial films on extremely vicinal substrates) we create a low-symmetry phase of BFO that acts as a structural bridge between the rhombohedral-like and tetragonal-like polymorphs. Interferometric displacement sensor measurements reveal that this phase has a 2.4x enhanced piezoelectric coefficient compared with typical rhombohedral-like BFO.

Second, by combining BFO with STO in carefully designed superlattices, we demonstrate ferroelectric solitons in this popular multiferroic system. High-resolution piezoresponse force microscopy and Cs-corrected high-angle annular dark-field scanning transmission electron microscopy uncover a zoo of topologies, and polarization displacement mapping of planar specimens reveals centre-convergent/divergent topological defects as small as 3 nm. Phase field simulations reveal that some of these structures can be classed as “bimerons” with a topological charge of ± 1 , and effective Hamiltonian computations show that the coexistence of such structures can lead to non-integer topological charges, a first observation in a BiFeO_3 -based system.

Our results once again highlight the versatility and power of epitaxy for the creation of novel phases in oxide thin films, and open new opportunities in multiferroic topotronics.

7:00 PM EL03.16.02

Investigation of Rare Earth Lean Sm-(Fe,Co)-Mo Alloys for Permanent Magnets Yitong Xu and George Hadjipanayis; University of Delaware, United States

R-(Fe,Co)-Mo compounds with the ThMn_{12} crystal structure have been studied recently as potential candidates for high-performance magnets, due to their low rare-earth (R) content which are considered as critical elements. The compounds with high Fe content, are expected to be strong magnets, because of their large magnetization M_s , high Curie temperature as well as strong uniaxial magnetocrystalline anisotropy when $R=\text{Sm}$. In this study, bulk alloys with composition $\text{Sm}_1\text{Fe}_{10.5-x}\text{Co}_x\text{Mo}_{1.5}$ ($x=0,1,2$) were prepared with the tetragonal ThMn_{12} structure. The effects of Co on the magnetic properties, including the Curie temperature, saturation magnetization M_s , anisotropy field, and energy product $(\text{BH})_{\text{max}}$, have been investigated. It was found that the Curie temperature shows a linear increase with the Co substitution; also, an increasing Co content increases M_s but decreases the anisotropy field. In order to develop high coercivity, the cast samples were high-energy-ball-milled followed by hot-compaction at 650 °C under 275 MPa. Annealing of compacted samples was done from 700 to 1000 °C to optimize the magnetic properties. Our studies showed that the $\text{Sm}_1\text{Fe}_{10.5-x}\text{Co}_x\text{Mo}_{1.5}$ alloy with $x=1$ has a coercivity $H_c=2.8$ kOe and the highest energy product $((\text{BH})_{\text{max}}=2.8$ MGOe) after annealing at 750 °C for 48 h, marking a 22% enhancement relative to the specimen without cobalt substitution. These properties are attractive for their future development into permanent magnets via sintering. This work was supported by the U.S. Department of Energy under Grant DE-FG02-90ER45413.

7:05 PM EL03.16.03

Surface-Sensitive and Bulk-Suppressed Raman Scattering by Transferable Nanoporous Plasmonic Membranes Sebastian Heeg¹, Roman Wyss^{1,2}, Günter Kewes¹, Martin Frimmer², Karl-Philipp Schlichting², Markus Parzefal², Eric Bonvin², Martin F. Sarott², Morgan Trassin², Lala Habibova¹, Giorgia Marcelli¹, Marcela Giraldo², Jan Vermant², Lukas Novotny² and Mads Weber³; ¹Humboldt-Universität zu Berlin, Germany; ²ETH Zürich, Switzerland; ³Le Mans Université, France

Raman spectroscopy is a powerful technique to characterize materials. It probes non-destructively chemical composition, crystallinity, defects, strain and coupling phenomena. However, the Raman response of surfaces or thin films is often weak and obscured by dominant bulk signals. Here we overcome this limitation by placing a transferable porous gold membrane (PAuM) on top of the surface of interest. Slot-like nanopores in the membrane act as plasmonic slot antennas and enhance the Raman response of the surface or thin film underneath. Simultaneously, the PAuM suppresses the penetration of the excitation laser into the bulk, efficiently blocking the bulk Raman signal. Using graphene as a model surface, we show that these two simultaneous effects lead to an increase in the surface-to-bulk Raman signal ratio by three orders of magnitude. We find that 90% of the Raman enhancement occurs within the top 2.5 nm of the material, demonstrating truly surface-sensitive Raman scattering. To validate our approach, we analyze the surface of a LaNiO_3 thin film. We observe a Raman mode splitting for the LaNiO_3 surface-layer, which is spectroscopic evidence that the surface structure differs from the bulk. This result underpins that PAuM give direct access to Raman signatures of surfaces and their structural properties.

7:20 PM *EL03.16.04

Ultrafast Activation of Hidden Phases in Antiferroelectrics, Relaxors, Quantum Paraelectrics and Ferroelectric Nanostructures Laurent Bellaïche; University of Arkansas, United States

One currently active and exciting research field explores the generation of “hidden” metastable states of matter by ultrafast optical excitation. Such states are referred to as hidden because they are not accessible via the tuning of thermodynamic variables, such as temperature or pressure. Optically-induced ultrafast transitions to hidden states have been found in superconductors (1), colossal magnetoresistance manganites (2), charge-density wave materials (3) and incipient ferroelectrics (4,5). A variety of optical excitation wavelengths have been used to trigger the transition to hidden phases, ranging from visible (3) to mid-infrared (1,2) to THz wavelengths (4,6). In an example most relevant to this Talk, ferroelectricity was induced in the quantum paraelectric SrTiO_3 by a THz optical pulse (4). These hidden metastable states often enable physical functionalities that do not exist in the equilibrium thermodynamic phase, such as novel electronic memory concepts (7).

The aim of this Talk is to demonstrate and explain why, via the use of first-principle-based atomistic effective Hamiltonians, that a variety of hidden states can be generated in antiferroelectrics, relaxor ferroelectrics, quantum paraelectrics and ferroelectric nanostructures, when applying THz pulses of electric fields [8]. Such hidden states can be of homogeneous nature in antiferroelectrics [9,10] versus of inhomogeneous character in relaxor ferroelectrics [11], while all having enhanced or novel physical properties and being also promising for neuromorphic computing. This talk will also report and discuss the ultrafast formation of ferroelectricity in quantum paraelectrics [12], as well as, of hidden states possessing electric topological defects, such as skyrmions or bubbles, in ferroelectric nanostructures [13].

The authors thank ONR Grant N00014-21-1-2086, the Vannevar Bush Faculty Fellowship (VBFF) from the Department of Defense, the MonArk NSF Quantum Foundry supported by the National Science Foundation Q-AMASE-I Program under NSF Award No. DMR-1906383, an Impact Grant from the Arkansas Research Alliance (ARA), the ARO Grants No. W911NF-21-1-011 and W911NF-21-2-0162 (ETHOS), the NSF Grant No. DMR-1554866, the French ANR through EXPAND project ANR-17-CE24-0032, the European Union’s Horizon 2020 research and innovation programme under Grant Agreement No. 964931 (TSAR), the U.S. Department of Energy (DOE), Office of Science, Basic Energy Sciences (BES), under Award # DE-SC0019273, the Ministry of Science and Technology of the People’s Republic of China (No. 2022YFA1402901) and from NSFC (No. 12274082).

References:

- [1] D. Fausti *et al.*, *Science* 331, 189 (2011).
- [2] M. Rini *et al.*, *Nature* 449, 72 (2007).
- [3] L. Stojchevska *et al.*, *Science* 344, 177 (2014).
- [4] X. Li *et al.*, *Science* 364, 1079 (2019).
- [5] T. F. Nova *et al.*, *Science* 364, 1075 (2019).
- [6] M. Liu *et al.*, *Nature* 487, 345 (2012).
- [7] I. Vaskivskiy *et al.*, *Nature Communications* 7, 11442 (2016).
- [8] S. Prosandeev *et al.*, *Neuromorphic Computing and Engineering* 3, 012002 (2023).
- [9] S. Prosandeev *et al.*, *Physical Review B* 105, L100101 (2022).
- [10] S. Prosandeev and L. Bellaïche, *Physical Review Materials* 6, 116201 (2022).
- [11] S. Prosandeev *et al.*, *Physical Review Letters* 126, 027602 (2021).
- [12] X. Li *et al.*, *Physical Review B* 107, 064306 (2023).
- [13] S. Prosandeev *et al.*, *Advanced Electronic Materials*, 2200808 (2022).

7:50 PM EL03.16.05

Characterizing Polarization Switching Kinetics of Ferroelectric $\text{Hf}_{0.5}\text{Zr}_{0.5}\text{O}_2$ at Cryogenic Temperature Jiacheng Xu¹, Jiajia Chen¹, Rongzong Shen¹, Chengji Jin¹, Minglei Ma^{1,2}, Haoji Qian¹, Gaobo Lin¹, Yian Ding¹, Yan Liu^{1,2}, Xiao Yu¹ and Genquan Han^{1,2}; ¹Zhejiang Lab, China; ²Xidian University, China

Properties of HfO₂-based ferroelectric at cryogenic temperature (T) are getting significant attention for various applications from high-performance computing to aerospace electronics. In this work, we characterize polarization (P) switching kinetics of Hf_{0.5}Zr_{0.5}O₂ (HZO) at cryogenic T down to 100 K. By nucleation limited switching (NLS) model with Lorentzian distribution fittings, the dependences of average switching time ($\log\tau_1$) and switching time distribution (ω) on T are extracted. As the T decreases from 300 K to 100 K, $\log\tau_1$ first rapidly decreases and then gradually stabilizes. Meanwhile, ω exhibits different trends under different applied electric fields (E), decreasing under low applied E while increasing under high applied E , eventually stabilizing at non-zero constants. Leakage, charge de-trapping, and imprint effect measurements are also carried out to reveal the possible mechanisms in the dependence of P switching kinetics on T . It is clarified that the less charge trapped by defects leads to the lower $\log\tau_1$ at lower T while the built-in E and domain wall motion induced by trapped charge result in the change of ω . With the further decrease of T (<100 K), due to the negligible charge trapping effect, $\log\tau_1$ and ω exhibited by HZO are saturated, indicating the intrinsic properties of ferroelectric domains, which are different from the prediction in previous literatures that $\log\tau_1$ and ω will linearly decrease as T decreases.

In this work, titanium nitride (TiN)/HZO(10 nm)/TiN structures are fabricated to study the switching kinetics. Firstly, the leakage measurements were carried out at different T . As the T decreases, the leakage current decreases ($3.49 \times 10^{-4}/1.21 \times 10^{-5}/4.70 \times 10^{-6}/2.66 \times 10^{-6}$ A/cm at 300/200/150/100 K under 3.0 MV/cm, 500 ms pulse), resulting in less trapped charge. Then, after 1000 cycles of triangular waves (± 4 MV/cm, 1 kHz) applied to fully release the trapped charge, $P-E$ curves (± 4 MV/cm, 1 kHz) at different T are readout for the first time. After a relaxing time (60 s), the $P-E$ curves are readout for the second time. We found that, the shift of coercive E after relaxing (0.442/0.126/0.040/0.002 MV/cm at 300/200/150/100 K) becomes much weak at low T . These results show lower leakage and less imprint at lower T and imply charge trapping effect can be ignored at deep cryogenic T (<100 K).

Finally, the switching kinetics of HZO are measured using a pulse sequence at 300/200/150/100 K. The P variations divided by the spontaneous P ($\Delta P(t)/2P_s$) are extracted under various writing pulses (0.1 μ s-1 ms, 0.5-4.0 MV/cm). The NLS model and the Lorentzian distribution are applied to fit all the experimental $\Delta P(t)/2P_s$ data. Lorentzian distribution includes two key parameters, i.e., $\log\tau_1$ and ω , representing the average switching time and half-width of the switching time distribution. For low applied E (1.5 MV/cm), the extracted $\log\tau_1$ and ω at $T=300/200/150/100$ K are -3.19/-4.66/-4.91/-5.06 s and 1.94/0.84/0.77/0.69, and the extrapolated $\log\tau_1$ and ω at $T<100$ K stabilize around -5.22 s and 0.60. For high applied E (4.0 MV/cm), the extracted $\log\tau_1$ and ω at $T=300/200/150/100$ K are -5.69/-5.87/-5.90/-5.90 s and 0.10/0.11/0.13/0.13, and the extrapolated $\log\tau_1$ and ω at $T<100$ K stabilize around -5.91 s and 0.15.

In summary, with the T decreases from 300 K to deep cryogenic, $\log\tau_1$ first rapidly decreases, attributed to the lower built-in E caused by charge trapping. Then it gradually stabilizes, representing the intrinsic switching speed of ferroelectric domains. ω decreases under low applied E , attributed to the more switching ferroelectric domains caused by the lower built-in E , while it increases under high applied E , due to the domain wall motion. Eventually ω stabilizes at non-zero constants, showing the intrinsic distribution of ferroelectric domains. These phenomena indicate that HZO will exhibit poly crystal properties described by NLS model as T down to deep cryogenic, which is different from the previous predictions.

8:05 PM EL03.16.06

Improvements in Ferroelectric Properties of Hf_{1-x}Zr_xO₂ Thin Film with Rapid Thermal Annealing under Alternating Electric Field ShoTanaka, TakumiHayakawa and MinoruNoda; Kyoto Institute of Technology, Japan

Various methods have been so far investigated to prepare the ferroelectric HfO₂ family film and to improve its properties. The origin of ferroelectricity of HfO₂ is considered to be the metastable orthorhombic phase, where, for example, this phase is thought to evolve during the process of cooling down in rapid thermal annealing (RTA) [1]. The volume fraction of the ferroelectric phase has a large relationship to the value of remanent polarization, so it is important to induce the o-phase as much as possible during the RTA. Regarding this, there are some reports of transformation from paraelectric tetragonal phase to the ferroelectric orthorhombic phase [2]. In this work, we newly propose applying an electric field on a HfO₂ family film during RTA process that would induce more effectively ferroelectric phases by way of field-induced phase transition, as hafnia is in the t-phase at high temperatures [3]. An alternating electric field was applied between a Pt substrate, contacting with a power supply, on the top electrode of HZO film capacitor and its bottom electrode. Hysteresis loops of $P-E$ and $J-E$ were measured at 1 kHz for samples RTA-annealed with and without electric field. The sample annealed with electric field showed nearly no imprint and larger remanent polarization by three times ($\sim 15 \mu\text{C}/\text{cm}^2$) than that without the field with a rather large imprint. Furthermore, it was noted from our XPS results that not only the phase change but the distribution of oxygen vacancies and/or constituent atoms especially near the film surface and interface at Hf_{1-x}Zr_xO₂(HZO)/TiN lower electrode gives influence on the electrical and ferroelectric properties of the HZO film. Finally, we found that the annealing with electric field leads to an enhancement in the ferroelectric o-phase and uniform diffusion of oxygen vacancies.

References:

- [1] M. H. Park et al., *Nanoscale*, 10, 716-725 (2018).
- [2] T. Shimizu et al., *Phys. Status Solidi RRL*, 15: 2000589 (2021).
- [3] T. D. Huan et al., *Phys. Rev. B* 90, 064111 (2014).

8:20 PM EL03.16.07

Enhancing Functionality of Lead-Free Ferroelectric BiFeO₃-BaTiO₃ based Piezoceramics through Chemical Modification and Site Engineering SrishitiPaliwal, ProsunMondal and AkhileshK. Singh; Indian Institute of Technology BHU, Varanasi, India

The urgent need for lead-free piezoceramics with superior ferroelectric and dielectric properties at high temperatures has spurred extensive research efforts, particularly for demanding environments such as oil drilling, process monitoring, nuclear, and space exploration. Despite the dominance of lead-based piezoelectric ceramics in commercial applications, concerns for the environment and human health necessitate the development of viable alternatives. BiFeO₃-BaTiO₃ (BF-BT) is one such extensively studied system that has attracted a lot of attention because of its properties like multiferroicity, high Curie temperature etc. In this study, we address this challenge by employing judicious chemical modification to develop two lead-free binary solid-solution of 0.67(Bi_{1.05}(Fe_{0.97}Ga_{0.03})_{1-x}Sc_xO₃)-0.33(BaTiO₃) and 0.67(Bi_{1.05-y}La_yFe_{0.97}Ga_{0.03}O₃)-0.33(BaTiO₃) with $x, y \leq 0.07$, through site engineering and the solid-state route using the air quenching sintering technique. The crystal structure analysis using X-ray diffraction (XRD) data reveals the pure perovskite phase formation. The Rietveld structure refinement confirms the presence of pseudocubic symmetry with space group Pm-3m as the majority phase. Microstructural analysis reveals a homogeneous and dense microstructure with a narrow grain size distribution of less than 3 μ m. The temperature dependent dielectric studies show strong frequency dependence of the dielectric constant resulting in diffuse phase transition peaks which indicates the relaxor ferroelectric behavior. In addition, the small grain size, low remnant polarization and coercive field values also confirm the relaxor like behavior for both systems. Furthermore, the dielectric peaks maxima temperature (T_m) shift to lower temperature side on increasing concentration of Sc³⁺. The freezing temperature (T_f) of ~ 633 K was obtained for $x=0.07$ while T_f follows an upward trajectory as accounted by the Vogel-Fulcher model, with the highest point observed at around 551 K for the composition containing $y=0.07$. In contrast, the activation energy exhibits a contrasting pattern, gradually decreasing from about 0.61 eV to 0.07 eV. The synthesized materials display promising characteristics, including remnant polarization ranging from 2Pr \sim 8-55 $\mu\text{C}/\text{cm}^2$ and coercive field (E_c) ranging from 2Ec \sim 27-91 kV/cm among different compositions. Improved resistivity on the order of 10¹⁰ was observed in leakage current measurements under an applied field of 1 kV/cm. Notably, the dielectric permittivity corresponding to peaks at 10 kHz experienced a remarkable boost from 4100 to 21832 as the concentration of La doping increased from 1 mol% to 7 mol%. These findings highlight the enhanced functional attributes and temperature stability achieved through site engineering, paving the way for the development of lead-free piezoceramics with enhanced performance in a wide range of industrial applications requiring reliable operation under harsh conditions.

8:25 PM EL03.16.08

Giant Electromechanical Response from Defective Non-Ferroelectric Epitaxial BaTiO₃ Integrated on Si (100) SandeepVura¹, ShubhamK. Parate¹, SubhajtPal², UpanyaKhandelwal¹, RajeevKumar Rai³, Sri HarshaMolleti¹, VishnuKumar¹, Rama SatyaSandilya¹, GirishPatil¹, MuditJain¹, AmbreshMallya¹, MajidAhmadi⁴, BartKooi⁴, SushobhanAvasthi¹, RajeevRanjan¹, SrinivasanRaghavan¹, SaurabhChandorkar¹ and PavanNukala¹; ¹Indian Institute of Science Bangalore, India; ²Queen Mary University of London, United Kingdom; ³University of Pennsylvania, United States; ⁴University of Groningen, Netherlands

Recently giant electromechanical (EM) responses have been observed in several defective systems due to the formation of site deficiency which is obtained either by creating geometrical or compositional modification. The idea of obtaining a giant EM response in the defective system gained tremendous attention owing to the observation of d_{33} value of $\sim 200,000$ pm/V even in centrosymmetric gadolinium-doped CeO_{2-x} films at milli Hz frequency owing to the mass migration of point defects under application of electric field leading to a local structural change from a cubic to tetragonal. Since large range motion of ions results in large EM response in Gd:CeO₂, its EM response is confined to very low frequency (\sim milli Hz). This response degrades to 25000 pm/V at 100 Hz and beyond that the response is almost zero, with different defect-induced mechanisms at play in different frequencies. Here we demonstrate silicon compatible Barium Titanate (BTO) system that shows an equivalent large electromechanical response at much higher frequencies (>1 kHz). These films are Barium and oxygen-deficient nature as revealed from XPS and TEM studies. X-ray Diffraction shows that the thermal expansion coefficient of these defective films is 3×10^{-5} (K⁻¹) one of the highest reported. We measure out-of-plane displacement while applying in-plane field using Laser Doppler Vibrometry (LDV) and report highest second order effective M_{31} (of the order 10^{-14} (m/V)²) for any material at high frequencies (>1000 Hz). We further performed small signal and large signal impedance measurements and correlate them with our structural data from TEM and XRD. Through simulations, we assess the effects of joule heating in mechanical displacements and attribute the rest to defect-based electro-strictive behavior.

8:40 PM EL03.16.09

A ReaxFF Reactive Force Field for Studying Ferroelectricity in Mg-Substituted ZnO AlirezaSepherinezhad and AdriVan Duin; Penn State, United States

Ferroelectric materials have emerged as a pivotal component in the realm of microelectronic devices, owing to their unique properties including robust spontaneous polarization, piezoelectric

and pyroelectric effects, and large dielectric constants. These materials have been used in nonvolatile memories, transducers, capacitors, and photovoltaic devices. Application of conventional perovskite ferroelectrics, however, faces prohibiting factors such as incompatible windows for synthesis and difficulties in scaling below 100nm. These limitations inspire looking beyond perovskite thin films. Recent research has attracted attention to the *Ferroelectrics Everywhere* hypothesis in the development of modern ferroelectrics. This hypothesis suggests that, in principle, one can observe ferroelectric behavior by distorting a polar structure through cation substitution, as long as the polar axes are re-orientable under an external electric field. In this study, we aim to demonstrate ferroelectricity in Mg-substituted ZnO slabs using the ReaxFF reactive force field. Specifically, we develop a ReaxFF reactive force field and utilize MD simulations to investigate reaction dynamics for $Zn_xMg_{1-x}O$ (ZMO). To develop the force field, we fit the force field parameters to a training set of data points from DFT calculations. The data points have been chosen to provide adequate descriptions of the phase transition path in ZnO. We then evaluate our force field against equations of state (compression and expansion) of ZMO from DFT derived data. The results show a strong agreement between DFT reference data and ReaxFF predictions. We then use the force field in NPT MD simulations to investigate ferroelectricity in the presence of an external electric field. Our findings show that Mg-substitution enables polarization reversal through lowering the coercive field. Specifically, an increase in Mg percentage consistently results in a decrease in coercive field. Moreover, we observe that coercive field magnitude in ZMO is strongly dependent to the temperature. In all cases, an increase in temperature is followed by a sharp drop in the coercive field. These findings would not only support the hypothesis of *Ferroelectrics Everywhere*, but also motivates how tunable ferroelectric properties of ZnMgO could be utilized in future applications.

SYMPOSIUM EL04

Materials and Devices for Neuromorphic Electronics and Bio-Interfaces
November 28 - December 6, 2023

Symposium Organizers

Simone Fabiano, Linköping University
Paschalis Gkoupidenis, Max Planck Institute
Zeinab Jahed, University of California, San Diego
Francesca Santoro, Forschungszentrum Jülich/RWTH Aachen University

Symposium Support

Bronze
Kepler Computing

* Invited Paper

+ JMR Distinguished Invited Speaker

SESSION EL04.01: Bio-Interfaces and Bioelectronics I
Session Chairs: Xenofon Strakosas and Fabrizio Torricelli
Tuesday Morning, November 28, 2023
Hynes, Level 3, Room 313

8:45 AM *EL04.01.03

Interfacing Neuronal Tissue with 3D Electrodes [Andreas Offenhaeusser](#)¹, [Jamal Shihada](#)^{1,2}, [Marie Jung](#)^{1,2}, [Simon Decke](#)^{1,2} and [Viviana Rincon Montes](#)¹; ¹Forschungszentrum Jülich, Germany; ²RWTH Aachen University, Germany

Neuronal signals obtained from 3D neural tissue using various - in vitro or in vivo - approaches lack the spatial resolution and high signal-to-noise ratio (SNR) required for a detailed understanding of neural network function and synaptic plasticity. To overcome these limitations, we used a highly customizable 3D printing process in combination with thin film technology and templated assisted electrodeposition to fabricate 3D-printed based microelectrode arrays on stiff and flexible substrates. We show devices with design flexibility and physical robustness for recording neural activity in different in vitro and in vivo applications: our microelectrode arrays successfully recorded neural activity in 3D neuronal cultures, retinal explants, and the cortex of living mice, thereby demonstrating the versatility of the 3D microelectrode platform while maintaining high-quality neural recordings. Customizable 3D microelectrode arrays provide unique opportunities to study neural activity under regular or various pathological conditions, both in vitro and in vivo, and contribute to the development of drug screening and neuromodulation systems that can accurately monitor the activity of large neural networks over time.

9:15 AM EL04.01.02

Three-Dimensional MnO₂ Nanoflowers Integrated into Flexible Optoelectronic Biointerfaces for Safe and Effective Neuronal Photostimulation [Lokman Kaya](#)¹, [Onuralp Karatum](#)¹, [Ridvan Balamur](#)¹, [Humeyra Nur Kaleli](#)¹, [Asim Onal](#)¹, [Sharadrao A. Vanalakar](#)², [Murat Hasanreisoglu](#)¹ and [Sedat Nizamoglu](#)¹; ¹Koç University, Turkey; ²Shivaji University, India

The utilization of optoelectronic biointerfaces for wireless and electrical control of neurons has garnered significant interest, particularly in the field of photovoltaic retinal implants. Three-dimensional pseudocapacitive nanomaterials with porous structures and large surface areas hold high promise for developing efficient optoelectronic biointerfaces that can effectively convert light into stimulating ionic currents because of their high electrode-electrolyte capacitance. In this study, we present the successful integration of flexible optoelectronic biointerfaces with three-dimensional manganese dioxide (MnO₂) nanoflowers, enabling the achievement of safe and effective photostimulation of neurons. The synthesis of MnO₂ nanoflowers involves a chemical bath deposition process on the return electrode, initially coated with a MnO₂ seed layer using cyclic voltammetry. The resulting nanoflowers exhibit remarkable interfacial capacitance (>10 mF.cm⁻²) and photogenerated charge density (>20 μC.cm⁻²) even at low light intensity (1 mW.mm⁻²). Significantly, the MnO₂ nanoflowers facilitate the generation of safe capacitive currents through reversible Faradaic reactions and exhibit no toxicity towards hippocampal neurons in vitro, making them a highly promising material for seamless biointerfacing with electrogenic cells. The functionality of the developed optoelectronic biointerfaces is validated through patch-clamp electrophysiology recordings conducted on hippocampal neurons in the whole-cell configuration and we observed repetitive and rapid firing of action potentials in response to light pulse trains. This study demonstrates the vast potential of electrochemically-deposited three-dimensional pseudocapacitive nanomaterials as a robust and versatile nanotool for optoelectronic control of neurons.

Reference

L. Kaya, O. Karatum, R. Balamur, H. N. Kaleli, A. Onal, S. A. Vanalakar, M. Hasanreisoglu, S. Nizamoglu, "MnO₂ Nanoflower Integrated Optoelectronic Biointerfaces for Photostimulation of Neurons," *Advanced Science* (2023). (Accepted)

Funding

SN acknowledges funding by the European Union (ERC, MESHOPITO, 101045289). Views and opinions expressed are however those of the author(s) only and do not necessarily reflect those of the European Union or the European Research Council Executive Agency. Neither the European Union nor the granting authority can be held responsible for them. S.N. also acknowledges the Scientific and Technological Research Council of Turkey (TUBITAK) with Project No.s 121C301, 120E329, and 121E376.

9:30 AM EL04.01.04

Ultra Low Impedance PEDOT:PSS Neural Electrode Array for Simultaneous Two Photon Imaging and Electrophysiology Analysis Hyun WooKim, Young UkCho and Ki JunYu; Yonsei University, Korea (the Republic of)

Understanding the intricate mechanisms of information processing in the brain requires precise electrophysiology recordings at the resolution of action potentials. Recent progress in optical technologies, notably the advancements in multi-photon microscopy, have brought about a paradigm shift in our capacity to observe and analyze neuronal activity. Integration of optical methodologies with electrical recordings assumes a crucial role in bridging the knowledge gap between animal models and human studies, which heavily rely on electrophysiological evaluations of brain activity. Nonetheless, this integration encounters obstacles such as the emergence of light-induced artifacts and the requirement for neural electrodes with low impedance. To address these challenges, we present transparent a poly(3,4-ethylenedioxythiophene):poly(styrenesulfonate)(PEDOT:PSS)-based neural interface array. This PEDOT:PSS neural array merges transparency, adaptability, and biocompatibility facilitating simultaneous acquisition of local field potentials (LFPs) and action potentials from superficial cortical neurons. By utilizing a flexible polyethylene terephthalate (PET) substrate, we enhance the convenience of electrocorticography (ECoG) measurements while maintaining a cost-effective and straightforward manufacturing process.

Transparent PEDOT:PSS electrode array ensure the integration of two-photon microscopy and ECoG recordings within a single in vivo experiment. To further enhance the functionality of the PEDOT:PSS electrode array, we have analyzed the charge transfer enhancement mechanism and developed a three-step post-processing technique. This technique effectively reduces the impedance of the electrode to an impressive value of 5.8 k Ω (at 1kHz) for a 50 \times 50 μm^2 electrode surface area without the use of traditional metal components. The transparent, low impedance PEDOT:PSS microelectrode array allows for depth-resolved two-photon imaging below the cortical surface, while simultaneous recordings of LFPs from the cortical surface and neuronal calcium activity provide a comprehensive understanding of neural dynamics. Our PEDOT:PSS electrode array offers a platform for integrating optical modalities with electrophysiology, enabling a wide range of experimental possibilities. The successful integration of diverse in vivo optical imaging and electrical recording with PEDOT:PSS electrode recordings exemplifies the versatility of this technology. Whether applied to depth-resolved two-photon imaging or the chronic monitoring of LFPs and action potentials of cortical neurons, our PEDOT:PSS electrode array offers a seamless and non-invasive solution that contributes to the advancement of our comprehension regarding brain function. These findings highlight the potential of our PEDOT:PSS microelectrode array as a effective tool for seamless and artifact-free integration of optical and electrical modalities, opening new avenues for comprehensive neuroscience research.

9:45 AM BREAK

10:15 AM *EL04.01.05

Organic Bioelectronic Circuits and Artificial Neurons for Biosensing and Biointerfacing FabrizioToricelli; University of Brescia, Italy

Organic bioelectronics based on organic mixed ionic-electronic materials and devices, can enable the direct communication and interfacing with ions, biomolecules, soft tissues, cells, and organs in the aqueous biological environment, opening opportunities for in-vitro and in-vivo applications. [1]

This talk will present emerging organic bioelectronics including technologies, devices and integrated architectures for enhanced applications. Starting from the fundamental properties of device operating principles and integrated bio-circuit configurations.[2,3] the talk will seamlessly move to a large set of applications including (i) multiscale ion detection,[4] (ii) selective multi-bio-marker detection at the single-entity limit,[5,6] (iii) real-time monitoring of cell layer integrity and tight junction modulation,[7] and (iv) artificial spiking neurons with electrochemical degrees of control for in situ neuromorphic sensing and biointerfacing.[8]

The talk will show the key achievements of a beautiful journey that I am doing with various multidisciplinary and geographically-distributed research groups, highlighting possibilities for next-generation multifunctional bioelectronics and neuromorphic bio-interfacing.

[1] F. Torricelli, et al. "Electrolyte-gated transistors for enhanced performance bioelectronics", Nature Reviews Methods Primers 1, 66 (2021)

[2] R. Granelli, et al. "High-Performance Bioelectronic Circuits Integrated on Biodegradable and Compostable Substrates with Fully-Printed Mask-less Organic Electrochemical Transistors", Small 18, 2108077 (2022).

[3] P. Romele, et al. "Ion buffering and interface charge enable high performance electronics with organic electrochemical transistors", Nature Communications 10, 3044, (2019).

[4] P. Romele, et al. "Multiscale real time and high sensitivity ion detection with complementary organic electrochemical transistors amplifier", Nature Communications 11, 3743 (2020).

[5] E. Macchia, et al. "A handheld intelligent single-molecule binary bioelectronic system for fast and reliable immunometric point-of-care testing", Science Advances 8, abo0881 (2022).

[6] E. Genco, et al. "Single-Molecule Bioelectronic Portable Array for Early-Diagnosis of Pancreatic Cancer Precursors", under review (2023).

[7] K. Lieberth, et al. "Real-Time Monitoring of Cellular Barrier Functionality with Dynamic-Mode Current- Driven Organic Electrochemical Transistor", Advanced Materials Technologies 8, 2201697 (2023).

[8] T. Sarkar, et al. "An organic artificial spiking neuron for in situ neuromorphic sensing and biointerfacing", Nature Electronics 5, 774-783 (2022).

10:45 AM *EL04.01.06

Enzymatic Polymerization of Thiophene-Based Oligomers for Soft Bioelectronic Interfaces XenofonStrakosas; Linköping University, Sweden

The field of Bioelectronics aims to integrate electronics and biology, offering promising opportunities in various domains. However, a major hurdle in this field is the mechanical mismatch between rigid electronics and the soft nature of living tissues. To overcome this challenge, soft and flexible bioelectronic devices are being developed using microfabrication and printing techniques. Alternatively, biological processes polymerize small molecules to create intricate micromachines. Inspired by these biological processes, we utilize thiophene-based oligomer building blocks and enzymatic processes for in vivo polymerization of organic conductors. By harnessing the advantages of this approach, we successfully achieved the in-situ formation of conducting polymer gels within living organisms. These gels exhibited soft mechanical properties that closely resemble those of natural tissues. Furthermore, we demonstrated the enzymatic construction of organic conductors in various tissues and their application as active materials in organic transistors. Our approach offers a solution to the limitations of conventional methods, providing opportunities for the development of novel, soft, and bio-compatible electronic interfaces. This advancement in Bioelectronics opens avenues for healthcare, bioengineering, and beyond.

11:15 AM EL04.01.07

Kirigami Electronics for Long-Term Electrophysiological Recording of Human Neural Organoids and Assembloids XiaoYang, CsabaForro, ThomasLi, YukiMiura, TomaszZaluska, Ching-TingTsai, SabinaKanton, JamesMcQueen, XiaoyuChen, SergiuPasca and BianxiaoCui; Stanford University, United States

Human stem cell-based organoids and assembloids have emerged as a promising platform to model aspects of nervous system development. Long-term, minimally invasive recordings in these three-dimensional (3D) multi-cellular systems are essential for developing disease models. Current technologies, such as patch clamp, penetrating microelectrodes, planar electrode arrays and substrate-attached flexible electrodes, do not, however, allow chronic recording of neural organoids in suspension, which is necessary to preserve their 3D architecture. Here, inspired by the art of kirigami, we develop flexible electronics that transition from a flat 2D pattern to a 3D basket-like configuration to accommodate the long-term culture of human neural organoids in suspension. We show that this novel platform named kirigami electronics (KiriE) integrates with and enables chronic recording of intact cortical organoids for 170 days while preserving their morphology, cytoarchitecture and cell composition. KiriE can be integrated with optogenetic and pharmacological stimulation and detect a disease-related hyperactive phenotype. Moreover, KiriE is compatible with simultaneous recordings from organoids in assembloid and can capture activity in emerging cortico-striatal circuits. Moving forward, this flexible electronics system could reveal disease phenotypes and the patterns of activity underlying the assembly of the nervous system.

11:30 AM EL04.01.08

High Aspect Ratio Au Nanotubes in Soft Bioelectronics YuyangLi and KlasTybrandt; Linköping University, Sweden

Soft bioelectronics offer a promising flexible and stretchable platform to engineer biomedical devices in healthcare applications, such as wearable health tracker, chronic neural interface probes, implantable electrophysiological sensors, electrical stimulator, etc. Much effort in decades has been devoted in materials science to the design of reliable soft bioelectronics. Typical flexible and stretchable devices utilize elastic polymers as substrate that are well conformable with human tissues, and fillers of conductive nanomaterials like carbon nanotubes (CNTs), Ag nanowires (NWs). These one-dimensional (1D) nanowires are proved to form highly percolated networks in the substrate, providing outstanding thermal, electrical, and mechanical properties. Of which Ag nanowires with high aspect ratio are easily accessible by facile large scale synthesis method. Up to now, Ag nanowires is one of the most popular materials as conductive fillers. Despite all of that, concerns of long-term biocompatibility hover around due to toxic Ag ions leaching from Ag nanowires-based devices, same on carbon nanotubes with plmonary toxicity. Researchers have turned to search for materials with high biocompatibility as well as uncompromised electromechanics properties.

Alternatively, Au nanomaterials show excellent optical-electrical properties and biological inertness. For instance, Au nanoparticles or nanorods could be obtained by well-developed synthetic routes, being applied in many biomedical applications such as cancer therapy, cell imaging, biosensing. Whereas, due to the low aspect ratio and poor percolation of Au nanoparticles, there is limited use in bioelectronics. The major challenge is that the insufficient conventional methods of synthesizing one-dimensional (1D) Au nanomaterials. The procedures are tedious for many

days with low yield, and includes toxic direction growth agent such as hexadecyltrimethylammonium bromide (CTAB), besides further purification needed to separate byproducts of nanoparticles and nanorods. The yielded Au NWs has limited aspect ratio, far less than that of Ag NWs. All these factors hinder the research and development of 1D Au nanomaterials based soft bioelectronics. Here we present a facile, large-scale, low-cost aqueous method to synthesis high aspect ratio Au nanotubes with controllable surface morphologies. It paves the way for future design and application of soft bioelectronics with high biocompatibility and electrical performance based on one-dimensional (1D) Au nanomaterials.

11:45 AM EL04.01.09

Self-Adhesive Organic Thin Film Transistors on Elastomeric Nanofilms[ChikaOkuda](#), SunghoonLee, TakaoSomeya and TomoyukiYokota; University of Tokyo, Japan

Devices that can be intimately contacted with our skin are increasingly gaining attention because of their huge potential in collecting long-term vital data for future healthcare, nursing, or sports activities. One of the key components is flexible or stretchable transistors, since they are necessary for signal amplification close to the body [1], or sensor matrixes to collect spatial data [2]. Flexible transistors in ultrathin form, especially below few-100 nm-thick, can conform to the complex shape of the skin surface [3], whereas thicker elastomeric transistors can also attach to the skin by their elastomeric property. Although these devices can contact well to the human skin, stability of the device-skin contact and robustness needed improvement in order to achieve long-term signal collection. Nanofilms, which are below few-100 nm thick and are made of elastomeric materials, have shown sufficient stability of the device-skin contact and robustness to be worn on skin for over a week [4]. These elastomeric nanofilms has become a candidate for wearable devices' interface, but only electrodes have been fabricated on them. Fabrication of transistors on them has remained a challenge, due to difficulty in handling and physical damages that occur during the fabrication.

In this work, we report novel device structure and process of organic thin film transistors (OTFT) on elastomeric nanofilms. Total device thickness is only 0.5 μm , enabling the devices to have stable contact on any parts of the body. The substrate film is ultrathin with average thickness of ~ 200 nm, enabling the film to be self-adhesive requiring ~ 130 $\mu\text{J}/\text{cm}^2$ for detachment from artificial skin. This film was fabricated by dip-coating electrospun polyurethane nanofibers into polydimethylsiloxane solution, according to ref.3. The fiber-reinforced structure enhances the robustness of the film. The film was then placed onto a flexible supporting substrate with release agent. Bottom gate was formed by thermally evaporating gold (50 nm) through a shadow mask, followed by chemical vapor deposition of parylene (200 nm) as the dielectric layer. Subsequently, organic semiconducting layer of dinaphthothienothiophene (DNTT) (30 nm) and gold contact electrodes (50 nm) were formed by thermal evaporation. Finally, OTFTs on nanofilms were delaminated manually from the supporting substrate to become free-standing state.

The fabricated transistors exhibited electrical characteristics comparable to those fabricated on conventional substrates. They showed excellent yield of 75/77, with mobility of 0.19 ± 0.02 cm^2/Vs and maximum on/off ratio of above 10^5 . To demonstrate stability, devices were laminated and then delaminated from a glass substrate, which showed negligible effect on the electrical characteristics.

[1] Sugiyama, M., *et al. Nat. Electron.* 2, 351–360 (2019).

[2] Wang, S., *et al. Nature* 555, 83–88 (2018).

[3] Viola, F.A., *et al. Nat. Commun.* 12, 5842 (2021).

[4] Wang, Y., *et al. Proc. Natl. Acad. Sci.* 118, e2111904118 (2021).

SESSION EL04.02: Bio-Interfaces and Bioelectronics II

Session Chairs: Simone Fabiano and Zeinab Jahed

Tuesday Afternoon, November 28, 2023

Hynes, Level 3, Room 313

1:30 PM *EL04.02.01

Wearable Ultrasound Technologies for Continuous Deep Tissue Monitoring[ShengXu](#); University of California, San Diego, United States

The use of wearable electronic devices that can acquire vital signs from the human body noninvasively and continuously is a significant trend for healthcare. The combination of materials design and advanced microfabrication techniques enables the integration of various components and devices onto a wearable platform, resulting in functional systems with minimal limitations on the human body. Physiological signals from deep tissues are particularly valuable as they have a stronger and faster correlation with the internal events within the body compared to signals obtained from the surface of the skin. In this presentation, I will demonstrate a soft ultrasonic technology that can noninvasively and continuously acquire dynamic information about deep tissues and central organs. I will also showcase examples of this technology's use in recording blood pressure and flow waveforms in central vessels, monitoring cardiac chamber activities, and measuring core body temperatures. The soft ultrasonic technology presented represents a platform with vast potential for applications in consumer electronics, defense medicine, and clinical practices.

2:00 PM EL04.02.02

A Fully Integrated Wearable Ultrasound System to Monitor Deep Tissues in Moving Subjects[MuyangLin](#), ZiyangZhang, XiaoxiangGao and ShengXu; University of California, San Diego, United States

Medical ultrasound is a powerful diagnostic and evaluation tool in hospitals and clinics due to its safety and versatility. Traditional ultrasound suffers from operator dependency and does not allow long-term usage. Recent advances in wearable ultrasound technologies have demonstrated the potential for hands-free data acquisition, but technical barriers remain as these probes require wire connections, can lose track of moving targets, and create data-interpretation challenges. Here we report a fully integrated autonomous wearable ultrasonic-system-on-patch (USoP). A miniaturized flexible control circuit is designed to interface with an ultrasound transducer array for signal pre-conditioning and wireless data communication. Machine learning is used to track moving tissue targets and assist the data interpretation. We demonstrate that the USoP allows continuous tracking of physiological signals from tissues as deep as 164 mm. On mobile subjects, the USoP can continuously monitor physiological signals, including central blood pressure, heart rate, and cardiac output, for as long as 12 h. This result enables continuous autonomous surveillance of deep tissue signals toward the internet-of-medical-things.

2:15 PM EL04.02.03

Conformable Ultrasound Patch for Cavitation Enhanced Transdermal Cosmeceutical Delivery[AasthaShah](#) and CananDagdeviren; Massachusetts Institute of Technology, United States

Increased consumer interest in healthy-looking skin demands a safe and effective method to increase transdermal absorption of innovative therapeutic cosmeceuticals. However, permeation of small-molecule drugs is limited by the innate barrier function of the stratum corneum. Here, we report a conformable ultrasound patch (cUSP) that enhances transdermal transport of niacinamide by inducing intermediate-frequency sonophoresis in the fluid coupling medium between the patch and the skin. The cUSP consists of piezoelectric transducers embedded in a soft elastomer to create localized cavitation pockets (0.8 cm^2 , 1 mm deep) over larger areas of conformal contact (20 cm^2). Multiphysics simulation models, acoustic spectrum analysis and high-speed videography are used to characterize transducer deflection, acoustic pressure fields and resulting cavitation bubble dynamics in the coupling medium. The final system demonstrates a 26.2-fold enhancement in niacinamide transport in a porcine model *in vitro* with a 10-minute ultrasound application, demonstrating suitability of the device for short-exposure, large-area application of sonophoresis for patients and consumers suffering from skin conditions and premature skin aging.

2:30 PM BREAK

3:00 PM *EL04.02.04

Mapping the Human Brain with High Spatiotemporal Resolution[ShadiA. Dayeh](#); University of California, San Diego, United States

Electrophysiological recording and stimulation are the gold standard for interrogating the nervous system for diagnostic and therapeutic purposes. Recording the human brain activity with microelectrode arrays enable broadband and high spatiotemporal resolution but are conventionally limited to a small cortical coverage. However, large cortical coverage together with the high spatiotemporal resolution are needed to advance our understanding of diseased and normal brain function to be able to develop effective therapies.

This talk will cover the challenges and latest developments in brain mapping and discuss the clinical translation of UCSD's multi-thousand channel platinum nanorod surface and depth microelectrode arrays to map the human brain activity. We will discuss considerations in the electrode-tissue interface for recording and stimulation and demonstrate mapping of functional units (cortical columns) across species including humans. Examples of large-scale microelectrode mapping of motor, language, and epileptogenic discharges from the human brain will be presented along with a perspective on future directions. Lastly, we will present the display of cortical activity directly from the surface of the human brain with the newly developed Brain-

intracranial electroencephalography-microdisplay (Brain-iEEG-microdisplay).

3:30 PM *EL04.02.05

Enhanced Photodetection and Resistant Switching in CVD Grown MoS₂: A Potential Neuromorphic Photo-memristor Pukhraj Prajapat^{1,2} and Govind Gupta^{1,2}; ¹National Physical Laboratory, India; ²Academy of Scientific & Innovative Research, India

The rapid development of neuromorphic computing has stimulated the research of novel materials and technologies to emulate the remarkable capabilities of the human brain. Two-dimensional transition metal dichalcogenides (2D-TMDs) have become interesting options in this scenario because of their distinctive electrical and optical characteristics. For its potential use in photodetection and memristive devices, molybdenum disulfide (MoS₂) has drawn much attention among them. MoS₂ is a viable material for future neuromorphic computing systems due to its unique qualities, which include its effective light-matter interaction, atomically thin structure, and customizable electrical characteristics. To establish an approach for advancing a neuromorphic photo-memristor, we examine the few layers of growth of MoS₂ using CVD and explore the potential for boosted photodetection and resistive switching. Photoluminescence and UV-Visible spectroscopy were used to characterize the optical characteristics of MoS₂, which demonstrated its potent excitonic emission and tunability concerning the number of atomic layers. The effective charge separation and transport in the atomically thin MoS₂ channel are responsible for the extraordinary photoresponsivity and low dark current displayed by the fabricated MoS₂ photodetectors. The enhanced photodetection performance was further demonstrated by measuring the responsivity under different light intensities (15mW to 2.85mW) and 532 nm wavelength. Additionally, the resistive switching behavior of MoS₂ was examined, which revealed potential memristive properties. The Au/MoS₂/Au device exhibits typical bipolar switching behavior with a low working voltage, extended retention time, high resistance ratio (~103), and strong endurance (104 cycles), which has enormous potential for neuromorphic computing applications. The analysis revealed the possibility of producing energy-efficient, brain-inspired computing platforms thanks to the integration of photodetection and resistant switching in a single chip.

4:00 PM EL04.02.06

Investigation of Opto-Electrical, Mechanical and Surface Properties of AgNWs-PEDOT: PSS Based Transparent and Conductive Electrodes for Bio-Sensing Applications Justin V. Dcosta, Sebastien Sanaur and Daniel Ochoa; École des Mines de Saint-Etienne, France

Ultra-flexible organic photodetectors (OPDs) have experienced a rapid development in recent years, making them increasingly significant in the field of flexible electronics, wearable technology and medical applications. They have emerged as promising optoelectronic devices for several applications including biosensing. For example, OPDs in the field of biosensing are used to monitor vital signs such as, heart rate, oxygen saturation and blood glucose levels. When fabricated on ultrathin flexible substrates organic photodetectors provide conformal surface contact thus allowing for efficient light absorption and detection, thereby enhancing the sensitivity and the performance. Transparent conductive electrodes (TCEs) are considered to be one of the most crucial components in OPDs as they play a significant role in improving their efficiency as they effectively take part in light transmission and charge extraction. Typically, TCEs are designed to exhibit high transparency in the visible spectrum thus allowing the incoming light to pass through them with minimum loss. The flexible nature of the TCEs will allow for the conformal contact on to curved or flexible substrates and thus allows the seamless integration of OPDs with biological tissues enabling for the continuous and real-time monitoring of the physiological parameters. Among the various available materials, one dimensional AgNWs are perceived as a promising candidate for TCEs for flexible OPDs due to some of their remarkable properties such as low percolation threshold, high electrical conductivity, high optical transparency and excellent flexibility. However, their long-term stability is still challenging as AgNWs are susceptible to oxidation thus limiting their reliability in flexible devices. Hence to solve this issue the combination of AgNWs with conducting polymers such as poly(3,4-ethylenedioxythiophene): poly(styrenesulfonate) (PEDOT: PSS) as transparent hybrid electrode has been explored. PEDOT: PSS alone offers excellent chemical stability and can therefore further contribute to the stability of AgNWs by preventing from oxidation, thus maintaining the overall integrity of the film from various environmental degradation conditions. Moreover, the hydrophobic properties of PEDOT: PSS helps to shield the AgNWs from the detrimental effects of moisture such as oxidation and loss in electrical conductivity. Additionally, PEDOT: PSS when incorporated in AgNWs will help to reduce the interfacial resistance between the nanowires thus help in the overall stability and electrical conductivity of the film. In this work, we have investigated the opto-electrical, mechanical and surface properties of silver nanowires/poly(3,4-ethylenedioxythiophene): poly(styrenesulfonate) (AgNWs-PEDOT: PSS) hybrid electrode fabricated on 5-µm ultrathin parylene C substrate. The fabricated electrode exhibits low sheet resistance of 27 Ω/Sq, and shows an average optical transmission of >85% throughout the visible spectrum which is suitable for optoelectronic applications. Besides the comparable work function of 5 eV with respect to standard ITO, the surface rms roughness of the electrode is effectively reduced from 8 nm to 4 nm by spin coating PEDOT: PSS as planarization layer. With a stable R/R₀ ≈ 1 over continuous 50k bending cycles at a radius of curvature of 0.1 mm, the electrode exhibits excellent mechanical characteristics suitable for ultraflexible and wearable applications. Utilizing this electrode, we have realized an ultraflexible organic photodetector that can be conformally adhere to human skin for biosensing applications. The OPD is fabricated in normal atmospheric conditions that can withstand 5k bending cycles when bent at a radius of curvature of 0.2 mm while maintaining similar values in ON/OFF ratio under white light illumination.

4:15 PM EL04.02.07

Intrinsically Stretchable Transistor Array Based on Pure Liquid Metal Electrodes for Biophysical Signal Monitoring on Skin Seungkyu Lee, Do Hoon Lee and Steve Park; Korea Advanced Institute of Science and Technology, Korea (the Republic of)

The human perception of auditory, tactile, and visual information is transformed into electro-physiological signals and transmitted to the brain, which processes these complex signals simultaneously. The development of electronic devices composed of intrinsic stretchable materials is essential to achieve seamless integration with the human skin and possess mechanical properties for human-machine interactions. The proposed research focuses on a stretchable transistor array, which consists of a flexible material-based output device and electronic circuits, providing opportunities for human-machine interaction. This research can be explained from three aspects: process and fabrication, measurement characteristics, and applications. Firstly, from the perspective of process and fabrication, liquid metals can exist in a liquid state at room temperature due to their low melting points and can exist as very small particles (spherical). They possess intrinsic flexibility and high electrical conductivity due to being metallic. The particle size is around 2-3 µm, the flexibility is 300%, and the electrical conductivity is 3.4 × 10⁶ S/cm. Coating pure liquid metals in film form on hydrophobic substrates is challenging due to their high surface tension. In this study, liquid metal particles are dispersed in two different hydrophilic solvents with different boiling points, and then coated on the substrate using the Marangoni flow principle. The boiling point of deionized water is 100 degrees Celsius, and the boiling point of ethyl acetate is 77.1 degrees Celsius. In the patterning of liquid metals through photolithography, the most crucial step is the etching process. To break the bonding between the thin metal oxide layer (approximately 5 nm) surrounding the liquid metal particles and the hydrophobic substrate, wet etching is conducted using an SC-2 (hydrochloric acid + hydrogen peroxide) solution. This is because gallium, which constitutes most of the liquid metal, is a metal and is etched by the reaction of hydrogen peroxide and hydrochloric acid. The resolution is <5 µm, and transistors using s-CNT (single-walled carbon nanotubes) and SEBS H10152 will be fabricated. From the perspective of measurement characteristics, a comparison will be made with previously reported stretchable transistors. The ultimate goal is to achieve a transistor device with an on/off ratio of 10⁵, an operating voltage of ~1V, a carrier mobility of 0.9 cm²/Vs, and maximum stretchability of 200%. Due to its high resolution, this transistor device is expected to be the smallest among the reported ones, enabling highly integrated mass production. It is also expected to have the advantage of low power consumption from an energy consumption perspective. Lastly, from the perspective of applications, the fabricated stretchable transistor array is highly flexible and can be attached to the skin. Its array characteristics will be verified for complex tasks such as signal processing, involving very small electro-physiological signals. Monitoring the electro-physiological signals of the stretchable transistor device enables applications in health monitoring, medical treatments/implants, etc. The intrinsic liquid metal-based stretchable transistors allow for the processing of weak electro-physiological signals (in the sub-millivolt range) with minimal interference from skin or tissue deformation. They enable the conversion of spike signals into analog-to-digital signals, enabling signal processing.

4:30 PM EL04.02.08

Fiber-Type Neural Probe with Balanced Mechano-Electrical Properties for Prolonged Electrophysiological Brain Signals Recording Chihyeon Won¹, Ui-Jin Jeong², Il-Joo Cho³ and Taeyoon Lee¹; ¹Yonsei University, Korea (the Republic of); ²Korea Institute of Science and Technology, Korea (the Republic of); ³Korea University, Korea (the Republic of)

Implantable neural probes that are inserted into the brain tissues are widely used in brain-machine interfaces (BMIs) for the analysis of brain circuits. They are implanted into specific brain regions such as Thalamus and Cerebellum, that generate neural signals related to electrophysiological information. Recently, flexible neural probes are developed to minimize the damage to brain tissues and nerves for reducing foreign body responses (FBRs) in the brain. To prevent FBRs between the probes and brain tissues, mechanical properties such as bending stiffness and Young's modulus of devices should be well matched with that of the brain. However, conventional flexible neural probes using a silicon substrate still induce damage in the brain due to their even high Young's modulus (> 1 MPa) than that of the brain (~ 1.8 kPa). Furthermore, the electrical properties of the devices such as conductivity and impedance could be deteriorated by focusing on only matching mechanical properties between the probes and the brain. Herein, we fabricated Au nanoparticles (AuNPs) embedded fiber-type neural probes with balanced mechanical and electrical properties for a long-term measuring brain signals. The fiber-type neural probe was fabricated by controlling the distribution of Au ions in polymeric networks to using osmotic pressure. After the Au ions were converted into AuNPs by the reducing agent, a core of the fiber-type neural probe was still remained as an original elastomer, and the AuNPs were formed on the exterior of the fiber. The proposed fiber showed remarkable electrical properties, including high conductivity (7.68 × 10⁴ S/m) and low impedance (2.88 × 10³ Ω at 1 kHz). In addition, the fiber exhibited brain tissue-like mechanical properties such as low Young's modulus (170 kPa) and low bending stiffness (22.2 N m⁻¹). We could successfully measure various electrophysiological signals from a mouse brain using a brain chip containing the developed fiber-type neural probe. Additionally, the fiber-type neural probe exhibited significantly reliable signal recording with an impedance of under 4 kΩ at 1 kHz over four months post-implantation with negligible FBRs in the brain. We suggest that the developed fiber-type neural

probe could be a crucial role in the field of neurological sciences and BMIs for understanding the mechanism of brain circuits and developing electronic devices in the treatment of chronic diseases.

4:45 PM EL04.02.09

A Perovskite Nanowire Array Based Spherical Bionic Eye with Filter-Free Color Vision, In-Device Neuromorphic Signal Preprocessing and Adaptive OpticsZhenghao Long and Zhiyong Fan; The Hong Kong University of Science and Technology, Hong Kong

Bio-inspired vision systems that utilize curved detector geometry have the potential to create miniaturized cameras with a wide field of view and low aberration. Nonetheless, integrating color vision, in-device signal preprocessing, and adaptive optics into spherical artificial eyes has always been a challenge. Herein, we developed a bionic eye that integrates all of the above functions. The device contains a hemispherical artificial retina and an optical sub-system.

The artificial retina is based on a hemispherical perovskite nanowire array, which possesses in-device color distinguishing and neuromorphic preprocessing abilities. The device structure incorporates a SnO₂/NiO double-shell nanotube filled with ionic liquid in the core, which is located on top of a CsPbI₃/NiO core-shell nanowire. It has been observed that under shorter (blue) or longer (green and red) wavelength illuminations, the positive surrounding gate effect of NiO due to photo hole injection can be partially or fully balanced by electrolyte, respectively. Thus, the device can yield either positive and negative photocurrent under shorter or longer wavelength illumination, respectively. Additionally, the color selectivity of such a structure can be adjusted by applying a small external bias, which allows for the acquisition of more detailed color information in multiple measurements. We demonstrated the reconstruction and classification of color patterns based on the artificial retina. Meanwhile, photo-generated carriers can accumulate in the SnO₂/NiO structure, resulting in a self-powered synaptic photo response that we used to demonstrate the neuromorphic preprocessing of noise filtering. The in-device signal preprocessing, along with the self-powered feature, can significantly reduce energy consumption.

The optical subsystem includes a fixed lens, an artificial crystalline lens, and an artificial iris, all of which mimic the optics of a human eyeball. The artificial crystalline lens is a liquid crystal Pancharatnam-Berry lens. Compared to conventional glass lenses, it exhibits reduced geometrical aberration and a much smaller thickness. The artificial crystalline lens can be switched between light refraction mode and transparent mode, allowing for the tuning of the focal length of the optical subsystem. Similarly, the artificial iris is based on liquid crystal technology, and it has five rings of liquid crystal. The transparency of each ring can be individually controlled from 0% to 95%, which enables the overall aperture size to be adjusted from 3.14 mm² to 78.50 mm². The electronic optics, which has reduced thickness and geometrical aberration, can assist with miniaturization and expand the depth of field and dynamic range of the system.

Overall, we have designed and developed a distinctive hemispherical bionic retina and spherical eye device that possesses the missing capabilities of color vision, optical adaptivity, and energy efficiency in previous research. This device presents a new paradigm by integrating structural and functional traits that are similar to biological eyes, and it highlights the potential for further exploration and optimization of artificial visual systems with biomimetic functionalities that can enhance the efficiency of machine vision and robotics.

SESSION EL04.03: Poster Session I
Session Chairs: Simone Fabiano and Xenofon Strakosas
Tuesday Afternoon, November 28, 2023
Hynes, Level 1, Hall A

8:00 PM EL04.03.01

Stacked One Selector-One Resistor 32x 32 Crossbar Array with Chalcogenide-Based OTS Selector for Neuromorphic ComputingSu Yeon Lee, Hyun Kyu Seo, Se Yeon Jeong and Min Kyu Yang; Sahmyook University, Korea (the Republic of)

Existing Resistive Random Access Memory (ReRAM) is a next-generation memory technology known for its high operating speed, low voltage operation, and higher density compared to other memory types. However, when implemented in a cross-point array structure, it can suffer from leakage currents that cause malfunctions in read and write operations. To overcome these limitations, structural changes were implemented by stacking a selector device on a resistor. The selector device utilizes an amorphous chalcogenide-based OTS (Ovonic Threshold Switching) technology.

By incorporating the amorphous chalcogenide-based threshold switching selection device onto the resistor (1R), it offers several advantages, including lower off-state current (I_{off}) compared to MIT-based selector devices. This makes it an attractive and optimal choice for stacking ReRAM with a 1 selector 1 resistor (1S1R) structure. The 1S1R architecture employs a W/Ti-TaOx/Pt structure for the resistor (1R) and a W/GeSeTe/W structure for the selector (1S). This crossbar resistance memory architecture is suitable for non-volatile, high-density, and low-latency storage class memory applications.

The reliability of each device was thoroughly evaluated, and a suitable material for the 1S1R structure was selected. Moreover, the 1S1R structure holds potential for application in neuromorphic computing, a novel conceptual architecture that aims to develop low-energy, high-speed neurons and synapses. In neuromorphic computing, an artificial neural network consists of low-power computing devices (neurons) and reconfigurable storage devices (synapses). This architecture offers the significant advantage of performing Multiply-Accumulate (MAC) operations in parallel, thereby reducing data transmission time and energy consumption.

In this study, the researchers demonstrated sufficient device yield in a 32 x 32 crossbar array structure using an auto-probe technique. They also showcased reliable MAC behavior, simulating neuromorphic computing.

8:00 PM EL04.03.02

Engineering Cell and Nuclear Morphology on Nano Topography by Contact-Free Protein MicropatterningEinollah Sarikhani¹, Dhivya Pushpa Meganathan¹, Keivan Rahmani¹, Ching-Ting Tsai², Abel Marquez-Serrano¹, Xiao Li^{2,3}, Francesca Santoro^{4,5,6}, Bianxiao Cui², Lasse Hyldgaard Klausen⁷ and Zeinab Jahed^{1,1}; ¹University of California, San Diego, United States; ²Stanford University, United States; ³Xi'an Jiaotong University, China; ⁴Istituto Italiano di Tecnologia, Italy; ⁵RWTH Aachen University, Germany; ⁶Forschungszentrum Juelich, Germany; ⁷Aarhus University, Denmark

Platforms with nanoscale topography have recently become powerful tools in cellular biophysics and bioengineering. Recent studies have shown that nanotopography affects various cellular processes like adhesion and endocytosis, as well as physical properties such as cell shape.

To engineer nanopillars more effectively for biomedical applications, it is crucial to gain better control and understanding of how nanopillars affect cell and nuclear physical properties, such as shape and spreading area, and impact cellular processes like endocytosis and adhesion. In this study, we utilized a laser-assisted micropatterning technique to manipulate the 2D architectures of cells on 3D nanopillar platforms. We performed a comprehensive analysis of cellular and nuclear morphology and deformation on both nanopillar and flat substrates. Our findings demonstrate precise engineering of cellular architectures through 2D micropatterning on nanopillar platforms. We show that the coupling between nuclear and cell shape is disrupted on nanopillar surfaces compared to flat surfaces. Furthermore, we discovered that cell elongation on nanopillars enhances nanopillar-induced endocytosis. These results have significant implications for various biomedical applications of nanopillars, including drug delivery, drug screening, intracellular electrophysiology, and biosensing. We believe our platform serves as a versatile tool for further explorations, facilitating investigations into the interplay between cell physical properties and alterations in cellular processes.

8:00 PM EL04.03.03

Low Voltage Organic Light-Emitting Synaptic Transistors for Neuromorphic In-Display ProcessingKwan-Nyeong Kim¹, Huan Yu Zhou¹, Dong-Yoon Kim¹, Hea-Lim Park², Yeongjun Lee³, Kyun Kyu Kim³, Min-Jun Sung¹, Yilei Xu³, Song Zhang³, Dae-Gyo Seo¹, Gyeong-Tak Go¹, Jinwoo Park¹, Zhenan Bao³ and Tae-Wool Lee¹; ¹Seoul National University, Korea (the Republic of); ²Seoul National University of Science and Technology, Korea (the Republic of); ³Stanford University, United States

Organic neuromorphic electronics using flexible organic semiconductors pave the way for the development of energy-efficient and intelligent devices, particularly in wearable applications. To create user-friendly systems, wearable neuromorphic devices need to provide outputs that are easily recognizable to user through light-emitting devices. The previous approach of employing external processing units to transmit signals from neuromorphic devices to display devices can give rise to limitations similar to those encountered in conventional electronic systems. Organic light-emitting synaptic transistors (OLESTs) offer a potential solution by integrating the functions of synaptic processing and light-emission in a single device. Despite this advantage, high voltage operation (>30V) in previous light-emitting synaptic transistors remains a main challenge that requires further investigation and improvement.

Here, we present low voltage OLESTs achieved through the electrochemical doping of semiconducting light-emitting polymers (LEPs). By utilizing surfactant molecules, we enhance the ion transport in the LEP channel, resulting in low turn on voltage ($|V_{DS}|=2.0V$ at $|V_{GS}|=1.0V$ that is lower than band gap of LEP ($E_g=2.17eV$) due to spontaneous band bending during the OFF state. With the low switching and channel voltage (2.5V), the synaptic plasticity with luminescent outputs was demonstrated. Finally, we show neuromorphic in-display processing using a sensory neuromorphic display system. This system utilizes a hierarchical structure consisting of temperature sensor, spike generator, and OLEST to provide intuitive visible warning signals to patients suffering from sensory disabilities. Our results present a new approach for the realization of user-friendly neuromorphic display systems in intelligent wearable electronics.

8:00 PM EL04.03.04

Biocompatible Multilayered Encapsulation of Organic Light-Emitting Diodes for Optogenetic ApplicationsSukyungChoi, Jin-WookShin, Jong-HeonYang, KukjooKim, Chun-WonByun, Dae-HyunAhn, Yong HeeKim and Sang-DonJung; Electronics and Telecommunications Research Institute (ETRI), Korea (the Republic of)

Organic light-emitting diodes (OLEDs) are gaining significant attention in the field of bioelectronics due to their advantages as thin and flexible light sources. However, OLEDs are highly susceptible to moisture and oxygen, making the development of protective encapsulation crucial. While conventional glass-based encapsulation has been suitable for rigid devices, it is not suitable for flexible bioelectronics that require flexibility. As a result, there has been extensive research on the application of thin inorganic or organic-inorganic hybrid encapsulations. Due to the unstable nature of OLED devices at temperatures above 100 degrees Celsius, low-temperature processes are required to develop encapsulation. In our study, we formed a high-density Al_2O_3 film using atomic layer deposition and deposited SiO_xN_y using low-temperature plasma-enhanced chemical vapor deposition to create a thin inorganic bilayer encapsulation. To enhance the biocompatibility of the device, we deposited parylene-c on the upper layer of the SiO_xN_y using chemical vapor deposition. The OLED device was fabricated as a blue-emitting component for optogenetic applications, specifically for stimulation using channelrhodopsin-2. The stability of the OLED devices was verified by dipping them into a phosphate-buffered saline solution, and it was observed that the OLEDs with a bilayer inorganic encapsulation of $\text{Al}_2\text{O}_3/\text{SiO}_x\text{N}_y$ exhibited significantly superior stability compared to OLEDs with only an Al_2O_3 encapsulation. However, it was found that the bilayer inorganic encapsulation of $\text{Al}_2\text{O}_3/\text{SiO}_x\text{N}_y$ alone exhibited cell toxicity, making it unsuitable for bio applications. To address this issue, parylene-c was introduced to assess cell viability. It was confirmed that OLED devices with an encapsulation of $\text{Al}_2\text{O}_3/\text{SiO}_x\text{N}_y/\text{parylene-c}$ demonstrated biocompatibility. HEK-293 and L-929 cells were used to assess biocompatibility, and both relative cell counting and MTT tests revealed cell viability of over 80%, demonstrating a high level of biocompatibility. Finally, the feasibility of optogenetic experiments was demonstrated by applying the OLED devices to neuronal cells.

8:00 PM EL04.03.05

Uncooled Self-Powered Hemispherical Biomimetic Pit Organ for Mid-to Long-Infrared ImagingYuchengDing and ZhiyongFan; The Hong Kong University of Science and Technology, Hong Kong

Infrared (IR) vision is a highly desirable capability for various applications, including medical instrumentation, surveillance, environmental monitoring, robotics, and space exploration. Among the few species with this exceptional visual capability, snakes stand out due to their advanced infrared perception assisted by pit organs. Inspired by the pit organ structure, we present a biomimetic hemispherical infrared imaging device that overcomes the limitations of conventional planar IR image sensors. Our innovative device employs high-density ionic thermoelectric polymer nanowire arrays as sensing nerve cells, demonstrating a notable voltage response to temperature variations in test objects. Unlike planar IR image sensors, which typically have a limited field of view (FoV) of less than 90° and require multiple lenses due to the Petzval field curvature, our hemispherical design effectively eliminates imaging aberrations and simplifies the optical system. This approach minimizes IR transmittance loss, preserves detection sensitivity, and reduces the form factor of the IR devices.

We successfully demonstrate an infrared sensor array with 625 pixels on a hemispherical substrate, achieving an ultrawide FoV of up to 135°, significantly larger than that of the pit organ. Furthermore, our device can image body temperature objects without the need for a cooling system or external power supply, thanks to the thermoelectric effect that enables a self-powered working mode. The device exhibits high responsivity (0.5 mV for a 40°C object at a 5-cm distance) and a reasonable response rate of 0.69 s. Despite the challenges associated with fabricating devices on curved substrates, our biomimetic hemispherical polymer-based ionic thermoelectric (PIT) image sensor effectively mimics thermal receptors in pit organs. Aided by an IR-absorbing layer, the PIT image sensor can detect and image mid- to long-wavelength IR light at room temperature. We also demonstrate the device's potential for practical applications, such as staring imaging of human hand gestures and heated symbols with approximately 60°C temperature. In conclusion, our hemispherical infrared imaging device not only mimics the pit organ both structurally and functionally but also surpasses it in terms of the density of the nanowire array. This work paves the way for the design and fabrication of a new generation of high-performance, bioinspired IR imaging devices based on emerging ionic thermoelectric materials, offering significant improvements over conventional IR sensing technologies.

8:00 PM EL04.03.06

Photopatternable OEETs for Scalable and High Resolution Organic ElectronicsCharles-ThéophileCoen and Yoerivan de Burgt; Technische Universiteit Eindhoven, Netherlands

The conjugated polymer PEDOT:PSS has been at the forefront of research in the field of organic mixed ionic-electronic conductors (OMIECs) thanks to its excellent conductivity, flexibility and biocompatibility. This material has found applications ranging from biosensing to neuromorphic computing.

Patterning OMIECs has however been one of the main challenges toward miniaturization and scalability of organic electronics. As these materials are sensitive to conventional photoresists, traditional microfabrication processes have to be adapted, leading to poorer reproducibility, scalability and resolution.

Nonetheless, the development of new materials and techniques in recent years, such as orthogonal photoresists and photopatterning, have led the way toward highly integrated organic circuits. Photopatterning of OMIECs offers a rapid and chemically compatible process. Two distinct strategies, namely interpenetrating network and direct crosslinking, are being investigated for the fabrication of organic electrochemical transistors (OEETs). Similarly, these two approaches are employed for patterning a solid-state electrolyte, enabling the creation of fully photopatternable solid-state and high performance OEETs. This type of device has great potential for applications in neuromorphic computing, such as hardware accelerators and artificial spiking neurons, and biosensing, including multiplexed electrode array and in-line trans-epithelial electrical resistance measurement.

8:00 PM EL04.03.07

Memristor Device Requirements Analysis and Update Thresholding Strategy for Accurate Neuromorphic Resistor (1R) Array ProgrammingGihoLee and JeehwanKim; Massachusetts Institute of Technology, United States

Neuromorphic computing, which draws inspiration from the functioning of the brain, offers several advantages such as minimizing data transmission, reducing power consumption, and enabling parallel computation. These remarkable properties of neuromorphic computing are expected to have a wide range of applications, including artificial intelligence (AI), scientific computing, and security. Particularly, neuromorphic computing powered by a memristor crossbar array has demonstrated promising capabilities as an AI inference accelerator, with various on-chip deep neural network inference demonstrations showing comparable inference performance to software-based approaches.

One common approach, known as the one-transistor one-resistor (1T1R) system, has been widely adopted to achieve precise programming of individual memristors and overcome the sneak path issue, thereby enhancing computing precision. However, this 1T1R system introduces compromises in terms of power consumption, computation speed, and design simplicity. These limitations can be addressed by employing the simplest one-resistor (1R) system. However, the effective utilization of the 1R system requires precise adjustment of the conductance values of each memristor on the cross-points. This task is often challenging due to the presence of asymmetry, selectivity, sneak path, and stochasticity in the conductance update process. In this study, we address this issue by developing the simplest automatic programming algorithm, which involves iterative conductance read and update sequences. Subsequently, we analyze the requirements of memristor devices for achieving high programming accuracy. We establish the relationships between array size and various requirements, such as the interconnect-to-memristor conductance ratio and illustrate how selectivity enhances the convergence speed. Additionally, we observe that the update asymmetry of memristor devices negatively affects programming performance when the target conductances deviate from the symmetry point of the memristors. To overcome this challenge, we demonstrate a simple update event thresholding algorithm that significantly improves the programming accuracy of an actual asymmetry device model. This requirement analysis and programming strategy have the potential to assist the 1R memristor array system in addressing programming challenges and implementing an ideal AI inference accelerator.

8:00 PM EL04.03.08

Optically and Electrically Modulated Optical Neuromorphic Transistor Based on Oxide Semiconductor with MgOx Oxygen Vacancy Forming LayerSujinLee, Min SeongKim, Hyung TaeKim, Young WookKim, Seok MinHong and Hyun JaeKim; Yonsei University, Korea (the Republic of)

As the Internet of Things (IoT) and artificial intelligence (AI) robot technologies have been developed, object recognition with artificial visual perception system is required to process massive data from the continuous light inputs in the environment. For the artificial visual perception system, an optical neuromorphic transistor (ONT) was proposed which combined the functionalities of an optical sensor and neuromorphic device to remove data movement between sensory and data storage components, minimize the required area for the system, and reduce the power consumption. The synaptic current of the ONT was modulated by the wavelengths and intensities of the light inputs, enabling the precise control of the synaptic weight at a low voltage. However, there was a limitation of the ONT in realizing the depression characteristics since the synaptic current showed an exponential decay rather than exhibiting various discrete states simply by removing the light inputs. To overcome this limitation, an additional input source was necessitated along with the light inputs. In this regard, an optically and electrically driven dual-functional neuromorphic transistor (DNT) was introduced which showed the potentiation characteristic by light inputs and the depression characteristic by electrical spikes. To achieve the aforementioned characteristics, we presented an oxygen vacancy forming layer (VFL) consisting of magnesium (Mg) which was introduced between the channel and the gate insulator of the amorphous indium-gallium-zinc oxide (a-IGZO) DNT. Since Mg has a high binding force with oxygen, the VFL attracted oxygen in the front channel, resulting in the formation of magnesium oxide (MgO_x) during the thermal treatment after the a-IGZO deposition. In other words, the VFL facilitated the creation of oxygen vacancies (V_{O}) in the front channel. Since the V_{O} acted as subgap states for visible light absorption and carrier trapping/de-trapping centers, the VFL conferred the potentiation and depression characteristics to the a-

IGZO DNT by light inputs and electrical spikes, respectively. To validate the optoelectronic characteristics with visible light inputs, the transfer characteristics of the a-IGZO DNT without and with VFL were measured without and with red light (635 nm) irradiation. The a-IGZO DNT with VFL showed improved optoelectronic characteristics including the maximum value of photoresponsivity (Max. PR), photosensitivity (Max. PS), and detectivity (Max. D*) from 1.51×10^{-4} to 1.13×10^2 A/W, 1.34×10^2 to 1.22×10^6 , and 2.69×10^4 to 2.93×10^{11} Jones compared to those of the a-IGZO DNT without VFL under red light irradiation with the light intensity of 5 mW/mm², respectively. In addition, to confirm the short-term plasticity characteristics, the synaptic current was measured over time by applying red light with the light intensity of 5 mW/mm² and the electrical spike with 10 V. As a result, it was confirmed that the a-IGZO DNT with VFL showed the potentiation and depression characteristics by light input and electrical spike, respectively.

8:00 PM EL04.03.09

Development of a Hand Tremor Monitoring System for Quantitative Diagnosis Criteria of Parkinson's Disease Chiwon Song, ChanPark, JeongbeomKang, CheoljeongPark, ByeongjunLee, JungminKim, HaranLee and Seong J.Cho; Chungnam National University, Korea (the Republic of)

Parkinson's disease is a neurodegenerative disorder that affects millions of people worldwide. One of the most common symptoms of PD is hand tremor, which is caused by involuntary muscle contractions. The frequency of hand tremor in PD patients is typically between 4 and 6 Hz. The current gold standard for diagnosing PD is the Movement Disorder Society Unified Parkinson's Disease Rating Scale (MDS-UPDRS). However, the MDS-UPDRS is a subjective assessment that is prone to human error. In addition, the MDS-UPDRS only assesses the severity of tremor, not the frequency. To address these limitations, we developed a new hand tremor monitoring system. Our system consists of a lightweight and flexible circuit, a portable device, and a flexible strain sensor. The flexible strain sensor has a skin-like Young's modulus (0.08 MPa), high readability (25,000 cycles), sensitivity (GF: 6.1 at 30% strain, which is the fracture strain of skin), self-adhesion, and a flexible circuit that experiences almost no change in electrical signal at 50% bending strain. We used our hand tremor monitoring system to assess the frequency and amplitude of hand tremor in a clinical trial of PD patients. The results showed that our system was able to accurately quantify the frequency and amplitude of hand tremor in PD patients. The development of our hand tremor monitoring system is a significant step forward in the diagnosis and management of PD. Our system can be used to objectively assess the severity of hand tremor, which can help clinicians to make more accurate diagnoses and to monitor the progression of the disease. In addition, our system could be used to develop new treatments for PD.

8:00 PM EL04.03.10

Tactile Neuromorphic Display Enabled by Block Copolymer Structural Color KyuhoLee, YeeunKim and CheolminPark; Yonsei University, Korea (the Republic of)

The development of tactile stimuli interactive display with a memory function in a single device is highly desired and holds promise for potential applications such as intelligent artificial electronic skin (e-skin) and human-machine interfaces. In this work, we report for the first time a tactile neuromorphic display integrated into a single device enabled by block copolymer (BCP) structural color capable of a dual output of optical signals by combining the functionality of reflective mode display with a synaptic transistor that allows for the sensing, storing, learning and visualizing the number and magnitude of external tactile stimuli. The proposed device is based on an ion-gel gated transistor with a dome-shaped gate electrode and periodically ordered block copolymer (BCP) lamellae which serve as both tactile-interactive color-tunable gate dielectrics and ion-moving pathways. The electrically switchable structural color (SC) of BCP is ascribed to the movement of hydrated Li⁺ ions to an electric field. As the structural color returns to its original state due to ion diffusion when the electrical field is removed, the conductance retention feature of the synaptic device can be observed intuitively through the display. Furthermore, we fabricated 4X4 arrays of tactile neuromorphic display (TND) devices to propose a novel dual personal locking device that can detect information using wavelength and current. The new locks are prohibited from being accessed if the pressing time and pressure of the pattern are different, even if the path of the pattern is known, by taking advantage of the difference in pressing time and pressure depending on the individual.

8:00 PM EL04.03.11

Retina-Inspired Ferroelectric-Based Photonic Synapses TingyuLong¹, HuanyuZhou¹, JaewanKo², DaehanKang¹, EojinYoon¹, Gyeong-TakGo¹, HyojunChoi¹, MinhyukPark¹, JoonaBang² and Tae-WooLee¹; ¹Seoul National University, Korea (the Republic of); ²Korea University, Korea (the Republic of)

Photonic synapses, combining sensing and processing in a single device, have received a lot of attention from photonic computing and neuromorphic computing in recent years. In particular, photonic synapses using ferroelectric polarization are receiving much attention due to their unique bidirectional polarization characteristics. However, there are few papers related to substituting ligands of quantum dots with ferroelectric material. Here, a photonic synapse using ferroelectric polarization is reported. The device shows some crucial synaptic functions, including paired-pulse facilitation, short-term potentiation, and long-term potentiation. Most importantly, compared to conventional ligand capped QDs, it is shown that the long-time retention is improved from 11% to 23%. It is expected that the development of this photonic synapse device will facilitate the next paradigm of neuromorphic electronics.

8:00 PM EL04.03.12

Synaptic Thin-Film Transistors Employing Titanium-Oxide-Based Dual-Channel ChohyeonPark^{1,2} and Jung-WookLim^{1,2}; ¹Electronics and Telecommunications Research Institute, Korea (the Republic of); ²University of Science and Technology, Korea (the Republic of)

Implementing neuromorphic computing systems in hardware has gained significant attention as an alternative to conventional Von-Neumann computer architecture, offering energy-efficient processing of large amounts of data. This study focuses on characterizing titanium-oxide-based synaptic thin-film transistors (TFTs) with a dual-channel structure, aiming to emulate biological synaptic behavior.

The dual-channel structure of the titanium-based synaptic TFTs consists of titanium oxide (TiO₂) and indium-titanium oxide (InTiO) prepared by plasma-enhanced atomic layer deposition (PEALD), which exhibit compatibility with the complementary metal-oxide-semiconductor (CMOS) process. In addition, different photo-sensitivity^[1] according to different energy bandgaps of each channel allows for synaptic behavior modulation based on the wavelength of the incident light.

Experimental results show various optical and electrical synaptic behaviors in the titanium-based dual-channel synaptic TFTs due to the different lifetimes of captured carriers at each interface. Moreover, various characteristics include excitatory postsynaptic currents, paired-pulse facilitation, and potentiation/depression of synaptic weights. These phenomena arise from trapping the carriers at the dielectric and channel interfaces. It provides potential applications for artificial synapses employing a dual-channel approach, paving the way for advancements in neuromorphic computing systems.

[1] Lim, J. W., Kim, T., Kim, J., Yun, S. J., Jung, K. H., Park, M. A., Photoinduced Synaptic Behavior of In_xTi_{1-x}O Thin Film Transistors. Adv. Electron. Mater. 2021, 7, 2001049.

Acknowledgements This work was supported by the Electronics and Telecommunications Research Institute (ETRI) grant funded by the Korean government [23YB1410].

8:00 PM EL04.03.13

In Vitro Implementation of Reconfigurable Logic-in-Memory using Crossbar Neuronal Networks YongheeBae, Kyo-SeokLee, Sun-MiLee and Kyung-HwaYoo; Yonsei University, Korea (the Republic of)

The proposal of a logical neural network by McCulloch and Pitts, along with Hebb's postulate of spike-timing-dependent plasticity (STDP) for learning, has greatly influenced the field of brain-inspired computing research. In order to examine the impact of these concepts on the computational principles of real neurons, researchers constructed 4x4 crossbar neuronal networks on multi-electrode arrays (MEA) using a microfluidic structure made of polydimethylsiloxane (PDMS). By recording neural activity spatiotemporally with MEA, it was observed that STDP learning caused a shift in the threshold voltage (V_{th}) required to activate neurons, as well as changes in the response time determined by the interval between the stimulus onset and the arrival of the evoked spike. Additionally, the crossbar neuronal network exhibited well-defined connections between neurons, enabling the successful implementation of reconfigurable AND/OR logic gates through STDP learning. These findings demonstrate the feasibility of implementing reconfigurable logic-in-memory in crossbar neuronal networks.

8:00 PM EL04.03.14

Synaptic Memory Properties of Micron-Scale Geopolymer-Based Memristors Mahmudul AlamShakib, ZhaolinGao and CaterinaLamuta; University of Iowa, United States

Memristors are electric components capable of emulating the memory and computational properties of biological synapses by remembering the current that flows through them. They are considered artificial synapses when they mimic the memory and sensing properties of biological synapses. Enormous efforts have been given to discover the most suitable memristor materials for different applications. Here we present the synaptic memory properties of geopolymer memristors. These properties make them excellent candidates for the development of artificial synapses, which represent the building blocks of neuromorphic computing. We recently demonstrated memristive properties of geopolymers, inexpensive ceramic materials obtained from alkaline activation of amorphous aluminosilicate precursors. We also proposed a physics-based model to describe the role of electroosmosis in the memristive properties of geopolymers. We followed-up with the demonstration of synaptic functions by geopolymer memristors. However, the samples were in millimeter scale. In this study, we present the synaptic functions of geopolymer memristors manufactured at micrometer scale. We have developed a simple fabrication method to device multiple geopolymer memristors with the help of double-sided adhesive layer sandwiched between two printed circuit boards (PCB). The memristors were analyzed with the help of single-channel pulsed excitations for Short-Term Plasticity (STP) and Long-Term Plasticity (LTP) behaviors. Additionally, Spike-Timing-Dependent Plasticity (STDP) in terms of Long-Term Potentiation (LTP) and Long-Term Depression (LTD) are also observed by stimulating the geopolymer memristors with pairs of pre-synaptic and post-synaptic pulses. All 4 types of Hebbian learning behaviors are demonstrated. Finally, Spike-Frequency-Dependent

Plasticity (SFDP) properties such as Paired-Pulse Facilitation (PPF) and Depression (PPD), Post-Tetanic Potentiation (PTP), and History-Dependent Plasticity are demonstrated. The reported findings pave the way for the use of geopolymers in novel and low-cost neuromorphic computing applications like analog switching, memristive neural network, computer vision, etc.

8:00 PM EL04.03.15

Direct Electrical Biointerfacing with Bioadhesive Polymer Semiconductors [NanLi](#) and [SihongWang](#); University of Chicago, United States

Polymer semiconductors have shown distinct promise for merging human-machine interfaces, owing to their solution processability and flexible mechanical nature. Polymer semiconductors-based organic electrochemical transistors (OECTs) as an advanced type of sensing devices, are highly desired for direct electrical biointerfacing due to their low operation voltage, high sensitivity, and signal-to-noise ratio. To interface with wet and dynamically moving tissues, conventional suturing causes tissue/device damage and cannot achieve good conformability; having the adhesive property will ease the attachment process and help achieve a conformable contact and high spatial sensing resolution.

Here, we develop an intrinsically bioadhesive semiconducting polymer by creating a rationally designed polymer network with interpenetrating semiconducting polymers and adhesive brush polymers to realize both high normalized maximum transconductance and good adhesion on wet biotissues. Benefiting from the brush polymer design, the semiconducting polymer network possesses soft and viscoelastic mechanical properties, moderate water absorption, and controllable swelling, which synergistically contribute to the adhesion on wet tissue surfaces. In addition, the semiconducting material shows abrasion resistance, high stretchability, and good biocompatibility. Furthermore, we fabricated an intrinsically bioadhesive and stretchable OECT and further demonstrated its use for monitoring electrophysiological signals consistently and reliably on wet heart surfaces and in vivo muscles.

8:00 PM EL04.03.16

CMOS-Compatible Linear and Symmetric Electrochemical Protonic Synapse Device with HfO₂ Electrolyte [LonglongXu](#), [MantaoHuang](#) and [BilgeYildiz](#); Massachusetts Institute of Technology, United States

Analog programmable resistors, as key components of hardware artificial neural network hardware, can help solve the high-energy-consumption challenge of conventional hardware in artificial intelligence applications. Three-terminal proton-based electrochemical synapse device, working as programmable resistors, are operated by the reversible electrochemical insertion and extraction of protons, modulating the channel conductance with nonvolatile conductance states. Achieving fast, energy efficient, and CMOS-compatible electrochemical synapse devices remain a challenge. Previous organic electrolytes in ionic synapses are not CMOS-compatible although having high proton conductivity. CMOS-compatible solid-state electrolyte with high proton conductivity is important for the integration of the synapse device for future applications. Meanwhile, achieving highly linear and symmetric conductance change are significantly important in order to improve the inference accuracy after the training process of hardware neural networks.

Herein, we investigated proton-based electrochemical ionic synapses using CMOS-compatible binary oxide Hafnium oxide (HfO₂) as the electrolyte. HfO₂ has a low electronic conductivity and high electric breakdown field, which can facilitate good retention and lower writing energy consumption. The devices are fabricated by an all-sputtering process, with shadow mask for patterning. It has reactive sputtered WO₃ as channel material, sputtered HfO₂ as electrolyte, Cr/Au as source and drain contact, and Palladium hydride as the gate and hydrogen reservoir.

The synapse devices can be programmed with hundreds of distinguishable conductance state with 0.1-10 microseconds, 1-2V voltage pulses. The conductance change exhibit repeatable and almost ideally symmetric and linear behavior for potentiation and depotentiation. The writing energy consumption of the device can be as low as ~100 femtojoule/um² per pulse.

This work not only achieved high performance programmable resistor, but also proved that undoped HfO₂ can work as a proton electrolyte, which is important in making protonic electrochemical device CMOS-compatible. We are now investigating thin film binary oxides proton kinetics including conductivity and proton conducting mechanisms. The next stage also includes further improving the device performance by scaling down and engineering the proton conduction properties of HfO₂ by structure modification.

8:00 PM EL04.03.17

Sub-Nanometer Interface Modifications for Conductance Modulation in Proton-Based ECRAM Devices [JordanMeyer](#), [MantaoHuang](#) and [BilgeYildiz](#); Massachusetts Institute of Technology, United States

Three-terminal electrochemical random-access memory (ECRAM) devices have gained interest for use as resistive elements in neuromorphic computing architectures, with promising nonvolatility, reversibility, and symmetric operation through solid-state ion intercalation of the channel. Engineering these ECRAM devices to be both fast and energy-efficient remains difficult, as even proton-based devices display operating voltages above 1 V and programming speeds on the order of μ s, above the desired ns programming speeds. Recent advances in high ionic conductivity electrolytes and decreasing electrolyte thickness have decreased the gap in operating voltages, but as electrolytes become increasingly thin, other optimizations are needed.

Modification of the interface between electrolyte and channel remains largely unexplored in ECRAM. Lithium-ion-based ECRAM devices may benefit from many of the same interface strategies used in solid-state lithium-ion batteries since the material systems are similar. For proton-based devices, much less is known about the interface reaction in solid-state proton transport. How device operation responds to interface modification may give insight towards faster, low-power ECRAM devices. This work reports attempts to modify the interface in a proton-based ECRAM device between the archetypal channel material WO₃ and proton-conducting electrolytes, HfO₂ and phosphosilicate glass, with sputtering of a range of metals and metal oxides. Differences in conductance modulation across interface-modified devices are presented, which could be relevant for the low operating voltage regime where interface-limited kinetics start to manifest. Electrochemical impedance spectroscopy (EIS) is employed to study charge-transfer features in symmetric cell configurations. Surface modification of WO₃ thin films is also examined with X-ray photoelectron spectroscopy (XPS) and sheet resistance measurements. In doing so, we demonstrate that some tunability of ECRAM device operation is possible using CMOS-compatible sputtering with sub-nanometer interface modifications.

8:00 PM EL04.03.18

Nanoparticles as Drug Delivery Vehicles for TLR7 Agonists and Their Influence of Anti-Inflammatory Activity [KiShawndaA. Parker](#); JSNN, United States

Nanoscale materials play an integral role in delivery of drugs to their targets. This project focuses on understanding how nanoparticles impact drug performance at the interface. Systemic Lupus Erythematosus (SLE) is an autoimmune disease that negatively influences the function of organs throughout the body. SLE is triggered by the toll-like receptor (TLR) gene TLR7, which is located on chromosome X and is responsible for activation of the immune system. TLR7 agonists have been effective in stimulating innate immune cells and can lead to anti-inflammatory activity. Consequently, the targeted delivery of TLR7 agonists to cells is an important process in the treatment of SLE. The design and synthesis of well-defined magnetic particles with nanoscale dimensions is opening new avenues in understanding their fundamental chemical and physical properties, and their biocompatibility for effective use as drug carriers. Our work describes a novel facile procedure for the synthesis of homogeneous isotropic and anisotropic magnetic and biocompatible nickel nanoparticles. These nanoparticles were produced using a wet-chemical process and characterized by transmission electron microscopy (TEM), high-resolution transmission electron microscopy (HRTEM), selected-area electron diffraction (SAED), powder x-ray diffraction (XRD), energy dispersive spectroscopy (EDS) and thermogravimetric analysis (TGA). While there is significant interest in using magnetic nanoparticles for biological applications, little is known about their size-dependent interactions with biological cells. We demonstrate the impact of TLR7 agonists anchored to magnetic nickel nanoparticle surfaces and the influence on the particle-cell interactions. We further compare the effect of anchoring TLR7 agonist molecules on magnetic nanoparticle surfaces relative to polymer nanoparticle surfaces and study their effect on cells. The results indicate that the surface and molecular orientation of the attached molecules play a significant role in cell interactions. The underlying mechanisms of these interactions will be discussed.

8:00 PM EL04.03.19

Gradient-Free Learning in Organic Neuromorphic Devices [SimoneSpolaor](#) and [Yoeirvan de Burtg](#); Eindhoven University of Technology, Netherlands

Organic electronics is paving the way towards a new generation of low-power, bio-compatible neuromorphic computing devices, implementing hardware neural networks that can directly interface with living matter. However, the lack of learning algorithms that work efficiently on online, in hardware learning still hampers their computing power and scope of application. On the one hand, offline learning on digital hardware requires precise computational modeling of the physical properties of the devices and limits the energy efficient computations done in hardware to the inference phase. On the other hand, conventional learning algorithms used to train software neural networks are difficult to implement in hardware, due to memory constraints, necessity to calculate gradients and share weight information across the whole network.

Here, we apply a gradient-free optimization algorithm, named Simulated Annealing, to train a network of electrochemical neuromorphic organic devices (ENODE) and perform classification tasks. The Simulated Annealing algorithm does not rely on gradient information, and it is co-designed to exploit the ENODE physical properties (e.g., number of conductance states, state-retention time, energy, and time required per state-switch). This novel learning algorithm could be employed to achieve online learning on emerging organic neuromorphic systems, enabling multi-sensory integration and actuation in biological environments.

8:00 PM EL04.03.20

Self-Assembled Networks at Avalanche Criticality in Ag-hBN PlatformAnkit S. Rao¹, SoorajSanjay¹, MajidAhmadi², AnirudhVenugopalrao¹, NavakantaBhat¹, BartKooi², SrinivasanRaghavan¹ and PavanNukala¹; ¹Indian Institute of Science, India; ²University of Groningen, Netherlands

Systems and networks which exhibit brain-like behavior can analyze information from intrinsically noisy and unstructured data with very low power consumption. Such characteristics arise due to the critical nature and complex interconnectivity of the brain and its neuronal network. We demonstrate that a system comprising of multilayer hexagonal Boron Nitride (hBN) films contacted with Silver (Ag), that can uniquely host two different self-assembled networks, which are self-organized at criticality (SOC). This system shows bipolar resistive switching between high resistance (HRS) and low resistance states (LRS). In the HRS, Ag clusters (nodes) intercalate in the van der Waals gaps of hBN forming a network of tunnel junctions, whereas the LRS contains a network of Ag filaments. The temporal avalanche dynamics in both these states exhibit power-law scaling, long-range temporal correlation, and SOC. These networks can be tuned from one to another with voltage as a control parameter. For the first time, different neuron-like networks are realized in a single CMOS compatible, 2D materials platform.

8:00 PM EL04.03.21

Identification of VCM Switching Mechanism and Synaptic Characteristics of CMOS-Compatible MemristorsFeiQin¹, YuxuanZhang¹, Han WookSong² and SunghwanLee¹; ¹Purdue University, United States; ²Korea Research Institute of Standard and Science, Korea (the Republic of)

Memristors are being increasingly recognized as prospective components in the realm of brain-like computing applications. However, gaining insights into their switching procedures, especially concerning valence change memristors (VCM), continues to be an actively debated issue due to the complexities involved in the direct visualization of conductive filaments via microscopy. In this work, we focus on an in-depth understanding of the switching behaviors and mechanisms of VCM, with an emphasis on the promising role of SiO₂-based memristors in neuromorphic computing. Firstly, our study presents findings on CMOS-compatible SiO₂-based memristors, showcasing an impressive on/off ratio exceeding 10⁵. We delve into an extensive analysis utilizing COMSOL Multiphysics simulations, aiming to illustrate the evolution of the oxygen vacancy-based conductive path in these memristors throughout the SET process. Furthermore, the theoretical findings are corroborated experimentally via electrochemical impedance spectroscopy, enabling the interpretation of the switching behavior in the context of the equivalent circuit. A core part of our study is the evaluation of synaptic characteristics with pulse measurements which were then integrated into neural networks for image recognition tasks, using the MNIST and Fashion MNIST datasets as benchmarks. In essence, this work provides an encompassing view of the fundamentals about VCM's switching mechanism as well as a potential application of low-cost and CMOS-compatible memristors towards neuromorphic computing.

References:

F Qin, Y Zhang, HW Song, S Lee "Enhancing Memristor Fundamentals through Instrumental Characterizations and Understanding Reliability Issues", Materials Advances 4, 1850-1875
F Qin, Y Zhang, H Park, CS Kim, DH Lee, ZT Jiang, J Park, K No, H Park, HW Song, S Lee "Factors Determining the Resistive Switching Behavior of Transparent InGaZnO-based Memristors" Physica Status Solidi (RRL) - Rapid Research Letters 16 (7), 2200075

Acknowledgments:

This work was partially supported by National Science Foundation, Award number ECCS-1931088 and CBET-2207302. S.L. and H.W.S. acknowledge the support from the Improvement of Measurement Standards and Technology for Mechanical Metrology (Grant No. 23011043) by KRISS.

8:00 PM EL04.03.22

Driving Flexible Electronics by Hybrid MaterialsRodrigo F. Martins and Elvira Fortunato; FCT UNL, Portugal

Printable electronics and flexible electronics are key areas of development worldwide, once offer the potential to add functionality to everyday objects at very low costs that would be difficult with conventional technologies. This was pushed by the large success of organic electronics over the past few decades due to their attractive features such as low process temperatures, good mechanical flexibility, light weight, and the possibility to use a wide range of substrates and being recyclable. Besides that, we can prepare these devices using inexpensive solution processes over large areas. These benefits offered by printable and embedded electronics have been recognized in many sectors. Nevertheless, the bottleneck here is the low electronics performance so far achieved.

On the other hand, metal oxide electronic materials are quite attractive since they are reliable, able to be processed at low temperatures and present excellent electronic performances at 1-2D scales, providing so a large variety of different and possible applications, going from low costs to high complex systems able to compete with silicon in applications like transparent electronics, optoelectronics, magneto electronics, photonics, spintronics, thermoelectrics, piezoelectrics, power harvesting, hydrogen storage and environmental waste management. In terms of production techniques RF magnetron sputtering has been well established and has demonstrated high-performance devices, as ALD. However, these require complex equipment, especially if we are targeting low-cost applications. In contrast, the solution process has many advantages such as large-area deposition, roll-to-roll capability, easy control of composition, atmospheric processing, and low cost.

In parallel, we have been observing a rapid and growing interest in the utilization of biological materials for a wide range of applications. One of the most representative examples is cellulose, not only in the form of raw material mainly for pulp and paper production but also in the development of advanced materials/products with tailor-made properties, especially the ones based on nanostructures, for low-cost and disposable applications. In this presentation we will review the main applications of vegetal and bacterial cellulose in electronics, either as substrate (passive) or as a real electronic material (active), considering the expertise as well as the major developments already done at CENIMAT|i3N in Paper Electronics.

SESSION EL04.04: Neuromorphic Devices I
Session Chairs: Imke Krauhausen and Duygu Kuzum
Wednesday Morning, November 29, 2023
Hynes, Level 3, Room 313

8:15 AM *EL04.04.01

Device Physics and Switching Speed in Polymer-Based Artificial Synapses: Towards "Iontronics"Alberto Salleo; Stanford University, United States

Polymer-based artificial synapses have shown outstanding performance in terms of switching speed, switching energy and endurance. Indeed, devices that can switch with 20 ns pulses and can undergo a read-write cycle in under 1 μs have been demonstrated. Furthermore, we have shown that they can be switched billions of times with no degradation. These are very unusual features for organic semiconductors, which are usually plagued with slow speeds and weak reliability. In order to understand the origins of this performance we have developed a suite of operando characterization techniques that allow to study the materials structural evolution during biasing. We show that the highest performance devices are permeated with electrolyte in the form of neutral pairs, essentially acting as internally-gated transistors. Furthermore, we show that despite intercalating and expelling large ions, switching occurs with minimal structural disruption. These features may enable the operation of a broader category of "iontronic" devices that rely on ionic motion yet achieve high speeds compatible with electronics.

8:45 AM *EL04.04.02

Neuromorphic Computing and 2D Materials for Neural InterfacesDuygu Kuzum, Mehrdad Ramezani, Madison Wilson and Ashwani Kumar; University of California, San Diego, United States

The next leap in implantable neural interfaces requires technological advances in materials, devices, and computing paradigms. Holistic approaches integrating optical and electrical sensing modalities using 2D materials can overcome spatiotemporal resolution limits of neural sensing as well as open up new avenues for non-invasive neural recording. Integration of sensing, computation on neuromorphic interfaces can enable real-time processing of neural signals for compact, low-power and high-throughput brain machine interfaces. Here, I present this vision, its challenges, and discuss recent advances in the areas of transparent neural interfaces for multimodal recordings, neuromorphic approaches for on-chip neural processing and computational co-design at the system level for minimally invasive neural interfaces.

9:15 AM EL04.04.03

Organic Neuromorphic Electronics for Local Learning and Control in RoboticsImke Krauhausen^{1,2}, Paschalis Gkoupidenis² and Yoerivan de Burgt¹; ¹Technische Universiteit Eindhoven, Netherlands; ²Max Planck Institute for Polymer Research, Germany

Biological systems learn by interacting directly with the environment and receiving positive and negative feedback from many different stimuli that influence the formation of dynamic associations inside their neuronal systems. These associations are encoded within the neuronal connections of the brain, specifically in the strength of the synaptic connection between neu-

rons. Recently, the organic electrochemical transistor (OECT) has emerged for its use as artificial synapse showcasing volatile and non-volatile tunable dynamics that emulate synaptic plasticity. This allows the mapping of (artificial) neural networks into hardware-based circuits as well as the development of specialized neuromorphic chips mimicking the efficient structure and function of the human brain. Organic neuromorphic electronics also operate on low voltage which make them ideal for integration in energy-restricted environments such as autonomous robots [1-6].

In this work, we aim to create a small-scale locally trained organic neuromorphic circuit connected to a robot. The robot is able to respond to different input signals adaptively and form behavioral associations based on its interaction with the environment. This on-chip adaptable integration of multiple stimuli with low-voltage organic neuromorphic electronics opens the way towards stand-alone, brain-inspired circuitry in autonomous and intelligent robotics.

References

- [1] C. Mead, *Neuromorphic electronic systems* (1990).
- [2] E. O. Neftci et al., *Nat Mach Intell*, 1, 3 (2019).
- [3] P. Gkoupidenis et al., *Advanced Materials*, 27, 44 (2015).
- [4] Y. van de Burgt et al., *Nature Materials*, 16, 4 (2017).
- [5] A. Melianas et al., *Science Advances*, 6, 27 (2020).
- [6] I. Krauhausen et al., *Science Advances*, 7, 50, (2021).

9:30 AM EL04.04.04

An Organic Spiking Neuron with Unconventional Form-Factor for Energy Efficient, Neurotransmitter-Mediated, In-Sensor Pre-Processing Functions Giovanni Maria Matrone¹, Xudong Ji¹, Abhijith Surendran¹, Zachary Laswick¹, Gang Ye², Francesca Santoro³, Yoerivan de Burgt⁴ and Jonathan Rivnay¹; ¹Northwestern University, United States; ²Shenzhen University, China; ³Forschungszentrum Juelich, Germany; ⁴Technische Universiteit Eindhoven, Netherlands

The fundamental mechanisms of signal communication within the human body rely on the spiking frequency of action potentials.¹ Through biological receptors and afferent neuronal cells, stimuli from the external world are encoded into a spiking pattern and transmitted to the central nervous systems where they are processed via interneurons: the “sensory coding” mechanisms. The fundamental goal of neuromorphic electronics is to emulate the architecture of the human brain to enable parallel computing with high energy efficiency² and local processing, thus advancing intelligent systems interfacing with the human body³.

Recently, organic materials have been employed to build electronic circuits that mimic both the spiking behaviour of neurons⁴⁻⁶ and their synaptic transmission⁷ thus replicating afferent neurons and interneurons functions. Indeed, a combination of bioelectronic devices may recreate a “neuronal pathway” that in nature relies on the cooperation of spiking (neurons and interneurons) and non-spiking elements such as mechano-chemical sensors (receptors), and neuromodulator junctions (chemical synapses)⁸. Although the most recent neuromorphic circuits emulate biological functions which are deemed essential for basic signal processing and computation capabilities (mimicking some retinal functions), i) these systems power consumption is 2-3 order of magnitude higher than the brain processors, ii) their footprint is still on a scale (tens of mm) impeding meaningful in-sensor applications, iii) the electrochemical detectors for neurotransmitter still show sensitivity and selectivity not suitable for tissue interfacing.

Here it is presented an integrated neuromorphic platform that replicates both afferent neurons “sensory coding” and synaptic transmission.

Exploiting a vertical transistor architecture comprising stacked n-p type polymer films, complementary inverters are fabricated with a lateral footprint of 50 nm and requiring low drain voltage (0.05 V), thus building an independent spiking unit. To allow neurotransmitter-mediated synaptic transmission with high sensitivity, a novel biohybrid synapse is developed exploiting a referenced-ENODE architecture⁹. This system allows the detection of neurotransmitters, such as dopamine and serotonin, with a sensitivity approaching sub-nanomolar concentrations and enhancement selectivity, facilitating tissue coupling and potentially avoiding molecular cross-talk.

Moreover, the total neuromorphic system energy consumption, as predicted by electronic circuit simulations, is reduced to 1 nJ¹⁰, with a synaptic transmission contribution depending on the device lateral dimension and an energy-per-spike depending on the materials selection and the dimension of the vertical inverters. Moreover, the integrate-and-fire neuron footprint is reduced to 200nm x 200nm. This system constitutes a fundamental building block for programmable neural pathways. It is compatible with in-sensor application footprint and sensitivity requirements for locally executing bio-inspired pre-processing functions while its unconventional architecture allows to dynamically communicate with the nervous system.

1 Kandel, E. R. *et al.* 4, (McGraw-hill New York, 2000)

2 Furber, S. J. *Neural Eng.* 13, 051001 (2016)

3 Yoo, J. *et al. Current Opinion in Biotechnology* 72, 95–101 (2021)

4 Mirshojaeian Hosseini, M. J. *et al. J. Phys. D: Appl. Phys.* 54, 104004 (2021)

5 Harikesh, P. C. *et al. Nat Commun* 13, 901 (2022)

6 Harikesh, P. C. *et al. Nat. Mater.* 22, 242–248 (2023)

7 Matrone, G. M. *et al. Adv Materials Technologies* 2201911 (2023)

8 Matrone, G. M. *et al.* (In Review, 2022)

9 Ji, X. *et al. Nat Commun* 14, 1665 (2023)

10 Lee, Y. *et al. Joule* 5, 794–810 (2021)

9:45 AM EL04.04.05

Overcoming the Trade-Off Between Electrochemical Doping Efficiency and Retention Time in Electrolyte-Gated Organic Synaptic Transistors Min-Jun Sung¹, Dae-Gyo Seo¹, Jingwan Kim², Ho Eon Baek², Gyeong-Tak Go¹, Seung-Je Woo¹, Kwan-Nyeong Kim¹, Hoichang Yang³, Yun-Hi Kim² and Tae-Woo Lee^{1,1,1}; ¹Seoul National University, Korea (the Republic of); ²Gyeongsang National University, Korea (the Republic of); ³Inha University, Korea (the Republic of)

The electrochemical doping efficiency and retention time of long-term potentiation (LTP) are essential for superior device performance such as fast operation speed, high on/off current ratio, and high state retention in electrolyte-gated organic synaptic transistors. However, these characteristics exhibit a trade-off relationship in general; faster and more efficient electrochemical doping can induce faster de-doping of ions, which is directly related to lower state retention, and vice versa. This work introduces an effective strategy to increase retention time while maintaining efficient electrochemical doping. Our approach involves blending two polymer semiconductors (PSCs) that have the same backbone but different types of side chains. Polymer synaptic transistors (PSTs) that used the blend film showed stronger potentiation under weaker presynaptic spikes and retained LTP longer than PSTs that used only one of the PSC films. We attribute this change to the increased redox activity of the blended PSC, which was confirmed by several electrochemical characterizations. Unlike the common belief in this field, this work is the first to enhance retention time in PSTs with neither increasing the crystallinity of polymer film nor sacrificing the electrochemical doping efficiency. This method provides an effective way to tune synaptic properties for various neuromorphic applications.

10:00 AM BREAK

10:30 AM *EL04.04.06

Memristive Technologies for Ultrasensitive and Advanced Bio/Chemical Sensing Systems Loulia Tzouvadaki; Ghent University, Belgium

Memristive technologies coupled with biological processes opened new perspectives in the role of bio-inspired sensors, bringing a new versatile approach for label-free and specific transduction with ultra-sensitivity. These emerging technologies hold great promise as intelligent bio-interfaces opening application perspectives in the biomedical field, particularly for implantable and lab-on-a-chip devices.

The recent developments on transduction and processing of chemical biomarkers of neural and endocrine functions will be discussed as well as the critical perspective on the future applicability of memristive devices as pivotal building blocks in advanced biosensing systems.

11:00 AM *EL04.04.07

Elucidating the Resistive Switching Mechanisms Taking Place in La₂NiO_{4+δ}-Based Devices by In Situ and Operando Spectroscopic Techniques Mónica Burriel; University Grenoble Alpes, CNRS, Grenoble INP, LMGP, France

Resistive switching (RS) devices have attracted increasing attention for their application as non-volatile memories and neuromorphic computing systems. In my talk, I will focus on the design of novel memristive heterostructures using a perovskite-related oxide with high oxygen mobility and p-type semiconducting electronic transport, namely La₂NiO_{4+δ} (L2NO4). Dense L2NO4 thin films were grown using pulsed-injection metal-organic chemical vapor deposition (PI-MOCVD) under optimized conditions. While our first studies were dedicated to epitaxial planar devices on single-crystal substrates,^{[1][2]} we then moved towards industrial-relevant substrates and thus fabricated vertical devices with polycrystalline L2NO4 films on Si-based CMOS-compatible wafers.^[3] The electrical response of these devices could be tuned both by changing the electrode materials and the amount of point defects (oxygen interstitials) of the sandwiched film. The chemical, structural, microstructural characterisation of the films will be presented, showing the high crystal quality, together with the change in Ni oxidation state and the

concomitant change in resistivity after annealing. Furthermore, by several electrical characterization measurements, the key role played by the oxygen interstitials on the initial resistance state, the initialization step, and the memristive characteristics of the devices will be presented and discussed. An analog bipolar counter-eightwise RS behavior with multiple resistance states has been proven using continuous sweeps and voltage pulses.

However, to ensure that the TiN/L2NO4/Pt devices are suitable for use in the neural networks (NN), certain additional properties should be investigated. Firstly, the device should exhibit reversible long-term potentiation/depression to enable learning in NN. In addition, requirements such as low current, low switching time, high endurance, and retention should also be met. Here we explore the possibility of device optimization by alternating varying both fabrication and measurement conditions for TiN/L2NO4/Pt devices. The use of post-deposition annealing allows tuning the memristive properties of the device, and potentially eliminating the forming process. On the other hand, we show that with adjustment of the pulse length and voltage amplitude the process of multilevel resistive switching can be strongly influenced. We demonstrate highly reproducible long-term potentiation and depression in TiN/L2NO4/Pt structures achieved with short voltage pulses, which allows the potential use of these devices as artificial hardware synapses in spiking neural networks.

Selected devices were further analyzed by X-ray absorption spectroscopy (XAS) using synchrotron radiation. Changes in the Ni K-edge were measured for different annealings, in different regions of the device and under *in situ* and *operando* conditions, allowing for a better understanding of the RS mechanisms taking place in the device. Furthermore, gradual changes in conductance after the application of repetitive DC sweeps, which can be regarded as the evolution of the synaptic weight between neurons, were obtained for these novel L2NO4-based devices. These results were complemented with *in situ* transmission electron microscopy (TEM) measurements combined with Electron Energy Loss Spectroscopy (EELS) carried out for "lamella-devices" using an adapted TEM sample holder, which allowed for the observation of chemical changes for different resistance states. These results go a step further towards the comprehension of the intricate switching mechanisms taking place, and open the door to the use of L2NO4-based memristors as artificial hardware synapses in spiking neural networks.

[1] K. Maas *et al.*, *J. Mater. Chem. C* **2020**, *8*, 464

[2] K. Maas *et al.*, *Adv. Funct. Mater.* **2020**, *30*, 1909942

[3] T. Khuu *et al.*, *Adv. Mater. Technol.* **2022**, 2200329

11:30 AM EL04.04.08

Single-Nanoparticle Based Memristors for Neuromorphic Computing Sabrina Artmeier¹, Jonathan Hiltz², Jonathan G. Veinot² and Marc Tornow¹; ¹Technical University of Munich, Germany; ²University of Alberta, Canada

During the last years, neuromorphic computing has emerged as a fascinating and important research area. As one of its key elements, which would mimic the biological synapses, memristors are among the most promising device candidates [1]. Due to their energy-efficient operation, which can be in the order of picojoule per synaptic event [2] and the perspective to solve the von Neumann bottleneck problem [3], these devices have become an extensive research topic. Important current directions of research and engineering include device down-scaling and 3D-integration. To address these challenges, single nanoparticle (NP) - based memristive devices offer a promising route as they can be chemically synthesized with a high yield [4; 5] and may form functional heterogeneous aggregates by bottom-up directed self-assembly [6].

In order to study the memristive electrical properties of oxide NPs, we have developed a nano-lithographic process to individually and permanently contact single nanoparticles by embedding them in-between two electrodes. Our fabrication process can be employed to investigate oxide nanoparticles of different material composition, shape and size.

A highly appealing active layer material for memristive devices is tungsten oxide [7]. In our research, we were able to chemically synthesize tungsten oxide NPs of size ca. 90x90x15 nm³ [8]. Our studies of these NPs included different contact material combinations such as Ti/Au-Ti/Au, Ti/Pd-W and Ti/Pd-TiN. Electrical characterization was performed in DC mode (range $\sim \pm 4$ V) where the results showed a forming-less and stable, gradual resistance switching behavior for hundreds of cycles. Pronounced potentiation and depression behavior was visible as a hysteresis with an in- or decreasing current, respectively, after repeated voltage sweeps for one fixed bias polarity. To mimic the function of a biological synapse, some devices were also investigated under pulsed operation, where the pulse parameters are currently adapted in a way to optimize device learning and forgetting behavior. We discuss the possible mechanism of the observed resistance switching in terms of conducting oxygen vacancy paths in the tungsten oxide, which can be reversibly strengthened or weakened.

As our studies are eventually aiming towards a directed self-assembly of nanoparticles, we have also undertaken first experiments to facilitate such aggregation via tailored surface functionalization. Via coating of our NPs with phosphonic acid molecules [9] comprising hydrophobic endgroups, we were able to demonstrate the formation of homogeneous, directed face-to-face agglomerates in hydrous environments. These agglomerates indicate a successful replacement of the initial capping layer by the phosphonic acid molecule layer. To support this hypothesis, element-specific analysis methods such as XPS are used alongside with scanning electron microscopy. As the second endgroup of the phosphonic acid molecules is variable, this process is anticipated to allow for the fabrication of the desired, heterogeneous NP stacks.

References

[1] Jeong, H. *et al.*, *Journal of Physics D: Applied Physics*, 2018, 52(2), 23003.

[2] Lei Deng *et al.*, *Physics Letters A*, 2016, 380(7), 903–909.

[3] Zidan, M. A. *et al.*, *Nature Electronics*, 2018, 1(1), 22–29.

[4] Li, F. *et al.*, *Sensors and Actuators B: Chemical*, 2017, 238, 364–373.

[5] Ouyang, J. *et al.*, *ACS Applied Materials & Interfaces*, 2014, 6(15), 12505–12514.

[6] Speckbacher, M. *et al.*, *ACS Applied Electronic Materials*, 2020, 2(4), 1099–1105.

[7] Qu, B. *et al.*, *Electronic Materials Letters*, 2016, 12(6), 715–731.

[8] Artmeier, S. *et al.*, 2022 IEEE 22nd International Conference on Nanotechnology (NANO), 2022, 504–507. Palma de Mallorca, Spain.

[9] Zhang, J. *et al.*, *Langmuir*, 2019, 35(29), 9554–9563.

11:45 AM EL04.04.09

2D Drift-Diffusion-Reaction Model of Organic Electrochemical Transistors for Biosensing and Neuromorphic Hardware Simulations Ugo Bruno^{1,2}, Bjorn Lussem³ and Francesca Santoro^{1,4,5}; ¹Istituto Italiano di Tecnologia, Italy; ²Università degli Studi di Napoli Federico II, Italy; ³University of Bremen, Germany; ⁴Forschungszentrum Jülich GmbH, Germany; ⁵RWTH Aachen University, Germany

Organic electronics, and in particular electrolyte-gated transistors, witnessed an exponential growth in the last decades, enabling a collection of different applications, ranging from biosensing to flexible digital circuits¹.

In particular, PEDOT:PSS-based organic electrochemical transistors (OECTs), have come to play an important role for their natural ionic-to-electronic signal transduction and biocompatibility².

In addition, thanks to the development of inexpensive, tuneable and energy efficient devices, organic neuromorphic engineering emerged as a promising approach to overcome conventional silicon technology limitations³. Notably, neuromorphic OECTs were shown to exhibit non-volatile and reproducible memory⁴, and the first biohybrid synapse was demonstrated, in which an artificial neuron could communicate with dopaminergic cells⁵.

As complex electrochemical mechanisms take place during doping/de-doping processes of OECT, several models were developed over the years^{6,7}, in order to guide device design of such complex devices. Still, while correctly describing several features of such devices, these modelling approaches rely on a 1D approximation of the transistor channel, neglecting import dynamics of ions and holes. Furthermore, a clear model of a neuromorphic OECT is still missing.

Here, starting from a newly developed 2D drift-diffusion model of an OECT⁸, we present a numerical model of a PEDOT:PSS-based neuromorphic OECT, working at the border with biology. First, drift-diffusion-reaction equations are solved, to describe redox reactions happening at the gate/electrolyte interface, and the subsequent faradic charge transfer that dopes/de-dopes the OECT.

In particular, dopamine oxidation, and the subsequent hydrogen release in the electrolyte of the OECT, were simulated.

Notably, the model predicts a dependence of the faradic reaction on the composition of the electrolyte, as it directly affects the voltage drop at gate/electrolyte interface, that drives the whole faradic reaction. In addition, experimental data are provided, validating the model.

Lastly, charge trapping is implemented in the model, enabling the simulation of a biohybrid synapse, in which PEDOT:PSS is de-doped by hydrogen ions in a non-volatile manner.

The proposed model aims to provide a tool to guide the design of the novel generation of organic sensors and neuromorphic hardware, enabling the modelling of the devices working at the interface with biological systems.

1. Rashid, R. B., Ji, X. & Rivnay, J. Organic electrochemical transistors in bioelectronic circuits. *Biosens. Bioelectron.* **190**, 113461 (2021).

2. Mariano, A. *et al.* Advances in Cell-Conductive Polymer Biointerfaces and Role of the Plasma Membrane. *Chem. Rev.* **122**, 4552–4580 (2022).

3. van de Burgt, Y., Melianas, A., Keene, S. T., Malliaras, G. & Salleo, A. Organic electronics for neuromorphic computing. *Nat. Electron.* **1**, 386–397 (2018).

4. van de Burgt, Y. *et al.* A non-volatile organic electrochemical device as a low-voltage artificial synapse for neuromorphic computing. *Nat. Mater.* **16**, 414–418 (2017).

5. Keene, S. T. *et al.* A biohybrid synapse with neurotransmitter-mediated plasticity. *Nat. Mater.* **19**, 969–973 (2020).

6. Friedlein, J. T., McLeod, R. R. & Rivnay, J. Device physics of organic electrochemical transistors. *Org. Electron.* **63**, 398–414 (2018).

7. Bernards, D. A. & Malliaras, G. G. Steady-State and Transient Behavior of Organic Electrochemical Transistors. *Adv. Funct. Mater.* **17**, 3538–3544 (2007).

8. Paudel, P. R., Skowrons, M., Dahal, D., Radha Krishnan, R. K. & Lüssem, B. The Transient Response of Organic Electrochemical Transistors. *Adv. Theory Simul.* **5**, 2100563 (2022).

1:30 PM *EL04.05.01

Time-Dependent Programming of Electrochemical Synapses Enabled by Nonlinear Voltage Kinetics Bilge Yildiz, Mantao Huang, JuLi and Jesus A. del Alamo; Massachusetts Institute of Technology, United States

The rapid rise in energy demand for computing motivates the search for new computing paradigms. The exploration and development of new architectures with brain-guided learning rules have the potential to offer substantial enhancements in energy efficiency and performance. Spiking neural networks (SNN) are one of such promising architectures for achieving highly energy-efficient machine intelligence. To effectively implement SNNs in hardware, one of the key components are programmable synaptic devices capable of time-dependent weight updates. Recent advance of electrochemical ionic synapses (EIS) has shown their promise as programmable synaptic weights in deep learning accelerators due to their exceptional energy efficiency and low variability. Here we propose a passive local circuit and crossbar array architecture that implements timing-dependent weight update of EIS in a parallel and asynchronous way, leveraging the intrinsic nonlinear kinetics of EIS. Our architecture accommodates a diverse range of STDP (spike-timing-dependent plasticity) learning rules, with time scales controllably ranging from milliseconds to nanoseconds. Moreover, the architecture offers the flexibility to choose different learning rules within the array, emulating the behavior of synaptic pathways in biological brains. This approach holds potential applicability across a wide range of ions and material systems for EIS, potentially enabling SNN hardware implementations with high energy efficiency and high throughput.

2:00 PM *EL04.05.02

Neuromorphic Organic Electronic Devices for Neural Signal Sensing, Recording and *In Situ* Processing Fabio Biscarini; University di Modena e Reggio Emilia, Italy

Organic electronic neuromorphic components and devices operated in electrolytes are being investigated *in vitro* and *in vivo* as tools for selective bio-sensing, as their frequency response is strongly affected by the dopamine content of the operational electrolyte,¹ and as signal recording and signal processing units, thanks to their frequency response which enables low-power computation at the hardware level.^{2,3}

These properties stem from the inherent matching of the relevant timescales, as well as the chemical nature of the active layer and its strong interactions with neurotransmitters on the one hand, and, on the other hand, the similarity between the signal processing logic paradigms in the brain and in organic neuromorphic devices. Nonetheless, the implementation of neuromorphic devices and concepts in neuroelectronic interfaces designed specifically for translation comes with number of practical and conceptual hurdles which should be addressed, at both sides of the biotic/abiotic interface.

In this presentation, I will discuss some of the hurdles to translation of neuromorphic devices to clinical settings, showing experimental examples of recordings of electrical and chemical signals, and present some device layouts and material processing strategies for overcoming them.

References

- Giordani M, Sensi M, Berto M, et al. Neuromorphic Organic Devices that Specifically Discriminate Dopamine from Its Metabolites by Nonspecific Interactions. *Adv Funct Mater.* 2020;30(28):1-13. doi:10.1002/adfm.202002141
De Salvo A, Rondelli F, Di Lauro M et al. *Organic electronics circuitry for in situ real-time processing of electrophysiological signals.* <https://www.researchsquare.com/article/rs-2775813/v1> (2023) doi:10.21203/rs.3.rs-2775813/v1.
Keene, S. T., Gkoupidenis, P. & Burgt, Y. van de. Neuromorphic computing systems based on flexible organic electronics. in *Organic Flexible Electronics* 531–574 (Elsevier, 2021). doi:10.1016/B978-0-12-818890-3.00018-7.

2:30 PM BREAK

3:30 PM EL04.05.03

A Phototransistor Leads to Artificial Synaptic Behaviors by Controlling Off-Current under Illumination Seungme Kang¹, Byungchul Jang², Sunyoung Sohn³ and Hocheon Yoo¹; ¹Gachon University, Korea (the Republic of); ²Kyungpook National University, Korea (the Republic of); ³Sangji University, Korea (the Republic of)

Organic phototransistors (OPTs) can amplify electrical output signals without additional devices and provide tunable optical spectral response. A lot of research is being conducted using the characteristic that the electrical characteristics of the OPT change depending on the light. Recent studies investigate the properties of these OPTs for various applications such as photodetectors, image sensors and neuromorphic devices. Here, we propose an organic semiconductor-based OPT device in which the off-current increases when light is applied to the OPT. The structure of OPT is a single transistor using p-type organic semiconductor dinaphtho[2,3-b:2',3'-f]thieno[3,2-b]thiophene (DNTT) as a channel layer by thermally depositing it on a SiO₂/Si substrate. In addition, the photoresponse was improved by doping the entire surface of the material 2,2',2''-(1,3,5-Benzinetriyl)-tris(1-phenyl-1-H-benzimidazole) (TPBi) used as the hole transport layer of the organic light emitting diode (OLED). As a result, when the electrical characteristics of a single DNTT transistor were checked, an increase in off-current could be observed only under illumination of 300 nm to 400 nm, which is the DNTT photoresponse region. On the other hand, the TPBi-doped DNTT phototransistor shows an increase in off-current in all broadband wavelength ranges from 400 nm to 1000 nm. In addition, the change of current over time, we imitated artificial synaptic behavior by applying a relatively slow light response speed. As a result, a recognition rate of over 70% was achieved in all wavelength bands.

3:45 PM EL04.05.04

Symmetric Electrochemical Ionic Synapses (EIS) Based on Mg²⁺-Intercalation Miranda Schwacke, Pjotr Zguns, Jesus A. del Alamo, JuLi and Bilge Yildiz; Massachusetts Institute of Technology, United States

Neuromorphic accelerators for deep learning applications, as well as other energy-efficient, brain-inspired computing hardware, can be enabled by low power programmable resistors which act as artificial synapses. Here we focus on artificial synapses in which the channel resistance is programmed by reversible electrochemical intercalation of small ions, allowing for dynamic doping of the channel. These devices are referred to as electrochemical ionic synapses (EIS). The use of protons as the working ions in EIS has enabled very fast and energy-efficient devices but limits the long-term retention of devices without encapsulation in ambient air. This motivates the search for an alternative working ion which is stable once intercalated into channel materials in air without requiring encapsulation. Here we provide a proof-of-concept for EIS based on intercalation of Mg²⁺ ions into tungsten trioxide (WO₃).

These proof-of-concept devices are symmetric, with Mg_xWO₃ serving as both the ion reservoir and channel materials. Increasing the Mg content x in Mg_xWO₃ from x = 0 to 0.3 continuously increases the electronic conductivity over several orders of magnitude. *Ex-situ* characterization of the channel confirms that the change in channel conductance is due to intercalation of Mg²⁺ ions and reveals the structural and chemical changes taking place in WO₃ during Mg²⁺ ion insertion. Compared to H₂WO₃, the conductance of Mg_xWO₃ rises much faster at low ion concentrations. Additionally, unlike H-EIS, Mg-EIS has good retention in air without any encapsulation. Computational results suggest that this stability is not thermodynamic but is enabled by very slow kinetics and/or the blocking nature of Mg-O reaction products. Mg²⁺ as a working ion with WO₃ as the channel material is a promising materials system for improving the retention of EIS devices without the need for encapsulation.

4:00 PM EL04.05.05

Vertical Bilayer Anti-Ambipolar Transistors for Tunable Electrochemical Neurons Zachary Laswick, Abhijith Surendran, Giovanni Maria Matrone and Jonathan Rivnay; Northwestern University, United States

The human brain deploys a complex network of interconnected spiking neurons featuring a variety of electrophysiological characteristics to perform complex classification and recognition tasks^{1,2,3}. Although machine learning algorithms implemented on traditional von Neumann electronics have emerged for diverse computing applications, they lag behind biological calculators in terms of performance and power consumption¹. This “technological gap” stems from the brain’s massively parallel event-based processing of information, via interconnected neuronal

8:00 PM EL04.06.01

Visible Light-Driven IGZO Optoelectronic Synaptic Transistors with Subgap State Enhanced by Sonication YoujinSeo, JusungChung, SujinJung, Sung MinRho, Min SeongKim and Hyun JaeKim; Yonsei University, Korea (the Republic of)

With the remarkable advancements in artificial intelligence (AI) and the internet of things (IoT), adeptly managing vast amounts of data has become imperative. However, conventional von Neumann architecture has intrinsic limitations such as high power consumption and data bottlenecks due to its reliance on sequential processing. As an alternative, neuromorphic computing has emerged which emulates the complex operations of the human nervous system. Similar to the parallel connection of neural synapses, neuromorphic computing enables the simultaneous execution of tasks like memory storage, reasoning, and learning while minimizing power consumption.

Among various neuromorphic devices, interest in optoelectronic synaptic transistors (OST) that regulate synaptic weight through the control of channel conductance has recently attracted attention due to wide bandwidth making them suitable for handling large amounts of data, low power consumption, and low susceptibility to surrounding signals. As an emerging candidate for channel material of OST, indium gallium zinc oxide (IGZO) has been attracted due to its low off-current, high photosensitivity, and large persistent photoconductance (PPC), which is responsible for neuromorphic characteristics. However, it is not feasible for IGZO-based OST to be driven by the entire range of visible light, resulting from the wide optical bandgap of IGZO (~ 3 eV). This limitation hinders the scalability of IGZO-based OST for various optical applications and recent research has focused on creating subgap states within the bandgap to expand the light absorption range.

Herein, we introduce complete visible light-driven OST by inducing subgap states in IGZO through a facile sonication method. This sonication process induces the cavitation phenomenon, the rapid collapse of bubbles, and the generation of shock waves, resulting in hydroxyl radicals. The interaction between IGZO and hydroxyl radicals leads to the formation of subgap states near the valence band maximum of IGZO. The optoelectronic properties of IGZO-based OST with subgap state enhanced by sonication (SES) are measured under red (635 nm), green (532 nm), and blue (405 nm) light irradiation. SES shows optoelectronic characteristics of the IGZO-based OST such as photoresponsivity of 1324.4 A/W, photosensitivity of 3.21×10^9 , and detectivity of 1.12×10^{13} Jones under red light irradiation of 635 nm with the light intensity of 5 mW/mm², respectively. Moreover, it is confirmed that IGZO OST with SES demonstrated neuromorphic characteristics such as pair-pulse facilitation (PPF), short term memory (STM), and long term memory (LTM). A maximum PPF index value of 150 % is shown for red-light pulses at 1 mW/mm² with time interval of 1 s. Light pulses are applied with the wavelength of 635 nm, pulse width of 0.5 s, and pulse number of 5, varying different light power density from 1 mW/mm² to 5 mW/mm². STM behavior is demonstrated, when red light pulses are applied with light power density of 1 mW/mm². However, LTM behavior is confirmed, when the same input pulses are applied with light power density of 5 mW/mm². The transition of STM-to-LTM occurs through repeated input pulses, depending on light power density.

As a result, a facile method is demonstrated to improve the optoelectronic performance of IGZO OST by controlling the photoresponse characteristics. This research proposes the introduction of a facile sonication fabrication for inducing subgap states in a-IGZO and suggests the implementation of an IGZO-based OST operating in the entire range of visible light, indicating the potential application in enhancing the functionality of artificial visual cells.

8:00 PM EL04.06.02

Bio-Interface for Actuation and Neuromorphic Devices Muhammad Yunusa¹, Mertcan Han¹, Muhammad TurabAli Khan¹, Erdost Yildiz¹, Andrés Rodríguez-Camargo², Amirreza Aghakhani³, Bettina V. Lotsch² and Metin Sitti¹; ¹Max Planck Institute for Intelligent Systems, Germany; ²Max Planck Institute for Solid State Research, Germany; ³Universität Stuttgart, Germany

Intrinsically soft materials are increasingly developed for biosensors and interfaces for neuromorphic bio-hybrid devices. Here, we developed new memristors material solution for soft and adaptive neural interfaces using a hybrid approach through the combination of organic polymers and inorganic liquid metals (such as gallium-indium). We have demonstrated the photo-charging mechanism and memristive behavior of such material interface with sensing and actuation capabilities. The electrically and thermally conducting inorganic liquid metal provides the possibility to design devices based on soft and deformable particles for integration with biological interfaces. Polymer conjugated micro- and nanodroplets of liquid metals are biocompatible as are previously been used in drug delivery and phagocytosis. The new approach presented in this work will provide a new material platform for biological interfaces, neural stimulation and neuromorphic computation.

8:00 PM EL04.06.03

Enhancing RRAM Device Performance: A Design of Experiments Approach Alireza Moazzeni, Md Tawfiq Rahman Chowdhury, Sakir Karakaya and Gozde Tutuncuoglu; Wayne State University, United States

Oxide-based Resistive Switching Random Access Memory (RRAM) devices hold significant promise as candidates for next-generation memory technology and novel brain-inspired computing applications. Among these, TaO_x (1 < x < 2.5)-based RRAMs have achieved substantial attention due to their promising performance in terms of durability and low energy consumption. However, these devices still suffer from instability and endurance degradation issues which hinder their large-scale adoption. One critical parameter is the forming voltage, which significantly influences resistive switching activation, device energy efficiency, and overall RRAM reliability but high forming voltage can increase the parasitic capacitance discharge which accelerates the degradation in the higher number of consecutive ON/OFF cycles. Intrinsic properties of TaO_x switching films such as film stoichiometry and oxygen vacancy profile play a pivotal role in shaping RRAM device performance metrics. The stoichiometry engineering of oxide films, enabled by varying the deposition parameters of a sputtering system, offers substantial advantages in optimizing RRAM behavior. However, the multitude of controllable and uncontrollable experimental parameters and potential interdependencies render this task challenging. In this work, we study the optimal processing conditions for sputtered TaO_x films that will yield the desired device metrics compatible with the algorithm requirements of neuromorphic computing. We employ a 2-level design of experiments (DOE) approach to examine the interactive impact of oxygen content on TaO_x films by varying the oxygen pressure and deposition power. Furthermore, we demonstrate how this set of parameters impact critical device performance metrics such as forming and set/reset voltages, the type of resistive switching (bipolar or unipolar, among others), initial resistance, memory window, and the endurance variation coefficient.

8:00 PM EL04.06.04

Double Dry-Etching Microfabrication of Flexible Neural Probes with Homogenous Glassy Carbon Microelectrodes and Interconnections Rabia Fatima¹, Austin Broussard¹, Daniel Rivera¹, Bingchen Wu², Emma-Bernadette Faul¹, Davis Bailey¹, Xinyan T. Cui² and Elisa Castagnola¹; ¹Louisiana Tech University, United States; ²University of Pittsburgh, United States

Glassy carbon (GC) has only recently been considered for implantable neural interfaces, mainly due to a key advanced technology that allows for pattern transfer and integration of pre-pyrolyzed GC electrodes into flexible circuits. Hybrid GC multielectrode arrays ("hybrid" GC-MEAs), with GC microelectrodes and metal interconnections, have shown promising performance in neural applications, such as highly sensitivity in multi-site neurotransmitter detection, and high quality acute single-unit recordings. Hybrid GC-MEAs on thin flexible SU-8 substrate have also been demonstrated to reduce tissue damage and inflammation compared to stiff silicon probe, showing that the flexible substrate preserves a healthy neural tissue interface that can facilitate long-term sensing measurements. However, the mechanical contact between the metal interconnects and the GC electrodes may not withstand prolonged and aggressive electrical stimulation and mechanical stresses in a chronic application.

Using GC as a homogenous material for both electrodes and interconnects eliminates this concern. MEAs with both electrodes and interconnects from a single and homogeneous GC layer ("all" GC-MEAs) have been previously fabricated and have shown outstanding electrochemical stability. However, their fabrication required a complex double-pattern lithography process that is a potential limitation for device miniaturization.

Here, we introduce an alternative double dry-etching process for the fabrication of "all" GC-MEAs and "all" GC-fibers with miniaturized features. First, we pattern the SU-8 precursor on a Si₃N₄ wafer followed by pyrolysis (900°C in an inert atmosphere) to obtain GC electrodes and interconnections. Dimensions of trace width (5 μm) and thickness (2-3 μm) are optimized to ensure practical conductivity (1.21 ± 0.26 Ω/sq). Second, we lithography pattern the SU-8 insulation of the device and we protect its features with a sacrificial hard mask. Then, we etch the 2 μm Si₃N₄ layer using CF₄ reactive ion etching (RIE), where not protected, leaving the Si exposed. Finally, we use a purely chemical isotropic XeF₂ etching, taking advantage of the > 100:1 Si versus Si₃N₄ selectivity, to release the Si₃N₄ insulated devices from the Si wafer.

The new double dry-etching process enables the batch fabrication of "all" GC-fibers and "all" GC-MEAs on ultra-thin substrate with miniaturized features. The bare GC microelectrodes of these "all" GC devices demonstrated promising electrochemical sensing capability in the detection of tonic dopamine levels using square wave voltammetry, *in vitro* and *in vivo* in the dorsal striatum of mouse brain. Next step will be the investigation of their chronic electrochemical and electrophysiological sensing performance.

8:00 PM EL04.06.05

Inspired by the human visual system, optoelectronic synaptic transistors have recently received a great deal of attention as a promising candidate for next-generation neuromorphic computing systems. To fully leverage the advantages of such systems, it is essential to address the challenges of developing low-cost, large-area, and solution-processable optoelectronic devices that can maintain long-term stability. In this study, we introduce an indium gallium zinc oxide (IGZO) based optoelectronic synaptic transistor by doping cadmium(Cd) using vertical diffusion process. By employing visible light stimulation, we successfully demonstrated a fundamental synaptic properties of the device, including excitatory post-synaptic current (EPSC), paired-pulse facilitation (PPF), and short-term plasticity(STP) to long-term plasticity(LTP) conversion. In addition, the Cd dopant act as an n-type dopant, resulting in improved electrical characteristics, such as field-effect mobility and on/off current ratio. Our findings offer a promising approach for advancing the development of visible light optoelectronic synaptic transistors for next-generation neuromorphic computing systems.

8:00 PM EL04.06.06

Expanding Dynamic Range of Ionic Liquid Based Physical Reservoirs by Utilizing High Molecular Design Flexibility AsahiArai, YumengZheng and KentaroKinoshita; Tokyo University of Science, Japan

In recent years, there has been a growing focus on reservoir computing (RC) due to its adaptability to edge computing. RC is composed of input, reservoir, and output layers, and is characterized by learning only in the readout part [1]. Furthermore, RC in which the reservoir is replaced with actual physical system is referred to as physical RC (PRC). Accordingly, PRC allows for physical implementation of the reservoir layer and is suitable for fast and low-load learning for time-series data processing. However, the time scale of input signal that can process is limited depending on the relaxation time peculiar to the selected physical system. We focus on ionic liquids (IL) that offer high molecular design flexibility, enabling fine- and wide-tuning of dynamics time scales.

In this study, we showed that the time constant of reservoir could be tuned by employing IL as a physical reservoir and controlling the dielectric relaxation time. In addition, we successfully expanded the dynamic range of PRC for short-term memory (STM) tasks [2] by mixing ILs or parallelizing IL reservoirs with different dielectric relaxation times.

IL reservoirs with EL/IL/EL structure were formed by supplying IL onto a gap between a pair of gold electrodes (ELs) deposited on a SiO₂ substrate. We employed four types of ILs with different cations of [C_nmim⁺] (n = 2, 4, 6, 8) each while fixing the anion to [Tf₂N⁻], in which the alkyl side chain length of the cation systematically becomes long with increasing n. Positive and negative triangular voltage pulses, which were defined respectively as binary data of “1” and “0”, were injected into the structure. The width (*t_w*) of the pulse was set in the range of 1-10 μs. We conducted STM tasks using the current response to the random binary data input, and estimated the performance of IL reservoirs as a function of *t_w*.

Impedance measurement revealed that the dielectric relaxation time of [C_nmim⁺][Tf₂N⁻] (n = 2, 4, 6, 8) increased with increasing the length of the cation alkyl side chain. Furthermore, it was confirmed that *t_w* at which each IL reservoir exhibits the best STM performance closely matches the dielectric relaxation time of each IL. This result enables us to optimize the STM performance of IL reservoirs by selecting IL with the dielectric relaxation time that is similar to *t_w*. However, once the IL is determined, it is difficult to learn input signals with *t_w* that is far from the dielectric relaxation time of the IL.

Then, we configured an IL reservoir by connecting all the IL reservoirs for n = 2-8 in parallel, which is called a parallel reservoir hereafter. The STM performance of the parallel reservoir was significantly improved in all the range of *t_w* compared to that of each single IL reservoir. This is thought to be the result that four IL reservoirs with different time constant provide feature vectors which are linearly independent to each other, creating a higher-dimensional feature vector space.

The above results suggest that a single reservoir which includes multiple relaxation time constants can process input signal with high performance over a wide range of *t_w*. Therefore, we evaluated the STM performance of an IL reservoir in which ILs for n = 2 and 8 were mixed at a ratio of 4:1, which is called a mixed IL reservoir hereafter. Although not as good as the parallel reservoir, the STM performance of the mixed IL reservoir improved over all the range of *t_w* compared to those of single IL reservoirs. It is interesting that by mixing two different types of IL, STM performance can be cooperatively improved without interfering with each other's learning.

The present study indicates the feasibility of wide dynamic range PRC with a single physical reservoir device.

[1] H. Jaeger, *GMD Technical Report* 148, 13 (2001).

[2] H. Jaeger, *GMD Report* 152 (2001).

8:00 PM EL04.06.07

Neuromorphic Applications Realized by a Free-Standing Multilayer Molybdenum Disulfide Memristor AmirhosseinHasani^{1,2}, AminAbnavi² and MichaelAdachi²; ¹Montana State University, United States; ²Simon Fraser University, Canada

Recently, there has been growing interest in ultra-thin two-dimensional materials called transition-metal dichalcogenides (TMDs) for their potential use in compact electronic and optoelectronic devices. These materials are appealing because of their extremely thin structure and high data storage capacity. In this study, we introduce a type of memristor created using suspended multiple layers of molybdenum disulfide (MoS₂). This memristor exhibits a substantial current on/off ratio of around ~1000 and maintains stable retention of data for at least ~3000 seconds. By adjusting the intensity of light shining on the suspended MoS₂ channel, we can further enhance the on/off ratio to approximately 10⁵. Additionally, we demonstrate that these devices can replicate essential functions of the human brain related to memory, both short-term and long-term. We found that short-term memory (STM) can be transformed into long-term memory (LTM) by increasing the power of the light stimulus, the duration of the light pulses, and the number of pulses. Our electrical measurements, conducted in both vacuum and ambient air conditions, suggest that the observed change in resistance in these memristors is due to the presence of oxygen and water molecules on both sides of the MoS₂ channel. Consequently, our free-standing two-dimensional MoS₂-based memristors offer a facile approach to creating energy-efficient and reliable resistive switching devices suitable for neuromorphic applications.

8:00 PM EL04.06.08

Self-Rectifying and Artificial Synaptic Characteristics of Amorphous Ta₂O₅ Thin Film Bilayer Memristor BumjooKim, In-SuKim and SahnNahm; Korea University, Korea (the Republic of)

Amorphous Ta₂O₅ (ATa₂O₅) film has different electrical properties depending on the growth conditions. ATa₂O₅ film, which was grown under the Ar/O₂ atmosphere with a high O₂ pressure, has insulating property and thus it can be used as a tunneling barrier. ATa₂O₅ film, which was grown under O₂ deficient condition, shows resistance random access memory (ReRAM) characteristic, indicating that it can be used for switching layer. ATa₂O₅ film for tunneling barrier was grown on TiN/SiO₂/Si (TSS) at room temperature and annealed under oxygen condition by RTA. ATa₂O₅ film for bipolar switching was grown on tunneling barrier. Self-rectifying characteristics were observed in an ATa₂O₅ bilayer memristor. The current conduction of this ATa₂O₅ bilayer memristor in the high-resistance state (HRS) is explained by Schottky emission, direct tunneling, and Fowler–Nordheim (FN) tunneling. In the low-resistance state (LRS), this ATa₂O₅ memristor shows insulating behavior, indicating that oxygen vacancy filaments were not formed. The current conduction of this memristor in the LRS was attributed to direct tunneling and FN tunneling. Moreover, ATa₂O₅ bilayer exhibited artificial synaptic properties. Therefore, the ATa₂O₅ bilayer memristor can be used as an artificial synapse for neuromorphic computing.

8:00 PM EL04.06.09

Improvement of Information Processing Performance in the Ionic Liquid-Based Physical Reservoir Device by Thermal and Electrical Pretreatment YukiKubo^{1,2}, MasaharuYonezawa^{1,2}, HisashiShima², YasuhisaNaitoh², HiroyukiAkinaga², ToshiyukiIto³, ToshiakiNokami⁴ and KentaroKinoshita¹; ¹Tokyo University of Science, Japan; ²National Institute of Advanced Industrial Science and Technology (AIST), Japan; ³Toyota Physical and Chemical Research Institute, Japan; ⁴Tottori University, Japan

Edge computing, where AI processing is carried out in the edge domain, is attracting considerable attention because it is expected to provide more energy-conservative information processing and more rapid (real-time) feedback of the processing results compared to a conventional cloud-based computing. The various machine learning models for edge AI, which is required to satisfy both of low processing cost and high performance, have been proposed.

One of the promising learning models that satisfies these requirements is reservoir computing (RC), which has a very simple network structure consisting of input, reservoir, and read-out layers. Physical reservoir computing is a device implementation of RC, which use the actual physical phenomenon as a reservoir, a non-linear data transformation layer. So far, a wide variety of physical systems have been investigated as the physical reservoir device (PRD) [1]. PRD can effectively handle time series data (TSD) by selecting the PRD having appropriate dynamics according to the time scale of the input signal.

We have developed PRD using faradaic currents generated by the redox reactions in metal ion doped ionic liquids (ILs), which is hereafter represented as IL-PRD [2]. The advantage of IL-PRD is to have the relaxation time constant around hundreds of milliseconds with adjustability and is suitable for processing TSD generated with biological activities. We have previously clarified that the information processing capability in IL-PRD was influenced by various parameters such as an input signal asymmetry [2], electrode size [3], water content in IL [4], and temperature [5]. Herein, we present the significant improvement of the information processing capability in IL-PRD by the simultaneous applications of thermal and electrical stimuli.

The present IL-PRD had a pair of input and output terminals made of a Pt thin film. The electrode size was 100 μm x 100 μm, and the electrode spacing was 124 μm. To clearly define the location at which the redox reactions take place, those terminals were covered by the insulating SiO₂ layer excepting the electrode area. A droplet of [C_nmim][Tf₂N] doped with 0.4 M Cu ions was placed over the electrode to form a Pt/IL interface. TSD consisting of “0” and “1” was input to the device as a triangular voltage pulse (TVP) (pulse height ±3.0 V, pulse width 500 ms),

and the output current was measured. The signs of the TVP for “0” and “1” were defined to be negative and positive, respectively.

The information processing capability was evaluated by performing a short-term memory (STM) task. In the present study, the output current dataset for the STM task was obtained under three different conditions. In condition 1, the dataset was acquired at room temperature (RT), i.e., without applying thermal stimulus. In condition 2, IL-PRD was heated to 100°C as a thermal stimulus and cooled down to RT without applying electrical stimulus, followed by the dataset acquisition at RT. In condition 3, IL-PRD was heated to 100°C and the external voltage was applied at 100°C before the dataset acquisition at RT. The atmosphere during the experiment under those conditions 1, 2, and 3 was high vacuum. The memory capacity (MC), which is a quantitative measure for the STM task accuracy, was 1.72, 1.68, and 2.38 under the conditions 1, 2, and 3, respectively. Namely, the learning performance was improved by about 40% by the simultaneous application of the thermal and electrical stimuli. This result suggests that thermally enhanced electrochemical reaction causes the change in IL and/or Pt/IL interface and improved the learning performance.

[1] G. Tanaka *et al.*, *Neural Networks*, **115**, 100 (2019).

[2] T. Matsuo *et al.*, *ACS Appl. Mater. Interface*, **14**, 36890 (2022).

[3] T. Matsuo *et al.*, *2022 MRS Fall Meeting*, EQ09.13.02.

[4] M. Yonezawa *et al.*, *2022 MRS Fall Meeting*, EQ09.13.03.

[5] M. Kobayashi *et al.*, *IEEE J. Electron Devices Soc.* **10**, 893 (2022).

8:00 PM EL04.06.11

Preparation and Characterization of Hf_{0.5}Zr_{0.5}O₂-Based Flexible RRAM Device [TurgunN. Boynazarov](#), [HoJinLee](#), [JoonbongLee](#) and [TaekjibChoi](#); Sejong University, Korea (the Republic of)

Flexible substrate-based non-volatile devices are even more desired than before for foldable tools and electronics. However, the use of flexible substrate and high-temperature growth of the Hf_{0.5}Zr_{0.5}O₂ thin films constitutes the main obstacles to using this kind of heterostructure in flexible computing devices. Here, we report the Hf_{0.5}Zr_{0.5}O₂ (HZO)-based flexible resistive random access memory (RRAM) fabrication process by water etching-based oxide membrane lift-off and the following transfer. We have fabricated HZO/La_{0.7}Sr_{0.3}MnO₃(LSMO)/Sr₂Al₂O₆ (SAO) on SiO₂/Si substrate by using pulsed laser deposition, in this case, we used SAO as a sacrifice layer for transferring HZO/LSMO heterostructure on a metal-coated PET flexible substrate. The RRAM device exhibited forming free bipolar switching characteristics with low power consumption and when it comes to practical applications, the ON/OFF ratio and long-term stability are two crucial concerns regarding flexible RRAM. Excellent RRAM performance in the bent state with radii of curvatures of 12, 10, and 8 mm. In addition, our flexible device shows memristor behavior by measuring multilevel switching. This study provides a promising candidate for flexible memory devices and wearable electronics. When it comes to practical applications, the ON/OFF ratio and long-term stability are two crucial concerns regarding flexible RRAM. Here, we report transfer method-based HZO deposition at a high temperature on silicon samples and transfer.

8:00 PM EL04.06.12

Crystalline NaNbO₃ Thin Films Grown on a Sr₂Nb₃O₁₀ Seed Layer at Low Temperature for Self-Rectifying and Self-Powered ReRAM Devices [SahnNahm](#), [In-SuKim](#) and [BunjooKim](#); Korea University, Korea (the Republic of)

Crystalline NaNbO₃ (NN) thin films were deposited on a Sr₂Nb₃O₁₀/TiN/Si substrate at 300 °C. The Sr₂Nb₃O₁₀ (SNO) nanosheets served as a template to form the crystalline NN films at low temperatures. When the NN film was deposited on one SNO monolayer, the NN memristor exhibited normal bipolar switching characteristics, which can be attributed to the formation and destruction of oxygen vacancy filaments. Additionally, the NN memristor with one SNO monolayer exhibited artificial synaptic properties. However, the NN memristor deposited on two SNO monolayers exhibited self-rectifying bipolar switching properties and two SNO monolayers behaved as a tunneling barrier in the memristor. The conduction mechanism of the NN memristor with two SNO monolayers in the HRS is attributed to Schottky emission, direct tunneling, and Fowler–Nordheim (FN) tunneling. Hence, the NN self-rectifying switching memory device with SNO multilayer can be attributed to fabricating high-density cross-bar devices. Moreover, the piezoelectric energy harvester (PEH) was fabricated using the [001]-oriented NN film grown on SNO/Ni at 250 °C and the NN ReRAM devices have been operated using the NN thin film PEH.

8:00 PM EL04.06.13

Rotating Janus Particles using Electric Field Gradients [Ji-YoungLee](#), [PatrickA. Sullivan](#) and [LeilaDeravi](#); Northeastern University, United States

Rotating particles using electric fields offers a platform to induce dynamic colors for display applications. We explore the rotational behavior of Janus structures comprising a metal and a dielectric material with different geometries, including matchstick-like and snowman-like configurations. We combine numerical analysis with experimental validation to gain insights into their dynamics. We investigate how different particle geometries influence rotational behavior under an applied electric field and highlight the role of high frequencies on the angular velocity and electric torque showing promise for controlling particle asymmetry for displays.

8:00 PM EL04.06.14

Integration of Local Neuromorphic Circuits in Soft Robotic Systems to Realize Learning and Memory [BobHuisman](#)¹, [Yoerivan de Burgt](#)¹ and [BasOvervelde](#)^{2,1}; ¹Eindhoven University of Technology, Netherlands; ²AMOLF, Netherlands

Organic electrochemical transistors (OECT) have shown to be promising components for neuromorphic computing. In particular, their ability to control stable conductance states over a large range, which can be used to emulate the synaptic weight in artificial neural networks (ANN), an important component in translating the network from digital to hardware, as to reduce operation power and to circumvent the von Neumann bottleneck. Simultaneously, the field of soft robotic systems has achieved inherently adaptive actuators by using compliant, soft materials, which makes them promising candidates to be used in non-conventional environments and for complex applications. However, they are typically pre-programmed and are subsequently not capable of adapting their behavior on longer time scales. Additionally, the weight and size of typical robotic learning systems do not make it suitable for integration in soft systems. Our goal is to integrate local neuromorphic circuits, as an alternative platform to achieve decentralized learning and memory in soft robotic systems for performance optimization and environment adaptability. Typical software-based ANN learning algorithms make use of backward propagation and gradient descent, the latter being particularly hard to achieve in hardware. A possible alternative route for the hardware-based ANN is to make use of a physical neural network (PNN), where the physical processes and local rules of the circuit are utilized to train the network.

8:00 PM EL04.06.15

The Impact of Sc-Substitution on the Switching Behavior in AlN-Based Memristor Devices [SeokgiKim](#), [JimyongYu](#) and [SungkyuKim](#); Sejong University, Korea (the Republic of)

Aluminum Nitride (AlN) has garnered significant interest as an active material for memristor devices due to its outstanding characteristics such as a tunable bandgap by doping, chemical/thermal stability, and high electrical resistivity (~ 10¹⁴ Ω-m). [1],[2] Since memristor devices for artificial intelligence learning must ensure low power consumption, fast write speed, and long-term stability, it is important to clearly identify the switching behavior and control the electrical path in active materials. [3] However, the strong electric field is required to generate the set state, and permanent breakdown by Joule heating occurs due to the high barrier of AlN/metal Schottky junction. [4] Therefore, it is necessary to lower the Schottky barrier *via* elemental doping and form the robust conductive path by soft breakdown for realizing a stable AlN-based memristor with multilevel resistance.

In this study, we fabricated the vertically stacked Au/Al_{0.7}Sc_{0.3}N/Cu device with a modified active layer in which 30% of Al sites is substituted with Sc to prevent permanent breakdown in Au/AlN/Cu device. The yield of Au/AlN/Cu is lower than Au/Al_{0.7}Sc_{0.3}N/Cu by 23% because of the excessive Joule heating induced by high forming voltage of AlN causes permanent breakdown. The irreversible migration of nitrogen ions in AlN active layer leads to the degradation of conductance. Compared to AlN-based device, Sc-substituted AlN (AlScN) with a 15% reduced bandgap exhibits a low forming voltage of 6.0 V due to Schottky barrier lowering. In addition, AlScN with a thickness of 30 nm shows stable switching behavior at a reduced set voltage of 2.1 V and a reset voltage of -1.3 V formed by relatively weak soft breakdown. We directly observed conductive path composed of nitrogen vacancies in a AlScN layer using atomic-resolution transmission electron microscopy. In addition, the resistance at low resistive state gradually decrease at the elevating temperature from 300 K to 400 K, indicating typical semiconductor behavior. Under various compliance current conditions ranging from 0.1 mA to 10 mA, all resistance states were maintained for a duration of 10⁵ seconds at a read voltage of 0.3 V without noticeable degradation. The analog switching characteristics of AlScN and AlN devices were measured by applying a 10 us positive/negative voltage pulse for potentiation/depression, and statistical values of non-linearity factors (NL) were obtained for its quantification. Compared to the average NL of AlN devices is 0.67, the average NL of AlScN devices is 0.36, which is explained by the reversible movement of nitrogen ions in AlScN matrix. Modification of junction properties by elemental substitution provides a specific method to improve the reliability of AlN-based memristor devices for future neuromorphic computing.

[1] Ravi Prakash *et al.*, *Vacuum* **143**, 102-105 (2017)

[2] Zhiping Zhang *et al.*, *IEEE ELECTRON devices LETTERS*, VOL. 36, NO. 1, JANUARY (2015)

[3] K. Moon *et al.*, *Faraday Discuss.*, 2019, 213, 421

[4] Eszter Piros *et al.*, *Appl. Phys. Lett.* **117**, 013504 (2020)

8:00 PM EL04.06.16

Leveraging Electrochromic Polymers for Organic Electrochemical Synaptic Devices by Unraveling Polymer-Ion Interactions. Heejung Roh¹, Shuwen Yue¹, Hang Hu², Ke Chen², Heather J. Kulik¹ and Aristide Gumyusenge¹; ¹Massachusetts Institute of Technology, United States; ²Purdue University, United States

Owing to low-power, fast and highly adaptive operability, as well as scalability, electrochemical random-access memory (ECRAM) technology is one of the most promising approaches for neuromorphic computing based on artificial neural networks. Despite recent advances, practical implementation of ECRAMs remains challenging due to several limitations including high write noise, asymmetric weight updates, and insufficient dynamic ranges. Here, inspired by similarities in structural and functional requirements between electrochromic devices and ECRAMs, we demonstrate high-performance, single-transistor and neuromorphic devices based on electrochromic polymers (ECPs). To effectively translate electrochromism into electrochemical ion memory in polymers, we systematically investigate polymer-ion interactions, redox activity, mixed ionic-electronic conduction, and stability of ECPs both experimentally and computationally using select electrolytes. The best-performing ECP-electrolyte combination is then implemented into an ECRAM device to further explore synaptic plasticity behaviors. The resulting ECRAM exhibits high linearity and symmetric conductance modulation, high dynamic range (~1 mS or ~6x), and high training accuracy (> 84% within 5 training cycles on a standard image recognition dataset), comparable to existing state-of-the-art ECRAMs. This work offers a promising approach to discover and design novel polymer materials for organic ECRAMs and demonstrates potential applications, taking advantage of mature knowledge basis on electrochromic materials and devices.

8:00 PM EL04.06.17

Flexible Electrochemical Neural Probes for *In Vivo* Recording of Neurotransmitters Mona Abdelmonem, Sina Gharahatekan, Abdulrahman Al-Shami, Farbod Amirghasemi, Ali Soleimani and Maral Mousavi; University of Southern California, United States

Catecholamines are a significant focus in research because they play a critical role in the brain's "reward" system, although their precise function is not yet fully comprehended. The quantification of catecholamines are vital as they regulate all cognitive processes in the brain and can aid in early detection, diagnosis, monitoring, and therapeutic interventions for complex neural disorders. Implantable neural interfaces are essential in expediting progress in neuroscience research and the practical application of clinical neurotechnologies. Electrochemical sensors offer several advantages for measuring catecholamines, including high sensitivity and selectivity, rapid response time, minimal sample preparation, non-invasiveness, and portability. The proposed design will be used to create the sensor. It includes a working electrode and a reference electrode with a reference membrane. The reference electrode is shared between the platinum electrodes and will be formed on a parylene C substrate that is 10-20 μm thick. The platinum electrodes have a 100-200 μm radius and a thickness of approximately 200 nm. The sensing membrane will be applied to the circular area of the platinum contact using drop-casting. For *in vivo* recording, parylene's flexibility is essential because it enables implanted devices to adapt to the shape of the brain or muscles and move with it without harming the surrounding tissue. While many *in vitro* catecholamine sensing electrodes utilize coatings made of enzymes, aptamers, and antibodies to increase their sensitivity, these coatings are prone to biofouling and quick degradation, reducing the sensor's lifespan *in vivo*. As a result, we are using a label-free surface-modified Pt electrode, which has been shown to be durable during long-term implantation, Figure 1. The expected peaks potential for different catecholamines are: Epinephrine (EP): around 0.1-0.3 V, Norepinephrine (NE): around 0.1-0.2 V, Dopamine (DA): around 0.2-0.4 V. We utilize cyclic voltammetry and square wave voltammetry for direct electrochemical detection of catecholamines. We are depositing a sensing membrane comprising an ionophore on the working electrode for acetylcholine and pH.

8:00 PM EL04.06.18

Improved Charge Trapping of Synaptic Flash Memory by TiO₂ Reinforcer Seong Hyun Lee, Lee Wangjoo, Jinha Kim, Jeong Woo Park and Dongwoo Suh; Electronics and Telecommunications Research Institute, Korea (the Republic of)

I. Introduction

As AI computing has come a long way in the last decade, synaptic devices in artificial neural networks (ANNs) are recently drawing more attention due to the role of connection between neurons. Among synaptic devices, flash memory has been thoroughly investigated because of high density of data storage and low-voltage operation. However, even conventional flash memory like SiO₂/Si₃N₄/Al₂O₃ (SONOS) device still has a serious issue of nonlinear responses limiting the ability to deal with complicated input patterns. In order to improve the linearity, synaptic devices should have a large window of conductance to afford various input signals. In the present study we suggest new solution to subdue the nonlinearity by enhancing charge trapping.

II. Main Body

2.1 Experimental

The present synaptic devices were fabricated on Si(100) wafers using ETRI's CMOS fab. Based on thermal oxide of 500 nm, deposition of polysilicon atop and ion implantation were performed in a row to make channel and source/drain. Dielectric complex including tunneling and blocking oxide was formed as SiO₂(3 nm)/Si₃N₄(3 nm)/TiO₂(2 nm)/Si₃N₄(3 nm)/Al₂O₃(9 nm) using plasma enhanced atomic layer deposition at 300°C. The incorporation of TiO₂, an additional charge-trapping layer in the middle of Si₃N₄, is the main feature of the solution suggested. Finally, we adopted TiN and aluminum as gate and electrode materials, respectively. Transfer properties of the implemented devices were measured using parameter analyzer for single and multiple pulse condition while keeping both programming (PRM) and erasing (ERS) voltages fixed. Input signal was a square-type pulse with duration of 2 sec in single pulse. On the other hand, we investigated conductance change under multiple pulses to simulate real ANNs by applying 10⁶ pulses with both duration and interval of 10 msec

2.2 Results and Discussion

We extracted from measured transfer curves conductance change between PRM and ERS states of TiN/Al₂O₃/Si₃N₄/SiO₂/poly-Si (TANOS) and TiN/Al₂O₃/Si₃N₄/TiO₂/Si₃N₄/SiO₂/poly-Si (TAXOS) devices. Both devices show much lower PRM and ERS voltage (9 V) than conventional SONOS device (~ 20 V). Furthermore both devices show largest conductance span near the gate voltage of 1 V, which is small enough to reduce the burden of power issue. The difference of conductance ΔG between PRM and ERS states are compared both for TANOS vs. TAXOS and single vs. multiple pulse condition, respectively. As a result, the conductance span of TAXOS is superior to TANOS both for single ($\Delta G_s = 3.6 \times 10^4$ S vs. 1.7×10^2 S) and multiple pulse condition ($\Delta G_m = 1.5 \times 10^4$ S vs. 2.6×10^3 S). The conductance span of TAXOS is one to two orders of magnitude higher than that of TANOS. The increased DG can keep more input signals contained in TAXOS device improving the linearity aforementioned. Furthermore, the wide tunability of conductance enables TAXOS synapse to catch even smaller change of input signals facilitating more accurate learning in ANNs. This improvement of conductance span in TAXOS is attributed to TiO₂ layer. TiO₂ has large dielectric constants of tens to hundreds depending on crystalline structure, thereby it can be regarded as a reinforcer of charge-trapping. Although we have not yet fully understood the trapping mechanism, its electron-deficient stoichiometry may be able to enhance the charge trapping capacity.

III. Conclusions

We suggested new synaptic flash device of TAXOS that enhances charge-trapping capacity due to TiO₂ layer. TAXOS shows larger conductance span (tens to hundreds times) between PRM and ERS states than TANOS, which would be able to improve linearity in synaptic response. Through this study we noted that very high-k electron-deficient TiO₂ plays a role of reinforcer in charge-trapping operation despite a necessity to explore theoretical mechanism yet.

8:00 PM EL04.06.19

MoTe₂ Neuromorphic Memory Devices Enabled by Metal Ion Intercalation Rifat Hasan Rupom¹, Moonyoung Jung², Dongseok Suh² and Wobong Choi¹; ¹University of North Texas, United States; ²Sungkyunkwan University, Korea (the Republic of)

Two-dimensional transition metal dichalcogenides (TMDs) have attracted a lot of attention as neuromorphic memory devices due to their phase-tuning properties at the atomic-level structure. Among 2D TMDs, Molybdenum ditelluride (MoTe₂) has shown a phase tuning property between its 1T' and 2H phases by a minimal energy change. We developed a large-scale MoTe₂-based synaptic memory device for neuromorphic computing by a simple sputtering and post-lithiation process. We observed that lithiation on sputtered MoTe₂ results in phase segregation by forming Te crystal structure, which has a negative effect on the phase tunability towards synaptic memory. We have developed a method for stabilizing MoTe₂ crystal structure under metal ion intercalation by using a passivation layer. When compared to non-lithiated pristine amorphous MoTe₂, the lithiated MoTe₂ effectively enhances I_{on}/I_{off} hysteresis current from 5 to >10² at lower sweep voltages of 5V with Pico joule power consumption. We will discuss the fundamental mechanism of phase transition by metal-ion intercalation and its neuromorphic characterization by stabilizing the phase in MoTe₂ in addition to the MoTe₂ synaptic memory device performance.

8:00 PM EL04.06.20

Tuneable Conductance Quantization in Crossbar Cu/Ta₂O₅/Pt Resistive Random Access Memory Devices Utkarsh Misra^{1,2}, Vikas K. Sahu^{2,3}, Amit K. Das², Ajimsha

Given the current demands of data-intensive and cost-efficient computing, there exists a need of a memory device that could offer low operating power in-memory computation capabilities and can redefine von Neuman computer architecture while still exhibiting compatibility with the current CMOS fabrication infrastructure. In the past decade, resistive random access memory (ReRAM), has emerged as a promising candidate for the logic-in-memory devices due to its excellent properties such as scalability, low power operation, multiple logic states, fast switching and CMOS compatibility. In addition, quantized conduction in ReRAM devices arising due to size quantization, presents an opportunity to realize high-bit multilevel resistive switching for ultra-high-density memory systems with in-memory computation applications. For device showing quantized conduction, the conductance (G) of the device can be expressed as $G=nG_0$, where n is integer or half integer, and G_0 is the fundamental unit of conductance ($G_0 \sim 77.5 \mu\text{S}$). Here, we report reliable and repeatable resistive switching behavior in crossbar Cu/Ta₂O₅/Pt ReRAM devices based on electrochemical metallization (ECM), wherein quantized conductance has been observed, investigated, and tuned in reset switching events.

The Cu/Ta₂O₅/Pt devices in 8x8 crossbar geometry were fabricated on SiO₂/Si substrates using RF magnetron sputtering. Platinum bottom electrodes of thickness ~ 20 nm and line width and separation $\sim 250 \mu\text{m}$ were patterned using a metal shadow mask, followed by ~ 100 nm thick Ta₂O₅ thin film. After the deposition of the Ta₂O₅ layer, about 45 nm thick copper line electrodes as top electrode were patterned again using the shadow mask orthogonal to the bottom electrode, forming an array of 64 individual RRAM devices. The devices showed robust bipolar resistive switching, where the set switching voltage was found in the range of ~ 0.6 - 0.8V and reset voltage $\sim (-) 0.5$ to $(-) 0.8\text{V}$ for 150 switching cycles at compliance current (I_C) of 200 μA . The mean resistances of the low and high resistance states were ~ 8.4 k Ω and ~ 828 k Ω , with variability of ~ 0.39 and 6.6 respectively. The reset currents were always found to be smaller than the compliance current confirming the ECM mechanism of the resistive switching, wherein the conducting filament (CF) is considered to have formed of Cu atoms which leads to low operating power per switching event. The variation in compliance current resulted in change in lateral dimension of the CFs leading to different low resistance states. Furthermore, integral and half integral quantized conduction (QC) states were clearly observed in the crossbar Cu/Ta₂O₅/Pt devices, where the number and magnitude (n) of the quantized states were found to ~ 6 and 3.5, respectively at I_C of $\sim 200 \mu\text{A}$. The distribution of the conductance was Gaussian which were centered at 1 G_0 , 1.5 G_0 , 2 G_0 , 2.5 G_0 , 3 G_0 , 3.5 G_0 . The magnitude and number of the QC states were found to increase from ~ 2.5 to 3.5 and from 4 to 6, respectively as the I_C increased from 50 to 200 μA . The increase in number and magnitude of QC steps with I_C was explained considering the fact that thicker CF obtained at higher I_C , when undergoes a gradual rupture during reset process, results in larger number of QC steps compared to a thinner CF. The diameter of the CF was calculated theoretically considering resistance contributions from Ohmic, Maxwell and Quantum point contact to the resistance of the low resistance states, and found to increase with increasing compliance current. In future work, the synaptic behaviour of Cu/Ta₂O₅/Pt devices for artificial learning will be explored via spike-time-dependent-plasticity, potentiation and depression characterisations. The observation of QC states in the ECM based crossbar Cu/Ta₂O₅/Pt device, and I_C controlled tuneability of magnitude and number may be useful for next generation high storage density resistive memory and electronic synapses for neuromorphic computing.

8:00 PM EL04.06.21

Closed-Loop Neuromorphic OECTs for Autonomous Reinforcement Learning in Robotics Ugo Bruno^{1,2}, Daniela Rana^{3,4}, Chiara Ausilio¹, Ottavia Bettucci⁵, Simon Musall³, Claudia Lubrano^{3,4} and Francesca Santoro^{1,3,4}; ¹Istituto Italiano di Tecnologia, Italy; ²Università degli Studi di Napoli Federico II, Italy; ³Forschungszentrum Jülich GmbH, Germany; ⁴RWTH Aachen University, Germany; ⁵University of Milano-Bicocca, Italy

Neuromorphic platforms are emerging as new computational paradigm¹, with the ultimate goal of building artificial neural system, by replicating the efficiency of the brain in terms of parallel computation.

Such technologies can mirror several aspects of the brain, by exploiting complex circuits² or by exploiting unique features of innovative materials³.

Among the plethora of the available materials and structures, organic electrochemical transistors (OECTs) have emerged as ideal candidates in the building of complex neuromorphic systems, able to interface with living organisms⁴ and to learn autonomously⁵.

Notably, PEDOT:PSS-based OECTs have been employed in the implementation of the first biohybrid synapse. Here, cells cultured *in vitro* could directly communicate with such artificial neurons by means of neurotransmitters, emulating a biological chemical synapse⁶.

In this scenario, while successfully recapitulating several features of the synaptic communication, current neuromorphic devices process information in an open-loop fashion, failing in the recapitulation of the intricate, redundant and closed-loop communication of the brain, that makes the human nervous system so fault-tolerant and energy efficient.

The present work demonstrates autonomous reinforcement learning mediated by biological-inspired signals, in a closed-loop neuromorphic system. Here a neuromorphic OECT will ultimately learn how to drive a robotic hand, in order to grasp objects of different sizes.

The OECT can communicate with a silicon microcontroller to drive the 3D-printer robotic hand that is required to execute the task of grasping a ball. A pressure sensor provides a feedback on the outcome of the task. If the OECT cannot elicit a complete grasp, a punishment signal is sent in the form of a dopaminergic signal, that oxidized the PEDOT:PSS channel of the transistor, changing its conductance and modifying the grasp. Conversely, if the grip is correctly executed, a reward signal is supplied.

In addition, even when the difficulty of the task is increased by changing using a progressively smaller object, the neuromorphic system can adapt and learn again to grasp the target. Notably, such learning is non-volatile.

In light of this, the present work paves the way towards a novel generation of hybrid devices able to combine decades of development of silicon-based technologies with innovative features of organic neuromorphic devices.

1. Hassan, S., Humaira & Asghar, M. Limitation of Silicon Based Computation and Future Prospects. in *2010 Second International Conference on Communication Software and Networks* 559–561 (2010). doi:10.1109/ICCSN.2010.81.

2. Merolla, P. A. *et al.* A million spiking-neuron integrated circuit with a scalable communication network and interface. *Science* **345**, 668–673 (2014).

3. Nandakumar, S. R. *et al.* A phase-change memory model for neuromorphic computing. *J. Appl. Phys.* **124**, 152135 (2018).

4. Harikesh, P. C. *et al.* Organic electrochemical neurons and synapses with ion mediated spiking. *Nat. Commun.* **13**, 901 (2022).

5. Krauhäuser, I. *et al.* Organic neuromorphic electronics for sensorimotor integration and learning in robotics. *Sci. Adv.* **7**, eabl5068 (2021).

6. Keene, S. T. *et al.* A biohybrid synapse with neurotransmitter-mediated plasticity. *Nat. Mater.* **19**, 969–973 (2020).

8:00 PM EL04.06.22

A Vacuum-Deposited Polymeric Dielectric for Intrinsically Stretchable Carbon Nanotube Transistors Ja Hoon Koo; Sejong University, Korea (the Republic of)

Stretchable devices based on high-performance inorganic materials require the use of stretchable device designs such as wavy interconnects and kirigami structures, which sacrifices the device density to achieve stretchability and complicates circuit design. For applications that require high resolution or complex circuit designs in stretchable formats, the inorganic-based stretchable devices based on the device design strategy are thus not suitable. Another strategy to achieve stretchability is to construct the devices using intrinsically stretchable materials, but significant progress is required as devices based on these materials generally exhibit low electrical/optoelectronic performance as compared to the inorganic-based devices. This is particularly due to the absence of a high-quality stretchable dielectric material that exhibit nanometer-scale thickness for easy gate control and excellent insulating/mechanical performances at the same time. As such, common stretchable dielectrics used for intrinsically stretchable devices exhibit micrometer-scale thickness, resulting in poor gate controllability and high operation voltages. In many cases, these stretchable dielectrics are solution-processed, susceptible to organic solvents, and have low dielectric constants, which are not desirable for fabrication of high-performance devices. Through this work, we report the development of nanoscale stretchable dielectric layer which is compatible with the current microfabrication tools such as photolithography, etching, and consequent film deposition. The dielectric layer can be deposited using vacuum-deposition technique (initiated chemical vapor deposition), thus allowing for excellent thickness controllability and high areal uniformity. Our nanoscale stretchable dielectric film with ~ 160 nm thickness exhibits high chemical, mechanical, and thermal stabilities. Wafer-scale transistor arrays employing the developed dielectric, semiconducting carbon nanotube networks (as channel), and Au nanomembranes exhibit comparable electrical performance as those fabricated using inorganic dielectric layers (Al₂O₃ layer deposited with atomic layer deposition), but with intrinsic stretchability (up to 40% strain).

8:00 PM EL04.06.23

Integration of Synaptic Optoelectronics and Quantum Dot Light-Emitting Diodes for The UV Visualization Moon Kee Choi; Ulsan National Institute of Science and Technology, Korea (the Republic of)

Synaptic photodetectors demonstrate photon-triggered synaptic plasticity, offering potential enhancements in image recognition rates by improving image contrast. However, the visualization and recognition of concealed ultraviolet (UV) patterns remain challenging due to significant background noise. In this study, drawing inspiration from the all-or-none potentiation of synapses, we introduce an integrated device comprising synaptic phototransistors (SPTs) and quantum dot light-emitting diodes (QLEDs) to address this issue. This device aids in noise reduction and the visualization of UV patterns through on-device preprocessing. The SPTs transform noisy UV inputs into a weighted photocurrent, which is subsequently applied to the QLEDs as a voltage input through an external current-voltage-converting circuit. The QLEDs' threshold switching characteristics result in amplified current and visible illumination in response to suprathreshold input voltage, while nearly zero current and no visible illumination occur below the threshold. Utilizing the SPT-QLED preprocessing for image data can effectively enhance image contrast, thereby facilitating high-accuracy image recognition.

8:00 PM EL04.06.24

Porous Organic Semiconductors for Geneless Optical Fine Tuning of Intracellular Reactive Oxygen Species in Endothelial Cells Camilla Marzuoli^{1,2}, Miryam Criado-Gonzalez³,

An imbalance in cellular redox status is intrinsically linked to the onset and progression of numerous diseases. ¹ In fact, Intracellular Reactive Oxygen Species (ROS) concentration plays a crucial role in the control and fine tuning of several physiological functions, from cell proliferation to differentiation, from migration to metabolic activity, to specific functionalities. ² As a consequence, a strong interest towards the concept of 'redox medicine' has been emerging in the few latest years. ²

Current available treatments to modulate the cell redox balance rely on the employment of chemically controlled methods. However, this strategy often fails to achieve accurate spatial and temporal control, is not reversible and is unsuitable for fine-tuned control of sub-cellular organelles. Employing optical excitation as a stimulus to finely modulate intracellular ROS concentration at non-toxic levels offers the opportunity to overcome these limitations, but requires the development of novel, photoelectrochemically active transducers.

To support the development of new tools for precise, non-toxic, non-invasive and on-demand modulation of intracellular ROS concentration it is therefore necessary to develop new biocompatible materials, characterized by highly tunable electrochemical efficiency and good stability in a biological environment. ^{4,5} Moreover, stimulation protocols should be as minimally invasive as possible.

Here, we propose a novel strategy, based on the use of semiconducting polymers. We demonstrate that photoelectrochemically active organic semiconductors potentially satisfy all these requirements and their application for bio-hybrid interfaces could lead to a reliable new medicine.

In more detail, our strategy is based on the development novel porous nanomaterials with an enlarged surface area that enhances their opto-electrochemical properties. ⁶ To that aim, graft copolymers, made of poly(3-hexylthiophene) (P3HT) and poly(lactic acid) (PLA) P3HT-g-PLA, are synthesized and employed for the fabrication of both porous thin films and porous nanoparticles (NPs). We employ FT-IR, TEM, AFM, DLS and water contact angle measurements to provide extensive characterization of morphology and composition. Importantly, sizable enhancement of photo-electrochemical efficiency is successfully achieved in porous P3HT-g-PLA materials, in both films and NPs, as demonstrated by photocurrent and Scanning Electrochemical Microscopy measurements.

Human Umbilical Vein Endothelial cells (HUVECs) are employed here as a physiologically relevant cell model. In endothelial cells, in fact, ROS production can regulate several aspects of vascular function, including angiogenesis. ^{7,8}

Internalization of porous NPs in HUVECs is successfully reported at different concentrations. For both thin films and NPs, intracellular, optically-modulated ROS production is demonstrated with high specificity and yield. Future work will aim at clarifying the functional interplay among biophysical pathways connecting intracellular ROS modulation, ion channels activation and Ca²⁺ dynamics, focusing on the potential application of these porous materials for therapeutic angiogenesis.

References

1. H. Sies et al., *J. Biol. Chem.* (2014)
2. J.P. Fruehauf et al., *Clin Cancer Res.* (2007)
3. H. Sies et al., *Nat Rev Mol Cell Biol.* (2020)
4. C. Bossio et al., *Front. Bioeng. Biotechnol.* (2018)
5. M.R. Antognazza et al., *Oxid. Med. Cell. Longev.* (2019)
6. M. Criado-Gonzalez et al., *ACS Appl. Mater. Interfaces* (2023)
7. E. Panieri et al., *Cell. Mol. Life Sci.* (2015)
8. S.C. Bir et al., *Free Radic Biol Med* (2013)

8:00 PM EL04.06.25

Development and Evaluation of Bioelectrode Array Devices for Monitoring Lower Back PainSeiichiTakamatsu, NaotoTomita and ToshihiroItoh; The University of Tokyo, Japan

In recent years, wearable devices like Fitbit and Apple Watch have gained popularity for health monitoring. Advances in e-textile technology have made fabric devices equipped with arrayed bioelectrodes particularly suitable for whole-body muscle activity monitoring. Specifically, it is suggested that back pain can be prevented or measured by capturing FRP signals in the lumbar region. Due to the need for monitoring in daily life, the longevity of these devices is becoming increasingly important. While there has been progress in developing long-lasting electrodes with low noise, the issue of electrode adhesion has remained a challenge. In this study, we propose a new method for securing electrodes using hot-melt sheets and have confirmed its effectiveness. Our results demonstrate that this approach ensures the electrodes do not detach, allowing for reliable electromyographic measurements. The device proposed in this study has a multi-layered structure in which various functional materials are laminated onto fabric. The composition of each layer. In the manufacturing process, silver paste is first screen-printed onto a polyurethane film (DUS-202, Seadam Co., Ltd.) to form the wiring layer. This wiring layer is then thermally bonded to the fabric using a hot-melt sheet (SHM101-PUR, Seadam Co., Ltd.). On top of that, another hot-melt sheet with holes opened in the via regions is thermally bonded to serve as the insulating and adhesive layer. Next, fabric cut into electrode shapes using a laser cutter is thermally bonded, and conductive plastic PEDOT:PSS and ionic liquid gel are then impregnated into this fabric piece and cured. We conducted mechanical characteristic evaluations as well as performance assessments as an electromyography (EMG) measuring device on the fabricated device. When wearing and using the device, it is anticipated that force will be applied to the electrodes from various directions, and it is required that the electrodes do not peel off under such conditions. Therefore, we evaluated the strength of the electrodes using tensile-shear tests and T-peel tests. During the evaluation, we prepared a sample based on the actual electrode structure by adhering a polyurethane film to a piece of fabric (10 mm x 30 mm) using a hot-melt sheet (10 mm x 10 mm). Another layer of fabric with electrode material applied was then attached using another hot-melt sheet. We also conducted tests on samples before the electrode material was applied for comparison. The strength was determined by clamping 10 mm x 10 mm sections on both ends of the fabric and investigating the relationship between the pulling amount and the load using a benchtop load tester (FTN1-13A, Iko Engineering Co., Ltd.). To assess the EMG measurement performance, the fabricated device was attached to the lower back and the lumbar EMG was measured. In the adhesive strength evaluation tests, two key findings emerged. First, when subjected to pulling forces, the fabric itself broke at around a strain level of 1.2 without any delamination at the adhesive interface. This indicates that the electrodes have sufficient tensile strength. Second, delamination began to occur when the strain exceeded 1, and the load plateaued. The peel strength was around 40 N before the electrode material was applied, and approximately 20 N after its application. Despite the reduction in peel strength due to the ionic liquid gel, it was confirmed that the electrode could withstand the types of force it would encounter in wearable use. In lumbar electromyography (EMG) measurements using the array electrodes, the data corresponded to a known physiological phenomenon. It is generally understood that no lumbar EMG activity is observed when maintaining a bent-over posture. This was confirmed in the current study, where a clear disappearance of EMG activity was observed between the 5 to 10-second interval, compared to the periods before and after.

8:00 PM EL04.06.26

Multilevel Resistance Modulation of Au-Nanodot Embedded Self-Rectifying Memristor for Neuromorphic HardwareTae GyunPark¹, JihunKim¹, Young JaeKwon¹, Hae JinKim² and Cheol SeongHwang¹; ¹Seoul National University, Korea (the Republic of); ²Myongji University, Korea (the Republic of)

The memristor-based materials have been researched as next-generation computing devices due to their simple metal-insulator-metal (MIM) structure and ease of device fabrication. The memristive crossbar array (CBA) is effective for the implementation of multiply-and-accumulate (MAC) operations by simply collecting current at the single bit line (BL) from the multiple biased memristors through word lines (WLs), which follows Kirchhoff's current law (KCL). Since the memristive CBA consists of multiple BLs, the multiple MAC operations can be performed in parallel, proving a more efficient computing device for ca. neuromorphic system as the size of the CBA increases.^[1,2]

Despite the promising structural advantages of memristive CBA for MAC operations, the non-ideal characteristics, such as sneak current, line resistance, variations, and electroforming, hinder more practical applications. Such a problem can be mitigated by introducing additional selecting devices, known as selectors or transistors, to the memristors.^[3] However, engineering the electrical characteristic to match the appropriate operational voltage and the current level is challenging, especially when processing variation exists throughout the CBA structure. Another aspect to consider for MAC operations is energy consumption. Introducing other three-terminal devices, however, often induces higher operational current levels in the range from several hundred μ A to mA and the operational voltage, resulting in significant additional energy consumption in the larger CBA structure.

To alleviate the difficulties, self-rectifying memristor (SRM)-based CBA is introduced that uses a bi-layered oxide structure instead of introducing the additional selecting devices and has a much lower operation current level with a range of sub- μ A to nA. Since the switching mechanism is governed by trap-rich and insulating layers with Schottky contact, the electroforming process is not required in the CBA structure, and the reversed current is significantly suppressed to prevent the sneak current.^[4,5]

However, SRM-based CBA still requires additional control in cycle-to-cycle variations and retention of states, resulting from the variation in the electronic trapping and detrapping in trap levels, which are essential parameters to determine the accuracy of the MAC operations and multilevel states in the implementation of the artificial synapse.

In this work, nanometer-sized gold nanodots (Au NDs) were formed at the interface of switching and rectifying layers to promote the electric field concentration in alignment with trap states. Enhancing the electric field concentration improves the overall cycle-to-cycle variations and retention characteristics. The conduction model to explain the improvement from Au NDs in Pt/Ta₂O₅/HfO₂/TiN structure is proposed based on the experimental result from the modulation of the size and position of Au NDs with transmission electron microscope (TEM) analyses. With conductive atomic force microscopy analysis and the finite element method simulations, the distribution of the internal electric field and the current density could be verified inside Au-NDs embedded SRM. Finally, the demonstration of MNIST classification in neural network application using eight stable states (3-bit) of the SRM-based CBA shows improved accuracy compared to non-inserted Au NDs SRM.

References

- [1] J. Kim, H. C. Woo, S. Lee, B. J. Lee, T. Park, *Adv. Intell. Syst.* **2022**, 4 (8), 2100256
- [2] T. Park, S. S. Kim, B. J. Lee, T. W. Park, H. J. Kim, C. S. Hwang, *Nanoscale* **2023**, 15, 6387-6395
- [3] H. C. Woo, J. Kim, S. Lee, H. J. Kim, C. S. Hwang, *Adv. Electron. Mater.* **2022**, 8 (12), 2200656
- [4] J. H. Yoon, S. S. Song, I.-H. Yoo, J. Y. Seok, K. J. Yoon, D. E. Kwon, T. H. Park, C.S. Hwang, *Adv. Funct. Mater.* **2014**, 24 (32), 5086-5095
- [5] S. S. Kim, S. K. Yong, J. Kim, J. M. Choi, T. W. Park, H. Y. Kim, H. J. Kim, C. S. Hwang, *Adv. Electron. Mater.* **2023**, 9 (3), 2200998

SESSION EL04.07: Emerging Materials for Neuromorphic Engineering I
Session Chairs: Kazuya Terabe and Myung-Han Yoon
Thursday Morning, November 30, 2023
Hynes, Level 3, Room 313

9:00 AM *EL04.07.01

Reconfigurable Logic Circuits Based on Organic Electrochemical Neuromorphic Devices Myung-Han Yoon; Gwangju Institute of Science and Technology, Korea (the Republic of)

Owing to the increasing demands of data-intensive applications, there exists an imperative need for next-generation electronic systems that are energy-efficient and possess low power consumption, facilitated by innovative architectures. In this study, we present the development of reconfigurable circuits built on organic neuromorphic devices. Our research focused on leveraging the learning capabilities of an organic electrochemical diode to execute multiple logic functions through high-performance reconfigurable logic circuits. A key feature of these devices is the tunability of their conductivity state, which can be modulated in response to the polarity of the drain-source voltage (V_{DS}), while the selective activation of various elements is governed by the manner in which the input voltage (V_{logic}) is utilized. Consequently, such manipulation facilitates the transition from an undefined state to selectively performing as either an AND or OR gate within the same hardware configuration. Additionally, it was demonstrated that the capacity for more sophisticated operations by integrating learnable AND and XOR circuits to construct a half-adder. We expect that our findings will provide an efficient approach toward novel digital circuitry through on-chip learning, thus surmounting the efficiency bottleneck that exists in conventional computing systems.

9:30 AM EL04.07.02

Characteristics of the Thermodynamics of Novel Ag-Cation Controllable Diffusive Memristors for Artificial Neuron Application Moonkyu Song, Sangheon Lee and Sanjay K. Banerjee; Microelectronics Research Center, The University of Texas at Austin, United States

Introduction: Diffusive memristors are essential elements for neuromorphic computing applications due to their ideal electrical characteristics such as high off-state resistance and a steep turn-on slope [1]-[2]. However, it is difficult to have characteristics with a large on/off ratio and a fast switching speed at the same time with conventional devices. Here, we reported a method to solve this problem using combination of Al_2O_3 metal oxide solid electrolyte layer and engineered defective graphene monolayer. We have also verified this characteristic through thermodynamic analysis for artificial neuron application.

Device Description: The devices for this study were fabricated using the same method as presented in our previous paper [3]. Silver active metal layer was deposited by e-beam evaporation on a SiO_2/Si wafer, followed by patterning with lift-off method. For the filament-control graphene interlayer, chemical vapor deposition (CVD) of graphene on copper foils was done, and then, CVD graphene was transferred onto a SiO_2/Si substrate with Ag bottom electrode using poly (methyl methacrylate) (PMMA) support layer. After the transfer of the graphene layer, the PMMA was removed with acetone. A hydrogen electrochemical reaction process and vacuum anneal were performed after the transfer process to form the defective area in the graphene and remove PMMA residue on the graphene film, and then the Al_2O_3 layer was deposited by atomic layer deposition (ALD). Finally, Pd inert metal was defined as the top electrode (TE). To analyze the characteristics of the thermodynamics of Ag-cation controllability with our system, MATLAB, and COMSOL Multiphysics were performed with the Ag-based threshold switching device measured parameters.

Results and Discussion: The DC current-voltage characteristics of Ag/Graphene-based novel diffusive memristor were performed. The initial states of devices were normally in the off-state and their resistances were about 10^{12} ohms at 0.1 V. When a graphene layer is placed between the active metal (Ag) and oxide electrolyte layer (Al_2O_3), the off-current was found to maintain its low value until the conductive filament is fully generated and the memristor is changed from off-state to on-state. The off-current of the novel memristor was $\sim 10^{-13}$ A. The on-current was $\sim 10^{-3}$ A, with self-compliance characteristics, as reported in our previous paper [3]. To elucidate the self-compliance characteristics, we investigated the dynamics of conductive filaments with limited Ag cation concentration using our defective graphene. We utilized MATLAB and COMSOL Multiphysics to calculate the relationship between chemical potential and filament radius during the turn-on process. The filament dynamics during turn-on were analyzed based on the minimization of free energy, which comprises thermal energy, electrostatic energy, surface chemical energy, and volume chemical energy. We calculated each term in the free energy equation using our device structures, and the total free energy was obtained by summing up these terms. The radius of the conductive filament was found to have the minimum value at the intersection of the thermal energy and volume chemical energy terms. This indicates that the radius of the filament can be fixed, resulting in the achievement of self-compliance characteristics at this fixed point. This limitation can be related to the filament dissolution time which makes the fast reset speed for artificial neuron applications.

[1] Z. Wang, *et al.*, *Nat. Mater.* 16, 101–108 (2017). [2] F. Ye, *et al.*, *Adv. Mater.*, 2204778 (2022). [3] M. Song, *et al.*, *Nano Lett.* 23, 2952–2957 (2023).

9:45 AM EL04.07.03

Lego-Like Heterogeneous Integration of Memristor Arrays using Optical Communication Min-Kyu Song, Hyunseok Kim, Junmin Suh and Jeehan Kim; Massachusetts Institute of Technology, United States

Conventional integration technologies have encountered issues including material deterioration due to the physical interaction between chips, fixed operation modes owing to the permanent connections to a single sensor, and limited data processing capabilities due to constraints when adding processors for various computing needs. In this study, we developed an innovative, reconfigurable 'Lego-style' 3D integration platform. This platform uses optoelectronic devices to facilitate communication between AI processors. We integrated freestanding GaAs/InGaP membranes into each chip via an epitaxial lift-off (ELO) process. Communication between chips was enabled by optical transmission between GaAs LEDs and InGaP photodiodes. By eliminating electrical interconnects, we not only avoided interference from physical contact, but also significantly enhanced chip configuration flexibility. We further incorporated memristor arrays into each stackable chip, serving as AI hardware accelerators and greatly improving processing efficiency. This innovative approach overcomes the limitations observed in previous 3D heterogeneous integration methods. By using this novel 'Lego-style' 3D heterointegration process based on a GaAs/InGaP stack, edge computing systems integrated with various sensors can provide infinite modality, exceptional computational efficiency, and adaptability for a variety of computing tasks.

10:00 AM BREAK

10:30 AM *EL04.07.04

Impact of Low-Voltage Resistive Switching Devices on Neuromorphic Computing Arka Mukherjee, Srikrishna Sagar and Bikas C. Das; IISER Thiruvananthapuram, India

The human brain is the most efficient machine around us in size, power efficiency, self-learning capability, decision-making, and simultaneous data storage and processing. Additionally, our brain performs all operations analogously by consuming energy of about 1 – 100 fJ per synaptic event. Even though the conventional computer works much faster than the brain, the von Neumann bottleneck and memory wall issues limit the performance and energy efficiency due to the physically separated storage and processing unit. After discovering the memristor (MR), a two-terminal device with multiple conducting states at a particular bias voltage, efforts are already underway toward developing machines similar to brain functionality. Despite massive progress in semiconductor technology, it is still challenging to mimic the functionality of synapses and neurons, the basic building blocks of our brain. Memristor (*memT*), a gate-controlled memristor or memory transistor, is also coming up rapidly to the limelight for mimicking functionalities of synapses and neurons more controlled way as the building block of the artificial brain. Among various approaches, the redox-controlled MR and *memT* are becoming very attractive to accomplishing the desired metrics for developing efficient neuromorphic computing tools. In this talk, I will introduce a few unconventional redox reaction-dependent molecular MR and organic *memT* devices that are very efficient for data storage and mimic various synaptic and neural functions electronically.

11:00 AM *EL04.07.05

Emergence of Neuromorphic Devices using Conductive Materials of Various Ion SpeciesKazuyaTerabe, TakashiTsuchiya and TohruTsuuoka; NIMS, Japan

The development of hardware-oriented artificial intelligence (AI), such as information terminals and brain computers that operate with small size and low power consumption, is expected to develop into the next generation of information technology. In order to realize such hardware-oriented AI systems that do not rely on conventional supercomputers and complex programs, new concept devices with diverse functions, such as memristive and neuromorphic devices, should be required. To this end, it is necessary not only to further develop conventional semiconductor devices with characteristics suitable for digital arithmetic processing, but also to create novel devices that operate based on new principles.

As you know, material properties can be significantly altered by slightly changing the composition and arrangement of its constituent atoms. Therefore, we have been actively searching for interesting nanophenomena arising from the control of composition and atomic configuration in nanostructures. Such nanostructure control can be achieved using ionic nanoarchitectonics techniques, which allow local control of ion transport and electrochemical reactions occurring at and near solid interfaces or surfaces. We have used the ionic nanoarchitectonics to create a variety of devices with unique electrical, magnetic, and optical functions and performance that cannot be obtained with conventional semiconductor devices^[1,2]. Some neuromorphic devices such as a decision-making device, artificial synaptic devices, multifunctional on-demand device, artificial vision device and physical reservoir devices^[3] have been fabricated using ion-conducting materials of various ion species. This talk will focus on the creation of various neuromorphic devices by ionic nanoarchitectonics using conductive materials of various ion species such as proton ions, lithium ions, silver ions, copper ions, and oxide ions.

Reference

[1] K. Terabe et al. *Adv. Electron. Mater.* **8**(8), 2100645, 2022

[2] K. Terabe et al. *Nanoscale* **148**(29), 13873-13879, 2016

[3] T. Nishioka et al. *Sci. Adv.* **8**, eade1156 (2022)

11:30 AM EL04.07.06

Tuning the Redox Properties of a Conducting Polymer for OECT-Based Zn Sensing: From Template to TargetTommasoNicolini^{1,2,3}, ShekharShinde^{4,3,2}, ReemEl-Attar^{5,6,3}, DamienThuau^{5,2,3}, MamatiminAbbas^{5,3,2}, JochenLang^{7,6,2}, EricCloutet^{4,3,2} and AlexanderKuhn^{1,2,3}; ¹Institut des Sciences Moleculaires, France; ²Bordeaux INP, France; ³Centre National de la Recherche Scientifique, France; ⁴Laboratoire de Chimie des Polymère Organiques, France; ⁵Laboratoire de l'Intégration du Matériau au Système, France; ⁶Université de Bordeaux, France; ⁷Chimie & Biologie des Membranes et de Nano-objets, France

Due to their ionic and electronic conducting capabilities, as well as their mechanical properties, conducting polymers have been at the forefront of organic bioelectronics,^[1] especially when integrated as active materials in organic electrochemical transistors^[2] (OECTs). Importantly, these devices allow developing analytical methods for a specific target mainly based on either amperometric or potentiometric sensing^[3]. Molecules or ionic species in solution can be quantified selectively and with high sensitivity due to the intrinsic amplification power of OECTs. Their sensing capabilities^[4] are based on the interaction of an analyte with either the channel or the gate electrode and the resulting modulation of the transistor readout, i.e. the drain current, I_d . Since the electrochemical doping/dedoping process is intimately governed by ion-aromatic backbone coupling^[5], some interest has been devoted to achieve selectivity towards ions of biological interest by using ion selective membranes^[6a-c] or through direct chemical modification of the conducting polymer^[7a-c]. In one of these latter examples^[7a], OECT-based membrane-free specific cation sensing has been achieved by implementing poly(3,4-alkoxy thiophene) (PEDOT) derivatives with added functionality at the gate electrode of an OECT through electropolymerization. Here, we present a novel conducting polymer allowing the selective sensing of Zn when implemented in the channel of an OECT. Interestingly, we use the target cation during electropolymerization to impart planarity and order to the polymer layer to modulate its electrochemical and electrical properties. This is the first instance of a OECT-based Zn-specific sensor and the limit of detection obtained is one order of magnitude lower than what has been achieved with membrane-free devices for other cations ($\approx 10^{-6}$ mol L⁻¹ vs. $\approx 10^{-5}$ mol L⁻¹). These results hold the promise to develop analytical methods for *in-vitro* and *in-vivo* applications investigating the numerous biological processes involving Zn²⁺.

References

[1] J. Rivnay et al., *Chem. Mater.* **2014**, *26*, 679.

[2] J. Rivnay et al., *Nat. Rev. Mater.* **2018**, *3*, 17086.

[3] E. Macchia et al., *Mater. Horizons* **2020**, *7*, 999.

[4] A. Marks et al., *Adv. Mater. Interfaces* **2022**, *9*, 2102039.

[5] A. Savva et al., *J. Mater. Chem. C* **2018**, *6*, 12023.

[6] a) S. T. Keene et al., *Adv. Healthc. Mater.* **2019**, *8*, 1901321; b) M. Sessolo et al., *Adv. Mater.* **2014**, *26*, 4803; c) Z. Mousavi et al., *Electroanalysis* **2009**, *21*, 472.

[7] a) S. Wustoni et al., *Adv. Funct. Mater.* **2019**, *29*, 1904403; b) A. Villarreal Marquez et al., *Macromol. Rapid Commun.* **2020**, *41*, 2000134; c) G. Salinas et al., *ChemElectroChem* **2020**, *7*, 2826.

11:45 AM EL04.07.07

Effects of Gamma on the Switching Performance of MoS₂ Based Resistive Random Access Memory (RRAM) DevicesArunNimmala^{1,2}, SakshiKapoor¹ and J. P. Singh¹; ¹Indian Institute of Technology Delhi (IIT-D), India; ²Indian Institute of Technology Delhi., India

Metal-Insulator-Metal (MIM) structures of a Non-volatile memory (NVM) devices were fabricated by sandwiching Molybdenum disulfide (MoS₂) thin film in between two metal electrodes. The top and bottom metal electrodes were deposited by using the thermal evaporation and the oxide layer was deposited by spin coating drop casting technique. A controlled resistive switching Resistive of random-access memory (RRAM) device structures such as Ag (or Au, Pt)/ MoS₂/Au (or ITO)/Si were fabricated and I-V characteristics for the pristine and gamma-irradiated devices with a few low doses were measured. The X-ray diffraction (XRD), Field emission scanning electron microscopy (FESEM) analysis measurements were performed to determine the crystallinity and stoichiometry of these films. The effects of gamma irradiation on the switching properties of these RRAM devices have been studied. The study also indicates the significance of radiation damage and reliability of these devices beyond a critical fluence. The electrical properties of these devices such as switching endurance cycling, retention time, and resistance ratio studied by using Agilent B1500 semiconductor device analyzer will be discussed in detail at the conference.

Key words: Resistive switching, 2-D materials, Gamma irradiation, RRAM, Endurance and Retention test.

SESSION EL04.08: Emerging Materials for Neuromorphic Engineering II

Session Chairs: Simone Fabiano and Francesca Santoro

Thursday Afternoon, November 30, 2023

Hynes, Level 3, Room 313

1:30 PM *EL04.08.01

Organic Neuromorphic Electronics for Sensory Coding and Biohybrid SystemsYoerivan de Burgt; Technische Universiteit Eindhoven, Netherlands

Neuromorphic engineering takes inspiration from the efficiency of the brain and focusses on how to utilise its functionality in hardware. Organic electronic materials have shown promising solutions for the manipulation and the processing of biological signals, with applications ranging from bioinformatics to brain-computer-interfaces and smart robotics.

This talk describes state-of-the-art organic neuromorphic devices and provides an overview of the current challenges in the field and attempts to address them. I demonstrate two device concepts based on novel organic mixed-ionic electronic materials and show how we can use these devices in trainable biosensors and smart autonomous robotics.

Next to that, organic electronic materials have the potential to operate at the interface with biology. This can pave the way for novel architectures with bio-inspired features, offering promising solutions for the manipulation and the processing of biological signals and potential applications ranging from brain-computer-interfaces to bioinformatics and neurotransmitter-mediated adaptive sensing. I will highlight our recent efforts for such hybrid biological memory devices and artificial neurons.

2:00 PM *EL04.08.02

Advances and Challenges in ECRAM-Based Resistive Crosspoint Arrays for AI ComputationSeyoungKim; Pohang University of Science and Technology, Korea (the Republic of

Artificial Intelligence (AI) technology, which heavily relies on deep neural networks, is having a significant impact on both business and society, transforming our daily lives. To support the

ever-increasing computation demands for AI applications, there has been a growing interest in novel analog computing architectures enabling massively-parallel neural network computation by adopting cross-point arrays of emerging non-volatile memory devices. Both device-level and system-level research efforts are actively pursued to achieve the promised power-efficiency and substantial performance improvements. Among various cross-point device candidates, electrochemical random-access memory (ECRAM) has recently attracted researchers owing to its 3-terminal nature and superior programmability [1-3]. In this talk, I will first introduce our recent device specification study when different training algorithms, optimized for practical resistive memory devices, are used to train neural networks in resistive cross-point arrays [4]. This quantitative study is expected to provide a guide for material and device research. I will continue the discussion on the recent advances and challenges in implementing large ECRAM-based cross-point arrays for analog AI computations with the consideration of the non-ideal device characteristics such as limited retention time and selector-less array-level operations.

[1] S. Kim et al., 2019 IEEE International Electron Devices Meeting, 2019. [2] H. Kwak et al., Semiconductor Science and Technology, 2021. [3] J. Tang et al., 2018 IEEE International Electron Devices Meeting, 2018. [4] C. Lee et al., Frontiers in Neuroscience, 2022.

2:30 PM EL04.08.03

Biomimetic Electrochemical Eye Based on Organic Optoelectronic Synapse KeChen and JianguoMei; Purdue University, United States

The human eye possesses remarkable abilities in sensing images, including a wide field of view, high resolution, sensitivity with minimal distortion. Moreover, the information captured by human eyes can be sent to the brain for processing, enabling image recognition and learning. Having biomimetic eyes or vision systems with such characteristics is highly desirable, particularly in fields like robotics and visual prostheses. Currently, most artificial eyes rely on rigid and brittle silicon electronics, which poses challenges for non-invasive implantation and seamless integration with soft biological tissues. In contrast, organic semiconducting materials have demonstrated biocompatibility, mechanical flexibility, and responsiveness to biological media, making them a promising candidate for the next generation of artificial eyes. In this talk, we present an organic electrochemical eye (E-eye) consisting of a high-density array of optically switchable synaptic devices. Within the device, light can control the insertion of ions into the photoactive layer, allowing for the modulation of multiple nonvolatile conductance states and the replication of ion flux-regulated synaptic activities observed in living systems. The device exhibits an unprecedented light-induced on/off ratio ($>10^4$), a wide range of wavelength detection (400-980nm), and high biocompatibility. Furthermore, we demonstrate the image-recognition capability of our E-eye by successfully distinguishing optical patterns projected onto it. This research has the potential to lead to the development of a biomimetic intelligent eye, which could find applications across a wide range of technologies.

2:45 PM BREAK

3:15 PM EL04.08.04

A Novel Electrical Bias Technique to Recover Degraded ReRAM Arrays for Deep Learning Fabia FarlinAthena^{1,2}, NanboGong², RamachandranMuralidhar², PaulSolomon², EricM. Vogel¹, VijayNarayanan² and TakashiAndo²; ¹Georgia Institute of Technology, United States; ²IBM T.J. Watson Research Center, United States

Resistive Random Access Memory (ReRAM) arrays based on HfO_x have shown promise for in-memory computing in deep neural network (DNN) training. A modified SGD algorithm [1, 2, 3], together with a co-optimized ReRAM material, can achieve respectable accuracy on a reduced Modified National Institute of Standards and Technology (MNIST) database classification task, approaching a floating point baseline [4]. However, as these arrays are used over time, they begin to degrade, which reduces their efficacy and impacts the performance of the systems that rely on them. As these arrays are leveraged for complex tasks like deep neural network training, the degradation issue becomes increasingly acute.

In an effort to better understand the degradation phenomena, we turned towards employing a 3D atomistic simulator that enables the simulation of processes such as bond breakage, ion and vacancy diffusion, and trap-assisted electronic tunneling between vacancies. The filament formation and subsequent switching are also simulated, providing valuable insights into the degradation process and the potential for recovery.

Building on this foundation, a unique electrical bias technique has been proposed to address the degradation issue and restore the precision of a deteriorated ReRAM array. We noticed that post-fatigue, the devices in the ReRAM array exhibited increased resistance and a diminished number of observable states. Our proposed electrical bias technique efficiently addresses both these challenges, reducing resistance and amplifying the number of states, thereby restoring the ReRAM array's accuracy to its initial pre-fatigue level.

In practice, this carefully controlled recovery method has demonstrated impressive results. The accuracy after recovery using the biasing technique reaches 98% on a reduced MNIST classification task, closely approaching the results from a floating point baseline, a notable benchmark in the field.

In summary, the proposed method offers a promising solution to a pervasive issue in neuromorphic computing. It underscores the potential for rejuvenating the performance of worn-out ReRAM crossbar arrays employed in in-memory deep neural network training. In addressing the immediate problem, it also significantly enhances the durability and reliability of these indispensable systems, promising more precise and reliable results over time. Moreover, this breakthrough sets a new direction for future developments in neuromorphic computing, paving the way for more resilient and enduring memory solutions that can withstand the rigorous demands of advanced computing tasks.

Reference:

- [1] Gokmen, Tayfun, and Wilfried Haensch. "Algorithm for training neural networks on resistive device arrays." *Frontiers in neuroscience* 14 (2020): 103.
- [2] Gokmen, Tayfun. "Enabling training of neural networks on noisy hardware." *Frontiers in Artificial Intelligence* 4 (2021): 699148.
- [3] Kim, Youngseok, et al. "Neural network learning using non-ideal resistive memory devices." *Frontiers in Nanotechnology* (2022).
- [4] Gong, Nanbo et al. "Deep learning acceleration in 14nm CMOS compatible ReRAM array: device, material and algorithm co-optimization." 2022 International Electron Devices Meeting (IEDM) (2022): 33.7.1-33.7.4.

Acknowledgment:

This work is supported by the IBM Research AI Hardware Center. The authors thank IBM Research and TEL Technology Center members in Albany for device fabrication.

3:30 PM EL04.08.05

Electrically Tunable Stochastic Devices via Magnetic Fluctuations in V-Doped WSe₂ Dinh LocDuong^{1,2}; ¹Montana State University, United States; ²Department of Physics, Montana State University, United States

Fluctuations are ubiquitous in magnetic materials and provoke random telegraph noise (RTN) that can be used for spiking neuron devices, random number generators, probability bits, and neuromorphic computing. Two-dimensional (2D) magnetic materials are thought to possess inherently stronger fluctuations than their three-dimensional (3D) counterparts, which yield weaker fluctuations that are more difficult to control with external forces. This has been demonstrated in 2D van der Waals (vdW) CrBr₃ utilizing the magneto-optic Kerr effect, but electrical measurement of these fluctuations has not yet been demonstrated. Moreover, these fluctuations only appear over a narrow range of transition temperatures centered around 22 K. For practical applications, such magnetic fluctuations in 2D materials should be well-described and electrically tunable across a wide range of temperatures, but there has been limited progress to date on this front. Here, we report magnetic fluctuations in a vdW-layered semiconductor with a magnetic dopant by investigating the giant RTN of resistance across the vertical tunnel junctions of a graphene/V-WSe₂/graphene (Gr/V-WSe₂/Gr) device. We identify bistable magnetic states from discrete Gaussian peaks of the RTN histogram, which were further confirmed by 1/f₂ features in the noise power spectrum. We detect three fluctuation categories in the resistance change: small changes from the intralayer coupling between magnetic domains at high temperatures, anomalous large resistance changes over a wide range of temperatures, and persistent large resistance changes originating from magnetic interlayer coupling at low temperatures. This device reveals high-amplitude RTN in resistance as large as 40% with a well-defined bistable state that can be tuned by magnetic and electric fields.

3:45 PM EL04.08.06

Nonvolatile Electrochemical Random-Access Memory Enabled by Phase Separation JingxianLi and YiyangLi; University of Michigan, Ann Arbor, United States

Electrochemical random access memory (ECRAM) is a promising recently developed device for analog computing. Like resistive random access memory (RRAM), ECRAM also stores and switches information through ion migration and the resulting change in valence and electronic conductivity. ECRAM is a three-terminal memory cell that electrochemically shuttles oxygen vacancy point defects between two transition metal oxides with a solid electrolyte sandwich. ECRAM enables analog, continuous retention state switching (~100 states) by deterministically modulating oxygen vacancy concentration. In the past, ECRAM suffered from poor retention, about several hours at room temperature and several minutes at 85C, substantially less than >10 years at 85C standard for most nonvolatile memory.

In this work, we utilize new materials that not only meet, but vastly exceed the 10 year retention time metric. We hypothesize that the poor retention in the previous ECRAM results from using solid solution materials; in contrast, our phase separating materials enable multiple equilibrium states and thereby substantially improve retention in ECRAM. Moreover, our results

show that a nonvolatile ECRAM with a retention time more than 12 hours at 400C, exceeds the performance of the best nonvolatile memory cell. Our work shows that harnessing phase separation can provide a powerful means to enable nonvolatile ECRAM to attain the necessary retention times and ECRAM's ability to electrochemically move point defects within solids for both analog and high-temperature memory.

4:00 PM EL04.08.07

Correlation Between Transient Response and Neuromorphic Behavior in P3HT based-Ion Gated Transistors. Ramin Karimi and Clara Santato; Polytechnique Montreal, Canada

Ion-gated transistors (IGTs), by perceiving dynamically the environment, can be studied and exploited as synaptic transistors in neuromorphic computing.

Depending on the permeability of the semiconducting channel to ions, IGTs undergo volumetric (three-dimensional) or electrostatic (field-effect, two-dimensional) doping, which leads to a wide range of response times. Long-term memory and high-speed data processing are essential for neuromorphic computing.

We propose a method to modulate the response time and synaptic plasticity of IGTs made up of poly(3-hexylthiophene, P3HT) gated by the [EMIM][TFSI] ionic liquid. We report on the effect of the frequency of the (gate-source voltage) V_{gs} pulses, the number of applied V_{gs} pulses, and the pulse duration time on the IGT response time. By increasing V_{ds} from -0.2 V to -1 V, we observed that the response time halves using a 200 ms-long square step $V_{gs} = -0.5$ V pulse. Moreover, increasing V_{gs} from -0.5 V to -1 V increases the response time by 27% in $V_{ds} = -1$ V. The methodology also includes the effect of the V_{gs} sampling time on the accuracy of electric measurements.

Our results shed light on the impact of various aspects of the input voltages on establishing the response time behavior and synaptic functions in organic IGTs, to reach low-power and fast-switching neuromorphic devices.

4:15 PM EL04.08.08

A Bio-Mimicking Synaptic Tactile Sensor Based on SWCNT Transistors Yan Huang, Angus Hawkey, Elisa Fresta and Jana Zaumseil; Heidelberg University, Germany

The skin is the largest organ in the human body, with a network of receptors that are essential for our perception of the surrounding environment. Among various receptors, the Merkel cell acts as the mechanoreceptor, and it forms a synapse called Merkel cell-neurite complex with an afferent neuron. With this complex, a tactile stimulus applied on the skin can be sensed, preprocessed, and then transmitted to the brain. To mimic the function of Merkel cell neurites, several devices such as sensors and synaptic transistors usually need to be integrated together. In this work, a synaptic tactile sensor capable of sensing and memorizing the stimulus in one device is demonstrated to imitate the main functions of the Merkel cell neurite. The synaptic sensor is based on a single-walled carbon nanotube (SWCNT) transistor with a surface patterned polymeric ionic gel as the solid electrolyte. We find that ions can be released from the ionic gel into the transistor channel when the ionic gel is compressed. Modulation of the post-synaptic current of the device is realized by electrochemically doping SWCNTs under presynaptic pressure spikes. Due to the unique morphology of SWCNTs and slow ion motion in the ionic gel, long-time conditioning up to 24 hours can be achieved. For sensing performance, the device also shows a high gate sensitivity (~ 14.24 kPa⁻¹) in a wide sensing range (~ 30 kPa). By combining the functions of mechanical sensors and synaptic transistors, the space and energy efficient design in this work can facilitate the development of next-generation electronic skin and artificial neuron systems.

4:30 PM EL04.08.09

Enabling The Formation of High Impedance Supported Lipid Bilayers on PEDOT:PSS for Biosensing Applications Jeremy Treiber¹, Zhongmou Chao², Reece McCoy³, Susan Daniel², Roisin Owens³ and Alberto Salleo¹; ¹Stanford University, United States; ²Cornell University, United States; ³University of Cambridge, United Kingdom

Supported lipid bilayer (SLB) electrochemical sensors are a promising platform to study analyte-ligand interactions that occur at the cell surface. Utilizing an organic mixed conductor, such as PEDOT:PSS, as the SLB supporting material has enabled this technology to be used for detection of biomolecules at physiological relevant concentrations by measuring impedances.

However, currently there is a lack in understanding of how the PEDOT:PSS surface facilitates SLB formation; a challenge which leads to significant device reproducibility issues. This talk will share our progress in investigating the PEDOT:PSS surface chemistry using x-ray photoelectron spectroscopy and correlating this to electrochemical impedance spectroscopy data of SLBs on microfabricated PEDOT:PSS electrodes. Results will be shared that show how we obtain a high yield of viable SLB devices by controlling aspects of the fabrication process, post-fabrication surface treatments, and electrolyte choice. This progress establishes guidelines necessary to realize high impedance SLBs on PEDOT:PSS electrodes.

4:45 PM EL04.08.10

Doping-Induced Assembly Interface for Non-Invasive *In Vivo* Local and Systemic Immunomodulation Baoning Sha^{1,2}; ¹Columbia University, United States; ²Shenzhen Institute of Advanced Technology, China

Peripheral neural interfaces exhibit considerable potential in the treatment of diseases by modulating both local and systemic immune responses. However, the mismatch between static electronic components and the dynamic, intricate tissue organization of the peripheral nervous system results in interface failure, hindering progress in circuit research and clinical implementation.

Jet-injectors are preferred by diabetic patients for insulin administration over syringes due to their enhanced diffusivity and reduced scar formation. By leveraging the diffusivity of jet-injection and *in vivo* polymerized neural interfaces, we aim to interface with the finely structured reticular nerve plexus, which has been demonstrated to possess unique capabilities in peripheral-central circuitry, such as systemic anti-inflammation, anxiety, and social disorders. However, recent *in vivo* polymerization systems are incompatible with this inherently diffusion-promoting injection method, as precursors, enzymes, and surfactants diffuse into the tissue and ultimately hinder the polymerization process.

To address these challenges, we developed a versatile, monocomponent cocktail strategy for the *in vivo* assembly of biodegradable, self-adaptive neural interfaces to achieve both local and global immunomodulation. To accomplish this regulation, we employed a propulsion flow-enhancing method—jet-injection—to interface with a series of reticular nerve plexuses. Additionally, we engineered ROS-triggered catalytic doping nanosheets with inherently low diffusivity to counteract tissue diffusion during jet-injection. MXene, a semi-metal, has been extensively investigated for its conductivity and catalytic properties. We harnessed MXene's catalase activity to catalyze the *in vivo* doping system, reconciling the conflict between catalyst and conductivity. Furthermore, we functionalized MXene with de-doped conductive polymer (CP)-PEDOT and dopant-benzenesulfonic acid. The doping of de-doped PEDOT is mediated by the ROS-MXene cascade, which occurs when the injection induces local microdamage, increasing ROS metabolites in tissue and subsequently triggering PEDOT doping by MXene. This doping process enhances the π - π interaction between nanosheets, driving *in vivo* assembly. Additionally, we employed a tissue cross-linking compound, PDA, to connect de-doped PEDOT and benzenesulfonic acid dopant, controlling spontaneous non-catalytic doping. This approach also allows nanosheets to form dynamic bonds during assembly, including hydrogen bonds, coordination bonds, cation- π interactions, and π - π interactions, further reducing diffusion.

Our neural interface can be deployed within 10 seconds, and the π - π mediated assembly process, along with the metabolic oxidation of MXene, enables biodegradation of the interface. The neural interface, established with the sciatic nerve, can promote peripheral tissue recovery through local regulation via electrical stimulation. In freely moving mice, the neural interface activated the vagal anti-inflammatory axis at ST36, releasing noradrenaline, adrenaline, and dopamine from adrenal chromaffin cells while reducing TNF and IL-6 levels in serum. We demonstrate that catalytic doping and cross-linking around peripheral tissue create degradable, self-adaptive interfaces with reticular nerve plexuses in peripheral-central circuitry.

SESSION EL02/EL04/EL16: Joint Virtual Session

Session Chairs: Peijun Guo, Francesca Santoro, ABM Hasan Talukder, Alexandre Tessier and Mukundan Thelakkat

Wednesday Morning, December 6, 2023

EL04-virtual

10:30 AM EL02/EL04/EL16.01

Unraveling the Relationship Between Molecular Weight and Long-Term Plasticity in IGOSTs Hyunhaeng Lee¹, Gyeong-Tak Go¹, Min-Jun Sung¹, Jaeho Lee^{2,1}, Hyunwoo Park^{3,1}, Tae-Lim Choi^{3,1} and Tae-Woo Lee^{1,4}; ¹Seoul National University, Korea (the Republic of); ²Korea Advanced Institute of Science and Technology, Korea (the Republic of); ³ETH Zürich, Switzerland; ⁴SN Display Co., Ltd., Korea (the Republic of)

Ion-gel Gated Organic Synaptic Transistors (IGOSTs) have been widely researched as a building block of neuromorphic computing due to low-energy consumption, large dynamic range, and high linearity. To realize hardware neural network using IGOSTs, long-term retention of updated synaptic weight is necessary. However, fast back diffusion of doped ions in semiconductor channel is the main limitation from achieving long-term retention. Poly(3-hexylthiophene-2,4-diyl) (P3HT) semiconductors can have high crystallinity, which allows long-term ion trapping. Therefore, fine control of morphology can be a solution to improve ion trapping time in semiconductor channels.

Here, we investigated the effect of molecular weight on morphology to achieve long-term retention of P3HT IGOSTs. The materials were synthesized through Living Anionic Polymerization, in which the molecular weight is controlled by degree of polymerization with extremely low polydispersity. As the chain length increased with molecular weight, the high-crystalline fibril morphology shifted to less-crystalline granular morphology which can show higher on current and transconductance due to elongated chains. The long-term plasticity of IGOSTs exhibited dependence on molecular weight, with distinct contributions from two different morphologies. High-crystalline fibril morphology in smaller molecular weight samples impeded ion back-diffusion, resulting in longer retention time. However, in higher molecular weight samples, granular morphology prolonged the retention time by promoting enhanced intergranular connectivity. This work could provide a fundamental understanding of the relationship between molecular weight and morphology of P3HT to achieve long-term retention for use in next-generation neuromorphic computing.

10:35 AM EL02/EL04/EL16.02

Dynamic Machine Vision with Retinomorph Photomemristor-Reservoir Computing[Hongwei Tan](#) and Sebastiaan van Dijken; Aalto University, Finland

Dynamic machine vision requires recognizing the past and predicting the future of a moving object based on present vision. Current image sensing and machine vision technologies accomplish this by analyzing massive frame-by-frame image sequences in multiple hardware blocks and complex software algorithms, engendering redundant data flows, high energy consumption, and latency. Photomemristors, or optoelectronic memristors, originally proposed for photosensing, processing, and memory functions [1], are ideal candidates for dynamic machine vision tasks. In recent years, photomemristors have been studied in neuromorphic vision and processing systems for static image classification [2-5] and human action recognition [5]. However, motion recognition and prediction within a compact dynamic sensing system, which is crucial for dynamic machine vision technology, has been elusive until very recently. Here, I will summarize a brief history of photomemristor, and show our recent works on photomemristors for sensing, processing, and memory. Then I will focus on the implementation of motion recognition and prediction in recurrent photomemristor networks [6]. In the retinomorph photomemristor reservoir computing system, a retinomorph photomemristor array, working as a dynamic vision reservoir, embeds past motion frames as hidden states into the single present frame through inherent dynamic memory. The informative present frame facilitates accurate recognition of past and prediction of future motions with machine learning algorithms. This in-sensor motion processing capability eliminates redundant data flows and promotes real-time perception of moving objects. Potential applications of the retinomorph photomemristor-reservoir computing system include video analysis, autonomous driving, and robotic vision.

References

1. H. Tan et al. *Adv. Mater.* **27**, 2797–2803, 2015.
2. H. Tan et al. *Nat. Commun.* **12**, 1120, 2021.
3. F. Zhou et al. *Nat. Nanotechnol.* **14**, 776–782, 2019.
4. Y. Meng et al. *Sci. Adv.* **6**, eabc6389, 2020.
5. Y. Sun et al. *Adv. Intell. Syst.* **5**, 2200196, 2023.
6. H. Tan et al. *Nat. Commun.* **14**, 2169, 2023.

10:50 AM EL02/EL04/EL16.03

Soft and Stretchable Wireless Skin Patch for Electrophysiological Recording[Alexandre Tessier](#), Anan Zhang and Shideh Kabiri Ameri; Queen's University, Canada

Developing soft and stretchable electronics that perform reliably during daily activity without limiting the users' physical movements during daily activities is a challenge. In most cases to improve stretchability of inherently rigid electronic components of a circuit, the use of off-the-shelf components in conjunction with stretchable interconnects to mitigate the strain is one method to address this issue. Several strategies have been reported to make such a hybrid platform including utilizing serpentine metal films on stretchable substrates, coating metal, or conducting films on pre-stretched polymers, using liquid metal filled microfluidic channels, etc. While such methods have indeed proved effective when low range of strain is applied, they fail at high level of strain. Further, the fabrication process for most of these methods often require microfabrication and access to clean-room facilities which is costly and time consuming. Here we report a wireless skin patch for electrophysiological recordings such as electrocardiography (ECG) and electromyography (EMG). This patch consists of self-adhesive stretchable sensor and circuit patches. The circuit consist of highly soft and stretchable interconnect with more than 600% stretchability and includes conditioning, wireless communication, and power circuits. Over 60,000 cycling test of the interconnects under 30% of strain showed no change in electrical conductivities of interconnects. Further, the fabrication process is low cost, scalable and done using bench top equipment.

In conclusion our approach is a low cost, time effective method of wireless circuit patches for electrophysiological recording. The low modulus and stretchability of the circuit patch allows the integration of ultrasoft sensors that can conform to the microscopic feature of skin and enables long term, mobile, low motion artifact, high quality health monitoring.

10:55 AM EL02/EL04/EL16.04

Analysis of Charge Transport in Narrow Amorphous Ge₂Sb₂Te₅ Line Cells Stressed and Stabilized at Room Temperature[ABM Hasan Talukder](#), Md Tashfiq Bin Kashem, Helena Silva and Ali Gokirmak; University of Connecticut, United States

Phase change memory (PCM) is considered as one of the most promising non-volatile memory technologies because of its high scalability, high endurance cycles, and long retention time [1]. The large resistivity contrast between amorphous and crystalline phases of phase change materials such as Ge₂Sb₂Te₅ (GST) opens up the possibility for multi-level-cell (MLC) operation to reduce the cost per bit. However, resistance in the amorphous phase spontaneously increases over time, known as resistance drift, making it difficult to implement MLC operation. We reported earlier on the stabilization of resistance drift by accelerating the drift with high-field stresses at cryogenic temperatures (≤ 200 K) [2] and established a charge transport model [3]. In this work, we have demonstrated the acceleration and stabilization of resistance drift by applying high field sweeps at room temperature in narrow GST line cells with ~ 20 -50 nm width and 20 nm thickness. Also, we performed analysis on the charge transport in these cells at a temperature range 300 K – 80 K.

We amorphized the GST cells using a ~ 200 ns rectangular pulse of 1.5 V amplitude at 300 K and monitored the resistance drift immediately (~ 1 s) after amorphization for an hour. Then we applied two high-field voltage sweeps with current compliance set to < 1 μ A not to cause any self-heating in the device. We observe a substantial acceleration in resistance drift during the high-field stresses. The device displays a slightly negative drift coefficient when we monitored the resistance drift after the stress. The device resistance reduces to the pre-stress level after 25 days. When another stress sweep is applied, the resistance comes back up to the previously stressed/stabilized level. We analyzed the I-V characteristics measured at temperatures 300 K to 80 K for different charge transport parameters and how they relate to the acceleration in resistance drift and stabilization with high field stresses.

Since we do not expect substantial self-heating to occur in the whole of the device at < 1 μ A, thermally induced structural relaxation is very unlikely to happen in the whole of the device. We expect that acceleration and stoppage of resistance drift is due to relaxation of the charges left in the traps within amorphous GST when devices were quenched [4].

Acknowledgment: This work is supported by NSF under award ECCS 1711626

References:

- [1] H. -S. P. Wong et al., 10th IEEE Intl. Conf. on Solid-State and Integ. Circ. Tech., 2010, pp. 1055 1060, doi: 10.1109/ICSICT.2010.5667542.
- [2] R. S. Khan et al., Dev. Res. Conf. (DRC), 2020, pp. 1-2, doi: 10.1109/DRC50226.2020.9135147.
- [3] M. T. B. Kashem et al., arXiv Pre-Print, doi:10.48550/arXiv.2210.14035.
- [4] R. S. Khan et al., Appl. Phys. Lett. **116**, 2020, doi: 10.1063/1.5144606.

11:00 AM EL02/EL04/EL16.05

Resistance Drift and Percolation Transport in Phase Change Memory[Md Samzid Bin Hafiz](#), Md Tashfiq Bin Kashem, ABM Hasan Talukder, Raihan Sayeed Khan, Helena Silva and Ali Gokirmak; University of Connecticut, United States

3D integration of electronic memories led to enormous storage capacity with substantially reduced cost, new processor architectures, and artificial neural network and artificial intelligence (AI) implementations dramatically improved performance and application space. However, the speed of typical data-heavy computations are still limited by memory access latencies between CPU and DRAM (dynamic random access memory), flash memory and magnetic drive^[1]. The next stage of improvements is expected to come from monolithic integration of memory and logic, and complementing silicon CMOS with new capabilities, which is likely to include devices with dynamic materials. The emerging resistive non-volatile memory (RRAM) technologies, such as phase change memory (PCM)^[2], conductive bridging RAM (CBRAM)^[3] and magnetic RAM (MRAM)^{[4],[5]}, offer the possibility of monolithic integration of processor and high-performance non-volatile memory.

PCM devices utilize reversible changes in resistance of a small volume of material (1000s of atoms) as it is thermally switched between amorphous and crystalline phases, which makes PCM (i) operable using signal polarity for set and reset, (ii) virtually immune to read disturbance, (iii) insensitive to point defects and thermodynamically stable down to $\sim (5$ nm)³ scale, (iv) have a large memory window (orders of magnitude) at a very desired resistance range for CMOS^[6].

The resistance of the reset (amorphous) state of the PCM cells increases over time, widening the memory window but hinders multi-bit-per-cell PCM. Although resistance drift has been commonly attributed to structural relaxation, resistance drift at lower temperatures (below 100 K) and its response to high-field stress and photoexcitation suggest an electronic origin to resistance drift. This is a promising finding for the potential mitigation strategies for resistance drift and the viability of multi-bit implementations of PCM^{[7], [8]} including neuromorphic computing.

In this study, we use our experimental results to construct a finite element model that captures electronic transport in amorphous Ge₂Sb₂Te₅ (GST)^[9] and investigate potential mitigation strategies. We model local hole-traps that are activated in time with a temperature dependent probability. The remaining fixed charges lead to local potential variations, which then give rise to formation of percolation paths in time. The changes give rise to resistance fluctuations (noise) along with the increase in resistance. Once the steady state is reached, resistance drift stops. Our experimental results show that the resistance drift can be dramatically accelerated with application of high-field stresses, which can be explained by acceleration of activation and removal of trapped holes in the amorphous material.

Acknowledgment: This work is supported by the US National Science Foundation award ECCS 1711626.

References

- [1] M. K. Qureshi, V. Srinivasan, and J. A. Rivers, *ACM SIGARCH Comput. Archit. News*, vol. 37, no. 3, 24–33, **2009**.
- [2] S. R. Ovshinsky, *Phys. Rev. Lett.*, vol. 21, no. 20, 1450–1453, **1968**.
- [3] M. N. Kozicki, M. Park, and M. Mitkova, *Nanotechnology*, *IEEE Trans.*, vol. 4, no. 3, 331–338, **2005**.
- [4] B. N. Engel *et al.*, *Magn. IEEE Trans.*, vol. 41, no. 1, 132–136, **2005**.
- [5] A. Deschenes, S. Muneer, M. Akbulut, A. Gokirmak, and H. Silva, *Beilstein J. Nanotechnol.*, vol. 7, no. 1, **2016**.
- [6] P. Cappellotti, R. Annunziata, F. Arnaud, F. Disegni, A. Maurelli, and P. Zuliani, *J. Phys. D: Appl. Phys.*, vol. 53, no. 19, 193002, **2020**.
- [7] R. S. Khan, F. Dirisaglik, A. Gokirmak, and H. Silva, *Appl. Phys. Lett.*, vol. 116, no. 25, 253501, **2020**.
- [8] R. S. Khan, A. H. Talukder, F. Dirisaglik, H. Silva, and A. Gokirmak, *arXiv Prepr. arXiv2002.12487*, **2020**.
- [9] A. Pirovano, A. L. Lacaita, A. Benvenuti, F. Pellizzer, and R. Bez, *IEEE Trans. Electron Devices*, vol. 51, no. 3, 452–459, **2004**.

11:05 AM *EL02/EL04/EL16.06

N-Heterocyclic Carbenes (NHCs) as Conductive and Stable Anchors for Au-Based Hybrid Materials and Devices Franziska Lisse^{1,2}; Technische Universität Hamburg-Harburg, Germany; ²Leibniz Institute for Polymer Research, Germany

Gold nanoparticles (Au NPs) have unique surface plasmonic resonances (SPR) and promise a broad variety of optical applications in sensors and imaging,¹ while combining them with organic components can give electronically functional hybrid materials.² Protecting surface ligands, carrying one or more functional anchor groups with a high affinity for gold, are needed to stabilize the Au NPs and prevent their irreversible aggregation. Thiols are ubiquitously used, yet the thermal instability and comparably low conductance of the S-Au contact limit the applications of the resulting Au NPs.³ N-heterocyclic carbenes (NHCs) have been used in surface chemistry as an high-performing alternative to sulfur-based ligands⁴: The NHC-Au linkage shows excellent stability under conditions that destroy the S-Au bond (e.g. high temperature, variable pH, and electrochemical redox), and is furthermore highly conductive.

We use NHC anchors as robust and conductive anchors to bind charge-conducting conjugated polymers (CPs) to Au NPs to obtain electronically functional hybrid materials.⁵ Br-NHC-Au-X (X=Br, Cl) complexes were synthesized, converted to Grignard monomers and used for a chain-growth Kumada polymerization to obtain regioregular poly-3-hexylthiophenes (P3HT) with a low polydispersity index. Direct reduction gave spherical Au NPs with P3HT as surface ligands. The presence of the NHC on the surface was confirmed by XPS. The P3HT-NHC@Au NPs have a remarkable thermal stability up to 24 h in 100 °C toluene solutions, while Au NPs stabilized by sulfur-based PEG fully degrade under the same conditions. Also, continuous CV scans show only a slight decay of peak current after 50 cycles, indicating the good electrochemical stability of P3HT-NHC@Au NPs. To investigate the conductive linker, electrochromism (EC) experiments were carried out. P3HT is electrochromically active, and one can assume that binding the polymer to Au NPs via a conductive NHC anchor group will increase the electrochromic response speed, allowing to estimate the organic/inorganic electron transfer of P3HT-NHC@Au NPs. We found that blending 10% of P3HT-NHC@Au NP into P3HT films improves the responsive speed significantly, from 1.21/1.05 s for neat P3HT to 0.79/0.52 s for the blend.

Reference

- 1 N. J. Halas, S. Lal, W.-S. Chang, S. Link, P. Nordlander, *Chem. Rev.* **2011**, 111, 3913
- 2 A. M. Steiner, F. Lissel, A. Fery, J. Lauth, M. Scheele, *Angew. Chem. Int. Ed.* **2020**, 60, 1152
- 3 M. S. Inkpen, Z.-F. Liu, H. Li, L. M. Campos, J. B. Neaton, L. Venkataraman, *Nat. Chem.* **2019**, 11, 351
- 4 P. Bellotti, M. Koy, M.N. Hopkinson, F. Glorius *Nat Rev Chem* 2021, 5, 711; C. M. Crudden, J. H. Horton, I. I. Ebralidze, O. V. Zenkina, A. B. McLean, B. Drevniok, Z. She, H.-B. Kraatz, N. J. Mosey, T. Seki, E. C. Keske, J. D. Leake, A. Rousina-Webb, G. Wu, *Nat. Chem.* **2014**, 6, 409
- 5 N. Sun, S.-T. Zhang, F. Simon, A. M. Steiner, J. Schubert, Y. Du, Z. Qiao, A. Fery, F. Lissel, *Angew. Chem. Int. Ed.* **2021**, 60, 3912

11:35 AM EL02/EL04/EL16.07

Probing Photosynthetic Light Harvesting with a Single Photon Quanwei Li¹, Kaydren Orcutt¹, Robert Cook¹, Javier Sabines-Chesterking², Ashley Tong³, Gabriela Schlau-Cohen³, Xiang Zhang¹, Graham Fleming¹ and K. Birgitta Whaley¹; ¹University of California, Berkeley, United States; ²Joint Quantum Institute, United States; ³Massachusetts Institute of Technology, United States

The process of converting light energy into chemical energy via photosynthesis sustains most of life on earth. However, fundamental questions remain open regarding the initial steps of photosynthesis, despite advances over the past several decades in understanding the dynamics of energy transfer in photosynthetic systems using ultrafast spectroscopies. Here, by developing a photon-counting quantum light spectroscopy that probes photosynthetic light harvesting with a single photon at a time, we experimentally demonstrate that photosynthesis begins and proceeds with a single quantum of energy [1]. We report the observation of individual single-photon absorption and emission events in spatially distinct regions in photosynthetic systems. We show that a complex material system can be prepared and studied with only a single excitation, without perturbation by other photons or averaged over many simultaneous excitations. The experiments were carried out on an ensemble of pigment-protein complexes light-harvesting 2 from purple bacteria *Rhodospirillum rubrum* under ambient conditions in vitro. Our results advance a true microscopic mechanism of energy conversion in photosynthesis at a fundamental single quantum regime, beyond the semi-classical picture of spectroscopy, and open a new domain of experiments using quantum light to probe complex material systems.

[1] Quanwei Li, Kaydren Orcutt, Robert L. Cook, Javier Sabines-Chesterking, Ashley L. Tong, Gabriela S. Schlau-Cohen, Xiang Zhang, Graham R. Fleming† & K. Birgitta Whaley†, Single-photon absorption and emission from a natural photosynthetic complex, *Nature*, in press.

11:50 AM EL02/EL04/EL16.08

Some Notes on Mixed Memristor-Resistor Model as Defined in [1] Kazimierz J. Plucinski; Military University of Technology, Poland

Edge network entropy as defined in [1] - inspired by the Shannon based entropy - proposed by Pershin et al [2] is analyzed, where the entropy is a measure of the number of possible configurations of a system. Notes on the Interpretation of the decrease of entropy as the consequence of the decreased number of equal resistance paths available in the network and the emergence of fewer low resistive paths for the current flow are presented.

References:

1. Cipollini D, and Schomaker LRB 2023 Conduction and entropy analysis of a mixed memristor-resistor model for neuromorphic networks *Neuromorph. Comput. Eng.* **3** 034001
2. Pershin Y V and Di Ventra M 2013 Self-organization and solution of shortest-path optimization problems with memristive networks *Phys. Rev. E* **88** 013305

11:55 AM *EL02/EL04/EL16.09

Heterogeneous Integration of Memristive HfO₂ Devices on 2D Van Der Waals Materials for Neuromorphic Computing Regina Dittmann; PGI-7, Germany

Based on their large dynamic range in resistance with analog tunability, memristive devices can act as ultra-dense, low power synapse in neuromorphic circuits. HfO₂ is one of the most common material for the use in redox-based memristive devices. It is usually grown on Si wafers or even integrated in the back-end of line of a CMOS process. In order to transfer Memristive HfO₂ cells to flexible or even biological substrates, we investigated to co-integrate HfO₂-based on graphene. The graphene serves as conductive bottom electrode and/or enables the transfer to arbitrary substrates.

To this end, we investigated both, the van der Waals epitaxy of HfO_2 thin films on graphene and the remote epitaxy on graphene-covered, lattice-matched Y-stabilized ZrO_2 (YSZ) substrates. We identified a growth window for the pulsed laser deposition of HfO_2 that preserves the graphene transferred to thermally oxidized Si wafers. This enabled us to successfully fabricate memristive HfO_2 cells with graphene bottom electrode on both substrates. Based on the crystalline growth of the HfO_2 on SiO_2 and the forming-free switching behaviour, likely caused by an oxygen deficiency of the HfO_2 , we conclude that graphene acts as diffusion barrier for both, Si and oxygen. Therefore, the growth on graphene offers high potential for the heterogenous integration of HfO_2 thin films on arbitrary substrates.

12:25 PM EL02/EL04/EL16.10

Accurate Predictions of the Stark Shifts of Nitrogen-Vacancy Optical Frequencies in Diamond [RodrickKuate Defo](#)¹, [AlejandroRodriguez](#)¹, [EfthimiosKaxiras](#)² and [StevenL. Richardson](#)^{3,2}; ¹Princeton University, United States; ²Harvard University, United States; ³Howard University, United States

Accurate prediction of the Stark shift of the optical frequencies of nitrogen-vacancy centers (NV) in diamond is generally hindered by uncertainties regarding the background environment. The nitrogen-vacancy center in diamond has, however, proven to be a very useful probe of the electric field within materials, which is important to determine to predict proper operation of semiconductor devices and performance of solid-state single-photon emitters embedded within the semiconductor devices. In this talk, we demonstrate accurate computation of the average electric field measured at the location of NV charged defects in diamond. Far away from the surface, we achieve this result by evaluating the leading-order contribution to the electric field, which comes from the Dirac delta function contribution to the dipole field generated as a result of the presence of the neighboring substitutional N (N_C) defects that induce the ionization of the NV centers. Our results use density-functional theory (DFT) and the principle of band bending. Our work has the potential to aid both in the prediction of the functioning of semiconductor devices and in the prediction and correction of the spectral diffusion that often plagues the optical frequencies of solid-state single-photon emitters upon repeated photoexcitation measurements.

12:40 PM EL02/EL04/EL06.11

Exploring the Interplay of Electro-Mechanical and Electro-Optical Signals in Neuristors [UpanyaKhandelwal](#)¹, [Rama SatyaSandilya](#)¹, [RajeevKumar Rai](#)^{2,1}, [Deepak](#)¹, [SmritiR. Mahapatra](#)¹, [DebasishMondal](#)¹, [NavakantaBhat](#)¹, [SushobhanAvasthi](#)¹, [SaurabhChandorkar](#)¹ and [PavanNukala](#)¹; ¹Indian Institute of Science, India; ²University of Pennsylvania, United States

Neuristor systems, as electro-mechanical counterparts, provides a valuable approach to explore and replicate the dynamics of biological neurons. Among them, VO_2 neuristors, characterized by insulator-to-metal transition (IMT) and negative differential resistance (NDR), have demonstrated diverse neuronal signals in the electrical domain. In this study, we investigate the intriguing behaviors of tonic spiking and tonic bursting in VO_2 neuristors, revealing their coupled electro-mechanical signals and unveiling additional electro-optical oscillations. The emergence of electro-mechanical and electro-optical oscillation arises from significant changes in the electrical, optical and mechanical properties of VO_2 during its phase transition from an insulator to a metal driven by joule heating. Laser interferometry is employed to analyze films with different thickness, allowing us to distinguish the contributions of optical and mechanical oscillations. Additionally, an analytical model is developed to effectively characterize these dynamics.

Our work highlights the multifaceted nature of self-oscillating neuristors, showing their coupled electro-mechanical and electro-optical behaviors. This research opens up the possibilities for utilizing neuristors as alternatives to conventional piezoelectric materials in MEMS applications and as potential replacements for Pockel's materials in electro-optic applications. By bridging the gap between biological neurons and engineered systems, neuristors offer versatile building blocks for bio-inspired electronics and opto-electronic technologies.

SYMPOSIUM EL05

Soft Optics

November 27 - December 5, 2023

Symposium Organizers

Michael Ford, Lawrence Livermore National Laboratory

Cindy Harnett, University of Louisville

Juejun Hu, Massachusetts Institute of Technology

Seungwoo Lee, Korea University

* Invited Paper

+ JMR Distinguished Invited Speaker

SESSION EL05.01: Eye-Inspired Soft Optics

Session Chairs: Juejun Hu and Seungwoo Lee

Monday Morning, November 27, 2023

Hynes, Level 2, Room 203

10:30 AM *EL05.01.01

Retinomorph Motion Detector and Supercapacitors Based on Organic Semiconductors [Tse NgaNg](#); University of California, San Diego, United States

Organic retinomorph sensors offer the advantage of in-sensor processing to filter out redundant static background and are well suited for motion detection. To improve this promising structure, here we studied the key role of interfacial energetics in promoting charge accumulation to raise the inherent photoresponse of the light-sensitive capacitor. Specifically, incorporating appropriate interfacial layers around the photoactive layer was crucial to extend the carrier lifetime, as confirmed by intensity-modulated photovoltage spectroscopy. Compared to its photodiode counterpart, the retinomorph sensor showed better detectivity and response speed due to the additional insulating layer, which reduced the dark current and the resistor-capacitor time constant. Lastly, three retinomorph sensors were integrated into a line array to demonstrate the detection of movement speed and direction, showing the potential of retinomorph designs for efficient motion tracking.

In addition to discussing the development of organic optical sensors, this presentation will also show the use of the same class of organic semiconductors in energy storage applications, in particular for redox supercapacitors as portable power sources. We developed multifunctional structures, which combine load-bearing and energy-storage functions in one, resulting in weight savings and safety improvements. We demonstrated a gradient electrolyte design to facilitate high ionic conductivity at the electrode-electrolyte interfaces and transitioned to a composition with high mechanical strength in the bulk for load support. The gradient design enabled the multilayer structural supercapacitors to reach state-of-the-art performance matching the level of mono-functional supercapacitors. Finally, the structural supercapacitor was made into the hull of a model boat to demonstrate its multifunctionality.

11:00 AM EL05.01.02

Bioinspired Compound Eye Camera for High-Resolution and Depth-Based Sensing Applications [SehuiChang](#)¹, [Min SeokKim](#)¹, [Gil JuLee](#)² and [Young MinSong](#)¹; ¹GIST, Korea (the Republic of); ²Pusan National University, Korea (the Republic of)

Machine vision has advanced to provide high-performance imaging for various fields in electronics and robotics such as smartphones, surveillance, and autonomous vehicles. The capabilities of high resolution, a small form factor, and functional imaging (e.g., depth extraction, object detection, etc.) are of major interest to modern vision platforms. However, conventional camera designs show an intrinsic trade-off between miniaturization and high-performance, including a wide field of view and low aberrations. In particular, a camera design requires multiple lenses to be compatible with a commercial planar CMOS sensor in order to compensate for optical aberrations (e.g., field curvature). This complexity of lens design originates from offsetting against an inherently curved focal plane, which eventually hinders the miniaturization of entire system.

Meanwhile, natural eyes carry out high-performance and functional imaging specialized to their natural habitat, despite having a compact, simple configuration of the ocular structure. For instance, the fish eye provides a wide field of view via a single spherical lens and a curved retina, and the eye of a fiddler crab enables clear imaging both on land and in water via a flat, graded refractive index microlens array. Thus, various animal eyes can inspire the development of enhanced vision systems with novel camera design strategies. Insect compound eye, *inter alia*, has inspired in various artificial vision systems due to their unique features of wide field of view with low aberrations, high sensitivity to motion, and infinite depth of field. However, most artificial compound eye cameras suffer from two major issues: low resolution caused by the use of a curved photodetector array, or limited field of view caused by the use of a planar image sensor.

Here, inspired by insect compound eyes, we propose a high-resolution compound eye camera for depth-based sensing applications. The artificial compound eye camera consists of a curved microlens array (cMLA), a tapered fiber bundle (TFB), and a commercial CMOS imager. The cMLA was fabricated using flexible polymer, polydimethylsiloxane (PDMS), to achieve the curvature of the MLA through a repeated molding process with a precisely machined flat MLA metal mold and a 3-D printed base mold, enabling wide field of view imaging. To relay sub-images of each microlens in the cMLA onto the planar image sensor plane, we utilized the TFB as a relay optics, which is tapered and polished to form each individual fiber facet perpendicular to its optical axis on its curved and flat sides. The fabricated systems demonstrated high-resolution imaging via the TFB with over 2 million fibers and the commercial sensor, while the entire microlenses of the cMLA provides focused images. Since each individual microlens is matched with ~5 thousands pixels, the acquired image data from the cMLA can provide depth information of objects by calculating disparities among adjacent microimages, while achieving wide field of view imaging. Unlike conventional light field cameras, the proposed artificial compound eye has a curved shape MLA. Therefore, geometrical calibration was conducted to convert the world coordinate into the camera's spherical coordinate for restoring the visual data in 3-dimensional space. By collecting and processing the image data of angular and distant objects, it is expected that the proposed camera system will pave the way for the development of bioinspired artificial vision specialized in depth sensing applications.

11:15 AM *EL05.01.03

Optics in Animal Eyes and Their Applications in Vision SystemYoung MinSong; Gwangju Institute of Science and Technology, Korea (the Republic of)

The development of bioinspired artificial cameras, through the application of optics and photonics, offers innovative designs inspired by diverse natural vision systems. The superior optical characteristics of these bioinspired devices often outperform traditional imaging systems, boasting heightened visual acuity, expanded field of view, unrestricted-wavelength imaging, enhanced aberration correction and depth of field, along with exceptional motion sensitivity. The evolution of soft materials, ultrathin electronics, and adaptable optoelectronics has ushered in an era of opportunity for crafting artificial eyes that closely emulate biological vision systems. This tutorial zeroes in on the recent progress and continuous efforts in the arena of bioinspired artificial eye research and development, specifically highlighting optical components and image sensors. The discussion kick-starts with an exploration of the structures of two key types of eyes from nature, namely, the single-chambered eye and the compound eye. The tutorial then progresses to delve into the recent developments in bioinspired optic components and image sensors, enveloping subjects like materials, optical and mechanical design approaches, and integration strategies.

11:45 AM EL05.01.04

Pupil-Scalable and Light Attenuating Soft Artificial Iris using Gradient Controlled Photochromic Effect Actuated by External LightHafiz SaadKhalig, AsadNauman, Young-MinCho, Jae-WonLee and Hak-RinKim; Kyungpook National University (KNU), Korea (the Republic of)

The constriction and dilation of human pupil diameter in reaction to the changes in ambient light are governed by the masculine components present in the iris tissue. This iris-mediated reflex mechanism controls the amount of light that reaches the retina, producing sharp and glare-free visual perceptions. Nonetheless, in cases where the iris is deficient in its inherent light-modulating capabilities due to congenital abnormalities or accidental damage, it can harm the retina's function and give rise to significant impairment in visual effects. The existing artificial iris designs documented rely on external circuitry to enable their activation or light-actuated mechanical opening and closing of the aperture. Moreover, with the development of photochromic materials, few groups presented remotely controlled artificial iris with chemical change at molecular level switching with no circuitry and mechanical movements involved. Meanwhile, the lack of a non-tunable aperture and dynamic response of reported artificial iris for active light regulation makes them difficult for practical implications. In this study, we present a novel artificial iris that exhibits dynamic light-regulating properties and can also scale its aperture size. In addition, iris patterns of different shapes are integrated, imitating the behavior of the different human iris. This innovative design enables the photochemical adjustment of light transmission and pupil size, leading to dynamic adaptation to diverse external lighting conditions. The cross-linking density of a hydrogel matrix containing a light-responsive photochromic dye is manipulated in a radially decreasing fashion. This radial control over cross-linking of hydrogel/photochromic dye composite is accomplished by employing a gradient-patterned UV light curing technique. The UV curing was achieved using UV curable resin mixed in the photochromic solution. The UV light is gradiently patterned using inject printed gray-scale patterns on transparent PET film as a photomask. This controlled cross-linking density results in varying switching speed of photochromic dye at the same UV intensity to realize the scalable aperture and hence the light transmission. The suggested self-regulating artificial iris exhibits the potential for customization in terms of color dyes and patterns, allowing for the replication of diverse iris colors and patterns mimicking specific regional and ethnic characteristics of the iris. Moreover, our proposed artificial iris shows consistent performance at body temperature under several on/off switching cycles with fast switching speeds.

SESSION EL05.03: Liquid Crystal Elastomer Optics
Session Chairs: Cindy Harnett and Juejun Hu
Tuesday Morning, November 28, 2023
Hynes, Level 2, Room 203

10:30 AM *EL05.03.01

Fully Solid, Dynamic Optical Filters via Mechanical Reconfiguration of Liquid Crystalline MaterialsTimothyWhite; University of Colorado, United States

Electrochromic devices have found widespread use in automotive, aerospace, and architectural implementations. This talk will detail our recent research of liquid crystalline compositions in which the selective reflection can be tuned, broadened, and switched by mechanical, thermal, or electrical stimuli. Enabled by the modularity of the formulation of the cholesteric liquid crystal phase, filters can be prepared throughout the electromagnetic spectrum (VIS, NIR, SWIR, MWIR).

11:00 AM *EL05.03.02

Pixelated Camouflage from Cholesteric Liquid Crystalline ElastomersShuYang; University of Pennsylvania, United States

In nature, there are full of creatures that will dynamically change their shapes and appearances to closely match their respective environments for camouflage, signaling, or energy regulation. Reflective structural colors can greatly enhance the appearance of their skin patterns, which are largely controlled by pigmented chromatophores. Meanwhile, bioorganisms are often sensitive to polarized light for navigation or communication. Cholesteric liquid crystalline elastomers (CLCEs) can assemble liquid crystal molecules into a helix, forming a 1D photonic crystal that can reversibly change the reflected colors upon mechanical deformation. Here, we demonstrate pneumatic inflation of the thin CLCE membranes with pixelated channels to achieve broadband color shift from near-infrared to ultraviolet wavelengths, where each channel is individually programmed as a color "pixel". We also 3D print CLCE filaments as color-changing smart wearables.

11:30 AM EL05.03.03

Reversible Selective Phase Patterning of Liquid Crystal Elastomer by Laser-Induced Dynamic CrosslinkingSeok HwanChoi¹, Kyung RokPyun¹, HuijaePark¹, Deog-GyuSeo¹, SangminSong² and Seung HwanKo^{1,1}; ¹Seoul National University, Korea (the Republic of); ²Korea Institute of Science and Technology, Korea (the Republic of)

Liquid crystal elastomers (LCEs) offer remarkable potential in various fields by enabling reversible transitions in mechanical and optical properties across polydomain, monodomain, and isotropic phases. However, the focus on the monodomain-isotropic phase transition has limited their applications to mechanical systems like soft robots and artificial muscles, overlooking their optical capabilities. This limitation arises from the absence of a local phase patterning method that can simultaneously pattern isotropic phases as well as monodomain and polydomain phases, hindering the utilization of LCEs in optical approaches. Furthermore, the lack of reversibility in conventional programming methods has impeded the widespread adoption of LCEs. To overcome these challenges, we introduce a novel laser-based technique termed laser-induced dynamic crosslinking (LIDC) for reversible selective phase patterning in LCEs.

LIDC leverages the precision and control offered by laser technology to achieve high-resolution patterning across various phases, enabling transmittance modulation while remaining compatible with conventional techniques. By crosslinking LCEs above the nematic-isotropic transition temperature (T_{NI}), the mesogenic units are immobilized, allowing for selective confinement in the isotropic configuration even upon cooling below T_{NI} , thus facilitating optical transmittance. Careful manipulation of laser parameters enables precise control over the degree of confinement and modulation of the optical and phase transition properties, including T_{NI} and ΔH , in LCE films. Combining LIDC with mechanical alignment methods enables the generation of patterns encompassing isotropic, polydomain, and monodomain phases within a single LCE film, facilitating visible patterns and actuation.

To introduce reversibility, allyl sulfide functional groups are incorporated into the LCE networks. Laser irradiation at higher power and temperature induces a relaxation process through the switching of bonds between allyl sulfide groups, leading to network reconfiguration and opaqueness upon cooling. The introduction of additional photoinitiators allows for repeated procedures, empowering LIDC to generate adaptive LCEs that can be configured into desired phases or used to create complex monolithic patterns that can be subsequently erased if necessary. Additionally, by incorporating allyl sulfide functional groups, T_{NI} is effectively reduced to near body temperature, expanding the thermal stimulus-responsive properties of LCEs for lower-temperature applications.

To demonstrate practical applications, particularly in human-related or skin-attachable contexts, we showcase a functional implementation of LIDC for easy information entry and deletion in LCE films, with information encryption triggered by body temperature. These findings open new avenues for the development of LCEs with enhanced versatility, functionality, and real-world applicability, paving the way for advanced applications across diverse fields.

11:45 AM EL05.03.04

Flexible, Fully Solid Tunable Filters via Cholesteric Liquid Crystalline Elastomer Stimuli-Response[Alexis T. Phillips](#) and Timothy White; University of Colorado Boulder, United States

Stretchable, soft optical materials are currently being explored for use in automotive, aerospace, and the wearable device industries as actuators, sensors, and light modulators. Cholesteric liquid crystalline elastomers (CLCEs) are a unique class of soft materials that self-organize into a helicoidal structure. The periodic nature of the hierarchical organization of these materials produces a 1-D photonic bandgap where periodicity in the refractive index causes the elastomer to exhibit selective reflection. This talk will entail the synthesis of CLCEs with high optical quality, a tunable modulus and reflection wavelengths. Stretchable, tunable light filters will be prepared that control light in the Visible-MWIR regions of the electromagnetic spectrum. We will detail how the tunability and polarization of the reflection can be controlled by the inherent optical and material properties of the elastomer and how the optical properties can be switched in response to mechanical, photothermal, and electrical stimuli.

SESSION EL05.04: Structural Optics with Soft Materials

Session Chairs: Michael Ford and Juejun Hu

Tuesday Afternoon, November 28, 2023

Hynes, Level 2, Room 203

1:30 PM *EL05.04.01

Electrically Tunable Structural Colors of Cholesteric Liquid Crystals[Oleg D. Lavrentovich](#), Kamal Thapa, Olena S. Iadlovskaya and Sergiy Shiyankovskii; Kent State University, United States

Cholesteric liquid crystals are soft materials capable of selective reflection and transmission of light thanks to a spatially varying refractive index associated with the helicoidal twist of the optic axis. An attractive feature of cholesterics for optical applications is that the pitch and, thus, the wavelength of reflected and transmitted light can be tuned by temperature or chemical composition. However, the most desired mode of pitch control, by electromagnetic fields, has been elusive. This presentation reports on a cholesteric liquid crystal with an oblique helicoidal structure, abbreviated as Ch_{OH} . In the helicoidal Ch_{OH} structure, the local director twists about a single axis but remains tilted to this axis (rather than being perpendicular to it, as in a conventional cholesteric). The Ch_{OH} forms when a chiral liquid crystal with a low bend elastic constant is acted upon by an electric (or a magnetic) field. The field tunes the pitch and the conical tilt angle without destroying the single-harmonic mode of periodic variation of the effective refractive index. As a result, a simple device in the form of a thin Ch_{OH} slab confined between two plates with transparent electrodes shows an extraordinarily broad range of electrically tunable robust selective reflection with structural colors reversibly shifting from ultraviolet to visible and infrared. For the oblique incidence of light, the slab shows total reflection with a tunable wavelength. The electric field controls both the bandwidth and the wavelength of reflection and transmission. The structure can also be used for electrically tunable retarders. The work is supported by the National Science Foundation grants ECCS-1906104 and ECCS - 2122399.

2:00 PM *EL05.04.02

Responsive Soft Photonic Materials from Cellulose Nanocrystals[Mark Maclachlan](#); University of British Columbia, Canada

Cellulose nanocrystals (CNCs) extracted from biomass such as cotton and wood pulp form stable colloidal suspensions in water. Above a critical concentration, the CNCs spontaneously form a chiral nematic liquid crystal. In the chiral nematic structure, the CNCs are organized into pseudolayers, whose orientation rotates with a helical pitch, P . This chiral nematic organization is retained in dried films of CNCs. When the pitch of the chiral nematic structure in the solid film corresponds to the wavelength of visible light, the materials exhibit selective diffraction of light and appear brightly iridescent.^[1] Moreover, the color of the material can be tuned by changing the helical pitch.

Our group has been active in using CNCs as a template to construct novel chiral nematic mesoporous materials with photonic properties.^[2] We have succeeded in preparing silica,^[3] organosilica,^[4] and polymeric materials^[5] through self-assembly or templating methods.

In this presentation, I will discuss our recent explorations of the liquid crystalline properties of CNCs, including shape-memory photonic materials^[6] and elastomers with tunable optical properties.^[5,7,8]

References:

- [1] J.-F. Revol et al., *J. Pulp Pap. Sci.*, **24**, 146 (1998).
- [2] M. Giese et al., *Angew. Chem. Int. Ed.*, **54**, 2888 (2015).
- [3] K. E. Shopsowitz et al., *Nature*, **468**, 422 (2010).
- [4] K. E. Shopsowitz et al., *J. Am. Chem. Soc.*, **134**, 867 (2012).
- [5] C. E. Boott et al., *Angew. Chem. Int. Ed.*, **59**, 226 (2020).
- [6] Boott, C. E. et al. *Adv. Funct. Mater.*, **31**, 2103268 (2021).
- [7] O. Kose et al., *Nature Commun.*, **10**, 510 (2019).
- [8] Boott, C. E. et al. *Liq. Cryst.*, in press (2023). DOI: 10.1080/02678292.2023.2200265

2:30 PM BREAK

3:00 PM EL05.04.03

All Water Processing for Multilayered Biomaterial-Based Nanostructures with High Refractive Index Contrast and Selectively Responsive Structural Color[Tae-hoon Kim](#)¹, Junyong Park² and Fiorenzo Omenetto¹; ¹Tufts University, United States; ²Kumoh National Institute of Technology, Korea (the Republic of)

Transparent multilayered nanocomposites, known as distributed Bragg reflectors (DBRs), offer effective light modulation control, making them vital for next-generation photonic materials and devices. While inorganic multilayer structures have been successfully manufactured using vacuum deposition techniques, the emergence of biopolymers as eco-friendly alternatives with advantages such as biocompatibility, flexibility, and stimuli-responsiveness presents new opportunities. However, substantial challenges remain in achieving high-resolution biopolymer-based DBRs suitable for optical functions, which require control down to the single nanometer scale.

Here, we present a fabrication strategy using aqueous SF and aqueous metal oxide (ZrO_2) precursor solutions to address these challenges. Control over the structural polymorphism of SF to tune its physicochemical properties. By inducing crystallization in the silk film, the coated silk layer becomes water-insoluble, enabling consecutive coating of the ZrO_2 precursor solution without dissolving the underlying film. The slightly hydrophobic surface of the crystallized silk film hinders spin coating coverage of the metal aqueous solution due to its high surface tension. To overcome this wetting issue, we utilize the amphiphilic nature of SF heavy chains. Adding a small amount of amphiphilic SF to the aqueous Zr solution dramatically improves surface coverage.

Through this optimized solution processing approach, we successfully demonstrate silk-ZrO₂ DBRs with a high index contrast ($\Delta n \sim 0.42@500 \text{ nm}$). The resulting DBR structure consists of eight pairs of silk/ZrO₂ bilayers, exhibiting uniformity and high reflectance of up to 85% at visible wavelengths. Additionally, by controlling the structural polymorphism of SF through UV light, the thickness and swelling behavior of the silk film can be modulated, enabling the fabrication of photo-patternable and stimuli-responsive DBRs.

These results showcase the potential of biopolymer-based multilayer structures for photonic applications, highlighting the importance of solvent design, large refractive index contrast, and precise control over layer thickness and roughness. The developed silk-ZrO₂ DBRs offer opportunities for diverse applications such as structural colors, colorimetric sensors, optical communication, and optoelectronic devices. Furthermore, we demonstrate the feasibility of utilizing stimuli-responsive silk polymorphism for structural color-based encryption, which holds promise for applications in colorimetric sensors and anti-counterfeiting technologies.

3:15 PM EL05.04.04

Solid-Phase Structural Coloration from Cholesteric Phases of Hydroxypropyl Cellulose-Parameter Space for a Full Color Palette Hongning Ren, Tadeusz Balcerowski, Camran Ali, Jordi Bures and Ahu Gumrah Dumanli; University of Manchester, United Kingdom

Hydroxypropyl cellulose (HPC) is a sustainable, cost-efficient and biocompatible cellulose derivative which can self-assemble into cholesteric mesophases at highly concentrated water solutions. Such cholesteric solutions reflect iridescent and metallic colors in the visible range (1.2-4). Retaining the vibrant coloration in the solid phase for the HPC has been widely studied by offering cross-linkers that are mostly toxic such as glutaraldehyde (3, 4), with the assistance of acid catalysts and the exact mechanism of cross-linking is still a subject of debate and ongoing research.

In this presentation, we will discuss the mechanisms behind retaining the solid-phase structural coloration in the HPC without cross-linking and by controlling the parameter space during the evaporation process to achieve a full color palette. (5) Our investigation revealed that during the evaporation process, at the early stages of the evaporation the HPC readily forms a disordered dense skin that controls the balance between the kinetic arrest of the cholesteric order and its thermal expansion. Increasing the sample thickness, applying higher curing temperatures, and exposing the samples to higher humidity during the evaporation all result in red-shift in the pitch values and the final coloration. Furthermore, we will also showcase our new findings which stems from the idea of implementing the steric repulsion that leads to fabricating solid phases of HPC with predictable coloration by adding linear dicarboxylic acids to the solution. The dicarboxylic acid additives causes further steric interactions between the cholesteric layers. Therefore changing the aliphatic chain length of the acid from 3 to 5 by using malonic acid (MA), succinic acid (SA) and glutaric acid (GA) allows an additional fine tuning ability at the molecular level for the color manipulation.

References

- Werbowski, R. S., & Gray, D. G. (1976). Liquid Crystalline Structure In Aqueous Hydroxypropyl Cellulose Solutions. *Molecular Crystals and Liquid Crystals*, 34(4), 97-103. <https://doi.org/10.1080/15421407608083894>
- Godinho, M. H., Gray, D. G., & Pieranski, P. (2017). Revisiting (hydroxypropyl) cellulose (HPC)/water liquid crystalline system. *Liquid Crystals*, 1-13. <https://doi.org/10.1080/02678292.2017.1325018>
- Chan, C. L. C., Bay, M. M., Jacucci, G., Vadrucchi, R., Williams, C. A., De Kerkhof, G. T., Parker, R. M., Vynck, K., Frka-Petescic, B., & Vignolini, S. (2019). Visual Appearance of Chiral Nematic Cellulose-Based Photonic Films: Angular and Polarization Independent Color Response with a Twist. *Advanced Materials*, 31(52), 1905151. <https://doi.org/10.1002/adma.201905151>
- Balcerowski, T., Ozbek, B., Akbulut, O., & Dumanli, A. G. (2023). Hierarchical Organization of Structurally Colored Cholesteric Phases of Cellulose via 3D Printing. *Small*, 19(8), 2205506. <https://doi.org/10.1002/sml.202205506>
- Ren, H., Balcerowski, T., & Dumanli, A. G. (2023). Achieving a full color palette with thickness, temperature, and humidity in cholesteric hydroxypropyl cellulose. *Frontiers in Photonics*, 4. <https://doi.org/10.3389/fphot.2023.1134807>

3:30 PM EL05.04.05

Xanthan-Induced Gelation in Cellulose Nanocrystal Suspensions: Tuning of the Self-Assembly and Optical Purity Tadeusz Balcerowski and Ahu Gumrah Dumanli; University of Manchester, United Kingdom

Cellulose nanocrystals (CNCs) are anisotropic nanoparticles that can undergo chiral self-assembly in aqueous suspension to produce vibrant structurally colored films with a helicoidal nanostructure resembling the cholesteric structures found in natural systems. Above a critical concentration, CNC suspensions form a cholesteric liquid crystal phase and small clusters of order called tactoids, with a periodicity (pitch) determined by the colloidal interactions between the CNCs, and further parameters affecting the dynamics of the evaporation. Upon further drying, the CNCs undergo kinetic arrest, which allows their helicoidal ordering to be preserved in the solid state. The color and the angular dependence in these films can be tuned using numerous experimental parameters. Such films can be used to produce optically active components or processed further. In this study, we explore two differently processed CNC colloidal suspensions and their interactions with a food-grade gelling agent with the aim to explore the onset of the gelation point. The Xanthan gum used here is produced by the fermentation of simple sugars by the bacteria *Xanthomas campestris*. While the presence of the complex polysaccharide gum brings flexibility to the CNC films, the films also demonstrate remarkable color uniformity and loss of iridescence due to the entrapment of the CNC tactoids into encapsulated structures to combine a surface texture and scattering of visible light within the co-assembled structure. In this talk, I will explain how in the evaporation stage Xanthan advances the onset of gelation and provides colloidal stability, thus restricting the expected phase separation into smaller-scale events as compared to pure CNC films. This work sheds new light on the gelation mechanisms in hybrid CNC systems, their interaction with an additive of alike chemistry, and self-assembly in a phase-stabilized environment.

3:45 PM EL05.04.06

Reflectin and Cellulose-Based Bragg Reflectors with Chiral Photonic Response Luz Carime GilHerrera, Jiaxin Hou, Tadeusz Balcerowski, Derren Heyes, Eriko Takano, Jonny Blaker, Nigel Scrutton and Ahu Gumrah Dumanli; University of Manchester, United Kingdom

Structural colors in nature are generated by elaborate hierarchical nanostructures, which have been exploited for the fabrication of functional bio-inspired photonic materials for sensing applications. One attractive model system for this is the structural coloration in cephalopods, which is achieved by the multilayer interference of periodically stratified reflectin platelets in iridophores that act as Bragg reflectors. Such multi-layered structures have the ability to respond to chemical stimuli via a complex response mechanism involving the change in the multilayer periodicity and absorbance through chromophores. While there are studies focused on using the reflectins in synthetic multilayered constructs, such optical materials are not scalable and the angular and polarisation response cannot be tuned easily. Here we designed a multilayered hybrid material system that is built by layer-by-layer (LbL) processing of reflectins and cellulose nanocrystals (CNCs). CNC films exhibit fascinating optical properties, mainly due to their chiral nematic structure and birefringence. The optical response of this hybrid system combines the chiral response from CNCs and is amplified by the addition of reflectins. LbL processing allows us to explore several parameters, such as dependence on the concentration, layer thickness, and the dynamics of cellulose suspension, in order to achieve optimal structural color-producing systems. The reflectance of these systems was analyzed by using an optical model based on the 4x4 Berreman matrix method (Mathematica®). In addition, the effect on the retention of the chiral optical response of the CNC by the building up of the thin film was evaluated. Our findings define the optimal points and the limitations of the optical response from these multilayer systems. The multilayer construct with thin layered reflectin and CNCs at the gelation point suggests that the chiral response is affected by the ability to retain the helicoidal morphology during the LBL process and can be non-uniform. Our results show good agreement between the theoretical model and experiments. Overall, we will demonstrate that the unique optical properties of cellulose materials can be combined with the dynamic coloration imparted by reflectin and this study will potentially broaden the application of these chiral photonic systems.

4:00 PM *EL05.04.07

Mechano-Responsive Color-Changing Photonic Materials Benjamin Miller, Andrew Blair, Max Thomsen and Mathias Kolle; Massachusetts Institute of Technology, United States

Color-changing photonic materials are promising candidates for the design of colorimetric sensors and wearable technology, which can for instance be used to quantify the pressure exerted on a patient's body with compression bandages. While efforts in research groups across the world have resulted in many interesting lab-scale implementations of dynamic photonic materials, the scalable and economically viable production of such materials with high throughput is still a challenge that remains to be addressed. This presentation will be focused on a scalable optical manufacturing approach for the generation of highly stretchable, color-changing photonic sheets on the square-meter scale. The design space that is accessible with this technique with regards to controlling the materials spatio-spectral reflection behavior, its angular scattering characteristics, and its strain-induced color dynamics will be discussed in detail. Potential application scenarios, including medical textiles will be presented.

4:30 PM EL05.04.08

Living Optical Networks for Light Redistribution Inspired by Orchid Leaves Giulia Guidetti and Fiorenzo Omenetto; Tufts University, United States

Plants and animals have developed sophisticated hierarchical systems that integrate physicochemical material properties with functional micro- and nanostructures to effectively manage energy, motion, and species survival. These biological systems, besides providing cues on bottom-up manufacturing of technological structures, can offer insight on strategies for efficient energy management. In this study, we investigate the light harvesting and redistribution capabilities of tropical orchid leaves, which employ a cell-based optical network. Unlike regular orchid

leaves, the outer epidermal cells of these leaves exhibit a distinctive hexagonally packed short-range order lattice and rounded shape, facilitating optical cross-communication. By replicating this optical network within a tunable biopolymer matrix, we can fabricate versatile devices such as omnidirectional light couplers, wavelength selective optical networks, and cryptographic systems including all-optical unclonable security tags. To reproduce this propagation mechanism, we mimic the leaf structure using free-standing silk fibroin films. The response of the bioinspired cell-based optical networks can be controlled through functionalization achieved by selective doping with pigments and absorbers, as well as by modulating the silk protein conformation. We explore the structure-function relationship of the bioinspired optical networks using finite-difference time-domain optical modelling, revealing that the lateral redistribution of light through cross-communication is not only geometrically but also wavelength dependent.

4:45 PM EL05.04.09

Photonic Crystals Built by Time in Ancient Roman Glass Giulia Guidetti¹, Roberta Zanini², Giulia Franceschin², Mauro Moglianetti², Taehoon Kim¹, Nathaniel Cohan³, Lisa Chan³, John Treadgold³, Arianna Travaglia² and Fiorenzo Omenetto¹; ¹Tufts University, United States; ²Center for Cultural Heritage Technology, Istituto Italiano di Tecnologia, Italy; ³Carl Zeiss Microscopy LLC, United States

Ancient glass artifacts, though not inherently soft materials, display intriguing optical phenomena resulting from environmental-induced physico-chemical transformations over time. Iridescence is a common optical signature and one of the distinctive signatures of glass aging that is often observed on the surface of excavated glass. This study presents the optical investigation of a Roman-era archaeological glass fragment, employing a correlated optical-morphological and elemental analysis approach. Specifically, the studied ancient glass fragment exhibits structural color through surface weathering resulting in iridescent patinas caused by silica reprecipitation in nanoscale lamellae with alternating low and high density. This archaeological artifact reveals an unusual hierarchically assembled photonic crystal with extremely ordered nanoscale domains, high spectral selectivity and reflectivity (~90%). When taken individually, these silica multilayer lamellar domains resemble Bragg-stacks with narrowband reflection; however, when taken collectively they behave like a gold mirror. Optical characterization paired with nanoscale elemental analysis further underscores the high quality of this structure providing a window into this sophisticated natural photonic crystal assembled by time. Significantly, this highly reflective patina consists of a rare example of a self-assembly, pH-driven fabrication process that involves top-down processes (glass network dissolution) followed by bottom-up nano- to micro-scale structuring (silica nanoparticles nucleation, growth, and assembly in ordered Bragg stacks) in a natural structure. The characterization of this Roman glass fragment opens new perspectives on the insights and inspiration provided by analyzing ancient materials at the nanoscale, enabling observations of phenomena occurring across temporal windows that are otherwise challenging to replicate with currently available artificial aging approaches.

SESSION EL05.05: Poster Session: Soft Optics
Session Chairs: Michael Ford and Cindy Harnett
Tuesday Afternoon, November 28, 2023
Hynes, Level 1, Hall A

8:00 PM EL05.05.01

Highly Sensitive Mid-Wavelength Infrared Linear Polarizers Based on Waste from Petroleum Refining Process Woongbi Cho^{1,1}, Jehwan Hwang², Sang Yeon Lee³, Zahun Ku⁴ and Jeong Jae Wie^{1,1}; ¹Hanyang University, Korea (the Republic of); ²Purdue University, United States; ³Inha University, Korea (the Republic of); ⁴Air Force Research Laboratory, United States

Infrared (IR) optics play a key role in detecting invisible objects in darkness as well as small gas molecules. For gas detectors in industries and night vision in the military, IR polarizers can provide high-resolution images by selectively reflecting the transverse electric (TE) field and transmitting the transverse magnetic (TM) field. In this presentation, we introduced a low-cost yet high-performance waste-based metal wire grid IR polarizer by deposition of Au on the sulfur-rich polymer-based 1D nano-gratings integrating with a spacer layer. For IR transparent materials, the sulfur-rich polymer is employed due to its economic feasibility and thermal/solution processability. The sulfur-rich polymers are synthesized through inverse vulcanization of elemental sulfur (S), waste from the petroleum refining process. To design an effective polarizer structure, we first simulated the variation of optical properties like transmission of TM and TE (T_{TM} and T_{TE}), and extinction ratio (ER), according to the geometries including pitch, height, a ratio of width and pitch, Au thickness, and spacer layer thickness. Then, we realized the sulfur-rich polymer-based polarizer having the simulated geometry by spin-coating, thermal nano-imprinting (NIR), and followed Au deposition. In detail, we precisely controlled spacer layer thickness from 50-5100 nm via spin-coating by tailoring the spin speed, and the concentration of sulfur-rich polymer solution. The high-fidelity 1D nano-grating was prepared by applying the systematically controlled thermal NIL conditions (temperature, pressure, and time), which are obtained by considering both temperature-dependent viscoelasticity and the correlation between time and pressure. Finally, the sulfur-rich polymer-based polarizer exhibited remarkably high T_{TM} of 0.59, and ER of 5.19×10^3 at 4 μm .

8:00 PM EL05.05.02

Controlling Optical Response of Hydrogel using Metallic Microstructures Fabricated with High-Speed Scanning of Femtosecond Laser Pulses Ken Kashikawa, Hirofumi Tomikawa, Hiroaki Onoe and Mitsuhiro Terakawa; Keio University, Japan

A temperature-responsive hydrogel shows reversible volume-phase transitions in response to changes in their surrounding temperature. By containing metal nanoparticles as light absorbers inside the temperature-responsive hydrogel, the hydrogel's transmittance can be changed by photo-thermal conversion of the metal nanoparticles stimulated by light irradiation. The multi-photon photoreduction (MPR) method can spatially and selectively fabricate metal microstructures consisting of metal nanoparticles inside the hydrogel. In the MPR method, metal microstructures can be fabricated by femtosecond laser pulses inside the hydrogel containing metal ions. However, temperature-responsive hydrogels are thermally affected by the irradiation of femtosecond laser pulses at high repetition rates during the structure fabrication process which induce an undesirable volume phase transition, resulting in the hindrance of fabricating the arbitrarily designed structures. In this study, we fabricated microstructures consisting of multiple gold thin lines inside a poly (N-isopropylacrylamide) (PNIPAM) hydrogel by laser scanning at high scanning speed and multiple times (hereinafter called "multiple scans") by using a galvanometer scanner system. Under the experimental conditions of low scanning speed at a single time (hereinafter called "single scan"), the density of gold nanoparticles in the gold microstructures was low and the lines formed curls, curves, and/or kinks. On the other hand, under the experimental conditions of high scanning speed and multiple scans, the density of gold nanoparticles in the gold microstructure was high and straight lines without curls and curves were fabricated. The temperature around the irradiated area during laser pulse irradiation was measured by a thermography camera (T865, FLIR), and it was confirmed that the maximum temperature at high scanning speed with multiple scans was lower than that at low scanning speed with a single scan. Next, transmittance control by light stimulation was performed using the PNIPAM hydrogel with the fabricated gold microstructure. The two laser diodes with wavelengths of 520 nm and 405 nm were used as a stimulating light and a signal light, respectively. When the stimulating light was illuminated to the fabricated gold microstructure, the transmittance of the signal light in the PNIPAM hydrogel significantly decreased. Furthermore, the rate of the decline in the hydrogel's transmittance of the signal light and the response time of the hydrogel around the gold microstructure during irradiation of the stimulating light depended on the laser parameters during the structure fabrication process. The gold microstructures fabricated with high scanning speed and multiple scans showed the lowest transmittance and the fastest response time during the stimulated light irradiation in this experiment. This result is attributable to the higher density of gold nanoparticles in the gold microstructures fabricated with high scanning speed and multiple scans than in the microstructures fabricated with low scanning speed with a single scan. In the case of high scanning speed and multiple scans, the hydrogel around the fabricated gold microstructure is easier to reach the phase transition temperature. In conclusion, we experimentally demonstrated that gold microstructures can be simply fabricated into the temperature-responsive hydrogel by scanning femtosecond laser pulses with a high scanning speed and multiple scans. The fabricated gold microstructure can increase the degree of the hydrogel's transmittance change and shorten the response time of the hydrogel.

8:00 PM EL05.05.03

Highly Selective Sensors for Carbonyl Groups via Ion-Pairing Dyes with Wide Visible Spectrum Donghyun Kim, Jinho Lee, Chungseong Park, Euichul Shin and Il-Doo Kim; Korea Advanced Institute of Science and Technology, Korea (the Republic of)

In sensor research, achieving selectivity to distinguish between different materials is crucial for sensor performance and practical application, albeit adding complexity to the sensor design. Here is a straightforward method to achieve selectivity: adjusting the amount of amine mixed into the sensor. Through visual observation, we can create a color change sensor that enables easy differentiation of carbonyl groups with similar structures (such as ketones, carboxylic acids, and aldehydes). This color change sensor generates different pH and chemical environment changes when exposed to different carbonyl materials, and these changes are detected using ion-pairing dyes with a broad range of colors. Notably, this change is particularly noticeable under high humidity conditions, allowing for the differentiation of concentrations at the ppm level. This feature enhances its potential use as an exhalation sensor in high-humidity environments. The presence of acetone in human breath is closely associated with fat burning, and the concentration of acetone at the ppm level varies depending on the extent of burning. Consequently, after transforming the sensor into nanofibers through electrospinning, it can be employed in a healthcare system capable of sensitively detecting acetone in human breath. Moreover, its high selectivity for acetone clearly distinguishes it from other gases produced through exhalation.

8:00 PM EL05.05.04

Na-fluorohectorite (Na-FHt), a synthetic clay mineral which spontaneously forms nematic phases of single 1-nm-thick nanosheets when immersed into water, show structural coloration. Our previous work has demonstrated that two single nanosheets pinned together by Cs⁺ (so-called Double Layers, DBLs) produce bright and non-iridescent structure coloration. In the present study, we demonstrate experimentally that a single acoustic levitated water droplet (with diameter around 2mm) containing clay DBL nanosheets can easily and rapidly present structure coloration. The color changes during droplet evaporation as the clay DBL concentration increases. In addition, we observe droplets with similar volume placed on non-wetting and wetting surfaces respectively. This study paves the way further for sustainable structural coloration design at the microscale.

Key words: nematic gel, structure, optical properties, environmental confinement, droplets and film

Acknowledgements: This work was funded by Norwegian University of Science and Technology grant 81771176 (PHMB), Research Council of Norway through the grant 250619 (BP, JOF, PHMB) and 315135 (YY, PHMB, JOF), German Science Foundation grant SFB 840 (B3) (JB) and Research Council of Norway project number 280643 (Petromaks2Program) (JOF, KA), CNPq 442599/2019-6, 401581/2016-0, 303137/2016-9 (KA), FAPESP 18/21489-1, 2017/50129-0 (KA) and Petrobrás 0050.0101557.16.9 (KA).

References:

- [1] Fossum, Jon Otto. "Clay nanolayer encapsulation, evolving from origins of life to future technologies." *The European Physical Journal Special Topics* 229 (2020): 2863-2879.
- [2] Michels-Brito, Paulo H., et al. "Bright, noniridescent structural coloration from clay mineral nanosheet suspensions." *Science Advances* 8.4 (2022): eabl8147.

8:00 PM EL05.05.05

Temperature-Dependent Self-Assembly Remodeling by a Polyether Perylene Diimide in Water [Adrian Fernandez](#)¹, Mireya McKee², Pedro Rodriguez¹, Sarah Weisbrodt¹, Krystal Ojumuada¹ and Sean M. Kerwin¹; ¹Texas State University, United States; ²The University of Texas at Austin, United States

We report a novel Perylene diimide (PDI) bearing polyether side chains that displays reversible, temperature depended remodeling of two spectroscopically distinct self-associated forms. We describe the synthesis of this PDI (TEL-045) and its self-association behavior in solution as determined by UV/Vis, fluorescence, and resonant light scattering spectral analysis. TEL-045 forms monomeric, emissive species in solution in organic solvents. In aqueous solution, TEL-045 undergoes self-association to produce a non-emissive state. As the temperature of aqueous solutions of TEL-045 are increased, the degree of self-association increases, leading to LCST behavior and a new type of self-associated, emissive species. This reversible, temperature-dependent switching between H- and J-type self-association of this simple, a non-chromophore-modified PDI leads to marked changes in fluorescence enabling temperature-sensing and other applications.

8:00 PM EL05.05.06

Near-Infrared Light Guidance Through a Long Length Hollow Core Polymer Optical Waveguide from a 3D Printed Preform [Mahmudur Rahman](#) and [Mustafa Ordu](#); Bilkent University, Turkey

Hollow-core polymer optical fibers have great significance due to wide range of applications, such as short distance data transmission, wideband light guidance, and chemical and biomolecule sensing. In this study, a novel hollow-core optical fiber design was proposed for visible and near-infrared light guidance. The fiber was drawn conventionally using thermal drawing tower using a 3D printed polymer preform. Light guidance was demonstrated through the air core surrounded by six-pointed star cladding tubes up to 57.8 cm with the lowest propagation loss of 0.11 dB/cm between 1.1 μm to 1.3 μm wavelength range.

8:00 PM EL05.05.07

Stretchable and Durable Electroluminescent Devices with Exceptional Luminance using In-Plane Electric Field and Ionogel Electrodes [Seongkyu Song](#) and [Soon Moon Jeong](#); Daegu Gyeongbuk Institute of Science and Technology, Korea (the Republic of)

The advantages of in-plane electric field-driven electroluminescent devices (IP-ACEL) over coplanar devices include reduced light loss and increased brightness due to the electrodes being embedded within the emissive layer. Previous research showed that using conducting fibers and silver nanowires as electrodes improved luminance, but had limitations in stretchability and transmittance [1,2]. In this study, we addressed these limitations by developing transparent and highly stretchable ionogel electrodes for IP-ACEL devices, resulting in bright, stretchable, and durable ACEL devices. Our ionogel electrodes-based IP-ACEL device achieved a maximum brightness exceeding 3,000 cd/m², the highest reported among flexible/stretchable type ACEL devices. Furthermore, the IP-ACEL device exhibited exceptional durability, enduring 5000 cycles of repeated stretching, and provided protection against various external factors such as water and light. This approach enhances device performance and holds potential for applications in sustainable light sources, soft robots, and actuators.

- [1] S. Song, H. -S. Choi, C. -H. Cho, S. K. Lim, S. M. Jeong, *App. Phys. Rev.* **9**, 011423 (2022).
- [2] S. Song, B. Song, C. -H. Cho, S. K. Lim, S. M. Jeong, *Mater. Today* **32**, 46-58 (2020).

8:00 PM EL05.05.08

The User-Friendly Foveated LED Smart Contact Lens for Realistic Metaverse [Jieun Yeo](#), [Sehui Chang](#) and [Young Min Song](#); GIST, Korea (the Republic of)

With the advancement of semiconducting technologies including optoelectronic devices and displays in internet of things (IoT) era, there is growing attention to realize a hyper-connected society where various subjects such as people, objects, and systems. A "metaverse" is of interest to seamlessly blend virtual and real world spaces, which enables users to experience not only a sense of reality but also a virtual information without constraints of space and time. In this regard, the demonstration of a hyper-realistic virtual space that blurs the boundary between real and virtual space has become crucial factor in the display technologies. The augmented reality (AR), the one of the major visualization technologies of metaverse, is a technology that synthesizes information of virtual objects or spaces onto the scene of the real world through the device. However, the most devices such as head-mounted display (HMD) for the AR have limitations of the need for additional displays and cameras to integrate virtual objects or information into the real world due to the blockage between the user and outer physical space during wearing the HMD. In addition, the HMD causes cybersickness, generating the discomfort to users due to visual occlusion and discrepancies between sensory inputs and visual stimuli. Thus, there is an emerging demand for alternative technologies that can effectively alleviate user's fatigue and seamlessly integrate metaverse visualization into daily life. Many studies in sunglasses-type displays to improve the large and heavy volume of HMD have been demonstrated, but fundamental issues (e.g., cybersickness) are remaining challenges. In this study, we present the foveated LED smart contact lenses system by incorporating transparent LED displays into the center of contact lenses. These smart contact lens-based technologies aim to achieve ultra-realistic virtual space that naturally blend the boundaries between the real world and the metaverse in user-friendly way.

The foveated imaging function in smart contact lens shows the maximum image quality in the main visual fields relating to the user's gaze, while having the background area in relatively low image quality to increase the user's immersion and reduce data processing speed. The foveated LED smart contact lens was designed by inserting the LED pixels to the human eye model through the commercial ray tracing software. The lens design was optimized with a basis of optical properties of the conventional contact lens polymer; refractive index (1.4-1.5), thickness (100-150 μm), and radius of curvature (8.5-8.9 mm). In particular, LED displays should be designed small enough not to cast their shadows on the retina, and the LEDs are assumed that emitted light goes in the vertical direction of the LED device along the waveguide structure, unlike general LEDs emit light in radial direction under the substrate. When the fovea area was set as a detector region, the curvature of the lens and the LED greatly affected the image formation of the fovea. At a curvature of 8.6-8.9 mm, which is mainly used as the RoC for commercial contact lenses, small images are focused on areas outside of the fovea. However, if the contact lens is flattened than this curvature, it occurs user's discomfort to actually wear it. Therefore, the LEDs is placed to flat only the center of the lens by dividing the layer, because the area occupied by the LED is sufficiently small, which is effective rather than controlling the curvature of the entire lens. As a result, we designed an optical system of the foveated LED smart contact lenses that is user-friendly and enables a realistic metaverse implementation. The proposed system is expected to open the way for the development and commercialization of user-friendly AR devices for metaverse.

8:00 PM EL05.05.09

Optical Physically Unclonable Function Based on Electrospun Fluorescent Random Fibrous Media [MinSeok Kim](#), [Joo Ho Yun](#), [Seungkyu Choi](#), [Dong Hyun Seo](#) and [Young Min Song](#); Gwangju Institute of Science Technology, Korea (the Republic of)

Physical Unclonable Functions (PUFs) are unique cryptographic mechanisms derived from non-deterministic random variables introduced during their fabrication process. PUFs have garnered significant interest in recent years, especially in combating counterfeit activities and ensuring privacy and confidentiality of sensitive information. Among the different categories of PUFs, those exploiting optical principles have gained prominence due to inherent benefits like high entropy, complex output patterns, and strong resistance against modeling and replication-based attacks. The use of random lasers provides an especially attractive aspect of optical-based PUFs that distinguishes it from conventional laser-based PUFs systems. This emission is a phenomenon of Anderson light localization, which occurs when light undergoes intense scattering within a disordered medium. However, the fabrication of large-scale random media that can induce random lasing remains a formidable challenge due to economic viability. In this study, we propose an innovative solution by capitalizing on electrospinning. We demonstrate the feasibility of fabricating an optical PUF device that incorporates random lasing properties using this method and investigate its potential use in security applications.

For implementing the optical PUFs, we employed the electrospinning technique to generate nano/microfibers. We created a solution by dissolving 2 g of polymethyl methacrylate (PMMA) in 9 g of dimethylformamide (DMF) and acetone, stirring it at 60 °C for eight hours. To acquire emission properties within the 560 nm to 640 nm, we used 4-(dicyanomethylene)-2-methyl-6-

(4-dimethylaminoethyl)-4H-pyran (DCM) dissolved in a 2 mM solution at 60 °C for two hours. This solution then underwent the electrospinning process through a 23 gauge nozzle, applying a high voltage of 14 kV and maintaining a dispensing rate of 1 mL/hr. The process resulted in the fabrication of random microfibers, with homogeneous diameter distribution and thickness. Despite uniform diameters, the fabricated samples showed different optical properties due to variations in fiber structures at separate locations within the sample. To verify the occurrence of random lasing, we initiated an optical stimulation procedure using a UV laser with a wavelength of 355 nm with 10 Hz repetition rate. The laser was concentrated on the fabricated sample using a convex lens. The wavelength information of the resulting random laser was collected using an objective lens and a spectrometer. We gathered wavelength data, which showed random peaks within the 580 nm to 620 nm range, indicating the occurrence of random lasing. We further processed the data to leverage the peaks acquired from optical PUF devices, removing the spontaneous emission with post-processing. Utilizing a De-biasing method, we extract random bits from the PUFs, thereby significantly enhancing the uniformity of the digitized data. To validate the uniqueness and reproducibility of the bits generated from the PUFs, we calculated the Hamming distance and applied the NIST Randomness Test Suite (NIST SP 800-22). The random laser-based PUFs show excellent performance in terms of randomness, uniqueness, and reproducibility. With an inter-Hamming distance near 0.5, there was a high level of differentiation between bits produced from different samples. Notably, the intra-Hamming distance approached zero, indicating the high reproducibility of the random laser-based PUF. This research brings to light the potential of creating large-scale optical PUFs with random lasing properties, offering a promising direction for future cryptographic applications.

This work was supported by the National Research Foundation of Korea funded by the Korean Government (grant RS-2023-00210438, NRF-2022M3C1A3081312)

8:00 PM EL05.05.10

Production of Stimuli-Responsive Microlens Arrays by Photografting Surface-Assembled Hydrogel Prepolymers John Kapitan¹, Grayson Minnick², Brennan Watts¹, Nengjian Huang¹, Mark Rose¹, Ruiguo Yang^{2,2,2} and Stephen A. Morin^{1,2,2}; ¹University of Nebraska-Lincoln, United States; ²University of Nebraska-Lincoln, United States

Hydrogels garner much interest due to their broad applicability to a wide range of fields such as soft robotics, biomaterials, and adaptive optics. Current manufacturing procedures for hydrogels, specifically those at the micro- and nanoscale, require the use of time consuming and expensive equipment. Moreover, often these microstructured hydrogels (microgels) lack strong interfacial adhesion to support materials limiting their applications. We developed a manufacturing scheme for hydrogel prepolymers that: 1) uses mechanically-driven coalescence to assemble prepolymer droplets into well-defined geometries and morphologies and 2) creates robust bonds with an elastomer support substrate using a "graft from" polymerization scheme. We used this technique with several hydrogel systems to manufacture large arrays of highly ordered microgels in minutes. The size and periodicity of the hydrogels was easily controlled by changing the surface chemical template. Hydrogel arrays demonstrated robust adhesion to the surface versus hydrogels assembled on surfaces without the necessary moieties for covalent attachment. Despite the strong adhesion the attached hydrogels maintained their stimuli responsive nature. We demonstrated optically dynamic hydrogel arrays whose refractive index could be adjusted by external stimuli, such as solvent or heat. We quantified the change in refractive index by measuring the magnification of an image projected through a hydrogel array. These microlens arrays can be applied as optical sensors in soft robotics or lens elements in wearable electronic devices.

8:00 PM EL05.05.11

Universal Self-Aligned Waveguide for an Amphibious Imaging System Inspired by the Compound Eye of the Fiddler Crab Hyuk Jae Jang, Jieun Yeo and Young Min Song; Gwangju Institute of Science and Technology, Korea (the Republic of)

Compound eyes of arthropods (e.g., insects) have remarkable features such as a wide field-of-view and high sensitivity to motion detection. [1] These characteristics are due to their unique optical unit, ommatidium, which consists of a corneal lens, crystalline cone, and rhabdom. In nature, the ommatidia have diversely evolved with their environments, such as a corneal lens for optical power and crystalline cone for optical guidance. Researchers have attempted to mimic the functionality of natural ommatidia using photosensitive polymer materials to create artificial ommatidia. [2] However, previous studies have not considered the effects of different environments, such as air and underwater, on the imaging performance of these artificial ommatidia. In typical optical systems, the refractive power of curved lenses is affected by the external refractive index (RI), leading to a loss of focusing power. In other words, curved lenses are not efficient in gathering optical rays when exposed to changing environments. Some imaging systems have addressed this limitation by modifying the lens shape or displacement (e.g., liquid lens). However, these optical accommodation systems tend to be bulky and complex, which is not suitable for compact configurations. To achieve more efficient vision in both air and water, an imaging system requires accommodation-free optical component. The fiddler crab, a semi-terrestrial crab, has compound eyes with flat corneal micro-lenses that possess a graded RI. Unlike traditional curved lenses, which rely on changes in shape or displacement for optical accommodation, the fiddler crab's flat micro-lenses maintain consistent optical power across various environments without the need for accommodation. Here, inspired by the fiddler crab's eye, we introduce an amphibious artificial ommatidium with self-aligned waveguide. The artificial ommatidium comprise a self-written waveguide (i.e., crystalline cone) and a flat micro-lens array (MLA) (i.e., corneal lens), achieved through a process involving the use of ultraviolet (UV) curing properties of a photosensitive polymer material (SU-8) and the light-focusing capability of the MLA. Prior to fabricating the SU-8 MLA, a polydimethylsiloxane (PDMS) mold with a sidewall was created using a quartz MLA mold etched through reactive ion etching. The temperature of the SU-8 material was gradually increased from 65 °C to 120 °C to ensure complete solvent evaporation, followed by spin-coating of an optical adhesive (Norland optical adhesive, NOA) onto the fabricated SU-8 MLA. Upon UV light irradiation, the exposed region underwent photo-crosslinking via post-exposure baking, resulting in an increase in RI. Meanwhile, the unexposed region experienced thermal-crosslinking through hard baking, leading to a reduction in RI (~0.008). Consequently, this process turned out to be RI change between a core and cladding structure for the waveguide ($\Delta n = 0.029$), with an additional spin-coating step to cover the outer layer. We successfully implemented the universal self-aligned waveguide by using flat MLA and the RI difference between the photo/thermal-crosslinked regions. The optical performance of the artificial ommatidium was evaluated, demonstrating its amphibious imaging capability. This amphibious artificial vision system represents a significant advancement in imaging applications, particularly in the field of amphibious motion detection.

References

- [1] Song, Young Min, et al. "Digital cameras with designs inspired by the arthropod eye." *Nature* 497.7447 (2013): 95-99.
- [2] Jeong, Ki-Hun, Jaeyoun Kim, and Luke P. Lee. "Biologically inspired artificial compound eyes." *science* 312.5773 (2006): 557-561.

8:00 PM EL05.05.12

Optical Fiber Probe based on Plasmonic Hydrogels for Continuous Glucose Sensing Irsar Ahmed, Amal AlGhaferi and Haider Butt; Khalifa University, United Arab Emirates

In recent years, the prevalence of diabetes mellitus (DM), a chronic metabolic disorder caused by excessive blood glucose levels, appears to have increased globally. Diabetes is not lethal, but its complications can result in serious illness or death. Consequently, cost-effective, rapid, and dependable sensing is required for diabetes control. Optical fiber sensors based on nanocomposite photonic hydrogel functionalized with phenylboronic acid (PBA) were developed here for continuous glucose monitoring. Optical fiber sensors were created by polymerizing PBA-based hydrogel on the tip of a commercial fiber. Subsequently, Au nanoparticles were incorporated into the polymerized OF sensor by immersing the sensor in a nanoparticle solution. In the physiological glucose range (0 - 20 mM), glucose sensors were studied using transmission and reflection modes. The transmission spectrum of the OF sensor exhibited a 27 percent variation. Also, a minor shift of 5 nm was seen in the SPR when the glucose concentration varied from 0 to 20 mM. An increase in the reflectance spectrum was also seen when glucose concentrations rose. These OF sensors were measured to have a rapid reaction time of 20 seconds and a saturation time of 3 minutes. Ultimately, the sensor's usability was validated using a smartphone readout. For this reason, the photodiode of a smartphone was utilized, and the change in optical power for various glucose concentrations was evaluated. These OF sensors may benefit continuous glucose monitoring systems in diabetic care.

8:00 PM EL05.05.13

Quantum Chemical Study of Electrogenerated Chemiluminescence Cell of Rubrene Solution with an Assist Dopant Nobuhiko Akino¹, Emiri Kato¹, Ryoichi Ishimatsu², Jun Mizuno³ and Takashi Kasahara¹; ¹Hosei University, Japan; ²University of Fukui, Japan; ³National Cheng Kung University, Taiwan

Recently, electrogenerated chemiluminescence or electrochemiluminescence (ECL) cells have been considerable attention for the use in future displays due to their simple device structure and also easy fabrication process.[1,2] In the previous study, we have shown that the ECL performances of 5,6,11,12-tetraphenyltetracene (rubrene)-based device was significantly improved by using 4-(di-*p*-tolylamino)-4'[(di-*p*-tolylamino)styryl]stilbene (DPAVB) as an emitting assist dopant, compared with the performance of device without it.[3] For example, the maximum luminance of the device with an emitting assist dopant was improved to 292 cd/m² at 6.0 V, which is approximately 3.4 times higher than the luminance of the device without it (86.2 cd/m² at 5.5 V).

From the cyclic voltammograms (CVs), both the highest occupied molecular orbital (HOMO) and the lowest unoccupied molecular orbital (LUMO) of DPAVB are shallower than HOMO and LUMO of rubrene. Based on the energy level configuration of neutral molecules, it seems energetically unfavorable for an electron on HOMO of rubrene radical anion to DPAVB radical cation in order to form the excited states of rubrene. The mechanism of the improvement in device performance has not been clear enough and it has been desired to understand deeply for further improvements.

In this study, we have utilized the quantum chemical calculations to shed some light on the mechanism in the device with an assist dopant. The geometry optimizations of molecules are performed using the density functional theory at the level of B3LYP and the solvent effects are incorporated using the polarizable continuum model (PCM). The calculated energy levels of the radical anion of rubrene and the radical cation of DPAVB are modified from the levels of the neutral molecules. Their relative positions support the energetically efficient electron transfer

from the former to the latter leading to the excited states of rubrene and the neutral state of DPAVB, which results in the luminance improvement in ECL device.

REFERENCES

- [1] S. H. Kong, J. I. Lee, S. Kim, and M. S. Kang, *ACS Photonics*, **5**, 267 (2018)
- [2] T. Nobeshima, T. Morimoto, K. Nakamura, and N. Kobayashi, *J. Mater. Chem.*, **20**, 10630 (2010)
- [3] E. Kato, R. Ishimatsu, J. Mizuno, and T. Kasahara, *Electrochemistry*, **91**(4), 047002 (2023)

SESSION EL05.06: Waveguides and Applications I
Session Chairs: Michael Ford and Cindy Harnett
Wednesday Morning, November 29, 2023
Hynes, Level 2, Room 203

8:00 AM *EL05.06.01

Soft, Side Emitting Optical Fibers by Multimaterial Printing Aránzazu Del Campo^{1,2}; ¹INM–Leibniz Institute for New Materials, Germany; ²Saarland University, Germany

Side-emitting optical fibers are used to illuminate large volumes of non-transparent material. Introducing a customized side-emission profile is a major challenge in the fabrication of side-emitting optical waveguides, requiring modulation of the guiding and emitting properties along the fiber length. This is particularly difficult to realize in continuous processing of soft materials. In this work we use extrusion-based multimaterial printing to generate segmented hydrogel optical fibers with tailored side emission. We print fibers with segments of different optical properties by switching between a waveguiding ink and its mixture with scattering particles. The method allows printing segment lengths below 500 microns. The length of the segments can be tailored by controlling the switching time between inks during printing, thereby achieving desired side-emission profiles along the fiber length. The presented technology and material combination allows unprecedented flexibility for designing optical fibers with customizable optical properties using simple processes and medical materials.

8:30 AM EL05.06.02

Thermally Reconfigurable Double Emulsions Droplets with Tunable Morphologies and Spherical Aberrations Zhang Wu¹, Brendan Deveney¹, Wenyun Wang¹, Stefano Aime², Mathias Kolle³, Joerg G. Werner⁴ and David Weitz¹; ¹Harvard University, United States; ²ESPCI – Paris FR, France; ³Massachusetts Institute of Technology, United States; ⁴Boston University, United States

Reconfigurable emulsions engineered with specific structure designs, present a promising avenue for achieving customized properties and advanced optical functionality. Tri-phase reconfigurable emulsion droplets hold significant promise as micro-lenses with the potential to revolutionize optics and photonics applications. Here we introduce a novel type of triple-phase emulsions characterized by thermally reconfigurable shells, consisting of hydrocarbon and fluorocarbon components. These components exhibit temperature-dependent miscibility and are stabilized with unique velcro-mimicking surfactants, resulting in the formation of solid-like water/oil interfaces and water-in-oil-in-water double emulsions at a high temperature above the critical point. We assess the viscoelastic properties of these interfaces by characterizing the droplet deformation as they flow through sinusoidal channels, essentially functioning as a rheometer within polydimethylsiloxane devices. Upon temperature change, the hydrocarbon and fluorocarbon components within the oil shell undergo phase separation, causing the droplets to adopt a new morphology of inner water core and hydrocarbon phase engulfed by fluorocarbon shell. The droplet morphologies can be fine-tuned by adjusting the hydrocarbon-fluorocarbon volume ratio and micelles used in the outer water phase, giving rise to diverse and exotic structures. We also perform two-dimensional ray-tracing simulations of visible light traversing through those morphologies to calculate the longitudinal and transverse spherical aberrations to inform the design and selection of fluid lenses for various applications, paving the way for expanding the scope of optical applications and future transformative technologies.

8:45 AM EL05.06.03

Evolution of The Geometry and Optical Anisotropy as Cellulose is Wet-Spun Pablo B. Sánchez¹, Jianyi Du², Javier Páez¹ and Pablo Otero¹; ¹University of Vigo, Spain; ²Massachusetts Institute of Technology, United States

It is critical to monitor the structural evolution of complex fluids for an optimal manufacturing performance. Thus, we increase the understanding of the underlying physics which drives the structural modifications and contribute to identify the variables triggering changes in the material properties. Also, in situ measurements facilitate the continuous optimization of the manufacturing process.

Since cellulose undergoes thermal degradation before melting, its processing requires a solvent media with the ability of dissolving cellulose without causing major harm to the polymer chains. The resulting dissolution, often named spinning dope, show slow dynamics with a significant shear thinning behavior which becomes larger as we increase cellulose concentrations. Under extension, spinning dopes experience strain softening behavior followed by a strain hardening trend as the strain grows larger (Sanchez et al, *Biomacromolecules*, 2022). The spinning dope is extruded through a nozzle as it is pulled by a rotating rod, so it undergoes combined shear and extensional strains. Immediately after, it is coagulated in water which acts as an anti-solvent and triggers the formation of a hydrogen bond network. While cellulose regenerates into a fiber, polymer chains aligned, and the formation of the hydrogen bond network induces a birefringent response in the material which depends on the spun material and the process variables. Traditionally, the performance of the spinning process is evaluated by measuring the target properties of the fiber (e.g. tenacity or elongation) and iterating over the spinning parameters in a heuristic loop which tends to be time consuming and neglects the insights of the different stages involved in the fiber formation. This approach seeks to establish a relation between the source material and the produced fiber and to optimize the process variables. However, information about the chemical and conformational changes undergone by the spinning dope are not accessible.

In this work we propose a new framework to determine the evolution of the fiber geometry and optical anisotropy along the spinning process by measuring diameter and birefringence at the selected points along the process. With this aim, we have built a customized spin-line enabling an easy-control of the critical variables involved in the spinning process: draw ratio and residence time. Then, a self developed optical device comprised of a charge couple device (CCD) and a liquid-crystal (LC) compensator with tunable retardation for rapid and accurate birefringence measurements was designed and built together with the spin line (Sanchez et al, *Carbohydrate Polymers*, 2023). Results substantiate the microstructural variation as the extensional strain increases. Noticeably, the drawing process occurs almost instantaneously at the nozzle while the fiber coagulation takes several minutes to be completed. Birefringent response grows linearly with the draw ratio and diminishes tenderly with the residence time proving the material relaxation when strain is not imposed. Superposition techniques were successfully applied to capture and describe the effect of draw ratio and coagulation time in terms of shifting factors. Finally, the fiber geometry and optical anisotropy obtained “in situ” are discussed together with the rheological analysis of the spinning dope and the mechanical properties of the obtained fibers.

9:00 AM *EL05.06.04

Thermally Drawn Soft Optical and Electrical Fibers as Wearable Sensors and Microrobots Xiaoting Jia; Virginia Institute of Technology, United States

Highly stretchable optical and electrical fibers have attracted significant attention in recent years due to their broad applications in wearable sensors, human-machine interfaces, and biomedical implantable devices. However, the scalable fabrication of submillimeter soft optical and electrical fibers with complex structures has been a challenge. Here we present a thermal fiber drawing method for the scalable fabrication of soft optical and electrical fibers with complex geometries and demonstrate the application of these fibers as wearable sensors and microrobots. This method allows for the production of hundreds of meters of continuous soft fibers per draw, and the resultant fibers can have optical, electrical, magnetic, and microfluidic functionalities within a submillimeter diameter. We first demonstrate an opto-electrical fiber sensor which can sustain at least 580% strain and up to 750% strain with a helix structure. The electrical fiber sensor simultaneously exhibits ultrahigh stretchability (400%), high gauge factors (≈ 1960), and excellent durability during 1000 stretching and bending cycles. We also show that the stretchable step-index optical fibers facilitate the detection of bending and stretching deformation through changes in the light transmission. By combining both electrical and optical detection schemes, multifunctional fibers can be used for quantifying and distinguishing multimodal deformations such as bending and stretching. Next, we demonstrate a soft robotic fiber that integrates navigation, sensing, and therapeutic functions at a submillimeter scale. These fiber robots consist of ferromagnetic, electrical, optical, and microfluidic components, and can navigate through complex and constrained environments, such as artificial vessels and brain phantoms. Moreover, we utilize Langendorff mouse hearts model, glioblastoma microplatforms, and in vivo mouse models to demonstrate the capabilities of sensing electrophysiology signals and performing localized treatment. Additionally, we demonstrate that the fiber robots can serve as endoscopes with embedded waveguides. These fiber robots provide a versatile platform for targeted multimodal detection and treatment at hard-to-reach locations in a minimally invasive and remotely controllable manner. These studies demonstrate the potential of using thermal fiber drawing as a versatile and powerful platform for fabricating soft optical and multifunctional fiber devices for a variety of applications.

9:30 AMBREAK

10:00 AM *EL05.06.05

Soft Multi-Material Optical Fibers and Metasurfaces: Innovative Fabrication Approaches and Novel Applications[Fabien Sorin](#)¹; Ecole Polytechnique Federale de Lausanne, Switzerland, Switzerland

The ability to realize advanced photonics systems on soft and deformable substrates can find tremendous opportunities in sensing and monitoring, health-care, soft robotics and smart textiles. The materials and processing challenges associated with imparting large, flexible and stretchable surfaces with state-of-the-art photonic performance remain however significant. Today, most existing photonics systems rely on rigid materials, with fabrication approaches that are not well adapted to soft substrates such as elastomers. In this talk, I will present novel fabrication strategies that we have been developing that rely on understanding and controlling viscous flow at various scales, from the fluid dynamics of optical fiber thermal drawing, to the nano-fluidics associated with thin-film dewetting¹⁻⁶. Both approaches, while seemingly very different, exhibit an interesting interplay between viscosity and surface tension, that can be elucidated via in-depth rheological analysis, thermomechanical characterization, and modeling. First, I will present the template dewetting of thin optical glass layers on textured flexible and stretchable substrates as a novel approach to realize advanced optical metasurfaces on stretchable substrates^{2,4}. Examples of structures and applications will include index and biosensing, second-harmonic generation, and soft metalenses. I will then make a parallel with thermal drawing, the fabrication process used to make optical fibers. I will show that an in-depth analysis of the rheological, thermomechanical and fluid dynamic aspects of this technique reveal similar features as dewetting, and has expanded the range of materials compatible with this approach. I will insist in particular on the recent ability to draw thermoplastic elastomers¹, metallic glasses³, as well as of complex and multi-functional optical fiber architectures with either mechanical⁵ or magnetic⁶ actuation. These advances in materials and processing is paving the way towards advanced state-of-the-art soft optics systems with multi-functionalities for applications in surgical diagnosis and intervention, wearable, soft robotics, bio-sensing and smart textiles.

References: [1] *Advanced Materials* 30, 1707251 (2018) ; [2] *Nature Nanotechnology* 14, 320 (2019); [3] *Nature Nanotechnology* 15, 875 (2020); [4] *Nanophotonics* 10, 3465 (2021); [5] *Advanced Science* 10, 2204016 (2022); [6] *Advanced Materials* 202212202 (2023).

10:30 AM EL05.06.06

Optofluidic Skins for Sustainable Buildings[Raphael Kay](#)¹, J. AlstanJakubiec², CharlieKatrycz², BenjaminHatton² and JoannaAizenberg¹; ¹Harvard University, United States; ²University of Toronto, Canada

Indoor climate control is among the most energy-intensive activities conducted by humans; more than 25% of the energy and 50% of the electricity we consume globally is spent heating, cooling, and lighting interior spaces to keep humans comfortable. At the core of this footprint is a fundamental design flaw in architecture: human comfort is predominantly curated internally, using air conditioners, furnaces, and electric lights. As an entirely different approach to keeping humans comfortable, a building 'skin' capable of achieving climate control directly could drastically reduce the use of the indoor heating, cooling, and lighting systems that drive energy consumption and greenhouse gas emissions globally. However, to date, the development of such a universally configurable building platform remains an unresolved scientific challenge.

Looking orthogonally to typical solid-state approaches, we have turned to a new class of material to achieve versatile climate control along the surfaces of buildings: liquids. Compared to solids, liquids have two important functional advantages. First, they flow. Liquids can be easily transported, overlapped, and exchanged, while quickly and reversibly filling the extents of their containers. Second, liquids can much more readily be tuned, and are able to hold a range of particles and molecules relevant to the manipulation of solar radiation. Taken together, the versatility of liquids allows us to explore a new set of optofluidic strategies for more comprehensively controlling environmental sunlight.

We develop simple fluidic devices capable of general solar configurability, and we treat rationally selected liquids as injectable solar filters, introducing them in different combinations and sequences to spatiotemporally regulate temperature and daylight distributions indoors. Altogether, using optical experiments and simulations, we demonstrate how a simple fluidic platform can synergistically control the amount, color, and position of transmitted sunlight over time – a universal solar toolkit not realized in traditional building technologies.

Importantly, because this fluid-based toolkit can curate much of the internal climate at the external skin, the need for indoor operational energy usage can be massively reduced. Compared to available alternatives, models demonstrate that our liquid wrappings can decrease heating, cooling, and lighting energy consumption in buildings by over 40%, suggesting the emergence of a liquid design paradigm toward net-zero buildings.

10:45 AM EL05.06.07

From Aberration Correction Elements to Liquid Space Telescopes-Theoretical Modeling of a Pinned Liquid Film in a Finite Domain[Israel Gabay](#)¹, VesnaBacheva², AntonioRamos³, MoranBercovici¹ and AmirGat¹; ¹Technion-Israel Institute of Technology, Israel; ²Cornell University, United States; ³University of Seville, Spain

Expanding beyond traditional applications in lubrication and coatings, thin liquid films now play pivotal roles in soft actuators and adaptive optical elements. These novel uses usually involve a finite volume of liquid within an impermeable domain, straying from the common models that mostly considered infinite or periodic boundary conditions. For example, researchers recently presented an adaptive optofluidic element that is based on a deformable membrane driven by an underlying layer of liquid enclosed with an impermeable chamber. The dynamics of these devices, due to the constraints of global mass conservation and a pinning boundary condition, significantly differ from those of infinite or periodic films. Mathematically, this constitutes non-self-adjoint problems. A theoretical framework is thus required in order to predict the performance of such devices.

In this work, we present a combined theoretical and experimental study to tackle this problem. We provide a time-dependent analytical solution for the linearized non-self-adjoint system that emerges from these boundary conditions. Our solution in the small deformations regime (i.e., the linearized equation) is particularly suitable in the context of diffractive optical components, which feature surface topography variations on the scale of a visible light wavelength. Unlike self-adjoint problems, this problem demands special attention to properly reconstruct the solution based on the system's eigenfunctions. Although our derivations primarily focus on a free interface, they apply directly to cases with a membrane under tension dominant regime and can readily be extended to include elastic bending of the membrane.

We compare our solutions with common models for self-adjoint thin-film problems, such as a pinned film in a permeable domain or periodic boundary conditions. We show that while the initial dynamics are almost identical, the boundary conditions eventually influence both the film topography of the entire domain and its response time. To validate our model, we designed an experimental setup that subjects a thin liquid film to a prescribed normal force distribution using dielectrophoresis, and measures the film deformation in real-time using high-frame-rate digital holography. The experimental results are in good agreement with our model, demonstrating that confined films behave differently from what existing self-adjoint models could predict.

Thin films in a finite domain have potential use as optical elements also in the other extreme of length scales; we are currently collaborating with NASA to explore their use for creating space telescopes on the scales of tens of meters. Aspects such as liquid settling time as stability under accelerations are particularly important for these applications and our model provides non-intuitive insights which guides the design. In my talk, I will also present our analysis for such applications and the most up-to-date experimental results on scaled-up systems that we are constructing.

11:00 AM EL05.06.08

Soft Waveguide Segments for Deformation Sensing[Tram Nguyen](#)¹, [Michael Han](#)² and [Cindy K. Harnett](#)²; ¹Hollins University, United States; ²University of Louisville, United States

This presentation looks at soft optical waveguides made from oils and gels for their potential in measuring curvature along paths that bend and twist. Mapping curvature along a path helps capture the shape of soft deformable objects. The focus of this presentation is on creating a defective segment in an otherwise transmissive optical waveguide, a segment with a light transmission level that is highly sensitive to deformation. Optical methods like this one are increasingly popular in soft robotics because their all-polymer construction matches the mechanical characteristics of the surface, and optical signals are less susceptible than electrical signals to temperature drift and electromagnetic interference. Aside from a few recent examples of distributed optical sensors, most examples are point sensors with one highly sensitive section, or integrating sensors that report deformation at an unknown location along the waveguide.

In the first implementation to be discussed, we change a point sensor into a deformation mapper by moving a sensitive segment along the waveguide. Here, the deformation-sensitive section is an air bubble in an oil-filled tube routed along a surface. Loss of total internal reflection at the air bubble means that when the bubble is positioned at a sharp curve, the overall transmission of the channel drops more than when the bubble is in a straight section. The signal is dominated by events at the sensitive segment, while the rest of the waveguide serves as a high transmission signal delivery channel. By circulating the oil through the waveguide with a pump, the sensitive segment is scanned over the waveguide to map out its local curvature, whether that curvature is caused by the static waveguide path layout or by dynamic bending motions of the underlying surface. We demonstrate that the scanned bubble is able to detect and localize the bending location of a soft robotic limb to within approximately 4 cm.

However, the scanned bubble method has a speed limit determined by the Weber number. Scanning faster than a few cm/s causes the air bubble to break up leading to an unreliable signal. Soft segments of silicone or hydrogel are investigated as an alternative low-index segment that can be scanned around the waveguide faster without breaking up. A related topic included in this presentation is verifying the location of scanned segments with a closed loop method. Measuring volumetric oil displacement gives segment location when things are flowing smoothly, but it is possible for solid segments to get stuck. We therefore investigate light reflection as a method to locate segment edges in the liquid core waveguide.

Twist is another aspect of path shape that isn't captured by a rotationally symmetric, cylindrical soft waveguide segment. We discuss soft waveguide segments with non-circular cross sections for their ability to detect left- and right-handed twisting along the waveguide path. In this example, the application is monitoring the state of a reconfigurable soft robotic actuator.

11:15 AM EL05.06.09

Highly Integrated Multi-Material Optical Fibers for Soft Robotics[Stella Laperrousaz](#), [Andreas Leber](#) and [Fabien Sorin](#); École Polytechnique Fédérale de Lausanne, Switzerland

Soft robotics is rapidly growing as a prominent research field, in particular when considering the development of safe biomedical devices where compliance is key to safely interact with delicate tissues and interfaces. While this is an attractive prospect, innovative scalable fabrication strategies are required to enable the incorporation of advanced functionalities into soft and compliant devices. In particular, the fabrication of soft systems with small diameters and high aspect ratios, that integrate optical but also electrical, microfluidics or actuation attributes, remains challenging. To alleviate this challenge, we propose to rely on the unique attributes of the thermal drawing technique. Despite being mostly known for the scalable production of optical fibers, thermal drawing can actually be adapted to yield 10s of meters long soft elastomeric fibers with intricate architectures and extremely high aspect ratios.^[1] In that regard, thermal drawing is a promising processing platform to realize highly integrated soft optical fibers imparted with multiple actuation and sensing modalities for soft robotics.

In this talk, we will present the thermal drawing of soft catheter-like fibers that can integrate optical waveguides but also microfluidic channels or electrical wires.^[2] We will first show how a careful analysis of the rheological attributes and mechanical compliance enables to select the best suited materials to realize a hybrid fiber structure with rigid conventional optical fibers embedded in an elastomeric cladding. Then, we will introduce a first example of application of such multifunctional architectures where autonomous fiber movement and obstacle avoidance are achieved through a closed-loop control based on the continuous measurement of reflected light intensity. In addition, the collected proximity signals can be used to map the surrounding environment in 3D, endowing the fiber with imaging capability. Moreover, the potential of thermal drawing to produce highly integrated fibers will be demonstrated through a complex design incorporating optical guides, but also metallic wires and microfluidic channels. This specific soft optical fiber is thus able to perceive and adapt to its environment, but also to stimulate, record or deliver fluids to spatially distributed targets.

Finally, we will explore the integration of sensing elements into soft optical fibers. More specifically, thanks to an in-depth rheological study, we identified soft electrically conductive composites compatible with the thermal drawing process.^[3] These piezoresistive composites can provide information about the fiber bending state and detect bending angles as small as 5°. By combining conventional rigid optical waveguides and soft piezoresistive composites into thermally drawn fibers, soft robotic fibers can accomplish both exteroception and proprioception. The advanced soft optical fibers we will present could be envisioned as the next generation of steerable endoscopes and catheters, endowed with multiple advanced functionalities, and thus promote the development of safe minimally-invasive procedures.

References:

[1] Y. Qu et al., *Advanced Materials* **2018**, *30*, DOI 10.1002/adma.201707251.

[2] A. Leber, et al., *Advanced Science* **2023**, *10*, DOI 10.1002/advs.202204016.

[3] S. Laperrousaz et al., *Advanced Science* **2023**, *10*, DOI 10.1002/advs.202207573.

SESSION EL05.07: Waveguides and Applications II

Session Chairs: Cindy Harnett and Juejun Hu

Wednesday Afternoon, November 29, 2023

Hynes, Level 2, Room 203

1:30 PM EL05.07.01

Characterization of Clear Urethane Plasticizer for Use in Optical Waveguide Strain Sensors in Soft Robotics[John Garrett Williamson](#), [Caroline Schell](#), [Scott Holmstrom](#), [Peter Lo Presti](#), [Michael Keller](#) and [Joshua Schultz](#); University of Tulsa, United States

One of the key challenges in soft robotics is proprioceptive sensing due to the robots' deformability and infinite degrees of freedom. Most often, soft robots rely on motion capture systems, which require external hardware like cameras. One of the proposed benefits of soft robots is their ability to navigate unstructured environments, however, the nature of these environments often leads to occlusions that interfere with motion capture sensing. Recently, researchers have proposed methods to integrate sensors into the robot body which have the potential to perform better in these environments; examples include galinstan and other liquid-metal resistive strain sensors. However, these sensors are prone to oxidizing, leading to hysteresis in sensor measurements over time.

We propose using optical strain sensors to sense motions within the robot body. These sensors are made by cladding a fiber made of clear, stretchable, high refractive index material with a low refractive index material. Light travels differently along the length of the fiber when it is deformed by stretching, bending, or locally applying lateral pressure. Prior work in this area has established methods to differentiate deformation modes based on the intensity and time of flight through these fibers.

Optical fiber strain sensors have little hysteresis or degradation over time, they are indifferent to electromagnetic interference and have large bandwidth. However, prior efforts to implement these sensors have been hampered by a mechanical mismatch between the core and cladding materials. One of the more stretchable versions of this type of sensor is made from urethane core material with silicone cladding. Most optically clear urethanes, however, are somewhat stiff. Clear Flex 30™ made by *Smooth-On* is a clear urethane with lower stiffness than most optically clear urethanes. It has been used in soft robotics in our work and the work of others. It is commercially available in shore hardnesses of 30, 50, or 90 A. Usually, the silicone is picked to match this material's mechanical properties as closely as possible. This avoids issues like fiber slip and non-uniform robot inflation due to the fibers acting as a local reinforcement to the robot wall. Matching silicone cladding stiffness to the urethane core fiber limits the material design options. Higher stiffness robots allow for greater lifting capacity, while lower stiffness robots are more deformable. It is also sometimes desirable to match the stiffness of something like human skin or an object to be manipulated.

To address these issues, new formulations of optically clear urethanes were created to match the mechanical properties of a range of cladding or substrate materials. Optical and mechanical analyses of urethanes modified with a commercial plasticizer (*Smooth-On* So-Flex II™) were performed to measure the basic properties of the new formulations and to determine suitability for sensing applications. Digital image correlation tensile testing shows that this additive can modify the 100% modulus from 380 kPa for the unmodified material to 200 kPa at a concentration of 20% by weight in Clear Flex 30™. At that concentration, spectrophotometer testing shows negligible optical loss compared to the unmodified material meaning the additive does not negatively affect usable fiber length. A refractive index test at 632.8 nm found that the refractive index of the modified material differed from the unmodified material by 0.01, dropping from 1.48 to 1.47. Further testing will establish a larger spectrum of refractive indices. A tensile specimen made of Dragon Skin 10™ silicone cladding and a Clear Flex 30™ core with So-Flex II™ showed adequate total internal reflection for a 12 cm long sensor; having approximately 0.14 dB additional loss under 50% strain.

1:45 PM EL05.07.02

Fatigue-Resistant Hydrogel Optical Fiber Enables Peripheral Nerve Optogenetics During Locomotion[Xinyue Liu](#)^{1,2}, [Siyuan Rao](#)^{3,2}, [Weixuan Chen](#)³, [Kayla Felix](#)³, [Jiahua Ni](#)², [Atharva Sahasrabudhe](#)², [Shaoting Lin](#)^{1,2}, [Qianbin Wang](#)³, [Yuanyuan Liu](#)⁴, [Zhigang He](#)⁵, [Polina Anikeeva](#)² and [Xuanhe Zhao](#)²; ¹Michigan State University, United States; ²Massachusetts Institute of Technology, United States; ³University of Massachusetts Amherst, United States; ⁴National Institutes of Health, United States; ⁵Harvard University, United States

We develop soft and stretchable fatigue-resistant hydrogel optical fibers that enable optogenetic modulation of peripheral nerves in naturally behaving animals during persistent locomotion. The formation of polymeric nanocrystalline domains within the hydrogels yields fibers with low optical losses of 1.09 dB cm⁻¹, Young's modulus of 1.6 MPa, stretchability of 200%, and fatigue strength of 1.4 MPa against 30,000 stretch cycles. The hydrogel optical fibers permitted light delivery to the sciatic nerve, optogenetically activating hindlimb muscles in Thy1::ChR2 mice during 6-week voluntary wheel running assays while experiencing repeated deformation. The fibers additionally enabled optical inhibition of pain hypersensitivity in an inflammatory model in TRPV1::NpHR mice over an eight-week period. Our hydrogel optical fibers offer a motion-adaptable and robust solution to peripheral nerve optogenetics, facilitating the investigation of somatosensation with implications in motor recovery and pain management.

2:00 PM *EL05.07.03

Toward Noninvasive Simultaneous Arterial and Venous Oxygenation Monitoring with an Optical E-Tattoo[Nanshu Lu](#); The University of Texas at Austin, United States

While noninvasive arterial blood oxygenation (SaO₂) is easily estimated using peripheral pulse oximeters, noninvasive venous blood oxygenation (SvO₂) monitoring is still a critical unmet

medical need. Critical conditions that lead to inefficient extraction of oxygen from the blood, such as sepsis or shock, can only be detected by analyzing the oxygen content of the venous blood. A fundamental assumption of photoplethysmography (PPG) and pulse oximetry is that only the arterial blood induces a pulsatile or alternating current (AC) signal. As a result, by analyzing only the pulsatile absorptivity changes of the tissue, arterial blood oxygenation alone will be isolated. However, this assumption may not hold outside of peripheral vasculature. Recent work has suggested that a venous pulse can be measured with a reflectance PPG probe placed over the jugular vein. A significant obstacle for simultaneous SaO₂ and SvO₂ extraction is the anatomic proximity of the artery and vein, thus leading to crosstalk. We characterize this crosstalk with simulation, in vitro, and in vivo experiments. We have devised a soft wearable optical e-tattoo sensor that simultaneously measures the arterial and venous pulses and used it to characterize how the PPG waveform morphology changes when the PPG sensor is shifted laterally over the carotid artery and jugular vein. We hypothesize that the venous and arterial pulses can be used to simultaneously extract SaO₂ and SvO₂, thus enabling noninvasive oxygen consumption estimation. This work offers a potential solution for minimizing the crosstalk through spatial filtering.

2:30 PMBREAK

3:30 PM *EL05.07.04

Flexible Integrated Photonics for On-Chip Sensing Based on Cascaded FSR-Free Cavities LanLi¹, YeLuo¹, ChunleiSun¹, MaoliangWei², HuiMa², ZequnChen¹, JialingJian¹, JunyingLi², KathleenRichardson³ and HongtaoLin²; ¹Westlake University, China; ²Zhejiang University, China; ³University of Central Florida, United States

High spatial resolution mechanical sensing within compact 3D space is important in healthcare, industrial automation, aerospace engineering, and intelligent robotics. Flexible optical sensors have received increasing attention due to their high sensitivity and measurement accuracy, electromagnetic interference immunity, and ability to conform to three-dimensional shapes. Compared to fiber and free-space flexible mechanical sensors, waveguide-integrated sensors exhibit superior performance due to their compact footprint, excellent sensitivity, high spatial resolution, scalability, and integration capability with electronics and other functional components. Here, we present a new flexible photonic integrated sensor concept that utilizes cascaded one-dimensional (1D) photonic crystal (PhC) micro-cavities. Due to the free-spectral-range (FSR) merit of the cascaded cavities, which eliminates restrictions on wavelength spacing, wavelength-division multiplexing technology has been utilized to fully utilize a wide band of optics. Additionally, mechanical sensing signals, like strain and position information, can be embedded into wavelength-dependent resonant dips, facilitating high spatial resolution quasi-distributed-strain sensing and two-dimensional shape sensing. The integrated photonic sensors exhibit ease of scalability, high sensitivity, and compact footprint, holding novel opportunities for on-chip and conformal sensing with high sensitivity and spatial resolution.

4:00 PM *EL05.07.05

Soft, Flexible and Biocompatible Technologies for Optical Sensing and Stimulation in Biomedical Applications JeroenMissinne¹, XavierDe Becker¹, FedericoPazzaglia¹, WouterVan Lysebetsens¹, AnastasiiaBabych^{1,2}, JeroenSpanoghe², MarijkeVergaelen², RobrechtRaedt², PieterBauwens¹, SandraVan Vlierberghe², JanVanfleteren¹ and GeertVan Steenberge¹; ¹Imec and Ghent University, Belgium; ²Ghent University, Belgium

Light-based therapies and optical sensing are rapidly gaining interest in the biomedical field. Currently, new therapeutic or diagnostic concepts are mainly relying on relatively large optical components made of standard rigid materials. For example in preclinical research, silica optical fibers are used for light delivery to and from brain tissue for both biosensing (fiber photometry, optoacoustic imaging,...) and therapy (optogenetics, optopharmacology,...). However, to bring these techniques to a clinical setting, the required technologies need to be made more biocompatible. Currently, chronic implantation of rigid large probes evokes gliotic scar formation, demyelination and neuronal loss near the probe. In addition, these biological responses have a negative influence on the efficacy and durability of triggered interventions. Therefore, small and soft probes are needed to limit gliotic scarring and cellular damage upon probe implantation. We address this need by developing miniaturized, soft wearable and implantable technology.

We give an overview of our technologies for realizing soft waveguides allowing guiding light to stimulate deeper regions (e.g. in the brain), and technologies for integrating miniature sources and detectors on flexible foils allowing non-invasive stimulation or on-body sensing.

To match mechanical properties of tissue, we investigate several (optically transparent) waveguide materials, ranging from 'standard' optical polymers (e.g. Ormocers®, epoxies), polydimethylsiloxane (PDMS), to ultra-soft hydrogels. Depending on the material of choice, and waveguide design (single mode or multimode), standard lithography, laser direct-write lithography, soft-lithography or moulding techniques are being used. We will report on planar multimode (stretchable) PDMS waveguides with low propagation loss for operation from near-UV (405nm), over visible, up to near-infrared wavelengths and planar single mode waveguides made of hybrid UV-curable polymers (OrmoClear®). Furthermore, the optically clear hydrogel materials that are under development (tuning mechanical, optical, biological properties) will allow even further improvements in softness of implantable waveguides.

While softness and flexibility are desired for long term implantation, a higher rigidity is required to successfully implant the probes. We are tackling this challenge from different angles, i.e. from the material science side (e.g. smart coatings) and the technological side (e.g. implantation aids).

For future wearable operation, implantable waveguides will need to be equipped with recording electrodes, driving electronics and light sources. Our focus is on combining such light sources in the least obtrusive way together with the flexible waveguides relying mainly on thin bare die (e.g. LEDs and VCSELs) integration on flexible foils. Similar in-house technologies can be applied to integrate the electrodes and driving circuitry. Alternatively, without waveguides, such patches can serve as standalone phototherapeutic minimally invasive flexible devices (e.g. for cortical stimulation or for skin monitoring).

Although the presented soft technologies have a wide applicability, our current focus is on optogenetic or optopharmacologic therapies of the brain e.g. in the context of epilepsy.

4:30 PM EL05.07.06

Flexible Carbon Nanotube-Based Optical Sensor Sheet Integrated with Ultra-Thin Organic Circuits ReiKawabata^{1,1}, KouLi², TeppeiAraki^{1,1}, MihokoAkiyama^{1,1}, NorikaTakahashi², DaikiSakai², YutoMatsuzaki², MinamiYamamoto², LeoTakai², YutoAoshima², NozomiMatsuoka^{1,1}, NaokoKurihira¹, TakafumiUemura¹, YukioKawano^{2,3} and TsuyoshiSekitani^{1,1}; ¹Osaka University, Japan; ²Chuo University, Japan; ³National Institute of Informatics, Japan

Flexible optical sensors have attracted considerable attention in the development of wearable and shape-adaptable devices for health monitoring, non-invasive inspection, and biochemical analysis [1–5]. This study develops an ultra-flexible optical sensor using carbon nanotube (CNT) films and organic circuits to detect wavelengths from near-infrared to THz. Owing to their formation on ultra-thin polymer substrates, the CNT films demonstrate a 21-fold increase in sensitivity when compared to those fabricated on rigid thick substrates; further, they exhibit durability against bending and crumpling. The CNT films are connected to organic circuits comprising organic thin-film transistors (OTFTs), with which CNT signals are selected and amplified. The functional CNT films are integrated into a flexible optical sensor as an active matrix, facilitating internal imaging from any surface using a broadband light, including THz. Flexible photodetectors have been intensively developed in recent years; for example, thin-film inorganic semiconductors, metal halide perovskites, and organic semiconductors have been employed as photodetector materials, demonstrating excellent sensitivity and flexibility [2–4]. While these flexible photodetectors are limited to detecting ultra-violet to near-infrared light, the detection of mid-infrared to THz for non-invasive inspection and chemical analysis is crucial. To address this issue, CNTs have garnered significant attention as flexible photodetectors; they can detect a broad range of electromagnetic waves (from visible light to millimeter waves) using the photothermoelectric effect at room temperature [5,6]. However, CNT optical sensors have been developed predominantly as single-element or small-scale sensors with low integration density. These types of sensors require signal processing via external circuits and spatial scanning for highly sensitive imaging, thereby limiting their portability, scalability, and scanning speed for imaging devices.

In this study, CNT films are fabricated on ultrathin Parylene substrates and exhibit broadband optical response from near-infrared to THz. The CNT films exhibit a 21-fold increase in sensitivity when compared with those on thick rigid substrates owing to the suppression of heat diffusion by an ultra-thin film. Furthermore, the photoresponse of CNT films is stable after bending and crumpling. The CNT films are connected to an organic amplifier and a matrix circuit that is constructed using OTFTs with the channel layer of dinaphtho [2,3-b:2',3'-f]thieno [3,2-b]thiophene. The organic amplifier circuit exhibits a 10-fold gain and successfully amplifies the THz detection signals. Finally, the active matrix is designed for a flexible broadband imager for non-invasive internal inspection from the surface of an object.

[1] Y. Luo, et al., ACS Nano 17 5211–95 (2023)

[2] Z. Rao, et al., Nat. Electron. 4 513–21 (2021)

[3] W. Wu, et al., Adv. Mater. 33 2006006 (2021)

[4] G. Simone, et al., Adv. Funct. Mater. 30 1904205 (2020)

[5] K. Li, et al., Sci. Adv. 8 eabm4349 (2022)

[6] M. Zhang, et al., ACS Nano. 13 13285-92 (2019)

8:15 AM *EL05.08.01

Stretchable Light-Emitting Polymers and OLEDs Based on Thermally Activated Delayed Fluorescence (TADF)[Sihong Wang](#); The University of Chicago, United States

The vast amount of biological mysteries and biomedical challenges faced by humans provide a prominent drive for seamlessly merging electronics with biological living systems (e.g. human bodies) to achieve long-term stable functions. Towards this trend, one of the key requirements for electronics is to possess biomimetic form factors in various aspects for achieving long-term biocompatibility. To enable such paradigm-shifting requirements, polymer-based electronics are uniquely promising for combining advanced electronic functionalities with biomimetic properties. Among all the functional materials, stretchable light-emitting materials are the key components for realizing skin-like displays and optical bio-stimulation. In this talk, I will mainly introduce our research in imparting stretchability onto "third-generation" electroluminescent polymers that can harness all the excitons through thermally activated delayed fluorescence (TADF), thereby with a theoretical near-unity quantum yield and high OLED efficiency. Our developments of fully stretchable OLED devices show the promise of achieving all the desired EL and mechanical characteristics, including high efficiency, brightness, switching speed, stretchability, and low driving voltage.

8:45 AM EL05.08.03

Structural Inclination for Next-Generation Mechano-Responsive Smart Windows[Haomin Chen](#)¹, [Gunho Chang](#)², [Taehee Lee](#)², [Kwonhwan Ko](#)², [Seokhwan Min](#)², [Jonghwa Shin](#)², [Jung-Wuk Hong](#)² and [Seokwoo Jeon](#)¹; ¹Korea University, Korea (the Republic of); ²Korea Advanced Institute of Science and Technology, Korea (the Republic of)

By implementing smart window technologies to regulate temperature and lighting conditions, an estimated 50% reduction in energy consumption for building services can be achieved. Promising candidates for smart windows are mechano-responsive membranes that exhibit tunable transmission through strain-controlled light scattering.

However, the state-of-the-art light scatterers have encountered a bottleneck. Achieving appreciable contrast still necessitates large strains which require additional space, occupying more than 15% of the original window area. Furthermore, recent improvements in contrast and strain reduction have come at the cost of complexity in composition and fabrication. Therefore, a new design principle is urgently needed to simultaneously achieve high visibility, strong regulation of irradiation, low operational lateral strains, and simplicity in composition and fabrication at a low cost.

One potential solution lies in manipulating pore sizes within a 3D structure through out-of-plane compression. The reversible opening and closing of pores provide the scatterer with opacity when released and transparency when compressed, accommodating changes in the in-plane area. This working mechanism inherently addresses the issue of large areal changes. The performance of a compression-driven scatterer relies on the optical density in the released state and its sensitivity to compressive strains. To tackle this, submicron 3D structures with inclined pores are proposed for the new scatterer. The array of submicron pores induces strong multiple scattering of visible light, resulting in a high optical density in the released state and thus a high achievable transmittance contrast. A novel 3D patterning technique based on a slanted exposure angle enables the realization of tailorable inclination angles in submicron structures. Experimental and multi-physics simulation results demonstrate that the inclined structures redistribute local compressive strains, facilitating pore closure and significantly increasing transmittance for a given compression. Scatterers based on the inclined 3D structures achieve high transmittance of 96% and an unprecedented transmittance contrast of 95%, all while experiencing minimal areal strains during operation. Compared to conventional driving modes, the out-of-plane compression mode brings the scatterer closer to practical use, enabling localized modulation of transmittance by selectively compressing specific positions of the scatterer that need to be transparent. The design principle and fabrication technique presented in this work for the compressive strain-responsive scatterer are expected to drive advancements in smart windows, transparent displays, and flexible pressure sensors.

9:00 AM EL05.08.04

Highly Efficient UV-Absorbing and Anti-Reflective PDMS Film for Improving Stability of Perovskite and Organic Photovoltaics[Han bin Lee](#) and [Hyo Jung Kim](#); Pusan National University, Korea (the Republic of)

Perovskite solar cells and polymer-based organic solar cells (OSCs) have emerged as promising next-generation solar cell technologies due to their high efficiency, utilization of low-cost materials, and large-area fabrication capabilities. Despite these advantages, the commercialization of these solar cells faces significant challenges, primarily concerning module reliability and lifespan. Notably, both perovskite solar cells and OSCs exhibit high sensitivity to the surrounding environment, including heat, moisture, and UV rays. Exposure to UV light has been identified as a cause of decomposition in perovskite solar cells, leading to the generation of ionized lead and interfacial separation. Additionally, UV light exposure has been associated with a burn-in phenomenon in organic solar cells. The importance of UV light blocking to prevent degradation has been reported through many research results. Hence, it is imperative to ensure stability against UV rays in order to successfully commercialize next-generation solar cells. Recently, the integration of UV-blocking materials into coatings and films has emerged as a promising strategy to address this issue of stability by effectively blocking UV light. Despite the significant improvement in a device, it leads to unavoidable photoconversion energy loss by blocking the UV region light. Consequently, the concept of blocking UV for stability requires additional techniques for keeping high photoconversion efficiency.

To overcome the inherent problem in this concept, we suggest an easily detachable multifunctional film for UV blocking without photoconversion energy loss. The multifunctional film was fabricated by incorporating a UV-blocking material (2,2'-dihydroxy-4-methoxybenzophenone) with polydimethylsiloxane (PDMS). By incorporating a UV absorber into the PDMS film, we could successfully block UV region light (< 380nm). As mentioned, the UV blocking induced the decrease of PCE of perovskite solar cells by 3.2% compared with reference cells. The decrease in PCE was compensated by the light-trapping effect from the surface texturing of the PDMS films. For the surface texturing, we used the soft lithography technique using a structured Si mold through Cu-assisted chemical etching. The light trapping effect was estimated by FDTD simulation and confirmed by the optical properties of textured films. The reflectance of structured PDMS decreased by ~ 4% compared with a flat PDMS surface. To increase the transmittance of the visible light region, we designed double-layered PDMS films, i.e., pure PDMS layer/UV block material embedded PDMS layer films. Our final multifunctional film was attached to the glass side of perovskite solar cells and showed 0.8% increased PCE compared with the reference cell. The UV-blocking effect was confirmed by 20 days test (10 days outdoor + 10 days UV irradiation). The solar cells with multifunctional PDMS films retained over 87% of their initial efficiency after 20 days test, in contrast to the rapid UV degradation observed in solar cells without the UV-blocking PDMS film.

9:15 AM EL05.08.05

Dynamic, Remote-Controllable Electroactive Hydrogel Waveguide Architectures[Oscar Alejandro Herrera Cortes](#); McMaster University, Canada

Remote-controllable waveguide architectures inspired by living organisms with unique flexible, camouflage and light guiding properties, were fabricated using self-trapped beams of incoherent light. Made of electroactive hydrogels, light-guiding structures are generated through a nonlinear, self-inscription process that utilizes visible beams from light-emitting diodes (LEDs). Due to irreversible refractive index changes experienced by photoinduced chemical reactions, these self-trapped beams permanently inscribe cylindrical waveguides along their paths. Taking advantage of this phenomena, we can fabricate macro-scale remote controllable waveguide structures in the form of planar rectangular prisms and arrays of cylindrical waveguides. We can also fabricate micro-scale structures for remote actuation, in the form of rectangular prisms embedded with thousands waveguide units. By applying and varying external electric fields, we can dynamically control the bending, angular orientation, and rotation (up to 360°) of these pliant light-guiding structures. This allows precise, remote control of the waveguided light output.

9:30 AM BREAK

10:00 AM EL05.08.06

3D-Structured Soft Microwave Plasmonic Resonators via Direct Ink Writing of Stretchable Conductors[Hoon Yeub Jeong](#) and [Seungjun Chung](#); Korea Institute of Science and Technology (KIST), Korea (the Republic of)

Beyond previous physical contact-based sensing technologies, emerging wireless sensing has gained significant interest in wearable electronics applications, particularly in monitoring human motion and acquiring data. However, existing wireless sensor systems face reliability and stability concerns when monitoring dynamic human motion due to the prevalent use of rigid integrated circuits (ICs) and wireless modules, along with complex wiring of electronic components. In this regard, developments of skin-attachable wireless sensor systems integrated with soft components are highly desirable. Recently, 2-dimensional (2D) flexible plasmonic resonators have been proposed to skin-attachable wireless sensors, but the coupling of their resonance to the lossy medium prevent from forming the robust resonances. Besides, additional initial calibration process is required due to the different dielectric properties of each individual and attached part. To address these challenges, we propose a novel approach: fully soft 3-dimensional (3D) plasmonic resonator structures enabling decoupled resonance from lossy substrates and the human body, thereby demonstrating reliable wireless sensing onto the human body.

In contrast to conventional 2D plasmonic resonators, our 3D plasmonic resonator structures allow resonance formation in a lossless free space. This achievement can be advanced by introducing an additional ground plane at the bottom of the resonators, enabling a perfect decoupling between the resonance and the lossy medium. Furthermore, we employ omnidirectional 3D printing to realize these 3D soft resonators using intrinsically stretchable conductor composites. Their composition and rheological properties were optimized to ensure that the conductivity and mechanical robustness of the stretchable conductor should be high enough to formulate high-quality factor resonance under mechanical deformation. Moreover, for the structural integrity of 3D free-form printed features, we introduced the emulsion phase into the conductive composite ink that achieves high storage modulus and yield stress, so the printed

resonators can maintain their own shapes after printing. In addition, high conductivity (10,000 S/cm) and low resistance variation during stretching (1.5 at 100 % strain) were successfully achieved by optimizing the ink formulation. This innovative material and fabrication method enables us to realize miniaturized free-form 3D resonator structures, which exhibit superior functionality and a high degree of design freedom compared to conventional 2D resonator structures.

We demonstrate highly robust wireless wearable strain sensors based on fully soft 3D microwave plasmonic resonators. The decoupling of resonance ensures that the resonant frequency shifting of these sensors is solely perturbed by geometric parameters, thereby enabling stable wireless strain sensing. A key merit of this approach is eliminating the initial calibration process, and compensating different dielectric properties among individuals or attachment parts. Our works will pave a promising pathway to develop lossless microwave metamaterials and resonators in wearable electronics, and we will present the state-of-the-art results of 3D-printed free-form plasmonic resonators opening up new avenues for highly efficient wireless sensing of human motion.

10:15 AM EL05.08.07

Unlocking Transparency in 3D Printing of Polysiloxanes Michael Ford, Colin Loeb, Lemuel X. Pérez Pérez, Stuart Gammon, Hawi Gameda, A. Melody Golobic, August Honnell, Justin Erspamer, Eric B. Duoss, Tom Wilson and Jeremy M. Lenhardt; Lawrence Livermore National Laboratory, United States

Silica-polysiloxane inks have been developed for 3D printing, but their opaqueness has limited their potential in some applications. We addressed this limitation by precisely adjusting the base polysiloxane composition to achieve transparency. When solidified, these inks transmit about 90% of 700 nm light through 1 cm, showcasing useful transparency. We explored the dependence of the ink's rheological properties on silica particle distribution, showing that these properties are influenced by silica functionality, weight content, and processing. This understanding enables precise control over printing and object quality. Furthermore, our research also unveiled a thermochromic effect, where ink opacity changes with refractive index mismatch and temperature. This effect was explored in further detail and will be highlighted in this talk. To demonstrate practicality, we successfully printed encapsulants for LEDs, scintillators, and microfluidic mixing devices. These transparent inks find applications in advanced lighting and cutting-edge medical devices.

This work was performed under the auspices of the U.S. Department of Energy by Lawrence Livermore National Laboratory under Contract DE-AC52-07NA27344. LLNL-ABS- 850030

10:30 AM EL05.08.08

Polymer-Based 4D-Printed Fresnel Lenses for Thermal Sensing Applications Murad Ali and Haider Butt; Khalifa University of Science and Technology, United Arab Emirates

The demand for additive manufacturing is on the rise in the optical industry. Notably, 3D printing overcomes the majority of the limitations inherent in traditional processes. 3D printing allows for the rapid and cost-effective design and fabrication of complex geometries. Here, we demonstrate the fabrication of polymer-based functionalized optical devices (4D Fresnel lenses) for the first time using a computer-aided design for 3D printing based on the digital light processing (DLP) technique. The fourth dimension is introduced by adding the thermochromic pigment powders (blue, green, and red) to a transparent resin that utilizes spectral color response to variations in temperature as an external stimulus. The thermally active powder added two functionalities to Fresnel lenses: selective color filtering at room temperature and thermal sensing (25°C to 32°C). Using homemade experimental setups, the printed lenses were assessed for light focusing performance and thermal sensing. Contact angle measurements revealed the hydrophilic nature of the lens material, while XRD confirmed no other phase formation during photopolymerization. The surface topography of lenses was investigated using scanning electron microscopy (SEM) and atomic force microscopy (AFM) characterizations that confirmed the surface integrity of our printing process (often used for lenses, $\lambda/4$ to $\lambda/10$). As a potential alternative to traditional optical devices, such as glass Fresnel lenses, 3D printing offers custom-built polymer-based optical devices with optimized materials for optical sensing applications.

<quillbot-extension-portal></quillbot-extension-portal>

10:45 AM *EL05.08.09

A Novel Electrochromic Platform that Integrates Dielectric Elastomers and Photonic Glasses Ming Xiao; Sichuan University, China

Electrochromic materials can change colors upon a voltage, which are based on either pigmentary or structural colors. The color changes of pigments originate from changes of absorption bandgap due to electrochromic redox reactions, while the structural color changes are caused by voltage-driven rearrangements of colloidal particles. So far, both types of electrochromic materials involve currents running through the materials and side electrochromic reactions, which limits cycling and performance lifetime. To address this issue, we develop all solid electrochromic materials by integrating dielectric elastomers and structural colors. We assemble colloidal particles in elastomers in ordered (photonic crystals) and disordered (photonic glasses) patterns to produce structural colors. With the voltages on, opposite charges accumulate on the two surfaces of elastomer composites, creating a Maxwell force to compress the elastomer without any currents running through the materials. The elastomers expand in area and shrink in thickness, leading to variations in spacing between colloidal particles and thus color changes. We achieve dramatic, rapid, and reversible color changes up to 10 Hz. The color of the photonic glass elastomer is not angle-dependent as typical photonic crystals. This avoids inhomogeneous colors when new curvatures are created with out-of-plane deformations, like wrinkling or buckling. To reduce the voltage and expand the color change range, we fabricate elastomer composites with lower modulus (~150 kPa) and higher stretchability (~250%) using lower volume fraction of silica nanoparticle and introducing a secondary aliphatic acrylate precursor into the matrix. We believe this novel electrochromic material will find wide applications in wide-angle color display, color-changing robots, military camouflage, and smart windows.

11:15 AM EL05.08.10

Unravelling the Governing Factors for Cholesteric Self-Assembly of Polysaccharides Cecile Chazot, Simona G. Fine and Eleanor C. Grosvenor; Northwestern University, United States

Thanks to their earth abundance and their ability to self-assemble in photonic crystals that can selectively reflect circularly polarized light, cholesteric polysaccharides have been investigated as the basis for colorimetric sensors responding to humidity, pressure, temperature, and other stimuli. However, cholesteric self-assembly requires a gel-like state, achieved by suspending the biopolymer in a strongly hydrogen-bonding solvent. Efforts to stabilize the cholesteric order in the solid-state have relied on controlled solvent evaporation or polymerization. However, the effects of polysaccharide chemistry and solvent-polymer interaction on the formation and solid-state retention of the cholesteric phase remain understudied. In this talk, we explain how different thermodynamic and chemical factors influence the self-assembly and optical properties of cholesteric mesophases constructed from suspensions of polysaccharides, such as cellulose ethers. Through a systematic data analysis framework we developed, we elucidate structure-property relationships linking solubility, viscosity, and hydrogen bonding to the cholesteric pitch and resulting optical properties. Then, we discuss how chemical factors such as molecular weight and repeat-unit chemistry affect kinetics of liquid-crystalline self-assembly and stabilization of the cholesteric order in a solid form. These relationships are expected to assist in the large-scale deployment of polysaccharide-based sensors with direct colorimetric assessment of temperature, mechanical strain, or humidity.

SESSION EL05.09: Soft Optical Emitters and Detectors

Session Chairs: Michael Ford and Juejun Hu

Thursday Afternoon, November 30, 2023

Hynes, Level 2, Room 203

2:00 PM *EL05.09.01

Soft Matter Infrared Photodetectors Jarrett Vella¹, Anthony Benasco² and Stefan Nikodemski³; ¹Air Force Research Laboratory, United States; ²NRC RAP at Air Force Research Laboratory, United States; ³KBR, United States

Infrared detection in the shortwave (1000-3000 nm), midwave (3000-5000 nm) and longwave (8000-14000 nm) regions has traditionally been dominated by compound semiconductors such as indium antimonide and mercury cadmium telluride, among others. These materials must be epitaxially grown and cooled to cryogenic temperatures before use. Alternative materials such as strained layer superlattices that are thermoelectrically cooled have been developed but still have complex and costly deposition processes. We have developed a new class of infrared photoconductive detectors active between 1000-14000 nm using disordered, soft matter semiconductors: conjugated polymers. Using both solution processing and vapor phase deposition, conductive polymers with direct, shortwave infrared bandgaps or degenerately doped effective bandgaps have been incorporated into IR detectors whose performance approaches that of inorganic compound semiconductor-based devices, but at room temperature and with no optimization. We have observed several unique morphologies, ranging from solid films to intercalated wires to isolated platelets, all of which function as effective infrared detectors for blackbody radiation. An extensive study was also undertaken to understand how deposition parameters affect electronic transport properties in the photoconductive films.

1. J. H. Vella, A. R. Benasco, S. Nikodemski, M. I. Vakil, and J. D. Azoulay, *Macromol. Rapid Commun.* **2023**, accepted.
2. J. H. Vella, S. Nikodemski, A. R. Benasco, T. A. Prusnick and V. Vasilyev, *Synth. Met.* **2023**, 293, 117277.
3. J. H. Vella, L. Huang, N. Eedugurala, K. S. Mayer, T. N. Ng and J. D. Azoulay, *Sci. Adv.* **2021**, 7, eabg2418.

2:30 PMBREAK

3:00 PM EL05.09.02

Morphology-Directed Light Emission from Fluorescent Janus Colloids for Pathogen SensingBradley D. Frank¹, Agata W. Baryzewska¹, Sara Nagelberg², Mathias Kolle² and Lukas Zeininger¹; ¹Max Planck Institute of Colloids and Interfaces, Germany; ²Massachusetts Institute of Technology, United States

Pathogen sensors which are accurate, sensitive, cost-efficient, quick, and with minimal training are a continuing healthcare need. The chemical orthogonality of Janus droplets connects nano-scale chemical events into a structural response that is sensitive, inexpensive, and quick. Utilizing this chemo-morphological coupling, the detection of e.g., antibodies, pathogens, enzymes, PFAS, and metal ions, have been reported. While the connection between environmental change and droplet morphology is established, a method for simple and quick measurement of polydisperse samples is required, which would enable the deployment of Janus emulsion-based sensors without the need for precise droplet generation. Spherical Janus colloids with a morphology-tunable interface can totally internally reflect light dependent on morphology. Gravity-aligned Janus droplets with an internal refractive index contrast induce environmental and structural effects that contribute mutually to programmable optical behaviors. We investigate total internal reflection at the internal droplet interface, and the resulting morphology-determined anisotropy of both incident and emissive light. Using this angular emission, we present a ratio-metric sensing scheme to measure monolayers of polydisperse emulsion droplets responding to their chemical environment. Using this ratio-metric sensing scheme, these droplets were successfully used to detect three pathogenic bacteria from polydisperse emulsion droplets generated on-site, selectively, sensitively, and quickly. The reference-free detection of droplet morphology from macro-scale measurement has implications for the transduction of many existing surfactant chemistries. Further understanding of directed anisotropic emission by spherical colloids has broad implications for the translation of nano-scale physical or chemical events into readily available macro-scale information.

3:15 PM EL05.09.03

Photoclickable Biopolymer for Soft, Spectrally-tunable and Reconfigurable Fluorescent Optical PatterningNicholas A. Ostrovsky-Snyder, Amanda Code and Fiorenzo Omenetto; Tufts University, United States

Patterned fluorescence has many applications in cell-tracking, fiducial markers and cryptography. Incorporating fluorescent patterning into soft and non-planar optics can be challenging with current rigid optical materials and planar fabrication techniques. Silk fibroin is a soft biomaterial that is highly transparent in the visible range with fair transmission in the near-UV and near-IR, and as such has been a proven optical material for waveguides, diffractive and refractive optics, photonic crystals and more¹. To make a patterned fluorescent material silk can be functionalized with methacrylate groups that allow it to participate in 2,5-diaryl tetrazole photoclick reactions. These photoclick reactions are catalyst-free, light-mediated, "click" reactions that produce highly fluorescent pyrazoline adducts from non-fluorescent reactants². In this work we have synthesized a library of photoclick-able tetrazoles with varying emission characteristics and environmental responses and integrated them into soft silk-based materials including films, hydrogels and nanoparticles. These materials display intense fluorescence and can be both implanted and patterned within biological media. The tunable secondary structure conformations of silk provide further control of the patterning, with selective wettability enabling diffusion restriction of the tetrazoles which act as a physical masking process. Alternatively, the intentional formation of di-tyrosine crosslinks acts in an auto-masking function to create soft and conformal photomasks well-tuned to the tetrazole excitation wavelength. The interplay of these mechanisms allows us to achieve complex multispectral patterns in multiple material formats of broad utility.

1. G. Guidetti, L. d'Amone, T. Kim, G. Matzeu, L. Mogas-Soldevila, B. Napier, N. Ostrovsky-Snyder, J. Roshko, E. Ruggeri, F. G. Omenetto, *Applied Physics Reviews*. **9**, 011302 (2022).
2. V. Pirota, A. Benassi, F. Doria, *Photochem Photobiol Sci.* **21**, 879–898 (2022).

3:30 PM EL05.09.04

TDDFT Study of Light Emitting Materials in OLEDsNobuhiko Akino; Hosei University, Japan

Recently, organic light emitting diodes (OLEDs) have been utilized in smartphones, large-size displays and solid-state lightings due to their desirable characteristics such as self-emission, high-speed response, light weight and so on. For the light emitting materials in OLEDs, the emission spectrum profile is one of the most important material properties as it determines not only the emission color, but also the device efficiency. Especially for the display applications, the material with sharp spectral profile is essential to achieve a better color gamut and also to avoid any loss by the energy filter. Hence, it has been highly desired to simulate the spectrum profile, that is, not only the peak wavelength of absorption and/or emission, but also its overall spectrum shape.

In order to study the spectrum profile of materials, the time dependent density functional theory (TDDFT) has been employed [1]. This is one of the most prominent and widely used methods for calculating excited states of medium-to-large molecules, and it is recognized as a powerful tool for studying electronic transition of molecules. The TDDFT code used in this study is based on the real-space and real-time (RSRT) formalism [2]. One of the advantages of this real-space and real-time formalism is that one can keep the code simple and understand physical meanings as directly as possible. Since this formalism is suitable for large-scale parallel computing, its MPI parallelized code has been developed and be applied to large molecules depending on the computer resources. Furthermore, the use of maximum entropy method has also been studied to extract spectrum peak information with limited real-time data [3].

This RSRT approach has been applied to some typical organic materials such as poly-(9,9'-dialkyl-fluorene) as a fluorescent material, tri(2-phenylpyridinato)iridium(III), Ir(ppy)₃, as a phosphorescent material, and 4CzIPN and DABNA-1 as a thermally activated delayed fluorescent (TADF) materials. The results have been suggesting that although some redshift of the peak wavelength is observed, the simulated spectral profiles agree very well with the experimentally observed profiles [4,5].

In the presentation, with utilizing both the RSRT-TDDFT and commercial quantum chemical software, TADF molecules will be studied in order to obtain design rules and possibly new molecules with desired spectrum profile in RGB region.

REFERENCES

- [1] E. Runge and E. K. U. Gross, *Phys. Rev. Lett.* **52**, 997 (1984)
- [2] K. Yabana and G. F. Bertsch, *Phys. Rev.* **B54**, 4484 (1996)
- [3] M. Toogoshi, S. S. Kano, Y. Zempo, *J. Phys.: Conf. Series.* **510**, 012027 (2014)
- [4] N. Akino and Y. Zempo, *J. Phys.: Conf. Ser.* **2207** 012039 (2022)
- [5] N. Akino, *MRS Advances* **7**, 310(2022)

3:45 PM EL05.09.05

Interfacial Triboelectricity Lights Up Phosphor-Polymer Elastic Composites: Mechanism of Bright Unwearying Mechanoluminescence in ZnS Microparticle-Embedded PDMS FilmsSung Jun Lim and Soon Moon Jeong; Daegu Gyeongbuk Institute of Science and Technology, Korea (the Republic of)

The composite of copper-doped zinc sulfide phosphor microparticles embedded in polydimethylsiloxane elastic polymer (ZnS:Cu-PDMS) has received significant attention over the past decade due to bright and durable mechanoluminescence (ML), but the underlying mechanism of this unique ML remained largely unclear. Here, we present a set of empirical and theoretical findings which prove that the ML of ZnS:Cu-PDMS composite is an electroluminescence (EL) of ZnS:Cu phosphor microparticle induced by triboelectricity generated at the interface of ZnS:Cu microparticle and PDMS matrix. We found that ZnS:Cu microparticles exhibiting bright ML are coated with alumina (AlO_x), an oxide with strong positive triboelectric properties, and the friction between this oxide coating and PDMS, a polymer with strong negative triboelectric properties, produces interfacial triboelectricity sufficient to turn on the EL of ZnS:Cu microparticles. Moreover, when changing the composition of this interface, the composite ML varies in a way that the ML intensity is proportional to the amount of interfacial triboelectricity. Based on these findings, we suggest a theoretical model that elucidates the ML process of phosphor-polymer elastic composite. Understanding such a mechanism will play a crucial role in exploring and advancing new materials beyond the ZnS:Cu-PDMS systems to achieve brighter and more durable ML composite systems.

8:15 AM EL05.10.01**Multimaterial 3D Printing Process for Color Blindness Correction Contact Lens Production** [MuhammedHisham](#) and HaiderButt; Khalifa University, United Arab Emirates

Multimaterial 3D printing is an emerging technology that allows for the production of 3D printed objects with controlled variations in material composition and properties. However, there have been very few studies on the use of multimaterial 3D printing for optical devices. In this work, a novel multimaterial 3D printing method is presented for the production of contact lenses with color blindness correction capabilities. The method utilizes vat-photopolymerization 3D printer and employs CAD file modifications along with a pause-material change step to enable material change within the contact lens. Using this method various dyes can be deposited at different regions within the contact lens in required patterns. Atto-565 and Atto-488 dyes were utilized for red-green and blue-yellow color blindness correction respectively. A suitable combination of hydroxyethyl methacrylate (HEMA) and polyethylene glycol diacrylate (PEGDA) served as the base resin for 3D printing. Good quality hydrogel contact lenses were obtained after 3D printing. The water absorption behavior, mechanical properties and surface quality of the contact lenses were evaluated. Good mechanical and material characteristics were observed for these lenses. Both Atto-488 and Atto-565 dyes were highly stable and did not leak from the crosslinked hydrogel matrix. Multimaterial contact lenses containing both dyes were found to be suitable for simultaneously correcting two types of color blindness. The contact lenses had light absorption spectra that closely matched commercially available color blindness correction glasses. The phenomenon of interface formation due material change was studied in detail and ways to reduce its intensity were explored. Contact lenses with dyes deposited in intricate patterns were also 3D printed, demonstrating the advanced capabilities of this technique. Multimaterial 3D printing enables the production of highly efficient aesthetically pleasing contact lenses with customizable color blindness correction capabilities.

8:30 AM *EL05.10.02**Soft Optical Fibers Made of Agar** [EricFujiwara](#)¹, [HiromasaOku](#)² and [CristianoM. Cordeiro](#)¹; ¹University of Campinas, Brazil; ²Gunma University, Japan

Biodegradable optical waveguides are emerging technologies for light delivery and sensing in various in-vivo applications, such as imaging systems, optogenetics, and the surveillance of intra-body parameters. In this context, agar extracted from red algae is a promising low-cost, renewable, and edible material for developing optical devices with remarkable characteristics, such as transparency, flexibility, moldability, and thermal reversibility.

This work introduces biocompatible optical fibers fabricated by pouring melted agar solutions into cylindrical molds. The solidified waveguides assume the mold geometry, allowing the manufacture of assorted waveguides, including no-core and structured holey fibers. Furthermore, the refractive index and mechanical strength are tailorable by choosing the agar concentration or adding glycerol to the precursor. Cutback tests with a 2 wt% agar, 60 wt% glycerol fiber revealed optical losses of ~0.8 dB/cm at 633 nm, comparable to waveguides made of typical biopolymers.

Subsequently, we investigate the ability of agar optical fibers to perceive physical and chemical stimuli. A coherent light excites multiple fiber modes due to the core dimensions, creating an output speckle field whose spatiotemporal distribution transcribes the fiber state. Besides traditional bending and strain measurements, one may explore the agar's swelling and syneresis behaviors to evaluate humidity, temperature, and its degradation over time. The electrical conductivity of agar also establishes current-driven modulation of the optical response. Moreover, the holey structure of agar waveguides can transport fluids and provide refractive index detection through interaction with the core modes.

The developed agar-based optical fibers are customizable, easy to fabricate, and exhibit versatile sensing capabilities, which inspires several applications as a biocompatible and degradable probe for medical, biochemical, and environmental measurements.

9:00 AM EL05.10.03**Simulation of Anisotropic Thermal Expansion Coefficient of Liquid Crystal Networks using Dreiding-Force Field** [Wei TingHsu](#), Yun HsiangChang, Nien JungChiang and Yu ChiehCheng; National Taipei University of Technology, Taiwan

The study presents molecular dynamics simulations employing the Dreiding force field in the open-source LAMMPS solver to investigate the thermal expansion coefficient of liquid crystal networks (LCNs). The LCNs were intentionally aligned unidirectionally, resulting in anisotropic variations in dimensions along three orthogonal directions. The calculated coefficients were subsequently imported into a structural mechanics module in the COMSOL solver to simulate the thermal deformation of the LCNs. The outcomes of the temperature-induced deformation simulation of LCNs were found to be in agreement with the experimental data.

9:15 AM *EL05.10.04**Conformable and Compact Multiaxis Tactile Sensor for Human and Robotic Grasping via Anisotropic Waveguides** [HuichanZhao](#) and JingyiZhou; Tsinghua University, China

Rich and accurate tactile perceptive capability is important for both humans and robots. Soft materials exhibit unique characteristics to construct high performance tactile sensors such as high sensitivity and high resistance to overload. In this work, a multiaxis tactile sensor based on a soft anisotropic waveguide that can distinguish normal force and shear force, which can greatly expand its potential uses in practice, is reported. First, the anisotropy of the waveguide sensor's response to vector forces is validated numerically and experimentally, and then two of those anisotropic units are embedded into one cladding with a crossed-over layout, to form a multiaxis sensor. Then, a calibration algorithm is implemented on this sensor and the reconstruction of vector forces is achieved at an average accuracy of 28.0 mN for normal forces and 81.1 mN for shear forces, both with the sensing range of 1 N. Using this device, three demonstrations are shown to give outlooks of its potential application in human and robotic grasping tasks: a wearable tactile sensor for collecting human's haptic data during operation, a uniaxial gyroscope, and a robotic gripper's tactile sensor for assisting an unlocking task with a key. This work is a step toward more functional soft waveguide-based force sensors.

9:45 AM EL05.10.05**Controlling Topological Defects and Disclinations in Liquid Crystals Through Structured Polymerization** [Adithya PradeepNair](#), SteveJ. Elston, CamronNourshargh, NathanSpiller and StephenMorris; University of Oxford, United Kingdom

Line singularities in nematic Liquid Crystals (LC) known as disclinations play an important role in the understanding of topography and electro-optic phenomena in LC technologies. Manipulating these singularities and defects in a precise and controlled way can unlock new functionality and electro-optic behavior in LC devices for a range of applications including tunable lasers and beam generators for optical communications. In this presentation, we demonstrate the control of disclinations and defects using a combination of bulk photopolymerization using an optical projection system and localized polymerization using direct laser writing. We use a so-called nematic LC Pi cell to show how this control of the disclinations and defects could be used as an effective template for transferring biological matter. An extensive study has been conducted to analyze the nucleation and growth processes, highlighting the significant influence of rubbing direction on the formation of random domains. By modulating the Pi cell, distinct states with varying boundary conditions are generated. This characteristic makes the Pi cell a promising platform for the manual manipulation of nanoparticles within an electro-optical waveguide. We anticipate that our disclination movement technique can lead to tunable metamaterials, LC plasmonic devices and more efficient optical phase modulators.

SYMPOSIUM EL06

Metamaterials Innovation in Photonics, Acoustics, Fluidics and Thermal Sciences
November 27 - December 7, 2023

Symposium Organizers

Artur Davoyan, University of California, Los Angeles
Lisa Poulidakos, Stanford University
Giulia Tagliabue, École Polytechnique Fédérale de Lausanne
Polina Vabishchevich, University of Maryland

* Invited Paper
+ JMR Distinguished Invited Speaker

SESSION EL06.01: Thermal and Radiative Properties of Metamaterials
Session Chairs: Guangxin Lv and Georgia Papadakis
Monday Morning, November 27, 2023
Hynes, Level 3, Room 308

10:30 AM EL06.01.01

Radiative Cooling and Thermoregulation in the Earth's Glow using Directional Emitters [Jyotirmoy Mandal](#) and Mathis DeGeorges; Princeton University, United States

Buildings exchange large amounts of heat with the environment as longwave radiation. Typical building envelopes are omnidirectional emitters and absorbers of this heat. However, vertical surfaces of buildings see a thermally oriented environment – the cold sky above and a seasonally hot or cold terrestrial environment near and below the horizon. Controlling radiative heat flows to and from such environments can yield large energy savings and thermal comfort in buildings, but remains unattained because it entails avoiding seasonal terrestrial heat gains and losses, while emitting heat skywards via the radiative cooling mechanism. As a solution, we propose micropatterned, directionally emissive facades (DEFs) which, on walls and windows, can achieve a skywards net heat loss through the long-wavelength infrared (LW-IR, $\lambda \sim 8\text{--}13\ \mu\text{m}$) atmospheric transmission window, while blocking terrestrial heat exchange near and below the horizon. Such DEFs can radiatively cool buildings by up to $100\ \text{Wm}^{-2}$ in the summer, and reduce overcooling by $20\ \text{Wm}^{-2}$ or more in the winter, relative to typical envelopes. This novel passive thermoregulation may yield similar or much greater energy savings per m^2 than cool roofs, depending on the type of facade. Furthermore, DEFs may cool urban canyons by $1\text{--}2^\circ\text{C}$, reducing heat island effects, and in turn lowering building cooling loads. Our design represents a new platform for tremendous and untapped energy savings.

10:45 AM EL06.01.02

Development of Highly Thermal Conductive Composites with Large Latent Heat [Yapeng Chen](#); The Hong Kong University of Science and Technology, Hong Kong

Investigating innovative methods for concurrently enhancing the thermal conductivity and preserving the high latent heat of phase change materials is crucial for improving their capacity to regulate the operating temperature of electronic devices by quickly collecting thermal energy within a small temperature range. Among these strategies, compositing the organic phase change matrix with prefabricated frameworks that provide high thermal conductivity and exceptional encapsulation capability is the most promising approach for efficiently boosting heat transfer while retaining its inherent high latent heat. Despite extensive efforts, constructing these frameworks using conventional casting methods remains challenging due to solid interlayer interaction and gravity-induced densification of high thermal conductivity nanosheet frameworks. In this study, a novel approach for the controllable casting of hierarchically aligned graphene frameworks was proposed by regulating the interface tension of the solvent, which imparted the eicosane matrix with a significantly enhanced thermal conductivity of up to $71.6\ \text{W m}^{-1}\ \text{K}^{-1}$ at 27.8 vol% graphene loading. Moreover, the constructed graphene-based framework featured numerous capillary channels that greatly enhanced the encapsulation capacity of the eicosane matrix, which exhibited a high composite latent heat of $129.6\ \text{J g}^{-1}$. We conducted visual and data-based characterizations as well as finite element-based simulations to confirm that our composites simultaneously improve thermal conduction and phase change matrix encapsulation capacity. We believe that our research will advance the construction paradigm of high thermal conductivity nanosheets toward controllable structures and contribute to enhancing the mechanical, electrical, and thermal properties of composites.

11:00 AM EL06.01.03

Photomolecular Effect: Visible Light Interaction with Air-Water Interface [Guangxin Lv](#), [Yaodong Tu](#), [Rohith Mittapally](#), [James H. Zhang](#) and [Gang Chen](#); Massachusetts Institute of Technology, United States

Despite that water is nearly transparent to visible light, we hypothesize that visible light can directly cleave off water molecular clusters at water-vapor interfaces via a process we call photomolecular effect. We had used this hypothesis to explain why some of the past experiments on solar-interfacial evaporation from porous materials can exceed the apparent thermodynamic limit, calculated based on the energy of the incident light and latent and sensible heat required for water evaporation. In this work, we show that this process happens at the air/water interface by measuring the dependence of photomolecular effect on the wavelength, the angle of incidence, and the polarization of the incident light. We further support the photomolecular effect by measuring the temperature response in water and the vapor phases, Raman and infrared spectroscopy, and multiple pump-probe measurements.

11:15 AM EL06.01.04

Mechanically Durable Camouflage Materials by Coating Polyimide Nanofilm with Controlling Radiative Energy [Namkyu Lee](#); Yonsei University, Korea (the Republic of)

Camouflage is an innate behavior observed in creatures that allows them to blend in with their surroundings, thereby increasing their chances of survival by evading predators [1]. The artificial camouflage materials is emerging from the inspiration from this natural phenomenon. These materials can be designed to exhibit specific electromagnetic properties across various domains such as acoustics, microwave, infrared (IR) waves, visible light, and ultraviolet light, depending on their intended applications. Among these domains, IR wave manipulation has gained significant attention due to its relevance in energy and military sectors [2-5].

Micro-nano structures show great promise in overcoming the limitations of conventional materials and realizing the designed properties for camouflage materials. However, these structures are susceptible to external stress such as mechanical or chemical, which can lead to a sudden degradation in material performance, making them challenging to use in practical applications. For this reason, various strategies have been explored, including chemical treatment, the implementation of hierarchical structures, and thin-film coatings for enhancing durability.

However, directly applying conventional methods to improve durability in the context of manipulating electromagnetic waves poses challenges. This is because electromagnetic properties are highly sensitive with residues on the surface, which can generate additional resonances and opaqueness in the target wave, resulting in different material performance. To meet requirements of IR camouflage materials, a polyimide nanofilm is used as a dielectric layer firstly. In the previous work, the polyimide nanofilm exhibits flexibility, anomalous dispersions, and, in particular, satisfies the IR camouflage requirements in the absorbed band based on atmospheric transmittance. Moreover, polyimide is chosen for its excellent mechanical properties and thermal stability. Based on these characteristics and optical properties, we utilize the nanofilm coating of polyimide on the structures, which can enhance mechanical durability.

In this study, we present durable camouflage materials specifically designed for IR radiative energy [6]. We coated ordinary metal-dielectric-metal (MDM) structures with a polyimide nanofilm to improve their mechanical durability. The electromagnetic performance of these durable materials was evaluated through measurements using Fourier transform infrared spectroscopy (FT-IR) and simulations using COMSOL Multiphysics. To check the mechanical durability, two methods, namely manual brushing and the root cause analysis (RCA) test, were employed for comparing conventional camouflage materials. Finally, the IR radiative energy was assessed by IR camera and calculation. We demonstrate that the mechanical stress doesn't change the IR camouflage performance.

References

- [1] Barnett, James B., et al. "Imperfect transparency and camouflage in glass frogs." *Proceedings of the National Academy of Sciences* 117.23 (2020): 12885-12890.
- [2] Kim, Taehwan, et al. "Hierarchical metamaterials for multispectral camouflage of infrared and microwaves." *Advanced Functional Materials* 29.10 (2019): 1807319.
- [3] Lee, Namkyu, et al. "Multiple resonance metamaterial emitter for deception of infrared emission with enhanced energy dissipation." *ACS applied materials & interfaces* 12.7 (2020): 8862-8869.
- [4] Lee, Namkyu, et al. "Transparent metamaterials for multispectral camouflage with thermal management." *International Journal of Heat and Mass Transfer* 173 (2021): 121173.
- [5] Lee, Namkyu, et al. "Flexible Thermocamouflage Materials in Supersonic Flowfields with Selective Energy Dissipation." *ACS Applied Materials & Interfaces* 13.36 (2021): 43524-43532.
- [6] Lee, Namkyu, et al. "Durable camouflage materials by polyimide nanofilm with thermal management." *Applied Surface Science* 608 (2023): 155107.

SESSION EL06.03: Metamaterials for Photonic and Optoelectronic Devices
Session Chairs: Qitong Li and Yu-Jung Lu
Tuesday Morning, November 28, 2023
Hynes, Level 3, Room 308

8:15 AM *EL06.03.01

Ultrafast and Nanoscale Photonics: From Metamaterial-Based All-Optical Switching to Plasmon-Driven Polaritonic Chemistry Nicolò Maccaferri; Umeå University, Sweden

Ultrafast control of light-matter interactions is fundamental to mark new technological frontiers, for instance in light-driven information processing and nanoscale photochemistry [1]. In this context, we have explored the possibility to use metal-dielectric nanocavities to achieve all-optical modulation of light states, such as reflectance, transmittance and polarization. Without the need of driving higher order effects, our system is based on linear absorption, provides large relative modulation exceeding 100% and switching bandwidths of few hundred GHz at moderate excitation fluence [2]. This archetypical system becomes even more interesting if the dielectric inclusion is not just a "passive" insulator material but an inorganic van der Waals bonded semiconductor, like a transition metal dichalcogenide (TMD). TMDs are subject of intense research due to their electronic and optical properties which are promising for next-generation optoelectronic devices. In this context, understanding ultrafast carrier dynamics, as well as charge and energy transfer at the interface between metals and semiconductors, is crucial and yet quite unexplored. By employing a pump-push-probe scheme, we experimentally study how optically-induced thermionic charge carrier injection affects the exciton formation dynamics in bulk WS₂ [3], disclosing excellent opportunities to control exciton formation and annihilation. The strong electric field associated with thermionic carriers excitation can have also important implications in polaritonic chemistry. In fact, if an electronic transition (e.g., exciton, singlet, etc.) strongly interacts with the optical modes of a resonator, we can tailor the energetics and the morphology of a molecular state. By combining quantum mechanical modelling and pump-probe spectroscopy, we recently shed new light on the ultrafast dynamics of a hybrid system composed of photo-switchable molecules coupled to optically anisotropic plasmonic nanoantennas, which allow us to selectively switch between two regimes where the light-matter interaction is either weak or strong [4]. Our synergistic approach is thus instrumental to devise new strategies for tailoring electronic states by using plasmons for applications in polaritonic chemistry on femtosecond timescales.

References

- A. N. Koya et al., *Appl. Phys. Rev.* (2023)
- J. Kuttruff et al., *Commun. Phys.* 3, 114 (2020)
- K. R. Keller et al., *ACS Photonics* 9, 2683 (2022)
- J. Kuttruff et al., *Nat. Commun.* (2023)

8:45 AM EL06.03.02

Artificial Intelligence Aided Rapid Design of THz Stereo-Metamaterials Based Polarization Conversion Devices for Highly Sensitive and Efficient Strain Sensors Patrick Kung, M.Zeki Güngördü, M. Reefaz Rahman, Anirban Swakshar, Abby Sanders, Callan Spooner and Seongsin M. Kim; University of Alabama, United States

Polarization conversion devices, pivotal in the field of photonics, are crucial for manipulating the polarization state of electromagnetic waves. These devices have significantly contributed to advancements in technology, specifically in the realms of communication, imaging, and remote sensing. They have facilitated applications ranging from space exploration to the detection of hidden objects, the identification of explosives, and even cancer detection using the Terahertz (THz) spectral range, which spans from 0.1 to 10 THz. Owing to its wide bandwidth and remarkable ability to penetrate dielectric materials, the THz wave is garnering more interest for noninvasive screenings, high-resolution imaging, and improved precision in data collection. Metamaterials (MM), which are artificially synthesized materials composed of repeated subwavelength-sized meta-atoms, offer a promising avenue for the advancement of these devices. Metamaterial-based THz polarization conversion devices have an advantage over conventional devices because of their thin and compact structure. They are not only easier to integrate but also offer flexibility, marking a new era in the evolution of polarization conversion technology. Stretchable electronics have recently obtained rising interest because the mechanical deformation of elastomeric substrates has been used to induce spectral shifts in the resonance of nanophotonic structures such as nanoparticle dimer extinction and gratings. With the advancement of polymer technology and lithographic techniques, it is possible to fabricate metamaterials on thin, flexible substrates, including Kapton polyimide or polyimide (PI), polyethylene naphthalate (PEN), and polydimethylsiloxane (PDMS). Research indicates that crumpling an unbending metamaterial on a soft backing layer surface can influence the response. The ability to realize such structures on elastic substrates presents further opportunities for tuning via mechanical straining.

In light of that information, we utilized a stereo-metamaterial (SMM) structure for new-generation THz polarizers converting the polarization from linearly to circularly and elliptically polarized wave at the THz frequency range in reflection mode. In this work, we present the processes and results of the inverse design of SMM using the artificial neural network (ANN), trained by various parameters, including polarization status and ellipticity angle, to achieve highly efficient device performance. Training and testing our ANN with the created datasets by simulation for the inverse design of the device, design parameters were obtained by giving an artificial EM response or ellipticity angle spectrum or vice versa more efficiently and rapidly. This study was designed to use a tandem neural network (TNN). It is created by two deep neural networks (DNNs); an inverse neural network (INN) predicts design parameters from the target spectrum, and a forward neural network (FNN) predicts the target spectrum from design parameters, as demonstrated in this work. During the training process of TNN, FNN is trained and tested first. Then, after FNN's weight freezes, it is cascaded with INN for training and testing TNN. The training error can be derived by comparing the target and prediction spectra, solving the non-unique input problem.

The SMM devices based on the ANN-powered design were successfully fabricated on the stretchable substrate. We demonstrated efficient sensing of different polarization statuses using THz polarimetry spectroscopy under the different strains. The sensitivity reaches to 0.1% strain sensing. More details on the results will be presented.

9:00 AM EL06.03.03

Inverse Design of Functionalized Photonic Patches for On-Chip Imaging and Spectroscopy Yilin Zhu, Tornike Shubitidze and Luca Dal Negro; Boston University, United States

In this talk, we present our work on the inverse design and experimental characterization of compact functionalized photonic structures, called “photonic patches”, using adjoint optimization coupled with the rigorous two-dimensional generalized Mie theory (2D-GMT) and validated by three-dimensional finite elements simulations. In particular, we demonstrate compact ($10\mu\text{m}\times 10\mu\text{m}$) silicon and silicon nitride structures that steer four different wavelengths into four predefined far-field directions with efficiencies close to 60%. Moreover, we inverse design structures for the compact spectrometers with nanometer-level spectral resolution. In addition, we demonstrate novel photonic patch geometries for near-field focusing at multiple focal lengths, achieving focusing efficiencies that exceed 70%. We also present our results on achromatic focusing devices with optimal aperiodic geometries and enhanced local density of states (LDOS) at predefined spatial and spectral locations. We show that our devices support localized optical modes with two-orders of magnitude enhancement of the Purcell factor for both TE and TM polarizations, enabling the fabrication of active photonic devices with ultracompact footprints. The performances of the fabricated devices are characterized experimentally using light emission spectroscopy and spectroscopic ellipsometry from the visible to the infrared spectral range. Leveraging on the rigorous mesh-free solution of the multiple scattering problem of dielectric cylinders, our approach provides an efficient and accurate inverse design methodology for the realization of novel aperiodic structures with optimal functionalities for nonlinear photonics, miniaturized light sources, and on-chip imaging and spectroscopic devices.

9:15 AM *EL06.03.04

Ultrafast Nonlinearities in Epsilon-Near-Zero Materials and Metasurfaces[Hayk Harutyunyan](#); Emory University, United States

In this talk I will review our recent progress in tailoring the ultrafast and nonlinear response in epsilon-near-zero materials and metasurfaces.

9:45 AMBREAK

10:15 AM EL06.03.05

Observation of Topological Phase Transition in Complex Momentum Space[Yung Kim](#)¹, [Sonu Verma](#)², [Minwook Kyung](#)¹, [Kyungmin Lee](#)¹, [Moon Jip Park](#)^{2,3} and [Bumki Min](#)¹; ¹KAIST, Korea (the Republic of); ²Institute for Basic Science, Korea (the Republic of); ³Hanyang University, Korea (the Republic of)

It is well known that topology of a periodic crystal can be characterized by calculating a topological invariant using the real Bloch wave vector. In systems governed by non-Hermitian Hamiltonians, however, this conventional knowledge is challenged due to a phenomenon known as the non-Hermitian skin effect, in which wave functions accumulate at the boundaries. To address the failure of Bloch's theorem in non-Hermitian systems, two representative approaches have been utilized: one involving complex spectral topology in the conventional Brillouin zone and the other revolving wave function topology in the generalized Brillouin zone. The complex spectral topology approach provides the topological information of a system by demonstrating the presence of point gap and line gap in the complex plane. On the other hand, the wave function topology provides a method to calculate non-Hermitian topological invariants using the complex Bloch wave vector, which hosts conventional topological boundary states. Recently, a new approach has been introduced - the intrinsic topology of the generalized Brillouin zone within the complex momentum plane. In this work, we present the first experimental demonstration of topological phase transition within the generalized Brillouin zone, occurring in complex momentum space, through a one-dimensional non-Hermitian electric circuit lattice. More specifically, we designed a one-dimensional non-Hermitian electric circuit lattice inspired by the Hatano-Nelson model with generalized boundary conditions. By adjusting the boundary conditions, specifically the onsite potentials and couplings of boundary nodes, we observed the emergence of topological boundary modes in complex momentum space. Furthermore, we identified that this topological phase transition, known as an exceptional transition, is accompanied by the manifestation of an exceptional point. To build upon and generalize our modified Hatano-Nelson model, we introduced next-nearest-neighbor hopping into the system and observed the emergence of multiple topological boundary modes within the complex momentum space. Our experimental findings hold significant promise for advancing the understanding of bulk-boundary correspondence within non-Hermitian systems, by highlighting the novel topological phase transition that occurs in complex momentum space.

10:30 AM EL06.03.06

Observation of Polaritonic Topological Nodal Line States in Natural Materials[Mingsong Wang](#)¹, [Xiang Ni](#)^{1,2} and [Andrea Alu](#)^{1,3,4}; ¹CUNY Advanced Science Research Center, United States; ²Central South University, China; ³Graduate Center of the City University of New York, United States; ⁴City College of the City University of New York, United States

Photonic topological systems have displayed significant potential for various applications, including robust wave propagation, topological lasers, non-Hermitian photonics, and nonlinear topological phases. A promising direction in the field of topological photonics is the exploration of interactions between photons and a diverse range of material excitations, such as excitons, plasma, and optical phonons. These interactions can give rise to half-light-half-matter quasiparticles called polaritons. Recent studies have unveiled the formation of topological exciton/phonon polaritons resulting from the strong coupling between photonic topological modes and excitons or optical phonons. However, most investigations into topological polaritons have focused on artificial structures or a combination of artificial topological structures with natural materials. These studies often require precise fabrication of sophisticated artificial structures, thus posing challenges for their practical implementation in real-world applications.

In this study, we report the observation of polaritonic topological nodal lines supported by unpatterned natural materials and experimentally characterize the associated surface polaritonic waves using scattering-type scanning near-field optical microscopy (s-SNOM). In electronic materials, topological nodal lines are manifested as one-dimensional lines in the electronic band structure, where the energy levels are doubly degenerate in three-dimensional momentum space, exhibiting a Berry phase of π . These nodal lines are topologically protected under specific spatial symmetries, rendering them robust against perturbations when these symmetries are preserved. The discovery of topological nodal lines has opened exciting opportunities for designing and synthesizing materials with intriguing electronic and optical properties. However, due to technical limitations and the delicate nature of their topology, the exploration of topological nodal lines in condensed matter experiments has been limited. More recently, the concept of topological nodal lines has been extended to classical wave systems, leading to a surge of interest in characterizing these modes and investigating their unique properties. Notably, the study of topological nodal lines in photonics and metamaterials has emerged as a rapidly growing field within topological photonics in recent years.

Through theoretical exploration and simulations, we have discovered that calcite crystal offers an outstanding platform for demonstrating polaritonic topological nodal line states in natural materials. The topological nodal line originates from a two-fold degeneracy within the upper Reststrahlen band of calcite when the crystal surfaces are oriented along the plane (001), forming angles θ of 90° with respect to the optical axis. At the interface of calcite, this topological nodal line gives rise to a novel type of topological surface polaritons, whose dispersion in momentum-energy space can be effectively characterized using s-SNOM. Additionally, we experimentally demonstrate optical spin-momentum locking for these new surface polaritons, with their propagation direction steered effortlessly through the handedness of circularly polarized excitations.

10:45 AM *EL06.03.07

Nanoscale Directional Photocurrents with Symmetry-Broken Optoelectronic Metasurfaces[Hou-Tong Chen](#); Los Alamos National Laboratory, United States

Light-driven electrical currents are of great importance in information science and microelectronics, particularly in emerging topological, magnetic, and low-dimensional materials, which introduce new speed limits and light-based control degrees of freedom. However, such photocurrents typically rely on the broken spatial or temporal symmetries, thus either intrinsic to the lattice and constrained to specific light-matter interaction geometries, or dependent upon applied static fields that are difficult to texture on small spatial scales. Artificially structured plasmonic systems can be utilized to overcome these spatial limitations and concentrate light down into deeply sub-diffractive nanometer scales. In this work, we show that hybrid plasmonic metasurface systems offer much broader capabilities for harnessing charge flows at previously inaccessible spatial scales. Nanoscale directional photocurrents in these systems are a universal manifestation of broken inversion symmetry, with patterned gold resonators on graphene serving as a testbed system. The rapidly-evolving nanoscale dynamics across the coupled photonic, electronic, and thermal responses introduces net photothermoelectric currents that are sensitive to the local symmetry of the light-matter interaction. The local (nanoscale) and global (millimeter-scale) photocurrents are highly responsive to the polarization and frequency of the ultrafast light pulses, leading to a combination of designer patterning and active control over ultrafast, nanoscale vectorial currents. As an immediate application, we exploit this scheme for efficient and versatile generation of broadband ultrafast terahertz radiation and terahertz vector beams.

SESSION EL06.05: Metamaterials for Next-Generation Imaging and Sensing Platforms

Session Chairs: Justus Ndukaife and Lisa Poulikakos

Tuesday Afternoon, November 28, 2023

Hynes, Level 3, Room 308

1:30 PM *EL06.05.01

Metallic Polymers as New Materials for Plasmonics and Active Metasurfaces: Video-Rate Beam Switching and Multi-Focal Metaobjectives[Harald Giessen](#); University of Stuttgart,

Miniaturizing optical components is key to achieve ultimate spatiotemporal control of light. Active subwavelength nanoantennas and metasurfaces are a prime candidate to achieve this goal, whose functionalities are currently limited by the proposed switching schemes.

We introduce nanoantennas and metasurfaces from *metallic polymers* which can be electrically switched in the infrared spectral range via CMOS-compatible voltages of $\pm 1\text{V}$ (Fig. 1A) [1]. The concept is based on an electrically driven metal-to-insulator transition. A positive voltage turns the polymer metallic and the nanoantennas exhibit a strong plasmonic resonance (right). In contrast, a negative applied voltage (left) switches the polymer into the insulating state with no nanoantenna resonance present. The electrical switching between ON- and OFF-state occurs fast, permitting video-rate switching frequencies of up to 30 Hz.

Using such nanoantennas we demonstrate, on the one hand, an electrically switchable metallic polymer metasurface for ultra-high-contrast active beam switching (Fig. 1B). On the other hand, we realize an electro-active metaobjective comprising two metalenses-on-demand [2]. The state of metalenses can be set fully independently. Non-volatile operation is used to set the refractive power of the individual metalenses either ON or OFF. Such, four different metaobjective states become possible. By using gel electrolytes, our metadevices can even be integrated into state-of-the-art on-chip electro-optic components [3,4].

Fig. 1 (A) Concept of electrically switchable nanoantennas made from metallic polymers. Right: Nanoantenna ON-state at applied voltage $+1\text{V}$, plasmonic resonance observed. Left: Antenna OFF-state at -1V , no plasmonic resonance observed. Switching is possible with video-rate frequencies of 30 Hz. (B) Metallic polymer plasmonic metasurface for ultra-high-contrast active beam steering. Camera images and intensity profiles in the ON- (left) and OFF-state (right). (C) Multi-focal metaobjective comprising two stacked metalenses-on-demand. The state of each metalens can be set individually in a non-volatile operation.

References

- [1] J. Karst et al., Electrically switchable metallic polymer nanoantennas, *Science* **374**, 612 (2021).
- [2] J. Karst et al., Electro-active metaobjective from metalenses-on-demand, *Nature Communications* **13**, 7183 (2022).
- [3] D. de Jong and J. Karst et al., Electrically switchable metallic polymer metasurface device with gel polymer electrolyte, *Nanophotonics* (2023), in press, <https://doi.org/10.1515/nanoph-2022-0654>.
- [4] Y. Lee, J. Karst, M. Ubl, M. Hentschel and H. Giessen, Dynamic beam control based on electrically switchable nanogratings from conducting polymers, *Nanophotonics* (2023), accepted.

2:00 PM *EL06.05.02

Scalable Classical and Quantum Light Sources Bouacar Kante; UC Berkeley, United States

The scaling of lasers and in-particular of surface emitting lasers is a multi-decade long question that has been investigated since the invention of lasers in 1958. It is an important question with numerous applications. In this talk, I will propose and discuss an intriguing solution to this question that we named the Berkeley Surface Emitting Laser (BerkSEL) and it is the world's first scale-invariant laser. In the second part of the talk, I will discuss our demonstration of the first deterministic quantum light source in silicon that emits single photons in the telecom band. The work opens unique perspectives for scalable quantum networks.

2:30 PM EL06.05.03

Multiplexed Immunoassays Enabled by Pixelated High-Quality Factor Metasurfaces and Acoustic Bioprinting Sajjad Abdollahramezani, Parivash Moradifar, Fareeha Safir, Sahil Dagli, Varun Dolia, Jack Hu, Hamish M. Carr Delgado, Kai Chang, Butrus T. Khuri-Yakub and Jennifer A. Dionne; Stanford University, United States

Nanophotonic biosensors hold the promise of early disease identification and continuous treatment monitoring due to their high sensitivity, fast response time, and possibility for label-free detection. Here, we leverage ultra-densely-pixelated high-quality factor (high-Q) metasurfaces in conjunction with acoustic bioprinting surface chemistry to enable scalable multiplexed immunoassays. Our platform capitalizes on a 2D array of finite-size all-dielectric metasurfaces supporting quasi-bound state in the continuum (qBIC) resonances to significantly enhance light-matter interaction with high spatial resolution. Unlike conventional metasurfaces, where sharp resonances are generally generated via the interference of sub- and super-radiant modes in a large 2D arrangement of metaunits, our high-Q metasurface exploits photonic mirrors to highly confine the collective qBIC mode of a 1D array of broken-symmetry resonators. Without comprising the optical performance, such small-scale (i.e., $15 \times 3\ \mu\text{m}^2$) metasurfaces provide high Q-factors (~ 3000) with a mode volume below $(\lambda/n_{\text{eff}})^3$. We demonstrate an ultradense array of pixelated biorecognition elements by introducing an acoustic bioprinting approach for the local functionalization of each metasurface resonator. In contrast to conventional surface functionalization approaches, which expose all sensing elements at once, our approach facilitates the realization of multiplexed biodetection by addressing individual elements at kHz rate. In combination with hyperspectral imaging, this sensitive label-free sensing platform allows for the simultaneous quantitative detection and kinetic analysis of multiple antibodies (e.g., SARS-CoV, Influenza A, and Influenza B) on a single chip. Further, we demonstrate how a single chip can also allow simultaneous detection of proteins and the associated gene fragments. Our AI-enhanced technique can capture two-dimensional spatially resolved images across contiguous spectral bands revealing subtle differentiation of spectral signatures associated with each linked bioanalyte, without relying on bulky and expensive spectrometers. The capability of our multiplexed immunoassay platform for parallel measurement of several biological targets of interest opens the door for easy-to-use and portable diagnostics.

2:45 PM EL06.05.04

A Simple Route for Generating Iridescent Retroreflective Color Filter Jieun Yeo, Joo Hwan Ko and Young Min Song; GIST, Korea (the Republic of)

Iridescent colors found in the body of various animals and insects, such as tails of birds or wings of butterflies, exhibit eye-catching visual information, enabling camouflage, predation, courtship, and communication in various environmental changes. In particular, certain living, *Papilio palinurus*, which has multilayer photonic structures on the concave structure of the wing surface, exhibits conspicuous light-matter interaction with both iridescent color reflection and retroreflection, which delivers vibrant visible information in the direction of light input¹. Conventionally, retroreflectors employ geometric structures, such as corner-cube shapes, to redirect incident light back toward its source. However, these structures typically yield non-iridescent colors and are challenging to apply in various applications due to these limitations. Moreover, the use of organic materials such as dyes and pigment for colorization compromises the color purity and durability of retroreflective materials. Based on a lesson from natural photonic structure, specific examples have been introduced to make an iridescent retroreflector inducing gap interference within biologically inspired microsphere structures or distributed Bragg reflector (DBR)². However, these methods still suffer from limitations such as intricate structures and time-consuming manufacturing processes. In this study, inspired by the structural properties of butterflies, we present a conspicuous iridescent retroreflective color filter that dynamically changes in response to the incident angle. The filter aims to overcome limitations in dynamic coloration and durability by utilizing an ultra-thin resonant layer (UTRL) on a metal film.

To implement the iridescent retroreflective filter, a metal film is deposited on a micro-concave array (MCA) designed to implement retroreflective behavior to form a UTRL. The round curvature of the MCA possesses different deposition angles at various locations, which consequently allows the UTRL to deposit with a gradual change in porosity, resulting in sequential color changes under modulated resonance conditions [4]. The fabricated UTRL converts white light into iridescent light that gradually changes with the curvature of MCA by turning the direction of light to the original light source. The resonance conditions were regulated by controlling the porosity of the absorption medium in the metal reflector, which means that when resonance occurs in the visible wavelength range, the change in porosity causes a color change³. The dynamic angle-sensitive color changes resulting from the difference between this porosity and the effective index are experimentally confirmed by the measurement of the reflection spectrum and its spectral color at a wide angle. Additionally, the retroreflective filter can analyze using a rotational linear polarizer. When the polarizer was located in front of the light source and the image sensor, the retroreflection can be confirmed by observing the near-field pattern. When the polarizer in front of the image sensor rotated 90° , the retroreflected light was detected in four segments of the concavity. As a result, we implemented a sustainable retroreflective structural color filter that is constructed using a self-graded porous medium comprising concave structures. The iridescent color filters can be used in various visual applications such as load signals or optical devices.

[1] Kolle, Mathias, et al., "Mimicking the colourful wing scale structure of the *Papilio blumei* butterfly," *Nat. Nanotechnol.* **5**, 511–515 (2010)

[2] Kats, Mikhail A., et al., "Nanometre optical coatings based on strong interference effects in highly absorbing media," *Nat. Mater.* **12**(1), 20–24 (2012).

[3] Ko, Joo Hwan, et al., "Flexible, Large-Area Covert Polarization Display Based on Ultrathin Lossy Nanocolumns on a Metal Film," *Adv. Funct. Mater.* **30**, 1908592 (2020).

3:00 PM BREAK

3:30 PM EL06.05.05

Plasmonic Metasurfaces for Taste Visualization Juhyeong Lee, Doeun Kim, Gyurin Kim, Juhwan Kim, Hyun Min Kim, Jang-Hwan Han and Hyeon-Ho Jeong; Gwangju Institute of Science and Technology, Korea (the Republic of)

Discriminating taste information before food consumption is vital for mitigating health risks associated with factors such as virus infection, radioactive pollutants, and drug abuse. Plasmonic

nanosensors based on refractive index sensing have emerged as a promising platform for taste molecular sensing due to their facile and modular sensing capabilities with low detection thresholds. However, a challenge for the plasmonic nanosensors lies in the lack of qualitative analysis of multiple target species.

Here, we present a breakthrough in plasmonic nanosensors that addresses the challenge of taste-sensing through a wafer-level plasmonic metasurface. This plasmonic metasurface is constructed in a scalable manner by coating metallic nanoparticles onto a metallic mirror, which are separated with a uniform solid nanogap. This design ensures an identical plasmonic cavity resonance (i.e., color) with enhanced sensitivity (> 100 nm/RIU) and uniform surface-wetting properties across the entire wafer. Leveraging this plasmonic metasurface, we introduce the concept of 'binding-free' multiple molecular sensing by simply capturing 2D projection images of molecular droplets on the single plasmonic metasurface using a conventional optical microscope. We are then able to extract two essential physical properties: the molecular refractive index and surface tension, obtained from the droplet's color and size, respectively. The combinatorial analysis of these two properties offers a scalable and intuitive means of detecting and visualizing the five basic tastes, otherwise impossible from either physical property alone. To showcase the utility of our surface-sensitive sensing platform, we successfully identify the tastes of various commercially available liquids. This breakthrough holds significant potential in establishing an end-user-friendly potable taste-sensing platform.

In this presentation, the fabrication method of the plasmonic metasurfaces will be discussed along with their theoretical and experimental optical features and sensing performance. Furthermore, we will demonstrate how to qualitatively model and mathematically analyze the colors and sizes of molecular droplets as a function of the molecular concentrations of each taste molecule for taste visualization and discrimination.

3:45 PM EL06.05.06

Procedural Metamaterials: A Unified Procedural Graph for Metamaterial Design [Liane Makatura](#)¹, [Bohan Wang](#)¹, [Yi-Lu Chen](#)², [Bolei Deng](#)¹, [Chris Wojtan](#)², [Bernd Bickel](#)² and [Wojciech Matusik](#)¹; ¹MIT, United States; ²IST Austria, Austria

Metamaterials have been architected to achieve a wide range of incredible material properties, from optical to acoustic, mechanical and beyond. These highly-performant metamaterials generally exhibit an equally wide range of structural "architectures", including diverse elements such as straight trusses, curved beams, thin shells, and solid bulks. Although this breadth is powerful -- as each architectural class offers a unique set of strengths -- it also complicates the process of metamaterial design, because no existing representation is well-suited for all classes. Generic representations like voxel grids can express any structure, but the specification is cumbersome and difficult to edit. Class-specific representations are often more practical, as each structure's description is compact and editable. However, the underlying specifications are as varied as the structures themselves, and they are generally incompatible with one another. These issues make it difficult to explore over the full space of interesting metamaterial architectures, which limits the set of structures that are easily accessible to engineers.

To alleviate these challenges, we propose a unified procedural graph representation that can succinctly represent the construction process for any structure using a simple thickness-annotated skeleton. Our high-level approach is intuitive and accessible: the designer builds a skeleton that describes a small fundamental piece of the desired structure; applies a sequence of mirror or rotation operations; and then thickens this skeleton to obtain the final volumetric object. Our low-level skeleton representation preserves this powerful simplicity, by leveraging intuitive, easy-to-specify elements like lines and surfaces. Each skeletal element is constructed from a small set of simple, high-level specifications comprised of vertices and edges, a bounding volume, and the type of skeletal element (e.g. line, surface) to be instantiated. Ultimately, the spatially-varying thickness function associated with each element determines how it should be thickened into a physically realizable volume (e.g., beam, shell, or solid bulk).

Despite its simplicity, our representation is expressive enough to capture a wide range of established structures, including those based on the complex *triple periodic minimal surfaces* (TPMS), which have traditionally been challenging to explore. Our representation can also seamlessly combine elements from various architectural classes. Moreover, our representation is compact, intuitive, and easily-editable, such that it is amenable to manual or automated design space exploration. As such, our approach streamlines the process of metamaterial design and greatly expands our capacity for exploration.

To demonstrate the expressiveness, accuracy and efficiency of our representation, we recreate a wide range of established structures with diverse architectures. We also conduct a user study to verify our representation's intuitiveness and ease-of-use. Finally, we demonstrate the potential of our approach by showing that random searches over our representation can efficiently produce large collections of novel structures with promising material properties.

4:00 PM EL06.05.07

Development of Spiropyran Immobilization and Characterization Protocols for Reversible Photo-Patterning of SiO₂ Surfaces [Bokun Zhou](#) and [Vincent Remcho](#); Oregon State University, United States

Spiropyran, a type of photochromic compound, is distinguished by its reversible transformation between its colorless, hydrophobic spiropyran (SP) form and the purple, hydrophilic merocyanine (MC) form. This transformation can be triggered by UV light and reversed by either visible light or heat. Spiropyran functionalized surface, therefore, present reversible contrast in properties such as color, fluorescence, and reactivity, rendering it optimal for a range of applications in chemical sensor, biosensor, drug delivery, and heavy metal extraction.

Despite the successful application of spiropyran attachment in various substrates: non-covalently in metal organic frameworks (MOFs), poly (ethylene glycol) (PEG) lipids, polydimethylsiloxane (PDMS), and covalently in poly (methyl methacrylate) (PMMA), polystyrene microbeads, silica microbeads, cellulose nanofibers, cellulose nanocrystals - its implementation on plain surfaces has been limited due to surface area constraints and insufficient characterization.

Our research focuses on a 3-step spiropyran immobilization protocol tailored for thermally grown SiO₂ surfaces. This process involves surface activation, amination using (3-aminopropyl) triethoxysilane (APTES) and spiropyran functionalization. We have also developed a robust characterization method utilizing techniques such as ellipsometry, X-ray photoelectron spectroscopy (XPS), Fourier transform infrared spectroscopy (FTIR), and fluorometric detections.

Our main results include comparing the effectiveness of various activation methods, such as H₂SO₄ acid, oxygen plasma, and piranha solution treatments. XPS and contact angle measurements show that the surface is clean and properly activated for all cases. We then monitored the uniformity and thickness of the APTES layer. By varying the reaction temperature, time, and concentration, we achieved a uniform and thin layer immobilization of APTES, verified by ellipsometry and XPS. A 1% APTES incubation for 5 minutes at room temperature yielded the best results. The functionalization step was verified by fluorescence microscopy, showing a clear contrast between SP and MC forms. FTIR monitors the change of functional groups after each step. The developed protocol demonstrated exceptional repeatability, with photo-patterning results showing reversibility over more than ten cycles and feature sizes of less than 20 μ m.

We also discussed the intrinsic limitations of immobilizing spiropyran onto a plain and rigid substrate, such as steric hindrance and effective activated surface sites, which greatly reduced the number of spiropyran immobilized. To address these challenges and expand the potential applications of our protocol, we propose several innovative directions for future research. One approach involves immobilizing spiropyran to a porous media that provides a larger surface area or finding a type of surface with more effective activated sites. Another strategy is to further modify the MC form to enhance the contrast between SP and MC forms.

In conclusion, our study highlights the potential of spiropyran in surface patterning applications and offers a comprehensive protocol for its immobilization on SiO₂ surfaces, which should also be applicable to other surfaces. These findings pave the way for the development of on-chip sensing and other applications.

SESSION EL06.07: Poster Session: Metamaterials Innovation in Photonics, Acoustics, Fluidics and Thermal Sciences

Session Chairs: [Jyotirmoy Mandal](#) and [Andrea Schirato](#)

Tuesday Afternoon, November 28, 2023

Hynes, Level 1, Hall A

8:00 PM EL06.07.01

Ductile Mode Machining Process of Piezoelectric Single Crystal for the Broad-Bandwidth Ultrasonic Transducer Applications [Jun Sae Han](#), [Dong-Hyun Seo](#), [Eun-Ji Gwak](#), [Tae-Jin Je](#) and [Doo-Sun Choi](#); Korea Institute of Machinery and Materials, Korea (the Republic of)

Ductile mode machining process was investigated with piezoelectric single crystal material based on laser assisted mechanical cutting process. For the fabrication of acoustic/ultrasonic metamaterials, micro/nano patterning of functional material has been widely researched. Especially for therapeutic ultrasound transducer, focusing and enlarging of ultrasonic wave have special interest to achieve high intensity. As a promising candidates for micro/nano hybrid patterning process of function piezoelectric single crystal, ductile mode machining process was

established and optimized. In this research, machinability of the relaxer based PMN-PT single crystal was investigated to achieve crack free cutting surface. Especially, effects of laser assisted cutting parameters were systematically investigated in the aspects of mechanical, chemical, crystallographic, and piezoelectric perspective. Based on the optimized process, crack-free high quality machined surface can be obtained with the roughness of 2.1 nm. Also, lens like curved structure was smoothly machined without showing any brittle crack defects. Fabricated structural PMN-PT single crystal was assembled as ultrasonic transducer and validated its ultrasonic transducer performance. Fabricated curved shape structure showed enhanced bandwidth properties which enable to achieve broad-bandwidth ultrasonic gas flow meter application. Based on established material processing technology, multi-scale patterning results will be presented for the advanced manipulation of ultrasonic wave.

8:00 PM EL06.07.02

High-Performance Transparent Radiative Cooling Integrated with Janus EmitterJunkyeongPark¹, DongwooChae², HeonLee² and JunsukRho¹; ¹Pohang University of Science and Technology, Korea (the Republic of); ²Korea University, Korea (the Republic of)

Passive daytime radiative cooling (PDRC) technology is a method that achieves cooling by reflecting incoming solar radiation and enhancing thermal radiation in the part of the atmosphere that allows radiation to pass through. Its ability to operate without consuming energy makes it a promising technology for future energy conservation, and it has gained significant interest in various research communities. In particular, the visible transparent radiative cooler offers advantages in a broad range of applications, including passive cooling for vehicles and buildings. In this study, we demonstrate the implementation of a high-performance transparent radiative cooler by attaching a broadband and selective emitter to both sides of the visible transparent film that blocks near-infrared (NIR) radiation. We conduct outdoor cooling experiments on the fabricated PDRC devices to demonstrate the cooling potential. This design not only achieves remarkable surface cooling but also provides space cooling when used as an energy-saving window. As a result, the proposed device can effectively counteract the greenhouse effect within enclosures while delivering surface cooling capabilities that are comparable to conventional radiative coolers.

8:00 PM EL06.07.03

Inverse-Designed Contact Lenses for Precise Correction of Color Vision DeficiencyYeTian and JianfengZang; Huazhong University of Science and Technology, China

Color vision deficiency affects more than 300 million people on the earth. Although no radical cure for the disorder exists now, some specialized color filtering glasses/lenses have been used on color vision deficiency management. However, as color vision deficiency patients usually diversify on their classification and severity, none of current glasses/lenses provides customized correction for various color vision deficiency patients, resulting in undesirable correction effects.

Here we demonstrated the new inverse-designed contact lenses based on nanoparticles for precise correction of color vision deficiency. Firstly, due to the diverse severity of color vision deficiency patients, the wavelength shift ($\Delta\lambda$) of patient's abnormal photoreceptors was measured to inversely design the best blocking wavelength and blocking rate of our contact lenses. The customized contact lenses were then fabricated by adding silica-coated gold nanoparticles (Au@SiO₂ nanoparticles) with appropriate sizes and concentrations to hydrogels or Polydimethylsiloxane (PDMS). Thus, contact lenses obtained a narrow optical absorption band due to the surface plasmonic resonance effect of the added Au@SiO₂ nanoparticles. The effect of customized inverse-designed contact lenses was then verified by the simulated color vision and practical human tests.

In summary, inverse-designed contact lenses for color vision deficiency correction were developed and testified in this work. The proposed concept of this work may open avenues to precise color vision correction, optical metamaterials in the wearable device and medical field, thereby addressing the challenge and unmet needs for color vision deficiency management.

8:00 PM EL06.07.04

Polarimetric Study of an Embeddable, Flexible, Textile-Compatible Ferromagnetic Microfiber PlatformSeokkeeMin¹, JosephPlumitallo¹, PetrMoroshkin¹, ZhengChen², RichardM. Osgood³, IhsanUluturk³ and JimmyXu¹; ¹Brown University, United States; ²Howtech, China; ³U.S. Army DEVCOM SC, United States

In the information age, much effort and attention remain focused on the processing and transmission of information. Of equal importance is data acquisition and execution, which is made even greater with today's big data and AI. In this work, we present an embeddable, flexible, wearable, and scalable sensing and actuation platform for monitoring, communicating physical and chemical conditionals, as well as extracting/delivering molecular substances. The platform is based on a novel ferromagnetic microfiber and can be configured into various embedded structures such as 2D arrays and 3D stacked sheets,

It offers many degrees of freedom to exploit, such as electrical, magnetic, and optical activities. The microfiber itself consists of a 30 μm diameter conductive ferromagnetic alloy (CoFeSiB) core, encased in a 10 μm thick borosilicate glass (Schott Duran) shell. This choice of materials and feature sizes allows us to exploit magnetic and electrical degrees of freedom, and strong polarization dependent electromagnetic activity that can be embedded in coating layers, fabrics and textiles and then read-out and/or activated from remote, over a broad spectral band from RF to visible to deep infrared while maintaining flexibility, chemical stability, cost effectiveness, and manufacturing lengths up to kilometers. In addition to individual fibers or their random ensembles, we can also structure them into 2-/3-dimensional arrays of these fibers (e.g. photonic band-gap engineering) to exploit their collective optical activities or functionalities, which are therefore variable via their spacings, fillings, and externally applied electric and/or magnetic fields.

Applications of these tunable degrees of freedom include but are not limited to sensing, actuation, remote-tracking, and thermal property management. Some configurations would also allow for delivering payloads (e.g., drug) via inductive heating of the conductive ferromagnetic core combined with thermal expansion and the Laplace force.

As an example, we report on a polarimetric study of a 1-D array of parallel microfibers, embedded between two PET double-sided acrylic adhesive layers, that are invisible to human eyes and indiscernible by touch. A polarimetric reflectance spectra, however, can read out this array and determine its structure features (e.g. optical thickness, orientation, and effective spacing). The experiment was conducted over the 600~1750 nm spectral range with a polarized broadband (Halogen) light source. To isolate the optical activity of the fibers from their 'concealing cover' (PET), the normalized reflectance spectra was subtracted from a control spectra of the PET films. The resulting spectra revealed a polarization-dependent cavity effect. When the polarization was both parallel and rotated 45° counterclockwise to the longitudinal axis of the fibers, we observed a free spectral range of 7.14 THz (optical thickness ~21 μm). When the polarization was both orthogonal and rotated 45° clockwise from the longitudinal axis of the fibers, we observed a free spectral range of 7.89 THz (optical thickness ~19 μm). The measured effective optical thickness of the array is consistent to the ~200 μm periodic spacing of the array. But the polarization preference off of the principal axes is curious. One contributor is the anisotropy of the PET films, resulting from a residual strain from the rolling and pressing process during manufacturing. Since the fiber spectrum was isolated from the control, the measurements also suggest an additional and likely mesoscopic physical origin (e.g. the ferromagnetic alloy grain/domains). However, the current 1D ferromagnetic array at a layer thickness of 50 μm already shows promise for a wide range of sensing and photonic management applications.

8:00 PM EL06.07.05

Anisotropic Metamaterials for Elastic Wave Mode Conversion Over a Wide Incidence Angle RangeJeseungLee, GihyunKim and Yoon YoungKim; Seoul National University, Korea (the Republic of)

The constitutive relation of an elastic medium requires a fourth-order elasticity tensor, leading to multi-modal characteristics in the elastic wave regime. As a result, elastic waves in solids carry not only longitudinal (pressure) but also transverse (shear) waves. This multi-modal characteristic complicates but enriches elastic wave phenomena, the most unique of which is the mode conversion between longitudinal and transverse waves. Early studies demonstrated that full-mode conversion between longitudinal and transverse waves could be realized by using anisotropic metamaterials with the non-zero mode coupling component in the elasticity tensor. However, the previously suggested anisotropic metamaterials for the mode conversion phenomenon operate only at normal incidence or oblique incidence with a specific incidence angle. Here, we present a novel anisotropic metamaterial with a spatially dispersive anisotropic tensor that converts longitudinal waves into transverse waves with high mode conversion efficiency over a wide range of incidence angles. The proposed anisotropic metamaterial was fabricated by drilling aperiodic holes with different sizes and angles in an isotropic base material. The mode conversion performance of the proposed anisotropic metamaterial was verified using ultrasonic-guided waves in aluminum plates.

8:00 PM EL06.07.06

Development, Fabrication and Characterization of Hyperbolic Flat Lensing in the X-Band using 3D Printing and Quasi-Conformal Transformation OpticsAlexandrosCooke-Politikos, AndrewRittenberg, DanielMartin and BrianM. Wells; University of Hartford, United States

Transformation optics is a well-established technique that can be used to design many novel electromagnetic and optical devices; some include cloaking, integrated optical components, focusing devices, and antennas. The method relies on the form-invariance of Maxwell's equations under a spatial coordinate transformation. Consequently, this approach can be difficult to implement in fabrication due to the complex material properties imposed, often requiring anisotropic lossy metamaterials. In this work, we restrict the transformation to a quasi-conformal mapping, requiring only dielectric isotropic materials. This allows for flat lens designs with varying focal lengths and thicknesses to be fabricated through 3D printing, experimentally tested, and compared with FEM numerical simulations.

Various flat hyperbolic lenses with controlled thicknesses and focal lengths have been designed for fabrication and experimental characterization in the X-band microwave regime. Standard Polymaker PLA 3D-printer filament has been optically characterized, allowing the refractive index to be modeled as a function of infill percentage. Quasi-Conformal transformation optics is used to transform modeled hyperbolic canonical lenses of various focal lengths into a planar lens of controlled thickness with variable refractive index. The varying refractive index regions of the flat lens are controlled through the 3D-printed infill percentage. After FEM numerical simulations verify the desired optical properties of this transformation, the lenses are fabricated using

3D printing. Both the flat lens and hyperbolic lens are created for experimental comparison. It is verified through this process that these flat lens variants are in excellent agreement with the FEM simulations and the experimental results from their hyperbolic canonical lens counterparts.

8:00 PM EL06.07.07

High-Performance Confocal Piezoelectric Energy Harvesting using the Achromatic Elastic Lens GeonLee¹, JeonghoonPark¹, WonjaeChoi², BonggyuJi², MisoKim³ and JunsukRho¹; ¹Pohang University of Science and Technology, Korea (the Republic of); ²Korea Research Institute of Standards and Science, Korea (the Republic of); ³Sungkyunkwan University, Korea (the Republic of)

In this study, we present a novel and high-performance confocal piezoelectric energy harvesting system that overcomes limitations observed in previous energy harvesting platforms. These limitations include changes in coal position with operating frequencies and impedance mismatch caused by inclusions or holes. To address these challenges, we developed a Mikaelian lens-based piezoelectric energy harvesting platform with a gradually distributed refractive index profile. This platform leverages the self-focusing ability based on conformal mapping theory and the achromatic ability based on the Kirchhoff-Love thin plate theory. The proposed platform demonstrates exceptional elastic wave focusing capabilities. Through the experimental validation, we achieved highly amplified output electrical power up to 1.44 mW within the frequency range of 40 kHz to 60 kHz, originating from confined elastic wave energy. Notably, the output electrical power extracted at the confocal position was up to 3.76 times higher than that extracted at the lens's input position. This highlights the effectiveness of our broadband achromatic piezoelectric energy harvesting platform. The remarkable performance and broad applicability of our platform lay a solid foundation for potential applications in wireless sensing, structural health monitoring, and biomedical devices.

8:00 PM EL06.07.08

Near-Infrared Signal-Based Sensor Platform with Wireless Data Transmission System for Accurate Detection of Infectious Disease Virus SuyeonKim, EunyoungJeon, SunghyunPark and JoonseokLee; Hanyang University, Korea (the Republic of)

Luminescent nanomaterial-based Lateral flow immunoassay (LFA) is widely used in on-site detection of infectious virus. Foot-and-mouth disease virus (FMDV) is a highly contagious infectious disease virus that can be spread over long distances in the air. The keys for reducing the risk of infectious disease spread and economic damage are: 1) rapid and sensitive on-site detection, and 2) real-time surveillance and remote monitoring in the field. However, on-site saliva samples from livestock are considerably opaque due to the high levels of contaminants and biological components such as food, feces, soil, and blood. These interfering agents in clinical saliva samples interfere with the detection of colorimetric signals of LFA by the naked eye. Commercial gold nanoparticle-based LFA, whose excitation and emission are located in the visible region, is limited in their low sensitivity affected by the background interference in the opaque sample. Here, we report a high sensitive detection of FMDVs in clinical samples and the wireless monitoring system of FMD's outbreak. We introduced near-infrared (NIR)-to-NIR upconversion nanoparticles (UCNPs) as a nanoprobe of the LFA platform for background-free sensitive detection of FMDV. The NIR-to-NIR UCNPs are effective in minimizing the interference noise of opaque biological samples because the interfering agents in the samples have low autofluorescence, scattering, and absorption within the NIR window. This NIR-to-NIR nanoprobe shows stable emission intensity at 800 nm without being disturbed by interfering agents under 980 nm excitation. The sensitivity of LFA assembled with NIR-to-NIR nanoprobe (denoted as NIR signal LFA) was improved in opaque clinical samples. The NIR signal LFA has 32-fold lower limit of detection (LOD) compared to a commercial gold nanoparticle-based FMDV LFA for assay using live FMDVs for all 7 serotypes. 148 clinical samples including saliva and vesicular fluid samples were used to validate the sensing performance of NIR signal LFA for FMDVs. The NIR signal LFA successfully detected FMDVs in clinical samples with a high sensitivity of 96.9%, and a specificity of 100.0%. In addition, information such as virus-detection results and infection location were successfully stored and transmitted in real-time through an online server. The developed platform is promising for establishing a quarantine linkage system that can effectively prevent and control the spread of FMDV at an early stage.

8:00 PM EL06.07.09

A Local Water Molecular-Heating Strategy for NIR Long-Lifetime Imaging-Guided Photothermal Therapy of Deep-Tissue-Bearing Tumor DongkyuKang, HyungshikKim, InaeLee, DongyunLee and JoonseokLee; Hanyang University, Korea (the Republic of)

1.0 μm near-infrared (NIR) is considered unsuitable as an imaging and analytical signal in biological environments owing to the strong absorption of water at around the regions. However, the 1.0 μm NIR can be converted to heat and used as a local water-molecular heating strategy for photothermal therapy of biological tissues. Herein, we designed a we developed Nd-sensitized 1.0 μm emissive core@shell NPs ($\text{NaYF}_4:50\% \text{Yb}@ \text{NaYF}_4:40\% \text{Nd}, 20\% \text{Yb}$, denoted as water-heating NPs) as a local water-molecular heating material as a strong 1.0 μm emissive NP to target the absorption band of water. Especially, the strong energy absorption coefficient derived from the overtones and the stretching vibrations of O-H oscillators matches the emission spectrum of water-heating NPs. Furthermore, introducing Tm ions into the water-heating NPs enabled the NIR lifetime, and it was developed as an NIR imaging-guided water-heating probe (water-heating NIR NPs). In the glioblastoma multiforme (GBM) mouse model, tumor-targeted water-heating NIR NPs reduced the tumor volume by 78.9% in the presence of high-resolution intracranial NIR long-lifetime imaging. Hence, water-heating NIR NPs can be used as a novel nanomaterial for imaging and photothermal ablation in deep-tissue-bearing tumor therapy.

8:00 PM EL06.07.10

Enhanced Thermoelectric Properties of $\text{Bi}_{0.4}\text{Sb}_{1.6}\text{Te}_3$ Through the Decoration of SnO_2 Nanoparticles SungWookYe¹, JeongminKim², SehoonSeo¹, Dae-HwangYoo¹ and JongWookRoh¹; ¹Kyungpook National University, Korea (the Republic of); ²Daegu Gyeongbuk Institute of Science and Technology, Korea (the Republic of)

Thermoelectric energy harvesting has emerged as a promising solution to mitigate global climate change by enabling the conversion of waste heat into electricity. The efficiency of thermoelectric devices relies heavily on the performance of thermoelectric materials, evaluated through the thermoelectric figure of merit (ZT). ZT is defined as $ZT = S^2\sigma T/\kappa$, where S, σ , T, and κ represent the Seebeck coefficient, electrical conductivity, absolute temperature, and thermal conductivity, respectively. To achieve high ZT values, thermoelectric materials must exhibit high σ and S values while minimizing κ , particularly κ_{elec} and κ_{lat} . However, independently controlling these parameters is challenging, making simultaneous optimization of these thermoelectric properties difficult.

Numerous studies over the past few decades have focused on enhancing the power factor (σS^2) by manipulating carrier density or conducting band engineering. Additionally, reducing κ_{lat} through nanostructuring or maximizing phonon scattering has been explored to achieve low thermal conductivity. Among various thermoelectric materials, $\text{Bi}_{0.4}\text{Sb}_{1.6}\text{Te}_3$ (BST) stands out as a material capable of converting temperature differences into electricity. Consequently, BST-based alloys have been investigated to improve thermoelectric performance by incorporating other materials as nanoparticles, aiming to increase the power factor and decrease thermal conductivity. However, the trade-off relationship between electrical and thermal properties presents challenges in simultaneous control.

To overcome this trade-off, we propose a novel approach called the metallization of surface reduction nanoparticle method. This method enables independent control of electrical and thermal properties, offering enhanced stability in the interface between the base material and the surface. SnO_2 , a typical n-type semiconducting oxide, exhibits unconventional behavior due to disruptions in the stoichiometric ratio of tin and oxygen caused by interstitial Sn atoms or O vacancies. The reduction reaction from the surface allows the existing base material (SnO_2) to form crystals without surface amorphousness, facilitating sequential arrangement ($\text{SnO}_2 - \text{SnO}_x - \text{Sn}$ rich) from SnO_2 (in the core) to metallic Sn (on the surface).

Based on this principle, we fabricate n-type SnO_2 -decorated BST alloys using a combination of microwave irradiation, ball milling, and spark plasma sintering processes. These processes prevent the synthesis of SnO_2 nanoparticles with other elements from BST, enabling the decoration of pure SnO_2 nanoparticles onto the surface of the BST matrix (BST- SnO_2). We confirm the presence of approximately 100nm-sized SnO_2 nanoparticles as a secondary phase on the BST matrix, exhibiting excellent dispersion. By decorating the surface with SnO_2 nanoparticles, the average thermoelectric figure of merit (ZT) improves from 0.78 to 1.24 at 400K. The observed enhancement in thermoelectric performance can be attributed to two primary factors. Firstly, in terms of electrical properties, the power factor improves due to a slight reduction in electrical conductivity and a significant increase in the Seebeck coefficient. Secondly, in terms of thermal properties, the total thermal conductivity experiences a slight reduction due to the reduced electrical thermal conductivity and the suppression of bipolar thermal conductivity.

8:00 PM EL06.07.11

Photonic Surface Energy Modification for Enhanced Flexible Substrate in Printed Electronics MohamadTaherian¹, ArjunWadhwa², KrunalShah², Francois-XavierFortier², SylvainG. Cloutier² and MartinBolduc¹; ¹Université du Québec à Trois-Rivières, Canada; ²École de Technologie Supérieure, Canada

This paper presents a comparative study on surface energy modulation to enable new types of enhanced surfaces from flexible polyimide that is necessary in printed electronics. The survey conducted in this research work focused on the impact of the surface structure modification on the surface energy of polyimide flexible substrates, which was measured through contact angle analysis using a calibration method from different liquids. We employed three distinct methods for the surface modification: from controlled mechanical abrasion with various sandpaper grit values to finer photonic irradiation methods using Laser-induced Periodic Surface Structures (LIPSSs) and Intense Pulse Light (IPL) with a sacrificial ceramic layer. The results revealed that these surface structure modifications had significant effects on the surface energy value, leading to improved wet-ability and adhesion strength. In addition, we found that optimizing surface energy values of the substrate to the proper printing ink is crucial, especially at the early stage of the printing work. The photonic process is shown to enable the control of surface structures size and periodicity, which provide control on ink spreading and allow an adequate interfacial bonding during printing. These findings bring valuable insights into the optimization of flexible substrates for printed electronics, offering higher performance and expanding the potential applications in this rapidly evolving field.

8:00 PM EL06.07.12

Modeling Vapor Transport in Nanoporous Materials for Solar-Interfacial Evaporating Materials James H. Zhang, Rohith Mittapally, Guangxin Lv and Gang Chen; Massachusetts Institute of Technology, United States

Fresh water scarcity is a growing challenge for many communities due to global warming. Solar desalination by direct evaporation is an attractive method to produce fresh water from brackish sources due to its simplicity and low capital costs. Many research groups have shown solar evaporation rates beyond the thermal limit by using porous materials that can efficiently utilize solar energy to evaporate water from its capillary pores. Although a lot of research has been focused on the material's development side, there is insufficient understanding on the heat and mass transport inside of the porous materials and how the internal geometry can be optimized to maximize evaporation into the ambient. In this work, a heat and mass transport model is proposed to understand the evaporation process inside of materials with microchannels surrounded by nanoporous walls. Results are compared with experimental studies on solar-interfacial evaporation from porous materials to show how this model can be used to optimize the material properties for solar desalination.

8:00 PM EL06.07.13

Highly Transmissive Scalable Colored Silica Nanoparticle Coatings for Photovoltaic Panels Akbar Syed¹, Clark Boyd² and Hani Elsayed-Ali¹; ¹Old Dominion University, United States; ²Evergreen Technologies, United States

Large area highly transmissive colored coatings were fabricated by roll coating of SiO₂ nanoparticles on glass substrates and on the photovoltaic cell glass covers. This coating is to maintain an attractive color appearance of the exterior surface for architecturally integrated photovoltaics and can be coated on fabricated photovoltaic panels. These nanoparticles form ordered layers with thickness that can be controlled from one layer of nanoparticles to several layers. The color and optical properties of the nanoparticle coating was investigated for different SiO₂ nanoparticles with diameters of 200, 300, and 400 nm, which showed blue, pink, and green colors, respectively. Multilayer coatings of the nanoparticles coated on polycrystalline silicon solar cells provided blue, pink, and green colors with solar cell power loss of 5.47 %, 15.61 %, and 10.73 % for the 200, 300, and 400 nm, respectively. Single-layers act as an antireflection coating enhancing solar cell power without a noticeable change in solar cell appearance. Power gain of 3.39 % and 3.21 % is observed for single-layer of 200 and 400 nm nanoparticles, respectively.

8:00 PM EL06.07.14

Thermal Radiative Switching Interface for Energy-Efficient Temperature Control Xuanjie Wang¹ and Shankar Narayan²; ¹Massachusetts Institute of Technology, United States; ²Rensselaer Polytechnic Institute, United States

Materials with dynamically switchable optical properties can modulate their interaction with sunlight, potentially saving significant energy for heating and air-conditioning if used as building exteriors. This study proposes a new technique for solar-thermal regulation using porous polytetrafluoroethylene (PTFE) layers integrated with a spectrally-selective absorber (PTFE-SS). This multilayered structure can provide tunable optical properties by wetting or dewetting the porous PTFE with a refractive index-matching liquid, allowing a highly reversible change in solar transmittance of 0.62. This variation allows the multilayered structure to switch between highly reflecting and absorbing states that is tunable using different PTFE thicknesses. With this multilayered structure as building exteriors, sunlight can be reflected or absorbed to reduce dependence on conventional heating and cooling systems driven by non-renewable primary energy sources. When exposed to 1 sun illumination under ideal conditions, this variation allows a 51 °C change in PTFE-SS steady temperatures. When applied to buildings as roofing materials, the PTFE-SS promises significant energy reduction with annual cooling and heating savings of around 77% and 27%, respectively. Hence, the proposed PTFE-SS structure presents a new paradigm for passive thermal management of buildings by controlling their interaction with sunlight and decreasing our dependence on fossil fuels.

Reference: X. Wang and S. Narayan, "Thermal radiative switching interface for energy-efficient temperature control," *Renew. Energy*, vol. 197, pp. 574–582, Sep. 2022, doi: 10.1016/j.renene.2022.07.143.

8:00 PM EL06.07.15

Plasmonic Controlled Nonreciprocal Transmission of Ultrasonic Waves in an Acoustic Meta-Atom Arup Neogi^{1,2}, Jiaxin Wang¹, Yuqi Jin², Teng Yang², Zhiming Wang¹ and Tae Choi²; ¹University of Electronic Science and Technology of China, China; ²University of North Texas, United States

Controlling the direction of energy flow in a matter-wave or vibrational mode of oscillation is challenging compared to electrons or electromagnetic waves. Vibrational or acoustic waves are dominantly longitudinal in nature and are not directly influenced by electric, magnetic, or electromagnetic fields. Effective control of the directionality of sound wave propagation and reversing the flow of energy can yield acoustic isolators, diodes, or rectifiers. Current nonreciprocal techniques use complex metamaterial systems or require large mechanical pumps for physical actuation of the medium to break the time-symmetry or require asymmetric structures that induce dissipation. The mechanical actuation process is also slow and cannot be precisely controlled. A new class of acoustic meta-atom-based laser-driven nonreciprocal acoustic devices is demonstrated. Novel light-controlled techniques are used to control the nonreciprocal transmission of sound waves. A photoacoustic or magneto-optical pump based on nanophotonic principles has been used to control fluid flow within meta-atom in the form of a ring resonator or linear Bragg cavity. Instead of mechanical actuation and flow pumps, a non-contact laser and or magnetic force field are applied for remote control of the acoustic energy to modulate the direction of the acoustic wave propagation transmitted through the fluid medium.

In the first case, a fluid-filled acoustic meta-atom cavity in the form of a 2cm diameter ring resonator was designed using 3D printing to confine acoustic modes excited by an external transducer as a probe wave. A photo-elastic process induced by lasers resonant to the plasmon frequency of Au-implanted quartz windows can induce pump ultrasonic waves within this meta-atom cavity. The plasmonic window was fabricated using metal-ion implantation or photo-thermal evaporation of metal to form plasmonic nanoparticles resonant to a 532nm laser source. The photo-elastic effect also acts as a fluid pump and induces an active motion of the fluidic medium within the cavity. The ponderomotive forces can drive the fluid within the meta-atom cavity that can either co-propagate or counter-propagate with acoustic waves in the cavity. The fluid motion within the cavity and the wave mixing between the laser-induced pump waves and the external probe waves can result in a nonreciprocal or unidirectional transmission of sound waves within the acoustic cavity. A fluid flow as fast as 6 cm/s was generated that can induce a nonlinear wave mixing and active motion for T-symmetry violation resulting in nonreciprocal wave transmission within the meta-atom resonator. A large nonreciprocity exceeding 25dB was observed. An optically controlled acoustic diode operation was realized and the transmission of the acoustic wave can be biased using the laser intensity. In the second case, a DBR cavity-like device design was used to demonstrate magneto-optically controlled acoustic nonreciprocity. In this case, a magneto-caloric force based on the temperature-dependent magnetization of the ferrofluid was used to drive the fluid in the presence of a magnetic field. Acoustic isolation due to nonreciprocity as large as 20dB was realized which can be controlled by the magnetic field strength and the laser intensity.

We used theoretical analysis, and numerical simulation for the design of additively manufactured ultrasonic devices which were then characterized using ultrasonic spectroscopy for the study of nonreciprocal acoustic wave transmission. Quantum optical effects such as Zeeman-like and Optical Stark-like effects on acoustic states have been observed. Ultrasonic spectroscopy characterized the optically driven diode and the isolator. This work is the first report on the realization of laser and magneto-optical control of ultrasonic acoustic diodes and isolators in a compact fluidic medium.

8:00 PM EL06.07.16

Micro-Structured Heat Exchangers for Energy-Efficient Control of Temperature and Humidity Rohith Mittapally, Yaodong Tu, James H. Zhang and Gang Chen; Massachusetts Institute of Technology, United States

As the climate extremities continue to rise, the demand for air-conditioning (AC) is expected to increase 3-fold in a few decades¹. To reduce the carbon-footprint of AC systems, it is necessary to make them more efficient. The conventional vapor-compression systems over-cool the process air for dehumidification, resulting in a low coefficient of performance (COP). Incorporating liquid desiccants into these systems can improve the COP by 2-fold². Recent efforts in this direction have resulted in efficient AC systems, but these large-scale demonstrations are not readily suitable for residential applications. Here, I will discuss the development of a heat exchanger with simultaneous heat and mass transfer characteristics, which can improve the efficiency of residential AC systems. In specific, the designed heat exchanger exhibits faster absorption-desorption kinetics with negligible carry-over of a liquid desiccant into the process air. In this talk, I will first discuss the fabrication of the heat exchanger and describe the development of a test chamber to characterize its performance. Our preliminary experiments on individual fins indicate an efficient moisture control at adsorption rates faster than state-of-the-art systems. Further, I will discuss a theoretical model that can predict the experimentally observed heat and mass transfer dynamics. Finally, I will discuss our efforts at scaling these techniques for low-cost mass production of heat exchangers for an efficient AC cycle.

(1) Campbell, I, Kalanki, A, Sachar, S, Solving the Global Cooling Challenge: How to Counter the Climate Threat from Room Air Conditioners; Rocky Mountain Institute: 2018

(2) Tu, Y, Wang, R, Ge, T, New concept of desiccant-enhanced heat pump. *Energy conversion and management*, 2018, 156, 568-574

8:15 AM *EL06.08.01

Broadband Nanophotonics: From Theory to Application [Aaswath P. Raman](#); University of California, Los Angeles, United States

While many applications of nanophotonic structures are geared towards narrow bandwidth applications, over the past decade there has been significant interest in better controlling the flows of broad spectrum light. From thermal imaging to solar cells and radiative cooling, interacting with broad spectrum light imposes numerous demands on nanophotonic structures and devices. In this talk we will introduce theoretical, computational and experimental demonstrations of the exceptional control and performance possible when optimizing for broadband applications. We will introduce approaches to enhance both transmissive and reflective optical components for thermal imaging, making use of resonant metasurfaces that enable high transmission through Silicon over infrared wavelengths, and a plasmonic reflective filter using a low-cost, solution-processed approach for a reflective optic. We will next explore machine learning approaches to optimizing broad spectral responses, and highlight how a multiscale approach to controlling broad spectrum emissivity is possible even in ultralight photonic structures that might be used for aerospace applications. Finally, we will introduce a coupled mode theory framework capable of accurately modeling multi-resonant systems that can control broad spectrum thermal emission from a bottom-up perspective.

8:45 AM EL06.08.02

Ultrafast Energy Transfer from Plasmonic Hot Carriers: Disentangling Injection Mechanisms in Pulsed Photocatalysis [Andrea Schirato](#)^{1,2,3}, Stephen K. Sanders³, Remo Proietti Zaccaria^{2,4}, Peter Nordlander^{3,3}, Giuseppe Della Valle^{1,5} and Alessandro Alabastri^{3,1}; ¹Politecnico di Milano, Italy; ²Istituto Italiano di Tecnologia, Italy; ³Rice University, United States; ⁴Chinese Academy of Science, China; ⁵Consiglio Nazionale delle Ricerche, Italy

Photocatalysis involves capturing energy from light to initialise and promote chemical reactions of industrial and environmental relevance. In the process, the photocatalyst absorbs and converts photons into charge carriers, driving thermodynamically favourable and non-spontaneous reactions. Since, as for natural photosynthesis, sunlight can be used, photocatalysis represents an attractive sustainable alternative to current chemical industrial processes, which often require intensive energy input, are fed by non-renewable sources and operate at high temperatures and pressures. In this framework, increasing attention has been drawn to plasmonic photothermal catalysis, offering opportunities for light-driven reactions under substantially milder conditions. At the interface between chemistry, nanophotonics and thermodynamics, this approach relies on plasmonic nanostructures and their peculiar optical properties. These nanostructured metallic materials couple strongly to light and support resonant oscillations of their free electrons, known as Localized Surface Plasmons. Their ability to concentrate electromagnetic visible radiation, excite highly energetic (hot) carriers, and locally convert their excess energy into heat via ultrafast non-radiative relaxation processes has made them crucial in various applications. In the context of catalysis, strong interaction between light and plasmonic nano- and metastructures (especially metasurfaces) provides the energy needed for photocatalytic conversion, and photoexcited nanoparticles can alter chemical reactions through both thermal and non-thermal pathways, close to the thermodynamic limit.

Among the mechanisms involved in photocatalysis, the hot carrier contribution is at the same time the most intriguing, as it leads to unique phenomena (e.g., changes in energy barriers for certain reactions) and the most challenging to control, mainly due to the carrier internal relaxation (which, on ultrafast timescales, brings them back to equilibrium). While promising advances have been reported on the carrier generation and ultrafast dynamics, a comprehensive theoretical description of their behaviour when interacting with nearby chemical species is missing. This is pivotal towards the accurate modelling of the energy harvesting from light to catalyse chemical transformations.

Here, we propose a novel approach to model the ultrafast dynamics and ensuing effects of hot carriers across extended plasmonic nanostructures in the presence of adsorbed molecules resonantly accepting energy from the photoexcited electrons. For that, we develop a numerical platform based on a rate-equation model of the excitation/relaxation of nonequilibrium carriers, where the injection of electrons to the molecule acts as an extra decay channel. Our approach combines the well-established quantum description of inelastic electron scattering with 'hot' adsorbate (generating transient negative ions) with a thermodynamics-like formalism (approximating the Boltzmann equation) for nonequilibrium electrons in metals. This results in a compact model enabling us to track over time and space, with a resolution of less than 1 fs and a few nm across nanostructures/meta-atoms of hundreds of nm, the evolution of the electronic energies in the metal upon pulsed illumination. The accurate modelling of the carrier spatio-temporal dynamics unlocks relevant information, e.g., reaction rates and quantum yields. Furthermore, with this model, we are able to disentangle the contributions arising from thermal effects and charge injection, and to quantify the impact of input variables such as pulse fluence and duration, photon energy, nanostructure dimension and shape. Our results are a promising step towards the design of photocatalytic platforms with enhanced electronic and thermal effects and provide a comprehensive, predictive approach suitable for directly comparing theory and experiments.

9:00 AM *EL06.08.03

Designing Chemical Reactivity in Plasmonic Nanogaps [Regina Ragan](#); University of California, Irvine, United States

I will present data on vibrational spectroscopy alongside state-of-the-art computational methods to 'visualize' chemical reactions in plasmonic nanogaps in order to understand physical and chemical cues governing reactions between functional groups on molecules. An experimental platform, using electrohydrodynamic (EHD) flow, which produces flow fields in solution with components parallel to an electrode surface in the presence of a perturbation, is used to facilitate interactions between plasmonic nanoparticles (NP). Au NP from colloid are first deposited using electrophoresis to seed EHD flow on a working electrode patterned with polystyrene-*block*-poly(methyl methacrylate) (PS-*b*-PMMA) copolymer. Au NP with ligands having carboxylic acid functional groups attach to ethylenediamine functionalized PMMA domains using carbodiimide coupling chemistry. After, an AC potential with a bias of 10 V_{pp} is applied resulting in EHD flow around Au NP seeds. Electron microscopy analysis of clusters chemically crosslinked during assembly shows deposition with a potential having an amplitude of 5 V and frequency of 500 Hz produces surfaces with a high density of Au NP trimers with 1 nm gap spacings controlled by crosslinking chemistry.

We have monitored crosslinking reactions between Au seeds and Au NPs deposited using EHD flow using surface-enhanced Raman scattering (SERS) *in situ*. Au NP functionalized with either lipoic acid, 4-mercaptophenylacetic acid and 4-mercaptobenzoic acid ligands may form anhydride bridges using carbodiimide crosslinking chemistry and reactivity appears governed by the proximity between the reactive carbon atom in the *O*-acylisourea intermediate and the deprotonated oxygen atom from molecular dynamics simulations. Comparing experimental spectra with that simulated using density functional theory simulations indicate that chemical reactions within nanogaps are promoted by the confined geometry, i.e., entropically driven sampling of molecular conformations in nanogaps leads to reactions. Reactions do not occur in the absence of EHD flow; the long range EHD driving force allows chemical reactions with high activation energy barriers to proceed in observable time frames. The temporal evolution of an acetylation reaction between analytes and anhydride bonds in plasmonic nanogaps will also be presented. Control of nanogap spacing and surface chemistry in plasmonic hotspots has numerous applications including molecular sensors, non-linear optics, and photocatalysis.

9:30 AM EL06.08.04

3D Interconnected Nanowire Scaffoldings that Increase the Thermoelectric Efficiency in Comparison to Similar Diameter 1D Nanowires [Marisol Martin-Gonzalez](#)¹, Alejandra Ruiz de Clavijo¹, Nicolas Perez², Olga Caballero¹, Kornelius Nielsch², Francesca Peiró³ and Segi Plana³; ¹Inst de Micro y Nanotecnologia, Spain; ²Ifw Dresden, Germany; ³Universidad de Barcelona, Spain

We will present how 3D interconnected nanowire scaffoldings can increase the thermoelectric efficiency in comparison to similar diameter 1D nanowires and films grown under similar electrodeposition conditions. Bi₂Te₃ 3D nanonetworks offer a reduction in thermal conductivity (κT) while preserving the high electrical conductivity of the films. The reduction in κT is modeled using the hydrodynamic heat transport equation, and it can be understood as a heat viscosity effect due to the 3D nanostructure or to additional scattering centers. The Seebeck coefficient is twice that of nanowires and films, and up to 50% higher than in a single crystal. This increase is interpreted as a nonequilibrium effect that the geometry of the structure induces on the distribution function of the phonons, producing an enhanced phonon drag. These thermoelectric metamaterials have higher performance and are fabricated with large areas by a cost-effective method, which makes them suitable for up-scale production. Other studies have also explored the transport properties of Bi₂Te₃ nanowires, including low temperature magnetoresistance measurements and local magnetic suppression of topological surface states. The crystalline structure and composition of the 3D Bi₂Te₃ nanowire network can be finely tuned by controlling the applied voltage and the relaxation. These findings have important implications for the development of macroscopic nanostructured thermoelectric materials based on scalable fabrication processes that could be directly integrated into devices. The study of the localization and directionality of electron transport in Bi₂Te₃ ordered 3D nano-networks is a fascinating area of research. In this study, the resistance of an ordered 3D-Bi₂Te₃ nanowire nano-networks were analyzed at low temperatures, and the increase in resistance below 50 K was found to be compatible with the Anderson model for localization.

The angle-dependent magnetoresistance measurements showed a unique weak anti-localization characteristic with a double feature, which could be associated with transport along two perpendicular directions dictated by the spatial arrangement of the nanowires. The coherence length obtained from the HLN model was about 700 nm across transversal nanowires, corresponding to approximately 10 nanowire junctions. The observed localization effects could be the reason for the enhancement of the Seebeck coefficient observed in the 3D-Bi₂Te₃ nanowire nano-network compared to individual nanowires. This research has important implications for the development of macroscopic nanostructured thermoelectric materials based on scalable fabrication processes that could be directly integrated into devices.

9:45 AMBREAK

10:15 AM EL06.08.05

Acoustic Metamaterials at the Microscale Rachel Sun, YunKai and [CarlosM. Portela](#); Massachusetts Institute of Technology, United States

Micro-architected materials allow for tunability of extreme static mechanical properties such as stiffness, Poisson's ratio, or strength. However, dynamic and acoustic properties of micro-architected materials remain largely unexplored, partially because it is challenging to measure their response at these scales. Dispersion resulting from Bragg scattering occurs at wavelengths which are dictated by the characteristic dimensions of the metamaterials, while local resonance remains wavelength-independent. Therefore, micro-architected materials have the potential to allow control of mechanical waves both at high (MHz) and medium-range (kHz) frequencies.

Here, we design, fabricate, and characterize micro-architected materials with tunable mechanical and acoustic properties in the megahertz regime. Using a two-photon lithography prototyping method, we explore the response of a class of architected material morphologies with varied mass distribution, features down to $\sim 1.5 \mu\text{m}$, and unit cell sizes of $15 \mu\text{m}$. We demonstrate that decoupling mass and stiffness by strategically placing micro-inertia affects the effective stiffness scaling of this class of acoustic metamaterials at the microscale. We present novel measurement techniques for wave velocity of three-dimensional architected materials that employ laser-ultrasonic principles, demonstrating a tunable range of wave velocities around 1000 m/s for different designs in a wide range of relative densities. We then validate their acoustic response numerically with Bloch wave analysis to determine their dispersion relation and rod-wave velocities. Our results provide a baseline to map the tunable acoustic metamaterial design space at the microscale and megahertz regime. These materials could have important implications in acoustic devices in microelectromechanical systems, biomedical imaging, and microscale waveguides.

10:30 AM EL06.08.06

Mechanical Metamaterials Enabling Knudsen-Pump-Based Propulsion for Novel Sensor-Based Mesosphere Exploration [ThomasCelenza](#), AndyEskenazi, ZhipengLu, LorenzoYao-Bate and IgorBargatin; University of Pennsylvania, United States

We propose a novel flight mechanism powered solely by light, with no moving parts, capable of photophoretically levitating metamaterials with kilogram-scale payloads. The ability to study certain atmospheric regions, such as the mesosphere, is hindered by current propulsion methods. The urgency to address climate change makes learning about all layers of the atmosphere imperative. For example, carbon dioxide in the mesosphere is critical due to its cooling effect, a crucial factor in climate prediction models [1]. Unfortunately, recording atmospheric data in the mesosphere is challenging due to air pressures that are too low for aerodynamic plane or balloon flight and too high for satellites. Developing an airborne platform operating in a low-density, low-pressure atmosphere on Earth for gathering atmospheric data related to wind patterns, temperature, pressure variations, and gas concentrations would be tremendous. Our proposed solution leverages the mesosphere environment through architected metamaterials to generate a high-speed gas jet due to Knudsen pumping [2], allowing controllable lift.

Nanocardboard, the metamaterial that achieved photophoretic flight, was created for tuning material properties such as increased bending stiffness and strength, shape recovery capabilities, and weight reduction [3]. Nanocardboard is a microfabricated analog of sandwich composites (like cardboard), made of Al_2O_3 . The structure consists of 0.1-micron face sheets on top and bottom, connected by several micron tall hollow rectangular channels, giving an area density of approximately 1 g/m^2 . For our purposes, we coated 1-cm wide nanocardboard plates with carbon nanotubes (CNTs). Due to the Al_2O_3 being an exceptional thermal insulator, a temperature difference between the top and bottom of the plates is introduced, given that CNTs absorb light and heat up. This temperature difference drives air through the channels and creates a lift force due to the Knudsen-pumping effect. Optimal at mesosphere air pressures, this phenomenon is known as photophoretic levitation. However, with such small plates, the experimentally recorded lift force is only a few milligrams [4]. Photophoretic levitation is not new for macroscale objects, but increasing payloads becomes more interesting.

Hence, we created a MATLAB model to scale the photophoretic force, employing nanocardboard on a large scale, simulating 3D structures with dimensions of tens of meters. The geometries included spheres, rockets, and cones, made of nanocardboard, with CNTs on the inner walls. When illuminated, CNTs heat up to Knudsen-pump air into the hollow inner chamber and out of a nozzle to create jet velocities, increasing lift. The model considers flight altitudes from sea level to 80 km in the atmosphere. We analytically solved a heat transfer system to calculate the temperature inside the structure. When the CNTs heat up, they heat the surrounding air in the inner chamber, decreasing its density and creating a buoyancy force. This solar buoyancy regime loses significance as the photophoretic regime starts dominating around 40 km, where balloons can no longer fly. We calculate the overall lift force from a characteristic equation discovered in our previous work [5] combined with the solar buoyant force. The results show a several-kg payload for a 30-meter radius spherical structure, which is comfortably sufficient to carry atmospheric data sensors like GPS and thermocouples from sea level to 80 km. These structures present brand-new flight mechanisms in the mesosphere, enabled by the unique mechanical and thermal properties of the nanocardboard metamaterial.

[1] Goessling, Helge, et al. *Earth System Dynamics* 7.3 (2016): 697-715

[2] Wang, Xiaowei, et al. *Microsystems & Nanoengineering* 6.1 (2020): 26

[3] Lin, Chen, et al. *Nature communications* 9.1 (2018): 4442

[4] Cortes, John, et al. *Advanced Materials* 32.16 (2020): 1906878

[5] Celenza, Thomas, et al. *arXiv preprint arXiv:2301.04281* (2023)

10:45 AM EL06.08.07

Laser-Based Ultrasound Spectroscopy for Characterization of Mechanical Metamaterials YunKai, ThomasPeziril and CarlosM. Portela; Massachusetts Institute of Technology, United States

Mechanical metamaterials, possessing custom-designed 3D structures at the nano- to microscale, exhibit exceptional properties that surpass those of their constituent materials. These structures unveil a diverse mechanical property landscape. Previous studies relied primarily on contact-based methods for mechanical characterization, such as nanoindentation, extracting static properties like stiffness and strength. These techniques often necessitate laborious sample preparation or specialized sample designs. There is a need for time-resolved characterization techniques to accelerate the process of characterizing the mechanical behavior of metamaterials and broaden our understanding of their dynamic response.

We present a characterization method for metamaterials that allows us to capture their effective dynamic elastic constants and linear dynamic response in a reliable and iterative manner. We fabricate architected materials using two-photon lithography with feature sizes on the order of $\sim 1 \mu\text{m}$ and unit cells on the order of $10 \mu\text{m}$. We employ a laser ultrasonic scheme to determine their effective elastic properties to excite elastic waves within the materials. We utilize a common-path interferometric setup to register the sample eigenvibrations. We experimentally reconstruct partial dispersion relations and attenuation properties of the 3D micro-architected materials, present their fully experimental dynamic elastic surfaces, and demonstrate the potential to use dynamic responses to identify defects in these materials. We validate this technique using a variety of 3D architectures along various crystallographic orientations. The field of mechanical metamaterials is in need of novel characterization techniques since, at this point, the design of new metamaterials has significantly outpaced efforts to construct structure-property relations. Our work addresses this need and provides a route for the accelerated data-driven discovery of materials and microdevices for dynamic applications such as protective structures, medical ultrasound, or vibration isolation.

11:00 AM EL06.08.08

Frequency Responsive Metamaterials for Contactless Acoustic Manipulation [SamKeller](#), MatthewStein, YujieLuo and OgnjenIlic; University of Minnesota-Twin Cities, United States

The radiation pressure of waves—such as acoustic waves or electromagnetic waves—enables mechanisms for entirely contactless actuation of objects with relevance spanning materials assembly, bioengineering and biomedicine, and imaging and sensing. However, the ability to control such motions is substantially limited by the way conventional objects scatter waves. For instance, acoustic actuation is often restricted to small (subwavelength) objects or objects with specific symmetries where actuating energy potentials are easy to create. Additionally, this form of contactless manipulation often features single-task devices that can only produce a single dynamic response. Here, we show how such wave force limitations can be overcome by embedding subwavelength metasurface patterns to alter the acoustic momentum of inaudible ultrasonic fields locally. Consequently, these metasurfaces can facilitate precise control of local acoustic forces independent of the size or shape of the object. We present the theory, modeling, and experiments to support the development of metasurfaces exhibiting novel dynamical behaviors, such as self-guiding metasurfaces and frequency-responsive metasurfaces. We survey several families of metasurface topologies and compare their advantages and limitations for contactless actuation. Additionally, we discuss the benefits and tradeoffs associated with ultralightweight acoustic metasurfaces. Our findings present a new approach to controlling radiation pressure forces and achieving dynamic behaviors that go beyond the limitations of traditional wave-matter interactions.

1:30 PM *EL06.10.01

Bound States in the Continuum in Dielectric and Plasmonic Metasurfaces: From Optofluidics to Thermal Emission Engineering Justus C. Ndukaife, Sen Yang, Guodong Zhu and Ikjun Hong; Vanderbilt University, United States

Recently, the concept of bound states in the continuum (BICs) has emerged as a promising approach to achieve sharp spectral resonances and strong electromagnetic field enhancements in plasmonic and dielectric metasurfaces. BICs represent eigenmodes that exist above the light cone but remain decoupled from the radiation continuum of free space. While true BICs, are completely invisible in the radiation spectrum and inaccessible, perturbations can lead to quasi-BIC modes characterized by a sharp spectrum peak and a finite quality factor (Q). In the first part of my talk, I will discuss the utilization of quasi-BIC modes to enable optofluidic control in all-dielectric metasurfaces. By exciting BIC modes, we can significantly enhance the speed of particle transport and assembly. The high-Q nature of quasi-BICs allows for precise tuning of particle assembly by adjusting the wavelength within a narrow spectral range. This enhanced optofluidic control enabled by quasi-BICs holds great potential for lab-on-chip applications, including analyte enrichment for sensing, on-chip mixing, and reconfigurable optically-active colloidal assembly. Moving on to the second part of my talk, I will introduce the use of plasmonic quasi-BICs for engineering thermal emission. Additionally, I will present a slotted quasi-BIC metasurface design that further enhances the quality factor of thermal quasi-BIC metasurfaces. Our numerical simulations demonstrate an ultra-narrowband emission peak with a Q factor of approximately 64 and near-unity absorptance over a broad band spanning more than 10 μm . By symmetrically introducing air slots, the Q factor can be further increased to around 100. Importantly, our experimental measurements confirm the remarkable stability of the resonance frequency in the face of temperature fluctuations. This research showcases the potential of plasmonic quasi-BICs in the design of ultra-narrowband thermal emitters that remain insensitive to temperature changes in the mid-infrared range. Furthermore, this concept can be readily adapted to other frequency ranges, such as near-infrared, Terahertz, and Gigahertz.

2:00 PM EL06.10.02

Enhanced Piezoelectric Energy Harvesting Through Multiband Elastic Wave Localization using Trampoline Metamaterials Geon Lee¹, Jeonghoon Park¹, Wonjae Choi², Bonggyu Ji², Miso Kim³ and Junsuk Rho¹; ¹Pohang University of Science and Technology, Korea (the Republic of); ²Korea Research Institute of Standards and Science, Korea (the Republic of); ³Sungkyunkwan University, Korea (the Republic of)

In this study, we investigate the efficient piezoelectric energy harvesting at both low and high frequency bands. Traditional energy harvesting platforms were limited to a narrow or high frequency range and showed insufficient electrical performances. To address this, we propose a novel piezoelectric energy harvesting platform based on a periodically arranged trampoline metamaterial with a defect. Our platform demonstrates exceptional electrical output at both low and high frequencies. By utilizing Bragg scattering, our platform expands the bandgap in the high frequency range, while the local resonance enables a wide bandgap in the low frequency range. Through the introduction of periodically broken structures, we create defect states that facilitate the trapping of flexural wave, capitalizing on fundamental physical phenomena. Through experimental validations, we confirm the localization of flexural waves within the defect cavity, which are efficiently converted into electrical energy using piezoelectric elements. Our measurements reveal an output voltage of 1.37 V and 4.05 V, as well as an output power of 24.4 μW and 1.28 mW at the 1st and 2nd defect modes, respectively. These values represent a significant improvement of 188% and 400% compared to the bare plate configuration. The high-power energy harvesting platform we present holds promising potential as a renewable and sustainable energy source in various applications, including structural health monitoring, signal processing, and sensors.

2:15 PM EL06.10.03

Glass Materials for Emission Stabilization Under High Temperatures Janet A. Elias¹, Luis A. Díaz-Torres², Gemma Perez-Cuellar¹, Pablo Reyes-Hernandez¹, Eduardo Montes¹ and Miguel Ángel Vallejillo Hernández¹; ¹Universidad de Guanajuato, Mexico; ²Centro de Investigaciones en Óptica, Mexico

By melt-quenching technique, sixteen samples of lithium diborate glass doped with Er^{3+} , Yb^{3+} , Dy^{+3} and containing Ag and Cu nanoparticles were synthesized. SEM micrograph is presented. X-ray diffraction patterns of all samples reveal their amorphous structure. Physical properties such as density, molar volume and boron-boron separation of amorphous materials are shown. UV-Vis-IR absorption spectra of all samples were recorded and display the characteristic bands of the used rare earths; all absorption bands present an enhancement with increasing metallic nanoparticles concentration. The estimated optical energy band gap of the samples was obtained using the Tauc plot method. Emission spectra of doped samples were collected in the temperature range from 30 to 180 °C. The results of emission under temperature indicate that the addition of metallic nanoparticles (Ag and Cu) in glass matrices are responsible for emission stabilization in samples when the temperature is increased creating a glass material for photonics and thermal sciences.

2:30 PM BREAK

3:30 PM *EL06.10.04

High-Temperature Thermal Energy Transport and Conversion using Photonic Nanostructures and Metamaterials Renkun Chen; University of California, San Diego, United States

High-temperature thermal energy transport, conversion, and management is fundamentally important for a multitude of energy processes, such as thermochemical, solar-thermal, thermophotovoltaic, thermal energy storage, and industrial heating, etc. Heat transfer physics at high temperature is also markedly different from its counterpart at room- and low-temperatures, including stronger phonon-phonon scattering leading to lower phonon thermal conductivity and the more prominent or even dominant role of radiation heat transfer. On the other hand, high temperature poses tremendous challenges on materials, especially on their thermal and chemical stability. Here we present two recent examples from our studies on photonic thermal energy transport and conversion at high temperature. First, we experimentally probed the more prominent role of surface phonon polariton (SPhP) in polar dielectric (e.g., SiO_2) nanostructures and studied their contribution to thermal radiation and conduction from room to high temperature. We show that the geometry of the polar dielectric nanostructures can be manipulated to engineer the SPhP-mediated thermal radiation and conduction. In particular, we observe photon-like heat conduction contributed by SPhP in SiO_2 nanoribbons. Second, we developed high-temperature selective emitters based on metamaterials. While metamaterial emitters have been widely explored, they are often not stable at high temperature due to the presence of nanoscale interfaces. We use novel material and structural designs to attain high temperature stability. These selective emitters could be used to more efficiently convert optical and electrical energy into thermal energy within a desirable spectrum that are useful for systems such as thermophotovoltaic and infrared heating.

4:00 PM *EL06.10.05

Thermal Photonics with Low-Dimensional Materials Georgia T. Papadakis, Michael Enders, Mitradep Sarkar and Maxime Giteau; ICFO – Institute of Photonic Sciences, United States

The blackbody spectrum for room temperature peaks at mid-infrared (IR) frequencies, making this spectral range of prominent importance for both fundamental science and technology. Examples include mid-IR thermal energy harvesting and radiative cooling, spectroscopy, molecular sensing and detection, thermal camouflage, and mid-IR free-space communications. Despite the relevance of mid-IR photonics, however, phase retardation, the process of rotating light's polarization and converting linear to circularly polarized light is limited to wavelengths up to approximately ten micrometers. Beyond this wavelength, due to the lack of strongly birefringent crystals and the prominent resonances in all polar media due to lattice vibrations (phonons), there exists no commercial phase retarder. In this talk, I will discuss how, by leveraging the strong frequency dispersion of a low-dimensional van der Waals crystal, a-molybdenum trioxide (a-MoO_3), we built the first deeply subwavelength phase retarders at mid-IR frequencies, achieving 90 degrees polarization rotation within a micrometer of material.

Using the strong frequency dispersion due to optical phonons in crystals, I will also discuss how one can build fully pattern-free heterostructures that can achieve directional control of thermal emission and absorption at mid-IR frequencies. By considering hexagonal boron nitride (hBN) as a thermal emitter, we theoretically predict thermal emission lobes that are comparable to those achievable with conventional gratings, yet without any lithography.

Furthermore, I will discuss approaches to leverage the strong anisotropy of several low-dimensional crystals to achieve deep-subwavelength control of optical chirality, without any nanopatterning. Chirality up to 0.8 is estimated with a-MoO_3 at mid-IR frequencies. I will discuss our current efforts to measure mid-IR chirality in the laboratory.

Furthermore, mid-IR-relevant low-dimensional materials, such as a-MoO_3 or hBN, are typically exfoliated in the laboratory, rather than grown in large scale. Exfoliated flakes are typically too small for mid-IR far-field optical experiments, due to the size mismatch between an IR beam and a flake. This introduces a major challenge: rather than being directly measured experimentally, for example via spectroscopic ellipsometry, the dielectric function of most low-dimensional materials is approximated by numerical fitting in experiments performed in the near-field, via scanning microscopy. I will introduce a robust method for retrieving the mid-IR dielectric properties of exfoliated flakes using far-field optics.

4:30 PM EL06.10.06

Controlled Growth of Titanium Oxynitride Thin Films for Plasmonic and Photovoltaic Applications Ikenna C. Chris-Okoro¹, Sheilah Cheron¹, Catalin Martin², Valentin Craciun^{1,3} and

Single crystalline pure titanium nitride (TiN) and partially oxidized titanium nitride (TiNO) thin films have been grown in a rock-salt structure using high vacuum conditions with and without intention oxygen ambience by a pulsed laser deposition (PLD) method. The films were grown under different vacuum conditions on different single-crystal substrates such as sapphire, silicon, and doped/undoped TiO₂. X-ray photoelectron spectroscopy (XPS) and Rutherford Backscattering spectroscopy analysis have shown that the oxygen content of the titanium oxynitride (TiNO) films increases with film thickness (or deposition time) and also with an increase in oxygen pressure during film deposition. The lattice constant of the TiNO films, measured using XRD, is found to increase with the oxygen content in the film. The lattice constant increase is explained using enhanced electrostatic repulsion between O²⁻ orbitals in the absence of vacant Ti³⁺ sites; in order to maintain charge neutrality within the lattice, one Ti³⁺ cation vacancy is created for every three substitutions of N³⁻ ions by O²⁻ ions. Despite the oxygen content, all films show metallic behavior, with a resistivity around 70-100 mW×cm and a carrier concentration of the order of $n_e \gg 10^{23} \text{ cm}^{-3}$, confirmed by (determined from) electrical transport, Hall effect and infrared spectroscopy measurements.

A spectroscopic ellipsometer was used to measure TiN/TiNO's spectroscopic optical properties and structural parameters. The reflection coefficient of TiN/TiNO films was measured within the electromagnetic spectrum range of 193 nm to 1690 nm by taking the ratio of perpendicular and parallel polarized light. The optical constants (refractive index, extinction coefficient, and film thickness) of the TiN/TiNO films were determined by analyzing the amplitude and phase difference components of the reflection coefficient where a line-shape analysis a point-by-point fit, or a parametrized function model were applied. A maximum in refractive index curves appears at a wavelength in the region of ~ 300 nm and a minimum at a wavelength range of 500-650 nm. The extinction coefficient plots of the films showed a minimum in the wavelength range of 300-400 nm. This result suggests that nitrogen present in the sample contributes to the additional critical point around 400 nm when compared to a pure TiO₂ layer in the literature. A widening of the absorption spectrum was seen, which indicates a narrowing of the bandgap when compared to TiO₂. We have observed a variation in the optical bandgap of the TiNO films as a function of film thickness. The band gap values obtained are suitable for the absorption of solar light in the full spectrum range, which indicates that the TiNO thin films can be used for converting solar light into electrical energy.

This work was supported by the NSF PREM on the Collaborative Research and Education in Energy Materials (CREEM) via grant # DMR-2122067 and the DOE EFRC on the Center for Electrochemical Dynamics And Reactions on Surfaces (CEDARS) via grant # DE-SC0023415.

4:45 PM EL06.10.07

Nanostructuring Plasmonic Dendron Core-Shell Nanoparticles: Energy and Charge Transfer Applications[Rigoberto C. Advincula](#); The University of Tennessee/Oak Ridge National Laboratory, United States

Organic-Inorganic hybrid nanomaterials and metamaterials accommodate interesting transport behavior when properly nanostructured by self-assembly or directed assembly. These hierarchical levels of relationships enable microscopic to the macroscopic transition of properties. Au nanoparticle plasmonics phenomena are well-known however, their utilizing beyond localized and propagating plasmons is the key to their appreciation of enhanced properties. This talk will highlight the use of dendron-based ligands of organic electro-active and electrochemically active organic molecules which can be used to enable specific energy and charge transfer properties with metal and quantum dot nanoparticles. Investigating these properties makes use of lateral ATR and surface-propagating plasmons methods, SPM, Electrochemistry, and fluorescence and scattering methods. The ability to control these transfer and transport properties enables new applications in sensing, solid-state display devices, sensors, and array structures that have macroscopic properties.

SESSION EL06.11: Novel Multiphysics Applications of Metamaterials

Thursday Morning, November 30, 2023

Hynes, Level 3, Room 308

8:15 AM *EL06.11.01

Three-Dimensional Colloidal Nanocrystal Metamaterials[Cherie R. Kagan](#); University of Pennsylvania, United States

Colloidal nanocrystals (NCs) have inorganic cores and organic or inorganic ligand shells. They are prized for their size- and shape-dependent properties and serve as building blocks of artificial materials and unconventional devices. Here, we describe NC-based, three-dimensional optical metamaterials constructed using imprinting techniques from single- and multiple-types of metal and metal oxide NCs. We focus on the chemical and thermal addressability of NCs, i.e., the ability to select, exchange, strip, or add atoms, ions, and molecules during or post-deposition, that is not accessible in bulk materials, and allows the control of metamaterial structure and properties. Through ligand engineering we tailor the dielectric function of metal NC assemblies through an insulator-to-metal transition.¹ By juxtaposing NC assemblies and bulk thin films to make bilayer heterostructures, we exploit ligand exchange to trigger folding of two- into three-dimensional structures,² which we use to achieve broadband^{3,4} and reconfigurable 3D chiral optical metamaterials. These structures can also be released from the surface to create and study active matter and its interface with microscale robotics.⁵

(1) Fafarman, A. T.; Hong, S.-H.; Caglayan, H.; Ye, X.; Diroll, B. T.; Paik, T.; Engheta, N.; Murray, C. B.; Kagan, C. R. Chemically Tailored Dielectric-to-Metal Transition for the Design of Metamaterials from Nanoimprinted Colloidal Nanocrystals. *Nano Lett.* **2013**, *13* (2), 350-357.

(2) Zhang, M.; Guo, J.; Yu, Y.; Wu, Y.; Yun, H.; Jishkariani, D.; Chen, W.; Greybush, N. J.; Kübel, C.; Stein, A.; Murray, C. B.; Kagan, C. R. 3D Nanofabrication via Chemo Mechanical Transformation of Nanocrystal/Bulk Heterostructures. *Adv. Mater.* **2018**, *30* (22), 1800233.

(3) Guo, J.; Kim, J.-Y.; Zhang, M.; Wang, H.; Stein, A.; Murray, C. B.; Kotov, N. A.; Kagan, C. R. Chemo- and Thermomechanically Configurable 3D Optical Metamaterials Constructed from Colloidal Nanocrystal Assemblies. *ACS Nano* **2020**, *14* (2), 1427-1435.

(4) Guo, J.; Kim, J.-Y.; Yang, S.; Xu, J.; Choi, Y. C.; Stein, A.; Murray, C. B.; Kotov, N. A.; Kagan, C. R. Broadband Circular Polarizers via Coupling in 3D Plasmonic Meta-Atom Arrays. *ACS Photonics* **2021**, *8* (5), 1286-1292.

(5) McNeill, J. M.; Choi, Y. C.; Cai, Y.-Y.; Guo, J.; Nadal, F.; Kagan, C. R.; Mallouk, T. E. Three-Dimensionally Complex Phase Behavior and Collective Phenomena in Mixtures of Acoustically Powered Chiral Microspinning. *ACS Nano* **2023**, *17* (8), 7911-7919.

8:45 AM *EL06.11.02

Nonlinear Optics via Multiple Linear Scattering[Demetri Psaltis](#); EPFL, Switzerland

We will describe how nonlinear operations can be optically implemented by multiple scattering with repeated data modulation.

9:15 AM BREAK

9:45 AM EL06.11.03

From Electrophonics to Photophonics—Controlling Heat Flux with External Fields[Claudio Cazorla](#)¹, [Sebastian Bichelmaier](#)², [Carlos Escorihuela Sayalero](#)¹, [Jorge Iniguez](#)³, [Jesús Carrete](#)² and [Riccardo Rurali](#)⁴; ¹Universitat Politècnica de Catalunya, Spain; ²Technische Universität Wien, Austria; ³Luxembourg Institute of Science and Technology, Luxembourg; ⁴Institut de Ciència de Materials de Barcelona, Spain

Dynamical tuning of the thermal conductivity in crystals, k , is critical for developing novel phononic devices able to perform logic operations with phonons, as well as for solid-state refrigeration, energy harvesting, and thermoelectrics. Such a desired k control can be achieved in functional materials that experience large structural and phonon variations as a result of field-induced phase transformations.

Current strategies to design materials with tailored thermal properties typically rely on the creation of structural inhomogeneities that scatter phonons and reduce the thermal conductivity (e.g., lattice defects, grain boundaries and nanostructure surfaces) and the engineering of periodic heterostructures (superlattices) in which wave interference induces the appearance of phonon frequency gaps. These approaches, however, yield changes in the thermal properties of materials that are static and irreversible. The design of *phononic* devices [1], capable of performing logic operations with phonons similarly to what their electronic counterparts do with charge carriers, on the other hand, relies on the possibility of dynamically tuning the thermal conductivity of materials, k .

A promising dynamical k tuning approach consists in using electric or magnetic fields to manipulate the lattice of polar and magnetic materials, respectively, ideally exploiting the effects of field-induced phase transitions on the thermal properties. The ensuing *electrophononic* [2-5] and *magnetophononic* [6-7] effects can provide fast and dynamical manipulation of the heat carriers, thus yielding *à la carte* thermal properties for on-demand applications.

Nevertheless, for these strategies to be practical, the operation conditions need to be close to zero-bias transition points, since otherwise the required driving fields may grow unfeasibly large

and the materials performances be seriously compromised owing to the presence of leakage/eddy currents and dielectric/magnetic losses. On the other hand, the possibility of manipulating k with light thus far has received very little attention. Light-driven control of the thermal conductivity could bypass some of the issues posed by the schemes described above (e.g., application of large driving fields) as well as simplify the design of logic devices (i.e., lack of electrical contacts) [8].

In this talk I will discuss our predictions, based on first-principles calculations, of each of these three effects: *electro-*, *magneto-*, and *photoponic* couplings as effective way to dynamically manipulate the thermal conductivity of materials with external fields.

References

- [1] N. Li, J. Ren, L. Wang, G. Zhang, P. Hänggi, and B. Li, *Rev. Mod. Phys.* 84 (2012) 1045
- [2] J. A. Seijas-Bellido, H. Aramberri, J. Íñiguez, and R. Rurali, *Phys. Rev. B* 97 (2018) 184306 (2018).
- [3] P. Torres, J. A. Seijas-Bellido, C. Escorihuela-Sayalero, J. Íñiguez, and R. Rurali, *Phys. Rev. Materials* 3 (2019) 044404
- [4] J. A. Seijas-Bellido, J. Íñiguez, and R. Rurali, *Appl. Phys. Lett.* 115 (2019) 192903
- [5] P. Torres, J. Íñiguez, and R. Rurali, *Phys. Rev. Lett.* 123 (2019) 185901
- [6] C. Cazorla and R. Rurali, *Phys. Rev. B* 105 (2022) 104401
- [7] C. Cazorla, M. Stengel, J. Íñiguez, and R. Rurali, *npj Comout. Mater.*, *accepted*.
- [8] C. Cazorla, S. Bichelmaier, C. Escorihuela-Sayalero, J. Íñiguez, J. Carrete, and R. Rurali, *in preparation*

10:00 AM *EL06.11.04

Scalable 2D Material-Based Plasmonic Phototransistors Yu-Jung Lu^{1,2}; ¹Academia Sinica, Taiwan; ²National Taiwan University, Taiwan

Monolayer transition metal dichalcogenides (TMDs) are promising materials for electronics and photonics at highly scaled lateral dimensions. However, their low photon absorption poses a challenge for high-performance optoelectronic devices. We present plasmonic phototransistors (photoFETs) that integrate monolayer molybdenum disulfide (MoS₂) with plasmonic metasurfaces [1-2], such as Ag, Bi, HfN, and TiN. These plasmonic photoFETs exhibit a significant enhancement in photocurrent compared to pristine 2D photoFETs, enabling high-performance devices with ultrahigh photoresponsivity. The enhancement is achieved through plasmonic nanostructures that enhance light absorption [1-4], photo-carrier generation, photo-gating, and hot-carrier transfer rates. We also discuss the design of 2D material-based plasmonic photodetectors that can be extended to other 2D materials, facilitating the development of ultrathin, high-performance scalable optoelectronic devices. Lastly, we explore the prospects for next-generation ultra-compact optoelectronic devices in the trans-Moore era, where traditional silicon-based electronics face limitations. The integration of monolayer 2D materials with plasmonic metasurfaces offers an avenue for enhancing optoelectronic device performance, while the design flexibility enables the utilization of various 2D materials. These advancements hold promise for developing ultrathin, high-performance optoelectronic devices for applications in telecommunications, sensing, and data processing.

Reference

- [1] Hao-Yu Lan, Yu-Hung Hsieh, Zong-Yi Chiao, Deep Jariwala, Min-Hsiung Shih, Ta-Jen Yen, Ortwin Hess, Yu-Jung Lu*, Gate-Tunable Plasmon-Enhanced Photodetection in a Monolayer MoS₂ Phototransistor with Ultrahigh Photoresponsivity. *Nano Lett.* 21, 3083–3091 (2021)
- [2] Ching-Han Mao, Chin-Chien Chung, Wei-Ren Syong, Yu-Chi Yao, Kai-Yuan Hsiao, Ming-Yen Lu, Mario Hofmann, Ya-Ping Hsieh, Yu-Jung Lu, and Ta-Jen Yen*. Bifunctional Semimetal as a Plasmonic Resonator and Ohmic Contact for an Ultrasensitive MoS₂ Photodetector. *ACS Photonics* 10, 1495–1503 (2023)
- [3] Z-Y Chiao, Y-C Chen, J-W Chen, Y-C Chu, J-W Yang, T-Y Peng, W-R Syong, H W H. Lee, S-W Chu, and Y-J Lu*. Full-Color Generation Enabled by Refractory Plasmonic Crystals. *Nanophotonics* 11, 2891-2899 (2022)
- [4] Y-H Hsieh, B-W Hsu, K-N Peng, K-W Lee, C W Chu, S-W Chang, H-W Lin*, T-J Yen*, and Y-J Lu*, Perovskite Quantum Dot Lasing in a Gap-Plasmon Nanocavity with Ultralow Threshold, *ACS Nano* 14, 11670 (2020).

10:30 AM EL06.11.05

Creating Superlattices for Interlayer Excitons with Metasurface Nanoelectrodes Qitong Li, Sze Cheung Lau, Tony F. Heinz and Mark L. Brongersma; Stanford University, United States

Atomically-thin transition metal dichalcogenide (TMDC) monolayers have attracted significant and broad interest in the last decade. They serve as a promising material platform for future low-dimensional electronics and optoelectronics because of their exceptional charge-carrier mobility and quantum yield, and provide a clean 2D system for fundamental physics study because of the enhanced quantum effects and correlations due to the reduction of the available states in the system. As compared with intralayer excitons in monolayers, interlayer excitons in TMDC heterostructures display longer lifetimes as their recombination rate is limited by the tunneling effect, resulting in a diffusion length of up to a few micrometers and creating an exciting playground for quantum many-body physics study.

Here, we propose that with state-of-the-art nanofabrication techniques, we can spatially control the energy level of interlayer excitons down to the nanometer scale via the DC Stack effect with the carefully designed metasurface nanoelectrodes. For instance, an electrode with patterned nano-holes (diameter ~ 30 nm) can trap interlayer excitons in quantum wells. The depth of the quantum wells can be scaled with the applied external vertical electric field up to ~ 100 meV. A superlattice can therefore be achieved with a periodically nanopatterned hole array (period ~ 50 nm), where its Hamiltonian can be described using a Bose-Hubbard model. By gradually tuning the depth of the quantum wells, a material phase transition (from insulating to conducting) is expected. What's more, a more complicated material phase (i.e., Hamiltonian), including but not limited to defect states, quasi-crystal, as well as general quantum metasurfaces, can all be simulated by engineering the geometry of the metasurface electrodes and associated DC electric field distribution.

10:45 AM EL06.11.06

Electromechanically Reconfigurable Optical Vortex Array Sanghyeok Park, Dongha Kim and Min-Kyo Seo; Korea Advanced Institute of Science and Technology, Korea (the Republic of)

An optical vortex (OV), which is a topological texture of the electromagnetic field with the intensity singularity and spiral phase rotation, has been garnering significant interest due to the supported orbital angular momentum [1]. The generation and modulation of OVs are important for applications that utilize the orbital angular momentum of light, such as multiplexing and multi-valued logic systems that aim to increase data capacity [2]. To date, active pixel arrays, including spatial light modulators or digital micromirror devices, have been typically employed to create and control a reconfigurable array of OVs [3]. However, these systems suffer from the modulation speed limited by the intrinsic response time of the materials used and the requirement to control each pixel individually. Moreover, the size of the pixel unit imposes constraints on achieving a compact OV array and increasing the number of OVs. Recently, the gradient thickness optical cavity (GTOC) has been proposed as an innovative platform for creating and controlling an array of reconfigurable OVs, capable of exhibiting quasi-particle-like behaviors [4]. The GTOC platform projects the parametrized space defined by the thicknesses of the employed dielectric spacers onto the real space through thickness gradients. The GTOC enables to spontaneously generate OVs and actively change their positions by engineering the optical thickness of the interlayer separating the dielectric spacers. In this study, we demonstrate the creation and high-speed manipulation of a reconfigurable OV array using an electromechanical GTOC (EM-GTOC). Employing a piezo-actuator to rapidly control the thickness gradients of the dielectric spacers, the EM-GTOC can control the position and periodicity of the generated OV array with a speed exceeding tens of kHz. The EM-GTOC is a multi-layered structure that includes a glass layer combined with a piezo-actuator, an air spacer, an 8-nm-thick Ni layer, a polymer layer (Norland Optical Adhesive), and an Al bottom mirror. The thickness of the air spacer between the glass and Ni layers changes with position, and the piezo-actuator electromechanically controls the thickness gradient. Phase distributions measured by a holographic interferometer reveal that the period of the OV array varies depending on the voltage applied to the piezo-actuator. Furthermore, the OVs can actively move in one dimension over distances of approximately 1.92 times of the period of the OV array. The high-speed piezo-actuator allows the rapid reconfiguration of the OV array at the region of interest. We assessed the reconfiguration speed of the EM-GTOC employing the orbital angular momentum dependent diffraction by a fork-grating. We observed that the EM-GTOC encodes the orbital angular momentum into the reflected light at a speed of 10 kHz, equivalent to the typical speed limit of the spatial light modulator, or potentially even faster. We also demonstrated a reconfigurable OV array of which the OVs move in two-dimensional space. Another piezo-actuator combined with a Ni-coated cover glass, which replaces the Ni/polymer/Al structure, provides the second OV driving axis. By applying voltage to the two piezo-actuators connected to the cover glass and the slide glass, we successfully maneuvered the vortex and anti-vortex within a space of 1.33 period 2.19 period. We expect that the EM-GTOC platform, which can rapidly reconfigure an array of OVs, can find applications in orbital angular momentum-based multi-level logic networks. We also anticipate that the use of Micro-Electro-Mechanical Systems (MEMS) techniques could potentially control OV arrays at sub-GHz speeds.

- [1] Y. Shen et al, *Light Sci. Appl.* (2019)
- [2] J. Wang et al, *Nat. Photon.* (2012)
- [3] S. Ngcobo et al, *Nat. Commun.* (2013)
- [4] D. Kim et al, *Nature*, (2022)

11:00 AM EL06.11.07

Laser Patterning of Semi-Transparent Oxide Nanotubes for Solar-Driven Processes Katarzyna Grochowska, AmeerNasih, Saiful IslamKhan and Katarzyna Siuzdak; Szwalski Institute of Fluid-Flow Machinery Polish Academy of Sciences, Poland

Novel and efficient renewable energy sources, solar cells or water splitting devices are hot topics within the society. The emphasis is put on the usage of solar energy, e.g. light-driven water splitting as well as its transformation into electrical energy by applying photovoltaic cells. Those devices require photoelectrode materials exhibiting wide absorption range overlapping solar spectrum, low recombination rate of photogenerated charges and photocorrosion resistance. Among different materials TiO₂ has been widely studied, in particular titania nanotubes (TiO₂ NTs) that provide unique set of geometrical and electrical properties as well as low production costs via anodization, chemical inertness and non-toxicity [1]. Though, it should be taken into account that it is a wide-bandgap semiconductor and some strategies should be undertaken to increase its absorption in visible range [2].

In this studies, we propose semi-transparent nanostructure fabricated via combined electrochemical and laser processing. In the first step the formation of flat metallic (pure Ti or Ti-Ni) layers onto the transparent conducting oxide substrate was realized via DC and RF magnetron sputtering. In order to obtain highly ordered metal oxide architecture anodization process was performed for applied voltage in the range of 30 – 60 V. SEM inspection confirmed the presence of nanotubes for both types of layers, i.e. Ti and Ti-Ni. Moreover, the outer NTs diameter increases with the anodization voltage, from 90 to 120 nm and 50 to 70 nm, for NTs formed out of Ti and Ti-Ni films, respectively. Interestingly, with the increase of the voltage value the length of NTs decreases from 1050 to 770 nm for the NTs obtained from Ti layers, while increases from 970 to 1100 nm for the ones obtained from Ti-Ni layers.

The optical band-gap values estimated for pure TiO₂ NTs vary in the range of 3.11-3.25 eV for different anodization voltage which is consistent with changes in geometrical features. Meanwhile, the band-gap values decrease for oxide nanotubes prepared out of Ti-Ni films confirming the correctness of undertaken strategy. Additionally, the presence of nickel in the anodizing layer led to the appearance of highly pronounced fringes in the UV-vis spectra of oxide NTs that were not observed for pure titania material. This phenomenon can be described by surface plasmon resonance, photonic behavior of the material and constructive and destructive interference of partially reflected light [3].

After calcination ensuring phase transition to anatase, the samples underwent laser processing (355 nm wavelength, 2 Hz repetition rate, 6 ns pulse duration) with varying fluence of 20-100 mJ/cm². Such processing resulted in the partial melting of the NTs tops with preservation of the tubular scaffold. The electrochemical measurements, such as cyclic voltammetry and linear sweep voltammetry, were performed for all the laser-treated and non-treated samples. All the samples show good electrochemical stability while the material treated with 40 mJ/cm² fluence exhibits 14.5 times higher photoactivity than the non-annealed one.

Overall, these findings suggest that the elaborated synthesis route can be successfully employed to form the systems exhibiting nature of the photonic crystal and plasmonic effect. Therefore, proposed material can be regarded as a promising electrode for utilization in optoelectronic devices, particularly solar cells and water photosplitting reactor.

Acknowledgements

The authors acknowledge the financial support of the National Science Centre (Poland) via grant no.: 2021/41/B/ST8/01849.

References

[1] P. Roy, S. Berger, P. Schmuki, *Angew. Chem.* 50 (2011) 2904

[2] L. Harynski, K. Grochowska, J. Karczewski, J. Ryl, K. Siuzdak, *ACS Appl. Mater. Interfaces* 12 (2020) 3225

[3] K. Grochowska, Z. Molenda, J. Karczewski, J. Bachmann, K. Darowicki, J. Ryl, K. Siuzdak, *Int. J. Hydrog. Energy* 45 (2020) 19192

SESSION EL06.15: Virtual Session
Session Chairs: Artur Davoyan and Giulia Tagliabue
Thursday Morning, December 7, 2023
EL06-virtual

8:00 AM *EL06.15.01

Dynamic Digital Control of the Translational Geometric Phase in Optical Metasurfaces Junghyun Park¹, Chunghwan Jung², Sun Il Kim¹, Byung Gil Jung¹, Minkyung Lee¹, Young Kim¹ and Junsuk Rho²; ¹Samsung Advanced Institute of Technology, Korea (the Republic of); ²POSTECH, Korea (the Republic of)

Dynamic metasurfaces facilitate on-demand wavefront shaping upon the control signal and can provide a versatile platform for various applications including light detection and ranging (LiDAR), free space optical communication, and holographic displays. There has been considerable research on the extension of the phase sweep range, increasing degree of freedom with complex amplitude modulation, and non-volatile tuning mechanism. However, the proposed configurations suffer in common from the analog property, where the device output is nonlinearly dependent on the input signal, giving rise to limited reliability and wavefront purity. The resulting wavefront with non-negligible grating lobes and background noises prevent us from achieving practical devices for real applications. In this presentation, we present a novel concept of the dynamic digital control of the translational geometric phase in the near infrared regime. Each pixel with independent functionality is composed of various sub-gratings, and the reflectivity of each grating can be electrically turned on and off. As a result, we can invoke apparent translation of the effective grating units. We show experimental measurement of the 4-step digital phases of 0°, 90°, 180°, and 270° with a constant amplitude at the wavelength of 1400 - 1550 nm regimes. We believe our work will shed light on innovative science and engineering toward high purity beam manipulation.

8:30 AM *EL06.15.02

Extreme Dissipation in Scalable Nanoscale Absorbers and Resonant Heat Transfer for Decentralized Solar Thermal Desalination Alessandro Alabastri; Rice University, United States

Thermal desalination is a flexible choice for water treatment, given its key advantages in robustness and limited salinity dependence. Light can power thermal desalination by carrying electromagnetic energy if efficiently turned into heat [1-2]. Solar-driven photothermal desalination (SDPD) can lead to decentralized water purification, improving accessibility and reducing the environmental impact over conventional, heavy infrastructure-based desalination practices like reverse osmosis. However, today's best decentralizable SDPD technologies barely surpass 10% of the thermodynamic limit for thermal desalination. A few years ago, we introduced the concept of nanophotonics-enabled solar membrane distillation, where solar-driven localized heat drives the distillation process [1]. Moreover, the desalination efficiency was increased by redistributing the photon flux incident on the membrane, suggesting the possibility of reducing the process footprint by utilizing miniaturized optics instead of more costly and bulky optical concentrators [2]. However, energy recovery is still a challenge.

Two key ingredients are necessary for practical solar desalination: 1) Input power (e.g., from direct sunlight) and 2) energy recovery. Light-heat conversion drives evaporation in solar thermal desalination, and I will show how properly designed large-scale ultrathin (~250nm) TiN-based metasurfaces allow extremely large (~GW/m³) and broadband (~90% of solar spectrum) dissipated power densities [3]. More recently, we have shown how thicker (~µm) nanoporous structures uniquely enhance light absorption thanks to deep subwavelength dissipative regions [4]. Such efficient absorbers allow exploiting the vast majority of sunlight as a heat source for desalination.

Heating and evaporating water is only one stage of the desalination process. Water vapor needs to be collected through condensation and latent heat recovered to make the process energy efficient. We have been developing desalination modules based on the concept of Resonant Heat Transfer (RHT), where a combination of conductive and convective heat transfer mechanisms allow the desalination process to be described as an oscillating thermal system where heat is re-utilized, thermal energy is stored, and losses are minimized [5,6]. Such an energy recovery method makes compact modules robust, performing and scalable.

We successfully demonstrated an RHT-based solar desalination module capable of delivering up to 20 L/m²/day [7], paving the way to realizing scalable and sustainable light-driven water purification systems. I will provide a perspective on the future opportunities and challenges of modular thermal desalination systems [8].

References

[1] P. D. Dongare, A. Alabastri et al., "Nanophotonics-Enabled Solar Membrane Distillation for off-Grid Water Purification," *PNAS* **114**, 6936 (2017).

[2] P. D. Dongare, A. Alabastri, et al., "Solar Thermal Desalination as a Nonlinear Optical Process," *PNAS* **116**, 13182 (2019)

[3] L. Mascaretti, A. Schirato et al., "Solar steam generation on scalable ultrathin thermoplasmonic TiN nanocavity arrays", *Nano Energy*, **83**, (2021)

[4] *Submitted*

[5] A. Alabastri, "Flow-Driven Resonant Energy Systems", *Phys. Rev. App.* **14**, (2020).

[6] Q. Ye, S. Sanders and A. Alabastri, "Resonant Energy Transfer and Storage in Coupled Flow-Driven Heat Oscillators", *PRX Energy*, **2**, (2023).

[7] A. Alabastri, P. D. Dongare, et al., "Resonant Energy Transfer Enhances Solar Thermal Desalination," *Energy Environ. Sci.* **13**, **968** (2020).

[8] W. Schmid et al., "Decentralized Solar-Driven Photothermal Desalination: An Interdisciplinary Challenge to Transition Lab-Scale Research to Off-Grid Applications," *ACS Photonics* **14**, 3764 (2022).

9:00 AM *EL06.15.03

Non-Linear and Non-Local Light-Matter Interaction in Quantum MaterialsGuru V. Naik and DingZhang; Rice University, United States

The optical response of quantum materials under illumination is interesting. The fine balance between many microscopic processes in quantum materials can be tipped by low-intensity light leading to a nonlinear response. Further, tipping such equilibrium also leads to an incommensurability of the quantum order resulting in domains with different electronic properties. This coexistence of multiple quantum many-body phases or electronic inhomogeneity is fundamental to quantum materials and gives rise to a nonlocal optical response. This optical nonlocality in quantum materials captures the competition between different electronic phases and serves as a useful material parameter. Here, we present a model to describe the optical non-linearity and nonlocality in quantum materials and validate it by optical experiments carried out on a charge density wave (CDW) material, 1T-TaS₂. 1T-TaS₂, a quasi-2D material, supports nearly commensurate CDWs at room temperature. CDW domain walls exist in every layer of 1T-TaS₂. Each CDW domain can now stack on top of the others in neighboring layers differently giving rise to a stacking order. This stacking order is sensitive to low-intensity incoherent light. Light tips the competition between center-to-corner and center-to-corner stacking types. As a result, the reflectance of TM polarized light changes with illumination intensity manifesting in an optical nonlinearity.

Apart from nonlinearity arising from the underlying competition between different orders, the optical response of quantum materials is also nonlocal. The nonlocality arises from spatial inhomogeneity. The existence of domains of different orders results in optical nonlocality. In 1T-TaS₂, the CDW domains in each layer corresponding to a particular stacking type are about 50 nm wide in any layer at room temperature. This level of spatial inhomogeneity at visible frequencies would result in appreciable nonlocality. Employing a single-shot energy-momentum microscopy, we capture the non-linear and non-local optical response of 1T-TaS₂ and infer the quantum order in this material. This work not only sheds light on light-matter interaction at low illumination intensities in quantum materials, but also demonstrates a quick and non-invasive technique to design, discover, and optimize quantum materials.

9:30 AM *EL06.15.04

Explorations into the Dynamics of Maxwell LatticesNicholasBoechler; University of California, San Diego, United States

In this invited talk, I will describe our recent collaborative studies into the dynamics of a class of mechanical metamaterial referred to as Maxwell lattices. Maxwell lattices are mechanical structures on the verge of instability, and they have drawn interest due to their capacity to support topologically protected, zero-energy modes of quasi-static deformation. Within this scope, I will show new phenomena observed in Maxwell lattices including: synthetically non-Hermitian deformation fields, the time evolution of said fields; backscattering free edge wave transport; and the interplay of finite energy thresholds with topologically protected localized modes, and their implications for active, and dynamic material phase transformation.

SESSION EL08.04/EL06.02/EL12.02: Joint Keynote Session
Session Chairs: Ho Wai (Howard) Lee and Lisa Poulikakos
Monday Afternoon, November 27, 2023
Hynes, Level 3, Room 312

1:30 PM KEYNOTE INTRODUCTIONS

1:40 PM *EL08.04/EL06.02/EL12.02.01

Optical Metasurfaces Saving Energy in Optical Computing and PhotovoltaicsAlbertPolman; AMOLF, Netherlands

I will present our recent collaborative work on the design, fabrication and operation of silicon-based optical metasurfaces that perform mathematical operations in an analog way, using light fields as input and output signals. We show how the interplay between scattering components in silicon metasurfaces creates a mathematical derivative on an input image. We then design and fabricate a silicon metasurface that solves an integral equation by using visible light in which we use grating orders as input and output ports on a periodic metasurface with a specially tailored unit cell. The new analog optical computing concepts operate with very low energy consumption, at the speed of light, and can form the basis of more complex geometries solving multiple equations and can be applied in optical neural networks, control systems, and more.

We then apply optical metasurfaces to control and enhance the interaction of free electrons and highly-localized optical near fields in scanning electron microscopy (SEM). Using angle-resolved cathodoluminescence spectroscopy we analyse the spatial modulation of Smith-Purcell radiation that results from the coherent interplay of free-electron driven optical excitations in a chirped metagrating. We embed cylindrically-shaped metagrating patterns onto the input facet of a multi-mode optical fiber to experimentally demonstrate the coupling of free electrons and guided fiber-optic modes via the Smith-Purcell effect.

In the last part of the talk I will introduce an integrated near field/far-field multiple scattering formalism to control the absorption of light in solar cells. We design and fabricate a metallodielectric metasurface back contact for an ultra-high efficiency InGaAs/InGaAsP/Si multi-junction solar cell and enhance the light trapping inside the silicon bottom cell by multiple scattering, creating a record photovoltaic energy conversion efficiency for silicon-based tandem solar cells of 36.1%.

2:20 PM *EL08.04/EL06.02/EL12.02.02

Tunable and Dynamic Photonics with Tailorable Conducting Oxides and Metal NitridesAlexandraBoltasseva; Purdue University, United States

Transparent Conducting Oxides (TCOs) and Transition Metal Nitrides (TMNs) are emerging material platforms for applications in tunable and nonlinear optics such as tailorable/tunable flat optics, all-optical switches and modulators, high harmonic generation as well as novel photonic time crystal concepts and beyond. We report on various approaches to both statically tailor the materials' properties and dynamically tune the optical response at the ultrafast time scales. We demonstrate remarkable control of the epsilon-near-zero response of TCOs such as aluminum-doped zinc oxide (AZO) and yttrium doped cadmium oxide. We also investigate the strong thickness dependence of the TCOs and TMNs optical properties. Employing the Berreman modes of TiN and AZO films on the same platform, we demonstrate variable switching speeds of an optically-pumped metasurface. We also demonstrate the nonlinear capabilities of undoped ZnO for all optical switching and third harmonic generation. To explore the realization of photonic time crystals, we investigate the fastest material response to an optical pump in AZO, showing sub-10 femtosecond rise time. Our approach paves the way to novel phenomena and device design with ultrafast tunable and tailorable materials.

2:50 PM BREAK

3:20 PM *EL08.04/EL06.02/EL12.02.03

Active Metasurfaces in Space and TimeHarry A. Atwater; California Institute of Technology, United States

Electro-optically tunable active metasurfaces that enable dynamic modulation of reflection and transmission amplitude, phase, and polarization using resonantly excited materials and phenomena are powerful design elements for meta-imaging and computation. As flat, low-profile optical elements, active metasurfaces have potential to serve as cascaded, programmable components in optical meta-imaging systems, such as lens-less cameras and single-photon imaging systems. In this talk, I will discuss metasurfaces with high quality factor, local, resonant elements capable of two-dimensional phase gradient generation, in both passive and active metasurface designs. I will also describe active metasurfaces with both spatial and temporal phase gradients, and an active metasurface as a lens-less imaging system, and compare the characteristics to conventional lens-coupled image sensors.

4:00 PM *EL08.04/EL06.02/EL12.02.04

Making Waves: Acoustic and Nanophotonic Platforms for Amplification-Free Cellular and Molecular DetectionJennifer A. Dionne¹, Mark Lawrence², Fareeha Safir¹, Jack Hu¹, Varun Dolia¹, Halleh Balch¹, Sajjad Abdollahramezani¹ and Parivash Moradifar¹; ¹Stanford University, United States; ²Washington University in St. Louis, United States

Infectious diseases are one of the leading causes of death in the 21st century, claiming the lives of over 16 million individuals each year. These staggering numbers highlight the need for rapid, sensitive, and multiplexed diagnostics to minimize the spread of infectious disease and guide appropriate treatment. Existing diagnostic methods often suffer from a need for sample culturing or molecular amplification, leading to long diagnostic times or high limits of detection when amplification is not possible. Here, we combine acoustic bioprinting with nanophotonics towards 1) culture-free detection and identification of bacteria in blood, sputum, and wastewater samples using surface enhanced Raman Spectroscopy and 2) enrichment-free detection of proteins using high-Q metasurfaces. While acoustic bioprinting allows for rapid, picoliter volume sample handling for isolation of analytes of interest from clinical samples, nanophotonics enables control of light at molecular scales and optical concentration that minimizes the need for sample enrichment or amplification.

First, I describe how acoustic bioprinting combined with surface enhanced Raman spectroscopy (SERS) can be used to rapidly detect and identify pathogens from complex multicellular samples. Acoustic droplet ejection allows for nozzle-free, kHz-rate printing of biological samples in ~2pL droplets while maintaining cell viability. We use our home-built 150 Mhz acoustic bioprinter to rapidly digitize droplets from solutions of blood, sputum, or wastewater. When the sample is infused with plasmonic gold nanorods, SERS enhancements of up to 1500x are achieved. We train a machine learning (ML) model on droplets consisting of either pure cells or mixed, multicellular species. We achieve ≥99% classification accuracy of droplets printed from cellularly-pure samples, and ≥87% accuracy in droplets printed from cellularly-mixed samples. Our combined acoustic droplet ejection, SERS and ML platform could enable clinical and industrial translation of SERS-based cellular identification for rapid pathogen detection.

Next, I describe a high quality-factor (“high-Q”) dielectric metasurface assay that, when coupled with our acoustic bioprinter for site-specific surface chemistry, allows for detection of multiple gene fragments and proteins. Our high-Q resonators produce a strong concentration of the electromagnetic field intensity within sub-wavelength-scale volumes. This platform can enable simultaneous read-out of the ~5 million independent sensor elements patterned per square cm. Unlike existing assays that rely on secondary tagging, our high-Q surfaces generate resonant scattering intensities that are proportional to minute refractive index changes from target protein load. We use hyperspectral imaging to demonstrate binding of Inf. A, Inf. B, and SARS-CoV2 gene fragments, as well as the associated IgG antibodies, with sub-femtomolar sensitivity and over 96% specificity. Together, this work provides a foundation for faster, higher-throughput, and more sensitive cellular and molecular diagnostics.

4:40 PM CLOSING REMARKS

SESSION EL08.09/EL06.06/EL12.06: Joint Keynote Presentation II
Session Chairs: Carlos Portela and Lisa Poulikakos
Tuesday Afternoon, November 28, 2023
Hynes, Level 3, Room 312

4:30 PM *EL08.09/EL06.06/EL12.06.01

Hydrogel Infusion-Based Additive Manufacturing of Nano- and Micro-Architected Materials for Photonics and Micro-Filtering Julia R. Greer^{1,2}, Wenyuan Chen^{1,2}, Sammy Shaker¹ and Andrii Syrota¹; ¹California Institute of Technology, United States; ²Kavli Nanoscience Institute, United States

Creation of reconfigurable and multi-functional materials can be achieved by incorporating architecture into material design. We design and fabricate three-dimensional (3D) nano-architected materials that can exhibit superior and often tunable thermal, photonic, electrochemical, biochemical, and mechanical properties at extremely low mass densities, lighter than aerogels, which renders them useful and enabling in technological applications. Dominant properties of such meta-materials are driven by their multi-scale nature: from characteristic material microstructure (atoms) to individual constituents (nanometers) to structural components (microns) and overall architectures (millimeters and above).

Additive manufacturing (AM) represents a set of processes that fabricate complex 3D structures using a layer-by-layer approach, with some advanced methods attaining nanometer resolution and the creation of unique, multifunctional materials and shapes derived from

photoinitiation-based chemical reaction of custom-synthesized resins and thermal post-processing. A type of AM, vat polymerization, has allowed for using hydrogels as precursors, and exploiting novel material properties, especially those that arise at the nano-scale and do not occur in conventional materials. The focus of this talk is on additive manufacturing of metal ion-containing hydrogels to create 3D nano- and micro-architected metals and metal oxides via vat polymerization for applications in nanophotonics and magneto-filtering.

Rapid development of medical imaging applications calls for the miniaturization of optical systems into ultra-compact micro-optical elements to allow for non-invasive and non-destructive examination of tissues. In the first case application, I will describe additive manufacturing of 3D nano-architected titanium dioxide (TiO₂) for meta-nano-optics that would allow us to redefine optical components. We use two-photon lithography and Ti-infused hydrogel photochemistry with subsequent calcination to produce 3D-sculpted TiO₂ structures with ~100nm resolution and characterize them using thermal analysis, FTIR, and finite difference time domain (FDTD) solver for NIR wavelengths.

The second part of the talk will be focused on the application of 3D micro-architected Fe (iron) as magnetofilters. Using multi-physics computational analyses of thermodynamic and magnetic forces, we model candidate device configurations that slow venous blood flow enough for magnetic interactions with filters but not cause flow stagnation and thrombosis under anticoagulated conditions. Micro-architected lattices made of iron alloys are first synthesized by hydrogel swell-in method and 3D printed using a photoresin composed of polyethylene glycol diacrylate (PEGda) dissolved in N,N-dimethylformamide (DMF). After exchanging DMF with water, the printed structures are swollen with aqueous metal nitrate solutions. Calcination and reduction transforms the metal ion-polymer structures into metal structures that are subsequently magnetized and tested in flow to capture magnetic microparticles. Using this approach, we fabricated twisted honeycombs, a theoretically predicted optimal geometry for particle capture, from iron and permalloy (80% nickel-20% iron) and characterized their microstructure and particle capture efficiency using X-ray diffraction (XRD), scanning electron microscopy (SEM), energy dispersive X-ray spectroscopy (EDS), magnetometry measurements, and flow experiments.

SESSION EL08.12/EL06.09/EL12.09: Joint Keynote Presentation III
Session Chairs: Lisa Poulikakos and Aaswath Raman
Wednesday Morning, November 29, 2023
Hynes, Level 3, Room 312

11:30 AM *EL08.12/EL06.09/EL12.09.01

Plasmon-Enhanced Photocatalysis for Green Chemistry Peter Nordlander; Rice University, United States

Plasmons can serve as efficient generators of hot electrons and holes that can be exploited in light harvesting applications. The physical mechanism for plasmon-induced hot carrier generation is plasmon decay. Plasmons can decay either radiatively or non-radiatively with a branching ratio that can be controlled by tuning the radiance of the plasmon mode. Non-radiative plasmon decay is a quantum mechanical process in which one plasmon quantum is transferred to the conduction electrons of the nanostructure by creating an electron-hole pair, i.e., excitation of an electron below the Fermi level of the metal into a state above the Fermi level but below the vacuum level. These hot carriers interact with all charge carriers in the system and eventually transfer their energy into phonons (heat). In my talk, I will discuss the time-dependent relaxation of plasmon-induced hot carriers including electron-electron scattering, fluorescence, and electron-phonon coupling [1] and show that the hot carrier lifetimes can exceed several picoseconds. I will also discuss recent applications of plasmon-induced hot carrier generation such as plasmon-enhanced photocatalysis, and how photocatalytic efficiencies can be enhanced and quantified by placing catalytic reactors in the nearfield of a plasmonic antenna in Antenna/Reactor geometries [2-6].

References

- [1] J.G. Liu *et al.*, “Relaxation of plasmon-induced ..”, ACS Photonics 5(2018)2584,
- [2] L. Zhou *et al.*, “Quantifying hot carrier and thermal ..”, Science 362(2018)69
- [3] H. Robotjazi *et al.*, “Plasmon-driven carbon–fluorine bond ..”, Nat. Catal. 3(2018)564
- [4] L. Zhou *et al.*, “Light-driven methane dry reforming ..”, Nat. Energ. 5 (2020)61, (2020).
- [5] M. Lou *et al.*, “Direct H₂S Decomposition by ..”, ACS Energ. Lett. 7(2022)3666
- [6] Y. Yuan *et al.*, “Earth-abundant photocatalyst for H₂ generation ..”, Science 378(2022)889

SYMPOSIUM EL07

1D and 2D Materials—Electronic Properties and Device Applications
November 27 - December 7, 2023

Symposium Organizers

Gabriela Borin Barin, Empa
Shengxi Huang, Rice University
Lain-Jong Li, The University of Hong Kong
Yuxuan Cosmi Lin, TSMC Technology Inc

Symposium Support

Silver

Montana Instruments

Bronze

Oxford Instruments WITec
PicoQuant
Raith America, Inc.

* Invited Paper
+ JMR Distinguished Invited Speaker

SESSION EL07.01: 1D and 2D Materials—Synthesis and Characterization I
Session Chairs: Taisuke Ohta and Pascal Ruffieux
Monday Morning, November 27, 2023
Hynes, Level 3, Ballroom B

10:30 AM *EL07.01.01

Polarity and Non-Linear Optics of Guided Nanowires Ernesto Joselevich, Regev Ben-Zvi, Omri Bar-Elli, Yael Soffer, Tommaso Salzillo, Maor Rosenberg, Omer Yaffe and Dan Oron; Weizmann Institute, Israel

The large-scale assembly of nanowires (NWs) with controlled orientation on surfaces remains one challenge toward their integration into practical devices. During the last decade, we have reported the growth of perfectly aligned, millimeter-long, horizontal NWs of GaN, ZnO, ZnSe, ZnTe, CdSe, CdS, ZnS, CsPbBr₃ and other materials, with controlled crystallographic orientations on different planes of sapphire, SiC, quartz, and spinel. The growth directions and crystallographic orientation of the NWs are controlled by their epitaxial relationship with the substrate, as well as by a graphoepitaxial effect that guides their growth along surface steps and grooves. We demonstrated the massively parallel self-integration of NWs into circuits via guided growth and the production of optoelectronic nanosystems, including photodetectors, photodiodes and photovoltaic cells. This talk will present systematic studies to map the crystallographic orientations and polarity of epitaxially guided NWs based on their nonlinear optical response under external electric fields [1]. Studies about epitaxially guided ZnO NWs on sapphire by Au-catalyzed vapor-liquid-solid (VLS) growth reveal interesting details about their formation mechanism and the role of the substrate and the catalyst in determining the polarity and morphology of the guided NWs. Studies done with epitaxial CsPbBr₃ perovskite NWs on sapphire by non-catalytic vapor-solid (VS) growth reveal an intriguing memory effect and a strong modulation of their photoluminescence under electric field [2]. These studies reveal the important interplay between epitaxy, polarity and optoelectronic behavior of guided NWs.

[1] *Nature Communications* **2021**, *12*, 3286.

[2] *ACS Nano* **2021**, *15*, 16130.

11:00 AM EL07.01.02

Short-Range Atomic Ordering and Unintentional Doping of Ge/Ge-Sn Semiconductor Alloy Core/Shell Nanowires John Lentz¹, Joe Woicik², Matthew Bergschneider³, Ryan Davis⁴, Apurva Mehta⁴, Kyeongjae Cho³ and Paul McIntyre^{1,4}; ¹Stanford University, United States; ²National Institute of Standards and Technology, United States; ³The University of Texas at Dallas, United States; ⁴SLAC National Accelerator Laboratory, United States

Ge-Sn alloys exhibit a tunable direct gap in the mid-infrared in an all-Group IV semiconductor system compatible with Si complementary metal-oxide-semiconductor (CMOS) technologies, presenting interesting possibilities for detectors and on-chip photonics. Ge-Sn films grown epitaxially around Ge nanowires result in core/shell structures with a strain-free Ge-Sn shell. In recent work, extended x-ray absorption fine structure (EXAFS) measurements detected short range order (SRO) in such structures, wherein Sn atoms are ~40% less likely to be nearest neighbors relative to a random alloy film¹. SRO has been shown to produce interesting mechanical properties in metals, but is not well-studied in semiconductors and has been predicted to substantially alter the electronic structure of Ge-Sn². EXAFS data are also consistent with a vacancy concentration in the Ge-Sn shells less than the detection limit. Vacancies produce acceptor levels in Ge and, therefore, are thought to be the origin of the high as-grown carrier concentrations in Ge-Sn films, often in the 10¹⁸ cm⁻³ range³. By lithographically patterning metal contacts onto single nanowires and performing four-point probe measurements, we have obtained electrical resistances corresponding to much lower carrier concentrations of about 10¹⁵ cm⁻³. This also suggests that the Ge core/Ge-Sn shell nanowire geometry promotes atypically small vacancy incorporation, reducing the unintentional hole doping compared to conventional, planar Ge-Sn films.

¹ J. Z. Lentz, J. C. Woicik, M. Bergschneider, R. Davis, A. Mehta, K. Cho, and P. C. McIntyre. *Appl. Phys. Lett.* **122**, 062103 (2023).

² B. Cao, S. Chen, X. Jin, J. Liu, and T. Li. *ACS Appl. Mater. Interfaces* **12**, 57245–57253 (2020).

³ O. Nakatsuka, N. Tsutsui, Y. Shimura, S. Takeuchi, A. Sakai, S. Zaima. *Jpn. J. Appl. Phys.* **49**, 04DA10 (2010).

11:15 AM EL07.01.03

Condensation-Driven Growth of Tellurene Nanosheets for Memristive Applications Sara Ghomi^{1,2}, Carlo Grazianetti¹, Alessio Lamperti¹, Christian Martella¹ and Alessandro Molle¹; ¹Consiglio Nazionale delle Ricerche, Italy; ²Politecnico di Milano, Italy

The increasing demand for the development of memories with low operating voltage, compatible with CMOS technologies and simple structure, has recently targeted the class of two-dimensional (2D) materials [1]. Novel 2D materials such as transition metal dichalcogenides like MoS₂ and MoTe₂ have inspired ultra-scaled layouts of non-volatile random-access memory (RAM) devices based on a resistive switching or phase change mechanism [2,3]. In this respect, mono-elemental 2D crystals, termed Xenes [4], may lead to a structural simplification with benefits in terms of energy consumption and performance. In this work, we report on the low temperature synthesis of tellurium nanosheets, known as tellurene, by condensation-driven vapor transport growth processing inside a chemical vapour deposition reactor towards the development of a tellurene-based memristive cell layout. First, we show that the process microscale tellurium structures like hexagonal pillars and nanotubes is scaled down to the 2D level by mastering the growth of tellurene sheet on SiO₂/Si substrates with lateral coverage on the order of tens of microns with a process temperature below 100°C, namely within BEOL compatible thermal regime. On the same line, we applied the same process to (111)-terminated metal templates like Au(111) and Ag(111) epilayer on mica as metallic substrates readily enabling the manufacture of a diode. For the case of tellurene growth on Au/mica substrate we can discriminate two different regimes depending on the substrate temperature T, i.e. a kinetically driven regime where tellurium grows as tellurene nanosheets with no interaction with Au with T < 350°C (condensation and nucleation) and a chemisorption regime where tellurene reacts with the Au surface to form AuTe₂ (tellurization) with T > 350°C. We characterized the two regimes by means of several probing techniques including Raman spectroscopy and atomic force microscopy, and we define the best condition for the growth by means of finite element simulation guidance. The tellurene nanosheet on Au(111)/mica stands out as an optimal configuration where to check a memristive behavior as reported in case of other 2D compounds like MoS₂ on metal substrates [5]. With this purpose in mind, we investigated the local current-voltage (I-V) response of tellurene nanosheet with thickness from 5 to 20 nm by means of conductive atomic force microscopy (C-AFM) with a sharp conductive diamond coated tip the Au substrate as top and bottom electrodes, respectively. A resistive switch behavior of tellurene was revealed by local C-AFM probing, i.e. by applying a linearly ramped voltage and measuring the current passing from the sample to the tip. A trap assisted space charge limited current conduction (SCLC) in the tellurene nanosheets was found to be consistent with the observed I-V behavior thus paving the way to store, read, and write a non-volatile information through tellurene. As such, the configurational details of the growth are accordingly developed for tellurene to be integrated as active layer in a memristor device, and thus transferred to a neuromorphic computing architecture.

This work has been financially supported by the European Commission under the H2020 ERC-COG grant n. 772261 “XFab”.

[1] W. Huh, et al., *Adv. Mater.* (2020) 32, 2002092.

[2] R. Ge, et al., *Nano Letters* (2018) 18, 434.

[3] I. M. Datye, et al., *Nano Letters* (2020) 20, 1461.

[4] “Xenes” Eds. A. Molle and C. Grazianetti, Woodhead Publ. (Elsevier), 2022.

[5] S. M. Hus, et al., *Nature Nanotechnol.* (2021) 16, 58.

11:30 AM +EL07.01.04

Low-Dimensional Neuromorphic Electronic Materials and Applications [Mark C. Hersam](#); Northwestern University, United States

The exponentially improving performance of digital computers has recently slowed due to the speed and power consumption issues resulting from the von Neumann bottleneck. In contrast, neuromorphic computing aims to circumvent these limitations by spatially co-locating logic and memory in a manner analogous to biological neuronal networks [1]. Beyond reducing power consumption, neuromorphic devices provide efficient architectures for image recognition, machine learning, and artificial intelligence [2]. This talk will explore how low-dimensional nanoelectronic materials enable gate-tunable neuromorphic devices [3]. For example, by utilizing self-aligned, atomically thin heterojunctions, dual-gated Gaussian transistors have been realized, which show tunable anti-ambipolarity for artificial neurons, competitive learning, spiking circuits, and mixed-kernel support vector machines [4]. In addition, field-driven defect motion in polycrystalline monolayer MoS₂ enables gate-tunable memristive phenomena that serve as the basis of hybrid memristor/transistor devices (i.e., ‘memtransistors’) that concurrently provide logic and data storage functions [5]. The planar geometry of memtransistors further allows multiple contacts and dual gating that mimic the behavior of biological systems such as heterosynaptic responses [6]. Moreover, control over polycrystalline grain structure enhances the tunability of potentiation and depression, which enables unsupervised continuous learning in spiking neural networks [7]. Overall, this work introduces foundational circuit elements for neuromorphic computing by utilizing the unique quantum characteristics of low-dimensional nanoelectronic materials [8].

[1] V. K. Sangwan, et al., *Matter*, **5**, 4133 (2022).

[2] V. K. Sangwan, et al., *Nature Nanotechnology*, **15**, 517 (2020).

[3] M. E. Beck, et al., *ACS Nano*, **14**, 6498 (2020).

[4] M. E. Beck, et al., *Nature Communications*, **11**, 1565 (2020).

[5] X. Yan, et al., *Advanced Materials*, **34**, 2108025 (2022).

[6] H.-S. Lee, et al., *Advanced Functional Materials*, **30**, 2003683 (2020).

[7] J. Yuan, et al., *Nano Letters*, **21**, 6432 (2021).

[8] M. I. B. Utama, et al., *Nature Communications*, **14**, 2193 (2023).

SESSION EL07.02: 1D and 2D Materials— Synthesis and Characterization II

Session Chairs: Gabriela Borin Barin and Ernesto Joselevich

Monday Afternoon, November 27, 2023

Hynes, Level 3, Ballroom B

1:30 PM *EL07.02.01

Nanoscale Heterogeneities at Transition Metal Dichalcogenide-Au Interfaces [Taisuke Ohta](#); Sandia National Laboratories, United States

Two-dimensional geometry renders unique screening properties in transition metal dichalcogenides (TMDs). Consequently, the electronic properties of TMDs are susceptible to extrinsic factors (e.g., substrate interactions, mechanical strains, and charge transfer), and display spatial nonuniformities as evidenced in recent reports. Thus, material combinations (i.e., TMD, dielectrics, and metals) and their nuanced interactions need to be considered when designing TMD-based devices. Of particular importance are the interfaces with metallic contacts. Uncovering the origin of heterogeneities at TMD-metal interfaces and establishing strategies to control TMD-metal interfaces could enable engineering pathways for future applications. In this presentation, we show that the electronic structures of mechanically exfoliated TMD-Au interfaces exhibit pronounced heterogeneity arising from the microstructure of the supporting metal. These electronic structure variations indicate spatially nonuniform doping levels and Schottky barrier height across the junction, which are pertinent for device applications. Through examination of the electronic structures of WS₂ and WSe₂ at 10s of nanometers spatial resolution via photoelectron emission microscopy (PEEM) we reveal key differences in work function and binding energies of the occupied states. Complemented with ab-initio calculation, electron backscatter diffraction, and scanning tunneling microscopy, our measurements show distinct variations in excess of 100meV due to the crystal facets of Au [namely (111), (112), and (110)]. Additionally, when multilayer WS₂ and Au(111) facets are azimuthally aligned, strong interactions induce mechanical slippage of the interfacing WS₂ layer, with respect to the rest of the WS₂ layers, resulting in local stacking variations with an occupied state energy shift of 20-50meV. Finally, we employed oxygen plasma treatment of Au to fabricate homogenous TMD-Au interfaces while also tuning the electronic properties of the TMDs. Our findings illustrate that the electronic properties of TMDs are greatly impacted by the interface interactions at energy and length scales pertinent to the operation of TMD-based electronics and optoelectronics.

The work presented in this talk is conducted in collaboration with A. Boehm, C. D. Spataru, K. Thürmer, J. D. Sugar, A. Kim, and C. J. Thomas at Sandia National Laboratories, and J. J. Fonseca and J. T. Robinson at US Naval Research Laboratory. We acknowledge insightful discussions with G. Copeland, N. Bartelt, F. Leonard, C. Smyth, and T. M. Lu at Sandia National Laboratories. The work at Sandia National Laboratories was supported by Sandia’s LDRD program and in part by the US Department of Energy, Office of Basic Energy Sciences, Division of Materials Sciences and Engineering (grant BES 20-017574). The work at the US Naval Research Laboratory was funded by the Office of Naval Research. Sandia National Laboratories is a multi-mission laboratory managed and operated by National Technology and Engineering Solutions of Sandia, LLC., a wholly-owned subsidiary of Honeywell International, Inc., for the U.S. Department of Energy’s National Nuclear Security Administration under contract DE-NA0003525. The views expressed in the article do not necessarily represent the views of the U.S. Department of Energy or the United States Government.

2:00 PM EL07.02.02

Cryogenic Nano-Imaging of Second-Order Moire Superlattices [Petr Stepanov](#); University of Notre Dame, United States

Magic angle twisted bilayer graphene has been realized as a new platform to study strongly correlated quantum states of matter such as superconductors, correlated insulators and topological

orders hosted by its native flat bands. Recent observations of anomalous Hall effect in MATBG revealed a non-zero Berry-curvature-induced orbital ferromagnetism and has been followed by extensive experimental and theoretical studies of its origin. Initial electronic transport studies demonstrated anomalous Hall effect at $\nu=+3$ electrons per moire unit cell in the samples aligned with the adjacent insulating hBN layer, which breaks MATBG moire inversion symmetry thus assisting in opening non-trivial insulating gaps with finite Chern numbers. Here we report on photovoltage scanning near-field imaging at cryogenic temperatures (10 K) of a MATBG device structurally aligned with hBN layer. We reveal a complex pattern of quasi-local photovoltage fringes attributed to the second-order superlattice (supermoire) potential modulated through the sample bulk. We assume that predominantly the photocurrent originates from PV generation mechanisms induced by the proximity of a hot spot formed on the metallic atomic force microscopy tip radiated by mid-infrared photons. Strikingly, we find a clear change of the PTE fringes' real-space orientation when the sample doping changes between the valence and conductance flat bands which may signal a nematic ordered state in a highly doping-dependent low-energy spectrum of MATBG. Our observation sheds a new light on the microscopic mechanisms of the inversion symmetry breaking on a mesoscopic lengthscale.

2:15 PM EL07.02.03

Raman Spectroscopy on 1D Graphene Nanoribbons: From Structure to Electron-Phonon Interactions Angel Labordet Alvarez¹, Mickael Perrin^{1,2}, Klaus Müllen³, Roman Fasel^{1,4}, Michel Calame^{1,5}, Gabriela Borin Barin¹ and Mirjana Dimitrijevska¹; ¹Empa-Swiss Federal Laboratories for Materials Science and Technology, Switzerland; ²ETH Zürich, Switzerland; ³Max Planck Institute for Polymer Research, Germany; ⁴University of Bern, Switzerland; ⁵University of Basel, Switzerland

Low-dimensional materials (1D and 2D) are promising candidates as building blocks of future electronics and optoelectronics. Controllable bandgap, strong light-matter interaction, and sub-nanometer thickness are among their favorable properties for various applications. In this regard, graphene nanoribbons (GNRs) are especially interesting, due to their remarkable physical properties that are critically determined by their width and edge structure [1]. A comprehensive characterization of these materials is a crucial learning step toward their reliable integration in devices.

In this work, we showcase the use of various types of Raman spectroscopy along with density functional theory (DFT) calculations, for the investigation of intrinsic and defect-induced structural, vibrational, and optoelectronic properties of GNRs, with special emphasis on probing the interaction in-between GNRs and with various substrates (metal and oxides). The 9-atom wide armchair GNR (9-AGNR) is chosen as an example system.

We start by using low-temperature, polarization Raman spectroscopy measured with multi-wavelength excitation (488, 532, and 785 nm) to investigate the differences in fundamental and defect-activated phonons of 9-AGNRs grown uniaxially aligned on gold (Au(788)) and transferred to oxide substrates using the process from [2]. We probe the possible interaction between the GNRs by investigating two samples with distinct surface coverages: a full monolayer (ML) and 0.3 ML assuming that the interaction between the GNRs decreases by decreasing the surface coverage. Raman measurements on these two samples show particular differences in the spectral region corresponding to C-H vibrations (1000 to 1400 cm^{-1}), suggesting possible activation of interaction-induced Raman peaks.

Next, we use temperature-dependent Raman measurements, in the range from 70 to 500 K, in order to probe phonon-electron and phonon-phonon coupling in these systems. We systematically investigate the dependence of Raman peak positions and widths of G, D and C-H related phonons with temperature. We show that, for the full monolayer GNRs on the Au (788) substrate, the electron-phonon coupling is dominating up to temperatures of 250 K. This is a surprising feature, considering that 9-AGNRs grown on Au substrates, have a semiconducting behavior with a bandgap of about 1.4 eV [3]. This should diminish electron-phonon coupling for all phonons with energies lower than 1.4 eV (11200 cm^{-1}). We explain this behavior in terms of interactions between adjacent GNRs and/or between GNRs and the substrate. Finally, we discuss how electron-phonon and phonon-phonon coupling can have a profound effect on the electronic properties of these materials, which can be especially crucial for device performances.

[1] Cai et al. Nature 466 (2010)

[2] Borin Barin et al. ACS Applied NanoMaterials 2 (2019)

[3] Talirz et al. ACS Nano 1, (2017)

2:30 PM EL07.02.04

Intercalation of Graphene Nanoribbons in Ultra-High Vacuum Towards Optimized Dry-Transfer into Devices Dominik Lüthi^{1,2}, Lin Yang³, JiMa³, Akimitsu Narita^{4,5}, Xinliang Feng³, Klaus Müllen⁴, Pascal Ruffieux¹, Roman Fasel¹ and Gabriela Borin Barin¹; ¹Empa-Swiss Federal Laboratories for Materials Science and Technology, Switzerland; ²University of Bern, Switzerland; ³Technische Universität Dresden, Germany; ⁴Max Planck Institute for Polymer Research (MPIP), Germany; ⁵Okinawa Institute of Science and Technology, Japan

Atomically precise graphene nanoribbons (GNRs) show exciting properties deriving from electron confinement and related band gap tunability. The ability to tune GNRs' electronic and magnetic properties at the single atom level makes them an ideal platform for a wide range of device applications, from classical transistors to spintronics. To achieve such control, atomic precision in the fabrication of the GNRs is indispensable.

On-surface synthesis, based on covalent coupling of specific precursors on a metallic surface, allows access to various types of GNRs including armchair-GNRs (AGNRs), [1] zig-zag-GNRs (ZGNRs) [2], and GNRs with specific edge-extensions [3].

Such edge topologies can give rise to intriguing physical properties such as spin-polarized edges with a long spin lifetime and topological quantum states, making these GNRs an interesting template for quantum-based technologies. [3]

To probe such properties in a device, GNRs need to be transferred from their metallic growth substrate to insulating ones.

However, the enhanced chemical reactivity of the zigzag edge states hinders the integration of these GNRs into devices, which so far has prevented any investigation on their (magneto) transport characteristics.

In this work we explore GNR-intercalation to achieve their decoupling (and decreased interaction) with the underneath metal, as a viable path to allow GNRs' dry-transfer in ultra-high-vacuum. Such method would allow better access to GNRs' electronic characterization decoupled from the metal substrate as well as their direct integration into different device architectures without any air exposure, therefore preserving GNRs' intrinsic properties.

Our first approach was to explore the intercalation of GNRs with carbenes (BIM) [4], as it has been shown to strongly interact with Au(111) by forming covalent bonds. The intercalation occurs due to the formation of a dense self-assembled monolayer (SAM) on the surface, causing stochastic intercalation of GNRs. We attribute a sterical argument to the intercalation, as the high excess of carbenes on the surface leads to some GNRs migrating to the top layer. Scanning tunneling microscopy and spectroscopy characterization of intercalated GNRs will be discussed.

Another exciting approach is the intercalation to open a pathway to study the interaction of GNRs with other surfaces. A promising template in this regard is the growth of transition metal halides with tuneable electronic and magnetic properties [5]. Intercalation of GNRs with transition metal halides allows to probe their interaction with magnetic layers by scanning tunneling spectroscopy (STS), while potentially keeping the advantage of decoupling GNRs for device integration via dry-transfer.

[1] Cai, J. et al. Nature 466, 470–473 (2010).

[2] Kan, Er-jun, et al. Journal of the American Chemical Society 130. 4224–4225 13 (2008):

[3] Gröning, O. et al. Nature 560, 209–213 (2018).

[4] Krzykawska, A. et al. P. ACS Nano 14, 6043–6057 (2020).

[5] McGuire, Michael A. Crystals 7.5: 121 (2017).

2:45 PM BREAK

3:15 PM *EL07.02.05

On-Surface Synthesis of Graphene Nanoribbons and Spin Chains Pascal Ruffieux; Empa-Swiss Federal Laboratories for Materials Science and Technology, Switzerland

Recent advances in on-surface synthesis has allowed the selective fabrication of a number of prototypical types of graphene nanoribbons. The thereby achieved properties include width-dependent electronic band gaps in armchair graphene nanoribbons, edge-localized states in zigzag graphene nanoribbons and topological band engineering in width-modulated topological graphene nanoribbons. More recently, on-surface synthesis of magnetic nanographenes has been reported. Here, the spin originates from unpaired electrons present in nanographenes with controlled sublattice imbalance or topological frustration. The corresponding magnetic moments live in π -orbitals and are hence largely delocalized, which allows for chemical control over their exchange interaction when covalently linking several molecular building blocks. Here, I will present synthesis of various prototypical magnetic nanographenes and the possibility to covalently link them to form coupled spin systems where exchange coupling can exceed 100 meV. Using halogen-substituted precursors, we achieve the on-surface synthesis-based deterministic bottom-up fabrication of various spin chains including a triangulene spin-1 chain revealing the predicted Haldane gap and fractional excitations at the chain termini or a strictly alternating spin- $\frac{1}{2}$ chain with chemically engineered coupling strengths J_1 and J_2 . Scanning tunneling microscopy and spectroscopy is used to determine the length- and site-dependent

magnetic excitations. Furthermore, we apply hydrogenation to achieve spin site passivation and controlled tip-based local reactivation to fabricate and characterize specific spin patterns in one-dimensional spin chains and spin clusters.

3:45 PM *EL07.02.06

Emerging Two-Dimensional Materials for Device Applications[JunLou](#); Rice University, United States

Two-dimensional (2D) materials, such as Graphene, h-BN and MoS₂, are promising candidates in a number of advanced device applications, owing to their exceptional electrical, optical and mechanical properties. Scalable growth of high quality 2D materials is crucial for their adoption in technological applications the same way the arrival of high-quality silicon single crystals was to the semiconductor industry. While CVD growth of wafer-scale monolayer graphene and TMDs has been demonstrated, considerable challenges still remain. In this talk, we first report a CVD method to grow fluorine rich 2D polymer (2DP-F) on various substrates for low-k dielectrics in 2D TMDs based devices. Using precursors with low vaporize temperature, a uniform and ultra-flat 2DP-F film with controlled thickness can be deposited on silicon oxide wafer, glass, sapphire and mica substrates. Dielectric properties and relevant mechanical properties were carefully characterized. These 2DP-F films were then used as the substrate for transition metal dichalcogenides (TMDs) based devices, and significant improvements in device performances were found, possibly owing to the ultra-smooth and dangling bond free surface of 2DP-F that can significantly reduce the interfacial scattering of carriers.

Next, we show that atomically thin Cs₃Bi₂I₉, an all-inorganic lead-free perovskite derivative with strong optical activity can be successfully synthesized by vapor growth method. Reducing the dimensionality of such perovskites could utilize the materials' advantages for solid-state information devices like valleytronics. By breaking the inversion symmetry, 2D Cs₃Bi₂I₉ flakes with odd-layer number exhibited persistent, optically addressable valley polarization. This study potentially opens generalizable CVD method for growing a broad range of 2D perovskites towards cost-effective and energy-efficient integrated device applications. Finally, we report a two-step vapor phase growth process for the creation of high-quality vdW heterostructures based on perovskites and TMDCs, such as 2D Cs₃Bi₂I₉/MoSe₂, with a large lattice mismatch. Supported by experimental and theoretical investigations, we discover that the Cs₃Bi₂I₉/MoSe₂ vdW heterostructure possesses hybrid band alignments consisting of type-I and type-II heterojunctions because of the existence of defect energy levels in Cs₃Bi₂I₉. More importantly, we demonstrate that the type-II heterojunction in the Cs₃Bi₂I₉/MoSe₂ vdW heterostructure not only shows a higher interlayer exciton density, but also exhibits a longer interlayer exciton lifetime than traditional 2D TMDCs based type-II heterostructures. Such vdW heterostructures provide promising platforms for exploring novel physics and cutting-edge optoelectronics and valleytronics applications.

4:15 PM EL07.02.07

In-Plane Polarization in 3R-β'-In₂Se₃ Grown by Molecular Beam Epitaxy[Derrick Shao HengLiu](#)¹, [SebastianCalderon](#)², [AlbertSuceava](#)¹, [ElizabethC. Dickey](#)², [VenkatramanGopalan](#)¹ and [JoanM. Redwing](#)¹; ¹The Pennsylvania State University, United States; ²Carnegie Mellon University, United States

Two-dimensional ferroelectrics have gained increasing attention due to their promising potential in new memory device applications, such as ferroelectric field effect transistors (FeFETs) and non-volatile memory (NVM). The In₂Se₃ family represents a promising system for 2D ferroelectrics that can be deposited at temperatures compatible with back-end-of-line processing and can enable an ultra-thin body due to the 2D layer structure. However, it is a complex material system with many combinations of polymorphs (a, b, and g) and polytypes. In the current scientific literature, phase assignment and phase characterization are still controversial. The phases are determined by the crystal structure of repeating quintuple layers, and the polytypes are determined by the stacking sequences of the quintuple layers. The α-In₂Se₃ has two polytypes (2H and 3R), and β-In₂Se₃ has three polytypes (1T, 2H, and 3R). γ-In₂Se₃ is not a 2D material, but has a distorted wurtzite structure leaving room for polarization in the tetrahedra. While existing reports suggest in-plane or out-of-plane polarization in In₂Se₃, many existing publications fail to discuss the specific phase or polytype when reporting the synthesis and ferroelectric properties. A deeper understanding of the In₂Se₃ phases and polytypes is crucial as ferroelectricity is directly coupled to the crystal structure. On top of that, not all of the phases and polytypes are noncentrosymmetric. Detailed studies are therefore needed to explore the synthesis and structural properties of specific phases and polytypes of In₂Se₃ to unambiguously connect to their respective ferroelectric properties.

This talk presents our findings on the growth and characterization of 3R-β'-In₂Se₃ films grown on c-plane sapphire and Si(111) substrates by molecular beam epitaxy (MBE). Single phase β-In₂Se₃ films were obtained on sapphire at 600°C and on Si(111) at 350°C. High Se/In flux ratio was required to suppress the formation of other indium selenide phases. In and Se atomic fluxes were calibrated with a quartz crystal microbalance (QCM) at the film growth position. The tooling factors of the QCM flux calibration were previously determined from physical thickness measurements on calibration samples using X-ray reflectivity (XRR) and scanning electron microscopy (SEM). An infrared (IR) camera was installed to serve as an additional substrate temperature metric along with the system's thermocouple installed behind the substrate. *In-situ* reflective high energy electron diffraction (RHEED) was used to monitor the structural formation of the films. Phase examination of the samples was determined by *ex-situ* X-ray diffraction (XRD) and Raman spectroscopy. Scanning transmission electron microscopy (STEM) carried out on the sample cross-sections revealed the films on sapphire and Si(111) to be the 3R polytype with small polytype impurities at the film/substrate interface. Furthermore, analysis of the STEM images indicated that the central Se atoms in the Se-In-Se-In-Se quintuple layer structure were slightly displaced in the in-plane direction, resulting in in-plane polarization and the phase assignment of the β' phase. The results were further supported by second harmonic generation (SHG) polar plots which were consistent with the observation of in-plane Se atoms displacement. I-V measurements and piezoresponse force microscopy (PFM) are being applied to capture the hysteresis behavior of 3R-β'-In₂Se₃ grown by MBE.

4:30 PM EL07.02.08

Characterisation of Monolayer MoS₂-Dielectric Interfaces[HanYan](#)¹, [YanWang](#)¹, [YangLi](#)¹, [SoumyaSarkar](#)¹, [DibyaPhuyal](#)², [JunghoKim](#)¹ and [ManishChowalla](#)¹; ¹University of Cambridge, United Kingdom; ²KTH Royal Institute of Technology, Sweden

The atomically thin nature of two-dimensional (2D) transition metal dichalcogenides (TMDs) makes them susceptible to the dielectric environment. Efforts on dielectrics for 2D semiconductors have been focused on gaining better gate control using high *k* dielectric STO or thin HfO₂ [1, 2]. While SiO₂, HfO₂, and ZrO₂ are widely employed as dielectrics, our understanding of how they influence the electronic properties of atomically thin semiconductors remains limited [3]. In this study, we investigated interfaces between monolayer MoS₂ and various dielectrics (SiO₂, HfO₂, ZrO₂ and hBN) using photoluminescence (PL), synchrotron X-ray photoelectron spectroscopy (XPS), and electrical transport measurements. PL results show that MoS₂ on SiO₂ gives the highest exciton peak energy at 1.91 eV and MoS₂ on ZrO₂ gives the lowest at 1.89 eV. Through XPS, we find that the Mo 3d_{5/2} core level binding energies are 231.05 eV, 230.6eV, and 230.22 eV, when MoS₂ is in contact with SiO₂, HfO₂, and ZrO₂, respectively. The results indicate monolayer MoS₂ has the highest electron doping when in contact with SiO₂ and the lowest when in contact with ZrO₂. Furthermore, we determined the band alignments at the interfaces between monolayer MoS₂ and the dielectric materials through angle-dependent XPS, elucidating the depth profile of elemental core-level binding energy and thus providing insights into the charge-transfer behaviour when atomically thin MoS₂ interacts with different dielectrics.

References:

- [1]: Huang J, Wan Y, Shi J et al. High-*k* perovskite membranes as insulators for two-dimensional transistors. *Nature*. 2022;605(7909):262-267.
- [2]: Chen T, Chuu C, Tseng C et al. Wafer-scale single-crystal hexagonal boron nitride monolayers on Cu (111). *Nature*. 2020;579:219-223.
- [3]: Wang Y, Chhowalla M. Making clean electrical contacts on 2D transition metal dichalcogenides. *Nature Reviews Physics*. 2021;4(2):101-112.

4:45 PM EL07.02.09

Replacing Hydrogen Sulfide with Di-tert-butyl Disulfide as an Atomic Layer Deposition Precursor for Synthesizing Transition Metal Dichalcogenides[IanCampbell](#), [DouglasHeine](#) and [AgeethBol](#); University of Michigan–Ann Arbor, United States

Sulfur-containing transition metal dichalcogenides (TMDs), like molybdenum sulfide, have proven to be promising materials for electrocatalysis, energy storage, and microelectronics applications that are demanding increasingly thinner films and smaller particles over large areas. Useful films of TMDs can be prepared via the process of exfoliating layers within TMDs, which suffers from poor scalability, or through approaches like chemical vapor deposition and atomic layer deposition (ALD). ALD is capable of depositing atomically thin layers of material by using self-limiting, surface-saturating reactions that make it uniquely capable of synthesizing subnanometer-scale layers and particles over large areas with variable topography. Currently, the dominant method for preparing sulfide TMDs via ALD is to alternately expose a substrate to a metalorganic precursor and a sulfur source, which is often hydrogen sulfide (H₂S) or a plasma containing H₂S. H₂S is a corrosive, toxic, and flammable gas that is heavier than air, which makes it hazardous and expensive to store, install, and transport. Additionally, the odor of H₂S is imperceptible at life-threatening concentrations, making it even more dangerous. Alternative sulfur precursors in the solid or liquid phase would be beneficial in terms of cost and safety and would require the installation of no additional hardware for most ALD reactors. In this contribution, the widely researched ALD process using bis(tert-butylimido)bis(dimethylamino)molybdenum(IV) ((^tBuN)₂(NMe₂)₂Mo) and H₂S plasma is compared to a novel ALD process using (^tBuN)₂(NMe₂)₂Mo, hydrogen plasma, and di-tert-butyl disulfide (TBDS), which is an inexpensive, liquid-phase sulfur precursor. The growth behavior of both ALD processes is characterized via continuous in-situ spectroscopic ellipsometry, which reveals saturating reactions for H₂S-plasma and TBDS exposures. The composition and stoichiometry of the deposited films are determined using X-ray photoelectron spectroscopy, Rutherford backscattering, and elastic recoil detection. The crystallographic structures of the films are assessed using Raman spectroscopy and selected-area electron diffraction in conjunction with transmission electron microscopy. Molybdenum sulfide films prepared using both sulfur precursors are compared for their abilities to catalyze the hydrogen evolution reaction and for their electronic resistivities and charge carrier mobilities as determined by van der Pauw measurements. Finally, it is demonstrated that the TBDS-based ALD process is transferrable to the synthesis of other TMDs like niobium sulfide.

8:00 PM EL07.03.01

Ag-Au-PANI Multilayered Nanowire Network Approach for Visible-To-Infrared Display and Data Encryption Kyung Rok Pyun¹, Yeongju Jung¹, Seok Hwan Choi¹, Huijae Park¹, Minjae Lee^{1,2}, Deog-Gyu Seo¹ and Seung Hwan Ko^{1,1}; ¹Seoul National University, Korea (the Republic of); ²Hyundai Motor Group, Korea (the Republic of)

Polyaniline (PANI) is a conductive polymer with distinct electrochemical characteristics that facilitate the functionalization of nanomaterials, enabling the development of various smart devices. In particular, it is known that its reversible redox process allows for the modulation of optical properties in the visible and infrared regions. While previous studies have explored the electrochromic properties of PANI, they utilized conventional electrodes such as ITO and Au sputtered electrodes, which restrict their application in flexible devices. To address this limitation, we present a novel approach that leverages metal nanowire networks, known for their high electrical conductivity and mechanical flexibility, as the electrode material. Specifically, we synthesize Ag-Au core-shell nanowires and employ a laser-based plasmonic welding process to enhance adhesion between the nanowire network and substrate. This prevents delamination during the electropolymerization of PANI in an aqueous solution, enabling the successful deposition of PANI onto the core-shell nanowire-based electrode. Furthermore, the Ag-Au core-shell nanowire network electrode exhibited excellent electrochemical stability, primarily attributed to the presence of Au outer shell. This characteristic facilitated the direct electropolymerization of aniline monomer on the Ag-Au core-shell nanowire network electrode, preventing the oxidation of core silver nanowires during the electropolymerization process. Thereby, the electrode successfully serves as both a current collector and a backbone for the electro-polymerization process. By optimizing the electrodeposition conditions, we can achieve variable optical properties in the Ag-Au-PANI multilayered nanowire network not only in the visible wavelength region (reflectance) but also in the infrared wavelength region (emissivity). In essence, our proposed flexible multispectral display can alter its visible color and apparent temperature in the visible and infrared wavelengths, respectively, by applying the desired electrical input. Furthermore, we have designed pre-patterned and multi-pixel displays for data encryption and confidential data visualization. This device provides the additional functionality of data encryption, making it highly suitable for diverse applications, including military camouflage, confidential data visualization, and secure communication systems.

8:00 PM EL07.03.02

Substitutional Oxygen-Mediated Se-Vacancy Healing in WSe₂: Enabling High-Mobility p-Type Field-Effect Transistors. Riya Dutta¹, Hae Won Cho¹, Younghyun Ju¹, Pavan Pujar¹, Young-Min Kim¹, Seongin Hong², Youngki Yoon³ and Sunkook Kim¹; ¹Sungkyunkwan University, Korea (the Republic of); ²Gachon University, Korea (the Republic of); ³University of Waterloo, Canada

Transition-metal dichalcogenides (TMDs) exhibit high carrier mobility and can be scaled down to sub-nanometer dimensions, presenting themselves as viable alternatives to silicon electronics. Among TMDs, WSe₂ stands out for its ability to facilitate both hole and electron carrier transport, making it a crucial component in CMOS logic circuits. However, the p-type electrical performance of WSe₂-field effect transistors (FETs) is still limited, prompting the exploration of various approaches to overcome this challenge. In this study, we employed a heterostructural multilayer WSe₂ channel and utilized solution-processed aluminum-doped zinc oxide (AZO) to modify the composition of WSe₂, resulting in a device with outstanding electrical properties. By introducing oxygen anions from AZO to the WSe₂ channel, we successfully eliminated subgap states through Se-deficiency healing, leading to enhanced transport capacity. Se vacancies, known to cause mobility degradation through scattering, were mitigated via ionic compensation. Consequently, the hole mobility reached high values, peaking at approximately 100 cm²/Vs. Furthermore, we systematically analyzed the transport behavior of the oxygen-doped WSe₂-FET using density functional theory simulations and photoexcited charge collection spectroscopy measurements.

8:00 PM EL07.03.03

Charge Transport Characteristics in Non-Van der Waals 2D Transition Metal Nitrides Synthesized via Atomic Substitution Approach Hongze Gao¹, Da Zhou², Zifan Wang¹, Lu Ping¹, Jun Cao¹, Mauricio Terrones² and Xi Ling¹; ¹Boston University, United States; ²The Pennsylvania State University, United States

Two-dimensional (2D) materials have been extensively explored in the past decade to advance the development of nanoelectronic devices by virtue of their exciting properties emerging at the reduced dimension. Numerous 2D crystals have been synthesized and studied, including graphene, transition metal dichalcogenides (TMDs), and h-BN, which are van der Waals (vdW) layered materials with vdW gaps between two adjacent atomic layers. Such vdW gaps result in an anisotropic bonding in the crystal and hence a weak interlayer interaction, which facilitates the separation of ultra-thin layers of these crystals. However, given the technological gaps in vdW 2D materials (e.g., absence of high-K dielectrics), exploring the non-vdW 2D crystals plays a vital role in advancing the development of 2D electronics. In contrast to vdW crystals, the isotropic strong bonding in non-vdW crystals imposes great challenges in downscaling these materials. Targeting on this technological challenge, our group developed an atomic substitution approach to prepare ultra-thin non-vdW 2D crystals, where vdW 2D crystals (e.g., MoS₂ and WSe₂) are used as precursors and converted into non-vdW materials through a chemical reaction. Non-vdW 2D metal nitrides (MN_x) (e.g., Mo₃N₆ and W₃N₆) with high crystallinity, smooth surface, and well controlled thicknesses have been successfully synthesized. Hereby, we further investigated the charge transport characteristics in these 2D MN_x prepared by the atomic substitution approach. A wide range of electrical conductivities of different MN_x were measured using four probe electrical measurements, and we also found high 2D carrier concentrations of the MN_x from Hall measurements. Temperature-dependent resistance (R-T) measurements further revealed the thermal excitation mechanisms and weak localization effect in the charge transport behaviors of the 2D MN_x. We comprehensively investigated the charge transport characteristics in MN_x and demonstrated their potential applications in nanoelectronic devices

8:00 PM EL07.03.04

Unusual Properties of TiO₂ Nanotube Arrays Formed Anodically in Alkanamide-Based Electrolytes Navneet Kumar, Kazi M. Alam, Damini Vrushabendrakumar, Harshitha Rajashekhar, John Garcia and Karthik Shankar; University of Alberta, Canada

The formation of highly ordered transition metal oxide nanotube arrays through electrochemical anodization of valve metals (Ti, V, Hf, Zr, Ta, Nb, etc) in fluoride-containing electrolytes is relatively well-established. Titanium dioxide nanotube arrays (TNTAs) have shown immense potential as photocatalysts, photoanodes, photodetectors and electron transport layers for photovoltaics. In the overwhelming majority of journal and conference papers on this topic, the TNTAs are grown in ethylene glycol-based organic electrolytes (eg-TNTAs) containing water and fluoride salt. Ethylene glycol is a polar protic solvent with a dense network of hydrogen bonds resulting in a high viscosity and a moderate dielectric constant of 37. On the other hand, alkanamides whilst polar protic solvents, have a polymer-like structure due to the availability of merely two hydrogen bonding sites in a *trans*-configuration. Furthermore, alkanamides exhibit large values of the dielectric constant - significantly higher than water e.g. formamide has ϵ_r of 111 while n-methylformamide has ϵ_r of 171 at room temperature. Herein, we present some unusual properties of TNTAs grown in formamide-based electrolytes (fa-TNTAs). Unlike eg-TNTAs which are self-organized into a closed honeycomb structure with a triangular lattice ordering, fa-TNTAs are non-periodic and have a more open structure with ready access to both the inner and outer nanotube walls. The fa-TNTAs absorb more visible light compared to eg-TNTAs, exhibit much lower lattice strain, differ in surface composition, possess a lower work function and demonstrate superior performance (3-fold improvement) in sunlight-driven transformation of carbon dioxide into carbon monoxide. Infrared spectroscopy indicated the dramatically different nature of adsorbates on fa-TNTAs compared to eg-TNTAs following CO₂ chemisorption. These differences in electronic properties and electronic device performance will be elaborated upon, and explained in the context of the different anodization electrolytes producing changes in morphology, composition, lattice strain and electronic band-structure.

8:00 PM EL07.03.05

Chemical Vapor Etching of Silicon Wafer for the Synthesis of Highly Dense and Aligned Sub-5 nm Silicon Nanowires Arrays Juyeon Seo¹, Sen Gao¹, Sanghyun Hong¹, Jianlin Li¹, Peiyun Feng¹, Ji Young Byun² and Yung Joon Jung¹; ¹Northeastern University, United States; ²Korea Institute of Science and Technology, Korea (the Republic of)

Silicon nanowires (SiNWs) have attracted great interest for applications in high-performance miniaturized devices and energy harvest and storage systems. Vapor-liquid-solid growth and metal-assisted chemical etching methods are the most commonly used approaches for synthesizing silicon nanowires. Still, using these catalyst-assisted methods, producing a large quantity of silicon nanowires with diameters less than 10 nm is elusive, and the removal of catalysts is a challenge for their practical applications. Recently, we reported the synthesis of highly dense and vertically aligned sub-5 nm silicon nanowires with a high aspect ratio of over 10,000 by a catalyst-free chemical vapor etching of silicon. In this paper, we systematically investigated the effect of key chemical vapor etching parameters that govern the morphology of silicon nanowires. We achieved highly aligned nanowire arrays with sub-5 nm diameter and a length of up to 52.1 μm by controlling the oxidant gas concentration, reaction temperature, and hydrogen concentration. The results demonstrate that ppm level of oxidant gases is crucial for silicon's steady-state etching into nanowires by passivating their surface with a silicon suboxide layer. Furthermore, the thermodynamic analysis combined with the experimental result suggests that anisotropic etching of silicon is also facilitated by increasing the reaction temperature and hydrogen concentration due to the increased ratio between two primary etchants (HCl/SiCl₄),

suggesting an optimum range of the etchant ratio (0.131–0.216) for the nanowire formation. Our results can help us understand the chemical vapor Si etching process and guide a scalable synthesis of ultra-narrow silicon nanowires for future scientific research and practical applications.

8:00 PM EL07.03.06

Structural Phase Transitions for Multi-Level In₂Se₃-Based Phase Change Memory [Nicholas D. Ignacio¹](#), [Yuqian Gu¹](#), [Sabah Hus²](#) and [Deji Akinwande¹](#); ¹The University of Texas at Austin, United States; ²Oak Ridge National Laboratory, United States

Layered materials such as In₂Se₃ and MoTe₂ have multiple crystal phases with differing electrical properties and can achieve reversible phase changes between them. Compared to transitions between amorphous and crystalline phase in conventional phase change memories (PCM), changes between crystalline phases are expected to have faster and low energy write operations for PCM even compared to interfacial PCM based Sb₂Te₃-GeTe superlattices due to the lower entropy of the crystalline-crystalline phase change. In₂Se₃ PCM have been demonstrated utilizing β and γ as the low and high resistance state respectively, however multilevel switching has not been extensively explored.

We report multi-level In₂Se₃ based PCM with device resistance covering a range of six-orders of magnitude. Local transport measurements conducted with scanning tunneling microscopy (STM) show the resistance of the vertical devices changes exponentially with the number of switching steps. These results indicate the existence of a layer-by-layer phase change in the structure of the material, rather than a lateral enlarging of low and high resistance phases as in conventional PCM. Compared to a planar PCM structure which only shows a three-orders of magnitude resistance change, tunneling like transport through the active material occurs in the vertical structure indicated by the six-orders of magnitude resistance change. The structural changes between crystalline β -In₂Se₃ and crystalline γ -In₂Se₃ phases of In₂Se₃ provide a high speed and low-entropy switching mechanism in conjunction with multi-level switching can allow for high density data storage and neuromorphic applications.

8:00 PM EL07.03.07

Flexible Gas Sensors Based on rGO and rGO-ZnO for NO₂ Detection at Room Temperature [Valmor R. Mastelaro](#) and [Amanda A. Komorizono](#); University of Sao Paulo, Brazil

With the progress in materials science, wearable devices have attracted great interest from the scientific community and the market. These devices can be integrated into watches, bracelets, glasses, clothes, and shoes and even adhered to the skin of the human body and monitor physiological and environmental conditions in real-time. Among the various types of wearable devices, flexible gas sensors have become an area of great importance due to the high demand for monitoring ambient air and exhaled air to identify possible environmental hazards or diseases, respectively [1]. Among toxic gases, NO₂ is one of the most harmful to health. When humans are exposed to a concentration above the safety limit, of 1 ppm for NO₂, this gas can be harmful to the human respiratory system, irritating the skin and eyes [2]. With this, the objective of this work is the manufacture of flexible gas sensors of rGO and rGO-ZnO for the detection of NO₂ at room temperature. ZnO was synthesized by the Pechini method using zinc nitrate hexahydrate as a precursor. The rGO used was the commercial one. Dispersions of rGO and rGO-ZnO with 1, 2 and 5% ZnO were prepared at a concentration of 0.2 mg/ml. For the fabrication of flexible gas sensors, the rGO and rGO-ZnO dispersions were deposited by drop-casting on the interdigitated electrode on the PET substrate. XRD analysis confirmed the formation of the wurtzite structure of ZnO. SEM images show that ZnO has quasi-spherical nanoparticles with an average diameter of 45 nm. SEM images from the rGO sensors show the rGO sheets with some folds due to the stacking of the sheets. For the rGO-ZnO sensors, the ZnO nanoparticles are anchored on the surface of the rGO sheets and surrounded by the rGO sheets. Measurements of NO₂ detection at room temperature show that the formation of composites with ZnO significantly increases the response of the sensors and reduces the response times of the sensors. Among the rGO-ZnO sensors, the rGO-5%ZnO sensor showed the best results in terms of response and response time. When exposed to 1.5 ppm of NO₂, the flexible rGO sensor showed a response and response time of 5.6% and 21 min, respectively. While the rGO-5%ZnO flexible sensor showed a response and response time of 18.5% and 14 min, respectively. Furthermore, the calculated limit of detection (LOD) of the rGO-5%ZnO sensor was 0.075 ppm, below the WHO recommended limit (1 ppm of NO₂).

Keywords: flexible gas sensor, rGO-ZnO gas sensor, PET substrate, NO₂ gas sensors

References

- [1] C. Zhou *et al.*, "Techniques for wearable gas sensors fabrication," *Sensors Actuators B Chem.*, vol. 353, no. November 2021, p. 131133, 2022.
- [2] Y. Huang *et al.*, "High Sensitivity, Humidity-Independent, Flexible NO₂ and NH₃ Gas Sensors Based on SnS₂ Hybrid Functional Graphene Ink," *ACS Appl. Mater. Interfaces*, vol. 12, no. 1, pp. 997–1004, 2020.

8:00 PM EL07.03.08

Multi-Ion Sensor Based on Carbon Nanotube Fibers for Wearable Electronic Tongue [Hocheol Gwac](#) and [Seon Jeong Kim](#); Hanyang University, Korea (the Republic of)

Wearable electronic tongue (e-tongue) sensors have garnered significant attention for their potential in enabling taste sensing in robotic systems and monitoring aberrant conditions, such as poor water quality, food spoilage (or freshness), and microbial contamination. Despite notable advancements in wearable multi-ion sensors, challenges persist in achieving stretchability and miniaturization of ion-selective sensors capable of detecting a wide range of ions for practical applications. In this study, we present a wearable multi-ion sensor based on ion-selective coiled fiber (ISCF) integrated with Carbon nanotubes (CNTs). The ISCFs were fabricated by coating CNT fibers with ion-selective membranes that include ionophores (valinomycin, sodium ionophore X, and Hydrogen ionophore I) corresponding to the target ions. In addition, the ISCF was fabricated in a coiled configuration to achieve stretchability without employing elastomers. Furthermore, they demonstrated selectivity for each target ions. Importantly, this sensitivity and selectivity were sustained even under mechanical deformations, such as a 25% strain, bending, and knotting. Furthermore, we endeavored to downscale the sensor into a single fiber (about 250 μ m) by plying three types of ISCFs and an all-solid-state reference electrode. This multi-ion potentiometric sensor was successfully woven into fabrics, such as clothing or gloves, demonstrating functional sensing performance in various solutions (sea, river, distilled waters, lemon, coconut, and grape juices) as practical applications. Collectively, these findings underscore the high potential of our potentiometric sensor as a taste sensor and monitoring device within the realm of e-tongues.

8:00 PM EL07.03.09

Side Gate Capacitive Coupling Reconfigurable Devices Based on BN-MoS₂ Van Der Waals Heterostructures [Miao Zhang](#), [Daobing Zeng](#), [Guanyu Liu](#), [Huihui Lu](#) and [Ziao Tian](#); Shanghai Institute of Microsystem and Information Technology, Chinese Academy of Sciences, China

As the traditional silicon-based device size has been miniaturized to its physical limits, to fulfill the requirements of big data and artificial intelligence technology, the devices with new materials and work principles are urgently required. Developing two dimensional (2D) reconfigurable multifunctional devices is of great potential in further miniaturizing the chip area and simplifying circuit design. Dissimilar atomically thin 2D materials can be vertically stacked to form van der Waals (vdW) heterostructures without being limited by lattice mismatch. Many previous reports have integrated various functions in a single 2D vdW heterostructures device. However, most of reconfigurable multifunctional devices are based on complex multilayer heterostructures (such as MoTe₂-MoS₂-BN-Graphene vdW heterostructures) or air-unstable ambipolar semiconductor channel materials (BP and WSe₂), inevitably limiting their application and manufacture in integrated circuits. Thus, it is urgent to develop 2D reconfigurable multifunctional devices with simple structures and stable electrical properties. MoS₂, one of the most air-stable 2D semiconductors, has shown great prospect to replace conventional silicon materials attributed to its high carrier mobility and tunable bandgap with thickness. Different from ambipolar semiconductors that polarity can be adjusted from ambipolar type to n or p type by electrostatic doping, MoS₂ generally behaves as an n-type semiconductor due to strong Fermi level pinning near the conduction band. Therefore, few works have reported reconfigurable multifunctional MoS₂ devices. Most of MoS₂-based reconfigurable devices are based on MoS₂ thickness engineering, potentially limiting their practicality and flexibility in reconfigurable multifunctional circuits. In this work, we propose a side gate capacitive coupling reconfigurable device based on simple Au-BN-MoS₂ heterostructures, in which Au, MoS₂ and BN serve as top semifloating gate, channel material and gate dielectric, respectively. Our work realize the integration of three different functions in a single device, including a diode, a double-side-gate reconfigurable logic transistor and a top floating gate memory. The side gate voltage can control the carrier concentration in the MoS₂ channel due to the capacitive coupling between the side gate and the extra extension of top semifloating gate. We demonstrate that the channel can switch between the deplete state, n⁺n junction, and accumulated state as the side gate voltage changes from negative to positive. The device exhibits rectification ratios of 10⁵ as a diode. The device can also be modulated by the two side gates simultaneously, in which the voltage of the two side gates and drain current serve as input signals and logic output respectively, reconfigurable logic operations (OR, AND) can be realized in a single device by switching the direction of source-drain voltage. The current on/off ratios of AND and OR logic reach about 10⁴. Moreover, the device demonstrates a large memory window and high on/off ratio (>10⁷) under a small back gate voltage (30V). Those results provide a way for integrating the same reconfigurable multifunctional devices to realizing complex electronic systems.

8:00 PM EL07.03.10

An Electrostatic Force Microscopy-Based Analysis for Metallic and Semiconducting Carbon Nanotubes [Indra Memdi Khoris¹](#), [Yuki Kuwahara¹](#), [Fahmida Nasrin¹](#), [Ryota Yuge²](#) and [Takeshi Saito¹](#); ¹National Institute Advanced Industrial Science and Technology, Japan; ²NEC Corporation, Japan

Carbon nanotubes (CNTs) have been known as a promising material for developing high-performance electronic devices. Depending on its chirality, CNTs can be semiconducting (s-type) and metallic (m-type). S-type CNTs have bandgaps, and high carrier mobility which is suitable as transistor, sensor, and logic nano-devices. On the other hand, m-type CNTs have near-ballistic conductance and high current density which is excellent as electrodes and interconnecting component in electrical circuits.^[1,2] In general, as-grown CNTs are composed of the mixture of m-

type and s-type. So, there is a need to quantify their m/s ratio. Optical methods, such as Raman spectroscopy and absorption spectroscopy, are widely used to characterize the m/s ratio and structure of CNTs.^[3] It is suitable for macroscopic analysis of multiple nanotubes in the bulk sample, but it is not easy for the optical methods to evaluate the microscopic analysis of individual CNTs. The direct observation of individual CNTs is a promising approach for visualizing and characterizing an individual CNT on the area of interest. Electrostatic Force Microscopy (EFM) has been reported to determine the metallicity of CNTs individually based on the line-shape of profile.^[4] Another work demonstrated the primary use of EFM to analyze the m/s fraction based on the counted number of CNTs.^[5] In this work, we demonstrated the determination of the m/s ratio of CNTs through the analysis of the topographic and EFM images, expressed as value of phase shift ($\Delta\Phi$).

The sample in this work was prepared by drop-casting as-grown CNTs on the APTES-functionalized Si wafer. Then, PtIr-coated cantilever were used to obtain the topographic images and EFM images. Then, the topographic image was analyzed to obtain the selections of all CNTs. The selection lines representing CNTs are drawn based on nearest end-to-end point selection of CNTs. Next, the selected lines were transferred to the EFM images to obtain the corresponding data of $\Delta\Phi$ from each of the selected CNTs. The ratio of the m-type and s-type CNTs were determined by two methods, direct contrast observation of the EFM images and the $\Delta\Phi$ average calculation. Based on the value of the phase shift, the height, and length of CNTs, we obtained the ratio of m-/s- type, the diameter and the length distribution of the as-grown CNTs.

By analyzing three data sets of topographic and EFM images, the developed EFM-based analysis showed the fraction of s-type CNTs in the as-grown sample around $67\% \pm 1\%$. The threshold of the sampling is determined to be around 600 units (line selection) to obtain 1% deviation. This result agrees to theoretical ratio of m-/s- type CNTs for as-grown samples. In addition, m-type and s-type CNTs showed asymmetric length distributions with mean length of 396.36 ± 10.93 nm and 232.85 ± 4.99 nm, respectively.

Further analysis and more experimental would be conducted to address characterization of CNTs' bundling, the non-straight CNTs analysis, and a simple quantification with precision down to 0.1% change of composition in the mixture of CNTs.

Acknowledgement:

This work was supported by ATLA Innovative Science and Technology Initiative for Security (Grant No. JPJ004596).

Reference:

Campidelli, S., et al. (2007). *Small*, 3(10), 1672-1676.

Wang, X., et al. (2016). *ACS nano*, 10(6), 6008-6019.

Miyazaki, J., et al. (2022). *The Journal of Physical Chemistry A*, 126(32), 5483-5491.

Barboza, A. P., et al. (2010). *Carbon*, 48(11), 3287-3292.

Lu, W., et al. (2009). *Nano letters*, 9(4), 1668-1672.

8:00 PM EL07.03.11

Performance Improvement of Thread Transistor using Carbon Nanotube Composite Thread with Ionic Gel Hiroki Kodaira and Takahide Oya; Yokohama National University, Japan

We propose a unique transistor based on carbon nanotube (CNT) composite threads with ionic gel.

It is known that the CNTs have many excellent properties such as highly electrical conductivity, highly chemical stability, electrical properties that can be metallic or semiconducting depending on their structure. Because of these properties, CNTs are expected to have a wide variety of applications. However, since the CNTs exist on a nanoscale, it is difficult to handle them on their own. For this reason, many approaches such as combining with other materials have been proposed. We have succeeded in developing "CNT composite threads" (CNTCTs), which combines CNTs with threads, a familiar material of our daily life. This material had good properties based on CNTs. In addition, we have also succeeded in producing metallic CNTCTs with a metallic property and semiconducting CNTCTs with a semiconducting property. Furthermore, by combining these, we succeeded in developing the "thread transistor" in our previous work. However, several problems have remained, including low performance.

In this study, we are aiming to develop ionic-gated thread transistors using CNTCTs.

Recently, ionic-gated transistors attracted attention because of its large capacitance and low operating voltage. Ionic liquids are suitable for gate dielectrics, but liquid state is not suitable for practical devices. Therefore, ionic gels are used as dielectrics, which is produced by combining ionic liquids and polymers. Because ionic gels have high mechanical toughness, we considered flexible transistors can be fabricated by combining them with CNTCTs.

The production method of our CNTCTs is based on the traditional dyeing method for threads. It is so simple method of dipping a thread in the CNT dispersion and drying in oven. Here we chose (6,5)-chirality CNT as the semiconducting CNT and multiwalled CNT (NC7000) as the metallic CNT. The method of preparing CNT dispersions was a typical one. Ionic gels are prepared by combining ionic liquids (EMI-TFSI), polymers (PVDF-HFP), and solvents (acetone). The solution is agitated until homogeneous. By combining the semiconducting CNTCT as a channel and the metallic CNTCT as a gate electrode, the thread transistor can be easily constructed. Here, a drop of the ionic gel is inserted between both CNTCTs to construct our ionic-gated thread transistor.

As results of measurements, the current-voltage characteristics of the thread transistor were p-type, and gate voltage dependency was improved compared to previous studies. Although the problem of high off-state current due to impurities in the CNTCTs still remains, we believe this approach is effective for performance improvement of our thread transistors.

By further developing this approach, we believe that our CNT composite thread will be used as a transistor in the near future.

8:00 PM EL07.03.12

Rapid Free-Patterning of Monolayer Graphene HaoCheng, TaeUkLim, JieHu, SangyouKim, YeongjunLee and WonsukJung; Chungnam National University, Korea (the Republic of)

The current methods for patterning graphene-based electrodes are complex and expensive, posing challenges for the commercialization of such electrodes due to repeated damage to the transferred graphene. In this study, we have devised a simple and efficient one-step free-patterning technique for graphene electrodes. This technique involves converting the C=C bonds in graphene to C-O bonds while pseudo-annealing the electrode. We compared the macroscopic and microscopic graphene electrodes produced using our method with those created using traditional techniques. Our evaluation included Raman spectroscopy, X-ray photoelectron spectroscopy, water contact angle measurements, field-emission scanning electron microscopy, and semi-auto probe station analysis. Moreover, we performed electron transport simulations and analyzed the results for both ideal graphene nanosheets (GNs) and GNs containing C-O bonds using a semi-empirical tightly coupled DFTB+ method based on density functional theory. Our findings demonstrate the feasibility and scalability of this proposed graphene patterning approach, which we anticipate will expedite the advancement and commercial availability of graphene-based devices.

8:00 PM EL07.03.13

Ferroelectric Field Effect Transistor Based on Graphene/CuInP₂S₆ Van Der Waals Heterostructures Maheera A. Ghani, Soumya Sarkar, Yan Wang and Manish Chowalla; University of Cambridge, United Kingdom

Ferroelectric field-effect transistors (FeFETs) demonstrate non-volatile hysteresis in transfer characteristics, which could be useful for logic and memory devices. FeFETs with two dimensional (2D) ferroelectric, Copper indium thiophosphate, CIPS (CuInP₂S₆) as the gate insulator and 2D semiconductor channels show variations (clockwise/anticlockwise hysteresis) in transfer characteristics.¹⁻³ It is therefore important to understand the influence of polarization, interface charge transfer and trap states on the performance of FeFETs based on CIPS van der Waals (vdW) heterostructures. Here, we investigate top gated 2D FeFET using ferroelectric CIPS and graphene channels with vdW contacts.⁴ We observed clockwise hysteresis in graphene FET with SiO₂ back gate due to interface trap states. This clockwise hysteresis can be mitigated by encapsulating graphene with hexagon boron nitride (hBN). We demonstrate the effect of charge transfer from CIPS by the shift of the Dirac point in graphene field effect transistor. Furthermore, we reveal anti-clockwise hysteresis in FeFET due to ferroelectricity of CIPS through minimising the influence of trap states at the interfaces.

Keywords: Ferroelectrics field-effect transistors, van der Waals heterostructure, charge transfer

References:

1. Si, M., Liao, P. Y., Qiu, G., Duan, Y. & Ye, P. D. Ferroelectric Field-Effect Transistors Based on MoS₂ and CuInP₂S₆ Two-Dimensional van der Waals Heterostructure. *ACS Nano* 12, 6700–6705 (2018).

2. Dey, A. *et al.* Memristive effects due to charge transfer in graphene gated through ferroelectric CuInP₂S₆. *2d Mater* 9, (2022).

3. Singh, P. *et al.* Two-Dimensional CIPS-InSe van der Waal Heterostructure Ferroelectric Field Effect Transistor for Nonvolatile Memory Applications. *ACS Nano* 16, 5418–5426 (2022).

8:00 PM EL07.03.14

Development of "Transpiration-Type Thermoelectric Power Generating Paper" using Carbon-Nanotube-Composite Papers Without Need for Heat Source Yudai Kamekawa¹, Koya Arai² and Takahide Oya¹; ¹Yokohama National University, Japan; ²Mitsubishi Materials Corporation, Japan

We propose a unique thermoelectric power generating device using carbon nanotube (CNT) composite paper, "transpiration-type thermoelectric power generating paper."

In recent years, thermoelectric power generation has been attracting attention because of its ability to effectively utilize heat that tends to be disposed of. However, the problem is that many of the thermoelectric materials currently in use are rare metals. Therefore, we focused on CNT, which has been shown to have high electrical conductivity and a high Seebeck coefficient. However, CNT is difficult to handle because they exist in powder form. For this, we have solved by developing CNT composite paper by combining paper and CNT. In this study, we are developing thermoelectric power generating devices based on the CNT composite papers.

Conventional thermoelectric power generating devices require a heat source to generate electricity. This research focuses on the capillary phenomenon of paper and aims to develop a new type of thermoelectric power generating paper that does not require a heat source and generates a temperature difference using the heat of vaporization when liquid evaporates from the CNT composite paper containing liquid.

The CNT composite paper is made using the modified Japanese washi paper making process. Specifically, a CNT dispersion consisting of single-walled CNT and SDS (sodium dodecyl sulfate) as dispersant dispersed ultrasonically in pure water is mixed with a pulp dispersion consisting of pulp, the raw material of paper, dispersed in pure water. Next, the water is removed from this mixed dispersion with a fine mesh. Finally, it is dried and molded to complete the process.

To conduct thermoelectric power generation without heat source, one end of this transpiration-type thermoelectric power generating paper is dipped in pure water filled in a container, and the other end is fixed from the top. At the top, the temperature is lower than at the bottom, which is immersed in water, due to the heat of vaporization caused by the evaporation of water lifted by capillary action. The difference in temperature causes the Seebeck effect. In the fabricated paper, a temperature difference of 0.9K was spontaneously generated, resulting in an electromotive force of 22 μ V.

As the next step in this research, we aim to further improve the output by changing the amount of material and the structure of the paper. Since our transpiration-type thermoelectric power generating paper obtained in this study does not require a heat source, we believe that it can be used as an environmental power generator in rivers and oceans in the near future.

8:00 PM EL07.03.15

CNFs/CNT-Prussian Blue/Chitosan Modified Thread Electrode for Non-Invasive Sensor of Glucose and Lactate Nadtinan Promphet¹, Chusak Thanawattano², Chatchai Buekban², Thidarut Laochai¹, Pranee Rattanawaleedirojn¹, Krisana Siralermukul¹, Pranut Potiyaraj¹, Juan Hinestroza³ and Nadnudda Rodthongkum¹; ¹Chulalongkorn University, Thailand; ²National Science and Technology Development Agency, Thailand; ³Cornell University, United States

Non-invasive diagnosis is an alternative approach to monitor health status without the patient painfulness. Among the flexible substrate materials, thread textile has become a promising substrate format for non-invasive wearable sensor fabrication owing to its small size, high flexibility, non-skin irritation, low-cost, and easy-to-use as an auto-microfluidic device. Herein, thread based non-invasive electrochemical sensor for sweat glucose and lactate was engineered. The cotton thread surfaces were modified by cellulose nanofibers (CNFs)/carbon nanotube (CNT) ink-Prussian blue/chitosan to enhance liquid adsorption, increase bioreceptor immobilization and improve sensor performance. The CNFs/CNT-prussian blue/chitosan modified cotton thread was characterized by laser scanning confocal microscopy, scanning electron microscopy, and fourier transform raman spectroscopy. Amperometric measurements using a hydrogen peroxide (H₂O₂) were applied for electrochemical characterization of the modified thread electrodes. A portable potentiostat was designed as a wristwatch and integrated with the modified thread electrode to provide a real-time detection of glucose and lactate. This sensor provides a linear range of 0.1–3 mM with the detection limit of 0.1 mM for glucose and a linear range of 1–35 mM with the detection limit of 1 mM for lactate which can distinguish the cut-off level of both glucose (0.3 mM) and lactate (25 mM) between the normal and high-risk people.

8:00 PM EL07.03.16

Enhancing Learning Accuracy with Floating-Gate Memristors in a Multi-Terminal Spiking Neurosynaptic Network Hosung Choi and Woojong Yu; Sungkyunkwan University, Korea (the Republic of)

Spiking neural networks (SNNs) are regarded as a more natural representation of artificial neural networks, distinguishing them from other types of networks. While several studies have been conducted to model SNNs, incorporating multiple connections between neurons has proven challenging due to the limited number of terminals in memristors. In this research, we propose a novel spiking neurosynaptic network that utilizes a multi-terminal floating-gate memristor.

Our memristor, named TRAM (Tunneling Random Access Memory), leverages the change in the Fermi energy level (E_f) of graphene, exhibiting desirable memory characteristics such as a high on/off ratio (>10⁵), excellent retention (>10,000 times), strong endurance (>100,000 times), and low energy consumption (120pJ). To emulate synapses and neurons, we adjusted the thickness of the insulating film layer (Al₂O₃). A thin layer (3nm) was used for neurons to demonstrate the Leaky Integrate-and-Fire (LIF) characteristic, while a thicker layer (7.5nm) was employed for synapses to exhibit Spike-timing-dependent Plasticity (STDP).

When voltage inputs are applied to multiple synapses, all inputs are transmitted to the neurons. If the cumulative input from the synapses fails to surpass the threshold voltage of a neuron, the neuron slowly discharges its voltage in accordance with its leaky properties. However, if the threshold voltage is exceeded, the neuron fires and generates an output signal to update the weight (conductance) of the synapse. The threshold and feedback voltage of the neuron are created using a comparator.

Through our multi-terminal spiking neurosynaptic network, we achieved a high learning accuracy of up to 83.08% on the unlabeled MNIST handwritten dataset.

8:00 PM EL07.03.17

Tuning of Ultrafast Carrier Dynamics in 2D GeS and GeSe by Cu Intercalation Sepideh Khanmohammadi¹, Kateryna Kushnir¹, Catherine Tran², Kristie Koski² and Lyubov V. Titova¹; ¹Worcester Polytechnic Institute, United States; ²University of California, Davis, United States

Germanium sulfide (GeS) and germanium selenide (GeSe) are 2D layered van der Waals semiconductors. These semiconductors have high carrier mobilities and moderate band gaps in the near-infrared (1.55-1.65 eV for GeS and 1.1 eV for GeSe, in the bulk)¹⁻⁴. Previously, we demonstrated that photoexcitation with either above or below the bandgap energy results in long-lived transient conductivity. Plus, photoexcitation above the bandgap results in emission of THz pulses in both materials due to shift current generation⁵. We found that 800 nm (1.55 eV) excitation results in longer-lived free photocarriers, lasting for hundreds of picoseconds to several nanoseconds. While it was in the order of hundreds of picoseconds for 400nm (3.1 eV) excitation⁶. Here, we focus on photoexcited carrier lifetimes by intercalation of zero-valent Cu into the van der Waals gaps of GeS or GeSe nanoribbons. We find that intercalation of copper drastically decreases carrier lifetime and introduces a much faster decay time. This behavior can be observed in both GeS and GeSe which can be promising for engineering optical properties of these materials for high-speed optoelectronic devices.

1. Vaughn, D. D., II; Patel, R. J.; Hickner, M. A.; Schaak, R. E., Single-Crystal Colloidal Nanosheets of GeS and GeSe. *Journal of the American Chemical Society* **2010**, *132* (43), 15170.
2. Elkorashy, A. M., Photoconductivity in single-crystal germanium sulphide. *Journal of Physics: Condensed Matter* **1990**, *2* (28), 6195.
3. Elkorashy, A. M., The indirect forbidden fundamental absorption edge in single-crystal germanium sulphide. *Journal of Physics C: Solid State Physics* **1988**, *21* (13), 2595.
4. Elkorashy, A. M., Indirect forbidden fundamental absorption edge in germanium selenide single crystals. *physica status solidi (b)* **1986**, *135* (2), 707.
5. Kushnir K, Wang M, Fitzgerald P, Koski KJ, Titova LV. Ultrafast zero-bias photocurrent in GeS nanosheets. In *Ultrafast Phenomena and Nanophotonics XXII* 2018 Feb 22 (Vol. 10530, pp. 59-62). SPIE.
6. Khanmohammadi S, Tran C, Colin-Ulloa E, Kushnir K, Koski KJ, Titova LV. Ultrafast carrier dynamics in 2D GeS in response to photoexcitation across the visible-NIR range. In *Ultrafast Phenomena and Nanophotonics XXVII* 2023 Mar 15 (Vol. 12419, pp. 114-117). SPIE.

8:00 PM EL07.03.18

Complementary Logic Circuit Based on Two-Dimensional Field-Effect Transistors with Ultrashort Gate Lengths Geonho Mun^{1,2}, Cheolhee Han^{1,2}, Heon-Su Ahn^{1,2} and Moon-Ho Jo^{1,2}; ¹Pohang University of Science and Technology, Korea (the Republic of); ²Institute for Basic Science, Korea (the Republic of)

As silicon transistors approach the sub-10-nm technology level and encounter increasingly complex technical obstacles, it becomes crucial to explore alternative device structures and new channel materials. Two-dimensional (2D) van der Waals semiconductors, which confine charge carriers within a 2D space, show promise as channel materials for transistors with gate lengths (L_G) below 10 nm, while maintaining a small subthreshold swing and low leakage current. Previous studies have demonstrated MoS₂ transistors with L_G of approximately 1 nm, utilizing a single-walled carbon nanotube or the edge of graphene as the gate electrode. However, the handling of these materials presents challenges, preventing the realization of ultra-scaled 2D transistors compatible with complementary logic circuits. In this study, we present high-quality 2D NMOS and PMOS transistors with a subthreshold swing of about 65 meV dec⁻¹ and an On/Off ratio of up to 10⁷, utilizing the MoS₂ mirror twin boundary as a gate electrode. These devices have an effective L_G below 10 nm, as the mirror twin boundary embedded in a MoS₂ bi-crystals acts as a one-dimensional metal with a width of only few atoms. Additionally, we demonstrate an array of CMOS inverters by controlling the nucleation sites of the MoS₂ bi-crystals,

offering prospects for a new generation of ultrashort electronic devices and their circuits that go beyond the limitations of Moore's law.

8:00 PM EL07.03.19

Mechanism of Magnesium Oxides Mg_xO_x Adsorption onto Pristine Graphene: Density Functional Theory Approach Mahlatse Matloga¹, MMTibane¹ and RRMaphanga²; ¹UNISA, South Africa; ²CSIR, South Africa

The demand for high energy storage systems has generated interest in metal-air batteries as a promising next generation battery technology due to their high theoretical energy density which surpasses that of metal-ion batteries. In this study, we investigated the adsorption mechanism of magnesium oxides (Mg_xO_x) onto pristine graphene during oxygen reduction reaction (ORR) for metal-air batteries operation using density functional theory. We studied different adsorption configurations, comprising the O_2 and Mg as ORR reactants and the MgO_2 , and Mg_2O_2 as ORR products and propose preferred pathways. Mg atom weakly adsorbed onto graphene with an adsorption energy of (-0.035 eV to -0.043 eV), whereas O_2 molecule adsorbed with an adsorption energy of (-0.101 eV to -0.134 eV) slightly stronger than Mg adsorption. Furthermore, the ORR product MgO_2 adsorbed strongly (-1.536 eV) than other reaction product Mg_2O_2 with a calculated adsorption energy of (-0.879 eV) onto graphene. Overall, the reaction product MgO_2 revealed strong stability than other configuration systems. Lastly, the electronic properties, i.e., the total and partial density of states were calculated to understand the electronic behaviour of graphene/ Mg_xO_x composites.

8:00 PM EL07.03.20

Study of n-Type Paper Transistor Fabrication using Carbon Nanotube Composite Paper Kaito Adachi^{hara} and Takahide Oya; Yokohama National University, Japan

We propose paper transistors using CNT composite papers. It is known that CNTs have many properties such as high electrical conductivity, light weight, high strength, and flexibility. Because of these properties, CNTs are expected to be applied in various fields. However, since CNTs exist in nanoscale and powder form, it is necessary to devise ways to apply them to devices. Therefore, we focus on paper, which is inexpensive, easy to process, and a familiar material. By combining CNTs and paper, we are applying CNTs to devices as the CNT composite paper, which has the properties of both CNTs and paper.

The method of making our CNT composite paper is described below. Our CNT composite paper is produced by using modified Japanese *washi* papermaking method. Specifically, CNT and Sodium Dodecyl Sulfate (SDS) are dispersed in pure water by ultrasonication to prepare CNT dispersion. Next, the pulp is placed in pure water and stirred to prepare pulp dispersion. The CNT dispersion and pulp dispersion are mixed, and then dehydrated on a fine mesh. After dehydration, the paper is formed in a heat press to complete the paper. By selecting metallic or semiconducting type CNTs when making the composite paper, it is possible to make the composite paper with each characteristic. Next, the paper transistor fabrication method is described below. Paper transistors can be made by cutting each part to the size used, moistening it with pure water, and then heat pressing it so that the paper fibers intertwine and adhere to each other. Since CNTs exhibit p-type semiconducting characteristics in air, it is known that fabricated paper transistors exhibit p-type characteristics. Therefore, n-type doping for CNTs should be used to prepare n-type semiconducting CNTs. By using the n-type doping to our paper transistors, they should show a n-type property. In previous research, our composite paper was dipped in a n-type doping solution and dried in an oven, was used. However, it failed to develop a desired n-type paper transistor because the dependence of the gate voltage could not be confirmed even after doping. One possible cause was that soaking the paper in the solution led to degradation of the paper fibers and the CNT network. Therefore, we adopted a new doping method, vapor deposition, to develop a desired n-type paper transistor. In this method, we do not immerse the paper in the solution, but instead uses the doping solution as a vapor to attach the dopant to the CNT composite paper. As a result of this deposition method, we obtained an on/off ratio of 1.82 with the deposition method compared to 1.51 with the previous doping method at a drain voltage of 2 V, showing a significant performance improvement. We were also able to confirm the gate voltage dependence and succeeded in developing a paper transistor with desired n-type characteristics, which could not be obtained in previous studies.

In the future, we will aim to realize paper logic circuits by combining p-type and n-type paper transistors. If this technology is realized, it will be possible to make every paper product have information processing functions, we believe.

8:00 PM EL07.03.21

Analytical Device Physics Model for the Design and Fabrication of a Nanowire-Based Betavoltaic Device Amanda Thomas and Ray R. LaPierre; McMaster University, Canada

The need for robust and versatile energy sources that surpass the lifespan limitations of traditional lithium-based devices have made betavoltaic (BV) devices a solution with promising potential. BV devices employ the direct conversion of radioactive decay energy into electrical power through a process analogous to the photovoltaic effect. In a BV device, the energy of the highly energetic electrons (beta particles) emitted from a radioisotope source generates electron-hole pairs (EHPs) within a target semiconductor material through impact ionization events induced by a series of scattering interactions between the betas and the semiconductor target. The separation and collection of the EHPs into the contact regions by the semiconductor p-n junction results in the generation of electrical power.

Given the extremely low flux of beta particles, BV devices generate very small current densities on the order of μAcm^{-2} to $nAcm^{-2}$. The half-life of the radioisotope used determines the lifetime of the device, allowing for device lifespans up to nearly 100 years. BV devices are also compact, occupying less than a cubic centimeter of volume. The temperature insensitivity of BV devices allows for continuous operation with minimal fluctuations in device performance in a variety of environmental conditions. The small footprint, long lifetimes, and operational robustness of BV devices make them highly suited for low power applications, particularly those that necessitate minimal or remote access. BV devices have found utility in a diverse range of fields, including health-care, space exploration, deep-sea operations, and military defense/intelligence industries.

Conventional BV devices employ a planar geometry, resulting in the loss of nearly half of the isotropically emitted beta flux, reducing device conversion efficiency. Planar BV devices are limited by the available surface area for source deposition. Increasing the available surface area for deposition increases the source thickness, resulting in the loss of beta flux due to self-absorption of the betas by the source material. In 2005, Sun et al. fabricated a tritium (3H) source BV device with a porous silicon (PS) diode structure, reporting improvement of the BV power-generation efficiency by a factor of 10 compared to planar devices [2]. The observed device performance improvements were attributed to the geometry increase from 2D to 3D, suggesting nearly every emitted beta entered a nearby PS BV junction as a result [2]. Many of the performance-limiting factors of planar BV devices can be mitigated by adopting a 3D interpenetrating device structure, in which the beta emitter source is embedded in the volume between the nanowires (NWs). This results in increased source deposition and overall device efficiency.

Unlike thin film BV devices, NW-based device material systems are not limited by the lattice mismatch constraint. In NWs, lattice mismatch-induced strain can be relaxed elastically at the NW free surface without the formation of dislocations [3], allowing for greater accommodation of lattice mismatch-induced strain within the NWs. As a result, NW hetero-structures can be readily grown on inexpensive silicon substrates, offering increased flexibility in materials system choice at reduced manufacturing costs. The limiting efficiency of a betavoltaic device can be approximated by the ratio of the active region bandgap and the effective ionization energy. Gallium phosphide's relatively large bandgap energy of 2.26 eV corresponds to a limiting efficiency of ~25%, exceeding that of conventional silicon-based BV devices. We introduce an analytical device physics model that simulates the current-voltage (J-V) characteristics of NW array-based betavoltaic devices for nanostructured and planar source configurations. This model serves as a roadmap to determine the ideal geometry and material properties of NW arrays, crucial for the development of a GaP "nanowire betavoltaic battery".

8:00 PM EL07.03.22

Ultralow-Power and Miniaturized X-Ray Sensor using the Single-Walled Carbon Nanotube Micro Network-Based Geiger Counter Design Hyehee Kim¹, Jianlin Li¹, Anthony Childress¹, Juyeon Seo¹, Poornaprakash Bathalavaram², Ahmed Busnaina¹, Sung-Hyun Moon³, Jihwan Boo⁴, Hak Soo Choi³, Geehyun Kim⁴, Young Lae Kim² and Yung Joon Jung¹; ¹Northeastern University, United States; ²Gangneung-Wonju National University, Korea (the Republic of); ³Massachusetts General Hospital and Harvard Medical School, United States; ⁴Seoul National University, Korea (the Republic of)

We present an ultralow-power, highly sensitive, and miniaturized X-ray sensor with micropatterned single-walled carbon nanotube (SWCNT) interdigitated networks inspired by the Geiger-Mueller counter design. Due to the unique nanostructured surface and superb electronic transport nature of assembled SWCNTs, a strong electric field is formed between and within highly organized SWCNT interdigitated electrodes, which effectively separates electrons and ionized ions created by incident X-rays into electrodes, facilitating electron detection. As a result, the device can detect a low X-ray dose rate ($9.97 \mu Gy s^{-1}$) with an extremely low power consumption of 80–90 fW, demonstrating a sensitivity of up to $203.96 \mu C Gy^{-1} cm^{-2}$. Furthermore, the interdigitated SWCNT electrode design produces a low noise level in the picoampere range, permitting exceptional real-time signal detection during X-ray exposure. These unique features of our SWCNT X-ray sensing device enable various low SWaP (size, weight, and power) radiation detectors in the fields of medicine, homeland security, and defense.

8:00 PM EL07.03.23

Quantitative Comparison of Conductivity and Piezoresistance in Networks of Graphene Nanosheets with Different Aspect Ratios Eoin Caffrey, Jose Munuera, Luke Doolan, Kevin Synnatschke, Cian Gabbett, Oran Cassidy, Tian Carey, Joseph Neilson, Adam G. Kelly and Jonathan N. Coleman; Trinity College Dublin, Ireland

Solution processed 2D nanosheet networks have found applications in printed transistors, batteries, photodetectors, catalysts and strain sensors. These networks are assembled from nanosheets in a liquid phase through a range of deposition techniques, yielding notably different structures. In this work, we prepared graphene inks by liquid phase (LPE) and electrochemical (EE)

exfoliation with very different nanosheet aspect ratios (~30 vs ~1000) and processed them into networks via spray coating and liquid-liquid interfacial assembly techniques. Top-down SEM and FIB SEM 3D imaging of the networks show clear differences in morphologies due to both nanosheet aspect ratio and deposition technique. Small, rigid LPE nanosheets form highly porous networks with point-like junctions, displaying different degrees of alignment depending on the deposition technique, while large, flexible EE nanosheets yield compact networks with large conformal junctions for every deposition technique. The electrical conductivities of these networks show a similar dependence on morphology, with a tenfold increase (~10⁴ to ~10⁵ S/m) for spray-coated LPE and EE nanosheets. Piezoresistance measurements show a strong dependence on the network morphology on gauge factor, as predicted by the percolation based model developed in previous work. Gauge factors of nanosheet networks were found to range between 0.4 and 350 depending on the network structure. This study casts light on the key tuning parameters to modify the network structure of nanosheet networks and the effect different structures have on the conductivity and piezoresistive response of the networks. Understanding these key electronic properties will pave pathways towards device applications using 2D materials, including strain sensors and printed flexible electronics.

References

- [1] Caffrey et al. ACS Appl. Mater. Interfaces 2022, 14, 5, 7141–7151
- [2] Kelly et al. Nature Reviews Materials 2022, 7, 217–234
- [3] Gabbett et al. Submitted 2023, arXiv:2301.11046
- [4] Carey et al. ACS Nano 2023, 17, 3, 2912–2922

8:00 PM EL07.03.24

Enhanced Photoelectrochemical Performance of CuBi₂O₄ Photocathodes by Constructing a Built-In VoltageJoon-SooYoon, Young-MinKim and Yun-MoSung; Korea University, Korea (the Republic of)

CuBi₂O₄ (CBO) is a p-type semiconductor showing numerous attractive features for photoelectrochemical (PEC) water splitting. Although the theoretical photocurrent density of the CBO photocathode is high enough to be practically applied to water splitting, the loss of charge carriers is considerable due to the recombination in the bulk. In this study, we designed a concentration gradient in a CBO photocathode where the Cu-rich phase is located at the top, and the Bi-rich phase is located at the bottom through the diffusion occurring during thermal annealing of CuBi thin film. The stacking order of Cu and Bi thin metal film was switched to analyze the effect of the gradient direction on PEC characteristics. UPS, UV-vis spectroscopy, and Mott-Schottky plots confirmed the resulting band structures of CBO photocathodes. The photocurrent densities of the CBO photocathode with Cu-rich top reveal -1.14 mA/cm² and -0.68 mA/cm² at 0.38 V vs. RHE in the electrolyte of 0.5 M NaOH purged with N₂ and O₂, respectively. These values are 33.8 and 49.7 % higher than the photocurrent densities obtained from the CBO photocathode with Bi-rich top. The enhancement was also verified by IPCE measurements. This is attributed to the internal electric field acting as a driving force for efficient charge separation and collection. The successful solid-state synthesis of CBO photocathodes having a built-in electric field demonstrates an effective and simple route toward band-engineered photoelectrodes for ternary oxide-based materials.

8:00 PM EL07.03.25

Enhanced PEC Water Oxidation of Rh-Decorated α -Hematite Through Reduced OverpotentialYoung-MinKim, Joon-SooYoon and Yun-MoSung; Korea University, Korea (the Republic of)

The photoelectrochemical behavior of Rh cluster-deposited hematite (α -Fe₂O₃) photoanodes (α -Fe₂O₃@Rh) was investigated and the interactions between Rh clusters and α -Fe₂O₃ nanorods were elucidated both experimentally and computationally. A facile UV-assisted solution casting deposition method allowed the deposition of 2 nm Rh clusters on α -Fe₂O₃. The deposited Rh clusters effectively enhanced the photoelectrochemical performance of the α -Fe₂O₃ photoanode, and electrochemical impedance spectroscopy (EIS) and Mott-Schottky analysis were applied to understand the working mechanism for the α -Fe₂O₃@Rh photoanodes. The results revealed a distinctive carrier transport mechanism for α -Fe₂O₃@Rh and increased carrier density, while the absorbance spectra remained unchanged. Furthermore, density functional theory (DFT) calculations of the oxygen evolution reaction (OER) mechanism corresponded well with the experimental results, indicating a reduced overpotential of the rate-determining step. In addition, DFT calculation models based on the XRD measurements and XPS results provided precise water splitting mechanisms for the fabricated α -Fe₂O₃ and α -Fe₂O₃@Rh nanorods. Owing to enhanced carrier generation and hole transfer, the optimum α -Fe₂O₃@Rh3 sample showed 72% increased photocurrent density of 1.06 mA/cm² at 1.23 V_{RHE} compared to that of the pristine α -Fe₂O₃ nanorods electrode.

8:00 PM EL07.03.26

Optical Blocking Layer and Field-Induced Junction on Silicon Nanowire Multispectral Photodetectors Toward High Quantum EfficiencyDeokjaeChoi, JungtaekLee and KwanyongSeo; Ulsan National Institute of Science and Technology, Korea (the Republic of)

Crystalline silicon nanowires (c-SiNWs) have unique optical characteristics that enable tuning of their spectral response depending on their diameter. However, real-world applications of c-SiNWs multispectral photodetectors are still hampered by their low selectivity and low quantum efficiency (< 30%). The primary obstacles include the broad-spectrum light absorption of the bottom crystalline silicon (c-Si) substrate underneath the c-SiNWs. In addition, it is difficult to form appropriate p-n junctions on c-SiNWs and it leads to severe recombination which makes low external quantum efficiency (EQE). In this study, a thin metal film was applied as an optical blocking layer to block light absorption in the bottom c-Si substrate, and atomic layer deposition (ALD)-based Al₂O₃ was employed to form a dopant-free p-n junction on diameter-controlled c-SiNWs. Consequently, the maximum EQE of the fabricated photodetector was 77.4% at 620 nm with remarkable wavelength selectivity. This work removes major stumbling blocks for the use of c-SiNW as selective light spectral bandpass photodetectors.

8:00 PM EL07.03.27

SAW-Induced Spin Wave Excitation in Ferromagnetic Epitaxial Thin FilmsAlfonsG. Schuck, SebastianKölsch, SwarnasreeBanik and MichaelHuth; Institute of Physics, Goethe-University, Germany

Surface acoustic wave (SAW) excitation of spin waves in ferromagnetic thin films has recently gained significance due to the potential for the realization of novel microwave devices and applications in magnonics.

So far, SAW excitation has commonly been accomplished by use of piezoelectric substrate materials, such as LiNbO₃, on top of which the ferromagnetic thin film is deposited. This approach has severe limitations with regard to studying SAW-spin wave coupling effects in epitaxial magnetic thin films. For epitaxy to occur, selected substrate materials and crystal orientations have to be used; and these substrate materials tend not to be piezoelectric.

Here we show how textured piezoelectric AlN thin film transducer structures can be fabricated on different substrate materials by means of reactive RF sputtering. By proper selection of the material for the interdigital transducer electrode structures and standard UV lithography, the frequency range up to about 3 GHz becomes available for spin wave excitation.

Selected examples of SAW-induced spin wave excitation in epitaxial magnetic thin films are presented and compared to results obtained on Nickel thin films as commonly used reference material.

8:00 PM EL07.03.28

Aptasensors Based on 2D Transition Metal Dichalcogenides for Label-Free and Ultrasensitive Detection of Cytokine Biomarkers.MiretteFawzy, ThushaniDe Silva, HamidrezaGhanbari, KarenKavanagh and MichaelAdachi; Simon Fraser University, Canada

Cytokines are small immune-system signaling proteins found in body fluids such as blood, saliva, and sweat, that are considered as biomarkers for numerous health conditions and diseases. An abnormal variation in cytokine concentrations is an indicator of uncontrolled inflammatory reactions that has been associated with diseases such as cancer, diabetes, Alzheimer's, rheumatoid arthritis, and cardiovascular diseases. Most diseases, particularly cancers, can often be cured if they are detected at an early stage. Thus, the ability to monitor and detect a slight change in cytokine levels is of great significance for early clinical diagnosis.

In this work, we report the development of aptasensors based on 2D transition metal dichalcogenides (TMDs) for rapid, label-free, highly sensitive and specific detection of tumor necrosis factor- α (TNF- α), a representative inflammatory cytokine biomarker.

Our biosensors employ mechanically exfoliated multilayer TMD flakes (MoS₂ and WSe₂) as the sensing channel, and aptamers (short single-stranded nucleic segments) as the bioreceptors. The sensing area is passivated with a thin aluminum oxide layer (around 5 nm) using atomic layer deposition technique (ALD) to provide available sites for facile functionalization with bioreceptors. The aptamers are immobilized on the sensor surface via surface chemical functionalization with (3-aminopropyl) triethoxysilane (APTES) and glutaraldehyde. A fluorescence measurement is used to confirm that the aptamers, labeled with a fluorescent dye (FAM dye), are successfully immobilized on the sensor surface. Aptamers were chosen as cytokine biomarker receptors since they bind specifically to the target cytokine forming G-quadruplex structures, bringing charged cytokines closer to the surface of the sensor. The change in the surface charge density can be used to detect the concentration of cytokines via a chemiresistive I-V measurement. The experimental results demonstrate that the cytokine aptasensor can rapidly (incubation time is around 2 mins) respond to the change in TNF- α concentration with a sub-picomolar limit of detection (LOD). The aptasensor showed good selectivity against other biomarkers such as IL-6 and C-reactive proteins. Therefore, our sensor has great potential for the early diagnosis of various human diseases.

8:00 PM EL07.03.29

Demonstration of Controlled Doping and Complementary Inverter Operation in Transition Metal Dichalcogenide Transistors using Self-Assembled Monolayers Dong Hyun Lee, Youngmin Han and Hocheon Yoo; Gachon University, Korea (the Republic of)

Transition metal dichalcogenides (TMDC) are attracting attention as next-generation semiconductor materials due to their theoretically high carrier mobility and excellent optical properties [1-3]. In addition, the TMDCs are extensively researched as an alternative that can overcome the limitations of integration in conventional silicon-based electronic devices. However, a method for controlling the electrical properties of TMDC-based electronic devices has not been established. The conventional ion implantation suitable for silicon-based electronic devices causes damage to the lattice structure of TMDC. As a countermeasure, the chemical doping method using self-assembled monolayer (SAM) minimizes damage to the lattice structure of the TMDCs and simultaneously controlling the energy band of the semiconductor. In this study, we demonstrated the p-type or n-type doping effect for ambipolar MoTe₂ transistors by applying the chemical doping method using SAMs. The SAM materials such as 1H,1H,2H,2H Perfluorooctyltriethoxysilane (PFOTES) and (3-Aminopropyl)triethoxysilane (APTES) doped onto MoTe₂ transistors accumulate holes or electrons in the channel due to their opposite electronegativity. As a result, the electron mobility and on/off ratio of n-type MoTe₂ transistor doped with APTES increased by 4.6 times and 79 times, respectively. On the other hand, MoTe₂ doped with PFOTES present p-type behavior had increased 18.4 times of the hole mobility and 159 times of on/off ratio. Finally, we demonstrated a complementary inverter using SAM-doped n-type and p-type MoTe₂ transistors, presenting a clearer full-swing operation compared to before SAM doping.

8:00 PM EL07.03.30

Advancements in Precise Atom Manipulation for Tailored One-Dimensional Molecular Arrays: Synthesis, Characterization and DFT calculations Orlando J. Silveira¹, Kewei Sun², Lauri Kurki¹, Jose Lado¹, Ondrej Krejci¹, Keisuke Sagisaka², Shohei Saito³, Shigehiro Yamaguchi⁴, Oscar Custance², Takashi Kubo⁵, Tomohiko Nishiuchi⁵, Takuya Kodama⁵, Yuan Zhang⁶, Adam Foster^{1,6} and Shigeki Kawai^{1,2}; ¹Aalto University, Finland; ²University of Tsukuba, Japan; ³Kyoto University, Japan; ⁴Nagoya University, Japan; ⁵Osaka University, Japan; ⁶Kanazawa University, Japan

The synthesis of one-dimensional molecular arrays with tailored stereoisomers presents a challenging yet highly promising avenue for molecular opto-, electronic-, and magnetic-devices, where the local array structure critically influences functional properties. This research showcases significant advancements in the synthesis and characterization of one-dimensional materials through precise atom manipulation. Utilising scanning tunnelling microscopy (STM) and spectroscopy (STS) with functionalized tips, coupled with density functional theory (DFT) calculations, we comprehensively characterised the materials. Firstly, we show that the magnetic states of a Boron substituted graphene nano ribbon (GNR) on an AuSi_x intercalation layer are suppressed by Si atoms adsorbed into the substituted areas, but can be recovered and controlled by tip-induced removal of the embedded Si atoms, as a clear Kondo resonance peak appears [1]. The successful control of such spin polarised states in an extended π carbon system holds great potential for spintronics application. Next, we describe the sequential tip-induced removal of bromine atoms on a linear array of 3D moieties with C-Br bonds protruding from the molecular plane [2]. Subsequently, an open-shell singlet diradical is observed, which undergoes an inelastic spin transition of 91 meV to a triplet state. Furthermore, we show the synthesis and characterization of one- and two-dimensional covalent orbital frameworks whose backbones contain 1,4-disilabenzene (C₄Si₂) linkers [3]. Substituting carbon with silicon in organic molecules and materials has long been an attractive way to modify their electronic structure and properties. Silicon-doped graphene-based materials are known to exhibit exotic properties, yet conjugated organic materials with atomically precise Si substitution have remained difficult to prepare. Our results for this part demonstrate the high generality of the C-Si on-surface coupling by depositing Si atoms and subsequent polyaromatic hydrocarbons on Au(111). These remarkable advancements pave the way for novel functional materials with vast scientific and technological implications.

[1] Manipulation of Spin Polarization in Boron-Substituted Graphene Nanoribbons, *ACS Nano* 2022, 16, 7, 11244–11250

[2] Local Probe Isomerization in a One-Dimensional Molecular Array, <https://arxiv.org/abs/2305.17703>

[3] On-surface synthesis of disilabenzene-bridged covalent organic frameworks. *Nat. Chem.* **15**, 136–142 (2023)

8:00 PM EL07.03.31

Selective Passivation of 2D TMD Surface Defects by Atomic Layer Deposited Al₂O₃ for Enhancement of Recovery Properties of Gas Sensor Lee Raeyoung¹, Sohn Inkyu¹, Wi Sungjoo¹, Kim Youngjun¹, Kim Myoungsub^{1,2}, Yoon Hwi¹, Shin Dain¹, Kim Jaehyeok¹, Seo Jeongwoo¹, Seungmin Chung¹ and Kim Hyungjun¹; ¹Yonsei University, Korea (the Republic of); ²SK Hynix, Korea (the Republic of)

Two-dimensional (2D) transition metal dichalcogenides (TMDs) which possess large surface-to-volume ratio have been widely used for room temperature gas sensing applications. [1] However, due to its intrinsic defect or vacancies on TMD surface, incomplete recovery of TMD gas sensors hinder the realization of reliable and repeatable use of 2D TMD gas sensors. [2] Here, we demonstrate improvement of recovery rate of TMD gas sensors by selectively passivating TMD surfaces' defect or vacancies with Al₂O₃ using atomic layer deposition. SEM analysis confirms that nucleation and growth procedure of atomic layer deposited Al₂O₃ occurs along the grain boundaries and defects of 2D MoS₂ and WS₂, not covering inert basal plane. Also, Raman, Photoluminescence and XPS spectra shows the slight n-doping effect of Al₂O₃, which attributes to improvement of gas sensor response as well as recovery rate. Our unique and unreported defect passivated TMD gas sensors show 400 % response toward 10 ppm of NO₂, and the recovery rate rises up from 74% to 96% as the number of ALD cycle increases even at room temperature. Also, the recovery rate toward NH₃, which is the reducing gas, shows an increase of more than 30% implying that our proposed method is a promising strategy for improving the recovery rate of 2D TMD gas sensors.

References [1] Late, D. J. *et al.* Sensing behavior of atomically thin-layered MoS₂ transistors. *ACS Nano* **7**, 4879–4891 (2013).

[2] Lee, K., Gatensby, R., McEvoy, N., Hallam, T. & Duesberg, G. S. High-performance sensors based on molybdenum disulfide thin films. *Adv. Mater.* **25**, 6699–6702 (2013).

8:00 PM EL07.03.32

Low Temperature Magneto-Transport Properties of ALD Grown TiN_xO_y Films Filipp Baron; SAAZ Micro Inc., United States

We report results of the magnetoresistivity and R(T) measurements of TiN_xO_y films with different N/O-content grown by ALD in magnetic fields up to 11 Tesla. Our results indicate that the films are amorphous metals, which follow the Mooij rule, they demonstrate both positive and negative magnetoresistivity, and some of them undergo superconductive transition below 4.2K. The technology for obtaining a compact temperature sensor for wide temperature range (liquid helium to +260deg C) based on 40 nm thick TiN_{0.87}O_{0.97} is presented. This technology is fully compatible with standard CMOS.

8:00 PM EL07.03.33

Development of Graphene Oxide with a Single Oxygen Functional Group and Applications for the Gas Barrier Membrane Tatsuki Sugawa, Kazuto Hatakeyama, Michio Koinuma and Shintaro Ida; Kumamoto University, Japan

Graphene oxide (GO) has a variety of oxygen functional groups on the surface, making it highly dispersible in various solvents such as water and N,N-dimethylformamide. This makes it possible to easily fabricate laminated membrane on the substrates of various shapes by using GO dispersion solution. Furthermore, GO has excellent potential for gas barrier applications due to high aspect ratio and flexibility. Therefore, GO has been investigated as gas separation membranes that can achieve both high flow rate and high selectivity, but in general, the many defects (nanopores) located in the nanosheet causes reduction in gas barrier performance. As a result, the gas barrier performance is significantly lower than that of graphene. Because of the uncontrolled introduction of these defects during GO synthesis, its use as a barrier membrane has been limited to large molecules or ions. In particular, the barrier performance for small molecules and ions such as H⁺ has only been achieved by graphitization using strong reducing agents, which was impractical given the damage and hazards to the substrate. In this report, we describe the GO with low defect density that sweep away this perception and barrier membranes based on it. The nanopores on the GO surface are formed by introducing COOH and C=O groups and breaking the C=C bonds of the graphene backbone during oxidation treatment. In other words, GO without nanopores can theoretically be obtained by introducing oxygen functional groups in-plane while maintaining the C-C bond. Oxygen functional groups that achieve these results include C-O-C (epoxy group) and C-OH (hydroxy group). It has been reported that graphite oxide treated with fuming HNO₃ and KClO₃ has almost only epoxy groups, and such GOs are considered to be free of nanopores. In this study, we succeeded in obtaining highly efficient monolayer nanosheets from this graphite oxide using a weakly basic solvent with the addition of ammonia, and clarified the detailed structure. It was found that the barrier performance against specific gases of GO without nanopores was found to be 10³ times higher than that of conventional GO and superior to Kapton and PET films in terms of gas permeability coefficient considering the film thickness. Furthermore, it was found that GO without nanopores exhibits 10⁶ times higher proton barrier performance than conventional GO.

8:00 PM EL07.03.34

Observation of Topological-Hubbard Phase Diagram in Twisted Homo-Bilayer MoTe₂ Moiré Superlattice Kaifei Kang¹, Yichen Qiu^{1,1}, Kenji Watanabe², Takashi Taniguchi², Jie Shan^{1,1,3} and Kin Fai Mak^{1,1,3}; ¹Cornell University, United States; ²National Institute for Materials Science, Japan; ³Kavli Institute at Cornell for Nanoscale Science, United States

At half-filling of a honeycomb lattice, competition between the onsite Coulomb repulsion and spin-orbit interaction leads to the Kane-Mele-Hubbard phase diagram, consisting mainly of a topological band insulating phase and an antiferromagnetic Mott insulating phase. Despite decades of theoretical efforts, experimental evidence is yet to be observed. Here we present the first

demonstration of such a phase diagram in a honeycomb moiré superlattice formed by small angle twisted MoTe₂ monolayers. A quantum phase transition from a quantum spin Hall insulator (QSHI) to an antiferromagnetic Mott insulator (AFMI) is realized by tuning the vertical electric field. In the QSHI state, we observe a resistance plateau of $\sim h/2e^2$ for temperatures below 10 K. In the AFMI state, we observe a zero Hall plateau and sharp magnetic transitions up to a Neel temperature of $T_N \sim 30$ K. At high magnetic fields of $B > 10$ T, both QSHI and AFMI are driven into Chern insulators with the quantized Hall resistance $R_{xy} = h/e^2$. A spin density wave state is further observed when the AFMI is electron doped. Our observation paves the way for realization of exotic phases of matter such as quantum spin liquid and heavy fermion superconductivities in moiré materials.

8:00 PM EL07.03.35

Charge Transport in Charge Transfer Cocrystal Nanoribbons Yuri Chung¹, Satwik R. Scott, Melis and Edward Van Keuren; Georgetown University, United States

Charge transfer cocrystals have interesting applications in the field of organic electronics due to their unique optical and electronic properties, and have potential advantages over inorganic materials, such as being flexible and biodegradable. Controlled evaporative self-assembly (CESA) is a technique that produces long, ordered ribbons of material on a substrate from an evaporating solvent, a more convenient method of fabrication than for many inorganic material devices. Charge transfer cocrystals were successfully grown using this method to form a neat arrangement of ribbons that were readily integrated with metal electrodes to create organic field-effect (OFET) transistors for electronic measurements. We show that the temperature dependence of device mobility can be described by a hopping mechanism for the charge transport in cocrystals such as phenothiazine and 7,7',8,8' tetracyanoquinodimethane (PTZ-TCNQ) and phenoxazine and TCNQ (PXZ-TCNQ). Ongoing work involves studying the semiconductor potential of other cocrystal pairs and superexchange modeling.

8:00 PM EL07.03.36

Ink-jet Printed Graphene-Silicon Schottky Diodes Alessandro Grillo¹, Zixing Peng¹, Aniello Pelella², Antonio Di Bartolomeo² and Cinzia Casiraghi¹; ¹University of Manchester, United Kingdom; ²University of Salerno, Italy

Integration of graphene (Gr) in silicon-based technology is of crucial importance for enabling the next generation electronics, photonics and sensors [1]. Although numerous works have reported devices based on Gr-Si junctions, the integration process relies on the use of high quality Gr produced by Chemical Vapour Deposition (CVD), making the fabrication steps expensive, time consuming and by limiting the large scale devices' reproducibility.

In this work we show that inkjet-printing enables simple and scalable integration of Gr into Si-technology [2]. We developed a simple fabrication procedure, based on the mechanical or chemical etching of the SiO₂ layer from a standard Si wafer, followed by the inkjet printing of water-based printable Gr inks [3] on the exposed area, leading to Schottky diodes with excellent rectifying behaviour and figures of merit, comparable to those produced with CVD graphene. We fully characterized the devices and applied several theoretical models achieving deep understanding of the underlying physics of the devices. We also investigated the optical response of the diodes by demonstrating a spatially selective photodetector.

Our results demonstrate that inkjet printing is a cost-effective and scalable method, which is also compatible with back-end-of-line fabrication processes for the integration of graphene in the modern Si-technology.

References

- [1] Akinwande et al, Nature, 573, 507–518 (2019)
- [2] Grillo et al, ACS Nano, 17, 2, 1533–1540 (2023)
- [3] McManus et al, Nature Nano, 12, 343 (2017)

8:00 PM EL07.03.37

On-Chip Electrocatalytic Microdevices: A New Platform for Electrochemical Interfacial and Micro-Kinetic Studies Mengning Ding; Nanjing University, China

Electrocatalysis has broad application prospects in the energy conversion and sustainable chemical synthesis, and thus has attracted considerable research attentions. For most electrocatalytic systems, the optimization and improvement of their electrocatalytic performances are usually generated from the reasonable construction of active sites and accurate descriptions of the catalytic mechanism. The continuous enrichment of measurement methodologies can greatly promote the in-depth studies and applications of electrocatalysis. In recent years, the continuous maturity and cross-disciplinary developments of micro-nano (device) processing technologies have provided a new and more sophisticated on-chip platforms for: 1) the *in situ* measurement/investigation of electrocatalytic materials and electrochemical interfacial processes; 2) the on-chip modulation of catalytic and sensing properties; and 3) the on-chip electrochemical fabrication of the novel functional devices. Here, we show some of the examples from our recent studies.

Reference

1. W. Wang, J. Qi, Z. Wu, W. Zhai, Y. Pan, K. Bao, L. Zhai, J. Wu, C. Ke, L. Wang, M. Ding*, Q. He*, On-chip electrocatalytic microdevices, *Nat. Protoc.* **2023**, DOI: 10.1038/s41596-023-00866-z.
2. Z. Mu, N. Han, D. Xu, B. Tian, F. Wang, Y. Wang, Y. Sun, C. Liu, P. Zhang, X. Wu, Y. Li*, M. Ding*, Critical role of hydrogen sorption kinetics in electrocatalytic CO₂ reduction revealed by on-chip *in situ* transport investigations, *Nat. Commun.* **2022**, *13*, 6911.
3. Y. Sun, H. Shin, F. Wang, B. Tian, C.-W. Chiang, S. Liu, X. Li, Y. Wang, L. Tang, W. A. Goddard III*, M. Ding*, Highly Selective Electrocatalytic Oxidation of Amines to Nitriles Assisted by Water Oxidation on Metal Doped -Ni(OH)₂, *J. Am. Chem. Soc.* **2022**, *144*, 15185-15192.
4. Y. Pan, X. Wang, W. Zhang, L. Tang, Z. Mu, C. Liu, B. Tian, M. Fei, Y. Sun, H. Su, L. Gao, P. Wang, X. Duan*, J. Ma*, M. Ding*, Boosting the performance of single-atom catalysts via external electric field polarization, *Nat. Commun.* **2022**, *13*, 3063.
5. B. Tian, H. Shin, S. Liu, M. Fei, Z. Mu, C. Liu, Y. Pan, Y. Sun, W. A. Goddard III*, M. Ding*, Double-Exchange-Induced *in situ* Conductivity in Nickel-Based Oxyhydroxides: An Effective Descriptor for Electrocatalytic Oxygen Evolution, *Angew Chem. Int. Ed.* **2021**, *60*, 16448-16456.
6. Y. Chen, B. Tian, Z. Cheng, X. Li, M. Huang, Y. Sun, S. Liu, X. Cheng, S. Li*, M. Ding*, Electro-descriptors for the performance prediction of electro-organic synthesis, *Angew Chem. Int. Ed.* **2021**, *60*, 4199-4207.

8:00 PM EL07.03.38

Visualizing the Electrochemical Microenvironment in Engineered Electrode Structures Yiming Wang, Mingxuan Zhu, Zhifei Yan, Sam Veroneau and Daniel Nocera; Harvard University, United States

The activity and selectivity of an electrocatalyst are intricately tied to the micro-environment at the electrochemical interface. While several factors influence the micro-environment, the impact of mesoscale electrode geometry remains relatively underexplored. Most electrocatalysts employ three dimensional structures to increase the electrochemical surface area. However, due to mass transport, local diffusional gradient emerges inside the pores or trenches of the catalyst layer, which creates the micro-environment distinct from that of the bulk. To fully understand the effect of electrode geometry, operando study is essential. Experimentally probing micro-environment in operating condition is challenging not only because it requires high spatial and temporal resolution but also because of the difficulty in systematically varying the mesoscale electrode geometry. Researchers have been using a variety of methods to elucidate the interplay between electrode structures and its micro-environment. However, most of the studies only provided qualitative insights, lacking the quantitative descriptors vital for the rational design of electrode architectures and the corresponding local environment. To address the above-mentioned challenges, we use fabricated micro-wire arrays to systematically study the effect of electrode architecture on local pH near the electrocatalyst. By varying the shape, size and spacing of the micro-wires we aim to attain a quantitative understanding of the influence of diverse geometric descriptors. We use confocal fluorescence microscopy to map pH near the micro-wire arrays in operando conditions. Our findings hold potential applications across numerous proton-coupled electron transfer reactions. The experimental design could also be easily adapted to study other elements within the microenvironment.

8:00 PM EL07.03.39

WS₂ & MoS₂ from 3D to 1D Structures: curvature and Chirality Induced Properties of Nanotubes S. Ghosh¹, C. Pallellappa¹, Yijin Zhang², Y. Iwasa², Antonio Di Bartolomeo³, Ifat Kaplan-Ashiri⁴, V. Bruser⁵, Y. Gao⁶ and Alla Zak¹; ¹Holon Institute of Technology, Israel; ²The University of Tokyo, Japan; ³University of Salerno, Italy; ⁴Weizmann Institute of Science, Israel; ⁵Leibnitz Institute of Plasma, Germany; ⁶Beijing Institute of Technology, China

Study of the multiwall WS₂ nanotubes (NTs) behaviour for numerous applications has been demonstrated that rolling of the WS₂ molecular layers into co-nanocylinders promotes modifications in their structure. This results in unusual mechanical, chemical and electrical properties, which appear not only due to size reduction and quantum confinement, but mainly due to strain in the lattice, curvature and chirality of the layers, inherent to the tubular structure. Thus, rare bulk photovoltaic effect (BPVE) was recently discovered in WS₂ NTs and exhibited the photocurrent in the nanotube-based devices orders of magnitude larger than in other BPVE materials. BPVE appears due to the intrinsic properties of NTs: the small band gap (1.4-2.1 eV), broken inversion symmetry and polar structure [1]. An exponential increase of the NTs' resistivity with tensile strain up to a recorded elastic elongation of 12 % was revealed, thereby making WS₂ NTs suitable for piezoresistive sensor applications [2]. Bandgap engineering via size and number of layers control was recently demonstrated via cathodoluminescence measurements of these NTs [3]. Moreover, a fully operated artificial vision system was built based on the memory ability, produced by discovered programmable photoeffect and sliding ferroelectricity in

multiwalled WS₂ NTs [4]. Such a wide investigation of this nanomaterial, became possible due to the breakthrough in their vapor-gas-solid (VGS) synthesis, which result in a pure phase and macroscopic amounts [5]. Special efforts were applied to complete extremely complicated synthesis of MoS₂ NTs from molybdenum trioxide (MoO₃) nanowhiskers in three-step high-temperature reaction with H₂/H₂S gases [6]. The availability of MoS₂ semiconductor NTs will enable their wide investigation in the future.

[1] Y.J. Zhang, et al., *Nature*, **570**, 349 (2019).

[2] A. Grillo, et al., *Small*, 2002880-1 (2020).

[3] S. Ghosh, et al., *Applied Physics Reviews*, **7**, 041401 (2020).

[4] Y. Sun, et al., *Nature Communication*, 2022.

[5] A. Zak, et al., *Fullerenes, Nanotubes, and Carbon Nanostructures*, **19**, 18 (2011).

[6] C. Pallellappa, et al., *ACS Nano*, **14**, 3004 (2020).

SESSION EL07.04: 1D and 2D Materials—Ab Initio Simulation

Session Chairs: Xi Ling and Zafer Mutlu

Tuesday Morning, November 28, 2023

Hynes, Level 3, Ballroom B

8:00 AM *EL07.04.01

Emerging Functionalities of Carbon-Based 1D and 2D Nanoarchitectures [Aran Garcia-Lekue](#)^{1,2}; ¹Donostia International Physics Center (DIPC), Ikerbasque, Basque Foundation for Science, Spain; ²Ikerbasque, Basque Foundation for Science, Spain

Nanostructuring graphene at the atomic scale is now possible by on-surface synthesis methods, which unite the sturdiness of covalently bonded networks with the easy tunability of molecular materials.[1,2] These experimental advances have boosted the research attempts to create novel 1D and 2D carbon-based structures aimed at the development of new nanoelectronic, spintronic or optoelectronic devices. However, before graphene nanostructures can be used in practical applications, an atomic level understanding and control of their properties is required. As such, *ab-initio* simulation has developed as an essential partner in the search of optimal carbon-based low dimensional materials.

In this talk, I will present some studies of prototype graphene nanostructures, such as graphene nanoribbons (GNRs) and nanoporous graphene (NPG), that we have recently performed in our group. Using mainly density functional theory (DFT), and in collaboration with our experimental colleagues, we have investigated their structural, electronic, magnetic and transport properties. On the one hand, we have explored the emergence of localized spins in metallic GNRs realized by substitutionally doping a narrow band gap GNR with boron atoms in its interior.[3] We have also reported on a novel NPG structure, which can be envisioned as GNRs laterally fused by phenylene bridges. Interestingly, electron transport simulations demonstrate the capability of modulating the interribon coupling by different degrees of freedom provided by the phenylene bridges.[4] Our results thus show that chemical doping offers the perspective of electronically controlling spins in 1D carbon nanoarchitectures, while molecular bridges emerge as an efficient tool to engineer quantum transport in 2D networks.

From a purely theoretical perspective, we have investigated prototypical hybrid GNRs formed using two existing carbon-based precursor molecules and a porphyrin center.[5] Our results reveal that narrow band gap hybrid GNRs might be achieved, and that embedding an iron atom in the porphyrin center gives rise to a spin-polarized ground state. Besides, our electron transmission calculations demonstrate how strain or chemical adsorption on the Fe atom gives rise to spin-crossover. This work highlights the potential of porphyrin-based hybrid GNRs as a highly tunable and flexible platform for spintronics and sensing applications.

References

[1] Cai *et al.*, *Nature* 466, 470 (2010)

[2] Moreno *et al.*, *Science* 360, 199 (2018)

[3] Friedrich *et al.*, *ACS Nano* 16, 14819 (2022)

[4] Moreno *et al.*, *J. Am. Chem. Soc.* 145, 8988 (2023)

[5] Gao *et al.*, *Comm. Phys.* 6, 115 (2023)

8:30 AM EL07.04.02

Topological Radical Pairs Produce Ultrahigh Conductance in Long Molecular Wires [Liang Li](#), Shayan Louie, Austin Evans, Elena Meirzadeh, Colin Nuckolls and Latha Venkataraman; Columbia University, United States

In the field of molecular electronics, it has been a challenge to make highly conductive long molecular wires. Typically, the conductive wires made to date are mostly designed and built from conjugated units, which conduct through a coherent and off-resonant mechanism. Within this mechanism, the conductance decays exponentially with increasing length. Therefore the conductance becomes low when more units are added to lengthen the wires. To overcome this problem, a new class of molecular wires with topological radical states at the edge sites (so-called edge states) can be created following the Su-Schrieffer-Heeger (SSH) model. These wires are one-dimensional topological insulators (1D TIs) and conduct through the energetically low-lying edge states that are localized to the wire ends. As a result, such 1D TI wires feature a reversed conductance decay, that is, the conductance increases exponentially with increasing wire length (*Nat. Chem.* **2022**, *14*, 1061-1067.). However, the reversed conductance decay only appears for short wires, as when the wire length increases beyond a threshold, the localized edge states become decoupled and no longer support electron transport. To extend the wire length at which these properties can be observed, we designed topological oligo[*n*]emeraldine wires, using short 1D TIs as building blocks (*J. Am. Chem. Soc.* **2023**, *145*, 2492-2498.). As the wire length increases, so does the number of topological states, resulting in an enhanced electronic transmission along the wire with increasing length. In our experiments, we successfully drove a current of over a microampere through a single ~5 nm molecular wire, significantly surpassing the performance of previously reported long wires. With DFT calculations, we demonstrated that the longest topological oligo[7]emeraldine exhibits over 10⁶ enhancements in the transmission compared to its isostructural non-topological molecular wire. Furthermore, there is no theoretical limit to the number of 1D SSH TI repeat units that can be incorporated with a single chain. Therefore, it is reasonable to expect that longer analogues of topological oligo[*n*]emeraldine (*n* > 7) will achieve higher currents and conductances. This discovery represents a significant breakthrough in implementing molecules into complex, nanoscale circuitry, as it overcomes a fundamental hurdle that their structures become too insulating at practical lengths for designing nanoscale circuits.

8:45 AM EL07.04.03

Leveraging Density Functional Theory in the Design of Novel Metal Organic Chalcogenide Assemblies (MOChAs) [Adriana Ladera](#), Aria Mansouri Tehrani and Tess Smidt; Massachusetts Institute of Technology, United States

In this work, we use density functional theory (DFT) and geometric algorithms to propose hypothetical low-energy metal organic chalcogenide assemblies (MOChAs) to aid synthesis efforts. MOChAs are hybrid organic-inorganic, self-assembled Van der Waals crystals where low-dimensional transition-metal chalcogenide (TMC) inorganic structures are scaffolded by organic ligands, which insulate the TMC structures from one another.

Despite being bulk crystals, MOChAs, like other low-dimensional TMC materials, host excitonic properties relevant to optoelectronic applications. The choice of organic ligand can control the geometry of the inorganic structure which drives the optoelectronic properties of the MOChAs. This tunability and ease of synthesizability makes MOChAs a compelling material class for exploring structure-property relationships.

We propose hypothetical MOChA structures by systematically generating hypothetical combinations of inorganic structures, organic ligands, and corresponding stacking patterns and evaluating their energetics with DFT. We benchmark our methods on experimentally synthesized MOChAs. In this talk we (i) discuss the efficacy of using DFT as a computational aid to evaluate MOChA structure feasibility, (ii) relate changes in MOChA geometry to electronic properties, and (iii) present a library of energetically favorable hypothetical MOChAs.

9:00 AM *EL07.04.04

Quantum Theory of Sputtering Rates in 2D Materials by Transmission Electron Microscopy [Vincent Meunier](#); Penn State University, United States

Many computational models have been developed to predict the rates of atomic displacements in two-dimensional (2D) materials under electron beam irradiation. However, these models often drastically underestimate the displacement rates in 2D insulators, in which beam-induced electronic excitations can reduce the binding energies of the irradiated atoms. This bond softening leads to a qualitative disagreement between theory and experiment, in that substantial sputtering is experimentally observed at beam energies deemed far too small to drive atomic dislocation by many current models. To address these theoretical shortcomings, this paper develops a first-principles method to calculate the probability of beam-induced electronic excitations by

coupling quantum electrodynamics (QED) scattering amplitudes to density functional theory (DFT) single-particle orbitals. The presented theory then explicitly considers the effect of these electronic excitations on the sputtering cross section. Applying this method to 2D hexagonal BN and MoS₂ significantly increases their calculated sputtering cross sections and correctly yields appreciable sputtering rates at beam energies previously predicted to leave the crystals intact. The proposed QED-DFT approach can be easily extended to describe a rich variety of beam-driven phenomena in any crystalline material.

9:30 AMBREAK

10:00 AM *EL07.04.05

Nonlinear Probing of Structural and Electronic Phase Transition in 2D Quantum Materials[Xiaofeng Qian](#); Texas A&M University, United States

2D quantum materials have demonstrated a plethora of novel physical properties with complex structural and electronic phase transition and potential applications. It is thus highly desirable to understand the underlying mechanism associated with those phase transitions. In this talk, I will report our recent theoretical effort on predicting nonlinear responses in 2D quantum materials, demonstrating nonlinear probe for structural and electronic phase transition, and showing the promise for quantum nonlinear electronics. Specifically, I will present microscopic theory of ferroelectric nonlinear Hall effect in time-reversal invariant layered topological materials and discuss the complex interplay of symmetry, electronic structure, and Berry curvature, and briefly report the experimental demonstration of Berry curvature memory effect as a high-order multiferrocity. Second, I will also present our recent theoretical work on magnetic shift photocurrent and magnetic injection photocurrent as the counterparts of normal shift current and normal injection current in time-reversal symmetry and inversion symmetry broken systems, and demonstrate how these nonlinear photocurrent responses can help decipher magnetic structures and interactions which could be particularly fruitful for probing and understanding magnetic topological quantum materials and phase transition.

10:30 AM EL07.04.06

Giant Rectification in Strongly-Interacting Driven Tilted Systems[Juan J. Mendoza-Arenas](#)^{1,2} and Stephen Clark²; ¹University of Pittsburgh, United States; ²University of Bristol, United Kingdom

Correlated quantum systems feature a wide range of nontrivial effects emerging from interactions between their constituting particles. In nonequilibrium scenarios, these manifest in phenomena such as many-body insulating states and anomalous scaling laws of currents of conserved quantities, crucial for applications in quantum circuit technologies. In this work [1] we propose a giant rectification scheme in one-dimensional systems based on the asymmetric interplay between strong particle interactions and a tilted potential, each of which induces an insulating state on their own. While for reverse bias both cooperate and induce a strengthened insulator with an exponentially suppressed current, for forward bias they compete generating conduction resonances; this leads to a rectification coefficient of many orders of magnitude. Based on numerical and analytical calculations, we uncover the mechanism underlying these resonances as enhanced coherences between energy eigenstates occurring at avoided crossings in the system's bulk energy spectrum. Furthermore, we demonstrate the complexity of the many-body nonequilibrium conducting state through the emergence of enhanced density matrix impurity and operator space entanglement entropy close to the resonances. Our proposal paves the way for implementing a perfect diode in currently-available electronic and quantum simulation platforms.

[1] J.J. Mendoza-Arenas and S.R. Clark, arXiv:2209.11718 (2022).

10:45 AM EL07.04.07

A Many-Body Diffusion Monte Carlo and DFT+U Study of Monolayer VSe₂[Daniel Wines](#)¹, Kayahan Saritas², Jaron T. Kroger², Nishwanth Gudibandla^{3,1}, Kamal Choudhary¹, Francesca Tavazza¹ and Can Ataca³; ¹National Institute of Standards and Technology, United States; ²Oak Ridge National Laboratory, United States; ³University of Maryland Baltimore County, United States

Previous works have controversially claimed near-room temperature ferromagnetism in two-dimensional (2D) VSe₂, with conflicting results throughout the literature. For T-phase VSe₂, competing magnetic and non-magnetic states are predicted to exist, which can drive charge density wave (CDW) formation. Although density functional theory (DFT) calculations can capture the differences in chemical composition and polymorphism, strong coupling between the magnetic and structural properties in this material makes it difficult to trust the results from approximate density functionals. For example, T and H-VSe₂ have a close lattice match and similar total energies, which makes it difficult to determine which phase is being observed experimentally. In this study, we used a combination of density functional theory (DFT), highly accurate diffusion Monte Carlo (DMC) and a surrogate Hessian line-search optimization technique to resolve the previously reported discrepancy in structural parameters and relative phase stability. With DMC accuracy, we determined the freestanding geometry of both phases and constructed a phase diagram. In addition, we studied the energy differences between the ferromagnetic, antiferromagnetic and CDW phases through a many-body lens to resolve these discrepancies for T-VSe₂. Going one step further, we also studied the effect of strain and Se vacancies on the electronic and magnetic properties of these competing magnetic states. Our findings demonstrate the successes of the DMC method when applied to a correlated 2D magnetic system such as VSe₂.

[1] *J. Phys. Chem. Lett.* 2023, **14**, 14, 3553–3560 (2023)

[2] *Phys. Rev. B* **106**, 085117 (2022)

11:00 AM EL07.04.08

A New Strategy to Develop p-Type Semiconductivity in Transition Metal Dichalcogenides: A First-Principles Study[Nikhil Sivasdas](#), Mahdi Amachraa and Yongwoo Shin; Advanced Materials Lab, United States

Over the years, silicon has been the preferred choice of channel material in transistors due to its simplicity and scalability. However, the performance of Si-based transistors degrades significantly as the channel thickness is reduced below 4 nm [1]. TMDs with group formula MX₂, where M = Mo, W and X = S, Se are a class of two-dimensional (2D) semiconductors that can replace Si in the next-generation transistors. Recently, it was shown that the mobility of monolayer TMDs are comparable with 4 nm thick Si channels [1]. Therefore, integrating TMDs into existing hyper-scaler geometries has the potential to leapfrogging decades on Moore's law time scale [2]. However, strategies to p-dope TMDs have been largely unsuccessful. Conventional approaches like substitution doping creates inhomogeneity such as charged defects within the channel layer that limits the transistor mobility [3].

In this talk, we propose a new strategy to p-dope TMDs via a surface charge transfer mechanism (SCTM) using inorganic oxides. Using physics based HT screening we identify 11 element that when doped into the high-k dielectric oxide layer (e.g. HfO₂) can p-dope TMDs without creating channel defects. To validate these finding, we demonstrate p-doping of WSe₂ using Ni-doped HfO₂ using first-principles density functional theory (DFT) calculation. We also discuss practical device geometries for implementing this SCTM induced doping and strategies to control the concentration of dopants. Thus our holistic approach proves the feasibility of p-dope TMDs while retaining the advantages of having a high-k gate-dielectric layer. Demonstrating p-doping in atomically-thin TMDs can allow us to save decades in Moore's law scaling, and can usher in the post-Si era for transistors. This approach can be easily generalized to tackle a broad array of materials design challenges. Our results provide a new strategy for p-doping TMDs.

[1] S. Su et al., Layered Semiconducting 2D Materials for Future Transistor Applications. *Small Struct.*, 2: 2000103, 2021.

[2] S. Datta et al., Toward attojoule switching energy in logic transistors. *Science*, 378.6621, 733, 2022.

[3] Z. Hu et al., Two-dimensional transition metal dichalcogenides: interface and defect engineering. *Chemical Society Reviews*, 47, 3100, 2018.

11:15 AM EL07.04.09

Tunability of Doping in 2D Material Heterostructures using High Work Function RuCl₃: A First Principles Study[Dakotah M. Kirk](#) and Marcelo Kuroda; Auburn University, United States

The facile formation of heterostructures based on two-dimensional (2D) materials permits controlling the electronic properties of the resulting systems [1,2,3,4]. In particular, charge transfer between adjacent layers may be exploited to dope layers that improve charge carrier injection and engineer band alignments [3,4,5,6,7]. Here we quantify how large work function RuCl₃ alters the electronic properties of heterostructures formed with various 2D materials: semiconducting transition metal dichalcogenides (TMDs), and few layer graphene structures. To this end we produce first principles calculations within the density functional theory (DFT) accounting for the on-site Coulomb interaction and spin-orbit. In the proximity of RuCl₃, TMD and graphene layer(s) become heavily p-doped with carrier densities of $\sim 5 \times 10^{13} \text{cm}^{-2}$, in agreement with prior experiments on RuCl₃ on graphene and WSe₂ [7]. We successfully rationalize our first principles results employing an analytical model based on properties of individual constituents. Study of the structural and electronic properties of the heterostructure upon application of vertical strain on these systems reveals that strain barely alters charge transfer but yields a stronger hybridization between layers. Additionally, accounting for the magnetic order in the RuCl₃ also results in similar doping when adjacent to semiconducting TMDs or graphene layers. The results of this work show that 2D material heterostructures may improve charge injection efficiency and band engineering in these systems.

The authors gratefully acknowledge the support from the National Science Foundation (NSF) through Grant No. NSF-1848344.

1. Novoselov et al., "2D materials and van der Waals heterostructures", *Science* 353, aac9439 (2016).
2. Geim et al. "Van der Waals heterostructures", *Nature* 499, (2013).
3. Zutic et al., "Proximitized materials", *Materials Today* 22, (2019)[MK1].
4. Lotsch "Vertical 2D Heterostructures", *Annual Review of Materials Research* 45, (2015)[MK2].
5. Solís-Fernández et al., "Synthesis, structure and applications of graphene-based 2D heterostructures", *Chemical Society Reviews* 46, (2017)
6. Yoo et al., "Recent Advances in Electrical Doping of 2D Semiconductor Materials: Methods, Analyses, and Applications", *Nanomaterials* 832, (2021).
7. Wang et al., "Modulation Doping via a Two-Dimensional Atomic Crystalline Acceptor", *Nano Letters* 20, 8446 (2020).

11:30 AM EL07.04.10

First Principles Study of Nernst Effect in 2D Materials [Emad S. Rezaei](#) and [Peter Schindler](#); Northeastern University, United States

The rapidly growing demand for replacing fossil fuels with clean energy harvesting methods necessitates research in renewable energy generation and management. Two-dimensional materials have attracted much attention in energy conversion applications due to their unique transport properties, more enticingly, when a thermoelectric power factor greater than 5 was reported in $\text{Fe}_2\text{V}_{0.8}\text{W}_{0.2}\text{Al}$ thin films [1]. Similar to the Seebeck effect, the ratio of the developed voltage to the temperature gradient in the presence of a magnetic field is called the Nernst effect [2] which has been utilized in cryogenic cooling [3], thermopile systems [4], and radiation detector applications [5]. The Nernst effect was observed in Bismuth for the first time and then further studied in semiconductors such as silicon, germanium, and indium antimonide. The Nernst effect in topological semimetals has been of focused interest, more recently. However, data of the Nernst coefficient of 2D materials has been very limited. Here, we present on large-scale screening of 2D structures using high-throughput density functional theory (DFT) calculations to discover promising new materials candidates with high Nernst coefficients. Our preliminary theoretical results show that some 2D materials could exhibit relatively considerable Nernst coefficients. The discovery of new ultra-high Nernst coefficient 2D materials (larger than Bismuth) could pave the way towards more efficient radiation detectors and more productive cryogenic cooling designs.

References

- [1] B. Hinterleitner *et al.*, "Thermoelectric performance of a metastable thin-film Heusler alloy," *Nature* 2019 576:7785, vol. 576, no. 7785, pp. 85–90, Nov. 2019, doi: 10.1038/s41586-019-1751-9.
- [2] S. E. Rezaei, M. Zebarjadi, and K. Esfarjani, "First-principles-aided evaluation of the Nernst coefficient beyond the constant relaxation time approximation," *Comput Mater Sci*, vol. 225, p. 112193, Jun. 2023, doi: 10.1016/j.commat.2023.112193.
- [3] S. Bogason, J. Heremans, and A. Sandip Mazumder, "Cryogenic Cooling with a Single Crystal Bismuth Nernst-Ettingshausen Cooler," 2018, Accessed: Jun. 11, 2023. [Online]. Available: <https://kb.osu.edu/handle/1811/86859>
- [4] M. Mizuguchi and S. Nakatsuji, "Energy-harvesting materials based on the anomalous Nernst effect," <http://www.tandfonline.com/action/journalInformation?show=aimsScope&journalCode=tsta20#VmBmuzZFCUk>, vol. 20, no. 1, pp. 262–275, Jan. 2019, doi: 10.1080/14686996.2019.1585143.
- [5] H. J. Goldsmid and K. R. Sydney, "A thermal radiation detector employing the Nernst effect in $\text{Cd}_3\text{As}_2\text{-NiAs}$," *J Phys D Appl Phys*, vol. 4, no. 6, p. 869, Jun. 1971, doi: 10.1088/0022-3727/4/6/319.

SESSION EL07.05: 1D and 2D Materials—Logic Devices and Interconnects I

Session Chairs: Xiaofeng Qian and Xu Zhang

Tuesday Afternoon, November 28, 2023

Hynes, Level 3, Ballroom B

1:30 PM *EL07.05.01

Graphene Nanoribbon-Based Field-Effect Transistors for High-Performance Logic Technology [Zafer Mutlu](#); University of Arizona, United States

Silicon has powered computing for decades through miniaturization, facilitated by innovations such as strained silicon, high-k dielectrics, fin field-effect transistor (FinFET), and the latest industry trend: gate-all-around FET (GAAFET) architectures. However, silicon is reaching its limits as miniaturization yields diminishing benefits. This necessitates a new 'wonder' material that can potentially take some pressure off silicon's shoulders and meet the increasing demands of computationally intensive technologies such as AI. Bottom-up synthesized, atomically precise graphene nanoribbons (GNRs) feature extremely high theoretical charge carrier mobility and on-state drive current capability at the atomic scale, making them highly promising transistor channel materials over silicon for high-performance logic applications. In this invited talk, I will begin with an introduction to GNRs, explaining the features that make them promising for FETs, detailing the bottom-up synthesis, discussing techniques used for their characterization and device fabrication, presenting the current state of the art with transistors made from them, and addressing the remaining key issues. In the next part, I will detail our recent studies, involving enhancing electrostatic control of the GNR channel through the deposition of an ultrathin high-k top HfO_2 dielectric layer, ultimately scaling transistors with GNRs, and optimizing the channel-contact interface through contact engineering to reduce contact resistance. Finally, I will address the remaining challenges and potential enhancements in materials, processes, device integration, and related areas that could enable GNRs to approach outstanding theoretical predictions and explore future opportunities in the field.

2:00 PM *EL07.05.02

Self-Assembly of Dense, Aligned, Semiconducting Carbon Nanotube Arrays for High Performance Transistors [Michael S. Arnold](#); University of Wisconsin–Madison, United States

Carbon nanotubes conduct more electricity per width than silicon and more rapidly switch between on and off states with less voltage, making them ideal for next-generation fast, low-energy logic and high-speed, linear RF devices. However, despite carbon nanotubes' promise, no one has yet been able to create a process for employing nanotubes in high-performance electronics commercially. Since their discovery more than 25 years ago, nanotubes' commercialization has been delayed by manufacturing challenges in purifying, aligning, and uniformly assembling them with precision over large areas. For nanotubes to be most useful, they must be purified by their electronic type (semiconducting versus metallic) and then lined up in the same direction in a dense layer with the thickness of a single nanotube, so that electricity can rapidly and efficiently travel through them.

This talk will present recent discoveries on (1) purifying and aligning semiconducting nanotubes into massively parallel arrays and (2) the research and development of semiconducting carbon nanotubes for logic and radio frequency devices. We have pioneered nanotube array fabrication technologies that enable the (a) partial alignment of nanotubes ($\pm 30^\circ$) via shear (demonstrated 100 mm wafer-scale); (b) finer alignment ($\pm 6^\circ$) at liquid-liquid interfaces (demonstrated 100 mm size-scale); and, (c) the selected-area deposition of nanotube arrays ($\pm 7^\circ$) in lithographically-defined patterns combining topographical and chemical features (demonstrated 25 mm size-scale). Most recently, we have discovered a powerful new mechanism for driving the self-assembly of nanotubes into aligned arrays, by coaxing them to form two-dimensional liquid-crystals. We have uncovered that when nanotubes are segregated to liquid-liquid interfaces, mesogenic interactions cause them to self-align (within ± 5.7 degrees so far) and self-assemble into dense arrays (> 100 per micron) like those needed for microelectronics. The assembled nanotubes are easily integrated on silicon substrates at room-temperature and integrated into high-performance devices. Work on the development of novel multifunctional polymer wrappers and the removal of these wrappers will also be presented.

APL (2014); ACS Nano (2014); Langmuir (2014); Science Advances (2016); Langmuir (2017); Adv Elect Materials (2019); Science Advances (2021); Nanoscale Advances (2021); JAP (2022); Submitted (2023). Highlights by Bloomberg News https://youtu.be/VsUF_CBJq50 (2022); US Patents 11,631,814; 10,873,026; 10,074,819; 9,938,149; 9,786,853; 9,728,734; 9,673,399; 9,425,405; 9,368,723; 9,327,979.

2:30 PM *EL07.05.03

Anchoring to Prevent Bundling in Dense CNT Array Device Process [Shengman Li](#); Stanford University, United States

Carbon nanotubes (CNTs) are highly promising candidates for replacing silicon (Si) in digital devices due to their remarkable characteristics, including a 1-nm thin body, high mobility/velocity, and low capacitance. To achieve high-performance devices, there is a demand for high-density aligned CNT arrays with a pitch size of 2–4 nm. Significant progress has been made recently in CNT array assembly through the dimension-limited self-alignment method, along with the use of small molecule additives to suppress CNT bundling.

However, the various processing steps involved in fabricating CNT field-effect transistors (CNTFETs) introduce extrinsic defects, such as lateral aggregation and vertical stacking, into the as-prepared CNT arrays. The presence of such CNT bundles can severely impact the ability of the transistor gate to effectively control the flow of charge carriers in the CNT channel, leading to considerable device-to-device variability.

In response to these challenges, this study proposes the incorporation of dielectric anchors to prevent CNT bundling. Through the use of Atomic Force Microscopy (AFM) and Transmission Electron Microscopy (TEM), we investigate the CNT bundling conditions after essential processing steps, including post-evaporation, post-Atomic Layer Deposition (ALD), post-resist spin-coating, post-developing with the anchor layer, and without the anchor layer.

By implementing the anchoring-first approach, we demonstrate reduced subthreshold slope variation (SS) and higher drain current (Ion) in CNTFETs. These findings present a promising process flow to construct high-performance CNTFETs, thereby advancing CNTFET fabrication towards practical applications in digital devices. The elimination of CNT bundling and improved device characteristics achieved through this study are crucial steps towards the realization of high-performance CNT-based electronics.

3:00 PMBREAK

3:30 PM *EL07.05.04

One-Dimensional Graphene Devices[HerreS. van der Zant](#); TU Delft, Netherlands

One-dimensional devices made of graphene are of great interest to study mesoscopic quantum transport phenomena. On one hand, one can define one dimensional channels by electrostatic gating with the advantage that the edges do not play a significant role in the transport characteristics. On the other hand, atomically precise graphene nanoribbons (GNRs) are predicted to exhibit exceptional edge-related properties, such as localized edge states, spin polarization, and half-metallicity. However, creating a good contact between electrodes and GNRs has been a longstanding challenge as it requires the controlled fabrication of sub-20 nm metallic gaps, a clean GNR transfer minimizing damage and organic contamination during the device fabrication, as well as work function matching to minimize the contact resistance. Here, I will discuss examples of both approaches: electron focusing and collimation experiments in bi-layer graphene channels defined by electrostatic gating and our progress in contacting 9-atom-wide armchair-edged GNRs with Pt, MoRe and Pd contacts. The two latter metals are known to provide low-contact resistance to carbon nanotubes. Density functional theory (DFT) calculations combined with the non-equilibrium Green's function method (NEGF) explain the observed p-type electrical characteristics using Pt electrodes and demonstrate that Pt gives a strong coupling and higher transmission in comparison to other materials such as graphene. Detailed electrical characterizations of the MoRe and Pd nanogaps, at various bias/gate voltages and temperatures allow us to investigate the formation of Schottky barriers at metal-GNR interface and extract the activation energies.

4:00 PM EL07.05.05

Non-Volatile Doping of Graphene Transistors using a Solid Polymer Electrolyte Crosslinked by Field Effect for Polymorphic Electronics[Dnyanesh Deepak Sarawate](#)¹, [Priscilla Prem](#)¹, [Ke Xu](#)^{2,2}, [Eric Beckman](#)¹ and [Susan Fullerton](#)^{1,1}; ¹University of Pittsburgh, United States; ²Rochester Institute of Technology, United States

Hardware security comes at a high price in the U.S. at \$200 billion annually. Polymorphic electronics provide a potential solution to hardware security threats by preventing unauthorized parties from accessing circuitry information through reverse engineering. The goal of this work is to obscure a device's function by taking advantage of electric double layer (EDL) gating to reconfigure NAND gates to/from NOR gates on-demand. The key innovation is a custom-synthesized polymer electrolyte that reacts under an electric field created by the EDL (~V/nm), retaining charges in the channel by crosslinking the polymer electrolyte. Ion mobility is confirmed in a lateral, parallel-plate capacitor geometry, and graphene field effect transistors (GFETs) are used to test non-volatile doping. Preliminary evidence of non-volatile doping is observed by programming GFETs at positive gate voltages ($V_G > +2$ V), and then sensing the Dirac point shift and ON/OFF ratio change. Positive programming voltages less than +2 V showed no effect on the doping; however, the device becomes more n-type, and ON/OFF increases as V_G increases from +2 to +5 V. Note that in the absence of a non-volatile doping mechanism, grounding the gate would dissipate the EDL and reverse the doping effect; however, in the case of our custom synthesized electrolyte, the doping effect persists even after the gate bias is grounded, confirming non-volatile doping at the graphene channel. Applying a negative V_G demonstrates a semi-permanent - but reversible - doping effect. Specifically, as V_G increases from -1 to -5 V, the Dirac point shifts less n-type and ON/OFF decreases, implying that the doping effect is reversible but non-volatile. We will also report on the sheet carrier densities measured by Hall effect to quantify the doping, along with chemical characterization of the polymer electrolyte. The work is supported by the National Science Foundation (NSF, U.S.) under Grant No. ECCS-EPMD-2132006

4:15 PM EL07.05.06

Electronic Transport in Twisted Nanoporous Graphene/Graphene Van Der Waals Heterostructures[Xabier Diaz de Cerio](#)¹, [Aleksander Bach Lorentzen](#)², [Mads Brandbyge](#)² and [Aran Garcia-Lekue](#)^{1,3}; ¹Donostia International Physics Center (DIPC), Spain; ²Technical University of Denmark, Denmark; ³Ikerbasque, Basque Foundation for Science, Spain

Nanoporous graphene (NPG) is a promising candidate for the development of next generation electronic devices [1]. Recent advances in bottom-up on-surface chemistry have allowed the fabrication of increasingly large atomically precise samples of various NPG geometries, which can be thought as lateral arrays of weakly coupled semiconducting graphene nanoribbons [1,2]. Besides, the highly anisotropic electronic structure of NPG causes injected currents to flow according to the so-called Talbot effect interference pattern [3]. Such phase coherent phenomenon can be tuned by the introduction of structural and chemical modifications, making this 2D material appealing to control currents at the nanoscale [2,4]. On the other hand, van der Waals heterostructures have attracted great interest in the last decade due to their unconventional electronic properties and the high level of control achieved in the stacking of 2D materials. In this regard, the stacking of NPG over graphene has emerged as a noteworthy strategy to tune the electronic and transport properties of the latter [5,6]. However, the potential control of nanoscale currents in such heterostructure remains largely unexplored.

In this work, we theoretically study the electronic anisotropy and transport properties of twisted NPG/graphene van der Waals heterostructures. Combining Non-Equilibrium Green's Functions with a tight-binding approach, we model devices comprising ~200,000 atoms and lengths over 50nm. In particular, we simulate the current flow in various commensurate and incommensurate geometries corresponding to different interlayer twist angles. The response of currents to the twist angle parameter is rationalized by means of the evolving interlayer coupling. Our findings showcase the versatility of NPG/graphene heterostructures for electronic applications and open new prospects for the realization of carbon nanocircuitry.

[1] C. Moreno et al., Science 360, 199 (2018)

[2] C. Moreno, X. Diaz de Cerio et al., J. Am. Chem. Soc. 145, 8988 (2023)

[3] G. Calogero et al., Nano Lett. 19, 576 (2019)

[4] I. Alcón et al., Adv. Funct. Mater., 2104031 (2021)

[5] A. Antidormi and A. W. Cummings, AIP Advances 11, 115007 (2021)

[6] B. Lee and J. Kang, Adv. Electron. Mater., 2200252 (2022)

4:30 PM *EL07.05.07

Atomic Substitution Approach for Electronic Non-vdW 2D Materials[Xi Ling](#); Boston University, United States

Atomically thin materials often exhibit extraordinary chemical, optical, electronic, and magnetic properties compared with their bulk 3D counterparts, enabling a variety of applications for next generation electronics and quantum information technologies. While extensive research has been conducted on 2D van der Waals (vdW) materials such as graphene, transition metal dichalcogenides (TMDs), and hexagonal boron nitride (hBN), little attention has been given to non-vdW materials, which make up the majority of materials in nature. One significant challenge is the lack of an effective synthesis method to access them. In this talk, I will introduce an atomic substitution approach that we have developed to convert vdW layered materials to ultrathin non-vdW materials. This approach is universal, enabling the synthesis of diverse unconventional 2D materials with tunable thicknesses, desired dimensions, and properties for fundamental physics investigations and nanodevices. As a model system, we will investigate the conversion process from TMDs (e.g. MoS₂ and WS₂) to corresponding metal nitrides (e.g. MoN_x and WN_x), characterize the electronic properties of the obtained metal nitrides, and highlight the advantages of this approach in creating new 2D heterostructures as desired building blocks for 2D electronics.

8:00 PM EL07.06.01

Montmorillonite/Graphene Composite Based Resistive Humidity Sensor [Juhyoeng Yu](#), Jin Woo An and Seung-Ki Lee; Pusan National University, Korea (the Republic of)

The needs about precise humidity sensor are getting higher gradually in numerous major industries for insuring optimal performance of electrical devices and safety in diverse environments. Graphene, the two-dimensional material, has extraordinary electrical properties due to its π -bonding of sp^3 hybrid orbital. Recent study has shown possibility of graphene-based material as the humidity sensing material because of its ultrahigh surface area. However, the results reported thus far are limited in recovery time and long-term stability due to irreversible adsorption of water molecules on graphene's surface during humidity sensing. Its high price also can be challenge for the practical application. Although doping other sensitive material to graphene is one of the possible ways that can improve recovery property, but it not that effective way to improve sensor's sensitivity.

In this study, we propose a stable humidity sensor based on a montmorillonite/graphene composite to overcome these recovery, stability, and price problem. As a natural clay mineral, montmorillonite has attracted interest because of its abundance and unique ability to absorb large amounts of water by an increase in the c-axis of the layer lattice structure.

The incorporation of graphene into montmorillonite, at the point where graphene's concentration exceeds electrical percolation threshold, forms a cost-effective composite material compared to carbon materials like GO or rGO that exhibits enhanced electrical resistance changes for humidity sensing. Additionally, the hydrophilic nature of montmorillonite facilitates the absorption of water molecules into the composite, whereas the hydrophobic nature of pristine graphene facilitates the desorption of water molecules. This combination of properties can contribute to the reduction of both response and recovery time in the composite.

The montmorillonite/graphene composite was fabricated using a simple solution-based method. The composite was then coated on an electrode deposited substrate. The best ratio of montmorillonite/graphene of composite sensor was confirmed through observation of distinct electrical resistance change in variation of ratio. And then, the sensor was characterized by measuring its resistance in response to different humidity levels ranging from 20% to 80%. The results showed that the sensor had a linear response to humidity, with a sensitivity of 10% per RH. Moreover, we find out the sensor was reversible and stable over time.

Overall, the montmorillonite/graphene composite is a promising candidate for highly efficient humidity sensor with plenty of advantages over traditional humidity sensors. The sensor is highly sensitive, reversible, and inexpensive. It is also easy to fabricate and can be scaled up for mass production. The sensor has potential applications in a wide range of fields, including civil engineering, agriculture, and industrial processes.

8:00 PM EL07.06.02

Blue-Emitting Core/Crown Nanoplatelets of CdSe/CdS for LED Application [Matilde Cirignano](#)^{1,2}, Hossein Roshan¹, Alessio Di Giacomo³, Davide Piccinotti¹, Iwan Moreels³ and Francesco Di Stasio¹; ¹Istituto Italiano di Tecnologia, Italy; ²Università degli Studi di Genova, Italy; ³Ghent University, Belgium

Colloidal inorganic nanocrystals are an attractive class of nanomaterials for both fundamental research and technical applications thanks to their size- and shape-dependent properties, but also because of their excellent chemical processability.¹ In particular, colloidal CdSe nanoplatelets (NPLs) are fascinating nanocrystals to explore the potential of two-dimensional (2D) materials for next generation optoelectronic devices.² The strong quantum confinement in the vertical direction leads to peculiar optical properties that depend on their thickness,³ such as, narrow emission, large exciton binding energy, relatively small dielectric constant, giant oscillator strength, large linear/nonlinear absorption cross sections and short radiative fluorescence lifetime.⁴ In addition, the large volume of NPLs makes Auger recombination less efficient.⁵ All of these advantages make NPLs promising for application in Light-Emitting Diodes (LEDs). However, application of CdSe NPLs in the ultraviolet/blue region remains an open challenge due to charge trapping leading to limited photoluminescence quantum yield (PLQY) and sub-bandgap emission in core-only NPLs.⁶

Furthermore, for LEDs based on II-VI semiconductor quantum dots (QDs), the efficiency and stability of red and green QD based devices is close to standards for commercial applications, while blue QLEDs (Quantum dots-LEDs) lag behind in terms of device efficiency and stability.⁷

The specific problems of blue QLEDs are as follows: surface defects and lattice mismatch of blue QDs, carrier injection imbalances, high absorption coefficient of charge injection layers, fluorescence quenching caused by exciton dissociation induced by an electric field, instability of the organic transport layer, and the loss of light caused by plane-laminated structures.⁸

We recently focused on the synthesis of 3.5 ML CdSe/CdS core/crown blue emitting nanoplatelets developed in 2023.⁹ After a significant improvement in core-only synthesis¹⁰ with a precise control over the aspect ratio (length/width), we raised the PLQY of core/crown NPLs up to 60% with complete elimination of trap state band and undesirable second phases. More specifically, our crowning procedure increases the quantum efficiency of 4 times with respect to the core-only using much less material than a core/shell structure.

Using CdSe/CdS core/crown NPLs emitting in the pure blue region of electromagnetic spectrum (2.7 eV = Eg, $\lambda = 460$ nm), we then obtained the highest EQE (2.8%) existing for blue core/crown structured CdSe-based material in Light-Emitting Diodes fabrication.

We take advantage of some important strategies to improve EQE in our proposed LED. In contrast to the majority of works present in the literature, we avoid using ZnO film as ETL due to its absorption in the same region of NPLs emission and in order to reduce self-absorption in NPLs, we use a very low thickness of NPLs as emissive layer. The electroluminescence measurement shows a 460 nm peak with a turn-on voltage of 3.3 V.

Our results show an effective way for the PLQY improvement of core-crown CdSe/CdS NPLs and good performances in hybrid organic-inorganic Light Emitting Diodes application.

1. Chem. Rev. 2010, 110, vol. 1, 389–458.

2. Energy Mater. Adv. 2022, ID 857943.

3. Nature Mater 10, 2011, 936–941.

4. Light Sci Appl 10, 2021, 112.

5. Physical Review Letters, 2003, vol. 91, no. 22, 227401.

6. ACS Appl. Nano Mater. 2022, vol. 5, 1367–1376.

7. Adv. Optical Mater. 2023, 2203152.

8. J. Mater. Chem. C, 2020, 8, 10160.

9. Nano Lett. 2023, 23, 8, 3224–3230.

10. Chem. Mater. 2020, 32, 21, 9260–9267.

8:00 PM EL07.06.03

Various Frequency Band Electromagnetic Shielding Film by Internal Multi-Reflection Between ITO Nano-Branched [Youngho Kim](#)¹ and Hakki Yu^{2,2}; ¹Korea University, Korea (the Republic of); ²Ajou University, Korea (the Republic of)

Electromagnetic wave interference (EMI) means that electromagnetic waves generated from the outside interfere with the operation of some device. As various industries develop, the contamination by electromagnetic waves increases and the risk also increases day by day. In particular, such interference in communication equipment or the space industry can lead to failure of huge capital projects from causing inconvenience in daily life. Shielding this interference is called electromagnetic wave interference shielding (EMI shielding), and various materials or processes are being studied. Representative materials studied so far include carbon, ferrite, perovskite, silicon carbide, and conducting polymer series. It is usually in the form of a composite composed of two or more materials without using a single material. What these composites have in common is that they basically use reflection by electron conductivity or absorption by dielectric or magnetic property. In addition, the effect of dielectric properties occurring at interfaces or internal scattering occurring between surface can be expected. For application to various fields, the thickness of the EMI shielding film should be thin, but considering only absorption by dielectric properties, it cannot be thinner than the skin depth, so the aforementioned additional effects are inevitable. In this study, ITO nano branches were used, and a film capable of EMI shielding on various regions was produced by increasing the density of the rods constituting the nano branches. Consequently, 22.31 dB (X band), 21.88 dB (K_u band), 21.09 dB (K band), and 17.81 dB (K_a band) shielding effect were shown for each region at a thickness of about 3 μ m. It has a very high shielding efficiency compared to a very low thickness. Therefore, it is expected that it can be used in various fields.

8:00 PM EL07.06.04

2D Materials-Based Ink to Develop Meta-Structures for Electromagnetic Interference (EMI) Shielding [Suwarna Datar](#); Defence Institute of Advanced Technology, India

2-D transition metal-chalcogenides which are semiconductor materials of the type MX₂, where M is a transition metal atom (like Ni, Fe, or Co) and X is a chalcogen atom (such as S or Se) are emerging class of materials which have excellent properties like atomic scale thickness, strong spin-orbit coupling, ability to form 2D nanosheets, direct band gap which 2D carbon based materials lack and many other mechanical and electronic properties. They are actively used in the fields like flexible electronics, opto-electronics, energy harvesting spintronics, personalised medicines etc. These properties make 2D materials lucrative for EMI shielding applications because of strong electronic polarization and enhanced dielectric loss. Research on hybrid materials like magnetic metal oxides with transition metal-chalcogenides like magnetic core-shell nanomaterials, Fe doped MoS₂, doped MoS₂-rGO composite, MoS₂/CoSe₂ hybrids, among several others suggests, these materials have high reflection loss. Further, magnetic transition metal dichalcogenides such as NiSe₂, CoSe₂ and their heterostructures, expediate multiple reflections and scattering of the incident wave, thereby elongating the course of transmission of the incident microwave, and thereby increasing dissipation efficiency, along with large specific surface area, which caters to EM absorption. In the present work inks have been developed base on these materials to make them versatile for several applications where it can be coated or screen printed.

The second part of this work involves development of meta structures using these paints as Radar absorbing materials. The tunability of material properties like permeability and permittivity

by changing meta structure thickness and dimension allows the user to manipulate the electric and magnetic resonance at different frequencies independently, therefore, frequency selective structures can be made. In the present work we screen printed different geometries of structures using 2D material paints and tested for its capability as EMI shielding paint in X Band.

8:00 PM EL07.06.05

Morphological Characterisation of Printed Networks of Nanomaterials using FIB-SEM Nanotomography Luke Doolan, Cian Gabbett, Kevin Synnatschke, Emmet Coleman, Adam G. Kelly, Shixin Liu, Eoin Caffrey, Jose Munuera, Catriona Murphy, Lewys Jones and Jonathan N. Coleman; Trinity College Dublin, Ireland

Networks of nanomaterials find applications in a wide variety of fields such as printed electronics, sensors, and energy storage [1]. While it is known that the morphology of the network plays a dominant role in determining their physical properties, quantitative measurements of morphology have proven difficult [2]. It has been demonstrated that changing nanomaterial size changes the network's electronic properties, however, its effect on network morphology is not well understood [3]. Utilizing FIB-SEM nanotomography we characterize the morphology of networks of nanomaterials. 3D-images with a voxel size of $5 \times 5 \times 15$ nm were obtained from printed networks of graphene with different nanosheet length. Using machine learning, 3D images were segmented into nanosheet and pore components and a wide range of morphological properties of the networks, including porosity, pore shape, nanosheet alignment, nanosheet aggregation and pore and nanosheet tortuosity were calculated. These properties were used to distinguish between the effect of network morphology and nanosheet size on the electrical properties of the networks, allowing calculation of the resistance of the junctions between the nanosheets. The same methodology was applied to printed networks composed of silver nanoplatelets, silver nanowires and tungsten disulphide with varying nanomaterial length. The technique was then extended to investigate the interfaces within vertical printed heterostacks, allowing measurement of the interfacial roughness and material penetration into subsequent layers, demonstrating the ability of this technique to characterize printed heterostacks devices [4].

[1] F. Bonaccorso, A. Bartolotta, J.N. Coleman, C. Backes, *Adv Mat.*, 28, 6136-3166, (2016)

[2] A.G. Kelly, D. O'Suilleabhain, C. Gabbett, and J.N. Coleman, *Nature Reviews Materials*, 7.3, 217-234 (2022).

[3] S. P. Ogilvie *et al.*, *Nanoscale*, 2022, 14, 320

[4] C. Gabbett, L. Doolan *et al.*, preprint, <https://doi.org/10.21203/rs.3.rs-2723977/v1>.

8:00 PM EL07.06.06

Oxidative Chemical Vapor Deposition of Highly Conductive and Transparent Polymer Layers for Contact Fabrication in 2D-MoS₂-Based FET Structures Jinmei Zhu, Florian Meierhofer and Tobias Voss; Braunschweig University of Technology, Germany

For 2D MoS₂ field-effect transistors (FETs), contact fabrication easily results in damaging the MoS₂ channel due to the fragility of the atomically thin structure, making it difficult to reliably achieve high-performance devices. To overcome this challenge, the deposition of highly conductive and transparent polymer layers from the gas phase (oxidative chemical vapor deposition (oCVD) [1]), is a promising approach that can lead to low-resistivity Ohmic contacts. In this work, we demonstrate a method for fabricating 2D MoS₂ bottom-gated FETs with poly (3, 4-ethylenedioxythiophene) (PEDOT) electrodes. PEDOT is a conductive polymer widely used as transparent electrode material. We used lithography to pattern oCVD-grown PEDOT layers and transferred them onto MoS₂ channels without aggressive chemical and physical treatments. This method allowed us to achieve a damage-free MoS₂ channel with a clean and smooth interface of the PEDOT electrodes, significantly decreasing the charged impurity and interface-roughness scattering processes. This universal approach could be applied to different 2D materials, thus enabling the fabrication low-resistivity Ohmic contacts in high-performance FETs without damaging the atomically thin crystals.

[1] Krieg, Meierhofer, Voss, *et al.*, *Nature Communications* 11, 5092 (2020).

8:00 PM EL07.06.07

Designing Natural Hyperbolic Materials: Expanding the Possibilities of Two-Dimensional Systems Mingwen Zhao; Shandong University, China

Hyperbolic materials (HMs) have garnered significant interest for their unique electromagnetic response characteristics, including optical nanoscale cavities, spontaneous emission enhancement, nanoscale imaging, and full-angle negative refraction. While initially achieved in metamaterials, the development of meta hyperbolic surfaces through intricate substrate patterning has enabled the support of highly-directional hyperbolic surface plasmons, crucial for optoelectronic devices. In this study, we introduce the concept of hyperbolicity into natural two-dimensional (2D) materials exhibiting highly-anisotropic electronic band structures. We demonstrate that these materials present intriguing scenarios similar to those observed in meta hyperbolic surfaces. Notably, natural hyperbolic 2D materials possess advantages over meta-surfaces, leveraging their small atomic-scale periodicity to yield large wavevectors and easy predictability without the need for complicated surface patterning. Based on orbital anisotropy, we propose a design principle for 2D hyperbolic materials and predict a family of candidate materials using first-principles calculations. Our computational results showcase the broadband hyperbolic regimes exhibited by these natural 2D-HMs across the near-infrared to ultraviolet spectrum, enabling the propagation of highly directional hyperbolic surface plasmons. By simulating the directional propagation of surface waves with hyperbolic dispersion relations through the solution of Maxwell's equations, we establish a correlation between the fascinating plasmonic properties and the unique electronic structures of these highly-anisotropic 2D materials. The findings presented in this study offer a promising strategy for the design of 2D hyperbolic materials, paving the way for advancements in optoelectronic devices and expanding the possibilities of utilizing natural materials with remarkable electromagnetic characteristics.

8:00 PM EL07.06.08

The Effect of 2D Nanosheet Size on the Performance of Printed Devices Anthony Dawson, Jose Munuera, Kevin Synnatschke, Joseph Neilson and Jonathan N. Coleman; Trinity College Dublin, Ireland

Printed networks of materials such as few layer MoS₂ enable the production of low-cost but poorer performance devices. This poor performance is due to low nanosheet network mobility of about 0.1 cm²/Vs, this is in part due to inter-nanosheet junctions. To improve network mobility of printed networks, we must better understand these junctions. To achieve this, this project sees the development of size-controlled networks by separating nanosheets into discrete size selected samples.

Recently developed Electrochemical Pellet Intercalation (ECPI) methods enable the scalable exfoliation of nanosheets from cheap, widely available powders. The development of size-controlled networks from commercially available powders via ECPI could transform access to the development of 2D material-based device development. [1,2]

The electrical performance of these networks is characterised, and these measurements are used to refine printing parameters to optimise network morphology, toward reducing junction resistance and thus improving mobility. Applying this knowledge, transistors are developed using these optimised networks and their performance assessed. [3]

8:00 PM EL07.06.09

Borophene and Silicene-Based Humidity Sensors using Quartz Crystal Microbalance Ahmet Gulsaran^{1,1}, Bersu Bastug Azer^{1,1}, Nevin Tasaltin^{2,2,3}, Cihat Tasaltin⁴ and Mustafa Yavuz^{1,1}; ¹University of Waterloo, Canada; ²Maltepe University, Turkey; ³Consens Inc., Turkey; ⁴Tubitak Marmara Research Center, Turkey

Humidity sensors, fundamental to a wide array of applications ranging from environmental monitoring to healthcare, have seen innovative advancements with the advent of two-dimensional (2D) materials. This study explores the promising potentials of borophene and silicene, two emergent 2D materials, as effective elements in humidity sensing when integrated into a Quartz Crystal Microbalance (QCM) platform.

These sensors, fabricated by transposing atomically thin layers onto a QCM surface, operate based on the detection of mass variations as a consequence of water molecule adsorption or desorption, thereby causing a resonant frequency shift in the quartz crystal. Leveraging the exceptional surface-to-volume ratio and ultrathin attributes of borophene and silicene, these sensors exhibit a marked sensitivity to ambient humidity levels.

Our rigorous examination of the borophene and silicene sensors' humidity sensing performance showed significant shifts in the QCM's resonant frequency in relation to humidity changes, demonstrating their high moisture sensitivity.

We have also analyzed the borophene and silicene's surface structure and morphology for their applications in humidity sensing. We employed Scanning Electron Microscopy (SEM) and Brunauer-Emmett-Teller (BET) analysis to determine atomic arrangements, topographical features, specific surface areas, and pore size distributions. The integrative use of SEM and BET has provided an in-depth characterization of these 2D materials, expanding our understanding of their potential applicability.

In conclusion, our research emphasises borophene and silicene as potent candidates for humidity sensing applications, with their great sensitivity and atomically thin composition demonstrating a new era in sensor development. This study's insights could guide the design and optimization of advanced 2D material-based humidity sensors.

8:00 PM EL07.06.10

First Demonstration of VGA Format Microbolometer FPAs using Semi-Conducting SWCNT Networks for Uncooled LWIR Image Sensor Tomo Tanaka^{1,2}, Masahiko Sano¹, Masataka Noguchi^{1,2}, Takashi Miyazaki^{1,2}, Megumi Kanaori², Toshie Miyamoto^{1,2}, Naoki Oda¹ and Ryota Yuge^{1,2}; ¹NEC Corporation, Japan; ²AIST, Japan

Uncooled infrared sensors of bolometer type have a wide range of applications such as security, military, food inspection, health care, and automotive night vision system. Currently, the highly sensitive device development is the key issue for further expansion of demand. The bolometer is an infrared detector of long wave infrared (LWIR) region for radiant heat by means of an infrared absorber having a temperature sensitive electrical resistance material. Infrared radiation strikes the absorber material heating it and thus changing resistor material resistance. Therefore, bolometer's performance is strongly limited by temperature coefficient of resistance (TCR) of the resistor. The conventional resistor is generally based on vanadium oxide (VO_x) with TCR of about $-2\%/K$ [1] and an outstanding resistor is essential to achieve highly sensitive infrared detectors. Recently, single-walled carbon nanotubes (SWCNTs) have been expected as promising materials with high TCR and high chemical stability. We have reported that semi-conducting SWCNT networks extracted by the "Electric-field inducing Layer Formation (ELF)" method [2] show high TCR which is close to $-6\%/K$ [3]. The pristine SWCNTs are fundamentally a mixture of both semi-conducting and metallic SWCNTs. The ELF method is the remarkable promising technique to extract semi-conducting SWCNTs with high purity, which show stable device performance and excellent electrical transportation property.

In this study, we fabricated the Video Graphics Array (VGA) format focal plane arrays (FPAs) with semiconducting SWCNTs for the first time and characterized them. Previously, we have developed a VO_x microbolometer with a suspended structure for thermally separation between the infrared absorber and the substrate by micro electro mechanical system (MEMS) process [4]. By utilizing this technology and constructing a new MEMS structure suitable for the CNT networks, we have successfully developed a SWCNT microbolometer FPAs. Device chip which was mounted on the ceramic carrier was installed in a vacuum dewar. For responsivity measurement, infrared radiation from cavity type blackbody was irradiated onto the microbolometer through the ZnSe optical window. This radiation was chopped by an optical chopper and the response signal of microbolometer was measured by lock-in amplifier.

The responsivity of LWIR region was estimated to be around 10^5 V/W in our FPAs with semi-conducting SWCNTs. This is about three times higher than that in FPAs with VO_x . TCR of our semi-conducting SWCNT networks was above $-6\%/K$, which is approximately three times higher than that of VO_x . Therefore, it means high TCR of semi-conducting SWCNT network was responsible for the increased sensitivity.

In conclusion, we showed the high-purity semi-conducting SWCNT networks extracted by ELF method effectively work for higher responsivity of microbolometer FPAs. In the future, we will evaluate the performance in more detail and obtain infrared images by combining a microbolometer and a readout circuit.

Acknowledgments: Part of this study was supported by Innovative Science and Technology Initiative for Security Grant No. JPJ004596, ATLA, Japan.

[1] C. Chen, et. al., *Sen. Act. A. Phys.* 90, 2001, 212.

[2] K. Ihara, et. al., *J. Phys. Chem. C*, 115, 2011, 22827.

[3] T. Tanaka, et. al., 2022 MRS Fall Meeting, NM02.09.08.

[4] N. Oda, et. al., *Proc. SPIE* 6940, Infrared Technology and Applications XXXIV, 69402Y (2008).

8:00 PM EL07.06.11

Spatially Heterogeneous Optical Emission from MoSe_2 Nanoribbons Ona Ambrozaite¹, Zhe Zhang¹, Sarah Hiestand², Leo Sun³, Atac Imamoglu², Adam Friedman³, Aubrey Hanbicki³ and Thomas J. Kempa^{1,3}; ¹Johns Hopkins University, United States; ²ETH Zürich, Switzerland; ³Laboratory for Physical Sciences, United States

In order to fully exploit the unique physical properties of 2D materials, one must precisely control their dimensionality, composition, strain state, and edge structure. Achieving these goals through a rational chemical synthesis strategy is a compelling but challenging prospect. Here we present detailed optoelectronic characterization of atomically-thin MoSe_2 nanoribbons synthesized through a directed growth strategy on phosphine treated Si surfaces. Temperature-dependent photoluminescence studies reveal both systematic shifts in the emission energy of the MoSe_2 nanoribbons relative to their 2D monolayer counterparts, and previously unobserved regular spatial variations in the photoluminescence intensity across the nanoribbon crystals. Transport measurements on a MoSe_2 nanoribbon field-effect transistor device are used to examine how edge effects manifest in changes of the channel and Hall conductance. This study pushes the boundaries of 2D materials synthesis by revealing that precise control over the structural attributes (dimensionality and edge states) of these crystals gives rise to unprecedented physical properties, and thereby paves the way for harnessing their novel phenomena to advance optics, electronics, and quantum sensing.

8:00 PM EL07.06.12

Transition-Metal Doped Ceria Nanoparticles Loaded Metal Oxide Nanofibers: Heightened Surface Activity for Chemiresistors Jong Won Baek and Il-Doo Kim; Korea Advanced Institute of Science and Technology, Korea (the Republic of)

Oxide semiconductor chemiresistors have shown promise as powerful gas sensors. However, their low surface reactivity limits sensitivity and selectivity. To address this issue, the functionalization of noble metal catalysts on oxide supports has been proposed, but challenges such as scarcity, agglomeration, and poisoning effects hinder practical application. In this study, we present a solution by introducing the highly promising physical and chemical properties of transition metal-doped cerium oxide (Co-CeO_2) as an alternative catalyst. To achieve uniform functionalization, we propose an elaborate design principle that employs an electrospinning technique to integrate Co-CeO_2 catalysts onto nanostructured metal oxide nanofibers. Through a single-step liquid-phase reaction involving organic solvents, we have developed sub-2 nm-sized Co-doped CeO_2 nanoparticle colloids, which can be conveniently and efficiently used for functionalizing the SnO_2 surface through solution-based electrospinning. The synthesized particles possess distinct physicochemical properties and exhibit active catalytic behavior, characterized by high purity and crystallinity. The resulting composite exhibits superior gas sensing characteristics, specifically for isoprene (C_5H_8), with low detection limit and excellent long-cycling stability. Notably, the high catalytic activities of Co-CeO_2 facilitate the spillover process of chemisorbed oxygen species, resulting in a 27.4-fold higher response towards the target analyte with exceptional selectivity. Furthermore, to gain further insights into the mechanisms behind the chemisorption of oxygen species and selective gas adsorption facilitated by the Co-CeO_2 sensitizers, we employed density functional theory (DFT) calculations and X-ray photoelectron spectroscopy (XPS) analyses. Altogether, our findings demonstrate the potential of transition metal-doped CeO_2 functionalization for highly sensitive chemiresistive gas sensors.

8:00 PM EL07.06.13

Imprinted 2D/3D Perovskite Film with Gradient Phase Distribution Toward High-Performance Polarization-Sensitive Photodetector Dustin Liu, Qi Wei, Lyuchao Zhuang and Shu Ping Lau; The Hong Kong Polytechnic University, Hong Kong

Polarization-sensitive perovskite photodetectors (PSPDs) are attracting wide attention due to their potential application in remote sensing, optical radar, astronomy detection, and military. The current mainstream of PSPDs is forming perovskites into anisotropy structures, especially nanowires (NWs). However, synthesizing high-quality perovskite NWs can be a challenging process. Two-dimensional (2D) Ruddlesden-Popper perovskites with the multilayered structure have emerged as promising candidates in optoelectronic devices for their higher oxygen and moist resistance than their three-dimensional (3D) counterparts. Previous research suggested that the spontaneously formed multiple phases of 2D perovskite films are always inhomogeneously distributed, hindering radiative recombination. It is an effective method to modulate perovskite phase distribution to facilitate the separation of charge carriers and improve carrier lifetime. This work reports a PSPD with high optoelectronic performance based on a 2D/3D perovskite heterojunction with a facile preparation process. The vertical gradient phase distribution of synthesized $(\text{PEA})_2(\text{MA})_{n-1}\text{Pb}_{n-1}\text{I}_{3n-1}$ film was determined by transient absorption (TA). This ordered phase distribution causes a progressive band energy alignment, which promotes the separation of photogenerated carriers, thereby enhancing the photodetector responsivity. Furthermore, the imprinting method was adopted to form NW-like nanoscale linear patterns on the film surface, realizing polarized light detection. The responsivity of the PSPD reaches almost 90 A/W, and the detectivity reaches the order of 10^{12} Jones. The photoluminescence intensity of the perovskite film with nanoscale linear patterns presents an anisotropy ratio of 2.2, and the photocurrent of the PSPD exhibits an anisotropy ratio of 1.6.

8:00 PM EL07.06.14

Investigation of Structural Regularity of Graphene Oxide by Experimental and Computational Methods Kazuto Hatakeyama¹, Takashi Taniguchi², Tatsuki Tsugawa¹ and Shintaro Ida¹; ¹Kumamoto University, Japan; ²National Institute for Materials Science, Japan

Graphene oxide (GO) is a well-known multifunctional 2D material. Owing to its highly useful properties, GO and reduced GO (rGO) are applied to a wide range of applications such as batteries, catalysts, and functional membranes. Furthermore, GO is easily produced via a liquid process from inexpensive natural graphite, and normally obtained as monolayer nanosheet well-dispersed in many kinds of solvents; thus, it is recognized that GO is a 2D material that is closest to practical use. However, the complex structure, which contains many types of functional groups and defects (nano-pores), has become a major impediment to studying GO. For example, its complex structure has prevented the elucidation of GO's useful properties and research using theoretical calculations. In addition, lack of repeatability, accuracy, and controllability is induced by its complex structure, which causes differences in results and discussions between papers. Moreover, rGO with the same characteristics as graphene has not been achieved because graphene structure cannot be restored perfectly using any reduction process. Recently, we developed an monolayer GO with low defect density and one type of oxygen functional group prepared by effective exfoliation of graphite oxide oxidized using Brodie's method. The high structural regularity of developed GO allows for detailed discussions in theoretical calculations and other methods that were not possible in the past. Herein, combining experimental results from FT-IR and UV-vis absorption measurements with DFT calculations, the structure of the developed GO is discussed in more depth. The experimental FT-IR and UV-vis absorption spectra were best explained by modelling a graphene backbone with regularly arranged epoxy groups. When slight structural defects were introduced in the model structure, inconsistencies

arise in the experimentally obtained spectra. The high structural regularity of the developed GO was also discussed from the experimental results of carrier mobility and electrical properties.

8:00 PM EL07.06.15

Hall Scattering Factors for Surface Termination Group Detection in Semiconducting MXenes: Unraveling Transport Behavior in 2D Materials Satadeep Bhattacharjee¹, Namitha AnnaKoshi¹, Anup KumarMandia¹, BhaskaranMuralidharan² and Seung-CheolLee¹; ¹Indo Korea Science and Technology Center, India; ²Indian Institute of Technology Bombay, India

Magnetotransport phenomena, especially in two-dimensional (2D) materials, have attracted a lot of attention due to their unique electronic properties and potential applications in various fields [1,2,3,4]. Understanding the transport behavior in these materials is crucial to elucidating their underlying physics and developing advanced electronic devices. In this study, we focus on developing a method to calculate the Hall scattering factor, a key parameter in magnetotransport studies, using Rodes' iterative approach. Our goal is to enable the calculation of this factor as part of *ab initio* calculations, thus providing a valuable tool for studying the transport properties of 2D materials. We formulate the Hall scattering factor in the context of the *ab initio* method [5] and present it in the calculation of Hall scattering factors of semiconducting MXenes such as Sc_2CF_2 , Sc_2CO_2 and $\text{Sc}_2\text{C}(\text{OH})_2$. By including elastic (acoustic and piezoelectric) and inelastic (polar optical phonon) scattering mechanisms, we model the electrical transport in these MXenes [6]. In particular, we find that polar optical phonon scattering is the most important mechanism in these materials. Interestingly, we observe a clear behavior of the Hall factor over a range of carrier concentrations. Specifically, Sc_2CF_2 exhibits an exceptionally high Hall factor of 2.49, while Sc_2CO_2 displays a relatively small value of approximately 0.5. In contrast, $\text{Sc}_2\text{C}(\text{OH})_2$ achieves the ideal value of 1. This fascinating behavior of the Hall factor holds significant promise for surface group identification in MXenes, addressing a longstanding challenge that has perplexed researchers in the field. Furthermore, our findings shed light on the role of various scattering mechanisms and highlight the intriguing behavior of the Hall factor in different materials. This work contributes to the understanding of magnetotransport phenomena in 2D materials and offers a pathway towards harnessing their unique properties for future electronic applications.

References:

- [1] Gehring P, Gao B, Burghard M, Kern K. Two-dimensional magnetotransport in $\text{Bi}_2\text{Te}_2\text{Se}$ nanoplatelets. *Applied Physics Letters*. 2012 Jul 9;101(2):023116.
- [2] Desai DC, Zviadzynski B, Zhou JJ, Bernardi M. Magnetotransport in semiconductors and two-dimensional materials from first principles. *Physical Review B*. 2021 Apr 7;103(16):L161103.
- [3] Ling X, Wang H, Huang S, Xia F, Dresselhaus MS. The renaissance of black phosphorus. *Proceedings of the National Academy of Sciences*. 2015 Apr 14;112(15):4523-30.
- [4] Akinwande D, Huyghebaert C, Wang CH, Serna MI, Goossens S, Li LJ, Wong HS, Koppens FH. Graphene and two-dimensional materials for silicon technology. *Nature*. 2019 Sep 26;573(7775):507-18.
- [5] Mandia AK, Koshi NA, Muralidharan B, Lee SC, Bhattacharjee S. Electrical and magneto-transport in the 2D semiconducting MXene Ti_2CO_2 . *Journal of Materials Chemistry C*. 2022;10(23):9062-72.
- [6] Koshi NA, Mandia AK, Muralidharan B, Lee SC, Bhattacharjee S. Can magneto-transport properties provide insight into the functional groups in semiconducting MXenes?. *Nanoscale*. 2023.

8:00 PM EL07.06.16

Effects of Vanadium Substitution on the Structure and Humidity Sensing Behavior of Microporous Titanosilicate ETS-10 Ramona Davoudnezhad, Duygu Kuzyaka and Burcu Akata Kurc; Middle East Technical University, Turkey

Humidity sensors hold an imperative role due to increased demand to control the indoor ambient environment, food and medicine storage, agriculture, health, industry, textile, and even space environments. There has been a rapid increase in developing humidity sensors with enhanced sensitivity at low and high relative humidity (RH) ranges for monitoring moisture, temperature, and chemical gases in various application fields.

Zeo-type Titanosilicate ETS-10 is microporous material that shows competitive sensitivity to TiO_2 . However similar to TiO_2 at low humidity range it needs some modifications. To achieve this, vanadium (V)-incorporated titanosilicate microporous thin films were successfully fabricated to investigate their performances as humidity sensors. A structure with both vanadium and titanium atoms of differing coordinations in the quantum wire of ETS-10 was used to better understand the sensing mechanism. The results indicated that vanadium incorporation led to structural changes in ETS-10, resulting in the formation of Ti^{3+} centers along with Ti^{4+} states with a more significant amount of V^{5+} as the incorporated vanadium level increased. Vanadium incorporation also resulted in the decreased bandgap, suggesting the introduction of disorders created along the -Ti-O-Ti- chains. The developed sensors showed full range sensitivity at an optimized amount of vanadium into the -Ti-O-Ti- quantum wires in ETS-10. It was observed that V-incorporated samples with an optimized amount of V/Ti+V ratio of 0.2 showed enhanced sensitivity at particularly low relative humidity (RH) levels for the first time. These results demonstrated that titanosilicate ETS-10 has potential application in fabricating humidity sensors, and the sensing performance is enhanced, particularly at an optimized vanadium amount.

Keywords: Humidity Sensor, Titanosilicates, V-incorporated ETS-10, Impedance Spectroscopy

8:00 PM EL07.06.17

Band Tunable Saturable Absorber Built from MoS_2 -Printed D-Shaped Fiber Mingfei Xiao¹, Amar Nath Ghosh², Jinrui Chen¹, Guolin Yun¹, Noel Healy³, Anna Claire Peacock² and Tawfique Hasan¹; ¹University of Cambridge, United Kingdom; ²Optoelectronics Research Centre, University of Southampton, United Kingdom; ³Emerging Technologies and Materials Group, School of Mathematics, Statistics and Physics, United Kingdom

Low-temperature additive fabrication techniques, such as inkjet printing, provide the ability to precisely deposit functional materials onto designated locations, helping to reduce costs in large-scale manufacturing. This research outlines a highly controllable materials deposition method for micro precision jetting a wide range of 2D nanocrystal inks onto nearly any surface, including plastic, glass, ceramics, silicon, and flexible substrates. Researchers can utilize interchangeable cartridges to fabricate thin films for applications such as flexible circuits, sensors, and photonics.

We use liquid phase exfoliation and solvent exchange processes to prepare the MoS_2 ink for inkjet printing. This ink contains few-layer MoS_2 flakes with ~50 nm lateral size and ~3 nm thickness, in a binary solvent combination of IPA and 2-butanol. This binary solvent ink suppresses coffee ring formation after inkjet printing.

To demonstrate the versatility of the process, we deposit the ink onto the side polished regions of D-shaped fibers. By printing the inks with different numbers of printing paths, the material thickness can be tuned, before sealing with a 1 μm thick parylene-C passivation layer. The devices demonstrate the transmittance covering the near-infrared region, with the position of absorption peak position tuned by the different number of printing paths, indicating their applicability as a band-tunable saturable absorber for the creation of ultrafast fiber lasers.

8:00 PM EL07.06.18

Enhancement of Electrochromic Performance of $\text{W}_{18}\text{O}_{49}$ NWs Through Instantaneous Acceleration of Ion and Electron Transport via $\text{Ti}_3\text{C}_2\text{Tx}$ (MXene) Addition Muhammad Hassan and Kemal Celebi; Zhejiang University, China

The field of flexible electrochromic materials has garnered considerable attention due to their potential applications in emerging technologies like smart windows, wearable displays, and electronic paper. Transition metal oxides (TMOs) show promise as electrochromic materials for smart windows and displays. However, the challenge remains to achieve simultaneous improvements in flexibility, coloration efficiency, and response time. Effective strategy to simultaneously boost the transport kinetics of electrons and ions in TMOs thin films is critical. One effective approach is the utilization of nanostructured materials in the form of 2D nanosheets, which significantly enhance electrical and ionic transport due to their increased surface-to-volume ratio. The high contact area between adjacent nanosheets facilitates even redistribution of induced strain, leading to improved mechanical strength and film flexibility. In this regard, we present advancements in the development of a promising material, the MXene- $\text{W}_{18}\text{O}_{49}$ nanowires (NWs) composite, and its interfacial assembly for flexible electrochromic applications. These assembled nanometer-thick heterostructures exhibit well-balanced alignment and connectivity, enabling fast and efficient transport of ions and electrons, as well as superior mechanical and electrochemical stability. Furthermore, we demonstrate the feasibility of large-area flexible devices that can be seamlessly integrated onto curved and flexible surfaces, paving the way for future global electronics.

<quillbot-extension-portal></quillbot-extension-portal><quillbot-extension-portal></quillbot-extension-portal>

8:00 PM EL07.06.19

The Development of Multifunctional Adhesive Point of Care Sensors Muthamilselvan T and Titash Mondal; Indian Institute of Technology Kharagpur, India

The development of multifunctional adhesive point of care sensors

Muthamil Selvan T,^a, Titash Mondal^{a*}

The 1D and 2D conductive nanomaterials have contributed to an increase in interest in the advancing development of flexible and wearable electronics over the past decade [1]. The current and next generational span presents wide opportunity for the advancement of printable flexible sensors for use in human healthcare assessment [2]. The existing metal-based sensors for medical diagnostics lack human comfort because of low flexibility, and poor conformity with the skin, and offer significantly less stretchability [3]. The carbon nanotubes (CNTs) are unique electrical properties, high intrinsic current mobility, and high performance and combination with elastomer provides wide benefits. In our work, the stencil printable elastomeric nanocomposite adhesive-based formulations were used to create multifunctional printed sensors [4]. The Liquid isoprene rubber (LIR) with methyl ester of succinic acid functionality and carboxylated (c-CNT) was selected as the material to develop adhesive-based multifunctional sensors. The formulation is designed to bond with various substrates including plastics, metals, glass, and wood. We picked the highest sensitivity formulation associated with the volume fraction of CNT using the rheological and electrical percolation model. The selected formulation could respond to a wide range of stimuli, such as changes in temperature, pressure, and strain. The developed sensors show a temperature sensitivity of 0.347%/°C and strain sensitivity of 62.4 up to 40%. As a result of these benefits, these sensors are being used in a variety of human health monitoring applications at the point of care. The developed sensors are capable of detecting low- to high-strain movements associated with monitoring human motion, such as twitching, frowning, eye blinking, and finger and elbow bending. In addition, the sensors were able to accurately track vital signs like pulse rate and respiration rate as well as track vocal patterns for use in diagnostics of human health.

References

- [1] J. Park, J. C. Hwang, G. G. Kim, and J. U. Park, "Flexible electronics based on one-dimensional and two-dimensional hybrid nanomaterials," *InfoMat*, vol. 2, no. 1. Blackwell Publishing Ltd, pp. 33–56, Jan. 01, 2020.
- [2] W. Gao, H. Ota, D. Kiriya, K. Takei, and A. Javey, "Flexible Electronics toward Wearable Sensing," *Acc. Chem. Res.*, vol. 52, no. 3, pp. 523–533, Mar. 2019.
- [3] S. Wagner and S. Bauer, "Materials for stretchable electronics," *MRS Bull.*, vol. 37, no. 3, pp. 207–213, Mar. 2012.
- [4] M. Selvan T. S. Sharma, S. Naskar, S. Mondal, M. Kaushal, and T. Mondal, "Printable Carbon Nanotube-Liquid Elastomer-Based Multifunctional Adhesive Sensors for Monitoring Physiological Parameters," *ACS Appl. Mater. Interfaces*, vol. 14, no. 40, pp. 45921–45933, Oct. 2022.

<quillbot-extension-portal></quillbot-extension-portal>

8:00 PM EL07.06.20

Thermal Conductivity and Dielectric Behavior of Nanobrick Wall Thin Films: A New Generation of High-Performance Insulation Ethan T. Iverson¹, Hudson Legendre¹, Shubham Vasant Chavan², Anil Aryal¹, Maninderjeet Singh², Sourav Chakravarty¹, Kendra Schmiegel¹, Hsu-Cheng Chiang¹, Patrick Shamberger¹, Alamgir Karim² and Jaime Grunlan¹; ¹Texas A&M University, United States; ²University of Houston, United States

Various high voltage electronics for aerospace, defense, and energy storage and conversion have experienced a significant increase in their miniaturization, complexity, power draw, and heat generation. Current insulation systems are inadequate to meet the demands of these rapidly evolving electronics due to subpar thermal conductivities, dielectric properties, and conformability to complex part geometries. Little research has focused on creating novel insulation systems that excel at both dissipating heat and withstanding high voltages (i.e., have both high thermal conductivity and superior dielectric breakdown strength) due to the inverse relationship between the material's thermal conductivity and insulating dielectric properties. Electronics often require specific combinations of thermal and dielectric properties that are difficult to obtain with one material. Layer-by-layer (LbL) deposition of polyelectrolytes and inorganic nanoplatelets, yields nanocomposite coatings with a high degree of conformality and ordered structures, with unique properties which rival Kapton. Properties can be controlled by adjusting solution concentration, chemistry, and pH, which directly alters the system's nanostructure. Thermal conductivity as high as 1.87 W/m*K and impressive dielectric constant, losses, and breakdown strength (3, 0.05, and 140 kV/mm, respectively) have been achieved. These novel insulation systems also demonstrate impressive dielectric properties at elevated temperatures, with breakdown strengths ranging from 180-270 kV/mm and low dielectric losses (<<0.1). This unique application of LbL assembly provides a practical route for the precise production of high performance, thermally conductive insulation systems for high voltage electronics.

8:00 PM EL07.06.21

Structural and Electronic Properties of α -Borophene Scrolls Guilherme Fabris¹, Douglas S. Galvao² and Ricardo Paupitz³; ¹Federal University of Pelotas, Brazil; ²State University of Campinas, Brazil; ³University of São Paulo –UNESP, Brazil

Since the advent of graphene, there is a renewed interest in low-dimensional materials. Among the structures related to graphene, it is worth mentioning the carbon nanoscrolls (CNS). CNS can be topologically described as graphene sheets rolled up into a spiral shape (papyrus-like) [1]. CNS and scrolls of other elements have already been obtained. Recently, borophenes (single-layer boron structures) were predicted and experimentally realized [2,3]. A natural question is whether stable borophene scrolls can exist. In the present work [4], we proposed and investigated the structural and electronic properties of boron-based nanoscrolls (armchair and zigzag) using the DFTB+ method. The electroactuation process (injecting and removing charges) was also investigated. Our results showed a giant electroactuation, similar to what was reported for carbon nanoscrolls [5]. Our results also show that the borophene scrolls are thermally and structurally stable for a large range of temperatures (up to 600K), and the electroactuation process can be easily tuned and can be entirely reversible for some configurations.

- [1] Braga, S. F.; Coluci, V. R.; Legoas, S. B.; Giro, R.; Galvao, D. S.; Baughman, R. H. *Nano Letters* 2004, 4, 881–884.
- [2] Penev, E. S.; Bhowmick, S.; Sadrzadeh, A.; Yakobson, B. I. *Nano Lett.* 2012, 12, 2441–2445.
- [3] Feng, B.; Zhang, J.; Zhong, Q.; Li, W.; Li, S.; Li, H.; Cheng, P.; Meng, S.; Chen, L.; Wu, K. *Nature Chem.* 2016, 8, 563–568.
- [4] Fabris, G. S. L.; Galvao, D. S.; Paupitz, R. *arXiv:2306.05602*.
- [5] Rurali, R.; Coluci, V. R.; Galvao, D. S. *Phys. Rev. B* 2006, 74, 085414.

8:00 PM EL07.06.22

New Paradigm of Label-Free Biosensor Enabled by Two-Dimensional Hexagonal Titanium Oxide Yange Luan, Bao Yue Zhang and Jianzhen Ou; RMIT University, Australia

Biosensors with high sensitivity and selectivity are increasingly in demand, especially in the fields of medical devices, health monitoring, and treatment, etc. Two-dimensional (2D) materials-enabled nanotechnology has brought promising pathways in rapid, highly sensitive, and selective cancer biomarker sensors. The recently developed 2D planar hexagonal titanium oxide (h-TiO₂) monolayer derived from the metal-gas interface exhibited a unique narrowed bandgap and extraordinary carrier transport performance up to 950 cm² V⁻¹s⁻¹ at room temperature, compared to that of conventional bulk phased ones. The findings show exciting opportunities in realizing high-performance electronic biosensors. Herein, we demonstrated the sensing capability of 2D h-TiO₂ by FET-based biosensor for carcinoembryonic antigen (CEA) detection—a representative broad-spectrum tumor marker. The h-TiO₂ nanosheets FET devices were functionalized with monoclonal CEA antibody using the probe linker of 3-aminopropyltriethoxysilane. The dissociation constant between anti-CEA and CEA protein was estimated to be approximately 1.03 × 10⁻¹⁰ M by hill model, showing high affinity between CEA protein and anti-CEA. Multiple techniques including XPS, and KPFM were carried out to investigate the surface condition at each of the functionalization stages. The real-time measurement of 2D h-TiO₂ FET biosensor showed a high specificity of and an ultralow limit of detection (LOD) down to 0.23 pg ml⁻¹, exceeding the performance enabled by conventional 2D systems including graphene, black phosphorus (BP), transition metal dichalcogenides (TMDs), etc. The outcome of this work demonstrates the significant potential of 2D hexagonal metal oxide in biological sensing applications.

8:00 PM EL07.06.23

Significantly Improving CNT-Fiber Thermal Conductivity via Ultra-Fast Pulsed Laser Annealing Rachel Martin¹, Zachary Piontkowski¹, Mitchell Trafford², Wyatt Hodges¹, Anthony McDonald¹, Lyle Brunke³, Matteo Pasquali² and Michael Siegal¹; ¹Sandia National Laboratories, United States; ²Rice University, United States; ³Oak Ridge National Laboratory, United States

We studied pulsed laser annealing (PLA) via an ultraviolet excimer laser with a 248 nm wavelength to perform ultra-rapid thermal annealing to coalesce or merge adjacent carbon nanotubes (CNTs) within graphitic CNT-fibers; this results in > 30% improvements to the overall fiber thermal conductivity. CNT-fibers are comprised of aligned, high aspect ratio (length/diameter > 3,000) CNT bundles held together with weak Van der Waals interactions. While individual CNTs have thermal conductivities > 3000 W/m*K, CNT-fiber thermal conductivities are only ~350 W/m*K. The lower conductivity is attributed to poor thermal contact between adjacent CNTs that act as phonon scattering sites. We hypothesized that coalescing adjacent CNTs in the contact regions to form larger diameter CNTs would reduce phonon scattering sites and improve the overall fiber thermal conductivity, although the CNTs would become somewhat more defective. CNT coalescence was recently demonstrated by furnace annealing to temperatures > 1700°C. Instead, we perform PLA, with ~ 20 ns pulse durations, to achieve rapid, targeted heating of fibers to induce CNT coalescence at a greatly reduced thermal budget. We operated the laser at a 20 Hz pulse frequency; hence 5 seconds of laser operation results in 2 microseconds of total annealing time.

PLA uses modest energy to anneal at high temperatures due to strong UV absorbance by opaque CNTs. Radial breathing modes (RBMs), found in Raman Spectroscopy data at low wavenumber, identify the various CNT diameters within the fiber. The degree of CNT coalescence within a fiber is assessed via increases in CNT diameters as a function of PLA conditions

(whereby laser energy density and total pulses are analogous to temperature and time respectively). We measure fiber thermal conductivities using the 3ω method, where AC current induces Joule heating of the sample, resulting in a 3ω output voltage correlating to the sample thermal conductivity. We find that the CNT-fiber thermal conductivity indeed increases with optimized PLA exposure, reaching values $> 500 \text{ W/m}^2\text{K}$, surpassing that of even the best metals. This work was supported by the Laboratory Directed Research and Development program at Sandia National Laboratories (SNL). SNL is managed and operated by NTESS under DOE NNSA contract DE-NA0003525.

8:00 PM EL07.06.24

Role of Carbon-Based Nanocomposites for Energy Storage[Jake Irvin](#), DuyPham, MasonCox and AshishAphale; Kennesaw State University, United States

Certain allotropes of carbon have unique properties that have the potential for clean energy storage systems, healthcare, aerospace, and energy conversion applications. In this work, graphene-based nanocomposites (GNCs) were synthesized and investigated for their use in an ultracapacitor device. GNCs were selected for use as an electrode material for the supercapacitor due to their superior electrochemical properties and high surface area which is promising to provide superior energy storage performance. GNCs will be synthesized using an electrochemical deposition technique and the performance will be evaluated using various electrochemical studies in the presence of various three different aqueous electrolytes. Distinct Faradaic and non-Faradaic charge transfer mechanisms will be investigated using cyclic voltammetry (CV), electrochemical impedance spectroscopy (EIS), and galvanostatic charge-discharge (GCD) studies. Results of different percentages of dopants in the nanocomposite during synthesis and their effect on ultracapacitor performance will be presented. Lifecycle testing of the ultracapacitor device will be discussed and its post-test analysis will be presented. The role of different substrates, electrolytes, and their effect on the device performance will be discussed. Mechanisms of charge storage and transfer between the electrolyte and GNC surface will be presented.

8:00 PM EL07.06.25

Mist CVD Modulated High- κ a-Al_{1-x}Ti_xO_y Films for p-WS_{2-x}Se_{1.7}-Channel Metal Oxide Field Effect Transistors (MOSFETs)[AbdulKuddus](#)¹, KojunYokoyama², ShinichiroMouri^{1,1}, KeijiUeno² and HajimeShirai²; ¹Ritsumeikan University, Japan; ²Saitama University, Japan

Introduction: High- κ amorphous (a)-AlO_x, and a-TiO₂ thin films from Al(acac)₃ and Ti(acac)₂OiPr₂ precursors dissolved in alcohol solvent investigated by mist CVD method in our previous reports [1,2]. In addition, the AlO_x, and TiO₂ alloy of a-Al_{1-x}Ti_xO_y (ATO) films revealed an adjustable dielectric constant of 6.23-25.12 and band gap of 4.25-6.38 eV studied. Further, an exfoliated MoSe₂-channel MOSFET on Al_{0.74}Ti_{0.26}O_y thin film as gate insulator with Au as the source and drain electrodes showed a mobility of 85 cm²/Vs, the threshold voltage of 0.92 V, and an on/off current ratio of 10⁸ [3]. However, a consistent fabrication of TMDCs such as MoS₂, MoSe₂, and WS₂, WSe₂, or their alloys such as WS_{2-x}Se_x film and the high- κ dielectric is highly promising toward large-scale device fabrication. To date, the synthesis of high-quality defect-free large-area TMDCs films and transfer-free device fabrication are major hindrances to further advancing in TMDCs-based devices technology. In this study, we investigated a consistent fabrication technique of metal oxide and TMDCs films as high- κ dielectric and channel layers in MOSFETs toward transfer-free large-scale TMDCs device fabrications.

Experiment: A 0.015 M Al(acac)₃ and Ti(acac)₂OiPr₂ solution with CH₃OH dilution was placed directly above a 3 MHz atomizer, N₂ was used as a generator, and dilution gas (500 and 2400 sccm) was used to transport the mist. A cleaned Si substrate was placed 16 cm inside the tube furnace in the open air. On the other hand, ammonium tetrathiotungstate (NH₄)₂WS₄ dissolved in N-methyl-2-pyrrolidone (NMP) solvent was used as a precursor of WS_{2-x}Se_x. The WS_{2-x}Se_x films were synthesized by mist CVD with Ar gas containing H₂ (25%) at a T_f of 400-600 °C at atmospheric pressure. Subsequent selenization of mist CVD WS_x was executed to further improve the flake's quality at T_f of 600 °C for 20 min. The p-WS_{2-x}Se_x channel MOSFETs on ATO dielectric were fabricated with Pt source and drain electrodes [4].

Results and Discussion: The deposition rates were found of 11 nm/min for Al_{0.74}Ti_{0.26}O_y with an adjustable dielectric constant of 6.23-25.12 and band gap of 4.25-6.38 eV. While, an average flake size of over 700-800 μm on ATO substrate, the mobility over 40 cm²/Vs, the threshold voltage around 0.30 V, and an on/off current ratio in the range of 10⁶ were obtained in p-WS_{0.3}Se_{1.7}-channel MOSFETs on ATO dielectric retaining reduced leakage current. Thus, a strong potential is revealed by the mist CVD to be used as a consistent manufacturing process for the fabrication of metal oxides and TMDCs films as high- κ dielectric and channel layers in MOSFETs toward transfer-free, large-scale TMDCs device technology.

References

- [1] A. Rajib *ACS Appl. Electron. Mater.* 3, 2, 658-667 (2021).
- [2] A. Rajib et al., *J. Appl. Phys.* 131, 105301 (2022).
- [3] K Yokoyama et al., *ACS Appl. Electron. Mater.* 4, 5, 2516–2524 (2022).
- [4] A. Kuddus et al., *Semicond. Sci. Technol.* 37 095020 (2022).

8:00 PM EL07.06.26

Atomic Layer Etch of Tungsten Disulfide Semiconductor using Downstream Plasma Treatment and Wet Etch Removal[Young-Hyun You](#), JoonyupBae and JihyunKim; Seoul National University, Korea (the Republic of)

Silicon has been used as a channel material for field-effect transistor (FET), driving the growth of the semiconductor industry. However, in modern technology where the channel size has been reduced to several nanometers, silicon has shown limitations such as short channel effects. Since numerous defects such as dangling bonds exist on the surface of silicon, the movement of carriers is hindered by the defects in channel with atomic-scale thickness. High-performance transistors with smaller form factor require the next-generation semiconductors to replace silicon. Recently, two-dimensional (2D) materials have drawn considerable attention due to their unique layered structure. Since layer-to-layer bonding is achieved through van der Waals (vdW) interaction, layer-to-layer separation can be easily achieved with relatively weak force. The separated monolayer has a complete structure and no defects on surface compared to silicon. Several semiconductor chip manufacturers have reported results of applying 2D materials as channels in various structures of next-generation transistors.

Transition-metal dichalcogenides (TMDCs) are one of the most actively studied 2D materials. Among them, WS₂ has a very high electron mobility of ~234 cm²V⁻¹s⁻¹ and generally exhibits n-type behavior due to its sulfur vacancy. WS₂ can also be used as a p-channel through p-doping and it is possible to implement a single semiconductor-based complementary metal-oxide-semiconductor (CMOS). Thickness-dependent energy band gap and excellent mechanical properties of WS₂ enable multiple device applications such as photo detectors and wearable devices. However, various problems exist in the fabrication process of electrical devices using TMDCs. In general, the mechanical exfoliation is used for interlayer separation of TMDCs and it is difficult to obtain the materials with accurate thickness due to its randomness. Photoresists or contaminants may also remain on the surface of TMDCs, which can cause interface defects and reduce device reliability. WS₂ can be oxidized in atmosphere and the oxide layer gives an unwanted doping effect. The fabricated devices exhibit different electrical properties from those originally designed because of the above problems.

In this study, we propose a method to accurately control the thickness and restore the contaminated surface to the pristine state through atomic layer etching of WS₂. Only the outermost layer of WS₂ can be oxidized by self-limiting reaction using downstream O₂ plasma. Subsequent KOH solution treatment selectively removes only the oxide layer (WO_x) for layer-by-layer control of thickness. A back-gate FET using WS₂ as a channel material was fabricated to confirm the changes of physical and electrical properties by atomic layer etching. The etch rate of WS₂ channel measured with atomic force microscope (AFM) was approximately 0.65 nm/cycle, equivalent to the thickness of WS₂ monolayer. Micro-Raman spectroscopy and high-resolution transmission electron microscopy (HR-TEM) showed that atomic layer etching had a minor effect on the crystallinity of WS₂. Finally, the n-type behavior was recovered through the surface cleaning effect and the recessed-channel WS₂ FET with improved output current on/off ratio higher than 10⁶ was realized. This method, which provides a facile approach to thickness control and surface cleaning, allows TMDCs to be precisely engineered, increasing their potential as channel materials for next-generation transistors.

8:00 PM EL07.06.27

Electrochemical Sculpting of Phosphorene Nanoribbons: Unleashing the Anisotropy of Black Phosphorous[Jacek B. Jasinski](#), UsmanAbu, SharminAkteer, BimalNepal, GaminiSumanasekera, BadriNarayanan and HuiWang; University of Louisville, United States

In recent years, phosphorene, a two-dimensional (2D) form of black phosphorus (BP), has garnered significant research attention due to its exceptional properties, including high carrier mobility (2,000 cm² V⁻¹s⁻¹), thickness-dependent bandgap (0.3 – 2.0 eV), and strong in-plane anisotropy. Moreover, phosphorene nanoribbons (PNRs) exhibit even more impressive characteristics owing to their one-dimensional (1D) nanostructure, which gives rise to additional quantum confinement effects, density of states redesign, and a high density of active edge sites. While several methods for producing PNRs have been explored, scalable synthesis with narrow widths remains challenging.

Here, we present our recently developed method termed "electrochemical sculpting" to synthesize PNRs through an electrochemical process utilizing the highly anisotropic ion diffusion in BP along the [001] (zigzag) direction. In this method, BP flakes are nanostructured via an electrochemical process into bundles of parallel PNRs separated by narrow amorphous phosphorus channels running along the zigzag direction, as confirmed by transmission electron microscopy (TEM) and in-situ Raman spectroscopy. A subsequent ultrasonic treatment in a solvent can be used to separate the PNR bundles into individual, well-defined PNRs. Using this low-cost and scalable electrochemical method, we were able to fabricate PNRs with confined widths (< 10 nm) that are significantly narrower than those produced by most previous methods. Our fabricated PNRs exhibit a highly confined structure with a suppressed B_{2g} vibrational mode. Notably, when employed in field-effect transistors (FETs), the PNR bundles demonstrate n-type behavior, which differs from that of BP flakes.

In our ongoing study, we focus on understanding this process and extending it to other anisotropic 2D layered materials. So far, the obtained results indicate that electrochemical sculpting and the fabrication of nanoribbons can also be achieved in black arsenic-phosphorus (b-AsP) alloys, i.e., 2D layered materials where some of the phosphorus atoms in the BP structure are

substituted by arsenic atoms. This is significant because b-AsP alloys are promising 2D materials, exhibiting unique electronic and optical properties. However, the fabrication of their nanoribbons using chemical approaches is particularly challenging due to the low solubility of arsenic in many solvents and the difficulties in controlling the crystal structure of the resulting material. While the overall mechanism responsible for electrochemical sculpting in BP and b-AsP alloys is similar, our study indicates several significant differences between these materials. These differences can be attributed to the variation in in-plane anisotropy as well as the disparity in defect formation energy between these systems.

Our study provides valuable insights into this novel synthesis approach for PNRs, opening up new possibilities for the development of nanoribbons using BP and other anisotropic 2D layered materials. The demonstrated electrochemical sculpting method offers improved scalability and holds promise for advancing the applications of PNRs in various fields.

8:00 PM EL07.06.28

Preparation of 2D MoS₂ Atomic Layers from Precursor Solution Formulation and Simple Thermal Annealing for Patterned MoS₂ TFT Thi Thu TuyCan and [Woon-SeopChoi](#); Hoseo University, Korea (the Republic of)

Due to unique properties such as high carrier mobility and innate band gap, two-dimensional (2D) transition metal dichalcogenides (TMDs) have attracted great attention in optoelectronic and nanoelectronic fields as well. Among those atomically thin materials, molybdenum disulfide (MoS₂) has become an emerge candidate because of the indirect to direct band gap transition in monolayer limit. Chemical vapor deposition (CVD) with sulfur gas is the most popular method for synthesizing large-scale 2D materials with high quality. Various MoS₂ can be obtained from this method using various precursors with different properties, process temperatures, and substrate materials. Solution process methods show advantages for preparing films with large size, high throughput, low cost, thickness control, and an environmentally friendly process.

We developed a Mo-based solution formulation for solution-processed synthesis of MoS₂ with large-scale and uniformity. The precursor solution can be converted to atomic layer films using simple thermal annealing without using chemical vapour process. A MoS₂ thin film was prepared by a simple jet printing and one-step annealing method. Three atomic layers of MoS₂ were obtained with 0.0125 M of precursor solution, which was confirmed by STEM. The atomic layers of the synthesized MoS₂ were identified as 2 layers for 0.0070 M, 3 layers for 0.0125 M, and 5 layers for 0.0250 M of MoS₂ solution by STEM-FIB. A printed MoS₂ TFT shows a high current ratio of approximately 10⁶, a good mobility of 27.5 cm²V⁻¹s⁻¹, a threshold voltage of 1.76 V, and a subthreshold slope of 1.32 Vdec⁻¹.

8:00 PM EL07.06.29

Observation of Intrinsic Seebeck Coefficient of 2D PtSe₂ Semiconducting Films Through Two-Step Annealing Process MinjeongKim, YunhoKim, Jae WonChoi, JungminCho, HyeokjunKwon, Gil-SungKim, SangkwonLee and [No-WonPark](#); Chung-Ang University, Korea (the Republic of)

The Seebeck coefficient is an important indicator of the thermoelectric (TE) properties of a material, so accurately measuring the Seebeck coefficient is essential. However, it is challenging to evaluate the Seebeck coefficient of a 2D film having extremely high resistance. Here, we propose a simple method to measure the intrinsic Seebeck coefficient of a 2D PtSe₂ thin films with high electrical resistance over 2 MΩ by two-step thermal annealing process. After two-step annealing process, the electrical resistance was decreased from ~2 MΩ to ~400 kΩ and the intrinsic Seebeck coefficient could be measured, and the value is exceeding 159 μVK⁻¹, which is approximately 400% higher than that of single crystalline PtSe₂ bulk. Furthermore, the power factor of the sample was calculated up to 44 μWm⁻¹K⁻². Additionally, it was observed that the measured intrinsic Seebeck coefficient was independent of the top metal electrode. We discuss the role of thermal annealing process in high resistance 2D semiconducting films based on the atomic crystallographic characteristics and contact resistance between the film and electrode. Our findings demonstrate significant achievements in measuring and understanding the Seebeck effect of 2D transition metal dichalcogenide (TMDC) materials.

SESSION EL07.07: 1D and 2D Materials—Logic Devices and Interconnects II

Session Chairs: [Lain-Jong Li](#) and [Yuxuan Cosmi Lin](#)

Wednesday Morning, November 29, 2023

Hynes, Level 3, Ballroom B

8:00 AM *EL07.07.01

1D Topological Systems for Next-Generation Electronics [JudyCha](#); Cornell University, United States

Topological nanowires, topological materials confined in one dimension (1D) at the nanoscale, hold great promise for robust and scalable quantum computing and low-dissipation interconnect applications, which will transform current computing technologies. To do so, research in topological nanowires must continue to improve their synthesis and properties.

In this talk, I will discuss my group's efforts to develop a synthesis method that is high throughput, scalable, and well controlled to fabricate 1D topological systems with precision in crystalline phase, morphology, and dimensions [1]. I will highlight our results on topological semimetal nanowires that can rival current state-of-the-art Cu interconnects for low-resistance interconnect applications. Specifically, we experimentally demonstrate that the resistivity scaling of MoP nanowires is superior to those of the latest Cu interconnect technologies and Cu alternative metals [2], presenting MoP as a breakthrough metal for the low-resistance interconnect applications.

[1] Matter doi:10.1016/j.matt.2023.03.023 (2023)

[2] Adv. Mater. 35, 2208965 (2023)

8:30 AM EL07.07.02

Unconventional Resistivity Scaling in Nanocrystalline NbP and TaP sub-5 nm Thin Film [Asir IntisarKhan](#)¹, [EmilyLindgren](#)¹, [XiangjinWu](#)¹, [Hyun-MiKim](#)², [AkashRamdas](#)¹, [ByoungjunWon](#)³, [FelipeJornada](#)¹, [Il-KwonOh](#)³, [H.S. PhilipWong](#)¹, [YuriSuzuki](#)¹ and [EricPop](#)¹; ¹Stanford University, United States; ²Korea Electronics Technology Institute (KETI), Korea (the Republic of); ³Ajou University, Korea (the Republic of)

The electrical resistivity of ultrathin metal films typically increases with decreasing film thickness due to electron scattering from the film surfaces. This behavior limits the performance of metal-based interconnects in all modern nanoelectronics [1]. To overcome this bottleneck, novel quantum materials like topological semimetals with disorder-tolerant conductive surface states have been suggested in the ultrathin film limit [2, 3].

Here we uncover the reduction of electrical resistivity with decreasing film thickness of ultrathin nanocrystalline NbP and TaP films, probed by detailed transport measurements, material characterization, and modeling. These materials have been demonstrated to be topological Weyl semimetals in the bulk [2], a class of materials wherein surface conduction is predicted to dominate thin-film transport even in the presence of disorder [3].

NbP and TaP thin films are sputtered on both r-plane sapphire and MgO substrates at 400 °C, a process compatible with back-end-of-the-line (BEOL) semiconductor fabrication. A thin seed layer of Nb (or Ta) is used to reduce lattice mismatch between the substrate and sputtered NbP (or TaP) thin films. High-angle annular dark-field (HAADF) scanning transmission electron microscope (STEM) imaging reveals nano-crystallinity of the ultrathin NbP films with short-range ordering at the NbP surface, irrespective of the film thickness. The compositional homogeneity of the NbP thin films is further confirmed by energy-dispersive X-ray analysis.

Our measured resistivity of NbP at room temperature decreases from 207 to 149 μΩ-cm (from ~18 nm down to ~2.3 nm film thickness), unlike conventional metals. We further confirm the decreasing resistivity trend with decreasing thicknesses of NbP film irrespective of the thickness of the seed layer. For example, with a 4 nm Nb (Ta) seed layer, we find that the resistivity of NbP thin films decreases from 135 μΩ-cm (18 nm thick film) to ~34 μΩ-cm (~1.5 nm thin film). On the other hand, the measured resistivity for ~1 nm thin TaP film is ~12 μΩ-cm. For both cases, the resistivity is significantly lower than the bulk single-crystal resistivity. We also note that the resistivity of NbP (TaP) thin films with a 4 nm seed layer is lower compared to their thinner seed layer counterparts due to possible charge transfers from the thicker metal seed layer to the NbP (TaP) thin films.

Temperature-dependent electrical resistivity measurements of NbP show a significantly weaker temperature dependence of resistivity in the thin NbP compared to control metal Nb. This behavior suggests a disorder-driven localization of conduction instead of phonon-dominated transport. To understand our measurements, we present a transport model in terms of a surface channel and bulk conduction in all films with surface-dominated conduction in the thinner NbP films leading to a decrease in effective electrical resistivity. Our measured Hall resistance is nearly linear with the magnetic field. This is a signature of transport dominated by single carriers (holes for NbP).

In summary, we demonstrated an unconventional resistivity scaling trend with the film thickness in sub-5 nm NbP and TaP thin films. Our transport measurements suggest surface-dominated conduction in such materials even at room temperature, which is promising for next-generation nanoelectronics. This work was supported in part by the Stanford Graduate Fellowship (A.I.K.) and the Stanford SystemX Alliance.

Refs: [1] D. Gall et al., *MRS Bulletin* (2021). [2] C. Shekhar et al., *Nat. Phys.* (2015). [3] N. Lanzillo et al., *Phys. Rev. Appl.* (2022). [4] Y-B. Yang et al., *Phys. Rev. Lett.* (2019).

8:45 AM EL07.07.03

Synthesis of Thin Film Weyl Semimetal TaPArkaChatterjee and ShengxiHuang; Rice University, United States

Topological Weyl semimetals (WSMs) have opened up a new horizon in physics and materials science due to their unique electronic, optical, and thermal properties. So far, experimental studies of WSMs have mainly focused on bulk samples. However, it has been predicted that thin films of WSMs could generate unique phenomena unachievable by bulk crystals, such as the unusual twisting of the Fermi surface, a metal-insulator transition upon thickness confinement, and the emergence of Floquet topological insulator phase modes. Furthermore, the synthesis of WSM thin films could potentially open up opportunities for creating heterostructures and functional interfaces with other materials, such as superconductors, ferromagnetic or antiferromagnetic materials, and ferroelectric materials. These interfacial interactions have been found to be promising for applications in spintronics and superconducting devices. Thus, the synthesis of thin film WSMs would be impactful from both fundamental and practical standpoints.

TaP, a type of WSM, has attracted significant attention due to its cleanest carrier pockets close to the Weyl fermions dominated Fermi energy and unsaturated negative magnetoresistance (MR), highlighting its potential for electronic applications. Here, we report the successful synthesis of thin films of TaP using a fast thermal process. State-of-the-art characterization techniques were employed to confirm the high quality of the synthesized TaP thin films. The electronic and optical properties were also obtained. Our synthesis method also offers the potential for wafer-scale manufacturing of thin film TaP. In summary, our synthesized TaP thin films hold great promise in both fundamental topological physics and novel electronic applications.

9:00 AM *EL07.07.04

Electronic Transport in 2D Semiconductors and Interconnect MetalsChenmuZhang, ZhongcanXiao, RongjingGuo and YuanYueLiu; The University of Texas at Austin, United States

The performance of many electronic devices heavily relies on how fast the electrons can transport. Thus there is a critical need to understand and improve electronic transport. Here I will present our recent progress in developing and apply first-principles methods to accurately calculate and understand the electronic transport in 2D semiconductors as well as interconnect metals. I will also present new materials with improved transport properties.

Ref: [1] C. Zhang, Y. Liu, "Electron-surface scattering from first principles", under review; [2] Z. Xiao, R. Guo, C. Zhang, Y. Liu, "Point defects limited charge mobility in 2D transition metal dichalcogenides", under review; [3] C. Zhang, R. Wang, H. Mishra, Y. Liu, "Discovering and Understanding 2D Semiconductors with High Intrinsic Charge Mobility at Room Temperature", *Phys. Rev. Lett.*, 2023, DOI: 10.1103/PhysRevLett.130.087001; [4] L. Cheng, C. Zhang, Y. Liu, "Why two-dimensional semiconductors generally have low electron mobility", *Phys. Rev. Lett.*, 2020, DOI: 10.1103/PhysRevLett.125.177701

9:30 AM BREAK

10:00 AM *EL07.07.05

MoS₂ Transistors with Sub-10nm Channel LengthXuZhang; Carnegie Mellon University, United States

As the lateral dimensions of silicon based transistors scale down, their vertical dimensions, i.e. semiconductor body thickness and dielectric thickness, have to be simultaneously shrunk to maintain a tight electrostatic control over the channel and avoid short channel effects (SCE). However, as silicon thickness is scaled down to sub-3 nm, its unavoidable surface dangling bonds will strongly scatter with charge carriers and dramatically degrade its carrier mobility. The atomically thin body thickness of two-dimensional (2D) semiconductors, especially 2D transition metal dichalcogenides (TMDs), makes it ideal to scale while maintaining a tight gate electrostatic control over channel. In this talk, we will share our recent results on the scalable fabrication of MoS₂ electronics devices with sub-10-nm channel length. A combined experimental and theoretical investigation was done to systematically study their short channel effects and performance limits.

10:30 AM EL07.07.06

Transport and Electron-Phonon Coupling of 2D Electrons in Layered ElectridesVahidAskarpour and JesseMaassen; Dalhousie University, Canada

Layered electrides are ionic solids comprised of weakly-interacting atomic layers in which the conducting 2D electrons are confined to the interstitial region between the atomic planes, or on their surfaces when exfoliated to form 2D electrides. Because the conducting electrons are physically separated from the lattice, layered electrides display high conductivity, low electron-phonon (el-ph) coupling, and low work function. As a result, they are promising material candidates for applications in transparent conductors, electron emitters, ohmic contacts to 2D semiconductors, and interconnects.

In this talk, we present our first-principles study exploring the transport and electron-phonon scattering characteristics of seven layered electrides of the form M₂X, where M is an alkaline earth metal (M = Ca, Sr, Ba) and X is a pnictogen (X = N, P, As, Sb). Our density functional theory calculations reveal that Sr₂N and Ca₂N have the lowest electrical resistivity and el-ph scattering rates among this group of electrides. To better understand what controls these properties, we analyze and compare their scattering phase space, average el-ph coupling, distribution of modes, average velocity, and mean-free-path for backscattering. Interestingly, while Ca₂N shows some of the lowest el-ph collision rates, resulting from its small scattering phase space, it has the largest el-ph interaction strength. Repeating these calculations for the metals Al, Au, and Cu reveals that their el-ph coupling can be an order of magnitude greater than the electrides. The decoupling of the conducting 2D electrons from the lattice in layered electrides, leading to weak el-ph interaction, suggests that these materials may be promising interconnects in nanoelectronic circuits.

10:45 AM EL07.07.07

Monte Carlo Simulation of Joule Heating in Monolayer MoS₂ DevicesMarithaA. Wang and EricPop; Stanford University, United States

Two-dimensional (2D) transition metal dichalcogenides (TMDs) like monolayer MoS₂ have emerged as promising semiconductors for nanoscale transistors and electronics due to their good charge mobilities at small thicknesses compared to ultrathin silicon [1]. However, to engineer high-performance 2D transistors, a detailed understanding of charge scattering and heat generation in TMDs is needed. When electrical current passes through a transistor, heat is generated due to electron-phonon scattering, an effect known as Joule heating. This effect occurs even in nanoscale transistors, where charge transport is partially ballistic [2]. Joule heating leads to increased phonon occupation, causing additional electron-phonon scattering, and thus a degradation of electrical transport; it also causes reliability concerns [2].

Here, we employ Monte Carlo simulations to investigate charge transport in monolayer MoS₂ transistors with Joule heating, inspired by earlier approaches with silicon [3]. We consider intravalley and intervalley electron-phonon scattering using the deformation potentials from [4]. To incorporate Joule heating, we consider the back-gated transistors frequently used in experimental transport studies on 2D semiconductors. The thermal resistance R_{th} of such a device is estimated as the sum of 1) the thermal boundary resistance of the MoS₂-SiO₂ interface, 2) the thermal resistance of the underlying oxide (SiO₂), and 3) the thermal resistance of the back-gate (Si) [5]. Such a thermal model can be easily modified to include heat loss through a top-gate or gate-all-around geometry for more general device structures [6].

The Monte Carlo approach is advantageous because it provides rich details on the contributions of different phonon modes to heating. With this approach, we simulate electron drift along the MoS₂ channel as the transistor heats up due to Joule heating. At steady-state, the average temperature rise is $\Delta T = PR_{th}$, where P is the power generated in the MoS₂ channel. This P is computed by summing the heat generated from electron-phonon scattering events and agrees with the expected $P = IV$, where I is the current and V is the potential across the channel. At 300 K ambient temperature, carrier density of 10^{13} cm⁻², and lateral electric fields in the velocity saturation regime (~4-5 V/μm), our simulations show that Joule heating leads to a transistor temperature rise of $\Delta T \approx 200$ -250 K during steady-state operation. This heating decreases the electron saturation velocity by >50% compared to when heating is not considered, indicating that high-field measurements of transistor operation must consider self-heating during analysis [7].

Overall, this work highlights the important consequences of Joule heating on charge transport in monolayer MoS₂ transistors. These simulations can further be extended to other TMDs and transient (i.e. digital) operation to identify design parameters for high-performance TMD devices that minimize Joule heating. This work was in part supported by the NSF Graduate Research Fellowship and Shoucheng Zhang Fellowship (M.A.W.) and by the SRC ASCENT JUMP Center (E.P.).

[1] C. English, et al., *Nano Lett.* **16**, 3824-3830 (2016).

- [2] E. Pop, et al., *Proc. IEEE*, **94**, 1587 (2006).
 [3] E. Pop, et al., *Appl. Phys. Lett.* **86**, 082101 (2005).
 [4] X. Li, et al., *Phys. Rev. B* **87**, 115418 (2013).
 [5] E. Yalon, et al., *Nano Lett.* **17**, 3429-3433 (2017).
 [6] A. Daus, et al., *Nat. Electron.* **4**, 495-501 (2021).
 [7] K. Smithe, et al., *Nano Lett.* **18**, 4616-4522 (2018).

11:00 AM EL07.07.08

Intact Electrical Contact to Air-Sensitive Atomically Thin Semiconductors and Their Optoelectronic ApplicationsHaeYeonLee, ZhiyingWang, YangLiu and JamesHone; Columbia University, United States

Two-dimensional semiconductors have been extensively explored with remarkable potential for applications in electronics and optoelectronics, however, high contact resistance and disorders in the monolayer still constrain harnessing their novel optoelectronic properties. There have been a lot of efforts to overcome these challenges such as using semimetal or low temperature metal deposition. Unfortunately, these approaches are not applicable for air-sensitive materials such as MoTe₂ or NbSe₂, as they require exposing the materials to deposit metal on top. Therefore, degradation is unavoidable unless the materials are completely encapsulated throughout the entire fabrication process. In the monolayer limit, this degradation issue becomes more critical. While the introduction of a protection layer between metal and the monolayer can prevent exposure of the monolayer to the air, it can inadvertently impede charge transfer, resulting in deteriorated performance.

Here, we present a novel technique that enables intact electrical contact to air-sensitive monolayer semiconductors while simultaneously achieving high performance by tackling both two issues. Our approach involves the perfect sealing of the air-sensitive monolayer MoTe₂ throughout the process by fluorinated graphene layer. At the same time, fluorine atoms improve the charge transmission between metal and MoTe₂ by reducing the interatomic spacing. As a result, monolayer MoTe₂ field effect transistor exhibits more than two orders of magnitude improvement in contact performance with excellent ambipolar behavior. By taking advantage of low contact resistance, intrinsic electrical properties of monolayer MoTe₂ are comprehensively elucidated. Furthermore, efficient charge transfer of both electrons and holes enables fabricating lateral p-n homojunction. The small band gap (1.1 eV) of monolayer MoTe₂ coupled with its compatibility with silicon holds promising potential for optoelectronic application including photodetector. Moreover, the electrical contact technique introduced in this study can be extended to other air sensitive materials, broadening its applicability.

11:15 AM EL07.07.09

Heat Dissipation in 2D Material Transistors: The Role of Interfaces and ContactsCagilKoroglu, Alexander J.Gabourie and EricPop; Stanford University, United States

While promising candidates for next-generation transistors, two-dimensional (2D) semiconductors like MoS₂ suffer from unique challenges due to the van der Waals gaps at their interfaces. These have made it difficult to achieve good electrical contacts, and they also result in relatively high thermal boundary resistances (TBR) to adjacent materials [1, 2]. In much the same way the electrical contact resistance is a key limiter of performance for nanoscale 2D transistors, the TBR is a major bottleneck for the cooling of these devices [2]. Coupled with their atomically thin channel which has limited capability of in-plane heat transport, this results in elevated temperatures during operation, reducing mobility [3] and posing thermal degradation and reliability concerns [4].

Here, we present fast analytical thermal models for common 2D transistors, carefully taking into account their thermally-resistive interfaces, contact geometry and other non-idealities. We first develop a steady-state thermal model for simple back-gated transistors, which quantifies the device temperature for a given power input. This model elucidates the cooling mechanisms for a wide range of device geometries and material combinations, highlighting in particular the crucial role of the contacts. Notably, scaling down the channel length does not necessarily lead to improved cooling performance as commonly assumed, because metal contacts are not ideal heat sinks for typical 2D material TBR and thermal conductivity values. Next, we extend this work into frequency-dependent models that can estimate the complex-valued device thermal impedance, which characterizes the amplitude and phase of temperature oscillations for sinusoidally-varying power. These models can be used to predict device thermal time constants, as well as to compute the temperature response to arbitrary power pulses, through an inverse Fourier transform. Finally, we generalize our models to top-gate and dual-gate FETs by accounting for the heat transferred to the contacts via the top gate. We validate our models against finite-element method simulations, with a worst-case temperature error of < 18% across typical device geometries and material/interface properties.

Key insights gained from this work include: (1) the thermal resistance of 2D transistors is relatively insensitive to channel length for sub-100 nm devices, which are dominated by their contact thermal resistance, (2) the short-channel transistor thermal resistance is influenced equally by the 2D material TBRs and the in-plane thermal conductivity, while also depending on contact geometry, (3) due to their ultrathin channel, thermal time constants of 2D transistors are often sub-nanosecond, making it difficult to probe intrinsic device performance (i.e. not limited by self-heating) with pulsed electrical measurements, and (4) top gates can lower temperatures by as much as 30% and 50% for wide and narrow (~50 nm width) devices, respectively.

In addition to their utility in guiding transistor design and optimization, predicting temperatures, estimating transient heating and cooling rates, and detailing pathways for heat flow, our fast analytical thermal models for 2D transistors can also be packaged into direct-current (DC), alternating-current (AC) and transient electrical compact models which incorporate self-heating. This work was supported in part by the Stanford SystemX Alliance, by the Semiconductor Research Corporation (SRC) and DARPA JUMP Centers, and by the National Science Foundation (NSF) Engineering Research Center for Power Optimization for Electro-Thermal Systems (POETS).

- [1] E. Yalon, E. Pop et al., *ACS Appl. Mater. Interfaces* **9**, 43013 (2017). [2] A. J. Gabourie, Ç. Köroğlu, E. Pop, *J. Appl. Phys.* **131**, 195103 (2022). [3] C. J. McClellan, E. Pop et al., *ACS Nano* **15**, 1587 (2021). [4] E. Yalon, E. Pop et al., *Nano Lett.* **17**, 3429 (2017).

11:30 AM EL07.07.10

Observing Aharonov-Bohm Oscillations in CVD-Grown, Parallel Graphene Nanoribbons at 4KZitaoTang¹, SiweiChen¹, Cynthia. Osuala¹, Abdus SalamSarkar¹, AronCummings², GregorzHader¹, StefanStrauf¹, ChunleiQu¹ and Eui-HyeokYang^{1,1}; ¹Stevens Institute of Technology, United States; ²Catalan Institute of Nanoscience and Nanotechnology, Spain

The Aharonov-Bohm (AB) effect demonstrates that the orbital wave function of a charged particle picks up a different phase when it moves along two different paths in the presence of an external magnetic field, which is proportional to the magnetic flux of the enclosed area divided by Planck's constant. While the AB effect has been studied in various semiconductors, including GaAs, InP, InAs, AlGaSb, phosphorene, and Bi₂Se₃ [1-3], graphene is an ideal material for studying the AB effect owing to its long coherence length of electrons: The electron coherence length in graphene is stated as 3-5 μm at 260 mK, and 765 nm-1.25 μm at 4 K [4] For this reason, several studies have been conducted on the AB effect in mechanically exfoliated graphene rings at temperatures ranging from 36 mK to 3.5 [5-10]. To date, only ring geometries have been studied to demonstrate the AB effect.

Here, we present the magnetoconductance measurements in parallel graphene nanoribbons (GNRs) for observing AB oscillations. We fabricated chemical vapor deposition (CVD)-grown GNRs and characterized their two-terminal magnetoconductance oscillations at 4 K under out-of-plane external magnetic fields up to +/-5.6T. Incorporating a baseline subtraction of the original conductance data enabled the observation of two-terminal conductance oscillations with a spacing of ΔB_{AB} from 4.14 mT to 6.46 mT, as expected for two GNRs conjoined at the start and the end, with the spacing between the GNRs of 800 nm and the arm width of 200 nm. The fast-Fourier transform (FFT) data showed a broad band of AB oscillation frequencies that constitute the interval of the h/e fundamental mode given by the sample geometry ranging from 155 to 242 1/T, and the interval of the h/2e fundamental mode is from 310 to 484 1/T. This work shows the AB oscillations in the lower mobility, non-suspended monolayer GNRs at a significantly high temperature (4K). We are currently working on modifying and improving the GNR design based on modeling inputs, including fabricating cascaded-parallel GNRs to seek amplifying oscillation signals.

References:

- [1] *Journal of applied physics*, **89** (11), 5815-5875, (2001).
 [2] *Physical Review B*, **74** (11), 115416, (2006).
 [3] *Physical Review B*, **105** (16), 165309, (2022).
 [4] *Science*, **317** (5844), 1530-1533, (2007).
 [5] *Physica Status Solidi (b)*, **246** (11-12), 2756-2759, (2009).
 [6] *Applied Physics Letters*, **100** (20), 203114, (2012).
 [7] *Physical Review B*, **76** (23), 235404, (2007).
 [8] *Solid State Communications*, **152** (15), 1411-1419, (2012).
 [9] *Physical Review B*, **96** (20), 205407, (2017).
 [10] *Physical Review B - Condensed Matter and Materials Physics*, **77** (8), 085413, (2008).

1:30 PM *EL07.08.01**2D Materials Design for Angstrom-Scale Multi-Stack Devices** Hyeon Jin Shin; Samsung Advanced Institute of Technology, Korea (the Republic of)

Due to our life style changes, data created exponentially and continuously increases. To respond to the huge Data created, conventional Si device scaling down for angstrom era, and 3D stacking device and introduction of disruptive device should be considered [1]. However, the process technology and material performance of Si devices are gradually reaching their limits, and the development of new materials, processes and device architectures is required to overcome these limitations. Graphene and 2D Materials have an ultra-thin crystal structure with a stable surface state. For example, among diverse 2D materials, MoS₂ has a great potential in logic transistor because of its high mobility, and no short channel effect [2]. In this talk, we will introduce 2D material and integration designs via interface property control to realize the Angstrom-scale multi-stack device: (i) adhesion/pattern [3], and (ii) Interconnect with a low resistance metal barrier [4] and ultralow dielectric material [5].

[1] M. C. Lemme, et al., “2D materials for future heterogeneous electronics” *Nat. Comm.* 13, 1392, 2022

[2] Y. Liu, H.-J. Shin et al., “Promises and prospects of two-dimensional transistors” *Nature*, 591 (7848), 43-53, 2021

[3] V. L. Nguyen, H.-J. Shin* et al., “Wafer-scale integration of transition metal dichalcogenide field-effect transistors using adhesion lithography” *Nat. Electron.* 5 (12), 2363, 2022

[4] C.-S. Lee, H.-J. Shin* et al., “Fabrication of metal/graphene hybrid interconnect by direct graphene growth and their integration properties” *Adv. Electron. Mater.*, 12 (4), 1700624, 2018

[5] S. Hong, H.-J. Shin* et al., “Ultralow-dielectric-constant amorphous boron nitride” *Nature*, 582 (7813), 511, 2020

2:00 PM EL07.08.02**Significant Device Performance Enhancement of 1L MoS₂ nMOSFETs by Van Der Waals Contact Formation with Sb₂Te₃** Wen Hsin Chang¹, Shogo Hatayama¹, Yuta Saito¹,

Naoya Okada¹, Takahiko Endo², Yasumitsu Miyata² and Toshifumi Irisawa¹; ¹National Institute of Advanced Industrial Science and Technology, Japan; ²Tokyo Metropolitan University, Japan

Recently, Bi semimetal contacts were found to be effective for the suppression of metal-induced gap states (MIGS), the origin of Fermi-level pinning, leading to extremely low contact resistance and enhanced device performance for MoS₂ nMOSFETs.^[1] However, Bi contacts suffer from thermal stability issues owing to its low melting point (~270 °C).^[2] To satisfy the VLSI back-end-of-line (BEOL) thermal compatibility requirement, the survey of a thermal stable contact up to 400 °C, while maintaining semimetal properties is still needed for MoS₂ devices. Therefore, we focused on Sb₂Te₃ as a possible contact candidate for MoS₂ devices, which melting point is higher than 600 °C^[3] and can maintain layered structure at least at 450 °C.^[4,5] Besides, Sb₂Te₃ is a degenerate semiconductor, and the Fermi-level of Sb₂Te₃ usually resides around its valence band maximum, resulting in a semimetallic behavior like that of Bi. Therefore, Sb₂Te₃ has great potential for reducing contact resistance of MoS₂ devices, while maintaining good thermal stability. In this work, ideal van der Waals (vdW) Sb₂Te₃/MoS₂ contacts are achieved by sputtering with low thermal budget annealing at 200 °C. The thermal-induced crystallization of Sb₂Te₃ helps to align Sb₂Te₃ with monolayer (1L) MoS₂ atomically. Significant device performance enhancement of 1L MoS₂ nMOSFETs is found owing to the vdW contact formation. Sb₂Te₃ is a very promising contact candidate for MoS₂ devices for future VLSI electronics and optoelectronics applications.

Acknowledgment: This work is supported by JST-MIRAI (JPMJMI22708192), JST FOREST Program (JPMJFR213X), NICT (05901), and Kakenhi Grant-in-Aid (JP21H05232, JP21H05234, JP22H04957) from the Japan Society for the Promotion of Science (JSPS).

References: [1] P. C. Shen et al., *Nature* **593**, 211 (2021). [2] A. S. Chou et al., *IEDM* 150 (2021). [3] P. Buffat et al., *Phys. Rev. A* **13**, 2287 (1976). [4] W. H. Chang et al., *Adv. Electron. Mater.* 2201091 (2023). [5] Y. Saito et al., *Mater. Sci. Semicond. Process.* **135**, 106079 (2021).

2:15 PM EL07.08.03**Demonstration of Ambipolar Transport in WS₂ via a Heterojunction-Based Charge Transfer Doping** Joonyup Bae¹, Jihyun Kim¹, Young-Hyun You¹ and Dongryul Lee²; ¹Seoul National University, Korea (the Republic of); ²Korea University, Korea (the Republic of)

Although higher device integration density is required, Si-based electronics reached the physical limits of their electrical property. The down-scaling of Si-based devices is restrained by several problems: punch-through, drain-induced barrier lowering, etc. Increment of the surface area-to-volume ratio of semiconductor devices and maintaining robust mechanical and electrical properties are prerequisites for next-generation materials.

To overcome the limitation of Si, atomically thin 2D transition-metal dichalcogenides (TMDs) have gained significant attraction due to their unique mechanical, optical, and electrical properties. TMDs layers are held by the weak van der Waals interaction and can be mechanically exfoliated into thin layers without surface dangling bonds. WS₂ belongs to the group of TMDs, which feature bandgaps that vary depending on the number of layers present (bulk: 1.44 eV, monolayer: 2.13 eV). WS₂ undergoes indirect-to-direct bandgap transitions as its thickness decreases from bulk to monolayer, which is appropriate for optoelectronic device applications. WS₂ possesses electron mobility of ~234 cm²/Vs and hole mobility of ~39 cm²/Vs. Ambipolar transport in WS₂ allows the modulation of both n-type and p-type channel operation under gate voltage. However, the n-dominant property exerted in intrinsic WS₂ results from the sulfur vacancy-induced trap states near the conduction band level.

In this study, a p-doping method for WS₂ is proposed using WSe₂ as a charge transfer layer. Back-gated WS₂ FETs with Ti/Au source and drain electrodes were fabricated, and WSe₂ flakes were dry-transferred onto the WS₂ FET channel. The surface of the WS₂/WSe₂ FET was oxidized by UV-ozone treatment. Previous studies have reported degenerate p-doping of WSe₂ through UV-ozone exposure. The tungsten oxide (WO_x) layer with high electron affinity effectively induces p-type doping in the underlying WS₂/WSe₂ upon oxidation. Ambipolar transport was observed with an on/off ratio of ~10⁸ for the p-branch and ~10⁷ for the n-branch and the hole mobility of 143 cm²/Vs after oxidation. WS₂/WSe₂ FETs with varying WS₂/WSe₂ channel coverage ratios were fabricated to examine the behavior of the formed WO_x on the WSe₂ surface. Electrical characteristics were measured using 3-terminal measurements with back gate modulation. Crystallinity and lattice structures of the oxidized channel layers were analyzed using micro-Raman spectroscopy and high-resolution transmission electron microscopy (HR-TEM), respectively. The current fabrication of Si-based CMOS devices involves multiple processes of thermal annealing and diffusion doping. Ambipolar materials such as WS₂ can be expected to reduce process complexity with a single-channel CMOS device structure. Therefore, the proposed p-doping methods in this study enable the fabrication of complementary metal-oxide semiconductor (CMOS) devices with down-scaled architectures.

2:30 PM BREAK**3:30 PM *EL07.08.04****What Are 2D Materials Good For?** Eric Pop; Stanford University, United States

This talk will present my (biased!) perspective of what two-dimensional (2D) materials could be good for. For example, they could be good for applications where their ultrathin nature gives them distinct advantages, such as flexible electronics [1] or light-weight solar cells [2]. They may not be good where conventional materials work sufficiently well, like transistors thicker than a few nanometers. I will focus on 2D materials for 3D heterogeneous integration of electronics, which presents major advantages for energy-efficient computing [3]. Here, 2D materials could be monolayer transistors with ultralow leakage [4] (due to larger band gaps than silicon), used to access high-density memory [5]. Recent results from our group [6,7] and others [8] have shown monolayer transistors with good performance, which cannot be achieved with sub-nanometer thin conventional semiconductors, and the 2D performance could be further boosted by strain [9]. I will also describe some unconventional applications, using 2D materials as thermal insulators [10], heat spreaders [11], and thermal transistors [12]. These could enable control of heat in “thermal circuits” analogous with electrical circuits. Combined, these studies reveal fundamental limits and some unusual applications of 2D materials, which take advantage of their unique properties.

Refs: [1] A. Daus et al., *Nat. Elec.* 4, 495 (2021). [2] K. Nassiri Nazif, et al., *Nat. Comm.* 12, 7034 (2021). [3] M. Aly et al., *Computer* 48, 24 (2015). [4] C. Bailey et al., *EMC* (2019). [5] A. Khan et al. *Science* 373, 1243 (2021). [6] C. English et al., *IEDM*, Dec 2016. [7] C. McClellan et al. *ACS Nano* 15, 1587 (2021). [8] S. Das et al., *Nat. Elec.* 4, 786 (2021). [9] I. Datye et al., *Nano Lett.* 22, 8052 (2022). [10] S. Vaziri et al., *Science Adv.* 5, eaax1325 (2019). [11] C. Koroglu & E. Pop, *IEEE Elec. Dev. Lett.* 44, 496 (2023). [12] M. Chen et al., *2D Mater.* 8, 035055 (2021).

4:00 PM EL07.08.05**High-Mobility Flexible Transistors with Low-Temperature Solution-Processed Tungsten Dichalcogenides** Tian Carey, Oran Cassidy, Kevin Synnatschke, Eoin Caffrey, James Garcia, Shixin Liu, Harneet Kaur, Adam G. Kelly, Jose Munuera, Cian Gabbett, Domhnall O'Suilleabhain and Jonathan N. Coleman; Trinity College Dublin, Ireland

Solution-processed electronic inks with two-dimensional (2D) materials have the potential to enable the next generation of low-cost printed digital electronics. [1] Here we will present the advances in fabricating printed complementary inverters achieving a voltage gain $|A_v| \approx 0.1$ with liquid phase exfoliated (LPE) flakes and discuss the limitations of the technology. [2] The electrochemical exfoliation of large-aspect-ratio (>100) semiconducting flakes of tungsten diselenide (WSe_2) and tungsten disulfide (WS_2) as well as molybdenum disulfide (MoS_2) will be necessary to create a library of high-mobility solution-processed networks that conform to substrates, remain functional over thousands of bending cycles and can be utilised in complementary solution-processed circuits.

We will present the use of Langmuir-Schaefer coating to achieve highly aligned and conformal flake networks of flakes, with minimal mesoporosity ($\sim 2\text{--}5\%$), at low processing temperatures (120°C) and without acid treatments. [3] Our processing enables the fabrication of state-of-the-art flexible transistors in ambient air, achieving average mobilities $\mu > 10\text{ cm}^2\text{V}^{-1}\text{s}^{-1}$, with a current on/off ratio of $I_{\text{on}}/I_{\text{off}} \approx 10^3 - 10^4$. [3] We will also demonstrate subthreshold slopes as low as 182 mV/dec , essential for maintaining power efficiency and examine the performance of our WSe_2 transistors after 1000 bending cycles at 1% strain. [3] Additionally, we will demonstrate air-stable, low voltage ($<5\text{ V}$) operation of inkjet-printed CMOS with MoS_2 , with a voltage gain above unity $|A_v| \approx 1.4$. [4] The results represent a critical enabling step towards ubiquitous long-term stable, low-cost solution-processed digital integrated circuits. [4]

[1] Torrisi, F. & Carey, T. Graphene, related two-dimensional crystals and hybrid systems for printed and wearable electronics. *Nano Today* **23**, 73-96 (2018).

[2] Carey, T. *et al.* Fully inkjet-printed two-dimensional material field-effect heterojunctions for wearable and textile electronics. *Nature Communications* **8**, 1202 (2017).

[3] Carey, T. *et al.* High-Mobility Flexible Transistors with Low-Temperature Solution-Processed Tungsten Dichalcogenides, *ACS Nano*, **17**, 3, 2912–2922 (2023).

[4] Carey, T. *et al.* Inkjet Printed Circuits with 2D Semiconductor Inks for High-Performance Electronics. *Advanced Electronic Materials* **7**, 2100112 (2021).

4:15 PM EL07.08.06

Bi-MoSe₂ Contacts in the Ultraclean Limit: Closing the Theory Experiment Loop [Zhiying Wang](#)¹, [Yang Liu](#)¹, [Song Liu](#)¹, [Amirali Zangiabadi](#)² and [James Hone](#)¹; ¹Columbia University, United States; ²University at Buffalo, The State University of New York, United States

Achieving robust electrical contacts has emerged as a key challenge to realizing the promise of monolayer two-dimensional (2D) semiconductors, such as semiconducting transition metal dichalcogenides (s-TMDs) in next-generation electronic technologies. While recent work has reported breakthroughs in achieving low contact resistance using defective s-TMDs, there still exists a lack of fundamental understanding of the contact interfaces, especially, the role of defects within the s-TMD and external disorder in achieving the reported low contact resistance is not well understood.

In this work, we study bismuth (Bi) semimetal contacts to monolayer molybdenum diselenide (MoSe_2), utilizing a device platform that combines ultrahigh-purity MoSe_2 , damage- and strain-free interfaces, and encapsulation of the channel within hexagonal boron nitride (hBN). The ultrahigh-purity MoSe_2 crystal is characterized through dedicated STM imaging. Gaps etched in the hBN define the contact regions and stabilize the structure. We characterize the damage-free and strain-free metal-semiconductor junction with atomically sharp interface by cross-sectional STEM imaging. We quantify the contact characteristics using contact-front and contact-end measurements that go beyond the basic transfer length method. These measurements reveal large differences between sheet resistance inside the channel (R_{sh}) and underneath the contacts (R_{sk}), which are assumed to be equal in the standard transfer length method. We employ a charge transfer model to gain further insight into the microscopic mechanism of vertical transport across the van der Waals metal-s-TMDs interface. In deeply scaled contacts, we directly observed a steep increase in end resistance when the contact length downscaled to around 40 nm , in agreement with the experimental and theoretical model derived characteristic length. This integrated approach can be readily expanded to other clean semiconductors to allow better comparison between theory and experiment.

SESSION EL07.09: Poster Session III
Session Chairs: Gabriela Borin Barin and Yuxuan Cosmi Lin
Wednesday Afternoon, November 29, 2023
Hynes, Level 1, Hall A

8:00 PM EL07.09.01

Large-Area, Pulsed Laser Deposition of MoS₂/a-BN Heterostructures for Back-Gate Field Effect Transistors Applications [Andres A. Forero Pico](#), [Jyoti Yadav](#), [Junsen Gao](#) and [Manisha Gupta](#); University of Alberta, Canada

Transition metal dichalcogenides (TMDCs) have emerged as alternative 2D materials for field effect transistor fabrication. Molybdenum disulfide (MoS_2) is a TMDC with semiconducting properties with monolayer (1ML) MoS_2 having a 1.8 eV direct bandgap and multilayer ($>2\text{ML}$) MoS_2 a 1.2 eV indirect bandgap [1]. Sulphur vacancies tend to form on the top sulphur layer which gives MoS_2 a natural n-type doping. However, exposure to ambient oxygen and humidity oxidizes the surface of MoS_2 and, along with increased number of defects from the sulphur vacancies, MoS_2 -based devices can lose performance. Therefore, encapsulation with different materials has been suggested as a solution for improving the device performance [2]. Hexagonal boron nitride (h-BN) is a 2D material with a 6.1 eV band gap [3] which can be utilised as an encapsulation material and also an insulator. The weak basal plane van der Waals forces of h-BN will not modify the surface of MoS_2 and hence improve the device performance.

One of challenges of 2D materials is the lack of scalable and reproducible large area 2D material growth. We propose to utilise pulsed laser deposition (PLD) as an alternative to high-quality, large-area growth of 2D materials capable of depositing uniform, large-area, thin-films with good control of the deposition parameters. High quality MoS_2 thin films can be grown with PLD [4], on the other hand, h-BN is difficult to grow with PLD because it needs temperatures above 1000°C . Therefore, amorphous boron nitride (a-BN) is grown as encapsulation, featuring large dielectric strength and low refractive index [5].

In this work, PLD was used to deposit a-BN thin-films on SiO_2/Si substrates. Subsequently, PLD was used to deposit the $\text{MoS}_2/\text{a-BN}$ heterostructure on $\text{SiO}_2/n^+ \text{Si}$ substrates with optimized deposition parameters for MoS_2 [4] and a-BN, varying the thickness of MoS_2 (1ML, 2ML, 4ML, 10ML, 15 ML). Back-gated field effect transistors (FETs) were fabricated on the $\text{MoS}_2/\text{a-BN}$ heterostructure samples using standard lithography techniques, followed by e-beam evaporation of Ti/Au contacts and rapid thermal annealing to reduce the contact resistance. The $\text{MoS}_2/\text{a-BN}$ back-gated FETs were electrically characterized, resulting in mobilities increasing one order of magnitude when compared to back-gated MoS_2 FETs without encapsulation. The devices can turn on and off, although their leakage current is still significant ($\sim 10^2 - 10^3\text{ nA}$), which can be attributed to the large voltages needed to control the gate ($>50\text{ V}$). Density functional theory (DFT) studies to understand the material interface will also be conducted and the results will be presented. DFT simulations of MoS_2 -based back-to-back Schottky devices will be shown to compare the measured output characteristics with the calculated ones. The effect of h-BN encapsulation on the back-to-back Schottky devices was also calculated.

References

[1] J. Gao, D. Nandi, and M. Gupta, "Density functional theory—projected local density of states—based estimation of Schottky barrier for monolayer MoS_2 ," *J. Appl. Phys.*, vol. 124, no. 1, p. 14502, Jul. 2018.

[2] S. Roy *et al.*, "Structure, Properties and Applications of Two-Dimensional Hexagonal Boron Nitride," *Adv. Mater.*, vol. 33, no. 44, p. 2101589, Nov. 2021.

[3] M. J. Molaei, M. Younas, and M. Rezakazemi, "A Comprehensive Review on Recent Advances in Two-Dimensional (2D) Hexagonal Boron Nitride," *ACS Appl. Electron. Mater.*, vol. 3, no. 12, pp. 5165–5187, Dec. 2021.

[4] D. Gudi, P. Sen, A. A. Forero Pico, D. Nandi, and M. Gupta, "Optimization of growth parameters to obtain epitaxial large area growth of molybdenum disulfide using pulsed laser deposition," *AIP Adv.*, vol. 12, no. 6, p. 065027, 2022.

[5] S. Hong *et al.*, "Ultralow-dielectric-constant amorphous boron nitride," *Nature*, vol. 582, no. 7813, pp. 511–514, 2020.

8:00 PM EL07.09.02

A Study of Transport and Optical Properties of Liquid Nitrogen-Assisted Deposition of Titanium Oxynitride Thin Films [Abiodun Odusanya](#), [Dhananjay Kumar](#) and [Valentin Craciun](#); North Carolina A&T State University, United States

This study presents a method to prevent an undesirable oxygenation process that occurs during the deposition of Ti-N thin films using the pulsed laser deposition technique. Nitrogen gas at various pressures from 0 mTorr to 50 mTorr was utilized during deposition and the oxygenation process occurred because of the presence of residual oxygen in the deposition chamber or oxygen impurities in the N_2 gas used during the film deposition. The method involves using a metal trap kept at liquid nitrogen temperature to condense the residual/impurity oxygen, which helps control the oxygenation process and results in desired transport and optical properties of the Ti-N-O thin films. The optical, electrical, and stoichiometric properties of the films depend on their N/O ratio. Direct band gap transition was observed in the material, and we also take note of other important properties like stacking faults, texture coefficient, Urbach energy,

dielectric constants, optical conductivity, refractive index, extinction coefficient, and skin depth. The x-ray diffraction measurements show a reduction in the intensity and shift of the (111) and (222) TiNO peaks to higher angles with increasing nitrogen pressure during growth. The study also found that increasing the deposition N₂ pressure of the TiNO thin films resulted in increased metallicity of the films as indicated by the reduction in bandgap from 2.64 eV to 1.70 eV, however, an increase in resistivity from 133 μΩcm to 3177 μΩcm was observed due to increase in surface scattering induced by increase in dislocation density.

This work was supported by the National Science Foundation, NSF-PREM through MRSEC [grant No. DMR-2122067].

8:00 PM EL07.09.03

High-Performance Electromechanical Power Generation of Lithography-Free Large-Scale MoS₂ Monolayer Film HarvestersYe SeulJung, Ji YeonKim and Yong SooCho; Department of Materials Science and Engineering, Yonsei University, Korea (the Republic of)

Recently, two-dimensional (2D) transition metal dichalcogenide (TMD) materials have been recognized to possess high piezoelectricity due to the lack of inversion symmetry. Because of the limited availability of large-area MoS₂ monolayer, however, the energy-harvesting performance of 2D TMD materials has not been fully understood. Only single-crystalline TMD with dimensions on the order of a few micrometers has been investigated as an electromechanical energy harvesting device so far. Here, we introduce a defect-controlled synthesis of centimeter-scale polycrystalline MoS₂ monolayers with the assistance of a Na₂S film. Beyond the known effect of Na as a growth promoter, extra sulfur supplied by the Na₂S critically passivates sulfur vacancies, enabling the preparation of a high-quality monolayer film. As a result, a millimeter-scale energy harvester with nonconventional interdigitated electrodes, which was fabricated without e-beam lithography, exhibited the unexpectedly high piezoelectric energy harvesting performance of ~402.9 mV output voltage and ~41.2 nA output current under a bending strain of ~0.47 %. These values are ~20 and ~1,370 times greater, respectively, than the reported best values for single-crystal 2D TMD materials.

8:00 PM EL07.09.04

Carrier Transport Comparison Between Inkjet Printed and Filtrated Ti₃C₂Tx-Ti₃AlC₂ Nanosheet Thin FilmsMi-JinJin; Institute for Basic Science, Korea (the Republic of)

Magnetoconductance studies of thin-film MXenes are important to understanding their electronic transport properties and charge carrier dynamics, and also to appraise their potential for spintronics applications. Also, it is desirable to develop deposition strategies such as inkjet-printing, filtration that would enable direct patterning with complex structures/networks. Here, we investigate the extrinsic negative magnetoconductance of inkjet printed and simply filtrated Ti₃C₂Tx-Ti₃AlC₂ nanosheet thin film. Functional process such as inkjet-printing and filtration have strong advantage of direct patterning for thin film devices. Importantly, we report a crossover from weak anti-localization (WAL) to weak localization (WL) near 3 K for both thin-film systems. Comparably, they show strong scale dependence depends on process. The crossover from WAL to WL is consistent with strong, extrinsic, spin-orbit coupling. From the magnetoconductance analysis, we estimate that the printed MXene thin-film has a strong spin orbit coupling field. Our results and analyses offer detailed understanding into microscopic charge carrier transport in Ti₃C₂Tx dominant, and Ti₃C₂Tx-Ti₃AlC₂ thin films and shows strong importance of process engineering.

8:00 PM EL07.09.05

Macroporous Nb₂O₅ as a Binder-Free Anode for Hybrid SupercapacitorSeungUkCheon, JaewooLee and SungOhCho; Korea Advanced Institute of Science and Technology, Korea (the Republic of)

The Li-ion hybrid capacitor (LHC) is an electrochemical energy-storage device that bridges the gap between lithium-ion batteries (LIBs) and supercapacitors (SC). It combines a battery-like anode and a capacitive cathode to achieve substantial energy and power densities. The anode provides high specific capacity, while the cathode delivers high power density, making the LHC suitable for high-performance electrochemical energy storage applications that require both high energy and power densities.

However, the sluggish reaction kinetics of the battery-like anode during the Li-ion intercalation/deintercalation process, compared to the non-faradaic adsorption/desorption process of the cathode, necessitates a Li-insertion type electrode with fast ion diffusion to minimize the kinetic gap between the two electrodes in LHCs. Among the investigated anode materials like TiO₂, Li₄Ti₅O₁₂, MnO₂, and Nb₂O₅, Nb₂O₅ shows particular promise due to its favorable kinetics of intercalation reaction, unaffected by Li-ion solid-state diffusion limitations. Consequently, Nb₂O₅ exhibits rapid Li-ion intercalation, pseudocapacitive behavior, and fast reversible electrochemical kinetics.

Previous approaches to create Nb₂O₅-based electrodes involved blending active Nb₂O₅ materials with a binder and conductive carbon black, applied to a current collector. However, the use of an insulating binder led to decreased energy/power densities due to the larger proportion of binder and carbon black. To construct a superior Li-ion hybrid supercapacitor (Li-HSC) with higher volumetric energy and power densities, researchers prefer a binder-free and freestanding Nb₂O₅-based film electrode, where all materials contribute to charge storage. In this study, an anodization technique was employed to fabricate a binder-free Nb₂O₅ electrode by directly generating a Nb₂O₅ oxide layer on a niobium metal substrate, controlling its nanostructure and thickness through adjustments in electrolyte, duration, voltage, and temperature.

The resulting oxide produced by anodization exhibits an amorphous state, offering superior characteristics compared to crystalline structures. The amorphous oxide demonstrates enhanced lithium ion mobility and higher capacity due to defects and vacancies. The primary objective of this research was to enhance electrochemical performance by creating a binder-free electrode utilizing amorphous Nb₂O₅ with a controlled nanostructure achieved through anodization.

The anodized samples were examined using Scanning Electron Microscope (SEM) and Focused Ion Beam (FIB) techniques to verify the formation of a macro-porous structure and measure the oxide layer's thickness. Electrochemical analysis, specifically cyclic voltammetry (CV) measurements, revealed a pore size of 87.1 nm and an oxide layer thickness of 11.0 μm, indicating rapid reaction kinetics. The sample exhibited the highest specific capacitance value of 469.9 F/g, confirming its superior performance compared to other electrode configurations.

Additionally, annealing was performed to compare the amorphous and crystalline states. X-ray Diffractometer (XRD) analysis confirmed the formation of Orthorhombic-Nb₂O₅ (T-Nb₂O₅) after annealing. CV measurements and rate capability tests were conducted, revealing that amorphous Nb₂O₅ displayed faster reaction kinetics compared to T-Nb₂O₅. At a C-rate of 0.5 C, amorphous Nb₂O₅ demonstrated a capacity of approximately 310 mAh/g, while at a C-rate of 20 C, it maintained a capacity of 260 mAh/g, exhibiting better capacity retention than T-Nb₂O₅. Moreover, compared to previously developed Nb₂O₅, the amorphous Nb₂O₅ electrode exhibited higher capacity and improved capacity retention.

8:00 PM EL07.09.06

An Investigation of Lithium and Cobalt Intercalation Method in 2D Transition Metal DichalcogenidesYonghaShin and WoojongYu; Sungkyunkwan University, United States

In recent studies, it has been confirmed that 2D van der Waals (vdW) materials, including magnetic elements such as CrI₃, Fe₃GeTe₂, Cr₂Ge₂Te₆, VS₂, and VSe₂, exhibit long-range ferromagnetic order. In addition, the previous studies have explored improving electrical properties by injecting magnetic dopants into 2D transition metal dichalcogenide (TMD) materials with semiconductor properties or chalcogen defects. However, the intercalation method of inserting a magnetic element between the van der Waals planes of 2D TMDs has rarely been explored.

This study proposes implementing ferromagnetism by inserting Cobalt (Co) between layers of Molybdenum ditelluride (MoTe₂) using a wet chemical method that sequentially proceeds with Li intercalation and Co intercalation. n-Butyllithium diluted in hexane is widely used as a reagent for Li intercalated complexes because Li has a small atomic radius, high reactivity, and can react at room temperature. 2D TMD materials can exist in a 2H (semiconducting) or 1T' (metallic) phase. MoTe₂ typically exists in a 2H phase under atmospheric conditions and has the lowest equilibrium energy difference between 2H-1T' among TMD materials. Pristine 2H-MoTe₂ undergoes a phase transition to 1T'-MoTe₂ by Li intercalation for 48 hours. This phase transition is confirmed by the 1T' peak observed in the Raman spectrum and the change in gap distance from 6.97 to 6.95 Å measured by X-ray diffraction (XRD) analysis.

Li-intercalated 1T'-MoTe₂ induces ionic exchange during secondary Co intercalation due to its strong reducing ability, effectively allowing zero-valent Co to settle within the vdW gap instead of Li ion. Dicobalt octacarbonyl, Co₂(CO)₈, is used as a precursor to provide Co.

8:00 PM EL07.09.07

Effect of Hot-Wire Oxidization and Sulfur Annealing on Layered p-MoS₂ for TFT ApplicationKousakuShimizu; Nihon University, Japan

High-quality p-type Thin Film Transistors have drawn considerable attention for switching elements in active matrix displays such as OLEDs and LCDs. We are investigating sputtered amorphous p-MoS₂ thin films for one of the good candidates. Hot-wire oxidation and sulfur annealing have been done to improve TFT performances. Raman spectroscopy and XPS were employed to characterize the film structure and compared with Id-Vg characteristics.

The sputtered amorphous MoS₂ is generally p-type [1], and the film consists of a stack of small two-dimensional MoS₂ pieces. To reduce the valence mismatch between metals and MoS₂, Cr/Cu double-layered electrode was employed. According to the TFT simulations, ATLAS, the mobility of TFT with Cr/Cu source-drain electrodes was the highest performance, around 9.95 cm²/Vs. After annealing at 200°C for one hour in air, it increased by 51.42 cm²/Vs. It has found that the sputtered film had many sulfur defects according to the TFT simulation and XPS study. To compensate for the defects, we have tried oxidation by the How-Wire method. As a result, the mobility increased to 62.73 cm²/Vs. The effect of oxygen introduction has been investigated by first-principles calculations [2]. Furthermore, it was found that the sulfur defects exist between the layers must be reduced in order to reduce the off-current. It was annealed at 200°C for 1 hour in a metal-sealed container containing S powder. We have succeeded in suppressing the off-current less than 10⁻¹⁰ A.

[1] Adam T. Neal, Ruth Pachter, and Shin Mou, Appl. Phys. Lett. 110, 193103 2017,

8:00 PM EL07.09.08

Photoelectrochemical Polymerization (PEP) of EDOT for Formation of Pattered PEDOT at Specific Arbitrary Regions on Hematite (α -Fe₂O₃) MisolHwang, TaeyoonKim and JoohoonKim; Kyung Hee University, Korea (the Republic of)

We performed photoelectrochemical polymerization (PEP) on hematite (α -Fe₂O₃) to synthesize PEDOT (poly(3,4-ethylenedioxythiophene)) in specific arbitrary regions with a high 2D flexibility. PEDOT is a conductive polymer that is highly attractive due to its ability to enhance conductivity and stability of electrical activity when used as crosslinkers or fillers. Hematite, as a semiconductor material with a bandgap of 1.9-2.2 eV, generates minority charge carriers (holes) with a short diffusion length when exposed to visible light. We confirmed the synthesis of PEDOT on hematite using cyclic voltammetry, which exhibited similar characteristics to PEDOT synthesized on Pt and ITO electrodes. Furthermore, we demonstrated the synthesis of PEDOT at lower voltages via PEP compared to voltages in the absence of light illumination. Additionally, by applying the appropriate voltage and utilizing a digital mirror device (DMD) to expose patterned light at specific arbitrary regions, we generated patterned PEDOT at the regions with a high 2D flexibility. We expect that these results can be utilized to enhance sensitivity and improve the fine-tuned functionalities of various semiconductor-based devices, including solar cells, supercapacitors, and biosensors.

8:00 PM EL07.09.09

Spatially Resolved and *In Situ* Electrochemical Imaging on Two-Dimensional Materials using Scanning ElectroChemical Cell Microscopy (SECCM) LuYang-Sheng¹, YuChun-Hung², ChengYu-Chieh³, ChenChun-Wei² and LiShao-Sian¹; ¹Institute of Materials Science and Engineering, National Taipei University of Technology, Taiwan, Taiwan; ²Department of Materials Science and Engineering, National Taiwan University, Taiwan, Taiwan; ³Department of Electro-Optical Engineering, Taipei Tech, Taiwan

In recent years scientists have used microelectrode technology to probe the electrochemical properties of a surface of interest through position feedback, allowing direct topographic and electrochemical imaging. It is especially important to determine the topological information correlated to the electrochemical activity of atomically thin 2D materials. Many researches have revealed that two-dimensional materials possess a promising potential for electrochemical catalytic reactions, such as Hydrogen Evolution Reaction (HER), Oxygen Evolution Reaction (OER), Carbon Dioxide Reduction (CO₂RR), Nitrogen Reduction Reaction (NRR), Iodide oxidation reaction (IOR). However, the topological correlation with electrochemical reactivity is relatively less reported due to a lack of high spatial resolution electrochemical measurement techniques. In this work, an advanced scanning electrochemical cell microscope (SECCM) is used to probe the microscale electrochemical reactivity of 2D materials for HER. With minuscule electrolyte droplets and surface feedback signals to adjust the surface-to-probe height, a highly spatial resolved topological correlation with electrochemical reactivity for 2D materials is revealed.

We have previously used SECCM to evaluate the activity of MoS₂, identifying the HER activity differences between edge areas and basal areas. Besides the defect related active sites, some processes were also applied to manipulate the surface properties of 2D materials for enhanced reactivity, such as light modulation, strain, or surface polarization. The morphological and topological properties that correlated to the water splitting performance of 2D materials were visually revealed through the measurements of Kelvin probe (KPFM), piezo response force microscopy (PFM), and SECCM. This work fills the gap between electrocatalytic HER and topological properties of 2D materials, and provides a microscopic understanding to further improve water splitting performance for clean energy.

8:00 PM EL07.09.10

Nanowire-Based Sensor Platform for Breath Analysis MariosConstantinou, SotiriosChristodoulou, AgapiosAgapiou and ChrysafisAndreou; University of Cyprus, Cyprus

Nanomaterials, such as nanowires (NWs), are enabling new directions in nanotechnology with significant applications in the biomedical sector. With the use of Surface-Enhanced Raman Spectroscopy (SERS) as an analytical technique for rapid biomarker identification, nanomaterials can play a pivotal role in shaping the next generation of non-invasive, rapid, and pain-free diagnostic devices. Potential applications include breath analysis for cancer screening.

SERS is an ultrasensitive vibrational spectroscopic technique used as a tool to detect volatile organic compounds (VOCs) near the surface of plasmonic metal nanoparticles with sharp features ('hot spots'). Conventional bottom-up approaches for sensing applications are based on the self-assembly of nanoparticles, which offers a simplistic, quick, and low-cost SERS substrate preparation. However, this approach demonstrates low reproducibility, hampering the sensor's performance. Top-down approaches use micro- and nanofabrication techniques with better uniformity and reproducibility, but with higher manufacturing costs.

We present a hybrid approach using NWs as the backbone of the SERS sensor – decorated with nanoparticles (NPs) – acting as 3D 'hot-spot' network for maximizing the available SERS-active surface of the device while achieving signal reliability and reproducibility.

We employed this new architecture for SERS-based gas sensing. The NWs are derived from fast and cost-effective solution processing, and form higher-order structures via dielectrophoresis (DEP)-based self-assembly. DEP offers unique features, including NW alignment on predefined locations, preferential orientation, and most importantly, controllable deposition and NW densities for precise 'hot-spot' distribution. The self-assembly technique will be discussed and compared to conventional SERS-sensor approaches. Our solution-based technique for the rapid gold (Au) nanoparticle decoration of the 1D titanium oxide (TiO₂) NWs will be described. This novel architecture further increases the overall 'hot-spot' availability, and combines strong SERS signal amplification with increased sample capture, allowing the detection of analytes at low concentrations.

The performance of the developed sensor was assessed by investigating the SERS signal of 4-aminothiophenol (4-ATP) in gas phase, at concentrations as low as 10 parts-per-billion (ppbv), and in liquid phase down to 24 picomolar (pM). Additionally, the SERS signals successfully separated - using the principal components analysis (PCA) – samples of exhaled breath from healthy volunteers. These findings demonstrate the applicability and potential of 1D nanomaterials in conjunction with state-of-the-art solution-processed techniques for the development of breath analysis platforms for cancer screening.

The developed non-invasive NW-based breath sensor platform can provide mobile, low-cost, miniaturized, and rapid breath analysis, making it suitable for clinical deployment. The sensor is suitable for real-time point-of-care (PoC) diagnosis and can significantly improve the understanding of the complex relationship between the exhaled VOC profile and disease, and lead the way to a new clinical breath-based diagnostic tests.

8:00 PM EL07.09.11

Sensitive Microwave Spectroscopy of Van der Waals Materials with Coplanar Waveguides VincentStrenzke, ChristianElsässer, IsabellGrandt-Ionita, JanStelzner, LarsTiemann and RobertBlick; Universität Hamburg, Germany

Strongly correlated states in graphene and transition metal dichalcogenides give rise to electrically tunable insulating, metallic and superconducting phases, making them of great interest for fundamental research and potential applications. Probing the electronic structure of such correlated systems is essential to understand their phase transitions and isospin order. Microwave spectroscopy has proven to be a powerful technique for resolving low energy gaps and studying spin interactions in large area graphene. However, implementing exfoliated van der Waals (vdW) materials into sensitive microwave measurements presents several technological challenges, including optimizing contact resistances, impedance matching, and the small area of exfoliated flakes. Microstructured transmission lines called coplanar waveguides (CPW) allow to efficiently couple microwaves to a two-dimensional material that rests nearby. Graphene Josephson junctions embedded in such a planar microwave circuit are commonly used as microwave bolometer devices, enabling detection of microwaves at the single-photon level due to graphene's broadband absorption and low heat capacity.

Generally, CPWs have to be designed and optimized for a specific purpose to minimize the attenuation (losses) in the desired frequency range. Here, we discuss design choices of CPWs that are optimized for sensitive microwave spectroscopy in two-dimensional vdW materials. We highlight different approaches and their associated technological challenges in coupling microwaves to vdW materials via CPWs. Simulations and fabrication approaches are presented along with the characterization of the finalized CPW. Our designs can be applied in various applications ranging from the investigation of strongly correlated phases and isospin physics in vdW materials using microwave spectroscopy to bolometric applications.

8:00 PM EL07.09.12

Ultrasensitive PFAS Detection using Amplifying Fluorescent Polymers AlbertoConcellón, JesusCastro Esteban and TimothyM. Swager; MIT, Department of Chemistry, United States

Per- and poly(fluoroalkyl) substances (PFAS) are environmentally persistent pollutants that are of growing concern due to their detrimental effects at ultratrace concentrations (ng/L) in human and environmental health. Suitable technologies for on-site ultratrace detection of PFAS do not exist and current methods require complex and specialized equipment, making the monitoring of PFAS in distributed water infrastructures extremely challenging.

Herein, we describe amplifying fluorescent polymers (AFPs) that can selectively detect perfluorooctanoic acid (PFOA) and perfluorooctane sulfonate (PFOS) at concentrations of ng/L. The AFPs are highly fluorinated and have poly(*p*-phenylene ethynylene) and polyfluorene backbones bearing pyridine-based selectors that react with acidic PFAS via a proton-transfer reaction. The fluorinated regions within the polymers partition PFAS into polymers, whereas the protonated pyridine units create lower-energy traps for the excitons, and emission from these pyridinium sites results in red-shifting of the fluorescence spectra. The AFPs are evaluated in thin-film and nanoparticle forms and can selectively detect PFAS concentrations of ~1 ppb and ~100 ppt, respectively. Both polymer films and nanoparticles are not affected by the type of water, and similar responses to PFAS were found in milliQ water, DI water, and well water. These results demonstrate a promising sensing approach for on-site detection of aqueous PFAS in the ng/L range.

8:00 PM EL07.09.13**Radiation Synthesis of Multimetallic Nanoparticles on 1-D Metal Oxide Nanotubes via Carbothermal Shock of Carbon Nanofibers for Highly Sensitive Acetone Gas Sensors** JaehyunKo and Il-DooKim; Korea Advanced Institute of Science and Technology, Korea (the Republic of)

Multi-metallic nanoparticles (MMNPs) have generated significant interest in various fields such as catalysis, bioimaging, and gas sensors due to their improved catalytic performance. Therefore, it is crucial to develop an efficient, cost-effective, and straightforward synthesis method for MMNPs, as the synthetic approach directly affects their applicability, stability, and performance. Traditional methods often involve intricate and expensive experimental procedures. Among the various approaches to synthesizing MMNPs, the carbothermal shock (CTS) synthesis has gained attention for its simple yet sophisticated mechanism. However, the CTS synthesis has a limitation, as it requires oxygenated, conductive carbon as a supporting material. To broaden the range of suitable substrates, we propose a novel and uncomplicated method that utilizes carbon support solely as a heat generator for the direct synthesis of MMNPs on SnO₂ nanotubes. The experimental procedure involves synthesizing SnO₂ nanotubes using the conventional electrospinning method, followed by loading Pt, Pd, and Ni precursors onto the synthesized SnO₂ nanotubes through immersion of SnO₂ powders in Pt, Pd, and Ni precursor solutions. The precursor-loaded SnO₂ nanotubes are then covered with a carbon nanofiber (CNF) film, and electrically-triggered Joule heating of the CNF film in a vacuum induces carbothermal shock. The successful deposition of Pt, Pd mono-metallic, PdPt, PtNi bi-metallic, and PdPtNi tri-metallic nanoparticles on SnO₂ nanotubes has been demonstrated using double Cs-corrected transmission electron microscopy and energy dispersive X-ray analysis. The nanoparticle synthesis mechanism has been investigated using various analytical techniques. The MMNP-decorated SnO₂ nanotubes exhibit highly sensitive gas sensing performance, indicating the feasibility and potential of this research. This work expands the applicability of the conventional CTS synthesis method and enables the straightforward decoration of different combinations of MMNPs onto various non-carbon supports, including semiconducting metal oxide substrates.

8:00 PM EL07.09.14**Direct Writing of Nanowires: New Opportunities to Study Shape- and Morphology-Dependent Effects** SvenBarth, FabrizioPorrati, FelixJungwirth and MichaelHuth; Goethe University Frankfurt, Germany

The fabrication of free-shaped 3D objects with very high accuracy using focused electron beam and focused ion beam-induced deposition (FEBID and FIBID) has been demonstrated in recent years.[1] For instance, we demonstrate the formation of free-form ferromagnetic 3D nanostructures and nanowires that can be used as functional devices and at the same time can emulate different morphologies in terms of magnetic properties.[2] Moreover, the direct writing also enables the growth of core-shell heterostructures by combination of 3D-nanowire FEBID scaffolds and the successive site-selective chemical vapor deposition (CVD). In particular, conductive 3D nanowire-based bridges are printed by FEBID and used as resistors allowing deposition induced by Joule heating. This hybrid-approach allows tailoring the cross section, shape and material combination for specific purposes. The applicability of the nano-CVD onto FEBID-nanowires has been demonstrated for two material systems of specific physical properties.[3] The fabrication of complex 3D core-shell heterostructures promises to add new functionalities by combining free-shaped 3D nanostructure writing with thin film deposition of different functional materials.

References:

- [1] *J. Appl. Phys.* **2021**, *130*, 170901.
 [2] *Nature Communications*, submitted.
 [3] *ACS Nano* **2023**, *17*, 4704–4715.

8:00 PM EL07.09.15**Tuning Electromigration Forces on Adsorbates on Low-Dimensional Materials** AnshulSaxena^{1,2} and NarayanaAluru^{1,2}; ¹University of Texas at Austin, United States; ²The University of Texas at Austin, United States

Electromigration, the movement of atoms induced by electrical currents, is a phenomenon of significant importance in various nanoscale applications. This study focuses on analyzing and optimizing electromigration forces on adsorbates, by considering the direct force resulting from the electric field and the electron wind force due to interactions with current-carrying electrons. Recent research has highlighted the influence of energy level alignment of adsorbates with the Fermi level of the current carrying system on the nature of electromigration forces. By altering the electronic structure of current carrying membranes, fine-tuning and optimization of electromigration forces becomes possible, facilitating migration of adsorbates on membrane surfaces. This property finds diverse applications in nanofluidic systems, including mass transport and ionic current generation. Using Density Functional Theory and Non-equilibrium Green's function calculations, we investigate the nature of electromigration forces on adsorbates across a range of low-dimensional systems such as Graphene, MoS₂, MXenes, etc. This study explores the impact of membrane characteristics, including semiconducting, metallic, or insulating properties, on electromigration forces. The results provide valuable insights into the underlying mechanisms and offer guidelines for designing and optimizing nanofluidic systems with tailored electromigration properties.

8:00 PM EL07.09.16**Reveal Atomic Phase Transition via Nanomechanical Resonator** YuluMao, FanFei, MojueZhang, DajunZhang, YangchenHe, Daniela. Rhodes, ChuMa, JiamianHu, JunXiao and YingWang; University of Wisconsin Madison, United States

The diverse interactions between lattice symmetry and layer stacking orders make transition metal dichalcogenides (TMDs) especially potentially effective to detect for investigating novel topological states and quantum phase transitions. A case in point is transition metal dichalcogenides, notable for its diverse phases: hexagonal (2H, α -phase), monoclinic (1T', β -phase), and orthorhombic (Td, γ -phase). The 2H phase exhibits semiconductors behavior while the 1T' phase and Td phase is semimetal. Current approaches to reveal the phase transition between those phases are limited to electrical and optical approaches, in which the contrast is low [1]. For example, the 1T' and Td phases are structurally commensurate[2]-[4], in which the structural difference refers to layer-to-layer stacking orders. In this experimental study, the phase transitions in transition metal dichalcogenides is studied by nanomechanical resonators. Phase transition is clearly revealed by the frequency shift of the resonators. Modeling has been established to qualitatively correlate the frequency of the nanomechanical resonator with the phase change. Accompanied by a high-quality factor exceeding 1000, the high sensitivity of the resonator shows small sliding transition, providing the possibility of the new application degree for 2D resonators combining with materials' phase diagram investigation and the potentiality to extract the thermodynamics information during the phase transition.

- [1] Qi, Y., Naumov, P., Ali, M. et al. Superconductivity in Weyl semimetal candidate MoTe₂. *Nat Commun* **7**, 11038 (2016). <https://doi.org/10.1038/ncomms11>
 [2] H. P. Hughes and R. H. Friend, "Electrical resistivity anomaly in β -MoTe₂ (metallic behaviour)," *J. Phys. C Solid State Phys.*, vol. 11, no. 3, pp. L103–L105, Feb. 1978, doi: 10.1088/0022-3719/11/3/004.
 [3] K. Zhang et al., "Raman signatures of inversion symmetry breaking and structural phase transition in type-II Weyl semimetal MoTe₂," *Nat. Commun.*, vol. 7, no. 1, p. 13552, Dec. 2016, doi: 10.1038/ncomms13552.
 [4] S.-Y. Chen, T. Goldstein, D. Venkataraman, A. Ramasubramaniam, and J. Yan, "Activation of New Raman Modes by Inversion Symmetry Breaking in Type II Weyl Semimetal Candidate T'-MoTe₂," *Nano Lett.*, vol. 16, no. 9, pp. 5852–5860, Sep. 2016, doi: 10.1021/acs.nanolett.6b02666.

8:00 PM EL07.09.17**Investigations of WSe₂/Graphene Heterostructures with Raman Spectroscopy** ArianeMarchese¹, YangLiu², ThiagoSeniuk³, ArieteRighi³, JamesHone¹ and MarcosPimenta³; ¹Columbia University, United States; ²Peking University, China; ³Universidade Federal de Minas Gerais, Brazil

Recent work has highlighted the potential for using tungsten diselenide (WSe₂) to modify the properties of graphene, including spin-orbit coupling (Island et al., 2019), superconductivity (Su et al., 2022), and electron-phonon scattering (Banszerus et al., 2019). Here we study interaction between WSe₂ and graphene using Raman spectroscopy. We observe blue-shifting of the 2D mode of 1.6 cm⁻¹ for heterostructures of graphene and few-layer WSe₂. The shift doubles with top and bottom WSe₂ coverage. The G mode for these measurements remains consistent at 1588 cm⁻¹, indicating the shifts were not due to strain. Further investigations will study the renormalization of the Fermi velocity in these heterostructures.

8:00 PM EL07.09.18**Electrical Behavior of Thin Film Devices Exposed to a Magnetic Field** GuinevereStrack¹, Jin HoKim², AlkimAkyurtlu^{1,1} and RichardM. Osgood²; ¹University of Massachusetts Lowell, United States; ²US Army Combat Capabilities Development Command Soldier Center, United States

The exploration of novel, magnetically controlled thin film devices can enable a range of technologies. For example, we demonstrated that the incorporation of ferromagnetic materials into a diode-type device can enable changes in electrical behavior in the presence of a weak, permanent magnet.[1] The diode, when combined with an antenna array, could serve as a rectification device. Magnetic control of the rectenna was referred to as mem(ory)rectification, which would not increase the electrical burden given that the permanent magnet did not require an external power source. Another application is the generation or storage of code in a series of magnetic thin film devices. An applied magnetic field could write or erase an electrical message that is

stored in the thin film devices. The materials properties of an array of devices could be varied to store a code that could be decrypted or erased via the application of a magnetic field.

Moving forward, the study of the device behavior in a stronger magnetic field in different configurations with respect to the direction of the applied field (in-plane vs. out-of-plane) would enable a better understanding of how the magnetic field influences the average electronic motion through the device. We will use a dipole electromagnet with adjustable pole gap and coil spacing to apply the field, which can be at least 1T, depending on the pole gap spacing. This builds upon our previous work in which the relatively weak magnetic field (~690 Oe) was roughly perpendicular to the film stack and therefore roughly parallel to the electronic transport across the layers. For this MRS presentation, we will measure and understand the transport when the magnetic field lies roughly in the plane of the sample, roughly perpendicular to the electronic flow between layers in the Metal-Insulator-Metal (MIM) diode stack. We will also report the impact of the fabrication techniques on device quality and performance. Dielectric layer (niobium oxide (NbOx)) deposition using atomic layer deposition (ALD) can enable single layer deposition and the deposition of a few layers. Preliminary characterization of the ALD-deposited NbOx using x-ray photon spectroscopy (XPS) revealed that the deposited layer was in the Nb₂O₅ oxidation state, with peaks found at 208.4 eV and atomic percentages of 29% niobium and 71% oxygen.

[1] Strack, G., Kim, J.H., Giardini, S. Akyurtlu, A. and Osgood, R. III Application of a magnetic field to ferromagnetic diodes. *MRS Advances* (2023). <https://doi.org/10.1557/s43580-023-00520-6>

8:00 PM EL07.09.19

One-Dimensional WO₃ Nanorods Loaded by Lead Halide Perovskites Nanocrystals for Ammonia Sensors Stimulated by Visible Light Luis F. da Silva¹, Frank Güell², Ariadne C. Catto¹, Pedro Atienzar³, Rocío García-Aboal³ and Eduard Llobet⁴; ¹Universidade Federal de São Carlos, Brazil; ²Universitat de Barcelona, Spain; ³Universitat Politècnica de València, Spain; ⁴Universitat Rovira i Virgili, Spain

The development in industrial and agricultural activities, mainly in emerging economies, has increased the toxic gases dumped into the atmosphere, such as CO, NO₂, NH₃, etc. Regarding ammonia (NH₃), it is considered a health hazard because it is highly corrosive. The Occupational Safety and Health Administration recommends avoiding exposure to NH₃ levels above 100 ppm (parts per million). Semiconducting metal oxides (SMOx) have been successfully used as a sensing layer to detect toxic gases. Among the SMOx, the WO₃ compound has exhibited excellent sensing performance, however, at operating temperatures above 200°C, which enhances the power consumption of such devices. An alternative way to get sensors working favorably at room temperature has been the photo-stimulation of the sensing element. The presence of photocarriers generated by the irradiation of the SMOx favors the chemisorption processes. The WO₃ pure has been widely used as a sensing layer under photoactivation, however, the fast recombination of charge carriers reduces its sensing activity. Thus, the loading of WO₃ by lead halide perovskites may contribute to improving the sensing performance. Note that these perovskites exhibit interesting properties, mainly the long charge carriers' lifetime. Based on these considerations, we report herein an investigation of the blue-light-assisted gas-sensing properties of 1D-WO₃ nanorods decorated with APbBr₃ (A= MA, FA, and Cs) towards NH₃ gas. The 1D nanorods were synthesized by aerosol chemical vapor deposition while the perovskite nanocrystals were synthesized through the hot injection method. The WO₃/APbBr₃ nanocomposites were prepared via spray coating. HRTEM images revealed that the APbBr₃ nanocrystals had an average size of less than 10 nm, and they were successfully loaded onto the WO₃ nanorods. Regarding the gas-sensing performance, it was found a significant enhancement of the NH₃ sensing response for nanorods loaded by perovskites, especially by FAPbBr₃ nanocrystals. This nanocomposite was sensitive towards different NH₃ levels, i.e., from 10 to 100 ppm under blue-light irradiation and at room temperature. Also, the experiments revealed that loaded nanorods presented total reversibility, good repeatability, and stability after consecutive exposure cycles. These findings demonstrate the potential of 1D WO₃ nanorods loaded by perovskites nanocrystals as sensing material to manufacture NH₃ gas sensor devices operating at room temperature.

8:00 PM EL07.09.20

Unravelling Spin-Manipulated Magneto-Photo-Electrochemical Water Splitting in Janus 2D-Material's Heterostructures Praveen Kumar^{1,2} and Krishnendu Roy¹; ¹Indian Association for the Cultivation of Science, India; ²Drexel University, United States

Manipulation of photogenerated electron-hole pairs towards low recombination and efficient transport is one of the key strategies to achieve high efficiency in photoelectrochemical water splitting. External magnetic fields have been reported for spin-to-charge conversion using either chiral molecules or magnetic elements-assisted photoelectrodes in spin-dependent electrochemistry (SDE). Herein we demonstrate a proof-of-concept for spin-manipulated charge transport in Janus MoSSe heterostructured with p-GaN as a photocathode under the influence of an external magnetic field. It is worth mentioning that we have neither used chiral molecules nor magnetic elements in the proposed photocathode. Our approach provides a new, effective, and affordable path-way to improve the catalytic performance of asymmetric 2D materials in PEC water splitting. Further, this proposed approach can be utilized for other asymmetric/disordered alloys for a wide range of applications.

Among two-dimensional (2D) materials, asymmetric Janus structure (MoSSe, WSSe) has exhibited many exciting properties, such as a significant Rashba effect, out-of-plane piezoelectricity, and spatial isolation of charge carriers. However, the critical gap that remains to be addressed yet is whether the spin properties of these asymmetric 2D materials can be combined with their optical and catalytic properties to establish more efficient photoelectrochemical (PEC) water splitting along with exploring some more fascinating science. Herein, we demonstrate a proof-of-concept for spin-manipulated PEC water splitting using Janus MoSSe. Magneto-photoelectrochemical properties have been critically investigated through lifting spin degeneracy by combined Rashba-Dresselhaus spin-orbit coupling and energy band splitting in Janus MoSSe/GaN heterostructure. Delaminated 2D-MXene (Ti₃C₂T_x) was decorated on top of MoSSe/GaN for efficient electron channelling. The optimized Ti₃C₂T_x/MoSSe/GaN device showed ~35% photocurrent enhancement as well as ~40% enhancement in the product (H₂/O₂) formation in PEC water splitting under a low applied magnetic field (0.4T). The external applied magnetic field helps spin manipulation even under unpolarized light by combining Zeeman and Rashba-Dresselhaus splitting by spin-to-charge conversion in Janus MoSSe/GaN heterostructure. Density functional theory (DFT) simulations were carried out to understand the role of the Rashba-Dresselhaus effect for efficient charge transport. This proposed concept of "spin manipulated charge transport" can be extended for various other asymmetric alloys for a wide range of applications, including selective CO₂ reduction, photodetection, photovoltaics, etc. Therefore opens new research domains like "Spin Manipulated Electrochemistry (SMPE)" using asymmetric materials.

References:

1. Journal of Physical Chemistry Letters 13 (2022) 1334
2. Chemical Engineering Journal 435 (2022) 134963
3. Progress in Energy 4 (2022) 022001
4. Nano Energy 87 (2021) 106119

8:00 PM EL07.09.21

Polyvinylpyrrolidone/CNTs Electrospun Composites for Advanced Applications Fatima TuzZahra¹, Adeolu Ajayi², Quincy Quick¹ and Richard Mu¹; ¹Tennessee State University, United States; ²Columbia University in the City of New York, United States

Electrospinning has attracted the attention of the scientific community since it is a simple yet effective technique to prepare fibers and their composites for various applications. Moreover, it provides a variety of choices in materials as compared to other methods that are used for fiber fabrication. The composites of interest in this study are CNT-based composites, as they hold a great significance in various applications due to their superior physical properties. There are various studies that confirm the potential of carbon nanotube (CNT)-based composites for advanced applications such as superconductors, microwave absorbers, and biomedical field. In the presented study, polyvinylpyrrolidone (PVP) and CNTs have been utilized to prepare composites using electrospinning technique. The purpose of this study is to prepare wire-like fibers which have good thermal and electrical conductivity and for that, the alignment of CNTs encapsulated in the fibers is one of the main features that was aimed. PVP and CNTs composites are believed to have high thermal and electrical conductivity along with good mechanical strength. Moreover, PVP has proven to be a good source of dispersion for CNTs. Generally, the PAN based CNTs are utilized during electrospinning, however, in the presented study we propose the simplified way to encapsulate CNTs directly in PVP nanofibers by using electrospinning technique. PVP with lower molecular weight (10,000 mol/gm) is utilized to attain fine nanofibers by optimizing the molarity, flow rate, voltage and needle to collector distance. The CNTs of length range 5-20 μm and diameters 15±5 nm, 30±10 nm were dispersed ultrasonically in the PVP and ethanol solution. The optimized process parameters were used for electrospinning. Scanning electron microscopy (SEM) and transmission electron microscopy (TEM) were utilized to study the morphology and structural properties of the prepared composites. The thermal and electrical conductivities of the samples were also analyzed. The CNTs tend to align along the length of the fibers, which led to enhanced thermal and electrical conductivities. Furthermore, considering the good dielectric properties of PVP, increasing the PVP content can lead to high potential of the study in microwave absorption applications.

8:00 PM EL07.09.22

Graphene-Enabled Selective Wetting of Liquid Metal on Polyamide Substrate for the Fabrication of Soft Wearable Electronics Wedyan Babatatin, Ozgun Kilic Afsar and Hiroshi Ishii; Massachusetts Institute of Technology, United States

The development of soft wearable electronics has gained significant attention due to their potential for seamless integration with the human body. This study presents a novel approach for fabricating soft wearable electronics using a graphene-enabled selective wetting of liquid metal on a polyimide substrate. Specifically, we leverage the growth of laser-induced graphene (LIG) on polyimide substrate as a surface modification functional material to allow precise patterning of liquid metal, offering control over the deposition process. The patterned liquid metal devices can be subsequently transferred from polyamide to various flexible and stretchable substrates, making them suitable for wearable applications. In order to study the interfacial behavior of LM

on top of the LIG substrate, scanning electron microscopy images of the patterned traces were reported, Raman spectrum of the grown LIG layer was obtained and scrolling angles of the LIG/LM interfaces was measured. Through a series of experiments and characterization, we demonstrate the successful fabrication of soft wearable electronics, including sensors using the proposed method. The selective wetting behavior of liquid metal on the polyimide substrate allows for the creation of intricate and functional patterns with excellent resolution producing LM traces up to 200 μm . The resulting devices exhibit remarkable mechanical robustness, enabling them to withstand bending, stretching, and other mechanical deformations for 1000 cycles without compromising their performance, allowing them to stretch up to 40% and bend with radii as small as 5 mm. The combination of graphene-enabled selective wetting and soft polymeric substrates offers several advantages for fabricating soft wearable electronics such as pressure sensors and touchpads. It provides a versatile and accessible approach that can be scaled up for mass production. The resulting devices exhibit excellent electrical conductivity, mechanical flexibility, and conformability, making them highly suitable for applications in healthcare monitoring, sports tracking, and soft human-machine interfaces.

8:00 PM EL07.09.23

Synthesis and Electronic Transport of Superconducting Molybdenum Nitride Ultrathin Crystalline Platelets DaZhou¹, David Sanchez¹, Alexander J. Sredenshek¹, Jiayang Wang¹, Lingrui Mei², Yuxin Gao¹, Luis Balicas², Susan B. Sinnott¹ and Mauricio Terrones¹; ¹The Pennsylvania State University, United States; ²Florida State University, United States

Transition metal carbides (TMCs) and transition metal nitrides (TMNs) have been intensively studied in their bulk form due to their outstanding properties such as superior hardness, high melting point, high metallic conductivity with superconductivity at low temperatures in certain phases, and chemical resistance.¹ Xu et al.² established a liquid-metal-assisted chemical vapor deposition (LMCVD) method to grow large-area ultrathin Mo₂C and studied their robust superconducting properties down to a few nanometers in thickness. Wang et al.³ implemented a similar LMCVD approach to grow ultrathin MoN_x and studied their catalytic properties. However, to the best of our knowledge, the electronic properties such as the superconductivity of ultrathin MoN_x crystalline platelets have not been studied to date.

In our study, ultrathin MoN_x nanoplatelets were grown by LMCVD, and the morphology was characterized by optical microscopy, scanning electron microscope (SEM), atomic force microscopy (AFM), and scanning/transmission electron microscope (s/TEM). Using a semi-dry deterministic transfer method, we stamped nanometer-thick MoN_x flakes onto pre-patterned Hall bar/4-probe electrodes and conducted electronic transport measurements. For 120 nm thick platelets, the onset superconducting transition temperature was 12.11 K which is comparable to the bulk T_c values, showing a sharp transition width smaller than 0.1 K, indicating a high degree of crystallinity. A magnetic field in the out-of-plane direction was applied and series of R-T measurements were performed under different fields and the corresponding T_c values were extracted. The critical field exhibited a linear temperature dependence which is consistent with the 2D Ginzburg-Landau formalism for fields perpendicular to the planes, which supports the 2D nature of the superconducting state. By linear fitting the H_c with T_c, we extrapolated the zero-temperature critical field to be around 3.79 T and the Ginzburg-Landau coherence length at zero temperature to be around 9.3 nm. By analyzing the results from Hall measurements and the longitudinal resistance measurements, the mean free path was estimated to be > 500 nm, orders of magnitude higher than the Ginzburg-Landau coherence length, exceeding the superconducting clean limit.

In summary, we have successfully synthesized ultrathin MoN_x nanoplatelets through a LMCVD method and conducted electronic transport measurements. The thickness dependence of superconducting transitions was also probed. We will also show how the superconducting transitions in chromium doped/alloyed MoN_x platelets get modulated by the introduction of magnetic impurities.

References

- Jauberteau, I. et al. Molybdenum Nitride Films: Crystal Structures, Synthesis, Mechanical, Electrical and Some Other Properties. *Coatings* 5, 656-687 (2015).
Xu, C. et al. Large-area high-quality 2D ultrathin Mo₂C superconducting crystals. *Nature Materials* 14, 1135-1141 (2015).
Wang, L. et al. Ultrafast Growth of Thin Hexagonal and Pyramidal Molybdenum Nitride Crystals and Films. *ACS Materials Letters* 1, 383-388 (2019).

8:00 PM EL07.09.24

Changes in Crystals of Two-Dimensional Materials According to Growth Conditions in the CVD Process and Consequent Changes in Their Properties Dokyong Yun and Woojong Yu; Sungkyunkwan University, Korea (the Republic of)

In this paper, we saw the change of crystal structure according to the change of the growth conditions of the 2D material. For the growth of the 2D material we used, a large-scale array resistive memristor device in which the crystallinity of the thin film was controlled by adjusting the growth conditions of hBN was used.

The structure of the device we used is a MIM (Metal/Insulator/Metal) vertical 2-terminal resistive switching device composed of Au/hBN/Au. Here, the growth conditions such as growth temperature, growth time, distance and amount of ammonia borane were adjusted to analyze the change in the state, thickness, and crystal structure of the thin film. It can be seen that they have slightly different characteristics. When a voltage is applied to the RRAM's non-conductive material, filaments are created and ions can clump together, allowing current to flow. RRAM with high electrical characteristics was realized by controlling the growth conditions.

8:00 PM EL07.09.25

2D InGaO_x Transistors Printed by Cabrera-Mott Oxidation of Liquid In-Ga Alloys Simon A. Agnew, Anand P. Tiwari and William J. Scheideler; Dartmouth College, United States

Next-generation flexible electronics will require low-temperature fabrication of high-mobility 2D semiconductors. Continuous liquid metal printing (CLMP) powered by Cabrera-Mott oxidation can support this goal by offering rapid (< 3 s) processing of large-area (> 20 cm²) 3 nm thick '2D' layers of semiconducting oxides with high mobility. However, their high intrinsic carrier density demands new mechanisms of electrostatic control. We present a strategy for controlling transport in 2D In₂O₃ via doping with trace Ga inclusions (0.1–0.001 wt.%) in precursor metal alloys. We use these alloys to print indium gallium oxide (IGO) transistors at < 200 °C with enhanced subthreshold slope and near 0 V turn on by reducing the electron concentrations 10–1000X with Ga-doping in the resultant channels (5–70 at. %). Printed 2D IGO transistors exhibit exceptional field effect mobility, with champion devices achieving up to 17 cm²/Vs and I_{on}/I_{off} up to 10⁶, with enhanced bias-stress stability over pure In₂O₃. Moreover, through a combination of experiments and finite element simulation, we demonstrate the synergy between 2D IGO and ultrathin high-k Al₂O₃ dielectrics for achieving low-voltage transistors with steep switching.

We apply detailed materials characterization including XPS to quantify Ga doping and oxygen stoichiometry in the 2D IGO channels and EDS to analyze the Ga-rich surface oxide of the liquid precursor alloys. IGO films were investigated by XRD to evaluate the doping threshold for amorphization and by UV-Vis to analyze modulation of the optical bandgap and effects of quantum confinement. Collectively, these results illustrate the power of liquid metal alloy printing to control 2D semiconductor electrostatics and crystallinity for developing high performance flexible electronics and next-generation display technologies.

8:00 PM EL07.09.26

Van der Waals SbSeI Quasi-1D Nano-Columns for Advanced Photonic Applications Ivan Caño Prades, Alejandro Navarro Güell, Edoardo Maggi, Joaquim Puigdollers, Sergio Giraldo, Zacharie Jehl, Marcel Placidi and Edgardo Saucedo; Universitat Politècnica de Catalunya, Spain

There is an increasing interest in novel van der Waals materials such as Sb₂(S,Se)₃ and (Sb,Bi)(S,Se)(Br,I) systems, thanks to their natural ability to form low dimensional structures with exotic properties. This is strongly related to their highly anisotropic crystal structure, which results in unique electrical and optical properties when the materials are correctly oriented. In addition, these semiconductors can cover a plethora of different possible technological applications including sensors, supercapacitors, piezoelectric generators, and solar cells. Amongst this family of largely overlooked materials, (Sb,Bi)(S,Se)(Br,I) pnictogen chalcogenides are highly attractive due to their wide range of possible bandgaps between 1.2 eV up to 2.2 eV, customizable optical properties by using different halides or chalcogenides while retaining their quasi-1D structure, defect-tolerance, and ferroelectric properties. Nevertheless, the progresses in the development of these pnictogen chalcogenide semiconductors are being limited by the complexity to synthesize compounds containing halogens and chalcogens in the same structure, due to the very different elemental vapor pressure.

The first attempts to synthesize these materials have been essentially focused on low temperature (<300 C) and atmospheric pressure solution-based chemical routes, resulting in columnar films with poor crystalline quality and very limited morphology tunability. Aiming towards a more controlled, reproducible and versatile system, in this work SbSeI, one of the most relevant materials amongst this family, has been synthesized by a novel procedure based on the selective iodination of co-evaporated Sb₂Se₃ films at high pressures (between 2 atm up to 20 atm), developing extremely uniform, single-crystal nano-columnar structures. We will show how the thickness, height, and density of these 1D nano-columns can be tuned by finely varying annealing temperature and pressure. The resulting nano-columns were characterized using microscopy imaging techniques, Raman spectroscopy and X-ray diffraction, demonstrating the formation of SbSeI single phase with orthorhombic structure (space group Pnma), and with excellent crystalline quality and compositional homogeneity. To study the potential of this material for different photonic applications, electrical and optoelectronic measurements have been performed on micro-scale devices, connecting nano-columnar crystals to Pt and Au contacts on a SiO₂/Si wafer. Interestingly, a clear diode response has been observed with Au-Au and Au-Pt, which is greatly enhanced under illumination. Memory effect, capacitance-voltage and ferroelectric measurements have also been performed. Kelvin probe microscope analysis has been used to determine its work function, observing that different facets of the crystals yield distinct surface potential, supporting our hypothesis that the quasi-1D growth of the material gives rise to anisotropic transport properties.

Overall, this work presents to the best of our knowledge, the first study of the physical vapor deposition synthesis and characterization of novel SbSeI chalcogenide compound, demonstrating the tunability of the SbSeI nano-columns morphology by varying synthesis pressure and temperature, as well as the potential of low dimensional chalcogenides to be implemented into innovative architectures and advanced functionalities (such as for enhanced carrier collection and light trapping), pointing the way to develop defect-tolerant and ferroelectric absorbers with anisotropic electrical properties for advanced photonic applications.

8:00 PM EL07.09.27

An *Ab Initio* Study of Vertical Heterostructures Formed by CdO and SnC Monolayers Bilal Tanatar, Mahsa Seyedmohammadzadeh, Arash Mobaraki and Oguz Gulseren; Bilkent University, Turkey

Assembling two-dimensional (2D) materials in vertical heterostructures is one of the main techniques for tuning electronic and optical properties. In most cases, known as van der Waals heterostructures (vdWHs), the interlayer distances are larger than typical covalent bond lengths resulting in weak interlayer interactions. It has been shown that reducing the distance between the layers can significantly alter the properties of separated layers, which is not so noticeable in vdWHs and thus creates a new platform for controlling the physical properties of 2D materials. Motivated by enhanced properties of 2D vertical heterostructures, employing *ab-initio* calculations based on density functional theory we examined CdO/SnC systems in four different configurations. Our results reveal that in spite of the thermodynamic and mechanical stabilities of all considered structures, according to the calculated phonon frequencies, only the structure formed by placing the Sn atom on the O atom and the C atom on the Cd atom is dynamically stable at zero temperature. This structure has an interlayer distance of 2.52 Å which is smaller than the interlayer distance in typical vdWHs. We investigated the electronic and optical properties of this dynamically stable structure utilizing GW approximation and solving the Bethe-Salpeter equation. Unlike the monolayer CdO which possesses a single optical absorption peak close to the red light energy, the considered CdO/SnC structure has an optical band gap of 1.14 eV, and it can absorb 13% of incident light in the blue light region.

8:00 PM EL07.09.28

The study of the intense pulsed light sintering process of BaTiO₃ nanoparticles added with graphene oxide for the realization of a high-k dielectric layers. Seok-hoon Jeong¹, Jong-Whi Park¹ and Hak-Sung Kim^{1,2}; ¹Hanyang University, Korea (the Republic of); ²Institute of Nano Science and Technology, Korea (the Republic of)

Abstract

Conventional photolithography technology is a technology for manufacturing existing devices, and has disadvantages such as complicated process problems, material loss, and expensive equipment. On the other hand, printed electronics technology is attracting attention because it can easily implement patterns through printing and coating processes using ink and solution materials. The material loss could be reduced through exposure and etching processes for patterning. However, high-temperature and long-term annealing and sintering process were required to realize high quality electrode and semiconductor layer. Accordingly, various annealing/sintering methods have been developed. Among the various methods, the thermal annealing process has disadvantages of complicated facilities for maintain the high temperature and long process time. In the case of laser annealing method, the process time could be shortened, but the disadvantage of the expensive equipment and the small annealing area. In addition, the deep-ultraviolet (UV) irradiation method can also reduce damage to the substrate material, but the process time is long and additional facilities such as inert gas was required. On the other hand, the IPL sintering method can sinter the material of a large area in millisecond units at room temperature and normal pressure using a visible ray xenon lamp. The BaTiO₃ has a high dielectric constant but a relatively low band gap. The low band gap has the disadvantage of a large leakage current, so the other materials, which has the adequate band gap, was used for recent industry. In this study, the disadvantages of BaTiO₃ was compensated by adding the graphene oxide. In addition, the hybrid layer composed of BaTiO₃ and graphene oxide was sintered by using IPL irradiation process. Through various analysis, the sintering characteristics, dielectric properties, and crystallinity of this hybrid layer were investigated.

Acknowledgment

This work was supported by Korea Institute of Energy Technology Evaluation and Planning (KETEP) grant funded by the Korea government (MOTIE) (2021020800090, Development and Demonstration of Energy-Efficiency Enhanced Technology for Temperature-Controlled Transportation and Logistics Center) and this work was supported by the Korea Institute of Energy Technology Evaluation and Planning (KETEP) and the Ministry of Trade, Industry & Energy (MOTIE) of the Republic of Korea (No. 20206910100160).

8:00 PM EL07.09.29

Enhancement of p-type Behavior of Inkjet-Printed Single-Walled Carbon Nanotube Transistors from Phenylphosphonic acid Coating Dong Hyun Lee¹, Siwon Hwang², Bongjun Kim² and Hocheon Yoo¹; ¹Gachon University, Korea (the Republic of); ²Sookmyung Women's University, Korea (the Republic of)

Single-walled carbon nanotube (SWCNT) had interest over the past decade as a high potential material due to their thermal stability and high conductivity [1-2]. In particular, SWCNTs had high carrier mobility and advantages of solution processing lead to their development for applications in electronic devices such as transistors and logic circuits [3-4]. However, the doping technology for controlling the charge carrier transport of SWCNT is still immature. The chemical doping method is a process that modulates the Schottky barrier without damaging SWCNT. In this paper, we present p-type behavior enhanced SWCNT transistor by patterning semiconductors and electrodes using inkjet printing technology and doping them with the self-assembled monolayer (SAM) material phenylphosphonic acid (PPA). The benzene rings of PPA coated on the SWCNTs without annealing process fill the voids in the channels by π -stacking interaction. As a result, SWCNTs connected through PPA form additional pathway for charge carrier transport. The p-type current of the SWCNT transistor is enhanced 4.3 times due to the improved hole injection resulting from PPA doping effect. In addition, the 10 PPA-doped SWCNT transistors increased the hole mobility by an average of 8.25 cm² V⁻¹ s⁻¹. Finally, the positive-shifted threshold voltage of 0.55 V indicates the potential for application in depletion mode of PPA-doped SWCNT transistor.

8:00 PM EL07.09.30

Anti-cancer Drug Delivery by Janus WSSe Monolayer: A First-Principles Study Md Tahmid Kabir and Ahmed Zubair; Bangladesh University of Engineering and Technology, Bangladesh

Two-dimensional Janus transition metal dichalcogenide (TMD) have a large surface-to-volume ratio that provides a variety of suitable anchoring points for active drug loading and incorporates distinct physicochemical properties for efficient, controlled, and selective drug delivery. Carmustine, an alkylating agent, treats several types of brain cancer. In this work, we investigated the compatibility of 1H-WSSe, a Janus TMD with hexagonal lattice, as a smart delivery vehicle in the human body. The first-principles calculations based on density functional theory were performed using periodic boundary conditions to calculate the electronic and optical properties of carmustine/WSSe drug complex. After investigating the spatial interaction between it and WSSe Janus sheet, four plausible configurations of carmustine emerged. These configurations are carmustine horizontally adsorbed on S (C-I) and Se (C-II) sides and vertically adsorbed on S (C-III) and Se (C-IV) sides. Drug complexes were relaxed until appropriate total energy and force convergence thresholds were attained. C-I and C-II had similar adsorption distance resulting in comparable adsorption energies of -0.93735 eV and -0.94177 eV, respectively, which were notably higher compared to previous reports. However, the S sheet for C-III has a closer adsorption interaction with the carmustine than Se sheet for C-IV resulting in better adsorption for C-III. We calculated E-k band diagrams, orbital projection of the bands and density of states for all configurations. As the bands near the band gap were primarily contributed by W, S, and Se of Janus WSSe, the band gap (E_g ~ 1.7 eV) remained unchanged compared to pristine Janus WSSe except for C-II. Both valence and conduction band edges were largely contributed by the d orbitals of W. In C-I, orbital projection revealed 32.23% d_{x²-y²} and 34.3% d_{xy} contribution at valence band maxima (K-point), and the conduction band edge had ~90.7% d_{z²} contribution. However, the emergence of a highly localized state near the conduction band edge in C-II resulted in band gap reduction to 1.642 eV. This state originated from the p orbitals of O and N atoms of carmustine. Mulliken charge analysis revealed that C, N, and O atoms of carmustine experienced an accumulation of electronic charge, and the electronic charge was depleted from H and Cl after interaction with the WSSe monolayer. The electron-dense region in the carmustine above has influenced the electron deficit region in the Janus sheet below and vice versa. Moderate to low charge transfer levels implied that carmustine was physisorbed on WSSe monolayer. Moreover, electron localization function calculation demonstrated no bonding between carmustine and Janus sheet. All drug complex configurations had a non-zero anisotropic absorption coefficient near the band gap. Finite absorption in the IR range and drug-independent absorption of the 2D Janus WSSe made it appropriate for drug delivery. Phonon dispersion and quasi-harmonic vibrational free energy were investigated to gain insight into the practical drug release under exogenous stimuli (i.e., temperature increase). We estimated the temperature effect on adsorption energy by incorporating quasi-harmonic vibrational free energy correction. Increasing temperature from 0 to 350 K produced an ~0.2954 eV upward shift for adsorption energy which indicated enhancement of the anti-cancer drug release rate. The adsorption energy was reduced by ~31.51% which was significantly higher than those of literature for 2D nanomaterials. The high adsorption energy of the drug complex enables the effective anchoring of carmustine avoiding accidental release and the capability to make a steep adsorption energy reduction by thermal radiation allows selective release. Therefore, the 2D Janus WSSe is a perfect candidate for controlled drug release into the cancer cell by photothermal therapy.

8:00 PM EL07.09.31

The Influence of ZnO Thin Film Thickness on Anion Exchange Membrane Fuel Cell PerformanceRohanSuri¹, SamuelChen², KristeAn³, HaoyanFang⁴, Md FarabiRahman⁴ and MiriamRafailovich⁴; ¹Ladue Horton Watkins High School, United States; ²Ed W. Clark High School, United States; ³Harvard-Westlake School, United States; ⁴Stony Brook University, The State University of New York, United States

In response to the global challenge to find a clean and sustainable power source, scientists have turned their attention to anion exchange membrane fuel cells (AEMFCs). Though significant progress has been made in the development of AEMFCs, several obstacles impede their application¹. Poor water management in AEMFCs, for example, leads to anode flooding and cathode dehydration, causing cell deterioration to occur over time. Additionally, platinum will ionize and migrate during operation, causing the AEM to degrade, leading to eventual cell failure². Left unmitigated, these problems could easily render a possible solution to the energy crisis useless. Herein, we report that depositing ZnO thin films on an AEM using Atomic Layer Deposition (ALD) can lead to increased maximum power outputs for AEMFC's. For testing, ALD was used to deposit 5, 10, 15, 20, and 30 layers of ZnO onto anion exchange membranes (Sustainion grade T). Atomic Force Microscopy (AFM) was used to verify that a uniform layer formed a flat topography, proving that ZnO was successfully coated on the surface. Our results demonstrated that there appears to be an optimal thickness of the ZnO thin film layer, with 10 cycles yielding the highest observed maximum power density of 0.430 W/cm² (a 28.7% increase from the control cell). Further addition of ZnO began to reduce maximum power densities, with 30 layers of ZnO causing a maximum power density of 0.274 W/cm² (an 18.0% decrease). Afterward, XRD measurements were performed, demonstrating the amorphous nature of the ZnO deposited, giving further insights into how the nanostructure could affect possible results. A possible explanation for our observations could be that ZnO improves the electrochemical durability of the AEM, allowing it to function for longer periods of time and become more resistant to the osmotic gradient created within the cell during operation. Future research should include further spectroscopic and microscopic characterization of the membrane and electrodes before and after the performance tests to gain a deeper understanding of our results. Regardless, the scientific community must continue to work with ZnO as a possible solution to many of the problems that plague AEMFC's, furthering humanity's goal to find sustainable energy sources.

Support from the Office of Naval Research [N00014-29-1-2858] is gratefully acknowledged.

¹ Felseghi, Raluca-Andreea, et al. "Hydrogen fuel cell technology for the sustainable future of stationary applications." *Energies* 12.23 (2019): 4593.

² Raut, Aniket Madhukar, et al. "Migration and Precipitation of Platinum in Anion Exchange Membrane Fuel Cells." *Angewandte Chemie International Edition* (2023): e202306754.

8:00 PM EL07.09.32

Study of Silver Nanoparticles Deposition on Proton Exchange Membrane Fuel CellPrishaJain¹, AnnaHeimowitz², JonathanSacolick³, HaichuanWang⁴, Md FarabiRahman⁵, HaoyanFang⁵ and MiriamRafailovich⁵; ¹Irvington High School, United States; ²Stella K. Abraham High School for Girls, United States; ³Hebrew Academy of Five Towns and Rockaway High School, United States; ⁴Shanghai Jianping High School, China; ⁵Stony Brook University, United States

Hydrogen fuel cells are an innovative technology capable of producing electricity from hydrogen gas and air. The fuel cell's electrolytic reaction emits only water, making hydrogen fuel cells a more sustainable energy technology¹. Proton exchange membrane fuel cells (PEMFCs) are known for their low operating temperature, high power density and longer durability². Existing PEMFCs utilize a platinum (Pt) catalyst for better efficiency while the performance of PEMFCs can be enhanced by adding comparatively low-cost non-Pt group nanocatalysts.

This study aims to research the impact of silver nanoparticles on the power density of PEMFCs. Silver nanoparticles, synthesized using the Brust-Schiffrin method, were capped with octanethiol or dodecanethiol. The thiol caps prevent nanoparticle interactions, reducing agglomeration, one of the main challenges with silver nanoparticles³. The synthesized particles were examined employing Transmission Electron Microscopy (TEM); they were spherical nanoparticles with an average diameter of about 4 nm for both octanethiol-capped (AgC₈) and dodecanethiol-capped (AgC₁₂) nanoparticles. The Langmuir-Blodgett Trough (LBT) produced isothermal curves for the AgC₈ and AgC₁₂ nanoparticles respectively and exploiting the data from there we deposited the silver nanoparticles on the Nafion-117 membrane at surface pressures of 2, 5, and 10 mN/m using LBT. The PEMFC was assembled employing a 0.1mg/cm² Pt loading on both the electrodes (anode and cathode) and the Nafion-117 membrane was placed in between the electrodes.

Data from the PEMFC demonstrated that octanethiol-capped silver nanoparticles at surface pressures of 2 mN/m achieved slight improvement in performance; however, at 5 mN/m and 10 mN/m, a 16% and 33% increase in power density was observed respectively. For dodecanethiol-capped silver particles a similar trend was observed. There was no significant power density increase at surface pressures of 2 mN/m but there was about a 16% increase in power density at 5 mN/m and a 33% increase at a pressure of 10 mN/m. The performance of the fuel cell increased at higher surface pressure deposition as it likely increased the quantity of silver nanoparticles deposited, increasing catalytic activity. TEM data demonstrated that AgC₈ nanoparticles were more uniform than AgC₁₂ nanoparticles which tended to be more agglomerated. However, both thiol-capped nanoparticles resulted in an equivalent increase in power, suggesting that the evenness of the monolayer did not impact the ability of the silver nanoparticles to catalyze the reaction. In the future, carbon monoxide test will be conducted to determine if the deposition of silver nanoparticles prevents the poisoning of the Pt catalyst.

Support from the Office of Naval Research [N00014-29-1-2858] is gratefully acknowledged by us.

¹ Wang, Likun et al. "Designing nanoplatelet alloy/nafion catalytic interface for optimization of PEMFCs: performance, durability, and CO resistance." *ACS Catalysis* 9.2 (2019): 1446-1456.

² Ryan O'Fayre et al. *Fuel Cell Fundamentals*. 3rd ed., Wiley, 2016

³ Connie Manz et al. Dispersibility of organically coated silver nanoparticles in organic media, *Colloids and Surfaces A: Physicochemical and Engineering Aspects*, Volume 385, Issues 1–3, 2011, Pages 201-205, doi.org/10.1016/j.colsurfa.2011.06.009.

8:00 PM EL07.09.33

Schiff Base Ligand-Based Mononuclear Co(II) / Ni(II) Complexes as Electrocatalysts for Hydrogen ProductionFatimahA. Hussein; University of Delhi, Iraq

Solar energy harnessing is a promising way to meet the increasing global energy needs.¹⁻⁷ An important approach in this context is artificial photosynthesis (AP) wherein water is split into hydrogen and oxygen using electrocatalysts incorporating different chromophores.⁸⁻⁹ For the reductive side of AP (H₂ generation), a highly active catalyst, stable in the presence of water and designed using earth abundant materials is preferable. Identifying a robust, active, and efficient electrocatalyst is hence, a crucial first step in this direction. Though Pt is active for proton reduction, the widespread application of Pt is limited due to its rare nature. Keeping this in mind, efforts have focused on using abundant elements such as Fe, Co, Ni, Mo and different combinations of ligands for designing the proton reduction catalysts. For the ligand platforms in developing the catalysts with inexpensive components, Schiff base ligands have received special attention in the past few years.

Based on the above-mentioned facts, tetradentate Schiff base ligands N, N'- Bis (salicyldiene)ethylenediamine(L1),2,2'-(1E-1'E)-(ethane1,2diybis(azanylydene))bis(ethane-1-yl-1-ylidene)diphenol(L2) and 3-(2-(E)-(hydroxynaphthyl)methyl)imidopropylamine (L3) were reacted with MCl₂.6H₂O (M = Co, Ni). The synthesized Schiff base complexes [CoII(L1/L2/L3)] 1-3 and [NiII(L1/L2/L3)] 4-6 were characterized by FTIR, NMR and UV-Vis spectroscopic techniques, mass spectrometry, elemental, and thermal analysis. The reported complexes 10 1, 2, 4-6 and the new complex 3 were investigated for electrocatalytic proton reduction to dihydrogen in the presence of weak acid (acetic acid) in homogenous media (CH₃CN)

8:00 PM EL07.09.34

Boosting the Electrochemical Reduction of CO₂ to Acetylene via Ultrathin 2D Conjugated Copper-Nickel Phthalocyanine-Por COFAbebeB. Workie; National Taiwan University of Science and Technology, Taiwan

Current research efforts are focused on developing a feasible strategy to mitigate global warming while enhancing C-C coupling and multi-carbon production from the electrochemical conversion of carbon dioxide (CO₂). Metallomacrocyclic materials are among those that have shown potential for catalyzing the conversion of CO₂ into high-value chemicals. But thus far, it has been constrained by low current density, weak activity, product selectivity, and stability. Herein, we report a stable and conductive ultrathin 2D conjugated Copper-Nickel Phthalocyanine-Por Based COF via nitrogen-rich linker-assisted strategy. The distance of adjacent metal atoms can be tuned by adjusting the functionality and size of ligands to promote the formation of ultrathin 2D conjugated tandem Copper-Nickel Phthalocyanine-Based COF, leading to improved atom utilization efficiency, tailored catalytic activities, and high catalytic selectivity, which surpassing C-C coupling and multi-carbon products. The synthesized COF electrocatalysts could exhibit outstanding selectivity for acetylene production demonstrated in an H-type cell. A conductive ultrathin 2D conjugated Copper-Nickel Phthalocyanine-Por Based COF delivers Faradaic efficiencies (FEs) for the CO₂ reduction at 0.57 V (vs. RHE) to acetylene of over 91%, with a current density exceeding 80 mA cm⁻² in a 0.5 M KHCO₃ solution, outstripping the performances of the majority of the reported CO₂ electrocatalysts. This study offers a practical strategy for developing future designs of novel, inexpensive dimeric electrocatalysts with exceptional efficiency and C₂⁺ selectivity for electrocatalytic reduction of carbon dioxide processes.

8:00 PM EL07.09.35

The Turbine Blades-Embedded Electrolyzer for Boosting CO₂RR PerformancesTa-ChungLiu¹, Jing RueiLin², You SyunLyu² and Yung ChiChang²; ¹National Yang Ming Chiao Tung University, Taiwan; ²Industrial Technology Research Institute, Taiwan

Aqueous CO₂ electrolysis is a promising technology for closing the carbon cycle and de-fossilizing industrial processes. In addition to vigorously developing advanced materials for electrocatalysts and ion-exchange membranes, challenges such as media flow management, module stability, and force distribution are highly associated with improving the process performance and developing a stackable cell concept to meet industrially relevant levels. The design of the “zero-gap” membrane electrolyzer assembly achieved a prevailing position in laboratory and primary industrialization. However, the utilization of CO₂ is less than 50% despite using a cationic ion-exchange membrane or bipolar membrane to reduce the CO₂ crossover between anode and cathode, making it economically less attractive. This could be attributed to the gas path architectures in the gas chamber, which touches the gas diffusion electrode (GDE) from both sides of the electrode. Herein, we reported a promising modified electrolyzer architecture concept with hierarchically continuous flow channels and GDEs. The meticulous turbine blades were introduced in the cylindrical-shaped gas path architecture to increase the CO₂ media vortex for compulsive reaction with electrocatalysts, thereby enhancing CO₂ utilization, reduction of applied cell voltage, and selectivity. The structure was built by powder bed fusion-based 3D printing and embedded with electrochemically restructured zinc oxide nanoparticles as cathode electrocatalysts. The effect of these modifications on the cell voltage, selectivity, and overall conversion was investigated at 100 mA/cm² with varying CO₂ feed gas flow, concentration, and humidity. This as-fabricated electrolyzer was designed to be modular and provide the cell with mechanical integrity and allowed an ionic and electric contact over the entire active cell area, which is required for both stacking and upscaling of the cell. This concept-proof configuration promises ~70% CO₂ utilization and displayed 95% CO₂ to CO conversion at 3V with 180 mA/cm², showing efficient and scalable CO₂ electrolysis without a notable increase in operation cost, and has high potential for practical application.

SESSION EL07.10: 1D and 2D Materials—Spintronic, Topological and Quantum Devices I
Session Chairs: Susan Fullerton and Haozhe Wang
Thursday Morning, November 30, 2023
Hynes, Level 3, Ballroom B

8:15 AM EL07.10.01

Interlayer and Spin Coupling in Magnetic Topological Insulator MnBi₂Te₄ Wenjing Wu, Junichiro Kono and Shengxi Huang; Rice University, United States

The emergence of magnetism in topological insulators introduces fascinating spin-related characteristics. This magnetism disrupts time-reversal symmetry, consequently fostering unique quantum states that can lead to extraordinary phenomena such as the quantum anomalous Hall effect. We will highlight our research on MnBi₂Te₄ (MBT), a two-dimensional van der Waals antiferromagnetic material demonstrating layer-dependent magnetism. Using magneto-Raman spectroscopy, we have studied the interlayer coupling and spin collective motion in MBT flakes, ranging from 1 to 5 septuple layers thick. Notably, we have detected strong interlayer phonon peaks between MBT thin layer and substrates. We also observed the spin-phonon interaction in flakes with different thicknesses and a distinct peak featuring magnons below the Néel temperature with external magnetic fields. Our work facilitates a deeper understanding of the spin and phonon characteristics in this emerging topological magnetic material, promising for quantum computing and spintronics applications.

8:30 AM EL07.10.02

Quantum-Coherent Electron Transport in Carbon Nanotube Fibers and Bundles with Ultrahigh Conductivity Shengjie Yu, Natsumi Komatsu, Liyang Chen, Nicolas M. Peraca, Xinwei Li, Renjie Luo, Oliver Dewey, Lauren Taylor, Ali Mojibpour, Geoffrey Wehmeyer, Matteo Pasquali, Matthew Foster, Douglas Natelson and Junichiro Kono; Rice University, United States

Macroscopic fibers of aligned carbon nanotubes (CNTs) with exceptional electrical conductivity (>10 MS/m) have emerged as potential alternatives to conventional metal-based electrical cables. However, to optimize their conductivity, a comprehensive understanding of the microscopic electronic transport processes within these CNT fibers is important, encompassing considerations of disorder, doping, and electron-electron interactions. This study presents the outcomes of temperature- and magnetic field-dependent conductivity measurements performed on solution-spun aligned CNT fibers and bundles. At high temperatures, all examined fiber and bundle samples exhibited metallic behavior, with conductivity increasing monotonically as the temperature was reduced from room temperature to a sample-specific temperature between 30 and 100 K. Below this characteristic temperature, the conductivity exhibited a gradual decrease with further decreases in temperature. Additionally, pronounced negative magnetoresistance manifested at low temperatures, signifying the presence of weak localization—a hallmark of quantum coherence in electron transport. Furthermore, investigations on individual bundles exfoliated from the fibers revealed fluctuations in conductivity as a function of magnetic field at temperatures below 50 K. These fluctuations, recognized as universal conductance fluctuations, provide further substantiation of the quantum-coherent nature of electron transport in the examined CNT bundles. By unraveling the interdependencies between temperature, magnetic field, and conductivity in CNT fibers and bundles, this study enhances our understanding of quantum-coherent electron transport phenomena, thereby contributing to the advancement of ultrahighly conductive materials for prospective applications.

8:45 AM *EL07.10.03

Controlling Quantum Interference in Molecular Materials Hatem Sadeghi; University of Warwick, United Kingdom

Thanks to their sub-10 nanometre size, molecules offer a fantastic platform for exploiting quantum effects at room temperature. Recently, it was shown that molecular wires can mediate long-range, phase-coherent tunnelling with remarkably low attenuation beyond a few nanometres, even at room temperature [1]. This opens up the possibility of using quantum interference (QI) to control the transport of electrons, spins and phonons through molecular junctions consisting of a single or a few molecules between electrodes.

In this talk I will present evidence for room-temperature QI in molecular junctions and discuss the agreement and disagreement between experiments and predictions based on phase-coherent quantum transport theory [2]. Then, I will discuss strategies to control QI in molecular junctions [3] and their applications for quantum switching, quantum sensing and quantum energy conversion.

[1] *Chem. Mater.* 25 (21), 4340, 2013; *Nano Lett.* 22 (18), 7682, 2022.

[2] *PNAS*, 112(9), 2658, 2015; *Nature Mat.*, 18(4), 364, 2019; *JACS*, 137(13), 4469, 2015; *Nano Lett.*, 18(7), 4482, 2018; *JACS*, 140(40), 12877, 2018; *Nanotechnology*, 29, 373001, 2018.

[3] *Nano Lett.*, 23, 9, 3748, 2023; *Nano Lett.*, 22, 3, 948, 2022; *PNAS*, 119, 46, e2211786119, 2022; *JPCL*, 13(39), 9156, 2022; *Nanoscale Adv.*, 2(3), 1031, 2020; *Nature Comm.* 11, 5905, 2020; *Angewandte Chem*, 61, e2021169, 2022; *ACS Nano*, 14(5), 5754, 2020; *Nanomaterials* 10 (8), 1544, 2020; *JACS*, 143(25), 9385, 2021; *PCCP*, 21, 2378, 2019; *Nano Lett.*, 20(11), 7980, 2020.

9:15 AM EL07.10.04

Abnormal Nonlinear Hall Effect in Thin-Film Weyl Semimetals Haotian Jiang, Yangchen He, Daniel A. Rhodes, Jun Xiao and Ying Wang; University of Wisconsin–Madison, United States

Type II Weyl semimetal possess exotic electronic properties arising from its unique topological structure near the Weyl nodes. Nonlinear Hall effect (NLH) is one of the most intriguing phenomenon in these materials which originated from the crystal inversion symmetry breaking. In NLH, the transverse Hall-like double-frequency voltage can be generated without the presence of any magnetic field and this unique electronic property is determined by quantum geometry, which is known as Berry curvature. In this presentation, we will show an abnormal nonlinear Hall behavior in a layered Type II Weyl semimetal TaIrTe₄. From the temperature dependent NLH measurement, we find that the nonlinear response is greatly enhanced up to 2 orders below a critical temperature. We will also show angle-dependent and layer-dependent NLH measurements to reveal the mechanism of enhancing the NLH effect and how it is related to quantum geometry. A theoretical model is also established to explain the abnormal NLH effect.

9:30 AM BREAK

10:00 AM *EL07.10.05

Novel Atomically Materials formed via Confinement Heteroepitaxy Joshua A. Robinson; The Pennsylvania State University, United States

The last decade has seen an exponential growth in the science and technology of two-dimensional materials. Beyond graphene, there is a huge variety of layered materials that range in properties from insulating to superconducting. Furthermore, heterogeneous stacking of 2D materials also allows for additional “dimensionality” for band structure engineering. In this talk, I will discuss recent breakthroughs in two-dimensional atomic layer synthesis and properties, including novel 2D heterostructures and realization of unique 2D allotropes of 3D materials (e.g. 2D metals, nitride, oxides). I will introduce a novel synthesis method, dubbed confinement heteroepitaxy (CHet), that utilizes graphene to enable the creation of atomically thin metals, enabling a new platform for creating artificial quantum lattices with atomically sharp interfaces and designed properties. By shrinking these traditional metals to atomically thin structures, we find that their properties are completely different than their bulk counterparts, lending themselves to unique quantum and optical applications not possible before.

10:30 AM EL07.10.06**A Novel Approach for Achieving Highly Clean Interfaces in 2D Material Spin Valves** Ting-ChunHuang and MarioHofmann; National Taiwan University, Taiwan

Spintronics is expected to revolutionize traditional electronics by harnessing the intrinsic spin property of electrons, but the spin manipulation requires high quality junctions between materials with different magnetic properties. 2D materials hold great promise for such junctions due to their atomically sharp interfaces. However, the current experimental results still fall short of meeting the theoretical expectations. This observed difference is primarily attributed to undesirable oxidation of the interfaces during the fabrication process. We here demonstrate a novel approach, called the asymmetrical deposition, to fabricate FM/graphene/FM spin valves (as-GSV) with unprecedented quality. This method achieves all necessary fabrication steps in-vacuo and thus eliminates any possibility for oxidation at the interface. The resulting spin-valve structure exhibits excellent layer conformity and low contamination. This advance yields a current density of the as-GSV that is four orders of magnitude higher than conventional spin valves. Parallel and antiparallel magnetic measurements confirm the high quality of the interface and highlight the importance of lattice-induced effects on spin transport. Furthermore, nearly identical amplitudes of magnetoresistance along two mutually perpendicular magnetic fields demonstrate a novel transport regime. Our results open up new routes for the integration of 2D materials in spintronics and provide inspiration for unprecedented device functionality.

10:45 AM EL07.10.07**Stimuli-Controlled Magnetism in Molecular 2D Magnets**ZhongxuanWang¹, ShenqiangRen¹ and YulongHuang²; ¹University of Maryland - College Park, United States; ²The State University of New York at Buffalo, United StatesZhongxuan Wang¹, Yulong Huang², Shenqiang Ren¹ *¹Department of Materials Science & Engineering University of Maryland—College, Park 4418 Stadium Drive College Park, MD 20740, USA²Department of Mechanical and Aerospace Engineering University at Buffalo The State University of New York Buffalo, NY 14260, USA

*E-mail:sren@umd.edu

Two-dimensional (2D) magnets provoke a surge of interest in large anisotropy and long-range magnetic ordering, and are promising for next-generation information technology where dynamic magnetic tuning is essential. Here, the controllable transformation of low-temperature magnetic order into room-temperature hard magnetism and pressure-controlled magnetism in LCPC is reported. The chemical tuning via electrochemical lithiation and solvation/desolvation exhibits continuously variable magnetic features from cryogenic magnetism to the room-temperature optimum performance of coercivity (Hc) of 8500 Oe and energy product of 0.6 MGOe. Due to the interlayer coupling of these two-dimensional magnets, interlayer magnetic coupling of molecular layered compounds also can be tuned by applied pressure via chromium-pyrazine coordination. Room-temperature long-range magnetic ordering exhibits pressure tuning coercivity coefficient, while pressure-controlled interlayer magnetism also presents a strong dependence on alkali metal stoichiometry and composition. Chemical tuning and pressure-controlled magnetism pave a pathway toward the understanding of room-temperature 2D magnetism in molecule-based systems.

11:00 AM EL07.10.08**Long-Lived Electronic Spin Qubits in Single-Walled Carbon Nanotubes**Jia-ShiangChen^{1,2}, Kasidet JingTrerayapiwat³, LeiSun¹, MatthewD. Krzyaniak², MichaelR. Wasielewski², TijanaRajhi⁴ and XuedanMa^{1,2,5}; ¹Argonne National Laboratory, United States; ²Northwestern University, United States; ³Boston University, United States; ⁴Arizona State University, United States; ⁵The University of Chicago, United States

Electron spins in solid-state systems offer the promise of spin-based information processing devices for quantum communication and computing. The key to preserving the encoding information is realized by the robust coherent spin state which acts against decoherence from losing the phase information. Single-walled carbon nanotubes (SWCNTs), an all-carbon one-dimensional material whose spin-free environment and weak spin-orbit coupling promise long spin coherence times, offer diverse freedom for extended functionality not available to bulk systems. Here, we report the creation of highly confined electron spins in SWCNTs by chemical functionalization through a bottom-up approach. The record long coherence time of 8.2 μs and spin-lattice relaxation time of 13 ms of these electronic spin qubits allow demonstration of quantum control operation manifested as Rabi oscillation. Investigation of the decoherence mechanism reveals an intrinsic coherence time of tens of milliseconds. These findings show that combining molecular approaches with one-dimensional crystalline systems provides a powerful route for reproducible and scalable quantum materials suitable for qubit applications.

11:15 AM EL07.10.09**Single-Photon Detection using a Graphene-Josephson Junction Calorimeter Part I**EthanArnault¹, BevinHuang¹, WochanJung², CalebFried³, KenjiWatanabe⁴, TakashiTaniguchi⁴, LeonardoRanzani⁵, Gil-HoLee², DirkEnglund¹ and Kin-ChungFong⁵; ¹Massachusetts Institute of Technology, United States; ²Postech, Korea (the Republic of); ³Harvard University, United States; ⁴National Institute for Materials Science, Japan; ⁵Raytheon BBN, United States

Single photon detectors (SPDs) are an enabling technology for quantum networks and quantum state readout. However, current implementations of SPDs often operate in narrow bandwidths, are limited in the tradeoff between the quantum efficiency and dark count, and many lack the ability to resolve photon number. The orthogonal approach of single-photon calorimetry based on graphene material properties can serve as an interesting option because it has 1) no band gap allowing for light absorption from optical down to microwave frequencies, 2) a vanishing density of states providing a low electronic heat capacity and 3) short electron-electron interactions (~100 fs). This makes graphene an ideal candidate for single photon calorimetry, where an incident photon is absorbed by the graphene and sensed through the temperature rise of the electrons.

In this two part talk, we will discuss our graphene-Josephson junction single-photon detector, which operates by measuring the heat deposited by a single photon. We are able to resolve single infrared (1550 nm) photons with a maximum quantum efficiency of ~90% and a dark count rate on the order of an hour. We can detect single-photons up to 1.2 K, paving the way to operate at liquid Helium-4 temperatures after further optimization. We further explore the heat propagation in our graphene. Using a milliKelvin optical scanner, we spatially resolve the heat propagation due to an incident single photon and find no substantial variation in switching rate over ~25 μm, indicating that the thermal length scale is substantially larger. Further, by varying backgate, the efficiency of the detector wanes as the device is tuned away from the Dirac peak, confirming that we are measuring the electronic temperature rise due to a single photon.

Part one of this talk highlights the mechanisms and verification of single photon detection.

11:30 AM EL07.10.10**Single-Photon Detection using a Graphene-Josephson Junction Calorimeter Part II**BevinHuang¹, EthanArnault¹, WochanJung², CalebFried³, TakashiTaniguchi⁴, KenjiWatanabe⁴, LeonardoRanzani⁵, Gil-HoLee², DirkR. Englund¹ and Kin-ChungFong⁵; ¹Massachusetts Institute of Technology, United States; ²Pohang University of Science and Technology, Korea (the Republic of); ³Harvard University, United States; ⁴National Institute for Materials Science, Japan; ⁵BBN Raytheon Technologies, United States

Single photon detectors (SPDs) are an enabling technology for quantum networks and quantum state readout. However, current implementations of SPDs often operate in narrow bandwidths, are limited in the tradeoff between the quantum efficiency and dark count, and many lack the ability to resolve photon number. The orthogonal approach of single-photon calorimetry based on graphene material properties can serve as an interesting option because it has 1) no band gap allowing for light absorption from optical down to microwave frequencies, 2) a vanishing density of states providing a low electronic heat capacity and 3) short electron-electron interactions (~100 fs). This makes graphene an ideal candidate for single photon calorimetry, where an incident photon is absorbed by the graphene and sensed through the temperature rise of the electrons.

In this two part talk, we will discuss our graphene-Josephson junction single-photon detector, which operates by measuring the heat deposited by a single photon. We are able to resolve single infrared (1550 nm) photons with a maximum quantum efficiency of ~90% and a dark count rate on the order of an hour. We can detect single-photons up to 1.2 K, paving the way to operate at liquid Helium-4 temperatures after further optimization. We further explore the heat propagation in our graphene. Using a milliKelvin optical scanner, we spatially resolve the heat propagation due to an incident single photon and find no substantial variation in switching rate over ~25 μm, indicating that the thermal length scale is substantially larger. Further, by varying backgate, the efficiency of the detector wanes as the device is tuned away from the Dirac peak, confirming that we are measuring the electronic temperature rise due to a single photon.

Part two of this talk focuses on the working mechanism of the graphene calorimeter, specifically thermal propagation, and the benchmarking of the calorimeter as a single-photon detector.

1:45 PM *EL07.11.01**Atomic Layer Smoothing for Quantum Materials: An Initial Investigation** Haozhe Wang; Duke University, United States

In the realm of quantum devices such as qubits and microwave kinetic inductance detectors, surface imperfections in metallic and dielectric films have been identified as a root cause of non-ideal behaviors. Despite significant investigations into surface-induced decoherence and low-frequency fluctuations, current nanofabrication techniques remain inadequate in addressing these issues. We introduce a novel surface smoothing technique utilizing a 'reversal' mechanism in atomic layer deposition (ALD), specifically isotropic plasma atomic layer etching (ALE), to mitigate Angstrom-level defects in quantum materials. Our approach focuses on minimizing surface roughness and native oxides, thereby enhancing device performance. This talk provides insights into the application of atomic layer smoothing in the processing of aluminum nitride, with observed smoothing effects at the Angstrom scale, offering potential improvements to AlN-based quantum optical devices. Further discussion will cover advancements in ALE for metallic aluminum, a material frequently used in superconducting circuits. We propose an integrated ALE-ALD approach to achieve smoother and oxygen-free surfaces.

2:15 PM EL07.11.02**Charge and Magnetotransport in Hybrid Molecule/Quantum Material Van der Waals Heterostructures** Emanuele Orgiu; Université du Québec/Institut National de la Recherche Scientifique, Canada

2D Quantum Materials are held together by weak interplanar van der Waals (vdW) interactions. The incorporation of molecules in such materials holds an immense potential to understand and modify the fundamental physical properties of the pristine materials while creating new artificial materials. Whilst nature offers a finite number of 2D materials, an almost unlimited variety of molecules can be designed and synthesized with predictable functionalities. The possibilities offered by systems in which continuous molecular layers are interfaced with inorganic 2D materials to form hybrid organic/inorganic van der Waals heterostructures (H-vdWH) are emphasized. Similar to their inorganic counterpart, the hybrid structures have been exploited to suggest novel device architectures. Moreover, specific molecular groups can be employed to modify intrinsic properties and confer new capabilities to 2D materials. In particular, I will highlight how molecular self-assembly at the surface of 2D materials can be mastered to achieve precise control over position and density of (molecular) functional groups, paving the way for a new class of hybrid functional materials.

In particular, I will show how the presence of ordered supramolecular assemblies bearing different functional groups can modify the pristine Shubnikov-De Haas oscillations [1] occurring in graphene or tune the magnetoresistance in a given transition metal dichalcogenide [2].

[1] A. Pezeshki, A. Hamdi, Z. Yang *et al.*, ACS Appl. Mat. Interf. 13, 26152 (2021).

[2] A. Hamdi, A. Pezeshki, ... E. Orgiu, Manuscript in preparation.

2:30 PMBREAK

SESSION EL07.12: 1D and 2D Materials—Memory Devices and Neuromorphic Computing

Session Chairs: Asir Intisar Khan and Lain-Jong Li

Thursday Afternoon, November 30, 2023

Hynes, Level 3, Ballroom B

3:00 PM *EL07.12.01**Monolayer Electrolyte for an All-Solid-State Non-Volatile Memory: Local Switching and Speed** Susan Fullerton, Huiran Wang and Shubham S. Awate; University of Pittsburgh, United States

Using an electrolyte that is a single molecule thick, our group previously demonstrated a non-volatile, solid-state, one-transistor (1T) memory by electric double layer (EDL) gating of WSe₂ field-effect transistors (FETs), Nano Letters 19, 8911 (2019). The "monolayer electrolyte" consists of cobalt crown ether phthalocyanine (CoCrPc) molecules and LiClO₄ wherein each crown ether solvates a cation. The cations are positioned by field-effect at either the surface of the WSe₂ channel or a h-BN capping layer to achieve a low resistance or high-resistance state, respectively. Our prior work focused on the combination of LiClO₄ and 15-crown-5 CoCrPc, giving rise to non-volatile threshold voltage shifts corresponding to a change in charge density of $\sim 2.5 \times 10^{12} \text{ cm}^{-2}$. Here, we report the impact of salt and solvent identity on the monolayer electrolyte deposition quality and electrical characteristics. First, we demonstrate that bistability is not limited to LiClO₄ – it is also detected for NaClO₄, Ca(ClO₄)₂ and LiCl in 15-crown-5. However, the change in charge density varies by more than one order of magnitude depending on the identity of the salt. Specifically, the top performers are the perchlorate-based salts with charge densities in the range of $1 - 2.5 \times 10^{12} \text{ cm}^{-2}$. In contrast, LiCl only induced a charge density modulation of $1 \times 10^{11} \text{ cm}^{-2}$, suggesting that the perchlorate anions may play an important, but unknown, role in the switching mechanism. Second, we demonstrate local ion switching with sheet densities on the order of $1 \times 10^{13} \text{ cm}^{-2}$ using electric force microscopy (EFM). Specifically, the EFM tip is used as a mobile top electrode to read, write, and erase the monolayer electrolyte on a heterostack of graphene/monolayer electrolyte/h-BN. This new approach to modulating the charge density provides insight on the lateral extent of switching which is critical for scaling the area of channel, and the energy barrier to switching. Lastly, we report on the switching speed having replicated prior results showing switching on the order of tens of nanoseconds. The interplay between device geometry and speed will be discussed. The work is supported by the National Science Foundation (NSF, U.S.) under Grant No. DMR-CAREER-1847808.

3:30 PM EL07.12.02**Role of Mobile Point Defects, Trap States and Joule Heating in Lateral Memristive Devices Based on Two-Dimensional TMDCs** Benjamin Spetzler¹, Dilara Abdel², Zhansong Geng¹, Frank Schwierz¹, Patricio Farrell² and Martin Ziegler^{1,1}; ¹Immenau University of Technology, Germany; ²Weierstrass Institute, Germany

Two-dimensional (2D) layered transition metal dichalcogenides (TMDCs) are promising materials for memristive devices and have gained significant attention because of their potential use in neuromorphic computing systems. However, despite extensive experimental work (e.g., [1,2]), the underlying resistive switching mechanisms in 2D TMDCs are still not understood, impeding progress in material and device functionality. This study discusses the contributions of various mechanisms to the current-voltage hysteresis and switching dynamics in 2D TMDC materials in detail and reveals the dominant role of mobile point defects [3]. Here, the switching process is governed by the formation and annihilation dynamics of a local vacancy depletion zone.

Moreover, minor changes in the interface potential barriers cause fundamentally different device behavior previously thought to originate from multiple mechanisms. The key mechanisms are identified with a numerical charge transport model for electrons, holes, and ionic point defects, including image-charge-induced Schottky barrier lowering, Joule heating, and charge trapping dynamics. The model is validated by comparing simulations with measurements for various 2D MoS₂-based and HfS₂-based lateral devices, which also allows us to identify the characteristic dynamic behavior as a fingerprint of the underlying physical mechanism. Our results strongly corroborate the relevance of vacancies in lateral TMDC devices and offer a new perspective on the switching mechanisms and the influence of Joule heating. The insights gained from this work can be used to extend the functional behavior of 2D TMDC memristive devices in future neuromorphic computing applications.

Funding by the Deutsche Forschungsgemeinschaft (DFG, German Research Foundation)–Project-ID 434434223–SFB 1461, the Carl-Zeiss Foundation via the Project MemWerk, and the Leibniz competition 2020 (NUMSEMIC, J89/2019) is gratefully acknowledged.

1. Bessonov, A.A.; Kirikova, M.N.; Petukhov, D.I.; Allen, M.; Ryhänen, T.; Bailey, M.J.A. Layered memristive and memcapacitive switches for printable electronics. *Nat. Mater.* **2015**, *14*, 199–204, doi:10.1038/nmat4135.

2. Da Li; Wu, B.; Zhu, X.; Wang, J.; Ryu, B.; Lu, W.D.; Lu, W.; Liang, X. MoS₂ memristors exhibiting variable switching characteristics toward biorealistic synaptic emulation. *ACS Nano* **2018**, *12*, 9240–9252, doi:10.1021/acsnano.8b03977.

3. Spetzler, B.; Abdel, D.; Schwierz, F.; Ziegler, M.; Farrell, P. The Role of Mobile Point Defects in Two-Dimensional Memristive Devices **2023**, doi:10.48550/arXiv.2304.06527.

3:45 PM *EL07.12.03**Nanoscale Devices Based on Van der Waals Ferroelectric Materials** Zijing Zhao¹, Kai Xu¹, Wei Jiang², Hojoon Ryu¹, Junzhe Kang¹, Tony Low², Shaloo Rakheja¹ and Wenjuan Zhu¹; ¹The University of Illinois at Urbana-Champaign, United States; ²University of Minnesota, United States

Van der Waals (vdW) ferroelectrics have emerged in recent years as a new class of ferroelectric materials, which have many intriguing properties, such as excellent size scaling, tunable

bandgap, negative piezoelectric coefficient, and high mechanical flexibility. Many vdW ferroelectrics can retain ferroelectricity down to 1 unit-cell thickness and can be grown or transferred on any material, which makes them promising building blocks for designing functional heterostructures. These new materials and heterostructures enable a wide range of emerging applications, including nonvolatile memories, steep slope transistors, programmable junctions, photodetectors, and pressure sensors. In this talk, we will discuss our recent work in developing reconfigurable and multifunction devices based on vdW ferroelectric materials [1-6].

Non-volatile reconfigurable logic transistors can be used to address the memory bottleneck in data-intensive applications because circuits based on these devices can realize various functions without changing the layout. We developed non-volatile reconfigurable transistors based on 2D $\text{CuInP}_2\text{S}_6/\text{MoTe}_2$ heterostructures [1]. The polarity (n-type or p-type) of these logic transistors can be dynamically programmed, while the configuration is non-volatile in nature. Utilizing these ferroelectric devices, we demonstrate reconfigurable logic gates with NAND/NOR dual functions, whose input-output mapping can be transformed in real-time without changing the layout. These reconfigurable circuits will serve as important building blocks for high-density data-stream processors and reconfigurable Application-Specific Integrated Circuits.

Content addressable memory (CAM) is one of the promising in-memory computing circuits widely used in high-speed search applications. However, traditional SRAM-based CAM needs ten transistors (10T) per bit, which imposes severe limits on the area and energy efficiency. We developed a novel 1-transistor-per-bit CAM based on the ferroelectric reconfigurable transistor. By exploiting the switchable polarity of the ferroelectric reconfigurable transistor, XOR/XNOR-like matching operation in CAM can be realized in a single transistor. By eliminating the need for the complementary circuit, these non-volatile CAMs based on reconfigurable transistors can offer a significant improvement in area and energy efficiency compared to conventional CAMs.

Furthermore, we developed multifunctional devices based on semiconducting ferroelectrics (In_2Se_3), which can concurrently serve as an electronic memory, photonic memory, logic gate, and photodetector [2]. This dual electrical and optical operation of the memories can simplify the device architecture and offer additional functionalities, such as ultrafast optical erasing of large memory arrays. We also demonstrated reconfigurable Schottky diodes based on $\text{In}_2\text{Se}_3/\text{graphene}$ heterostructures, where the diode polarity is reversible via switching the In_2Se_3 polarization. The current ratio between ON and OFF states at a given read voltage can be as high as 100. These results indicate that ferroelectric In_2Se_3 and other semiconducting ferroelectric materials have great potential for multifunctional devices.

Acknowledgment: The authors would like to thank the support from Semiconductor Research Corporation (SRC) under grant SRC 2021-LM-3042.

References:

- [1] Z. Zhao, S. Rakheja, and W. Zhu, Nano Letters, vol. 21, no. 21, pp. 9318, 2021.
- [2] K. Xu, W. Jiang, X. Gao, Z. Zhao, T. Low, and W. Zhu, Nanoscale, vol. 12, no. 46, pp. 23488, 2020.
- [3] J. Liu, H. Ryu, and W. Zhu, IEEE Transactions on Electron Devices, vol. 68, no. 3, pp. 1334, 2021.
- [4] Z. Zhao, K. Xu, H. Ryu, and W. Zhu, ACS Appl Mater Interfaces, vol. 12, no. 46, pp. 51820, 2020.
- [5] H. Ryu, K. Xu, D. Li, X. Hong, and W. Zhu, Applied Physics Letters, vol. 117, no. 8, p. 080503, 2020.
- [6] H. Ryu, H. Wu, F. Rao, and W. Zhu, Sci Rep, vol. 9, no. 1, p. 20383, 2019.

4:15 PM EL07.12.04

Application of Van der Waals CuInP_2S_6 in Multifunctional Devices YiqunLiu, YonghuangWu, HaojieHan, RuixuanPeng, HetianChen, DiYi, KaiLiu, Ce-WenNan and JingMa; Tsinghua University, China

CuInP_2S_6 (CIPS) has gained widespread attention as an emerging room-temperature two-dimensional ferroelectric material due to its novel physical properties. There is a growing demand for achieving diverse and complex functional features in simpler device structures, aiming to simplify peripheral circuit design and reduce overall production costs. Memristors play a crucial role in realizing the in-memory computing. Versatile memristors, which can achieve non-volatile and volatile performances in a single device, holds the potential for achieving selector and memory functions simultaneously, also opening up possibilities for emulating artificial neural networks (ANN) and spiking neural networks (SNN) in a single cell. In CIPS-based versatile memristor, electrochemically active Ag is utilized as the top electrode, and resistive switching is achieved by the formation and rupture of conductive filaments under the electric field. By controlling the compliance currents (CCs) during the test, both volatile and non-volatile resistive switching can be realized in the single device. Stable diode-like volatile behaviors with notable rectification ratio of 10^3 are exhibited with CCs = $10 \mu\text{A}$. In the same device, non-volatile memory performances with on/off ratio of 10^3 and remarkable retention time up to 10^4 s are acquired under CC = 5 mA. A 3×3 crossbar memory array is also fabricated, demonstrating the potential pattern learning in actual application. What's more, optoelectronic synapses are receiving a burgeoning amount of interest due to their ability to mimic the functionality of the human visual system. Integrating electronic and optoelectronic synapses into a single device enables their applications in more complex scenarios while maintaining low power consumption. In simple graphene/CIPS/Au device configuration, the migration of Cu^+ ions under electrical stimuli and persistent photoconductivity under optical stimuli were leveraged to demonstrate the simultaneous realization of electronic and optoelectronic synapse functionalities. Taking advantage of optical-electrical cooperative effect, information perception, processing, memorizing and light adaption behavior were efficiently demonstrated in such simple-structure electronic/optoelectronic synapse, paving a prospective way towards achieving artificial visual system. The findings presented contribute to the advancement of CIPS-based devices and their potential for various applications in the field of multifunctional electronic devices.

4:30 PM EL07.12.05

Monolayer Electrolytes for Nonvolatile Memory: Impact of Salt Identity on Electrical Characteristics HuiranWang, ShubhamS. Awate and SusanFullerton; University of Pittsburgh, United States

A solid-state, non-volatile memory based on electric-double-layer (EDL) gating using a monolayer electrolyte (ME) has been developed in our lab. This ME comprises cobalt crown ether phthalocyanine (CoCrPc), with four, 15-crown-5 ethers (15C5) attached, and a lithium salt that forms an ordered array on the two-dimensional (2D) semiconductor surface. The monolayer electrolyte is capped with h-BN. Each crown solvates one metal cation that is stable in two distinct states in the crown: one near the 2D semiconductor, creating a low-resistance state, and the other near h-BN, creating a high-resistance state. The switching mechanism is triggered by an electric field via a back-gated field-effect transistor (FET). Prior work focused exclusively on LiClO_4 deposited with ethanol. Here, we report on additional salt/solvent systems and their impact on switching, including LiCl , LiI , NaClO_4 , and $\text{Ca}(\text{ClO}_4)_2$. The surface roughness (R_q) of bare WSe_2 flakes before electrolyte deposition is typically 0.2 ± 0.01 nm, and after 15C5-CoCrPc/ LiClO_4 deposition, the R_q increases by a factor of 2 to 3. Therefore, for electrical characterization, we select salts for which the R_q remains within this range: LiCl , NaClO_4 , $\text{Ca}(\text{ClO}_4)_2$ in ethanol. Non-volatile subthreshold voltage shifts (ΔV_S) in the range of 9 – 15 V are observed for all three salts measured, indicating that all three are bistable in 15C5-CoCrPc. Specifically, ΔV_S of 9.1 ± 1.4 , 14 ± 2.1 , and 9.2 ± 0.3 V for LiCl , NaClO_4 , and $\text{Ca}(\text{ClO}_4)_2$, respectively, correspond sheet carrier densities (Δn_S) of 1.4×10^{11} , 1.2×10^{12} , $1.0 \times 10^{12} \text{ cm}^{-2}$. Thus, the best performing salts are those containing perchlorate anions with doping densities on the order of 10^{12} cm^{-2} , suggesting that the anion may play an important role in the switching mechanism. ON/OFF ratios of $< 10^3$, $\sim 10^3$, and $\sim 10^3$ are measured for LiCl , NaClO_4 , and $\text{Ca}(\text{ClO}_4)_2$, respectively. These ratios are similar to what we observe in LiClO_4 , indicating two distinguishable resistance states in MERAM. Retention measurements will be reported. These findings advance our goal of developing a high-speed, non-volatile memory at the limit of scaling. This work is supported by the NSF under Grant # NSF-DMR-EPM CAREER: 1847808.

4:45 PM EL07.12.06

Highly Nonlinear Memory Selectors with Ultrathin $\text{MoS}_2/\text{WSe}_2/\text{MoS}_2$ Heterojunction HongyeChen¹, TianqingWan¹, YueZhou¹, JianminYan¹, HongyuYu² and YangChai¹; ¹The Hong Kong Polytechnic University, Hong Kong; ²Southern University of Science and Technology, China

Two-terminal (2D) resistive random access memory (RRAM) crossbar arrays require the highly nonlinear selector with high current density to address a specific memory cell and suppress leakage current through the unselected cell. Three-dimensional (3D) monolithic integration of RRAM array requires selector devices with a small footprint and low-temperature processing for ultrahigh-density data storage. Here, we design an ultrathin two-terminal n-p-n selector below 10 nm with 2D transition metal dichalcogenides (TMDs) by a low-temperature transfer method. The van der Waals (vdW) contact between transferred Au electrodes and 2D TMDs reduces the Fermi level pinning and retains the intrinsic transport behavior of TMD. The selector with single type of TMD exhibits a trade-off between the current density and nonlinearity depending on the barrier height. By controlling the thickness of p-type WSe_2 in $\text{MoS}_2/\text{WSe}_2/\text{MoS}_2$ n-p-n selector and tuning the Schottky barrier height for a punch-through transport, the selector shows high nonlinearity (~ 230) and high current density ($2 \times 10^3 \text{ A/cm}^2$) simultaneously. We further integrate the n-p-n selectors with a bipolar hexagonal boron nitride (h-BN) resistive switching memory and calculate the maximum crossbar size of the 2D material-based 1S1R according to a 10% read margin, which offers the possible realization of future 3D monolithic integration.

8:15 AM EL07.13.01

Electrical Transport in Carbon Nanotubes and Junction Conductance [Vasili Perebeinos¹](#), [Davoud Adinehloo¹](#), [Weilu Gao²](#), [Ali Moji pour³](#) and [Junichiro Kono³](#); ¹University at Buffalo, United States; ²The University of Utah, United States; ³Rice University, United States

In the study of carbon nanotubes (CNTs), we simulate the junction conductance within a tight-binding model approach. The interplay of intertube and intratube conductance as a function of temperature and CNT chirality explains the experimental measurements in CNT films of separated CNT chirality [1]. By using Anderson model, we were able to calculate the conductance in different types of CNTs. Our findings showed that intratube conductance dominates conductance in CNTs with small localization lengths. In the case of armchair CNTs, we find that at room temperature, phonon-assisted intertube junction conductance dominates the transport properties of the films. We performed a comprehensive study of the dependence of junction conductance on different factors, such as the angle between the CNTs, the twist angle, the sliding shift of the CNTs, the Fermi energy, and the applied bias voltage between CNTs [2]. Using a single geometrical fitting parameter, our calculations perfectly matched the temperature-dependent conductance measurements.

[1] W. Gao, D. Adinehloo, X. Li, A. Moji pour, Y. Yomogida, A. Hirano, T. Tanaka, H. Kataura, M. Zheng, V. Perebeinos, J. Kono, "Band structure-dependent electronic localization in macroscopic films of single-chirality single-wall carbon nanotubes", *Carbon* 183, 774 (2021).

[2] D. Adinehloo, W. Gao, A. Moji pour, J. Kono, and V. Perebeinos, "Phonon-Assisted Intertube Electronic Transport in an Armchair Carbon Nanotube Film," *Phys. Rev. Lett.* 130, 176303 (2023).

8:30 AM *EL07.13.02

Low-Thermal-Budget Synthesis of MoS₂ on 8" Wafers for BEOL and FEOL Transistors [Jiadi Zhu](#), [Ji-Hoon Park](#), [Jing Kong](#) and [Tomas Palacios](#); MIT, United States

The development of low-thermal-budget (<300C) synthesis technologies for two-dimensional materials such as Molybdenum Disulfide (MoS₂) enables both new architectures for front end of the line (FEOL) transistors, but also the integration of these devices on new substrates as well as at the back end of the line (BEOL) of Silicon chips. This paper describes our recent work on the synthesis of MoS₂ below 300C and its applications to electronic devices. The trade-offs between growth temperature, precursor partial pressures and flows, substrate diameter, mobility and grain size will be discussed. Several device applications of the low temperature MoS₂ material will be presented, including FEOL single and multi-channel MoS₂ transistors, BEOL memory circuits, and high performance RF harvesting devices.

Acknowledgements.- This work has been partially supported by the MIT/Army Institute for Soldier Nanotechnologies, the NSF Center for Integrated Quantum Materials, the SRC CHIMES and SUPREME JUMP 2.0 Centers, Ericsson, and the Army Research Office.

9:00 AM EL07.13.03

Chip-Less Wireless Electronic Skin Sensors Enabled by Epitaxial Freestanding Compound Semiconductors [Yeongin Kim^{1,2}](#), [Junmin Suh¹](#), [Jiho Shin¹](#), [Yunpeng Liu¹](#), [Jiyeon Han³](#) and [Jeehan Kim¹](#); ¹Massachusetts Institute of Technology, United States; ²University of Cincinnati, United States; ³Amorepacific R&D Center, Korea (the Republic of)

Electronic skin (e-skin) has been developed with a goal to obtain a non-invasive human health monitoring electronic system with its imperceptibility. So far, one of the major shortcomings in this field is the bulky wireless communication system that severely affects its wearability. In this work, we introduce a single-crystalline non-Si-based e-skin system where fully conformable, ultrathin, piezoelectric, compound semiconductor membranes are incorporated as power-efficient wireless communication modules and extremely high sensitivity sensors without needing for bulky chips and batteries. The developed GaN surface acoustic wave-based device successfully measured wirelessly three different inputs including strain, ultraviolet light, and ion concentrations. The consistency and accuracy of the measured heart rate and pulse waveforms over a 7-day period, during which the e-skin was re-attached 7 times, strongly demonstrate the reusability and long-term wearability of our device. This study will change the paradigm of e-skins by providing versatile wireless platforms for fully imperceptible e-skins with very high sensitivity and low power consumption.

9:15 AM EL07.13.04

Large-Scale Integrated Vector-Matrix Multiplication Processor Based on Monolayer MoS₂ [Guilherme Migliato Marega](#), [Hyun Goo Ji](#), [Zhenyu Wang](#), [Mukesh Tripathi](#), [Aleksandra Radenovic](#) and [Andras Kis](#); Ecole Polytechnique Federale de Lausanne, Switzerland

In recent years, data-driven algorithms took the spotlight promising new and efficient ways for processing and extracting meaningful information from ever-growing amounts of generated data. Although the von-Neuman architecture was the backbone of the data revolution, the separation of the memory and processing units makes the current processors spend a significant amount of energy moving data compared to the energy spent in computing [1]. This motivated the research in emerging computer architectures which could provide energy benefits while performing data-driven algorithms, such as artificial neural networks or signal and image processing. Among the different proposals, in-memory computing has been systematically shown to be beneficial for the previously mentioned applications [2]. Despite the intense research efforts put into the types of memory devices used in this architecture, no technology has been able to satisfy all the requirements [3]. The lack of a universal memory platform for performing computation has led to the investigation using two-dimensional materials as a promising material system for this emerging architecture [4]. In this light, here, we fabricated a 32x32 vector-matrix multiplier with 1024 floating-gate field-effect transistors (FGFET) that use atomically thin MoS₂ as the semiconducting channel material. This large-scale integration device is developed in a wafer-scale fabrication process, achieving high yield and low device-to-device variation. Due to the low device variability, an open-loop programming scheme can be employed while obtaining multi-level memory behavior. Finally, our in-memory processor is used to demonstrate discrete signal processing based on vector-matrix multiplications. Our findings lay the foundations for creating complex in-memory processors that can harvest all the advantages of 2D materials.

[1] G. Kestor, R. Gioiosa, D. J. Kerbyson, and A. Hoisie, "Quantifying the energy cost of data movement in scientific applications," in 2013 IEEE International Symposium on Workload Characterization (IISWC), Sep. 2013, pp. 56–65. doi: 10.1109/IISWC.2013.6704670.

[2] S. Yu, "Neuro-inspired computing with emerging nonvolatile memories," *Proceedings of the IEEE*, vol. 106, no. 2, pp. 260–285, Feb. 2018, doi: 10.1109/JPROC.2018.2790840.

[3] H.-S. P. Wong and S. Salahuddin, "Memory leads the way to better computing," *Nature Nanotech.*, vol. 10, no. 3, Art. no. 3, Mar. 2015, doi: 10.1038/nnano.2015.29.

[4] G. Migliato Marega et al., "Low-Power Artificial Neural Network Perceptron Based on Monolayer MoS₂," *ACS Nano*, vol. 16, no. 3, pp. 3684–3694, Mar. 2022, doi: 10.1021/acsnano.1c07065.

9:30 AM *EL07.13.05

Van der Waals Integration beyond the Limits of Van der Waals Forces [Farnaz Niroui](#); Massachusetts Institute of Technology, United States

Heterostructures of dissimilar materials are core building blocks of nanoscale devices. Their growth through common chemical epitaxy or physical vapor deposition often poses strict chemical and physical compatibility constraints, limiting accessible heterostructures due to potential disorder and damage. Physical stacking provides an alternative approach to hetero-integration. This has been the foundation of the growing discipline of van der Waals (vdW) integration for 2D materials and materials of varying other dimensionalities. However, vdW integration faces a fundamental limit due to vdW forces being dependent on the intrinsic materials' optical and electrical properties and thus not readily tailorable to allow direct integration of arbitrary layers. Here, we introduce the adhesive matrix transfer approach to overcome this fundamental limit to enable direct fabrication of conventionally-forbidden vdW heterostructures and single-step 2D material-to-device integration. As no solvents, high-temperatures or sacrificial layers are involved, our platform yields pristine surfaces and interfaces uniquely suited for studying the intrinsic properties of 2D materials and leveraging them in device applications which will be discussed.

10:00 AM BREAK

10:30 AM EL07.14.01

NIL, Nanopatterning and Etching of Nanopillars for GaN-Based microLEDs [Nabil Labchir](#)¹, [Saber Hammami](#)², [Kilian Baril](#)³, [Maya Wehbe](#)³, [Sébastien Labau](#)¹, [Camille Petit-Etienne](#)¹, [Blandine Alloing](#)³, [Matthew Charles](#)², [Jesus Zuniga Perez](#)³ and [Cécile Gourgou](#)¹; ¹LTM/CEA, France; ²CEA Leti, France; ³CRHEA_CNRS, France

At present, GaN-based μ LED optoelectronic devices are progressing beyond solid-state lighting, inspiring a fascinating new category of applications. Indeed, the μ display sector has reached a highly dynamic expansion phase. Unlike conventional displays, μ displays require image magnification to be seen by the human eye. However, they must be able to display an image of similar quality to that of standard in terms of definition, i.e. number of pixels. To display as many pixels on a smaller surface, we need to reduce the pixel pitch, i.e. the distance between two pixels, from a few hundred micrometers to only a few micrometers. At present, controlling the internal crystal quality of the GaN substrate permits the development of smaller, more efficient μ LEDs. However, the μ LED lifetime is highly dependent on the density of dislocations inside GaN which behave as non-emissive zones on the μ LED surface. In this context, nanoimprint lithography (NIL) will be deployed to nanotexture silicon-on-insulator (SOI) substrates in order to achieve a high density of GaN growth sites. The regrowth on these SiO₂-based sites enhances the GaN quality and therefore the μ LEDs performance. The innovation in our strategy is based on the nanopatterning of deposited GaN/AlN layers on 3 cm² SOI surface for fabricating 200 nm nanopillar arrays with zero defect and that possess SiO₂ at the bottom, using both NIL and plasma etching techniques. Here, I have developed a process without lift-off that is compatible with industrial transfer by using metal hard mask etching. In this process, I have controlled pillar arrays with 150 nm in diameter at the bottom, and I have carefully optimized the plasma etching of materials at all the different steps, especially at the NIL and hard mask sections. For transferring our zero-defect protocol to large-scale production, we are working on extending our strategy to fabricate μ LEDs on 200-300 mm wafers. This research will provide a breakthrough for the future optoelectronics industry of displays.

10:45 AM EL07.14.02

Polarity-Reversible 2D MoTe₂ Field-Effect Transistors and Their Logic Applications [Byoung-Soo Yu](#)^{1,2}, [Jongtae Ahn](#)¹, [Wonsik Kim](#)¹, [Soohyung Park](#)¹ and [Do Kyung Hwang](#)^{1,2}; ¹Korea Institute of Science and Technology, Korea (the Republic of); ²University of Science and Technology, Korea (the Republic of)

2H-type molybdenum ditelluride (MoTe₂) has been greatly spotlighted as a semiconducting TMDC material which facilitates polarity transition between high performance n- and p-type characteristics due to its small bandgap of ~ 1.0 eV. However, the reversible polarity control between unipolar n- and p-type conduction in MoTe₂ is still challenging, which causes difficulties for device strategies which require unlimited manipulation of carrier transport properties of MoTe₂ devices. Here, we demonstrate reversible polarity transition between unipolar n- and p-type characteristics in MoTe₂ FETs by controlling annealing environment. Fermi level shift and formation/removal of oxygen relevant phases in the MoTe₂ layer are repetitively occurred with the change of annealing atmospheres. Also, the polarity modulations in well-designed MoTe₂ devices are compatible with the phenomena presented in MoTe₂ material. This precise polarity control in MoTe₂ FETs eventually permits to realize functional logic application such as an inverter circuit.

11:00 AM *EL07.14.03

Graphene Nanoribbons for Optical Applications: Insights from *Ab Initio* Simulations [Deborah Prezzi](#); Consiglio Nazionale delle Ricerche, Italy

To be sent

11:30 AM EL07.14.04

Micro-Heater Integrated Nanotube Array Gas Sensor for Parts-Per-Trillion Level Gas Detection and Single Sensor-Based Gas Discrimination [Wenying Tang](#) and [Zhiyong Fan](#); The Hong Kong University of Science and Technology, Hong Kong

Ensuring chemical safety and safeguarding human health require real-time monitoring and discrimination of trace gases using appropriate gas sensors. Typically, these tasks involve expensive, bulky, and power-hungry devices such as optical and electrochemical gas sensors. Metal oxide (MOX) semiconductor gas sensors possess several attractive features, such as low cost, small size and long lifespan, making them promising candidates for highly integrated sensor systems. Unfortunately, the mainstream MOX sensors suffer from poor selectivity and sensitivity, which have limited their application.

Researchers have made great efforts to address the limitations of MOX-based gas sensors. Various strategies have been explored to improve the poor sensitivity and LOD of MOX-based gas sensors, such as adding a porous overlayer on top of the sensing films as a molecular sieve or functionalizing the surface with noble metals or oxides as catalytic sites. For selectivity issue, gas sensor array with various sensing pixels has been broadly applied to discriminate multiple gases. However, the construction of complicated gas sensor arrays and the processing of high-dimensional sensing data pose significant challenges, which highlights the urgent need for gas discrimination based on a single sensor. Temperature modulation, which can provide temperature-dependent kinetic information, has been widely utilized to trigger single-sensor based gas discrimination. Nonetheless, most of the related studies discriminated gas species with the sensor responses under different operation temperatures using the continuous heating (CH) mode, which is difficult to realize real-time gas recognition due to the long operation periods. In contrast, pulse heating, featuring periodic transient thermal cycle, has great potential for real-time gas discrimination since it provides the transient characteristics emerging from gas diffusion and gas-solid surface reactions between gas molecules and sensing materials. However, most of the proposed pulse-driven MOX sensors focused on reducing power consumption and improving gas sensing performance. The gas discrimination capability of pulse-driven MOX sensors through extracting transient features has been rarely explored in the past.

In this study, we demonstrated a novel gas sensor called micro-heater integrated nanotube array gas sensor (MINA sensor), which can operate in dual modes. The sensor can detect multiple gases at parts-per-trillion (ppt) level under the CH mode and distinguish multiple gases under the PH mode. We constructed the MINA sensor on the nano-porous anodic aluminum oxide (AAO) templates with a top-bottom electrode structure, which significantly increases the sensor's surface area for molecular access. To create the sensing material layer, we used atomic layer deposition (ALD) to deposit an ultrathin and conformal SnO₂ thin film and decorated it with Pd nanoparticles (NPs). When operating under the CH mode, the MINA sensor could detect hydrogen, acetone, toluene and formaldehyde with measured LODs as low as 100 ppt, 100 ppt, 100 ppt, 4 ppb, with the corresponding theoretical LODs as 6.96 ppt, 11.88 ppt, 16.52 ppt, 70.06 ppt, respectively. Under PH mode, the MINA sensor provided varying transient responses to different gases due to the variations of gas diffusion and surface reaction activation energy of the gases. By analyzing the conductance amplitude and slope features of a single pulse, different concentrations of hydrogen, acetone, toluene, and formaldehyde can be distinguished. Furthermore, the PH mode saved 66.7% energy compared to the traditional CH mode. The remarkable capabilities of the MINA sensor make it highly appealing for various applications, including distributed low-power sensor networks and battery-powered mobile sensing systems for chemical safety, environmental monitoring, and healthcare.

11:45 AM EL07.14.05

High-Performance Infrared Light-Emitting Diodes Based on Chirality-Sorted Carbon Nanotube Films [Bing Han](#) and [Sheng Wang](#); Peking University, China

An important goal in the carbon nanotube (CNT) optoelectronics is to achieve a high-performance near-infrared (NIR) light source. But there are still many challenges such as CNT chirality purity, defects, thin film quality and device structure design. Here, we realized high-performance infrared light-emitting diodes (LEDs) based on the high chirality purity (10, 5) single-walled carbon nanotubes (SWCNTs) network film. Asymmetric palladium (Pd) and hafnium (Hf) contacts were used as the holes and electrons injection electrodes of the LEDs, respectively. However, the large Schottky barrier between the Hf electrode and CNTs, resulting from the polymer wrapped on the CNT surface during the sorting process, leads to difficult electron injection and low efficiency of electroluminescence (EL). We found that the electron injection efficiency could be improved by the local doping of the CNT channel with dielectric layers of YOX-HfO₂, which reduced the Schottky barrier for electron injection from Hf electrodes. At last, our CNT LED device exhibits a high external quantum efficiency (EQE) of about 5×10⁻⁴ without any optical coupling structure. It shows an EL peak at the optical communication O band of 1290 nm with a simple structure and low work voltage. It's believed that the chiral CNT infrared light source has great application potential in the field of the CNT monolithic optoelectronic integrated system and on-chip optical interconnection.

SESSION EL07.15: 1D and 2D Materials—Sensors and Actuators II

Session Chairs: [Farnaz Niroui](#) and [Haozhe Wang](#)

Friday Afternoon, December 1, 2023

Hynes, Level 3, Ballroom B

1:30 PM EL07.15.01

Enhancing Electrochemical Sensing via Hybridization of 2-D Mxene and Transition Metal Dichalcogenides [Lia Stanciu](#), [Winston Y. Chen](#) and [Dimitrios Stanciu](#); Purdue University, United States

The exceptional conductive properties, flexibility, and surface functionality of two-dimensional (2D) transition-metal carbides/nitrides (MXenes) position them as prospective electronic materials for electronic devices and electrochemical sensors specifically. Nonetheless, strategies to amplify MXene's sensitivity to volatile organic compounds (VOCs) in particular remain relatively uncharted. In this study, we elucidate a novel methodology involving surface treatment and exfoliation to fabricate a hybrid material of 2D WSe₂ and Ti₃C₂T_x.

By employing scanning electron microscopy, transmission electron microscopy, X-ray diffractometry, and dynamic light scattering, we characterized the microstructure, size, and surface charge states (zeta potential) of WSe₂ and Ti₃C₂T_x nanosheets. This extensive analysis facilitated the optimal processing of the WSe₂ and Ti₃C₂T_x hybrid, enabling its use as ink for ink-jet printing of flexible Ti₃C₂T_x/WSe₂ electrochemical sensors, which are integrated into wireless systems.

VOCs were selected as the test subject to elucidate the functional properties of these 2D nanohybrids for electrochemical sensing. Within this configuration, the Ti₃C₂T_x scaffold contributes high electrical conductivity while the WSe₂ nanoflakes impart remarkable sensitivity and enhanced selectivity to VOCs.

Contrasted with other Ti₃C₂T_x reference sensors and 2D materials-based sensors, the Ti₃C₂T_x/WSe₂ sensors exhibit superior resilience after numerous bending cycles. They also demonstrate exceptional electrochemical durability and sustained response, with distinct selectivity for detecting model VOCs (ethanol, methanol, acetone, hexane, benzene and toluene) across a broad concentration range (1–40 ppm) at room temperature.

This work is expected to illuminate a path for future exploration into the hybridization of 2D MXenes, paving the way for the creation of high-performance electrochemical sensing devices.

1:45 PM EL07.15.02

Meniscus-Guided Control of Highly Wrinkled Reduced Graphene Oxide-Based Electrodes for Sensing ER Stress-Related Antibodies [Su Yeong Kim](#), Jeong Chan Lee and Steve Park; KAIST, Korea (the Republic of)

As the aging society emerges, the market for point-of-care (POC) biosensing platforms that can quickly and efficiently diagnose diseases like cancer and diabetes is rapidly expanding. Implantable electrochemical biosensors within the body enable rapid and continuous detection and facilitate prompt personalized medical treatments. Recent research has focused on flexible fiber or wire-based implantable biosensors coated with nanostructured conductive materials. This innovation addresses the degradation of the signal-to-noise ratio caused by the mechanical mismatch between the biosensor and the surrounding tissues. By overcoming this challenge, these biosensors enable accurate and continuous monitoring of biomarkers and drug delivery over extended periods. However, wire-based electrochemical biosensors face several obstacles in detecting target biomarkers within tissues. These include (1) degradation of sensing performances (i.e., sensitivity, specificity) and shelf-life of the biosensor due to non-specific binding and biofouling of various biomolecules, (2) false positive and negative increment during diagnosis, and (3) potential inflammation caused by the low bio-compatible nanomaterials. Addressing these challenges is crucial for the successful development of effective wire-based electrochemical biosensors for clinical applications.

Here, we designed the wire-based electrochemical biosensor by coating the highly porous antifouling matrix composed of cross-linked bovine serum albumin (BSA) and pentaamine-functionalized reduced graphene oxide (prGOx). The conventional antifouling coating still has an issue of high electrochemical impedance because the coating is thick to improve the antifouling properties, such as the blocking layer with the BSA solution and PEG hydrogel-based coating. Unlike these coatings, we optimized the composition of cross-linker, or glutaraldehyde (GA), to contain high porosity and durability while maintaining the biocompatibility of the antifouling matrix. Coated through a solution process on gold wires, this coating showed a BET surface area two-folds higher than conventional BSA structure and provided the micro-level electrochemical signal and high antifouling property of 95 % under serum conditions. This wire-based biosensor was used to confirm the real-time glucose detection with a dynamic concentration range of 0.4 mM to 0.9 mM. In addition, we demonstrated the in-vitro stability of this sensor by detecting glucose with constant sensitivity in the presence of various nonspecific substances from the serum. As a result, this highly durable wire-based electrochemical biosensor enables various applications of implantable biosensing and customized diagnosis and treatment with high accuracy.

2:00 PM EL07.15.03

Rational Design of Graphene Quantum Dots for Light-Activation in Organic-Inorganic Hybrid Nanostructure: Toward Room Temperature Gas Sensing [Jinho Lee](#), Minhyun Kim, Seyeon Park and Il-Doo Kim; Korea Advanced Institute of Science and Technology, Korea (the Republic of)

The demand for power-efficient, high-performance gas sensors operating at room temperature has promoted research into light-activated gas sensors for Internet of Things (IoT) applications. While semiconducting metal oxides have been extensively employed due to their suitable electronic band structure for light absorption, their low gas response with light-activation mechanism still requires improvement with effective strategies such as catalyst decoration for enlarging light absorption. Recently, graphene quantum dots (GQDs) have newly proven their catalytic ability for room temperature gas sensing with their tunable electronic band structure and surface functional groups. Herein, we decorated high-quality GQDs on In₂O₃ nanofibers with varying the size of GQDs (2 nm to 20 nm) for enhancing light-absorption of In₂O₃ nanofiber. The electronic band gap of GQDs was tuned from ~ 2 eV to 3.5 eV to facilitate optimized light absorption and electronic transfer. The gas sensing performance of GQDs decorated In₂O₃ nanofiber was investigated with NO₂ gas under different light illumination (UV, violet, blue, green) at room temperature. Regardless of the GQD size, the GQD decoration improves NO₂ gas responses compared to bare In₂O₃. Notably, pristine In₂O₃ nanofibers exhibited their highest gas response under violet light. However, upon decoration with graphene quantum dots (GQDs), a notable shift in the activation wavelength toward a longer wavelength, specifically blue light. The most significant enhancement was observed with 5 nm-sized GQD under blue light, resulting in a remarkable 5-fold improvement in NO₂ gas response. This improvement can be attributed to the modulation of GQD electronic band gaps, enabling enhanced light absorption and suitable band alignment. In addition, the oxygen functional groups in GQDs can lower the adsorption energy of NO₂ gases, realizing selective gas responses to NO₂ gas. Our findings offer fundamental insights into the potential of graphene quantum dots as catalysts for high-performance light-activated gas sensors, paving the way for advancements in IoT applications with their low-power consumption and room-temperature operation.

2:15 PM EL07.15.04

Thermoelectric Structure-Property Relationship Establishment in TiGaSe₂ [Tigran Simonian](#)¹, [Ahin Roy](#)¹, [Zdenek Sofer](#)² and [Valeria Nicolosi](#)¹; ¹Trinity College Dublin, Ireland; ²University of Chemistry and Technology Prague, Czechia

Layered 2D materials are increasingly investigated for their often highly anisotropic properties, such as thermoelectricity. Such a property is useful in electronics, such as transistors and sensors, where wasted heat is not only economically and environmentally unsustainable, but can also be detrimental to device performance. It is repeatedly assumed that planar defects, such as stacking faults, affect the thermoelectric properties of these materials [1-2]. However, to date, no comprehensive study into establishing this relationship has been performed.

In this work, the ternary chalcogenide TiGaSe₂ serves as a prototypical example of this type of analysis. TiGaSe₂ is characterized via (scanning) transmission electron microscopy (STEM) and density functional theory (DFT) simulations. Streaking in selected area diffraction patterns are correlated to simulations which indicate the presence of stacking faults in the growth direction [3]. High resolution STEM confirms these stacking faults and indicates a lack of long-range order to the stacking. DFT calculations reveals a high preference for the system to include these faults. This is then coupled with phonon dispersion and electron transmission simulations to confirm their relationship to the thermoelectric properties of the material.

References:

- [1] A. Cengiz, Y. M. Chumakov, M. Erdem, Y. Sale, F. A. Mikailzade, and M. Y. Seyidov, "Origin of the optical absorption of TiGaSe₂ layered semiconductor in the visible range," *Semicond. Sci. Technol.*, vol. 33, no. 7, 2018.
- [2] M. Caydasi, M. F. Mintas, Y. M. Chumakov, S. Volz, A. Cengiz, and M. Y. Seyidov, "A Study of Thermoelectric Performance of TiGaSe₂ Layered Dichalcogenides from First-Principles Calculations: Vacancy Defects Modeling and Engineering," *Phys. status solidi*, vol. 259, no. 1, p. 2100409, Jan. 2022.
- [3] D. F. McMorrow, R. A. Cowley, P. D. Hatton, and J. Banys, "The structure of the paraelectric and incommensurate phases of TiGaSe₂," *J. Phys. Condens. Matter*, vol. 2, no. 16, pp. 3699–3712, 1990.

2:30 PM EL07.15.05

Extra Polarization-Engineered Power Generation of CNT/Halide Composite Nanofibers [Ju Han](#)¹, [Da Bin Kim](#)^{1,2} and [Yong Soo Cho](#)¹; ¹Yonsei University, Korea (the Republic of); ²University of Toronto, Canada

Diverse nanostructures have been widely applied for efficient energy generation in low-power consuming and self-powering devices. Herein, we explore the origin of bending-driven power generation in carbon nanotube (CNT)/halide/poly(vinylidene fluoride-trifluoroethylene) (P(VDF-TrFE)) nanofiber and their versatile applications in piezoelectric energy harvester, tactile sensor, and pressure sensor. Two effective fillers of inorganic halide perovskite CsPbBr₃ nanocrystals and CNT were incorporated in P(VDF-TrFE) matrix to demonstrate bending-driven energy harvesting performances and their ability to sense physiological signals from the human motions. Owing to the synergistic piezoelectric coupling between the fillers and the matrix, impressive harvesting outputs of ~15.9 V and 1,128 nA were achieved for the 0.3 wt.% CNT and 5 wt.% halide-incorporated samples, which are ~17.6 and 10.5 times better than the results achieved for the pure P(VDF-TrFE) nanofiber harvester. The values are also the best values reported using bending-driven operations. The origin of substantial enhancements in electromechanical energy generation under the bending motions is attributed to the extra dipolar polarization by embedded CsPbBr₃ and space-charge polarization by dispersed CNTs in contact with the piezoelectric polymer matrix. Wearable physiological and pressure sensors were successfully demonstrated to effectively sense the motions and convert them into electric signals. The optimal nanofiber sensors demonstrated a wide force detection range from 0.002 N to 600 N, and superior reliability and repeatability for 20,000 cycles under the periodic mechanical deformation. Nanofiber composites-based pressure sensor was further applied in the pressure signal-mapping system, demonstrating its promising possibility in the self-powered

2:45 PM EL07.15.06

Conductive 2D Metal-Organic Frameworks for Chemical Sensor ApplicationsSeon-JinChoi; Hanyang University, Korea (the Republic of)

Metal-organic frameworks (MOFs) are materials formed by the combination of metal nodes and organic linkers. They possess a large surface area and high porosity, making them promising materials for chemical sensing applications. Several MOFs have been synthesized and utilized as chemical sensing layers in combination with other sensing materials such as metal oxides, as demonstrated in our previous studies [1-4]. However, intrinsic 3D MOFs typically exhibit insulating properties, which limits their application in electrochemical sensing materials. In contrast, electrically conductive 2D MOFs have recently gained attention for chemiresistive-type gas sensor applications. These materials possess intrinsic electrical conductivity and show redox-reactive properties with gaseous analytes.

The presentation will highlight recent progress in the development of conductive 2D MOFs and their application in chemiresistive-type gas sensors. Various electrically conductive 2D MOFs were prepared by combining metal nodes (Cu^{2+} , Ni^{2+} , and Co^{2+}) with an organic linker (hexahydroxytriphenylene, HHTP). The result showed that the 2D $\text{Cu}_3(\text{HHTP})_2$ MOF film exhibited high sensitivity toward hydrogen sulfide and toluene at room temperature. To gain insights into the fundamental sensing mechanism, an in-situ spectroscopy analysis technique was established. This technique involved monitoring surface adsorbed species and by-products after chemical reactions using Raman spectroscopy and gas chromatography-mass spectroscopy (GC-MS), respectively. Through these investigations, a better understanding of the fundamental sensing mechanisms of 2D MOFs was obtained, paving the way for the development of high-performance chemical sensors for environmental monitoring and healthcare applications.

References

- [1] Seon-Jin Choi, Hack-Jong Choi, Won-Tae Koo, Daihong Huh, Heon Lee*, and Il-Doo Kim*, *ACS Applied Materials & Interfaces*, Vol. 9, No. 46, pp. 40593–40603, 2017.
- [2] Won-Tae Koo, Ji-Soo Jang, Seon-Jin Choi, Hee-Jin Cho, and Il-Doo Kim*, *ACS Applied Materials & Interfaces*, Vol. 9, pp. 18069-18077, 2017.
- [3] Won-Tae Koo, Seon-Jin Choi, Ji-Soo Jang, and Il-Doo Kim*, *Scientific Reports*, Vol. 7, No. 45074, 2017.
- [4] Won-Tae Koo, Seon-Jin Choi, Sang-Joon Kim, Ji-Soo Jang, Harry L. Tuller, and Il-Doo Kim*, *Journal of the American Chemical Society (JACS)*, Vol. 138, pp. 13431-13437, 2016.

3:00 PMBREAK

3:30 PM EL07.15.07

Hierarchical MoS_2 @Au/N, S-Graphene Quantum Dots Tubular Nanostructure for Impedimetric Detection of C-Reactive ProteinNareshK. Dega¹, AkhileshB.Ganganboina² and Ruyey-AnDoong¹; ¹National Tsing Hua University, Taiwan; ²National Institute for Materials Science, Japan

Molybdenum disulfide (MoS_2), one of the most often used transitional metal dichalcogenides (TMDs), has gained increasing attention in various fields including sensors, lithium batteries, catalysts, and cancer therapy because of its high surface area, notable mechanical strength, efficient electron transport capabilities, and satisfactory chemical stability. However, the low conductivity of MoS_2 has limited its electrochemical applications. To address this limitation, the incorporation of metal nanoparticles or graphene-based nanomaterials has been commonly employed as a strategy to enhance the conductivity of MoS_2 . Herein, a novel 1D hierarchical MoS_2 tubular structures (MoS_2 HT) doped with Au nanoparticles and N, S-coped graphene quantum dots (NSGQDs) was successfully fabricated as the sensing probe of immunosensor for impedimetric detection of C-reactive protein (CRP), a widely recognized serum biomarker used to evaluate the presence of acute inflammatory response in patients. Initially, MoS_2 HTs were synthesized by hydrothermal method, and then Au nanoparticles were formed homogeneously on MoS_2 HT in the presence of HAuCl_4 solution. After the deposition of 3-9 nm NSGQDs by Au-thiol linkage and drop-casting on the screen-printed electrode (Es), the $\text{Es}||\text{MoS}_2$ @Au/NSGQDs served as a bifunctional probe to enhance the electrochemical performance by facilitating rapid electron transfer as well as to anchor the CRP-Ab for specific detection of CRP protein. The $\text{Es}||\text{MoS}_2$ @Au/S, N-GQD immunosensor exhibits a wide linear range of 7 orders of magnitude for CRP detection, and the limit of detection can be lower to 0.04 pg/mL. Moreover, the immunosensor shows remarkable selectivity towards CRP detection over other biomarkers and biomolecules and superior reproducibility after long-term storage. The obtained results have demonstrated the superiority of the proposed $\text{Es}||\text{MoS}_2$ @Au/NSGQDs impedimetric immunosensor for highly sensitive and selective detection of CRP. These findings highlight the potential fabrication of MoS_2 HT-based nanocomposites for high-performance electrochemical applications including electrochemical sensor and energy storage.

3:45 PM EL07.15.08

Magnetic Phase Transition and Magneto-Mechanical Coupling in Layered CrSBr Probed by Nano-Optomechanical ResonatorsFanFei¹, YuluMao¹, WenhaoLiu², BingLv²,YingWang¹ and JunXiao¹; ¹University of Wisconsin–Madison, United States; ²The University of Texas at Dallas, United States

Recent progress in 2D magnetic materials represents an emerging research frontier. For example, various types of novel magnetic orderings at 2D limit have been discovered, including collinear ferromagnets/antiferromagnets, noncollinear spin textures, quantum spin liquid and magnetic topological insulators [1]. In addition, their spin excitations and the coupling with other quasiparticles are expected to be substantially enhanced due to the weak dielectric screening at the 2D limit [2,3]. In contrast to the abundant optical and electrical studies, the thermodynamic and mechanical properties for these rich quantum phases and unique coupling physics are important yet missing.

In this talk, I will present our study of the thermodynamic and mechanical properties in van der Waals magnets using nano-optomechanical resonators. In particular we have successfully developed nanoscale resonators based on target ultrathin magnetic membranes CrSBr, in which mechanical properties of the membrane can be electrically driven and sensed by precise optical interferometry. The nanomechanical response contains critical thermodynamic and information in magnetostriction in different spin orderings. Our work advances the understanding of magneto-mechanical coupling in 2D magnetic materials and enables new opportunities for coupling light, magnetism, and mechanics at the nanoscale.

[1] C. Gong and X. Zhang, *Science* 363, 706 (2019).[2] M. Gibertini, M. Koperski, A. F Morpurgo, and K. S. Novoselov, *Nat. Nanotechnol.* 14, 408 (2019).[3] H. Kurebayashi, J. H. Garcia, S. Khan, J. Sinova, and S. Roche, *Nat. Rev. Phys.* 4, 150 (2022).

4:00 PM EL07.15.09

Impact of Precursor Material on the Structural, Chemical and Gas Chemoresistive Properties of β - Ga_2O_3 NanowiresMarinaRojano-Mateos^{1,1}, AnnaEstany-Macià^{1,1,2}, GuillemDomènech-Gil³, ElenaLopez-Aymerich², PaoloPellegrino¹, ChristopheSerre^{1,1}, MauricioMoreno-Sereno^{1,1}, JanRomano-deGea⁴, IsabelGracia⁵, CarlesCané⁶ and AlbertRomano-Rodriguez^{1,1}; ¹Universitat de Barcelona, Spain; ²Danmark Technical University, Denmark; ³Linköping University, Sweden; ⁴Ecole Polytechnique Federale de Lausanne, Switzerland; ⁵Consejo Superior de Investigaciones Científicas (CSIC), Spain

Gallium oxide (β - Ga_2O_3) is a wide band gap semiconductor material used in the fabrication of high power, high temperature and gas sensing devices. For its use as gas sensor, Ga_2O_3 in form of thin films has been demonstrated to be sensitive towards oxygen and reducing gases at temperatures above 600°C. To decrease the working temperature to bring sensors based on this material towards their compatibility with the Internet of Things (IoT), different innovations have been proposed, mainly based on surface functionalization, material doping or the increase of the surface-to-volume ratio using the nanowire (NW) morphology.

In this work we report the synthesis, characterisation and gas sensing behaviour of β - Ga_2O_3 NWs. These nanowires are fabricated via a metal-assisted vapour liquid solid (VLS) mechanism using either gallium metal evaporation or carbothermal reduction of Ga_2O_3 nanopowders and employing Au as seed for the growth. The NWs have been grown on oxidised silicon or on fused silica substrates. For their use as gas sensors, the NWs have been removed from the substrates where they grew and were transferred to substrates containing microelectrodes. In some cases, these are on placed on suspended microhotplates containing a buried heater. In this way, individual NWs have been contacted using Focused Electron (FEB) and Focused Ion Beam (FIB) Induced Deposition techniques, giving rise to resistors whose value changes in the presence of different gases, i.e., they are chemiresistors.

The grown NWs are monocrystalline and almost defect free, with a diameter of few tens of nm and lengths in the range of several tens of micrometre, which increases with evaporation time. The NWs grown by carbothermal reduction present, in addition, a carbon-containing shell, which is the result of the use of graphite. From the electrical point of view, this shell gives rise to an important reduction of the resistance of the resistor. The electrical properties of these chemoresistive gas sensors have been measured in the presence of different gases, which will be described.

The structural and chemical properties grown materials, their sensing behaviour and the differences among them will be discussed as a function of the fabrication routes employed.

4:15 PM EL07.15.10

Interfacial Engineering of Reduced Graphene Oxide Sensing Layer for Remote Floating-Gate FET SensorsWenZhuang^{1,2}, Hyun JuneJang^{1,2}, XiaoyuSui^{1,2}, ByunghoonRyu²,YuqinWang^{1,2}, HaihuiPu^{1,2} and JunhongChen^{1,2}; ¹University of Chicago, United States; ²Argonne National Laboratory, United States

With the increasing demand for field-deployable, sensitive, and low-cost sensors, nanomaterial-based field-effect transistor (FET) sensors have been widely studied over the past decades, due to the advantages in rapid response, lower detection limit, miniaturized sensor chip and direct digital readout. Two-dimensional (2D) materials such as reduced graphene oxide have gained the attention for FET sensors due to excellent mechanical, electrical and physicochemical properties, which enables extremely higher sensitivity and stronger selectivity to analytes compared to

bulk counterparts. Despite numerous demonstrations of high sensitivity given by 2D reduced graphene oxide (rGO) FET sensors, there is a lack of fundamental understanding of rGO interfaces, especially to improve sensing performance by engineering the rGO interfaces.

In rGO-based sensors, it has been challenging to characterize the intrinsic properties of solution interfaces due to a lack of reliable analytical tool. In our previous work, a remote floating-gate (RFG) structure proposed for a 2D rGO layer eliminates non-reliable behaviours of solution interfacial properties while remaining in a high surface-to-volume ratio at the sensing zone. To be specific, the RFG structure enables to avoid any undesirable effects from interface traps, defects, and redox reactions of 2D rGO sensing membrane, which produces a high yield of signal reproducibility and could serve as a potential analytical platform to study the rGO interfaces.

In this work, we investigated properties of rGO-based sensors that are prepared with self-assembled layers such as (3-Aminopropyl) trimethoxysilane (APTMS) and hexamethyldisilazane (HMDS) through measurements of pH sensitivity of such APTMS- and HMDS-treated rGO layers. For this analysis, we adopted the remote floating-gate FET (RFGFET) configuration which enables the characterization of intrinsic properties of solution-rGO interfaces only. The HMDS-treated surface induces more hydrophobicity on the interface and lowers pH sensitivity of rGO layers by reducing the number of oxygen functional groups. On the other hand, the APTMS-treated surface contains more rGO layers with enriched oxygen functional groups, which leads to higher pH sensitivity and hydrophilicity. Finally, we also characterized interfacial potentials of rGO layers modified by 1-pyrenebutyric acid N-hydroxysuccinimide ester (PBASE) linker molecules during functionalization process and monitored the surface charge density of the solution-rGO interface brought by PBASE functionalization. These results suggest useful interface-engineering strategies to tailor the sensing performance and functionalities of FET-based sensing devices, which holds great promise for developing advanced chemical and biological sensors.

SESSION EL07.16: Virtual Session

Session Chairs: Gabriela Borin Barin and Yuxuan Cosmi Lin

Thursday Morning, December 7, 2023

EL07-virtual

8:00 AM EL07.16.01

Two-Terminal Floating-Gate Memristor Arrays for Neuromorphic Computing [Hongwoon Yun](#) and Woojong Yu; Sungkyunkwan University, Korea (the Republic of)

As deep learning has rapidly advanced, it required significant amounts of computational load. Computers which designed based on von Neumann architecture are not suitable for deep learning, because they have limitations in computational speed due to bottlenecks and waste a large amount of energy. To address the energy and speed issue, in-memory computing based on memristor arrays is emerging as a new alternative.

In this study, we present two-terminal (Drain, Source) floating-gate memristor array using van der Waals layered materials. To significantly reduce the set, reset voltage compared to previous works [1,2], we formed a layer of gold nanoparticles between the tunneling insulator (Al_2O_3) and the floating-gate (graphene).

Using the change of the Fermi energy level (Ef) of graphene, our memristor, Au-nanoparticle TRAM (Tunneling Random Access Memory), exhibits memory characteristic. Our device shows high on/off ratio over than 10^6 , retention more than 9 hours, multi-level retention of 2,500 seconds and robust endurance more than 80,000 times. Notably, our TRAM shows low cycle to cycle variability of $C_v = 3.6\%$ ($n = 90$, $C_v =$, = standard deviation, = mean value). Furthermore, non-linearity factor for long-term potentiation (LTP) ranges from 0.1 to 0.6 while for long-term depression (LTD), it ranges from 2.3 to 4.6 ($n = 15$), achieved through 100 potentiation (+4V, 0.5s) followed by 100 depression (-3V, 0.2s). A similar trend was shown even when the number of input pulses was changed (25, 50, 100, 150, 200 inputs for LTP, LTD).

With 400 input layers, 100 hidden layers, and 10 output layers of neural network, considering the non-linearity parameter, we were able to achieve an accuracy up to 89.56% in classifying handwritten digits of the MNIST database.

References

- [1] Q. A. Vu, Y. S. Shin, Y. R. Kim, V. L. Nguyen, W. T. Kang, H. Kim, D. H. Luong, I. M. Lee, K. Lee, D. S. Ko, J. Heo, S. Park, Y. H. Lee, W. J. Yu, *Nat Commun* **2016**, 7, 12725.
- [2] Q. A. Vu, H. Kim, V. L. Nguyen, U. Y. Won, S. Adhikari, K. Kim, Y. H. Lee, W. J. Yu, *Advanced Materials* **2017**, 29, 1703363.

8:05 AM EL07.16.02

Tunable Electronic Structure in Carbon-Based Shwarzites under Mechanical Strain [Paulo Rodrigo E. Raulino](#) and Cristiano F. Woellner; Federal University of Parana, Brazil

The Schwarzites were proposed by Mackay and Terrones in the 90s, and are obtained by adding rings of carbon with more than eight atoms between hexagonal regions, producing structures with negative curvatures [1]. Since their proposal, several studies have been demonstrate its electronic, thermal, mechanic, and optical properties [2]. In this work, we explored the variation of the electronic behavior of some members of the P-family Schwarzites under mechanical stress/strain. We used Density Functional Theory (DFT) and Density Functional based on Tight-binding (DFTB) computationally implemented via CASTEP and DFTB+ softwares. The P8-0 Schwarzite has semimetal behavior with two Dirac cones on the first Brillouin zone [2]. After applying the mechanical stress/strain, the Dirac cones merge into a single cone with parabolic dispersion. Under approximately 18% of stress/strain, the bands separate, forming a finite bandgap between the bands, which causes the structure to behave like a semiconductor. The P8-1 structure presenting a semiconductor behavior, we notice a significant reduction of the bandgap energy between conduct and valence bands [2]. We demonstrate that it is possible to change the electronic behavior of these structures under mechanical stress and strain. Breaking the crystal symmetry allow the production of the piezoelectricity effect from a centrosymmetric structure. This effect implies a separation of the positive and negative charges in the crystal, creating polarized charges or dipole [3]. Piezoelectricity has many applications in medical and microelectronic devices, resonators and sensors [3].

Acknowledgments: We thank the Physics Department at Federal University of Parana for computational and financial support. We also thank CNPq for the financial support.

References:

- [1] A. L. Mackay, H. Terrones, *Nature*. 352 (1991) 762.
- [2] F. Valencia et al, *New J. Phys.* 5 (2003) .
- [3] D. Park et al, *Science*. 375 (2022) 653-657 123.

8:10 AM EL07.16.03

High Thermal-Conductive Packaging Composites Based on Uniform Dispersion of 2D Materials [Chia-Lien Chao](#)¹, Yu-Chiao Chang¹, Rong-Teng Lin¹, Yun-Hong Yang¹, Bi-Xian Wu¹, Kuan-Yun Chi² and Tzu-Hsuan Chang^{1,2}; ¹Graduate Institute of Electronics Engineering, National Taiwan University, Taipei, Taiwan, R. O. C., Taiwan; ²Graduate School of Advanced Technology, National Taiwan University, Taipei, Taiwan, R. O. C., Taiwan

The scaling of integrated circuits (IC) has posed significant challenges, particularly when aiming for nanometer-level scales capable of accommodating billions of transistors. To keep up with Moore's Law, IC industry has shifted towards developing three-dimensional integration (3DICs). The use of 3D packaging technology has allowed chips to incorporate numerous additional functionalities. While the calculation capability increased substantially by dielet stacking, power density per area increased as well. In this way, the design of 3DIC has intensified the research focus on thermal management. While heat dissipation is managed through metals in the TSV design of 3DIC, the additional supporting approaches of thermal dissipation capability by IC packaging remain unsolved. Conventional packaging materials have shown poor thermal conductivity, typically ranging from only 1 to 2 W/mK for decades, despite having maximum contact area with the stacked dielets. Consequently, it is crucial to develop innovative strategies to tackle these problems, potentially utilizing packaging materials with high thermal conductivity. While commercially available packaging materials like polymer and epoxy are lightweight, inexpensive, and easy to process, they suffer from low thermal conductivity properties. This is primarily because conventional techniques are unable to address the issue of percolation, where the stuffed and isolated ceramic particles blended that were used to enhance the thermal conductivity can not form the continuous phonon conductive path. In this study, we have successfully tackled this issue by dispensing 2D materials as the filler of packaging materials to develop novel composites with high thermal conductivity. The filler incorporates graphene, which exhibits excellent thermal conductivity, weaves continuous networks inside the epoxy, and forms thermal conductive network. To maintain the structural integrity and successful dispersion of the graphene, cellulose nanofibers (CNF) with 1D structures were used. The resulting graphene/CNF structures can form continuous heat dissipation network. Through the blending of the graphene/CNF filler, the thermal conductivity of the polymer, polypropylene, can be increased by 270 times, rising from 0.2 W/mK to 54 W/mK, and epoxy can be increased by 66 times, rising from 0.14 W/mK to 9.35 W/mK. While keeping the superior high thermal conductivity, our composite still maintains low leakage that shows a promising candidate for the next generation packaging materials.

8:15 AM EL07.16.04

Insights from Ab-Initio Simulations on the Working Mechanism of Single-Layer MoS₂ Memristors [Gabriele Boschetto](#)¹, [Stefania Carapezzi](#)^{1,2} and [Aida Todri-Saniai](#)^{3,1}; ¹LIRMM, France; ²Silvaco Europe, France; ³Eindhoven University of Technology, Netherlands

Memristors are promising building blocks for important technological applications such as high-density memory, data encryption and neuromorphic computing. In this context, 2D memristors based on atomically thin single-layer molybdenum disulfide (MoS_2) are particularly interesting due to their extremely compact size and low-power operation [1,2]. Although few notable examples of working devices based on monolayer MoS_2 have been already reported in the literature, their working mechanism is still far from being understood, the main challenge being the great variability in terms of device architecture and quality of MoS_2 film. Nevertheless, regardless of the device architecture, intrinsic defects in MoS_2 are thought to be crucial for the functionality of memristors: for instance, S vacancies are highly abundant in CVD- MoS_2 and may impact non-trivially the properties at the interface with the metal contact, such as the contact resistance [3]. Moreover, in vertical $\text{Au/MoS}_2/\text{Au}$ memristors it has been argued that the resistive switching mechanism may be due to the migration of metal atoms from the electrode to fill such S vacancies in MoS_2 [4]. Here, we focus on such a device architecture and we carry out atomistic computer simulations in the framework of density functional theory (DFT). We employ surface calculations based on the Green's function formalism [5] to construct realistic interfaces and to compute relevant properties at the interface between MoS_2 and Au electrode. To elucidate the working mechanism of MoS_2 memristors, we consider defective MoS_2 either with S vacancies or with Au substitution (adatoms). Then, we investigate the effect of defect concentration and defect clustering on the physics and chemistry of MoS_2 interfaces. By exploring several possible case scenarios, we were able not only to better understand the pivotal role of the extra Au atoms for the resistive switch mechanism of MoS_2 memristors, but also to provide the theoretical justification on experimental findings.

[1] EU H2020 NeurONN Project, www.neuronn.eu.

[2] Horizon EU PHASTRAC Project, <https://phastrac.eu>.

[3] G. Boschetto et al. "Ab Initio Computer Simulations on Interfacial Properties of Single-Layer MoS_2 and Au Contacts for Two-Dimensional Nanodevices" *ACS Appl. Nano Mater.*, 5, 1092-1020, 2022.

[4] R. Ge et al., "Atomristor: Nonvolatile Resistance Switching in Atomic Sheets of Transition Metal Dichalcogenides," *Nano Lett.*, 18, 434-441, 2017.

[5] S. Smidstrup et al. "First-Principles Green's Function Method for Surface Calculations: A Pseudopotential Localized Basis Set Approach," *Phys. Rev. B*, 96, 195309, 2017.

8:30 AM EL07.16.05

A Preliminary Study on Implementation of Five-Qubit Quantum Information Processing in Silicon Devices [Junghee Ryu](#) and Hoon Ryu; Korea Institute of Science and Technology Information, Korea (the Republic of)

INTRODUCTION

An electrode-driven Silicon (Si) quantum dot (QD) system can be adopted to design scalable quantum processors with well-established industrial fabrication technologies [*Nat. Electron.* 5, 184 (2022)]. Recently, there have been experimental efforts to understand the physics of electron-spin qubits in Si QD systems whose confinement is manipulated with human controls, including a successful implementation of entangling logic operations up to six qubits [*Nature* 609, 919 (2022)]. Device designs & control engineering of physical systems consisting of many QDs, however, are still critical issues that must be uncovered with computational modeling to secure the scalability of quantum processors. Here we study the control engineering needed to initialize the linear five QD (FQD) system in Si and show the initialized spin states can be controlled to produce the magic state, one of quantum resource for realization of fault-tolerant quantum computing [*Nature* 510, 351 (2014)].

METHODS

Device simulations are conducted for the realistically sized Si FQD system with our multi-scale modeling approach integrating the bulk physics & the parabolic effective mass approximation. Qubits are encoded to electron spins that are created with quantum confinement driven by gate biases imposed on top electrodes. A static magnetic field is applied with a lateral gradient to make the Zeeman-splitting energies of electron ground states distinguishable. Once a set of five Zeeman-splitting energies and exchange interactions between nearest QDs is obtained from device simulations, the time-response of spin qubits is obtained from solutions of a time-dependent Schrödinger equation that is described with the Heisenberg spin Hamiltonian.

RESULTS AND DISCUSSION

We rigorously explored appropriate sets of biases imposed on the top electrodes, with which the FQD can be stably created satisfying the symmetric-biasing condition. Figuring out the bias condition that fills a single electron to each QD (qubit initialization), we engineered the sizes of nine electrodes to calibrate the distance between nearest electron spins to $\sim 100\text{nm}$. When the system is initialized, the five Zeeman-splitting energies come clearly distinguishable, and the four exchange interactions between nearest electron spins turn out to be weak enough to guarantee the individual address of five qubits. Then, as an application example, we show how a specific type of 5-qubit magic states can be prepared in the Si FQD platform, where we also present the detailed guideline of controls required to implement the non-Clifford T -gate and the Hadamard gate that are essential to generate the magic state. Robustness of the secured 5-qubit circuit (and so the magic state) to charge noise is also confirmed by simulation results that are obtained with unintentional random fluctuations in exchange energies.

8:35 AM EL07.16.06

Theoretical Exploration of Two-Dimensional Electrenes for Low-Resistance Metal-2D Semiconductor Contacts [Mohammad Rafiee Diznab](#), Erin R. Johnson and Jesse Maassen; Dalhousie University, Canada

Transition-metal dichalcogenides (TMDCs), including MoS_2 , have great potential in electronic applications. However, achieving low-resistance metal contacts is a challenge that impacts their performance in nanodevices, due to strong Fermi level pinning and the presence of a tunnelling barrier. As a solution, we explore a strategy utilizing two-dimensional (2D) alkaline-earth sub-nitride electrenes with a general formula of M_2X ($\text{M} = \text{Ca}, \text{Sr}, \text{Ba}$; $\text{X} = \text{N}, \text{P}, \text{As}, \text{Sb}$) as an intermediate material between the 2D TMDC and metal. Electrenes possess one excess electron per formula unit resulting in the formation of 2D sheets of charge on their surfaces. This charge can be readily donated when interfaced with a TMDC semiconductor, thereby lowering its conduction band below the Fermi level and eliminating Schottky and tunnelling barriers. Density-functional theory calculations were performed on metal-electrene- MoS_2 heterojunctions for all stable M_2X electrenes, and both Cu and Au metals. To identify the material combinations that provide the most effective Ohmic contact the charge transfer, band structure and electrostatic potential, among other quantities, were analyzed. In all cases, a linear correlation was found between the charge donated to the MoS_2 and the electrene surface charge. The electride Ca_3N is found to be most promising for achieving an Ohmic metal- MoS_2 contact, due to its high surface charge density.

This research was supported by SRC.

8:50 AM EL07.16.07

Doping-Controlled $\text{WSe}_2/\text{MoS}_2$ Lateral Heterostructure for High-Performance Photodetection [Sung Hyun Kim](#) and Woojong Yu; Sungkyunkwan University, Korea (the Republic of)

A two-dimensional material having an atomic thickness has an advantage in miniaturization of next-generation sensors. Some transition metal dichalcogenide (TMD) materials with semiconducting properties exhibit high light absorption in addition to their thin thickness. However, the optical properties of the current 2D heterostructure are dependent on the inherent properties of the material, and as a way to solve this, it is possible to improve it by forming an ideal PN diode by using the doping control of the 2D heterostructure. To confirm this, we fabricated a WSe_2 (Nb-doped)/ MoS_2 PN heterostructure photodetector and confirmed its characteristics. In our experiment, ammonium metatungstate (AMT) hydrate and ammonium niobium oxalate (ANO) ($\text{C}_4\text{H}_4\text{NNbO}_9 \cdot x\text{H}_2\text{O}$) were used as precursors of W and Nb, and sodium hydroxide (NaOH) was used as a promoter to increase the growth rate. Stock solutions of AMT, ANO, and NaOH were obtained by dissolving the calculated amount of powder in DI water. Medium solution (iodixanol)-Opti was used to improve adhesion to the substrate during the spin coating process. Various mixed solutions (AMT, ANO, NaOH and opti) with different molar ratios of Nb/(W+Nb) were prepared from stock solutions. MoS_2 growth is similar to WSe_2 growth. Our device exhibits a high Ilight / Idark ratio (10^5), which is about 100 times higher than the reported lateral 2D PN heterostructured photodiodes. These excellent performances indicate that the doping-controlled transition metal dichalcogenide PN heterostructure is a promising candidate for optoelectronic engineering.

8:55 AM *EL07.16.08

Integrating 2D Materials in Silicon Microchips [Mario Lanza](#); King Abdullah University of Science and Technology, Saudi Arabia

Two-dimensional layered materials (2D-LMs) materials have outstanding physical, chemical and thermal properties that make them attractive for the fabrication of solid-state micro/nano-electronic devices and circuits. However, synthesizing high-quality 2D-LMs at the wafer scale is difficult, and integrating them in semiconductor production lines brings associated multiple challenges. Nevertheless, in the past few years substantial progress has been achieved and leading companies like TSMC, Samsung and IMEC have started to work more intensively on the fabrication of devices using 2D-LMs. In this talk, I will discuss the state-of-the-art on micro/nano-electronic devices made (entirely or partially) of 2D-LMs, the most sophisticated circuits ever constructed, and the fabrication of CMOS/2D hybrid microchips. I will put special emphasis on devices that employ hexagonal boron nitride, the only 2D-LM with an enough high band gap to be employed as dielectric. I will also discuss the main technological challenges to face in the next years and provide some recommendations on how to solve them.

9:25 AM *EL07.16.09

Room Temperature Photoluminescence Mediated by Sulfur Vacancies in 2D Molybdenum Disulfide [Manish Chhowalla](#); University of Cambridge, United Kingdom

Atomic defects in monolayer transition metal dichalcogenides (TMDs) such as chalcogen vacancies significantly affect their properties. In this work, we provide a reproducible and facile strategy to rationally induce chalcogen vacancies in monolayer MoS₂ by annealing at 600 °C in argon/hydrogen (95%/5%) atmosphere. Synchrotron X-ray photoemission spectroscopy shows that a Mo 3d_{5/2} core peak at 230.1 eV emerges in the annealed MoS₂ associated with non-stoichiometric MoS_x (0 < x < 2), and Raman spectroscopy shows an enhancement of the ~380 cm⁻¹ peak that is attributed to sulfur vacancies. At sulfur vacancy densities of ~2.4 × 10¹⁴ cm⁻², we observe a defect peak at ~1.72 eV (referred to as LX_D) at room temperature in the photoluminescence (PL) spectra. The LX_D peak is attributed to excitons trapped at defect-induced in-gap states and is typically observed only at low temperatures (≤ 77 K). Time-resolved PL measurements reveal that the lifetime of defect-mediated LX_D emission is longer than band edge excitons, both at room and low temperatures (~2.77 ns at 8 K). The LX_D peak can be suppressed by annealing the defective MoS₂ in sulfur vapor, which indicates that it is possible to passivate the vacancies. Our results provide insights into how excitonic and defect-mediated PL emission in MoS₂ are influenced by sulfur vacancies at room and low temperatures.

9:55 AM EL07.16.10

Atomically Thin SnO-Based p-Channel Thin-Film Transistor and Low-Power Complementary Inverter Chi-Hsin Huang¹, Yalun Tang², Tzu-Yi Yang³, Yu-Lun Chueh³ and Kenji Nomura^{2,2}; ¹University of California, San Diego, United States; ²University of California San Diego, United States; ³National Tsing Hua University, Taiwan

Atomically thin oxide semiconductors play a crucial role in the development of next-generation, cost-effective, and energy-efficient electronics. In this study, we successfully developed a high-performance, fully depleted-type p-channel oxide thin-film transistor (TFT) utilizing an atomically thin p-type tin monoxide (SnO) channel with a thickness of approximately 1 nm. The SnO channel was grown using a vacuum-free, solvent-free, metal-liquid printing process at a remarkably low temperature of 250 °C in an ambient atmosphere. To enhance the performance of the p-channel SnO TFTs, we employed oxygen vacancy defect terminations for both the bulk-channel and back-channel of the SnO channel. As a result, the presented p-channel SnO TFTs exhibited favorable characteristics, including a reasonable TFT mobility of ~0.47 cm²V⁻¹s⁻¹, a high on/off current ratio of ~10⁶, a low off current (< 10⁻¹² A), and a subthreshold swing of ~2.5 V decade⁻¹, which was improved compared to the conventional p-channel SnO TFTs. Furthermore, we successfully developed a low-power oxide-TFT-based complementary metal-oxide-semiconductor (CMOS) inverter using the ultrathin p-SnO and n-In₂O₃ TFTs. The CMOS inverter demonstrated a high voltage gain of approximately 120 and achieved low-power operation, consuming less than 58 nW, for the p-SnO/n-In₂O₃-TFT-based CMOS inverter. This work highlights the significant potential of oxide-TFT-based CMOS logic development by leveraging atomically thin oxide material channels. It offers new opportunities for next-generation, energy-efficient, and cost-effective oxide TFT technology, with the added benefits of vacuum-free, solvent-free, and low-temperature processing techniques.

SYMPOSIUM EL08

Emerging Material Platforms and Fundamental Approaches for Plasmonics, Nanophotonics and Metasurfaces
November 26 - December 5, 2023

Symposium Organizers

Viktorii Babicheva, University of New Mexico
Ho Wai (Howard) Lee, University of California, Irvine
Yu-Jung Lu, Academia Sinica
Benjamin Vest, Institut d'Optique Graduate School

Symposium Support

Bronze

ACS Photonics | ACS Publications
APL Quantum | AIP Publishing
Enli Technology Co., LTD
Nanophotonics | De Gruyter
Taiwan Semiconductor Manufacturing Company Limited (TSMC)

* Invited Paper

+ JMR Distinguished Invited Speaker

SESSION EL08.01: Plasmonic/Nanophotonic Imaging and Spectroscopy
Session Chairs: Ho Wai (Howard) Lee and Yu-Jung Lu
Sunday Morning, November 26, 2023
Hynes, Level 2, Room 200

10:00 AM *EL08.01.01

Nanophotonic Force Nanoscopy for Ultrafast Dynamic Imaging of Nanostructures Yang Zhao; University of Illinois Urbana-Champaign, United States

Light and plasmonic nanoparticle interaction creates many physical effects, including the generation of non-equilibrium charge carriers, enhanced electromagnetic near-field, and photothermal effect. Particularly, the plasmonic photothermal effect, given by the optical absorption induced by surface plasmons, is well studied because of its broad applications. The plasmonic photothermal effect has been associated with fields as diverse as near-field optics, cell biology, drug delivery, cancer therapy, chemical reactions, nanofabrication, biomedical imaging, sensing, and so on. The photothermal effect of nanoparticles has been characterized by various tools and techniques. For example, photothermal dynamics of nanoparticles have been observed with optical microscopy using the pump and probe approaches but are diffraction limited. At the single particle level, electron microscopy can assess the nanoparticle's morphology, surface potential, and phase transformations, and cathodoluminescence has been used for probing the thermal profiles of nanowires. However, these methods based on electron microscopy require a vacuum environment and a conductive substrate. The measured thermal profiles oftentimes do not represent the nanoparticles in an ambient condition because the thermal properties of nanoparticles are highly associated with the environment. Moreover, because of the slow scanning speed of the electron beam, the dynamical evolution of the thermal profile due to non-stationary heat transfer is unmeasurable. On the other hand, nanoscopic thermal profiles have been measured using micromechanical probes, where the near-field energy extinction and the thermal relaxation govern the thermal field and heat flow. The thermal expansion triggered by a modulated laser resonantly drives a micromechanical cantilever, through which one can assess the thermal profile of nanoparticles in situ. However, the dynamic information can be lost due to the relatively slow response of the cantilever. Although improved mechanical designs of the scanner have enabled a high-speed atomic force microscope (HS-AFM) that can reach up to 1300 frames per second, a single image/frame still takes hundreds of microseconds, significantly longer than the thermal relaxation time of nanoparticles, which is in the nanosecond regime.

In this talk, I will introduce an ultrafast visualization of dynamic heat transfer in the nanosecond temporal regime with a spatial resolution of around 10 nm. We show the heating and cooling stages of a single gold nanoparticle using nearfield optical force imaging, termed decoupled optical force nanoscopy (Dofn). Our technique, different from conventional near-field scanning

optical microscopy, probes optical forces originating from the interactions between the illuminated nanoparticle and the probe.

10:30 AM EL08.01.02

Boosting the Efficiency of Passive Upconversion Imaging using Engineered Nanostructures RabeeyaHamid¹, DemengFeng¹, EmmaBelliveau², ManchenHu², PourmimaNarayanan², ChenghaoWan², JustinEdwards¹, DanielCongreve² and MikhailKats¹; ¹University of Wisconsin-Madison, United States; ²Stanford University, United States

Most existing technologies to enable vision in the near infrared (NIR) region rely on cameras, displays, and other powered optoelectronics. These devices capture NIR images and convert them to the visible. In contrast, we are working on a passive frequency-upconversion imaging system that directly converts NIR light to visible light, thereby eliminating the need for external power sources or electronic components. We use a photon upconversion process that involves a sequential transfer of energy from two low-energy incident photons, resulting in the emission of a higher-energy photon via triplet-triplet annihilation [1], enabling solid-state upconverting thin films [2]. However, the previously demonstrated efficiency of this upconversion process is not sufficient for passive night-vision imaging systems.

We designed and demonstrated several types of nanostructures that enhance the absorption, emission, and collection efficiencies of upconverting films, with the ultimate goal of enabling a wearable, all-passive, NIR-to-visible imaging system.

In our design, the upconverting material is a 100-nm thick bulk heterojunction comprising organic molecules Y6 (sensitizer) and rubrene (emitter; here, doped with DBP [2]), similar to the materials in the bilayer structure in ref. [3]. Our bulk heterojunction passively converts incident NIR light to orange light with peak emission at ~600 nm; however, the emission is incoherent and isotropic. To enable imaging, the directionality of rays needs to be preserved through the upconversion process. We address this issue by positioning the upconverter at the focal plane of a Keplerian telescope system, a strategy that we previously demonstrated for a down-conversion imaging system [4].

To enhance light extraction while operating in transmission mode, we developed a dichroic substrate that reflects visible light while transmitting NIR light, which allows us to recover visible light otherwise emitted backwards towards the source. To further improve the efficiency of the upconverter, we designed a superstrate that is transparent in the visible range but reflects in the NIR, enabling the recycling of unabsorbed NIR light back into the upconverting film, thereby enhancing the absorption and the subsequent emission.

We designed the multilayer substrates and superstrates such that they provide a consistent spectral response across a broad range of viewing angles (here, up to 30 degrees) for the desired wavelengths (500 – 650 nm in the visible, and 750 – 900 nm in the NIR). This functionality was implemented using niobium pentoxide (Nb₂O₅) and silicon dioxide (SiO₂) layers. To maintain our imaging resolution, we limited the total thickness of the combined structure to 2 microns, thus ensuring that we remain within the depth of focus of our imaging system.

Our approach has yielded an approximately 2-fold enhancement in collection efficiency and a 2.5-fold increase in absorption. As of this writing, we have verified the collection-efficiency enhancement in experiments using both a laser source (at 852 nm) and a broadband NIR source. We anticipate presenting the absorption-enhancement data at the conference.

In addition to power measurements, we have demonstrated imaging through the upconverter with the engineered substrate, observing an approximate doubling in brightness without compromising spatial resolution. We anticipate that our approach will be useful for a variety of incoherent upconverting schemes beyond the all-organic chemistry presented here (e.g., those based on inorganic nanocrystals [2, 4]) and can enable all-passive vision even under low-power NIR illumination and longer wavelengths.

We acknowledge funding from DARPA under Grant No. HR00112220010

[1] T. N. Singh-Rachford et al, *Coord. Chem. Rev.* 254, 2560–2573 (2010).

[2] M. Wu et al., *Nat. Photonics* 10, 31–34 (2016).

[3] S. Izawa et al, *Nat. Photon.* 15, 895-900 (2021).

[4] J. Salman et al., *J. Opt.* 23, 054001 (2021).

10:45 AM EL08.01.03

Optical Loss Measurements of Silicon-Nitride Membranes using Photothermal Common-Path Interferometry TanujKumar¹, DemengFeng¹, ShenweiYin¹, PhyoLin², MerlinMah², MargaretFortman¹, GabrielJaffe¹, ChenghaoWan¹, ChengyuFang¹, RonaldWarzoha³, VictorBrar¹, JosephTalgahder² and MikhailKats¹; ¹University of Wisconsin-Madison, United States; ²University of Minnesota Twin Cities, United States; ³U.S. Naval Academy, United States

Materials that feature low optical loss and relatively high refractive index are important for applications such as on-chip photonics¹, free-space optics for sensitive experiments like LIGO^{2,3} and, more recently, laser-driven light sails comprising thin membrane-like structures that efficiently reflect a high-power drive laser⁴. We have been investigating stoichiometric silicon nitride (Si₃N₄) membranes as a candidate material for such laser-light sails, due to its [a] low loss in the near infrared, [b] a moderately high refractive index (~2), [c] a large bandgap (~4.5 eV) that prevents two-photon absorption^{5,6}, and [d] vibrational resonances in the mid infrared that can enable radiative cooling⁷. To our knowledge, the optical absorption of Si₃N₄ membranes has not been directly measured.

We used photothermal commonpath interferometry (PCI)⁸, a sensitive pump-probe technique, to measure the absorption of Si₃N₄ membranes in the near infrared. We characterized membranes because they are the closest form factor to laser sails, and conventional techniques such as variable-angle spectroscopic ellipsometry are not sensitive enough to measure optical absorption in such thin low-loss membranes. PCI characterizes optical loss in a material by measuring the effect of the sample's absorption of a chopped pump beam on a probe beam via the thermo-optic effect. The amount of modulation in the probe beam carries information about the sample's absorptivity at the pump wavelength.

Translation of the PCI signal to the actual absorption value depends on the sample geometry and material properties, including the thermo-optic coefficient and thermal conductance of the sample. The translation is most-easily done using a reference similar to the sample in terms of optical and thermal properties, except with a higher, known absorbance. Here, we transferred a monolayer of graphene onto the SiN membranes we want to measure. Because it is thin and grown by chemical vapor deposition, the graphene does not significantly affect the overall thermal conductance of the sample; however, the presence of graphene increases the optical absorption from the ppm level to the ~1% level (the latter easily measurable using ellipsometry or reflection/transmission spectroscopy), and thus the resulting graphene/SiN structure can be used as a reference for PCI measurements of the SiN alone. To our knowledge, this technique of using a highly absorbing monolayer as a reference for PCI measurements has not been proposed or demonstrated previously.

Using graphene-referenced PCI, we found the absorption coefficient of stoichiometric Si₃N₄ to be ~1.3 × 10⁻² cm⁻¹ and that of non-stoichiometric SiN_x (x~1) to be ~6.7 cm⁻¹. These values of absorption are close to those reported in literature for waveguides.¹⁻³ Based on our measurements, stoichiometric Si₃N₄ is indeed a promising candidate for laser-light sails and other applications where low optical absorption is required.

¹ X. Ji, et al., *APL Photonics* 6(7), (2021).

² J. Steinlechner, et al., *Class Quantum Gravity* 32(10), (2015).

³ J. Steinlechner, et al., *Physical Review D* 96(2), 022007 (2017).

⁴ K.L.G. Parkin, *Acta Astronaut* 152, 370–384 (2018).

⁵ H.R. Philipp, *J Electrochem Soc* 120(2), 295 (1973).

⁶ G.R. Holdman, et al., *Adv Opt Mater* 10(19), 2102835 (2022).

⁷ K. Luke, et al., *Opt Lett* 40(21), 4823 (2015).

⁸ A. Alexandrovski, et al., in *Solid State Lasers XVIII: Technology and Devices*, edited by W.A. Clarkson, N. Hodgson, and R.K. Shori (SPIE, 2009), p. 71930D.

11:00 AM *EL08.01.04

Hybrid Plasmonic-Dielectric Geometric Metasurfaces for Emission Control and Chiral Sensing Wen-Hui (Sophia)Cheng, Yu-ChiaWang and Si-ChenLi; National Cheng Kung University, Taiwan

Metasurface has advanced the field of optics for the past decade thanks to the great tunability with multiple degree of freedom. By coupling the geometric plasmonic metasurfaces with the dielectric Si cavity mode, the direction and polarization of photon emission can be controlled. The hybrid structure with desired configuration presents the highest electric field and the best cross-polarization conversion efficiency while maintaining the Purcell factor. The Pancharatnam-Berry (PB) phase construction to manipulate the emission wavefront of both dipole emitter and chiral emitter is successfully demonstrated with simulation. The enantiomeric interaction between circular polarized light and the chiral molecule offers the significant feature for sensing application. To increase the selectivity for real-time chiral sensing, we employ the P-B phase antenna with silicon disk metamaterials. The improvement of Circular Dichroism (CD) measurement is also realized with the L-glucose and D-glucose.

1:30 PM *EL08.02.01

Properties and Control of Excitons in 2D Semiconductor Heterostructures Tony F. Heinz^{1,2}; ¹Stanford University, United States; ²SLAC National Accelerator Laboratory, United States

In this paper we will describe some of our recent progress in understanding fundamental aspects of excitons in 2D heterostructures in the transition metal dichalcogenide (TMDC) family. For many of these systems, type II band alignment is obtained in stacked layers, causing the lowest-lying optical excited state to be an interlayer exciton. Because of the static dipole moment of these charge-separated states, they are highly tunable by external electric fields, making them interesting sources with readily tunable photon energy by gating available in the visible and infrared spectral ranges. In addition, for crystallographically aligned samples, the moiré potential leads to distinctive exciton localization effects. We will present recent advances in characterizing these states, both through direct optical absorption measurements and through the use of time-resolved, angle-resolve photoemission spectroscopy (tr-ARPES). These methods give us new insight into the radiative lifetime of these states and the degree and nature of exciton localization in moiré structures. In addition to their intrinsic interest, the ability to transfer

2:00 PM EL08.02.02

Paradigms for Realizing Symmetry-Guaranteed Pairs of Bound States in the Continuum and Identifying Super-Mossian Materials Chloe F. Doiron; Sandia National Laboratories, United States

Over the last decade, all-dielectric metasurfaces have emerged as a powerful platform for enhancing light-matter interactions, enabling device performance improvements across a range of applications. To increase light-matter interactions, photonic states with long lifetimes (high-quality factors) are desirable, requiring improvements in photonic designs, material quality, and fabrication tolerances. In this talk, I will present one structural design paradigm and one material search heuristic for improving all-dielectric metasurfaces.

Bound states in the continuum are states that are completely decoupled from a continuum leading to infinitely long lifetimes. In practice, while states with infinitely long lifetimes are undesirable, they enable a design paradigm that solves the photonic design component leaving material quality and fabrication tolerances as the primary means to achieve arbitrary lifetimes. Demonstrations using bound states in the continuum have enabled improvements for lasers, sensors, and frequency mixers. However, many applications require degenerate or nearly degenerate high-quality factor (Q) states, such as spontaneous parametric down conversion, non-linear four-wave mixing, and intra-cavity difference frequency mixing for terahertz generation. I will present a group theory approach based on lattices with six-fold rotational symmetry for creating symmetry-guaranteed pairs of bound states in the continuum. Using this design paradigm, the splitting and Q-factors can be independently and robustly controlled creating new pathways for improving metasurfaces for frequency conversion, heralded single-photon production, and sensing.

Finally, I will discuss a search heuristic for materials with refractive indices that surpass the common form of the Moss rule ($n^2 E_g \approx 95$ eV) leading to the creation of super-Mossian materials. With this heuristic, I will present an experimental realization of a super-Mossian metasurface using iron pyrite (FeS₂), with refractive index greater than 4.37 and a bandgap of 1.03 eV, surpassing the common form of the Moss rule by nearly 40%.

Work supported by the US Department of Energy, Office of Basic Energy Sciences, Division of Materials Sciences and Engineering (grant BES 20-017574). The work was performed, in part, at the Center for Integrated Nanotechnologies, an Office of Science User Facility operated for the US Department of Energy, Office of Science. Sandia National Laboratories is a multi-mission laboratory managed and operated by National Technology and Engineering Solutions of Sandia LLC, a wholly owned subsidiary of Honeywell International Inc., for the US Department of Energy's National Nuclear Security Administration under contract DE-NA0003525. This paper describes objective technical results and analysis. Any subjective views or opinions that might be expressed in the paper do not necessarily represent the views of the US Department of Energy or the United States government.

2:15 PM EL08.02.03

Understanding the Origins of Low-Frequency Instability in Thin-Film Lithium Niobate Nanophotonic Devices David R. Barton¹, Matthew Yeh¹, Gavin Smith², Evelyn Hu¹ and Marko Loncar¹; ¹Harvard University, United States; ²University of New Hampshire, United States

Thin-film lithium niobate on insulator (TFLN) is a promising platform for integrated classical and quantum photonics due to its intrinsically large electro-optic effect and wafer-scale availability. The direct connection between driving electric fields and refractive index in this platform has enabled new schemes for creating pulsed lasers on chip, high-bandwidth and energy-efficient modulators, and devices for integrated nonlinear photonics. However, it is generally recognized that the reliability of thin-film lithium niobate modulators is subject to unstable electro-optic response at low frequencies, and undesired photorefractive index changes due to defect absorption at high optical powers. Post-processing methods such as annealing have been developed to reduce these deleterious effects, but their microscopic origins remain unclear. It is also not known if these effects relate to fundamental materials issues, might be exacerbated for materials in thin-film form with possible strain inhomogeneities, and indeed might arise from thin-film preparation, which involves ion implantation, and chemical-mechanical polishing.

Here, we use a combination of materials characterization (XPS, Atom Probe Tomography, and electronic transport) and optical device characterization to explore the structure-device-processing parameter space in integrated lithium niobate devices and attempt to identify a mechanistic insight for low-frequency instability in our devices. All our devices are fabricated on 600 nm thick x-cut Lithium Niobate on insulator wafers, and we explore fabrication processes that impact both the bulk and interfaces in our devices. First, we show through XPS that the etch conditions and standard acid cleans used in our thin-film processing dramatically impact the surface by removing lithium from the surface, locally reducing Nb⁵⁺ to Nb⁴⁺, and creating a damaged amorphous Lithium Niobate layer. Specific chemical cleans remove the damaged layer, while annealing at moderate temperatures in an oxygen environment restores the surface Li:Nb ratio to its unprocessed status. We gained additional insight by using APT to map out the material composition in 3D with ~nm-scale resolution. Surprisingly, we find that the lithium composition within the unprocessed material varies substantially over length scales on the order of 10 nanometers, suggesting that local defect structures such as the small polaron may exist in appreciable concentrations that could give rise to photorefractive. Annealing our samples temporarily increases quality factors and reduces photorefractive, indicating that diffusion of mobile species such as Lithium or Hydrogen may indeed play a role in long-term stability of our devices.

Finally, we find that the metal-Lithium Niobate interface is important for the low-frequency response of our devices. Etching through the oxide cladding in our structures dramatically improves the electro-optic response but leaves behind an amorphous lithium niobate interface for the electrical contacts. Surprisingly, any attempts to remove redeposition or clean the surface semiconductor-metal interface reduces the low-frequency response and degrades the response flatness. Together, these results point to the importance of surface and bulk conductivity within our electro-optic devices for stable low-frequency tuning, a requirement for deployable devices and systems in thin-film Lithium Niobate.

2:30 PM BREAK

3:00 PM *EL08.02.04

To Be, or Not to Be: Labeled and Label-Free Raman Based Pathogen Detection in Water and Clinical Samples Loza Tadesse^{1,2}; ¹Massachusetts Institute of Technology, United States; ²Ragon Institute, United States

Raman spectroscopy promises a rapid and accurate pathogen detection alternative compared to complex and tedious culture dependant alternatives. Although spontaneous Raman measurements could provide enough signal for detection, some applications such where a hand full of pathogen are present compared to liters of surrounding sample volume, may require specific labeling and isolation of cells. In this talk, I will discuss how the limits of Raman spectroscopy for biosensing can be pushed further in its resolution by demonstrating ~98% accurate classification of presence of anti-TB drug resistance using spontaneous Raman to expansion in its sample volume reach by demonstrating rapid magnetic isolation and detection of hand full of pathogenic bacteria from water and food contaminants using polymer coated magnetic beads as Raman reporters. We also demonstrate detection on home built hand held Raman systems for ease of deployment to clinical end users. Lastly, I will cover new territories Raman spectroscopy can serve in next generation disease therapeutics. Clinical and field translation of Raman based cell detection calls for careful analysis of the application at hand as either labeled or label free alternatives would best serve the target.

3:30 PM EL08.02.05

Plasmonic Ammonia Synthesis with a AuRu Bimetallic Alloy Lin Yuan, Briley Bourgeois, Alan X. Dai, Peiwen Ren, Felipe Jornada and Jennifer A. Dionne; Stanford University, United States

The Haber-Bosch process has had a significant impact on global food production, enabling ammonia synthesis for nearly all agricultural fertilizers. However, ammonia production generally requires high operating temperatures (exceeding 300 °C) and high pressures (100 atm), leading to over 3% of annual global greenhouse gas emissions. To promote sustainable chemistry, ammonia synthesis must be accomplished under milder conditions while also eliminating the greenhouse gas footprint. In this presentation, we describe bimetallic plasmonic nanoparticles that enable high-efficiency and sustainable nitrogen fixation at room temperature and pressure. We utilize AuRu metallic nanoparticles, where Au serves as the plasmonic optical absorber, and Ru

acts as the catalyst for nitrogen bond-breaking. We develop a colloidal synthesis to create AuRu nanoparticles with controlled phases, including the fcc phase and hcp phase. We vary the Au and Ru composition from 1:0.1 to 1:0.3. We then load the nanoparticles onto a commercial MgO substrate at 5% mass-loading. Using UV-Vis spectroscopy, the nanoparticles show strong optical absorption at wavelengths of 520 nm. We use our bench-scale photoreactor to characterize the ammonia synthesis ($N_2+3H_2\rightarrow NH_3$), using nitrogen and hydrogen as a feeding gas, at various temperatures, pressures, and under various illumination conditions. Our observations indicate an ammonia rate of 60 $\mu\text{mol/g/h}$ under 100 mW/cm^2 visible light irradiation, and a 0.12% external quantum efficiency on our fcc AuRu_{0.2} catalyst. By correlating the wavelength-dependent reactivity and electromagnetic hot carrier calculations, we have identified the potential contributions from phonon-assisted intraband and interband transitions in driving the photochemical transformation. Our study provides a solution for designing photocatalysts to drive nitrogen fixation under mild conditions and an understanding of the mechanisms that can inform future applications.

3:45 PM EL08.02.06

Single Particle Plasmonic Nanocavity-Based Strong Coupling with Intrananogap Nanostructure Kyungwha Chung^{1,2}, Soohyun Lee², Nathan Grain³, Subin Yu¹, Seokhyoung Kim³, Sung Ho Park² and Luke Lee^{1,2}; ¹Harvard University, United States; ²Sungkyunkwan University, Korea (the Republic of); ³Michigan State University, United States

Achieving strong coupling in practical applications of cavity quantum electrodynamics (CQED) often poses significant challenges due to the delicate conditions required. In particular, the realization of strong coupling with single nanoparticles has been predominantly demonstrated using J-aggregate dye molecules. In this work, we present a novel CQED probe capable of transforming a nanocavity within a single nanoparticle. Our approach utilizes a plasmonic CQED structure based on a gold double nanoring (Au DNR) that incorporates an intraparticle nanogap. Through dark-field measurements on individual particles, we observe the emergence of exciton-plasmon polaritons, known as plexcitons, evidenced by the bifurcation of the scattering peak into two distinct resonances. Finite-element modeling is employed to elucidate the correlation between the Au DNR morphology and the cavity resonance wavelength relative to the exciton absorption, while temporal coupled-mode theory quantifies the strength of coupling. Verification of plexciton states is accomplished through photoluminescence measurements, which demonstrate light emission from the lower plexciton state. The proposed CQED nanocavity serves as a promising nanoprobe for the detection of small molecules within cells and offers a platform for groundbreaking biomolecular studies.

4:00 PM EL08.02.07

Crystalline AuNP with Strain-Controlled Morphologies and Optical Properties Qiaomu Yao and Peter K. Petrov; Imperial College London, United Kingdom

Metallic nanoparticles (NP) decorated with thin films have been extensively studied and exhibit promising performance in a wide range of applications, including biosensing, electrical devices, photocatalysis, and solar cells. For perovskite thin films, the decoration can produce an enhanced plasmonic response, which indicates a promising future in nano-waveguides, energy harvesting, and chemical sensing applications. The morphologies and chemistries of NPs strongly govern plasmonic performance. The size and density of AuNPs dramatically influence the absorption, surface plasmonic resonance peak intensity, and the second harmonic generation responses. It also alters the so-called epsilon-near-zero (ENZ) effects, where the interplay between real and imaginary parts of permittivity results in the strong enhancement and local confinement of the normal field inside ENZ materials.

Here we present a study of the formation of gold nanoparticles (AuNP) grown by PLD onto perovskite strontium niobate (SNO) thin films deposited on both MgO and SrTiO₃ substrates. The strain-free SNO₃ ($a = 4.023 \text{ \AA}$) has a -3.0% lattice mismatch with the STO ($a = 3.905 \text{ \AA}$) and 4.5% with MgO ($a = 4.212 \text{ \AA}$) which leads to compressive and tensile in-plane residual strains, respectively. We observed that the formation of Au NPs and their morphology depends on the structure of the underlying SNO film. It conveys the surface structure and controls nanoparticle formation. The morphologies of AuNPs were measured using SEM and AFM. The residual strain in the SNO thin films and AuNPs was evaluated by X-ray diffraction (XRD). Finally, the complex permittivity of AuNP-decorated SNO films was measured using Variable Angle Spectroscopic Ellipsometry (VASE).

In summary, AuNP-decorated SNO/MgO and SNO/STO thin films exhibit different optical properties with only gold-decorated SNO/MgO samples showing nano particles' size-dependent epsilon-near-zero behaviour. These results provide an additional route to control the structure of AuNPs. They can be used for the design and development of strain-engineered gold nanoparticle decorated devices for surface-enhanced Raman spectroscopy (SERS) and photocatalysis.

4:15 PM EL08.02.08

Scalable Plasmonic Superstructures for Colorful Dichroism Jang-Hwan Han, Juhwan Kim, Gyurin Kim, Hyun Min Kim and Hyeon-Ho Jeong; Gwangju Institute of Science and Technology (GIST), Korea (the Republic of)

Flat optics based on metasurfaces or reflectors as a promising approach to achieve compact and efficient optical systems.[1,2] However, the development of optical color filters using single or multilayered thin film resonators or reflectors has received less attention, although their structural thickness still needs to exceed at least a quarter of a wavelength, resulting in bulky optical system.

Herein, we present scalable plasmonic superstructures comprising randomly but uniformly distributed metallic nanoparticles embedded within a glass matrix. These superstructures are fabricated using a metal-dielectric co-deposition method with substrate cooling, allowing for precise control over the sizes, densities, and materials of the plasmonic nanoparticles in the form of wafer-scale nanocomposite film. Crucially, we introduce 'scattering-free' plasmonic resonators with diameters below 10 nm,[3] so the reflected colors from these superstructures can be engineered primarily based on the film thickness, covering a wide range from ultraviolet to near-infrared regions, analogous to the conventional dielectric thin film reflectors. In contrast, the transmitted colors through the same structures exhibit weak dependence on the film thickness, but give rise to the vibrant colors due to strong plasmonic absorptions. This unique property of the plasmonic superstructure films enables independent engineering of reflected and transmitted colors by controlling their thickness and materials, thus demonstrating applications such as dichroic imaging and encryption systems.

In this presentation, the design rule, fabrication method, and optical features of the plasmonic superstructures will be discussed. Especially, we will demonstrate how to achieve full colors in both the reflection and transmission modes, featuring their potential for colorful imaging applications.

4:30 PM EL08.02.09

Simulation and Fabrication of Tunable Metal-Insulator-Metal Bow-Tie Antenna Arrays for Surface Enhanced Raman Scattering Sümevra Vural Kaymaz^{1,2}, Hasan Sarigül², Caner Soyulukan², Selim Tanrıseven², Hasan Kurt³ and Meral Yuçe²; ¹Sabancı University, Turkey; ²SUNUM Nanotechnology Research and Application Center, Sabancı University, Turkey; ³Imperial College London, United Kingdom

Surface plasmons in metal/dielectric interfaces provide significant levels of electric field enhancements in the subwavelength resolution, enabling a wide range of applications. One such application is surface-enhanced Raman scattering (SERS), a powerful analytical method for label-free molecular fingerprinting of various analytes. A careful design and nanofabrication of SERS substrates with a considerable Raman enhancement factor (EF) at the wavelength of interest are imperative for SERS applications. SERS substrates based on noble metal colloids, roughened nanosurfaces, nanospheres, and nanotips have been previously reported. Nevertheless, the low reproducibility of electric field hot spots has limited the utilization of these inherently random structures with high EF. The period arrays of plasmonic nanostructures offer the potential for generating reproducible SERS substrates. Specifically, metal-insulator-metal (MIM) based nanostructures exhibit substantial gap resonance due to the coupling of localized fields between two metal layers underlying the dielectric layer. By adjusting the geometric parameters of metal nanostructures and dielectric layer thickness, gap resonance can be tuned for application-specific requirements. In this work, we investigated the performance of gold (Au) bow-tie antenna arrays on insulator-metal substrates for SERS applications. The Finite-difference time-domain (FDTD) method was used to simulate the effects of parameters such as bow-tie apex angle, gap size, length, and dielectric layer thickness. We achieved an electric field enhancement of up to 630 times the incoming electric field intensity, corresponding to a SERS EF factor improvement of $\sim 3.9 \times 10^5$ in our final optimized design at an excitation wavelength of 785 nm. Later, we fabricated Au MIM bow-tie antenna arrays using electron beam lithography and investigated their optical characteristics with an in-house modular reflection/transmission-based Microspectroscopy system.

4:45 PM EL08.02.10

Electro-Optical Chromophores and Polymers for Short NIR-Wavelengths – Materials to Application Florens R. Kurth^{1,2}, Sophie-Luise Hachmeister¹, Li Zhao^{1,2}, Anna K. Rüsseler^{3,2}, Jonas N. Matthes³, Tasje Schwenke^{4,2}, Ons Amira⁴, Emil Agocs^{1,2}, Marco Jupé^{3,2}, Hans-Hermann Johannes^{1,2}, Henning Menzel^{1,2} and Wolfgang Kowalsky^{1,2}; ¹TU Braunschweig, Bienroder Weg 94, Germany; ²Leibniz University Hannover, Welfengarten 1a, Germany; ³Laser Zentrum Hannover e.V., Hollerithallee 8, Germany; ⁴TU Braunschweig, Hagenring 30, Germany

The development of photonics in communication and sensing, particularly in integrated circuits, relies heavily on functional optical materials. These materials play a central role in converting external impulses into optical signals and vice versa. Examples include piezo-optic, elasto-optic, magneto-optic, acousto-optic, and electro-optic materials, which find applications in modulators, sensing resonators, and beam steering devices.

In the field of electro-optics (EO), traditionally dominated by periodically poled LiNbO₃, there is an ongoing demand for alternative materials with distinct properties to cater to specialized applications. Organic electro-optic chromophores, as part of composite polymer materials, exhibit the Pockels effect. This effect occurs when electrons move along the molecular axis within a donor-acceptor structure in response to external stimuli in an electric field. These chromophores can be easily integrated into waveguides using common spin-coating and molding techniques, offering convenient fabrication.

This work specializes on the 980 nm wavelength at the short end of the NIR spectrum. The active component of such materials are electro optical (EO) chromophores, which are integrated in a suitable host polymer, mostly amorphous polycarbonate (APC) and methacrylate polymers/copolymers and are electroopted to achieve the parallel orientation necessary for a strong electro-optic effect. A range of chromophores has previously been synthesized, guided by DFT calculations, with consideration on high-dipole moments μ , good hyperpolarizability β , optical

transmission in the desired spectral window and shielded side-groups that improve electroplating quality due to decreased intermolecular interactions. These materials also exhibit strong solvatochromism with differences in absorption maxima ranging between 60 nm and 90 nm depending on solvent polarity. The materials are characterized regarding their optical and materials property, specifically the electro-optical coefficient r_{33} , which is measured using Teng-Man ellipsometry. These materials have been successfully used in electro-optical Fabry-Pérot switches in a cooperation with the Laser Zentrum Hannover e.V. to translate an electrical field-shift into a transmission wavelength shift of up to 20 nm with the desired application of miniaturized optical switches. With the transition from materials research towards device applications, long-term stability has come into focus. Different polymer host-materials and covalently integrated chromophore polymer composite materials have been exposed to high-temperature aging experiments to compare their ability to maintain the parallel chromophore orientation that was obtained during the electroplating step.

SESSION EL08.03: Advanced Nanophotonic Materials and Devices
Session Chairs: Ho Wai (Howard) Lee and Yang Zhao
Monday Morning, November 27, 2023
Hynes, Level 3, Room 312

10:30 AM *EL08.03.01

Low-Cost and Scalable Manufacturing of Optical Metasurfaces in the Visible using Engineered Optical Materials (PER, Low-Loss a-Si:H, and Hybrid ALD Structural Resin) JunsukRho; Pohang University of Science and Technology, Korea (the Republic of)

Here, we demonstrate low-cost, scalable manufacturing of optical metasurfaces with three approaches: 1) increasing a refractive index of resin with dielectric particle embedding for single-step nanoimprinting, 2) suppressing optical losses of hydrogenated amorphous silicon (a-Si:H) to apply complementary-metal-oxide-semiconductor technologies, and 3) high-index atomic layer deposited (ALD) structural resin. We demonstrate the effectiveness of these materials in creating optical metasurfaces operating at different wavelengths in the infrared, visible, and ultraviolet spectra. Firstly, we achieve high efficiencies of up to 90.6%, 47%, and 60% with a-Si, TiO₂, and ZrO₂ PER at wavelengths of 940, 532, and 325 nm, respectively. Furthermore, we obtain a measured efficiency of 30% at a wavelength of 248 nm using ZrO₂ PER metasurfaces. Secondly, by adjusting the deposition conditions of plasma-enhanced chemical vapor deposition, we engineer the bandgap of a-Si:H to enable low-loss operation, with minimum extinction coefficients as low as 0.082 at 450 nm. Using low-loss a-Si:H, we demonstrate efficient beam-steering metasurfaces with measured efficiencies of 42%, 65%, and 75% at 450, 532, and 635 nm, respectively, marking the first Si-typed metasurfaces working at the full visible. Finally, we manufacture highly efficient metalenses using hybrid ALD structural resin with deep-ultraviolet lithography at visible wavelengths. Their measured efficiencies approach 60.9%, 77.8%, and 64.8% at 450, 532 and 635 nm, making them suitable for ultrathin virtual reality devices. Our approaches using PER, low-loss a-Si:H, and hybrid ALD structural resin enables the low-cost, large-area manufacturing of efficient optical metasurfaces across different wavelengths, facilitating the commercialization of metasurface-based photonic devices.

11:00 AM EL08.03.02

3D Interior Plasmonic Nanocavities for Sensitive and Selective Recognition of Hazardous Substances in Plastic Products Sung-GyuPark; Korea Institute of Materials Science, Korea (the Republic of)

Surface-enhanced Raman scattering (SERS) utilizing plasmonic nanomaterials and nanostructured substrates has been extensively investigated to directly recognize substances because the energy differences between the incident and scattered lights correspond to the molecular vibrational energy states of the substances. SERS performance is dominantly derived from electric fields confined in dielectric media, called hotspots, between adjacent plasmonic nanostructures. Recently, the 3D interior hotspots templated with dielectric media surrounded by plasmonic materials have attracted great attention [1]. Various electrochemical techniques such as catalytic reaction, electrodeposition, and galvanic reaction (GR) have been exploited to realize the 3D interior hotspots. Particularly, a GR process spontaneously originates from energy differences in the reduction potential of two or more materials [2]. An imbalanced atomic exchange strategically defines narrow hollow regions which have dual functions of electric field confinement domains and molecular diffusion paths. For deeper comprehension of interior hotspots, the Ag nanocavities galvanically replaced by Au (Au/AgNC) on the silicon substrates were prepared. The proposed Au/AgNC platforms were used to trace hazardous substances such as phthalates. The activation of interior hotspots with superior density in a unit volume enabled reliable sensing operations at ppb levels. From the collected dataset, a machine-learning model was designed to predict various combinations (i.e., single, binary, ternary, and quaternary) of four major phthalates. Subtle differences in the phthalates' spectral characteristics were successfully classified using a machine learning algorithm based on a principal component analysis-linear discriminant analysis model.

References

I.-B. Anshah, S.-H. Lee, J.-Y. Yang, C.W. Moon, S. Jung, H.S. Jung, M.-Y. Lee, T. Kang, S. Lee, D.-H. Kim, S.-G. Park, In-situ fabrication of 3D interior hotspots templated with a protein@Au core-shell structure for label-free and on-site SERS detection of viral diseases, *Biosens. Bioelectron.* **220** 114930 (2023).
I.-B. Anshah, S.-H. Lee, C.W. Moon, J.-Y. Yang, J. Park, S.-Y. Nam, S. Lee, D.-H. Kim, S.-G. Park, Nanoscale crack generation of Au/Ag nanopillars by in situ galvanic replacement for sensitive, label-free, and rapid SERS detection of toxic substances, *Sens. Actuators, B.* **379** 133172 (2023).

11:15 AM EL08.03.03

Multifractal Photonic Membranes for Random Lasing Devices TornikeShubitidze, YilinZhu and LucaDal Negro; Boston University, United States

Random lasers are at the center of an intense research activity due to their ease of fabrication and robustness combined with small-size (micron-scale) of the order of the lasing wavelength as well as their unique characteristics that include low-spatial coherence, lack of directionality, and bio-compatibility. In particular, non-resonant random laser devices rely on uncorrelated random fluctuations of the dielectric environment that give rise to traditional photon diffusion. On the other hand, anomalous light transport phenomena with significantly slower dynamics, or sub-diffusive transport, occur in engineered random media with correlated disorder, providing opportunities to further enhance optical amplification and reduce device footprints. In this talk, we present our work on the design and fabrication of active photonic membranes with multifractal structural correlations and we characterize their optical emission properties using leaky-mode and photoluminescence spectroscopy.

Photonic multifractals are heterogeneous optical media with complex spatial fluctuations at multiple length scales characterized by a rich spectrum of local scaling exponents, i.e., a multifractal spectrum. Differently from well-known fractal structures, which possess only one global scaling quantified by a single fractal dimension, multifractals feature a continuous distribution of generalized fractal dimensions and can be considered as "intertwined sets" of self-similar structures. While the optical properties of fractal structures are well-understood, photon transport and light emission in multifractals remain fundamentally open problems. Here, we discuss photonic structures with tailored multi-scale correlations generated by iterative and multiplicative cascades of random fields. Localization and transport properties are explored and optimized using rigorous multi-particle Mie theory in combination with efficient tight-binding models. Based on this approach, using electron beam lithography and high-quality deep reactive ion etching, we demonstrate multifractal nano-hole arrays in both passive (a-Si:H, Si₃N₄) and active (ZnO) photonic membrane geometries. We report on the characterization of the optical and structural properties of each membrane structure with variable angle spectroscopic ellipsometry (VASE), photoluminescence spectroscopy, x-ray diffraction measurements, scanning electron microscope imaging (SEM) and atomic force microscopy.

11:30 AM EL08.03.04

Eu,O-Codoped GaN-Based High-Q Two-Dimensional Photonic Crystal Cavities in the Red Region TakenroiIwaya¹, ShuheiIchikawa^{1,2}, DolfTimmerman¹, JunTatebayashi¹ and YasufumiFujiwara¹; ¹Osaka University, Japan; ²Research Center for Ultra-High Voltage Electron Microscopy, Osaka University, Japan

Eu,O-codoped GaN (GaN:Eu,O) is an efficient red light emitting material based on the GaN platform. We have demonstrated red light-emitting diodes using GaN:Eu,O grown by organometallic vapor phase epitaxy method and reported a high light output power of 1.25 mW at 20 mA operation with a maximum external quantum efficiency over 9% [1,2]. Furthermore, we have shown that GaN:Eu,O has a moderate value of gain of 6.6 cm⁻¹ [3]. This observation suggests the possibility to develop a novel GaN:Eu,O-based red laser diodes (LDs). The emission wavelength from Eu³⁺ ions is highly stable with respect to the surroundings, thus GaN:Eu,O-based red LDs have a large potential applications including high-resolution laser displays and optical communications. In this contribution, we designed and fabricated an optical cavity with a high Q-factor in the red region, which is required for the realization of a laser based on this material [4].

Although two-dimensional photonic crystal (2D-PhC) cavities are prominent candidates to achieve high Q-factors, they typically show relatively low Q-factors (< 5000) due to structural disorder that is inevitably introduced during the fabrication stages [5]. From an extensive analysis of the influence of such disorder for various cavity designs, we have shown that especially H3-type cavities are much less sensitive to optical losses, when compared to linear (LN) cavities [4]. We have fabricated H3-type cavities and demonstrated a highest value of Q of 7900. This value is much higher than previously reported Q-factors (~5500) of III-nitride-based 2D-PhC cavities in the visible range, and approaches the theoretical Q-factor of this cavity design. These results demonstrate that H3-type cavities can indeed effectively suppress the disorder-induced optical losses, and that a further improvement of the design is required with a higher

theoretical Q -factor, in order to achieve higher experimental values.

We propose a 2D-heterostructure with core, trans and clad region. By designing the radii as $r_{\text{core}} > r_{\text{trans}} > r_{\text{outer}}$, the photonic band structure is modified and light at the photonic band-edge is well confined in the core region. For the optimal design parameters, a theoretical value of the Q -factor of 1.1×10^5 was obtained.

The fabricated structure of this design shows a few resonant modes, with the mode with the largest Q -factor reaching a value of $Q = 10500$ [6], which is almost twice that of previously reported values. Thus, we conclude that this type of III-nitride-based 2D-PhC cavity is effective for confining light, and has a great promise for obtaining ultrahigh Q -factors in the visible region. This study shows the guideline to achieve high Q -factors with III-nitride-based 2D-PhC cavities in the red region, which would open up a larger potential application.

Acknowledgments

This work was supported by JSPS KAKENHI Grant Nos. 18H05212, 22K14614 and No.23H05449, and by Nanotechnology Platform of MEXT, Grant Number JPMXP09F20OS0026 and JPMXP09S20OS0021.

References

- [1] A. Nishikawa, Y. Fujiwara *et al.*, *Appl. Phys. Express* **2**, 071004 (2009).
- [2] B. Mitchell, Y. Fujiwara *et al.*, *J. Appl. Phys.* **123**, 160901 (2018).
- [3] A. Takeo, Y. Fujiwara *et al.*, *Jpn. J. Appl. Phys.* **60**, 120905 (2021).
- [4] T. Iwaya, Y. Fujiwara, *et al.*, *Appl. Phys. Express* **14**, 122002, (2021).
- [5] R. Butté and N. Grandjean, *Nanophotonics* **9**, 569, (2020).
- [6] T. Iwaya, Y. Fujiwara, *et al.*, *Opt. Express* **30**, 28853, (2022).

11:45 AM EL08.03.05

Gate-Tunable Optical Anisotropy in Wafer-Scale, Aligned Carbon Nanotube Films Jason Lynch¹, Evan Smith², Adam Alfieri¹, Baokun Song^{1,3}, Cindy Yueli Chen¹, Chavez Lawrence¹, Cherie R. Kagan¹, Honggang Gu³, Shiyuan Liu³, Lian-Mao Peng⁴, Shivashankar Vangala², Joshua Hendrickson² and Deep M. Jariwala¹; ¹University of Pennsylvania, United States; ²Air Force Research Laboratory, United States; ³Huazhong University of Science & Technology, China; ⁴Peking University, China

Modern telecommunications and polarimetry systems require active control of the polarization of light. This is currently done by either combining an intrinsically anisotropic material with a tunable isotropic one in a heterostructure or by nano-patterning a tunable material to give it optical anisotropy. Both of these processes complicate the fabrication process of real-world devices. Although materials that are both highly anisotropic and highly tunable can actively control the polarization of light on their own, materials that possess both properties are scarce and rarely available in high-quality thin films over wafer scales. Here, we present optical anisotropy and gate-tunability in semiconducting, highly-aligned, single-walled carbon nanotubes (SWCNTs) over 4" wafers in the visible and near infrared (IR) regimes. SWCNTs were found to have a normalized birefringence value of up to 0.09 in the near IR which is larger than common anisotropic crystals such as liquid crystals (0.06), calcite (0.05), and LiNbO₃ (0.02). The optical selection rules of SWCNTs result in a large optical band gap difference in the ordinary and extraordinary directions of 210 meV enabling its normalized dichroism to reach 0.58 which is only exceeded bulky, unstable crystals. SWCNTs were found to have record normalized birefringence and dichroism values for thin films (< 4 nm thick). Additionally, the optical properties of SWCNTs can be modulated using carrier injection to induce the plasma dispersion effect. The real and imaginary parts of the extraordinary refractive index were tuned by 5.9% and 14.3% in the near infrared at 2200 nm and 1660 nm, respectively. This outperforms popular semiconductors for near IR telecommunications systems such as Si, LiNbO₃, and graphene. Highly-aligned SWCNTs are among the most optically anisotropic and tunable materials and promise to open new avenues for their application in integrated photonics and telecommunications.

SESSION EL08.05: Poster Session I: Nanostructure Design, Fabrication and Characterization

Session Chairs: Ho Wai (Howard) Lee and Benjamin Vest

Monday Afternoon, November 27, 2023

Hynes, Level 1, Hall A

8:00 PM EL08.05.01

Characterization of Iridium Films for Emerging Optical Applications Zachary Kranefeld, Pan Menasuta, Kevin Grossklaus, John McElearney and Thomas Vandervelde; Tufts University, United States

Iridium (Ir) is a refractory metal with optical properties that make it an excellent candidate for a wide range of optical applications, including metamaterials; such as, selective-emitters for thermophotovoltaic (TPV) cells. Metamaterial applications require patterning with nanofabrication techniques, but these processes are still relatively unexplored for Ir films. In this work, various density Ir films were characterized throughout wet and dry etch fabrication processes. Electrical properties were measured as a function of film thickness via 4-point probe. Complex refractive index (n and k) was measured with variable angle spectroscopic ellipsometry (VASE) and reported as a function of film thickness and density. Surface morphology was determined by AFM and SEM, as a function of etch depth. Additionally, well-defined etch rates as well as etchant selectivity are reported for each etch recipe.

8:00 PM EL08.05.02

Hydrogen-Free PVD SiN for Low-Losses 300 Mm Photonics Waveguides Eleonora Garoni¹, Laura Sauze², Quentin Wilmart¹, Lavinia E. Nistor², Dominique Cerqueira², Ahmed Gharbi¹, Vincent Mathieu¹, Tristan Dewolf¹, Christophe Lecouvey¹, Rémi Coquand¹ and Guillaume Rodriguez¹; ¹University Grenoble Alpes, CEA, LETI, France; ²Applied Materials France Sarl, France

Silicon nitride (SiN) has recently become a particularly successful material for integrated photonics platforms. Its use as an optical waveguide has been reported for a wide range of applications: LiDAR, microwave optics, quantum photonics, neuromorphic computing, telecommunication and sensors. Indeed, SiN can be a possible substitute of silicon waveguides for applications requiring ultra-low optical losses, thermal stability or in wavelength regimes where silicon is non-transparent (<1.1 μm). It can also be integrated in a silicon photonic platform to combine the properties of both materials. [[1]]

In addition, SiN photonics offers a good level of versatility depending on the integration constraints and the targeted application. However, the combination of low deposition temperature and low optical losses is still elusive. In particular, the presence of hydrogen in SiN film deposited by chemical vapor deposition (CVD) causes optical absorption in the C-band. [[2]]

Contrarily to CVD, physical vapor deposition (PVD) technique for SiN film growth has two main advantages: the ability to deposit a hydrogen-free film and a low deposition temperature.

Intuitively, propagation losses in the near-infrared region are expected to be low. On the other hand, PVD SiN can be highly stressed, which can be detrimental for integration. [[3]]

In this work, the process, characterization and integration in devices for waveguides applications of a PVD-deposited SiN thin film will be discussed.

The films were prepared by magnetron reactive pulsed-DC sputtering on 300 mm silicon wafers at low temperature (200°C) in an Ar/N₂ gas mixture. Deposited film thicknesses were in the range from 400 nm to 800 nm.

By tuning the Ar/N₂ gas ratio, we managed to obtain a film with refractive indexes corresponding to the targeted stoichiometric Si₃N₄, also confirmed by RBS-NRA measurements.

The film stress was found to be compressive and can be tuned close to zero by increasing the power and the pressure in the deposition chamber. The gas ratio and pressure conditions needed to achieve lower stress also give a film with optical properties adapted for the waveguides applications specifications.

In-film particles are detrimental for waveguides performances, since they can increase scattering phenomena and thus enhance waveguide losses. We managed to minimize in-film particles by improving the deposition sequence, succeeding in keeping low values even for 800 nm thick films.

FTIR analysis allowed to assess the absence of N-H and Si-H absorption bands, visible between 1150 cm⁻¹ and 3500 cm⁻¹ in CVD deposited SiN films to which PVD SiN was compared, confirming that the latter is hydrogen-free.

In a second time, waveguides integration will be discussed. SiN deposited by PVD is known to be rougher than CVD SiN: the waveguides side roughness can be improved thanks to lithography and etching optimization. Side roughness values comparable to CVD were obtained, for the same film thickness and design.

Finally, we will present some optical results including propagation losses in the C-band for three PVD-deposited SiN film thicknesses (400 nm, 600 nm, 800 nm) on a 300 mm photonic platform. PVD SiN waveguides outperform CVD SiN waveguides in the C-band where the presence of hydrogen in the SiN film is critical for optical losses.

[[1]] Rahim, A. *et al.*, *J. Lightw. Technol.* **2017**, 35, 639–649. C. Xiang *et al.*, *Photon. Res.* **2022**, 10, A82–A96. Q. Wilmart *et al.*, *Appl. Sci.* **2019**, 9, 255. <https://doi.org/10.3390/app9020255>

[[2]] Bauters, J. F. *et al.*, *Opt. Express* **2011**, 19 (4), 3163. Roeloffzen, C. G. H *et al.*, *IEEE J. Select. Topics Quantum Electron.* **2018**, 24 (4), 1–21.

[[3]] Zhang, Z. *et al.*, *Science and Technology of Advanced Materials* **2017**, 18 (1), 283–293. Frigg, A. *et al.*, *Opt. Express* **2019**, 27 (26), 37795. E. Kempf *et al.*, 2020 22nd International Conference on Transparent Optical Networks (ICTON), Bari, Italy, **2020**, 1–4.

8:00 PM EL08.05.03

Organic solar cells provide many hopes for the future: potential for mass manufacturing, cheap materials, flexible substrates. However, they also pose many problems that have yet to be solved, namely relatively low efficiency and instability. This work attempts to improve the efficiency of organic solar cells by using a quasi-random nanostructured active layer. While many methods exist for manufacturing nanostructures, we utilize a soft lithography approach using Digital Video Disks (DVDs) as molds. DVDs provide a low cost, programmable alternative to conventional manufacturing methods, which aligns with the goals and prospects of organic solar cells. Previous papers have explored this DVD soft lithography method, but we propose further improvements by using the optimized quasi-random sequence into the DVD before the soft lithography process. The optimized quasi-random structure increases the local surface randomness thus increasing the light trapping properties of the active layer. Additionally, the tiered structures generated by DVD nanoimprinting reduce reflectance at higher angles of incidence, leading to improved performance at all angles.

8:00 PM EL08.05.04

Enhancing the Electrical and Optical Properties of Thermochromic VO₂: The Impact of Nanostructuring and Gold Nanoparticles Gregory Savorianakis¹, Stephanos Konstantinidis¹, Michel Voué¹, Bjorn Maes¹, Nicolas Martin², Cedric Rousseau¹ and Gilles Rosolen¹; ¹UMONS, Belgium; ²Femto-ST, France

Monoclinic VO₂ (m-VO₂) exhibits a Metal-Insulator Transition (MIT) at around 67°C, earning it the label of a thermochromic material. In this study, we show how to optimize the magnetron sputtering process using a vanadium target in an Ar/O₂ mixture to synthesize 200 nm thick films composed of m-VO₂ crystals. Our synthesis method involves regulating the oxygen flow rate and annealing the samples for 120 minutes at 500 °C in an O₂ environment, as confirmed by Raman spectra and XRD.

In the second part of our study, we validate the numerical results obtained using the Cavity Modelling Framework (CAMFR) by comparing them to the optical properties of the synthesized films. Through simulations, we demonstrate the ability to improve the properties of the films for use as smart windows by tuning the nanostructures of a VO₂ nano-ribbons configuration. By adjusting the width, periodicity, and thickness of the nano-ribbons, we can achieve improved energy efficiency and a less opaque appearance which means it's a stronger contender, when compared to a dense film of the same thickness, for smart windows application.

In the final part of our research, we experimentally combine dense m-VO₂ films with gold nanoparticles (AuNPs) to achieve a tunable plasmonic signal based on temperature changes. We demonstrate the use of (3-aminopropyl) trimethoxysilane (APTMS) linkers for grafting AuNPs onto the surface of VO₂ films. By optimizing the protocol, we can obtain a well-spread monolayer of NPs without clustering. From the absorption spectra, we observe a 10nm shift in the plasmonic peak wavelength as a function of temperature. Furthermore, resistivity and optical hysteresis measurements reveal that AuNPs amplify by one order of magnitude the resistivity drop and by 15% the transmission drop, as well as decreasing the critical temperature by 5°C and narrowing the hysteresis width. Additionally, by depositing a second m-VO₂ layer above the AuNPs, we created another hybrid platform, which lead to even greater improvements in resistivity and transmission modulation compared to bare m-VO₂. Hall measurements were performed on these hybrid platforms, revealing the important role played by AuNPs in improving carrier density. About the plasmonic wavelength shift according to the temperature, it reaches now a value of 60 nm. This second platform have been simulated as well in order to optimize the plasmonic shift by varying the NPs size and their coverage. Here again, an optimized plasmonic wavelength shift of 130 nm is obtained for a coverage around 60%.

The here-mentioned work may pave the way towards the elaboration of thin film materials with high optical accordability which can potentially be used in applications as color display, protection against counterfeiting and opto-electronics chips.

8:00 PM EL08.05.05

Improvement of Light Extraction Efficiency and Viewing Angle Characteristics of Organic and Quantum Dot Light Emitting Diodes with Spontaneously Formed Buckling Patterns of Soft Materials Yoon-Jeong Choi, Jeong-Yeol Yoo and Byung Doo Chin; Dankook University, Korea (the Republic of)

There exist a lot of technologies for a light extraction (LE) of organic light emitting diodes (OLEDs). However, for the successful commercial application, the restriction on the cost of manufacturing, directionality of color, and the requirement to maintain a high-quality image are severe for devices with LE structure. Insertion of scattering medium in the OLED with microcavity (mostly popular for commercial panels) can be generally effective but reduces the function of polarization, which blocks the reflection from the external light. Recovering of the lost power from surface plasmon (SP) is also effective strategy for an enhancement of LE, and a method of grating coupling by a generation of corrugate the organic/metal interface causes Bragg scattering. Several kinds of periodically corrugated or "buckled" patterns were proposed, showing a reduction of light loss (LE effect) by a scattering of SPs [1,2]. In this work, simple fabrication processes for the micro-scale LE pattern formation is introduced. For a top-emitting OLED (TOLED), a useful platform of commercial panels for high-resolution mobile on the non-transparent polymeric substrates, colors and spectra are significantly sensitive to those specific LE structures and intrinsic micro-cavity effects of TOLED having translucent electrodes. Here, a quasi-periodic and controllable buckling patterns with broad size/scale distribution are described in detail [3,4]. The formation of buckling patterns is spontaneously driven by the mismatch of thermal expansion coefficient of the stacked organic and polymeric layers, which are easily deposited by a simple deposition process in the vacuum or solution coating environment on top of the translucent cathode of TOLED structure. Further experimental studies on the effect of molecular weight, glass transition temperature with segmental softness/rigidity, and phase separation behavior of material combination will be presented for the understanding of the mechanism of quasi-periodic 3-dimensional buckling structure formation. As for OLED and QD-LED performance with buckling LE structure, luminous efficiency of device with buckling patterns in a various position of device was characterized. The results on the microcavity-driven, top-emitting type OLED showed the improvement of the luminous efficiency of phosphorescent device (68 cd/A) more than 40% of the pattern-less control devices (47 cd/A). Such a result, observed in case of optimum buckling structure formed on top of the translucent electrode of device, can be explained by the suppression of light loss by the SP mode at semi-transparent metal/air interface without losing the control of polarization of light. Moreover, the shift of the maximum peak of electroluminescence for buckling patterned device was less than 4nm with the viewing angle range of 0 to 75 degree (>20nm shift for control device), securing a negligible change of the spectral characteristics and color stability (robust viewing angle behavior) [5]. Our corrugated pattern structure was also successfully applied to the electroluminescent quantum dot (QD) device, where the intrinsic pure and saturated emission colors and narrow FWHM (full width at half maximum) could be further improved.

[1] T. Schwab, C. Fuchs, R. Scholz, A. Zakhidov, K. Leo, M. C. Gather, *Optics Express*, (2014) 22, 7524-7537

[2] Y. Zhang, R. Biswas, *ACS Omega* (2021) 6, 9291-9301

[3] W. H. Koo, S. M. Jeong, F. Araoka, K. Ishikawa, S. Nishimura, T. Toyooka, and H. Takezoe Lastname, F. M. and F. M. Lastname, *Nature Photonics* (2010) 4, 222-226

[4] W. H. Koo, B.D. Chin, S. M. Jo, *Korea Patent* (2021) 10-2293473

[5] E. Kim, J. Chung, J. Lee, H. Cho, N. S. Cho, S. Yoo, *Organic Electronics* (2017) 48, 348-356

8:00 PM EL08.05.06

Flexible Route to AuNP-Cluster Arrays for Plasmonic Sensing Pooria Golvari¹, Tyrone Morales¹, Stephen M. Kuebler^{1,1,1} and Jimmy Touma²; ¹University of Central Florida, United States; ²Air Force Research Laboratory, United States

Periodic assemblies of gold-nanoparticle (AuNP) clusters are attractive as tunable substrates for surface-enhanced Raman spectroscopy (SERS)¹, as well as analyte sensors based on coupled localized surface plasmon resonance (LSPR)² and diffractively-coupled plasmonic surface lattice resonances (SLR)^{3,4}. We report an approach for fabricating two-dimensional lattices selectively filled with mono- or multi-layers of AuNP films. The lattices are prepared using e-beam lithography and then transferring the pattern into fused silica by reactive ion etching. Centrifuge-aided deposition assisted by a protein binder is then used to load dense mono- and multi-layers of AuNPs into the silica arrays, in one tenth of the time required for immersion methods. Post-assembly cross-linking of the binder prior to drying the AuNP film is used to control the spacing between the deposited layers and to tune the LSPR coupling. Masking and lift-off can be used to selectively deposit AuNP-clusters inside the prepatterned arrays. The AuNP-filled arrays are optically characterized in reflection and transmission modes in the visible and near-infrared. The method provides a means for independently controlling properties of the AuNP-clusters (e.g., size and interparticle spacing) and properties of the lattice (e.g., symmetry, the size, the depth, and periodicity). As such, the method should be useful for preparing sensors based on hybrid-LSPR with controlled coupling between AuNPs and SLR modes.

1. Matricardi, C.; Hanske, C.; Garcia-Pomar, J. L.; Langer, J.; Mihi, A.; Liz-Marzán, L. M., Gold Nanoparticle Plasmonic Superlattices as Surface-Enhanced Raman Spectroscopy Substrates. *ACS Nano* **2018**, *12* (8), 8531-8539.

2. Halas, N. J.; Lal, S.; Chang, W.-S.; Link, S.; Nordlander, P., Plasmons in Strongly Coupled Metallic Nanostructures. *Chemical Reviews* **2011**, *111* (6), 3913-3961.

3. Cherqui, C.; Bourgeois, M. R.; Wang, D.; Schatz, G. C., Plasmonic Surface Lattice Resonances: Theory and Computation. *Accounts of Chemical Research* **2019**, *52* (9), 2548-2558.

4. Kravets, V. G.; Kabashin, A. V.; Barnes, W. L.; Grigorenko, A. N., Plasmonic surface lattice resonances: a review of properties and applications. *Chemical reviews* **2018**, *118* (12), 5912-5951.

8:00 PM EL08.05.07

Hot-Carrier Multi-Junction Solar Cells: The Best of Both Worlds Maxime Giteau^{1,2}, Samy Almosny^{1,3}, Jean-François Guillemoles^{1,4} and Daniel Suchet^{1,4}; ¹NextPV, CNRS, The University of Tokyo, Japan; ²ICFO, Spain; ³Saule Technologies, Poland; ⁴CNRS, Ecole Polytechnique, ENSCP, Institut Photovoltaïque d'Ile de France (IPVF), UMR, France

Conventional single-junction solar cells are limited in power conversion efficiency at around 33% (Shockley-Queisser limit) due to the mismatch between the broadband solar spectrum and the fixed bandgap of the cell. Multijunction solar cells (MJSCs) can overcome this limit by combining multiple subcells with decreasing bandgaps, allowing them to extract more energy per

photon. These are the most efficient cells manufactured today, but they remain expensive and offer limited material combinations. An alternative approach is the hot-carrier solar cell (HCSC), which converts the extra kinetic energy of the (hot) carriers into electricity before it is dissipated by interaction with the lattice, in a process called thermalization. However, despite significant progress, thermalization rates remain too fast for hot-carrier devices to operate efficiently as solar cells. In essence, the main issue is that HCSCs should be ultrathin to significantly reduce thermalization, while nonetheless absorbing most of the incident illumination (optically thick).

To alleviate this issue, we introduce the hot-carrier multi-junction solar cell (HCMJSC) concept [1,2], a 2-junction MJSC in which the top subcell is an HCSC. With this configuration, photons not absorbed in the ultrathin hot-carrier subcell can be harvested by the bottom subcell, thereby not sacrificing absorption. As a result, HCMJSCs make it much easier to benefit from hot-carrier effects than HCSCs, leading to large efficiency gains for realistic thermalization rates. HCMJSCs also offer a significant advantage over MJSCs: the efficiency shows little dependence on the bandgap of the subcells. As a result, HCMJSCs can be designed for whatever bandgap combination is most practically achievable, which is especially relevant for lattice-matched III-V multi-junction devices. We will highlight some promising material combinations, including double homo-junction configurations, in which both subcells use the same material. After illustrating the advantages of HCMJSCs over both MJSCs and HCSCs, we will look at their resilience under operation conditions, focusing on the influence of the cell temperature and variations in the illumination spectra [3].

References:

- [1] Giteau, M., Almosni, S. & Guillemoles, J.-F., Hot-carrier multi-junction solar cells: A synergistic approach, *Appl. Phys. Lett.* **120**, 213901 (2022).
- [2] Almosni, S., Giteau, M., Guillemoles, J.-F. & Suchet, D., CELLULES SOLAIRES MULTI-JONCTIONS A PORTEUR CHAUD, French patent filed on 19/05/2022 (application number FR2204325)
- [3] Giteau, M., Almosni, S., Guillemoles, J.-F. & Suchet, D., Hot-carrier multijunction solar cells: sensitivity and resilience to nonidealities, *JPE* **12**, 032208 (2022).

8:00 PM EL08.05.08

Gap-Plasmon CrystallographyPeeranuchPoungsripong, VyshnavKannampalli, LionelSantinacci, DominiqueChatain, OlivierMargeat and BeniaminoSciaccia; Aix-Marseille Université, France

Plasmonic nanocavities have the ability to confine light in extremely small volumes, enhancing the electromagnetic field and providing a highly sensitive and reproducible platform. Using plasmonic nanocrystals, this tunability is achieved by adjusting the nanoparticle size, the gap spacing, and the gap spacer refractive index. These phenomena are receiving increasing attention by the nanophotonics and nanoelectronics communities due to their potential applications in optoelectronics, quantum optics, and novel nanophotonic and plasmonic-circuit devices. In this study, we investigated gap plasmon resonators made of silver nanocubes separated from a gold mirror by thin dielectric layers (Al₂O₃, TiO₂). First, we studied the impact of dielectric thickness, refractive index and nanocube size on individual resonators, supported by correlative SEM microscopy. This enabled us to gain insights on the system sensitivity to various parameters. Next, we show that this platform can be used to assess the removal of residual capping ligands (such as PVP) on the nanocube surface, which hampers use in nanoelectronics applications. Finally, by performing polarisation-resolved measurements on birefringent anatase layers (2-10nm), we show that we can identify their crystal orientation with a sub-100nm spatial resolution, despite their extremely small thickness. We found a wide range of possible orientations and no specific epitaxial relationships with the underlying polycrystalline gold film. EBSD measurements on thicker anatase layers confirmed these findings. This work further extends the use of gap-plasmons to a new domain.

References

1. Barbillon, G., Plasmonics and its Applications. Materials 2019, 12 (9), 1502.
2. Kim, J.-M.; Lee, C.; Lee, Y.; Lee, J.; Park, S.-J.; Park, S.; Nam, J.-M., Synthesis, Assembly, Optical Properties, and Sensing Applications of Plasmonic Gap Nanostructures. Advanced Materials 2021, 33 (46), 2006966.
3. Li, G.-C.; Zhang, Q.; Maier, S. A.; Lei, D., Plasmonic particle-on-film nanocavities: a versatile platform for plasmon-enhanced spectroscopy and photochemistry. Nanophotonics 2018, 7 (12), 1865-1889.
4. Chikkaraddy, R.; Zheng, X.; Benz, F.; Brooks, L. J.; de Nijs, B.; Carnegie, C.; Kleemann, M.-E.; Mertens, J.; Bowman, R. W.; Vandenbosch, G. A. E.; Moshchalkov, V. V.; Baumberg, J. J., How Ultranarrow Gap Symmetries Control Plasmonic Nanocavity Modes: From Cubes to Spheres in the Nanoparticle-on-Mirror. ACS Photonics 2017, 4 (3), 469-475.
5. Dufond, M. E.; Chazalviel, J.-N.; Santinacci, L., Electrochemical Stability of n-Si Photoanodes Protected by TiO₂ Thin Layers Grown by Atomic Layer Deposition. Journal of The Electrochemical Society 2021, 168 (3).

8:00 PM EL08.05.09

Engineering Exciton Emission in Monolayer MoS₂ by using Electroplated Gold Plasmonic NanodiscsAbhayA. V S¹, MihirK. Sahoo¹, FaihaMujeeb¹, AbinVarghese¹, SubhabrataDhar¹, SaurabhLodha¹, SandipGhosh² and AnshumanKumar¹; ¹Indian Institute of Technology Bombay, India; ²Tata Institute of Fundamental Research, India

Transition metal dichalcogenides (TMDCs), such as MoS₂, hold great promise as 2D semiconductors, making them suitable for various applications in optics and novel electrical devices. However, their atomically thin thickness and low quantum yield have hindered their practical application due to limited light absorption. Integrating subwavelength plasmonic nanostructures with monolayer TMDCs is a promising method to address these challenges effectively and manipulate the optical properties. In this study, we utilized electron beam lithography and electroplating techniques to fabricate an array of gold nanodiscs (AuNDs) capable of significantly enhancing the photoluminescence (PL) of monolayer MoS₂. The monolayer MoS₂ on the gold nanodisc array resulted in an impressive photoluminescence enhancement compared to as-grown MoS₂ on sapphire and a monolayer MoS₂ on a plane gold film. To gain insights into the underlying mechanism behind this enhancement, we conducted Finite-Difference Time-Domain (FDTD) simulations.

8:00 PM EL08.05.10

Highly Efficient Near-Infrared Light-Emitting Diode Based on CdHgSe/ZnCdS Core/Shell NanoplateletsHosseinRoshan¹, AnatolPrudnikau², FabianPaulus^{2,3}, BeatrizMartín-García⁴, RenéHübner⁵, HoumanBahmani Jalali^{1,1}, ManuelaDe Franco¹, MirkoPrato¹, FrancescoDi Stasio¹ and VladimirLesnyak⁶; ¹Istituto Italiano di Tecnologia, Italy; ²Helmholtzstraße, Germany; ³Universitat Dresden, Germany; ⁴Tolosa Hiribidea, Spain; ⁵Helmholtz-Zentrum Dresden-Rossendorf e.V., Germany; ⁶Technische Universität Dresden, Germany

Luminescent Quantum dots (QDs) have gathered significant attention over the past decade. Their distinct chemical and optical properties, including size-adjustable light emission, remarkable photostability, and a range of fluorescence colors, have motivated extensive investigations. In recent years, near-infrared (NIR) quantum dots have emerged as a promising avenue for a new generation of optoelectronic devices including infrared detectors and light sources. This study presents the fabrication of NIR-LEDs operating at the o-band optical telecommunication wavelength (1300 nm) using novel CdHgSe/ZnCdS core/shell nanoplatelets with a photoluminescence quantum yield of 70%. The nanoplatelets achieve a remarkable external quantum efficiency (EQE) of 7% in the final device. Notably, the resulting EQE of the fabricated NIR-LED sets a new benchmark for mercury-based QD LEDs.

8:00 PM EL08.05.11

Utilizing Short-Pulsed Laser Ablation to Create Plasmonic Colloidal Nitride Nanoparticles for Biomedical ApplicationsNikolaosPliatsikas, SpyridonKassavetis, StavrosPanos, TamaraOdutola, IliasFekas, ChrysanthiPapoulia, JohnArvanitidis, DimitrisChristofilos, MariaGiotti and PanosPatsalas; Aristotle University of Thessaloniki, Greece

The field of plasmonics is currently witnessing rapid growth and advancement, offering exciting prospects for various scientific and technological applications. In particular, metal nanoparticles (NPs) exhibiting plasmonic behavior in the Near-Infrared (NIR) spectral range have gained significant attention for their potential in biological applications. These NPs possess exceptional abilities to efficiently absorb and generate heat within a highly confined volume surrounding them. However, conventional plasmonic metal NPs like gold (Au) and silver (Ag) face limitations when exposed to the high temperatures and intense electric fields required for biomedical applications involving NIR concentrated light [1]. To overcome these challenges and unlock new possibilities in plasmonic bio-applications, the fabrication of refractory transition metal nitride NPs has emerged as a promising avenue. Among them, Titanium Nitride (TiN) stands out, as it offers plasmonic performance that extends into the NIR spectral range through stoichiometry variations and/or doping [2]. Pulsed laser ablation in liquids (LAL) has emerged as the most favorable method for producing plasmonic TiN NPs, offering advantages in terms of reproducibility and scalability. LAL ensures that the ablated NPs maintain the elemental composition of the solid target, a crucial factor considering the sensitivity of NIR plasmonics to the stoichiometry and doping of TiN. By leveraging LAL, researchers can explore and optimize the plasmonic properties of TiN NPs, paving the way for groundbreaking advancements in the field of plasmonic biomedical applications.

In this study, we demonstrate the fabrication of refractory and stable plasmonic TiN NPs with absorption characteristics within the NIR biological window using LAL. To achieve this, we initially developed target materials through reactive Magnetron Sputtering at room temperature. Subsequently, the colloidal NPs were shaped using a nanosecond Nd:YAG pulsed laser system at different wavelengths (1064, 532, and 355 nm) via the LAL. To assess the structure, morphology, and material quality of the TiN NPs, we conducted comprehensive analyses employing Raman spectroscopy, scanning electron microscopy (SEM), atomic force microscopy (AFM), and X-ray photoelectron spectroscopy (XPS). Additionally, the optical properties of the TiN target materials were evaluated using NIR-Vis-UV spectroscopic ellipsometry, while optical absorbance characterization was performed on the colloidal TiN NPs. Furthermore, we investigated the photothermal properties of these colloidal NPs and conducted preliminary biocompatibility tests using proteins such as albumin and fibrinogen in a PBS solvent.

[1] P. Patsalas, N. Kalfagiannis, S. Kassavetis, Materials 8 (2015) 3128–3154.

[2] P. Patsalas, N. Kalfagiannis, S. Kassavetis, G. Abadias, D. V. Bellas, C. Lekka, E. Lidorikis, Mater. Sci. Eng. R Reports. 123 (2018) 1–55.

We gratefully acknowledge support of the Hellenic Foundation for Research and Innovation (H.F.R.I.) under the “2nd Call for H.F.R.I. Research Projects for supporting Post-Doctoral Researchers” (Project Number: 1099).

8:00 PM EL08.05.12

Novel Synthesis and Characterization of Magneto-Plasmonic Core-Shell Nanoparticles Carlos A. Marquez Ibarra¹, Natasha Engel¹, Gesuri Morales-Luna², Nicolas Large¹, Nancy Ornelas-Soto³ and Kathryn Mayer¹; ¹The University of Texas at San Antonio, United States; ²Universidad Iberoamericana, Mexico; ³Tecnológico de Monterrey, Mexico

Advancements in numerous technologies including chemical sensing are spurring progress in the development of novel composite nanostructures that integrate magnetic and plasmonic materials. These nanostructures exhibit a unique amalgamation of plasmonic and magnetic properties, positioning them at the forefront of scientific research. The magnetic properties facilitate precise control and manipulation of the nanoparticles in the presence of magnetic fields. Furthermore, materials with plasmonic activity, such as gold, offer outstanding biocompatibility, along with exceptional optical features that include enhanced scattering and high sensitivity to changes in refractive index. The aim of this research is to analyze and describe core-shell nanoparticles (CS-NPs) comprising a magnetite core enveloped by a gold shell (Fe@Au CS-NPs). These nanoparticles are synthesized through a novel method that integrates established wet lab synthesis techniques under ambient conditions. A comprehensive characterization approach was employed. Electron microscopy techniques including Scanning Electron Microscopy (SEM) and Transmission Electron Microscopy (TEM) were utilized to examine and analyze the structure and surface morphology of the investigated materials. Additionally, analytical techniques including Energy-Dispersive X-ray Spectroscopy (EDS) and Fourier Transform Infrared Spectroscopy (FTIR) were employed to investigate the chemical composition of the samples and the presence of surface ligands. Furthermore, computational methods including finite difference time domain (FDTD) and finite element method (FEM) modeling were applied to confirm the plasmonic properties of the composite materials. Calculated optical properties of light absorption and scattering cross-sections were compared with experimental characterization data obtained via techniques including UV-vis absorbance spectroscopy and darkfield scattering microspectroscopy. By employing these extensive characterization methods, the research aims to obtain valuable insights into the composition and properties of the materials under investigation. These insights will serve as a foundation for the development of sensing technology for water quality monitoring.

8:00 PM EL08.05.13

Simulating the Co-Assembly of Cellulose Nanocrystals and Gold Nanorods - Effect of Size Distribution and Density Jiaxin Hou, Yuchen Zhu, William Sampson and Ahu Gumrah Dumanli; University of Manchester, United Kingdom

The self-assembly of anisotropic particles holds great potential in fabricating multifunctional optical materials through cholesteric structures. Specifically, cholesteric structures formed by these particles can exhibit unique optical properties, making them ideal for various applications for sensing and fabrication of optical security features. In particular, integrating plasmonic materials into cholesteric phases that can interact with the visible spectrum can be used in building metasurfaces that can alter the interaction of the light completely. While there have been efforts to validate this hypothesis, the experimental work on combining the self-assembly of gold nanorods (Au-NRs) with cellulose nanocrystals (CNCs) had limited success as the plasmonic particle loading was minimal and didn't allow coupling between the plasmonic states of the Au-NPs possible without disrupting the cholesteric order. To understand the physical and theoretical limitations of this co-assembly system, we used molecular dynamic coarse-grained methods with Gay-Berne potential with anisotropic particle systems of different aspect ratios and densities to complement our experimental work.

Our experimental and modeling work demonstrated good agreement with regard to identifying the surface charge and the density of Au-NRs as the main driving force on the co-assembly. Negatively charged AuNRs can distribute uniformly and align in the same direction with CNCs and the particle systems with higher aspect ratio distributions would have successfully co-assembled, as AuNRs would prefer to fill the vacancy between the cholesteric structures formed by CNC particles. Our further studies explain the limit of maximum concentration from density, as lighter particles (CNCs) would reach assembly conditions compared to the AuNRs. Our work sheds new light on the understanding of the self-assembly of multi-component systems with polydispersity and charge variations and takes our understanding one step further in developing optical materials.

8:00 PM EL08.05.14

Organic Microcrystal Synthesis: Effects of Composition and Environment Ashleigh K. Wilson, John N. Munga, Tori Furlow, Violet MacAuley, Asia Jones, Chantel Johnson and Natalia Noginova; Norfolk State University, United States

Luminescent organic crystals suitable for thin film fabrication present interest for nanophotonic applications. Using simple solution growth technique, we grow crystals with phenanthroline as a ligand and various rare earth ions, such as thulium (Tm), ytterbium (Yb), gadolinium (Gd), lanthanum (La), neodymium (Nd), europium (Eu), and erbium (Er). We explore effects of and various conditions on crystal formation and growth, and demonstrate that composition and local environment strongly affect the size and shape of microcrystals.

8:00 PM EL08.05.15

Photoinduced Electric Effects in Magnetic Metasurfaces of Various Geometry MD Afzalur Rab, Sean Nesbit and Natalia Noginova; Norfolk State University, United States

Permalloy metasurfaces with design-controlled magnetic uniaxial anisotropy have been fabricated and studied for plasmonic behavior and photoinduced electric effects. Significant photovoltages are observed as the response to the pulsed laser illumination, and are maximized at the plasmon resonance conditions. The voltage sharply changes its polarity at certain fields which are different for systems of different geometry. The switching fields are found to be in good correlation with the magnetic anisotropy fields determined by the ferromagnetic resonance method. The effects are discussed taking into account non equilibrium heating of the electron subsystem by the laser pulse and the Nernst effect.

8:00 PM EL08.05.16

Optical Characteristics of Superconducting Plasmonic Transition Metal Nitrides Li-Chung Yang^{1,2}, Jingwei Yang¹, Jing-Yuan Chen³, Tzu-Yu Peng^{1,2}, Chung-Ting Ke¹ and Yu-Jung Lu^{1,2}; ¹Academia Sinica, Taiwan; ²National Taiwan University, Taiwan; ³National Taiwan University of Science and Technology, Taiwan

Transition metal nitrides (TMNs) exhibit exceptional promise due to their elevated melting points, metallic optical characteristics, and superconductivity at cryogenic temperatures. Recent attention has turned toward TMNs as potential substitutes for conventional plasmonic materials like gold and silver due to their unique plasmonic properties. However, the optical properties of plasmonic TMN films in the superconducting state have remained uncharted territory. In the past, we have demonstrated the utility of plasmonic TMN films (including TiN, ZrN, HfN, and NbN) as alternative plasmonic materials for various applications [1-3]. Here, we sputtered a thin film of NbN onto a MgO (100) substrate at 800°C, revealing a measured critical temperature (T_c) of 10.5 K. Employing temperature-dependent spectroscopic ellipsometry, we systematically characterized the optical behavior of NbN films from 4 K to 300 K within a wavelength range spanning 300 nm to 2 μ m. As the temperature decreased, we observed a remarkable reduction in the magnitude of the imaginary part of the permittivity, the magnitude dropped by 13.8 times at 1550 nm. Subsequently, we applied the Drude-Lorentz model for parameter fitting, elucidating that the substantial reduction in the imaginary component primarily resulted from a sharp increase in the relaxation time. These findings underscore NbN's potential as a highly promising material for the development of low-loss superconducting plasmonic devices.

Reference

- [1] M-J Yu, C-L Chang, H-Y Lan, Z-Y Chiao, Y-C Chen, H W H. Lee, Y-C Chang, S-W Chang, T. Tanaka, V. Tung, H-H Chou*, and **Y-J Lu***, Plasmon-Enhanced Solar-Driven Hydrogen Evolution Using Titanium Nitride Metasurface Broadband Absorbers. *ACS Photonics* **8**, 3125–3132 (2021).
- [2] Z-Y Chiao, Y-C Chen, J-W Chen, Y-C Chu, J-W Yang, T-Y Peng, W-R Syong, H W H. Lee, S-W Chu, and **Y-J Lu***, Full-Color Generation Enabled by Refractory Plasmonic Crystals. *Nanophotons* **11**, 2891-2899 (2022)
- [3] Sheng-Zong Chen, Jing-Wei Yang, Tzu-Yu Peng, Yu-Cheng Chu, Ching-Chen Yeh, I-Fan Hu, Swapnil Mhatre, Yu-Jung Lu*, and Chi-Te Liang*, Disorder-Induced 2D Superconductivity in a NbTiN Film Grown on Si by Ultrahigh-Vacuum Magnetron Sputtering. *Superconductor Science and Technology* **35**, 064003 (2022)

8:00 PM EL08.05.17

Light Extraction and Stability of Fluorescent and Phosphorescent Organic Light-Emitting Diodes Incorporating Plasmonic Ag Nanoparticles Sneha Sreekumar¹ and Deirdre O'Carroll^{2,1}; ¹Rutgers University, United States; ²Rutgers, The State University of New Jersey, United States

In recent years, organic light-emitting diodes (OLEDs) have gained great popularity in the display industry due to their thin form factor, high color quality and the ability to be fabricated onto flexible substrates. However, OLED stability and efficiency, particularly at blue wavelengths, need significant improvement for future, more demanding display applications, such as micro displays. Several methods have been employed to increase the light-extraction efficiency (LEE) and stability in OLEDs, including the development of new active-layer materials, interfacial layer modifications, addition of nanoparticles or nanopatterns into various layers of the devices, optimization of the structural design and the application of microlens arrays. The LEE in an OLED is typically ~20% with the rest of the 80% of photon energy being lost to substrate, surface plasmon and thin-film waveguide modes. While these approaches are effective for improving LEE of red and green OLEDs, very few of these approaches have significantly improved the efficiency of blue OLEDs. We have shown in previous studies that plasmonic Ag enhances the quantum yield in fluorescent materials through the Purcell effect and improves the photostability of phosphorescent OLED materials by a factor of 3.6 by reducing the triplet emission lifetime. Here, we present a study of the use of silver nanoparticles introduced at different device interfaces and within different layers from the anode to the cathode to combat the various optical losses that reduce LEE. The results show improvements in blue OLED stability and luminescence lifetime in addition to improved LEE. We have chosen a blend of PFO: F8BT to study fluorescent OLEDs and a blend of PVK:FIrpic to study blue phosphorescent OLEDs as a function of different nanoparticle additions. The devices are built on ITO on glass substrates

with different formulations of PEDOT:PSS to get the highest conductivity. We vary the Ag nanoparticle size from 15-50 nm and introduce them into different layers of the OLED including: (i) on ITO directly, through spin coating or de-wetting methods, (ii) doped into the PEDOT:PSS layer; (iii) grown on the PEDOT:PSS layer; (iv) within and on top of active layer; and finally (v) deposited on top of the active layer before depositing the Ca/Al cathode. We present current-density measurements, luminance, electroluminescence measurements, external quantum efficiency and stability measurements in addition to lifetime and quantum yield measurements to investigate how positioning of the plasmonic structures effects the stability and lifetime of the OLEDs. We are hoping to contribute to solving the issue of low efficient blue OLEDs by improving the lifetime and stability of the devices as well as achieving the required "true blue" color that is required by the display industry by manipulating the interactions between the plasmonic Ag particles and the emissive layers.

8:00 PM EL08.05.18

Ultra Short Pulse Laser Ablation of Titanium Nitride Nanoparticles in Solvent for Biomedical Applications [Ilias Fekas](#), Nikolaos Pliatsikas, Spyridon Kassavetis, Stavros Panos, Tamara Odutola, Evi Rampota, Chrysanthi Papoulia, Christos Kapnopoulos, Maria Gioti, Stergios Logothetidis and Panos Patsalas; AUTH, Greece

Titanium Nitride (TiN) has emerged as a promising alternative plasmonic material that may outperform the traditional plasmonic metals, such as Au and Ag in terms of durability to high temperatures and/or to the high electric fields of concentrated light present in most realistic plasmonic applications. TiN is a well-known conductor of high mobility, widely used in the mainstream microelectronics industry, and it owes its electronic conductivity to the partially filled valence d orbitals that are not completely hybridized with the N-2p electrons and presents high optical response similar to that of Au, hence its golden optical appearance, when in stoichiometric form; non-stoichiometric TiN_{x-1} films are also reported and are predicted to exhibit Localized Surface Plasmon Resonance (LSPR) in red and Near-Infrared (NIR) ranges. TiN is usually grown in thin film form by sputter deposition, its bottom-up nanostructuring was not successful so far, and the formation of colloidal TiN is exceptionally rare, both due to the refractory character of TiN, which is a major obstacle for its wide range implementation [1, 2]. The scope of this work is the fabrication of colloidal TiN nanoparticles with tunable LSPR from the visible to the NIR spectral ranges, thus covering the biological window, a property that can find use in many different biomedical applications. The TiN nanoparticles were fabricated by Ultra Short Pulse Laser ablation (USPL) of TiN in liquid media irradiated at 532nm laser wavelength [1, 3].

USPL corresponding to a shorter thermal relaxation time and would be expected to more effective than nanosecond. USP lasers can reach a higher peak intensity and induce a stronger photoacoustic effect than nanosecond lasers, they can be used with reduced laser fluence compared to that utilized for nanosecond lasers for the TiN nanoparticles fabrication.

The TiN films were grown by reactive magnetron sputtering at room temperature. The chemistry, crystallinity, optical properties, and the point defects of the target materials were evaluated by X-Ray Diffraction, X-Ray Photoelectron Spectroscopy and Scanning Electron Microscopy, respectively.

Then, the major laser ablation parameters were investigated, in particular, low power (up to 2 W) and solvent (water, acetone, and isopropanol). The optical properties, the size, and the structure/defects of the produced nanoparticles were assessed by optical transmittance spectroscopy, Scanning Electron Microscopy and atomic force microscopy, respectively.

[1] P. Patsalas, N. Kalfagiannis, S. Kassavetis, *Materials* 8 (2015) 3128–3154.

[2] P. Patsalas, N. Kalfagiannis, S. Kassavetis, G. Abadias, D. V. Bellas, C. Lekka, E. Lidorikis, *Mater. Sci. Eng. R Reports*. 123 (2018) 1–55.

[3] Kassavetis, S., Kaziannis, S., Pliatsikas, N., Avgeropoulos, A., Karantzalis, A.E., Kosmidis, C., Lidorikis, E., Patsalas, P., *Applied Surface Science* 336 (2015) 262-266.

We gratefully acknowledge support of the Hellenic Foundation for Research and Innovation (H.F.R.I.) under the "2nd Call for H.F.R.I. Research Projects to support Post-Doctoral Researchers" (Project Number: 1099).

8:00 PM EL08.05.19

IGZO Based Oxide Heterostructured Phototransistor for Widening The Detection Limit up to 1000 nm Wavelength [Jun Hyung Jeong](#) and Seong Jun Kang; KyungHee University, Korea (the Republic of)

On the rapidly developing technologies for light communication, night vision system, invisible security system, and health care system industries, detecting near infrared (NIR) wavelength light is becoming a crucial component for electronic devices. Among various structures of photodetectors, such as phototransistors, photodiodes, and photoresistors, phototransistors possess much higher potential compared to other structures photodetectors, such as ultra-low dark current, facile tunable photocurrent by modulating gate and drain bias, which leads to the much higher photodetection characteristics. Numerous materials, such as organic semiconductors (OSCs), quantum dots (QDs), or perovskite materials have widely investigated for transparent NIR detection owing to their adequate photon-electron conversion efficiency maintaining relatively high transparency. However, these materials are intrinsically suffered from environmental moisture or oxygen, which leads to the accelerated degradation of the device. Here, to avoid the above issues, oxide phototransistor with IGZO/Ag₂O was fabricated for the detection of NIR wavelength light. The detectable wavelength range of IGZO phototransistor was highly enlarged from ultraviolet (UV)-visible (vis, 450 nm) to UV-vis-NIR (1000 nm). The device exhibited high photoresponsivity and photodetectivity characteristics of 9.9 A/W and 5.55×10¹⁴ Jones, respectively. Our results suggest a useful method for fabricating metal oxide hetero-structured NIR phototransistors.

SESSION EL08.06: Tunable Metasurfaces and Nanophotonics

Session Chairs: Deep Jariwala and Benjamin Vest

Tuesday Morning, November 28, 2023

Hynes, Level 3, Room 312

8:15 AM EL08.06.01

Plasmonic Tip-Enhanced Probing of Excitonic Materials and Heterostructures [Deep M. Jariwala](#); University of Pennsylvania, United States

Two-Dimensional (2D) chalcogenides of Mo and W are semiconductors that show strong excitonic responses due to their highly quantum-confined character.^{1, 2, 3, 4} This talk will discuss our recent work on optical phenomena and electronic phenomena in 2D semiconductors when they are placed in close proximity on plasmonic substrates such as Au, Ag and Al. For a bulk of this talk, I will be presenting our work on near-field optical spectroscopy using a plasmonic tip. I will also show how using a plasmonic tip once can use near-field tip based micro-spectroscopy to probe defects,^{5, 6} interfaces^{7, 8} and hybrid states in 2D excitonic semiconductors. I will start by showing how tip-enhanced micro-spectroscopy can be used to probe buried metal-semiconductor interfaces in 2D MoS₂.⁷ Specifically, I will focus on how scanning potential probe and scanning conductance probe can be correlated with near-field photoluminescence (PL) to understand the nature of contact between metal and the semiconductor. Next, I will show that the same technique can be used to probe defects,⁵ heterointerfaces, heterogeneities and strain⁹ in 2D semiconductor layers. I will also show how strong-light matter coupling between excitons and plasmonic gap modes can be probed directly using this technique¹⁰ including observation of interlayer excitons.^{11, 12}

References:

1. Jariwala, D.; Marks, T. J.; Hersam, M. C., Mixed Dimensional van der Waals Heterostructures. *Nature Materials* **2017**, *16*, 170-181.
2. Jariwala, D.; Sangwan, V. K.; Lauhon, L. J.; Marks, T. J.; Hersam, M. C., Emerging device applications for semiconducting two-dimensional transition metal dichalcogenides. *ACS Nano* **2014**, *8* (2), 1102–1120.
3. Brar, V. W.; Sherrott, M. C.; Jariwala, D., Emerging photonic architectures in two-dimensional opto-electronics. *Chemical Society Reviews* **2018**, *47* (17), 6824–6844.
4. Jariwala, D.; Davoyan, A. R.; Wong, J.; Atwater, H. A., Van der Waals Materials for Atomically-Thin Photovoltaics: Promise and Outlook. *ACS Photonics* **2017**, *4*, 2692-2970.
5. Moore, D.; Jo, K.; Nguyen, C.; Lou, J.; Muratore, C.; Jariwala, D.; Glavin, N. R., Uncovering topographically hidden features in 2D MoSe₂ with correlated potential and optical nanoprobe. *npj 2D Materials and Applications* **2020**, *4* (1), 44.
6. Chowdhury, T.; Kim, J.; Sadler, E. C.; Li, C.; Lee, S. W.; Jo, K.; Xu, W.; Gracias, D. H.; Drichko, N. V.; Jariwala, D.; Brintlinger, T. H.; Mueller, T.; Park, H.-G.; Kempa, T. J., Substrate-directed synthesis of MoS₂ nanocrystals with tunable dimensionality and optical properties. *Nature Nanotechnology* **2020**, *15* (1), 29-34.
7. Jo, K.; et al. Jariwala, D., Direct Optoelectronic Imaging of 2D Semiconductor–3D Metal Buried Interfaces. *ACS Nano* **2021**, *15* (3), 5618-5630.
8. Krayev, A.; et al. Jariwala, D., Dry Transfer of van der Waals Crystals to Noble Metal Surfaces To Enable Characterization of Buried Interfaces. *ACS Applied Materials & Interfaces* **2019**, *11* (41), 38218-38225.
9. Kim, G.; et al. Jariwala, D., High Density, Localized Quantum Emitters in Strained 2D Semiconductors. *ACS Nano* **2022**, *16* (6), 9651–9659.
10. Jo, K.; et al. Jariwala, D., Direct Nano-Imaging of Light-Matter Interactions in Nanoscale Excitonic Emitters. *Nature Communications* **2023**, *14*, 2469.
11. Rahaman, et al. Jariwala, D., Tunable Localized Charge Transfer Excitons in a Mixed Dimensional van der Waals Heterostructure. *arXiv preprint arXiv:2210.12608* **2022**.
12. Rahaman, M.; Kim, G.; Ma, K. Y.; Song, S.; Shin, H. S.; Jariwala, D., Tailoring Exciton Dynamics in TMDC Heterobilayers in the Quantum Plasmonic Regime. *arXiv:2306.06337* **2023**.

8:30 AM *EL08.06.02

Materials with Ultrastrong Light-Matter Coupling using Nanooptical Building Blocks Stephanie Reich¹, Niclas S. Mueller² and Eduardo B. Barros³; ¹Freie Universität Berlin, Germany; ²Fritz-Haber-Institut, Germany; ³Universidade Federal de Ceará, Brazil

The localized excitations of nanooptical building blocks such as molecules, quantum dots, and plasmonic nanoparticles may be used to design complex optical excitations and engineer light-matter coupling in materials. The underlying concept is that excitation centered on different particles interact through dipole-dipole coupling of their transition moments creating hybridized optical excitation in a similar way as the electrons of atoms hybridize into molecular or crystal states. A second important ingredient is the interaction between photons and the optically excited states. It has been engineered through photonic and plasmonic cavities that locally change the density of electromagnetic states as well as their dispersion.

In this talk we discuss how to obtain three-dimensional materials out of nanooptical building blocks and what kind of properties to expect for such systems. We show that three-dimensional lattices of localized optical excitations create materials with superior strength of light-matter coupling, often reaching the regime of ultrastrong interaction, where light-matter coupling affects the material ground state. We discuss how to realize such optically driven materials artificially, but also show that light-matter coupling is surprisingly strong in most naturally occurring crystals. We envision photonic degrees of freedom as a powerful general tool for materials tailoring and manipulation.

9:00 AM EL08.06.03

Multi-State Control Of Spectral Response In Coupled 2d Material Systems Yujie Luo and Ognjen Ilic; University of Minnesota, United States

Reconfigurable optical systems capable of reproducing complex spectral profiles have broad relevance across optics and photonics. Here, we present a framework for designing reconfigurable metamaterials using active cells that incorporate gate-tunable two-dimensional (2D) materials. Due to their reduced dimensionality, 2D materials exhibit high sensitivity to electric fields, allowing for the tuning of their optical properties through the application of external voltage. By assembling nanopatterned 2D materials into coupled arrays, a single solid-state device can be used to synthesize a wide range of spectral responses. However, the design of such multi-state devices is challenging due to the inherently high-dimensional parameter space involved.

To address this challenge, we present a coupled-mode analytical framework to model the relationship between system control inputs (e.g., voltage) and the manifold of optical outputs embodying multiple spectral resonances. Using graphene as a model 2D material, we investigate the potential for synthesizing complex thermal-infrared spectral absorption profiles within the spectral range where graphene supports surface plasmon polaritons. By employing this coupled framework, we demonstrate that a single judiciously designed array of graphene resonators can dynamically switch between distinct absorption spectra of multiple gases, mimicking both narrow spectral features and broad spectral envelopes. We validate our model by comparing it to full numerical EM simulations, demonstrating a high level of agreement with orders of magnitude speed up in computation time. In addition, through the integration of auto-differentiation algorithms, our model enables efficient gradient-based optimization over the multi-state, multi-spectral design space. We elucidate the tradeoffs between the device complexity, number of resonators and their spectral performance, in both planar and stratified configurations. This approach has potential for various applications in sensing, energy harvesting, and signature management.

9:15 AM EL08.06.04

Photonic Properties of Thin Film BaTiO₃ Grown via Molecular Beam Epitaxy Larissa Little, David R. Barton, Keith Powell, Ashley Cavanagh, Neil Sinclair, Jason Hoffman, Charles Brooks, Robert Westervelt, Marko Loncar and Julia Mundy; Harvard University, United States

Electro-optic modulators form the backbone of efficient data transfer necessary for modern optical communications. These modulators directly connect a driving electric field with optical properties of a material, efficiently converting an electrical signal to an optical signal. Modern data centers and high speed internet, as well as sensing systems, heavily rely on these devices. The electro-optic modulators are often bulk crystals of lithium niobate with indiffused waveguides, limiting their size, speed, and efficiency.

Although thin film lithium niobate offers improved scalability and higher bandwidth over its bulk counterpart, lithium oxides are not CMOS compatible and there is a growing need for higher bandwidth modulators with lower voltage requirements. Barium titanate (BaTiO₃) is an alternative material platform which exhibits an extremely high electro-optic coefficient ($r_{42} \sim 900$ pm/V), a reasonably high band gap (> 3 eV), a relatively high refractive index ($n = 2.4$), and is compatible with traditional CMOS processing. Scalable methods for creating high quality, single ferroelectric domain films of barium titanate are therefore extremely attractive for highly efficient modulators and integrated optical devices.

In this work, we use molecular beam epitaxy to grow high quality BaTiO₃ films on a variety of substrates and use electron microscopy, electronic measurements, and confocal optical measurements to evaluate the optical and electro-optic properties.

9:30 AM BREAK

10:00 AM *EL08.06.05

Quantum Photonics with Emerging Single-Photon Emitters in Silicon Nitride Alexander Senichev, Zachariah O. Martin, Samuel Peana, Demid Sychev, Xiaohui Xu, Omer Yesilyurt, Vahagn Mkhitaryan, Alexei S. Lagoutchev, Alexandra Boltasheva and Vladimir M. Shalaev; Purdue University, United States

The use of photonic-based quantum platforms shows great potential in both fundamental research and practical applications in the field of quantum information science. This is primarily due to the inherent advantages of photons, such as their extremely high speed, weak interactions with matter, and resistance to decoherence. To make practical quantum photonic information processing a reality, it is crucial to have thousands of optical components working together in a controlled and reconfigurable manner. This level of integration can only be achieved using integrated photonics. Hence, there is an urgent need to discover and explore on-chip photonic elements that can efficiently generate, manipulate, and detect quantum states of light.

Additionally, it is essential to enhance light-matter interaction to speed-up quantum photonic processes such as single-photon generation rate employing optical resonators and metamaterials. Silicon nitride (SiN) is one of the most promising and established material platforms for integrated nanophotonics and an emerging platform for quantum applications. It possesses ultra-low losses, absence of two-photon absorption in the telecommunication bands, high refractive index, strong optical Kerr nonlinearity, and CMOS-compatible and foundry-friendly fabrication.

However, until recently, SiN lacked an intrinsic atomic-like source of single photons, which are essential resources for quantum photonic applications. Hence, it required probabilistic nonlinear sources or hybrid heterogeneous integration with other materials hosting quantum emitters. Recently, we discovered intrinsic color centers in the low-autofluorescence SiN material platform [1],[2]. We established methods of creation of these quantum emitters and performed foundational photophysical studies at room and cryogenic temperatures. These emitters exhibit high single-photon purity and brightness at room temperature and narrow zero-phonon lines (ZPL) at cryogenic temperature [3]. Furthermore, they can be monolithically integrated with the technologically favorable silicon nitride photonics platforms, which holds great potential for various applications in the quantum domain [2]. Moreover, we developed a novel technique for the site-controlled fabrication of quantum emitters in SiN achieving high yield with a sub-100-nm lateral placement accuracy. In our study, we explore the possibility of generating indistinguishable photons at high repetition rates at cryo-temperatures as well as at non-cryogenic temperatures, with the use of plasmonic metamaterials, which may enable broader applications of SiN quantum emitters. Plasmonic speed-up of spontaneous emission rate beyond the rate of quantum decoherence processes may enable the generation of indistinguishable photons that could lead to important quantum photonics applications, including quantum communication and quantum computing even at non-cryogenic temperatures. In my talk, I will delve into our research effort to engineer these novel quantum emitters in SiN and explore potential avenues for their improvement and application.

References

- [1] Senichev et al., Sci. Adv. 7, eabj0627 (2021)
- [2] Senichev et al., ACS Photonics, 9(10), 3357–3365 (2022)
- [3] Martin et al., ArXiv, 2301.10809 (2023)

10:30 AM EL08.06.06

Novel Tunable Low-Index Materials for Metaphotonics Applications Kristian W. Munnikhuis¹, Smridhi Chawla¹, Tornike Shubitidze¹, Wesley Britton², David Woolf² and Luca Dal Negro¹; ¹Boston University, United States; ²Physical Sciences Inc, United States

Low refractive index and epsilon-near-zero (ENZ) materials give rise to many fascinating optical properties driven by strongly enhanced nonlinear optical processes such as harmonic generation, frequency mixing and conversion, electro-optical modulation, and order-unity light-induced refractive index changes. These effects are important requirements to enable reconfigurable optical devices and metamaterials with ultrafast (sub-picosecond) response times for active devices in the photonics and metaphotonics domains. However, ENZ materials operating in the near- and mid-infrared spectral ranges often rely on metallic components with limited tunability of the optical permittivity and high absorption losses. Likewise, they traditional platforms are not compatible with the widespread silicon technology, severely limiting their scalability and device integration. Here we report on a novel and largely tunable Si-compatible low-index material platform based on zirconium silicon oxynitride (ZrSiON). In particular, using co-deposition RF magnetron sputtering with Nitrogen gas, we have developed ZrSiON thin films and investigated their structural and optical properties using X-ray diffraction (XRD) and variable angle spectroscopic ellipsometry (VASE) in a broad spectral range. We find that resistivity decreases as SiO₂ incorporation is increased, becoming a dispersionless dielectric material with n approx. 2.5 and negligible dispersion losses in the infrared spectral ranges. On the other hand, when SiO₂ incorporation is comparable to Zr, we found the material becomes metallic with an ENZ transition in the near-infrared spectrum around 830 nm. We found that upon post-deposition annealing at 500C these materials exhibit a transition to the metallic regime that can be controlled with the sputtering and annealing conditions. In addition, we

measure the optical bandgaps and resistivity and the nonlinear optical responses of the fabricated materials via Z-scan technique. Finally, we identify optimal etching conditions for achieving resonant nanostructures for integration into nonlinear optical devices and metasurfaces.

10:45 AM EL08.06.07

Full-Colored, Large-Area, Electrically Reconfigurable Photonic Resonator with Low-Power Consumption Hyo EunJeong, Joo HwanKo, Se RimKim, Hyeon-HoJeong and Young MinSong; Gwangju Institute of Science and Technology, Korea (the Republic of)

Display technology plays an essential role in effectively delivering visual information in contemporary daily life. Reflective display, which uses external ambient light as a source, can operate without a backlight panel electronic paper, enabling low energy consumption. In the past few years, there have been various approaches implemented to improve the performance of electronic paper (e-paper), particularly in terms of switching time and on/off ratio. As a result, leading electronics companies (e.g., *Amazon Kindle*) have introduced e-papers with enhanced capabilities. While e-papers serve as excellent display devices, they have certain limitations, such as the necessity of high operating voltages and monochromatic image operation, restricting colorful output. Recently, a new strategy has emerged focusing on the active modulation of plasmonic structural colors based on nanostructured photonic systems [1]. This progress successfully demonstrates the switchable structural colors based on the optically active materials, including phase change materials and conducting polymers, which modulate its complex refractive index by external energy [2]. Especially, conducting polymer, which controls the optical property by an electrochemical redox reaction, has attracted great attention due to its low power consumption. However, the limited complex refractive index and minimal variation levels impede strong interaction between light and matter on plasmonic structures, leading to a diminished ability to express vibrant colors [3].

In this study, we present the milliwatt-level controllable electrochromic thin-film resonator capable of full-color generation based on polyaniline (PANI). To overcome the low complex refractive index variation level of PANI ($\Delta n \sim 0.6$), we designed a highly resonant planar photonic structure based on a refractive index engineered layer on the metal film, resulting in diverse coloration over an entire visible wavelength range. In particular, the electrochemical redox reaction is enabled by the exchange of proton, which controls the doping level of PANI, leading to the fast/efficient modulation of optical properties. The protonation process is achieved in the narrow voltage range from -0.2 V to 0.8 V. The voltage level significantly contributes to low power consumption ($\sim 1.32 \text{ mW cm}^{-2}$), which is 20 times lower than commercial displays such as OLED, and even half the power consumption of e-paper. In addition, the active resonant structure based on PANI demonstrates stable reversibility without any degradation over 200 cycles. Moreover, this device achieves a fast-switching time ($\sim 34 \text{ ms}$), and also, shows operation capability compared to a commercial video rate of 30 Hz. In conclusion, we present an electrochemically switchable reflective display based on PANI, enabling remarkably efficient and dynamic coloration. We also suggested a passive matrix display module; thus, the pixel-by-pixel control of potential enables diverse pattern generation. We believe that our suggested platform will be utilized as a promising display application including smart windows, electronic wallpapers, attachable displays, and many types of electronics based on its ultra-thin scale, large color space, and low power consumption.

[1] Peng, J., Jeong, H. -H., Lin, Q. *et al.* Scalable electrochromic nanopixels using plasmonics. *Sci. Adv.* **5**, eaaw2205 (2019)

[2] Duan, X., Kamin, S. & Liu, N. Dynamic plasmonic colour display. *Nat. Commun.* **8**, 14606 (2017)

[3] Wang, Z., Wang, X., Cong, S. *et al.* Towards full-colour tunability of inorganic electrochromic devices using ultracompact fabry-perot nanocavities. *Nat. Commun.* **11**, 302 (2020)

11:00 AM *EL08.06.08

Colloidal Crystal Engineering for Programmable and Stimuli-Responsive Optical Metasurfaces and Metamaterials KorayAydin; Northwestern University, United States

Metasurfaces and metamaterials emerged as promising nanophotonic material and device platforms to control light-matter interactions at the nanoscale. In such materials, the collective and effective optical response is dictated by individual building blocks and controlled by the geometrical parameters forming the crystal structure. I will introduce DNA-assembly of gold nanoparticles as a fabrication method to realize bottom-up, programmable, and stimuli-responsive nanophotonic hybrid metamaterials and metasurfaces. The ability to control the distance, size, shape, architecture of nanoparticles and overall crystal structure enables access to optical properties that are not accessible readily in nature. I will highlight wide range of functional nanophotonic device architectures including epsilon-near-zero metasurfaces, negative index metamaterials and broadband absorber meta-films. The synthesis of plasmonic nanoparticle architectures with structures and stimuli-responsive behavior that are not accessible in lithographically defined plasmonic nanostructures provides an opportunity to design materials with emergent optical properties that offer new fundamental insights and previously inaccessible functionalities.

SESSION EL08.08: Tunable Plasmonics/Nanophotonics and Breaking News Presentation

Session Chairs: Koray Aydin and Yu-Jung Lu

Tuesday Afternoon, November 28, 2023

Hynes, Level 3, Room 312

1:30 PM *EL08.08.01

Plasmonic Transmission-Line-Based Logic Circuitry Pei-YuanWu and Chen-BinHuang; National Tsing Hua University, Taiwan

We experimentally demonstrate OR, XOR, NOT, and AND Boolean operations can be achieved in plasmonic two-wire transmission-line devices. A plasmonic half-adder is also designed and realized. In all operations, only four predefined polarizations of a single laser beam are required. All devices and circuits operate with greater than 12.5 THz optical bandwidth.

2:00 PM EL08.08.02

High Quality Ordered Titanium Nitride Nanotriangles and Nanowires for Plasmonic Applications SpyridonKassavetis, EviRampota, StavrosPanos, NikolaosPliatsikas, DespinaTselekidou and PanosPatsalas; Aristotle University of Thessaloniki, Greece

Novel and cost-efficient fabrication techniques of alternative plasmonic nanostructures pave the pathway for practical applications in various fields such energy harvesting, microelectronics and medicine. Transition metals nitrides (TMNs) emerge as alternative plasmonic nanomaterials suitable for a wide range of applications from photovoltaics to photonics and medicine. The TMNs are conductive ceramics that combine exceptional properties such as substantial electronic conductivity, high melting point ($>3000 \text{ K}$) and tunable work function, while the TMNs are particularly stable in hostile chemical environments, high temperature, and strong electric fields, such as in lasers. Among them, Titanium Nitride (TiN) is emerging as significant candidate material for practical plasmonic applications (biosensors, catalysis and photochemistry, solar energy harvesting, photo-detection, and optical storage of information).

In this work, we focus on the low-cost fabrication of TiN nanotriangles with controlled spacing and tunable dimensions (thickness and lateral dimensions) using a combination of Nanosphere Lithography (NSL) and several reactive magnetron sputtering (MS) deposition techniques such as DC, Closed-Field Unbalanced MS or Highly Power Impulse MS (HIPMS) on rigid and flexible substrates and with the aim to study the fundamentals that will unlock the fabrication of high quality TMNs nanotriangles and nanowires for plasmonic applications.

NSL appears as a very promising approach, due to its rapid implementation and compatibility with wafer-scale processes, combines the advantages of both top-down and bottom-up approaches and includes: (a) development of the nanospheres monolayer colloidal mask, (b) deposition of the desired material in the empty space between the nanospheres and (c) removal/lift-off of the nanosphere colloidal mask to "reveal" the deposited material that keeps the ordered patterning of the mask interstices. Specifically, a suspension of monodisperse polystyrene nanospheres (diameter, $d=552 \text{ nm}$ or $d=175 \text{ nm}$) was spin coated on a substrate (such as Si (001), glass, flexible PET) to form the colloidal mask. A UV ozone process was used to confine the triple-junction vias of the polystyrene mask. Subsequently, the selective growth of TiN was made by the above mentioned MS in Ar/N atmosphere by varying the TiN thickness from 10 to 30 nm, while the MS process parameters were also fine-tuned to increase the directionality of deposited species, and the TiN crystal quality (low concentration of point defects). In particular, the substrate-to-target distance was maximized to improve geometrical directionality, and a negative bias voltage during the growth of the TiN was used to "guide" the ionic species deep into the vias between the nanospheres.

The arrays of ordered TiN nanostructures and nanowires appear after the lift-off of the mask. Atomic Force Microscopy characterization of the samples showed the fabrication of TiN nanotriangles, with low concentration of point defects, similar structure with the continuous TiN films of high electrical conductivity and plasmonic performance, and durability at least up to 400° C .

Refs.: P. Patsalas, N. Kalfagiannis, S. Kassavetis, G. Abadias, D.V. Bellas, Ch. Lekka, E. Lidorikis, Materials Science and Engineering R 123 (2018) 1–55.

Panos, S., Tselekidou, D., Kassavetis, S., Fekas, I., Arvanitidis, J., Christofilos, D., Karfaridis, D., Dellis, S., Logothetidis, S. and Patsalas, P., Phys. Status Solidi B, 258 (2021) 2000573

2:15 PM EL08.08.03

Tunable Plasmonic Properties in Silicon Nanostructures RosariaA. Puglisi¹, AntoninoLa Magna¹, GiovanniMannino¹ and JostAdam²; ¹CNR-IMM, Italy; ²Mads Clausen Institute, Denmark

The scientific literature on plasmon resonances in metallic nanostructures is quite extensive thanks to their interesting physical characteristics and for their numerous applications. It is known that their plasmonic properties can be controlled by changing the metallic nanostructure geometry and the characteristics of the medium surrounding it, allowing for the tunability of the plasmonic response. The possibility to exploit these properties in semiconducting nanomaterials, particularly in silicon, thanks to its exceptional CMOS compatibility, would allow for an extensive industrial application. Electron plasma oscillations have been demonstrated in Si/SiO₂ nanowires, in structures with diameters as large as 100 nm. But some of their properties are still not deeply investigated or understood, for the limits of the standard characterization techniques, and for the difficulty to interpret the data. Moreover, despite the potential to deliver an intense optical energy below the diffraction limit offered by a plasmon-induced resonant cavity smaller than 100 nm, little is known about the plasmon properties of silicon nanostructures smaller than this size. In this talk we will present the results of an experimental and theoretical investigation performed on silicon nanowires as small as 30 nm and less. Thanks to the use of a high-resolution STEM coupled with electron energy loss spectroscopy in situ, supported by finite-element method simulations to model the optical response, we will present a study on the plasmonic resonances in such small nanostructures. We will demonstrate how it is possible to change their features by changing the nanostructure size and where the plasmon effect stops, in terms of energy and geometry, to give space to other concurring phenomena.

2:30 PM EL08.08.04

Tunable Anisotropic Plasmonics with Shape-Symmetric Conducting Polymer Nanoantennas [Yulong Duan](#); Linköping University, Sweden

Plasmonic nanoantennas with polarization-dependent resonances have widespread application in photonics, yet their design has been limited to antennas with anisotropic shapes such as nanorods. We proposed an alternative approach to overcome this limitation, wherein shape-symmetric nanoantennas are fabricated from aligned conductive polymer materials possessing anisotropic permittivity.

Conventional plasmonic metals, like gold and silver, possess highly cubic symmetry and exhibit isotropic permittivity. Although researchers can artificially induce anisotropy in various isotropic metallic materials using nanoscale lateral gratings which results in hyperbolic metasurfaces, materials with naturally in-plane hyperbolic permittivity or in-plane anisotropic negative permittivity, along with in-situ tunability, are rare. We have recently introduced a new type of tunable plasmonic material based on conducting polymers of PEDOT:Sulf (poly[3,4-ethylenedioxythiophene]:sulfate) (1). The unique capability to switch the material between metallic and dielectric states via its redox state enables the reversible operation of plasmonic nanoantennas, as validated both chemically and electrically (2, 3). Moreover, research in the field of stretchable electronics has shown that adding strain to these materials can align the polymer chains in certain directions, resulting in different conductivities in different in-plane directions. The molecular alignment of the conducting polymer not only influences anisotropic charge mobility but also induces anisotropy in the effective mass of the charge carriers. Consequently, we achieve a material with polarization-dependent plasma frequency and an accompanying region of in-plane hyperbolic permittivity.

Utilizing this unique characteristic, we present the design of circularly symmetric nanoantennas capable of exhibiting anisotropic localized plasmonic resonances in parallel and perpendicular orientations to the polymer alignment direction. The anisotropic nanoantennas are further tuneable via the redox state of the polymer. Notably, the polymer alignment can blue-shift the plasma wavelength by several hundreds of nanometers, thereby forming a novel approach towards reaching the goal of redox-tunable conducting polymer nanoantennas for visible light.

1. S. Chen *et al.*, Conductive polymer nanoantennas for dynamic organic plasmonics. *Nature Nanotechnology* **15**, 35-40 (2020).
2. A. Karki *et al.*, Doped semiconducting polymer nanoantennas for tunable organic plasmonics. *Communications Materials* **3**, 48 (2022).
3. A. Karki *et al.*, Electrical Tuning of Plasmonic Conducting Polymer Nanoantennas. *Advanced Materials* **34**, 2107172 (2022).

2:45 PM BREAK

3:15 PM *EL08.08.05

Moiré Nanoplasmonics [Teri W. Odom](#); Northwestern University, United States

Moiré patterns can be described as the superposition of two or more periodic structures rotated by a relative twist angle. These patterns can be formed either from the vertical stacking of periodic lattices or the projection of two periodic lattices into the same horizontal plane. Photonic moiré lattices have exhibited broadband light trapping, optical chirality, and spatially-confined as well as long-range lasing. This talk will describe optical moiré phenomena in different plasmonic architectures. First, we will discuss how to design moiré nanostructures using scalable nanofabrication tools. Next, we will characterize and model their optical properties at different twist angles. Finally, we will integrate the plasmonic moiré nanopatterns with emissive materials and discuss potential applications of their short-range and long-range responses.

3:45 PM EL08.08.06

Reaching a Strong Coupling Regime between Quantum Emitters and Plasmonic Resonators using DNA [Jeanne Heintz](#) and [Sebastien Bidault](#); ESPCI Paris, France

Light-matter interactions in condensed media at room-temperature are fundamentally limited by electron-phonon coupling. For instance, while the excitation cross-section of an isolated atom, or of a single quantum emitter at cryogenic temperatures, can reach one half of the wavelength of light squared (the so-called unitary limit); this value is reduced by 6 orders of magnitude for a fluorescent molecule or for a colloidal quantum dot at room temperature because of homogeneous phonon broadening. In order to render the exceptional optical properties of single quantum systems (such as single-photon emission and nonlinearities) efficiently accessible at room temperature and in condensed media, it is essential to enhance and optimize these interaction cross-sections.

Over the last decade, gold nanostructures have shown amazing promise towards this goal thanks to their ability to enhance optical fields by several orders of magnitude in deeply sub-wavelength volumes. However, the nanoscale dimensions of these field enhancements mean that it is extremely difficult to address them in a controlled and reproducible way. To this end, we exploit DNA molecules to create plasmonic resonators with a control over both their nanoscale dimensions and their chemical environment. Using this strategy, we were able to enhance single-photon emission from fluorescent molecules by more than two orders of magnitude in a weak-coupling regime (ACS Nano 10, 4806 (2016)) and to reach a strong-coupling regime between a plasmonic resonator and 5 organic molecules, albeit with low reproducibility (ACS Nano 15, 14732 (2021)). We propose the DNA-based assembly of dimers of plasmonic nanocubes in order to provide reproducible single-molecule strong coupling and to make the coherent interaction of light with single quantum emitters feasible at room temperature (J. Phys. Chem. Lett. 13, 11996 (2022)).

4:00 PM EL08.08.07

Photon Avalanches in Nanoparticles [Bruce E. Cohen](#); Lawrence Berkeley National Laboratory, United States

While the original applications of nanoscience to bioimaging used luminescent nanocrystals whose properties largely mirrored those of traditional probes, newer nanocrystals have been engineered with optical properties unlike anything found in organics or proteins. These include perfect photostability, multiphoton emission a billion-fold more efficient than standard multiphoton techniques, and most recently, photon avalanches hosted within nanostructures. In two recent studies,^{1,2} we describe the engineering and imaging of avalanching nanoparticles (ANPs), which are Tm³⁺-doped NaYF₄ upconverting nanoparticles that efficiently convert near infrared excitation to higher energy emission. Avalanches are steeply nonlinear events in which outsized responses arise from a series of minute inputs and, with light, photon avalanching had been observed only in bulk materials, often at cryogenic temperatures. The extreme nonlinearity of ANP emission enables sub-70 nm spatial resolution using only simple scanning confocal microscopy and before any computational analysis. Two-way NIR photoswitching of ANPs enables full optical control of photodarkening and photobrightening, and we find indefinite photoswitching of individual nanoparticles in ambient or aqueous conditions without measurable photodegradation. This enables unlimited photon collection for calculation of sub-Ångström localization accuracies, and we can distinguish individual ANPs within tightly packed clusters.

1. Lee, C. *et al.* Giant nonlinear optical responses from photon-avalanching nanoparticles. *Nature* **589**, 230–235 (2021).
2. Lee, C. *et al.* Indefinite and bidirectional near-infrared nanocrystal photoswitching. *Nature* **618**, 951–958 (2023).

4:15 PM EL08.08.08

Strong Emission Enhancement of Rare Earth Quantum Emitters in an Integrated Waveguide Nano De-Focusing Platform [Nicholas A. Gusken](#)¹, [Ming Fu](#)², [Maximilian Zapf](#)³, [Michael Nielsen](#)⁴, [Robert Röder](#)³, [Stefan Maier](#)^{5,2}, [Mark L. Brongersma](#)¹, [Carsten Ronning](#)³, [Rupert Oulton](#)² and [Alex Clark](#)⁶; ¹Stanford University, United States; ²Imperial College London, United Kingdom; ³Friedrich-Schiller-Universität Jena, Germany; ⁴University of New South Wales, Australia; ⁵Monash University, Australia; ⁶University of Bristol, United Kingdom

As demonstrated in our recent publication, we present a novel reverse nanofocusing platform which allows to boost, extract and guide quantum emission at and from the nanoscale efficiently.

Enhancing fluorescence of quantum emitters while allowing for efficient extraction of emission in an integrated fashion is of great interest for future photonic quantum networks. Optical and electrical control at the emitter level is important in different fields of research and applications ranging from sensing and quantum networks to active metasurfaces. Dielectric as well as metallic cavities can accelerate radiative transitions of emitters by orders of magnitude based on the Purcell effect. For dielectric cavities, emission enhancement can be achieved by efficient modal coupling to high quality cavities. One drawback of this approach however is the fundamental limit in bandwidth and mode size. Plasmonic metal structures in contrast, are not diffraction limited and allow for the creation of cavities with mode volumes far below the wavelength scale and electrical control for direct emitter manipulation. One emitter which has raised significant interest is erbium, due to its C-band emission which is of strong technological significance for optical communications.

Here we demonstrate a strong radiative emission enhancement of Er^{3+} ions based on efficient coupling to and de-focusing from a hybrid plasmonic waveguide platform. Our results show acceleration of quantum emission over several orders of magnitude across the entire C-band based on a single hybrid plasmonic waveguide. Additionally, efficient coupling to a highly confined waveguide mode allows to resolve single electric dipole transitions which can be attributed to Stark-split energy levels of Er^{3+} .

SESSION EL08.10: Poster Session II: Advances in Plasmonics, Nanophotonics and Metasurfaces I
Session Chairs: Yu-Jung Lu and Benjamin Vest
Tuesday Afternoon, November 28, 2023
Hynes, Level 1, Hall A

8:00 PM EL08.10.01

Core-Shell Au@ZnO Nanocomposite for the Photocatalytic Degradation of Toxic Dyes Anjali Vijeata^{1,2}, Ganga Ram Chaudhary¹, Alastair Wark² and Savita Chaudhary¹; ¹Panjab University, Chandigarh, India, India; ²University of Strathclyde, United Kingdom

Abstract

An advanced synergistic Au nanorods and metal oxide (ZnO) nanoparticles-based nanocomposite was synthesized in order to get insight into plasmonic control over photocatalysis. The absorption power of the complex shifts towards the visible range of the spectrum due to the interference of plasmonic effects of Au nanorods with the surface defects in ZnO nanoparticles. Manipulating such design gives highly active surface sites and results in productive outcomes. In this report, the positively charged ZnO nanoparticles are coated with poly-tannic acid to make the surface highly negatively charged which was then bonded to Au nanorods through thiol linkage. The surface chemistry of CTAB-stabilized Au nanorods was altered with a small chain cysteamine group which can readily bind to the surface-active sites of PTA-coated ZnO nanoparticles. We demonstrated that the plasmonically active nanocomposite efficiently supports the catalytic activity under a 300W xenon lamp. Notably, surface plasmonic energy-based electron transfer boost up the light absorption power of the nanocomposite during the process of photocatalysis. This metal oxide and nanorods complex provides a breakthrough in generating free radicals which can readily degrade the cationic dyes with outstanding reproducibility. This work exploited the promising aspects of using plasmonic nanoparticles in the photocatalysis of toxic dyes.

8:00 PM EL08.10.02

Precision Patterning of ZnO using Femtosecond Laser: Opening Doors to Nanophotonic Device Innovations Ajinkya B. Palwe, Sonu K. Singh, Gaurav P. Singh, Soumi Mukherjee, Sweta Rani, Arun Jaiswal, Shobha Shukla and Sumit Saxena; IIT Bombay, India

Patterned nanostructure exhibits interesting optoelectronic characteristics due to light-matter interaction at comparable dimensions. The optical response of the nanostructure-based devices is modulated by the size and the periodicity of the structure. Numerous techniques based on top-down and bottom-up approaches are used to obtain patterned nanostructure. However, top-down methods provide more precise control over the patterning of the surfaces. Recently patterned structures of metal oxide semiconductors are getting attention for various electronic devices like photodetectors, solar cells, etc. The femtosecond laser has shown the capability to precisely pattern the surfaces with regular and smaller structures. In this work, we have fabricated ZnO nanopillars by patterning the ZnO thin film using a femtosecond laser. ZnO film (thickness ~600 nm) is deposited on a glass slide using an organic salt solution of zinc in isopropanol and annealed at 400°C. The ultrafast mode-locked Ti: sapphire-based femtosecond pulsed laser (Coherent made, Chameleon Ultra I) with fixed pulse width (140 fs) and a repetition rate (80 MHz) is used for this patterning. The laser beam of 800 nm with a beam diameter of 1.2 mm at $1/e^2$ tightly is focused onto the ZnO film for the selective patterning (ablation). The patterns are prominent after increasing the laser power beyond 1.5 W. ZnO is patterned in a square mesh with a periodicity of 1 μm , which resulted in the formation of ZnO nanopillars with a side of ~500 nm and a height of 600 nm. The fabricated structure exhibits different colors at different angles due to the scattering of the light. These reflected colors are analyzed with the camera by varying the incident angle of the white light. It is observed that the photo emitted light colour changes from colourless to blue, orange, pink, green, red, and finally deep red. Due to the multiple scattering, the overall path length of the light inside the active material increases. Also, the total surface area of the active material in the patterned film is larger as compared to the plane film. The array of semiconducting ZnO nanopillars exhibits unique electronic and optical characteristics for optoelectronic and photonic applications. Similarly, the femtosecond laser can pattern different metal oxide layers and incorporate the fabricated structures in optoelectronic devices to improve their performances.

8:00 PM EL08.10.03

Computational characterization of optical response in noble metals and plasmonic ceramics Xiao Zhang and Emmanouil Kioupakis; University of Michigan at Ann Arbor, United States

Understanding the optical response of plasmonic materials is essential for understanding the physics and functionality of plasmonic devices. While traditional plasmonic materials such as noble metals have shown great success, the search of alternative materials for high-temperature applications remains open in the community. In recent years, several transition-metal nitrides and carbides have emerged as a promising new family of plasmonic materials. Benefiting from their high thermal stability, these materials are expected to be promising for easy processing and for high-temperature applications. To better understand and guide the discovery of new plasmonic materials, a reliable computational first-principles framework to characterize optical properties of metallic systems is important. These characterizations require a predictive treatment of free-carrier absorption considering both inter- and intra-band single particle excitation, and the collective oscillation of electrons (Drude contribution) on the same footing.

In this work, we present a computational framework that combines density functional theory, density functional perturbation theory, many-body perturbation theory, the maximally localized Wannier function approach, and the special displacement method to capture the direct and phonon-assisted single-particle process, as well as the Drude contribution, to provide a consistent, predictive description of the optical response of metallic systems. We show that with our framework, we can characterize the optical response both of noble metals (Ag, Au, and Cu) and of TiN, a promising plasmonic ceramic material. We achieve excellent agreement with experimentally measured dielectric functions, and we successfully characterize the temperature dependence of the optical response of TiN. We show that in the IR to visible region, both single-particle phonon-assisted indirect transitions and the Drude contribution are important to understand optical response of metals. Our framework is general and is available as a community tool implemented in the open source EPW code. It can be extended to other metallic materials, thus provides a general platform to accurately model the optical properties of metallic materials. Our platform creates an excellent opportunity to enable rational design of new plasmonic materials for nonconventional applications.

This work was supported as part of the Computational Materials Sciences Program funded by the U.S. Department of Energy, Office of Science, Basic Energy Sciences, under Award No. DE-SC0020129. It used resources of the National Energy Research Scientific Computing (NERSC) Center, a DOE Office of Science User Facility supported under Contract No. DE-AC02-05CH11231.

8:00 PM EL08.10.04

Low-Powered, Electrically Controllable Tamm Plasmons for High On/Off Ratio Optical Switch Joo Hwan Ko¹, Dong Hyun Seo¹, Sejeong Kim² and Young Min Song¹; ¹Gwangju Institute of Science and Engineering, Korea (the Republic of); ²The University of Melbourne, Australia

Recent advances in reconfigurable photonics have attracted attention for enabling the active manipulation of light, facilitating rapid information transfer and high-density multi-spectral operations. The fundamental requirements of active photonics are the photonic structure, which confines a specific wavelength range at the target resonance, and the active material that modifies the condition of light-matter interaction using external stimuli or control mechanisms [1]. To confine and propagate electromagnetic waves effectively, these resonators rely on photonic structures. Specifically, in metasurfaces-driven reconfigurable photonics, photonic structures have emerged as highly promising, leveraging resonant properties to interact with light and enable localized manipulation, detection, or confinement at subwavelength scales. However, the intricate design and complexity of fabrication processes have posed challenges. Alternatively, thin-film-based optical modulators have shown significant potential for strong light-matter interaction, even with simplified configurations. Tamm plasmon (TP) structures, as powerful planar plasmonics, offer efficient light absorption. Optical TPs can occur at the interface between distributed Bragg reflectors (DBRs) and an absorbing layer with layers of optical thickness half the light wavelength [2]. While the lossy layer efficiently absorbs the confined electric field density at the interface in the Tamm plasmon state, complete elimination of the lossy property is necessary to deactivate the absorption. To unlock their active functionality, the ability to perform optical mode conversion between lossless and absorption states is essential.

In this study, we introduce the active Tamm resonator, which utilizes poly(3,4-ethylenedioxythiophene):polystyrene sulfonate (PEDOT:PSS) as the active material for optical modulation. By applying a voltage range of ± 1 V, the resonator transitions from a Tamm resonant state (complete absorption) to a mirror state (total reflection). PEDOT:PSS possesses optical characteristics that enable efficient and rapid conversion of the optical mode between a lossless state (dielectric) and an absorption state (metallic) through a redox electrochemical reaction [3]. This conversion is achieved through an electrochemical redox reaction involving proton exchange, facilitated by self-aligned Au nanocolumns acting as a membrane between TPs and electrode for

fast proton permeability. The active Tamm resonator exhibits reversible and fast response, characterized by triggered stimulation. Notably, cyclical writes and erase states generate a hysteresis loop, enabling the development of a non-volatile memory device. By sequentially programming the input electrical signal, the fabricated device demonstrates optically readable information with excellent retention. Moreover, by designing a circuit that can address each pixel, we have developed an information storage system that uses square pulsed potentials for optical recording and reading. Overall, this research emphasizes the design of optical structures and material selection for the active Tamm resonator as a powerful tool in reconfigurable photonics.

[1] J. Karst, M. Floess, M. Ubl, C. Dingler, C. Malacrida, T. Steinle, S. Ludwigs, M. Hentschel, H. Giessen, "Electrically switchable metallic polymer nanoantennas," *Science*. 374, 612-616 (2021).

[2] S. H. Kim, J. H. Ko, Y. J. Yoo, M. S. Kim, G. J. Lee, S. Ishii, Y. M. Song, "Single-Material, Near-Infrared Selective Absorber Based on Refractive Index-Tunable Tamm Plasmon Structure," *Adv. Opt. Mater.* 10, 2102388 (2022).

[3] J. H. Ko, Y. J. Yoo, Y. Lee, H.-H. Jeong, Y. M. Song, "A review of tunable photonics: Optically active materials and applications from visible to terahertz," *iScience* 25, 104727 (2022).

8:00 PM EL08.10.05

Design of Plasmonic Nanoantennas Coupled to Ultra-Fast Molecular Diodes to Produce Electricity Halidou Halidou Abdoul-Yasset¹, Peeranuch Pongsrirong¹, Beniamino Sciacca², Olivier Margeat^{2,1}, David Duché^{3,1} and Judikael Le Rouzou^{3,1}; ¹Aix-Marseille Université, France; ²CINAM-CNRS, France; ³IM2NP, France

Current PV technologies are the leading technologies used to harvest visible light with good efficiencies. However, their overall performance is limited by the band gap of the semiconducting material used as an active layer.

A promising way to overcome this limitation is to rely on a technological breakthrough, mostly known as rectenna solar cells. Rectennas or rectifying antennas are devices that capture light as a wave, then generate an alternating current which is rectified by a diode producing finally usable or storable direct current. Rectennas are not a recent concept. They have been developed since the '60s for microwave frequencies and were able to yield efficiencies close to 90% [1]. Today, the challenge is to translate their high efficiencies from microwaves to infrared and optical frequencies. The primary obstacle lies in designing and fabricating rectifying diodes that can rectify high-frequency optical signals efficiently.

A rectenna composed of patch nano-antennas associated with molecular diodes has been fabricated using an original bottom-up process which has been patented [2]. Thanks to this design, we demonstrated a photo-electrical effect at a bias voltage higher than 0.3V resulting from rectification of light under illumination at 1,55µm. These promising results allow IM2NP to be one of the few groups in the world able to rectify optical frequencies. In the present work, we explore the possibility of using plasmonic nanocubes and molecular diodes to have a functional device. Our rectenna architecture enables us to leverage the unique properties of nanostructures such as surface plasmons and gap plasmons. By coupling these nanoantennas with ultrafast molecular diodes, we exploit the diodes' unique nonlinear electron transport properties to convert gap plasmons into electrical currents. To this end, we employ advanced bottom-up fabrication techniques to self-assemble patch nano-antennas made of plasmonic nanocubes with tailored sizes, optimizing their resonant characteristics to efficiently capture and concentrate optical frequencies of light. In addition, we integrated self-assembled molecules by click chemistry as ultra-fast diodes. Finally, we investigate the performance of the plasmonic nanoantenna-molecular diode system through rigorous theoretical simulations and experimental characterizations.

8:00 PM EL08.10.06

Combining Plasmonic Nanostructures and Diamond for Emission of Electrons using Visible Light Daniele Catone¹, Giuseppe Ammirati¹, Alessandro Bellucci¹, Valerio Campanari¹, Faustino Martelli², Matteo Mastellone¹, Patrick O'Keeffe¹, Silvia Orlanducci³, Alessandra Paladini¹, Riccardo Polini³, Francesco Toschi¹, Daniele Trucchi¹, Stefano Turchini¹ and Veronica Valentini¹; ¹Istituto di Struttura della Materia - CNR, Italy; ²CNR, Italy; ³Università di Roma "Tor Vergata", Italy

Combining plasmonic metal nanoparticles with wide bandgap semiconductor materials has been demonstrated to be an effective way to sensitize these materials to sub bandgap light.¹ This is often used as a strategy to improve the photocatalytic properties of these materials.

In this work we focus our efforts on diamond as it has the very interesting property of having a negative electron affinity at its surface when it is hydrogenated. The result is that when electrons are excited into the conduction band in the vicinity of a diamond/vacuum or, indeed, a diamond/water interface they are ejected from the diamond into the vacuum or water. This property can lead to numerous useful applications such as a cold cathode or as a clean source of solvated electrons. The problem is that diamond has a band gap of 5.5 eV and therefore this process only works with VUV light (wavelength < 213 nm).

We have fabricated two separate systems based on the combination of plasmonic nanoparticles with diamond which show that the exciting the plasmonic resonance of the metal nanoparticles can lead to a strong enhancement of the emission of electrons from the diamond surface. The process is demonstrated using an array of nanoparticles embedded below the surface of a thin film of diamond for the emission of electrons into vacuum using visible light. The increased electron emission efficiency was verified by photoemission and photoconduction measurements. Initial attempts with Aluminum as the plasmonic material were not successful² while successive fabrication using silver showed the required properties. Furthermore, a second system involving detonation nanodiamonds coupled with gold nanoparticles in aqueous solution has been shown to be source of solvated electrons following interaction with visible light. In this case the presence of solvated electrons was verified by using an ultrafast pump-probe experiment in which a visible light pump was used to excite the plasmon resonance of the gold nanoparticles while the white light probe was used to optically detect the formation of the solvated electron in the first picoseconds after the excitation.

Based on the details of the above measurements we propose slightly different mechanisms to explain the photoemission in the AgNP@Diamond system with respect to the formation of hydrated electrons in the AuNP@Nanodiamond system.

References

[1] D. Catone, L. Di Mario, F. Martelli, P. O'Keeffe, A. Paladini, J.S. Pelli Cresi, A.K. Sivan, L. Tian, F. Toschi, S. Turchini "Ultrafast optical spectroscopy of semiconducting and plasmonic nanostructures and their hybrids." *Nanotechnology*, Vol. 32, 025703, 2020.

[2] A. Bellucci, V. Campanari, M. Mastellone, P. O'Keeffe, A. Paladini, R. Polini, D.M. Trucchi, "Optical characteristics of nanostructured aluminium/diamond composite systems in the visible range," *Diamond and Related Materials*, Vol. 132, 109669, 2023.

8:00 PM EL08.10.07

Thermal Radiation Around a Nanobubble Generated by a Heated Gold Nanoparticle Sreyash Sarkar, Jérôme Sarr, Olivier Merchiers and Pierre-Olivier Chapuis; University Lyon, CNRS, INSA Lyon, Université Claude Bernard Lyon 1, France

By injecting metallic nanoparticles into a liquid, localized heating without physical contact is achieved, facilitated by steady-state or pulsed illumination that generates nanobubbles around the particles. This technique has applications [1] in optical hyperthermia for local therapy, microbiology, and solar thermal water heating. The complex dynamics of bubble formation involve vaporization, heat transfer by vapor molecules, and multiple scattering [1]. However, the thermal radiation between nanoparticles and the liquid has not been adequately studied due to the size of the nanoparticles being below the characteristic wavelength (Wien's wavelength). To accurately assess the sub-wavelength thermal radiation emission, fluctuational electrodynamics calculations are necessary. These calculations reveal that the effective emissivity of small objects can exceed unity [2]. Furthermore, due to the small distance between the nanoparticle and the fluid, the radiative transfer occurs through photon tunneling, in the near field. Fluctuational electrodynamics provides also a suitable approach for considering this phenomenon. This work focuses on evaluating these radiative contributions. The analysis considers the dipole approximation, encompassing both electric and magnetic dipole cases within a cavity immersed in a dissipative medium. Multireflection scattering solutions account for wave-related effects in the vacuum cavity. The results obtained in spherical geometry, using the Mie theory, demonstrate the significance of both wave effects. The volumetric near-field absorption in water varies as almost a sixth power of the distance from the origin and as a third power of the cavity radius, exhibiting observable interferences when approaching the far-field regime. Spectral signature resonances of water dominate the radiative exchange in this scenario. This work will contribute to a more comprehensive understanding of radiative exchange in nanoparticle-liquid systems ultimately aiding the development of thermal engineering, bioengineering, and biomedical applications

Keywords: near-field thermal radiation, nanobubbles, nanoparticles.

Acknowledgments: The authors acknowledge the support of ANR research funding in the frame of the CASTEX project and valuable discussions with Dr. Samy Merabia.

References:

1. Yifan Zhang, Wei An, Chang Zhao, and Qingchun Dong. Radiation-induced plasmonic nanobubbles: fundamentals, applications, and prospects. *AIMS Energy*, 9(4):676–713, 2021.
2. KL Nguyen, Olivier Merchiers, and P-O Chapuis. Temperature-dependent and optimized thermal emission by spheres. *Applied Physics Letters*, 112(11):111906, 2018.

8:00 PM EL08.10.08

Furthering Nano-Optical Techniques by Integrating Tapping-Mode AFM and TCSPC Kevin W. Kwock¹, Thomas P. Darlington¹, Emanuil Yanev¹, Matthew C. Strasbourg², James Hone¹, Nicholas J. Borys² and P. James Schuck¹; ¹Columbia University, United States; ²Montana State University, United States

Scanning tip-enhanced optical spectro-microscopy techniques are powerful tools for investigating the opto-electronic properties of materials surfaces. However, the improved resolution comes at the significant expense of optical signal, requiring the use of higher excitation powers which can be detrimental to samples and nano-optical probes.^{1,2} This current experimental paradigm is heavily dependent on fabrication of extraordinary nano-optical probes that can simultaneously tolerate high excitation densities and greatly enhance the signal of interest for a measurement's duration. Methods to increase signal/noise in a system without high photon fluences on the sample/tip are thus needed for imaging weak optical interactions, including Raman and nonlinear optical (e.g. SHG) scattering signals. In this study, we present efforts to improve our nano-optical studies through the incorporation of lock-in detection of tip-enhanced signals using tapping-mode atomic force microscopy scanning. We correlate fast single photon sensitive avalanche photodiodes and time-correlated single photon counting electronics, following the system design first demonstrated by Gerton et al.³ We show successful imaging of the nano-PL from a nanobubble in monolayer WSe₂ on Au, achieving resolutions ~ 10 nm. Our results show the viability for lock-in detection in tip-enhanced experiments and show a potential path for high-sensitivity nano-optical measurements utilizing photon correlations.

[1] Neacsu, C.C., van Aken, B.B., Fiebig, and Raschke, M.B. 2005. *Phys. Rev. B* **79**, 100107.

[2] Yao, K., Zhang, S., Yanev, E., McCreary, K., Chuang, H., Rosenberger, M.R., Darlington, T., Krayev, A., Jonker, B.T., Hone, J.C., Basov, D.N., and Schuck, P.J. 2022. arXiv:2111.06955.

[3] Gerton, J.M., Wade, L.A., Lessard, G.A., Ma, Z., and Quake, S.R. 2004. *Phys. Rev. Lett.* **93**, 180801.

[4] Darlington, T.P. et al. 2020. Imaging strain-localized excitons in nanoscale bubbles of monolayer WSe₂ at room temperature, *Nature Nanotechnology*, **15**(10), 854-860.

SESSION EL08.11: Lasing and Radiation Engineering with Metasurfaces and Metamaterials

Session Chairs: Ho Wai (Howard) Lee and Yu-Jung Lu

Wednesday Morning, November 29, 2023

Hynes, Level 3, Room 312

8:00 AM *EL08.11.01

Bioinspired Colorimetric Metasurfaces for Next Generation, On-Chip Imaging of Tissue Microstructure Lisa V. Poulikakos, Zaid Haddadin, Paula Kirya, Shahrose Khan, Dev Shah and Loren Phillips; University of California, San Diego, United States

The origin and progression of a variety of leading health challenges, encompassing Alzheimer's disease, heart disease, fibrosis and cancer, are directly linked to changes in the presence and orientation of fibrous matter in biological tissue. Fibrous biological tissue exhibits distinct anisotropic optical properties, which can be leveraged for selective imaging. However, these naturally occurring light-matter interactions are inherently weak, posing barriers to their visualization in a clinically translatable manner. Existing imaging techniques which visualize the fibrous properties of biological matter face challenges in complexity, cost, destructiveness, or precision. Thus, innovation in imaging technology of fibrous tissue with facile clinical implementation is urgently needed.

To address this challenge, we develop a new class of anisotropic, colorimetric metasurfaces to selectively visualize disease-relevant fiber density and orientation in biological tissue. We draw inspiration from iridescent structural color which is abundant in nature, arising in the saturated blues of the Morpho butterfly wing or the greens of jeweled beetle shells. At the micrometer scale and smaller, these naturally occurring, three-dimensionally (3D)-architected photonic crystals are composed of ordered, geometrically anisotropic features which exhibit distinct interactions with light at varying angles of incidence or polarization state. Due to their 3D hierarchical architecture, these nature-derived systems are unique sources of polarization-sensitive structural color with high color purity and brightness. Based on these principles, our colorimetric metasurfaces are designed to exhibit a high sensitivity to varying polarization states of light. We implement our colorimetric metasurfaces as a next-generation tissue microstructure imaging technology. Starting with the example of breast cancer diagnostics, we then expand our view to the rich palette of fiber-affecting diseases where metasurfaces hold great potential to achieve rapid, precise and low-cost tissue diagnostics with facile clinical implementation.

8:30 AM *EL08.11.02

Metamaterials Concepts for Active Photonics and Laser-Based Nanofabrication Gennady Shvets; Cornell University, United States

Theoretical and experimental results demonstrating reversible and irreversible regimes of light-metasurface interactions will be described. First, I will describe how all-dielectric metasurfaces can be combined with liquid crystals to develop a new class of electrically-controlled varifocal metalenses operating at multiple wavelengths. New design strategies aimed at simplifying metalens fabrication and producing high-NA tunable meta-optics will be discussed. Finally, I will demonstrate how semiconductor metasurfaces enable the strongly-driven regime of laser-metasurface interactions manifested as (a) enhanced high harmonics generation, and (b) laser-assisted material nanostructuring.

9:00 AM EL08.11.03

Active Metal-Dielectric Photonic Crystals David Alameier; Boston University, United States

Metal-dielectric photonic crystals (MDPCs) are periodic structures realized by vertically stacked metallic microcavities, resulting in alternating layers of semi-transparent metals and relatively thick dielectrics. Unlike plasmonic metamaterials, MDPCs rely on the hybridization of the underlying microcavity states rather than the coupling of surface plasmons, which produces multiple optical Bloch states arranged in photonic bands. This hybridization can be accurately described using coupled-mode theory, exactly analogous to the formation of molecular orbitals and the electronic energy bands in atomic crystals.

The high conductivity and carrier density of the metallic layers makes MDPCs ideal for active photonic devices and enables a significant reduction in physical thickness due to the high reflectivity at the metal-dielectric interfaces. We have recently exploited this to develop organic light-emitting diodes (OLEDs) that directly express the photonic band structure in their electroluminescence spectrum in the weak coupling regime. In this presentation, we discuss the theoretical foundations of MDPCs using quasi-normal mode formalism and coupled-mode theory. We apply this theory to demonstrate control over the emission spectrum of electrically-driven MDPC OLEDs in both simple and binary crystal configurations by varying the density-of-states and introducing a photonic band gap.

9:15 AM DISCUSSION TIME

9:30 AM BREAK

10:00 AM EL08.11.04

Plasmonic Optomechanical Switch Irene Castro Fernández¹, Daniel R. Vega¹, Antonio Garcia-Martin² and Manuel Marques³; ¹Materials Science Institute of Madrid (Spanish National Research Council), Spain; ²Instituto de Micro y Nanotecnología (CSIC), Spain; ³Universidad Autónoma de Madrid, Spain

In this work we theoretically demonstrate the use of a two-level optomechanical system actuated by plasmon-mediated optical forces as a reconfigurable nanophotonic switch. We have simulated a nanostructured suspended gold membrane allowing the normal excitation of a Surface Plasmon Polariton by patterning an air nanohole array. By placing the membrane in a close proximity of a reflecting substrate, we observe a mode splitting which provides two stable mechanical states accessible by tuning the illuminating wavelength.

In recent years the active control of optical forces is attracting more and more attention from the scientific community ranging from the fundamental physics [1] to diverse applications such as optical (and plasmonic) tweezers [2], optically reconfigurable nanophotonic devices and cooling and/or amplification of the mechanical modes to reach the fundamental ground state [3] or to increase the sensitivity of inertial sensors [4]. In this work, we present a two level optomechanical system that can be statically or dynamically manipulated to act as an optical bit in photonic nanoprocessors or as an optical switcher. The accomplishment of the optical force modulation is theoretically demonstrated by means of the mechanical excitation of a suspended membrane consisting of an array of air nanoholes in a gold layer supporting surface plasmon polariton modes [5]. The nanostructured membrane is suspended over a silicon substrate assembling a Fabry-Perot microcavity that enables strong coupling between cavity and plasmonic modes [6].

We simulate the whole optomechanical device through finite element simulations, including the coupled Fabry-Perot cavity. The optical force is calculated by the asymmetries in the integral of the Maxwell stress tensor over a closed surface around the suspended membrane. The Surface Plasmon Polariton and its influence on the optical force is calculated as a function of the cavity length. From the force calculation at a fixed wavelength a double potential well is obtained, showing two stable states with a central energy barrier. It is possible to dynamically actuate on the length of the cavity by introducing a mechanical actuation on the membrane by means of a harmonic displacement. The oscillatory movement of the suspended membrane can be modeled by a Duffing non-linear mechanical oscillator whose amplitude can be manipulated via optomechanical amplitude modulation (cooling or amplification). Therefore, the final state

(stable) of the dynamical system can then be actively chosen, opening the door for the development of an optomechanical switch.

1. Kim, E., Zhang, X., Ferreira, V. S., Banker, J., Iverson, J. K., Sipahigil, A., Bello, M., González-Tudela, A., Mirhosseini, M. Painter O. "Quantum Electrodynamics in a Topological Waveguide" Phys. Rev. X 11, 011015, 2021.
2. Ashkin, A. "Optical trapping and manipulation of neutral particles using lasers" Proc. Natl. Acad. Sci. 94, 4853–4860, 1997.
3. Chan, J., Alegre, T. P., Safavi-Naeini, A. H., Hill, J. T., Krause, A., Gröblacher, S., Aspelmeyer, M. and Painter, O. "Laser cooling of a nanomechanical oscillator into its quantum ground state" Nature 478 (7367), 89–92, 2010.
4. Ramos, D., Gil-Santos, E., Pini, V., Llorens, J. M., Fernández-Regúlez, M., San Paulo, A., Calleja, M. and Tamayo J. "Optomechanics with silicon nanowires by harnessing confined electromagnetic modes" Nano letters 12 (2), 932–937, 2012
5. Ramos, D., Malvar, O., Davis, Z. J., Tamayo, J. and Calleja, M. "Nanomechanical plasmon spectroscopy of single gold nanoparticles" Nano Letters 18 (11), 7165–7170, 2018.
6. Castro, I., Garcia-Martin, A. and Ramos, D., "Plasmon Optomechanical Switch" In press.

10:15 AM *EL08.11.05

Controlling Spontaneous Emission from Semiconductor Metasurfaces: From Reconfigurability to Single Photon Sources[PrasadIyer](#); Sandia National Labs, United States

The ability to achieve spatiotemporal control of incoherent (thermal and quantum) light emission has been a critical challenge in the field of optics with far ranging applications from remote sensing, holographic displays and quantum information processing. Here we present our results on two light emitting metasurfaces systems: 1) Ultrafast dynamic steering of spontaneous light emission from high-density InAs quantum dots (QDs) embedded inside GaAs resonators under structured optical pumping and 2) Enhancement of single-photon emission from single GaAs local-droplet epitaxial QDs from within AlGaAs Huygens' metasurfaces.

Spatially varying refractive index profiles are the key to steer incoherent light, since reconfigurable metasurfaces operating as phased-antenna arrays can only steer coherent (laser) light. We discover spatial refractive index profiles beyond human intuition that enable high efficiency (77%) steering of incoherent emission from reconfigurable dielectric metasurfaces over an 80° field of view, using generative models and active learning. We developed a machine learning framework where an active learning agent drives a generative model (variational autoencoder-VAE) to predict a spatially structured optical pump pattern which, when imaged onto the metasurface, generates a highly directional emission of incoherent light. This was achieved by creating a dynamic spatially varying resonant phase gradients across the metasurface using an ultrafast (80fs, 1 KHz rep rate, 3mJ/cm²) 800nm pump which images the pattern from a spatial light modulator (SLM) onto the metasurface. The photoluminescence (beam) steering is initially demonstrated using a periodic blaze (saw-tooth) grating patterns, which created a periodic refractive index profile using Drude free-carrier refraction, resulting in a spatial phase gradient on the metasurface and ultimately directing the momentum of the light emission. We find that AI-generated pump patterns are 10x more efficient in beam steering compared to the initial periodic blaze grating pump pattern designed using human intuition. Our work provides a novel machine learning driven closed-loop platform to understand and discover the physics of incoherent emission steering from metasurfaces with potential applications for augmented and virtual reality displays.

Epitaxially grown III-V QDs are promising sources for single photons with some of the highest metrics in purity, emission efficiency, brightness and indistinguishability reported to date. Here, we explore Al₃₀Ga₇₀As Huygens' resonators with spectrally overlapping the electric and magnetic dipole modes at the emission wavelength of a GaAs local droplet etching quantum dot for enhancing the emission of single photons. We enhance the emission rate of a single QD by an order of magnitude in comparison to an unstructured layer. We demonstrate anti-bunched single photon emission ($g^{(2)}(0) < 0.2$) under continuous wave (515nm) pumping with less than 45nW of pump power. Additionally, we report a 5x life-time reduction of the GaAs QD emission under increased pump fluence from 45 to 400nW. Finally, we demonstrate that the enhancement of the QD emission is independent of the position of the QD within the metasurface which alleviates a major challenge of placing these QDs with resonant nano-cavities. For semiconductor metasurfaces, the control of mode properties can open incredible opportunities in quantum information sciences, for manipulation of single photon qubits, and for enabling photon entanglement schemes and architectures.

10:45 AM EL08.11.06

Nanoimprinted PEDOT:PSS Polymer Metasurfaces with Metal-Like Infrared Optical Properties[HaydeePacheco](#) and [DeirdreO'Carroll](#); Rutgers, The State University of New Jersey, United States

Polymer plasmonics offer exciting opportunities for the development of infrared nanophotonic devices. Notably, the high conductivity of heavily doped polymers allows for plasmonic properties and local electric field enhancement, resulting in enhanced infrared absorption and antenna effects. Understanding and controlling the shift in the plasma frequency of doped conductive polymers is crucial for designing and optimizing plasmonic devices and metasurfaces with tailored optical properties in various spectral ranges, including the infrared region.

Here, we report the fabrication and characterization of a nanoimprinted poly(3,4-ethylenedioxythiophene) polystyrene sulfonate (PEDOT: PSS) polymer metasurfaces with metal-like optical properties in the infrared and high electrical conductivity. We focus on investigating the shift in the plasma frequency of nanoimprinted PEDOT:PSS polymer metasurfaces relative to planar-doped and undoped PEDOT:PSS surfaces. By adding dopants, such as DMSO, aniline, and ethanolamine, during film fabrication, we significantly enhance the film conductivity while inducing a corresponding shift in the plasma frequency. The heavily doped PEDOT:PSS films exhibit high electrical conductivities ranging from 10 to 1000 S/cm, making them suitable for plasmonic applications. Doped PEDOT:PSS metasurfaces were fabricated by spin-coating dopant-PEDOT:PSS solutions into films onto glass substrates and nanoimprinting the film using a custom-designed mold with a periodic array of nanostrips. We find that the resulting metasurface exhibits infrared absorption peaks in the 1.5 μm to 15 μm wavelength range, which we attribute to the excitation of surface plasmon resonances. We also characterize the metasurfaces using scanning electron microscopy (SEM) to confirm the morphology of the nanostrips, and Fourier-transform infrared (FTIR) spectroscopy to identify the chemical composition of the various doped PEDOT:PSS films. Our results show metasurface-induced significant changes in the reflection spectrum, with a pronounced dip at the resonance wavelengths, demonstrating efficient manipulation of infrared light by the metasurface structure.

11:00 AM EL08.11.07

Optical and Structural Characterization of ScO_xN_y and ScSi_xO_xN_y Thin Films as Dispersion Engineered Optical Materials[SmridhiChawla](#)¹, [KristianW. Munnikhuis](#)¹, [TornikeShubitidze](#)¹, [WesleyBritton](#)², [DavidWoolf](#)² and [LucaDal Negro](#)¹; ¹Boston University, United States; ²Physical Sciences, Inc., United States

The development of compact diffractive optical elements with tailored optical phases has revolutionized the field of photonics, enabling the creation of high-efficiency photonic components with unprecedented functionalities. This research contributes to developing novel ScO_xN_y and ScSi_xO_xN_y thin films, providing valuable insights into their optical properties, structural characteristics, and patterning potential. We studied the optical and structural properties of ScO_xN_y and ScSi_xO_xN_y thin films, synthesized using reactive RF magnetron sputtering. By modulating the growth conditions and incorporating SiO₂ components through co-deposition and post-deposition annealing, we achieve tunability in the optical constants of the materials with refractive indices ranging from 1.7 to 3 with negligible absorption losses across the visible spectral range. Variable angle spectroscopic ellipsometry (VASE) is employed to determine the dielectric function of each sample in a broad spectral range extended from the ultraviolet to the mid infrared wavelengths. Furthermore, the structural properties of the thin films are investigated using atomic force microscopy (AFM), X-ray diffraction (XRD), and scanning electron microscopy (SEM). These characterization techniques provide insights into the surface morphology, crystal structure, and composition of the films, essential for understanding their optical performances. In addition, our study explores the suitability of different reactive ion etching (RIE) processes for the fabrication of nanopatterns in these materials. The etching behaviour and selectivity of the thin films is investigated with an aim to identify optimal etching conditions for achieving precise patterning and integration into functional photonic devices such as ultracompact imaging components and broadband dielectric metasurfaces.

1:30 PM EL08.13.01

Nonreciprocal Free Space Electromagnetic Wave Propagation Enabled by Magnetic Metasurfaces Weihao Yang, Shuang Xia, Yucong Yang, Wei Yan, Jun Qin and Lei Bi; University of Electronic Science and Technology of China, China

Controlling the propagation of free space electromagnetic (EM) waves is of key importance in wireless communication, LIDAR and thermal energy harvesting applications. Nonreciprocal metasurfaces break Lorentz reciprocity, which may enable higher communication bandwidth and thermal energy harvesting efficiency. Nevertheless, experimental study on such devices have just emerged. In this report, I will present our recent progress on magnetic nonreciprocal metasurfaces. We demonstrate nonreciprocal phase gradient metasurfaces in the microwave frequencies (X and Ku bands) by using ferrite (BaM, YIG) based metaatoms. We designed the metaatoms by simulating their forward and backward scattering cross-section, amplitude and phase under the magnetized state. We designed the nonreciprocal metasurface by forming different phase gradients in the forward and backward directions based on the digital coded metasurface design method. In one experimental demonstration, we fabricated magnetic-bias-free metasurfaces using self-biased BaM materials, showing unidirectional EM wave transmission, nonreciprocal beam steering, nonreciprocal wave focusing and nonreciprocal holography at around 15 GHz. (Nat. Electron. 6,225, 2023) In a second work, we demonstrated reflection phase modulation in YIG meta-atoms by shifting their Larmor precession frequency using gradient magnetic fields, realizing nonreciprocal beam steering up to 28 deg. at 6.5 GHz. I will also present preliminary results on how to fabricate such devices in optical and thermal infrared frequencies. Our work provides a general strategy for design and fabrication of magnetic nonreciprocal metasurfaces, providing a practical solution for nonreciprocal EM wave propagation manipulation for wireless communication, LIDAR and thermal energy harvesting applications.

1:45 PM EL08.13.02

Light Source Engineering of Directive Photoluminescent Metasurfaces with the Local Kirchhoff's Law Elise Bailly, Jean-Paul Hugonin, Benjamin Vest and Jean-Jacques Greffet; Institut d'Optique Graduate School, France

Controlling spontaneous emission is the key to build efficient sources with controlled spectrum, angular emission pattern or polarization. This can be traditionally performed by adding external components, such as filters, lenses or polarizers that shape the wavefront emitted by an external source – but this all results in bulky and expensive system.

Over the past few years, progress in nanophotonics showed the extreme versatility of metasurfaces, designed as thin multifunctional components operating via the interaction between an incident wavefront and periodic elements covering the surface. The shaping of light features comes from the local scattering of a coherent wavefront by meta-atoms. Spatial coherence is therefore critical to engineer directional light sources, and is challenging to maintain when working with ensembles of emitters, as required in order to build bright sources delivering enough sufficient levels of optical power.

In this presentation, we investigate designs of light-emitting metasurfaces, or in other words, nanostructured surfaces covered with emitters. In these systems, the interaction between emitters and the metasurface enables a precise control of the emission properties. In particular, spatially extended modes can be exploited to restore spatial coherence between initially independent emitters, and therefore to shape the angular distribution of emitted light.

A first part of our presentation will comment on our design approach. The standard approach way to proceed is to calculate the field emitted by a dipole placed in the electromagnetic environment of the structure, and by summing and averaging out incoherently over all positions of the dipole. We follow here a radically different approach that exploit reciprocity : we use the local Kirchhoff's law to optimize the emission features in terms of spectrum, polarization and directivity by optimizing the absorption features of the same structure in the reciprocal picture.

This approach gives us the possibility to access quantitatively to the performances of the structure, in terms of efficiency or total emitted power. The latter for instance can be maximized by maximizing the local absorptivity of the structure within the active layer, and making it as close as possible to unity.

In a second part, we will present devices consisting of a 2D metallic (silver) grating covered with a thin layer of nanoplatelets deposited by spin coating on the metasurface. The samples were designed following the Kirchhoff's approach, then fabricated in a clean room environment. Our samples provide highly directional photoluminescence at 605 nm, both in s and p polarizations, with an emission cone around 13.4° half angle.

This work paves the way towards new paradigms in metasurface designs and to a new generation of ultra-thin photoluminescent sources providing highly-controlled wavefront all in a device incorporating both the active medium and the electromagnetic environment that shapes the emission.

References :

E. Bailly, J.-P. Hugonin, B. Vest, and J.-J. Greffet. Spatial coherence of light emitted by thermalized ensembles of emitters coupled to surface waves. Phys. Rev. Res., 3 :L032040, Aug 2021

E. Bailly, K. Chevrier, C. Perez de la Vega, J.-P. Hugonin, Y. De Wilde, V. Krachmalnicoff, B. Vest, and J.-J. Greffet. Method to measure the refractive index for photoluminescence modelling. Opt. Mater. Express, 12(7) :2772–2781, Jul 2022.

H. Monin, A. Loirette-Pelous, E. De Leo, A. A. Rossinelli, F. Prins, D.J. Norris, E. Bailly, J.-P. Hugonin, B. Vest, and J.-J. Greffet. Controlling light emission by a thermalized ensemble of colloidal quantum dots with a metasurface. Opt. Express, 31(3) :4851–4861, Jan 2023

2:00 PM EL08.13.03

Adaptive Photonic Platforms for Radiative Thermal Management in Near-Space and Space Environments Daniel K. Kindem, Karl Pederson, Sam Keller and Ognjen Ilic; University of Minnesota, United States

Materials with tunable optical properties offer exciting opportunities for dynamic control of thermal emission and radiative heat transfer. Among such materials, solid-state chalcogenide glasses are characterized by a reversible amorphous-crystalline phase change process with benefits such as substantial refractive index contrast, stability of both phases over a broad range of temperatures, and the ability to maintain state without the use of energy. In this work, we discuss how these desirable properties can be implemented into photonic platforms for near-space and space environments where the radiative contribution to heat transfer is dominant.

We present a systematic approach for modeling and optimizing multi-state thermal emissivity spectral profiles that are relevant in this radiative environment. Using this model, we explore viable candidate metamaterial and metasurface platforms capable of minimizing or maximizing their temperature profiles, depending on the desired target behavior. Our analysis further elucidates the appropriate experimental parameters governing the thermal behavior of these photonic structures in near-space and space environments. This enables reliable prediction of temperature profiles of different adaptive photonic platforms under various heat transfer modes. The proposed approach has promise in realizing efficient and dynamic thermal management of satellites and spacecraft.

2:15 PM EL08.13.04

What Can a Laser-Induced Microbubble Do for Photonics? Monika Kataria and Zijie Yan; University of North Carolina at Chapel Hill, United States

Upconversion nanoparticles (UCNPs) have proven their remarkable versatility and importance in a wide range of applications, including displays, bio-imaging, sensing, optoelectronics, photovoltaics, photocatalysis, therapeutics, and diagnostics. These nanoparticles possess the unique capability to emit ultraviolet and visible photons by absorbing multiple near-infrared (NIR) photons, thanks to their multi-energy level systems derived from the 4fⁿ electronic configuration of lanthanides. However, their practical utilization is impeded by the low quantum yield of upconversion emission, resulting from limitations such as multiphoton processes and low absorption cross-section. To overcome this challenge, we have devised and successfully demonstrated an innovative strategy to enhance the emission of a UCNPs film utilizing laser-induced microbubbles. The microbubble shoulders multiple functionalities, including the collection of plasmonic silver nanoparticles (Ag NPs) via the Marangoni effect, their controlled deposition onto the UCNPs film to amplify emission through localized surface plasmon resonances (LSPR), and the creation of a bubble micro-resonator enabling optical whispering gallery modes (WGMs). The experimental setup involved an optical trapping system operating at $\lambda = 800$ nm, an upconversion excitation laser at $\lambda = 980$ nm, an optical microscope, and a spectrometer. The UCNPs (NaYF₄: 30 % Yb, 1 % Tm @ SiO₂) employed in this study were monodispersed with an average particle diameter of 24.7 ± 1.8 nm. Dispersed in ethanol, they exhibited multimodal upconversion emissions centered around 449 nm and 475 nm upon excitation at 980 nm. To achieve maximum extinction at approximately 450 nm, silver metal nanoparticles (Ag NPs) of size ~70 nm were selected based on localized surface plasmon resonance (LSPR) matching. The developed platform employs laser-induced bubbles to establish a micro-resonator atop a bilayer film composed of poly(methyl methacrylate) (PMMA) and

UCNPs within a sample cell. At the interface of the microbubble and the PMMA/UCNPs film, Ag NPs are efficiently collected. This integration synergistically enhances upconversion emissions by combining resonant plasmonic Ag NPs with the optical WGMs provided by the bubble micro-resonator. Consequently, the emission intensity from the UCNPs is amplified by over 200 times compared to the case of UCNPs alone. Moreover, the controlled growth and gradual disintegration of the bubble enabled the precise imprinting of Ag NPs onto the PMMA/UCNPs film, enabling the creation of intricate metallic nanoparticle patterns through bubble-pen lithography. The versatile properties exhibited by microbubbles make them highly suitable for the development of multifunctional devices that effectively address the prevailing demands of sustainable technologies. Furthermore, the integration of UCNPs films and laser-induced microbubbles in a solution successfully overcomes the challenges associated with the manipulation and control of micro-bubbles at solid-liquid interfaces, thereby presenting new opportunities for real-time applications. This interdisciplinary research not only highlights the immense potential of laser-induced microbubbles but also underscores their promising applications in the fields of photonics and biomedicine.

2:30 PMBREAK

3:30 PM EL08.13.05

Advances in Strong Coupling Between CdSe Nanoplatelets and Fabry-Pérot Microcavities Robert Collison, Nicole M. Cogan, Ovishek Morshed, Mitesh Amin, Liangyu Qiu, Trevor Tumieli, Trevor Ollis, William F. Girten, Farwa Awan, Pengfei Huo, Todd Krauss and Nickolas Vamivakas; University of Rochester, United States

Fabry-Pérot (FP) cavities containing CdSe nanoplatelets (NPLs) were fabricated by three methods. In the first method, NPLs were dispersed in a polymer film on top of a distributed Bragg reflector (DBR), and overcoated with silver¹. The resulting cavity exhibited strong coupling, with a Rabi splitting of 50 meV and a Q-factor of 270. However, the presence of the polymer and resulting phase segregation between polymer and NPLs limited the concentration of NPLs within the cavities, thereby limiting the strength of the coupling between the NPLs and the cavity photon.

In the second method, the NPL/polymer layer was replaced with a single layer of neat NPLs. These cavities exhibited larger Rabi splittings, up to 80 meV, but with Q-factors around 50, lower than the Q of the NPL/polymer cavity, which we attribute to the increased absorption and scattering losses of the concentrated NPL films, and to the roughness of silver mirror deposited onto the neat NPL film.

To improve the Q factor of the cavities, a third iteration of cavities were made having thinner layers of neat NPLs enclosed between two SiO₂ spacer layers. This arrangement reduced the average absorption and scattering losses of the film stack and planarized the Ag top mirror. A Rabi splitting of up to 60 meV and a Q of 360 was achieved.

These results demonstrate the importance of concentration and uniformity in the assembly of FP microcavities with colloidal semiconductor nanoplatelets, and how these factors meaningfully affect the degree of strong coupling.

(1) Qiu, L.; Mandal, A.; Morshed, O.; Meidenbauer, M. T.; Girten, W.; Huo, P.; Vamivakas, A. N.; Krauss, T. D. Molecular Polaritons Generated from Strong Coupling between CdSe Nanoplatelets and a Dielectric Optical Cavity. *J. Phys. Chem. Lett.* **2021**, *12* (20), 5030–5038. <https://doi.org/10.1021/acs.jpcclett.1c01104>.

3:45 PM *EL08.13.06

Fundamental Limits of Optical Materials and Metamaterials Francesco Monticone; Cornell University, United States

In this talk, I discuss our recent research efforts on determining fundamental and practical limits to various properties of optical materials and metamaterials, including upper bounds on the refractive index of transparent media, universal bounds on reflection, and challenges and opportunities of time-varying metamaterials. Our findings provide insight into the physical constraints of natural and engineered materials and suggest ways to achieve significant improvements over the current state of the art.

4:15 PM *EL08.13.07

Quantum Nanoplasmonic Networks at Ambient Temperature Ortwine Hess; Trinity College Dublin, The University of Dublin, Ireland

Quantum technologies are widely expected to bring a revolution in communications and information technologies in the coming decade allowing, for example, un-paralleled levels of secure communications. For quantum communication, photonic quantum effects have played a central role, but most photonic solutions and systems based on light-matter interaction also require cryogenic environments. Strong coupling of light and matter at the single emitter level is a fundamental quantum resource offering deterministic energy exchange between single photons and a two-level system, and the possibility to achieve single-photon nonlinearities via the anharmonicity of the Jaynes-Cummings ladder. Until recently, however, the conditions for achieving strong light-matter coupling were most commonly met at cryogenic temperatures such that de-coherence processes are suppressed. As a major step forward, we have recently demonstrated room-temperature strong coupling of single molecules [1] and single quantum dots [2] to ultra-confined light fields in plasmonic resonators at ambient conditions. The fact that strong-coupling conditions may be reached at room temperature is of immense interest because it represents a clear route to a practical implementation and use of quantum behaviour in nanophotonic systems and its application in bio-sensing [3].

The talk will discuss how nanoplasmonics can be an enabler of ultrafast quantum nanophotonic networks via strong coupling and ultrafast quantum dynamics [4]. We will highlight the physics associated with recently demonstrated room-temperature strong coupling of single molecules in a plasmonic nano-cavity [1] and near-field generated strong coupling of single quantum dots [2] and single quantum emitter Dicke enhancement [5] paving the road towards single-photon quantum nonlinearities. The presentation will also explain near-field enhanced single-photon emission in near-zero index materials [6] and ultrafast multi-partite quantum entanglement [7]. This provides the foundation for unprecedented control over photon number, single photon dynamics, and dynamic multi-photon coherence. These properties are all imperative for the development of next-generation, nanoscale building blocks in ambient-temperature quantum communication technologies.

ACKNOWLEDGEMENTS

Supported by the Science Foundation Ireland (SFI) via grants 18/RP/6236 and 22/QERA/3821.

REFERENCES

- [1] R. Chikkaraddy, B. de Nijs, F. Benz, S. J. Barrow, O. A. Scherman, E. Rosta, A. Demetriadou, P. Fox, O. Hess, and J. J. Baumberg, *Single-Molecule Strong Coupling at Room Temperature in Plasmonic Nanocavities*, *Nature* **535**, 127 (2016).
- [2] H. Groß, J. M. Hamm, T. Tufarelli, O. Hess, and B. Hecht, *Near-Field Strong Coupling of Single Quantum Dots*, *Science Advances* **4**, eaar4906 (2018).
- [3] N. Kongsuwan, X. Xiong, P. Bai, J.-B. You, C. E. Png, L. Wu, and O. Hess, *Quantum Plasmonic Immunoassay Sensing*, *Nano Lett.* **19**, 5853 (2019).
- [4] X. Xiong, N. Kongsuwan, Y. Lai, C. E. Png, L. Wu, and O. Hess, *Room-Temperature Plexcitonic Strong Coupling: Ultrafast Dynamics for Quantum Applications*, *Appl. Phys. Lett.* **118**, 130501 (2021).
- [5] T. Tufarelli, D. Friedrich, H. Groß, J. Hamm, O. Hess, and B. Hecht, *Single Quantum Emitter Dicke Enhancement*, *Phys. Rev. Research* **3**, 033103 (2021).
- [6] F. Bello, N. Kongsuwan, J. F. Donegan, and O. Hess, *Controlled Cavity-Free, Single-Photon Emission and Bipartite Entanglement of Near-Field-Excited Quantum Emitters*, *Nano Lett.* **20**, 5830 (2020).
- [7] F. D. Bello, N. Kongsuwan, and O. Hess, *Near-Field Generation and Control of Ultrafast, Multipartite Entanglement for Quantum Nanoplasmonic Networks*, *Nano Lett.* **22**, 2801 (2022).

SESSION EL08.14: Poster Session III: Advances in Plasmonics, Nanophotonics and Metasurfaces II

Session Chairs: Ho Wai (Howard) Lee and Benjamin Vest

Wednesday Afternoon, November 29, 2023

Hynes, Level 1, Hall A

8:00 PM EL08.14.01

Design of Different Leaky MoS₂ Nanoresonators Focusing on Biosensing Application Dipanjan Nandi and Manisha Gupta; University of Alberta, Canada

Novel atomically thin layered two-dimensional transition metal-dichalcogenides (TMDCs) such as MoS₂ are a promising material for different for optoelectronic applications [1] as well as

biosensing [2,3]. In recent reported works, MoS₂ based field-effect transistor platform was demonstrated for sensing of protein and DNA molecules [4,5]. Stacked heterostructure of MoS₂ and graphene were also explored for detecting Rhodamine 6G (R6G) molecules [6] and DNA hybridization [7].

In this work, we propose different metasurface designs with MoS₂ for biosensing applications. The reason of using MoS₂ is due to its high refractive index ($n > 4$ [8]) contrast with air and low absorption ($k < 1$ [8]) in the visible wavelength range both at monolayer and bulk thicknesses. Also, MoS₂ surface favours bonding with carboxyl (-COOH) group, which makes it compatible for biofunctionalization. We have explored designs with MoS₂ split-nanorings and nanotriangles. Finite difference time domain (FDTD) simulations were performed to optimize the different design parameters such as, inner and outer diameter, pitch, and split gaps of nanorings and side length and gap between nanotriangles, height of MoS₂ to study the leaky resonances for biosensing applications. Simulations have been performed with polystyrene particles (100 nm diameter) distributed (Gaussian distribution) over the device surface and the resonance wavelength shift was calculated with respect to the number of particles. The size of polystyrene particles was chosen as 100 nm because, because it matches with the size of small virus such as, SARS-CoV-2 and Influenza (H1N1). Here, we have considered polystyrene particles as most of the bioanalytes have similar refractive index to the polystyrene [9].

One of the best design parameters for split-nanorings resonators are: diameter: nanoring's outer diameter- 200 nm, inner diameter- 100 nm, height of MoS₂ nanoring- 150 nm, split gap- 50 nm with gap between two adjacent nanorings- 200 nm, and sensitivity achieved 59.49 nm/decade. The best sensitivity achieved with MoS₂ nanotriangles array is 305.31 nm/decade with 100 nm side length of 100 nm of equilateral triangle. In this study our primary goal is to introduce a symmetry breaking structure to leak out the resonance field to attain high detection sensitivity for small size bioanalytes detection. Attachment of target bioanalytes on the MoS₂ nanoresonators surface disturbs the resonance field and induces a red-shift at the resonance wavelength and detection sensitivity is obtained by calculating the slope of resonance shift curve with respect to the bioanalytes concentrations. We will present the design optimization and comparison between different MoS₂ nanoresonators detection performances.

8:00 PM EL08.14.02

Photo-Induced Enhanced Raman Spectroscopy from β -glucan-AuNPs-Thiram Films Douglasd. Lopes¹, Rafaella F. Fernandes¹, Paola Corio¹ and Alexandre Brolo²; ¹University of Sao Paulo, Brazil; ²University of Victoria, Canada

Photo-Induced Enhanced Raman Spectroscopy (PIERS) is an exciting novel technique for the enhancement of the Raman signal of molecular adsorbates. By irradiating semiconductor and plasmonic nanoparticles hybrid substrates using UV photons, the vibrational signal can be enhanced beyond the typical electromagnetic mechanism of Surface Enhanced Raman Spectroscopy (SERS), through resonant Charge-Transfer (CT) transitions. The creation of oxygen vacancy defects (V_O) in semiconductor materials is universal to explain PIERS. The presence of such defects alters the local surface charge and is reported to be responsible for the increase in the density of donor electronic states within the semiconductor bandgap, leading to the absorption of visible radiation. During exposure to Raman laser radiation, electrons occupying V_O defect states can be promoted to the conduction band (CB) of inorganic semiconductors to be transferred to metallic nanoparticles on the semiconductor surface. This charge migration and consequent increase in charge density shifts the Fermi level of plasmonic nanoparticles and significantly increases the probability of CT transitions with molecular orbitals of the analyte under investigation. The synthetic approach to obtain semiconductor materials with such properties can be not as straightforward and time-consuming, usually requiring several steps and chemicals. Organic semiconductors can arise as an alternative material to more traditional semiconductors, such as TiO₂, as templates for PIERS-active substrates.

Herein, β -glucan films (extracted chemically from *Usnea* lichen (*Usnea* sp.) through a low-cost methodology) were used as an organic template for Gold Nanoparticles functionalized with Thiram (AuNPs-Thiram), a widely used dimethyl dithiocarbamate fungicide to prevent crop damage in the field and to protect harvested crops from deterioration in storage or transport. Thiram is cleaved upon interacting with the AuNPs' surface and its S-S bond is broken, yielding two dimethyldithiocarbamate ions. Thiram is chemically adsorbed on AuNPs through S-Metal bonds and results show that UV pre-irradiation of β -glucan-AuNPs-Thiram films leads to an enhancement of Thiram Raman signal beyond SERS intensities. Although the detailed mechanism for the PIERS effect in organic semiconductors and plasmonic nanoparticles hybrid substrates remains rather unclear, charge separation and migration between the β -glucan biopolymer phase and AuNPs were successfully probed in our experiments. Our results demonstrate that our substrate can be used as a greener alternative material to typical semiconductors employed for PIERS applications and could potentially provide a deeper understanding of the mechanism for the enhancement effect in alternative materials in which the typical UV photo-induced formation of V_O defects is not expected.

8:00 PM EL08.14.03

Geometrical Hierarchy-Derived Optical Asymmetry for Photovoltaic Application Byunghoon Kim¹, Gyu-Hee Kim², Lee Chihyung², Yong Jae Cho² and Doo-Hyun Ko²; ¹Princeton University, United States; ²Sungkyunkwan University, Korea (the Republic of)

In the quest for efficient and sustainable energy sources, a photovoltaic technique has emerged as a promising solution for harnessing solar energy. The primary strategy for facilitating this technique is to achieve efficient light absorption and/or manipulation of light propagation inside the media. This study presents a novel design to remarkably improve the efficiency of photovoltaic devices by incorporating the concept of optical asymmetry. The proposed structure features multidimensional and hierarchical geometry that differ hundreds of times, allowing anomalous light propagation within the media. It phenomenologically shows the notable light-trapping effect at a wide wavelength regime, thereby enhancing the overall short-circuit current by up to 46.19%. Taking a step forward, we explored the leverage of this structural design for the wavelength-converting material. Targeting the photon excitation regime of the photoactive layers, we observed a significant improvement of short-circuit current density up to 25.97% in the semi-transparent photovoltaic system at indoor light illumination. We believe this research opens up new avenues to externally optimize such photovoltaic systems, paving the way for more efficient and sustainable solar energy utilization.

8:00 PM EL08.14.04

Au@Ag Nanostructures for the Sensitive Detection of Hydrogen Peroxide I-Hsiu Yeh¹, Sirimuvva Tadepalli² and Keng-Ku Liu¹; ¹National Tsing Hua University, Taiwan; ²Stanford University, United States

Hydrogen peroxide (H₂O₂) is an important molecule in biological and environmental systems. In living systems, H₂O₂ plays essential functions in physical signaling pathways, cell growth, differentiation, and proliferation. Plasmonic nanostructures have attracted significant research attention in the fields of catalysis, imaging, and sensing applications because of their unique properties. Owing to the difference in the reduction potential, silver nanostructures have been proposed for the detection of H₂O₂. In this work, we demonstrate the Au@Ag nanocubes for the label- and enzyme-free detection of H₂O₂. Seed-mediated synthesis method was employed to realize the Au@Ag nanocubes with high uniformity. The Au@Ag nanocubes were demonstrated to exhibit the ability to monitor the H₂O₂ in the range of concentration from 0 μ M to 200 μ M with $r^2=0.904$ of the calibration curve and the limit of detection (LOD) of 1.11 μ M. In the relatively narrow range of the H₂O₂ concentration from 0 μ M to 40 μ M, the LOD was calculated to be 0.60 μ M with $r^2=0.941$ of the calibration curve of the H₂O₂ sensor. This facile fabrication strategy of the Au@Ag nanocubes would provide inspiring insights for the label- and enzyme-free detection of H₂O₂.

8:00 PM EL08.14.05

Plasmonic Nanomaterials-Based Flexible Strip for the SERS Detection of Gouty Arthritis Mei-Chin Lien, I-Hsiu Yeh, Yin-Cheng Lu and Keng-Ku Liu; National Tsing Hua University, Taiwan

Flexible biochips that enable sensitive detection and simultaneous quantification of biomarkers are of great importance in the field of point-of-care testing. Cellulose paper-based biochips have been employed for the diagnostics and biosensing owing to their unique advantages such as high specific surface area, flexibility, and abundance. Recently, surface-enhanced Raman scattering (SERS)-based flexible biochips have attracted a great deal of research attention for disease detection due to their rapid, sensitive, and noninvasive sensing abilities. Phenomenal progress in the synthesis of structure-controlled plasmonic nanomaterials has made SERS a powerful sensing platform for disease diagnosis and trace detection. Owing to their outstanding optical properties, noble metal nanomaterials are excellent candidates for chemical and biological sensing applications. Yolk-shell structured plasmonic nanomaterials, which consist of solid nanomaterials as the core and nanocage as the shell, have been demonstrated to exhibit extraordinary optical properties due to their high surface to volume ratio and the high density of the electromagnetic fields compared to their solid counterparts. Here, we demonstrate the flexible plasmonic biochips for the SERS-based detection of uric acid (UA). Flexible strips exhibited excellent sensing performance with a detection limit of around 10 μ M of UA, which is lower than the average level of UA in tears. This rapid and sensitive detection method enables the noninvasive diagnosis of gouty arthritis.

8:00 PM EL08.14.06

Comprehensive Development of Reactive Sputtering Parameters for High-Performing Zirconium Nitride Thin Films for Earth-Abundant Plasmonics Kyle Haas¹ and Vivek Subramanian^{1,2}; ¹École Polytechnique Fédérale de Lausanne, Switzerland; ²Institute of Electrical and Microengineering, Switzerland

Zirconium Nitride (ZrN) is a highly promising earth-abundant alternative for plasmonic materials due to its lower cost, high electrochemical stability, and greater mechanical durability than traditional metals like Au and Ag. While epitaxial films enable longer plasmonic propagation lengths than their polycrystalline counterparts, epitaxial ZrN has so far only been achieved with expensive, MgO substrates via unbalanced magnetron reactive sputtering. Therefore, research efforts have been focused on developing ZrN films on Si/SiO₂ substrates to achieve low-cost films with optical performance suitable for commercial plasmonic applications such as on-chip waveguiding and catalysis enhancement. However, a comprehensive understanding of the reactive sputtering deposition conditions necessary for high-performing ZrN thin films on Si/SiO₂ substrates is lacking; most research has relied on high-deposition temperatures and the tuning of N₂ flow rates to produce films of acceptable quality. Most notably, the influence of large substrate biases (>100V) on ZrN film formation and its corresponding optical properties has been largely unexplored; given the strong impact of the increased kinetic energy that results from bias, this is a shortcoming of the existing studies.

Herein, for the first time, we explore the systematic tuning and effect of deposition temperature, nitrogen flow rate, and substrate bias, on the optoelectronic properties of ZrN thin films via XRD, XPS, and spectroscopic ellipsometry. First, to optimize the nitrogen concentration and generate stoichiometric ZrN, the ideal gas flow rate was found to be 2.0:30sccm N₂:Ar at a plasma power of 150W. Next, we demonstrate that a large, applied RF bias of 400V to the Si substrate enables optimum film formation conditions, likely arising from increased film densification, as evidenced by improved optical properties and higher surface plasmon polariton figures of merit (Q_{SPP}). Lastly, we show the effect of moderate, elevated temperatures of 400C, on improved film performance likely from decreased microstrain as evidenced similarly.

As a result, our highest performing ZrN films demonstrate a Q_{SPP} over 50 in the VIS-IR spectrum rivaling the best silicon-based ZrN films across literature. Without relying on expensive MgO substrates or extremely high deposition temperatures, we demonstrate the comprehensive effect of sputtering conditions on film formation and plasmonic performance. Given the significant performance achievements, this work can open the door for widely accessible, earth-abundant plasmonic materials suitable for electrochemical and optoelectronic systems and devices operating within the VIS-IR spectrum.

8:00 PM EL08.14.07

Engineering Photonic Nanodevice by Prescribed Particles Organization and DNA-Based Self-Assembly AlexiaYun¹, BrianMinevich¹, HuajianJi¹, JiahaoWu^{1,1}, KaterinaDeOlivares¹, DanielRedeker¹, GloriaLee¹, NanfangYu¹ and OlegGang^{1,2,1}; ¹Columbia University, United States; ²Brookhaven National Laboratory, United States

Engineering novel optical properties via self-assembly is a promising approach for the fabrication of complex photonic devices with light harvesting, light manipulation, and optical communication capacities. The ability to organize nanoparticles with precise spacing at different scales can enable the structured nanomaterial with emergent optical properties. However, the realization of such materials remains a challenge. We use a DNA-based self-assembly platform to fabricate three-dimensional (3D) optical materials with ordered nanoparticles. DNA origami frames with DNA complementary bonds can capture selective nano-cargo in prescribed spatial positions with nano-scale precision. Programmable bonds enable DNA origami to serve as building blocks that can self-assemble into 3D lattices with repeating and highly organized nanoparticle motifs. By designing an organized structure that couples plasmonic and light-emitting nanoparticles, we investigated the light-emitting properties of the assembled 3D arrays. The optical properties were strengthened by the site-specific growing of the plasmonic particles within the lattice. To enhance stability, the assembled materials were silylated prior to advanced material characterization and optical measurements. To characterize the assembled materials and to achieve the desired optical response, we used electron microscopy and small-angle X-ray scattering (SAXS) to optimize the assembly process, particle sizes, and particle organization. We further investigated the optical properties by optical microscopy and spectroscopy.

8:00 PM EL08.14.08

Integration of Nanaphotonic Structures with a Metallic Nanoporous Air Filter for Particulate Matter Monitoring SeongjaeKim¹, GaabhinRyu¹, JihaeChang¹, YongtaekIm¹, JessieSungyunJeon¹, HanaLim², Hyun-JongKim² and SanhaKim¹; ¹Korea Advanced Institute of Science and Technology, Korea (the Republic of); ²Korea Institute of Industrial Technology, Korea (the Republic of)

The filtration and analysis of airborne particles have received substantial attention since the COVID-19 pandemic. Previous methods of analyzing airborne particles were conducted independently using a sampler, which requires a lengthy and complicated preparation process. In this research, we introduce a new concept of filter-type surface-enhanced Raman spectroscopy (SERS) substrate that allows the simultaneous collection and analysis of ultrafine nanoparticles in the air. SERS is an analytical technique that investigates small amounts of molecules without labeling, which predominantly utilizes the localization effect of an electric field on the nanophotonic surface. Such an analysis method is advantageous over conventional chemical sensors, as a wide range of analyte molecules are detectable. Furthermore, with the recent advance in the miniaturization of spectroscopic devices, there is an increasing potential for integration with Internet of Things (IoT) applications. The proposed substrate in this study is fabricated using the scalable electrochemical deposition of copper nano-dendrites followed by appropriate post-engineering processes to create a nanoporous metal membrane. The thin porous media is suitable for the physical filtration of small particulate matter in the air, and the excellent electrical conductivity of copper allows the capture of particles via electrostatic attraction. In addition, the SERS activation capability is achieved via electron beam deposition of gold. The gold-copper nanoporous membrane demonstrates a particle capture efficiency of ~96% for 300 nm particles under a charging condition of 5 kV with a differential pressure of 121 Pa. The captured particulates on the substrate can be monitored via Raman spectroscopy. We evaluate the performance of the substrate by measuring the Raman spectra of a 1 μM Rhodamine 6G solution and a bacterial sample (*P. aeruginosa*). Characteristic peaks are observed in both cases, which indicates successful detection. Additionally, we measure the Raman spectra from aerosolized Rhodamine 6G particles as small as 150 nm. The substrate exhibits excellent mechanical properties due to the roll pressing process, which simultaneously allows it to be reused via liquid phase rinsing. Even after undergoing repeated compression tests of ~22,000 cycles at 177 kPa, the substrate maintains functionality along with its filtering and sensing properties. We further conduct numerical simulations to elucidate the localized enhancement of the Raman signal from the nanoporous metal membrane. Finite-difference time-domain (FDTD) simulations of Maxwell's equations reveal amplification of the near field between the nanorod structures. Moreover, by analyzing the electrostatic potential using the finite element method (FEM), we confirm that the particles can be spontaneously transported toward the electromagnetic hotspot.

8:00 PM EL08.14.09

Plasmonic External Nanogap Dumbbells for On-Particle Direct Raman Assays KyunginChoi and Jwa-MinNam; Seoul National University, Korea (the Republic of)

Metal nanostructures with a plasmonic nanogap are useful for surface-enhanced spectroscopy, and many bio-applications like biosensing and bioimaging. The use of these structures as chemical and biological sensing/imaging probes typically requires an ultra-precise synthesis of the targeted nanostructure and skill in complex assay techniques are required. Here, we designed and synthesized a plasmonic nanostructure based on Au nanorod cores with two types of external nanogap particles with different gap positions. Au dual-gap nanodumbbells (AuDGNs) were synthesized via the anisotropic adsorption of polyethyleneimine (PEI) on Au nanorods to facilitate tip-selective Au growths on nanorod tips for forming mushroom-shaped dumbbell-head structures at both tips. The dual gaps (intra-head and inter-head gaps) were formed within a single particle. Au tip-intragap nanodumbbells (AuTIDs) were synthesized based on co-reduction and dealloying process of Ag and Au on the tip of Au nanorods. Two heads with closed intra-head gap were grown on the tips of Au nanorod and inter-head gap exposed to outer environment were formed within a single particle. Importantly, these particles enabled facile on-particle SERS detection assays in a short period of time through the diffusion of target molecules into the gap exposed to outer environment.

8:00 PM EL08.14.10

Phase Modulator Ellipsometry Based Biosensor for Detection of E. coli K12 SorayaZangenehzadeh¹, FenjaSchröder¹, SvenjaHerdan¹, EmilAgocs¹, NassimaAmroun¹, RebekkaBiedendieck², BernhardW.Roth³, Hans-HermannJohannes¹, DieterJahn² and WolfgangKowalsky¹; ¹Institute of High Frequency Technology, Germany; ²Braunschweig Center for Systems Biology, Germany; ³Hanover Center for Optical Technologies, Germany

In recent years, rapid detection of pathogenic microorganisms in human food and water resources has been widely investigated to reduce the number of deaths as well as economic loss. Surface plasmon resonance (SPR) sensors as an optical method is used for detection of biological and chemical targets. These biosensors are extensively applied for monitoring of microorganisms such as bacteria. While most strains of *E. coli* are harmless, there are certain pathogenic strains that can cause illnesses in humans. Due to the size of *E. coli* bacteria (~ 1 micron), detection of these microorganisms brings challenges in experimental measurement. In this study, we aim to apply phase-modulator based ellipsometer to enhance the performance of conventional SPR sensors for *E. coli* detection.

Surface plasmons as a surface charge density waves of free electrons at a metal surface propagate at metal-dielectric interface. In specific angle, the p-polarized incident light is strongly absorbed in consequence of coupling the evanescent wave generated at metal-dielectric interface and surface plasmon waves. Hence, the resonance can be observed as a sharp dip in reflectivity profile. Conventional SPR sensors monitor the changes in the intensity of reflected light according to the changes of refractive index of target sample. In resonance condition, not only the intensity of the incoming light changes, but also the phase change is strongly modulated. Due to the significant phase jump, this sharper shift can be studied to improve the performance of SPR sensors. Spectroscopic ellipsometry provides this opportunity to study both reflectance ratio and phase changes in reflected light from the sample of interest. Spectroscopic ellipsometry analyzes the changes in the polarization state of light after reflection or transmission from a surface and determines the optical properties and thickness of thin films. These changes in polarization states are studied by the amplitude ratio (Ψ) and the phase difference (Δ) between p- and s-polarized light, respectively. There are different measurement methods of ellipsometry based on the optical elements configuration and arrangement. Barium borate crystal based phase-modulator has been used in our optical setup to induce phase changes in the incoming light beam. Using a phase-modulator in optical design of ellipsometer makes it a faster measurement tool compared to the conventional ellipsometric measurement methods. Using this method each measurement takes around micro second. Therefore, this method can be used for detection of microorganisms with higher time resolution. This project has been focused on using conventional Kretschmann configuration including quartz prism and ~45 nm of homogenous gold film to support propagation of surface plasmon waves. Gold film is functionalized with porphyrin molecules as a linker with specific peptide group to bind with outer membrane of Gram-negative bacterium. This configuration has been used upon phase-modulator ellipsometer to monitor *E. coli* K12.

8:00 PM EL08.14.11

Abnormal In-Plan Epitaxy and Formation Mechanism of Vertically Aligned Au Nanopillars in Self-Assembled CeO₂-Au Metamaterial System JuanjuanLu¹, DiZhang², RobynneL. Paldi³, ZihaoHe¹, PingLu², JuliaDeitz³, AhmadAhmad¹, HongyiDou¹, XuejingWang², JunchengLiu¹, ZedongHu¹, BoYang¹, XinghangZhang¹, AnterA. El-Azab¹ and HaiyanWang¹; ¹Purdue

Metamaterials present great potential in the applications of solar cells and nanophotonics, such as super lenses and other meta devices, owing to their superior optical properties. In particular, hyperbolic metamaterials (HMMs) with exceptional optical anisotropy offer improved manipulation of the light-matter interactions as well as a divergence in the density of states and thus have enhanced performances in related fields. Recently, the emerging field of oxide-metal vertically aligned nanocomposites (VANs) suggest a new approach to realize HMMs with flexible microstructural modulations. In this work, a new oxide-metal metamaterial system, CeO₂-Au, has been demonstrated with variable Au phase morphologies from nanoparticle-in-matrix (PIM), nanoantenna-in-matrix, to VAN. The effective morphology tuning through deposition background pressure, and the corresponding highly tunable optical performances of three distinctive morphologies, were systematically explored and analyzed. A hyperbolic dispersion at higher wavelength has been confirmed in the nano-antenna CeO₂-Au thin film, proving this system as a promising candidate for HMM applications. More interestingly, a new and abnormal in-plane epitaxy of Au nanopillars following the orientation of CeO₂ matrix instead of the SrTiO₃ substrate, was discovered. Additionally, the tilting angle of Au nanopillars, α , has been found to be a quantitative measure of the balance between kinetics and thermodynamics during the depositions of VANs. All these findings provide valuable information in the understanding of the VAN formation mechanisms and related morphology tuning.

8:00 PM EL08.14.12

Alternative Platform for COVID-19 Diagnosis Based on AuNPs Modified Lab-On-Paper Pornchanok Punnoy, Tatiya Siripongprea, Trairak Pisitkun, Nadnudda Rodthongkum and Pranut Potiyaraj; Chulalongkorn University, Thailand

Since the SARS-CoV-2 virus was first discovered in 2019, it has spread over the world. Rapid testing is critical to retard the spread of the virus. Herein, a Lab-on-Paper for diagnosis of COVID-19 is developed applying a colorimetric method for screening test, along with high precision SARS-CoV-2 antigen detection on paper using a laser desorption/ionization mass spectrometry (LDI-MS). Gold nanoparticles (AuNPs) were modified on paper for both colorimetric and LDI-MS detection. The colorimetric detection is based on the color change occurring on the paper from pink to purple as a result of AuNP aggregation which can be regulated by antigen-antibody bioconjugation. AuNPs on paper can be used directly as an LDI-MS substrate for direct quantitation of SARS-CoV-2 antigen in saliva without sample preparation for SARS-CoV-2 quantitative detection. In comparison to RT-PCR, LDI-MS provides early diagnosis with high sensitivity, rapidly without sample preparation, as well as a lower cost/test, which is crucial for preventing mortality of patients with underlying conditions. This approach demonstrated linearity between 0.01 and 1 $\mu\text{g mL}^{-1}$, covering a cut-off value of 0.048 $\mu\text{g mL}^{-1}$ for COVID-19 indication in saliva. Hence, this platform might be a potential device for applying as non-invasive diagnosis of COVID-19 Omicron BA.2 variant.

8:00 PM EL08.14.13

In Vivo Real-time Multiplex Detection of Plant Signalling Molecules using Surface-Enhanced Raman Scattering Nanosensor Won Ki Son, Seon-Yeong Kwak and Dae Hong Jeong; Seoul National University, Korea (the Republic of)

To understand the biological and chemical dynamics of plants is essential in agriculture, and various sensor technologies have been studied. 'Plant signalling molecules' released against stimuli are drawing attention as a key to understand plant's status under stressors. Surface-enhanced Raman scattering (SERS)-based nanosensor has shown strong potential for its non-invasiveness and capability of real-time detection from fingerprint spectra. In our research, we fabricated PDDA-capped Ag nanoshell (AgNS@PDDA) and introduced it into plants through stoma. Due to AgNS@PDDA's optical activity in NIR, it was possible to evade chlorophyll's autofluorescence and obtain SERS signals with fine quality. Also, PDDA polymer effectively attracted signalling molecules by coulombic interaction.

Then, we studied the plant's reaction against biotic and abiotic stress with SERS signal monitoring. When plants leaf was under wound stress or cold stress, nasturlexin B, extracellular ATP and glutathione were successfully detected *in vivo* environment. Meanwhile, biotic stress was studied for the plants infected with fungal disease. *F. Graminearum* was injected into the plant, and signaling molecules was monitored with nanosensors according to the elapsed days after injection. Even only 2 hours after the fungi injection, when no lesion was detectable, SERS signals of eATP and salicylic acid related to systemic acquired resistance were successfully detected.

8:00 PM EL08.14.14

Pulsed Laser Ablation for Flexible Printed Electronics Applications: Harnessing the Power of Colloidal Nitride Nanoparticles Stavros Panos, Nikolaos Pliatsikas, Spyridon Kassavetis, Maria Gioti and Panos Patsalas; Aristotle University of Thessaloniki, Greece

Nitrides are of the most prominent families of materials dominating nowadays. They can be divided into two distinct sub-categories: i) III-nitride wide-gap semiconductors (GaN, AlN) and ii) Conducting nitrides of IIb-Vb transition metals (TiN, ZrN, Ti_{1-x}Sc_xN, Ti_{1-x}Ta_xN) that have recently emerged as important plasmonic materials.

Despite the intrinsically superior electrical and optical performance of nitrides compared to conductive oxides, there is a continued and strong prominence of oxides over nitrides in flexible printed electronics due to the compatibility of oxides with solution methods that provide enormous scale up and have allowed oxides to enter the field of printed electronics. The refractory nature of nitrides and the use of high vacuum, introduce industrial costs, reduced scalability and increased power consumption. Therefore, alternative technologies for the fabrication of nitrides are required to be adapted to the needs of printed electronics such as R2R printed sensors and optoelectronic devices.

In this study we propose a radical solution to overcome all the aforementioned obstacles by applying laser fabrication processes that promises to produce colloidal nitride nanoparticles with the desired optoelectrical or plasmonic performance compatible with printed technologies. The colloidal nanoparticles were fabricated through laser ablation of Titanium Nitride (TiN), Gallium Nitride (GaN) and Aluminum Nitride (AlN) thick coatings using a nanosecond Nd:YAG pulsed laser at 355, 532 and 1064 nm wavelengths in various liquids. The colloidal NPs' structure, morphology as well as quality have been analysed by Raman, SEM, AFM. The optical properties of the target materials have been evaluated by NIR-Vis-UV, Spectroscopic Ellipsometry, while an optical absorbance characterization was performed on the colloidal TiN NPs.

8:00 PM EL08.14.15

Color Purity Enhancement Through Effective Index Modulation of GST for Applications in Reconfigurable Displays Yubin Lee¹, Joo Hwan Ko¹, Sung-Hoon Hong² and Young Min Song¹; ¹Gwangju Institute of Science and Technology, Korea (the Republic of); ²Electronics and Telecommunications Research Institute Materials and Components Research Division, Korea (the Republic of)

Phase-change materials (PCMs) have been emerged owing to their reconfigurable physical properties such as refractive index, light absorption, electrical conductivity, and Young's modulus by switching between amorphous and crystalline phases [1]. Ge₂Sb₂Te₅ (GST), which consists of germanium, antimony, and tellurium, is one of the representative PCM materials and is widely studied for a dynamic color display or phase change memory by utilizing its great tunability in both optical and electrical properties. Due to the nature of the refractive index variation depending on the phase of GST, there have been tremendous suggestions for reconfigurable photonic structures, including photonic memory, thermal radiation modulator, and tunable structural color [2]. Typically, optical coating of dielectric thin films is based on Fabry-Perot or thin film interference. Recently, high-absorption dielectric films have been studied as optical coatings, and when metals are combined with high-absorption dielectrics, strong optical interference can be obtained with a small phase change of the reflected wave, which can significantly reduce the thickness compared to conventional coating layers. Resonance behavior impacting the structural color can be observed in structures consisting of a metal-coated substrate with an ultra-thin absorbing layer. The high color purity and feasible tuning functions of structural coloration has attracted attention due to its promising applicability as a next generation color display. Despite its great potential application, low chromaticity and limited intermediate step over phase change have been treated as a barrier to the efficient operation as a color display [3]. In this study, we present an ultrathin tunable color filter comprising GST. We modulate the effective index of GST by applying porosity (P_r) with anisotropic geometry, resulting in color purity enhancement and enhanced controllability based on polarization-driven modulation. Specifically, we deposit GST on top of an Au film using glancing angle deposition (GLAD) to manufacture self-aligned porous nanocolumns (PNCs) with varying P_r (0% 40%, 75%). In the amorphous GST/Au reflection spectrum, dip intensity decreases as P_r increases, and we find that color purity can be enhanced by controlling the P_r and phase. Particularly, the amorphous phase of GST exhibits a higher color purity and a wider color range than the crystalline phase. Additionally, mitigate the risk of surface oxidation and potential damage when depositing GST on an Au film exposed to ambient air, we conducted simulations to explore the effect of incorporating an oxide layer as a film passivation strategy. This additional dielectric layer serves noticeable shift in the dip position of the reflectance spectrum and changes in the phase condition, the color response can be dynamically adjusted, offering a wide range of color variations depending on the thickness of the oxide layer. Furthermore, GLAD technique induces atomic shadowing and creates inclined columnar structures on the substrate, resulting in an increased porosity. Due to the shadowing effect, the slanting plane direction of the PNCs has a higher P_r and varies with the polarization angle, causing a structural color change.

We confirm that the color purity can be improved with the P_r , phase, thickness of GST, and polarization angle. And the incorporation of the additional dielectric layer provides both protective benefits and enhanced control over color changes, presenting exciting possibilities for diverse applications. Our suggestions can be used as a way to improve optical properties in applications such as optical coating, optoelectronic displays, and optical storage devices.

References

- [1] P. Hosseini, C.D. Wright and H. Bhaskaran, *Nature*. 511, 206–211 (2014).
- [2] J. H. Ko, D. H. Kim, S. H. Hong, S. K. Kim and Y. M. Song, *iScience*. 26, 105780 (2023)
- [3] J. H. Ko, Y. J. Yoo, Y. Lee, H. H. Jeong and Y. M. Song, *iScience*. 25, 104727 (2022)

8:00 PM EL08.14.16

Infrared Thermal Management with Graphene-Ag Nanocubes Heterostructures¹ [Ihsan Uluturk](#)¹, Michael Leuenberger², Peter Capuzzi¹, Margaret Peters³, Jin Ho Kim¹, Michael J. Manser¹ and Richard M. Osgood¹; ¹U.S. Army, United States; ²University of Central Florida, United States; ³University of Massachusetts Lowell, United States

The main purpose of textiles throughout history is to regulate heat flow and provide warmth or decrease excessive heat for the wearer. In recent times, the textile industry has developed new materials that can ensure the wearer stays dry in hot environments and that repel moisture. The main downside of these new textiles, however, is that their electromagnetic response has not been fully optimized, allowing too much radiation to be absorbed and radiated back to the skin, causing the wearer to overheat. Our work is composed of two parts: simulation and experimentation. Simulations will first be conducted to better understand graphene chemistry, as graphene ink with Ag nanocubes, FeCl₃, and SU-8 are spin coated onto silicon wafers.

In this work, heterostructures made of Ag nanocubes-Graphene-FeCl₃-SU-8-Si wafer-Al mirror are considered. This system is a representative of a Fabry-Perot type of cavity, where incident infrared light interacts strongly with graphene and the Ag nanocubes. FeCl₃ is used to dope graphene to a Fermi energy of E_F=-0.6 eV. The thickness of SU-8 will be chosen to be a quarter of the infrared wavelength in order for the amplitude of the infrared light to be maximal at the position of the graphene sheet.

Finite-difference time domain (FDTD) simulations show narrow resonance peaks in the absorbance (=emittance) due to localized acoustic surface plasmons (AGPs) in the dielectric between graphene and the Ag nanocubes.

The positions of the resonance peaks can be tuned in the range between 3 μm and 12 μm by means of a gate voltage.

When the number of graphene layers is increased, the conductivity is multiplied by the number of layers, which results in a blueshift of the AGP peaks. By increasing the size of the Ag nanocubes and the period of the square lattice of Ag nanocubes, the AGP peaks are redshifted.

For highly doped graphene layers with a small layer of FeCl₃ of around 50 nm between graphene and the Ag mirror, the absorbance (emittance) between 3 μm and 12 μm is around 2%, independent of the number of graphene layers. Such heterostructures could be useful for thermal management systems.

Based on the simulation results, we will be fine tuning the graphene chemistry. Resultant graphene ink with Ag nanocubes will be spin coated onto Si wafers. The fabricated heterostructures made of Ag nanocubes-Graphene-FeCl₃-SU-8-Si wafer-Al mirror will be characterized using in-house developed Delta T measurement system. In this system, anodized Aluminum with an emissivity of 0.77 is used, which is smaller than the emissivity of human skin (95% to 98%). The anodized aluminum is placed on a hot plate and a thermocouple. The hot plate is heated up to 38 °C to simulate the body temperature and standoff is created between heterostructures and the hot plate. Thermocouples will be used to measure the temperature difference between the heterostructures and plain Al mirrors to see if the heterostructures have a significant effect on the thermal management property.

8:00 PM EL08.14.17

Genetic Algorithm Optimization of Mid-Infrared Nonreciprocity in Weyl Semimetal Planar Photonic Structures¹ [Hannah Gold](#), Simo Pajovic, Abhishek Mukherjee and Svetlana V. Boriskina; Massachusetts Institute of Technology, United States

Engineering thermal radiation from surfaces is usually limited by the constraints of Kirchhoff's law of radiation, which states that the spectral directional emissivity of a surface equals its spectral directional absorptivity at thermal equilibrium; This imposes fundamental limits on the efficiency of radiative- energy harvesting, as any absorber also acts as a thermal emitter in the same spectral and angular range. In turn, breaking this reciprocity enables breaking the barriers in thermal efficiency engineering [1,2]. In this work, we develop an algorithm to optimize the non-reciprocal infrared response and to enable breaking of the Kirchhoff's law in a one-dimensional (1D) planar photonic multi-layer stack composed of thin films of Weyl semimetals and dielectrics. The design space and parameters of this structure were traversed using a genetic algorithm to find a global optimal solution, and then the design was further refined with numerical gradient descent to find the local minimum thereafter. The resulting design achieves a large nonreciprocal absorption contrast in the near infrared wavelength range at positive and negative angles of incidence (55 and -55 degrees were used during the optimization). Differently from prior studies, our optimized design accounts for both s- and p- polarized reflection coefficients when calculating the non-reciprocal Figure of Merit (FOM), which is vital for applications in harnessing the thermal radiation from the structure. Because the non-reciprocity is governed by the excitation of the surface plasmon polariton modes at the interfaces between Weyl semimetal and dielectric layers, it is limited to the p-polarized optical response engineering. Thermal emission into the allowed s-polarized modes is still reciprocal and may degrade the overall figure of merit in the design of a non-reciprocal thermal emitter. Furthermore, our optimally designed 1D planar non-reciprocal absorber avoids the technical challenges of fabricating grating-based structures that require lithographic techniques. Finally, our optimum design offers the largest FOM while using much fewer layers in the heterostructure, which should significantly simplify its experimental realization. The use of the Weyl semimetals instead of the conventional magneto-optical materials in our design eliminates the need for an external magnetic field bias, thus allowing for a compact form factor and integrability. Applications of our work range from thermophotovoltaic cells to optical switches, circulators, and isolators.

The authors acknowledge support from ARO MURI (Grant No. W911NF-19-1-0279).

H.G. was supported by an MIT Presidential Fellowship, S.P. was supported by NSF GRFP.

[1] S.V. Boriskina, M. Blevins, S. Pajovic, The Nonreciprocal Adventures of Light, Optics and Photonics News, 33(9), 46-53, 2022.

[2] S. Pajovic, Y. Tsurimaki, X. Qian, S.V. Boriskina, Radiative heat and momentum transfer from materials with broken symmetries: opinion, Optical Materials Express, 11(9), 3125-3131, 2021.

8:00 PM EL08.14.18

Nanoimprinted Pyramid Scanning Probe for Nanoscale Optical Mapping¹ [Junze Zhou](#), Adam Schwartzberg and Alexander Weber-Bargioni; Lawrence Berkeley National Laboratory, United States

Tip-enhanced Photoluminescence (TEPL) enables the simultaneous collection of emission spectra and topographic information with sub-diffraction spatial resolution, providing valuable insights into the correlation between local material properties, structure, and macroscopic functionality of a material. In this study, we focus on the development of a novel near-field probe using a cost-effective and efficient nanoimprinting technique for investigating the optical properties of low-dimensional quantum materials. Through extensive experimental demonstrations, we showcase the performance of the nanoimprinted probe in terms of high-precision height sensing and high-resolution optical mapping on a 2-dimensional (2D) semiconductor. Additionally, we introduce advanced plasmonic designs and nanofabrication strategies based on the pyramidal probe, which facilitate the observation of nanoscale dark states and plexciton emission in 2D materials.

8:00 PM EL08.14.19

Ellipsometric Detection of Bacteria using Dielectrophoresis¹ [Fenja Schröder](#)¹, Soraya Zangenehzadeh^{1,2}, Emil Agocs^{1,2}, Marten Musiol¹, Nassima Amroun¹, Rebekka Biedendieck¹, Dieter Jahn¹, Hans-Hermann Johannes^{1,2} and Wolfgang Kowalsky^{1,2}; ¹Technische Universität Braunschweig, Germany; ²Leibniz Universität Hannover, Germany

The aim of this research is to detect bacteria by ellipsometry and evaluate if dielectrophoresis (DEP) can be useful to improve the limit of detection of optical biosensors.

Spectroscopic ellipsometry allows the non-destructive and contactless analysis of thin films or biological samples in a time range of seconds. Ellipsometry is based on the investigation of the polarization state of reflected or transmitted light. The measured parameters are the amplitude ratio (Ψ) and the phase difference (Δ) of s- and p-polarized light. Our measurement set-up consists of a flowcell that guides bacteria in liquid environment to a sensing surface, which consists of a glass substrate coated with thin film gold electrodes. Measurements were performed in Kretschmann configuration utilizing a quartz prism and gold electrode substrates. The bacteria studied in our experiments is the well-known, Gram-negative *E. coli* K12 strain.

The irradiation of the electrodes under a certain angle of incidence at a certain wavelength of light allows the excitation of surface plasmons resonance (SPR). Under this condition p-polarized light is coupled to the mode of surface plasmons at the metal-liquid-interface. This phenomenon can be monitored in the spectra of the ellipsometric parameters Ψ and Δ in form of a sharp dip, that correlates to the intensity minimum of the reflected p-polarized light. The excitation of SPR is highly dependent on the refractive index at the metal-liquid-interface. The presence of bacteria in a liquid changes the refractive index near the gold surface and therefore also changes the excitation condition of the SPR. Due to the penetration depth (~300nm) of the evanescent wave associated with the excitation of SPR, SPR-based sensors can only provide information on the refractive index very close to the metal interface. Therefore, it is of high importance to increase the number of bacteria at the metal-liquid-interface. To reach our goal of a highly sensitive SPR sensor we utilize the effect of dielectrophoresis.

Dielectrophoresis (DEP) describes the movement of dielectric particles in suspension due to the presence of inhomogeneous electric fields. DEP is divided into positive and negative DEP, depending on the different movement of particles due to the outer electric field. For positive DEP (pDEP) particles, such as bacteria, are accelerated to regions of high field inhomogeneity, which occur at the electrode edges. Hence bacteria are collected directly on the electrodes, the change in the spectra of Ψ and Δ magnified.

To explore the efficiency of bacteria collection by pDEP and the behavior of different electrode geometries in ellipsometry, a variety of electrode structures were designed. The structures vary in complexity and symmetry. Furthermore, the dependence of dielectrophoretic bacteria collection and SPR excitation on the gold film thickness was investigated. The designed electrodes and measurement set-up were able to visualize the influence of DEP on an ellipsometry based biosensor.

8:00 PM EL08.14.20

Hardware and Sensor Optimization of a Nanotechnology Enabled Implantable Sensor for Hormones in Marine Animals XiaojiaJin¹, VolodymyrKoman, MankiSon and MichaelS Strano; Massachusetts Institute of Technology, United States

Biologging has yielded tremendous insights in ecological biology by enabling the collection of data in animals free-roaming in their environments. However, measurements have largely been limited to temperature, pressure, and movement. Physiological data of animals' biomarkers would create valuable orthogonal datasets and produce more nuanced understanding of organisms in the context of their environments and behaviors. Nevertheless, successes in collecting such biochemical information remain absent. In this work, we explore hardware and sensor optimization of nanotechnology-enabled implantable sensor for tracking hormone levels in marine animals. We have extensively studied the performance of nanosensors based on polymer-wrapped single-wall carbon nanotubes (SWNT) embedded within a biocompatible poly (ethylene glycol) diacrylate (PEGDA) hydrogel under various temperatures, illumination conditions, and sensor concentrations. We have further prototyped a miniaturized fluorescent system integrated into commercially available acoustic tags used in marine biology. An integrated nanosensor hydrogel reached 100 nM limit of progesterone detection as an example of important hormone in marine animals. The developed form-factor will complement the presently collected data by providing insights into the physiological state of the animals in the context of their behavior and environments. With these new data, biologging studies will reach a new level of sophistication and nuanced understanding.

8:00 PM EL08.14.21

Using Cell Lensing and Nanosensor Chemical Cytometry to Characterize the Efflux Heterogeneity of Immune Cell Populations XiaojiaJin¹, XunGong¹, VolodymyrKoman¹, SooyeonCho² and MichaelS Strano¹; ¹Massachusetts Institute of Technology, United States; ²Sungkyunkwan University, Korea (the Republic of)

Cellular immune heterogeneities play a critical role in the progression and prevention of cardiovascular or neurodegenerative diseases. Thus, a tool that can profile the dynamic antigenic responses of different immune cell populations in terms of their chemical efflux and biophysical properties can enhance our understanding of past and future unknown microorganisms and diseases. Herein, we have developed a technique called Nanosensor Chemical Cytometry (NCC), that utilizes an optical nanosensor array embedded within microfluidics to interrogate chemical species efflux from individual cells in real-time. The NCC technique takes advantage of the cell itself as an informative Gaussian lens, projecting both the nIR emission of the single-walled carbon nanotube sensors as well as various cellular physical properties. Different nanosensor integration methods were investigated to optimize the signal readout.

Using the NCC technique, we have profiled both the heterogeneity of nitric oxide (NO) efflux from macrophage populations and hydrogen peroxide (H₂O₂) efflux from monocyte populations. The technique was able to profile immune heterogeneities at attomolar sensitivity in a completely non-destructive and real-time manner with a throughput rate of ~600 cells/hr. In addition, new phenotype correlations between real-time extracellular immune responses and multiple biophysical properties (cell size, eccentricity, RI) of cell populations were investigated with exact numerical values and distribution statistics. This work provides an efficient strategy for the chemical analysis of cell populations in manufacturing and biopharmaceutical engineering.

8:00 PM EL08.14.22

Core-Shell and Yolk-Shell Plasmonic Nanocrystals for Hydrogen Production Yung-JungHsu; National Yang Ming Chiao Tung University, Taiwan

With the inherently high degree of complexity, heterostructures composed of two or more materials joined in unique architectures may exhibit superior synergetic properties that are difficult or impossible to acquire from their individual constituents. For semiconductor heterostructures, the relative band alignment of the constituents promotes effective charge separation to bring them desirable properties for photocatalysis applications. Among the different types of heterostructures, core-shell and yolk-shell nanocrystals have received particular interest due to their fascinating properties. Several representative works from our lab will be introduced to demonstrate the promising potentials of core-shell and yolk-shell nanocrystals for hydrogen production applications, especially those involving localized surface plasmon resonance.

8:00 PM EL08.14.23

Optical Confinement in Silicon Nanowire: A Correlated Characteristics and Fabrication of Vertically Aligned Nanowire Mohammad KamaHossain¹ and AymanMukhaimar²; ¹King Fahd University of Petroleum & Minerals, Saudi Arabia; ²RMIT University, Australia

Here in this work, finite-difference time-domain (FDTD) analysis has been carried out to extract the optical characteristics of a single silicon nanowire (Si-NW) on a c-Si slab. Correlated absorption depth profile, electromagnetic field distribution, energy distribution and generation rate distributions of the Si-NW model showed the possibility of efficient light trapping within the nanowire. An experimental attempt has been taken to fabricate catalyst-induced vertically aligned Si-NWs. High-resolution field emission scanning electron microscope (FESEM) revealed the coverage of ca. $6.5 \times 10^8/\text{cm}^2$ with a diameter in the range of 50-200 nm. Si-based nanostructures, particularly Si-NWs exhibit strong optical absorption with reference to those observed in conventional Si-based solar cells. Henceforth, Si-NW is a promising candidate in confining incident light and contributes in designing efficient and miniaturized solar cells.

The sputtering technique was used to deposit a gold ultrathin film on the Si wafer and the film was annealed at a high temperature to achieve metal nanoparticles. Thereafter, a CVD reactor was used to grow Si-NWs. The morphology of as-fabricated Si-NWs was confirmed by SEM and high-resolution SEM investigations. Exciton generation rate distributions of vertically aligned Si-NWs of 50 and 200 nm diameters at 700 and 1100 nm solar spectral wavelengths have been simulated. Excitation rate distribution was found to be localized near the edges in both scenarios. At 700 nm wavelength confined spots were observed in a repeated fashion along with lower intensities, whereas at 1100 nm wavelength such spots increased in intensity and lower in repetition. Unlike those observed for Si-NW of 50 nm diameter, excitation rate distribution was found to be localized near the center with higher intensity at 700 nm solar wavelength, whereas at 1100 nm wavelength such distribution disappeared.

During the fabrication process adopted here in this work, it was observed that metal nanoparticles acted as catalysts and were the main ingredient to define the diameter of the Si-NWs. FESEM observations confirmed the diameter of the as-grown Si-NWs to be in the range of 50 to 200 nm. In the simulation we have considered four different sizes of Si-NWs, such as 50, 100, 150 and 200 nm in diameters. Due to space constraints, further details are out of this context and will be elaborated in the event as well as in the full manuscript.

Authors acknowledge Interdisciplinary Research Center for Renewable Energy and Power System (IRC-REPS), Research Institute, King Fahd University of Petroleum & Minerals (KFUPM), Dhahran 31261, Saudi Arabia (Grant # INRE2215).

<quillbot-extension-portal></quillbot-extension-portal>

SESSION EL08.15: Imaging and Sensing with Metasurfaces

Session Chairs: Ho Wai (Howard) Lee and Jason Valentine

Thursday Morning, November 30, 2023

Hynes, Level 3, Room 312

9:00 AM EL08.15.01

Nanoscale Imaging of Surface Plasmon Polaritons at Interface of Metal/Dielectric by UEM HaihuaLiu, Thomas E.Gage and IlkeArslan; Argonne National Laboratory, United States

Haihua Liu^{1,*}, Thomas E. Gage¹, Ilke Arslan¹

¹ Center for Nanoscale Materials, Argonne National Laboratory, Lemont, IL, USA

*Corresponding email: haihua.liu@anl.gov

Surface plasmon polaritons (SPPs) are collective oscillation of surface charge-density waves at the interface between a metal and a dielectric material. The SPPs that propagate along the interface and exhibits exponential decays perpendicular to the interface into an adjacent dielectric medium. With the unique properties of evanescence and surface localization, SPP's are non-radiative and can be transversely localized and guided into subwavelength metallic structures as small as a few nanometers. A new branch of photonics called plasmonics, based on control and manipulation of light using SPPs at the nanoscale, has the potential to break diffraction limit of light and exhibit significant advantages in nanophotonics device development by replacing electronic signals with light as information carriers is a prime motivation behind research on photonic circuits.¹ Therefore, it is of great importance to image the SPPs at the nanometer scale to give one deeper understanding of the guide and localization of light below the diffraction limit for nanophotonics applications.

Ultrafast Electron Microscopy (UEM) has been used to study the ultrafast dynamics of light-matter interactions in physics, chemistry and materials science with temporal resolution of hundreds of femtoseconds,² which is 10 orders better than that of conventional electron microscopy limited by the camera read-out rate. Other than light-matter interaction observed in UEM, the investigation of photon-electron interaction has been enabled by one unique technique called Photon-Induced Near Field Electron Microscopy (PINEM) developed in UEM to capture the evanescent electromagnetic field on its intrinsic time scale and nanometer scale.³ We recently established one state-of-art UEM scientific platform at the Center for Nanoscale Materials (CNM), Argonne National Laboratory. Besides the capabilities of imaging and diffraction, the UEM at the CNM is equipped with one GIF spectrometer, which enables it to work in energy filtering mode and record the PINEM image.⁴ Here, we investigated the excitation and localization of extended two-dimensional surface plasmon polaritons waves at the interface of metal and dielectric material including metal/dielectric interface with simple irregular nano holes or nano slots, and metal/dielectric interface with nanofabrication of nano hole array under excitation by ultrashort laser pulses using PINEM. The dependence of the SPPs on surface roughness, propagation distance, laser wavelength, fluence, and polarization was studied at the nanometer spatial scale and femtoseconds time scale. The results reveal that UEM is one powerful tool to study the SPPs at high spatiotemporal resolution of nanometer scale and femtoseconds time scale for the development and applications of SPPs-based photonic circuits such as waveguides, near-field optics, data storage, solar cells biosensing and optical communication.

1. Gramotnev, D.K.; Bozhevolnyi, S.I, Plasmonics beyond the diffraction limit. *Nature Photonics*, 4, 83-91 (2010).
2. Zewail A. H. Four-Dimensional Electron Microscopy. *Science*, 328, 187-913 (2010).
3. Barwick B., David J. Flannigan & Ahmed H. Zewail. Photon-induced near-field electron microscopy, *Nature*, 462, 902-904, (2009).
4. Haihua Liu, Thomas E Gage, Prem Singh, Amit Jaiswal, Richard D Schaller, Jau Tang, Sang Tae Park, Stephen K Gray, Ilke Arslan, Visualization of Plasmonic Couplings Using Ultrafast Electron Microscopy, *Nano Letters*, 21, 13, 5842–5849 (2021).

Work performed at the Center for Nanoscale Materials, a U.S. Department of Energy Office of Science User Facility, was supported by the U.S. DOE, Office of Basic Energy Sciences, under Contract No. DE-AC02-06CH11357.

9:15 AM EL08.15.02

ZnO-ZnWO₄ Eutectic Composites as Tunable Mid-IR Polaritonic Metamaterials Marco Centini¹, Emilija Petronijevic¹, Alessandro Bile¹, Dorota A. Pawlak², Concita Sibilila¹ and Maria Cristina Larciprete¹; ¹University of Rome, Italy; ²Ensemble3 sp. z o.o., Wolczynska, Poland

A wide branch of nanophotonics in the infrared (IR) range is based on the ability to excite surface plasmon polaritons (SPPs) at the interface between a metal and a dielectric. However, the use of metals restricts the SPP band to the visible/near IR, being the poor field confinement at longer wavelengths the main limitation. The development of a photonic platform in mid-IR range is crucial for applications like sensing the number of IR active vibrational fingerprints for the identification of trace levels of chemical and biological contaminants.

Recently proposed polarization sensitive applications in mid-IR relies on metamaterials and metasurfaces based on so called van der Waals (vdW) materials exhibiting strong anisotropy as well as natural hyperbolicity [1-2]. In the present work we investigated another interesting strategy, provided by the exploitation of self-assembled ZnO/ZnWO₄ eutectic composites [3]. In the visible range, the optical linear properties of these eutectic structures were found to exhibit a natural narrowband strong polarization dependence of the transmitted signal at $\lambda = (397 \pm 3)$ nm [4]. This effect is due to the refractive index matching of the two constituents so that, for some specific wavelength and polarization state, the composite medium appears homogenous while it produces strong scattering losses under all other conditions.

In the present work, we demonstrate that a similar polarization sensitive behaviour can be obtained, in reflection mode, at much longer wavelengths (around 11.6 μm).

We characterized the polarization dependent reflectivity spectra in the 2-16 μm range from several eutectic ZnO/ZnWO₄ samples [5]. The eutectic composites under investigation display a lamellar geometry with regions composed of ZnO alternating to regions of ZnWO₄. Reflectivity spectra have been recorded using a Fourier Transformed infrared interferometric (FTIR) microscope (Bruker Hyperion). During data acquisition, knife edge apertures were set to designate selected sample portion so to get defined area where lamellas display similar orientation. The obtained micro-FTIR spectra show that it is possible get a polarization sensitive reflection band by taking advantage of the optical phonon properties of ZnWO₄ and excitation of surface phonon polaritons at ZnO/ZnWO₄ interfaces.

Specifically, a high reflectivity band, corresponding to a phonon Reststrahlen band of the ZnWO₄ is located around 850 cm^{-1} (11.6 μm). The reflectance signal, measured under different polarization state of the incoming light, reaches its maximum value when the incident field is polarized along the direction of the lamellas. When the input field is polarized perpendicularly with respect to the lamellas direction, the corresponding reflectivity value is strongly attenuated. The strong reflectivity modulation of ZnO/ZnWO₄ system with polarization direction leads to reflectivity dynamic range as high as $\text{DR} = 72\%$.

Furthermore, preliminary optical images also indicate that improved lamellas thickness as well as area with better definition of lamellas lead to higher polarization sensitivity of the reflected signal.

In conclusion the complex, self-assembling, geometry arising in eutectic composites unveils extremely interesting optical properties both in the visible [4] and in the IR ranges [5].

The obtained experimental findings will make a valuable contribution in surpassing the wavelength limitations imposed by plasmonics. This advancement holds promise for a wide range of applications in the IR spectrum, including modulators, thermal radiators, tunable radiative cooling, thermal emitters, and advanced sensing capabilities.

1. Y. Poddubny et al. *Nat. Photon.* 7, 948 (2013)
2. S. Abedini Dereshgi et al., *Nat. Comm.* 11, 5771 (2020)
3. M. Tomczyc et al, *J Mater Sci*, 56,11219 (2021)
4. P. Osewski et al., *Adv. Opt. Mat.* 8, 7, 1901617 (2020).
5. E. Petronijevic, et al. *Adv. Mater.* f 2206005 (2022).

9:30 AMBREAK

10:00 AM EL08.15.03

Nonlocality and Loss in Nonreciprocal Photonics Enabled by Weyl Semimetals Morgan Blevins and Svetlana V. Boriskina; Massachusetts Institute of Technology, United States

Engineering new nonreciprocal optical devices is an important initiative in current photonics research. There is a desire to engineer new, nonreciprocal integrated photonic devices to replace the current standard of magneto-optic materials, which require bulky external magnets incompatible with many chip-scale device architectures [1]. Much research has been dedicated to modeling and designing nonreciprocal devices made from Weyl semimetals (WSMs) for next generation isolators and enhanced near-field radiative heat transfer devices [2]. However, as has been recently discussed [3], the impacts of nonlocality and loss on the proposed nonreciprocal Weyl devices close the window of one-way transport and render the realistic structures less useful than those initially proposed in the lossless, local regime. While loss and nonlocality are inherent to plasmonic devices, nonreciprocal Weyl devices with large figures of merit can be engineered by judicious combinations of external symmetry-breaking stimuli. To date, the qualitative impacts of loss and nonlocality have been mostly investigated in intrinsic time reversal-breaking WSM [4]. Here, we expand this analysis to time reversal- and inversion symmetry-breaking WSMs under a variety of *in situ* and *ex situ* stimuli, which either induce or enhance nonreciprocity. These stimuli include inhomogeneous strain and Fizeau drag via DC current bias. By evaluating the effect of various external stimuli that induce nonreciprocity in WSMs – as well as their combinations – we aim to identify a breadth of useful regimes for nonreciprocal and tunable WSM devices operation when realistic loss and nonlocality are accounted for.

[1] S.V. Boriskina, M. Blevins, S. Pajovic, There and Back Again: the nonreciprocal adventures of light, *Opt. Photon. News*, Sept. 2022.

[2] S. Pajovic, et al, Intrinsic nonreciprocal reflection and violation of Kirchhoff's law of radiation in planar type-I magnetic Weyl semimetal surfaces, *Phys. Rev. B* 102(16), 165417, 2020.

[3] Monticone and Gangaraj, Do Truly Unidirectional Surface Plasmon-Polaritons Exist?, *Optica* Vol. 6, Issue 9, pp. 1158-1165 (2019)

[4] Buddhiraju et al., Absence of Unidirectionally Propagating Surface Plasmon-Polaritons in Nonreciprocal Plasmonics., *Nat. Comm.* (2020) 11:674

This research has been supported by the Army Research Office (W911NF-13-D-0001), Lincoln Laboratory, Massachusetts Institute of Technology (ACC-777), and a Draper Fellowship to M.B.

10:15 AM EL08.15.04

An Active Metasurface Single-Pixel Lensless Imaging Device Julie Belleville, Prachi Thureja and Harry A. Atwater; California Institute of Technology, United States

We present a computational model that evaluates the performance of active metasurfaces as platforms for lensless imaging and find that an active metasurface with a 0.3 mm aperture size could capture images at >2 pixel/degree resolution across a wide field of view (FOV) of 120° . Our model optimizes the metasurface array configuration to obtain angular Hadamard and Fourier bases, and the results address the performance of an experimentally realized indium tin oxide (ITO)-based metasurface operating at telecom wavelengths.

Lens-coupled detector arrays are the basis for most of today's imaging systems but are not well suited to realized low-weight or small-footprint systems due to the weight and focal lengths of lenses. Lensless imaging—in which a modulator is coupled to a detector and modifies the detected light to enable computational image retrieval—offers an attractive alternative to lens-coupled detectors in applications requiring low SWaP (size, weight and power) devices or wide FOVs [1].

We investigate active metasurface elements to modulate light in a single-pixel imaging configuration. In contrast to passive metasurfaces that have set optical properties, the phases and amplitudes of active metasurface elements can be dynamically controlled via external stimuli which modulate their dielectric properties. In this study, we use the experimentally demonstrated performance of a field-effect tunable ITO-based metasurface at an operating wavelength of 1510 nm, with a phase tunability of 271°, covarying reflectance and phase, and modulation speeds exceeding 10 MHz [2][3]. The model and analysis, however, can be applied to various active metasurface platforms.

To determine the attainable performance of active metasurfaces in imaging, we use array-level inverse design, which was previously used to enhance beam steering performance [4]. We simulate the 1D far-field intensity of the metasurface using an array factor calculation and control the acceptance of light by optimizing the voltages applied at each element. Using a simulated aperture size of 0.3 mm (768 elements), we demonstrate a peak resolution of 4 pixel/degree and of 2 pixel/degree across a 120° FOV. We also show the suitability of active metasurfaces for compressed sensing, in which sparse images are recovered in fewer measurements than there are pixels. For this, we optimize the metasurface array configuration to obtain angular Hadamard and Fourier bases. In preliminary tests, our optimized Hadamard basis retrieves images with good agreement to the ground truth, with a power signal-to-noise ratio of 40 dB across 512 pixels. Additionally, we demonstrate the convolution of image processing filters across the FOV, which is desirable in classification applications. Our ability to produce grayscale filters distinguishes our platform from digital micromirror devices, which are often used in single-pixel imaging and support modulation speeds of ~20 kHz only for binary bases [5]. As resolution and FOV improve with metasurface size, we note that our current results are not an upper bound on performance.

As a next step, we will explore algorithms for 2D imaging and increase the realism of our model by modeling amplitude/phase errors, voltage discretization, and component reaction times. We will also report on an analysis of which imaging bases are best suited to active metasurfaces, and on the use of machine learning to correct for imperfections in basis construction. Finally, we will discuss the potential of active metasurfaces in multi-pixel lensless imaging applications.

- [1] V. Boominathan *et al.*, *Optica*, vol. 9, no. 1, p. 1, 2022.
- [2] Y.-W. Huang *et al.*, *Nano Lett.*, vol. 16, no. 9, pp. 5319–5325, 2016.
- [3] G. K. Shirmanesh *et al.*, *ACS Nano*, vol. 14, no. 6, pp. 6912–6920, 2020.
- [4] P. Thureja *et al.*, *ACS Nano*, vol. 14, no. 11, pp. 15042–15055, 2020.
- [5] G. M. Gibson *et al.*, *Opt. Express*, vol. 28, no. 19, p. 28190, 2020.

10:30 AM EL08.15.05

Biomaterial-Based Optical Metasurfaces and Cavities - Analysis and Sensing Richard M. Osgood, Jin Ho Kim, Peter Capuzzi, Margaret Peters, Ihsan Uluturk and Richard Pang; CCDC-SC, United States

New optical biomaterials such as biopigments and biominerals enable fascinating optical properties, such as bright and structural color and advanced camouflage. Arrays of isoxanthopterin nanoparticles in reflectors within shrimp eyes cause significant photonic backscattering, optimizing the sensitivity and spectral coverage of shrimp eyes. [1] Biominerals such as silicate in diatoms, strontium sulfate in radiolarians, goethite in limpets, magnetite in magnetotactic bacteria, and calcium phosphate in bones provide mechanical structure, sense magnetic and gravitational fields, and can store and mobilize iron. Biominerals are primarily non-toxic and environmentally friendly materials, generally with very high indices of refraction, especially for organic compounds. Biominerals are good candidates for optically sensing materials, because of their high index of refraction and non-toxic, scalable, and manufacturable properties. They are expected to be unregulated in the future due to lack of toxicological concern, unlike metal oxide nanoparticles, which are facing increasing amounts of regulation in manufacturing settings, due to concerns about potential carcinogenic nature from chronic exposure to workers in a manufacturing plant. Biominerals should be supply-chain resilient as well because they are straightforward and relatively simple to fabricate.

We have chemically synthesized the biomineral goethite (α-FeOOH), using a mixture of iron nitrate and tetramethylammonium hydroxide with an initial pH around 13. The reactant has a pure yellowish color, forms spinel rods that have 10-30 nm diameters and lengths in the range of 100-300 nm as determined by Scanning Electron Microscopy (SEM), exhibits the correct elemental composition for goethite in Electron Dispersive Spectroscopy (EDS), and powder x-ray analysis matches reference data from x-ray crystallographic data. 2-D photonic crystals were formed using 508 nm PS beads and were very iridescent, producing different colors at different angles. These photonic crystals had a bandgap in the red and transmitted light therefore had a yellowish-green color. A film of goethite was dropcast onto this 2-D array and registered an interesting drop in signal intensity when exposed to ethanol vapor, the analysis of which will be reported in this presentation. 1-D photonic crystal arrays consisting of alternating 70 nm PVA and 100 nm goethite layers were fabricated, show the expected multilayer peaks in reflectivity (7 maxima between 800 nm and 2500 nm), and considerable backscattering above 1100 nm. For wavelengths less than 1100 nm, the silicon substrate attenuated the backscattered light. Exposing this multilayer to glucose liquid, ethanol vapor, and humidity all results in an attenuated signal and possibly a peak shift. This peak shift was modeled and the wavelength shift per refractive unit change at the surface estimated, for detecting molecules like ethanol, water, and glucose. Single Fabry-Perot cavity films of goethite were also fabricated, thickness and optical indices measured with profilometry, spectrophotometry, and ellipsometry, and sensing results from these F-P cavities will be reported. We will also explain how, in the future, to make the biomineral-based sensing more sensitive and selective, using an embedded specific receptor in the photonic crystal and in thin films. Potential optical systems and detection methods using biominerals will be discussed.

- [1] Nat. Nanotech. 15 138 2020.

10:45 AM *EL08.15.06

Pushing the Limit of Multiplexing Capacity in Photonic Metasurfaces Yongmin Liu; Northeastern University, United States

Over the past decades, we have witnessed tremendous progress and success of photonic metasurfaces. By tailoring the geometry of the building blocks of metasurfaces and engineering their spatial distribution, we can control the amplitude, polarization state, phase and trajectory of light in an almost arbitrary manner. For practical applications such as high-capacity optical display, information encryption, and data storage, it is crucial to encode distinct functionalities into a single meta-device and increase the information channels. In this talk, I will present our recent works that aim to push the multiplexing limit in photonic metasurfaces through both physics-guided and data-driven approaches. In the first part of my talk, I will show that we can break the fundamental limit of polarization multiplexing capacity of metasurfaces by introducing the engineered noise to the precise solution of Jones matrix elements [*Science* 379, 294 (2023)]. We experimentally demonstrate up to 11 independent holographic images using a single metasurface illuminated by visible light with different polarizations. To the best of our knowledge, it is the highest capacity reported for polarization multiplexing. Combining our noise engineering method with the position multiplexing scheme, we design and demonstrate another metasurface that can generate 36 distinct images, forming a holographic keyboard pattern. In the second part of my talk, I will show that machine learning enables us to accelerate the development of complex metasurfaces (and other photonic structures) with high efficiency, accuracy and fidelity [*Nature Photonics* 15, 77 (2021)]. The developed machine learning models, after training, can evaluate the optical responses of metasurfaces and inversely design them in less than seconds. We propose to embed machine learning models in both gradient-based and non-gradient optimization loops for the automatic implementation of multifunctional metasurfaces [*Advanced Materials* 34, 2110022 (2022)]. Fundamentally different from the traditional two-step approach that separates phase retrieval and meta-atom structural design, the proposed end-to-end framework facilitates full exploitation of the prescribed design space and pushes the multifunctional design capacity to its physical limit. With a single-layer structure that can be readily fabricated, metasurface focusing lenses and holograms are experimentally demonstrated in the near-infrared region. They show up to eight controllable responses subjected to different combinations of working frequencies and linear polarization states.

11:15 AM EL08.15.07

Undoped Organic Semiconductors as a New SERS Platform Antonio Facchetti; Northwestern University/Flexterra Inc, United States

Nanostructured molecular organic semiconductor films are promising Surface-Enhanced Raman Spectroscopy (SERS) platforms for both fundamental and technological research. In this presentation we report that nanostructured films of oligothiophenes functionalized with different fluorinated alkyl or aryl groups demonstrate unprecedented Raman enhancement factor (>10⁵) and a low limit of detection (10⁻⁹ M) for the methylene blue probe molecule. This data is comparable to those reported for the best inorganic semiconductors and even intrinsic plasmonic metal-based SERS platforms. Photoluminescence spectroscopy and computational analysis suggest that both charge-transfer energy and effective molecular interactions, leading to a small but non-zero oscillator strength in the charge-transfer state between the organic semiconductor film and the analyte molecule, are required to achieve large SERS enhancement factors and low molecular sensitivities in these systems. Our results provide not only a considerable experimental advance in organic SERS figure-of-merits but also guidance for the molecular design of more sensitive SERS platforms based on organic (macro)molecules.

1:30 PM *EL08.16.01

Intelligent Meta-Imagers for Machine Vision Jason G. Valentine¹, Hanyu Zheng¹, Brandon Swartz¹, Xiaomeng Zhang¹, Greg Forcherio² and Yuankai Huo¹; ¹Vanderbilt University, United States; ²Naval Surface Warfare Center Crane Division, United States

Rapid developments in machine vision have led to advances in a variety of industries, from medical image analysis to autonomous systems. These achievements, however, typically necessitate digital neural networks with heavy computational requirements, which are limited by high energy consumption and further hinder real-time decision-making when computation resources are not accessible. Here, we demonstrate an intelligent meta-imager that is designed to work in concert with a digital back-end to off-load computationally expensive convolution operations into high-speed and low-power optics. The key to these architectures are the new freedoms afforded by metasurfaces such as optical edge isolation, polarization discrimination, and the ability to spatially multiplex, and demultiplex, information channels. I will discuss how these freedoms can be utilized for accelerating optical segmentation networks and objection classifiers, both based on incoherent illumination. This approach could enable compact, high-speed, and low-power image and information processing systems for a wide range of applications in machine-vision and artificial intelligence.

2:00 PM EL08.16.02

Inverse-Designed Metasurfaces with Oblique Helicoidal Cholesterics for Active Multicolor Holography Jooheon Kim and Junsuk Rho; Pohang University of Science and Technology, Korea (the Republic of)

Metasurfaces are composed of arrays of subwavelength structures and can provide fine wavefront-shaping platform with a compact form factor, resulting in both capability of diverse functionality and drastic miniaturization of the optical device. However, due to their low information capacity and passive nature, extensive studies focusing on overcoming these limitations have been conducted to achieve high information capacity [Science 379, 294-299 (2023)], spatial (wavefront) tunability [Science 364, 1087-1090 (2019)], and spectral (wavelength) tunability [Nat. Nanotechnol 16, 795-801 (2021)]. However, previous approaches cannot simultaneously achieve all these features. This manuscript provides the first report of simultaneous spatial and spectral tunable metasurface with high information capacity and its applications in dynamic multicolor holography. To this end, we propose unique combination of an inverse designed metasurface and a layer of oblique helicoidal cholesteric liquid crystal (ChOH) layer. The inverse design method enables the single-phase map encoding of 10 independent holographic images at different wavelengths. To the best of our knowledge, this represents the highest capacity reported for a single-cell metasurface. ChOH provides precise and free modulation of the reflected wavelength with a wide spectral range (420 nm ~ 720 nm) and narrow bandwidth (13 ~ 32 nm). Therefore, both holographic image and its color can be varied by applying programmed stimuli (electric field and temperature). Further, we believe that it is a simple and generalizable approach for interactive metasurface with high information capacity, spatial and spectral modulation. Moreover, this work can also be applied to a wide range of novel applications, including secret-sharing platform, hyperspectral imaging, and full-color 3D display.

2:15 PM EL08.16.03

3D Plasmonic Nanoarchitecture on Paper-Based Strip for Deep Learning-Assisted Human Urine Sensing and Cancer Screening Ho Sang Jung; Korea Institute of Materials Science, Korea (the Republic of)

Practical human biofluid sensing device is required to screen the patient from the normal group with high sensitivity and specificity. Especially, urine metabolite detection of cancer patient provides insights for early diagnosis and finding of new biomarkers. Here, 3D coral-like plasmonic nanoarchitecture (3D-CPN) is fabricated on a paper substrate as a urine test strip via direct one-step gold reduction process, which is available for quick urine absorption and metabolite filtration. The coral-like nanoarchitecture was grown with multiple grain boundaries forming particle-like protrusions (PPs), which were characterized by scanning electron microscopy (SEM), transmission electron microscopy (TEM), X-ray diffraction (XRD) and so on. The coral-like structure formation mechanism can be explained by successive primary particle-to-particle attachment process, such as oriented attachment and coalescence, following atomic diffusion. After preparation of the nano-structural model using conjugated gaussian random particle generation method, the optical characteristics of the 3D-CPN was investigated and compared with the experimental results. For clinical validation, the prepared 3D-CPN urine strip was used for label-free surface-enhanced Raman scattering (SERS) sensor to obtain metabolite signals from normal, prostate and pancreatic cancer urine. Statistical analysis was performed to verify the meaningful Raman peak positions related with cancer metabolites and then matched with metabolite candidates reported in previous literatures. Then, a typical deep learning method of convolutional neural network (CNN) was applied to classify the normal, prostate and pancreatic cancer after oversampling the train, validation and test sets. The confusion matrix showed the 95~97% accuracy for patient classification. This technology is expected to be applied for non-invasive multi-cancer analysis and also for other diseases after training the urinary signal.

2:30 PM EL08.16.04

Optical Fourier Surfaces for Holography Yannik M. Glauser¹, Patrick Benito Eberhard¹, Hannah Niese¹, Juri G. Crimmann¹, Valentina G. De Rosa¹, Nolan Lassaline^{1,2}, Daniel Petter¹ and David J. Norris¹; ¹ETH Zürich, Switzerland; ²Technical University of Denmark, Denmark

Controlling light is crucial for modern technologies, such as solar cells, biosensors, and optical communication. A common approach involves the fabrication of nanostructured surfaces with sub-wavelength feature sizes to manipulate electromagnetic fields through diffraction. However, current lithographic methods are typically restricted to “binary” surface profiles with only two depth levels, limiting their optical performance. Here, we overcome this limitation by exploiting thermal scanning-probe lithography to fabricate grayscale diffractive surfaces, known as optical Fourier surfaces (OFSs) [1]. We utilize these OFSs as reflective phase-only holograms in silver to control the amplitude and phase of the diffracted wavefront in the far field. Due to the non-trivial relation between the surface profile and diffraction output [2], an adapted Gerchberg–Saxton algorithm [3] is applied to inversely design the OFS holograms. Furthermore, we extend the concept of OFS holograms to diffract bound electromagnetic modes, such as surface-plasmon polaritons [4] and waveguided photons [5], to free space. This approach may provide expanded possibilities for holography, beam shaping, and optical display technology.

References:

- [1] Lassaline, N. et al. Optical Fourier surfaces. *Nature* **582**, 506–510 (2020).
- [2] Harvey, J. E. & Pfisterer, R. N. Understanding diffraction grating behavior, part II: parametric diffraction efficiency of sinusoidal reflection (holographic) gratings. *Opt. Eng.* **59**, 017103 (2020).
- [3] Gerchberg, R. W. & Saxton, W. O. A practical algorithm for the determination of the phase from image and diffraction plane pictures. *Optik* **35**, 237–246 (1972).
- [4] Dolev, I., Epstein, I. & Arie, A. Surface-plasmon holographic beam shaping. *Phys. Rev. Lett.* **109**, 203903 (2012).
- [5] Huang, Z. Q., Marks, D. L. & Smith, D. R. Out-of-plane computer-generated multicolor waveguide holography, *Optica* **6**, 119–124 (2019).

2:45 PM BREAK

3:15 PM *EL08.16.05

Van der Waals Nanophotonics for Deeply Subwavelength Optics Artur Davoyan; University of California, Los Angeles, United States

Van der Waals materials are of great promise for photonics and optoelectronics. In this talk I will discuss use of bulk van der Waals materials for controlling visible and infrared radiation. I will show that strong light-matter interaction within excitonic transition metal dichalcogenides, such as MoS₂, allows deeply subwavelength light confinement and manipulation. I will demonstrate passive nanophotonic devices that can confine and guide light in structures that are more than 16 times smaller than the wavelength. I will further present a combined near and far field imaging and discuss device efficiency. I will then discuss use of hexagonal boron nitride for controlling mid-infrared radiation. Specifically, manifestations of strong light-phonon coupling in hBN will be discussed and their use for creating deeply subwavelength resonators will be shown. I will then present first in-kind measurement of tunable hBN metasurface emitters which can cover over 2-micron band. Our studies suggest that smaller and more efficient devices may be created with the use of van der Waals materials.

3:45 PM EL08.16.06

Experimental Demonstration of Deep Learning-enabled Ultra-Broadband Epsilon-Near-Zero Perfect Absorbers David Dang, Sudip Gurung, Juan Manuel Raffo Calixto, Xuguo Zhou, Aleksei Anopchenko and Ho Wai (Howard) Lee; University of California, Irvine, United States

Epsilon near zero (ENZ) materials have gained interest in recent years due to their unique optical properties, such as their large optical nonlinearity, non-reciprocal magneto-optical effects, and specifically, perfect absorption of light. Transparent conducting oxides, in particular, hold promise as ideal ENZ material due to their tunable optical properties during the fabrication process. Broad perfect absorption of light can be achieved by creating a thin film stack of ENZ materials. However, the design of multilayer ENZ stacks is challenging due to the many

parameters involved, including the number of layers, thicknesses, ENZ wavelength, and optical losses.

Our machine learning-based approach enables us to efficiently search through the vast design space and experimentally verify the performance of the resulting thin film stack. In particular, we use a physics inspired generative neural network to optimize the thickness and optical properties of the thin film stack. Once we obtained the optimized thickness and optical properties, we used atomic layer deposition and spectroscopy techniques to fabricate and measure the meta-material. The resulting 2-layered AZO ENZ thin film stack achieved perfect absorption of light (> 98%) in the near-infrared region from 1500 nm to 2500 nm, highlighting the potential of machine learning techniques in designing ENZ materials for various applications.

SESSION EL08.18: Quantum Photonics and Emission Control
Session Chairs: Wen-Hui (Sophia) Cheng and Ho Wai (Howard) Lee
Friday Morning, December 1, 2023
Hynes, Level 3, Room 312

9:30 AM EL08.18.01

Highly Confined Surface and Epsilon-Near-Zero Phonon Polaritons in SrTiO₃ Nanomembrane Yin Liu¹, Alexey Kuzmenko², Ruijuan Xu¹, Iris Crassee² and Hans Betchelet^{1,3}; ¹North Carolina State University, United States; ²Université de Genève, Switzerland; ³Lawrence Berkeley National Laboratory, United States

Free-standing, wafer-scale, single-crystalline complex oxide membranes have enabled a new set of optical, electrical, and magnetic functionalities and structural and quantum phase transitions. Recent theoretical studies suggest that oxide perovskites nanomembranes support surface phonon polaritons with low-loss and strong confinement. In this work, we explore the SrTiO₃ nanomembrane as a photonic platform for phonon polaritons in the far-infrared regime. Our combined far-field and near-field infrared spectroscopic and nanoscopic studies reveal two types of phonon polaritons on a SrTiO₃ membranes transferred on gold and thermally oxidized silicon substrate, namely surface phonon polaritons and epsilon-near-zero (ENZ) polaritons. Radiative Berreman modes and bound ENZ polaritons confined within the nanomembrane are detected in the frequency window with epsilon zero, resulting from the deep subwavelength thickness of the membrane. Moreover, we reveal highly confined, propagating surface phonon polaritons through real-space hyperspectral nanoimaging. Surface polaritons with up to 7 times increased momenta as compared to surface polaritons of the same energy in bulk SrTiO₃ are detected. Our results suggest that perovskite oxide nanomembranes are promising two-dimensional polaritonic platforms within the terahertz regime.

9:45 AM EL08.18.02

Non-Local Effects in Epsilon Near-Zero Photonic Gap Antennas Boost Field Enhancement Felix Thouin¹, David M. Myers², Ashutosh Patri², Bill Baloukas², Antonio I. Fernández-Domínguez³, Ludvik Martinu² and Stephane Kena-Cohen²; ¹Photon etc, Canada; ²Polytechnique Montréal, Canada; ³Universidad Autónoma de Madrid, Spain

A material's non-local response to an electromagnetic field becomes important when its dimensions are comparable to the Fermi wavelength of electrons within. This regime is particularly relevant for optical antennas, where fields are confined to deep subwavelength regions of the device. Particularly, optical antenna devices based on epsilon-near zero (ENZ) materials are further susceptible to non-localities, given their long electronic Fermi wavelengths. Simulating the extent to which non-localities affect the performance of these devices is challenging as it requires a proper account of this complex phenomena along with conventional electromagnetics.

We observed the impact of non-localities on the far-field and near-field optical properties of epsilon near-zero photonic gap antennas (ENZ PGA). These devices consist of dielectric pillars (a-Si) within which a 10-nm thin slab of indium tin oxide (ITO) material is embedded. In these, hybrid dielectric-ENZ modes emerge from the strong coupling between the dielectric antenna modes and the thin film's ENZ mode. These hybrid modes efficiently couple to free space and strongly confine the incident electric field within the ITO slab over nearly an octave bandwidth. The far-field response of single ENZ PGAs is probed using hyperspectral dark field scattering spectroscopy (DFSS) and their near-field response using third-harmonic generation (THG). Sharp resonances invisible in DFSS are observed atop of a broad band in the THG efficiency spectra and shift when changing the dimensions of the antennas. Local simulations using conventional electromagnetics fail to reproduce this phenomenon and instead predict broad featureless THG efficiency spectra. However, in addition to yielding a better agreement with the experimental DFSS, non-local simulations using a local analogue model qualitatively capture the resonant character of THG efficiency spectra as well as their dependence on device geometry. This work opens up the possibility of leveraging non-local effects to further enhance electromagnetic field confinement in optical antennas. It shows how a proper theoretical account of non-localities in simulations is crucial to guide the design of these non-local devices.

10:00 AM BREAK

10:30 AM EL08.18.03

Simultaneous Control of Spectral and Directional Emissivity with Gradient Epsilon-Near-Zero InAs Photonic Structures Jae Seung Hwang, Jin Xu and Aaswath P. Raman; University of California, Los Angeles, United States

Controlling the spatial distribution of broadband far-field radiation is a challenging, but a fundamentally enabling capability in a broad range of applications such as thermophotovoltaics, thermal imaging and IR sensing. Here, we discuss a III-V semiconductor-based broadband directional thermal emitter where the angular and spectral response of the nanophotonic structure can be decoupled, in contrast to conventional beliefs. We demonstrate this capability by using the concept of plasmonic gradient ENZ materials, where the epsilon-near-zero (ENZ) frequency of the constituent plasmonic thin films vary spatially along the depth dimension. To show that plasmonic thin film based gradient ENZ materials enable arbitrary and simultaneous tuning of the spectral peak and operation range of the thermal emitter by changing the doping concentration range of the gradient ENZ layer, we compare two plasmonic gradient ENZ structures with the same total thickness of 300nm but different doping profiles. We compare two structures, structure 1 with a doping concentration of the gradient ENZ thin film ranging from $1.010^{18} \text{ cm}^{-3}$ to $1.910^{18} \text{ cm}^{-3}$ and structure 2 ranging from $2.010^{18} \text{ cm}^{-3}$ to $4.510^{18} \text{ cm}^{-3}$; the first structure demonstrating thermal beaming between 17.5 to 19.5 μm and the second structure between 12.5 to 15 μm . Here, we also observe that it is possible to control the operational bandwidth of the thermal emitter by introducing a larger spatial gradient of the doping concentration of the gradient ENZ layer. This highlights the remarkable control over spectral emissivity bandwidth that plasmonic gradient ENZ structures can provide by controlling the doping concentration profile of the gradient ENZ layer. Furthermore, we demonstrate the directional tunability of plasmonic thin film based gradient ENZ materials by controlling the total thickness of the gradient ENZ layer, where a third structure with the same doping concentration range as structure 2 but larger thickness of 900nm is used as the test sample: the high emission angular range of the 300nm structure was centered at 74, whereas the 900nm structure was centered at 66. This response originates fundamentally from the spatial shift of the optical mode supported by the thicker gradient ENZ photonic structure relative to the thinner one. As the total thickness of the gradient ENZ layer increases, the dispersion curve of the broadband Berreman mode moves to the left and thus will couple to modes from angles of incidence that are closer to normal incidence. We emphasize that in our approach a directional emitter has emissivity that is highly directional to the same set of angles, across an arbitrary bandwidth. By constraining directional emission to particular angular ranges over arbitrary spectral ranges, improved performance may be possible for a range of applications, including thermophotovoltaics, radiative cooling, and waste heat recovery. It is noteworthy that the lithography/patterning free, chip-scale geometry suggests that the plasmonic gradient ENZ structure can be incorporated with conventional scattering structures, opening up exciting possibilities to observe new optical phenomena where the narrowband resonance condition is relaxed. Ultimately, since these plasmonic gradient ENZ materials exhibit extraordinary modulation of their complex refractive indices as their carrier concentrations can be controlled by orders of magnitude by applying external fields, we believe that this configuration provides an avenue for on-demand control of broadband directional thermal emission, beam steering, as well as broadband non-reciprocal thermal emission.

10:45 AM EL08.18.04

Dimensional Patterning of CdO Thin Films for Plasma Frequency Tunability in Mid-IR Plasmonic Metamaterials Maxwell Tolchin¹, Angela Cleri¹, Mingze He², Kevin Wynne³, Khalid Hattar^{4,5}, Bhavesh Kumar Kamaliya⁶, Nabil Bassim^{6,6}, Joshua D. Caldwell^{2,7} and Jon-Paul Maria¹; ¹The Pennsylvania State University, United States; ²Vanderbilt University, United States; ³University at Albany, State University of New York, United States; ⁴The University of Tennessee, Knoxville, United States; ⁵Sandia National Laboratories, United States; ⁶McMaster University, Canada; ⁷Sensorium Technological Laboratories, United States

Dimensionally patterned monolithic cadmium oxide (CdO) thin films are accessible by high-power impulse magnetron sputtering (HiPIMS) coupled with donor defect doping via ion-beam modification. Although compositional platforms exist to dope graded structures in transparent conducting oxides (TCOs), they are conventionally complex and mostly limited in interface and structural competency. However, we demonstrate two ion-beam techniques of high energy ion bombardment (1-3 MeV) across micron-area grating masks and nanometer-scale ion implantation via focused ion beam (FIB) as facile approaches to spatially modulate CdO permittivity and effectively tune CdO plasma frequency in the mid-IR regime. High-energy bombardment generates donor dopant defects with exceptional transport properties: carrier densities of $2.5 \times 10^{19} \text{ cm}^{-3}$ to $2.5 \times 10^{20} \text{ cm}^{-3}$ and mobilities of up to 200 cm^2/Vs relative to the ion's displacement damage dose (DDD). Even upon pattern removal, well-defined optical and morphological interfaces are observed by far-field variable-angle reflectance spectroscopic dispersion maps. Near-field and atomic force microscopy supported by transfer matrix method (TMM) simulations. To further reduce grating feature size, preliminary FIB implantation indicates generated local and

controllable donor defects thermally activated with nanometer resolution between doped and undoped regions. These are indicated by Raman shifts and peak sharpness as carrier density and mobility are enhanced respectively. Also, we are currently systematically investigating mechanisms to CdO defect healing and donor activation based on temperature and environment. Overall, these ion-beam modification methods facilitate new dimensional patterning capabilities of CdO for tunable mid-IR plasmonic metamaterials.

11:00 AM EL08.18.05

Deterministic Positioning of Aqueous Quantum Dots for Single-Photon Emission Deepshikha Arora¹, Muhammad T. Pambudi^{2,3}, XiaoLiang³, LuDing² and JoelYang¹; ¹Singapore University of Technology and Design, Singapore; ²A*STAR, Singapore; ³Nanyang Technological University, Singapore

Colloidal semiconductor nanocrystals (NCs), commonly referred to as quantum dots (QDs), represent an innovative class of materials distinguished by their unique electrical and optical properties as well as notable antibunching behavior.¹ Consequently, colloidal QDs emerge as indispensable contenders for deployment in single photon devices, a crucial component facilitating various emerging applications in quantum information technology, quantum sensing, and quantum communication.² A pivotal advantage lies in their amenability to solution processing, offering substantial versatility and scalability for seamless integration across a diverse spectrum of material platforms and nanocavities.³⁻⁵ A significant aspect of nanophotonics is the coupling of NCs and nanoantennas. Realizing their full potential requires that the emitter be deterministically placed in the nanoantenna hotspot. Thus, the controlled assembly of nanocrystals is imperative for the incorporation of these materials into solid-state devices. Numerous assembly techniques have been explored, aiming to achieve precise nanocrystal positioning, high process controllability, scalability, and universality. However, most existing methods fall short of simultaneously accomplishing all of these objectives. In this work, we present a facile and universally applicable, high-yield method for depositing core-shell CdSe/CdS/CdZnS/SiO₂ QDs. This method leverages capillary-assisted slow evaporation in a saturated vapor environment induced by Marangoni flow, for deposition. Herein, polymer cavities are fabricated through lithographic techniques on various substrates. Following this, QDs are deposited into these cavities, and a lift-off process is then utilized to attain a clean background. Therefore, this technique can be effortlessly implemented for photonic integration on various substrates, including silicon (Si), gold (Au), and silicon nitride (SiN). Noteworthy advantages of this method encompass minimal sample requirements and the preservation of the QDs' optical properties through the requisite processes. We demonstrate a high-yield deterministic deposition, with ~60% representing single particles. Furthermore, this approach not only enables precise single nanocrystal patterning but also opens avenues for deposition and optical studies on both individual and small nanocrystal clusters, holding great significance for various applications.

References:

- (1) Nguyen, H. A.; Sharp, D.; Fröch, J. E.; Cai, Y.-Y.; Wu, S.; Monahan, M.; Munley, C.; Manna, A.; Majumdar, A.; Kagan, C. R.; Cossairt, B. M. Deterministic Quantum Light Arrays from Giant Silica-Shelled Quantum Dots. *ACS Appl. Mater. Interfaces* **2023**, *15* (3), 4294–4302.
- (2) Eich, A.; Spiekermann, T. C.; Gehring, H.; Sommer, L.; Bankwitz, J. R.; Schrunner, P. P. J.; Preuß, J. A.; Michaelis de Vasconcellos, S.; Bratschitsch, R.; Pernice, W. H. P.; Schuck, C. Single-Photon Emission from Individual Nanophotonic-Integrated Colloidal Quantum Dots. *ACS Photonics* **2022**, *9* (2), 551–558.
- Manfrinato, V. R.; Wanger, D. D.; Strasfeld, D. B.; Han, H.-S.; Marsili, F.; Arrieta, J. P.; Mentzel, T. S.; Bawendi, M. G.; Berggren, K. K. Controlled Placement of Colloidal Quantum Dots in Sub-15 Nm Clusters. *Nanotechnology* **2013**, *24* (12), 125302.
- (4) Xie, W.; Gomes, R.; Aubert, T.; Bisschop, S.; Zhu, Y.; Hens, Z.; Brainis, E.; Van Thourhout, D. Nanoscale and Single-Dot Patterning of Colloidal Quantum Dots. *Nano Lett.* **2015**, *15* (11), 7481–7487.
- (5) Zhang, Q.; Dang, C.; Urabe, H.; Wang, J.; Sun, S.; Nurmikko, A. Large Ordered Arrays of Single Photon Sources Based on II–VI Semiconductor Colloidal Quantum Dot. *Opt. Express* **2008**, *16* (24), 19592.

11:15 AM EL08.18.06

Near-Field Scanning Optical Spectroscopy of Known Gold Nanoaggregate Mohammad Kamal Hossain; King Fahd University of Petroleum & Minerals, Saudi Arabia

Nanoassembly of noble metal nanoparticles facilitates surface plasmon confinements and such localizations can coalesce and percolate due to a small variation in local nanogeometry. However, realizing such confinement by conventional microscopic and spectroscopic techniques has been challenging until now. We report near-field optical confinement observed by an aperture near-field scanning optical microscopy (a-NSOM). Three typical constructs of gold nanoparticles, viz., archetype dimer, nano-assembly of few nanoparticles and long-range two-dimensional (2D) nano-assembly were investigated. Surface-sensitive techniques such as near-field surface-enhanced Raman scattering (SERS) and near-field surface-enhanced two-photon-induced photoluminescence (TPI-PL) have been recorded using a-NSOM. Well-correlated optometry was confirmed amongst SERS, TPI-PL and shear-force topography of the abovementioned constructs tapping simultaneously at the very same spot of interest. Distinctive aggregates and 2D nano-assemblies of gold nanoparticles (~100 nm diameter) were fabricated by the “sandwich technique”, wherein the droplet on a silane treated cover-slip was sandwiched by another glass slide. Monomers, dimers and nano-assemblies of various sizes were confirmed by a field-emission scanning electron microscope. The specimens were spin-coated with Raman active dyes, Rhodamine 6G. A fs-Ti:sapphire laser ($\lambda=800\text{nm}$, $<100\text{fs}$, 80MHz) and He-Ne laser ($\lambda=632.8\text{nm}$) were coupled to the a-NSOM to carry out TPI-PL and SERS measurements. Au-coated tapered optical fibre was used to carry the excitations and act as an apertured probe (aperture ~ 50-100 nm) to scan the specimen. The emitted signals were collected by an objective lens and transferred to an avalanche photodiode (for single-channel detection) and/or to a polychromator-CCD (for multichannel detection). As expected, optical signals from SERS and TPI-PL were found to be confined and localized at the interstitials of dimers, whereas coalescence and hybridization of such nearby confinements for nano-assemblies were observed. For long-range 2D nano-assembly, optical confinements were more complex and homogeneously distributed apart from the edge effect in this context. Finite-difference time-domain (FDTD) simulations were carried out to validate the results obtained in this investigation. FDTD models were designed in such a way that the geometries and parameters closely represent the constructs under investigation and the a-NSOM setup. Such a direct observation with high spatial resolution is required to comprehend the origin of the localized electromagnetic (EM) field at the “hot-site” and the EM amplification factor in surface-sensitive optical processes. The author acknowledges the Interdisciplinary Research Center for Renewable Energy and Power Systems (IRC-REPS), Research Institute, King Fahd University of Petroleum and Minerals (KFUPM), Dhahran 31261, Saudi Arabia (Grant # INRE2215).

<quillbot-extension-portal><quillbot-extension-portal><quillbot-extension-portal><quillbot-extension-portal>

SESSION EL08.19/EL06.14/EL12.16: Joint Keynote Presentation V
Session Chair: Ho Wai (Howard) Lee
Friday Morning, December 1, 2023
Hynes, Level 3, Room 312

11:30 AM *EL08.19/EL06.14/EL12.16.01

Polaritonic Metastructures Andrea Alu; City University of New York, United States

In this talk, I will discuss our recent progress in the area of polaritonics, and its role in advancing the field of metamaterials and metasurfaces. Tailored material resonances, based on excitons, phonons, magnons and electronic transitions, can be strongly coupled to light in engineered metastructures, unveiling new degrees of freedom for the control of light-matter interactions and enhancing optical nonlinearities. In particular, I will discuss our recent progress on metasurfaces strongly coupled to vibrational and excitonic modes of van der Waals crystals, and control of magnon-exciton polaritons through the magnetic bias in tailored metastructures.

SESSION EL08.20: Quantum Photonics and Emission Control
Session Chairs: Andrea Alu and Ho Wai (Howard) Lee
Friday Afternoon, December 1, 2023
Hynes, Level 3, Room 312

2:00 PM EL08.20.01

In silico programming the atomic-scale metal gap junctions over wafer-scale substrates Kexin Wang¹, Yuhyeon Jung¹, Zhaoxuan Zhang¹, Suhui Zhang², Ling-Dong Sun¹, Chun-Hua Yan¹ and Wei Sun¹; ¹Peking University, China; ²Xiamen University, China

The ability of site-specific programming few atoms-spaced metal gap junctions on wafer enables the volume production of future atomic-scaled high-performance devices. Towards this projected milestone, bottom-up self-assembly of solution-synthesized nanoparticles exhibits unique capabilities in atomic-smooth interface and mesoscale programmable junction geometries, suggesting an alternative approach to conventional top-down lithography. Here, we report an effective strategy, i.e. deterministic assembly of nanoparticle arrays (DANA), to program the assembly of billion oriented nanoparticles on 2-inch wafer. Different from previous bottom-up approaches, DANA defines the geometries of diverse designer atomic-scale gap junctions and their positionings without using directional molecular linkers. DANA is generalizable to wide material selections and complex asymmetric patterns. Assembled gap junctions exhibit average spacing down to sub-10 atoms, smaller than the 12-nm gap spacing in the projected 2 nm technology node. The atomic-spacing gap junctions facilitate efficient charge transport different from direct tunneling, with performance superior to lithography-defined or thin film-assembled analogs. Hence, DANA bridges the atomic-smooth solution synthesis/assembly into wafer-scale high-performance devices, and complements to the resolution limit of conventional lithography.

2:15 PM EL08.20.02

Active Exciton Resonance Tuning for Ultrathin Free-Space Optical Modulators Tom Hoekstra and Jorik van de Groep; University of Amsterdam, Netherlands

Emergent optoelectronic technologies such as augmented reality and free-space optical communications call for ultracompact devices with dynamic control over their optical functionalities. This presents a problem, since conventional optoelectronics require bulky optical elements and filters to operate, thereby limiting the minimal device footprint. In recent years, optically resonant nanostructures and metasurfaces have enabled highly compact devices and optical coatings with tailored spectral, angular, and polarization responses. Nevertheless, active tuning of the optical response remains challenging, owing to the weak electro-absorptive and electro-refractive effects in traditional semiconductors and noble metals.

Here, we leverage highly tunable exciton resonances in 2D quantum materials to realize hybrid metasurfaces for active wavefront manipulation. We greatly enhance the excitonic light-matter interaction through coupling with guided mode resonances in dielectric metasurfaces. More specifically, we embed atomically thin WS₂ in an asymmetric Van der Waals heterostructure cavity and integrate it with a subwavelength grating. The resulting hybrid-2D metasurface exhibits highly tunable and near-unity excitonic light absorption at room temperature, which we leverage to realize an ultrathin free-space optical modulator.

We fabricate a heterostructure comprised of atomically thin WS₂ encapsulated by hBN on a Au back-reflector using an all-dry deterministic stamping technique. This method enables sequential stacking of the 2D layers onto the back-reflector, which we prepatterned on a SiO₂/Si substrate. As such, we circumvent direct lithography on the WS₂ flake, thereby largely preserving its pristine optical and electronic properties. Encapsulation of the monolayer with hBN also limits degradation caused by oxidation, environmental adsorbates, and nanofabrication of the grating.

Next, we integrate the heterostructure cavity with a nonlocal dielectric metasurface to maximize the excitonic light-matter interaction. We fabricate a subwavelength grating in the top hBN layer using electron-beam lithography and reactive-ion etching. The grating allows free-space radiation to couple efficiently to a guided mode resonance of the structure. The guided mode confines the field in the structure and therefore interacts strongly with the monolayer. By tailoring the modal dispersion to spectrally overlap with the exciton resonance, we greatly enhance the coupling efficiency at the operation wavelength. In fact, we achieve near-unity excitonic absorption at room temperature through critical coupling to the cavity mode.

Lastly, we employ electrostatic gating to actively manipulate the exciton resonance amplitude. In our device, the WS₂ monolayer is connected to ground, while the Au back-reflector is attached to a voltage source. By applying a gate voltage, we actively modulate the carrier density in the WS₂ via the field effect. By inducing strong n- or p-type doping in the monolayer, the Coulombic electron-hole interaction is effectively screened, and we observe a 90% reduction in excitonic emission at room temperature. We can actively and reversibly switch the device out of the critically coupled state by suppressing the exciton state, allowing for a large modulation depth in reflection. Altogether, our results demonstrate how exciton resonance tuning combined with strong light-matter interaction in hybrid-2D metasurfaces enables dynamically tunable and ultracompact optoelectronic devices.

2:30 PM BREAK

3:00 PM EL08.20.03

Plasmonically Enhancing 2D WSe₂ Light Absorption for Photodetection Serene Kamal¹, Andrew Bennett-Jackson², Rohit Srivastava³, Robert Bruce², Ekin G. Ozaktas¹, Chris Khoury¹, Ramesh Budhani³, David Shrekenhamer² and Susanna M. Thon¹; ¹Johns Hopkins University, United States; ²Johns Hopkins University Applied Physics Laboratory, United States; ³Morgan State University, United States

2D material semiconductors, specifically transition metal dichalcogenides (TMDs), have gained attention in recent years due to their unique and tunable electronic and optical properties at the monolayer and few-layer thicknesses. Because these materials are thin, low loss, and lightweight, TMDs such as WSe₂ are good candidates for flexible photodetector technology. However, unlike traditional semiconductors, TMD films cannot simply be made thicker to increase their absorptivity because their spectral response is a function of their thickness. Surface plasmonics are a nanoscale, size-tunable solution for enhancing light absorption in certain materials. By incorporating a periodic pattern consisting of nanoplasmonic structures on top of WSe₂ and tuning its design parameters, the performance of a WSe₂ photodetector can be greatly improved at targeted wavelengths.

In this work, Finite Element Method (FEM) simulations are first performed in CST Microwave Studio to design gold nanoellipse arrays as enhancement structures for 2D WSe₂ photodetectors. We simulate the coupling between the WSe₂ layer and the localized surface plasmon resonances of the patterned metal layer, and we show that the WSe₂ thickness (number of WSe₂ monolayers) strongly affects the behavior of these plasmonic resonances. By varying the Au nanoellipse size and lattice spacing in the plasmonic layer, we optimize the WSe₂ absorption enhancement at a targeted wavelength of 690 nm. We demonstrate an absolute theoretical WSe₂ absorption of 26% in a 5-layer WSe₂ film, which is over 3 times greater than the WSe₂ absorption without the plasmonic structures.

In addition to investigating traditional nanoellipses in our simulations, we also investigate their inverses, elliptical nanohole arrays. At a wavelength of 690 nm, we show that inverted nanohole arrays achieve a theoretical WSe₂ absorption of 24%, which is comparable to the optical enhancement achieved by the inverse nanoellipse design. These designs can be directly incorporated into the interdigitated electrodes of WSe₂ photoconductive photodetectors. This multifunctional electrode strategy could allow for more efficient charge extraction due to the generation of hot carriers associated with plasmonic excitation precisely at the charge extraction point, causing increased photocurrent.

We use our simulated designs to fabricate WSe₂ photoconductive photodetectors enhanced by plasmonic nanoellipse and nanohole arrays, and we investigate the impact of these designs on the light absorption, photoresponsivity and sensitivity in the devices. We fabricate devices consisting of Au nanoplasmonic arrays on epitaxially-grown WSe₂ using electron-beam lithography, and we characterize the photodetectors' photocurrent response and polarization dependence at 690 nm.

We demonstrate designs for plasmonic Au nanoellipse and nanohole arrays and calculate theoretical enhancement factors of up to 3 for absorption in 2D WSe₂. We use electron beam lithography to fabricate plasmonically-enhanced 2D WSe₂ photoconductive photodetectors and investigate these designs experimentally. These results should advance the field of next-generation sensors for flexible and wearable applications, and could be further applied to optical communications, photovoltaic, and environmental sensing technologies.

3:15 PM EL08.20.04

Plasmonic SERS Biosensor for Rapid and Accurate Bacterial Identification Jiwoo Ko and Yeon Sik Jung; Korea Advanced Institute of Science and Technology, Korea (the Republic of)

In 2019, an estimated 7.7 million people died from bacterial infections, accounting for 13.6% of all global deaths. This means that more than 1 in 8 deaths were due to bacterial infections, making it the second leading cause of death worldwide. Deaths from pathogenic bacterial infections are predicted to reach 10 million per year by 2050 due to the emergence of superbugs. Identifying the correct type of bacteria is critical for proper prevention and treatment.

Bacteria are categorized into cocci, bacillus, vibrio, spirilla, and spirochaetes based on their shape. While most bacillus (rod-shaped) bacteria are harmless, some, like Bacillus anthracis (causing anthrax) and Bacillus cereus (causing food poisoning), are deadly to humans. Identifying Bacillus species accurately is challenging due to their structural and genetic similarities (99.2-99.6%). PCR analysis is the industry standard, but it is accurate yet time-consuming. Rapid and accurate identification is crucial for high-risk pathogens, prompting the need for a faster analysis method.

Surface-enhanced Raman spectroscopy (SERS) is emerging as an alternative to PCR analysis for the detection of biomaterials. SERS is a rapid, highly sensitive, accurate, and selective identification of extremely trace amounts of analytes by significantly enhancing the Raman signal from plasmon resonance on metal nanosurfaces. However, because the SERS effect is strongest at the metal nanosurface and decreases with distance, SERS-based measurements of bacteria can only utilize information about limited outer regions such as the cell wall, cell membrane, and membrane proteins. Therefore, SERS is not known to be a suitable method for the analysis of relatively large biomaterials such as cells or bacteria.

In this study, we propose a bacterial pretreatment process to apply the high-potential SERS technique to bacterial identification and analyze the obtained Raman spectra to discriminate

between structurally and genetically similar bacteria. The proposed pretreatment process suitable for SERS is a hybrid lysis process consisting of a mechanical lysis process and a chemical lysis process.

Bacillus, Gram-positive bacteria, have a relatively thick cell wall layer, so mechanical lysis is primarily used to reduce the size of the macromolecule bacteria while releasing intracellular components. Alkaline lysis is used to further reduce the size of the analyte, including the crushed cell wall and intracellular components, and in particular, to denature the released DNA into single strands, making it suitable for SERS analysis.

In parallel, for Raman signal enhancement, we fabricated a 20 nm three-dimensional nanowire network using nanotransfer printing technology to fabricate nanodevices with ultra-high density hotspot regions where electromagnetic fields are enhanced. The presence of numerous factors in the pretreated bacterial samples, including small crushed cell walls and intracellular components, which can be located in the ultra-high density hotspot regions formed on the fabricated nanodevices, resulted in new signal peaks or enhanced signal results.

Finally, principal component analysis, which is used to analyze high-dimensional data, was performed to verify that discrimination of five structurally and genetically similar Bacillus bacteria was possible, confirming its applicability as a next-generation biosensor.

The proposed mechanical/chemical hybrid lysis process, which is an appropriate pretreatment process for SERS analysis of macromolecules, is applicable to large biological materials such as cells as well as bacteria. In addition, as a rapid analysis method with high accuracy, it can be applied beyond the public health industry to the high-tech bioindustry, and high-tech defense industry and is expected to be used in the medical field, such as early diagnosis of diseases.

3:30 PM EL08.20.05

Lattice Kerker Effect and Out-Of-Plane Anisotropic Radiation of Photoluminescence from Nanoparticle Array of Titanium Oxide with Tuned Packing Volume Makoto Higashino, Shunsuke Murai, Tien-Yang Lo and Katsuhisa Tanaka; Kyoto University, Japan

Surface lattice resonance (SLR) is a collective resonance induced by radiative coupling between localized resonances in periodically arranged nanoparticles. When the local scattering elements are Mie-resonators such as dielectric nanoparticles, Mie-SLRs are formed by coupling between local Mie resonances mediated via in-plane diffraction [1]. Because of the orthogonality of local magnetic and electric dipoles excited in each Mie resonator, their scattering fields extend to the orthogonal direction and couple to the diffraction modes that match the direction of field expansion. Especially, in rectangular lattice the spectral positions of magnetic and electric SLRs are tunable independently via periodicities along two axes.

The multipolarity of Mie resonances can cause an optical response known as the Kerker effect. In this effect, interference between the far fields deriving from electric and magnetic polarizations suppresses either forward or backward scattering. Rectangular lattices of Mie resonators are very suitable platforms for inducing the Kerker effect, i.e., lattice Kerker effect, because of the independent tunability of spectral position of magnetic and electric SLRs. Zero-backscattering has been reported numerically by carefully tuning the periodicity of one axis [2]. In this study, we focused on Photoluminescence control by utilizing the Lattice-Kerker effect in the square array of rectangle-shaped TiO₂ nanoparticles. We fixed the lattice periodicity while changing the length of one axis of TiO₂ nanoparticles in order to achieve mode crossing of electric and magnetic SLRs. We found asymmetric out-of-plane PL radiation from the light-emitting layer deposited on top of the array at the spectral and angular point where the lattice Kerker effect is achieved.

As a precursor of TiO₂, titanium nanoparticle array was fabricated on SiO₂ substrate by utilizing nanoimprint lithography. Then TiO₂ nanoparticle array was obtained by thermal oxidation of titanium nanoparticle array [3]. Excited resonances were attributed by measured and calculated optical extinction. PL enhancement of TiO₂ nanoparticle array was obtained by measured PL intensity of these arrays embedded in polymethyl methacrylate (PMMA) containing coumarin 153.

The optical extinction of TiO₂ nanoparticle array was measured through optical transmission at various incident angles. By using in-plane diffraction conditions that dominate SLR and calculated extinction through the finite element method, the peaks in the extinction spectra were attributed to electric and magnetic SLRs. In the angle-resolved extinction spectra, we confirmed the intersection of electric and magnetic SLR due to changes in the dispersion relation near $\theta_{in} = 0^\circ$ with increased packing factor of nanoparticles. The PL enhancement in the front and back of the array as a function of the emission angle was evaluated for each thickness of the emitter layer. Significant PL enhancement was observed at the intersection of electrical and magnetic SLR independent of film thickness. In addition, the PL enhancement at the front of the array was greater than at the back, given a certain film thickness. This result suggests a coupling of Lattice-Kerker effect and PL.

[1] S. Murai et al., *Adv. Opt. Mater.* **8**, 10902024 (2020)

[2] V. E. Babicheva et al., *Laser Photonics Rev.* **11** 1700132 (2017)

[3] S. Murai et al., *J. Appl. Phys.* **129**, 163101 (2021)

SESSION EL08.21: Virtual Session I
Tuesday Morning, December 5, 2023
EL08-virtual

10:30 AM *EL08.21.01

Lasing Polarization Control and Imaging with Reflective Metasurfaces Pin Chieh Wu; National Cheng Kung University, Taiwan

In this presentation, I will discuss two specific applications that utilize nanophotonic metasurfaces in reflection. Firstly, we propose the active modulation of the polarization state of a lasing emission at the source using a metasurface-engaged microcavity. This approach allows for generating highly circularly polarized, linearly polarized, or elliptically polarized lasing emissions. By leveraging the strong optical feedback produced by the Fabry-Perot optofluidic microcavity, we can enhance the interactions between light and metasurface atoms, resulting in polarized lasing emissions with high purity and controllability.

Secondly, we introduce and demonstrate a compact snapshot hyperspectral imaging system that incorporates the concept of meta-optics with small-data deep learning theory. Our snapshot hyperspectral imager utilizes a single multi-wavelength metasurface chip operating in the visible window of 500 to 650 nm, significantly reducing the device footprint. To showcase the high performance of our imaging system, we employ a multispectral imaging dataset as the input and through the deep learning-driven imaging system. We generate a hyperspectral data cube with exceptional fidelity through such an approach.

By elegantly integrating multi-resonant metasurfaces with other techniques, such as microcavities and computational imaging, we anticipate the development of low-profile advanced instruments for fundamental science studies and laser physics. This integration will bridge the gap between metasurfaces and microlasers, opening up new possibilities for practical applications.

11:00 AM *EL08.21.02

Exploring Light Absorption and Light Emission with Gold Microflakes Giulia Tagliabue; École Polytechnique Fédérale de Lausanne, Switzerland

In the last decade, optical nanoantennas have revolutionized light manipulation and control at the nanoscale. In particular, by engineering material and morphology it has become possible to shape light absorption and emission. While light absorption was initially considered a purely detrimental process in plasmonic nanostructures, the discovery of hot carriers has sparked great interest, leading to novel light-energy conversion pathways.

Monocrystalline gold microflakes offer interesting possibility for the study of light absorption and emission processes, seamlessly going from bulk metals to plasmonic nanostructures. We recently developed an advanced synthesis method that breaks the proportionality between lateral size and thickness of the gold microflakes [1]. As a result, it becomes possible to obtain on-substrate growth of large area (>100 μm) and ultra-thin (<30nm) gold monocrystalline films, uniquely bridging bottom-up and top-down nanofabrication processes. I will thus discuss the distinct features of hot carrier generation in these monocrystalline films as well as their performance in plasmonic photoelectrochemical devices. I will also show comparison with cm-scale plasmonic photoanodes for solar-driven redox cells [2]. Finally, I will report interesting experimental observations on photoluminescence emission from the flakes as well as theoretical analysis of these results.

References

[1] Kiani F., Tagliabue G. High Aspect Ratio Au Microflakes via Gap Assisted Synthesis, *Chemistry of Materials* 34 (3), 1278-1288

[2] Ma J., Oh K., Tagliabue G. Understanding Wavelength Dependent Synergies between Morphology and Photonic Design in TiO₂-Based Solar Powered Redox Cells, *Journal of Physical Chemistry C* 2022

11:30 AM *EL08.21.03

Tailored Spectro-Temporal Dynamics in Hot-Carrier Plasmonics Wenshan Cai; Georgia Institute of Technology, United States

Plasmonic metamaterials and metasurfaces can serve as a versatile arena for the investigation and utilization of optically excited, or plasmonically induced, energetic carriers. This is particularly intriguing when the decay pathways of hot carriers are rationally engineered with purposeful selections of the constituent materials and geometrical symmetries. The generation, transport, and relaxation of hot carriers also provide a novel route to active and nonlinear optical effects with ultrafast response rates.

Ultrafast optical switching in plasmonic platforms relies on the third-order Kerr nonlinearity, which is tightly linked to the dynamics of hot carriers in nanostructured metals. Although extensively utilized, a fundamental understanding on the dependence of the switching dynamics upon optical resonances has often been overlooked. Here we employ all-optical control of resonance bands in a hybrid photonic-plasmonic crystal as an empowering technique for probing the resonance-dependent switching dynamics upon hot carrier formation. Differential optical spectral measurements reveal an enhanced switching performance near the anti-crossing point arising from strong coupling between local and nonlocal resonance modes. Furthermore, entangled with hot-carrier dynamics, the nonlinear correspondence between optical resonances and refractive index change results in tailorable dispersion of recovery speeds which can notably deviate from the characteristic lifetime of hot carriers.

We further exploit hot-carrier dynamics to facilitate the creation of handedness-selectable transient chirality in achiral optical metasurfaces. As much as chiral metasurfaces are significant in stereochemistry and polarization control, tunable chiroptical response is important for their dynamic counterparts. A single metasurface device with invertible chiral states can selectively harness or manipulate both handedness of circularly polarized light upon demand, where in fact chiral inversion in molecules is an active research field. Tactics for chirality switching can be classified into geometry modification and refractive index tuning. However, these generally confront slow modulation speed or restrained refractive index tuning effects in the visible regime with forbidden 'true' inversion. Here, we reconfigure the 'optical' geometry through inhomogeneous spatiotemporal distribution of hot carriers as a breakthrough, transforming a plasmonic achiral metasurface into an ultrafast transient chiral medium with near-perfectly-invertible handedness in the visible. The photoinduced chirality relaxes through the fast spatial diffusion process of electron temperature compared to electron-phonon relaxation, empowering hot-carrier-based devices to be particularly suitable for ultrafast chiroptics.

Our comprehensive understanding provides new protocols for optically characterizing hot-carrier dynamics and optimizing all-optical light modulation and chirality manipulation for operations across the visible spectrum.

12:00 PM EL08.21.04

Large Magneto-Optic Response from Transparent Conducting Oxide Films near Their Epsilon-Near-Zero Frequency Jonathon Schrecengost¹, Angela Cleri¹, Maxwell Tolchin¹, Ramya Mohan², John P. Murphy¹, Sara Adamkovic¹, Alex J. Grede¹, Mario Imperatore¹, Patrick E. Hopkins², Jon-Paul Maria¹ and Noel Giebink^{1,3}; ¹The Pennsylvania State University, United States; ²University of Virginia, United States; ³University of Michigan—Ann Arbor, United States

Transparent conducting oxide (TCO) materials are promising for a variety of plasmonic and nanophotonic applications because their plasma frequency can be varied across the near- and mid-infrared spectrum via doping. In this work, cadmium oxide thin films doped with In or Gd ions are demonstrated as a promising magneto-optic (MO) material for integration of MO isolators, circulators, non-reciprocal linear to circular polarizers ("Faraday retarders"), and sensors in NIR-MIR Si photonics. Near the epsilon-near-zero (ENZ) condition, applied magnetic fields induce large differences between the refractive index of right and left-hand circularly polarized light, leading to correspondingly large Faraday rotations. Experimental data supported by theory show that doped CdO films have Verdet constants in the range of 10^5 - 10^6 deg T⁻¹ m⁻¹ that increase with wavelength up to the ENZ condition. The high optical mobility of CdO leads to >10x the Verdet constant and >100x MO figure of merit (rotation/loss) compared to other TCOs such as indium tin oxide (ITO). CdO films offer additional advantages over current state-of-the-art materials, such as high saturation fields (>3 T) that are achievable in photonic chip applications, an ENZ condition that is tunable over a broad range of mid-infrared wavelengths (2-10 microns), and the ability to sputter high quality films on Si.

12:15 PM EL08.21.06

Fabrication of Multi-Emissive Nanostructures using Two-photon Lithography for Photonics Applications Gaurav P. Singh¹, Arun Jaiswal¹, Sarika Joshi^{1,2}, Sweta Rani^{1,2}, Ajinkya Palwe¹, Sumit Saxena^{1,2} and Shobha Shukla^{1,2}; ¹Indian Institute of Technology Bombay, India; ²IITB-Monash Research Academy, India

Nanoscale structures enable unprecedented opportunities in innovating multifunctional devices, especially in nanophotonics, optoelectronics, and other related fields. It is desirable to tailor electromagnetic wave response by tuning size and morphology for niche photonics applications. The realization of such nanostructures depends on sophisticated, complex, time-consuming, serial, and conventional nanofabrication techniques like mask-based photolithography, electron beam deposition, and reactive ion etching. Additionally, precise fabrication of 3D nanostructures, especially control over z-axis features with the subwavelength resolution is challenging using above mentioned methods. There is a need to develop a facile three-dimensional fabrication protocol using new material formulations with embedded functionalization capabilities. In this context, we report the fabrication of multi-emissive nanostructures via two-photon lithography of multifunctional resin.

In this work, we present a multi-emissive polymeric resin comprising a commercially available acrylate-based resin and carbon nanomaterial (CNM). The formulated composite resin was exposed using a femtosecond (fs) laser to induce nonlinear absorption at the focal volume, which helps to create nanostructures with three-dimensional characteristics. The CNMs are multi-emissive with its optical activity retained in resin form as well as in polymerized micro/nanostructures under ultraviolet (UV) excitation. The fabricated structures, when examined under a fluorescence microscope at varying depths, exhibit uniform, bright emission, indicating uniform distribution of CNMs present in the composite resin. These multi-emissive micro/nanostructures are potential building blocks for photonics and can be applied in many areas, such as sensing, optoelectronics, and frequency-selective devices. These multi-emissive properties of the micro/nanostructures have a big impact on improving the field of photonics. Further, tailoring the dimensions of the micro/nanostructures pave the way towards the development of optically engineered next-generation photonic devices.

SYMPOSIUM EL09

2Ds Go Hybrid—Properties and Applications of Dimensionally Hybrid Systems
November 27 - December 7, 2023

Symposium Organizers

Valerio Piazza, Ecole Polytechnique Federale de Lausanne
Frances Ross, Massachusetts Institute of Technology
Alessandro Surrente, Wroclaw University of Science and Technology
Hark Hoe Tan, Australian National University

* Invited Paper
+ JMR Distinguished Invited Speaker

SESSION EL09.01: Quantum Platforms
Session Chairs: Anna Fontcuberta i Morral and Prineha Narang

1:30 PM *EL09.01.01

Layered Materials as a Platform for Quantum Technologies[Andrea C. Ferrari](#); University of Cambridge, United Kingdom

Layered materials are taking centre stage in the ever-increasing research effort to develop material platforms for quantum technologies. We are at the dawn of the era of layered quantum materials. Their optical, electronic, magnetic, thermal and mechanical properties make them attractive for most aspects of this global pursuit. Layered materials have already shown potential as scalable components, including quantum light sources, photon detectors and nanoscale sensors, and have enabled research of new phases of matter within the broader field of quantum simulations. I will discuss opportunities and challenges faced by layered materials within the landscape of material platforms for quantum technologies, with focus on applications that rely on light-matter interfaces [1].

1. A. R. P. Montblanch et al. *Nature Nano* 2023, 10.1038/s41565-023-01354-x

2:00 PM *EL09.01.02

Predicting Signatures of Unconventional Transport in Low Dimensional and Topological Quantum Materials[Prineha Narang](#); University of California, Los Angeles, United States

The re-invigorated field of electron hydrodynamics in quantum matter has recently garnered considerable scientific interest, both due to its technological promise of designing near dissipationless nanoelectronics, as well as its fundamental importance as an experimental probe of strong electron-electron interactions. Investigating the capacity to which observations of electron hydrodynamic flows can inform the nature of electron-electron interactions is particularly important and timely with the advent of spatially-resolved transport measurements which, having demonstrated the hallmark spatial signature of electron hydrodynamic channel flow, must now turn their attention to studying more spatially-complex geometries, enabling the observation of intricate fluid phenomena such as vortices. Recently we have explored the effects of crystal symmetry on electron fluid behaviors starting from the most general viscosity tensors in two and three dimensions, constrained only by crystal symmetry and thermodynamics. In our work we demonstrate the anomalous landscape for electron hydrodynamics in systems beyond graphene, highlighting that previously-thought exotic fluid phenomena can exist in both two-dimensional and anisotropic three-dimensional materials with or without breaking time-reversal symmetry. In this context, the first part of my talk will discuss our recent predictions of hydrodynamics beyond graphene, especially the role of phonons in hydrodynamics in Weyl semimetals. We identify phonon-mediated electron-electron interactions, computed with techniques recently developed that I will discuss in this talk, as critical in a microscopic understanding of hydrodynamics. The second part of my talk will introduce a new theoretical and computational transport framework, the SpARtANS (Spatially Resolved Transport of Nonequilibrium Species) framework. I will discuss applications of this method in nonequilibrium electron and phonon transport in low dimensional and layered quantum matter.

2:30 PM *EL09.01.03

Hexagonal Boron Nitride—An Intriguing Platform for On Chip Quantum Technologies[Igor Aharonovich](#); University of Technology-Sydney, Australia

Engineering robust solid-state quantum systems is amongst the most pressing challenges to realize scalable quantum photonic circuitry. While several 3D systems (such as diamond or silicon carbide) have been thoroughly studied, solid state emitters in two dimensional (2D) materials are still in their infancy.

In this presentation I will discuss hexagonal boron nitride (hBN) as an emerging platform for integrated quantum photonics. In particular, I will focus on emerging ways to deterministically engineer quantum emitters in hBN and discuss their photophysical properties. I will also highlight scalable pathways for integration of these emitters with on chip optical and photonic resonators. I will conclude by discussing a new class of spin defects in hBN, that operate as quantum sensors and can be used at room temperature. Hosted by an atomically thin lattice, the new spin defects poised to revolutionise the field of quantum sensing, by enabling true atomic proximity between the sensor and the analyte.

I will summarize by outlining challenges and promising directions in the field of quantum nanophotonics with hBN and its integration with other van der Waals structures.

3:00 PM BREAK

3:30 PM *EL09.01.04

2D Meets 1 and 3D: Opportunities and Open Questions.[Anna Fontcuberta i Morral](#); Ecole Polytechnique Federale de Lausanne, Switzerland

Since the discovery of graphene 2D materials have opened a new world of opportunities in a large variety of applications, ranging from electronics to energy harvesting. In this talk we walk through several examples in which 2D materials have enabled new functionality. We start by outlining the use of commercial graphene to integrate materials that otherwise would not exhibit any commercial lattice-matched epitaxial substrate. We then move by explaining how 2D materials can be integrated to 3D and 1D materials, forming heterostructures of hybrid dimensionality that involve highly heterogeneous materials. We explain how the functional properties of each part, strain and interface characteristics dictate the functionality of the whole and provide several examples.

4:00 PM *EL09.01.05

Control of Magneto-Optic Response in Van Der Waals Magnets via Strong Light-Matter Coupling[Vinod Menon](#)^{1,2}; ¹The City College of New York, United States; ²Graduate Center, The City University of New York, United States

van der Waals (vdW) magnets that host electronic excitations (excitons) correlated to the magnetic order present a unique opportunity to realize strongly coupled magneto-exciton-polaritons and thereby manipulate electronic and spin degrees of freedom via light. Here we report our recent work on such strongly coupled polaritons that show signatures of the underlying magnetic order. Specifically, we will discuss the formation of polaritons in antiferromagnetic insulator NiPS₃ and the use of polariton nonlinear spectroscopy to shed light on the nature of excitons in this system [1]. Following this, we will present our work on magnetic semiconductor, CrSBr where the excitons are naturally dressed by photons forming self-hybridized polaritons. We demonstrate the signature of coherent magnon oscillations on these polaritons and the potential to modify magneto-optical response by tuning the photon fraction of the polariton states [2].

[1] "Observation of spin-correlated exciton-polaritons in a van der Waals magnet, F. Dimberger, et al. *Nature Nanotechnology* 17, 1060 (2022).

[2] "Cavity-controlled magneto-optical properties of a strongly coupled van der Waals magnet," F. Dimberger et al. *arXiv:2301.07593* (2023) [in press - Nature].

SESSION EL09.02: Advances on Growth
Session Chairs: Young Joon Hong and Ernesto Joselevich
Tuesday Morning, November 28, 2023
Hynes, Level 2, Room 202

8:30 AM *EL09.02.01

Dimensionally Hybrid Nanostructures by Van Der Waals Epitaxy[Ernesto Joselevich](#), [Yarden Danieli](#), [Noya R. Itzhak](#), [Olga Brontvein](#), [Katya Rechav](#), [Lothar Houben](#), [Ifat Kaplan-Ashiri](#), [Iddo Pinkas](#), [Hagai Cohen](#), [Irit Rosenhek Goldian](#) and [Sidney Cohen](#); Weizmann Institute, Israel

Mixed-dimensional heterostructures with unusual optoelectronic properties are created by placing two materials of different dimensionalities together, but often without control of their interface at the atomic level. Nanoribbons and nanofins combine in themselves the 2D character of their atomically thin constituents with the 1D character that arises from their elongated structure. They can have unique optoelectronic properties too, but are difficult to produce with well-defined geometries and to assemble into ordered arrays for integration into devices. Our group has developed a series of epitaxial approaches for the guided growth of 1D nanostructures like nanotubes and nanowires with exquisite control of their orientation on surfaces. Here we extend this approach to create a variety of epitaxial mixed-dimensional nanostructures, including nanoribbons, nanofins and nanoplatelet-2D material heterostructures with a high degree of control at the atomic, nanoscopic and macroscopic levels, which enable their integration into devices. Under certain conditions, MoS₂ grows epitaxially on sapphire forming oriented hybrid nanoribbon-nanofin structures, which possess an advantageous geometry for fast and efficient photodetectors. CsPbBr₃ perovskite grows on ReSe₂ forming aligned rectangular nanoplates. Despite the highly symmetric cubic structure of the CsPbBr₃ perovskite, the nanoplatelets are elongated in one principal direction due to the broken symmetry of the ReSe₂ substrate. The CsPbBr₃ nanoplatelets on ReSe₂ have highly anisotropy tribological properties: They easily slide along their long axis, but are firmly locked along their short axis. Cross-sectional TEM shows

that the CsPbBr₃/ReSe₂ interface is highly mismatched and incommensurate in the long axis direction, as typical of van der Waals epitaxy, but it is highly coherent with very low mismatch in the perpendicular direction. This explains the anisotropic growth and sliding of the CsPbBr₃ nanoplatelets on ReSe₂. The electronic and optoelectronic properties of the mixed-dimensional heterostructure are characterized by a series of methods. Our work underscores the potential and richness of van der Waals epitaxy for the creation of dimensionally hybrid nanostructures and heterostructures with controlled shapes and orientations and their integration into devices.

9:00 AM EL09.02.02

Enhanced Crystallinity of ZnO Columns Grown on Monolayer MoS₂ via Compliant Substrate and Combinatorial Epitaxy YeonjooLee^{1,2}, XuejingWang¹, KyungtaeKim¹, BenjaminDerby¹, TerrenceMcGuckin³, GabrielCalderón⁴, MichaelT. Pettes¹, JinwooHwang⁴, YeonhooKim⁵, JeongwonPark⁶, AipingChen¹, KibumKang⁶ and JinkyongYoo¹; ¹Los Alamos National Laboratory, United States; ²University of Minnesota, United States; ³Ephemeron-Labs, United States; ⁴The Ohio State University, United States; ⁵Korea Research Institute of Standards and Science, Korea (the Republic of); ⁶Korea Advanced Institute of Science and Technology, Korea (the Republic of)

Numerous multi-dimensional architectures have been studied to realize reusable substrates using remote and van der Waals (vdW) epitaxy techniques. In order to prepare high-quality and transferrable semiconductor films, it is mandatory to understand behaviors of two-dimensional (2D) and three-dimensional (3D) materials in epitaxy techniques. We investigated growth behavior of a 3D material on a 2D material by growing ZnO on monolayer MoS₂ which is known that this 2D/3D heterogeneous integration is out of scope for remote and van der Waals epitaxy. We performed high-resolution transmission electron microscopy, grazing incidence wide-angle X-ray scattering, electron beam absorbed current microscopy, Raman microscopy, and photoluminescence measurements to correlate the microstructures and functional properties. This study revealed that random in-plane ordering was preserved while ZnO grew across the monolayer MoS₂ layers. By stacking multiple ZnO/MoS₂ layers, it was shown that inversion of crystallinity occurred; the crystallinity of the top ZnO layer was improved compared to that of the middle ZnO layer. This complex heterostructure can be explained by combinatorial epitaxy, grain alignment across atomically sharp interface, and a compliant substrate. The growth study enabled to form ZnO/MoS₂ heterostructure with type-I band alignment as the narrow band gap of monolayer MoS₂ serves as a charge carrier sink. Our findings provide insight to realize the 2D/3D heterostructure for highly functional device applications.

9:15 AM EL09.02.03

CMOS Compatible Single-Crystal 2D Material Growth by Geometric Confinement KiseokKim¹, DoyoonLee¹, SeunghwanSeo¹, JunyoungKwon², ChanghyunKim², MinsuSeo², Jin-HongPark³ and JeehwanKim^{1,2}; ¹Massachusetts Institute of Technology, United States; ²Samsung Advanced Institute of Technology, Korea (the Republic of); ³Pohang University of Science and Technology, Korea (the Republic of)

The innovations in Si-based complementary metal-oxide-semiconductor (CMOS) technology have a fundamental limit, which precludes achieving ultimate scaling and thereby meeting consumers' demands in the era of data explosion. Thus, for innovation beyond Si-based CMOS scaling, back end of line (BEOL) compatible new materials and the development of next generation transistors are urgently required. Recently, 2D TMD materials are attracting attention as channel materials for next-generation CMOS logic semiconductor devices, as they can outperform Si-based counterparts in terms of the scaling length and carrier mobility. However, despite the excellent performance of 2D TMDs, major obstacles remain in the commercialization of 2D materials; i) Deterioration of channel performance due to polycrystalline growth, ii) Requirement of epitaxial high-temperature growth and transfer process to form single-crystal channels etc.

In this study, we demonstrated the growth of non-epitaxial single-crystal 2D TMD materials at low temperatures by fabricating trenches on amorphous HfO₂-coated Si wafers. This technology enables the direct growth of single-crystal 2D materials on a Si wafer without a separate transfer process. This advancement significantly enhances the potential for integrating 2D materials into commercial CMOS technology.

9:30 AM EL09.02.04

Remote Epitaxy-Assisted Mixed-Dimensional Integration of 3D Complex-Oxides and 2D Materials SanghoLee, Jung-ElRyu, KiseokKim, XinyuanZhang, CelestaS. Chang, Min-KyuSong and JeehwanKim; Massachusetts Institute of Technology, United States

A new method for growing and releasing three-dimensional (3D) complex-oxide layers in a single crystal form through an atomically thin graphene interlayer, known as remote epitaxy, has revolutionized the heterogeneous integration strategies, which were previously limited due to stringent lattice and processing restrictions. However, the transfer of graphene, which is a typical process for forming graphene on growth substrates, inevitably introduces a significant number of unwanted defects such as wrinkles, holes, process residues, and interfacial contamination. Such defects can disturb the remote interaction between the substrate and epitaxial layer through graphene, reducing the crystal quality and exfoliation yield of membranes. Recently, we developed a direct synthesis method for growing alternative two-dimensional (2D) materials, such as transition metal dichalcogenides (TMDs), on epitaxial substrates, which enables the creation of wafer-scale, defect-free 2D interlayers for reliable remote epitaxy of spinel CoFe₂O₄ (CFO) and garnet Y₃Fe₅O₁₂ (YIG) thin films of high-quality. The atomically clean van der Waals interfaces formed by direct growth of TMDs onto epitaxial substrates offer an ideal platform for high-throughput production of single-crystalline, freestanding complex-oxide membranes that can be released from substrates, but also for facile fabrication of a new class of mixed-dimensional heterogeneous systems that exhibit emergent physical phenomena at well-defined 3D/2D heterointerfaces. Based on this unique approach to integrating mixed-dimensional heterostructures in a scalable and controlled manner, we demonstrate new device concepts that take advantage of unusual physical coupling or decoupling at exotic 3D/2D interfaces, which are both fundamentally intriguing and practically useful.

Acknowledgement

This work was supported by Korea Institute for Advancement of Technology (KIAT) grant funded by the Korea Government(MOTIE) (P0017305, Human Resource Development Program for Industrial Innovation(Global))

9:45 AM BREAK

10:15 AM +EL09.02.05

2D Materials-Based Remote & Van Der Waals Epitaxy for Heterogeneous Vertical Integration of RGB LEDs and Flexible LEDs Young JoonHong; Sejong University, Korea (the Republic of)

Epitaxy, a process to grow single-crystalline overlayers on wafers of diverse materials, has facilitated the commercial deployment of superior heterostructured electronic and optoelectronic devices. Increasing demand for multifunctional, high-performance devices on a single chip has led to a technological transition from miniaturization to high-density hetero-integration. This shift has catalyzed the development of stamping-printing and transfer-assembly techniques [1]. One approach to heterogeneous integration employs transfer-based assembly methods, requiring the delamination of epi-layers fabricated through different batches and procedures. This process encounters two significant technical obstacles when aiming for high-density integration of high-performance devices. Firstly, traditional epitaxial growth methods produce epi-layer devices strongly bonded to the substrate, making their separation challenging without resorting to high-power laser irradiation or chemical etchants. These separation techniques are known to cause damage to both the substrate and epi-layers, and their strict requirements restrict improved device performance and productivity [2]. Secondly, during the transfer and assembly process, diverse functional devices need to be divided into tiny chips before their precise transfer and assembly onto the target surface (or substrate). Even slight misalignment during chip bonding to backplane circuits can disrupt device interconnects with underlying layouts, thereby increasing the manufacturing costs of micro-LED displays. Additionally, fabricating higher-density vertical stack devices presents a formidable challenge, not only for high-resolution display production (such as augmented reality (AR) and metaverse devices) but also for hetero-integrated electronics. In this presentation, we examine an emerging epitaxy technique that eliminates chemical bonds between the epi-layer and wafer [3-5]. This method offers a potential solution via simple delamination of epi-layers and subsequent stacking of these layers, supplemented with precise photolithographic patterning procedures [4]. We will showcase our recent work on high-density heterogeneously integrated vertical R/G/B micro-LEDs and flexible devices utilizing this innovative epitaxy approach, highlighting potential applications in AR [6]. The remote epitaxy of spatially isolated micro-crystal LEDs has enabled the fabrication of deformable lighting devices [7]. The emerging epitaxy without chemical bonds could be readily employed to broaden the scope of the semiconductor manufacture, potentially leading to a heterogeneous system on a chip for all-in-one electronic and optoelectronics.

References

- [1] J. A. Rogers et al., Science 327, 1603 (2010).
- [2] H. Kum et al., Nat. Electron. 2, 439 (2019).
- [3] H. Kim et al., Nat. Rev. Methods Primers 2, 40 (2022).
- [4] Y. Kim et al., Nature 544, 340 (2017).
- [5] Y. J. Hong et al., Nano Lett. 12, 1431 (2012); Y. J. Hong and T. Fukui, ACS Nano 5, 7576 (2011).
- [6] J. Shin et al., Nature 614, 81 (2023).
- [7] J. Jeong et al., Sci. Adv. eaaz5180 (2020); J. Jeong et al., Nano Energy 86, 106075 (2021).

10:45 AM *EL09.02.06

Reduction in the size of devices is no longer an option for enhancing the performance of next-generation electronic products. Vertical stacking of wafers containing electronic devices, known as 3D heterogeneous integration, is being considered as the most promising strategy for further performance enhancement. However, this technique requires the following complex processes: i) drilling holes through the wafer (TSV), filling the holes with Cu, and bonding the wafers through bumps. Omitting wafers during such a complicated 3D stacking process would greatly simplify the process and minimize device loss. However, there are almost no options available to transfer active devices detached from the wafer and restack them together. The direct growth of device layers on top of finished circuitry is even more challenging. In this talk, I will discuss the unique strategies to transfer active device layers from the substrate and ultimately direct grow single-crystalline films on BEOL-processed wafer based on our signature 2D material-based layer transfer technique.

11:15 AM EL09.02.07

Area-Selective Deposition of Germanium on Patterned Graphene/Molybdenum Disulfide Stacks[JinkyungYoo](#)¹, [TowfiqAhmed](#)², [XuejingWang](#)¹, [MichaelT. Pettes](#)¹, [YeonhooKim](#)³, [YeonjooLee](#)^{1,4}, [JeongwonPark](#)⁵, [Woo SeokYang](#)⁶, [KibumKang](#)⁵ and [Young JoonHong](#)⁷; ¹Los Alamos National Laboratory, United States; ²Pacific Northwest National Laboratory, United States; ³Korea Research Institute of Standards and Science, Korea (the Republic of); ⁴University of Minnesota, United States; ⁵Korea Advanced Institute of Science and Technology, Korea (the Republic of); ⁶Korea Electronics Technology Institute, Korea (the Republic of); ⁷Sejong University, Korea (the Republic of)

Advances in multi-dimensional structures via epitaxy techniques have revealed that two-dimensional (2D) materials can be substrates of the conventional semiconductors, called as three-dimensional (3D) materials, for economical manufacturing and delivering novel functionalities. Integration of 2D materials into the existing device architectures is a key approach for 'More Moore' and 'Beyond Moore'. However, transfer of 2D materials onto the device architectures has been hindered by unintentional formation of wrinkles and absence of a way to remove the support media for the transfer. Therefore, direct growth of 2D materials on conventional materials and vice versa is a scalable and promising way to integrate 2D and 3D materials in an architecture. Growth of 3D materials on 2D materials has been hindered by low nucleation efficiency due to low density of surface dangling bonds on a 2D material. Here, we present area-selective deposition of germanium (Ge) on patterned graphene/MoS₂ stacks. Stacking graphene onto monolayer MoS₂ induces out-of-plane dipole moment due to charge transfer between the 2D materials. The out-of-plane dipole moment results in higher adsorption of germanium precursors. We performed density functional theory calculations of the out-of-plane dipole moment in the graphene/MoS₂ stack, chemical vapor deposition of Ge, and processing-dependent Ge nucleation behaviors on the graphene/MoS₂ stack.

11:30 AM EL09.02.08

Remote Epitaxial Growth of GaN Thin Films on Graphene Buffer Layer on SiC Substrates using Metalorganic Vapor-Phase Epitaxy[SeokjeLee](#)¹, [HanikKim](#)¹, [Bo-InPark](#)², [JekyungKim](#)², [HyunseokKim](#)², [Gyu-ChulYi](#)¹, [KysangLee](#)³ and [JeehwanKim](#)²; ¹Seoul National University, Korea (the Republic of); ²Massachusetts Institute of Technology, United States; ³University of Virginia, United States

High-quality inorganic thin films on flexible substrates are crucial for advancing the field of flexible devices such as wearable sensors, flexible displays, and electronic devices. Remote epitaxy on graphene-coated substrates has emerged as a promising methodology for creating these thin films, offering the potential for mass production of superior material platforms. However, the remote epitaxy of GaN thin films using the widely favored metalorganic vapor-phase epitaxy (MOVPE) has been challenging, mainly due to the degradation of the graphene by the harsh MOVPE growth environment and poor nucleation of GaN on graphene.

In this study, we demonstrate the successful remote epitaxial growth of GaN thin films on graphene buffer layer (GBL) on SiC substrates using MOVPE. The unique properties of GBL, including its strong adhesion to the SiC substrate and the quasi-2D surface that allows for epilayer release, make it a suitable candidate for enduring the harsh growth conditions of MOVPE and remote epitaxy. Moreover, the step edges of GBL, naturally formed by the SiC substrate during the graphitization process, provide numerous nucleation sites for GaN.

To identify the optimum conditions for GaN film growth on GBL, we investigated the nucleation and lateral growth of GaN, with an emphasis on varying growth parameters such as temperature, pressure, and precursor flow rates. Notably, we found that the step edges of GBL served as effective nucleation sites for GaN. The resultant films exhibited smooth surface morphology, and their high crystalline quality was confirmed through XRD and EBSD analyses. Additionally, we successfully exfoliated and transferred these films onto different substrates, fully preserving their properties.

This study opens new horizons for the large-scale production of high-quality, freestanding GaN membranes by overcoming previous challenges related to the remote epitaxy of GaN in the harsh MOVPE environment.

11:45 AM EL09.02.09

Engineering Defects in III-V Semiconductors Grown by Remote Epitaxy on Thin Amorphous Carbon[Ne MyoHan](#), [KuangyeLu](#), [HyunseokKim](#), [Seong HoCho](#) and [JeehwanKim](#); Massachusetts Institute of Technology, United States

Remote epitaxy has emerged as a facile technique for producing freestanding, wafer-scale membranes of single-crystalline semiconductors. However, it still encounters challenges but also presents other benefits when compared to direct epitaxy. In the case of growing epitaxial layers on the same or lattice-matched substrates, remote epitaxy results in lower material quality and higher defect density due to the attenuated atomic registry from the substrate. To address this issue, we propose the incorporation of thermal cycle annealing (TCA) and strained layer superlattice (SLS) into the growth process, which effectively reduces the threading dislocation density by a few orders of magnitude.

Conversely, when the substrate and epitaxial layer have a high lattice mismatch, remote epitaxy offers an advantage through the van der Waals interface, which provides an additional pathway to relax the strain developed in heteroepitaxial layers. This spontaneous relaxation mechanism significantly reduces the occurrence of misfit dislocations that are commonly observed in direct heteroepitaxy. By directly growing thin amorphous carbon (TAC) on GaAs, bypassing the need for a 2D layer transfer process, we can create an ultra-thin van der Waals interface that enhances the atomic registry of the epitaxial layer to the substrate while facilitating strain relaxation. In this study, we investigate the impact of TAC growth time on the material quality of remote heteroepitaxial InGaAs layers grown on GaAs substrates. The inherent strain relaxation capabilities offered by remote epitaxy enable the heteroepitaxy of high-quality membranes on lattice-mismatched substrates, paving the way for the fabrication of diverse electronic and optoelectronic devices.

SESSION EL09.03: Excitonic Platforms
Session Chairs: Michal Baranowski and Dehui Li
Tuesday Afternoon, November 28, 2023
Hynes, Level 2, Room 202

1:30 PM *EL09.03.01

Energy and Charge Transfer in Novel Hybrid Transition Metal Dichalcogenides/2D Perovskite Heterostructures[MichalBaranowski](#); Wroclaw University of Science and Technology, Poland

Van der Waals heterostructures are currently the focus of intense investigation, this is essentially due to the unprecedented flexibility offered by the total relaxation of lattice matching requirements, and their new and exotic properties compared to the individual layers. In this study, we present experimental and theoretical findings on hybrid transition metal dichalcogenide (TMD)/2D perovskite heterostructures. Our density functional theory (DFT) calculations reveal distinctive band alignment in these structures. Specifically, we observe that direct electron transfer between layers is hindered by the presence of the organic spacer in the 2D perovskite. However, the valence band forms a cascade from the TMD monolayer through the organic spacer to the PbI₄ octahedral layer, facilitating hole transfer. Optical spectroscopy studies further support these predictions, providing compelling evidence for both charge transfer and energy transfer between the layers.

Moreover, we demonstrate the presence of long-lived interlayer excitons in these structures, which inherits unique valley properties of WSe₂. By successfully achieving circular polarization of interlayer excitons, we highlight the efficient spin injection from WSe₂ into the 2D perovskite layer. These findings underscore the ability of TMD/2D perovskite heterostructures to engineer the band alignment for diverse excitation transfer processes, as well as spin injection and manipulation.

2:00 PM EL09.03.02

Magnetic Exciton-Polariton with Strongly Coupled Atomic and Photonic Anisotropies[QiuyangLi](#)¹, [XinXie](#)¹, [AdamAlfrey](#)¹, [YangLu](#)¹, [JiaqiHu](#)¹, [WenhaoLiu](#)², [BingLv](#)², [LiuyanZhao](#)¹, [KaiSun](#)¹ and [HuiDeng](#)¹; ¹University of Michigan, United States; ²The University of Texas at Dallas, United States

Anisotropy plays a key role in science and engineering. However, the interplay between the material and engineered photonic anisotropies has hardly been explored due to the vastly different

length scales. Here we demonstrate a matter-light hybrid system, exciton-polaritons in a 2D antiferromagnet, CrSBr, coupled with an anisotropic photonic crystal (PC) cavity, where the spin, atomic lattice, and photonic lattices anisotropies are strongly correlated, giving rise to unusual properties of the hybrid system and new possibilities of tuning. We show exceptionally strong coupling between engineered anisotropic optical modes and anisotropic excitons in CrSBr, which is stable against excitation densities a few orders of magnitude higher than polaritons in isotropic materials. Moreover, the polaritons feature a highly anisotropic polarization tunable by tens of degrees by controlling the matter-light coupling via, for instance, spatial alignment between the material and photonic lattices, magnetic field, temperature, cavity detuning and cavity quality-factors. The demonstrated system provides a prototype where atomic- and photonic-scale orders strongly couple, opening opportunities for photonic engineering of quantum materials and novel photonic devices, such as compact, on-chip polarized light sources and polariton lasers.

2:15 PM EL09.03.03

Bandgap Tunable Metal Oxynitride Nanosheets and Functions of Oxynitride/Oxide Superlattices-Like Hybrids[Shintaro Iida](#) and Kazuto Hatakeyama; Kumamoto University, Japan

Nanosheets have been studied as multi-functional nanomaterials for a wide range of applications. Controlling the bandgap of nanosheets remains a major challenge. Herein, we report bandgap tunable lanthanum niobium oxynitride nanosheets, which was prepared by exfoliation of layered perovskite oxynitride ($K_{1-x}LaNb_2O_{7-x}N_x$) via ion-exchange and two-step intercalation processes. The resulting $[LaNb_2O_{7-x}N_x]^{(1+x)-}$ nanosheets had homogeneous thickness (1.6 nm) and exhibited a variety of chromatic colors depend on the nitridation temperature including yellow, orange, and brown. The band gap energy of the nanosheet was tunable from 2.03 to 2.63 eV, and their band structures were determined by UPS, Mott-Schottky and photoelectrochemical measurement. In addition, well-organized superlattices are successfully prepared by a layer-by-layer assembly using two different oxynitride/oxide perovskite nanosheets ($LaNb_2O_{7-x}N_x/Ca_2Nb_3O_{10}$). Moreover, the superlattices-like restacked $Ca_2Nb_3O_{10}/LaNb_2O_6N$ hybrid showed proton conductivity and dielectric properties strongly influenced by the oxynitride nanosheets, and enhanced photocatalytic activity under visible light irradiation.

2:30 PM BREAK

3:00 PM *EL09.03.04

Interlayer Excitons in 2D Perovskite/Transition Metal Dichalcogenide Heterostructures[Dehui Li](#); Huazhong University of Science and Technology, China

The emergence of two-dimensional (2D) materials has intrigued a great deal of research on novel physical phenomena and various functional applications due to their particular crystal structures and reduced dimensionality. Chemical bonds between two layers of 2D materials are replaced by van der Waals forces, which are weak and do not require lattice match. Therefore, unlike 3D materials, bulks of 2D materials can be easily thinned to atomic thickness by mechanical exfoliation and atomically thin 2D materials can be arbitrarily stacked to form vertical van der Waals (vdW) heterostructures, which could inherit the unique characteristics of the constituent layers and even exhibit new properties not possessed by them. Particularly, when type-II vdW heterostructures are excited, the positive and the negative charges would reside in the different layers after the charge transfer but be limited within a short distance due to the strong quantum confinement effect of 2D materials, leading to strong Coulomb interaction and the formation of interlayer excitons (IXs). IXs are generally equipped with orientated dipole moment and long lifetime. Currently, studies on IXs are mainly focused on the vdW heterostructures formed by monolayers of transition-metal dichalcogenides (TMDs). Here, I will first talk about an alternate system, vdW heterostructures formed by 2D perovskites and TMDs, for studying IXs. Stacking different kinds of 2D perovskites and TMDs, formation of IXs is confirmed by excitation-power-, temperature-, electric-field-dependent and time-resolved photoluminescence (PL) studies. Notably, robust IX emission can be observed regardless of the stacking sequence and geometric alignment of the constituent layers, showing great advantages over the TMD/TMD vdW heterostructures, which require special twist-angle and thermal annealing. Then, I would like to give a brief introduction on widely tuning the IX emission energy by changing the layer number of the 2D perovskite or the TMD, which shed light on the application of 2D perovskite/TMD vdW heterostructures in broad-spectrum optoelectronics. Besides the layer number, I would like to next talk about how the selection of organic chains in 2D perovskites influences the properties of the IXs. By using chiral 2D perovskites, the IX emission shows substantial circular polarization and the polarization direction is only related to the chirality of the molecules regardless of the excitation scheme or any other external field, which could open up new passages for controlling valley- or spin-polarization of IXs. By introducing molecules with different dielectric constants, the dielectric screening strength in the vdW heterostructure is changed and hence the binding energy of the IXs is also modified, which offers great opportunities for exploiting tunable excitonic devices. Finally, I will also introduce IX as a non-destructive tool for probing the local phase transition at the surface of the 2D perovskite $(BA)_2PbI_4$ flakes. By spatially PL mapping of the $(BA)_2PbI_4/WSe_2$ heterostructure, two different IX species can be observed to distinguish the low-temperature and the high-temperature phase respectively, which offer a new route to regulate the phase transition of $(BA)_2PbI_4$.

3:30 PM EL09.03.05

Hybrid Charge Transfer Exciton at WS₂-Rubrene Interface[Yuchen Kan](#), Zhengyang Lyu and Parag Deotare; University of Michigan, United States

The low dimensionality and van der Waals nature of organics and transition metal dichalcogenides (TMDs) provide a unique opportunity to combine two disparate excitonic systems. This can lead to hybrid interfaces with photophysical properties that do not normally coexist in the individual material systems.

In this work, we investigate a hybrid type-II heterointerface formed between monolayer tungsten disulfide (WS_2) and single crystal Rubrene using optical spectroscopy at cryogenic temperature. We find that hybrid charge transfer excitons (HCTEs) are formed only when WS_2 monolayer is transferred onto the *bc* facet of orthorhombic Rubrene thin film single crystal. In addition, we observe that HCTE formation efficiency and energy is dependent on the twist angle between the monolayer and Rubrene crystal axes. Finally, polarization measurements reveal that HCTEs preserve spin-valley polarization of the WS_2 monolayer.

SESSION EL09.04: Poster Session
Session Chairs: Frances Ross and Alessandro Surrente
Tuesday Afternoon, November 28, 2023
Hynes, Level 1, Hall A

8:00 PM EL09.04.01

Van Der Waals Epitaxy and Thin Film Transfer using Sputter-Grown Two-Dimensional α -MoO₃[Sangho Han](#)¹, Sangho Lee², Xinyuan Zhang², Dohyun Ko¹, Deokyeon Lee¹, Sehyun Oh¹, Jeehwan Kim², Caroline A. Ross² and Dong Hun Kim¹; ¹Myongji University, Korea (the Republic of); ²Massachusetts Institute of Technology, United States

The manipulation of electronic, optoelectronic, and magnetic properties of oxide thin films by applying strain provides powerful functionality for future electronic devices. Strain originated from lattice or thermal expansion mismatches changes the physical properties of epitaxial thin films. But external strain by mechanical deformation of rigid substrates has been prohibited due to the low mechanical stability of single crystalline substrates, which limited the application of the epitaxial layers to flexible electronics. The low thermal stability of polymer-based flexible substrates has motivated the development of advanced lift-off technique of van der Waals or remote epitaxy using two dimensional layers.

We present the epitaxial growth of α -MoO₃ layers using sputtering for low cost and large area devices. The films grown at lower temperature and oxygen-free atmosphere showed randomly oriented growth while, they grew epitaxially on SrTiO₃ (001) substrates due to the coherent lattice constant along the in-plane at optimized deposition conditions. We detailed microstructure was investigated using an electron backscatter diffraction mapping and high-resolution transmission electron microscopy.

We also report the transfer of high temperature grown thin films using sputter-grown α -MoO₃ layers consisting of MoO₆ sheets with normal along the [010] direction bonded by weak van der Waals forces while the bonds within each layer are covalent and ionic. The metallic Au films on α -MoO₃ layer can be easily transferred to flexible supports by cracking the weak interface between the sheets using tapes or by dissolving the α -MoO₃ layer in heated water. We demonstrate that spinel-structured CoFe₂O₄ thin films with high crystallinity can be grown on α -MoO₃ layers and can be separated from substrates via mechanical exfoliation, which allows for the modulation of magnetic anisotropy of freestanding CoFe₂O₄ films by bending.

8:00 PM EL09.04.02

Collective States in 2D Molecular Monolayers[Sabrina Juergensen](#)¹, Moritz Kessens¹, Charlotte Berrezueta-Palacios¹, Nikolai Severin², Sumayyafland², Jürgen Rabe², Niclas S. Mueller³ and Stephanie Reich¹; ¹Freie Universität Berlin, Germany; ²Humboldt-Universität zu Berlin, Germany; ³University of Cambridge, United Kingdom

Molecules (0D) have long been known to interact through the dipole moments of their excited states, which may be exploited to create complex optical excitations. In recent years, great interest arose in combining them with 2D materials to design hybrid heterostructures with greatly tunable optical properties. Of particular interest are lattices of molecular monolayers that mimic 2D systems through ordered arrangement of 0D monomers. They can be thought of as a new material platform to replace and expand existing optically active 2D monolayers such as transition metal dichalcogenides (TMDs). Most organic monolayers are grown out of planar dye molecules that tend to form J-aggregates. In J-aggregates the transition dipole moments of the molecules are aligned resulting in a strong coupling of the molecules, forming a collective state. The photonic excitation of the collective states to higher electronic levels will result in a very

narrow and strong emission peak.

Theoretically and experimentally, we show how robust the collective state is against spatial disorder excited state quenching, and inhomogeneous broadening of the molecular transitions. Therefore, we grew monolayers of N,N'-Dimethyl-3,4,9,10-Perylene-tetracarboxylic diimide (MePTCDI), a perylene derivative, on two different van der Waals materials, few-layer hexagonal boron nitride and graphene. Both materials have a flat surface promoting the growth of dye monolayers providing a perfect platform to study the fundamental mechanism of collective states. High resolution AFM was used to determine the lattice structure that the molecules form in a monolayer. Showing a dense packed and highly ordered molecular structure. Optical spectroscopy and light scattering were used to characterize the collective state of the grown 2D material. We were able to measure the characteristic fluorescence for closely packed molecules, further we observed the vanishing Stokes shift between absorption and emission spectrum which is another characteristic for the presence of a collective dipole state. These findings make the molecular monolayers exciting platforms to implement designs of quantum optics in scalable devices.

8:00 PM EL09.04.03

Amorphous 2D Materials – A Novel Platform for Remote Epitaxy and Nanopatterned Epitaxy of III-V Semiconductors with Low Decomposition Temperatures KuangyeLu, HyunseokKim, Ne MyoHan, SanghoLee, YunpengLiu and JeehwanKim; Massachusetts Institute of Technology, United States

III-V semiconductor materials such as indium phosphide (InP) offer outstanding photonic properties that outperform silicon. However, the cost of InP wafers is considerably higher compared to commonly used semiconductor wafers like gallium arsenide (GaAs). While reusing original wafers can effectively reduce costs, traditional techniques for wafer recycling, such as chemical or mechanical lift-off, introduce significant expenses during fabrication, negating the cost savings achieved through wafer reuse. Besides, unlike other III-V materials such as GaAs, the epitaxial lift-off method for wafer recycling has not been extensively investigated for InP due to the lack of lattice-matched sacrificial layers with sufficient etching selectivity. Consequently, the reuse of InP wafers becomes more challenging.

Remote epitaxy and nanopatterned epitaxy have emerged as novel methods capable of facilitating the growth of III-V semiconductor membranes with single-crystal quality, as well as enabling easy exfoliation of these films. These breakthroughs offer a promising avenue for cost-effective wafer reuse. However, traditional approaches for transferring two-dimensional (2D) materials, utilizing polymethyl methacrylate (PMMA) or metal stressor layers to transfer materials grown on foreign substrates like copper (Cu) or silicon carbide (SiC), have been found to introduce defects and damages to both the 2D layer and the substrates during the transfer process. As a result, remote epitaxial and nanopatterned epitaxial films grown on these damaged 2D layers or substrates exhibit lower crystal quality and imperfect exfoliation, hampering wafer reusability and device performance. Additionally, the method of using grown thin amorphous carbon (TAC) for AlGaAs/GaAs is not suitable for InP, since the decomposition temperature of InP (< 600°C) is significantly lower than the growth temperature of TAC (700°C). Here we report the MBE growth of amorphous boron nitride (a-BN) on InP wafers at low temperature that enabled improved quality of remote epitaxial and nanopatterned epitaxial films and their perfect exfoliation. We show fully covered a-BN on InP substrates despite their low decomposition temperatures. The surface of a-BN coated InP substrate remains smooth with a RMS roughness of around 3Å. We also demonstrate 100% coverage of single-crystal InP thin films grown on a-BN, with the film's quality significantly improved compared to the case of transferred 2D materials. In addition, the growth and exfoliation were successfully repeated multiple times, proving the feasibility for InP wafer recycling. Through this low temperature MBE growth approach with remote epitaxy and nanopatterned epitaxy, we successfully demonstrate large-scale flexible thin film exfoliation and recycling of InP substrates, which will lead to new opportunities in InP thin film-based photonics and novel heterostructures with significantly reduced cost.

8:00 PM EL09.04.04

Remote Epitaxy of III-N Membranes on Amorphous Boron Nitride YunpengLiu¹, KuanQiao², WeiKong³, Bo-InPark¹, JekyungKim¹ and JeehwanKim¹; ¹Massachusetts Institute of Technology, United States; ²Intel Corporation, United States; ³Westlake University, China

Gallium Nitride (GaN) is a wide bandgap binary semiconductor material, which can be fabricated by epitaxy crystal growth such as MBE. GaN owns many physical properties such as wide bandgap and high breakdown electric field. These merits make GaN a promising material for devices such as Light-Emitting diode (LED) and High-Electron-Mobility Transistor (HEMT). Knowing the merits of GaN compared with other semiconductor materials, remote epitaxy appears as a new way to manufacture free-standing GaN films recently. Compared with other methods of fabricating free-standing film such as Laser Lift Off (LLO), Controlled Spalling and Epitaxial Lift Off (ELO), remote epitaxy has smoother lift-off interface, higher substrate reusability, thinner membranes and faster process.

So far, both graphene and Hexagonal Boron Nitride (hBN) have been shown in previous papers as promising 2D materials for remote epitaxy growth. Graphene can be transferred to the substrate from Copper (Cu) foil or SiC substrate or directly grown on the substrate by Chemical Vapor Deposition (CVD). Graphene transferred by PMMA (wet transfer) always results in polymer residuals on the graphene surface, which leads to bad epitaxial film quality. Although less residuals appear during dry transfer process (transferred by Nickle), the process results in the holes on the graphene, which can finally lead to the spall of the substrate during exfoliation. CVD grown graphene shows better graphene quality compared with transferred graphene. However, contaminations generated during sample transferring process between chambers, and graphene leads to high Carbon doping concentration. Besides graphene, hBN is also reported as the platform for remote epitaxy. However, unlike graphene, hBN is a polar material, which means epilayer is guided by the ionic field of the substrate as well as the hBN interlayer. Depending on the thickness of the transferred hBN, the epitaxial layer can be dominated by either of the two phases.

Aiming to solve the problems mentioned above, in situ MBE grown amorphous Boron Nitride (aBN) is developed as the 2D material for remote epitaxy. aBN is grown in MBE chamber with the help of high temperature effusion Boron cell and plasma assisted nitrogen source. aBN is a more transparent 2D material with no ionic field compared with hBN. Epilayer is purely seeded by the substrate in the remote epitaxy process. This MBE in situ grown aBN fully eliminates the contaminations generated during 2D material transferring process and sample reloading process. This technique enables the growth of ultrathin free-standing single crystalline GaN films. This high-quality free-standing film enables the high sensitivity Surface Acoustic Wave (SAW) sensor which can make a conformal contact on human skin. By transferring the GaN on a substrate with higher heat conductivity, GaN based device heat dissipation can be improved. Multiple GaN/aBN layers can be stacked together with single MBE growth to enhance the fabrication rate of the free-standing films. Furthermore, unlike normal epitaxy methods, the epilayer of remote epitaxy spontaneously relaxes due to the slippery surface of the 2D material. The Van der Waal force on the 2D material doesn't limit the relaxation like the covalent bond. Therefore, high quality relaxed InGaN can be obtained with this method.

The synthesis temperature of MBE grown aBN can go as low as 300 °C, which broadens the application field of aBN based remote epitaxy. In the future, this technique has the potential to be applied to more semiconductor materials.

8:00 PM EL09.04.05

Transfer-Free Graphene for High-Quality Wafer-Scale Free-Standing GaN Membrane by Remote Epitaxy JekyungKim, Bo-InPark, YunpengLiu, HyunseokKim, SeokjeLee and JeehwanKim; Massachusetts Institute of Technology, United States

To fabricate universal platforms for electronic and photonic devices with significantly reduced material costs, it is highly essential to realize free-standing membranes with successful separation of active materials from substrates. However, conventional techniques have their own drawbacks considering poor interface quality, difficulty in stack-up, or materials limitations. Recently, remote epitaxy has posed a remarkable potential that can ultimately overcome the existing challenges and produce high crystalline quality even with the simplicity in choosing the materials. 2D material (e.g. graphene) enables remote interaction between two materials and results in the "remote" epitaxial growth of the material (III-N, III-V, or complex oxides). In this study, we demonstrated an ultra-stable and transfer-free 2D platform using pseudo-graphene(pGr)/SiC in remote epitaxy of GaN. Our approach removed the process for fabricating conventional pGr by exfoliation and achieved wafer-scale high-quality free-standing GaN membrane. This can pave the way for realizing multiple wafer-scale GaN free-standing membranes with high-quality using a single SiC.

8:00 PM EL09.04.06

III-N Remote Epitaxy on Epitaxial 2D Materials Bo-InPark, JekyungKim, YunpengLiu, HyunseokKim and JeehwanKim; Massachusetts Institute of Technology, United States

The demand for semiconductor technology is rapidly increasing alongside the significant growth of industries such as communication, military, aviation, automobile, and high electric power. GaN and SiC-based compound semiconductors, known for their cutting-edge optical and power devices, are being recognized as the next-generation semiconductors with the potential to revolutionize the world. These compound semiconductors are already extensively utilized in various industries. Recently, the principle of "Remote epitaxy" technology has been discovered, capturing the attention of researchers in different epitaxy-related fields. Remote epitaxy, developed specifically for the epitaxial growth of high-quality compound semiconductor materials, takes advantage of the unique surface and physical characteristics exhibited by certain two-dimensional (2D) materials. Unlike existing epitaxy techniques, remote epitaxy stands out by enabling the production of freestanding membranes through easy separation and transfer from the substrate. Over the past few years, we have successfully demonstrated the viability of this technology and acquired scientific knowledge in fabricating diverse high-quality compound semiconductor materials.

In this research, we introduce the implementation of remote epitaxy for producing freestanding, high-quality single crystalline GaN membranes. We present the manufacturing process involving optimized 2D materials obtained through various epitaxy methods and thoroughly analyze their characteristics. The development of defect-free 2D materials through remote epitaxy has facilitated the fabrication of high-quality single crystalline membranes on a wafer scale.

8:00 PM EL09.04.07

Generalising Murray's Law for Materials BinghanZhou¹, QianCheng¹, ZhuoChen¹, ZeshengChen¹, DongfangLiang¹, EricA. Munro¹, GuolinYun¹, YoshikiKawai², JinruiChen¹,

Hierarchically porous materials benefit from their multi-level and interconnected pore networks by combining the advantages of efficient mass transfer and high specific surface area. Recently, Murray's law has garnered significant research interest as a promising tool for optimising hierarchy in porous materials.[1] This biomechanics principle describes optimal biological networks for transport.[2] The bio-inspired synthetic porous materials following this law, Murray materials, have been reported to excel in applications involving mass transfer processes. However, Murray's law is based on branching tubular networks found in biological systems, whereas synthetic pores in materials often exhibit complex geometries. This discrepancy in architecture undermines the strict application of Murray's law to synthetic materials.

Here we expand Murray's law for hierarchically porous materials. We extend Murray's law into a universal form and demonstrate its use in other hierarchical structure and transfer type. We further discuss the structural optimisation of several typical hierarchical networks and transfer types in porous materials, demonstrating this law's remarkable applicability and universality. We verify the optimal laminar flow predicted by Universal Murray's law in freeze-casted graphene oxide aerogel through experiments and simulations. Additionally, we demonstrate the practical value of this principle in gas sensors, where simply adjusting the macroscopic shape according to Murray's law improves response and recovery time. Our study therefore establishes a solid theoretical foundation for future Murray material development.

Reference:

[1] Zheng, X. et al. Bio-inspired Murray materials for mass transfer and activity. *Nat. Commun.* 8, 14921 (2017).

[2] Murray, C. D. The physiological principle of minimum work. I. The vascular system and the cost of blood volume. *Proc. Natl. Acad. Sci. U. S. A.* 12, 207-214 (1926).

8:00 PM EL09.04.08

Shape-Driven Variation of Photon Emission in Dimensionally Hybrid ML-TMDs/III-V NWs HeterostructuresClaireBlaga¹, MicheleZendrini¹, OsmanBalci², SachinShinde², SohamJoshi¹, VictorBugnion¹, AndreaC. Ferrari², AnnaFontcuberta i Morral^{1,3} and ValerioPiazza¹; ¹Ecole Polytechnique Federale de Lausanne, Switzerland; ²University of Cambridge, United Kingdom; ³École Polytechnique Fédérale de Lausanne, Switzerland

Transition metal dichalcogenides (TMDs) have high spin-orbit coupling (spin splitting energies between 0.1 and 0.5 eV [1]), exciton funneling [2] and strain modulation [3] which may allow them to be core semiconductors in a wide variety of devices. The ability to tune their properties by applying localized strain is appealing in fields ranging from electronics [4] to photonics [5], from spintronics [6] to optoelectronics [7]. The combination with 1D nanostructures could be used to control the strain distribution in monolayers (1Ls) as the morphological reshaping of the TMDs on nanowires (NWs) results in a localized strain [5,6]. III-V NWs can enable control over charge and exciton injection into 1L-TMDs. Heterostructures made of 1L-TMDs on horizontal III-V NWs exhibit interesting optical properties in view of the design of quantum emitter arrays [8]. However, the impact of material stacking, geometry and NW size on the strain distribution and the consequent effect on the optical properties must be clarified.

Here, we report on hybrid heterostructures made of 1L-WSe₂ on horizontal GaAs NWs. The 1L-WSe₂ is grown on sapphire by water-assisted chemical vapor deposition (CVD) using WSe₂ bulk as the precursor. Selective area epitaxy molecular beam epitaxy (SAE-MBE) is used to grow ordered arrays of faceted III-V NWs, differing by width and height and NW-to-NW distance. After GaAs surface passivation with ammonium sulphide, 1L-WSe₂ is placed on the horizontal NWs via wet transfer using polymethyl methacrylate as the support layer. Micro-photoluminescence and Raman mapping are performed at room and low temperature to outline the variation of optical features with the NW array parameters. Numerical simulations support the strain distribution description, consistently with the experimental optical maps.

References

[1] Bangar et al., *ACS Appl. Mater. Interfaces* 14, (2022)

[2] Moon et al., *Nano Lett.* 20, (2020)

[3] Manzeli et al., *Nat.Rev.Mater.* 2, (2017)

[4] Datye et al., *Nano Lett.* 22, (2022)

[5] Palacios-Berraquero, *Nat. Commun.* 8, (2017)

[6] Mukherjee et al., *Nat. Commun.* 11, (2020)

[7] Lopez-Sanchez et al., *ACS Nano* 8(3), (2014)

[8] Jasinski et al., *2D Mat.* 9, (2022)

8:00 PM EL09.04.09

Low-Barrier Heterojunction of Layered Sb₂Te₃ on Si for Low Resistance n-Type ContactsNaoyaOkada, ShogoHatayama, Wen HsinChang, YutaSaito and ToshifumiIrisawa; National Institute of Advanced Industrial Science and Technology, Japan

In advanced CMOS, the transistor performance is becoming highly dependent on the contact resistance at the source/drain with recent extreme scaling. To reduce the specific contact resistivity, a low Schottky barrier height at the metal/semiconductor interface is required; however, it is well known that most metal/Si junctions always show a high electron Schottky barrier height to n-Si owing to the Fermi-level pinning in the range between the mid gap and the valence band edge. This fact imposes a fundamental difficulty in obtaining low contact resistance and further high performance in Si n-FET.

We have recently demonstrated van der Waals stacking of Sb₂Te₃ on MoS₂, and additionally achieved significant device performance enhancement of MoS₂ n-FET using the Sb₂Te₃ contact at source/drain thanks to the significant reduction of the contact resistance [1]. These findings motivated us to investigate the junction properties of Sb₂Te₃ on Si. In this work, we demonstrate the low barrier height of the Sb₂Te₃/n-Si junction. To evaluate potentials of Sb₂Te₃ as the source/drain contacts in n-FET and p-FET, we prepared the W/Sb₂Te₃/Si junctions. Here, the Sb₂Te₃ with a thickness of 20 nm was prepared by magnetron sputtering in pure Ar onto the n- and p-type Si substrates (~1-10 Ωcm), and then the W electrode with a thickness of 30 nm was successively formed onto Sb₂Te₃ in the same deposition system. The formed Sb₂Te₃ films have a layered structure on Si, and they are stable against annealing up to 400 °C. Control samples of W/Si direct junctions showed a high electron barrier height of 0.65 eV and hole barrier height of 0.41 eV, owing to the Fermi-level pinning at the Si surface. These resulted in rectifying behavior both for n- and p-Si. In contrast, the current-voltage characteristics of Sb₂Te₃/n-Si junction was found to become ohmic, while the only Sb₂Te₃/p-Si junction was rectifying with the hole barrier height of 0.81 eV. These results suggest that the Fermi level in the Sb₂Te₃/Si junction is close to the conduction band edge of Si.

In conclusion, a clear reduction in an electron barrier height was obtained by the insertion of Sb₂Te₃ between W electrodes and n-Si substrates. This low electron barrier height will be useful in the n-FET. Thus, the Sb₂Te₃ film is a promising contact material for the source/drain in the advanced Si CMOS transistors.

Reference: [1] W. H. Chang et al., *Adv. Electron. Mater.* 2201091 (2023).

8:00 PM EL09.04.10

Composition Control of Two-Dimensional Cu_{2-x}S/CdS Heterostructured Nanoplates via Cation Exchange Reaction for Photocatalytic Hydrogen Generation under Visible LightKodongBang, BumjinPark and HyunjoonSong; Korea Advanced Institute of Science and Technology, Korea (the Republic of)

Solar-to-fuel conversion using semiconductor materials has long been studied as a promising sustainable and clean energy solution. Among various reactions, photocatalytic hydrogen generation holds significant potential for the development of clean and renewable energy sources. To enhance the efficiency of photocatalytic activity, heterostructures has been explored to reduce electron-hole recombination and promote increased charge separation efficiency. In this study, we present the controlled metal ratio of two-dimensional Cu_{2-x}S/CdS heterostructured nanoplate achieved through a cation exchange reaction. By adjusting the composition ratio, we investigated the photocatalytic activity and focused on the optical and photochemical properties. Notably, a 65% of Cd content of Cu_{2-x}S/CdS heterostructured nanoplate exhibited the highest photocatalytic activity, surpassing that of a similar one-dimensional Cu_{2-x}S/CdS system. Our observation provides a guideline to the rational design of semiconductor-semiconductor heterojunctions in two-dimensional nanostructures for enhanced photocatalytic activity.

8:00 PM EL09.04.11

Synthesis and Characterization of TiO₂-GO Hybrid via Femtosecond Laser Irradiation in Liquid for Enhanced Photocatalytic Applications under Visible-LightBersuBastug Azer, AhmetGulsaran, RezaKarimi, JosephSanderson, MichaelPope and MustafaYavuz; University of Waterloo, Canada

In the pursuit of efficient photocatalytic materials, the integration of titanium dioxide (TiO₂) with graphene oxide (GO) has emerged as a promising strategy. Herein, we present a novel and environmentally friendly method for synthesizing a TiO₂-GO hybrid through laser irradiation in liquid. This technique offers simplicity, greenness, and remarkable control over the heterostructure's properties depending on the laser parameters.

The TiO₂-GO hybrid was fabricated by ultrasonication of TiO₂ nanoparticles and GO in a liquid medium, followed by femtosecond laser irradiation. The resulting heterostructure was

characterized using various techniques. The structural properties were investigated through X-ray diffraction (XRD), Raman spectroscopy, and BET analysis. The XRD patterns confirmed the successful integration of TiO₂ and GO, while Raman spectroscopy revealed a strong interface formation between the two materials. BET analysis demonstrated increased surface area in the hybrid structure. To evaluate the optical properties, UV-Vis spectroscopy was employed. The absorption spectra exhibited enhanced light absorption in the visible range, indicating efficient utilization of visible light for photocatalytic processes. The band gap energy of the TiO₂-GO hybrid was estimated using the Kubelka-Munk function, revealing a reduced band gap compared to pure TiO₂. This band gap narrowing enables the hybrid to harness a broader spectrum of light, enhancing its photocatalytic activity under visible light illumination. Moreover, the morphology of the TiO₂-GO hybrid was examined using scanning electron microscopy (SEM). The SEM images showcased a well-dispersed and interconnected structure with intimate contact between TiO₂ nanoparticles and GO sheets.

In summary, our laser irradiation in liquid synthesis approach enables the fabrication of a TiO₂-GO hybrid with outstanding properties for photocatalytic applications. This green and straightforward technique results in a heterostructure that exhibits enhanced photocatalytic performance under visible light, surpassing the capabilities of TiO₂ and GO individually. The comprehensive characterization of the hybrid's optical, structural, and morphological properties validates its potential for highly efficient photocatalytic applications.

8:00 PM EL09.04.12

Artificially Intelligent Formaldehyde Sensing using Printed Graphene-Based Aerogels[ZhuoChen](#), BinghamZhou, TyneeBhowmick and TawfiqueHasan; University of Cambridge, United Kingdom

The identification and analysis of formaldehyde as a hazardous air pollutant in indoor environments present an immediate and critical concern. The endeavour to achieve real-time recognition of formaldehyde in the presence of interfering gases represents a formidable challenge, particularly for room temperature sensors that are susceptible to noise and baseline drift. Exploring the unique properties of dimensionally hybrid systems based on graphene and leveraging artificial intelligence (AI) offer promising pathways.

In this study, we tackle these challenges by utilising the 3D-printed porous structure of graphene-based aerogels as interconnected frameworks for rapid gas diffusion and sensitising the aerogels with tin oxide quantum dots (QDs) for high-performance chemical sensing at room temperature. Through reaction-coupled diffusion modelling of both filament-structured and film-like aerogels, we explain and experimentally demonstrate the superior gas-sensing capabilities of thinner filaments with higher surface porosity. With optimised morphology and doping of the printed structures, we achieve an outstanding response of 15.23% towards 1 ppm formaldehyde at room temperature.

Furthermore, we explore the versatility of different structures and chemical doping to construct gas sensor arrays capable of distinguishing formaldehyde from ammonia and nitrogen dioxide. To enable real-time gas species classification, we develop gas recognition algorithms based on dynamic response features that are independent of steady-state response or testing sequences. These algorithms demonstrate remarkable accuracies, even in the presence of significant noise and baseline drift. Our findings present a novel artificially intelligent solution for the detection and real-time identification of formaldehyde at room temperature, offering promising prospects of graphene-based aerogels for addressing this pressing environmental issue.

8:00 PM EL09.04.13

Introduction of Low Dimensional Charge-Boosters into Graphene Oxide Nanochannels for Energy Harvesting[Ki HyunLee](#), HyeonhooLee, WoojaeJeong and Tae HeeHan; Hanyang University, Korea (the Republic of)

Osmotic energy, a potential source of electricity from salinity differences in water, relies on ion-exchange membranes to convert salt gradient energy into electric power. However, these membranes encounter challenges, including inadequate charge densities and resistance to mass transfer. Recent efforts have focused on enhancing ion-selective membranes using materials like polymers, metal oxides, and frameworks. Two-dimensional (2D) nanosheets, such as graphene and boron nitride, have shown promise, featuring nanochannels with controlled thickness. These structures exhibit an electrical double layer that enhances ion transport. Utilizing reverse electrodialysis (RED), 2D nanochannel membranes demonstrate high ion conductance and osmotic power extraction. However, the challenges also arise from the intrinsic limitations of 2D nanomaterials, including relatively low surface charge densities and mass-transfer resistance, which hinder their effective integration into RED systems. In this study, we used negatively charged graphene quantum dots (GQDs) and polyelectrolyte nanorods to boost the charge density of graphene oxide (GO) nanochannels. Charged GQDs and polyelectrolyte nanorods can be integrated into GO fibers and films to increase the charge density and improve energy harvesting performances. Moreover, by aligning nanoscale charge boosters onto GO nanochannels through a blade-coating technique, the charge density can be precisely directed to optimize ion transport. Our study introduces an innovative and efficient approach to refining ion transport characteristics of 2D GO nanochannels, ultimately enhancing ion selectivity for proficient osmotic energy generation.

SESSION EL09.05: Functional Properties I
Session Chairs: Kirill Bolotin and Jennifer Dionne
Wednesday Morning, November 29, 2023
Hynes, Level 2, Room 202

8:30 AM *EL09.05.01

Phonons and Thermal Transport in Two-Dimensional Systems[IlariaZardo](#)^{1,2}; ¹University of Basel, Netherlands; ²Universität Basel, Switzerland

Phonon engineering leads to a controlled modification of phonon dispersion, phonon interactions, and transport. However, engineering and probing phonons and phonon transport at the nanoscale is a non-trivial problem. In this talk, we discuss how phononic properties and thermal transport can be engineered and measured in low dimensional systems. In particular, a fundamental difference in the phononic properties of 2D and 3D polar materials is predicted to be the long-wavelength dispersion of longitudinal (LO) and transverse (TO) optical phonon modes [1]: in 2D systems these modes become degenerate at the zone center, at variance with the well-known splitting they exhibit in bulk 3D materials. Besides the fundamental importance of understanding how the phonon modes of polar materials change when dimensionality is reduced, we stress two applicative reasons for this investigation: *i*) the peculiar characteristics of the phonon modes have an impact on thermal and electrical transport and optical coupling of 2D materials; *ii*) Raman spectroscopy is one of the most important non-destructive tools used to determine the thickness of the flakes [2], and thus it is essential to interpret correctly the experimental measurements by identifying all the observed phonon modes. We provide the experimental proof of the collapse of the TO-LO splitting in polar 2D materials [3], predicted by ref. [1]. We also investigate the effect of the parity of the number of layers and the role of inversion symmetry. Once all the proper theoretical tools required to fully account for all the experimental features of the Raman spectra of 2D materials are assessed, we exploit them to unveil the lattice dynamics of WSe₂ [4], which is, among the most diffused transition metal dichalcogenides, the one having the most controversial phononic properties, due to a very small thickness-dependence of the main phonon modes (A_{1g} and E'_{2g}). We show that conventional first order Raman spectroscopy has a limited validity in the determination of the number of layers in WSe₂ and we propose an alternative, more general approach, based on multi-phonon bands, which enables to distinguish between 1L, 2L, and 3L [4]. Finally, we present a method to investigate thermal transport in two-dimensional systems using multi-terminal suspended SiN_x membranes with resistive elements. These devices enable us to probe thermal transport along different directions as a function of thermal bias.

References

- [1] Sohier T, Gibertini M, Calandra M, et al., *Nano Lett.* **17**, 3758 (2017)
- [2] Zhang X, Qiao X-F, Shi W, et al., *Chem. Soc. Rev.* **44**, 2757 (2015)
- [3] De Luca M, Cartoixa X, Indolese D, et al., *2D Materials* **7**(3), 35017 (2020)
- [4] De Luca M, Cartoixa X, Martín-Sánchez J, et al., *2D Materials* **7**(2), 025004 (2020)

9:00 AM *EL09.05.02

Generating and Exploring the Effects of Ultrastrong Electric Field in 2D Material/molecule Heterostructures[KirillBolotin](#); Freie University Berlin, Germany

We consider a new type of heterostructure: a 2D material with donor molecules on one side and acceptor molecules on the other. The charge transfer between the molecules generates an electrical field inside the 2D material. We experimentally measure the field produced by this "molecular gating" and show that it reaches >4V/m, the highest field measured in a solid-state device. We then explore the effect of this intense field. First, we demonstrate that the field suffices to modify and eventually completely close the bandgap in bilayer 2D semiconductors driving a semiconductor-to-metal transition. Second, we show that the field lifts degeneracies between excitons in semiconductor 2D bilayer and brings different excitons into resonance. Finally, we demonstrate new types of excitonic states that arise because of that.

9:30 AM EL09.05.03

Role of the Anion in an Ionic Liquid-Gated MoS₂ Transistor[AnoirHamdi](#)¹, Iréné Bérenger AmicheEssomba², KanaIshisone², RaminKarimi³, TianLan³, ClaraSantato³, MauroBoero²,

Electrical double layer gating is employed to achieve ultra-high charge carrier accumulation in a semiconductor material operating as the active layer in a transistor. Such strategy allows to overcome the problem of low carrier density and high operating voltage in field-effect transistors (FETs) due to low capacitance and electrical breakdown of the gate dielectric. In the present work, electrical double-layer transistors based on molybdenum disulfide (EDLT- MoS₂) and an ionic liquid (IL) were fabricated to achieve a higher carrier density and lower operating voltage than those in the FET-MoS₂ transistor. EDLT-MoS₂ were obtained by combining a three-terminal back-gated MoS₂ FET with an ionic liquid while disabling the back-gate effect and using the ionic liquid as a top-gate dielectric. A heavily p doped silicon layer Si⁺⁺ with thermally grown 285 nm thick SiO₂ was used as substrate, while gold (Au) with chromium (adhesion layer) were used to fabricate the source and drain electrodes of the EDLT-MoS₂. Activated carbon was chosen as the gate electrode. Two different ionic liquids [EMIM][anion1] and [EMIM][anion2] were used as gate dielectrics in order to: obtain high performance transistors, study the IL/MoS₂ interface and identify the anion/cation pair most capable of injecting a high density of charge carriers on the surface of the molybdenum disulfide channel. The results of electrical characterizations showed that both [EMIM][anion1] and [EMIM][anion2] allow us to achieve a higher carrier density in the MoS₂ channel than what usually achieved by means of conventional gating with insulating oxides such as SiO₂. This allows to use our transistors at lower operating voltage. Comparing the results obtained by the two ILs, it was found that although the gating occurs through the [EMIM] cation, [anion1] achieves the highest electric double layer capacitance over [EMIM][anion2]. Surprisingly, we found that the anion plays a role in the gating efficiency of our devices in spite of the fact that it is the cation that actually recalls charge carriers (electrons in this case) within the FET channel. This is in agreement with theoretical predictions and modeling carried out by using classical and first-principles molecular dynamics simulations. Furthermore, the performances of FET gated by [EMIM][anion1] were found to be stable over time. This work explored from a theoretical and an experimental point of view the role of the anion in an ionic liquid. This paves the way for the choice of suitable pairs of ILs for applications in electronics or superconductivity.

9:45 AM EL09.05.04

Electrostatic Self-Assembly of GO-CNT Nano-Hybrid StructuresLokeshSoni, Kamendra PSharma and Ajay SinghPanwar; Indian Institute of Technology Bombay, India

Carbon-based hybrid nanostructures consisting of graphene oxide (GO) and carbon nanotubes (CNT) could potentially provide superior properties relative to their individual components. However, the fabrication of such nanostructures at this length scale is found to be an arduous task, due to restacking of GO sheets and aggregation of CNTs. By using CNTs as anchoring material to prevent restacking of GO sheets, a hybrid nanostructure can be synthesized which can show synergistic properties from both materials[1], [2]. In this study, we report a scalable approach to develop highly ordered CNT intercalated GO hybrid nanostructures in an aqueous medium with an electrostatic self-assembly process. The GO-CNT hybrids were synthesized by first modifying the GO and CNT with polyelectrolytes such as Poly(diallyldimethylammonium chloride) (PDDA) and Poly(styrene sulfonate) (PSS) via non-covalent interactions, resulting in highly stable dispersions of mGO, and mCNT respectively. The hybrid nanostructures were synthesized by homogeneous mixing of mGO and mCNT constituents with varying volumetric ratios with ultrasonication. The hybrid nanostructures were characterized by zeta potential, dynamic light scattering, scanning electron microscopy (SEM), and transmission electron microscopy (TEM). From SEM the hybrid nanostructure with 1:0.5 mGO:mCNT (v/v) ratio was found with highly organised stacking of CNT intercalated GO sheets, owing to the charge neutralization point of the dispersion as studied with zeta potential study. TEM micrographs also show homogeneous distribution of CNTs on the exfoliated GO sheets. Strengthened electrostatic interaction on the GO and CNT with adsorbed polyelectrolytes prevents restacking and aggregation of GO sheets and CNTs and further facilitates the self-assembly of oppositely charged nanoparticles into the formation of layered hybrid nanostructures. The mobility of polyelectrolyte chains also facilitates the ordered arrangement of CNTs with their anisotropic shapes and extends the electrostatic interaction to a much greater length scale to produce a compact yet strengthened nanostructure. The proposed process provides a highly cost-effective method against processes such as CVD, and large-scale production of a highly ordered arrangement of CNTs than the conventional Layer-by-layer assembly method to produce GO-CNT hybrid nanostructures for membrane and high surface area application in aqueous media.

References

- [1] J. K. Wu *et al.*, "Synergistic effects of CNT and GO on enhancing mechanical properties and separation performance of polyelectrolyte complex membranes," *Mater Des*, vol. 119, pp. 38–46, 2017
- [2] C. Min *et al.*, "Unique synergistic effects of graphene oxide and carbon nanotube hybrids on the tribological properties of polyimide nanocomposites," *Tribol Int*, vol. 117, no. May 2017, pp. 217–224, 2018

10:00 AMBREAK

10:30 AM *EL09.05.05

Nanoscale Optoelectronic Characterisation of Hybrid Heterostructures via Scattering-Type Scanning-Near-Field Optical MicroscopyJessicaL. Boland^{1,2}; ¹University of Manchester, United Kingdom; ²National Physical Laboratory, United Kingdom

Dimensionally hybrid semiconductor heterostructures and 2D heterostructures have enormous promise for a range of functional technologies. Indeed, heterostructures of planar 2D materials have already found applications in photonics, optoelectronics, straintronics, valleytronics and twistronics; where pushing towards 2D/1D and 2D/0D systems have shown exciting optoelectronic phenomena [1,2]. To understand the effect of this hybridisation, characterisation techniques with high spatial resolution, temporal resolution and depth selectivity are required in order to examine the optoelectronic and chemical properties of individual layers and components of the heterostructure. In this talk, we present scattering-type scanning near-field optical microscopy (s-SNOM) as a powerful tool for non-destructive optoelectronic characterisation of hybrid heterostructures [3,4]. By coupling radiation to the apex of an atomic force tip, we achieve spatial resolutions way beyond the diffraction limit of light down to 10 nm across wavelengths from the visible to the terahertz range. We perform both imaging and spectroscopy to extract the local material dielectric function on nanometre length scales. By oscillating the tip and changing the tapping amplitude, we can also alter the probing depth to perform nanotomography, enabling us to observe differences in optoelectronic properties in different layers of a material. Here, we present s-SNOM on a range of example heterostructures, including: interlayer charge transfer between 2D TMDC heterostructures [5]; identification of surface layer in InN nanoparticles; nanoscale 3D mapping of dielectric function in topological insulator thin films and nanowires [6].

- [1] Pei-Yu Huang *et al* 2D–1D mixed-dimensional heterostructures: progress, device applications and perspectives, *J. Phys.: Condens. Matter* 33 493001 (2021)
- [2] Basov, D., Averitt, R. & Hsieh, D. Towards properties on demand in quantum materials. *Nature Mater* 16, 1077–1088 (2017). <https://doi.org/10.1038/nmat5017>
- [3] F. Keilmann and R. Hillenbrand, Near-field microscopy by elastic light scattering from a tip, *Philos. Trans. R. Soc. London. Ser. A Math. Phys. Eng. Sci.*, vol. 362, no. 1817, pp. 787–805, Apr. 2004, doi: 10.1098/rsta.2003.1347.
- [4] Yao, Ziheng, et al. Nanoimaging and nanospectroscopy of polaritons with time resolved s-SNOM. *Advanced Optical Materials* 8.5 1901042 (2020)
- [5] Plankl, M., Faria Junior, P.E., Mooshammer, F. et al. Subcycle contact-free nanoscopy of ultrafast interlayer transport in atomically thin heterostructures. *Nat. Photon.* 15, 594–600 (2021). <https://doi.org/10.1038/s41566-021-00813-y>
- [6] F. Mooshammer *et al.*, Nanoscale Near-Field Tomography of Surface States on (Bi 0.5 Sb 0.5) 2 Te 3, *Nano Lett.*, vol. 18, no. 12, pp. 7515–7523, Dec. 2018, doi: 10.1021/acs.nanolett.8b03008.

11:00 AM *EL09.05.06

New Optical Features of Designer 2D Materials and Machine-Learning Assisted CharacterizationShengxiHuang; Rice University, United States

2D materials offer enormous opportunities to build designer structures with widely tunable properties. The precise atomic engineering and quick characterization approach are critical to advance the application of designer 2D materials. This talk will introduce new optical features of designer 2D materials [1-4] with a focus on atomic substitution in monolayer WS₂ [1]. The engineering of 2D materials presents unique opportunities for optoelectronic device and quantum information platform. When designing optoelectronic devices of 2D materials, spectroscopic permittivity of 2D material is a key parameter. While ellipsometry has been used to measure permittivity, it requires simple device structure, non-trivial parameter fitting, and special setup. This talk will also present a new machine-learning assisted approach to measure permittivity of 2D materials embedded in complex device structures without model fitting, which can facilitate a quick, accurate, and in-situ characterization of 2D and other thin film materials [5].

References

- [1] Q. Qian, et al. "Photoluminescence Induced by Substitutional Nitrogen in Single-Layer Tungsten Disulfide," *ACS Nano*, 16 (5), 7428-7437 (2022).
- [2] K. Zhang, et al. "Enhancement of van der Waals Interlayer Coupling Through Polar Janus MoSSe," *Journal of the American Chemical Society*, 142 (41), 17499-17507 (2020).
- [3] K. Zhang, et al. "Spectroscopic signatures of interlayer coupling in Janus MoSSe/MoS₂ heterostructures," *ACS Nano*, 15 (9), 14394-14403 (2021).
- [4] Q. Qian, et al. "Chirality-Dependent Second Harmonic Generation of MoS₂ Nanoscroll with Enhanced Efficiency," *ACS Nano*, 14 (10), 13333-13342 (2020).
- [5] Z. Wang, et al. "Measuring complex refractive index through deep-learning-enabled optical reflectometry," *2D Materials*, 10, 025025 (2023).

11:30 AM EL09.05.07

Tailored Epitaxial Growth and Morphology of 1D/2D Heterostructures Kate Reidy¹, NoyaR. Izhak², MayaLevy-Greenberg², PaulMiller¹, YasenHou¹, FedericoPanciera³, JagadeeshMoodera¹, ErnestoJoselevich² and FrancesM. Ross¹; ¹Massachusetts Institute of Technology, United States; ²Weizmann Institute of Science, Israel; ³Université Paris-Saclay, France

Controlling emergent phenomena at the nanometer regime requires unprecedented precision, resolution, and uniformity not readily feasible through conventional top-down fabrication techniques. This is particularly true in the growth and design of van der Waals (vdW) bonded 'mixed dimensional' heterostructures, where two-dimensional (2D) and nD (where n is 0, 1 or 3) materials adhered primarily through non-covalent interactions are highly dependent on local structure.¹ Direct visualization of atomic-scale structures and interfaces allows the determination of growth mechanisms and routes towards tailoring morphology.

Here, we explore how vdW-bonded 2D substrates influence complex epitaxial growth modes of 1D tellurium (Te) nanostructures using a combination of *in-situ* growth and *ex-situ* analysis via atomic resolution scanning transmission electron microscopy (STEM). Te is a p-doped semiconductor that can exhibit a chiral atomic structure and is emerging for application in next-generation electronic, optoelectronic, and piezoelectric applications. First, we utilize vdW epitaxy to tailor Te nanostructure growth on a variety of 2D substrates, exhibiting both hexagonal symmetry and more asymmetric surface structures. We then elucidate the role of temperature in the resulting nanostructure morphology, moving towards faceted islands at higher temperature with well-defined interfaces and morphologies. We compare the growth morphologies of chiral Te with the case of higher symmetry crystal structures, such as Au, Ti, and Hf, examining the role of symmetry on nanostructure morphology. Such understanding of tailored growth mode allows versatile design of heterostructures for next generation nanoscale devices, and we discuss mechanisms by which optimizing this 1D/2D interface is crucial for improving existing devices as well as generating novel mixed-dimensional heterostructures.

1. Jariwala, D., Marks, T. J. & Hersam, M. C. Mixed-dimensional van der Waals heterostructures. *Nat. Mater.* **16**, 170–181 (2017).

11:45 AM EL09.05.08

Epitaxial MoS₂ Nanofins and Nanoribbons for Optoelectronics YardenDanieli, LotharHouben, KatyaRechav and ErnestoJoselevich; Weizmann Institute of Science, Israel

2D materials are a versatile platform for optoelectronics, memory and energy-harvesting devices owing to their high-carrier mobility and strong light-matter interaction. Scientific efforts were invested during the last decade to tailor the physical properties of these materials by gaining control over their dimensionality. The synthesis of new structures with mixed dimensionalities, such as nanoribbons or nanofins, with controlled orientations, can give rise to a change of physical behavior and has many potential applications in electronics and optoelectronics. However, efficient synthetic methods for the bottom-up creation of aligned single-crystal nanoribbons and nanofins are still lacking. Our group gained substantial knowledge regarding the aligned growth of 1D nanowires of different semiconductors, guided by different crystalline substrates, as part of the general guided-growth approach. This work aims to implement the guided growth approach to induce 1D growth of MoS₂ nanofins-nanoribbons with controlled orientations. Synthesized in a CVD system by epitaxy on sapphire, the formation of these unique hybrid structures is discussed in terms of crystal structure and morphology. Optical properties such as photoluminescence and Raman spectroscopy are also presented. The MoS₂ nanoribbons-nanofins were integrated into arrays of visible-light photodetectors, showing high responsivity and short response times with respect to previously reported MoS₂-based photodetectors. Such growth of nanofins-nanoribbons can be generalized to other 2D materials, suggesting new structures that enable various device architectures with improved performance.

SESSION EL09.06: Functional Properties II
Session Chairs: Hannah Joyce and Alessandro Surrente
Wednesday Afternoon, November 29, 2023
Hynes, Level 2, Room 202

1:30 PM *EL09.07.01

Controlling Valley-Selective Absorption and Emission from Monolayer Materials with High-Q Metasurfaces JenniferA. Dionne, FengPan, YinLiu, Sze CheungLau, FangLiu, MarkL. Brongersma and TonyF. Heinz; Stanford University, United States

Atomically thin two-dimensional (2D) materials, transition metal dichalcogenides (TMDCs), graphene, and hexagonal boron nitride as well as their heterostructures, have recently found wide applications in optoelectronic devices, condensed matter physics, and quantum information science (QIS). Among these 2D materials, excitons in atomically-thin TMDCs have large exciton binding energies (>500 meV) and provide bright and sharp photoluminescence (PL) emission. More importantly, the presence of spin-orbit coupling and broken inversion symmetry renders the spin/valley polarization addressable through optically-circular polarization control. The valley-polarized PL can be observed and characterized by the degree of circular polarization, defined as $DOP = [I(\sigma+) - I(\sigma-)] / [I(\sigma+) + I(\sigma-)]$, where $I(\sigma\pm)$ are right and left circularly polarized PL intensities. Achieving high DOP is important for high-fidelity quantum information processing and generating high-quality chiral light sources. However, their short spin coherence time due to intervalley scattering, i.e. a few ps even at low temperatures (4 K or 100 K), prevents them from being employed as on-chip valley-selective devices for wide applications in valleytronics.

Here, we integrate the TMDC MoS₂ with high-quality-factor silicon metasurfaces to enhance and control valley-specific absorption and emission. By varying the metasurface disk diameter, we tune the frequencies of Mie scattering modes to match the exciton frequency in MoS₂. When the electric and magnetic Mie modes overlap (a Kerker-like condition), the photoluminescence (PL) intensity of MoS₂ is enhanced by over 30 times on the metasurface in contrast to that on flat sapphire substrate. The MoS₂ emission spectra are also markedly modified via the coupling of neutral excitons, trions and defect bound excitonic states with the metasurface Mie modes. At the Kerker condition, we also demonstrate the symmetric enhancement of the degree-of-polarization (DOP) of neutral exciton and trions via valley-resolved PL measurements, and find that the DOP can be as high as 24% for exciton emission and 34% for trion emission at 100K. These results can be understood by analyzing the near-field impact of metasurface resonators on both the chiral absorption of MoS₂ emitters as well as the enhanced emission from the Purcell effect. Combining Si-compatible photonic design with large-scale (mm-scale) 2D materials integration, our work makes an important step towards on-chip valleytronic and QIS applications approaching room-temperature operation.

2:00 PM EL09.06.02

Interfacing 2D Transition-Metal Dichalcogenides with III-V Substrates and Nanostructures MicheleZendrini, MichelePonso, ClaireBlaga, JinJiang, MitaliBanerjee, ValerioPiazza and AnnaFontcuberta i Morral; Ecole Polytechnique Federale de Lausanne (EPFL), Switzerland

Two-dimensional transition metal dichalcogenides (2D-TMDs) figure as promising candidates for new generation optoelectronics, ranging from flexible electronics to single-photon emitters and strain-tunable devices. Their functionalization through the integration with a suitable substrate is a key factor as 2D materials are strongly influenced by both the substrate morphology and the dielectric environment. The heterostructures of 2D-TMDs and III-V materials have shown to induce sharper and more stable emission with respect to their counterparts on oxides [1]. A clear understanding of the band alignment between the 2D material and the specific III-V material is still needed to outline the most suitable material coupling for functional devices. In this context, one must also consider the impact of the strain on the band structure of the 2D-TMDs and thus on the heterojunction. The substrate morphology is therefore of primary importance as it can be engineered to induce various strain configurations [2].

In our work, we transfer MoS₂ and WSe₂ monolayers (ML) on different III-V substrates such as GaAs and related ternary alloys. We grow the III-V semiconductors by molecular beam epitaxy in form of a thin film or an ordered array of 1D nanostructures such as horizontal nanowires. Selective area epitaxy allows obtaining arrays with precise morphology and size. In the case of thin films, the TMD/III-V stacking is explored to evaluate the effective band alignment. In the latter case of nanostructures, the extent of strain-induced modification is investigated. The heterojunction properties are defined both optically and electrically. On the one hand, micro-photoluminescence and Raman spectroscopy are utilized to evaluate the evolution of emissions and vibrational modes respectively when transitioning from unstrained to strained MLs. On the other hand, conductive atomic force microscopy and electrical contacts patterned by electron-beam lithography provide comprehension of the electrical response of the different heterojunctions.

[1] Iff, Oliver, et al. "Substrate engineering for high-quality emission of free and localized excitons from atomic monolayers in hybrid architectures." *Optica* 4.6 (2017): 669-673

[2] Jasinski, Jakub, et al. "Strain induced lifting of the charged exciton degeneracy in monolayer MoS₂ on a GaAs nanomembrane." *2D Materials* 9.4 (2022): 045006

2:15 PM EL09.06.03

Laser Induced Incorporation of CNTs in Graphene Electrodes Improves Flexibility and Conductivity AsmitaDutta; Ariel University, Israel

Laser processing of nanocarbon films emerges as the preferred technique to prepare carbon-based electrodes. A great effort focuses on exploiting this fast, sustainable, and cost-effective method on a broader range of nanomaterials. This study describes the laser-induced production of reduced graphene oxide with carbon nanotube (rGO/CNT) composites and their application as flexible electrodes. Conductive carbonized films were imprinted on a flexible substrate by laser-carbonization. The composites formation is supported by a detailed microstructural and

chemical analysis, which confirms the structural integration of rGO with CNTs. Electrodes containing CNTs exhibit 7.5-fold increase in conductivity compared to only rGO electrodes. Importantly, when the electrodes are bent, the conductivity retention of the composite is significantly superior compared to the only rGO electrodes. Upon bending, the change in conductivity is lowered from 0.62 to 0.19. Furthermore, when used as electrodes in flexible supercapacitor devices, the composites with CNTs show 98.45 % retention in specific capacitance while maintaining structural integrity. In contrast, rGO electrodes without CNT addition deform upon bending and retain only 63.88 % of the relaxed specific capacitance.

SESSION EL09.07: Towards 2Ds Applications
Session Chairs: Jessica Boland and Ilaria Zardo
Thursday Morning, November30, 2023
Hynes, Level 2, Room 202

8:30 AM *EL09.06.01

Heterostructuring in Mechanically Deformed Van Der Waals Crystals Antonio Polimeni¹, Elena Blundo¹, Salvatore Cianci^{1,2}, Marzia Cuccu^{1,2}, Federico Tuzi¹, Giorgio Pettinari³ and Marco Felici¹; ¹Sapienza Università di Roma, Italy; ²TU Dresden, Germany; ³Italian National Research Council (CNR), Italy

Heterostructures (HSs) of van der Waals (vdW) crystals are created by stacking atomically thin layers with different compositions and relative angular alignment thus prompting an endless number of combinations and novel physical phenomena. Another key feature of vdW HSs, and of their constituent layers, is their highly sensitive response to mechanical deformations stemming from their virtually two-dimensional (2D) structure. Strain indeed has been demonstrated to be a most powerful tool to modify controllably the electronic properties of 2D materials [1].

Here, we report two exemplary cases, where the interplay between heterostructuring and strain add new functionalities to and improve the optoelectronic characteristics of 2D crystals and their HSs.

In the first instance, we consider HSs formed by strained transition metal dichalcogenide (TMD) monolayers (MLs) and hexagonal boron nitride (h-BN). Strain is achieved by proton irradiation of TMD bulk flakes, in which protons lead to a local blistering of the crystal just beneath the topmost plane and hence to the formation of highly strained ML micro/nano-domes filled with H₂ [2]. The capping with h-BN promotes an elastic energy transfer from the domes to h-BN that eventually prevents the dome deflation at the liquefaction temperature of H₂ (~33 K). In turn, this preserves the dome strain field and enables the fabrication of spatially controlled quantum emitters [3].

In the second case, InSe/TMD dome HSs are presented. InSe features excellent transport properties but poor emission efficiency in the few layer limit. We exploit the strain-induced transition of the valence band maximum from K to Γ in MS₂ (M=Mo,W) ML domes [4] to create a type-I HS with InSe. Therein, a direct transfer of holes from the Γ point of the ML dome to that of the InSe occurs, while electrons undergo a defect-assisted tunnelling from the conduction band of the strained ML to that of InSe. As a result of these processes an increase by up to two orders of magnitude in the emission efficiency of InSe is observed.

[1] E. Blundo *et al.*, *Appl. Phys. Rev.* **8**, 021318 (2021)

[2] E. Blundo *et al.*, *Phys. Rev. Lett.* **127**, 046101 (2021)

[3] S. Cianci *et al.*, *Adv. Opt. Mater.* DOI:10.1002/adom.202202953

[4] E. Blundo *et al.*, *Phys. Rev. Res.* **2**, 012024 (2020)

9:00 AM *EL09.07.02

Engineering Hybrid Nanowire/2D Systems for (Opto)Electronics Hannah J. Joyce, Tom Albrow-Owen, Oliver Burton and Jack Alexander-Webber; University of Cambridge, United Kingdom

The combination of nanowires with two-dimensional (2D) systems is an exciting one enabling new growth approaches, new (opto)electronic device functions and new systems. Here we present two such examples, firstly a nanowire-graphene spectrometer, and secondly an array of single nanowires addressed through a two-dimensional electron gas.

Semiconductor nanowires of graded composition are prime candidates for miniaturised spectrometers [1]. In these devices, the nanowire's bandgap varies with position along the nanowire's axis, and photons of sufficient energy will selectively excite particular regions depending on the local bandgap. Multiple electrode pairs placed laterally at intervals along the nanowire axis are used to detect local changes in conductivity induced by photoexcitation, with the graded bandgap giving a means to discriminate incoming wavelengths. This concept is powerful, but complicated by the diffusion of photoexcited charge carriers into lower bandgap regions. To overcome this problem, we instead use graphene channels at intervals in contact with the graded bandgap nanowire, and measure the conduction through the graphene. Efficient transfer of photoexcited carriers from the nanowire into the graphene alters its chemical potential and conductivity, which provides a measure of the wavelength-dependent intensity of incident light.

Multiplexed arrays of single InAs nanowires were achieved using a quantum multiplexer chip [2] with individual InAs nanowires transfer printed onto each of the chip's channels. The quantum multiplexer itself consists of a two-dimensional electron gas (2DEG) patterned into a cascaded structure with arms that can be depleted by the application of a gate bias. Depletion prevents conduction through the associated channels. Using the multiplexer, measurements of conductance and quantum transport through 16 individual nanowire channels were achieved with just 9 electrodes. The multiplexer permits a reduction in the number of electrodes needed, with the number of devices scaling as $2^{(n-1)/2}$ with n being the number of electrodes. This multiplexer is particularly beneficial for experiments at cryogenic temperatures in which the number of leads entering a cryostat is limited, and for large statistical studies of nanowires.

[1] Z Yang *et al.*, *Science* **365**: 1017-1020 (2019)

[2] L Smith *et al.*, *ACS Nano* **14**: 15293-15305 (2020)

9:30 AM BREAK

10:00 AM EL09.07.03

Hybrid Carbon Materials: Synthesis, Properties and Electrochemical Sensor Potential Carolina Rojas Michea^{1,2}, Neida Santacruz³, Frank Mendoza-Centeno³, Gerardo Morell^{3,2}, Brad Weiner^{1,2} and Ana R. Guadalupe^{1,2}; ¹University of Puerto Rico at Río Piedras Campus, United States; ²Molecular Science Research Center, University of Puerto Rico, United States; ³University of Puerto Rico at Río Piedras, United States

This research presents a hybrid carbon material foam developed by chemical vapor deposition technique, with acetone as a carbon source and Ni as scaffolds. Carbon poses some interesting allotropes, and this material exhibits some of them. Graphene and graphene oxide are valuable in the sensors field due to their electrical and conductive properties. However, there are essential applications in gas and liquid media that can benefit from the unique properties of graphene but require a 3D structure able to interact thoroughly with the medium. We studied how the structural properties of the graphene hybrids foams depend on the growth parameters, such as temperature, precursor concentration, and Ni foams thickness. This material will be used as an electrode in sensing some enzymes or other biological molecules which are at low concentrations.

The high purity and yield of the material fabrication would enable further applications for research and industrial processes, such as catalysis and environmental remediation.

10:15 AM EL09.07.04

Multi-Walled Carbon Nanotubes and Graphene Oxide Decorated Pitch-Derived Carbon Foam Composites for Enhanced Structural and Catalytic Performances Muhammad Khan and Husnu E. Unalan; Middle East Technical University, Turkey

Various amounts of multi-walled carbon nanotubes (MWCNTs) and graphene oxide (GO) were synergistically dispersed into the pitch-derived carbon foam (CF) matrix via direct pyrolysis. The structural and catalytic behaviors of prepared CF composites were investigated. Results showed porous morphology with compressive strength and Young's modulus of 19.3 MPa and 57.4 MPa, respectively, after an additive loading of 2%. Excellent thermal and electrical conductivities of 30.92 W/m.K and 27.4×10^3 S/m were obtained from the CF sample with an additive loading of 2%. Furthermore, the catalytic decolorization performance of the CF samples against methyl orange (MO) dye was investigated and reported. Results revealed that the CF sample with an additive loading of 4% decolorized about 76% MO dye under exposure to UV light within 60 min. The decolorization of MO dye increases by increasing additive loading in the nanocomposite while dye decolorization decreases with increasing the initial dye concentration.

10:30 AM *EL09.07.05

Understanding and Enhancing the Color Center Emission in hBN Coupled to Photonic Circuits Henry Roberts¹, Scott Wicker, Jr.¹, apratim Khandelwal² and [Xiuling Li](#)¹; ¹The University of Texas at Austin, United States; ²University of Illinois at Urbana-Champaign, United States

Defects embedded in solids or thin films function as attractive quantum sensors. For example, negatively charged nitrogen vacancies NV⁻ in diamond films can be used for detecting electric, magnetic, and strain fields with promising sensitivity and resolutions. Here we explore the color center emission in van der Waals (vdW) materials, particularly hexagonal boron nitride (hBN), and in silicon carbide nanostructures, coupled to photonic circuits. We will discuss the design, photonic structure fabrication, deterministic spin defect generation, and characterization.

11:00 AM *EL09.07.06
(Clarifying) A Few Alternative Facts about 2D Materials [Eric Pop](#); Stanford University, United States

Great interest in the science and engineering of two-dimensional (2D) materials has led to a great rush of publications, some stating or propagating a number of “alternative facts” about 2D material and device properties (with thanks to Kellyanne Conway for coining this term). An “alternative fact” (AF) is a statement, a number, or a belief that is presented as “fact”, despite reasonable uncertainty or evidence to the contrary. Common examples include the 0.65 nm thickness and 1.8 eV band gap of monolayer MoS₂, or various exaggerated mobility values. Unfortunately, such AFs have propagated in the 2D literature perhaps by accident, perhaps because some form a compelling story, or perhaps due to convenience. Here we try to address and hopefully clarify a few AFs, especially as they pertain to basic 2D material parameters or simple device applications. The presentation will be incomplete, yet will hopefully provide some useful guidance for researchers working with 2D materials. The audience will be encouraged to participate and contribute their favorite AFs (and corrections), which will be published online for the benefit of new students and others entering the broad and exciting field of 2D materials.

SESSION EL01/EL09/EL12: Joint Virtual Session
Session Chairs: Guru Naik, Junghyun Park and Alessandro Surrente
Thursday Morning, December 7, 2023
EL09-virtual

8:00 AM *EL01/EL09/EL12.01
Enhanced Interactions of Interlayer Excitons in Free-Standing Hetero-Bilayers [Yuerui Lu](#); Australian National University, Australia

Strong, long-range dipole-dipole interactions between interlayer excitons (IXs) can lead to novel multi-particle correlation regimes that drive the system into distinct quantum and classical phases¹ including dipolar liquids, crystals, and superfluids. Both repulsive and attractive dipole-dipole interactions have been theoretically predicted between IXs in a semiconductor bilayer^{2,3}, but only repulsive interactions have been experimentally reported so far^{4,5}. This study⁶ investigated free-standing, twisted (51°, 53°, 45°), tungsten diselenide/tungsten disulfide (WSe₂/WS₂) hetero-bilayers, where we observed a transition in the nature of dipolar interactions among IXs from repulsive to attractive. This was caused by quantum-exchange-correlation effects, leading to the appearance of a robust interlayer biexciton (formed by two IXs) phase that was theoretically predicted⁷ but never observed in experiments before. The reduced dielectric screening in a free-standing hetero-bilayer not only resulted in a much higher formation efficiency of IXs, but also led to strongly enhanced dipole-dipole interactions, which allowed us to observe the many-body correlations of pristine IXs at the two-dimensional (2D) quantum limit. In addition, we first observed multiple emission peaks from moiré-trapped IXs at room temperature in a well-aligned, free-standing WSe₂/WS₂ hetero-bilayer. Our findings can open avenues for exploring new quantum phases with potential for application in nonlinear optics. <!--!endif]---->

8:30 AM *EL01/EL09/EL12.02
Two-Dimensional Materials for Next-Generation Electronics and Optoelectronics Technologies—From Fundamentals to Applied Industrial Solutions [Sumeet Walia](#); RMIT University, Australia

Atomically-thin materials possess unique intrinsic properties and are amenable to a range of tuning techniques. We harness these properties underpinned by application demand and work with industry to translate into end-user products.

Firstly, we synthesise a variety of atomically-thin metal oxides, mono/dichalcogenides and elemental 2D materials using solid, liquid and vapour phase techniques guided by application. Our fundamental advances have been uncovering the origins of oxidative degradation in few-layer black phosphorus (BP) and subsequently proposing an ionic liquid-based approach to prevent ambient degradation of BP. Using defect engineering, we have demonstrated light operated artificial- synaptic and logic devices and neural networks that can recognise numbers and patterns. We have explored the use of hybrids of dissimilar materials to enhance electronic and optical performance. Ultra-thin layers have been used to develop one of the world's thinnest photodetectors that can sense all shades of light from UV-infrared. We further study strain-tunability in low-dimensional structures via integrating them onto elastomeric platforms and engineer optoelectronic functionalities.

Using a cross-disciplinary approach, we deploy multifunctionality of these new material systems into solving technological challenges for a range of industry partners.

9:00 AM EL01/EL09/EL12.03
Correlated KPFM and TERS Imaging to Elucidate Defect-Induced Inhomogeneities in Oxygen Plasma Treated 2D-MoS₂ Layers [Sanju Gupta](#); Penn State University, United States

Modulating physical and chemical properties of two-dimensional (2D) transition metal dichalcogenides (TMDC) by defect-engineering induced by oxygen plasma is actively pursued. In this work, exfoliated 2D MoS₂ layers treated by medium power oxygen plasma for different times (0, 10, 20, 40, and 60 s) are investigated using Kelvin Probe Force microscopy and tip-enhanced Raman spectroscopy (TERS) besides micro-Raman and photoluminescence (PL) spectroscopy. Under oxygen plasma, defects (mono- and di-sulfur vacancies) and chemical oxidation is predominant from 0s (native defects) up to 40s, while etching becomes dominant beyond 40 s, for mono- (1L), bi- (2L), and tri- (3L) layer MoS₂ with optimal defect density for four- (4L) and more layers. While Raman spectra exhibited lattice distortion (broadening of phonon bands) and surface oxidation by the presence of sub-stoichiometric molybdenum trioxide MoO₃ (*i.e.*, MoO_{3-x} or Mo₅O_{2-x}) the increased spectral weight of trions and quenching in PL spectra are observed with treatment time. The localized nanodomains (~20-40 nm) and aggregated vacancies as nanovoids and intermixed MoS₂/MoO_{3-x} alloy are identified in near-field Raman spectra. The atomic force microscopy also showed defects aggregation and Kelvin probe force microscopy revealed the work function (WF) increase from 4.98 eV to 5.56 eV, corroborating the existence of MoO_{3-x} phase which enables doping and shift Fermi level. We also highlight the unique interaction between the gold substrate and the formed MoO_{3-x} facilitating Mo⁶⁺ cation reduction to lower oxidation (*i.e.*, Mo⁴⁺) thereby yielding intermediate oxidation states responsible for lower WF (*ca.* theoretical 6.3 eV for stoichiometric MoO₃). Strong correlations among the work function, vibrational and optical responses are established while exploring the oxygen plasma-induced defects and changing the landscape on oxygen doping at the nanoscale with varying MoS₂ layers, which are useful for heterogeneous electrocatalysis and applicable to other 2D TMDCs.

9:15 AM *EL01/EL09/EL12.04
Manufacturing of Meta Optics by Nanoimprint Lithography [Niklas Hansson](#); NIL Technology, Denmark

Metalenses have gained significant attention in various fields such as augmented reality (AR), automotive technology, and consumer electronics. Their unique properties, including high thermal stability, fewer lens components, and focal lengths that closely match design values in production. These aspects lead to simplified camera modules, and make meta lenses highly desirable for these applications.

The efficiency of metalenses is crucial, as low-efficiency metalenses result in undesirable diffraction of light. To achieve high efficiency, it is important that the fabricated meta atoms, typically in the form of pillars, closely match the intended design. Even small deviations in the order of a few nanometers can lead to noticeable decreases in efficiency. Nanoimprint lithography (NIL) is a manufacturing technique employed for mass producing metalenses. We have investigated how closely the fabricated pillar diameters align with the design specifications. In the case of a focusing lens designed for 940 nm, the deviations in pillar diameters were found to be within the range of +/-10 nm for repeated fabrication on a single wafer and between consecutive manufactured wafers.

The corresponding focusing efficiencies of these metalenses were measured to be between 85% and 90%. This indicates that NIL is a valid manufacturing method for producing metalenses suitable for the aforementioned applications. The high efficiency of the manufactured metalenses suggests that they effectively mitigate the issue of light diffraction into unwanted orders, making them a promising choice for AR, automotive, and consumer electronics.

SYMPOSIUM EL10

Understanding the Inorganic-Organic Interface—The Case of Colloidal Nanoscale Materials
November 27 - December 7, 2023

Symposium Organizers

Tae-Woo Lee, Seoul National University
Liberato Manna, Istituto Italiano di Tecnologia
Hedi Mattoussi, Florida State Univ
Vincent Rotello, University of Massachusetts Amherst

Symposium Support

Silver

Science Advances | AAAS

* Invited Paper
+ JMR Distinguished Invited Speaker

SESSION EL10.01: Growth and Characterization I
Session Chairs: Hedi Mattoussi and Elena Shevchenko
Monday Morning, November 27, 2023
Hynes, Level 3, Ballroom A

10:30 AM *EL10.01.01

Effect of Ligands on the Structure and Mechanical Properties of Three-Dimensional Nanoparticles Superlattices [Elena Shevchenko](#)^{1,2}; ¹Argonne National Laboratory, United States; ²The University of Chicago, United States

Extensive research has been conducted on the self-organization of uniform nanoparticles, leading to the formation of various types of periodic structures. Numerous instances of both single and multicomponent periodic assemblies have been successfully demonstrated. It has been established that the self-assembly process of nanoparticles is highly intricate, involving a wide range of attractive and repulsive interactions between particles and their ligands.

In this study, we will explore the influence of nanoparticle purification, ligand solvation, and the type of ligands on the self-assembly of nanoparticles and their impact on the structure and properties of the resulting structures. Furthermore, we will discuss the effect of size distribution on the structure of periodic superlattices.

We will present combined quasi-hydrostatic high-pressure small-angle X-ray scattering (SAXS) and X-ray diffraction (XRD) studies on faceted 3D supercrystals self-assembled from colloidal nanoparticles. To investigate the overall mechanical characteristics of the assembled structures, we employed the diamond anvil cell technique, allowing us to examine the contributions of solvated ligands and inorganic ligands. Additionally, we will discuss the role of ligand solvation in the mechanical properties of periodic structures, as well as the structural transformations that occur upon compression for supercrystals obtained using different nonsolvents and ligands.

11:00 AM EL10.01.02

How General are Changes in Excited State Surface Chemistry of Colloidal Quantum Dots for Photocatalysis? [John B. Asbury](#); Pennsylvania State University, United States

The ligand-nanocrystal boundaries of colloidal quantum dots (QDs) mediate the primary energy and electron transfer processes that underpin photochemical and photocatalytic transformations at their surfaces. These boundaries also protect nanocrystal surfaces from photochemical degradation and maintain their colloidal stability. In recent work, we demonstrated using time-resolved infrared (TRIR) spectroscopy that certain types of ligand-nanocrystal interactions on PbS QDs exhibit marked reduction in surface bonding strength in the excited states of the nanocrystals, which may provide a pathway to modulate ligand bonding during photocatalytic reactions. In this work, we examined changes in the excited state surface chemistry of CdSe QDs passivated with stearic acid ligands to test the generality of this phenomenon. Transient absorption and photoluminescence spectroscopies were used to characterize the vibrational spectra of the ligands in the excited states of the QDs and to compare their time-dependence to the dynamics of the electronic states. The transient vibrational spectra of the symmetric and antisymmetric stretch modes of the carboxylate anchoring groups of the ligands indicated a net reduction of their higher frequency antisymmetric stretch and an enhancement of the lower frequency symmetric stretch modes. These changes were consistent with the influence that image dipoles created by the polarizable excited excitonic states of the QDs have on the transition dipole moments of the carboxylate anchoring groups. Importantly, a lower frequency transient vibrational feature around 1330 cm⁻¹ appeared in the TRIR spectra that was not present in the ground state infrared absorption (FTIR) spectrum of the QDs. This feature corresponded to the C–O single bond of more weakly bonded carboxylate groups in the monodentate bonding geometry. The shorter excited state lifetime of CdSe in comparison to PbS QDs allowed us to directly observe the reattachment of ligands to their original bonding geometries on much longer time scales. These findings suggest that changes in excited state surface chemistry may be general to metal chalcogenide QDs and motivates continued work to elucidate the origins and means to control the phenomenon for photocatalytic applications.

11:15 AM EL10.01.03

Density Functional Theory Investigation of Trap States in III-V Quantum Dots [Ezra A. Alexander](#)¹, [Matthias Kick](#)¹, [Alexandra McIsaac](#)² and [Troy Van Voorhis](#)¹; ¹Massachusetts Institute of Technology, United States; ²University of California, Berkeley, United States

Cadmium selenide, one of the premier quantum dot (QD) materials for light emission, solar cells, and biomedical imaging, is highly toxic to both humans and the environment. Alternative nontoxic III-V QDs are held back by a high density of surface-localized mid-gap states, which trap photoexcited charge carriers and reduce device efficiency. Despite the prevalence of density functional theory (DFT) in past research on surface trapping in the II-VI family of QDs, very few studies have applied DFT to the substantially different III-V family of QDs. In this work, we survey a broad range of realistic, carefully selected InP and GaP QDs of different sizes, shapes, and surface terminations. By utilizing orbital localization techniques to deconvolute the dense manifold of states at the band edges, we create a framework for understanding the complex surface trapping in these III-V QDs. Not only can trap states form from under-coordinated surface atoms as in II-VI QDs, but we also identify localized midgap states that originate from atomic dimers and distorted four-coordinate surface atoms. We discuss several factors that influence the depth of both electron and hole traps in these materials, including potential avenues for removing such localized states from the band gap. Finally, we identify key differences between the surface reconstruction and electronic structure of InP and GaP QDs.

11:30 AM EL10.01.04

Surface Chemistry, Optoelectronic Properties and Methods for Enhancing the Photoluminescence Quantum Efficiency of InP-based Core/Shell Quantum Dots Pieter Schiettecatte, Ben Cruysaert, Luca Giordano, Hannes Van Avermaet and Zeger Hens; Ghent University, Belgium

Colloidal quantum dots (QDs) possess spectrally narrow and tunable emission lines, making them highly attractive for applications in displays, light sources, and energy devices. However, to meet the stringent demands of efficient and sustainable devices, it is essential for QDs to exhibit high photoluminescence quantum efficiencies (PLQY) that are close to unity. In this study, we, therefore, focus on enhancing the PLQY of InP-based core/shell QDs by investigating the relationship between their surface chemistry and their optoelectronic properties.

Our approach involves saturating the surface of InP-based QDs using a zinc acetate complex. This surface passivation step can be carried out either during QD synthesis or after synthesis. We have successfully applied this method to over 25 QD samples with diverse compositions synthesized by different collaborators, demonstrating its robustness and versatility. Additionally, we develop a ligand exchange technique that enables the transfer of InP-based QDs from apolar to polar media while preserving their high PLQY. This method opens up new possibilities for utilizing QDs in both polar and apolar environments without sacrificing their photoluminescence efficiency.

By significantly enhancing the PLQY of InP-based QDs, our findings offer promising prospects for their application in optoelectronics and photonics. These advancements can contribute to the development of more efficient and high-performance devices in different fields.

11:45 AM EL10.01.05

Solid-State Synthesis and Solution-Processable MB₆ Nanocrystals Suhas Mutalik; University of Groningen, Netherlands

Metal hexaborides (MB₆) are of high technological interest as they show a wide range of bulk physical properties depending on the metal ion in the structure. Boron-rich compounds like CeB₆ and LaB₆ possess low work functions (2.5-2.7 eV), while CaB₆ and SrB₆ possess high-temperature thermoelectric properties.¹ The MB₆ is reported to have very high hardness (9.5 on the Mohs hardness scale) with nanoindentation hardness of 16-18 GPa.² The existing literature reports the solid-state synthesis of MB₆ nanocrystals below 500 °C, but so far, no studies have been reported on solution-processable MB₆ hexaborides. Herein we report a solid-state synthesis of LaB₆ and SrB₆ nanocrystals performed at 440 °C and a novel post-processing technique of treating the nanopowders obtained from solid-state reaction to form a colloidal stable ink. Through the surface modification of the nanocrystals, we can exchange the surface ligands from inorganic short-chain ligands to organic long-chain ligands, making them solution processable in both polar and non-polar solvents. The colloidal stable MB₆ nanocrystals have great potential to be used as thermoelectric devices or ultra-hard protective coatings, which can be fabricated at low cost by solution-based mass production processes.

References

(1) Takeda, M.; Fukuda, T.; Miura, T. Thermoelectric Properties of Metal-Hexaborides. International Conference on Thermoelectrics, ICT, Proceedings 2002, 2002-Janua, 173–176.

<https://doi.org/10.1109/ICT.2002.1190293>.

(2) Qin, M.; Yan, Q.; Liu, Y.; Wang, H.; Wang, C.; Lei, T.; Vecchio, K. S.; Xin, H. L.; Rupert, T. J.; Luo, J. Bulk

High-Entropy Hexaborides. J Eur Ceram Soc 2021, 41 (12), 5775–5781. <https://doi.org/10.1016/J.JEURCERAMSOC.2021.05.027>.

SESSION EL10.02: Growth and Characterization II
Session Chairs: Andrew Greytak, Zeger Hens and Liberato Manna
Monday Afternoon, November 27, 2023
Hynes, Level 3, Ballroom A

1:30 PM *EL10.02.01

Ligands on Nanocrystal Surfaces - What Ligand Stripping Can Tell Us Zeger Hens; Ghent University, Belgium

Colloidal semiconductor nanocrystals are in most cases synthesized as hybrid inorganic/organic objects where organic ligands passivate the surface of the inorganic crystallite. This organic ligand shell helps controlling the growth of nanocrystals during synthesis, stabilizes nanocrystal dispersions by steric hindrance, contributes to the electronic passivation of surface-localized electronic states and determines the mobility of charge carriers in nanocrystal films. Hence, the importance of understanding the binding and packing of ligands to nanocrystal surfaces in nanocrystal science.

In this contribution, we focus on the binding of metal salts such as cadmium oleate, zinc oleate or zinc halides to semiconductor nanocrystals surfaces. We first discuss how the displacement of such Lewis acids through the addition of Lewis bases can be used to probe the binding energy of these metal salts to the nanocrystal surface. By gradually increasing the concentration of the Lewis base, displacement isotherms can be recorded and analyzed using surface-adsorption models. Using this approach on core nanocrystals, such as CdSe, CdS and ZnSe, we show that Z-type ligands can be ranked according to their binding strength. In a second step, we use the method to probe the distribution of binding energies across the nanocrystal surface, where in the case of 2D colloidal nanoplatelets, the weakest ligands could be localized at the nanoplatelet edges. Finally, we extend the method to InP/ZnSe core/shell nanocrystals, where we relate the progressive displacement of zinc halides from the shell outer surface to the creation of a non-radiative recombination channel that can still compete with the radiative recombination of electron-hole pairs to quench the photoluminescence. This result contrasts starkly with colloidal CdSe nanoplatelets, where the passivation of edge states by a CdS crown suffices to eliminate non-radiative recombination related to ligand desorption.

We conclude by highlighting the relation between progressive ligand stripping and photoluminescence quenching as a most useful stress test to evaluate the emission characteristics of colloidal semiconductor nanocrystals.

2:00 PM EL10.02.02

Designer Zwitterionic Phospholipid Capping Ligands for Structurally Soft Metal Halide Nanocrystals Viktoriia Morad^{1,2}, Andriy Stelmakh^{1,2}, Mariia Svyrydenko^{1,2}, Leon G. Feld^{1,2}, Marcel Aebi^{1,2}, Joel Affolter¹, Christop J. Kaul¹, Nadine J. Schrenker², Sara Bals³, Ihor Cherniukh^{1,2}, Gabriele Raino^{1,2}, Andrij Baumketner⁴ and Maksym V. Kovalenko^{1,2}; ¹ETH Zurich, Switzerland; ²Empa—Swiss Federal Laboratories for Materials Science and Technology, Switzerland; ³University of Antwerp, Belgium; ⁴National Academy of Sciences of Ukraine, Ukraine

The success of colloidal semiconductor nanocrystals (NCs) in science and commercial optoelectronic devices is inextricable from their surfaces. A versatile and robust surface functionalization of lead halide perovskite (LHP) NCs and NCs of other structurally soft metal chlorides, bromides, and iodides poses a formidable challenge. Compared to conventional semiconductors, surface capping ligands bind in a non-covalent, rather ionic manner; furthermore, they may readily engage in adverse solubilization equilibria with the ions constituting the labile inorganic cores of these NCs. We posited that the vast and facile molecular engineering of phospholipids as zwitterionic surfactants make for an attractive platform to deliver highly customized surface chemistries for diverse metal halide NCs. Molecular dynamics simulations inferred that ligand-NC surface affinity is primarily governed by the structure of the zwitterionic head group, particularly by the geometric fitness of the anionic and cationic moieties into the surface lattice sites, as corroborated by the solid-state nuclear magnetic resonance (NMR) spectroscopy. Lattice-matched primary ammonium phospholipids enhance the structural and colloidal integrity of hybrid organic-inorganic LHPs – FAPbBr₃ and MAPbBr₃ (FA-formamidinium; MA-methylammonium), as well as a range of other functional metal halides. The molecular structure of the organic ligand tail instead governs the long-term colloidal stability and compatibility with solvents of diverse polarity, from hydrocarbons to acetone and alcohols. These NCs exhibit photoluminescence quantum yield (PL QY) above 96% in solution and solids, retained after repetitive purification steps, and minimal PL emission intermittency at the single particle level with an average ON fraction as high as 94%, as well as bright and high-purity (ca. 95%) single-photon emission.

2:15 PM EL10.02.03

Conformational Entropy Mediated Orientation of Ligated Nanocrystals Eliza Price and William Tisdale; Massachusetts Institute of Technology, United States

Colloidal nanocrystals (NCs) are often assembled into ordered superlattices (SLs) for incorporation into optoelectronic devices. For some NCs, self-assembly is dominated by the inorganic core, depending on NC size and shape. However, when NCs are coated in a soft ligand layer, self-assembly behavior can become unpredictable due to the competing interactions of the inorganic and organic components. To address this knowledge gap, we investigated how the conformational entropy of organic ligands mediates the orientation of non-spherical NCs in self-assembled SLs.

With a framework combining numerically derived ligand density distributions and analytical expressions for the freely jointed chain model, we predict NC orientation for several polyhedral shapes, self-assembled structures, and ligand lengths. Additionally, we compare rotationally ordered and disordered NC SLs to estimate the driving force for nanocrystal orientation, finding a strong dependence on both NC shape and ligand length. We test the predictive ability of this framework by comparing model results to the experimentally observed orientation of truncated octahedral PbS NCs in BCC and FCC superlattices. Our work offers a tractable starting point for the thermodynamic understanding of polyhedral NCs with competing core-ligand interactions and may inform experimental efforts to achieve the self-assembly of coherently oriented NCs for high-quality devices.

2:30 PM EL10.02.04

Selective Agglomeration for 2D-Separation: Insights into the Surface Interaction in Colloids[AzitaRezvani](#)¹, ZhuangWang¹ and DorisSegets^{1,2}; ¹Institute for Energy and Materials Processes (EMPI), Germany; ²Universität Duisburg-Essen, Germany

Small semiconductor nanoparticles (NPs), known as quantum dots (QDs), have a wide range of applications in various fields, including electronics, optoelectronics, photovoltaics, biotechnology, and medicine. The unique properties of QDs, such as size-tunable emission, high photostability, and high quantum yield are intricately linked to their size, shape, composition, and surface chemistry [1]. Hence, the dispersity of a sample in all these dimensions becomes one of the most crucial factors to tailor the final product properties. Although the synthesis of colloidal QDs has seen impressive progress in the past two decades, even with sophisticated synthetic techniques, the obtained sample always exhibits a certain dispersity [2]. It can be assumed that this will be even more dominant in large-scale productions which makes it essential to narrow down the dispersity in different dimensions by post-processing approaches. However, there is a clear lack of scalable post-synthetic separation strategies for such small colloids, even in terms of size. In recent studies, selective agglomeration has shown promise as an effective approach with the potential to be scaled up in continuous setups for size-classification of ZnS QDs smaller than 5 nm [3, 4]. It is based on the titration of an already existing dispersion by a poor solvent to selectively flocculate one colloidal component.

A highly relevant case in this context is the post-synthetic classification after the larger-scale synthesis of core-shell QDs, where the shell thickness directly influences the final performance of the product. Therefore, we studied a mixture of InP QDs (first colloidal component) and InP/ZnS (core-shell) QDs (second colloidal component), both having oleylamine on the surface [5]. Considering the small size of QDs, the main challenge in such a binary system is the characterization of the coarse and the fine fraction after separation regarding the mixture composition and particle size distribution of each individual component, in each fraction. To achieve this, we developed a combination of UV-Visible spectroscopy, X-ray photoelectron spectroscopy, analytical ultracentrifugation, and inductively coupled plasma optical emission spectroscopy. Their combination resulted in a toolbox for the characterization of such a complex system which is applicable to similar and potentially even more complex multinary colloids. Finally, the toolbox enables a systematic study of important parameters including the type of good and poor solvents and their volume ratios, and to establish a stability map for the binary mixture.

In conclusion, we developed a strategy to characterize binary colloids of ultrasmall QDs during their selective separation. We successfully established a stability map that provides a fundamental understanding of surface interactions and driving forces in binary colloids in solvent mixtures. This is so far not addressed but it is the main step towards the design of multidimensional classification processes reliant on selective agglomeration. Finally, based on these findings we reported the results of the 2D-separation of ultrasmall QDs in terms of size and composition.

References

- [1] D. Vak et al., Adv. Energy Mater. 2015, 5, 1401539.
- [2] D. Segets et al., Journal of Physical Chemistry C. 2015, 119, 4009–4022.
- [3] C. Menter and D. Segets, Advanced Powder Technology 2019, 30, 2801–2811
- [4] D. Zhitomirsky et al, Nano Lett. 2012, 12, 2, 1007–1012
- [5] Z. Wang and D. Segets, React. Chem. Eng., 2023, 8, 316

2:45 PM EL10.02.05

Expedition Nanoparticle Transfer via Combinatorial Electrostatic Engineering[DoeunKim](#), Ji YeongMa, JuhyeongLee, GyurinKim, Jang-HwanHan, Hyun MinKim and Hyeon-HoJeong; Gwangju Institute of Science and Technology, Korea (the Republic of)

The versatility of solution chemistry offers exceptional flexibility in synthesizing functional nanoparticles with tailored materials, shapes, and surface properties. However, the translation of these colloidal nanoparticles into the industrial domain remains a significant challenge due to the lack of a rapid and uniform transfer technique for achieving 2D-like monolayered coating – an essential requirement for various applications, particularly photonic devices for plasmonics (metals), down- and up-conversion luminescence (semiconductors), and Mie resonance (dielectrics).

We here present a significant advancement in scalable nanoparticle transfer techniques, enabling the efficient transport of nanoparticles from liquid to a 2-inch wafer remarkably within 10 seconds to reach over 40% surface coverage in a 2D monolayered fashion. This transfer rate, to the best of our knowledge, represents the record, reaching 2.03 cm²/s with 30% nanoparticle coverage – an order of magnitude faster than the currently reported results in the literature. Our success lies in the refinement of the well-established electrostatic coating method, where we combinatorially engineer electrostatic features of both the nanoparticles and the surface. This electrostatic engineering leads to enhanced potential differences and thus generates strong electrostatic attraction forces between the nanoparticle and the substrate. Notably, electrostatic repulsion also plays a crucial role, self-limiting the coating process to a single layer due to repulsive interactions between nanoparticles. This charge-sensitive dynamic further offers ‘one-shot’ nanoparticle patterning when the surface is patterned with two opposite charges, i.e. the nanoparticles are selectively coated only on the oppositely charged area. Furthermore, our approach can be seamlessly extended to various surface materials, including dielectrics, conducting metal oxides and polymers, and 3D-printed polymers, without requiring conventional surface functionalization and treatment processes specific to individual materials.

In this presentation, we will discuss the nanoparticle coating method in which the electrostatic features are engineered, highlighting its key features such as rapid coating speed, large-area uniformity, charge-sensitive selectivity, and flexibility in surface materials and geometries. We will indeed demonstrate how this coating technique enables the realization of novel functional plasmonic metasurfaces, exhibiting consistent resonating colors across diverse material and geometrical platforms.

3:00 PM BREAK

3:30 PM *EL10.02.06

Ligand Exchange Equilibrium at Quantum Dot Surfaces in Polar and Aqueous Solvent Environments[AndrewB. Greytak](#); University of South Carolina, United States

Our group and many others have contributed to an increasingly detailed understanding of the surface chemistry of representative compound semiconductor quantum dots, including metal chalcogenides, pnictides, and halide perovskites with effective bandgaps spanning much of the visible and infrared spectrum. Such particles are frequently stabilized by organic molecules with nucleophilic or anionic headgroups that coordinate surface atoms. To date, the greatest understanding has been achieved in non-polar or less polar solvents in which charge balance helps to simplify the range of surface reactions that must be considered. Techniques such as NMR and infrared spectroscopy, mass spectrometry, and isothermal titration calorimetry have helped to reveal the chemistry at such surfaces, including the importance of ligand interactions that can govern the composition and local organization of the surface monolayer.

It is critically important to extend the understanding of such nanocrystal surfaces to polar solvents, including aqueous solution required for biological applications and polar organic mixtures favored for storable nanocrystal inks for electronic devices. However, polar solvents and buffers introduce additional challenges for fundamentals studies due to charge stabilization, acid-base equilibria, protic buffer components, oxidation, and the need for core/shell structures to achieve good photoluminescence quantum yield.

I will describe our group’s efforts to quantify ligand association and exchange reactions on nanocrystal surfaces in polar and aqueous solutions, including coordination of quantum dots by imidazoles, thiolates, and polymeric ligands, and prospects for extending these studies to additional classes of materials including magnetic oxides and halide perovskites. I will also emphasize the advantages and limitations of isothermal titration calorimetry as a tool to study the surfaces of colloidal nanostructures and compare the binding of different ligand architectures in polar environments.

4:00 PM EL10.02.07

Non-Einsteinian Viscosity Reduction in Water-Based Nanofluids of Boron Nitride Nanotubes, Graphene Nanoflakes and Carbon Nanotubes[AndreGuerra](#), MilanMaric, AlejandroD. Rey and PhillipServio; McGill University, Canada

Introduction: Nanoparticles have multiple applications, including drug delivery systems, biosensing, and carbon capture. Non-Einstein-like viscosity reduction has been reported in

nanoparticle-polymer blends at low nanoparticle concentrations. More recently, a similar non-Einsteinian viscosity reduction effect has been observed in aqueous ultra-low concentration carbon-based nanofluids of graphene nanoflakes (GNF) and multi-wall carbon nanotubes (MWCNT)[1,2]. The use of nanoparticles as promoters of the growth of gas hydrates has been an active research field in the past decade[3–6]. This study aimed to explore the viscosity of ultra-low concentration boron nitride nanotube (BNNT) nanofluids in the presence of air and methane.

Methods: We use a boron nitride nanotube functionalized with hydrophilic groups in rheological experiments to investigate the viscosity reduction in ultra-low concentration nanofluids (0.1–10 ppm). We measure the dynamic viscosity in an air atmosphere and methane (0–5 MPa) at low temperatures (0–10 C).

Results: A negligible effect on the temperature dependence of viscosity was found. Ultra-low concentrations of BNNT reduced the viscosity of the nanofluid by up to 29% at 10 ppm in the presence of methane. The results presented here were compared to similar studies on O-GNF and O-MWCNT nanofluids, which also reported significant viscosity reductions. The non-Einsteinian viscosity reduction measured in BNNT nanofluids in the present work was higher than the effect measured for O-GNF and O-MWCNT nanofluids.

Conclusions: This work identified a non-Einsteinian viscosity reduction in BNNT nanofluids, exacerbated by methane dissolved in the nanofluid. In a previous study, we suggested the role of nanoparticles in viscosity reduction by disrupting hydrogen bond networks and facilitating energy dissipation through enhanced density fluctuations. At ultra-low concentrations, these effects may dominate over conventional drag and viscous forces present higher-concentration nanofluids and colloidal suspensions, which lead to increased viscosity with particle loading (Einsteinian behavior). The effects measured for the three different nanoparticles studied so far indicate the role of nanoparticle geometry and surface chemistry on the disturbance of hydrogen bond networks in water leading to the reduction in dynamic viscosity. We suggest computational modeling to investigate molecular scale interactions to elucidate the non-Einsteinian viscosity reduction.

References:

1. McElligott A, Guerra A, Du CY, Rey AD, Meunier J-L, Servio P. Non-Einsteinian Viscosity Behavior in Plasma-Functionalized Graphene Nanoflake Nanofluids and Their Effect on the Dynamic Viscosity of Methane Hydrate Systems. *ACS Appl Energy Mater.* 2022;5: 12977–12990.
2. McElligott A, Guerra A, Du CY, Rey AD, Meunier J-L, Servio P. Dynamic viscosity of methane hydrate systems from non-Einsteinian, plasma-functionalized carbon nanotube nanofluids. *Nanoscale.* 2022;14: 10211–10225.
3. McElligott A, Meunier J-L, Servio P. Effects of nitrogen-doped graphene nanoflakes on methane hydrate formation. *Journal of Natural Gas Science and Engineering.* 2021;96: 104336.
4. McElligott A, Uddin H, Meunier JL, Servio P. Effects of Hydrophobic and Hydrophilic Graphene Nanoflakes on Methane Hydrate Kinetics. *Energy and Fuels.* 2019;33: 11705–11711.
5. Pasięka J, Coulombe S, Servio P. Investigating the effects of hydrophobic and hydrophilic multi-wall carbon nanotubes on methane hydrate growth kinetics. *Chem Eng Sci.* 2013;104: 998–1002.
6. Pasięka J, Jorge L, Coulombe S, Servio P. Effects of As-Produced and Amine-Functionalized Multi-Wall Carbon Nanotubes on Carbon Dioxide Hydrate Formation. *Energy and Fuels.* 8 2015;29: 5259–5266.

4:15 PM EL10.02.08

Engineering the III-V/II-VI Interface in Core-Shell Heterostructures in Colloidal Nanocrystals Yields Bluer Emission [Anirajit Gupta](#), Jun Hyuk Chang, Justin Ondry, Zirui Zhou and Dmitri V. Talapin; University of Chicago, United States

A persistent red shift and broadening of the emission peak during the shelling step renders obtaining blue emission from III-V colloidal nanocrystals difficult, despite significant efforts invested in improving synthetic protocols. Previous studies of the type-I core-shell III-V/II-VI interface have ascribed this red shift to factors such as the thickness and shape of the II-VI shell, the band energy alignment of the core-shell, surface dangling defects, surface oxidation, and structural disorder associated with lattice defects. In particular, in-depth studies of the InP/ZnS interface have established that Zn²⁺ ions incorporated at substitutional or interstitial sites introduce internal disorder, observed via broadened Raman lines that are accompanied by a pronounced increase in Stokes shift of the emission. In contrast, when the long-chain organic ligands on as-synthesized InP QDs are exchanged for S²⁻ ligands, the sulfide-capped nanocrystals show little change in the Raman spectrum even after high-temperature annealing. We hereby employ the knowledge from the InP system to ternary alloyed In_{1-x}Ga_xP nanocrystals that are synthesized in a molten halide salt reaction medium. We optimize the III-V/II-VI interface in bright In_{1-x}Ga_xP/ZnS core-shell nanocrystals at the shelling step, allowing us to yield bluer emissions from systems that are otherwise very similar in size and composition.

4:30 PM EL10.02.09

Multilayer Diffraction: A New Tool for Probing the Interparticle Region in Nanocrystal Superlattices [Stefano Toso](#)¹, [Dmitry Baranov](#)^{2,1}, [Umberto Filippi](#)¹, [Cinzia Giannini](#)³ and [Liberato Manna](#)¹; ¹Istituto Italiano di Tecnologia, Italy; ²Lund University, Sweden; ³Consiglio Nazionale delle Ricerche, Italy

Owing to their hybrid nature, the properties of nanocrystals are determined by both their inorganic core and their organic shell. This is particularly true when nanocrystals are packed into superlattices, where the ligands surrounding each particle stop being just a surface coating and become an actual component of a more complex nanostructured material. Thanks to these organic spacers, each nanocrystal can retain its non-bulk characteristics while also interacting with neighbors through a variety of coupling mechanisms.

Since these phenomena take place at short distances (electronic coupling = neighboring particles; optical coupling = dozens of nanometers), quantifying parameters like the interparticle distance and the degree of disorder at very local scales is crucial for understanding the superlattice properties. This, however, is far from trivial: the grazing-incidence diffraction techniques usually employed for such studies provide an average response over a much wider volume of the sample, and the diffracted signal comes mainly from the inorganic core, overshadowing the contribution of the inter-nanocrystal region.

In our research, we propose a novel approach to answer such questions. Our method is based on Multilayer Diffraction, an intriguing collective interference effect known for epitaxial thin films but never reported for colloidal nanocrystals before.[1] This phenomenon occurs when X-rays are diffracted by nanocrystals stacked vertically: the radiation scattered by each particle interferes with that diffracted by neighbors, creating fringes of constructive interference. Since the interfering radiation comes from nanocrystals, the fringes are convoluted by their Bragg peak profile, thus retaining information on the nanocrystals structure, size, and orientation. However, the position of the fringes depends on the overall stacking periodicity, which includes the inter-nanocrystal spacing, while their broadening provides a direct quantification of the stacking disorder.

We will retrace our journey into the understanding of Multilayer Diffraction, from its serendipitous discovery in CsPbBr₃ nanocubes superlattices,[2] to the development of open-source pattern fitting algorithms,[3] and their application to films of colloidal nanoplatelets,[4] where the unique advantages of Multilayer Diffraction can be appreciated at their best. Finally, with the help of literature and simulations we will show that Multilayer Diffraction is a much more common phenomenon than one might think, and is routinely observed without being recognized in a variety of appealing nanomaterials behind the borders of halide perovskites.

[1] Toso, S. et al. Collective Diffraction Effects in Perovskite Nanocrystal Superlattices. *Accounts of Chemical Research* 2023 56 (1), 66-76

[2] Toso, S. et al. Multilayer Diffraction Reveals That Colloidal Superlattices Approach the Structural Perfection of Single Crystals. *ACS Nano* 2021, 15 (4), 6243–6256.

[3] Toso, S. et al. Structure and Surface Passivation of Ultrathin Cesium Lead Halide Nanoplatelets Revealed by Multilayer Diffraction. *ACS Nano* 2021, 15 (12), 20341–20352.

[4] Toso, S. et al. Collective Diffraction Effects in Perovskite Nanocrystal Superlattices. *Accounts of Chemical Research* 2023 56 (1), 66-76

4:45 PM EL10.02.10

Combining Organic or Inorganic Dyes with Lanthanide Nanoparticles to Overcome the Weak Absorption of Lanthanide Ions [Zhongzheng Yu](#); University of Cambridge, United Kingdom

Lanthanide-based nanoconstructs have gained increasing attention in recent decades due to their unique optical and magnetic properties. The design of lanthanide-based nanosystems is expected to contribute to various applications including biomedical applications, data storage, optical communications, remote sensing, super-resolution fluorescence microscopy, and night vision etc., due to their advantageous properties such as excellent photostability, non-photobleaching, low cytotoxicity, large Stokes/anti-Stokes shift, narrow and tunable emission peaks. There are two major limitations for lanthanide ions, including weak absorption and low photon conversion efficiency. Developing novel lanthanide-based nanoconstructs and uncovering new insights of the energy conversion pathways are key to the advancement of the field. Combining organic or inorganic dyes with lanthanide nanoparticles to form nanohybrids is highly possible to overcome the weak absorption of lanthanide ions. In this talk, I will introduce our recent work about a) dye-sensitized lanthanide-doped nanoparticles, b) novel nanocomposites as photothermal agents and their corresponding applications in light-controlled release, light-activated photomedicines, sensing, multiplexing imaging, photoacoustic imaging and photothermal therapy. I hope the strategies and studies presented in this talk could further enhance the attractiveness of lanthanide-based nanoconstructs towards clinical translation and applications influencing our daily life.

8:30 AM *EL10.03.01

Semiconductor Nanocrystals and Copper Clusters for Radiotherapy: The Importance of the Coating and Composition for the Radio Incorporation of Cu-64, Their Photo-and Colloidal- StabilityTeresa Pellegrino; Italian Institute of Technology, Italy

Cation exchange (CE) reactions on nanocrystals consists of the replacement of cations in the nanocrystalline structure with different metal ions while maintaining in place the anion framework. This technique has been extensively used for the synthesis of nanocrystals at different compositions. Here, we exploit CE reactions to radiolabel cadmium-free semiconductor NCs of ZnS, ZnSe and chalcopyrite (CuFeS₂) NCs with Cu-64 radioisotope. [1] To make it possible a one-step CE protocol that is straightforward and highly efficient while maintaining good NC colloidal stability, the type of ligand coating to be chosen as water soluble stabilizer agents and the amount of Copper-64 to be exchanged were the key factors. This enabled to obtaining ⁶⁴Cu:CuFeS₂ in very high yields which did not require any further work out for the purification thus speeding up the radiolabeled NCs preparation. This unique approach of CE reaction enables to tune the specific activity in a wide range (from 2 to 100 TBq/g) with an unprecedentedly record value of specific activity up to 100 TBq/g. In addition, among the NCs explored, CuFeS₂ NCs [2] even after partial-CE reaction with Copper-64 were promising heat mediators for photo-thermal therapy (PPT). The synergic toxicity of photo-ablation and ⁶⁴Cu mediated radiotherapy ionization is here used to eliminate the glioblastoma and epidermoid carcinoma tumor cells. Further, as demonstrated with preliminary and unpublished results, the dual therapy is evaluated on xenograft mice models bearing epidermoid carcinoma tumor, resulting in elimination of solid tumor mass in mice. A modified version of this protocol was also established to obtain copper-64 radio-clusters of sub nanometer size and having also radio and photoluminescent properties. The optical stability of the copper clusters was tuned by controlling the size, coating and composition of the clusters and it will be also discussed.

References

- [1] Avellini, T. et al, Adv. Funct. Mat. 2020, 30, 2002362
[2] Ghosh, S. et al, Chem. Mater. 2016, 28, 13, 4848.

9:00 AM EL10.03.02

Conjugation of Quaternary Zn-Cu-In-S/ZnS Quantum Dots to Porphyrins and Their Photodynamic Therapy and Antibacterial ActivitiesSamuel O. Oluwafemi; University of Johannesburg, South Africa

Photodynamic therapy (PDT) is a non-invasive treatment modality that uses photosensitizing drugs (PS) to generate reactive oxygen species for the destruction of abnormally growing cells or microorganisms. Porphyrins are the most widely used PS in PDT, their clinical application is limited by poor water solubility, which often results in aggregation and their low quantum yield of ROS generation after light absorption in the near infra-red region (NIR). To overcome these limitations and improve PDT efficacy, we herein report the conjugation of Zn-Cu-In-S/ZnS (ZCIS/ZnS) quantum dots (QDs) to porphyrins and evaluated their PDT efficiency and antibacterial potency. The ZCIS/ZnS QDs and porphyrins were evaluated to determine the optimized reaction conditions for the formation of QDs-porphyrin conjugates. The PDT efficiency of ZCIS/ZnS QDs, porphyrin and NIR emitting QDs-Porphyrin conjugates was evaluated against murine metastatic melanoma (B16 F10 Nex 2) cell line in the absence of light and under LED irradiation. B16 F10 Nex 2 exhibited the highest reduction in cell viabilities following exposure to the conjugate under LED light irradiation compared to the bare QDs and porphyrins (1%). The antimicrobial therapy studies were tested by exposing Escherichia coli (ATCC 25922) to ZCIS/ZnS QDs, porphyrin and the conjugate. The conjugate showed greater antibacterial effects compared to the bare ZCIS/ZnS QDs even in the absence of light. The results of this study show that the as-synthesized conjugate is a suitable and promising class of material for dual anticancer and antimicrobial PDT.

9:15 AM EL10.03.03

Multimodal Nanoparticle Bioengineering for X-Ray Fluorescence ImagingGiovanni Marco Saladin¹, Bertha Brodin¹, Carmen Vogt¹, Kian Shaker¹, Nuzhet Inci Kilic¹, Yuyang Li¹, Kenth Andersson¹, Idris Yazgan², Marie Arsenian-Henriksson³, Muhammet S. Toprak¹ and Hans M. Hertz¹; ¹KTH Royal Institute of Technology, Sweden; ²Kastamonu University, Turkey; ³Karolinska Institutet, Sweden

Multimodal nanoparticles (NPs) are promising contrast agents for multiscale and complementary bioimaging. It is essential to study the interactions between the cellular environment and NPs in order to evaluate their functional and toxic properties. Here, we present a methodology for complementary imaging to evaluate the biocompatibility and biodistribution of dual-mode hybrid NPs *in vitro* and *in vivo*. These inorganic NPs are composed of an X-ray fluorescent (XRF) active element, complemented with dye-doped silica coating, conjugated carbon quantum dots, or decorated superparamagnetic iron oxide NPs. We investigated the advantages of whole-animal XRF imaging and local XRF computed tomography (XFCT), characterized by high specificity and sensitivity. The complementary properties enabled the multiscale visualization of the NPs *in vitro* and in tissues from excised organs via optical fluorescence microscopy and correlative imaging with *in vivo* magnetic resonance imaging (MRI). The optimization of the hybrid NP surface chemistry and colloidal stability led to biocompatible contrast agents for XRF molecular imaging.

9:30 AM *EL10.03.04

Zwitterionic Polymer Coatings for Stable and Stealthy Nanocrystals in Bioimaging and MicromanipulationThomas Pons; LPEM ESPCI/CNRS/SU, France

Inorganic nanocrystals such as gold, iron oxide and semiconductor nanocrystals have unique optical or magnetic properties that make them very promising for cancer detection, imaging and therapeutic applications. The surface ligands of these nanoparticles play a critical role in their application and control the nanoparticle interaction with biomolecules and cells. I will present the development of zwitterionic copolymer ligands containing a multidentate anchoring block, adaptable to the type of nanoparticle, and that provide a stable binding to the surface of different inorganic nanocrystals, enabling prolonged biological applications. The nature of the zwitterion group has a strong influence on antifouling properties, ranging from specific interactions with some biomolecules to a complete suppression of interactions with serum biomolecules, cytosolic components and macrophage cells. This enables various applications including intracellular targeting of fluorescent quantum dots, *in vivo* tracking of individual circulating cells, or micromanipulation in the nucleus of living cells using magnetic nanoparticles.

10:00 AM BREAK

10:30 AM *EL10.03.05

Peptidic Bioactivable Au Nanoclusters for Extracellular Vesicles and Cellular Labelling and BiosensingValerie Marchi-Artzner¹, Regina Cheichio¹, Solene Ducarre¹, Ester Butera¹, Pascale Even-Hernandez¹ and Celia Ravel²; ¹University Rennes, France; ²CHU Rennes, France

We present an overview of the interaction between ultrasmall luminescent gold nanoclusters and lipidic or biological membranes, showing that it is possible to induce a large change in membrane structures or not. The synthesis of original aqueous bioactivatable and PEGylated AuNC suspensions of various charges were performed by using synthetic short peptides. This chemical platform provides various charged AuNC with potential sensitivity to the environment for biosensing applications.

Extracellular vesicles (EVs) are well-known membrane-limited particles that are secreted by healthy and cancerous cells. EVs are heterogeneous in size and three subtypes are described depending on the location of secretion: microvesicles, myelinosomes and exosomes. EVs are identified in human follicular fluid as a mode of communication in the ovarian follicle (Neyroud A. S. et al. Int. J. Molecular Sci. **2022**). In addition EVs involved in cell-cell communication are considered as biomarkers for early cancer diagnosis. The analysis of their content and their labeling with easily detectable nanoparticles could enable the development of a powerful tool for the early diagnosis of specific diseases.

In this view, Gold nanoclusters (AuNCs) appear as a recent class of non-toxic fluorophores. Their brightness, their ultrasmall size (< 2 nm) and large window of fluorescence lifetime (1 ns – 1 ms) and their good biocompatibility make them an attractive alternative as fluorescent probes for biological labeling and bioimaging.

Following incubation of the AuNCs with oppositely charged vesicles, either liposomes or EVs, the strong electrostatic attraction resulting in the adsorption of AuNCs to the membranes was evidenced by complementary techniques such as zetametry, fluorescence optical microscopy, SAXS, and cryo-TEM. In the presence of an excess of oppositely charged AuNCs, the liposomes strongly adhere to each other without disrupting their membrane whereas the EVs extracted from human follicular fluid rearrange into a hybrid lamellar phase. Instead, in the presence of a membrane surface excess, AuNCs do not change the size of the membrane thickness, so they are positioned between the polar headgroups of the membrane phospholipids. As opposed to larger gold nanoparticles, the smaller size of AuNCs not only prevents the deformation of biological membranes but also allows labeling with higher spatial resolution (R. Cheichio et al. J. Phys. Chem. Lett. **2022**).

By adjusting the surface ligands, these probes are easily internalized into cells and *in vivo* organisms such as Arabidopsis plant or cancerous cell lines. We demonstrated their *in vivo* targeting ability because of specific recognition groups (R. Cheichio et al. ACS Nano materials **2023**) and biosensing by fluorescence because of their sensitivity to microenvironment.

In addition their small size make them attractive to encapsulate them into liposomes without damaging the compartment integrity and then to be delivered into the extracellular vesicles. We demonstrated first the possible encapsulation of the AuNC into liposomes for drug delivery. Cell-like-sized vesicles (GUVs) encapsulating red or blue Au NCs were successfully obtained by

an innovative method using emulsion phase transfer. Finally, exosome-like-sized vesicles (LUVs) containing Au NCs were obtained with an encapsulation yield of 40%, as estimated from ICP-MS (R. Chiechio et al. *Nanomaterials* **2022**). Finally the lipidic membranes composition was optimized with ionizable lipids so that the mixture of the liposomes and EVs results in efficient fusion and delivery of AuNC into the lumen of EVs. The lipid exchange was demonstrated by FRET experiments and fusion was revealed by the increased size and the fluorescent labelling of the fused EVs. The fused EVs encapsulating the AuNC were successfully separated by size exclusion chromatography. Such nanostructures offer promising candidates for fluorescent in vivo biosensing and biolabeling.

11:00 AM EL10.03.06

Lithographic Synthesis of Anisotropic Nanomagnetic Bars for *In-Vivo* Magnetic Particle Imaging and Spectroscopy Noah Kent¹, Eli Mattingly², Keisuke Nagao¹ and Polina Anikeeva¹; ¹Massachusetts Institute of Technology, United States; ²Harvard University, United States

Magnetic Particle Imaging (MPI) is an imaging modality where a field free point is scanned over magnetic nanoparticle (MNP) tracers generating a temporally resolved spatial map of particle distribution, and velocity [1]. MPI tracers are designed to be biocompatible enabling in-vivo MPI. Additionally, by analyzing the spectral frequency response of MPI tracers as their magnetization reverses, information about their local environment can be extracted (e.g. temperature, viscosity). This approach, termed magnetic particle spectroscopy (MPS), leverages the changes in the Neel and Brownian behavior of a tracer as a function of the external parameter being measured [2].

In MPS the resolution (the spectral information available) is highly dependent on the magnetic properties of the magnetic tracer. To achieve high spatial resolution, the magnetic field range over which a particle reverses its magnetization should be small. For a strong MPS signal, the particle should be physically anisotropic (to have a more pronounced Brownian rotation) and the dynamics of magnetic switching behavior should be independent of drive field frequency.

Guided by nanomagnetic simulations in MuMax3, we lithographically fabricated Permalloy (PY, Ni80Fe20) nanomagnetic bars of varying sizes with a length to width ratio of 5:1 and layered structure that is Ti 5nm/ PY 30nm/ Ti 5nm. Due to shape anisotropy PY structures of these dimensions are strongly uniaxial ferromagnetic with the magnetic hard axis along the length of the bars. These bars were released into solution via dissolution of a sacrificial layer. To enhance colloidal stability and enable biocompatibility, the bars were chemically coated with silica using the modified Stöber method. The silica coating also allowed the bars to be passivated with poly(ethylene glycol) via ester-carbodiimide chemistry. The resultant mixture is colloidally stable, biocompatible lithographically fabricated magnetic nanoparticles.

Initial MPS measurements show that due to the uniaxial ferromagnetic switching behavior demonstrated in the bars, the magnetic field range over which MPI signal is measured is a factor of 5 smaller than the current state of the art particles (Synomag®). This is directly correlated with the particle's spatial resolution as a tracer. For MPS, comparison between a large number of spectral harmonics gives information about the local environment. State of the art MPI tracers lose harmonic signal around the 15th harmonic, but anisotropic magnetic bars retain strong harmonic signal until the 24th harmonic. Additionally, harmonic strength relative to overall magnetic signal is stronger in bar particles when compared to Synomag®. Current work is focused on further optimizing the bar particles for their future applications in vivo.

References

[1] Talebloo, N. et al. *J. Magn. Reson. Imaging*. 2020, 51: 1659-1668.

[2] Wu, K. et al, *ACS Appl. Nano Mater.* 2020, 3: 4972-4989.

11:15 AM EL10.03.07

Subak: A Novel Color-Switching Reporter for Nuclease Activity and Nucleic Acid Detection Soonwoo Hong, Jada Walker, Aaron Luong, Yu-An Kuo, Yuan-I Chen, Trung Duc Nguyen, Yujie He, Anh Thu Nguyen, Jennifer S. Brodbelt and Tim Yeh; The University of Texas at Austin, United States

The COVID-19 pandemic has underscored the importance of nucleic acid amplification tests for reliable and sensitive detection of pathogens. While recent advancements have eliminated the need for specialized equipment, the fluorescence readout remains crucial in highly accurate nucleic acid assays. However, existing fluorescent reporters, such as TaqMan and DNaseAlert, which solely rely on fluorescence resonance energy transfer (FRET), have limitations in terms of cost, quantitative sensing, and dual labeling requirements. We introduce Subak, a novel DNA-templated silver nanocluster (DNA/AgNC) probe to address these challenges. Subak exhibits green fluorescence emission when intact but undergoes a remarkable color-switching to bright red upon fragmentation by nuclease activities, distinct from other fluorescent nanomaterials.

Compared to conventional FRET reporters, Subak offers significant advantages, including a cost reduction of over 60-fold (\$1 vs. \$62 per nanomole) and the ability to support ratiometric sensing of nuclease activities. Subak reporters are synthesized using a 37-nt long hairpin DNA strand, silver salt (AgNO₃), and a reducing agent (NaBH₄). As none of the starting materials are inherently fluorescent, purification steps to remove excess products are unnecessary. Addition of DNase I to Subak results in a discernible color change within 20 minutes, visible to the naked eye under a UV lamp due to the effective excitation of DNA/AgNCs by UV light.

Subak reporters enable both single-color detection and ratiometric sensing. In single-channel detection, fluorescence enhancement ratios of up to 20-fold are achieved upon Subak reporter digestion (using Subak and DNase I). For ratiometric sensing, Subak and Cas12a demonstrate a remarkably low limit of detection (~1.19 pM) for SARS-CoV-2 strands in a DETECTR assay without the need for pre-amplification steps. Notably, this performance is comparable to DNaseAlert under the same conditions, exhibiting 15 times higher fold changes (221-fold vs. 14-fold).

The color-switching mechanism of Subak reporters arises from a combination of altered base-cluster coordination geometry and the modified size/shape of the fragmented AgNC. Electrospray ionization mass spectrometry (ESI-MS) analysis identifies preferred cleavage sites on Subak reporters and determines silver stoichiometries before and after fragmentation. The intact Subak reporters emit green fluorescence due to an Ag₁₃ cluster, while fragmented Subak reporters emit red fluorescence attributed to an Ag₁₀ cluster. This color-switching property results from the breakdown of Ag₁₃ into Ag₁₀ and Ag₃. Traditional nucleation-and-reduction methods that yield Ag₁₀ clusters only exhibit low fluorescence or green emission, necessitating postprocessing steps such as complementary strand hybridization and nuclease fragmentation. These steps alter the AgNC stoichiometry and transform the AgNC into a new geometry within the DNA host, previously unachievable using traditional methods. The combined altered base-cluster coordination geometry and changed size/shape of the fragmented AgNC ultimately contribute to the color-switching phenomenon in Subak reporters.

While some AgNC reporters have been reported for nuclease activity detection, they either operate as turn-off sensors based on fluorescence quenching or require multiple steps in detection, involving digestion by nucleases followed by AgNC nucleation. Our findings demonstrate that DNA/AgNC probes, such as Subak, can be simple and versatile reporters for detecting nuclease activities in nucleic acid detection assays. Moreover, this study presents a promising strategy to create novel AgNC fluorophores that were previously unattainable using traditional nucleation-and-reduction processes.

11:30 AM EL10.03.08

Ultrafast Dense DNA Functionalization of Quantum Dots and Rods for Scalable 2D Array Fabrication on DNA Origami with Nanoscale Precision Chi Chen, Xin Luo, Alexander E. Kaplan, Mouni G. Bawendi, Robert J. Macfarlane and Mark Bathe; Massachusetts Institute of Technology, United States

Quantum dots (QDs) and quantum rods (QRs) have attracted extensive interest in next-generation display systems due to their bright and tunable narrowband photoluminescence (PL). Moreover, QDs are also key candidates for quantum computing, quantum sensing, and quantum metrology through integrated quantum photonics. Scalable fabrication of QD/QR arrays possessing controlled spacing and orientation with nanometer precision on a device substrate is essential to the advancement of such research and applications. DNA origami technology has offered a scalable bottom-up strategy to organize nanoparticles at the nanoscale with unparalleled programmability and versatility. However, multiplexing QDs and QRs with DNA origami structures has been challenging, primarily due to the low DNA conjugation density to QDs/QRs from existing methods, which often leads to poor colloidal stability and low binding efficiency. Here, we developed an ultrafast strategy to prepare high-density DNA functionalized QDs/QRs (0.17–0.21 DNA per nm²) directly from their organic solution using a dehydration and rehydration process that reduces the fabrication time from hours to a few minutes. As prepared QDs/QRs were stable in a range of buffer conditions and able to hybridize to DNA origami structures with excellent efficiency and precision. To fabricate QD/QR arrays, we further developed a Surface-Assisted Large-Scale Assembly (SALSA) method to construct 2D origami lattices directly on a solid substrate for QD/QR templating, which circumvents problems in transferring solution-assembled soft 2D materials to a device surface. We designed a 6-helix-bundle (6HB) rhombic-shaped wireframe origami structure with high structural fidelity, planarity, and rigidity. With unique anisotropic crossover designs between neighboring origami structures, 2D origami lattices up to micrometer scale were produced by tuning origami surface diffusion, hybridization error correction and landing face selection. QDs and QRs were then assembled to the origami lattices with precisely controlled positions, inter-particle distances and orientations, with a loading yield over 90%. We further fabricated a monolayer QR array with aligned QR orientations, which can function as a polarized light source due to the PL emission anisotropy along the long axis of QRs and their alignment on surface. Our approaches can enable scalable fabrication of DNA-programmed QD and QR devices with nanoscale orientation and positioning accuracy for advanced applications in display, sensing and photonics.

11:45 AM EL10.03.09

Evaluating the Catalytic Activity of the Enzyme Matrix Metalloproteinase (MMP-14, a Cancer Marker) using AuNP–Peptide Conjugates Zhicheng Jin, Narjes Dridi, Qing-Xiang A.

Proximity-driven interactions between plasmonic nanostructures and fluorescent dyes yield efficient quenching of the dye photoluminescence (PL). This has provided researchers with an effective strategy to develop analytical biosensors.

We report on the use of polyethylene glycol-stabilized gold nanoparticles (AuNPs) covalently coupled to several dye-labelled peptides, as sensitive optically-addressable sensors for determining the catalytic efficiency of the human matrix metalloproteinase-14 (MMP-14), a known molecular marker of select metastatic cancers. We exploit the time-dependent recovery of the dye emission triggered by hydrolysis of the AuNP-tethered peptide-dye by added MMP-14, to extract quantitative analysis of the proteolysis kinetics. Sub-nanomolar limit of detections for the target enzyme has been achieved using these constructs. In addition, we have used conceptual rationales that consider the effects of the AuNP size, reduced Brownian diffusion combined with surface crowdedness of the AuNP-peptide conjugates, compared to peptide only system, to gain additional insights into the kinetic of the PL recovery. We derive enzyme substrate hydrolysis equations and evaluate the catalytic efficiency ($[endit] \rightarrow$) for these platforms. This allowed us to describe the complexity of enzyme activity interacting with nanosurface-bound substrates. Our findings offer a great strategy for the development of highly sensitive and stable biosensors for cancer detection and imaging.

SESSION EL10.04: Semiconductor QDs, Structure and Photophysics
Session Chairs: Mounji Bawendi, Ou Chen and Lakshminarayana Polavarapu
Tuesday Afternoon, November 28, 2023
Hynes, Level 3, Ballroom A

1:30 PM EL10.04.01

Electrically Pumped Colloidal-Quantum-Dot Sources of Amplified Spontaneous Emission Namyoung Ahn, Clément Livache and Victor I. Klimov; Los Alamos National Laboratory, United States

Electrically pumped lasers employing solution-processable optical gain media will be a game changer in numerous technological areas including on-chips photonics and electronics, optical communications, lab-on-a-chip devices, displays, and projectors. Colloidal quantum dots (QDs) are a promising class of materials for realizing laser diodes. In addition to being compatible with standard solution-based processing techniques, they feature size-controlled emission energies, low optical-gain thresholds, and high temperature stability of lasing characteristics originating from atomic-like character of electronic states.

Despite their promising characteristics, QDs are difficult lasing materials, especially in the case of electrical pumping. One challenge is fast nonradiative Auger recombination of multicarrier states needed to achieve optical gain. Other challenges include poor stability of QD solids under high current densities required for lasing and unfavorable balance between modal gain produced by a thin electroluminescence (EL) active QD layer and large optical losses in charge injection/transport layers.

Recently, the problem of Auger recombination has been alleviated using continuously-graded QDs (cg-QDs) that exhibit strong suppression of Auger decay.¹ Here we resolve the remaining challenges on a path to a QD laser diode. In particular, we develop “current-focusing” EL devices capable to sustain without damage current densities (j) of more than 1 kA cm⁻².^{2,3} Next, we integrate an ultra-high- j charge-injection architecture with a low-loss Bragg-reflection photonic waveguide which allows us to improve optical field distribution within the device and thereby realize the regime when net optical gain is positive.⁴ Finally, we develop devices that exhibit strong edge emitted amplified spontaneous emission (ASE) under electrical pumping. The next important milestone – the demonstration of a QD laser oscillator – can be accomplished by supplementing the developed structures with an optical resonator implemented, for example, as an in-plane distributed feedback grating.

1. J. Lim, Y.-S. Park, V.I. Klimov, *Nature Materials* **17**, 42-49 (2018)
2. H. Jung, Y.-S. Park, N. Ahn, J. Lim, I. Fedin, C. Livache, V. I. Klimov, *Nature Communications*, **13**, 3734 (2022)
3. H. Jung, N. Ahn, V. I. Klimov, *Nature Photonics*, **15**, 643-655 (2021)
4. N. Ahn, Y.-S. Park, C. Livache, J. Du, K. Gungor, J. Kim, V.I. Klimov, *Adv. Mater.* **35**, 2206613 (2023)
5. N. Ahn, C. Livache, V. Pinchetti, H. Jung, H. Jin, D. Hahm, Y.-S. Park, V.I. Klimov, *Nature* **617**, 79-85 (2023)

1:45 PM EL10.04.02

Inter-Shell Structure-Dependent Optimization of Electroluminescence and Driving Performance of Colloidal Quantum Dots Geun Woo Baek¹, Seung G. Seo², Donghyo Hahm³, Wan Ki Baek³, Sung Hun Jin² and Jeonghun Kwak¹; ¹Seoul National University, Korea (the Republic of); ²Incheon National University, Korea (the Republic of); ³Sungkyunkwan University, Korea (the Republic of)

Colloidal quantum dots (QDs) have attracted attention as promising emitters owing to their excellent optical properties, such as broad absorption, narrow emission bandwidth with near-unity photoluminescence quantum yield, size-dependent tunable bandgap, and high stability. Due to these advantages, QD-based light-emitting diodes (QLEDs) have been investigated as the next-generation display devices. In this work, we investigated the effects of the inter-shell structure on the device performance of QLEDs by comparing two different giant QDs, i.e., CdSe/Cd_{1-x}Zn_xSe/ZnS QDs (Se-QDs) and CdSe/CdZn_yS_{1-y}/ZnS QDs (S-QDs). Through the systematic analysis of Se-QDs and S-QDs, we found that the modification of the inter-shell structure can improve the device efficiency and operational stability. In particular, the QLEDs with Se-QDs exhibited a maximum external quantum efficiency and an operational half-lifetime (at 100 cd/m²) of 21.2% and 38,100,000 h. We further investigated the optimal configuration of QLEDs by changing the device structure and circuit geometry for practical display application.

2:00 PM EL10.04.03

A Generalized Approach for Colloidal Synthesis of Chalcogenide Perovskites and Related Materials as Emerging Photoabsorbers for Optoelectronic Applications Daniel C. Hayes, Shubhanshu Agarwal, Izoduwa Aimiwu, Madeleine C. Uible, Apurva Pradhan, Ryan N. Swope, Suzanne Bart and Rakesh Agrawal; Purdue University, United States

Among thin-film technologies, the perovskite crystal family (of the form ABX₃), most of which has been dominated by the lead-halide perovskites (where typically A = CH₃NH₃⁺, B = Pb²⁺, and X = I), has seen an unprecedented growth both in the sheer number of contributions from the research community, but also in improvements to the power conversion efficiencies (PCEs). From a modest 3.8% to an impressive 26.0% for a single-junction device, lead-halide perovskites have achieved, in just over a decade, what has taken silicon technologies over six decades. While lead-halide perovskites are incredibly high performing, they suffer from one crucial flaw: they are incredibly air and moisture sensitive. This vital flaw severely limits their commercial applicability where multiple decades of service are required.

Because of this, a different class of perovskites has gained interest, namely the chalcogenide perovskites (A = Ca²⁺, Sr²⁺, Ba²⁺, ..., B = Ti⁴⁺, Zr⁴⁺, Hf⁴⁺, ..., and X = S²⁻ or Se²⁻). Of these, BaZrS₃ has been the most widely studied chalcogenide perovskite to date due to its favorable bandgap, experimentally reported between ~1.7-1.9 eV, for photoabsorbing applications. Traditionally, chalcogenide perovskites, BaZrS₃ included, have required rigorous synthesis conditions, both in high temperature (>1000 °C) and/or significant residence times (>2 weeks). These demanding conditions consequently would prevent this material from being used with traditional conductive substrates such as gold or molybdenum. More recently, work has been done to synthesize these materials at less extreme conditions. Over just the past two years, procedures have been developed to synthesize the material well below 1000 °C, and in some cases via solution-deposited methods below 600 °C, and through a bottom-up, colloidal nanoparticle approach at temperatures from 330-365 °C. As a result, the possibility of using these materials in thin-film devices is on the horizon.

In this work, we report a generalized approach to synthesize an array of chalcogenide perovskites and related ternary materials as colloidal nanocrystals. Colloidal syntheses provide us the unique advantage of relatively easy size- and shape-control which allows us to optimize these nanomaterials for downstream fabrication methods, such as in use for thin-film devices. Like previous reports, we show that BaZrS₃ can be synthesized at similar conditions ranging from 340 °C to below 300 °C. These comparatively mild conditions make the use and scale-up of such a process more attractive for other researchers as the field of chalcogenide perovskites continues to grow. In addition to BaZrS₃, we also show that the synthesis approach can be translated to other materials like BaHfS₃, BaTiS₃, and SrZrS₃ nanomaterials, owing to the versatility of the approach.

2:15 PM EL10.04.04

Biexciton Auger Recombination in Strongly Confined Perovskite Quantum Dots and its Correlation to Photoluminescence Blinking Yitong Dong, Chenjia Mi, Gavin Gee and Matthew Atteberry; The University of Oklahoma, United States

Lead halide perovskite quantum dots (QDs) are promising single photon emitters owing to their high room temperature luminescence efficiency and solution processibility. Moreover, strongly confined perovskite QDs (SCPQDs), whose physical sizes are much smaller than their Bohr diameters, are predicted to have high single photon emission purity due to their ultra-fast biexciton Auger recombination rates. Recent advances have demonstrated that reducing the sizes of perovskite QDs leads to higher single photon emission purities. It is also known that biexciton emission quantum yield can be estimated by the $g_2(0)$ values from the second-order photon correlation measurements. However, studies on single perovskite QDs have witnessed unexpectedly low single photon emission purities with $g_2(0)$ values varying dramatically. Additionally, perovskite QDs often show severe fluorescence intensity fluctuations. Recently, we have developed a

QD-in-matrix method that can successfully passivate and disperse SCPQDs with improved photostability. By controlling the surface passivation conditions, we have studied over 1000 single SCPQDs and correlated their fluorescence blinking behaviors with their $g^2(0)$ values. We found that perovskite QDs with high "ON" time fraction show significantly lower biexciton emission efficiency. The biexciton emissions from perovskite QDs with high "OFF" fraction are more efficient. Such a positive correlation between QD "OFF" time fractions and biexciton emission quantum yields is opposite to what has been revealed in CdSe core-shell QDs, and it suggests that the Auger recombination rate can change with respect to the surface conditions of the perovskite QDs. We propose a model that combines both exciton trapping and exciton-surface lattice interaction for different biexciton emission quantum yields observed in SCPQDs.

2:30 PM *EL10.04.05

Colloidal Quantum dots as Single Photon Quantum Emitters Mounqi G. Bawendi; Massachusetts Institute of Technology, United States

The spectroscopic riddles of quantum confined colloidal quantum dots (CQDs) initially fueled synthetic advances following their birth at the end of the last millennium. As the 1990's turned into the 2000's, the synthesis had developed rapidly and commercial applications of CQDs emerged, first as bright and robust emitters for biological imaging, and later as the source of saturated green and red light in displays widely sold around the world. From the beginning the fluorescent properties of CQDs has been central to both their academic study as well as to their commercial success. As the tools to probe the photo-physics of individual CQDs have become more sophisticated, an appreciation of their properties as nano-emitters has grown. CQDs are now showing potential as quantum emitters, sources of single indistinguishable photons. It is this new direction that will be the focus of my presentation. Cesium lead halide perovskite CQDs, an emergent nano-material with unique optical properties, have now shown potential as colloidal sources of coherent single photons at cryogenic temperatures. We report that large CsPbBr₃ CQDs (~20nm in size) show direct evidence of interference between indistinguishable single photons sequentially emitted from a single nanocrystal through Hong-Ou-Mandel interference in the absence of any radiative enhancement or photonic architecture.

3:00 PM BREAK

3:30 PM *EL10.04.06

Synthesis and Applications of Two-Dimensional Cs₂AgM(III)X₆ Double Perovskite Nanoplatelets OuChen; Brown University, United States

Lead-free double perovskite nanocrystals have emerged as a promising class of materials with potential to be integrated into a wide range of optical and optoelectronic applications. In this regard, composition engineering and morphology control are the two effective means to tune and optimize their properties. In this talk, I will discuss about the synthesis of high-quality Cs₂AgM(III)X₆ (M(III) = In, Bi, and X = Cl, Br, I) two-dimensional nanoplatelets through our newly developed synthetic method. By analyzing the optical, morphological, and structural evolutions of the samples during synthesis, we elucidated that the growth mechanism of lead-free double perovskite nanoplatelets followed a lateral growth process from mono-octahedral-layer cluster-based nanosheets to multilayer nanoplatelets. Through controlling composition, the optical properties of double perovskite nanoplatelets can be tuned and optimized with the highest photoluminescence quantum yield reaching over 40%. Importantly, the synthesized double perovskite nanoplatelets possess large surface areas, and high colloidal and solid-phase stabilities, which allow them to be applied for photocatalytic CO₂ reduction and light emitting diode applications.

4:00 PM EL10.04.07

Post-Synthetic Doping and Surface Ligand Engineering of Lead-Free Perovskite Nanocrystals: Tuning the Composition, Dimensionality and Dopant Characteristics Lacie Connelli and OuChen; Brown University, United States

Doping in perovskite nanocrystals (NCs) offers effective means to alter and improve the magnetic, optical and optoelectronic properties of the perovskite NCs. Unlike traditional direct-synthetic doping methods, post-synthetic perovskite NCs doping reactions provide a facile doping method with the possibility of providing insights into intermediate states and reaction mechanisms through highly controllable reaction kinetics and minimum side products. As such, the previous development of post-synthetic doping reactions focused on the phase (i.e. solid or liquid) dependence of both the precursor and NC to determine dopant incorporation and diffusion kinetics. Herein, I will show a detailed study of post-synthetic doping of perovskite NCs within three distinct aspects: NCs composition, dopant interactions and the perovskite crystal dimensionality. More specifically, diffusion dynamics of Mn²⁺ dopants were interpolated and compared between lead-based and lead-free perovskite NCs. Furthermore, post-synthetic ligand engineering characterized by 1D and 2D NMR techniques was applied to enhance both the particle stability and optical properties of the doped perovskite NCs.

4:15 PM EL10.04.08

Multicomponent Functional Superlattices Co-Assembled from Shape Anisotropic Lead Halide Perovskite Nanocrystals Taras Sekh^{1,2}, Gabriele Rainò^{1,2}, Ihor Cherniukh^{1,2}, Etsuki Kobiyama^{1,3}, Modestos Athanasiou⁴, Andreas Manoli⁴, Thomas Sheehan⁵, William Tisdale⁵, Thilo Stoeferle⁵, Rolf Erni², Grigoris Itsoos⁴, Maryna Bodnarchuk^{2,1} and Maksym V. Kovalenko^{1,2}; ¹ETH Zürich, Switzerland; ²Empa-Swiss Federal Laboratories for Materials Science and Technology, Switzerland; ³IBM Research-Zurich, Switzerland; ⁴University of Cyprus, Cyprus; ⁵Massachusetts Institute of Technology, United States

With the development of new approaches in synthetic chemistry over the last few decades, various colloidal nanocrystals were obtained in the monodisperse form, which, in turn, fostered the extensive research and application possibilities of novel nanomaterials. To this end, self-assembly of colloidal nanocrystals via a bottom-up approach holds great promise for creating metamaterials with programmable functionalities which originate from not only ensemble-average properties but also from diverse synergistic and collective effects, including conductivity enhancement, dipolar interactions, plasmonic couplings as well as collective light emission-superfluorescence [1]. The last was recently shown on the single-component perovskite nanocrystal superlattices [2]. Such peculiar optical properties, together with a high degree of monodispersity, size tunability, and shape anisotropy of perovskite nanocrystals, stimulated research in exploring multicomponent superlattices [3]. Thus, a whole plethora of superlattice types has become accessible, encompassing the superlattices comprised of perovskite nanocubes and spherical, truncated cuboid, or disc-shaped nanocrystals acting as spacers between fluorescent nanocrystals [4]. The superlattices can be fabricated as films on different flat substrates, including at the liquid-air interface, or as spherically confined 3-dimensional supraparticles [5]. A particular interest lies in studying superlattices containing a few light emitter types, wherein promising collective phenomena are expected to emerge. For such systems exemplified on lead perovskite nanocrystal superlattices, we observed the Foster-like energy transfer with accelerated exciton diffusion.

[1] Michael A. Boles *et al.* *Chem Rev.* **2016**, 116, 11220-11289.

[2] Gabriele Rainò *et al.* *Nature*, **2018**, 563, 671-675.

[3] Ihor Cherniukh *et al.* *Nature*, **2021**, 593, 535-542.

[4] Ihor Cherniukh *et al.* *ACS Nano*, **2021**, 15, 16488-16500.

[5] Ihor Cherniukh *et al.* *ACS Nano*, **2022**, 16, 7210-7232.

4:30 PM EL10.04.09

Accurate TDDFT Absorption Spectra of Molecules on Surfaces over Full Spectral Range Matthias Kick, Ezra A. Alexander and Troy Van Voorhis; Massachusetts Institute of Technology, United States

Theoretically, electronic excitations can be obtained by analysing the frequency components of the time-dependent dipole moment obtained from real-time time-dependent density functional theory (RT-TDDFT) simulations. Yet, an exact treatment of electronic excitations in large systems with TDDFT is computationally prohibitive. Super-resolution techniques such as compressed sensing typically fail due to the presence of a quasi-continuum of electronic excitations. We present a new approach where we combine exact short time dynamics with approximate frequency space methods. As a prototypical test system, we use an organic dye-molecule adsorbed on a semi-conductor quantum-dot surface. We calculate the entire electronic absorption spectrum of this system and find that our approach can accurately capture narrow features and a quasi-continuum of states at the same time. We see a reduction of the required amount of data points up to a factor of 40 compared to standard Fourier analysis. By doing so, our method allows us to study electronic properties of large systems in ways that are not currently possible.

4:45 PM EL10.04.10

Lanthanide Doping into All-Inorganic Heterometallic Halide Layered Double Perovskite Nanocrystals for Multimodal Visible and Near-Infrared Emission Tong Cai^{1,2} and OuChen¹; ¹Brown University, United States; ²Northwestern University, United States

The introduction of rare earth lanthanide ion (Ln³⁺) impurities into all-inorganic lead-free halide perovskites has captured significant research attention and exhibited great promise in a range of optoelectronic applications. Nevertheless, the successful achievement of Ln³⁺ doping within heterometallic layered double perovskite (LDP) nanocrystals (NCs) remains as an unexplored frontier, accompanied by a lack of understanding. Herein, we report the first colloidal synthesis of Ln³⁺ (Yb³⁺, Er³⁺) doped LDP NCs utilizing a modified hot-injection method. The resulting NCs exhibited proficient NIR PL profiles encompassing both the NIR-I and NIR-II regions, achieved *via* energy transfer down-conversion mechanisms. Density function theory (DFT) calculations reveal that Ln³⁺ dopants exhibit a preference for substituting Sb³⁺ cations, occupying within the LDP crystal lattice while maintaining its structural stability. By leveraging sensitizations of intermediate energy levels, we delved into the mechanisms of energy transfer between the host and dopants, and between different types of dopants, across a series of

designed Ln^{3+} doped $\text{Cs}_4\text{CdSb}_2\text{Cl}_{12}$ or $\text{Cs}_4\text{MnSb}_2\text{Cl}_{12}$ LDP NCs. Interestingly, doping Er^{3+} ions into $\text{Cs}_4\text{MnSb}_2\text{Cl}_{12}$ LDP NCs yielded distinct photophysical responses, *i.e.*, brightening the pre-dark states of Er^{3+} dopants, owing to the role of Mn component played as an intermediate energy bridge. This study not only presents a novel model system that advances our understanding of sensitization-induced energy transfer mechanisms in doped semiconductor NCs, but also propels the potential applications of all-inorganic lead-free LDP NCs across a wide array of optoelectronic domains, such as optical data encryption, optical telecommunication, multiplexed NIR detection and imaging.

SESSION EL10.05: Poster Session I
Session Chairs: Tae-Woo Lee and Hedi Mattoussi
Tuesday Afternoon, November 28, 2023
Hynes, Level 1, Hall A

8:00 PM EL10.05.01

All-Solution Processed Green Quantum-Dot Lighting Device with PEDOT:PSS:PMA P-Type Conducting Layer Guanning Shao^{1,2} and Young Joon Hong^{1,2}; ¹GRI-TPC International Research Center, Korea (the Republic of); ²Sejong University, China

Quantum dot light-emitting diodes (QLEDs) have drawn substantial interest over the past few decades as potential large-area display devices, thanks to their remarkable quantum efficiency, pure and highly saturated RGB color expression, and broad process adaptability. Typically, the colloidal quantum dots (QDs) are spin-coated to form an emissive layer (EML) sandwiched between the hole and electron transport layers (HTLs and ETLs), essential for crafting p-n junction lighting devices. Despite their simple solution casting process, QLEDs show high efficiency and long lifetime, qualifying them for practical devices and displays. However, the overall efficiency of QLEDs is determined not just by the internal quantum efficiency of QDs, but also significantly by the carrier transport and injection capabilities of the HTLs and ETLs. Particularly, the electron mobility and concentration often surpass those of holes by orders of magnitude. This carrier imbalance leads to the accumulation of excess electrons at the interfaces around light EML, causing exciton quenching and leakage current overflow in the devices. Additionally, surplus electrons intensify the Auger recombination of quantum dots, resulting in further fluorescence quenching, which is a principal factor behind the reduced efficiency of QLED devices. Thus, the carrier imbalance poses a significant challenge in the fabrication of high efficiency devices. In this presentation, we highlight the improved p-type conductivity in solution-processed green QLEDs, achieved through the use of mixed solution of poly(3,4-ethylenedioxythiophene):poly(styrene-sulfonate) (PEDOT:PSS) and phosphomolybdic acid (PMA) as an HTL. The mixing ratio of PEDOT:PSS to PMA was progressively adjusted from 1:0 to 1:0.5 to determine the optimal mixing ratio for maximizing p-type conductivity and QLED lighting efficiency. Ultraviolet photoelectron spectroscopy (UPS) and x-ray photoelectron spectroscopy (XPS) were used to investigate the actual energy level shift of hole transport layers in the junction device structure. Moreover, the redox of Mo in various valence states in the mixed solution was explored concerning work function and energy level via UPS, suggesting the modulation of hole injection and electron blocking abilities. The work function of PEDOT:PSS:PMA was evaluated as well. The optimized energy level mitigates the hole transport barrier, leading to a decrease in driving voltage and an enhancement in electroluminescent efficiency. The p-type conductivity of the mixture was further validated by assessing the electrical properties of hole-only devices. This approach to enhance the hole conduction can be extended to the fabrication of many other solution-processed QLEDs, thereby advancing practical display applications.

8:00 PM EL10.05.02

Intense Pulsed Light Annealing of All Printed Thin Film Transistors using Solution-Based Indium-Gallium-Zinc-Oxide Semiconductor and Printed Silver Electrodes Jong-Whi Park¹, Chang-Jin Moon¹ and Hak Sung Kim^{1,2}; ¹Hanyang University, Korea (the Republic of); ²Institute of Nano Science and Technology, Korea (the Republic of)

In this study, intense pulsed light (IPL) annealing process for printed multi-layered Indium-Gallium-Zinc-Oxide (IGZO) and silver (Ag) electrode structure was developed for high performance all printed inorganic thin film transistor (TFT). Through solution-process using IGZO precursor and Ag ink, the bottom gate structure TFT was fabricated. The spin coating method was used for the forming IGZO semiconductor layer on heavily-doped silicon wafer covered with thermally grown silicon dioxide. The annealing process of IGZO layer was proceeded using optimized IPL irradiation process. The Ag inks were printed on the IGZO layer by screen printing, so the source and drain (S/D) pattern was formed. This S/D pattern was dried by near infrared radiation (NIR), and the dried S/D pattern was sintered with the intense pulsed light varying the irradiation energy. The performances of all-printed TFT such as field effect mobility and on-off ratio electrical transfer properties were measured by parameter analyzer. The interfacial analysis such as contact resistance and the cross-sectional microstructure analysis was essential, because the diffusion phenomenon can occur during annealing and sintering process. Consequently, this TFT device shows noteworthy performance, it was similar performance compared to conventional TFT, which is expected to open a new path in the printed metal oxide based TFT field.

Acknowledgment

This work was supported by Korea Institute of Energy Technology Evaluation and Planning (KETEP) grant funded by the Korea government (MOTIE) (20212020800090, Development and Demonstration of Energy-Efficiency Enhanced Technology for Temperature-Controlled Transportation and Logistics Center) and this work was supported by Korea Institute of Energy Technology Evaluation and Planning (KETEP) grant funded by the Korea government (MOTIE) (20202020800360, Innovative Energy Remodeling Total Technologies (M&V, Design, Package Solutions, and Testing & Verifications Technologies) for the Aging Public Buildings)

8:00 PM EL10.05.03

Nature-Inspired Superhydrophobic/Water-Repellent Surface on PCB/Semiconductor Based on Automatic Coating Process using Functional Nanoparticles Seungchul Park, Seon Ju Yeon and Bo-Yeon Lee; Korea Institute of Machinery and Materials, Korea (the Republic of)

We demonstrate a simple generic principle of constructing superhydrophobic and water-repellent surfaces, which is the biomimic of Lotus-leaf, based on automatic spray coating on PCB substrate. Using the low surface energy nanoparticles such as fluorinated silicon dioxide nanoparticles, atomized spray equipment can help to generate superhydrophobic and water-repellent surface with in large area and high-uniformity. The coating pathway can be controlled by the 3D image of the target substrate, PCB substrate in our case, and the nanoparticle coated PCB substrate can show the water-repellency without additional process such as thermal treatment due to the functional of our fluorinated silicon dioxide nanoparticle. We expect that our coating process with functional nanoparticles can increase the stability of electronic devices.

8:00 PM EL10.05.04

Functionalization Platform of Magnetic Nanoparticles Through Silica Shell Formation Katherine Lei, Keisuke Nagao, Robert J. Macfarlane and Polina Anikeeva; Massachusetts Institute of Technology, United States

Magnetic nanomaterials enable transduction of weak magnetic fields into biological signals including force, heat, and force or heat-mediated chemical release. However, biochemically benign ferrites, including iron oxide, pose challenges to surface modification offering limited surface functionalization options for cell targeting. We hypothesized that functionalization of magnetic nanomaterials with silica, for which numerous surface chemistries are established, would offer a versatile and robust route to their surface engineering. Although prior work suggested the use of the Stöber and reverse microemulsion methods to functionalize magnetic nanomaterials with silica, formation of thin uniform shells necessary to preserve the particles' functional properties remained challenging. Furthermore, during functionalization reactions multiple nanoparticles are readily encapsulated in a single silica shell, which similarly compromises performance. To overcome these challenges, we develop a novel, robust protocol for a reverse microemulsion method to create uniform shells with tunable thickness on magnetic nanoparticle cores. Our protocol uses oleic acid as a secondary surfactant to prevent the formation of multi-core particles and control the rate of silica shell growth. We demonstrate that our protocol is adaptable to a wide range of particles of different shapes/sizes and compositions such as spherical nanoparticles with high heat-dissipation rates in magnetic fields, hexagonal ferrite nanodiscs (>200 nm in diameter), and semiconductor quantum dots. Additionally, the surface chemistry of our coated nanoparticles can be readily modified with desired functional groups. Our protocol can be used to form uniformly coated core-shell nanoparticles of a desired thickness as a platform for applications in materials research, chemistry, and biomedicine.

8:00 PM EL10.05.05

Photoelectrochemical Behavior of Gold Nanocluster-Sensitized TiO₂ Electrodes Modulated by Interfacial Engineering Minwook Jeon and Jin Ho Bang; Hanyang University, Korea (the Republic of)

Metal nanoclusters (NCs) are a newly emerging photosensitizer in light-conversion devices due to their unique physicochemical properties. While many aspects of NC-sensitized photoelectrodes have not fully been elucidated to date, recent reports uncovered exotic photoelectrochemical (PEC) behavior that has not been observed in conventional photosensitizers, thus attracting great interest in this newly devised system. Susceptibility of the PEC behavior of NC-sensitized photoelectrodes to surface states of the photoelectrodes is subtle; hence a systematic investigation is urgently required to obtain a better understanding of charge separation and charge recombination events occurring at the interface. In this work, we revealed that a simple pH change during the sensitization of NCs to TiO₂ can have a significant effect on charge injection and charge recombination kinetics. In-depth-time-resolved spectroscopy combined with

potential-dependent electrochemical impedance spectroscopy shed new light on these interfacial events. We envision that the newly acquired insight from our investigation would be crucial for the development of the NC-TiO₂ system because its PEC behavior is intimately altered by even a subtle change in the interface.

8:00 PM EL10.05.06

Direct Patterning of Colloidal Quantum Dots Through Blending with a Photo-Cross-Linkable Functional Polymers Jaeyoop Lee¹, Seon Lee Kwak¹, Woon Ho Jung², Chaegwang Lim¹, Jaehoon Lim², Do-Hoon Hwang¹ and Jeongkyun Roh¹; ¹Pusan National University, Korea (the Republic of); ²Sungkyunkwan University, Korea (the Republic of)

Colloidal quantum dots (QDs) have been spotlighted in advanced display technologies due to their unique ability to adjust emission colors based on their core size, along with their excellent color reproducibility (*Advanced Materials* n/a, 2212220, 2023). Numerous researchers have made significant strides in developing high-performance quantum dot light-emitting diodes (QD-LEDs) by optimizing the device structure (*Organic Electronics* 108, 106593, 2022), achieving charge balance (*ACS Photonics* 10, 500-507, 2023), and refining emissive mechanisms (*Small* 15, 1905162, 2019). However, despite these impressive advancements, the commercialization of QD-LEDs still lags behind, primarily due to the absence of suitable patterning technologies for QDs (*The Journal of Physical Chemistry Letters* 12, 3522-3527, 2021). Optical lithography has often been employed to produce high-resolution QD arrays, but direct exposure to UV light often leads to the degradation of QDs by surface oxidation (*Advanced Materials* 31, 1804294, 2019).

In this study, we addressed this challenge by blending QDs with a photo-cross-linkable functional polymer to mitigate oxidation during the patterning process. By adopting this method, we successfully achieved patterned QD films with a minimum line width of 2 μm . Furthermore, we demonstrated high-resolution RGB full-color QD pixels, surpassing 1,000 pixels per inch (ppi). Importantly, the pixelated QD-LEDs exhibited negligible degradation during the patterning process thanks to the protective presence of functional polymers surrounding the QDs. This result presents a readily accessible solution for QD patterning, effectively overcoming the challenges associated with the oxidation of QDs under UV exposure. This significant advancement in patterning technology holds tremendous potential for the development and commercialization of high-resolution RGB full-color QD-LEDs.

8:00 PM EL10.05.07

The Synthesis of Colloidal Au Nanocrystals with Unconventional Crystal Phase and Their Optical Applications Chen Ma and Ye Chen; The Chinese University of Hong Kong, China

Gold nanocrystals have attracted considerable research attention due to their potential applications in energy conversion, catalysis, electronics, and biomedicine. However, previous studies mainly focused on tuning the morphology, facet, size, and dimensionality of Au nanomaterials. Recently, research in phase engineering of nanomaterials has highlighted the significance of the crystal phase in modulating the physicochemical properties of nanomaterials. Interestingly, most of the reported Au nanomaterials with unconventional crystal phases were prepared starting from [Au(I)-oleylamine] system because oleylamine exhibits unique adsorption behaviors with Au nanocrystals. Based on the [Au(I)-oleylamine] system, we developed a facile colloidal method to synthesize Au nanocrystals with unconventional crystal phases in high phase purity, high yield, and high shape uniformity. The crystal phase of as-synthesized Au nanocrystals was evidently revealed by selected area electron diffraction, X-ray diffraction, and high-resolution transmission electron microscopy. In addition, Au nanocrystals with different morphology were obtained via a simple ligand exchange method. More importantly, it is found that Au nanomaterials with unusual crystal phases possess unique optoelectronic properties compared with their thermodynamically stable face-centered cubic phase. Our work not only can pave a new avenue to the colloidal synthesis of nanocrystals with unconventional crystal phases but also promote the fundamental understanding of crystal phase-dependent optical properties of noble metal nanomaterials.

8:00 PM EL10.05.08

Stoichiometric Engineering of Ag₂S Nanocrystals to Realize High-Performance Organic-Inorganic Hybrid Photomultiplication-Type Photodiode Jisu Kwon, Kyu Min Sim, Daesung Chung and Sungjee Kim; POSTECH, Korea (the Republic of)

Heavy metal-free Ag₂S nanocrystals (NCs) were synthesized for a novel class of sensitizing center of photomultiplication (PM)-type photodiodes in which polymeric semiconductor poly(3-hexylthiophene) (P3HT) was co-used. The key role of PM sensitizing center is considered as efficient charge separation and trapping, which requires prolonged capturing of minority carriers and advantageous band-bending at the cathode interface for continuous tunneling injection of majority carriers. To this end, the surface stoichiometry of Ag₂S NCs was strategically tuned as Ag-rich, stoichiometric, or S-rich. The Ag₂S NCs are designed to have more acceptor-like states when the stoichiometry is dominated by Ag atoms. Conversely, they have more donor-like states when S atoms prevail. In addition to the elemental analyses, the surface stoichiometry of NCs was further characterized by time-resolved photoluminescence and space-charge limited current analyses. An optimal PM-type photodiode was demonstrated by the structure of ITO/PEDOT:PSS/P3HT:Ag₂S NCs/Al with the holes as the majority carriers, Ag-rich Ag₂S NCs as the sensitizing centers. The Ag-rich Ag₂S NCs showed enhanced electron trapping and minimized hole trapping rate due to the high density of acceptor-like states. We showcased that fine-tuning the surface stoichiometry of Ag₂S nanocrystal enables high external quantum efficiency (EQE) of the PM-type photodiode. The optimized hybrid PM-type photodiode exhibited a high peak EQE of 170,000%, responsivity of 580 A/W, and specific detectivity of 3 X 10¹³ Jones. Sophisticated control of NC stoichiometry is important for the photophysical properties of sensitizing centers which guarantees successful applications to optoelectronic devices such as photodiodes.

8:00 PM EL10.05.09

Nanoparticle Accelerants for Liquid-Liquid Phase Separation (LLPS) of Intrinsically Disordered Proteins Ryan M. Doherty, Xiaoting Guo and Vicki L. Colvin; Brown University, United States

Biomolecular condensates, also known as membraneless organelles, play a critical role in cellular organization, and their dysregulation has been linked to multiple disorders including neurodegenerative diseases and cancers. They form through a liquid-liquid phase separation process (LLPS) that occurs when LLPS-forming proteins demix into higher concentration and lower concentration phases within a cellular environment. Understanding what triggers LLPS formation and the role that protein structure may play remains an active area of research. Previous studies have shown that some small molecules and polymers may promote LLPS paving the way for generating druggable targets for this important class of biomolecules. This study evaluates whether nanoparticles can serve as accelerants for this important biological process ex-situ.

Gold nanoparticles coated with polyethylene glycol (PEG) have previously been shown to be crowding agents able to accelerate protein-protein interactions during crystallization processes. Given that crystallization requires a liquid-liquid phase separation (LLPS) step, we expected that these same materials would also accelerate the LLPS of candidate proteins. Au-PEG nanoparticle conjugates (AuNP-PEG) also can expand the set of conditions that allow for protein-protein interactions to occur.

This study looks to understand how the inorganic core diameter of AuNP-PEG and the PEG chain length — both important variables in designing agents that are efficient accelerants — can change the rate of liquid-liquid phase separation (LLPS) and the properties of condensates. Such design and modulation of this organic-inorganic interface allow us to create better tools to promote LLPS ex-situ. AuNP-PEG of various core diameters was prepared and functionalized with varying chain lengths of polymers from 1,000 to 40,000 molecular weight. The polymer coating has different properties; short-chain PEG is tightly packed and has a high grafting density whereas long-chain PEG adopts mushroom configurations and is less dense. Previous work with protein crystallization showed that nanoparticle core diameter did not play a significant role in the nucleation rate, a finding expected for the rate of LLPS. But, protein crystallization occurred faster at high PEG-chain lengths, so we expected AuNP-PEG to accelerate LLPS. Longer PEG length would increase the LLPS rate due to the more crowded environment, hydrophobicity, and multivalency, which are key LLPS-promoting factors associated with longer polymer chains. Optical microscopy was used to evaluate the kinetics of LLPS in addition to other spectroscopic tools. We also analyzed biomolecular condensate diameter, density, and other material properties.

Materials that accelerate the liquid-liquid phase separation (LLPS) should also promote LLPS under less extreme solution phase conditions. Typically, LLPS is brought about ex-situ by placing intrinsically disordered proteins into solutions of high ionic strength and/or low pH and then mixing with a low-salt buffer, producing a limited phase space. In the presence of accelerants, this phase space should be expanded. A screening procedure was performed at various protein and salt concentrations to determine if the presence of AuNP-PEG would induce LLPS in a larger set of conditions. From this, a phase map was developed to understand the expanded range of phase separation.

8:00 PM EL10.05.10

Reversibly Controlling Assembly/Disassembly of Plasmonic Nanoparticles by Electrochemical Redox of Copper-Coordinated Surface Ligands Taeyong Ha¹, Sanghwa Jeong² and Sungjee Kim¹; ¹Pohang University of Science and Technology (POSTECH), Korea (the Republic of); ²Pusan National University, Korea (the Republic of)

Plasmonic nanoparticles (NPs) show dramatically different scattering properties by the assembly/disassembly of the NPs due to the notable change between the collective and individual plasmonic modes. Reversible and on-demand control of such assembly and disassembly states of plasmonic modes is of great importance for potential optoelectronic and display applications. Control of assembly/disassembly of plasmonic NPs have been demonstrated by changing the pH, light exposure, or temperature. However, such cues are not very practical for device applications because of the limited reversibility and necessity of extended time. We report reversible and electro-tunable control of assembly/disassembly of metal NPs by electrochemical redox reactions of copper complexes. The copper complex moiety is tethered to the surface ligands of metal NPs. The reversible control of assembly/disassembly of metal NPs was attained by switching the oxidation states between Cu(I) and Cu(II). Cu(I) state prefers tetrahedrally-coordinated complexes which form inter-NP sandwich structures and induces the assembled NP state. Whereas Cu(II) takes octahedral ligand geometry which results in individually and freely dispersed NP state. Our control does not need external chemical reagents, and the reversible change can be made quite rapidly. The electrochemical control was also demonstrated by using a low operating voltage less than a couple of volts. We believe our design can be useful in

optoelectronic display applications such as smart windows because it provides reversible bistability between transmittance and reflectance.

8:00 PM EL10.05.11

Trap-Induced Excitation “Memory” Enable High-Speed Modulation of Quantum-Dot Light-Emitting Diodes Yunzhou Deng^{1,2}, Xiuyuan Lu² and Yizheng Jin²; ¹University of Cambridge, United Kingdom; ²Zhejiang University, China

Quantum-dot light-emitting diodes (QLEDs), a class of solution-processed EL devices based on organic-inorganic hybrid structures, show great potential in next-generation optoelectronics. Understanding their transient response dynamics is essential for developing high-speed devices for EL display, light communications [1] and potentially electrically-pumped lasing [2].

Here, we report that the transient responses of the QLED can be accelerated by the “memory” of its excitation history, distinguishing QLEDs from conventional inorganic LEDs. We elucidate that this transient behavior originates from the interplay between transient EL processes and deep-level fast traps in the organic hole-transport layer, which generates a new fast-response EL channel that occurs in high-frequency operations. Finally, we harness this transient response pathway on a micro-QLED, demonstrating high-speed modulations up to 100 MHz at a moderate excitation level of $\sim 200 \text{ mA cm}^{-2}$.

This work highlights a universal transient EL behavior dominated by trap-related processes in the organic charge-transport materials, which is found to generally exist in solution-processed LEDs employing organic hole-transport materials, including perovskite LEDs and polymer LEDs. We expect that the excitation-memory induced fast-response dynamics could facilitate the realization of solution-processed, low-power, and fast-response EL devices.

[1] Ren, A., et al., “Emerging light-emitting diodes for next-generation data communications”. *Nat. Electron.* **4**, 559-572 (2021).

[2] Ahn, N., et al., “Electrically driven amplified spontaneous emission from colloidal quantum dots”. *Nature*, **617**, 79-85 (2023).

8:00 PM EL10.05.12

Aqueous Synthesis of Copper Plates Based on Anisotropic Growth of Copper Crystals with Bromide Ions Yusaku Noda, Shun Yokoyama and Hideyuki Takahashi; Tohoku University, Japan

Copper micro/nanoplates (Cu MNPs) have been studied intensively for potential applications in optical devices and electronic wiring due to their low cost, unique optical properties, and high conductivity. Aqueous chemical reduction from Cu complexes to Cu crystals is used to produce Cu MNPs with halogen ions and surfactants as capping agents¹. During the chemical reduction, halogen ions are predicted to adsorb on (111) facets of Cu crystals and the surfactants work as stabilizer for the halogen adsorption and consequently Cu crystals grow anisotropically, leading to plate-shaped particles. While the capping agents also adsorb on (100) facets depending on the synthesis conditions, leading to wire-shaped particles. It is unclear what triggers the wire and plate-shaped particle syntheses. Although we previously developed an environmental-friendly synthesis method of Cu nanowires with chloride ions and polymers as the capping agents, plate-shaped particles are never synthesized in the method. While reduction speed of the chemical reduction and types of capping agents are reported to greatly affected the anisotropic growth. In this study, we controlled types of capping agents and the reaction speed in the environmental-friendly synthesis method for selectively synthesizing Cu plate particles and revealing their formation mechanism. We selected bromide (Br) ions as the capping agent and no other capping agents are used. We used ascorbic acid and lactic acid (LA) as the reducing and complexing agent, respectively. We changed the reduction pass from Cu-LA complexes to Cu and the reduction rate by controlling pH and concentrations of Br and LA based on pH-potential diagrams. The synthesized particles were analyzed by SEM for particle morphologies and XPS for surface conditions.

In the calculated pH-potential diagrams, Cu-LA complexes are expected to be stable at wide pH region and then reduced to Cu through CuBr below pH 6 and through Cu₂O above pH 6.0. Micro-sized wire and plate particles were mainly synthesized at pH 3.5 and between pH 4.5 and 5.5, respectively. Above pH 6.0, polyhedral particles were mainly synthesized. From XPS results of particle surfaces obtained at various pH values, the amount of Br ions on particle surfaces obtained below pH 6.0 is larger than that above pH 6.0. These results indicate that low pH values facilitate adlayer formations of Br ions on Cu crystal surfaces because CuBr is more stable than Cu₂O, resulting in syntheses of wire and plate particles. Br ions could be adsorbed on (100) facets for wire particle formations and (111) facets for plate particle formations. To examine why this difference arose between pH 3.5 and pH 4.5 to 5.5, the reduction rate of Cu complexes at 3.5 and 5.5 was evaluated. The reduction rate at pH 3.5 was much slower than that at pH 5.5 due to changes in redox potentials of ascorbic acid with pH, indicating the reduction rate affected the adsorption of Br ions on Cu crystal facets. The details about the growth mechanism of wire and plate particles will be introduced.

1. Kim MJ, Cruz MA, Chen ZH, Xu H, Brown M, Fichthorn KA, et al. Isotropic Iodide Adsorption Causes Anisotropic Growth of Copper Microplates. *Chemistry of Materials*. 2021;33(3):881-91.

SESSION EL10.06: Applications in Biology II
Session Chairs: Wolfgang Parak, Vincent Rotello and Andrew Smith
Wednesday Morning, November 29, 2023
Hynes, Level 3, Ballroom A

8:30 AM *EL10.06.01

New Syntheses for Aqueous and Processable Nanocrystals Suresh Sarkar, Opeyemi Arogundade and Andrew M. Smith; University of Illinois Urbana-Champaign, United States

Many classes of nanocrystals are synthesized by reactions in solvents composed of aliphatic hydrocarbons, resulting in products dispersible only in nonpolar media. To disperse these nanocrystals in aqueous and other polar solvents, secondary processing steps are used to exchange ligands or encapsulate the particles within amphiphilic polymers. This report will focus on new processes to increase the efficiency, scalability, and environmental waste profile for the production of hydrophilic nanocrystals. In particular, new types of coordinating ligands and processing steps will be described that may increase access to diverse nanocrystals stable in biological media for diverse applications in imaging and sensing.

9:00 AM EL10.06.02

Chloride Ligands on DNA-Stabilized Silver Nanoclusters Anna Gonzalez Rosell¹, Sami Malola², Rweetuparna Guha¹, Nery Arevalos¹, María Francisca Matus², Meghan Goulet¹, Esa Haapaniemi², Benjamin Katz¹, Tom Vosch³, Jiro Kondo⁴, Hannu Häkkinen² and Stacy Copp¹; ¹University of California, Irvine, United States; ²University of Jyväskylä, Finland; ³University of Copenhagen, Denmark; ⁴Sophia University, Japan

DNA-stabilized silver nanoclusters (Ag_N-DNAs) are magic-sized nanoclusters of 10-30 silver atoms stabilized by one to three short DNA oligomers. The stabilizing DNA ligand's sequence sculpts the size and shape of the tiny nanocluster, thereby selecting its shape-tuned fluorescence excitation and emission peaks. The combinatorially large space of DNA sequence enables DNA ligands to stabilize a wide range of nanocluster structures with sequence-tuned optical properties. These emitters are promising for sensing and biomedical imaging applications, but until recently, the inorganic-organic interface of Ag_N-DNAs was not well-understood. Here, we report our recent work on characterizing the surface chemistry of a new class of Ag_N-DNAs with hybrid ligands and superior optical properties.

We investigate a set of five atomically precise Ag_N-DNA species with near infrared emission and previously reported X-ray crystal structures. Using high-resolution mass spectrometry, we determine the molecular formula of these nanoclusters to be (DNA)₂[Ag₁₆Cl₂]⁸⁺. This is the first time that chloride ligands have been ever reported for Ag_N-DNAs. [1] Chloride ligands can be exchanged for bromide ligands, leading to a redshift in the optical spectra of the emitters. DFT calculations confirm the stability of chloride ligands on the Ag₁₆ nanocluster core, yield qualitative agreement between computed and measured UV-vis absorption spectra, and provide interpretation of the ³⁵Cl-nuclear magnetic resonance spectrum of the (DNA)₂[Ag₁₆Cl₂]⁸⁺. A reanalysis of the X-ray crystal structure confirms that two previously assigned low-occupancy silvers are, in fact, the two chloride ligands. Finally, using the unusual stability of (DNA)₂[Ag₁₆Cl₂]⁸⁺ in biologically relevant saline solutions as an indicator of chloride ligands on Ag_N-DNAs, we use high-throughput screening to identify an additional new Ag_N-DNA with mixed DNA/chloride ligand chemistry. Inclusion of chlorides on Ag_N-DNAs presents a promising new route to expand the diversity of Ag_N-DNA structure-property relationships and to imbue these emitters with significantly enhanced stabilities for *in vivo* biomedical imaging applications. This work also demonstrates the power of combining high-resolution mass spectrometry, optical spectroscopy, nuclear magnetic resonance, and DFT to characterize the ligand interface of metal nanoclusters and to understand how this interface influences optical properties of these novel emitters.

[1] A. González-Rosell, et al., *J. Am. Chem. Soc.* 2023, 145, 19, 10721–10729

9:15 AM EL10.06.03

Polydopamine Coated Gold Nanorods: Photothermal and Photocatalytic Mechanism Study Daniel Aguilar Ferrer^{1,2}, Emerson Coy¹, Mikhael Bechelany^{2,3}, Thomas Vasileiadis¹,

IgorIatsunskyi¹, MarcinZiolek¹, SergioMoya⁴, KlaudiaZebrowska¹, OlenaIvashchenko¹, RaquelPazos⁵, BartoszGrzeskowiak¹ and PaulinaBlaszkievicz⁶; ¹Adam Mickiewicz University, Poland; ²Université de Montpellier, France; ³Gulf University for Science and Technology, Kuwait; ⁴Soft Matter Nanotechnology, Centre for Cooperative Research in Biomaterials (CIC biomaGUNE), Basque Research and Technology Alliance (BRTA), Spain; ⁵Chromatography & Mass Spectrometry Platform, CIC biomaGUNE, Spain; ⁶Poznan University of Technology, Poland

The strong photothermal effect made by the combination of localized surface plasmon resonance (LSPR) presented by gold nanorods (AuNRs) with polydopamine (PDA) makes them appeal nanomaterials for biomedical applications. Here, by seed-mediated growth and a further self-polymerization of dopamine (DA), a reproducible hybrid nanoplatform combining these two materials have been synthesized (AuNRs/PDA). PDA shell thickness was controlled as well as LSPR, besides, their effect on temperature and the photocatalytic response was examined towards Rhodamine 6G (Rh6G) degradation showing a final depletion of 51% during 60 minutes of irradiation and a catalyst concentration of 7.4 µg mL⁻¹. Moreover, the kinetics of the reaction were studied through the Langmuir-Hinshelwood model which in combination with time-resolved spectroscopy, and finite-element method simulations of plasmons unveiled low thermalization and enhanced charge carrier at the composite resulted from the combination of AuNRs plasmons and low thermal conductivity presented by PDA [1].

1. Daniel Aguilar-Ferrer et al. Understanding the Photothermal and Photocatalytic Mechanism of Polydopamine Coated Gold Nanorods. Accepted at Advanced Functional Materials Journal.

9:30 AM *EL10.06.04

Role of the Ligand Structure Around Nanomaterials for Chemical ReactionsWolfgangParak and FlorianSchulz; Universität Hamburg, Germany

Ligands at the surface of nanomaterials can influence chemical reactions, as will be discussed for 3 different examples. 1) In case ion-responsive ligands are attached to nanomaterial surfaces, the binding properties and such working point can shift. As example, when pH-responsive fluorophores are attached with negatively charged ligands to a surface, then there is a local attraction of H⁺, i.e. the pH at the surface is lower than in bulk. 2) Ligands may restrict the available space for reactions. 3) Ligands may change the adsorption properties of molecules to surfaces. One interesting example here is the formation of a protein corona. With different coating different proteins can be "fished" from the environment.

References:

[1] F. Schulz, J. Hühn, M. Werner, D. Hühn, J. Kvelstad, U. Koert, N. Wutke, M. Klapper, M. Fröba, V. Baulin, W. J. Parak, "Local environments created by the ligand coating of nanoparticles and their implications for sensing and surface reactions", Accounts of Chemical Research, in revision.

10:00 AMBREAK

10:30 AM *EL10.06.05

Engineering the Inorganic-Living InterfaceBruceE. Cohen¹, CassioPedroso¹, VictorMann¹, EmmaXu², ChanghanLee², P. JamesSchuck² and EmoryChan¹; ¹Lawrence Berkeley National Laboratory, United States; ²Columbia University, United States

Surface functionalization of nanocrystals is essential for their practical application in living systems, but introducing biocompatibility can come at the cost of diminished nanoparticle optics, diminished colloidal stability, or massive increases in probe size. In addition, the cell presents a remarkably complex chemical environment, rich in metal ions, amines, thiols, and other compounds that can disrupt nanoparticle complexes that are perfectly stable *in vitro*. Inorganic nanocrystals such as quantum dots (QDs),^{1,2} upconverting nanoparticles (UCNPs),³ and avalanching nanoparticles (ANPs)^{4,5} are uniquely suited for quantitative live-cell imaging and are typically functionalized with ligands to study specific receptors or cellular targets. Antibodies are among the most useful targeting reagents owing to their high affinities and specificities, but common nanocrystal labeling methods may orient antibodies incorrectly, be reversible or denaturing, or lead to antibody-nanoparticle complexes too large for some applications. We have shown that SpyCatcher proteins, which bind and spontaneously form covalent isopeptide bonds with cognate SpyTag peptides, can conjugate engineered antibodies to nanoparticle surfaces with control over stability, orientation, and stoichiometry.⁶ Compact SpyCatcher-functionalized QDs and UCNPs may be labeled with short-chain variable fragment antibody (scFv) engineered to bind urokinase-type plasminogen activator receptors (uPAR) that are overexpressed in many human cancers. Confocal imaging of anti-uPAR scFv-QD conjugates shows the antibody mediates specific binding and internalization by breast cancer cells expressing uPAR. Time-lapse imaging of photostable scFv-UCNP conjugates shows that antibody binding causes uPAR internalization with a ~20 min half-life on the cell surface, and uPAR is internalized to endolysosomal compartments distinct from general membrane stains and without significant recycling to the cell surface. With Tm³⁺-doped upconverting ANPs functionalized with these scFv antibodies, the extreme nonlinearity of ANP emission leads to sub-100 nm spatial resolution using only simple scanning confocal microscopy and before any computational analysis. Quantification of ANP spot intensity across multiple z planes then yields a high-resolution 3D map of uPAR distribution on the cell surface. The controlled and stable conjugation of engineered antibodies to nanoparticles enables targeting of diverse receptors for quantitative live-cell study of their distribution, trafficking, and physiology

1. Mann, V. R., Powers, A. S., Tilley, D. C., Sack, J. T. & Cohen, B. E. Azide-Alkyne Click Conjugation on Quantum Dots by Selective Copper Coordination. *ACS Nano* **12**, 4469–4477 (2018).

2. Wichner, S. M. *et al.* Covalent Protein Labeling and Improved Single-Molecule Optical Properties of Aqueous CdSe/CdS Quantum Dots. *ACS Nano* **11**, 6773–6781 (2017).

3. Tian, B. *et al.* Low irradiance multiphoton imaging with alloyed lanthanide nanocrystals. *Nat. Commun.* **9**, 3082 (2018).

4. Lee, C. *et al.* Giant nonlinear optical responses from photon-avalanching nanoparticles. *Nature* **589**, 230–235 (2021).

5. Lee, C. *et al.* Indefinite and bidirectional near-infrared nanocrystal photoswitching. *Nature* (2023) doi:10.1038/s41586-023-06076-7.

6. Pedroso, C. C. S. *et al.* Immunotargeting of nanocrystals by SpyCatcher conjugation of engineered antibodies. *ACS Nano* **15**, 18374–18384 (2021).

11:00 AM EL10.06.06

Unravelling the Relationship Between Degradation and Toxicity of Copper Chalcogenide Nanocrystals via Ligand Control and Compositional ChangesXingjianZhong^{1,2} and AllisonM. Dennis²; ¹Boston University, United States; ²Northeastern University, United States

Copper chalcogenide nanocrystals with a doped composition of Cu_xM_yS_z (M = doping element), are promising agents for biomedical imaging and therapeutic applications. These nanocrystals include direct bandgap semiconductors such as copper indium sulfide (CIS) and stoichiometric Cu₂S quantum dots (QDs) exhibiting photoluminescence and indirect bandgap materials like vacancy-doped copper sulfide (Cu_{2-x}S) and iron-doped copper iron sulfide (CuFeS₂) that exhibit plasmonic features. Compositionally, copper chalcogenide nanomaterials like CIS were thought to have better translational potential than the prototypical QDs that contain the heavy metals cadmium and lead. However, we found that CIS QDs are only biostable and biocompatible when coated with a protective zinc sulfide (ZnS) outer shell; bare CIS QDs degrade rapidly causing acute toxicity *in vivo*. These findings link the nanotoxicity of CIS nanocrystals to their degradation; expanding on these results will provide a framework for the concerted design of biocompatible and optically active copper chalcogenides by controlling the degradation products and rate.

In this study, we quantitatively analyze the toxicity and biodegradation of similarly sized copper chalcogenide nanocrystals with compositional differences (CIS, Cu_{2-x}S, CuFeS₂) as well as the impact of coating and ligand differences (lipid-PEG micelle, poly-*iso*-maleic anhydride polymer, etc.) on CIS. We first observe the degradation of different chalcogenide species coated with the same DSPE-PEG_{2k} micelle encapsulation in biological media to examine the impact of composition on degradation rate. The rate of copper release into the solution is gradual and comparable between compositions. Release of indium and iron mimics that of copper in neutral and chelator-free biological media, but both indium and iron rapidly dissociate from the particles at very early time points upon exposure to the artificial lysosomal fluid containing citric acid, which is prevalent in the lysosomal compartment of cells. When testing the cellular toxicity of these particles on a HepG₂ cell line following 24-hour incubation, CIS exhibits severe toxicity with an estimated IC₅₀ of 124.1 mg/mL total cation concentration. Cu_{2-x}S shows moderate toxicity with IC₅₀ cation concentration of 401.3 mg/mL, and CuFeS₂ demonstrates the least cytotoxicity with over 75% cell viability at 1 mg/mL cation concentration. We hypothesize that the chelation effect of citric acid in the artificial lysosomal fluid rapidly leaches the indium and iron from the particles. This high local concentration of indium ions appears to be detrimental to the cells, while the strong homeostasis mechanisms used to buffer iron bioavailability may prove protective even in the face of burst release. We found that the surface coating (lipid-PEG micelle encapsulation vs polymer wrapping) alters the rate of oxidation of the surface and particle degradation, inspiring further study into the effect of ligand coating on the degradation and toxicity of CIS QDs. We hypothesize that a covalently bonded ligand will slow the rate of CIS degradation in biological environments and will therefore lead to reduced acute nanotoxicity. This study informs the design of biocompatible nanocrystals by elucidating the relationship between nanoparticle surface ligands, particle degradation, and cytotoxicity for copper chalcogenide nanomaterials.

11:15 AM EL10.06.07

Multidentate Hybrid Ligand for Efficient and Robust Hydrophilic Quantum DotsJisuHan^{1,1}, YeonghoChoi^{1,1}, HyeonjunLee^{2,2} and JaehoonLim^{1,1}; ¹Sungkyunkwan University, Korea (the Republic of); ²Korea Advanced Institute of Science and Technology, Korea (the Republic of)

Colloidal quantum dots (QDs) are promising nanomaterials in various fields thanks to high photoluminescence quantum yield (PLQY), band gap tunability and spectrally pure emission profile. To utilize QDs to various applications, surface functionalization, exchanging original surface ligands with functional moieties, is typically demanded for solvent exchange, orthogonal

processing capability, long-term colloidal stability, morphology control, and so on. However, typical ligand exchange protocols are likely to deteriorate innate properties of QDs owing to surface etching by excessive use of introducing ligands, for instance, a reduction in PLQY and colloidal stability during/after the fabrication of aqueous QDs. Adopting multidentate bindings in the functional molecules are one of promising approaches for resolving such troubles as an increased binding affinity allows for effective ligand exchange with minimal amount of ligands. However, the limited number of multidentate ligands and complex synthesis routes for granting multidentate nature obstruct their pervasive use. Herein, we propose the facile synthesis of multidentate hybrid composed of zinc thiolate backbone and functional hydrocarbon branches. For demonstration, zinc chloride (ZnCl₂) and 3-mercaptopropionic acid (MPA) were chosen for preparing hydrophilic hybrid ligands. ¹H nuclear magnetic resonance spectroscopy and Fourier transformed infrared spectroscopy revealed two different configurations of linear and toroidal structure. Their multidentate binding on QDs was confirmed in two-dimensional ¹H nuclear Overhauser effect spectroscopy displaying clear negative cross peaks from propionate branches bound on surface. Titration of CdSe QDs using the hybrid ligands revealed enhanced binding affinity of the hybrid ligands, enabling effective aqueous phase transfer with ~70-fold fewer binding groups compared to MPA. The aqueous QDs using the hybrid ligands featured sustained PLQY and photochemical stability; the hybrid-capped InP/ZnSe/ZnS QDs displayed ~90% of PLQY that is the record efficient to our best knowledge. Prolonged shelf-life and resistance to ultraviolet irradiation were also achieved. We attribute these enhancements to the robust, thick hybrid ligand shell prohibiting invasion of oxygen and water molecules. We believe that our hybrid ligands are expected to serve as useful building blocks for nanocrystal functionalization.

11:30 AM EL10.06.08

How Giant ZnSe-Alloyed Shell Realizes Nearly Unity Quantum Yield Byong Jae Kim^{1,1}, Hyeonjun Kim^{1,1}, Yeongho Choi^{1,1}, Woon Ho Jung^{1,1}, Hyeonjun Lee², Ji-Sang Park³ and Jaehoon Lim^{1,1}; ¹Sung Kyun Kwan University, Korea (the Republic of); ²Korea Advanced Institute of Science and Technology, Korea (the Republic of); ³Sungkyunkwan University Advanced Institute of NanoTechnology, Korea (the Republic of)

Core/shell heterostructure has become one of essential formulae in various applications of colloidal quantum dots (QDs). Heteroepitaxy of wide band gap materials passivates mid-gap states derived from the surface dangling bonds of cores and confines carrier wavefunctions to the inside, allowing for realizing near unity photoluminescence (PL) quantum yield (QY). In addition, the extended shell thickness (typically, 4–10 nm), so-called giant QDs, enables us to manipulate ultrafast carrier dynamics in QDs such as nonradiative Auger recombination or energy transfer in densely packed QD films. In the early stages of giant QDs, CdSe/CdS heterostructures have been exclusively spotlighted as the only suitable pair capable of extended shell thickness due to their minimal lattice mismatch. However, recent research has successfully demonstrated giant ZnSe or its alloyed shells for CdSe cores despite the large lattice mismatch that generally deteriorates PL QY as a shell thickness increases. Unfortunately, there are no reasonable explanation for how such new giant QDs are possible.

Here, we scrutinize the origin of unexpectedly high PL QY observed in giant CdSe QDs with ZnSe-alloyed shells. In the synthesis of QDs growing the graded thick Cd_{1-x}Zn_xSe (average x = 0.3) or ZnSe shell up to ~10 nm, careful heteroepitaxy reaction accomplished nearly unity PL QY at moderate shell thickness (H ~ 4 nm) followed by the gradual reduction, understood as defect formation by compressive lattice strain of shell. However, it was found that more intense strain provided by ZnSeS or ZnS shell recovered the PL QY of giant QDs. To understand such counter-intuitive phenomenon, we investigate the development of strain in the heterostructure and consequent derivation of electronic states. Along the accumulation of compressive strain applied to CdSe core, probed from the CdSe phonon mode shift and altered exciton dynamics, we observed the emergence of low-energy tail in cryo-PL spectra regardless of shell thickness. Retarded decay dynamics at this tail states and Ab-initio calculation suggest that Zn vacancy in ZnSe shell (V_{Zn}) introduced during the shell growth forms shallow hole traps that is 0.05–0.1 eV higher than the 1S_h state of CdSe core. The formation of V_{Zn} and partial strain relaxation seems to prevent the excessive strain accumulation and consequent misfit dislocation. As long as the catastrophic strain is avoided, additional hydrostatic compressive strain lifts the 1S_h state of CdSe core and the shallow traps in the shell become deactivated. Our study proposes the bright side of defects that they can mitigate the lattice strain in the growth of thick ZnSe-based shells to prevent the destruction of QDs by the excessive stress.

11:45 AMA SHORT PRESENTATION IN THE MEMORY OF MARCEL BRUCHEZ, MAXIME DAHAN AND NIKOCLAI GAPONIK. PRESENTED BY H. MATTOUSSI AND ELENA SHEVCHENKO

SESSION EL10.07: Energy Flow in Colloidal QDs
Session Chairs: Sandrine Ithurria, Prashant Kamat and Lea Nienhaus
Wednesday Afternoon, November 29, 2023
Hynes, Level 3, Ballroom A

1:30 PM *EL10.07.01

Effect of Surface Chemistry in Cation Exchange of NPLs Sandrine Ithurria; Sorbonne Université, France

II-VI semiconductor nanoplatelets have attracted lot of interest due to their narrow optical properties controlled by the thickness of these 2D particles. Working with Cadmium chalcogenide semiconductor enables to cover the visible range both with homostructures and heterostructures. In order to extend the optical properties, it is required to use semiconductors with narrow band gaps. However, controlling the shape of the nanoparticles remains challenging and one option that has been explored for a number of years is cation exchange. One more time preserving the anisotropic shape may be challenging in the case one of the dimensions is very small. Here, we will show that ligands in NPLs, not only control the lateral dimensions of NPLs during a growth, but also the shape of the NPLs and the cation exchange rate such that NPLs with narrow band gap semiconductors with optical properties in the NIR may be obtained.

2:00 PM EL10.07.02

Controlling Electronic Coupling of Acene Chromophores on QD Surfaces Through Variable Concentration Ligand Exchange Marissa Martinez¹, Michelle Nolen^{1,2}, Nicholas Pompetti^{3,1}, Lee Richter⁴, Carrie Farberow¹, Justin Johnson¹ and Matthew C. Beard¹; ¹National Renewable Energy Laboratory, United States; ²Colorado School of Mines, United States; ³University of Colorado Boulder, United States; ⁴National Institute of Standards and Technology, United States

Controlling the binding of functional organic molecules on quantum dot (QD) surfaces and the resulting ligand/QD interfacial structure determines the resulting organic-inorganic hybrid behavior. In this study, we vary the binding of tetracene di-carboxylate ligands bound to PbS QDs cast in thin films by performing solid-state ligand exchange of as-produced bound oleate ligands. We employ comprehensive FTIR analysis coupled with UV-Vis spectrophotometric measurements, transient absorption and DFT simulations to study the QD/ligand surface structure and resulting optoelectronic properties. We find that there are three primary QD/diacid structures, each with a unique binding mode dictated by the QD-ligand and ligand-ligand intermolecular and steric interactions. They can be accessed nearly independently from one another via different input ligand concentrations. Low concentrations produce mixed oleate/tetracene ligand structures where the tetracene carboxylates tilt towards QD surfaces. Intermediate concentrations produce mixed oleate/tetracene ligand structures with ligand-ligand interactions through intramolecular hydrogen bonding with the ligands perpendicular to the QD surface and weaker QD/ligand electronic interactions. High concentrations result in full ligand exchange, and the ligands tilt towards the surface while the QD film compacts. When the tetracene ligands tilt or lie flat on the QD surface the benzene ring pi-system interacts strongly with the p-orbitals at the PbS surface and produces strong QD-ligand interactions evidenced through QD/ligand state mixing, with a coupling energy of > 700 meV.

2:15 PM EL10.07.03

Charge-and-Energy-Transfer Processes in Two-Dimensional Supramolecular Materials Ruggero Emmanuele¹, Hiroaki Sai², Darien Morrow¹, Saw Hla^{1,3}, Samuel I. Stupp² and Xuedan Ma^{1,4,2}; ¹Argonne National Laboratory, United States; ²Northwestern University, United States; ³Ohio University, United States; ⁴The University of Chicago, United States

Synthetic soft materials could overcome the limitation of biological structures in terms of robustness, making them appealing for practical applications related to photovoltaics and photocatalysis.¹ Understanding of charge- and energy-transfer mechanisms is often required to build efficient devices from such synthetic soft materials. In this work, we self-assemble 2D supramolecular systems into 2D ribbons and investigate both Frenkel and charge-transfer excitons (FEs and CTEs, respectively) using optical spectroscopy. We discover that the presence of defects intentionally inserted into these nanoribbons leads to variations in the CTEs / FEs emission ratio. Moreover, we find that propagations of the CTEs and FEs are closely related to the compositions and lattice structures of the 2D ribbons. These results were well reproduced by our numerical simulations based on a charge-transfer model. Our findings have important implications for utilizing soft materials in photovoltaics and photocatalytic applications.

1. O. Dumele, J. Chen, J. V. Passarelli, and S. I. Stupp, "Supramolecular Energy Materials" Adv. Mater., 32, 1907247 (2020)

2:30 PM BREAK

3:30 PM *EL10.07.04

CdSe Nanoplatelet Sensitized Upconversion—(Lateral) Size Matters Lea Nienhaus; Florida State University, United States

In photon upconversion, the energy of two photons is combined to generate a higher energy state. A popular pathway for upconversion is triplet-triplet annihilation as it can become efficient at low solar-relevant powers. Here, two triplets are combined to form the desired high energy singlet state. However, since triplet states are 'spin-forbidden', sensitizers are required to indirectly populate the triplet state.

Here, we investigate the effect of material dimensionality on the triplet generation mechanism at the interface of two-dimensional CdSe nanoplatelet sensitizers and surface-bound anthracene carboxylic acid and the resulting effect on triplet-triplet annihilation in the annihilator diphenylanthracene.

We find an unexpected anti-correlation between the upconversion quantum yield and power threshold I_{th} as the NPL lateral size increases. This result is attributed to differences in the triplet-triplet annihilation mechanism: one is mediated by molecular diffusion and the other by triplet energy diffusion.[1,2]

[1] VanOrman, Z.A.; Weiss, R.; Bieber, A.S.; Chen, B.; Nienhaus, L., Mechanistic Insight into CdSe Nanoplatelet-Sensitized Upconversion: Size and Stacking Induced Effects. *Chem Commun.*, **2023**, 59, 322-325.

[2] VanOrman, Z.A.; Bieber, A.S.; Wieghold, S.; Nienhaus, L., Green-to-Blue Triplet Fusion Upconversion Sensitized by Anisotropic CdSe Nanoplatelets. *Chem. Mater.*, **2020**, 32, 4734-4742.

4:00 PM EL10.07.05

Fluorescence Energy Transfer Processes Involving CsPbBr₃ PQD-Dye Assemblies Selin Donmez¹, Sisi Wang^{1,2} and Hedi M. Mattoussi¹; ¹Florida State University, United States; ²ASM International, United States

Fluorescence resonance energy transfer (FRET) is a well-known technique that exploits the non-radiative transfer of excitation energy from an excited donor fluorophore to a proximal ground-state acceptor molecule. FRET is highly sensitive to small changes in the separation distance between the donor and acceptor molecules which offers the use of FRET as a platform for a range of applications such as protein conformation studies and biological assays.

Colloidal lead halide perovskite quantum dots (PQDs) have gained interest, over the past few decades, owing to their unique photophysical properties, including tunable and narrow photoluminescence (PL) profiles, high PL quantum yields (PLQY), high tolerance for structural defects, along with relatively easy to implement synthesis. Energy transfer interactions using these colloidal materials is a highly important, yet underexplored process, for practical applications relying on energy harvesting as well as for addressing fundamental questions. Questions of whether resonance energy transfer interactions relying on the dipole-dipole approximation apply to colloidal QDs (including conventional nanocrystals) have persisted. Another serious challenge that has impeded a better understanding of energy transfer processes with PQDs is the implementation of controlled conjugation of acceptor molecules.

We hereby exploit the ionic nature of CsPbBr₃ QDs to achieve controlled coupling, through electrostatic interactions, of sulfo-cyanine dyes bearing zwitterionic moieties. This has allowed us to control among others the spectral overlap function between PQD emission. We combined steady-state and time-resolved photoluminescence experiments using these assemblies to measure highly efficient energy transfer interactions. This manifested in pronounced losses in PQD emission along with shortening of the PQD PL lifetime. Energy transfer rates were also strongly dependent on the spectral overlap. We will detail our synthetic approach, compare our findings to available theories on energy transfer process, and address potential contributions from charge transfer-induced quenching.

4:15 PM EL10.07.06

Enhancing SWIR Emission: Gradient Alloying and Auger Recombination Suppression in High-Performance Heavy-Metal-Free Colloidal Quantum Dots Hyunjin Cho and DohChangLee; Korea Advanced Institute of Science and Technology, Korea (the Republic of)

The short-wave infrared (SWIR) region, which indicates light in the 1.4 to 3 μm wavelength range, is utilized in various fields such as bio-imaging, telecommunication, and surveillance. However, there has been limited research on the light emission characteristics in the SWIR region using heavy-metal-free colloidal quantum dots. Light Detection and Ranging (LiDAR) is a method that utilizes lasers to determine ranges by measuring the time it takes for the reflected light to return to the receiver. The use of colloidal quantum dots as light emitters in LiDAR can significantly reduce costs and enhance detection capabilities by leveraging the long wavelengths in the SWIR region.

Here, we successfully synthesized InAs/In(Zn)P/ZnSe quantum dots using a one-batch method, suppressing the vulnerability to oxidation, which is a common issue with III-V quantum dots. We controlled various parameters such as initial volume, injection rate, ligand, and temperature to create quantum dots that emit light in the SWIR region. The resulting quantum dots exhibited emission at 1550 nm in the SWIR region. Notably, these quantum dots achieved a photoluminescence quantum yield (PLQY) of 3% at a wavelength of 1400 nm, which represents the highest reported value thus far. To gain insights into the carrier dynamics, we conducted ultrafast time-resolved photoluminescence and transient absorption spectroscopy experiments. These investigations revealed energy variations attributed to the mid-shell gradient alloy and suppressed Auger recombination within the quantum dots. Moreover, the formation of an outer shell on the InAs quantum dots confirmed the passivation of interfacial traps.

Overall, these findings contribute to the development of heavy-metal-free colloidal quantum dots with excellent performance, particularly in the SWIR region at 1550 nm, where the Auger recombination is effectively suppressed. This research provides valuable insights into SWIR region emissions using colloidal quantum dots, furthering the understanding and application of these materials.

4:30 PM *EL10.07.07

Tuning the Energy Flow in Halide Perovskite-Molecular Hybrids AkshayaChemmangat, JishnuChakkamalayath, JeffreyDuBose and PrashantKamat; University of Notre Dame, United States

The flow of energy and electron transfer processes in semiconductor nanocrystal based light harvesting assemblies is governed by the nature of the excited state interactions. Surface interaction of chromophore or redox active molecule with semiconductor nanocrystals dictate the efficiency of photoinduced energy/electron transfer processes. Metal halide perovskite nanocrystals are interesting in the sense that they can either transfer singlet or triplet energy, or selectively transfer electrons or holes to the adsorbed molecules. The presentation will show how one can direct the flow of energy to achieve desired results in a semiconductor-molecular hybrid assembly. The presentation will focus on two specific scenarios of the flow of energy and electron processes in CsPbBr₃ nanocrystal-molecular hybrids. The energy transfer is probed through three molecular acceptors – rhodamine B (RhB), rhodamine isothiocyanate (RhB-NCS), and rose Bengal (RoseB), which contain an increasing degree of heavy atom pendant groups. When interacting with CsPbBr₃ as an energy donor, photoluminescence excitation spectroscopy reveals that singlet energy transfer occurs with all three acceptors. The acceptor functionalization directly influences several key parameters that dictate the excited state interaction (CsPbI₃) is employed as a sensitizer we observe triplet energy transfer to RoseB and other rhodamine dyes. A basic understanding of the fundamental differences between the two excited deactivation processes (energy and charge transfer) and ways to modulate them should enable design of more efficient light harvesting assemblies with semiconductor and molecular systems.

SESSION EL10.08: Poster Session II

Session Chairs: Tae-Woo Lee and Liberato Manna

Wednesday Afternoon, November 29, 2023

Hynes, Level 1, Hall A

8:00 PM EL10.08.01

Heat-Up-Assisted Precursor-Conversion Synthesis of Ultra-Monodisperse Perovskite Colloidal Nanocrystals Igeon Kim¹, YounghoonKim² and Min JaeKo¹; ¹Hanyang University, Korea (the Republic of); ²Kookmin University, Korea (the Republic of)

Colloidal quantum-confined semiconducting nanocrystals are extraordinarily unique photo-active materials, with electronic energy structures, such as optical bandgap energy, that can be tailored by altering their size and dimensionality. Among them, lead halide perovskite nanocrystals (PNCs) have exhibited superior light-harvesting and emitting features, owing to their exceptional optical, photophysical, and optoelectronic properties. Therefore, the PNCs have been extensively studied for their optoelectronic applications such as solar cells, photo-detectors, and light-emitting diodes. Traditionally, the PNCs have been easily prepared at laboratory scale through precursor-injection synthetic methods such as hot-injection methods and ligand-assisted reprecipitation methods. However, the precursor-injection synthetic methods, using highly reactive ionic-salt-type precursor solutions, induce various synthetic variables such as temperature and precursor concentration gradients, leading to the inseparable and unmanageable nucleation and growth process. In this study, we design a precursor-conversion synthetic approaches to homogeneously control the nucleation and growth mechanism of CsPbX₃ PNC crystallizations by using the heat-up methods. In this approach, the highly monodisperse CsPbX₃ (X = Cl, Br, I) PNCs can be successfully synthesized by supplying halide reactants through S_N2 reactions of various haloalkanes in homogeneously blended precursor solutions (denoted as heat-up PNCs). The heat-up synthetic approaches accelerate the halide conversion rates by promoting the S_N2 reactions, and thereby lead to the crystallizations of photo-active CsPbX₃ crystal phases, suppressing the undesired production of photo-inactive and halide-deficient Cs₃PbX₆ phases. During the heat-up process, we monitored the production yield of

halide reactants and the nucleation and growth mechanism along with the increasing reaction temperature. Through this observation, we found that the nucleation and growth stages could be separated in the heat-up process and the heat-up CsPbX₃ PNCs are size-focused into highly narrow size distribution during diffusion-controlled growth. The size and dimensionality of the heat-up PNCs can be easily tuned by precisely adjusting the precursor feeding ratios. Furthermore, the heat-up approaches enable the synthesis of CsPbX₃ PNCs with diverse halide compositions by promoting the S_N2 reactions of various haloalkanes. As a result, ultra-monodisperse heat-up CsPbX₃ PNCs are obtained through the S_N2-based heat-up synthetic approaches, and their high monodispersity and optical features are maintained even in large-scale synthesis.

8:00 PM EL10.08.02

Gate Tunable High-Performance Broadband Phototransistor Based on Organic-Inorganic Vertical Heterojunctions Sourabh Pal, Rajinder S. Deol, Reem Alshambari, Megan Noga, Oliver A. Durnan, Vikrant Kumar and Ioannis Kymissis; Columbia University, United States

In recent times broadband photodetectors find widespread applications in environmental surveillance, optical imaging, spectroscopy, and sensing. A remarkable photodetection performance over a broadband spectral range can be successfully achieved through two primary methods. The first approach involves the utilization of semiconductor materials with broad detection ranges. However, the selection of suitable broadband photoabsorbing materials, especially inorganic ones, is often limited. The second commonly adopted method is the development of hybrid systems by combining nanomaterials with distinct photoabsorption bands, thereby achieving a heterostructured system with a broad photodetection range. Amorphous Indium Gallium Zinc Oxide (a-IGZO) is one of the most widely researched oxide semiconductors owing to its high carrier mobility, good uniformity, and facile synthesis process.¹ However, as an active photosensitive material, a-IGZO also has its own limitation such as the large bandgap (~ 3.3 eV) leading to its limited light absorption capability and response to long-wavelength light.² On the other hand, organic semiconductor materials have garnered significant attention in the field of optoelectronics due to their favourable intrinsic properties, together with the simple and easy synthesis processes, making them cost-effective for large-scale fabrication. One promising area of exploration involves the utilization of organic-inorganic heterostructures, which combine the optoelectronic attributes of both constituent materials. This novel device structure allows for synergistic advantages, enabling extensive applications in the fields of electronics as well as optoelectronics.³ Herein, we report a high-performance broadband phototransistor exploiting the concept of organic-inorganic heterostructure, in which conjugated polymer J71:ITIC with narrow band gap is used as a visible photosensitizer, whereas a-IGZO with high mobility acts as conducting channel as well as active UV sensing material. The favourable energy band alignment between J71:ITIC and a-IGZO effectively contributes to the high-efficiency separation of photogenerated carriers across the interface, resulting in ultrahigh photoresponsivity of ~10⁴ A/W and specific detectivity of ~10¹⁴ Jones at an applied gate bias of ~ -7.5 V for incident light illumination of ~ 680 nm together with an adequate UV photoresponse owing to the UV light sensitivity of active channel layer. These results validate that the fabricated J71:ITIC/a-IGZO heterostructure based phototransistor can be an ideal prototype for the next-generation broadband photodetection applications.

References:

- 1 J. Troughton and D. Atkinson, *J. Mater. Chem. C*, 2019, **7**, 12388–12414.
- 2 D. H. Lee, K. Kawamura, K. Nomura, T. Kamiya and H. Hosono, *Electrochem. Solid-State Lett.*, 2010, **13**, H324.
- 3 B. Yang, Y. Wang, L. Li, J. Zhang, J. Wang, H. Jiao, D. Hao, P. Guo, S. Zeng, Z. Hua and J. Huang, *Adv. Funct. Mater.*, 2021, **31**, 2103787.

8:00 PM EL10.08.03

Triplet Energy Transfer from CdS QDs Enhances Organometallic Eu(III) Emission Tingting Huang¹, Sheng He², Tianquan Lian² and Ming Lee Tang¹; ¹The University of Utah, United States; ²Emory University, United States

Europium (III) complexes are of interest for bioimaging because of their long-lived, narrow emission in the visible and near-IR wavelengths. Since the direct absorption of light by Eu³⁺ ions is intrinsically poor, the photoluminescence (PL) intensity for Europium (III) complexes are usually low. Their PL quantum yield is improved by coordinating ligands that absorb photons. These coordination ligands are usually excited to their singlet state. Intersystem crossing to the ligand triplet state allows for energy transfer to the central Eu³⁺ ions. Therefore, excitation of the ligands requires high-energy photons and only UV light can be used. Here, we show for the first time that quantum dots (QDs) can serve as triplet photosensitizers for Europium (III) complexes. We make use of the high extinction coefficients of CdS QDs for excitation after 400 nm. Energy transfer occurs through a dark triplet state, eliminating the need for high-energy photon excitation. 1-Naphthoic acid (1-NCA) is used to enhance energy transfer because its triplet state is higher than ⁵D₀ state of Eu³⁺ (2.16 eV) and lower than QDs' band edge. 1-NCA is critical in mediating the energy transfer between QDs and the Europium (III) complex. Transient absorption spectroscopy confirms triplet energy transfer between QDs, mediator, and Eu(III) complex. The Eu(III) photoluminescence quantum yield is enhanced up to 21.4 times, the highest value reported in literature.

8:00 PM EL10.08.04

Surface Passivation of Blue-Emitting Perovskite Nanoplatelets using Polysalt Ligand Complexes Unaisah Vorajee, Selin Donmez, Sisi Wang and Hedi M. Mattoussi; Florida State University, United States

Colloidal CsPbBr₃ nanoplatelets (NPLs) exhibit blue and narrow photoluminescence emission, which makes them highly promising for use in applications such as light-emitting diodes. However, these materials tend to be colloidal and structurally unstable under normal storage conditions. In addition, the presence of surface defects increases the exciton nonradiative recombination rates for as-grown nanocrystals, resulting in modest to small photoluminescence quantum yields (PLQYs).

In this presentation, we detail the use of a set of Br-based polysalt-complexes as stabilizing ligand-complexes that enhance the PLQY while preserving the morphology and the crystal structures of these NPLs. More precisely, we find that while application of the polysalts (made of imidazolium or ammonium bromide motifs and solubilizing alkyl chains) alone can improve the PL, it also tends to progressively etch the NPL surfaces and damages their structural integrity. In contrast, mixing bromide-based salts, namely PbBr₂, SnBr₂, CoBr₂, MnBr₂, and ZnBr₂, with the polymer prior to ligand substitution forms polymer-complexes, which promote electronic passivation and simultaneously impart morphological stability to the NPLs. Optical and spectroscopic results show a PL enhancement of about one order of magnitude measured compared to as-grown NPLs, with high color purity profiles at 460 nm. Furthermore, structural characterization and monitoring of NPL dispersions over time have proved long-lasting colloidal stability together with preserved structural integrity of these materials.

8:00 PM EL10.08.05

Engineered Hybrid Organic-Inorganic Perovskite/Ag Contact for Preventing Ag Diffusion using Buffer Barriers Ji Myeong Yu, Yunhwa Hong, Seokgi Kim, Sungkyu Kim and KwangHeo; Sejong University, Korea (the Republic of)

CH₃NHPbI₃(MAPbI₃), one of the organic-inorganic halide perovskite materials, has attracted strong interest in various optoelectronic devices due to its high absorption coefficient, tunable band gap, and fast charge transport. [1] However, halide perovskite not only causes reliability issues in temperature and humidity environments but also is decomposed into CH₃NH₃⁺ and PbI₂ by an electron-induced reduction reaction at the metal/MAPbI₃ interface. [2] Although various candidates such as oxide thin films, 2D perovskites, and polymers were proposed as protective layers to prevent the deformation of MAPbI₃, [3] the effects of diffused metal ions on structural deformation and phase transition in the metal/MAPbI₃ contact have not been clearly understood yet.

Here, we directly confirmed the diffusion of metal ions and phase deformation in Ag/MAPbI₃ contact using transmission electron microscopy and energy dispersive x-ray spectroscopy. The PbI₂ phase is formed in the MAPbI₃ matrix contacted with metal and gradually transformed into PbI₂ and I⁻ due to Gibbs free energy, which is confirmed by diffracted peaks of the PbI₂ phase at 12.6°, 28.2°, and 29.4°. Furthermore, thermodynamically stable Ag-I bonding is generated by energy barrier, forming an AgI interfacial layer at the Ag/MAPbI₃. Because non-protective MAPbI₃ with the damaged surface shows reduced grain size by 20% and the formation of deep pinholes, we inserted various protective layers to passivate the surface and maintain the MAPbI₃ matrix. In order to prevent penetration of Ag, SnO₂ thin films with a thickness of 30 nm were deposited onto MAPbI₃ by atomic layer deposition. Because anions of the SnO₂ precursor are bonded with the most reactive MA⁺ at the early stage, only hexagonal and orthorhombic PbI₂ phases were identified in the as-deposited structure. The physically deposited C₆₀ layer with a 30 nm thickness damages the MAPbI₃ matrix, resulting in the formation of PbI₂ phases and a 15% reduction in the grain size of MAPbI₃. PMMA of the 30 nm thickness was coated on the MAPbI₃ layer for surface protection and prevention of diffused Ag ions. The penetrated Ag ions through the PMMA layer generate AgI phase inside the MAPbI₃ matrix though the MAPbI₃ was effectively protected for 30 days without the formation of PbI₂ phase. Two types of structures composed of C₆₀ and PMMA are suggested for the anti-diffusion barrier and passivation layer, respectively. Although the C₆₀/PMMA bilayer structure effectively prevents the formation of PbI₂ and AgI phases for 50 days, the grain size of MAPbI₃ decreased by 5%. Compared to the bilayer structure, MAPbI₃ matrix protected by C₆₀-PMMA complex is well maintained in its original structure even after 60 days without phase deformation and grain shrinking. Because the uniform and cohesive hydrophobic PMMA film not only effectively protects the MAPbI₃ structure but also the diffusion of Ag ions is controlled by the C₆₀ layer, our findings suggest advanced buffer layers to protect the surface of MAPbI₃ and prevent structural deformation caused by metal diffusion in various metal/MAPbI₃ contact.

[1] A. Babayigit et al., *Nat. Mater.* **15**, 247 (2016)

[2] K. Hong et al., *J. Mater. Chem. C*, **9**, 15212 (2021)

[3] Abd. Rashid et al., *Energy Environ. Sci.* **14**, 2906 (2021)

8:00 PM EL10.08.06

Self-Healable Quantum Dot/Polymer Composite Film for Quantum Dot Light-Emitting Diodes Ji Su Kim and Dae-Hyeong Kim; Seoul National University, Korea (the Republic of)

Highly stretchable, self-healable material engineering is key for next-generation stretchable light-emitting devices. Despite recent progress in intrinsically stretchable materials for light-

emitting layer (EML), the formation and propagation of irreversible cracks on the EML remain a significant challenge, leading to rapid device failure. Here we report material design of self-healable and stretchable quantum dot (QD) based EML for stable and stretchable quantum dot light-emitting diodes (QLEDs). We fabricated a homogeneous ternary composite film by blending QDs, self-healable elastomer, and a semiconducting polymer. Upon optimization of the composition, the composite film exhibited autonomous self-healing ability at room temperature, and high stretchability while the optical properties of QDs remained intact. The resulting intrinsically stretchable QLED with self-healable EML demonstrated enhanced stability under repeated deformations.

8:00 PM EL10.08.07

Bright Visible Luminescence of Dimethylformamide-Stabilized Niobium Oxide Nanoparticles Shohei Murotani, Akito Mizobata, Moegi Nomura, Honami Iguchi, Mahito Yamamoto, Yasushi Obara and Mitsuru Inada; Kansai University, Japan

Inorganic metal oxides are expected to be candidates for new functional materials because they exhibit a wide variety of physical properties. For transition metal oxides, slight differences in structure, composition, and oxidation state can cause completely different physical properties, due to the flexibility of their crystal structures and the diversity of their electronic structures. While it is well known that nanostructures exhibit different physical properties than bulk materials due to quantum size and surface effects. Therefore, metal oxide nanoparticles are suitable for novel functional materials. However, it has been difficult to synthesize nano-sized particles of niobium because of its easy oxidation and aggregation.

Recently, we have succeeded in synthesizing niobium oxide nanoparticles (Nb NPs) with a particle size of less than 4 nm by DMF reduction method. The surface of the Nb NPs is terminated with DMF molecules, which is extremely stable and has excellent re-dispersibility in water and alcohol solvents. We have modified the surface of the nanoparticles by adding chlorides. We compared the physical properties of the nanoparticles with and without the addition of chlorides: XPS and XANES analyses showed that the addition of chlorides resulted in a lower average oxidation state of niobium. The both Nb NPs with and without chloride additive showed bluish-white luminescence in the visible light range, but the nanoparticles with chloride additive showed a larger luminescence intensity. The broad emission spectrum could be divided into about four emission origins. As the concentration of nanoparticles in solution was increased, the peak emission wavelength was red-shifted. This shift was due to Förster-type resonant energy transfer. A light emitting device was fabricated by using Nb NPs. The EL devices showed different emission colors depending on the materials in contact with the nanoparticles: red emission was obtained for the Al/p-Si/Nb NPs/ITO structure and blue emission was obtained for the ITO/PEDOT:PSS/Polysilane-TPD/Nb NPs/TPBi/Al structure. These results suggest that the EL mechanism and origin can be controlled by the interface conditions between Nb NPs and the electron (hole) transport layer.

8:00 PM EL10.08.08

Development of Highly Fluorescent Copper and Silver Chalcogenides for SWIR Imaging via Surface Control Yidan Sun¹, Xingjian Zhong^{2,1} and Allison M. Dennis¹; ¹Northeastern University, United States; ²Boston University, United States

Ag₂S nanoparticles are promising candidates as short-wave infrared (SWIR) imaging agents due to their low toxicity, high photostability, small size, and tunable fluorescent properties in the second near infrared biological window (NIR-II). They have been widely studied for preclinical imaging with high resolution and signal-to-noise ratio. However, Ag₂S nanoparticles suffer from potential heavy-metal toxicity as well as poor fluorescence efficiency due to surface defects. To overcome these limitations, we are optimizing Ag₂S surface treatments while also investigating alternative heavy-metal-free compositions like Cu-based nanocrystals. While copper sulfide nanocrystals are more commonly known for their localized surface plasmon resonance behavior, recent research shows that stoichiometric Cu₂S nanocrystals fluoresce with a peak between 900 to 1100 nm; more effort is needed to optimize their fluorescence properties and stability. A common factor influencing the photophysical behavior of nanoparticles is their surface properties, including the presence of surface defects and the ligands at the interface between the nanoparticle and the surrounding media. Energy transition processes are highly correlated with these interfacial interactions, impacting both radiative and non-radiative recombination and thus photoluminescence. By modifying the ligand coating and shelling, nanoparticles can be protected from defect-derived nonradiative relaxation and energy loss during interaction with the environment.

In this study, we synthesize fluorescent Ag₂S and Cu₂S nanoparticles and manipulate their optical properties through surface treatment. We explore the impact of different shelling and ligands on surface traps, stability, and optical properties. Enhanced fluorescence intensity of Ag₂S demonstrates the removal of surface defects, while surface treatment of Cu₂S reduces surface oxidation, preventing the shift from fluorescent to plasmonic nanocrystals. By acknowledging the impact of surface conditions on nanoparticle behavior, we can pursue the deliberate design of high-quality contrast agents for SWIR imaging.

8:00 PM EL10.08.09

Photocatalytic Properties of Perovskite Quantum Dots and Their Role in the Degradation of Alkyl Halide Molecules Selin Donmez, Sisi Wang and Hedi M. Mattoussi; Florida State University, United States

Since the first successful implementation of solution phase growth of colloidal cesium lead halide perovskite nanocrystals (PNCs), interest in these materials has steadily grown. This has been driven by their unique photophysical properties and the ionic nature of the semiconducting cores. One of the most interesting properties of PNCs is the ability to forego anion exchange reactions with the surrounding medium, which offers an alternative route for tuning the photophysical properties of these materials.

We present a detailed study on the photo catalytically assisted anion exchange reaction of CsPbBr₃ PQDs dispersed in alkyl chloride solutions. We found that electron transfer from photoexcited PNCs to the surrounding alkyl chloride molecules triggers their electrochemical degradation which produces alkyl radicals and reactive Cl⁻ anions in the medium. The resulting reactive chlorides engage in halide exchange reaction with the PNC cores, resulting in blue shift in the absorption and PL emission properties of the samples. We probe the efficiency of the reaction by varying the nature of the photoexcitation source (e.g., laser source vs UV reactor or sunlight) and the relative reduction potential of the alkyl halide molecules used. We supplement our findings with thorough characterization of the nanocrystal intermediates to track changes in the crystal structure and stoichiometry during irradiation, using optical and fluorescence spectroscopy, powder X-ray diffraction and x-ray fluorescence spectroscopy. These findings bode well for testing the photocatalytic properties of PNCs in general and may have implications in the degradation of chlorinated molecules.

8:00 PM EL10.08.10

Doping Colloidal Quantum Dots Marissa Martinez and Matthew C. Beard; National Renewable Energy Laboratory, United States

Doping has been an important method for tuning semiconductor electronic and optical properties, yet doping quantum dots (QDs) still presents a challenge. Herein, we report a facile method to dope PbS, CdSe, and CsPbBr₃ quantum dots with Ag, Na and Bi using ligand chemistry. Adding a solution of the metal oleates to a QD solution produces a bleach in the QD exciton absorption in the UV-VIS spectrum, and an intraband absorption in the FTIR. We found a higher free-carrier conductivity in solution-doped coupled QD films, compared to as-synthesized, using sheet resistance measurements. This study demonstrates the ability to dope QDs in solution while maintaining colloidal stability and increasing conductivity of the QD solids.

8:00 PM EL10.08.11

Spatial Composition Tuning of Colloidal NiMgO Hole Transport Materials for All-Inorganic Quantum Dot Light-Emitting Diodes Woon Ho Jung^{1,1}, Byong Jae Kim^{1,1}, Jisu Han^{1,1}, Jaehoon Lim^{1,1}, Yeongho Choi^{1,1}, Yong Woo Kwon^{1,1} and Hyeonjun Lee²; ¹Sungkyunkwan University, Korea (the Republic of); ²Korea Advanced Institute of Science and Technology, Korea (the Republic of)

Rapid progress in the device performance of colloidal quantum dot (QD) based light-emitting diodes (QD-LEDs) proposed the new technical opportunity for next-generation displays. Beyond the premise of QD-LEDs in displays, scientists in this field are now looking forward to realizing brighter and robust lighting sources based on QDs, previously achieved solely by inorganic LEDs and laser technologies. Unfortunately, the state-of-the-art QD-LEDs employing the hybrid device architectures, organic hole transport layers (HTLs) and inorganic electron transport layers (ETLs), seem to be incapable of the direction toward high power devices due to limited hole conductivity and thermal instability of organic HTLs. This intrinsic demerit of organic HTLs naturally calls for the development of inorganic HTLs featuring enhanced hole conductivity and stability. Among various candidates, nickel oxide (NiO_x, x < 1) has gained attention due to its wide band gap and p-type conductivity granted by Ni vacancy (V_{Ni}). However, prior attempts to implant NiO_x in QD-LEDs have exhibited suboptimal performance due to the large hole injection barrier and difficulty to match electrical property of ETL counterparts.

To address the disparity of valence band maximum (VBM) and conductivity of NiO_x to typical ETLs, herein, we propose the colloidal NiMgO nanocrystals (NCs) with spatially controlled Mg content. The NiMgO NPs was synthesized by co-condensation of Ni(OH)₂ and Mg(OH)₂ at elevated temperature. X-ray photoelectron spectroscopy (XPS) and photoluminescence yield spectroscopy (PYS) confirmed that the incorporation of Mg to the Ni-O lattice increased the amount of V_{Ni} within and on the NCs, and lowered VBM position. We verified that the internal Mg content was limited to ~2% and residual Mg(OH)₂ coordinated to V_{Ni} sites on NCs. Interestingly, V_{Ni} on NCs' surface had a marginal effect on the hole concentration but significantly suppressed hole mobility by an order of magnitude. Maneuvering the spatial Mg content, we successfully optimized NiMgO NCs to minimize the energy offset between the VBM of NiMgO and the 1S_B state of QDs, and to achieve suitable hole mobility similar to that of ZnMgO ETLs. This optimization was also beneficial to reduce photo-induced hole transfer from QDs to NiMgO that was identified as a serious efficiency-limiting process at NiO_x-QD junctions. All-inorganic QD-LEDs employing our NiMgO HTLs exhibited a record peak efficiency of 16.3% and T₅₀ of 382,239 hr (at 100 nit), surpassing previous benchmarks. Our achievement highlights the potential of inorganic HTLs in paving the way for high power QD-LEDs in the future.

8:00 PM EL10.08.12

Recently, quantum dot light-emitting diodes (QLEDs) have extensively utilized electron transport layers (ETLs) based on the metal oxides such as ZnO, which stands out for their high performance in QLEDs. Despite the successful implementation of metal oxide-based ETLs, there is still a puzzle surrounding how they effectively drive QLEDs. Previous studies have primarily attributed this advancement to the modification of energy levels within the ETLs. However, despite the energetic considerations, several reports on metal oxide-based QLEDs have shown driving voltages lower than the optical bandgap of quantum dots (QDs). Additionally, the efficiencies of QLEDs often surpass the theoretical limit dictated by the emissive probability of neutral QDs. This intriguing finding suggests the existence of a concealed mechanism behind the performance improvement of QLEDs. In this study, we demonstrate that the charge transfer between ZnO-based ETLs and QDs not only affects the energy alignment of QDs in QLEDs but also influences their optical properties. The study for ultraviolet photoelectron spectroscopy represents the overall energy landscape of QLEDs being rearranged centered on the surface states of QDs. The consequence of charge transfer from ZnO-based ETL to the QD surface increases the work function of QDs, providing electrostatic potential gain for hole injection. The spectrally-resolved photoluminescence and electroluminescence results show that carriers injected into individual QDs regulate the injection rate of opposite carriers through Coulombic interaction. By carefully assessing the carrier occupation in QDs, we are able to quantify the emissive probability of QDs on metal oxides. The transfer of electrons from the metal oxides to QDs electrically passivates the surface trap states on QDs, thereby increasing the emissive probability of QDs. The electrobrightening of QDs by metal oxide ETLs pushes the efficiency envelopment of QDs by surface defects. Our series of analyses indicate an oversimplification in considering the QD ensemble as a single emitter and the ligand-passivated surface as a mere insulator within QLEDs. From a practical perspective, we emphasize the importance of considering individual QDs as discrete emitters and the optoelectronic changes resulting from charge exchange. We believe this consideration would pave the way for the design of efficient QLEDs.

8:00 PM EL10.08.13

Characterization and Optimization of Gold Nanoparticles Synthesized via Environmentally Benign Electrochemical Synthesis on Chitosan Layers [Harjaisal S. Brar](#)^{1,2}, [Daniell. Lu](#)^{1,3}, [Claire Kang](#)^{1,4}, [Jacob Zerykier](#)^{1,5} and [Michael Cuffio](#)¹; ¹Stony Brook University, The State University of New York, United States; ²Stockdale High School, United States; ³Westview High School, United States; ⁴Canyon Crest Academy, United States; ⁵Massachusetts Institute of Technology, United States

Previously, palladium and other noble metal nanoparticles have been synthesized on chitosan-coated stainless steel [1][2]. These metal nanoparticles have been shown to have both antibacterial and catalytic properties. Finding ways to synthesize potentially catalytic noble nanoparticles (gold, palladium, and silver) while maintaining their stability under atmospheric conditions is an important goal of materials research. Electrochemically deposited chitosan layers on steel are used as an environmentally benign nucleation support structure for the creation of stable metal nanoparticles. Utilizing electrochemistry to create an abundance of activation sites on the chitosan structure, we have synthesized pure metal nanoparticles of gold. 1µm mirror finish 304 stainless steel purchased from McMaster-Carr was cut into 1 square inch samples (6.45 cm²). The steel samples were ultrasonicated in deionized (DI) water for 10 minutes, briefly rinsed, and ultrasonicated for another 10 minutes in isopropyl alcohol to remove greases and other contaminants. The steel samples were then allowed to air dry and prepared for electrochemical deposition.

A chitosan solution with a concentration of 1.00 to 3.00 grams of chitosan per 120 mL DI water was prepared, and the pH was lowered to less than 5 by adding HCl dropwise to the solution. The solution was stirred overnight so that the chitosan could fully dissolve. A potassium gold (III) chloride solution with a concentration of 0.01 M was prepared in a volumetric flask using high purity (>18mΩ/cm) DI water.

Electrochemically deposited chitosan layers on steel are used as an environmentally benign nucleation support structure for the creation of stable metal nanoparticles. The steel samples were electrochemically coated with a layer of chitosan using controlled potential coulometry. A constant potential of -3.0 V was applied for 60-120 seconds. Each sample was air dried overnight. The chitosan-coated steel samples were used for electrochemical reduction of the gold (III) ions to synthesize nanoparticles on the chitosan layer at voltages ranging from -1.5 V to +1.5 V for 60-120 seconds in order to determine the optimized parameters for gold nanoparticle synthesis, as electrochemistry creates an abundance of activation sites on the chitosan structure. Once the process was complete, the samples were air dried overnight or placed in a vacuum chamber for several hours.

Various methods of analysis were employed to image and quantify the nanoparticles including Optical Microscopy, Scanning Electron Microscopy (SEM), Fourier Transform Infrared (FTIR) spectroscopy, X-Ray Fluorescence (XRF), Energy Dispersive Analysis by X-rays (EDAX), and cyclic voltammetry. It was also discovered that the nanoparticles created were protected by a thin film or coating of chitosan which prevented oxidation while maintaining viability for catalytic reactions and possibly antimicrobial and antibacterial applications [3]. Exposure to ultraviolet (UV) light following electrochemical deposition was found to enhance abundance and dispersion of nanoparticles formed. However, the amount of pure metal nanoparticles was found to decrease with exposure to UV light due to an increase in the formation of metal oxide nanoparticles. The elimination of trapped hydrogen gas bubbles formed during the cathodic polarization via heating was found to eliminate nucleation sites and lead to the formation of micron-sized clusters, oxides, and little to no pure gold metal. The surface of these mixed nanoparticles was found to be highly chemically reactive.

Future work will include X-Ray Photoelectron Spectroscopy (XPS) to determine the oxidation states of the nanoparticles and more experimentation with concentrations and voltages to optimize the parameters for electrochemistry.

8:00 PM EL10.08.14

Nearly 100% Radiative Lifetime Enhancement Through Polymer-Blend-Assisted Defect Passivation and Morphology Regulation in Inorganic Halide Perovskite LEDs [Parvez Akhtar](#), [Raman Aggarwal](#), [Nidhi Dua](#), [Henam S. Devi](#), [Md.S. Hassan](#) and [Madhusudan Singh](#); Indian Institute of Technology Delhi, India

All-inorganic halide perovskite light-emitting diodes (LEDs) exhibit color purity comparable to organic LEDs with significantly greater operational stability. However, owing to the rheological properties of inks of CsPbBr₃ with commonly used solvents such as dimethyl sulfoxide (DMSO) deposited on hole injection layers such as poly(3,4-ethylenedioxythiophene) polystyrene sulfonate (PEDOT:PSS), formation of pinhole-free thin films is a challenge. Further, in the perovskite structures (ABX₃)[1], surface and grain-boundary defects play a critical role in determining transport and the degree of non-radiative energy loss. In this work, we report on the impact of the use of inexpensive polymers (poly(ethylene) glycol (PEG) and polyvinylpyrrolidone (PVP)) on passivating defect states in nanocrystalline CsPbBr₃. Precursors cesium bromide (CsBr) and lead bromide (PbBr₂) (in DMSO) were heated under vigorous stirring, and then optionally combined with the blend PEG:PVP in DMSO and dimethyl formamide (DMF) in a 1:1 ratio to form an ink[2]. X-ray diffraction (Rigaku, Cu-Kα 1.54Å) reveals an orthorhombic phase (ICDD 96-153-3063) with the stoichiometric composition confirmed using energy dispersive X-ray (EDX) analysis. Thin films of control (CsPbBr₃) and test (CsPbBr₃:PEG:PVP) formed with spin-coating exhibit different nanocrystallite sizes using field-emission scanning electron microscopy (FESEM, JEOL): ~204 nm (control) vs ~101 nm (test). The polymers are seen to assist in regulation of grain sizes, resulting in a narrower size distribution for the test film, and lead to a lower pinhole density (>99% coverage) in the test film vs control (<80% coverage) estimated using image processing techniques on FESEM scan data. However, owing to the increase of surface to volume ratio for the test film, we should expect an increased defect density, leading to a deterioration of the radiative efficiency. To investigate the impact on carrier lifetimes, we carried out time-resolved photoluminescence (TRPL) using time-correlated single-photon counting (TCSPC) with a pulsed laser (377 nm) (Edinburgh Instruments FLSP920). Interestingly, measurements and analysis using a bi-exponential model on the test thin film show a higher radiative lifetime (17.82 ns) vs control (9.10 ns). There is a nearly four-fold reduction in the relative strength of the nonradiative tail for the test sample when compared to control, with a ~4.5-fold enhancement in the relative intensities of measured photoluminescence. These results strongly suggest effective passivation of dangling bonds, grain boundaries, etc, which suggests potential Lewis acid-base interactions between Pb²⁺ and π-bonds in the polymer chains. This interaction was confirmed using a Fourier Transform Infrared (FTIR, Thermo-Fischer) spectrophotometer. Finally, LED devices (PEDOT:PSS/CsPbBr₃:PEG:PVP/2,2',2''-(1,3,5-Benzinetriyl)-tris(1-phenyl-1-H-benzimidazole (TPBi)/LiF/Al) were fabricated using a combination of spin coating and thermal evaporation at a pressure 2.3 x 10⁻⁶ Torr (Angstrom Engineering, Evovac). Device characterization yields significant enhancement in electroluminescence (EL, green:518 nm, FWHM: 17nm) of test devices vs control in a manner consistent with the observed enhancement in PL. Briefly: peak brightness (7204 vs 2371 Cd/m²), current efficiency (4.19 vs 0.54 cd/A) and efficacy (2.32 vs 0.29 lm/W), with a slight reduction in the turn-on voltage (2.9 vs 3.3 V), etc. can be attributed to effective defect-passivation despite a seemingly adverse increase in surface to volume ratio. Future work will involve quantification of any device lifetime changes arising from passivation of defects as we expect that the increase of current efficiency is likely to limit degradation of LEDs in demanding applications such as lighting, and high brightness displays.

[1] Ye, J. et al *Angew Chem Int Ed Engl* **2021**, 60 (40), 21636–21660.

[2] Akhtar, P. et al *Thin Solid Films* **2023**, (minor revisions submitted).

8:00 PM EL10.08.15

Enhanced Interfaces for Higher Efficiency and Lifetime of Quantum Dot Light-Emitting Diodes [Jeonghun Kwak](#), [Geun Woo Baek](#) and [Taesoo Lee](#); Seoul National University, Korea (the Republic of)

Owing to the superior optical properties of quantum dots (QDs), QD-based light-emitting diodes (QLEDs) are becoming established as the next generation of displays and light sources. In recent years, device performance has been steadily enhanced by improving the charge balance within the device as well as increasing the photoluminescence quantum yield of QDs. However, the light-emitting mechanism of QLEDs, the mechanism of carrier injection into QDs, and the factors affecting their operational lifetime are still not clearly understood. Research on these issues is crucial for the practical application of QLEDs. In this work, we show our recent research results on the influence of various interfaces on the efficiency and lifetime of the QLEDs, including the core/shell interfaces of QDs and the charge transport layer/QD interfaces.

8:00 PM EL10.08.17

Hydrodynamically-Modulated Dewetting of Colloidal Solution for Physical Unclonable Functions Yeonjin Cho, Jeongsu Pyeon, Hyoungsoo Kim and Yeon Sik Jung; Korea Advanced Institute of Science and Technology, Korea (the Republic of)

Traditional methods of blocking counterfeiting are prone to detection by potential attackers. In response, Physical Unclonable Function (PUF) has emerged as an alternative security measure. PUF is a specialized function that leverages the inherent unpredictability of physical processes to yield unique responses to specific challenges. PUF offers hardware-based security, mitigating vulnerabilities inherent in software-based systems susceptible to hacking and signal jamming. Recent efforts have aimed to develop optical PUF labels using various randomness sources. These PUF's non-deterministic fabrication process ensures a substantial encoding capacity for robust data security. However, excessively disorderly PUF codes disseminated across the information space might exhibit a deficiency in possessing a distinguishing fingerprint key. Using random optical features for security keys mandates statistical image processing for digitization and key generation. Unfortunately, the processing of analog signals to digitized codes may compromise authentication accuracy resulting from an arbitrary threshold during an image analysis.

We tackle this by utilizing the geometric multi-bit patterning technique, manipulating dewetting of colloidal solution for advanced optical PUFs that exhibit both high randomness and determinism. By placing agglomerated dots of colloidal particles at a specific vertex within geometrically confined polygons, these two contrasting features can be provided to the PUF system through the hydrodynamic modulation of the dots as visual cues. Exploiting binary solvent flow unpredictability in confined spaces during dewetting, we fabricate sophisticated PUF labels in periodic pixel arrays. The fundamental principle stems from instability arising from imbalanced solutal-Marangoni flows in evaporating polygonal droplets. Importantly, the dynamic coating procedures have the capability to induce unforeseeable fluctuations in contact angles at every vertex during each coating iteration. These fluctuations perturbed the radial symmetry of the solutal-Marangoni flows within polygonal-shaped droplet, introducing randomness to the final PUF pattern—a phenomenon supported by statistical parameters. This pattern achieves an entropy of 0.977, a uniqueness value of 0.759, and a correlation coefficient of 0.009, all of which are close to the ideal values. It successfully passes the statistical test for random number generators conducted by NIST (National Institute of Standards and Technology), confirming its true randomness, unpredictability, and unclonability. These random PUF labels with quantized signals at deterministic sites enable efficient, accurate, and swift authentication in both encoding and decoding. They also offer reconfigurability, transferability to diverse surfaces, and the potential for enhanced security through fluorescent molecule dyeing.

8:00 PM EL10.08.18

Silica-Encapsulated Quantum Dots with Thiol Ligand Exchange for High Thermal and Photo-Stability Against Moisture Yoon-Jeong Choi, Jeong-Yeol Yoo and Byung Doo Chin; Dankook University, Korea (the Republic of)

Colloidal quantum dots (QDs) have attracted attention in various fields including light emitters for the next-generation display due to their high photoluminescence quantum yield (PLQY) and excellent color purity.¹ However, their low stability under harsh conditions, such as exposure to heat and oxygen, limits their wide-scale applications. Barrier films for QD-sheet are widely used but are expensive and dimensionally less effective. Encapsulation of QDs with silica is regarded as one of the reasonable surface modification methods, which has many advantages such as optical transparency, excellent chemical/mechanical stability, and ease of making chemical modifications.² The encapsulation of QDs with silica is based on the use of a silane precursor in a solution containing water, ethanol, ammonia, and amines. However, general QDs are extremely sensitive to their surrounding environment and undergo quenching at these solution conditions. As a result, the development of a waterless silica coating method has become a new strategy.^{3,4} Using the waterless method, the thickness of the silica shell can be controlled by the catalyzed hydrolysis and condensation of silane precursors and requires initial surface modification of the QDs with a silane source followed by condensation on the QD surface. However, the QDs often exhibit decreased quantum efficiencies. To address this issue, a reverse microemulsion method has been applied to facilitate the formation of silica-encapsulated QDs.

In this study, red-emitting QDs were coated with silica to enhance their thermal and photo-stability via a two-step involving ligand exchange and a reverse microemulsion method. Especially, native oleic-acid-capped hydrophobic QDs were substituted with strongly binding thiol-functionalized ligands, namely, (3-mercaptopropyl) methyltrimethoxysilane (MPMDMS). Then, partially-MPMDMS ligand-exchanged-QDs (MQDs) were coated with silica, and additional ligand substitution reaction with hydrophilic properties ligands such as 3-mercaptopropionic acid were conducted to enhance the incorporation of the QDs in the reverse microemulsion system. The final silica-coated QDs obtained using these two steps showed only a 6-13% reduction in their PLQYs after UV irradiation and upon high-temperature exposure for 7 days, compared to that of the untreated QDs showing a huge drop of 72-80%. Through this research, we see the great potential of our work that QDs with high stability can be used in the color-conversion layer in various ways such as spin coating, inkjet printing, and film manufacturing, expecting significant enhancement of lifetime compared with pristine QDs.

SESSION EL10.09: Self-Assemblies and Catalysis I
Session Chairs: Maryna Bodnarchuk, Jie He and Geoffrey Strouse
Thursday Morning, November 30, 2023
Hynes, Level 3, Ballroom A

8:30 AM *EL10.09.01

Spinel Plasmonic Metal Oxide Nanocrystals, The Role of Antisite Occupation and Faceting on the Observed Plasmon Properties Geoffrey F. Strouse; Florida State University, United States

Plasmonic metals have been a rich area of research for over two decades, exhibiting shape and size dependent extinction spectra. In n-doped wide band gap metal oxide semiconductors, a plasmon feature (ω_p) is observed due to the introduction of carriers. In these plasmonic semiconductor nanocrystals (PSNC), the plasmon frequency and spectral shape are correlated with the number of free carriers (n) at the Fermi level, the carrier effective mass (m^*), and the faceting of the metal oxide nanocrystal. The stability of the free carrier in these materials is impacted by the nature of the surface passivation. Solid state NMR, high field EPR, and optical techniques allow the free carrier to be probed, the carrier mass measured, and the impact of faceting and surface interfaces to be evaluated. In the presentation, the role of surface, shape, faceting magneto-optical and synthetic approaches to address fundamental questions in classical oxygen vacancy PSNCs WO_{3-x} , and spinel antisite PSNCs $CdSn_2O_4$ will be explored.

9:00 AM EL10.09.02

Thermal-Response of Promesogenic-Ligands Functionalized Nanocrystals Shengsong Yang¹, Yifan Ning¹, Yi-Yu Cai¹, Ruipeng Li², Yugang Zhang², Cherie R. Kagan¹ and Christopher B. Murray¹; ¹University of Pennsylvania, United States; ²Brookhaven National Laboratory, United States

Limited by the mobility of building units, assembled superstructures often lack dynamics, narrowing the potential for applications in smart materials. Here we introduce a novel approach using a specially designed dendritic ligand that exhibits liquid crystal-like behavior at the interface to enable the realization of dynamic superlattices. The ligands act as a thermally triggered lubricant between nanocrystals. It allows the substrate-bounded (dried) nanocrystal solids to transform from poorly ordered aggregates to superlattices with high crystallinity and preferred orientation simultaneously when subjected to thermal activation. With the help from *in situ* X-ray scattering, the process of the reorientation of the superlattices are revealed and the bottom-to-top transition was observed. The superlattice also prefer to expose the most stable facet at the interface to the substrate.

9:15 AM EL10.09.03

Hydrosilylation on Hydrogen-Terminated Silicon Surfaces using Pt(dvs): From Efficient Grafting of Olefins to Platinum-Coated Silicon Nanoparticles for Catalysis Pooria Golvari, Khaled Alkameh, Azina Rahmani, Titil Jurca and Stephen M. Kuebler; University of Central Florida, United States

Hydrosilylation is an effective method for functionalizing the surface of hydrogen terminated Si substrates and Si nanoparticles (H-SiNPs). We report on the efficiency of Pt-catalyzed hydrosilylation using Karstedt's catalyst on H-SiNPs and H-Si(100) surfaces. In contrast to the well-established catalytic cycle for the hydrosilylation of olefins using tertiary silanes, we observe that the addition of Pt(0) onto H-SiNPs through oxidative addition is irreversible at room temperature. Optimal reaction conditions are reported for effective hydrosilylation of 1-octene. Higher temperature enable hydrosilylation of 1-octene on the surface of H-SiNPs by favoring reductive elimination of the catalyst. Trapping the catalyst at low temperatures opens a route for the synthesis of Pt(II)-loaded SiNPs that can undergo ligand exchange. Pt-on-Si ensembles were analyzed using Fourier-transform infrared spectroscopy, X-ray photoelectron spectroscopy, transmission electron microscopy, energy-dispersive X-ray spectroscopy, and atomic force microscopy. Calcination renders Pt-on-Si nanostructures catalytically active towards hydrogenation of phenyl acetylene. These robust Pt nanocatalysts are anchored on SiNPs which enables their facile recovery and reuse through centrifugation or filtration.

9:30 AM *EL10.09.04

Polymers on Metal Nanoparticles—Deficient Ligand Exchange and Site-Specific Grafting Jie He; University of Connecticut, United States

Symmetry-breaking nanoparticles (NPs) are important building blocks showing directional interparticle interaction as a key that enable precise macroscopic organization of NPs. We demonstrate a facile post-synthetic approach to prepare symmetry-breaking plasmonic NPs through deficient ligand modification. Our research highlights the patterning of isotropic gold spherical NPs (AuNPs) or anisotropic nanorods (AuNRs) with controlled surface coverage by polymer domains. The concentration of thiol-terminated polystyrene (PS-SH) ligands plays a dominant role in tuning the surface patterns through hydrophobicity-driven phase segregation. Through a gradual reduction in the concentration of polymer ligands, a distinct morphological transition from core-shell structures to site-specific grafting of AuNPs and/or AuNRs is observed. This transition arises from the interplay between the conformational entropy of PS-SH ligands and the interfacial energy between polymer ligands and the solvent. The method we have developed shows high yield, high quality, and remarkable selectivity in a one-step process for modifying NPs with polymer domains at precise locations. These polymer-patched NPs, serving as fundamental building blocks, exhibit controlled supracolloidal self-assembly as guided by polymer ligands.

10:00 AMBREAK

10:30 AM *EL10.09.05

Advancements in Synthesis and Multicomponent Superlattices of Highly Luminescent Lead Halide Perovskite Nanocrystals Maryna Bodnarchuk^{1,2}, Ihor Chemiukh^{1,2}, Taras Sekh^{1,2}, Alex Travesset³, Rainer Mahrt⁴, Thilo Stoefler⁴, Gabriele Raino^{2,1}, Rolf Ermi¹ and Maksym V. Kovalenko^{2,1}; ¹Empa-Swiss Federal Laboratories for Materials Science and Technology, Switzerland; ²ETH Zürich, Switzerland; ³Iowa State University of Science and Technology, United States; ⁴IBM Zurich, Switzerland

Colloidal lead halide perovskite nanocrystals (LHP NCs, APbX_3 , where $\text{A}=\text{Cs}^+$, FA^+ , $\text{FA}=\text{formamidinium}$; $\text{X}=\text{Cl}$, Br , I) have become a research spotlight owing to their spectrally narrow (~100 meV) fluorescence, tunable over the entire visible spectral region of 400-800 nm, as well as facile colloidal synthesis. These NCs are attractive single-photon emitters and building blocks for creating controlled, aggregated states exhibiting collective luminescence phenomena. Attaining such states through the spontaneous self-assembly into long-range ordered superlattices (SLs) is a particularly attractive avenue. The atomically flat, sharp cubic shape of LHP NCs is also of interest because the vast majority of prior work had invoked NCs of spherical shape. Long-range ordered SLs with the simple cubic packing of cubic perovskite NCs exhibit sharp red-shifted lines in their emission spectra and superfluorescence (a fast collective emission resulting from coherent multi-NCs excited states).

When CsPbBr_3 NCs are combined with spherical dielectric NCs, perovskite-type ABO_3 binary NC SLs form, wherein CsPbBr_3 nanocubes occupy B- and/or O-sites, while spherical dielectric Fe_3O_4 or NaGdF_4 NCs reside on A-sites. When truncated-cuboid PbS NCs are added to these systems, ternary ABO_3 -phase form (PbS NCs occupy B-sites). Such ABO_3 SLs, as well as other newly obtained SL structures (binary NaCl , AlB_2 - and ABO_6 types, columnar assemblies with disks, etc.), exhibit a high degree of orientational ordering of CsPbBr_3 nanocubes. These mesostructures also exhibit superfluorescence, characterized, at high excitation density, by emission pulses with ultrafast (22 ps) radiative decay and Burnham-Chiao ringing behavior with a strongly accelerated build-up time. Co-assembly of steric-stabilized CsPbBr_3 nanocubes with disk-shaped LaF_3 NCs yields six columnar structures with AB , AB_2 , AB_4 , and AB_6 stoichiometry, not observed before with NC systems comprising spheres and disks. Combining CsPbBr_3 nanocubes with large and thick NaGdF_4 nanodisks results in the orthorhombic SL resembling CaC_2 structure with pairs of CsPbBr_3 NCs on one lattice site. Additionally, we have also implemented two substrate-free methods of SL formation. The first method involves oil-in-oil templated assembly that leads to the formation of binary supraparticles, while the second method utilizes self-assembly at the liquid-air interface.

11:00 AM EL10.09.06

Type-I CdS/ZnS Core/Shell Quantum Dot-Gold Heterostructural Nanocrystals for Enhanced Photocatalytic Hydrogen Generation NaJin¹, Yonglei Sun², Wenwu Shi³, Ping Wang⁴, Yasutaka Nagaoka¹, Tong Cai¹, Rongzhen Wu¹, Yuzi Liu⁵, Tomoyasu Mani², Xinzhong Wang⁶, Jing Zhao² and Ou Chen¹; ¹Brown University, United States; ²University of Connecticut, United States; ³Southwest University, China; ⁴Jilin Normal University, China; ⁵Argonne National Laboratory, United States; ⁶Shenzhen Institute of Information Technology, China

The rapid industrialization has led to serious problems of environmental pollution and energy shortages, necessitating the need for exploring renewable energy sources that can be produced ecologically without further releasing pollutants, such as molecular hydrogen (H_2). Type-I core/shell quantum dot (QD) systems have been long recognized and utilized as efficient, stable, and sustainable light harvesting and emitting materials. Nevertheless, the application of Type-I core/shell QDs in photocatalysis has been restricted due to the strongly confined photogenerated charges within the core, making them catalytically "inert". In this project, we found that through the decoration of Au satellite-type domains on the surface of Type-I CdS/ZnS core/shell quantum dots, the energy barrier introduced by the wide-bandgap shell material can be effectively overcome and an over-four-hundred-fold enhancement of the photocatalytic H_2 evolution rate was achieved compared to bare CdS/ZnS quantum dots. Transient absorption spectroscopic studies indicated that the charges can be effectively extracted and subsequently transferred to surrounding molecular substrates in a sub-picosecond timescale in such hybrid nanocrystals. Based on density functional theory calculations, the ultrafast charge separation rates were ascribed to the formation of an intermediate Au_2S layer at the semiconductor-metal interface, which can successfully offset the energy confinement introduced by the ZnS shell. Our findings not only provide insightful understandings of charge carrier dynamics in semiconductor-metal heterostructural materials but also pave the way for the future design of quantum dot-based hybrid photocatalytic systems.

11:15 AM *EL10.09.07

PbS Nanocrystal Surfaces and Their Assemblies William Tisdale; Massachusetts Institute of Technology, United States

PbS quantum dots (QDs) have been widely pursued in applications ranging from solar cells to IR LEDs to photon up/down conversion systems and thermoelectrics. Despite their rich history we continue to learn new things about PbS QD chemistry, photophysics, and self-organization into ordered solids. In this talk, I will highlight recent work from my lab at MIT on the structure of PbS QD surfaces. In particular, I will demonstrate neutron scattering as a powerful emerging tool for the characterization of colloidal QDs and the detailed information that small-angle neutron scattering (SANS) can provide about the ligand layers surrounding QDs. Additionally, I will demonstrate the underappreciated role of unbound – or "free" – ligand in mediating the structure of self-assembled QD superlattices.

SESSION EL10.10: Self-Assemblies and Catalysis II
Session Chairs: Rigoberto Advincula and William Tisdale
Thursday Afternoon, November 30, 2023
Hynes, Level 3, Ballroom A

2:00 PM EL10.10.02

Extended Size-Tunable Synthesis of Gold Nanorods and its Application in Catalysis Jun Zhu and R.B. Lennox; McGill University, Canada

The role of silver ions in silver-aided seed-mediated gold nanorod (AuNR) syntheses has been investigated and the key silver intermediate which controls the AuNR aspect ratio (AR) was identified to be a CTA-Ag-Br complex. The CTA-Ag-Br complex has a characteristic UV absorption peak which enables an *in situ* spectroscopy study of the roles the silver has in AuNR formation. Previous assumptions have held that silver is only involved in the symmetry breaking of the seed growth step. However, this is the case only a small fraction of the silver present is involved in the process, whereas the AuNR aspect ratio (AR) can be controlled by varying the Ag:Au ratio. The current work however provides direct experimental evidence for the first time that the silver intermediate is consumed at the same rate as gold nanorod growth. The silver intermediate also plays an important role during the AuNR growth step and becomes a size-limiting reagent due to its limited solubility. However, addition of a limited quantity of acetonitrile (2% v/v) leads to a significant increase in the solubility of the silver intermediate, leading to AuNR with a greater range of characteristic AR values. The LSPR of the resulting AuNR can be increased from 880 nm (AR = 4.5) to 1200 nm (AR = 8). The catalytic property of the resulting AuNRs for nitrophenol reduction was tested and this reduction reaction showed AR dependant. This work provides new insight into the mechanism of seed-mediated growth of AuNRs as well as the synthesis of AuNRs having a greater AR range (1.5 - 8) using the same seed-mediated growth method. The catalytic property of AuNRs was also tested and gave insight for the catalytic active site on AuNRs.

2:15 PM EL10.10.03

Harvesting of Photons in a Broad Spectrum via Quantum Dot Integration in a Polymer Based Solar Cells Idris Candan; Kocaeli University, Turkey

The narrow absorption range and the energy loss associated with the spectral mismatch of materials are among the main challenges in conventional solar cells. To use solar energy effectively, solar cells must absorb photons across a broad spectrum, from UV to IR. New approaches are required to enhance the power conversion efficiency (PCE) of solar devices. The main goal of this work is to increase efficiency by extending the absorption range and absorbing photons throughout a broad spectrum. We added a quantum dot (QD) thin film layer within the inverted polymer solar cell (IPSC) structure as a novel approach to accomplish broadband absorption and gather photons specifically toward the IR region for effective use of solar energy. The efficiency of the solar cell devices was much improved by sandwiching a thin layer of lead sulfide quantum dots (PbS QDs) between the photoactive polymer layer and the metal oxide

electron transport layer. The optical, structural, and morphological measurements were carried out using the transmission, absorbance, photoluminescence (PL), XRD, Raman spectroscopy, SEM and TEM measurements to characterize the PbS QDs thin film layer. Measurements of photoconductivity, Hall effect, external quantum efficiency (EQE), current-voltage (I-V), capacitance-voltage (C-V), and impedance spectroscopy were performed to ascertain the contribution of the PbS QDs thin film layer to the device parameters. The quantum dot thin film has greatly enhanced the parameters of solar cells, resulting in increases in power conversion efficiency (PCE). The PCE improvements were found to be largely dependent on the QD thin film thickness. Additionally, an increase in external quantum efficiency (EQE) was seen as carrier concentration and mobility increased. Our findings provide a novel approach for enhancing IPSC device parameters and the PCE by adding a QD thin layer to the solar cell architecture.

2:30 PM EL10.10.04

Solution-Processed Flexible Broadband Photodetectors[XiongGong](#) and TaoZhu; University of Akron, United States

Broadband photodetectors (PDs) with high detectivities are widely utilized in telecommunications, day/night surveillance, thermal imaging, interconnects, and medical instruments. Today, separate sensors or materials are required for different sub-bands within the ultraviolet (UV) to infrared (IR) wavelength (λ) range. To obtain the desired sensitivities, IR PDs must be operated at low temperatures (for example, at 4.2 K). Moreover, the PDs with different spectral response are required to be integrated together to cover the spectral range from 250 to 2600 nm. Therefore, it would be advantageous to have a solution-processed low-cost multicolor PDs with high sensitivity and high-speed response over the broad spectral range from the UV to IR and the PDs do not require cooling to obtain high detectivity. In this presentation, I will report room-temperature solution-processed photodetectors with spectral response from 300 to 2600 nm based on the solution-processed polymeric thin film electrodes, which is with transparency ranging from 300 to 7000 nm and superior electrical conductivity. Solution processed flexible broadband photodetectors with a "vertical" device structure incorporating a perovskite/PbSe quantum dot bilayer thin film based on the above solution-processed transparent polymeric electrode are demonstrated. The utilization of perovskite/PbSe quantum dot bilayer thin film as the photoactive layer extends spectral response to infrared region and boosts photocurrent densities in both visible and infrared regions through the trap-assisted photomultiplication effect. Operated at room temperature and under an external bias of -1 V, the solution-processed flexible photodetectors exhibit over 230 mA W⁻¹ responsivity, over 10¹¹ cm Hz^{1/2}/W photodetectivity from 300 to 2600 nm and \approx 70 dB linear dynamic ranges. It is also found that the solution-processed flexible broadband photodetectors exhibit fast response time and excellent flexibility. All these results demonstrate that this work develop a facile approach to realize room temperature operated ultrasensitive solution-processed flexible broadband photodetectors with "vertical" device structure through solution-processed transparent polymeric electrode.

2:45 PM EL10.10.05

Opposite Charge Separation-Induced DUV/Visible Bipolar Photo-Response of Organic/Inorganic Heterojunction Self-Powered Photodetector[TaehyunPark](#), JuhungSeo and HocheonYoo; Gachon University, Korea (the Republic of)

Recently, bipolar dual-band photodetectors (BDPD) have been spotlighted for emerging applications such as optoelectronic logic gates and machine vision owing to their wavelength-dependent output signals. Compared to conventional unipolar photodetectors, BDPD devices provide clearly distinguishable spectral output signals based on opposite charge separation mechanism to verify the input optical information without further wavelength selection filters or multi-devices. This special ability of BDPDs offers higher device densities by reducing the number of unit components, and multi-functionality in a single optoelectronic device. However, challenges such as limited photo-active material combination or complicated device architecture to achieve opposite charge separation still limits the widespread use of BDPDs.

Herein, we present the wavelength-dependent bipolar photo-responsive organic/inorganic heterojunction photodiode based on dually stacked Schottky and pn junctions. The proposed BDPD was fabricated through a simple and cost-effective sequential spin-coating process. To generate oppositely charged two built-in electric fields, back-to-back diode system was demonstrated with only 4 stacked layers consisting of bottom ITO electrode, p-type fluorene copolymer (Poly(9,9-dioctylfluorene-alt-benzothiadiazole), F8BT), n-type tin-oxide (SnO₂) quantum dots (QDs) and transparent conductive polymer electrode (poly(3,4-ethylenedioxythiophene) polystyrene sulfonate (PEDOT:PSS)). Based on wavelength selective light absorption in Schottky and pn junctions, the proposed BDPD exhibited clearly distinguishable positive and negative photo responses in deep-ultraviolet (DUV) and visible blue wavelength. Finally, we demonstrated BDPD-based emerging applications including NOT, OR, and XOR optoelectronic logic gates, and true random number generation with arc discharge.

3:00 PM BREAK

3:30 PM EL10.10.06

Organic Ligands Mediated Carrier Dynamics in Photochromic Nanoparticles[AdamF. Gross](#), ShirellKlein, GregoryP. Rutkowski and ErikD. Crenshaw; HRL Laboratories LLC, United States

Photochromic materials are useful for glare reduction, optical switches, and laser dazzling protection. While many photochromics darken rapidly, their reversal to a clear state is governed by ambient temperature or a sequence of optical excitations. Slow detinting times limit their use in many applications where a rapid return to a clear state is needed for retaining visibility for safe operation or faster cycling rates. Photochromic Cu-doped ZnS nanoparticles were recently discovered where darkening occurs via the reversible oxidation of the dopant (J. Am. Chem. Soc. 2021, 143, 2239–2249; J. Phys. Chem. Lett. 2021, 12, 8129–8133). However, the detinting time depends on the concentration of environmental water and temperature to mediate the capture of a photoexcited hole. Instead of the environment regulating detinting times, ligand engineering can provide a more direct and controllable route to tune detinting. The nanoparticles' high surface area and small diameters enable placing hole traps on the surface that affect carrier dynamics; conjugated ligands trap photoexcited holes and return the material to a clear state. Control of the amount of conjugation in the ligand and proximity to the surface reduces the detinting time by up to 8 fold. Furthermore, while ZnS is a known photochromic material, we show that Cu-doped ZnS' darkening mechanism applies more broadly to additional materials. We employed a fundamental computational pipeline to hunt for fingerprints of photochromicity, which enabled us to identify and validate novel visible and NIR photochromic material compositions.

3:45 PM EL10.10.07

Two in One: Ni-Doped CsPbBr₃ Nanocrystals Enabling Photocatalytic Dehydrogenation of Diaryl Hydrazines[HaipengLu](#); The Hong Kong University of Science and Technology, Hong Kong

Colloidal semiconductor nanocrystals, also known as quantum dots (QDs), have demonstrated remarkable abilities as photocatalytic systems for organic transformations, with efficiencies that can rival those of traditional molecular catalysts. However, the unique potential of QDs for photocatalysis, which stems from their large surface-volume ratio, tunable chemical composition, and quantum confinement, has yet to be fully explored. In this presentation, we will discuss our recent work on the design of colloidal CsPbBr₃ QDs for acceptorless dehydrogenation of diaryl hydrazines under mild conditions. We achieved this by doping CsPbBr₃ QDs with Ni²⁺, creating a dual-catalysis system. Specifically, our catalyst combines visible-light active CsPbBr₃ as the photoredox catalyst and Ni²⁺ as the proton-reduction catalyst. This dual-catalytic strategy exhibits a broad substrate scope. Transient absorption spectroscopy indicates an ultrafast electron transfer step from the QD to Ni²⁺ dopants upon photoexcitation, which serves as the proton reduction centers. Our work demonstrates a new design strategy for challenging photocatalytic organic transformations using proton-coupled multiple electron transfer processes.

4:00 PM EL10.10.08

Bifunctional Electron-Transporting Agent for Red Colloidal Quantum Dot Light-Emitting Diodes[HaoyueWan](#)¹, YakunWang¹, JianXu¹, YunZhong¹ and EdwardH. Sargent^{1,2}; ¹University of Toronto, Canada; ²Northwestern University, United States

Indium phosphide (InP) quantum dots have enabled light-emitting diodes (LEDs) that are heavy-metal-free, narrow in emission linewidth, and physically flexible. However, ZnO/ZnMgO, the electron-transporting layer (ETL) in high-performance red InP/ZnSe/ZnS LEDs, suffers from high defect densities, quenches luminescence when deposited on InP, and induces performance degradation that arises due to trap migration from the ETL to the InP emitting layer. We posited that the formation of Zn²⁺ traps on the outer ZnS shell, combined with sulfur and oxygen vacancy migration between ZnO/ZnMgO and InP, may account for this issue. We synthesized therefore a bifunctional ETL (CNT2T, 3',3''',3''''-(1,3,5-triazine-2,4,6-triyl)tris((1,1'-biphenyl)-3-carbonitrile)) designed to passivate Zn²⁺ traps locally and *in situ* and to prevent vacancy migration between layers: the backbone of the small molecule ETL contains a triazine electron-withdrawing unit to ensure sufficient electron mobility (6 × 10⁻⁴ cm² V⁻¹ s⁻¹), and the star-shaped structure with multiple cyano groups provides effective passivation of the ZnS surface. We report as a result red InP LEDs having an EQE of 15% and a luminance of over 12,000 cd m⁻²; this represents a record among organic-ETL-based red LEDs.

4:15 PM EL10.10.09

Development of Molten Salt Solvents for Synthesis of Ternary and Quaternary III-V Colloidal Nanocrystals via Cation Exchange[JustinOndry](#)¹, Jun HyukChang¹, ArirajitGupta¹, ZiruiZhou¹ and DmitriV. Talapin^{1,2}; ¹The University of Chicago, United States; ²Argonne National Laboratory, United States

For the most part, colloidal nanocrystals made of III-V materials (*e.g.*, GaAs, InP, GaSb, *etc.*) are less developed than their corresponding II-VI and IV-VI counterparts in terms of synthetic control and optoelectronic performance. Despite this, colloidal III-V nanocrystals are desirable since these materials have many impressive optoelectronic properties in bulk, they are less toxic than many II-VI and IV-VI phases, and they may have higher chemical and thermal stability. So far only the indium-based III-V materials (*e.g.*, InAs, InP, and InSb) have been prepared as

colloidal nanocrystals with high quality. Gallium- and aluminum-based III-V nanocrystals are difficult to synthesize via traditional colloidal synthesis due to the high temperatures needed to crystallize the more covalent III-V materials and the extreme reactivity of Ga^{3+} and Al^{3+} cations towards organic solvents at elevated temperatures. To address this, we have developed molten salt solvents as reaction media to synthesize several important alloy III-V nanocrystal phases via cation exchange from their corresponding indium pnictide colloidal nanocrystals. In this presentation we will discuss how colloidal In-pnictide nanocrystals can be transformed to their respective InGa-pnictide and InGaAl-pnictide alloy phases via processing in gallium and aluminum containing molten salts. Further we will discuss the importance of the molten salt composition, elucidated using *in-situ* high temperature UV-vis absorption and Raman spectroscopy, for ensuring chemical stability of III-V nanocrystals in molten salt solvents. From this, we identify Lewis neutral alkali tetrahalogallate (MGaX_4) molten salts are the key reactive phase which engender chemical stability of colloidal InAs nanocrystals and allows their subsequent transformation to InGaAs and InGaAlAs using Lewis neutral alkali tetrahaloaluminate (MAiX_4) molten salts. Additionally, we will describe how controlling the redox potential in the molten salt solvents by using reduced gallium halide molten salts is key to protecting InSb from decomposition and thus enabling the synthesis of InGaSb colloidal nanocrystals. Finally, we describe an atomically precise colloidal atomic layer deposition approach to grow wide band gap II-VI shell materials which precisely passivate surface traps enabling bright band edge photoluminescence from molten salt synthesized InP nanocrystals and quaternary InGaPAs nanocrystals. The materials synthesized by the molten salt methods provide access to continuously tunable light emission from the visible to mid IR suggesting these materials could have broad impact in many applications. Together our work provides key insights into strategies to prepare a diverse family of III-V alloy nanocrystals and will likely enable future development of all-III-V colloidal nanocrystals heterostructures via growth of wide band gap shell materials in molten salt solvents.

4:30 PM EL10.10.10

Short-Wave Infrared Quantum Dots with High Quantum Yield Through Mercury Cation Exchange Wonseok Lee and Andrew M. Smith; University of Illinois at Urbana-Champaign, United States

Colloidal semiconductor nanocrystals (NCs) are photonic materials with a combination of unique properties such as size-tunable electronic/optical energy levels, high absorption cross-section, high photoluminescence quantum yield (PLQY), long-term photochemical/photophysical stability, and versatile solution-based processability. NCs with optical transitions in the infrared are currently being developed to reduce the cost of infrared optoelectronic devices, which are currently limited to a few high-tech specialized areas, including defense and astronomy. Among the candidate NC materials, mercury chalcogenide (HgE) and mercury cadmium chalcogenide ($\text{Hg}_x\text{Cd}_{1-x}\text{E}$) are leading candidates for infrared optics. In comparison with alternative infrared NCs (e.g., InAs and lead chalcogenides), these materials provide extremely wide spectral tunability across the near, mid, and far infrared spectra. Nevertheless, challenges remain in their advancement due to the low reduction potential of mercury ions that limit the high-temperature solvothermal synthesis and difficulties in the precise selection of mercury-to-cadmium ratios in alloys.

The cation exchange (CE) reaction can create new functional NCs by replacing one type of cation with another. The product materials which often cannot be synthesized *de novo*, can inherit the structural integrities of the parent nanomaterials in terms of size, shape, crystal phase, and homogeneity. However, due to the diffusion-limited CE reaction mechanism, achieving fine control of the radial composition of host and guest cations has been challenging. In addition, for some material systems, the slow diffusivity of cations significantly impedes the CE reaction and requires a high reaction temperature, resulting in a loss of structural homogeneity. In this research work, we developed a new CE method that can bypass the diffusion-limited reaction pathways. In particular, we developed a CE conversion of CdSe NCs to HgSe NCs and evaluated the reaction mechanism. Through the improved reaction, $\text{Hg}_x\text{Cd}_{1-x}\text{Se}$ NCs exhibit a homogeneous radial distribution of cation species and enhanced overlap of electron and hole wavefunctions, as well as improved PL properties tunable across the short-wave infrared spectrum (~1000–1700 nm wavelength). After shell overcoating, these $\text{Hg}_x\text{Cd}_{1-x}\text{Se}/\text{CdS}/\text{ZnS}$ NCs exhibited excellent optical properties: the PLQY was above 85% and photoluminescence full-width-at-half-maximum (FWHM) was below 110 meV, properties matching those of the parental CdSe-based core/shell NC emitters.

4:45 PM EL10.10.11

Stability Assessment of Binary Mixture of Small Colloidal Nanoparticles Azita Rezvani¹, Osama Anwar¹ and Doris Segets^{1,2}; ¹Institute for Energy and Materials Processes (EMPI), Germany; ²Universität Duisburg-Essen, Germany

Over the past few decades, extensive research has been conducted on the stability and surface interactions of colloidal dispersions consisting of a single component. However, practical formulations in the real world often involve mixtures of colloidal nanoparticles with different components, such as binders and additives. Therefore, it is crucial to have precise control over the stability of these mixtures, as it plays a vital role in various applications like the self-assembly of nanoparticles into complex structures [1, 2] and the recycling or separation of nanoparticles after synthesis [3–4]. However, studies on handling and stability regulation are scarce in the literature, even for binary colloids. This lack is particularly evident for small nanoparticles (< 20 nm), which are highly interface-dominated. This can be attributed to significant challenges in characterizing and comprehending the surface interactions in such complex systems of small colloidal nanoparticles.

In this work, we studied the stability regulation of a mixture of colloidal Au nanoparticles (< 20 nm) and an aqueous dispersion of ZnS quantum dots (< 5 nm) as a binary colloid made of nanoparticles of different sizes and compositions. This is a practically relevant model system and of great interest in this context when we try to recycle the smallest nanostructures from complex mixtures, for instance during the recovery of metals from fuel cell or battery electrodes, in a true circular economy. Here, we investigated how the surface ligand and the purification process of Au nanoparticles affect the stability of the hetero-colloid. To do this, we investigated the stability of Au nanoparticles with three different ligands on the surface after mixing them with ZnS QDs, each before and after functionalization of the Au NPs by bis (p-sulfonatophenyl) phenyl phosphine (BSPP). To characterize the mixture, UV-visible spectroscopy as the main method was combined with dynamic light scattering and analytical centrifugation to assess and monitor the stability of both colloidal components over time. This enabled us to understand the stability-controlling parameters and tailor the surface interactions.

Our work presents a general strategy to understand and tailor the stability of a binary mixture of small colloidal nanoparticles which is a challenge. We successfully created a stable binary mixture of BSPP-capped Au nanoparticles with ZnS QDs as a representative model system. We consider this achievement to be a significant initial stride in the characterization and understanding of the surface interactions of real-world multicomponent formulations.

References

- [1] J. Zhang et al., *Advanced Materials*. 31 (2019) 1901485. <https://doi.org/10.1002/ADMA.201901485>
- [2] S.K. Ghosh et al., *Macromol Chem Phys*. 220 (2019). <https://doi.org/10.1002/MACP.201900196>
- [3] K.K. Brar et al., *Environ Res*. 207 (2022) 112202. <https://doi.org/10.1016/J.ENVRES.2021.112202>
- [4] D. Segets et al., *Journal of Physical Chemistry C*. 119 (2015) 4009–4022. <https://doi.org/10.1021/jp508746s>

SESSION EL10.11: Growth and Characterization III
Session Chairs: Jonathan Owen and Loredana Protesescu
Friday Morning, December 1, 2023
Hynes, Level 3, Ballroom A

8:30 AM *EL10.11.01

Passivation and Stabilization of InP Nanocrystals with Organic Halide Ion Salts Rodolphe Valleix, Abrahm Jordan, William Zhang and Jonathan S. Owen; Columbia University, United States

The surface coordination chemistry of InP nanocrystals prepared from oleylamine, indium chloride and aminophosphines was investigated following synthesis, purification, and ligand exchange. ^1H , ^{31}P , and ^{19}F nuclear magnetic resonance and Fourier transform infrared absorption spectroscopy were used to quantify the surface ligand coverages and to monitor the ligand reaction with ammonium halides, diethyl zinc, phosphine, and chlorotrimethyl silane reagents. The coverage of tetralkylaminophosphonium chloride, alkylammonium fluoride, metal halide surface ligands were determined. The findings will be discussed in light of the metal rich stoichiometry and the steric constraints of packing surface passivating ligands.

9:00 AM EL10.11.02

Low-Cost Synthesis of Silicon Quantum Dots and Their Applications on Luminescent Solar Concentrators Jingjian Zhou; Uppsala University, Sweden

Here, we developed a cost-effective batch synthesis method for silicon quantum dots (Si QDs) with large Stokes shift and high quantum yield (>50% in polymer nanocomposite) for efficient light conversion. These Si QDs were fabricated from an inexpensive commercial precursor (triethoxysilane, TES), using optimized annealing and etching processes. The optical properties of such QDs are similar to those prepared from state-of-the-art precursors (hydrogen silsesquioxane, HSQ) yet featuring an order of magnitude lower cost. FTIR revealed that the surface oxide on Si QD was closely related to its light conversion efficiency. Based on this mass production method, we are able to investigate many factors when applying Si QDs as fluorophores in luminescent solar concentrators (LSCs), such as the thickness of polymer interlayer, the appropriate UV dose for curing polymer to avoid haze etc. Eventually, we are aiming at transparent

large-area light-harvesting devices serving as "solar windows".

9:15 AM EL10.11.03

Composition-Defined Optical Properties and the Direct to Indirect Transition in Core-Shell $\text{In}_{1-x}\text{Ga}_x\text{P/ZnS}$ Colloidal Quantum Dots Justin Ondry¹, Artrajit Gupta¹, Kailai Lin², Richard Schaller³, Eran Rabani^{2,4} and Dmitri V. Talapin^{1,3}; ¹The University of Chicago, United States; ²University of California, Berkeley, United States; ³Argonne National Laboratory, United States; ⁴Lawrence Berkeley National Laboratory, United States

Semiconductors are commonly divided into materials with direct or indirect band gaps based on the relative positions of the top of the valence band and the bottom of the conduction band in crystal momentum (**k**) space. It has, however, been debated if **k** is a useful quantum number to describe band structure in strongly quantum-confined nanocrystalline systems, which blur the distinction between direct and indirect gap semiconductors. In bulk III-V semiconductor alloys like $\text{In}_{1-x}\text{Ga}_x\text{P}$, the band structure can be tuned continuously from direct to indirect gap by changing the value of *x*, where for $x > 0.75$, the material behaves as an indirect gap semiconductor. The effect of strong quantum confinement on the direct-to-indirect transition in this system has yet to be established because high-quality colloidal nanocrystal samples have remained inaccessible. Herein we report one of the first systematic studies of ternary III-V nanocrystals by utilizing an optimized molten salt In-to-Ga cation exchange protocol to yield highly emissive $\text{In}_{1-x}\text{Ga}_x\text{P/ZnS}$ core-shell particles with photoluminescence quantum yields exceeding 80%. As the gallium content is increased in these systems, we observe the quantum yield decreases and the PL lifetime *increases* indicating the radiative lifetime increases with increased gallium content. This indicates the oscillator strength of the excitonic transition decreases as gallium is incorporated, consistent with increased indirect-like character of the band edge states. Transient absorption spectroscopy on $\text{In}_{1-x}\text{Ga}_x\text{P/ZnS}$ nanocrystals enables direct identification of the direct-like or indirect-like character of the band edge in $\text{In}_{1-x}\text{Ga}_x\text{P/ZnS}$ nanocrystals based on the presence or absence of a band edge bleach feature respectively. Further we study the biexciton lifetimes of $\text{In}_{1-x}\text{Ga}_x\text{P/ZnS}$ nanocrystals across a broad size and composition range. We identify that biexciton dynamics are dominated by volume scaling explanations, rather than composition effects, which is consistent with what is observed for many strongly quantum confined binary semiconductor systems. Finally, atomistic electronic structure calculations based on the semi-empirical pseudopotential model are used to calculate absorption spectra, radiative lifetimes, and evaluate band edge degeneracy. The resulting calculated electronic properties are consistent with experimental observations and provide considerable insight into the underlying band character of the excitonic transitions in these systems. Altogether our results provide a detailed picture of the electronic structure of strongly confined alloy III-V nanocrystals which point to key design principles for optimizing optoelectronic properties of strongly confined semiconductor emitters.

9:30 AM *EL10.11.04

Unlocking the Potential of Metal Borides Nanocrystals—A Journey Through Synthesis and Surface Modification Loredana Protesescu; University of Groningen, Netherlands

Metal borides, a versatile class of materials used in various industrial applications such as superconductors, magnetic materials, and hot cathodes, remain under-explored at the nanoscale due to the challenges in synthesizing single-phase nanocrystals (NCs). Their small size, high surface area-to-volume ratio, and well-defined surfaces exhibit unique physical and chemical properties, making them appealing for various applications, including catalysis, energy storage, electronics, and biomedical imaging. While metal-rich borides, like Ni_3B , are mainly used in electrocatalysis, boron-rich metal borides (metal hexaborides, MB_6) are highly valued for their broad range of physical properties that vary based on the metal ion present in their structure. For example, CeB_6 and LaB_6 have low work functions, while CaB_6 and SrB_6 exhibit high potential for high-temperature thermoelectric applications. Additionally, they are known for their high hardness, making them suitable for ultra-hard protective coatings.

In this presentation, we will showcase a novel method for synthesizing boron-rich M_1B_6 ($\text{M}_1 = \text{Sr, Ca, Ba, La, Ce}$) and metal-rich M_2B_6 ($\text{M}_2 = \text{Ni, Co, Fe, } x=2,3$) [1] NCs through solid-state synthesis at low temperatures (380–440°C), as well as a strategy for stabilizing these crystals for use in solution-based mass production processes. Our discussion will highlight the reaction mechanisms in both classes of nanomaterials, demonstrating the versatility of boron chemistry. By using specific surface modifications, including inorganic and organic ligands, we have achieved stable suspensions of these nanocrystals in both polar and non-polar solvents, with the potential for implementation in cutting-edge technologies.

1. Hong J., Mutalik S., Miola M., Gerlach D., Mehrabi K. R., Ahmadi M., J. Kooi B., Portale G., Rudolf P., P. Pescarmona P., Protesescu L., Chemistry of Materials, 2023.

10:00 AM BREAK

10:30 AM *EL10.11.05

Organic-Inorganic Supramolecular Photosynthesis: The Quantasome Vision Marcella Bonchio^{1,2}; ¹University of Padova, Italy; ²INSTM unit of Padova, Italy

The use of solar-activated $\text{H}_2\text{O}/\text{CO}_2$ routines as a feed-stock for photosynthetic processes is nowadays a breakthrough concept for sustainable energy, solar fuels, green chemistry and food security. [1-2] The enormous potential of this vital cycle is far from being adequately exploited. An extraordinary research effort has been dedicated to elucidate the structural and mechanistic prerogatives of the natural oxygen evolving complex embedded within the photosystem II enzyme (PSII-OEC). [2] In the early studies, on Oxygenic Photosynthesis, the "quantasome hypothesis" led to seminal discoveries correlating the structure of natural photosystems with their complementary photo-redox functions. [1] Indeed, and despite the vast bio-diversity footprint, just one protein complex is used by Nature as the H_2O -photolyzer: photosystem II (PSII). Man-made systems are still far from replicating the complexity of PSII, showing the ideal co-localization of Light Harvesting antennas with the functional Reaction Center (LH-RC). A recent breakthrough in the field of artificial photosynthesis is the discovery of totally inorganic multi-redox clusters, as analogs of the PSII-OEC, with a common functional-motif, i.e. a redox-active, tetranuclear, metal-oxo core boosting H_2O oxidation to O_2 with unprecedented efficiency. Our vision points to a careful choice/design of the catalytic core, of its ligand set and of the surrounding nano-environment. We report herein a synthetic, spectroscopic and mechanistic study on the use multi-metal catalysts for water oxidation and their combined use with visible light sensitizers and carbon-based nanostructures (CNS). [3-4] In particular we will report on the design of multi-erylenebisimide (PBI) networks shaped to function by interaction with a polyoxometalate water oxidation catalyst (Ru_4POM). [5-7] Our results point to overcome the classical "photo-dyad" model, based on a donor-acceptor binary combination, with integrated artificial "quantasomes" formed both in solution and on photoelectrodes, showing a: (i) red-shifted, light harvesting efficiency ($\text{LHE} > 40\%$), (ii) favorable exciton accumulation and negligible excimeric loss; (iii) a robust amphiphilic structure; (iv) dynamic aggregation into large 2D-paracrystalline domains. Photoexcitation of the PBI-quantasome triggers one of the highest driving force for photo-induced electron transfer applied so far. The outcome is a hybrid organic-inorganic nanomaterial, showing a hierarchical supramolecular structure with a striking resemblance to the natural plasmid membranes, enabling water splitting using low energy green photons at overpotentials as low as the natural protein. [5-7]

References

- [1] Scheuring, S., Sturgis, J. N. Chromatic Adaptation of Photosynthetic Membranes. Science 309, 484–487 (2005);
- [2] Sartorel, A., Carraro, M., Toma, F. M., Prato, M., Bonchio, M. Shaping the beating heart of artificial photosynthesis: oxygenic metal oxide nano-clusters. Energy Environ. Sci. 5, 5592 (2012);
- [3] Piccinin, S.; Sartorel, A.; Aquilanti, G.; Goldoni, A.; Bonchio, M.; Fabris, S. Water oxidation surface mechanisms replicated by a totally inorganic tetraruthenium-oxo molecular complex. Proc. Natl. Acad. Sci. 110, 4917–4922 (2013)
- [4] Toma, F. M.; Prato, M.; Bonchio, M. et al. Efficient water oxidation at carbon nanotube–polyoxometalate electrocatalytic interfaces. Nature Chemistry 2, 826-831 (2010).
- [5] Bonchio, M.; Sartorel, A.; Prato, M. et al. Hierarchical organization of perylene bisimides and polyoxometalates for photo-assisted water oxidation. Nature Chemistry 11, 146-153 (2019).
- [6] Gobbo, P.; Bonchio, M.; Mann, S. et al. Catalytic processing in ruthenium-based polyoxometalate coacervate protocells Nature Commun 11, 41 (2020).
- [7] Gobbo T.; Rigodanza F.; Benazzi, E.; Prato, M.; Bonchio M. et al. J. Am. Chem. Soc. 144, 14021-14025 (2022).

11:00 AM EL10.11.06

Alignment of Colloidal Metal-Oxide Based Nanoparticles Embedded in Polymer-Based Nanofibers via Electrospinning for Electrochemical Biosensing of Microbial Pathogens Bianca Seufert, Arash Takshi and Nirmita Roy; University of South Florida, United States

The aeronautics industry continues to evolve its approach to deep space exploration and therefore the growing need for rapid accurate biosensing is becoming more and more relevant. Along with size, weight, and various technology constraints making a nano-scale biosensor is critical to furthering this exploratory venture. Furthermore, to expand this endeavor the proposed research chiefly investigates the viability of the design of an electrochemical biosensor to detect microbial pathogens. Through embedding colloidal metal oxide-based nanoparticles (MOx) in electrospun polymer-based nanofibers one can further investigate the interfacial passivation between the biomolecule under study and the MOx embedded nanofibers. The unique characteristics of these adjoined nanomaterials such as large surface areas can provide many opportunities for manipulating their shape, size, and other properties. Which is why the use of several different metal oxide (MOX) based electrodes aptly placed as a bio-field effect transistors (bioFET) are used in this study as electrochemical sensors for a specific antigen/antibody detection. This study utilizes the testing methods of Cyclic voltammetry (CV) and electrochemical impedance spectroscopy (EIS) using the VersaStat 4 Potentiostat to measure the sensors' responses. It will be necessary to analyze and identify the effect on sensitivity, response time, and LOD of each sensor.

11:15 AM EL10.11.07

Zinc Chalcogenide Based Colloidal Nanoplatelets Muhammed S. Es, Cagatay H. Aldemir, Ebrar Colak, Nehir Ergezer and Yusuf Kelestemur; Middle East Technical University, Turkey

Two-dimensional colloidal nanoplatelets have become an attractive class of colloidal nanocrystals. With their thickness dependent excitonic properties, they exhibit exciting performance in optoelectronic devices. However, the most widely studied family of colloidal nanoplatelets are based on cadmium chalcogenides, which are considered as toxic materials and their optical properties cover very limited range of the electromagnetic spectrum. To overcome these limitations, we studied the synthesis of zinc chalcogenide based nanoplatelets with two different approaches: cation exchange and direct synthesis. For the cation exchange experiments, we firstly synthesized CdSe/ZnS core/shell NPLs and then performed cation exchange. With this approach, we can achieve core/shell nanoplatelets emitting in the blue spectral region (450 – 480 nm) by preserving their narrower emission linewidth (< 30 nm). In the second approach, we tried direct synthesis of zinc chalcogenide based nanoplatelets. We demonstrated that it is also possible to synthesize ZnSe nanoplatelets having zinc-blende crystal structure with direct synthesis approach. With our optimized synthesis conditions, we synthesized two different population of ZnSe nanoplatelets having absorption peaks at 347 and 369 nm.

SESSION EL10.12: Virtual Session
Session Chairs: Liberato Manna and Vincent Rotello
Thursday Morning, December 7, 2023
EL10-virtual

10:30 AM *EL10.12.01

Exploring Interplay of Engineered Materials with the Living by Label-Free Analytical Imaging Inge K. Herrmann; ETH Zurich, Switzerland

The well-controlled synthesis of nanoscale materials is arguably one of the most important achievements of material science in the past decades. Nanoscale materials find growing applications also in biomedicine. Fascinating therapeutic performances have been achieved by employing metal, metal oxide, and metal organic framework nanoparticles as drug delivery vehicles, radio-enhancers, and antimicrobial agents. Although recent studies have recognized the limited stability of nanomaterials in biological environments, analytical techniques have not yet been harnessed to their full potential to assess the biological fate engineered nanomaterials in complex biological environments. Despite fascinating achievements, the current limited understanding of the molecular interplay between engineered materials and the surrounding tissue remains a major obstacle in the rational development of medical materials, which is reflected in their modest clinical approval rate.

In this presentation, I will present a multiscale multimodal analytical imaging approach for the label-free assessment of nanomaterial fate and alterations to tissue. I will, in a first example, demonstrate that cerium oxide-based nanozymes preferentially accumulate in tissue macrophages after topical application to the subcutis and partially biotransform into catalytically inactive cerium phosphate over time. In a second example, I will present a methodological approach for the analysis of iron-based nanoparticles after systemic administration and reveal accumulation of iron particles in splenic macrophage subpopulations co-accumulating endogenous iron. Finally, I will showcase the application of multimodal analytical imaging in the assessment of the stability and fate of a diverse set of metal organic framework nanoparticles. Taken together, this presentation discusses how modern analytical methodologies can be harnessed for the label-free tracking of nanomaterials in complex biological environments with single particle sensitivity. Comprehensive assessment of material alterations and changes in the local tissue surrounding at unprecedented sensitivity decisively contributes to a rational and safer nanomaterial design and development for health applications.

11:00 AM EL10.12.02

Cathodoluminescent Rare-Earth-Doped Nanoprobes as Bright Labels in Electron Microscopy Sebastian Habermann^{1,2}, Mathieu Kociak³, Alexander Gogos^{1,2}, Lukas Gerken^{1,2}, Christian Monachon⁴, Kerda Keevend^{1,2} and Inge K. Herrmann^{1,2}; ¹Swiss Federal Laboratories for Materials Science and Technology (Empa), Switzerland; ²ETH Zurich, Switzerland; ³Université Paris-Saclay, CNRS, France; ⁴Attolight AG, Switzerland

Progress and achievements in the natural sciences are fundamentally linked to appropriate analytical tools. By unlocking previously unattainable scales, microscopy laid the foundation for many future-shaping discoveries and enabled the emergence of whole scientific fields. Due to its widespread usage in biological and medical laboratories, (fluorescence-)microscopy significantly contributed to our today's understanding of the fundamental processes in living systems. Intensive work with and on the improvement of microscopy techniques allowed ever-new milestones, primarily by enhancing contrast and resolution by exploitation of optical labels and physical phenomena. However, understanding the interactions of biomolecules at the nanoscale and put them in a cellular context remains a major challenge. Electron microscopy (EM) as a non-Abbe limited technique gives access to the cellular ultrastructure yet results in low-contrast grey-scale images and is not able to (co-)localize biomolecules without electron-dense labels or correlative microscopy approaches.

In this work, we demonstrate the feasibility of nanoparticle-based immunolabels for correlative cathodoluminescence electron microscopy (CCLEM). By introducing rare-earth-doped labels, the challenging sample preparation and resolution mismatch of correlative (light-)microscopy methods is addressed. Further, incorrect assignment of electron-dense labels due to their low-contrast and similarity with cell features is prevented. Hereby, we exploit the single-particle cathodoluminescence (CL) of sub-20 nm nanoparticles as a unique spectral fingerprint to identify their precise location and enable the separation from second labels and cell components without additional investigations. To maximize the nanoparticle's emission intensity, the dopant was incorporated in a sodium gadolinium fluoride host lattice and separated from the environment using a passivating shell. Both folic acid and caffeic acid decorated nanoparticles were prepared using terbium and europium as their characteristic signature dopants. Their potential for immunolabeling in CCLEM and easy (co-)localization was successfully demonstrated using HeLa cells, as both embedded particle populations demonstrated strong single-particle emission and therefore added a color contrast to the previously grey-scale EM image. Taken together, these results open a route to color immunolabelling based on cathodoluminescence electron microscopy.

11:15 AM EL10.12.03

Selective On-Off-On Polymer Bonded Quantum Dot-Nitroxide Radical Fluorescent Sensor to Detect Cd²⁺ Ion in Aqueous Media Merve Karabiyik and Ozgenc Ebil; Izmir Institute of Technology, Turkey

One of the most important problems of recent years is heavy metal pollution, which has great harm to the environment and human health. Especially, Cd²⁺ ion selectivity of quantum dot (QD)-nitroxide radical nanoprobe developed in this study was found as higher than the other heavy metal ions (Al³⁺, Co²⁺, Cu²⁺, Mn²⁺, Ag⁺, Fe³⁺, Ni²⁺, Pb²⁺, Cr³⁺, Hg²⁺, Mg²⁺, Zn²⁺). Cadmium is widely used in industry, agriculture and many other fields. Recently, serious environmental and health problems caused by Cd²⁺ ion have made it a great need to develop methods for detecting and monitoring cadmium levels. Due to the simplicity and high sensitivity features, fluorescent methods have become powerful tools to monitor target heavy metal ions in different sources. The main aim of this study is to develop cross-linked copolymer-based fluorescent sensor with high mechanical strength, sensitivity and selectivity that can detect Cd²⁺ ion in aqueous media. In the literature studies, different types of fluorophores have shown selective properties against different heavy metal ions, and in general, only turn-off and turn-on sensors have been developed. Compared to the studies in the literature, in this study, it is planned to go one step further than the liquid-phase and disposable sensors that have been made so far, and develop a fluorescent sensor with a more functional and high mechanical strength and on-off-on feature. Today, solventless vapor phase deposition methods are most commonly used techniques for production of polymeric thin film coatings. Initiated chemical vapor deposition (iCVD) is a suitable method for the fabrication of crosslinked copolymer thin film coatings and it has many advantages such as low production cost, low temperature, 3D geometry coating performance and high deposition rate. Therefore, production of crosslinked copolymer thin films of glycidyl methacrylate (GMA) and 2,4,6,8-tetramethyl-2,4,6,8-tetravinylcyclohexane (V4D4) via iCVD system was performed in this study. Also, experimental studies for investigations of quantum dot-nitroxide radical nanoprobe formation, attachment of this nanoprobe on iCVD deposited crosslinked copolymer film, interaction between the nanoprobe and target heavy metal ion and some parameter effects on the Cd²⁺ ion detection with developed fluorescent sensor were carried out. Fluorescence Spectroscopy, Fluorescence Microscopy, UV-Vis Spectroscopy, Fourier Transform Infrared Spectroscopy (FTIR) and Electron Paramagnetic Resonance Spectroscopy (EPR) analyses were performed to examine the formation of QD and nitroxide radical nanoprobe due to electron transfer between them, QD-nitroxide radical nanoprobe attachment to the thin polymeric film surfaces and interaction between polymer bonded nanoprobe and target heavy metal ion. Under optimal conditions, a good linear relationship between the fluorescence response and concentration of Cd²⁺ ion was obtained in the range from 0.5 to 15 µM. The detection limit (LOD) of Cd²⁺ ion with QD-nitroxide radical nanoprobe was found as 0.223 µM showed that sensor nanoprobe developed in this study can be comparable with the other Cd²⁺ ion detection studies made so far in literature. Cd²⁺ ion detection study was performed with nanoprobe connected to the developed cross-linked copolymer film and according to the results, Cd²⁺ ion detection was successfully performed with the novel polymer-bonded fluorescent sensor nanoprobe because the desired fluorescence recovery (~ 88%) was obtained from analysis results.

11:30 AM EL10.12.04

Design of Dendritic Promesogenic Ligands for Liquid Crystal-Nanoparticle Hybrid Systems Yifan Ning, Zhe Liu, Shengsong Yang, Yuma Morimitsu, Chinedum Osuji and Christopher B. Murray; University of Pennsylvania, United States

Liquid crystal-nanoparticle (LC-NP) hybrid systems allow synergistic interactions between LC matrixes with anisotropic alignment and NP dopants with versatile functionalities. A uniform, well-dispersed, and highly stable thermotropic LC-NP mixture paves the way for further applications. In this work, a linear promesogenic ligand and two types of dendritic promesogenic ligands with alkyl or oligo ethylene glycol (OEG) chains are designed and synthesized to facilitate incorporating NPs into the thermotropic 4-cyano-4'-pentylbiphenyl (5CB) LC matrix. A comparison study between the linear and the dendritic ligands on the capability to promote miscibility and stability of NPs in LCs is conducted. Miscibility test results show that the linear

ligand and the OEG-chained dendrimer both perform well in uniformly dispersing NPs in LCs. Dynamic assemblies of NPs assisted by dendritic ligands and driven by aligning and equilibrating of mesogens are captured, showing the potential of manipulating the assembly of NPs through external thermal stimuli. The stability test shows that both types of dendrimers can significantly enhance the shelf-life time and thermal stability of NPs compared to the linear ligand. In particular, Au NPs capped with OEG-chained dendrimers are stable in 5CB for 6 months at room temperature and over 10 h at 50 °C. The synthesis of dendritic ligands is highly modulated and can be generalized onto NPs with different dimensions and properties. Tied by the dendritic promesogenic ligands, this LC-NP hybrid system with good uniformity and stability could be further applied to tunable optical displays, responsive materials, etc.

SYMPOSIUM EL11

Ultra-Wide Bandgap Materials, Devices and Applications
November 27 - December 7, 2023

Symposium Organizers

Stephen Goodnick, Arizona State University
Robert Kaplar, Sandia National Laboratories
Martin Kuball, University of Bristol
Yoshinao Kumagai, Tokyo University of Agriculture and Technology

Symposium Support

Silver

Taiyo Nippon Sanson

* Invited Paper

+ JMR Distinguished Invited Speaker

SESSION EL11.01: Characterization and Defects

Session Chairs: Jack Flicker and Robert Kaplar

Monday Morning, November 27, 2023

Hynes, Level 2, Room 210

10:30 AM *EL11.01.01

Lifetime Limiting Degradation Mechanisms of State-Of-The-Art UVC LEDs Enrico Zanoni¹, Francesco Piva¹, Matteo Buffolo¹, Nicola Trivellin¹, Carlo De Santi¹, Nicola Roccatò¹, Norman Susilo², David Hauer Vidal², Antoni Muhin², Luca Sulmoni², Tim Wernicke², Michael Kneissl², Gaudenzio Meneghesso¹ and Matteo Meneghini¹; ¹University of Padova, Italy; ²Technische Universität Berlin, Germany

In recent years, an increasing interest was generated in ultraviolet (UV) light-emitting diodes (LEDs), owing to their several fields of application, such as sanitation and disinfection, and to their superior efficiency and lower environmental impact compared to traditional UV light sources. Despite that, these devices still suffer from several problems that lead to a limited lifetime compared to their visible counterpart.

Nowadays, state-of-the-art commercial UV-C LEDs emitting in the 265 to 275 nm wavelength range show a limited lifetime that decreases, together with EQE, with decreasing emitting wavelengths. This could not be a problem if the useful lifetime of the source is determined based on the total number of deliverable doses for the disinfection of a specific virus species, for instance. If we consider the example of Sars-CoV-2, the disinfection energy required is relatively low, and it was demonstrated that by reducing the operating current of the device, the number of provided doses could be six times higher, in the L70 standard. At the same time, considering the disinfection efficiency as a function of the emitting wavelength, a 265 nm LED with an L70 20% lower could provide higher doses with respect to a 275 nm device.

To better understand the physical mechanisms behind this limited lifetime, specific experiments were carried out on research-grade single quantum well (SQW) LEDs. The analysis highlights the correlation between the physical phenomena observed from electro-optical characterizations and degradation processes detected and modeled by means of capacitance deep-levels transient spectroscopy (C-DLTS), deep-levels optical spectroscopy (DLOS), and numerical simulations based on TCAD models. These studies on SQW LEDs were conducted to identify the types of degradation mechanisms, which can be divided into optical and electrical ones.

Regarding the degradation of the optical characteristics, two different trends can typically be observed comparing high and low bias levels. By using conventional rate equations, it was demonstrated that a simple increase in non-radiative recombination is not sufficient to reproduce the experimentally-observed changes in the L-I curve but is required the consideration of a decreasing injection efficiency. While the first degradation mechanism is confirmed by several works, the latter is still under investigation, though most preliminary investigations relate it to the accumulation of charged centers in the active region, and to the subsequent formation of a higher injection barrier for holes.

Regarding the electrical degradation mechanisms, the worsening of p-contact conductivity and the increase in the concentration of deep-levels participating favoring trap-assisted tunneling (TAT) and sub-turn-on conduction are commonly identified during aging. The former process, associated with an increase in the device turn-on voltage can typically be ascribed to the current-induced deactivation of the magnesium (Mg) dopant located in the proximity of the region-S interface. The reduction in effective dopant concentration causes the increase in the width of the space-charge region (SCR) of the p-Schottky contact, thus lowering the hole tunneling probability from the metal to the semiconductor.

The stress-induced de-activation of Mg in the p-GaN contact layer was also confirmed by C-DLTS measurements and by TCAD simulations.

TAT-assisted conduction was simulated with TCAD models, placing traps in the interlayer region, with an increasing concentration toward the EBL. The energy of these traps was extracted from DLOS measurements, and using their concentration as a fitting parameter allowed to match the I-V curves during the ageing. Moreover, their increase can be associated with a diffusion process from the p-side toward the n-side ascribable to the hydrogen diffusion.

11:00 AM EL11.01.02

Defect Control Strategies for AlN-Based Alloys Naseem Ud Din¹, Cheng-Wei Lee¹, Keisuke Yazawa^{1,2}, William Nemeth², Rebecca Smaha², Nancy Haegel² and Prashun Gorai^{1,2}; ¹Colorado School of Mines, United States; ²National Renewable Energy Laboratory, United States

Tetraedrally-bonded III-N and related alloys are useful for a wide range of applications, from optoelectronics to dielectric electromechanics. Heterostructural AlN-based alloys offer unique properties for piezoelectrics, ferroelectrics, and other emerging applications. Atomic-scale point defects and impurities can strongly affect the functional properties of materials, and therefore, it is crucial to understand the nature of these defects and mechanisms through which their concentrations may be controlled in AlN-based alloys. In this study, we employ density functional theory with alloy modeling and point defect calculations to investigate native point defects and unintentional impurities in $\text{Al}_{1-x}\text{Gd}_x\text{N}$ and $\text{Al}_{1-x}\text{Sc}_x\text{N}$ alloys in the wurtzite phase. We find that the native defect chemistry in both AlN-based alloys is generally similar while differences can be attributed to their electronic band gaps. Among the native defects that introduce deep mid-gap states, nitrogen vacancies (V_N) are predicted to be in the highest concentration, especially under N-poor growth conditions. We predict and experimentally demonstrate that V_N formation can be suppressed in thin films through growth in N-rich environments [1]. Like AlN, we also find that both $\text{Al}_{1-x}\text{Gd}_x\text{N}$ and $\text{Al}_{1-x}\text{Sc}_x\text{N}$ alloys are prone to high levels of unintentional O incorporation, which indirectly leads to even higher concentrations of deep defects. Growth under N-rich/reducing conditions is predicted to minimize and partially alleviate the effects of O incorporation. The results of this study provide valuable insights into the defect behavior in wurtzite nitride-based alloys, which can guide their design and optimization for various applications.

[1] Ud Din N, et al., *ChemRxiv* 10.26434/chemrxiv-2023-prmw

11:15 AM EL11.01.03

Time-Resolved Cathodoluminescence Spectroscopy of Oxygen Related Defects in AlN Layers Barbara Szafranski, Lukas Peters, Andreas Waag and Tobias Voss; Braunschweig University of Technology, Germany

For the fabrication of AlGaIn UV LEDs, a high quality AlN buffer layer on sapphire substrate is a prerequisite for increasing the quantum efficiency. However, in MOVPE it is challenging to achieve a low threading dislocation density (TDD), high transparency of the AlN buffer layer and high light outcoupling efficiencies at the same time. Additional processing challenges arise due to excessive wafer bow caused by differences in thermal expansion coefficients between LED stack and substrate. AlN is one of the few compound semiconductors where annealing at high temperatures (HTA) leads to a substantial improvement of the crystal quality without dissociation of the compound. At the same time, the optical transparency is increased and bowing problems are reduced, since much thinner AlN HTA layers can be used in comparison to thick MOVPE-grown buffers. Typical HTA AlN thicknesses are below 500 nm. However, during the annealing process, a large number of point defects is introduced. Among those, oxygen is one of the most prominent ones due to the higher chemical affinity of aluminum for oxygen than for nitrogen.

We analyzed the influence of oxygen defects in AlN layers with cathodoluminescence (CL) spectroscopy. For all experiments, we used an AlN sample fabricated by PVD on *c*-oriented sapphire substrates. The 425 nm thick AlN layer was treated with HTA at 1680°C for 2 hours in N_2 atmosphere at normal pressure. SIMS measurements revealed a high oxygen concentration of $2 \times 10^{20} \text{ cm}^{-3}$ for the studied AlN sample.

At room temperature, CL spectroscopy shows a broad (FWHM ~ 400 meV) oxygen related luminescence band centered at about 3.54 eV (350 nm). To study the charge carrier dynamics of the oxygen-related defects in AlN, time-resolved CL measurements have been performed. The defect related emission is characterized by a complex multiexponential decay with a fast component of less than 100 ns and a slow component of longer than 10 μs . We attribute the short decay time to the radiative transition from the conduction band-edge states to $(\text{V}_\text{Al}-\text{O}_\text{N})^-$ or $(\text{V}_\text{Al}-\text{O}_\text{N})^{2-}$. The long recombination times might be related to carriers deeply trapped in spatially separated regions of the sample by the impurity-derived electric fields. Further we will discuss the influence of the oxygen concentration in AlN on the recombination times.

11:30 AM EL11.01.04

Microscale Electronic Properties of Epitaxial Gallium Nitride Surface Defects Andrew Winchester¹, Michael Mastro², Travis Anderson², Jennifer Hite² and Sujitra Pookpanratana¹; ¹National Institute of Standards and Technology, United States; ²U.S. Naval Research Laboratory, United States

The wide bandgap material GaN is desired for next-generation high power electronics beyond Si and SiC. However, the vertical structures needed for scalable devices suffer from issues related to dislocations and defects, which propagate from the substrate into the epitaxially grown device area. Substrate developments such as strain patterning to coalesce dislocation bundles and alternate scalable growth methods such as the ammonothermal process have produced higher structural quality substrates. However, in both cases, the remaining dislocations and defects are still a major concern for high power device performance and reliability. For example, threading dislocations with screw components are known to exhibit leakage current and are predicted to have mid-bandgap states, while newer ammonothermal GaN substrates may exhibit different defect densities and distributions compared to GaN grown on foreign substrates. Therefore, determining the electronic properties of dislocations and defects at the microscale will provide valuable information for identifying “killer” defects.

Here, we use a combination of laser-based photoemission electron microscopy (PEEM) and conductive atomic force microscopy (cAFM) to investigate the local surface electronic properties of defects and dislocations in GaN epitaxially grown via MOCVD on different substrates. In epitaxy on patterned substrates, we identify surface defects located near strain centers that have a star-shaped appearance with central pits and extending cracks. These star defects exhibit a larger work function and a shifted valence band maximum, and further, show increased reverse bias leakage current compared to the surrounding GaN. For epitaxy on ammonothermal GaN substrates, we instead observe elongated triangular patches that sporadically occur on a face of certain growth ridges. These regions also show altered electronic structure compared to the surrounding GaN, but are instead more resistive under both forward and reverse bias conditions. Our results provide evidence for defective sites likely related to extended dislocations that will lead to degraded device performance.

11:45 AM EL11.01.05

Defects in Gallium Oxide Imaged by Photoluminescence Microscopy Matthew D. McCluskey, Cassandra Remple, Benjamin Dutton and John S. McCloy; Washington State University, United States

Photoluminescence (PL) spectroscopy is an important method to characterize dopants and defects in gallium oxide. Common features in the PL spectrum include the intrinsic UV band, blue and green bands that involve donor-acceptor pairs, and red emission due to Cr^{3+} impurities. PL mapping with excitation wavelengths ranging from 266 to 532 nm reveals the spatial distribution of these features with submicron resolution. In Czochralski-grown $\beta\text{-Ga}_2\text{O}_3\text{:Fe}$, the Cr^{3+} emission intensity shows striations that are attributed due to inhomogeneities during growth. Ir^{4+} can also be imaged through resonant Raman scattering. By comparing the two signals, we can gain insight into Fermi level variations across the sample. In addition to defects in the bulk, PL microscopy has revealed several specific defects on the surface. Some of these localized centers are very bright UV emitters. Raman scans of these bright emitters revealed hydrocarbon peaks, which may point toward the origin of the light emission.

SESSION EL11.02: UWBG RF and Power Devices
Session Chairs: Alan Doolittle and Robert Kaplar
Monday Afternoon, November 27, 2023
Hynes, Level 2, Room 210

1:30 PM *EL11.02.01

UWBG Semiconductors—The Next Leap in RF and Power Electronics Thomas EKazior¹ and Sharon Woodruff²; ¹DARPA, United States; ²Booz Allen Hamilton, United States

Just as the wide bandgap (WBG) semiconductors, GaN and SiC, are revolutionizing RF and power electronics for defense and commercial applications, the unique properties of the ultra-wide bandgap (UWBG) semiconductors hold promise to create the next revolution. However, these materials are in their infancy, and many technical challenges must be overcome before their promise can become a reality. This invited talk will provide an overview of several UWBG research areas of interest to DARPA. These include: 1) methods to integrate dissimilar semiconductor materials, such as UWBG and narrow bandgap (NBG) semiconductors, to create new device structures that leverage the unique properties of the individual material layers, funded under the Heterogeneous Heterostructures (H2) program; 2) methods to integrate high thermal conductivity UWBG materials with WBG and NBG materials to overcome thermal and electric field bottlenecks in traditional RF power devices, funded under the Technologies for Heat Removal in Electronics at the Device Scale (THREADS) program; 3) new approaches to create large diameter, low defect density, single crystal diamond substrates, funded under the Large Area Device-Quality Diamond Substrates (LADDIS) program; 4) the synthesis of doped UWBG materials, the creation of novel UWBG heterostructures and the engineering of electrical and thermal interfaces funded under various smaller efforts; and 5) exploiting the high breakdown field of UWBG materials to achieve unprecedented levels of RF power handling.

2:00 PM *EL11.02.02

Bridging the Gap: Overcoming Materials and Device Challenges that Limit UWBG Semiconductor Progress David J. Meyer, Virginia Wheeler, Matthew Hardy, Eric Jin, Andrew Lang,

Ultrawide bandgap semiconductors (UWBGs) offer a myriad of electrical, optical, thermal, and mechanical properties that have the potential to unlock previously unattainable levels of performance in coupled-phenomena devices. Despite their known theoretical advantages, progress in UWBG materials and devices has been inhibited by a number of challenges over the past few decades. Practical considerations such as cost, size and consistency of substrate material have made it difficult for the research community to systematically study technical questions that exist with the synthesis and processing of UWBGs. It is exciting to see recent progress in wafer size and affordability of UWBG substrates such as single crystal diamond, AlN, and Ga₂O₃; however, proof-of-concept device demonstrations that clearly display the performance benefits of these materials are still needed to further attract interest in the technology.

While the breakdown strength advantages of UWBGs have been clearly verified in the lab by several groups, there are additional challenges that need to be overcome in order to establish this technology's long-term applicability. This talk will discuss a few of these challenges along with potential approaches being explored to provide solutions:

Challenge #1: Realizing highly mobile electronic charge at sufficient density within UWBG channels and thin films – Conventional approaches such as impurity doping in UWBGs are difficult because many impurities form deep levels within the bandgap (typically 0.2 eV or deeper), resulting in low room-temperature ionization efficiency. Additionally, conventional thin film growth approaches may not provide an energetically favorable environment for the incorporation of dopant atoms on the desired lattice site. Lastly, UWBG materials often have high levels of point or extended defects that can serve as compensation dopants, limiting the concentration of free carriers. A synthesis approach that has been studied by a few groups is the use of metal-modulated molecular beam epitaxy (MME) for the kinetically-controlled incorporation of impurities in AlN thin films. We will discuss our group's efforts involving Si-doping of AlN with MME.

Challenge #2: Managing high electric fields present in UWBG devices – Common device passivation layers such as SiN_x and gate dielectrics such as HfO₂ have electric field breakdown strengths in the ~5-10 MV/cm range. As the breakdown strength of UWBG materials exceeds this range and devices start to operate at 100's and 1000's of volts, passive dielectrics in the device will quickly become potential points for catastrophic failure. As much effort as the community is investing in UWBG thin films, it should also be working to develop complementary dielectrics necessary for device passivation or gate insulation to support long-term reliability. In this talk, we will discuss the concept of relative permittivity engineering for dielectric superjunctions and their use to spread the peak electric fields in UWBG devices.

Challenge #3: Improving the thermal management of high power UWBG devices – A potential future application of UWBGs is in the area of RF power transistors. The current state-of-the-art, GaN, is typically operated in a backed-off power state to prevent acceleration of failure mechanisms due to excessive self-heating during operation, limiting its ultimate RF output power density. While the physics of failure mechanisms in UWBG devices are largely unknown at present, it is likely that thermal management of these devices will need to be co-designed alongside electrical considerations in order for the technology to realize performance benefits. This talk will discuss strategies for device integration with diamond for improved thermal management.

2:30 PM *EL11.02.03

Comparative Operation of Ultra-Wide Bandgap Devices for Voltage/Power Conversion Jack D. Flicker¹, Robert J. Kaplar¹, Jonah Shoemaker² and Stephen M. Goodnick²; ¹Sandia National Laboratories, United States; ²Arizona State University, United States

Ultra-Wide-Bandgap (UWBG) semiconductors hold great promise for future power conversion applications, especially for incorporation at grid-level currents and voltages (10s-100s of kV, 100s of A). Figures of Merit (FOMs) are often used as a first means to understand the impact of semiconductor material parameters on power semiconductor performance, and, in particular, the Unipolar (or Baliga) FOM is often cited for this purpose. However, the use of UWBG materials in a given application requires the fabrication of devices followed by system insertion. While the benefit of UWBG incorporation in power converters should roughly scale with the UFOM, there are several factors of importance for UWBG incorporation in switching power converters that are not explicitly included in UFOM-type calculations including switching behavior, incomplete ionization, mobility, and temperature dependence.

This talk will give an overview of work under the Ultra Materials for a Resilient, Smart Electricity Grid, a Department of Energy Basic Energy Sciences Energy Frontier Research Center, dedicated to evaluating the impact of UWBG materials in grid-level power electronic converters. Toolsets and modeling efforts will be introduced to evaluate how material characteristics of UWBG semiconductors percolate up to system-level improvements, especially regarding power dissipation for different material systems and device types in switching power converters. An optimization technique for two- and three-terminal devices will be introduced that calculates the minimum power dissipation in a switching power converter for a given system operational regime (reverse voltage, forward current density, frequency, duty cycle, and temperature), thereby allowing utilization of the optimal material/device combination for that application. A variety of UWBG device types and materials systems will be directly compared, e.g. diamond, gallium oxide, and aluminum nitride. This gives an overall roadmap for materials systems and device structures that can be utilized to target UWBGs to specific application areas.

3:00 PM BREAK

3:30 PM *EL11.02.04

Semiconducting AlN Electrical Devices Alan Doolittle^{1,1} and Samuel Graham²; ¹Georgia Institute of Technology, United States; ²University of Maryland, United States

Aluminum nitride (AlN) is a material of great interest for high performance power electronics, extreme environment semiconductor devices, radio frequency devices, and deep ultraviolet (DUV) optoelectronics due to its excellent electrical and thermal properties. Compared to other commonly used semiconductors (i.e., Si, SiC, GaN, and β-Ga₂O₃), AlN has the highest critical electric field and theoretical breakdown voltage, which lead to the highest Baliga's and Johnson's figures-of-merit (BFOM & JFOM)³. AlN also has the second highest saturation velocity, and thermal conductivity among semiconductors with a commercially available substrate³. However, AlN has traditionally only been an insulator without the ability to be converted to a semiconductor via doping. We recently demonstrated substantial bulk doping (carrier concentrations above 10¹⁸ cm⁻³) for both p- and n-type AlN using Be and Si dopants, respectively. From these results, we also demonstrated rectification and a 6 V turn-on in AlN PN diodes^{1,2,3}.

Electrical characterization of homojunction aluminum nitride (AlN) PIN diodes is presented along with an update on the prospects for an AlN FET. Recently, using the metal modulated epitaxy (MME) variation of molecular beam epitaxy that controls the surface chemistry to enable low temperature, high quality epitaxy, substantial bulk n- and p-doping in AlN as well as AlN homojunction PN diodes are demonstrated, overcoming the longstanding barrier to doping of AlN^{1,2}. P-type (p=4.4x10¹⁸ cm⁻³, 0.04 ohm-cm) and N-type (n=3x10¹⁸ cm⁻³, 0.02 ohm-cm) bulk conducting AlN is demonstrated with a narrow window for substrate temperatures for achieving semiconducting AlN. With proper surface cleaning procedures, MME grown AlN is indistinguishable from the HVPE AlN on sapphire template via TEM. Current-voltage-temperature (IVT) data from 25 °C to 300 °C is used to investigate these diodes. Diodes with poor substrate cleaning shows a kinked, temperature independent IV behavior in the low forward voltage range associated with defect assisted tunneling originating from stacking faults near the re-growth interface. No such kink, no stacking faults but still temperature independent IV is observed for properly cleaned substrates. These quasi-vertical devices consist of 1 μm highly n-type AlN:Si, a lightly Si-doped intrinsic AlN layer with varied thickness, and a 200 nm highly p-type AlN:Be.

IVT measurements from 25 °C to 300 °C in deep forward bias is presently limited by high series resistance originating from contacts to the plasma etched n-type AlN layer which has ~100x higher contact resistance than as-grown n-type AlN. However, the current increases by ~2 orders of magnitude as temperature increases with contact limited specific-resistance improving by >250x with an activation energy of ~0.3 eV. Forward current below the turn on voltage appear to be dominated by tunneling as suggested by temperature independence. Transistor structures will be discussed and at present are, again, contact limited to ~0.1 A/mm and only modest current modulation. Contact metallization, surface preparation of the AlN templates, and various device geometry parameters as important areas for future optimization in order to allow AlN devices to eventually push the limits in the field power electronics.

References:

- 1 H. Ahmad, J. Lindemuth, Z. Engel, C. Matthews, T. McCrone, W.A. Doolittle, Adv. Mater. 33, 2104497 (2021).
- 2 H. Ahmad, Z. Engel, C.M. Matthews, S. Lee, and W.A. Doolittle, J. Appl. Phys. 131, 175701 (2022).
- 3 W. Alan Doolittle, et al, Accepted in Appl. Phys. Lett. (2023)

4:00 PM EL11.02.05

Impact of Buffer Layer on the Thermal Performance of Multi Channel AlGaIn/GaN Transistors Georges Pavlidis¹, Muhammad Jamil¹, Bivek Bista¹, Francis Vasquez¹ and Andrea Centrone²; ¹University of Connecticut, United States; ²National Institute of Standards and Technology, United States

The formation of the two dimensional electron gas (2DEG) in AlGaIn/GaN high electron mobility transistors (HEMTs) has enabled devices that can operate at both high frequencies (> GHz) and high voltages (> 3 kV). These advantageous characteristics have translated to the commercialization of superior DC converters and high-power density radio frequency (RF) devices. The current record performances of single channel AlGaIn/GaN RF transistors, however, have been thermally limited to power densities that are significantly lower than the expected theoretical

limits. One approach to improve the power density is the implementation of superlattice based multichannel transistors. The stacking of adjacent 2DEGs has been proven to increase the current density and transconductance of HEMTs.

To maintain a low ON-resistance, the heat generated in these nanostructured devices must be efficiently removed which requires in-depth knowledge of nanoscale thermal transport. Two challenges to overcome include the low cross plane thermal conductivity of superlattices and the high thermal resistance of a thick AlGaIn buffer layer. This study investigates the impact of implementing a thinner GaN buffer layer with higher thermal conductivity. Furthermore, to assess the feasibility of simplifying the thin film structure, the thermal performance of non-castellated multichannel HEMTs is assessed via two techniques: scanning thermal microscopy (SThM) and Raman thermometry. For direct comparison, a multichannel device with a thin GaN buffer layer is demonstrated to achieve the similar thermal resistance to a device that is epitaxially grown on a AlGaIn buffer layer that has fewer number of channels. A thermal finite element model (FEM) is developed to explain the discrepancy between the temperatures measured via SThM (surface temperature) and Raman thermometry (depth average). The peak temperature is found to be in the proximity of the topmost channel which highlights the importance of surface temperature techniques, such as SThM, for accurate extraction of thermal resistance. Finally, the challenges associated with SThM measurements on structures with small channel spacing and thick metal contacts is discussed and a numerical solution via FEM modelling is proposed.

4:15 PM EL11.02.06

X-Band AlGaIn/GaN HEMT with Output Power over 20 W/mm and PAE over 50% using High Purity GaN Channel[Kenji Homma](#), Maciej Matys, Atsushi Yamada, Toshihiro Ohki and Norikazu Nakamura; Fujitsu Limited, Japan

An AlGaIn/GaN high electron mobility transistor (HEMT) is still attractive devices for high frequency amplifier applications due to excellent properties of nitride materials like a wide band gap and large breakdown field. In the recent years, several reports concerning the high output power characteristics of AlGaIn/GaN HEMT for X-band applications have been published [1,2]. Practical devices are required to satisfy not only high output but also power saving performance by high efficiency. In this work, we report on our success in simultaneously achieving a power density of more than 20 W/mm and an efficiency of more than 50% in the X-band.

A high-performance X-band AlGaIn/GaN HEMT were grown by metal-organic chemical vapor deposition (MOCVD) on a SiC substrate. The devices exhibited a peak transconductance (Gm) of 335 mS/mm and high maximum drain current of 1.34 A/mm. The load-pull measurements performed at 8 GHz corresponding to the target device operating frequency in X-band for devices with gate lengths of 0.25 μ m demonstrated a peak power added efficiency (PAE) of 52.6% and a maximum output power density of 21.2 W/mm at 60 V. To the best of our knowledge this is the highest power ever reported for X-band AlGaIn/GaN HEMT at $V_{ds} = 60$ V. We achieved these results by improvement of the current collapse (dc-RF dispersion) in terms of optimizing the growth conditions of the GaN channel on top of the Fe-doped GaN buffer in AlGaIn/AlN/GaN heterostructures. In particular, we investigated the impact of growth parameters of the GaN channel layer, such as the growth rate, and V/III ratio on the AlGaIn/AlN/GaN HEMT performance. We found that the GaN channel layers grown with the high V/III ratio (about 5000) lead to a suppression of the current collapse in AlGaIn/AlN/GaN HEMTs. Based on the photoluminescence (PL) measurements, we attributed the current collapse suppression to the reduction of GaN channel acceptor-like traps related to the carbon impurities. More precisely, for the GaN channel layers grown with the V/III ratio of about 5000, we observed a significant decreases of yellow luminescence from the AlGaIn/AlN/GaN heterostructure, which directly correlated with the current collapse improvement. We believe that the achieved progress represents an important step toward the development of high power AlGaIn/GaN HEMTs.

References

- [1] J. Kotani et al., "24.4 W/mm X-Band GaN HEMTs on AlN Substrates With the LPCVD-Grown High-Breakdown-Field SiNx Layer," in IEEE Journal of the Electron Devices Society, vol. 11, pp. 101-106, 2023,
- [2] K. M. Bothe et al., "Improved X-Band Performance and Reliability of a GaN HEMT With Sunken Source Connected Field Plate Design," in IEEE Electron Device Letters, vol. 43, no. 3, pp. 354-357, March 2022,

4:30 PM EL11.02.07

Ultra-Wide Bandgap AlGaIn-Based N-Polar High Electron Mobility Transistors: From Materials to Devices[Maliha Noshin](#), Xinyi Wen, Rohith Soman, Xiaoqing Xu and Srabanti Chowdhury; Stanford University, United States

Ultrawide bandgap (UWBG) materials are being widely investigated for high-power and high-frequency electronics [1,2]. While emerging UWBG materials like Ga₂O₃ possess large bandgap and high critical electric field, AlGaIn compositions can potentially have larger Figure of Merit owing to higher sheet carrier concentration and larger mobility. Recently, using N-polar all AlGaIn-HEMT we showed simultaneously large drive current, low on-state leakage current as well as > 400 V breakdown voltage [3].

In this work, we discuss the growth and optimization as well as the characterization of N-polar AlGaIn channel HEMT with varying Al concentrations. We also probe the composition-dependent surface morphology and transport in these materials, aided by simulation and Hall measurements.

For the growth of the N-polar all-AlGaIn HEMT structures, we used the metal-organic chemical vapor deposition (MOCVD) method. We used c-plane sapphire substrates with a 4° miscut towards a-plane for achieving smooth and high-quality epitaxy. We demonstrated four different HEMT structures with Al mole fraction $x=20\%$, 30%, 59% and 73% in the Al_xGa_{1-x}N channel layer. The growth of such MOCVD-grown N-polar all-AlGaIn HEMT was optimized at higher temperatures with higher TMAI flow to achieve a crack-free growth and lower dislocation density within the structures.

We measured the stoichiometries of the structures using both symmetric and asymmetric 2 θ - ω scans in X-ray diffraction to incorporate strain effect. After KOH etching the N-polar HEMT showed hexagonal hillock-like structures, confirming the N-polarity of our grown samples. Atomic force microscopy imaging confirmed the good surface morphology with a root mean square surface roughness of <1 nm under 5 μ m x 5 μ m scan size. We also found that the surface roughness increased for HEMTs with the higher Al mole fraction AlGaIn in the channel and barrier layers which can be from strain due to larger lattice mismatch between layers.

To develop a fundamental understanding of the material property and device performance, we explored the effect of Al mole fraction in the transport characteristics of the HEMT structures using Hall measurement. We found a decreasing trend in the mobility with increasing Al mole fraction in the AlGaIn channel that can be correlated to alloy-scattering [4] and optical phonon-scattering dominated transport, further explored in our TCAD simulations. Our simulation showed that beyond 73% Al mole fraction, the mobility increases again. Comparing our simulation with the Hall mobility numbers, we can discern that mobility degradation due to surface undulation might be more pronounced for HEMT structures with higher Al percentages. We also fabricated N-polar all-AlGaIn HEMT devices with 20% Al composition in the channel. A 10 μ m channel length device offered a drive current of ~250 mA/mm. The high drive current can be attributed to the formation of better contacts on the lower-bandgap material and the natural formation of a back-barrier.

To summarize, in this work we reported experimental demonstration of device-quality epitaxial growth of N-polar all-AlGaIn HEMT. The success of this study which will be discussed at the presentation led to the first demonstration of >400V breakdown voltage N-polar AlGaIn HEMTs. We also explored the correlation between the material surface morphology and transport properties for varying Al compositions. This work will deepen our understanding of the optimization of N-polar AlGaIn HEMT for high-power applications.

We acknowledge the funding from ONR (Award No N00014-19-1-2611- P00004) and Dr. Paul Maki for supporting this work.

- References: [1] R. J. Kaplar et al. *ECS J Solid State Sci Technol* 6, 3061 (2016). [2] J. Y. Tsao, S. Chowdhury et al., *Adv. Electron. Mater.* 4(1), 1600501 (2018). [3] M. Noshin, S. Chowdhury et al., *IEEE Electron Dev. Lett.*, DOI: 10.1109/LED.2023.3279400 (2023). [4] M.E. Coltrin et al., *ECS J Solid State Sci Technol* 6, S3114 (2017).

4:45 PM EL11.02.08

Polarity Inversion of Scandium Aluminum Nitride (ScAlN) Piezoelectric Thin Films via Addition of Element in Group IVB (C, Si, Ge or Sn)[Sri Ayu Anggraini](#), Masato Uehara, Kenji Hirata, Hiroshi Yamada and Morito Akiyama; National Institute of Advanced Industrial Science and Technology, Japan

The discovery of scandium aluminum nitride (ScAlN) piezoelectric thin film has successfully brought promising improvement to the performance of modern wireless communication technology, particularly radio frequency (RF) filter [1,2]. The shift toward 6G communication system demands RF filter that can work at much higher frequency and wider bandwidth to allow efficient data transmission. Since integrating multilayers of piezoelectric thin films with different polarities enable an RF filter to function at much higher frequency [3], stacking Al-polar and N-polar ScAlN thin films is expected to be an effective strategy to achieve high-performance RF filter. As a result, controlling the polarity of ScAlN has become paramount for the development of next generation RF filter. Addition of element such as silicon (Si) or germanium (Ge) into AlN was reported to capable of inverting the polarity of aluminum nitride (AlN) [3,4] as well as ScAlN [5,6]. Therefore, in this study, we investigated the effect of addition of each element in group IVB (carbon (C), Si, Ge, tin (Sn)) on the polarization direction of ScAlN thin films.

All thin films were deposited on Si (100) wafer by using radio frequency magnetron sputtering system. Our study reveals that addition of C into ScAlN resulted in thin films with positive piezoelectric coefficient (d_{33}), which means addition of C into ScAlN maintained the polarity of ScAlN to be Al-polar. However, addition of either Si or Ge into ScAlN resulted in thin films

with negative d_{33} and the d_{33} values have similar magnitude with that of ScAlN. This suggested that addition of Si or Ge could inverse the polarity of ScAlN from Al-polar into N-polar, without significantly decreasing the value of d_{33} . In case of Sn, the negative d_{33} that was obtained upon the addition of Sn into ScAlN is an indication that addition of Sn could led to thin films with N-polarity. However, the d_{33} values of ScSnAlN are lower than that of ScAlN. Our study confirmed that the formation of N-polar ScAlN is largely controlled by both concentration of each additive element (in this case: Si, Ge, Sn) and the concentration of Sc. Effect of addition of each element on polarity distribution, crystal structure and surface states were also investigated in this study.

Acknowledgement: This work was supported by JSPS KAKENHI Grant Number JP21K04168.

References:

- [1] M. Akiyama et al, *Adv. Mater.* (2009) 21, 593.
- [2] M. Moreira et al, *Vacuum*, (2011) 86, 23.
- [3] Mizuno, T. et al. *2017 19th International Conference on Solid-State Sensors, Actuators and Microsystems (TRANSDUCERS)*. 1891.
- [4] S. A. Anggraini et al, *Scientific Reports* (2020) 10, 4369.
- [5] S. A. Anggraini et al, *JSAP Spring Meeting 2021*.
- [6] S. A. Anggraini et al, *JSAP Fall Meeting 2021*.

SESSION EL11.03/EL14.05: Joint Session I: Diamond Electronic Devices
Session Chairs: David Moran and Mariko Suzuki
Tuesday Morning, November 28, 2023
Hynes, Level 2, Room 210

8:30 AM *EL11.03/EL14.05.01

Prospects of Diamond Devices in High-Temperature and High-Power Applications Srabanti Chowdhury; Stanford University, United States

Electrification is driving us closer to our goal of a sustainable society. Highly efficient and reliable ways of converting, delivering, and conditioning power call for innovations at every level, from systems to semiconductors. Beyond Si, GaN, and SiC, Diamond, with a bandgap of 5.47eV is being explored for its large critical electric field (3x more than SiC), and high thermal conductivity (6x more than SiC). Doping diamond p-type has been less challenging than n-type. However, in comparison with other wider bandgap materials such as Ga₂O₃ and AlN, n-type diamond has shown promises demonstrating high blocking voltage (>2kV) Schottky/p-i-n diodes quite routinely [1-2]. We have studied three notable features of diamond to help us understand its scope and applicability in power electronics - first, its voltage handling capability, second its high-temperature operability, and lastly its role as an optical switch and an isolator. While PIN diodes fabricated on (100) and (111)-samples, demonstrated a higher blocking voltage in (100) compared to (111) viz. 1kV, the maximum electric field of ~4MV/cm was registered in (111). We also noted that P incorporation, along with surface stability, was greater in (111) over (100), the latter leading to Schottky-PIN diodes in (100), while PIN behavior was intact in (111) [1-4]. We studied and reported up to 600°C operation in Schottky-PIN diodes for operation under harsh and high-temperature environments [5]. With a proper packaging scheme, the devices were stable to handle high temperatures. This could lead to unprecedented advantages for high-voltage electronics where local junction temperatures in devices can rise to 300°C or more under specific operating conditions. Furthermore, to study the possibility of the diamond as a photoconductive switch, or optically triggered device, we fabricated and characterized planar interdigitated photoconductive switches using a single crystalline diamond with 30 μm, electrode gaps [6]. 532 and 1064 nm Nd: YAG laser pulses with energies up to 3.5 mJ/pulse were used to trigger the switches. Photoresponses with sub-bandgap excitation were measured at bias voltages ranging from 10 to 100 V, corresponding to electric fields of 3.3–33 kV/cm. The ratio of resistances measured under dark and under illumination was of the order of 10¹¹. While this value is comparable to those achieved by other wide bandgap materials, the minimum resistances of the devices could be improved. Based on these three studies, along with reverse recovery analysis [2,7] that we conducted over the past seven years, we envision a diamond-based platform to be suitable for delivering high-temperature tolerant power electronics platforms that can transform the field. Although there remain significant challenges, such as designing edge termination and tackling surface reconstructions, the results so far are remarkably promising.

References:

1. M. Dutta, F. A. M. Koeck, W. Li, R. J. Nemanich and S. Chowdhury, *IEEE Electron Device Letters*, vol. 38, no. 5, pp. 600-603, 2017
2. M. Dutta, M., S. Mandal, R. Hathwar, A.M. Fischer, F.A.M. Koeck, R.J. Nemanich, S.M. Goodnick, and S. Chowdhury, *IEEE Electron Device Letters*, vol. 39, no. 4, pp. 552-555, 2018
3. R. Hathwar, M. Dutta, F. A. M. Koeck, R. J. Nemanich, S. Chowdhury, and S. M. Goodnick, *J. Appl. Phys.*, vol. 119, no. 22, pp. 225703, 2016.
4. M. Dutta, F. A. M. Koeck, R. Hathwar, S. M. Goodnick, R. J. Nemanich, and S. Chowdhury, *IEEE Electron Device Lett.*, vol. 37, no. 9, pp.1170-1173, 2016.
5. M. Malakoutian, M. Benipal, F. A. Koeck, R. J. Nemanich and S. Chowdhury, *IEEE Journal of the Electron Devices Society*, vol. 8, pp. 614-618, 2020.
6. K. Woo, M. Malakoutian, B. A. Reeves, and S. Chowdhury, *Applied Physics Letters*, vol. 120, no. 11, p. 112104, 2022.
7. K. Woo, B. Shankar, M. Malakoutian, F. Koeck, R. Nemanich and S. Chowdhury, *2022 Compound Semiconductor Week (CSW)*, Ann Arbor, MI, USA, 2022, pp. 1-2, doi: 10.1109/CSW55288.2022.9930407.

9:00 AM *EL11.03/EL14.05.02

Diamond for Next Generation Power Electronic Devices Etienne Gheeraert^{1,2}; ¹University Grenoble Alpes, France; ²University of Tsukuba, Japan

The key to the efficient transmission and conversion of low-carbon electrical energy is the improvement of power electronic devices. Diamond is considered to be the ultimate wide bandgap semiconductor material for applications in high power electronics due to its exceptional thermal and electronic properties. Two recent developments - the emergence of commercially available electronic grade single crystals and a scientific breakthrough in creating a MOS channel in diamond technology, have now opened new opportunities for the fabrication and commercialisation of diamond power transistors.

This will result in substantial improvements in the performance of power electronic systems by offering higher blocking voltages, improved efficiency and reliability, as well as reduced thermal requirements thus opening the door to more efficient green electronic systems.

In the literature, several diamond-based field-effect-transistors (FETs) have already revealed good on state performance and high blocking voltage capability (~3kV) in a wide range of operating temperatures. The possibility of generating an inversion regime in diamond metal-oxide-semiconductor FET (MOSFET), and the new Deep Depletion regime (D2MOSFET) specific to wide bandgap semiconductors pave the way for a new generation of power devices. The critical part of the transistor is the gate oxide, with electrical charge traps located within the oxide or at its interface with the semiconductor. These traps can screen the gate potential and shift the threshold voltage, making the devices unusable.

The current research carried out mainly in Japan and Europe will be presented, with the various device architectures explored, including MOSFET, MESFET, D2MOSFET and rectifiers.

9:30 AM EL11.03/EL14.05.03

High Breakdown Voltage Diamond Schottky Barrier Diode via Submicron Fin Channel Shumiao Zhang and Hong-Xing Wang; Xi'an Jiaotong University, China

Diamond electric devices have potential to be apply for high power applications owing to superior physics and electrical properties. For diamond-based Schottky barrier diode(SBD), the research focus on high breakdown voltage to achieve high power devices. In previous studies, field plate, floating diffused guard rings, fluorine termination, and trench MOS structure have been used to improve reverse blocking characteristic. Trench MOS with fin width is a novel method to improve the capacity of SBD to withstand high voltage. On account of extremely narrow mesa, the lateral depletion at sidewall wide enough to pinch-off leakage current through mesa. In addition, charge-coupling effect is strong for fin channel MOS SBD and can uniform distribution of electric field effectively. Thus, fin channel MOS structure is beneficial to alleviate electric field crowding at the edge of the electrode and avoid premature breakdown. In this work, submicron fin channel diamond SBD is fabricated by anodic aluminum oxide(PAA) and inductively coupled plasma (ICP) technology. And SiO₂ dielectric layer is deposited on fin channel to realize MOS structure and adjust electric field distribution in diamond. Furthermore, the impact of width of the mesa on breakdown characteristics for diamond SBD has also been investigated.

9:45 AMBREAK

1:30 PM *EL11.05.01

Theoretical Models of High-Field Transport and Impact Ionization in Ultra-Wide Band Gap Semiconductors Enrico Bellotti, Mike Zhu and Masahiko Matsubara; Boston University, United States

Theoretical models that attempt to predict high-field carrier transport parameters and the values of the carriers' ionization coefficients are important since they provide an estimate of the expected values and a first order evaluation of the material performance. The direct measurement of ionization coefficients in wide and ultra-wide band gap semiconductor materials is challenging due to the need to operate at high field strengths and the requirement of specific test structures that enable single carrier injection. More often than not, ionization coefficients are inferred from current multiplication data measured in p-n junctions or transistors structures. Unfortunately, sub-par material quality, processing issues and inappropriate measuring techniques have led to ionization coefficients values that are contradictory and with large variation among different datasets.

Developing theoretical models presents its own set of challenges. The established approach is based on a full electronics structure description of the semiconductor material and a suitable model to quantify the interaction of carriers with phonons, impurities and material imperfections. While this methodology has been successful with conventional elemental and compound semiconductors, and it has been applied to some wide band gap materials such as GaN, 4H-SiC [1,2] and diamond, a number of open issues still exists. The main difficulty is the determination of the carrier-phonon scattering strength at high electric field strengths that cannot be inferred from low-field mobility measurements.

Among all wide band gap semiconductors, 4H-SiC [3] and GaN [4] are the material for which ionization coefficients have been measured by several groups. In the case of GaN, different measured ionization coefficients datasets are available and seems to provide a consistent indication of the expected values. Corresponding theoretical models based on full-band Monte Carlo simulations have been able to predict the correct trends, namely the fact that holes dominate the ionization process, but a quantitative agreement between predicted and measured values has only been achieved recently [5].

This talk will provide an overview of the currently available experimentally measured ionization coefficients for wide band gap semiconductors and compare them to the ones obtained with theoretical models of different complexity. Specifically the development of the theoretical models for high-field transport for 4H-SiC, GaN will be discussed. Three different approaches, one based on empirical carrier-phonon scattering rates, one using the rigid pseudo ion model, and the direct evaluation of the interaction parameters based on an ab-initio DFT approach will be compared, and the outcome for each one of them benchmarked against the measured values. Additionally, the models will be applied to determine the ionization coefficients in ultra-wide band-gap semiconductors including AlGaN alloys, cubic BN [6] and diamond.

[1] E. Bellotti et al., J. Appl. Phys., 87, (8), p.3864, 15 April 2000.

[2] F. Bertazzi et al., J. Appl. Phys., Vol.106, N6, p.063719, 15 September 2009.

[3] A.O. Kostantinov, Appl. Phys. Lett. 71, 90, 1997, T. Hatakeyama, Appl. Phys. Lett. 85, 8, 2004

[4] Cao et al., APL, N.112, 2018, Maeda et al., JAP, N.129, 2021, McClintock et al., APL, N.90, 2007, Ji et al., APL, N115, 2019

[5] E. Bellotti and M. Matsubara, unpublished.

[6] M. Zhu, M. Matsubara, and E. Bellotti, Phys. Rev. App. Under review.

2:00 PM EL11.05.02

Quantitative Disorder Metrics and Structure-Property Relationships in Ga-Based Ultra-Wide Bandgap Semiconductors Robert Makin¹, Andrew S. Messecar¹, Nancy S. Muiyanja², Kate Wislang³, Rodrigo Martinez-Gazoni³, Martin Allen³ and Steve Durbin¹; ¹Western Michigan University, United States; ²University of Michigan-Ann Arbor, United States; ³University of Canterbury, New Zealand

In the context of epitaxial semiconductor layers prepared for electronic devices, disorder is frequently an important consideration. One well-known model for quantifying disorder was developed by Bragg and Williams in the early 1930s, who were concerned with accurately describing the varying degrees of atomic ordering in metal alloys. In their formulation, a numerical order parameter (S) is defined as having a value between 0 (fully randomized lattice) and unity (fully ordered lattice). Traditionally this order parameter is measured using x-ray diffraction techniques, but we have recently demonstrated that electron diffraction, Raman spectroscopy and electron microscopy are equally viable experimental methods. Following the approach of Laks, Wei and Zunger as applied to semiconductor alloys, it is possible to employ spin-based modeling in conjunction with cluster expansion theory (out to pair-interaction terms) to express a material property P as $P(x,S) = [P(x=0.5, S=1) - P(x,S=0)]S^2 - P(x,S=0)$, provided that P is dominated by pair interactions. Here, S is the Bragg-Williams order parameter, and x represents the composition (e.g., $x = [\text{Ga}]/([\text{Ga}]+[\text{N}])$). Consequently, the expectation is that some properties may exhibit a linear dependence on S^2 provided that composition is properly accounted for; in fact, this is what has been observed in the case of a number of different semiconductor materials.

In the present study, forty-four Ga_2O_3 and twenty-eight distinct GaN samples were considered. Ga_2O_3 layers were grown either by plasma-assisted molecular beam epitaxy or a sol-gel method; GaN was grown by plasma-assisted molecular beam epitaxy. An additional set of samples identified in the literature was also included. The Bragg-Williams order parameter was measured using either in-situ reflection high-energy diffraction, Raman spectroscopy, or electron microscopy image analysis, with several samples characterized by multiple techniques (with S typically agreeing to three decimal places). For the GaN samples measured, S^2 ranged from approximately (0.02 to 0.52), with both nitrogen-rich and gallium-rich compositions in addition to stoichiometric material included. For Ga_2O_3 , experimentally-determined values of S^2 ranged from (0.08) to (0.53). As would be expected, a range of band gap energies was measured for the GaN samples, including evidence of inverted bands for some gallium-rich samples as indicated by the observed temperature dependence. In the case of Ga_2O_3 , only stoichiometric samples were included in the initial study, with a range of measured band gap energy between 3.2 eV at $S^2 = 0.53$ to 5.0 eV at $S^2 = 0.08$. For the GaN samples, Hall effect mobility values were also measured, with a linear relationship between mobility and S^2 and higher mobility values for Ga-rich samples at the same value of S^2 . Extrapolation of the experimental points suggests that further tuning of S could lead to slightly higher mobility values than what have been reported for undoped epitaxial layers. There are several ways to tune S in a plasma-assisted molecular beam epitaxy process, with a weak dependence on temperature and a stronger dependence on plasma conditions. In contrast, for Ga_2O_3 grown by PLD, a strong dependence of S^2 on oxygen partial pressure is observed, with a weaker dependence on sapphire substrate plane. For Ga_2O_3 grown by dehydroxylation of GaOOH , a linear relationship between temperature and S^2 is observed. Consequently, process parameters can be tuned during epilayer growth to achieve a specific value of S and composition (x), and thereby engineer a desired value of band gap and potentially mobility.

This work was partially supported by a grant from the National Science Foundation (DMR-2003571).

2:15 PM EL11.05.03

Deciphering 3d Transition Metal Dopants in GaN (and Wide Band Gap Materials) using Ground State and Excited State Density Functional Theory Peter A. Schultz¹, Jesse J. Lutz¹, Renee Van Ginhoven² and Arthur H. Edwards²; ¹Sandia National Laboratories, United States; ²Air Force Research Laboratory, United States

Doping of gallium nitride (GaN) and (ultra-)wide band gap, (U)WBG, materials is used to control the Fermi level and create functional defects for optoelectronic and spintronic applications. Harnessing the greater temperature tolerance, faster switching speeds, and larger breakdown voltages possible with III-nitrides would profoundly improve the performance of power electronics. To exploit the technological potential of 3d-doped (U)WBG requires greater understanding of 3d defects than currently exists. Firm identification and characterization of defects in (U)WBG remains fraught. The mismatch between what experiment can measure and definitively identify and what theory can reliably compute is a particularly acute challenge in 3d-doped GaN. Using a generalized gradient approximation (GGA) to density functional theory (DFT) along with a non-jellium local moment countercharge (LMCC) treatment of the charge boundary conditions, we demonstrate accurate predictions of defect levels of magnetic 3d dopants in GaN unhindered by a band gap problem and in agreement with available experimental data. We implement an occupation-constrained DFT (occ-DFT) to self-consistently obtain excited state total energies, and thereby predict vertical and adiabatic optical excitation energies corresponding to photoluminescence (PL) data. These GGA excited-state results agree quantitatively with PL measurements, whereas literature hybrid functional calculations fail qualitatively. In concert, ground state (defect levels) and excited state (PL) calculations mandate wide reinterpretation of GaN experimental literature. The Mn dopant is shown to take charge states as deep as (2+), with corroborating evidence anchored at one end by accurate prediction of the 1.4 eV PL for the Mn(0) and the other end by accurate prediction of PL for a d^2 Mn(2+) defect. The 1.19 eV PL in n-type GaN, attributed to Cr^{4+} and touted as a promising candidate for a quantum color center, cannot be the $\text{Cr}(1+)$ —the $\text{Cr}(1+)$ is stable only in midgap. A combined ground-state/excited-state modeling approach enables more confident chemical identification of defects in (U)WBG, aiding the search to identify, characterize, and design doping regimens to create functional defects with auspicious electronic properties.

— Sandia National Laboratories is a multimission laboratory managed and operated by National Technology and Engineering Solutions of Sandia, LLC., a wholly owned subsidiary of

2:30 PM EL11.05.04

Yellow Luminescence in GaN: Predictions for Candidate Defects at Zero and 12 GPa Hydrostatic Pressure Arthur H. Edwards¹ and Peter A. Schultz²; ¹Air Force Research Laboratory, United States; ²Sandia National Laboratories, United States

Yellow luminescence (YL) has held great interest in GaN. The identity(ies) of the YL defect(s) has been controversial for many years. Recent experimental work by Zvanut *et al.* and by Narita *et al.* proved that carbon substituting on a nitrogen (C_N) site is at least one of the components. This identification is supported by recent theoretical results, buttressed by the photoluminescence studies of Reshchicov and coworkers, who resolved the zero phonon line (ZPL) and other phonon replicas. These theoretical studies have found other defect candidates predicted to have PL_{max} and ZPL close to experiment for YL. There is prior data for YL obtained at high hydrostatic pressure, showing that YL band strongly shifts and broadens, making assignment to a single defect untenable. We perform a detailed study of C_N, as well as other candidate defects (V_{Ga}, C_N:O_N, V_{Ga}:O_NH₂, V_{Ga}:H₃) at 0 GPa and 12 GPa using the standard PBE exchange correlation functional with the local moment counter charge (LMCC) method, an alternative to the standard *jellium* approximation for electrostatic boundary conditions. Prior published LMCC results show that the method reproduces a reasonable proxy for the band gap (3.56 eV (LMCC), vs. 3.3 eV (exp.)) bounding by the span of all defect levels arising from localized charge states for an extensive set of intrinsic and extrinsic defects. We use this "defect band gap" both to estimate the change in the experimental gap as a function of pressure, and to assign new band edges for calculation of PL_{max} at 12 GPa. At 0 GPa our results agree well with Lyons *et al.*: V_{Ga}, V_{Ga}:O_NH₂, and C_N have PL_{max} within ~0.1 eV of experiment (2.18 eV), and also yield accurate prediction for the ZPL. We are in reasonable agreement with Lyons *et al.* that V_{Ga}:H₃ is within 0.2 eV of experiment ZPL. Our new results at 12 GPa provide crucial chemically differentiating information. First, we find that the prediction of the slope of E_G vs. pressure using the extremal defect levels as band edge bounds (36 meV/GPa) is in very good agreement with several experimental values (36-47), where the larger values were taken from the linear coefficient of a quadratic fit, and the lowest was taken from a purely linear fit. For V_{Ga}, V_{Ga}:O_NH₂, and C_N, we find that predicted PL_{max} are no longer close in energy: the values range from 2.51 eV to 2.83 eV. Almost all of the change in PL_{max} is in the ZPL. Even though the Frank-Condon shifts (FCS), the energy difference between PL_{max} and the ZPL, are quite different for each defect, ranging from 0.2 to 0.55 eV, the changes in FCS with pressure are minimal--~10-20 meV. These results point to using hydrostatic pressure, combined with computational predictions, to chemically discriminate PL.

2:45 PM EL11.05.05

Stability and Molecular Pathways to The Formation of Spin Defects in Wide Band Gap Semiconductors for Quantum Technologies Elizabeth M. Lee; University of California, Irvine, United States

Spin defects in wide-bandgap semiconductors provide a promising platform to create qubits for quantum technologies. Their synthesis, however, presents considerable challenges, and the mechanisms responsible for their generation or annihilation are poorly understood. Here, we elucidate spin defect formation processes in a solid-state crystals for leading qubit candidates—the divacancy complex in silicon carbide [1] and the nitrogen vacancy (NV) center in diamond. Using *ab initio* molecular dynamics with enhanced sampling techniques, we characterize the formation mechanism of spin defects. We then predict the conditions favoring the formation of spin defects over the competing process of other undesirable defects. Moreover, we identify pathways to create new spin defects and determine their electronic properties using hybrid density functional calculations. The detailed view of the mechanisms that underpin the formation and dynamics of spin defects presented here may facilitate the realization of qubits for designing room temperature quantum devices.

[1] E. M. Y. Lee, A. Yu, J. J. de Pablo, and G. Galli. *Nature Communications*, **12**, 6325 (2021)

3:00 PM BREAK

3:30 PM *EL11.05.06

Rutile GeO₂ and GeSnO₂ Alloys: A New Family of Ultra-Wide-Band Semiconductors for Power Electronics SieunChae¹, HanjongPaik², KelseyMenge¹, KyleBushick¹, JohnT. Heron¹ and EmmanouilKioupakis¹; ¹University of Michigan, United States; ²The University of Oklahoma, United States

Ultra-wide-band-gap (UWBG) semiconductors are promising for higher efficiency, reduced size, and lower cost in power-electronics applications. UWBG materials such as diamond, cubic boron nitride (cBN), β-Ga₂O₃, and AlGaN alloys promise orders-of-magnitude improvements in power density compared to current technologies (Si, SiC, and GaN). However, none of the above UWBG materials offers all the desired properties needed for high-performance electronics and, despite decades of research, very few alternative UWBG semiconductors have been developed to date. There is therefore a pressing need to develop synergistic methods that combine predictive theory with experimental synthesis and validation in order to discover and design new UWBG semiconductors that can overcome the limitations of current technologies.

In recent years, our team has advanced the development of rutile GeO₂ and its alloys with SnO₂ as a novel family of UWBG semiconductors that can surpass the state of the art in power electronics. Our predictive atomistic calculations demonstrate that these alloys exhibit superior fundamental properties that can overcome the limitations of current materials. Their band gaps fall in the ultra-wide range, spanning from 3.6 eV for SnO₂ to 4.68 eV for rutile GeO₂. They exhibit ambipolar dopability, with Sb_{Ge}, As_{Ge}, Ta_{Ge}, H, and F_O acting as shallow donors, while Al_{Ge} and Ga_{Ge} acting as acceptors. The predicted carrier mobilities are high (up to 377 cm²/Vs for electrons and up to 29 cm²/Vs for holes at room temperature), while the relatively light carrier effective masses prevent the formation of self-trapped polarons. The predicted thermal conductivity is high (up to 51 W/m K at room temperature) and surpasses β-Ga₂O₃, a prediction that we verified experimentally with thermal measurements in unoptimized polycrystalline bulk samples. Overall, we find that the Baliga figure of merit of rutile GeO₂, modified to account for donor ionization, surpasses all known semiconductors, demonstrating its unique potential for energy-efficient power electronics.

Experimentally, we demonstrate the synthesis of single-crystalline GeO₂-based thin films and substrates, which are prerequisites for the fabrication of epitaxial devices. Our results demonstrate the epitaxial stability of GeSnO₂ alloys over their entire composition range, while the demonstration of epitaxy on high-quality rutile GeO₂ substrates opens up the possibility of epitaxial single-crystalline thin films. Overall, our work demonstrates the promise of rutile GeO₂-based materials for advancing the state of the art in power electronic devices.

4:00 PM EL11.05.07

Influence of Local Coordination on the Electronic Structure of Ga₂O₃ AnnaRegoutz¹, LauraRatcliff², TakayoshiOshima³, FelixNippert⁴, BenjaminJanzen⁴, EliasKluth⁵, RuedigerGoldhahn⁵, MartinFeneberg⁵, PieroMazzolini⁶, OliverBierwagen⁶, CharlotteWouters⁷, MosbahNofal⁷, MartinAlbrecht⁷, JackSwallow⁸, LeanneJones⁸, PardeepThakur⁹, Tien-LinLee⁹, CurranKalha¹, ChristophSchlueter¹⁰, TimVeal⁸, JoelB. Varley¹¹ and MarkusWagner^{4,6}; ¹University College London, United Kingdom; ²University of Bristol, United Kingdom; ³Saga University, Japan; ⁴Technische Universität Berlin, Germany; ⁵Otto von Guericke Universität Magdeburg, Germany; ⁶Paul-Drude-Institut für Festkörperelektronik, Germany; ⁷Leibniz Institute for Crystal Growth, Germany; ⁸University of Liverpool, United Kingdom; ⁹Diamond Light Source, United Kingdom; ¹⁰DESY, Germany; ¹¹Lawrence Livermore National Laboratory, United States

Ga₂O₃ is a key ultra-wide band gap oxide offering a rich structural space, with a number of accessible polymorphs. Its most stable form is monoclinic β-Ga₂O₃, but other polymorphs, including hexagonal α-Ga₂O₃, cubic γ-Ga₂O₃, and orthorhombic ε(κ)-Ga₂O₃, are of increasing interest. Although this wealth of possible structures opens opportunities to control and tune structure, electronic structure, and ultimately physical characteristics, the polymorphs beyond β-Ga₂O₃ remain comparatively unexplored. Experimental results are particularly scarce due to current limitations in producing high-quality materials and the lack of theoretical results for the more structurally complex polymorphs.

This study presents an in-depth exploration of the relationship between local coordination environments and the electronic structure of the α, β, γ, and ε(κ) polymorphs of Ga₂O₃. The samples investigated are either bulk single crystals or epitaxial films grown using molecular beam epitaxy (MBE) or atomic layer deposition (ALD), selecting the highest quality samples available for each of the polymorphs. We report high-resolution valence band spectra from soft and hard X-ray photoelectron spectroscopy (SXPS and HAXPES) which are directly compared to theoretical partial and total electronic densities of states as calculated within the framework of density functional theory (DFT). Both deep and shallow core level spectra are also compared to DFT results to explore the influence of structure, rather than solely the oxidation state, on the core level behavior. X-ray absorption spectroscopy (XAS) is used to probe the unoccupied states and in combination with SXPS is used to gain an estimate of the changes in the band gaps of the polymorphs. For the highly disordered γ-Ga₂O₃ polymorph, we combine DFT with machine learning to screen one million potential structures of γ-Ga₂O₃ to develop a robust atomistic model. We can clearly show that only the lowest energy structural models are able to describe the experimental results from SXPS and HAXPES, providing a new avenue to understand disordered oxides.

Ultimately, this work presents a systematic and comprehensive study of the electronic structure of Ga₂O₃ polymorphs, providing an insight into electronic trends and their relationship to crystal structure. This comparative study helps to discern trends between the different structures and advances our understanding of this polymorphic material. It lays the foundation for further exploration of Ga₂O₃ in applications beyond its β phase.

4:15 PM EL11.05.08

The nitrogen vacancy (NV-) center in diamond is a prototypical spin defect with favorable properties, such as long coherence times, and optical addressability and readout. However, the drawbacks of this defect, including incompatibility with telecommunication fiber optics infrastructure and manufacturing challenges, continue to prompt investigations into other host material systems. Recent predictions [1] suggest that several oxides, including CeO₂, CaO, and MgO, may possess long coherence times and thus could serve as promising hosts for quantum applications. However, the defects in these oxide hosts that exhibit such long coherence times are yet to be identified. By leveraging a high-throughput first principles workflow [2], we have identified that MgO and CaO can host NV-like centers with promising electronic and optical properties. Using first principles methods including constrained occupation density functional theory and time-dependent density functional theory [3], we report that these defects have a stable spin triplet state and report their absorption, emission, and zero-phonon lines. Interestingly, we also find that strain can tune the excited state potential energy surface of these defect, changing their optical transition energies and ionic displacements by altering the interaction with higher energy excited states. This work provides crucial insight into point defects in a class of promising oxide host materials for quantum applications, as well as points to routes to further engineer them through strain.

- [1] Shun Kanai, et al. "Generalized scaling of spin qubit coherence in over 12,000 host materials." Proceedings of the National Academy of Sciences 119.15 (2022): e2121808119.
[2] Joel Davidsson, et al. "ADAQ: Automatic workflows for magneto-optical properties of point defects in semiconductors." Computer Physics Communications 269 (2021): 108091.
[3] Yu Jin, Marco Govoni, and Giulia Galli. "Vibrationally resolved optical excitations of the nitrogen-vacancy center in diamond." npj Computational Materials 8.1 (2022): 238.

4:30 PM EL11.05.09

Efficient and Accurate Calculations of Electronic Excited States of the Negatively Charged NV-Center in Diamond Hannes Jonsson; University of Iceland, Iceland

Electronic structure calculations of the properties of ultra-wide-bandgap materials and the effect of dopants in such materials can play an important role in the development of high-performance devices for e.g. quantum information science and ultraviolet optoelectronic emitters and detectors. Results of calculations based on the most commonly used method for electronic structure calculations of solids, density functional theory (DFT), reported in the literature on one of the most commonly used systems, the negatively charged NV-center in diamond, have been contradictory and controversial, leaving the impression that much more computationally intensive methods are needed to get accurate results [1]. This applies in particular to the excited states of the defect relevant for optical generation a pure spin state where DFT calculations from different groups have not even agreed on the ordering of the relevant energy levels, the two excited singlet states and the first excited triplet state. A new approach for calculating excited electronic states using density functionals based on direct optimisation and convergence on saddle points on the energy surface [2,3] has, however, been found to give remarkably close results to 'beyond RPA' embedding calculations and experimental data [4]. This is an important result as it opens the door for large scale, reliable calculations of other doped ultra-wide-bandgap materials without excessive computational effort. The approach presented makes calculations of excited states in materials similar in computational effort as ground state DFT calculations.

- [1] Churna Bhandari, Aleksander L. Wysocki, Sophia E. Economou, Prathiba Dev, and Kyung-wha Park, "Multiconfigurational study of the negatively charged nitrogen-vacancy center in diamond", Phys. Rev. B 103, 1 (2021).
[2] A. V. Ivanov, G. Levi, E. Ö. Jónsson and H. Jónsson, "Method for Calculating Excited Electronic States Using Density Functionals and Direct Orbital Optimization with Real Space Grid or Plane-Wave Basis Set", J. Chem. Theory Comput. 17, 5034 (2021).
[3] A. V. Ivanov, Y. L. A. Schmerwitz, G. Levi and H. Jónsson, "Electronic Excitations of the Charged Nitrogen-Vacancy Center in Diamond Obtained Using Time-Independent Variational Density Functional Calculations", SciPost Physics scipost_202303_00008v1 (2023).
[4] He Ma, Marco Govoni, and Giulia Galli, "Quantum simulations of materials on near-term quantum computers", npj Computational Materials 6, 85 (2020).

4:45 PM EL11.05.10

Theory of Optically Detected Magnetic Resonance of a Silicon Vacancy in Silicon Carbide David Fehr and Michael E. Flatte; University of Iowa, United States

Optically detected magnetic resonance (ODMR) is one tool that can be used to probe the spin character of optically-active color centers in a nondestructive manner, with applications including the identification of radiation-induced defects in semiconductors and quantum magnetometry [1,2]. In ODMR, a color center is optically pumped while a Zeeman magnetic field is swept and the resulting photoluminescence (PL) is measured on a detector. A microwave field is also applied to induce resonant Rabi oscillations, seen as extrema in the PL contrast, and creates a characteristic and reproducible curve. A detailed and fully quantitative simulation of the ODMR of a color center would provide confidence that the foundations of nonequilibrium optical and spin dynamics relevant for ODMR are sufficiently understood, while allowing for the extraction of reliable parameters for spin coherence times, optical transition rates, and microwave coupling strengths.

In this work we simulate room-temperature ODMR of the negatively charged silicon vacancy V_{Si}^- V(2) site in 6H-SiC, an emerging candidate for quantum magnetometry, using Lindblad master equations and density matrix populations and compare with experimental results [2]. V_{Si}^- in 6H-SiC ODMR can be described as a synthetic atom with $S=3/2$ ground and excited spin manifolds, separated by 1.397 eV, and a metastable state in the energy gap between these manifolds [2,3]. The Hamiltonian of each spin manifold can be divided into terms which cause coherent transitions between states and subsequent resonances, the magnetic and electric components of the microwave field, and terms that dictate the positions of the resonances, the Zeeman field and zero field splitting. In ODMR the ground and excited spin manifolds are coupled via absorption, spontaneous emission, and nonradiative pathways through the metastable state and we simulate these processes, as well as pure dephasing, with a Lindblad master equation [4]. Using the steady-state solution of the master equation and excited manifold density matrix populations, we calculate ODMR curves to compare with experimental results [2].

Through comparison of our calculations with experimental results [2], we show that a vast amount of information is contained in a single ODMR curve. By fitting our model to experimental results [2] we are able to extract spin Hamiltonian parameters such as zero field splitting, g-factors, microwave electric and magnetic field strengths, Stark coupling coefficients [5], and hyperfine couplings. We are also able to extract absorption, spontaneous emission, and intersystem crossing rates as well as coherence times T_2^* . Finally, we stress the flexibility of these calculations and their natural extension to ODMR theories of other color centers and polytypes of SiC, and their natural extension to color centers in other wide or ultra-wide bandgap materials, which would be desirable for quantum sensing applications or radiation-induced defect identification.

We acknowledge support from NSF DMR-1921877 and AFOSR MURI "REDESIGN".

- [1] Kraus, H., Soltamov, V., Fuchs, F. et al. Magnetic field and temperature sensing with atomic-scale spin defects in silicon carbide. *Sci Rep* 4, 5303 (2014).
[2] Kraus, H., Soltamov, V., Riedel, D. et al. Room-temperature quantum microwave emitters based on spin defects in silicon carbide. *Nature Phys* 10, 157–162 (2014).
[3] Biktagirov, T., Schmidt, W., Gerstmann, U. et al. Polytypism driven zero-field splitting of silicon vacancies in 6H-SiC. *Physical Review B* 98, 195204 (2018).
[4] Breuer, H. and Petruccione, F. The Theory of Open Quantum Systems. Vol. 9780199213900. Oxford: Oxford University Press, (2007).
[5] Falk, A., Klimov, P., Buckley, B. et al. Electrically and Mechanically Tunable Electron Spins in Silicon Carbide Color Centers. *Physical Review Letters* 112, 187601, (2014).

SESSION EL11.06/EL14.09: Joint Session III: Diamond Doping and Electronic Devices
Session Chairs: Stephen Goodnick and Lionel Rousseau
Wednesday Morning, November 29, 2023
Hynes, Level 2, Room 210

8:00 AM *EL11.06/EL14.09.01

Diamond P-i-N and Schottky P-i-N Diodes for High Power Limiters Josephine Chang¹, Harshad Surdi², Mason Bressler¹, Franz Koeck², Bryce Winters¹, Stephen M. Goodnick², Trevor Thornton² and Robert J. Nemanich²; ¹Northrop Grumman Corporation, United States; ²Arizona State University, United States

Diamond P-i-N and Schottky P-i-N diodes are a promising new technology for high power limiters. Receivers, solid-state amplifiers, and detectors commonly use P-i-N and/or Schottky

diodes for protection from high power incident signals. Limiters reflect the majority of excess RF power, but inevitably absorb some portion of the incoming power as well. As dissipated power converts to heat, the thermal impedance and temperature resilience of the limiter diode becomes the primary factor determining device lifetime, reliability, and power handling. Si and GaAs-based P-i-N and Schottky diodes and even SiC-based Schottky diodes suffer non-recoverable thermal overload upon excess power dissipation. Diamond, by contrast, offers superior thermal conductivity and temperature resilience. Diamond also provides good charge carrier mobility and high electric breakdown field making it an ideal material for next generation high power RF limiters.

Power limiter circuits frequently rely on solid-state P-i-N and/or Schottky diodes to act as a protective buffer for microwave components that are susceptible to damage from high-power signals. Limiters must transmit low power signals with minimal attenuation or distortion, while attenuating high power signals so as not to exceed a prescribed maximum. While solid state power limiters offer the advantages of a long operating life, small size, and flexible use, including integration with other MMIC components, they often require a pre-limiter stage due to limitations in power handling and spike leakage. Diamond diodes with high power handling and low spike leakage promise to eliminate the need for a pre-limiter stage by offering significantly enhanced power handling and reduced spike leakage.

In a shunt-connected diode power limiter circuit, the diode remains off for low input signals, with any diode off-capacitance (C_{off}) contributing to insertion loss (attenuation of low power signals) and limiting the frequency bandwidth. When the magnitude of the input signal exceeds a threshold, the shunt-connected diode turns on. In the on state, the diode acts as a short to ground, resulting in reflection of most incoming RF power. However, on-resistance (R_{on}) in the diode results in dissipation of some portion of incident power through the limiter circuit. As incident power increases, the power absorbed by the power limiter circuit increases as well. Device overheating from this dissipated power is the primary failure mechanism that sets the maximum power handling of a diode. Using a larger diode can increase power handling at the expense of greater C_{off} and thus greater insertion loss.

The cutoff frequency figure of merit captures the tradeoff between C_{off} and R_{on} , and can serve as a useful metric for evaluating the suitability of limiter device technologies for RF applications. Commercially available high power Si P-i-N diodes have an F_{CO} of around 700GHz. The F_{CO} figure of merit, however, does not account for the power dissipation capability of a device. Two devices with the same F_{CO} may dissipate the same power under the same incident conditions, but if one device can handle a greater heat load, it will have better power handling. Therefore, fabricating diodes in a material such as diamond offers a route to dramatically increasing power handling without insertion loss penalty. Compared to the conventional materials systems used for diodes—including Si, GaAs, and SiC—diamond offers over 20x higher thermal conductivity and 2-3x higher maximum operating temperature. While significant material growth and processing challenges remain before diamond matures as an electronics material, the advent of single-crystal substrates and breakthroughs in bipolar dopant incorporation have spurred rapid advances in recent years. If diamond diodes can be achieved with F_{CO} of several hundred GHz, they could be a viable high power-handling alternative for the Si or GaAs diodes in use today.

8:30 AM EL11.06/EL14.09.02

Improved Nitrogen-Doped Diamond Photoconductivity by Electrode Design KellyWoo, MohamadaliMalakoutian, BhawaniShankar and SrabantiChowdhury; Stanford University, United States

In photoconductive semiconductor switches (PCSS), the conductance between two terminals on a semiconductor is modulated by the absorption of optical radiation in the gap between the electrodes. This switching device can be applied to pulsed power technology for high speed and jitter free switching. These may include radar, particle acceleration, and pulsed high-power lasers. More recently, as we move towards electrification of the grid, trigger isolation enabled by PCSSs may enable safer mechanisms for making and breaking high power circuits as well. However, typical materials studied for photoconductive switching, such as Si and GaAs suffer from thermal runaway effects at high power [1]. Since diamond is an ideal material for high power electronics due to its large bandgap (5.47 eV), high breakdown electric field (10 MV/cm), high carrier mobility, high thermal conductivity (10-20 W/cm.K), and low coefficient of thermal expansion (~1.1um/mK) [2], we chose to study its photoconductive properties and potential as a high power optoelectronic switch.

Past studies have shown photoconductivity in intrinsic diamond by UV-band excimers in high electric fields up to 2 MV/cm [3]. In our devices, however, we utilize nitrogen doped substrates to excite carriers by sub-bandgap photon energies while maintaining the desirable properties of diamond that would facilitate higher breakdown field and better thermal management [4]. In this case, a lower energy, a below bandgap Vis-NIR excitation source is sufficient, which increases the feasibility of PCSS integration. In designing extrinsic PCSS, on/off current ratios should be maximized for high performance switching. In the off state, the material conductance primarily depends on the number of ionized dopants, which is very low in the case of nitrogen doped diamond due to the high activation energy. In the on state, the conduction is increased due to the photogeneration of free carriers through ionization of dopants and traps. In this work, we aim to increase the on-state conductivity by using different metal electrode stacks on both lateral and vertical PCSS configurations. In the vertical configuration, we also aim to demonstrate the higher power capabilities of an extrinsic diamond PCSS.

Testing of the extrinsic diamond PCSS was performed by optically exciting with a frequency doubled Nd:YAG pulsed laser (532 nm) with an output energy of <1 mJ and a full width half maximum (FWHM) of 10 ns. The nitrogen diamond HPHT substrates from Element Six had an average doping concentration on the order of 10^{19} . Our experiments have shown pulsed photoresponses with FWHMs like those of the laser pulse itself, thus nanosecond order rise and fall times were observed. Two different contact stacks were tested: Ti/Pt/Au and Ti/ITO. Because a thin Ti adhesion layer was used, the Ti/ITO contact was measured to be transparent to 532 nm light. In vertical PCSS devices, the on state current was observed to be as much as 70% higher when using Ti/ITO instead of Ti/Pt/Au. This is due to the reduced shadowing effect by opaque contacts and reduced contact resistance by the photogeneration of carriers beneath the contacts. Furthermore, the devices were tested up to biases of 500 V across a drift region of 300 um, resulting in >0.8 A peak photocurrent and showed no signs of breakdown. Through this study, Ti/ITO was established as an effective contact metal for high power PCSS applications, which can be further developed and optimized for higher performance.

This work was supported by ULTRA, an Energy Frontier Research Center funded by the U.S. DOE.

[1] S. Feng, et al., IEEE Transactions on Electron Devices, 37, 12, 2511-2516, (1990).

[2] Tsao, J. Y., et al., Adv. Electron. Mater., 4, 1600501 (2018).

[3] Yoneda, H., et al., Appl. Opt. 40, 6733-6736 (2001)

[4] Woo K., et al., Appl. Phys. Lett. 120, 112104 (2022).

8:45 AM EL11.06/EL14.09.03

Formation of Ohmic Contacts to (001) Diamond with Nitrogen-Doped Nanocarbon Surface Layers EvangelineAmonoo, VishalJha, TrevorThornton, FranzKoeck, RobertJ. Nemanich and TerryL. Alford; Arizona State University, United States

The electrical properties of Ohmic contacts (*i.e.*, the specific contact resistance) was investigated using the transfer length method (TLM). In this study, the TLM method was employed to analyze the properties of Ohmic contacts using a tri-layer stack of Ti/Pt/Au contacts on a nitrogen-doped n-type conducting nanocarbon (nanoC, Patent No.: US 11,380,763 B2) epitaxial film grown on a (001) diamond substrate. Samples were annealed to monitor any changes in electrical conductivity and specific contact resistance values between the electrode and the nanoC layer were $8 \times 10^{-5} \Omega \text{cm}^2$. This is significantly lower than previously reported values by almost two orders of magnitude. The improved contact resistivity was attributed to two factors. Firstly, the increased amount of nitrogen incorporation into the nanocarbon film enhanced the electrical conductivity. Nitrogen doping also introduced additional charge carriers, improving conduction properties in the nanocarbon layer. Secondly, the presence of electrically active defects in the film further contributed to the increase in conduction. These findings demonstrate the potential for improved Ohmic contacts in nanocarbon-based electronic devices, offering opportunities for enhanced performance.

9:00 AM *EL11.06/EL14.09.04

Schottky Barrier Diodes Based on B-Doped Single Crystal Diamond Films – An Experimental and Theoretical Methodology KenHaenen^{1,2}; ¹Hasselt University, Belgium; ²IMEC vzw, Belgium

The growth of high quality heavily (p+) B-doped single crystal diamond (SCD) layers is prerequisite for the successful realisation of diamond-based high-power electronics. This presentation will zoom in on a combined experimental and theoretical approach of the impact of methane concentration on the deposition of heavily boron-doped (p+) single crystal diamond (SCD), in turn influencing the performance of Schottky barrier diodes based on said layers.

Using (100)-oriented high-pressure high-temperature substrates, optimized CVD growth conditions led to ~ 1.6 μm lightly B-doped (p-) SCD films with an acceptor concentration of $(1.0 \pm 0.5) \times 10^{16} \text{ cm}^{-3}$ on top of the p+ layers [1]. To fabricate pseudo-vertical Schottky barrier diodes, Ohmic and Schottky contacts were sputtered on the p+ and p- layers, respectively.

It was already observed that the forward operation current of the diodes increased proportionally with increasing [CH₄]/[H₂] ratio (from 0.5 % to 3 %) used for the CVD of p+ layer. This increase in current is associated with an increase in the doping level of the p+ layers, a direct result of the increase of CH₄ concentration in the CVD plasma [1]. The Schottky barrier height and ideality factor of the diodes were determined and compared with theoretical calculations, where an ideal diode (n = 1) with a barrier height variation over the Schottky diode area agreed reasonably well with our experimental results. The diodes fabricated on samples with the p+ layers grown at higher [CH₄]/[H₂] behaved similarly, except for their non-ideality (n > 1) [2]. To conclude, the voltage-dependent ideality factor of the Schottky diodes will be discussed.

References

[1] R. Rouzbahani, et al., Carbon 172 (2021), 463-473.

9:30 AMBREAK

SESSION EL11.08/EL14.11: Joint Session V: Diamond Electrochemical Devices
Session Chairs: Robert Bogdanowicz and Julien Pernot
Wednesday Afternoon, November 29, 2023
Hynes, Level 2, Room 210

1:30 PM *EL11.08/EL14.11.01

Electrochemical Application of Boron-Doped Diamond Electrodes—Electrochemical Sensors and CO₂ Reduction Yasuaki Einaga; Keio University, Japan

Boron-doped diamond (BDD) electrodes are very attractive material, because of their wide potential window, low background current, chemical inertness, and mechanical durability.[1] In these years, we have reported several examples for electrochemical sensor applications including novel microsensing systems for in vivo real time detection of local drug kinetics.[2] Furthermore, applications for electrochemical organic synthesis[3] and electrochemiluminescence (ECL) systems[4] are also reported. Here, recent developments on electrochemical CO₂ reduction using BDD electrodes are presented. In 2018, we investigated the electrochemical reduction of CO₂ in a flow cell using BDD electrodes. The faradaic efficiency (FE) for the production of HCOOH was as high as 94.7%. Furthermore, the selectivity for the production of HCOOH was more than 99%. The rate of the production was increased to 473 $\mu\text{mol m}^{-2}\text{s}^{-1}$ at a current density of 15 mA cm⁻² with a FE of 61%. The FE and the production rate are almost the same as or larger than those achieved using Sn and Pb electrodes. In addition, the stability of the BDD electrodes was confirmed by 24 hours operation.[5] Then, in 2019, we were able to control the selectivity and efficiency with which carbon monoxide (CO) is produced by optimizing certain parameters and conditions used in the electrochemical process with BDD electrodes, such as the electrolyte, the boron concentration of the BDD electrode, and the applied potential. With a BDD electrode with 1% boron used for the cathode and KClO₄ for the catholyte, the selectivity for producing carbon monoxide was high. On the other hand, with a BDD electrode with 0.1% boron used for the cathode and KCl for the catholyte, the production of formic acid was the most evident. *In-situ* ATR-IR measurements during electrolysis showed that CO₂ anion radical intermediates were adsorbed on the BDD surface in the KClO₄ aqueous solution. Here, switchable product selectivity was achieved when reducing CO₂ using BDD electrodes.[6] Recently, in order to operate on a large scale for industrial applications, an intermittent flow cell system was presented. A stop-start motion of the flow conditions in the intermittent cell was created using a piston pump, and this considerably increases the rate of electrochemical conversion of CO₂ to HCOOH compared to a continuous flow system.[7] Furthermore, we found that an initial electrochemical CO₂ reduction reaction could significantly improve the reaction current and Faradaic efficiency of the CO₂ reduction on BDD electrodes.[8] The effect is referred to as the “self-activation” of BDD. Here, the mechanisms and the effect of self-activation is discussed.

References

- [1] (a) “Diamond Electrodes”, Springer Nature (2022). (b) Bull. Chem. Soc. Jpn. 91, 1752 (2018).
- [2] Nature Biomed. Eng. 1, 654 (2017).
- [3] Angew. Chem. Int. Ed. 51, 5443 (2012).
- [4] (a) J. Am. Chem. Soc. 138, 15636 (2016). (b) J. Am. Chem. Soc. 142, 1518 (2020).
- [5] Angew. Chem. Int. Ed. 57, 2639 (2018).
- [6] J. Am. Chem. Soc. 141, 7414 (2019).
- [7] ACS Sustainable Chem. Eng. 9, 5298 (2021).
- [8] JACS Au 2, 1375 (2022).

2:00 PM EL11.08/EL14.11.02

High Production of Hydrogen Peroxide from Carbonated Water Through Electrochemical Synthesis by Boron-Doped Diamond Yusuke Tatsumi¹, Andrea Fiorani¹, Irkham Irkham² and Yasuaki Einaga¹; ¹Keio University, Japan, Japan; ²Universitas Padjadjaran, Indonesia

Introduction H₂O₂ is recognized as a powerful oxidizing, bleaching and water treatment agent. It attracts great interest as a green oxidant because it decomposes to water and oxygen. Most of H₂O₂ is nowadays produced by large-scale anthraquinone auto-oxidation (AO) process, but recently efforts have been made to establish alternative synthetic strategies, because AO process employs anthraquinone, known as a carcinogen, in addition to organic solvents. Electrochemical methods offer some advantage, such as direct synthesis in aqueous electrolytes, and oxygen and water as starting reagents. The boron-doped diamond (BDD) electrode is physically and chemically stable, and it is known for its specific electrochemical property to produce OH radical easily¹. For the purpose of analytical applications, we previously demonstrated that BDD electrode can produce H₂O₂ from water oxidation. Here, we focused our attention on the optimization of H₂O₂ production on BDD.

Experimental Electrochemical experiments were conducted in a two-chamber cell separated by a Nafion membrane with a three-electrode setup (working electrode and counter electrode: BDD with 1% B/C ratio, reference electrode: Ag/AgCl). H₂O₂ was produced by electrochemical oxidation in chronoamperometry (CA) at 2.5 V. We investigated the effect of electrolyte solution on the H₂O₂ production by comparing the electrolyte salt (phosphate and carbonate), and by pH variation. H₂O₂ was detected by UV-visible spectrophotometry after the reaction with KMnO₄.

Results & Discussion CA was conducted for 2 hours in 1 M KHCO₃ and 1 M K₂CO₃ aqueous solution respectively as the anolyte, and time production was compared. The maximum production was 16.8 $\mu\text{mol cm}^{-2}$, whereas it was 118 $\mu\text{mol cm}^{-2}$ with K₂CO₃. This suggests that CO₃²⁻ anion was superior to HCO₃⁻ anion for H₂O₂ formation. Due to their equilibrium between CO₃²⁻ and HCO₃⁻, the ratio of their presence changes with pH. To verify the contribution of CO₃²⁻ to increased H₂O₂ production, 1 M KHCO₃ solution and 1 M K₂CO₃ solution were mixed to reach the desired pH. CA performed from pH 8 to 12 demonstrated that the amount of H₂O₂ production increased concurrent to the CO₃²⁻ fraction. To confirm whether this was due to the effect of the basic solution or carbonate ions, hydrogen peroxide production was conducted either by using 1 M K₂CO₃ or 1 M K₃PO₄ solutions (pH 11.9 and 12.9, respectively), and it was found that only the K₂CO₃ solution produced hydrogen peroxide. Concerning the mechanism, our laboratory suggested that OH radicals generated by electrochemical oxidation of OH⁻ on BDD oxidized CO₃²⁻ to C₂O₆²⁻, that reacts with water finally producing hydrogen peroxide by hydrolysis.^{2,3} Hydrogen peroxide formation in this work can be considered to have proceeded by a similar reaction pathway. In addition to the BDD electrode, glassy carbon (GC), fluorinated tin oxide (FTO), and Ni electrodes were used in a 2-hour electrolysis to compare the time dependence of hydrogen peroxide production. The results showed that BDD >> GC > FTO > Ni. Characterization of GC and BDD by SEM after electrolysis demonstrated that the surface of GC electrode was clearly damaged and corroded, while BDD did not reveal any apparent change confirming the high stability of BDD surface. From these results, we demonstrated that BDD can be used profitably to synthesize hydrogen peroxide with a high production rate from aqueous solutions containing carbonate.

References

- P-A. Michaud, *et. al.*, *J. Appl. Electrochem.*, **2003**, 33, 397.
- Irkham, *et. al.*, *J. Am. Chem. Soc.*, **2020**, 142, 1518.
- Irkham, *et. al.*, *Anal. Chem.*, **2021**, 93, 2336.

2:15 PM EL11.08/EL14.11.03

Ammonia Synthesis by Electrochemical Reduction of Nitrate Anion using Boron-Doped Diamond Electrode Satoru Kuramochi, Andrea Fiorani and Yasuaki Einaga; Keio University, Japan

Introduction Ammonia is currently in great demand as fertilizer or as industrial raw material, however environmental pollution caused by reactive nitrogen species emitted from factories and agricultural wastewater might be an issue. ⁽¹⁾ This is in fact true for nitrate, one of the reactive nitrogen species. Therefore, electrochemical nitrate reduction which produces ammonia is a twofold attracting method: 1) abatement of pollutant (nitrate), and 2) highly useful product (ammonia). In addition, it works under mild conditions. Currently, several metal electrodes and many highly complexed catalysts have been reported for electrochemical nitrate reduction. ⁽²⁾ On the other hand, we focused our attention on boron-doped diamond (BDD) electrodes, which have the advantages to be metal-free and a simple bulky material lend high durability to BDD. Therefore, the objective of this study is to generate ammonia by electrochemical nitrate

reduction by using BDD electrodes.

Experimental The working electrode was a BDD electrode which was fabricated by Microwave Plasma assisted Chemical Vapor Deposition method, the counter electrode was a platinum plate, the reference electrode was a Ag/AgCl KCl saturated, and the electrolyte was sodium nitrate in water. The optimum potential was determined by performing 1-hour potentiostatic reduction in a cell divided by a Nafion membrane. The mass transport effect on ammonia production was determined by changing the cell setup and stirring conditions. The effect of pH and the composition of the supporting electrolyte (e.g., sodium hydroxide concentration) on the Faradaic efficiency of ammonia production was also investigated. In addition, the time dependence of ammonia production by electrochemical nitrate reduction was measured over several hours. Ammonia, nitrite and nitrate were quantified by spectrophotometric method.

Results & Discussion The results of constant potential reduction in a divided flow cell showed that ammonia production and Faradaic efficiency were highest at -1.8 V vs. Ag/AgCl. Comparing Faradaic efficiencies by cell and stirring conditions, the divided batch cell with stirring had the highest ammonia production and Faradaic efficiency. This is because the products are not oxidized at the counter electrode in a divided batch cell and the reduction of nitrate anions is diffusion-controlled reaction. When the pH was changed in a phosphate buffer electrolyte, the ammonia Faradaic efficiency was around 70-80% regardless of the pH, without a significant difference. On the other hand, raising the concentration of the supporting electrolyte, in this case sodium hydroxide, increased the Faradaic efficiency of ammonia production. In particular, the ammonia production Faradaic efficiency reached 96.4% when 0.1 M sodium nitrate solution was added of 1 M sodium hydroxide. We found a positive correlation between concentration of sodium hydroxide and charge transfer resistance. During the several hour reduction in 0.1 M sodium nitrate solution, ammonia production was slower than nitrite production at the beginning, but as time progressed, the amount of ammonia production increased while that of nitrite production leveled off. This result suggests that ammonia production by electrochemical nitrate reduction includes sequential reactions. During the 6 hours reduction in 0.1 M sodium nitrate solution added with 1 M sodium hydroxide solution, ammonia production was faster than nitrite production. This result suggests that high concentration of sodium hydroxide promote nitrite reduction to ammonia.

(1) P. H. Langevelde, I. Katsounaros, and M. T. M. Koper, *Joule*, **2021**, 5, 290-294.

(2) W. Chen, X. Yang, Z. Chen, Z. Ou, J. Hu, Y. Xu, Y. Li, X. Ren, S. Ye, J. Qiu, J. Liu, and Q. Zhang, *Adv. Funct. Mater.* **2023**, 2300512.

2:30 PMBREAK

SESSION EL11.09: Optoelectronics
Session Chairs: Jack Flicker and Robert Kaplar
Wednesday Afternoon, November 29, 2023
Hynes, Level 2, Room 210

3:30 PM EL11.09.01

High-Temperature Annealed Al(Ga)N Templates Deposited by PLD for Optimized Epitaxial Growth of UV-C LEDs Kevin Guy¹, Aly Zaiter², Mathieu Bernard¹, Julien Brault², Jean-Yves Duboz², Guy Feuillet¹ and Florian Dupont¹; ¹University Grenoble Alpes, CEA, LETI, France; ²Centre de Recherche sur l'Hétéro-Epitaxie et ses Applications, CNRS, France

UV-C LEDs are intended to replace Hg-based UV lamps in sterilization and bacterial/viral decontamination systems. UV-C LEDs are currently not efficient enough to consider their use on a large scale, due to a poor external quantum efficiency up to 10%. One of the main issues concerns the high dislocation density in the epitaxial Al(Ga)N layers constituting the active layers of the diode. Using Al(Ga)N templates instead of regular AlN templates could be a solution to increase UV-C LEDs efficiency.

This work focuses on the realization of cost-effective Al(Ga)N templates on sapphire by low-temperature sputtering and PLD (Pulsed Laser Deposition). For the first time, AlGaN layers are deposited directly on sapphire substrates by PLD. A great effort has been made to optimize both the deposition conditions and the substrate preparation. Al(Ga)N templates were characterized by XRD (X-Ray Diffraction), AFM (Atomic Force Microscopy) and SEM (Scanning Electron Microscopy). The pros and cons of sputtering and PLD will be discussed by comparing the roughness and the crystallinity of Al(Ga)N templates. The high temperature face-to-face annealing technique is used to strongly increase the crystallinity of the materials. Modifying the annealing temperature and atmosphere can greatly affect the surface morphology and the roughness of Al(Ga)N, which is of great interest for the subsequent growth of UV-C LEDs.

This work is part of the LABEX GANEXT, and realized in close collaboration between CEA-Leti (Grenoble) and CNRS-CRHEA (Valbonne).

3:45 PM EL11.09.02

Self-Powered DUV Photodetectors and Their Emerging Applications Taehyun Park and Hocheon Yoo; Gachon University, Korea (the Republic of)

Among the various range of ultraviolet rays (400 nm – 10 nm), the deep ultraviolet (DUV) region (280 nm – 200 nm) has been recently spotlighted in risk factor monitoring, chemical, and biological sensing fields owing to its specific light-matter interaction in biomaterials, noise-free detection based on solar blindness, and limited environmental generation conditions including partial discharge, missile plume, and flame. However, there are still challenges to using DUV photodetectors (PDs) in practical applications mentioned above as follows. First, material selection with appropriate energy bandgap, and cost-effectiveness for large-scale fabrication is limited. Second, efficient DUV transparent electrodes to reduce the transmittance loss are absent. Third, high-power consumption issues during the operation limit the use of DUV PDs as a unit sensor of the comprehensive range monitoring system. Here, we introduce our recent efforts implementing cost-effective solution-processed self-powered DUV PDs by systematic strategies including widened energy bandgap through size modulation to quantum dots, synthesizing ultra-wide bandgap oxide semiconductors with great stability, and controlling junction characteristics for effective self-powered operation. We also present our representative DUV PDs-based emerging applications: (i) partial discharge detection [1], (ii) flame sensing for fire monitoring [2], and (iii) blood component identification [3] through facile, and real-time optoelectronic approach. By introducing comprehensive strategies for solution-processed self-powered DUV PDs, this talk suggests the significance and future aspects of the DUV PDs for various emerging applications.

References

- [1] Park, Taehyun, and Jaehyun Hur. "Self-powered low-cost UVC sensor based on organic-inorganic heterojunction for partial discharge detection." *Small* 17.28 (2021): 2100695.
- [2] Park, Taehyun et al. "Calcium Titanate Orthorhombic Perovskite-Nickel Oxide Solar-Blind UVC Photodetectors with Unprecedented Long-Term Stability Exceeding 500 Days and Their Applications to Real-Time Flame Detection." *ACS Photonics* (2022).
- [3] Park, Taehyun, et al. "Facile, Real-Time Identification of Blood Components with Self-Powered Organic-Inorganic Heterostructure Photodetectors." *Advanced Optical Materials* 10.7 (2022): 2102542.

4:00 PM EL11.09.03

Reliability Investigation on 265 nm UV-C LEDs from a Commercial Point of View Francesco Piva, Matteo Buffolo, Carlo De Santi, Gaudenzio Meneghesso, Enrico Zanoni, Matteo Meneghini and Nicola Trivellin; University of Padova, Italy

The reliability of ultraviolet light-emitting diodes (UV LEDs) has acquired relevant importance over the last few years, thanks to increasing requests for disinfection systems, particularly against the Sars-CoV-2 virus. For this reason, it is important to understand how these LEDs perform over time, to identify the criticalities that system designers had to consider. UV-C LEDs are the perfect solution as a UV light source because they are smaller, lighter, with a faster start-up, and environmentally friendly with respect to the classical mercury-based UV lamp. However, these LEDs do not have the same performance as their visible counterparts, showing a still limited lifetime and a low emitted optical power. In this work, we studied four interesting devices found on the market, with a nominal emitting wavelength of 265 nm and promising electrical-optical characteristics and lifetimes. We carried out accelerating lifetime tests on each sample, choosing as stress current their absolute maximum reported in the datasheet, and evaluating their electrical (J-V), optical (L-J) and spectral (PSD-J) characteristics.

From the characteristic characteristics, we found: (i) an increase in subthreshold leakage current in all devices, corresponding to an increase in parasitic conduction paths in the active region associated with an increase in defect generation. (ii) The high operating voltages, from 6 to 8 V, implied elevated power dissipation over time, which led to a fast decrease in optical power. (iii) To provide useful data for the design phase, we extrapolated the junction temperatures, obtaining values from 44 to 84 °C.

Optical characteristics represented an interesting turning point: two devices reached an L90 higher than 140 h, and three of them presented an L70 of at least 650 h. Just one LED showed a limited L70 of 190 h, aligned with classical results reported in the literature. It is interesting to note that one LED does not show significant degradation after 330 h of stress test, caused by a conservative choice of the manufacturer, which indicated an absolute maximum current density much lower with respect to the other devices. For this reason, we decided to exclude this sample from the following analyzes. In terms of emitted optical power, a LED (called LED S) distinguished itself from the others by an OP an order of magnitude higher at the same current density, although it was not the best for lifetime duration.

To conclude our analyses, we decided to compare the most promising LED with emitting wavelength of 265 nm with the most promising LED at 275 nm, studied in previous tests. From the J-V comparison, we noted similar behaviors, with a lower turn-on voltage for the 265 nm device; OP-J followed similar trends, with a higher optical recovery for the 275 nm LED, which implies a slightly longer lifetime. Instead, PSD-J characterization highlighted the same parasitic spectral peaks in both samples, suggesting similar issues in structure optimization. Other interesting results came when we compared the total number of doses to disinfect the Covid-19 virus that an LED can provide during its lifetime. Considering a dose of 3 mJ/cm², the best 265 nm LED can provide double doses with respect to the 275 nm LED, but their cost is higher, due to the elevated cost of the device. In fact, normalizing these results for device expense, we found that 275 nm LED is the right choice for a disinfection system. But both results are outdated if we consider LED S: despite its lower lifetime, the higher total emitted optical power allowed it to provide 6.5 times the number of doses per LED with respect to the best 265 nm LED, and 3 times the number of doses per LED per Euro with respect to the best 275 nm LED.

These results are important design considerations because they show the importance of achieving the best trade-off between wavelength, optical power, and reliability to build an efficient disinfection system.

4:15 PM EL11.09.04

Device Design Considerations for a Monolithically Integrated III-Nitride Infrared-Visible Detector-Emitter [AlirezaLanjani](#)¹, BenjaminMcEwen¹, EmmaRocco¹, VincentMeyers¹, DavidHill², W.K. Chan² and Fatemeh (Shadi)Shahedi-pour-Sandvik¹; ¹University of Albany, United States; ²SRI International, United States

Quantum well infrared photodetectors (QWIPs) have been used for applications such as telecommunication and thermal imaging in astronomy and defense. Recently, III-nitride materials have attracted much attention in the design of QWIPs owing to their large conduction band offset (CBO) up to 2 eV [1], which makes it suitable for a variety of intersubband transition (ISBT) energies [2]. The system's polarization in the c-direction offers additional design flexibility, permitting further tuning of band offset and therefore of ISBT energies.

One of the challenges impeding the use of III-nitride QWIPs in many applications, such as thermal imaging, is the need for wavelength up-conversion to permit emission in the visible range. Without integrated up-conversion, the QWIP must have an additional readout circuit, which increases the device complexity, size, and weight which is undesirable in many applications such as handheld devices. This challenge was overcome in another material system where monolithic integration of a GaAs/AlGaAs QWIP and light emitting diode (LED) was proposed in 1997 [3] and successfully demonstrated [4]. The principle of integrated QWIP-LED for wavelength upconversion is the photoexcitation of carriers from IR spectral radiation in quantum wells by ISBT and then injection of excited carrier towards the LED for generation of visible light [5]. Such structures require precise control over the thickness of layers and interfaces. Growth of several nm thick layers with high quality interfaces (e.g., in QWIP) is quite challenging in metal organic chemical vapor deposition (MOCVD) of III-nitrides. Of key importance in interface quality is the RMS roughness of each layer, controlled by the time lapse between growth of barrier/well/barrier and growth rate in the layers. Thicknesses of less than 5 nm were required in our QWIP design.

In this work, we present for the first time a design for a monolithically integrated III-N detector-emitter with a target absorption wavelength of 1.5 μm and emission in the visible range. Parametric tuning of QWIP layers compositions and thicknesses is performed with parallel simulations using classical (Sentaurus TCAD) and quantum mechanical (nextnano) modelling. The impact of doping and polarization charges at heterointerfaces of the QWIP structure on the band alignment and absorption are discussed. It is found that p-type doping of the QWIP superlattice is required for absorption of TE polarized light. Doping and composition of the transition layers between QWIP and LED were optimized to promote higher carrier injection efficiency. Experimental limitations and experimental material characteristics are considered to achieve a realistic design. We will present characterization of initial proof-of-concept structures grown by MOCVD, comparing simulated design to experimental characteristics.

[1] A. N. Westmeyer et al., J Appl Phys, vol. 99, no. 1, p. 013705, 2006

[2] S. D. Gunapala et al., "IEEE Journal of Selected Topics in Quantum Electronics, vol. 20, no. 6, pp. 154–165, 2014

[3] L. B. Allard, et al., Appl Phys Lett, vol. 70, no. 21, pp. 2784–2786, 1997

[4] E. Dupont et al., Semicond Sci Technol, vol. 23, no. 5, p. 055006, 2008

[5] T. Rao, et al., Coatings, vol. 12, no. 4, p. 456, Mar. 2022

4:30 PM EL11.09.05

Broadband Photodetectors with Zinc Gallate Spinel Structure for Broadband IR-Vis-UV Wavelength Detection [SeungmeKang](#), WangmyungChoi and HocheonYoo; Gachon University, Korea (the Republic of)

The detection range of light wavelengths is a crucial factor for photodetectors (PDs) since they need to be capable of detecting a wide spectrum of optical signals. The active layer, located between the electrodes, plays a significant role in the photodetection performance of broadband photodetectors (BPDs). Recent studies have focused on exploring photosensitive materials that can generate electron-hole pairs from photon energy using simple fabrication techniques and are stable in air. Among these materials, metal oxides show promise as active layers for BPDs. However, previously reported metal oxide BPDs have limitations, such as lower photodetection performance and the need for external bias at specific target wavelengths, when compared to narrow-band PDs. In this study, we propose a BPD with a spinel structure capable of detecting a wide range of wavelengths from ultraviolet (UV) to infrared (IR) by synthesizing zinc gallate (ZnGa₂O₄) using a solution process. The BPD device was fabricated through a straightforward spin-coating process and thermal evaporation. We formed an n-type ZnGa₂O₄ layer and a top titanium (Ti) electrode on p-type silicon. The resulting BPD demonstrated distinct photoresponse across various wavelengths, ranging from UV-C to the visible and IR regions. Notably, we achieved an IPhoto/IDark ratio of up to 105 AA-1 at 0 V, indicating that our BPD is suitable for self-powered operation without the need for any external voltage application. To assess the uniformity of the BPD, we fabricated a 10 x 10 array and confirmed the possibility of broadband detection in all 100 devices.

SESSION EL11.10: Poster Session: UWBG
Session Chairs: Stephen Goodnick and Robert Kaplar
Wednesday Afternoon, November 29, 2023
Hynes, Level 1, Hall A

8:00 PM EL11.10.01

Achieving Highly Reliable, High Mobility Spinel SinglePhase IZTO Thin-Film Transistors at a Low Temperature of 300°C [Gwang-BokKim](#); Hanyang University, Korea (the Republic of)

In this study, In_{0.22}Zn_{0.78}Sn_{0.78-d}O_{1.89-d} [d = 0.55] films featuring a spinel single phase are effectively produced at a low temperature of 300 °C by meticulously designing the cation composition and employing a catalytic chemical reaction. Thin-film transistors (TFTs) with an amorphous In_{0.22}Zn_{0.78}Sn_{0.78-d}O_{1.89-d} [d = 0.55] channel exhibit a respectable mobility of 41.0 cm²/Vs, which is a result of the cooperative intercalation of In and Sn ions. On the other hand, TFTs with polycrystalline spinel In_{0.22}Zn_{0.78}Sn_{0.78-d}O_{1.89-d} [d = 0.55] channel layers, created through metal-induced crystallization at 300 °C, display an impressive field-effect mobility of approximately 83.2 cm²/Vs and outstanding stability against external gate bias stress. This can be attributed to the consistent formation of the highly ordered spinel phase. We deduce that the cubic spinel phase of Zn_{2-y}Sn_{1-y}In_yO₄ (y = 0.45) film holds great potential as a replacement for semiconducting polysilicon in the backplane channel components of mobile active-matrix organic light-emitting diode displays.

8:00 PM EL11.10.02

Effects of Sn Doping Concentration of α-Ga₂O₃ Films Grown by Mist-CVD [Jang hyeokPark](#) and You SeungRim; Sejong University, Korea (the Republic of)

Recently, gallium oxide (Ga₂O₃) has been considered the next-generation power semiconductor materials because it has a wide band-gap of 4.9-5.3eV. For the growth of epitaxial Ga₂O₃ films, hydride vapor phase epitaxy, metal organic chemical vapor deposition, molecular beam epitaxy, and mist chemical vapor deposition (Mist-CVD) have been proposed. Among them, Mist-CVD has several advantages. It can easily control the chemical compositions and phases as well as does low-cost deposition due to simple equipment and can grow high quality Ga₂O₃ epitaxial films without vacuum systems. Especially, hetero-epitaxial growth we did is essential because it enables high quality thin film growth while the integration of different materials.

In this work, Sn-doped α-Ga₂O₃ (006) thin films are grown on c-plane sapphire (006) substrates by mist-CVD. And then, we conducted analysis of Sn-doped α-Ga₂O₃ thin films with varying doping concentration. The crystal structure and orientation were investigated by XRD θ–2θ. When Sn doping concentration of α-Ga₂O₃ was increased from undoped to 10% and 20%, the calculated FWHM were 421.236arcsec, 600.372arcsec and 292.14arcsec. It showed crystallinity of high quality Ga₂O₃ films despite of doping concentration. When the Sn doping concentration of α-Ga₂O₃ was increased from undoped to 10% and 20%, the calculated optical band gaps were 4.90eV, 4.95eV and 5.65eV. Blue shift in band gap which is believed to be

caused by the Burstein-Moss shift was observed in Sn-doped α -Ga₂O₃ films. Carrier concentration and electrical characteristics were extracted from fabricated Sn-doped α -Ga₂O₃ Schottky barrier diodes (SBDs).

We analyzed Sn-doped α -Ga₂O₃ thin films and carrier concentration control of α -Ga₂O₃ by increasing the Sn doping concentration. This allowed us to demonstrate doping control of Mist-CVD-based α -Ga₂O₃ epitaxial films and revealed the great potential of α -Ga₂O₃ SBDs.

Acknowledgments

This work was supported by the National Research Foundation of Korea (NRF) grant funded by the Korea government (MSIT) (No. 2020R1A2C1013693), Korea Institute for Advancement of Technology (KIAT) grant funded by By the Ministry of Trade, Industry & Energy (MOTIE, Korea) (P0012451, The Competency Development Program for Industry Specialist) and the Technology Innovation Program - (20016102, Development of 1.2kV Gallium oxide power semiconductor devices technology, RS-2022-00144027, Development of 1.2kV-class low-loss gallium oxide transistor) funded by MOTIE.

References [1] Kazuaki Akaiwa, *et al.* Electrical Properties of Sn-Doped α -Ga₂O₃ Films on m-Plane Sapphire Substrates Grown by Mist Chemical Vapor Deposition. *Phys. Status Solidi A* 2020, 217, 1900632.

[2] Yaoqiao Hu, *et al.* First Principles Design of High Hole Mobility p-Type Sn–O–X Ternary Oxides: Valence Orbital Engineering of Sn²⁺ in Sn²⁺–O–X by Selection of Appropriate Elements X. *Chem. Mater.* 2021, 33, 1, 212–225.

[3] Malleshham Bandi, *et al.* Effect of Titanium Induced Chemical Inhomogeneity on Crystal Structure, Electronic Structure, and Optical Properties of Wide Band Gap Ga₂O₃. *Cryst. Growth Des.* 2020, 20, 1422–1433

8:00 PM EL11.10.03

Site-Selective Laser-Induced Crystallization of Amorphous GaO_x for the Micropatterning of Ga₂O₃ Thin Films Daishi Shiojiri¹, Ryoya Kai², Satoru Kaneko^{1,2}, Akifumi Matsuda² and Mamoru Yoshimoto²; ¹Kanagawa Institute of Industrial Science and Technology, Japan; ²Tokyo Institute of Technology, Japan

Wide-gap semiconducting materials have been investigated for practical use in various devices because of advantages in these materials' excellent electronic and optical properties, such as a combination of visible light transparency with electrical conductivity, high voltage resistance, and ultraviolet (UV) light emission and absorption. In past decades, materials with band gaps (E_g) in the 3–4 eV range, such as GaN and SiC, have been the main focus of research efforts. To extend the range of applications using high-power deep-UV light, it is necessary to exploit semiconductors with an E_g above 4 eV.

Ga₂O₃ has been identified as a great potential wide-gap semiconductor with an E_g of > 4 eV. Ga₂O₃ thin films are promising for a variety of UV optoelectronic applications and technologies, such as deep-UV-transparent conductive oxides, UV photodetectors, and high-breakdown-voltage field-effect transistor devices. Among the Ga₂O₃ polymorphs, β -Ga₂O₃ (monoclinic, space group: C 2/m) is identified as thermodynamically stable phase. Its crystalline thin films have been mostly prepared at moderate to relatively high temperatures (> 400°C) by processes such as pulsed laser deposition, metal-organic vapor phase epitaxy, molecular beam epitaxy, and others. In addition, the surface-structure patterning of the single-crystalline β phase is important for device applications, but there are few reports of low-toxicity and low-temperature fabrication methods, especially for those at room temperature.

Excimer laser annealing (ELA) has been widely used for the solid-phase crystallization of amorphous thin films at low temperatures, such as in the manufacturing of poly-Si thin film transistors with large areas in industrial. The laser annealing process exhibits the advantages of high photon energy and a lack of thermal effects in unirradiated areas, and these features would be applicable to the crystallization of amorphous materials of oxide materials with large band gaps.

Previously, we reported the room-temperature fabrication of highly oriented β -Ga₂O₃ thin films on α -Al₂O₃ substrates [1]. We have also reported the fabrication of epitaxial β -Ga₂O₃ films on epitaxial NiO(111)-buffered α -Al₂O₃ substrates using the ELA process [2, 3]. In this study, we report the effects of laser intensity, annealing time, and film thickness on the crystallinity, surface morphology, and optical properties of Ga₂O₃ thin films to discuss the mechanisms of the excimer laser crystallization. In addition, we also report on a fully room-temperature surface-patterning method for wide-gap β -Ga₂O₃, characterized by the site-selective laser-induced crystallization of amorphous GaO_x thin films and by acid-solution etching processes.

References

[1] D. Shiojiri, R. Yamauchi, D. Fukuda, N. Tsuchimine, S. Kaneko, A. Matsuda, and M. Yoshimoto, "Room-temperature fabrication of highly oriented β -Ga₂O₃ thin films by excimer laser annealing," *Journal of Crystal Growth* 424 (2015) 38–41.

[2] D. Shiojiri, D. Fukuda, R. Yamauchi, N. Tsuchimine, K. Koyama, S. Kaneko, A. Matsuda, and M. Yoshimoto, "Room-temperature laser annealing for solid-phase epitaxial crystallization of β -Ga₂O₃ thin films," *Applied Physics Express* 9 (2016) 105502.

[3] H. Morita, T. Matsushima, K. Nakamura, K. Kaneko, S. Kaneko, A. Matsuda, and M. Yoshimoto, "Solid-phase epitaxial crystallization of β -Ga₂O₃ thin film by KrF excimer laser irradiation from backside of NiO (111)-buffered α -Al₂O₃ (0001) substrate at room temperature," *Journal of Vacuum Science & Technology A* 39 (2021) 043414.

8:00 PM EL11.10.04

Remote Epitaxy of 4H-SiC on Epitaxial Graphene/SiC Doyoon Lee, Bo-In Park, Kiseok Kim and Jeehwan Kim; Massachusetts Institute of Technology, United States

Remote epitaxy technique has the possibility of impacting many research areas including SiC and GaN SMART power, integration of opto- and electronic devices, HEMT performance, flexible electronics and quantum sciences. SiC, a wide band gap semiconductor, has attracted attention because of its various band gap depending on its polytype, superior thermal conductivity and chemical stability which enable SiC to outperform GaN for applications in extremely harsh operating conditions such as high temperature, aerospace, radioactive environment, etc. In addition, SiC recently has been used as a template for state-of-art such as topological insulator and color center for quantum applications. In spite of its usefulness, the expensive wafer cost of SiC has hindered its scalability and commercialization. Even though the remote epitaxy has proven that it can dramatically reduce wafer cost by reusing substrate, the remote epitaxy of SiC has not been demonstrated.

In this work, we focus on the remote epitaxy of 4H-SiC, which is directly grown on epitaxial graphene (EG) on 4H-SiC (0001) substrate using a chemical vapor deposition (CVD) reactor. The epitaxial graphene was grown via Si sublimation of 4H-SiC substrate. Both on-axis (4H-SiC) and off-axis (4H-SiC cut 4° off-axis towards the [11-20]) substrates were investigated. Following the epitaxial graphene growth, SiC growth was performed. Growth parameters were modified to eliminate SiC polytype conversion and other extended defects and to preserve the graphene at elevated temperatures during the growth for successful remote epitaxy. The epitaxial SiC films were characterized using scanning electron microscopy (SEM), transmission electron microscopy (TEM) and electron backscattering diffraction (EBSD). To evaluate the ability to grow 4H-SiC remote-epitaxially, a Ni metal stessor technique was used to exfoliate the SiC epitaxial film and demonstrated exfoliation yields of up to 50 – 70 %.

8:00 PM EL11.10.05

Color Spectroscopy for Failure Analysis of Silicon Carbide Single Crystals using Energy Level Analysis Hyoungseuk Choi; Korea Institute of Ceramic Engineering and Technology, Korea (the Republic of)

Single crystal silicon carbide (SiC), which has a closed-packed crystal structure, is a wide-bandgap (WBG) material applicable to power electronic devices. During crystal growth, many types of SiC stacking order can be produced within the bulk of a single crystal because of temperature fluctuations in the crucible. The different stacking-order types are called "polytypes". These SiC polytypes have the same densities and share a single Gibbs free energy, but the electronic band structures vary, resulting in different ultraviolet photoluminescence (UVPL) wavelengths. The inclusion of the wrong polytype in SiC single crystals is an issue of interest because it is one of the causes of degradation in the reliability of power devices that use them. For example, 4H-SiC is widely used for the fabrication of power electronics, and the inclusion of 3C-SiC within 4H-SiC crystals has been the subject of considerable research with much effort directed toward the control of polytype formation. Therefore, a rapid testing procedure for polytype analysis is important for the mass production of SiC crystals.

Commercial SiC may be categorized as either conductive SiC or high-purity semi-insulating (HPSI) SiC. HPSI SiC includes very few dopant atoms, and hence it has an intrinsic bandgap in the ultraviolet range, corresponding to colorless photoemission. Conductive SiC may be doped with N, P, Al, or B to generate additional energy levels with different colors, depending on their polytype. In conductive SiC, N and P dopants result in shallow donor levels, and Al-doping results in a shallow acceptor level. However, doping with B creates a deeper acceptor level, allowing a donor-acceptor pair (DAP) with an energy difference in the visible range to be created. These B-doping-induced DAP recombination energies result in UVPL emission from conductive SiC.

Color spectroscopy can measure energy levels via transformation of ultraviolet photoluminescence (UVPL) color images into a color space in which emission energies have been indexed. It can be applied to the measurement of electronic energies in various materials that have energy-level differences in the visible range (1.65–3 eV). We demonstrate that color spectroscopy provides potential for cost-effective, simple, non-destructive, and full-field measurement of energy levels and can be applied widely, including in laboratories and on production lines. In this study, we developed a new spectroscopic technique named "color spectroscopy" and applied it to the analysis of the different polytypes of silicon carbide single crystals. Raman and photoluminescence spectroscopy data are compared with the results of our method to verify its accuracy. We show that color spectroscopy can provide very accurate energy-level measurements and has potential as a characterization tool in many fields.

8:00 PM EL11.10.06

Ozone Gas Sensing and Photo-Refreshing in Solution-Processed IGZO-TFTs Hiroharu Sasajima, Takaaki Morimoto and Keisuke Ishii; National Defense Academy, Japan

In recent years, flexible devices, in which semiconductor circuits are fabricated on polymer film or paper, have been attracting much attention. One of the leading candidates of material for them is Indium Gallium Zinc Oxide (IGZO). Because of higher mobility and lower leakage current than conventional a-Si, it is used as a material for thin-film transistor (TFT) on flat panel displays. Since the connective fabrication process, namely vacuum process is not cost-effective for fabricating large electronic devices, solution processes such as coating and printing one promising as the inexpensive preparation methods. We have reported that IGZO-TFTs can be fabricated by the solution process. On the other hand, flexible devices should consist of not only TFTs but also various devices such as sensors, which have never been reported as solution-processed IGZO devices.

Although ozone gas is widely used in various industrial fields, since high concentration ozone is harmful to the human body, the concentration should be exactly controlled. We are developing an ozone gas sensor based on solution-processed IGZO-TFTs. We have already detected high concentration ozone (100 ppm) by using these TFTs successfully. However, for practical use, they have to detect ozone at less than 10 ppm, at which ozone becomes harmful. In this study, the sensitivity of solution-processed IGZO-TFTs to 5 ppm ozone was evaluated. In order to improve the ozone detection sensitivity, we also optimized the fabrication conditions and elucidated the reaction mechanism of this sensor. In addition, we clarified that the refresh behavior essential for repeated use as a sensor is induced by the irradiation of visible photons (1.7-3.1 eV).

The precursor solutions for the fabrication of solution-processed IGZO-TFTs were prepared by dissolving nitrate hydrates of In, Ga, and Zn in 2-methoxyethanol and mixing each solution at a ratio of In: Ga: Zn = 6: 1: 3. This precursor solution was dropped onto a p-type Si substrate with a SiO₂ thermal oxide film, spin-coated, and fired in air for 1 hour. Then, the Al drain and source electrodes were formed by vapor evaporation on this IGZO film to fabricate a TFT. Here, p-Si is also used as a gate electrode.

To evaluate the ozone detection sensitivity, the drain current (I_D) was measured with and without ozone exposure, while the TFT was turned on by applying +40 V to the gate and drain electrodes. Here, the reduction rate of I_D by ozone exposure for 1 minute was defined as the ozone detection sensitivity S . At samples spin-coated at 2000 rpm and fired below 340 °C, S exceeds 10³ even when the ozone concentration is as low as 5 ppm. In the O 1s XPS spectrum, the intensity of a peak due to OH groups becomes larger in the samples measured with high S. The FT-IR peak intensity due to the stretching vibrations of the OH shows a similar trend. This indicates that the OH groups in the IGZO film contribute to the reaction mechanism to ozone.

To recover the I_D reduced by ozone, IGZO-TFTs in the on-state were irradiated with photons at energies of 1.7 to 3.1 eV for 5 min. After photon irradiation above 2.6 eV, I_D recovered significantly, indicating that these TFTs can be reused as a sensor. This threshold is slightly smaller than the band gap energy of 3.05 eV estimated from the optical absorption spectrum. Considering the reported band diagram, the recovery of I_D can be caused by the excitation of electrons from a state near the valence band to the donor level of IGZO. Furthermore, the ozone-induced I_D reduction can be caused by the reverse reaction, i.e., the electron desorption in the donor level by ozone.

8:00 PM EL11.10.07

Theoretical Analysis of Threshold Voltage Shift with Operating Temperature of Self-Aligned Coplanar IZTO Thin Film Transistors Minjae Kim; Hanyang University, Korea (the Republic of)

With the rise of the Internet-of-Things and 5G networks, electronic devices with low power consumption are crucial. However, as FETs are downscaled to meet performance demands, self-heating-induced instability becomes a challenge due to limited heat dissipation paths. This leads to thermally accelerated degradation and increased power consumption. The self-heating effect in TFTs, especially those used in organic light-emitting diode (OLED) displays, has not been extensively studied. The study focuses on amorphous indium-zinc-tin oxide (a-IZTO) TFTs, which offer high field-effect mobility and low off-current. The study identifies intrinsic and extrinsic factors contributing to temperature-dependent VTH instability, including subgap density-of-state (DOS) and interface traps. The paper presents an analytical model for temperature-dependent VTH instability and validates it through experiments, DOS extraction, and simulations. The diffusion of hydrogen in a-IZTO TFTs is also examined, and optimal hydrogen incorporation is found to improve performance and thermal VTH stability. The study highlights the importance of material and device design parameters, such as subgap DOS, channel thickness, and gate capacitance, in optimizing oxide semiconductor TFTs for applications like OLED displays, augmented and virtual reality, memory, and logic devices.

In this study, we investigated the impact of temperature on the stability of the threshold voltage (VTH) in self-aligned coplanar amorphous indium-zinc-tin oxide (a-IZTO) thin-film transistors (TFTs). We developed an analytical model that revealed the importance of device geometry and reducing the subgap density-of-state (DOS) in achieving high stability in a-IZTO TFTs. The validity of the model was confirmed through experiments and computer simulations. The study also examined the role of hydrogen impurities in the performance and VTH stability of a-IZTO TFTs. It was found that incorporating hydrogen in the a-IZTO channels improved TFT performance and thermal stability due to hydrogen acting as a passivation center. However, excessive hydrogen incorporation increased the subgap DOS distribution, resulting in a slight deterioration in thermal stability. Consequently, two strategies were identified to improve the temperature stability of VTH in oxide TFTs. Firstly, minimizing the subgap DOS distribution can be achieved through a post-deposition annealing (PDA) temperature of 320 °C, resulting in reduced subgap DOS and improved thermal stability. This can be attributed to the passivation effect of hydrogen during PDA. Secondly, geometrical engineering of the channel thickness (Tch) and oxide capacitance (COX) can help mitigate the effect of temperature on the VTH shift. A thinner channel and/or higher COX were shown to be effective in achieving stable VTH at varying temperatures. The study discussed the use of careful thermal annealing, mass ensification of the channel layer, and interface matching between the channel and gate dielectrics to obtain super-steep IV characteristics in metal oxides, which can further reduce subgap DOS distribution and enhance thermal stability. The findings of the study have implications for future designs of stable oxide semiconductor TFTs, particularly in applications such as organic light-emitting diodes, augmented and virtual reality, memory, logic, and monolithic three-dimensional devices. Experimental results and computer simulations validated the analytical model, providing valuable insights for the design of oxide TFTs with improved temperature stability of VTH.

8:00 PM EL11.10.08

Selective Deposition of Fluid Skin Restorer Passivation Layers for IGZO TFTs using Electrohydrodynamic Jet Printing for Enhanced Electrical Characteristics and Stability Young Wook Kim, Min Seong Kim, Jong Hyuk Ahn, Hyung Tae Kim, Sujin Lee and Hyun Jae Kim; Yonsei University, Korea (the Republic of)

Amorphous oxide semiconductors (AOSs) are commonly used as active layer materials in thin-film transistors (TFTs) due to their notable advantages. Especially, indium-gallium-zinc-oxide (IGZO) based TFTs among AOS-TFTs include attractive mobility (~ 10 cm²/Vs), low off current (< 100 pA), and high transparency (> 80%) in the visible region, making them suitable for display backplanes. However, IGZO TFTs exhibit critical instability issues when exposed to light, temperature variations, bias stress, and ambient gases. One of the significant challenges is the threshold voltage (V_{th}) shifts caused by O₂ and H₂O exposure in the atmosphere. The adsorption/desorption of O₂ and H₂O molecules can shift the V_{th} of IGZO TFTs in a positive or negative direction, acting as donor-like or acceptor-like states, respectively. To mitigate this problem, optimal passivation layers (PVLs) are required to prevent the IGZO channel layer from coming into contact with the ambient environment, and numerous studies have focused on developing inorganic and organic material PVLs to address these challenges. Inorganic materials such as SiO₂ and Al₂O₃ have been commonly used, but they require high temperatures and expensive vacuum processes. These conditions are unsuitable for flexible display devices, which are typically manufactured on polymer substrates with low glass-transition temperature (< 200°C). Moreover, the limited flexibility and brittle properties of inorganic PVLs pose further constraints. In order to overcome the limitations of inorganic PVL, PVL utilizing organic materials such as polydimethylsiloxane (PDMS) and Poly (methyl methacrylate) (PMMA) have been studied. However, due to its unique material properties, organic PVL is inferior to inorganic PVL in the view of barrier performance against ambient gases.

In this study, organic material fluid skin restorer (FSR) with low gas permeability was introduced as PVL of IGZO TFT. To reduce the viscosity of FSR, the solution was prepared by dissolving FSR in ethanol to a concentration of 2 wt% at room temperature with physical stirring. The FSR PVL has an advantage in minimizing the thermal degradation on the device by annealing for 5 min at a low temperature of 100°C compared to PMMA PVL which required 150°C, and 20 min. The electrical characteristics and stability under positive bias stress (PBS) exhibited improvement compared to the devices without FSR PVL, specifically in terms of field-effect mobility 7.22 to 18.95 cm²/Vs, on/off current ratio 2.23 10⁸ to 7.54 10⁸, and subthreshold swing 0.46 to 0.43 V/decade. The Vth shift under PBS of FSR PVL for 10,000s decreased from 6.16V to 4.67V compared to the devices without PVL. These improvements are expected to be due to the diffusion of atoms, such as nitrogen and oxygen from the FSR to the channel layer, and the blocking of the adsorption/desorption of ambient gases such as O₂ and H₂O. Moreover, the electrohydrodynamic (EHD) jet printing method enables selective deposition of FSR on IGZO TFTs. Given its selectivity, transparency, and impressive performance, this material holds a great promise as a valuable resource in the field of printing electronics and transparent devices (e.g., flexible displays, wearable sensors).

8:00 PM EL11.10.09

Thin Films of Zn(S, O) and (Zn, Mg)O as Wide-Band Gap Components in SnS Solar Cells Luis A. López Cruz, P. Karunakaran Nair and M.T. Santhamma Nair; Universidad Nacional Autónoma de México, México

Thin films of sulfides and oxides of zinc such as Zn(S, O) and (Zn, Mg) O as wide band gap buffers are known to provide better band alignments than CdS in heterojunction solar cells with SnS absorber. We used chemical bath deposition for obtaining thin films of Zn(O, S) and RF sputtering for (Zn, Mg)O films. Thin films of zinc sulfide deposited from aqueous chemical baths of soluble complexes of Zn(II) and thioacetamide or thiourea as sulfide-ion source, are Zn(O, S) with a sulfur to zinc ratio of 0.28 to 0.34. The optical bandgap of these films deposited on quartz substrates is around 4 eV. Variations in crystal structure, chemical composition, and band gaps occur in the films when the films are heated with S- and Se-vapor at 400 – 500 °C. For example, the films showed XRD peaks characteristic of cubic ZnS and a S/Zn of 0.89 after they are annealed in presence of S at 500 °C under nitrogen. The thin films of (Zn, Mg)O obtained by co-sputtering showed hexagonal crystal structure with band gap 3.2 to 3.8 eV. The electrical conductivity in both these films is of the order of 10⁻⁸ Ω⁻¹ cm⁻¹. Photovoltaic structures incorporating these films with chemically deposited SnS of cubic and orthorhombic structures as absorber components showed V_{oc} of 480 mV in the case of Zn(O,S) and 508 mV in the case of (Zn, Mg)O buffers.

8:00 PM EL11.10.10

Characterization of Gold-Catalyzed Gallium Oxide Nanowires Geordan Dorsey¹, Antonio Moore¹, Warren Collins¹, Akira Ueda^{1,2}, Virginia Lorenz³, Arend M. van der Zande³ and

The growth of β -gallium oxide (Ga_2O_3) nanowires has been achieved by the vapor-solid-liquid method on silicon wafer substrates. In Argon atmosphere, pure gallium was heated to produce gallium vapor and oxidized by background impurities, inside a vertical tube furnace. Since β - Ga_2O_3 is the most thermodynamically stable phase of Ga_2O_3 at standard temperature and pressure, and has the monoclinic crystal structure, β - Ga_2O_3 nanowires were grown in a specific direction. For the growth of β - Ga_2O_3 , the substrates were prepared by treating silicon wafers with hydrofluoric acid, then sputter-coated with a 2 nano meter gold layer. The correlation between the gold nanoparticle diameter and the morphology of the Ga_2O_3 nanowires was studied. The growth orientation was also investigated for nanowires on these two kinds of substrates via Transmission Electron Microscopy (TEM) characterization. The elemental composition was also verified using Energy-dispersive X-ray spectroscopy (EDS).

The authors acknowledge the support of the NSF through the Partnership for Research and Education in Materials (PREM) program DMR-2122169, the University of Illinois at Urbana-Champaign Materials Research Science and Engineering Center DMR-1720633, and NSF HBCU-RISE Program HRD-1924241

8:00 PM EL11.10.11

Epitaxial Growth and Semiconductor Properties of Novel UWBG Oxides for Power Electronic Devices Kingsley O. Egbo¹, Emily Garrity², Cheng-Wei Lee², Brooks Teltekamp¹, Vladan Stevanovic² and Andriy Zakutayev¹; ¹National Renewable Energy Laboratory, United States; ²Colorado School of Mines, United States

Electronic devices suitable for high power, high voltage operation and which can withstand high-temperature environments are required for applications in electric vehicles, gas turbines, gas and oil drilling, and other energy-dense systems. For these devices, the active layer determines the application space possible, and ultrawide bandgap semiconductors with suitable carrier mobility and power figure of merit ensure a high breakdown field and limited temperature-induced leakage which are required for high-voltage and high-temperature applications respectively. Among ultrawide bandgap materials, most oxides offer further advantages for operation in oxidizing and reducing conditions as they are chemically robust. A recent high throughput search predicted thirty candidate oxide materials with properties suitable for power electronic applications and among these candidate materials, InBO_3 , Mg_2GeO_4 , and $\text{In}_2\text{Ge}_2\text{O}_7$ were identified as having the best potential in high-power device application¹. Here, we explore the thin film growth and properties of these three novel ternary oxides. Thin films of these novel ternary oxides are grown by Pulsed laser deposition using a KrF Excimer laser of wavelength 248 nm in a vacuum chamber with a base pressure of 10^{-8} Torr. Ceramic targets of these ternary oxides were ablated at an average pulse repetition rate of 8Hz and laser energy of 300mJ on different single crystalline substrates. Structural, composition and optoelectronic properties of the thin films are explored by x-ray diffraction, x-ray fluorescence, spectroscopic ellipsometry, and x-ray photoelectron spectroscopy. Structural characterization shows that epitaxial spinel-type $\text{Mg}_2\text{GeO}_4(100)$ is obtained on $\sim 1.8\%$ lattice mismatch $\text{MgAl}_2\text{O}_4(100)$ and $\text{MgO}(100)$ substrates. $\text{In}_2\text{Ge}_2\text{O}_7(220)$ is grown on $\text{Al}_2\text{O}_3(00.6)$ and InBO_3 thin films on $\text{Al}_2\text{O}_3(00.6)$ and $\text{YSZ}(100)$ are polycrystalline. Spectroscopic ellipsometry analysis gives a bandgap value of 4.9 eV, 4.0 eV, and 5.1 eV for InBO_3 , $\text{In}_2\text{Ge}_2\text{O}_7$, and Mg_2GeO_4 respectively which matches closely to theoretical predicted values¹. Preliminary transport measurement for undoped thin films shows that both InBO_3 and Mg_2GeO_4 are semi-insulating while $\text{In}_2\text{Ge}_2\text{O}_7$ shows sheet resistance $> 1\text{M}\Omega$. However, detailed defect chemistry calculations further provide insight into the dopability of these materials. Results show that InBO_3 has defect chemistry that allows n-type doping under In-rich/O-poor synthesis. Zr also acts as a donor in both InBO_3 and $\text{In}_2\text{Ge}_2\text{O}_7$. These results provide the basis for further material exploration and characterization of these new set of ultra-wide bandgap ternary oxide materials and will pave the way for their potential integration in high-power devices.

¹Garrity E.M. *et al.* Computational identification of ternary wide-bandgap oxides for high power electronics. PRX Energy 1, 033006 (2022).

8:00 PM EL11.10.12

Study on Enhanced Electron Field Emission Properties of Graphene Quantum Dots Synthesized by Pulsed LASER Ablation Vincent R. Walsh Rivera, Muhammad Shehzad Sultan, Amanda M. Gracia Mercado, Brad Weiner and Gerardo Morell; University of Puerto Rico - Río Piedras, United States

Graphene quantum dots (GQDs) and Nitrogen doped graphene quantum dots (N-GQDs) were synthesized by Pulsed LASER Ablation method. The nanostructure and chemical composition of the GQDs were analyzed by means of TEM, HRTEM, Raman, XPS, and FT-IR spectra. Field emission is a quantum mechanical phenomenon where electrons tunnel from the cathode to the anode through vacuum upon an applied electric field. So far field emission properties of two-dimensional (graphene) and one-dimensional (CNT) carbon nanostructures have been extensively studied. For the first time, to the best of our knowledge, the field emission behavior of GQDs and N-GQDs, deposited on n-Si (100) substrates, is studied. As a candidate of cold cathode, the GQDs display good field emission performance. The field emission properties of GQDs and N-GQDs were studied by measuring turn-on field (E) and field enhancement factor β . The results show that nitrogen doping improved the field emission properties of GQDs by reducing turn-on field from $13.1\text{V}/\mu\text{m}$ (GQDs) to $7.9\text{V}/\mu\text{m}$ (N-GQDs) and enhancing the field enhancement factor β from 1427 (GQDs) to 2511 (N-GQDs). The field emission behavior of pristine GQDs and N-GQDs is explained in terms of change in the effective microstructure as well as a reduction in the work function as probed by measured characterizations. The enhanced emission properties of N-GQDs are mainly attributed to the upshifting of fermi energy level and defects produced as a result of Nitrogen doping. The good emission performance of the GQDs field emitters suggests promising applications in next generation vacuum micro and nano electronic devices

<quillbot-extension-portal></quillbot-extension-portal>

8:00 PM EL11.10.13

Luminescence characteristics of low-voltage thick-film ELs with evaporated ZnS:Mn and spin-coated BaTiO₃ dielectrics and microLEDs Shin-ichi Yamamoto¹, Koichi Wani¹, Taisei Kitawaki¹, Oliver A. Durnan², Vikrant Kumar², Reem Alshambari² and Ioannis Kymissis²; ¹Ryukoku University, Japan; ²Columbia University, United States

Thin film electroluminescent (TFEL) devices have been mainly applied as all-solid-state flat panel displays and other light sources. A thin film EL display consists of an emission layer which is an inorganic phosphor, insulator layers, and top and bottom electrodes. The phosphor layer emits light when its luminescent center is excited by hot electrons accelerated by the applied voltage across the electrodes. Because of its rigid structure, high resistance to humidity, and self-emissive property, TFEL displays have a long life, good visibility, wide operating temperature range, and a thin profile.

The well-established structure of the TFEL is a double insulator type in which the phosphor layers are sandwiched by insulation layers. As TFELs are usually driven by an ac power supply, the double insulator structure assures a stable operation and long life. Variations of TFEL have been intensively investigated over decades. When a transparent conductor such as ITO is used for both electrodes, a transparent display is manufacture, which is commercially available aiming at head-up displays or automotive applications. Recently, new types of TFEL using quantum dots as the phosphor material are actively investigated.

Despite the above features, TFEL displays are not available as large size monitors or televisions because the operating voltage is high ($>150\text{V}$), brightness is not enough for television applications, and full-color devices are not ready. A variation of TFEL known as a thick dielectric EL or TDEL was developed to solve these problems. In this structure, a thick dielectric layer, which is a laminate of high-k material powders, replaces the thin film dielectric in TFEL. The dielectric powder in TDEL is well crystallized through its manufacturing process. It exhibits higher relative permittivity or dielectric constant k than a thin film dielectric, usually deposited by e-beam evaporation or sputtering. Such thick film dielectric layers have a high breakdown voltage and eventually bring about good reliability and high luminance for blue phosphors, which is inevitable for a full-color display. As thick dielectric layers are manufacture by an atmospheric process, the manufacturing cost can be lower than TFELs. On the other hand, thick dielectric layers require a high temperature sintering process, and a planarization measure is needed on its surface to grow the phosphor layer on it. These constraints in the process prevent the TDEL from being commercialized as a display product.

In this paper, we investigated a structure and process of TDEL having high luminance with lower operating voltage than TFEL. Although the reported TDEL displays so far have a top emission structure, we employed a bottom emission structure instead. As for the thick film dielectric, paste material, which is a mixture of dielectric powders, a binder resin with solvent, and is curable at low temperatures, is employed. The phosphor layer is a conventional ZnS:Mn deposited by an electron beam evaporator and annealed in a sulfur environment. Aiming at a low operating voltage below 100V, the layer thicknesses are minimized. On the other hand, by using MOCVD GaN thin film, microELD was fabricated and compared with low voltage driving.

Acknowledgment

This study is the result of an experiment conducted at Columbia University in the city of New York by a visiting researcher from Ryukoku University.

8:00 PM EL11.10.14

Manufacturing 2-Inch AlN and Beyond - The Road to 4-Inch AlN Substrates Kasey Hogan, Robert Bondokov, Justin Mark, Griffin Norbury and James Grandusky; Crystal IS, United States

The bulk crystal growth process for aluminum nitride (AlN) has had significant development over the past decade and is now at manufacturing scale. Currently, Crystal IS produces multiple thousands of high quality 2-inch AlN substrates per year. These substrates have demonstrated symmetric (0002) X-ray rocking curve FWHM values as low as 6.7 arcseconds, low UV absorption coefficients of $<10\text{ cm}^{-1}$ at 265 nm, and high room temperature thermal conductivities of $294\text{ W m}^{-1}\text{ K}^{-1}$. AlN has thrived in the UVC LED market as a better suited substrate over sapphire by providing closer lattice matching to $\text{Al}_{1-x}\text{Ga}_x\text{N}$ -based epitaxial layers. There exists a desire for larger diameter (4-inch) substrates to realize the potential for AlN technology in power device applications. In 2022, Crystal IS demonstrated similar quality 3-inch AlN and has since continued to expand to the 4-inch diameter. We demonstrate the growth of 4-inch diameter AlN boules and subsequent wafer characterization, signaling the first commercially available 4-inch substrate to be realized in the near future.

8:00 PM EL11.10.15

High Performance Self-Powered UV Photodetector Based on Nitrogen-Doped Graphene Quantum Dot Schottky Diode Muhammad Shehzad Sultan¹, Wojciech Jadwisieniczak², Brad Weiner¹ and Gerardo Morell¹; ¹University of Puerto Rico at Río Piedras, United States; ²Ohio University, United States

We report a straightforward bottom-up approach for the synthesis of high-quality nitrogen-doped graphene quantum dots (NGQDs). This approach is cost-effective, environmentally friendly, and suitable for production of high quality NGQDs on large-scale. The as-synthesized NGQDs have high crystalline quality with an average size of 3.26 nm, are water soluble, and show strong fluorescence. The UV-vis spectra indicate that N-doping introduces new energy levels into the electronic structure of graphene, which tune the optical properties resulting in photoluminescence quantum yield (PLQY) of 73%. The NGQDs show excitation wavelength-dependent fluorescence with a maximum excitation and emission at 340 and 431 nm, respectively. Using the as-synthesized NGQDs, we fabricated a high-efficiency fast-response self-powered UV photodetector. Under the illumination of 365 nm UV light with power density of 25 mW/cm², the NGQD photodetector shows a high photoresponsivity of 37 A/W, detectivity of 1×10^{11} Jones, and external quantum efficiency (EQE) of 12.6×10^3 %. This UV photoresponse is fast, with rise time of 0.29 s and fall time of 0.33 s. This work paves the way for the development of graphene-based high-performance optoelectronic devices.

8:00 PM EL11.10.16

Novel Synthesis and Tuning Optical Properties of High Quantum Yield Nitrogen Doped Graphene Quantum Dots Muhammad Shehzad Sultan¹, Wojciech Jadwisieniczak², Alejandra P Flores Rivera¹, Brad Weiner¹ and Gerardo Morell¹; ¹University of Puerto Rico at Río Piedras, United States; ²Ohio University, United States

The graphene quantum dots (GQDs) have attracted the attention of researchers due to their excellent properties and potential applications in biomedicines, energy storage devices and photovoltaics. The photoluminescence is one of the most important characteristics of GQDs. The doping of GQDs with Nitrogen atoms is one of the most effective ways to tune their photoluminescence emission and to increase quantum yield. In this work, high-quality Nitrogen-doped graphene quantum dots (N-GQDs) were synthesized by using pulsed laser synthesis method at various irradiation powers of pulsed laser and changing the concentration of nitrogen doping to effectively tune the photoluminescence emission and improve the quantum yield (QY) of as synthesized N-GQDs. The TEM, HRTEM, XPS, XRD, Raman spectroscopy and FTIR were carried out to observe the morphology, size distribution, crystalline structure and to prove successful doping of GQDs with nitrogen atoms. To observe optical properties of as synthesized N-GQDs, the UV-vis and Photoluminescence measurements were carried out. The as-synthesized NGQDs exhibit high quality crystalline structure of graphene. A high quantum yield was exhibited by the obtained N-GQDs as compare to the pristine GQDs. The obtained N-GQDs with oxygen-rich functional groups exhibit a strong emission. This work may be helpful to expand the scope of GQDs especially in biomedical applications.

8:00 PM EL11.10.17

Mechanisms Unveiled: A Comprehensive Study on Boosting Efficiency in GaN-Based Micro-LEDs Mengyuan Zhanghu, Byung-Ryool Hyun and Zhaojun Liu; Southern University of Science and Technology, China

Micro Light Emitting Diodes (Micro-LEDs), with a size of 100 μm or less, are predominantly utilized in display and lighting applications, thanks to their foundation in III-nitrides. Key materials used include GaN/InGaN for blue and green emissions, and AlGaInP for red. GaN-based LEDs are celebrated for their exceptional traits, such as self-illumination, high brightness, low power consumption, rapid response time, and enduring lifespan. When juxtaposed with traditional LEDs, which are over 100 μm in size, Micro-LEDs shine for their superior efficiency. This stems from enhanced thermal distribution, optimal current density distribution, and reduced junction temperature.

However, numerous studies have revealed a downside to Micro-LEDs. As the size of these devices becomes smaller, there's a notable decrease in external quantum efficiency (EQE) - a crucial measure of LED performance. This is attributed to sidewall damage incurred during plasma-assisted dry etching in device fabrication, causing non-radiative recombination centers at the surface of the active layers. Given the large perimeter-to-area ratio of smaller devices, they are particularly susceptible to such sidewall damage.

A prevalent technique to mitigate the impact of this damage involves the utilization of sidewall passivation via dielectric materials. Such treatment increases EQE, a combination of internal quantum efficiency (IQE) and light extraction efficiency (LEE), primarily by curtailing surface recombination according to the ABC model. Hence, devices equipped with passivation layers are anticipated to show higher IQE. Determined by the ratio of radiative recombination rate to total recombination rate, the IQE of an LED holds a significant correlation with the diode's ideality factor in the Shockley model. Micro-LEDs with improved IQE should, therefore, demonstrate an ideality factor approximating one - a physical expectation yet to be comprehensively explored!

To systematically probe this conjecture, we fabricated green GaN-based Micro-LEDs, varying in size from 20 to 100 μm and emitting at 520 nm, on a commercially available sapphire substrate. A 50 nm thermal ALD Al₂O₃ layer was then deposited at 300°C to passivate residual sidewall dangling bonds. Our findings unequivocally demonstrate that this passivation layer bolsters the EQE of Micro-LEDs. An increase in EQE/IQE of Micro-LEDs leads to a decline in ideality factors. As the size decreases, the EQE increases, while the ideality factor descends. It's been observed that the radiative ideality factor of Micro-LEDs can reach 1, aligning with the expectations of the Shockley model. Additionally, we found that the LEE of Micro-LEDs with a passivation layer increases as the device size diminishes. Optical simulations indicate that depositing a dielectric layer with a lower refractive index than III-nitride bolsters light extraction by enlarging the critical angle. In this discourse, we will share a comprehensive presentation of experimental outcomes, along with a detailed analysis of the correlation between the ideality factor and IQE, LEE, and their size dependence, as informed by the ABC and Shockley models.

SESSION EL11.11: Oxide Materials and Devices I
Session Chairs: Stephen Goodnick and Robert Kaplar
Thursday Morning, November 30, 2023
Hynes, Level 2, Room 210

8:30 AM *EL11.11.01

β-Gallium Oxide: Progress in Epitaxial Materials and Power Devices Sriram Krishnamoorthy, Saurav Roy and Arkka Bhattacharyya; University of California, Santa Barbara, United States

The availability of shallow donors and large area melt-grown bulk substrates are the key enablers for next-generation power devices based on β-Ga₂O₃. Three key results will be highlighted in this presentation. (1) We demonstrate a hybrid low temperature - high temperature (LT-HT) buffer/channel stack growth using metal organic vapor phase epitaxy with record carrier mobility values (range of 196–85 cm²/Vs) over four orders of doping range (2×10^{16} – 1×10^{20} cm⁻³). Record electron mobility of 110 cm²/Vs is also demonstrated in delta-doped (2D) channels ($n_s = 9.2 \times 10^{12}$ cm⁻²). The improvement in transport properties was achieved mainly by realizing pristine doped channels, eliminating undesired parasitic conduction paths, and minimizing carrier compensation. Lateral transistors utilizing these uniformly Si-doped channels with LT buffers exhibit exceptional device performance. Planar and tri-gate transistors showed very low reverse leakage for breakdown voltages up to 3 kV. Due to enhanced electron mobility, these devices were able to exhibit low on-state resistances for a given device dimension. In conjunction with effective electric-field management (achieved max average breakdown field of over 4 MV/cm with tri-gate architectures), these devices were able to deliver a high power figure of merit of ~1 GW/cm². (2) We report on the growth and characterization of in-situ Al₂O₃ dielectric on (010) β-Ga₂O₃ deposited using metalorganic chemical vapor deposition (MOCVD) to enhance the dielectric quality and lifetime. The dielectrics grown at 600 °C exhibited higher interface trap densities ($D_i = 3.2 \times 10^{12}$ cm⁻²) and lower breakdown fields ($E_{BR} = 6$ MV/cm) when compared to the dielectrics grown at 800 °C ($E_{BR} = 10$ MV/cm, $D_i = 5.4 \times 10^{11}$ cm⁻²) as is evident from the hysteresis and the trap density vs energy characterization which were determined using deep-UV assisted CV measurements and the current-voltage characteristics of the MOS capacitor test structures. The temperature-modulated dielectric sample (interfacial layer grown at 800 °C, and the bulk dielectric grown at 600 °C) has higher breakdown strength ($E_{BR} = 7.7$ MV/cm) and lower trap density ($D_i = 1.1 \times 10^{12}$ cm⁻²) compared to the dielectric grown at 600 °C. Time dependent dielectric breakdown (TDDB) (current vs stress time) was performed to characterize the long-term reliability of the grown dielectrics. This approach of in-situ dielectric deposition on β-Ga₂O₃ can pave the way for promising robust gate dielectrics for future β-Ga₂O₃ based high performance MOSFETs due to its promise of improved interface and bulk quality and long-term reliability compared to other conventional dielectric deposition techniques. (3) We report large area (1mm² and 4mm²) β-Ga₂O₃ trench Schottky barrier diodes with high-k dielectric RESURF. The breakdown voltage of the BTO field-plated SBD increases to 2.1 kV from 816 V (planar SBD) whereas the breakdown voltage increases to 2.8-3kV for the trench SBD with high-k RESURF. The 1 mm² trench SBD exhibits a current of 3.7A(Pulsed)/2.9A(DC) and the 4mm² trench SBD exhibits a current of 15A(Pulsed)/9A(DC) at 5V. The breakdown (catastrophic) voltage of the 1mm² and 4mm² trench SBDs are measured to be 1.4 and 1.8kV, respectively. The rapid progress in the realization of high purity materials, high quality dielectrics, experimentally demonstrated high electric field handling capability along with a pathway to scaling to high absolute current ratings, indicates the promise and potential of Gallium Oxide for next-generation power electronics. This material is based upon work supported by the II-VI Block Gift Program and the Air Force Office of Scientific Research MURI award

9:00 AM EL11.11.02

Evaluating Both Gallium Oxide Wafer Growth Method Economics and Cost Comparison to other Wide Bandgap Materials Samantha Reese¹, Karen Heinselman¹, Drew Haven² and

Gallium oxide (Ga_2O_3) is an emerging ultra-wide bandgap semiconductor which shows promise for use in high-power, high-temperature, optoelectronic, and sensing applications. Ga_2O_3 's wider bandgap enables increased breakdown voltages and lower on-state resistances making it potentially superior to current commercially available materials such as silicon carbide and gallium nitride. Economically Ga_2O_3 is cost-competitive with the ability to be grown from melt. To best understand cost drivers and opportunities for research to enable cost reductions we present a techno-economic analysis that projects the cost of 6" β - Ga_2O_3 wafers fabricated from crystals grown via edge-defined film-fed growth (EFG). We compare it to previously reported epi-wafers grown via the Czochralski (CZ) method. We further explore what are currently key drivers of cost, such as the historically high iridium prices and present cost-sensitivity analysis of other various drivers' impact on the final cost. The key result presented is that EFG has a 2 \times cost advantage compared to epi-wafers grown via the CZ method.

9:15 AM EL11.11.03

Thermodynamic Phase Control of Highly Crystalline and Oriented Ga_2O_3 Thin Films using Pulsed Laser Deposition Amit K. Khare and Igor Shvets; Trinity College Dublin, The University of Dublin, Ireland

Among possible candidates to be the base materials for power electronics, Ga_2O_3 is particularly interesting owing to its excellent material properties (e.g. high-voltage blocking capability and high-temperature operation) that guarantee higher efficiency and lower loss with excellent compatibility with industrial production processes. Although, some of the fundamental materials issues, such as understanding the electronic structure and controllability of composition, require a focused effort to unravel its full potential. Here we present the phase control, stability and growth mechanisms of highly crystalline Ga_2O_3 thin films. β - and γ - Ga_2O_3 thin films are deposited on c-plane sapphire and MgO (100) substrates using pulsed laser deposition in ambient from the vacuum (1e-7 Torr) to oxygen partial pressure (OPP, 2 mTorr). Highly oriented γ - and β - Ga_2O_3 phases are stabilized at the same temperature, only changing the ambient during the film growth. Reflection high-energy electron diffraction and ex-situ high-resolution x-ray diffraction (HRXRD) confirmed the formation of single-phase films with excellent crystalline quality. It is found that the films crystallize in monoclinic β -phase with (-201)-orientation when deposited in oxygen ambient, while it crystallizes in the γ -phase with (111)-orientation when deposited in the vacuum. We observe that the difference between the lattice spacings of the (-201) β -phase and the (111) γ -phase is very subtle; therefore, HRXRD alone is not sufficient in identifying the distinct phases. All the films are electrical insulators at room temperature, suggesting minimal defect related to oxygen vacancies in β - Ga_2O_3 , further supported by x-ray photoemission spectroscopy studies. Additionally, the Raman spectra revealed the phase control in Ga_2O_3 films because Raman active modes are present only in the β -phase, in contrast to the γ -phase.

9:30 AM EL11.11.04

Vertical α - Ga_2O_3 Device Applications Enabled by Same Crystal Structured Indium Tin Oxide Electrode via Mist Chemical Vapor Deposition Kazuki Shimazoe, Hiroyuki Nishinaka, Temma Ogawa and Masahiro Yoshimoto; Kyoto Institute of Technology, Japan

Extensive research has been conducted on gallium oxide (Ga_2O_3), an ultra-wide bandgap material, in the field of power electronics and deep UV optoelectronic devices. The band gap of Ga_2O_3 ranges from 4.4 to 5.3 eV, surpassing the bandgap of Si, SiC, and GaN, thus indicating its potential for enhanced device performance. Among the polymorphs of Ga_2O_3 , namely α , β , δ , γ , and κ , α - Ga_2O_3 is characterized by the highest bandgap of 5.3 eV. [1] This α phase exhibits promising potential in power-switching and deep-UV optoelectronics devices, such as Schottky barrier diodes and photodetectors, owing to its ultra-wide bandgap. [2-3] A vertical device structure can provide low on-resistivity and rapid response. One way to realize vertical structure is by inserting a conductive layer under the active layer. However, the growth of metastable α - Ga_2O_3 necessitates an epitaxial growth on other substrates, and an insulating α - Al_2O_3 substrate is usually used, making realizing vertical structure challenging. To address this issue, we featured high-conductive rhombohedral indium tin oxide (rh-ITO) as the bottom electrode. This rh-ITO exhibits the same crystal structure as α - Ga_2O_3 ; therefore, it is expected that α - Ga_2O_3 is grown epitaxially on the rh-ITO electrode. This study demonstrates heteroepitaxial growth of α - Ga_2O_3 on rh-ITO electrode and its device applications.

Mist CVD was utilized for the epitaxial growth of oxide thin films. Initially, we investigated the growth of α - Ga_2O_3 on rh-ITO, however, orthorhombic κ - Ga_2O_3 was grown on bare rh-ITO thin films because of the large lattice mismatch between α - Ga_2O_3 and rh-ITO (-9.2%). Therefore, to decrease the lattice mismatch, α - Fe_2O_3 buffer layers with a small lattice mismatch (-1.0 %) were utilized for the growth of α - Ga_2O_3 thin films. XRD 2θ scans determined that the α - Fe_2O_3 buffer layer allowed the growth of α - Ga_2O_3 thin films on rh-ITO thin films. Furthermore, XRD phi scans revealed that α - Ga_2O_3 thin films were successfully grown in the same in-plane orientations as rh-ITO and c-plane sapphire substrates. These XRD measurements indicated that α - Ga_2O_3 thin films were epitaxially grown on the rh-ITO/c-plane sapphire substrates.

Next, we conducted device operations using α - Ga_2O_3 thin films with rh-ITO thin films as bottom electrodes, and fabricated two device architectures, deep-UV photodetectors, and Schottky barrier diodes. For photodetectors, PEDOT:PSS thin films, exhibiting high transparency in the deep UV region to the visible light region, high conductivity, and large work function were utilized for top electrodes. PEDOT:PSS thin films were deposited by mist deposition [4]. The n-type α - Ga_2O_3 and PEDOT:PSS showed Schottky behavior enabling the separation of the photo-excited hole-electron pairs. The spectral photoresponsivity of the photodetector was measured using a short-circuit current and demonstrated the ability to detect UV-C region light without any bias voltage. The photoresponsivity at 220 nm was 9.7×10^{-4} A/W, exceeding that of a self-powered lateral structured α - Ga_2O_3 photodetector, thereby suggesting its association with the vertical structure, which can reduce the recombination of photogenerated carriers [3]. Furthermore, we investigated the Schottky barrier diode based on α - Ga_2O_3 with Ni/Au electrode deposited by thermal evaporation. Current-voltage measurements confirmed the rectification characteristics of the diode, which can be attributed to the Schottky contact between Ni and α - Ga_2O_3 . These results demonstrate the device applications of α - Ga_2O_3 grown on rh-ITO bottom electrodes using mist chemical vapor deposition, including deep-UV photodetectors and Schottky barrier diodes.

References

- [1] D. Shinohara, and S. Fujita, Jpn. J. Appl. Phys. 47, p. 7311 (2008)
- [2] M. Oda, et al., Appl. Phys. Express 9, p. 021101 (2016)
- [3] J. Bae, et al., APL Mater. 9, p. 101108 (2021)
- [4] T. Ikenoue, et al., Thin Solid Films, 520, p. 1978 (2012)

9:45 AM EL11.11.05

High-Temperature Characteristics of β - Ga_2O_3 -Based p-i-n Heterojunction Rectifiers Kingsley O. Egbo¹, William Callahan¹, Brooks Tellekamp¹, Ryan O'Hayre² and Andriy Zakutayev¹; ¹National Renewable Energy Laboratory, United States; ²Colorado School of Mines, United States

Electronic device performance and reliability under extreme conditions such as at very high temperatures is essential for several applications in the industrial, energy, and automotive sectors. Wide band gap semiconductor devices using SiC and GaN have demonstrated operation in the 400-600°C temperature range for prolonged periods of time. However, >600°C operation in oxidizing and reducing conditions requires the next generation of chemically robust ultra-wide band gap semiconductor devices where GaN and SiC fail. Wide bandgap β - Ga_2O_3 , an important material for high-power device applications, also shows promise for high-temperature electronics due to reduced temperature-activated parasitic leakage and chemical stability. Ga_2O_3 is not p-type dopable therefore currently studied devices use heterojunction architectures, often with p-type NiO. Unfortunately, NiO and Ga_2O_3 are not predicted to be thermodynamically stable at high temperatures. NiGa_2O_4 , however, is stable in contact with Ga_2O_3 at high temperatures and is investigated for the first time in this work.

Here, we explore the high-temperature characteristics of vertical heterojunction NiO/ β - Ga_2O_3 and NiGa_2O_4 / β - Ga_2O_3 p-i-n diodes fabricated using commercial HVPE grown drift layers (Novel Crystal Technology). For both heterojunctions pulsed laser deposition (PLD) was used to grow ~200 nm thick p-layer on a 1 μm thick HVPE β - Ga_2O_3 (001) ($\sim 3.5 \times 10^{16} \text{cm}^{-3}$) layer deposited on an Sn-doped β - Ga_2O_3 wafer ($\sim 2 \times 10^{18} \text{cm}^{-3}$). The device was processed using photolithography and the device area mesa isolation was achieved by argon dry etching¹. Anode top contacts on the p-type layers were formed by depositing 30 nm Ni / 100 nm Au via e-beam evaporation while stable Ohmic back contact to Ga_2O_3 was formed by 5 nm Ti / 100 nm Au annealed under N_2 at 550 °C for 90 seconds². Temperature-dependent current-voltage (I-V) characteristics were measured in vacuum ($\leq 10^{-4}$ Torr) for temperature setpoints in the range of RT-800°C using a custom-built high-temperature probe station.

The rectification ratio was found to be 10^8 (2V) at room temperature (RT) for both the NiO/ Ga_2O_3 and NiGa_2O_4 / Ga_2O_3 devices, however, a lower turn on-voltage is observed for NiGa_2O_4 (1.4V compared to 1.8V) and is attributed to a smaller barrier height in NiGa_2O_4 / Ga_2O_3 . The turn-on voltage for both device stacks decreased monotonously with increasing temperature. However, while the specific on-resistance decreased rapidly with temperature for the NiO/ Ga_2O_3 device, the decrease in specific on-resistance in NiGa_2O_4 / Ga_2O_3 device was negligible. Thus, while the rectification ratio of the NiO/ Ga_2O_3 device was $>10^3$ at 600°C, the NiGa_2O_4 / Ga_2O_3 device showed a lower ratio of 10^2 due to small forward current attributed to low carrier density in NiGa_2O_4 compared to NiO. The measured reverse leakage current increased with temperature due to increasing intrinsic carriers, nonetheless, both devices maintained a leakage current density of $<10^{-3} \text{A/cm}^2$ at 600°C.

To explore long-term continuous operation at high temperatures, the device was soaked at 600°C (>100 hours) and subjected to repeated thermal cycling (30 times) between room temperature and 550°C in flowing N_2 and in laboratory ambient air. Both devices show good stability however the NiO- Ga_2O_3 device had better performance compared to the NiGa_2O_4 - Ga_2O_3 device due to a higher built-in voltage. These results suggest that irrespective of thermally driven leakage current increase, Ga_2O_3 -based p-i-n diodes hold great potential for high-temperature operation with $<10^{-3} \text{A/cm}^2$ leakage current density at $>600^\circ\text{C}$ operating temperature.

¹Sohel, S. H. *et al.* Gallium Oxide Heterojunction Diodes for Improved High-Temperature Performance. Preprint at <http://arxiv.org/abs/2204.00112> (2022).

²Callahan, W. *et al.* Ultrathin stable ohmic contacts for high-temperature operation of β - Ga_2O_3 devices. Preprint at <https://arxiv.org/abs/2304.02161> (2023).

10:00 AMBREAK

10:30 AM *EL11.11.06

Innovative Solutions to Overcome Challenges in Gallium Oxide TechnologySrabantiChowdhury; Stanford University, United States

In any electronics application today, higher power density is desired. Switches are an integral part of every power converter, impacting its efficiency directly. RF transistors are the backbone of high-frequency power amplifiers for base stations or radars, impacting not only the sustainability of 5G but also national security and resilience. Although Silicon has been the backbone of electronics, it is simply clear when high temperature, high frequency, and high-power density when required simultaneously for an application, wide bandgap semiconductors like Silicon Carbide (SiC) and Gallium Nitride (GaN) are the forerunners. Already commercialized in some RF and power applications, they have pushed the roadmap further beyond Si, owing to their superior material quality. While SiC and GaN are making impressive headway, even wider bandgap semiconductors are being evaluated in labs to understand their role in electronics and optoelectronics. One of the emerging ultra-wide bandgap (UWBG) materials is Ga₂O₃. Vertical MOSFET was a critical milestone in the gallium oxide (Ga₂O₃) roadmap that was recently achieved [1]. Due to the lack of an effective current blocking layer in Ga₂O₃, which is essential for any DMOS-like (double-diffused MOSFET) the achievement of a vertical MOSFET has been difficult. Using two novel findings first, a selective diffusion doping technique utilizing magnesium (Mg) doping spin-on-glass (SOG) as a dopant source to form a current blocking layer (CBL), and second, the first demonstration of a vertical Ga₂O₃ MOSFET with the Mg diffused CBL- Vertical Diffused Barrier Field-Effect-Transistor (VDBFET). At its very first stage of development, the device exhibited an excellent field effect-transistor (FET) behavior with a high on-off ratio of 10⁹ and a decent saturation. If successful, this technology can lead to at least a 3x increase in power density in vertical switches over and above SiC and GaN, and at a lower cost per die.

Besides the lack of p-type Ga₂O₃, thermal management has been a challenge. For achieving high power density at high frequencies, with aggressive device scaling heat generation is unavoidable. However, the room temperature thermal conductivity of β -Ga₂O₃ (anisotropic; 11-27 W/mK) is the lowest among the technologically relevant semiconductor materials [2]. Polycrystalline diamond epitaxial growth on β -Ga₂O₃ for device-level thermal management was performed and reported in our recent study. Our study focused on establishing diamond growth conditions on β -Ga₂O₃ accompanying the study of various nucleation strategies [3]. A growth window was identified, yielding uniform-coalesced films while maintaining interface smoothness. In this first demonstration of diamond growth on β -Ga₂O₃, a diamond thermal conductivity of $110 \pm 33 \text{ W m}^{-1} \text{ K}^{-1}$ and a diamond/ β -Ga₂O₃ thermal boundary resistance of $30.2 \pm 1.8 \text{ m}^2 \text{ K G}^{-1} \text{ W}^{-1}$ were measured. The film stress was managed by growth optimization techniques preventing delamination of the diamond film. It marked a significant step toward device-level thermal management of β -Ga₂O₃ electronic devices.

These two recent experimental studies set the stage to systematically study and understand the challenges of Ga₂O₃ technology and create a road map beyond GaN

References

1. K. Zeng, R. Soman, Z. Bian, S. Jeong, and S. Chowdhury, "Vertical Ga₂O₃ MOSFET With Magnesium Diffused Current Blocking Layer," in *IEEE Electron Device Letters*, vol. 43, no. 9, pp. 1527-1530, Sept. 2022
2. S. Choi, S. Graham, S. Chowdhury, E. R. Heller, M. J. Tadjer, G. Moreno, and S. Narumanchi, "A perspective on the electro-thermal co-design of ultra-wide bandgap lateral devices", *Appl. Phys. Lett.* vol. 119, p. 170501, 2021.
3. M. Malakoutian, Y. Song, C. Yuan, C. Ren, J. S. Lundh, R. M. Lavelle, J. E. Brown, D. W. Snyder, S. Graham, S. Choi, and S. Chowdhury, "Polycrystalline diamond growth on β -Ga₂O₃ for thermal management," *Applied Physics Express*, vol. 14, no. 5, p. 055502, 2021

11:00 AM EL11.11.07

Electrical and Thermal Properties of BeO Gate Dielectrics for β -Ga₂O₃ Power DevicesDohanJung¹, YoonseongJang¹, PrakashR. Sultane², ChristopherW. Bielawski² and JungwooOh¹; ¹Yonsei University, Korea (the Republic of); ²UNIST, Korea (the Republic of)

Monoclinic gallium oxide (β -Ga₂O₃) is a promising wide-bandgap semiconductor for power device application. β -Ga₂O₃ demonstrates superior material performance, including an ultra-wide bandgap of 4.8-4.9 eV, a high breakdown field of approximately 8 MV/cm, and a remarkable bulk electron mobility of $\sim 300 \text{ cm}^2 \text{ V}^{-1} \text{ s}^{-1}$, showing a Baliga's Figure of Merit (BFOM) of up to 3444. Despite these properties, the primary drawback of β -Ga₂O₃ lies in its heat management capabilities. It exhibits a low thermal conductivity of 10-30 Wm⁻¹K⁻¹, which is significantly lower compared to other power semiconductors such as GaN (220 Wm⁻¹K⁻¹) and SiC (280-342 Wm⁻¹K⁻¹), which potentially makes β -Ga₂O₃ susceptible to malfunctions under high-temperature operation.

The use of conventional gate dielectrics for β -Ga₂O₃ power devices might worsen the thermal dissipation issue. Oxides typically possess low thermal conductivity. For instance, SiO₂ exhibits approximately 1.4 Wm⁻¹K⁻¹, and HfO₂ exhibits approximately 1.2 Wm⁻¹K⁻¹ of thermal conductivity. To address these challenges, we propose beryllium oxide (BeO) gate dielectrics for β -Ga₂O₃ power devices. BeO possesses unique properties, including a bandgap energy of 10.6 eV, a high dielectric constant of 6.8, and most importantly, an extraordinarily high thermal conductivity of approximately 330 Wm⁻¹K⁻¹ coupled with high thermal stability. Its thermal conductivity is the highest among oxides, surpassing that of most metals except for copper and silver. Consequently, BeO holds significant potential in improving the heat dissipation capabilities of β -Ga₂O₃ power devices. However, its application to nanoscale front-end devices has been constrained by the absence of well-established thin film deposition techniques.

In this work, we developed the atomic layer deposition (ALD) of BeO. This technique enables the precise and high-quality deposition of thin film on the substrates. ALD BeO gate dielectrics were successfully grown on β -Ga₂O₃ substrates. We comprehensively analyzed the physical and electrical properties of ALD BeO deposited on β -Ga₂O₃. A BeO on β -Ga₂O₃ was confirmed via a survey scan of X-ray Photoelectron Spectroscopy (XPS). The cross-section TEM image revealed a uniform thickness and a sharp interface between BeO and β -Ga₂O₃. The crystalline growth of BeO in the (102) diffraction on the β -Ga₂O₃ substrate was confirmed using Grazing Incidence X-ray Diffraction (GI-XRD). In addition, we analyzed the electrical properties of BeO gate dielectrics on β -Ga₂O₃ power devices. We determined the conduction band offset (3.4 eV) between the BeO film and β -Ga₂O₃ substrate using Kraut's method, which involved the determination of the valence band offset (0.5 eV) using the XPS core level and valence band maximum energies of the BeO film and β -Ga₂O₃ substrate. The bandgap energies of BeO (8.6 eV) and β -Ga₂O₃ (4.7 eV) were determined using reflection electron energy loss spectroscopy (REELS). The large conduction band offset of ALD BeO on the β -Ga₂O₃ substantially lowered the gate leakage current of β -Ga₂O₃ MOS capacitors. The forward leakage current was $2.21 \times 10^{-9} \text{ A/cm}^2$ at 1 MV/cm for 100 nm Mo electrodes/24 nm BeO dielectrics/ β -Ga₂O₃ substrates, demonstrating the potential of ALD BeO as gate dielectrics for high-performance β -Ga₂O₃ power devices.

11:15 AM EL11.11.08

Vertical Van Der Waals Heterojunction Diodes Comprising 2D Semiconductors on 3D β -Ga₂O₃ChloeLeblanc¹, DinushaHerath Mudiyansele², SeungukSong¹, HuairuoZhang^{3,4}, AlbertV. Davydov³, HouqiangFu² and DeepM. Jariwala¹; ¹University of Pennsylvania, United States; ²Arizona State University, United States; ³National Institute of Standards and Technology, United States; ⁴Theiss Research, Inc., United States

Monocyclic Gallium oxide β -Ga₂O₃ is a promising candidate for high-power and high-temperature electronics and UV-range optoelectronic devices. Its advantageous properties include an ultra-wide bandgap, high critical electric field, and affordable bulk single crystal melt-growth techniques at the large production scale. However, single crystalline β -Ga₂O₃ substrates are seldom explored, in part due to the uncertain effects of the semiconductor's proven anisotropy. In this study, we fabricated 2D/3D β -Ga₂O₃ vertical heterojunctions and comprehensively assessed the effect of the choice of 2D material, contact metal and substrate crystalline orientation on their performance. Three orientations of degenerately n-doped β -Ga₂O₃ were considered: (001), (010) and (-201). Tungsten diselenide (WSe₂), tungsten disulfide (WS₂) and black phosphorus (BP) were chosen as 2D semiconductor materials for their popularity in high-performing optoelectronic devices, field-effect transistors (FETs) and light-emitting diodes (LEDs) among others. We compared Electron beam (E-beam) evaporated titanium (Ti), molybdenum trioxide (MoO₃) and palladium (Pd) as candidates for electrical contacts, with thicknesses based on previous reports of low-resistance: Ti/Au (10/90nm), MoO₃/Au (3/30nm), Pd/Au (30/70nm). The structure and properties of our fabricated devices were then evaluated using current-voltage (I-V) measurements at varying temperatures, atomic-force microscopy (AFM) techniques and technology computer-aided design (TCAD) simulations. Scanning transmission electron microscopy (STEM) cross-sectional images verified the clean interfaces of the heterostructures. We were able to realize high-performing diodes, whose ideality factors ranged from 1 to 3. Our findings suggest that heterojunction performance is optimized by the β -Ga₂O₃ orientation (-201), combined with 2D WS₂ exfoliated layers and Ti metal contacts, and show record rectification ratios ($> 10^6$) concurrently with ON current density ($> 10^3 \text{ A/cm}^2$) for application in power rectifiers. The lowest ideality factors along the (-201) orientation were 1.18 (BP & Ti/Au contacts), 1.22 (WS₂ & Ti/Au contacts) and 1.43 (WS₂ & Pd/Au contacts) in line with some of the best 2D/3D van der Waals heterojunction diodes reported in the past. The TCAD simulations were able to verify this, and accurately mimic the (-201) heterostructures' behavior. At large biases and before the junctions reach saturation, the exponential current density increase matches the strongly rectifying property of ideal diodes. In such a linear regime, the devices are driven by the diffusion current across the internal 2D/3D potential barrier. Moreover, the reverse and low forward bias regions present current densities that are both very low ($< 10^{-10} \text{ A}/\mu\text{m}^2$) and independent of the applied voltage. Our findings demonstrate a facile fabrication of strongly rectifying and high ON current density Ga₂O₃-based heterojunction diodes and enables this material's potential for new avenues in solid state devices.

11:30 AM EL11.11.09

Implantation and Activation of Ge and Si Shallow Donors in β -Ga₂O₃ for Improved Ohmic Contact FormationKorneliusTetzner¹, AndreasThies¹, PalvanSeyidov², NicoThiele¹, Ta-ShunChou², JanaRehm², InaOstermay¹, ZbigniewGalazka², AndreasFiedler², AndreasPopp², JoachimWürl¹ and OliverHilt¹; ¹Ferdinand-Braun-Institut, Germany; ²Leibniz-Institut für Kristallzüchtung, Germany

The recent developments in the fabrication of electronic devices based on the semiconductor β -Ga₂O₃ have demonstrated the high potential of this material to be used in next-generation power electronics applications. Due to the ultra-wide bandgap of 4.8 eV, a high breakdown strength of 8 MV/cm is expected, which could pave the way for power devices with even higher

breakdown voltages and efficiencies than are possible with the SiC and GaN counterparts. One major key requirement for high performance electronic devices based on ultrawide bandgap semiconductors such as $\beta\text{-Ga}_2\text{O}_3$ is the formation of low ohmic contact resistances in order to reduce conduction losses inside the devices. This becomes even more important for RF devices, where the channel resistance is much lower as in high-voltage devices. An effective way to reduce ohmic contact resistances is the use of ion implantation of shallow donors for local n-type doping of the contact region prior to ohmic metal deposition.

In this presentation, we report on the optimum annealing conditions for the activation of Ge-implanted (100) $\beta\text{-Ga}_2\text{O}_3$ in order to reach low ohmic contact resistances. In this regard, the influence of rapid thermal annealing treatment at temperatures between 900 and 1200 °C on the structural and electrical properties were analyzed. Our studies reveal significant changes in the surface morphology after high-temperature annealing above 1000 °C involving an increase in the surface roughness which is accompanied with a steady increase of the activation efficiency up to almost 20% at annealing temperatures of 1200 °C. Optimum annealing conditions were identified at 1100 °C at which the specific contact resistance is reduced by one order of magnitude down to $4.8 \times 10^{-7} \Omega\text{cm}^2$ in comparison to non-implanted samples. In contrast to these findings, the surface morphology of Si-implanted (010) $\beta\text{-Ga}_2\text{O}_3$ with a comparable doping profile remains almost unchanged even after annealing at 1100 °C. Furthermore, the highest activation efficiency of around 60 % is reached at annealing temperatures between 900 and 1000 °C whereas higher temperatures lead to significant reduction. Our investigations verify the severe impact of the anisotropic nature of $\beta\text{-Ga}_2\text{O}_3$ on implantation processes of shallow donors which is particularly emphasized by the implantation instability of (100) $\beta\text{-Ga}_2\text{O}_3$ at high beam currents. Comparative experiments on $\beta\text{-Ga}_2\text{O}_3$ samples with different crystal orientations revealed a massive destruction of the (100) $\beta\text{-Ga}_2\text{O}_3$ surface after Ge implantation using beam currents around 1 μA whereas no damage was observed for (010) $\beta\text{-Ga}_2\text{O}_3$ using the same implantation conditions.

In summary, our results will reveal and identify important challenges but also the huge potential of ion implantation of shallow donors into $\beta\text{-Ga}_2\text{O}_3$ in order to reach low ohmic contact resistances.

11:45 AM EL11.11.10

Optimizing Si Implantation and Annealing in $\beta\text{-Ga}_2\text{O}_3$ and $\beta\text{-(Al}_x\text{Ga}_{1-x})_2\text{O}_3$ Katie R. Gann¹, Naomi Pieczulewski¹, Cameron Gorsak¹, Karen Heinselmann², Kathleen Smith¹, Thaddeus Asel³, Brenton Noesges³, Huili G. Xing¹, Debdeep Jena¹, David Muller¹, Hari P. Nair¹ and Michael O. Thompson¹; ¹Cornell University, United States; ²National Renewable Energy Laboratory, United States; ³Air Force Research Laboratory, United States

Optimizing thermal activation anneals for silicon ion implantation in $\beta\text{-Ga}_2\text{O}_3$ is critical for achieving low resistance contacts and selective area doping for advanced device structures. While activation has been widely reported, annealing conditions vary significantly and systematic annealing studies are lacking. We report the impact of time, temperature, and especially the annealing ambient, on the activation of Si in $\beta\text{-Ga}_2\text{O}_3$ at concentrations from $5 \times 10^{18} \text{ cm}^{-3}$, to $1 \times 10^{20} \text{ cm}^{-3}$, and in $\beta\text{-(Al}_x\text{Ga}_{1-x})_2\text{O}_3$ ($x \leq 25\%$) at concentrations up to $5 \times 10^{19} \text{ cm}^{-3}$. Under optimized conditions, nearly full activation (>80%) and high mobility (>70 $\text{cm}^2/\text{V-s}$) are achieved in $\beta\text{-Ga}_2\text{O}_3$ at implant concentrations to $1 \times 10^{20} \text{ cm}^{-3}$, with contact resistances below 0.16 $\Omega\text{-mm}$ for $5 \times 10^{19} \text{ cm}^{-3}$. Similar optimized anneal conditions for $\beta\text{-(Al}_x\text{Ga}_{1-x})_2\text{O}_3$ show promising results with high activation (50%) and mobility recovery (>60 $\text{cm}^2/\text{V-s}$) at 9% Al.

Unintentionally doped (UID) $\beta\text{-Ga}_2\text{O}_3$ films (>400 nm) were grown by plasma assisted molecular beam epitaxy, and $\beta\text{-(Al}_x\text{Ga}_{1-x})_2\text{O}_3$ layers by metal-organic chemical vapor deposition, on Fe-doped (010) $\beta\text{-Ga}_2\text{O}_3$ substrates. Samples were ion implanted with Si at multiple energies to yield 65 or 100 nm box profiles with concentrations of $5 \times 10^{18} \text{ cm}^{-3}$, $5 \times 10^{19} \text{ cm}^{-3}$, or $1 \times 10^{20} \text{ cm}^{-3}$. Dopant activation was achieved by annealing as-implanted films in a load-locked ultrahigh vacuum compatible quartz tube furnace at 1 bar pressure with precisely controlled gas ambient.

The impact of O_2 (partial pressure $< 10^{-6}$ to 1 bar) and H_2O (to 25 ppm) in the annealing ambient condition was determined by mixing trace gases in research plus grade nitrogen (< 1 ppm total impurities). To maintain the stability of the $\beta\text{-Ga}_2\text{O}_3$, P_{O_2} must be greater than 10^{-9} bar, with annealing in vacuum or forming gas resulting in poor activation or decomposition, respectively. The upper limit for P_{O_2} is strongly dependent on Si concentration: P_{O_2} below 10^{-4} bar ensures Si activation (>85%) at $5 \times 10^{19} \text{ cm}^{-3}$ while lower concentration implants ($5 \times 10^{18} \text{ cm}^{-3}$) maintain high carrier activation to oxygen partial pressures above 10^{-2} bar. Water vapor is even more critical at ppm concentrations; 25 ppm H_2O reduces active carriers by an order of magnitude $5 \times 10^{19} \text{ cm}^{-3}$ implants. The effect is reversible, and activation can be recovered by annealing in a “dry” ambient. Optimal results were consistently obtained with the gas ambient intentionally dried below 10 ppb of H_2O .

Recovery of the mobility requires annealing temperatures above 900 °C, with increasing carrier activation and mobility to temperatures as high as 1050 °C, though SIMS shows substantial Si diffusion at temperatures above 1000 °C. 950 °C is identified as an optimized temperature with minimal Si diffusion, with optimal times between 5 and 30 minutes; shorter times show lower mobilities with longer durations showing carrier deactivation. “Over-annealing” behavior is observed at all temperatures and becomes increasingly significant with higher Si concentrations.

Lattice damage and recovery were determined using Rutherford Backscattering Channeling (RBS/C), scanning transmission electron microscopy (STEM), and X-ray diffraction (XRD). XRD showed no evidence of second phase formation and RBS/C and STEM show only partial damage from even $1 \times 10^{20} \text{ cm}^{-3}$ implants. In STEM, damage regions remain crystal-like with no evidence of full amorphization. The remnant aligned $\beta\text{-Ga}_2\text{O}_3$ is hypothesized to volumetrically seed lattice recovery during thermal annealing. Varying implant doses and implant temperatures (from liquid nitrogen cooled to 600 °C) were used to assess the impact of implant damage on lattice recovery.

In conclusion, we demonstrate the importance of optimizing anneal conditions to activate implanted Si carriers in $\beta\text{-Ga}_2\text{O}_3$ and extend this understanding to higher concentration Si implants and to activating implants in $\beta\text{-(Al}_x\text{Ga}_{1-x})_2\text{O}_3$.

SESSION EL11.12: Oxide Materials and Devices II
Session Chairs: Srabanti Chowdhury and Sriram Krishnamoorthy
Thursday Afternoon, November 30, 2023
Hynes, Level 2, Room 210

1:30 PM *EL11.12.01

The Applied Science of Gallium Oxide: Lessons, Challenges and Goals Daniel M. Dryden; Air Force Research Laboratory, United States

Gallium oxide ($\beta\text{-Ga}_2\text{O}_3$) is an emerging ultra-wide band gap semiconductor which shows promise across a range of applications due to its high critical breakdown field, readily available n-type dopant species, and low native substrate cost. The Air Force Research Laboratory is particularly interested in $\beta\text{-Ga}_2\text{O}_3$ for applications including high-frequency converter operation, power switching, and on-chip power conversion, all of which serve to improve the size, weight, power, and cost of sensors systems. Realizing the potential of $\beta\text{-Ga}_2\text{O}_3$ in prototype devices has necessitated clever solutions to challenging problems in materials science and materials engineering. In this talk, we will discuss some of the materials science and engineering challenges $\beta\text{-Ga}_2\text{O}_3$ has faced, as well as the solutions that have been implemented. We will discuss the identification and mitigation of Si contamination sources in $\beta\text{-Ga}_2\text{O}_3$ epitaxy, optimizing regrowth and liftoff for ohmic contact formation, defect engineering of the oxide-semiconductor interface in $\beta\text{-Ga}_2\text{O}_3$ MOSFETs, and challenges in device design for high-temperature applications. We will also discuss open challenges in $\beta\text{-Ga}_2\text{O}_3$ that may have solutions in future materials science research.

2:00 PM EL11.12.02

Computational Thermochemical Stability Analysis of Metal/ $\beta\text{-Ga}_2\text{O}_3$ Interface Cheng-Wei Lee¹, Andriy Zakutayev^{2,1} and Vladan Stevanovic^{1,2}; ¹Colorado School of Mines, United States; ²National Renewable Energy Laboratory, United States

Thermochemical stability of metal terminal contacts with wide-band-gap (WBG) semiconductors poses challenges for device fabrication. During the operation at high power and high temperature, such metal/oxide contacts can react and form interfacial layers that are electronically insulating. Experimental database of standard formation enthalpy of semiconductors can be used to estimate the stability of these metal/semiconductor interfaces but is mostly limited to binary materials. Furthermore, such estimation fails when a competing multi-component oxides (number of metal elements > 2) has a lower formation enthalpy per oxygen. On the other hand, density functional theory (DFT) databases include not only the binary but also most of the multi-component compounds documented in ICSD. Several efforts in the past, including the approach of fitted elemental-phase reference energies[1], has enabled prediction of formation enthalpy of these compounds using DFT results within chemical accuracy (~50 meV/atom).

Using $\beta\text{-Ga}_2\text{O}_3$ as an example, and building on these theoretical models, we perform thermochemical analysis to predict the stability of metal/ $\beta\text{-Ga}_2\text{O}_3$ interfaces. $\beta\text{-Ga}_2\text{O}_3$ has great n-type performance as power electronics and electron affinity (EA) around 4.0 eV. Based on the Schottky-Mott rule, metals with work functions (WF) around 4.0 eV will be ideal as Ohmic contact for $\beta\text{-Ga}_2\text{O}_3$. From the stability analysis, we found that Cd, In, Sn, Tl, Pb, and Bi are stable with $\beta\text{-Ga}_2\text{O}_3$ and the difference in WF from 4.0 eV is ≤ 0.3 eV. But we also notice that these metal candidates have low melting temperatures (<400 °C) and require very low oxygen partial pressure ($< 10^{-10}$ atm) to avoid oxidation when in contact with $\beta\text{-Ga}_2\text{O}_3$. Our results are also consistent with experimental findings [3,4] that the commonly used Ti contact is not stable with $\beta\text{-Ga}_2\text{O}_3$ at elevated temperature (~400 °C).

Based on the results for $\beta\text{-Ga}_2\text{O}_3$, we also identified a trend: Metals with smaller work functions, i.e. Fermi levels closer to vacuum level, are generally more reactive with oxygen molecules.

Such observation suggests that if a metal oxide's EA is smaller than the WF of its constituent metal, other metals with WF close to its EA will likely oxidize in contact with the metal oxide. For $\beta\text{-Ga}_2\text{O}_3$, the WF of Ga is ~ 4.3 eV from the vacuum level, which is larger than its EA at ~ 4.0 eV. To form Ohmic contacts, metals with EA around 4.0 eV are needed but the observed trend suggests that these metals are also likely to oxidize when in contact with Ga_2O_3 . On the other hand, metals with WF > 4.3 eV are needed to have stable interfaces but these form Schottky contacts. Such dilemma suggests that alternative approaches are needed for $\beta\text{-Ga}_2\text{O}_3$ and one alternative is to heavily dope the region near stable Schottky contacts to balance conductivity and stability at metal/semiconductor interfaces. This computational approach can be also used to identify suitable metal contacts for other UWBG semiconductors.

[1] Stevanović *et al.*, *Phys. Rev. B* 85, 115104 (2012)

[2] <https://materials.nrel.gov/>

[3] Heinselman *et al.*, *Journal of Vacuum Science & Technology A* 39, 040402 (2021)

[4] Callahan *et al.*, *Journal of Vacuum Science & Technology A*, Preprint at <https://arxiv.org/abs/2304.02161> (2023)

2:15 PM EL11.12.03

Computationally Predicted Electronic Structure of $\beta\text{-Ga}_2\text{O}_3(001)$ Interfaces with NiO Cheng-Wei Lee¹, Andriy Zakutayev^{2,1} and Vladan Stevanovic^{1,2}; ¹Colorado School of Mines, United States; ²National Renewable Energy Laboratory, United States

$\beta\text{-Ga}_2\text{O}_3$ is a promising ultra-wide band-gap oxide ($E_g \sim 4.9$ eV) due to its excellent n -type performance. Furthermore, high-quality and low-cost bulk single crystal can be grown from melt, making it particularly attractive for device fabrication and commercialization. However, no p -type doping has been realized for $\beta\text{-Ga}_2\text{O}_3$, preventing applications that involve homoepitaxial p - n junction. Instead, heterojunction is needed to fabricate device like MOSFET and $\beta\text{-Ga}_2\text{O}_3(001)/\text{NiO}$ heterojunction have been shown to have better rectifying performance than $\beta\text{-Ga}_2\text{O}_3/\text{Ni}$ Schottky diodes. Experimental J-V curve indicates existence of interfacial states but their identities remain unclear [1]. Furthermore, recently reported band alignment of the $\beta\text{-Ga}_2\text{O}_3(001)/\text{NiO}$ heterojunction strongly depends on the synthesis conditions [2]. Therefore, a computational study connecting atomic details at the interfaces and band alignment is critical for further engineering of the heterojunctions. However, an atomistic interface model, which is non-trivial to construct, is needed to computationally study the electronic structure of a heterojunction. We found that the experimentally observed orientations of (001) and (111) are among the top three NiO surfaces that best match the $\beta\text{-Ga}_2\text{O}_3(001)$ substrate, utilizing the recently developed atom-to-atom structure-matching algorithm [3]. Such consistency provides the credibility for the atomistic interface model for the subsequent electronic-structure calculation. Furthermore, we estimated the energetics of oxygen incorporation at the interface under different synthesis conditions to identify the most relevant atomistic interface models.

Another critical challenge of modeling such heterojunction lies in the selection of proper exchange-correlation functionals that can correctly describe the band gaps of $\beta\text{-Ga}_2\text{O}_3$ and antiferromagnetic rock-salt NiO simultaneously. Hybrid functionals like HSE06 are known to reproduce the band gap of $\beta\text{-Ga}_2\text{O}_3$ when an adjusted mixing parameter ($\alpha=0.32$) is used. But HSE06 requires a significantly smaller mixing parameter ($\sim\alpha=0.19$) to reproduce the band gap of NiO (~ 3.5 eV). The nature of homogeneous screening for HSE06 makes it challenging to find a mixing parameter that can describe the electronic structure of the whole heterojunction correctly at the same time [4]. Fortunately for NiO, its conduction band edge near minimum is mostly composed of localized Ni d orbital, which can be adjusted via on-site potential [5].

In this talk, we will show that HSE06+U method can simultaneously reproduce the respective band gaps of $\beta\text{-Ga}_2\text{O}_3$ and NiO within the interface. We predicted that the estimated built-in potentials for $\beta\text{-Ga}_2\text{O}_3(001)/\text{NiO}(111)$ and $\beta\text{-Ga}_2\text{O}_3(001)/\text{NiO}(001)$ are 1.9 and 2.9 eV, respectively, which are consistent with experimental measurements [1,2]. We also compared band alignments based on our atomistic models to results based on electron affinity rule and branch-point energy. The significant differences between different methods support the necessity to calculate band alignments based on atomistic interface models. Lastly, our findings suggest that a single-phase $\beta\text{-Ga}_2\text{O}_3(001)/\text{NiO}(001)$ heterojunction can have larger built-in potential and thus better rectifying performance than $\beta\text{-Ga}_2\text{O}_3(001)/\text{NiO}$ with mixed NiO orientations.

[1] Sohel *et al.* arXiv:2204.00112

[2] Xia *et al.* *J. Phys. D: Appl. Phys.* 55 385105 (2022)

[3] Therrien *et al.*, *Phys. Rev. Applied* 16, 064064 (2021)

[4] Zheng *et al.*, *Phys. Rev. Materials* 3, 073803 (2019)

[5] Ivády *et al.*, *Phys. Rev. B* 90, 035146 (2014)

2:30 PM EL11.12.04

Growth of Ga_2O_3 Nanowires Directly on Top of Interdigitated Electrodes for Their use as Chemoresistive Gas Sensor Anna Estany-Macià^{1,1}, Marina Rojano-Mateos^{1,1}, Jan Román-de Gea², Paolo Pellegrino^{1,1}, Mauricio Moreno-Sereno^{1,1} and Albert Romano-Rodríguez^{1,1}; ¹Universitat de Barcelona, Spain; ²Ecole Polytechnique de Lausanne (EPFL), Switzerland

Monoclinic $\beta\text{-Ga}_2\text{O}_3$ is a wide bandgap (4.9 eV) semiconducting material that is used for the fabrication of high power and high temperature electronic devices. Like other metal oxides, this material can also be used for the fabrication of gas sensing devices. For this, chemiresistive thin films of $\beta\text{-Ga}_2\text{O}_3$ have been demonstrated to respond to different gases, like oxygen, hydrogen, methane, and carbon monoxide, at temperatures above 600 °C. With the aim of lowering the operation temperature of this material to make it compatible with Internet-of-Things (IoT) applications, $\beta\text{-Ga}_2\text{O}_3$ nanowires (NWs) have been reported to respond, i.e., to change their resistance, to relative humidity at room temperature.

Following this last idea, in this work we present a fabrication route that allows the direct growth and integration of $\beta\text{-Ga}_2\text{O}_3$ NWs on top of substrates containing interdigitated electrodes.

Here, the $\beta\text{-Ga}_2\text{O}_3$ has been directly synthesized on top of fused silica substrates containing interdigitated electrodes made from Cr/Pt. The growth of the nanowires was performed at atmospheric pressure and temperatures above 800 °C inside a quartz tube inserted in a tubular furnace via a Vapor-Liquid-Solid mechanism, using gold as catalyst and a flux of 500 ml/min of argon as carrier. Two different methods for the generation of the precursor vapor have been used: either metallic gallium or a mixture of gallium oxide and graphite, for which a carbothermal reduction takes place. Structural and chemical characterization has been carried out using scanning (SEM) and transmission electron microscopy (TEM), and X-ray photoelectron spectroscopy (XPS). Furthermore, the samples have been mounted in a home-made stainless-steel miniaturized gas chamber and connected to a gas injections system through mass-flow controllers.

Alternating pulses of different gases (diluted relative humidity (RH), CO and NO₂) and dry synthetic air have been introduced into the chamber while resistance changes were measured.

SEM confirms that long (above 10 micrometer) and thin (below 50 nanometer) nanowires have been synthesized, which bridge the gap between the interdigitated electrodes. Furthermore,

TEM confirms the monocrystalline and almost defect-free nature of the NWs. A subtle difference between the NWs grown from the two precursor generation methods: for the carbothermal reduction, a carbon-rich shell layer is formed around the $\beta\text{-Ga}_2\text{O}_3$ NWs. This is confirmed by XPS and by Electron Energy Loss Spectroscopy inside the TEM. From an electrical point of view, the major difference is the value of the resistance in dry synthetic air, which is orders of magnitude lower for the NWs with the carbon shell. At room temperature, both type of sensors is sensitive to relative humidity and selective to almost all other gases.

In the presentation, the complete gas sensing behavior of these sensors will be presented and the differences will be discussed taking into account the differences in structural and chemical properties of the NWs.

2:45 PM EL11.12.05

Sol-Gel Synthesized $\beta\text{-Ga}_2\text{O}_3$ Nanostructures for Selective Detection of Formaldehyde Soumen Giri, Bidesh Mahata, Prasanta K. Guha and Prof. Pallab Banerji; IIT Kharagpur, India

Selective and accurate detection of formaldehyde (HCHO), one of the volatile organic compounds (VOCs), is crucial for various applications such as indoor air quality monitoring. Gallium oxide (Ga_2O_3) is a promising material due to its wide bandgap and distinctive physical and chemical properties for sensing applications. This study proposes a novel approach utilizing sol-gel technique to synthesize Ga_2O_3 nanostructures for VOC sensing such as formaldehyde, ethanol, acetone, 2-propanol, and toluene; and to investigate the kinetic parameters of the sensing materials using the Eley-Rideal model.

$\beta\text{-Ga}_2\text{O}_3$ was prepared by dissolving gallium (III) nitrate hydrate in different polar solvents at four different temperatures, viz. at 65 °C, 95 °C, 115 °C, and 135 °C for 5 h while the solution pH was kept at 10. It was found that cocoon-shaped nanostructures of $\beta\text{-Ga}_2\text{O}_3$ were formed at a temperature of 65 °C through the stacking of small nanoplates. As the temperature was increased to 95 °C, the nanoplates began to merge and grow thicker and wider due to Ostwald's ripening. At 115 °C, further Ostwald's ripening occurred, leading to the transformation of the multi-layered structures into rod-shaped structures of length 0.97 μm and diameter 0.15 μm . When the temperature reached to 135 °C, the growth process resulted in the formation of nanorods, with an average length of 10 μm and diameter of 1.0 μm .

Drop casting was used to deposit the sensing materials, $\beta\text{-Ga}_2\text{O}_3$ onto a ceramic substrate with interdigitated electrodes made of gold. Compared to other nanostructures, such as nanoparticles, cocoon-like structures, nanoplates, and high aspect ratios of nanorods, a sensor based on $\beta\text{-Ga}_2\text{O}_3$ nanorod with a diameter of 150 nm, showed outstanding selectivity and sensitivity towards HCHO, even in the presence of other volatile organic compounds. The maximum response, $R = [(R_g - R_a) / R_a] \times 100\%$, where R_g and R_a has their usual meaning, for formaldehyde at 300 °C at a concentration of 300 ppm was found to be 23.2%. The Eley-Rideal model considers the direct interaction of gas molecules adsorbed on the sensor surface with the pre-adsorbed species. By fitting experimental data to theoretical response transient curves, key kinetic parameters such as adsorption and reaction rates were determined. The activation energy determined by the model for HCHO sensing at concentrations ranging from 50 to 300 ppm is found to be 0.05972 eV. The low activation energy indicates that the sensing method is reasonably efficient, needing low energy for HCHO molecules to react with the $\beta\text{-Ga}_2\text{O}_3$ nanorods and generate observable signals or changes.

$\beta\text{-Ga}_2\text{O}_3$, an n -type semiconductor, surprisingly exhibits p -type conductivity in our experiments. XPS analysis reveals that the overall concentration of absorbed oxygen, including oxygen vacancies and chemisorbed oxygen, exceeds that of lattice oxygen. A significant number of electrons in the conduction band are captured when oxygen species are adsorbed. Consequently, the electron concentration is reduced relative to the hole concentration, leading to the formation of an inversion layer and enabling $\beta\text{-Ga}_2\text{O}_3$ to display p -type conductivity. The electrons from the conduction band are efficiently trapped by adsorbed oxygen species, leading to a bending of the energy band and the creation of an inversion layer. At elevated temperatures (300 °C), the sensor reacts with reducing gases like HCHO to create H₂O, CO₂ and e⁻. The subsequent annihilation of released electrons with holes reduces the thickness of the hole accumulation layer, causing a decrease in the conductivity of $\beta\text{-Ga}_2\text{O}_3$ nanorods. When HCHO is removed, the released holes return to the valence band, increasing the hole concentration and decreasing the

resistance.

<quillbot-extension-portal></quillbot-extension-portal>

3:00 PMBREAK

3:30 PM *EL11.12.06

Epitaxial Growth and Phase Stability of α -(Al,Ga)₂O₃RienaJinno; The University of Tokyo, Japan

In recent years, ultra-wide bandgap (UWBG) semiconductor materials ($E_g > 3.4$ eV) have attracted much attention as materials for high-power electronics and ultraviolet photonics. α -(Al,Ga)₂O₃ is an oxide family possessing a UWBG energy spanning 5.4 to 8.6 eV [1]. At the present stage, n-type conductivity control is possible in the Ga-rich region ($E_g \sim 5.5$ eV). However, a recent first-principles study predicts that Si can be an efficient shallow donor up to a bandgap of 7.5 eV (Al compositions of 0.71) for α -(Al_{1-x}Ga_x)₂O₃ [2]. The UWBG larger than 6 eV is unachievable in the nitride semiconductor family, offering the possibility to take semiconductor electronics and photonics into regimes that currently remain out of reach. This talk will focus on the recent progress of phase stability and plasma-assisted molecular beam epitaxy (PAMBE) of α -(Al_{1-x}Ga_x)₂O₃.

The challenge of α -(Al_{1-x}Ga_x)₂O₃ is related to the metastable characteristic of α -Ga₂O₃. The ground-state crystal structure of Al₂O₃ is rhombohedral corundum (α phase), while Ga₂O₃ takes the monoclinic β -gallia (β -phase). A theoretical study using hybrid density functional theory calculations elucidated that the β -phase is the preferred structure up to an Al concentration of 71%, and α -(Al_{1-x}Ga_x)₂O₃ is stable at $x > 0.7$ [3]. In experiments, α -(Al_{1-x}Ga_x)₂O₃ with Al contents lower than 70% converted to the β -phase, while the Al-rich α -(Al_{1-x}Ga_x)₂O₃ is stable, in good agreement with the theoretical stability [4].

The epitaxial growth of α -(Al_{1-x}Ga_x)₂O₃ is typically conducted on sapphire (α -Al₂O₃) substrates. The growth of α -(Al_{1-x}Ga_x)₂O₃ by MBE suffered due to the inclusion of the β -phase, especially for growth on c-plane substrates. The c-plane facet was found to enhance the growth of β -Ga₂O₃ in MBE. The sapphire crystal plane perpendicular to the c-plane, such as a- or m-planes, allowed the growth of phase-pure α -(Al_{1-x}Ga_x)₂O₃ by avoiding the facets. Interestingly, the homoepitaxial growth of α -Al₂O₃ also required preventing the c-plane facet. The crystal orientation dictated epitaxy was also useful for metal-organic chemical vapor deposition and pulsed laser deposition [5,6]. If Al-rich α -(Al_{1-x}Ga_x)₂O₃ can be controllably doped, it would pave the way for α -(Al_{1-x}Ga_x)₂O₃-based high-power heterostructure electronic and photonic devices at bandgaps far beyond all materials available today.

This work was partially supported by NEDO Feasibility Study Program Uncharted Territory Challenge 2050.

[1] R. Jinno, *et. al.*, *Sci. Adv.* **7**, eabd5891 (2021).

[2] D. Wickramaratne, *et. al.*, *Appl. Phys. Lett.* **121**, 042110 (2022).

[3] H. Peelaers, *et. al.*, *Appl. Phys. Lett.* **112**, 242101 (2018).

[4] R. Jinno, *et. al.*, *JJAP* **60**, SBBD13 (2020).

[5] A F M A. U. Bhuiyan, *et. al.*, *APL Mater.* **9**, 101109 (2021).

[6] M. Kneiß, *et. al.*, *J. Mater. Res.* **36**, 4865 (2021).

4:00 PM EL11.12.07

MOCVD Grown High-Al Content β -(Al,Ga)₂O₃ for Enabling 2DEGsCameronGorsak, JonathanP. McCandless, KatieR. Gann, HuiLiG. Xing, DebdeepJena, MichaelO. Thompson and HariP. Nair; Cornell University, United States

The unique properties of β -Ga₂O₃ including its ultra-wide bandgap of ~4.8 eV, critical breakdown field of ~8 MV/cm, availability of large-area native substrates, and controllable n-type doping have enabled rapid development in both growth and device processing. However, compared to other wide bandgap semiconductors, the intrinsic channel mobility is relatively low. A potential pathway to overcome this mobility limit is through two-dimensional electron gas (2DEG) formed at the interface of δ -doped β -(Al,Ga)₂O₃ and undoped β -Ga₂O₃. In this work, abrupt and smooth heterojunctions were grown at high Al concentrations using metal organic chemical vapor deposition (MOCVD) with TEGa and TEAL precursors.

Prior to growth, (010) β -Ga₂O₃ substrates were etched in hydrofluoric acid (HF) for 30 minutes to minimize parasitic interfacial Si doping. In pure β -Ga₂O₃, we have demonstrated mobilities of 156 and 114 cm²/Vs for 1x10¹⁷ and 1x10¹⁸/cm³ Si doping, respectively, with sub-nm RMS roughness. However, as the Al concentration increases, multiple material challenges must be addressed including potential segregation, dopant activation, and maintaining film smoothness. Using TMAI and TEGa precursors, we demonstrate sub-2 nm RMS roughness for 130 nm β -(Al_{0.09}Ga_{0.91})₂O₃ films. However, the growth temperature of 900 °C is too high for δ -doping; to reduce the growth temperature, TMAI was replaced with TEAL as the Al precursor due to the reduced cracking temperature. Additionally, TEAL shows potentially lower carbon incorporation because it pyrolyzes via β -hydrogen elimination whereas the pyrolysis of TMAI can leave behind highly reactive methyl radicals that may incorporate into the film.

Surface roughness, carrier activation, and mobility as a function of Al concentration and doping conditions are reported.

Combining effective substrate etching to remove a parasitic conducting channel with smooth highly doped β -(Al_{1-x}Ga_x)₂O₃ will enable high mobility 2DEGs which will open the opportunity for devices with high switching speeds to operate in extreme environments.

4:15 PM EL11.12.08

Monoclinic (In_xGa_{1-x})₂O₃ Alloys Investigated by Cyclical Molecular Beam Epitaxy Growth and *In-Situ* EtchStephenSchaefer, AndriyZakutayev and BrooksTeltekamp; National Renewable Energy Laboratory, United States

Gallium oxide (β -Ga₂O) has attracted attention as a candidate material for high-power diodes and transistors due to its wide bandgap, high breakdown voltage, controllable n-type dopability, and scalable melt growth of substrates. Its bandgap energy and electronic properties can be tuned by alloying with isoelectronic cations Al and In, however growth of the In-containing monoclinic alloy (In_xGa_{1-x})₂O₃ is challenging due to suboxide kinetics and the tendency for bixbyite In₂O₃ to phase separate.

This work uses cyclical growth and *in-situ* etching to rapidly investigate the (In_xGa_{1-x})₂O₃ growth space. Plasma-assisted molecular beam epitaxy (MBE) is used to grow (In_xGa_{1-x})₂O₃ on (010) oriented Fe doped Ga₂O₃ substrates at temperatures ranging from 590 to 770 °C and Ga and In beam equivalent pressures (BEP) ranging from 5x10⁻⁸ to 1x10⁻⁶ torr. Reflection high energy electron diffraction (RHEED) monitors the surface reconstruction and associated changes in streak d -spacing and FWHM during (In_xGa_{1-x})₂O₃ growth. The epilayer is then etched back *in-situ* by exposure to Ga flux without supplying oxygen plasma. Formation of the volatile suboxide Ga₂O and desorption of metallic In decomposes the (In_xGa_{1-x})₂O₃ film and recovers the initial Ga₂O₃ surface as evidenced by the FWHM of the RHEED streaks. Over 40 growth/etch cycles are achieved on a single substrate without degradation of RHEED surface reconstruction, and we achieve approximately 5x throughput improvement over traditional growth and characterization.

The [001] surface reconstruction remains a streaky 2x pattern typical of monoclinic Ga₂O₃ growth for high growth temperatures, high Ga flux, and low In flux. Conversely, the surface reconstruction becomes spotty with a reduced d -spacing for low growth temperatures, low Ga flux, and high In flux, suggestive of formation of bixbyite In₂O₃. In this manner the growth conditions corresponding to the lowest growth temperature, lowest Ga BEP, and highest In BEP that stabilize a streaky 2x-RHEED reconstruction are rapidly identified, and targeted thick (In_xGa_{1-x})₂O₃ growths are carried out under these conditions.

400 – 500 nm thick (In_xGa_{1-x})₂O₃ epilayers were grown using conditions identified by the rapid throughput experiment. X-ray diffraction measurements of these films show pseudomorphic alloys with a graded composition that is initially In-rich with ~10% mole fraction. Reciprocal space maps indicate partial relaxation, in agreement with calibrated RHEED diffraction spot spacings. The RHEED d -spacing increases rapidly before slowly relaxing back to the Ga₂O₃ lattice c -plane spacing, suggesting growth is initially In-rich with reduced In content as growth progresses. Interestingly, growth at very high In fluxes results in slight contraction of d -spacing suggesting In-catalyzed Ga₂O₃ growth and negligible In incorporation. Depth-sensitive characterization including SEM and SIMS will be presented to demonstrate the competing In incorporation and suboxide kinetics for MBE growth of Ga₂O₃ alloys. Rapid identification of suitable Ga₂O₃ alloy growth conditions will lead to improved material quality, electrical properties, and bandgap tunability for ultra-wide bandgap devices.

4:30 PM EL11.12.09

Schottky Barrier Diode and MESFET based on Ge-Doped α -Ga₂O₃ Thin Film Grown by Mist-CVDTakeruWakamatsu¹, YukiIsobe¹, HitoshiTakane¹, KentaroKaneko^{1,2} and KatsuhisaTanaka¹; ¹Kyoto University, Japan; ²Ritsumeikan University, Japan

Gallium oxide (Ga₂O₃), which is one of the ultra-wide bandgap semiconductors, has attracted considerable attention because of its potential applications for power electronics. Among polymorphs of Ga₂O₃, β -Ga₂O₃ is the most stable phase. Although β -Ga₂O₃-based devices such as Schottky barrier diode (SBD), MESFET and MOSFET have been reported thus far, the fact that β -Ga₂O₃ substrate is expensive and has a low thermal conductivity is a problem from a point of view of practical applications. On the other hand, α -Ga₂O₃, which is one of the metastable phases, can be grown on a sapphire substrate by heteroepitaxial growth techniques such as mist-CVD, HVPE and MEB. The sapphire substrate is cost-effective and has a high thermal conductivity, which is preferable for device applications. Nonetheless, there are not so many reports on the α -Ga₂O₃-based devices including SBD, MESFET and MOSFET. This is partly because the control of carrier density and achievement of high mobility are not so easy compared with β -Ga₂O₃. Recently, we successfully obtained Ge-doped α -Ga₂O₃ thin films by using mist-CVD method with the wider carrier density ranging from 10¹⁶ to 10¹⁹ cm⁻³ and the higher mobility 65.9 cm²V⁻¹s⁻¹ than previous reported Sn-doped α -Ga₂O₃.^[1] In this work, we report on the fabrication of SBD and MESFET based on the Ge-doped α -Ga₂O₃ thin films and confirm that the resultant devices exhibit high performance.

Ge-doped α -Ga₂O₃ thin films were grown on *m*-plane sapphire substrates by mist-CVD method. An α -Ga₂O₃ n⁺ layer (900-1000 nm thick, the donor density, $N_d = 1 \times 10^{19}$ cm⁻³) and an α -Ga₂O₃ n⁻ drift layer (500-600 nm thick, UID) were grown on the *m*-plane sapphire substrate for SBD. To make a mesa structure, the n⁻ layer was etched by ICP-RIE following photolithography. As an ohmic electrode, Ti/Au (20 nm/100 nm thick) or Ti/Al/Ti/Au (30 nm/100 nm/30 nm/30 nm thick) was deposited on the n⁺ layer by electron beam (EB) deposition. After that, the samples were annealed at 400, 450, 470 and 500 °C for 1 min in an N₂ atmosphere. Then, Ti/Au (20/100 nm thick) Schottky electrode was formed by EB deposition. The *I*-*V* characteristic of the resultant SBDs was measured and analyzed in terms of the thermionic emission model. The *n* value and the barrier height are 1.06-1.19 and 0.95-1.13 eV, respectively. The on-resistance decreases as the annealing temperature is increased. The lowest on-resistance is 3.7 mΩcm² achieved for the device with Ti/Au/Ti/Au ohmic electrode annealed at 500 °C. Also, we prepared MESFET as follows. First, Fe-doped buffer layer (800 nm thick), Ge-doped channel layer (300 nm thick) and n⁺ layer (30 nm thick) were grown on an *m*-plane sapphire substrate. For the mesa device isolation, 500 nm-thick α -Ga₂O₃ was etched by ICP-RIE. A Ti/Au (20/100 nm thick) was deposited as source and drain electrodes. The n⁺ layer on the channel layer was etched by ICP-RIE. A Ni/Au (30/100 nm thick) was deposited as a gate electrode. From the Hall effect measurements, the carrier concentration, the sheet carrier density, and the electron mobility were evaluated to be 2.1×10^{17} cm⁻³, 4.9×10^{12} cm⁻² and 44 cm²V⁻¹s⁻¹, respectively. The *I*-*V* measurements were conducted for the device with $L_{GS}/L_G/L_{GD} = 3/3/12$ μm, where L_{GS} , L_G , and L_{GD} are gate-to-source, gate and gate-to-drain lengths, respectively. From the output curve (V_{DS} - I_D characteristic), the maximum I_D and the on-resistance were estimated to be 24 mA/mm and 587 Ωmm (at $V_{GS} = 2$ V), respectively. The break down voltage is 364 V (at $V_{GS} = -10$ V). From the transfer curve (I_D - V_{GS} characteristic), the threshold voltage, the subthreshold slope and the on-off ratio were evaluated to be -9 V, 164 mV/dec and 10⁹, respectively. These values are superior compared to α -Ga₂O₃-based MESFET reported previously, for which the break down voltage, the on-off ratio and the maximum I_D are 48 V, 2×10^7 and 35 mA.^[2]

[1] *Phys. status solidi A* **217**, 1900632 (2020). [2] *IEEE Trans. Electron Devices* **62**, 3640 (2015).

4:45 PM EL11.12.10

Demonstration of 3 kV Schottky Barrier Diodes on AlN Epilayers Grown on Bulk AlN Substrates by MOCVD [Dinusha Herath](#), [Mudiyanselage, Dawei Wang](#), [Ziyi He](#), [Bingchen Da](#) and [Houqiang Fu](#), Arizona State University, United States

Aluminum Nitride (AlN) is a promising material for next-generation power electronics due to its remarkable attributes, including an ultra-wide bandgap (6.2 eV), robust breakdown field (~12-15 MV/cm), and superior thermal conductivity (340 W/mK). AlN power devices have already shown promising development with high temperature stability and potential to improve energy efficiency and reduce system size for various power conversion applications. Nevertheless, several challenges persist in the growth and fabrication processes, including the high cost and lack of conductive substrates for AlN substrates, growth of high-quality AlN epilayers, and the need for proper Ohmic and Schottky contacts.

In this study, we have grown AlN epilayers on AlN bulk substrates with high Si doping concentration (~ 1×10^{19} cm⁻³) to demonstrate lateral Schottky barrier diodes (SBDs) with kV-class capabilities. The device configuration incorporates Ti/Al/Ni/Au as Ohmic contacts and Pt/Au for the Schottky contact. The AlN epilayers were grown via metal-organic chemical vapor deposition (MOCVD), utilizing trimethylaluminum (TMAI) and ammonia (NH₃) as the Al and N sources, with SiH₄ employed as the *n*-type dopant Si precursor. The device structure entails a 1-μm-thick resistive UID AlN underlayer, a 200 nm Si-doped *n*-AlN layer, and a 2 nm UID GaN capping layer, to prevent the oxidation of underlying AlN epilayers. High-resolution X-ray diffraction (HRXRD) confirmed the crystallographic quality of the epilayers. Device fabrication started with rigorous cleaning using acetone, isopropyl alcohol and D.I. water aided by sonication, and HCl:H₂O (1:2) solution treatment. Subsequently, the Ohmic contacts were patterned using standard photolithography, followed by e-beam evaporation of Ti/Al/Ni/Au (25/50/25/50 nm) and liftoff. After that, 1000 °C, 1-minute annealing process in N₂ ambient was performed using rapid thermal annealing. Schottky contacts were subsequently patterned, with Pt/Au (30/120 nm) metal deposition and liftoff. The distance between Schottky and Ohmic contacts were varied between 50-350 μm. The devices were tested with a 4200 semiconductor parameter analyzer equipped with a controllable thermal chuck. High voltage measurements were carried out using a Keysight B1505A Power Device Analyzer. The devices exhibit remarkable ON/OFF ratios ranging from 10⁵ to 10⁸ across a temperature range of 298 - 623 K, exhibiting their robust temperature stability. The current of the devices increases linearly with temperature as more carriers are excited and enabled the current transport. The devices maintain a Schottky barrier height of approximately 0.9 eV, with this value increasing from 0.9 - 2.2 eV as temperature rises, while the ideality factor decreases from 4.8 - 2.5. This deviation from the thermionic emission model indicates a unique current transport mechanism mainly governed by the resistive nature of the AlN epilayers. Furthermore, temperature-dependent C-V measurements verify an increase in carrier concentration with rising temperature. The devices demonstrate decent forward characteristics and exhibit breakdown voltages exceeding 3 kV. At -3 kV, the devices display a low leakage current of 200 nA. The observed leakage current variation with the area of the Ohmic contact region suggests that surface leakage governs the reverse leakage current. This work serves as a valuable reference for the development of kV-class AlN high-voltage, high-power devices, showcasing significant progress in the field.

SESSION EL11.13: Boron Nitride
Session Chairs: Jack Flicker and Robert Kaplar
Friday Morning, December 1, 2023
Hynes, Level 2, Room 210

8:30 AM *EL11.13.01

High-Temperature Molecular Beam Epitaxy of Hexagonal Boron Nitride and hBN-Based Lateral Heterostructures [Sergei V. Novikov](#)¹, [Tin S. Cheng](#)¹, [Jonathan Bradford](#)¹, [Tyler James](#)¹, [Christopher Mellor](#)¹, [Kenji Watanabe](#)², [Takashi Taniguchi](#)², [Igor Aharonovich](#)³, [Luiz F. Zagonel](#)⁴, [Bernard Gil](#)⁵, [Guillaume Cassabois](#)⁵ and [Peter Beton](#)¹; ¹The University of Nottingham, United Kingdom; ²National Institute for Materials Science, Japan; ³University of Technology Sydney, Australia; ⁴Institute of Physics, University of Campinas, Brazil; ⁵Laboratoire Charles Coulomb, CNRS-Université de Montpellier, France

There has been a surge of interest in hexagonal boron nitride (hBN) due to its technological potential for deep ultraviolet (DUV) photonics, single photon emitters (SPEs) and through its incorporation into van der Waals (vdW) two-dimensional (2D) heterostructures as either a substrate, tunnel barrier or capping layer.

We have developed high-temperature molecular beam epitaxy (HT-MBE) of hexagonal boron nitride with the thicknesses up to 70 nm at growth temperatures from 1100°C to 1700°C using high-temperature sublimation and e-beam MBE sources for boron and nitrogen RF-plasma sources. By growing hBN on highly oriented pyrolytic graphite (HOPG) substrates, we have produced monolayer and few-layer thick boron nitride with atomically flat hBN surfaces, which are essential for 2D and DUV applications. The hBN coverage can be reproducibly controlled by the growth time, substrate temperature and boron to nitrogen flux ratios. We will discuss our recent measurements of a direct optical energy gap of ~6.1 eV [1] and electronic band gap of ~6.8 eV [2] in single monolayer hBN.

We will present data demonstrating that the single-photon emitters in hBN are related to carbon (C) incorporation [3] and will discuss different C-doping techniques that we are currently using in HT-MBE.

In addition to the conventional hBN-based vertical vdW heterostructures, recent studies worldwide have focused on the development of novel 2D lateral heterostructures. These vdW lateral heterostructures consist of multiple connected monolayer-thick materials within the same atomic plane and can have novel and unique transport and optical properties. Integration of graphene and hBN in lateral heterostructures can provide a route to engineer the material properties by quantum confinement of electrons or introduction of novel electronic and magnetic states at the interface. Whereas vertical 2D heterostructures can be produced by epitaxy or by exfoliating and stacking of 2D layers, lateral 2D heterostructures can only feasibly be produced by an epitaxial growth process.

We have demonstrated that lateral heterojunctions of hBN and graphene can be grown *in-situ* using HT-MBE. We used different types of the MBE carbon sources, including a sublimation carbon source, atomic carbon source and e-beam carbon source, to grow graphene monolayers on hBN substrates and hBN epitaxial layers at temperatures between 1000°C and 1700°C.

We will discuss HT-MBE of graphene monolayers in crystallographically oriented hBN trenches, formed *ex-situ* by catalytic Ni-nanoparticle etching. High-resolution atomic force microscopy (AFM) reveals that graphene monolayers grow epitaxially from the hBN etched trench edges, and merge to form a graphene nanoribbon network.

We will also discuss *in-situ* HT-MBE of monolayer-thick lateral hBN-graphene heterostructures. Monolayer-thick hBN, grown at a higher temperature of ~1400°C, exhibited armchair edges, minimal aggregate presence, and a reduced but significant width of the hBN monolayer sheet. We have shown that in HT-MBE graphene grows preferentially laterally from the edges of hBN in a mode of step-flow growth, which results in the formation of lateral hBN-graphene heterojunctions. The graphene and hBN regions show a clear epitaxial relationship through the alignment of atomic lattices. Sequential HT-MBE growth of hBN, graphene and a second cycle of hBN growth resulted in the formation of monolayer-thick lateral hBN-graphene-hBN heterostructures, in which a strip of graphene is laterally embedded between monolayers of hBN.

References

- [1] C. Elias et al., *Nat. Commun.* **10** 2639 (2019).
 [2] R.J.P. Roman et al., *2D Mater.* **8** 044001 (2021).
 [3] N. Mendelson et al., *Nat. Mater.* **20** 321 (2020).

9:00 AM EL11.13.02

Direct MOVPE Growth of High-Quality h-BN on the Wafer-Scale Sapphire: The Role of Substrate Off-Cut Mateusz Tokarczyk, Aleksandra Dabrowska, Grzegorz Kowalski, Rafal Bozek, Jakublwanski, Johannes Binder, Roman Stepniewski and Andrzej Wyszomolek; Faculty of Physics, University of Warsaw, Poland

Hexagonal boron nitride (h-BN) is an attractive wide bandgap 2D material for possible applications in electronic and optoelectronic devices based on van der Waals heterostructures [1], but direct growth of high-quality h-BN on the wafer-scale is still the bottleneck for future successful implementation of h-BN in industry. Although the synthesis of h-BN by metal-organic vapor phase epitaxy (MOVPE) has already been reported [1-3], there is a fundamental lack in understanding of many basic aspects of this process affecting obtaining a good structural quality and a smooth surface. In particular the role of the substrate off-cut, although well known as being of major importance for the growth of other materials, has not yet been fully addressed so far. In this communication, we present a study that addresses the influence of the sapphire substrate off-cut angle on the final quality of h-BN obtained in a two-step growth procedure [3]. The main process starts with a self-limiting continuous flow growth (CFG) of a BN buffer followed by flow-modulated epitaxy (FME) in the second step of one MOVPE process and is used to study substrates with five different off-cuts angles for three different CFG times.

Based on results obtained by x-ray diffraction and x-ray reflectometry, Raman and Fourier-transform spectroscopy, atomic force microscopy and scanning electron microscopy, we present a comprehensive study that shows that the quality of h-BN epilayers dramatically depends on the off-cut angle of the c-plane sapphire substrate [4]. We demonstrate that the highest quality of h-BN layers is obtained for a sapphire substrate off-cut angle of 1 degree. Samples with this off-cut have the lowest amount of debris, 3D grains consisting of mostly h-BN material [5], on the surface. They also have most intense x-ray diffraction signal, minimal Raman phonon linewidth and thinnest amorphous BN part. We are able to explain these results by following the evolution of the whole interface, which includes a thin AlN layer coming from initial nitridation step at the beginning of MOVPE process. This AlN layer is shown to smooth out the surface forming (with sapphire) a kind of "effective substrate" which leads to the observed increase in quality.

A detailed analysis of the crystallographic structure of the h-BN obtained layers and mechanisms responsible for the existence of an optimal off-cut angle will be discussed.

Acknowledgments: This work was supported by the National Science Centre, Poland, under decisions 2019/33/B/ST5/02766 and 2020/39/D/ST7/02811.

- [1] A. E. Naclerio and P. R. Kidambi, *Adv. Mater.* **35**, 2207374 (2023).
 [2] Y. Kobayashi, T. Akasaka, *J. Cryst. Growth* **310**, 5044 (2008).
 [3] A. K. Dabrowska, et al. *2D Materials* **8**, 015017 (2020).
 [4] M. Tokarczyk, et al. *2D Materials* **10**, 025010 (2023).
 [5] D. Chugh, et al. *2D Materials* **5**, 045018 (2018).

9:15 AM EL11.13.03

Towards Growth of High Quality Cubic Boron Nitride using Fluorine Chemistry Ali Ebadati Yekta, Avani Patel and Robert J. Nemanich; Arizona State University, United States

Boron Nitride (BN) is an ultra-wide bandgap material having a bandgap of 6.4 eV and 5.9 eV for the cubic (c-BN) and hexagonal (h-BN) phases, respectively. The ultra-wide bandgap of both BN phases indicates a high breakdown voltage, possibly even greater than diamond [1]. Moreover, epitaxial c-BN on diamond is expected to have high thermal conductivity. Diamond and c-BN have a small lattice mismatch of 1.4 percent [2]. Therefore, diamond is a candidate for use as a substrate for growth of c-BN. However, the choice of an appropriate substrate among different types of diamond as well as crystallographic orientation can affect the quality of the grown c-BN films. Also, depending on the growth technique, it might be essential to use either p-type or n-type diamond to achieve high-quality c-BN films. The last but not the least in growing high-quality c-BN films is the method utilized to clean the substrate which is of great significance, too.

Physical vapor deposition (PVD) is one of the techniques that has shown success in growing c-BN layers. Magnetron sputtering, ion-assisted pulsed laser deposition (IAPLD), ion beam-assisted deposition (IBAD) and mass selected ion beam deposition (MSIBD) are some methods under PVD category that have been exploited to grow pure c-BN [3]. However, utilizing high energy ion bombardment as well as high bias voltage is a must in such methods. Therefore, we should expect high compressive stress on the films which leads to defect formation and delamination of very thick films. Also, slow growth rate of PVD methods, few nm/hrs, prevent us from getting thick, pure c-BN films. To overcome the above obstacles Chemical vapor deposition (CVD) is also suggested for growing c-BN. These methods include DC jet plasma CVD, RF plasma CVD, inductively coupled PECVD and electron cyclotron resonance microwave plasma CVD (ECR MPCVD). The advantage of CVD over PVD is that ion bombardment and high bias voltage are not present to impose compressive stress and the resulting defects. Besides that, faster growth rate of CVD techniques opens up a lot of opportunities to get thick films of c-BN in short processing times [3]. Among the CVD methods, ECR MPCVD has been the most successful technique in getting thick and pure c-BN films due to the fact that processing is done in very low pressure environment down to even Torr. This reduces the contaminants that can interfere with the reaction and improves the precursors reaction on the substrate surface.

In this study we have explored achieving both thick and high quality c-BN films on polycrystalline boron-doped diamond at fast, 100 nm/hrs, and slower, 50 nm/hrs, growth rate. ECR MPCVD method in combination with Fluorine chemistry using H₂, BF₃, N₂, He and Ar gases was utilized. Substrate is negatively biased, i.e. -60 V, with respect to the grounded chamber to facilitate growth of c-BN layers. Fluorine atoms that manage to reach the substrate etch the sp² B-N bondings formed during the growth facilitating sp³ B-N bond formation. That is achieved by use of limited H₂ flow rate. On the other hand, Cleaning the substrate is critical in getting a high quality interface. High flow rate of H₂ plasma cleaning in ECR MPCVD chamber resulted in damage to diamond surface and that prevented us from getting smooth interface. However, when H₂ flow rate was reduced we observed fewer damage to the substrate and that improved the quality of c-BN/diamond interface.

Then, we increased flow rates of the gas precursors while keeping gas ratios and applied voltage bias fixed. This resulted in growth of c-BN at a faster rate. The H₂:BF₃ ratios of 2:2 and 4:4 sccm resulted in 50 nm/hrs and 100 nm/hrs of BN, respectively. We then utilized in-situ X-ray photoemission spectroscopy (XPS) to confirm the presence of only sp³ bonding states at the surface of the grown film (Fig. 1). Also, data acquired from ellipsometry confirms the growth rates of the two scenarios mentioned above.

9:30 AM EL11.13.04

Computational Investigation of Optical Properties of Boron Nitride Quantum Dots Chandler Martin and Arindam Chakraborty; Syracuse University, United States

Boron nitride (BN) is a promising material for bright single photon source with applications in optical quantum technologies. The photoluminescence properties of BN can be modulated by optimizing the size and dopant characteristics of BN quantum dots. This work presents a systematic investigation of emission characteristics of BN quantum dots in the size range of 1-10nm. The electron-hole binding energies and radiative and non-radiative electron-hole recombination rates were calculated for dots in the size range of 1-10nm. First-principles quantum mechanical calculations were performed using the frequency-dependent geminal screened electron-hole interaction kernel (FD-GSIK) method, and the recombination probability was evaluated from the correlated electron-hole reduced density matrix. The FD-GSIK method is a real-space method that uses an explicitly-correlated operator to include many-body quasiparticle correlation effect in the electronically excited state calculation. The scaling of electron-hole binding energies and electron-hole recombination probability as a function of dot size will be presented, and the impact of surface defects on radiative electron-hole recombination will be discussed.

9:45 AM BREAK

SESSION EL11.14: Characterization and Computation
 Session Chairs: Robert Kaplar and Z. Sitar
 Friday Morning, December 1, 2023
 Hynes, Level 2, Room 210

10:15 AM *EL11.14.01

Pushing the Limits of Diffraction Imaging in the Scanning Electron Microscope for the Structural Characterisation of Semiconductor Thin Films and Microstructures Carol Trager-Cowan¹, Jochen Bruckbauer¹, Ryan McDermott¹, Dale Waters¹, Kieran Hiller¹, Ben Hourahine¹, Grzegorz Cios² and Aimo Winkelmann^{2,1}; ¹University of Strathclyde, United Kingdom; ²AGH University of Science and Technology, Poland

To achieve the best performance from the next generation of wide bandgap semiconductor-based devices, it is crucial that we understand and optimise the structural properties (i.e., crystal structure, extended defects, misorientation and strain) of the new materials used in their manufacture. Many new materials are produced using non-planar growth techniques such as selected area growth or epitaxial overgrowth, resulting in material where defect densities, misorientation and strain vary on the micron and/or nanoscale. To fully understand and optimise subsequent devices requires a characterisation tool capable of rapidly and non-destructively mapping structural properties on the micron and nanoscale. Using advanced electron diffraction techniques in the scanning electron microscope (SEM), namely electron channelling contrast imaging (ECCI) and electron backscatter diffraction (EBSD) imaging, together with bespoke analysis software utilising pattern matching to accurate simulations of EBSD patterns and novel strain and defect analysis software, we are now able to map microstructure, defects, misorientation and strain in semiconductor thin films and 3-D microstructures with a spatial resolution of order 100 nm, a misorientation resolution of order 0.5 mrad (0.03°) and a strain resolution of order 5×10^{-4} . To date, we have characterised GaN thin films containing both wurtzite and zincblende material; mapped polarity in GaN microstructures; determined dislocation density and types in planar and non-planar GaN, AlGaIn and AlN thin films; imaged misfit dislocations in AlGaIn HEMT structures; imaged stacking faults in non-polar and semi-polar wurtzite GaN; and mapped strain in GaN thin films [1-5]. The benefits of imaging in the SEM include minimal sample preparation and the ability to produce images from areas ranging in size from square microns to square centimetres. Diffraction analysis can also be combined with energy dispersive X-ray spectroscopy; hyperspectral cathodoluminescence imaging; and electron beam induced current to provide complementary, non-destructive high resolution information on the structural, compositional, luminescence and electrical properties of materials [1-3]. In our presentation we will illustrate our present capabilities with recent results and explore the potential of diffraction imaging in the SEM to underpin fast optimisation of new materials and device structures.

[1] C. Trager-Cowan et al., *Semicond. Sci. Technol.* **35** 054001 (2020).

[2] F. C.-P. Massabuau et al., in "Characterisation and control of defects in semiconductors". Ed. F. Tuomisto (Institution of Engineering and Technology) (2019).

[3] J. Bruckbauer et al., *J. Appl. Phys.*, **127** 035705 (2020).

[4] A. Vilalta-Clemente et al., *Acta Mater.* **125** 125 (2017).

[5] G. Naresh-Kumar et al., *Mater. Sci. Semicond. Process* **47** 44 (2016).

10:45 AM EL11.14.04

Evaluation of Band Alignment of Rutile-Sn_{1-x}Ge_xO₂ by XPSYoNagashima¹, AkiraChikamatsu², DaichiOka³ and YasushiHirose³; ¹The University of Tokyo, Japan; ²Ochanomizu University, Japan; ³Tokyo Metropolitan University, Japan

Introduction: An alloy of rutile-type SnO₂ and GeO₂ (Sn_{1-x}Ge_xO₂: SGO) is an ultrawide-gap oxide semiconductor. SGO is expected to be applicable for power electronic and ultraviolet optoelectronic devices because of its wide tunability of bandgap from ~3.7 eV to ~4.7 eV [1, 2]. A unique feature of SGO is a possibility of ambipolar doping, originating from shallow valence band maximum (VBM) of rutile GeO₂ (x=1), predicted by first-principles calculations [3, 4]. Although the band alignment (band edge position) of SGO is important for considering dopability in SGO as well as for designing SGO-based heterostructure devices, it has not been experimentally investigated yet. In this study, therefore, we evaluated the position of VBM of a series of SGO epitaxial thin films (x=0-0.6) using X-ray photoelectron spectroscopy (XPS) and determined its band alignment.

Methods: The (001)-oriented SGO thin films (x=0-0.6) were epitaxially grown on Nb:TiO₂ (001) substrates by the pulsed laser deposition [1]. Crystal structure and Ge/Sn ratio of the films were confirmed by X-ray diffraction and energy-dispersive X-ray spectroscopy, respectively. In the XPS measurements, valence band and O 2s spectra of the SGO films were measured at 300 K with an Al-K α X-ray source. The variation of the VBM from the vacuum level as a function of the chemical composition was evaluated using the position of O 2s peak as a reference. Before the XPS measurement, the SGO thin films were annealed at 800 °C for 6 hours in air to remove Sn²⁺ component from the surface.

Results: VBM of the SGO films became shallower monotonically by 0.5 eV with increase of x from 0 to 0.6, which qualitatively agreed with the prediction by first-principles calculations [3]. On the other hand, the position of VBM was still deeper than the practical level of Fermi energy pinning level for p-type doping, requiring further increase of Ge to realize ambipolar doping. We also estimated the position of conduction band minimum (CBM) using the band gap of SGO determined from the optical absorption spectroscopy. As x increased from 0 to 0.6, CBM also became shallower by 0.8 eV. This rise of CBM position can explain the reduction of donor activation ratio with increasing x, observed in Ta-doped SGO thin films. These results also indicated that a heterostructure consisting of SGO thin films with different Sn/Ge ratio will become a type-II heterojunction.

References:

[1] Y. Nagashima et al., *Chem. Mater.* **34**, 24, 10842–10848 (2022)

[2] H. Takane et al., *Phys. Rev. Mater.* **6**, 8, 084604 (2022)

[3] C. A. Niedermeier et al., *J. Phys. Chem. C* **124**, 47, 25721–25728 (2020)

[4] S. Chae et al., *Appl. Phys. Lett.* **114**, 102104 (2019)

11:00 AM EL11.14.05

Low-Temperature Electrical Properties of r-Ge_xSn_{1-x}O₂ Alloy FilmHitoshiTakane¹, ItsuhiroKakeya¹, HirokazuIzumi², TakeruWakamatsu¹, YukiIsobe¹, KentaroKaneko³ and KatsuhisaTanaka¹; ¹Kyoto University, Japan; ²Hyogo Prefectural Institute of Technology, Japan; ³Ritsumeikan University, Japan

Rutile-type wide and ultrawide band-gap oxide semiconductors, such as r-GeO₂ and r-SnO₂, are emerging materials for high-power electronics and deep ultraviolet optoelectronics devices [1,2]. Recently, their alloy (r-Ge_xSn_{1-x}O₂) has also gained attentions due to the possibility to modulate its bandgap and electrical properties by tuning the Ge:Sn compositional ratio [2-4]. In addition, Sn-rich r-Ge_xSn_{1-x}O₂ exhibits excellent n-type conductivity, which is favorable for future device-oriented researches [2,3]. However, details of its electrical properties including carrier transport mechanisms have not been elucidated yet.

In this study, we investigated low-temperature electron transport properties of Sn-rich r-Ge_xSn_{1-x}O₂ thin films (x=0.28 and 0.41). Temperature-dependent Hall effect measurements suggest that the hopping conduction is dominant at low temperatures (< 100 K) in both r-Ge_{0.41}Sn_{0.59}O₂ and r-Ge_{0.28}Sn_{0.72}O₂. Temperature-dependent resistivity measurements indicate that the hopping mechanism at low temperatures ($T \leq 15$ K) is explained by the Efros-Shklovskii variable-range hopping (ES VRH), that is, hopping over the states within the Coulomb gap. In the temperature region, both r-Ge_{0.41}Sn_{0.59}O₂ and r-Ge_{0.28}Sn_{0.72}O₂ exhibit both negative and positive magnetoresistances. Based on the theory of quantum interference that includes effects of both frozen- and free-electron spins [5], it is found that the negative and positive components are attributed to the quantum interference and field-induced spin-alignment, respectively, and the transport mechanism at $T \leq 15$ K for both r-Ge_{0.41}Sn_{0.59}O₂ and r-Ge_{0.28}Sn_{0.72}O₂ corresponds to the ES VRH with large number of scattering centers. The results are coincident with those obtained by the temperature dependence of resistivity. At $T \geq 30$ K, the negative magnetoresistance induced by the quantum-interference effect decreases as the temperature increases. Moreover, at $T \geq 150$ K, both r-Ge_{0.41}Sn_{0.59}O₂ and r-Ge_{0.28}Sn_{0.72}O₂ show temperature-independent positive magnetoresistance induced by the Lorentz force. It is considered that these results indicate a mixture of the Mott VRH and thermally activated band conduction ($T < 100$ K) and almost pure thermally activated band conduction ($T \geq 150$ K).

We believe that our experimental and analytical results provide a basis for the development of not only r-Ge_xSn_{1-x}O₂, but also all the other rutile-type wide and ultrawide band-gap oxide semiconductors.

This work was, in part, supported by JSPS KAKENHI under Grant Number 21H01811 and 20H02606.

[1] S. Chae et al., *Appl. Phys. Lett.* **118**, 260501 (2021).

[2] H. Takane et al., *Phys. Rev. Mater.* **6**, 084604 (2022).

[3] Y. Nagashima et al., *Chem. Mater.* **34**, 10842 (2022).

[4] F. Liu et al., *Commun. Mater.* **3**, 69 (2022).

[5] A. V. Shumilin et al., *Phys. Rev. B* **85**, 115203 (2012).

11:15 AM EL11.14.06

Investigation on Electronic and Magnetic Properties of Ti Doped Diamond Nanowire using First-PrinciplesJianingSu and Hong-XingWang; Xi'an Jiaotong University, China

The dilute magnetic semiconductor (DMS) has attracted significant attention as it unifies the characters of semiconductor and magnetism into single hybrid devices for spintronic applications. The key issue of current research is to search for DMS materials with ferromagnetic ordering at or above room temperature due to that the low Curie temperatures (T_c) prevents spintronic devices from being used at room temperature. Dietl's theoretical investigations showed that the T_c of a DMS varied with the host lattice constant as $1/a^3$, indicating that semiconductor with small lattice constant would be a potential candidate for ferromagnetic ordering at room temperature. Diamond possesses the smallest lattice constant among semiconductors ($a=3.567$ Å), which makes it an excellent candidate DMS material for spintronic applications at room temperature. In addition, one-dimensional (1D) magnetic nanowire can limit all spin rotations to a single axis, which makes it to be potential candidate for spin transistor.

In this work, the electronic and magnetic properties of Ti-doped diamond nanowire were investigated by first-principles calculation. The results revealed that Ti-doped diamond nanowire with vacancy possessed stable ferromagnetism with a magnetic moment of 2 μ_B , while Ti-doped diamond nanowire without vacancy was non-magnetic. Moreover, The Ti-doped diamond nanowire with vacancy exhibited the half metallic behavior and the spin polarization of 100% near the Fermi level with half-metal bandgap of 0.236 eV, while Ti-doped diamond nanowire without vacancy has metallic property. The density of states implied that magnetism originated from the p-d hybridization between the Ti-3d, Ti-2p and C-2p states. The p-d hybridization leads to that the spin-down DOS is pushed above the Fermi level while the spin-up DOS is moved lower than Fermi level, which increases the occupation probability of electrons in the spin-up DOS and results in the spin polarization. Therefore, the Ti-doped diamond nanowire with vacancy would be a promising novel type of dilute magnetic semiconductor and could possess a great potential application in spintronic devices.

1:30 PM *EL11.15.01

Electrical Conductivity in Ultra-Wide Bandgap Materials P.Reddy¹, R.Kirste², JTweedie², RamonCollazo¹ and Z.Sitar^{1,2}; ¹North Carolina State University, United States; ²Adroit Materials, Inc., United States

AlN is a UWBG material ($E_g = 6.1$ eV) for the realization of UV optoelectronics and high-power, high-frequency electronics. Although most challenges in crystal growth and epitaxy of AlN have been overcome, achieving controlled electrical conductivity of technological interest has proven to be challenging. While controlling the chemical and electrochemical potentials during doping has been crucial for achieving doping and compensation control, the obtained conductivity was still modest. The presumed DX formation has been considered an insurmountable killer defect as it pins the Fermi level and imposes a low limit on the achievable free carrier concentration. We have developed several novel equilibrium and non-equilibrium approaches for doping and point defect management in AlN and shown that donors in AlN do not undergo a DX transition but rather are distributed between a shallow and deep state. We have shown that the shallow state can be kinetically stabilized to obtain highly-conducting n-type AlN with mobilities approaching $400 \text{ cm}^2/\text{Vs}$. These results have enabled the first demonstration of AlN Schottky diodes capable of $>3 \text{ kAcm}^{-2}$ with a critical breakdown field exceeding 10 MVcm^{-1} .

Zlatko Sitar is a Kobe Steel distinguished Professor of Materials Science and Engineering, Physics, and Electrical Engineering at NCSU. His research is concerned with bulk and thin film growth, characterization, property control, and device development in ultrawide bandgap semiconductors. He has developed and commercialized processes for growth of AlN crystals, epitaxy on AlN wafers, and doping control in this material. Based on his research, he founded HexaTech, Inc., focusing on AlN wafer technology, and Adroit Materials, Inc., focusing on high performance devices on native GaN and AlN substrates slated for DoD and NASA applications.

2:00 PM EL11.15.02

Surface, Structural and Optical Studies of GaN Grown on Si by MOCVD Manika TunNafisa, IkramTalukder, Zhe ChuanFeng, BenjaminKlein and IanT. Ferguson; Kennesaw State University, United States

In the last two decades, there has been considerable research focused on investigating GaN films grown on silicon as a wide bandgap semiconductor material. Optical techniques, such as ellipsometry, have been widely employed for characterizing thin films and bulk materials, enabling the determination of layer thicknesses and surface roughness. X-ray diffraction (XRD) has proven to be an essential tool for analyzing semiconductor crystal structures, while Raman spectroscopy provides insights into the composition and homogeneity of epitaxial semiconductor samples. This study examines four GaN thin films grown on silicon substrates using metalorganic chemical vapor deposition (MOCVD). Variable angle spectroscopic ellipsometry (VASE) measurements were conducted to determine film thickness and surface roughness as well as the dependence of n & k versus wavelength in 250-1000 nm for these GaN on Si samples. The obtained results indicate specific values for each sample: the first sample has a film thickness of 180 nm and a surface roughness of 47 nm, the second sample has a thickness of 106 nm and a surface roughness of 8 nm, the third sample has a thickness of 1004 nm and a surface roughness of 3 nm, and the fourth sample has a thickness of 1510 nm and a surface roughness of 2 nm, as derived from Spectroscopic ellipsometry (SE) fits. The highest recorded refractive index among the four samples is 2.76, XRD measurements were performed on the first two samples, while Raman scattering measurements were conducted on the remaining two samples. The XRD experiments involved wide scans and fine scans with step sizes of 0.1° and 0.005° , respectively. The XRD analysis revealed distinct peaks corresponding to silicon (002) and (004) orientations at approximately 28° and 90° , respectively, in the first sample. Additionally, a weak peak at around 35° indicated the presence of the GaN (0002) peak. In the second sample, the XRD analysis demonstrated clear peaks for the Si substrate (002) and (004) orientations at 28° and 90° , respectively, along with distinct peaks corresponding to GaN at (0002), (0004), and (0006) orientations. Notably, the first-order GaN peak was observed at approximately 34.6° , the second-order peak at around 73° , and the third-order peak at approximately 127° , providing valuable information about the crystallographic properties of the GaN films. Raman scattering measurements were conducted on two samples under a microscope at room temperature, employing different excitation laser powers (5%, 1%, and 0.5%). The first Raman experiment revealed characteristic peaks at 520 cm^{-1} for Si, confirming its crystalline nature, while peaks at 565 cm^{-1} corresponded to the GaN crystallinity characteristics of the E_2 (High) and A_1 (LO) vibrational modes. In the second Raman experiment, distinctive peaks at 520 cm^{-1} , 567 cm^{-1} , and 734 cm^{-1} were identified for Si, GaN E_2 (High), and GaN A_1 (LO), respectively, further supporting the exceptional crystalline purity of the GaN films grown on silicon substrates. Through these comprehensive surface, structural, and optical characterizations, our study provides compelling evidence of the exceptional crystalline purity of the investigated GaN films on silicon substrates. These findings, achieved through Ellipsometry, XRD, and Raman spectroscopy techniques, enhance our understanding of the surface, structural, and optical properties of GaN films and open up exciting possibilities for their utilization for high-power and spintronic applications.

<quillbot-extension-portal></quillbot-extension-portal>

2:15 PM EL11.15.03

Direct Growth of Wafer-Scale Self-Separated GaN on Reusable Two-Dimensional Material Substrate Chang HsunHuang¹, Chia-YiWu² and Yi-ChiaChou¹; ¹National Taiwan University, Taiwan; ²National Yang Ming Chiao Tung University, Taiwan

Gallium nitride (GaN) is extensively employed in light-emitting diodes, lasers, and high-power electronic devices due to its wide direct band gap and chemical stability.¹ Given the difficulty of obtaining high-quality GaN substrates, most current GaN-based devices are heteroepitaxially grown on foreign substrates, such as sapphire, Si, and silicon carbide.² However, the conventional growth of GaN films on these substrates generates a high defect density and considerable biaxial strain, attributed to the large lattice and thermal mismatch between the GaN films and their substrates. Thus, the lack of GaN native substrates is the main obstacle for the extending development of GaN-based devices. Although several conventional methods exist for obtaining free-standing GaN, such as laser lift-off, void-assisted separation, and chemical etching of the intermediate layer between GaN and the original substrate, the process of removing the substrate from a thick GaN film is complicated, expensive, and time-consuming. Furthermore, the original substrate can be damaged or contaminated during this process.³

Recently, the van der Waals epitaxial growth of III-V films on two-dimensional (2D) materials has been proposed to effectively mitigate the lattice mismatch effect caused by the weak bonds between III-V films and 2D materials.⁴ Fluorophlogopite mica is a thermally stable material with a flexible atomic flat surface and low commercial cost, making it an ideal 2D material substrate. However, the dangling bond-free surface of 2D materials suppresses the nucleation of the III-V film, limiting the growth of large-area single crystals. Although some studies have proposed graphene as an intermediate layer in bridging techniques for growing and lifting off III-V films,⁵ the integration of GaN growth with mica for self-separation is a relatively unexplored area.

In this research, we successfully grew a 2-inch thick GaN film with high uniformity on a fluorophlogopite mica substrate via hydride vapor phase epitaxy. The 2-inch thick GaN film easily self-separated from the mica substrate during rapid cooling. After the film growth process, the residual GaN on the mica substrate was effectively eliminated through deionized water, owing to the hydrophilic characteristic of mica and the weak bonding between GaN and mica. Moreover, we demonstrated the capability of reusing the mica substrates by repeatedly growing self-separated GaN films on the same substrate. Additionally, to verify that the thick GaN film was of device quality, we demonstrated a completely functional ultraviolet light-emitting diode with a wavelength of 378 nm. In summary, our proposed approach may facilitate the epitaxy of large-area single-crystalline GaN on 2D materials, offering a new substrate option in the self-separation technology of III-V materials.

References

1. W. Han et al. Synthesis of gallium nitride nanorods through a carbon nanotube-confined reaction. *Science*, 1997, 277, 1287-1289.
2. S. J. Pearton et al. GaN: Processing, defects, and devices. *Journal of Applied Physics*, 1999, 86, 1-78.
3. H. Kum et al. Epitaxial growth and layer-transfer techniques for heterogeneous integration of materials for electronic and photonic devices. *Nature Electronics*, 2019, 2, 439-450.
4. J. Yu et al. Van der Waals epitaxy of iii-nitride semiconductors based on 2D materials for flexible applications. *Advanced Materials* 2020, 32, 1903407.
5. H. Kim et al. Graphene nanopattern as a universal epitaxy platform for single-crystal membrane production and defect reduction. *Nature Nanotechnology*, 2022, 17, 1054-1059.

2:30 PM EL11.15.04

New Insights into Q-Carbon: Novel Interlayer in Gan-Diamond Integration for Improved Heat Dissipation Saif Al ArafinTaqy, Pallab KumarSarkar and ArifulHaque; Texas State University, United States

The recent surge in high-power electronic device research has led to the development of various wide bandgap materials. GaN is such a material with immense potential due to its many impressive characteristics, such as high electron mobility and high breakdown voltage, leading to smaller device footprints with better power densities and high efficiency. However, heat dissipation has become a significant concern in high-power semiconductor devices made of GaN, which stems from the combination of low thermal conductivity and increasing power density. This study aims to resolve this issue by incorporating a Q-carbon (quenched form of carbon) interlayer to form continuous diamond films, which have the highest thermal conductivity of any material. Q-carbon is a novel form of carbon that has been rapidly cooled after melting, resulting in its unique properties and potential for use in electronic applications and device fabrication. The growth of large-area Q-carbon has been restricted to low thermally conductive substrates due to the non-equilibrium nature of the synthesis process and a narrow range of parameters. This study addresses the abovementioned limitations by conducting a comprehensive parameter optimization of diamond-like carbon (DLC), the fundamental structure necessary for synthesizing Q-carbon. Initially, the deposition of DLC films onto sapphire substrates is accomplished through the utilization of graphitic carbon targets via pulsed laser deposition (PLD), and subsequent pulsed laser annealing (PLA) is employed to generate Q-carbon, with a comprehensive regulation of laser, deposition, and annealing parameters. The DLC films deposited in their as-formed state exhibit an sp³ content ranging from 15% to 82%, which is achieved by optimizing the laser energy density, frequency, and deposition temperature during the process of PLD. SLIM simulation is employed to determine the optimal energy level of pulsed laser annealing (PLA) necessary for the synthesis of extensive Q-carbon. The experimental outcomes are then replicated by subjecting diverse diamond-like carbon (DLC) films to PLA with varying energy densities, spanning from 0.3 J/cm² to 1.2 J/cm², to obtain Q-carbon. The present study demonstrates that the synthesis of large-area Q-carbon can be achieved by adjusting the parameters of PLD and PLA. This research broadens the scope of feasible thermally conductive substrates and provides fundamental parameters for future investigations on Q-carbon. Subsequently, we focus on GaN as a relatively higher thermally conductive substrate (conductivity ~200 Wm⁻¹K⁻¹) compared to the other substrates in the existing literature to employ the knowledge of large-area Q-carbon growth on various DLC films. This study incorporates a thin Q-carbon interlayer by utilizing low sp³ DLC film as the precursor and attempts to provide a solution to address the challenges associated with the integration of diamond and GaN for necessary thermal management capability. Incorporating a low thermally conductive DLC film and appropriate annealing parameters assist in achieving a Q-carbon interlayer on GaN. The utilization of Q-carbon on GaN serves as a nucleation substrate for producing high-quality HFCVD diamond with uniformity while protecting the GaN layer from deterioration and resolving the thermal mismatch between GaN and diamond. The distinctive combination of features possesses the capability to address the predicament of heat management in GaN devices, thereby advancing the attainment of GaN's theoretical potential in the domains of wireless/5-g communications, high-power devices, and other intricate microelectronic systems.

2:45 PM EL11.15.05

Molecular Beam Epitaxy of Superconducting ZrN Thin Films on GaN Substrates [Brelon J. May](#), Kevin D. Vallejo, David Hurley and Krzysztof Gofryk; Idaho National Laboratory, United States

Group III-Nitride materials have found applications in optoelectronics and photonic devices due to the large variation in direct bandgap spanning from the infrared to the deep ultraviolet. Recent research has pursued the integration of this well-established material system with transition-metal nitrides to create complex heterostructures with additional magnetic or superconducting functionality. ZrN is a well-known refractory conductor with high oxidation resistance, high hardness, and has been shown to be a superconductor at low temperatures. The estimated lattice mismatch of ZrN with InN, GaN, and AlN is 8.5%, -1.5%, and -4.2%, respectively, suggesting strain free as well as strain-tunable growth on the ternary III-Ns. This work focuses on the epitaxial growth of ZrN on c-plane GaN substrates via molecular beam epitaxy. An electron beam evaporation source and an RF-plasma source were used to supply the Zr and active nitrogen, respectively. Neither reflection high energy electron diffraction (RHEED) and X-ray diffraction (XRD) revealed any crystallographic texture of ZrN deposited on fused silica at temperatures >700°C. However, growth of ZrN on c-plane GaN substrates at similar temperatures was epitaxial. RHEED revealed that the ZrN maintains the symmetry of the underlying GaN throughout the entire deposition, and post-growth examination via XRD showed (111) oriented ZrN thin films. RHEED patterns during the regrowth of GaN directly on thicker layers of higher symmetry ZrN suggest a preference for the formation of rotational domains and a slight degree of surface faceting. The electrical transport as a function of temperature and magnetic field of ZrN films has been measured. Initial results of uncapped ZrN thin films reveal a superconducting phase with a critical temperature of <10 K and a critical field of 2 T. The critical temperature of the films is lower than reports of bulk ZrN, which could be attributed to strain, the presence of off stoichiometry or structural disorder, and is under investigation. These results pave the way for integration of additional superconductors and quantum phenomena in existing III-N systems.

3:00 PM EL11.15.06

Reduction of Lattice Mismatch Induced Strain and Critical Thickness Identification for Long-Range Crystallinity Niobium Nitride on 6H-SiC for High Quality SNSPD Detectors [Annaliese Drechsler](#)^{1,2}, Patrick Shea² and Aristos Christou¹; ¹University of Maryland, United States; ²Northrop Grumman Corporation, United States

Niobium nitride (NbN) films have garnered significant attention and research recently due to their high critical temperature (T_c) and their usage in infrared-sensitive superconducting nanowire single photon detectors (SNSPDs). Devices fabricated from NbN have demonstrated single photon detection to mid-wave infrared wavelengths, which unlocks possibilities for novel applications such as long-range laser detection and ranging (LiDAR), interferometry of signals in planetary emissions, quantum key decryption, and optical communications. Due to their polycrystalline nature, NbN films are sensitive to defects stemming from the deposition and fabrication processes referred to as constrictions. These film constrictions effectively reduce the cross-sectional area of the detector nanowire, which in turn limits the critical current and resultant detection efficiency and jitter. NbN films are still, however, among the most promising for practical use and array development due to their high T_c approaching 16K, thus necessitating the development of methods to reduce film defectivity.

NbN films utilized for SNSPD fabrication must be thin, typically <100 nanometers. As a result, the film quality and defectivity are highly correlated to the interface between the NbN film and underlying lattice, lattice-mismatch strain, and deposition parameters of the NbN processing. To optimize this interface, a material with similar lattice structures and parameters to NbN must be chosen to minimize intrinsic defect sources. Then the deposition process can be optimized to reduce extrinsic defects.

Silicon carbide (SiC) 6H polytype substrates were selected for use as the deposition substrate. 6H-SiC has an in-plane lattice parameter a=3.08Å, leading to a 3.57% lattice mismatch with hexagonal NbN with in-plane lattice parameter of 2.98Å and minimizing strain from lattice matching below the critical thickness. SiC can be later utilized to fabricate semiconductor components necessary for focal plan array (FPA) development. NbN films were sputtered onto the substrates in an AJA ATC Orion 8 sputtering tool utilizing a non-reactive RF magnetron process in an inert argon atmosphere to control resultant film stoichiometry. Deposition conditions such as temperature, gas flow, and pressure were modified, and the resultant films were characterized through x-ray diffraction to determine phase, orientation, crystallinity, and stress.

The temperature of the substrate during deposition runs was increased from ambient temperature to 600C. As temperature increased, XRD peak intensity increased, and crystallite size calculated from peak FWHM increased linearly from 26.07nm to 1618.1nm for P6m2 NbN. This substantial increase in crystallinity stemming from increased energy promoting nucleation and growth of higher order crystallites reduces the number of grain boundaries and resultant constrictions within a SNSPD to improve efficiency. High temperatures, however, are not always compatible with semiconductor fabrication necessary for FPA development so pressure modifications were also explored as an alternative. The deposition pressure was increased from 3mTorr linearly to 8mTorr. Similar improvements in crystallinity to temperature were observed. The critical thickness where the film stress cannot be accommodated through lattice matching was measured to extract the stress of these films. 3mTorr films demonstrated a critical thickness of 475Å, while films with higher pressures increase that to >750Å. This improvement points towards reduced film stress and reduced formation of threading dislocations to accommodate strain.

In conclusion, we studied the impact of substrate lattice matching and non-reactive sputtering of NbN films on 6H-SiC. Modifying the deposition temperature and pressure allowed for the development of films with long range crystallinity and low stress to enable defectivity reduction and facilitate the development of high-quality long wavelength SNSPDs.

3:15 PM EL11.15.07

Scalable Low Temperature Perovskite Epitaxy in Open Atmosphere [Zhuotong Sun](#), Nives Strkalj, Ziyi Yuan and Judith L. Driscoll; University of Cambridge, United Kingdom

Epitaxial growth of single-crystalline oxides is one of the fundamental ways to integrate perovskite structures on semiconductors and other oxides, being very attractive for applications as well as fundamental studies, where the film uniformity is greatly enhanced in comparison to polycrystalline films with reduced grain boundaries, superior interfacial conductivity and integration with silicon. However, large-scale epitaxial implantation of complex oxides in consumer electronic devices remains a challenge. Epitaxial deposition techniques, such as molecular beam epitaxy (MBE) and pulsed laser deposition (PLD), require high-temperature and high vacuum systems, with a limited deposition area, which pose problems when during production. Other techniques, such chemical vapor deposition (CVD), can also be used to deposit complex oxides, but generally at growth or post-deposition annealing temperatures over 500°C to achieve epitaxy. Therefore, a thin-film growth technique with reduced complexity and less-energy-intensive conditions, giving epitaxial films in a short growth time is highly desired. Herein, we use an open atmospheric deposition technique, Spatial Atmospheric CVD, mimicking the film growth by PLD, to deposit highly crystalline, epitaxial binary oxide, on various single crystal substrates at 350°C, with similar electrical properties of PLD grown film. Thus, opening the possibility the low cost, large scale, high throughput of epitaxial devices commercially.

8:00 AM EL11/EL13.01

CuI Based p Type Thin Film Transistor WeiWei, MingGao, WangZhiyong and ChunxiangZhu; National University of Singapore, Singapore

CuI is a wide bandgap p type transparent semiconductor and owns a high potential to be used in the fields like thin film transistor, Optoelectronic, and memory devices etc. It has many advantages like high hole mobility, good electrical property with a structure disorder. However, a high hole concentration in the CuI leads to a low Current On-Off ratio (I_{ON-OFF}) for CuI TFT devices. To solve this issue, Br doping technique is proposed to lower down the hole concentration in the CuBr film so that a better TFT device performance can be obtained. The density functional theory (DFT) results show that the copper vacancy formation energy increases with the CuBr content in the Br-doped CuI film, resulting in lower hole concentration. The CuBr TFTs with different Br content were then fabricated. All the CuBr films were synthesized by the solution method. When the Br concentration increases from 0% to 10%, the hole mobility decreases while the I_{ON-OFF} ratio increases from the order of 10^2 to 10^4 . A Br doping concentration of 7.5% shows the best device performance with hole concentration about $5\text{ cm}^2\text{V}^{-1}\text{s}^{-1}$ and I_{ON-OFF} ratio of 10^4 . The good p type CuI TFT device performance is a good foundation for the later application of CuI in the fields, including Logic circuits, Optoelectronic etc.

Corresponding Author: Chunxiang Zhu, Email: elezhucx@nus.edu.sg

This work was supported by Ministry of Education (MOE), Singapore under its Tier 1 grant (WBS no. A-0009043-01-00) and NUS ARTIC WDSS-RP3 (WBS no: A-0005943-33-00).

8:05 AM EL11/EL13.02

Polarization-Dependent Optical Properties of Ce-Implanted Quartz YuichiroAbe^{1,2}, ShunKanai^{1,3,4}, ManatoKawahara^{1,2}, JunIshihara⁵, MakotoKohda² and ShunsukeFukami^{2,6}; ¹Tohoku University, Japan; ²Graduate School of Engineering, Tohoku University, Japan; ³PRESTO, Japan Science and Technology Agency, Japan; ⁴National Institutes for Quantum Science and Technology, Japan; ⁵Department of Applied Physics, Tokyo University of Science, Japan; ⁶Inamori Research Institute for Science, Japan

Nitrogen-Vacancy centers in diamonds and divacancies in SiC are the representative material systems composing solid-state spin qubits with a long coherence time at room temperature [1-4]. While various functionalities, e.g., remote entanglement, quantum sensing, and quantum communications, have been achieved, new qubit material systems may offer a new range of opportunities. One of the most critical material parameters for many quantum applications is the relaxation time T_2 . Here, we focus on quartz as a host material, the most common mineral on the earth, and has been predicted to have a long T_2 without nuclear purification [5]. We choose the Ce^{3+} center as a spin center, which often composes a stable spin center in the widegap oxides, e.g., in $\text{Y}_3\text{Al}_5\text{O}_{12}$, whose spin state can be controlled through the circularly polarized laser [6].

We implant Ce ion into a naturally abundant single-crystal quartz substrate at room temperature in the air. The implantation dose and energy are $1.0 \times 10^{14}\text{cm}^{-2}$ and 100 keV, respectively. Subsequently, the samples are annealed in Ar for 0-9 hours at 700-1000°C. First, we investigate the unpolarized optical properties of Ce-implanted quartz. The unpolarized photoluminescence (PL) spectra are measured with unpolarized He-Cd laser excitation at 325 nm. The unpolarized PL shows similar spectra with the previous studies on the sputter-deposited $\text{SiO}_2:\text{Ce}$ [7]: unpolarized PL spectra have a prominent peak at around 445 nm, which corresponds to the $4f-5d$ transitions with different spin-orbit interaction of the Ce^{3+} center. We investigate the unpolarized PL of the samples with various annealing conditions. Up to 800°C, as the annealing temperature increases, PL intensity increases, suggesting the formation of luminescent Ce^{3+} , while the further increase of the annealing temperature decreases the unpolarized PL intensity, suggesting the formation of the Ce clusters without bright luminescence.

Next, we investigate the polarized optical properties with the samples annealed at 800°C. In a single Ce^{3+} center of YAG: Ce^{3+} , the polarization-dependent PL signal corresponding to the spin-dependent $4f-5d$ transition and the pulsed optically-detected magnetic resonance (ODMR) have been reported at 5 K [6]. We observe that a polarization-dependent optical signal of the Ce-implanted quartz is consistent with the $4f-5d$ transition of the isolated Ce^{3+} centers: σ^+ excitation offers a larger σ^+ PL emission than that with σ^- at the peak wavelength, and the more prominent σ^- emission at the shoulder wavelength (~560 nm). The degree of circular polarization (DOCP) reaches 15% (5%) at peak (shoulder) wavelength at 5 K. The DOCP monotonically decreases with increasing the measurement temperature, which suggests that the spin-lattice relaxation time T_1 limits T_2 in this material system.

[1] A. Gruber *et al.*, Science **276**, 2012 (1997).

[2] L. Childress *et al.*, Science **314**, 281 (2006).

[3] W. F. Kohel *et al.*, Nature **479**, 84 (2011).

[4] D. J. Christle *et al.*, Nature Mater. **14**, 160 (2014).

[5] S. Kanai *et al.*, Proc. Natl. Acad. Sci. **119**, e2121808119 (2022).

[6] P. Siyushev *et al.*, Nat. Commun. **5**, 3895 (2014).

[7] J. Weimskirch-Aubatin *et al.*, J. Alloys Compd. **622**, 358 (2015).

Acknowledgment: We thank Hideo Ohno, Fumihiko Matsukura, F. Joseph Heremans, C. P. Anderson, S. E. Sullivan and G. Wolfowicz for the fruitful discussion. This work was supported in part by Shimadzu Research Foundation; Takano Research Foundation; RIEC Cooperative Research Projects; JSPS Kakenhi Nos. 19KK0130 and 20H02178; and JST-PRESTO No. JPMJPR21B2.

8:20 AM EL11/EL13.03

Optical Control of Spin in Amorphous $\text{SiO}_2:\text{Ce}^{3+}$ ShunKanai^{1,2,3}, YuichiroAbe¹, ManatoKawahara¹, JunIshihara¹, MakotoKohda¹ and ShunsukeFukami^{1,4}; ¹Tohoku University, Japan; ²Japan Science and Technology Agency, Japan; ³National Institute for Quantum Science and Technology, Japan; ⁴Inamori Research Institute for Science, Japan

Defect centers in diamond and SiC are the most established spin centers as optically accessible solid-state qubits [1-4]. To develop other widegap host materials with new qubit functionalities [5], based on the Liouville-von Neumann equation and the cluster correlation expansion (CCE), we have predicted the spin coherence time T_2 of the oxide host materials and found that (1) single crystal α -quartz (SiO_2) has a long coherence time ($T_2 \sim 3.4$ ms) without nuclear purification and (2) T_2 does not significantly depend on the crystalline structure of the host material as long as the T_2 is limited by the interaction between electron spin – nuclear spin bath [6]. Here we focus on the amorphous SiO_2 , namely glass, as a host material for its possible application to the qubit.

As an optically accessible spin center, we choose Ce^{3+} center because it often composes a stable spin state, and its spin state can be controlled through the circularly polarized laser in the widegap oxides [7]. We introduce Ce into pure SiO_2 glass substrate by ion implantation with a dose of $1.0 \times 10^{14}\text{cm}^{-2}$ and an energy of 100 keV. Subsequently, we anneal the samples in Ar for 2 hours at 500-1000°C. The unpolarized photoluminescence (PL) spectra are measured with a He-Cd laser with an excitation wavelength of 325 nm. The PL shows similar spectra with the previous works on the sputter-deposited $\text{SiO}_2:\text{Ce}$ [7]: PL spectra have a relatively broad peak over 400 – 550 nm and show a prominent peak at 430 nm and a shoulder at 460 nm, consistent with the $4f^2(F_{5/2})-5d$ and $4f^2(F_{7/2})-5d$ transitions in tetrahedral coordinate, respectively. We investigate the PL of the samples with various annealing conditions. The PL intensity gradually increases with annealing temperature up to 700-900°C with the formation of luminescent isolated Ce^{3+} center and decreases with increasing the annealing temperature to 1000°C due to the Ce cluster formation. Further increase of the annealing temperature increases the PL intensity again, corresponding to the formation of luminescent Ce silicate.

For the optical control of the spin, we investigate the polarization dependence of the optical properties of the samples annealed at 800°C at 4 K. In a single Ce^{3+} center of YAG: Ce^{3+} , the polarization-dependent PL signal corresponding to the spin-dependent $4f-5d$ transition and the pulsed optically-detected magnetic resonance (ODMR) have been reported at 5 K [7]. Even in our sample with the Ce-implanted glass SiO_2 , we observe a polarization-dependent optical signal is consistent with the $4f-5d$ transition of the isolated Ce^{3+} centers: the degree of circular polarization (DOCP) reaches 12% and -5% at peak and shoulder wavelengths, respectively. Our result shows that an isolated Ce^{3+} center can be formed in the glass substrate, and helicity-dependent optical property suggests that it takes a similar crystalline coordination to YAG: Ce^{3+} due to its short-range order.

References

[1] A. Gruber *et al.*, Science **276**, 2012 (1997).

[2] L. Childress *et al.*, Science **314**, 281 (2006).

[3] W. F. Kohel *et al.*, Nature **479**, 84 (2011).

[4] D. J. Christle *et al.*, Nature Mater. **14**, 160 (2014).

[5] G. Wolfowicz *et al.*, Nat. Rev. Mater. **6**, 906 (2021).

[6] S. Kanai *et al.*, Proc. Natl. Acad. Sci. **119**, e2121808119 (2022).

[7] P. Siyushev *et al.*, Nat. Commun. **5**, 3895 (2014).

[8] J. Weimskirch-Aubatin *et al.*, J. Alloys Compd. **622**, 358 (2015).

Acknowledgment

We thank H. Ohno, F. Matsukura, K. Takano, F. J. Heremans, C. P. Anderson, S. E. Sullivan, and G. Wolfowicz for the fruitful discussion. This work was supported in part by Shimadzu Research Foundation; Takano Research Foundation; RIEC Cooperative Research Projects; JSPS Kakenhi Nos. 19KK0130 and 20H02178; and JST-PRESTO No. JPMJPR21B2.

8:25 AM EL11/EL13.04

Approximate Quasiparticle DFT+A-1/2 Method Applied to Ga_2O_3 and In_2O_3 Polymorphs ClaudioR. da Silva¹, FriedhelmBechstedt², LaraK. Teles¹ and MarceloMarques¹; ¹Aeronautics

Gallium oxide (Ga₂O₃) and indium oxide (In₂O₃) are at the forefront of the recent progress in power semiconductor devices, which extend the range of power semiconductors from wide bandgap semiconductors (WBS) such as GaN and SiC to ultra-wide bandgap semiconductors (UWBS) such as Ga₂O₃ and Al₂O₃, sometimes alloyed with In₂O₃. These oxide semiconductors currently find themselves at a stage of development similar to that of the WBG semiconductors in the 1980s and therefore, several challenges related to the understanding of their properties have to be settled yet. Specifically for these oxides the well-known underestimation of DFT-based bandgap prediction is more complicated because it is also connected with the wrong position of the d-level in disagreement with the experimental results. Several techniques can be used to overcome these difficulties, but, in general, state-of-the-art methods (such as GW and hybrid functionals), are computationally extremely expensive, which makes them impractical for more complex systems as it is required for a deep investigation for these oxides with pronounced polymorphism and the need for large unit cells.

In this study we investigate the structural, optical and electronic properties of ten polymorphs of Ga₂O₃ and In₂O₃ using a fast and efficient approximate quasiparticle method called DFT+ $A^{-1/2}$ which at the same time could deal with the delocalized d-levels and the problem in underestimation of the energy bandgap. We provide approximate quasiparticle band structures and binding energies even for very complex systems such as defective spinel phase of Ga₂O₃ containing 160 atoms in a cell. Our results are in line with the state-of-the-art methods and experimental data providing energy bandgaps of about 4.6 eV to 5.1 eV for Ga₂O₃ polymorphs and, 2.4 eV to 3.3 eV for In₂O₃ polymorphs. Band edge optical properties including excitonic effects are explained in terms of effective masses and dielectric constants. Furthermore, we predict pressure-induced phase transitions between polymorphs of the same oxides derived from equations of state.

8:30 AM EL11/EL13.05

Fully Solution-Processed Ultraviolet Photodetector Based on Hydrothermally Grown ZnO Nanorod Array Ajinkya B. Palwe, Tapesh Kumar, Sweta Rani, Shobha Shukla and Sumit Saxena; IIT Bombay, India

Patterned nanostructures exhibit interesting optoelectronic characteristics due to light-matter interaction at the comparable dimension of incident light and material. At a comparable dimension, the optoelectronic response of the nanostructure-based devices is modulated by the size and the periodicity of the structure. Numerous techniques based on top-down and bottom-up approaches are used to obtain patterned nanostructure. However, the solution-based technique is considered to be best due to cost-effectiveness as well as large-area processing. Recently patterned structures of metal oxide semiconductors are getting attention for various optoelectronic devices like photodetectors, solar cells, etc. ZnO is an abundantly available metal oxide that has high absorption coefficient and is highly appropriate for low-cost ultraviolet photodetectors. The hydrothermally patterned ZNA was achieved in two steps of deposition starting with ZnO quantum dots (QDs) seed layer followed by hydrothermal reaction. The as-grown ZNA was treated with ZnO QDs to remove any pin-holes or trap sites. P-type polymer PEDOT:PSS was used for making heterojunction with n-type ZNAs. The carbon electrode at the top was deposited by screen printing of carbon paste.

The optical bandgap increases with decreasing the size/periodicity of the ZNA. ZNR based film and heterojunction devices are investigated for different sizes/periodicity using surface morphology and optoelectronic properties. The ZNA based heterojunction photodetectors have shown improved photoresponse under ultraviolet (UV) light. The maximum photoresponsivity of 9.2 A/W and external quantum efficiency of 3144% are achieved for the ZNA obtained by 20 mM precursor solution. The response time is also fast due to the reduction in surface pin-holes/traps.

KEYWORDS: Hydrothermal deposition; Patterned ZnO; P-N junction, UV photodetector;

ACKNOWLEDGEMENT: The authors express their gratitude for support from SAIF and IRCC, IIT Bombay, and funding from DST (India); SERI (grant no. DST/TM/SERI/2k10/12/(G)), TMD (grant no. DST/TM/WTI/WIC/2K17/100(C)), and SERB (grant no. EMR/2017/005144).

References:

- Kasani, S., Curtin, K. and Wu, N. (2019), *Nanophotonics*, 8(12), pp. 2065–2089.
 Kumar, C. et al. (2020), *IEEE Photonics Technology Letters*, 32(6), pp. 337–340.
 Kumar, C. et al. (2022), *IEEE Electron Device Letters*, 43(2), pp. 260–263.
 Sørensen, M. W. and Sørensen, A. S. (2008), *Physical Review A*, 77, p. 013826.

8:45 AM *EL11/EL13.06

WITHDRAWN 11/13/2023 EL11/EL13.06 2D Van Der Waals Multiferroics Designed by Layer Stacking Evgeny Y. Tsybmal; University of Nebraska–Lincoln, United States

Van der Waals (vdW) assembly of two-dimensional (2D) materials allows polar layer stacking accompanied by the emergence of a switchable out-of-plane electric polarization. The vdW polar stacking can be employed to engineer 2D multiferroics from the recently discovered 2D magnets, whose magnetic properties can be controlled by the induced electric polarization. Here, we predict novel phenomena in the 2D magnets MnBi₂Te₄ and CrI₃ that are not present in their bulk form. We demonstrate that broken space-inversion (*P*) and time-reversal (*T*) symmetries produce a magnetoelectric effect. While the effect is small, in case of antiferromagnetic MnBi₂Te₄, symmetry couples electric and magnetic polarizations resulting in the reversal of an uncompensated magnetic moment with reversal of electric polarization. The broken *PT* symmetry in a polar-stacked MnBi₂Te₄ bilayer produces an intrinsic anomalous Hall effect (AHE) driven by the non-vanishing Berry curvature, which can be reversed by ferroelectric polarization. In a three-layer MnBi₂Te₄ film, switchable polarization at one of the interfaces drives a metal-insulator transition, as well as switching between the AHE and quantum AHE (QAHE). In case of ferromagnetic CrI₃, we predict that polar layer stacking of this 2D material supports antiskyrmions – topological quasiparticles with a swirling spin texture. Unlike the widely investigated skyrmions, antiskyrmions combine opposite spin helicity across the structure driven by the anisotropic Dzyaloshinskii-Moriya interaction (DMI). We show that the polar layer stacking of two monolayers of CrI₃ efficiently lowers the symmetry, resulting in the required anisotropic DMI. The DMI is reversible with ferroelectric polarization switching, offering the ability to control antiskyrmions by an electric field. Overall, this work emphasizes the topological properties in 2D vdW magnets induced by polar layer stacking which do not exist in bulk materials and can be controlled by an electric field. The work is supported by the grant DE-SC0023140 funded by the U.S. Department of Energy, Office of Science.

9:15 AM EL11/EL13.07

Magnetoelectric Heterostructure for Passive Internet of Things Vibration Sensor Node Application Yifan He, Cunzheng Dong, Xiaxin Liu, Melania St. Cyr, Haoling Li and Nian Sun; Northeastern University, United States

Vibration detection have been widely applied in multiple fields including mechanical machine malfunctioning diagnosis, structural health monitoring (SHM) as well as human activity monitoring. For many of the sensing applications, the vibration sensing data collected needs to be transmitted and further analyzed. This requires the vibration sensor being integrated with long-lasting or self-powered power source and compact, highly efficient data transmitting/receiving antenna as an Internet of Things (IOT) sensor node, especially in rather inaccessible and harsh environment such as sea water or deep soil. Some efforts [1,2] have been made to build a passive vibration sensor node, the researchers utilized ambient vibration as the potential power source, however, a separate antenna is still needed in those cases for data communication wireless module in an IOT sensor node. With demonstrated near field communication capability [3], the potential of magnetoelectric (ME) heterostructure as an IOT vibration sensor node has been investigated by conducting the vibration detection test and stray magnetic field energy harvesting test. The PZT-8 based ME heterostructure showed a vibration detection sensitivity of 188 mV/g and 163 mV/g with 0 and button magnet bias at corresponding frequencies, respectively. The vibration limit of detection with button magnet bias was 4 μ g at 21.18 kHz. The magnetically tunable vibration performance is desirable for broadband operation. The energy harvesting test showed a maximum 94% of wireless power transfer (WPT) efficiency with a planer coil as magnetic field source. Compared to coil-to-coil WPT link, the ME heterostructure-coil link has ~7 times higher efficiency at rather long distance considering the magnetic flux concentration effect brought by the high permeability Metglas material in ME heterostructure.

- [1]. Rubes, O., Chalupa, J., Ksica, F. and Hadas, Z., 2021. Development and experimental validation of self-powered wireless vibration sensor node using vibration energy harvester. *Mechanical Systems and Signal Processing*, 160, p.107890.
 [2]. Chen, X., Guo, H., Wu, H., Chen, H., Song, Y., Su, Z. and Zhang, H., 2018. Hybrid generator based on freestanding magnet as all-direction in-plane energy harvester and vibration sensor. *Nano Energy*, 49, pp.51-58.
 [3]. Dong, C., He, Y., Li, M., Tu, C., Chu, Z., Liang, X., Chen, H., Wei, Y., Zaimbashi, M., Wang, X. and Lin, H., 2020. A portable very low frequency (VLF) communication system based on acoustically actuated magnetoelectric antennas. *IEEE Antennas and Wireless Propagation Letters*, 19(3), pp.398-402.

9:20 AM EL11/EL13.08

Study on Doping Effect of Copper and Chromium Ions on the Magnetic and Magnetocaloric Properties of Single Crystal Mn₃O₄ Md Farhan Azim¹, Pramanand Joshi² and Sanjay Mishra¹; ¹University of Memphis, United States; ²The University of Texas at Arlington, United States

Magnetic refrigeration technology, which works on the magnetocaloric effect (MCE) of magnetic materials, has attracted the interest of numerous research groups over traditional gas refrigeration. It has several advantages, including being highly energy-efficient, environmentally friendly, and cost-effective. The major effort is directed in improving the magnetic entropy change along with the relative cooling power (RCP) of transition metal oxide magnetocaloric materials. This study reports the structural and magnetocaloric properties of Cr_{1.5}Mn_{1.5}O₄ and Cu_{1.5}Mn_{1.5}O₄ which were synthesized via the facile autocombustion technique. The second-order phase transition temperature may be supposed to appear at the temperature-dependent field-

cooled magnetization curve near room temperature. These compounds with individual ferromagnetic phase transition temperatures may vary between 40K and 80 K that consequently enhances the RCP value. Moreover, ferromagnetic ordering can be observed in these mixed-metal compounds due to the presence of uncompensated electronic state of Mn^{2+} and doped transition metal ions. The difference in the super exchange pathway between the metal ions via the oxygen can give rise to a large ferromagnetic interaction. The fundamental key of this work is to demonstrate the potentiality of enhancing the magnetic phase transition temperature and magnetocaloric effect in the framework via spin coupling mechanism of transition metal doped Mn_3O_4 nanocomposites.

9:25 AM EL11/EL13.09

Study on Doping Effect of Cobalt and Zinc Ions on the Magnetic and Magnetocaloric Properties of Single Crystal Mn_3O_4 Md FarhanAzim¹, PramanandJoshi² and SanjayMishra¹; ¹University of Memphis, United States; ²The University of Texas at Arlington, United States

Magnetic refrigeration technology, which works on the magnetocaloric effect (MCE) of magnetic materials, has attracted the interest of numerous research groups over traditional gas refrigeration. It has several advantages, including being highly energy-efficient, environmentally friendly, and cost-effective. The major effort is directed in improving the magnetic entropy change along with the relative cooling power (RCP) of transition metal oxide magnetocaloric materials. This study reports the structural and magnetocaloric properties of $CoMn_2O_4$ and $ZnMn_2O_4$ which were synthesized via the facile autocombustion technique. The second-order phase transition temperature may be supposed to appear at the temperature-dependent field-cooled magnetization curve near room temperature. These compounds with individual ferromagnetic phase transition temperatures may vary between 80K and 120 K that consequently enhances the RCP value. Moreover, ferromagnetic ordering can be observed in these mixed-metal compounds due to the presence of uncompensated electronic state of Mn^{2+} and doped transition metal ions. The difference in the super exchange pathway between the metal ions via the oxygen can give rise to a large ferromagnetic interaction. The fundamental key of this work is to demonstrate the potentiality of enhancing the magnetic phase transition temperature and magnetocaloric effect in the framework via spin coupling mechanism of transition metal doped Mn_3O_4 nanocomposites.

9:30 AM EL11/EL13.10

Advances in Multiferroic Composites: Expanding the Horizons of Ferroelectric-Ferromagnetic Materials ProsunMondal, SrishtiPaliwal and Akhilesh KumarSingh; IIT (Bhu) Varanasi, India

Multiferroic composites have attracted significant attention due to their ability to exhibit both ferroelectric and ferromagnetic properties. These materials hold great promise for a wide range of technological applications, including memory devices, sensors, actuators, and energy harvesting. Multiferroic composites typically consist of a ferroelectric material and a ferromagnetic material, either as a composite structure or as a multi-layered system. The coupling between the ferroelectric and ferromagnetic properties can be achieved through strain-mediated, magnetoelectric, or exchange interactions. One common approach is to combine a ferroelectric material, such as $Pb(Zr,Ti)O_3$, $Bi(Na,K)TiO_3$, $(K,Na)NbO_3$ with a ferromagnetic material, such as cobalt ferrite ($CoFe_2O_4$), $NiZnFe_2O_4$, $MnFe_2O_4$ etc. These composites exhibit magnetoelectric coupling, where an applied magnetic field induces an electric polarization and vice versa. Other combinations of ferroelectric and ferromagnetic materials have also been explored, including bismuth ferrite ($BiFeO_3$) with a variety of ferromagnetic materials. The challenges associated with achieving strong coupling between the ferroelectric and ferromagnetic phases are addressed here along with ongoing efforts to optimize material compositions and processing techniques. Another area of research focuses on exploring new multiferroic materials beyond the commonly studied systems. Identifying novel materials with improved properties and higher operating temperatures is essential for expanding the range of applications for multiferroic composites. Additionally, efforts are being made to understand the fundamental mechanisms behind the coupling between ferroelectric and ferromagnetic properties. This includes studying the role of defects, interfaces, and domain structures in the overall behavior of multiferroic composites. In summary, the abstract highlights the promising future of multiferroic composites as advanced functional materials. It underscores the importance of ongoing research and development efforts to address existing challenges and explore new avenues for their applications. By harnessing the full potential of multiferroic composites, it is anticipated that they will contribute to the development of innovative technologies with enhanced performance, functionality and efficiency.

SYMPOSIUM EL12

Perspective on Applications of Metasurfaces—Advances in Metasurface Design, Fabrication, Integration and Material
November 27 - December 6, 2023

Symposium Organizers

Yongmin Liu, Northeastern University

Guru Naik, Rice University

Junghyun Park, Samsung Advanced Institute of Technology

Junsuk Rho, Pohang University of Science and Technology

* Invited Paper

+ JMR Distinguished Invited Speaker

SESSION EL06.12/EL12.12: Joint Keynote Presentation

Session Chairs: Yongmin Liu and Guru Naik

Thursday Morning, November 30, 2023

Hynes, Level 3, Room 312

11:30 AM *EL06.12/EL12.12.01

Active Epsilon-Near-Zero Photonics Aleksei Anopchenko, Quynh Dang, David Dang, Christopher MGonzalez, Yu-Hsun Chen, Juan Manuel Raffo Calixto, Sudip Gurung and Ho Wai (Howard) Lee; University of California, Irvine, United States

Epsilon-near-zero materials have been shown to be as one of the most promising optical materials in the recent years as the electromagnetic field inside media with near-zero permittivity has been shown to exhibit unique optical properties. I will review our recent studies on the active linear, nonlinear, and emission properties of conducting oxide and metallic nitride epsilon-near-zero materials.

Discovery of novel active materials is fundamental for photonic applications. The epsilon-near-zero (ENZ) materials have been shown to be as one of the most promising optical materials in the recent years as the electromagnetic field inside media with near-zero permittivity has been shown to exhibit unique optical properties, including strong electromagnetic wave confinement, enhanced quantum emission near ENZ media, non-reciprocal magneto-optical effects, unique topological properties, and abnormally large optical nonlinearity. While ENZ optics have been investigated extensively in the last few years, the current commonly used ENZ materials suffer from limited optical enhancement because of the lack of precise control of ENZ frequency, loss, and thickness for efficient ENZ mode excitation. In addition, the active tunability and enhanced nonlinearity and emission properties in ENZ materials have yet been fully experimentally

explored.

This talk will review our recent studies on the active linear, nonlinear, and emission properties of conducting oxide and metallic nitride epsilon-near-zero materials in planar and optical fiber platforms [1-7]. I will present a method to engineer the field intensity enhancement of the Al-doped zinc oxide (AZO) ENZ thin films synthesized by atomic layer deposition (ALD) technique. I will then discuss the observation of abnormal nonlinear temporal dynamic of hot electrons and enhanced optical nonlinearity in AZO and ITO ENZ thin films under different pump fluences and excitation angles using a degenerate pump-probe spectroscopy technique. Finally, I will also discuss the first experimental demonstration of optically confined ENZ resonance excitation in an optical fiber waveguide uniformly coated with AZO nanolayer. These studies enrich the fundamental understanding of emission and nonlinear properties on ENZ thin films and the integration of ENZ materials and optical fiber will open the path to revolutionary ultracompact in-fiber optical devices for optical communication, imaging, sensing/laser applications.

This work was supported in part by the National Science Foundation (grant number: 2113010), and Air Force Office of Scientific Research (FA9550-21-1-02204) (AFOSR-AOARD, FA2386-21-1-4057)

Reference:

A. Anopchenko, L. Tao, C. Arndt, H. W. Lee, "Field-effect tunable and broadband Epsilon-near-zero perfect absorbers with deep subwavelength thickness," *ACS Photonics* 5, 2631 (2018).

A. Anopchenko, S. Gurung, L. Tao, C. Arndt, , 5, 014012 (2018).

S. Gurung, A. Anopchenko, S. Bej, J. Joyner, J. Myers, J. Frantz, H. W. Lee, "Atomic layer engineering of epsilon-near-zero ultrathin films with controllable field enhancement," *Advanced Materials Interfaces* 2000844 (2020).

K. Minn, A. Anopchenko, J. Yang, 2342 (2018).

J. Yang, K. Minn, A. Anopchenko, S. Gurung, H. W. Lee, "Coupling to Epsilon-near-Zero Mode on Ultrathin Atomic Layer Deposited Conducting Oxide Film in Optical Fiber", submitted (2022).

A. Anopchenko, S. Gurung, S. Bej, H. W. Lee, "Field Enhancement of Epsilon-near-Zero Modes in Realistic Ultra-Thin Absorbing Films," submitted (2022).

K. Minn, A. Anopchenko, C.W. Chang, R. Mishra, J. Kim, Z. Zhang, Y. J. Lu, S. Gwo, and H. W. Lee "Enhanced Spontaneous Emission of Monolayer MoS2 on Epitaxially Grown Titanium Nitride Epsilon-Near-Zero Thin Films," *Nano Letter* 21, 4928 (2021).

SESSION EL08.07/EL06.04/EL12.04: Joint Keynote Presentation I

Session Chairs: Ho Wai (Howard) Lee and Lisa Poulikakos

Tuesday Morning, November28, 2023

Hynes, Level 3, Room 312

11:30 AM *EL08.07/EL06.04/EL12.04.01

From Structuring Light to High-Volume Manufacturing with Flat OpticsFedericoCapasso; Harvard University, United States

An overview of passive and active metasurfaces, encompassing complex supercell multifunctional types, and structuring light and darkness; inverse designed RGB metalenses specifically for virtual reality, combined organic/silicon telecommunication modulators, metacavities intended for holographic lasing, and XUV metalenses by vacuum guiding will be presented, along with a brief description of high volume semiconductor manufacturing of flat optics for consumer electronics (<https://www.electronicweekly.com/news/business/metalenz-to-move-into-volume-production-with-umc-2023-06/>)

SESSION EL08.17/EL06.13/EL12.14: Joint Keynote Presentation IV

Session Chairs: Guru Naik and Junsuk Rho

Thursday Afternoon, November30, 2023

Hynes, Level 3, Room 312

4:30 PM *EL08.17/EL06.13/EL12.14.01

Flat Optics for Dynamic Wavefront ManipulationMarkL. Brongersma; Stanford University, United States

Since the development of diffractive optical elements in the 1970s, major research efforts have focused on replacing bulky optical components by thinner, planar counterparts. The more recent advent of metasurfaces, i.e. nanostructured optical coatings, has further accelerated the development of flat optics through the realization that nanoscale antenna elements can be utilized to facilitate local and nonlocal control over the light scattering amplitude and phase. In this presentation, I will highlight recent efforts in our group to realize electrically-tunable metasurfaces employing nanomechanics, tunable transparent oxides, electrochemistry, microfluidics, phase change materials, and atomically-thin semiconductors. Such elements are capable of dynamic wavefront manipulation for optical beam steering, holography and future display technologies. The proposed optical elements can be fabricated by scalable fabrication technologies, opening the door to a wide range of commercial applications.

SESSION EL12.01: AI-Empowered Metasurface

Session Chairs: Yongmin Liu and Junsuk Rho

Monday Morning, November27, 2023

Hynes, Level 3, Room 305

10:30 AM *EL12.01.01

Novel Machine-Learning Approaches Based on Metric Learning and Manifold Learning for the Design and Knowledge Discovery in NanophotonicsMohammadrezaZandehshahvar and AliAdibi; Georgia Institution of Technology, United States

This talk is focused on using the machine-learning (ML) approaches based on dimensionality reduction and manifold learning for considerably reducing the dimensionality of the forward and inverse problems in relating the input and output of a nanophotonic system. It is shown that by using manifold learning techniques and simplifying the resulting networks using pruning, the computation complexity of the underlying ML algorithms will be considerably reduced. Furthermore, the importance of using an optimally defined loss function (or metric) for ML algorithms in obtaining priceless information about the properties of photonic nanostructures will be emphasized. It is shown that by moving from conventional mean-squared error to more intelligent metrics, knowledge discovery in nanophotonics will be facilitated along with better visualization of the input-output relationship in these nanostructures. In addition to knowledge discovery, the resulting manifold-learning algorithms can be optimally trained to facilitate the inverse design of such nanostructures while minimizing the structural complexity. As such, this talk will provide the foundation for both knowledge discovery and design in photonic nanostructures using manifold learning and metric learning and their application to the highly desired metaphotonic structures as an example platform.

11:00 AM *EL12.01.02

Machine Learning Methods for Freeform Metamaterial DesignJonathanA. Fan; Stanford University, United States

We will discuss computational algorithms based on deep neural networks that can accelerate the design and simulation of nanophotonic devices, using metasurfaces and metamaterials as a model system. We will discuss the use of generative networks to perform population-based optimization and elucidate how the neural network architecture can be tailored to effectively perform freeform optimization. We will also discuss how physics-augmented deep networks can be trained with a combination of data and physics constraints to serve as accurate surrogate electromagnetic solvers. A principal challenge involves configuring the algorithms in a manner that enables application to a wide range of problems, and we show how these concepts can generalize to the simulation and optimization of photonic devices involving a range of domain sizes, fitting parameters, and functions. Together, these algorithms can effectively search for the

global optimum three to four orders of magnitude faster than with conventional methods. We anticipate that with proper co-design of the neural network architecture with the scientific computing task, our surrogate solver and optimizer concepts can be adapted to large scale three-dimensional photonic systems.

11:30 AM *EL12.01.03

Three-Dimensional Metamaterial Absorber for Gas Molecular Sensing [Takuo Tanaka](#)^{1,2,3}; ¹RIKEN Center for Advanced Photonics, Japan; ²RIKEN Cluster for Pioneering Research, Japan; ³Tokushima University, Japan

Metamaterials have attracted considerable attention due to their capabilities to manipulate light. Recently we applied metamaterial light absorber for improving the sensitivity of IR spectroscopy. Owing to its plasmonically resonant interaction with incident light wave, and molecules, unwanted background and noises in IR spectroscopy were suppressed, and molecular signals are enhanced and clearly observed at the bottom of the suppressed background. This technique has already been applied for self-assembled monolayer of 16-mercaptohexadecanoic acid molecules on the surface of metamaterial absorber and atto-molar (10^{-18} mol) level molecular sensitivity was realized [1]. For liquid samples, to introduce target molecules into the hot spot region of the metamaterial absorber, we proposed a metamaterial absorptive device that incorporates with nanofluidics and demonstrated an ultra-high sensitivity of IR absorption detection [2, 3, 4]. In this paper, we introduced metamaterial absorber with three-dimensional vertical-oriented metal-insulator-metal (v-MIM) structure for ultra-sensitive infrared spectroscopic gas molecule sensing [5]. We designed the v-MIM structure with a nano-gap of 25 nm channel which enabled the delivery of small molecules into hot-spot region. We developed the fabrication technique to realize v-MIMs on the surface of Si substrate using electron-beam lithography and reactive ion etching techniques. Owing to small footprint of v-MIM comparing conventional lateral MIM structure, the density of hot spots was dramatically increased resulting in strong signal enhancement and efficient suppression of background light. This metamaterial was applied to carbon dioxide and butane detection designing to exhibit a resonance at 4033 cm^{-1} and 2945 cm^{-1} which spectral overlap with the C=O and $-\text{CH}_2$ vibration mode, respectively. The mutual coupling of these two resonant modes creates a Fano resonance, and their distinct peaks are clearly observed in the corresponding transmission dips. In addition, owing to its small footprint, v-MIM structure allows the detection of a 20 ppm concentration with suppressed background and high selectivity in the mid-infrared region.

[1] A. Ishikawa and T. Tanaka, *Scientific Reports* 5, 12570 (2015).

[2] T. Le and T. Tanaka, *ACS Nano* 11, 9780 (2017).

[3] T. Le, A. Morita, K. Mawatari, T. Kitamori, and T. Tanaka, *ACS Photonics* 5, 3179 (2018).

[4] T. H. H. Le, A. Morita, and T. Tanaka, *Nanoscale Horiz.* 5, 1016 (2020).

[5] D.-S. Su, D. P. Tsai, T.-J. Yen, and T. Tanaka, *ACS Sensors* 4, 2900 (2019).

SESSION EL12.03: Industrial Perspective on Metasurface

Session Chairs: Yongmin Liu and Junsuk Rho

Tuesday Morning, November 28, 2023

Hynes, Level 3, Room 305

8:30 AM *EL12.03.01

Large Scale Manufacturing Techniques for Metamaterials and Their Industrial Applications [Ragip Pala](#); Meta Materials Inc., United States

Development of a scalable nanofabrication technique is essential for the practical realization of nanostructured materials in functional transparent films. META® has developed discrete platform-specific proprietary technologies for large-scale lithography, allowing the manufacture of nanostructures to be carried out with high uniformity and low cost. Using these manufacturing techniques at META®, we design and mass-produce nano-technology-based films with applications in a wide variety of products and markets.

In this talk, I will present large-scale manufacturing techniques at META® including nanoimprinting, roll-to-roll processing, and holographic lithography. I will also discuss various industrial applications in automotive, authentication, 5G communication and consumer electronics. Our customizable patented nano-optics include visual authentication technology, KolourOptik® Stripe, with a unique combination of multiple colors, 3D depth and omni-directional movement. I will describe NANOWEB®, META®'s Roll to roll lithographically fabricated conductor with superior electrical and optical properties. This functional film is configured as a nanostructured conformable metal wire mesh, that is transparent to the naked eye. I will explain how we utilize NANOWEB® to enable smart solutions for distinct functions including electro-optical dimming, transparent antennas, anti-fog heaters and EMI Shielding.

In addition, we are also using a first of its kind Plasma Fusion® deposition technology, which enables high speed coating of any alloy on any type of thin flexible plastic substrate. Large scale and efficient metallization coating of ultra-thin substrate with zero defect, is a critical step for example toward volume production of safe reliable lightweight battery materials, requiring hundreds of millions of square meters per year. We use this metallization step in our roll-to-roll production process for functional films, which for solid state NCORE™ battery current collectors will reduce battery weight, increase safety, significantly accelerate line speed, and hence reduce cost.

9:00 AM *EL12.03.02

A Scalable Technology Platform for Creating Meta-Surface Based Optics and Waveguide Combiners for Augmented Reality [Robert J. Visser](#), [Ludovic Godet](#), [Rutger Thijssen](#), [Jinxin Fu](#), [Rami Hourani](#), [Sage Doshay](#) and [Guannan Chen](#); Applied Materials, United States

Optics is increasingly important in modern life, and advances in nanostructure-based flat optical devices hold great promise for revolutionary new opportunities in the display space. Augmented and Virtual Reality (AR/VR) are expected to enable the next ubiquitous computing and communication platform.^[1] Augmented Reality, Optical metasurfaces also leverage engineered nanostructures to offer the possibility of extreme wavefront control, enabling further miniaturization of imaging and display optical systems and exciting new applications not achievable with conventional optics.^[2,3]

The Engineered Optics™ group at Applied Materials is enabling thinner, light-weight optical systems with precise wavefront engineering to make possible novel optical devices. We have leveraged Applied Materials' materials engineering expertise to develop a platform for the precision fabrication of nanostructured optical devices on 300mm glass wafers, as well as metrology, optical performance characterization, and back-end assembly of these devices. With this platform, we are producing waveguide combiners for AR/VR applications and optical metasurfaces for multi-functional wavefront control in the near infrared. An essential element in designing the process and making choices for equipment is scalability, laying the foundation for large scale industrial manufacturing in a later stage. We have opted to focus on the use of optical lithography Nano Imprint Lithography and a 300 mm equipment for all the etch and deposition steps. This leverages all the experience and the availability of equipment from the Semiconductor Industry.

Waveguide combiners are a key component in lightweight augmented reality headset or glasses systems, but are difficult to fabricate to the high precision required for simultaneous high optical image quality of the AR content and clear vision of the real world.^[1]

The Engineered Optics platform includes a fully integrated front-end process flow to make surface relief grating-based waveguide combiner devices for our customers. All our tools are customized to enable handling of transparent substrates of a variety of refractive indices and thicknesses. We produce binary and slanted nanostructures using UV or nanoimprint lithography and etch in high-quality, low-loss optical materials. We can process single- or double-sided devices with high alignment fidelity, and can create desired features with global and local-area processing techniques.

The Engineered Optics platform offers full end-to-end capabilities: after front-end fabrication on 300mm substrates, we optically characterize device performance at the wafer level, then complete back-end singulation, edge blackening, stacking assembly, and final testing. Completed waveguide combiner devices can then be integrated with light engines and appropriate electronics, power sources, and housings to create final AR glasses or headset devices.

The Engineered Optics platform also enables direct fabrication of optical metasurfaces on transparent substrates, without transfer from silicon substrates. We can fabricate the extremely high aspect-ratio structures required for full 2π phase control in a variety of extremely low-loss, high-refractive index optical materials.

We are also looking at photonic integrated circuits, optical computing, optical data communication, and beyond.

References

B. C. Kress and I. Chatterjee, *Nanophotonics*, 10 (1), 41-74 (2021).

F. Capasso, *Nanophotonics*, 7 (6), 953-957 (2018).

V.-C. Su, C. H. Chu, G. Sun, and D. P. Tsai, *Opt. Express* 26, 13148-13182 (2018).

9:30 AM BREAK

10:00 AM *EL12.03.03

Highly Efficient Color Separation and Focusing in Various Color Pattern Arrays of CMOS Image Sensor Sookyoung Roh, Sungmo Ahn, Choonlae Cho, Hongkyu Park, Sangeun Mun, Sangyun Lee, Junho Lee and Seokho Yun; Samsung Advanced Institute of Technology, Korea (the Republic of)

We designed various types of nanoscale metaphotonic color-routing (MPCR) structures that can significantly improve the low-light performance of CMOS image sensors. Fabricated on a 1.12 μ m Dual pixel sensor and a 0.64 μ m Quad-pixel sensor, the MPCR structure separates the incident light energy into the respective color pixels, resulting in a notable increase in quantum efficiency of up to 20%. Our experimental demonstration confirmed a luminance SNR improvement of +1.0 dB under low light condition of 20 lux. Furthermore, this improvement was consistently achieved across different types of color pattern arrangements, further validating the versatility and effectiveness of our MPCR structures. Pixel miniaturization has been the main driver of product innovation in CMOS image sensors (CIS) for many years, and now pixel sizes are approaching the sub-wavelength diffraction limit. While downsizing pixels enables higher pixel densities and smaller form factors, there is a trade-off between pixel miniaturization and signal-to-noise ratio (SNR). Consequently, the overall performance of CIS is adversely affected due to the reduction in light-receiving areas [1]. To address these inherent physical limitations, alternative approaches involving efficient redistribution of incident light energy can be pursued through the integration of appropriately designed sub-wavelength scale photonic structures. Recent attempts to replace conventional color filters with metasurface structures are noteworthy in this regard [2-4], yet the performance and the process compatibility of the demonstrated devices have been far from commercialization, suffering from severe color crosstalk, poor angular response, complex or impractical fabrication processes, and additional color correction that resulted in lower-than-expected SNR gains. In this work, we present a new approach to revolutionize current optical stack layers by incorporating sub-wavelength scale metaphotonic color-routing (MPCR) structures. Our research efforts have yielded a wide range of nanoscale MPCR structures with remarkable capabilities to significantly improve the low-light performance of CMOS image sensors. By integrating these structures, we aim to improve sensor performance by manipulating the incoming light more efficiently. We have directly integrated the MPCR structures onto both of Samsung's 1.12 μ m dual-pixel CIS and 0.64 μ m quad-pixel CIS. And we characterized the imaging properties along with quantum efficiency compared to the reference sensor. The fabrication process is 100% CMOS-compatible, promising commercialization of high-performance sub-wavelength-pixel CIS.

10:30 AM *EL12.03.04

Metasurfaces: From Lab to Mass Markets Robert Devlin; Metalenz, United States

Optical metasurfaces enable unprecedented control over all aspects of light (phase, wavelength, intensity, and polarization) with a single, planar semiconductor layer. Comprised of subwavelength nanostructures, a single metasurface can carry out optical functions typically requiring four or more conventional refractive and/or diffractive optics, bringing new forms of sensing to mobile form factor for the first time. In addition to the expanded functionality they provide, they also open a route to the manufacture of optical devices in the semiconductor foundry, because they are constructed from CMOS-compatible materials on a planar substrate. This presentation will discuss metasurfaces from fundamental concepts to commercialization and will explore how the performance and large-scale manufacturing advantages of this technology will ultimately allow Metalenz to proliferate forms of sensing that have previously only been accessible in scientific or industrial laboratories.

11:00 AM TRAVEL TIME TO KEYNOTE SESSION

SESSION EL12.05: Wavefront Shaping, Metalens and Applications
Session Chairs: Yongmin Liu and Junsuk Rho
Tuesday Afternoon, November 28, 2023
Hynes, Level 3, Room 305

1:30 PM *EL12.05.01

Circularly Polarized Photoluminescence from Chiral Metamaterials and Large Area Fabrication Vivian Ferry; University of Minnesota, United States

Chirality controls light polarization, leading to emerging applications ranging from 3D displays to anti-counterfeiting to sensing. In the first example, I will show patterned, light-emitting metasurface structures, combining plasmonic structures and patterned, photoluminescent quantum dots. I will show how strategically placing these nanocrystals results in highly tailored circularly polarized photoluminescence, which realize simultaneously high polarization control and photoluminescence intensity. The light-emitting meta-atoms, which consist of cross-linked nanocrystals, are fabricated using direct-write electron beam lithography, realizing lateral feature sizes as small as 30 nm and heights in excess of 100 nm without degradation of the photoluminescence. I will then discuss an alternative strategy that uses additive manufacturing to create large-area metamaterials, and is roll-to-roll compatible. Finally, I will discuss the optical properties of chiral metamaterials formed by block co-polymer assembly and the effects of both the surface termination and bulk structure. I will show that it is possible to realize circular dichroism even in structures that are achiral in the bulk, due to the surface termination.

2:00 PM *EL12.05.02

Nanoscale 3D Printing of Structural Colors and Micro Optics Joel Yang; Singapore University of Technology and Design, Singapore

Structural colors are generated from nanoscale structures of various materials due either to interference or optical resonance effects. The ability to achieve a wide range of colors by simply tuning geometric properties opens fascinating opportunities to the nanoengineer or nanoscientist to design colors using material properties, sizes and shapes as input parameters. This physical approach contrasts with the chemical approach for synthesizing pigments and dyes. Using semiconductor fabrication methods, 2D structures based on metals and high index dielectrics have been realized, e.g. nanodisks, ellipses, etc. defined with electron-beam lithography and vacuum deposition methods.

Recently, we have extended the generation of structural colors from 3D nanostructures created using two-photon polymerization lithography (TPL). The use of TPL, an additive manufacturing process with sub-micron print resolutions, to produce structures for optical effect is a relatively new endeavor [1]. We have previously shown the fabrication of nanopillars, gratings, mesh-like, and wood-pile photonic crystal structures that appear colorful under white-light illumination.

We now demonstrate the integration of these structural colors with other micro-optical elements, such as microlenses and spiral phase plates. Equipped with TPL as a nanoscale 3D printer, structural color geometries are conveniently integrated in a single print run with other user-defined optics. Doing so enables one to produce structured light from incoherent light sources, holographic color prints, and control of the light-field for 3D representation. We will discuss the use of structural colors combined with micro-optics for enhanced information content and optical security [2].

References

Hao Wang, Wang Zhang, Dimitra Ladika, Haoyi Yu, Darius Gailevičius, Hongtao Wang, Cheng-Feng Pan, Parvathi Nair Suseela Nair, Yujie Ke, Tomohiro Mori, John You En Chan, Qifeng Ruan, Maria Farsari, Mangirdas Malinauskas, Saulius Juodkazis, Min Gu, Joel K. W. Yang, "Two-Photon Polymerization Lithography for Optics and Photonics: Fundamentals, Materials, Technologies, and Applications", *Adv. Funct. Mater.* 2214211(2023)
Hongtao Wang, Hao Wang, Qifeng Ruan, John You En Chan, Wang Zhang, Hailong Liu, Soroosh Daqiqeh Rezaei, Jonathan Trisno, Cheng-Wei Qiu, Min Gu, Joel KW Yang, "Coloured vortex beams with incoherent white light illumination", *Nature Nanotechnology* 18, 264–272(2023)

2:30 PM BREAK**3:00 PM EL12.05.03**

High-Numerical Aperture Metalenses with High Quality Factor Claudio U. Hail, Morgan Foley, Ruzan Sokhoyan, Lior Michaeli and Harry A. Atwater; California Institute of Technology, United States

In highly resonant optical elements, attaining a high quality factor typically comes at the cost of limited spatial control over the wavefront. Here, we report on dielectric, higher-order Mie-resonant metasurfaces that break this paradigm by realizing high-numerical aperture wavefront manipulation with high-quality factors. Our structure consists of high-index dielectric nanoparticles exhibiting a spectrally overlapped electric dipole and electric octupole mode, which allows for local wavefront manipulation. By appropriately tailoring the nanoparticle dimensions over a range of 545 – 555 nm with a period of 736 nm, we imposed a paraboloidal phase profile at an interface to realize radial metalenses for operation at near-infrared wavelengths with linear TE or TM polarization. The structures were fabricated from an amorphous silicon thin film on a glass substrate by a single step electron beam lithography and dry

etching process. We have experimentally demonstrated dielectric metalenses with numerical apertures of up to 0.8 and quality factors of up to 880, in some cases with diffraction-limited performance. Our findings represent a significant advancement compared to previous approaches that have been limited to low numerical apertures or one-dimensional wavefront manipulation.

3:15 PM *EL12.05.04

Wide Field-Of-View Metasurface Optics—From Fundamentals to Applications[Juejun Hu](#); Massachusetts Institute of Technology, United States

Wide field-of-view (FOV) is a much coveted feature in many optical systems with wide applications ranging from automotive sensing to biomedical imaging. In this talk, we will start by introducing our work formulating the analytical design frameworks for wide FOV metasurfaces with two distinctive and yet related configurations: imaging and projection optics. We will then proceed to discuss several device implementations guided by the analytically derived designs with applications spanning 3-D sensing, extended depth-of-field imaging, and full-color projection display.

3:45 PM EL12.05.05

Hybrid Metalens Platform for Nanoparticle Levitation and Control in Vacuum[Mohamed S. Mohamed](#); ETH Zürich, Switzerland

Levitated nanoparticle systems have emerged as a promising approach for studying fundamental forces, investigating non-Gaussian quantum states, and probing material properties at the nanoscale. When operated under ultra-high vacuum (UHV), damping of nanoparticle mechanical motion is kept sufficiently low, reducing decoherence and sustaining a high-quality-factor mechanical oscillator which can be exploited for quantum-limited sensing.

One of the main challenges towards implementing nanoparticle levitation in vacuum is the required level of control over trapping potentials, feedback forces, and sources of noise. Control schemes should additionally satisfy vacuum-compatibility and stability requirements. A compact design implementation, especially in an integrated form factor, can further enable a wide range of experiments such as acceleration sensing in dynamic testing or quantum state manipulation in cryogenic systems.

Here, a hybrid chip-scale platform for trapping and control of dielectric nanoparticles in vacuum is presented. The platform features a primary optical trap generated through an optimized polarization-insensitive dielectric metalens which features focal length in the range of 50 – 200 μm and numerical aperture values of up to 0.98. Individual silicon meta-atoms are designed to provide complete 2π phase coverage in the near-infrared wavelength range, with average transmission values exceeding 90%. The near diffraction-limited performance of the metalens alleviates requirements on input power for stable optical trapping. The metalens is patterned in an epitaxial silicon-on-sapphire layer, which exhibits reduced optical losses in comparison to silicon layers prepared by alternative deposition methods. The sapphire substrate provides a broad transparency window for the incident trapping laser beam, while preventing heat build-up given its thermal properties.

The hybrid device design features metallic electrodes embedded within the metalens layer. A dual-ring electrode configuration serves to create a tunable-height Paul trap, where the trapping volume overlaps the focal spot of the optical metalens trap. This is to assist with the loading of nanoparticles into the device by virtue of the deep potential well of the Paul trap. Furthermore, the electrode layer comprises pads for nanoparticle feedback cooling by means of cold damping. The overall architecture can additionally accommodate customized static and dynamic electromagnetic potentials which can be readily applied to the trapped nanoparticle. The overall electrode design enables the above functionalities without significantly perturbing the generated optical potential of the metalens near the trapping zone.

The proposed design was fabricated using a refined approach relying on electron-beam patterning and etching, combined with metal lift-off. Initial testing confirmed UHV compatibility of the device down to a pressure of $\approx 10^{-7}$ mbar, at the limit of the experimental vacuum chamber. Optical trapping was demonstrated with the device using femtogram SiO_2 nanoparticles, down to a pressure of 1 mbar. The collected forward scattering signal allowed for nanoparticle motion tracking using split detection.

The demonstrated platform provides a robust approach for chip-scale nanoparticle levitation and control, which opens the door to highly promising applications in both fundamental and applied science.

SESSION EL12.07: Poster Session
Session Chairs: Yongmin Liu and Junsuk Rho
Tuesday Afternoon, November 28, 2023
Hynes, Level 1, Hall A

8:00 PM EL12.07.01

Stretchable Dielectric Metasurfaces with Electrical Control[Hyunjung Kang](#), [Joohoon Kim](#), [Dongmin Jeon](#) and [Junsuk Rho](#); Pohang University of Science and Technology, Korea (the Republic of)

Metasurfaces are a type of structured surface composed of subwavelength-sized elements that can manipulate light at the nanoscale. Structural colors of metasurfaces are engineered by manipulating light to produce color without relying on dyes. They utilize microscopic or nanoscale structures to interact with light and selectively reflect or transmit certain wavelengths. By designing the size and shape of the sub-wavelength structures, metasurfaces can exhibit a wide color gamut, high color saturation, and even iridescence through precise control over the interaction of light. To improve the tunability, some techniques using phase-transition materials and active materials have been developed. In addition, a stretchable structural color via mechanical stretching has been reported. However, mechanical stretching is difficult to achieve precise and localized stretching. Also, mechanical stress can cause emergency structural damage, material fatigue and deformation. Here, we demonstrate electrically tunable structural color pixels with full-spectrum in the range from 450 to 650 nm. Electrical stretching allows for enhanced control and uniform/reversible deformation of the metasurfaces. By embedding a SiN metasurface in a polydimethylsiloxane (PDMS) substrate and stretching it in radial direction, the distinct reflection colors are tuned. As the period of the meta-atom increases from 310 nm to 450 nm, red-shift of the reflection spectrum is realized, covering from blue color to red color. In addition, since the intensity of light can be adjusted using a polarizer, it shows high-resolution images by adjusting the contrast. The reversible structural colors are promising in anti-counterfeiting, and strain-sensing applications.

8:00 PM EL12.07.02

Single-Step Manufacturing of UV Metasurface using ZrO_2 Nano-PER[Joohoon Kim](#) and [Junsuk Rho](#); Pohang University of Science and Technology, Korea (the Republic of)

UV light, essential in scientific and technological fields, has various applications ranging from spectroscopy and quantum optics to photolithography and biosensing. Traditional UV optics rely on large optical components, which offer limited functionality and versatility. In contrast, flat optics consisting of subwavelength optical scatter offer compact platforms for precise wavefront manipulation. They enable significant downsizing of optical components and provide diverse functionalities. Nonetheless, UV metasurfaces encounter persistent challenges such as the scarcity of UV materials with low-loss and high-index properties, exorbitant manufacturing costs, and low throughput associated with electron beam lithography [Adv. Mat. 30, 1802632, 2018]. Therefore, low-loss and high-index materials for UV metasurface have been actively studied in recent years: hafnium oxide [Light Sci. Appl. 9, 55, 2020], zinc oxide [Sci. Adv. 8, abn5644, 2022], silicon nitride [ACS Nano 16, 3546-3553, 2022], and niobium pentoxide [Laser Photonics Rev. 13, 1800289, 2019]. However, fabrication processes of the aforementioned materials include not only electron beam lithography but also multi-step etching with a high aspect ratio or atomic layer deposition of a thick layer. In this manuscript, we fully address this long-standing challenge by introducing a zirconium dioxide (ZrO_2) nanoparticle-embedded resin (nano-PER) for a one-step printable platform for UV metasurface. The ZrO_2 nano-PER is synthesized by dispersing ZrO_2 nanoparticles in a UV-curable resin which makes nano-PER printable. Owing to the large bandgap and high refractive index of ZrO_2 nanoparticles, the ZrO_2 nano-PER has a high refractive index and low extinction coefficient over the broad UV regime. Thus, a designed meta-atom has a conversion efficiency of 88% ($\lambda=325$ nm) and 81% ($\lambda=248$ nm), respectively. In this method, high-efficiency UV metasurface can be replicated repeatedly using a single step of nanoimprint lithography without any secondary operations, resulting in high throughput and low cost. This method will provide real opportunities for practical applications of UV metasurfaces.

8:00 PM EL12.07.03

Metasurface Selective Nanoimprint by Continuous Lithography with Laser-Induced Graphene on Metal Thin Film[Timothy Yee Him Chan](#) and [Mitch Guijun Li](#); The Hong Kong University of Science and Technology, Hong Kong

Efficient and cost-effective fabrication of metasurfaces is crucial for their widespread application in thin film technologies such as optical modulation and chemical sensing. In this study, we propose a laser-based selective nanoimprint method that enables faster and more controlled fabrication of metasurfaces, facilitating the application of different molds onto the target surface with ease. Laser-induced graphene is deposited on a metal thin film, and it is placed on the flexible mold, then the metal thin film will be used to absorb the laser energy to provide pressure on the mold for nanoimprinting the mold pattern onto the target surface. The pressure from the laser source can be controlled precisely, and the target surface can be cured at the same time to stabilize the nanostructure imprinted. By pausing the laser irradiation during the curing process, the mold will return to its original position to create a pulling effect on the nanostructure, this can enhance the height of the nanostructure on the target surface to 2 times or more of the mold structure, from 2.54 μm of the original mold to 7.74 μm on the target surface. The presented approach offers a simple fabrication method with outstanding performance for the construction of selective metasurfaces. It utilizes laser-induced transfer techniques and laser-induced pressure to enable the efficient manufacturing of optical metasurfaces and other 2D-nanostructure-based applications. The demonstrated capabilities of this technique hold great promise for the advancement of metasurface technology and its integration into various thin film devices.

SESSION EL12.08: Tunable Metasurfaces
Session Chairs: Yongmin Liu and Junsuk Rho
Wednesday Morning, November 29, 2023
Hynes, Level 3, Room 305

8:00 AM *EL12.08.01

Optical Metasurfaces for Dynamic Wavefront Control in the Visible RangeRamon Paniagua Dominguez; Institute of Materials Research and Engineering (A*STAR), Singapore

The ability to dynamically manipulate propagating light is critically important in various applications, from optical communications, precision manufacturing or adaptive optics, to metrology and displays. While Spatial Light Modulator technologies offering dynamic control of wavefronts have been around for a long time, they have faced severe difficulties in increasing the spatial precision at which this can be done. As an alternative platform to common liquid crystals or micromirror-based devices, optical metasurfaces have opened a possible pathway to achieve dynamic wavefront control with sub-wavelength spatial resolution by endowing resonant nanoantennas with different tuning mechanisms. In this talk, we will present some of our recent efforts in this regard, particularly in two of the mechanisms that we find most promising for visible light manipulation, namely interfacing nanoantennas with liquid crystals and using low-loss phase-change materials with and without memory.

8:30 AM EL12.08.02

Dynamic Polarization Control across the Poincaré Sphere with Black Phosphorus MetasurfacesSamuel K. Seah, Souvik Biswas, Meir Grajower and Harry A. Atwater; California Institute of Technology, United States

Controlling polarization of light on-demand can unlock a multitude of applications in optical imaging, sensing, and computing. The electrically tunable crystalline anisotropy of black phosphorus (BP) holds promise for miniaturizing polarization modulators. Here, we report on plasmonic metasurfaces combined with van der Waals heterostructures incorporating twisted BP layers. This design builds on previous single BP layer Fabry-Pérot devices and increases the tuning range from linear trajectories to nearly half the area on the Poincaré sphere.

The proposed device leverages two independently electrically tunable BP layers that have their crystal axes orthogonally aligned, while careful design of the plasmonic nano-disks on top of the heterostructure allows critical coupling of light for enhanced dynamic range of polarization tuning. By incorporating boron-nitride spacer layers and capacitively gating the BP stacks against graphene gates within the heterostructure, we achieve the two degrees of freedom needed to tune polarization across the Poincaré sphere. We will discuss the effects of metasurface design and electronic doping on the Poincaré sphere, as well as highlight our efforts on the fabrication advances of the proposed device.

8:45 AM EL12.08.03

Free-Space Electro-Optic Modulators using High Quality Factor MetasurfacesSahil Dagli, Halleh Balch, Sajjad Abdollahramezani, Hamish M. Carr Delgado, Varun Dolia, Jefferson Dixon, Elissa Klopfer, Jung-Hwan Song, Jack Hu, Babatunde Ogunlade and Jennifer A. Dionne; Stanford University, United States

Metasurfaces advance optical communications and imaging technologies through their highly miniaturized control of the amplitude, phase and polarization of light. Achieving active tunability within a compact footprint represents a step towards power-efficient, ultrafast data processing and computation. Here, we design, fabricate, and characterize high quality factor metasurfaces as an electro-optically tunable element for photonic devices. Our device uses a hybrid materials platform of silicon on lithium niobate, taking advantage of the high index and lossless properties of silicon and the electro-optic Pockels effect in lithium niobate. We design subwavelength (400 nm width) nanobars of 300 nm thick silicon atop a 300 nm lithium niobate thin film that are fabricated by well-established top-down lithography and wafer bonding techniques in 150x150 μm metasurface devices. By introducing subtle geometric perturbations into each constituent nanobar, we enable leaky guided mode resonances coupled to normally-incident free-space light. These guided mode resonances enhance light-matter interactions by exciting strongly localized optical fields in the lithium niobate, with mode quality factors exceeding 1000 in both theoretical and experimental demonstrations. Applying a voltage across individual nanoantennas shifts the spectral position of the high-Q resonance, modifying the amplitude of the scattered light from the antenna. We measure an electro-optic coefficient of 3 pm/V when switching the applied voltage between 0 and 20 V. To decrease the nanoantenna length required to generate high-Q resonances, we pattern the ends of the notched bar with photonic bandgap mirrors, enabling the lateral light recirculation of leaky guided waves without causing significant radiation leakage. This allows us to achieve compact (<15 μm), high quality factor (>1000) resonator pixelated nanoelements. Our high-Q electro-optic devices provide a foundation for light-weight, reconfigurable, solid-state information processing.

9:00 AM BREAK

9:30 AM *EL12.08.04

GSSe and ITO: Novel Materials Combination for Metasurface and Optical CircuitsNicola Peserico and Volker J. Sorger; University of Florida, United States

With the increasing pressure driven by novel machine learning applications, new computing systems are required to match the need for low latency, low power consumption, and high capacity. The combination of novel materials, such as the Phase Change Material GSSe and the semiconductor ITO, can provide a strong boost for multiple applications. Here, we show how we leverage the integration of the two materials over several different applications, from building tunable metalens to architect an energy-efficient optical circuit accelerator for machine learning.

10:00 AM EL12.08.05

Toward High-Endurance Nonvolatile Reconfigurable MetasurfacesHyun Jung Kim¹, Kiumars Aryana¹, Scott Bartram¹, Stephen Borg¹, William Humphreys¹, Cosmin-Constantin Popescu², Tian Gu², Juejun Hu², Hyung Bin Bae³ and Taewoo Lee³; ¹NASA LaRC, United States; ²Massachusetts Institute of Technology, United States; ³KAIST Analysis Center for Research Advancement, Korea (the Republic of)

The applications of adaptive optics extend across multiple sectors, encompassing areas such as LiDAR, biological and chemical sensing, and free-space optical communications. The advent of metasurfaces optics with reconfigurability has offered a versatile platform for the design of compact optical components, offering a compelling alternative to their conventional bulky counterparts. In this study, we introduce the PROWESS (Phase change Reconfigurable Optical Wavefront Synthesis System) project at NASA LaRC, electrically reconfigurable metasurfaces using low-loss, high-contrast phase change material (PCM), $\text{Ge}_2\text{Sb}_2\text{Se}_4\text{Te}$ integrated with IR-transparent silicon microheater for various practical applications.

The talk covers a reliable platform for switching large-scale PCM-based devices utilizing a microheater and an architecture for the metasurface switching within an integrated circuit configuration, which is compatible with standard foundry fabrication processes. The utilization of near- to midinfrared transparent silicon microheater in the proposed architecture opens possibilities for the development of reconfigurable transmissive optics such as filters, zoom lenses, and beam steering modules. We demonstrated switching of 140 μm \times 140 μm PCM pixel, on a 200 μm \times 200 μm silicon microheater for several thousand cycles. Further, we performed an in-depth investigation into the failure mechanism utilizing techniques such as transmission electron microscopy and thermal modeling. Guidelines for device performance improvement are proposed, and an improved design with larger endurance is shown in progress. With further progress, we aim to unlock the full potential of PCM-based devices and advance the field of adaptive optics with demonstrable examples including a reconfigurable beam steerer for ocean surface flash LiDAR and Navigation Doppler LiDAR for precise lunar landing missions.

10:15 AM EL12.08.06

Toward Accurate Thermal Modeling of Phase Change Material Based Photonic DevicesKiumars Aryana¹, Hyun Jung Kim¹, Cosmin-Constantin Popescu², Steven Vitale³, Hyung Bin Bae⁴,

Reconfigurable or programmable photonic devices are rapidly growing and have become an integral part of many optical systems. The ability to selectively modulate electromagnetic waves through electrical stimuli is crucial in the advancement of a variety of applications from data communication and computing devices to environmental science and space explorations. Chalcogenide-based phase change materials (PCMs) are one of the most promising material candidates for reconfigurable photonics due to their large optical contrast between their different solid-state structural phases. While significant efforts have been devoted to accurately simulating PCM-based devices, there are important aspects that have not been captured in prior models. In this study, we will highlight three key parameters that strongly influence the thermal and phase transition behavior in PCM-based devices: the enthalpy of fusion, the heat capacity change upon glass transition, as well as the thermal conductivity of liquid-phase PCMs. The PCMs studied here for examining the amorphization process are Ge₂Sb₂Se₄Te and Ge₂Sb₂Te₅ with areal size on the order of 140 μm × 140 μm. We further investigated the important topic of switching energy scaling in PCM devices, which also helps explain why the three above-mentioned effects have long been overlooked in electronic PCM memories but only become important in photonics. Our findings offer insight to facilitate accurate modeling of PCM-based photonic devices and can inform the development of more efficient reconfigurable optics.

10:30 AM EL12.08.07

Embeddable and Steerable Metasurfaces for Active Control of Light SteeringSeung YeolLee, YujieLuo and OgnjenIlic; University of Minnesota Twin Cities, United States

Photonic surfaces, such as metasurfaces and metagratings, offer precise control of optical properties such as wavelength, intensity, and polarization, with a crucial role in efficiently focusing and directing light for various applications, ranging from imaging and communication to LiDAR and display technologies. However, typical platforms for metasurface steering and focusing are static and macroscopic, which limits their ability for adaptive control and embedding. To overcome these challenges, we propose a novel design for a microscale magneto-photonic metasurface capable of actively delivering light with high efficiency to a specific location through remote manipulation of its translational or rotational motion using an external magnetic field. This composite particle consists of a tailored photonic surface integrated with a magnetic core. To enable effective beam steering during rotation, the photonic surface incorporates metagrating patterns designed to achieve high efficiencies (~90%) for both TM and TE polarizations. The magnetic core, incorporated through a lift-off method, consists of an anisotropic cobalt layer that facilitates programmable collective translational and rotational motion. We describe a control mechanism for positioning and orienting such metasurfaces to deliver light to the targeted spot. We present modeling and experimental data to demonstrate active light steering, and we discuss the tradeoffs associated with scaling the size of this magneto-photonic metasurface. The proposed approach offers a particle-based platform that enables high-fidelity light delivery within the biological transparency window, presenting promising potential for biophotonic applications.

10:45 AM EL12.08.08

Creation of Frequency Selective Absorbing (FSB) Metasurfaces using 2D Transition Metal Dichalcogenides (TMD)SuwarnaDatar, BishakhaRay and SiyadRahim; Defence Institute of Advanced Technology (DIAT), India

Combining 2D materials and metastructures is a promising field of research with exotic outcomes like entangled quantum sources, enhanced non-linear effects and application in many interdisciplinary fields. 2-D transition metal-dichalcogenides (TMDs) which are semiconductor materials of the type MX₂, where M is a transition metal atom (like Ni, Fe, or Co) and X is a chalcogen atom (such as S or Se) are emerging class of materials which have excellent properties like atomic scale thickness, strong spin-orbit coupling, ability to form 2D nanosheets, direct band gap and many other mechanical and electronic properties. These properties make 2D materials lucrative as frequency selective absorbers (FSBs) because of strong electronic polarization and enhanced dielectric loss. By changing M in MX₂ one can achieve tunable microwave metadevices. In the present work we have developed inks made of 2-D TMDs. Research on hybrid materials like Fe doped MoS₂, doped MoS₂-rGO composite, MoS₂/CoSe₂ hybrids, among several others suggests that these materials have high reflection loss. Further, magnetic transition metal dichalcogenides such as NiSe₂, CoSe₂ and their heterostructures, expediate multiple reflections and scattering of the incident wave, thereby elongating the course of transmission of the incident microwave. This increases dissipation efficiency, along with large specific surface area, which caters to EM absorption. In the present work inks have been developed base on these materials to make them versatile for several applications. Metastructures using these paints have tunability of material properties like permeability and permittivity by changing meta structure thickness and dimension allowing to manipulate the electric and magnetic resonance at different frequencies independently, therefore, frequency selective structures can be made. Furthermore, in the present work, the structures have been made using 2D TMD whose conductivity has peaks depending on the percolation threshold at a given frequency for a particular concentration of the 2D structure in the paint. The analysis of the absorption by structures made of such composites is complex. Interestingly, it has been observed that unlike the meta structures created by metals where the absorption bandwidth and frequency, solely depend on the structures made, here they seem to also depend on the composition of 2D TMD which is encouraging. This provides an additional method to modulate the properties of FSA. The results are discussed to understand the role of 2D TMD in metadvice fabrication.

SESSION EL12.10: Nonlocal Metasurface in Frequency Space, BIC and Its Application for Tuning

Session Chairs: Yongmin Liu and Junsuk Rho

Wednesday Afternoon, November 29, 2023

Hynes, Level 3, Room 305

1:30 PM EL12.10.01

High Quality Factor Meta-Reflect-Arrays for Electrical Programmable Wavefront ShapingLinLin^{1,1}, JackHu², SahilDagli², YuanMeng¹, ZhihaoXu¹, JenniferA. Dionne² and MarkLawrence¹; ¹Washington University in St. Louis, United States; ²Stanford University, United States

LiDAR technology allows high-resolution 3D mapping and object identification for distance measuring, revolutionizing remote sensing. It is crucial for autonomous vehicles, AR/VR devices, and AI robots. Among components of LiDAR systems, beam steering is the most crucial part for precise control of the laser beam's trajectory and scanning pattern. The existing techniques, including mechanically rotating mirrors or prisms, microelectromechanical systems (MEMS), liquid crystal (LC), digital micro-mirror devices (DMD), and optical phased arrays (OPAs) have slow response time, mechanical complexity, and bulkiness. For instance, the number of optical elements and the challenge of aligning additional optical elements limit OPA's achievable steering range and resolution. Recent flat optics or phase gradient metasurface spatial light modulators (SLMs) offer promising alternatives. Metasurfaces, which consist of densely arranged diffractive nanoantennas, can manipulate light with enhanced light-matter interaction on a subwavelength scale. However, achieving high diffraction efficiencies with strong modulation is still one of the greatest obstacles for metasurface SLMs. Narrowband resonances, characterized by a high quality factor (Q-factor), are well known to increase the efficiency of modulation. With Q-factor up to 10⁷, micro-ring resonators used in integrated electro-optical modulators have achieved unity extinction modulation up to 40 GHz with a few volts. However, Q-factors for free-space light modulation with metasurfaces having subwavelength elements are typically on the order of 10.

To address the challenge of this weak modulation, a new class of silicon nanoantennas supporting high-Q dipolar guided mode resonances (DGMR) has been reported. By subtly breaking translational symmetry, DGMR nanoantennas are guided mode standing waves that can leak into free space and result in high-Q resonances with dipole radiation patterns perpendicular to the antenna. This makes them the ideal element for the efficient modulation of light scattering. While many interesting transfer functions have been explored using this scheme, universal wavefront shaping has yet to be experimentally demonstrated.

Here, we present a universal meta-reflect-array platform made from only high-Q DGMR nanoantennas acting as independent extremely sensitive pixels, enabling strong responses to weak structural tuning. When post-processed to incorporate a reflective ground plane, changes of <2.6% volume fraction across the array are found to facilitate efficient beam steering. To demonstrate that these devices are acting as phase gradient optics and not gratings, we realize beam steering to angles 32.3°, 25.3°, and 20.9°. To apply this concept to dynamic wave-shaping, we replace the structural perturbations with electro-thermal biasing. Although the thermo-optic coefficient of silicon is only 1.8x10⁻⁴ K⁻¹, the extreme sensitivity of DGMRs with high-Q of 2088 can be red-shifted efficiently with minimal temperature change. We exploit the temperature sensitivity by realizing a prototypical electrically programmable multi-element transmissive amplitude display consisting of a structurally uniform Si high-Q meta-reflect array with Ni resistive heating elements encapsulated above silica. With the second Au circuit patterned above, three distinct groups of Ni wires are separated and connected into three Au pads. Applying individual bias voltages to the conducting pads using an SMU, we can tune the intensity transmitted by each high-Q pixel. We have measured the electrically tunable transmission pattern resulting from different voltage distributions using an imaging spectrometer. This compact and efficient dynamic wave shaping prototype with programmable capability can be extended in the future to quicker mechanisms such as carrier injection and the Pockels effect with higher tuning speed, shedding light on high resolution modern flat display technologies and LiDAR beam-steering.

1:45 PM EL12.10.02

Eliminating Nearfield Coupling in Dense High-Quality-Factor Phase Gradient MetasurfacesSamuelAmevaw, LinLin and MarkLawrence; Washington University in St. Louis, United States

Recent developments in optical technologies call for precise wavefront manipulation and miniaturized and lightweight optical components. Phase gradient metasurfaces, have over the years proven to be a strong candidate for the realization of novel technologies especially in AR, VR, and LIDAR applications¹. Resonance is a key property of the nanostructured building blocks of a phase gradient metasurface. Boosting the light-matter interaction over subwavelength volumes allows many nanoscale objects to be combined to impose smooth spatially varying phase profiles on incident light waves².

A crucial metric by which to evaluate the performance of phase gradient metasurface is resolution, as it directly influences the accuracy achievable in wavefront shaping as well as the angular field of view. The resolution of phase gradient metasurfaces is predominantly limited by nearfield coupling between neighboring meta-atoms, preventing them from scattering light independently and generating crosstalk. The fact that the impact of coupling scales with Q typically forces a tradeoff between resolution and Q-factor. Coupling can be reduced by shrinking the evanescent decay lengths of the individual modes, thereby reducing the mode overlap. However, there will still be a Q for which the remaining coupling is a problem.

Here we show that extremely dense silicon metasurfaces supporting dipolar guided mode resonances can be engineered to entirely suppress near-field coupling for arbitrarily high Q. We reveal a zero-coupling regime occurs when nanoantennas are separated by anisotropic nanofins³. Rather than decreasing the field overlap, the fins enhance the longitudinal electric field, allowing it to interfere with the transverse electric field. For a specific nanoantenna width we demonstrate that the interference is perfect, effectively decoupling the high Q dipolar-guided mode resonators in proximity, enabling deep resolution and efficient diffraction.

To demonstrate the power of this new platform, we show how decoupled DGMR metasurfaces, backed by a mirror, can efficiently shape reflected diffraction when independent adjustments are applied to the refractive indices of each nanoantenna. Varying the refractive index of the outer pixels of a three pixel metasurface by only 1.7×10^{-5} , we achieve steering to the +1st diffraction order with an efficiency of 85%. The tiny index modulation needed is a direct consequence of the giant Q of 192,474. Having a pixel pitch of $\lambda/1.6$, the steering also occurs at a large angle of 32°. In beamsplitting we achieve diffraction efficiency of 99% with Q greater than 257,000 and δn of 1.5×10^{-5} . Importantly, we believe the Q can be much higher, but such structures become increasingly difficult to model. By increasing the thickness of the silicon film to 383nm, the decoupled regime can even be found with sub-diffraction resolution, pixel pitch $\approx \lambda/2.2$.

In this case, beamsteering of incident light is achieved to the +1st diffraction order at an angle of 47° with an efficiency of 85%. As the elements in this device have a Q of 68,797, the refractive index bias was only 1×10^{-4} . Another symptom of nearfield coupling is angular dispersion. With the decoupled nanoantennas, we have been able to achieve angle independence such that the resonant shift of a DGMR with Q~45k stays below the FWHM for an angle of incidence from -45° to 45°. Our platform provides a route for dense high Q metasurfaces with independent addressability of the constituent meta-atoms paving the way for highly efficient nonlinear and dynamic wavefront shaping.

References

1. Yu, N. & Capasso, F. Flat optics with designer metasurfaces. *Nature Materials* vol. 13 139–150 Preprint at <https://doi.org/10.1038/nmat3839> (2014).
2. Lawrence, M. *et al.* High quality factor phase gradient metasurfaces. *Nat Nanotechnol* **15**, 956–961 (2020).
3. Mia, M. B. *et al.* Exceptional coupling in photonic anisotropic metamaterials for extremely low waveguide crosstalk. *Optica* **7**, 881 (2020).

2:00 PM EL12.10.03

Magneto-Optic Control of Brewster Quasi Bound States in the Continuum [Antonio Garcia-Martin](#); Instituto de Micro y Nanotecnología, CSIC, Spain

Bound states in the continuum (BICs) emerge throughout Physics as leaky/resonant modes that remain, however, highly localized^[1]. They have attracted much attention in Photonics, and especially in metasurfaces^[2,3]. One of their most outstanding features is their divergent Q-factors, indeed arbitrarily large upon approaching the BIC condition (quasi-BICs) ^[4,5]. Here we investigate how to tune quasi-BICs in magneto-optic (MO) all-dielectric metasurfaces. The impact of the applied magnetic field in the BIC parameter space is revealed for a metasurface consisting of Si spheres with MO response. Through our coupled electric/magnetic dipole formulation, the MO activity is found to manifest itself through the interference of the (MO-induced) out-of-plane electric/magnetic dipole resonances with the in-plane magnetic/electric (directly induced) dipole, leading to a rich, magnetically-tuned quasi-BIC phenomenology, resembling the behavior of Brewster quasi-BICs for tilted vertical-dipole resonant metasurfaces. Such resemblance underlies our proposed design for a fast MO switch of a Brewster quasi-BIC by simply reversing the driving magnetic field. This MO-active BIC behavior is further confirmed in the optical regime for a realistic YIG nanodisk metasurface through numerical calculations. Our results present various mechanisms to magneto-optically manipulate BICs and quasi-BICs, which could be exploited throughout the electromagnetic spectrum with applications in lasing, filtering, and sensing ^[6].

References

- [1] Chia Wei Hsu, *et al.*, *Nat. Rev. Mater.* **1** 16048, (2016).
- [2] D.C. Marinica, *et al.*, *Phys. Rev. Lett.*, **100**, 183902 (2008).
- [3] Chia Wei Hsu, *et al.*, *Nature* **499**, 188 (2013).
- [4] Kirill Koshelev, *et al.*, *Phys. Rev. Lett.* **121**, 193903 (2018).
- [5] Diego R. Abujetas, *et al.*, *Sci. Rep.* **9**, 16048 (2019).
- [6] Diego R. Abujetas, *et al.*, *Nanophotonics* **10**, 42232 (2021).

2:15 PM EL12.10.04

Thermal and Electro-Optic Control of High-Q Metasurfaces for Dynamic Lensing [Hamish M. Carr](#) ¹, [Elissa Klopfer](#) ¹, [Sahil Dagli](#) ¹, [Jennifer A. Dionne](#) ^{1,1} and [Mark Lawrence](#) ²; ¹Stanford University, United States; ²Washington University in St. Louis, United States

Metasurfaces—arrays of subwavelength nanoantennas that control the phase, amplitude, and polarization of light—are a promising platform for novel and compact optical technologies and communication. However, dynamic control of metasurfaces remains challenging due to weak light-matter interactions and in compact, nanoscale devices. Here, we design and characterize a dynamically-tunable metasurface lens, with a high-quality-factor (high-Q) resonance working as both the basis of the lensing behavior and means for efficient modulation with thermal or electrical biasing. Our high-Q lens is constructed via a zone plate architecture consisting of alternating regions with and without resonant character. Both regions consist of 500 nm tall and 320 nm wide silicon nanobars atop a sapphire substrate. Nanobars in non-resonant regions are highly reflective, while nanobars in resonant regions are highly transmissive on resonance due to the inclusion of periodic perturbations, which enable a guided mode resonance with measured Q-factors up to ~1350. By leveraging the thermo-optic effect of silicon, we dynamically control the spectral position of the high-Q resonance to achieve wavelength selectivity of the focusing behavior. Due to the sharp spectral linewidth and amplitude variation of the high-Q resonance, thermal tuning can further result in metasurface switching, where the lensing behavior is changed between on and off states in response to thermal stimuli. For a device utilizing only moderate Q-factors of ~350, the resonance's FWHM can be shifted with temperature changes of only 50 C, and the device can be fully switched off when operating at 100 C. These experiments provide a foundation for dynamic control of a local high-Q wavefront shaping metasurface. Next, to overcome the low switching speeds of thermal tunability, we simulate and fabricate silicon metasurfaces with a silicon nitride straining layer, which breaks the inversion symmetry of the silicon crystal, enabling a non-zero electro-optic coefficient. The stress imparted by the silicon nitride layer can be tuned by varying the deposition conditions to maximize the induced electro-optic effect in silicon. Simulations show a tunability in the resonant wavelength of ~44 pm per applied volt in a vertical bias configuration for an induced second order susceptibility of 40 pm/V, which can be achieved with moderate film strains. For resonances with quality factors ~7,000 in simulation, it is thus possible to switch the device from highly reflective to highly transmissive with low voltages ~15 V due to the narrow linewidth of the resonance. These devices provide a CMOS compatible platform for lightweight, compact, and reconfigurable solid state information processing.

SESSION EL12.11: Bottom-up Fabrication
Session Chairs: Junsuk Rho and Shuang Zhang
Thursday Morning, November 30, 2023
Hynes, Level 3, Room 305

9:15 AM EL12.11.01

Self-Assembled Designer Monocrystalline Metasurfaces [Beniamino Sciacca](#) ^{1,2}; ¹CNRS, France; ²Aix-Marseille Université, France

High-quality monocrystalline materials and nanostructures are key to high-efficiency optoelectronic devices, plasmonic materials and metasurfaces. A large variety of materials can be synthesized at low temperature in solution as colloidal single crystals, combining the advantages of high-quality material and low-cost fabrication, but the potential for large area integration into nanophotonic and plasmonic devices via nanoparticle assembly techniques still remain elusive. The two major bottleneck are:

- 1) Difficulty to achieve defect-free colloids self-assembly in truly arbitrary patterns
- 2) Poor optical and electronic properties resulting from the discreteness of individual building blocks.

In this talk I will present recent breakthroughs from our team tackling both challenges with a new approach that we have introduced based on nanocube epitaxy. In the first part I will focus on advances on directed-assembly with detailed insight into the mechanisms. I will show for the first time the fabrication of complex and truly arbitrary organisation of nanocubes on a large surface, with a single nanocube resolution. Examples includes 1D linear assembly (A. Capitaine et al., *Small Methods* 2023), 2D nanocube grid arrays for transparent electrodes (A. Capitaine et al., *ACS Nano* 2023), highly dense split-ring resonator absorbers and Pancharatnam–Berry metasurfaces (M. Fajri et al., in prep).

In the second part I will focus on advances on nanocube epitaxy, showing a general methodology to transform an arbitrary assembly of nanocubes (Ag, Au, Cu₂O, core-shell) into defect-free continuous nanostructures and *operando* mechanistic insights (B. Sciacca et al. *Adv. Mat.* 2017, A. Capitaine et al. *Adv. Mat.* 2022). This approach enables to obtain monocrystalline plasmonic and nanophotonic surfaces that can be readily printed on any substrate (flat, microstructured), but also to make nanocrystals with unconventional (à la carte) geometries, that can be used as colloids to go beyond Platonic solids. Finally, I will show optical characterisation of the resulting large area metasurfaces, supported by numerical simulations.

I believe that this constitute a major breakthrough in the field, can inspire many scientists and lead the way for a new generation of bottom-up metasurfaces and their spread in industrially-relevant products.

9:30 AM EL12.11.02

Self-Assembled TiN-Based Metamaterials with Anisotropic Properties and Magneto-Optical Coupling Effects Jiawei Song¹, Di Zhang², Ping Lu³, Haohan Wang⁴, Yizhi Zhang¹, Xiaoshan Xu⁴, Julia Deitz³, Xinghang Zhang¹ and Haiyan Wang¹; ¹Purdue University, United States; ²Los Alamos National Laboratory, United States; ³Sandia National Laboratories, United States; ⁴University of Nebraska-Lincoln, United States

Transition metal nitrides (e.g., TiN) have shown tremendous promise for nanophotonic devices due to their low-loss plasmonic properties and superior high-temperature stability compared to noble metals. Coupling other functionalities with plasmonic nitrides as multifunctional nitride-based hybrid metamaterials presents an enormous opportunity for advanced integrated photonic devices. In this talk, we present a novel approach for creating TiN-based hybrid metamaterials in vertically aligned nanocomposites (VANS) form with anisotropic properties and magneto-optical coupling effects. First, we present a two-phase nanocomposite design that combines ferromagnetic CoFe₂ nanosheets within the plasmonic TiN matrix. The resulting hybrid metamaterials exhibit obvious anisotropic optical and magnetic responses, along with a pronounced magneto-optical coupling response, owing to the unique vertically aligned structure. Second, we demonstrate a complex three-phase nanocomposite design of Au-TiN-CoFe₂ nanocomposites. Compared to the co-growth method that yields three distinct morphologies of Au-CoFe₂ core-shell nanopillars, the templated growth resulted in the formation of highly ordered and uniform single-type core-shell nanopillars (i.e., the CoFe₂ shell with an Au core) in the TiN matrix. Both the co-growth and templated growth TiN-CoFe₂-Au films exhibit excellent epitaxial quality, hyperbolic dispersion, magnetic anisotropy, and magneto-optical coupling effects. These findings open up exciting opportunities for the development of advanced nanophotonic devices and applications that leverage the enhanced functionalities of plasmonic-magnetic hybrid metamaterials.

9:45 AM EL12.11.03

Fabrication of Spiky Gold Nanoparticles in Ordered Arrays with Tunable Nanofeatures JinJia, Nadia Metzko, Sang-Min Park, Yuhao L. Wu, Alexander D. Sample, Bundit Diloknawarit, Insub Jung and Teri W. Odom; Northwestern University, United States

Anisotropic gold nanoparticles (AuNPs) with branched spikes, known as spiky AuNPs, are attractive plasmonic materials due to their localized surface plasmon (LSP) resonances. Achieving precise control over the morphology and optical response of spiky AuNPs, as well as arranging AuNPs in ordered arrays on substrates are important for designing metamaterials, biosensors and optoelectronics. This talk will describe a substrate-bound seed-mediated synthesis approach to fabricate spiky AuNPs in ordered arrays with tunable nanofeatures. We will discuss advances in nanofabrication techniques that enable the patterning of AuNP seeds with designed shape and size. We will describe how different growth conditions can lead to the formation of different nanofeatures on the seeds, resulting in different LSP resonances. Finally, we will discuss the prospects of using spiky AuNP arrays for surface-enhanced Raman spectroscopy (SERS).

10:00 AM BREAK

10:30 AM EL12.11.04

Nanocube Assembly à La Carte Muhammad Luthfi Fajri¹, Ibtissem Bouanane², Frédéric Bedu¹, Peeranuch Pongsripong¹, Olivier Margeat¹, Judikaël Le Rouzo², Patrice Genevet³ and Beniamino Sciacca¹; ¹Aix Marseille University, CNRS, CINaM UMR 7325, France; ²Aix Marseille University, CNRS, IMN2P UMR 7334, France; ³Université Côte d'Azur, CNRS, CRHEA, France

Arrays of nanopatterns are of high interest in the multidisciplinary field of nanoscale photonics. Conventionally there are two approaches to fabricating such nanopatterns: top-down nanofabrication via electron beam lithography and bottom-up self-assembly. The former can create complex structures but lacks control over crystallinity, introduces surface roughness due to etching¹, is expensive and time-consuming, making it unfavorable for large-scale fabrication. Conversely, the latter is typically straightforward, affordable, and has better control over atomic composition and crystallinity. However, it struggles to fabricate complex nanopatterns due to thermodynamic constraints². This has been partially circumvented with directed assembly strategies, which consist of colloidal nanoparticles in PDMS templates replicated from a nanofabricated master³. However, the nanopattern geometry that could be achieved effectively is still strongly limited to individual particles or low-density 1D arrays^{4,5}, whereas precise and deterministic arrangement of nanoparticles in truly complex and arbitrary nanopatterns (needed for nanophotonics and plasmonics applications) have so far remained elusive.

Here, we offer a new approach to obtain arbitrarily complex nanostructure arrays with a single nanoparticle resolution with no need for advanced equipment. Nanoparticles are first deposited at the air/water interface in a compact film and then transferred into a nanopatterned template. This highly versatile technique is independent from the specific nanopattern and can apply to a plethora of materials and shapes. We will show assembly of various materials (Ag, Au, Au-Cu₂O core-shell nanoparticles and nanocubes) into various complex nanopatterns, such as U-shapes, L-shapes, cross-shapes, S-shapes, T-shapes, Pancharatnam–Berry metasurfaces, and also split-ring resonators on PDMS, that cannot be obtained with conventional assembly techniques. Among other nanoparticle shapes, we focus on nanocubes because they are ideal building blocks for obtaining monocrystalline nanostructures^{6,7}. We will show that such assemblies, in which each nanocube unit is precisely assembled as a Lego brick in complex extended arbitrary motifs, can subsequently be transformed into continuous nanostructures via nanocube epitaxy and then transfer-printed to various substrates, including flat and microstructured substrates. Finally, we will show optical characterizations and simulations of the metasurfaces obtained. This strategy potentially offers an alternative to a bottom-up fabrication for metal nanostructuring, which can then be applied to optoelectronic applications.

References:

1. Agrawal & Garnett. *ACS Nano* **2020**, 14 (9).
2. Ostrovsky et al. *Langmuir* **2021**, 37 (30).
3. Kraus et al. *Nat. Nanotechnol.* **2007**, 2 (9).
4. Flauraud et al. *Nat. Nanotechnol.* **2017**, 12 (1).
5. Capitaine & Sciacca. *Adv. Mater.* **2022**, 34 (24).
6. Sciacca et al. *Adv. Mater.* **2017**, 29 (26).
7. Capitaine et al. *ACS Nano* **2023**, 17 (10).

10:45 AM EL12.11.05

Meta-Structure IR Absorber Applied Microbolometer for Perfect Absorbance and Responsivity Improvement Jeongeun Mo^{1,2}, Dasom Wang¹, Ji-Hun Kang³, Jeong Min Baik² and Won Jun Choi¹; ¹Korea Institute of Science and Technology, Korea (the Republic of); ²Sungkyunkwan University, Korea (the Republic of); ³Kongju National University, Korea (the Republic of)

In recent years, the demand for high-performance infrared image sensors has increased significantly in various fields, including military applications, medical imaging, and Advanced Driving Assistance Systems (ADAS). Microbolometers, which are cooler-free infrared image sensors, have gained popularity due to their affordability and convenience. However, to enhance the performance of microbolometers, it is crucial to achieve high responsivity and detectivity. Effective infrared (IR) absorption is essential for microbolometers to efficiently transfer heat to the thermistor layer and achieve high responsivity ($R_v = \alpha \eta I_b R_0 / G(1 + \omega^2 \tau^2)^{(1/2)}$). To address this requirement, we applied a meta-structured IR absorber to enhance the IR absorbance of microbolometers.

In this study, we employed an alternating metal-dielectric multilayer films with different refractive index as the IR absorbing medium. A periodic circular structure is introduced to multilayer

films for higher absorptance. This structure has been designed to decrease total volume of IR absorbing medium in order to get lower thermal mass so that heat can easily transfer to the thermistor layer. FDTD simulation is conducted to compare the dependence of different sizes of periodic circles and intervals on absorptance of meta-structured multilayered absorber. This result revealed significant improvement in the absorptance of incident light in LWIR region (8-14 μ m), which is commonly used for object detection. For experimental demonstration, IR absorber is deposited by electron beam evaporator based on reported previous research. The experimental results confirmed that the meta-structured IR absorber exhibited higher absorptance compared to the non-meta-structured counterpart. Consequently, we expect that the application of meta-structured IR absorber to microbolometers will facilitate the temperature increase of the thermistor material, leading to a notable improvement in responsivity. In conclusion, the presented research will give an idea of increasing responsivity of microbolometer with drawing up absorptance of IR absorber with meta-structure.

11:00 AM EL12.11.06

Wafer-Scale Manufacturing of Centimeter-Sized Metasurfaces Down to the Deep-Ultraviolet RegionJoohoonKim and JunsukRho; Pohang University of Science and Technology, Korea (the Republic of)

UV optics play a vital role in both science and technology, from spectroscopy and quantum optics to photolithography and biosensing. Conventional UV optics are primarily based on bulky optical components and have limited functionality and diversity. As an alternative, metasurfaces can provide fine wavefront-shaping platforms with a compact form-factor, resulting in drastic miniaturization of the device and capability of diverse functionality. However, metasurfaces operating in the UV regime face long-standing challenges, such as the scarcity of low-loss and high-index UV materials and patterning limitations (small patterning area, high cost, and low throughput). Recently, UV-transparent materials such as zinc oxide [Sci. Adv. 8, abn5644, 2022], silicon nitride [ACS Nano 16, 3546-3553, 2022], and hafnium oxide [Light Sci. Appl. 9, 55, 2020] have been actively studied; however, the fabrication process of these materials is not scalable or easy to manufacture because they include e-beam lithography and multi-step etching with thick layer deposition. Recently, our group developed a scalable manufacturing platform that can produce visible metasurfaces on the wafer scale [Nat. Mater. 22, 474-481 (2023)]. However, a UV-transparent material compatible with our scalable method and patterning resolution remains a challenge for scalable manufacturing of UV metasurfaces. In this work, we fully address this long-standing challenge and mass-produce centimeter-scale UV metalenses by introducing a zirconium dioxide (ZrO₂)–polymer hybrid material and high-resolution ArF photolithography. We find that ZrO₂ has both a high refractive index and low absorption in the UV regime, and is compatible with our scalable method using atomic layer deposition (ALD). Using scalable and easily manufacturable ZrO₂–polymer hybrid material, we succeed in mass-producing centimeter-scale UV metalenses for the first time. Owing to the high repeatability of nanoimprint lithography, our method can fabricate wafer-scale UV metalenses at extremely low cost and high throughput. Notably, thin-film coatings in hybrid materials enable strong light confinement, resulting in high efficiency of fabricated metalenses. The proposed method fully addresses the long-standing challenges in the field of UV metasurfaces and presents a practical possibility for the first time that UV metasurfaces can be applied in real life.

SESSION EL12.13: Advanced Nanophotonic Design Strategies

Session Chairs: Zhaowei Liu and Junsuk Rho

Thursday Afternoon, November 30, 2023

Hynes, Level 3, Room 305

1:30 PM *EL12.13.01

Comprehensive Design of Metasurfaces: The Role of Symmetries in the Position of Complex Frequency Zero SingularitiesPatriceGenevet; Université Côte d'Azur, France

Metasurfaces are artificial optical interfaces designed to control the phase, the amplitude and the polarization of an optical wavefront. These optical surfaces rely on the coherent scattering of light by a sizable distribution of nano-scatterers of various shapes and material compositions. Metasurfaces hold great potential for on-chip integration of photonic components, significantly promoting the development of miniaturized optoelectronic systems.

Genevet group is working on the physics of Metasurfaces and their applications for directional light collection and emission (imaging systems and VCSEL arrays), and LiDARs. The group recently pioneered disruptive research on the developments in topological and tunable nanophotonics systems. This talk will concern fundamental properties of metasurfaces with emphasis on topological and vectorial metasurfaces. Our work starts from the observation from the fact that because of their radiative coupling to the environment, all optical components are intrinsically non-Hermitian systems, often described by reflection and transmission matrices with complex eigenfrequencies [1,2]. The control and the creation of zero singularities are shown to be the key ingredients to achieve full phase modulation of light. In particular, we rely on complex-frequency analysis to draw conclusions on the physics of metasurfaces and guide the designs towards the engineering of innovative nanophotonic devices. Symmetry breaking -- either explicit or spontaneous -- thus plays significant role in the response of the system, moving the position of Zero singularities of the reflection or transmission matrices from the real axis to the upper part of the complex frequency plane. A universal 0 to 2 π -phase gradient needed for wavefront modulation of an output channel as a function of the real frequency excitation is shown to be linked to the presence of discontinuity branch bridging a Zero and a Pole, i.e a pair of singularities, crossing the real axis[2]. This basic understanding helps us engineering electromagnetic fields at interfaces, including, but not limited to, metasurfaces[3-6]. Non-Hermitian topological features associated with exceptional degeneracies or branch cut crossing are shown to play a surprisingly pivotal role in the design of resonant photonic systems. With our works, we establish a general framework to predict and study the response of resonant systems in photonics and metaoptics.

Relevant publications:

[1] "Asymmetric phase modulation of light with parity-symmetry broken metasurfaces"

Elena Mikheeva, Remi Colom, Karim Achouri, Adam Overvig, Felix Binkowski, Jean-Yves Duboz, Sebastien Cuff, Shanhui Fan, Sven Burger, Andrea Alu and Patrice Genevet, Optica Open. Preprint. <https://doi.org/10.1364/opticaopen.22828976.v1>

[2] "Crossing of the branch cut: the topological origin of a universal [Equation]-phase retardation in non-Hermitian metasurfaces"

R Colom, E Mikheeva, K Achouri, J Zuniga-Perez, N Bonod, O JF Martin, S Burger, and P Genevet
Laser Photonics Rev. 220097 (2023)

[3] "Exploiting Extraordinary Topological Optical Forces at Bound States in the Continuum"

H. Qin, Y. Shi, Z. Su, G. Wei, Z. Wang, X. Cheng, A. Q. Liu, P. Genevet, Q Song
Science Advances 8 eade7556 (2022) <https://www.science.org/doi/10.1126/sciadv.ade7556>

[4] "Getting topological photonics out of the laboratory"

P Genevet, Nature Communications 13: 2249 (2022) invited "Q&A"

[5] "Space &/or Time modulation of light with metasurfaces: recent progress and future prospects"

E. Mikheeva, C. Kyrou, F. Bentata, S. Khadir, S. Cuff, and P Genevet ACS Photonics <https://doi.org/10.1021/acsp Photonics.1c01833> (2022) invited "perspective article"

[6] "Plasmonic Topological Metasurface by Encircling an Exceptional Point"

Q. Song, M. Odeh, J. Zúñiga-Pérez, B. Kanté, and P. Genevet
Science, 373, 1133-1137 (2021)

2:00 PM *EL12.13.02

Overcoming Optical Losses of Superlenses with Synthetic Waves of Complex FrequencyShuangZhang; University of Hong Kong, Hong Kong

In conventional optical imaging, Abbe diffraction limits the resolution of feature sizes to larger than half the wavelength. This limit is due to the loss of the subwavelength information carried by evanescent waves. To overcome this limitation, a negative refractive index lens has been proposed to enhance the evanescent waves to recover the deep-subwavelength resolution of imaging. Subsequently, superlenses, made of either natural materials with negative permittivities, or hyperbolic materials with mixed signs of dielectric constants along different directions, have been proposed to attain sub-diffractive limited imaging. Nevertheless, losses are non-negligible in materials with negative parameters, which reduces the deep-subwavelength information of the superlenses and seriously affects the resolution of imaging. To compensate the losses, it has been proposed that gain materials could be incorporated into metamaterial designs or plasmonics, but the setup is extremely complicated and the gain will inevitably introduce instability and noise into the system. Recently, complex-frequency waves with temporally growing or attenuating behaviors have been treated as virtual absorption or gain waves. Some theoretical proposals have been put forward to recover the deep-subwavelength information

carried by surface plasmons via excitation of complex-frequency waves (CFW) with temporal attenuation. However, synthesizing CFW is challenging in optical systems from a practical perspective.

To address this challenge, we synthesize CFW signals using a multi-frequency approach. We exploit the fact that a truncated CFW can be expressed as combination of multiple frequency components with coefficients following a Lorentzian spectral lineshape through the Fourier transformation. We perform measurements at multiple real frequencies and numerically synthesize the field distribution under CFW illumination by combining the measured field plots at different frequencies according to the Lorentzian lineshape. As a proof of the concept, both a SiC slab operating at optical frequencies and a bulk hyperbolic metamaterial operating at microwave frequencies are used as superlenses. We show that, while the spatial resolution of imaging at real frequencies is poor, caused by the inevitable material loss in these systems, an ultra-high resolution imaging can be obtained with the synthesized CFW consisting of multiple frequency components. Our approach successfully overcomes the challenges of experimentally implementing CFW in the time domain, which include the need for precise CFW synthesis and time-gated measurements after reaching the quasi-steady state, and holds great potential for high-resolution microscopy. Furthermore, the synthesized complex-frequency approach can be extended to other areas of optics, such as plasmonic sensing applications. By leveraging the enhanced quality factor of plasmonic structures, our approach has the potential to significantly improve sensitivity in sensing applications. In addition, the approach can be tailored to different systems and geometries, providing a flexible and versatile tool for improving optical performance.

2:30 PM *EL12.13.03

Disordered Optical Metasurfaces to Create New Visual Effects[PhilippeLalanne](#); CNRS, France

The visual appearance of flat surfaces and curved objects is paramount in life and technology for fine and applied arts.

The ERC project **UNSEEN** aims at creating metasurfaces that offer new visual appearances, unseen in nature so far. The metasurfaces are composed of disordered monolayers of high-index resonant nanoparticles, either deposited from a colloidal solution on solid support or fabricated with ebeam lithography.

We have developed two models to predict the scattering properties of disordered metasurfaces. They allow us to predict design the scattering properties for all wavelength and incident angles. We have validated the models by testing them with experimental data, we have also been able to design a metasurface that generate only two distinct colors (green and violet) under all incidence and viewing angles, a quite strange phenomenon if we consider that usual iridescence provides a continuous variation of color as the incident and viewing angles changes (think to a thin film). For more details on the topic, please refer to

K. Vynck et al., Nat. Mater. 21, 1035–41 (2022).

A. Agreda et al., ACS Nano 17, 6362–72 (2023).

3:00 PMBREAK

3:30 PM EL12.13.04

Analysis of the Effect of Material Choice on the Performance of Metasurfaces[JunkyeongPark](#), [YounghwanYang](#), [HyunjungKang](#) and [JunsukRho](#); Pohang University of Science and Technology, Korea (the Republic of)

A metasurface is a thin layer that operates at a scale smaller than the wavelength of light. It controls light by using meta-atoms, which are small structures arranged in a specific pattern. These meta-atoms are typically made of plasmonic or dielectric nanoantennas and have the ability to change the properties of light, such as its phase, amplitude, and polarization. As a result, metasurfaces find applications in various fields, including advanced displays, lenses, and sensors in the next generation. Particularly, due to their low optical losses, broadband operation, and compatibility with complementary technologies, dielectric metasurfaces are a promising platform for various photonic applications. Generally, dielectric materials with high refractive indices and low optical losses are favored for the development of highly efficient metasurfaces, which enable the creation of wide-angle beam steering and near-unity numerical aperture metalenses. Despite the intuitive choice of such materials, the relationship between material properties and metasurface performance remains unclear. In this presentation, we aim to determine the correlation between the refractive index and the performance of metasurfaces. Specifically, we investigate metalenses operating within the visible spectrum and evaluate their efficiency and full width at half maximum (FWHM). By examining these parameters, we aim to gain quantitative insights into how the refractive index influences the effectiveness of metasurfaces in manipulating light in the visible regime.

3:45 PM EL12.13.05

Breaking the Limitation of Polarization Multiplexing in Optical Metasurfaces with Engineered Noise[RuwenPeng](#)¹, [YongminLiu](#)² and [MuWang](#)^{1,3}; ¹Nanjing University, China; ²Northeastern University, United States; ³American Physical Society, United States

Noise is usually undesired yet inevitable in science and engineering. However, by introducing the engineered noise to the precise solution of Jones matrix elements, we break the fundamental limit of polarization multiplexing capacity of metasurfaces that roots from the dimension constraints of the Jones matrix. We experimentally demonstrate up to 11 independent holographic images using a single metasurface illuminated by visible light with different polarizations. To the best of our knowledge, it is the highest capacity reported for polarization multiplexing. Combining the position multiplexing scheme, the metasurface can generate 36 distinct images, forming a holographic keyboard pattern. This discovery implies a new paradigm for high-capacity optical display, information encryption, and data storage.

Ref: Bo Xiong et al., *Science* **379**, 294-299 (2023).

4:00 PM EL12.13.06

Algorithmic Optimization of Disordered Plasmonic Metasurfaces using Far-Field Wavefront Shaping[GauthierRoubaud](#)¹, [SylvainGigan](#)², [SamuelGréssillon](#)¹ and [SebastienBidault](#)¹; ¹ESPCI Paris, France; ²Sorbonne Université, France

Plasmonic metasurfaces have broad applications in wavefront control, surface-enhanced spectroscopy or sensing. However, deterministic nanostructures do not allow an active tuning of these optical properties. By comparison, wavefront shaping techniques in disordered media have shown tremendous flexibility in actively modulating the propagation and focusing of light in space and time. We demonstrate here that delocalized modes in disordered plasmonic metasurfaces can be controlled using far-field wavefront shaping and algorithmic optimization schemes in order to locally modulate their optical responses.

By controlling the phase of an incoming femtosecond pulsed laser on a disordered gold metasurface, we optimize the two-photon induced luminescence (TPL) at a chosen position with a typical two-order of magnitude enhancement, indicating a far-field optimization of the optical near-field. The optimization process is performed using a random genetic algorithm and provides the highest enhancement when the metasurface features the highest degree of morphological complexity, close to the percolation threshold (Nano Lett. 20, 3291 (2020)).

Far-field wavefront shaping also provides new degrees of freedom to provide statistical imaging schemes that offset the structural complexity of disordered nanophotonic systems. For instance, using nonlinear luminescence images measured with randomly wavefront-shaped femtosecond excitations, we can independently map the localized and delocalized plasmonic modes on a disordered gold metasurface (ACS Photonics 8, 1973 (2021)).

SESSION EL12.15: Nonlocal Metasurfaces in Momentum Space

Session Chairs: Yongmin Liu and Junsuk Rho

Friday Morning, December 1, 2023

Hynes, Level 3, Room 305

9:45 AM *EL12.15.01

Metasurfaces for Edge Detection and Quantitative Phase Imaging[ZhaoweiLiu](#); University of California, San Diego, United States

Microscopy has been playing a crucial role in many science and engineering fields. Metasurface as a new emerging tool has shown its unique capability to manipulate light at scales previously thought impossible, opening doors for optical microscopy systems with ultracompact footprint. In my talk, I will present some of our recent development by using metasurfaces to build various compact microscopy systems. Specifically, I will discuss metasurface enabled edge detection, Fourier optical spin splitting microscopy, and various schemes to achieve quantitative phase imaging. Some biological imaging results will be presented by using such metasurface based microscopes.

10:15 AM EL12.15.02

Image processing is of fundamental importance for many emerging technologies such as AR/VR glasses, autonomous driving, and biometric identification. Conventionally, image processing tasks are performed by digital computers. However, the processing time and power consumption of digital computers become a limiting factor with the increasing demand for real time, continuous data processing. With the advent of metamaterials and metasurfaces, optical computing platforms emerged as promising candidates to perform such image processing tasks. In recent years, numerous examples based on spin Hall effect, Pancharatnam–Berry phase, photonic crystals, and surface plasmons were realized. These studies have shown that metasurfaces offer real time image processing with low to none power consumption. However, the previous demonstrations suffer from one or few of the several limitations that are requiring angled incidence, polarization dependence, requiring additional polarizers, narrow operation band, being limited with 1D processing, requiring coherent light, and requiring digital post-processing.

Here, addressing these problems, we propose and demonstrate metasurfaces for 2D isotropic and polarization independent edge detection based on Fourier optics principles. We designed sub-wavelength metallic metasurfaces to perform edge detection. The metasurface consist of co-centric metallic rings that create a spatial transmission profile matching the Fourier transformation of the second order differentiation. We experimentally confirm polarization independent, broadband edge detection with high transmission efficiency under both coherent and non-coherent illumination along the visible range. By further simulations and measurements, we show that the operation range of the metasurface also covers the 800 nm to 1600 nm wavelength range in the near IR. Our results constitute an important step towards the application of metasurfaces for real-life image processing tasks.

10:30 AM EL12.15.03

Generation of Arbitrarily Directed Out-Of-Plane Split Beams with Reflective Metasurfaces[Brian M. Wells](#), Joseph F. Tripp and Richard J. Williams; University of Hartford, United States

Metasurfaces, the planar equivalent of metamaterials, have recently gained significant attention due to their physically compact nature, versatility, and ultrathin thickness in the wave propagation direction, significantly suppressing undesirable losses and exotic electromagnetic properties in manipulating propagating waves. In recent years, metasurfaces have been applied to anomalous reflection and refraction, perfect absorption, flat lensing, wave plates, and cloaking. In this work, we present an out-of-plane beam-splitter reflector metasurface design that is not confined to the gradient metasurface paradigm and, as such, is not restricted to beam-splitting into diffraction orders. Instead, we can generate metasurface beam-splitters with arbitrary split beam directionality, including combined in-plane and out-of-plane splitting, such that one of the split beams remains in the plane of incidence while the other split beam is generated outside the plane of incidence.

A reflective metasurface exhibiting simultaneous in-plane and out-of-plane beam-splitting was designed using an approach based on the Fourier transform method of array synthesis. This method involves supplying the desired far-field scattering pattern of the metasurface, in this case, a far-field pattern with two main beams scattering in different planes, and then performing the inverse discrete Fourier transform on this far-field pattern to determine the spatially dependent reflection properties of the metasurface. To validate the approach, an impedance sheet-based simulation is performed to verify the desired beam-splitting phenomena as an initial step in the design process. This technique involves casting the spatially dependent complex reflection coefficients calculated from the Fourier transform method into a spatially dependent surface impedance. The metasurface is then simulated as a 2D plane, defined by the surface impedance. This allows for a fast-initial simulation of the metasurface beamsplitter before unit cell simulations. Both approaches are compared to full-wave, unit cell 3D FEM numerical simulations using realistic material parameters. An excellent agreement can be shown between all three approaches, thus illustrating the usefulness of the impedance sheet-based simulations method to obtain the metasurface far-field profile.

10:45 AM *EL12.15.04

Manipulating the State of Polarizations at the Nanoscale using a Nonlocal Metasurface[Soo Jin Kim](#); Korea University, Korea (the Republic of)

Recent development of chiral metasurfaces attracts significant attention from researchers due to their unique abilities to manipulate the spin state of light at the nano-scale. Such functionalities can have potential applications in diverse fields, including quantum communications, biosensing, CD spectroscopy, and nano-scaled imaging. However, despite the progress in developing efficient and compact configurations, there still remain challenges in realizing an effective metasurface with strong circular dichroism (CD) and a spectrally narrow bandwidth of response for the potential applications of spectropolarimetrics.

In this presentation, I will show the nonlocal metasurfaces with a high-Q resonance and how such metasurfaces can be tailored to have the capability to effectively control the polarization state of incident light at a relatively narrow spectral range. We first demonstrate the conversion of polarizations in transmitted light using a GMR-based nonlocal metasurface to achieve near-perfect flat-top transmission spectra in simulation and efficiency over 0.8 in experiments using a method of electro-optic-based wavelength-scanning laser at a narrow spectral bandwidth. Following this, we also focus on the detection of the state of polarization using an ultrathin chiral metasurface by inducing collective chiral resonances in the constituent nanostructures. We design and show the selective transmission of the spin state of light using a nonlocal chiral metasurface, which experimentally features a CD value over 0.8 at a bandwidth less than 10 nm by judiciously arranging the nano-units to induce chirality without the need for precise fabrication of nano-chiral geometry. We further demonstrate that the minimally perturbed geometries of nano-units can efficiently detect the full Stokes parameters by directly tracking the azimuthal and ellipticity paths of the Poincare sphere at a spectrally narrow bandwidth. We believe that the proposed approaches could pave an alternative pathway to realize efficient nonlocal metasurfaces for diverse, nano-scaled polarimetric applications.

SESSION EL12.17: Quantum, Nonlinear and Chiral Metasurfaces

Session Chairs: Yongmin Liu and Junsuk Rho

Friday Afternoon, December 1, 2023

Hynes, Level 3, Room 305

2:15 PM *EL12.17.01

Scalable Classical and Quantum Photonics[Giovanni Scuri](#); Stanford University, United States

Novel computational techniques such as photonics inverse design, along with new nanofabrication approaches, play a crucial role in building scalable integrated classical and quantum photonics. Inverse design, a departure from the traditional photonics design approach, can lead to photonics much better than state of the art in many metrics (smaller, more efficient, more robust, a much higher density of integration). This is enabled by development of a computer software which efficiently searches through the space of all possible and fabricable photonic geometries, in any material of interest. On the other hand, future photonic systems also require integration and fabrication of traditional and non-traditional photonic materials, including silicon, silicon-carbide, diamond, sapphire, and strong electro-optic materials such as lithium niobate, strontium and barium titanate.

2:45 PM EL12.17.03

Surface Enhanced Raman Spectroscopy of 19th Century Japanese Artworks via Silver Nano-Island Films[Omari Kirkland](#)¹, Marco Leona² and John R. Lombardi³; ¹CUNY Graduate Center, United States; ²Metropolitan Museum of Art, United States; ³The City College of New York, United States

Surface Enhanced Raman Spectroscopy (SERS) is an extremely sensitive analytical technique. It is powerful enough to detect the presence of single molecules. As powerful as the technique is, there are limitations when applying SERS to the study of heritage objects. Many SERS experiments use citrate-stabilized silver nanoparticle (AgNP) colloids. The citrate groups present at the surface of the silver nanoparticles can interfere with a target analyte's absorption onto the substrate surface. This interference can lead to very low Raman signals of the target analyte leading to spectra that are dominated by citrate. Here we show that thermally evaporated silver nano-island films (AgNIFs) deposited on glass slides outperform the traditionally used AgNP colloids for the identification of the colorants present in textile samples from 19th century Japanese artworks. The presence of cochineal, lac dye, acid fuchsin, and shikonin were detectable via SERS using the AgNIFs substrate where the AgNP colloid spectra were dominated by citrate. A development chamber was also designed to transport dye molecules from the textile fiber sample onto the AgNIFs surface via a thin film liquid mobile phase created by a liquid-vapor equilibrium maintained within. The use of AgNIFs could prove successful with other textile heritage objects that were not possible to measure with SERS via AgNP colloids. The sensitivity of SERS may elucidate complex mixtures of colorants that are otherwise too trace in concentration to detect with other analytical methods, such as HPLC and GC-MS.

3:00 PM BREAK

3:30 PM EL12.18.01

Water-Soluble Smart-Labeling Platform using Nanoimprint Lithography [Hyunjung Kang](#), [Joohoon Kim](#), [Hongyoon Kim](#) and [Junsuk Rho](#); Pohang University of Science and Technology, Korea (the Republic of)

The food packaging industry is increasingly focusing on sustainability and origin security. Biodegradable plastics and traceability systems like QR codes have been developed to address these concerns. However, there are challenges in ensuring sustainability and traceability. Biodegradable plastics have drawbacks such as specific conditions for degradation, greenhouse gas emissions, higher costs, and recycling difficulties. To overcome these challenges, a new sustainable and anti-counterfeit labeling platform is necessary. Also, traditional coloration methods using dyes and pigments have limitations, but structural coloration inspired by nature offers high resolution, color saturation, wide gamut, and resistance to fading. Recent advancements have demonstrated water-soluble structural colors using materials like polyvinyl alcohol (PVA) and hydroxypropyl cellulose (HPC). However, it has previously been limited by the need for silver deposition due to its low refractive index. We report a new water-soluble nanocomposite ink composed of HPC and TiO₂ nanoparticles to increase the refractive index. This ink allows for vivid colors, a wide gamut palette, high saturation, and brightness. The ink is used to print QR codes via nanoimprint lithography. The methods are cost-effective techniques and have minimal environmental impact. This labeling platform has the potential to address waste issues, enhance consumer trust, and provide accurate information about products.

3:45 PM EL12.18.02

Fabrication of Crystalline-Silicon Metasurfaces for Atom Trapping [Minjeong Kim](#)¹, [Chengyu Fang](#)¹, [David A. Czaplowski](#)², [Hongyan Mei](#)¹, [Zhaoning Yu](#)³, [Sanket Deshpande](#)¹, [Yuzhe Xiao](#)^{1,4}, [Xuting Yang](#)³, [Alan M. Dibos](#)², [Mark Saffman](#)³, [Jennifer T. Choy](#)^{1,3,3} and [Mikhail Kats](#)^{1,3,3}; ¹University of Wisconsin - Madison, United States; ²Argonne National Laboratory, United States; ³University of Wisconsin - Madison, United States; ⁴University of North Texas, United States

Optical bottle beams, distinguished by their localized light intensity minima surrounded by areas of higher intensity, can be used to trap neutral atoms and lower-index particles [1]. In particular, bottle beams are required for blue-detuned trapping of cold atoms, where the atoms are localized within low-intensity regions, resulting in smaller perturbation of the atoms by the trapping laser compared to the more-conventional, red-detuned traps where the atom is in a high-intensity region [2]. Complex beam profiles such as optical bottle beams can be synthesized using optical metasurfaces constructed from arrays of subwavelength structures that locally control the amplitude, phase, and/or polarization response at an interface [3]. Crystalline silicon, characterized by its indirect bandgap, exhibits moderate loss at wavelengths longer than about 500 nm [4], while polycrystalline and amorphous silicon have much higher absorption coefficients these wavelengths [5]. Here, we designed, fabricated, and characterized optical metasurfaces comprised of crystalline silicon for atom trapping, using silicon-on-sapphire (SOS) technology.

We employed a figure of merit to assess the effectiveness of our optical bottle-beam traps [1]. Through the simulation of a single unit cell, characterized by a pillar height of 500 nm and a periodicity of 360 nm, we designed metasurfaces for a wavelength of 770 nm, which is suitable for blue-detuned trapping of rubidium atoms. We fabricated bottle-beam-generating metasurfaces that are 2 mm on a side using a combination of electron beam lithography and silicon etching. In our process, the silicon thickness is 500 nm and the smallest lateral feature is 130 nm, resulting in an aspect ratio of 4:1. Our process is as follows: (1) A SiO₂ hard mask is deposited using plasma-enhanced chemical vapor deposition (PECVD); (2) ZEP520A resist is spun onto the wafer; (3) E-beam exposure and development; (4) Etching of the SiO₂ layer using CHF₃ and O₂ to defined the features in the hard mask; (5) Removal of the resist residue with O₂ plasma; (6) Etching of the Si layer using HBr to produce pillars on sapphire; (7) Removal of the SiO₂ hard mask with buffered oxide etchant (BOE).

The optical performance of the fabricated bottle-beam-generating metasurfaces was evaluated using a 795 nm distributed-Bragg-reflector (DBR) laser normally incident on the metasurface. Using a camera with an objective lens with a numerical aperture of 0.65, we observed the formation of an optical bottle beam with a diameter of 6 μm, in agreement with our electromagnetic modeling. Future work will include the design of more-complex atom-trapping field distributions, and the incorporation of these metasurfaces into atom trapping setups.

Acknowledgment

This material is based upon work supported by the U.S. Department of Energy, Office of Science, National Quantum Information Science Research Centers. Work performed at the Center for Nanoscale Materials, a U.S. Department of Energy Office of Science User Facility, was supported by the U.S. DOE, Office of Basic Energy Sciences, under Contract No. DE-AC02-06CH11357 (Proposal #82158).

References

- [1] Y. Xiao et al., "Efficient generation of optical bottle beams," *Nanophotonics*, vol. 10, no. 11, pp. 2893–2901, 2021. doi:10.1515/nanoph-2021-0243
- [2] P. Xu, X. He, J. Wang, and M. Zhan, "Trapping a single atom in a blue detuned optical bottle beam trap," *Optics Letters*, vol. 35, no. 13, p. 2164, 2010. doi:10.1364/ol.35.002164
- [3] N. Yu and F. Capasso, "Flat optics with designer metasurfaces," *Nature Materials*, vol. 13, no. 2, pp. 139–150, 2014. doi:10.1038/nmat3839
- [4] Z. Zhou et al., "Efficient silicon metasurfaces for visible light," *ACS Photonics*, vol. 4, no. 3, pp. 544–551, 2017. doi:10.1021/acsp Photonics.6b00740
- [5] D. Sell, J. Yang, S. Doshay, K. Zhang, and J. A. Fan, "Visible light metasurfaces based on single-crystal silicon," *ACS Photonics*, vol. 3, no. 10, pp. 1919–1925, 2016. doi:10.1021/acsp Photonics.6b00436

4:00 PM EL12.18.03

Laser-Based Selective Nanoimprint Method for Fabrication of Optical Metasurfaces as Modulating Layers for Fluorescent Materials [Timothy Yee Him Chan](#) and [Mitch Guijun Li](#); The Hong Kong University of Science and Technology, Hong Kong

The enhancement of fluorescent materials' performance is a significant research area aimed at expanding their utility and versatility. Optical metasurfaces have emerged as a viable solution to manipulate the optical properties of fluorescent material media. In this study, we propose a laser-based selective nanoimprint method that enables fast and controlled fabrication of metasurfaces specifically tailored as optical modulating layers for fluorescent crystals. The fabrication process involves depositing laser-induced graphene on a metal thin film, then it is placed on the flexible PDMS mold. The mold will undergo laser irradiation for pressurizing the photoresist, the metal thin film will be used as a protective layer to absorb the laser energy, and the laser energy will be converted to kinetic energy to provide pressure on the mold for nanoimprinting the mold pattern onto the photoresist. Precise control of laser-induced pressure allows for accurate replication of the mold pattern, while concurrently curing the photoresist to stabilize the imprinted nanostructures. The photoresist can be cured at the same time to stabilize the nanostructure imprinted, afterwards, we can apply the fluorescent solution to the photoresist by spin-coating. The fabricated metasurface can improve the absorption of the fluorescence materials and it can act as a better gain medium for the fluorescence crystal layer. We are also working on forming the metasurface directly on the crystal by replacing the photoresist with the solution, and then thermal treating the solution to promote fast crystallization.

This innovative approach presents a simple yet highly effective fabrication method for constructing selective metasurfaces as optical modulating layers for fluorescent materials. It utilizes laser-induced transfer techniques and laser-induced pressure to enable the efficient manufacturing of optical metasurfaces so that different metasurface structures and designs can be used for testing. The demonstrated capabilities of this technique hold great promise for the advancement of the integration between metasurface technology and fluorescent materials. The development of optimized metasurfaces as modulating layers can significantly enhance the optical properties and performance of fluorescent materials, paving the way for new applications in fields such as sensing, imaging, and optoelectronic devices.

8:00 AM *EL12.19.01

Extreme Micro/Nanomanufacturing for Metasurface Applications [Huihao Duan](#); Hunan University, China

Micro/Nanomanufacturing has been playing a key role in the integrated-circuits industry and developing micro/nanosystems. Pushing the micro/nanomanufacturing towards ultrasmall dimension and ultrahigh precision is of great interest and importance for various applications. In this presentation, I will share our efforts in developing new processes such as sketch and peel

lithography, greyscale lithography and conformal filling with ion beam polishing portfolio to achieve the multiscale, multidimensional and high-precision fabrication capabilities for functional micro/nanostructures. Novel applications on metasurfaces, transparent electrodes, and optical metadevices will be demonstrated.

8:30 AM *EL12.19.02

Plasmonic Structural Color PaintDebashisChanda; University of Central Florida, United States

In nature, vibrant colors as those of many butterflies, birds, octopuses, or fishes, arise from microscopically textured surfaces. These vivid colors result from the coherent interaction between light and the structural arrangement of colorless materials found in their skin. In contrast, all manmade colors are pigment based and rely on the molecular absorption of their constituents, with each color requiring a different molecule. While traditional pigment-based colorants offer a viable commercial platform for large-volume and angle-insensitiveness, they are limited by their resolution, instability in atmosphere, color fading, and severe environmental toxicity. However, till date all attempts to industrial production of polarization and angle independent full-range structural colors have failed due to the angle-dependent colors and fabrication challenges. In this talk, we present a subwavelength plasmonic cavity that generates color by the hybridization of a metallic self-assembly with an ultrathin optical cavity. This configuration offers both polarization and angle insensitiveness, while simultaneously providing a full-color gamut of vibrant structural color paints. In this work, we presented this unique structural color generation mechanism and demonstrated color generation of these structures across the entire visible spectrum by tuning just the structural parameters. The self-assembly facilitates growing the stack on a sacrificial layer we produce a self-standing nanostructured color platform that, when mixed with a binder, can be transferred to any surface to impart full coloration with a single sub-micron layer of pigment. This structural color platform offers a highly integrable ultra-lightweight solution that bridges the gap from proof-of-concept to real-world industrial applications of non-toxic, fade resistant, and environmentally friendly colorants.

9:00 AM EL12.19.03

Multimode Coupling and Bound States in the Continuum in High-Index MetasurfaceVahidKarimi¹, NealRaney², AaronHolzer¹, Md SakibulIslam¹ and ViktoriiBabicheva¹; ¹University of New Mexico, United States; ²Central New Mexico Community College, United States

Metasurfaces based on high-refractive-index materials have emerged as a promising platform for manipulating light at the nanoscale, enabling a wide range of applications in optics, photonics, and beyond. Through careful control of nanoantenna dimensions and arrangement, one can achieve tunable optical functionalities in high-index metasurfaces. By harnessing the unique properties of these materials, such as their strong light-matter interactions and efficient light confinement, metasurfaces offer unprecedented control over the propagation, polarization, and phase of light. This control opens up new possibilities for developing compact and versatile optical devices with enhanced functionalities, paving the way for advancements in areas such as imaging, sensing, communication, and integrated photonics.

Our investigation focused on a high-refractive-index metasurface, which offers exciting possibilities for manipulating light at the nanoscale. Through careful analysis, we discovered that this metasurface enables multimode coupling and bound states in the continuum, resulting in the emergence of narrow Fano resonances. By examining the reflection and transmission spectra obtained from our experiments, we observed the presence of multiple mode excitations and witnessed the occurrence of the generalized Kerker effect within the nanoantenna array. This highlights the metasurface's remarkable capability to control and manipulate light propagation at the nanoscale.

In addition to studying the metasurface, we also explored the influence of silicon quality on its optical properties. Our findings indicate that the rate of material deposition and subsequent rapid thermal annealing play pivotal roles in enhancing the optical properties of silicon. By mitigating oxidation and minimizing material defects, we observed a significant improvement in silicon quality. This improvement was characterized by an increase in the real part of the refractive index and a decrease in the imaginary part. These insights provide a deeper understanding of the interplay between metasurface design, light manipulation, and silicon quality. They open up avenues for further advancements in the field of metasurfaces, unlocking new possibilities for developing innovative photonic devices and systems with enhanced functionalities and improved performance.

The rapid thermal annealing process at high temperatures plays a vital role in reducing defects and impurities within the silicon material. This results in a more uniform and crystalline structure, leading to decreased light absorption, reduced optical losses, and enhanced light-matter interactions. These improvements in silicon quality enable precise tuning of collective modes within the metasurface, leading to the emergence of new photonic functionalities and improved sensing capabilities across various optical applications. Our investigation demonstrates the potential of high-index metasurfaces for achieving enhanced photonic functionalities. By controlling nanoantenna dimensions and optimizing silicon quality through rapid thermal annealing, we successfully manipulate light at the nanoscale, enabling the emergence of narrow Fano resonances and the realization of tunable optical functionalities. These findings open up exciting opportunities for advanced optical devices and applications, ranging from sensing to data communication and beyond.

This work was performed, in part, at the Center for Integrated Nanotechnologies, an Office of Science User Facility operated for the U.S. Department of Energy (DOE) Office of Science by Los Alamos National Laboratory (Contract 89233218CNA000001) and Sandia National Laboratories (Contract DE-NA-0003525).

SESSION EL12.20: Virtual Session II: Topological and Chiral Metasurfaces
Session Chairs: Yongmin Liu and Junghyun Park
Wednesday Morning, December6, 2023
EL12-virtual

8:00 AM *EL12.20.01

Single-Metaatom-Driven Tri-Channel Metaholographic DisplaysMuhammad QasimMehmood and Muhammad AsharNaveed; Information Technology University of the Punjab, Lahore, Pakistan, Pakistan

Multi-functional metadevices promise enormous potential in realizing ultra-compact optical and photonics systems. One of the effective techniques to achieve multi-functionalities is the merger of holographic information and nano-printing. Such multiplexing can significantly enhance the information encoding capacity. Most current methodologies focus on interleaving or multilayer stacking to achieve this goal. These techniques combine the functionalities of multiple metaatoms at the cost of reduced efficiency, design complexity, and challenging fabrication. This work introduces a unique way of introducing tri-channel capacity in a single-layered metadevice. The proposed resonators combine a geometric phase-based spin-decoupling and Malus's law intensity modulation to achieve such a tri-functional. The proposed strategy effectively improves information capacity owing to the orientation degeneracy of spin-decoupling rather than layer stacking or super-cell designs. To validate the proposed method, a metadevice demonstrating two helicity-dependent holographic outputs is presented in the far field, whereas a continuous nano-printing image is in the near field.

8:30 AM *EL12.20.02

Some Novel Topological Surface WavesBaileZhang; Nanyang Technological University, Singapore

Topological surface waves are the topological modes on the surface of a 3D topological insulator or semimetal. Typically in a 3D topological insulator, the topological surface states exhibit Dirac cones, while a Weyl topological semimetal can support Fermi arc surface states. Here we discuss some novel types of topological surface states.

The first type is the topological surface states on a 3D Chern insulator. It is known that a 3D bandgap can be characterized by three Chern numbers, defined for three perpendicular planes in momentum space, forming a Chern vector. The vectorial nature of the Chern vector gives rise to novel structures of topological surface states, including torus knots and links. We have implemented a 3D photonic Chern insulator and demonstrated a (2,2) torus Hopf link for such topological surface states.

The second type is the topological surface states on a 3D valley crystal. Valley degree of freedom (DOF) is widely used as a binary DOF in valleytronic materials, and has recently been introduced into acoustic crystals and photonic crystals. Here we generalize the valley DOF into a 3D crystal and demonstrate 3D valley contrasting physics.

9:00 AM *EL12.20.03

Chiral Metaphotonics and ManipulationsCheng-WeiQiu; National University of Singapore, Singapore

In this talk, we will report the recent progress on how chirality could assist and transcend the designs of advanced metasurfaces, sensing, strong coupling, BIC photonics and optical micromanipulations. In particular, we will report our very recent results on realizing intrinsic chiral metasurfaces where the engineered slant geometry breaks both in-plane and out-of-plane

symmetries. Our result achieves intrinsic chiral bound states in the continuum with near-unity CD of 0.93 and quality factor exceeding 2300 for visible frequencies. We will also cast new perspectives on using photonic orbit angular momentum to effectively discriminate single-size and multi-scale chiral nanostructures.

9:30 AM *EL12.20.04

Optical Metasurfaces for Generating and Manipulating Grafted Vortex BeamsXianzhongChen and HammadAhmed; Heriot-Watt University, United Kingdom

Inspired by plant grafting, the technique of generating a grafted vortex beam involves combining two or more spiral phase profiles of optical vortex beams. Recently, there has been significant interest in grafted perfect vortex beams (GPVBs) and perfect vector vortex beams (PVVBs) due to their distinctive optical properties and potential applications. GPVBs exhibit a constant intensity profile and a radius irrespective of topological charges. PVVBs are structured light beams with inhomogeneous polarization and spiral phase profiles. However, the existing method used for generating and manipulating these beams suffers from the complex optical system, large volume, and high cost. These optical systems are impractical for numerous applications, thus creating an urgent need for a compact, simple, and efficient approach to generating and manipulating these beams.

We propose and experimentally demonstrate a metasurface approach to generating and manipulating these beams. A single metasurface is used to generate various GPVBs in multiple channels and PVVBs without relying on the complicated optical setup. The uniqueness of this method is that the superimposed GPVBs have nonuniform orbital angular momentum and asymmetric singularity distributions in different channels, which can be further modulated by introducing initial phase difference in the metasurface design. Our work has demonstrated a compact metasurface platform that performs a sophisticated optical task that is extremely challenging or impossible with conventional optics, opening opportunities for the investigation and applications of these structured beams in a wide range of emerging application areas such as singular optics and quantum science.

SYMPOSIUM EL13

Multiferroics and Magnetoelectrics
November27 - November30, 2023

Symposium Organizers

Tianxiang Nan, Tsinghua University
Eckhard Quandt, University of Kiel
Caroline Ross, Massachusetts Institute of Technology
Nian Sun, Northeastern University

* Invited Paper

+ JMR Distinguished Invited Speaker

SESSION EL13.01: Multiferroic Materials I
Session Chairs: Caroline Ross and Nian Sun
Monday Morning, November27, 2023
Hynes, Level 2, Room 201

10:30 AM *EL13.01.01

Trompe L'oeil FerromagnetismSang WookCheong and Fei-TingHuang; Rutgers University, United States

Ferromagnetism can be characterized by non-zero magnetization (inducing magnetic attraction/repulsion), diagonal piezomagnetism, nonreciprocal circular dichroism (such as Faraday effect), odd-order (including linear) anomalous Hall effect, and magneto-optical Kerr effect. We identify all broken symmetries requiring each of the above phenomena, and also the relevant magnetic point groups (MPGs) with those broken symmetries. All of ferromagnetic point groups, relevant for ferromagnets, ferri-magnets and weak ferromagnets, can certainly exhibit all of those phenomena, including non-zero magnetization. Some of true antiferromagnets, which are defined as magnets whose MPGs do not belong to ferromagnetic point groups, can show those phenomena through magnetization induced by external perturbations such as applied current, electric fields, light illumination, and strain. Such MPGs are identified for each external perturbation. A number of exemplary materials for specific ferromagnetic-like phenomena will be discussed. Since high-density and ultrafast spintronic technologies can be enabled by antiferromagnets, our findings will be an essential guidance for the future magnetism-related science as well as technology.

11:00 AM *EL13.01.02

Controlling the Topologically-Protected Magnetoelectric Switching in Multiferroic GdMn₂O₅AndreiPimenov¹, LouisPonet², JanekWettstein¹, AnnaPimenov¹, MaksimRyzhkov¹, KefengWang³, Sang WookCheong³, MaximMostovoy⁴ and SergeyArtyukhin⁵; ¹TU Vienna, Austria; ²Ecole Polytechnique Federale, Switzerland; ³Rutgers, The State University of New Jersey, United States; ⁴University of Groningen, Netherlands; ⁵Istituto Italiano di Tecnologia, Italy

Manipulating magnetic moments by electric fields has been an everlasting goal for fundamental research. Recently, we could demonstrate a peculiar magnetoelectric behavior in multiferroic GdMn₂O₅ showing a switching through a cycle of four states when the magnetic field is ramped up and down [1]. In this sequence, half of the spins undergo a rotation of about 90° each time the magnetic field is ramped leading to a full-circle 360° rotation when applying and removing a magnetic field two times in a series. GdMn₂O₅ thus acts as a magnetic crankshaft that converts the back-and-forth variations of the magnetic field into a circular spin motion. This peculiar four-state magnetoelectric switching emerges as a topologically protected boundary between two different series, 1→2→3→4→1 and 1→4→3→2→1, respectively.

Further on, in a certain range of experimental parameters the 4-state sequence becomes topologically trivial. In this regime, the external electric field adds a key parameter of the switching. We show that in such case the electric voltage allows a full control over the four magnetoelectric states in GdMn₂O₅.

[1] L. Ponet, S. Artyukhin, Th. Kain, J. Wettstein, Anna Pimenov, A. Shuvaev, X. Wang, S.-W. Cheong, M. Mostovoy, and A. Pimenov, "Topologically protected magnetoelectric switching in a multiferroic", Nature **607**, 81 (2022). <https://rdu.be/ddZaF>

11:30 AM *EL13.01.03

Thermodynamics of MultiferroicsLong-QingChen; The Pennsylvania State University, United States

Multiferroics, by definition, are material systems, either as single phases or composites of multiple phases, that exhibit more than one ferroic orders such as ferroelectric, ferromagnetic, or ferroelastic order. One of the objectives of this presentation is to conceptually connect among the classical first and second laws of thermodynamics, the Maxwell relations relating various and multiferroic properties, the Landau theory description of multiferroic phase transitions, as well as thermodynamics and phase-field method of multiferroic domain structures and responses to external fields. It will start from the classical first and second laws of thermodynamics to establish the fundamental equation of thermodynamics for a multiferroic system as a function of its

basic thermodynamic variables. According to Gibbs, the fundamental equation of thermodynamics contains all the information about the equilibrium thermodynamic properties of a system, i.e., one can derive all the equilibrium ferroic and multiferroic properties of a system and their mutual relations from its fundamental equation of thermodynamics. On the other hand, irreversible thermodynamics considers all the ferroic phase transitions as internal irreversible thermodynamic processes within a material which generate entropy and dissipate chemical energy, allowing one to establish an energy function of both basic thermodynamic variables and the ferroic order parameters, e.g., through a Landau-type description, for a given multiferroic system. The thermodynamic description of a homogeneous system can be extended to inhomogeneous systems by introducing the contributions of ferroic domain wall energies through gradient or exchange energies as well as long-range elastic, electrostatic, and magnetic energies and by assuming that a local point of a domain structure can be described by the fundamental equation of thermodynamics in terms of both basic thermodynamic variables and ferroic order parameters. One can then apply the thermodynamic energy functions or functionals to construct multidomain and multiphase diagrams in the space of thermal, mechanical, electric, and magnetic variables using thermodynamic analysis, in analogy to the well-known temperature-composition phase diagrams or model the static and dynamic responses of a multiferroic domain structure to external stimuli using computational methods, such as the relaxational or dynamic phase-field method.

SESSION EL13.02: Magnetoelectric Heterostructures and Nanostructures I

Session Chairs: Tianxiang Nan and Eckhard Quandt

Monday Afternoon, November 27, 2023

Hynes, Level 2, Room 201

1:30 PM *EL13.02.02

Two-Step Phase Transition Enabled Superelasticity in Quasi-Two-Dimensional Freestanding Perovskite Ferroelectric Films Mingjie Xu and Xiaoqing Pan; University of California, United States

Perovskite ferroelectric materials have garnered significant attention due to their unique properties, including ferroelectricity, piezoelectricity, and high stability, making them promising for diverse applications in memory devices and sensors. However, the inherent weak elasticity and brittleness of most perovskite ferroelectrics pose challenges for their integration into flexible electronic devices.

In this study, we present the observation of superelasticity induced by a two-step phase transition in an 8-nm thick freestanding BiFeO₃ (BFO) film. Through atomically resolved in situ transmission electron microscopy (TEM) combined with in situ scanning transmission electron microscopy (STEM), we investigate the lattice deformation and atomic rearrangement in the film under mechanical stress, revealing reversible phase transitions and continuous evolution of the *c/a* ratio. Notably, we observe a remarkably large *c/a* ratio of approximately 1.53 in a super-tetragonal (S) phase under a lattice strain of approximately 34.4%, surpassing the highest strain reported for freestanding BFO films. This exceptional superelasticity arises from reversible 2-step phase transitions: R-T-S phase transitions, rather than conventional R-T transitions. Density functional theory (DFT) calculations support the crucial role of these 2-step phase transitions in facilitating such unusually large strain.

The experimental results obtained through in situ TEM and STEM techniques provide a comprehensive understanding of lattice deformations and phase transitions occurring in the BFO film under mechanical stress. This work unveils unprecedented superelasticity in freestanding BiFeO₃ films and elucidates its fundamental mechanisms, offering novel insights for the design of advanced flexible electronic devices. The exceptional superelastic behavior demonstrated by quasi-two-dimensional freestanding perovskite ferroelectric films highlights their immense potential for a wide range of applications, including flexible electronics, solid-state actuators, and other innovative technologies.

2:00 PM *EL13.02.03

Achieving High Performance Magnetoelectrics using Nanostructured Thin Films Judith L. Driscoll¹, Muireann A. de Hora¹, Markus Hellenbrand¹ and Adnan Mehonic²; ¹University of Cambridge, United Kingdom; ²University College London, United Kingdom

As the basic elements of computation are approaching their fundamental limitations, data intensive computation is shifting from being logic-centric to being memory centric. Current memory technologies are either volatile or if they are non-volatile have limitations. A very large body of work has been conducted on multiferroic/magnetoelectric materials for high performance non-volatile memory, particularly in oxides but the systems are complex and typically don't give high performance at room temperature. Here we show how to nanoengineer thin film composite systems to have strong magnetoelectric effects at room temperature, either via strain coupling or ionic coupling. We compare the performance with novel resistive switching composites grown at CMOS compatible temperatures.

2:30 PM *EL13.02.04

Nanoscale Ferroelastic Writing of Ferroelectric Domains Kathrin Dorr; Martin-Luther-Universität-Halle-Wittenberg, Germany

There is a growing effort towards nanomechanics approaches using a scanning probe microscopy (SPM) tip in order to define patterns of ferroic properties. Next to micromachining, pressure-induced phase transitions or the flexoelectric effect, there is the emerging field of ferroelastic nanoscale manipulation. Ferroelasticity can provide access to mechanical manipulation of a local ferroic order parameter (such as magnetization or ferroelectric polarization), if the order parameter is coupled to a distinct lattice distortion. After giving an introduction to recent advances in the field, the talk addresses our work on mechanical tip-induced definition of ferroelectric domains in a prototype ferroelectric copolymer, P(VDF-TrFE). While there is an increasing track record of nanomechanical manipulation by SPM tip in fully crystalline ferroic films, semi-crystalline polymers offer a unique advantage because of their elasticity supporting damage-free strains of several percent.

The ferroelectric copolymer P(VDF-TrFE) (here with 22% TrFE) is one of the most often applied ferroelectric organic materials. The pseudo-hexagonal lattice of P(VDF-TrFE) supports six stable ferroelectric polarization orientations, and, strikingly, the lattice shrinks substantially along the polarization direction. As-prepared films show multiple few-nanometer-wide ferroelectric domains. The electric dipolar disorder is highly critical, leading to strong suppression of the functional electric responses such as dielectric permittivity, direct or inverse piezoelectric effects. In addition, electric poling and switching of P(VDF-TrFE) films require relatively large electric fields, preventing precise electric nanoscale domain writing because of the tip stray fields.

Our spin-coated P(VDF-TrFE) films consist of very densely packed fine crystalline lamellae of the ferroelectric beta-phase. There is a well-defined (110) out-of-plane texture, but no in-plane texture. After vertical electric poling, complex deliberate in-plane domain patterns with tip-related resolution of 50 nm have been defined [1] by scanning with moderate mechanical tip forces (100-300 nN). The mechanical treatment leaves the semicrystalline lamellar structure essentially unchanged, and the surface roughness remains below 3 nm (rms). Importantly for various functional devices, the in-plane piezoelectric response in written domains is massively enhanced, indicating the achievement of efficient ordering of electric dipoles. I will discuss opportunities to exploit mechanically defined nanoscale polarization patterns in functional devices. This work was partially funded by Deutsche Forschungsgemeinschaft (DFG), CRC 762 and TRR 102.

[1] R. Roth et al., *Adv. Electron. Mater.* 2022, **8**, 2101416

3:00 PM BREAK

SESSION EL13.03: Magnetoelectric Spintronics I

Session Chairs: Tianxiang Nan and Eckhard Quandt

Monday Afternoon, November 27, 2023

Hynes, Level 2, Room 201

4:00 PM *EL13.03.01

Spin Hall Magnetoresistance and Quadratic Magneto-Optic Studies of Antiferromagnets Kang L. Wang; University of California, Los Angeles, United States

Antiferromagnets with two sets of spins against each other pushes the operation of spintronics memory frequencies up to terahertz with a higher areal density, compared with the traditional

ferromagnets due to the absence of the stray field and the strong coupling among spins. However, the net zero magnetic moment makes it difficult in probing and controlling the spin state in antiferromagnet. In this presentation, we discuss electrical and optical approaches to detect and manipulate spins, which pave the way for utilizing antiferromagnet in novel spintronic devices. First, we will discuss the use of magneto-transport or unidirectional spin Hall magnetoresistance (USMR) in Fe_2O_3 bilayer AFM bilayer. USMR has been widely reported in the heavy metal / ferromagnet (HM/FM) bilayer systems. We observed USMR in Pt/ α - Fe_2O_3 bilayers where the α - Fe_2O_3 is an antiferromagnetic (AFM) insulator. Systematic field and temperature-dependent measurements confirm the magnonic origin of the USMR. The appearance of AFM-USMR is driven by the imbalance of creation and annihilation of AFM magnons by spin-orbit torque due to the thermal fluctuation field. Theoretical modeling reveals that the USMR in Pt/ α - Fe_2O_3 is determined by the antiferromagnetic magnon number with a non-monotonic field dependence as compared with that of ferromagnetic materials. The magnonic origin of USMR is further confirmed by temperature-dependent measurements. This first evidence of USMR in other HM/AFM bilayers may be expanded to include the large family of AF insulators and paves the way for the highly sensitive detection of AF spin states in emerging the AF spintronics. Second, we will discuss the use of the quadratic magnetic-optical Kerr effect (QMOKE) to study dynamics of several AFMs. We will describe the experiments of e.g., α -MnTe; This antiferromagnet has a hexagonal close-packed structure with antiferromagnetic ordering along the c-axis. It is a collinear antiferromagnet with three in-plane easy axes, and its Néel temperature is approximately 310K [1,2], which is also known recently as an altermagnet, hosting anti-ferromagnetism in macroscopic scale and ferromagnetism in k space [3,4]. The hexagonal NiAs phase of MnTe (α -MnTe) is obtained by MBE on GaAs. We employ the time resolved pump-probe laser quadratic magnetic-optical Kerr effect (QMOKE) to study MnTe. The QMOKE of α -MnTe is more visible due to the spin splitting of electronic states in the k space. The pump process puts the Néel vector deviate from its equilibrium state. The pump results in the loss of the Néel order, referred to as the fast demagnetization, which endures for about 20 ps; the energy is redistributed between the electron, phonon and the magnon. This dynamics of the change of the Néel order is investigated through quadratic MOKE, reflecting the magnon dynamics. The dynamic study will also be used for other materials to compare the differences of the AFM dynamics.

- [1] Ferrer-Roca, C., Segura, A., Reig, C., & Munoz, V. (2000). Temperature and pressure dependence of the optical absorption in hexagonal MnTe. *Physical Review B*, 61(20), 13679.
[2] Yin, G., Yu, J. X., Liu, Y., Lake, R. K., Zang, J., & Wang, K. L. (2019). Planar Hall effect in antiferromagnetic MnTe thin films. *Physical review letters*, 122(10), 106602.
[3] Mazin, I. I. (2023). Altermagnetism in MnTe: Origin, predicted manifestations, and routes to detwinning. *Physical Review B*, 107(10), L100418.
[4] Gonzalez Betancourt R.D. et al, Spontaneous Anomalous Hall Effect Arising from an Unconventional Compensated Magnetic Phase in a Semiconductor, *Phys. Rev. Lett.* 130, 036702(2023).

4:30 PM *EL13.03.02

Ferroelectric Control of Spin-Charge Interconversion and Magnetism in Oxide Two-Dimensional Electron Gases [Manuel Bibes](#); CNRS/Thales, France

Two-dimensional electron gases (2DEG) based on SrTiO_3 (STO) display fascinating properties such as low-temperature superconductivity and Rashba spin-orbit coupling allowing to interconvert spin and charge currents through the Edelstein effect. We have introduced ferroelectricity in these 2DEGs in order to achieve a non-volatile electrical control of their properties. Practically, we replaced STO by Ca-substituted STO (Ca-STO) which is ferroelectric up to about 30 K and generated 2DEGs either by sputtering a thin Al film or growing perovskite overlayers by pulsed laser deposition. We will present spin-charge and charge-spin conversion measurements and their control by the ferroelectric state. We will also show how magnetism can be introduced in the system and use x-ray absorption spectroscopy and magnetotransport to demonstrate the coexistence of ferroelectricity and magnetism with metallicity. Our data evidence the non-volatile control of polar displacements, magnetization and anomalous Hall effect upon switching the polarization direction, indicating a magnetoelectric coupling. Our results provide new opportunities in quantum matter arising from the interplay between ferroelectricity, ferromagnetism, metallicity, and Rashba spin-orbit coupling in low dimensions.

SESSION EL13.04: Poster Session
Session Chairs: Tianxiang Nan and Eckhard Quandt
Monday Afternoon, November 27, 2023
Hynes, Level 1, Hall A

8:00 PM EL13.04.01

Leveraging Colloidal Assembly to Texture Hexaferrites to Enable Better Performance in RF Devices [Jose A. Martinez](#) and [Randall M. Erb](#); Northeastern University, United States

With the implementation of 5G, the telecommunications industry desires enhanced performance of incumbent radio-frequency (RF) devices. Non-reciprocal devices, circulators, and isolators are integral to RF communication systems by isolating the incoming signals from the outgoing signals, exhibiting different electromagnetic wave propagation characteristics in the forward and reverse directions. Such devices rely on soft and hard ferrite materials currently limited in performance by the current achievable saturation magnetization and coercive field levels. Significant work has been applied toward improving the materials synthesis of these ferrite materials to achieve better performance. Specifically, M-type hexagonal ferrites, such as $\text{SrFe}_{12}\text{O}_{19}$ (SrM) and $\text{BaFe}_{12}\text{O}_{19}$ (BaM), have been studied for their large coercivity, high Curie temperature, good chemical stability, and high corrosion resistance. Here, we investigate the role that both the composition and microstructure of these materials have on the material performance. We tailor the saturation magnetization and the particle geometry of SrM and BaM through hydrothermal synthesis and thermal treatment. Further, we investigate the role of microstructure texturing by aligning ferrite particles in the pre-sintered state by leveraging a colloidal assembly technique that takes advantage of anisotropic morphology, magnetic fields, and vibrational stimulus. We additionally provide perspective on the current materials limitations and opportunities in these magnetic RF devices.

8:00 PM EL13.04.02

Enhancement of Magnetic Properties of NdFeB Sintered Magnet by Grain Boundary Diffusion Process with TbAlCu [Dong Hyun Lee](#)^{1,2}, [Seong Chan Kim](#)^{1,3}, [Juyoung Baek](#)¹, [Donghwan Kim](#)⁴, [Sang Hyub Lee](#)⁴, [Hyesun Yoo](#)², [Dalhyun Do](#)³, [Dong Hwan Kim](#)¹, [Jong Wook Roh](#)² and [Jeongmin Kim](#)¹; ¹Daegu Gyeongbuk Institute of Science and Technology, Korea (the Republic of); ²Kyungpook National University, Korea (the Republic of); ³Keimyung University, Korea (the Republic of); ⁴Star Group Ind. Co., Ltd., Korea (the Republic of)

A strong coercivity enhancement of the commercial NdFeB magnets with the magnetic properties of $H_c = 22.76$ – 22.48 kOe and $(BH)_{\max} = 48.61$ – 48.58 MGOe is demonstrated by the grain boundary diffusion (GBD) process with low-melting point $\text{Tb}_{80}\text{Al}_{(x-20)}\text{Cu}_x$ ($x = 0$ – 20) alloys. The maximum coercivity enhancement was obtained from the diffused magnet with $\text{Tb}_{80}\text{Al}_{15}\text{Cu}_5$, in which the value increased from 12.25 to 22.76 kOe by GBD process. Microstructural investigation with the electron probe micro analysis reveals that the enhancement of coercivity in the GBD magnets is mainly due to magnetic isolation by continuous Nd-rich grain boundary phases and Tb-rich shells. Tb diffusion through grain boundaries at a lower temperature than 900 °C, and consequently developed continuous and thin Tb-rich shell structures. Especially, the partial replacement of Tb by Al and Cu in diffusion sources resulted in higher coercivity with consuming fewer Tb elements (0.8 wt%) in the samples with $\text{Tb}_{80}\text{Al}_{(x-20)}\text{Cu}_x$ which are much lower than that in the samples with Tb metal (1.0 wt%). The results show that Cu and Al addition in diffusion source can effectively improve Tb diffusion efficiency by modifying intergranular Nd-rich phase. This work may shed light on the reduction of heavy rare earth in NdFeB sintered magnets.

8:00 PM EL13.04.03

Evolution of Antiferromagnetic Spin Texture in MBE-Grown Epitaxial Multiferroic BiFeO_3 [Maya Ramesh](#)¹, [Peter Meisenheimer](#)², [Isaac Harris](#)², [Sajid Husain](#)², [Shiyu Zhou](#)³, [Zhi Yao](#)⁴, [Paul Stevenson](#)⁵, [Lucas Caretta](#)³, [Ramamoorthy Ramesh](#)⁶ and [Darrell Schlom](#)¹; ¹Cornell University, United States; ²University of California, Berkeley, United States; ³Brown University, United States; ⁴Lawrence Berkeley National Laboratory, United States; ⁵Northeastern University, United States; ⁶Rice University, United States

Bismuth ferrite (BiFeO_3) is a lead-free magnetoelectric multiferroic showing antiferromagnetic order and a large spontaneous polarization at room temperature. This antiferromagnetic order in BiFeO_3 is complex, where, as a consequence of the Dzyaloshinskii-Moriya interaction (DMI), a small canting of the antiferromagnetic order forms a chiral spin cycloid in bulk samples. Understanding the interplay between the ferroelectric polarization and the spin cycloid, as well as its electric field manipulation, is of significant interest for antiferromagnetic spintronics and next generation computation. There is still much to learn about BiFeO_3 's intrinsic antiferromagnetic structure in thin films, where epitaxial strain imposed by an underlying substrate can influence the spin texture. As a model system, we have synthesized epitaxial thin films (2–100 nm) of BiFeO_3 on (110) TbScO_3 substrates via oxide molecular-beam epitaxy (MBE). This allows us to synthesize BiFeO_3 thin films with an unparalleled structural quality where even small amounts of strain (0.1% in the case of TbScO_3) can have a large impact on the spin texture. In this work, we explore how epitaxial strain from the substrate affects the formation and orientation of the spin texture in BiFeO_3 using nitrogen-vacancy magnetometry (NV magnetometry) and spin transport measurements. NV magnetometry uses a nitrogen vacancy implanted at the tip of a diamond cantilever which acts as a single-spin magnetometer to sensitively map nanoscale surface stray fields. By correlating the spin texture to ferroelectric information measured using piezoresponse force microscopy, we are able to explore coupling between the two order parameters. Electric-field-dependent transport shows that the spin cycloid can be manipulated by switching the ferroelectric polarization, which is of great interest in low dissipation magnonics and spintronics.

8:00 PM EL13.04.04

Sputter Deposited Ni-Based Intrinsic Magnetic Topological Insulator Thin Films RuiHuang¹, BinLuo¹, AlexandriaWill-Cole¹, SerhiyLeontsev², ValeriaLauter³, MichaelMcConney², MichaelPage² and NianSun¹; ¹Northeastern University, United States; ²Air Force Research Laboratory, United States; ³Oak Ridge National Laboratory, United States

Three-dimensional topological insulators (TIs) exhibit unique properties such as topologically protected Dirac surface states (TSS) that enable metallic surface states while the bulk remains insulating. These TIs, including Bi_{1-x}Sb_x alloys and hexagonal X₂Q₃ compounds (X = Bi, Sb, Bi_{1-x}Sb_x; Q = Se, Te), also demonstrate the quantum anomalous Hall effect (QAHE). The QAHE occurs when a gap is created in the TSS by introducing perpendicular magnetic order and breaking time reversal symmetry, resulting in spin polarized, chiral edge currents while maintaining an insulating bulk state. Magnetic order can be introduced through compositional doping, stoichiometric intrinsic magnetic TI (MTI), or proximity-induced magnetization (PIM) methods. Although the QAHE has been observed in experiments for each of these methods, the temperatures involved are currently impractical for technology, being in the milliKelvin range. A phenomenological trend is that the magnetic ordering temperature (Curie temperature, T_C, or Néel temperature, T_N) is typically at least ten times higher than the observed QAHE temperature. In our previous work, we studied the interfacial magnetic phases of sputtered Bi₂Te₃/Ni₉₀Fe₁₀ and confirmed with selected area diffraction the existence of the NiBi₂Te₄ phase. We found a relatively high T_N of 63 K; thus, this phase is very promising to exhibit a high QAH state. Here we expand our work on Ni-based MTI materials through sputtering single-phase Ni-doped Bi₂Te₃ films, an intrinsic MTI. We present crystallographic structure characterization and temperature dependent magnetometry. To further understand the depth-dependent nuclear and magnetic structure we performed polarized neutron reflectometry.

8:00 PM EL13.04.05

Heterogeneous Strain Control by Interlayer Addition in Multiferroic Bi₃Fe₂Mn₂O_x Resulting in Thick Film Growth James P. Barnard¹, Jianan Shen¹, Yizhi Zhang¹, Juanjuan Lu¹, Jiawei Song¹, Aleem Siddiqui², Raktim Sarma^{2,3} and Haiyan Wang^{1,1}; ¹Purdue University, United States; ²Sandia National Laboratories, United States; ³Center for Integrated Nanotechnologies, United States

In recent work on electronic devices based on multiferroic and ferroelectric materials, thicker films have become a necessity for certain applications, including MEMS magnetic actuators, magnetoelectric antennas designed for energy harvesting, and optical metasurface fabrication. A common roadblock for the synthesis of thicker films is the loss of film-substrate strain effects as the strain relaxes over the larger thickness. For example, the Bi₃Fe₂Mn₂O_x (BFMO) Aurivillius supercell (SC) phase is a multiferroic system that depends on substrate strain to initiate the growth of the phase. In our work, a new re-seeding technique has been developed that utilizes a heterogeneous film topology to reestablish the required strain to maintain SC phase growth. This is done by the insertion of CeO₂ interlayers, which reintroduce the heteroepitaxial strain in the BFMO. The thick BFMO SC phase also maintains the desired ferroelectric and ferromagnetic properties as well as anisotropic optical properties. This technique allows for thicker growths of the BFMO SC phase (over 100 nm) and can also be applied to other supercell Aurivillius or strain-dependent films for device applications, effectively eliminating the current thickness limitations.

8:00 PM EL13.04.06

Studies of Structural, Magnetic and Dielectric Properties of Zinc Doped Nickel Ferrites for Spintronics Applications Sunny Choudhary, Mohan Bhattarai, Satyam Kumar and Ram Katiyar; University of Puerto Rico, Puerto Rico

This study investigates the impact of zinc doping at the nickel site in the parent nickel ferrite of stoichiometric formula Ni_(1-x)Zn_xFe₂O₄ (0 ≤ x ≤ 1); NZFO. The high-quality samples were prepared using a solid-state reaction route, employing the highly energy ball-milling. It has garnered considerable interest due to its versatile applications in the fields of electronics, telecommunications, and spintronic devices.

Experimental results of structural characterization show that there is no signature of impurity phase and confirmed the single phase with a characteristic cubic spinel structure by XRD analysis. We studied the vibrational modes of NZFO by Raman Spectroscopy which corroborated XRD analysis. Elemental analysis was carried out by EDS and XRF technique in which primary atomic stoichiometric ratios and percentages are approximately similar in both the analysis. SEM imaging revealed the morphology and microstructure of the prepared samples, exhibiting uniform particle distribution and well-defined grain boundaries. Dielectric measurements were performed across a wide frequency (100 Hz to 1 MHz) and temperature range (200 to 600 K) exhibited high dielectric constant and low loss tangent. The Temperature dependent magnetic behaviour of prepared samples were studied by Physical Property measurement system (PPMS).

<quillbot-extension-portal></quillbot-extension-portal>

8:00 PM EL13.04.07

Thin Film Surface Acoustic Wave Magnetic Field Sensors: Impact of the Thickness of the Magnetostrictive Layer Jana M. Meyer¹, Lars Thormählen², Stefan Moench³, Thorsten Giese¹, Simon Fichtner^{1,2}, Vadim Lebedev³, Agne Zukauskaitė⁴, Eckhard Quandt² and Fabian Lofink^{1,2}; ¹Fraunhofer ISIT, Germany; ²Kiel University, Germany; ³Fraunhofer IAF, Germany; ⁴Fraunhofer FEP, Germany

For the fabrication of surface acoustic wave (SAW) sensors the use of piezoelectric single-crystal substrates (e.g., quartz) is established. Utilizing thin-film technology benefits from larger material flexibility, reduction in chip size, better integrability in standard MEMS and CMOS fabrication technology and thus better scalability. Additionally, it is possible to design multilayer stacks to customise the wave properties to the application purpose. [1] In this context, a piezoelectric AlScN thin film is a promising material, as it combines the advantages from AlN (e.g., high wave velocity, good mechanical and dielectric properties, high thermal conductivity, and high breakdown voltage) with improved electromechanical coupling due to alloying with Sc [2]. AlScN can be fabricated with standard semiconductor technology at reasonable cost on 200 mm silicon wafers.

By combining a SAW sensor with a magnetostrictive film, a magnetic field sensor can be realized that is based on the change of the Young's modulus (E effect) of magnetostrictive films in the presence of an external magnetic field that can be detected as a phase change of the SAW. [1] The SAW is generated by interdigital transducers on top of the piezoelectric AlScN thin film. By the application of a CMP polished SiO₂ layer on top of the AlScN, the magnetostrictive film quality is improved by reducing the roughness of the surface. The SiO₂ layer also acts as a guiding layer and is used to excite new surface confined SAW modes. High sensitivities of the SAW magnetic field sensor can be obtained by using magnetically soft magnetostrictive films with high magnetostriction like FeCoSiB or FeCoB. [3]

Different layer properties of the sensor stack can be varied (e.g., thickness) and different SAW modes aside from the fundamental Rayleigh mode (e.g., Sezawa mode or shear modes) can be excited in layered thin film structures. Crucial is the thickness of the magnetostrictive FeCoSiB film as it was shown that the sensitivity of the sensor is increasing with the magnetostrictive film thickness [4]. In contrast to the use of bulk piezoelectric substrates like quartz, a post annealing step to induce a uniaxial magnetic anisotropy is possible and the deposition temperature can be elevated to improve the magnetic anisotropy alignment. The influence on the phase shift induced by the applied magnetic field, on the corresponding sensitivity and especially on the frequency dependent noise behaviour of the sensor is investigated and the influence on the different SAW modes compared.

The SAW sensors can be used to measure weak fields at low frequencies as required for biomagnetic applications [5] but is also well suited for current sensing and control applications, such as power electronics [6], benefitting from the large dynamic range (up to 8 orders of magnitude), high bandwidth (> 1 MHz) and the possibility of an isolated measurement. [6]

[1] Meyer, J. M. et al. "Thin-Film-Based SAW Magnetic Field Sensors". Sensors, 21(24), 8166, 2021.

[2] Fichtner, S. et al. "Identifying and overcoming the interface originating c-axis instability in highly Sc enhanced AlN for piezo-electric micro-electromechanical systems". J. Appl. Phys., 122, 035301, 2017.

[3] Schell, V. et al. "Exchange biased surface acoustic wave magnetic field sensors". Sci Rep 13, 8446 2023.

[4] Kittmann, A., et al. "Sensitivity and noise analysis of SAW magnetic field sensors with varied magnetostrictive layer thicknesses". Sensors and Actuators A: Physical, 311, 111998, 2020.

[5] Kittmann, A.; et al. "Wide band low noise love wave magnetic field sensor system". Scientific reports, 8 (1), 278, 2018.

[6] Moench, S.; Meyer, J. M. et al. "AlScN-Based SAW Magnetic Field Sensor for Isolated Closed-Loop Hysteretic Current Control of Switched-Mode Power Converters". IEEE Sensors Letters, 6 (10), 1-4, 2022.

8:00 PM EL13.04.08

The Structural, Dielectric and Ferromagnetic Analysis of (BF)_(1-x)(BST)_xO₃ for Magnetic Applications Satyam Kumar, Mohan K. Bhattarai, Sunny Choudhary, Shweta Shweta and Ram Katiyar; University of Puerto Rico- Rio Piedras, United States

In this work, we studied the effect of doping BST (Ba_{0.75}Sr_{0.25}TiO₃)_(1-x) in BFO (BiFeO₃). The (BF)_(1-x)(BST)_xO₃ (0 < x < 0.2) were synthesized by the solid state reaction route. The XRD spectra exhibited the pure perovskite phase and Raman spectroscopy analysis supported it. The SEM image reveals the uniform size of grains ~ 3 μm and EDS analysis shows the stoichiometry of various compositions, which is further supported by the XRF results.

The temperature-dependent dielectric measurement was carried out over a wide frequency band (100Hz- 1MHz) obtained high dielectric constant and low loss. The electrical measurement analysis shows the reduced leakage current due to Ba, Sr, and Ti doping on BFO. The electric field polarization (P-E hysteresis) shows a ferroelectric behavior, and the magnetic properties of the material were studied with the Physical Property Measurement System (PPMS) in VSM mode.

8:00 PM EL13.04.09

Experimental Investigation of Multiferroic Cobalt-Doped Bismuth Ferrite Nano-Composites for Sensitive Electric Field Detection Isha Sharma and Partha Roy Chaudhuri; Indian

In this study, we present an experimental investigation on the utilization of cobalt-doped bismuth ferrite, viz. $\text{BiFe}_{0.9}\text{Co}_{0.1}\text{O}_3$ nano-composites as a novel class of multiferroic materials for sensitive electric field detection. The choice is due to the fact that it has been established that bismuth ferrite (BFO: BiFeO_3) is the only known multiferroic material that exhibits substantial coupling between magnetic and ferroelectric order at room temperature. Hence, the same platform facilitates the efficient detection of low magnetic fields also.

The experimental approach involves the thorough fabrication of the bismuth ferrite nano-composite sample, followed by a comprehensive characterization of its structural properties. To enhance the sensitivity of our device, we prioritized the gain multiplication factor to amplify the response of our sensing system. Hence, we employed an approach that involved the multiple routing of the light signal through the implementation of a variable cavity all-fiber Fabry-Perot configuration. In this configuration, we have coated an optimized composition of $\text{BiFe}_{0.9}\text{Co}_{0.1}\text{O}_3$ on the tip of an optical fiber, serving as a transducer. The fiber tip is placed like a cantilever, with its coated end remains freely suspended.

The detection of electric fields in our experimental scheme relies on the phenomenon that when the coated fiber is placed in an electric field, the induced polarization of the probe material leads to a bending effect, thereby resulting in the modulation of the cavity length. This modulation is utilized as a sensitive measure of the applied electric field.

Furthermore, we have presented a theoretical model that accurately predicts the experimentally obtained results, taking into account the multiple reflection-transmission processes occurring within the Fabry-Perot circuit integrated with the beam-deflection based cavity. Significantly, from the output transmitted profile of our developed electric field sensing scheme, we can estimate the polarisation properties of sample materials under varying electric field conditions. The detailed methodology of calculation of the polarisation values is reported in our previous research work. While performing the experiment, we kept 3.0 cm long cantilever length with coated thickness of 0.31 mm.

The electric field sensing device based on beam deflection that we propose in this study exhibits excellent performance characteristics and represents a highly promising approach for the design and implementation of all-dielectric electric field sensors. Also, being an all fiber product, it offers a range of advantageous features when compared to conventional techniques. These advantages include enhanced safety, flexibility, small size and immunity to electromagnetic interference (EMI) etc.

8:00 PM EL13.04.10

Thermoelectric Study of CsMnBi [Shubham R. Singh](#)¹, [Nirpendra Singh](#)² and [Udo Schwingenschlogl](#)¹; ¹King Abdullah University of Science and Technology (KAUST), Saudi Arabia; ²Khalifa University of Science and Technology, United Arab Emirates

We have studied antiferromagnetic and ferromagnetic CsMnBi at room temperature using the linearized Boltzmann transport equation. First-principles calculations show for the antiferromagnetic phase a direct band gap of 0.23 eV when the spin-orbit coupling is considered, while metallicity is found for the ferromagnetic phase. A Seebeck coefficient of 0.58 mV/K is achieved by p-doping. The phonon band structure shows overlap in energy between the acoustic and low-frequency optical branches, resulting in strong scattering and low lattice thermal conductivity (0.09 and 0.34 W/mK for the antiferromagnetic and ferromagnetic phase, respectively). This points to a high figure of merit.

8:00 PM EL13.04.11

A Miniaturized Magnetolectric Wireless Power Transfer System with an Integrated DC Magnetic Bias [Hao Ren](#); ShanghaiTech University, China

In this abstract, we present a miniaturized magnetolectric wireless power transfer (MEWPT) system with a MEWPT receiving antenna and a spiral-coil-based transmitter. Four DC magnets are integrated onto the MEWPT receiving antenna to significantly reduce its overall dimension while providing a DC magnetic bias of 190 Oe for optimal performance. Electrochemical polarization characterizations are adopted to analyze the performance of the WPT receiving antenna, which reveal that maximum output power of 4.096 and 1.155 mW are obtained when the distance between the transmitter and receiving antenna are 0 and 0.5 cm, respectively, which corresponds to record energy conversion efficiency (ECE) of 2.64% and 0.654%, the highest among all MEWPT systems to date. The output power is improved by at least 49.3 times compared with the MEWPT system without integrated DC magnets. We demonstrate that the MEWPT system can power low power electronics, showing its potential applications in internet of things (IoT) and implantable medical devices (IMD).

Wireless power transfer (WPT) system, which transfers energy without a physical link, has received significant research interest. Due to the advantages of small dimension, low operation frequency and low transmission loss, MEWPT systems have been presented in the past few years as a promising technology. However, MEWPT systems require a DC magnetic bias for optimal performance and prior arts have implemented large electromagnets, Helmholtz coils or externally positioned magnet bias systems, which increases the system dimension. Furthermore, prior MEWPT studies report low energy conversion efficiency (ECE). In this paper, we report a miniaturized MEWPT system with an integrated DC magnetic bias, which significantly reduces the MEWPT system dimension. A 10-turn spiral coil is implemented as the WPT transmitter and a ferrite plate backplate is integrated on the spiral coil to enhance its transmitting performance. Electrochemical polarization characterizations, including the output voltage versus current characterization and output power versus current characterizations are adopted to systematically analyze the performance of the MEWPT receiving antenna. The equivalent internal resistance of the MEWPT receiving antenna is obtained by linearly fitting the output voltage versus current curve. The MEWPT receiving antenna shows an output power of 4.096 mW and 1.155 mW when the distance between the transmitter and receiving antenna is 0 cm and 0.5 cm, which corresponds to record ECE of 2.64% and 0.654% among all MEWPT systems to date. The equivalent internal resistance of the MEWPT receiving antenna is measured to be 5.04 k Ω when the output power is at 4.096 mW. We demonstrate that the MEWPT system can wirelessly power low power light emitting diodes and microchips at a distance of 0.5 cm, which demonstrates the potential applications in IoT and IMD. As the input voltage to the inductive coil transmitter decreases, the output voltage of the receiving antenna linearly decreases. The directivity and off-axis characteristics of the MEWPT receiving antenna are also measured, which shows that the directivity and off-axis distance have a significant impact on the MEWPT receiving antenna performance.

8:00 PM EL13.04.12

Electrical Control of Magnetic Texture in a Multiferroic Oxide [Peter Meisenheimer](#)¹, [Shiyu Zhou](#)², [Hongrui Zhang](#)¹, [Sajid Husain](#)¹, [Isaac Harris](#)¹, [Lucas Caretta](#)², [Paul Stevenson](#)³ and [Ramamoorthy Ramesh](#)^{1,4}; ¹University of California, Berkeley, United States; ²Brown University, United States; ³Northeastern University, United States; ⁴Rice University, United States

Materials for antiferromagnetic spintronics are becoming a popular topic due to their potential applications in next generation technologies. A primary advantage lies in their stability with external magnetic fields and potentially ultrafast spin dynamics, making them promising candidates for high-speed data storage and processing. A key challenge in this field, however, is the control of the antiferromagnetic order parameter on the nanometer scales applicable to solid state technologies. Bismuth ferrite is a multiferroic material that exhibits both ferroelectric and antiferromagnetic properties at room temperature, making it a unique candidate in the development of electrically controllable magnetic devices. In this material, the magnetic moments are arranged into a long-range spin cycloid, resulting in a unique set of magnetic properties that are intimately tied to the ferroelectric order parameter. Here we show that the propagation axis of this spin cycloid can be deterministically controlled with careful tuning of the ferroelectric order. Through precise application of electric fields, we show reversible control of the spin texture in BiFeO_3 thin films and deterministic spin transport that can be traced back to changes in the nanoscale magnetic structure.

8:00 PM EL13.04.13

Influence of K Substitution on Electronic, Structural and Magnetic Properties of $\text{La}_2\text{FeMnO}_6$: Experimental and Theoretical Study [Suman Mondal](#)¹, [Vishal Kotha](#)² and [Amrita Bhattacharya](#)¹; ¹Indian Institute of Technology Bombay, India; ²Weizmann Institute of Science, Israel

The study investigates the influence of monovalent substitution on the electronic, structural, and magnetic properties of $\text{La}_2\text{FeMnO}_6$ (LFMO) through a combination of experimental techniques and first principles Density Functional Theory (DFT) calculations. A low temperature (270 °C) one step hydrothermal process was employed to control the synthesis of K substitution within the LFMO lattice. Simultaneously, primitive LFMO samples were synthesized using the molten salt synthesis (MSS) process. The hydrothermal process yielded well-defined microcubes, while the MSS LFMO exhibited faceted nanocubes with an average size below 100 nm. Raman spectroscopy analysis revealed a noticeable shift in phonon modes with K doping, indicating a strong spin-lattice coupling. DFT calculations of the cubic phase of LFMO in a checkerboard configuration confirmed the ground state to be ferromagnetic, which was further validated through experimental investigations and theoretical calculations. Furthermore, the study highlights the significant impact of particle size on the magnetic properties and Curie temperature of LFMO, providing detailed insights into this phenomenon.

8:00 PM EL13.04.14

Creating a Three-Dimensional Intrinsic Electric Dipole on Rotated CrI_3 Bilayers [Shiva Prasad Poudel](#); University of Arkansas, Fayetteville, United States

New multiferroic platforms by sliding or rotation are being explored in two-dimensional (2D) materials [1,2,3]. Antiferromagnetically-coupled CrI_3 bilayers are one of the most studied magneto-electric multiferroic 2D materials [4]. Without considering magnetism, those bilayers possess a crystalline point of inversion, which can only be removed by antiparallel spin configuration between their two monolayers [4]. However, relative rotations between layers break the crystalline point of inversion, resulting in an inherent electric dipole moment \mathbf{P} . Magnetolectric couplings can be enhanced this way on a two-dimensional bilayer that is experimentally accessible [5].

This work was funded by MonArk NSF Quantum Foundry, supported by the National Science Foundation Q-AMASE-i program under NSF Award DMR-1906383. Calculations were performed on Cori at the National Energy Research Scientific Computing Center (NERSC), a U.S. Department of Energy Office of Science user facility operated under contract No. DE-AC02-05CH1231, the Arkansas High-Performance Computing Center's Pinnacle supercomputer, and the Tempest Research Cluster at Montana State University.

References:

- [1] Wu et al. ACS Nano, **11**, 6382-6388, 2017.
- [2] Marmolejo-Tejada et al. Nano Lett. **22**, 19, 2022.
- [3] Junyi Ji et al. Phys. Rev. Lett. **130**, 146801, 2023.
- [4] Sun et al. Nature **572**, 497, 2019.
- [5] Poudel et al. Phys. Rev. B **107**, 195128, 2023.

SESSION EL13.05: Multiferroic Materials II
Session Chairs: Caroline Ross and Mingzhong Wu
Tuesday Morning, November 28, 2023
Hynes, Level 2, Room 201

8:00 AM *EL13.05.01

Interfacial Néel Temperature Tuning for Voltage-Controlled Antiferromagnetic Spintronics Christian Binek^{1,2}, Ather Mahmood^{1,2}, Jamie L. Weaver³, Syed Qamar Abbas Shah^{1,2}, Jeffrey W. Lynn³ and Peter Dowben^{1,2}; ¹University of Nebraska-Lincoln, United States; ²Nebraska Center for Materials and Nanoscience, United States; ³National Institute of Standards and Technology, United States

Nonvolatile, voltage-controlled Néel vector rotation in the absence of an applied magnetic field is a much-desired material property in the context of antiferromagnetic spintronics. It enables ultra-low power, ultra-fast, nonvolatile memory, and logic device applications. We achieve this voltage-control by Boron (B) alloying the magnetoelectric antiferromagnet Cr₂O₃. It transforms Cr₂O₃ into a multifunctional single-phase material enabling electric field driven $\pi/2$ rotation of the Néel vector.

Voltage-controlled Néel vector rotation is detected with the help of heavy metal (Pt) Hall-bars in proximity of pulsed laser deposited B:Cr₂O₃ films. Together with results from scanning probe microscopy measurements which are sensitive to topography and surface boundary magnetization, the mechanism of voltage-controlled Néel vector reorientation is explained in terms of voltage-induced orientation of polar nanoregions. Their macroscopic orientation polarization is accompanied by piezoelectric straining which causes reorientation of the magnetic easy axis due to magnetoelastic coupling.

To facilitate operation of B:Cr₂O₃-based devices in CMOS environments, the Néel temperature, T_N , of the functional film must be tunable to values significantly above room temperature. Cold neutron depth profiling and x-ray photoemission spectroscopy depth profiling reveal thermally activated B-accumulation at the B:Cr₂O₃/vacuum interface in thin films deposited on Al₂O₃ substrates. We attribute the B-enrichment to surface segregation. Magnetotransport data confirm thermally controlled B-accumulation at the interface where the device properties reside. The increased B-concentration increases T_N from 334 K pre annealing to $T_N=477$ K post annealing within an interface layer of about 50 nm thickness. Scaling analysis determines T_N as a function of the annealing temperature. Stability of post-annealing device properties is evident from reproducible Néel vector rotation at 370 K performed over the course of weeks.

This work was supported by the National Science Foundation through EPSCoR RII Track-1: Emergent Quantum Materials and Technologies (EQUATE), Award OIA-2044049. The research was performed in part in the Nebraska Nanoscale Facility: National Nanotechnology Coordinated Infrastructure and the Nebraska Center for Materials and Nanoscience, which are supported by NSF under Award ECCS: 2025298, and the Nebraska Research Initiative.

8:30 AM *EL13.05.02

A Lattice Perspective on Bismuth Ferrite Doru C. Lupascu; University of Duisburg-Essen, Germany

Bismuth ferrite is our Drosophila system for multiferroicity at room temperature. One of the facts that has been giving the society large headaches is its low magnetoelectric coupling. In this presentation it is shown that this decoupling of the magnetic and electric orders happens fundamentally at the unit cell level. Antiferromagnetism and the cycloidal ordering of the Dzyaloshinskii–Moriya interaction generated magnetic moments are not even necessary to be considered for explaining the low coupling.

Our data from a nuclear solid state technique show that the magneto-electric coupling in the magnetic sub-lattice is actually enormous. The oxygen octahedral around the iron site experience a large tilt due to the onset of magnetic ordering. The Bi-containing complementary sub-lattice on the other hand is practically unaffected by this large structural change in its direct vicinity. Relation to classical magnetoelectric coupling schemes are drawn.

The second part of the presentation will then deal with applications of this knowledge to the tuning of magnetic, electric and photon interaction properties in custom designed nanoparticles. Photocatalytic applications, hyperthermia treatment and net magnetization studies will be shown for nanoparticles differently doped on the two sub-lattices tuning strain and magnetic coupling. Surface effects will be considered.

9:00 AM *EL13.05.03

Dynamical Multiferroicity and Magnetic Topological Structures Induced by Orbital Angular Momentum of Light in a Non-Magnetic Material Lingyuan Gao, Sergei Prokhorenko, Younsu Nahas and Laurent Bellaïche; University of Arkansas, Fayetteville, United States

Many efforts have been made in studying effective magnetization resulting from the temporally varying electric polarization [1, 2]. Such dynamical polarization can be produced by driving collective motions of ions, usually termed as “phonons” in solid-state language. Moreover, numerous recent studies show that light can control the magnetization in crystals by driving optical phonon modes and tuning structural distortions [3-6]. At the zone center of reciprocal space, infrared (IR)- and Raman-active modes, related to electric polarization and polarizability, respectively, can be excited with an ultrafast Terahertz (THz) laser pulse.

In this Talk, we will present an alternative approach to induce effective magnetic field established on the mechanism of dynamical multiferroicity. Instead of focusing on coherently excited chiral phonons, we drive real-space circular motions of ions with a particular type of light–optical vortex (OV) beam. Such light carries an orbital angular momentum (OAM) [7-9], and can manipulate the motion of microparticles as an optical tweezer [10-12]. As a prototype example, we use first-principles-based simulations and demonstrate that in ultrathin ferroelectric Pb(Zr, Ti)O₃ films, microscopic electric dipoles indeed rotate with the time-varying OAM field. As a result, orbital magnetic moments of ions are effectively generated resulting in a non-negligible magnetic field even in non-magnetic materials. More intriguingly, we will show that the microscopic magnetic moments on a single layer of this quasi 2D system are arranged in a vortex-type configuration, proving that topological magnetic structures—magnetic merons—can also be produced out of orbital magnetic moments of ions and dynamical multiferroicity.

The authors acknowledge the support from the Grant MURI ETHOS W911NF-21-2-0162 from Army Research Office (ARO) and the Vannevar Bush Faculty Fellowship (VBFF) Grant No. N00014-20-1-2834 from the Department of Defense. We also acknowledge the computational support from the Arkansas High Performance Computing Center for computational resources.

References:

- [1] D. M. Juraschek et al., Physical Review Materials 1, 014401 (2017)
- [2] D. M. Juraschek et al., Physical Review Materials 3, 064405 (2019)
- [3] T.F. Nova et al., Nature Physics 13, 132 (2017)
- [4] D. Afanasiev et al., Nature materials 20, 607 (2021)
- [5] A. Stupakiewicz et al., Nature Physics 17, 489 (2021)
- [6] M. Basini et al., arXiv:2210.01690 (2022)
- [7] L. Allen et al., Physical Review A 45, 8185 (1992)
- [8] S. Franke-Arnold, Nature Review Physics 4, 361 (2022)
- [9] G. F. Q. Rosen et al., Review of Modern Physics 94, 035003 (2022)

- [10] L. Paterson *et al.*, *Science* 292, 912 (2001)
[11] M. P. MacDonald *et al.*, *Science* 296, 1101 (2002)
[12] D. G. Grier, *Nature* 424, 810 (2003)

9:30 AM *EL13.05.04

Three's Company: On Order Parameters in Magnetic Ferroelectrics Manfred Fiebig; ETH Zurich, Switzerland

In magnetic ferroelectrics ("multiferroics"), magnetic and electric orders emerge independently ("type I"), or the former induces the latter ("type 2"). For type I, magnetic and electric order parameters are independent, and for type II, they are rigidly coupled. I argue that multiferroics with a coexistence of three order parameters combine the best of the type-I and type-II worlds. We have rigidly coupled order parameters, yet with a certain freedom to link magnetization and polarization to each other. Inversion, magnetoelectric transfer of domain patterns, or antiferromagnetic domain vortex formation are among its consequences. While these examples are of a predominantly conceptual nature, there are also connections to device applications that I will discuss.

10:00 AMB BREAK

10:30 AM *EL13.05.05

The Spin Spiral in Multiferroic BiFeO₃—Effects of Strain and Electric Field Ramamoorthy Ramesh¹ and Peter Meisenheimer²; ¹Rice University, United States; ²University of California, Berkeley, United States

The multiferroic BiFeO₃ (BFO) system seems to have an unending fountain of scientific and technological questions that the community is able to focus on. With the advent of NV-diamond based ultrahigh resolution magnetic probes, it is now possible to image with very high spatial resolution the spatial mapping of the spin spiral. Using epitaxial thin films (prepared by MBE, PLD and Sputtering), we are attempting to answer two questions: 1. What happens to the spin spiral as we impose epitaxial strain on the BFO layer through heteroepitaxy? This is being studied by using substrates of different lattice mismatch with BFO as well as the thickness of the BFO layer. 2. The second question pertains to what happens to the spin spiral when the ferroelectric polarization is switched by applying an electric field. This we are exploring using a combination of NV diamond based imaging as well as nonlocal spin transport studies. These studies are providing us with a wealth of information on the intrinsic magnetoelectric coupling in this system. These experimental studies are being complemented with theoretical studies to throw light on the origins of the spin transport behavior.

11:00 AM EL13.05.06

Switchable, Anisotropic Magnon Propagation Through the Spin Cycloid in Multiferroic BiFeO₃ Isaac Harris^{1,2}, Sajid Husain^{2,1}, Maya Ramesh³, Peter Meisenheimer⁴, Darrell Schlom³, Zhi Yao² and Ramamoorthy Ramesh^{4,1}; ¹University of California, Berkeley, United States; ²Lawrence Berkeley National Laboratory, United States; ³Cornell University, United States; ⁴Rice University, United States

Magneto-electric spin orbit (MESO) devices have been proposed as an alternative to CMOS devices for computational logic and memory, providing a possible solution to greatly reduce the energy consumption of conventional computers. This is expected to be done by electric field control of the magnetic order parameter of a ferromagnet through the magnetoelectric coupling of a BiFeO₃ (BFO) multiferroic attached to a ferromagnet. Here, we demonstrate a simplified version of a MESO device where we remove the ferromagnet entirely, and directly manipulate and measure the antiferromagnetic order of the BFO with electric fields and magnon detection, respectively. Using only the antiferromagnetic BFO in the MESO device is an attractive proposal for such a spintronic memory element due to its robustness against external fields, its lack of stray fields, and its fast switching dynamics. Furthermore, the insulating nature of BFO greatly reduces Ohmic losses in the transfer of spin information via magnons, creating a pathway for realizing ultra-low power spintronics. First, we present a bi-stable state switching of the AFM order, controlled by electric fields and measured using the inverse spin Hall effect in a platinum detector wire. Second, we demonstrate anisotropic magnon propagation in BFO, where the direction of magnon transport relative to the propagation of the spin cycloid in BFO – made visible by novel nitrogen vacancy center imaging techniques – is paramount to the retention of magnon spin information. With a better understanding of the controllable magnons in BiFeO₃, we aim to demonstrate novel AFM memory devices for energy efficient spintronic applications.

11:15 AM EL13.05.07

Observation of Optical Magnetolectric Effect in an Antiferromagnetic Metal TbB₄ Takeshi Hayashida¹, Keito Arakawa¹, Kenta Kimura^{1,2}, Ryusuke Misawa¹, Tatsuya Miyamoto¹, Hiroshi Okamoto¹, Fumitoshi Iga³ and Tsuyoshi Kimura^{1,1}; ¹The University of Tokyo, Japan; ²Osaka Metropolitan University, Japan; ³Ibaraki University, Japan

In media breaking space-inversion and time-reversal symmetries simultaneously, intriguing cross-couplings between electric and magnetic properties emerge. A representative example is the linear magnetoelectric (ME) effect, that is, the induction of electric polarization P (magnetization M) by an applied magnetic field H (electric field E). The linear ME effect can be extended to optical frequency ω , known as the optical magnetoelectric effect (OME), in which $P(\omega)$ [$M(\omega)$] is induced by oscillating $H(\omega)$ [$E(\omega)$] of an electromagnetic wave [1]. The OME effect induces nonreciprocal optical phenomena, which will be effective for probing the ME coupling in metallic systems, where the linear ME effect responding to a static field is ill-defined. In this study, we investigate the OME effect in an antiferromagnetic (AFM) metal TbB₄.

TbB₄ exhibits two successive AFM phase transition at $T_{N1} = 44$ K and $T_{N2} = 24$ K [2]. The magnetic structure in the AFM1 phase at $T_{N2} \leq T \leq T_{N1}$ breaks both space-inversion and time-reversal symmetries (magnetic point group: $4/m'm'm'$) and allows for the diagonal ME coupling ($\alpha_{11} = \alpha_{22}$, and α_{33} , where α_{ij} is the ME tensor defined as $P_i = \alpha_{ij} H_j$). The diagonal terms of the ME tensor induce nonreciprocal rotation of reflected light (NRR), which refers to the rotation of the polarization of reflected light [3,4]. In the AFM1 phase of TbB₄, there are two distinct AFM domain states, and the rotation directions of NRR are opposite between the two. Therefore, for the detection of NRR in TbB₄, spatial distribution measurements are suitable. Here, we obtain two-dimensional maps of NRR, with magnitudes ranging from 10^{-5} to 10^{-4} rad in the visible light region, by adopting a difference image sensing technique using polarization modulation of incident light [5,6]. As a result, we have successfully detected NRR and visualized AFM domains in TbB₄. We expect that our achievement will further promote understanding of ME effects in metallic compounds.

References

- [1] Y. Tokura and N. Nagaosa, *Nat. Commun.* **9**, 3740 (2018).
[2] Z. Fisk *et al.*, *Solid State Commun.* **39**, 1189–1192 (1981).
[3] B. B. Krichevskov, *et al.*, *J. Phys.: Condens. Matter* **5**, 8233–8244 (1993).
[4] B. B. Krichevskov, *et al.*, *Phys. Rev. Lett.* **76**, 4628–4631 (1996).
[5] T. Hayashida, *et al.*, *Phys. Rev. Research* **4**, 043063 (2022).
[6] T. Ishibashi, *et al.*, *J. Appl. Phys.* **100**, 093903 (2006).

11:30 AM EL13.05.08

Lattice Distortions, Electronic and Magnetic Orders in Multiferroic BiFeO₃ Valeri Petkov; Central Michigan University, United States

The presence of a spin cycloid and zero net magnetization negate any linear magnetoelectric coupling (MEC) between the polarization and magnetization in BiFeO₃ (BFO), hampering its usage in practical applications. It has been found that the problem can be alleviated by reducing BFO to nanoscale dimensions or chemical substitution but the underlying physics behind the improved MEC remains unknown. In the talk, we will show results from recent total x-ray scattering studies on nanosized [1] and La substituted [2] BFO indicating that both approaches have a common structural origin. That is, both approaches induce lattice distortions, which reduce the lattice symmetry leading to nonzero magnetization while largely preserving the ferroelectricity. We argue that lattice degrees of freedom in multiferroics often appear as lattice distortions which entangle their electronic and magnetic orders, providing a convenient mechanism to manipulate them as desired.

- [1] V. Petkov and S. Shastri "Lattice symmetry breaking transition and critical size limit for ferroic orders in nanophase BiFeO₃" *Phys. Rev. B* 104, 054121 (2021).
[2] V. Petkov, A. Zafar, P. Kenesei, and S. Shastri "Chemical compression and ferroic orders in La substituted BiFeO₃" *Phys. Rev. Mater* 7, 054404 (2023).

Acknowledgments: The reported research was supported by DOE under Award No. DE-SC0021973 and used resources of the Advanced Photon Source at the Argonne National Laboratory provided by the DOE under Contract No DE-AC02-06CH11357.

11:45 AM EL13.05.09

Efficient Voltage Control of Two-Dimensional Magnetic Insulators Shanchuan Liang¹, Ti Xie¹, Nicholas Blumenschein², Tong Zhou³, Thomas Ersevim¹, Zhihao Song¹, Jierui Liang¹, Michael A. Susner⁴, Benjamin Conner⁴, Shi-Jing Gong⁵, Jian-Ping Wang⁶, Min Ouyang¹, Igor Zutic³, Adam Friedman², Xiang Zhang⁷ and Cheng Gong¹; ¹University of Maryland, United States; ²Laboratory for Physical Sciences, United States; ³University at Buffalo, The State University of New York, United States; ⁴Air Force Research Laboratory, United States; ⁵East China

Magnetic insulators (MI), possessing long-range magnetic order while being electrically insulating, allow spin propagation without electrons' motion and thus promise a unique paradigm of next-generation dissipationless magnetoelectric and magneto-optical devices. While two-dimensional (2D) MIs usher the prospects into the atomic-thin region, efficient electrical control as an essential prerequisite for practical devices remains elusive; fundamental obstacles arise from the difficulty of electrostatically doping insulators and the inability of external electric fields to effectively modify materials' crystal fields. Here, by constructing a heterostructure consisting of a functional thin film and a 2D magnetic insulator, we achieved a strong and reversible electrical control of magnetism. The wavefunction overlaps at the heterostructure interface differs greatly under opposite voltages applied, leading to effective control of the coercivities in magnetic hysteresis loops of the 2D magnets. The layered dependence study confirmed that this effective control occurs exclusively for 2D magnets instead of the bulk counterpart, owing to the electrically controllable interfacial wavefunction overlap that could effectively alter the interfacial crystal field. Our work opens up new avenues to usher 2D MIs towards future nanoscale spintronic, magnonic, and magneto-optical applications.

SESSION EL13.06: Magnetoelectric Sensors and Actuators I
Session Chairs: Tianxiang Nan and Eckhard Quandt
Tuesday Afternoon, November 28, 2023
Hynes, Level 2, Room 201

1:30 PM *EL13.06.01

Removing Magnetic Noise from Composite Magnetoelectric Sensors Jeffrey McCord; Kiel University, Germany

Magnetic field sensors are devices that detect and measure magnetic fields around permanent magnets, electrical conductors, and electrical devices. As such, they are particularly relevant for magnetic applications in IoT, 5G, smartphones, energy, and biomedical engineering. In this context, dedicated research is currently being carried out on novel thin film magnetoelectric (ME) sensor concepts for the detection of magnetic fields down to the picotesla range.

Advanced wide-field magneto-optical Kerr effect microscopy [1] with high temporal resolution is used to study local effects in operating ME composite sensor structures. The realized magnetospatial analysis of working devices sheds light on magnetization changes due to domain nucleation, domain wall resonances, domain wall bending modes, precessional magnetization effects and spin-wave-like phenomena. Each of these is specific to different types of composite ME sensors, ranging from resonance to modulated to DE to SAW sensor systems. Complementary ME response, noise and detection limit analyses reveal the different magnetic noise mechanisms with different magnetic domain activities for the different sensor types (e.g. [2-5]). By understanding the complex magnetic interactions, strategies and implementations are identified to optimize sensor structures. Single magnetic domain layers are the basis for low noise magnetic thin film sensors due to the absence of magnetic domain walls.

The design and application of magnetic layered structures with minimal noise performance sensitivity is discussed. Beyond magnetic domain engineering [6], other schemes of magnetic noise suppression, based on a combination of sensing and pinning magnetic multilayer stacks are discussed. By introducing magnetic sensing layers with subtractive response to carrier excitations while maintaining sensitivity, the influence of the electrical carrier signal to noise is virtually eliminated [7]. The magnetically enforced reduction of the electrical background signal paves the way for ultra-low noise ME sensor applications capable of detecting picotesla magnetic fields. Fundamental limitations of composite ME sensors beyond magnetic domain activity will be further discussed [5].

Funding by the DFG for the CRC 1261 "Magnetoelectric Sensors: From Composite Materials to Biomagnetic Diagnostics" and collaborations within the CRC are acknowledged.

References

- [1] J. McCord, Journal of Physics D: Applied Physics 48, 333001, 2015.
- [2] N. O. Urs, I. Teliban, A. Piorra, et al., Applied Physics Letters 105, 202406, 2014.
- [3] N.O. Urs, E. Golubeva, V. Röbisch, et al., Physical Review Applied 13, 024018, 2020.
- [4] C. Müller, P. Durdaut, R.B. Holländer, et al., Advanced Electronic Materials, 2200033, 2022.
- [5] E. Spetzler, B. Spetzler, J. McCord, under review.
- [6] M. Jovičević Klug, L. Thormählen, V. Röbisch, et al., Applied Physics Letters 114, 192410, 2019.
- [7] D. Seidler, P. Hayes, E. Spetzler, et al., in preparation.

2:00 PM *EL13.06.02

Dynamically Tunable, Narrowband Terahertz Emitters Designed by Tailoring Magnon-Phonon Interaction in Multilayer Heterostructures Jiamian Hu; University of Wisconsin-Madison, United States

A dynamically tunable, narrowband terahertz (THz) source is much needed for an accurate identification and imaging of chemical and biological species, with wide-ranging applications from security screening to medical imaging and to semiconductor inspection. However, existing pulsed THz sources are mostly single-cycle, broadband, and difficult to tune dynamically. In this presentation, the speaker will first introduce an approach that permits converting a femtosecond laser pulse into a multi-cycle, narrowband THz pulse via resonant magnon-phonon interaction. The peak frequency of the emitted THz pulse can be tuned by up to 50% through a varying bias magnetic field. The speaker will then present computational demonstration of this approach in several carefully designed ferromagnet and antiferromagnet based multilayer heterostructures, which allows us to cover without gaps different frequency ranges (deep millimeter-wave, sub-THz, and >1 THz) of the THz spectrum, tune the polarization, duration, and power of the emitted THz pulse. The demonstration was performed based on an in-house dynamical phase-field model that incorporates the coupled dynamics of magnons, phonons, photons, and plasmons in multiphase systems.

2:30 PM *EL13.06.03

Imaging of Magnetic Particles by Magnetic Susceptibility Particle Mapping (MSPM) Christine Selhuber-Unkel; Heidelberg University, Germany

The imaging of magnetic particles is highly relevant in many biomedical investigations, including disease detection, diagnosis, and treatment. Magnetic Susceptibility Particle Mapping (MSPM) has the potential to emerge as an important tool in this context, as it can be used to detect magnetic nanoparticles in a lab scale device. The system is based on magnetoelectric (ME) sensors that make use of the Delta-E effect, in combination with a permanent magnet, which generates a bias field for the sensor and at the same time magnetizes the SPIONs. The SPIONs in the sample are magnetized by the permanent magnet and generate an additional magnetic field, which is recorded by the ME sensor. To demonstrate the capability of the MSPM as an imaging technique, magnetic particle distributions are assessed in 3D printing scaffolds. In addition, 3D microtumors based on MCF-7 and MDA-MB-231 breast cancer cells were labelled with magnetic nanoparticles assessed by MSPM. The data show the potential of the device as well as new avenues towards a lab scale investigation of biomedically relevant samples at the standard lab scale.

3:00 PM BREAK

3:30 PM *EL13.06.04

Nonreciprocity and Nonlinearity in Hybrid Magnetoacoustic Devices Derek Bas¹, Roman Verba², Piyush Shah¹, Serhiy Leontsev¹, Abbass Hamadeh³, Michael Wolf¹, Andrew Franson¹, Alexei Matyushov⁴, Michael Newburger¹, Philipp Pirro³, Mathias Weiler³, Nian Sun⁴, Vasyly Tyberkevych⁵, Andrei Slavin⁵ and Michael Page¹; ¹Air Force Research Laboratory, United States; ²Institute of Magnetism, Ukraine; ³Technische Universität Kaiserslautern, Germany; ⁴Northeastern University, United States; ⁵Oakland University, United States

Nonreciprocity, the property of merit for a variety of RF components such as isolators and circulators, is typically difficult to achieve with the magnitude required for applications. To this end, I will discuss discoveries of non-reciprocity and non-linearity in surface acoustic waves interacting with magnetic materials. Giant Nonreciprocity of 48.4 dB (ratio of 1:100,000) is achieved in the transmission of surface acoustic waves on a lithium niobate substrate coated with ferromagnet/insulator/ferromagnet (FeGaB/Al₂O₃/FeGaB) multilayer structure. This same structure has now also demonstrated very large phase shifts due to a similar interaction, and the nature of the magnetic ordering and coupling to the acoustic system will be discussed. Nonlinearity will also be discussed and is demonstrated using focused interdigitated transistors employing curved fingers, in contrast to the straight fingers typically used. These transducers are engineered to concentrate acoustic energy towards a small region in the center of the device allowing driven magnetic precession much higher than was previously possible. Enhanced acoustic absorption

and modeling of the response will be shown. These devices promise functionality which outperforms current state of the art high frequency devices in a novel acoustic wave system that facilitates unprecedented size, weight, and power reduction.

4:00 PM EL13.06.05

Miniaturized Delta-E Effect Magnetic Field Sensors Fatih Hlgaz¹, Patrick Wiegand¹, Benjamin Spetzler², Rober Rieger¹ and Franz Faupel¹; ¹Kiel University, Germany; ²Ilmenau University of Technology, Germany

Magnetolectric delta-E effect sensors utilize the change in the elastic modulus of the magnetostrictive material upon applying a magnetic field, resulting in a shift in the resonance frequency. Such sensors have demonstrated the potential to detect small-amplitude and low-frequency magnetic fields. It was also shown that the limit of detection can be improved by using sensor arrays including a large number of sensor elements [1]. However, building compact arrays and achieving high spatial resolutions using mm-sized sensors is challenging. Moreover, the reproducibility of the sensors is significantly impacted by the anisotropic stress developing in the magnetic layer upon releasing the resonator during the fabrication process [2]. Additionally, sensors with a cantilever design suffer from inhomogeneous magnetic properties caused by different stress relaxation at the clamping region affecting their performance [3]. Here, we present an experimental and theoretical investigation of μm -sized delta-E effect sensors employing a free-free beam design that overcomes the limitations and challenges encountered in previous approaches. To control and minimize the residual stress in the magnetic layer, we use a shadow-mask deposition technique where the magnetic layer is deposited on the released resonators. The spatial stress distribution can be accurately determined by combining displacement measurements with a magneto-mechanical model. Different resonance modes are identified, and the dependency of the resonance frequency shift and the sensitivities on these modes are established. The influence of the anchors and the stiffness tensor components on the resonance frequency shift are analyzed by combining a magnetoelastic macrospin model and an electromechanical finite element model. Noise performance and the limit of detection of different sensor geometries are investigated to gain general insight into the relationship between geometry, resonance mode, and sensor performance. We demonstrate extreme stress control with a minimal change of smaller than 8 MPa in the normal stress components (σ_{11} and σ_{22}) and smaller than 2 MPa in the shear stress component (σ_{12}) following the deposition of the magnetic layer. We find that the delta-E effect and sensitivities exhibit strong dependence on resonance modes, attributed to distinct variations in local magnetic and mechanical properties specific to each mode. We identify the optimum mode shape and achieve detection limits below 300 pT/Hz^{1/2} at 10 Hz, comparable to macroscopic sensors [4,5]. Overall, we demonstrate the successful production and miniaturization of delta-E effect sensors with high reproducibility and similar performance to the macroscopic sensors using the proposed manufacturing process and sensor design. The achieved miniaturization and reproducibility represent a significant step toward developing fully integrated sensor arrays and emphasize the potential for high spatial resolution and improved detection limits with large sensor arrays or using flux concentrators.

[1] B. Spetzler, P. Wiegand, P. Durdaut, M. Höft, A. Bahr, R. Rieger, F. Faupel, *Sensors* **2021**, *21*, 7594

[2] A. D. Matyushov, B. Spetzler, M. Zaeimbashi, J. Zhou, Z. Qian, E. V. Golubeva, C. Tu, Y. Guo, B. F. Chen, D. Wang, A. Will-Cole, H. Chen, M. Rinaldi, J. McCord, F. Faupel, N. X. Sun, *Adv. Mater. Technol.* **2021**, *6*, 2100294.

[3] B. Spetzler, E. V. Golubeva, R. M. Friedrich, S. Zabel, C. Kirchof, D. Meyners, J. McCord, F. Faupel, *Sensors* **2021**, *21*, 2022.

[4] S. Zabel, C. Kirchof, E. Yasar, D. Meyners, E. Quandt, F. Faupel, *Appl. Phys. Lett.* **2015**, *107*, 152402.

[5] P. Durdaut, J. Reermann, S. Zabel, C. Kirchof, E. Quandt, G. Schmidt, R. Knöchel, F. Faupel, M. Höft, *IEEE Trans. Instrum. Meas.* **2017**, *66*, 2771.

4:15 PM EL13.06.06

Love Wave Magnetic Field Sensor Operating Without External Bias Field Felix Weisheit¹, Viktor Schell¹, Elizaveta Spetzler¹, Jeffrey McCord¹, Dirk Meyners¹, Eckhard Quandt¹ and Susana Cardoso de Freitas²; ¹University of Kiel, Germany; ²INESC Microsystems and Nanotechnologies, Portugal

Surface acoustic wave (SAW) technology is widely utilized in electronics as e.g. filters and sensors. One notable application is their implementation for magnetic field detection [1]. Currently, magnetic field sensors have achieved a limit of detection (LOD) below 40 pT*Hz^{1/2} within the frequency range of 1 Hz to 1 kHz. However, these sensors require an external bias field of approximately 0.4 mT to achieve the desired sensitivity [2]. Alternatively, newly developed SAW sensors incorporate a sensing layer of FeCoSiB deposited through ion beam deposition. These sensors can achieve a LOD of 71 pT*Hz^{1/2} at 10 Hz without the need for an external bias field. This eliminates the requirement for an additional magnetic field source during operation. The SAW sensor is constructed on a substrate of piezoelectric ST-cut quartz with gold interdigital transducers (IDTs) for generating the acoustic wave. A waveguiding layer made of amorphous SiO₂ is placed on top to confine the wave to the surface, resulting in Love waves. They exhibit an in-plane displacement perpendicular to the direction of propagation. The IDTs are arranged sequentially to create a delay line, and a magnetostrictive sensing element is positioned between them. This sensing layer consists of a single-layer amorphous (Fe₈₀Co₂₀)₇₈Si₁₂B₁₀ thin film deposited using ion beam deposition. If a magnetic field is present, it induces changes in the elastic properties of the FeCoSiB due to the ΔE effect. This alteration in properties leads to a phase shift in the Love wave. The sensitivity of the sensor to the magnetic field is determined by measuring this phase shift. This measurement is carried out using a Zurich Instruments UHFLI lock-in amplifier, which employs dynamic phase detection. The phase noise analysis is performed using a Rhode & Schwarz FSWP phase noise analyzer. The FeCoSiB coating on the new sensor does not exhibit ideal soft magnetic behavior, but instead displays a more hysteretic behavior with a coercivity field of 0.5 mT. Consequently, this leads to a shift in the sensitivity curve, wherein the maximum sensitivity of 1410 °/mT is achieved at a bias field of 0.75 mT. But, even in the remanence state, the sensor retains a sensitivity of 640 °/mT, whereas other sensors with a more ideal soft magnetic film have a sensitivity below 100 °/mT. To determine the LOD, the phase noise is divided by the sensitivity. The best sensor, in this case, achieves a LOD of 71 pT*Hz^{1/2} at 10 Hz and 24 pT*Hz^{1/2} at 100 Hz. The magnetic properties, as well as the findings when considering the sensitivities, will be presented. Furthermore, advances in utilizing LiNbO₃ single crystal substrate, which possesses a significantly higher electromechanical coupling factor than quartz, will be discussed. LiNbO₃ also allows higher excitation frequencies to be used, which is expected to result in a further increase in sensitivity.

[1] A. Kittmann, P. Durdaut, S. Zabel, J. Reermann, J. Schmalz, B. Spetzler, D. Meyners, N. X. Sun, J. McCord, M. Gerken, G. Schmidt, M. Höft, R. Knöchel, F. Faupel, and E. Quandt, "Wide Band Low Noise Love Wave Magnetic Field Sensor System" *Scientific Reports*, *8*, 278, 2018.

[2] V. Schell, E. Spetzler, N. Wolff, L. Bumke, D. Meyners, L. Kienle, J. McCord, E. Quandt, "Exchange biased surface acoustic wave magnetic field sensors" *Scientific Reports*, *13*, 8446, 2023.

4:30 PM EL13.06.07

Temperature Stability of Magnetic Materials for Highly Sensitive Magnetolectric Sensors Lars Thormählen¹, Bin Luo², Nian Sun², Eckhard Quandt¹ and Dirk Meyners¹; ¹University of Kiel, Germany; ²Northeastern University, United States

The detection of magnetic signals is a significant research area where numerous magnetolectric sensor systems, such as antennas, filters, and magnetometers, are being developed and tested [1]. The use of magnetic signals has the advantage over electrical signals that they are not affected by water, for example, which simplifies communication with underwater vessels and the measurement of biomagnetic signals [1, 2].

The development and fabrication of magnetolectric cantilever sensors, based on microsystem techniques, are among the primary research focuses of the Collaborative Research Center 1261 at Kiel University [2, 3]. To construct such highly sensitive magnetic field sensors, a wide range of material parameters must be considered. For instance, piezoelectric layers require high piezoelectric coefficients, while magnetic layers should possess soft magnetic properties combined with high magnetostriction. Commonly used magnetostrictive materials are FeCoSiB and FeGaB. Amorphous magnetic materials have the advantage of avoiding undesired crystal anisotropies. To further enhance the magnetic behavior, exchange-bias multilayer systems are employed to minimize magnetic noise resulting from domain wall activity. Imprinting anisotropy in the multilayers is crucial for optimal performance, which can be achieved through sputter deposition in a magnetic field, as well as subsequent heat treatment at approximately 250 °C for FeCoSiB. However, higher annealing temperatures may be necessary depending on the blocking temperature of the selected antiferromagnet for biasing, which could lead to crystallization of the amorphous magnetic layers.

Another potential source of unintentional crystallization is the packaging of the devices at the end of production to protect them from environmental influences and facilitate handling. This common method typically requires temperatures of about 400 °C to create a vacuum-sealed capsule.

This study focuses on investigating different magnetostrictive materials such as FeCoSiB, FeGaB, FeGaC, and CoFeB, which are fabricated through sputter deposition with multicomponent targets and co-deposited layers [1]. The materials are evaluated using XRD, VSM, and magnetostriction measurements at different temperatures. The study aims to determine the temperature ranges at which a negative magnetic change occurs. For example, significant changes in the magnetic behavior of FeCoSiB are observed at temperatures above 300 °C, resulting in a degradation of sensor properties and rendering them unsuitable for vacuum encapsulation by standard wafer bonding.

[1] Tu, C.; Chu, Z.-Q.; Spetzler, B.; Hayes, P.; Dong, C.-Z.; Liang, X.-F.; Chen, H.-H.; He, Y.-F.; Wei, Y.-Y.; Lisenkov, I.; et al. **Mechanical-Resonance-Enhanced Thin-Film Magnetolectric Heterostructures for Magnetometers**, *Mechanical Antennas, Tunable RF Inductors, and Filters. Materials* **2019**, *12*, 2259

[2] E. Elzenheimer, P. Hayes, L. Thormählen, E. Engelhardt, A. Zaman, E. Quandt, N. Frey, M. Höft, G. Schmidt: **Investigation of Converse Magnetolectric Thin Film Sensors for Magnetocardiography**, *IEEE Sensors Journal*, Volume 23, Number 6, Pages 5660-5669, 2023

[3] P. Hayes, M. Jovičević Klug, S. Toxværd, P. Durdaut, V. Schell, A. Teplýuk, D. Burdin, A. Winkler, R. Weser, Y. Fetisov, M. Höft, R. Knöchel, J. McCord & E. Quandt: **Converse Magnetolectric Composite Resonator for Sensing Small Magnetic Fields**, *Sci Rep* **9**, 16355, 2019

8:00 AM *EL13.07.01

Exploiting Structural and Electronic Coupling in Transition Metal Oxide Heterostructures Jean-Marc Triscone¹, Hugo Meley¹, Duncan T. Alexander², Clémentine Thibault¹, Lucia Varbaro¹, Lukas Korosec¹, Claribel Dominguez¹, Bernat Mundet³, Jennifer Fowlie⁴, Marta Gibert⁵, Marcus Schmitt⁶, Philippe Ghosez⁶ and Stefano Gariglio¹; ¹University of Geneva, Switzerland; ²EPFL, Switzerland; ³Institut Català de Nanociència i Nanotecnologia (ICN2), Spain; ⁴SLAC National Accelerator Laboratory, United States; ⁵TU Wien, Austria; ⁶Université de Liège, Belgium

In this talk, I will illustrate through some examples how electronic and structural coupling can lead to exciting novel properties in oxide films and heterostructures.

I will first recall how tri-linear coupling of structural instabilities can lead to improper ferroelectricity in PbTiO₃/SrTiO₃ superlattices [1]. I will then discuss how such a coupling of instabilities can be used to design artificial ferroelectric and possibly multiferroic materials with a focus on vanadate-based structures [2,3]. In these structures, it was found that the competition between the strain state and the coupling of oxygen octahedra rotations leads to an interesting “transition layer” and a reorientation of the orthorhombic long-axis. This competition can be used for designing an artificial interface with possibly designed electronic properties. The reorientation of the orthorhombic long-axis is also observed in SmNiO₃/NdNiO₃ nickelate superlattices [4,5] - when an additional insulating spacer layer of LaAlO₃ is introduced [6].

[1] E. Bousquet et al. *Nature* 452, 732 (2008)

[2] See, for instance, J. M. Rondinelli and C. J. Fennie, *Adv. Mater.* 24, 1961 (2012)

[3] H. Meley et al. *APL Materials* 6, 046102 (2018)

[4] C. Dominguez et al. *Nature Materials* 19, 1182 (2020)

[5] B. Mundet et al. *Nano Letters* 21, 2436 (2021)

[6] L. Varbaro et al. *Advanced Electronic Materials* 2201291 (2023).

8:30 AM *EL13.07.02

Interface-Dependent Magnetotransport Properties of Perovskite Lanthanum Manganite Thin Films Pinku Roy^{1,2}, Aiping Chen² and Quanxi Jia¹; ¹University at Buffalo, United States; ²Los Alamos National Laboratory, United States

Enhanced functionalities and/or emergent behavior, often not accessible from the individual constituents, could be produced by interfacing certain materials at different length scales. Over the years, major advances have been made to synthesize high crystallinity epitaxial perovskite lanthanum manganite films with controlled microstructures and to gain a fundamental understanding of their physical properties. In this talk, we will discuss our strategies in the synthesis and characterization of epitaxial lanthanum manganite films. Using perovskite lanthanum manganite as the model system, we examine interface-dependent magnetotransport properties by creating both vertically aligned nanocomposite films and layered heterostructures. Specifically, we will discuss the effect of interfaces (both vertical and lateral interfaces) on the magnetotransport properties of lanthanum manganite films.

9:00 AM *EL13.07.03

Novel Tetragonal Phase and Multiferroism in (1-x)BiFeO₃-(x)BaTiO₃ Films Lane W. Martin^{1,2,3}; ¹Rice University, United States; ²Lawrence Berkeley National Laboratory, United States; ³University of California, Berkeley, United States

While bulk BiFeO₃ has a rhombohedral perovskite structure with the polarization lying along the {111}, the room temperature structure and polarization can be manipulated using strain and chemistry due to the presence of numerous structural polymorphs. Under sufficiently large compressive (tensile) strains researchers have found super-tetragonal-like (orthorhombic) structures. Changing the structure can also change the resulting polarization and magnetism and thus the study of the polymorphism in this system has been a matter of great attention. Considerable work has been done on the super-tetragonal-like structure (with large $c/a \approx 1.25$ and predicted polarization as large as $\sim 150 \mu\text{C}/\text{cm}^2$), but it has been found that growing a phase-pure version of this material is challenging and limited to very thin films before it relaxes back to the parent structure. On the other hand, chemical substitution has also been widely used to modify BiFeO₃ since the polarization (structure) is strongly influenced by the 6s² lone pair electrons of bismuth meaning that A-site substitution can greatly impact the structure and properties.

Here, we explore such concepts by examining the evolution of the structure and polar and magnetic properties of (1-x)BiFeO₃-(x)BaTiO₃ (x = 0-0.3) solid solution thin films. Films of varying compositions have been deposited using pulsed-laser deposition on a range of perovskite substrates. While for all values of x films grown on scandate substrates exhibit the expected rhombohedral (monoclinic) structure seen in most films (albeit with slightly larger lattice parameter), growth of films with x = 0.1, 0.2, and 0.3 on SrTiO₃ (001) substrates produces a new phase. Detailed X-ray diffraction, piezoresponse force microscopy, and scanning transmission electron microscopy reveal this new phase to be tetragonal and different from the previously observed super-tetragonal-like phase. Insights on this new structure are gleaned from first-principles calculations. Subsequent dielectric and polarization-electric field hysteresis loop studies show that the novel tetragonal phase exhibits a lower dielectric constant and increased polarization (as large as 120 mC/cm²) and coercive field ($\sim 500 \text{ kV}/\text{cm}$) as compared to parent-phase BiFeO₃. In turn, the magnetic nature of the material is studied via inelastic light scattering, exchange bias, SQUID magnetometry, angle-dependent X-ray absorption spectroscopy and magnetic linear and circular dichroism, and scanning NV magnetometry measurements. A comparatively large in-plane magnetization is observed. Finally, the potential for magnetoelectric coupling in this system is probed. Overall, these findings suggest the discovery of a new phase of BiFeO₃ that, to the best of our knowledge, has not been observed before and works to provide understanding for why it forms and how it evolves from the parent phase.

9:30 AM BREAK**10:00 AM *EL13.07.04**

Superconductivity in Layered Square Planar Nickelates Julia Mundy; Harvard University, United States

Since the discovery of high-temperature superconductivity in copper oxide materials, there have been sustained efforts to both understand the origins of this phase and discover new cuprate-like superconducting materials. One prime materials platform has been the rare-earth nickelates; indeed, superconductivity was recently discovered in the doped compound Nd_{0.8}Sr_{0.2}NiO₂ [1]. Undoped NdNiO₂ belongs to a series of layered square-planar nickelates with chemical formula Nd_{n+1}Ni_nO_{2n+2} and is known as the ‘infinite-layer’ (n = ∞) nickelate. Here, we report the synthesis of the quintuple-layer (n = 5) member of this series, Nd₆Ni₅O₁₂, in which optimal cuprate-like electron filling ($d^{8.8}$) is achieved without chemical doping [2]. We observe a superconducting transition beginning at $\sim 13 \text{ K}$. Electronic structure calculations, in tandem with magnetoresistive and spectroscopic measurements, suggest that Nd₆Ni₅O₁₂ interpolates between cuprate-like and infinite-layer nickelate-like behaviour. By engineering a distinct superconducting nickelate, we identify the square-planar nickelates as a new family of superconductors that can be tuned via both doping and dimensionality. [3]

[1] D. Li, K. Lee, B. Y. Wang, M. Osada, S. Crossley, H. R. Lee, Y. Cui, Y. Hikita, and H. Y. Hwang, *Superconductivity in an Infinite-Layer Nickelate*, *Nature* **572**, 7771 (2019).

[2] G. A. Pan et al., *Superconductivity in a Quintuple-Layer Square-Planar Nickelate*, *Nat. Mater.* **21**, 2 (2022).

[3] We acknowledge support from the US Department of Energy under award no. DE-SC0021925.

10:30 AM EL13.07.05

Structural and Electronic Properties of Nickelate Based Superlattices Lucia Varbaro¹, Claribel Dominguez¹, Jennifer Fowlie², Lukas Korosec¹, Bernat Mundet³, Duncan T. Alexander⁴ and Jean-Marc Triscone¹; ¹University of Geneva, Switzerland; ²SLAC National Accelerator Laboratory, United States; ³Institut Català de Nanociència i Nanotecnologia (ICN2), Spain; ⁴École Polytechnique Fédérale de Lausanne, Switzerland

Rare-earth nickelates belong to the wider family of perovskite oxides. These materials display a characteristic temperature-dependent metal-to-insulator transition (MIT) together with a lowering of the crystal symmetry related to the onset of a breathing distortion of the NiO₆ octahedra units [1,2]. Furthermore, below the Néel temperature ($T_N < T_{MI}$ for R = Lu - Sm and $T_N = T_{MI}$ for R = Nd, Pr), these compounds were found to exhibit antiferromagnetic order with the (1/4,1/4, 1/4) pseudocubic propagation vector [3-4]. In theory, it has been predicted that the coalescence of breathing distortion and non-centrosymmetric magnetic order could result in a breaking of inversion symmetry within the crystal lattice. Consequently, this would lead to the emergence of an electric dipole, classifying nickelates as type-II multiferroics. [5]. Raman spectroscopic data of RNiO₃ single crystals by Ardizzone and al. [6], show that, entering the magnetically ordered phase, additional vibrational modes appear as a possible signature of breaking of inversion symmetry.

In this work, we investigate nickelate thin films and superlattices. Raman experiments were performed on NdNiO₃ and SmNiO₃ thin films, revealing temperature evolution of the Raman spectra rather similar to the one reported in [6].

Moreover, the structural and electronic properties of nickelate superlattices were studied to investigate the characteristic length scale over which a metallic or an insulating phase can be established and the physics that sets it [7]. By growing $\text{SmNiO}_3/\text{NdNiO}_3$ superlattices and using experimental and theoretical methods we showed that this length scale depends on the interplay between the energy cost of the boundary between metallic and insulating phases and the energy gain of the bulk phases [7]. To further understand this unusual coupling and the evolution of the structural and electronic order parameters across these phase boundaries, $\text{SmNiO}_3/\text{NdNiO}_3$ superlattices were grown with additional insulating LaAlO_3 spacer layers, that should lead to a progressive decoupling of the nickelate layers. Furthermore, the phase boundary cost of maintaining an interface between a metal and an insulator will be exploited as an additional parameter to tune the electronic properties of this class of materials, specifically alternating metallic layers and layers displaying a metal-to-insulator transition within a superlattice, with the aim of forcing a metal into an insulating phase by increasing the density of interfaces. All the samples were grown using RF off axis magnetron sputtering, and are morphologically and structurally characterized using atomic force microscopy (AFM), X-ray diffraction (XRD) and STEM-EELS. Temperature dependent transport measurements will be presented for each different system, giving an overview on electronic and structural couplings, and more generally on the properties of these complex heterostructures.

[1] M. L. Medarde, J. Phys.: Condens. Matter 9, (1997) 1679
 [2] G. Catalan, Phase Transitions 81, (2008) 729
 [3] J. L. García-Muñoz, J. Rodríguez-Carvajal, and P. Lacorre, Phys. Rev. B 50, (1994) 978
 [4] M. T. Fernández-Díaz, J. A. Alonso, M. J. Martínez-Lope, M. T. Casais, and J. L. García-Muñoz, Phys. Rev. B 64, (2001) 144417
 [5] Gianluca Giovannetti, Sanjeev Kumar, Daniel Khomskii, Silvia Picozzi, and Jeroen van den Brink, Phys. Rev. Lett. 103, (2009) 156401
 [6] I. Ardizzone, J. Teyssier, I. Crassee, A. B. Kuzmenko, D. G. Mazzone, D. J. Gawryluk, M. Medarde, and D. van der Marel, Phys. Rev. Research 3, (2021) 033007
 [7] Domínguez, C., Georgescu, A.B., Mundet, B. et al., Length scales of interfacial coupling between metal and insulator phases in oxides. Nat. Mater. 19, 1182–1187 (2020)

10:45 AM EL13.07.06

Ferromagnetism and Ferroelectricity in a Superlattice of Antiferromagnetic Perovskite Oxides Without Ferroelectric Polarization Avijeet Ray, Paresh C. Rout and Udo Schwingschlögl; King Abdullah University of Science and Technology, Saudi Arabia

Using density functional theory with onsite Coulomb interaction, we study the structural, electronic, and magnetic properties of the $\text{SrCrO}_3/\text{YCrO}_3$ superlattice and their dependence on epitaxial strain. We discover that the superlattice adopts A-type antiferromagnetic (A-AFM) ordering in contrast to its constituents (SrCrO_3 : C-AFM; YCrO_3 : G-AFM) and retains it under compressive strain while becoming ferromagnetic ($5 \mu_B$ per formula unit) at +1% strain. The obtained ferroelectric polarization is significantly higher than that of the $\text{R}_2\text{NiMnO}_6/\text{La}_2\text{NiMnO}_6$ ($R = \text{Ce to Er}$) series of superlattices [Nat. Commun. 5, 4021 (2014)] due to a large difference between the antipolar displacements of the Sr and Y cations. The superlattice is a hybrid-improper multiferroic material with a spontaneous ferroelectric polarization ($13.5 \mu\text{C}/\text{cm}^2$) approaching that of bulk BaTiO_3 ($19 \mu\text{C}/\text{cm}^2$). The combination of ferromagnetism with ferroelectricity enables multistate memory applications. In addition, the charge-order-driven p-type semiconducting state of the ferromagnetic phase (despite the metallic nature of SrCrO_3) is a rare property and interesting for spintronics. Monte Carlo simulations demonstrate a magnetic critical temperature of 90 K for the A-AFM phase without strain and of 115 K for the ferromagnetic phase at +5% strain, for example.

Acknowledgment: The research reported in this publication was supported by funding from King Abdullah University of Science and Technology (KAUST).

11:00 AM EL13.07.07

Giant Magnetolectric Effect and Interactive Control of Magnetic Anisotropy Driven by a Ferroelectric Phase Transition in Ferromagnetic-Piezoelectric Heterostructure Thomas R. Mion^{1,2}, Margo Staruch², Peter Finkel² and Konrad Bussmann²; ¹NOVA Research, United States; ²U.S. Naval Research Laboratory, United States

Magnetolectric materials and, to a larger extent, multiferroic heterostructures offer a novel route for electric field control of magnetism. We explored the induced magnetic anisotropy of an FeCo/Ag multilayer thin film deposited on the surface of 001 poled $\text{Pb}(\text{In}_{1/2}\text{Nb}_{1/2})\text{O}_3\text{-Pb}(\text{Mg}_{1/3}\text{Nb}_{2/3})\text{O}_3\text{-PbTiO}_3$ PIN-PMN-PT single crystal as it is electrically driven through a ferroelectric-ferroelectric phase transition. In PIN-PMN-PT an effective giant piezoelectric coefficient $>10,000 \text{ pm}/\text{V}$ occurs during the phase transition providing strain $>0.25\%$ along a principle strain direction. This effect translates into anisotropic strain to the magnetoelastic thin film inducing a giant magnetoelastic effect driven by the induced magnetic anisotropy along the principle strain direction. We measured an effective converse magnetoelectric coefficient $\sim 1.4 \times 10^{-5} \text{ s}/\text{m}$ when driven through the phase transition which was more than double the values obtained in the linear piezoelectric rhombohedral phase. The controllable and repeatable nature of the phase transition allows an interactive driving of the induced magnetization making the phenomenon attractive for application in spintronic devices.

SESSION EL13.08: Magnetolectric Spintronics II

Session Chairs: Tianxiang Nan and Eckhard Quandt

Wednesday Afternoon, November 29, 2023

Hynes, Level 2, Room 201

1:30 PM *EL13.08.01

Recent Advances and Future Opportunities with Magnetic X-Ray Spectromicroscopies Peter Fischer^{1,2}; ¹Lawrence Berkeley National Lab, United States; ²University of California, Santa Cruz, United States

Spin textures in magnetic materials, and polarization textures in multiferroic materials hold the key to understand and control properties and behavior, that offer tremendous potential for novel applications in future information processing technologies with significant improvements in energy efficiency, processing speed, functionalities, and miniaturization of future microelectronic devices.

An emerging research field in nanomagnetism is the scientific and technological exploration of 3-dimensional magnetic nanostructures that opens the path to exciting novel physical phenomena, originating from the increased complexity in spin textures, topology, frustration, and tailored geometries in three dimensions. This has attracted significant scientific interest and led to intense research addressing a broad spectrum, including stability, dynamics, nucleation, and transport in novel spin textures, such as vortices, skyrmions, chiral bobbers, hopfions, torons, skyrmion tubes, etc. [1]. Analogous structures are also found in multiferroic (polar) materials, such as polar vortices [2], skyrmions [3] and hopfions [4].

Advanced characterization tools that provide magnetic sensitivity to spin textures, disentangling the role of individual components in heterogeneous material at high spatial resolution, ultimately at buried interfaces and in all three dimensions [5], and at high temporal resolution to capture the spin dynamics across scales, are required to address those questions, and are therefore of large scientific interest.

Various magnetic soft X-ray spectro-microscopies [6] using polarized soft x-rays provide unique characterization opportunities to study the statics and dynamics of spin textures in magnetic materials combining X-ray magnetic circular dichroism (X-MCD) as element specific, quantifiable magnetic contrast mechanism with spatial and temporal resolutions down to fundamental magnetic length, time, and energy scales.

Current developments of x-ray sources aim to increase dramatically the coherence of x-rays opening the path to new techniques, x-ray photo-correlation spectroscopy (XPCS) [7] that allow unprecedented studies of nanoscale heterogeneity, complexity, and fluctuations.

I will review recent achievements and future opportunities with magnetic x-ray spectro-microscopies. Examples will address static properties and dynamic behavior of magnetic hopfions [8] and a 3D metrology of skyrmions using soft x-ray laminography [9].

This work was supported by the U.S. Department of Energy, Office of Science, Office of Basic Energy Sciences, Materials Sciences and Engineering Division Contract No. DE-AC02-05-CH1123 in the Non-Equilibrium Magnetic Materials Program (MSMAG).

REFERENCES

- [1] C.H. Back, et al, J Phys D: Appl Phys 53 (36), 363001 (2020)
- [2] A. Yadav et al, Nature 530 198 (2016)
- [3] S. Das et al, Nature 568 368 (2019)
- [4] I. Luk'yanchuk et al, Nature Comm 11 2433 (2020)
- [5] P. Fischer et al, APL Materials 8 010701 (2020)
- [6] P. Fischer and H. Ohldag, Report on Progress in Physics 78 094501 (2015)
- [7] M. H. Seaberg, et al, Phys Rev Lett 119 067403 (2017)
- [8] N. Kent et al, Nature Comm 12 1562 (2021)

2:00 PM *EL13.08.02

Imaging Magnetic Skyrmions and Perpendicular Domains under Voltage Control in Metallic Multilayers and 2D Materials. Massimo Ghidini^{1,2,3}; ¹University of Parma, Italy; ²Diamond Light Source, United Kingdom; ³University of Cambridge, United Kingdom

X-ray Photoemission electron microscopy and Magnetic Force Microscopy permit to image strain-coupled ferroelectric and ferromagnetic domains with submicron spatial resolution, thus revealing novel magnetoelectric effects in multiferroic heterostructures.

Here, we employ these complementary techniques to demonstrate voltage manipulation of skyrmions and perpendicular domains in magnetic multilayers and 2D materials overlying PMN-PT ferroelectric substrates. The resulting local magnetoelectric effects include transition from worm-like to skyrmion states, stripe domain displacement, nucleation/annihilation of isolated skyrmions and local magnetisation reversals.

2:30 PMBREAK

3:30 PM EL13.08.03

Electrical Tuning of Spin-Wave Transport in Magnetic Insulators Hossein Taghinejad^{1,2} and James G. Analytis^{1,3}; ¹University of California, Berkeley, United States; ²Kavli Energy NanoScience Institute, United States; ³Lawrence Berkeley National Laboratory, United States

Spin-waves have recently gained popularity to replace electrons as carriers of information in emerging computing and signal processing technologies. Collective excitations of magnetic materials promise low-power operation and potentially faster data processing in a wide range of materials including insulators, which have traditionally been employed as only passive elements in the mainstream microelectronic technology. However, controlling the transport of spin-waves often requires the use of an external magnetic field, a major drawback that has hindered its widespread use in practice. Here, we introduce an all-electrical approach for full control over the transport of spin-waves in the archetype magnetic insulator Yttrium Iron Garnet (YIG), eliminating the use of external magnetic field. In our study we employ the spin-Hall physics at the interface of a heavy metal with YIG for the excitation and detection of spin waves at room temperature. We will discuss the potential applications of our developed technique for the design of practical devices based on spin-waves.

3:45 PM EL13.08.04

Enhancement of Spin-Orbit Torque in Pt/Co/HfO_x Heterostructures with Voltage-Controlled Oxygen Ion Migration Shuo Wu, Tianli Jin, Funan Tan, Ching Ian Ang, Gerard Joseph Lim and Wensiang Lew; Nanyang Technological University, Singapore

Spin-orbit torque (SOT) induced magnetization switching and SOT modulation have been intensely pursued and developed in recent years for efficient spintronic devices. Research has shown that the magnetic anisotropy of ferromagnet (FM) layers can be modified via inducing surface charges or orbital occupancy by interfacing with an oxide layer. Moreover, voltage-controlled oxygen migration can reduce the energy barrier for magnetization switching. The electric-field-driven interfacial oxygen mobility can affect both the SOT strength and sign. However, more research on the oxidation effects at the interfaces of the voltage-controlled magnetism in FM/oxide systems needs to be investigated. In this work, we report the enhancement of damping-like field and SOT efficiency of up to 60% and 23%, respectively, in perpendicularly magnetized Pt/Co/HfO_x heterostructures over Pt/Co system at an optimal thickness of 2 nm HfO_x. We further verify this enhanced SOT by applying voltages across the Pt/Co/HfO_x structure, which allows the O²⁻ migration from HfO_x to the Co layer. By using voltage-controlled oxygen ion modulation of interfacial oxidation, we show that the gate voltage affects not only coercivity and anisotropy fields but also the SOT efficiency at room temperature. Our work promotes the SOT enhancement and modulation by oxidation effects for energy-efficient spintronic devices.

SESSION EL13.09: Magnetoelectric Sensors and Actuators II

Session Chairs: Tianxiang Nan and Eckhard Quandt

Wednesday Afternoon, November 29, 2023

Hynes, Level 2, Room 201

4:00 PM *EL13.09.01

Simulation of Magnetoelectric Sensors in Inhomogeneous Magnetic Fields Mohsen Samadi, Julius Schmalz, Mesut Ömür Özden, Giuseppe Barbieri and Martina Gerken; Kiel University, Germany

Thin-film magnetoelectric (ME) sensors have the potential for room-temperature, magnetic-shielding-free measurement of a variety of biomagnetic fields from magnetocardiography over deep-brain stimulation signals (DBS) to magnetomyography [1, 2]. Approaches for modelling and simulation of the behavior of different types of magnetoelectric sensors are discussed. Besides the standard excitation with homogeneous magnetic fields, inhomogeneous magnetic-field excitation is considered as found in biomedical applications.

As a first sensor type, cantilever sensors based on strain-coupled thin-film magnetostrictive and piezoelectric layers and their response to inhomogeneous magnetic fields are reviewed [3]. A linear material model is used to calculate the small-signal behavior of sensors at the working point. The elastic, magnetic and electric properties are included in a coupled finite-element-method (FEM) simulation. Second, the magnetic-field response of electrically-modulated magnetoelectric cantilever sensors is investigated [4]. These sensors are electrically excited and operate in a mechanical mode with bending in the short cantilever direction (U-mode). They exhibit a high-quality factor and a promising limit of detection in the pico-Tesla range. It is demonstrated that for specific sensor dimensions and clamping structures a homogeneous response is obtained across the sensor. As a third sensor type, surface-acoustic-wave (SAW) magnetic-field sensors are considered. Our previous results [5] are extended to include microstructuring of the delay line to realize phononic crystals. It has been shown that resonances appear due to the acoustic-crystal structure [6, 7] and here their suitability to magnetic-field sensing is investigated. For all three types of sensors FEM simulation models and results are discussed.

In the next part of the talk, a multiscale simulation approach is introduced for a full system simulation including magnetoelectric sensors, a human head model and electric-dipole excitation to model deep-brain stimulation (DBS). Due to the thin layers in the sensor structure as well as the intricate structure of the brain with different types of tissues this is a highly challenging task. The head model is implemented based on MRI data [8]. Since mesh management is crucial for successfully running simulations, the three-dimensional model is extrapolated and morphological operations are used for filtering and smoothing. The trade-off between surface idealness and performance needs to be considered. The complexity is increased stepwise by starting with a simple three-shell model and proceeding to an increasing number of compartments and more detail. With the multiscale model we calculate electromagnetic field propagation through the head and the magnetoelectric sensor response. The combined calculations allow for the investigation of field concentration effects and inhomogeneous sensor excitation in a realistic geometry, secondary-source effects due to conductivity, as well as field effects in the human head caused by the sensor system.

Acknowledgment:

This work was supported by the German Research Foundation (DFG) through the Collaborative Research Centre CRC1261.

References:

- [1] E. Elzenheimer et al., MDPI Sensors 22, 1018 (2022). <https://doi.org/10.3390/s22031018>
- [2] S. Zuo et al., IEEE Trans Biomed Circuits Syst. 14(5), 971-984 (2020). <https://doi.org/10.1109/TBCAS.2020.2998290>
- [3] M.-Ö. Özden et al., AIP Adv., 10(2), 025132 (2020). <https://doi.org/10.1063/1.5136239>
- [4] J. Schmalz et al., MDPI Sensors 23(11), 5012 (2023). <https://doi.org/10.3390/s23115012>
- [5] J. Schmalz et al., MDPI Sensors 20(12), 3421 (2020). <https://doi.org/10.3390/s20123421>
- [6] A. Khelif et al., Phys. Rev. B, 81(21), 214303 (2010). <https://doi.org/10.1103/PhysRevB.81.214303>
- [7] Y. Liu et al., J. Appl. Phys. 124, 145102 (2018). <https://doi.org/10.1063/1.5040069>
- [8] Y. Huang et al., Neuroimage 140, 150-162 (2016). <https://doi.org/10.1016/j.neuroimage.2015.12.019>

4:30 PM EL13.09.02

Negligible Magnetic Losses at Low Temperatures in Liquid Phase Epitaxy Grown Y₃Fe₅O₁₂ Films Alexandria Will-Cole¹, James L. Hart², Valeria Lauter³, Alexander Grutter⁴, Carsten Dubs⁵, Morris Lindner⁶, Timmy Reimann⁷, Nichole Valdez¹, Charles Pearce¹, Todd Monson¹, Judy Cha², Don Heiman^{6,7} and Nian Sun⁶; ¹Sandia National Laboratories, United

Yttrium iron garnet ($\text{Y}_3\text{Fe}_5\text{O}_{12}$, YIG) has a unique combination of low magnetic damping, high spin wave conductivity, and insulating properties that make it a highly attractive material for a variety of applications in the fields of magnetism and spintronics. While the room temperature magnetization dynamics of YIG have been extensively studied, there are limited reports correlating the low temperature magnetization dynamics to the material structure or growth method. Here we investigate liquid phase epitaxy grown YIG films and their magnetization dynamics at temperatures down to 10 K. We show there is negligible increase in the ferromagnetic resonance linewidth down to 10 K which is unique when compared with YIG films grown by other deposition methods. From the broadband ferromagnetic resonance measurements, polarized neutron reflectivity, and scanning transmission electron microscopy, we conclude that these liquid phase epitaxy grown films contain negligible rare-earth impurities present, specifically the suppression of Gd-diffusion from the $\text{Gd}_3\text{Ga}_5\text{O}_{12}$ substrate into the $\text{Y}_3\text{Fe}_5\text{O}_{12}$ film, and therefore consequently insignificant magnetic losses attributed to the slow relaxation mechanism. Overall, liquid phase epitaxy YIG films have a YIG/GGG interface that is 5 times sharper and has 10 times lower ferromagnetic resonance linewidths below 50 K than comparable YIG films produced by other deposition methods. Thus, YIG films grown by liquid phase epitaxy are ideal for low temperature experiments/applications that require low magnetic losses, such as quantum transduction and manipulation via magnon coupling. SNL is managed and operated by NTESS under DOE NNSA contract DE-NA0003525.

SESSION EL13.10: Magnetolectric Sensors and Actuators III
Session Chairs: Tianxiang Nan and Eckhard Quandt
Thursday Morning, November 30, 2023
Hynes, Level 2, Room 201

8:30 AM *EL13.10.01

Ferroics, Multiferroics and Magnetolectrics: Reconsidering New Paths to Large Transduction, Ultra-Low Power Sensors and Giant Energy Conversion Peter Finkel, Margo Staruch, Thomas R. Mion and Konrad Bussmann; Naval Research Laboratory, United States

The ability to tune both magnetic and electric properties concomitantly in magnetolectric (ME) composite heterostructures, consisting of magnetostrictive and piezoelectric phases coupled through strain with orders-of-magnitude larger ME coupling coefficient than single-phase multiferroics due to additional functionalities and makes them very promising in many applications and devices [1,2]. This has generated a revived interest in multiferroics, and is projected to play a critical role in next-generation applications ranging from transducers, tunable inductors, gyrators, magnetic sensors to high-frequency filters and communication devices. In this talk we highlight different approaches to achieve maximum ME coupling in heterostructures of magnetostrictive films deposited on domain-engineered relaxor ferroelectric single crystals. Much work has been done over the past decade to maximize the magnetolectric (ME) coupling coefficient, α_{ME} , the figure of merit for these composites that can be enhanced through deliberate choice of materials as well as carefully controlling the interface. For the piezoelectric phase, relaxor ferroelectrics have attracted much attention recently due to a piezoelectric coefficient an order of magnitude larger than conventional lead zirconate-titanate [3] especially in proximity to morphotropic phase boundary. In the ME heterostructures we demonstrated that by exploiting the large ferroelectric phase transitional strain in piezoelectric substrate, the converse magnetolectric coupling coefficient is expected to be greatly up to 4x enhanced as compared to linear piezoelectricity [4,5]. In this presentation, the impact of this enhancement will be examined and a path for utilization of this phenomenon in ME composites will be discussed. Magnetolectric (ME) resonators are of significant interest for next generation near-dc magnetic field sensors, as the direct coupling of highly magnetostrictive (FeCo- or FeGa-based alloys) and piezoelectric phases (AlN) enables high magnetic field sub-nT sensitivity with exceptionally low operational power requirements. This talk highlights several programs within the Materials Science & Technology Division at US Naval Research Laboratory focused on the investigation and understanding physics of these ferroic and multiferroic materials, and how current research presents another opportunity to advance acoustic transduction devices, magnetic sensors and electrically small antennas.

References:

1. R. Ramesh and N.A. Spaldin, Nat. Mater. **6**, 21–29 (2007).
2. J.M. Hu, Z. Li, L.Q. Chen, and C.W. Nan, Nat. Comm. **2**, 553 (2011).
3. Finkel et al Sci. Rep. **5**, 13770 (2015)
4. M. Staruch et al., Applied Physics Letters **105**, 152902 (2014)
5. M. Staruch et al., Sci. Rep. **6**, 37429 (2016)

9:00 AM EL13.10.02

Voltage Control of Exchange Coupling: A Novel Way to Switch MRAM Devices Bhagwati Prasad¹, Akash Surampalli¹, Rajesh V. Chopdekar², Alan Kalitsov², Lei Wan², Jordan Katine², Derek Stewart² and Tiffany Santos²; ¹Indian Institute of Science, India; ²Western Digital Corporation, United States

Traditional memory devices based on spintronics leverage electric current to ingeniously regulate the direction and movement of electrons' spin, albeit at the expense of high energy consumption and limited device durability [1, 2]. As a result, with the increasing demand for faster, smaller, and extremely energy-efficient electronic devices, the pursuit of magnetism controlled by voltage has notably intensified. This field offers the potential to create ultra-low-power, non-volatile memory solutions for future computing systems [3, 4]. In this context, we present our latest research on magnetism controlled by voltage via voltage-controlled exchange coupling (VCEC) [5, 6]. To explore the control of exchange coupling through an electric field, we have fabricated magnetic heterostructures with varying thicknesses of Ru and Ir spacer layers. In these layered structures, two ferromagnets (free and reference layers) possessing perpendicular magnetic anisotropy are separated by a non-magnetic Ru and Ir spacer layer. This separation creates an oscillatory interlayer exchange coupling (IEC) as the Ru or Ir layer's thickness varies, as predicted by the RKKY theory. To quantify the VCEC effect, a bias field is applied across the MgO layer, and resistance-magnetic field loops are measured while a DC bias voltage is in effect. This results in a visible gating effect in the minor loops of resistance-magnetic field plots, thus demonstrating the manipulation of exchange interactions between the free and reference layer via an applied electric field. In this way, we demonstrate modulation of the interlayer exchange coupling with the Ru and Ir spacer layers using non-ionic liquid gating such as MgO [6]. These findings provide a route for modifying the resistance states of spintronic devices, thereby paving the way for the creation of a new generation of energy-efficient computing devices.

References

- [1] Wong, H-S. Philip, and Sayeef Salahuddin. "Memory leads the way to better computing." *Nature Nanotechnology* 10.3 (2015): 191-194
- [2] Song, Cheng, et al. "Recent progress in voltage control of magnetism: Materials, mechanisms, and performance." *Progress in Materials Science* 87 (2017): 33-82.
- [3] Prasad, Bhagwati, et al. "Ultralow voltage manipulation of ferromagnetism." *Advanced materials* 32.28 (2020): 2001943.
- [4] Heron, J. T., et al. "Deterministic switching of ferromagnetism at room temperature using an electric field." *Nature* 516.7531 (2014): 370-373.
- [5] Kossak, Alexander E., et al. "Voltage control of magnetic order in RKKY coupled multilayers." *Science Advances* 9.1 (2023): eadd0548
- [6] Kalitsov, A. and Prasad, Bhagwati. "Voltage-controlled interlayer exchange coupling magnetoresistive memory device and method of operating thereof" *US Patent: US 11049538 B2* (June, 2021)

9:15 AM EL13.10.03

Proving the Suitability of Polymer-Based Magnetolectrics for Spintronic Applications Pedro Martins¹, Senentxu Lanceros-Mendez² and Rui Carvalho¹; ¹Universidade do Minho, Portugal; ²BCMaterials, Basque Center for Materials, Applications and Nanostructures, Spain

The rapid advancement of technology has generated significant requirements for electrical energy to power electronic devices. A pivotal aspect of this technological progress, for sensors, actuators, and memory devices, involves harnessing the spin of electrons in electronics, known as spintronics. However, a considerable portion of the electric power utilized in spintronics is dissipated as heat through the Joule effect (3–5% of the energy: thousands of millions of dollars annually). Consequently, there is a pressing need to explore novel approaches to develop energy-efficient devices, making it a prominent research topic within the realm of spintronics.

To address concerns regarding energy efficiency and the control of spin states, alternatives to the energy-consuming external magnetic field have been explored: the spin-polarized current injection. However, this approach still generates heat, negatively impacting the overall power efficiency of the device. In this scope, the utilization of applied voltages represents a promising strategy to reduce energy requirements. Materials with magnetolectric (ME) properties have emerged as leading contenders for future spintronic advancements, as their magnetization and ferromagnetism can be controlled by an electric field.

By incorporating an additional magnetolectric (ME) layer into the conventional three-layer spin-valve spintronic structure, it becomes possible to create electrically tunable spintronic

devices. This is achieved by exploiting the interface between the ME layer and the ferromagnetic-free layer. The introduction of this ME layer brings about a significant reduction in power consumption, estimated to be two orders of magnitude lower when compared to traditional devices. In the broader context of the global technological landscape, which is witnessing the rapid and widespread implementation of revolutionary advancements such as Industry 4.0, the Internet of Things, and digitalization, the production of ME materials is facilitated by additive manufacturing tools. These tools not only enable the efficient manufacturing of ME materials but also ensure safety during the production process, productivity, reduced time requirements, miniaturization, and sustainability. Among the different & available ME materials, polymer-based ME materials have been specifically selected to demonstrate their suitability for spintronic applications, due to their flexibility, high ME coupling, and printability, making them ideal for integration into spintronic devices. In particular, P(VDF-TrFE) (poly(vinylidene fluoride-trifluoroethylene)) has been selected as the piezoelectric matrix material due to its exceptional piezoelectric response, which is the highest among all polymers ($d_{33} \approx 30$ pC/N). Three different types of magnetostrictive fillers were incorporated into the polymer matrix: CoFe_2O_4 nanoparticles, Fe_3O_4 nanoparticles, and NdFeB microparticles. Results show that an AC electric field of $10 \text{ V/f} \approx 13 \text{ MHz}$ applied on samples with 20 wt.% of magnetic filler produced magnetic fields of $\approx 8 \text{ Oe}$ in all three composites, that correspond to converse ME coefficients of 4.1, 4.4, and 6.5 mG.cm.V^{-1} , respectively for P(VDF-TrFE) composites with NdFeB, Fe_3O_4 and CoFe_2O_4 fillers. CoFe_2O_4 fillers induced the highest converse ME coefficient due to their highest magnetostriction (≈ 250 ppm) Such performance holds promise for spintronic (low field sensing and memory applications) once the generated magnetic fields are greater than the ones needed for recently reported spin-valve structures (0.4 Oe).

9:30 AM EL13.10.04

2.87 GHz SAW Delay Lines for Efficient Spin Control of NV⁻ Centers Bin Luo¹, Andreas Winkler², Hagen Schmidt², Benyamin Davaji¹, Derek Bas³, Michael McConney³, Michael Page³, Beaver Nathaniel¹, Paul Stevenson¹ and Nian Sun¹; ¹Northeastern University, United States; ²Leibniz Institute for Solid State and Materials Research, Germany; ³Air Force Research Laboratory, United States

Motivation

Owing to long coherence time, high fidelity and easy optical initiation and readout of quantum states tuned by magnetic excitations over a broad temperature range, NV⁻ centers are intriguing solid-state platforms for quantum computing, communication, information processing and sensitive non-invasive nanoscale magnetic sensors. The SAW delay line driven spin wave enabled by magnon-phonon interactions exhibits superior properties of high-power efficiency, low noise and small footprint, leading to efficient voltage control of NV⁻ center and quantum transduction between hybrid quantum systems. In this work, we present a 2D finite element (FEM) model for a fabricated SAW delay line with S11 minima at 2.87 GHz and ~ -10 dB insertion loss for NV center excitation. The consistency of S parameters between simulation and probing experiments makes the model prospective for SAW delay line design for chemical, biomedical, RF and quantum applications.

Methods

The transmission and receiving IDT Al electrodes with a fundamental mode of ~ 2.87 GHz were patterned on bulk LiNbO_3 substrate via laser lithography, e-beam lithography, e-beam metal evaporation and lift-off technique. The S parameters were measured by RF probes connected to a vector network analyzer. A 1:1 2D finite element model was built in COMSOL Multiphysics. The electrostatic module was combined with solid mechanics module to simulate piezoelectrically induced Rayleigh wave excited by SAW delay line under different attenuation conditions.

Results

The fabricated SAW delay line shows a low insertion loss of ~ -10 dB at 2.87 GHz, which is excellent to control the ground states of NV⁻ centers. The simulated S parameters agree well with probe measurement. The displacement and electric field profile demonstrate a high transmission between IDT electrodes. The increased mechanical damping results in decreased Sxy magnitude and diminished modulation of the SAW resonance peak ("triple transit echo") caused by reflections between the IDTs near fundamental mode.

9:45 AM EL13.10.05

Highly Cyclable Voltage Control of Magnetism in Cobalt Ferrite Nanopillars for Memory and Neuromorphic Applications Muireann A. de Hora¹, Aliona Nicolenco², Monalisha Peda³, Tuhin Maity⁴, Bonan Zhu⁵, Shinbuh Lee⁶, Zhuotong Sun¹, Jordi Sort³ and Judith L. Driscoll¹; ¹University of Cambridge, United Kingdom; ²Cidetic, Spain; ³Universitat Autònoma de Barcelona, Spain; ⁴Indian Institute of Science Education and Research Thiruvananthapuram, India; ⁵University College London, United Kingdom; ⁶DGIST, Korea (the Republic of)

Research in digital memory is growing with the increase in popularity of artificial intelligence, machine learning, Internet of Things, and Big Data. This in turn has caused an energy demand that has triggered innovation towards non-volatile memory technologies that do not require continuous power supply. Magnetic memory is a promising non-volatile technology for storing data, but conventional magnetic memory concepts use electrical current to control magnetic properties (i.e. through electromagnets or spin-torque effects) and this can lead to significant energy loss by heat dissipation. On the other hand, tuning the properties of magnetic materials by voltage-driven ion migration (magneto-ionics) gives potential for energy-efficient, non-volatile magnetic memory and neuromorphic computing.

Our study shows large changes in both the magnetic moment at saturation (m_s) and coercivity (H_c), of 34% and 78%, respectively, in an array CoFe_2O_4 (CFO) epitaxial nanopillar electrodes (~ 50 nm diameter, ~ 70 nm pitch, and 90 nm in height) with applied voltage of -10 V in a liquid electrolyte cell. Furthermore, a magneto-ionic response faster than 3 s and endurance $> 2,000$ cycles are demonstrated. The response time is faster than for other magneto-ionic films of similar thickness, and cyclability is around two orders of magnitude higher than for other oxygen magneto-ionic systems. Using a range of characterisation techniques, the magnetic switching is shown to arise from modulation of oxygen content in the CFO. Also, the highly cyclable, self-assembled nanopillar structures were demonstrated to emulate various synaptic behaviours, exhibiting non-volatile, multilevel magnetic states for analog computing and high-density storage. Overall, CFO nanopillar arrays offer potential to be used as interconnected synapses for advanced neuromorphic computing applications.

10:00 AM EL13.10.06

Imaging of Voltage-Controlled Switching of Magnetization in Highly Magnetostrictive Epitaxial Fe-Ga Microstructures on PMN-PT Maite Goirienea^{1,2}, Zhuyun Xiao^{3,4}, Rachel Steinhart⁵, Victor Estrada³, Nobumichi Tamura⁴, Rajesh V. Chopdekar⁴, Alfredo García-Arribas², Abdón Sepúlveda³, Darrell Schlom^{5,6}, Rob N. Candler^{3,6} and Jeffrey Bokor^{1,4}; ¹University of California, Berkeley, United States; ²University of the Basque Country, Spain; ³University of California, Los Angeles, United States; ⁴Lawrence Berkeley National Laboratory, United States; ⁵Cornell University, United States; ⁶California NanoSystems Institute, United States

The magnetoelectric behavior of epitaxial Fe-Ga microstructures on top of (001)-oriented PMN-PT piezoelectric substrate is investigated under magnetic electron microscopy (XMCD-PEEM). Additionally, micron-scale strain distribution in PMN-PT is characterized by X-ray microdiffraction and examined with respect to the results of the Fe-Ga magnetoelectric switching. The magnetic reorientation is found to be strongly correlated with the size, shape and crystallographic orientation of the microstructures. In the case of square-shaped structures, size dictates the degree of influence of the strain distribution on both the initialization of the ground state and on the dynamics of the magnetic reorientation during application of voltage. On the other hand, the case of the elliptical microstructures demonstrates the importance of the orientation of the long axis with respect to the crystallographic directions of the PMN-PT, which leads to completely different magnetic responses. This study demonstrates that engineering highly magnetostrictive epitaxial microdevices is possible. It further elucidates that voltage-induced actuation can be largely tuned to achieve the desired type of magnetic switching ranging from vortex circulation reversal, domain wall motion, to a large rotation of magnetization. Because of the outstanding properties of the investigated material system, the reported findings are expected to be of great interest for the realization of next-generation energy-efficient magnetic memory, sensing and actuation devices.

10:15 AM EL13.10.07

Hidden Order in Cr_2O_3 and $\alpha\text{-Fe}_2\text{O}_3$ as a Predictor for (anti-)Magnetoelectricity Xanthe H. Verbeek, Andrea Urru and Nicola Spaldin; ETH Zürich, Switzerland

With first-principles calculations of Cr_2O_3 and its iron-based analog, $\alpha\text{-Fe}_2\text{O}_3$, we show that the different magnetoelectric effects in these materials result from the ordering of hidden magnetic multipoles [1]. Starting from the established connection between ferroically-ordered magnetic quadrupoles and the linear magnetoelectric effect in Cr_2O_3 , we explore the presence of additional multipoles. We reveal for the first time anti-ferroically ordered magnetic multipoles in both Cr_2O_3 , and isostructural $\alpha\text{-Fe}_2\text{O}_3$, in which the global inversion symmetry is preserved by the different magnetic dipolar ordering. Using symmetry considerations, we can relate each of these multipoles and their ordering to linear, quadratic, and cubic (anti-) magnetoelectric effects, where in an anti-magnetoelectric effect the induced moments are ordered antiferromagnetically in the unit cell. We confirm the predicted induced moments using first-principles calculations, showing the lowest response in $\alpha\text{-Fe}_2\text{O}_3$, a centrosymmetric magnetic material, to be a linear anti-magnetoelectric effect, revealing the presence of the magnetoelectric coupling despite the preserved global inversion symmetry. Our results demonstrate the existence of hidden magnetic multipoles leading to local linear magnetoelectric responses, even in centrosymmetric magnetic materials, and broaden the definition of magnetoelectric materials by including those showing such local magnetoelectric responses.

References:

[1] X. H. Verbeek, et al., arXiv:2303.00513

<!--[if !supportLineBreakNewLine]-->

SYMPOSIUM EL14

Diamond Electronics, Devices and Sensors
November27 - December7, 2023

Symposium Organizers

Philippe Bergonzo, Seki Diamond Systems
Chia-Liang Cheng, National Dong Hwa University
David Eon, Institut Neel
Anke Krueger, Stuttgart University

Symposium Support

Platinum

Great Lakes Crystal Technologies

Gold

Element Six

Silver

Qnami AG
SEKI DIAMOND SYSTEMS

Bronze

Applied Diamond, Inc.
DIAMFAB
Fraunhofer USA, Inc.

* Invited Paper
+ JMR Distinguished Invited Speaker

SESSION EL11.04/EL14.06: Joint Session II: Diamond Transfer Doping and MOSFETs
Session Chairs: Srabanti Chowdhury and Hiroshi Kawarada
Tuesday Morning, November28, 2023
Hynes, Level 2, Room 210

10:15 AM *EL11.04/EL14.06.01

New Developments in Transfer-Doped and Accumulation Channel Diamond Electronic Devices [David A. Moran](#); University of Glasgow, United Kingdom

Transfer-doping of diamond has proven to be an attractive alternative to substitutional doping of diamond for the production of high-performance diamond electronic devices, such as Field Effect Transistors. The process, which relies in a low/negative electron affinity chemical termination of the diamond surface e.g. with hydrogen, combined with the application of a surface electron acceptor material of sufficiently high electron affinity, generates a high carrier density, shallow, sub-surface 2D hole gas that may be exploited as a conductive channel in several device applications.

Significant progress has been made recently in the further development of transfer doping processes in diamond, virtually eliminating previous issues such as inherent temperature and atmospheric sensitivity and associated instability. Through engineering of surface acceptor materials, charge mobility in the diamond has also seen significant improvement, leading to significant reduction in material resistivity. Alternative chemical surface terminations of diamond have also more recently demonstrated additional routes for the production of high performance electronic devices.

This presentation will attempt to provide an overview of these recent and exciting developments in the diamond electronic devices, and speculate on future directions and the potential impact of this accelerating area of research.

10:45 AM EL11.04/EL14.06.02

MOSFETs on (111) Highly Oriented Polycrystalline 1-Inch Diamond Substrate [Yukihiro Chou](#)¹, [Fuga Asai](#)¹, [Kosuke Ota](#)¹, [Atsushi Hiraiwa](#)¹, [Yoshiki Nishibayashi](#)² and [Hiroshi Kawarada](#)^{1,1}; ¹Waseda University, Japan; ²Sumitomo Electric Industries, Ltd., Japan

We fabricated 2DHG diamond MOSFETs on a (111) highly oriented polycrystalline 1-inch diamond substrate and confirmed that the devices correctly functioned as a FET. The area of the 1-inch substrate is about 55 times larger than that of conventional 3mm square substrate. In this work, we fabricated 220 devices on the 1-inch diamond substrate, and the yield rate was about 95 percent. We found that the yield rate on the 1inch substrate tends to be much higher than that on the 3mm square substrate.

Diamond has outstanding characteristics as a semiconductor, such as wide band gap (5.5 eV), high thermal conductivity (22 W/cmK), and high breakdown field (10 MV/cm). Therefore,

diamond is expected to be applied to the next generation's RF amplifier and power device. However, a problem in fabricating diamond devices is the low yield rate due to the small substrate size. In this work, we fabricated 2DHG diamond MOSFETs on the polycrystalline 1-inch diamond substrate, and we found that the yield rate was greatly improved. The highly oriented (111) polycrystalline substrate was fabricated by Sumitomo Electric Industries, Ltd. All the devices on the 1-inch substrate are double-finger structure. Firstly, source and drain electrodes were deposited Ti/Pt/Au (20 nm/ 30 nm/ 90 nm). After H-termination and isolation, 200 nm of Al₂O₃ was deposited as the gate insulator. After that, 300 nm of Al was deposited as the gate electrode. 80 percent of all the devices have the gate length L_G = 5 μm and the others have L_G = 2 μm. There are 3 kinds of source-drain length L_{SD}, 10 μm, 15 μm, and 20 μm. Also, there are 3 kinds of total gate width W_{GT}, 1 mm, 2 mm, and 3 mm. The highest maximum drain current density was obtained from the device of L_G = 2 μm, L_{SD} = 10 μm, and W_{GT} = 1 mm at V_{GS} = -40 V and V_{DS} = -40 V, and the result was 151 mA/mm. For all the devices that correctly functioned as a FET, the drain current density was in the range of 100 mA/mm to 150 mA/mm. The decrease in current density was observed as the gate width expanded, but it is assumed that the effect of the grain boundary on the devices is not serious. About 95 percent of yield rate was achieved in this work, and the distribution of the devices that did not function were impartial on the 1-inch substrate. This is because, thanks to the substrate size, photoresists uniformly coated the whole substrate in the fabricating process. In this work, we fabricated 2DHG diamond MOSFETs on a (111) highly oriented polycrystalline 1-inch diamond substrate and confirmed that the devices correctly functioned as a FET. The highest maximum drain current density was 151 mA/mm, and the yield rate of devices on the 1-inch substrate was greatly improved. Fabricating 2DHG diamond MOSFETs on polycrystalline 1-inch diamond substrate is possible and it contributes to the yield rate improvement.

11:00 AM EL11.04/EL14.06.03

Normally-Off H-Diamond Field Effect Transistors with ZrO₂/Zr Stack GateFeiWang; Xi'an Jiaotong University, China

A normally-off hydrogen-terminated diamond (H-diamond) field effect transistor (FET) with ZrO₂/Zr stack gate was realized via electron beam evaporation. The threshold voltages range from -0.4 V to -2.5 V with different gate lengths, indicating ZrO₂/Zr could deplete the hole carrier densities at channel area, due to the difference of work function between Zr and hydrogen-terminated diamond and the fixed positive charges in ZrO₂ layer. The on/off ratio and subthreshold swing of device 2 are found to be 10⁹ and 128 mV/decade, respectively. The device exhibits a relatively low drain-source leakage current of 10⁻⁸ mA/mm and an effective mobility as high as 652 cm²/Vs is obtained at V_{GS} = -2 V. The 2 μm-gate length device shows a maximum drain current density of -74 mA/mm. This work reveals a simple fabrication process for ZrO₂/Zr/H-diamond FET, which will provide an alternative approach for low power device applications.

11:15 AM EL11.04/EL14.06.04

Gate Leakage Suppression of Normally-OFF Diamond FET by Hybrid GateGenqiangChen and Hong-XingWang; Xi'an Jiaotong University, China

Diamond is a promising material to develop high-power and high-frequency device owing to its wide-band gap, high carrier mobility and extremely high thermal conductivity. Nevertheless, diamond can release its potential on the basis of its n-type doping. Luckily, diamond field-effect transistor was survived from its hydrogen termination, which can induce a two-dimension hole gas (2DHG). However, the present hydrogen-terminated diamond field-effect transistor based on 2DHG, naturally demonstrates normally-on operation, which goes against energy saving and safety. Normally-OFF FET is critical for logical circuit and switch systems. Metal-semiconductor (MES) FET with Schottky gate is a good approach to achieve normally-OFF hydrogen-terminated (C-H) diamond FETs, but the drawback is large gate leakage. In this work, a MOS-MES hybrid gate diamond FET (HGFET) with normally-OFF operation and low gate leakage current were attained. The hybrid gate was realized by adding nanoparticles Al₂O₃(nano-Al₂O₃) between Al/C-H diamond interface. The MES formed by Al/C-H plays a role of realizing normally-OFF operation. Of 57 devices, 100% shows normally-OFF operation and the threshold voltage varied from -0.2 V to -1.2 V. The MOS gate Al/nano-Al₂O₃/C-H diamond is used to lower the gate leakage current, which is 10²-fold lower than that of FET without nano-Al₂O₃. The HGFET was expected to be a member in FET community.

11:30 AM EL11.04/EL14.06.05

High Quality Al₂O₃/(111) (OH)-Terminated Diamond Interface for MOSFETs FabricationPietroArgenton¹, MartinKah¹, MarineCourte², NicolasRouger², DavidEon¹ and JulienPernot¹; ¹University Grenoble Alpes, CNRS, Grenoble INP, Institut Néel, France; ²Université de Toulouse, LAPLACE, CNRS, INPT, France

The efficiency of power devices is critical nowadays for the rise of renewable energy. Wide-bandgap semiconductors, such as silicon carbide (SiC) and gallium nitride (GaN), have advantages over silicon due to their high breakdown electric field and high-temperature operation. However, p-channel wide-bandgap FETs have poor performance compared with their n-channel counterparts due to low hole mobility, which leads to a high ON resistance and high conduction loss. This has constrained the production of complementary circuits with integrated n-channel and p-channel transistors. Diamond is a wide-bandgap material that has a bulk intrinsic hole mobility very high respectively to SiC and GaN, which makes it promising for use in high-mobility p-channel transistors. Due to the high optical phonon frequency and high acoustic phonon velocity of diamond, the number of phonons that participate in carrier scattering is small. Having all the others wide band gap semiconductors characteristics like high electric field, high breakdown voltage and high thermal conductivity also makes diamond attractive for power applications.

Most diamond power metal-oxide-semiconductor field-effect transistors (MOSFETs) have been fabricated using H-terminated diamond surfaces (and afterwards the surface transfer doping) with their unique properties of two-dimensional hole gas (2DHG). The downside of this concept comes from the close proximity of the negatively charged surface acceptors with the 2DHG, the carrier mobility is limited by surface impurities, and increasing the carrier concentration dramatically decreases the hole mobility. Moreover, the negative charges cause a positive shift in the threshold voltage, leading to normally ON characteristics.

In this work we try to find an alternative by realizing p-type OH-terminated diamond surface, taking advantage of the fact that applying a negative potential to a MOS stack leads to an accumulation regime of holes on the diamond surface. However, this happens only if the Fermi level is not pinned due to interface states. Therefore, a good interface quality between diamond and oxide is needed. We realized a p-type diamond with a boron concentration approximately 10¹⁷ atom/cm³ and a thickness of 0.5 μm on (111) EDP substrate followed by a OH-termination using a wet vapour annealing^[1]. We have then realized some metal-oxide-semiconductor capacitors (MOSCAP) on top of it and studied their behaviour.

The frequency-dependent capacitance-voltage (C-V) characteristics were examined from depletion to accumulation regimes. The latter one was clearly observed with a very small leakage current. Moreover, we reached accumulation regime around 0V which can lead to a realization of a MOSFET with normally OFF characteristics with very high current in ON state, thanks to the 2DHG. With these promising results, we finally fabricate MOSFETs using the same procedure as MOSCAPs.

In the first part of this presentation, the method will be described in details. Then, the C-V characteristics will be reported and deeply analysed. Lastly, we will show and discuss the first results obtained regarding the MOSFETs and comparing them with finite element simulation as well.

References

[1] Ryo Yoshida et al, "Formation of atomically flat hydroxyl-terminated diamond (111) surfaces via water vapor annealing", Applied Surface Science, 458 (2018)

11:45 AM EL11.04/EL14.06.06

Normally-Off Hydrogen-Terminated Diamond FET with High Temperature ALD Grown HfO₂DevanshSaraswat, MohamadaliMalakoutian, KellyWoo and SrabantiChowdhury; Stanford University, United States

Diamond is one of the best candidates for high-power, high-frequency applications due to desirable properties like high breakdown electric field (10 MV/cm), high carrier mobility (3800 cm² V⁻¹s⁻¹ for holes and 4500 cm² V⁻¹s⁻¹ for electrons) and high saturation velocity (>10⁷ cm/s) [1].

Due to the difficulty in doping by conventional methods, the two-dimensional hole gas (2DHG) layer below the hydrogen-terminated diamond surface has been widely explored for fabricating field effect transistors. Prior studies have reported sheet density in the range of 10¹²-10¹⁴ cm⁻² [2] and mobility of 50-200 cm² V⁻¹s⁻¹ [3] for the 2DHG, including integrated CMOS operation at high temperatures[4]. For FET fabrication, it is essential to choose a dielectric that can minimize the gate leakage current as well as preserve the 2DHG in the channel. Various dielectrics such as Al₂O₃, ZrO₂, AlN and MoO₃ have been used as a gate dielectric for diamond HFETs. HfO₂ is a widely used high-k dielectric material due its superior dielectric properties, high breakdown field and large band offsets (ΔE_c=2.29 eV and ΔE_v=1.98 eV) with respect to H-terminated diamond [5]. In this work, Al₂O₃ and HfO₂ were compared as gate dielectric for HFETs. Normally off operation with two orders of higher current was achieved with high-temperature atomic layer deposition (ALD) grown HfO₂ in comparison with Al₂O₃ counterpart, as the gate dielectric.

For device fabrication, a (100) CVD-grown diamond substrate was used. The sample was first oxygen terminated by boiling in a 3:1 mixture of H₂SO₄ and HNO₃ at 200°C for 30 minutes. Then, hydrogen termination was performed in a microwave plasma CVD reactor at 850°C. This was followed by photolithography and oxygen plasma treatment for device isolation. Then, Ti/Pt/Au adhesion pads were deposited using e-beam evaporation. This was followed by gold deposition on hydrogen terminated regions to form the source and drain ohmic contacts. Subsequently, a 10 nm thick HfO₂ layer was deposited at 300°C using ALD. Then, Al/Au gate metal contact with a gate length (L_G) of 1.5 μm was formed. The gate to drain distance (L_{GD}) varied from 1.75 μm to 3.25 μm. Finally, source and drain contacts were opened using a 6:1 buffered oxide etchant (BOE) wet etch.

After device fabrication, DC output characteristics were measured using a probe station. A maximum drain output current of 2.05 mA/mm was achieved for a V_{GS}=-4V. Gate leakage current ≤ 10⁻⁶ mA/mm and a current on/off ratio of 10⁷ were measured. A maximum transconductance (g_m) of 2.06 mS/mm was obtained at V_{GS}=-2V. The threshold voltage was determined to be -1.2V, indicating a normally-off performance. In contrast, our Al₂O₃-based FETs showed poor performance which requires further investigation.

The normally-off behavior in this device is likely due to the decrease in the upward band bending at the H-diamond surface. This is possibly a result of the desorption of acceptor species during the high-temperature ALD growth. Dielectrics grown at high temperatures are thermally more stable, making the device suitable for high-temperature applications. Further

improvement in the device performance can be possible by exposing the substrate to a NO₂ gas environment and by using multiple dielectric layer stacks to improve the channel mobility. The current results show the potential of using high-temperature ALD grown HfO₂ for achieving normally-off behavior in diamond HFETs[6].

References:

1. C. J. H. Wort et al, Mater. Today, vol. 11, Issues 1-2, pp. 22–28, 2008.
2. H. Sato et al, Diamond and Related Materials, Volume 31, 2013.
3. C.E. Nebel et al, Diamond and Related Materials, Volume 13, Issues 11–12, 2004.
4. C. Ren et al, ACS Applied Electronic Materials, Oct. 2021.
5. Z. Ren et al, AIP Advances 11, 035041 (2021).
6. J. W. Liu et al, Appl. Phys. Lett. 103, 092905 (2013).

SESSION EL11.07/EL14.10: Joint Session IV: Diamond Wafers and Wafer Bonding
Session Chairs: Philippe Bergonzo and Stephen Goodnick
Wednesday Morning, November 29, 2023
Hynes, Level 2, Room 210

10:00 AM *EL11.07/EL14.10.01

Two-Inch High Quality Diamond Heteroepitaxial Growth on Sapphire Seong-Woo Kim; Orbray Co, Ltd, Japan

Diamond semiconductors, owing to their superior properties compared to SiC and GaN, can be used to develop high-end applications, such as power devices, high frequency devices, quantum devices, and sensors. However, the inch-scaled diamond wafer is essential. In this study, Two-inch-diameter high-quality diamond (001) layers were grown on sapphire (11-20) A-plane misoriented substrate. Step-flow growth in diamond is realized thanks to misoriented substrate, and releases tensile strain in diamond layer. Consequently, even if microneedle technique^[1] is not used, without breakage, diamond layer naturally was delaminated from the sapphire substrate. The FWHM of (004) and (311) X-ray rocking curves of the diamond layer grown on sapphire substrate misoriented by 7° towards [1-100] direction were 75 and 140 arcsec, respectively, the lowest ever.

In this study, results on 3 types of high-end applications will be discussed. One of them is the world largest diamond detector with the dimensions of 20 mm ' 20 mm ' 0.5 mm was fabricated from a 30 mm ' 30 mm heteroepitaxial diamond wafer. The device demonstrated a nuclide discrimination capability for ¹³³Ba, ¹³⁷Cs and ⁶⁰Co based on the pulse-height difference. The electrode was used as a cathode to apply -500 V bias voltage. The anode on another side was connected to a charge sensitive preamplifier. The anode was maintained at ground potential. The output signal from the preamplifier was acquired with a digitizer. A digital trapezoidal filter was applied to the waveforms to obtain pulse height spectra.

[1] S.-W. Kim et al., Appl. Phys. Lett. 117, 202102 (2020).

10:30 AM *EL11.07/EL14.10.02

Wide Bandgap Material Transfer as a Flagship Technology for Future High Power Devices Julie Widiez, Guillaume Gelineau, Jérémie Chrétien, Cédric Masante, Alexandre Moulin, Vladimir Prudkovskiy, Nicolas Troutot, Emmanuel Rolland, Patrice Gergaud, Denis Mariolle, Sophie Barbet, Lucie Corbin, Vincent Amalbert, Pierrick Gilles, Frédéric Milesi, Frédéric Mazen and Lucie Le Van-Jodin; CEA-LETI, France

Today's environmental requirements for energy efficiency call for better management of electrical energy with minimum leakage at all levels: from DC phone chargers to power transmission via electrical vehicles. Wide bandgap (WBG) semiconductors are better suited for high-voltage and low-loss power devices than traditional Si-based power devices. The most commonly used are SiC, GaN and diamond with bandgap values of 3.2 eV, 3.4 eV and 5.5 eV respectively. However, the challenge of producing these competitive materials economically and efficiently remains. For example, the fabrication of SiC substrates is very energy-intensive, since it is carried out at 2400°C, i.e. 1000°C higher than for Si. To cite another example, the size of diamond substrates today is no more than a few square millimeters, while 300 mm Si wafers are on the market, limiting the appeal of such a material.

The ability to transfer only a thin layer of high-quality WBG material on a substrate that offers either the advantage of being less expensive or the advantage of its own function (thermal, electrical or insulating...) is therefore very interesting. The Smart Cut™ process combines an ion implantation with a bonding step and allows to create a structure that otherwise could not be made using deposition techniques. Relatively new direct covalent bonding techniques now make it possible to relax the draconian characteristics imposed on surfaces and substrates to enable such bonding with materials renowned for their outstanding properties. This opens up new possibilities in terms of assembly.

Significant improvements in electrical performance have been achieved by combining the advantages of a polycrystalline substrate with very low resistivity and a high-quality 4H-SiC transferred layer [1, 2]. However, the H⁺ ion implantation used for the Smart Cut™ process leads to electrical deactivation and partially disorders the material. We report studies of healing and reactivation mechanisms of a transferred 4H-SiC thin film over a wide range of temperatures. After 950°C (splitting temperature), the thin SiC layer is still insulating. A 1300°C anneal allows the material to fully relax and reorganize with no further evolution beyond this temperature. The dopant reactivation takes place at higher thermal budgets. The transferred layer then recovers the donor doping level and electrical conductivity after 1700°C [3].

We also develop the transfer of IIa diamond onto larger and less expensive substrates [4]. The two key technological steps of the Smart Cut™ process (ion implantation and bonding) are studied:

A simplified process using a single ion implantation step at high temperature has been developed [5]. The diamond material after such implantation is studied in terms of sp²/sp³ ratio (XPS), hydrogen concentration (SIMS) and exfoliation capability.

A wide range of bonding conditions are studied: direct bonding (manual, Surface Activated Bonding - SAB -), metal bonding (Ti, Au...) with a special care on bonding parameters (the flatness, the coefficient of thermal expansion and the roughness values). This part is particularly difficult because of the remarkable properties of diamond: its low coefficient of thermal expansion and its hardness make surface preparation and adhesion very challenging.

Acknowledgements: This work has received funding from the Key Digital Technologies (KDT) under Grant Agreement No 101007237 and from the French Agence Nationale de la Recherche (ANR) under the grant ANR-19-CE05-0025.

[1] S. Rouchier, et al., *Mat. Sci. Forum*, vol. 1062, pp. 131–135, 2021

[2] W. Schwarzenbach et al., *ICICDT conference*, pp. 55–56, 2022

[3] G. Gelineau et al., *Materials Science Forum*, vol. 1089, pp. 71–79, 2023

[4] C. Masante et al., *Diamond and Related Materials*, Vol. 126, 2022

[5] C. Masante et al., *27th Hasselt Diamond Workshop*, March 2023.

11:00 AM *EL11.07/EL14.10.03

Low-Temperature Direct Bonding of Diamond—Approach for Fabricating Low-Thermal-Resistance Widegap Devices Naoteru Shigekawa¹, Ryo Kagawa¹, Jianbo Liang¹, Yasuo Shimizu², Yutaka Ohno² and Yasuyoshi Nagai²; ¹Osaka Metropolitan University, Japan; ²Tohoku University, Japan

Characteristics of semiconductor electron devices such as output powers are limited by their temperature rise due to Joule heating in operation (self-heating effects). Device structures with the lowest thermal resistance are, consequently, one of the most important topics in R&D for advanced devices, especially for devices with widegap semiconductors that handle high output powers with high frequencies. Diamond is assumed to be the ideal material as heat spreader because of its high thermal conductivity and excellent electrical properties. In this presentation, we describe results that we obtained by directly bonding of diamond to Si and GaN and discuss the future prospective of direct bonding of diamond. We used surface activated bonding (SAB) technologies, in which two wafers are bonded after removing native oxides on their surfaces by irradiating them with fast atom beams of Ar (surface activation process). In SAB, bonding process is completed without heating bonded wafers in most cases, i.e., junctions of semiconductors with different coefficients of thermal expansion (CTE) can be fabricated.

We bonded a high-pressure high-temperature (HPHT) diamond (001) wafer and a Si (100) wafer using SAB. We found that the diamond/Si junction withstood a 1000-°C annealing in spite of a large difference in CTEs between diamond and Si. A high-resolution TEM observation revealed that a poly crystalline SiC intermediate layer was formed at the bonding interface after the annealing, which was assumed to play a role of reducing impacts of the difference in CTEs.

We prepared a GaN/diamond junction by bonding a GaN (0001) surface grown on Si (111) wafer to a diamond (001) wafer and removing the Si (111) wafer for the growth of nitride. We annealed the GaN/diamond junctions at temperatures up to 1000 °C and found that the junctions were also tolerant against such a high-temperature annealing.

Recently we transferred an AlGaIn/GaN epi layer to diamond using SAB and subsequently fabricated HEMTs. Ohmic contacts on nitride were formed by an annealing at 800-°C after bonding to diamond. The temperature rise of the GaN-on-diamond HEMTs was found to be lower than that of on-Si HEMTs with the same nitride structure. The results imply that direct bonding of diamond is promising for fabricating low-thermal-resistance semiconductor devices, especially after transferring active device layers to diamond wafers.

Acknowledgement—This work was supported by the Feasibility Study Program of New Energy and Industrial Technology Development Organization (NEDO) and JSPS KAKENHI. TEM samples were fabricated at The Oarai Center and at the Laboratory of Alpha-Ray Emitters in IMR under the Inter-University Cooperative Research in IMR of Tohoku University. The observation of the TEM samples was supported by Kyoto University Nano Technology Hub. AlGaIn/GaN epi layers were grown and supplied by Air Water Inc.

11:30 AM EL11.07/EL14.10.04

Direct-Bonded Diamond Membrane Heterostructures for Quantum and Electronic TechnologiesXinghanGuo¹, MouzheXie¹, AnchitaAddhya¹, AveryLinder¹, UriZvi¹, TanviD. Deshmukh¹, YuziLiu², IanN. Hammock¹, ZixiLi¹, ClaytonT. DeVault^{2,1}, AmyButcher¹, AaronEsser-Kahn¹, DavidAwschalom^{1,1,2}, NazarDelegan^{2,1}, PeterC. Maurer^{1,2}, F. JosephHeremans^{2,1} and AlexanderA. High^{1,2}; ¹The University of Chicago, United States; ²Argonne National Laboratory, United States

Diamond has unique material properties well suited for a broad range of quantum and electronic technologies. However, heterogeneous integration of diamond with other materials remains a challenge, mainly due to limited heteroepitaxial growth of single-crystal diamond. Here, we discuss a directly bonded single-crystal diamond membrane technique that enables a wide variety of materials integration, including bonding diamond to silicon, fused silica, sapphire, thermal oxides, and lithium niobate. Our direct bonding process combines diamond overgrowth, membrane transfer, and dry surface functionalization, resulting in minimal contamination for high yield and scalable integration. We have demonstrated direct-bonded diamond membranes with thicknesses as thin as 10 nm, and observe a sub-nanometer interfacial region. We demonstrate the use case for integrating these direct-bonded membranes for high-quality nano-photonics, and total internal reflection fluorescence (TIRF) microscopy applications. The demonstrated process provides a key advance in the necessary toolkit needed to realize heterogeneous diamond-based hybrid systems for quantum and electronic technologies.

* The authors acknowledge funding from DOE QNEX, NSF AM-2240399, NSF OMA-1936118, NSF OMA-2121044, NSF OMA-2016136, and NSF DMR-2011854.

11:45 AM EL11.07/EL14.10.05

Diamond Integration on GaN HEMTs: Overcoming the Challenges for Device-Level Thermal ManagementMohamadaliMalakoutian, RohithSoman, KellyWoo, AnnaKasperovich, JeongkyuKim and SrabantiChowdhury; Stanford University, United States

In the realm of higher frequency devices, where the gain is of utmost importance, the effective management of heat becomes crucial to maintain Power Added Efficiency (PAE) [1]. Ensuring efficient heat removal necessitates minimizing the thermal boundary resistance (*TBR*) between the heat source and the heat spreader, as well as establishing a low thermal resistance path to the heat sink [2]. The integration of diamond near the hot spot holds excellent potential due to its exceptional thermal properties. By incorporating diamond, heat can be effectively spread, thereby enhancing the heat transfer coefficient [3, 4]. The integration of diamond onto GaN HEMTs poses significant challenges, regardless of whether a diamond-first or device-first approach is employed.

In the diamond-first approach, the primary challenge lies in diamond surface roughness, which imposes a limitation on gate length <2 μm through lithography, non-uniformity in the diamond etching, and contacts/pads damage after diamond etching. To address this issue, we have implemented a polishing technique through ion-milling, achieving a surface smoothness of less than 10 nm RMS roughness before carrying out E-beam lithography, and developed a more selective etching process using O₂/SF₆ mixture in RIE. Additionally, a slanted etching technique was developed for rough diamond surfaces that starts with a 2 μm opening at the top and achieves a gate footprint of less than 100 nm, suitable for X- to W-band applications.

In the device-first approach, two key challenges arise: gate dielectric leakage (2-10 mA/mm) and ohmic loss ($R_c=1.4 \Omega/\text{mm}$, $R_{sh}=250 \Omega/\text{mm}$). To overcome gate leakage, we have modified the gate metal stack from Au/Ni to Mo and employed a low-temperature (LT) diamond growth technique at 350-400°C [5], effectively reducing the leakage to <1 μA/mm. As for ohmic loss, we have successfully tackled it by incorporating a thicker N+ regrown region and using a 400°C diamond growth temperature ($R_c=0.24 \Omega/\text{mm}$, $R_{sh}=225 \Omega/\text{mm}$). These combined measures have proven to be effective solutions in mitigating gate dielectric leakage and reducing the ohmic loss for higher current capabilities ~ 1 A/mm.

We have successfully integrated LT diamond on GaN HEMTs using the above-mentioned approaches. By implementing the all-around diamond scheme and connecting the top diamond to the heat sink through diamond vias, the channel thermal resistance (R_{th}) was reduced by 34% from 6.9 to 4.6 K.mm/W, realizing a higher heat transfer coefficient from the channel. This integration resulted in no dispersion (pulsed I-V at 400 ns gate pulse) and lower channel temperature (T_{ch}) compared to the case without diamond. With low *TBR* (3-5 m²K/GW) and high thermal conductivity (*TC*:300-1000 W/m/K depending on the grain size and thickness), the average and peak T_{ch} dropped by 35% (200 to 130°C at 25 W/mm, measured by I-V thermometry) and over 50% (120°C at 20 W/mm, measured by thermoreflectance imaging), respectively [6]. Our technique not only addresses thermal management challenges for GaN-based power amplifiers but is also compatible with other technologies such as InP, Ga₂O₃, SiC, and Si. Proper thermal management can enhance the device's reliability and lifetime while providing a higher power at higher frequencies.

[1] A. Nigam et al., AIP Advances, 7 (8), 085015, 2017.

[2] D. Shoemaker et al., IEEE Trans. Compon. Packaging Manuf. Technol., 11 (8), 1177-1186, 2021.

[3] M. Malakoutian et al., Cryst. Growth Des., 21 (5), 2624–2632, 2021.

[4] M. Malakoutian et al., ACS Appl. Mater. Interfaces, 13 (50), 60553–60560, 2021.

[5] M. Malakoutian et al., Adv. Funct. Mater., 32, 2208997, 2022.

[6] R. Soman et al., IEDM, San Francisco, CA, USA, 30.8.1-30.8.4, 2022.

SESSION EL14.01: Keynote Session
Session Chairs: Philippe Bergonzo and Alastair Stacey
Monday Morning, November 27, 2023
Hynes, Level 2, Room 209

10:30 AM *EL14.01.01

Engineering Diamond Sensors for Quantum MetrologyAniaBleszynski Javich; University of California, Santa Barbara, United States

Defects in diamond constitute a versatile and powerful platform for quantum sensing and simulation. Here I discuss nitrogen-vacancy (NV) center-based imaging experiments aimed at revealing condensed matter phenomena on the nanoscale. I also discuss developments in diamond growth, NV formation, and diamond nanofabrication of NV-containing sensing platforms that enable sensing experiments with higher spatial resolution and improved sensitivity, as well as progress towards entanglement-assisted metrology with strongly interacting spins in diamond.

11:00 AM *EL14.01.02

Diamond/Graphene (carbon sp³-sp²) Heterojunctions for Neuromorphic Electronic DevicesKenjiUeda; Waseda University, Japan

Diamond/graphene (carbon sp³-sp²) interfaces have attracted much attention because they are sources of various interesting electronic phenomena. Many theorists suggest hybrid structures of diamond and graphene exhibit interesting electronic characters, however there are only limited experimental reports on electronic characters of carbon sp³-sp² interfaces.

Recently, we newly found that diamond/graphene heterojunctions became photo-controllable memristors (photomemristors), which are optically controllable memory-resistors with both photo-switching and memory functions [1, 2]. The junctions also showed characteristic response to optical pulses, and brain mimic memory functions, that is, change of photomemory time from shorter to longer memory time depending on irradiated numbers of optical pulses [3]. These behaviors are analogous to transitions from short to long-term memory states of biological synapses. In addition, arrays using the diamond/graphene junctions can function as special types of image sensors which have selective memory function of optical information depending on the relative importance of the data as human brains perform.

These results suggest the diamond/graphene (C sp³-sp²) junctions are promising for fabricating novel neuromorphic visual information processing systems that are modulated by specific interests.

Ref.:

[1] K. Ueda et al., J. Mater. Res., 34 (2019) 626.

[2] K. Ueda et al., Appl. Phys. Lett. 117 (2020) 092103.

11:30 AM *EL14.01.03

Diamond Material Pave the way for the Next Generation of Neuronal Implants Lionel Rousseau¹, Emmanuel S. Scorsone², Gaëlle Lissorgues¹, Patrick Poulichet¹, Olivier François¹, Blaise Yvert³, Clement Hebert³, Serge Piccaud⁴ and Julie Zhang⁴; ¹Université Gustave Eiffel - ESIEE Paris, ESYCOM UMR 9007, France; ²Université Paris-Saclay, CEA, France; ³GIN, France; ⁴Sorbonne Université/INSERM UMR_S968/ CNRS UMR 7210, France

Brain Computer Interface (BCI) offers a way to restore neuronal dysfunction due to degenerative diseases or accidents. Thus, it becomes possible to restore vision with retinal implant or to offer a way for tetraplegic to control a robot by thinking with electrodes implanted in the cortex and recently to do a digital bridge for paraplegic patient to stand-up and walk. But today these systems are limited by their insufficient stability. Neuronal implants require to operation during 10 years of lifetime, and collect data 24/7 and for 10 hours or more every day. But after several months of implantation, some modification can appear such as swelling of the passivation polymers thus inducing current leakage, or degradation of the electrode material.

With the last development of diamond growth process, it is now possible to integrate this material in micro and nano fabrication process as a standard material to produce sensors or neuronal implants. Diamond properties are very attractive for medical application. Diamond is a biocompatible material and it has no native oxide, so there is no degradation when the structure is placed in water or harsh environment. Diamond is also a high density material, so there are no species that can migrate inside diamond. In addition, conductive diamond, boron doped diamond (BDD) has a wide electrochemistry window that allow to give possibility to inject more current compare to classical metallic electrode.

We have developed a specific process to achieve a very thin full diamond implant combine conductive diamond for the electrode and intrinsic diamond as protective layer. With this structure we take advantages and strength of conductive and intrinsic diamond to achieve an hermetic implant. To validate our full diamond implant, we have done electrical characterizations impedance Spectroscopy and Cyclic Voltammetry. In-vivo experiments have been conducted on several set-ups to record Visual Evoked Potential and Auditory Evoked Potential, assessing the proper functionality of our implants.

To demonstrate their stability, we developed an accelerate long life set-up. The devices placed on PBS solution at a temperature of 77°C. Follow Arrhenius law, at this temperature acceleration factor is around 16, that means for one month in solution, is equivalent to one year and 4 months. This set up is composed of hotplate, and aluminum piece where we placed a hermetic containers with Phosphate Bovine Solution (PBS) and samples. To control integrity of samples an impedance meter is used to record periodically impedance. This type of set-up is also answer at ethical issue and reduce number of animal experimentation.

With this ageing setup, we compared InterDigited Electrodes (IDE) composed of metallic IDE covered with either intrinsic diamond or polymer like SU8. After 29 weeks (around 9 years), diamond is more stable with a variation of 3 % at 1 kHz (frequency of interest for neurons recording), compared to SU8 with 50 % of variation.

Therefore, intrinsic and doped diamond are very attractive for the next generation of neuronal implants.

SESSION EL14.02: Superconductive Diamond Devices

Session Chairs: David Eon and Kenji Ueda

Monday Afternoon, November 27, 2023

Hynes, Level 2, Room 209

2:00 PM *EL14.02.01

Superconducting Diamond Microwave Resonators Georgina M. Klemencic, Jerome Cuenca, Thomas Brien, Soumen Mandal, Scott Manifold, Simon Doyle, Adrian Porch and Oliver A. Williams; Cardiff University, United Kingdom

Superconducting microwave resonators form the foundation of an increasing number of superconducting technologies for quantum information processing¹ and radiation detection.² A specific example is the Kinetic Inductance Detector (KID), which uses a high-Q resonator as a photon detector for purposes ranging from astronomy to security.³

In a KID, radiation is detected when an incoming photon breaks a Cooper pair which decreases the frequency of the microwave resonator. The relative size of this shift increases with the penetration depth of the material. Noise in the form of random fluctuations in the resonant frequency can occur due to two-level systems (TLSs), generally ascribed to dangling bonds in amorphous oxides that form at the surface of metallic superconductors. For practical applications, optimising for both sensitivity and signal-to-noise ratio, the superconducting material used for a microwave resonator should ideally have a high penetration depth and a low population of TLSs.

Here, I will present our results on a detailed characterisation of a $\lambda/2$ microwave resonator with a fundamental frequency of 409 MHz at 300 mK patterned from boron-doped nanocrystalline diamond (BNCD).⁴ We compare the observed resonant frequency to simulations based on the device geometry alone and show that the frequency is reduced by more than half, indicating a very large penetration depth enabled by the granularity of the material. I will also present early measurements of the effect of noise on this resonator and make a comparison to a single crystal equivalent device.

Our data show that BNCD is a good candidate for fabricating microwave resonators requiring a high kinetic inductance fraction. Knowledge of the penetration depth of a material is also vital for the design of low-frequency superconducting devices, including SQUIDS. Our results, therefore, pave the way for more complex superconducting circuits based on BNCD.

References

- [1] L. Grünhaupt, *et al. Nat. Mater.* **18** (2019): 816-819.
- [2] S. Doyle, *et al. J. Low Temp. Phys.* **151** (2008): 530-536.
- [3] S. Rowe, *et al. Rev. Sci. Instrum.* **87** (2016): 033105.
- [4] J. A. Cuenca, *et al. Carbon* **201** (2023): 251-259.

2:30 PM EL14.02.02

Reduction of Etching Damage and SQUID Operation of Single-Crystalline Diamond Josephson Junctions by Ridge Conduction Structure Yutaro Hashimoto¹, Chiyuki Wakabayashi¹, Yasuhiro Takahashi¹, Yoshihiko Takano², Minoru Tachiki², Shuichi Ooi² and Hiroshi Kawarada^{1,3}; ¹Waseda University, Japan; ²National Institute for Materials Science, Japan; ³The Kagami Memorial Research Institute for Materials Science and Technology, Japan

Josephson junctions (JJs) are weak junctions between two superconductors and have been applied to various devices such as transmon qubits and superconducting quantum interference devices (SQUIDs). SQUIDs are extremely sensitive magnetic sensors. Typical materials for JJs, such as Nb and Al, are weak against oxidation and abrasion. In contrast, superconducting boron (B)-doped diamond has high resistance to oxidation and abrasion. So, it is expected to be applied to robust and highly resistant to degradation superconducting devices.

The first SQUID using superconducting B-doped diamond was reported by S. Mandal[1]. This SQUID using nanocrystalline diamond consists of JJs with 250 nm to 100 nm linewidth weak links. The operating temperature was 400 mK at low magnetic field and 40 mK at high magnetic field, and the maximum voltage modulations (V_{p-p}) to magnetic field, which is a parameter related to magnetic sensitivity, was 0.35 μ V. While the first SQUID using single-crystalline diamond was constructed by JJs with a step edge structure[2]. Operating temperature and V_{p-p} of up to 2.6K and 1.1 μ V were reported for this type SQUIDs. Single-crystalline superconducting diamonds have different superconducting transition temperatures T_c depending on the growth orientation[3]. (001) B--doped diamond with low T_c (<4.2 K) grows on the step with 230 nm slope 50° produced by etching and regrowth of un-doped diamond, and the discontinuity with the heavily boron doped (B: $8 \times 10^{21} \text{cm}^{-3}$) (111) layer with high T_c (10 K) forms the step edge JJ. For operating temperatures above the liquid He temperature (4.2 K), it was necessary to fabricate JJs and SQUIDs using only the heavily B-doped (111) layer. SQUIDs consisting of trench-type JJs with the boundaries of discontinuous (111) sectors on trenches formed by focused ion beam (FIB) operated at 10 K and the maximum V_{p-p} was 4.0 μ V [4]. However, the trench shape formed by FIB was unstable, and it was difficult to obtain uniform JJs characteristics. Therefore, JJs with a single-step structure, consisting of a discontinuity in the heavily B-doped (111) layer deposited on top of a minute step of about 40 nm formed by reactive ion etching (RIE), has been proposed[4][5]. SQUID with single-step JJs is simple and highly reproducible, and operation at 9.5 K has been achieved. However, the V_{p-p} of single-crystal diamond SQUIDs was still small compared to SQUIDs made of other materials. Therefore, we have tried to improve V_{p-p} by increasing the normal resistance of JJs through JJ width miniaturization. For SQUIDs with single-step JJs, V_{p-p} increased significantly from 1.4 μ V to 47.7 μ V by miniaturizing JJs width from 15um to 5um. In the JJs miniaturized down to less than 5 um, however, the etching damage

became prominent, and V_{p-p} could no longer be expected to improve with this type of miniaturization.

In this study, we propose a new JJ structure, the ridge conduction structure, which is unaffected by etching damage. In ridge conduction structure JJs, first a narrow ridge structure is formed on the undoped substrate by RIE, and then the heavily B-doped diamond has been grown along the ridge. JJs with a 40 nm step as in single-step JJs are formed on top of the ridge structure. The flow path of superconducting current can be restricted on the ridgelines of (111) surface, because growth sectors different from (111) sector show low T_c superconducting on sidewalls without etching the B-doped layer. As a result, we confirmed the operation of JJs and SQUIDS with a minimum JJs width of 3 μm using this structure. Also, we confirmed that the ridge conduction structure reduces etching damage by reducing the residual resistance at 300 nm nanobridges with this structure.

2:45 PMBREAK

SESSION EL14.03: Quantum Sensing Platforms
Session Chairs: Ania Bleszynski Jayich and Cyril Popov
Monday Afternoon, November 27, 2023
Hynes, Level 2, Room 209

3:15 PM *EL14:03.01

Diamond Quantum Devices: Surface Termination Characterization and Methods Alastair Stacey, RMIT University, Australia

Diamond quantum devices are being increasingly explored for technological applications, with a common need being quantum defects - such as NV centres - very near to the diamond surface. These surfaces are known to host crystalline defects and a range of crystal termination chemistries, all of which can affect the near-surface defect centres in a variety of ways. In this talk we will present our efforts to quantify these defects, while simultaneously engineering the diamond surface with chemical and electronic functionalities.

3:45 PM EL14:03.02

Environmental Control of Shallow Nitrogen-Vacancy Sensors in Oxygenated (100) Diamond Surface Adam Gali^{1,2}, Anton Pershin^{1,2} and Peter Udvarhelyi^{1,2}; ¹Wigner Research Centre for Physics, Hungary; ²Budapest University of Technology and Economics, Hungary

Quantum sensing with nitrogen vacancy (NV) center in diamond is an emerging technology to detect nuclear spins and chemical species with nearly atomistic resolution. This is achieved by translating the magnetic- and electric-field fluctuations from the respective sources directly to an optical signal, detected by a change in the fluorescence intensity of the NV center. In this work, we develop realistic models of the diamond-solvent interfaces to elucidate new sensing applications for the NV center, which are based on the reversible variations in the surface potential. More specifically, we show that aqueous diamagnetic electrolyte solutions such as sodium chloride can be sensed by an increase of the spin relaxation time of near-surface NV-center ensembles. Our first principles calculations combined with interface modeling identify a critical role of the interfacial band bending which leads to a stabilization of fluctuating charges at the interface of an oxygen-terminated diamond. In addition, we demonstrate that aqueous environment enables to recover a contrast in the optically detected magnetic resonance experiment for the shallow NV centers at cryogenic temperatures. Both predicted phenomena were directly confirmed in experiments by observing the optically detected magnetic resonance and spin relaxation times of the ensemble and single NV-centers.

This work was supported by the National Research, Development, and Innovation Office of Hungary (NKFIH) grant No. KKP129866 of the National Excellence Program of Quantum-coherent materials project and the Quantum Information National Laboratory supported by the Ministry of Innovation and Technology of Hungary, the QUANTERA II MAESTRO project, and the Horizon Europe EIC Pathfinder QuMicro project (grant No. 101046911).

4:00 PM EL14:03.03

Pick-Flip-And-Place Hybrid Integration of a Single-Crystal Diamond Nanobeam with an Ensemble of Nitrogen-Vacancy Centers Ryota Katsumi^{1,2}, Kosuke Takada¹, Shun Naruse¹, Kenta Kawai¹, Daichi Sato¹, Takeshi Hizawa¹ and Takashi Yatsui^{1,2}; ¹Toyoashi University of Technology, Japan; ²The University of Tokyo, Japan

Nitrogen-vacancy (NV) centers in single-crystal diamond have been intensively studied for various quantum applications such as quantum sensing, quantum communication, and quantum simulation. To accelerate advances in quantum technologies based on NV centers, implementing micro/nanostructures in diamonds is essential. Because of recent advancements in etching technologies for diamond photonics, various nanophotonic structures, including photonic crystals, ring resonators, and disk resonators, have been successfully fabricated to date. Combining color centers in diamond with well-developed integrated photonics using hybrid integration techniques such as transfer printing provides a powerful route toward large-scale and multifunctional quantum devices. However, the existing etching technology for diamond photonics is inherently not compatible with reported hybrid integration approaches. For example, the bottom of a diamond nanostructure fabricated using angled etching is a triangular shape that makes it difficult to place on other substrates using conventional pick-and-place techniques. Therefore, it is significant to develop hybrid integration techniques with high yields for scalable diamond quantum photonics, irrespective of the sample structure. In this work, we propose "pick-flip-and-place" transfer printing for the hybrid integration of a diamond NV triangular nanobeam on chip in a deterministic manner. This approach provides a flat diamond-chip interface and allows for the integration of NV centers on chip with a near-unity success rate, irrespective of the width and shape of the diamond nanostructures. In experiment, we demonstrate that an integrated diamond nanobeam containing an ensemble of NV centers can function as a nanoscale quantum sensor. We believe that the proposed approach paves the way for the realization of scalable diamond quantum photonics assisted by cutting-edge integrated photonic technologies. We describe the basic procedure for the proposed nanofabrication and hybrid integration processes based on transfer printing. First, triangular nanobeam containing NV centers with high density (300 ppb) were prepared via vertical dry etching of diamond substrate, followed by a diamond undercut process based on angled etching. We then used transfer printing to select a suitable diamond nanostructure from the processed diamond substrate using a polydimethylsiloxane (PDMS) film with weak adhesion. This "weak" PDMS was flipped to lift off the nanostructure from the flipped film using a PDMS film with strong adhesion. This process allows for a flat interface between the diamond nanostructures and photonic chip, which is necessary for high-yield integration. Finally, the transferred diamond nanobeam was integrated by slowly peeling off the film onto an SiO₂ substrate, which is a common low-refractive-index material in integrated photonics for efficient light confinement in a waveguide. It is notable that we can perform hybrid integration irrespective of device structure and target materials by using the proposed "pick-flip-and-place" integration approach, enabling us to combine diamond quantum photonics and state-of-the-art photonic integration technology. To experimentally show that the fabricated device could function as a nanoscale quantum sensor, we performed optically detected magnetic resonance (ODMR) measurements on integrated NV centers. We confirmed an ODMR dip at a microwave frequency of 2.88 GHz with an ODMR contrast of ~0.006 and the linewidth of 7.8 MHz, which is comparable to those measured for bulk diamond. Therefore, we, for the first time, succeeded in the hybrid integration of a diamond nanobeam with an ensemble of NV centers on a chip for quantum sensing. The proposed approach based on transfer printing provides a deterministic route toward a scalable combination of diamond quantum photonics and cutting-edge integrated photonics technologies.

4:15 PM EL14:03.04

Characterization of Nitrogen Aggregation in CVD-Grown Diamond Eveline Postelnicu¹, Christine Jilly-Rehak¹, Lillian B. Hughes², Simon Meynell², Haoxue Yan¹, Tri Nguyen¹, Ania Bleszynski Jayich² and Kunal Mukherjee¹; ¹Stanford University, United States; ²University of California, Santa Barbara, United States

Understanding the mechanisms behind incorporation of dopants in chemical vapor deposition (CVD)-grown diamond is paramount to optimizing nitrogen vacancy (NV)-center based quantum devices and those for power electronics. The mechanism of nitrogen incorporation during CVD growth, and the resulting density and spatial distribution of the nitrogen are not well understood. In the context of limited incorporation of dopants such as nitrogen, there is evidence that features on the growth surface of diamond, like step bunching and hillocks, strongly segregate these impurities. A spatially resolved study of dopant distribution around these growth features would provide more insight into the impact on devices and point to strategies to obtain higher densities of dopants. To this end, we have studied nitrogen aggregation in hillocks formed in (100) homoepitaxial diamond grown via plasma-enhanced chemical vapor deposition (PECVD). [1] ¹⁵N enriched nitrogen gas was utilized during growth to form a near-surface, 7 nm-thick delta-doped ¹⁵N layer. Hillock growth has been studied extensively in diamond and has been attributed to a variety of mechanisms, including spiral growth on a screw dislocation core [2], heterogeneous nucleation at foreign crystallite sites [3] and penetration twins [4], as well as repeated 2D nucleation on miscut diamond substrates. [5] Meynell et al confirmed an inverse relationship between hillock density and substrate miscut and also observed nitrogen accumulation in hillock defects which correlated to a higher NV density. [6] Using panchromatic and spectrally resolved cathodoluminescence (CL) mapping, we observed greater NV emission from hillock edges in particular. We utilized nanoscale secondary ion mass spectrometry (nanoSIMS) to spatially resolve ¹⁵N concentration (measured as the ¹²C¹⁵N⁻ ion) with ~50-70 nm resolution, using a 20 pA Cs⁺ ion beam and a mass resolution greater than 9000 to resolve nearby isobaric interferences. NanoSIMS confirmed ¹⁵N aggregation in hillock edges, which we conclude directly correlates to an increase in NV center density. Previous broad-area SIMS measurements identified $2 \times 10^{16} \text{ cm}^{-3}$ ¹⁵N density in the uniform regions of the delta-doped layer. By comparing the local ¹²C¹⁵N⁻ counts per volume in the hillock defect to that of the uniform regions, we identified ¹⁵N density of $1.2 \times 10^{18} \text{ cm}^{-3}$ in the hillock defects, a nearly two order of magnitude increase compared to the delta-doped layer. We will show how volumetric SIMS scans using nitrogen as a tracer provide additional insight into the growth mechanism of these

surface features. Understanding these can lead to future NV-based device applications that intentionally harness dopant aggregation.

1. Hughes, L. B. et al. Two-dimensional spin systems in PECVD-grown diamond with tunable density and long coherence for enhanced quantum sensing and simulation. *APL Mater.* 11, (2023).
2. Tokuda, N. Homoepitaxial diamond growth by plasma-enhanced chemical vapor deposition. in *Novel aspects of diamond: from growth to applications* 1–29 (2014).
3. Van Enckevort, W. J. P. et al. Thermal chemical vapour deposition of homoepitaxial diamond: dependence of surface morphology and defect structure on substrate orientation. *Surf. Coatings Technol.* 47, 39–50 (1991).
4. Tsuno, T et al. Twinning Structure and Growth Hillock on Diamond (001) Epitaxial Film. *Jpn. J. Appl. Phys.* 33, 4039 (1994).
5. Lee, N. & Badzian, A. A study on surface morphologies of (001) homoepitaxial diamond films. *Diam. Relat. Mater.* 6, 130–145 (1997).
6. Meynell, S. A. et al. Engineering quantum-coherent defects: The role of substrate miscut in chemical vapor deposition diamond growth. *Appl. Phys. Lett.* 117, (2020).

4:30 PM EL14:03.05

Two-Dimensional Spin Systems in PECVD-Grown Diamond with Tunable Density and Long Coherence for Enhanced Quantum Sensing and Simulation Lillian B. Hughes¹, Simon Meynell¹, Zhiran Zhang¹, Weijie Wu², Emily Davis², Zilin Wang², Bingtian Ye², Norm Yao², Kunal Mukherjee³ and Ania Bleszynski Jayich¹; ¹University of California, Santa Barbara, United States; ²Harvard University, United States; ³Stanford University, United States

Solid-state spins constitute a powerful platform for quantum technologies. Dense ensembles of coherent spins provide a starting point for investigating strongly interacting spin systems in which novel, many-body states can arise with applications in both quantum simulation and sensing. Dimensionality plays a critical role in the nature of many-body states, with reduced dimensionality giving access to unique phases and phenomena such as interaction-driven localization or dipolar-driven spin squeezing. For sensing applications, a dense 2D layer of sensors in close proximity to a sensing target exhibits enhanced spatial resolution (set by the depth of the layer) compared to a 3D ensemble at the same volumetric density, while benefiting from either $1/\sqrt{N}$ classical sensitivity enhancements or entanglement-driven enhancements. Lastly, dense 2D ensembles could serve as a starting point for targeted, on demand formation of individual, optically resolvable defects at specific locations, such as inside nanostructures. Altogether, creating thin spin layers with tunable density is of intense current interest but has been minimally explored in solid-state electronic spin systems to date.

Defects in diamond, such as nitrogen-vacancy (NV) centers and substitutional nitrogen (P1 centers), are particularly promising solid-state platforms to explore. However, the ability to controllably create coherent, two-dimensional spin systems and characterize their properties, such as density, depth confinement, and coherence has been an outstanding materials challenge. We present a refined approach to engineer dense ($> 1 \text{ ppm} \cdot \text{nm}$), 2D nitrogen and NV layers in both (100) and (111) diamond using delta-doping during plasma-enhanced chemical vapor deposition (PECVD) epitaxial growth. We employ both traditional materials techniques, e.g., secondary ion mass spectrometry (SIMS), alongside NV spin decoherence-based measurements to characterize the density and dimensionality of the P1 and NV layers. We present depth confinement of the spin layer down to $< 4 \text{ nm}$, high (up to 0.74) ratios of NV to P1 centers, and reproducibly long NV coherence times which are dominated by dipolar interactions between the engineered P1 and NV spin baths. Altogether, the results of our joint materials and qubit-based approach are key elements in the engineering of solid-state-spin systems for the next generation of quantum technologies.^{1,2}

References

- [1] L. B. Hughes, Z. Zhang, C. Jin, S. A. Meynell, B. Ye, W. Wu, Z. Wang, E. J. Davis, T. E. Mates, N. Yao, K. Mukherjee, A. C. B. Jayich, “Two-dimensional spin systems in PECVD-grown diamond with tunable density and long coherence for enhanced quantum sensing and simulation.” *APL Mater.* 11, 021101 (2023) <https://doi.org/10.1063/5.0133501>
- [2] E. Davis, B. Ye, F. Machado, S. Meynell, T. Mittiga, W. Schenken, M. Joos, B. Kobrin, Y. Lyu, D. Bluvstein, S. Choi, C. Zu, A. C. B. Jayich, and N. Y. Yao, “Probing many-body noise in a strongly interacting two-dimensional dipolar spin system,” *Nat. Phys.* 19, 836-844 (2023). <https://doi.org/10.1038/s41567-023-01944-5>

4:45 PM EL14:03.06

Photophysics of the SnV Center in Diamond Philipp Fuchs¹, Soniya Nuchikkat¹, JanFait¹, JohannesGoerlitz¹, MichaelKieschnick², JanMeijer² and ChristophBecher¹; ¹Universität des Saarlandes, Germany; ²Universität Leipzig, Germany

For many applications in the field of quantum information processing stationary qubits are required, providing long-lived spin coherence and suitable level schemes for coherent control and efficient optical read out. Color centers in diamond, more specifically the group-IV-vacancy centers, have emerged as promising candidates among solid state qubits. They exhibit favorable properties such as individually addressable spins with long coherence times and bright emission of single, close to transform limited photons. Recent experiments have shown that the negatively charged tin-vacancy center (SnV) [1] combines long spin coherence times at conveniently achievable cryogenic temperatures ($> 1 \text{ K}$) [2,3] with truly lifetime-limited transition linewidths down to 20 MHz [1].

However, exploiting these properties requires active stabilization of the charge state, as the SnV center upon resonant laser illumination can be easily ionized to its double negative charge state (SnV^{2-}) which is optically inactive [3]. To prevent ionization, illumination with a second light field in the blue spectral range is required. We find that the charge stabilization requires the presence of additional defects in the vicinity of the SnV center such as di-vacancies [3] in the bulk or sp^2 defects on the surface [4].

Here, we propose a simple rate equation model for the SnV center photophysics that includes this ionization process. We apply the model to an extensive set of measurements on different SnV centers, along with a thorough characterization of the efficiency of our measurement setup. We conclude that a charge-stabilized SnV^- center is a nearly ideal single photon source in terms of quantum efficiency, since we can describe any reduced photon rate by ionization to the optically inactive SnV^{2-} charge state without assuming other non-radiative decay channels. We further discuss the occurrence of fluctuating background emission, its suppression via thermal oxidation in air atmosphere and the role of surface defects in the charge transition cycle.

References

- [1] T. Iwasaki et al., *Phys. Rev. Lett.* 119 (2017), 253601; J. Görlitz et al., *New J. Phys.* 22 (2020), 013048.
- [2] R. Debroux et al., *Phys. Rev. X* 11 (2021), 041041
- [3] J. Görlitz et al., *npj Quantum Inf* 8 (2022), 45.
- [4] A. Stacey et al., *Adv. Mater. Interfaces* 6 (2019), 1801449.

SESSION EL14.04: Poster Session
Session Chairs: David Moran and Mariko Suzuki
Monday Afternoon, November 27, 2023
Hynes, Level 1, Hall A

8:00 PM EL14.04.01

Disposable Electrochemical Biosensor for Ultrasensitive Detection of Salivary Cortisol on a Non-Covalently Modified Laser-Induced Graphene Surface for Stress Monitoring Atul Sharma, Alia Wolff, Ayanna Thomas and Sameer R. Sonkusale; Tufts University, United States

Monitoring stress indicators (such as cortisol) is crucial for understanding and managing the root cause of several cognitive, neurological, cardiovascular and endocrinological diseases. Cortisol negatively affects the regulation of various physiological processes such as carbohydrate metabolism and blood glucose levels. Long-term stress can disrupt homeostasis in the cardiovascular, renal, skeletal, and endocrine systems, leading to the development of chronic diseases [1,2]. Because of its central role, continuous monitoring of cortisol levels in the human body is critical for health and wellness. Current diagnostic techniques are complex and performed at centralized facilities by qualified specialists rather than at the site of therapy, which is critical for real-time monitoring. Electrochemical biosensors based on graphene's conductivity and flexibility are appealing in such contexts. Towards the goal of routine stress-level monitoring, this work realizes the design and development of an ultrasensitive and disposable immunosensor based on vertically aligned laser-induced-graphene (LIG) electrodes as a transducer surface for non-invasive salivary cortisol monitoring via differential pulse voltammetry (DPV) signal transduction mechanism. The LIG electrode was used due to its wide scalability, high electrochemical stability, increased number of reaction sites, efficient electrical conduction owing to the increased surface area and structurally more uniform alignment of the graphene layer conductivity, and low cost [3]. The LIG electrodes were fabricated using a laser ablation technique (in-house). Before use, the surface of the electrode was cleaned by cyclic voltammetry in 0.50 M sulphuric acid containing 0.10 M KCl as electrolyte. Later, the LIG electrode surface was chemically functionalized with a self-assembled monolayer of pyrene-NHS (1-Pyrenebutyric acid N-hydroxy succinimide) ester incorporating an NHS-activated functional group for the receptor (antibody) immobilization. Furthermore, a monoclonal antibody to

salivary cortisol (mAb) was incubated on the Pyr-NHS-LIG electrode surface and immobilized via peptide bond formation between the carboxyl terminal of the crosslinker and the amine terminal of the antibody. This step is followed by electrode passivation to incorporate an antifouling layer. LIG's structure and electrical conductivity were preserved by using the non-covalent functionalization of Pyr-NHS ester. Cortisol complexation with immobilized mAb-Cort resulted in ferri/ferro redox electrochemistry-mediated measurement. Under optimum experimental settings, the immunosensor performance exhibited a dynamic working range from 100 fg/mL⁻¹ to 10.0 ng/mL⁻¹ ($R^2 = 0.9982$) with a detection limit of 10.0 fg/mL⁻¹ for cortisol (n=3). The developed immunosensor was successfully deployed to assay human salivary cortisol and showed a strong correlation with established laboratory methods (e.g., ELISA). This offers great promise for point of care monitoring of diseases.

KEYWORDS: Laser induced graphene, Cortisol, Human Saliva, Electrochemical- Immunosensor, Pyrene-NHS ester, Stress monitoring

8:00 PM EL14.04.02

Reliable Formation of Diamond p-Type Channel by Additional Negative Ions Formed from Corona DischargeXueZhenJia¹, KentoNarita¹, KosukeOta^{1,2}, AkiraTakahashi¹, RyoukeYamamoto¹, AtsushiHiraiwa¹, TatsuyaFujishima² and HiroshiKawarada^{1,2,3}; ¹School of Fundamental Science & Engineering, Waseda University, Japan; ²Power Diamond Systems, Inc., Japan; ³The Kagami Memorial Laboratory for Materials Science and Technology, Waseda University, Japan

The hydrogen-terminated (C-H) diamond surface has been used in diamond MOSFETs for its p-type high conductivity[1][2]. So far, we have reported diamond MOSFETs using 2-dimensional hole gas (2DHG), which is induced by the surface dipole formed by hydrogen-carbon bonds. The negatively charged adsorbates are also considered to have an important role to obtain high surface conductivity[3]. In the fabrication of diamond MOSFETs, even if C-H surface is preserved, we noticed that the surface conductivity decreases after several device processing sequences, because of different ambient and high temperature processing condition. In this work, we developed the recovering method of conductivity by irradiating extra negative ions in air on the hydrogen-carbon (C-H) surface to enhance the current density of the C-H diamond surface. The low conductivity of C-H diamond substrate was improved successfully. This result indicates the necessity of negatively charged adsorbates on the C-H diamond surface. It also makes the fabrication of C-H diamond FET more reliable by intentionally introducing additional negative ion formed by corona discharge to the C-H diamond surface.

In this study, the surface of (001) undoped diamond was hydrogen-terminated. Ti/Pt/Au (30nm/20nm/100nm) was evaporated as source/drain electrodes to define the channel length. Before introducing additional negative ion, the current density was 8 mA/mm at $V_{DS} = 30$ V, with $L_{ch} = 5$ μ m, $W_{ch} = 70$ μ m, which is more than 1 order of magnitude below the current density of C-H diamond channel reported [4]. To increase the conductivity of C-H surface, we introduced a large amount of negative ion by corona discharge near the substrate surface to provide additional negative charge on the hydrogen-carbon surface for 30 min[5]. The change of current density over time was measured. With additional negative ion in the air, the current density increased rapidly from 9 mA/mm to 164 mA/mm in 30 min and saturated. Sheet resistance decreased from 656 k Ω /sq to 38k Ω /sq. The current density maintained the maximum for more than 3 days. All the experiment and measurement were performed in regular air.

The increase of current density indicated the amount of negative charge on the C-H surface has a great influence on the density of polarization-induced 2DHG. The desorption of negatively charged adsorbates in the device processing probably leads to a low density of 2DHG, which results in low conductivity of hydrogen-terminated surface. It takes more than several hours for negatively charged adsorbates to cover the surface. This low conductivity issue can be simply improved by introducing additional negative ion to the C-H surface. This process only takes about 30 minutes in air without using toxic gas such as NO₂. Introducing additional negatively charged adsorbates in the device fabrication process is recommended to secure the higher density of polarization-induced 2DHG, higher p-type conductivity and a higher yield of C-H diamond p-FET.

[1] H. Kawarada, Makoto Aoki, Masahiro Ito, Appl. Phys. Lett. 65(12): 1563–1565. (1994)

[2] H. Kawarada, Surface Science Reports. 26(7), 205-259 (1996)

[3] K. Hirama, H. Kawarada, H. Umezawa, et al., Appl. Phys. Lett., 92(11), 112107-1~112107-3 (2008)

[4] K. Kudara, H. Kawarada, et al., Carbon, 188, pp.220-228. (2022)

[5] D.K.Schroder, *Semiconductor Material and Device Characterization*, 3rd ed. John Wiley & Sons Inc., 2005, pp.438-439.

8:00 PM EL14.04.03

High Breakdown Voltage Diamond Schottky Barrier Diode with HfO₂/ Al₂O₃ Multilayer Field Plate StructureQiLi and Hong-XingWang; Xi'an Jiaotong University, China

Diamond Schottky barrier diodes (SBDs) have been studied by many researchers because of its high current, low turn-on voltage and fast switching frequency. However, the edge electric field crowding effect will lead to premature breakdown of SBD under large reverse voltage, which will result in large leakage current. There are some termination structures have been reported to improve the blocking capacitance, such as field plates (FP), junction termination extension (JTE), metal guard rings. Among those structures, FP is the most common structure because it can alleviate the electric crowding without reducing the forward current and increasing the turn-on voltage. Al₂O₃ has been used as FP of diamond SBD because of its large band offset for oxygen-termination diamond. The HfO₂ has a high dielectric constant (k) of 25-30 and can withstand higher voltage than Al₂O₃. However, due to the large positive fixed charge density in the bulk HfO₂, the barrier between HfO₂ and diamond is low.

In order to solve the weak points of single Al₂O₃ and HfO₂ FP, we fabricated a diamond SBD with HfO₂/Al₂O₃ multilayer FP. The k value of the HfO₂/Al₂O₃ multilayer was larger than that for single Al₂O₃. The leakage current of HfO₂/Al₂O₃ multilayer FP diamond SBD was always smaller than that of single oxide FP SBD. Compared with HfO₂ FP, there was a better interface between diamond and HfO₂/Al₂O₃ multilayer FP. And the diamond SBD has higher breakdown voltage than single oxide FP SBD. We also investigated the effect of annealing on this diamond SBD. The breakdown voltage was improved and the leakage current was reduced after annealing. These results show that the HfO₂/Al₂O₃ multilayer FP and annealing can effectively improve the reverse breakdown voltage of the diamond SBD, and the forward characteristics do not decrease significantly.

8:00 PM EL14.04.04

Carbon Ink Printed Flexible Glove-Based Aptasensor using Zinc Nanorods for Rapid and Point of Care Detection of Chikungunya VirusPradakshinaSharma; Jamia Hamdard, India

Printed electronic technologies have sparked interest worldwide because of their capacity to transcend the limitations of existing high-cost electronics based on the fabrication of various devices deploying flexible substrates. As a crucial component of flexible electronics, electrodes fabricated on soft, stretchable, and bendable substrates are significant. Hence this study demonstrates an electrochemical flexible substrate-based aptamer sensor for CHIKV antigen over an extensive range of concentrations. In brief, ZnO nanorods were chemically synthesized and characterized by FESEM, UV-Vis spectroscopy, FTIR analysis, and X-Ray Diffraction(XRD) providing biocompatibility to the biorecognition element called aptamer. The aptasensor showed a wide dynamic range (1ng/ml-10 μ g/ml), employing a voltammetric identification in the presence of 10mM methylene blue act as a redox-transition substance, with an estimated detection limit in the range of 1ng/ml and 25secs as its optimal response time. The sensor's applicability was also demonstrated by introducing CHIKV-Antigen into human serum samples. The built-in sensor has a shelf-life of more than a month. A portable platform for diagnosing CHIKV-Antigen has a fast response time and high sensitivity. Therefore, this allows for the diagnosis of CHIKV in a timelier manner, allowing for more effective treatment options.

8:00 PM EL14.04.05

Investigation of Intracellular Thermogenesis Dynamics using Mitochondria-Targeted Nanodiamond Quantum ThermometryYoobeenLee¹, KihoKim², DohunKim² and Jin SeokLee¹; ¹Hanyang University, Korea (the Republic of); ²Seoul National University, Korea (the Republic of)

Intracellular thermometry techniques provide valuable information into biological processes by detecting temperature variations within specific organelles under different physiological conditions. However, miniaturizing biocompatible thermometers to submicrometer sizes and attaching them to organelles pose significant challenges. In this study, we present a novel approach utilizing organelle-targeting nanodiamond quantum thermometry, using nitrogen-vacancy (NV) color centers, to monitor temperature changes during ATP generation within living human skin fibroblast cells. To enable this monitoring, we developed a microscopy system that integrates a coplanar waveguide-incubating chamber and a real-time particle tracking system, facilitating the tracking of nanodiamonds within cells while simultaneously measuring temperature. Using this system, we induced temperature rise based on the thermogenic response by inhibiting ATP synthesis, and measured the resulting changes in temperature within mitochondria, nucleus, and membrane. Our technique can achieve spatially resolved temperature measurements related to mitochondrial thermodynamic and gain insights into the distinct thermodynamic properties in specific organelles within cells.

8:00 PM EL14.04.06

Homoeptitaxial Diamond Growth Initiation on Smooth CMP Surfaces at Various Mis-Cut AnglesS Masaduzzaman and TimothyA. Grotjohn; Michigan State University, United States

Homoeptitaxial diamond growth by microwave plasma-assisted CVD is used to grow both doped and intrinsic epilayers of diamond for electronic and quantum applications. Often when different doping types or concentrations are desired, the deposition is done in different diamond deposition systems due to avoiding doping memory effects in the deposition system. This requires that the growth process be re-initiated when the sample is moved to a different deposition system. The initiation of the growth process has been shown to often have defects at the growth initiation boundary as evidenced by optical microscopy, photoluminescence and/or cathodoluminescence. This study aims to investigate the growth process at the initiation of the diamond deposition to improve the boundary between different doped epilayers. An objective in many applications is to have abrupt junction between diamond doped with different concentrations or types.

Experiments were performed on the growth initiation on single crystal diamond substrates with various mis-cut angles from the (001) surface. The mis-cut angle was varied from 0 to 4 degrees as determined by X-ray diffraction measurements. To prepare the smooth diamond surface before growth the substrates were chemical mechanical polishing (CMP) polished to achieve a surface roughness of less than 0.3 nm RA. The CMP process was done by polishing the diamond substrate with a slurry of boron carbide, potassium permanganate, and phosphoric acid at a rate of about 100 nm/hr. The surface roughness was measured with AFM. Prior to CMP the substrate was mechanically polished on a Scaife, and the surface was then plasma etched to remove about 2 μm of diamond that may have polishing damage.

The diamond deposition was performed with a hydrogen, methane, and carbon dioxide feed gas mixture that gives a growth rate of 2-6 $\mu\text{m/hr}$. The diamond deposition was done with only a short time between deposition system turn on and growth initiation. This short time is important to minimize any surface etching/roughening before the growth starts. The growth was allowed to proceed for short periods of time so that 1-2 μm of diamond or less were grown. When the short growth is finished the surface is examined with AFM, optical microscopy, and SEM to look for island growth and step-terrace growth features as a function of the mis-cut angle. Also diamond deposition runs are done under the same growth conditions for various times to see how the growth surface evolves at the start.

The work has observed the smooth surface getting rougher at the initiation of the growth. We will report on the evolution of the surface versus growth time and mis-cut angle. For small mis-cut angles island-like growth occurs and we will quantify the growth of the island size versus growth time. For larger mis-cut angles the transition to step-flow growth will be quantified in terms of terrace and step size evolution. The steps will also be analyzed in terms of step facet height and direction. We will also look at the implications of the growth initiation on doping spatial uniformity in the grown layer.

Acknowledgement: The Energy Frontier Research Center on Ultrawide Bandgap Materials (EFRC-UWBG) funded by the U.S. Department of Energy (DOE), Office of Science, Basic Energy Sciences (BES) division under award number DE-SC0021230.

<quillbot-extension-portal></quillbot-extension-portal>

8:00 PM EL14.04.07

Fabrication of Polymeric Microresonators Embedded with NV Color Centers in Nanodiamonds using Two-Photon Polymerization Filipe A. Couto, Marcelo B. Andrade, Adriano Otuka, Sebastião Prata Vieira, Sérgio Muniz and Cleber Mendonça; São Carlos Institute of Physics, University of São Paulo, Brazil

The NV-color center in diamond is a fluorescent defect that shows great potential for quantum information technologies. It acts as a single-photon emitter at room temperature, offers optical spin state preparation and readout capabilities, and exhibits long coherence time and photostability. Integration of these emitters into photonic structures is essential for various applications and can be achieved through the use of nanodiamonds as a platform. Nanodiamonds enable the incorporation of these quantum emitters into a wide variety of host materials and structures. This work focuses on the fabrication of polymeric cylindrical microresonators embedded with NV color centers using the two-photon polymerization (2PP) technique on a nanodiamond-doped photoresist. The fabricated resonators are 50 μm tall, with radii ranging from 30 μm to 15 μm , and the average size of the nanodiamonds is 40 nm. The positions of the nanodiamonds are located using laser scanning microscopy (LSM), and a homemade confocal fluorescence setup is used to map and measure the spectra of the fluorescent spots. Different concentrations of nanodiamonds were tested, and it was observed that concentrations above 0.5 wt% of nanodiamonds in the photoresist made fabrication impossible. Fabrication was achieved for concentrations ranging from 0.1 wt% to 0.01 wt%, resulting in the identification of multiple fluorescent spots in the structures. However, the quality factors of the resonators were in the range of 10^2 to 10^3 . For a concentration of 0.002 wt%, resonators with quality factors in the range of 10^4 to 10^5 containing around three emitters per structure were successfully fabricated. Raman spectroscopy measurements were carried out on a previously mapped resonator, where the characteristic diamond peak at 1332 cm^{-1} could only be observed in the spots where fluorescence was previously detected, confirming the presence of nanodiamonds at specific positions within the resonators. In summary, this work highlights the utilization of the 2PP technique to fabricate polymeric microresonators embedded with fluorescent nanodiamonds. Various characterization techniques were employed to analyze the position and fluorescence of the nanodiamonds. The findings pave the way for the fabrication of photonic devices integrated with nanodiamonds for applications in sensing and quantum optics.

8:00 PM EL14.04.08

Normally-Off Hydrogen-Terminated Diamond Field Effect Transistors with Nd/NdO_x Gate Dielectric Formed by Thermal Oxidation of Nd Jianing Su and Hong-Xing Wang; Xi'an Jiaotong University, China

Hydrogen-terminated diamond (H-diamond) with p-type conductivity, high carrier mobility and large carrier density (10^{13} cm^{-2}) accumulated on the surface which makes it can fabricate the diamond-based field effect transistor (FET). However, H-diamond FET usually shows normally on operation. In terms of the consideration of fail-safe system and energy saving for the logic circuits, the normally-off H-diamond FET are urgently required.

In this work, a normally-off H-diamond FET is realized by using Nd/NdO_x gate dielectric formed by thermal oxidation of Nd. The threshold voltage of Al/Nd/NdO_x/H-diamond FET is demonstrated to be -2.3 V , indicating that this device has the normally-off characteristics. The normally-off mode could be greatly ascribed to the work function difference between Nd and H diamond, and positive fixed charge in NdO_x layer. The maximum gate leakage current density value at -7.0 V is $3.3 \times 10^{-5}\text{ A/cm}^2$, which is lower than previously reported H-diamond FET with other gate dielectrics. The maximum drain-source current, maximum transconductance, current on/off ratio, and subthreshold swing are calculated to be -6.6 mA/mm , 1.8 mS/mm , 10^8 , and 112 mV/dec , respectively. Additionally, the small hysteresis voltage extracted from the C-V characteristic exhibits low trapped charge density in NdO_x layer, which indicated that the Al/Nd/NdO_x/H-diamond structure has good control on the two-dimensional hole gas (2DHG) channel. This work suggests that Nd/NdO_x gate dielectric could possess a great potential to achieve a high-performance H-diamond FET and also supplies a simple approach to realize normally-off devices.

8:00 PM EL14.04.09

Detection of CA125 by Hydrogen-Diamond Solution Gate Field Effect Transistor Minghui Zhang, Wei Wang and Hong-Xing Wang; Xi'an Jiaotong University, China

In this work, the concentration of CA125 has been detected by a hydrogen-diamond solution gate field effect transistor (H-terminated diamond SGFET). The linker molecular 1-pyrenebutyric acid-N-hydroxy succinimide ester (Pyr-NHS) has been utilized to modify the H-terminated diamond surface by π - π bonding. Then, the anti-CA125 antibody has been immobilized with Pyr-NHS. Finally, the specific binding of CA125 with anti-CA125 antibody leads an obviously shift of the transfer characteristics, which exhibiting a promising application of H-terminated diamond SGFET in CA125 detection.

8:00 PM EL14.04.10

Spin-Photon Interfaces based on Spin Defects in Diamond Coupled to an Optical Microcavity Andrea Corazza, Yannick Fontana, Viktoria Yurgens, Josh Zuber, Brendan Shields, Minghao Li, Mark Kasparczyk, Patrick Maletinsky and Richard Warburton; University of Basel, Switzerland

Optically-active spins in diamond attracted considerable attention as spin-photon interfaces to establish remote spin-spin entanglement among the nodes - a key building block in a quantum network. A prominent example of a highly coherent and optically addressable electron spin is the negatively charged Nitrogen-Vacancy (NV) center. However, its long radiative lifetime, the small branching ratio into the zero-phonon-line (ZPL) of the emitted photons (2.5-3%) and the inefficient photon extraction out of the diamond limit the entanglement rates and hence the scalability to a few network nodes. We demonstrate efficient selective coupling of the ZPL transition of a coherent NV center to the optical mode of an open Fabry-Perot optical microcavity, mitigating these problems. The coupling of a solid-state spin to a microcavity acts on its radiative lifetime via the Purcell effect, on its branching ratio via the cavity coupling and it efficiently funnels the coherent photons out of the diamond [1]. We present an improved NV creation protocol, carbon implantation post-fabrication, which yields to NV centers with excellent optical coherence even in membranes thinner than 2 μm , with over 50% of the emitters showing optical linewidths below 150 MHz [2]. We then embedded one of these diamond membranes (1.6 μm thick) in an open Fabry-Perot optical microcavity. The ZPL count rates are as high as 140 kcts/s under off-resonant excitation, exceeding the state-of-the-art achieved for photonic interfaces based on solid-immersion lenses (SILs). The high photonic flux is achieved through a net Purcell enhancement of 1.8, increasing the fraction of ZPL photons from 3% to 44.7%, an improvement by a factor of 17.5 compared to the NV Debye-Waller factor of 2.55%. By efficient suppression of the resonant excitation, we measure resonance fluorescence from an NV for the first time without relying on time-bin filtering and extract an NV linewidth of 159 MHz. In two-photon protocols for spin-spin entanglement, our platform would increase the entanglement success probability by more than an order of magnitude, and by more than two orders of magnitude with feasible system improvements.

Our versatile cavity design enables us to use any optically-active spin, which ideally combines excellent optical and long spin coherences. To this regard, the neutral charge state of the Silicon-Vacancy centre emerged as a promising defect in diamond and it exhibits cardinal properties required from an optically active solid-state spin such as long spin coherence and stable, strong optical transitions thanks to its high Debye-Waller factor of and its inversion symmetry which makes it insensitive to electric field noise. While the isolation and stabilization of the neutral SiV charge state has recently been made possible using Boron doping, the method is technologically challenging as it requires careful fine-tuning of the B concentration [3]. Using a versatile approach based on hydrogen surface termination, we demonstrate that the charge state of the SiV can be switched between SiV⁻ and SiV⁰ in a reliable way, even for diamond structures with low surface-to-volume ratios [4]. We present the method by creating single SiV⁰ centres in 0.5-3 μm thin diamond membranes. These structures can be readily integrated in optical microcavities, making them a promising spin-photon interface and an ideal host for a quantum memory. In conclusion, we propose two different approaches to manipulate coherently

spin defects and to generate coherent single photons resonantly and with high probability, making our systems attractive spin-photon interfaces - an important step towards quantum networks based on spin defects in diamond.

- [1] D. Riedel et al., Phys. Rev. X 7, 031040 (2017)
- [2] V. Yurgens et al., Appl. Phys. Lett. 121, 234001 (2022)
- [3] B. Rose et al., Science 361, 6397 (2018)
- [4] Z. H. Zhang et al., Phys. Rev. Lett. 130, 166902(2023)

8:00 PM EL14.04.12

High Lateral Breakdown Field in Ib HPHT Diamond SubstratesPietroArgenton, MartinKah, DanialMajidi, MarineCourret, NicolasRouger, DavidEon and JulienPernot; CNRS, France

The efficiency of power devices is critical nowadays for the rise of renewable energy. A great effort is being put into trying to optimize both energy dissipation and blocking capability. In the latter respect the goal is to increase as much as possible the voltage breakdown of devices in the off-state. Because the breakdown voltage increases with the semiconductor bandgap, Ib HPHT diamond substrate, with a bandgap of 5.5 eV, is a candidate as the ultimate substrate for power devices. In particular Ib HPHT diamond substrates are widely used for lateral Field Effect Transistors (FET) thanks to its insulating properties at room temperature.

In this work, the blocking characteristics of diamond Ib nitrogen-doped substrates are investigated through the use of metallic contacts separated by different gap widths in order to apply large range of electric field (from V/cm to MV/cm). Thanks to the electron beam lithography technique, several metallic structures separated by different gaps down to 500 nm were deposited on an Ib HPHT diamond substrate. The I-V characteristics between two electrodes have been measured up to reach the breakdown voltage of each structures. In order to understand the breakdown mechanism underlying within the structure, electron beam induced current (EBIC) has been used in order to map the electric field between two successive electrodes. This experiment is particularly useful for voltages close to the breakdown voltage.

In the first part of this presentation, the method will be described in details. Then, the I-V characteristics for different breakdown voltages and fields up to 10 MV/cm will be reported and compared with previous theoretical and experimental results. Finally, the mechanism causing the breakdown of the material will be discussed and compared with finite element simulation.

SESSION EL14.07: Laser Processing for Novel Devices

Session Chairs: David Eon and Franz Koeck

Tuesday Afternoon, November 28, 2023

Hynes, Level 2, Room 209

1:30 PM *EL14:07.01

Femtosecond Laser Writing Inside DiamondPatrickSalter¹, PilarVillar², CalumHenderson³, MartaKruger¹, FernandoLloret², DanielReyes², DanielAraujo² and RichardB. Jackman³; ¹University of Oxford, United Kingdom; ²Universidad de Cadiz, Spain; ³University College London, United Kingdom

Laser writing with pulses of duration less than a picosecond presents a diverse platform for the functionalisation of diamond, with a range of different modification regimes for internal structuring beneath the diamond surface. The laser is tightly focused beneath the surface where non-linear absorption leads to a perturbation of the diamond structure on a scale less than a micrometre, without any damage to the surrounding material or surface. At higher laser pulse energy, the light-matter interaction breaks down the diamond to create a graphitic phase. At lower laser pulse energy, a finer process is accessible which can yield a vacancy ensemble, without breakdown of the diamond lattice. These processing regimes are applied for the fabrication of a range of devices, ranging from detectors for harsh environments, through to quantum technology and security inscription within gemstones.

We focus this talk on our new results for laser written vias passing through a diamond wafer, and the influence of laser dose on the electrical conductivity. Surprisingly, increasing the laser dose delivered to the sample causes a transition from a regime in which the written structures display ohmic conductivity into a regime in which they are insulating in nature. We show that a combination of these regimes can be achieved with laser over-writing to give asymmetric conduction characteristics for the vias. A high-resolution structural characterisation of the laser written features by transmission electron microscopy reveals a diverse range of carbon nanostructures embedded within the diamond, and can be used to explain some of these phenomenon

2:00 PM *EL14:07.02

Direct Laser Writing of Nanochannels Between Ultra-Thin Nanocrystalline Diamond Films and Glass SubstratesStoffelD. Janssens, DavidVázquez-Cortés and EliotFried; Okinawa Institute of Science and Technology Graduate University, Japan

The fabrication of nanofluidic devices, which have one dimension below the 100 nm cornerstone, is complex, expensive, and time-consuming due to the small length scales involved. Direct femtosecond laser writing of nanochannels might overcome the inherent challenges; however, progress in this field is limited. Still, encouraging developments have been made. For example, laser writing can produce nanocavities in thin nickel films [1]. Films with such cavities may offer a wide range of possibilities for magnetism-related research but are not transparent in the visible spectrum, which excludes optical microscopy for nanofluidic research. Laser writing can also produce nanochannels in fused silica substrates [2]. These channels are usually perpendicular to the surface of the substrates, have variable diameters, are open on one side, and are typically no more than ten micrometers long.

This talk presents a method for fabricating nanofluidic devices through the direct femtosecond laser writing of arbitrary long nanochannels between nanocrystalline diamond (NCD) films and glass substrates. Laser writing transforms a portion of the sample into a nanostrip, and the nanostrip is surrounded by two nanochannels generated by film delamination. For an NCD film with an as-deposited thickness of 300 nm, the mean height and the width of a nanochannel made in this way are on the order of 30 nm and 2 μ m, respectively, and are tunable to a certain extent by laser pulse energy. Experiments indicate that a nanostrip consists of NCD, non-diamond carbon, and glass particles, which might be mixed with carbon due to laser ablation. It is found that the expansion of the sample material shapes a nanostrip and causes delamination and nanochannel formation. Such an expansion happens, for example, during the transformation of diamond to carbon of other forms [3]. Since the pulse energy needed to ablate the bare glass substrate is much greater than those used for nanochannel writing, one can deduce that nanostrip formation is initiated in the NCD film near the film-substrate interface. The origin of this phenomenon might be the presence of low-quality NCD at that location, which is bound to absorb more light than high-quality NCD [4]. By fabricating a nanofluidic device and performing simulations, it is shown that the nanochannels fill with water through capillary action.

NCD is an appealing material for applications due to its biocompatible, chemical, mechanical, electrical, optical, and quantum properties. Low-cost diamond films can be achieved by plasma-assisted chemical vapor deposition with methane gas diluted in molecular hydrogen as a precursor mixture. With this deposition technique, NCD films are commonly synthesized on substrates seeded with nanodiamonds [5]. NCD can also be doped to make it electrically conductive, paving the way for various applications [6]. Being inexpensive, transparent, and chemically inert, glass is a natural choice for research in micro- and nanofluidics. The coefficient of thermal expansion can also be tuned towards that of other materials, allowing the fabrication of structures with relatively low residual stress. Since NCD films are inert to hydrofluoric acid (HF), NCD can act as an etch stop during the HF etching of glass [7]. Here, we rely on this property for fabricating the nanofluidic device.

- [1] V. V. Temnov et al., Nano Lett. 2020, 20, 7912–7918.
- [2] Y. Li et al., Adv. Photon. Nexus 2022, 1, 026004.
- [3] A. Courvoisier et al., Appl. Phys. Lett. 2016, 109, 031109.
- [4] V. V. Kononenko et al., Appl. Phys. Lett. 2019, 114, 251903.
- [5] S. Mandal, RSC Adv. 2021, 11, 10159–10182.
- [6] S. D. Janssens et al., Appl. Phys. Lett. 2014, 104, 073107.
- [7] S. D. Janssens et al., Appl. Phys. Lett. 2020, 116, 193702.

2:30 PM EL14:07.03

Femtosecond Direct Laser Writing for Diamond NV Centers PlacementCleberMendonca¹, LucasNolasco¹, FilipeCouto¹, JulianaAlmeida², CarlieOncebay³ and SergioMuniz¹; ¹University of Sao Paulo, Brazil; ²UFSCar, Brazil; ³National University of Engineering, Peru

The integration of devices for applications in photonics and quantum information technologies requires the development of platforms combining basic elements, such as resonators and waveguides. One promising solid-state optically active systems currently studied for such applications is the nitrogen-vacancy (NV) center in diamond, which is usually produced by irradiating diamond with beams of electrons or nitrogen ions. NV centers can be optically initialized and read out, present long coherence times at room temperature and allows creating

protocols to manipulate its spin-state by combining optical and magnetic methods. Furthermore, NV centers can also be used as quantum sensors to detect temperature and magnetic and electric fields. The controlled production and placement of NV centers in photonic structures is of high relevance to engineer devices. In this direction, this work presents results obtained from our efforts to use of fs-laser pulses to generate active and spatially localized NV centers in CVD diamond, as well as the fabrication of polymeric optical microcavities, via two-photon polymerization, incorporated with nanodiamonds containing NV centers. Upon excitation of diamond using 150-fs pulses from a Ti:sapphire laser at 775 nm, with a repetition rate of 1 kHz, we have determined that active defects, with the least damage to the surface, can be generated using pulse fluence in the range of 11 – 34 mJ/cm², as observed by the typical fluorescent emission of NV center. For fluences higher than 34 mJ/cm² the damage on the diamond's surface started to get too severe, also resulting in lower emission. Our results also revealed that the density of NV centers grows with the number of fs-pulses. The generation process, however, is stochastic. Furthermore, fs-pulse at ~800 nm (86 MHz repetition rate) were used to fabricate, via the two-photon polymerization (2PP), cylindrical resonators incorporated with nanodiamonds presenting centers. Even though the cavity quality factor (Q) decreases with the amount of nanodiamonds, for a cavity with 0.01 wt% of nanodiamonds Q ~10³ is achieved. More interestingly, we were able to collect the NV-center emission from specific positions in such microvities, that display the typical features of the NV-centers. In summary, The results reported here demonstrate the use of fs-laser pulses to generate localized center in diamond by using 150-fs pulses (775 nm) with fluences higher than 11 mJ/cm². Also 2PP was successfully used to fabricate microresonators containing nanodiamonds, with Q of about 10³. The authors acknowledge FAPESP (grants 2018/11283-7, 2020/08715-2, 2019/27471-0, 2015/17058-7, 2013/07276-1, and 2009/54035-4), Air Force Office of Scientific Research, CNPq, and CAPES for financial support.

2:45 PMBREAK

SESSION EL14.08: Florescent NanoDiamond and ND for Bio Applications
Session Chairs: Bohuslav Rezek and Stepan Stehlik
Tuesday Afternoon, November 28, 2023
Hynes, Level 2, Room 209

3:15 PM *EL14.08.01

Shape Induced Enhanced Fluorescence in Fluorescent Nanodiamond Revealed by Correlative Transmission Electron Microscopy and Photoluminescence Microscopy SheryChang¹, HaotianWen¹, DavidKodah² and ChristianDwyer³; ¹University of New South Wales, Australia; ²Centenary College of Louisiana, United States; ³Electron Imaging and Spectroscopy Tools, Australia

Fluorescent nanodiamonds (FNDs) are diamond nanoparticles containing color centers that emit visible light at room temperature. Among the color centers in FNDs, the nitrogen-vacancy centers (NV) have drawn the most attention due to its exceptionally stable optical properties and great prospect in sensing and biomedical diagnostic applications.

The current understanding of the optical properties of the FNDs relies largely on the optical measurement methods from either ensemble of materials or from few single particles. As most of the FND fabrication is a top-down process where larger diamond crystals are milled to desired nanometer size, FNDs generally have broad size distribution and irregular shapes. Therefore understanding of FNDs structure-property relationship using ensemble measurements only is insufficient.

We have developed a new method based on correlative transmission electron microscopy and photoluminescence (TEMPL). TEMPL allows a direct correlation of the fluorescence brightness and three-dimensional size and shape of individual nanoparticles. PL provides optical information with exquisite energy resolution, and TEM provides structural information with exquisite spatial resolution. Unsupervised machine learning (ML) with the generalized 3D shape descriptors, is used to analyse correlations between the PL brightness and 3D shape of FND particles. The automation provided by machine learning allows TEMPL to be applied to large sample areas (2-3 orders of magnitude larger than a typical TEM field of view) containing a statistically significant number of particles.

Using this new method, we directly reveal that the volume-averaged PL brightness of thin, flake-like nanodiamond particles is up to several times greater than that of three-dimensional-shaped, thicker particles provided the particle diameter is less than the sub-wavelength limit. With the assumption that the number of NVs within a particle is proportional to its volume, this implies that individual NVs within thinner particles are brighter. This experimental observation is supported by the theoretical simulations on simplified particle geometries on a range of supporting substrate and surrounding medium. The simulations indicates that the comparative brightness of thinner particles, either on a thin supporting substrate or in a low-index medium, is attributable, at least in part, to the constructive interference of partial light waves in these particles. With increasing particle thickness, such an effect becomes damped. The sub-wavelength dimension of the substrate plays an important role, as it results in higher effective reflectivity comparable to diamond particles in a low-index medium (e.g., a low-index solution).

In addition to correlative PL with TEM, we have also carried out correlative SEM and AFM for the study of FNDs supported on bulk substrate. Our overall results help to guide new routes of enhancing fluorescence brightness of FNDs for broad sensing applications.

3:45 PM EL14.08.02

Enhanced Photophysical Transition Dynamics of NV Centers in Nanodiamond on Structured Metamaterial Platforms PengZheng and IshanBarman; Johns Hopkins University, United States

While promising as photostable solid-state quantum emitters for biological sensing and imaging applications, nitrogen-vacancy (NV) centers in nanodiamond are limited by their intrinsically inefficient photon generation and extraction from excited NV centers, which restrict the achievable sensitivity and temporal resolution. To overcome these challenges, judiciously structured metamaterials are developed, which can support broadband Purcell enhancement and spatially extended local plasmonic fields for effective plasmon-NV centers coupling. With fluorescence lifetime imaging microscopy characterizations, a simultaneous amplification to the photophysical transition dynamics and emission intensity of NV centers are observed. We envision that the structured metamaterials pave the way for developing superior biological sensing platforms with enhanced sensitivity as well as augmented spatial and temporal resolution.

4:00 PM *EL14.08.03

High-Efficiency Tractable Nanodiamond-Mediated Gene Editing System Development and Application Chia-ChingChang^{1,1,2}, Shih-HwaChiou^{3,1} and YonhuaTzeng⁴; ¹National Yang Ming Chiao Tung University, Taiwan; ²Academia Sinica, Taiwan; ³Taipei Veterans General Hospital, Taiwan; ⁴National Cheng Kung University, Taiwan

Nanodiamonds (NDs) are biocompatible crystalline carbon nanomaterials for biomolecules or small molecules delivery into the target cells especially for NDs smaller than 5 nm. By conjugating NDs with red fluorescence protein, mCherry, the distribution of these nano-fluorescence nanoparticles (ND-mCherry) can be traced in the cells or tissues. Moreover, by conjugating linear DNA fragments with all the components of the CRISPR/Cas9 genome editing system, the NDs particles became a gene-editing device. X-linked retinoschisis (XLR) is an inherited retinal disorder disease that leads to reduced visual acuity in affected persons. Genetic analysis indicated that XLR is caused by mutations c.625T in the RS1 gene. Therefore, RS1 serves as a target for gene editing systems. The low transfection efficiency is one of the major challenges of conventional CRISPR/Cas9 genomic editing systems. In this study, we developed an ND-mCherry-CRISPR / Cas9 gene editing system (ND-mCherry-CRISPR / Cas9). The size of ND is approximately 3 nm, which contained both a target gene sequence and an extra green fluorescence protein gene as a gene expression reporter. This tractable ND-mediated gene editing system is not only delivered genes into hiPSCs and mouse retina but also mediates gene editing events. Therefore, the structure of the mouse photoreceptor layer was loose, and cone/rod cells were also found to be abnormal by the ND-mediated gene editing system introduced. The effective gene editing efficiency is about 10 times higher than conventional CRISPR / Cas9. Namely, ND-mediated gene editing systems can be used as a way to quickly establish animal models of hereditary diseases. Furthermore, by conjugating with the gene correction sequences and our system will be a potential medical device for disease treatment.

4:30 PM EL14.08.04

Controlling the Interaction of Nanodiamond Surfaces with Physiologic Environments ElisabethMayerhoefer¹, JuliaPuck², Daniela ElenaCostea³, Harsh NitinDongre³ and AnkeKrueger¹; ¹Stuttgart University, Germany; ²Wuerzburg University, Germany; ³University of Bergen, Norway

The application of nanodiamond in quantum sensing, tissue engineering or drug delivery requires a highly defined interaction of the diamond surface with the surrounding medium. The uncontrolled formation of a protein corona is one of the major challenges. Furthermore, the denaturing of surface bound functional moieties as well as the attachment of serum components can lead e.g. to a loss of function, masking of functional moieties, the uncontrolled agglomeration of the particles as well as alteration in the uptake mechanism for the introduction of diamond nanoparticles into cells.[1] We have recently reported on the use of a complex zwitterionic moiety for the inhibition of the protein corona formation and the efficient uptake of such functionalized fluorescent nanodiamonds into cells.[2,3]

Here, we discuss the control of these undesired effect by the highly defined modification of the diamond surface using different zwitterionic moieties based on differently charged small peptides as well as crown ethers immobilized using short organic linker molecules.

The resulting nanodiamond conjugates have been investigated regarding their dispersibility, colloidal stability and inhibition of protein adsorption.

Uptake experiments and cell based assays confirm the low toxicity and high biocompatibility of these functionalized nanodiamonds and elucidate the efficient uptake and release into the cytosol without substantial agglomeration. The influence of differently charged surface moieties will be discussed. Such functionalized nanodiamonds are a promising tool for biomedical and sensing applications as the modular approach allows to introduce additional functional moieties, which can then be used to deliver drug molecules, provide specific interactions for targeting and tissue engineering.

[1] E. Mayerhoefer, A. Krueger, *Acc. Chem. Res.* **2022**, *55*, 3594.

[2] V. Merz, J. Lenhart, Y. Vonhausen, M. E. Ortiz Soto, J. Seibel, A. Krueger, *Small* **2019**, 1901551.

[3] A. Sigaeva, Viktor Merz, R. Sharmin, R. Schirhagl, Anke Krueger, *J. Mater. Chem. C* **2023**, *11*, 6642.

4:45 PM EL14.08.05

Nanodiamond Facilitated Drug Delivery for Drug Resistant Breast CancersC.-Y.Huang, Y.-J.Su and Chia-LiangCheng; National Dong Hwa University, Taiwan

Nanodiamond (ND) has been considered as a biocompatible and feasible platform for efficient cancer drug delivery. Examples have been successfully demonstrated for various cellular and animal models. However, to date, very few or none studies had included the assessment on the effects and efficiency in a quantitative fashion; and the transportation of these ND-drugs to the cancer/tumor sites are still in a less understood state. In cancer therapy, drug resistance may arise due to intercellular microenvironment, cytoskeletal structure, and drug resistance genes causing limited therapeutic effect in cancer treatment.

In this study, we use nanodiamond (ND) as a carrier to improve drug delivery in the 3D cellular model which has been observed drug resistant characterization due to the structure of cellular model. The aim of this study is to compare the penetration ability of ND-drug complex and free anticancer drug treatment in 2D and 3D breast cancerous cells model (MCF-7 and MDA-MB-231). Several variations of the Multi cellular tumor spheroid (MCTS) cocultures were used to examine the effect of the extra cellular matrix (ECM) to the drug delivery and drug entering mechanisms. ND-drug complex is formed by conjugating Human Serum Albumin (HSA) and doxorubicin (DOX) with ND. Cytotoxicity of the drug complex is determined by MTT assay and Quantitative analysis in 2D cellular model. Growth inhibition assay evaluated the drug efficacy in 3D cellular model. Results show that ND-complexes are more efficient to deliver the drug in 3D cellular model.

SESSION EL14.12: Nanodiamond Synthesis and Applications

Session Chairs: Shery Chang and Chia-Liang Cheng

Wednesday Afternoon, November 29, 2023

Hynes, Level 2, Room 209

3:30 PM EL14.12.01

Nucleation Layer Formation and Properties of 5 nm Hydrogenated Boron-Doped HPHT NanodiamondsStepanStehlik^{1,2}, KaterinaDragounova Aubrechtova², EkaterinaShagieva², RostislavMedlin¹, PetrBelsky¹, TomasKovarik¹, EvgenyEkimov³, StepanPotocky⁴, BohuslavRezek⁴ and AlexanderKromka²; ¹New Technologies – Research Centre, University of West Bohemia, Czechia; ²Institute of Physics, AS CR, Czechia; ³Institute of High Pressure Physics, Russian Academy of Sciences, Russian Federation; ⁴Faculty of Electrical Engineering, Czech Technical University in Prague, Czechia

Boron-doped diamond is an excellent electrode material due to its large potential window, robustness, and antifouling properties. While boron-doped diamond in the form of CVD-grown mono or polycrystalline diamond films is already a well-established material, reports on boron-doped nanodiamonds (BNDs) are rare, and BNDs are not broadly accessible. Yet, their potential is tremendous e.g. in (photo)catalysis and biomedicine. BNDs were at first obtained by delamination and milling of CVD films (10.1021/nn500573x), showing also some positive effect on conductivity when used for nucleation (10.1016/j.carbon.2014.07.048). A more scalable and promising technique for making of BNDs is a high-pressure high-temperature (HPHT) synthesis from organic molecular precursors. This process offers unprecedented control of the ND size, enables the dopant incorporation in a high concentration, and provides monocrystalline NDs (10.1021/acsbiomaterials.0c00505). Here we investigate whether a nucleation layer from these HPHT BNDs, can potentially lead to better quality (morphology, electrical properties) of the thin (50-200 nm) boron-doped CVD diamond films compared to the standard nucleation with detonation nanodiamonds (DNDs).

We used the BNDs that were synthesized from borabicyclo[3.3.1]nonane dimer C₁₆H₃₀B₂ under HPHT conditions (8-9 GPa, 1250°C). The obtained black powder was analyzed by Raman and FTIR spectroscopies, which showed relatively high sp²-C content and an abundance of C-H₃ bonds. To obtain pure BNDs, the powder was boiled under reflux in a mixture of H₂SO₄ and HNO₃ (3:1) for 6 hours until the bubbling of the mixture disappeared. Surprisingly, boiling in acids led to complete breakage of the interparticle bonds, and after the centrifugal acid removal, well-dispersed deep blue BND colloid was obtained just by gentle shaking of the sediment. Raman spectroscopy showed a spectrum typical for highly boron-doped diamond without any significant sp²-C content. FTIR and zeta potential analysis showed an oxidized surface (presence of C-O and C=O bonds and negative zeta potential of -31 mV). To determine the BND size we used small angle X-ray scattering (SAXS) that showed the mode particle size to be 5 nm. TEM analysis confirmed well-crystalline and well-dispersed BNDs. In order to reverse the zeta potential of the BNDs to become positive, the oxidized BNDs were lyophilized and then hydrogenated at 700°C for 3h. After hydrogenation, the zeta potential of BNDs indeed became positive (44 mV), i.e., similar to the intrinsic NDs after hydrogenation which is important for the achievement of densely seeded substrates with a negative zeta potential. The nucleation layer was created on Si substrates as well as on SiO₂/Au interdigital electrodes. The morphology and density of the nucleation layers obtained with H-BNDs was investigated by AFM and SEM. Finally, boron-doped CVD diamond film was grown over the nucleation layer on both substrate types, and its morphology, structure, and electrical properties were characterized and compared to the standard nucleation obtained with DNDs.

3:45 PM EL14.12.02

Accuracy Estimation of All-Optical Thermometry Between 283–373 K using the NV⁻-Center Zero-Phonon Line Spectrum of Diamond MicroparticlesTaiichiShikama¹, TakatoWatanabe¹, MasayaZetsu¹, YoshikazuHirai¹, MazinJouda² and MasahiroHasuo¹; ¹Kyoto University, Japan; ²Karlsruhe Institute of Technology, Germany

The temperature dependences of the intensity, peak wavelength, and width of the zero-phonon line (ZPL) spectrum from diamond nanoparticles have been used for all-optical thermometry of microscale objects [1-3]. The method is especially effective when it is challenging to apply the thermometry using the optically detected magnetic resonance [4-5]. However, the ZPL spectrum shape varies particle-to-particle due to presumably the difference in the particle shape [3], which produces a different magnitude of the strain in the diamond lattice, and the variation requires calibration of the particle dependence of the three parameters mentioned above. To establish the calibration procedure and estimate the accuracy of the all-optical thermometry, we measured the particle-to-particle variation in the ZPL spectrum between 283–373 K.

In the experiments, we used commercial diamond microparticles of 150 μm and 0.75 μm average diameters (Adamas Nanotechnologies). The microparticles were used instead of nanoparticles for the ease of particle-to-particle spectroscopy. Approximately 100 particles were dispersed on a silicon wafer mounted on a temperature-controlled stage of an epifluorescent microscope. 594 nm laser was used as an excitation light source, and the photoluminescence spectrum of each particle was measured using a spectrometer (1.5 nm resolution). In the measured spectra, a wavelength range near the ZPL was fitted using an analytical function based on the theoretical shapes of the ZPL and phonon side band spectra [6].

The three parameters were evaluated from the fitting result, and we made histograms of them at every 10 K between 283–373 K. Among the three parameters, the peak wavelength has the smallest variance compared with the temperature dependence suggesting that better accuracy of the thermometry can be obtained by using the peak wavelength. We found that particles with close ZPL spectrum shape at 293 K have close temperature dependences of the peak wavelength between 283–373 K. Thus, the calibration could be done at one temperature condition by sorting particles having close ZPL spectrum shapes.

[1] T. Plakhotnik, *et al.*, *Nanotechnology* **26**, 245501 (2015).

[2] P. C. Tsai, *et al.*, *Angew. Chem. Int. Ed.* **56**, 3025 (2017).

[3] Y. Y. Hui, *et al.*, *J. Phys. Chem. C* **123**, 15366 (2019).

[4] M. Fukami, *et al.*, *Phys. Rev. Appl.* **12**, 014042 (2019).

[5] L. Ishikawa, *et al.*, *Rev. Sci. Instrum.* **93**, 083705 (2022).

[6] T. Shikama, *et al.*, *Jpn. J. Appl. Phys.* **60**, 012001 (2020).

4:00 PM EL14.12.03

Enhancement of NV⁻-Center Coherence Times via Suppression of the Surface Noise in Coated NanodiamondsDenisR. Candido¹, UriZvi², PeterC. Maurer² and MichaelE. Flatte¹; ¹The

The emergence of Nitrogen-Vacancy centers (NVs) as a candidate for quantum sensing and metrology has recently attracted significant attention in the quantum information science community. While it is optimal to have shallow NV to increase its sensitivity to the external signal, this conflicts with the rapid increase of the noise near the surface – decreasing the signal-to-noise ratio. Accordingly, efforts have been devoted to explore techniques aiming to reduce the surface noise.

In this work we first model and study the interplay between bulk and surface electric and magnetic noise for NVs implanted in nanodiamonds [1]. Furthermore, we theoretically obtain the corresponding signatures of both surface and bulk noises on the evolution of NV-coherence [1,2,3]. By contrasting these findings with our experimental data, we show that while the surface noise is the dominant source in bare nanodiamonds, silica-coated nanodiamonds show a dominant bulk noise source [3]. This evidences a suppression of the surface noise via coating processes, with corresponding 3.5-fold increase in the NV-coherence time [3]. Our findings evidences the potential of engineering spin coherence using fundamental nanoscience principles to significantly improve the sensitivity of real-world nanoscale quantum sensors.

[1] D. R. Candido, M. E. Flatté, arXiv:2303.13370

[2] D. R. Candido, M. E. Flatté, arXiv:2112.15581

[3] U. Zvi, D. R. Candido, A. Weiss, A. R. Jones, L. Chen, et al., arXiv:2305.03075

The work was supported as part of the Center for Molecular Quantum Transduction, an Energy Frontier Research Center funded by the U.S. Department of Energy, Office of Science, Basic Energy Sciences, under Award Number DE-SC0021314.

4:15 PM EL14.12.04

Growth of Nanocrystalline Diamond Thin Films from Detonation and HPHT Nanodiamonds: Correlative Microscopy Study StepanStehlik^{1,2}, KaterinaDragounova Aubrechtova², EkaterinaShagieva², RostislavMedlin¹, PetrBelsky¹, TomasKovarik¹, AlexanderKromka², StepanPotocky³ and BohuslavRezek³; ¹University of West Bohemia, Czechia; ²Czech Academy of Sciences, Czechia; ³Czech Technical University in Prague, Czechia

The nucleation layer formed by diamond nanoparticles (nanodiamonds, NDs) is nowadays probably the most common approach how to facilitate polycrystalline diamond growth on diverse substrates by chemical vapor deposition (CVD). Yet the formation of thin and ultrathin functional diamond films [Stehlik et al., doi 10.1021/acscami.7b14436] gives rise to numerous challenges in terms of adhesion, surface uniformity, layer density, sp²/sp³ carbon phases, grain sizes, grain boundaries, etc. A recent study with oxidized nanodiamonds showed that the nanodiamond material quality (determined by origin and surface modifications) has a pronounced effect on the diamond CVD growth and resulting properties, including the brightness of SiV color centers [Zhang et al., doi 10.1039/d2tc01090a].

Thus, in this work we compare the effect of several types of hydrogenated nanodiamonds (being principally more suitable) for nucleation and growth of nanocrystalline diamond thin films with SiV centers. We employ detonation nanodiamond (DND) solutions from standard 4 nm DNDs and novel size-reduced 2 nm DNDs and 4 nm DNDs with reduced nitrogen content (< 0.05 at.%), all obtained from pre-production stock (OZM Research). We also employ HPHT NDs of 0-30 nm size (MSY30, Pureon) purified by annealing in air (450°C, 5h). All NDs were hydrogenated by annealing in a hydrogen atmosphere, providing them positive zeta potential and stability in a colloidal solution [Kolarova et al., doi 10.1016/j.diamond.2023.109754]. The nucleation solutions were prepared by sonication of 100 mg NDs in 20 mL water and subsequent centrifugation to remove larger aggregates. Nucleation layers were formed on Si substrates and Si self-sensing AFM probes which were immersed in the nucleation solution and sonicated for 10 min. We applied CVD diamond growth for 5-30 min (10 - 80 nm thickness) using microwave plasma SEKI SDS6K reactor with standard growth conditions (hydrogen 300 sccm, methane 15 sccm, 60 mbar, 3 kW, 800 °C).

We characterize the morphology, material, and functional properties of the nucleation layers and resulting CVD diamond thin films by correlative microscopy combining SEM, AFM, Raman, and photoluminescence measurements. We show the dependence of these features on the specific properties of the 4 types of employed nanodiamonds. The work has been supported by the Technology Agency of the Czech Republic (TACOM project) and the Czech Science Foundation.

SESSION EL14.13: PIN Junctions and Vertical Devices
Session Chairs: Seong-Woo Kim and Mohamadali Malakoutian
Thursday Morning, November 30, 2023
Hynes, Level 2, Room 209

8:45 AM EL14.13.01

Fabrication of Q-Carbon Nanostructures and Subsequent Formation of High-Quality Diamond on β -Ga₂O₃ Pallab KumarSarkar, Saif Al ArafinTaqy and ArifulHaque; Texas State University, United States

The ultrawide bandgap (UWBG) oxides and nitrides, particularly beta-gallium oxide (β -Ga₂O₃), are promising material systems for next-generation power devices in commercial and military applications. For most electronic and RF applications, UWBG semiconductor-based devices, including β -Ga₂O₃, can operate at much higher voltages, frequencies, and temperatures than commercially available options, including silicon carbide and gallium nitride. However, the remarkably low anisotropic thermal conductivity of β -Ga₂O₃ (11-27 Wm⁻¹ K⁻¹) is a significant bottleneck for high-power device applications as it affects the device performance and results in self-heating effects (SHE), which severely limits output power density and maximum current flow of the circuit. To address this issue, the incorporation of a diamond layer that can operate as a heat spreader in Ga₂O₃-based devices has been investigated due to its extraordinarily high thermal conductivity (~ 2000 W/m.k). The deposition of high-quality diamond coatings onto non-diamond substrates, such as β -Ga₂O₃ films, is a complex task due to several inherent nucleation, growth, stress, and adhesion-related issues. The absence of carbon solubility in β -Ga₂O₃, a large mismatch in surface energies with a significant difference in thermal expansion coefficient between β -Ga₂O₃ and diamond, and unfavorable decomposition phenomena during CVD make it difficult to achieve uniform diamond layers with suitable adhesion and nucleation density. This study introduces a novel method for depositing diamond on β -Ga₂O₃ films using a diamond-like carbon (DLC) through pulsed laser deposition (PLD) and successive pulsed laser annealing (PLA) to form a quenched carbon (Q-carbon) layer, demonstrating improved precision and control in the synthesis of diamond coatings for optoelectronic and electronic devices. In this investigation, we have created strong Q-carbon/ α -carbon and Q-carbon/nanodiamond heterostructures on β -Ga₂O₃ films using laser annealing of amorphous carbon films with nanosecond laser pulses above the melt threshold. The energy density required for the PLA is calculated by modeling the laser-solid melt interaction, and a maximum melt regrowth velocity of 12.5 m/s is achieved at a laser energy density of 0.4 J/cm². Raman studies and X-ray photoelectron spectroscopy (XPS) demonstrate the presence of a high sp³ content of ~ 81% in the Q-carbon region. Nanodiamonds formed by the PLA process exhibit a distinct Raman peak at 1320 cm⁻¹, with a red shift of approximately 12 cm⁻¹ due to the phonon confinement effect. This research reveals a considerable increase in the nucleation density during diamond deposition by hot filament chemical vapor deposition (HFCVD). A very high seeding density with high-quality delamination-free diamond film growth is possible on the Q-carbon region of the film due to the presence of densely packed diamond tetrahedra in Q-carbon which act as nucleation sites for diamond growth. The nucleation density, diamond quality, and stress values were compared for diamonds on Q-carbon coated β -Ga₂O₃ and uncoated β -Ga₂O₃ films. The incorporation of a Q-carbon intermediate layer significantly reduces the compressive stress in diamond films on β -Ga₂O₃ to 0.37 GPa, compared to 1.23 GPa for films deposited on uncoated substrates. The phase purity of the diamond can be measured by its FWHM of signature Raman peak, with a manually calculated value that matches the direct value obtained from the deconvoluted signal. The values obtained were 11 cm⁻¹ and 16.66 cm⁻¹ for Q-carbon coated β -Ga₂O₃ and uncoated β -Ga₂O₃, respectively. Thus, this study addresses the critical challenges, i.e., poor adhesion and large thermal mismatch between diamonds and β -Ga₂O₃ films, which has tremendous implications in realizing efficient β -Ga₂O₃-based high power devices.

9:00 AM EL14.13.02

Progress on Doped Diamond Electronics AnnaM. Zaniewski, ManpunetBenipal and JesseBrown; Advent Diamond, United States

The promise of diamond as a semiconducting material has long been understood, but this promise for commercial applications has only recently begun to be realized. Advent Diamond and collaborators have been engaging in substantial research and development efforts to bring diamond-based components to targeted applications. In this presentation, we will demonstrate how an initial focus on serving niche applications, such as a diamond-based x-ray beam monitor for scientific facilities, specialized detectors, quantum materials, and diodes, creates a platform for addressing the required technology development and the scientific advances that underpin diamond electronics development.

9:15 AM *EL14.13.04

Current Status of Diamond Power Devices for High Voltage Applications - Prospects of Vertical Devices MarikoSuzuki; University of Cádiz, Spain

The global demand for energy savings through improved power conversion efficiency is creating a tremendous opportunity for high-performance power devices. Ultra-high-voltage and high-efficiency power devices will offer a significant reduction in size, weight, and cooling for power systems and grid-scale power conversion applications. Diamond, an ultra-wide-bandgap semiconductor, is an ideal candidate for ultra-high-voltage devices due to its exceptional characteristics such as the high thermal conductivity, the mechanical strength, high carrier mobilities (both of electrons and holes), and the high dielectric breakdown strength. Diamond devices have been remarkably developed thanks to the establishment of microwave plasma chemical vapor deposition (MPCVD) growth techniques including doping control and characterization techniques. In this decade, several diamond power devices have exhibited excellent performances beyond other semiconductors based on the material advantages. Vertical devices have advantages for high power devices, such as low on-resistance, high blocking voltage and high operation current. However, there are not many reports on vertical diamond power devices due to inadequate device fabrication techniques and difficulty in obtaining doped substrates especially with high-quality. In this talk, current status and prospects of diamond power devices will be introduced focusing on vertical devices.

9:45 AMBREAK

SESSION EL14.14: Diamond Wafers for Electronic Devices
Session Chairs: Etienne Gheeraert and Robert Nemanich
Thursday Morning, November 30, 2023
Hynes, Level 2, Room 209

10:15 AM *EL14.14.01

$10^6 \text{ cm}^2/(\text{V}\cdot\text{s})$ Carrier Mobility Measured in Ultra Pure Diamond by Time of Flight Electron Beam Induced CurrentAlexandrePortier^{1,2}, FabriceDonatini², DenisDauvergne¹, Marie LaureGallin Martel¹ and JulienPernot²; ¹University Grenoble Alpes, CNRS, Grenoble INP, LPSC-IN2P3, France; ²University Grenoble Alpes, CNRS, Grenoble INP, Institut Néel, France

Diamond is a very promising material for various applications, and understanding its basic properties is key for the development of future devices. In particular, the low-field mobility of holes has never been measured below ~ 80 K in ultra-pure diamond. In order to measure this mobility, we developed an innovative Time of Flight electron Beam Induced Current (ToF-eBIC) technique. A 1 ns pulsed electron beam was made to impact the diamond semiconductor, inducing charge carrier creation and motion through the 546 μm thick bulk diamond, under the influence of an applied electric field. The resulting signal was analysed using the transient time technique. Thus, the velocity of electrons and holes was assessed as a function of the temperature from 13 to 300 K and as a function of the electric field with values ranging from 1.5 to 9200 V/cm. A low-field mobility value of $1.03 \times 10^6 \text{ cm}^2/(\text{V}\cdot\text{s})$ was measured for holes at 13 K, demonstrating that diamond is a suitable material to transport charge carriers in a ballistic regime at a scale of ten micrometers.

10:45 AM EL14.14.02

Effects of Modulated Boron Doping on the Carrier Transportation Characteristics of Single Crystal Diamond MOSFETsRuozhengWang, QiLi and Hong-XingWang; Xi'an Jiaotong University, China

Diamond has superior physical properties for power devices such as ultra wide band-gap (5.45eV), high breakdown field voltage (10MV/cm), high thermal conductivity (22 W/cmK) and high carrier mobility. Nowadays, Boron (B) doped diamond devices has been widely studied since boron atoms acted as a shallow acceptor impurities in diamond (0.37eV). However, the B doping concentration is hardly to be controlled because of the unintentional doping, leading to the poor electrical properties of devices. Delta doping technology could solve this issue by the alternating growth of heavily doped and intrinsic diamond films within the range of a few nanometers for fully activating doped carriers. However, the fabricating of high-quality delta doping diamond is rarely studied. In addition, the electrical properties of delta doping diamond film is not very high, inhibiting the practical application from materials to devices. In this work, the high-quality growth, modulated doping and carrier transportation characteristics based on (100) single crystal diamond (SCD) boron delta doping are studied, followed by the verification of vertical structures of boron-doped diamond MOSFETs. Firstly, high quality B-doped (100) SCD has been worked out owing to the priority of high crystallinity intrinsic layer. The growth rate of B-doped layer is 3 $\mu\text{m}/\text{h}$, the RMS, Raman and XRD FWHM were 0.35 nm, 4.0 cm^{-1} and 28.4 arcsec, respectively. Then, the results of carrier concentration and mobility have been calculated for B-doped diamond at 300k by four-probe Hall tests. Then, the consecutive boron delta doping diamond film has been fabricated, adjusting the doping density of heavily ($\text{P}^+, 10^{19} \text{ cm}^{-3} \sim 10^{20} \text{ cm}^{-3}$) and lightly ($\text{P}^-, 10^{16} \sim 10^{17} \text{ cm}^{-3}$) B-doped SCD layers. Finally, the multi-vertical structures of boron-doped diamond MOSFETs have been realized by I-V and C-V measurements. The details will be presented in the conference.

11:00 AM EL14.14.03

Electron Contact Strategies for Diamond Enabled with a Nitrogen Doped Nano-Carbon InterlayerGabrielB. Munro-Ludders, SaurabhVishwakarma, DavidJ. Smith, RobertJ. Nemanich and FranzKoeck; Arizona State University, United States

Ohmic metal contacts to n-type diamond have historically posed a challenge to the fabrication of diamond devices, due to the formation of a rectifying Schottky barrier, which limits the practicality and scope of diamond devices. Nitrogen-doped nanoCarbon films have recently been explored as ohmic interface layers to enable low-resistance ohmic contact with N-type diamond [1]. In this work the electronic interface between nitrogen-doped nanoCarbon interlayers and metals is investigated using photoelectron spectroscopy and transmission electron microscopy, to determine the mechanism of ohmic contact.

Titanium and molybdenum layers were deposited on nanoCarbon films, and each respective metal/nanoCarbon interface was characterized via X-ray Photoelectron Spectroscopy (XPS) and Ultraviolet Photoelectron Spectroscopy (UPS). The n-type SBH was determined to be $\Phi_B = 3.7 \text{ eV}$ and $\Phi_B = 4.1 \text{ eV}$ for the titanium-nanoCarbon and molybdenum-nanoCarbon interfaces, which indicates a partial pinning of the fermi level. Characterization via TEM and electron energy loss spectroscopy reveal the presence of $\sim 4 \text{ nm}$ diameter sp^3 -bonded diamond grains surrounded by a matrix of sp^2 bonded carbon, indicating a mixed phase material with non-crystalline states. Two models of the contact mechanism, contingent on the density of unfilled surface states after metal deposition, are proposed to understand the ohmic contact mechanism. A sufficiently low surface state density coupled with a high inter-bandgap density may reduce band bending and allow for flat-band contact by filling surface states, unpinning the fermi level. Alternatively, hopping-type conduction near the Fermi level through π^* -bonded states into the conduction band may also reduce the effective SBH.

Future work will investigate the electronic interface between nanoCarbon interlayers and n-type diamond substrates, to enable ohmic contact with n-type single-crystalline diamond. Switching between pinned and unpinned contact regimes through modulating the inter-bandgap state density via modifying morphology, doping concentration, and non-carbon chemical composition in the film also presents an avenue for future investigations.

Research supported by the NSF under Award No. 2003567 and by ULTRA, an Energy Frontier Research Center funded by the DOE Office of Science, Basic Energy Sciences (BES) under Award No. DE-SC0021230.

11:15 AM EL14.14.04

Improving Off-State Performance of Schottky Barrier Diodes Through Enhanced Apparent Schottky Barrier using Nitrogen-Doped LayersHusseinKassem, DavidEon and JulienPernot; Institut Néel, France

Diamond Schottky barrier diodes (SBDs) are commonly affected by an imperfect metal/semiconductor interface, resulting in an interface-dependent Schottky barrier height (SBH) inducing large reverse leakage current and premature breakdown voltages [1]. To remediate this issue, more advanced device structures and various metals have been explored to find the ideal trade-off between reduction of leakage current in reverse, and high current at low voltage in forward [2] [3].

The presents work aims to investigate and compare the electrical characteristics of diamond Schottky-np diode (SNPD) and classical diamond SBDs that were fabricated on the same sample. Our hypothesis is that after nitrogen-selective growth, the dopants are ionized conducting to an opposite band bending, and increasing the apparent Schottky barrier. The objective is to assess the influence of a thin nitrogen layer under the SBDs.

In advance of that, a numerical modeling study was carried out on a SNPD using nitrogen layers of different thicknesses. The aim was to evaluate the band structure and bending at proximity of the contact, as well as to quantify the electric field at the interface. According to the simulation results, an increase in the apparent Schottky barrier ($V_b = V_{b0} + \Delta V$) was observed in front of holes in the semiconductor. We also observed that the interface electric field is increasing with the nitrogen layer thickness, which is making the sharp field peak in the material rather

than at the interface when reverse bias is applied, allowing to prevent early reverse leakage current. Further characterization with different parameters will be described.

The fabrication process involves depositing a heavily doped layer with a thickness of 500 nm and a lightly boron-doped layer with a thickness of 2.4 μm on a diamond substrate. A thin n-type layer is selectively grown on half part of the lightly boron-doped layer, followed by treating both the nitrogen-type and boron-type layers with an OH-termination process. Zirconium Schottky metal is then deposited on each layer to form the SNPDs and SBDs, respectively. The ohmic contact on the highly boron-doped layer exhibits metallic behavior.

The electrical characteristics of SNPDs and SBDs have been investigated using current voltage and capacitance-voltage methods. The forward state of SBDs in boron-type diamond showed better performance than SNPDs, while SNPDs exhibit superior performance in the reverse state. Furthermore, the comparison, of SNPDs and SBDs, fabricated on the same sample is performed in order to validate the model.

The important parameters for temperature-dependent adjustments, such as the ideality factor, apparent Schottky barrier, and serial resistance, were extracted by fitting the curve of the current density-voltage of SNPDs using the thermionic emission model. The observations indicate an increase in the barrier, which is intriguing. The overall resistance is generally low, with slight variations between the SNPDs and SBDs. However, the ideality factors are less favorable, suggesting the need for further understanding at the interface level. Therefore, to address the high ideality factor and its impact on the thermionic current reduction, a series of measures will be implemented to examine the interface quality accurately.

In conclusion, SNPD structures present a promising approach for power electronics to improve the breakdown and reduce leakage.

References

- [1] Journal of Applied Physics, 10 (1965), 3212-3220.
- [2] Diamond & Related Materials 16 (2007) 1033-1037.
- [3] Journal of Applied Physics. 51 (2012), 090116

11:30 AM EL14.14.05

Improved Diamond Schottky Barrier Diode Breakdown Voltage using High Resistance and High Quality Diamond Double-Stack Field Plate Structure Qi Li and Hong-Xing Wang; Xi'an Jiaotong University, China

The application of diamond in Schottky barrier diodes (SBD) has attracted more and more attention due to its excellent electrical and physical properties. However, because of edge electric field crowding of Schottky electrode, the breakdown electric field is far below the limit of diamond. The field plate (FP) structure is a simple method to alleviate the crowding of edge electric field, but due to the limitation of the withstand voltage capability of the FP material, the edge of the device will still be broken down in advance. Homoepitaxial diamond has the highest breakdown electric field of at least 20MV/cm, so it is suitable to choose diamond as the field plate. However, since boron atoms can diffuse from the boron-doped diamond substrate to the epitaxial layer during growth, making the epitaxial layer conductive. Therefore, we prepared high-resistance(H-R) nitrogen-doped diamond, and then grew a high-quality(H-Q) diamond protective layer as the field plate to improve the withstand voltage. The H-R and H-Q diamond is achieved by selective growth method. We have reported that the H-R diamond field plate structure can effectively increase the breakdown voltage of diamond SBDs. We reduced the thickness of the H-R layer from 800 nm to 400 nm, resulting in an increase in the breakdown voltage from 113 V to 322 V due to the introduction of fewer defects. Compared with the nitrogen-doped diamond H-R field plate, the defect density on the diamond surface will be reduced after adding the H-Q layer, thereby improving the withstand voltage. This structure will further alleviate the edge electric field crowding effect. Therefore, H-R and H-Q diamond double-stack field plate structure is expected to greatly improve the reverse breakdown characteristics of the device.

SESSION EL14.15: Engineering Quantum Devices
Session Chairs: Robert Bogdanowicz and Lillian Hughes
Thursday Afternoon, November 30, 2023
Hynes, Level 2, Room 209

1:45 PM EL14.15.01

Fabrication of Diamond Membranes and Photonic Nanostructures for Integration of Color Centers Julia Heupel, Lukas Wolfram and Cyril Popov; University of Kassel, Germany

Single-crystal diamond (SCD) in form of thin membranes with incorporated color centers, such as nitrogen-vacancy (NV) centers or silicon-vacancy (SiV) centers, has gained an ever-increasing interest over the years as a highly promising platform for photonic integrated devices or for envisioned applications in quantum information technologies (QITs). To achieve the desired long optical and spin coherence times for QIT applications, such membranes need to be free from lattice defects, paramagnetic impurities, and charge traps. This requires an initial removal of the damaged surface layers from the cut and polished starting material. Additionally, further processing of diamond by e.g., dry etching for fabrication of photonic structures, can lead to higher roughening of the surface due to a micro-masking effect from particles, originating from the polishing procedure. In our work we address the importance of the SCD surface preparation to overcome the above mentioned challenges, which affect the structuring process and critically influence the final quality of the membrane or structured photonic devices as well as their performance.

The fabrication process of SCD membranes with various diameters and thicknesses, exhibiting a low surface roughness down to 0.2 nm, applying inductively coupled plasma reactive ion etching (ICP-RIE) with Ar/Cl₂ and O₂ plasma will be demonstrated. By a variation of the major etching parameters, an enhanced planarization of the surface can be obtained, especially due to a low etch rate of a few nm/min and the Ar/Cl₂ chemistry. These planarized SCD membranes can be successfully bonded via van der Waals forces or via PMMA on plane cavity mirrors and optically characterized in a fiber-based Fabry-Pérot microcavity system regarding their mode structure and finesse. They can be also used as starting material for fabrication of 1D or 2D photonic crystal structures applying electron beam lithography (EBL).

The work is financially supported by the German Federal Ministry of Education and Research (BMBF) under the Project "Quantenrepeater.Link" (QR.X).

2:00 PM EL14.15.02

The Highest Concentration NV Ensembles Formed by Heavily Nitrogen-Doping CVD System with Plasma Confinement and High Density Vacancy Formation by Focused Electron Beam Irradiation Yudai Asano¹, Kyosuke Hayasaka¹, Mayu Ueda¹, Kyotaro Kanehisa¹, Kosuke Kimura², Takashi Tani¹, Shinobu Onoda², Shinpei Enomoto³ and Hiroshi Kawarada^{1,3}; ¹Waseda University, Japan; ²National Institutes for Quantum Science and Technology, Japan; ³Waseda University, Japan

Highly concentrated NV ensembles are expected to be applied to magnetic sensing. Only method for high concentration of nitrogen above 10²⁰ cm⁻³ in diamond is limited to CVD method, because the damage of heavily implanted diamond cannot recover easily.

We have successfully fabricated diamond thin films with the world's highest nitrogen concentration of 8.0 × 10²⁰ cm⁻³ [1] using a microwave plasma chemical vapor deposition (MPCVD) system that is specially designed to confine plasma to the thickness of a microwave waveguide. This method can also introduce 1 × 10²² cm⁻³ of boron, and diamond with the world's highest superconducting transition temperature has been synthesized. HPHT synthetic (111)-oriented diamond substrates were used. That's because (111) diamond substrate has the high impurity incorporation efficiency [2]. These CVD films exhibit extremely high crystallinity, as indicated by the Raman spectrum measurement (Laser 532nm), which shows a diamond peak FWHM of 8.6 cm⁻¹, comparable to HPHT diamonds. After fabricating the films, we performed electron beam irradiation using a 300 keV TEM with an electron fluence of 10¹⁸⁻²² cm⁻², resulting in the world's highest NV concentration of 8.5 × 10¹⁸ cm⁻³ [3]. This method is necessary for electron irradiation for high density nitrogen above 1 × 10²⁰ cm⁻³. The quantification of NV concentration was done using the DEER (Double Electron-Electron Resonance) based on NV interactions. DEER is a method of measuring NV concentration from the magnetic dipole interaction strength between NV's four orientation groups by applying microwaves simultaneously to groups of each different resonance frequencies, so this method utilizes the fact that the decay rate of coherence time is proportional to the number of resonant NV groups in the concentration range of 8.5 × 10¹⁷ ~ 1.7 × 10¹⁹ cm⁻³, as confirmed by simulations and experiments [4]. By manipulating the number of resonant NV groups, we determined the NV concentration [3]. Previously, the concentration was estimated from the emission intensity, but when the NV concentration exceeded 10¹⁸ cm⁻³, the saturation of NV concentration occurred without an increase in irradiation fluence. As a result, the estimated values from the emission intensity using the DEER method were higher than those estimated from the emission intensity. However, the obtained NV concentration of 1.0 × 10¹⁸ cm⁻³ is only about 1% yield relative to the nitrogen concentration. Understanding the behavior of nitrogen in CVD diamond could potentially lead to higher NV concentrations. Despite such a high nitrogen concentration, the T₂^{*} was 50 ns, and T₂ remained at 0.5 μs measured by Ramsey and Hahn echo, respectively. This value is long compared to experimentally reported values [5]. This is because many reports showed that coherence time is inversely proportional to nitrogen concentration between 2 × 10¹⁶ and 1 × 10²⁰ cm⁻³. At the nitrogen concentration of our nitrogen-doped CVD diamond ([N] = 8.0 × 10²⁰ cm⁻³), the coherence time is calculated to be approximately 0.03 μs , which is much shorter than our measured value, suggesting that CVD diamond has advantages for high-density NV ensemble.

This work was supported by MEXT Quantum Leap Flagship Program (MEXT Q-LEAP) Grant Number JPMXS0118067395.

[1] M. Ueda, H. Kawarada, et al., 2022 MRS Fall Meeting, EQ07.08.01

[2] J Hiromitsu Kato, Toshiharu Makino, Satoshi Yamasaki and Hideyo Okushi. Phys. D: Appl. Phys. 40 (2007) 6189- 6200

[3] K. Hayasaka, H. Kawarada, et al., 2022 MRS Fall Meeting, EQ07.05.04

[4] G. Kucsko, M. D. Lukin, et. al., Phys. Rev. Lett. 121 (2018).

[5] E. Bauch, R. L. Walsworth, et al., arXiv:1904.08763 (2019).

2:15 PM EL14.15.03

Exploring Magnetism in Multiferroics with Scanning NV Magnetometry Paul Stevenson¹, Peter Meisenheimer², Hongrui Zhang² and Ramamoorthy Ramesh³; ¹Northeastern University, United States; ²University of California, Berkeley, United States; ³Rice University, United States

Multiferroic materials hold great promise for next-generation devices, offering a route towards low-power, voltage-based control of magnetic ordering. Realizing this potential, however, requires understanding the coupling between magnetic and ferroelectric degrees of freedom. Using scanning NV magnetometry (SNVM), we are able to resolve the wide range of antiferromagnetic textures in the multiferroic BiFeO₃, revealing previously hidden heterogeneity and allowing us to directly image the effect of applied electric fields.

We also show how SNVM can be used to image multiple field components simultaneously – without ambiguities normally present in reconstructions – by optimizing magnetic field conditions, and how local variations in the refractive index of BiFeO₃ can be imaged below the diffraction limit. These new capabilities demonstrate the broad utility of SNVM for exploring magnetic textures in multiferroic materials.

2:30 PM EL14.15.04

Analysis of Ferro- and Antiferromagnetic Memory Bits by Scanning NV Magnetometry Peter Rickhaus¹, Vicent Borrás¹, Robert Carpenter², Sebastien Couet², Liza Zaper^{1,3}, Alexander Stark¹, Mathieu Munsch¹, Marco Nordmann¹, Paul Lehmann², Kai Wagner³, Christoph Adelman², Oleksandr Pylypovskiy⁴, Paul van der Heide², Denys Makarov⁴ and Patrick Maletinsky^{3,1}; ¹Qnami AG, Switzerland; ²Imec, Belgium; ³University of Basel, Switzerland; ⁴Helmholtz-Zentrum Dresden-Rossendorf, Germany

Storing information in magnetic bits requires excellent control over their nanoscale magnetic properties. A prime example of this challenge are STT-MRAM (spin transfer torque magnetic random access memory) devices - which have rather high failure rates. In order to investigate the sources of potential failure, a technique that can resolve small magnetic fields with high spatial resolution is required. The request is even more urgent for next-generation magnetic memory materials, such as antiferromagnets, which generate even smaller magnetic signals.

Scanning NV magnetometry (SNVM) is an emerging quantum sensing technique that offers the required sensitivity. Here, we will look at the local magnetic properties of bits in state-of-the-art STT-MRAM devices using scanning-NV magnetometry [1]. Furthermore, we will demonstrate magnetic images of a few hot candidate materials for future magnetic memory devices including antiferromagnetic chromia, BFO [2] and ultra-scaled CoFeB nanowires [3]. We will reveal magnetic textures that are undetectable with more standard characterization techniques and discuss implications on device fabrication.

References:

[1] P. Rickhaus et al., <https://arxiv.org/abs/2306.15502>

[2] H. Zhong et al, Phys. Rev. Applied 17, 044051 (2022)

[3] U. Celano et al, Nano Lett. 21, 24, 10409–10415 (2021)

2:45 PM BREAK

SESSION EL14.16: Diamond Bio-Devices and Sensors

Session Chairs: Philippe Bergonzo and Anke Krueger

Thursday Afternoon, November 30, 2023

Hynes, Level 2, Room 209

3:15 PM *EL14.16.01

An Ultra-Sensitive Biosensor Based on Mid-Infrared Diamond Waveguide Spectroscopy Pontus Forsberg and Mikael Karlsson; Uppsala University, Sweden

In this presentation, our latest work in the development and the use of an ultra-sensitive biosensor based on diamond waveguides will be highlighted. We have during the last years been working on the design and fabrication of mid-infrared (MIR) diamond waveguides. The diamond MIR waveguides together with a broadband tunable quantum cascade laser (QCL), emitting in the so called molecular fingerprint region, are the two key elements in our newly developed label free MIR biosensor. In our approach MIR light is coupled into microfabricated diamond waveguide structures, which are purposefully designed to sustain single or multimode standing waves. The associated evanescent waves that are created at the waveguide surface will extend into the surrounding media and interact with the analyte thus provide the sensing volume. In existing commercial technologies, attenuated total reflection IR (ATR-IR) spectroscopy, IR light from a thermal emitter is coupled through a millimeter sized diamond crystal, with up to 10 internal reflections in the diamond crystal. This is a powerful technology and is today used for i.e. quality control in medical and food industry, protein analysis, forensics, etc. However, the relatively low sensitivity of this technique hinders its use in many applications. Our biosensor achieves unsurpassed sensitivity due to the large number of standing waves nodes created in our waveguides which roughly can be translated to the number of internal reflections per length unit is maximized. Moreover, the use of a bright QCL laser as a light source further increases the sensitivity of our biosensor – therefore an ultra-sensitive sensor is realized. Finally, the diamond waveguide material facilitates further functionalization by means of organic chemistry thus extending the capabilities of traditional silicon or gold based biosensor technologies, and we demonstrate here one possible route to fabricate selective affinity layers for protein fishing from complex mixtures.

Several designs of diamond waveguides are discussed, ranging from thin film diamond slab waveguides, rib waveguides, to microfabricated free hanging diamond waveguides. We have recently showed how AlN can be used as cladding layer to overcome earlier difficulties in guiding light at longer wavelengths (5-10 μm). We will also present how we significantly can increase the sensitivity of the diamond waveguide sensor by depositing a high index film on the diamond waveguide. Using silicon as the high index film also opens up for easy functionalization of the sensor.

The diamond waveguide sensor has been tested on different analytes, such as acetone and isopropanol, showing a very stable performance and very high sensitivity. We have therefore starting to work on “real-world” chemical sensing applications. Currently, we are analyzing different forms of the protein alpha-synuclein, which is relevant in understanding the mechanism behind Parkinson’s disease. We have previously shown that ATR-IR spectroscopy can be used to analyze the secondary structure of different alpha-synuclein aggregates. Moreover, it is also possible to see the difference in the IR-spectra between the native state and the neurotoxic misfolded state of the protein. However, the ATR element is impractical to functionalize and the sensitivity of the ATR-IR spectroscopy is too low to be used on relevant samples from patients. In contrast, our diamond waveguide biosensor exhibits the desired key properties to analyze the secondary structure of alpha-synuclein at biologically relevant concentrations. Future work includes the functionalization of the diamond waveguide sensor surface to selectively adsorb alpha-synuclein from cerebrospinal fluid, with the ultimate goal to detect Parkinson’s disease at an early stage.

3:45 PM *EL14.16.02

Electronic Properties and Memristive Behavior in Undoped Diamond Foils for Artificial Neurons-On-A-Chip Application Adrian Nosek¹, Adrian Olejnik², Marc Bockrath³ and Robert Bogdanowicz²; ¹University of California Riverside, United States; ²Gdansk University of Technology, Poland; ³The Ohio State University, United States

The electronic properties of chemical vapor deposited undoped polycrystalline diamond foils are investigated via continuous and pulsed mode measurements. In continuous mode, our diamond thin foil operates as a bipolar memristor with a variable onset voltage and internal nanobattery effect. We attribute the memristive properties to a filamentary redox-based resistive switching mechanism with ionic and electronic charge transport within our diamond foil. In order to explain the occurrence of this dip, we consider the hydrogen redox-based switching model. In this model, hydrogen ions are separated from the conductive filament and migrate towards the negatively charged electrode through atomic vacancies and produce a build-up internal nanobattery voltage. This diffusion process is accelerated by local high temperatures produced by the current carrying filament. While current compliance is not necessary for this effect to occur, it is certainly beneficial because a fixed part of the voltage drop occurs due to electrons travelling towards the positive electrode and the rest of the voltage drop occurs due to protons migrating and accumulating at the negative electrode. After the pulse is turned off, a current in reverse direction flows due to the build-up internal voltage as well as repulsion of accumulated positive charge carriers. In pulsed mode operation, our diamond foils exhibit synaptic behavior, similar to the interface between two neurons. Our memristors exhibit high retention times with high on/off ratios up to 10⁴ required for logic operations. As an inorganic synapse, our foil exhibits sensory, short-term, and long-term memory effects according to a psychological human

memory model. Spike-timing dependent plasticity supports our findings. Furthermore, we observe functionalities commonly found in neurons, such as a mimicked refractory period where our conductive filament corresponds to an axon. We anticipate that our study paves the way for future artificial-neurons-on-a-chip application. Our research findings constitute an important step towards artificial-neurons-on-a-chip application, as well as organic-inorganic brain-electronics interfaces.

4:15 PM EL14.16.03

Rapid Measurement of Plasma Molecular-Targeted Drug Concentration with Boron-Doped Diamond Electrode Genki Ogata¹, Takuro Saiki², Yasuo Saio², Yasuaki Einaga¹ and Hiroshi Hibino^{3,4}; ¹Keio University, Japan; ²Niigata University, Japan; ³Osaka University, Japan; ⁴AMED, Japan

Compared to conventional cytotoxic anti-cancer drugs, molecular-targeted medications exhibit reduced toxicity. These drugs are administered to patients at fixed doses, without the need for adjustments based on biomedical indices such as body surface area. However, this therapeutic approach leads to considerable variability in plasma concentration among individuals, often resulting in significant adverse events that necessitate dosage reduction. Recent clinical studies have sought to quantify the correlation between drug concentration and clinical efficacy or toxicity. To enable personalized administration of molecular-targeted drugs, it is imperative to determine plasma concentrations directly at the clinical site. In recent years, advancements in medical engineering have yielded various portable or wearable biosensors capable of rapid on-site monitoring. Nonetheless, the widespread utilization of these devices has been hindered by insufficient evaluation of accuracy using clinical samples, variability between sensors, and the need for complex and costly fabrication processes. To overcome these challenges, we propose a straightforward approach utilizing untreated boron-doped diamond (BDD), an electrochemical material known for its sustainability. As a proof-of-concept, we selected pazopanib, a molecular-targeting anticancer drug recommended for monitoring. By employing a BDD plate chip measuring approximately 1 cm², our sensing system accurately detected pazopanib concentrations in rat plasma samples within the clinically relevant range. Furthermore, the response of the chip remained stable throughout 60 consecutive measurements, demonstrating its excellent repeatability. When we examined plasma samples collected from orally administered healthy rats and cancer patients using our system, the measured concentrations closely matched those obtained through liquid chromatography with mass spectrometry. Additionally, we evaluated the reproducibility of the BDD chips. Finally, we constructed a portable system featuring a palm-sized sensor housing a chip to facilitate practical implementation. This setup successfully determined drug concentrations from approximately 40 µL of whole blood obtained from dosed rats within a short turnaround time of approximately 10 minutes. By employing this "reusable" sensor-based approach, we can accelerate point-of-care drug monitoring, advance personalized medicine, and potentially reduce medical expenses.

4:30 PM EL14.16.04

Fabrication of Diamond/Metal Oxide Hybrid Structures: Towards Gas Sensors with Enhanced Sensitivity and Selectivity Petr Ashcheulov¹, Marina Davydova¹, Andrew Taylor¹, Neda Neykova¹, Alexandr Laposa², Jaromír Kopeček¹ and Pavel Hubík¹; ¹FZU, Czechia; ²CVUT, Czechia

The release of hazardous compounds such as NO_x, SO_x, CO, NH₃, other nitrogen or sulfur-containing compounds, and volatile organic compounds (benzene, toluene, methanol, etc.) in the atmosphere is of significant concern for human health. Therefore, there is a rising demand for advanced chemiresistor sensors, which need to satisfy the following requirements: high sensitivity, selectivity, stability and reproducibility. In recent years, various metal oxides (e.g., ZnO, SnO₂, CeO₂) have been recognized as promising materials for the detection/sensing of toxic pollutants and hazardous gases. Yet, chemiresistor sensors based on metal oxides have exhibited rather poor selectivity (i.e., simultaneous sensitivity to reducing and oxidizing gases) along with the necessity of high temperature (> 300 °C) operation.

In this work we demonstrate fabrication of hybrid structures based on diamond (intrinsic and boron-doped) and metal oxides (MOx) for their application as active components in gas chemiresistor sensors. We investigate the effect of doping and the diamond structure (planar and/or 3D geometries) on the sensing characteristics of hybrid structures (e.g., sensitivity and selectivity) towards various gases. Fabricated diamond/MOx structures were characterized via various microscopic and spectroscopic techniques, and the effect of their electrical characteristics on the sensing properties is discussed.

This work was supported by the Czech Science Foundation grant GACR 22-04533S.

4:45 PM STUDENT PRIZES AND CONCLUDING REMARKS

SESSION EL14.17: Virtual Session
Session Chairs: Ania Bleszynski Jayich and Alastair Stacey
Thursday Morning, December 7, 2023
EL14-virtual

9:00 AM EL14.17.01

Normally-Off Vertical Diamond MOSFETs with Drain Current Density over 200 mA/mm using Oxidized Si Terminated Diamond Channel Formed by Si Molecular Beam Deposition Approaches Kento Narita¹, Kosuke Ota^{1,2}, YuFu¹, Chiyuki Wakabayashi¹, Atsushi Hiraiwa¹, Tatsuya Fujishima² and Hiroshi Kawarada^{1,2,3}; ¹Waseda University, Japan; ²Power Diamond Systems, Inc., Japan; ³The Kagami Memorial Research Institute for Materials Science and Technology, Japan

For realization of high-power high-speed miniaturized complementary inverters [1], development of p-type field-effect transistors (p-FETs) corresponding to SiC or GaN n-FETs is essential. Normally-off operation with threshold voltages (V_{th}) more negative than -3 V are required for power devices with operating voltage above 500 V, but the conventional vertical diamond FETs are normally-on operation (V_{th} : +15 ~ +30 V) using hydrogen-terminated diamond (C-H) channel [2,3]. In contrast, we have fabricated (001) vertical diamond MOSFETs with oxidized Si terminated diamond (C-Si-O) channel by the reaction of chemical vapor deposition (CVD) SiO₂ with diamond and achieved the first normally-off operation (V_{th} : -9.0 V) in vertical diamond FETs with a maximum drain current density ($I_{D,max}$) of 108 mA/mm [4]. In this study, by Si molecular beam deposition (MBD) method, we fabricated C-Si-O side-wall channel in vertical diamond MOSFETs for the first time. We obtained the V_{th} of -4.5 V and the $I_{D,max}$ of 214 mA/mm, which is the highest $I_{D,max}$ among the normally-off vertical diamond FETs.

The C-Si-O channel formation method is as follows. After 200 nm regrown undoped layer was deposited by microwave plasma CVD, SiO₂ was deposited 400 nm as a mask by tetraethyl orthosilicate based plasma-enhanced CVD. A p⁺ layer (IB): 1×10²¹ cm⁻³ was selectively deposited by MPCVD after etching 400 nm of the SiO₂ mask and 40 nm of the regrown undoped layer by inductively coupled plasma reactive ion etching. After SiO₂ mask removal, the diamond surface was treated with hydrogen termination. 0.5 nm-silicon was deposited and followed by in-situ annealing at 1193 K for 15 min in the MBD apparatus. During the annealing in high vacuum, the reaction between C-H and Si occurred and C-Si- happened [5,6]. The C-Si- surface was naturally oxidized and transformed to C-Si-O after the C-Si- channel was exposed to air [7].

The vertical device dimensions for source-source length (L_{SS}), effective channel length (L_{ch}), trench width (W_T), gate-drain length (L_{GD}), trench depth (D_T) and gate width (W_G) are 8 µm, 5.2 µm, 4 µm, 0.4 µm, 3 µm and 25 µm, respectively. The $I_{D,max}$ normalized by the W_G was 214 mA/mm, and the $I_{D,max}$ normalized by the active area ($L_{SS} \times W_G$: 2.0 × 10⁻⁶ cm²) was 5350 A/cm² at V_{DS} : -45 V and V_{GS} : -40 V, and the on-resistance (R_{on}) was 8.1 mΩcm². The on/off ratio was 10⁷ and gate leakage current was less than 10⁻⁵ mA/mm at V_{DS} : -10 V. The maximum transconductance ($g_{m,max}$) was 15 mS/mm, and the maximum field-effect mobility ($\mu_{FE,max}$) was 68 cm²/Vs. The V_{th} was -4.5 V at V_{DS} : -10 V. As a result, we achieved the normally-off operation of $|V_{th}| > 3$ V, and the $I_{D,max}$ of over 200 mA/mm. The V_{th} shifted more than 20 V in the negative direction compared to conventional C-H channel vertical diamond FETs [2,3]. The negative electron affinity of C-Si-O surface (-0.25 eV) [7] is weaker than that of C-H surface (-1.3 eV) [8] and the negative fixed charge of Al₂O₃ on the C-Si-O interface is less than that on the C-H interface. The large negative shift of V_{th} is due to the smaller band offset and the smaller band bending between diamond and Al₂O₃ in the C-Si-O channel than in the C-H channel. In the near future, by introducing a p⁻ drift layer, and C-Si-O channel only on the sidewalls, we will realize vertical diamond devices with high breakdown voltage over 1000 V and normally-off operation.

[1] K. Okuda, N. Iwamuro, et al., EPE'16 ECCE Europe, 1-10. (2016)

[2] N. Oi, H. K. et al., Sci. Rep., 8, 1-10. (2018)

[3] J. Tsunoda, H. K. et al., Carbon 176, 349-357. (2021)

[4] K. Ota, K. Narita, H. K. et al., Carbon, in press. (2023)

[5] A. Shenk, C. Pakes, et al., Appl. Phys. Lett., 106(19), 191603. (2015)

[6] Y. Fu, H. K. et al., IEEE TED, 69(5), 2236-2242. (2022)

[7] A. Schenk, C. Pakes, et al., J. Phys., Conds. Matt, 29, 025003. (2017)

[8] J. B. Cui, J. Ristein, and L. Ley, Phys. Rev. Lett. 81, 429. (1998)

9:05 AM EL14.17.02

Atomic Hydrogen Effects on Chemical Bonding of Diamond-Like Carbon Films Prepared by Pulsed Laser Deposition Takahiro Kawabata; Public University Corporation Toyama Prefectural University, Japan

1. Introduction

Tetrahedral amorphous carbon (ta-C) films have been prepared by pulsed laser deposition (PLD) [1-4]. Stock et al. [1] reported that the sp^3 carbon ratio [$sp^3 C / (sp^3 C + sp^2 C)$] in the ta-C film prepared using an ArF excimer laser (198 nm) was 80% or more, which was higher than the sp^3 ratio (~60%) in the film deposited using a KrF excimer laser (248 nm). Yoshitake et al. [2] reported that the ta-C film prepared in a hydrogen atmosphere had a higher sp^3 ratio than the film deposited in an oxygen atmosphere. Cheng et al. [3,4] performed postdeposition-annealing of ta-C with atomic hydrogen irradiation and found that atomic hydrogen etching accelerated crystallization of micro/nano graphite as the annealing temperature rose. In this study, we have deposited diamond-like carbon (DLC) films by PLD using a KrF excimer laser and investigated atomic hydrogen effects on the chemical bonding of the DLC films. We clarified the optimum deposition conditions to promote sp^3 -bonded carbon atoms in the films. The novelty of this study is that the hydrogen effects were investigated by varying the deposition parameters systematically.

2. Experimental methods

DLC films were prepared on Si(100) substrates by PLD using a KrF excimer laser with a wavelength of 248 nm. The DLC film was deposited at a substrate temperature of RT, a laser repetition rate of 20 Hz, a laser intensity of 0.25 J/pulse using an atomic hydrogen source (hydrogen pressure: 0.01 Pa, tungsten filament current: 4 A) for 60 min as a standard sample. One of the substrate temperature, laser repetition rate, hydrogen pressure, and filament current was varied with the other parameters fixed. The sp^3 ratio [$sp^3 C / (sp^3 C + sp^2 C)$] was determined from C 1s core-level spectra obtained by X-ray photoelectron spectroscopy (XPS).

3. Results and discussion

The DLC films prepared with atomic hydrogen irradiation had higher sp^3 ratios than those prepared in a vacuum. Especially, the DLC film deposited at a filament current of 4 A exhibited the highest sp^3 ratio. The hydrogen pressure at which the sp^3 ratio reached a maximum was found to be 0.01 Pa. When the substrate temperature was increased from RT to 700 °C, the sp^3 ratio decreased. It was found that the sp^3 ratio in the film deposited at a repetition rate of 20 Hz was higher than that in the film deposited at 10 Hz. The maximum sp^3 ratio of 57% was obtained in this study, which was close to that reported in Ref. 1, in which PLD using a KrF excimer laser was employed.

Yasui et al. [5] have reported that the amount of atomic hydrogen generated using a tungsten filament source increases with the filament temperature. C.-L. Cheng et al. [3] have shown that hydrogenated, disordered carbon films are deposited at RT, whereas the graphitization of the films occurs at substrate temperatures above 500 °C, which is facilitated by hydrogen etching. When the filament temperature and hydrogen pressure increase, the amount of atomic hydrogen increases, leading to the acceleration of the formation of C-H bonds and selective etching of sp^2 -bonded carbons by atomic hydrogen. When the substrate temperature decreases or the repetition rate (the flux of C atoms) increases, the surface diffusion length of C atoms decreases. In this case, C atoms adsorbed on the surfaces are not able to arrive at stable sites, and the film becomes a metastable form of amorphous carbon.

4. Summary

The maximum sp^3 ratio of 57% was obtained when the hydrogen pressure, substrate temperature, laser intensity, and laser repetition rate were 0.01 Pa, RT, 0.25 J/pulse, and 20 Hz, respectively.

References

- [1] F. Stock et al., Appl. Phys. A **123** (2017) 590.
- [2] T. Yoshitake et al., Diam. Relat. Mater. **9** (2000) 689.
- [3] C.-L. Cheng et al., Appl. Surf. Sci. **174** (2001) 251.
- [4] C.-L. Cheng et al., Diam. Relat. Mater. **11** (2002) 262.
- [5] K Yasui et al., Jpn. J. Appl. Phys. **44** (2005) 1361.

9:10 AM EL14.17.03

All-Optical Modulation of Fluorescent Nanodiamonds for Practical Applications [LingzhiWang](#) and ZhiqinChu; The University of Hong Kong, Hong Kong

Because of ultrahigh photostability, nanoscale volume emitting strong fluorescent signal, and low cytotoxicity, fluorescent nanodiamonds (FND) containing nitrogen vacancy (NV) centers are regarded as promising fluorescent markers in various applications. Here, based on optical polarization-selective excitation phenomenon of NV centers, we provided FNDs with more useful functions, including orientation measurement and providing high-dimensional anticounterfeiting information. Particularly, our scheme showed two characteristics: 1) easy-to-implement solution; 2) useful functions. Specifically, our scheme can be conveniently achieved based on mature commercial sample and common microscope with slight modification. Utilizing the orientation measurement of FNDs, we provided the information for cell traction force in a new dimension (rotational dimension). Based on the 3D anticounterfeiting information from FNDs, we achieved physical unclonable function labels, well satisfying common commercial and anticounterfeiting requirements. In above application scenarios, our scheme has little negative influence due to all-optical manipulation.

9:25 AM *EL14.17.04

Non-Invasive Quantum Sensing and Coherent Control of Surface-Supported Spin Systems [AparajitaSingha](#); Max Planck Institute for Solid State Research, Germany

Controlling individual atoms and molecules at their native spatio-temporal limit has an indispensable appeal that has driven fundamental research for decades. Atomic-scale interactions and correlations are also the basis of all timeless technological progress, ranging from nanoelectronics to information processing. In particular, a new attractive avenue has recently emerged for nanoscale quantum bits made of individual lanthanide atoms and molecules. The intrinsic large magnetic moment, nontrivial intra- as well as inter-atomic electron correlations, and long-term quantum coherence in these model systems altogether offer a myriad of new exciting possibilities across molecular magnetism and quantum computing research.

My present scientific effort is devoted to understand and control quantum mechanical properties of such smallest building blocks of matter, especially by probing them in the least invasive manner. However, addressing the spin states in such quantum systems is an extremely challenging task. So far, only scanning tunneling microscopy (STM) with subatomic spatial resolution is capable of achieving this, albeit being highly invasive and limited with the scope of operational temperature (< 4 K). Atomic force microscopy (AFM) using novel defect centers in diamond (NV) has the potential to overcome these limitations, given their unparalleled magnetic sensing capability, high-fidelity optical readout, and broad operational range of temperature. However, this method currently suffers from insufficient resolving power (tens of nm) primarily due to fluorescence quenching in so-called shallow NV centers. In this talk, I will discuss each of these techniques in view of access and quantum control at the atomic scale, highlighting our efforts to surpass the current capabilities of STM in this context, while simultaneously generalizing the scopes of scanning NV-magnetometry for addressing solid-state spin systems.

9:55 AM EL14.17.05

Room Temperature sub-THz (300 GHz) Plasma Wave Generation in p-Diamond TeraFET [Muhammad MahmudulHasan](#)¹, [NezihPala](#)¹ and [MichaelShur](#)²; ¹Florida International University, United States; ²Rensselaer Polytechnic Institute, United States

The growing demand for efficient and compact terahertz (THz) sources operating at room temperature is driven by their wide-ranging applications in spectroscopy, imaging, and communication systems. Hydrodynamic transport modeling of TeraFETs (Terahertz Field-Effect Transistors) has revealed that p-diamond is a promising material for sub-THz applications beyond 5G. P-diamond, characterized by its large carrier effective mass, exhibits longer momentum relaxation times compared to other semiconductor materials, rendering it advantageous for generating THz radiation at lower frequencies. This paper presents a comprehensive hydrodynamic modeling study of a p-diamond-based TeraFET acting as a THz source. Our simulations show that p-diamond TeraFETs could support channel carrier oscillations at THz frequencies below 1 THz at room temperature operating as THz sources enabled by the Dyakonov-Shur instability.

To investigate the performance of the p-diamond TeraFETs, we conducted a thorough numerical analysis using a 1D hydrodynamic model. This model incorporates viscosity effects and considers damping resulting from electron scattering by impurities and phonons. Our simulations conclusively demonstrate the efficacy of the p-diamond TeraFET in emitting resonant THz radiation at a frequency of 300 GHz at room temperature when biased by a DC current. We explored the dependencies of the resonant oscillations on the channel length, drift velocity, and gate bias. These dependencies guide precise tuning of the emitted THz radiation. Our analysis predicts the minimum drift velocity necessary to overcome the decay factor caused by scattering and viscosity effects, ensuring robust resonant oscillation. These findings shed light on the p-diamond TeraFET's operation and aid in optimizing its performance as a sub-THz source.

SYMPOSIUM EL15

Chiral Materials—New Structures and Properties
November 27 - November 30, 2023

Symposium Organizers

Clarice Aiello, University of California, Los Angeles
Matthew Beard, National Renewable Energy Lab
Jian Shi, Rensselaer Polytechnic Institute
Hanyu Zhu, Rice University

* Invited Paper
+ JMR Distinguished Invited Speaker

SESSION EL15.01: Synthesis of Chiral Materials from Molecular Level
Session Chairs: Clarice Aiello and Jian Shi
Monday Morning, November 27, 2023
Hynes, Level 2, Room 207

10:30 AM EL15.01.01

Iodine Doping in Tetrathiafulvalene Twisted Crystals St. John Whittaker, Merritt C. McDowell, Shin Kim, Bart Kahr and Stephanie Lee; New York University, United States

Tetrathiafulvalene (TTF), a workhorse of the organic electronics community since its superconductor tetracyano-p-quinodimethane co-crystal was discovered in 1973,[1] is an optically inactive centrosymmetric molecule that crystallizes in an optically inactive centrosymmetric space group $P-1$ when grown from the melt. We recently discovered that growth-actuated crystal twisting breaks this symmetry to render TTF twisted crystals optically active and thus promising candidates for chiroptoelectronics.[2] In this work, tetrathiafulvalene (TTF) banded spherulites comprising helicoidal fibrils are doped with iodine to improve their conductivity for (chir)optoelectronics. Within five minutes of exposure to iodine vapor, TTF film conductivity increased by six orders of magnitude, from 100 pA to 100 μ A, accompanied by a color change from pale yellow to dark red. Grazing incidence x-ray diffraction patterns also revealed a change in crystal structure upon iodine doping. The rate of iodine doping was found to depend on the local crystal face presented at the film surface, which alternates between faces as the crystalline fibrils twist about the growth direction, forming concentric "bands" surrounding the spherulite center. Crystal face-dependent iodine intercalation was observed by optical microscopy, light absorbance spectroscopy, and electron dispersive x-ray spectroscopy. Faces corresponding to fast iodine intercalation were previously identified as the 1-11 face.[3] Mueller Matrix imaging revealed that crystal twisting is not disrupted by iodine intercalation, with circular dichroism and birefringence retained after five minutes of film exposure to iodine vapor. Combined with the orders of magnitude improvement in electrical conductivity, optically active doped TTF banded spherulites will provide a platform to examine chiral-induced anisotropies in electron and photon interactions in molecular semiconductor twisted crystals.

[1] J Am Chem Soc (1973) 95. 948-949

[2] MSDE (2022) 7. 569-576

[3] In preparation

10:45 AM EL15.01.02

Blending Chiral Small Molecules to Achiral DPP-Based Conjugated Polymer to Induce Chiroptical Properties Jeongwoo Beak, Yina Moon, Jeongjin Hong and Dong-Yu Kim; Gwangju Institute of Science and Technology, Korea (the Republic of)

Conjugated polymers have been developing due to their electrical and optical properties. Furthermore, the chiroptical properties with conjugated polymer have distinguished characteristics of selectivity based on handedness. There are many methods to induce chirality to conjugated polymers, but blending chiral small molecules to achiral conjugated polymers is one of promising and simple methods via supramolecular interactions. By utilizing this method, the induced chirality to conjugated polymer can be applied to optoelectronic devices for multiple signal due to differences in absorption depending on right or left circularly polarized light at the same wavelength.

In this study, diketopyrrolopyrrole (DPP) based polymers with charge transport, NIR absorption property, PDVT-10 is blended with chiral small molecules, (*R*)- or (*S*)-1,1'-Binaphthyl-2,2'-diamine (*R*)- or (*S*)-BN. The chiroptical characteristics are based on the blending ratio and opposite properties between (*R*)- and (*S*)-BN with PDVT-10 in solution. In thin films, the presence of (*R*)- or (*S*)-BN affects PDVT-10, leading to the emergence of a new peak in circular dichroism on near-infrared range and a peak shift in UV-Vis spectrometer. Moreover, it is possible to invert the absorption of circular dichroism and shift UV-Vis peaks through annealing condition. The formation of helical structures through supramolecular assembly on blended films is observed on AFM images and the chiral orientation of BN is transferred to the morphology of PDVT-10 confirmed by 2D-GIWAXS analysis. Moreover, a phototransistor based on an organic field-effect transistor (OFET) demonstrates difference sensitivity to right or left circularly polarized light with a wavelength of 850 nm in the near-infrared range. In particular, the optical activity of semiconductors in the near-infrared range, combined with chirality, is significantly important due to their ability for long-range optical communication, skin penetration, and night vision. In conclusion, this blending method could be proposed as a simple and straightforward approach to induce new chiroptical properties to achiral conjugated polymers.

11:00 AM EL15.01.03

Twisted Hydrogen-Bonded Frameworks Rochelle B. Spencer, Anna Yusov, Alexandra Dillon, Wantong Wu, Bart Kahr, Michael D. Ward and Stephanie Lee; New York University, United States

Directing the assembly of molecules within hydrogen-bonded frameworks is being extensively explored as a modular crystal engineering strategy to access novel molecular packing arrangements of target molecules. Crystal twisting, a common but little-known phenomenon in molecular crystals, of these frameworks provides an additional handle to not only interrogate crystal orientation-dependent properties but also to impart chirality for chiroptoelectronics. Here, we demonstrate crystal twisting in solution-processed bis(guanidinium) naphthalene-1,5-disulfonate (G_2)(1,5-NDS) films in which molecular assembly is driven by hydrogen bonding between guanidinium and sulfonate moieties. When deposited from ethanol in conditions that

favor low nucleation densities but high branching rates, (G)₂(1,5-NDS) crystallizes as banded spherulites of helicoidal fibrils emanating radially from a single nucleation center and twisting in concert with one another about the growth direction. Scanning electron micrographs (SEMs) reveal tightly packed fibrils that alternate between flat-on and edge-on orientations with respect to the substrate surface with a twisting pitch of ~ 3 - 4 μm. 2D x-ray diffraction (XRD) patterns collected on (G)₂(1,5-NDS) banded spherulites confirm that the crystals adopt a bilayer packing motif with ethanol as guest molecules. These banded spherulites further exhibit band-dependent linear dichroism and birefringence, as well as circular dichroism and birefringence as a consequence of twist-induced loss of symmetry. Given the modular nature of these hydrogen-bonded frameworks to incorporate a broad range of molecular pillars and guests, combining hydrogen bond-directed assembly with crystal twisting will open unexplored avenues in the design of chiroptoelectronic materials.

11:15 AM EL15.01.04

Spinning Around You: Using Organic Doublet Systems with Rotameric Chirality to Your Benefit in Optoelectronics and Spintronics Rituparno Chowdhury¹, Petri Murto², Craig Yu², Pratyush Ghosh¹, Yao Fu², Clare P. Grey², Akshay Rao¹, Hugo Bronstein² and Richard Friend¹; ¹The University of Cambridge, United Kingdom; ²University of Cambridge, United Kingdom

Over the last decade a large fraction of materials and optoelectronics research has been focussed on the development of methods to mitigate and manage triplet states in organic optoelectronics devices while a comparably large effort is also ongoing in engineering the spin-optical interface for the design of molecular qubit systems. Intermediate exchange-coupled high spin states are very counter-productive to the optical activity of a material, but they turn out as a hero instead of a villain if you want to make quantum computing units out of them. The discovery of the CISS effect was pivotal in showing a chirality mediated effect in light elements that can serve as a proxy to spin-orbit coupling without the presence of any heavy atom has now allowed us to access exotic spintronic properties which would otherwise remain untapped in chiral organic molecules. Even better, this opens up further possibilities to utilise chiral molecules with an open shell ground state. In this work I will walk you through the many ways that we are doing so with carbon centered tris(2,6-chloro-4-mesitylphenyl)methyl (MTTM) radicals. We first start off simple by showing that doublet organic molecules can achieve deep red, NIR-1 and NIR-2 photoluminescence with high quantum efficiency. We then address the topic of redox stability, a big issue in standard open shell molecules, and we show successfully that these doublet materials are exceptionally redox stable and redox reversible. Finally we dive deeper into the magnetic properties of the doublets when connected in different ways and show how this can interchange the spin multiplicity of the ground state and allow exceptional control of both the ground and excited state exchange couplings. We finally embark on the journey to unravel how chirality plays a role in these systems bearing in mind that all along chirality was inherent to these systems by virtue of the rotameric bond joining the donor and acceptor fragments of these molecules, this inherent chirality gives the possibility to design all-organic spin valves, which would be an unprecedented achievement. By taking you through this story I aim to show you the versatility of our materials and their potential for extensive application in quantum information sciences and spintronics setting the stage for an era of radical organic semiconductors.

This work encompasses multiple publications and manuscripts from our group:

- [1] Murto, P., Chowdhury, R., et al, 'Mesitylated trityl radicals as a new platform for doublet emission: symmetry breaking, charge-transfer states and conjugated polymers' Nat. Comm, 2023(Accepted)
- [2] Yu, C., Chowdhury, R., Fu, Y., Ghosh, P., et al 'High-spin open-shell π-conjugated near-infrared emitters with distinct spin dynamics' (Submitted, 2023)
- [3] Chowdhury, R., Murto, P., Ghosh, P., et al 'Brightening up the dark: Synthesis and photophysical exploration of series of new highly emissive chichibabin molecules' (Submitted, 2023)

11:30 AM EL15.01.05

Chiral Organic Semiconductors – Lending a Hand in Photocatalysis Aisha Mumtaz, Rebecca Ingle and Bob Schroeder; University College London, United Kingdom

Society's ever-growing energy demands and simultaneous rapid depletion of current greenhouse gas-emitting resources showcase the need to find clean, renewable alternatives. Generation of hydrogen through the combined action of sunlight, water and a photocatalyst, the water splitting reaction (WSR), offers a promising solution to this long-standing problem. However, the WSR suffers from uncontrolled spin alignment of OH radicals, producing hydrogen peroxide (H₂O₂) as a by-product, which greatly hinders the efficacy and scalability of this process.[1] As chiral molecules are sensitive to electron spin orientation, due to the Chiral Induced Spin Selectivity (CISS) effect, they could behave as spin filters in photocatalysis, thus providing a unique pathway to cleaner energy by impeding hydrogen peroxide formation.[1],[2]

Conjugated polymers are a class of material that have gained increasing attention due to their applications in many electronic devices such as transistors, organic light emitting diodes (OLEDs) and flexible organic photovoltaics (OPVs). This is owing to their tuneable optoelectronic properties, intrinsic flexibility, solution-processability, low cost and abundance. Application of these features to photocatalysis, in combination with the spin selectivity of chiral molecules, could result in efficient, scalable production of hydrogen for clean energy resources.[2],[3]

This work focuses on the synthesis and spectroscopic characterisation of a series of novel, chiral conjugated polymers to generate the desired CISS effect for the suppression of H₂O₂ in the WSR. Development of these systems relies on gaining a deeper understanding on how the nanoscale chirality impacts the overall chiral expression. We therefore investigate the effect of chiral centre positioning on the polymer microstructure. In addition to pursuing renewable, cleaner energy for society, this work could also have a profound impact on our understanding between the interplay of chiral centres and polymer microstructure.

References:

- [1] W. Mtangi et al., *J. Am. Chem. Soc.*, 2017, 139, 2794–2798.
- [2] R. Naaman et al., *J. Phys. Chem. Lett.*, 2012, 3, 2178–2187.
- [3] J. Kosco et al., *Nat. Mater.*, 2020, 19, 559-565.

11:45 AM EL15.01.06

Can We Still Measure Circular Dichroism with Circular Dichroism Spectrometers: Anisotropic Artifacts in Multiscale Hierarchically Structured Films from Magic-Sized Clusters Thomas J. Ugras¹, Yuan Yao¹, Talisi Meyer¹, Da Wang², Arantxa Arbe³, Sara Bals², Bart Kahr⁴ and Richard Robinson¹; ¹Cornell University, United States; ²University of Antwerp, Belgium; ³Spanish National Research Council, Spain; ⁴New York University, United States

Chiral materials with strong linear anisotropies are difficult to accurately characterize with circular dichroism (CD) because of artifactual contributions to their spectra from linear dichroism (LD) and birefringence (LB). Recently, we have discovered that CdS magic-sized clusters (MSC) can self-assemble into ordered films that have a hierarchical structure spanning seven orders of length-scale [1]. Because of the small size of MSCs and because of their high organic-ligand/core ratio, these hybrid materials have “softer” inter-particle interactions, with access to a richer phase diagram beyond the classical close packed structures seen with larger nanoparticles, resulting in self-organization into anisotropic patterns. These films have a strong CD response, but the chiral origins are obfuscated by the hierarchical architecture and LDLB contributions. Here, we derive and demonstrate a method for extracting the “chiroptic” CD signal (CD generated by structural dissymmetry) from hierarchical MSC films and identify the chiral origin [2]. The theory behind the method is derived using Mueller matrix and Stokes vector conventions, making use of a second-order Taylor series expansion to extract the CD. The method is verified experimentally before it is applied to hierarchical MSC and nanoparticle films with varying macroscopic orderings. Each film's extracted chiroptic CD shares a bisignate profile aligned with the exciton peak, indicating the assemblies adopt a chiral arrangement and form an exciton coupled system. Interestingly, linearly aligned MSC films possess one of the highest g-factors (0.05) among semiconducting nanostructures reported. Further, we derive an expression to model the measured CD using a third order Taylor series expansion which introduces “pairwise interference” contributions to CD spectra that, unlike LDLB contributions, cannot be averaged out of the signal. We find that the third order pairwise interference terms can make noticeable contributions to the simulated CD spectra. Using numerical simulations of the measured CD across a broad range of linear and chiral anisotropy parameters, the LDLB interactions are most prominent in samples that have strong linear anisotropies (LD, LB) but negligible chiral anisotropies, where the measured CD strays from the chiroptic CD by factors greater than 10³. Media with moderate-to-strong linear anisotropy are in great danger of having their CD altered by these effects in subtle manners. These experimental and theoretical studies provide a simple means to extract the chiroptic CD from spectra anisotropically structured samples and highlight the significance of considering distortions in CD measurements through higher order interference effects in highly anisotropic nanomaterials.

- [1] H. Han, S. Kallakuri, Y. Yao, C.B. Williamson, D.R. Nevers, B.H. Savitzky, R.S. Skye, M. Xu, O. Voznyy, J. Dshemuchadse, L.F. Kourkoutis, S.J. Weinstein, T. Hanrath, R.D. Robinson, Multiscale hierarchical structures from a nanocluster mesophase, *Nat. Mater.* 21 (2022) 518–525. <https://doi.org/10.1038/s41563-022-01223-3>.
- [2] Y. Yao, T.J. Ugras, T. Meyer, M. Dykes, D. Wang, A. Arbe, S. Bals, B. Kahr, R.D. Robinson, Extracting Pure Circular Dichroism from Hierarchically Structured CdS Magic Cluster Films, *ACS Nano*. (2022) [acsnano.2c06730](https://doi.org/10.1021/acsnano.2c06730). <https://doi.org/10.1021/acsnano.2c06730>.
- [3] T.J. Ugras, Y. Yao, R.D. Robinson, Can We Still Measure Circular Dichroism with Circular Dichroism Spectrometers: the Dangers of Anisotropic Artifacts, *Chirality*. (2023) DOI: 10.1002/chir.23597.

2:00 PM *EL15.02.01

Chirality-Induced Quantum and Topological Properties in 2D Tellurium ChangNiu and PeideP. Ye; Purdue University, United States

Chirality is increasingly recognized as a critical property in various aspects of human life, spanning fields such as biological chemistry and physics. The disruption of chiral symmetry significantly influences the properties of matter, particularly in pharmaceuticals, biochemistry, and materials science. Thus, a comprehensive understanding and manipulation of chiral materials are crucial for advancing cutting-edge technologies, including chirality-based sensors, optical devices, and electronic systems.

Trigonal Tellurium (Te) possesses one of the simplest crystal structures, consisting of a unit cell where three Te atoms form a covalently bonded spiral chain. The chirality of the Te crystal is determined by the helicity of these atomic Te chains, classified into different space groups: $P3_121$ (right-handed) and $P3_221$ (left-handed). Recently, hydrothermally grown two-dimensional (2D) Tellurium (Te) with a thickness of about 10 nanometers has attracted considerable attention due to its excellent electrical, thermal, and optical properties. The chemical potential of 2D Te can be electrostatically tuned by applying a gate voltage, enabling systematic studies of the quantum and topological properties induced by chirality.

Under ambient pressure, the conduction band minimum and valence band maximum of Te are located at the $H(H')$ point in the first Brillouin zone. Due to Te atoms' strong spin-orbit interaction and the unique chiral crystal structure characterized by three-fold screw symmetry, the conduction bands split and cross at the $H(H')$ point, leading to a Weyl node. This node produces a radial-like spin texture in k -space, where spin polarization aligns parallel to the direction of electron momentum. This characteristic distinguishes it from the spin texture observed in Rashba semiconductors or the surface states of topological insulators, where the spin polarization is perpendicular to the electron momentum direction. Importantly, the spin polarization and charge of the Weyl nodes reverse in different enantiomers, a consequence of the mirror symmetry of left- and right-handed Te crystals.

Our investigations of the chirality-induced properties in 2D Te involved electrical and photoelectric responses. The chirality of 2D Te flakes was determined and verified using hot sulfuric acid etch pits and high-angle tilted high-resolution scanning transmission electron microscopy (HR-STEM). At low temperatures (0.3 K), we observed gate-tunable nonlinear electrical responses in 2D Te, including nonreciprocal electrical transport along the longitudinal direction and a nonlinear planar Hall effect along the transverse direction when subjected to a magnetic field. At room temperature, we discovered tunable chirality-dependent circular photogalvanic and photovoltaic effects, stemming from the interaction between circular-polarized light and the chiral crystal structure of 2D Te. These findings highlight the ability to control and manipulate the degree of chirality in materials.

2:30 PM EL15.02.02

Nonlocal Spin Transport Property of Chemical Vapor Deposition - Grown Tellurium Crystal ZixuWang and JianShi; Rensselaer Polytechnic Institute, United States

Chiral crystalline materials have a unique and robust spin-momentum relation allowing the design of energy-efficient spintronic devices. For example, when electrons flow in chiral materials, the electron spin is polarized either parallel or antiparallel to the current direction. In this work, we report the nonlocal spin transport characteristics of chemical vapor deposition - synthesized single crystalline Te crystal. We apply inversion spin hall effect to measure the current-induced spin in Te crystal. We find that the spin polarization can transport several hundreds of micrometers at room temperature. This work provides resilient testbeds for future development of practical spintronic devices.

2:45 PM EL15.02.03

Anisotropic and Bilinear Magnetoresistance of Bulk Doped GaAs ZhizhuoLiang and JianShi; Rensselaer Polytechnic Institute, United States

Basic understanding of the anisotropic and bilinear magnetoresistance (BMR) of GaAs is crucial for the design of spin-active devices. For BMR, it shows a linear dependence on the electric current and the magnetic field. BMR has been reported in topological insulators, two-dimensional electron gas, topological semimetals, 3D Rashba materials, etc. Here we report the observation of BMR in bulk n-type GaAs with a doping concentration of $1 \times 10^{18} \text{ cm}^{-3}$. We measure the anisotropic magnetoresistance and BMR at 2.4 K, 4 K, and 10 K. During measurement, we vary the magnetic field from -14 T to 14 T. Magnetoresistance dependency on the current intensity, the magnetic field strength, direction of the magnetic field, and angle between the magnetic field and the current are studied. The work suggests the existence of non-trivial BMR in bulk GaAs.

3:00 PM BREAK

3:30 PM *EL15.02.04

Novel Topological Chiral Materials and Quantum Properties M. ZahidHasan; Princeton University, United States

Abstract Body: In this talk I present experimental realizations and properties of several chiral topological materials in novel Weyl, Dirac and Kagome systems building up on earlier results on topological insulators (Hasan & Kane, RMP 2010) and "Topological quantum properties of chiral crystals" (Nature Materials (2018)); "Topological Hopf and Chain Link Semimetal States" (Physical Review Letters 119, 156401 (2017)); "Magnetic Weyl fermion semimetals in the R-AlGe family of compounds" (Physical Review B (2018)); "Giant and anisotropic many-body spin-orbit tunability in a strongly correlated kagome magnet" (Nature 562, 91-95 (2018)), Chern magnets (Nature 2020, Nature Physics 2020) and "Unconventional chiral charge order (magnetic) in the normal state of kagome superconductor KV3Sb5" (Nature Materials 2021). I conclude by indicating the new frontiers of research opened by the discovery some of these chiral materials.

4:00 PM EL15.02.05

Atomically Sharp Internal Interface in a Chiral Weyl Semimetal Nanowire NitishMathur¹, Fang Yuan¹, GuangmingCheng², SahalKaushik³, InigoRobredo⁴, MaiaG. Vergniory⁴, JenniferCano^{5,6}, NanYao², SongJin⁷ and LeslieSchoop¹; ¹Princeton University, United States; ²Princeton Institute for Science and Technology of Materials, United States; ³Nordita, Stockholm University and KTH Royal Institute of Technology, Sweden; ⁴Max Planck Institute for Chemical Physics of Solids, Germany; ⁵Department of Physics and Astronomy, Stony Brook University, United States; ⁶Center for Computational Quantum Physics, Flatiron Institute, United States; ⁷University of Wisconsin--Madison, United States

Internal interfaces in Weyl semimetals (WSMs) are predicted to host distinct topological features that are different from the commonly studied external interfaces (crystal-to-vacuum boundaries). However, the lack of atomically sharp and crystallographically oriented internal interfaces in WSMs makes it difficult to experimentally investigate hidden topological states buried inside the material. In this talk, I will first discuss the presence of a unique internal interface known as *merohedral* twin boundary in chemically synthesized single-crystal nanowires (NWs) of CoSi, a chiral WSM of space group $P2_13$ (No. 198). Secondly, I will show the material characterization techniques to confirm the nature of lattice symmetry breaking inside the CoSi NWs due to the presence of this internal interface. Finally, I will conclude with showing why these interfaces are topologically relevant and how these *merohedrally* twinned NWs could be ideal material systems to probe unexplored topological properties associated with internal interfaces in chiral nanostructures.

4:15 PM EL15.02.06

A Room-Temperature Polar Magnetic Metal HongruiZhang¹ and RamamoorthyRamesh^{1,2,3}; ¹University of California, Berkeley, United States; ²Lawrence Berkeley National Laboratory, United States; ³Rice University, United States

Multiferroic (-like) materials-based electric/magnetic devices hold great promise for the realization of ultra-low power logic-memory elements.[1] However, multiferroic (like) materials are elusive.[2] In this talk, we present the successful synthesis of a room-temperature polar magnetic metal, $\text{Fe}_{2.5}\text{Co}_{2.5}\text{GeTe}_2$ (FCGT).[3] The breaking inversion symmetry in FCGT induces an in-plane Dzyaloshinskii-Moriya interaction and spin-orbit torque when a charge current is applied. Thus, the FCGT system with perpendicular magnetic anisotropy demonstrates various novel magnetic properties that hold potential for spintronic devices. Our experimental results demonstrate the observation of a Néel-type skyrmion lattice at room temperature and zero field [4]. Additionally, by utilizing the confinement effect through stacking two flakes, we created an ordered skyrmion lattice [5]. Furthermore, we achieved current-induced magnetization self-switching in a few-layered flake at room temperature. This discovery of a non-centrosymmetric layered magnet operating at room temperature opens up new possibilities for layered spintronic device applications.

[1] S. Manipatruni *et al.* Nature 565, 35-42 (2019)

[2] R. Wilkinson, Physics 15, s44 (2022)

[3] H. R. Zhang *et al.* Physical Review Materials 6 (4), 044403 (2022)

[4] H. R. Zhang *et al.* Science advances 8 (12), eabm7103 (2022)

[5] P. Meisenheimer *et al.* Xiv:2210.02546

8:00 AM *EL15.03.01

Inorganic Chiral Nanoparticles—A Promising Chiral Trigger to Induce Homochirality[ZhifengHuang](#); The Chinese University of Hong Kong, Hong Kong

Origin of homochirality is a fundamentally important but yet unanswered question. One of the keys to answer this question is to understand external chiral forces to trigger symmetry breaking, which has been believed to induce the homochirality. Diverse chiral forces have been proposed, but one is missing: inorganic chiral surfaces have an enantiospecific interaction with prochiral molecules, considering the fact when the Earth formed about 4.5 billion years ago, it was prebiotically composed of inorganic minerals, mostly crystalline in nature and some are chiral, followed by the existence of organic life. We are studying chiral forces contributed from inorganic atomically chiral surfaces.

We use glancing angle physical vapour deposition to fabricate inorganic chiral nanoparticles (or CNPs), which have adjustable optical activities in the UV-visible-near infrared region. Inorganic CNPs are made of diverse metals, alloys and oxides, and composed of chiral structures at the atomic scale, including chiral twisting of multi-layers of achiral facets, high-index chiral facets, and chiral defects. Inorganic CNPs enantiospecifically interact with prochiral molecules, leading to an enantiospecific amplification of molecular optical activity, an enantioselective photoinduced cyclodimerization of a prochiral anthracene derivative, and reliable manipulation of symmetry breaking of prochiral helicenes. Our works shed light on the origin of homochirality (or life) stemming from the atomically chiral surfaces of minerals through the enantiospecific interactions with prochiral molecules.

8:30 AM EL15.03.02

Origins of Chirality in II-VI Semiconductor Nanoclusters via Symmetry Breaking[ChenjieZeng](#); University of Florida, United States

Chiral semiconductor nanostructures have potential applications in chiral optoelectronics, spintronics, sensors, and catalysis. Compared to organic molecules, the origins of chirality in semiconductor nanomaterials are less understood due to many possible chiral geometries at hierarchical levels. Here, we unveil the intrinsic origins of chirality in II-VI semiconductor nanoclusters by achieving atomic precision in a tetrahedral-shaped CdSe nanocluster and X-ray crystallographic analysis. We show that the chirality emerges from the incorporation of tetrahedral coordination of individual ions into the icosahedral packing of the lattices, breaking the symmetry of the inorganic core from an achiral I_h to a chiral T . The chirality in the CdSe core further propagates to the metal-ligand interface, as manifested in the clockwise and counter-clockwise rotations of the interfacial coordination patterns. The asymmetric assembly of ligands on the tetrahedral facets further breaks the cluster symmetry from T to C_3 . The left- and right-handed enantiomers are co-crystallized as a 1:1 racemic mixture. The resolved atomic structure of the chiral CdSe clusters shed light on the chiral structures observed in the larger semiconductor nanocrystals and their assemblies.

8:45 AM EL15.03.03

Inducing Chiral Photoluminescence in Single Photon Quantum Emitters using Chiral Induced Spin Selectivity Effects.[SuryakantMishra](#), [JenniferHollingsworth](#), [EricBowes](#), [HanHtoon](#) and [AndrewC. Jones](#); Los Alamos National Laboratory, United States

Chiral quantum emitters or non-reciprocal single photon devices have the potential for playing a significant role in future quantum communication-based infrastructure. To date, the realization of circularly polarized quantum emitters generally requires complex and bulky experimental infrastructures such as high magnetic/electric fields and cryogenic-temperatures. One potential means of realizing chiral quantum emission in solid-state systems is Chiral-Induced Spin Selectivity (CISS). This effect is a well-known physical phenomena known to enable control over electronic spins via the asymmetric transport of electronic spins in chiral organic and inorganic systems. We have explored the utilization of CISS effects as a means of manipulating the circular polarization of photoluminescence from single quantum emitters. Here, cadmium selenide-quantum dots are immobilized on a chiral surface prepared using electrodeposition of aniline. We observe both the inducement a significant degree of circular polarized photoluminescence emission and a magnetization-dependent photoluminescence quenching by using a ferromagnet valve in the chiral substrate. These observations illustrate the potential of a CISS-based mechanisms for realizing chiral single photon emission sources in solid-state material devices. By further exploring the dependence of circularly polarized emission on the quantum dot shell thickness and the thickness of the chiral films, we develop and demonstrate a model for the energy transfer pathways experienced by differing spin orientations in this system.

9:00 AM EL15.03.04

Structure-Property Relationships of Electrospun CdS Quantum Dot Fibers with Mechanically Modulated Reversible Chirality[HansadiJayamaha](#), [ThomasJ. Ugras](#), [TobiasHanrath](#), [RichardRobinson](#) and [LarissaShepherd](#); Cornell University, United States

Over the last three decades, electrospinning has gained increasing interest as a synthesis technique for micro and nano fibers due to its tunability and versatility. For the first time, electrospinning induced self-assembly of Cadmium Sulfide (CdS) magic sized clusters (MSCs) and their resulting chiroptical properties are discussed. The MSCs assemble into hexagonal mesophase during synthesis and the higher-level structures arise during the evaporation process. Through electrospinning, multiple hexagonal mesophase bundles are postulated to form twisted nanofibrils. These nanofibrils collectively constitute the microfiber as the result of self-assembly. Using Field emission scanning electron microscopy (FE-SEM), and atomic force microscopy (AFM) the morphology of the microfibers and the arrangement of the observed fibrillar structures are studied. The chiroptical properties of the fiber mats are extensively studied using Circular dichroism (CD) spectroscopy.

We improve the uniaxial fiber orientation, thereby synthesizing chiral microfibers with high dissymmetric factors (~ 0.02) and linear dichroism (LD), comparable to thin films of the same material. Reversible changes in CD signals and reduced electron dipole alignment (i.e., LD) occur on stretching of the fibers embedded in elastomeric films. To study the alignment of the mesophase filaments and inter-filament distance upon stretching, Synchrotron based small angle X-ray scattering (SAXS) was used. We confirm a 4-scan method for removing Linear Dichroism-Linear Birefringence (LD-LB) and photo elastic modulator contributions and isolating true CD is applicable for such fibrous webs. This work provides the groundwork for further study of electrospun chiral fibers by bringing forth new research questions regarding the assembly of MSCs into fibrous structures.

9:15 AM EL15.03.05

Room-Temperature Electrically Switchable Rashba-Dresselhaus Effect in a Van Der Waals Ferroelectric Crystal with Persistent Spin Helix[JianShi](#); Rensselaer Polytechnic Institute, United States

Here we show the discovery of the persistent spin helix in an organic-inorganic hybrid ferroelectric halide perovskite whose layered nature makes it intrinsically like a quantum well. We demonstrate that the spin-polarized band structure is switchable at room temperature via an intrinsic ferroelectric field. We reveal valley-spin coupling through a circular photogalvanic effect in single-crystalline bulk crystals. The favoured short spin helix wavelength (three orders of magnitude shorter than in III-V materials), room-temperature operation and non-volatility make the hybrid perovskite an ideal platform for understanding symmetry-tuned spin dynamics, towards designing practical spintronic materials and devices that can resolve the control-relaxation dilemma.

9:30 AM BREAK

10:00 AM *EL15.03.06

Noncentrosymmetric and Chiral 2D Quantum Materials Through Screw Dislocations and Structural Tuning[SongJin](#); University of Wisconsin--Madison, United States

Rationally controlling the structures of two-dimensional (2D) layered materials allows us to tune the electronic structures and quantum states of matter, discover new physical properties, thus enable new applications. We show how the phase, layer stacking and thus physical properties of 2D MX₂ materials can be influenced by screw dislocations. Noncentrosymmetry of these MX₂ materials and 2D Ruddlesden-Popper (RP) lead halide perovskites could be enabled at the monolayer and bulk crystal structure level by structural tuning and screw dislocations. Furthermore, chiral microplates of MX₂ and 2D RP perovskites can be produced via a screw dislocation growth mechanism and the resulting chiroptical properties of individual chiral objects are studied using fluorescence detected circular dichroism (FD-CD) microscopy and other polarized spectroscopic/nonlinear optical techniques. Moreover, we achieved systematic interlayer twisting of MX₂ spiral layers grown via screw dislocations due to mismatched geometry between Euclidean crystal lattices and non-Euclidean (curved) surfaces to form moiré superlattices, which could lead to novel quantum phenomena. The ability to enable and control noncentrosymmetry, chirality, and twisting of 2D materials open up new dimensions of quantum materials for the study of nonlinear and chiral optical properties, valleytronics and twistronics.

10:30 AM EL15.03.07

Enabling Chiroptical Properties in Achiral 2D Perovskites via Spiral Morphology Willa Mihaljic-Koch, Katherine Parrish, Randall H. Goldsmith and Song Jin; University of Wisconsin–Madison, United States

Chiral 2D halide perovskites are promising semiconducting materials for chiroptoelectronic and spintronic applications. Chirality is typically imparted into 2D perovskites through the incorporation of chiral ammonium spacer cations, resulting in a chiral crystal structure. However, the extent of chirality transfer from the chiral organic cations to the inorganic perovskite network remains debated. In this work, we present another approach to introduce chirality and chiroptical properties into 2D perovskites through nanostructure morphology. By tuning crystallization conditions at an air–water interface, a large family of 2D perovskites with achiral crystal structures can be directly grown into spiral microplates via a screw dislocation growth mechanism. We demonstrated the versatility of this method by synthesizing spiral microplates of 10 different 2D Ruddlesden–Popper lead halide perovskites with various spacer cations, A-site cations, *n* number, and halide anions. The microplates can then be transferred to arbitrary substrates and characterization with atomic force microscopy clearly revealed the spiral centers. Fluorescence-detected circular dichroism (FD-CD) microscopy was used to investigate the resulting chiroptical properties of individual chiral objects and large, spatially dependent *g*-factors on the order of 10^{-3} were observed from (BA)₂(MA)₂Pb₃I₁₀ spiral microplates. These results show that screw dislocation-driven growth can be used as a generally applicable method for enabling chirality and chiroptical properties in 2D perovskites without the need for chiral cations.

10:45 AM EL15.03.08

Ligand-Induced Chirality in Zig-Zag Topography of Two-Dimensional Iron Hydroxide for Spin-Polarized Photon Absorption Control Bumchul Park^{1,1}, Sung-Chul Kim², Dae Beom Lee³, Jun Lu^{1,1}, Ji-Young Kim^{1,1}, Sang Hyun Lee^{1,1}, Young Keun Kim³ and Nicholas A. Kotov^{1,1}; ¹University of Michigan–Ann Arbor, United States; ²Korea Institute of Science and Technology, Korea (the Republic of); ³Korea University, Korea (the Republic of)

Chiroptical nanomaterials capable of combining magnetism and chirality are of the cutting-edge engineering for spin-polarized light–matter interaction because they can modulate circularly polarized light through a magnetic field or conversely modulate the excited state and spin state of a material with circularly polarized light. However, most chiral nanomaterials, including noble metals, semiconductors, and ceramics, have a strong chiroptical response but a weak net magnetic moment, limiting to induce strong coupling with the magnetic field of photons in polarized light–matter interaction. Transition metal oxides such as Co, Fe, Ni, and Mn can offer a strong magnetic dipole moment from the exchange coupling of 3d electron spins but rarely have optical activity in the UV–Vis range. Antiferromagnet has been marginalized in spin-polarized light modulation because the net magnetic moment is canceled out by antiparallel spin sublattice leading to negligible Zeeman effect. However, unlike ferromagnetism, which is usually limited to metals, antiferromagnets offer a much greater degree of freedom to control atomic topography and spin configuration.

Here, we identified that previously unknown two-dimensional (2D) topography of iron oxyhydroxide enables the arrangement of low-dimensional antiferromagnet spin chains, which can be leveraged in a magnetically tunable spin-polarized photon absorption. We found a new type of nanoscale iron oxyhydroxide, layered ferric rust (LFR), with a monoclinic structure forming in the crystallization in the presence of acetate anion. The acid ligands coordinating iron atoms induce an unexpected zig-zag stacking of dimerized FeO octahedra, leading to a layered crystal structure with extended interlayer spacing. Topotactic intercalation of enantiomeric amino acids between the sheets breaks mirror symmetry in the crystal lattice and introduces screw axis symmetry, enabling transfer chirality of amino acid to LFR crystallization, producing chiroptical active LFRs. Achiral and chiral LFRs reserve low dimensional antiferromagnet spin chains where some portion of spins can be excited into parallel spin arrangement even under low external magnetic fields at room temperature. Therefore, the chiral LFR enables spin-polarized photon absorption in the UV–Vis wavelength range by the Zeeman effect in addition to the chiroptical activity contributed by the ligand-induced mirror symmetry breaking, as manifested by magnetic circular dichroism measurement. We believe our results would be a cornerstone for designing inorganic–organic hybrid two-dimensional nanomaterials for the various chiral spintronics, optoelectronics, and catalyst fields.

11:00 AM EL15.03.09

Exceptionally Large Chiroptic Dissymmetry Factors in Films of Supramolecular Magic-Sized Clusters Thomas J. Ugras, Yuan Yao, Reilly Lynch and Richard Robinson; Cornell University, United States

A key goal of optical materials science is to develop self-assembling hierarchical materials from nanoparticle building blocks with interesting properties. Understanding the structure–property relationships within these systems will enable the rational design of advanced optical devices. Recently, our group has discovered that CdS magic-sized clusters organize into hexagonal fibers which can self-assemble into ordered films that have a hierarchical structure spanning seven orders of length-scale [1]. These films have demonstrated strong linear and circular dichroism (LD, CD) responses originating from transition dipole alignment and cluster-to-cluster coupling, respectively, but further characterization of the optical properties using lab-based measurements are obscured by the samples' mixed linear and chiral anisotropies [2, 3]. In this work, we pair two synchrotron techniques, microfocussed small-angle x-ray scattering (SAXS) and synchrotron radiation Mueller Matrix polarimetry (MMP) mapping, to unravel the structural and optical anisotropies present in the self-assembled nanocrystal films. These studies have revealed local chiroptical properties stronger than previous measurements from lab instruments; in fact, our measured dissymmetry factors (i.e., absorption *g*-factor) are the largest reported for inorganic semiconductors, and only an order of magnitude smaller than the theoretical maximum limit of 2. The MMP mapping reveals that the self-organized films contain millimeter-scale domains with a constant CD magnitude and handedness, whereas isotropic films (non-self-assembled) present much smaller micron-scale domains. Further, MMP and SAXS measurements show that within self-assembled, anisotropic films the transition dipoles of the clusters are macroscopically oriented in the same direction as the nm-scale fibers. In summary, these experiments have revealed a relationship between the self-assembly process, the orientation of supramolecular nanocrystal fibers, and the handedness of a film's response. These results - anomalously large chiral anisotropy, orientational control of the clusters and their transition dipoles, and enantiomeric control of chiral domains within nanocrystal films - enable chiral light control for a range of emerging technologies.

[1] H. Han, S. Kallakuri, Y. Yao, C.B. Williamson, D.R. Nevers, B.H. Savitzky, R.S. Skye, M. Xu, O. Voznyy, J. Dshemuchadse, L.F. Kourkoutis, S.J. Weinstein, T. Hanrath, R.D. Robinson, Multiscale hierarchical structures from a nanocluster mesophase, *Nat. Mater.* 21 (2022) 518–525. <https://doi.org/10.1038/s41563-022-01223-3>.

[2] Y. Yao, T.J. Ugras, T. Meyer, M. Dykes, D. Wang, A. Arbe, S. Bals, B. Kahr, R.D. Robinson, Extracting Pure Circular Dichroism from Hierarchically Structured CdS Magic Cluster Films, *ACS Nano*. (2022) *acs.nano.2c06730*. <https://doi.org/10.1021/acsnano.2c06730>.

[3] T.J. Ugras, Y. Yao, R.D. Robinson, Can We Still Measure Circular Dichroism with Circular Dichroism Spectrometers: the Dangers of Anisotropic Artifacts, *Chirality*. (2023) DOI: 10.1002/chir.23597

11:15 AM EL15.03.10

Decomposition of Layered Double Hydroxides for Accessing Chiral Metal Oxides Áine Coogan¹, Lucia Hughes^{1,1,1}, Finn Purcell-Milton^{1,2,3}, Seán Cardiff^{1,1}, Valeria Nicolosi^{1,1,1} and Yuri K. Gun'ko^{1,3,1}; ¹Trinity College Dublin, The University of Dublin, Ireland; ²Technological University Dublin, Ireland; ³University College Dublin, Ireland

In recent years, significant research efforts have been directed towards the development of chiral and chiroptically active inorganic nanomaterials, resulting in many new nanomaterials of various forms and morphologies, including quantum dots, nanowires, and tetrapods, among others.^{1–3} Layered double hydroxides (LDHs) have emerged as a distinct class of ionic two-dimensional (2D) nanomaterials, renowned for their exceptional anion exchange properties, allowing for the incorporation of diverse species within their interlayer spaces, including chiral molecules. Surprisingly, despite this unique characteristic, there is a notable absence of reported studies exploring the utilisation of LDHs treated with chiral ligands to induce chiroptical activity.

While chiral copper (II) oxide (CuO) nanostructures have previously been documented in literature, their synthesis often requires harsh, high-temperature synthetic conditions and the inclusion of expensive surfactants and symmetry-breaking agents to induce circular dichroism (CD) responses in the visible range.^{4,5} Prior to this work, the room temperature synthesis of chiral CuO has remained un-explored to the best of our knowledge. Additionally, the potential for chirality transfer from chiral ligands to LDH-based nanostructures has not been reported. Herein, we present the unique facile approach to the synthesis of chiral CuO nanostructures through an alkaline room-temperature, aqueous treatment of carbonate-intercalated copper–aluminium LDHs (CuAl–CO₃ LDHs) with L- and D-Phenylalanine (L- and D-Phe). The resulting 2D CuO nanosheet bundles display remarkable chiroptical activity, with *g*-factors up to 0.0035. Time-dependent circular dichroism (CD), powder X-ray diffraction (pXRD) and Fourier transform infrared spectroscopy (FT-IR) studies reveal that the initial chirality transfer arises from Phe coordination to the Cu²⁺ sites, leading to decomposition of the CuAl–CO₃ LDH to CuO. Self-assembly of the Phe-functionalised CuO nanosheets results in enhancement of the chiroptical activity. This work represents a novel, facile route of accessing chiral metal oxides through decomposition of LDH precursors. The ease of synthesis and induction of strong chiroptical activity in the visible range (400–800 nm) highlights the significance of this work. The resultant new chiral metal oxides hold promise for potential applications in enantiomeric separation and asymmetric catalysis, paving the way for advancements in chiral nanomaterial research.⁶

References:

1 - F. Purcell-Milton, R. McKenna, L. J. Brennan, C. P. Cullen, L. Guillemeney, N. V. Teplakov, A. S. Baimuratov, I. D. Rukhlenko, T. S. Perova, G. S. Duesberg, A. V. Baranov, A. V. Fedorov and Y. K. Gun'ko, *ACS Nano*, 2018, **12**, 954–964.

2 - D. Kehoe, E. Mates-Torres, P. Samokhvalov, M. García-Melchor and Y. K. Gun'ko, *J. Phys. Chem. C*, 2022, **126**, 434–443.

3 - J. E. Govan, E. Jan, A. Querejeta, N. A. Kotov and Y. K. Gun'ko, *Chem. Commun.*, 2010, **46**, 6072–6074.

4 - Y. Duan, X. Liu, L. Han, S. Asahina, D. Xu, Y. Cao, Y. Yao and S. Che, *J. Am. Chem. Soc.*, 2014, **136**, 7193–7196.

5 - C. Hao, A. Qu, L. Xu, M. Sun, H. Zhang, C. Xu and H. Kuang, *J. Am. Chem. Soc.*, 2019, **141**, 1091–1099.

6 - Á. Coogan, L. Hughes, F. Purcell-Milton, S. Cardiff, V. Nicolosi and Y. K. Gun'ko, *J. Phys. Chem. C*, 2022, **126**, 18980–18987.

11:30 AM EL15.03.11

DNA-Templated Silver Nanoclusters with Strong Chiroptical Response in the Visible Spectral Region Rweetuparna Guha, Anna Gonzalez Rosell, Malak Rafik and Stacy Copp; University of California, Irvine, United States

DNA can template the chemical synthesis of few-atom silver nanoclusters with defined chiralities and strong electronic circular dichroism (CD) response. These "Ag_N-DNAs" have a diversity of sizes, shapes, and optical properties that are selected by the nucleobase sequence of their DNA ligands. Composed of just 10–30 Ag atoms and 1–3 short DNA oligomers, most studies of Ag_N-DNAs have focused on their bright visible to near-infrared fluorescence. The DNA sequence-selected chiroptical properties of Ag_N-DNAs are also of both fundamental and applied interest and have been far less studied. As an inherently chiral ligand, DNA selects for nanocluster chirality without the need for intensive separation techniques that are typically required for metal nanocluster enantiomer separation, such as chiral chromatography. The chiral properties of Ag_N-DNAs hold promise for biomolecular sensing and nanophotonics applications. However, studies of the chirality of Ag_N-DNAs prepared to atomic precision are limited to date, and few X-ray crystallographic structures have been reported.

To understand the chiral properties of Ag_N-DNAs, we investigated a large set of 19 different atomically precise Ag_N-DNA species with emission at the far red/NIR spectral border [1]. The molecular formula of each purified species is determined by high-resolution mass spectrometry and correlated to its optical absorbance, emission, and CD spectra. We find that these Ag_N-DNAs are either 6-electron clusters or 8-electron clusters (corresponding to the oxidation state of the silver nanocluster), with distinct absorbance and CD spectral features for these two classes of nanoclusters. 8-electron Ag_N-DNAs are stabilized by two DNA oligomer copies and display complex CD spectra with multiple distinct UV and visible transitions. The electron count of these "magic-sized" 8-electron nanoclusters suggests quasispherical geometries. 6-electron Ag_N-DNAs, which past studies support have rod-like shapes, exhibit three different ligand compositions, each with its own characteristic CD signatures. Ag_N-DNAs stabilized by two oligomer copies exhibit a distinct positive or negative monosignate CD signature aligned with the longest visible absorbance peak of the nanocluster, suggesting a chiral nanocluster core whose handedness is selected by the specific DNA template sequence. Ag_N-DNAs stabilized by three oligomer copies exhibit the same visible CD signature but distinct UV CD signatures, suggesting that DNA ligands adopt similar conformations around nanoclusters with three DNA ligands. Finally, Ag_N-DNAs stabilized by two oligomer copies and additional chlorido ligands exhibit significantly suppressed visible CD signatures, supporting that the additional atomic ligands suppresses nanocluster chirality. The distinct chiroptical signatures and compositions of these four classes of Ag_N-DNAs also correlate to distinct excited state emission properties, suggesting that nanocluster electron count and chirality influences both ground and excited state processes in these emitters. This study illustrates the diversity of structure-property relationships for NIR-emissive Ag_N-DNAs, which could be harnessed to precisely tune these emitters for applications that exploit their DNA sequence-selected chiral properties. Moreover, the results show that the chiroptical properties of Ag_N-DNAs are highly sensitive to nanocluster composition and ligand conformation.

References: [1] Guha, Rweetuparna, et al. "Electron count and ligand composition influence the optical and chiroptical signatures of NIR-emissive DNA-stabilized silver nanoclusters." (2023). DOI: 10.26434/chemrxiv-2023-hftx9

SESSION EL15.04: Interaction Between Spin and Structural Chirality in Materials

Session Chairs: Matthew Beard and Hanyu Zhu

Tuesday Afternoon, November 28, 2023

Hynes, Level 2, Room 207

1:30 PM *EL15.04.01

Magnetic Chirality Sang Wook Cheong and Xianghan Xu; Rutgers University, United States

Chirality, which arises from the breaking of mirror symmetries combined with any spatial rotations, is a fundamental concept that plays a pervasive role in a wide range of phenomena from the functionality of DNA, vine climbing to the piezoelectricity of quartz crystals. It is worth noting that chirality does not always involve a twisting resembling a screw. In the context of magnetic systems, chirality refers to the presence of chirality in spin ordered states or mesoscopic spin textures. The term "chirality" has been extensively used in the physics community in recent years, often leading to confusion due to its various interpretations. To provide clarity, we define that in steady states, chirality (C) remains unchanged under time-reversal operations, whereas chirality prime (C_⊥) represents the breaking of both time-reversal and mirror symmetries combined with spatial rotations. This colloquium aims to explore different examples of magnetic chirality and chirality prime, along with the emergent phenomena associated with them. These phenomena include self-inductance, directional nonreciprocity in magnetic fields, current-induced magnetization, chirality-selective spin-polarized current, Schwinger scattering, magneto-optical Kerr effect, and linear magnetoelectricity. While some of these exotic phenomena have been recently observed, many others still require experimental confirmation in the future.

2:00 PM *EL15.04.02

Chiral States of Electrons and Spins and Their Electromagnetic Signatures Joel Moore^{1,2}; ¹University of California, Berkeley, United States; ²Lawrence Berkeley National Laboratory, United States

Chiral crystal structures allow optical effects such as natural optical activity, which has long been used to identify chirality. While the symmetry analysis of structural chirality and optical response was carried out many years ago, the details of how microscopic electron wavefunctions generate observed chirality were not completely understood even in the linear case. Studies motivated by the experimental discovery of Weyl semimetals clarified the origin of chirality at low frequency in all chiral metals (the chiral or gyrotropic magnetic effects) and the importance of the orbital magnetic moment. Weyl semimetals are more unique in their *nonlinear* optical properties, where chiral Weyl semimetals show an exciting kind of quantization in their chiral photocurrent or chiral magnetic effect at the non-interacting level. The second part of the talk concerns how interactions between electrons or spins can lead to the spontaneous development of a chiral order parameter. The specific example discussed in detail is the behavior of triangular lattice Mott insulators, where a chiral spin liquid is shown numerically and analytically to be a competitive state arising near the Mott transition. Experimental signatures of this state, and the rapidly developing experimental situation of triangular lattice compounds, are discussed as an example of how new techniques allow greater understanding of correlated lattice problems.

2:30 PM EL15.04.03

Chiral Magneto-Optical Properties and Chiral Spintronics Based on Chiral Halide Perovskites Lan-Sheng Yang, Pei-Hsuan Lo, Chin-An Hsu, Yi-Hsiu Hua and Yu-Chiang Chao; National Taiwan Normal University, Taiwan

Chiral halide perovskites can be prepared by solution processing using a mixture of a lead halide and a chiral organic halide as a precursor. Examples of chiral organic halides are *R*- and *S*-methylbenzylammonium halide and *R*- and *S*-1-(2-naphthyl)ethylammonium halide. In this presentation, we will present the chemical composition, morphology, absorption, photoluminescence, quantum yield and carrier lifetime of chiral perovskite films prepared from precursor solutions with different stoichiometric ratios and different halide ratios. The chiral halide perovskite films exhibit chiroptical properties, such as circular dichroism and circularly polarized luminescence, in the absence of an external magnetic field. Symmetrical circular dichroism spectra were obtained. The energy level splitting induced by chiral molecules was estimated by using multiple Gaussian fitting. Once the magnetic field is applied, the magnetic field-induced CD features are superimposed on the intrinsic chirality-induced CD features. In addition, spin organic light-emitting diodes were realized by using chiral halide perovskite film as the spin-polarized hole transport layer. At room temperature, circularly polarized electroluminescence was observed from the spin organic light-emitting diodes in the absence of an external magnetic field.

2:45 PM EL15.04.04

Evaluation of the Spin Splitting of Chiral Perovskites via Circular Photogalvanic Effect Taishi Noma¹ and Daigo Miyajima^{1,2,3}; ¹RIKEN, Japan; ²The University of Tokyo, Japan; ³The Chinese University of Hong Kong, China

In materials that exhibit spin splitting, a zero-bias photocurrent can be generated by circularly polarized light. This phenomenon is called circular photogalvanic effect (CPGE), and CPGE had been investigated exclusively in inorganic materials.^[1] However, recently, CPGE has been observed also in chiral perovskites, where chiral organic molecules are incorporated into inorganic

perovskite frameworks.^[2,3] It is reported that the direction of the CPGE current in chiral perovskites is reversed depending on the chirality, which could provide novel functionalities for spintronic devices. Nevertheless, the CPGE of chiral perovskites has not been well investigated. The chirality-dependent CPGE of chiral perovskites originates from Dresselhaus effect, which is caused by the inversion asymmetry at crystal structures. However, Rashba effect, which is caused by the inversion asymmetry at surfaces or interfaces, can also occur in chiral perovskites with strong spin-orbit coupling (SOC). Rashba effect is promising for spintronic application because the strength of SOC can be tuned by external voltages. Therefore, it is of great importance to clarify the contribution of Rashba and Dresselhaus effects in the observed CPGE currents. In this study, we observe the CPGE of ((R/S)-(-)-1-cyclohexylethylamine (R/S-CYHEA))₈Pb₃I₁₄ single crystals possessing chiral-polar crystal structures (space group is *P*₂), and evaluate the contribution of Rashba and Dresselhaus effects.

To evaluate the contribution of Rashba and Dresselhaus effects, we compared the CPGE currents of (R-CYHEA)₈Pb₃I₁₄ and (S-CYHEA)₈Pb₃I₁₄, generated along the nonpolar axis in the crystals. As reported in our previous work,^[3] we observed the chirality-dependent CPGE current of the (R/S-CYHEA)₈Pb₃I₁₄ based on the Dresselhaus effect, by obliquely irradiating light in the incident plane parallel to the measurement direction of photocurrent. In our experiment, in theory, the CPGE current based on Dresselhaus effect can be generated regardless of the incident planes of light, whereas the CPGE current based on Rashba effect can be generated only in the direction perpendicular to the incident plane of light. Therefore, by obliquely irradiating light in the incident plane perpendicular to the measurement direction of photocurrent, it is possible that we can observe the CPGE current induced by both Rashba and Dresselhaus effects. Results showed that the CPGE of (R-CYHEA)₈Pb₃I₁₄ was negligibly small, whereas that of (S-CYHEA)₈Pb₃I₁₄ was significantly large. Importantly, the direction of the CPGE current based on the Rashba effect is identical regardless of the chirality, which is in contrast to that based on the Dresselhaus effect. Hence, it could be reasonable that the magnitudes of the CPGE currents of (R-CYHEA)₈Pb₃I₁₄ and (S-CYHEA)₈Pb₃I₁₄ were significantly different due to the contribution of both Rashba and Dresselhaus effects.

We investigated the contribution of Rashba and Dresselhaus effects to the CPGE of chiral perovskites. In the presentation, we will quantitatively discuss the contribution of Rashba and Dresselhaus effects.

References

- [1] S. D. Ganichev, W. Prettl, *J. Phys. Condens. Matter* **15**, R935–R983, 2003.
- [2] P. Huang et al., *Adv. Mater.* **33**, 2008611, 2021.
- [3] T. Noma et al., *Angew. Chemie Int. Ed.* **2023**, DOI: 10.1002/anie.202309055.

3:00 PMBREAK

3:30 PM *EL15.04.05

Chiral Discrimination and Dispersion Intermolecular Forces Vladimiro Mujica¹ and Rafael Gutierrez²; ¹Arizona State University, United States; ²Dresden University of Technology, Germany

Intermolecular London dispersion forces, responsible for van der Waals (vdW) interactions, are due to induced-electric dipole induced-electric dipole interaction. They can be affected by molecular chirality in an unexpected way that is connected to the Chiral-Induced Spin Selectivity (CISS) effect, which provides a physical mechanism for the onset of an effective vdW interaction that depends on the relative orientation of the two enantiomers associated to a chiral molecule. This argument provides a path for chiral discrimination, which plays a fundamental role in molecular recognition of bio-molecules and the design of chiral material interfaces.

In this contribution, we will explicitly describe a simple model to explore the influence of the CISS effect in vdW forces, and the way this leads to molecular chiral discrimination.

4:00 PM EL15.04.06

Theoretical Perspective on Chirality-Induced Spin Selectivity and Chiroptical Properties in Layered Halide Perovskites Mikael Kepenekian¹, Claudine Katan¹, Simon Thébaud², Jacky Even², Shangpu Liu³, Felix Deschler³, Alexandre Abhervé⁴ and Nicolas Mercier⁴; ¹University of Rennes, France; ²INSA Rennes, France; ³Heidelberg University, Germany; ⁴University of Angers, France

3-dimensional (3D) halide perovskites AMX₃ (A: organic cation, M: metal ion, X: halide) have shown spectacular results in optoelectronic devices. However, they offer limited choice of metals and organic cations, which limits the chemical design of optimal materials. This is not the case of lower dimensional materials, e.g. layered (2D) halide perovskites (LHPs) [1], that impose far less constraints over the organic spacer. It then become possible to associate the exceptional optoelectronic properties of halide perovskites with chiral cations to reach promising materials for chiroptical and magnetochiral applications [2].

Here, we report joint experimental and theoretical investigations of LHPs with exceptional (i) chiroptical, and (ii) magnetochiral properties. Firstly, the enantiopure 3BrMBA₂PbI₄ (MBA = methylbenzylammonium) perovskite thin films exhibit external photoluminescence quantum efficiency as high as 39% and circularly polarized photoluminescence up to 52%, at room temperature [3]. Next, we consider a series of chiral lead-bromide networks which crystallize in enantiomorphic polar space groups P4₁2₁2 and P4₃2₁2 for the R and S enantiomers, respectively [4]. Chirality-induced spin selectivity (CISS) effect measurements performed over those materials by magnetic conducting-probe atomic force microscopy (mc-AFM) reveal a spin polarization of about 40% [4].

We use a set of experimental characterizations (e.g. single-crystal x-ray diffraction), and theoretical tools (semi-empirical modeling and density-functional theory based calculations) to describe the chiral-related properties of these LHPs and help the cation engineering of efficient chiral halide perovskites.

Acknowledgment. The work was performed with funding from Agence Nationale pour la Recherche under grant ANR-18-CE05-0026 (MORELESS project), the European Union's Horizon 2020 program, through an innovation action under grant agreement no. 861985 (PeroCUBE) and a FET Open research and innovation action under the grant agreement no. 899141 (PoLLOC). This work was granted access to the HPC resources of TGCC under the allocations 2022-A0130907682 made by GENCI.

- [1] B. Saparov, D. B. Mitzi, *Chem. Rev.* **2016**, *116*, 4558; L. Pedesseau, M.K. et al., *ACS Nano* **2016**, *10*, 9776; C. Katan, N. Mercier, J. Even, *Chem. Rev.* **2019**, *119*, 3140.
- [2] Y.-H. Kim et al., *Science* **2021**, *371*, 1129; M. K. Jana et al., *Nat. Commun.* **2021**, *12*, 4982; G. Long et al., *Nat. Rev. Mater.* **2020**, *5*, 423; H. Lu, Z. V. Vardeny, M. C. Beard, *Nat. Rev. Chem.* **2022**, *6*, 470.
- [3] S. Liu, M.K. et al., submitted manuscript.
- [4] A. Abhervé, M.K. et al., submitted manuscript.

4:15 PM EL15.04.07

Spin Polarized Current Injection from Chiral Halide Perovskites into III-V LEDs Matthew Hautzinger, Kirstin M. Alberi and Matthew C. Beard; National Renewable Energy Laboratory, United States

Spintronic applications integrating conventional group IV and III-V semiconductors suffer from a lack of efficient spin injection techniques. Most works rely on a ferromagnetic layer in combination with a tunnel oxide barrier, to avoid the conductivity mismatch, to inject spin polarized current into the semiconductor. These complicated interfaces are susceptible to defect chemistries inhibiting efficient spin polarized carrier injection. Here, we integrate semiconducting chiral halide perovskite, (R/S-MBA)₂PbI₄ (MBA = alpha-methylbenzylammonium) with III-V AlGaInP LEDs. The semiconducting (R/S-MBA)₂PbI₄ injects spin polarized current into the AlGaInP via the chirality induced spin selectivity effect. The spin polarized current produces circularly polarized electroluminescence, with efficiencies regularly achieved of 10 +/- 3% at room temperature and no external magnetic field applied. This remarkable efficiency is due to the pristine semiconductor-semiconductor interface between the (R/S-MBA)₂PbI₄ and AlGaInP which avoids the problematic conductivity mismatch of ferromagnetic-semiconductor interfaces. We characterized this interface with TEM, XPS, and cross sectional KPFM to show it has excellent interfacial properties with no unintentional barriers introduced. We further prove the circularly polarized emission is the result of spin polarized current injection by measuring the Hanle effect. We observe a decrease in circularly polarized light emission with the application of a magnetic field, as expected from spin polarized current injection. These results present a new method of spin polarized current injection, enabled by a semiconducting CISS layer, which can be applied to numerous spintronic applications.

9:00 AM *EL15.05.01

Structure-Property Tunability using Chirality and Symmetry Breaking in Hybrid 2D Perovskites David B. Mitzi; Duke University, United States

Hybrid organic-inorganic perovskite (HOIP) semiconductors based on metal halide frameworks offer unprecedented opportunity to tailor structural and materials properties using the full flexibility afforded by the associated inorganic and organic components,¹ and such tunability offers wide-ranging potential for applications including solar cells, light-emitting devices, detectors, transistors and advanced computing devices. In this talk we will focus on examining the role that the organic cation can play in introducing or impacting chirality, symmetry breaking and associated phase transitions within HOIPs, as well as on the resulting chiroptical (e.g., circularly dichroism),² spin-selective charge transport (e.g., chirality-induced spin selectivity),³ and electronic structure (e.g., spin splitting of the conduction band)⁴ characteristics of these systems. Recent examples of such symmetry-related tunability highlight the promise of using the organic component to control light, charge and spin within the wide-ranging HOIP family.

1. D. B. Mitzi, K. Chondroudis, C. R. Kagan, *IBM J. Res. & Dev.* 45, 29 (2001).

2. L. Yan, M. K. Jana, P. C. Sercel, D. B. Mitzi, W. You, *J. Am. Chem. Soc.* 143, 18114 (2021).

3. H. Lu, C. Xiao, R. Song, T. Li, A. E. Maughan, A. Levin, R. Brunecky, J. J. Berry, D. B. Mitzi, V. Blum, M. C. Beard, *J. Am. Chem. Soc.* 142, 13030 (2020).

4. M. K. Jana, R. Song, Y. Xie, R. Zhao, P. C. Sercel, V. Blum, D. B. Mitzi, *Nature Comm.* 12, 4982 (2021).

9:30 AM EL15.05.02

Proximity-Effect-Induced Remote Chirality Transfer in Halide Perovskites Md Azimul Haque¹, Roman Brunecky¹, Junxiang Zhang², Yifan Dong¹, Matthew P. Hautzinger¹, Steven P. Harvey¹, Seth R. Marder², Matthew C. Beard¹ and Joseph Luther¹; ¹National Renewable Energy Laboratory, United States; ²University of Colorado Boulder, United States

Hybrid organic/inorganic halide perovskites are intriguing chiral material systems owing to their excellent optoelectronic properties and potential to impart chirality with the organic A-site cation. Typically, chiroptical properties arise due to structural symmetry breaking from chiral A-site organic cation to the inorganic framework. In the present work, we demonstrate a proximity effect of remote chirality transfer to induce chirality in otherwise achiral 2D halide perovskites. A chiral organic ligand is introduced in the perovskite lattice without altering the structure, thus introducing chirality into existing 2D perovskites. Furthermore, we construct a chirality-composition library with varying the A, B, X-sites, along with the dimensionality, revealing the essential role of each atomic component in the perovskite structure. This approach of remote chirality transfer in halide perovskites could lead to new prospects in terms of composition, spin transport properties, and devices without extensive chemical modifications.

9:45 AM EL15.05.03

The Real Origin of Apparent Circular Dichroism in Chiral Perovskites Sunih Ma¹, Bumchul Park¹, Sang Hyun Lee¹, Jooho Moon² and Nicholas A. Kotov¹; ¹University of Michigan–Ann Arbor, United States; ²Yonsei University, Korea (the Republic of)

Chirality, a fundamental concept for matters that cannot be super-imposed with their mirror images, is ubiquitous in almost all branches of natural science. Due to significance of chirality and wide versatility of chiral materials, in recent years, the concept of chirality can be successfully expanded to variety of different material including quantum dots, liquid crystals, and organic-inorganic hybrid system. Especially, chiral perovskite materials have attracted unprecedented attention as a new type of chiral semiconductors since the first report of chiroptical response in 2017. Different from the inherent chiral organic materials, chirality transfer from chiral organic spacer to achiral inorganic frameworks should be preceded to achieve chiroptical activity in chiral perovskite. Although extensive studies have reported the circular dichroism (CD) in chiral perovskite, the origin of chiroptical response in chiral perovskite ambiguous. Furthermore, several groups reported CD sign inversion behavior when flipping thin films samples, implying that the observed CD signal from chiral perovskite thin films might be originated from linear effects. However, due to the poor understanding of CD mechanism and inherent limitation of commercial CD spectrometers, the macroscopic origin of apparent CD behavior has been incorrectly interpreted. From this point of view, we investigate the real origin of apparent and genuine CD response in chiral perovskite thin films by using our home-made Mueller matrix polarimeter (MMP). Interestingly, based on experimental results from MMP and theoretical decomposition of Mueller matrix parameters, we found that apparent CD behavior is primarily originated from linear birefringence (LB) effects rather than linear dichroism (LD) behavior which is attributed to microscopy preferred orientation of thin films. Furthermore, polarization optical microscopy confirmed that LB effect is closely related with second-order ferroelectric phase transition behavior. To the best of our knowledge, this is first systematic study to clarify the real origin of apparent CD behavior based on the decomposition of Mueller matrix parameter, which is different from the interpretation based on ambiguous LDLB effect. Our study unveils the importance of the LB effect on the CD behavior of thin films and provide an in-depth understanding between ferroelectricity and chiroptical response.

10:00 AM BREAK

10:30 AM EL15.05.04

Fluorinated Structural Isomers in 2D Chiral Perovskites Enabling Efficient Stable Spin-Dependent Oxygen Evolution Reaction Jaehyun Son¹, Sunih Ma², Hyungsoo Lee¹, Gyumin Jang¹, Chan Uk Lee¹, Seongyeon Yang¹, Subin Moon¹, Junwoo Lee¹, Wooyong Jeong¹ and Jooho Moon¹; ¹Yonsei University, Korea (the Republic of); ²University of Michigan–Ann Arbor, United States

Spin-dependent electrochemistry is introduced as an innovative concept for boosting overall photoelectrochemical (PEC) efficiency. Especially, the performance of oxygen evolution reaction (OER) can be improved by the chirality-induced spin-selectivity (CISS) phenomenon based on chiral materials. The CISS can effectively reduce the overpotential of the OER process by aligning the electron spins with specific directions. The parallel-aligned electron spins favor the generation of triplet oxygen (³O₂), which is energetically more stable than the singlet oxygen state (¹O₂), while refraining from the formation of competitive by-product of hydrogen peroxide. In this regard, the chiral 2D organic-inorganic hybrid perovskites (OIHP) are considered as a promising spin filter due to their exceptional spin-polarization capability of over 80%. However, there are still underlying intrinsic obstacles to exploit chiral 2D OIHPs as spin filters for OER devices. The 2D OIHPs structures have poor conductivity along with out-of-plane direction where multiple spin-alignment occurs, which restricts further enhancement of OER performance. Such a problem stems from the multi-quantum well structures of OIHPs composed of two repeating building blocks, namely organic cations and inorganic frameworks. In addition, the vulnerability of 2D OIHPs to water is attributed to the hygroscopic nature of the organic cations, which becomes another hindrance to accomplishing the long-term operational stability of OER devices. Therefore, it is essentially necessary to develop groundbreaking materials that can promote electrical properties and moisture instability while maintaining the chirality of OIHPs.

Herein, we introduce chiral 2D OIHPs fluorinated methyl-benzylamine (F-MBA) chiral structural isomer cations, which have different structures according to the fluorine location of ortho-, meta-, and para- on the benzene ring. The chirality of the 2D OIHPs can be augmented according to the specific chiral cation structures originating from the intensified organic-inorganic halogen-halogen interactions. Moreover, the fluorinated chiral organic cations can not only endow hydrophobic characteristics to OIHP systems but also enhance the out-of-plane conductivity by reducing the exciton binding energy. As a result, we have implemented the fluorinated 2D OIHPs film on top of BiVO₄ photoanode for oxygen production. The fluorinated OIHPs spin filter dramatically reduces the overpotential with improved operational stability. Our results suggest a promising material design rule to fabricate stable and efficient chiral 2D OIHPs spin filter for spin-dependent applications.

10:45 AM EL15.05.05

Chiral Cation Doping for Modulating Structural Symmetry of 2D Perovskites Yi Xie^{1,2}, Jack Morgenstein¹, Benjamin Bobay¹, Ruyi Song¹, Naidel Caturello², Peter C. Sercel³, Volker Blum^{1,2} and David B. Mitzi^{1,2}; ¹Duke University, United States; ²Federal University of ABC, Brazil; ³Center for Hybrid Organic Inorganic Semiconductors for Energy, United States

Cation-mixing in two-dimensional (2D) hybrid organic-inorganic perovskite (HOIP) structures represents an important degree of freedom for modifying organic templating effects and tailoring inorganic structures. However, the limited number of known cation-mixed 2D HOIP systems generally employ a 1:1 ratio of cations for stabilizing the 2D perovskite structure. Achieving more general cation mixing ratios should allow greater control over accessing lower symmetry structures and therefore opportunities for modulating and enhancing emergent symmetry-sensitive properties. Here we demonstrated a chiral-chiral mixed-cation system wherein a controlled small amount (<5 %) of chiral cation S-2-MeBA (S-2-MeBA = (S)-(-)-2-methylbutylammonium) can be doped into (S-BrMBA)₂PbI₄ (S-BrMBA = (S)-(-)-4-bromo- α -methylbenzylammonium), modulating the structural symmetry from a higher symmetry (C₂) to the lowest symmetry state (P1). This structural change occurs when the concentration of S-2-MeBA, measured by solution nuclear magnetic resonance, exceeds a critical level—specifically, for 1.4 ± 0.6 %, the structure remains as C₂, whereas 3.9 ± 1.4 % substitution induces the structure change to P1. Atomic occupancy analysis suggests that one specific S-BrMBA cation site is preferentially substituted by S-2-MeBA in the unit cell, which rearranges the organic layer to break C₂ rotational symmetry. Density-functional theory calculations indicate that the spin splitting along different k-paths can be modulated by cation doping. A true circular dichroism band at the exciton energy of the 3.9% doping phase shows polarity inversion and a ~45 meV blue shift of the Cotton-effect-type line-shape relative to (S-BrMBA)₂PbI₄. A trend toward suppressed melting temperature with higher doping concentration was observed. The chiral cation doping system and the associated doping-concentration-dependent structural transition provide a material design strategy for controlling and enhancing symmetry-related properties, such as chiroptical, non-linear optical, spin-related, and ferroelectric properties.

11:00 AM EL15.05.06

Boosting Non-Centrosymmetric Distortion and Magnetic Properties in Chiral Metal Halide Perovskites SanghyunNam¹, JaewookAn², In HyeokPark² and Young HoonKim¹; ¹Hanyang University, Korea (the Republic of); ²Chungnam National University, Korea (the Republic of)

Control of spin-polarized currents and magnetic properties in materials are important to demonstrate various spintronic applications such as MRAM and spin LEDs. In conventional semiconductors and metals, spin polarization and magnetization occur by the application of external magnetic fields or fabrication of ultra-thin (<5 nm) layer of the materials, which complicate the fabrication process and device structure. Here, we report novel materials system, hybrid chiral metal-halide perovskites (MHPs), which can control the spin polarization and magnetic properties via simple solution process. MHPs consist of three different atoms or molecules in various crystal structures (representations are ABX₃ and A₂BX₄ where A is an organic ammonium, B is a transition metal cation and X is a halide anion). First, we synthesize chiral lead (Pb)-based MHPs ((R-/S-MBA)₂PbI₄ where MBA is methylbenzylammonium) and find that R-/S-MBA cations transfer the chirality to the inorganic metal-halide octahedra (PbI₆) by the asymmetric electrostatic interaction between ammonium group in MBA and halide in inorganic octahedra. (R-/S-MBA)₂PbI₄ polycrystalline thin films show circular dichroism (CD) signals with opposite directions which are dependent on the chiral direction of MBA. Furthermore, (R-/S-MBA)₂PbI₄ show efficient spin selectivity > 80% without external magnetic fields by the chiral-induced spin selectivity (CISS) effect. Second, to solve the toxic problem in Pb-based MHPs, we synthesize Pb-free chiral MHPs that use palladium (Pd) in B site cation. Pd-based MHPs have 0-dimensional orientation of Pd-halide square-planar, where the direction of the orientation depends on the chiral direction in A-site cation, and increased CD signals when mixed halides are used in X-site (anisotropy g-factor (g_{CD}) = 3.3 × 10⁻³ in pure chloride, 1.2 × 10⁻² in pure bromide, 1.8 × 10⁻² when Br_{0.5}Cl_{0.5}). We also measured the spin selectivity in Pd-based chiral MHPs. Third, to induce magnetic properties in MHPs in addition to the chirality, we synthesize iron (Fe)-based chiral MHPs with different Fe compositions. Fe-based chiral MHPs show CD signals in the absorption range of metal-halide tetrahedra, which clarify that R-/S-MBA transfers its chirality to the metal-halide tetrahedra. Furthermore Fe-based chiral MHPs exhibit paramagnetism at low temperature, which demonstrate the potential of future MHP materials which have both chirality and magnetic properties.

11:15 AM EL15.05.07

Highly Efficient Chiral 2D/3D Perovskite Artificial Leaf for Spin-Dependent Photoelectrochemical Overall Water Splitting HyungsooLee, Chan UkLee, JuwonYun, WooyongJeong, Chang-SeopJong, JaehyunSon, Young SunPark, SubinMoon and JoohoMoon; Yonsei University, Korea (the Republic of)

The intricate nature of the multi-step oxygen evolution reaction (OER) continues to pose a challenge in achieving bias-free photoelectrochemical water-splitting systems. Several theoretical and experimental studies have suggested that OER efficiency can be significantly improved in chiral material-based photoanodes by utilizing the chirality-induced spin selectivity (CISS) phenomenon. The final product at the photoanode is the oxygen molecules, where the spin alignment of intermediate radicals is favorable to the generation of triplet ³O₂ (most stable molecular oxygen species). Considering the energy difference between a singlet ¹O₂ and triplet ³O₂ (the energy of a singlet ¹O₂ is approximately 100 kJ mol⁻¹ higher than that of triplet ³O₂), spin-dependent chemical reactions combined with the CISS phenomenon can play a crucial role in facilitating the OER process. Especially, by promptly aligning the spin distribution of photo-generated charges within the absorber, it could effectively prevent the formation of hydrogen peroxide, leading to a dramatic reduction in overpotential. In this regard, the incorporation of a chiral spin-filter layer on top of the absorber has been recognized as a promising strategy to achieve a significant enhancement on the PEC performance of the solar-driven water splitting system.

Chiral 2D OIHPs have been conventionally employed as spin-filter layer with two distinct enantiomers, namely R- and S-methyl benzylamine (R- and S-MBA). Owing to the weak π-π interaction of the MBA organic cation, however, the coupling effect between the π-electron and p-orbital of the halide in the inorganic framework is relatively weak in chiral 2D OIHPs. To reinforce the coupling effect of chiral 2D OIHPs, we utilized naphthyl ethylamine (NEA) capable of stronger π-π stacking interaction between naphthalene rings. Moreover, the introduction of NEA organic cations can simplify the molecular arrangement of chiral 2D OIHPs, leading to enhanced film crystallinity and improved chiroptical properties. Herein, we demonstrated that the CISS phenomena can become a remarkable approach by adopting NEA-based chiral 2D OIHPs as a spin-filtering layer on the 3D OIHPs photoanode. Our chiral 2D OIHPs exhibited an impressive CISS efficiency of approximately 95%, indicating a remarkable achievement in spin controlling when compared to other chiral materials. Moreover, chiral 2D/3D OIHPs-based water-splitting device achieved enhanced oxygen evolution performance with a reduced overpotential of 0.2 V, high fill factor, and increased photocurrent of 22 mA cm⁻² at 1.2 V_{RHE} compared to a device without a spin-filtering layer. For unbiased water splitting, a perovskite-based photocathode decorated with a spatially decoupled hydrogen evolution reaction catalyst was fabricated. This decoupled geometry was adopted to enable the physical protection of the perovskite layer from the electrolyte, thus allowing excellent stability for over 100 h. To implement the bias-free water splitting performance, this perovskite photocathode was connected in parallel with spin-filtering layer adopted 2D/3D OIHPs-based photoanode. Overall solar-driven water splitting was achieved using all the OIHP photoelectrodes, resulting in a remarkable unassisted solar-to-hydrogen efficiency of ~13% and a continuous 100 h stable operation.

SESSION EL15.06: Chiral Photonic and Optoelectronic Materials

Session Chairs: Jian Shi and Hanyu Zhu

Wednesday Afternoon, November 29, 2023

Hynes, Level 2, Room 207

1:30 PM *EL15.06.01

Leveraging Chirality for Extreme Control of Light AndreaAlu; City University of New York, United States

In this talk, I will discuss our recent progress in tailored broken geometrical symmetries to control the interaction of light with structured materials and metasurfaces. In particular, I will discuss our theoretical and experimental work on nonlocal metasurfaces supporting chiral eigenstates, locally structured with subwavelength resolution. I will also discuss the unique opportunities that chirality and rotational broken symmetry enables in the context of polaritonic systems and time metamaterials.

2:00 PM EL15.06.02

Active Chiral Plasmonic Metasurfaces JuhwanKim, Jang-HwanHan, GyurinKim and Hyeon-HoJeong; Gwangju Institute of Science and Technology, Korea (the Republic of)

Chiral plasmonics offers a powerful means to control light-matter interactions based on their unique polarization-sensitive chiroptical characteristics, enabling a wide range of applications, including molecular sensing, holographic encryption, and optical filters.[1] In order to fully exploit the potential of chiral plasmonics for industrial applications, it is crucial to develop their active system that can respond to external stimuli and thus allow us to dynamically control their chiroptical responses. However, such active chiral plasmonics are still in their early stages of development.

Here, we present an active chiral plasmonic metasurface capable of dynamically controlling the chiroptical response through combinatorial modulation of both the state of light polarization and an external electrical input. The metasurface consists of a wafer-scale array of chiral nanohelices grown using a physical shadow growth technique, with a conductive polymer shell polymerized around the entire surface of helices. The intrinsic dissymmetry factor of this chiral plasmonic metasurface exceeds 0.1, leading to rich polarization-dependent colors. To achieve further extended color dynamics, we electrochemically control the redox state (i.e., refractive index) of the conductive polymer shell, thereby inducing changes in the plasmonically resonating colors of the nanohelices.[2] Remarkably, in conjunction with controlling the state of the light polarization, we achieve full-color dynamics from the single chiral plasmonic metasurface, driven by just input voltages of less than 1 V, highlighting its potential applications in electrochromic displays and filters.

In this presentation, we will discuss the successful fabrication of these chiral plasmonic metasurfaces and provide a comprehensive characterization of their active chiroptical properties. The proof-of-concept applications will also be presented, featuring their impressive fidelity for active coloration.

[1] J. H. Han et al, Adv. Mat. 2023

[2] J. Peng et. al, Sci. Adv. 2019, 12, eaw2205

2:15 PM EL15.06.03

Chirality Induced Second Harmonic Generation in Aligned and Enantiomer Enriched Carbon Nanotubes RuiXu¹, YuanTian², JacquesDoumani¹, AndreyBaydin¹, WeiranTu¹, YoheiYomogida³, FuyangTay¹, JiamingLuo¹, JunLou¹, KazuhiroYanagi³, RiichiroSaito², JunichiroKono¹ and HanyuZhu¹; ¹Rice University, United States; ²Tohoku University, Japan; ³Tokyo Metropolitan University, Japan

Aligned assemblies of single-chirality semiconducting carbon nanotubes (CNTs) are ideal materials for developing nanoelectronic, optoelectronic, and quantum photonic devices. Although left- and right-handed CNTs have identical properties in many aspects, enantiomer-dependent properties can manifest in magneto-transport, optical polarization selection, and nonlinear optics. For example, theoretical studies have predicted a large, resonance-enhanced second-order nonlinear optical susceptibility up to nm/V in perfect chiral CNT ensembles, but the value has never been experimentally verified due to mixed chirality components, poor alignment, and low densities. Here, we report the synthesis of centimeter-scale single-enantiomer, highly packed, and

aligned (11,-5) CNT thin films using the controlled vacuum filtration method. We observed giant second harmonic generation (SHG) from the samples with effective second-order nonlinear optical susceptibility up to 70 pm/V, which corresponds to 350 pm/V for an enantiomerically pure, densely packed and perfectly aligned solid as predicted when the fundamental frequency resonates with the transition of the CNTs at 1000 nm. We confirmed that the SHG signal originates from the inversion symmetry breaking from the intrinsic chirality of the film, instead of surface defects, by angle and polarization dependent SHG measurements. Our findings provide a fast and scalable method for characterizing the alignment and enantiomer purity of CNT films, and establish them as an excellent material for nonlinear optical studies and applications.

2:30 PMBREAK

3:30 PM *EL15.06.04

Chiral Materials from Perylene Diimide Building Blocks: Twistacenes and Helicenes[Colin Nuckolls](#); Columbia University, United States

This presentation will detail our efforts to create materials from contorted aromatic molecules. In particular, I will discuss how to create helicenes and twistacenes from perylene diimide building blocks. These materials have extraordinary properties as materials. The helicenes have the largest chiroptic response of any molecular species. The twistacenes helicity is dynamic and can be controlled by light and chemical/electrochemical reductions. These materials excel as photovoltaics, photodetectors, batteries, and pseudocapacitors. The presentation will discuss these opportunities.

4:00 PM EL15.06.05

Bringing Sensitive Circularly Polarized Luminescence Spectroscopy to the Time Domain[Antti-Pekka M. Reponen](#)¹, [Marcel Mattes](#)¹, [Winald Kitzmann](#)² and [Sascha Feldmann](#)¹; ¹Harvard University, United States; ²Johannes Gutenberg-Universität, Germany

Materials capable of emitting circularly polarized light (CPL) are promising for breaking efficiency limits in existing optoelectronic applications and may enable entirely new photonic and spintronic technologies [1]. However, reliably detecting CPL with the necessary sensitivity to quantify low dissymmetry factors, while being able to identify and ideally circumvent artefacts arising from linear dichroism, linear birefringence or linearly polarized emitted or scattered light is experimentally challenging [2].

Here we report on our recent efforts to develop CPL detection with the additional dimension of time evolution to achieve broadband, calibration-free CPL spectroscopy with nanosecond time resolution [3]. This technique will serve as a powerful tool to study the dynamics of chiral emitters and to understand how chirality evolves in the excited state.

[1] Crassous, Fuchter, Freedman, Kotov, Moon, Beard, Feldmann, *Nat. Rev. Mater.* 8, 365 (2023).

[2] Kitzmann, Freudenthal, Reponen, VanOrman, Feldmann, *Adv. Mater. in press* (2023).

[3] Reponen *et al. to be submitted* (2023).

4:15 PM EL15.06.06

Twisting Photons with Chiral Metal-Halide Semiconductors[Haipeng Lu](#); The Hong Kong University of Science and Technology, Hong Kong

Chiral metal-halide semiconductors (MHS) have recently developed as promising candidates for spin- and polarization-resolved optoelectronic devices. Although several chiral MHS with rich chemical and structural diversity have been reported lately, the fundamental mechanisms governing their chiroptical activity, namely, circularly polarized absorption and emission, remain elusive. In this talk, I will discuss our recent progress in understanding and tuning the chiroptical activity in chiral MHS. I will first discuss how the chirality is transferred from organic to inorganic component through asymmetric covalent bonding interactions. Their endowed molecular chirality was then studied by circular dichroism (CD). However, we found that the previously reported "apparent" CD in chiral MHS thin films is not an intrinsic chiroptical property, but rather, arising from an interference between the film's linear birefringence and linear dichroism. We verify the presence of LB and LD effects in both one-dimensional and zero-dimensional chiral MHS thin films. We then establish spectroscopic methods to decouple the genuine CD from other spurious contributions, which allows a quantitative comparison of the intrinsic chiroptical activity across different chiral MHS. The relationship between the structure and the genuine chiroptical activity is then uncovered, which is well described by the chirality-induced spin-orbit coupling in the chiral structures. Meanwhile, we found that high CD signals do not necessarily lead to high circularly polarized luminescence as most of the current chiral MHS display very low photoluminescence quantum yields (PLQY). We will then discuss the reasons of low PLQY in these materials. Finally, we will show our strategies to turn on the circularly polarized luminescence by introducing extrinsic self-trapped excitons in a 0D chiral MHS, and by tuning the inorganic layer thickness in perovskite nanoplatelets.

4:30 PM EL15.06.07

Twisted Organic Semiconductor Crystals for Chiroptoelectronics[Schee Jeong](#), [St. John Whittaker](#), [Yongfan Yang](#), [Akash Tiwari](#), [Alexander Shtukenberg](#), [Bart Kahr](#) and [Stephanie Lee](#); New York University, United States

We present crystal twisting, a common albeit little known phenomenon in molecular crystals, as a generalizable strategy to repurpose optically inactive organic semiconductors for chiroptoelectronics. This phenomenon is not limited to specific chemical structures or crystal space groups - twisting has been observed in inorganic, polymer, and small molecule crystals grown from vapor, solutions and melts. Because crystal twisting introduces repeating patterns of crystal orientations perpendicular to the substrate surface as crystals twist about the fast growth direction, <hkl>-dependent material properties are likewise patterned on the microns to millimeter length scale. Twisting also imparts chirality - crystals twist either clockwise or counterclockwise about the growth direction - rendering them optically active. The commonality of crystal twisting enables potentially hundreds of centrosymmetric organic semiconductors designed over the past fifty years to be incorporated into devices that discriminately transmit, emit and detect circularly polarized light. Here we characterize the (chir)optoelectronic properties of several molecular semiconductors, including triisopropylsilyl ethynyl anthradithiophene (TIPS ADT) and tetrathiafulvalene (TTF), and test their performance in resistors, transistors and photodetectors.

4:45 PM EL15.06.08

Chiroptical Synaptic Heterojunction Phototransistors: Noise-Reduced Detection of Circularly Polarized Light via Self-Assembled Supramolecular Nanohelix of π -Conjugated Molecules[Jung Ah Lim](#)¹, [Hanna Lee](#)¹, [Changsoo Choi](#)¹ and [Eunji Lee](#)²; ¹Korea Institute of Science and Technology, Korea (the Republic of); ²Gwangju Institute of Science and Technology, Korea (the Republic of)

Chiroptical photodetectors have become increasingly important in a range of fields, including chiral imaging, spintronics, and quantum optics. To enable practical chiroptical optoelectronics, it is essential to develop high-performance chiroptical photodetectors with high responsivity, sensitivity, polarization direction identification, and device integration feasibility. This study presents the successful demonstration of high-performance chiroptical synaptic phototransistors utilizing heterojunctions comprising a self-assembled nanohelix of a π -conjugated molecule and a metal oxide semiconductor. In this work, heterojunction devices consisting of a chiral nanomaterial and semiconductor offer a promising strategy for developing high-performance chiral optoelectronic devices. To impart strong chiroptical activity, a novel diketopyrrolopyrrole-based, donor-acceptor type π -conjugated molecule decorated with chiral glutamic acid was newly synthesized, capable of supramolecular self-assembly through noncovalent intermolecular interactions. Through hydrogen-bonding-driven, gelation-assisted self-assembly, we obtained supramolecular nanohelix structure consisting of intertwining fibers with strong and stable chiroptical activity in solid-film form. Phototransistors based on interfacial charge transfer at the heterojunction from the chiroptical nanohelix to the metal oxide semiconductor exhibited exceptional chiroptical detection, with a high photocurrent dissymmetry factor and remarkable photoresponsivity. Interestingly, the chiroptical phototransistor displayed photonic synapse-like behavior, generating time-dependent photocurrents and persistent photoconductivity attributed to interfacial charge trapping. Leveraging the synaptic functionality advantage, a trained convolutional neural network achieved over 89 % accuracy in recognizing noise-reduced circularly polarized images of handwritten alphabetic characters.

5:00 PM EL15.06.09

Ionically Modified Cellulose Nanocrystals Chiral Structures for Electronics[Diana Gaspar](#)¹, [Paul Grey](#)², [Bruno Mendes](#)², [Madalena Roque](#)², [Rodrigo F. Martins](#)² and [Luis Pereira](#)^{1,2}; ¹AlmaScience, Portugal; ²Cenimat@3N, School of Science and Technology (FCT-NOVA), Universidade NOVA de Lisboa and CEMOP/UNINOVA, Portugal

Many approaches exist in the quest for efficient, abundant, cheap and eco-friendly photonics that can be easily integrated with other platforms for practical applications.

Approaches using 3D metamaterials, mesoporous semiconductors, or plasmonics are promising. Nevertheless, these methods often involve complicated fabrication processes that need high energy consumption (such as vacuum and physical vapour deposition) to deposit these materials, which are often not so green, sustainable, typically expensive, and colour-limited. Researchers have sought eco-friendly materials with similar performance and lower energy costs during the past few years, and Nature offers many examples of such materials for our innovation. Natural micro and nanostructures, such as the ones found in beetles or butterflies, have evolved over millions of years to produce periodic patterns that can reflect light. These structures served as inspiration to create artificial analogues using cellulose nanocrystals (CNCs), which can form a chiral nematic liquid crystalline phase when dispersed in water. The chiral order is preserved as the water evaporates, and solid films with 1D photonic crystal properties and iridescent colours are obtained. The intrinsic left-handedness of such structures can interact

selectively with left and right-circular polarized light (LCPL and RCPL).

The pitch control and, therefore, the reflected colour is particularly interesting. This manipulation can be done using external stimuli such as magnetic and electric fields, drying processes with different interfaces or playing with the chemistry behind the acid hydrolysis. With this work, we demonstrate that CNC suspensions with low concentrations (~4-5wt.%) with proper evaporation-induced self-assembly conditions lead to the formation of films with interesting photonic properties with a left-handed twisted arrangement. The use of strong acid cation resins to mediate the counterion exchange on commercial CNCs. It was observed that adding different alkali salts to the CNCs anisotropic suspension results in a blue shift of the photonic bandgap with higher salt concentrations and proper distinction between LCPL and RCPL ($\Delta\text{CPL} \approx 42\%$).

Combining the photonic character of the tailored CNC films, whose photonic bandgap can be matched with the bandgap of light sensitivity of semiconductors, it will be possible to create devices capable of discrimination between LCPL and RCPL signals in the blue region.

SESSION EL15.07: Poster Session: Chiral Materials with Novel Properties

Session Chairs: Matthew Beard and Rui Xu

Wednesday Afternoon, November 29, 2023

Hynes, Level 1, Hall A

8:00 PM EL15.07.01

Anisotropic Circular Photogalvanic Response in Chiral Weyl Semimetal RhSi Byunghoon Kim¹, Tyler Cochran¹, Zi-Jia Cheng¹, Gyu-Hee Kim², Xian Yang¹, Doo-Hyun Ko², Prashant Padmanabhan³ and M. Zahid Hasan¹; ¹Princeton University, United States; ²Sungkyunkwan University, Korea (the Republic of); ³Los Alamos National Laboratory, United States

Weyl semimetals have been a hot topic in the condensed matter physics community due to their unconventional linear band crossing from the bulk characters. Breaking of time-reversal or inversion symmetry allows Dirac fermions to split into a pair of Weyl fermions with an opposite chirality at a non-high symmetry point in momentum space. The circular photogalvanic effect in which the incident helicity determines the generated current vector is direct evidence from the topology and band structure of the chiral Weyl semimetals. Notably, in optical transition near a Weyl node, it has recently been predicted that the magnitude of the CPGE is associated with its monopole charge. Since the nodes with opposite charges are nondegenerate, it also hints at the CPGE response stemming from the Berry monopole charge. Here, we explore the helicity-dependent optoelectronic response of the topological/Weyl semimetal RhSi via time-domain terahertz emission spectroscopy. The remarkable CPGE behavior in in-plane mode was experimentally demonstrated, whereas it did not exhibit notable signatures in out-of-plane mode. We further perform the photoemission measurement, together with optical simulation, to investigate the physical properties of chiral Weyl semimetal RhSi.

8:00 PM EL15.07.02

Chiral Pyrrole-Based Polyaromatics Abdusalam A. Suleymanov and Timothy M. Swager; Massachusetts Institute of Technology, United States

In recent years, there has been significant interest in incorporating heteroatoms into polycyclic aromatic hydrocarbons (PAHs). This exploration of heteroatom-doped variants of extended π -conjugated materials has revealed their distinct and enhanced electronic and photophysical properties. Among the various five-membered aromatic heterocycles, pyrrole stands out as the most electron-rich when compared to its isoelectronic counterparts, furan and thiophene. The synthetic versatility and strong redox activity of pyrrole enable the creation of synthetic frameworks with enhanced p-doping and other desirable material properties.

Our research has focused on the synthesis and characterization of novel chiral pyrrole-based PAHs. These include twisted azacoronenes and helicenes incorporating pyrrole units. We are currently investigating their chiroptical, electrochemical, and magneto-optical properties.

8:00 PM EL15.07.03

Chiral Phonons in α -HgS Nanocrystal Sang Hyun Lee, Bumchul Park and Nicholas A. Kotov; University of Michigan, Ann Arbor, United States

Chiral phonon is a quantized particle that represent collective atomic motions with broken reflection and inversion symmetries. Chiral phonons have gathered significant interest due to their unique properties observed in various types of materials such as two-dimensional (2D) materials, biomolecular complexes, and inorganic chiral crystals [1,2,3]. Here, we observe chiral phonons in mercury sulfide cinnabar (α -HgS) nanocrystals with terahertz time-domain polarimetry (THz-TDP). α -HgS has two enantiomeric crystal structure that belongs to space group P3₁21 or P3₂21 depending on the rotational direction of the helical crystal lattice. By employing phonon dispersion calculations, we identify the IR active phonon modes in α -HgS that lies in the spectral range of 1 ~ 10 meV, specifically the A₂ (1.16 THz) and E modes (1.3 THz), which can be experimentally measured using THz-TDP. Mirror-symmetrically synthesized P/M α -HgS nanocrystals show identical THz absorption (TA) peaks, while their THz circular dichroism (TCD)/THz optical rotary dispersion (TORD) signals exhibit opposite characteristics, corresponding to the A₂ phonon mode. This clearly proves the existence of chiral phonons in α -HgS nanocrystals. Moreover, it is important to mention that strong TCD signals can be measured despite the substantial disparity in scales between the THz wavelength (~300 μm) and α -HgS nanocrystals (~20 nm). Chiral phonons of α -HgS nanocrystals within the THz range not only provide new insights for THz photonics/phononics, but also bridges the gap between THz photonics and nano-engineering, opening a new door for various applications.

8:00 PM EL15.07.04

Banded Spherulite Formation in Chiral Halide Perovskites Matthew Hautzinger, Qitong Ge and Matthew C. Beard; National Renewable Energy Laboratory, United States

Halide perovskites containing chiral organic moieties have been recognized recently for their remarkable chirality induced spin selectivity properties. Notably, the compounds exhibit chirality transfer from the chiral organic to the inorganic metal halide components. Here, we investigate the growth of the chiral halide perovskites as textured thin films containing banded spherulite structures. The compound, (S-NPB)₂PbBr₄ in particular, exhibits robust banded spherulite formation when the processing conditions are optimized. These banded spherulites containing extrinsic chirality of helical twists in them leading to their mesoscopic structure. We show the temperature control over these structures during the growth and characterize the pitch and growth of the helical twists within these films. The results presented here have implications for the chirality induced spin selectivity of these materials, as the compound contains meta chirality, not only in the crystallographic structure, but also in the mesoscale banded spherulites formed.

8:00 PM EL15.07.05

Growth-Actuated Twisting of Photochromic Crystals Merritt C. McDowell¹, Natercia Barbosa², Helen Zardus¹, Alexander Shtukenberg¹, Johanna Brazard², Bart Kahr¹, Takuji Adachi², St. John Whittaker¹ and Stephanie Lee¹; ¹New York University, United States; ²University of Geneva, Switzerland

1,2-bis(2-methyl-5-phenyl-3-thienyl)perfluorocyclopentene (BpFCP) single crystals grown from the vapor phase were previously discovered to dynamically twist and coil when irradiated with UV light due to mechanical strain associated with a reversible, light-induced ring closure [1]. Here, we form BpFCP twisted crystals through growth-actuated twisting during crystallization from the melt. At high undercoolings, i.e. large crystallographic driving forces, BpFCP forms banded spherulites comprising helicoidal fibrils that twist in concert with one another as they grow radially from the spherulitic nucleation center. As-crystallized films appear transparent when viewed using unpolarized light. When imaged between crossed polarizers, on the other hand, concentric bands of interference colors are visible due to continuously rotating refractive indices as the crystals twist about the growth direction. Upon irradiation with UV light to induce the photochromic ring closure, alternating bands in BpFCP spherulites turn dark blue, creating a vibrant stripe pattern. Local Raman spectroscopy on adjacent bands revealed this patterning to be a result of orientation-dependent dichroism of photocyclized crystals, as opposed to orientation-dependent photoreactivity. Film cracking upon UV light exposure suggests that fibrils experience internal stress from photoisomerization-induced shifts in crystal lattice parameters. Mueller Matrix imaging further revealed strong circular dichroism (CD) and birefringence (CB) in BpFCP banded spherulites, with local CD and CB signals changing dynamically during photocyclization. Because banded spherulites expose different crystal orientations at the film surface, they provide a unique opportunity to investigate orientation-dependent chiroptoelectronic properties in these dynamic crystals.

[1] D. Kitagawa, H. Tsujioka, F. Tong, X. Dong, C.J. Bardeen, S. Kobatake. Control of Photomechanical Crystal Twisting by Illumination Direction. *J. Am. Chem. Soc.*, 140, 4208 (2018).

8:00 PM EL15.07.06

Supramolecular Chirality Induced by Self-Assembly in Novel Quinoid Conjugated Molecules Jeongjin Hong, Yeonsu Choi, Yunseul Kim, Yina Moon, Jeongwoo Beak and Dong-Yu Kim; Gwangju Institute of Science and Technology, Korea (the Republic of)

Molecular assemblies with supramolecular chirality have been developed for decades due to their distinctive chiroptical properties. Among the versatile approaches to induce supramolecular chirality, self-assemblies using non-covalent interactions have considered as a great potential for applying biological field and chiroptical devices owing to their high tunability and controllability.

In this work, we designed and synthesized novel quinoid conjugated molecules QuEDOT-(S)-Cn and QuPheDOT-(S)-Cn employing enantiopure alkyl side chains. Quinoidal moieties are suitable for constructing supramolecular chirality through self-assembly due to their strong π - π stacking property of highly planar structure. QuEDOT-(S)-Cn and QuPheDOT-(S)-Cn had different chiroptical properties in solution and film states depending on the external stimuli (solvents, temp) as well as different chemical structures. Then we conducted diverse analyses such as AFM, POM, SEM, CD, GIWAXS to determine the reason for the difference in anisotropic factors between two molecules. We will explain and discuss the relationship between the behavior of supramolecular chirality and chemical structures. These results suggest chemical designing strategies of organic semiconducting materials in forming supramolecular chirality using self-assembly.

8:00 PM EL15.07.07

Chiral-Induced Surface-Enhanced Raman Optical Activity on Nanoparticle-On-Mirror Substrate Sung GunLee; Seoul National University, Korea (the Republic of)

Raman Optical Activity (ROA) has emerged as a valuable tool for characterizing stereostructural changes in both organic and inorganic compounds, offering complementary steric information to traditional spectroscopic methods. In particular, ROA has garnered attention as a chiral-selective method for analyzing biomolecules such as nucleic acids, and peptides, overcoming the limitations of conventional spectroscopy. However, due to the inherently low cross-section of ROA, which is three to five orders of magnitude lower than typical Raman, achieving sufficient signal sensitivity remains a challenge. To address this issue, efforts have been made to measure ROA signals using SERS, which utilizes plasmonic materials to enhance the Raman signal of analytes via the electric field concentrated around nanoparticles (SEROA). However, biomolecules typically have low Raman cross-sections and poor signal stability at high laser intensity and long measuring times, limiting the utility of SEROA. Recently, chiral-induced ROA has been proposed as a breakthrough, leveraging the "sergeants-and-soldiers" principle to induce chirality in a trace chiral compound, enabling the measurement of chirality with shorter measuring times and lower laser intensities.

This study demonstrates the possibility of a nanoparticle-on-mirror (NPoM) substrate and measurement configuration for ROA, which isolates hotspots from particle aggregation. To confirm the reliability of the NPoM configuration for ROA, chirality was induced in a self-assembled monolayer of 4-mercaptopyridine on a gold nanofilm surface.

SESSION EL15.08: Tunable Structural Chirality in Materials

Session Chairs: Clarice Aiello and Matthew Beard

Thursday Morning, November 30, 2023

Hynes, Level 2, Room 207

9:00 AM *EL15.08.01

Bio-Enabled Chiral Flexible Nanomaterials—From Chiral Emitting Sources to Photonically-Assisted Multilevel Logic Vladimir Tsukruk^{1,2}; ¹Georgia Institute of Technology, United States; ²Institute for Human and Machine Cognition, United States

Bio-enabled hybrid nanomaterials represent a novel class of functional materials, which uses bio-derived materials, bioinspiration and biomimetic approaches to design functional nanomaterials and structures with co-assembled biological and synthetic components to bring best of two worlds: adaptive photonic functions and chiroptical activity, flexibility and mechanical strength, potential sustainability and scalability [1]. Here, we summarize our recent results on functional bio-derived chiral nematic polysaccharides co-assembled with graphene oxides, organic semiconductors, magnetic nanoparticles, and quantum dots for adaptive chiroptical materials, magnetic materials and photonic multi-value logic thin film electronics.

Firstly, we discuss robust photonic nanomaterials from cellulose nanocrystals and nanofibers decorated with highly photoluminescent organic dyes, quantum dots and quantum nanowires for tailored emission of linear and circular polarized light [2, 3]. Secondly, we present results on magnetically steerable uniform photonic organization of cellulose nanocrystals decorated with superparamagnetic nanoparticles to achieve uniform organization [4]. Assembly under weak magnetic field gradients enables transformation from helicoidal cholesteric to uniaxial nematic phase with near-perfect orientation order parameter was achieved across large areas, enhanced mechanical robustness, and fast actuation ability. Finally, we demonstrate biophotonic field effect transistors mediated by circularly polarized excitation with multi-valued logic elements for dramatically elevated encryption ability [5].

References

- [1] D. Nepal, S. Kang, K. M. Adstedt, K. Kanhaiya, M. R. Bockstaller, L. C. Brinson, M. J. Buehler, P. V. Coveney, K. Dayal, J. A. El-Awady, L. C. Henderson, D. L. Kaplan, S. Keten, N. A. Kotov, G. C. Schatz, S. Vignolini, F. Vollrath, B. I. Yacobson, V. V. Tsukruk, H. Heinz, New Frontiers of Structural Bioinspired Nanocomposites: Advances and Opportunities, *Nature Mat.*, **2023**, 22, 18; D. Bukharina, R. Xiong, M. Kim, X. Zhang, S. Kang, V. V. Tsukruk, Chiral Nematic Liquid Crystal Organization of Natural Polymer Nanocrystals, *Liquid Crystals*, **2023**, <https://doi.org/10.1080/02678292.2023.2168776>
- [2] S. Kang, Y. Li, D. Bukharina, M. Kim, H. Lee, M. L. Buxton, M. J. Han, D. Nepal, T. J. Bunning, V. V. Tsukruk: Bio-organic chiral nematic materials with adaptive light emission and on-demand handedness, *Adv. Mater.*, **2021**, 2103329
- [3] S. Kang, G. M. Biesold, H. Lee, D. Bukharina, Z. Lin, V. V. Tsukruk, Dynamic chiro-optics of bio-inorganic nanomaterials via seamless co-assembly of semiconducting nanowires and polysaccharide nanocrystals, *Adv. Funct. Mater.*, **2021**, 2104596.
- [4] X. Zhang, S. Kang, K. Adstedt, M. Kim, R. Xiong, J. Yu, X. Chen, X. Zhao, C. Ye, V. V. Tsukruk, Uniformly aligned flexible magnetic films from bacterial nanocelluloses for fast actuating optical materials, *Nature Com.*, **2022**, 13, 5804; <https://doi.org/10.1038/s41467-022-33615-z>;
- [5] M. J. Han, M. Kim, V. V. Tsukruk, Multi-Valued Logic Structures for Optical Computing with Photonically Enabled Chiral Bio-Organic Structures, *ACS Nano*, **2022**, doi.org/10.1021/acsnano.2c04182; M. J. Han, M. Kim, V. V. Tsukruk, Chiro-Optoelectronic Encodable Multilevel Thin Film Electronic Elements with Active Bio-Organic Dielectric Layer, *Small*, **2023**, <https://doi.org/10.1002/sml.202207921>

9:30 AM EL15.08.02

Switching Chirality in Microarrays Enabled by Shape-Reconfigurable Spindle Microparticles MingzhuLiu, XingyueHan, So HeeNah, TianweiWu, YuchenWang, LiangFeng, LiangWu and ShuYang; University of Pennsylvania, United States

Giant circular photo-galvanic effect has been realized in chiral metals when illuminated by the circularly polarized light. However, the structure itself is not reconfigurable nor can we tune the crystal chirality in the adjacent domains. Here we synthesize spindle-shaped liquid crystalline elastomer microparticles that can continuously change shape from prolate to spherical to oblate upon heating above the nematic to isotropic transition temperature. The shapes are reversed upon cooling. When arranged the microparticles in a honeycomb lattice, the lattice can be switched from a right-handed chiral state to achiral one, then to a left-handed chiral state, without breaking the translational symmetry. Accordingly, the sign of rotation of the polarized light passing through the lattices changes as measured by time-domain terahertz (THz) spectroscopy. Further, we can locally alter the chirality in the adjacent domains using near-infrared (NIR) light illumination. The ability to controllably create chiral states at the boundary of the achiral/chiral domains will allow us to explore complex structures through the interplay of symmetry and topology.

9:45 AM EL15.08.03

Artificial Photosynthesis Empowered by PSII-Inspired Supramolecular Qantasomes with Chiral Architectures MarcellaBonchio^{1,2,3}; ¹University of Padova, Italy; ²INSTM, Italy; ³ITM-CNR, Italy

Being the natural-born photoelectrolyzer for oxygen delivery, Photosystem II (PSII) is hardly replicated with man-made constructs. In particular, the PSII organization in natural thylakoids sets key guidelines to rethink the molecular design of groundbreaking artificial photo-electrolysers. Building on the early "qantasome" hypothesis (*Science* 1964, 144, 1009-1011), PSII mimicry can be pared down to essentials by shaping a photocatalytic ensemble (from the Greek term "soma" = body) where light-quanta trigger water oxidation. We have recently reported on PSII-inspired nanodimensional qantasomes (QS) that readily self-assemble into hierarchical photosynthetic nano-stacks, made of bis-cationic perylenebisimides (PBI²⁺) as chromophores and deca-anionic tetrathionate polyoxometalates (Ru4POM) as water oxidation catalysts (*Nature Chem.* 2019, 11, 146–153). A combined supramolecular and click-chemistry strategy allows to interlock the multi-lamellar architecture emerging from the perylene aromatic stacking in water, while installing tetraethylene glycol (TEG) cross-linkers thus enhancing water harvesting and transport in proximity of the oxygen evolving center (*J. Am. Chem. Soc.* 2022, 144, 14021-14025). Our breaking new results deal with the introduction of sugar-based substituents as asymmetry effectors for the assembly of chiral qantasomes evolving oxygen using low energy green photons ($\lambda > 450$ nm, $\text{FEO}_2 > 95\%$). Action spectra, mass-activity, light-management, photoelectrochemical impedance spectroscopy (PEIS) together with Raman mapping of hydration shells, point to a key role of the supramolecular structure nano-arrays, where the interplay of hydrophilic, hydrophobic and chiral domains is reminiscent of PSII-rich natural thylakoids.

References

- [1] Scheuring, S., Sturgis, J. N. Chromatic Adaptation of Photosynthetic Membranes. *Science* 309, 484–487 (2005); Sartorel, A., Carraro, M., Toma, F. M., Prato, M., Bonchio, M. Shaping the beating heart of artificial photosynthesis: oxygenic metal oxide nano-clusters. *Energy Environ. Sci.* 5, 5592 (2012);
- [2] Piccinin, S.; Sartorel, A.; Aquilanti, G.; Goldoni, A.; Bonchio, M.; Fabris, S. Water oxidation surface mechanisms replicated by a totally inorganic tetraruthenium-oxo molecular complex. *Proc. Natl. Acad. Sci.* 110, 4917–4922 (2013)
- [3] Toma, F. M.; Prato, M.; Bonchio, M. et al. Efficient water oxidation at carbon nanotube–polyoxometalate electrocatalytic interfaces. *Nature Chemistry* 2, 826-831 (2010).
- [4] Bonchio, M.; Sartorel, A.; Prato, M. et al. Hierarchical organization of perylene bisimides and polyoxometalates for photo-assisted water oxidation. *Nature Chemistry* 11, 146-153 (2019).
- [5] Gobbo, P.; Bonchio, M.; Mann, S. et al. Catalytic processing in ruthenium-based polyoxometalate coacervate protocells *Nature Commun* 11, 41 (2020);
- [6] GobboT.; Rigodanza F.; Benazzi, E.; Prato, M.; Bonchio M. et al. *J. Am. Chem. Soc.* 144, 14021-14025 (2022).

10:00 AMBREAK

10:30 AM EL15.08.04

A Multi-Functional Full-Polarized Light Emitting and Controlling Device [Jiawei Lyu](#) and Ki Tae Nam; Seoul National University, China

Nanomaterials emitting polarized light directly without using the traditional polarizers are believed to simplify the design of polarization optics and afford higher efficiency, showing great potential in practical applications such as 3D display, hologram, anti-counterfeiting and light communication. While most efforts are focused on improving the polarized light emission performance of specific nanomaterials, of paramount importance is to interface these excellent materials with state-of-the-art industrial technology to make functional devices. Herein, we propose and demonstrate an efficient route to fabricate full-polarized emitting and controlling devices via integrating 3D printing technique with the (micro) LED display technology. We achieved an extraordinarily high degree of linearly and circularly polarized luminescence (CPL) through precise control of the nanomaterial assembly structure. Moreover, we realized efficient spatio-temporal modulation of various polarization states. These features enable multiple applications including a secured visible light communication (VLC) system and polarization-based multichannel displays.

10:45 AM

Solution Synthesis of Halide Chiral Crystal with Controlled Dimension and Morphology [Zhihao Zhang](#); Rensselaer Polytechnic Institute, United States

Recently, there has been a surge of research interest in understanding the intriguing spin-related phenomena in chiral materials. In this work, we present a solution-based approach for growing ferromagnetic chiral halide crystal. By tuning the temperature, growth time and concentration, we optimize the growth morphologies. We use X-ray diffraction and Raman spectroscopy to characterize the crystal structure and phase. The chirality is investigated by circular dichroism spectroscopy. The integration of ferromagnetism and chirality in the same crystal provides a rich platform for understanding spintronic phenomena.

11:00 AM EL15.08.06

Unprecedented Intrinsic Chirality in CsPbBr₃ Nanoplatelets Tunable Through Synthetic Conditions [Progna Banerjee](#), [Jia-Shiang Chen](#), [Xuedan Ma](#) and [Elena Shevchenko](#); Argonne National Laboratory, Center for Nanoscale Materials, United States

This work reports on the intrinsic chiral behavior in colloidal ultrathin CsPbBr₃ nanoplatelets with unprecedented quantitative s-handed value as studied using circular dichroism measurements. Through adjusting various synthetic parameters, such as temperature, Cs and Pb reagent ratios, reaction solvents and stirring direction, we are able to tune the quantitative chiral properties in these nanomaterials. Additionally, the functional aspects such as the handedness of these nanoplatelets can be tuned using brominated methylbenzylamines with suitable r/s chirality. We utilize the advantageous procedure of single particle photoluminescence studies to attain insights into the lifetimes and correlate them with the presence and the type of ligands. We reach qualitative arguments based on surface defects and Pb extraction through selected area electron microscopy, and rigorous x-ray diffraction accompanied with Rietveld refinement analyses- to explain the atomic arrangements at the surface of these nanoplatelets which can be tuned through synthetic factors. Optical characterization by absorption and circular dichroism extends these ideas into correlation with microscopy and diffraction results. These remarkable control of chiral parameters without external stimuli in untreated/as prepared nanoplatelets; and through choice of the ligation combinations hence accomplished highlight the suitability of these ultrathin CsPbBr₃ nanoplatelets for applications in a wide range of optical and mechanical applications including chiral superstructures.

11:15 AM EL15.08.07

Tuning Chiroptical Properties of Chiral 2D Hybrid Organic-Inorganic Perovskites Through Mixing Halogen [Lan-Sheng Yang](#), [Chun-Yao Huang](#) and [Yu-Chiang Chao](#); National Taiwan Normal University, Taiwan

Chiral 2D halide perovskites have attracted increasing attention due to their exceptional photoluminescence properties, tunable bandgap, and various crystallized structure. However, tuning chiroptical properties of chiral 2D hybrid halide organic-inorganic perovskites have not yet been extensively studied. Here, we report the chirality of chiral 2D halide perovskites through circular dichroism (CD) and circularly polarized photoluminescence (CPL). By varying the mixing ratio of chlorine, bromide, and iodide anions in S- or R-(MBA)₂PbI₄(1-x)Br_{4x} or S- or R-(MBA)₂PbBr₄(1-y)Cl_{4y}, the mixing of halide ions allows a tunable band gap of the chiral OIHPs, leading to a shift of the CD signal from 495 to 320 nm and the CPL signal from 530 to 485 nm. Moreover, it is noticed that the CD signal ascends from x=0 to x=1 and descends from x=1 to x=4. Successively, the CD signal ascends from y=0 to y=4. This difference can be explained that the phase transition of the crystalline structure occurred. Chiral optical asymmetry (g-factor) at y=4 has a maximum value of 0.015 compared to other mixing ratios. The CPL signal becomes greatly small after the phase transition because of structural distortion in the inorganic framework and instability. Additionally, the CD sign conversion is discovered as well through mixing halogen. These properties can take advantage of the structural engineering of high-performance chiroptical materials for spin-polarized light-emitting devices. Spin organic light-emitting diodes were achieved by using chiral 2D hybrid halide perovskites film as the spin filter layer. Circularly polarized electroluminescence was observed at room temperature in the absence of an external magnetic field.

11:30 AM EL15.08.08

Telling Left From Right using Electron Microscopes [Assaf Ben Moshe](#); Bar Ilan University, Israel

In 1848 Louis Pasteur reported his findings on the separation of a racemic mixture of chiral molecules during their crystallization from the solution phase. Left and right molecules crystallized separately in crystals that exhibited left- and right- handedness at the macroscopic level, as portrayed by their overall chiral habit. This monumental experiment is considered by many to have helped setting the foundations of modern stereochemistry.

Determination of absolute configurations of molecules, and relation between microscopic and macroscopic handedness in chiral crystals became a key challenge. This is often addressed using chemical assays with chiral additives, x-ray crystallography and chiroptical spectroscopy. At a later stage in history the advent of electron microscopy led to many studies of (nano)crystals using powerful high-resolution techniques, yet the problem of handedness determination often remains untreated and elusive.

In this project a nanoscale crystalline system that exhibits chirality at the atomic arrangement, as well as its overall habit was studied.¹ We showed that the mechanism that determines shape chirality in this material is not trivial, and is not the result of the chiral crystallographic symmetry of the crystal. While doing so, we also developed approaches for determination of shape and crystal structure handedness using electron microscopy.

- [1] Ben-Moshe, A.; da Silva, A.; Mueller, A.; Abu-Odeh, A.; Harrison, P. J.; Cho, Waelder, J.; Niroui, F.; Ophus, C.; Minor, A. M.; Asta, M.; Theis, W.; Ercius, P.; Alivisatos, A. P. "The chain of chirality transfer in tellurium nanocrystals" *Science* **2021** 379, 729-733.

11:45 AM EL15.08.09

Leveraging The Preferences in Transition Metal-P/Si Bonding to Design Novel Chiral Materials [Kirill Kovnir](#); Iowa State University, United States

Non-centrosymmetric chiral intermetallic compounds with antisymmetric spin-orbit coupling exhibit a plethora of emergent properties. Chemical bonding preferences in the transition metal silicon-phosphides TM-Si-P create the asymmetric environment around metal atoms resulting in high abundance of non-centrosymmetric chiral and polar crystal structures. The synthesis of those phases is hampered by inertness of TM and Si in contrast to high reactivity and vapor pressure of phosphorus. We developed a comprehensive synthetic strategy allowing to produce single crystals and phase-pure polycrystalline samples of metal tetrel-pnictides. The correlation between the crystal structure, chemical bonding, and optical and properties will be discussed with focus of earth abundant TM for applications.

1:30 PM *EL15.09.01

Chirality-Induced Spin Selectivity Effect in 2D Chiral Hybrid Perovskites: Chiral-Phonon-Activated Spin Seebeck EffectDaliSun; North Carolina State University, United States

The Chirality-Induced Spin Selectivity (CISS) effect, a unique ‘spin filtering’ effect arising from the structural handedness of organic compounds (i.e., chirality) and their assemblies that lack inversion symmetry [1]. It utilizes chirality to generate robust spin information from chiral (left- (S) or right-handed (R)) molecules without the need for common magnetic elements. The CISS effect provides a strong coupling between spin and electronic properties without the need for magnetic ordering. Recently, the CISS effect has been reported in 2D chiral hybrid perovskites (2D-chiral-HOIPs), a resurgent class of solution-processed hybrid semiconductors consisting of alternating layers of chiral organic compounds and inorganic framework of corner-sharing metal halide octahedra. Although considerable progress has been made in understanding many features of the CISS response in chiral-HOPs [2,3] and other chiral materials, an adequate quantitative description of (i) the CISS effect, (ii) its strong manifestation for spin selectivity at ambient temperatures, and (iii) its mechanistic origins, is still lacking. It comes to our attentions that angular momentum in condensed matter systems, including rigid rotation and elastic deformation, can be viewed as an information vector [4]. At the microscopic scale, the lattice vibrations, i.e., phonons, can carry angular momentum and mimic the well-known information-carrying photons [5]. This phonon angular momentum, i.e., *chiral phonon* displays a non-zero phonon angular momentum when the system is displaced from equilibrium, offering a high potential for producing the CISS effect at elevated temperatures. Here we show the observation of spin currents generated by chiral phonons in a 2D chiral HOIP implanted with chiral cations when subjected to a thermal gradient [6]. The generated spin current shows a strong dependence on the chirality of the film and external magnetic fields, of which the coefficient is orders of magnitude larger than that produced by the reported spin Seebeck effect. Our findings indicate the potential of chiral phonons for spin caloritronic applications and offer a new route toward spin generation in the absence of magnetic materials. Demonstration of the chiral-phonon-activated spin Seebeck effect in 2D chiral HOIPs may aid in solving the paradoxical diversity of CISS models, shedding light on CISS-related responses observed in a wide variety of chiral systems.

References

- [1] B. Göhler *et al.* *Science* **331**, 894–897 (2011).
- [2] Z. Huang *et al.*, *ACS Nano* **14**, 10370 (2020).
- [3] Y.-H. Kim, *et al.* *Science* **371**, 1129 (2021).
- [4] L. Zhang & N. Qiu. *Phys. Rev. Lett.* **115**, 115502 (2015).
- [5] H. Zhu *et al.*, *Science*, **359**, 6375 (2018).
- [6] K. Kim *et al.*, *Nature Materials* **22**, 322 (2023).

2:00 PM EL15.09.02

Chiral Phonon-Induced Spin PolarizationHanyuZhu, JiamingLuo, TongLin, JunjieZhang, XiaotongChen, ElizabethBlackert, RuiXu and BorisI. Yakobson; Rice University, United States

Controlling spins on very short time scales may enable novel non-equilibrium magnetic physics as well as ultrafast spintronics for energy-efficient information processing. Chiral phonons, where atoms rotate unidirectionally around the equilibrium position inside crystalline lattice, break time reversal symmetry and are expected to directly couple with magnetization. We excited chiral phonons using circular-polarized terahertz pulses and observed a prominent transient magneto-optic Kerr effect in rare-earth trihalides. The effective magnetic field needed to polarize the paramagnetic spins is on the order of 1 T under very moderate pump fluence of 0.2 mJ/cm². The temperature dependence of the spin dynamics indicates the magnetic field indeed is generated by the phonons, as opposed to a pure electromagnetic inverse Faraday effect. Our result may open a new route to investigate spin-phonon interaction in ultrafast magnetism and chiral transport properties for quantum devices.

2:15 PM EL15.09.03

Terahertz Excitation of Chiral Phonons to Induce Dynamical MultiferroicityMeganNielsen, Enoch (Sin Hang)Ho, AldairAlejandro, MatthewLutz, ClaytonMoss and JeremyA. Johnson; Brigham Young University, United States

Circular motion of ions in solid materials has been posited as a means to dynamically induce or control magnetic properties. This circular motion fundamentally requires the excitation of “chiral” phonon modes, and the ability to excite and control transient crystal chirality could have a significant impact on condensed matter physics.

Pairs of phonon modes in ferroelectric materials can be excited to create circular or elliptical motion of ions. Depending on the charge of the ions and magnitude of their motions, these ion loops with right or left handedness can induce a magnetic moment, even in originally non-magnetic materials. Therefore, exciting ion loops in ferroelectric solids to dynamically induce magnetic ordering, will make them transiently multiferroic.

We have recently had much success in controlling the waveform and polarization of high-field, broadband terahertz (THz) pulses. This waveform control is driven by the capability to perform two-dimensional (2D) THz spectroscopy, including the ability to create circularly polarized THz pump pulses. In this presentation, we report how we generated intense pulses of circularly polarized THz light to excite pairs of degenerate phonon modes. As the phonon modes are excited with proper relative phase (provided by the circularly polarized THz pulses), circular phonon motion results. The transient magnetic moment induced by these excited ions loops is then measured with the ultrafast Faraday effect.

To generate circularly polarized light, we combine two linearly polarized THz pulses with adjustable relative delay. A differential chopping scheme enables us to readily measure the sample response from a single (vertically polarized) THz pulse, the other individual (horizontally polarized) THz pulse, and the combined THz pulse with controllable polarization state, all in a succession of four laser shots; the probe response in the absence of a THz pump pulse is measured with the fourth laser shot.

To probe the sample response, we direct an 800-nm probe pulse through the excited region of the sample and measure the modification of the probe polarization with a transient birefringence detection scheme. This allows us to measure the transient Faraday effect to detect the creation of an ultrafast magnetic moment. However, it can also measure other ultrafast birefringence signals, like the THz Kerr effect. Fortunately, by controlling the relative polarization angles between THz and probe pulses, we can isolate the Faraday signal from the Kerr signal.

With circularly polarized THz pulses, we excite a z-cut sample of LiNbO₃. The lowest frequency E symmetry phonon modes are doubly-degenerate with perpendicular mode effective charge vectors that can be driven with THz pulses polarized along the crystallographic x and y directions. Exciting pairs of E-modes with circularly polarized THz pump pulses induces ion-loop motion, leading to a transient magnetic moment in LiNbO₃. While the chiral phonon motion takes place, a transient magnetic moment is induced that can be detected with the Faraday rotation of a probe pulse. We observe a transient signal persisting for ~3 ps, which is longer than the THz pump pulse duration (<1 ps), confirming that this isn’t just the THz inverse Faraday effect. The magnetic moment signal also switches sign as the THz polarization and subsequent chiral phonon motion changes handedness.

In summary, using a 2D THz experimental setup, we can create high-field circularly polarized THz pulses. These circularly polarized THz pulses excite chiral phonon motion in LiNbO₃, transiently inducing a magnetic moment that persists longer than the THz excitation pulses. Isolating the Faraday signal from the Kerr signal confirms that the excited chiral phonon motion, so-called ion loops, induces magnetic ordering in non-magnetic LiNbO₃. The ability to use circularly polarized THz pulses to control chiral phonon motion will provide many new avenues in the study of condensed matter systems.

2:30 PM BREAK

3:00 PM *EL15.09.04

Phonons and Phase Symmetries in Non-Symmorphic Twisted and Layered MaterialsLucasLindsay; Oak Ridge National Laboratory, United States

Structural complexity underlies a variety of novel quasiparticle behaviors that can have profound impacts on material functionalities. Here I will discuss the role of structural twisting and translational symmetries in determining the vibrational behaviors of non-symmorphic chiral and achiral materials and how these translate into spectral features and functionalities. We advance

a dynamical theory that incorporates the various symmetries internal to the lattice unit cell directly into the description of the phonon frequencies and eigenvectors. This naturally elucidates phase conservation relations in twisted structures and layered materials. We apply this theory to build insights into vibrational dynamical structure factors and spectral observations from inelastic neutron and x-ray scattering experiments, and provide a fresh perspective on symmetry-enforced crossings, quasiparticle interactions, and band topologies.

L.L. acknowledges support from the U. S. Department of Energy, Office of Science, Basic Energy Sciences, Materials Sciences and Engineering Division.

3:30 PM EL15.09.05

Towards Chiral Acoustoplasmonics Beatriz Castillo Lopez de Larrinzar¹, Chushuang Xiang², Edson Rafael Cardozo de Oliveira², Norberto Daniel Lanzillotti-Kimura² and Antonio Garcia-Martin¹; ¹Instituto de Micro y Nanotecnología, CSIC, Spain; ²Centre de Nanosciences et de Nanotechnologies (C2N), France

The possibility of creating and manipulating nanostructured materials encouraged the exploration of new strategies to control electromagnetic properties. Among the most intriguing nanostructures are those that respond differently to helical polarization, i.e., exhibit chirality.[1] Circularly polarized light can be used to probe and determine the chiral nature of a plasmonic structure, which is usually reflected as quantitative differences in the values of the absorption or scattering cross-sections. However, reaching maximum absorption and minimum scattering for one helicity, and the opposite for the other is not usually found to occur at the same wavelength.[2]

In the present work, we propose a simple chiral plasmonic structure based on crossed elongated bars where light-handedness defines the dominating cross-section absorption or scattering, as it identifies the two different enantiomers in a chiral structure which determine how the system interacts with its environment. The system is yet maintained simple enough to understand the actual nature of the response observed, be open to future developments, and warrant fabrication for future experimental verification [3,4]. Based on this structure, our work demonstrate that, not only through the interactions between different elements it is possible to make the absorption and scattering cross-sections radically and qualitatively different for the two circular polarizations, but also that the dominating cross-section can be switched from absorption to scattering by simply changing the polarization of the impinging beam. Also, we theoretically propose a simple pump-probe experiment using circularly polarized light. [5] In the reported structures, the generation of acoustic phonons is optimized by maximizing the absorption, while the detection is enhanced at the same wavelength -and different helicity- by engineering the scattering properties [6]. Thus, the presented results constitute one of the first steps towards harvesting chirality effects in the design and optimization of efficient and versatile acoustoplasmonic transducers.

References

- [1] S. L. D. Barron, *Molecular Light Scattering and Optical Activity*, Cambridge, Cambridge University Press, (2004)
- [2] B. Hopkins, et al., *Laser Phot. Rev.* 10, 137 (2016).
- [3] B. Auguie, et al., *J. Phys. Chem. Lett.* 2, 846 (2011)
- [4] C. de Dios, et al., *Opt. Express* 27, 21142 (2019)
- [5] B. Castillo López de Larrinzar, et al., *Nanophotonics* 12, 1957 (2023)
- [6] N. D. Lanzillotti-Kimura, et al., *Phys. Rev. B* 83, 201103 (2011)

3:45 PM EL15.09.06

Preparation and Characterization of Chiral Mechanical Metamaterials Wenbing Wu and Nicholas A. Kotov; University of Michigan, United States

Chirality of nanostructures and nanocomposites have been instinctively associated with their chiroptical activities, e.g., circular dichroism and optical rotation. Chiral effects have also been predicted to exist in the mechanics of materials by theories more than 50 years ago.^[1] Two key phenomena have been identified: 1) A chiral material can rotate the linear polarization plane of a transverse mechanical wave, analogous to the optical rotation of electromagnetic waves. 2) A moment is induced when a chiral solid is subjected to longitudinal stress. Notwithstanding the theoretical achievements, it has only been recently that a few experimental progresses have emerged, because challenges remain in both the preparation and characterization of such materials. The goal of this talk is to present our most recent work in addressing these two challenges.

Currently reported chiral mechanical structures were mostly created via 3D printing. We propose a material engineering strategy to fabricate chiral mechanical composites with helical inclusions. A variety of chiral nano- and micro-particles and assemblies can be obtained self-assembly methods.^[2] The morphology of these particles, including their size and twisting pattern, can be tuned by the self-assembly process. The chiral particles are then included in an aerogel matrix of aramid nanofibers.^[3] The micro-rotation of the particles, induced by external linear mechanical waves, transmits through the nanofiber network and couples into a collective macroscopic rotation, which can be experimentally measured.

In contrast to electromagnetics, there are few commercially available tools for the detection of the polarization of mechanical waves. We built up a digital image correlation (DIC) system that enables the measurements of the displacement vector of a surface with nanometer resolution.^[4] A piezoelectric transducer, on which a chiral solid is mounted, produces a linear transverse mechanical wave up to 250 kHz. The DIC measurements are used to identify the polarization directions of the transverse waves on the piezoelectric transducer and the sample surface. The twisting angle between the two directions is an indication of the mechanical chirality of the solids. This presentation outlines our ongoing efforts on the preparation and characterization of chiral mechanical effects in self-assembled composite metamaterials.

- [1] A. C. Eringen, *Microcontinuum Field Theories*, Springer New York, New York, NY, 1999.
- [2] W. Jiang, Z. Qu, P. Kumar, D. Vecchio, Y. Wang, Y. Ma, J. H. Bahng, K. Bernardino, W. R. Gomes, F. M. Colombari, A. Lozada-Blanco, M. Veksler, E. Marino, A. Simon, C. Murray, S. R. Muniz, A. F. de Moura, N. A. Kotov, *SCIENCE* 2020, 368, 642+.
- [3] M. Yang, K. Cao, L. Sui, Y. Qi, J. Zhu, A. Waas, E. M. Arruda, J. Kieffer, M. D. Thouless, N. A. Kotov, *ACS Nano* 2011, 5, 6945.
- [4] T. Frenzel, J. Köpfler, A. Naber, M. Wegener, *Sci Rep* 2021, 11, 2304.

SYMPOSIUM EL16

Carrier-Dopant Interactions in Organic Semiconductors—From Fundamentals to Applications
November 27 - November 30, 2023

Symposium Organizers

Nagarjuna Gavvalapalli, Georgetown University
Mukundan Thelakkat, Univ of Bayreuth
Dhandapani Venkataraman, University of Massachusetts Amherst
Luisa Whittaker-Brooks, University of Utah

* Invited Paper

+ JMR Distinguished Invited Speaker

10:30 AM *EL16.01.01

The Interplay Between Dopants and Charge Carriers in Organic Semiconductors Lambert Jan AntonKoster; University of Groningen, Netherlands

In order to make rational improvements of the charge transport properties of doped organic semiconductors, a thorough understanding of this rather complex process is needed. The efficacy of doping is governed by a multitude of steps, including the interactions between (ionized) dopants and charge carriers. In this contribution, we explore the effects of carrier-dopant and carrier-carrier interactions and strategies to mitigate them.

We use kinetic Monte-Carlo simulations to better understand the effects of carrier-dopant and carrier-carrier interactions. Such simulations predict that a larger host-dopant distance can result in a higher Seebeck coefficient for a given electrical conductivity. In order to realize such a system, we use amphiphatic side chains in an n-type donor-acceptor copolymer. The amphiphatic side chain contains an alkyl chain segment that acts as a spacer between the polymer backbone and an ethylene glycol type chain segment. The use of this alkyl spacer can not only reduce the energetic disorder in the conjugated polymer film but can also properly control the dopant sites away from the backbone, which minimizes the adverse influence of counterions. We find that this selectively increases the Seebeck coefficient and the power factor by a factor of ~ 5 .

While it has been recognised that Coulomb interactions between dopants and charge carriers are important, carrier-carrier interactions—interactions among charge carriers—in doped organics have received less attention. In a doped organic semiconductor, however, the number of (free and bound) charge carriers equals the number of reacted dopants. As a result, both types of interactions are of importance for a proper description of the transport properties of doped organic semiconductors.

To study the transport properties in the presence of dopants and including both carrier-carrier and carrier-dopant interactions we once again use kinetic Monte-Carlo simulations. While the conductivity is indeed affected by carrier-dopant interactions, the effect of carrier-carrier interactions appears to be even stronger, especially so at high doping concentrations. Experimentally, we observe that the electrical conductivity of a large number of organic semiconductors shows a maximum: Upon increased doping levels the conductivity decreases. This type of behaviour is commonly attributed to changes in the microstructure as a consequence of doping. However, we find that even when using vapour doping, where there are no observable changes in the microstructure, this behaviour persists. The experimental findings match the Monte-Carlo data very closely, which suggests that the Coulomb interactions among charge carriers is at the root of the limited conductivity at high doping densities.

11:00 AM *EL16.01.02

Dopant-Carrier Coulomb Interactions in Organic Electronics: DOS Shape, Transport, and Carrier Screening Zlatan Aksamija; University of Utah, United States

Organic electronic materials, specifically conjugated polymers, are a cost-effective and environmentally friendly alternative to inorganics. However, they do not possess intrinsic free carriers, which means they must be doped to increase the number of free carriers and boost conductivity. Simultaneously, their low dielectric constant means electrostatic Coulomb interactions between free carriers and dopant counterions are poorly screened. These dopant-carrier interactions dramatically alter the energetics of the states available for transport as well as the dynamics of free carriers. The importance of Coulomb interactions and their impact on the density of states (DOS) via dopant-induced disorder is now well established. In this invited talk, I will discuss our results arising from coupling a model for modification of the electronic density of states (DOS) in the presence of dopants with a phonon-assisted carrier hopping simulation through those states. We expanded the model initially proposed by Arkhipov et al. to include the finite dopant size and minimum dopant-carrier separation, which limit the deepest traps in the tail of the DOS. We use the DOS model as input to the hopping transport simulation to analyze the transport properties of doped conjugated polymers and extract both conductivity and Seebeck coefficient at each doping concentration. We also vary the parameters of the dopants, including their size, energy level, and charge distribution on the dopant counterion to quantify their impact on conductivity.

However, previous studies of hopping transport within the Gaussian Disorder Model did not consider the role of screening the dielectric interactions by the carriers. In our work, we implement screening in the Debye-Hückel formalism and calculate dopant-induced disorder with the resulting electrostatic potential. For a point dopant, this gives the well-known Yukawa potential, which we generalize for dopant charge distributions other than the point charge. Then we solve Pauli Master Equation with Miller Abrahams hopping rates with states from the resulting screened DOS. Our results show that screening has a significant impact on the Seebeck coefficient and shape of the DOS. The thermoelectric power factor increases almost by a factor of 2 at higher doping. We also observe that the log slope of the Seebeck coefficient plotted against the electrical conductivity for different doping concentrations, which was previously thought to have a universal value ($-1/4$), increases for a more energetically disordered system. By including screening, we were able to reproduce and explain these curves obtained in measurements and connect the change in slope with the change in structure of the host polymer. We conclude that carrier screening of dopant Coulomb interactions plays an important role in transport and thermoelectric properties of polymers, especially at high doping concentrations. Our work refines the understanding of fundamental processes in doped polymers and enables their easier engineering for thermoelectric, photovoltaic and other applications.

11:30 AM EL16.01.03

The Effects of Doping on Transport in Organic Electronics: Analyzing the Dopant-Induced Disorder Andrew Tolton and Zlatan Aksamija; University of Utah, United States

Organic electronic materials, specifically conjugated polymers, are a cost-effective and environmentally friendly alternative to inorganics. However, their low intrinsic conductivity means they must be doped to increase the number of free carriers. Characterizing the effects of doping on organic thermoelectrics has proven to be a long-standing problem. Doping introduces both structural and energetic changes to the polymer, changing the shape of the electronic Density of States (DOS) through the creation of band tails and widening the DOS, resulting in a type of energetic disorder termed dopant-induced disorder (DID). The shape of the DOS resulting from doping can be captured through two parameters: the width of the DOS, termed energetic disorder, and the shape of the DOS, which is quantified by a shape parameter p , which can take on values of 1 for an exponential DOS to 2 for a Gaussian one. In our previous work, we showed that DID causes energetic disorder to increase while the p value simultaneously decreases from 2 to below 1 in heavily doped polymers, implying heavy tails. The resulting carrier mobility is impaired by the presence of heavy tails and the deep trap states in them. Doping then simultaneously increases DID, affecting the shape of the DOS, but fills the deepest tail states first, partially countering their effect.

To decouple the influences of each of these effects, we fix the shape of the DOS to simulate doping without DID. We then compute both conductivity and thermoelectric Seebeck coefficient at each DOS and carrier concentration using a numerical simulation of phonon-assisted carrier hopping between localized states. The simulation iteratively solves the Pauli master equation with Miller-Abrahams hopping rates. The iteration converges on an out-of-equilibrium distribution function, from which carrier and energy currents are computed, from which we extract conductivity and Seebeck coefficient, respectively. The Seebeck coefficient is a convenient and readily measurable proxy for the carrier concentration as it scales with the position of the Fermi level in the DOS. The Seebeck vs conductivity plot thus reveals the tradeoff induced by doping and captures the impact of the DOS on transport. We find distinct behavior of the Seebeck vs conductivity relation across doping regions, and these behaviors can be described in terms of carrier concentration in conjunction with the key parameters of the DOS: its width (energetic disorder) and shape parameter. The distinct regions on the Seebeck-conductivity curve come from surprisingly simple relationships between doping and several transport parameters, which also allow us to provide qualitative expressions for difficult-to-measure quantities like carrier concentration and carrier-dependent mobility. Ultimately, this analysis clearly displays the underlying effects of doping without the simultaneous obfuscation of DID, allowing us to gain a clearer understanding of the effects of both influences. This work will impact the design of polymer-dopant complexes for reaching higher carrier mobility in future organic electronics.

11:45 AM EL16.01.04

A New Strategy to Greatly Improve The Seebeck Coefficient and Overall Thermoelectric Properties of Conducting Polymers Jianyong Ouyang; National University of Singapore, Singapore

Conducting polymers emerge as the next-generation thermoelectric materials because of their merits including high conductivity, high mechanical flexibility, low cost and solution processability. However, their Seebeck coefficient is notably lower than inorganic thermoelectric materials by about one order in magnitude. The conventional methods to increase the Seebeck coefficient of conducting polymers including partial dedoping with a reducing agent or base and energy filtering. Nevertheless, these methods are not very effective, and the overall thermoelectric properties of conducting polymers are not very high. Here, I will present a new strategy to greatly improve the Seebeck coefficient and thus the overall thermoelectric properties of conducting polymers. The zT value can be comparable to the best inorganic thermoelectric materials at room temperature.

1:30 PM EL16.02.01

Doping-Enabled Photomultiplication in Narrowband Near-Infrared Organic Photodetectors for Enhanced Detectivity [Louis Conrad Winkler](#)¹, [Jonas Kublitski](#)², [Johannes Benduhn](#)¹ and [Karl Leo](#)¹; ¹Technische Universität Dresden, Germany; ²Universidade Tecnológica Federal do Paraná, Brazil

Continuous monitoring of food quality, blood oxygen, or industrial processes requires high-throughput near-infrared photodetectors. Due to excellent properties like low-cost, flexibility, and narrowband response, organic photodetectors (OPDs) have vast market potential for such applications.

In this work, we utilize the emerging absorption feature of a weakly doped C60 bulk for photo-responses above 1000 nm, circumventing the difficulties of obtaining molecules with a low optical gap and low molecular mass. The unavoidable increase of band-to-band recombination for low-gap systems, which is detrimental to the external quantum efficiency (EQE), is overcome by combining two mechanisms to achieve a strong photocurrent gain. Trap-assisted accumulation, realized by very low doping, and energetic blocking of holes, are utilized to achieve a spectral response (SR) of 15 AW⁻¹ at 1092 nm.

Furthermore, spatial doping variations are implemented into the device to boost the absorption within the optical cavity, resulting in a narrow response of 18 nm. This approach allows easy tuning of the resonant wavelength by bulk thickness variations and thus allows spectrally highly resolved measurements. Contrary to OPDs working in the self-powered mode, this detector is optimized for operation under reverse bias. With its high spectral response, low-cost readout circuitry based on CMOS technology could be used for signal detection.

1:45 PM EL16.02.02

Control of Resistance Temperature Change of Solution-Processed Conductive Polymers for Strain Sensor Applications [Yu Kato](#)¹, [Kenjiro Fukuda](#)^{2,2}, [Takao Someya](#)^{1,2,2} and [Tomoyuki Yokota](#)^{1,1}; ¹The University of Tokyo, Japan; ²RIKEN, Japan

Organic materials are used in flexible electronics due to their excellent flexibility and simple fabrication using solution processes. Because the resistance of organic materials changes with strain and temperature, flexible strain^[1] and temperature^[2] sensors using organic materials have been studied. In such sensors, control of conductivity and resistance temperature change is important. When the device is used as a strain sensor, the resistance temperature change needs to be small to make the sensor less susceptible to temperature. In contrast, when the device is used as a temperature sensor, the resistance temperature change should be large to increase sensitivity. Low conductivity makes the device more sensitive to electronic noise. In this study, we evaluated the influence of the fabrication conditions on the conductivity and temperature characteristics of devices using conductive polymers. Then, we selected a condition and applied it to a strain sensor.

Chromium and gold were evaporated on substrates as electrodes. Conductive polymers were spin-coated on the substrates followed by annealing under a nitrogen atmosphere. Conductive polymers consisted of a polymer material and a p-type dopant. The doping concentration in this experiment was 12%, which means that twelve dopant molecules were added per one hundred monomeric units of the polymer. The standard conditions in this experiment were P3HT for the polymer, BCF for the dopant, and 70 °C for the annealing temperature, and the effects of changing these conditions were evaluated. Temperature coefficient of resistance (TCR) is defined as the ratio of resistance change to temperature change. In this study, TCR was calculated using the resistances at 25 and 40 °C. When the device was applied to the strain sensor, a 1- μ m-thick parylene was deposited on the device as a passivation layer. A gauge factor, defined as a ratio of resistance change to applied strain, was measured.

By adding BCF to P3HT, the conductivity increased by four orders of magnitude, and the TCR changed from -1.3%/K to -0.9%/K. Increasing the annealing temperature from 70 to 150 °C reduced the conductivity by two orders of magnitude and changed the TCR to -2.0%/K. Similar results were obtained when F4-TCNQ was used as a dopant, indicating that the influence of the dopant type on the characteristics was small. When other polymers such as DPP-DTT, PTB7 and PBDTT-DPP were mixed with F4-TCNQ, the TCRs were -2.0%/K, -2.3%/K, and -2.7%/K, respectively. Subsequently, we fabricated a strain sensor using P3HT/BCF annealed at a low temperature, which was a condition that exhibited a small resistance temperature change and high conductivity. The gauge factor of the sensor was 5.9 when a tensile strain of 6.6% was applied. The sensor was attached to an arm and detected resistance change during arm bending.

<Reference>

[1] S. Watanabe *et al. Adv. Sci.* **8**, 2002065 (2021) [2] Y. Wang *et al. Scientific Reports* **10**, 2467 (2020)

<Abbreviation of materials>

P3HT: poly(3-hexylthiophene-2,5-diyl), BCF: tris(pentafluorophenyl)borane, F4-TCNQ: 2,3,5,6-tetrafluoro-7,7,8,8-tetracyano-quinodimethane, DPP-DTT: poly[[2,3,5,6-tetrahydro-2,5-bis(2-octyldodecyl)-3,6-dioxopyrrolo[3,4-c]pyrrole-1,4-diyl]-2,5-thiophenediylthieno[3,2-b]thiophene-2,5-diyl-2,5-thiophenediyl], PTB7: poly[[4,8-bis[(2-ethylhexyloxy)benzo[1,2-b:4,5-b']dithiophene-2,6-diyl]]3-fluoro-2-(2-ethylhexyl)carbonyl]thieno[3,4-b]thiophenediyl], PBDTT-DPP: poly[2,6'-4,8-di(5-ethylhexylthienyl)benzo[1,2-b:3,4-b']dithiophene-alt-5-dibutylthio-3,6-bis(5-bromothiophen-2-yl)-pyrrolo[3,4-c]pyrrole-1,4-dione]

2:00 PM *EL16.02.03

Interplay of Electrical and Mechanical Properties of Doped Conjugated Polymers [Christian Müller](#); Chalmers University of Technology, Sweden

Chemical and electrochemical doping are widely used to modulate the electrical properties of conjugated polymers. Doping of thin films facilitates fundamental spectroscopic studies and, ultimately, is important for the operation of devices from transistors to solar cells. However, some applications such as thermoelectrics and wearable electronics require bulk materials, which complicates doping processes and mass transport, limiting the performance of devices. This talk will explore some of the fundamentals of doping of both thin films and bulk materials. The impact of doping on the electrical as well as mechanical properties will be discussed, and it is shown how doping can be used to tune both the conductivity and stiffness of conjugated polymers. Finally, strategies are explored that permit to decouple the effect of doping on the electrical and mechanical properties, which can be used to prepare a variety of conducting bulk materials, from stiff composites and foams to hydrogels and stretchable fibers.

2:30 PM BREAK

3:00 PM *EL16.02.04

Role of Confinement in Enhancing Electrical Transport of Conducting Polymers [K.S. Narayan](#), [Sukanya Das](#) and [Chandan Pramanik](#); JNCASR, India

Confined conducting polymers (CPs) such as in nanocylinder geometries have been shown to exhibit enhanced conductance that is primarily attributed to factors such as chain alignment, increased crystallinity, and/or pi-pi stacking. We address the significance of these factors of polymers confined in alumina nanocylinders of diameters ranging from 20 nm to 100 nm and compare them with properties of bulk films. A conducting substrate of suitable work function and a common top contact was used to examine the macroscopic electrical transport of the CPs in these regularly patterned structures. Isolated nanopores were examined using conducting atomic force microscopy methods. A series of conducting polymers that include in-situ polymerized PEDOT:Tos, other forms of PEDOT from aqueous dispersion, and n-type doped polymers were examined. The enhanced vertical conductivity that is normally not observed in thick PEDOT films due to the transport barriers also points to the reduced degree of disorder. The difference in electrical charge transport of polymer blend PEDOT:PSS and polymer-monomer blend PEDOT:Tos in alumina scaffold in terms of σ as a function of ϕ and T highlights the efficacy of this approach to reduce disorder in tailored systems. The high-resolution transmission electron microscopic technique illustrates the picture of structural disorder present in the nanochannels and the variation of connecting pathways between the ordered regions on an amorphous matrix in two types of CPs with similar electronic PEDOT backbone. The confinement facilitates microstructures as the in-situ polymerization of PEDOT:Tos proceeds. The utility of these geometry-induced properties is demonstrated in the context of photodetection and thermoelectric applications.

3:30 PM EL16.02.05

Electric Field Induced Negative Capacitance in Semiconducting Polymer [Sougata Mandal](#) and [Reghu Menon](#); Indian Institute of Science Bangalore, India

Electric field dependent capacitance and dielectric loss in poly(3-hexylthiophene) are measured by precision capacitance bridge. Carrier mobility and density are estimated from fits to current-voltage and capacitance data. The capacitance varies largely at lower frequency, and it decreases at higher electric fields. The negative capacitance at low frequency and high field is due to the negative phase angle between the dipole field and the ac signal. The intrinsic carrier density is calculated from fits to the Mott-Schottky equation, and this is consistent with I-V data analysis. At higher frequency, the carriers do not follow the ac signal and their density drops; and the flatband potential increases mainly due to the build-in potentials within ordered and amorphous regions in the sample.

3:45 PM EL16.02.06

A Close Look at Organic Magnetoresistance in Conjugated Polymers [Zuchong Yang](#) and [Emanuele Orgiu](#); Institut National de la Recherche Scientifique (INRS), Canada

Migratory animals in nature can amazingly sense Earth's extremely weak magnetic field (~50 micro-tesla) and use it as a compass for the precise navigation during their long-distance migration. It has been shown that this mysterious magnetoreception capability is closely related to the quantum spin dynamics of radical pairs from their magnetically sensitive proteins¹. Intriguingly, some lab-synthesized organic semiconductors (OSCs) can also show a similar magnetic field response but to a much wider range (from sub-milli-tesla to tens of tesla), even at room temperature. The electrical current of organic-based devices can exhibit a noticeable variation when the latter ones are immersed in a magnetic field, which is called the organic magnetoresistance (OMAR). As OMAR is believed to be originated from bipolaron formation, which is intimately coupled with the charge transport, it represents an attractive playground for understanding the fundamental spin physics in OSCs and further exploring its potential for organic spintronics.

So far, most of the previous studies on OMAR have been based on limited kinds of model OSCs such as Alq₃, polyfluorene with a relatively disordered charge transport, which also serve as the active layer in the organic light-emitting diode². Compared with a diode, a 3-terminal field-effect transistor (FET) adds a powerful electrical knob to tune the charge density inside the semiconductor via electrostatic doping. Furthermore, by functionalizing with different self-assembled monolayers, the structure of additional semiconductor-dielectric interface can also have an impact on the charge transport and spin dynamics through van der Waals interaction. Thus, an extensive study on state-of-the-art OSCs and more importantly, from the perspective of FET, could provide insights for understanding the effect of magnetic field-dependent spin pair configuration on charge transport. Herein, we chose three high-performance semiconducting polymers with the microstructure ranging from semi-crystalline to semi-amorphous, and representative of p-, n-, and ambipolar-type, respectively. Exploiting the transistor configuration, we studied the magnetic field effect on charge transport in these conjugated polymers under both low (100 milli-tesla) and high magnetic field (up to 9 tesla). A systematic investigation of the temperature-, electric field-, and interface-dependent magnetoresistance will be presented in detail.

References

1. J. Xu, P. J. Hore, *et al.* Magnetic sensitivity of cryptochrome 4 from a migratory songbird. *Nature* 594, 535-540 (2021).
2. M. Gobbi, E. Orgiu. The rise of organic magnetoresistance: materials and challenges. *J. Mater. Chem. C* 5, 5572-5580 (2017).

4:00 PM EL16.02.07

Amorphous Poly-3-Hexylthiophene Thin Films via Electro Spray Deposition under High Vacuum Shubham Bhagat and Ingo Salzmann; Concordia University, Canada

Conjugated polymers (CPs) are heavily explored for their application in flexible organic electronic devices such as organic photovoltaics, organic light emitting diodes, organic transistors and organic thermoelectrics. This interest in CPs mainly stems from their high flexibility and ease of processibility on the large-scale by using cost-efficient solution-based techniques. Moreover, unlike their inorganic counterparts, the materials class of organic semiconductors offers the striking advantage that their optoelectronic properties can be easily tuned by their chemical structure including the chain length. However, CPs are thermally fragile thus intrinsically inhibiting vacuum deposition by thermal evaporation. Therefore, CPs are typically processed by solution-based techniques only. There, however, the extent of polymer pre-aggregation and film growth is substantially influenced by the choice of the solvent and other difficult to control experimental factors. The resulting microstructure in CP films can, in addition, not be improved by processing at elevated temperatures, which are largely inaccessible for common solvents. In contrast to conjugated organic molecules (COMs) that can be processed in-vacuo to form crystalline films of high coherence lengths, prototypical CPs such as regioregular poly(3-hexylthiophene) (P3HT) are semi-crystalline when grown from solution with the ratio of crystalline to amorphous film portion being hard to control.

For CPs, molecular doping enables tuning the thin-film conductivity over orders of magnitude. However, the film crystallinity has huge impact on the charge carrier mobility in CP heterostructures as well as pristine and doped CP films, where it has been argued that amorphous and crystalline film portions react differently to dopant exposure. Due to the intrinsic semi-crystalline nature of CPs such as P3HT in thin films, information experimentally gained comprises superimposed signatures from the crystalline and amorphous regions of the CP. Therefore, preparing amorphous CP films represents the most straightforward experimental approach to disentangle this information. In contrast to *improving* the structural properties of semi-crystalline CP films, however, deliberately *reducing* their crystallinity and achieving *amorphous* films has not been achieved so far. Here, we demonstrate that room-temperature high vacuum electro spray deposition (HV-ESD) of P3HT enables reproducibly establishing such films and provide evidence for their amorphicity by synchrotron grazing-incidence X-ray diffraction (GIXRD). In addition to details of the experimental procedure of HV-ESD and the properties of pristine P3HT films established therewith, we will discuss their doping phenomenology with the strong electron acceptor 2,3,5,6-Tetrafluoro-tetracyanoquinodimethane (F4TCNQ).

4:15 PM *EL16.02.08

Tuning the Properties of Poly(3-alkylthiophene)s via Side Chain Engineering Genevieve Sauve; Case Western Reserve University, United States

Regioregular poly(3-alkylthiophene)s (P3ATs) constitute an important class of conjugated polymers (CPs) for organic electronic applications. In particular, poly(3-hexylthiophene) (P3HT) is one of the most studied and accessible CPs due to its simple synthesis that enables kilogram scale production. One way to potentially tune CPs properties without affecting electronic properties is to introduce functional groups several carbons away from the conjugated backbone. However, such modifications can affect CPs self-assembly, crystallinity and π - π stacking, making it challenging to optimize properties while maintaining good charge carrier mobility. It is thus essential to better understand how side chain modifications affect desirable properties. Here, we explore using side chain engineering to increase the relative dielectric constant (ϵ_r) and to improve the mechanical properties of P3ATs. Results give us guidelines to tune properties while maintaining favorable film morphology for charge carrier mobility.

Conjugated polymers typically have low ϵ_r (3-4), which limits their application. Increasing ϵ_r could enhance device performance by promoting exciton dissociation, reducing bimolecular charge carrier recombination, and enhance charge carrier mobility via charge screening. Here, we introduced highly polar methylsulfinyl and methylsulfonyl groups at the end of P3AT side chains. This placement should allow the polar groups to efficiently rotate and increase orientational polarization. High ϵ_r values were achieved for these functionalized P3ATs based on an accurate capacitance measurement using a gold/semiconducting polymer/SiO₂/n-doped Si configuration. The ϵ_r at megahertz and room temperature increased from 3.8 for P3HT to 7.4 for the sulfinylated and 8.1-9.3 for sulfonylated P3ATs. These values are among the highest ϵ_r reported for CPs. Grazing-incident wide-angle X-ray diffraction results showed that these polar groups decreased the crystallinity for the polythiophene backbones and interfered with the π - π stacking in the crystalline structure, especially the methylsulfonyl groups. From this study, we conclude that the methylsulfinylated polymers may be promising to provide a balance between high ϵ_r and preserving favorable π - π stacking structure for device applications.

Like most CPs, P3ATs tend to be brittle, limiting their application. Interestingly, one of the polymers with high dielectric constant had unusual mechanical properties. We hypothesized that the improved properties were due to the ester group six carbon away from the backbone. To better understand the effect of ester groups on both mechanical and electronic properties, we synthesized two random copolymer series: poly(3-alkylthiophene-2,5-diyl)-*ran*-(3-(6-pentanoatehexyl)thiophene-2,5-diyl) where alkyl is either hexyl (P3HT series) or dodecyl (P3DDT series). In both series, the ester-functionalized side chain content was varied. The copolymer's optical, thermal, structural, electrical and mechanical properties were investigated. Optimal mechanical and electrical properties were obtained with 10% ester content, and the mechanical property improvements were maximized when the co-side chain was shorter (hexyl) than the ester-functionalized side chain. The best combination of robustness and charge carrier mobility was thus obtained for the P3HT random copolymer with 10% ester-functionalized side chain: a high fracture strain (29±6%) combined with a high tensile strength (3.9±0.6 MPa) was achieved while maintaining the same high charge carrier mobility than a similar MW P3HT (0.12±0.01 cm²/Vs). These exciting results demonstrate the feasibility of using ester-functionality in optimizing both mechanical and electrical properties of poly(3-alkylthiophene)s.

4:45 PM EL16.02.09

Tuning Work Function and Device Efficiency in Nanostructured Organic Layered Interfaces—From Electrochemical Crosslinking to Hybrid Dendrimers Rigoberto C. Advincula; The University of Tennessee/Oak Ridge National Laboratory, United States

The introduction of organic and polymer layers in bulk heterojunction solid-state devices, displays, and transistor devices, plays a central role in mediating device performance. It is often associated with thin-layered nanostructuring and control of energy/electron transport corresponding to mobility with the active layers. In this talk, we emphasize our studies in the use of nanostructuring methods and rational electrochemically active dendrimer synthesis to fine-tune the work function in organic semiconductor devices, i.e. to increase device performance and efficiency. Several examples of this approach in exploring the role of electro-active species include 1) synthesis and electrochemical crosslinking of precursor polymers, 2) grafting of polymer brushes and patterning, 3) utilizing surface plasmon resonance spectroscopy to probe transport phenomena, and 4) LED, PV and sensor device development.

SESSION EL16.03: Poster Session: Carrier-Dopant Interactions in Organic Semiconductors—From Fundamentals to Applications III

Session Chairs: Nagarjuna Gavvalapalli, Mukundan Thelakkat, Dhandapani Venkataraman and Luisa Whittaker-Brooks

Monday Afternoon, November 27, 2023

Hynes, Level 1, Hall A

8:00 PM EL16.03.01

Role of Polymer-Dopant Distance on Charge Transport in Amorphous and Crystalline Domains in Doped Conjugated Polymers Michael Lu-Díaz¹, Muhamed Duhandzic², Subhayan Samanta¹, Simon Harry¹, Zlatan Aksamija² and Dhandapani Venkataraman¹; ¹University of Massachusetts Amherst, United States; ²The University of Utah, United States

Conjugated polymers lack free carriers and thus need to be chemically doped to increase conductivity. This process, however, introduces energetic disorder and charge traps. Therefore, there is a compelling need to identify factors that affect dopant-polymer interactions and modify them suitably for improved charge transport. The effect of Coulomb interaction of charged polymer and dopant counterion is one such factor. In literature, some studies ascribe reduced Coulomb interactions to increased counterion size while others to increased molecular ordering. We resolve this apparent conflict by evaluating the impact of doping the crystalline and amorphous domains on the density of states (DOS) and how each domain type contributes to charge transport. We measured Seebeck coefficient (α) and electrical conductivity (σ) of gradually dedoping of regioregular and regiorandom P3HT films and their blends. We used wide angle X-ray scattering and UV-Vis-near IR spectroscopy to characterize the doped P3HT films and fitted data to a phonon-assisted hopping model of charge transport to extract the dopant-induced disorder from the calculated DOS. We show that the regiorandom and regioregular domains in the doped polymer simultaneously contribute to the charge transport with their individual contribution depending on their doping level. We also show that any observable impact of counterion size or paracrystallinity on charge transport can be correlated to polymer-dopant distance, R_s . Our two-DOS model of crystalline and amorphous regions connects well to the observed trends in the α - σ curves of regiorandom and regioregular P3HT blends. Our work shows the amorphous domain encounters a larger dopant-induced disorder and also contributes to charge transport significantly. Thus, it is important to take into account the effect of dopant-induced disorder on particular structural regions while designing polymers and dopants for improved charge transport.

8:00 PM EL16.03.02

Enhancing the Power Factor of SWNT Thin Films for Organic Thermoelectrics Sooyon Chang and Zhiting Tian; Cornell University, United States

Thermoelectrics are regarded as one solution that upcycles waste heat to convert it into a useful resource; electricity. A thermoelectric device utilizes the Seebeck effect across a p-type and n-type material to create a voltage difference from a temperature gradient. Unlike many developments in the area of p-type, many conventional n-type materials have been restricted to inorganics that are toxic and expensive. Here, we focus on organic n-type material through doping and post-treatment which allows us to tune the power factor (PF) even further. Organic single wall carbon nanotubes (SWNT) are known for their high electrical conductivity through electron hopping of valence electrons and have shown potential for thermoelectrics. We have fabricated micron-thick SWNT films using a surfactant to induce an n-type behavior and doped them to further increase the electrical conductivity. The films were measured over 3 months and retained a stable negative Seebeck coefficient, which proves as a promising candidate for long-term thermoelectric devices. We have found that the different annealing temperatures and doping times of the dopant resulted in a distinguished surface morphology where we could improve the electrical conductivity with no diminishing of thermopower.

8:00 PM EL16.03.03

Large Area Scalable HTL-Free Organic Solar Cells with Phosphotungstic Acid Solid Additives Jahandar Muhammad, Soyeon Kim and Dong Chan Lim; Korea Institute of Materials Science, Korea (the Republic of)

The interfacial layers play a crucial role in enhancing the performance and stability of organic solar cells (OSCs). Despite achieving high efficiency in OSCs, the challenges associated with large-area manufacturing and the need for nanoscale uniformity during coating have hindered large-scale production. To address these issues, we propose the concept of hole transport layer (HTL)-free OSCs to simplify fabrication processes and enable more efficient production. In this study, we explore the potential of phosphotungstic acid (TWA) as a promising alternative for the HTL and as a solid additive in HTL-free OSCs to enhance device performance and scalability from cell-to-module. Remarkably, incorporating TWA as an annealing-free HTL and as a solid additive into the photo-active layer (PM6:Y6:PC71BM) significantly boosts the power conversion efficiency (PCE) up to 17.28% and 16.33%, respectively, compared to the reference device with PEDOT:PSS (15.88%). We successfully fabricated a large-area OSC module with an impressive PCE of 15.18% and an active area of 54 cm², achieving approximately 85% of the effectiveness of small-area OSCs. The improved performance is attributed to the enhanced transmittance, excellent carrier-dynamic capacity, suppressed carrier recombination, and reduced trap-states in the ternary-bulk heterojunction OSCs. This study demonstrates the promising versatility of TWA for OSCs, offering potential enhancements for device performance and scalability in future applications.

SESSION EL16.04: Design of Dopants and Polymers I
Session Chairs: Nagarjuna Gavvalapalli and Dhandapani Venkataraman
Tuesday Morning, November 28, 2023
Hynes, Level 2, Room 205

8:30 AM EL16.04.01

Stability of FeCl₃ as a p-Type Dopant for Semiconducting Polymers Meghna Jha, Joaquin Santana and Adam J. Moule; University of California, Davis, United States

Molecular doping of semiconducting polymers has garnered significant attention in the field of organic electronics. FeCl₃ has emerged as a promising, cost-effective p-type dopant for "hard-to-dope" polymers like DPPs. In this study, we investigate the stability of FeCl₃ as a dopant by cycling the doping and de-doping process. Specifically, DPP-4T is doped with FeCl₃ and subjected to temporal de-doping in air and darkness. Our observations reveal a degradation of neutral peaks and a subsequent reduction in absorbance during the de-doping process.

To gain deeper insights into the doping mechanism at the atomic level, we employ UV-Vis-NIR spectroscopy, Four-probe sheet resistance measurements, and X-ray absorption near-edge structure (XANES) spectroscopy. Our results indicate the involvement of two distinct Fe ions in charge transfer and charge stabilization reactions during the doping process.

Furthermore, we explore the impact of different solvents on the properties of the dopant. Our findings highlight the crucial role of solvent dielectric constant and electron donor effects in controlling the degree of polymer doping.

Additionally, we discuss the application of anion exchange doping and perform lifetime measurements to assess the long-term stability of the doped polymers. Finally, we present an analysis of the advantages and disadvantages of molecular doping, including a comparison to simple molecular doping techniques.

This study provides valuable insights into the stability of FeCl₃ as a dopant, elucidates the atomic-level mechanisms of the doping process, and underscores the significance of solvent choice. The findings contribute to the understanding of molecular doping in organic electronics and pave the way for further advancements in the field.

8:45 AM EL16.04.02

Quasi-Instantaneous Doping Mechanism of Organic Semiconductors by a Strong Lewis Acid Melissa Berteau-Rainville¹, Shubham Bhagat², Thomas Baumgartner³, Emanuele Orgiu¹, Christopher Caputo³ and Ingo Salzmann^{2,2}; ¹Institut National de la Recherche Scientifique, Canada; ²Concordia University, Canada; ³York University, Canada

The doping of organic semiconductors (OSCs) is of crucial importance for applications in electronic devices, where it is used to alter the opto-electronic properties of OSCs. P-type doping is generally achieved via the admixture of strong electron acceptors, i.e. molecules that feature a high electron affinity, in order to remove a full electron from the OSC. Because of their typically conjugated nature such molecules tend to form supramolecular complexes with the organic semiconductor instead of promoting electron transfer, which quenches the efficiency of the dopant. Furthermore, control over structure in doped systems, which is paramount to performances in applications, is difficult to achieve because these molecules do not interact covalently.

In this light, trivalent group XIII Lewis acids (boron, aluminum centers) have been used as dopants, paired with OSCs that contain hard nitrogen atoms to which they can bind covalently. This resulted, for example, in the possibility to tune the bandgap of OSCs by employing acids of different strengths, but not in full electron transfer. In other systems where OSCs do *not* feature hard basic sites to which LAs can bind covalently, however, full electron transfers were reported, notably in the poly(3-hexylthiophene) (P3HT) - tris(pentafluorophenyl)borane (BCF) system. This came as a surprise as the electron affinity of BCF is thought to be insufficient to induce such electron transfers. As such, it was more recently proposed that this doping proceeds via a proton transfer that can be introduced by water traces even in inert environments, through a mechanism that was calculated to be highly endergonic.

Considering all these findings, we will report on the surprising observation that BCF can readily dope three different thiophene-containing OSCs of relatively low ionization energy in a quasi-instantaneous manner that is at odds with a highly endergonic mechanism. We investigated more closely the doping behavior of several Lewis acids analogous to BCF with P3HT in order to understand the factors determining the ability of Lewis acids to produce such doping. We performed supporting DFT calculations to assess the energetics involved in different possible mechanisms. Altogether, our data strongly suggest that this quasi-instantaneous doping is not mediated by a proton transfer alone, which we will discuss in the framework of the previously suggested doping processes known to be at work for organic semiconductors.

9:00 AM *EL16.04.03

The traditional vision of the dopant-semiconductor interaction, including organic and polymeric semiconductors, is direct electron transfer between the two, leaving a charge carrier on the semiconductor in the form of a mobile radical ion and an oppositely charged counterion. In this presentation, we explore a two-step alternative doping mechanism, by which the dopant forms a covalent adduct with a conjugated polymer segment, and that adduct subsequently participates in the electron transfer that leads to the charge carrier generation. We investigated both p-type and n-type versions of this process, using tris(pentafluorophenyl)borane (TPFB) and fluoride anion (F⁻), respectively, as the adduct-forming species. Many structures of conjugated segments were used as models for the polymer segments that might form adducts with TPFB or F⁻. Evidence that adducts could serve as dopants was obtained from conductivity and Seebeck coefficient measurements, electron paramagnetic resonance (EPR) spectroscopy, optical absorbance spectroscopy, and Density Functional Theory calculations. Furthermore, we paired the F⁻ dopant with a pyridinium polymer to create an n-type analog of PEDOT-PSS, where the charge transporter and dopant counterion in the conducting composition are both macromolecular, and the electronic conductivity was especially high compared to that obtained from single-molecule dopants.

9:30 AMBREAK

10:00 AM +EL16.04.04

Inhomogeneous Dopant Distribution in Organic Semiconductors: Causes and Consequences for Charge Transport Martijn Kemerink; University of Heidelberg, Germany

While the effect of the incorporation of dopant molecules on the microstructure of the host material has been intensely investigated, translating these results to electronic properties has received less attention. Here, we will show two case studies of inhomogeneous dopant distribution in organic semiconductors, for which we do a quantitative comparison between experimental data of dopant distributions and conductivity and numerical simulations thereof. For the latter we developed two intuitive tools to produce simplified yet realistic morphologies of doped organic polymers, accounting for the effects of (a) aggregation and phase separation in the semiconducting host material and of (b) diffusion and preferential incorporation in specific phases of the dopant. The created morphologies are then used as starting point for kinetic Monte Carlo simulations of charge transport. Importantly, the case studies can be generalized to design rules to achieve high conductivity at low dopant concentrations.

10:30 AM EL16.04.05

Stable and Tunable Chemical Doping for Organic Semiconductors in Aqueous Solution under Ambient Conditions Masaki Ishii^{1,2}, Yu Yamashita^{1,3}, Shun Watanabe³, Katsuhiko Ariga^{1,2,3} and Jun Takeya^{1,3}; ¹National Institute for Materials Science, Japan; ²Tokyo University of Science, Japan; ³The University of Tokyo, Japan

Doping levels in chemical doping of organic semiconductors are determined by semiconductor and dopant energy levels. While precise control of doping is required to fabricate advanced devices, as seen in silicon semiconductors, control in doping levels at a scale of thermal energy (25 meV) has been challenging for organic semiconductors. Most of dopants are unstable under ambient conditions owing to the reactivity with water or oxygen in air, which further decreases precision in doping levels. Low precision in doping levels and need for inert processing environment have been bottlenecks for developing and manufacturing advanced organic semiconductor devices employing chemical doping.

In this study, doping levels of organic semiconductors were controlled reproducibly and precisely in aqueous dopant solution under ambient conditions [1]. In our method, chemical doping is based on proton-coupled electron transfer (PCET) reactions that are widely observed in biochemistry, unlike conventional methods that employ single electron transfer reactions. Our aqueous dopant solutions contain dopant salts, pH adjusting agents and PCET-based redox couples. As a PCET-based redox agent, for instance, Benzoquinone/Hydroquinone (BQ/HQ) couple was employed. Through redox reactions, BQ gets transformed into HQ by accepting two electrons and two protons, where its redox potential depends on proton activity, pH, of the aqueous solution following the Nernst equation. A well-known p-type semiconducting polymer, poly[2,5-bis(3-tetradecylthiophen-2-yl)thieno[3,2-b]thiophene] (PBTTT), was doped by BQ/HQ doping solutions. PBTTT got oxidized when the redox potential of BQ/HQ exceeded the Fermi level of PBTTT in a low pH environment. The positive charge introduced into PBTTT was compensated by intercalation of anions in aqueous solution similarly to anion-exchange doping in organic solvents [2]. Bis(trifluoromethanesulfonyl)imide (TFSI) or bis(nonafluorobutanesulfonyl)imide (NFSI) was employed as dopant anion introduced into PBTTT, which would realize stable doped state owing to their closed-shell structures and hydrophobicity [3].

Doping level of PBTTT was controlled by the pH value of dopant aqueous solution, where the redox potential of BQ/HQ showed pH dependence of 59 mV/pH. According to the optical absorption and conductivity measurement, the doping level of PBTTT increases with decreasing solution pH. Tuning of doping levels were also confirmed by structural analysis based on X-ray diffraction and elemental analysis based on X-ray photoelectron spectroscopy measurements. Doping levels of one PBTTT film were modulated repeatedly by cycles of increase and decrease in solution pH, which demonstrates that both of oxidation and reduction of organic semiconductors take place in our system that develops chemical equilibrium. It was verified that one can control the Fermi level of organic semiconductors reproducibly with a high degree of precision, *ca.* thermal energy of 25 meV at RT, over a few hundred meV around the band edge. This is a critical range to control electronic properties of semiconductors.

Our PCET-based system provides a facile, scalable, precisely controlled, reproducible and reliable chemical doping method, which would lead to ambient processed organic electronics and bioelectronics.

[1] M. Ishii, Y. Yamashita, S. Watanabe, K. Ariga, J. Takeya, *under review*, preprint DOI: 10.21203/rs.3.rs-2011544/v1.

[2] Y. Yamashita, J. Takeya, S. Watanabe et al., *Nature* **572**, 634–638 (2019).

[3] Y. Yamashita, J. Takeya, S. Watanabe et al., *Commun. Mater.* **2**, 45 (2021).

10:45 AM EL16.04.06

Effect of Dipolar Dopants on Charge Carrier Transport in Ordered Molecular Semiconductors with Order Parameters Akira Ohno, Tsukasa Nakamura, Yukiko Takayashiki, Jun-ichi Hanna and Hiroakifilino; Tokyo Institute of Technology, Japan

We have investigated the orientational and translational order effect of dipolar molecules on carrier transport. Random orientation of dipolar or polar molecules interacting with carriers provides static disorder in organic semiconductors. We examined the doping effect of dipolar dopants using liquid crystalline organic semiconductors, which provides us with a useful model system for examining the effect in both experiments and simulations: we doped molecules with electrostatic dipoles or molecular polarization in smectic liquid crystal, e.g., phenyl naphthalene derivatives, which show the layered structure and resulting 2D carrier transport. The dopants such as organic cyanides and ketones are controlled in their orientation and translational ordering in the smectic liquid crystals where they are either mixed in intralayer or microphase separated in the interlayer, while the others are inserted into the interlayer and behave in a three-dimensional random orientation and coordination in the alkyl chain of liquid crystal.

Obtained mobilities by time-of-flight experiments have characteristic temperature and field dependence and can be analyzed by Gaussian disorder formalism. These effects are successfully analyzed by using our theoretical model based on calculating the N-th moment of the total Coulomb potential contribution of dipoles for an ordered molecular alignment. We found that the dipole dopants degrade the carrier transport in the 2D-ordered layer structure and gave the additional energetic disorder σ_d proportional to a square root of the dipole concentration $\sim C^{1/2}$. Therefore, it should be noted that the carrier transport is less sensitive to the dipoles compared with that in the 3D conduction system. We also confirmed the phenomena by carrier transport simulation of kinetic Monte Carlo for a snap-shot of hopping sites decided by MD simulation with generated energetic disorder landscape.

This dependence shows us that the effect on carrier transport is limited in highly ordered materials, even if there is an origin that causes a large static disorder. This gives us an insight into why the behavior of carrier transport is different between crystal and semi-ordered phases such as liquid crystals or polymers. Intrinsic mobilities measured in various liquid crystalline (LC) materials reported in the last few decades, do not change much from material to material but do change much from mesophase to mesophase: for example, typical mobility is on the order of $\sim 10^{-2}$ - 10^{-3} cm²/Vs in crystal B and E phases, of $\sim 10^{-2}$ cm²/Vs in hexatic B phase, and 10^{-3} cm²/Vs in smectic A and C phases [1] regardless chemical structures of liquid crystal. On the other hand, a wide variation of mobilities from 10^{-3} to 10 cm²/Vs depending on chemical structures is often observed in crystals. It is true even for liquid crystalline molecules, benzothienobenzothiophene (BTBT) derivatives, such as Cn-BTBT and Ph-BTBT-Cn in crystalline phase: in fact, high mobility of over 10 cm²/Vs reported in their crystalline phase. [2] These facts indicate a clear contrast in carrier transport between the ordered and semi-ordered phases. For investigating the origin of differences, we introduced the Gaussian disorder model restricted by the order parameters as static disorder into the charge transport model with the dynamic disorder. This model can be consistently applied for both crystalline and liquid crystalline phases and made it possible to discuss the difference in carrier transport between crystal and semi-ordered materials. These fundamental studies are very important for the functional design of organic semiconductors, especially for the operation of printable electronics.

References

[1] Jun-ichi Hanna, Akira Ohno, Chap.3 in Self-Organized Organic Semiconductors: From Materials to Device Applications, edited by Quan Li, WILEY, (U.S.) 2011.

[2] H. Iino, T. Usui, and J. Hanna, *Nature Comm.*, **6**, 6828 (2015).

11:00 AM EL16.04.07

Minimizing Molecular-Dopant-Induced Disorder in Emerging Semiconductors Keehoon Kang; Seoul National University, Korea (the Republic of)

Doping has been one of the most essential methods to control charge carrier concentration in semiconductors. Excess generation of charge carriers is a key route for controlling electrical

properties of semiconducting materials and typically accompanies alteration of electronic structure by the introduction of dopant impurities, both of which have played pivotal roles in making breakthroughs in inorganic microelectronic and optoelectronic devices both at research and industrial levels, especially for Si-based technology. Molecular doping is a facile and effective doping method for various semiconducting materials since it is relatively non-invasive compared to high-energy implantation of ionic impurities used in Si. However, there are main challenges remaining in fully utilising molecular doping in emerging semiconducting materials such as π -conjugated polymer semiconductors, two-dimensional materials and metal-halide perovskites due to the difficulties in preventing dopant-induced disorder effects while maintaining a high carrier mobility. This talk will introduce concepts that we have developed to minimizing the dopant-induced disorder [1, 2, 3] while mitigating current injection and doping stability issues in electronic devices [4, 5], and finally outline the future challenges remaining in the field to fully uncover the potentials.

- [1] K. Kang, et. al., "2D Coherent Charge Transport in Highly Ordered Conducting Polymers Doped by Solid State Diffusion", *Nat. Mater.*, Vol. 15, p. 896, 2016.
- [2] J. Jang, et. al., "Reduced dopant-induced scattering in remote charge-transfer-doped MoS₂ field-effect transistors", *Sci. Adv.*, Vol. 8, No. 38, p. eabn3181, 2022.
- [3] J. Lee, et. al., "Bulk Incorporation of Molecular Dopants into Ruddlesden-Popper Organic Metal-Halide Perovskites for Charge Transfer Doping", *Adv. Funct. Mater.*, doi:10.1002/adfm.202302048.
- [4] Y. Kim, et. al., "Enhanced Charge Injection Properties of Organic Field-Effect Transistor by Molecular Implantation Doping", *Adv. Mater.*, Vol. 31, p. 1806697, 2019.
- [5] Y. Kim, et. al., "Highly Stable Contact Doping in Organic Field Effect Transistors by Dopant-Blockade Method" *Adv. Funct. Mater.* (2020) Vol. 30, p. 2000058

11:15 AM EL16.04.08

Self-Doped Conjugated Polymers and Copolymers - Feasibility and Advantages in Devices [Julian Hungenberg](#), Adrian Hochgesang, Florian Meichsner and Mukundan Thelakkat; University of Bayreuth, Germany

Mixed ionic-electronic conductors are widely studied for accumulation mode (undoped systems) or depletion mode (doped systems) devices. PEDOT:PSS has been established as the working horse for depletion mode organic electrochemical transistors (OECTs) as it consists of the conjugated polymer PEDOT⁺ which is intrinsically doped and stabilized by PSS⁻ counterions. It is neither soluble in water nor organic solvents, wherefore thin films are processed from aqueous dispersion. This results in a nonuniform film morphology consisting of doped PEDOT-rich domains surrounded by an insulating PSS matrix. This particular structure leads to several drawbacks such as long-term instability. Furthermore, its complex structure hampers the ability for chemical modification.

In contrast to PEDOT:PSS, most conjugated polymers are intrinsic (pristine or undoped) semiconductors and hence show very low electrical conductivities. Therefore, doping is necessary to increase the charge carrier density and thus the electrical conductivity. Upon molecular doping, active redox species are added to the OSC which can donate (n-type) or accept electrons (p-type) generating free charge carriers. For p-type doping, this means a transfer of electrons from the highest occupied molecular orbital (HOMO) of the OSC to the lowest unoccupied molecular orbital (LUMO) of the dopant. Issues here are the requirement of deep-lying dopant LUMO, thus stability against air/water, and the need for high amounts of dopants for charge carrier formation which ultimately disturbs the film morphology.

To address these challenges, our group took high efforts in the field of molecular doping of conjugated polymers. The first concept published takes advantage of HOMO-HOMO doping by mixing two donor materials (OSC-1 and OSC-2). OSC-2 is a chemically oxidized small molecule semiconductor namely Spiro-OMETAD(TFSI)₂ which is capable to oxidize the OSC PDDPP[*T*]₂-EDOT (OSC-1). Thereby, the doping takes place by an electron transfer from the HOMO_{OSC-1} to the partly occupied HOMO_{OSC-2}.¹ A second work extends this concept through the use of multielectron acceptor salts. For this, oxidized triphenylamines were linked to form multielectron acceptor dopants, which can accept up to four electrons per dopant. This strategy allows for significantly reducing the number of dopant molecules compared to common single electron acceptor dopants.²

Here, we present a novel synthetic strategy of a conjugated polyelectrolyte (CPE) based on a polythiophene-derivative toward a stable self-doped system which can be solution-processed from water as well as organic solvents. Our new CPE is intrinsically doped after synthesis, which is promoted by the stabilization of free charge carriers by its ionic side chains. We present self-doping as an elegant way to avoid the use of molecular dopants fully, while still maintaining high and stable conductivity. This was investigated by time-resolved spectroelectrochemistry in aqueous electrolytes, UV-vis spectroscopy in thin films in the dry state as well as conductivity measurements. We were furthermore able to employ our self-doped CPE as a mixed conductor and showed its application in a depletion mode OECT device with high transconductance and currents. By copolymerization with a comonomer, which is not self-dopable, we were able to tune the self-dopability and therefore to switch the transistor's mode of operation towards a well-performing accumulation mode device with a low threshold voltage.³ These findings could help to study the self-doping processes and to develop new CPEs with low threshold voltages towards innovative device applications.

- (1) Goel, M.; Siegert, M.; Kraus, G.; Mohanraj, J.; Hochgesang A.; Heinrich, C. D.; Fried, M.; Pflaum, J.; Thelakkat, M. *Adv. Mater.* **2020**, 32, 2003596
- (2) Kraus, G.; Hochgesang A.; Mohanraj, J.; Thelakkat, M. *Macromol. Rapid Commun.* **2021**, 42, 2100443
- (3) Hungenberg, J.; Hochgesang, A.; Meichsner, F.; Thelakkat, M. *To be submitted.*

11:30 AM *EL16.04.09

Challenges in Doping of Organics: Small Molecules vs. Polymers [Karl Leo](#); IAPP, Germany

Controlling the charge carrier densities is a key feature of any semiconductor electronic device. In inorganic semiconductors, general understanding of doping has been achieved early on and research has concentrated on finding dopants in large-gap systems like nitrides. In organic materials, doping is now a routine technique for mass-produced OLED displays and organic solar cells. However, it is still far from a microscopic understanding. Furthermore, doping in organic systems where both electronic and ionic transport happen has recently generated much interest. In this talk, I will address these two very different systems: I will discuss recent progress in understanding the doping in small-molecule semiconductors, touching new dopants and high mobility materials, allowing to realize devices like the first organic bipolar transistors.

I will compare to recent work on the doping of organic electrochemical transistors (OECTs). These devices have recently been investigated broadly since they offer switching and sensing functionality in an electrolytic environment compatible with biological systems. The mixed electron-ion transport of the devices has consequences for the doping process, making it significantly different from the electrostatic doping of standard FET devices.

SESSION EL16.05: Impact on Carrier-Dopant Interactions Thermoelectric Properties and Charge Transport
Session Chairs: Mukundan Thelakkat and Luisa Whittaker-Brooks
Tuesday Afternoon, November 28, 2023
Hynes, Level 2, Room 205

1:30 PM EL16.05.01

Molecular Doping of Conjugated Polymers for Flexible and Printed Organic Thermoelectric Generators [Boseok Kang](#); Sungkyunkwan University, Korea (the Republic of)

Organic thermoelectric generators (OTEGs) have received significant attention as a promising independent energy harvesting solution in the era of the Internet of Things. The OTEG device is attached directly to the surface of heat energy sources and transforms waste heat energy into valuable electricity based on the principle of the Seebeck effect. Several attempts have been made to achieve high-efficiency solution-processed OTEG devices, but there still remains a challenge to improve the thermoelectric figure of merits and the solution processibility for the device fabrication. In particular, doping is essential for controlling the charge carrier concentration in the conjugated organic media and governing charge transport physics, resulting in optimized device performance. In this talk, I will discuss various doping and molecular design strategies for improving the thermoelectric efficiency and solution processibility of conjugated polymers for flexible and printed OTEGs.

<quillbot-extension-portal></quillbot-extension-portal>

1:45 PM EL16.05.02

Enhancing the Performance of DPP-Based n-Type Thermoelectrics: The Role of Precise Solvent Selection for Mitigating the σ -S Trade-Off [Soyeong Jang](#)¹, [Diego Rosas Villalva](#)¹, [Guorong Ma](#)², [Anirudh Sharma](#)¹, [Andrew Bates](#)², [Abdel H. Amwas](#)², [Xiaodan Gu](#)² and [Derya Baran](#)¹; ¹Kaust, Saudi Arabia; ²The University of Southern Mississippi, United States

The solubility of conjugated polymers (CPs) significantly determines their device performance. Consequently, understanding the relationship between the solubility of n-type host polymer-dopant-solvent systems and their electronic properties is vital within the CPs realm. This study delves into the impact of various halogenated solvents on the solubility and morphological

properties of a novel pyridine-flanked DPP n-type polymer (2PyDPP-2CNTVT) and Tetrabutylammonium fluoride (TBAF) as the dopant system. We utilized Hansen Solubility Parameter (HSP) for the solubility study. We employed Grazing Incidence Wide Angle X-ray Scattering (GIWAXS) and Atomic Force Microscopy (AFM) to probe the doped polymer thin films' molecular structural disorders and surface morphology. Our findings indicate that Dichlorobenzene (DCB) solvent has superior solubility affinity for the polymer backbone and dopant. This affinity fosters improved host-dopant miscibility, excellent dopant accommodation, and enhanced film processability. Consequently, this leads to increased electron mobility (μ_e) of 2.3 cm² V⁻¹ s⁻¹ and conductivity (σ) of 2.64 S cm⁻¹ compared to films made with alternative halogenated solvents in this study. Additionally, our multidisciplinary experimental approach reveals an improved doping efficiency resulting from the lowest activation energy in the DCB system. These insights propose the DCB solvent as the optimal choice for achieving high μ_e and electrical conductivity σ in TBAF-doped 2PyDPP-2CNTVT CP film. This work underscores the importance of selecting solvent based on HSP evaluation to maximize the potential of molecular doping into n-type DPP-based CP, mitigating the trade-off between σ and Seebeck coefficient (S).

2:00 PM *EL16.05.03

Advancements in Molecular Doping of Semiconducting Polymers: Applications in Organic Thermoelectrics [Shravyesh Patel](#); University of Chicago, United States

Molecular doping of semiconducting polymers holds significant promise for organic thermoelectrics, offering tunable electronic properties and ease of processability. In the first part of the talk, we delve into the fundamental structure-property relationships of sequentially doped thiophene-based polymers, shedding light on dopant segregation, microstructure, and their impact on conduction limits and stability. In the second part, we explore the potential of molecular doping in the development of functionally graded materials (FGMs) for organic thermoelectrics. Specifically, we demonstrate precise compositional control in thin film FGMs through sequential vapor doping of polythiophene derivatives with 2,3,5,6-tetrafluoro-7,7,8,8-tetracyanoquinodimethane (F4TCNQ). Utilizing techniques such as grazing incidence wide angle X-ray scattering (GIWAXS) and Raman spectroscopy, we spatially resolve dopant compositional profiles within the FGM thin films. Additionally, we quantify the lateral distribution of electronic conductivity and Seebeck coefficient, providing insights into the spatial distribution of transport parameters. Our research advances the understanding of structure-transport properties and contributes to the development of efficient organic thermoelectric materials through sequential doping and functional grading.

2:30 PM BREAK

3:00 PM *EL16.05.04

Enhancing Thermoelectric Properties and Optimization Through Coulombic Interactions and AI-Driven High-Throughput Experiments [Kedar Hippalgaonkar](#)^{1,2}; ¹Nanyang Technological University, Singapore; ²Institute of Materials Research and Engineering, Singapore

Our studies propose a novel approach to enhance thermoelectric properties in conducting polymers by controlling coulombic interactions, without regulating morphology. We observe a significant three-fold enhancement in the thermoelectric power factor of OD-PDPP2T-TT compared to PBTTC-Cl₂, attributed to improved counterion screening, verified experimentally by measuring the dielectric constant of the films, and explaining the enhancement through Boltzmann Transport Equations [1]. We establish a correlation between optical absorption signatures and thermoelectric properties, extracting carrier concentration and confirming the importance of charge mobility amidst structural disorder. Furthermore, we demonstrate the benefits of combining high-throughput experiments with machine learning for materials and process optimization, especially by consider optical signatures that directly provide information about doping [2]. Our automated setup enables rapid thin film preparation and characterization, achieving a >10× improvement in learning cycles. By combining regio-regular poly-3-hexylthiophene with carbon nanotubes, we identify optimal compositions achieving high electrical conductivities [3]. This integrated approach offers insights into enhancing thermoelectric properties and accelerates materials optimization in organic thermoelectrics.

[1] Pawan Kumar et al (2023) unpublished, under review

[2] A. Abutaha et al (2023) ACS Applied Energy Materials 6 (7), 3960-3969

[3] D. Bash et al (2021) Advanced Functional Materials 31 (36), 2102606

3:30 PM EL16.05.05

Beyond Doping: Self-Induced Anisotropy Breaks the σ -S Coupling Towards High Performance N-Type Conjugated Polymer Thermoelectrics [Diego Rosas Villalva](#)¹, Deniss Derewjanko², Yongcao Zhang¹, Ye Liu¹, Andrew Bates³, Anirudh Sharma¹, Soyeong Jang¹, Xiaodan Gu³, Martijn Kemerink² and Derya Baran¹; ¹King Abdullah University of Science and Technology, Saudi Arabia; ²Heidelberg University, Germany; ³The University of Southern Mississippi, United States

In recent years, there has been continuous progress in the development of N-type organic thermoelectrics (OTE) due to the synthesis of new conjugated polymers and dopants. The primary focus of most designs has been to enhance doping efficiency and increase electrical conductivity, resulting in values surpassing 102 S cm⁻¹. Although effective, doping encounters limitations because of the inherent inverse relationship between the properties that determine the figures of merit in thermoelectric materials. To advance the field further, alternative approaches are needed beyond optimizing doping efficiency and the host:dopant ratio. In this study, we propose the concept of self-induced anisotropy as a solution to overcome the inverse coupling between electrical conductivity and Seebeck coefficient in N-type OTEs. Previous research has suggested methods like rubbing and drawing to induce anisotropy in p-type OTEs based on thiophenes. In our work, we exploit the interactions between solvent, host, and dopant to induce a preferential orientation. This orientation increases the in-plane delocalization length, thereby improving electrical conductivity while maintaining the Seebeck coefficient. By adopting this approach, we have achieved promising results in the 2DPP-2CNTVT:N-DMBI system. At room temperature, we obtained a Power Factor of 115 μ W m⁻¹ K⁻² and a figure of merit of 0.17, which further increased to 188 μ W m⁻¹ K⁻² and 0.36, respectively, at 105 C. To explain the origin of self-induced anisotropy, we utilized Hansen Solubility Parameters and established guidelines for formulating solvent-host-dopant systems that can achieve a similar effect. This discovery opens new possibilities for advancing N-type OTEs.

3:45 PM EL16.05.06

Elucidating Design Rules Towards Enhanced Solid-State Charge Transport in Oligoether-Functionalized Dioxithiophene-Based Alternating Copolymers [Abigail A. Advincula](#)^{1,2,3}, Amalie Atassi¹, Shawn A. Gregory¹, Karl Thorley⁴, James Ponder^{2,1,5}, Guillaume Freychet⁶, Austin Jones¹, Gregory Su⁷, Shannon Yee^{1,1} and John R. Reynolds^{1,1}; ¹Georgia Institute of Technology, United States; ²Air Force Research Laboratory, United States; ³ARCTOS Technology Solutions, United States; ⁴University of Kentucky, United States; ⁵UES, Inc., United States; ⁶Brookhaven National Laboratory, United States; ⁷Lawrence Berkeley National Laboratory, United States

Understanding solid-state charge transport in chemically doped, electrically-conductive conjugated polymers (CPs) is important to emerging applications which include organic thermoelectrics, transparent electrodes, and bioelectronics. The synthetic tunability of CPs, e.g., backbone or side chain modulation, affords high control over energy levels (i.e., ionization energy/electron affinity), doping processes, and microstructures, factors which influence the electrical conductivity of a given CP system.

This study investigates the solid-state charge transport properties of the oxidized forms of dioxithiophene-based alternating copolymers consisting of oligoether-functionalized 3,4-propylenedioxythiophene (ProDOT) copolymerized with different aryl groups, dimethyl ProDOT (DMP), 3,4-ethylenedioxythiophene (EDOT), and 3,4-phenylenedioxythiophene (PheDOT) respectively, to yield the copolymers P(OE3)-D, P(OE3)-E, and P(OE3)-Ph. At a dopant concentration of 5 mM FeToS₃, electrical conductivities for these copolymers vary significantly (ranging between 9 S cm⁻¹ and 195 S cm⁻¹) with the EDOT copolymer, P(OE3)-E, achieving the highest electrical conductivity. UV-vis-NIR and X-ray spectroscopies show differences in both susceptibility to oxidative doping and extent of oxidation for the P(OE3) series, with P(OE3)-E being the most doped. Wide angle X-ray scattering measurements indicate that P(OE3)-E generally demonstrates the lowest paracrystallinity values in the series, as well as relatively small π - π stacking distances. The significant (i.e., order of magnitude) increase in electrical conductivity of doped P(OE3)-E films versus doped P(OE3)-D or P(OE3)-Ph films can therefore be attributed to P(OE3)-E exhibiting both the highest carrier ratios in the P(OE3) series as well as good π - π overlap and local ordering (low paracrystallinity values). Furthermore, these trends in extent of doping and paracrystallinity are consistent with the reduced Fermi energy level and transport function prefactor parameters calculated using the semi-localized transport (SLoT) model. Observed differences in carrier ratios at the transport edge (c_e) and reduced Fermi energies [$\eta(c_e)$] suggest a broader electronic band (better overlap and more delocalization) for the EDOT-incorporating P(OE3)-E polymer relative to P(OE3)-D and P(OE3)-Ph. Ultimately, we rationalize improvements in electrical conductivity due to microstructural and doping enhancements caused by EDOT-incorporation, a structure-property relationship worth considering in the future design of highly electrically conductive systems.

4:00 PM EL16.05.07

Ion-Exchange Doping of Semiconducting Single-Walled Carbon Nanotubes [Angus Hawkey](#), Aditya Dash, Zhiyong Zhao, Anna Champ, Michael Zharnikov, Martijn Kemerink and Jana Zaumseil; Heidelberg University, Germany

Due to their unique electronic and thermoelectric properties, networks of purely semiconducting single-walled carbon nanotubes (SWNTs) are a promising material for thermoelectric generators, which convert a temperature difference produced by waste heat into an electrical current. Dense films of SWNTs can be deposited from dispersion (e.g., by printing) and are mechanically flexible. They reach high electrical conductivities upon p- or n-doping and retain a high Seebeck coefficient. To introduce the charge carrier densities relevant for thermoelectric applications, chemical doping is typically used. However, the remaining dopant counterions are often unstable and the impact of the counterion on the thermoelectric properties of the SWNTs

is still not fully explored. The recently developed technique of ion-exchange doping provides a means to exchange the dopant counterion with anions or cations from a huge library of commercially available salts and ionic liquids that do not possess the redox potential to reduce or oxidize the SWNTs themselves. In this work, we fabricated thin film networks of polymer-sorted small and large diameter SWNTs (>99% semiconducting) and chemically p-doped them using ion-exchange doping with a range of dopant counterions at low and high doping levels. Optical and electrical measurements reveal the ion-exchange efficiency and the influence of the counterion size on the electrical and thermoelectric properties.

4:15 PM *EL16.05.08

The Influence of Counterion Structure and Doping Level on the Optical, Electronic, and Thermoelectric Properties of π -Conjugated Polymers Kyle N. Baustert, Ashkan Abtahi, Joel H. Bombile, Ahmed Ayyash, Chad Risko, Augustine O. Yusuf and [Kenneth R. Graham](#); University of Kentucky, United States

Many organic electronic devices use chemical or electrochemical doping to introduce charge carriers into π -conjugated polymers (CPs) and change their optical and electronic properties. As these charge carriers are introduced into a CP, counterions are either created (chemical doping) or injected (electrochemical doping) into the CP to balance the charge associated with the polaron on the CP. The structure of these counterions can exert a pronounced influence on the properties of doped CPs. Understanding how dopants and counterions interact with CPs to influence their optical and electronic properties is thus critical to designing new dopants and electrochemically doped CPs. Here, we focus on the influence of counterion size on the optical, electronic, and thermoelectric properties of selected CPs, including P3HT derivatives and PDPP4T. At the small and large ends of the spectrum we use tetrafluoroborate (BF_4^-) and tetrakis[3,5-bis(trifluoromethyl)phenyl]borate (BARF^-), respectively, where BARF^- has a molar volume that is eight times larger than BF_4^- . We find that the electrochemical doping behavior and polaron absorbance of *regioregular*-poly(3-hexylthiophene), *rr*-P3HT, differs significantly depending on whether BF_4^- or BARF^- is the counterion. Through comparing *rr*-P3HT to *regiorandom*-P3HT, *rra*-P3HT, we attribute the counterion-dependent properties of *rr*-P3HT partly to the ability of the counterion to penetrate the crystalline regions. The large counterion BARF^- cannot penetrate the crystalline regions and as a result a higher potential is needed to oxidize *rr*-P3HT with BARF^- . Counterion distribution is not the only influential parameter, as the low energy polaron absorbance peak (P1) appears at lower energy with BARF^- for both *rr*- and *rra*-P3HT, which density functional theory calculations indicate is due to the larger size of BARF^- relative to BF_4^- and the resulting increased distance between the charged counterion and charged polaron. Through electron paramagnetic resonance (EPR) measurements we show that the smaller counterion BF_4^- , which can penetrate the crystalline regions, results in increased bipolaron formation relative to BARF^- as a counterion in *rr*-P3HT. Additionally, we find that the choice of counterion impacts both the electrical conductivity and Seebeck coefficient reached at a given charge-carrier concentration for P3HT derivatives and PDPP4T. These results highlight the influential interplay between counterion structure, polymer morphology, and resulting optical, electronic, and thermoelectric properties.

SESSION EL16.06: Design of Dopants and Polymers II
Session Chairs: Dhandapani Venkataraman and Luisa Whittaker-Brooks
Wednesday Morning, November 29, 2023
Hynes, Level 2, Room 205

8:30 AM EL16.06.01

Changing the Charge Transport Mechanism in Conjugated Polymers via Post-Processing Side Chain Removal James Ponder^{1,2}, Shawn Gregory³, Amalie Atassi³, Abigail Advincula^{1,4}, Joshua M. Rinehart³, Shannon Yee³ and John R. Reynolds³; ¹Air Force Research Laboratory, United States; ²UES, Inc., United States; ³Georgia Institute of Technology, United States; ⁴Arctos, United States

As the processability of electroactive conjugated polymers (CPs) is essential to their application in a range of devices, balancing solubility, processability, and film properties has become a key point of research. Solubilization of the conjugated backbone is typically achieved by introduction of relatively long branched hydrocarbon or oligoether side chains, which allows many degrees of conformational freedom. Such side chains, while enabling a wide range of processing conditions, reduce the relative fraction of active material in the film and obstruct π - π intermolecular interactions, leading to increased localization of charge carriers and compromise many of the desirable properties of the material (such as electrical conductivity). To counteract the deleterious effects introduced by side chains, we report that post-processing side chain removal, exemplified here via ester hydrolysis, significantly increases the electrical conductivity of chemically doped CP films with a corresponding decrease in Seebeck coefficient. In a model alkyl ester functionalized 3,4-propylenedioxythiophene (ProDOT) system, we found that the electrical conductivity of oxidatively doped films increased 10-fold upon side chain removal via hydrolysis. A combination of X-ray photoelectron spectroscopy (XPS), profilometry, and grazing incidence wide angle X-ray scattering (GIWAXS) results show that improvement in electrical conductivity and reduced Seebeck values are not due to an increase in carrier ratio (i.e., number of charge carriers per repeat unit ring), but instead results from an increase in charge carrier density (i.e., number of charge carriers per unit volume) due to densification and increased ordering of active polymer backbone material following side chain removal. This increase in charge carrier density leads to a reduction in charge localization, thereby improving charge transport, as contextualized using the newly developed semi-localized transport (SLoT) model. Applying this method to 3,4-ethylenedioxythiophene (EDOT) copolymer and homopolymer structures, synthesized via direct arylation polymerization, significantly higher average electrical conductivities are attained, with values ranging from 450 to ~1200 S/cm, depending on the repeat unit structure, in thick (> 600 nm) films. In an all EDOT-based system, we observe a change in transport mechanism, from a low electrical conductivity and thermally activated (hopping-like) regime to a high electrical conductivity and thermally deactivated (metal-like) regime. Finally, these results are compared to those of matching oligoether functionalized polymers for a direct comparison of the differences in charge transport between these two reported methods of conductivity enhancement.

8:45 AM EL16.06.02

Maleimide-Substituted Polyacetylene: A New Highly Conductive n-Type Polymer Harrison M. Bergman and Timothy M. Swager; Massachusetts Institute of Technology, United States

The development of highly conductive organic semiconductors has been a longstanding goal in materials science due to their chemical tunability, solution processability, mechanical flexibility, and other unique properties. Conjugated polymers are some of the most promising materials in this respect and have been widely employed in diverse device architectures such as organic field effect transistors (OFETs), organic light emitting diodes (OLEDs), and organic photovoltaics (OPVs). These applications generally require both n-type and p-type semiconducting materials, but the development of p-type conducting polymers has greatly outstripped that of n-type and ambipolar systems. Specifically, n-type materials generally display lower conductivities and mobilities in their doped states and are less stable due to oxidation under ambient conditions.

This bottleneck is largely synthetic. Stability against oxidation requires decreasing LUMO levels well below -4.0 eV, yet there are relatively few building blocks that are sufficiently electron withdrawing to achieve this. Furthermore, there are limited design strategies for assembling these building blocks into polymers that retain high backbone planarity and electron delocalization, which are both critical to high mobility and conductivity. Thus, the development of new polymer scaffolds is critical to closing the performance gap between n-type and p-type conjugated polymers.

Polyacetylenes (PAs) are attractive as high conductivity polymers, holding the record for highest reported conductivity in an organic semiconductor. However, they are inherently p-type materials. Although the introduction of strongly withdrawing groups to the PA core is straightforward conceptually, there are several practical challenges. Many standard withdrawing groups are too sterically bulky to preserve backbone planarity, and those that remain are generally incompatible with traditional PA syntheses.

We address this issue by developing a new class of PAs consisting of an alternating sequence of maleimide and vinylene units, dubbed maleimide-polyacetylene or mPA. This structure achieves high backbone planarity while still introducing a high density of strongly withdrawing groups, furnishing a highly conductive polymer with a low LUMO of -4.2 eV. The maleimide unit is also a facile synthetic handle, which enables the introduction of diverse functionality without perturbing backbone conformation. These polymers were accessed via a new synthetic approach, where a nonconjugated precursor polymer was synthesized via ring opening metathesis polymerization (ROMP), followed by an efficient elimination to furnish the final polyacetylene. This strategy is scalable and efficient and enables the synthesis of low dispersity polymers with highly controllable molecular weights. Beyond mPA, it should be generalizable to a range of other electron-deficient polyacetylenes, opening the door to a new class of n-type organic semiconductors.

9:00 AM *EL16.06.03

Negative Polaron in an n-Doped Polymer Semiconductor: Energy Levels and Hubbard *U* Interactions Dominique Lungwitz¹, Syed Joy², Ahmed E. Mansour³, Andreas Opitz³, Chamikara Karunasena⁴, Hong Li⁴, Naitik A. Panjwani⁵, Karttikay Moudgil⁶, Kan Tang⁷, Jan Behrends⁵, Stephen Barlow^{7,6}, Seth R. Marder^{7,6}, Jean-Luc Brédas⁴, Kenneth R. Graham², Norbert Koch^{3,8} and [Antoine Kahn](#)¹; Princeton University, United States; ²University of Kentucky, United States; ³Humboldt-Universität zu Berlin, Germany; ⁴University of Arizona, United States; ⁵Freie Universität Berlin, Germany; ⁶Georgia Institute of Technology, United States; ⁷University of Colorado Boulder, United States; ⁸Helmholtz-Zentrum Berlin, Germany

Doping organic semiconductors leads to the formation of polarons, positive in the case of p-doping and negative for n-doping. The released carrier polarizes neighboring molecular sites and induces intra- and inter-molecular relaxation. In the traditional picture, the formation of a negative polaron results in two localized levels within the gap: a half-occupied level below the

LUMO/CBM, and a doubly occupied level above the HOMO/VBM. Conversely, the formation of a positive polaron results in an empty level below the LUMO/CBM and a half-occupied level above the HOMO/VBM. Recent experimental and theoretical studies have challenged this original interpretation.[1-3] In the case of an added electron (hole), the new picture points to a half-occupied (empty) level below the semiconductor LUMO/CBM, split from an unoccupied (half-occupied) level positioned above (below) the LUMO/CBM (HOMO/VBM). The split corresponds to the intra-molecular Coulomb interaction, also known as Hubbard interaction U . In this work, we investigate n-doping of the polymer P(NDI2OD-T₂) with the molecular dopants [RhCp* Cp]₂ and [N-DMBI]₂ as well as Cs, using ultra-violet and low-energy inverse photoemission spectroscopy (UPS, LEIPES) aided by EPR measurements and DFT computations.[4] The UPS data show that all three dopants induce the growth of a DOS in the former empty gap of the polymer while LEIPES shows an additional DOS above the polymer CBM. In agreement with the above-mentioned new interpretation, the additional DOS is assigned to the formation of the singly occupied and unoccupied levels, and allows the direct determination of the Hubbard U .

[1] Winkler et al., *Mater Horiz* **2015**, 2, 427–433

[2] HeimeI, *ACS Cent Sci* **2016**, 2, 309–315

[3] Png et al, *Nat Commun* **2016**, 7, 11948

[4] Lungwitz et al., *J. Phys. Chem. Lett.* (in press)

9:30 AMBREAK

10:00 AM *EL16.06.04

The Role of Redox Doping in Organic Electronics and Opto-Electronics Seth R. Marder; University of Colorado Boulder, United States

Organic semiconductors and hybrid/organic materials have attracted interest for electronic applications due to their potential for use in low-cost, large-area, flexible electronic devices. Here we will report on recent developments pertaining to n-dopants that could impact the charge injection/collection processes in organic light emitting diodes, organic field effect transistors, and organic photovoltaic and hybrid organic/inorganic perovskite devices. I will highlight the application of n-doping for the development of electron injection layers for organic light emitting diodes (OLEDs), and their use for doping of electron transport materials which result in high conductivities and in some cases good thermoelectric performance. In the case of OLEDs, it will be shown that photoactivation (as illustrated in the cartoon at the right) can lead to stable doping of materials (i.e. the doping induced conductivity remains relative constant over hundreds of hours) beyond the expected thermodynamic limit, which would be predicted based on an assessment of the effective reduction potential of the n-dopant and the reduction potential of the electron transport material. We will also highlight some of the differences between approaches based upon “dimeric” dopants, vs. hydride donor dopants.

10:30 AM EL16.06.05

Deprotonation-Based n-Doping of a New Acceptor-Acceptor Conjugated Polymer Andreas Erhardt^{1,2}, Adrian Hochgesang², John Mohanraj² and Mukundan Thelakkat²; ¹Monash University, Australia; ²University of Bayreuth, Germany

Doped organic semiconductors have proven to be viable materials for heat-to-electrical energy conversion (TE: thermoelectrics). For working large-scale thermoelectric generator devices, the synergistic use of p- and n-type components is necessary. However, as common for organic semiconductors, stable, n-doped polymers are sparse. Besides approaches to solve intrinsic stability issues of the doped acceptor towards ubiquitous oxidizing agents (H₂O and O₂), the choice and underlying mechanism of suitable n-dopants is an open field of research.

Our very recent works report the design and synthesis of an acceptor-acceptor low LUMO copolymer (“DPP-TPD”, [1]) in conjunction with bulk n-doping using Cs₂CO₃. [2] We present a novel acceptor-acceptor copolymer synthetic strategy using direct arylation polymerization and demonstrate excellent viability for n-doped systems for TE applications.

In contrast to previous reports about Cs₂CO₃ n-doped systems, we elucidate the mechanism, that our copolymer is doped via a solid-state acid-base interaction between the polymer and the basic carbonate. The resulting increase of the backbone electron density by deprotonation of the thiophene moiety is accompanied by the formation of bicarbonate. The crucial role of the basicity was demonstrated by comparative doping studies of the host polymer with further organic and inorganic carbonates. The general viability of the concept was evaluated with the strong base n-butyl lithium, which, in agreement with our findings, induces outstanding electron conductivity after thermal annealing. Comparable to N-DMBI hydride/electron transfer, Cs₂CO₃ proton abstraction doping shifts the polymer work function towards the LUMO. Thereby, the anionic doped state is resilient against O₂ but is highly susceptible to H₂O. Based on GWAXS, Cs₂CO₃ is mainly incorporated into the amorphous region of the film with the help of hydrophilic side chains and has a minor impact on the crystallinity. Together, the synergy between Cs₂CO₃ proton abstraction doping and acceptor-acceptor copolymer strategy creates an n-doped system with promising properties for thermal energy conversion, as evidenced by a remarkable maximum power factor of $(5.59 \pm 0.39) \times 10^{-6} \text{ W m}^{-1} \text{ K}^{-2}$ in n-type thermoelectric element.

The main implications and novelty of our work are a: the viability of copolymers, following an acceptor-acceptor design principle, and b: the possibility to n-dope suitable copolymers via deprotonation reactions using simple carbonate dopants, opening a vast field of new n-type dopants.

References

[1] *Adv. Electron. Mater.* **2023**, 9, 2300026

[2] *Adv. Funct. Mater.* **2023**, 33, 2300614

10:45 AM *EL16.06.06

Factors Promoting or Inhibiting Charge Transfer in Doped Organic Semiconductors Ingo Salzmann; Concordia University, Canada

To control the conductivity of organic semiconductors (OSCs) and their energy level alignment in heterostructures and at interfaces, OSCs are being electrically doped by introducing guest species into the semiconductor host. Common doping agents added to initiate electron transfer include strong molecular donors/acceptors and Lewis acids. Complementary to direct integer charge transfer between OSC and dopant to form ion pairs (the ultimate goal of doping OSCs), fractional charge transfer can occur forming ground-state charge transfer complexes instead via intermolecular orbital rehybridization of OSC and dopant, which is detrimental to the doping efficiency [1]. For OSCs including oligothiophenes of different chain length p-doped with strong electron acceptors [2, 3], I will discuss the role that (i) thin film structure plays for the respective doping scenario, (ii) that of the dopant strength, and (iii) of OSC conjugation length. These findings suggest exploiting steric hindrance to suppress CPX formation which we recently demonstrated for a non-planar p-dopant of 3D shape [4]. Finally, I will contrast above doping scenarios to those that have been proposed to be at work for the doping of OSCs using Lewis acids as alternative doping agents.

[1] I. Salzmann et al., *Acc. Chem. Res.* **49**, 370 (2016)

[2] H. Hase et al., *J. Phys. Mater.* **6**, 014004 (2023)

[3] J.T. Liu et al., *Angew. Chem. Int. Ed.* **59**, 7146 (2020)

[4] S. Charoughchi et al., *Angew. Chem. Int. Ed.*, DOI: 10.1002/anie.202304964 (2023, in press)

11:15 AM *EL16.06.07

Engineering Carrier-Dopant Interactions to Improve Charge Transport Properties in Highly-Doped Semiconducting Polymers Kilwon Cho; Pohang University of Science and Technology, Korea (the Republic of)

Doping is a powerful technique that can easily tune the electrical properties of semiconducting polymers and hence, grant flexibility to their applications. Highly-doped semiconducting polymers with high electrical conductivity have found extensive use in thermoelectric materials and bioelectronics. However, the low dielectric constant of semiconducting polymers causes strong Coulomb interactions between carriers and dopants. As a result, carriers cannot be effectively transported through the host polymer network and tend to localize within a few monomer units or π -stacks. These limitations, distinct from those observed in conventionally doped inorganic semiconductors, necessitate novel engineering strategies to not only generate more charge carriers but also reduce unfavorable electrostatic interactions between carriers and dopants in doped semiconducting polymers. This talk will explore straightforward engineering methods to reduce Coulomb interactions between carriers and dopants in highly-doped semiconducting polymers. The corresponding reduction in charge localization and improved transport achieved through these methods will be discussed. Additionally, I will explore the effects of molecular structures that exhibit resilience to the energetic disorder caused by electrostatic carrier-dopant interactions on charge transport properties. Lastly, the talk will introduce the significant thermoelectric performance achieved in our research and discuss the potential of thermoelectric materials based on doped semiconducting polymers for the near future.

1:30 PM *EL16.07.01

Quantifying Polaron Populations in Sequentially Doped Conjugated Polymers Adam L. Moule¹, Tucker L. Murrey¹, Melissa Berteau-Rainville², Meghna Jha¹, Ingo Salzmänn³ and Mark Mascall¹; ¹University of California, Davis, United States; ²Institut National de la Recherche Scientifique, Canada; ³Concordia University, Canada

Conjugated polymers can be chemically tailored for a variety of electronic device applications. Sequential solution doping with high electron affinity (EA) molecular dopants is the processing technique that has produced molecularly doped polymeric films with the highest conductivity. In spite of numerous studies quantifying the conductivity of molecularly doped polymers as a function of processing conditions, there is no established method to quantify the charge density. The consequence is that the relationship between conductivity, mobility, and charge density is poorly understood, prohibiting meaningful quantitative comparisons between different polymers and dopants. Here we demonstrate a practical method to quantify the polaron density using the material density, molecular volumes, and optical measurements. Importantly, this method enables quantitative comparisons between multiple different polymer and dopant combinations as we demonstrate using P3HT and a series diketopyrrolopyrrole (DPP) co-polymers doped with a series of ultra-high EA cyano- and ester-substituted cyclopropane-1,2,3-triylidene-based dopants. The Langmuir isotherm is used to fit the solution concentration dependence of the film polaron mole fraction, which enables characterization of the sequential doping process using a single equilibrium constant. The saturated polaron mole fraction saturates with respect to the energetic driving force for doping, indicating that simply increasing the EA of the dopant is not an effective strategy for obtaining 100% ionization of the polymer monomers. To ground this thermodynamic model, we simulated the density of states (DOS) using Gaussian energy distributions. This DOS model predicts the experimental saturated doping level for every polymer/dopant pair within uncertainty. This data and model demonstrate conclusively that increasing the polaron density has a larger effect on increasing both conductivity and charge mobility than the polymer chemistry or structure.

2:00 PM *EL16.07.02

Considerations on "Double Doping" and an Enhanced *p*-Dopant Complex Norbert Koch^{1,2}; ¹Humboldt-Universität zu Berlin, Germany; ²Helmholtz-Zentrum Berlin, Germany

The double ionization of molecular dopants enables the doping efficiency to rise above 100%. This means increased conductivity can be achieved with fewer dopant molecules, resulting in less disruption to the semiconductor film's structure. However, current models of doped organic semiconductors based on Fermi-Dirac statistics with two distributions that represent the host and dopant density of states, fail to explain double dopant ionization, and also the analogous situation of bipolaron formation on a host semiconductor polymer. This shortcoming is addressed by considering the energy level renormalization of the frontier molecular orbital levels upon electron transfer between host and *p*-dopant. Varying the model parameters host-dopant energy level offset, energetic disorder, reorganization energy, and Hubbard *U* sublevel splitting, robust trends in the fractions of doubly-ionized, singly-ionized, and neutral species are found. The conventionally used *p*-dopants based on tetracyanoquinodimethane (TCNQ) and its derivatives feature limited oxidation strength especially for modern polymer semiconductors with high ionization energy (IE). These small molecular dopants also exhibit pronounced diffusion in polymer hosts. A facile approach is presented to increase the oxidation strength of several TCNQ-derivatives by coordination with four tris(pentafluorophenyl)borane (BCF) molecules, using a single-step solution mixing process, resulting in bulky dopant complexes. Using a series of polymer semiconductors with IE up to 5.9 eV, the efficiency of doping using such complexes is found to be significantly higher compared to using either of the dopants alone. Additionally, the bulkier structure of the complexes is shown to result in a higher stability against dopant drift in thin films under an applied electric field. The simple approach of solution-mixing of readily accessible molecules thus offers access to enhanced molecular *p*-dopants.

2:30 PM BREAK

3:30 PM EL16.07.03

Unlocking the Full Potential of Electron Acceptor Molecules for Efficient and Stable Hole Injection into Organic Semiconductors Takuo Oono, Takuya Okada, Tsubasa Sasaki, Takahisa Shimizu and Hirohiko Fukagawa; Japan Broadcasting Corporation, Japan

Improving the hole injection property are of pivotal importance in the future development of organic optoelectronic devices. Electron acceptor molecules with high electron affinity (EA) are widely used in electronic applications, such as hole injection, *p*-doping and charge generation. Although *p*-doping and charge generation have generally been discussed in terms of matching the ionization energy (IE) of organic semiconductors with the EA of acceptor molecules, it has been demonstrated that the EA depends on the charged states of acceptor molecules in recent years [1,2].

In this study, we report a strategy to maximize the potential of acceptor molecules for efficient and stable hole injection into organic semiconductors [3]. This strategy has been developed based on the correlation between the HIL-dependent properties of OLEDs and the actual energy levels around the anodes as determined by both low-energy inverse photoemission spectroscopy and ultraviolet photoemission spectroscopy. Efficient and stable hole injection into an organic semiconductor with a relatively high IE of 5.8 eV is possible by stacking acceptor molecules with EAs of 4.3 and 5.0 eV. This superior hole injection property enables direct hole injection even into materials used as the emitting host for pure blue thermally activated delayed fluorescence (TADF) emitters with a large band gap. A pure blue TADF organic light-emitting diode (OLED) that has both a Commission internationale de l'éclairage (CIE) *y* coordinate of less than 0.10 and a low turn-on voltage of only 2.67 V was realized by employing a device architecture with no energy barrier in the OLED. The findings are expected to have a wide range of organic electronic applications, such as the efficient hole injection into materials with high IE used in perovskite LEDs, organic thin-film transistors, and organic semiconductor laser diodes.

[1] J. Li *et al.*, *Mater. Horiz.* 2019, 6, 107.

[2] D. Kiefer, *et al.*, *Nat. Mater.* 2019, 18, 149.

[3] T. Oono *et al.*, *Adv. Mater.* 2022, 35, 2210413.

3:45 PM EL16.07.04

Imaging the Effect of Nanoscale Morphology on Molecular Doping Efficiency in Conducting Polymers Sung-Joo Kwon¹, Rajiv Giridharagopal¹, Shinya Chen¹, Ramsess Quezada¹, Jiajie Guo¹, Justin Neu², Wei You² and David S. Ginger¹; ¹University of Washington, United States; ²University of North Carolina at Chapel Hill, United States

Understanding the mechanisms underpinning doping of conducting polymers (CPs) is critical for improving their performance in next-generation organic electronic devices. Although a number of studies have investigated molecular or electrochemical doping of conducting polymers, most work has focused primarily on understanding doping via device-level operation using macroscopic probes. Conducting polymers (CPs) are inherently nanostructured, with a mixture of crystalline and amorphous domains. Thus, understanding the underlying mechanisms behind doping can benefit from nanoscale real-space imaging. Here, we investigate the molecular and electrochemical doping on two CPs with very different reported doping efficiencies (# charges/dopant molecules) using functional atomic force microscopy methods. Specifically, we compare the morphology dependence behind the well-known poly(3-hexylthiophene) (P3HT) polymer, with alkyl sidechains, to a more state-of-the-art polymer p(g₃2T-TT) that has been reported to exhibit substantially higher doping efficiencies. We use scanning Kelvin probe microscopy and conductive AFM to investigate local doping and visualize the morphology-dependence of local dopant/counterion accumulation. We use these methods to provide a link between optical measurements of doping with spectroelectrochemistry and local work function variations for films that have been molecularly and electrochemically doped. These results show that doping efficiency is linked to the polymer's ability to accommodate the dopant in its three-dimensional structure, where P3HT exhibits significant surface aggregation of molecular dopants that limits its ultimate efficiency compared to p(g₃2T-TT). We validate these results chemically via time-of-flight secondary ion mass spectrometry, providing a comprehensive view of the interplay between the local structure and ion ingress. This work provides guidance for optimizing future combinations of polymeric materials and molecular dopants to maximize conductivity

4:00 PM EL16.07.05

Thermal Stability of Organic Hole Transport Layers Stephanie A. Buchholz, Tobias Antrank, Hans Kleemann and Karl Leo; Dresden Integrated Center for Applied Physics and Photonic Materials, Germany

The electrical conductivity of amorphous doped organic hole transport layers, as used in organic light-emitting diodes (OLEDs), solar cells, or photodetectors, increases with temperature due to the dominant hopping-like transport mechanism. However, the conductivity irreversibly breaks down at a certain temperature. For example, OLEDs and organic photovoltaics have operating temperatures up to 80°C and 145°C, respectively. In addition, the active layer of an organic solar cell is deposited on the hole transport layer and has to be annealed at temperatures up to 140°C for a higher efficiency. The reasons for this breakdown are unknown, impeding the development of more stable devices. Here, we show a relation between the breakdown of the conductivity and the glass transition of the small molecule host materials and find that the choice of the dopant and the doping concentration significantly affects the thermal stability of the layer. Based on our investigations, we develop different hypotheses about the cause of the breakdown. With our results, we devise strategies to improve the thermal stability of organic hole transport layers.

4:15 PM *EL16.07.06

Counterion Control and the Electronic Structure of Polarons and Bipolarons in Doped Conjugated Polymers Benjamin J. Schwartz; UCLA, United States

When an electron is removed from a conjugated polymer, such as poly(3-hexylthiophene-2,5-diyl) (P3HT), the remaining hole and associated change in the polymer backbone structure from aromatic to quinoidal are referred to as a polaron. Bipolarons are created by removing the unpaired electron from an already-oxidized polymer segment. In electrochemically-doped P3HT films, polarons and bipolarons are readily observed, but in chemically-doped P3HT films, bipolarons rarely form. We explain this observation by studying the effects of counterion position on the formation of polarons, strongly coupled polarons, and bipolarons using both spectroscopic and X-ray diffraction experiments and time-dependent density functional theory (TD-DFT) calculations. The counterion positions control whether two polarons spin-pair to form a bipolaron or whether they strongly couple without spin-pairing. When two counterions lie close to the same polymer segment, bipolarons can form, with an absorption spectrum that is blueshifted from that of a single polaron. Otherwise, polarons at high concentrations do not spin-pair, but instead J-couple, leading to a redshifted absorption spectrum. The counterion location needed for bipolaron formation is accompanied by a loss of polymer crystallinity, so that bipolarons can form only in disordered regions of conjugated polymer films. Our TD-DFT calculations of polarons and bipolarons predict absorption spectra that match well with experiment, providing strong evidence that TD-DFT is correctly capturing the electronic structure of the doped material. Several groups, however, who looked at the energies of the Kohn-Sham orbitals from (non-time-dependent) DFT calculations, have recently argued that the traditional band picture is incorrect for doped conjugated polymers. Instead, these non-time-dependent DFT calculations suggest that polaron creation causes only one unoccupied state to move into the band gap near the valence band edge while half-filled states in the conduction and valence bands bend downward in energy. To understand the discrepancy, we also performed an analysis using natural transitional orbitals (NTOs) that shows that our TD-DFT calculations indeed reproduce the traditional band picture of polarons and bipolarons. Taken together, our experimental and theoretical results argue that controlling the counterion location and using the properly level of theory is critical to understanding the electronic structure of polarons and bipolarons on doped conjugated polymers.

SESSION EL16.08: Applications of Doped Organic Semiconductors
Session Chairs: Mukundan Thelakkat and Dhandapani Venkataraman
Thursday Morning, November 30, 2023
Hynes, Level 2, Room 205

8:30 AM EL16.08.01

Electrical Doping Stabilizes Organic Nanoparticle Dispersions for the Eco-Friendly Fabrication of Solar Cells Felix Manger, Jonas Armleder, Philipp Marlow, Karen Fischer, Holger Roehm, Christian Sprau and Alexander Colsmann; Karlsruhe Institute of Technology, Germany

Nanoparticle dispersions allow the use of eco-friendly processing agents for the solution deposition of organic semiconductor thin-films for photovoltaic and other optoelectronic applications. Omitting surfactants, which are commonly used to stabilize dispersions, is essential to not jeopardize the solar cell performance. In this work, electrical doping is used to charge the organic nanoparticles. The resulting electrostatic repulsion between the nanoparticles stabilizes the dispersion. Different doping concepts are deployed, compared and their effect on the nanoparticle stabilization is explored. Preference is given to volatile dopants which evaporate from the nanoparticulate light-harvesting layer after thin-film deposition. Finally, using electrical doping and the corresponding electrostatic stabilization, novel surfactant-free nanoparticle dispersions from high-performance organic semiconductors are synthesized by nanoprecipitation, giving rise to record solar cell power conversion efficiencies beyond 10%.

F. Manger et al., *Adv. Funct. Mater.* 2202566 (2022); F. Manger et al., *Adv. Energy Mater.* 2202820 (2023)

8:45 AM EL16.08.02

Efficient N-Doping in Organic Semiconductors by Novel Approaches and Materials Design Antonio Facchetti; Northwestern University/Flexterra Inc, United States

In this presentation we will report new strategies to efficiently n-doped organic semiconductor films. Thus, starting from initial work investigating molecular n-doping of naphthalenediimide (NDI) and isomeric benzothiadiazole (isoBT) based polymers we explored how variations in polymer backbone composition, regiochemistry, thin-film processing, and doping affect major film morphology and charge transport characteristics in transistor and diode architectures. For instance, we showed that NDI-(TVT)_x(TET)_y [x+y=100%; TVT = thienyl-CH=CH-thienyl; TET = thienyl-CH₂CH₂-thienyl] charge transport in transistor has a unique dependence on the x,y values. Thus, we explored how charge transport is affected in diodes as well as how NDI-(TVT)_x(TET)_y (polymer acceptor) + polymer donor solar cells perform. Finally, we recently discovered new approaches to enhance doping efficiency and conductivity via 1, tuning film morphology by favoring molecule dopant penetration and, 2, using catalysts that promote the semiconductor+dopant reaction. The latter strategy enables excellent doping efficiencies and conductivities for several organic semiconductors.

9:00 AM *EL16.08.03

The Role of Carrier Density and Morphology on Charge Transport Anna Kohler; University of Bayreuth, Germany

Charge carrier mobility is a decisive factor in controlling the efficiency of organic solar cells (OSCs) and field effect transistors (OFETs). This presentation will discuss how the mobility will be influenced by factors including aggregation, local morphology or carrier density. We employ kinetic Monte-Carlo simulation to study the charge transport¹.

1 T. Meier, H. Bässler, A. Köhler, *Advanced Optical Materials* 9 (14), 2100115 (2021)

9:30 AM BREAK

10:00 AM *EL16.08.04

Models of Polymeric Mixed Ionic and Electronic Conductors Alessandro Troisi¹, Alessandro Landi², Colm A. Burke¹ and Hesam Makki¹; ¹University of Liverpool, United Kingdom; ²University of Salerno, Italy

In organic polymeric materials with mixed ionic and electronic conduction (OMIEC), the excess charge in doped polymers is very mobile and the dynamics of the polymer chain cannot be accurately described with a model including only fixed point charges. Ions and polymer are comparatively slower and a methodology to capture the correlated motions of excess charge and ions is currently unavailable. Considering a prototypical interface encountered in this type of materials, we constructed a scheme based on the combination of MD and QM/MM to evaluate the classical dynamics of polymer, water and ions, while allowing the excess charge of the polymer chains to rearrange following the external electrostatic potential. We used this methodology to study the timescale for electronic charge rearrangement and the change in static and dynamic disorder as the doping level increase. We also propose a microscopic mechanism for reversible charging of OMIEC materials that can be used for designing new materials and rationalizing the current experimental observations.

Landi A et al., *J. Mater. Chem. C*, 2023, <https://doi.org/10.1039/D2TC05103F>

Keen S.T. et al, *J. Am. Chem. Soc.*, 2022, <https://doi.org/10.1021/jacs.2c02139>

Makki H. and Troisi A., 2022, *J. Mater. Chem. C*, 2022, <https://doi.org/10.1039/d2tc03158b>

10:30 AM *EL16.08.05

MURI: Doping in Organic and Printed Electronics Center (DOPE Center) Wei You; University of North Carolina at Chapel Hill, United States

Doping of organic semiconductors plays an important and growing role in organic electronics, ranging from organic light emitting diodes and organic solar cells to thermoelectrics and bioelectronics. However, unlike Si, where parts per million dopant concentrations can significantly alter conductivity, doping organic semiconductors with molecular dopants typically requires a much higher concentration. Complex interplay between the microstructure, electronic structure and molecular interactions of the polymer and dopants has prevented systematic understanding. Progress is largely dependent on heuristically guided, slow, trial-and-error experimentation. Furthermore, only *p*-type doping has been widely implemented in organic semiconductors, and *n*-type doping has met with limited success. Thus, developing air-stable *n*-dopants is an important objective for the field of molecular dopants.

Supported by the DoD MURI program, the DOPE Center aims to transform the field of solution-processed, doped conducting polymers by 1) co-designing optimized *p*- and *n*-doped conducting polymer systems and achieving facile *n*-doping, 2) extending our recent, paradigm-changing discovery of photoredox doping in conjugate polymers, 3) accelerating the pace of data generation by collaborative workflow integration of robotic experimentation and machine learning (ML) and artificial intelligence (AI) approaches, 4) creating fundamental knowledge that informs novel materials synthesis and system optimization.

This talk will introduce the DOPE Center, and progress made up to this point. Importantly, the DOPE Center welcomes collaboration, and hopes to serve as a coalescing point to work with the large community to rapidly advance the field.

11:00 AM *EL16.08.06

Nanomechanics of Materials used in Flexible Electronics Deepak Venkateshvaran and Leszek J. Spalek; University of Cambridge, United Kingdom

Organic semiconductors are multifunctional soft electronic materials that play an impactful role in the flexible electronics industry. Their use spans printed electronic circuits, large area displays, flexible solar energy harvesters, and implantable bioelectronics. For their competitive optical, electronic, thermoelectric, and spin-based properties, these soft electronic materials attract significant academic engagement, seeding new technologies for the future. ^[1, 2, 3]

Although macroscopic flexibility on the centimetre to metre scale is a unique selling point for organic semiconductor technology, not much is known about their mechanical properties on the nanoscale. Quantification of these nanomechanical properties, together with an understanding of nanoscale stiffness tunability and homogenisation, holds significant potential for fundamental and applied science. ^[4, 5]

During the last decade, the development of high precision atomic force microscopes has made it possible to quantify the mechanical properties of organic polymers on the scale of a few polymer chains. Techniques such as higher eigen mode imaging make it possible to visualise molecular ordering on the nanoscale under ambient conditions with ease. These techniques allow one to correlate molecular ordering with the stiffness that such ordering manifests.

In this talk, the science and technology of precision nanoscale measurement of mechanics will be spotlight. The interrelation between molecular organisation and nanomechanical properties in high-performance polymers used for organic electronics will be shown. ^[6, 7] A quantification of differences in strain within organic nanocrystal polymorphs will also be demonstrated. The measurement techniques demonstrated in this talk are extendable to a wide variety of multifunctional materials with a broad range of elastic properties and have significant use in both academia and industry.

[1] D. Venkateshvaran, M. Nikolka *et al.*, Nature **515**, 384–388 (2014)

[2] S. J. Wang, D. Venkateshvaran *et al.*, Nature Electronics **2**, 98–107 (2019)

[3] P. Skalski, O. Zadvorna *et al.*, Physical Review Materials **6**, 024601 (2021)

[4] L. Ouyang, C. Kuo *et al.*, J. Mater. Chem. B **3**, 5010 (2015)

[5] C. D. Gerardo *et al.*, Microsystems and Nanoengineering **4**, 19 (2018)

[6] V. Panchal, I. Dobryden ... D. Venkateshvaran, Advanced Electronic Materials **8**, 2101019 (2022)

[7] I. Dobryden, V. V. Korolkov ... D. Venkateshvaran, Nature Communications **13**, 3076 (2022)

SYMPOSIUM EL17

Synthesis, Properties and Applications of 2D MXenes
November 27 - December 6, 2023

Symposium Organizers

Majid Beidaghi, University of Arizona
Abdoulaye Djire, Texas A&M University
Seon Joon Kim, Korea Institute of Science and Technology
Xuehang Wang, Delft University of Technology

Symposium Support

Silver
INNOMXENE Co., Ltd.
Nanoplexus Limited

Bronze
King Abdullah University of Science
MSE Supplies LLC

* Invited Paper

+ JMR Distinguished Invited Speaker

SESSION EL17.01: MXene Synthesis and Structure I
Session Chairs: Majid Beidaghi and Abdoulaye Djire
Monday Morning, November 27, 2023
Hynes, Level 2, Room 208

10:30 AM *EL17.01.01

MXene Synthesis – Pros and Cons of Various Methods Yury Gogotsi; Drexel University, United States

MXenes (carbides, nitrides, oxycarbides and carbonitrides of early transition metals) are a very large family of 2D materials. They have a chemical formula of $M_{n+1}X_nT_x$, where M is a transition metal (Ti, Mo, Nb, V, Cr, etc.), X is either carbon and/or nitrogen (n=1, 2, 3 or 4), and T_x represents surface terminations (O, OH, halogens, chalcogens). The large variety of structures and compositions, availability of solid solutions on M and X sites, and control of surface terminations offer a plethora of materials to produce and investigate.¹ Combining their plasmonic properties with ease in aqueous processing, high electronic conductivity (over 20,000 S/cm), biocompatibility, and excellent mechanical properties, which exceed other solution-processable 2D materials, MXenes have the characteristics enabling numerous applications. However, the properties of MXenes depend on their synthesis method. Selective etching of Al, Si or Ga in acidic electrolytes is the most common approach. However, the use of molten salts for selective etching has been gaining momentum, as MXenes with uniform halogen surface terminations can be produced. Hydrothermal and electrochemical selective etching methods have been introduced. Finally, CVD synthesis and topochemical synthesis using graphene/graphite or metal oxide add a new dimension. A critical overview of various synthesis techniques will be provided.

References

A. VahidMohammadi, J. Rosen, Y. Gogotsi, The World of Two-Dimensional Carbides and Nitrides (MXenes), *Science*, 372, eabf1581 (2021)

11:00 AM EL17.01.02

Progress in the Direct Synthesis of Two-Dimensional Transition Metal Carbides and Nitrides (MXenes) DiWang¹, ChenkunZhou¹, AlexanderS. Filatov¹, WoojeCho¹, FranciscoLagunas², MingzhanWang¹, Young-HwanKim¹, SuriyanarayananVaikuntanathan¹, ChongLiu¹, RobertF. Klie² and DmitriV. Talapin¹; ¹University of Chicago, United States; ²University of Illinois at Chicago, United States

MXenes are a large family of two-dimensional (2D) transition metal carbides and nitrides with a general formula of $M_{n+1}X_nT_x$ ($n = 1-4$), where M stands for early transition metal (such as Ti, V, or Nb), X is C or N, and T is surface terminations (for example, -OH, -F, and -Cl). Their structures can be described as $n+1$ close-packed M layers interleaved with n layers of X atoms, then sandwiched between surface groups. MXenes have been actively studied for their potential applications in energy storage, electromagnetic interference (EMI) shielding, and catalysis. MXenes are typically synthesized from a series of non-van der Waals precursors (MAX phases, where A is typically Al) by selectively extracting A atoms with hydrofluoric acid-containing solutions. This process is relatively time-consuming and generates hazardous waste, both of which may limit the scalability of MXene manufacture.

We demonstrated two direct ways, bypassing the MAX phase intermediates, to prepare one of the most widely used MXenes, Ti_2CCl_2 . One is based on the high-temperature reaction of a stoichiometric mixture of precursors. The other uses chemical vapor deposition (CVD), where gaseous reagents flow through a heated substrate to form a thin film of product. We even pushed MXene bottom-up synthesis to a new level by expanding the scope of MXene available through direct synthesis, tuning the morphology of MXene products from stacks to spheres. The direct synthesis routes save time and minimize hazardous waste production. Besides, these new routes offer synthetic modalities not compatible with traditional methods, especially in cases where corresponding MAX phases are not available. Considering the extensive possibility of element combinations, the direct synthesis method could substantially expand the variety of MXene family. These benefits are expected to improve the efficiency of scaling production and expedite converting lab-scale discoveries into industrial-level applications.

References:

1. D. Wang *et al.*, *Science* **379**, 1243 (2023).

11:15 AM EL17.01.03

Synthesis of Three Families of Titanium Carbonitride MXenes TengZhang, ChristopherE. Shuck, KaterynaShevchuk, MarkAnayee and YuryGogotsi; Drexel University, United States

Layered MAX phases and 2D MXenes derived from them are among the most studied materials due to their attractive properties and numerous potential applications. The tunability of their structure and composition allows every property to be modulated over a wide range. Particularly, elemental replacement and forming a solid solution without changing the structure allows fine tuning of material properties. While solid solutions on M (metal) site have received attention, the partial replacement of carbon with nitrogen (carbonitrides) has received little attention. By applying this concept, herein we report the synthesis of three families of titanium carbonitride $Ti_{n+1}Al(C_{1-y}N_y)_n$ MAX phases and $Ti_{n+1}(C_{1-y}N_y)_nT_x$ MXenes with one, two and three C/N layers. This greatly expands the variety of known MAX phases and MXenes to encompass 16 titanium carbonitrides with tunable X-site chemistries and different 2D layer thicknesses, including MXenes in the $Ti_4(C_{1-y}N_y)_3T_x$ system, which have not been previously reported. We further investigated the relationship between the composition, structure, stability, and synthesis conditions of the MXenes and their respective Al-based MAX phases. This range of materials will enable fundamental studies of the N:C ratio effect on optoelectronic, electromagnetic and mechanical properties of MXenes, as well as tuning those properties for specific applications

11:30 AM *EL17.01.04

Synthesis Science Between MAX Phases and MXenes ChristinaS. Birkel^{1,2}, RoseSnyder¹ and CarinaBüchner^{2,1}; ¹Arizona State University, United States; ²Technische Universität Darmstadt, Germany

The synthesis of MAX phases and their two-dimensional siblings MXenes, especially when pushing beyond Ti-based compounds, is far from trivial. Our group uses diverse preparation techniques to access new versions of these intriguing types of materials, recent examples include Cr_2GaC in the shape of carbonaceous microwires,¹ hollow and full microspheres² as well as hitherto unknown carbonitride phases, such as $Cr_2GaC_{1-x}N_x$ and $V_2GaC_{1-x}N_x$.³ We specialize in non-conventional methods, such as sol-gel chemistry⁴⁻⁶ and microwave heating⁷ to synthesize the MAX phases.

In this talk, I will highlight two of our recent projects: (i) Our work on a unique “514” MAX phase $(Mo_{0.75}V_{0.25})_5AlC_4$, its structural investigation and transition to the respective MXene including its electrocatalytic properties. (ii) The transition from a MAX-like “221” compound Mo_2Ga_2C to the fully exfoliated MXene Mo_2CT_x as well as Mn-doped variants.

All materials are structurally characterized by diffraction and microscopy techniques and a deeper understanding of their chemical composition, formation mechanism and stability is obtained through spectroscopy and thermogravimetric methods.

1 J. P. Siebert, D. Hajra, S. Tongay and C. S. Birkel, *Nanoscale*, 2022, **14**, 744–751.

2 J. P. Siebert, M. Flores and C. Birkel, *ACS Org. Inorg. Au*, 2, 59–65.

3 N. Kubitzka, A. Reitz, A. M. Zieschang, H. Pazniak, B. Albert, A. Regoutz, U. Wiedwald and C. S. Birkel, *Inorg. Chem.*, 2022, **61**, 10634–10641.

4 J. P. Siebert, L. Bischoff, M. Lepple, A. Zintler, L. Molina-Luna, U. Wiedwald and C. S. Birkel, *J. Mater. Chem. C*, 2019, **7**, 6034–6040.

5 J. P. Siebert, K. Patarakun and C. Birkel, *Inorg. Chem.*, **61**, 1603–1610.

6 J. P. Siebert, M. Juelsholt, D. Günzing, H. Wende, K. Ollefs and C. S. Birkel, *Inorg. Chem. Front.*, 2022, **9**, 1565–1574.

7 J. P. Siebert, C. M. Hamm and C. S. Birkel, *Appl. Phys. Rev.*, 2019, **6**, 041314.

SESSION EL17.02: MXene Synthesis and Structure II
Session Chairs: Seon Joon Kim and Ruocun (John) Wang
Monday Afternoon, November 27, 2023
Hynes, Level 2, Room 208

1:30 PM *EL17.02.01

MXenes: Science, Applications and Hype MichelW. Barsoum; Drexel University, United States

At this juncture there is no doubt that MXenes have captivated the world's interest and with good reason. The number of potential applications is quite numerous and diverse. The use, or addition, of MXenes can boost some properties sometimes to record levels; in other cases it allows for herewith new applications for 2D materials. Their chemical diversity is also a huge attractor. As MXenes - like other new materials - get more popular, they are accompanied by hype. With hype comes responsibility. Hying, or overpromising, is bad for the field in general and should be curtailed. In this talk I differentiate between work done in the name of science that has little chance of applicability and other work that may lead to applications. The fundamental, and quite difficult problem to solve, with MXenes is that because we are dealing with essentially a few - 2, 3, 4 - of highly reactive transition metals layers interleaved with C or N, it will be very difficult indeed to render them oxidation resistant. It follows that applications where MXenes are placed in *open*, aqueous-based systems will be few and far between. Hying such applications - while not simultaneously solving the stability conundrum for times commensurate with the time of use in said applications - is irresponsible since they fall under the purview of science. Another example of hype is work on MXene-based supercapacitors. To date, most of supercapacitor work on MXenes makes use of dilute aqueous-based electrolytes. We have shown that when using such electrolytes, such as sulphuric acid, the self-discharge rate is quite high which, in turn, would again greatly limit the scope of applicability of such devices. Other potential pitfalls will be discussed.

2:00 PM EL17.02.02

High-Entropy Laminate Metal Carbide (MAX Phase) and its Two-Dimensional Derivative MXene JieZhou¹, QuanzhengTao¹, JustinasPalisaitis¹, SuaPark¹, MichelW. Barsoum², PerO. Persson¹ and JohannaRosen¹; ¹IFM, Sweden; ²Drexel University, United States

High-entropy (HE) ceramics, by analogy with HE metallic alloys, are an emerging family of multi-elemental solid solutions. These materials offer a large compositional space, with a corresponding large range of properties. We here report the experimental realization of a 3D HE MAX phase, $Ti_{1.0}V_{0.7}Cr_{0.05}Nb_{1.0}Ta_{1.0}AlC_3$, and corresponding 2D HE MXene in the form of free-standing flakes of average composition $Ti_{1-x}V_{0.7-x}Cr_xNb_{1.0}Ta_{0.6}C_3T_z$ ($T_z = -F, -O, -OH$), as produced by selective removing of Al from the HE MAX phase in aqueous hydrofluoric acid (HF). Initial tests on the HE MXene “paper” electrodes show high potential as electrode material in supercapacitors through a volumetric and gravimetric capacitance of 1688 F/cm³ and 490

F/g, originating from a combination of diffusion- and surface-controlled charge storage processes. The introduction of the HE concept into the field of 2D materials suggests a wealth of future 2D materials and applications. Moreover, we found that the thickness/atomic arrangement of MC slabs within the HE MAX phases and MXenes can be tuned by adding the fifth element to the quaternary M (Ti-V-Nb-Ta)-Al-C system, which may provide an insight into the future design, synthesis, and application of HE MXenes.

2:15 PM EL17.02.03

M₅X₄: A Family of MXenes [MarleyDownes](#)¹, Christopher E. Shuck¹, Robert Lord¹, Mark Anayee¹, Mikhail Shekhirev¹, Ruocun (John) Wang¹, Tetiana Hryhorchuk¹, Martin Dahlqvist², Johanna Rosen² and Yury Gogotsi¹; ¹Drexel University, United States; ²Linköping University, Sweden

MXenes are two-dimensional (2D) transition metal carbides, nitrides, and carbonitrides typically synthesized from layered MAX-phase precursors. With over 50 experimentally reported MXenes and a near-infinite number of possible chemistries, MXenes are the fastest-growing family of 2D materials. They offer a wide range of properties, which can be altered by their chemistry (M, X, T_x) and the number of metal layers in the structure, ranging from two in M₂XT_x to five in M₅X₄. Only one M₅X₄T_x MXene, Mo₄VC₄, has been reported. Herein, we report the synthesis and characterization of two new phase-pure M₅AX₄ mixed transition metal MAX-phases, (TiTa)₅AlC₄ and (TiNb)₅AlC₄, and their successful topochemical transformation into (TiTa)₅C₄T_x and (TiNb)₅C₄T_x MXenes. The resulting MXenes were delaminated into single-layer flakes, analyzed structurally, and characterized for their thermal and optical properties. This establishes a family of M₅AX₄ MAX phases and their corresponding MXenes. These materials were experimentally produced based on guidance from theoretical predictions, opening the door to exciting new applications for MXenes.

2:30 PM *EL17.02.04

Tailoring of Vacancy Concentration and Pore Size in MXenes [Johanna Rosen](#); Linköping University, Sweden

MXenes show great prospects for surface-related applications owing to their large surface area and unique physical and chemical properties. MXenes with vacancies, whether ordered or randomly distributed, have shown a significant property enhancement, particularly in energy storage devices. Generally, randomly ordered vacancies in 2D monolayers have the possibility to conglomerate and form pores of different size. The performance can then be further enhanced, allowing interaction with various inorganic and organic species depending on the pore size. I will present a general experimental approach for tailoring vacancy concentration and pore size in a selection of well-known MXenes, inspired by theoretical calculations. The method is based on alloying of the parent MAX phases, where the concentration of the alloying element is directly correlated to the vacancy concentration (pore size) in the resulting MXene. The synthesized MXenes are shown to have a large surface area, and are further characterized with respect to structure, composition, and selected properties. The formation of pores is shown to significantly enhance the capacitance, and the materials are predicted to have selectivity towards inorganic and organic chemical species which can play an important role in molecular separation and energy related applications.

3:00 PM BREAK

SESSION EL17.03: MXenes Electrochemical and Optical Properties I

Session Chairs: Majid Beidaghi and Abdoulaye Djire

Monday Afternoon, November 27, 2023

Hynes, Level 2, Room 208

3:30 PM *EL17.03.01

MXenes for Solid-State Electrochemical Energy Storage [Masashi Okubo](#); Waseda University, Japan

Layered transition-metal carbides/nitrides (MXenes) are an emerging family of electrochemical energy storage materials. When used as an electrode material with a liquid electrolyte, MXenes exhibit Li⁺ intercalation without large structural changes, which enables fast ion transport as well as dense charge storage in the open interlayer space between MXene nanosheets. It is well known that the Li⁺ intercalation of MXene electrodes is significantly affected by liquid electrolytes. However, the charge storage using MXene electrodes in inorganic solid electrolytes has rarely been investigated. Especially, the strain-free property of MXene should be beneficial to maintaining solid-solid interface, which enabling long-term cycling of all-solid-state batteries.

In this work, we investigate the charge storage behavior of various MXene electrodes with solid electrolytes. After clarifying the strain-free charge storage mechanism through the MXene-solid electrolyte interface, we exploit it for the stable operation of a strain-free ASSB using MXene as a negative electrode material.

4:00 PM EL17.03.02

Bringing Together Laser Treated MXene and Titania Nanotubes Towards Composite Electrode Material Active under Visible Light [Katarzyna Siuzdak](#)¹, Duje Jaric Kouao¹, Mirosław Sawczak¹, Wit Stranak², Petr Sezemsky³, Jan Hanus³, Ondrej Kylian³ and Katarzyna Grochowska¹; ¹The Szwalski Institute of Fluid-Flow Machinery Polish Academy of Sciences, Poland; ²University of South Bohemia in České Budějovice, Czechia; ³Charles University, Czechia

For the past 20 years, taking into account as the starting date the discovery of the extraordinary properties of a single layer graphene, finally the materials exhibiting 2D architecture have gained more attention. Among family of chalcogenides and boron nitrides that became so popular, the carbides and nitrides of transition metals became a rising star due to the attractive properties [1]. In MXene flake one can find a layer of transition metal and interlayer of carbon with some termination (O, OH, F or Cl) that are linked also to the metallic part. Most of known MXene synthesis routes involved fluoride-containing compounds, either aqueous or molten salts treatment of the MAX phase. Despite individual sheets are obtained they are still formed in a specific stack of several micrometers providing some problem when the composite with other materials should be achieved.

To overcome this problematic issue we propose laser treatment as an additional step in the fabrication route. The fabrication of Ti₃C₂T_x is performed in a quite typical way including mixing of MAX phase with HF and HCl solution and further delamination supported with NaCl. Microscopic investigation revealed that MXene sheets form agglomerates and additional efforts should be undertaken. Therefore, the MXene powder was frozen using liquid nitrogen and on such frozen material a liquid isopropanol was poured. Then beam of 1064 nm generated by pulsed Nd:YAG laser was irradiating frozen Ti₃C₂T_x. The interaction between laser and this material results in its ablation and its capture in a liquid medium. During the process the solution above the frozen material become grayish and such liquid was collected after different periods of time. Both the resonant peak at 120 cm⁻¹ and the out-of-plane vibrations at 736 cm⁻¹ of Ti₃C₂T_x are clearly visible on the Raman spectrum confirming the preservation of the MXene structure.

Finally, the material was used for the modification of surface provided by titania nanotubes obtained via anodization of Ti plates and Ti sputtered layer. The modification was carried out via treatment with TiCl₄/Ti₃C₂T_x solution followed by thermal annealing. The SEM inspection revealed that the initially smooth and thin walls of titania were uniformly overgrown and more porous but any agglomerates clogging the tubular interior were not detected. Cyclic voltammetry curves recorded for the series of modified titania electrodes indicated enhanced photoresponse under both visible and UV-vis light. In a particular case when the electrode was exposed to visible light, almost 20 times higher photocurrent at 0 V vs. Ag/AgCl/0.1M KCl comparing to bare titania was reached.

Apart from the improved photoresponse, the electrochemical activity of modified titania in the cathodic range was significantly changed, namely the cathodic current was much higher than the one registered for bare titania. For example at -1.0 V, bare titania exhibits nearly 0.1 mA/cm² whereas for the modified substrate the recorded current equals 2.6 mA/cm². It should be underlined that when the treatment of titania was carried out with TiCl₄ solution but without addition of laser treated MXene, such electrochemical response was not achieved. It indicated that the presence of MXene is crucial for greatly improved electrochemical and photoelectrochemical properties of the composite electrode material.

Summarizing we would like to show the unique laser treatment of 2D metal carbide material and its possible usage for formation of the composite with inorganic platform exhibiting promising electrochemical and photoelectrochemical properties being of high importance for development in the research area of water splitting and photoconversion.

[1] G. Sha, Z. Ding, Y. Gogotsi, *Frontiers of Physics* 18 (2023) 13604

Acknowledgements

The authors acknowledge the financial support of the National Science Centre (Poland) via grant no.: 2020/02/Y/ST8/00030

4:15 PM EL17.03.03

Investigation of Electrochemical Properties of Carbonitride MXenes with Different Nitrogen Contents [Chun-Pei Cho](#)^{1,2}, Teng Zhang², Kateryna Shevchuk², Ruocun (John) Wang² and Yury Gogotsi²; ¹National Chi Nan University, Taiwan; ²Drexel University, United States

Carbonitride MXenes with different nitrogen-to-carbon ratios have been fabricated. As the nitrogen content increases, the plasmonic resonance and A_{1g} characteristic peaks in the Raman spectra become weaker, indicating successful nitrogen substitution in the carbon (X) sublattice of MXene. An additional redox pair in the cyclic voltammetry (CV) curves further confirms the

presence of nitrogen species in the carbonitride MXenes. When utilized as the anode material in a supercapacitor with a 3M aqueous sulfuric acid electrolyte, the highest specific capacitance achieved by a carbonitride MXene is approximately 370 Fg^{-1} at a scan rate of 2 mVs^{-1} . The fitting results of XPS spectra demonstrate the reduction in both carbide and nitride signals, and C-Ti-F becomes the dominant surface termination after electrochemical cycling. The carbonitride MXene with the highest nitrogen level exhibits the best rate capability but the worst cyclic stability. It also shows inferior Coulombic efficiency at lower scan rates. In contrast, the Lithium-delaminated Ti_3C_2 material has the best cyclic stability. The results of Electrochemical Impedance Spectroscopy (EIS) align with the CV results for the carbonitride MXenes. It has been demonstrated by Staircase Potentiometric Electrochemical Impedance Spectroscopy (SPEIS) that, with a higher nitrogen content, a less negative applied potential is required to achieve smaller impedance and interlayer spacing.

4:30 PM *EL17.03.04

V_2C and Nb_2C MXenes: An Emerging Tunable Platform for Nanophotonics [Alexandra Boltasheva](#)¹, [Jeffrey Simon](#)¹, [Colton Fruhlin](#)¹, [Stefano Ippolito](#)², [Dan Zhen Zhang](#)² and [Yury Gogotsi](#)²; ¹Purdue University, United States; ²Drexel University, United States

MXenes, or transitional metal carbides, carbon nitrides, and nitrides, have recently emerged as a fascinating class of two-dimensional nanomaterials. These materials follow the chemical formula Mn+1XnTx . A prototypical MXene, $\text{Ti}_3\text{C}_2\text{Tx}$ has been studied extensively over the past two decades demonstrating remarkable electrical and optical properties and utilized for linear optical devices such as broadband absorbers, and nonlinear devices like saturable absorbers in lasing cavities. Here, we expand upon our groups' previous work with $\text{Ti}_3\text{C}_2\text{Tx}$ to new members in the MXene family, specifically V_2C and Nb_2C . By employing ellipsometry, we investigate the optical response of V_2C and Nb_2C . Our findings reveal a metallic transition for V_2C at longer wavelengths, while Nb_2C retains its dielectric nature due to the higher carrier concentration in V_2C . This transition from dielectric to metallic behavior is marked by the permittivity ϵ crossing zero in a region known as epsilon-near-zero (ENZ), which holds significant implications for optical technology. Furthermore, our research demonstrates that the ENZ point can be manipulated by adjusting the film thickness of V_2C , thereby affecting both its linear and nonlinear properties. These findings lay the foundation for future device development utilizing various members of the MXene family, including the creation of layered metamaterials.

SESSION EL17.04: Poster Session I
Session Chairs: [Majid Beidaghi](#), [Abdoulaye Djire](#) and [Seon Joon Kim](#)
Monday Afternoon, November 27, 2023
Hynes, Level 1, Hall A

8:00 PM EL17.04.01

Etching Mechanism of Aluminum Layers during 2D MXene Synthesis [Chi Won Ahn](#); NNFC, Korea Advanced Institute of Science and Technology, Korea (the Republic of)

Understanding the etching mechanisms of MXene and obtaining direct insights into the influence of etchants on structural features and defects are of critical importance for improving MXene properties, optimization of etching protocols, and exploring new MXene compositions. Despite their importance, such studies have been challenging because of the monoatomic thickness of the A-element layers being etched and aggressive etchants that hinder in situ studies. Here, we visualize the etching behavior of the Ti_3AlC_2 MAX phase in different etchants at the atomic scale using focused ion beam and electron microscopy. We also report on the structural changes in the Ti_3AlC_2 phase as a function of etching time and etchant type (LiF/HCl , HF, or NH_4HF_2) to reveal the etching mechanism for the first time.
[Ref] Chemistry of Materials 33(16) 2021.

8:00 PM EL17.04.02

Controlling the Interlayer Spacing of Two-Dimensional Titanium Carbide (MXene) Membranes for Selective Ion Separations in Water [Yaguang Zhu](#), [Austin J. Booth](#), [Kimberly Ventura-Martinez](#) and [Kelsey B. Hatzell](#); Princeton University, United States

MXenes are an emerging class of two-dimensional nanomaterials with promising applications in critical resource recovery, energy storage, and desalination. Specifically, MXene membranes are able to selectively separate cations based on charge and ionic radius¹, with low permeation rates for large and/or multivalent cations but high permeation rates for alkali-metal cations such as Li^+ . Fine-tuning of this ion sieving behavior could enable the energy-efficient recovery of lithium and other critical metals from wastewater. More recently, aluminum ions (Al^{3+}) have shown the ability to "lock" the interlayer spacing of MXene membranes² via intercalation between MXene nanosheets, preventing other cations from intercalating and preserving the selectivity of these membranes over time. Other ions³, as well as water molecules⁴, can also readily intercalate between MXene layers; furthermore, intercalation can strongly affect water adsorption/desorption³.

The exchange rates and mechanisms of ions and water within these confined interlayer spaces remain poorly understood, yet understanding these mechanisms is critical to the use of MXenes for advanced ion sieving technologies. To explore these processes, we have examined the changes in MXene membranes' interlayer spacing in response to intercalation (and exchange after pre-intercalation) with a variety of metal cations, including hydrophilic ions such as Mg^{2+} as well as more hydrophobic cations such as Cs^+ . We have also investigated the effects of water intercalation on interlayer spacing, especially the ability of hydrophilic cations to introduce additional layers of water between MXene nanosheets. Understanding how to reliably control the interlayer spacing (i.e., pore size) of MXene thin films will improve our ability to design selective ion sieves for metal recovery from water.

[1] Ren, C.E. et al., *J. Phys. Chem. Lett.* **6**, 4026-4031 (2015).

[2] Ding, L. et al., *Nat. Sustain.* **3**, 296-302 (2020).

[3] Zaman, W. et al., *Proc. Natl. Acad. Sci. U.S.A.* **118**, e2108325118 (2021).

[4] Muckley, E. S. et al., *ACS Nano* **11**, 11118-11126 (2017).

8:00 PM EL17.04.03

Development of Rapid Synthesis Method of MAX Phase Composites by Combination of Induction Heating and Self-Propagating High-Temperature Synthesis [Daisuke Nishine](#), [Ryosuke Numata](#), [Riku Sawamura](#), [Taro Shimomura](#), [Mahito Yamamoto](#) and [Mitsuru Inada](#); Kansai University, Japan

MXene, a two-dimensional layered material, is expected to be applied in a wide variety of fields. Generally, MXene is prepared by etching MAX phase. Therefore, it is very important for MXene research to develop a low-cost and simple method to synthesize the MAX phase. In most cases, the MAX phase is synthesized by high-temperature heating at around 1500°C under high pressure. Hot-pressing, spark plasma sintering, and other methods are used to satisfy these synthesis conditions, but they are specialized, expensive, and sometimes require several hours to synthesize the MAX phase. Therefore, it is desirable to develop a simple, low-cost and rapid synthesis method.

We have developed an original, low-cost and simple MAX-phase synthesis equipment by combination of the induction heating (IH) and the self-propagating high-temperature synthesis method. The IH method can rapidly heat a sample in a carbon crucible up to about 2000°C . This rapid heating induces local chemical reactions. The heat of the chemical reaction then propagates throughout the sample and then the MAX phase is synthesized. We have tried to synthesize two types of MAX phases using this equipment. One is Ti_3AlC_2 and the other is V_2AlC . XRD measurements and SEM observations showed that both MAX phases were successfully synthesized. It should be noted that this method can synthesize both in vacuum and in inert gas atmosphere. And it took less than a minute from the start of heating to the end of synthesis. These results indicate that this method is one of the candidates for a low-cost, simple, and rapid MAX phase synthesis method that can be applied to various types of MAX phase synthesis.

8:00 PM EL17.04.04

Synthesis of MXenes via Dry Selective Extraction from MAX Phases [Mark Anavee](#), [Ervin Rems](#), [Eiara Fajardo](#), [Robert Lord](#), [David Bugallo](#) and [Yury Gogotsi](#); Drexel University, United States

MXenes are a rapidly growing family of two-dimensional (2D) transition metal carbides and nitrides which are promising for various applications, including energy storage and conversion, electronics, and healthcare. Hydrofluoric acid-based etchants are typically used for large-scale and high-throughput synthesis of MXenes. Herein, we present a computational thermodynamic model with experimental validations to explore the feasibility of fluorine-free synthesis of MXenes by dry selective extraction (DSE) from precursor MAX phases using iodine vapors at elevated temperature. A range of MXenes with iodine surface terminations are systematically screened using first-principles calculations to find candidates with high phase stability and low etching energy. We further demonstrate a thermodynamic model based on the CALculation of PHase Diagrams (CALPHAD) approach, using $\text{Ti}_3\text{C}_2\text{I}_2$ as an example, to assess the Gibbs free energy of the reaction and the state of the byproducts (e.g., gas or solid) as a function of temperature and pressure. Based on the assessment, the optimal etching temperature and vapor

pressure are predicted, and further verified by experiments. This work opens an avenue for scalable, fluorine-free dry synthesis of MXenes with compositions and surface chemistries that are not accessible using wet chemical etching.

8:00 PM EL17.04.05

Microwave-Assisted Hydrothermal Synthesis of MXene-Derived Bilayered Vanadium Oxides for Aqueous Zinc Ion BatteryShang-TungChiang and MajidBeidaghi; Auburn University, United States

V₂O₅ shows great promise as a cathode material in zinc-ion batteries (ZIBs) due to its impressive theoretical capacity of 589 mAh/g, which is based on a two-electron transfer mechanism. However, its limited conductivity poses a significant challenge to its widespread application. In this study, we propose a universal approach to produce high-rate cathodes by creating heterostructures through a single-step process of ion intercalation and phase transition of MXene-derived hydrated vanadates. In our experiment, we introduced Zinc ions (using ZnCl₂) into the V₂C MXene precursor to increase the spacing between layers, and then applied hydrothermal treatment using a microwave. This significantly reduced the synthesis time from several hours to 15 minutes while maintaining the excellent conductivity of MXene and the high theoretical capacity of V₂O₅. The resulting material, denoted as Zn-V₂C-V₂O₅, exhibits a high specific capacity of 352 mAh/g at 0.1 A/g and demonstrates remarkable cycling stability. These findings position Zn-V₂C-V₂O₅ as a promising candidate for cathode materials in Zinc-ion batteries, offering a new approach for enhancing zinc ion storage in vanadium-based materials.

8:00 PM EL17.04.06

Reaction Barrier and Desorption Energy Co-Determined CO₂ Electroreduction Selectivity on Mo₂C-Based Catalysts by Modulating Terminations Species and DefectsCaihongLiang, ZhonghanZhang, ZhengLiu, ShuzhouLi and Yeng MingLam; Nanyang Technological University, Singapore

Using electrocatalysts to convert CO₂ to useful products via CO₂ reduction reaction (CO₂RR) is one of the solutions to greenhouse gases problems. Recently, MXenes have been recognised as potential CO₂RR electrocatalysts for its efficiency and tunability. However, comprehensive understanding on the relationship between CO₂RR performance and terminations of MXenes still remains open. For the sake of rational design for effective catalysts, Mo₂CT_x, a widely applied type of MXenes, is used as the model to systematically investigate the effect for CO₂RR from terminations via density functional theory (DFT) calculations. In this study, it is verified that different terminations over Mo₂CT_x exhibit different CO₂RR performances. This work puts forward that the selectivity is co-determined by desorption energy and reaction barrier of each product. Slabs completely covered with -O- or -F are tended to produce HCOOH, while slab with full -OH coverage are inclined to generate CO. Furthermore, results from a reconstructed slab based on one published experimental work with mixture terminations of 5.5% F, 5.5% Vacancy, 33.5% O, and 55.5% OH shows good consistency for the major products (selectivity towards C₁ products as HCOOH >> CO >> CH₄ >> CH₃OH). Additionally, this study predicts CO₂RR performance of Mo₂CO₂ with 0%, 5.6%, 11.1%, and 100% oxygen vacancy (Ov). The models with 5.6% or 100% Ov are beneficial to generate more valuable final products - methanol or methane, respectively, while the model with medium Ov (11.1%) tend to produce CO. This work provides useful insight and guidance to future research that utilizing terminations of MXene to design CO₂RR electrocatalysts, especially for Mo₂CT_x systems.

8:00 PM EL17.04.07

Broad-Wavelength Light-Driven Hybrid MXene/Molecular Crystal Actuators Actuated inside Tissue-Like PhantomsDong WookKim¹, YukiHagiwara², HidekoKoshima² and MetinSitti¹; ¹Max Planck Institute for Intelligent Systems, Germany; ²Waseda University, Japan

Significant progress has been made in the research of molecular crystals that can undergo light-driven actuation. This progress has been achieved through the development of different molecules and the identification of driving mechanisms. However, the crystals that have been developed so far have primarily been driven by ultraviolet (UV) or blue light, and the use of red or near-infrared (NIR) light for actuation has not been explored. In this study, we have successfully created molecular crystals that can be actuated by light across a broad range of wavelengths, including UV, visible, and NIR light, using the photothermal effect. To achieve this, we incorporated titanium carbide (Ti₃C₂T_x) MXene nanosheets into salicylideneaniline crystals. Unlike the original thin molecular crystals, which only exhibited slow bending under UV light due to photoisomerization, the addition of the MXene layer enabled rapid actuation of the molecular crystals at various thicknesses and wavelengths. The hybridization of MXene with molecular crystals not only provides strong biocompatibility but also allows for the bending of the hybrid crystals within agar phantoms that mimic biological tissue. Furthermore, we demonstrated that this MXene hybridization approach can be extended to other common molecular crystals, including different derivatives of salicylideneaniline and anisole.

8:00 PM EL17.04.09

Probing the Thermoelectric and Thermodynamic Properties of Hexagonal M3AC2 MAX-Phase by First-Principles CalculationsNaziaNasr; Northwestern Polytechnical University China, China

The thermodynamic and thermoelectric properties of hexagonal M3AC2 (M = Ti, V; A Al, Si) within MAX-phases have been investigated by first-principles calculations. The considered properties of M3AC2 compounds at 0 GPa were in reasonable agreement with available experimental and other theoretical data. The investigation probed into the thermodynamic attributes of M3AC2 (M = Ti, V; A = Al, Si) MAX-phases across diverse temperature and pressure conditions, elucidating the impact of these factors on heat capacity, bulk modulus, thermal expansion coefficient, Debye temperature, enthalpy, entropy, and Gibbs free energy. Notably, the bulk modulus and Debye temperature exhibited inverse trends with increasing temperature and direct trends with rising pressure. The impact of pressure and temperature on heat capacity (C_v and C_p) were found to be operated in opposing manners, devoted by the elevated atomic thermal velocity. The impact of the Seebeck coefficient and electrical conductivity also becomes evident at higher temperatures. At 200 K, the power factor (PF) sequence among M3AC2 (M = Ti, V; A = Al, Si) compounds is Ti3SiC2 > Ti3AlC2 > V3AlC2.

8:00 PM EL17.04.10

Enhancing The Ion Intercalation of MXene in Molecular Crowding ElectrolytesChaofanChen, Albertde Kogel and XuehangWang; TU Delft, Netherlands

The charge storage mechanism and performance of the MXenes electrode are highly dependent on the electrode and electrolyte composition. For example, Ti₃C₂T_x has shown rapid pseudocapacitive (de)intercalation of protons and transformation between the oxygen surface groups (=O) and hydroxyl (-OH) groups in acidic aqueous electrolytes.¹ As a result, Ti₃C₂T_x exhibit an ultrahigh volumetric capacitance of 1500 F cm⁻³ in H₂SO₄ electrolyte.² In less corrosive neutral aqueous electrolytes, the cation intercalation is accompanied by negligible charge transfer, leading to ultrafast charge storage.³ Consequently, a moderate capacitance with superior cycling stability is reported in neutral electrolytes compared to acidic electrolytes. Compared to dilute aqueous electrolyte, which has a limited electrochemical stability window (ESW), the water-in-salt (WIS) electrolyte possesses a large ESW owing to the depressed activity of free water. Besides, the unique solvation structure of WIS electrolyte induces novel solvation-free Li⁺ intercalation and increases capacitance.⁴ As a result, WIS electrolyte helps overcome the drawback of the low energy density of MXene in neutral aqueous electrolytes. We further explored the electrochemical behavior of 2D Ti₃C₂ MXene in safe, low-cost, and environmentally benign polyethylene glycol (PEG)-based molecular crowding electrolytes (MCE). The addition of PEG-based molecular crowding agents can also widen the potential window of the MXene electrode up to 1.6 V due to the suppressed hydrogen evolution reaction. Additionally, a pair of redox peaks at -0.25 V/-0.05 V vs. Ag (cathodic/anodic) emerged in cyclic voltammetry after adding the PEG, yielding an additional 25% capacitance. We used in-situ XRD to reveal the charge storage mechanism in MCE electrolytes. Interestingly, we observed the co-insertion of the molecular crowding agent PEG-400 during the Li⁺ intercalation process. As a result, Ti₃C₂T_x electrodes presented a large interlayer space change of 4.7 Å during a complete charge/discharge process.

Reference

- [1] Mu, X. *et al. Advanced Functional Materials* **29**, 1902953 (2019).
- [2] Lukatskaya, M. R. *et al. Nat Energy* **2**, 1–6 (2017).
- [3] Ando, Y., *et al. Advanced Functional Materials* **30**, 2000820 (2020).
- [4] Wang, X. *et al. ACS Nano* **15**, 15274–15284 (2021).

8:00 PM EL17.04.11

MXene Functionalized Kevlar Yarn via Automated Dip CoatingLingyiBi¹, WilliamPerry¹, RobertLord¹, Ruocun (John)Wang¹, TetianaHryhorchuk¹, AlexInman¹, OleksiyGogotsi², VitaliyBalitskiy², VeronikaZahorodna², IvanBaginskiy², StepanVorotilo¹, GenevieveDion¹ and YuryGogotsi¹; ¹Drexel University, United States; ²Materials Research Center, Ukraine

The rise of the Internet of Things (IoT) has spurred extensive research on integrating conductive materials into textiles to turn them into sensors, antennas, energy storage devices, and heaters. MXenes, owing to their high electrical conductivity and solution processability, offer an efficient way to add conductivity and electronic functions to textiles through simple dip coating. However, manual development of MXene-coated textiles restricts their quality, quantity, and variety. Here, we developed a versatile automatic yarn dip coater tailored for producing continuously high-quality MXene-coated yarns and conducted the most comprehensive MXene-yarn dip coating study to date. Compared to manual methods, the automatic coater provides lower resistance, superior uniformity, faster speed, and reduced MXene consumption. It also enables rapid coating parameter optimization, resulting in a thin Ti₃C₂T_x coating uniform over a 1 km length on a braided Kevlar yarn while preserving its excellent mechanical properties (over 800 MPa) and adding Joule heating and damage sensing to composites reinforced by the yarns. By dip-coating five different yarns of varying materials, diameters, structures, and chemistries, we gained new insights into MXene-yarn interactions. Thus, the automatic dip coating presents

ample opportunities for scalable integration of MXenes into a wide range of yarns for diverse functions and applications.

SESSION EL17.05: MXenes Electrochemistry and and Electrochemical Applications

Session Chairs: Abdoulaye Djire and Seon Joon Kim

Tuesday Morning, November 28, 2023

Hynes, Level 2, Room 208

8:00 AM *EL17.05.01

MXenes and Two-Dimensional Transition Metal Carbo-Chalcogenides as Electrocatalysts for Hydrogen Evolution Reaction Elham Loni¹, Ahmad Majed¹, Kun Liang², Anika Tabassum³ and Michael Naguib¹; ¹Tulane University, United States; ²Ningbo Institute of Materials Technology and Engineering, Chinese Academy of Sciences, China; ³University of the District of Columbia, United States

MXenes are a group of two-dimensional (2D) materials composed of transition metal carbide, nitrides, and carbonitrides denoted as $M_{n+1}X_nT_x$; M is an early transition metal, X is carbon/nitrogen, and T_x stands for surface terminations. These materials are created by selectively etching thin metal layers from layered ceramics. MXenes have shown great promise in various electrochemical energy storage and conversion applications. For instance, Ti_3CNT_x MXene demonstrated an onset overpotential of 53 mV and an overpotential of 148 mV at 10 mA/cm² when used as an electrocatalyst for the hydrogen evolution reaction (HER). Another class of 2D materials called transition metal carbo-chalcogenides (TMCCs) combines characteristics of MXenes and transition metal dichalcogenides on an atomic scale. They are synthesized via solid-state synthesis at ambient pressure, followed by intercalation and delamination in water without the use of surfactants. The conductive carbide core and catalytically active chalcogenides surface of TMCCs make them appealing as electrocatalysts. In this study, we will present the large-scale synthesis and characterization of various TMCCs (e.g., Ta_2Se_2C , Ta_2S_2C , Nb_2S_2C , and their solid solutions: $(Ta_yNb_{1-y})_2S_2C$; $y = 0.25, 0.5, \text{ and } 0.75$). Additionally, we will discuss the electrochemical performance of MXenes and TMCCs as electrocatalysts for the HER.

8:30 AM EL17.05.02

Tuning the Structure of MXene-Based Composites for Electrochemical Carbon Dioxide Reduction Guangxin Sun^{1,2}, Chunnian He³ and Andrew B. Wong^{1,1}; ¹National University of Singapore, Singapore; ²The Joint School of NUS-TJU, China; ³Tianjin University, China

The electrochemical CO₂ reduction reaction (CO₂RR) is a promising way to valorize CO₂ and realize net-zero CO₂ emissions. For CO₂RR, MXene is a good candidate that can adsorb CO₂. However, one of the critical challenges for CO₂RR is the control of selectivity. In our case, titanium carbide-based MXene materials were usually found to have high competing hydrogen evolution reaction (HER) performance, where HER is a competing reaction to CO₂RR. Therefore, to improve selectivity to CO₂RR products, we tuned the electronic structure of MXene to suppress HER and enhance the CO₂RR performance via a cations-alloying method. Through systematic investigations, we found that the MXene electronic structure can be tuned, which accompanies microstructure evolution, which is dependent on the reduction potentials of introduced cations. Additions of cations with lower reduction potentials, e.g., Na⁺, Co²⁺, Ni²⁺, did not change performance significantly, while Cu²⁺ and Ag⁺ have significant effects, which was confirmed by systematic characterizations.

Taking the *in-situ* reduced Ag nanoparticle decorated MXene as a model system, we demonstrate that these materials showed a significant improvement in CO₂RR performance. The ratio of CO to H₂ in the product can be tuned in the range of 1:3 to 1:1 by changing the added amount of Ag⁺. The result can be attributed to the change in electronic structure. With a moderate addition of cations and moderate redox reaction between MXene and cations, the electronic structure can be tuned while the MXene microstructure is maintained. Therefore, with the well-kept MXene structure, the electrons can be transferred from MXene to Ag nanoparticles, and the HER performance is suppressed. With much more cation addition, the MXene structure was degraded, which resulted in nearly 100% HER.

8:45 AM EL17.05.03

Rational Selection of Transition Metals in M₄C₃ MXenes to Control the Electrocatalytic Hydrogen Evolution Reaction Anupma Thakur, Nithin Chandran B S, Brian Wyatt and Babak Anasori; Indiana University-Purdue University Indianapolis, United States

2D MXenes have shown great promise as active materials in electrocatalytic hydrogen evolution reaction (HER). In this work, we present the selection of transition metal elements (V, Nb, Ta) in three M₄C₃T_x MXenes (V₄C₃T_x, Nb₄C₃T_x, Ta₄C₃T_x) to control their electrocatalytic performance for HER using an experimental approach. We synthesized V₄C₃T_x, Nb₄C₃T_x, Ta₄C₃T_x MXenes from their parent MAX phases via a selective etching route using hydrofluoric acid, followed by an organic intercalant (tetramethylammonium hydroxide)-assisted delamination. Further, we used an ion exchange process to modify the MXenes' surface chemistry and interlayer spacing by replacing (TMA⁺) with Li⁺ cations. By comparing the electrocatalytic HER performance of the resulting V₄C₃T_x, Nb₄C₃T_x, Ta₄C₃T_x MXenes, we demonstrate the role of exposed transition metals (V, Nb, Ta) on the basal plane. Notably, V₄C₃T_x MXenes exhibit the lowest HER overpotential of ~248 mV at 10 mA/cm² under acidic conditions (0.5 M H₂SO₄), surpassing Nb₄C₃T_x (~317 mV at 10 mA/cm²) and Ta₄C₃T_x MXenes (~426 mV at 10 mA/cm²). This improved performance can be attributed to the catalytically active vanadium basal planes in V₄C₃T_x. Our findings provide insight into the design of efficient and cost-effective catalysts through the rational selection of transition metals in MXenes for application as HER catalysts and tailoring electrocatalytic properties of 2D materials for sustainable energy applications.

9:00 AM EL17.05.04

Elucidating the Interactions Between Different Transition Metal Cations and Ti₃C₂T_x MXene Through Intercalation Method for Electrochemical Applications Shianlin Wee, Dario Gomez Vazquez and Maria Lukatskaya; ETH Zurich, Switzerland

MXenes, are a family of two-dimensional (2D) transition metal carbides, nitrides and/or carbonitrides.[1] The intercalation of different metal cations and organic molecules into MXenes for tuning MXenes' electronic and electrochemical properties have been widely reported.[2][3][4] However, transition metals (TMs) which have distinct electrochemical behaviors[5][6] have not been explored in the literature of MXenes' intercalation. Therefore, we herein compared the intercalation effects of different TM cations including (Ni²⁺, Co²⁺, Zn²⁺, Mn²⁺) on Ti₃C₂T_x, for offering a general insight on the influences of multi-valent, redox-active TMs on MXenes. In particular, the changes on the physicochemical and electrochemical properties of MXenes were investigated using different in-situ and ex-situ methods, for a better understanding on the interfacial interactions between TM cations and MXenes in the confined environment of MXenes' multilayer structures. Additionally, we studied the TM-intercalated MXenes in hydrogen evolution reaction to further explore their electrocatalytic performances. This work serves as a foundation for the fine-tuning of MXenes' properties by utilizing a variety of TM cations intercalation for different electrochemical systems.

[1] B. Anasori, M. R. Lukatskaya, Y. Gogotsi, Nature Reviews Materials 2017, 2, 16098.

[2] M. R. Lukatskaya, O. Mashtalir, E. Ren Chang, Y. Dall'Agness, P. Rozier, L. Taberna Pierre, M. Naguib, P. Simon, M.W. Barsoum, Y. Gogotsi, Science 2013, 341, 1502-1505.

[3] J. Li, H. Wang, X. Xiao, Energy & Environmental Materials 2020, 3, 306-322

[4] M. Ghidui, S. Kota, J. Halim, A. W. Sherwood, N. Nedfors, J. Rosen, V. N. Mochalin, M. W. Barsoum, Chemistry of Materials 2017, 29, 1099-1106.

[5] D. Göhl, H. Rueß, M. Pander, A. R. Zeradjanin, K. J. J. Mayrhofer, J. M. Schneider, A. Erbe, M. Ledendecker, Journal of The Electrochemical Society 2020, 167, 021501.

[6] M. Esmailirad, A. Baskin, A. Kondori, A. Sanz-Matias, J. Qian, B. Song, M. Tamadoni Saray, K. Kucuk, A. R. Belmonte, P. N. M. Delgado, J. Park, R. Azari, C. U. Segre, R. Shahbazian-Yassar, D. Prendergast, M. Asadi, Nature Communications 2021, 12, 5067.

9:15 AM EL17.05.05

Electrochemical Charge Storage Process of Ti₃C₂T_x in Neutral Aqueous Electrolyte Chaofan Chen¹, Glenn Quek², Albertde Kogel¹, Ruipeng Li³, Xuehang Wang¹ and Guillermo Carlos Bazan²; ¹Department of Radiation Science and Technology, Delft University of Technology, Netherlands; ²Departments of Chemistry and Chemical & Biomolecular Engineering, National University of Singapore, Singapore; ³Brookhaven National Laboratory, United States

MXenes, a group of two-dimensional transition carbides/nitrides, have demonstrated remarkable performance as pseudocapacitive electrodes, owing to their unique transition metal oxide-like surface, large interlayer spacing and high electrical conductivity^[1]. The charge storage behavior of MXene electrodes are strongly dependent on the interaction between MXene surface chemistry and the electrolyte solution^[2]. In acidic electrolyte, the (de)intercalation of hydrated H⁺ (from) into Ti₃C₂T_x interlayer leads to a reversible conversion between =O and -OH surface groups, which is accompanied by the Ti valence change^[3]. Consequently, Ti₃C₂T_x displays a pseudocapacitive behavior with a mirrored redox peaks emerged in the CV curve. In contrast, Ti₃C₂T_x electrodes typically exhibit EDL-like behavior in neutral aqueous electrolytes, with a rectangular CV and a sloping GCD curve within a narrow (ca. 1.2 V) potential window, resulting in a relatively lower capacitance (80 -120 F g⁻¹)^[4]. Recently, it has been found that the charge storage mechanism of MXene electrodes in different electrolytes can be elucidated through in-

situ UV-Vis spectroscopy^[5].

Engineering the MXene electrode and optimizing the electrolyte composition have the potential to further enhance the pseudocapacitive performance of MXene. An extended potential window of 1.6 V can be obtained by employing water-in-salt electrolyte (WIS). Using WIS electrolyte also induces a novel intercalation process that fully solvated Li⁺ ions intercalate into MXene layer at positive potential^[6]. Partially oxidizing Ti₃C₂T_x in the WIS electrolyte can further enhance the pseudocapacitance in the neutral aqueous electrolyte by activating a new surface redox reaction at <-0.2 V. This is due to the higher valence of Ti (+2.86) in the partially oxidized Ti₃C₂T_x, which is more prone to be reduced than the Ti (+2.43) in the pristine MXene^[7]. In our recent research, we try to improve the electrochemical performance of Ti₃C₂T_x by employing PEG-based Molecular crowding electrolyte (MCE) and designing MXene-based heterostructure. By introducing PEG as the molecular crowding agent into dilute LiTFSI electrolyte, a 25% increase in capacitance (100.8 F g⁻¹) is obtained in MCE. The capacitance increase is possibly due to additional intercalation process of fully-solvated Li⁺, accompanied by the co-insertion of the PEG molecules. Furthermore, We construct a Ti₃C₂@Naphthalenediimide (NDI) heterostructure, in which a n-type conjugated polyelectrolyte is incorporated with Ti₃C₂T_x MXene through a facial self-assemble process. Contributing from both the faradaic reaction from NDI and the pseudocapacitance from MXene, a high specific capacitance of 126.1 F g⁻¹ is obtained in 1 M NH₄Cl electrolyte, which is 1.5 times higher than that of pristine Ti₃C₂T_x. Benefiting from the unique structure, Ti₃C₂@NDI also showed a superior rate performance of 102.8 F g⁻¹ at 10 A g⁻¹ (81% capacitance retention of 0.1 A g⁻¹) and a great cycling stability of 89% capacitance retention upon 10 000 cycles for NH₄⁺ storage.

Reference:

[1]Anasori et al., *Nature Reviews Materials*. **2017**, 2, 16098.

[2]Bergman et al., *Advanced Energy Materials*. **2023**, 202203154.

[3]Shao et al., *ACS Energy Letters*. **2020**, 5, 2873.

[4]Lukatskaya et al., *Science*. **2013**, 341, 1502.

[5]Zhang et al., *Nature Energy*. **2023**, 8, 567.

[6]Wang et al., *ACS Nano*. **2021**, 15, 15274.

[7]Wang et al., *ACS Energy Letters*. **2022**, 7, 30.

9:30 AM *EL17.05.06

Tuning the Electrochemical Response of MXenes Through Cation Intercalation [MariaLukatskaya](#); ETH Zurich, Switzerland

As electronic technology advances, there is an increasing demand for safe and compact energy storage devices with long-lasting performance. Pseudocapacitors offer a promising solution by providing short charging times, ranging from several seconds to minutes, and energy densities comparable to batteries. Pseudocapacitors belong to the subclass of supercapacitors, where capacitance is mediated through fast redox reactions. They have the potential to store at least an order of magnitude more energy compared to typical electrical double-layer capacitors. Common examples of pseudocapacitor materials include transition metal oxides (e.g., RuO₂, MnO₂) and conducting polymers (e.g., polyaniline). However, these materials often suffer from high cost and/or low cycling stability. Consequently, there is an ongoing search for new pseudocapacitive materials, which represents a crucial research direction.

In this talk, I will delve into how the key performance metrics of pseudocapacitors – capacitance and charging rates – can be pushed to the limits in the materials that combine good electrical and ionic conductivities (ensuring fast charge transfer and hence charging rates) with high density of redox-active and ionically accessible sites (enabling high capacitance and charging rates). In particular, the electrochemistry of 2D transition metal carbides (MXenes), with an emphasis on the mechanism of charge storage and factors affecting the overall capacitive response in these materials will be discussed. Moreover, I will discuss the role of cation intercalation in layered MXenes to tune their electrochemical response.

<quillbot-extension-portal></quillbot-extension-portal>

10:00 AMBREAK

SESSION EL17.06: MXenes Chemistry and Electrochemistry

Session Chairs: Majid Beidaghi and Michael Naguib

Tuesday Morning, November 28, 2023

Hynes, Level 2, Room 208

10:30 AM *EL17.06.01

MXene Chemistry and Applications [VadymMochalin](#); Missouri University of Science and Technology, United States

A large family of two-dimensional transition metal carbides and nitrides (MXenes) raises interest for many applications due to their high electrical conductivity, mechanical properties [1], potentially tunable electronic structure [2], nonlinear optical properties [3], and the ability to be manufactured in the thin film state [4]. However, their chemistry that is key to development of these applications, still remains poorly understood [5,6]. In this presentation we will discuss recent progress in understanding fundamental MXene chemistry and harnessing it for suppressing unwanted reactions and prolonging stability of these materials.

For example, suppressing oxidation and hydrolysis at high pH was demonstrated as an effective way to prolong shelf-life and stability of MXene aqueous colloids [7]. Use of polyphosphate also has been shown to improve chemical stability of MXene aqueous colloids [8].

Other selected examples illustrating connections between understanding MXene chemistry and development of their applications will also be considered.

References

1. Y. Li, S. Huang, C. Wei, C. Wu, V. N. Mochalin, *Nature Communications*, 10, 3014 (2019)

2. M. Naguib, V. N. Mochalin, M. W. Barsoum, Y. Gogotsi, *Advanced Materials*, 26(7), 992-1005 (2014)

3. J. Yi, L. Du, J. Li, L. Yang, L. Hu, S. Huang, Y. Dong, L. Miao, S. Wen, V. N. Mochalin, et al., *2D Materials*, 6, 045038 (2019)

4. Y. Dong, S. Chertopalov, K. Maleski, B. Anasori, L. Hu, S. Bhattacharya, A. M. Rao, Y. Gogotsi, V. N. Mochalin, R. Podila, *Advanced Materials*, 30(10), 1705714 (2018)

5. S. Huang, V. N. Mochalin, *Inorganic Chemistry*, 58(3), 1958 (2019)

6. S. Huang, V. N. Mochalin, *ACS Nano* 14(8), 10251-10257 (2020)

7. S. Huang, V. N. Mochalin, *Inorganic Chemistry*, 61(26), 9877 (2022)

8. S. Huang, V. Natu, J. Tao, Y. Xia, M. W. Barsoum, V. N. Mochalin, *Journal of Materials Chemistry A* 10 (41), 22016 (2022)

11:00 AM EL17.06.02

Atomistic Insights into the Degradation Mechanism of Ti₃C₂T_x [ValentinaNesterova](#) and [KonstantinKlyukin](#); Auburn University, United States

Understanding the degradation mechanism at the molecular level is increasingly needed for a variety of clean energy applications, including membranes, batteries, and catalysts. MXenes, a family of 2D transition metal carbides and nitrides, demonstrate outstanding electrochemical performances and intriguing mechanical properties. However, the stability of MXenes remains a concern because of their fast degradation in water solution or air under ambient conditions. The mechanisms responsible for the oxidative degradation of MXenes remain elusive. In this work, we use ab initio molecular dynamics (AIMD) and density functional theory (DFT) simulations to resolve the atomistic mechanism of oxidative degradation of titanium carbide layers in the presence of water molecules and elucidate the role of surface chemistry on its stability. To reveal factors controlling the degradation rate, we correlate activation barriers of oxidation processes to chemical and physical traits of MXene surfaces.

11:15 AM EL17.06.03

Effect of Synthesis Conditions on the Morphology, Stability and Electrochemical Properties of Nb₂CT_x MXenes [YeonjinBaek](#) and Majid Beidaghi; Auburn University, United States

MXenes have gained significant attention in recent years for their unique properties and potential applications. Among several compositions of MXenes synthesized so far, Niobium carbide (Nb₂CT_x) MXene has shown promise for use in batteries, supercapacitors, photocatalysts, and fuel cells. However, despite many studies on the properties of this material, the effect of the synthesis process on the morphology, stability, and electrochemical properties of single-layer Nb₂CT_x MXenes, has not been extensively studied before. In this study, we have explored various etching and delamination processes for Nb₂CT_x and propose an improved synthesis process. Etching of the Nb₂AIC MAX phase was performed in two different etchants and followed

by delamination with TBAOH or TMAOH. Our results show that the synthesis yield is highly dependent on the composition of the etchant. Also, the size and quality of the produced MXene can be tuned by adjusting the etching and delamination conditions. To evaluate the electrochemical properties of Nb_2CT_x synthesized using different methods, free-standing films of the MXene were fabricated and tested as supercapacitor electrodes. These studies also showed the dependence of the electrochemical properties and stability of produced MXenes on the synthesis condition.

11:30 AM *EL17.06.04

Hybrid Organic-Inorganic MXenes Chenkun Zhou, Di Wang, Young-Hwan Kim and Dmitri V. Talapin; University of Chicago, United States

Two-dimensional (2D) transition-metal carbides and nitrides (MXenes) show impressive performance in applications, such as supercapacitors, batteries, electromagnetic interference shielding, or electrocatalysis. These materials combine the electronic and mechanical properties of 2D inorganic crystals with chemically modifiable surfaces, and surface-engineered MXenes represent an ideal platform for fundamental and applied studies of interfaces in 2D functional materials.

The comprehensive understanding of MXene surfaces is required for prescriptive engineering of their physical and chemical properties. We discuss general strategies to install and remove surface groups by performing substitution, reductive elimination and oxidative addition reactions. Successful synthesis of MXenes with oxo-, imido-, thio-, seleno-, or telluro- terminations, as well as bare MXenes (no surface termination), and hybrid organic-inorganic MXenes are demonstrated. The description of MXene surface structure requires a mix of concepts from the fields of coordination chemistry, self-assembled monolayers and surface science. MXene surface groups control biaxial lattice strain, phonon frequencies, electrochemical performance, the strength of electron-phonon coupling, making MXene surfaces not spectators but active contributors to conductivity, superconductivity, and catalytic activity.

SESSION EL17.07: MXenes Applications
Session Chairs: Seon Joon Kim and Maria Lukatskaya
Tuesday Afternoon, November 28, 2023
Hynes, Level 2, Room 208

1:30 PM *EL17.07.01

Bioelectronics and Beyond: MXenes for Sensing, Treating and Restoring Human Health Flavia Vitale; University of Pennsylvania, United States

MXenes have sparked a rapidly growing interest for applications in biomedical research and medicine. Alongside with the remarkable combination of properties and scalable processability, the growing selection of tunable MXene species, and the increasing recognition of their broad biocompatibility are paving the way for the integration of MXenes in high-performance sensing and therapeutic platforms.

In this talk I will first highlight the most recent developments of MXene-based biomedical technologies, particularly in the areas of sensing, therapeutics, and regenerative medicine. Then, I will present our most recent work on $\text{Ti}_3\text{C}_2\text{T}_x$ MXene-based wearable and implantable bioelectronics for recording and stimulating brain and muscle activity. Due to the combination of high conductivity and low electrochemical impedance, these human-scale MXene bioelectronics can establish highly conformable interfaces with the body without the need for any conductive adhesives and gels that are typically required with conventional metal-based electrodes. Furthermore, the low density and low magnetic susceptibility mismatch between $\text{Ti}_3\text{C}_2\text{T}_x$ and biological tissues enable artifact-free clinical imaging with magnetic resonance (MRI) and computed tomography (CT), which is precluded when using metals such as Pt. Finally, we recently demonstrated that $\text{Ti}_3\text{C}_2\text{T}_x$ films and devices can be effectively sterilized with clinical thermal and chemical sterilization processes, without any degradation of their properties and structure. To illustrate the potential of $\text{Ti}_3\text{C}_2\text{T}_x$ MXene bioelectronics, I will review examples of application in cognitive neuroscience research, clinical neurological monitoring, and neuromuscular rehabilitation. In conclusion of the talk, I will discuss the opportunities and challenges for clinical translation and commercialization of MXene-based medical technologies.

2:00 PM EL17.07.02

3D Microporous $\text{Ti}_3\text{C}_2\text{T}_x$ MXene for Electrochemical Sensing of Antibiotics in Tissue Engineered Scaffolds Anand P. Tiwari, Katie Hixon and William J. Scheideler; Dartmouth College, United States

3D continuous mesoscale architectures of nanomaterials provide opportunities to enhance performance and integration of electrochemical biosensors through control over the distribution of active sites and facilitation of ion transport. We present 3D printed microporous electrochemical biosensors integrating biocompatible 2D $\text{Ti}_3\text{C}_2\text{T}_x$ MXenes to monitor antibiotic drug release in tissue engineering scaffolds. The 3D microporous $\text{Ti}_3\text{C}_2\text{T}_x$ MXene is synthesized by a simple deposition of MXene ink on a microscale 3D-printed polymer scaffold coated in conductive ZnO:Al. Due to the microporous hybrid structure of $\text{Ti}_3\text{C}_2\text{T}_x$ MXene, direct electron transfer is facilitated and the 3D biosensors displayed efficient detection of common antibiotics such as gentamicin and vancomycin. The engineered 3D pore structure exposes more electrochemically active surfaces of MXene, resulting in remarkable sensitivity for detecting gentamicin concentrations from 10 nM to 1 mM and vancomycin concentrations from 100 nM to 1 mM, which are 1000 times more sensitive than planar 2D films of MXene. Additionally, this study characterized the suitability of these implantable sensors for bone tissue regeneration applications. Osteoblast-like (MG-63) cells are seeded on the microporous 3D MXene architectures for 3, 5, and 7 days. An increased concentration of cells is noted over the 7 days along both the edges and pores where MXene had been deposited, demonstrating biocompatibility and clinical translation potential. Based on these results, this combination of 3D scaffolds with biocompatible 2D $\text{Ti}_3\text{C}_2\text{T}_x$ MXene materials can provide a platform for mediator-free biosensing, enabling new applications for *in vivo* monitoring of drug elution.

2:15 PM EL17.07.03

MXene-Based Stimuli-Responsive Transdermal Patches for Wound Healing Fateme Fayyazbakhsh, Lev Suliandziga, Vadym Mochalin, Yue-Wern Huang and Ming C. Leu; Missouri University of Science and Technology, United States

MXenes, a recent large family of 2D materials, are now intensely researched for various biomedical applications including drug delivery and release via intercalation/deintercalation mechanisms. Through a unique combination of high hydrophilicity with excellent electrical conductivity and strong photothermal response, MXenes offer unique capabilities to trigger and regulate drug release, while being compatible with hydrogels that are widely used in wound healing. In this talk, we will present our results on MXene-hydrogel stimuli-responsive transdermal patches for alleviating inflammatory response during wound healing. Hydrogel-based transdermal patches (HTPs) can serve as effective drug carriers for localized delivery of various therapeutic agents, while leveraging their inherent healing properties as wound dressings. The incorporation of anti-inflammatory and antibacterial agents empowers the therapeutic activity of HTPs to alleviate pain and combat bacterial infection. However, their application is limited by low stability, inadequate therapeutic effect, and systemic side effects caused by excessive drug release. To address these limitations, we developed novel stimuli-responsive HTPs capable of on-demand drug release. For this development we incorporated a titanium carbide MXene into gelatin-alginate hydrogel mixture. After loading with ibuprofen (IBU), the obtained bioinks were 3D printed and characterized. The drug release was measured after applying electric current to the samples. In addition, we assessed the biocompatibility, cell migration, and *in vitro* wound healing functionality of MXene-HTPs using a scratch test with human dermal fibroblasts, and measured the level of inflammatory markers. We will discuss our results in terms of correlations between the drug release and external stimuli (e.g., applied current), as well as immunomodulatory activity of MXene, which are the two important factors improving the progression of wound care products. Overall, these findings position MXene incorporating hydrogels as promising candidates for alleviating inflammatory response and enabling other external-stimuli responsive functionality in the field of smart wound care.

2:30 PM EL17.07.04

Sustained Superlubricity in Mo_2TiC_2 MXenes Facilitated by Tribocatalytic Reaction at The Sliding Interfaces Sai Varun Sunkara¹, Brian Wyatt², Yuzi Liu¹, Subramanian Sankaranarayanan¹, Babak Anasori², Andreas Rosenkranz³ and Anirudha Sumant¹; ¹Argonne National Laboratory, United States; ²Purdue University, United States; ³University of Chile, Chile

The materials community has witnessed remarkable progress over recent decades in exploring various attractive properties of MXenes due to their excellent, physical, chemical, and mechanical properties. These properties encompass its outstanding physical, chemical, and mechanical attributes, all of which have demonstrated exceptional potential across diverse application domains, ranging from energy storage, and electromagnetic shielding, to advancements in biological and medical technology. Recent interest in exploring their tribological properties is rooted in their layered structure and ability to shear easily coupled with their robust mechanical properties. While numerous studies have been published showcasing MXenes' promise as an additive under lubricated conditions or as a solid lubricant in dry environments, the critical factor of long-term stability as a reliable lubricant in either scenario has remained unproven, thereby constraining its full application potential within the lubrication industry.

In this current work, we study an ordered double transition metal MXene (Mo_2TiC_2) and demonstrate its exceptional tribological performance in dry nitrogen atmosphere using macro-scale pin-on-disc tribo-testing. We demonstrate sustained superlubricity, with a friction coefficient as low as 0.005, persisting over the extensive course of linear sliding, spanning an astonishing distance of 86 kilometers, with no signs of failure and minimal wear rates. We will elucidate the intricate mechanisms governing wear and friction, which underpin such extraordinary

tribological performance. Additionally, we explain the pivotal role played by tribo-catalytic reactions at the sliding interface, which yield a stable, lubricious tribolayer. This milestone achievement represents a game-changer across a spectrum of tribological applications and marks a significant leap forward in the development of innovative solid lubricants based on MXene.

Work performed at the Center for Nanoscale Materials, a U.S. Department of Energy Office of Science User Facility, was supported by the U.S. DOE, Office of Basic Energy Sciences, under Contract No. DE-AC02-06CH11357.

2:45 PM EL17.07.05

Effect of 2D MXenes on The Densification and Stability of Boron Carbide-Ti₃C₂ Composites Nithin Chandran B S^{1,2,3}, Kartik Nemani^{2,1}, Anupma Thakur^{2,1} and Babak Anasori^{1,2}; ¹Purdue University, United States; ²IUPUI, United States; ³Indian Institute of Technology Madras, India

MXenes are explored as additive materials for structural and high-temperature applications due to high temperature stability and two-dimensional (2D) layered morphology. Boron carbide (B₄C) holds significance as a structural ceramic due to its superior hardness (up to 43 GPa) along with low density (2.52 g cm⁻³), and high melting point (2763 °C). However, poor sinterability of B₄C is attributed to the presence of strong covalent bonds between boron and carbon, the presence of nanoscale B₂O₃ on the surface, and low self-diffusion coefficients. Incorporating 2D MXenes in the B₄C matrices can improve the fracture toughness. MXenes' layered morphology combined with colloidal stability due to their high negative zeta potential (-35 to -50 mV) allows additive-free self-assembly on ceramic grains, leading to their uniform distribution in the sintered ceramic composite. In this work, we demonstrate the preparation of green bodies of B₄C with nanometer-thin Ti₃C₂T_x MXene flakes via electrostatic self-assembly. The prepared green bodies of MXene-wrapped B₄C, up to 10 wt.% MXene, are sintered by pressure-assisted spark plasma sintering. We also discuss the effect of MXene flake concentration on the improvement of B₄C sinterability and mechanical properties. Our study presents the first use of MXene in B₄C manufacturing and MXenes effects on the densification and stability of boron carbide sintered ceramics and offers insights into the potential of MXenes as sintering additives in ceramic systems.

3:00 PM BREAK

SESSION EL17.08: MXenes Catalysis and Sensing Applications
Session Chairs: Vadym Mochalin and Ruocun (John) Wang
Tuesday Afternoon, November 28, 2023
Hynes, Level 2, Room 208

3:30 PM *EL17.08.01

Applications of 2D Metal Carbides in Catalysis Yue Wu; Iowa State University, United States

Many novel applications have been discovered for 2D metal carbides (MXenes), among which catalysis is a unique one. Due to their different crystal structures, MXenes behave differently from conventional bulk carbides. In this presentation, we will discuss the metal-support interactions observed in different MXene systems and how they alternate the catalytic reactions, including alkane dehydrogenation, methane coupling, and electrochemical reactions, from both experimental studies and theoretical modelings. These newly-discovered metal-support interactions could enable MXenes as exciting platforms for reactions important to petrochemical industry and low-carbon energy development.

4:00 PM EL17.08.02

Environmentally Stable Organo-MXene Gas Sensors Based on Surface Chemical Functionalization Seon Joon Kim; Korea Institute of Science and Technology, Korea (the Republic of)

The demand for low-power chemical sensing has been increasing due to the emergence of flexible, portable, and wearable devices. To achieve this, two-dimensional (2D) nanomaterials have drawn attention due to their high surface area, and high tunability, and room-temperature operation. Among them, MXenes especially show outstanding performance due to their simultaneous existence of high electrical conductivity and high-density surface functional groups. However, issues such as limited environmental stability need to be addressed for further utilization. Here, we introduce ligand-grafting surface chemical functionalization methods to develop organo-MXene gas sensors that have enhanced environmental stability over pristine MXene gas sensors. Based on the good dispersibility of organo-MXenes in organic solvents, a self-assembly method was designed and employed to fabricate nanometer-scale thin film gas sensors. Gas responses were greatly enhanced compared to that of pristine MXene where the modification of surface tail groups allowed tunable selectivity toward various VOC gases. Furthermore, organo-MXene gas sensors showed good stability in ambient environments for extended periods of time.

4:15 PM EL17.08.03

Three-Dimensional MoS₂/MXene Heterostructure Aerogel for Chemical Gas Sensors with Superior Sensitivity and Stability Hamin Shin¹, Seulgi Kim², Jaewoong Lee¹, Jihan Kim¹, Dongju Lee² and Il-Doo Kim¹; ¹Korea Advanced Institute of Science and Technology, Korea (the Republic of); ²Chungbuk National University, Korea (the Republic of)

The concept of integrating diverse functional 2D materials into a heterostructure provides unparalleled platforms for exploring novel physics not accessible in a single 2D material. Here, physical mixing two 2D materials, MXene and MoS₂, followed by freeze drying is utilized to successfully fabricate a 3D MoS₂/MXene van der Waals heterostructure aerogel. The low temperature synthetic approach effectively suppresses significant oxidation of the Ti₃C₂T_x MXene, and results in a hierarchical, and freestanding 3D heterostructure composed of high-quality MoS₂ and MXene nanosheets. Functionalization of MXene with MoS₂ catalytic layer substantially improves sensitivity and long-term stability toward detection of NO₂ gas, and computational studies are coupled with experimental results to elucidate that the mechanism behind enhancements in the gas sensing properties is effective inhibition of HNO₂ formation on MXene surface, due to the presence of MoS₂. Overall, this study has a great potential for expansion of applicability to other classes of two-dimensional materials as a general synthesis method, thus laying a foundation to be applied in future fields of catalysis and electronics.

4:30 PM EL17.08.04

MOF-MXene Heterostructure for Promising Detection of Asthma Through H₂S Biomarkers Sakshi Kapoor¹, Hilal Ahmad² and J. P. Singh¹; ¹Indian Institute of Technology Delhi, India; ²Jamia Millia Islamia, India

Chronic wheezing and dyspnea episodes, which differ in intensity and frequency from person to person, are hallmarks of asthma. Asthma is thought to have a biomarker called H₂S. Here, a 5 ppb detection limit ultrasensitive chemiresistive H₂S gas sensor based on a MOF-MXene heterostructure has been created. This sensor reveals, pathologically, that the concentration of H₂S in one's exhaled breath steadily rises when asthma is treated. This sensor may be used to monitor the severity of asthma since it can precisely detect this minute concentration fluctuation of H₂S. This sensor may be combined with circuits to create a low-cost, clever, and portable H₂S detecting device. This device can be easily accessed by asthmatic patients and can make asthma severity monitoring simple, especially for young people and the elderly. Nitric oxide (NO), obtained as a biomarker of asthma and utilized in clinical diagnosis, is one effective example. H₂S is also thought to be a biomarker for halitosis, chronic obstructive pulmonary disease, and asthma. A more thorough explanation of the asthma phenotypes may be provided by further research into this substance, which may also result in advancements in the diagnosis and management of this condition. Although H₂S may be found in serum, sputum, and exhaled breath, there is still no consistent standard procedure for analysis. According to reports, the amounts of exhaled H₂S are influenced by airway inflammatory processes. A high-performance H₂S gas sensor is characterized and modelled by fusing the distinctive properties of various materials.

<quillbot-extension-portal></quillbot-extension-portal><quillbot-extension-portal></quillbot-extension-portal>

4:45 PM EL17.08.05

Mxene-Based Engineering for Photoelectrochemical Detection by Combining Nanozyme and Oxygen Reduction Akhilesh B. Ganganboina; National Institute of Materials Sciences, Japan

Efficient photoelectrochemical (PEC) detection requires a deep understanding of the processes involved in generating, separating, and reacting photoinduced carriers at interfaces. However, slow interfacial reactions and the need for appropriate photoactive layers pose significant challenges to constructing advanced PEC platforms. In this study, platinum single-atom catalysts (Pt SACs) were integrated onto CuO₂ and two dimensional Mxene as a proof of concept, amplifying PEC signals by boosting oxygen reduction reactions. As a newly emerging class of 2D materials, Ti₃C₂T_x MXene was used as fantastic support to uniformly anchor Cu₂O nanoparticles due to its electronegative surface. Pt SACs were also shown to exhibit efficient peroxidase-like activity, depressing PEC signals through Pt SACs-mediated enzymatic precipitation reactions. By utilizing the oxygen reduction and peroxidase-like activity of Pt SACs, a robust PEC

sensing platform was successfully constructed for the sensitive detection of SARS-CoV-2. This research provides valuable insights into the use of SACs for sensitive PEC analysis.

SESSION EL17.09: Poster Session II
Session Chairs: Majid Beidaghi, Abdoulaye Djire and Seon Joon Kim
Tuesday Afternoon, November 28, 2023
Hynes, Level 1, Hall A

8:00 PM EL17.09.01

The Adsorption Ability of Urea on Single 3d Metal Doped MXene ($Ti_3C_2T_x$) via DFT Calculations and Experiments Caihong Liang, Zhihao Yen, Teddy Salim and Yeng Ming Lam;
Nanyang Technological University, Singapore

Dialysis is a process used to remove excess urea toxins from the body through adsorption or conversion. Urea adsorption by emergent 2D materials such as MXenes is one probable approach. However, MXenes synthesized by the safer and easier MILD method (MILD $Ti_3C_2T_x$) has lower affinity to urea, which can be improved by surface modifications. Density Functional Theory (DFT) studies indicate that oxygen-terminated $Ti_3C_2O_2$, which is the dominant species on MILD $Ti_3C_2T_x$, have a much better urea adsorption ability when introduced with Cu, Co, and Ni dopants and the corresponding adsorption energy (E_{ads}) are -2.16 eV, -1.91 eV and -1.78 eV respectively. These adsorption energies are much more favourable than the undoped one ($E_{ads} = -0.52$ eV). Experimentally, the adsorption studies found that low concentration of Cu, Co, Ni on $Ti_3C_2T_x$ showed a removal efficiency of 21.9 %, 6.0 % and 0.2 %, respectively, much better than 0 % removal efficiency of unfunctionalized $Ti_3C_2T_x$. Both DFT calculations and experiment showed that various metal functionalized MXenes has similar trend for urea adsorption, highlighting the feasibility of using computational approach to predict urea adsorption and further opening a new promising direction for the urea adsorption.

8:00 PM EL17.09.02

Langmuir-Like Adsorption Behavior of Amine Ligand for Surface Chemistry of MXene Woojae Jeong, Hwansoo Shin and Tae Hee Han; Hanyang University, Korea (the Republic of)

Surface chemistry is important to comprehend the stability of oxidation and dispersion of MXene in different organic media, thereby expanding its potential applications. Amine ligands is a potential candidate to modify the surface of MXene nanosheets due to strong interaction between Amine functionalities and MXene surface. Among those, Oleylamine (OAm) is a promising ligand due to its amine functionalities and commercial availability. The OAm is grafting onto MXene by covalent bonds through nucleophilic reactions and hydrogen bonding at room temperature. Furthermore, the OAm develop monolayer on MXene surface behavior by Langmuir-like adsorption. It is finely confirmed by that the slope decreases as the OAm concentration (C_1) increases in coverage vs C_1 . The monolayer formation occurs in two distinct steps: a lying-down phase followed by an ordered monolayer. The OAm grafted MXene nanosheets (OAM-MX) represent highly stable dispersion in various organic solvents including non-polar solvents, as well as excellent oxidation stability. This be attributed to the hydrophobic properties and steric stabilization induced by the long alkyl chain of OAm on the MXene surface. Moreover, the OAM-MX nanosheets was facially assembled by solution process on the various substrate, demonstrating enhanced coating performance. Therefore, this study provides key comprehension of the adsorption behavior and interaction between amine ligands and MXene nanosheets for the surface chemistry of MXene.

8:00 PM EL17.09.03

High Performance Waste-Based Triboelectric Nanogenerators with Sulfur-Rich Polymer and MXene Sungsu Kim^{1,1}, Woongbi Cho^{1,1}, Hyeonhoo Lee^{1,1}, Minbaek Lee², Tae Hee Han¹ and Jeong Jae Wie^{1,1,1}; ¹Hanyang University, Korea (the Republic of); ²Inha University, Korea (the Republic of)

Recently, we reported utilization of inverse-vulcanized sulfur-rich polymer (SRP) prepared by surplus annually generated 7 million tons during petroleum refining processes, as tribo-negative materials for a triboelectric nanogenerator (TENG). Since the TENG generates power by charge separation on friction surfaces, utilization of fluorine with the highest electronegativity induced excellent electron-withdrawing ability is widely used in the TENG. Previous studies employed F2 gas or fluorine-rich polymers to enhance SRP tribo-negative characteristics. However, F2 is toxic, and the TENG with fluorine-rich polymers requires higher output current to stably operate electronic devices. Herein, we introduce MXene as a filler for the reinforcement of SRP tribo-negative characteristics. MXene is a metallic 2D nanomaterial with a high electronic conductivity and specific surface area. Hence, the inclusion of minute amount of MXene can significantly improve the electric properties of composites. In a same area 12.5 cm²-sized, incorporating 0.4 wt% MXene into the SRP composite in the TENG without using toxic gas had shown output voltage and current 2-fold and 3-fold higher compared to the neat SRP. We believe that the SRP/MXene composites will contribute to the advancement of waste-based and self-powered devices in the form of the TENG.

8:00 PM EL17.09.04

Revolutionizing Greenhouse Gas Monitoring with Layered MXenes: Room-Temperature Chemoresistors Niravkumar J. Joshi, Sachin T. Navale and Albert Romano-Rodriguez; University of Barcelona, Spain

Greenhouse gas (GHG) emissions, particularly carbon dioxide, methane, and nitrous oxide, are the primary cause of global warming and climate change. To effectively monitor the actual impact of emission of these gases, specialized gas measurement systems that are specifically adapted are necessary. Currently, National surveillance agencies rely on highly sensitive, selective, complex, bulky, and expensive systems to monitor the environment. These systems serve as reference units and are only installed in a few specific, mostly fixed, key locations. However, in order to achieve a more comprehensive monitoring approach and develop climate change models, it is essential to have a distributed network of sensing system. This can be achieved through the deployment and connection of numerous gas sensing systems enabled by the Internet of Things (IoT). These devices need to be sensitive, selective, and energy-efficient, although they may have lower accuracy and precision compared to the reference instruments. Existing commercial sensors do not meet all the necessary requirements, highlighting the need for new and enhanced functional nanomaterials and sensors.

The objective of this research is to demonstrate the current state of development regarding advanced miniaturized gas sensing devices for monitoring GHG emissions. For this, we have developed a chemiresistive sensor platform that utilizes a layered structure of 2D MXenes, serving as an advanced sensing platform for detecting GHGs. The layered MXenes were synthesized using a chemical etching method involving a strong HF etchant, resulting in the formation of multilayered $Ti_3C_2T_x$ (MXene) sheets. These MXene sheets were then integrated onto a chip with interdigitated electrodes to form a microsensor. In this way, a low-cost gas-sensitive sensor for methane (CH₄) was developed, which exhibited superior selectivity in front of other gases.

Throughout this research, a comprehensive investigation of the synthesis and of greenhouse gas detection application of these 2D MXenes has been conducted. This study is expected to pave the way for the utilization of a broad range of MXenes as highly sensitive sensors for greenhouse gases.

SESSION EL17.10: MXenes Structures and Properties I
Session Chairs: Babak Anasori and Seon Joon Kim
Wednesday Morning, November 29, 2023
Hynes, Level 2, Room 208

8:00 AM *EL17.10.01

Tailoring MXene Crystal Defects & Surface Terminations for Electronic and Energy Applications Chong Min Koo; Sungkyunkwan University, Korea (the Republic of)

Surface chemistry and defect engineering play a crucial role in determining not only the physicochemical, electrochemical, and optoelectronic properties, but also environment stability and processability of 2D MXene nanomaterials. MXenes, transition metal carbides/carbonitrides/nitrides, are a very large family of 2D materials with the general formula $M_{n+1}X_nT_x$, where M, X, T_x, and n represent transition metal(s), carbon or nitrogen, surface terminal groups such as -OH, -O and -F, and integers ranging from 1 to 4, respectively. MXenes have been attracted in many electronic, electrochemical, and optoelectronic applications, due to their high electronic conductivity, and solution processability. However, achieving high quality MXenes with precise stoichiometry remains a challenge due to difficulties in controlling the oxygen substitution in both the precursors and final MXene products. Furthermore, the presence of complex oxidation states, surface terminal groups, and interactions with the environment pose obstacles to post-surface functionalization of MXenes. As a result, the establishment of robust surface chemistry and defect engineering protocols for MXenes is still in progress, impeding practical applications. This presentation will briefly demonstrate recent our progress in controlling the surface

chemistry and crystal defects of MXenes.

8:30 AM EL17.10.02

The Effect of Carbon Compounds on MXene Surfaces Yusuke Ogawa, Seiji Kawasaki, Yasuaki Okada and Takeshi Torita; Murata Manufacturing Co. Ltd., Japan

MXene can be used in a wide range of material applications because of its diverse material properties, derived from its various compositions and surface termination groups. Surface terminations, such as -F, -O, -OH, are introduced by the etching process, and many works related to surface terminations have already been published. One publication has already explored how surface terminations affect the resulting material properties, as well as how to control surface termination groups.^[1] However, in reality, MXene also captures carbon compounds spontaneously by electrostatic interaction. Therefore, we should also take these factors into account. XPS is a useful method for evaluating surface properties. Generally, we use Ar sputtering to remove contaminants on the sample surface, but sputtering also affects the inherent surface condition. In such case, gas cluster ion beam (GCIB) provides an alternative way to clean the sample surface, while causing less damage.^[2] Accordingly, herein we present on GCIB treatment of MXene samples, and outline property differences before and after carbon compounds are removed from the MXene surface.

References

^[1] James L. Hart, Kanit Hantanasirisakul, Andrew C. Lang, Babak Anasori, David Pinto, Yevheniy Pivak, J. Tijn van Omme, Steven J. May, Yury Gogotsi & Mitra L. Taheri, Nature Communications vol. 10, 2019, 522

^[2] Isao Yamada, Jiro Matsuo, Noriaki Toyoda, Allen Kirkpatrick, Materials science and Engineering, R 34, 2001, 231-295

8:45 AM EL17.10.03

Enhancing Heating Efficiency and Protection of MXene Through Graphene Skin Dongjun Kang and Tae Hee Han; Hanyang University, Korea (the Republic of)

Ti₃C₂T_x MXene has outstanding characteristics of high electrical conductivity and facile processability in benign water solvents, and has been highlighted as a versatile Joule heating material with low-voltage operation with stable heating performance. However, MXene can be easily oxidized in warm and damp environments due to its plentiful hydrophilic functional groups on sheets. In addition, the high convective heat loss from the MXene surface limits their heating efficiency. Therefore, we tailored a multifunctional graphene skin (with a thickness of ~370 nm) for MXene, to protect the venerable surface properties of MXene. Both MXene and graphene layers have tortuous pathways with similar layered structures; however, the water impermeability of graphene was ~70 times higher than that of bare MXene due to narrow d-spacing and the hydrophobic nature of graphene skin. In addition, we found that the heat loss regulation effect of graphene skin increased the heating efficiency, indicating that the graphene skin is promising for developing adaptive heating materials. Our research has inspired a new hybrid skin strategy that exploits the full potential of materials for developing functional coatings for various applications.

9:00 AM EL17.10.04

Hybrid MXene-Polydopamine Nanocomposites for Targeted and Effective Photothermal Therapy Igor Iatsunskiy¹, Daniel Aguilar-Ferrer¹, Maksym Pogorielov^{2,3}, Oleksiy Gogotsi⁴ and Emerson Coy¹; ¹Adam Mickiewicz University, Poland; ²University of Latvia, Latvia; ³Sumy State University, Ukraine; ⁴Materials Research Center, Ukraine

Hybrid MXene-Polydopamine (PDA) nanocomposites have emerged as a promising targeted and effective photothermal therapy (PTT) platform. PTT utilizes light-absorbing materials to convert light energy into heat, resulting in localized hyperthermia that selectively damages cancer cells. However, challenges such as limited photothermal conversion efficiency, inadequate tumor targeting, and potential side effects hinder the clinical translation of PTT.

MXenes, a class of two-dimensional transition metal carbides/nitrides, possess exceptional optical absorption properties in the near-infrared (NIR) region, where biological tissues exhibit maximum transparency. The combination of MXenes with PDA offers synergistic advantages for enhanced PTT. MXenes serve as efficient photothermal agents, while PDA provides a versatile coating that promotes biocompatibility and allows surface functionalization for targeted therapy.

The hybrid MXene-PDA nanocomposites exhibit excellent photothermal conversion efficiency due to the strong light absorption of MXenes and efficient heat transfer facilitated by the PDA coating. The nanocomposites can be easily functionalized by targeting ligands or biomolecules, enabling selective accumulation and internalization in cancer cells. Moreover, the MXene-PDA nanocomposites can be further engineered to release therapeutic agents, such as chemotherapy drugs, in response to the photothermal effect, achieving combined photothermal-chemotherapy treatment.

This research highlights experimental results in developing MXene-PDA nanocomposites for targeted and effective PTT. The synthesis methods employed to fabricate the nanocomposites, including surface modification and functionalization, are discussed, along with their photothermal conversion efficiency and biocompatibility. We explored the effect of PDA layer thickness over MXene flakes on PTT. Antibodies for various types of cancers were used as targeting ligands. We demonstrated that the hybrid MXene-PDA nanocomposites are promising to advance PTT as a cancer treatment modality. Their unique properties, such as high photothermal conversion efficiency and surface functionalization capabilities, make them attractive candidates for targeted therapy.

9:15 AM EL17.10.05

Electrochemically Modulated Interaction of MXenes with Microwaves Danzhen Zhang, Meikang Han, Christopher E. Shuck, Bernard McBride, Teng Zhang, Ruocun (John) Wang, Kateryna Shevchuk and Yury Gogotsi; Drexel University, United States

Controlling the reflection and absorption of incident electromagnetic waves at gigahertz frequencies in thin films is important for protecting electronics and humans. The ability to dynamically depress electromagnetic wave jamming is significant for enabling communication while protecting electronics. However, conventional electromagnetic interference (EMI) shielding materials don't offer this capability. MXenes, as a large family of two-dimensional transition metal carbides and nitrides, have shown a broad range of EMI shielding performance as well as different energy storage mechanisms from electric-double-layer capacitance to pseudocapacitive behavior. Herein, we report a method for active control of electromagnetic wave interactions with various MXene films, including Ti₃C₂T_x, Ti₂CT_x, V₂CT_x, V₄C₃T_x and Nb₄C₃T_x, leading to EMI shields with unprecedented bidirectional modulation of shielding capability. The reversible tunability of EMI shielding effectiveness was achieved by electrochemically driven ion insertion/desertion and charge transfer in MXene layers with different electrolytes, accompanied by expansion and shrinkage of layer spacing, as well as a change in the oxidation state of the transition metal. An EMI shielding 'switch' was demonstrated through the electrochemical oxidation of MXene films. Our results offer opportunities to develop smart EMI protection with active modulation, which is different from conventional 'static' shielding and can adapt to demanding environments.

9:30 AM *EL17.10.06

Enhancing MXene's Heating Functionality Through Surface Modification Tae Hee Han; Hanyang University, Korea (the Republic of)

MXenes are a class of two-dimensional materials with potential applications in fields such as thermal management and high-temperature materials. In this talk, I focus on two key aspects: the thermal evolution of Ti₃C₂T_x MXene during annealing and the grafting behavior of amine ligands for MXene surface modification. (1) The thermal decomposition behavior of MXene is explored using X-ray photoelectron spectroscopy (XPS) and two-dimensional correlation spectroscopy (2D-COS), providing insights into its structural changes, providing practical information for thermal applications of MXene. (2) Surface modification strategies are employed to enhance MXene's stability and dispersibility. Oleylamine (OAm) is grafted onto MXene nanosheets, resulting in improved oxidation and dispersion stability. The modified MXene exhibits excellent solution processability and coating performance. Additionally, the potential of OAm-MX as a heating element is investigated, leading to the development of a scalable electrothermal heating membrane with high efficiency. These advancements broaden the applications of MXene in thermal management and water desalination.

10:00 AM BREAK

SESSION EL17.11: MXenes Electrochemical and Optical Properties II

Session Chairs: Majid Beidaghi and Ruocun (John) Wang

Wednesday Morning, November 29, 2023

Hynes, Level 2, Room 208

10:30 AM *EL17.11.01

Plasmonic Properties of 2D MXenes Sarah B. King¹, Joseph Spellberg¹, Janek Rieger¹, Calvin Raab¹, Francisco Lagunas², Robert F. Klie², Di Wang¹, Dmitri V. Talapin¹ and Jordan A.

Despite their tremendous potential as plasmonic materials because of their 2D metallic properties, very little is known about the fundamental plasmonic resonances of MXenes. This is primarily due to irregularity in plasmonic responses from mixed surface terminations and varying material shape and thickness. In this talk I will discuss experimental methods we are using in my group to probe the nanoscale plasmonic response of MXenes, both traditional mixed-terminated $Ti_3C_2T_x$ as well as singly terminated MXenes synthesized by both CVD and molten salt synthesis, Ti_2CCl_2 and $Ti_3C_2Cl_2$. Leveraging the time-resolution and spatial-resolution of time-resolved photoemission electron microscopy we are investigating the evolution of plasmonic fields in MXenes in space and time. Using the (MAC)-STEM/EELS facility at ORNL we can directly image energy-resolved plasmonic resonances of MXenes, where we find that surface oxidation substantially decreases the plasmonic response of $Ti_3C_2Cl_2$. Together our experiments highlight the variation in nanoscale plasmonic properties of MXenes and opportunities for control.

11:00 AM *EL17.11.02

Ultrafast Photoexcitations in 2D MXenes Lyubov V. Titova; Worcester Polytechnic Institute, United States

MXenes are 2D transition metal carbides and nitrides with electronic properties that can be tuned by their chemistry and structure. Metallic-like conductivity, flexibility, high optical damage threshold and ease of processing owing to their hydrophilicity, make MXenes candidates for a host of electronic and optical applications. We use ultrafast optical and THz spectroscopic techniques to investigate the nature and behavior of photoexcitations in MXenes of different chemistries. We show that electronic and optical properties of MXenes can be engineered by choices of the transition metals and their order as well as by controlling the intercalants in the interlayer gaps [1,2]. Furthermore, we demonstrate that MXenes with high free carrier density show promise as polarizers and tunable electromagnetic interference shields in the THz range [3,4].

[1] G. Li, V. Natu, T. Shi, M.W. Barsoum, L.V. Titova, "Two-Dimensional MXenes $Mo_2Ti_2C_3T_z$ and $Mo_2TiC_2T_z$: Microscopic Conductivity and Dynamics of Photoexcited Carriers," *ACS Applied Energy Materials* 3, 1530-1539 (2020).

[2] E. Colin Ulloa, A. Fitzgerald, K. Montazeri, J. Mann, V. Natu, K. Ngo, J. Uzarski, M.W. Barsoum, L.V. Titova, "Ultrafast Spectroscopy of Plasmons and Free Carriers in 2D MXenes," *Adv. Materials* 35, 2208659 (2023).

[3] G. Li, N. Amer, H.A. Hafez, S. Huang, D. Turchinovich, V.N. Mochalin, F.A. Hegmann, L.V. Titova, "Dynamical Control over Terahertz Electromagnetic Interference Shielding with 2D $Ti_3C_2T_y$ MXene by Ultrafast Optical Pulses," *Nano Lett.* 20, 636-643 (2020).

[4] G. Li, K. Montazeri, M.K. Ismail, M.W. Barsoum, B. Nabet, L.V. Titova, "Terahertz Polarizers Based on 2D $Ti_3C_2T_z$ MXene: Spin Cast from Aqueous Suspensions," *Adv. Photonics Research*, 2000084 (2020).

11:30 AM EL17.11.03

Stability of Pseudocapacitive Energy Storage in $Ti_3C_2T_x$ MXene over Wide Temperature Range Ruocun Wang, Mark Anayee, Teng Zhang, Yuan Zhang, Mikhail Shekhirev, Kateryna Shevchuk and Yury Gogotsi; Drexel University, United States

Pseudocapacitors have the potential to achieve high energy and high power density simultaneously, a holy grail for electrochemical energy storage. However, one obstacle facing pseudocapacitors is their shorter lifetime compared to commercial supercapacitors using the double-layer charge storage mechanism. In MXene-based pseudocapacitors, this concern is pronounced particularly at high temperatures due to the limited stability of the active material in contact with aqueous solutions, which can lead to oxidation and hydrolysis. This work shows that $Ti_3C_2T_x$ MXene thin-film electrodes in 5 M H_2SO_4 possess excellent rate capabilities from -50 °C to 100 °C but also a sufficient lifetime at 70 °C using a float test holding at -0.9 V vs. Hg/Hg_2SO_4 reference electrode. Post-mortem characterization using X-ray photoelectron spectroscopy, Raman spectroscopy, and scanning electron microscopy with energy-dispersive X-ray spectroscopy showed no signs of oxidation in the bulk of the film. This work suggests sufficient electrochemical stability of $Ti_3C_2T_x$ MXene as a negative electrode in protic aqueous electrolytes across a wide temperature range, making it promising for pseudocapacitor energy storage.

SESSION EL17.12: MXenes Structures and Properties II

Session Chairs: Abdoulaye Djire and Seon Joon Kim

Wednesday Afternoon, November 29, 2023

Hynes, Level 2, Room 208

1:45 PM *EL17.12.01

High-Temperature Stability and Phase Transformation of 2D $Ti_3C_2T_x$ and $Mo_2TiC_2T_x$ MXenes Brian Wyatt¹, Kartik Nemani¹, Matthew Boebinger², Raymond R. Unocic² and Babak Anasori¹; ¹Purdue University, United States; ²Oak Ridge National Laboratory, United States

2D MXenes have a wide array of impressive properties due to their inherent transition metal carbide cores with abundant surface functionalities. While MXenes can be rapidly oxidized in air at high temperatures, they can be transformed into ultra-high temperature carbides when annealed under an inert atmosphere or vacuum. By annealing stacks of 2D MXene flakes, we can fabricate refractory carbides with controlled morphologies and crystal orientations. In this talk, we present our current understanding of the phase transformation of different MXenes, including $Ti_3C_2T_x$ and $Mo_2TiC_2T_x$, by annealing them in the 600 °C to 2000 °C range under argon. We used a combination of ex-situ and in-situ characterization techniques and identified the effect of defects, such as vacancies and cation decorations, on phase stability and transformation of MXenes to refractory carbides. Our results suggest that MXenes can be used as nanosized building blocks for ultra-high temperature coatings or ceramic composite additives.

2:15 PM EL17.12.02

Prediction of Stable Titanium Carbonitride Alloy MXenes using a Cluster Expansion Approach Krishnamohan Thekkepat^{1,2,3} and Seung-Cheol Lee^{1,2,3}; ¹Korea Institute of Science and Technology, Korea (the Republic of); ²KIST School, Korea University of Science and Technology, Korea (the Republic of); ³Indo-Korea Science and Technology Center, India

MXenes are the largest and rapidly growing class of 2D materials with a general chemical formula $M_{N+1}X_NT_x$ where N=1,2 or 3 represents the number of layers; M is a transition metal; X is either Carbon or Nitrogen; and T represents surface terminations. Over the last decade since they were first synthesized, several different MXenes have reported with different transition metals, thickness and surface terminations. They exhibit a versatile and distinct set of properties ranging from high strength and stiffness, high electrical conductivity, redox active surface sites. These properties make them stand out among other 2D materials and make them promising candidates in energy storage, wireless communications, electrocatalysis and gas sensing applications.¹ Moreover, these properties can be tuned by forming alloys of transition metal elements at the M site or by changing the surface terminations as demonstrated in various experimental and theoretical reports.^{2,3,4} However, very little attention has been given to carbonitride alloys, although they have shown outstanding promise, especially in wireless communications.⁵ MXenes are synthesized from precursor MAX phases. They are layered hexagonal ternary ceramics formed by stacking MXenes, with a layer of A group metals (usually Al) in between. MXenes are separated from MAX phases by selectively etching out the A layers. Hence stability of MAX phases is very important for the synthesis of MXenes.

In this work, we carried out a comprehensive study of the phase stability of 3 types of titanium carbonitride MXenes $Ti_2(C,N)$, $Ti_3(C,N)_2$ and $Ti_4(C,N)_3$ and their corresponding Al based MAX phase precursors $Ti_3Al(C,N)$, $Ti_4Al(C,N)_2$ and $Ti_5Al(C,N)_3$. We train cluster expansion Hamiltonians for each of the pseudo-binary alloys using state-of-the-art machine learning algorithms implemented in the LACOS package developed in-house. These Hamiltonians are then used to search for low energy stable structures from among thousands of possible carbon/nitrogen ordered configurations. Temperature and composition dependent ordering behaviour and phase stability is also assessed using Monte Carlo simulations sampled with the cluster expansion Hamiltonians. We theoretically predict 3 new types of stable ordered titanium carbonitride MAX phases, $Ti_2Al(C_{1-x}N_x)$, $Ti_3Al(C_{1-x}N_x)_2$ and $Ti_4Al(C_{1-x}N_x)_3$ which have not been reported previously. Additionally, we predict new MXenes with different layer thicknesses and nitrogen compositions that are synthesizable from these MAX phases. We also find stable MAX phases consisting of 2 different MXene layers with different atomic arrangements and nitrogen compositions. To aid experimental efforts to synthesize and characterize these new MXenes, we checked the effect of surface terminations on their stability and carried out lattice dynamics calculations to identify Raman active vibration modes. This is the first comprehensive study of Titanium carbonitride MXene alloys and their synthesizability. Identifying a new family of alloys of varying X-site composition would open up new opportunities to further fine tune properties for promising applications.

References

- Gogotsi, Y., & Anasori, B. *ACS Nano*, 13(8), 8491–8494.
- Tan, T. L., Jin, H. M., Sullivan, M. B., Anasori, B., & Gogotsi, Y. *ACS Nano*, 11(5), 4407–4418
- Nemani, S. K., Zhang, B., Wyatt, B. C., Hood, Z. D., Manna, S., Khaledialidusti, R., Hong, W., Sternberg, M. G., Sankaranarayanan, S. K. R. S., & Anasori, B. *ACS Nano*, 15(8),

2:30 PMBREAK**SESSION EL17.13: MXenes Structures and Properties III**

Session Chairs: Majid Beidaghi and Anupma Thakur

Wednesday Afternoon, November 29, 2023

Hynes, Level 2, Room 208

3:30 PM *EL17.13.01**Electroactive Soft Actuators Based on MXene-MOF Nanoarchitectures** [IkkwonOh](#); Korea Advanced Institute of Science and Technology, Korea (the Republic of)

Electro-ionic soft actuators, capable of continuous deformations replacing non-compliant rigid mechanical components, attract increasing interest in the field of next-generation metaverse interfaces and soft robotics. Here, we report a novel MXene ($\text{Ti}_3\text{C}_2\text{T}_x$) electrode anchoring manganese-based 1,3,5-benzenetricarboxylate metal-organic framework (MnBTC) for ultrastable electro-ionic artificial muscles. By a facile supramolecular self-assembly, the $\text{Ti}_3\text{C}_2\text{T}_x$ -MnBTC hybrid nanoarchitecture forms coordinate bond, hydrogen bond, and hydrophilic interaction with the conducting polymer of poly(3,4-ethylenedioxythiophene) polystyrene sulfonate (PEDOT:PSS), resulting in a mechanically flexible and electro-ionically active electrode. The superior electrical and electrochemical performances of the electrode stem from the synergistic effects between intrinsically hierarchical nanoarchitecture of MnBTC and rapid electron transport behavior of MXene, leading to fast diffusion and accommodation of ions in the ion-exchangeable membrane. The developed artificial muscle based on $\text{Ti}_3\text{C}_2\text{T}_x$ -MnBTC is found to exhibit high bending displacement (12.5 mm) and ultrafast response time (0.77 s) under a low driving voltage (0.5V), along with wide frequency response (0.1 to 10 Hz) and exceptional stability (98% retention at 43,200 s) without any distortion of actuation performance. Furthermore, the designed electro-active artificial muscle was successfully used to demonstrate mimicry of eye motions including eyelid blinking and eyeball movement in a doll.

4:00 PM EL17.13.02**Salt-Assisted Assembly of $\text{Ti}_3\text{C}_2\text{T}_x$ Nanosheets on Arbitrary Polymers** [LiangZhao](#)¹, [LingyiBi](#)², [JiayueHu](#)³, [GuanhuiGao](#)⁴, [DanZhenZhang](#)², [YunLi](#)¹, [AidanFlynn](#)¹, [Ruocun \(John\)Wang](#)², [LingLiu](#)³, [YuryGogotsi](#)² and [BoLi](#)¹; ¹Hybrid Nano-Architectures and Advanced Manufacturing Laboratory, United States; ²A.J. Drexel Nanomaterials Institute, Drexel University, United States; ³Temple University, United States; ⁴Shared Equipment Authority, Rice University, United States

MXenes are promising materials for next-generation flexible electronics and wearable systems due to their excellent conductivity, low infrared emissivity, and high mechanical properties. However, in a solution-based assembly process, hydrophilic MXenes are not compatible with many polymers, especially some high-performance polymers with inert and/or hydrophobic surfaces, such as Kevlar. Unlike many harsh surface treatment methods that induce dangling bonds on the polymer surface, we proposed a universal solution-processed salt-assisted assembly (SAA) strategy that enables ultra-thin and uniform $\text{Ti}_3\text{C}_2\text{T}_x$ MXene coatings with high conductivity on diverse polymers without their modification. The salt added to the MXene aqueous solution neutralizes the charge, coagulates the colloid, and deposits MXene aggregates, leading to the ultrafast assembly of MXene from the solution on arbitrary polymer substrates. A library of salts has been demonstrated to be effective. Importantly, our method enables $\text{Ti}_3\text{C}_2\text{T}_x$ assembly on high-performance thermally stable polymers such as Kevlar fabric. This SAA strategy may significantly broaden the applications of MXene coatings.

4:15 PM EL17.13.03**Metal Ion-Driven Gelation in MXenes for Multiproperty and Multifunctional Hydrogels and Aerogels** [StefanoIppolito](#) and [YuryGogotsi](#); Drexel University - Drexel Nanomaterials Institute, United States

To date, MXenes include over fifty different structures and compositions, with more than a hundred compositions predicted computationally (more than a thousand if surface terminations are also taken into account), being the largest known family of 2D materials. Owing to their extremely versatile structural and chemical composition, as well as surface chemistry, MXenes are one-of-a-kind materials in many research fields, embodying a true revolution in materials science. They introduce a large number of 2D building blocks in materials science, providing an exciting and wide-ranging portfolio of physicochemical properties and promoting the production of several MXenes-based hybrid systems for numerous applications. Here, we will discuss the production of all-MXene hydrogels and aerogels, where the gelation process is induced by metal ions. Taking advantage of the coordination chemistry between -OH groups on the surface of MXene flakes (resulting from the wet chemical etching steps) and metal ions, the gelation (in aqueous environment) is very fast (< 5 min) and the physicochemical properties of the resulting hybrid systems are strongly related to the nature of the MXene/metal ion dyad. Rheological measurements show a strong relationship between the metal ion and the loss tangent $\tan\delta$ (equal to the ratio between loss Modulus and storage Modulus, namely viscous modulus and elastic modulus) of the related hydrogel, where the main parameter seems to be represented by the charge density of the selected ion. Such a dependence is also observed in the surface area of corresponding aerogels (prepared from hydrogel by means of freeze-drying), where metal ions with higher charge density return lower surface area, glimpsing the chance to tune the latter parameter based on the envisaged final applications. In this regard, pore shape and aerogel structure are strongly affected by the chemical nature of the metal ions too, as a result of the different coordination geometry. Considering the extremely high versatility of such all-MXene hydrogels and aerogels (in terms of chemical and structural composition, as well as physicochemical properties), many different applications are being tested. For instance, the different and tunable electrostatic behavior of MXene aerogels could result crucial to produce gas and/or particle capture and sensing systems, whose regeneration *via* Joule heating might be possible because of their high electrical conductivity and versatile thermal properties. Also, the metal ions trapped within the MXene porous structure can be converted to metal clusters by simple thermal annealing (performed at 300°C, under Ar/H₂), allowing the formation of ferromagnetic particles for electromagnetic sensing and other related applications. Moreover, due to their tunable porosity, mechanical properties, and composition, MXene aerogels are being tested for acoustic insulation/damping and sensing as well. Finally, thanks to the abovementioned gelation process, MXene hydrogels and aerogels can be shaped in many forms, including fibers that might be use for bioelectronics and sensing. Finally, this versatile approach can be employed for several metal ions and MXene structures, leading to the production of hybrid systems with tunable properties according to envisaged applications.

4:30 PM EL17.13.04**Developing Vitrimer-MXene Laminated Sheets for Stimuli-Responsive Coatings and Improved Composite Functionality** [AbigailA. Advincula](#)^{1,2}, [JustinBrackenridge](#)^{3,1}, [PhilipBarnett](#)⁴, [ChristopherMuratore](#)³, [MadelineBuxton](#)⁵, [VladimirTsukruk](#)⁵, [YuryGogotsi](#)⁶ and [DhritiNepal](#)¹; ¹Air Force Research Laboratory, United States; ²ARCTOS, United States; ³University of Dayton, United States; ⁴University of Tennessee Knoxville, United States; ⁵Georgia Institute of Technology, United States; ⁶Drexel University, United States

Organic-inorganic hybrid structures found in nature, e.g., nacre (“mother-of-pearl”), are often remarkably tough and exhibit multi-functional properties due to highly ordered arrangements of organic and inorganic components in such structures at the nanometer-to-micron length scale. Inspired by these hierarchical biological structures, this work details our efforts to fabricate a hybrid composite of ordered, alternating layers of organic vitrimer polymer and inorganic MXenes. Vitrimers, as a new class of polymers, ideally exhibit thermoset-like behavior at lower temperatures and thermoplastic-like reformability at higher temperatures due to their permanent yet dynamic polymer networks. MXenes, as a class of inorganic two-dimensional (2D) transition metal carbides and nitrides, exhibit excellent metallic conductivity, good transparency in the visible wavelength range, and high photon-to-phonon conversion efficiency.

In this work, we demonstrate the fabrication of highly ordered, ultra-thin (nearly single to a few layers) MXene films onto thin, free-standing sheets of vitrimer, yielding electrically conductive, highly transmissive vitrimer-MXene sheets for self-healing coatings and multi-functional composites. Large area (20 x 20 cm), thin (<65 μm) free-standing vitrimer sheets are first obtained utilizing industrially-relevant compression molding techniques. Thermomechanical testing (TGA, DSC, DMA, TMA, micro-indentation) indicates excellent spot-to-spot consistency in the fabricated sheets. Subsequently, a thin film of MXene is deposited onto the vitrimer sheet surface using an advanced deposition technique that leverages Rayleigh-Benard convection and the Marangoni effect. Surface morphology and mechanical properties of the vitrimer-MXene sheets are investigated at different length scales using micro-indentation testing and quantitative nanomechanical (QNM) analysis. UV-vis measurements and electrical conductivity measurements additionally indicate reasonably good transparency (>75 % T in the visible spectrum) and electrical conductivity values (~100 S/cm) for the vitrimer-MXene layers. Self-healing mechanisms of the vitrimer-MXene sheets in response to light are demonstrated, leveraging the high photon-to-phonon conversion efficiency of MXene. Finally, compression molding of multiple individual MXene-coated vitrimer layers together yields a hybrid composite with alternating ordered layers of vitrimer and MXene. DMA and tensile testing are subsequently used to evaluate modulus, creep resistance, and toughness. This work presents a novel approach to accessing composites with ordered layers of vitrimer and MXene, techniques useful towards further enhancing vitrimer functionality towards structurally robust electronic applications.

4:45 PM EL17.13.05

Ti₃C₂T_x MXene for Enhancing Hydrogel Adhesion and Structural IntegrityElham (Ellie)Jafarigol and NaderTaheri-Qazvini; University of South Carolina, United States

Self-adhesive hydrogels are lauded for their tunability and ability to stick to a range of surfaces without needing extra adhesives, making them highly promising for tissue engineering and regenerative medicine. However, their relatively weak adhesion limits their application in load-bearing uses. This study aims to address this limitation by integrating Ti₃C₂T_x MXene, a two-dimensional nanomaterial recognized for its exceptional mechanical properties and conductivity, to improve hydrogel flexibility and adhesion. We utilized a simple synthesis process to create MXene-based hydrogels at different concentrations. The results revealed substantial enhancements in the mechanical strength and interfacial toughness as the MXene concentration increased. Impressively, the molecular interactions of MXene within the hydrogel network resulted in high stretchability, reaching up to 1600% of their initial value. The inclusion of MXene also shifted the bond fracture mechanism from adhesion failure to cohesion failure. This shift confirmed the increased structural integrity and crosslinking density. With excellent extrudability and shape fidelity, these MXene-based hydrogels are ideally suited for 3D printing applications. Overall, introducing MXene into hydrogels is a promising strategy for improving their robustness and self-adhesiveness, while maintaining their injectability. This advancement holds significant advantages for biofabrication and biomedical engineering.

KEYWORDS: MXene, hydrogels, adhesion, cohesion failure, injectability, flexibility

SESSION EL17.14: MXenes Structures and Properties IV

Session Chairs: Abdoulaye Djire and Ruocun (John) Wang

Thursday Morning, November 30, 2023

Hynes, Level 2, Room 208

8:00 AM *EL17.14.01

MXetronics: Integrated Electronics using MXenesHusamN. Alshareef¹, XiangmingXu¹, TianchaoGuo¹, MrinalK. Hota¹ and HalaA. Al-Jawhari²; ¹King Abdullah University of Science and Technology, Saudi Arabia; ²King Abdulaziz University, Saudi Arabia

This talk will focus on MXenes and their development for integrated electronic device applications. MXenes can be considered as 2D metal contacts with tunable conductivity and tunable work function which makes them in principle suitable for a variety of electronic devices. To realize electronic devices, we have been developing deposition processes, transfer techniques, interface engineering, surface functionalization, photolithographic and e-beam patterning, wet and plasma etching of MXenes. In this talk, I will discuss the various aspects of device fabrication methods to integrate MXenes in several types of electronic devices. The benefits and challenges of using MXenes in each device type will be discussed, with particular focus on the role of interface. Example devices that will be discussed include using MXenes as electrical contacts in thin-film electronics, quantum dot electronics, CMOS devices, GaN high electron mobility transistors (HEMT), memristors, and solar cells. We show that the device performance strongly depends on the quality of the interface between MXene and the semiconductor material, whose control is critical for achieving good device performance. We have also integrated MXene films as active materials for photodevices, photothermal devices, and sensors.

8:30 AM EL17.14.02

Structural Strategies of MXene-Based Materials for Thermoconductive Electromagnetic Interference Shielding Materials with Excellent Mechanical FlexibilityCanhM. Vu; University of Chicago, United States

MXenes, which are a type of 2D transition metal carbides and nitrides, have shown great potential as electromagnetic interference (EMI) shielding materials owing to their properties of electrical conductivity, low density, and flexibility. However, the weak interfacial interaction and the low thermal conductivity of MXenes resulted in poor mechanical flexibility and heat-dissipating capability. In this study, we developed structural strategies of MXenes-based carbon nanomaterials to fabricate MXenes films with enhanced mechanical strength, electromagnetic interference (EMI) shielding, and thermal conductivity properties. Compared to MXene films, the resulting hybrid MXenes films exhibited significantly improved mechanical strength of over 270 MPa, a toughness of 5 MJ m⁻³, EMI shielding effectiveness of 70 dB, and an ultrahigh in-plane thermal conductivity of 110 W m⁻¹ K⁻¹. This study presents a promising methodology for the development of high-performance materials that exhibit mechanical flexibility, electrical conductivity, electromagnetic interference shielding, and thermal conductivity properties.

8:45 AM EL17.14.03

Development of Polymeric/MXene Composites Towards 3D Printable ElectronicsAlejandraSalas Chavez¹, IgnazioRoppolo¹, MatteoCocuzza¹, HannaPazniak², JesusGonzalez-Julian³, StefanoBianco¹, JuliaAmici¹ and ThierryOuisse²; ¹Politecnico di Torino, Italy; ²Institut Polytechnique de Grenoble, France; ³RWTH Aachen University, Germany

[Accepted Manuscript]

3D printing is an emerging technology for many applications, including electronics. On the other hand, to gather the applications' requirements with the possibility to produce complex 3-dimensional structures, the development of novel 3D printable materials is necessary. In this context, we studied the synthesis of 3D printable photocurable resins embedding Ti₃C₂T_x-MXenes, a class of 2D layered materials with outstanding electrical and electronic properties.

Starting from the pioneering works of Y. Gogotsi and M.W. Barsoum, MXenes envisage promising performances in different fields like energy storage[1], electromagnetic shielding[2], photodetectors[3], sensors[4] and electrocatalysis[5]. Nevertheless, their translation to devices nowadays is mainly limited to 2D configuration or conventional production processes.

Herein the motivation for this work stands for the development of stable polymeric inks suitable for Digital Light Processing (DLP) 3D printing technology using Ti₃C₂T_x-MXenes as functional fillers. Those were successfully synthesized using Ti₃AlC₂ as a MAX phase precursor etched by a strong acid (hydrofluoric acid- HF) and using tetrabutylammonium hydroxide (TBAOH) as an intercalator, providing a few layered flakes presentation. Then, employed to fabricate complex 3D composite structures with high printing fidelity. To enhance the material's electrical conductivity, annealing treatments have been performed, followed by a complete characterization of the so obtained. The results show that objects with improved electrical conductivity have been successfully obtained. To this end, this achievement would open new perspectives towards developing complex 3-dimensional electronic applications.

References:

- [1] Shanto MAH, Chowdhury MI, Antu AB, Niloy NR, Alam N, Ullah MA, et al. MXene based Heterostructures for electrode materials of Batteries: A Review. IOP Conf Ser: Mater Sci Eng. 2022;1225(1):012018.
- [2] Wan H, Liu N, Tang J, Wen Q, Xiao X. Substrate-Independent Ti₃C₂T_x MXene Waterborne Paint for Terahertz Absorption and Shielding. ACS Nano. 2021.
- [3] Tao N, Zhang D, Li X, Lou D, Sun X, Wei C, et al. Near-infrared light-responsive hydrogels via peroxide-decorated MXene-initiated polymerization. Chem Sci. 2019;10(46):10765-71.
- [4] Chia HL, Mayorga-Martinez CC, Antonatos N, Sofer Z, Gonzalez-Julian JJ, Webster RD, et al. MXene Titanium Carbide-based Biosensor: Strong Dependence of Exfoliation Method on Performance. Anal Chem. 2020;92(3):2452-9.
- [5] Liu H-J, Dong B. Recent advances and prospects of MXene-based materials for electrocatalysis and energy storage. Mater Today Phys. 2021;20.

9:00 AM EL17.14.04

MXene and Their Surface Functionalization for the Development of Functional MXene Organic InksTae YunKo; Korea Institute of Science and Technology, Korea (the Republic of)

Due to their unique metallic conductivity, transparency, and outstanding solution processability in water, MXenes have been attracted to many potential applications such as EMI shielding, energy storage, and electronic applications. However, oxidation instability of aqueous MXene dispersions and poor dispersion stability in organic solvents prevent the utility of MXenes in potential applications. Surface functionalization of MXene is critical for controlling the dispersion system, surface chemistry, processing, physicochemical properties, and applications. Herein, we designed and conceptualized various organic ligands that can improve oxidation stability and organic dispersibility of the functionalized MXene. The recently developed surface functionalization methods demonstrate a range of processes for synthesizing MXene organic inks into composites with different polymer and metal nanoparticles without chemical oxidation issues. Moreover, utilizing these functional inks as highly efficient electrodes, it is also possible to achieve fine patterning and direct writing on hydrophilic or hydrophobic substrates with excellent conductivity.

9:15 AM EL17.14.05

Controlling Aerosol-Jet Printed Mxene Flakes Morphology for Neural and Energy Storage ApplicationsJavierGutierrez Gonzalez^{1,2,3}, DahnnaSpurling¹, TaraMcGuire², KeLi¹, IanWoods^{2,3}, AdrianG. Dervan², ValeriaNicolosi^{1,3} and FergalO'Brien^{2,3}; ¹Trinity College, Ireland; ²Tissue Engineering Research Group, Royal College of Surgeons in Ireland (RCSI),

MXenes are a class of 2D layered materials consisting of carbides and nitrides of transition metals which has found application in a wide range of fields due to their excellent electrical conductivity, charge storage, and biocompatibility. Mainly used as aligned flakes, under certain processing conditions these 2D flakes can also fold in crumpled 3D structures. Despite being occasionally associated with faulty deposition, crumpled MXenes hold untapped potential, harboring intriguing properties that remain largely unexplored. Thus, the main goal of this study was to investigate the uncharted role that crumpled MXenes can play in both neural and energy storage applications.

In this work, the production of crumpled and aligned MXene ($Ti_3C_2T_x$) flake morphologies was systematically studied by using high-resolution Aerosol Jet 3D printing, while assessing their novel physical properties, such as roughness, conductivity, and optical properties. Furthermore, cell line -derived and primary neurons were plated on either morphology to examine the ability of both forms to support neuronal growth and development. In addition, to assess the potential utility of crumpled MXenes for energy storage applications, crumpled MXene flakes were used as a conductive spacer between aligned MXene layers for developing an all-MXene supercapacitor.

By modifying several 3D printing parameters, MXene flakes could both align and crumple at specific mass and sheath flow regimes, depending on the nozzle size, speed, and solvent mixture, while flake morphology was rapidly monitored using the in-built camera.

To assess biocompatibility, mouse neurons were seeded on printed crumpled and aligned MXene films, revealing distinct behavior depending on the flake morphology: crumpled MXene facilitated higher cell adhesion (as indicated by DNA count and immunostained cells), whereas neurons grown on aligned MXene films possessed longer neurite outgrowth. Further analysis using mouse primary neurons, resulted in healthy neuronal growth on both types of MXene for 8 days, while crumpled surfaces elicited decreased expression of GFAP, as observed in image analysis, suggesting reduced astrocytic reactivity.¹

MXene supercapacitors were aerosol jet printed with the first layer being a highly conductive aligned MXene current collector, followed by alternating layers of crumpled and aligned MXene, resembling a *lasagne* structure. This hierarchical architecture effectively prevented excessive restacking of the flakes by smartly combining both morphologies, preserving a nanoporous network and achieving up to 65 (F/g) gravimetric capacitance, 193 (F/cm³) volumetric capacitance and 88 (mF/cm²) areal capacitance.

Taken together, these results demonstrate that crumpled and aligned MXenes can be easily 3D printed with Aerosol Jet printing; both MXene morphologies exhibited unique characteristics when supporting neuronal growth, and also powered energy-dense *lasagne* structured supercapacitors. This study highlights the need for precise management of MXene deposition and customized flake design, encouraging material scientists to intensify the study of crumpled MXenes and other 2D materials, and their application in multiple fields including biomedicine, electronics and energy storage.

References:

[1] Woods, I. *et al.* Biomimetic Scaffolds for Spinal Cord Applications Exhibit Stiffness-Dependent Immunomodulatory and Neurotrophic Characteristics. *Adv. Healthc. Mater.* **11**, 2101663 (2022).

9:30 AM EL17.14.06

Understanding Light-Matter Interactions of MXene Family of 2D Materials [Hyunho Kim](#)^{1,2}, [Danzen Zhang](#)^{1,2}, [Teng Zhang](#)^{1,2} and [Yury Gogotsi](#)^{1,2}; ¹A.J. Drexel Nanomaterials Institute, United States; ²Drexel University, United States

The MXene family, two-dimensional transition metal carbides, nitrides, and carbonitrides, have been the subject of extensive research activities for the past decade. Recent developments in the molten-salt route have enabled the engineering of MXenes' surface termination groups. For example, molten-salt route synthesized $Ti_3C_2Cl_2$ is found to have a vis-NIR absorption band centered at ~880 nm, which is red-shifted from 770–800 nm for the acid route prepared $Ti_3C_2T_x$ with O, OH, and F terminations. The origin of this vis-NIR absorption band is yet to be understood, and the red-shift is difficult to explain by carrier density with the surface plasmon concept. Instead, we adapt an interband transition mechanism with consideration of light polarization to explain both UV and vis-NIR absorption bands of MXenes. The light-matter interactions of MXenes will be analyzed by using in-situ UV-vis spectroscopy under electrochemical modulation and Raman spectroscopy, and correlated with the literature on nonlinear optics, ultrafast terahertz spectroscopy, and pump-probe transient absorption. The important relationships between photons, electrons, and phonons in MXene, which are important for numerous applications of those materials, will be discussed.

9:45 AMBREAK

SESSION EL17.15: MXenes Separation Applications
Session Chairs: [Majid Beidaghi](#) and [Anupma Thakur](#)
Thursday Morning, November 30, 2023
Hynes, Level 2, Room 208

10:15 AM *EL17.15.01

Application of Two-Dimensional Metal Carbides (MXenes) for the Removal of Emerging Contaminants from Water [Khaled Mahmoud](#); Hamad Bin Khalifa University, Qatar

Characteristic properties of two-dimensional (2D) transition metal carbides and nitrides (MXenes), such as high conductivity, hydrophilicity, and catalytic activity have led to a growing research interest in their use in environmental remediation and water treatment applications. The ability to process MXenes into flexible films with negative surface charge and hydrophilicity adds a possibility to control ion flux and biofouling by applying a small potential to the membrane. MXene shows a much higher antibacterial efficiency toward both Gram-negative and Gram-positive bacteria as compared with other 2D nanomaterials. Consequently, MXene membranes demonstrated outstanding water flux, and selective rejection of salts and organic molecules, which makes them ideal UF/NF membrane materials. Moreover, MXene has been successfully used for the efficient adsorption and removal of heavy metals such as Hg, and Cu. This talk summarizes the recent advances in the applications of MXenes as adsorbents, desalination membranes, electrodes for electrochemical deionization, and catalytic or antibacterial agents for water purification and other environmental remediation processes. The overview also features discussions on the computational attempts, biocompatibility, and environmental impact in the exploration of MXenes for water applications, highlighting the challenges and opportunities of these advanced 2D materials. The biocompatibility and cytotoxicity assessment of MXene and its impact on the environment will be highlighted.

10:45 AM EL17.15.02

The Effect of Lateral Size and Surface Functional Groups on Membrane Performance of the $Ti_3C_2T_x$ MXenes [Kian Dokht Pakravan](#) and [Majid Beidaghi](#); Auburn University, United States

The applications of MXenes in membrane-based separation technologies have been rapidly expanding in recent years due to their hydrophilicity, exceptional flexibility, superior thermal stability, high electrical conductivity, and large surface area. In this presentation, we demonstrate significant enhancement in the performance of MXenes ($Ti_3C_2T_x$) membranes through understanding the effects of lateral sizes and surface chemistry of MXenes on the permeability and separation properties of the fabricated membranes. Single-layer $Ti_3C_2T_x$ nanosheets with different lateral sizes were obtained by applying high-power sonication with varying times to MXene dispersion. The resulting MXene dispersions were used to fabricate membranes for studying the effect of lateral size on the membrane performance. Also, to investigate the effect of surface chemistry on membrane performance, $Ti_3C_2T_x$ was synthesized by two different methods. The first method was the conventional MXene synthesis based on the MILD etching method, where delamination and etching were performed in a single step using a mixture of LiF and HCl as the etchant. The second method used a mixed acid etchant (HF/HCl) followed by delamination with LiCl. The existence of HF in the mixed acid method results in a higher concentration of -F functional groups, which can decrease the hydrophilicity of MXene membranes. Our initial permeability measurements indicate that membranes fabricated using MXenes with smaller lateral sizes have higher permeability compared with MXenes membranes with larger flakes. Also, the permeability of the MXene membrane varies across different methods.

11:00 AM EL17.15.03

Highly Efficient Electrochemical Performance of MXene-Based Nanocomposites for Capacitive Deionization of Metals and Cations [Ruey-An Doong](#), [Nai-Ying Wang](#) and [Thi Kim Anh Nguyen](#); National Tsing Hua University, Taiwan

MXenes, a promising 2D materials derived from MAX phases, have been potentially applied to energy storage devices and pollution purification systems including ion-sieving membranes and ion removal. MXene has also established its prospective as electrodes for capacitive deionization (CDI) application for water purification and reuse due to the similar principle of charge storage in supercapacitors that uses the faradaic ion intercalation phenomenon. Electrode materials for asymmetric capacitive deionization, by combining carbonaceous materials with metal oxides, have emerged as a potential electrode material for CDI applications, which enable high ion removal capacity in comparison with devices containing only carbon materials. In this study, MXene based nanocomposites including $MoS_2@MXene$ and Prussian blue analogues (PBA) $@MXene$ have been fabricated to serve as the electrode materials for symmetric and asymmetric CDI applications. Results show that all the developed nanocomposites have a high surface area, suitable pore texture, and low electrical conductivity to accelerate the electron and

ion transfer rate. The specific electrosorption capacities (SECs) of the MXene-based nanocomposites are in the range of 39.5 – 43.8 mg/g with a charge efficiency of > 82%. Additionally, the as-developed MXene nanosheet has an excellent selective adsorption capacity toward heavy metal and ammonium ions removal. The Ti_3C_2 MXene can selectively electroadsorb NH_4^+ with the SEC of 40 mg/g. When combining the vanadium aluminum carbide ($V_2AlC-OH_x$) with activated biochar (AB), the asymmetric $AB||V_2AlC-OH_x$ device exhibits a superior deionization performance for Cr(VI) removal. These results clearly demonstrate the superiority of the as-developed MXene nanocomposites and can pave a gateway for combining MXene materials with novel metal oxides for highly efficient deionization of salty water as well as toxic metal and inorganic ions in water and wastewater treatment.

11:15 AM EL17.15.04

Synergistic Effect of Combining UiO-66 Nanoparticles and Mxene Nanosheets in Pebax Mixed Matrix Membranes for CO₂ Separation Eyasu G. Ajebe; National Taiwan University of Science and Technology, Taiwan

Membrane gas separation has received much attention due to its low cost, high efficiency, and environmental benefits. Mixed matrix membranes (MMMs) can significantly improve the performance of gas separation membranes, but poor filler-matrix interactions and the aggregation of highly loaded fillers in mixed matrix membranes limit the benefit of overcoming the trade-off limitation. Therefore, how to regulate the state of fillers in the membrane becomes a key factor in the development of MMMs. In this work, Mxene ($Ti_3C_2T_x$) nanosheets and UiO-66 nanoparticles were prepared and used as combined fillers with Pebax-1657 matrix to synthesize MMMs for CO₂ capture. As-prepared MMMs were used to capture CO₂; the large porosity of UiO-66 served as a highway to enhance CO₂ permeability, and Mxene nanosheets were used as selective channels to achieve high selectivity via the terminal polar surface groups of Mxene. The combination of UiO-66 and Mxene not only enhanced selectivity but also increased solubility and diffusivity via the CO₂ adsorbing carboxylate group of UiO-66 and the tortuous pathway provided by Mxene nanosheets. As a result, adding Mxene and UiO-66 in Pebax can help MMMs break through the trade-off limit. Pebax-based MMMs incorporated with 10-wt% Mxene/UiO-66 provide CO₂ permeability of 214 barrers and CO₂/N₂ selectivity of 102. The as-prepared MMMs showed enhanced CO₂ permeability and CO₂/N₂ selectivity, compared to pristine Pebax membrane. The CO₂ capture performance of Mxene/UiO-66/Pebax membrane has been successfully exceeded the upper limit of Robeson (2008) which indicates that Mxene/UiO-66/Pebax MMMs has great potential for CO₂ capture. This work provides a roadmap to fabricate high performance MMMs for CO₂ capture.

Keywords: Mxene, UiO-66, Pebax, mixed matrix membranes, CO₂ separation

SESSION EL17.16: Virtual Session
Session Chairs: Majid Beidaghi and Xuehang Wang
Wednesday Morning, December 6, 2023
EL17-virtual

8:00 AM EL17.16.01

Deciphering the Dominant Activity Origin of a Single-Atom Catalyst Anchored on a MXene Membrane for Recalcitrant Deterioration Mohammed Askar Deen F; Indian Institute of Technology Guwahati, India

Water is an elixir of life, but only about 0.5% of freshwater is available in an accessible form, resulting in enormous demand for the freshwater supply. A substantial increase in the need for wastewater treatment to meet its demand arises. Though many wastewater treatment technologies exist, advanced oxidation processes (AOPs), particularly sulfate radicals-based AOPs, offer a complete deterioration of recalcitrant. These sulfate radicals are highly oxidizing species that can be activated by the single-atom catalysts (SACs) in the presence of persulfate (SO₂-5). The utmost efficiency of SACs can be attained by tracking down their superior activity origin. This elusive knot can be untied by computational modelling to determine the superior activity origin of SACs. Computational modelling using first principle calculations unveils the specific catalytic site at which the SACs activity can be enriched for the maximum radicals' generation. This method results in one of the most active catalysts for PS conversion in recalcitrant deterioration. Transition-metal carbides (MXenes) incorporated with the membrane are active support that can result in unique properties combining inherent polymer characteristics and inorganic materials, offering a potential platform for efficient catalytic processes for sustainable wastewater treatment. In this work Ti_3C_2 MXenes mixed matrix membrane will be used to support SACs to overcome the synthesis challenge and pave the way for an efficient catalytic process. This study will use computational modelling and simulations to determine the specific type of transition metal atom, i.e. SACs and its electronic configuration that results in superior activity for generating highly oxidizing reactive species. Moreover, it will be followed by the synthesis of TCM3 and anchoring of SACs on the TCM3 for maximum recalcitrant deterioration.

8:15 AM EL17.16.02

Operando Synchrotron Radiation X-Ray Diffraction Study on Phase Evolution of Nb₂GaC MAX during Molten Salt Etching Changda Wang; University of Science and Technology of China, China

Lewis acidic molten salt method is a promising synthesis strategy to achieve MXenes with controllable surface terminations from numerous MAX materials. However, the molten salt etching strategy is not totally controllable and most experimental parameters are usually set empirically due to the unclear reaction process. Understanding the phase evolution chemistry and time-dependency during etching and post-processing is highly desirable, but still a key challenge due to the lack of operando characterizations and the complexity of the reaction process. Herein, we introduce an operando synchrotron radiation X-ray diffraction (SRXRD) technique to unveil the phase evolution process of Nb₂GaC MAX under molten-salts ambient. Several critical steps are demonstrated, including ultra-fast evolution from Nb₂GaC to Nb₂CuC, quick extraction of Cu atoms to form Nb₂CT_x MXene, and interlayer expansion caused by Cl grafting. Accordingly, we propose a controllable synthesis of Nb₂CT_x through precise temperature-controlling and time-adjusting. Afterward, the phase structure of Nb₂CT_x is also successfully tailored from hexagonal to amorphous by the time-dependent subsequent persulfate oxidation. The amorphous Nb₂CT_x with well-patterned morphology and numerous chloride terminations exhibits highly improved specific capacity, rate, and long cycling capability in lithium-ion batteries (LIBs). In conclusion, the operando SRXRD with online devices is promising for the dynamic study of the Lewis acid molten salt etching process such as phase evolution, lattice change, and etching time scale, which could not be provided by ex-situ methods.

8:30 AM *EL17.16.03

MXene Label-Free Detection and Immune-Based Applications Lucia G. Delogu^{1,2}, Laura Fusco^{1,3,4}, Arianna Gazzini¹, Christopher E. Shuck³, Marco Orecchioni⁵, Sènan Mickael D'Almeida⁶, Darawan Rinchai⁴, Eiman Ahmed⁴, Leeat Keren⁷, Davide Bedognetti⁴ and Yury Gogotsi³; ¹University of Padua, Italy; ²New York University Abu Dhabi, United Arab Emirates; ³A.J. Drexel Nanomaterials Institute, United States; ⁴Sidra Medicine, Qatar; ⁵La Jolla Institute for Allergy and Immunology, United States; ⁶Flow Cytometry Core Facility, School of Life Sciences Ecole Polytechnique Fédérale de Lausanne (EPFL), Switzerland; ⁷Department of Molecular Cell Biology, Weizmann Institute of Science, Israel

Two-dimensional (2D) transition metal carbides, nitrides, and carbonitrides (MXenes) are rapidly growing as nanoplatforms in biomedicine.[1-3] Considering the central importance of the immune response for any clinical translation of nanomaterials, we explored the potential biomedical applications of MXenes and their immune impact exploiting our expertise on the biological effects of 2D materials.[1-4]

To satisfy a critical unmet need to detect 2D materials at the single-cell level while measuring multiple cell and tissue features, we proposed the "Label-free sIngle-cell tracking of 2D matErials by mass cytometry and MIBI-TOF Design" (LINKED) strategy, enabling nanomaterial detection while surveying a high degree of information from single samples.[5] This strategy is based on single-cell mass cytometry (CyTOF) and ion-beam imaging by time-of-flight (MIBI-TOF). MXenes ensured mass detection within the cytometry range while avoiding overlap with more than 70 available tags. We demonstrated their detection in 15 human immune cell populations. We used mass cytometry to capture MXene biocompatibility and cytokine production after their uptake. *In vivo* biodistribution experiments using a mixture of MXenes in mice confirmed the versatility of our strategy and revealed MXene accumulation in the main organs. In addition, envisaging future MXene-based biomedical nanotools and drug nanoformulations we further explored MXene immune modulation and antiviral activity taking SARS-CoV-2 as a model.[6,7] We analyzed four SARS-CoV-2 genotypes. When viral inhibition was tested *in vitro*, Ti_3C_2 was able to reduce infection in SARS-CoV-2/clade GR-infected Vero E6 cells. Among the other MXenes tested, $Mo_2Ti_2C_3$ also showed antiviral properties. Proteomic and functional annotation analysis revealed that MXene-treatment exerts specific inhibitory mechanisms. The immune impact of MXenes was evaluated on human primary immune cells by flow cytometry and CyTOF on 17 distinct cell subpopulations. Moreover, 40 secreted cytokines were analyzed by Luminex technology. MXene immune profiling revealed i) the excellent bio and immune compatibility of the material, as well as the ability of MXene ii) to inhibit monocytes and iii) to reduce the release of pro-inflammatory cytokines, suggesting an anti-inflammatory effect elicited by MXene.

Finally, we considered that although vanadium-based metalloids have been recently explored for their effective anti-inflammatory activity, they frequently cause undesired side effects. Therefore, we hypothesized that vanadium immune properties could be extended to MXene compounds.[8] Therefore, we synthesized V_4C_3 , evaluating its biocompatibility and immunomodulatory effects. By combining multiple experimental approaches, we investigated the effects on hemolysis, apoptosis, necrosis, activation, and cytokine production. We demonstrated the ability to inhibit T cell-dendritic cell interactions, evaluating the modulation of CD40-CD40 ligand interaction, two key co-stimulatory molecules for immune activation. We confirmed the biocompatibility at the single-cell level on 17 human immune cell subpopulations by single-cell mass cytometry. Finally, we explored the molecular mechanism underlying V_4C_3 immune modulation, demonstrating a MXene-mediated downregulation of antigen presentation-associated genes. Our findings set the basis for further V_4C_3 investigation as a negative

modulator of the immune response in inflammatory and autoimmune diseases.

Taken together, our results provide a compendium of knowledge on the biocompatibility of MXenes for the safe development of multi-functioning nanosystems in biomedicine.

References:

1. Gogotsi Y & Anasori B. *ACS Nano*, 2019
2. Fusco L *et al. Theranostics*, 2020
3. Gazzì A *et al. Front Bioeng Biotechnol*, 2019
4. Gazzì A *et al. J Phys materials*, 2020
5. Fusco L *et al. Advanced Materials*, 2022
6. Unal MA *et al. Nano Today*, 2021
7. Weiss C *et al. ACS Nano*, 2020
8. Fusco L *et al. Small Methods*, 2023

9:00 AM EL17.16.04

Achieving of High Power MXene Electrode through Laser-Driven treatment[Asmita Dutta](#); Ariel University, Israel

MXenes-based compounds, particularly Ti_3C_2Tx , were studied intensively as electrodes for supercapacitors due to their layered structure and high conductivity, enabling facile ions diffusion and charge transfer. However, tight restacking of the 2D layers limits their practical, accessible surface area, thereby impeding their capacity and rate capability performance. To mitigate this phenomenon, we present in this study a processing method based on laser beam irradiation on Ti_3C_2Tx film. The laser induces chemical and morphological changes in the 2D material, optimizing the stacking arrangement of the MXene layers, resulting in considerably improved electrochemical of the treated MXenes. In concentrated neutral aqueous electrolytes (7 M LiCl), the laser treatments increase the electric double layer (EDL) capacitance by 126%, from 96 F/g to 121.23 F/g at a scan rate of 5 mV/s. In acidic aqueous electrolytes (3 M H_2SO_4), capacitance enhanced by 132%, from 214 F/g to 284 F/g. Furthermore, the laser-modified MXene electrodes demonstrate excellent rate capabilities of 84% retention at extreme rates of 0.5 V compared to only 33% of the original Ti_3C_2Tx electrodes. Finally, we discuss the chemical and physical changes induced by the laser treatments and their influence on the electrochemical behavior of the lasered MXene.

SYMPOSIUM EL18

Fundamentals of Mixed Ionic-Electronic Conductors
November 27 - November 29, 2023

Symposium Organizers

Laure Kayser, University of Delaware

Scott Keene, Stanford University

Christine Luscombe, Okinawa Institute of Science and Technology

Micaela Matta, King's College London

* Invited Paper

+ JMR Distinguished Invited Speaker

SESSION EL18.01: Understanding Charge Transport in Mixed Ionic-Electronic Conductors

Session Chairs: Laure Kayser, Christine Luscombe and Micaela Matta

Monday Morning, November 27, 2023

Hynes, Level 1, Room 111

10:30 AM *EL18.01.01

The Influence of Hydration on the Mixed Charge Conduction of Conjugated Polymer Films[Sahika Inal](#); King Abdullah University of Science and Technology, Saudi Arabia

Organic mixed (ionic and electronic) charge conductors and electrochemical phenomena at the solid-liquid interface have garnered significant attention for applications in bioelectronics, electrochromics, energy storage/generation, neuromorphic computing, and thermoelectrics. These devices operate in electrolytes that render ions mobile in the film, making the coupling between electronic and ionic charges crucial. An example of such a device is the organic electrochemical transistor (OECT), a high-gain transducer commonly used to monitor bioelectronic signals. In this talk, I will show that the ions entering the semiconducting polymer channel are hydrated, and the water they bring inside the channel significantly affects OECT performance, which can be traced back to changes in the overall structural order. I will show the generality of this phenomenon with p and n-type materials. I will demonstrate how the amount of water the film takes governs its dielectric constant and the polaronic species formation. I will introduce one synthetic method and one postprocessing approach that can limit the water uptake of the film during device operation. These approaches enhance the mixed conductivity of polymers while preventing material degradation with oxygen, leading to OECTs with longer shelf life and operational stability.

11:00 AM EL18.01.02

Are Existing OECT Models Broad Enough? The Role of the Counter Ion and Ionic Contact Blocking[Sapir Bittons](#) and [Nir Tessler](#); Technion-Israel Institute of Technology, Israel

OECTs have many advantages making them a promising technology for the future of electronics and bio-electronics. They have high transconductance which leads to a high sensitivity [1], and low operating voltage [2]. They can be fabricated on flexible substrates, [3] are scalable, and cost-effective for mass production. [4] The above attributes make them suitable for various applications, including healthcare (biosensors, drug delivery devices), robotics (sensors and actuators), and flexible electronics (e-skins, displays). However, they have limitations and challenges, such as stability and reversibility issues, manufacturing complexity, and the need for further optimization in certain applications. [5]

In our study, we simulated an OECT with PEDOT: PSS as the semiconductor layer. At the ON state, no cations are present in the bulk, resulting in a hole current within the PEDOT: PSS bulk. Conversely, at the OFF state, cations penetrate the bulk, depleting it and causing a significant drop in current. The above is well-known and detailed modeling has already revealed the importance of the ions' distribution with the semiconducting layer. [6,7]

Here we expand on previous studies using the industry-standard device simulator Sentaurus by Synopsys. Using the ion ("hydrogen") diffusion module allows for self-consistent simulation of the ionic electronic conduction as well as the contact phenomena. The first new observation to report is that, like in some memory technologies, ion accumulation close to the contact interface blocks the contact injection. In fact, this contact blocking plays an important role in obtaining low enough off currents.

Next, since the counterions (anions) are explicitly incorporated into the model, we report their influence on the OECT's conductance. We will present hole, cation, and anion distributions in

the electrolyte and semiconductor for ON and OFF states under three scenarios: (1) Anions can move freely in the electrolyte but are blocked by the semiconductor, (2) Anions can move freely in the electrolyte and penetrate the semiconductor, and (3) Anions are static in the electrolyte (as in solid electrolytes). We identify the scenario resulting in the highest transconductance and demonstrate the potential role of the electrolyte's counter ions (anions) in achieving best-performing OECTs.

We will discuss how our new findings suggest that the models used abundantly to describe OECT's performance may not be general enough. [8]

References:

1. Khodagholy, D., et al., *High transconductance organic electrochemical transistors*. Nature Communications, 2013. **4**(1): p. 2133.
2. Chen, S., et al., *Contact Modulated Ionic Transfer Doping in All-Solid-State Organic Electrochemical Transistor for Ultra-High Sensitive Tactile Perception at Low Operating Voltage*. Advanced Functional Materials, 2020. **30**(51): p. 2006186.
3. Wang, L., et al., *Flexible organic electrochemical transistors for chemical and biological sensing*. Nano Research, 2022. **15**(3): p. 2433-2464.
4. Basirić, L., et al., *Electrical characteristics of ink-jet printed, all-polymer electrochemical transistors*. Organic Electronics, 2012. **13**(2): p. 244-248.
5. Li, Y., et al., *Ion-Selective Organic Electrochemical Transistors: Recent Progress and Challenges*. Small, 2022. **18**(19): p. 2107413.
6. Paudel, P.R., et al., *Tuning the Transconductance of Organic Electrochemical Transistors*. Advanced Functional Materials, 2021. **31**(3): p. 2004939.
7. Kaphle, V., et al., *Finding the equilibrium of organic electrochemical transistors*. Nature Communications, 2020. **11**(1): p. 2515.
8. M. Shahi et al., Nature Materials, in press, 2023

11:15 AM *EL18.01.03

Ion-Associated Charge Transport in Conjugated/Non-Conjugated Polymer Layers for Wet and Dry Electronic Devices[Takeo Suga](#); Waseda University, Japan

Electro-active organic polymers (*i.e.* p-conjugated polymer conductors/semi-conductors) have attracted increasing interest for organic electronics applications, such as solar cells, field-effect transistors, and batteries, because of their facile integration to soft/flexible device configurations, and environmentally benign/sustainable feedstock compared with rare metals, etc. Non-conjugated, redox-active polymers such as radical polymers have also attracted research attention to their utilization as an electrode-active material for rechargeable batteries and a charge-transport layer for electronic devices. Any of these applications, the role of associated ion transport is indispensable for efficient charge injection, transport, and storage. Here we take three examples: a) stable charge-storage in radical/conducting polymers, b) modulated charge-transport in the radical-containing resistive memory, and c) efficient charge collection through polymer semiconductors in the perovskite solar cells, and discuss each role of ions for charge-transport in electro-active polymers.

11:45 AM EL18.01.04

Elucidating Oxygen Reduction Mechanisms on Organic Mixed Ionic-Electronic Conducting Polymers[Ana De La Fuente Duran](#)¹, [Allen Yu-Lun Liang](#)¹, [Ilaria Denti](#)¹, [Emily Penn](#)¹, [Adam Marks](#)¹, [William C. Chueh](#)¹, [Alberto Sallero](#)¹, [Alexander Giovannitti](#)² and [J. Tyler Mefford](#)¹; ¹Stanford University, United States; ²Chalmers University of Technology, Sweden

Atmospheric oxygen is an attractive oxidant for the generation of electricity from chemical fuels and for the electrochemical production of hydrogen peroxide. Although not universal, it is generally assumed that an electrocatalyst is needed to reduce oxygen. Recently, a variety of organic mixed ionic-electronic conducting polymers (OMIECs) have been reported to exhibit catalytic behavior for both the 4-electron/4-proton and the 2-electron/2-proton oxygen reduction reaction (ORR).

This work sets out to identify the operative oxygen reduction mechanism of OMIECs through a multi-faceted experimental and theoretical approach. We primarily focus our efforts on p(NDI-T2 P75)—a random copolymer comprised of naphthalene diimide (NDI) and bithiophene (T2) units with 75% polar sidechains—and then expand the understanding built on this system to a range of other OMIECs. Using rotating ring disk electrochemistry, we find that the OMIECs investigated exhibit a high selectivity towards the 2-electron ORR product. Using *operando* UV-Vis and Raman spectroscopy measurements, we identify changes in OMIEC performance when in the presence of O₂. To gain further insights about the catalytic reaction path, we construct and test a microkinetic model. Through this model, we show that the performance of our tested OMIECs can be rationalized through an EC'D reaction mechanism. Our results suggest that these materials do not operate as electrocatalysts for the initial reduction of oxygen to superoxide but do function as catalysts for the disproportionation of superoxide.

SESSION EL18.02: Structure-Property Relationships in Mixed Ionic-Electronic Conductors

Session Chairs: Laure Kayser and Micaela Matta

Monday Afternoon, November 27, 2023

Hynes, Level 1, Room 111

1:30 PM EL18.02.01

Asymmetric Side-Chain Engineering of Thiophene-Based Polymers for Organic Electrochemical Transistor Applications[Preeti Yadav](#) and [Christine Luscombe](#); Okinawa Institute of Science and Technology Graduate University, Japan

Conjugated polymers with mixed ion-conducting properties have recently gained considerable attention due to their potential applications in various emerging technologies spanning from bioelectronics to energy harvesting and storage. The soft and biocompatible nature of conjugated polymers coupled with their mixed conduction properties has been leveraged to develop many organic bioelectronic devices including organic electrochemical transistors (OECTs), neural probes, organic electronic ion pumps, and conducting polymer actuators. Among these, an OECT device comprising of a redox-active organic semiconductor layer interfacing a source, a drain electrode, and an electrolyte solution is capable of directly transducing small ionic fluxes into electrical signals making it ideal for sensing biomolecules. To achieve a high-performing OECT device, carrier mobility, and ion transport should be balanced in such a way that maximum transconductance is achieved, highlighting the crucial role played by crystallinity and morphology in mixed conduction. Therefore, it is important to establish an in-depth understanding of the chemical structure of the semiconducting polymer, charge transport, and morphology for designing high-performance OECT materials. In this work, we have synthesized polythiophene derivatives and explore how the polymer morphologies will affect carrier mobility and ion transport. The fundamental design idea is to obtain a highly planarized polymer structure by enhancing the side-chain organization through the incorporation of asymmetric side chains. Specifically, we investigate the effect of the enhanced side-chain organization on film morphologies, carrier mobility, and ion transport. Thiophene monomer is synthesized using Stille coupling and subsequently polymerized using Kumada catalyst transfer polymerization. The obtained polymer is characterized using NMR, MALDI, DSC, TGA, UV-vis absorption spectroscopy, and cyclic voltammetry. The morphologies and microstructure of the polymer films are examined using AFM and GIWAX followed by OECT device fabrication and characterization.

1:45 PM *EL18.02.02

Operando Studies of Organic Mixed Ionic-Electronic Conductors: Structure, Composition and More...[Jonathan Rivnay](#); Northwestern University, United States

Organic mixed ionic-electronic conductors (OMIECs) have gained considerable interest in bioelectronics, power electronics, circuits and neuromorphic computing. These organic, often polymer-based semiconductors rely on a combination of ionic transport, electronic transport, and high volumetric charge storage capacity. Despite recent progress and a rapidly expanding library of new materials, a full understanding of fundamental processes of OMIECs remains largely unexplored. Critically, useful studies require us to probe these systems in device-relevant conditions, fully considering the effects of ions and solvent on microstructure and transport. To this end, we report on recent efforts towards structure/composition-property relations in high performance organic mixed conductors using ex-situ, in-situ, and operando scattering and spectroscopic techniques. We use a combination of GIWAXS, GISAXS, XPCS, E-QCMD, UV-Vis, XRF, as well as device measurements to explore kinetics, composition, and structural evolution during electrochemical operation. Importantly, these findings provide insights into materials design for enhancing device performance and stability.

2:15 PM EL18.02.03

Probing Polarons in Mixed Conductors via the Photoinduced Stark Effect[Christopher Grieco](#), [Abdul Rashid Umar](#) and [Austin Dorris](#); Auburn University, United States

Conjugated polymers are promising candidates for high performance bioelectronics due in part to their ability to conduct ions and charge carriers simultaneously. However, the fundamentals of mixed ion and charge transport, including their complex dependence on polymer structural dynamics occurring *in operando*, remain unclear due to limited characterization methods. Using ultrafast transient absorption spectroscopy, we demonstrate a new approach to probing the nature and local environment of polarons in a mixed conducting, electrochromic polymer, 3,4-propylenedioxythiophene-*co*-3,4-ethylenedioxythiophene (ProDOT-*co*-EDOT).[1] Selectively photoexciting hole polarons via the P1 and P2 polaronic transitions causes spatial separation of the hole from its counterion during thermalization. The resulting electric field, which induces a Stark shift of the bandgap transition of nearby polymer chains, creates signals in the transient spectrum that reflect the electronic structure and environment of the charge carrier. As a first step, we show how this optical spectroscopy method, which effectively senses polarons in both

amorphous and crystalline domains, can be implemented in spectroelectrochemical measurements to elucidate mixed conduction mechanisms.

[1] Umar, AR., Dorris, A.L., Kotadiya, N.M., Giebink, N.C., Collier, G.S., and Grieco, C.: Probing Polaron Environment in a Doped Polymer via the Photoinduced Stark Effect, *J. Phys. Chem. C* **127**, 9498-9508 (2023)

2:30 PM EL18.02.04

Swelling of Side Chain Free Polymers upon Electrochemical Cycling Lucas Flagg¹, Lee Richter¹, Jiajie Guo², David S. Ginger² and Jianguo Mei³; ¹NIST, United States; ²University of Washington, United States; ³Purdue University, United States

Organic mixed ionic-electronic conductors (OMIECs) are an exciting class of new materials with a range of potential applications including biosensors, electrochromics, and neuromorphic computing. For many of these applications the performance of n-type materials trails p-type materials by at least an order of magnitude. Recently, a pair of side-chain less polymers have been demonstrated as promising n-type OMIECs. These materials challenge the existing understanding of this class of materials, where polar (often ethylene glycol) side chains enable electrolyte and ion ingress, which subsequently enables volumetric doping. Here, we seek to understand the swelling during electrolyte contact and during redox cycling of these side chain less materials using *in-situ* GIWAXS. These measurements reveal drastic differences in how the two polymers swell in response to applied bias. In water-based electrolytes, BBL shows a redox induced swelling upon first passage, and remains swollen during subsequent doping cycles. In contrast, PBDF does not show any lattice expansion when in contact with water regardless of doping state. However, in propylene carbonate electrolyte PBDF shows a reversible melting during dedoping to the point where all diffraction peaks disappear. Upon electrochemical redoping, the crystallinity returns to its original level. Additionally, in the partially doped state the lattice spacing depends strongly on the exact doping state. We investigate this melting/recrystallization and swelling phenomena in relation to conductivity of the system. Overall, this work provides insights into the role of swelling in side-chain less OMEIC materials which can inform design rules moving forward.

2:45 PM BREAK

SESSION EL18.03: New Materials for Mixed Ionic-Electronic Conduction

Session Chairs: Laure Kayser and Julia Schneider

Monday Afternoon, November 27, 2023

Hynes, Level 1, Room 111

3:15 PM *EL18.03.01

Electronic and Ionic Conduction in Radical-Containing Small Molecules and Polymers Bryan W. Boudouris; Purdue University, United States

Optoelectronically active small molecules and polymers have made critical inroads in many solid-state electronic devices (e.g., organic field-effect transistors), and excitingly, organic molecules capable of providing mixed electronic and ionic conduction offer unique opportunities in many application areas including bioelectronic devices. Here, we describe electronic and ionic conduction in both low molecular weight and polymeric materials containing stable open-shell sites. While the chemical nature of the two classes of materials differs, the key premise is that controlling the spatial distance between the radical groups is critical for electronic transport and that the redox behavior of open-shell species allows for facile ion transport if it is controlled appropriately.

First, we demonstrate how control of the local structure in radical-containing small molecules and polymers impacts charge transport in these materials. In one example, we implement radical polymers, which are macromolecular materials that have flexible polymeric backbones and pendant groups that bear stable open-shell moieties. In contrast to almost all other optoelectronically-active polymers, radical polymers lack backbone conjugation and are completely amorphous in the solid state. Despite this shift in macromolecular design archetype, we demonstrate that the solid-state electrical conductivity of a designer radical polymer exceeds 20 S m⁻¹, and this places this nonconjugated polymer conductor in the same regime as many grades of common commercially-available, chemically-doped conjugated conducting polymers. Thus, this work presents an alternate design paradigm for next-generation organic electronic materials. In a second example, small molecules that bear stable radical groups and form macroscopic single crystals are evaluated. Specifically, we quantified the electrical conductivity in two organic radical single crystals and demonstrated that a subtle change in atomic connectivity drastically alters the macroscopic electronic properties of the materials. One radical-based crystal had an electrical conductivity of ~3 S m⁻¹, which is the highest value for nonconjugated radical conductors over a 1 μm-scale reported to date. However, the other radical crystal has a 1,000-fold lower conductivity despite their extremely similar molecular structures. The temperature-dependent conductivity follows the variable range hopping mechanism for both radical crystals, and the difference in effective charge mobility is the reason for the conductivity difference. These results present a clear picture of the design rules and charge transport mechanism for radical-based materials.

Next, we describe how a blend of a common conjugated polymer, poly(3-hexylthiophene) (P3HT), and a radical polymer (i.e., a macromolecule with a nonconjugated backbone and with stable open-shell sites on its pendant groups), poly(4-glycidyl-2,2,6,6-tetramethylpiperidine-1-oxyl) PTEO, allows for the creation of high-performance organic electrochemical transistors (OECTs) through a unique mixed conduction mechanism. Second, we will discuss how this type of archetype can be translated to biomedical device applications through a practical demonstration of a stretchable and flexible polymer-based biosensor. This bioelectronic device is inkjet-printed atop a commercial soft contact lens in a high-throughput manner, and our electroretinogram (ERG) sensor shows performance that is superior to current clinical gold standards in human subjects. In this way, we couple the materials science mixed organic electronic conductors to translational performance to demonstrate clear patient impact.

3:45 PM EL18.03.02

Generalised Framework for Controlling and Understanding Ion Dynamics with Passivated Lead Halide Perovskites Tomi Baikie¹, Philip Calado², Krzysztof Galkowski¹, Samuel D. Stranks¹ and Piers R. Barnes²; ¹University of Cambridge, United Kingdom; ²Imperial College London, United Kingdom

Metal halide perovskite solar cells have gained widespread attention due to their high efficiency and high defect tolerance. The absorbing perovskite layer is as a mixed electron-ion conductor that supports high rates of ion and charge transport at room temperature, but the migration of mobile defects can lead to degradation pathways. We combine experimental observations and drift-diffusion modelling to demonstrate a new framework to interpret surface photovoltage (SPV) measurements in perovskite systems and mixed electronic ionic conductors more generally. We conclude that the SPV in mixed electronic ionic conductors can be understood in terms of the change in electric potential at the surface associated with changes in the net charge within the semiconductor system. We show that by modifying the interfaces of perovskite bilayers, we may control defect migration behaviour throughout the perovskite bulk. Our new framework for SPV has broad implications for developing strategies to improve the stability of perovskite devices by controlling defect accumulation at interfaces. More generally, in mixed electronic conductors our framework provides new insights into the behaviour of mobile defects and their interaction with photoinduced charges, which are foundational to physical mechanisms in memristivity, logic, impedance, sensors and energy storage.

4:00 PM EL18.03.03

Ion- and Charge Transport in Dense Films of Semiconducting Single-Walled Carbon Nanotubes Daniel Heimfarth, Merve Balci Leinen, Xuqiang Xu and Jana Zaumseil; Heidelberg University, Germany

Dispersions of purely semiconducting single-walled carbon nanotubes (SWCNTs) can be sorted and purified by polymer-wrapping and subsequently printed into thin or thick SWCNT films that are suitable for various electronic devices. Here, we demonstrate that these porous composites of conjugated polymer and semiconducting nanotubes enable mixed ionic and electronic transport with high charge carrier mobilities in electrochemical transistors with different electrolytes. The ionic transport and hence also the effective volumetric capacitance of the nanotube network can be increased substantially by changing from a hydrophobic polyfluorene copolymer with alkyl sidechains to one with tetraethylene glycol sidechains, thus reaching over 200 F cm⁻¹ V⁻¹ s⁻¹ as the product of carrier mobility and volumetric capacitance (*ACS Appl. Mater. Interfaces* 2022, 14, 8209). We find that the maximum transconductance for hole transport in SWCNT networks also depends on the size of the electrolyte anions, suggesting a direct impact on the delocalization of charge carriers along the nanotubes. Furthermore, we monitor the ion movement and thus charge carrier concentration within a nanotube network by spatially resolved *in-situ* Raman- and photoluminescence spectroscopy and explore the role of the network morphology and density for both charge and ion transport. Finally, we demonstrate the direct sensing of cupric ions and indirectly of glyphosate in water-gated transistors with polyfluorene copolymer-wrapped nanotubes (*Nanoscale* 2022, 14, 13542).

4:15 PM EL18.03.04

Semiconducting polymers bearing hydrophilic glycol side chains can transport aqueous electrolytes through their bulk, allowing for the simultaneous movement of electronic and ionic charges during electrochemical doping (therefore called organic mixed ionic-electronic conductors, or OMIECs). Their mixed charge transport properties, chemical tuneability and easy synthetic scalability make them attractive materials for bioelectronic devices such as transistors [1] and charge storage devices [2]. While hydrophobic alkylated polythiophenes have demonstrated favourable charge transport properties [3] and the ability to operate stably in devices such as field-effect transistors, upon glycolation (making them into OMIECs) some of these favourable properties are deteriorated. For example, heavily glycolated polythiophenes have shown to excessively swell when electrochemically doped in the presence of an aqueous electrolyte [4], damaging their operational stability and charge transport properties. We explore how amphiphilic chemical design strategies can be leveraged to design OMIECs that retain their operational stability and high charge transport properties. We explore two strategies – 1) the random copolymerisation of alkylated and glycolated repeat units together and 2) using homopolymers with both alkyl and glycol moieties on their side chains. In the first case we find that a small level of alkylation leads to a large increase in the electrochemical cycling stability of the OMIEC, while leaving the electrochemical doping characteristics broadly unchanged. When using homopolymers with mixed alkyl/glycol side chains, we show how the size of the alkyl group on the side chain can control the polymer backbone conformation, impacting its electronic transport properties. Through a joint experimental/theoretical approach we identify the underlying microstructural mechanism behind both the inhibited swelling in alkyl/glycol copolymers and the effect on the backbone morphology in amphiphilic homopolymers. We identify the driving forces causing them to adopt their particular microstructure and draw parallels between the formation of micelles and vesicles in surfactants. Identifying these mechanisms and their driving forces in OMIEC systems will aid in the design of future polymers which optimise the transport of both ionic and electronic charges, while having high operational stability and charge transport properties.

- [1] Giovannitti, Alexander, et al. "Controlling the mode of operation of organic transistors through side-chain engineering." *Proceedings of the National Academy of Sciences* 113.43 (2016): 12017-12022.
- [2] Moia, Davide, et al. "Design and evaluation of conjugated polymers with polar side chains as electrode materials for electrochemical energy storage in aqueous electrolytes." *Energy & Environmental Science* 12.4 (2019): 1349-1357.
- [3] McCullough, Richard D., et al. "Design, synthesis, and control of conducting polymer architectures: structurally homogeneous poly(3-alkylthiophenes)." *The Journal of Organic Chemistry* 58.4 (1993): 904-912.
- [4] Gladisch, Johannes, et al. "Reversible electronic solid-gel switching of a conjugated polymer." *Advanced Science* 7.2 (2020): 1901144

SESSION EL18.04: Poster Session: Fundamentals of Mixed Ionic-Electronic Conductors
Session Chairs: Christine Luscombe and Micaela Matta
Monday Afternoon, November 27, 2023
Hynes, Level 1, Hall A

8:00 PM EL18.04.01

Enhanced Thermoelectric Performance of PEDOT:PSS-Based Composites by Constructing Sequential Energy-Filtering Interfaces and Energy Barriers Siqui Liu¹ and Chaobin He^{1,2}; ¹National University of Singapore, Singapore; ²Institute of Materials Research and Engineering, Singapore

Among all reported organic thermoelectric materials, poly(3,4-ethylenedioxythiophene):poly(styrenesulfonate) (PEDOT:PSS) has drawn extensive attention owing to its high electrical conductivity. However, the Seebeck coefficient of PEDOT:PSS needs to be enhanced without sacrificing electrical conductivity. As one approach, modulating the energy filtering effect at the component interfaces can enhance the Seebeck coefficient with only a slight reduction in electrical conductivity. In this presentation, I will report an effective strategy to significantly enhance the thermoelectric properties of PEDOT:PSS by integrating core-shell PEDOT/polypyrrole (PPy) nanowires to form multiple sequential interfaces and enabling more effective energy filtering process in between. By tailoring the energy barriers among PEDOT/PPy/PEDOT:PSS interfaces, the Seebeck coefficient of the PEDOT:PSS composites was increased by ~46% with only a slight decrease in electrical conductivity. As a result, a significant improvement of over 85% in power factor was achieved compared with pristine PEDOT:PSS.

8:00 PM EL18.04.02

Textile-Embeddable Fibriform Organic Electrochemical Diodes with Rectifying, Complimentary Logic and Transient Voltage Suppression Function for Wearable E-Textile Circuits Kwang-Hun Choi^{1,2}, Soo Kin Kim^{1,2}, Ho Won Jang^{2,2}, Changsoo Choi¹, Hyunsu Ju¹ and Jung Ah Lim^{1,3}; ¹Korea Institute of Science and Technology, Korea (the Republic of); ²Seoul National University, Korea (the Republic of); ³Korea University of Science and Technology of Korea, Korea (the Republic of)

Electronic textile (E-textile) are considered ideal wearable platforms for human-machine interaction due to their flexibility and flexible, comfortable-wearing textile properties. For realization of a multi-functional, fully integrated E-textile circuit system, fibriform electronic devices become a key component that can merge a multifunctionality of integrated circuits and a textile nature. Here, we propose a fibriform electrochemical diode (fOED) as a building block for E-textile circuits. The fOED is fabricated by twisting metal/polymer semiconductor/ion gel coaxial microfibers and microfiber electrodes. The fOED exhibits a prominent asymmetrical current flow similar to that of the diode, with a rectification ratio of over 10². From the fundamental studies on the electrochemical interaction between polymer semiconductors and ions, we reveal that the faradaic current by electrochemical reaction originates an abrupt current increase under a forward bias. Then, the threshold voltages of devices are determined by the redox potential of the polymer semiconductor. The fOED exhibit great bending and washing robustness, and was embeddable on the textile platform by its one-dimensional architecture (diameter < 300 μm). It also could be expanded to integrated circuit systems by simply merging the electrode threads, the full-wave rectifiers and logic gates (AND/OR) could be easily accomplished on textiles. Furthermore, it was also confirmed that fOED could be utilized as a protection diode, a fOED integrated electrocardiogram monitoring system could be protected from circuit damage by instant transient voltages. Our approach offers a new form factor for electrochemical diodes and we believe that this work will contribute to the development of next-generation wearable E-textile circuit systems.

8:00 PM EL18.04.03

Aerosol Jet Printed Organic Electrochemical Transistors using n-Type Naphthalene Dimide-Based Small-Molecule Organic Mixed Ionic-Electronic Conductor Seongdae Kang¹, Paul Lavryshyn¹, Jiaxin Fan² and Manisha Gupta¹; ¹University of Alberta, Canada; ²Polytechnique Montréal, Canada

Organic semiconductors are capable of transporting both the ionic and electronic charges representing a new class of material: organic mixed ionic-electronic conductor (OMIECs). OMIECs have been used for a variety of organic electronics, including organic electrochemical transistors (OECTs) and energy conversion/storage devices. Most reported OMIECs are hole-transporting p-type polymeric material, such as PEDOT:PSS and polythiophene derivatives. In contrast, electron-transporting n-type OMIECs are less reported and often have poorer performance and stability, despite their need in fabricating complementary circuits or biosensors that require electron transfer. Compared to polymeric OMIECs, small-molecule mixed conductors offer significant potential thanks to their mono-dispersity and synthesis simplicity.¹⁾

We recently reported the first naphthalene-diimide-based n-type small-molecule organic mixed ionic-electronic conductors and their utilization as a channel material in accumulation mode organic electrochemical transistors. The glycolated naphthalene diimide n-type OMIEC, gNDI-Br₂, was characterized for its electrochemical behaviour and used to fabricate an OECT via a simple drop-casting technique. The gNDI-Br₂ OECT operated as an n-type accumulation mode and showed a maximum transconductance ($g_{m, \max}$) of $814 \pm 124.2 \mu\text{S}$ and a mobility capacitance product (μC^*) of $0.23 \pm 0.04 \text{ F cm}^{-1} \text{V}^{-1} \text{s}^{-1}$.²⁾

The transconductance of the OECT is affected by its intrinsic material figure-of-merit (μC^*) and channel geometry.³⁾ Drop-casted gNDI-Br₂ devices pose a challenge for practical applications due to their unpredictable channel geometry and hence their repeatability. To resolve this issue, we fabricated gNDI-Br₂ OECTs using an aerosol-jet 3D printing technique with the Optomec Aerosol Jet 5X 3D printer. This method creates the sub-micron size aerosols using ultrasonic atomization which are deposited onto the substrate via a nozzle.⁴⁾ Owing to the AJ5X 3D printing system, we were able to manipulate the OECT channel geometry and fabricate repeatable OECT devices.

Additionally, for the aerosol jet printing, the gNDI-Br₂ solution with low evaporation rate was required while transitioning to an aerosol. By using low-volatile solvent for the solution and aerosol-jet 3D printing, the gNDI-Br₂ molecules were evenly distributed onto the substrate, resulting in higher crystallinity as compared to the drop-casted OECTs. This resulted in an improved performance of the gNDI-Br₂ OECT ($g_{m, \max} = 1.12 \text{ mS}$, $\mu\text{C}^* = 0.75 \text{ F cm}^{-1} \text{V}^{-1} \text{s}^{-1}$). Moreover, we achieved a fully printed n-type OECT by printing other component, including metal electrodes onto flexible polymer substrates. Using this gNDI-Br₂ OECT, we were able to fabricate aerosol-jet printed complementary logic circuit with a PEDOT:PSS p-type counterpart.

Reference

- 1) S. Yu, C.J. Kousseff, C.B. Nielsen, n-Type semiconductors for organic electrochemical transistor applications, *Synth. Met.* 293 (2023) 117295.
2) S. Kang, J. Fan, M. Gupta, Naphthalene diimide-based n-type small molecule organic mixed conductors for accumulation mode organic electrochemical transistors, *RSC Adv.* 13 (2023) 5096-5106.

3) D.A. Bernards, G.G. Malliaras, Steady-state and transient behavior of organic electrochemical transistors. *Adv. Funct. Mater.* 17 (2007) 3538-3544.

4) E.B. Secor, Principles of aerosol jet printing. *Flex. Print. Electron.* 3 (2018) 035002.

8:00 PM EL18.04.04

Ionic Liquid Driven Enhancements in the Electromagnetic Interference Shielding Capabilities of Carbon-Based Polymer Composites Paul Al Malak^{1,2}, Cedric Vancaeyzeele¹, Pierre-Henri Aubert¹, Frédéric Vidal¹, Giao T.M. Nguyen¹, Paolo Bondavalli² and Cédric Plesse¹; ¹CY Cergy-Paris Université, France; ²Thales Research & Technology, France

Electromagnetic interference (EMI) has emerged as a crucial problem in the modern world because of the rapid proliferation of electronic and telecommunication systems, which emit electromagnetic radiation that may perturb the performance of electronic devices on one hand, and could be harmful to the human body on the other [1]. As a result, considerable endeavors have been devoted to the development of efficient materials for EMI shielding/absorption. Polymers and polymeric composites with a wide array of fillers, especially carbon-based fillers have been widely used as promising candidates in the development of commercially viable EMI shielding materials. Lately, extensive research efforts have been put forward, towards effective dispersion of the fillers throughout the matrix. Ionic liquids have emerged as a promising dispersing agent for CNTs through non-covalent functionalization by interacting with the CNTs surface through π - π , cation- π or even Van der Waals interaction [2]. They have been also used as fillers in metamaterial structures, where they actively engage in attenuating the electromagnetic wave thanks to their polarity [3]. Accordingly, it would be really interesting to develop a shield where we can take advantage of the already proven excellent EMI shielding capabilities of carbon based composites and in exploring the capabilities of ionic liquids in a more active manner in a polymer matrix.

Here, we demonstrate the use of carbon-based nanomaterials (MWCNT, Graphene derivatives) incorporated in ionogels as effective EMI shields. These ionogels combine the unique properties of ionic liquids and their ability to attenuate the electromagnetic wave through dipole reorientation and translational motion (movement of the ions). The structural support is provided by the gel matrix, which also aids in matching the impedance of the shield with the surrounding environment, while the presence of carbon-based nanomaterials not only facilitated the formation of conductive pathways but also introduced interfacial polarization and dipole polarization between them and the ionic liquid-gel matrix. The ionogels exhibited remarkable performances across a wide frequency range, where the presence of the ionic liquid led to an enhanced absorption of the electromagnetic wave, with over 97% attenuation, of which over 55% is by absorption. Morphological characterizations revealed the homogeneous envelopment of the CNTs by the ionic liquid enhancing the interfacial polarization. The electrical conductivity measurements confirmed the conductive behavior of the carbon-based nanomaterial incorporated ionogels, which is essential for effective EMI shielding.

[1]: S. Driessen et al. *Ep Europace*, vol. 21, no. 2, p. 219-229, (2019).

[2]: Lopes Pereira, et al. *Journal of Applied Polymer Science*, vol. 133, no. 38 (2016).

[3]: Yang, Fulong, et al. *Applied Physics A*, vol. 125, p. 1-9 (2019).

8:00 PM EL18.04.05

Elucidating the Role of Side-Chain Polarity of Conjugated Polyelectrolytes by Doping Through Organic Electrochemical Transistor Sung Hyun Lee¹, Changwha Jung¹, Hyunho Jeong¹, Chaeyeon Park², Soonyong Lee², Han Young Woo² and Hyunjung Lee¹; ¹Kookmin University, Korea (the Republic of); ²Korea University, Korea (the Republic of)

Conjugated polyelectrolytes (CPEs) exhibit a novel structure composed of electron or hole conducting π -conjugated backbone and ion conducting pendant ionic functionalities. Anionic narrow-band-gap CPE named poly[2,6-(4,4-bis-potassium butanysulfonate-4H-cyclopenta-[2,1-b:3,4-b0]-dithiophene)-alt-4,7-(2,1,3-benzothiadiazole)] (PCPDTBTSO3K, or CPE-K) is well known for self-doped property which is fabricated as a channel material for organic electrochemical transistor (OECT).

In this work, electronic and ionic transport is studied by OECT system. Different types of polarity of side chain attached to the same backbone that contains an alternating D-A units of cyclopentadithiophene (CPDT) and benzothiadiazole (BT) were synthesized. The affect of different polarity was examined as a channel material by using gel-type ionic liquid electrolyte (1-Ethyl-3-methylimidazolium bis(trifluoromethylsulfonyl)imide or [EMIM]⁺[TFSI]⁻) which allows wider range of gate voltage and constant measurement conditions etc. All three channel materials each showed ON and OFF state both in accumulation and depletion mode only by changing the polarity of gate and drain voltage. Ion transport mechanism was compared through OECT system by measuring transfer/output curve, μC^+ value and response time etc. Our work allows for maximizing doping effect through ion penetration and utilize as a dual mode switching system.

8:00 PM EL18.04.06

Study on the Impact of Ions Uptake on the Thermoelectric Performance in Organic Electrochemical Transistors Hyunho Jeong¹, Changwha Jung¹, Sung Hyun Lee¹, Chaeyeon Park², Soonyong Lee², Han Young Woo² and Hyunjung Lee¹; ¹Kookmin university, Korea (the Republic of); ²Korea University, Korea (the Republic of)

The aim of our research is to explore the effects of penetrated ions in the polymer matrix by electrochemical doping on the thermoelectric performance in organic electrochemical transistors (OECTs). Controlling the Seebeck coefficient and electrical conductivity values of organic thermoelectric (TE) materials has been widely studied. However, earlier works were primarily conducted based on the chemical doping method. In terms of controlling the TE performance, the electrochemical doping method has the advantage of finely tuning doping levels by changing the applied gate voltage (V_g). Anions or cations from ionic liquid penetrate the polymer matrix depending on the sign of applied gate voltage and modulating the conductivity. This method provides an easy way to study the TE performance of organic TE materials.

Generally, the focus is on the doped organic TE materials by penetration of mobile ions, and penetrated ions induced Seebeck coefficient is seldom considered. The temperature gradient causes not only the potential difference created by the polymer film but also the potential difference due to ions in the ionic liquid moving by the Soret effect. Thus, it is essential to clarify the contribution of ions to TE performance for further application.

Here, we demonstrate the influence of the uptake of mobile ions in an electrolyte (1-Ethyl-3-methylimidazolium bis(trifluoromethylsulfonyl)imide, ([EMIM]⁺[TFSI]⁻)) on TE performance using different polarity side chain polymers. We characterize the time-dependency of the potential difference between the cold side electrode and the hot side electrode based on the OECT system to investigate the ionic and electronic induced Seebeck coefficient separately.

8:00 PM EL18.04.07

Molecular Design for Tunable Ionic Thermopower with High Stretchability Minju Park; Korea Research Institute of Chemical Technology, Korea (the Republic of)

Wearable and stretchable electronics have attracted tremendous attention due to their wide applications in various areas. However, the lack of efficient, light-weighted and environmental friendly power sources has been the bottleneck that hinders the wide applications of wearable technologies. One of the attractive solutions is the thermoelectric generators (TEGs), which can directly convert waste heat from human body or environment into electricity. Though great development has been achieved with conventional TEGs, present inorganic thermoelectric materials still suffer from rigid properties and low Seebeck coefficient (several hundred $\mu\text{V}/\text{K}$ scale), which requires an integration of hundreds of elements. To overcome these challenges, ionic thermoelectric materials utilizing ionic transport open up new possibilities for the recuperation of waste heat due to their enormous Seebeck coefficient, which can operate supercapacitors by energy harvesting.

Herein, we introduce intrinsically stretchable acrylamide based polymers (PAM) as the ion conductive materials comprising graphene derivatives, which possess high stretchability and excellent thermoelectric performance. Interestingly, ionic conductivity and thermopower could be tunable according to the molecular structure of graphene-based additives. Chemical structure of graphene-based additives was successfully modified by covalent functionalization with phenylsulfonic acid (SGO) and amine species (NGO), resulting in strong positive and negative charged graphene nanosheets, respectively. Induced charge could significantly affect to Coulombic interaction between ion and polymer, or ion and solvent, rendering in large difference in ion concentration under temperature gradient. As a result, the proposed materials exhibit excellent and tunable Seebeck coefficient (up to 39.7 mV/K) as well as remarkable stretchability. The ionic thermoelectric performance was sustained during multiple stretch-release cycles (50% strain, 1000 cycles), which demonstrates high durability under severe deformation. Furthermore, we fabricate ionic thermoelectric supercapacitors (ITESC) with ionogels, demonstrating the heat-to-electricity conversion was successfully established. These findings show a promising strategy to obtain multifunctional ionic thermoelectric materials by engineering the molecular structures, and demonstrate the great potential of ionogels for harvesting low-grade heat in human-comfortable humidity environments.

8:00 PM EL18.04.08

Pyrene Dianhydride Condensation Ladder Polymer: Synthesis and Film Characterization. Katherine Johnston, Emma Mikita and Julia A. Schneider; Fordham University, United States

Organic materials that display mixed-conductance—the ability to conduct both ions and electrons—are actively sought after for their possible use in organic electrochemical transistors and sodium-ion batteries, among many other applications. Of only a few n-type polymers reported to display mixed-conductance, poly(benzobisimidazobenzophenanthrolinedione) (BBL) is the most promising to date. Its conjugated ladder structure makes it very environmentally stable and its ability to maintain a planar backbone when swelling in ionic media has led to high capacitance and electron mobility. The success of BBL in terms of its mixed-conductance has renewed interest in the study and development of n-type ladder polymers. We will present the synthesis of a new mixed-conducting material, a pyrene-based ladder polymer, poly(benzimidazobenzod(e,e,f)phenanthrenedione) ladder (BPyL), formed from the polycondensation reaction between our pyrene dianhydride monomer unit and 1,2,4,5-tetraaminobenzene tetrahydrochloride (TAB.4HCl). The larger aromatic core of BPyL vs. BBL influences the packing of the

polymer, and therefore, how well the polymer can form films and perform in electronic devices. We will study and present how **BPyL** and **BBL** differ in regard to their film making abilities using spectro-electrochemical analysis, UV-Vis, and TEM. The capacitance of **BPyL** will also be measured and reported.

Through our synthesis of the pyrene dianhydride monomer, two isomers are produced. We will present the synthesis and characterization of each isomer in its diimide forms. The pyrene diimide dyes themselves and their spectral and electrochemical properties are useful to study for future incorporation into conjugated polymers. Pyrene is impactful as a core for these molecules due to its unique fluorescence property: excimer formation. Excimer formation causes a shift in fluorescence when the molecule is close to a neighboring molecule and can be a useful way to visualize the molecule's ability to stack or congregate. Determining the monomers' ability to form excimers can help with determining their ability to pack when in the polymer form. The synthesis of both pyrene diimide isomers will be presented with their fluorescence spectrum, which demonstrate excimer formation at higher concentrations.

8:00 PM EL18.04.09

Nanoscale Perspective on Charge Carrier Transport in Sepia Melanin [ShahidKhaleel](#), Anthony Camus, Joaquin Isasmendi and Clara Santato; Polytechnique Montreal, Canada

Sepia melanin, a naturally occurring pigment found in the ink sac of cuttlefish, has garnered significant interest for its intriguing electrical properties and potential as an organic semiconductor material. Sepia melanin exhibits properties of disordered organic semiconductors which display charge transport behavior attributable to a combination of band-like and hopping transport mechanisms¹. The electrical conduction in Sepia melanin is influenced by its complex hierarchical structure, which consists of melanin nanoparticles self-assembled into granules. These nanoparticles result from variety of arrangements of pi-pi stacked molecules².

Understanding charge carrier transport in organic materials at the nanoscale is key for the advancement of emerging optoelectronic technologies. In this study, we investigate the charge transport properties of Sepia melanin at the nanoscale. The unique properties of Sepia melanin, including its moisture dependent electrical response³ and broadband optical absorption⁴, make it a promising material for applications in organic electronics, energy harvesting, and bioelectronics. By understanding the charge transport phenomena at the nanoscale, we aim to unlock the full potential of Sepia melanin for these technological applications.

We focus our investigations on an inter-digitated planar geometry of patterns (inter-electrodes distance ~200-700 nm) as we try to catch signals from individual granules of Sepia melanin. Patterns are fabricated by Electron Beam Lithography.

Preliminary findings from our ongoing study reveal the influence of structural disorder on charge carrier transport in Sepia melanin, such as charge carrier localization and trapping effects, which offer opportunities for tailored charge transport characteristics in devices.

Work is in progress to study the Electrochemical Impedance Spectroscopy (EIS) response in different atmospheres to confirm the nature of the charge carriers. Temperature dependent electrical characterization are helping us to shed light on aspects pertaining to hopping transport (e.g. to calculate the activation energy).

The insights gained from this research have the potential to advance the field of organic electronics and open up new avenues for the development of bioinspired electronic devices and sensors.

1. Haneef, Hamna F., Andrew M. Zeidell, and Oana D. Jurchescu. "Charge carrier traps in organic semiconductors: a review on the underlying physics and impact on electronic devices." *Journal of Materials Chemistry C* 8, no. 3 (2020): 759-787.

2. Clancy, Christine MR, and John D. Simon. "Ultrastructural organization of eumelanin from *Sepia officinalis* measured by atomic force microscopy." *Biochemistry* 40, no. 44 (2001): 13353-13360.

3. Wuunsche, Julia, Yingxin Deng, Prajwal Kumar, Eduardo Di Mauro, Erik Josberger, Jonathan Sayago, Alessandro Pezzella et al. "Protonic and electronic transport in hydrated thin films of the pigment eumelanin." *Chemistry of Materials* 27, no. 2 (2015): 436-442.

4. Pullman, Alberte, and Bernard Pullman. "The band structure of melanins." *Biochimica et biophysica acta* 54 (1961): 384-385.

8:00 PM EL18.04.10

Enhancing Adhesion of PEDOT Coatings on Metal Electrodes: A Promising Approach [SaraEbrahimi](#), Fabio Cicoira and Sadaf Khoomortezaei; Polytechnique Montreal, Canada

The use of electrodes as biomedical devices in healthcare is undergoing innovative advancements, employing novel techniques that bridge the gap between biological systems and electronics. Nonetheless, traditional metallic electrodes encounter a substantial hurdle in the form of impedance, impeding the smooth transmission of electrical signals within living tissues. To tackle this challenge, recent breakthroughs suggest the utilization of poly(3,4-ethylene dioxythiophene) (PEDOT), an organic conducting polymer, as a solution to overcome the impedance obstacle [1]. PEDOT exhibits favourable qualities that make it an excellent candidate for bioelectronic devices. These desirable characteristics include its ability to maintain low impedance, high conductivity, excellent electrochemical stability, and biocompatibility, rendering it an optimal material for such applications [2]. When left uncoated, copper electrodes are susceptible to rapid oxidation, which challenges their direct compatibility with a PEDOT coating. To address this limitation, we propose applying nickel-phosphorus and gold/nickel-phosphorus layers onto the copper electrodes (Au/Ni-P/Cu). This coating approach helps overcome the oxidation issue and enhances the compatibility between the electrodes and the PEDOT material [3]. Afterward, the process involves depositing PEDOT onto the surface of the electrodes. The primary goal is to develop cutting-edge biomedical electrodes that exhibit enhanced conductivity, minimized impedance, and improved mechanical adhesion to the underlying metal substrate. However, it has been observed that PEDOT does not adhere adequately to the metal substrates [4]. In this work the main strategy employed for enhancing adhesion is etching the substrate.

The Ni-P/Cu electrodes were prepared through electroless plating, and applied gold and PEDOT layers onto the Cu electrodes. The deposition of PEDOT onto the electrodes was achieved using galvanostatic chronopotentiometry (CP) electropolymerization, gradually transforming the electrodes into a dark blue colour. The chronoamperometric method yielded PEDOT films that were uniform and consistent across the electrodes. To analyze and characterize the PEDOT coatings on both Ni-P/Cu and Au/Ni-P/Cu electrodes, several techniques were employed, including electrochemical impedance spectroscopy (EIS) and cyclic voltammetry (CV) in a phosphate-buffered saline solution (PBS), X-ray photoelectron spectroscopy (XPS), and scanning electron microscopy (SEM). The adhesion of the coatings to the substrate was evaluated through sonication and a tape test, demonstrating their robustness and strong adherence. Furthermore, the electrochemical and mechanical stability of the PEDOT material, doped with LiClO₄, on the metal electrodes was successfully demonstrated by optimizing the conditions of the electropolymerization process and pre-treatments of the substrates.

References:

1. N. Rossetti, ACS Appl. Bio Mater. 2(11): p. 5154-5163(2019).

2. C.m. Bodart, . ACS applied materials interfaces. 11(19): p. 17226-17233(2019).

3. J. Son, Ind. Eng. Chem. Res. 7. 59(16): p. 8086-8092(2020).

4. B. Wei, ACS applied materials interfaces., 7(28): p. 15388-15394 (2015).

8:00 PM EL18.04.11

Advanced in Operando Atomic Force Microscopy Studies of the Gating Mechanisms at Metal Oxide Ion-Gated Transistors [LuanP. Camargo](#)^{1,2}, LarieI.C. Neres^{1,3}, MartinS. Barbosa⁴, RaminKarimi¹, JoseR. Herrera¹ and ClaraSantato¹; ¹Polytechnique Montreal, Canada; ²State University of Londrina, Brazil; ³State University of São Paulo (UNESP), Brazil; ⁴Federal University of Goias, Brazil

Characterization of interfaces by advanced techniques *in operando*, including Atomic Force Microscopy (AFM), are gaining significance in the scientific investigation of electrochemical devices since they permit to follow materials' dynamics, which in turn are linked to device performance.

Ion-Gated Transistors (IGTs) enable the modulation of electronic conductivity in a semiconducting channel upon the application of an electrical bias between the channel material and the gate electrode, through an ionic medium. Metal oxides such as WO₃ and TiO₂ as channel materials interfaced with ionic liquids, such as 1-ethyl-3-methylimidazolium bis(trifluoromethylsulfonyl)imide ([EMIM][TFSI]), shows great promise for low-power, large-area electronics but also, at the fundamental level, the study insulator-to-metal transitions. The presence of Li⁺ ions in the ionic liquid can enhance the versatility of IGTs in terms of the degree of doping and time response^{1,2}.

The doping mechanisms establishing the effectiveness of the ion gating mechanism are not well understood. Gaining insight into the structure of the electric double layer (EDL) forming at the channel ionic medium interface is expected to advance such understanding.

We report on a nanoscale study at interfaces between WO₃ and TiO₂ films and ionic liquids, possibly including Li ions, by AFM, force-distance profiling. The aim of the study is to shed light on phenomena and processes such as ion layering, ion packing density and shrinking, and ion reorientations. Scanning probe studies have been paralleled by computational efforts (Molecular Dynamics, MD). AFM force-distance profiling in conjunction with simulation methods, allows the characterization and understanding of the structure of the EDL and its evolution with the applied bias, thus permitting optimizing device performance.

8:00 PM EL18.04.12

Investigating Doping/Dedoping Processes in Electropolymerized Organic Mixed Ionic-Electronic Conductors [MeijingWang](#)^{1,2}, JanineMauzerol² and FabioCicoira¹; ¹Polytechnique

Organic electrochemical transistors (OECTs) based on organic mixed ionic-electronic conductors (OMIECs), which possess both electronic and ionic transport capabilities, have shown promising application potentials in bioelectronics.¹ OECTs utilize the reversible doping/dedoping properties of active OMIEC channel materials by applying a gate voltage across the electrolyte to modulate the channel conductance.² Although there has been extensive research to understand the working principle which involves mixed ionic and electronic transport, the study on the fundamental understanding of ionic transport and injection/ejection is still limited. For example, in one of the model OMIECs, poly(3,4-ethylenedioxythiophene) (PEDOT) doped with organic polyanions poly(styrenesulfonate) (PSS), the dedoping mechanism is believed to be mainly due to the insertion of cations from the electrolyte to the PEDOT:PSS film. However, when small anion-based dopants, such as ClO₄⁻ and BF₄⁻, are used in the PEDOT system, the anions may be released from the material to the electrolyte.² The doping/dedoping mechanisms are therefore becoming more complicated. To better understand these doping/dedoping processes, we utilized an *in situ* film fabrication method, electropolymerization, to prepare PEDOT-based films with various dopants, such as PSS⁻, ClO₄⁻ and BF₄⁻. This approach allows the material properties to be readily adjusted by controlling the dopant type, dopant concentration, and other electropolymerization parameters.³ The polymer films were deposited on the source and drain electrodes and grow gradually to cover the gap in between. The effects of dopant type, concentration, and deposition time on the performance of OECTs were systematically studied. Next, the electrochemical quartz crystal microbalance (EQCM), which can monitor the mass exchange between the film and electrolyte, was incorporated to explore the doping/dedoping behavior. Our work contributes to a deeper understanding of the ionic charge transport in small anion-doped OMIECs and the working mechanism of corresponding OECTs.

References:

- (1) Nawaz, A.; Liu, Q.; Leong, W. L.; Fairfull-Smith, K. E.; Sonar, P. Organic Electrochemical Transistors for In Vivo Bioelectronics. *Adv Mater* **2021**, *33* (49), e2101874. DOI: 10.1002/adma.202101874.
- (2) Rivnay, J.; Inal, S.; Salleo, A.; Owens, R. M.; Berggren, M.; Malliaras, G. G. Organic electrochemical transistors. *Nature Reviews Materials* **2018**, *3* (2). DOI: 10.1038/natrevmats.2017.86.
- (3) Heinze, J.; Frontana-Urbe A. B.; Ludwigs, S. Electrochemistry of Conducting Polymers-Persistent Models and New Concepts. *Chemical Reviews* **2010**, *110* (8). DOI: 10.1021/cr900226k.

8:00 PM EL18.04.13

Dynamic Surface Phases Controlling Asymmetry of High-Rate Lithiation and Delithiation in Phase-Separating ElectrodesBonhoKoo¹, JinkyuChung¹, JuwonKim¹, MartinZ. Bazant² and JongwooLim¹; ¹Seoul National University, Korea (the Republic of); ²Massachusetts Institute of Technology, United States

Lithium-ion batteries (LIBs) are a cornerstone of modern energy storage systems due to their ability to store and release electrical energy as chemical energy. However, at high cycling rates, the conversion becomes irreversible, resulting in higher overpotential and decreased capacity. This is particularly pronounced during lithiation compared to delithiation and is a major challenge for electrodes undergoing phase transitions. Despite attempts to understand the root cause of this asymmetry, the impact of these electrochemical conditions on the dynamics and pathways of lithium ion insertion and extraction remains unclear.

In this study, we used *operando* X-ray microscopy to observe the surface and bulk Li compositions in [100]-oriented Li_{1-x}FePO₄ sub-micron particles over a wide range of currents, 0.07C-7C. We clearly visualised anisotropic and rate-dependent phase-transformation pathways, revealed how surface and bulk phase separation strongly depend on the direction and magnitude of the current, and thereby reconciled contradictions among existing models. The dynamical asymmetry between fast lithiation and delithiation is attributed to autoinhibitory (negative self-feedback on reaction rate) Li-rich and autocatalytic (positive self-feedback) Li-poor domains, respectively. These domains are stabilised in proximity to the active crystal surface, which is the origin of asymmetry in the overpotential and rate capability between fast lithiation and delithiation.

New insights on how dynamic phase transition controls the lithium ion transport kinetics can be applied to a variety of electrode materials undergoing phase transitions, such as Li_{4/5}Ti_{5/3}O₄ and LiCoO₂, Ni-rich LiNiMnCoO₂, LiNiO₂ etc., paving the way for improved performance and stability in future LIBs. Moreover, our study may also have applications in lithionic memristors that can store information by modulating the electronic conductivity of Li surface phases (*e.g.*, in LTO and LCO), which have to be visualised at the nanoscale.

8:00 PM EL18.04.14

The Role of Alky Spacers and Functionality in Polar Carboxylated Functionalized Polythiophene for High-Performance Organic Electrochemical TransistorsZeyuanSun¹ and BrianKhou²; ¹Lehigh University, United States; ²The University of Chicago, United States

Side chain engineering of polar hydrophilic substituents on the mixed conductor backbones has been proved as a successful strategy in developing robust bioelectronic devices, including organic electrochemical transistors (OECTs). However, prevailing design principles rely heavily on the ethylene glycol moiety, limiting the ability to tailor chemistry to serve the vast application space for OECTs. In this work, we report a family of carboxylic acid functionalized polythiophenes, poly [3-(4-carboxyalkyl) thiophene-2,5-diyl], processing with a varying carboxyalkyl chain lengths (propyl, butyl, and pentyl) as a novel hybrid alkyl-polar side chain moiety. With the aid of a fully aqueous processing strategy, this family of material provides an opportunity for a comprehensive evaluation of both the length effect of alkyl spacer and the impact of carboxylic acid functionality on the electrochemical characteristics in aqueous environment. Our results show that longer alkyl spacers in carboxylic acid functionalized side chain yield disadvantages for achieving higher volumetric capacitance (C*), however, significantly reducing detrimental swelling, with P3C(Pe)T exhibiting a thickness change upon passive swelling of only +1.9%. By integrating these high-performance mixed conductors into planar OECT architectures, it has been found that polymer bearing with butyl spacer exhibits the highest performance (= 128.6 5.5), which render them as one of the best performing conjugated polyelectrolytes. By integrating these high-performance mixed conductors into both interdigitated and planar OECT architectures, material dependent properties were evaluated, including device performance and stability as well as geometry dependent effects. Furthermore, *in-situ* Raman spectroscopy and spectroelectrochemistry studies are also conducted which provide meaningful insights into structural reorganization and optical progression upon electrochemical doping/de-doping, yielding a molecular level understanding toward ionic-electronic coupling and device operation upon varying side chain length. Overall, through these extensive and methodical investigations, we were able to uncover distinct properties associated with the increased alkyl length in these carboxylated polythiophenes. Our study highlights that even minor alterations and structural variation in the side chain can have a significant impact on electrochemical, optical, microstructural, and electrical properties of a polymeric mixed conductor.

8:00 PM EL18.04.15

High-throughput microfluidic-assisted machine learning to investigate vertical phase separation of small molecule:polymer blendJun HeeWoo and StevePark; Korea Advanced Institute of Science and Technology, Korea (the Republic of)

Solution-based thin-film processing has been deemed as a promising technology that enables the fabrication of various devices such as field-effect transistors (FETs), solar cells, and sensors in a cost-efficient, facile, and scalable manner. One key feature of solution-based processing is the tunability of the ink formulation, through which the thin-film coating process and device performance can be controlled. Also, blending solutions containing different solutes has been shown to significantly improve the performance of the resulting devices compared to that of their unmixed counterparts. When small molecule organic semiconductor is mixed with insulating polymer, bilayer structure can be formed by the induction of vertical phase separation during drying process, which yields drastically improved charge transport properties, and hence the transistor performance. Despite the advantage of having controllability of ink formation, there also exists the critical challenge of finding the ideal ink composition that yields optimum device performance amongst numerous possible compositions. To generate a thin-film large enough to conduct device testing, several to hundreds of microliters of solution is required. However, since precisely controlling the ink formulation at this volume is difficult, several milliliters of solution is typically prepared. Therefore, ink formula optimization is inevitably a highly time-consuming and resource-intensive process. Added on top of this issue is the fact that the coating process parameters (*e.g.*, substrate temperature, coating speed) also changes the thin-film properties and therefore the device performance, resulting in orders of magnitude increase in the number of possible combinations of experimental parameters (*e.g.*, different combinations of ink composition, substrate temperature, coating speed) that need to be tested. The sheer number of combinations renders it impractical to test all combinations. Hence, researchers typically resort to iterative experiments based on intuition and heuristic approach, which limits or prolongs the optimization process and results in poor understanding of process-performance correlations. Resolving this challenge involves addressing two important questions. Firstly, how can thin-films of varying combinations of experimental parameters (*i.e.*, various experimental conditions, where condition refers to a set of specific values of parameters under which thin-film was formed) be made in a time-efficient and resource-efficient manner so that data can be collected rapidly and economically? Secondly, how can the correlation between experimental parameters and device performance be systematically analyzed without reliance on human intuition? In this work, microfluidic screening-embedded thin-film processing technique is developed, through which thin-films of varying ratios of small molecule semiconductor:polymer blend were simultaneously generated and screened in a time- and resource-efficient manner. The vertical phase separation of C8-BTBT and PS blend solution was demonstrated, and was shown to have relatively high transistor performance, owing to the high intrinsic mobility of C8-BTBT and high viscosity of PS-added solution. Moreover, utilizing the thin-films of varying combinations of experimental parameters, machine learning models were trained to predict the transistor performance. Gaussian Process Regression (GPR) algorithms tuned by Bayesian optimization showed the best predictive accuracy amongst the trained models, which enables narrowing down of the combinations of experimental parameters and investigation of the degree of vertical phase separation under the predicted parameter space. Our technique can serve as a guideline for elucidating the underlying complex parameter-property-performance correlations in solution-based thin-film processing, thereby accelerating the optimization of various thin-film devices in the future.

8:00 PM EL18.04.16

Vertical-Structure Improves The Strain Limit of OMIEC-TransistorsShileiDai, ZhongruiWang and ShimingZhang; The University of Hong Kong, Hong Kong

Organic mixed ionic-electronic conductors (OMIECs), also known as organic mixed conductors, such as PEDOT:PSS, are becoming increasingly important materials in various applications. One typical application is the development of organic electrochemical transistors (OECTs), which enable high sensitivity at low power consumption. PEDOT:PSS OECTs find significant applications in diverse fields, including brain-machine interfaces and ubiquitous wearable biosensing.

To enhance the robustness for skin-integrated applications, stretchable OECTs (sOECTs) have been developed [1]. However, most sOECTs require OMIECs films to possess good mechanical properties, which limit their use in this emerging area.

In this study, we introduce the design of vertical sOECTs [2]. The unique vertically sandwiched structure between the source, OMIEC channel, and drain electrodes enables significantly higher stretchability, surpassing the strain limit of OMIECs. sOECTs developed with this design can be stretched in arbitrary directions, making them suitable for a wide range of skin-interfaced bioelectronic applications.

References:

- [1]. Zhang S, Hubis E, Tomasello G, et al. Patterning of stretchable organic electrochemical transistors[J]. *Chemistry of Materials*, 2017, 29(7): 3126-3132.
- [2]. Dai S, Zhang S, Submitted.

8:00 PM EL18.04.17

Dual Gate Electrochemical and Transistors and Inverters based on WO₃ for Improved Transconductance and Dynamic ResponseLuisPereira^{1,2}; ¹FCT NOVA, Portugal; ²AlmaScience, Portugal

Electrolyte-gated transistors (EGTs) and electrochemical transistors (ECTs) have received special attention over the last decade due to their advantages, deriving from using electrolytes as gate dielectrics. These include low operating voltages, printability and solution processability, low contact resistances, and the possibility of fabricating new device architectures. High driving currents due to electric double layer (EDL) capacitance (C_{DL}) in EDL transistors (EDLTs) or 3D-channel formation in ECTs, complement the list and open routes for their application in biosensors, electrochemical logic gates, wearable electronics, or low-power consumption and flexible devices.

This work shows a novel architecture of ECTs based on the electrochromic material WO₃. Introducing a fourth electrode behind the channel (Back-electrode -BE) stabilized drain current, as electrons can be channeled into the active layer for electrochemical reactions. Additionally, control over the ion movement in the channel and the electrolyte and, consequently over the occurring redox reactions is possible. As a consequence thereof, it was found that V_{on} can be controllable through the applied voltage at the BE (V_{BE}) and that V_{on} can be shifted from any negative V_G up to 0 V and possibly beyond. The devices can be 'programmed' to work in normally-off (enhancement) or normally-on (depletion) mode. On-Off ratios of 10⁵ and transconductances of 0.35 mS were achieved. Dynamic characterization with an asymmetric square (V_G between -6 and 4 V) wave potential demonstrated On-Off ratios of 4 orders of magnitude for frequencies up to 1 Hz. Data suggests that the cut-off frequency lies way beyond that value. It was demonstrated that with precise control over V_{on}, electrochemical logic inverters with two identical devices are feasible, presenting very high and controllable gains. The possibility of keeping load and driver transistors respectively at normally-on and normally-off makes transistor sizing redundant. Further, with this transistor architecture, problems like small logic swings or small noise margins, usually related to enhancement-load inverters, can be counteracted.

8:00 PM EL18.04.18

Unraveling The Critical Hydration Effect on Size-Dependent and Ion-Specific Ion Pairing Inside Sub-1nm Graphene NanoslitsFanFeng, ZheLiu and DanLi; The University of Melbourne, Australia

The intriguing phenomena of ion pairing and salt aggregation inside two-dimensional nanoslits have recently been reported in experiments and numerical simulations, leading to the anomalous gate-voltage modulated ion transport and memoresistive properties. An in-depth grasp of the intricate mechanisms governing this ion pairing effect is imperative for engineering advanced materials with specific functionalities and heightened performance. Nevertheless, despite extensive investigations into the dielectric properties of confined water and its confining medium, a unified understanding of how ion-pairing effects are governed by the interplay of hydration effect and nanoconfinement has remained elusive.

This study delves into the ion pairing effect within sub-1nm graphene nanoslits and offers a novel insight into the mechanisms driven by hydration effects. Conducting atomic-level molecular dynamics (MD) simulations of alkali ion electrolytes within multilayered graphene membranes, we unveil a nuanced dependence on slit size and ion-specific behaviors influencing the ion pairing phenomenon, which are confirmed in our experiments. Furthermore, we conclude that the complicated dehydration and renormalization processes primarily determine the propensity for nanoconfined ion-pairing effects, by displaying a comprehensive analysis of the structural and energetic characteristics of water molecules within the hydration shells. We validate this mechanism by elucidating both slit-size and ion-specific effects: as the slit size decreases from 1nm to 7 Å, the structure of the hydration shell becomes increasingly ordered, resulting in a corresponding reduction in entropic free energy; on the other hand, the ion-specific effect is driven by distinct enthalpic changes associated with the formation of larger ion clusters, rather than the mere presence of individual ion pairs.

8:00 PM EL18.04.19

Ultrafast Dynamics of n-Type Organic Mixed Ionic-Electronic Conductors for Photoelectrochemical Transistor ApplicationsChristopherE. Petoukhoff¹, VictorDruet¹, LatifahAlmullah¹, NisreenAlshehri¹, CatherineDe Castro¹, SophieGriggs², MaryamAlsufyani², IainMcCulloch², Sahikamal¹ and FredericLaqui¹; ¹King Abdullah University of Science & Technology (KAUST), Saudi Arabia; ²University of Oxford, United Kingdom

Conjugated polymer-based organic mixed ionic-electronic conductors (OMIECs) have been widely employed as the active materials in the channel of organic electrochemical transistor (OECT) devices, which are ideal for electronic devices in aqueous media. Due to their ease of chemical functionalization, tunable softness, and flexibility, polymer OMIECs are uniquely suited for biological applications, where OECT devices are expected to play a major role. Although the photosensitivity of conjugated polymers has been widely studied and applied for solar cells, photodetectors, and photocatalysts, the light-sensitivity of polymer OMIECs has been largely underexplored in OECT devices. While there have been several reports on light-sensitivity of organic photoelectrochemical transistors (OPECTs) employing OMIECs, these have largely relied on incorporation of additional light-sensitive inorganic materials at the gate terminal. Very recently, we have demonstrated that a single n-type OMIEC can serve as the photoactive material in OPECT devices, without additional materials in the gate terminal [1]. We then demonstrated for a variety of different n-type OMIEC polymers that the intrinsic photosensitivity of the polymer is critically important for achieving large open circuit potentials, which must be balanced against the transconductance for the best performance of OPECT devices [2].

In this breaking news contribution, we discuss the origin of the photosensitivity of five different OMIECs. We combine doping-induced absorption (DIA), femtosecond transient absorption (TA), time-resolved photoluminescence (TRPL), and time-resolved THz (TRTS) spectroscopies to investigate the excited state dynamics. We compare the photoexcited species in dry, intrinsic OMIEC films and demonstrate that the instantaneous formation of intramolecular charge transfer (ICT) excitons is largely responsible for facilitating charge dissociation at interfaces, such as either at the ITO or electrolyte interface. We demonstrate that the exciton lifetime plays a critical role in determining the open-circuit potential of photoelectrochemical cells. However, the responsivity of OPECT devices is balanced by the dark transconductance, which is orders of magnitude larger for self-doped polymers, having conductivities on the order of 190 ohms-per-cm. Finally, we show that the exciton-to-charge conversion process is faster when the OMIEC is immersed in electrolytic solutions, which we attribute to the increased dielectric constant of the medium.

[1] V. Druet, D. Ohayon, C. E. Petoukhoff, *et al.*, "A single n-type semiconducting polymer-based photo-electrochemical transistor," *Nature Communications*, **14**, 5481 (2023).

[2] L. Almulla, V. Druet, C. E. Petoukhoff, *et al.*, "N-type Polymeric Mixed Conductors for All-in-One Photoelectrochemical Transistors" (*under review*).

8:00 PM EL18.04.20

Navigating The Complex Hole-Transport Material Additive Cocktail: Doping Methodologies for Small-Molecule HTMsBenjaminVella, MadeleineMcRoberts, GraemeCooke and PabloDocampo; University of Glasgow, United Kingdom

Most organic molecular hole transporters used in perovskite solar cells require effective doping to reach conductivity values necessary to achieve maximum device efficiencies. This is typically achieved by incorporating a cocktail of additives including tert-butylpyridine, ionic salts (LiTFSI, Zn(TFSI)₂) and metal complexes (FK209) which results in the partial oxidation of the semiconducting material, introducing additional free holes within the HTL and thus providing effective hole transport. However, a detailed study of the relationship between doping level and the quantity of free holes within the matrix has not been carried out. Indiscriminately adding the same additive cocktail to different HTM systems can lead to sub-optimal doping and an excess of reactive substances within the film that can catalyse degradation mechanisms. In this study, we investigate a range of HTMs possessing amide or imine linker groups. Our research highlights that oxidation and doping are not synonymous, and while oxidation generally leads to doping, this is not always the case. In addition, we reveal the intricate relationship between the different additives and the doping mechanism as a function of the chemical structures used. We conclude that a 'one size fits all' approach to HTM doping can lead to the misdiagnosis of effectively oxidised molecules, and therefore propose spectroscopic techniques to monitor the efficacy of doping, promoting rational HTM design and expediting the characterisation of new

HTMs.

8:00 PM EL18.04.21

Regioregularity Effects on Mixed Conduction in a Glycolated Polythiophene[DilaraMeli](#)¹, [EllaKelly](#)², [JoshuaTropp](#)^{1,3}, [RuihengWu](#)¹ and [JonathanRivnay](#)^{1,1}; ¹Northwestern University, United States; ²Kalamazoo College, United States; ³Texas Tech University, United States

Organic mixed ionic/electronic conductors (OMIECs) are a versatile class of materials that have found use in a wide variety of applications, from bioelectronics to neuromorphic computing. Much effort has been devoted in recent years to improve OMIEC performance, primarily focusing on systematic side chain and backbone engineering. Usually, novel OMIECs are characterized in organic electrochemical transistor (OECT) test beds from which the figure of merit, μC^* (mobility \times volumetric capacitance), is extracted. μC^* is an attractive metric for comparison, as it scales with device dimensions. However, care must be taken to emphasize that μC^* is not only dependent on synthetic chemistry, but also processing conditions and operating electrolyte environments.

Most prominent high-performing OMIECs synthesized to date are only available at the lab scale, leading to large batch-to-batch variability. Such issues of replicability further hinder systematic structure-property studies. To this extent, we herein study a commercially available glycolated polythiophene OMIEC, P3MEEET. Previous work on this polymer has revealed strong dependence of μC^* on operating electrolyte environment, an effect found to also be molecular weight dependent. It was shown that doping occurred with cation expulsion in KTFSI electrolytes, but via traditional anion uptake in NaCl electrolyte. This had dramatic impacts on charge percolation, which ultimately resulted in large observed differences in mixed conductivity.

To further probe the interplay between microstructure and electrolyte choice, we study regiorandom (RRA) and regioregular (RR) P3MEEET operated in two model electrolytes, aqueous KCl and KTFSI. Surprisingly, we observe little difference in μC^* for as-cast microstructures between the RRA and RR polymers. GIWAXS of as-cast RRA films reveals strong lamellar diffraction and DSC shows distinct side-chain melting. RRA P3MEEET is found to preferentially order edge-on, while the RR polymer shows more distinct face-on scattering. We further conduct electrochemical quartz crystal microbalance (EQCM) measurements to probe doping kinetics in both polymers.

Studies of post-processing treatments on other RR glycolated polythiophenes, in particular annealing, have previously been shown to dramatically affect swelling and thus mixed conduction. Here, we find strong dependence of μC^* on structural changes when operated in KCl electrolytes, whereas in KTFSI electrolytes μC^* appears relatively unchanged given the same post-processing conditions. In particular, annealed RRA polymers in KCl show improved performance, whereas RR polymers exhibit a decrease in μC^* . For the RRA polymer, this enhancement is primarily driven by an increase in C^* due to annealing, which is in contrast to the RR polymer which experiences a decrease in C^* .

In summary, we find that post-processing tunes mixed conductivity differently given differences in polymer regioregularity. However, these effects are also dependent on electrolyte environments, further emphasizing that μC^* must be treated as a system figure of merit.

SESSION EL18.05: Characterizing Mixed Ionic-Electronic Conductors
Session Chairs: Gitti Frey and Micaela Matta
Tuesday Morning, November 28, 2023
Hynes, Level 1, Room 111

8:30 AM *EL18.05.01

Controlling Volume and Mechanical Properties of Polythiophenes via Electrochemical Doping[EleniStavriniidou](#); Linköping University, Sweden

The properties of organic mixed ionic-electronic conductors such as conductivity, volume and even mechanical properties can be tuned via electrochemical doping. These dynamic processes rely on exchange of ions with the surrounding electrolyte combined with injection or extraction of electronic carriers through the addressing electrode. Polythiophenes with glycol side chains are single component OMIECs where the glycolated chains facilitate the ion transport. We demonstrated that a polythiophene with tri-ethylene glycol side chains reversibly expands by 300% upon electrochemical addressing, relative to its previous contracted state, while the first irreversible actuation can achieve values of 10000%, outperforming any other conjugated polymers. Here I will present our findings on how the molecular structure impacts the volume change based on a study with series of polythiophenes that differ in the length and/or in the distribution of the ethylene glycol side chains. Furthermore, I will discuss the effect of the electrolyte and molecular design not only on the volume change but also on the mechanical properties of the polymer. Molecular Dynamics also provide insight on the mechanisms involved at the nanoscale correlating the volume changes with ion and water molecule intercalation to the polymer matrix as well as conformational changes of the polymer chains. Finally, I will present our results on applying these materials for dynamic microfiltration and drug delivery.

9:00 AM EL18.05.02

Magnetic Resonance Studies of Highly Doped Polymeric Semiconductors[TariqMustafa](#), [Dionisius Hardjo LukitoTjhe](#), [IanJacobs](#), [XinglongRen](#), [YaoFu](#), [ClareP. Grey](#) and [HenningSirringhaus](#); University of Cambridge, United Kingdom

Doped organic semiconductors have proved attractive for future device applications such as thermoelectrics, bioelectronics and spintronics. At low doping levels, coulombic trapping of intercalated counter ions is believed to limit charge transport while at high doping levels conductivity is limited by disorder in the material.¹ However, a more detailed understanding of the couplings between the charge/spin carrying polarons of these materials and their environment remains sought after. Work has been done to understand such interactions in undoped materials by means of field induced Electron Spin Resonance (ESR) and has yielded valuable insight into the intimate couplings between charge, spin and structural dynamics.² Here, we extend that work to the study of systems systematically doped in-situ by means of an electrochemical transistor architecture and investigate the effects of interactions between polarons and with the counterions as function of temperature and varying doping levels. We complement the ESR measurements with Nuclear Magnetic Resonance (NMR) characterisation which has been shown to be a powerful technique for characterising ion dynamics in polymeric semiconductors.³ We therefore use NMR to understand ionic motion and interactions in these systems and explore how they could impact the electronic properties of the material.

References

1. I. Jacobs et al., *Journal of the American Chemical Society*, doi:10.1021/jacs.1c10651.
2. S. Schott et al., *Nature Physics*, doi:10.1038/s41567-019-0538-0.
3. D. Lyu et al., *Nature Materials*, doi: 10.1038/s41563-023-01524-1.

9:15 AM *EL18.05.03

Mixed Electron-Ion-Solvent Transfer in Conjugated Polymers Monitored using Quartz Crystal Microbalance with Dissipation Monitoring[RatulThakur](#) and [JodieLutkenhaus](#); Texas A&M University, United States

Conjugated polymers have promising applications in electronics and energy storage due to the polymer's tunable conductivity and redox activity. For example, the conductivity of poly(3-hexylthiophene) (P3HT) is heavily dependent upon the doping level and the dopant type. This feature becomes especially important when considering P3HT or similar conjugated polymers for devices that require switching between electronic states (conductive vs insulating). In this study, the mechanism of mixed ion-electron transfer studied using electrochemical quartz crystal microbalance with dissipation monitoring (EQCM-D) is discussed for P3HT and poly(3,4-ethylenedioxythiophene):polystyrene sulfonate (PEDOT:PSS). During cyclic voltammetry and galvanostatic charge-discharge experiments, the mass change of the polymer film is monitored in real time. Distinct mass transfer regions are quantified as a function of doping level and potential, which are then correlated to changes with *in situ* conductance and spectroelectrochemical response. To identify the time scale at which the doping reaction transitions from kinetic to diffusion control, electrochemical impedance spectroscopy is coupled with EQCM-D. Combining these insights with an electron and mass balance on the process, the number of solvent molecules per ion are estimated. This work gives valuable insight into the nature of mixed ion-electron transfer, including its time scale, as it relates to the electronic properties of conjugated polymers.

9:45 AM EL18.05.04

Ion Trapping and Induced Ordering of Regiorandom Poly(3-hexylthiophene) upon Repeated Electrochemical Doping[SethJackson](#), [RandKingsford](#), [GarrettCollins](#) and [ConnorG. Bischak](#); University of Utah, United States

Conjugated polymer organic mixed ionic electronic conductors (OMIECs) are promising materials for bioelectronics and other organic electronic devices. How these materials behave with repeated electrochemical doping matters for the stability and longevity of these devices. In this work, we employ a combination of grazing incidence wide-angle X-ray scattering (GIWAXS), UV-vis spectroelectrochemistry, and nanoscale imaging of the ions with photoinduced force microscopy (PiFM) to monitor film morphology changes in regiorandom poly(3-hexylthiophene) (RRa P3HT) when exposing the polymer film to various aqueous electrolytes upon repeated electrochemical doping. When using potassium bis(trifluoromethanesulfonyl)imide (KTFSI) as our electrolyte, we see increased ion trapping and an increase in crystalline order in RRa P3HT, as well as the crystallization of TFSI⁻ ions, upon repeated electrochemical doping. Upon thermal annealing at 120 °C after continuous doping of RRa P3HT with TFSI⁻, we see a significant increase in lamellar stacking intensity compared to the film without thermal annealing. When comparing less chaotropic ions to TFSI⁻, we see these ions do not order RRa P3HT to the same extent as TFSI⁻. Overall, this study shows that both ion trapping and structural reorganizations occur in disordered conjugated polymers upon repeated electrochemical cycling.

10:00 AMBREAK

SESSION EL18.06: Mixed Ionic-Electronic Conductors Device Performance and Mechanical Properties

Session Chairs: Laure Kayser and Micaela Matta

Tuesday Morning, November 28, 2023

Hynes, Level 1, Room 111

10:30 AM *EL18.06.01

Improvement of the Electrical, Mechanical and Adhesive Properties of PEDOT:PSSJianyong Ouyang; National University of Singapore, Singapore

Poly(3,4-ethylenedioxythiophene):Polystyrene sulfonate (PEDOT:PSS) is a popular mixed ion-electron conductor, and it can have important application many areas. However, its electrical, mechanical and adhesive properties must be greatly improved for the practical application in some areas. Here, I will present some of our methods to significantly improve the electrical, mechanical and adhesive properties. We also demonstrate their application in wearable/flexible electronics.

References. (1) H. He, R. Chen, S. Yue, S. Yu, J. Wei, and J. Ouyang, Salt-induced ductilization and strain-insensitive resistance of an intrinsically conducting polymer, *Science Advances*, 2022, 8, abq8160; (2) J. Cao, X. Yang, J. Rao, A. Mitriashkin, X. Fan, R. Chen, H. Cheng, X. Wang, J. Goh, H. L. Leo, and J. Ouyang, A Stretchable and Self-adhesive PEDOT:PSS Blend with High Sweat Tolerance as Conformal Biopotential Dry Electrodes, *ACS Applied Materials & Interfaces*, 2022, 14, 39159; (3) L. Zhang, S. K. Kirthika, H. He, C. J. Cai, X. He, H. Gao, S. Yue, C. Li, R. C.-S. Seet, H. Ren, J. Ouyang, Fully Organic, Skin-compliant, Self-adhesive and Stretchable Dry Electrodes for Long-term Motion-robust Epidermal Biopotential Monitoring, *Nature Communications*, 2020, 11, 4683.

11:00 AM EL18.06.02

Tailored Design of Mixed Ionic-Electronic Conductors for both P-Type and N-Type OECTSMukundan Thelakkat^{1,2}, Adrian Hochgesang¹, Andreas Erhardt¹, Gert Krauss¹, Florian Meichsner¹ and Philip Schmode¹; ¹University of Bayreuth, Germany; ²Bavarian Polymer Institute, Germany

Mixed ionic electronic conductors (MIECs) were designed by various strategies of polymer architecture. For all materials, Cyclic voltammetry (CV), spectroelectrochemistry (SEC), ultraviolet photoelectron spectroscopy (UPS), Ultraviolet-Visible (UV-Vis) absorption spectroscopy, and organic field effect transistor (OFET) characterization were carried out and these properties demonstrate the suitability for OECT (organic electrochemical transistor) devices.

For p-type OECTs, conjugated polyelectrolytes and their copolymers based on polythiophene family was first designed and studied [1-2]. The concept was extended to hydrophilic polythiophenes carrying different oligoethylene glycol (OEG) substituents [3]. The advantage of the latter class is that no crosslinking is necessary to prevent the thin films from delamination. The concept of OEG substitution and the required degree of OEG substitution was further applied in the class of poly(diketopyrrolopyrrole) copolymers using different comonomers [4]. For this, four Polydiketopyrrolopyrroles (PDPPs) with increasing ethylene glycol (EG) content and varying nature of comonomer were synthesized. The studies of these hydrophilic PDPPs in NaCl electrolyte-gated OECTs reveal that a high amount of OEG on the DPP moiety is essential for MIEC. The PDPP containing 52 wt.% EG exhibits a high volumetric capacitance of 338 Fcm⁻³ (at 0.8 V), a high hole mobility in aqueous medium (0.13 cm²V⁻¹s⁻¹) and a μC^* product of 45 Fcm⁻¹V⁻¹s⁻¹. OECTs using this polymer retained 97 % of its initial drain-current after 1200 cycles (90 min of continuous operation). In cell-growth medium, the OECT-performance was fully maintained as in NaCl electrolyte. In vitro cytotoxicity and cell viability assays reveal the excellent cell compatibility of these novel systems, showing no toxicity after 24 h of culture. Due to the excellent OECT performance with a considerable cycling stability for 1200 cycles and an outstanding cell compatibility, these PDPPs render themselves viable for in vitro and in vivo bioelectronics.

For the n-type OECTs, two different classical acceptor motifs diketopyrrolopyrrole (DPP) and thienopyrrolodione (TPD) are copolymerized to yield the acceptor-acceptor polymer, Poly(DPP-TPD) [5]. The fundamental design idea is to maximize the electron affinity, thus increasing the ambient stability of the reduced state against oxygen and water while ensuring high ion compatibility through the incorporation of hydrophilic oligoethylene glycol N-substituents. Additionally, a highly planarized polymer structure is anticipated, due to the extended non-covalent interactions (conformational locking) between the carbonyl oxygen and the thiophene protons. The acceptor-acceptor system poly(DPP-TPD) for n-type devices exhibit high electron affinity (EA), and good electron mobility ($\mu_{e(OEFT)}$), in addition to the electrochemical reduction of polymer films in aq. electrolyte. In n-type OECTs, poly(DPP-TPD) demonstrates a moderate threshold voltage of $V_{th} = 0.58$ V, and an outstanding μC^* value of 7.62 F cm⁻¹ V⁻¹ s⁻¹. Cycling studies consisting of pulsed on- and off-switching of the device at gate voltages between $V_g = 0.6 - 0.8$ V in the saturation regime reveal high stability for more than 2700 cycles with rapid switching kinetics.

[1] Brendel et al. *Chem. Mater.* 2014, 26, 1992–1998

[2] Schmode et al. *Chem. Mater.* 2019, 31, 14, 5286–5295

[3] Schmode et al., *ACS Appl. Mater. Interfaces*, 2020, 12, 13209–13039

[4] Krauss et al., *Adv. Funct. Mater.* 2021, 31, 2010048

[5] M Thelakkat et al., *Adv. Electron.Mater.*2023, 2300026

11:15 AM EL18.06.03

Mechanically Adaptive Mixed Ionic-Electronic Conductors Based on a Polar Polythiophene Reinforced with Cellulose NanofibrilsYoungeok Kim¹, Mariza Mone^{1,2}, Sozan Darabi^{1,2}, Sepideh Zokaei¹, Lovisa Karlsson¹, Mariavittoria Craighero¹, Simone Fabiano^{3,4}, Renee Kroon^{3,4} and Christian Müller^{1,2}; ¹Chalmers University of Technology, Sweden; ²Wallenberg Wood Science Center, Chalmers University of Technology, Sweden; ³Linköping University, Sweden; ⁴Wallenberg Wood Science Center, Linköping University, Sweden

Conjugated polymers with oligoether side chains are considered as one of the promising active materials for organic electrochemical devices due to their ability to facilitate mixed ionic-electronic conduction in the electrolyte. However, they tend to have a low glass transition temperature and, consequently, a low elastic modulus, which prevent their use if mechanical robust materials are required. Carboxymethylated cellulose nanofibrils (CNF) are found to be a suitable reinforcing agent for a soft polythiophene with tetraethylene glycol side chains. Dry nanocomposites feature a Young's modulus of more than 400 MPa, which reversibly decreases to 10 MPa or less upon passive swelling through water uptake. The presence of CNF results in a slight decrease in electronic mobility but enhances the ionic mobility and volumetric capacitance, with the latter increasing from 164 to 197 F cm³ upon the addition of 20 vol% CNF. Overall, organic electrochemical transistors (OECTs) feature a higher switching speed and a transconductance that is independent of the CNF content up to at least 20 vol% CNF. Hence, CNF reinforced conjugated polymers with oligoether side chains facilitate the design of mechanically adaptive mixed ionic-electronic conductors for wearable electronics and bioelectronics.

11:30 AM EL18.06.04

Engineering Response Time and Synaptic Behavior of Organic Ion-Gated Transistors Through Structural ModificationsRamin Karimi¹, Zhaojing Gao¹, Afzal-Ahmed Dar¹, Lariel C. Neres^{1,2}, Patrick Dang¹ and Clara Santato¹; ¹Polytechnique Montreal, Canada; ²State University of São Paulo (UNESP), Brazil

The von Neumann architecture was designed for processing tasks serially. The amount of data produced in the present *intelligent* era renders this architecture unable to keep up. As a result, new solutions, such as neuromorphic parallel computing, are being developed to increase data storage and processing speed. There are concerns, however, about the sizes of the chips composed of synaptic transistors and their parallel computing capacity.

In this work, we present the effect of poly(3-hexylthiophene) (P3HT) film thickness on the synaptic behavior and response time of ion-gated transistors (IGTs) based thereon. The P3HT films' thickness varies from 50 to 300 nm. The drain-source current, I_{ds} , and charge carrier mobility increase with thickness, likely due to an increased degree of crystallinity in the films with the thickness. The presence of crystalline domains is expected to increase the de-doping time (time to remove the anions from the p-type P3HT channel). In turn, this increases the transistor response time and permits to achieve transition from short-term plasticity (STP) to long-term plasticity (LTP). Further, increasing the thickness of the channel increases the plasticity and

paired-pulse facilitation (PPF) index.

The molecular weight (MW) is another parameter that we consider to control synaptic functions and response time. The XRD patterns of films obtained from three different MW, low (ca. 24 kDa), intermediate (ca. 42 kDa), and high (ca. 91 kDa), show that the degree of crystallinity decreases with increasing MW. This is expected to strongly affect ion permeability, and therefore the advancement of doping and redistribution time of anions.

In conclusion, we propose a methodology to control the response time and synaptic functions of IGTs with changing P3HT MW at constant film thickness or varying the thickness of channel fixing MW.

11:45 AM EL18.06.05

Surface Functionalization for High-Performance and Water-Stable PEDOT:PSS Thin Films for Bioelectronics Peter O. Osazuwa, Abigail Nolin, Chun-Yuan Lo, XuFeng, Charles Dhong and Laure V. Kayser; University of Delaware, United States

Organic mixed ionic-electronic conductors such as poly(3,4-ethylenedioxythiophene):poly(styrene sulfonate) (PEDOT:PSS) have attracted attention as materials for the fabrication of organic electrochemical transistors (OECTs) for bioelectronics. The PEDOT:PSS dispersions are typically blended with (3-glycidyloxypropyl)trimethoxysilane (GOPS) before spin-coating to ensure strong adhesion of the films to device substrates and maintain their long-term stability in aqueous solutions. However, blending with GOPS changes the morphology of PEDOT:PSS films, affecting their electrical properties and significantly reducing the performance of OECTs. Here, we functionalized the surface of the substrates with GOPS to introduce a silane monolayer with epoxy groups before spin-coating PEDOT:PSS. The resulting films were compared to those obtained by blending and showed similar long-term stability in aqueous solutions under passive conditions and electrochemical cycling. However, the surface functionalization approach led to increased electronic conductivity ($2650 \pm 467 \text{ S cm}^{-1}$), higher transconductance ($24 \pm 4 \text{ mS } \mu\text{m}^{-1}$), and $[\mu\text{C}^*]$ value ($376 \pm 74 \text{ F cm}^{-1} \text{ V}^{-1} \text{ s}^{-1}$) in OECT devices, and larger volumetric capacitance ($109 \pm 5 \text{ F cm}^{-3}$). Detailed characterization using time of flight secondary ion mass spectrometry (TOF-SIMS), atomic force microscopy (AFM), and X-ray photoelectron spectroscopy (XPS) confirmed that the silane crosslinker was not present in the bulk of the film which allowed an increased phase separation between PEDOT and PSS, and the formation of enlarged PEDOT-rich domains. We expect that this study will strengthen the case for the functionalization of substrates with GOPS instead of the conventional blending approach for the development of stable films in water and high-performance organic mixed ionic-electronic conductors for biological interfaces.

SESSION EL18.07: Theory and Simulations for Mixed Ionic-Electronic Conductors

Session Chairs: Laure Kayser and Micaela Matta

Tuesday Afternoon, November 28, 2023

Hynes, Level 1, Room 111

1:30 PM EL18.07.01

Operando Experiments and Continuum Modeling of Mechanical Breathing and Multiphysics Coupling in Organic Mixed Ionic-Electronic Conductors Kejie Zhao; Purdue University, United States

Organic mixed ionic-electronic conductors (OMIECs) are the core functioning component in electrochemical devices such as organic electrochemical transistors (OECTs) and bioelectronics owing to their unique capability of mixed conduction. In electrochromic polymers, the cyclic redox reaction is associated with a mechanical breathing strain, which deforms the OMIECs and degrades the device reliability. We measure the breathing strain, the evolution of the mechanical properties of electrochromic thin films, and mechanical damage using customized environmental nanoindentation. Further, we formulate a continuum theory following the thermodynamics framework to describe the concurrent transport of charge carriers, mechanical swelling, and phase separation in the OMIEC. The free energy consists of contributions from the deformation of the polymer chains, the mixing of the polymer with salts and solvents, the electrostatic field, and the two-phase interfaces. We implement the theory into a finite element model and study the mechanics and electrochemistry of the OMIEC channel in an electrolyte-gated OECT. The computational model replicates the electrochemical performance of an OECT which agrees well with the experiments. Overall, this work provides a basic understanding of electrochemical and mechanical behaviors of organic mixed conductors.

1:45 PM EL18.07.02

Modelling the Performance of a Novel Mixed Ionic-Electronic Conductor Based on SmCoO_3 Nora H. de Leeuw; University of Leeds, United Kingdom

One of the main challenges facing solid oxide fuel cell (SOFC) technology is the need to develop materials capable of functioning at intermediate temperatures (500–800°C), thereby reducing the costs associated with SOFCs. Here, a novel SOFC cathode material is presented, predicted through a holistic approach of a combination of complementary computational techniques to optimise the material properties. This approach is transferrable to any material optimisation problem and allows the effect of A/B-site doping to be understood, on the scale of the individual property, but also the device as a whole. The electronic, magnetic, and physical properties as well as the thermal behaviour of $\text{Sm}_{0.75}\text{A}_{0.25}\text{Co}_{1-x}\text{Mn}_x\text{O}_{2.88}$ (A = Ca, Sr; x = 0.125, 0.25) is systematically described, showing important trends and correlations that are directly coupled to its potential practical application in sustainable energy generation. The magnetic and electronic structures of these materials were directly coupled to the electronic conductivity, a finding that is applicable to other perovskite systems and to the wider energy materials community. Furthermore, evaluating the ionic conductivities of $\text{Sm}_{0.75}\text{A}_{0.25}\text{Co}_{1-x}\text{Mn}_x\text{O}_{2.88}$ (A = Ca, Sr; x = 0.125, 0.25), a distinct improvement is identified in comparison to both SmCoO_3 and the traditional cathode material strontium-doped lanthanum manganate. By coupling the electronic and ionic conductivity properties to the thermal expansion coefficients, we have shown that this material is compatible with traditional SOFC electrolytes. Combining all these insights from density functional theory calculations and molecular dynamics simulations strongly suggests that $\text{Sm}_{0.75}\text{A}_{0.25}\text{Mn}_{0.25}\text{Co}_{0.75}\text{O}_{2.88}$ possesses the necessary properties that are desirable in an efficient intermediate temperature SOFC cathode material.

2:00 PM EL18.07.03

Proton and Small Polaron Association and Migration in $\text{H}_x\text{V}_2\text{O}_5$, $\text{H}_x\text{Ta}_2\text{O}_5$, H_xMoO_3 , H_xWO_3 Pjotr Zeguns and Bilge Yildiz; Massachusetts Institute of Technology, United States

Neuromorphic computing based on electrochemical random access memory (ECRAM) enables low-energy computing and nanosecond timescale operation [1–3]. The nanosecond switching relies on fast proton and small polaron diffusion in the working channel materials, transition metal oxides. Here we investigate the fundamental limit of mixed proton–polaron diffusion in $\text{H}_x\text{V}_2\text{O}_5$, $\text{H}_x\text{Ta}_2\text{O}_5$, H_xMoO_3 , and H_xWO_3 by means of first-principles calculations. We apply the DFT+U method to describe the electronic structure and polaron localization in the host oxide lattice. By investigating various spatial arrangements of these defects, we identify the ground state configuration of the proton–polaron. We probe microscopic factors that control carrier mobility, viz. the migration barriers and proton–polaron association energy (i.e., the energy required to break the pair). Our results indicate that the polaron migration barrier is comparable to the association energy (in V_2O_5 , on the order of 0.1 eV–0.2 eV), highlighting that the attraction between polarons and protons plays an important role in diffusion. Altogether, these computations will help us to identify the most suitable oxide for nanosecond switching of ECRAM devices.

References

- [1] X. Yao, K. Klyukin, W. Lu, M. Onen, S. Ryu, D. Kim, N. Emond, I. Waluyo, A. Hunt, J.A. del Alamo, J. Li, B. Yildiz, Protonic Solid-State Electrochemical Synapse for Physical Neural Networks, *Nat. Commun.* **11**, 3134 (2020)
- [2] M. Onen, N. Emond, J. Li, B. Yildiz, J.A. del Alamo, CMOS-Compatible Protonic Programmable Resistor Based on Phosphosilicate Glass Electrolyte for Analog Deep Learning, *Nano Lett.* **21**, 14, 6111–6116 (2021)
- [3] M. Onen, N. Emond, B. Wang, D. Zhang, F.M. Ross, J. Li, B. Yildiz, J.A. Del Alamo, Nanosecond protonic programmable resistors for analog deep learning, *Science* **377**, 6605, 539–543 (2022)

2:15 PM *EL18.07.04

Influence of Chemical Structure on Properties of Mixed Conducting Conjugated Polymer Electrodes Jenny Nelson¹, Nicholas D. Siemons¹, Hang Yu¹, Iona Anderson¹, Sachetan Tuladhar¹ and Alexander Giovannitti²; ¹Imperial College London, United Kingdom; ²Chalmers University, Sweden

Organic mixed electronic and ionic conductors based on conjugated polymers with polar side chains are attractive candidates for electrodes in electrochemical devices. Their electrochemical and redox properties can be tuned through choice of polymer backbone and side chain [1, 2] while the processible nature of the polymer materials facilitates both manufacture and recycling. When applied as electrodes in electrochemical energy storage devices, conjugated polymer electrodes show excellent charging and discharging rates, high coulometric efficiency and compatibility with simple aqueous electrolytes. However, their specific capacity and their operational stability need to be improved [3]. In this work, we use electrochemical measurements and modelling to investigate the relationship between polymer chemical structure and the redox properties, charging behaviour and cycling stability of the polymer electrodes. We focus on the

effect of side chains, since small changes in side-chain composition or structure can significantly influence the electrode properties. We use molecular dynamics simulations for series of polymers, to investigate how the side chain polarity influences polymer packing [4]; how the composition of mixed polar and non-polar side chains influences film swelling and stability; how backbone and side-chain structure influence electronic transport properties; and how polymer-ion interactions depend on the ion type. Finally, we consider design strategies for enhancing specific capacity. The findings can help to develop chemical designs for improved conjugated polymer electrodes for aqueous environments.

[1] A. Giovannitti et al. (2018) <https://doi.org/10.1021/acs.chemmater.8b00321>

[2] A. A. Szumska et al. (2021) <https://doi.org/10.1021/jacs.1c06713>

[3] D. Moia et al. (2019) <https://doi.org/10.1039/C8EE03518K>

[4] N. Siemons et al (2022) <https://doi.org/10.1002/adma.202204258>

2:45 PMBREAK

SESSION EL18.08: Processing Mixed Ionic-Electronic Conductors

Session Chairs: Christine Luscombe and Christian Nielsen

Tuesday Afternoon, November 28, 2023

Hynes, Level 1, Room 111

3:15 PM EL18.08.01

In-Plane Orientation of Organic Mixed Ionic-Electronic Conductors to Enhance Charge Transport Properties [Sabelle Holzer](#)¹, [Demetra Tsokkou](#)¹, [Shubhradip Guhait](#)², [Badr Jismy](#)², [Martin Brinkmann](#)², [Nicolas Leclerc](#)² and [Natalie Banerji](#)¹; ¹University of Bern, Switzerland; ²CNRS University of Strasbourg, France

Organic mixed ionic-electronic conductors (OMIECs) are perfectly suited to interface biology and electronic devices as they enable both ionic and electronic transport; feature mechanical flexibility; can be successfully fabricated in versatile processing conditions; and are synthetically tunable.¹ While most recent progress in bioelectronics has been focused on device fabrication and comparing performance of different materials, there is still a lack of a more in-depth understanding of the fundamental processes occurring in functioning OMIECs.² The charge transport is happening mainly on the π -conjugated backbone of the organic semiconductor, while ions penetrate the bulk material. In PBTTT, a polymer with high charge-carrier mobility, ion uptake in the polymer matrix can be facilitated by incorporating alkyl side chains with an ether group, further improving the performance.^{3,4} Therefore, in this study we use high temperature rubbing to orient PBTTT-⁸O films helping to unravel the fundamental processes of both the charge and ion transport. For comparison the same experiments were carried out with an OMIECs model material P3HT, which was already characterized by multiple different research groups.⁵

Combining electrochemical and chemical doping with spectroscopic techniques and chronoamperometry the oxidation behavior of the OMIECs was investigated. Foremost, with *in-situ* terahertz (THz) spectroscopy we can detect the scattering frequencies of charge carriers in semiconductors, this allows us to get the intrinsic nanoscale conductivity and short-range mobility of the studied OMIECs, which is not affected by any grain boundaries or electrodes. The analysis of the complex THz conductivity unveils the mobility and density of charges altogether. We were able to get conductivities of more than 1000 Scm⁻¹ for P3HT and PBTTT-⁸O for electrochemical doping. Furthermore, with chemical doping conductivities of more than 2000 Scm⁻¹ were obtained and band like transport behavior was observed for PBTTT-⁸O, showing the large effect of high in plane orientation of OMIECs.

[1] J. Rivnay, R. M. Owens and G. G. Malliaras, *Chem. Mater.*, 2014, **26**, 679-685.

[2] J. Chung, A. Khot, B. M. Savoie and B. W. Boudouris, *ACS Macro Letters*, 2020, **9** (5), 646-655.

[3] J. E. Cochran, M. J. N. Junk, A. M. Gludell, P. L. Miller, J. S. Cowart, M. F. Toney, C. J. Hawker, B. F. Chmelka and M. L. Chabiny, *Macromolecules*, 2014, **47**, 19, 6836-6846.

[4] P. Durand, H. Zeng, T. Biskup, V. Vijayakumar, V. Untilova, C. Kiefer, B. Heinrich, L. Herrmann, M. Brinkmann and N. Leclerc, *Adv. Energy Mater.* 2022, **12**, 2103049.

[5] D. Khodagholy, J. Rivnay, M. Sessolo, M. Gurfinkel, P. Leleux, L. H. Jimison, E. Stavrinidou, T. Herve, S. Sanaur, R. M. Owens and G. G. Malliaras, *Nat. Commun.*, 2013, **4**, 2133.

3:30 PM *EL18.08.02

Blend-Based Organic Electrochemical Transistors [Gittul Frey](#); Technion - Israel Institute of Technology, Israel

Organic electrochemical transistors (OECTs) are building block devices for applications in a variety of fields including bioelectronics, energy storage, mechanical actuators, sensors etc. OECTs utilize organic mixed ionic-electronic conductors (OMIECs) and rely on the injection/extraction of ions from an electrolyte into an OMIEC material to modulate its bulk conductivity. Recently, we introduced a new strategy for the design of OECTs where the bulk includes a blend of two OMIECs endowing the device with multifunctionality. For example, we demonstrated that judicious selection of p- and n-type OMIECs and optimization of the blend ratio can lead to a fully balanced ambipolar OECT where both ions and cations are modulated in a single device. A variety of characterization methods including optical and impedance spectroscopy, x-ray diffraction, and device measurements were used to gain insights on the structure-property relationships in the system. The blend strategy was further extended to offer multifunctional performance by blending components that operate in different conditions such as solvents, temperature, and ions. To study multifunctionality in OECTs we used a series of judiciously synthesized non-fullerene small molecules and blended each with a commercial n-type mixed conducting polymer. We investigated the effects of blend composition, electrolyte and ion type, and thermal treatments on the electrochemical performance using spectro-electrochemistry, cyclic voltammetry, electrochemical quartz crystal microbalance, and OECTs. The blends were also characterized using X-ray scattering and electron microscopy to reveal film morphology. We find that the small differences in the structure of the small molecules have significant effects on both the morphology and the electrochemical performance of the blends. For example, ion selectivity and reversibility can be modulated by the type and composition of the blend. A better understanding of these systems will allow us to design a new generation of materials and device structures for multifunctional bioelectronic applications.

4:00 PM EL18.08.03

Influence on the Performance of Organic Electrochemical Transistors of PEDOT:PSS Blends with Polyethylene Oxide of Different Molecular Weight [Chun-Yuan Lo](#)¹, [Lucas Flag](#)² and [Laure V. Kayser](#)¹; ¹University of Delaware, United States; ²National Institute of Standards and Technology, United States

The addition of polyethylene oxide (PEO) to organic mixed ionic-electronic conductors, such as PEDOT:PSS, is commonly done to increase biocompatibility, hydrophilicity, or stretchability. In particular, when blended with PEDOT:PSS, PEO has been shown to change the microstructure of the thin films. In this study, we were interested in the effect of PEO on mixed ionic-electronic transport properties, particularly when the films are immersed in aqueous solutions such as for organic electrochemical transistors (OECTs). PEO is water soluble and therefore could easily leached out of the films when immersed in water or an aqueous electrolyte. We studied PEO of two different molecular weights (MW), 400 Da (low MW) and 20,000 Da (high MW), in PEDOT:PSS:PEO blends at 5 wt% PEO in solution, and crosslinked with GOPS. We monitored the composition of the spin-coated films by X-ray photoelectron spectroscopy (XPS) over a period of 4 hours of immersion in water. We found that most, if not all low MW PEO is removed from the films after 2 hours of immersion, while for high MW PEO, nearly 50% was still present in the films with a stable concentration after 1-2 h. In both cases, we noted the removal of excess PSS in the films, which is common for PEDOT:PSS immersed in water. The removal of PEO and PSS following water immersion was also confirmed by a significant reduction in film thickness, as measured by profilometry and atomic force microscopy. We then performed transconductance measurements on OECT devices to extract the mobility-capacitance product, $[\mu C^*]$, of our PEDOT:PSS formulations. In all cases, without PEO, or with low or high MW PEO, the transconductance increased significantly after immersion in water, consistent with the removal of insulating material. What was more surprising, however, was a much higher $[\mu C^*]$ when low MW PEO was used as an additive and then removed by soaking in water. The $[\mu C^*]$ values obtained, which have yet to be validated externally, are higher than those obtained when doping with ethylene glycol and close to that of previously reported crystalline PEDOT:PSS obtained by sulfuric acid treatment. We are still exploring the exact reasons for this increase, but it seems to stem from both an increase in the charge mobility and volumetric capacitance (up to $129 \pm 22 \text{ F cm}^{-3}$). GIWAXS measurements did not indicate a change in film crystallinity, but spectroelectrochemistry revealed a higher charge density which is consistent again with the removal of PSS and PEO from the films. This study provides an avenue towards improving the performance of PEDOT:PSS electrodes without using sulfuric acid. We also hope to encourage others to study the fate of polymeric additives and small molecules in devices operating under aqueous conditions.

4:15 PM EL18.08.04

Phase Separation in Mixed Ionic and Electronic Conductors for Information Storage [Yiyang Li](#); University of Michigan, United States

Mixed ionic and electronic conductors (MIECs) enable vast changes in chemical composition induced by electrochemical currents and voltages. This electrochemically-induced change in chemical composition enables a substantial chemical capacitance, which can be harnessed for energy storage and emerging microelectronic devices. This change in composition can yield phase transformations and spinodal decomposition in MIEC materials due to materials thermodynamics. In this presentation, we show how this phase separation in metal oxide MIECs enables

the coexistence of multiple physical states that are identical in energy. By switching between these physical states, we can provide a thermodynamically nonvolatile form of information storage. We demonstrate this phenomenon in two types of memory cells: resistive memory and electrochemical memory. We anticipate that phase separation can be broadly generalized to other forms of MIECs.

SESSION EL18.09: New Materials and Characterization Tools for Mixed Ionic-Electronic Conductors
Session Chairs: Laure Kayser and Jianyong Ouyang
Wednesday Afternoon, November 29, 2023
Hynes, Level 1, Room 101

1:30 PM EL18.09.01

Understanding the Disparity Between Doping and Dedoping Kinetics in Organic Electrochemical Transistors with Operando Optical Microscopy Jiajie Guo¹, Shinya Chen¹, Rajiv Giri¹, Connor G. Bischak^{1,2}, Jonathan W. Onorato¹, Kangrong Yan³, Ziqiu Shen³, Chang-Zhi Li³, Christine Luscombe^{4,1} and David S. Ginger¹; ¹University of Washington, United States; ²The University of Utah, United States; ³Zhejiang University, China; ⁴Okinawa Institute of Science and Technology, Japan

Organic electrochemical transistors (OECTs) operate via electrochemical doping, where an applied gate potential in an aqueous electrolyte modulates the channel conductivity through counterion injection into and expulsion from the semiconducting polymer. This doping process, and the resulting current in OECT devices, is far from instantaneous and exhibits significant disparity between doping and dedoping kinetics. Existing models of device operation cannot explain the experimental observations that turn-off times are generally much faster than turn-on times in accumulation mode OECTs, yet this difference in kinetics has significant practical implications for devices where designing for optimal switching times is critical. We address this shortcoming through operando optical microscopy, where we directly image the local doping level of the transistor channel (in real time) in combination with device measurements to present a comprehensive view of the physical process. We use these microscopy data to show that device turn-on occurs in two stages, while turn-off occurs in one stage. We attribute the faster turn-off to a combination of engineering as well as physical and chemical factors including channel geometry, differences in doping and dedoping kinetics, and carrier density-dependent mobility. We further show that ion transport is limiting the device operation speed in our model devices. Our study provides insights into the asymmetric kinetics in OECTs and gives practical guidelines for rationally engineering faster OECTs.

1:45 PM *EL18.09.02

Application Guided Design of Conjugated Polymers Towards Next-Generation Iono-Electronic Devices Aristide Gumyusenge; Massachusetts Institute of Technology, United States

Conjugated polymers, particularly organic mixed ionic-electronic conductors (OMIECs), continue to shine as promising conductors for applications requiring coupled conduction, particularly in bioelectronics. However, only a few mixed conductors are implemented in functional devices to date and a one-material-fits-all bottleneck continues to hamper rapid advancements. The challenge lies in the lack of a cross-disciplinary design approach for high-performance materials. Establishing the needed balance between the two antagonistic modes of transport (ion permeability and electronic charge transport) to yield high performance devices has not only become an exciting field of fundamental research, but also a conduit towards advanced electronics. My research group at MIT (the laboratory of organic materials for smart electronics, OMSE Lab) employs polymer modularity to design novel iono-electronic semiconductors. We employ an application-guided approach and create tailored structures for integrating into devices. In this talk, I will share our ongoing efforts in designing new semiconductors with varying degrees of ion-responsiveness and the scope of applications enabled by their molecular tuning. We utilize copolymerization as a facile route to yield a library of mixed conductors enabling a variety of applications ranging from rapidly switching electrochemical transistors to high-fidelity artificial synapses. We have shown that by systematically tethering polar side groups onto known excellent electron conductors, we can probe the contribution from both ionic and electronic conduction to the resulting device performance and determine suitable applications. We have also studied a hybridization strategy between different polymer components to yield extrinsic properties especially environmental robustness. This hybridization strategy has also shown effective for widening the scope of target analytes toward which our mixed conductors can respond, thus enabling new electronic designs.

2:15 PM EL18.09.03

In-Situ Characterization of Ordering/Disordering in Electrochemically Doped Oligo-Ether Sidechain Modified Polythiophenes Lee Richter¹, Lucas Flag¹, Maximilian Moser², Iain McCulloch², Jonathan W. Onorato³ and Christine Luscombe⁴; ¹National Institute of Standards and Technology, United States; ²University of Oxford, United Kingdom; ³University of Washington, United States; ⁴Okinawa Institute of Science and Technology, Japan

Organic mixed ionic and electronic conductors (OMIECs) are a novel material class, emerging as potential enablers for devices as diverse as actuators, biosensors and neuromorphic computing. In an OMIEC, volumetric doping (gating) of the active material is achieved through ingress of electrolyte ions, under potential control. This opens unique transduction modalities due to the mixed (ionic and electronic) modes of conduction. However, the complex changes in film structure: swelling by both electrolyte and counter ion coupled with electrochemical doping, requires in-situ and in-operando measurements to develop quantitative process-structure-function relationships. Side-chain modification, typically by the introduction of oligoethylene glycol (oEG) units, of traditional semiconducting polymers, has emerged as a powerful paradigm for OMIEC material design. We have applied in-situ grazing incidence X-ray diffraction (GIXD) to the study of 3 oEG modified polythiophenes, p3MEEMT[1], p(g3T2) and p(g1t2-g5t2).[2] All are regio-regular, but differ in terms of the length of the oEG side chain (2 units for P3MEEMT, 3 units for p(g3T2), and up to 5 units for p(g1T2-g5T2)) and in repeat unit symmetry. While the optoelectronic properties of these polymers are similar, consistent with the common backbone, the swelling behavior of the polymers were notably distinct. With moderate thermal annealing, all polymers exhibit semicrystalline behavior, typical of polythiophenes, with an edge-on habit of pi-stacked lamella. When characterized in-situ we find a remarkable disordering of the p(g3T2) in the neutral, dedoped state. Effectively no diffraction can be observed. However, a degree of order comparable to that observed ex-situ (dry) is obtained upon doping. This severe doping induced ordering is similar to that observed in doped regio-random P3HT[3] and is consistent with the enhanced pi-pi interaction (evidenced by a decrease in the interchain separation) typically observed for doped polythiophenes. This electrolyte induced "melting" is also present in the asymmetric sidechain p(g1T2-g5T2) but is absent in the shorter side chain polymer. While significant effort has been placed on characterization of swelling in OMIECs, the observation of nominal melting of semicrystalline material has not been extensively discussed and may limit the oEG content. In general, order within the polymer is considered important to electronic transport [4] thus the doping induced ordering may be essential to the final device performance.

[1] Flag, L.Q. et al. J. Am. Chem. Soc. 2019, 141, 4345, DOI:10.1021/jacs.8b12640

[2] Moser, M. et al. Adv. Mater 2020, 32, 2002748, DOI: 10.1002/adma.202002748

[3] Lim, E. et al. Adv. Elec. Mater 2019, 5, 1800915, DOI: 10.1002/aelm.201800915

[4] Jacobs, I.E. J. AM. Chem. Soc. 2022, 144, 3005, Doi: 10.1021/jacs.1c10651

2:30 PM BREAK

3:30 PM *EL18.09.04

Tailoring Organic Semiconductors for Mixed Ionic and Electronic Transport Christian Nielsen; Queen Mary University, United Kingdom

The emerging research field of organic bioelectronics has developed rapidly over the last few years and elegant examples of biomedically important applications including for example in-vivo drug delivery and neural interfacing have been demonstrated.

The organic electrochemical transistor (OECT), capable of transducing small ionic fluxes into electronic signals in an aqueous environment, is an ideal device to utilise in bioelectronic applications. Initially, nearly all OECTs were fabricated with commercially available PEDOT:PSS, heavily limiting the variability in performance. We have previously shown that tailor-made semiconducting polymers are fully capable of matching the performance of PEDOT:PSS and over the last few years the library of mixed ionic-electronic conductors for OECT applications have expanded significantly. To capitalise on this development and the versatility of the organic chemistry toolbox, further materials development is needed. In my talk I will discuss our recent work in this area covering examples of both molecular and polymeric semiconducting materials and their performance in organic electrochemical transistors.

4:00 PM EL18.09.05

Nanoscale Mapping of Ions, Polarons and Bipolarons in Organic Mixed Conductors Seth Jackson, Garrett Collins and Connor G. Bischak; The University of Utah, United States

Organic mixed ionic-electronic conductors have emerged as promising materials for biosensors, bioelectronics, neuromorphic computing, and electrochromics. These technologies all operate based on electrochemical doping of organic mixed ionic-electronic conductors, which are most commonly conjugated polymers. The locations of ions, polarons, bipolarons directly impact how electronic charge carriers move through the OMIEC matrix. Using photoinduced force microscopy (PiFM) with visible, near-infrared, and infrared wavelengths, we generate maps of ion,

polaron, and bipolaron densities with ~10 nm spatial resolution. In poly(3-hexylthiophene), we demonstrate using a combination of UV-vis spectroelectrochemistry, grazing incidence wide angle X-ray scattering (GIWAXS), nanoscale stiffness mapping, and PiFM, that ions and polarons reside preferentially in crystalline regions. We extend these initial studies to other OMIEC polymers with oligo(ethylene glycol) side chains to visualize the arrangement of ions, polarons, and bipolarons in the polymer matrix.

4:15 PM *EL18.09.06

Effect of Backbone Linearity on Mixed-Conductance in New Pyrene Dianhydride-Based Conjugated Ladder Polymers Julia A. Schneider, Katherine Johnston, Emma Mikita and Emil Jaffal; Fordham University, United States

We report the synthesis of a new organic n-type ladder conjugated polymer, poly(benzimidazobenzod(e,f)phenanthrene-dione) (**BPyl**), for applications utilizing mixed ionic-electronic semiconductors. This pyrene-based ladder polymer is an exciting core-expansion of the high performing naphthalene-based polymer, poly(benzimidazobenzophenanthroline) **BBL**, but unlike **BBL**, it allows for structural variety in the conjugated backbone. Electronic charge transport and ion diffusion in organic conjugated polymers are both dependent on interchain interactions, yet maximizing these processes equally is a significant challenge toward achieving mixed conductance. The crystalline assemblies necessary for charge transport can often limit ion diffusion and hinder the capacitance of the material. While studies have shown that amorphous films perform better due to uniform swelling by the electrolyte, the insertion of conjugation-break spacers or hydrophilic side chains leads to decreased charge transport. With **BPyl**, we present a new approach for controlling polymer crystallinity by tuning backbone linearity using “linear” and “bent” isomeric monomers. We have synthesized two isomers of pyrene dianhydride for the polycondensation with 1,2,4,5-tetraaminobenzene tetrahydrochloride (TAB.4HCl) into conjugated ladder polymers. By tuning the ratio of pyrene comonomers we can impact film-formation ability and performance. We will present comparisons of **BBL** and **BPyl** (linear and bent) via spectro-electrochemical analysis, TEM imaging, electrochemical characterization, and organic electrochemical transistor (OECT) devices.

4:45 PM EL18.09.07

Revealing The Microstructure of Hydrated Conjugated Polymers using Cryogenic Electron Microscopy Masoud Ghasemi and Enrique Gomez; The Pennsylvania State University, United States

Organic mixed ionic-electronic conducting (OMIEC) polymers have attracted a tremendous amount of attention due to their easy tunability and potential for various applications, such as neuromorphic computing and biosensing. Among different OMIECs, poly(3,4-ethylenedioxythiophene):polystyrene sulfonate (PEDOT:PSS) is the most widely used polymeric system due to its commercial availability and ease of processibility as an aqueous dispersion. PEDOT is a p-type conjugated polymer with poor solubility in both polar and nonpolar solvents, hence it is usually processed along with PSS which also serves as a dopant to induce positively charged electronic carriers in PEDOT. It has been shown that both the electronic and mechanical properties of PEDOT:PSS can be modulated through post-processing or the application of different additives. Despite its wide range of applications the underlying mechanisms behind the improvement in the mechanical properties of PEDOT:PSS in the presence of additives remains poorly understood. In this work, we use cryogenic electron microscopy (Cryo-EM) to investigate micro- and nano-structure of PEDOT:PSS in different hydrated and swollen states. Our results suggest that in a hydrated state PSS rich regions of the PEDOT:PSS swell while the PEDOT-rich phases maintain an interconnected network which highlights the importance of a charge percolation pathway as well as the amorphous phase connectivity to achieve high mobility and stretchable OMIECs. Our findings may pave the way to a deeper understanding of OMIECs and their structure-function relationships.

SYMPOSIUM EL19

Atomically-Thin 2D Materials and Heterostructures—Synthesis, Properties and Applications
November 27 - December 7, 2023

Symposium Organizers

Sanjay Behura, San Diego State University
Kibum Kang, Korea Advanced Institute of Science and Technology
Andrew Mannix, Stanford University
Hyeon Jin Shin, Gwangju Institute of Science and Technology

* Invited Paper

+ JMR Distinguished Invited Speaker

SESSION EL19.01: Applications of Wafer-Scale 2D Materials—Electronics I
Session Chairs: Kibum Kang and Andrew Mannix
Monday Morning, November 27, 2023
Hynes, Level 3, Room 309

10:30 AM *EL19.01.01

Monolithic Integration of Single-Crystalline 2D Standalone Circuitry Enabled by Ultra Low Temperature Growth Jeehwan Kim; Massachusetts Institute of Technology, United States

It is necessary to find a strategy obtain single-crystalline TMDs on a Si wafer without transfer for seamless integration of TMDs for CMOS technologies. However, so far, epitaxial methods has been an only way to obtain single-crystalline TMDs which requires a single-crystalline hexagonal substrate and transfer them onto the Si wafer. Here my team at MIT has succeeded to directly grow single-crystalline MoS₂ and WSe₂ on a HfO₂-coated Si wafer without needing to have an epitaxial seeding. We geometrically confine the growth of the first set of nuclei by defining selective growth trenches before the second set of nuclei is introduced. By utilizing the edge of trenches as a heterogeneous nucleation site, we were able to grow TMDs as low as at 380 oC which will enable monolithic integration of logic devices on various circuitry. Also, such low temperature direct non-epitaxial single-crystalline growth methods lay foundations to finally obtain vertically stacked complementary FETs by monolithic integration of MoS₂ nMOS on top of WSe₂ pMOS.

11:00 AM EL19.01.02

Area-Selective Atomic Layer Deposition on a 2D Monolayer Lateral Superlattice Jeongwon Park¹, Seung Jae Kwak², Won Bo Lee², Yong Joo Kim³ and Kibum Kang¹; ¹Korea Advanced Institute of Science and Technology (KAIST), Korea (the Republic of); ²Seoul National University (SNU), Korea (the Republic of); ³Kookmin University, Korea (the Republic of)

Recently, area-selective atomic-layer-deposition (AS-ALD), which allows the direct deposition of target materials on the desired area using a deposition barrier, has emerged as an advanced patterning process. In conventional AS-ALD (CAS-ALD), various barriers, including self-assembled monolayers, surface terminations, and inherent selectivity in metal-insulator combinations, have been deployed. Nevertheless, these barriers have not yielded satisfactory results when confronting highly reactive ALD precursors or when handling diverse materials in AS-ALD. Furthermore, CAS-ALD, which selectively deposits materials in predefined regions through top-down patterning, has not successfully reduced pattern sizes beyond the resolution of

optical lithography.

In this research, we report a novel superlattice-based AS-ALD (SAS-ALD) using a 2D lateral superlattice as a patterning template. The lateral superlattice is grown by coherent lateral epitaxy of monolayer MoS₂ and MoSe₂ with chemical vapor deposition (CVD) process. Due to the unique feature of lateral growth in 2D materials, the superlattice is composed of linear patterns of MoS₂ and MoSe₂. Interestingly, we have discovered that when various materials (Al₂O₃, HfO₂, Ru, Te, Sb₂Se₃, and TiN) are deposited via ALD on the MoS₂-MoSe₂ lateral superlattice, they selectively deposit only on the MoSe₂ regions, resulting in linear patterns of target materials.

Since the width of linear pattern is determined by the duration time of gaseous CVD precursors, a scaling down is significantly easier compared to conventional patterning methods. As a result, we patterned target materials on the lateral superlattice template with a sub-10 nm half pitch size. Furthermore, unlike CAS-ALD, which controls the chemisorption of ALD precursors, SAS-ALD has a completely new mechanism that utilizes physisorption differences and diffusions. Through molecular dynamics (MD) simulations and density functional theory (DFT) calculations, we confirmed that the adsorption energy of ALD precursor on 2D transition dichalcogenides (TMDs) is influenced by local strain and curvature of TMDs. Importantly, we observed that the most stable adsorption of the precursors occurs on the compressed MoSe₂ valley region, which has compressive strain and concave surfaces. The computational results were further supported by experimental evidence showing initial nucleation of ALD materials on the compressed MoSe₂ valley region. Based on the physisorption differences and diffusion of ALD precursors, SAS-ALD has been able to selectively deposit various materials such as Al₂O₃, HfO₂, Ru, Te, Sb₂Se₃, and TiN. Additionally, we successfully achieved Al₂O₃ AS-ALD using a trimethyl aluminum, the highly reactive precursor, and this was possible even at a few nanometer scales.

SAS-ALD, based on a novel mechanism, allows for patterning of target materials in a linear shape using a 2D lateral superlattice template. From a patterning perspective, the width is controlled by the duration time of CVD precursor, making scaling down very easy. In addition, in terms of AS-ALD, we were able to effectively fabricate various materials in very narrow patterns. This technology is expected to have even greater potential when combined with guide patterns created through photolithography for precise positioning. Additionally, since SAS-ALD utilized 2D TMDs as pattern templates, we anticipate that various 2D/3D hybrid structures can be created.

11:15 AM EL19.01.03

Reconfigurable Mixed-Kernel Heterojunction Transistors for Personalized Support Vector Machine Classification Justin Qian¹, Xiaodong Yan¹, Jiahui Ma², Aoyang Zhang², Stephanie Liu¹, Matthew Bland¹, Kevin Liu¹, Xuechun Wang², Vinod K. Sangwan¹, Han Wang² and Mark C. Hersam¹; ¹Northwestern University, United States; ²University of Southern California, United States

The continual increase in the volume of data generated by sensors, robots, and mobile devices poses a challenge for cloud computing centers in terms of power costs, efficiency, accessibility, and scalability. In particular, artificial intelligence (AI) based classification has shown tremendous potential in a variety of applications such as signal processing and image recognition but often has huge data and energy costs due to the underlying von Neumann architecture of complementary metal-oxide-semiconductor (CMOS) chips. In contrast, the use of edge computing to locally analyze and process data has the potential to alleviate the burden on large data centers, while also improving latency, security, and privacy. Because edge computing resources are often limited, edge-based hardware needs to be more power-efficient than conventional graphics processing units (GPUs), application-specific integrated circuits (ASICs), or field programmable gate arrays (FPGAs).

This presentation will discuss edge computing at the device level using a highly reconfigurable mixed-dimensional dual-gated MoS₂/carbon nanotube (CNT) van der Waals heterojunction device achieved in a self-aligned manner. By tailoring the degree of electric-field screening through control over CNT density and overlapping heterojunction area, the heterojunction device is shown to generate tunable Gaussian, sigmoid, and mixed Gaussian/sigmoid functions. These heterojunction-generated functions are then used as kernels for support vector machine (SVM) based arrhythmia detection from electrocardiogram (ECG) signals. For a single device, mixed kernels were found to outperform purely Gaussian and purely sigmoid kernels. Bayesian optimization was further used to determine the optimal Gaussian/sigmoid hyperparameters and mixing ratio for a full mixed-kernel library that was generated from the integration of two devices, resulting in exceptionally high classification accuracies. Compared to existing literature on Gaussian transistors and CMOS circuits, our mixed-kernel heterojunction (MKH) transistors show unprecedented tunability in a compact four-terminal geometry with close to two orders of magnitude fewer circuit elements. In this manner, CNT-MoS₂ MKHs have the potential to be widely applicable to SVM classification in diverse wearable and edge applications.

11:30 AM *EL19.01.04

Hexagonal and Amorphous Boron Nitride Thin Films Hyeon Suk Shin; Ulsan National Institute of Science and Technology, Korea (the Republic of)

Hexagonal boron nitride (hBN) is a promising two-dimensional (2D) material owing to its unique optical properties in the deep-UV region, mechanical robustness, thermal stability, and chemical inertness. hBN thin films have gained significant attention for various applications, including nanoelectronics, photonics, single photon emission, anti-corrosion, and membranes. Thus, wafer-scale growth of hBN films is crucial to enable their industrial-scale applications. In this regard, chemical vapor deposition (CVD) is a promising method for scalable high-quality films. To date, considerable efforts have been made to develop continuous hBN thin films with high crystallinity, from those with large grains to single-crystal ones, and to realize thickness control of hBN films by CVD. However, the growth of wafer-scale high crystalline hBN films with precise thickness control has not been reported yet. The hBN growth is significantly affected by substrate, in particular the type of metals, because the intrinsic solubilities of boron and nitrogen depend on the type of metal. In this talk, state-of-the-art strategies adopted for growing wafer-scale, highly crystalline hBN are summarized, followed by the proposed mechanisms of hBN growth on catalytic substrates [1]. Furthermore, various applications of the hBN thin films are demonstrated, including a dielectric layer, an encapsulation layer, a wrapping layer of gold nanoparticles for surface enhanced Raman scattering, a proton-exchange membrane, a template for growth of other 2D materials or nanomaterials, and a platform of fabricating in-plane heterostructures. In addition, amorphous BN (aBN) as a counterpart of crystalline hBN is introduced [2]. Detailed structural characterisation indicates that a-BN is sp²-hybridised, with no measurable crystallinity, and mechanically robust, with excellent diffusion-barrier characteristics. The aBN thin film shows ultra-low dielectric constant (< 2.5), indicating great potential for its applications in Cu interconnects of integrated circuits.

[1] K. Y. Ma et al., Nature 606, 88 (2022).

[2] S. Hong et al., Nature 582, 511 (2020).

SESSION EL19.02: Advances in the Assembly of Van der Waals Heterostructures

Session Chairs: Andrew Mannix and Hyeon Jin Shin

Monday Afternoon, November 27, 2023

Hynes, Level 3, Room 309

1:30 PM *EL19.02.01

Ultraclean Layer Transfer and Atomic Reconstruction in Twisted TMD Lattices Roman Gorbachev; University of Manchester, United Kingdom

Layer-by-layer assembly of van der Waals (vdW) heterostructures underpins new discoveries in solid state physics, material science and chemistry. Despite successes, all current assembly techniques use polymeric supports which limit their cleanliness, ultimate electronic performance, and potential for optoelectronic applications. In the first part of the talk, I will introduce a polymer-free platform for heterostructure assembly using re-usable flexible silicon nitride membranes. This approach enables production of heterostructures with interfaces free from interlayer contamination and correspondingly excellent (opto)electronic behaviour. In addition, eliminating polymeric supports allows new possibilities for vdW heterostructure fabrication: assembly at temperatures up to 600°C, and in different environments including ultra-high vacuum (UHV) and liquid submersion. We demonstrate UHV heterostructure assembly for the first time and show the reliable creation of moiré superlattices with over x10 improvement in homogeneity.

In the second part of the talk, I will review our recent progress on twisted bilayer TMDs bilayers in the reconstruction regime. I will discuss their atomic structure observed in STEM, which is strikingly different for aligned (R) and anti-aligned (H) TMD monolayer orientations. This difference gives rise to correspondingly different optoelectronic properties, with ferroelectric domains arising in the former case and piezoelectric charge texturing in the latter. I will report our recent investigation of sliding ferroelectricity, and its switching behaviour observed in double gated structures using the electron channelling contrast SEM.

2:00 PM *EL19.02.02

More Magic with Atomic Crystals Jiwoong Park; University of Chicago, United States

Atomically thin crystals, that are grown, combined, and integrated in large scale, can enable novel properties previously unimaginable. Such "magical" properties can span functional dimensions that go beyond widely-explored electronic phenomena, resulting in extreme thermal, photonic, and mechanical properties. In this talk, I will discuss latest examples with such magical properties realized with atomic crystals. First, we demonstrated three atom thick photonic waveguides, named delta-waveguide, that can generate light plane waves that propagate freely along the waveguide plane but confined along the out-of-plane direction. This enables integrated two-dimensional photonics and seamless mode matching with free-beam optics. Second, we demonstrated the fabrication and measurements of wafer-scale atomic crystal membranes on water that behave like a freestanding mechanical film. We discover that these

membranes are not flat; instead they self-wrinkle with the wrinkle morphologies following a universal scaling law, as shown by continuum mechanics theory. This enables a tuning of their mechanical moduli over multiple orders of magnitude.

2:30 PMBREAK

3:00 PM EL19.02.03

Exploring the Inter-Layer Interactions of 2D Materials with Sub-Angstrom Resolution Modulated Nanoindentation[RyanKhan](#), DanielVizoso, FrankDelrio and RemiDingreville; Sandia National Laboratories, United States

As the field of 2D materials continues to grow, more intriguing and complex structures will be discovered, increasing the demand for techniques to properly characterize the local nanoscale mechanical properties of any and all varieties of materials. While traditional nanoindentation can measure the in-plane modulus of suspended films over holes, the technique fails to accurately determine the out-of-plane modulus, requiring such large indentation depths that substrate effects cannot be distinguished. We employ modulated nanoindentation with Angstrom resolution (MoNI/ÅI), a novel technique that enables non-destructive measurements of the out-of-plane elasticity of ultra-thin materials with sub-angstrom level indentation depths. With such high resolution, even atomically thin materials can be examined in their most practical state on any underlying substrate, without erroneous contributions from the substrate. MoNI/ÅI has been previously used to explore local pressure induced phase transformations only possible in few layer 2D materials. In our work we explored the multi-layer stiffness dependence of deposited graphene and uncovered a peak transverse stiffness in bilayer graphene that was previously unknown. We complemented these findings with MD simulations and other characterization techniques to further elucidate this phenomenon providing a deeper insight of the inter-layer forces and interactions in graphene and other 2D materials.

3:15 PM *EL19.02.05

Electronic and Electrochemical Properties of Moiré Superlattices[DanielK. Bediako](#); University of California, Berkeley, United States

The formation of moiré superlattices alters the electronic band structure in a manner that is systematically dependent on the interlayer twist angle, but spontaneous strain relaxation has considerable impact on the resulting physics. This talk will focus on the use of four-dimensional scanning transmission electron microscopy measurements to map lattice relaxation in bilayer and trilayer moiré superlattices and how these structural perturbations impact both the correlated electron physics of the materials as well as their interfacial electrochemical behavior measured by scanning electrochemical cell microscopy.

3:45 PM *EL19.02.06

Introduction to the MonArk NSF Quantum Foundry[HughChurchill](#); University of Arkansas, United States

The MonArk Quantum Foundry is an NSF program jointly led by Montana State University and the University of Arkansas with a mission to accelerate two-dimensional materials research for quantum technologies. The rapid prototyping and characterization capabilities of the foundry will be used to serve a broad range of collaborators and users interested in the development of 2D materials and devices for quantum technologies. In this talk I will provide an introduction to the goals and capabilities of MonArk, which are centered on robotic and AI-assisted creation, identification, and fabrication of 2D quantum materials and devices. I will provide a status report on the development of these capabilities and an outlook for the collaborator and user program that will begin in 2024.

4:15 PM *EL19.16.07

Upconversion Electroluminescence in Plasmonic Van der Waals Tunnel Diodes[GokiEda](#); National University of Singapore, Singapore

Plasmonic tunnel junctions comprising van der Waals semiconductor are an attractive platform where the interplay between inelastically tunneling electrons, surface plasmons, and excitons is expected to give rise to novel light emission phenomena. Here, we report observation of peculiar upconversion electroluminescence in van der Waals tunnel diodes comprising a monolayer transition metal dichalcogenide (TMD) in the electron tunneling pathway. The device exhibits bimodal electroluminescence with a broad low energy band and a narrow high energy band. Interestingly, the high energy emission, which is attributed to the TMD ground exciton, is found to turn on at applied biases significantly lower than the threshold defined by its emission energy, whereas the low energy emission, which arises from plasmonic emission, strictly obeys the quantum cut-off. We examine several possible model and show that momentum-indirect excitation of high energy carriers enabled by inelastic electron tunneling is a key component enabling the apparent energy gain.

SESSION EL19.03: Poster Session I: 2D Materials—Liquid-Phase Deposition and Growth

Session Chairs: Kibum Kang and Andrew Mannix

Monday Afternoon, November 27, 2023

Hynes, Level 1, Hall A

8:00 PM EL19.03.01

Ultra-Low Gas Permeability of Irreversibly-Bonded Two-Dimensional Polyaramid (2DPA-1) Films[CodyRitt](#), QuienMichelle, YuwenZeng, Yu-MingTu and MichaelS. Strano; Massachusetts Institute of Technology, United States

Polymers that extend covalently in two dimensions (2D) have attracted recent attention as a means of combining the mechanical strength and in-plane energy conduction of conventional 2D materials with the low densities, synthetic processability, and organic composition of polymeric materials. Our recent synthesis of irreversibly-bonded, solution-phase 2D polyaramid (2DPA-1)—exhibiting exceptional mechanical strength and chemical stability—presents a new material class for thin films. Here, we report spin-coated 2DPA-1 films, between 4 to 65 nm in thickness, with gas permeability on the order of 10^{-4} Barrer. Gas permeation measurements are enabled by atomic force microscopy (AFM) of inflated bulges over microwells. We find the gas barrier properties of 2DPA-1 thin films, which are commensurate with liquid crystal polymers, are largely immutable over the span of two years. The resistance of 2DPA-1 to degradation contrasts its hygroscopic 1D polyaramid counterparts. Further, the inflation of 4-nm-thick bulges suspended across microwells indicates the absence of defects such as pinholes that commonly plague graphene-based thin films. Despite the intrinsic porosity of a single 2DPA-1 platelet, the ultralow permeability, negligible BET surface area, and orientation-dependent fluorescence of its films suggests 2DPA-1 platelets align anisotropically in a tightly packed and staggered order. Overall, our work elucidates the potential of 2DPA-1 as a next-generation gas barrier material and warrants its further exploration for selective gas separations.

8:00 PM EL19.03.02

Scalable Solution Synthesis and Photocatalytic Activity of Layered ZnO and MoS₂ Heterostructures[MariaSushko](#), LiliLiu, LiborKovarik, JunLiu and XinZhang; Pacific Northwest National Laboratory, United States

Numerous inorganic materials have been identified as potential candidates for high-performance photocatalysts. However, their solar-to-energy conversion efficiencies still fail to meet commercial requirements. The main hurdle is the rapid recombination of photoexcited electrons and holes in single-phase materials. A viable predicted approach to suppress charge recombination is coupling two materials to form a two-dimensional (2D) heterostructure that physically separates photoinduced electrons and holes in different layers. In this work, the heterostructure-based paradigm was tested and a scalable solution synthesis of epitaxial ZnO-MoS₂ heterostructure was developed. A 2D ZnO-MoS₂ heterostructure was synthesized under hydrothermal conditions by stabilizing intermediate Zn-hydroxide states on a functionalized MoS₂ surface. Detailed characterization showed the formation of multilayer heterostructure with MoS₂ flakes intercalated between large size ZnO plates. The performance of this heterostructure was evaluated using photocatalytic degradation of rhodamine B. A degradation efficiency of 70% was measured within 90 minutes of visible light irradiation, almost doubling the efficiency of the corresponding single-phase materials or their physical mixtures.

8:00 PM EL19.03.03

Synthesis, Exfoliation and Characterization of 2D Materials[Nasimul AlamSyed](#), ArkaGhosh, NityanandaSahoo and UddeshyaShukla; National Institute of Technology Rourkela, India

Abstract

Two-dimensional (2D) materials, also known as single-layer materials, consisting of a single or few atomic layers in which the in-plane interaction is much stronger than the interaction between the planes stacked over each other have excellent mechanical, electrical, optical and thermal properties. Since the discovery of graphene in 2004, 2D materials have attracted enormous attention due to their unique properties. 2D materials have a wide range of application in areas like flexible electronics, semiconductors, energy storage, nanoelectromechanical

systems (NEMS), water purification, gas sensing and several others. In a 2D material, the atomic layers stacked over each other, are held together by weak van der Waals forces. By breaking the van der Waals forces between the adjacent layers, the 2D materials can be exfoliated. Understanding the exfoliation mechanism can provide useful information to optimize and improve the parameters of the exfoliation technique in order to obtain high quality as well as higher yield of 2D materials. The properties of 2D materials are highly dependent on the number of layers it is made up of. Ultrasonication, shear exfoliation, micromechanical cleavage, ball milling, mechanical processes, hydrothermal processes, electrochemical processes, laser-assisted and microwave-assisted methods and chemical vapour deposition (CVD) are some of the most commonly used techniques to separate layers of 2D materials and exfoliate them. The choice of the technique depends on the exfoliation yield and quality of the exfoliated 2D materials. It is essential to know how the parameters of these techniques affect both the yield and quality of the exfoliated materials. This paper presents the results of the exfoliation of materials like graphene, hexagonal boron nitride (hBN) and molybdenum disulphide (MoS₂) by mechanical methods like high energy ball milling, by chemical routes through the synthesis of graphite intercalation compound (GIC), ultrasonication technique and centrifugation will be discussed in detail. The various conditions under which these processes were carried out will be discussed. Here, the effectiveness of these techniques in exfoliating different types of 2D materials has been analyzed and the exfoliated 2D materials have been characterized by several analytical techniques to determine the number of atomic layers stacked together in the exfoliated 2D materials. Apart from this, the functional groups that were attached to the surfaces of the 2D materials and their thermal stability were also determined. Using various characterization techniques like x-ray diffraction (XRD), scanning electron microscopy (SEM), high resolution transmission electron microscopy (HRTEM), Raman spectroscopy, atomic force microscopy (AFM) and ultraviolet-visible (UV-vis) spectroscopy and photoluminescence (PL) it is possible to determine the number of layers stacked over each other in a 2D material. Other characterization techniques like Fourier transform infrared spectroscopy (FTIR) and differential scanning calorimetry and thermogravimetric analysis (DSC/TGA) can determine the functional groups attached to their surfaces and the thermal stability of the 2D material. The results show that the exfoliation techniques used here were highly successful in exfoliating the 2D materials. The synthesis of graphene from bulk natural flake graphite (NFG) by the formation of a graphite intercalation compound will also be discussed. The synthesis of graphene oxide (GO) by modified Hummers' method and its thermal reduction to obtain reduced graphene oxide (rGO) will also be discussed in detail.

8:00 PM EL19.03.04

Electrochemically Exfoliated BCN-Cu Nanosheet Electrocatalysts for Efficient Green Hydrogen Evolution: Tuning the Intermolecular Electron Transfer[NagehK. Allam](#); American University in Cairo, Egypt

The search for materials with superior electrocatalytic performance has attracted attention during the past few years aiming to identify a convenient material that works at a low overpotential with long-term stability. Herein, we introduce an innovative technique to fabricate two-dimensional BCN heterostructure nanosheets with various Cu:BCN weight ratios. The fabricated composites showed unique electrocatalytic properties for hydrogen evolution reaction (HER). The morphology and structure of the electrocatalysts were characterized using field emission scanning electron microscopy, Raman, Fourier transform infrared spectroscopy, and X-ray photoelectron spectroscopy techniques. Remarkably, this study reveals the effect of electrochemical chronopotentiometry on facilitating electrochemical exfoliation and hence enhancing the catalytic activity of the fabricated nanosheets. This effect was further confirmed via density functional theory (DFT) calculations, unveiling the effect of the formed oxide layer on the charge transfer process. The overpotential of the 0.125 Cu-BCN composite at a current density of -10 mA/cm² vs RHE is 50% lower than that of pristine BCN. These findings were also affirmed by the DFT calculations, which showed that incorporating copper on BCN has significantly reduced the G_{H^+} value of the HER and subsequently accelerates the kinetics of the reaction and the overall catalytic activity of the material.

8:00 PM EL19.03.05

Predicting Mechanical Properties of Nanocomposites Embedded with Carbon-Based Low Dimensional Materials[AbigailL. Eaton](#), [MarcoFielder](#) and [ArunK. Nair](#); University of Arkansas, United States

Carbon-based low dimensional materials, such as 1D carbyne and 2D cyclo[18]carbon (C₁₈), offer a broad range of material properties that may be beneficial for the development of metal-matrix nanocomposites. However, the interface properties of these carbon-based materials with metal matrix could affect the nanocomposite mechanical properties. Thus, it is important to study the interface properties and perform mechanical testing of the nanocomposites embedded with carbon-based low dimensional materials to determine the most efficient material combinations to improve the mechanical properties.

Using molecular dynamics and density functional theory methods, we develop and study the interface properties of carbon-based materials embedded in Cu metal matrix. We focus on the use of 1D carbyne, 2D C₁₈, and 2D C₁₈-carbyne hybrids due to their low dimensionality and range of strength and elasticity. We then conduct uniaxial tensile testing of the nanocomposites to determine if the nanomaterials improve their mechanical properties when compared to single crystal Cu. From the mechanical property prediction and interface analysis, it is possible to determine the nanocomposite that would be most compatible for future development and applications.

8:00 PM EL19.03.06

Synthesis of Atomically Thin Yellow Pearl: An Impetus for Non-Linear Optical Effects Assisted Light Scattering Applications[NabarunMandal](#), [VidyaKochat](#) and [ChandraS. Tiwary](#); Indian Institute of Technology Kharagpur, India

Synthesis of 2D materials from natural resources, and having unique functionalities have created enormous research interest among material scientists. Naturally occurring organic gemstones such as pearl are found to have a van der Waal's heterostructure with alternating layers of aragonite and complex organic compound conchiolin. In modern laser generation setups, simple optical mirrors on either side of an optical gain medium are being replaced by Bragg's mirrors since such heterostructures increase reflectivity significantly. Hence, 2D pearl, owing to its Bragg's mirror like structure, can replace conventional passive scatterers such as 2D-hBN, 2D-TiO₂ and graphene in generation of amplified spontaneous emission (ASE) and random lasing (RL) applications. Such 2D materials can be used as impetus for light scattering to generate continuous wave (CW) pumped random laser (RL) emission even at room temperature. In this work, defects-free 2D yellow pearl (2D-YP) has been synthesized from bulk south sea pearl using liquid-phase exfoliation (LPE) technique. Thereafter, 2D-YP has been employed as passive scatterer to achieve CW pumped RL emission from a conventional gain molecule. Compared to other semiconductor (TiO₂) and 2D (Graphene and h-BN) passive scatterers, ~25 times improvement in gain volume is observed for the disordered system consisting of 2D-YP, and is due to the formation of a large refractive index gradient via thermal nonlinear optical (NLO) interaction. Hence, incoherent RL (ic-RL) emission ~591 nm is reported at a lowest threshold input pump power and a linewidth of 65 mW and 3 nm, respectively. Additionally, a clear transition from ic-RL to mode tunable coherent RL (c-RL) emission is also demonstrated by altering the pump configuration. Therefore, the newly designed van der Waals heterostructure, i.e., 2D-YP with intrinsic photon trapping capability may pave an avenue towards developing exciting optoelectronic devices.

8:00 PM EL19.03.07

Synthesis of Layered Conducting Polymer Electrode for Superior Ultracapacitor Performance[DuyPham](#); Kennesaw State University, United States

Ultracapacitors (UCs) are electrochemical energy storage (EES) devices that provide fast charge-discharge capabilities and large storage capacity. UCs are comprised of two electrodes that house an electrolyte solution with a porous separator. Electrochemical double layer capacitors (EDLC) that are comprised of carbon-based materials such as activated carbons have an electrostatic charge storage mechanism, also known as non-Faradic charge transfer. The other well-known UCs are pseudocapacitors that are comprised of conducting polymers or metal oxides and have a redox charge storage mechanism, known as Faradic charge transfer. Currently, pseudocapacitors are thoroughly researched, however, the role of conducting polymer structure and property as a function of the deposition method currently remains limited. In this work, conducting polymer electrodes, polypyrrole (PPy) are synthesized using electrochemical depositions with controlled cycles and their performance is investigated. The UCs will be tested using cyclic voltammetry (CV), electrochemical impedance spectroscopy (EIS), and galvanostatic charge/discharge (GCD) to understand the role between deposition cycles and electrochemical performance. Material characterization such as XRD and FT-IR with surface morphology such as SEM are analyzed to give more insights into this charge kinetics between these variations of cycles.

8:00 PM EL19.03.08

Graphene Based Nanofibrous Scaffold for Embedding Bacteriorhodopsin for Bioengineered Memory Application[PhilipByrne](#), [EvanMcCarthy](#) and [IsaacMacwan](#); Fairfield University, United States

The photoactive protein, Bacteriorhodopsin (bR), is being implemented into optical memory applications, most notably for its photochemical and thermal stability. Due to this photochemical stability, bR can remain in one of two stable photostates, bR (ground state) and Q (elevated state), which are used to designate binary bits '0' and '1'. The challenge with this phenomenon is that the Q photo state has a low quantum yield, meaning that bR will not absorb enough photons to undergo photoisomerization. To increase the quantum yield of the photocycle, a molecular dynamics simulation involving graphene monolayer and crystal structure of the bR protein was performed to study the adsorption and preservation of the photostates of bR, where it was found that graphene has a potential to increase the quantum yield. However, a major challenge is to have a porous surface with even distribution of graphene nanoparticles to employ it as a scaffold to anchor the bR protein. The porosity of the surface would help anchor the protein onto the surface and the distribution of graphene nanoparticles would ensure proper chemical interactions. Such a porous surface is achieved through electrospinning where nanofibrous scaffold of poly vinyl alcohol (PVA) with graphene nanoparticles is utilized to immobilize the bR protein. Four different scaffolds on aluminum and Indium Titanium Oxide (ITO) surfaces are fabricated with and without graphene having PVA as a common matrix with optimized electrospinning parameters including flow rate, nozzle collector distance, voltage between nozzle and collector, viscosity of the polymer solution and type and configuration of the collector. It is found that the synthesized nanofibers have average diameters of ~200nm with graphene monolayers embedded within the nanofibrous scaffolds. The resulting scaffolds are characterized using scanning electron microscopy (SEM), profilometry and electrochemical impedance spectroscopy (EIS) to quantify its physical and electrical properties and are compared to the control PVA-bR

scaffolds without graphene. The distribution of the purple membrane discs containing bR embedded within the nanofibers is also quantified based on the fiber diameter, porosity and collector surface. The synthesized scaffolds are also tested using lasers with wavelengths ranging from 380nm to 640nm to drive the bR molecules to the branched photostates to demonstrate their use as a bioengineered memory device.

8:00 PM EL19.03.09

Faradaic and Non-Faradaic Charge Transfer Mechanism for Energy Storage Systems BenMcKinney, SonnettKowalski, AshishAphale and DuyPham; Kennesaw State University, United States

Faradaic and non-Faradaic charge transfer mechanisms play an essential role in energy storage and conversion processes. The faradaic charge transfer mechanism involves electrochemical reactions that result in the exchange of electrons between the electrode and the electrolyte. Whereas the non-faradaic charge transfer mechanism involves charge storage without significant chemical reactions at the electrode-electrolyte interface. In this work we report a hybrid nanocomposite material operating on both Faradaic and non-Faradaic mechanisms simultaneously. The hybrid electrodes containing conducting polymer and graphene oxide were synthesized using electropolymerization process and the effects of graphene oxide (GO) on polypyrrole were studied. Details of electrode synthesis, electrochemical testing, and fabrication of device as a button cell will be discussed. Polypyrrole and graphene oxide (PPy/GO) films were tested using electrochemical methods such as cyclic voltammetry (CV), Electrochemical Impedance Spectroscopy (EIS), and Galvanostatic Charge Discharge (GCD) to assess electrode performance. The results generated from such tests will provide insights into the ohmic, non-ohmic, and Warburg resistances along with specific capacities and charge discharge behavior of the electrodes. These insights will be discussed and compared with electrodes with different levels of graphene oxide.

8:00 PM EL19.03.10

Solar Assisted Expansion of Graphite Flakes for an Effective Exfoliation of Graphene Sheets ShanavasShajahan^{1,1}, RamiA. Elkaffas¹ and YarjanAbdul Samad^{1,1,2}; ¹Khalifa University of Science and Technology, United Arab Emirates; ²University of Cambridge, United Kingdom

Synthesis of scalable monolayer or few-layered graphene sheets is challenging due to the complex production processes [1-3]. Liquid phase exfoliation is considered as one of the most feasible techniques to produce industrially scalable [1] defect-free graphene sheets [4,5]. In ultrasonic exfoliation techniques, long exposure (up to 48 hours) [6] of graphene sheets to the ultrasonic waves considerably decreases its lateral size [7], which limits the mechanical and electrical properties of produced graphene [8]. In this study, we successfully achieved the preparation of graphene sheets with high (4-5 mm) lateral sizes by pre-expanding the graphite through solar-assisted expansion process [9]. The graphite flakes with a lateral size of about 600 μm are intercalated with the perchloric acid (HClO_4) at 120 °C for 30 min to prepare stage II intercalated graphite (S_2IG). In the S_2IG , HClO_4 is intercalated in between every two layer of graphene sheets, which can be confirmed through Raman analysis [10]. The S_2IG is expanded by focusing sunlight on its surface using a simple magnification lens (diameter = 75 mm, focal length = 10 cm). The solar expansion process (SEP) resulted in the formation of expanded graphite with an expansion ratio of about 1:240 (graphite: solar expanded graphite) and lateral size of solar expanded graphite is about 400 μm , which is similar to the intercalated graphite flakes. The solar expanded graphite is exfoliated through probe sonication (500-watt, 20 kHz) for 20 min to obtain few-layer graphene sheets [11]. Raman analysis confirms the formation of defect-free solar expanded graphite as well as few-layer graphene sheets. The obtained results clearly show that the lateral size of graphene sheets can be enhanced by pre-expanding the graphite sheets through solar irradiation before the probe sonication process.

*Corresponding authors

Dr Yarjan Abdul Samad (yarjan.abdulsamad@ku.ac.ae)

Dr Shanavas Shajahan (shanavas.shajahan@ku.ac.ae)

References

1. A Zurutuza et al., *Nat. nanotech.*, **9** (2014), 730.
2. EJ Siochi et al., *Nat. nanotech.*, **9** (2014), 745.
3. KR Paton et al., *Nat. mater.*, **13** (2014), 624.
4. Z Li et al., *ACS nano*, **14** (2020), 10976.
5. Y Hernandez et al., *Nat. nanotech.*, **3** (2008), 563.
6. M Sandhya et al., *Ultrason. Sonochem.*, **73** (2021), 105479.
7. P Turner et al., *Sci. rep.*, **9** (2019), 8710.
8. L Lin et al., *Nat. mater.*, **18** (2019), 520.
9. L Zhu et al., *Mater. Chem. Phys.*, **137** (2013), 984.
10. Li Yuqi et al., *Chem. Soc. Rev.*, **48** (2019), 4655.
11. AV Tyurnina et al., *Carbon* **168** (2020), 737.

SESSION EL19.04: Poster Session II: 2D Materials—Properties of 2D Semiconductors and Heterostructures

Session Chairs: Kibum Kang and Hyeon Jin Shin

Monday Afternoon, November 27, 2023

Hynes, Level 1, Hall A

8:00 PM EL19.04.01

First-Principles Study of Electronic Structure and Nonlinear Optical Responses of Novel Two-Dimensional Materials and Moiré Superlattices AlexStrasser and XiaofengQian; Texas A&M University, United States

Janus two-dimensional (2D) materials and moiré superlattices exhibit rich physical properties and novel fundamental effects. In addition, the recent discovery and synthesis of MA_2Z_4 2D materials prompt further exploration of a new family of van der Waals materials, as well as their Janus counterparts. We investigate and compare the electronic structure and nonlinear optical responses in transition metal dichalcogenides (TMDCs) and Janus TMDCs, MA_2Z_4 and Janus MABZ_4 ($\text{M} = \text{Mo}, \text{W}$; $\text{A}, \text{B} = \text{Si}, \text{Ge}$; $\text{Z} = \text{N}, \text{P}$), as well as twisted multilayer graphene systems. Using first-principles density functional theory, we show that the Janus structuring of TMDCs and MABZ_4 leads to out-of-plane nonlinear responses in both second harmonic generation and shift current, enabling applications for nonlinear electronics and optoelectronics. Furthermore, phosphorous-based MA_2Z_4 2D crystals exhibit enhanced nonlinear response in both low- and mid-frequency of second harmonic generation and shift current, comparable to and beyond that of 2D transition metal dichalcogenide MX_2 materials. These phosphorous materials present strong Rashba spin splitting as evidenced in spin texture. Finally, a Wannier tight-binding model of twisted multilayer graphene is used to calculate nonlinear optical response, including k-point resolved shift vector. The data reveal intense shift current in twisted bilayer graphene on hexagonal boron nitride. In summary, our theoretical results suggest that 2D Janus materials and twisted moiré superlattices offer significant opportunities for the design and manipulation of optoelectronic responses and devices.

8:00 PM EL19.04.02

Long-Lived Charge Separation in Large-Area, Single Crystal MoS_2 Monolayers Interfaced with Non-Fullerene Acceptor Y6 ChristopherE. Petoukhoff, ZhengYang, ShahidulAlam, NisreenAlshehri, JoseP. Jurado Carlin, CatherineDe Castro, VincentTung and FredericLaquai; King Abdullah University of Science & Technology (KAUST), Saudi Arabia

Semiconductor heterojunctions based on 2D transition metal dichalcogenides (TMDs) have displayed record thickness-normalized current densities and absorption coefficients, particularly when interfaced with organic semiconductors [1]. As such, 2D TMDs have been employed as both charge transport layers in organic [2] and perovskite photovoltaics [3], as well as the active layer in mixed dimensional organic-2D heterojunctions [4]. MoS_2 and WS_2 have been demonstrated as alternative hole transport layers in high-efficiency organic photovoltaics (OPVs), leading to devices having greater than 17% power conversion efficiencies [5,6]. However, these works have focused on either mechanically-exfoliated, single-crystal TMDs or liquid-phase exfoliated films, which either limit the size or the homogeneity of the resulting devices. There have not yet been works incorporating large-area, single crystal TMD monolayers as hole transport layer materials for OPVs.

In recent years, the advancement of OPV efficiencies has largely been driven by the development of non-fullerene acceptor materials, such as the molecule BTP-4F (i.e., Y6). This molecule has sub-units of electron donating (D) and accepting (A) groups, in the form of A-DA'D-A structure, which give rise to large exciton delocalization with excitons having charge-transfer-like character. In fact, there has been growing evidence that neat Y6, unlike most neat organic semiconducting materials, can generate charge-separated states even without a donor/acceptor interface typical for OPVs.

In this work, we investigate the charge generation, transfer, and separation processes that occur when neat Y6 is interfaced with large-area, single crystal MoS₂ monolayers. We explore these processes using femtosecond transient absorption (TA) and time-resolved photoluminescence (TRPL) spectroscopies. Our results demonstrate that MoS₂/Y6 interfaces lead to long-lived charges in both the MoS₂ and Y6 layers. We will compare the impact of MoS₂ on charge separation in neat Y6 compared to a typical donor:acceptor blend, PM6:Y6. These results demonstrate the viability of using MoS₂ as an effective hole transport layer in high-efficiency solar cells, particularly for single component OSCs fabricated from Y6-type materials.

1. T. A. Shastry *et al.*, *ACS Nano* **10**, 10573-10579 (2016).
2. X. Gu *et al.*, *Adv. Energy Mater.* **3**, 1262-1268 (2013).
3. U. Dasgupta *et al.*, *Sol. En. Mat. Sol. Cells* **172**, 353-360 (2017).
4. H. Liu *et al.*, *Materials* **14**, 3206 (2021).
5. B. Adilbekova *et al.*, *J. Mater. Chem. C* **8**, 5259-5264 (2020).
6. Y. Lin *et al.*, *Adv. Mater.* **31**, 1902965 (2019).

8:00 PM EL19.04.03

Monolayer 2D Material-Polymer Nanohybrid Crystals Mingyuan Sun¹, Dong Zhou¹, Akash Singh², Lu An¹, Jan Michael Y. Carrillo³, Jong K. Keum^{3,3}, Miguel Fuentes-Cabrera³, Raymond R. Unocic³, Kunlun Hong³, Ilija Ivanov³, Christopher M. Rouleau³, Feng Gang¹, Kai Xiao³, Jihua Chen³, Yumeng Li² and Bo Li¹; ¹Villanova University, United States; ²University of Illinois at Urbana Champaign, United States; ³Oak Ridge National Laboratory, United States

Ultrathin and mechanically robust structures and devices with nanoscale dimension resolution are critical for miniaturized nanoelectromechanical systems (NEMS) and integrated circuit (IC). It is extremely challenging to achieve such structures from hybrid inorganic-organic systems because the lack of controllability of depositing/assembly organic structures. The attainment of precise fabrication control and comprehension of atomic-level interactions stands as the principal objectives of this research. Here, we propose the utilization of monolayer two-dimensional (2D) materials, such as graphene and MoSe₂, synthesized through chemical vapor deposition (CVD), as 2D atomic templates to induce the epitaxial assembly of orthorhombic polyethylene (PE) crystals. By meticulously regulating the assembly temperature and time, the growth of PE lamellar crystals can be modulated, ranging from a few nanometers to hundreds of nanometers with an accuracy of sub-nanometer resolution. Adding PE will not only increase the mechanical robustness of 2D materials in fabricating the suspended structures, but also create a dielectric layer with controlled thickness to realize ultrathin device fabrication. The incorporation of polymer nanocrystals, monolayer graphene, and MoSe₂ yields a pioneering category of hybrid nanostructures, wherein the crystalline architectures of both constituents are highly controlled, thereby potentially reshaping the paradigm for manufacturing superior materials and devices with precisely engineered structures and properties.

8:00 PM EL19.04.04

2D Materials Junction-Templated Photoelectrochemistry Radha Raman^{1,2,3}, Ya-Ping Hsieh² and Mario Hofmann³; ¹National Central University, Taiwan; ²Academia Sinica, Taiwan; ³National Taiwan University, Taiwan

In recent years, the development of lateral junctions between 2D materials has enabled a new class of nanostructures with precise transitions in electronic structure. In this study, we have utilized the unique carrier transport properties of lateral junctions to conduct electrochemistry with unprecedented spatial resolution and dynamic controllability. By electrostatically confining electrons within the junction, we were able to localize electrochemical reactions with nanometer precision in their lateral position. We have also developed a scalable process for the formation of graphene pn-junction networks that is compatible with various materials and techniques, including dielectrophoretic deposition. The high spatial selectivity of the deposition process allowed us to create complex 1D fractal-shaped nanostructures with ultrahigh Raman enhancement.

Furthermore, we have extended our study to utilize MoS₂ junctions to photo-deposit gold nanoparticles. The incorporation of MoS₂ lateral junctions facilitated the deposition of gold nanoparticles with high spatial resolution. The resulting nanostructure morphology can be used for various applications including surface-enhanced Raman spectroscopy and nanoelectronics. These results offer exciting possibilities for the assembly of a new type of neural network based on axon-like guided growth of interconnected neurons. Such a network could have significant applications in the development of evolvable, brain-like future electronics. The potential of this technology highlights the importance of continued research in the field of photoelectrochemically deposited nanostructures on 2D material lateral junctions.

8:00 PM EL19.04.05

Exploring Two-Dimensional Indium Oxide for Memristive Switching: Fabrication, Characterization and Potential Applications Kuan-Hung Chen¹, Chang Hsun Huang¹, Chen-Yuan Weng², Chen-Chih Hsiang¹, Yi-Hsiang Yen¹ and Yi-Chia Chou¹; ¹Nation Taiwan University, Taiwan; ²National Yang Ming Chiao Tung University, Taiwan

Since its groundbreaking discovery in 2004, graphene has captivated the scientific community[1], igniting an unprecedented interest in the exploration of two-dimensional materials (2DMs). These materials have garnered immense attention due to their exceptional properties resulting from their reduced dimensions, charge carrier confinement, and dangling-bond-free surface. Their distinctive van der Waals nature holds tremendous potential for applications in the scaling era of semiconductor[2], propelling researchers into a realm of innovation. In particular, liquid indium and its alloys have emerged as highly promising candidates in the realm of printed electronics, owing to their low melting point, high stability and remarkable conductivity. A novel top-down technique called liquid metal printing (LMP) has ushered in a new era for the production of 2D metal-oxide films, operating at lower temperatures and simplifying the fabrication process compared to traditional deposition methods. By skillfully tailoring the temperature and oxidation time during LMP, researchers can fashion films of varying thicknesses while preserving their 2D attributes. The striking electrical behavior observed in liquid indium-based metals, stemming from their oxide interfaces, has paved the way for exciting prospects in electronic device design. Among these devices, memristors stand out, offering an array of advantages including rapid operation speed, low power consumption, and the ability to retain multiple memory states.

This study embarks on an exploration of the untapped potential of two-dimensional indium oxide (InO_x) as a medium for memristive switching, a territory that has thus far remained relatively unexplored. We successfully extracted InO_x from liquid indium and adeptly transferred it onto a SiO₂/Si substrate utilizing the LMP technique. The resultant InO_x showcased a considerable area coverage along with an ultra-thin atomic thickness, emphasizing its remarkable properties. A thorough analysis validated the presence of high-quality, structurally stable InO_x. To expand the horizons of this investigation, the fabrication process encompassed the creation of InO_x memory device, revealing distinct memristive characteristics. Delving further into the intricacies of the relationship between defect and fabrication temperature, we uncovered a direct correlation between oxygen vacancies and temperature, thereby influencing the memristive behavior of InO_x. To elucidate the switching mechanism, an elaborate model was constructed, unraveling the indispensable role played by preferential oxygen segregation along the grain boundaries. Besides, the memristor exhibited outstanding performance in terms of low power consumption and retention, holding its on/off ratio over multiple operating cycles with remarkable stability. Furthermore, the InO_x memristor showcased the ability to assume multi-level states under specific conditions, highlighting its potential for diverse applications. An intriguing revelation emerged from this study: the behavior of oxygen vacancies within the InO_x memristor exhibited a resemblance to the behaviors observed in ion migration within bionic neurons. This striking similarity opens up new vistas for the application of InO_x devices in constructing artificial neural network. This discovery holds immense significance as it enhances our understanding of the precise characteristics of oxygen defects and our ability to control the oxygen vacancies in atomically thin oxide films. Moreover, it carries substantial implications for the field of memory technology.

Reference:

1. Novoselov, K.S., et al., *Electric field effect in atomically thin carbon films*. science, 2004. **306**(5696): p. 666-669.
2. Lemme, M.C., et al., *2D materials for future heterogeneous electronics*. Nature communications, 2022. **13**(1): p. 1392.

8:00 PM EL19.04.06

Spontaneous Enthalpy-Uphill Exciton Dissociation at Organic/2D Heterostructures Fatimah H. Rudayni^{1,2}, Kushal Rijal¹, Neno Fuller¹ and Wai-Lun Chan¹; ¹The University of Kansas, United States; ²Jazan University, Saudi Arabia

Bound interlayer excitons (IXs) at type-II transition-metal dichalcogenide (TMD) heterostructures are usually stable against thermal dissociation because of their large binding energy. In this work, we show that by combining TMD with organic molecules, IXs can dissociate spontaneously into free carriers despite it is an enthalpy-uphill process. Time-resolved photoemission spectroscopy is used to probe the exciton dynamics at the fluorinated zine phthalocyanine (F₈ZnPc)/monolayer-WS₂ heterostructure. It is found that bound IXs can gain an energy of 240 meV in 50 ps without any external driving force. We attribute this anomalous enthalpy-uphill process to the entropy-driven IX dissociation. The face-on orientation of F₈ZnPc molecules on TMD allows the electron within the IX to delocalize along a direction perpendicular to the interface. This geometry reduces the density of bound IXs and enhances the entropic driving force. This kind of organic/2D heterostructures is advantageous to applications that require the generation of free carriers from bound excitons.

8:00 PM EL19.04.07

The Electrical, Optical, Structural and Chemical Properties of Molybdenum Ditetelluride Film (MoTe₂) using Ion-Beam Assist Magnetron Sputtering for the Device Application of Phototransistor Hyeon Gi Park¹ and Jae-Hyun Lee²; ¹Ajou Kiuri Research Center, Korea (the Republic of); ²Ajou University, Korea (the Republic of)

In this study, we investigate transition metal dichalcogenide materials as active layers for heterojunction phototransistors and optimize their physical properties through numerical simulation programs. Numerical analysis was performed using the AFORS-HET 1D program, and we optimized the parameters of MoTe₂, WS₂, and other materials for the active layer along with Si, SiC, and GaAs substrates to improve the external and internal quantum efficiency. We deposited the MoTe₂ by ion-beam assisted magnetron sputtering. Tuning of the Fermi level in MoTe₂ leads to phototransistors with excellent electrical, structural, chemical and optical properties. Specifically, we investigated the different parameters such as power, pressure, temperature and gas atmosphere by sputtering process. Subsequently, we illuminated n-type MoTe₂ sample with ion-beam source under Ar, oxygen (O₂) and nitrogen (N₂) gas environment and then transversed the carrier type into p-MoTe₂. However, unveil of the doping mechanism effect on various thicknesses using ion-beam is still challenging. In addition, we investigated the photoresponse of MoTe after illumination of ion beam. After that, the phenomenon of carrier modulations and photoresponse paves the way for wide applications of MoTe₂ in optoelectronic devices.

8:00 PM EL19.04.08

Two-Dimensional Transition Metal Dichalcogenide Nanosheets for Therapeutic Drug Monitoring of Human Blood Samples TaeG. Lee¹, SunhoJoh¹, Hee-KyungNa¹, Jin GyeongSong¹, JaekakYoo^{1,2}, A YoungLee¹, Cheol-HeeAhn³, Da-JeongJi³, Jung-subWi⁴, Mun SeokJeong⁵ and Sang-GukLee³; ¹KRISS, Korea (the Republic of); ²Sungkyunkwan University, Korea (the Republic of); ³Yonsei University College of Medicine, Korea (the Republic of); ⁴Hanbat National University, Korea (the Republic of); ⁵Hanyang University, Korea (the Republic of)

Two-dimensionally layered transition metal dichalcogenides (TMDs) have been widely used in various biomedical applications such as biosensing and cancer therapy due to their characteristics including UV absorbance, photoinduced thermal effect, tunable bandgap and photoluminescence.¹ However, their applications in therapeutic drug monitoring, which is essential for individualizing drug dosage regimens, is rarely reported. In this regard, we exemplarily present a facile platform for rapid quantitative determination of therapeutic drugs and biomarkers that can satisfy clinical diagnostic demands. Two-dimensionally layered TMDs including tungsten disulfide (WS₂), tungsten ditelluride (WTe₂) and molybdenum ditelluride (MoTe₂) were fabricated by chemical exfoliation and incorporated as matrices for laser desorption/ionization mass spectrometry (LDI-MS) to promote the ionization efficiency of the analytes. The WS₂ nanosheet allowed for a sensitive detection of commonly prescribed immunosuppressive drugs including cyclosporine A and tacrolimus in the blood of organ transplant patients by LDI-MS, up to nanomolar concentration with a good linear response within the therapeutic concentration range.² Quantification of antiepileptic drugs in human blood was achieved using WTe₂ and MoTe₂ nanosheets, while they also facilitated the concentration determination of vitamin D3, which is a well-known biomarker for osteoporosis, Parkinson's disease, and cancers.³ The validity of our method was further verified by performing statistical agreement assessment to compare our results with those of conventional analytical techniques such as liquid chromatography tandem mass spectrometry. The contribution of the physicochemical properties of TMDs to the ionization efficiency was studied by performing density function theory (DFT) calculations. The results of DFT calculations indicated that the WTe₂ and MoTe₂ tend to assist the ionization of small molecules more efficiently by yielding greater proton affinities for the anti-epileptic drugs, suggesting that the metallic nature of telluride is one of the contributing factors. It is anticipated that our LDI-MS based method would expand the applicability of TMDs in diagnostic medicine, while it can also provide the evidences to elucidate their roles in ionization properties under laser irradiation.

References

1. V. Agarwal and K. Chatterjee. *Nanoscale*, 2018, **10**, 16365.
2. S. Joh *et al.* *ACS Nano*, 2021, **15**, 19141-10152.
3. Manuscript in preparation

8:00 PM EL19.04.09

Trace Detection of Ciprofloxacin in Milk by Label-Free Raman Enhancement using Two-Dimensional Magnesiocromite AnyeshaChakraborty, ChandraS. Tiwary and BasudevLahiri; Indian Institute of Technology, Kharagpur, India

Exploring the noteworthy features of the non-Van der Waals two-dimensional (2D) metal oxide, 2D-Magnesiocromite (2D-MgCr₂O₄), we have developed a simple, flexible, and scalable optical sensing method. The presence of antibiotics in food products is no doubt a concerning issue these days, increasing the risk of the formation of antibiotic-resistant bacteria, which can lead to severe infections and allergies in the human body that can be challenging to cure. Ciprofloxacin (CFX, C₁₇H₁₈FN₃O₃) is a second-generation fluoroquinolone that is highly effective in treating several bacterial infections affecting the urinary tract, respiratory tract, skin, and gastrointestinal tract. Its broad-spectrum activity has made it a popular choice for treating a wide range of organisms, including humans, livestock, and aquaculture. Due to incomplete metabolism within the body, the drug's residue is expelled through urine and faeces, resulting in significant environmental pollution. Besides, due to drug overdoses in cattle, traces of the drug can often be found in the milk produced by them. To eliminate the antibiotic from the milk supply chain, early detection of the drug is necessary. To meet the demand, 2D-MgCr₂O₄ has been used for its biocompatibility, high thermal stability, abundance of surface defects, high density of surface oxygen ions which act as active binding sites, and ease of availability. We used a real-time label-free Raman enhancement mechanism for antibiotic detection, along with a Raman spectral mapping method for clear chemical fingerprint imaging for rapid identification. Here, we have used UV-Visible spectroscopy, Raman spectroscopy, and Raman imaging to analyse the 2D material's detection potential in water initially and finally in milk. The sensor has over a month-long shelf life, even when stored in typical atmospheric conditions, and the acquired detection limits are 260 ng/ml by UV-Visible spectroscopy and 120 ng/ml by Raman spectroscopy in milk. Such methods can be extended to the detection of other toxic ingredients in near future.

8:00 PM EL19.04.10

Evolution of Bandgap in WS₂ from Monolayer to Multilayer XuHe, JinpengTian, SaïenXie and AntoineKahn; Princeton University, United States

Transition metal dichalcogenides (TMDs) are 2D van der Waals materials with a chemical formula MX₂, where M represents a transition metal such as tungsten (W) or molybdenum (Mo) and X represents a chalcogen atom such as sulfur (S) or selenium (Se). TMDs are layered compounds and can be stacked from mono- to multi-layer films. Unlike graphene, which has a zero gap, TMDs are more versatile in their applications in electronics due to their sizable electronic gaps, tunable with composition and thicknesses. Many theoretical works have been done to study and predict the electronic structures of these materials. It is now a consensus that TMD electronic gaps decrease as the number of layers increases. However, no experimental study has been completed to show how the electronic gap evolves from monolayer to multilayer structures.

In this work, we explore the evolution of optoelectronic properties such as energy level positions, electronic gap (E_G), and exciton binding energy (E_B) using ultraviolet and inverse photoelectron spectroscopies (UPS / IPES), complemented with Raman spectroscopy and photoluminescence (PL) measurements. High-quality large-scale monolayer and multilayer continuous films of WS₂ are grown by chemical vapor deposition on p-Si (with a native SiO₂ layer). Raman spectroscopy and PL help differentiate between mono- and multi-layer films. UPS and IPES are used to measure occupied and unoccupied states and determine valence band maximum (VBM), conduction band minimum (CBM), Fermi level position, and associated ionization energy, electron affinity, and E_G. We find that the valence (conduction) states shift toward (away from) the vacuum level from mono- to multi-layer films, decreasing the electronic gap from 2.29 eV to 1.61 eV. The optical gap (E_{OPT}) measured by PL for the monolayer film is 1.96 eV. Finally, by subtracting E_{OPT} from E_G, we determine E_B for the monolayer film to be ~0.33 eV. Further studies are being conducted on other TMDs, including WS₂, to confirm our findings. These experimental studies will shed light on understanding TMDs bandgap evolution, making predictions on bandgap and energy levels possible for new TMD materials. This will help better decide on TMDs for appropriate band alignments in devices such as LEDs and solar cells where suitable energy levels are of essential importance.

8:00 PM EL19.04.11

High Drift Velocity in Multilayer Indium Selenide at High Electric Fields YongwookSeok^{1,2}, HanbyeolJang², YiTaekChoi², HeungsoonIm², KenjiWatanabe³, TakashiTaniguchi³, JunghyoNah⁴ and KayoungLee¹; ¹Korea Advanced Institute of Science and Technology (KAIST), Korea (the Republic of); ²Gwangju Institute of Science and Technology (GIST), Korea (the Republic of); ³National Institute for Materials Science, Japan; ⁴Chungnam National University, Korea (the Republic of)

Creating a high-frequency electron system demands a high saturation velocity (v_{sat}). Herein, we report high-field transport properties of multilayer van der Waals indium selenide (InSe). The InSe is on a hexagonal boron nitride substrate and encapsulated by a thin, non-continuous indium layer, resulting in an impressive electron mobility that approaches 3000 cm²/Vs at room temperature. Along with the high mobility, the temperature dependence characteristics of the insulating state reveals the presence of minimal disorder and impurities in our InSe. By utilizing four-terminal pulsed measurements, the drain current (I_{DS}) at high drain bias (V_{DS}) was accessed, reaching up to 3.8 mA at 8 V. I_{DS} vs V_{DS} was measured at different carrier densities and temperatures, which are converted into electron drift velocity (v_d) vs electric field (F). v_d vs F data allow us to extract v_{sat} values, which are as high as 1.8×10^7 cm/s at room temperature, superior to those of other gapped 2D semiconductors. Finally, we suggest an optical phonon emission model modified for parabolic dispersion to explain the current saturation, and determine the optical phonon energy of InSe as 22.9 meV, which is close to the theoretically expected value of monolayer InSe.

8:00 PM EL19.05.01

Applications of Ambipolar Molybdenum Disulfide with Van der Waals Contacts Jungi Song¹, Suyeon Lee¹, Yongwook Seok¹, Yeonghyeon Ko¹, Hanbyeol Jang² and Kayoung Lee¹; ¹KAIST, Korea (the Republic of); ²Gwangju Institute of Science and Technology, Korea (the Republic of)

Two-dimensional (2D) materials are promising to replace silicon because they do not exhibit performance degradation when scaled down to the nanoscale. However, their high contact resistance and Fermi-level pinning hinder the modulation of a single 2D semiconductor into n-type and p-type, and restrict their potential applications. To overcome those limitations, ambipolar transistors, which can dynamically switch the type of majority carriers, have been proposed. However, a few semiconductors with small bandgaps, such as graphene, black phosphorus, and tungsten diselenide, have shown ambipolar properties. Achieving ambipolar characteristics in 2D materials with a relatively large bandgap remains challenging. Here, we show ambipolar molybdenum disulfide (MoS₂) transistors by employing van der Waals contacts. MoS₂ shows great potential for the future semiconductor industry, thanks to its sufficient bandgap (1.2–1.9 eV), decent mobility, stability, and mature large-area growth technology. Our devices achieve outstanding ambipolar current characteristics, with both PMOS and NMOS On/Off current ratios > 10⁶ and two-point hole mobility > 23 cm²/V*s. By utilizing the ambipolar current characteristics, we have designed a new multifunctional electronics that is reconfigurable between an ambipolar transistor, an n-type transistor, a rectifier (rectification ratio of ~10⁶), a reversible negative breakdown diode (On current of ~0.1 mA), and a photodetector. The talk will be concluded with a brief discussion regarding our demonstration of a complementary inverter based on ambipolar MoS₂ homojunction.

8:00 PM EL19.05.02

Modification of Mono-layer MoS₂ Through Post-Deposition Treatment and Oxidation for Enhanced Optoelectronic Properties Jonathan Rommelfangen¹, Marco A. Gonzalez-Angulo², Devendra Pareek², Levent Gütağ², Phillip J. Dale¹ and Alex Redinger¹; ¹University of Luxembourg, Luxembourg; ²Carl von Ossietzky University of Oldenburg, Germany

Atomic layer deposition is a great tool for growing large-scale high-quality mono-layer (ML) MoS₂ and with a dedicated high temperature post-deposition treatment the amount of sulfur vacancies can be controlled. Sulfur-containing atmospheres, such as H₂S, lead to MoS₂ with low number of sulfur vacancies and increased stability against oxidation in air, whereas post-annealing treatments in N₂ increase the number of vacancies and the material is more prone to oxidation. Post-deposition annealing treatments thereby offer a great possibility to tune the properties of the 2D layer.

Here we show that the sulfur vacancy-rich ML MoS₂ films oxidize already at room temperature, which strongly affects the photoluminescence yield, the MoS₂-Al₂O₃ substrate interaction and the structural integrity of the films. We used X-ray photoelectron spectroscopy to monitor the formation of MoO₃ and possibly MoS_{2-x}O_x after exposure to air and to quantify the number of sulfur defects in the films. Atomic force microscopy (AFM) measurements allow us to pinpoint the exact regions of oxidation and to develop a dedicated low temperature heating procedure to remove the oxidized species, leading to MoO₃-free MoS₂ films. Interestingly, AFM and Kelvin probe force microscopy show that the MoS₂-Al₂O₃ substrate coupling is changed, which also affects the ML MoS₂ work function significantly (variations by approximately 300 meV). In addition, the reduction in MoS₂-substrate coupling leads to a 10-fold increase in the PL intensity, and the ratio between trions and neutral excitons is changed.

Our work highlights the importance of oxidized sulfur vacancies and provides useful methods to measure and manipulate the number of vacancies on MoS₂. Furthermore, the changes in the MoS₂-substrate interaction via sulfur vacancies and oxidation offer a new pathway to tune the optoelectronic properties of the 2D films.

8:00 PM EL19.05.03

Band Alignment Tunability of 2-Layer MoS₂/SiO₂ Interface with The Use of Inorganic Salts in Liquid-CVD Sulfurization Alessio Lamperti¹, Pinaka Pani Tummala^{1,2,3}, Alessandro Cataldo¹, Sara Ghomi^{1,4}, Christian Martella¹, Valeri Afanas'ev² and Alessandro Molle¹; ¹IMM-CNR Agrate Brianza, Italy; ²KU Leuven, Belgium; ³Università Cattolica del Sacro Cuore, Italy; ⁴Politecnico di Milano, Italy

Among two-dimensional (2D) transition metal dichalcogenides (TMDs), molybdenum disulfide (MoS₂), in the semiconducting 2H phase, is one of the most extensively studied, because of its stability, versatility, and applicability in several fields, such as electrochemistry, optoelectronics, and microelectronics [1, 2]. To achieve sustainable exploitation of 2D-MoS₂, a scalable synthesis over large macroscopic areas is required. In this respect, chemical vapor deposition (CVD) is a versatile and cost-effective method to address the deposition of high-quality few-to-single layers MoS₂ with controlled thickness, uniformity and defectivity up to the wafer scale and with satisfactory carrier mobility [3]. Having 2D-MoS₂ based microelectronic devices as target, the electron band alignment at MoS₂/SiO₂ interface is a key-parameter dictating the electrostatic properties of the stacks such as built-in voltages, transistor thresholds, as well as the tunneling barrier heights. Therefore, the electrostatic control of the MoS₂/SiO₂ interface, entailing the energy barrier height at the junction and the emergence of interface dipoles, is essential to overcome parasitic or undesired short-channel effects in ultra-scaled field-effect transistors (FETs) based on MoS₂ [1], or to fabricate compliant stacks in ultra-steep sub-threshold slope tunneling FET [4].

Despite previous attempts proved that the use of inorganic salts, such as NaCl, is effective in promoting selective extended 2D-MoS₂ growth [5], no attention has been put on the electrical properties at the MoS₂/SiO₂ interface. Here, we performed internal photoemission (IPE) spectroscopy, a method successfully applied to 2D layered materials interfacing [6], on large-area (cm²) bi-layers MoS₂ directly grown on SiO₂/Si substrates via liquid precursor CVD (L-CVD) sulfurization, where the ammonium heptamolybdate (AHM) Mo precursor, is provided via solution deposition with inorganic salts (NaCl, NaOH, KCl, KI) spun over the substrate, to assess any possible effect of these inorganic molecules on the MoS₂/SiO₂ interface properties, in particular to determine the energy band alignment of MoS₂ with SiO₂. We measured IPE thresholds from 3.9 to 4.2 eV, depending on the type of inorganic salt in solution, which in any case disagrees with the 3.6 eV value obtained in CVD grown MoS₂ from MoO₃ and S powders with the assistance of organic perylene-3,4,9,10-tetracarboxylic acid tetra-potassium salt (PTAS) [7]. To in-depth elucidate the origin of such discrepancy, we performed structural, morphological, and chemical analysis (SEM, AFM, Raman, XPS). For the case of NaOH, we revealed the presence of Na and OH residuals. Our findings are consistent with the emergence of Si-OH dipoles at the interface that individually dependent with each surface treatment in use, thus explaining the observed 0.6 eV energy widening in the IPE threshold.

Our study evidence the impact of the junction characteristics, and thus the need to consider them, on the real electrical behavior of devices integrating 2D materials, with critical implications on proposed models and reported values so far. We also report a relatively easy route to tune the band alignment at 2D-MoS₂/SiO₂ interface, a fundamental property to consider in the perspective of direct integration of 2D materials in the process flow for microelectronic devices.

This study was supported by the Government of Italy through Ministero dell'Università e della Ricerca (MUR) under the PRIN projects "aSTAR", n. 2017RKTMY and "PHOTO" n. 2020RPEPNH.

References

- [1] C. Martella et al., *Nanomaterials* 12, 4050 (2022)
- [2] M. Bhatnagar et al., *Nanoscale* 12, 2 24385 (2020)
- [3] C. Martella et al., *Adv. Mater. Interf.* 7, 2000791 (2020)
- [4] I. Shlyakhov et al., *APL Mater* 6, 026801 (2017)
- [5] L. Huang et al., *J. Am. Chem. Soc.* 142, 13130 (2020)
- [6] V. V. Afanas'ev et al., *J. Phys.: Cond. Matter* 32, 413002 (2020)
- [7] P.P. Tummala et al., *Materials* 13, 2786 (2020)

8:00 PM EL19.05.04

Galvanic Displacement Across Single-Layer Graphene for The Fabrication of Metal Nanostructures Isabelle Cunitz and Rohit Karnik; Massachusetts Institute of Technology, United States

This work aims to advance the scientific and engineering understanding of galvanic displacement reactions as buffered by a monolayer of graphene, specifically by investigating palladium deposition on graphene on a copper foil substrate via galvanic displacement between the copper and palladium (II) ions in solution. To understand palladium nanoparticle deposition and determine how this process can be controlled, electrochemical thermodynamics and classical nucleation theory are first synthesized into a thermodynamic model of the system. Next, scanning electron microscopy is used to characterize palladium deposition on the graphene/copper surface after galvanic displacement. Copper etch pits are observed to form during the reaction, maintaining contact between the deposition solution and the copper and thereby ensuring that the reaction is not self-limiting under the conditions studied. Palladium is observed to preferentially deposit along atomic steps in the copper foil, at graphene defects where the copper is exposed to the deposition solution, and at etch pits. The effects of varying palladium concentration and graphene/copper surface treatments are characterized, and these results are synthesized to propose a mechanism of palladium deposition via galvanic displacement through graphene. Finally, galvanic displacement is investigated in a novel engineering application, as a method of sealing graphene defects for the synthesis of centimeter-scale nanoporous atomically thin membranes. Palladium nanoparticles deposited on the graphene surface are observed to largely survive graphene transfer to a support membrane substrate, as well as mounting and use in

aqueous diffusion cell experiments. However, diffusion experiments show that graphene treated via galvanic displacement has higher leakage than untreated graphene, indicating that under the reaction conditions studied here, galvanic displacement has a net effect of graphene defect enhancement rather than defect sealing. This work contributes new insights regarding galvanic displacement as a method of modifying monolayer graphene, as well as exploring this method in the novel application of membrane separations. With further development, this simple, quick, and inexpensive technique for the fabrication of 2D material/nanoparticle composites may have a myriad of applications relevant to sustainability and beyond.

8:00 PM EL19.05.05

Substrate Effects on Spin Defects in Two-Dimensional Hexagonal Boron Nitride Chi-Che Wu and Elizabeth M. Lee; University of California, Irvine, United States

Two-dimensional (2D) hexagonal boron nitride (hBN) is a single atom thick wide band gap semiconductor with high thermal conductivity and chemical stability. Negatively charged boron vacancies (V_B^-) in hBN have recently emerged as a promising platform for quantum sensing and quantum information science applications, owing to their long spin coherence times even at room temperature. Here, we investigate electronic structure properties of V_B^- in 2D hBN on top of solid-state substrates using density functional theory calculations and *ab initio* molecular dynamics simulations. By using substrates ranging from metals (e.g., copper) to insulators (e.g., silica), we discuss how the substrates and their surface chemistry can greatly impact the electronic and mechanical stability of V_B^- . Our results suggest ways to control the spin defect properties for 2D materials using substrate engineering and surface modification.

8:00 PM EL19.05.06

Synthesis of V-Doped WTe_2 Nanolayers and Single Crystals Vera M. Gospodinova¹, Dimitre Dimitrov^{1,2}, Peter Rafailov², Nikola Malinowski¹, J.F. Sierra³ and Sergio Valenzuela³; ¹IOMT-BAS, Bulgaria; ²ISSP, Bulgaria; ³Catalan Institute of Nanoscience and Nanotechnology (ICN2), Spain

The discovery of 2D topological insulator in monolayer $1T'-WTe_2$ indicates great potential for novel electronic, spintronic, and quantum metrology. Theoretically, the interaction between the topological states and the magnetic ordered states of $Td-WTe_2$ enables the modulation of Weyl semimetal states by an external magnetic field and potentially the creation of a quantum anomalous Hall phase [1-3]. However, currently, ferromagnetism in layered $1T'-WTe_2$ is still not observed. We are attempting to synthesize nanolayers/ flakes of $1T'-WTe_2$ with vanadium doping in order to induce magnetism. V-doped WTe_2 nanolayers/ flakes were synthesized in an atmospheric pressure CVD (APCVD) quartz tube reactor with three independent thermal zones. LP (liquid precursors) method based on ammonium metavanadate hydrate (AMT) and ammonium metavanadate (AMV) or vanadium(IV) oxide sulfate ($VOSO_4$) with addition of PTAS was used for the synthesis. The obtained nanolayers/clusters/flakes were studied by optical microscopy and Raman spectroscopy.

In addition, we are reporting growth of V-doped WTe_2 single crystals by using flux (high-temperature solution) method. Particularly the self-flux method was used for crystal growth, and tellurium was used as a solvent (flux). The grown crystals were studied by XRD, XPS and Raman spectroscopy and the typical for WTe_2 X-ray diffraction patterns and Raman modes were observed. Vanadium incorporation (1.8 at. %) in the crystal structure was detected by XPS measurements. The estimated overall elemental composition in at. % confirms the presence of vanadium.

Acknowledgement: We acknowledge the support of the European Union's Horizon 2020 FET-PROACTIVE project TOCHA under grant agreement 824140.

References:

[1] Wu, S. et al. Science 359, 76–79 (2017)

[2] Yu, R. et al. Science 329, 61–64 (2010)

[3] Li, Y. et al. Adv. Funct. Mater., 31 (2021) 2008116

SESSION EL19.06: Poster Session IV: 2D Materials—Epitaxial and Van der Waals Heterostructures
Monday Afternoon, November 27, 2023
Hynes, Level 1, Hall A

8:00 PM EL19.06.01

Photogeneration at a Dirac/Charge-Compensated Semimetal Heterojunction based on Graphene and WTe_2 Farima Farahmand, Ao Shi and Nathaniel Gabor; University of California, Riverside, United States

The unique photocurrent characteristics of pure semimetal heterojunctions composed of atomically thin materials remains a new frontier in optoelectronics. A novel pairing of a Dirac semimetal and a charge-compensated semimetal provides an opportunity to investigate photogeneration when photo-thermoelectric, photovoltaic, and other important photogeneration effects coexist. We employ near-infrared scanning photocurrent microscopy to investigate the dynamics of photoexcited electrons that control the electrical and optical conductivities at the interface to clarify the heterojunction band alignment between WTe_2 and graphene, which have charge compensated electron-hole bands and a Dirac point, respectively. Our findings highlight the important role that the photo-thermoelectric effect plays in the photocurrent distribution, alongside other phenomena such as the photovoltaic effect that have been seen earlier in p-n junctions. Our measurements not only define the essential photocurrent and band alignment characteristics of this combined Dirac-Weyl system but also provide valuable insights for the design and enhancement of highly sensitive infrared sensors based on van der Waals heterostructures. These discoveries pave the way for exciting advancements in the field of quantum optoelectronics.

8:00 PM EL19.06.02

Atomic Reconstruction of Large-Lattice-Mismatched Transition Metal Dichalcogenides Heterobilayers into Strained-Commensurate Structures Seongchul Hong¹, Ji-Hwan Baek¹, Yunyeong Chang¹, Hong M. Nguyen², Changheon Kim¹, Yeonjoon Jung¹, Hyeonseo Lee¹, Kenji Watanabe³, Takashi Taniguchi³, Jangyup Son⁴, Hyeonsik Cheong², Miyoung Kim¹ and Gwan-Hyoung Lee¹; ¹Seoul National University, Korea (the Republic of); ²Sogang University, Korea (the Republic of); ³National Institute for Materials Science, Japan; ⁴Korea Institute of Science and Technology, Korea (the Republic of)

Moiré superlattices between vertically stacked van der Waals (vdW) layers with twist angle or lattice mismatch generate periodic moiré potentials, which induce renormalization of electronic band structures and corresponding modulation of electrical and optical properties of moiré crystals. In addition, lots of attentions have been paid for spontaneous atomic reconstruction of small-mismatched vdW layers into periodic commensurate domains separated by incommensurate boundaries because of unprecedented physical properties of these unique vdW layers. Unlike small-mismatched vdW layers, the spontaneous reconstruction has not been observed in large-mismatched vdW layers owing to their large formation energy of commensurate structures. Here, we report thermally induced atomic reconstruction of a large-mismatched $MoS_2/MoSe_2$ heterobilayer (lattice mismatch = 3.88%) into a strained-commensurate (SC) heterostructure that has angle- and lattice-matched commensurate domains separated by saddle point (SP) structures through hBN-encapsulation annealing. We verified that the SP structure has large dilatational and shear strains of 4% and the SC structure exhibited splitting of the intralayer excitons owing to the inhomogeneous strain distribution. Our work verifies that even hetero-bilayers with large lattice mismatches can transform into lattice-aligned heterostructures regardless of twist angle and expands our understanding for electrical and optical properties of vdW heterostructures with new stacking sequences.

8:00 PM EL19.06.03

A High- κ Wide-Gap Layered Dielectric for Two-Dimensional Van der Waals Heterostructures Aljoscha Söll¹, Edoardo Lopriore^{2,3}, Asmund Ottesen^{2,3}, Jan Luxa¹, Gabriele Pasquale^{2,3}, Jiri Sturala¹, František Hájek⁴, Vitězslav Jary⁴, David Sedmidubský¹, Kseniia Mosina¹, Andras Kis^{2,3} and Zdenek Sofer¹; ¹University of Chemistry and Technology, Czechia; ²Institute of Electrical and Microengineering, Switzerland; ³Institute of Materials Science and Engineering, Switzerland; ⁴Institute of Physics of the Czech Academy of Sciences, v.v.i., Czechia

Van der Waals heterostructures of two-dimensional materials have opened up new frontiers in condensed matter physics, unlocking unexplored possibilities in electronic and photonic device applications. However, the investigation of wide-gap high- κ layered dielectrics for devices based on van der Waals structures has been relatively limited. In this work, we demonstrate an easily reproducible synthesis method for the rare earth oxyhalide LaOBr, and we exfoliate it as a 2D layered material with a measured static dielectric constant of $\epsilon_{0,\perp} \approx 9$ and a wide bandgap of 5.3 eV. Furthermore, our research demonstrates that LaOBr can be used as a high- κ dielectric in van der Waals field-effect transistors with high performance and low interface defect concentrations. Additionally, it proves to be an attractive choice for electrical gating in excitonic devices based on 2D materials. Our work demonstrates the versatile realization and functionality of 2D systems with wide-gap and high- κ van der Waals dielectric environments.

8:00 PM EL19.06.04

Synthesis and Characterization of (3D/2D) $\alpha-Fe_2O_3$ /Graphene Heterostructure for Application as a Toxic Gas Sensor Ariadne C. Catto¹, Luis F. da Silva¹, Eduard Lobet² and Elson Longo¹; ¹Federal University of Sao Carlos, Brazil; ²Universitat Rovira i Virgili, Spain

Metal semiconducting oxides (MOXs) have been widely employed in gas sensors due to their potential features, such as high sensitivity, selectivity, rapid gas detection, and stability. N-type

MOXs (e.g. SnO₂, WO₃, ZnO, and α -Fe₂O₃) have been successfully applied as sensing elements in gas sensor devices for the detection of a variety of toxic gases, such as NO₂, NH₃, O₃, and H₂S. Among the n-type MOXs, hematite (α -Fe₂O₃) nanostructures have gained attention due to their high oxygen ion mobility at the material surface, excellent chemical and thermal stability under ambient atmosphere, and low cost. Despite its advantages, few studies have investigated the sensing activity of hematite. Therefore, efforts have been paid to improving the sensing performance of α -Fe₂O₃ by using distinct strategies, such as combination with other components including noble metals, semiconductors, and carbon-based materials. Among these, graphene has received considerable attention due to its unique two-dimensional (2D) structure, high electron conductivity and mobility, and high surface area. Also, various MOXs may be combined with GO and/or rGO resulting in a self-assembled heterostructure with unique properties for the most diverse applications. Regarding gas sensing applications, hydrophobic graphene-based materials have been cited as an effective way to be employed in gas sensor devices leading to high sensitivity and selectivity even in high humidity conditions. Motivated by these considerations, we report here a versatile approach towards the production of advanced materials based on (3D/2D) α -Fe₂O₃/graphene sheets heterostructure to be applied as a resistive NO₂ gas sensor. The effect of different amounts of addition ratios of graphene on the sensing performance has been studied. The α -Fe₂O₃/Gr heterostructures were obtained by hydrothermal method and the crystalline phase, morphological, and surface properties were studied by XRD, FESEM, TEM and XPS techniques. Additionally, we successfully combined experimental and DFT calculations to understand the role played by the heterointerface and the chemical environment along the exposed surfaces α -Fe₂O₃/Graphene sheets in the sensing properties towards NO₂ gas. The gas sensing experiments show that the α -Fe₂O₃/graphene heterostructure gas sensor has better sensing performance for NO₂ than the pristine graphene, such as high response, excellent selectivity, and low detection limit. The effects of temperature and moisture on the NO₂ sensitivity of α -Fe₂O₃/graphene heterostructures were also investigated. The optimal operating temperature for the highest gas response is around 150 °C, and the formation of α -Fe₂O₃/graphene heterostructure improved the NO₂ sensitivity against moisture. Furthermore, the selectivity was also evaluated by exposing the heterostructures to different gases such as O₃, NH₃, and CO. These findings show that (3D/2D) α -Fe₂O₃/Graphene sheets heterostructures have a remarkable potential for practical applications as NO₂ gas sensor in environmental monitoring devices.

8:00 PM EL19.06.05

High-Performance Self-Powered UV Photodetector Based on NGQD/Graphene Schottky Diode Muhammad Shehzad Sultan¹, Wojciech Jadwisieniczak², Alejandra P Flores Rivera¹, Brad Weiner¹ and Gerardo Morell¹; ¹University of Puerto Rico at Río Piedras, United States; ²Ohio University, United States

Nitrogen doped graphene quantum dots (GQDs) have been widely used for various optoelectronic devices as a photoactive material due to their high absorption coefficient and tunable bandgap. However, the low mobility of NGQD films results in poor charge collection and device performance. By combining NGQDs with graphene into hybrid NGQD/Graphene photodetectors, photocarriers from NGQDs are transferred to graphene, improving charge collection and transport, and drastically increasing the photoresponsivity. In this study, we report the preparation of a NGQD/Graphene heterostructure in order to investigate the effect of NGQD on the photoactive response of graphene. Using UV-vis absorption and photoluminescence (PL) spectra, the optical properties of NGQD/Graphene heterostructure were measured. Moreover, to investigate their electronic and charge transfer properties, we fabricated the photodetectors with pristine graphene quantum dots and NGQD/Graphene heterostructure to analyze and compare their photoactive electrical properties. Under illumination, NGQD/Graphene PD showed an increase in both current and carrier mobility as compared to NGQD PD. The increased current and carrier mobility of NGQD/Graphene PD is due to the presence of a large number of photoexcited charge carriers. This is explained by NGQDs' n-type doping effect on graphene, which reduces the accumulation of holes in the active p-channel near the insulating layer and causes charge to be transferred from the NGQDs to the graphene. As a result, we discovered a charge transfer effect in the NGQD/Graphene heterostructure, which could be used in optoelectronic devices.

SESSION EL19.07: 2D Semiconductors—Quantum Emitters and Dopants

Session Chairs: Kibum Kang and Andrew Mannix

Tuesday Morning, November 28, 2023

Hynes, Level 3, Room 309

8:30 AM EL19.07.01

Macroscopic Transition Metal Dichalcogenides Monolayers with Uniformly High Optical Quality Qiuyang Li, Adam Alfrey, Jiaqi Hu, Nathaniel Lydick, Eunice Paik, Bin Liu, Haiping Sun, Yang Lu, Ruoyu Wang, Stephen R. Forrest and Hui Deng; University of Michigan, United States

The unique optical properties of transition metal dichalcogenide (TMD) monolayers have attracted significant attention for both photonics applications and fundamental studies of low-dimensional systems. TMD monolayers of high optical quality, however, have been limited to micron-sized flakes produced by low-throughput and labor-intensive processes, whereas large-area films are often affected by surface defects and large inhomogeneity. Here we report a rapid and reliable method to synthesize macroscopic-scale TMD monolayers of uniform, high optical quality. Using 1-dodecanol encapsulation combined with gold-tape-assisted exfoliation, we obtain monolayers with lateral size >1 mm, exhibiting exciton energy, linewidth, and quantum yield uniform over the whole area and close to those of high-quality micron-sized flakes. We tentatively associate the role of the two molecular encapsulating layers as isolating the TMD from the substrate and passivating the chalcogen vacancies, respectively. We demonstrate the utility of our encapsulated monolayers by scalable integration with an array of photonic crystal cavities, creating polariton arrays with enhanced light-matter coupling strength. This work provides a pathway to achieving high-quality two-dimensional materials over large areas, enabling research and technology development beyond individual micron-sized devices.

8:45 AM EL19.07.02

Unraveling the Role of Dopant Clustering in Magnetic Impurity Doped Monolayers of Transition Metal Dichalcogenides Rehan Younas, Guanyu Zhou and Christopher L. Hinkle; University of Notre Dame, United States

Efforts to achieve above room temperature ferromagnetism in monolayers of transition metal dichalcogenides (TMDs) through substitutional doping with magnetic impurities are actively being pursued for energy-efficient logic and memory devices. However, the current limitations stem from phase separation and multi-layered growth at heavy doping levels, restricting the doping in monolayers to levels well below the threshold established by density functional theory (DFT) for above room temperature Curie temperature. On the other hand, room temperature magnetism has been frequently observed at significantly lower doping levels (0.1-1%), but this magnetism arises from a combination of substitutional dopants, point defects, contaminants, interstitials, or edge states. As a result, the origin of purely substitutional doping-induced ferromagnetism remains a subject of debate.

Towards this end, this study employs molecular beam epitaxy to achieve up to 30% substitutional doping of vanadium (V) and iron (Fe) in a monolayer of tungsten diselenide, surpassing the doping requirements (>15%) indicated by DFT for room temperature ferromagnetism. Magnetometry measurements, however, reveal the absence of ferromagnetism down to a temperature of 4 K in these phase-pure films, with only the phase-separated films exhibiting any room temperature ferromagnetic behavior at Fe doping levels exceeding 30%. Structural characterization utilizing plan-view transmission electron microscopy reveals significant dopant clustering, even at modest doping levels (~5%), which serves as the primary factor responsible for the absence of ferromagnetism in phase-pure films. Remarkably, these observations align with DFT calculations, which predict a low formation energy for dopant clustering, leading to a weakened exchange interaction that subsequently suppresses ferromagnetism. The insights gained from this exploratory study offer a promising pathway to attain high doping densities in monolayer TMDs while emphasizing the influence of dopant clustering on the magnetic properties of the films.

9:00 AM *EL19.07.03

Structure-Property Relations of Quantum Emitters in 2D Materials Su Ying Quek; National University of Singapore, Singapore

Quantum emitters in the form of point defects in 2D materials are of interest as scalable single photon sources for photonics-based quantum technologies. It is important to know the optical signatures of intrinsic defects, but also critical to be able to controllably synthesize quantum emitters with desirable and known optical properties. In this work, we use state-of-the-art first principles calculations to elucidate the structure-property relations of quantum emitters in the wide-band-gap hexagonal boron nitride (hBN) layer, as well as in transition metal dichalcogenide (TMD) monolayers. Defects in hBN can be controllably created by carbon implantation and electron or ion bombardment. We present the photophysical properties of defects derived from boron vacancies and carbon impurities [1], as well as preliminary results on other point defects created by the electron or ion bombardment process. Comparisons are made with recent experiments. In the second part of the talk, we discuss the optical properties of unintended oxygen-related defects and intentional substitutional defects in TMDs. We find that chalcogen vacancies in WSe₂ are readily passivated by oxygen, and oxygen interstitials are a possible source of single photons in WSe₂ [2]. For both Re [3] and Nb dopants in WS₂, we present theoretical and experimental evidence of optical defect-to-bulk state transitions that partially preserve the valley polarization. We will also touch on preliminary results on THz quantum emitters in TMDs.

[1] Y. Chen and S. Y. Quek, "Photophysical Characteristics of Boron Vacancy-Derived Defect Centers in Hexagonal Boron Nitride", *Journal of Physical Chemistry C*, 125, 21791 (2021)

[2] Y. J. Zheng, Y. Chen, Y. L. Huang, P. K. Gogoi, M.-Y. Li, L.-J. Li, P. E. Trevisanuto, Q. Wang, S. J. Pennycook, A. T. S. Wee, S. Y. Quek, "Point Defects and Localized Excitons in 2D

WSe₂”, ACS Nano 13, 6050 (2019)

[3] L. Loh, Y. Chen, J. Wang, X. Yin, C.S. Tang, Q. Zhang, K. Watanabe, T. Taniguchi, A.T.S. Wee, M. Bosman, S.Y. Quek, and G. Eda, “Impurity-Induced Emission in Re-Doped WS₂ Monolayers”, Nano Letters, 21, 5293 (2021)

Funding Acknowledgement:

Supported by the Singapore Ministry of Education under grant number MOE2018-T3-1-005.

9:30 AM EL19.07.04

Magnetic Fluctuations in V-Doped WSe₂Dinh LocDuong^{1,2}, Lan-AnhT. Nguyen³, JinbaoJiang⁴, Tuan DungNguyen³, PhilipKim⁵, Min-kyuJoo⁶ and Young HeeLee³; ¹Department of Physics, Montana State University, United States; ²Montana State University, United States; ³Center for Integrated Nanostructure Physics, Institute for Basic Science, Korea (the Republic of); ⁴National University of Defense Technology, China; ⁵Harvard University, United States; ⁶Sookmyung Women's University, Korea (the Republic of)

Vanadium-doped tungsten dichalcogenide (V-doped WSe₂) reveals ferromagnetic order at room temperature, which can be controlled by a gate bias. In this presentation, we report electrically tunable magnetic fluctuations associated with RTNs in V-doped WSe₂ at a low doping concentration using vertical tunneling graphene/V-WSe₂/graphene devices. We identify bistable magnetic states from discrete Gaussian peaks of the RTN histogram, which were further confirmed by 1/f² features in the noise power spectrum. Three fluctuation categories in the resistance change were detected: small changes from the intralayer coupling between magnetic domains at high temperatures, anomalous large resistance changes over a wide range of temperatures, and persistent large resistance changes originating from magnetic interlayer coupling at low temperatures. We demonstrate the switching of the bistable state and further modulate the cut-off frequency of RTNs with bias. The observed electrical switching of a tunable bistable state in magnetic 2D materials can be utilized for low-power spintronics.

9:45 AM EL19.07.05

Elucidating Ferromagnetic Properties of Fe-Doped MoS₂, WSe₂ and WS₂ at Various TemperaturesMengqiFang¹, Hee SukChung², Jae HyuckJang², ChunliTang³, WencanJin³ and Eui-HyeokYang¹; ¹Stevens Institute of Technology, United States; ²Korea Basic Science Institute, Korea (the Republic of); ³Auburn University, United States

Transition metal-doped transition metal dichalcogenides (TMDs) have attracted significant attention due to their potential for spintronic and magneto-optical applications [1, 2]. By introducing transition metal dopants, such as vanadium [3], rhenium [4], and iron [5, 6], into TMDs, it is possible to create new electronic and magnetic properties, leading to the emergence of diluted magnetic semiconductors (DMS). These DMS materials combine the advantages of semiconductors with ferromagnetic behavior, enabling the development of spintronic devices for efficient information storage and processing [7, 8].

In this study, we present the synthesis and characterization of Fe:MoS₂, Fe:WSe₂, and Fe:WS₂ to elucidate their magnetic properties. The Fe-doped TMD materials were synthesized using contact-growth, of which detailed synthesis methods are reported elsewhere [5, 9]. To determine the ferromagnetic properties of synthesized materials, various techniques were employed: The structural and morphological characterizations were carried out using techniques such as optical, atomic force microscopy (AFM), and scanning transmission electron microscopy (STEM), confirming their successful synthesis and the presence of desired structural features. Furthermore, vibrating sample magnetometry (VSM) measurements were performed to determine the macroscopic magnetic properties, including coercivity and saturation magnetization. These measurements indicate that Fe:WSe₂ displays a more pronounced ferromagnetic signal than that from Fe:MoS₂. Further investigation is needed to gain deeper insights into the underlying mechanisms responsible for these observations.

This research may pave the way for developing novel TMD materials with tailored magnetic properties for low-power spintronics applications and quantum information science.

Reference

- [1] *Advanced Materials*, **33** (6), 1907818, (2021).
- [2] *Advanced Science*, **8** (9), 1–26, (2021).
- [3] *Advanced Science*, **7** (9), 1903076, (2020).
- [4] *Advanced Materials*, **2005159**, 1–9, (2020).
- [5] *Nature Communications*, **11** (1), 6–13, (2020).
- [6] *ACS nano*, **14** (4), 4636–4645, (2020).
- [7] *MRS Bulletin*, **13** (6), 32–36, (1988).
- [8] *Journal of Magnetism and Magnetic Materials*, **414**, 45–48, (2016).
- [9] *Nanotechnology*, **32** (9), 095708, (2021).

10:00 AMB BREAK

10:30 AM *EL19.07.06

Controlling Quasiparticle Excitations in 2D Solids Through Atomically Precise HeterostructuresAlexanderWeber-Bargioni; Lawrence Berkeley National Laboratory, United States

In this presentation, we investigate how atomically defined heterostructures, such as 2D stacks, 1D boundaries within a 2D material, and 0D vacancies and substitutes in 2D materials, localize new protected states that host quasiparticle excitations. Quasiparticles are emergent excitations in condensed matter systems that behave like particles, but are not elementary particles like electrons or protons. In 2D solids, a wide variety of quasiparticle excitations can be experimentally accessed, including localized electrons, excitons, superconducting states, and polaritons, as well as more exotic systems like Tomonaga Luttinger liquid. Each specific quasiparticle excitation is a result of a specific crystalline symmetry. By inducing atomically defined 0D, 1D, and 2D heterostructures, it is possible to localize, protect, and create novel quasiparticle excitations.

We demonstrate how to engineer heterostructures into 2D Transition Metal Dichalcogenides and visualize the resulting electronic structure using Scanning Tunneling Microscopy. We discuss the resulting quasiparticle excitations that we directly capture using Scanning Tunneling Microscopy, as well as Time Resolved optical Spectroscopy. We show how 0D heterostructures or defects in 2D MoSe₂ and 2D WS₂ carry intrinsic point defects that substantially modify electronic properties. For instance, individual S vacancies create two-level systems within the band gap with extremely high spin-orbit coupling, and can mediate single photon emission via optical or electric stimulation. We also demonstrate how C-H for S or Se substitutes in 2D WS₂ and 2D WSe₂ form locally charged hydrogen-like states. Upon deprotonation, the localized carbon radical hosts a deep in-gap state with a net spin and electron-phonon coupling that is similar to NV color centers in diamond, but with atomistic control. Furthermore, individual Chalcogen Vacancies can be decorated with a variety of different adatoms, creating new types of 0D heterostructures, such as Co-S substitutes that could become relevant for Quantum Information Science.

In 1D heterostructures, such as Mirror Twin Boundaries in MoSe₂ or WS₂, we discovered atomically thin metallic conductors that undergo a quantum phase transition at low temperature to form a Tomonaga Luttinger Liquid (TTL). TTLs are correlated electron systems, where electrons couple to form a bosonic system, and that can foster partial electron and spin transport. As a 2D heterostructure, we explore WS₂/WSe₂ stacks, where we study the formation and recombination channels of interlayer excitons formed in WS₂/WSe₂ stacks, which may relate to the recently reported formation of excitonic Bose-Einstein condensates. Another fascinating area of research is coupling quasiparticles to form new quasiparticles. By stacking 2D WSe on linear plasmonic cavities, we were able to couple excitons to plasmons, creating plexcitons. We use techniques such as photo low-temperature Scanning Tunneling Microscopy, near-field optical microscopy, and low-temperature time-resolved optical spectroscopy to investigate the properties and behavior of these quasiparticle excitations.

11:00 AM *EL19.07.07

Moiré Minibands, Interlayer Coupling and Hybridization in vdW Stacks from Optical SpectroscopiesUrsulaWurstbauer; University of Münster, Germany

Two-dimensional (2D) materials exhibit unique properties due to their atomically thin structure and weak van der Waals (vdW) coupling between layers. This vdW nature allows for the precise engineering of 2D quantum systems through stacking, twisting, and inducing defects. External stimuli, such as electric or magnetic fields and charge doping, enable in-situ control of these systems.

In this study, we employ advanced optical spectroscopy methods to characterize interlayer coupling, interfacial quality, interlayer hybridization, and miniband formation in twisted vdW homo- and heterobilayers prepared from semiconducting transition metal dichalcogenides (TMDCs) such as MoSe₂ or WSe₂. Photoluminescence and spectroscopic imaging ellipsometry (SIE) provide insights into the hybridization of band-edge and higher-lying interband transitions [1,2]. Non-resonant Raman spectroscopy is used to study the phonon fingerprint, which is sensitive to interlayer coupling, strain, and doping [3-4].

Resonant Raman spectroscopy (RRS) is found to be highly sensitive to exciton-phonon coupling [5,6], and electronic Raman known as resonant inelastic light scattering (RILS) allows spectroscopy of Moiré mini-bands by probing collective electronic inter-miniband excitations [7]. Our research aims to deepen our understanding of the interplay between interlayer coupling,

hybridization, and mini-band formation in 2D materials. These findings have implications for the design and development of novel quantum devices and applications.

We acknowledge funding by the Deutsche Forschungsgemeinschaft (DFG, German Research Foundation) under projects Wu 637/4- 1, 4 – 2, 7-1 and SPP 2244.

- [1] J. Kiemle, et al. Phys. Rev. B 101, 121404(R) (2020).
- [2] F. Sigger et al. Appl. Phys. Lett. 121, 071102 (2022).
- [3] B. Miller et al. Appl. Phys. Lett. 106, 122103 (2015).
- [4] I. Niehues et al. Phys. Rev. B 105, 205432 (2022).
- [5] B. Miller et al. Nature communications 10 (1), 807 (2019).
- [6] H. Lambers et al. in preparation.
- [6] N. Saigal et al. in preparation.

11:30 AM *EL19.07.08

Overcoming Industrial Challenges in Implementing 2D Materials in CMOS ByunKyung-Eun, MinsuSeol, JunyoungKwon, AlumJung and Min SeokYoo; Samsung Advanced Institute of Technology, Korea (the Republic of)

Two-dimensional (2D) transition metal dichalcogenides (TMDs) have received great attention for their potential role as the channel material in electronic devices. Although 2D materials have demonstrated exceptional promise in academic research, significant industrial challenges must be confronted to integrate them into next-generation Complementary Metal-Oxide-Semiconductor (CMOS) technologies. In this talk, we highlight the significant challenges that the industry faces in implementing 2D materials into current semiconductor devices. These include issues related to material synthesis with high-throughput, fast and nondestructive characterization, proper integration processes for TMDs. We'll present the ongoing research about growth, characterization and integration. We demonstrate high-throughput production of 8-inch wafer-scale MoS₂ and WS₂. Utilizing our TMD, we have successfully achieved the TMD FETs on an 8-inch wafer scale through a conventional CMOS process, demonstrating consistent electrical performance with a high yield of over 99%. Through our research on TMD FET structures, we have achieved remarkable advancements in device performance. We're also accelerating the Lab to Fab transition by using artificial intelligence (AI), which proves beneficial in predicting material behaviors and optimizing processing parameters. The talk will provide insights into the extensive efforts companies are making to navigate these challenges.

SESSION EL19.08: 2D Semiconductors—Synthesis I
Session Chairs: Andrew Mannix and Hyeon Jin Shin
Tuesday Afternoon, November 28, 2023
Hynes, Level 3, Room 309

1:30 PM EL19.08.01

Unconventional vdW Heterostructures Assembled from Bespoke 2D Atomic and Molecular Lattices ThomasJ. Kempa, ReynoldsDziobek-Garrett, OnaAmbrozaitė, YifeiZhu and DaraWeiss; Johns Hopkins University, United States

Quantum materials have the potential to revolutionize sensing, analytical instrumentation, information processing, and energy conversion. Unconventional vdW superlattices assembled from precisely tailored 2D atomic and molecular lattices encode heterointerfaces which can provide an unprecedented control over charge, exciton, and spin states leading to unique artificial quantum solids. Realizing such superlattices requires not only rational, mechanism-driven chemical synthesis of atomically-precise 2D crystals, but also careful optical spectroscopy and device studies for rigorous determination of fundamental properties and intrinsic limits. In this talk I will discuss our key prior achievements and emerging results towards the assembly of these unconventional superlattices. First, we show that innovative surface-treatments and precursor chemistries can dramatically alter the dimensionality, morphology, and defect level of 2D transition metal dichalcogenides (TMD) grown by chemical vapor deposition (CVD). Second, we demonstrate the promise of gas-phase methods for the synthesis of single monolayer 2D molecular lattices (e.g., metal-organic frameworks), and also demonstrate their response to chemical, optical, and electrical stimuli through device transport and scanning probe measurements. Finally, we show that the merger, through direct CVD deposition or exfoliation and transfer, of these 2D crystals yields unique heterointerfaces that can elicit photon upconversion, modulation of lattice phonons, and control of exciton dynamics. Ultimately, the unprecedented array of chemical, dielectric, and mechanical potentials that such superlattices can support open unique opportunities for breakthroughs in optics, sensing, information processing, and sustainability.

1:45 PM *EL19.08.02

Epitaxial Mechanism of Two-Dimensional Materials on Crystalline Substrates YiWan, Cheng YangLi, Yu-MingChang and Lain-JongLi; The University of Hong Kong, Hong Kong

One key challenge with two-dimensional semiconducting transition metal dichalcogenides (2D-TMD) channel materials or insulating hexagonal boron nitride (hBN) for industry applications is the large-scale batch growth on substrates with continuous single crystallinity, and spatial homogeneity. To achieve large-area and grain boundary-free growth of 2D materials, it is critical to understand the fundamentals of the substrate-2D interaction to enable the mono-orientation of these 2D domains.

Taking a few examples including 2D TMD, hBN, and perovskites, we like to discuss the factors that control the epitaxy. Detailed analysis will be provided to illustrate the following points. (1) In the situation that 2D seeds strongly bind to the atomic substrates edges (eg. hBN on Cu(111); TMD on Ga₂O₃(100)), seed nucleation and orientation are controlled by the step edges. (2) In the circumstance that 2D seeds do not strongly bind to the step edges (eg. TMD on C- or M-sapphire; TMD on Ga₂O₃ (001)), the epitaxy of 2D is governed by the atomic structures (and symmetry) of the substrates. Hence, the reconstruction the surfaces of substrates to only a single type (symmetry) is necessary for the single-crystal epitaxy of monolayer TMDs without the aid of step edges. (3) Precursors may react with the substrate surfaces to change the substrate atomic structures and thus the orientation of 2D materials. For example, the surface sulfurization of sapphire or surface metallization of Ga₂O₃ drastically change the orientation preference. In summary, the substrate symmetry, step edges and chemical modification of substrates (or edges) need to be taken into consideration when reconstructing the substrates for successful epitaxial growth of 2D materials.

2:15 PM EL19.08.03

Metalorganic Chemical Vapor Deposition of Epitaxial MoS₂ and WS₂ on Group III-Nitrides ShaliniKumari, DorotaKowalczyk, ChenChen, NicholasTrainor, SeungH. Lee, TimMirabito, NicholasD. Redwing and JoanM. Redwing; The Pennsylvania State University, United States

Scalable vapor phase deposition methods are rapidly developing enabling epitaxial growth of transition metal dichalcogenides (TMDs) monolayer and few-layer films on wafer-scale substrates. C-plane sapphire has been the primary substrate used so far for TMD epitaxy as it is crystallographically compatible with the hexagonal TMD lattice, is thermally stable at high temperatures and is available in large area at low cost. However, the direct lattice mismatch between the TMDs and sapphire is large and while there is commensurability which reduces the effective mismatch, the lattice off-sets lead to translational line defects between coalescing domains. In contrast, the group III-nitrides (GaN and AlN) are nearly directly lattice matched to MoS₂ and WS₂ making them intriguing substrates for TMDs epitaxial growth. WS₂ and MoS₂ have a lattice mismatch of only 1.1 % and 0.8 % to the lattice parameter of GaN, whereas WS₂ and MoS₂ have a lattice mismatch of only 1.3 % and 1.6 % to the lattice parameter of AlN respectively. In addition, direct growth of TMDs on GaN opens up prospects for novel 2D/3D heterostructures for bipolar and hot electron transistors and optoelectronics.

In this work, we present the growth, structural, and optical properties of fully coalesced MoS₂ and WS₂ monolayer to few layer films grown on GaN and AlN epitaxial templates on sapphire via Metalorganic Chemical Vapor Deposition (MOCVD). Molybdenum hexacarbonyl (Mo(CO)₆), tungsten hexacarbonyl (W(CO)₆) and hydrogen sulfide (H₂S) were used as precursors in a N₂ and H₂ carrier gas for the growth of MoS₂ and WS₂ on 1 x 1 cm² GaN and AlN substrates. The relative thermal and chemical stability of GaN and AlN can significantly affect the epitaxial growth of TMDs. For example, in the absence of NH₃, GaN begins to decompose at elevated temperatures in H₂ while AlN remains relatively stable. Therefore, for TMD growth on GaN, the samples were heated in N₂ to prevent decomposition and the growth temperature and flow rate/growth rate were tuned to prevent GaN decomposition and pit formation before the MoS₂/WS₂ covers the surface. In this study, the growth temperature was varied from 900 to 1000 °C, growth time from 10 to 25 minutes, and molybdenum and tungsten precursor flow rates from 0.0006 to 0.003 sccm whereas the H₂S flow rate was maintained at 400 sccm. All the growths were done with a moderate reactor pressure of 50 Torr using N₂ and H₂ as the carrier gas. AFM and FESEM were carried out to characterize the surface coverage and morphology of the layers. Spatially resolved Raman and photoluminescence spectroscopy were used to investigate the uniformity of the growth across the sample. The TMD films were continuous with thicknesses of mono- to few layers although pits were present in films grown on GaN at elevated temperature and reduced growth rate. The presence of A_{1g} and E_{2g} Raman modes for MoS₂ and WS₂ were observed at room temperature. The MoS₂ and WS₂ films exhibits strong photoluminescence at room temperature centered around 1.9 eV and 2 eV respectively. The structural, microscopic, and optical properties of the MoS₂ and WS₂ monolayers on GaN and AlN will be discussed in detail in the meeting. We emphasize the opportunities for the compatible integration of 2D/3D TMDs/III-V nitrides heterostructures without any transfer process by a fine-

tuned deposition, which can have wide implications for the performance of future electronic and optoelectronic devices.

2:30 PM EL19.08.04

Multiscale Structural Analysis of Epitaxially Grown 2D Layers using Four-Dimensional Scanning Transmission Electron Microscopy Hanako Okuno, Djordje Dosenovic, Samuel Dechamps, Matthieu Jamet and Alain Marty; CEA-Grenoble, France

Epitaxial growth is a route to achieve highly crystalline continuous 2D layers. In recent years, large scale epitaxial growth of graphene and various transition metal dichalcogenides (TMDs) have been demonstrated by many research groups. However, high quality layer production with expected electrical properties is still challenging due to the imperfection of nucleation control. For instance, slight misalignment and symmetrical crystal inversion in neighbouring nucleation sites result in domain junctions, at the stage of coalescence, containing a large number of atomic defects and which drastically degrades material quality. The presence of polymorphs, such as 2H and 1T' in the TMDs, also modifies their electronic properties.

In order to control growth process and to predict intrinsic properties of grown material up to wafer scale as a patchwork of defect structures, multiscale structural analysis should be accessible in routine way. X-ray diffraction (XRD) gives a precise information on material quality regarding the crystallinity and the angular distribution at mm scale, while scanning transmission electron microscopy (STEM) imaging offers today the capability to study the detailed local atomic structures such as vacancies, grain boundaries as well as the associated chemical composition at atomic scale. However, these techniques do not reveal complete material characteristics because of the gap in scale between the information obtained by different techniques. Four dimensional (4D)-STEM is a new acquisition technique allowing to simultaneously record 2D images in real and reciprocal spaces. Multiple information, from structure to electric field, at different scales can be reconstructed from signals appearing in diffraction pattern acquired at each pixel of the beam scan.

In this work, we demonstrate an analytical process using 4D-STEM to study epitaxial 2D materials grown in both laboratory and industrial scales. Orientation, polarity and phase maps in various TMD monolayers, such as WSe₂ and WS₂, are reconstructed at micron scale from 4D-diffraction datasets and directly correlated with both large scale XRD analysis and related atomic defect structures revealed by STEM imaging. This structural mapping technique allowed the localization of various domain junctions as well as quantitative information on their density. In addition, the technique was also applied in epitaxial vdW heterostructures for mapping local twist angles. The results show the capacity to construct structural overview of synthesized materials from large scale down to atomic scale, which provides reliable information necessary to develop high quality 2D materials and further to enable theoretical prediction of material properties basis on large-scale realistic structure models.

2:45 PM BREAK

3:15 PM *EL19.08.05

Understanding Salt-Promoted Metal Organic Chemical Vapour Deposition of Transition Metal Dichalcogenides Jinfeng Yang, Ryo Mizuta, Ye Fan, Vitaly Babenko and Stephan Hofmann; University of Cambridge, United Kingdom

Scalable integrated process pathways remain a key challenge for ultrathin 2D device materials particularly for potential opto-electronic device applications. For transition metal dichalcogenides (TMDC), the use of salts to enhance chemical vapour deposition (CVD) has become widespread, yet the underpinning understanding remains limited. We employ operando scanning electron microscopy (SEM) and environmental X-ray photoelectron spectroscopy (XPS) to systematically study the role of salt-based growth promoters. We focus on WS₂ as a model system and explore surface-based mechanisms linked to sodium tungstates, NaOH and NaCl on SiO₂ and sapphire substrates in conjunction with widely used gaseous (MO)CVD precursors. We report various hot salt substrate corrosion phenomena that lead to the substrate spreading of W intermediates and significantly influence the growth mechanisms. We can directly resolve the formation and wetting behaviour of liquid droplets and show that the growth scenario particularly for mono-layers is not following a vapour-liquid-solid (VLS) model. Holistic calibration of SE contrast allows us to reveal WS₂ nucleation and in-plane growth kinetics. Our discussion brings together the wider literature including mechanisms of 1D TMDC nanotube formation.

3:45 PM EL19.08.06

Modified Self-Flux Synthesis of Centimeter-Scale Transition Metal Dichalcogenides Luke Holtzman, Madisen Holbrook, Nicholas Olsen, Xiaoyang Zhu, Abhay Narayan Pasupathy, James Hone and Katayun Barmak; Columbia University, United States

Two-dimensional transition metal dichalcogenides (TMDs) are a highly attractive class of materials due to their novel electronic and optoelectronic properties and the ability to use them as a platform for assembling heterostructures. Self-flux crystal growth of TMDs has been shown to grow bulk TMDs with the lowest defect densities of any synthesis technique, maximizing the ability to study their unique, intrinsic phenomena [1-3]. However, the current self-flux crystal growth method produces TMD crystals smaller than 1 mm² on average, making monolayer-exfoliation difficult and limiting applications to single devices. Additionally, these crystals are too small to use macroscopic exfoliation techniques such as gold-assisted exfoliation, which require crystals greater than 2 mm in diameter and can isolate entire monolayers from every layer of a bulk crystal. [4]

In this work, we use a modified flux-synthesis thermal cycle containing an optimized dwell temperature and temperature cycling Ostwald ripening to increase the crystal area of ultralow defect density TMDs by more than ten-fold. The crystal growth kinetics as a function of temperature are determined, enabling increased cooling rate steps and shorter synthesis times. An additional post-processing self-flux recrystallization step is added and further increases the crystal size of TMDs and reduces the defect density. Lastly, gold-assisted exfoliation is used to isolate several centimeter-long monolayers from one modified self-flux synthesis MoSe₂ crystal, displaying monolayer yields per crystal more than five orders of magnitude greater than traditional scotch-tape exfoliation techniques. These self-flux synthesis modifications provide a route towards reproducibly exfoliating ultralow defect density TMD monolayers at the centimeter scale with high yields, greatly increasing the scalability of high-quality self-flux TMD bulk crystals for mass production.

[1] D. Rhodes, *et al.*, *Nat. Mater.* 18 (2019), pp. 541-549, <https://doi.org/10.1038/s41563-019-0366-8>

[2] D. Edelberg, *et al.*, *Nano Lett.* 19 (2019), pp. 4371-4379, <https://doi.org/10.1021/acs.nanolett.9b00985>

[3] S. Liu, *et al.*, *arXiv preprint arXiv:2303.16290* (2023).

[4] F. Liu, *et al.*, *Science* 367 (2020), pp. 903-906, <https://doi.org/10.1126/science.aba1416>

4:00 PM EL19.08.07

Wafer-Scale Fabrication of Extremely Narrow Nanowires of 2D Materials Quynh Sam¹, Qishuo Tan², Mehrdad Kiani¹, Xi Ling² and Judy Cha¹; ¹Cornell University, United States; ²Boston University, United States

Many van der Waals (vdW) layered two-dimensional (2D) materials host exotic transport phenomena such as topologically protected surface states¹ and quantum Hall effects¹ which exhibit strong size dependence at nanoscale dimensions.² When formed into 1D nanowires, additional materials property engineering via lateral confinement can be achieved.³ The tunability of 2D materials with nanowire morphology makes them an attractive platform for studying fundamental physics and for use in next generation microelectronics; however, reliable fabrication methods that can produce narrow nanowires with high aspect ratios are currently lacking.¹

Here, we report the thermomechanical nanomolding (TMNM) of bulk vdW layered materials to make nanowires with consistent crystal orientation, narrow widths under 40 nm, and high aspect ratios. In TMNM, elevated temperatures and pressures are used to extrude a material through a nanoporous mold to form nanostructures.⁴ Until now, TMNM has been reported for metallic glasses and 3D crystalline materials to form 1D nanowires.⁴ We demonstrate the use of this technique to successfully fabricate nanowires with widths ranging from 10 – 120 nm of four vdW layered materials: Te, In₂Se₃, Bi₂Se₃, and Bi₂Te₃. Atomic resolution scanning transmission electron microscopy (STEM) imaging shows the high crystalline quality of the molded nanowires. While the molding direction was perpendicular to the layer planes in the bulk crystal, crystal rotation occurs during TMNM such that the layers consistently lie along the growth axis of the molded nanowire. We find that the length of the nanowires increases with decreasing width during molding, suggesting that interfacial diffusion along the pores of the mold is the growth mechanism. This work expands the capabilities of TMNM as a straightforward approach to fabricate nanowires of 2D materials with uniform morphology and crystallographic orientation. Furthermore, lateral confinement of the nanowires afforded by TMNM provides an additional tuning knob for materials properties.

References

1. *National Science Review* 9 (2022) nwab164.

2. *Nature Reviews Materials* 4 (2019) 669–684.

3. *Physical Review Letters* 98 (2007) 206805.

4. *Progress in Materials Science* 125 (2022) 100891.

4:15 PM EL19.08.08

Effects of Nucleation Temperature on the Properties of Wafer-Scale Epitaxial WS₂ on Sapphire Grown by Metalorganic Chemical Vapor Deposition Chen¹, Nicholas Trainor^{1,1}, Shalini Kumari^{1,1}, Nicholas D. Redwing^{1,1}, Yuxi Zhang^{1,1}, Anuj Bisht¹, Stephen Revesz², Synda Labidi², Meghan E. Leger^{1,1}, Thomas V. McKnight^{1,1}, Andrew R. Graves¹, Hebin Li², Nasim Alem^{1,1} and Joan M. Redwing^{1,1}; ¹The Pennsylvania State University, United States; ²Florida International University, United States

Wafer-scale epitaxial growth of single crystal TMD monolayers is of significant interest to advance 2D device applications. MOCVD is a promising approach for TMD growth on c-plane sapphire as it enables the use of high substrate temperatures (800-1000°C) and chalcogen/metal ratios (10³-10⁵) which are beneficial for epitaxy. Previously we reported a multi-step process for MOCVD growth of WS₂ on sapphire which involves nucleation, ripening and lateral growth. The nucleation temperature was found to be crucial for achieving single orientation domains and coalesced layers with minimal inversion domain boundaries. In this study, we report the effects of nucleation temperature and film microstructure on the resulting optical and electrical properties of the monolayers.

Coalesced WS₂ monolayers were grown on 2" diameter c-plane sapphire in a cold-wall horizontal MOCVD reactor with an inductively heated graphite susceptor with gas-foil wafer rotation. W(CO)₆ was used as the metal precursor while H₂S was the chalcogen source with H₂ as the carrier gas at 50 Torr reactor pressure. The multi-step process consisted of a 30sec nucleation at temperatures ranging from 800°C to 950°C followed by 10min ripening in H₂S, and then lateral growth for 20min at 1000°C, which gives rise to a coalesced monolayer across the entire 2" wafer. After growth, the substrate was cooled in H₂S to 300°C to inhibit the decomposition of the obtained WS₂ films. A coalesced monolayer of WS₂ was achieved on 2" c-plane sapphire over the nucleation temperature ranges from 800°C to 950°C. AFM indicates that the WS₂ monolayers are fully coalesced, with a bilayer coverage of less than 20%. Interestingly, stripe-pattern contrasts due to variations in the adhesion of the WS₂ monolayer to the underlying sapphire were observed under FESEM and the density of stripes increased as the nucleation temperature was raised from 800°C to 950°C. In-plane XRD *phi*-scans confirm that the films are epitaxially oriented with respect to the sapphire over the nucleation temperatures from 800°C to 950°C with the (11-20) of WS₂ aligned with the (11-20) of α-Al₂O₃. The FWHM of both the *phi*-scan peak and 2*theta*-scan peak of WS₂ decreased as the nucleation temperature was reduced. The sample nucleated at 800°C demonstrated the lowest FWHM of ~0.26° in the *phi*-scan peak, indicating larger crystalline domains and reduced in-plane rotational misorientation of the WS₂ domains compared to the higher temperature samples. Room temperature photoluminescence measurements of the films on sapphire reveal an increase in the PL peak position from 1.9eV to 2.0eV as the nucleation temperature was increased from 800°C to 950°C. The variations in the structural and optical properties of the WS₂ films with nucleation temperature are attributed to differences in the extent of coupling of the WS₂ to the underlying sapphire. The WS₂ grown at 800°C nucleation temperature exhibits the strongest coupling to the underlying sapphire as evidenced by the narrow FWHM of the in-plane XRD *phi*-scan peak, the lack of stripe contrast from buckling in the FESEM image and the red-shift in the PL peak indicating residual strain in the layer. In contrast, the WS₂ grown at 950°C nucleation temperature exhibits weaker coupling consistent with buckling contrast in the FESEM image, a broader FWHM for the XRD *phi*-scan peak and a PL peak at 2.0eV. To test this hypothesis, the films were transferred from the growth substrates and onto sapphire to remove the coupling arising from epitaxy. For the transferred WS₂ film grown at 800°C, a substantial increase in the PL intensity and a blueshift in the PL peak position to 1.95eV were observed, indicating a reduction in strain within the film after the transfer process. Additional results correlating the structural and optical properties of the WS₂ monolayers to the transport properties of field-effect devices will be reported.

4:30 PM EL19.08.09

Large-Area Epitaxial Hexagonal Boron Nitride for Hydrogen Generation by Radiolysis of Interfacial Water Johannes Binder, Aleksandra Dabrowska, Mateusz Tokarczyk, Katarzyna Ludwiczak, Rafal Bozek, Grzegorz Kowalski, Roman Stepniewski and Andrzej Wyszomolka; Faculty of Physics, University of Warsaw, Poland

Hydrogen is an important building block in global strategies toward a future green energy system. To make this transition possible, intense scientific efforts are needed, also in the field of materials science. Hexagonal boron nitride (h-BN) is a very promising candidate for such applications, as it has been demonstrated that micrometer-sized flakes are excellent barriers to molecular hydrogen. However, it remains an open question whether large-area layers fabricated by industrially relevant methods preserve such promising properties.

We address this issue and show results on the growth of epitaxial h-BN on 2-inch sapphire wafers by metalorganic vapour-phase epitaxy (MOVPE) [1-5], which is currently regarded as one of the most promising growth techniques. This technique allows to grow hBN layers, with thicknesses of tens of nm [1,3], and can serve as a substrate for the direct growth of van der Waals heterostructures on the wafer-scale [4].

In this work, we show that electron-beam-induced splitting of water creates hBN bubbles that effectively store molecular hydrogen for weeks [5]. The bubble formation can be observed in-situ in a scanning electron microscope, giving us the unique possibility to visualize the hydrogen generation process. Raman spectroscopy proves the presence of molecular hydrogen and experiments with heavy water provide evidence that hydrogen generation is triggered by the radiolysis of water captured at the van der Waals interface. By performing a stress test we could also demonstrate that H₂ remains in the bubble even after extreme wear and deformation (over 500 cycles of deflation and inflation by changing the ambient pressure), highlighting the suitability of our large-area epitaxial material for possible hydrogen storage applications.

Our findings show that epitaxial h-BN by MOVPE is not only a potential candidate for the growth of large-area van der Waals heterostructures and hydrogen storage but also holds promise for the development of unconventional hydrogen production schemes [5].

References:

- [1] M. Tokarczyk, A. K. Dabrowska, G. Kowalski, R. Bozek, J. Iwanski, J. Binder, R. Stepniewski, A. Wyszomolka *2D Materials* **10**, 025010 (2023)
- [2] K. P. Korona, J. Binder, A. K. Dabrowska, J. Iwanski, A. Reszka, T. Korona, M. Tokarczyk, R. Stepniewski, A. Wyszomolka *Nanoscale* **15**, 9864 (2023)
- [3] A. K. Dabrowska, M. Tokarczyk, G. Kowalski, J. Binder, R. Bozek, J. Borysiuk, R. Stepniewski, A. Wyszomolka *2D Materials* **8**, 015017 (2021)
- [4] K. Ludwiczak, A. K. Dabrowska, J. Binder, M. Tokarczyk, J. Iwanski, B. Kurowska, J. Turczynski, G. Kowalski, R. Bozek, R. Stepniewski, W. Pacuski, A. Wyszomolka *ACS Appl. Mater. Interfaces* **13**, 47904 (2021)
- [5] J. Binder, A. K. Dabrowska, M. Tokarczyk, K. Ludwiczak, R. Bozek, G. Kowalski, R. Stepniewski, A. Wyszomolka *Nano Letters* **23**, 1267–1272 (2023)

4:45 PM *EL19.08.10

2D-3D Heterostructures for Low Power Logic and Memory Devices DeepM. Jariwala; University of Pennsylvania, United States

The isolation of a growing number of two-dimensional (2D) materials has inspired worldwide efforts to integrate distinct 2D materials into van der Waals (vdW) heterostructures. While a tremendous amount of research activity has occurred in assembling disparate 2D materials into "all-2D" van der Waals heterostructures and making outstanding progress on fundamental studies, practical applications of 2D materials will require a broader integration strategy. I will present our ongoing and recent work on integration of 2D materials with 3D electronic materials to realize logic switches and memory devices with novel functionality that can potentially augment the performance and functionality of Silicon technology. First, I will present our recent work on gate-tunable diode and tunnel junction devices based on integration of 2D chalcogenides with Si. I will extend that work to synthesizing high quality, homogenous phase 2D materials at back end of line compatible temperatures for logic applications. Following this I will present our recent work on non-volatile memories based on Ferroelectric Field Effect Transistors (FE-FETs) made using a heterostructure of MoS₂/AlScN and also introduce achieving ambipolarity and low contact resistance with a highly polar ferroelectric material.

SESSION EL19.09: Poster Session III: 2D Materials—Doping, Modification, Processing and Quantum Emitters

Session Chairs: Kibum Kang and Andrew Mannix

Tuesday Afternoon, November 28, 2023

Hynes, Level 1, Hall A

8:00 PM EL19.09.01

Surface Modifications and Hydrophilic Transformations of Hydrophobic InSe 2D Materials for Biological Applications Shreyasi Sengupta¹, Swapnil B. Ambade¹, Tana L. O'Keefe², Christy L. Haynes² and Zeev Rosenzweig¹; ¹UMBC, United States; ²University of Minnesota Twin Cities, United States

Nanosheets are solid, layered two-dimensional nanostructures having properties unique and different from their bulk precursors, due to which they find potential applications in various fields. Our material of interest is InSe due to its many advantages, especially because it is an emerging material for electronic applications and is a direct bandgap semiconductor with high photoresponsivity. Usage of InSe and other 2D materials is expected to increase exponentially in the next decade. However, their unique morphology and ability to produce reactive oxygen species (ROS) can be detrimental to the environment. To address this environmental concern, our studies aim to understand the impact of surface chemistry modifications on the stability and interactions of these 2D materials with model membranes and bacterial organisms relevant to human health and the environment. Initially hydrophobic InSe nanosheets are synthesized by a facile kinetically controlled semi-bottom-up approach and are subsequently made hydrophilic and suitable for biological studies by surface modifications with different molecular ligands

having varying toxicity via physisorption or chemisorption. A comparative study of the toxicity profiles of the differently modified hydrophilic InSe nanosheets is performed on *Shewanella oneidensis* MR-1, an environmentally relevant gram-negative bacterium. The goal is to understand the post-use fate of these materials on their disposal to the natural aqueous environment and design surface modification strategies to make them safer and sustainable for extensive environmental use. From a fundamental science perspective, this study should increase the molecular-level understanding of the interactions between hydrophobic 2D materials and their hydrophilic adsorbates.

8:00 PM EL19.09.02

Correlation-Induced Magnetism in Substrate-Supported 2D Metal-Organic Frameworks Bernard Field, Agustin Schiffrin and Nikhil Medhekar; Monash University, Australia

Two-dimensional (2D) metal-organic frameworks (MOFs) with a kagome lattice can exhibit strong electron-electron interactions, which can lead to tunable quantum phases including many exotic magnetic phases. While technological developments of 2D MOFs typically take advantage of substrates for growth, support, and electrical contacts, investigations often ignore substrates and their dramatic influence on electronic properties. Here, we show how substrates alter the correlated magnetic phases in kagome MOFs using systematic density functional theory and mean-field Hubbard calculations. We demonstrate that MOF-substrate coupling, MOF-substrate charge transfer, strain, and external electric fields are key variables, activating and deactivating magnetic phases in these materials. While we consider the example of kagome-arranged 9,10-dicyanoanthracene molecules coordinated with copper atoms, our findings should generalise to any 2D kagome material. This work offers useful predictions for tunable interaction-induced magnetism in surface-supported 2D (metal)-organic materials, opening the door to solid-state electronic and spintronic technologies based on such systems.

[1] B. Field, A. Schiffrin and N. V. Medhekar, NPJ Computational Materials 8, 227 (2022).

[2] D Kumar, J Hellerstedt, B Field, B Lowe, Y Yin, NV Medhekar, A Schiffrin, Advanced Functional Materials 31, 2106474 (2021).

8:00 PM EL19.09.03

Physical Adsorption and Oxidation of Ultra-Thin MoS₂ Crystals Yingchun Jiang, Zihan Liu, Huimin Zhou, Anju Sharma, Jia Deng and Changhong Ke; Binghamton University, The State University of New York, United States

The oxidation mechanism of atomically thin molybdenum disulfide (MoS₂) is critical to its nanoelectronics, optoelectronics and catalytic applications as these devices dissipate Joule heating and often operate in oxidative environments. Herein, we systematically investigate the oxidation of mono- and few-layer MoS₂ flakes in air with temperature of 23-525 °C and relative humidity of ~10-60% using atomic force microscopy (AFM), Raman spectroscopy and X-ray photoelectron spectroscopy. Our study reveals the formation of a uniform nanometer-thick physical adsorption layer on the surface of MoS₂, which is attributed to the adsorption of ambient moisture. This physical adsorption layer acts as a thermal shield of the underlying MoS₂ lattice to enhance its thermal stability and can be effectively removed by an AFM tip scanning in contact mode or annealing at 400 °C. Our study also shows that high-temperature thermal annealing and AFM tip-based cleaning result in chemical adsorption on sulfur vacancies in MoS₂, leading to p-type doping. Our study highlights the importance of humidity control in ensuring reliable and optimal performance for MoS₂-based electronic and electrochemical devices and provides crucial insights into the surface engineering of MoS₂, which are also relevant to the study of other two-dimensional transition metal dichalcogenide (TMD) materials and their applications.

8:00 PM EL19.09.04

Optothermal Properties and All-Around Encapsulation of Silicene Carlo Grazianetti¹, Daya Sagar Dhungana¹, Chiara Massetti^{1,2}, Eleonora Bonaventura¹, Emiliano Bonera², Christian Martella¹ and Alessandro Molle¹; ¹CNR-IMM, Italy; ²Università degli Studi di Milano Bicocca, Italy

Xenes, the mono-elemental family of two-dimensional (2D) materials, exhibit a variety of interesting physical properties with potential exploitation in nanotechnology [1]. Recently, 2D materials-based homo- and heterostructures, e.g. magic-angle twisted graphene and transition metal dichalcogenides van der Waals artificially stacked junctions, further provided additional momentum to this research field. In this framework, the realization of vertically stacked silicene-stanene heterostructures grown by molecular beam epitaxy turns out to be a viable route to access the properties of silicene [2]. Indeed, such a heterostructure scheme, where silicene is sandwiched in between an alumina encapsulation layer on the top surface and stanene on thin Ag(111) crystal at the bottom face, makes possible to step over the unavoidable interaction between silicene and silver substrate [3]. Therefore, the introduction of a stanene buffer layer enables to disclose the optothermal properties of silicene by means of power-dependent Raman spectroscopy [4], achieve a single-crystal silicene phase by means of template engineering [5], and develop an all-around encapsulation scheme to protect silicene in ambient conditions [6]. The photo-thermal Raman spectroscopy evidences the stark difference in the heat transport in silicene depending on the substrate, i.e. Ag(111) vs. stanene/Ag(111) [4]. The Ag substrate can be engineered by tin decoration, forming Ag₂Sn alloy, or by buffering the interface with a stanene layer, therein resulting in a promising way to master single crystal silicene layer on the cm²-scale [5]. The insertion of a stanene layer at the bottom of silicene allows to remove the silver substrate stabilizing silicene, that can be easily gated, for example, via the on the top oxide. Moreover, a full 2D encapsulation scheme, where top and bottom faces of silicene are protected by 2D tin layers, gives rise to an atomically thin and cm²-scaled membrane preventing degradation of silicene for months [6]. The all-around encapsulation of silicene thus constitutes an advancement for the silicene stability and encapsulation in ambient conditions and paves the way to further exploitation of silicene (but also all the Xenes) in flexible and wearable electronics [7].

The work is within the ERC-COG 2017 Grant N0. 772261 "XFab" and ERC-PoC 2022 Grant N. 101069262 "XMem".

References

[1] A. Molle and C. Grazianetti, "Xenes: 2D Synthetic Materials Beyond Graphene", Elsevier (2022).

[2] D. S. Dhungana, C. Grazianetti, C. Martella, S. Achilli, G. Fratesi, A. Molle, Adv. Funct. Mater. 31, 2102797 (2021).

[3] Tsoutsou et al., Appl. Phys. Lett. 103, 231604 (2013).

[4] E. Bonaventura, D. S. Dhungana, C. Martella, C. Grazianetti, S. Macis, S. Lupi, E. Bonera, and A. Molle, Nanoscale Horiz. 7, 924 (2022).

[5] S. Achilli, D. S. Dhungana, F. Orlando, C. Grazianetti, C. Martella, A. Molle, and G. Fratesi, Nanoscale, accepted (DOI: 10.1039/D3NR01581E).

[6] D. S. Dhungana, C. Massetti, C. Martella, C. Grazianetti, and A. Molle, under review.

[7] C. Martella, C. Massetti, D. S. Dhungana, E. Bonera, C. Grazianetti, and A. Molle, Adv. Mater. accepted (DOI: 10.1002/adma.202211419).

8:00 PM EL19.09.05

Graphene Origami: Evolution of the Morphology of Free-Standing Few-Layer Graphene in Plasma Synthesis Claudia-F. Lopez Camara, Paolo Fortugno, Markus Heidelmann, Hartmut Wiggers and Christof Schulz; University of Duisburg-Essen, Germany

Since discovered, graphene has shown to be a very versatile material due to its unique properties, which makes it suitable to multiple applications, ranging from sensing to batteries. Even though free-standing graphene flakes have traditionally been synthesized using exfoliation techniques, interest on gas-phase synthesis is on the rise due to its suitability for process scale-up and for generating graphene with very low oxygen content. Yet, the growth of free-standing few-layer graphene (FLG) during plasma synthesis leads to a variety of morphologies, such as turbostratic graphene (typically less than ten graphene layers), and the growth mechanism is essentially unknown.

Using spatially resolved thermophoretic sampling directly from the area of the graphene formation zone for transmission electron microscopy (TEM) analysis, we studied the morphology of graphene flakes in different growth stages. Single-layer and few-layer graphene were observed, and a morphology pattern evolution was discerned depending on time and reaction conditions. Based on these investigations, we propose a folding-based growth and structure formation process, leading to a conceptual mechanism of few-layer graphene formation and growth, starting from initial round single-layer graphene to, eventually, carbonaceous nanoparticles. The edges resulting from the folding have also been investigated, revealing that graphene does not seem to break at the bends but fold similar to rolling up carbon nanotubes and without opening new reactive sites for further growth.

8:00 PM EL19.09.06

Breathable MOFs Layer on Atomically Grown 2D SnS₂ for Stable and Selective Surface Activation Ji-Soo Jang; Korea Institute of Science and Technology, Korea (the Republic of)

Two-dimensional (2D) materials (MoS₂, SnS₂, MXene, black phosphorus (BP), and graphene oxide) with intriguing physicochemical properties such as abundant reactive edge-sites, tunable electrical properties, and mechanical flexibility, have been developed for broad applications in chemical sensing, electrocatalysis, filtration membrane, and energy storage system.[1] Among various 2D materials, SnS₂ (IV-VI A group), which is a semiconducting layered structure with a large bandgap of ~2.2 eV and has many advantages (low-cost, nontoxic, and environmental friendly properties), can be catered well into the broad applications.[2] Based on these interesting material properties of SnS₂, 2D SnS₂ is widely used as active surface reactor with rapid, sensitive, and selective surface reactivity to various molecules including ions, gases, and biomolecules. Even though the outstanding and exceptional characteristics of SnS₂ has been proved in many previous studies, its poor stability due to oxidation and degradation issues under the ambient operation conditions limits the practical usage of SnS₂.

In this work, we newly developed 'Sandwich' like hybrid materials platform, 2D SnS₂ layer covered by uniformly porous ZIF-8, employing in-situ growing methods. First of all, the 2D SnS₂ layer (1st layer) was directly grown on the Si based sensor substrate through ALD method, and as such, strong bonds between active material (SnS₂ in this case) and the sensor substrate are

able to be formed. Then, the in-situ growing of ZIF-8 was followed on the heterogeneous SnS₂ layers, so the defect free ZIF-8 covered the whole SnS₂ layers. The top-side of ZIF-8 membrane and bottom-side SnS₂ play critical role for molecular sieving and chemical detection, respectively. Due to the uniform pore distribution of ZIF-8 layer on the SnS₂ sensing layer, H₂O molecules can be reliably blocked by ZIF-8 breathable layer, while target NO₂ molecules can selectively penetrate through the ZIF-8 layer. Therefore, our hybrid materials exceptionally showed high stability and selective surface activity from the chemical sensing case study and the underlying mechanisms were further investigated in the atomistic level using theoretical calculations.

8:00 PM EL19.09.07

High-Throughput Production of an Atomically Thin Nano-Dot Array for Enhanced Exciton-Exciton Interactions JeongInYeo¹, SeungjaeLim², TaewanKim², Jae-UngLee² and JoonkiSuh^{1,†}; ¹Ulsan National Institute of Science and Technology, Korea (the Republic of); ²Ajou University, Korea (the Republic of)

Monolayer transition metal dichalcogenides (TMDs) are an appealing material platform for investigating and manipulating excitonic properties in the atomically thin limit due to their intrinsic strong Coulomb interactions and alleviated screening effects. To date, a number of such studies have been conducted to determine the excitonic physics or control their dynamics by diverse experimental approaches including electrostatic gating, magnetic field manipulation and strain engineering. However, physically confined excitonic transport through nanostructuring is not handled yet. Herein, we introduce a high-throughput nanofabrication of laterally confined monolayer TMDs in a hexagonal array. The fabricated nanodots of monolayer TMDs are approximately 20 nm wide far below typical exciton diffusion length of monolayer TMDs. We then investigated their photoluminescence (PL) characteristics by performing a series of power, wavelength (2.25–2.82 eV), and temperature dependent measurements. We observed the unconventional emission in sub-20 nm WS₂ nanodots, which is presumably associated with the physically confined excitonic transport behavior and reconstructed band structure. This platform is suitable tool for understanding of confined quasi-particle transport behavior and size-dependent PL study, providing a broader insight for fundamental excitonic many-body interactions and related dynamics.

8:00 PM EL19.09.08

A Practical Hydrogenated Graphene Gas Sensor for CO₂ Monitoring SolimarCollazo^{1,†}, SamuelEscobar^{1,2}, BradWeiner^{1,†} and GerardoMorell^{1,†}; ¹University of Puerto Rico at Río Piedras, Puerto Rico; ²National Institute of Standards and Technology, United States

The development of a practical gas sensor is of great interest for monitoring toxic and non-toxic gases that might endanger our safety and wellbeing in different settings. Here, we present a gas sensor based on hydrogenated graphene for monitoring carbon dioxide (CO₂). Hydrogenated graphene was synthesized using a single-step method directly onto an insulating substrate plated with gold. The material was characterized using Raman spectroscopy, X-ray photoelectron spectroscopy (XPS), and X-ray diffraction (XRD). The interaction of the hydrogenated graphene with CO₂ was systematically studied at different parts per million (PPM) to determine the detection limits of the sensor. Our results show that the hydrogenated graphene-based sensor is capable of sensing CO₂ at mid-PPM levels with a CO₂ responsivity of -176.21. The biosensor was also found to detect CO₂ at low ppm values, making it suitable for use as a biosensor for aerobic cellular respiration and regular CO₂ emission sensing. We have successfully developed a versatile and practical gas sensor based on hydrogenated graphene for CO₂ monitoring. The sensor's detection limits, and responsivity make it suitable for a wide range of applications, including monitoring of CO₂ emissions and aerobic cellular respiration. The simplicity of the synthesis method used also makes it a promising candidate for large-scale production.

SESSION EL19.10: Poster Session IV: 2D Materials—Epitaxial and Van der Waals Heterostructures

Session Chairs: Kibum Kang and Andrew Mannix

Tuesday Afternoon, November 28, 2023

Hynes, Level 1, Hall A

8:00 PM EL19.10.01

Van der Waals Heterostructures Containing Group-III Chalcogenides MichaelAltwater^{1,2} and NicholasGlavin¹; ¹Air Force Research Lab, United States; ²UES, Inc., United States

The group-III chalcogenides are an emerging class of van der Waals semiconductors with potential for applications in electronics, optoelectronics, and photonics. Further, material properties such as work function and band gap vary dramatically as the material is thinned toward the 2D limit. In this talk, we present experimental studies of the electronic and optical properties of van der Waals heterostructures containing the layered group-III chalcogenides. We analyze the effect of charge transfer within the structure as a function of layer thickness and compare the electronic performance with the more common TMD-based heterostructure devices.

8:00 PM EL19.10.02

Self-Catalyzed Vapor-Liquid-Solid Growth of GaS Nanobelt YukihiroEndo, YoshiakiSekine and YoshitakaTaniyasu; NTT Basic Research Laboratories, Japan

Among group-III chalcogenides, which are atomic-layered semiconductors, GaS shows a large layer-number-dependent bandgap energy from 2.5 eV (bulk) to 3.4 eV (monolayer) corresponding to blue and ultraviolet light wavelengths, respectively [1]. This unique property makes it a promising material for photonic devices and water-splitting photocatalysts [2, 3] and also an important component for group-III chalcogenide heterostructures. Furthermore, 1D structures of 2D layered materials, nanobelt or nanoribbon, would enable novel quantum devices and nanodevice integration. In this work, we demonstrate the synthesis of GaS nanobelt by means of self-catalyzed vapor-liquid-solid (VLS) growth. GaS was grown on a sapphire wafer by metalorganic chemical vapor deposition (MOCVD). Triethylgallium (TEGa) and diethylsulfide (DES) were used as Ga and S sources, respectively. VLS growth of 1D GaS-nanobelts occurs from Ga clusters, which can be formed under a Ga-rich surface growth condition obtained at high [TEGa]/[DES] supply ratios, while 2D GaS layers are grown at low [TEGa]/[DES] supply ratios. Thus, the dimension of the GaS structure can be controlled by MOCVD growth conditions. To evaluate the optical quality of the GaS nanobelt, we fabricated a photodetector (width: 900 nm, thickness: 100 nm, channel length: 2 μm). A photocurrent was generated under light irradiation with photon energies larger than 2.5 eV (wavelengths shorter than 500 nm), corresponding to the bandgap energy of GaS. The dark current was lower than the detection limit of our measurement system. A high ON/OFF ratio (> 1000) at a wavelength of 400 nm was obtained at the applied voltage of 10 V. This good photoresponsivity indicates that the VLS-grown GaS nanobelt has a high enough quality for device operation. The development of high-quality 1D GaS nanobelt synthesis on a wafer opens up opportunities for group-III chalcogenide nanodevice applications as well as the exploration of novel quantum phenomena.

References:

- [1] C. S. Jung *et al.*, ACS Nano **9**, 9585 (2015).
- [2] Y. Lu *et al.*, Adv. Mater. **32**, 1906958 (2019).
- [3] H. L. Zhuang *et al.*, Chem. Mater. **25**, 3232 (2013).

8:00 PM EL19.10.03

Engineered 0D-2D Heterostructure for Broad-Band Photodetectors Mukesh KumarThakur, AswinAsaithambi and IlkaKriegel; Istituto Italiano di Tecnologia, Italy

In the past decades, two-dimensional (2D) transition metal dichalcogenides (TMDs) like MoS₂, WS₂, WSe₂, etc., have drawn great research interest in various applications, such as phototransistors, light emitters, photocatalysis, solar cells, biomedical imaging, and many others due to their fascinating optical, electronic, and chemical properties. Although, monolayer (1L) TMDs, such as 1L MoS₂, have a direct band gap, the atomically thin nature of the 1L TMDs leads to very low optical absorption (< 5 %, mainly in the visible range). Consequently, devices made of such materials suffer from low photoresponse (mA/W) and their spectral range is limited to the visible spectrum. Additionally, TMDs have many defect states and are very sensitive to O₂/H₂O, affecting the device response time, which is a major drawback of TMD-based photodetectors. Integration with light-absorbing nanomaterials, such as zero-dimensional (0D) nanocrystals (quantum dots, perovskites, etc.) not only enhances photoresponse and spectral range, it also helps to passivate the defects in 2D materials, thereby improving the overall performance of the device.[1-3]

Here, we proposed two possible strategies to enhance the device performance of TMDs by coupling them with engineered 0D core-shell nanocrystals, such as InAs@ZnSe and Sn:In₂O₃@In₂O₃. In both cases, the resulting hybrid structures not only enhance the net absorption, they also help to build charge trap states, which allow efficient charge-transfer pathways for fast IR photodetection. The interaction is obtained through the spin coating of these 0D nanomaterials on the 1L TMDs, such as MoS₂ or WSe₂, which realizes the intimate and direct interfacing of 0D and 2D materials. I will also outline the impact of the surface ligands of such nanomaterials on the overall device performance and how selective excitation can give insight into the interaction mechanism between the two species. The spectroscopic results suggest the efficient charge transfer between 2D and 0D materials. For proof of concept, a photodetector device of these heterostructures is fabricated with improved photocurrent, detection range, and response time compared to the bare TMDs.

Key Words: 2D Materials, CVD, InAs, ITO nanocrystals, Infrared, Phototransistor

References:

1. A. Asaithambi, et al., *Adv. Optical Mater.* 2022, 10, 2200638
2. A. Asaithambi, et al., *Chem. Commun.*, 2023, 10.1039/D3CC01125A
3. Thakur et al., *ACS Appl. Mater. Interfaces* 2020, 12, 25, 28550–28560

8:00 PM EL19.10.04

Moiré Excitons in WS₂-MoSe₂ Heterobilayers [Yara Galvão Gobato](#)¹, Caique Serati de Brito¹, Andrey Chaves², M. A. Prosnikov³, T. Wozniak⁴, Shi Guo⁵, Ingrid Barcelos⁶, M. V. Milosevic⁷, Freddie Withers⁸, A. Beer⁸, J. Fuchs⁸, Christian Schueller⁸ and P. C. Christianen³; ¹Universidade Federal de São Carlos, Brazil; ²Universidade Federal do Ceará, Brazil; ³Radboud University, Netherlands; ⁴Wrocław University of Science and Technology, Poland; ⁵University of Exeter, United Kingdom; ⁶Brazilian Center for Research in Energy and Materials (CNPEM), Brazil; ⁷University of Antwerp, Belgium; ⁸Universität Regensburg, Germany

Twisted van der Waals (vdW) heterostructures exhibit periodic variations, leading to a new type of in-plane superlattice known as moiré superlattice/pattern which modifies considerably the optical properties of excitons in transition metal dichalcogenides (TMD) vdW heterostructures. Here, we report on optical and magneto-optical properties of WS₂/MoSe₂ heterobilayers with twist angles around 0° and 60° under out-plane magnetic fields up to 20 T [1]. We observed two neutral exciton peaks in the PL spectra: the lower energy one exhibits a reduced g-factor relative to that of the higher energy peak, and much lower than the recently reported values for interlayer excitons in other vdW heterostructures such as WSe₂-MoSe₂. In addition, similar values of g-factors are obtained for samples with twist angles of approximately 0° and 60° which indicates a weak hybridization between the intralayer and interlayer excitons for this heterostructure. Furthermore, time resolved PL experiments reveal that the lifetimes of the moiré exciton emission peaks are much shorter (< 50 ps) than the values reported in the literature for the interlayer excitons in other TMD heterostructures (≈ 2 ns), which also indicates a weak exciton hybridization. The observed reduction of the g-factor value for the moiré exciton was explained by the quantized center-of-mass momentum of the moiré-confined exciton resulting in an exciton momenta value away from the exciton band edge. In general, our experimental and theoretical results provide evidence that such a discernible g-factor stems from the spatial confinement of the exciton in the potential landscape created by the moiré pattern, due to lattice mismatch and/or inter-layer twist in heterobilayers [1].

References

- [1] Y. Galvão Gobato et al, *Nano Letters* 22, 8641 (2022)

8:00 PM EL19.10.05

Fabrication of Graphene/WC/SiC Heterostructures and its Electronic Properties [Kohei Otsuka](#)¹, Takahiro Ito¹, Akira Endo² and Wataru Norimatsu³; ¹Nagoya University, Japan; ²University of Tokyo, Japan; ³Waseda University, Japan

Graphene can be grown by thermal decomposition of SiC and other carbides, which means that we can easily fabricate graphene/carbide heterostructure [1]. In this study, we focus on tungsten carbide (WC) as the carbide. Recently, it is found that Hexagonal WC is one of the topological semimetals, and it has attractive properties such as Fermi-arc surface states, negative magnetoresistance, and dHvA oscillations [2, 3]. In graphene/topological semimetal heterostructures, nonlocal resistance originating from spin-polarized carriers has been observed, which is expected to be applied to spintronics [4]. Therefore, fabrication of graphene/WC heterostructures is expected to enable us to observe new electronic properties.

In this study, we fabricated graphene/WC/SiC heterostructure and investigate the electronic properties. Highly crystalline WC thin films were formed on 4H-SiC single-crystal substrates by pulsed laser deposition (PLD). Then, graphene was fabricated by thermal decomposition of the films. The fabricated graphene/WC/SiC samples were characterized by some measurements. The electronic state of the samples was measured by angle-resolved photoemission spectroscopy (ARPES). Transport measurements of WC/SiC and graphene/WC/SiC samples were also performed at low temperatures.

4H-SiC (000-1) single crystal substrate (5×5 mm², on-axis, CREE) was used as a substrate. The WC thin film was fabricated by the PLD method. Then, the substrate was heated at 1100°C for 10 minutes. The resulting WC thin film was heated at 1750°C for 10 minutes in a vacuum to fabricate graphene. Reflection high-energy electron diffraction (RHEED), atomic force microscopy (AFM), Raman spectroscopy, X-ray photoelectron spectroscopy (XPS), transmission electron microscopy (TEM), ARPES, and low-temperature transport measurements were performed on the prepared samples.

From the High-resolution TEM images after WC deposition, we observed a WC thin film deposited on the SiC substrate with a thickness of about 7 nm. Analysis of the electron diffraction showed that the relationship of the orientation between hexagonal WC and SiC substrate was (0001)_{WC}//(000-1)_{SiC} and [11-20]_{WC}//[11-20]_{SiC}.

ARPES measurements of the graphene/WC/SiC sample showed band dispersions of graphene and bulk WC. Furthermore, we observed a band near the Γ point of WC, which we cannot explain by the band structure of graphene and bulk WC. We think the band originate from the surface state of WC or the interface interaction between graphene and WC.

Transport measurements indicate that superconductivity of WC/SiC and graphene/WC/SiC sample. We estimated the transition temperature (T_c) of WC/SiC is about 1.8-2.2 K. We found that graphene/WC/SiC has smaller T_c than WC/SiC.

- [1] W. Norimatsu, et al., *Nanotechnology* **31**, 145711 (2020).

- [2] J. Z. Ma, et al., *Nat. Phys.* **14**, 349 (2018).

- [3] J. B. He, et al., *Phys. Rev. B* **95**, 195165 (2017).

- [4] Y. Wu, et al., *Adv. Mater.* **30**, 34 (2018).

8:00 PM EL19.10.06

Quasi Van der Waals Epitaxy of Cadmium Telluride on 2D Materials [Enguerrand Tourard](#); CEA Leti, France

Cadmium telluride is a key material for many technologies, such as energy production or infrared sensing, which makes the growth of free standing (strain free) layers of CdTe of particular interest. In 2017, Kim et al demonstrated that it is possible to guide the growth of a material through one or few monolayers of 2D material, given that the polarity of the substrate below the 2D material is strong enough. This technique, called “remote epitaxy”, has been applied successfully to a wide range of III-V / 2D systems, such as the epitaxial growth of GaN on hBN / GaN substrate, or GaAs on Graphene / GaAs substrate. Epitaxially grown layers are then easily transferred and the 2D coated substrate can be re-used for future growths. Despite this great success with III-V materials, remote epitaxy of II-VI semiconductors hasn't been studied much. From a purely theoretical point of view, CdTe with its higher ionicity than GaAs or GaN should be a good candidate for remote epitaxy. However, a transfer step is required to obtain 2D coated substrates, with its lot of difficulties (polymeric contamination, degradation of the 2D surface, oxidation of the substrate...), whereas high quality surface and interface are required to perform remote epitaxy.

Another approach to bypass the need of 2D material transfer would be to perform epitaxy on a reconstructed passivated surface. It has been proven recently (Jovanovic et al, 2020) that sapphire could act as a quasi van der Waals substrate for such a growth of CdTe via the in-situ formation of a monolayer of tellurium at the interface. In such a case, the substrate surface, free from dangling bonds, allows for an easy transfer of the epitaxially grown CdTe membrane. But, unlike with “remote epitaxy”, growth is not seeded by the polar substrate, and one can ask what is the impact on the crystalline quality of the epilayer?

In this communication, we will present the results of MBE grown CdTe film on both sapphire and graphene wet-transferred onto CdZnTe. The crystalline quality of the grown CdTe film is discussed based on SEM, AFM and X-ray diffraction. Graphene quality is checked out prior and after epitaxy based upon Raman spectroscopy. Additional XPS analysis were performed to evaluate substrate oxidation and graphene cleanliness. Results of CdTe layer removal and manipulation will also be presented.

8:00 PM EL19.10.07

Edge-Contacted In-Plane Mixed-Dimensional Heterostructures from Monolayer MoS₂ and Low-Dimensional Mo/Te Compounds [Hyeonkyeong Kim](#), Young Chul Kim, Yeong Hwan Ahn and Youngdong Yoo; Ajou University, Korea (the Republic of)

Mixed-dimensional heterostructures formed by combining 2D materials and other dimensional (0D, 1D, and 3D) materials have attracted attention due to their hybrid structures. However, in-plane mixed-dimensional heterostructures have been rarely investigated. Here, we report a novel sequential chemical vapor deposition method for synthesizing in-plane mixed-dimensional heterostructures composed of monolayer MoS₂ and low-dimensional molybdenum/tellurium (Mo/Te) compounds. The composition, dimension, and phase of the Mo/Te compounds interfaced with the monolayer MoS₂ were determined by adjusting the Te flux and growth time. While in-plane 2D/1D MoS₂/Mo₆Te₆ and 2D/2D/1D MoS₂/2H MoTe₂/Mo₆Te₆ heterostructures were synthesized with a low Te flux, in-plane 2D/2D MoS₂/mixed 2H-1T' MoTe₂ and 2D/2D MoS₂/2H MoTe₂ heterostructures were obtained with a high Te flux. We performed scanning photocurrent microscopy measurements for studying the transport properties and the electronic band structures of the devices fabricated with in-plane mixed-dimensional 2D/2D/1D MoS₂/2H MoTe₂/Mo₆Te₆ heterostructures. The composition-, dimension-, and phase-controlled synthesis method developed in this study will allow large-scale controlled fabrication of edge-contacted mixed-dimensional in-plane heterostructures.

8:00 PM EL19.10.08

Atomic-Layer-Deposited Wide Bandgap Metal Oxide Buffer Layers on the Eco-Friendly Thin Film Photovoltaics Cheng-Ying Chen¹, I-Jui Hsieh² and Pochun Chen²; ¹National Taiwan Ocean University, Taiwan; ²National Taipei University of Technology, Taiwan

In this work, atomic layer deposition (ALD) is conducted for growing Wide Bandgap Metal Oxides (ZnSnO) as buffer layers on p-type selenium (Se) absorbers, which was used in the first solid-state solar cell in 1883 and has a high absorption coefficient and mobility, making it a p-type absorber for wide energy gap (~1.8–2.0 eV) thin film solar cells. In addition, direct bandgap, earth-abundance, simple composition, non-toxicity, low melting point and environmental stability make Se inexpensive and developable for solar cells. However, in the n-type buffer layer perspective, so far, has not been found a suitable buffer layer for modulating conduction band offset (CBO) between n-type buffer layers and p-type Se absorbers. The benefit for using ALD growth ZnSnO can be summarized as the following points: (1) ZnSnO is wide band gap material (~3.2 eV); (2) Controllable of Zn and Sn ratio, which can intentionally modulate the CBO become spike type (i.e., $0 < \text{CBO} < 0.5$ eV); (3) ALD can effectively growth larger scale of thin-film and precisely control the thickness. Finally, the result presented the $\text{Zn}_{1-x}\text{Sn}_x\text{O}$ ($x=7\%$) under the optimization of ZnO and SnO ratio, the power conversion efficiency can be achieved at about 2.68%.

8:00 PM EL19.10.09

Coherently Stacked Van der Waals Semiconductor Heterostructures Jong Yun Choi^{1,2}, Hyun Je Cho^{1,2}, Suk-Ho Lee^{1,2}, Geonho Mun^{1,2}, Heon-Su Ahn^{1,2}, Hwang-Jung Chang^{1,2}, Hyunjin Jung^{2,3} and Moon-Ho Jo^{1,2}; ¹Center for Van der Waals Quantum Solids, IBS (Institute of Basic Science), Korea (the Republic of); ²Pohang University of Science and Technology, Korea (the Republic of); ³Center for Artificial Low Dimensional Electronic Systems, Institute for Basic Science (IBS), Korea (the Republic of)

We report atomically coherent layer-by-layer epitaxial growth of MoS_2/WS_2 van der Waals (vdW) heterostructure with metal-organic chemical vapor deposition (MOCVD) which enables vertical stacking of atomically thin semiconductors without interlayer atomic mixing. Engineering the miscut angle of c-plane sapphire substrate, we first achieved the epitaxial growth of single crystalline WS_2 monolayer (ML) template as base layer. Single crystalline texture was confirmed by microscopies and transmission electron microscope (TEM) studies. Moreover, low energy electron diffraction (LEED) measurements at several different points perfectly exhibited 3-fold symmetry without any angle deviation. We also demonstrated coherent ML-by-ML epitaxial growth of MoS_2 on top of single crystalline WS_2 film. VdW epitaxy is kinetically controlled in the near-equilibrium limit, resulting in the tunable two-dimensional (2D) vdW electronic systems. Coherent monolayer stacking was verified by transmission electron microscope studies and optical characterization. Our AA'(2H) and AB(3R) stacked MoS_2/WS_2 heterostructures showed strong interlayer coupling. Furthermore, electronic and optoelectronic properties of coherent vdW heterostructures were obtained. Our work suggests synthetic material platform of various 2D coherent heterostructures for future application in electronic and photonic nano devices.

References

1. Jin, G., Lee, C.S., Okello, O.F.N. et al. *Heteroepitaxial van der Waals semiconductor superlattices*. *Nat. Nanotechnol.* **16**, 1092–1098 (2021).
2. Li, T., Guo, W., Ma, L. et al. *Epitaxial growth of wafer-scale molybdenum disulfide semiconductor single crystals on sapphire*. *Nat. Nanotechnol.* **16**, 1201–1207 (2021).
3. Kim, Y., Cruz, S., Lee, K. et al. *Remote epitaxy through graphene enables two-dimensional material-based layer transfer*. *Nature* **544**, 340–343 (2017).

SESSION EL19.11: 2D Semiconductors—Synthesis II

Session Chairs: Kibum Kang and Andrew Mannix

Wednesday Morning, November 29, 2023

Hynes, Level 3, Room 309

8:30 AM *EL19.11.01

Metalorganic Chemical Vapor Deposition of Wafer-Scale Transition Metal Dichalcogenide Monolayer and Heterostructures Joan M. Redwing; The Pennsylvania State University, United States

Wafer-scale synthesis of transition metal dichalcogenide (TMDs) monolayers is of significant interest for device applications to circumvent size limitations associated with the use of exfoliated flakes. Metalorganic chemical vapor deposition (MOCVD) has emerged as a promising technique for scalable synthesis of TMD films as it enables growth at high temperatures and chalcogen overpressures which are beneficial for epitaxy and provides good control over precursor flux which is necessary for the synthesis of heterostructures.

Our work has focused on MOCVD growth of epitaxial semiconducting TMDs (MoS_2 , WS_2 and WSe_2) on 2" diameter c-plane sapphire substrates. Metal hexacarbonyls ($\text{Mo}(\text{CO})_6$, $\text{W}(\text{CO})_6$) and hydrides (H_2S , H_2Se) are used as precursors with H_2 as the carrier gas in cold-wall MOCVD reactor geometries. Pre-annealing the sapphire surface in H_2S or H_2Se modifies the nucleation behavior of TMDs on sapphire which is attributed to passivation of dangling bonds on the sapphire surface. Passivation of step terraces can drive nucleation to occur preferentially at step edges on sapphire leading to unidirectional domains and a concomitant reduction in mirror twin defects. In situ spectroscopic ellipsometry is demonstrated to be an effective real time monitor of TMD growth even at the sub-monolayer level which can be exploited to track surface coverage as a function of time under varying growth conditions. The ability to precisely control and modulate precursor flux during growth is used to synthesize in-plane heterostructures that enable localized exciton confinement and emission.

9:00 AM EL19.11.02

Structure and Phase Engineering of Novel Two-Dimensional Transition Metal Chalcogenides Bijun Tang and Zheng Liu; Nanyang Technological University, Singapore

Since the discovery of monolayer graphene in 2004, two-dimensional (2D) materials have attracted considerable attention owing to their potential applications in various fields such as optics, electronics, and catalysis. Numerous 2D materials have been developed in the past decade. Among them, 2D transition metal chalcogenides (TMCs) attract most of the attention, mainly attributed to their large spectrum of fascinating properties along with various crystal structures. In parallel with the discovery of new candidate materials and exploration of their unique characteristics, engineering 2D TMCs into designated structures and phases are also of great importance for meeting the requirement for different applications. In this talk, I will discuss how we use the chemical vapor deposition (CVD) method to engineer the structure and phase of 2D TMCs and as a result, to tune their electronic and magnetic properties. Several strategies will be particularly introduced including construction of heterostructure, alloying, phase-selective growth, and dimension tuning. Additionally, the feasibility and capability of using state-of-the-art machine learning (ML) techniques to guide the synthesis and engineering of 2D TMCs will also be discussed.

9:15 AM EL19.11.03

Growth of Width-Controlled Single Atomic Layer TMD Nanoribbons Xufan Li and Avetik R. Harutyunyan; Honda Research Institute USA Inc., United States

Controlling the width of single atomic layer transition metal dichalcogenides (TMDs) offers additional degree of freedoms for engineering their properties aiming applications in fields for next generations of optoelectronics, quantum computing, communication, and sensing. However, direct width-controlled synthesis of TMD nanoribbons, especially for the appealing width range below 30 nm, remains challenging. Therefore, developing facile methods for their direct and controllable synthesis is of central importance. We present a new growth method for single and double atomic layer of TMD nanoribbons with width down to sub-10 nm. Nanoribbons are grown via precipitation from the pre-deposited nanoparticles via vapor-liquid-solid mechanism in which the nanoparticle diameter also controls the width of nanoribbon. We also present the evolution of electrical and optical properties of the nanoribbons with their width reduction due to the corresponding dimension confinement and the results of their performance in the quantum electronics, particularly as a single electron transistor and single photon emitter.

References

- X. Li., et al. *ACS Nano* **14**, 6570 (2020).
- X. Li., et al. *Sci. Adv.* **7** (50), eabk1892 (2021).

9:30 AM BREAK

10:00 AM *EL19.11.04

The Impact of Boron and Nitrogen Isotopes on the Properties of Hexagonal Boron Nitride James H. Edgar, Eli Janzen and Thomas Poirier; Kansas State University, United States

Hexagonal boron nitride (hBN) is a two-dimensional dielectric material prized for its potential electronic, optoelectronic, and nanophotonic device applications. Here we describe how its properties are affected by changing its boron and nitrogen isotopes. hBN consists of 20% ^{10}B and 80% ^{11}B , and 99.6% ^{14}N and 0.4% ^{15}N when it is synthesized from sources with the natural distribution of isotopes (hBN^{nat}). Isotopic disorder is greatly reduced when hBN is synthesized using an isotopically enriched boron source, either ^{10}B or ^{11}B . Consequently, the phonon

polariton propagation length and lifetimes are increased by factors of eight and four times in monoisotopic hBN crystals. Due to reduced phonon scattering, the thermal conductivity is also increased, by as much as 50% to 650 Wm⁻¹K⁻¹ for h¹⁰BN at room temperature. Reducing the density of nuclear spin density motivates the synthesis of hBN with the ¹⁵N isotope: ¹⁴N and ¹⁵N have nuclear spins of 1 and ½ respectively. Thus, the DC sensitivity of the boron vacancy V_B to magnetic fields is increased by a factor of four with h¹⁰B¹⁵N over hBN^{nat}.

These hBN crystals with controlled isotope concentrations were grown at atmospheric pressure from molten metal solutions of nickel, chromium, and enriched boron in contacted with nitrogen gas at 1550 °C. By slow cooling (1–4 °C/h), hBN is synthesized and its crystals precipitate on the surface of the metal. This technique produces high quality hBN crystals, as indicated by their narrow E_{2g} Raman peak widths (<3 cm⁻¹ for h¹⁰BN) and strong photoluminescence intensities at energies great than 5.75 eV. This is a versatile, scalable technique for making high quality, large area, hBN single crystals with low residual impurity concentrations.

10:30 AM EL19.11.05

Optoelectronic Property of APCVD Grown 2D Non-Van der Waals Bi₂O₂Se NanosheetsSurajLakhchaura and AtikurRahman; Indian Institute of Science Education and Research (IISER), Pune, India

Bismuth oxyselelide has recently gained attention as a highly promising 2D material for next-generation digital electronics and optoelectronics due to its ultrahigh mobility, the moderate bandgap of 0.8eV, and exceptional environmental stability. Bi₂O₂Se-based field-effect transistors (FETs) have also shown excellent current on/ off ratios of >10⁶ with an almost ideal subthreshold swing (≈65 mV dec⁻¹), which is essential for low-power logic devices. In this study, we have synthesized ultrathin single crystalline nanosheets of Bismuth oxyselelide using a Homebuilt Atmospheric Pressure Chemical Vapor Deposition system. We transferred as-grown samples to different substrates using a non-corrosive dry transfer method. We have fabricated a back-gated Bi₂O₂Se Field Effect Transistor and examined its electronic transport properties. Furthermore, our investigations into its optoelectronic properties revealed that our device demonstrated an ultrahigh responsivity of 1.16×10⁶ A/W and detectivity of 2.55×10¹³ Jones. Our findings suggest that Bismuth oxyselelide is a promising material for applications in optoelectronics.

10:45 AM EL19.11.06

High Crystalline Quality PtSe₂ Films for High Frequency OptoelectronicsPierreLegagneux and EvaDesgue; Thales Research & Technology, France

Transition metal dichalcogenides (TMDs) are very attractive two-dimensional materials for optoelectronic applications, due to their various and tunable bandgaps, to the strong light-matter interaction per 2D layer and to the possibility to transfer and integrate these 2D materials on CMOS or photonic platforms.

While the most well-known TMDs (MoS₂, WSe₂,...) exhibit a bandgap in the visible range, PtSe₂ is an original and remarkable TMD particularly adapted for optoelectronics in the infrared (IR) domain. It exhibits a bandgap varying from 1.2eV (monolayer) to 0.2eV (bilayer) and becomes semi-metallic from few layers to bulk. Thus, PtSe₂ absorption can be easily tuned to absorb IR light by varying its thickness from two to multilayers.

PtSe₂ is air stable and particularly adapted for high-frequency optoelectronics with a very high theoretical (4000 cm²/V.s) and a high experimental (e.g. ~ 200 cm²/V.s) carrier mobility at room temperature (Note that larger mobilities are reported in the literature which remain however difficult to measure due to the difficulty to estimate actual carrier concentration in semimetal multi-layered PtSe₂).

Due to its high intrinsic qualities, PtSe₂ is studied to fabricate high frequency photodetectors operating at the 1.55 μm telecom wavelength. Based on transferred thin PtSe₂ films grown by CVD, 17 GHz bandwidth photodetectors have been fabricated on a SiO₂/Si substrate and 35 GHz bandwidth waveguide photodetectors have been realized on a silicon nitride platform.

High frequency optoelectronics requires both efficient photodetection and high-speed transport and thus materials exhibiting high crystalline quality.

PtSe₂ has been synthesized by mechanical exfoliation, CVD, thermally assisted conversion and molecular beam epitaxy (MBE). To evaluate PtSe₂ crystalline quality, most groups have studied the full width at half maximum (FWHM) of the in-plane Eg Raman peak and shown that thinner is the Eg peak, higher is the crystalline quality and the electrical conductivity.

Here, we have studied the growth of high quality PtSe₂ by MBE on sapphire, which is a low cost, insulating substrate and have fabricated high frequency optoelectronic devices on 2 inches sapphire substrates. We show 8-nm thick PtSe₂ films exhibiting average FWHM Eg values as low as 3.7 cm⁻¹ and electrical conductivities as high as 1.5 mS. Integrated in a coplanar wave guide, we demonstrated 1.55 μm photodetectors with a 60 GHz bandwidth and optoelectronic mixers exhibiting a flat response between 1 and 30 GHz. Optoelectronic mixing is a key technical enabler for future broadband and multifunctional RF systems such as radio-over-fiber communication systems, radar systems, and satellite payloads.

To further increase PtSe₂ crystalline quality, we are studying two methods: step-guided epitaxy and van der Waals epitaxy. Step-guided epitaxy on sapphire consists in growing on dedicated vicinal surfaces to favor the oriented nucleation of the crystals at the step edges (this method has been demonstrated by other groups for MoS₂ and WS₂ on sapphire). We will also show first results targeting van Der Waals (vdW) epitaxy of PtSe₂ on h-BN.

11:00 AM EL19.11.07

Reproducible Synthesis of Ultrahigh-Quality Graphene by Oxygen-Free Chemical Vapor DepositionXingzhouYan¹, JacobAmontree¹, ChristopherDiMarco¹, PierreLevesque², TehsenAde³, MadisenHolbrook¹, ChristianCupo¹, DihaoSun¹, KenjiWatanabe⁴, TakashiTaniguchi⁴, CoryDean¹, AngelaR. Hight Walker², KatayunBarmak¹, RichardMartel² and JamesHone¹; ¹Columbia University, United States; ²Université de Montréal, Canada; ³National Institute of Standards and Technology, United States; ⁴National Institute for Materials Science, Japan

Progress in translating advances in the growth of graphene films by chemical vapor deposition (CVD) to applications has been hindered by challenges in quality and reproducibility, as well as the lack of a simple model of growth kinetics. Here we show that eliminating trace oxygen leads to fast and highly reproducible CVD graphene growth. The dependence of growth rate on growth time, temperature, and CH₄ pressure follow straightforward trends, while previously unobserved behavior is seen for H₂ pressure. A compact kinetic model is constructed to describe the graphene growth behavior, which can be used to guide graphene synthesis. We confirm that ppm-level oxygen disrupts growth by etching the graphene edges, and map the boundary between growth and etching in the presence of H₂. We demonstrate that trace oxygen causes two major sources of disorder in CVD-grown graphene: pinholes and amorphous carbon deposition. Finally, we grow epitaxial graphene on sapphire-supported Cu(111) films. The graphene shows few wrinkles, no evidence of amorphous carbon, and an ultra-low defect density. After dry transfer and device assembly, this graphene shows electrical transport behavior virtually indistinguishable from that of exfoliated graphene, both at room temperature and at low temperature.

11:15 AM *EL19.11.08

In-Situ TEM of Atomic Reconstructions in 2D Transition Metal DichalcogenidesYichaoZhang¹, Chia-HaoLee¹, Ji-HwanBaek², HuijieRyu², GillianNolan¹, Gwan-HyongLee² and PinshaneY. Huang¹; ¹University of Illinois at Urbana-Champaign, United States; ²Seoul National University, Korea (the Republic of)

Scanning transmission electron microscopy (STEM) provides uniquely powerful tools to study the interfacial structure and transformations of 2D materials up to atomic resolution. Here, we utilize 2D multilayer stacks to create nanoscale laboratories for studying the atomic structure, structural transformations, and properties of 2D interfaces inside the STEM. We utilize graphene encapsulation in combination with a MEMS-based heating holder to conduct in-situ studies of solid-solid phase transformations and interfacial restructuring in 2D transition metal dichalcogenides. The graphene encapsulation protects the 2D materials from the vacuum environment of the STEM, enabling high temperature studies up to 1000°C. We use these structures to directly visualize the layer-by-layer phase transformation of MoTe₂ and the lattice reconstruction of 2D moirés.

First, we study the interfacial reconstruction mechanisms of twisted bilayer transition metal dichalcogenides (MoSe₂ and WSe₂) using *in situ* aberration-corrected STEM and dark-field transmission electron microscopy (DFTEM). We discover a new mechanism of local reconstruction from moiré patterns to parallel (3R) and/or antiparallel (2H) domains in twisted bilayer 2D transition metal dichalcogenides (TMDCs). Unlike previous reports, where the twist angle is altered by the rotation of a whole flake, we observe the nucleation and growth of commensurate domains through the formation and migration of grain boundaries. We capture the dynamic process of nucleation and growth of the aligned structure through a series of atomic resolution STEM images combined with atom-tracking analysis. These results provide new insights into the mechanisms of interlayer rotation at the atomic scale and potential methods for engineering the structure of moiré superlattices.

Second, we examine the atomic mechanisms of phase transitions of MoTe₂. MoTe₂ exhibits multiple structural and electronic phases at room temperature (2H, 1T', and T_d) that can be easily manipulated with different stimuli, making it a promising candidate for phase-change memories, high-performance transistors, and broadband photodetectors. We combine dark-field TEM and aberration-corrected STEM to image the phase transitions of few-layer MoTe₂ *in situ* from the micro- to atomic scales. We find that T_d-to-2H phase transitions initiate at the phase boundary at temperatures as low as 200-225 C, much lower than previously thought. The 2H-T_d interfaces propagate primarily along the b-axis of the T_d grain, producing an anisotropic, layer-by-layer phase transformation. These results should lead to new methods to manipulate the quantum and electronic properties within individual atomic layers.

1:30 PM EL19.12.01

Giant Magnetoresistance of Dirac Plasma in High Mobility Graphene Alexey Berdyugin^{1,2}, NaXin¹, James Lourembam¹, Piranavan Kumaravadivel¹, Alexander Kazantsev¹, Zefei Wu¹, Ciaran Mullan¹, Julien Barrier¹, Alexandra Geim¹, Irina Grigorieva¹, Artem Mishchenko¹, Alessandro Principi¹, Vladimir Falko¹, Leonid Ponomarenko³ and Andre Geim¹; ¹The University of Manchester, United Kingdom; ²National University of Singapore, Singapore; ³The University of Lancaster, United Kingdom

The most recognizable feature of graphene's electronic spectrum is its Dirac point, around which interesting phenomena tend to cluster. At low temperatures, the intrinsic behaviour in this regime is often obscured by charge inhomogeneity but thermal excitations can overcome the disorder at elevated temperatures and create an electron-hole plasma of Dirac fermions. The Dirac plasma has been found to exhibit unusual properties, including quantum-critical scattering and hydrodynamic flow. However, little is known about the plasma's behaviour in magnetic fields. Here we report magnetotransport in this quantum-critical regime. In low fields, the plasma exhibits giant parabolic magnetoresistivity reaching more than 100 per cent in a magnetic field of 0.1 tesla at room temperature. This is orders-of-magnitude higher than magnetoresistivity found in any other system at such temperatures. We show that this behaviour is unique to monolayer graphene, being underpinned by its massless spectrum and ultrahigh mobility, despite frequent (Planckian limit) scattering. With the onset of Landau quantization in a magnetic field of a few tesla, where the electron-hole plasma resides entirely on the zeroth Landau level, giant linear magnetoresistivity emerges. It is nearly independent of temperature and can be suppressed by proximity screening, indicating a many-body origin. Clear parallels with magnetotransport in strange metals and so-called quantum linear magnetoresistance predicted for Weyl metals offer an interesting opportunity to further explore relevant physics using this well defined quantum-critical two-dimensional system.

1:45 PM EL19.12.02

Two-Fold Anisotropic Superconductivity in Bilayer T_d -MoTe₂ Zizhong Li¹, Apoorv Jindal², Alex Strasser³, Yangchen He¹, David Graf⁴, Wenkai Zheng⁴, Kenji Watanabe⁵, Takashi Taniguchi⁶, Luis Balicas⁴, Xiaofeng Qian³, Abhay Narayan Pasupathy² and Daniel A. Rhodes¹; ¹University of Wisconsin Madison, United States; ²Columbia University, United States; ³Texas A&M University, United States; ⁴National High Magnetic Field Laboratory, United States; ⁵NIMS, Japan; ⁶Kyoto University, Japan

Non-centrosymmetric 2D superconductors offer an opportunity to explore superconducting behaviors with large values of anisotropy. Among the non-centrosymmetric families, T_d -MoTe₂ is a representative material because of its rich phases. Notably, T_d -MoTe₂ is the first 2D material that demonstrated a coupling between ferroelectricity and superconductivity, and this ferroelectric switching can be simply controlled by electrical gating. Here, we will present on the superconducting behavior in bilayer T_d -MoTe₂ under the application of an applied magnetic field along different directions in-plane and under differing displacement fields and doping densities. Importantly, we find that bilayer T_d -MoTe₂ has two-fold symmetric superconducting behavior as a function of in-plane magnetic field angle that maximizes along the a-axis, parallel to the mirror plane. The two-fold anisotropy is preserved in the entire superconducting region, even with the interaction of strong Rashba spin-orbit coupling, and we find that the two-fold symmetric superconductivity exists after the ferroelectric switching. Our findings generally agree with previously observed results in multilayer and monolayer T_d -MoTe₂ and the expected spin-orbit enhanced upper critical fields as found in DFT calculations.

2:00 PM *EL19.12.03

Few-layer 2M and T_d -TMDs: Topologically Nontrivial States, Superconductivity and Ferroelectricity Apoorv Jindal¹, Amartyajyoti Saha², Zizhong Li³, Yangchen He³, Takashi Taniguchi⁴, Kenji Watanabe⁴, James Hone¹, Turan Birol², Rafael Fernandes², Cory Dean¹, Abhay Narayan Pasupathy¹ and Daniel A. Rhodes³; ¹Columbia University, United States; ²University of Minnesota, United States; ³University of Wisconsin - Madison, United States; ⁴National Institute for Materials Science, Japan

I will discuss our most recent results on superconductivity in bilayer T_d -MoTe₂. For bilayer T_d -MoTe₂ the influence of an electrostatic gate allows us to identify a unique superconducting state that relies on Fermi surface nesting between hole and electron pockets. As a result, we show that the superconducting state can be completely quenched by an electrostatic gate. Concomitant to this effect, ferroelectricity resulting from interlayer sliding is also present in bilayer T_d -MoTe₂, resulting in a hysteretic behavior of superconductivity with respect to an applied out-of-plane electric field. This behavior allows for the first investigations of how internal polarization might conflict with or enhance superconductivity in the two-dimensional limit. Time allowing, I will discuss our results on a similarly structured TMD in the few-layer limit, the topologically nontrivial 2M-WSe₂.

2:30 PM BREAK

3:30 PM EL19.12.04

Van der Waals Josephson Junctions for 2D Superconducting Qubits Jesse Balgley¹, Xuanjing Chu¹, Jinho Park¹, Ethan Arnault², Martin V. Gustafsson³, James Hone¹ and Kin-Chung Fong³; ¹Columbia University, United States; ²Massachusetts Institute of Technology, United States; ³Raytheon BBN Technologies, United States

State-of-the-art superconducting qubits currently face numerous materials-limited roadblocks to increasing coherence times for fault-tolerant computing while shrinking form factors for scalability. Two-dimensional van der Waals (vdW) materials offer an ideal platform to circumvent these issues owing to their single-crystallinity, low defect density, and lack of dangling bonds. In particular, the vdW semiconductor WSe₂—whose band gap is ~5x smaller than that of vdW insulator hBN—can exhibit tunneling through ~10 layers, enabling Josephson junctions with exceptional tunnel barrier homogeneity and lower loss compared to deposition-grown junctions by confining fields in ultra-clean vdW interfaces while achieving 100x smaller qubit area. We characterize the electronic properties of vdW Josephson junctions with ultra-high-purity WSe₂ barriers and discuss their potential in small-footprint, long-coherence-time superconducting qubits.

3:45 PM EL19.12.05

Field-Free Superconducting Diode Effect in Fe(Se,Te) Van der Waals Josephson Junctions Gang Qiu^{1,2}, Hung-Yu Yang¹, Lunhui Hu³, Huairuo Zhang⁴, Chi-Yen Chen⁵, Yanfeng Lyu⁶, Peng Deng¹, Sergiy Krylyuk⁴, Albert V. Davydov⁴, Ruixing Zhang³ and Kang L. Wang¹; ¹University of California, Los Angeles, United States; ²University of Minnesota, United States; ³The University of Tennessee, Knoxville, United States; ⁴National Institute of Standards and Technology, United States; ⁵National Sun Yat-sen University, Taiwan; ⁶Nanjing University of Posts and Telecommunications, China

Iron-based high-Tc FeTe_xSe_{1-x} (FTS) has been proposed to host unconventional superconductivity. Recent scanning probe and ARPES experiments imply spontaneous time-reversal symmetry breaking in FTS systems. In this work, we report the field-free superconducting diode effect in FTS van der Waals Josephson junctions (vJJ). Non-reciprocal superconducting critical current can be observed in the absence of external magnetic field, which directly manifests spontaneous time-reversal symmetry breaking in FTS systems. The polarity and efficiency of the diode effect are also stochastic, which can be randomly reset by performing a thermal cycle above the superconducting critical temperature T_c. This suggests the time-reversal symmetry breaking ordering is closely tied to the superconducting states. The stochasticity also provides insights into ferromagnetic domain behaviors of superconducting surface states.

4:00 PM EL19.12.06

2D-Material-Based Superconducting Quantum Devices Xuanjing Chu¹, Jesse Balgley¹, Jinho Park¹, Ethan Arnault², Martin V. Gustafsson³, James Hone¹ and Kin-Chung Fong³; ¹Columbia University, United States; ²Massachusetts Institute of Technology, United States; ³Raytheon BBN Technologies, United States

Two-dimensional van der Waals (vdW) materials are promising platforms for superconducting quantum devices due to their single-crystallinity, low defect density, and lack of dangling bonds. Additionally, vdW materials offer a novel knob of gate-tunable electronic properties, including carrier density and superconducting gap energy, and can be readily combined into quantum device heterostructures such as Josephson junctions (JJs). JJs made from vdW materials can boast homogeneity across large (~1000 μm²) areas making them practical as novel sub-THz JJ emitters whose frequency can be tuned with a gate voltage as opposed to changing the bias current. We characterize the dc and microwave electronic properties of vdW materials and show they are compatible with high-quality-factor superconducting quantum devices. We also present numerical calculations of the emitting properties of gate-tunable Josephson junctions based on vdW superconductors and semiconductors and show that they can meet desirable performance criteria, including narrow linewidths < 1 MHz and appreciable output power at the microwatt level.

4:15 PM *EL19.12.07

Probing Complex Many-Body Interactions in 2D Heterostructures Jyoti Katoch; Carnegie Mellon University, United States

Two-dimensional (2D) materials provide unprecedented opportunity to engineer their physical properties by modification to the electronic structure utilizing external perturbations- strain, gating, adsorbates, defects, twist-angle, and interface engineering. This is expected to cause changes to the Hamiltonian describing the system and has resulted in exotic phenomena such as superconductivity, bound quasiparticles, topological states as well as magnetic phases, with implications for novel electronics and spin-device applications. In this talk, I will present our work on directly visualizing (without any assumption) the electronic structure of atomically thin systems utilizing *in-operando* angle-resolved photoemission spectroscopy with nanoscale spatial

resolution (nanoARPES) on 2D heterostructures and their fully functional devices. I will present the experiments which demonstrate on-demand tuning of the electronic band structure in atomically thin systems, such as transition metal dichalcogenides (TMDs) and graphene, by varying the twist-angle between the atomic layers and external dopants. Specifically, I will discuss the electric field tuning of the electronic interactions that result in van Hove singularity and flat bands in twisted bilayer graphene and twisted double bilayer graphene heterostructures. In addition, I will discuss our results where we observe the formation of quasiparticle polarons due to many-body interactions in graphene/TMDs heterostructures.

4:45 PM EL19.12.08

Polymer-Free Assembly of Van der Waals Heterostructures [Wendong Wang](#)^{1,2}, Nicholas Clark^{1,2} and Roman Gorbachev^{1,2,2}; ¹National Graphene Institute, United Kingdom; ²The University of Manchester, United Kingdom

2D heterostructures present an optimal approach for the synthesis of novel materials with highly adjustable properties, including electron topology and correlation effects. Currently, the prevailing method for constructing van der Waals heterostructures involves the "tear and stack" technique, wherein individual 2D layers are stacked using a polymer stamp. However, this approach easily traps contaminants at the heterostructure interface, leading to limitations in atomic cleanliness and electronic performance of the resulting heterostructures. To address this issue, we have developed a novel polymer-free stacking method that employs flexible, transparent, and thermally stable metallized silicon nitride membranes (SiN). These SiN membranes enable precise and rapid transfer of 2D flakes to desired locations in various environments, including air, argon glovebox, and ultrahigh vacuum, at elevated temperatures of up to 300°C. The elevated temperature during the fabrication process facilitates the removal of surface-absorbed contaminants from the 2D heterostructure interfaces. To showcase the merits of this polymer-free transfer technique, we successfully fabricated and assessed distinct heterostructures. In initial experiments, we achieved hBN/graphene/hBN heterostructures exhibiting remarkably bubble-free regions, accompanied by mobility values reaching $3 \times 10^6 \text{ cm}^2 \text{ V}^{-1} \text{ s}^{-1}$. Moreover, we demonstrated the fabrication of a more intricate LED structure with a bubble-free area $25 \times 30 \mu\text{m}$, completed within a mere 10-minute timeframe. Furthermore, a twisted monolayer/bilayer graphene on an hBN substrate displayed minimal variation in twist angles, with deviations of merely 0.016° over a length of 10 μm . Lastly, the SiN membrane method enables the large-scale transfer of 2D materials synthesized via chemical vapour deposition (CVD) from the growth substrate, devoid of any polymer involvement.

SESSION EL19.13: Poster Session V: 2D Materials—Characterization

Session Chairs: Sanjay Behura and Andrew Mannix

Wednesday Afternoon, November 29, 2023

Hynes, Level 1, Hall A

8:00 PM EL19.13.01

Twist Related Structure-Property Correlations in h-BN/SiC Heterostructures [Abhijit Biswas](#)¹, Rui Xu¹, Gustavo A. Alvarez², Jin Zhang³, Robert Vajtai¹, Hanyu Zhu¹, Zhiting Tian², Angel Rubio³ and Pulickel Ajayan¹; ¹Rice University, United States; ²Cornell University, United States; ³Max Planck Institute for the Structure and Dynamics of Matter and Center for Free-Electron Laser Science, Germany

Recently, "twistronics" in two-dimensional van der Waals (2D-vdW) materials and their heterostructures has become an emergent topic in materials science and condensed matter physics. Hitherto, ex-situ top-down mechanical stacking of individual monolayers of exfoliated single crystal 2D-vdW materials has been used for twistronics, which is technically challenging, non-trivial process, with the resultant interfacial impurity/contaminations. Therefore, future application of twistronics demands an alternative in-situ ultra-clean approach for the large-scale production of twisted nanomaterials.

Here we propose a simple and scalable alternative approach to investigate the twisted-interface-dependent properties in 2D-vdW nanomaterials. Two-dimensional hexagonal boron nitride (h-BN) thin films are grown directly on high in-plane lattice mismatched 3D silicon carbide (4H-SiC) substrate by using pulsed laser deposition (PLD), to explore possible twist-dependent structure-property correlations. In-depth investigations reveal that, concurrently, nanocrystalline h-BN exhibits unusually strong non-linear second-harmonic generation (SHG) and ultra-low cross-plane thermal conductivity. These properties are attributed to the inherent formation of twisted nano-domain edges between the 2D-vdW stacked h-BN nanocrystals with random in-plane orientations, exploited via their high in-plane lattice mismatch. Furthermore, first-principles time-dependent density functional theory (TDDFT) calculations reveal strong even-order optical non-linearity in twisted h-BN layers, supporting our observations.

Considering the uniqueness in growth and application-worthiness of h-BN, our work not only provides fundamental insights, but also demonstrates an alternate method for creating significant twisted-interface regions in directly deposited 2D nanocrystalline thin films (without the need of time-consuming, low-yield mechanical exfoliation processes with interfacial impurities), making it feasible to integrate the clean 2D twistronics into next-generation 3D materials devices.

[1] A. Biswas *et al.*, [arXiv:2304.12312](#).

8:00 PM EL19.13.02

Strain-Induced Stacking Order Change in Trilayer Graphene [Aditya Dey](#) and [Hesam Askari](#); University of Rochester, United States

The layer stacking order plays a crucial role in the physical properties of two-dimensional van der Waals heterostructures. In graphene, stackings have garnered significant attention due to their potential impact on future applications, as demonstrated by the recent discovery of superconductivity in twisted bilayer graphene. Trilayer graphene, with its Bernal (ABA) and rhombohedral (ABC) stackings, has recently emerged as an intriguing system. ABC-trilayer graphene (ABC-TLG) is particularly noteworthy due to its fascinating opto-electronic properties, including Mott insulator behavior, superconductivity, and ferromagnetism. However, achieving stable ABC stacking in trilayer graphene presents challenges due to its lower thermodynamic stability compared to the more prevalent ABA stacking. To address this, a novel approach utilizing strain engineering is proposed and the underlying interfacial mechanics driving this stacking order change are investigated. The results demonstrate that the transition from ABA to ABC-TLG can be achieved at a critical strain magnitude of 0.55%, resulting in a significant transformation of approximately 80% of the configuration from ABA to ABC stacking. The stability and preservation of the obtained ABC stacking are examined, revealing the resistance of the transformed ABC-TLG region to transition into other high-energy states. Overall, this comprehensive approach provides a robust and controllable method for achieving stable ABC domains in trilayer graphene. The findings open up possibilities for the development of advanced electronic and optoelectronic devices, further advancing our understanding of stackings in two-dimensional materials.

8:00 PM EL19.13.03

Interface Structure of Fe-Intercalated Graphene/SiC (0001) Revealed by Atomic-Resolution Electron Microscopy [Ryotaro Sakakibara](#)¹, Tomo-o Terasawa^{2,3} and Wataru Norimatsu⁴; ¹Nagoya University, Japan; ²Japan Atomic Energy Agency, Japan; ³The University of Tokyo, Japan; ⁴Waseda University, Japan

Thermal decomposition of SiC (0001) yields highly crystalline single-oriented graphene at the wafer scale [1]. There is a so-called buffer layer (BL) at the graphene/SiC interface, which is a reconstructed carbon layer on SiC (0001). It is possible to convert this BL to quasi-freestanding monolayer graphene by intercalation of a foreign element [2]. In this method, foreign atoms enter the BL/SiC interface to terminate the interfacial Si atoms, and the BL is decoupled from the substrate. The intercalated atoms are thus arranged in two-dimension and covered by graphene. The intercalation of the ferromagnetic element Fe can manifest intriguing physical properties such as perpendicular magnetic anisotropy and spin injection to graphene. Meanwhile, due to the affinity of Fe with Si and C, its intercalation is challenging. So far, several studies are reporting Fe intercalation in graphene/SiC [3]; however, the direct observation of its interface structure is missing. Here, we performed a uniform Fe intercalation and observed its interface structure at the atomic scale with cross-sectional transmission electron microscopy (TEM).

The uniform BL sample was prepared by annealing a single crystalline 4H-SiC (0001) substrate at 1500°C in an Ar atmosphere. Fe intercalation was carried out by vacuum deposition of Fe with a thickness of about 10 nm at room temperature, followed by annealing at around 660°C. The samples thus obtained were characterized by Raman spectroscopy ($\lambda=532 \text{ nm}$), X-ray photoemission spectroscopy (XPS, $h\nu=1486.6 \text{ eV}$), and TEM. The TEM observations were performed using a JEM-ARM200F-type microscope at an accelerating voltage of 200 kV. The thin specimen for TEM was prepared by the conventional Ar-ion thinning method.

From the Raman spectra of the sample, the BL was successfully converted to monolayer graphene. The Fe 2p spectrum of XPS suggests the presence of metallic Fe or Fe silicide on the sample surface, even after air exposure. A high-resolution TEM (HRTEM) observation of this sample revealed a layered contrast of graphene on the substrate surface. More importantly, uniform atomic layers of Fe were identified at the graphene/SiC interface by a high-angle annular dark field scanning TEM (HAADF-STEM) observation and energy dispersive X-ray spectroscopy (EDX) analysis. The number of these Fe layers was two to four over a wide range of observations. The interlayer distance between the first and second layers of Fe was $\sim 2.4 \text{ \AA}$. Such a structure has not been reported for Fe, Fe-oxide and Fe-silicide in their bulk form. In this Fe-intercalated graphene/SiC, modulation of the magnetic structure of Fe and spin injection to graphene can be expected.

- [1] W. Norimatsu and M. Kusunoki, *J. Phys. D: Appl. Phys.* **47**, (2014).
 [2] C. Riedl, *et al.*, *Phys. Rev. Lett.* **103**, 246804 (2009), N. Briggs, *et al.*, *Nat. Mater.* **19**, 637 (2020).
 [3] S. J. Sung, *et al.*, *Nanoscale* **6**, 3824 (2014), Z. Wang, *et al.*, *Appl. Phys. Lett.* **104**, 181604 (2014), M. V. Gomoyunova, *et al.*, *Phys. Solid State* **60**, 1439 (2018), K. Shen, *et al.*, *J. Phys. Chem. C* **122**, 21484 (2018).

8:00 PM EL19.13.04

Second-Harmonic Generation Imaging Microscopy with Ps Pulsed Lasers [Bita Rezaei](#), Volker Buschmann, Christian Oelsner and Maria Loidolt-Krueger; PicoQuant GmbH, Germany

Second harmonic generation (SHG) imaging microscopy is a nonlinear optical imaging technique that uses SHG as a contrast mechanism to produce high-resolution images. SHG occurs in materials with non-centrosymmetric crystal structures. Therefore, SHG imaging has been applied for characterization of 2D semiconductors, transition-metal dichalcogenides (TMDs) such as WS₂ and MoSe₂, lithium niobate crystals, PZT thin films, graphene, lanthanides, and even biological tissues. It provides information on the crystal lattice, assesses crystal quality and maps grain boundaries, defects, and mechanical strain. Furthermore, SHG imaging reveals the number of stacked layers as well as their orientation with respect to each other.

SHG imaging is commonly performed with a confocal laser scanning microscope using a high-power fs pulsed laser for excitation. In this study, we establish the use of high power ps pulsed lasers instead, with the aims of decreasing laser safety issues as well as reducing microscope complexity and cost. In addition, ps lasers offer high flexibility and tunability in terms of pulse duration, repetition rates, output power and external triggering.

We investigated two different 2D materials namely WSe₂ and MoS₂ on PDMS utilizing MicroTime 100 time-resolved confocal microscope. Reflection images and SHG images were acquired using a VisIR-1064 laser with 1064 nm wavelength, dimmed to laser class 3B and time-resolved photoluminescence (TRPL) images with 640 nm excitation.

The results set prove that ps pulsed lasers can replace fs lasers for SHG imaging. Moreover, the combination of ps lasers enables the collection of complementary datasets including reflection, SHG, TRPL and even two photon excitation (TPE) images collected from the same region of the sample using a single microscope setup. Thus, the optical properties of the materials can be characterized locally with several techniques to obtain a comprehensive understanding.

8:00 PM EL19.13.05

Imaging of Hyperbolic Plasmon-Phonon Polaritons in Twisted Double Bilayer Graphene [Anna Li](#)¹, William Wilson², Dania Haei² and Yue Luo²; ¹University of California, Berkeley, United States; ²Harvard University, United States

Complex van der Waals heterostructures can be assembled, layer-by-layer, via the deterministic transfer of selected two-dimensional layered materials. The transfer method used offers a significant degree of control and precision enabling assembly of new composite materials with engineered optical properties. Here, we have fabricated twisted double bilayer graphene using a new transfer system with far greater spatial resolution (20 nm) than the previous systems at Harvard. We transferred mechanically exfoliated graphene and hexagonal boron nitride (hBN) with this transfer system (which uses a polymer stamp consisting of Polydimethylsiloxane (PDMS) and polycarbonate (PC)) to form hBN encapsulated, twisted double bilayer graphene at very small (~0.03 degrees) twist angles. The top capping layers of hBN was between 5–10nm thick, as verified using atomic force microscopy, and the bottom layers ranged from 10–20nm thick. These stacks were subsequently imaged using scanning near field microscopy in the mid-infrared range to observe the interference fringes from the system's "mixed" hyperbolic plasmon-phonon polaritons. Excited with a tunable QCL laser, we were able to study the dispersion relation and propagation behavior of the hybridized polaritons in twisted double bilayer graphene.

8:00 PM EL19.13.06

Measurement of Thermoelectric Properties of Semimetallic Polycrystal PtSe₂ Film with Temperature Dependence [Jae Won Choi](#), No-Won Park, Gil-Sung Kim, Min-Sung Kang, Yunho Kim, Seungwon Yang and Sangkwon Lee; Chung-Ang University, Korea (the Republic of)

Hardness of measuring thermoelectric properties of nm-scale thickness thin film structure is one of the obstacles to research TMDC materials. We used a suspended bridge-type method and a strain gauge-controlled suspend platform to observe in-plane thermal conductivity and Seebeck coefficient of large-area platinum diselenide (PtSe₂) thin film. We found influence about thermoelectric properties difference with thickness and crystallinity changes. We observe the greatly suppressed in-plane thermal conductivity for 11-nm-thick polycrystalline PtSe₂ film as compared to that of exfoliated similar-thick in-plane single-crystalline PtSe₂ layer at 300 K. This reduction is attributed to the enhanced phonon scattering in polycrystalline PtSe₂ thin film. Our finding can pave the way toward an effective strategy for promising large-area TE energy harvesting devices with a high figure of merit in 2D semimetallic transition metal dichalcogenide materials.

8:00 PM EL19.13.07

Investigating the Trap-State Emission of CdTe Nanoplatelets [Tasnim Ahmed](#) and Justin R. Caram; University of California, Los Angeles, United States

Recently, two-dimensional II-VI semiconductor nanoplatelets (NPLs) have gained tremendous attention due to their exceptional photophysical properties including sharp emission spectra, tunable absorption and emission, large absorption cross section and giant oscillator strength etc. With the advancement of synthetic strategies, these NPLs now can be synthesized with controlled thickness even down to atomic precision. But while most of the progresses have been made with CdSe NPLs, the controlled synthesis of CdTe NPLs still remains challenging; even the detailed photophysics involving them remain unexplored. Here in this work we aim to synthesize CdTe NPLs with controlled thickness and decipher their carrier dynamics in single particle and ensemble level. With this aim we synthesized three monolayer NPLs which interestingly show a distinct excitonic emission and a broad emission band which can be related to trap states emission. The time resolved photoluminescence study reveal two distinct PL decay behavior when monitored at different probe wavelengths. The prolonged PL decay (>30ns) of the broad emission also suggests that it is related to trap emission. To dig deep into the mechanistic pathways of the photogenerated charge carriers, temperature dependent photoluminescence, single particle photoluminescence imaging and ultrafast pump-probe measurements are employed. Understanding the trap states nature will help us to find a key to manipulate them and these long lived trap states carriers can be utilized for their potential applications such as in photocatalysis.

8:00 PM EL19.13.08

Manipulating Charge Density Wave States in Lanthanum Tri-Telluride through Lithium Intercalation [Natalie Williams](#)¹, Shiyu Xu¹, Saif Siddique¹, Ratnadwip Singha², Judy Cha¹ and Leslie Schoop²; ¹Cornell University, United States; ²Princeton University, United States

The rare earth tri-tellurides belong to a group of two-dimensional (2D) materials that possess intriguing quantum characteristics, including magnetic ordering, superconductivity, spin-density waves, and charge density waves (CDWs).¹ These properties hold significant potential for controlling electronic phases, making them appealing for applications in electronics and spintronics with specific advantages in memory devices and supercapacitors.²

Lanthanum tri-telluride, where lanthanum is the first element in the rare-earth series, exhibits a unidirectional CDW along the c-axis at room temperature. Here, we modulate the CDW order of lanthanum tri-telluride by electrochemically intercalating lithium into the gaps of the exfoliated flakes of lanthanum tri-telluride. Lithium intercalation imparts strain and electron doping to the host material, inducing changes in materials properties and even phase transformations.^{3,4} We utilize in-situ Raman spectroscopy to investigate the structural alterations and CDWs of lanthanum tri-telluride flakes as consequence of lithium intercalation. These intercalation experiments hold the potential to uncover novel insights into the understanding of CDW states in rare earth tri-tellurides.

References

- [1] K. Yumigeta, Y. Qin, H. Li, M. Blei, Y. Attarde, C. Kopas, S. Tongay, *Adv. Sci.* **8**, 2004762 (2021).
 [2] Y. Xing, Y. Li, Z. Yang, Z. Wang, P. Yang, J. Ge, Y. Liu, Y. Liu, T. Luo, Y. Tang, and J. Wang, *Appl. Phys.* **128**, 073901 (2020).
 [3] M. Wang, A. Kumar, H. Dong, J. M. Woods, J. V. Pondick, S. Xu, D. J. Hynek, P. Guo, D. Y. Qiu, J. J. Cha., *Adv. Mater.* **34**, 2200861 (2022).
 [4] J. V. Pondick, S. Yazdani, A. Kumar, D. J. Hynek, J. L. Hart, M. Wang, D. Y. Qiu, J. J. Cha, *2D Mater.* **9**, 025009 (2022).

8:00 PM EL19.13.09

Tuning the Fermi Level of Graphene by Two-Dimensional Metals for Raman Enhancement [Na Zhang](#)¹, Kunyan Zhang^{2,3}, Wei Hu⁴, Rinu A. Maniyara¹, Timothy Bowen¹, Jonathon Schreengost¹, Arpit Jain¹, Da Zhou¹, Chengye Dong¹, Zhuohang Yu¹, He Liu¹, Noel Giebink¹, Joshua A. Robinson¹, Shengxi Huang⁵ and Mauricio Terrones^{1,1,1}; ¹The Pennsylvania State University, United States; ²Lawrence Berkeley National Laboratory, United States; ³University of California, Berkeley, United States; ⁴Qilu University of Technology, China; ⁵Rice University, United States

Graphene-enhanced Raman scattering (GERS) offers great opportunities to achieve optical sensing with high uniformity and superior molecular selectivity. The GERS mechanism relies on the charge transfer between molecules and graphene, which is difficult to precisely manipulate through varying the band alignment between graphene and molecules. In this work, we leveraged a few atomic layers of metal termed 2D metal to precisely and deterministically modify the graphene Fermi level. Using CuPc as a representative molecule, we demonstrated that the Fermi level tuning can significantly improve the enhancement and molecule selectivity of GERS. Specifically, aligning the Fermi level of graphene closer to the highest occupied molecular orbital (HOMO) of CuPc results in a more pronounced Raman enhancement. Density functional theory (DFT) calculations of the charge density distribution reproduce the enhanced charge transfer between CuPc molecules and graphene with a modulated Fermi level. Extending our investigation to other molecules such as Rhodamine 6G, Rhodamine B, crystal violet, and F_{16} CuPc, we showed that 2D metal-enabled Fermi level tuning can preferentially improve the GERS for molecules with better band alignment with graphene, contributing to an enhanced molecule selectivity. This underscores the potential of utilizing 2D metals for precise control and optimization of GERS applications, which will benefit the development of high sensitivity, specificity, and reliability sensors.

8:00 PM EL19.13.10

Structural Phase Patterning of MoS₂ Christopher A. Barns¹ and Scott Dietrich²; ¹West Chester University, United States; ²Villanova University, United States

Finding ways to protect our technology from intellectual theft has become increasingly needed in recent years. While most people think of technology security in terms of software, many neglect the need to bolster the protection of our hardware. With the U.S. pushing towards being a lead innovator in metal-oxide semiconductor field-effect transistors (MOSFETs), our innovations must have built-in protection to negate any chance of being stolen through reverse engineering. To aid this endeavor, we propose an alternative method of making MOSFETs by utilizing the structural phases of molybdenum di-sulfide (MoS₂). Using a 30kV electron beam at 500pA, we expose MoS₂ flakes mounted on an SiO₂ substrate to a variety of electron beam doses to create patterns of its 1T metallic phase surrounded by the rest of its 2H semiconductor phase. Through this method, di-material logic gates are possible which will substantially fortify device security as a result.

8:00 PM EL19.13.11

Spectrally-Resolved Polarization-Resolved Multiphoton Fluorescence and Second Harmonic Imaging in Low-Dimensional Materials Tolulope Ajuwon, Arik Ahmed and Steve Smith; South Dakota School of Mines and Technology, United States

Low-dimensional materials, especially two-dimensional (2D) materials, can have significantly enhanced nonlinear optical coefficients. In particular, the second-order nonlinear polarizability $\chi^{(2)}$, an important materials parameter for the generation of entangled photon pairs via parametric downconversion, can be notably enhanced in monolayer materials. The relationship between this nonlinear susceptibility and multi-layer stacking, orientation and material defects can be revealed by spectroscopic, polarization-resolved imaging. A spectrally-resolved multi-photon induced fluorescence (MPIF) and second harmonic generation (SHG) imaging system, based on a closed loop piezoelectric stage, a transmission grating and an EMCCD is used to examine the nonlinear optical properties of low-dimensional materials. From the spectrally-resolved multiphoton emission, we form ratiometric images of select spectral bands, reducing sensitivity to variations in intensity caused by scattering or attenuation of the excitation beam. We visualize the spectrally-resolved MPIF and SHG in the two-dimensional (2D) material WSe₂ and demonstrate the correlation between the symmetry-induced suppression of SHG for even-numbered layers, where inversion symmetry is established, and the presence of edge and localized defect states on the finite-sized 2D flakes, revealed by variations in the MPIF. The polarization-resolved SHG in the single and multi-layer 2D material identifies the symmetry and orientation of the layers. The application of the methods to determine $\chi^{(2)}$ in other low-dimensional materials is also described.

Acknowledgement: The authors acknowledge the MonArk NSF Quantum Foundry supported by the National Science Foundation Q-AMASE-i program under NSF award No. DMR-1906383

8:00 PM EL19.13.12

Multimodal Raman, Photoluminescence & SHG Imaging of 2D Materials Stuart Thomson; Edinburgh Instruments Ltd., United Kingdom

Transition metal dichalcogenides (TMDCs) are exciting next-generation 2D semiconductors with versatile layer-dependent optoelectronic properties. The spatial characterisation of lab-grown TMDCs is crucial to understanding their unique optoelectronic properties and optimising film growth conditions. In this work, we present a multimodal imaging platform that combines optical widefield, Raman, photoluminescence and second harmonic generation imaging for the characterisation of 2D materials.

The imaging platform was used to characterise CVD grown WSe₂ crystals. Using Raman imaging, the presence of both monolayer and multilayer WSe₂ could be identified through a change in the intensity and peak position of the E_{2g} / A_{1g} phonon modes. Photoluminescence imaging confirmed the presence of monolayer WSe₂ with exciton emission at 780 nm, and identified two distinct multilayer regions in the centre of the crystal through changes in the photoluminescence wavelength and intensity. Finally, second harmonic generation imaging with femtosecond laser excitation was used to obtain the relative layer orientation of the multilayer domains in the WSe₂ flake.

SESSION EL19.14: Poster Session VI: 2D Materials—New and Emerging Materials
Session Chairs: Sanjay Behura and Andrew Mannix
Wednesday Afternoon, November 29, 2023
Hynes, Level 1, Hall A

8:00 PM EL19.14.01

Exploring the use of Earth-Abundant Layered Materials in 2D-Based Studies: From Natural Mines to Van der Waals Applications Ingrid Barcelos¹, Raphaelade Oliveira¹, Yara Galvão Gobato², Raul Freitas¹, Helio Chacham³, Bernardo R. Neves³, Cristiano J. de Matos⁴ and Alisson R. Cadore⁵; ¹Brazilian Synchrotron Light Laboratory, Brazil; ²Universidade Federal de São Carlos, Brazil; ³Universidade Federal de Minas Gerais, Brazil; ⁴Universidade Presbiteriana Mackenzie, Brazil; ⁵Brazilian Nanotechnology National Laboratory (LNNano), Brazil

Phyllosilicates minerals are an emerging class of naturally occurring layered insulators with large bandgap energy that have gained considerable attention from the scientific community. This class of materials has been explored recently at the ultrathin two-dimensional level due to their specific mechanical and optoelectronic properties, which are crucial for engineering novel devices. Phyllosilicates have lamellar structures and can be embedded into van der Waals heterostructures (vdWHs) due to the possibility of exfoliation down to monolayers and easy handling. Here, we will present a high throughput characterization of some naturally occurring layered phyllosilicates by employing several experimental techniques, first-principles calculations, and will demonstrate that these layered materials can be mechanically exfoliated down to their monolayer limit and combined in the different vdWHs[1-5]. Due to these properties, phyllosilicates minerals can be considered as promising low-cost nanomaterials for electronics, photonics, and optoelectronics future 2D-based device applications. We will also present features of these nanomaterials that are relevant to their use in potential 2D-based applications, discussing the major challenges in working with them. Consequently, our results establish the basis of further studies tuning phyllosilicates properties to desired studies. Therefore, we expect our work to stimulate further exploration of layered phyllosilicate materials and provide the foundation for novel nanotechnological applications.

Acknowledgments:

Fundo Mackenzie de Pesquisa e Inovação (No. 221017), FAPEMIG, CAPES, CNPq, and FAPESP (No. 2020/04374-6).

References:

- [1] Barcelos I D, et. al., *J. Appl. Phys.* Accepted (2023)
- [2] de Oliveira R, et. al., *J. Opt. Soc. Am. A* 40, 153959 (2023)
- [3] Cadore A R, et. al., *2D Mater.* 9, 035007 (2022)
- [4] Longuinhos R*, Cadore A R*, et. al., *J. Phys. Chem. C*, 127, 5876 (2023)
- [5] de Oliveira R, et. al., *Appl. Surf. Sci.* 599, 153959 (2022)

8:00 PM EL19.14.02

Energy Harvesting using Few-Layer 2D Galena (galenene) R. Karthik¹, Appu Singh¹, P. R. Sreeram¹, Preeti L. Mahapatra¹, Douglas S. Galvao² and Chandra S. Tiwary¹; ¹Indian Institute of Technology, India; ²State University of Campinas, Brazil

Radiofrequency (RF) energy harvesting using 2D materials is receiving increased attention. In this work, we have demonstrated RF energy harvesting using 2D galena (galenene). Galenene was obtained from liquid exfoliation of bulk galena crystals (PbS), which is one of the naturally abundant metal chalcogenides, the primary ore of lead. Several characterization analyses, such as X-ray diffraction, atomic force microscopy, Raman spectroscopy, and XPS, were carried out to determine the physicochemical properties of the 2D galena structures. A galenene-based Schottky diode was fabricated, and the energy harvesting was demonstrated using a handheld radio transceiver with a carrier frequency of 140–170 MHz. The device extracts RF energy and produces an output DC voltage of a maximum of 1.8 volts and a corresponding output power of 38 mW at 150 MHz, and lights up an LED within a range of 100 cm. At 150 MHz, the device's power conversion efficiency was found to be 19%. DFT simulations were used to gain further insight into the galenene RF energy harvesting mechanism and support the experimental interpretations [1].

[1] R. Khartik, A. K. Singh, P. R. Sreeram, P. L. Mahapatra, D. S. Galvao, and C. S. Tiwary, *Nanoscale* 2023, 15, 9022.

8:00 PM EL19.14.03

Monolayer Amorphous Carbon as a 2D Barrier Ugur Karadeniz, Artem K. Grebenko, Zhang Hongji, Lucas M. Sassi, Alena A. Alekseeva, Chee-Tat Toh and Barbaros Oezylmaz; National University of Singapore, Singapore

Monolayer amorphous carbon (MAC) have emerged as a highly promising 2D material with exceptional properties. As the first amorphous 2D material, MAC possess a single atomic layer thickness and large area continuity over wafer scale. MAC can be synthesized conformally over a wide range of substrates at low temperatures (<300 °C). Its structure consists of complete in-plane sp² bonding and is free-standing at monolayer thickness. These unique attributes give MAC a range of properties that set it apart from its crystalline counterpart, graphene, and make it a compatible material for barrier applications.

This study presents research on the structural characterisation and barrier properties of atomically thin MAC films. By using laser-assisted chemical vapor deposition (LCVD), we successfully grew monolayer and multilayer MAC films, with precise control of the number of layers. By using Raman spectroscopy, X-ray photoelectron spectroscopy (XPS), and atomic resolution transmission electron microscopy (TEM), we show that MAC amorphous layered structure remains identical regardless of thickness. Multilayer MAC were found to be fully sp² bonded and lacked long-range order, exhibiting a distribution of 5-9-member carbon rings.

In our investigations, we explore the potential applications of MAC across various fields as a 2D barrier layer. The direct conformal growth of MAC onto the target substrate ensures defect-free, continuous coverage over large areas. Combined with the absence of reactive grain boundaries, this gives MAC films its exceptional chemical and mechanical stability despite their sub-nanometer thickness. The stability of MAC films is highly advantageous for barrier applications, where materials must remain structurally intact and free from degradation despite being sub-nanometer thick. We demonstrate the use of MAC films as ultrathin barrier films for copper interconnects in integrated circuits to impede metal ion diffusion. The findings of this study highlight the exceptional properties of atomically thin amorphous materials to overcome existing material bottlenecks. Together with its technologically relevant growth conditions, there is immense potential for enhancing device performance and addressing prevalent technological challenges.

8:00 PM EL19.14.04

Rational Design of Two-Dimensional Reduced Siloxene Metal-Free Semiconductor for Enhanced Photocatalytic Performance Nav Deepak, Shobha Shukla and Sumit Saxena; IIT Bombay, India

This study investigated the photocatalytic properties of Reduced siloxene nanosheets for the removal of organic pollutants from wastewater. Reduction of Siloxene resulted in a decreased band gap from 2.7 to 2.3 eV, allowing for better absorption of visible light, and quenched photoluminescence, indicating increased efficiency in the utilization of absorbed light energy for photocatalytic reactions. The catalytic activity of the Reduced siloxene nanosheets was examined through the degradation of Methylene Blue (MB), following a pseudo-second-order model, and exhibited an adsorption capacity of 9.6 mg/g for MB. The results demonstrate that reduced siloxene nanosheets have significant potential as an efficient and effective catalyst for removing organic pollutants from wastewater. The reduction process induced changes in the band gap and photoluminescence quenching that contributed to a 78% increase in catalytic activity compared to the pristine Siloxene material (53%).

8:00 PM EL19.14.05

Large Area Phase Selection in Silicene by Interface Engineering Daya Sagar Dhungana¹, Simona Achilli², Chiara Massetti³, Christian Martella¹, Carlo Grazianetti¹, Guido Fratresi² and Alessandro Molle¹; ¹Consiglio Nazionale delle Ricerche, Italy; ²Università degli Studi di Milano, Italy; ³Università degli Studi di Milano-Bicocca, Italy

The synthesis of two-dimensional (2D) silicene by direct growth on Ag(111) substrate is usually qualified by the formation of multiple phases and domains, posing severe constraints on the spatial charge conduction towards a technological transfer of silicene to electronic transport devices. Here we engineer the silicene/silver interface by two different schemes, namely through decoration with Sn atoms, forming a 2D Ag₂Sn surface alloy (surface decoration scheme), or through an epitaxially grown silicene-stanene heterostructure with stanene buffering the substrate (heterostructure scheme) [1]. Based on in situ low energy electron diffraction (LEED) we observe that phase selection is obtained via the two interface engineering schemes. In details, a 4×4 and √3×√3 single silicene phase are selectively stabilized in the surface decoration and heterostructure scheme, respectively. The two selected phases in both case separately, are well-distinguished by characteristic phase-sensitive Raman spectra taken after top encapsulation of silicene with a sequentially grown nanoscale Al₂O₃, and upon probing the surface by positional LEED and Raman scanning, they prove to be extended all over the whole growth area, namely on the cm² scale. Interface engineering by surface decoration also stabilizes the ordered growth of a √3×√3 phase in the multilayer range, featuring a single rotational domain instead of the multiple domain formation upon direct growth. Theoretical *ab initio* models are used to investigate low-buckled silicene phases (4×4 and a competing √13×√13 one) and various √3×√3 structures, supporting the experimental findings [2]. Interface engineering with the heterostructure scheme is also functional to design an all-around encapsulation of silicene, entailing the top and the bottom face of silicene [3]. This processing step is structurally preparatory to extract the silicene from its native Ag substrate with no occurring environmental degradation (e.g. oxidation). Stabilization of Ag-free silicene is explained in terms of the sacrificial role played by the bottom stanene layer. Based on close Raman spectroscopy monitoring, we are able to certify the endurance of the silicene in the monthly scale.

Interface engineering of silicene as reported in Ref. [2] provides new and promising technology routes to manipulate the silicene structure by controlled phase selection and single-crystal silicene growth on a wafer-scale, and enables us to develop an encapsulation scheme for the silicene preservation when its native Ag substrate is stripped off so as to create the condition for a full exploitation of silicene in durable operational devices like transistors and piezotransistors [4].

[1] D. S. Dhungana et al., *Adv. Funct. Mater.* (2021) 31, 2102797.

[2] S. Achilli et al., *Nanoscale* (2023) 15, 11005.

[3] D. S. Dhungana, et al., *Nanoscale Horiz.* (2023), doi: 10.1039/D3NH00309D.

[4] L. Tao, et al., *Nature Nanotech.* (2015) 10, 227; C. Martella et al., *Adv. Mater.* (2023), doi: 10.1002/adma.202211419.

SESSION EL19.15: Poster Session VII: 2D Materials—Vapor-Phase Growth

Session Chair: Sanjay Behura

Wednesday Afternoon, November 29, 2023

Hynes, Level 1, Hall A

8:00 PM EL19.15.01

Growth of Hexagonal Boron Nitride (h-BN) Films under Low Pressure by Chemical Vapor Deposition (CVD) Thais C. de Carvalho, Neileth Johanna S. Figueroa, Cesar Augusto D. Mendoza and Marcelo Eduardo H. Maia da Costa; Pontificia Universidade Catolica Do Rio De Janeiro, Brazil

Hexagonal Boron Nitride (h-BN) is a two-dimensional (2D) material that shares structural similarities with graphene. However, unlike graphene, h-BN consists of a honeycomb lattice with alternating B and N atoms. It possesses the distinction of being the thinnest insulating material, exhibiting an electrical bandgap of 5.9 eV. Atomically thin h-BN films are crucial for the development of emerging applications involving 2D devices based on Van der Waals heterostructures. These films exhibit desirable properties, including high thermal stability, chemical inertness, and mechanical flexibility, enabling their utilization in diverse applications such as serving as a dielectric substrate for transistors, flexible nanoelectronics, and nano-capacitors.

However, the production of large-area, high-quality monocrystalline h-BN using the chemical vapor deposition (CVD) method remains a significant challenge. The current study focuses on the synthesis of h-BN layers by employing the CVD method under low pressure, utilizing ammonia borane (AB) as a precursor to be deposited on Si (100) substrates. The objective is to overcome the existing obstacles and advance the fabrication of large-area, high-quality monocrystalline h-BN. Throughout the growth process, the precursor, ammonia borane (AB), was maintained at a temperature of approximately 95°C. Meanwhile, the substrate, in this case, was maintained at a much higher temperature of 1100°C. The gas atmosphere used during this process was a mixture of H₂ (flow of 2 sccm, standard cubic centimeters per minute) and Ar (100 sccm flow). The h-BN films undergo characterization using various spectroscopic techniques, including Raman spectroscopy, Atomic force microscopy (AFM), UV-visible spectroscopy, and X-ray photoelectron spectroscopy (XPS). The measured B:N ratio of the h-BN films obtained

in this study aligns well with the theoretical stoichiometric values of 1:1. The optical band gap of the hBN films grown on silicon substrate was determined to be 4.8 eV. Raman spectroscopy measurements were carried out and exhibited a peak at 1375 cm^{-1} , characteristic of the monolayer h-BN and corresponding to the E_{2g} vibration mode. The results showed that we were successful in the synthesis of h-BN films.

8:00 PM EL19.15.02

Synthesis and Properties of Atomically-Thin Width-Controlled TMD Quantum Nanoribbons Xufan Li¹, Samuel Wyss², Baichang Li³, Emanuil Yanev³, Yang Liu³, Yongwen Sun⁴, Zhiying Wang³, Matthew C. Strassburg², Raymond R. Unocic³, Yang Yang⁴, James Hone³, Nicholas J. Borys², P. James Schuck³ and Avetik R. Harutyunyan¹; ¹Honda Research Institute USA Inc., United States; ²Montana State University, United States; ³Columbia University, United States; ⁴The Pennsylvania State University, United States; ⁵Oak Ridge National Laboratory, United States

Width confinement and effect of edge structure add new freedoms for exploring exotic properties for already rich atomically-thin materials. Unique properties have already been discovered in graphene nanoribbons with width less than 5 nm. However, for transition metal dichalcogenides (TMDs), the effects by width confinement and edge structure have only been predicted in theoretical calculation due to challenges in synthetic methods to obtain nanoribbons with width less than ~30 nm. We develop a synthetic strategy to directly grow TMD nanoribbons with controllable width (down to sub-10 nm) and layers (single or double layer), from the pre-deposited seed nanoparticles. Width-dependent Coulomb blockade oscillation in the electron transfer behavior in the nanoribbons suggests formation of quantum-dot-like electronic states due to width confinement. Furthermore, combination of width confinement with strain engineering through sharp bending generates highly localized states in TMD nanoribbons, which is responsible for high purity, deterministic single photon emissions. The TMD nanoribbons add a new family of materials to the reservoir for future quantum electronics and photonics.

References

X. Li., et al. *ACS Nano* **14**, 6570 (2020).
X. Li., et al. *Sci. Adv.* **7** (50), eabk1892 (2021).

8:00 PM EL19.15.03

Room-Temperature Direct Growth of Wafer-Scale Transition Metal Dichalcogenide Films via Remote Plasma-Assisted Chemical Vapor Deposition Jina Lee, Soo Ho Choi, Seok Joonyun and Ki Kang Kim; Sungkyunkwan University, Korea (the Republic of)

Transition metal dichalcogenides (TMDs) offer potential solutions to address the challenges associated with silicon technology. To enable large-scale TMD film growth, chemical vapor deposition (CVD) techniques have been extensively studied. However, the transfer process required for device fabrication often degrades individual device performance and overall wafer reliability. In this work, we present a low-temperature, direct growth approach for TMDs using remote plasma-assisted chemical vapor deposition.

By employing hydrogen plasma, reactive precursor radicals are generated, enabling the growth of TMD films at temperatures as low as ~300°C. The thickness of wafer-scale TMD films can be easily controlled by adjusting the growth time. The direct growth of TMD films eliminates the need for transfer processes, preserving their uniform quality across the entire region, which is crucial for maintaining device performance.

Additionally, we demonstrate the successful growth of TMD films directly on high-k dielectric films such as Al₂O₃. This achievement opens up new possibilities for integrating TMDs with high-k materials, offering potential advantages for future device applications.

Overall, this work presents a low-temperature, direct growth method for TMDs using remote plasma-assisted chemical vapor deposition. The elimination of transfer processes and the ability to grow TMD films on high-k dielectric films contribute to improved device fabrication processes and enhanced device performance. This research lays the foundation for the scalable production of TMD-based devices, paving the way for the integration of TMDs into advanced electronic technologies.

8:00 PM EL19.15.04

On the Structural and Morphological of Graphene Layers Grown on Pt/Ti/SiO₂ by Hot Filament Chemical Vapor Deposition Angela Luis Matos¹, Tej B. Limbu², Ivan Castillo¹, Balram Tripathi¹, Brad Weiner³ and Gerardo Morell¹; ¹University of Puerto Rico at Río Piedras, Puerto Rico; ²University of Houston-Clear Lake, United States; ³University of Puerto Rico-Rio Piedras, Puerto Rico

Herein, we report large area single and bilayer graphene growth on Pt/Ti/SiO₂ substrate by hot filament chemical vapor deposition (HFCVD) with and without the assistance of Cu foil. The quality and the number of graphene layers deposited on the substrate were assessed by Raman spectroscopy, and X-rays photoelectron spectroscopy (XPS) analysis. Atomic force microscopy (AFM) was used for assessing the surface topography of the graphene films grown on the Pt/Ti/SiO₂ substrates. The microstructure and elemental analysis have been performed by Scanning electron microscopy (SEM), and Energy dispersive spectroscopy (EDS). Our results show that bilayer layer graphene growth is facilitated by the presence of a copper foil placed nearby Pt/Ti/SiO₂ substrate, or by a relatively high filament temperature in the HFCVD reactor. Monolayer graphene grows only when no copper foil was placed nearby the Pt/Ti/SiO₂ substrate at a low filament temperature. Our approach paves a novel pathway towards the layer-controlled growth of graphene on Pt/Ti/SiO₂ substrate by HFCVD reactor for frontier applications.

8:00 PM EL19.15.05

Low Pressure Chemical Vapor Deposition of 1T-TaS₂ Films on Sapphire for Controllable Charge Density Wave Phase Transitions Nicholas D. Redwing¹, Nicholas Trainor¹, Gabriel Martinez², Daniela R. Radu² and Joan M. Redwing¹; ¹The Pennsylvania State University, United States; ²Florida International University, United States

Metallic two-dimensional (2D) transition metal dichalcogenides such as TaS₂ can host charge density waves (CDWs), periodic modulations of electron density that arise in systems with strong electron-phonon coupling. CDWs can break crystal symmetry, mediate metal-insulator phase transitions and coexist with superconductivity. Furthermore, transitions between CDW phases can be tuned via strain, electric fields, etc. which can potentially be exploited for devices. Crystal disorder can inhibit CDWs, consequently, studies are typically carried out utilizing single crystal flakes exfoliated from bulk TMD crystals. Techniques to deposit large area, high crystal quality TaS₂ films are therefore needed to advance the field toward practical applications.

In this study, we report the synthesis and characterization of 1T-TaS₂ films on c-plane sapphire using low pressure chemical vapor deposition (LPCVD). The growths were carried out at 100 Torr in a horizontal hot wall CVD reactor using TaCl₅ and sulfur powder as sources in a 5% H₂/Ar carrier gas mixture. The sulfur powder was placed upstream of the substrate in the quartz tube and was maintained at 150 °C. The TaCl₅ powder was contained within a stainless steel bubbler external to the reactor that was heated to 80 °C and maintained at a pressure of 110 Torr. The TaCl₅ was transported to the reactor by passing the H₂/Ar carrier gas at a flow rate of 100 sccm through the bubbler and was introduced downstream of the sulfur boat in the reactor via a separate quartz injector tube. The effects of reactor temperature, gas flow rates and reactor pressure on the uniformity, deposition rate and properties of the films were investigated. Temperatures greater than ~800 °C and low reactor pressures (100 Torr) were required to decompose the TaCl₅ via reaction with H₂ and minimize pre-reactions upstream of the substrate. AFM, Raman spectroscopy and X-ray photoelectron spectroscopy were used to characterize the films after growth. The Raman spectrum of films grown at 900 °C and 100 Torr and cooled rapidly after growth exhibited Raman modes at ~90, ~240 and ~380 cm⁻¹, consistent with the 1T phase of TaS₂. Variable temperature Raman measurements are underway to investigate CDW phase transitions in the films.

8:00 PM EL19.15.06

Epitaxial Monolayer Growth of 2D ReS₂ via MOCVD Heewon Park^{1,2}, Yeon-Jeong Jang^{1,2} and Moon-Ho Jo^{1,2}; ¹IBS, Korea (the Republic of); ²POSTECH, Korea (the Republic of)

We report monolayer growth of epitaxial van der Waals semiconductor ReS₂ on sapphire substrate. ReS₂, a member of transition metal dichalcogenide (TMDC), exhibits unique 1T' structure with large anisotropy. Metal-organic chemical vapor deposition (MOCVD) enables the synthesis of atomically thin semiconductor by precisely controlling vapor pressure. ReS₂ film and crystal could be obtained on sapphire substrate depending on the growth condition. Growth parameters such as temperature, pressure, and precursor supply affect the result of MOCVD growth. Material characterizations including Raman spectroscopy, atomic force microscopy (AFM), and x-ray photoelectron spectroscopy (XPS) were conducted to verify the quality of film and triangular crystals. Also, field effect transistors were fabricated to assess the mobility of polycrystalline ReS₂ film. We discuss polycrystalline nature of ReS₂ grown on insulating substrate due to its low in-plane symmetry and weak interlayer coupling between layers.

8:00 PM EL19.15.07

Growth of Superconducting Sr₂RuO₄ Thin Films via Thermal Laser Epitaxy Brendan D. Faeth¹, Varun Harbola¹, Lena Majer¹, Hans Boschker², Felix Hensling¹, Wolfgang Braun^{1,2} and Jochen Mannhart¹; ¹Max Planck Institute for Solid State Research, Germany; ²Epiray GmbH, Germany

Thermal laser epitaxy (TLE) is a novel technique for thin film deposition which employs continuous wave lasers to simultaneously heat both the substrate and elemental sources. This laser heating approach allows for evaporation or sublimation of nearly all elements from the periodic table, ultrahigh substrate temperatures exceeding 2000 C, and broad compatibility with process gases at a wide range of pressures from UHV up to 1 Torr, among other benefits. As a result, TLE dramatically expands the parameter space available for thin film synthesis compared to existing epitaxy techniques. However, to date it has proven experimentally challenging to achieve simultaneous control of multiple laser based elemental sources with the flux stability and

systematic fidelity necessary for the growth of ternary or multinary systems of interest such as complex oxides.

In order to establish the capabilities of TLE for the growth of such complex materials, we demonstrate here the successful epitaxial synthesis of several Ruddlesden-Popper phases of the Sr-Ru-O ternary oxide system via TLE. Near instant thermalization of both source elements and substrates from laser heating allows the process of thermodynamic phase control to be achieved rapidly during film deposition without the need for physical shuttering of sources. Additionally, we find that the “n=1” phase Sr₂RuO₄ can be reliably synthesized at substrate temperatures in excess of 1200 C and in a background environment of pure molecular oxygen, within an adsorption-controlled growth window that is inaccessible to conventional MBE approaches. We show that Sr₂RuO₄ films grown under these conditions demonstrate extremely high structural, electronic, and chemical quality, as evidenced by the appearance of superconductivity at relatively high critical temperatures. A detailed accounting of the experimental approach, growth thermodynamics and film characterization will be discussed.

This work not only demonstrates the feasibility of TLE for the synthesis of high-quality complex oxide thin films, but also suggests new routes to achieving thin film growth in other materials systems that remain as-yet inaccessible to conventional epitaxy techniques.

8:00 PM EL19.15.08

Barium Titanate Thin Film Remote Epitaxy using Graphene Temazulu S. Zulu, Larissa Little and Julia Mundy; Harvard University, United States

Barium titanate (BTO) thin films present exciting opportunities for use in photonics due to their high refractive index (~ 2.4) and wide bandgap (> 3 eV). We can integrate these films onto silicon to make scalable and efficient optical devices. In order to integrate the films onto silicon, we use remote Molecular Beam Epitaxy (MBE). In our process, we grow BTO films on a strontium titanate (STO) substrate with a graphene intermediate layer and then transfer the BTO films onto a silicon substrate. We first transfer graphene onto an STO substrate, then grow the BTO directly on the graphene layer. The weak Van Der Waals bond between graphene and the BTO thin film allows us to remove the film from the substrate and transfer it to a silicon substrate. We propose this as an alternative to growing directly on silicon using an oxide layer, which requires careful control of oxygen pressure to maintain epitaxial growth. Our method allows the barium titanate to grow in a single epitaxial orientation since we have a nearly lattice matched oxide substrate, and allows us to reuse the substrates. We propose that this could be a potentially straightforward, scalable, and efficient method for the nanofabrication of integrated barium titanate films on silicon.

8:00 PM EL19.15.09

Controllable Growth of Large Area P-Type MoS₂ with Transition Metal Doping using Confined Space CVD Muhammad Suleman, Minwook Kim, Hyun-min Park and Yongho Seo; Sejong University, Korea (the Republic of)

2D Molybdenum Disulfide (MoS₂) has been used extensively as a semiconductor in recent years. Typically, MoS₂ demonstrates an N-Type Behavior as there are sulfur vacancies that are present in the material. However, the large-scale synthesis of P-Type MoS₂ and other 2D materials can still be challenging. Various methods can be used for doping the pristine MoS₂ to provide P-Type behavior and one of these methods is substitutional doping. Group VB Transition metals like Niobium (Nb), Vanadium (V) and Tantalum (Ta) can be used to achieve substitutional doping into the MoS₂ crystal lattice. In this work we have achieved P-Type behavior in CVD grown monolayer MoS₂ through a similar method. Moreover, the existence of doping atoms was confirmed by using XPS (X-ray photoelectron spectroscopy), EDX (Energy dispersive X-ray) and TEM (Transmission Electron Microscopy). The fabricated back gate FETs also confirm the behavior as a P-Type material. This proposed method for the synthesis of P-Type MoS₂ can have a lot of potential applications ranging from photodiodes, photodetectors, optoelectronics, field effect transistors, synaptic transistors, advanced materials heterostructures and energy harvesting.

8:00 PM EL19.15.10

Promoting Growth of Two-Dimensional Semiconductors by Preloaded Precursors Minsu Kim¹, Minkyun Son², Ki-Seok An² and Soonmin Yim²; ¹Kyonggi University, Korea (the Republic of); ²Korea Research Institute of Chemical Technology, Korea (the Republic of)

The recent implementation of alkali metal halide catalysts in the context of chemical vapor deposition (CVD) for synthesizing transition metal dichalcogenides (TMDs) has facilitated impressive growth of two-dimensional (2D) TMDs. However, there remains a need for further investigation into process development and growth mechanisms in order to amplify the impact of catalysts and comprehend the underlying principles. In this regard, a novel approach is proposed that involving the concurrent introduction of a metal source (MoO₃) and a salt (NaCl) through thermal evaporation. This technique yields notable growth behaviors, including enhanced 2D growth, regional selective growth, and expanded possibilities for diverse target materials. Employing a combination of sequential spectroscopy and morphological analyses, a comprehensive reaction pathway for MoS₂ growth is unveiled. Within this pathway, NaCl and MoO₃ react independently to generate intermediate compounds; Na₂SO₄ and Na₂Mo₂O₇. These intermediates play a crucial role in creating a conducive environment for 2D growth, characterized by augmented source availability and a liquid medium. Subsequently, through a self-assembly process, minute equilateral triangular grains amalgamate atop the liquid intermediates, culminating in the formation of substantial monolayer MoS₂ grains. This investigation is poised to become a fundamental point of reference, offering insights into the principles underpinning salt catalysis and the evolution of CVD techniques for producing 2D TMDs.

8:00 PM EL19.15.11

Direct Synthesis of Twisted WSe₂ Multilayers by B₂O₃-Assisted Chemical Vapor Deposition Jinwoo Kim and Gwan-Hyoung Lee; Seoul National University, Korea (the Republic of)

Moiré superlattices of stacked 2D layers have attracted a great attention, offering a unique platform for investigation of unprecedented quantum phenomena, such as superconductivity in twisted graphene bilayer and moiré excitons in twisted transition metal dichalcogenides (TMDs) bilayers. However, fabrication of twisted TMD bilayers still relies on a manual transfer process, which probably contaminates the interface of stacked layers and makes it difficult to precisely control the twist angle. Here, we present a direct synthesis method of twisted WSe₂ bilayers using chemical vapor deposition. We mixed small amount of B₂O₃ with the source materials to promote growth of WSe₂. In contrast to the WSe₂ grains produced by conventional CVD process, the WSe₂ grains grown in this work show the overlapping of neighboring grains, forming twist bilayer regions with various twist angles. Low-frequency Raman spectra of the twisted WSe₂ bilayers clearly shows the twist-angle-dependent layer breathing mode (LBM) and B_{2g} mode, indicating that the twisted bilayers have atomically clean van der Waals interface and no contamination. Our work shows a way to directly synthesize a large number of the twisted bilayers with different twist angles and provides a platform to investigate the twist-angle-dependent electrical and optical properties of the twisted bilayers.

8:00 PM EL19.15.12

Van der Waals Epitaxially-Grown Molecular Crystal Dielectric α -Sb₂O₃ for 2D Electronics Hyunjun Kim¹, Huijie Ryu² and Gwan-Hyoung Lee¹; ¹Seoul National University, Korea (the Republic of); ²Samsung Advanced Institute of Technology, Korea (the Republic of)

In the forefront of nanoelectronics, two-dimensional (2D) materials have garnered substantial attention as prospective channel materials. This is due to their surface properties featuring free-dangling bonds, along with their exceptional mobility and the capacity for precise gate control at the atomic layer level. Nevertheless, the advancement of 2D electronics faces a hurdle in creating a seamless van der Waals interface, particularly in the direct growth of a high-k dielectric with a high degree of crystallinity on a 2D channel material. Here, we report van der Waals epitaxial growth of the molecular crystal dielectric α -Sb₂O₃ on graphene. The α -Sb₂O₃ nanosheets show a high breakdown field of 18.6 MV/cm for bilayers of 1.3 nm and decrease of the breakdown field with increasing thickness. We achieved equivalent oxide thickness (EOT) of 0.77 nm for 3L-Sb₂O₃ and as low leakage current as the DRAM limit of 1×10⁻⁷ A/cm² at a gate voltage of 1 V. The epitaxially grown Sb₂O₃ on graphene has two dominant orientation so that two types of grain boundaries (GB) with orientation angles of 0° and 60° are generated between aligned grains. The 0°-GB with well-stitched boundary shows higher electrical and thermal stabilities than 60°-GB with disordered boundary. Our work shows a method to epitaxially grow the molecular crystals on 2D materials and a great potential of molecular crystals for van der Waals dielectric in 2D electronics.

SESSION EL19.16: Applications of Wafer-Scale 2D Materials—Photonics

Session Chairs: Sanjay Behura and Hyeon Jin Shin

Thursday Morning, November 30, 2023

Hynes, Level 3, Room 309

8:30 AM *EL19.16.01

Harnessing Exciton Dynamics for Tunable Polarization Conversion and Switchable Polarized Narrowband Emission Samuel K. Seah¹, Souvik Biswas¹, Joeson Wong¹, Hamidreza Akbari¹, Supavit Pokawanvit², Wei-Chang David Yang³, Huairuo Zhang³, Claudio U. Hail¹, Meir Grajower¹, Kenji Watanabe⁴, Takashi Taniguchi⁴, Felipe Jornada², Albert Davydov³ and Harry A. Atwater¹; ¹California Institute of Technology, United States; ²Stanford University, United States; ³National Institute of Standards and Technology, United States; ⁴National Institute of Materials Science, Japan

Light-matter interactions in anisotropic layered and two-dimensional semiconductors such as black phosphorus enables exploration of novel optical confinement phenomena at the atomic scale. Active polarization control, which has diverse applications in optical imaging, sensing, and computing, arises from the electrically tuneable crystalline anisotropy of black phosphorus (BP) which creates a mechanism for polarization modulation. I will discuss metasurfaces combined with van der Waals heterostructures incorporating twisted BP layers which open up further degrees of freedom in polarization conversion, and increases the polarization state tuning range to nearly half the Poincaré sphere. In other recent work, we discovered that certain edges of monolayer black phosphorus act as sites for localization and quantum confinement of quasi-1D excitons, resulting in discrete edge excitonic spectral emission lines with a nearly 10x reduction in linewidth relative to the surrounding 2D bulk. Integration of edge excitons into a gate-tunable heterostructure revealed a highly symmetric gate-dependence, enabling voltage-controlled turn-on/turn-off of polarized radiative emission.

9:00 AM EL19.16.02

Tunable Interlayer Excitons in Organic-Inorganic Van der Waals Heterostructures Aurelie Champagne^{1,2}, Olugbenga Adeniran³, Tomojit Chowdhury⁴, Mengyu Gao⁴, Jiwoong Park⁴, Zhenfei Liu³ and Jeffrey B. Neaton^{1,2,5}; ¹Lawrence Berkeley National Laboratory, United States; ²University of California, Berkeley, United States; ³Wayne State University, United States; ⁴The University of Chicago, United States; ⁵Kavli Energy NanoScience Institute, United States

Interfacing transition metal dichalcogenides (TMDs) into van der Waals heterostructure bilayers with type-II level alignment has led to recent reports of interlayer excitons with large binding energies, long lifetimes, and signatures of exciton condensation at elevated temperatures [1–4]. Atomically flat two-dimensional molecular crystals (MC) on TMD monolayers is an emerging interfacial quantum materials platform with tunable level alignment, exciton binding energies, and photoluminescence, given the heightened sensitivity of the organic layers to their environment [5]. In addition to non-local adsorbate/substrate screening, free charge carrier screening is particularly relevant in MC-TMD bilayer heterostructures, and controllably altering these distinct modes of screening can lead to new phenomena. Using a dielectric embedding ab initio GW plus Bethe-Salpeter equation (GW-BSE) approach [6], we compute energy level alignment as well as neutral excitations at MC-TMD interfaces (MC = PDI or PTCDA; TMD = MoS₂ or WS₂), exploring new emergent optical transitions, such as those associated with interlayer excitons characterized by electrons and holes separated between the MC adsorbate and the TMD, respectively. Combining the GW-BSE approach with a new model we have developed that reduces computational cost with no loss of accuracy [7], we further explore how the presence of free charge carriers can screen the electron-hole interactions and modify the quasiparticle energy level alignment and interlayer excitons.

This work is supported by the Center for Computational Study of Excited-state Phenomena in Energy Materials (C2SEP) and the Theory of Materials FWP at LBNL, funded by the US Department of Energy (DOE) under contract No. DE-AC02-05CH11231. Computational resources are provided by the National Energy Research Scientific Computing Center (NERSC).

[1] Fogler et al., Nat. Commun. 5, 4555 (2014); [2] Wilson et al., Nature 599, 383 (2021); [3] Rivera et al., Nat. Nanotechnol. 13, 1004 (2018); [4] Barré et al., Science 376, 406 (2022); [5] Ulman and Quek, Nano Lett. 21, 8888 (2021); [6] Liu et al., J. Chem. Theory Comput. 15, 4218 (2019); [7] Champagne et al., Nano Lett. 23, 4274 (2023).

9:15 AM EL19.16.03

Extremely Anisotropic Few-Atom-Thick Organic-Inorganic Bilayers with Wafer-Scale Uniformity Tomojit Chowdhury¹, Fauzia Mujid¹, Aurelie Champagne², CeLiang¹, Patrick Knüppel³, Nathan Guisinger⁴, Jeffrey B. Neaton², Kin Fai Mak³ and Jiwoong Park¹; ¹University of Chicago, United States; ²Lawrence Berkeley National Laboratory, United States; ³Cornell University, United States; ⁴Argonne National Laboratory, United States

Thin films featuring extreme optical anisotropy are an ideal platform that enables efficient light sensing, harvesting, and display functionalities. However, realizing large-scale thin films with controllable and predictable optical anisotropy remains a major challenge due to two formidable experimental hurdles. First, the non-triviality of producing high-quality large area thin films while preserving their global anisotropic response. Second, the lack of direct experimental evidence linking the films' structures and their anisotropic properties. In this talk, we introduce large-scale and highly crystalline few-atom-thick organic-inorganic bilayers (BL) comprising single-layer two-dimensional molecular crystals (2DMC) atop transition metal dichalcogenide (TMD) monolayers. By leveraging the design flexibility in non-covalent molecular crystals, we grow diverse BLs that exhibit fully deterministic linear dichroism, which is tunable within a 50% range as we vary the 2DMC structures. Through comprehensive optical and high-resolution scanning probe microscopies and analyses, we establish a direct correlation between the molecular unit cells' structures and the observed optical anisotropy. Intriguingly, temperature-dependent polarized optical imaging and spectroscopy unveil the existence of a highly anisotropic excitonic species in the BL, which is distinct from both the pristine molecular and TMD excitons, even under the substantial dielectric screening by the TMD monolayer. To gain insights into the nature of this anomalous excitonic species, we employ ab initio GW Bethe-Salpeter equation (BSE) calculations, which reveal a strong correlation between the electrons and the holes within the BL. This correlation gives rise to an anisotropic and significantly delocalized Wannier-like interlayer exciton that exhibits high sensitivity to the structure and composition of the 2DMC. These results underscore the potential of our organic-inorganic BL as an excitonically rich platform enabling the discovery of novel light-matter interactions beyond the confines of traditional covalent 2D materials. We will conclude this talk with an outlook on the prospects of creating exotic hybrid 2D systems, that includes the molecular analogue of the moiré superlattice.

9:30 AM BREAK

10:00 AM EL19.16.04

Interfacial Optical Sensing of Ferroelectricity in Freestanding Perovskite Oxides with Monolayer WSe₂ Jaehong Choi¹, Kevin Crust², Lizhong Li¹, Jae Pil So¹, Kenji Watanabe³, Takashi Taniguchi³, Harold Y. Hwang², Jie Shan¹, Kin Fai Mak¹ and Gregory Fuchs¹; ¹Cornell University, United States; ²Stanford University, United States; ³National Institute for Materials Science, Japan

Two-dimensional (2D) transition-metal dichalcogenides (TMDs) can be easily integrated with other functional materials such as ferroelectric materials due to their lack of dangling bonds. Also, owing to their atomic thickness, electronic and photoluminescence (PL) properties of 2D TMDs can be modulated by external perturbations, which opens new avenues for quantum sensing and tunable optoelectronic devices. In this work, we integrate monolayer WSe₂ with a free-standing BaTiO₃ (BTO) membrane and studied the ferroelectricity induced PL modulation in WSe₂. Perovskite oxide BTO has strong spontaneous polarization and moderate coercive field, but their epitaxial mother substrates often limit the range of device structures. Recent studies showed that BTO can be separated from its substrate by using a sacrificial oxide layer. By using this method, BTO is released from the substrate and transferred to a Si-based substrate. We pick up BTO membranes with an appropriate size by using a stamping method and fabricate a field effect device where the BTO polarization can be switched and sensed simultaneously with monolayer WSe₂ in-situ. We observe that the relative density of charge carriers in changes as the polarization switches, and this gives rise to the PL intensity modulation. The relative emission intensity of neutral excitons and trions show gate dependent hysteresis, which confirms that WSe₂ senses and optically reads out the ferroelectricity in BTO.

This work is supported by AFOSR MURI (FA9550-18-1-0480).

10:15 AM EL19.16.05

Revealing Photophysical Properties of 2D BA₂MAPb₂I₇/MoS₂ Type-II Heterostructures Alp Yilmaz¹, F. Gonca Aras¹ and Aydan Yeltek^{1,2}; ¹TOBB University of Economics and Technology, Turkey; ²UNAM – Institute of National Nanotechnology Research Center, Bilkent University, Turkey

Optoelectronic devices based on type-II heterojunction semiconductors have great potential to provide high-performance characteristics due to their superior charge separation capabilities[1]. Various type-II heterostructures have been studied to date by using different semiconductor materials[2,3], among which 2D organometal halide perovskite single crystals (OHPSCs) have recently gained intensive interest owing to their significant properties such as high absorption coefficient, adjustable bandgap, and high charge carrier mobility[4]. Single-layer transition metal dichalcogenides (TMDs) have been also used in optoelectronics due to their high carrier mobility, direct bandgap, flexible structural properties, and high stability[5]. However, by including two promising candidates of these material categories, the photophysical properties of BA₂MAPb₂I₇/monolayer-MoS₂ type-II heterostructure have not been studied yet. Herein, we studied the optical properties of BA₂MAPb₂I₇/monolayer-MoS₂ heterostructures for the first time. Detailed investigations were carried out using μ -PL and μ -Raman spectroscopies along with various other characterization techniques. 2D OHPSCs were synthesized via the solution temperature lowering method and 2D OHPSCs of different thicknesses, from atomic to multilayer thicknesses, were produced using the mechanical exfoliation method. Furthermore, the large-area continuous monolayer MoS₂ film was synthesized via the chemical vapor deposition method with a glass-assisted approach for the first time. PDMS-based dry-transfer method was used to produce the BA₂MAPb₂I₇/MoS₂ heterostructures. When excitation was performed with a 532-nm laser source, the PL intensities of both the MoS₂ and OHPSCs decreased compared to those of the bare materials due to type-II band alignment in the heterojunction region. We also report that the photophysical properties of the BA₂MAPb₂I₇/monolayer-MoS₂ type-II heterostructures are able to be controlled depending on the 2D OHPSC layer thickness. The fundamental insight is provided for the heterojunction materials investigated in this study for use in high-performance optoelectronic applications.

References

[1] Q. Xu, L. Zhang, J. Yu, S. Wageh, A.A. Al-Ghamdi, M. Jaroniec, Direct Z-scheme photocatalysts: Principles, synthesis, and applications, Materials Today. 21 (2018) 1042–1063. <https://doi.org/10.1016/j.mattod.2018.04.008>.

- [2] A. Yang, J.-C. Blancon, W. Jiang, H. Zhang, J. Wong, E. Yan, Y.-R. Lin, J. Crochet, M.G. Kanatzidis, D. Jariwala, T. Low, A.D. Mohite, H.A. Atwater, Giant Enhancement of Photoluminescence Emission in WS₂-Two-Dimensional Perovskite Heterostructures, *Nano Letters*. 19 (2019) 4852–4860. <https://doi.org/10.1021/acs.nanolett.8b05105>.
- [3] H. Zhou, H. Lai, X. Sun, N. Zhang, Y. Wang, P. Liu, Y. Zhou, W. Xie, Van der Waals MoS₂/Two-Dimensional Perovskite Heterostructure for Sensitive and Ultrafast Sub-Band-Gap Photodetection, *ACS Applied Materials & Interfaces*. 14 (2022) 3356–3362. <https://doi.org/10.1021/acsami.1c15861>.
- [4] C.C. Stoumpos, D.H. Cao, D.J. Clark, J. Young, J.M. Rondinelli, J.I. Jang, J.T. Hupp, M.G. Kanatzidis, Ruddlesden–Popper Hybrid Lead Iodide Perovskite 2D Homologous Semiconductors, *Chemistry of Materials*. 28 (2016) 2852–2867. <https://doi.org/10.1021/acs.chemmater.6b00847>.
- [5] F.G. Aras, A. Yilmaz, H.G. Tasdelen, A. Ozden, F. Ay, N.K. Perkoz, A. Yeltik, A review on recent advances of chemical vapor deposition technique for monolayer transition metal dichalcogenides (MX₂: Mo, W; S, Se, Te), *Materials Science in Semiconductor Processing*. 148 (2022) 106829. <https://doi.org/10.1016/j.mssp.2022.106829>.

10:30 AM EL19.16.06

Low-Power Optical Control of Two-Dimensional Magnets TiXie¹, JieruiLiang¹, HasithaS. Arachchige², DavidMandrus² and ChengGong¹; ¹University of Maryland, United States; ²The University of Tennessee, Knoxville, United States

A magnetic material, while dressed with different spin configurations, can host a variety of emergent phenomena such as chiral domain walls, skyrmions, and Majorana fermions. Traditional preparation of various spin textures in magnetic films by transforming an already established spin pattern demands intensive energy to cause spin flipping or domain wall motion. In contrast, engineering the phase transition kinetics potentially opens up new avenues to achieve desired spin configurations. The two-dimensional (2D) layered magnets, owing to the ultra-thinness, allow the magnetism control by various external stimuli, among which optical approaches promise non-destructive manipulation, both locally and globally. In this talk, I will introduce how we demonstrated a low-power optical control of 2D magnets. By perturbing the phase transition kinetics, we found that optical incidence on the order of tens of microwatt per micrometer can effectively control magnetic domain formation, and the orientation of the magnetic domain is highly dependent on optical helicity. Our low-power optical operation paves the new avenue to efficiently engineer 2D spin textures for a plethora of emergent quantum phenomena.

SESSION EL19.17: Scalable Processing for 2D Materials

Session Chairs: Andrew Mannix and Hyeon Jin Shin

Thursday Afternoon, November 30, 2023

Hynes, Level 3, Room 309

1:30 PM *EL19.17.01

Manufacturing 2D Materials at Large Scale and High Spatial Selectivity ZakariaAl Balushi; University of California, Berkeley, United States

The multitude of 2D materials in regard to composition, crystal structure and layer thickness leads to a variety of material properties covering all of the components necessary to address voltage, interconnect, energy, and dimensional scaling issues in a variety of applications. For 2D materials to be technologically competitive, it is imperative to develop manufacturable materials deposition protocols at low temperatures and at any location on demand without wafer transfer processing. In this talk, a low temperature spin coating process will be discussed to form transition metal dichalcogenides at low temperatures using a modified spin coating technique from low decomposition temperature molecules. Furthermore, to achieve spatial selectivity of grown 2D materials, this talk will also describe a novel process to spatially measure and modulate the surface energy of van der Waals surfaces at growth temperatures to achieve selective area growth of 2D materials into a variety of form factors.

2:00 PM EL19.17.02

Light Emission from Megasonically Solution-Processed MoS₂ Nanosheet Films VinodK. Sangwan, SonalV. Rangnekar, MengruJin, MaryamKhalaj, BeataM. Szydłowska, AnushkaDasgupta, LidiaKuo, HeatherKurtz, TobinJ. Marks and MarkC. Hersam; Northwestern University, United States

Electroluminescence (EL), the conversion of an electrical current into light, is the basis of ubiquitous technologies including lighting, displays, and data communication. Recently, two-dimensional (2D) monolayer semiconductors have been widely studied in the context of electroluminescent devices due to their tunable photonic and electrical properties. Specifically, transition metal dichalcogenides (TMDs) show a direct band gap at the monolayer scale, strong light-matter interactions, tightly bound excitons, trions, and multi-excitons that can be controlled by strain and doping. Layered TMDs are also amenable to solution-processibility for printed optoelectronics with high carrier mobility and mechanical flexibility in printed active layers. Furthermore, stacking arbitrary 2D materials in van der Waals heterojunctions has enabled a variety of light-emitting devices, including lateral p-n homojunctions, vertical p-n heterojunctions, and quantum well structures. On the other hand, a light-emitting capacitor (LEC) achieves light emission through bipolar carrier injection using an alternating-current (AC) gating scheme that avoids stringent materials selection for matching contact metals and is less sensitive to morphological nonuniformity in the semiconductor. However, challenges in isolating optoelectronic-grade monolayer TMDs using scalable liquid-phase exfoliation have thus far precluded the realization of large-area EL devices.

Here, we overcome these challenges and demonstrate EL in large-area solution-processed molybdenum disulfide (MoS₂) nanosheet films. Monolayer-rich MoS₂ ink is produced through electrochemical intercalation followed by megasonic exfoliation (i.e., sonication at megahertz frequencies) that has recently been shown to yield high-performance visible and near-infrared photodetectors.^{1,2} The MoS₂ ink is used to produce large-area, percolating nanosheet films for AC-gated transient-EL devices in a metal-insulator-semiconductor-metal geometry. Characteristic monolayer MoS₂ photoluminescence (PL) and EL spectral peaks at 1.88-1.90 eV are observed in thick MoS₂ films with the emission intensity increasing with film thickness over the range of 10-70 nm. A vertical LEC geometry produces highly uniform EL in large-area devices, thus confirming that megasonically exfoliated MoS₂ monolayers retain their direct bandgap character in electrically percolating thin films. This work establishes the potential of megasonicated 2D monolayer inks as an additive manufacturing platform for flexible, patterned, and miniaturized light sources.

References

- [1] L. Kuo, V. K. Sangwan, S. V. Rangnekar, T.-C. Chu, D. Lam, Z. Zhu, L. J. Richter, R. Li, B. M. Szydłowska, J. R. Downing, B. J. Luijten, L. J. Lauhon, and M. C. Hersam *Advanced Materials* **34**, 2203772 (2022).
- [2] D. Lam, D. Lebedev, L. Kuo, V. K. Sangwan, B. M. Szydłowska, F. Ferraresi, A. Söll, Z. Sofer, and M. C. Hersam *ACS Nano* **16**, 11315 (2022).

2:15 PM EL19.17.03

A Scalable Route for Composition-Tunable Transition Metal Dichalcogenide Nanosheets RebekahWells¹, NicolasDiercks¹, VictorBoureau¹, SimonNussbaum¹, MarcEsteve¹, MarinaCaretti^{2,1}, HannahJohnson^{2,1} and KevinSivula¹; ¹Ecole Polytechnique Federale de Lausanne, Switzerland; ²Toyota Motor Europe, Belgium

The alloying of 2D TMDs is an established route to robust semiconductors with continuously-tunable optoelectronic properties. However, a major obstacle in commercializing large-area, thin devices based on alloyed TMD nanosheets is their large-scale production.¹

In this presentation we describe major advances that address this issue. Firstly, we describe a new powder-based, solution processable method to produce high quality 2D TMD nanosheets using a pre-annealing step and electrochemical intercalation/exfoliation.² Compared to traditional methods (i.e., ultrasonication), 2D TMD nanosheets produced using our method show ameliorated optoelectronic properties owing to high aspect ratios and low defect densities. Next, we demonstrate how this innovative method can be adapted to afford production of ternary (Mo_{0.5}W_{0.5}S₂, Mo_{0.5}W_{0.5}Se₂, MoSSe, WSSe) and quaternary (Mo_{0.5}W_{0.5}SSe) alloyed TMD nanosheets from commercially available, pure-phase bulk TMD powders. We provide evidence of the atomic mixing within the nanosheets using atomic resolution scanning transmission electron microscopy (STEM) in combination with integrated differential phase contrast (iDPC) for the metal and chalcogenide atoms, respectively. Furthermore, we show that control over the final composition of the nanosheets can be exerted by tuning the feed ratios of the TMD powders. Accordingly, we examine the unique optoelectronic properties that arise as a function of the chemical composition of the alloy. Notably, the phenomena observed are consistent with nanosheets produced *via* chemical vapor deposition (CVD) and related methods, suggesting that this versatile method is an economically viable solution for making alloyed 2D TMD nanosheets. Indeed, the ability to produce controllably alloyed TMD nanosheets in large quantities is critical for the inexpensive production of next-generation, large-area optoelectronic devices.

In order to transform our exfoliated materials into large-area, thin films, we report the further advancement of our preparation methods toward a continuous roll-to-roll deposition of TMD-based thin films from nanosheet dispersions using a liquid-liquid self-assembly technique.³ We demonstrate reproducible printing of 100mm wide TMD nanosheet films on plastic substrates.

Thus, the advances presented here represent a comprehensive route towards large-area, tunable, and fully solution-processable 2D TMD-based devices.

[1] Wells, R.A.; Sivula, K. Assembling a Photoactive 2D Puzzle: From Bulk Powder to Large-Area Films of Semiconducting Transition-Metal Dichalcogenide Nanosheets. *Accounts of Materials Research*. **2023** 4 (4), 348-358. DOI: 10.1021/accounts.mr.2c00209

[2] Wells, R.A.; Diercks, N.J.; Boureau, V.; Wang, Z.; Zhao, Y.; Nussbaum, S.; Esteve, M.; Caretti, M.; Johnson, H.; Kis, A.; Sivula, K. Composition-Tunable Transition Metal Dichalcogenide Nanosheets via a Scalable, Solution-Processable Method. (*Submitted*) **2023**.

[3] Wells, R. A.; Johnson, H.; Lhermitte, C. R.; Kinge, S.; Sivula, K. Roll-to-Roll Deposition of Semiconducting 2D Nanoflake Films of Transition Metal Dichalcogenides for Optoelectronic Applications. *ACS Appl. Nano Mater.* **2019**, 2 (12), 7705–7712. <https://doi.org/10.1021/acsanm.9b01774>.

2:30 PMBREAK

3:00 PM EL19.17.04

Permeation Mechanisms Through 1 nm Thin Carbon Nanomembranes [Andrey Turchanin](#); Friedrich Schiller University Jena, Germany

Molecular thin carbon nanomembranes (CNMs) synthesized by electron irradiation induced cross-linking of aromatic self-assembled monolayers (SAMs) are promising 2D materials for the next generation of filtration technologies [1, 2]. Their unique properties including ultimately low thickness of ~1 nm, sub-nanometer porosity, mechanical and chemical stability are attractive for the development of innovative filters with low energy consumption, improved selectivity and robustness. However, the permeation mechanisms through CNMs resulting in, e.g., an ~1000 times higher fluxes of water in comparison to helium have not been yet understood [1]. Here we report a study of the permeation of He, Ne, D₂, CO₂, Ar, O₂ and D₂O using mass spectrometry in the temperature range from room temperature to ~120 °C. As a model system, we investigate CNMs made from [1',4',1',1]-terphenyl-4-thiol SAMs. We found out that all studied gases experience an activation energy barrier upon the permeation which scales with their kinetic diameters. Moreover, their permeation rates are dependent on the adsorption enthalpy on the nanomembrane surface. These findings enable us to rationalize the permeation mechanisms and establish a model, which paves the way towards the rational design not only of CNMs but also of other organic and inorganic 2D materials for energy-efficient and highly selective filtration applications [3].

[1] Y. Yang *et al.*, *ACS Nano* **2018**, 12, 4695

[2] Y. Yang *et al.*, *Adv. Mater.* **2020**, 32, 1907850

[3] V. Stroganov *et al.*, *Small* **2023**, <https://doi.org/10.1002/sml.202300282>

3:15 PM EL19.17.05

Topological Characterization of 2D Polymers and Thin Nanofilms: TEM Imaging Processing and Computational Analysis [Yu-Ming Tu](#), [Xun Gong](#), [Quien Michelle](#) and [Michael S Strano](#); Massachusetts Institute of Technology, United States

Recent research has shown an increased interest in the development of polymers that can extend covalently in two dimensions. This type of material has the potential to combine the mechanical strength and in-plane energy conduction of conventional two-dimensional (2D) materials with the low densities, synthetic processability, and organic composition of their one-dimensional counterparts. 2D polymers and materials possess unique properties such as ultra-thinness, well-organized pore structures, and high chemical stability, making them highly attractive for a range of applications, including nanotechnology and devices. One promising area of research involves altering the 2D layered structure of these materials to create barriers through staggered platelet stacking or perm-selective separation membranes via aligned pore structures. Nevertheless, comprehensive studies are required to validate the 2D formation and layered stacking structure, which necessitates combining material characterization techniques and computational tools. In our recent study, we designed and synthesized a 2D polyamide-1 (2DPA-1) using irreversible polycondensation chemistry. This approach offers mechanical processability and high chemical stability, making it an ideal candidate for further investigation. Our current work focused on exploring how the 2DPA-1 polymer molecules, which are covalently linked by interlayer hydrogen bonds, can be realigned into highly organized nanofilms using various techniques such as solvent retreatment, spinning coating, drop-casting, and scotch tape exfoliation. To analyze the resulting 2D structure, we used a combination of transmission electron microscopy (TEM) imaging and computational processing tools. These tools enabled us to examine the ultra-thinness sheet-like structure (0.4 nm thickness) and estimate possible 2D platelet orientation and layered structure. The image processing tools also allowed for high throughput structural analysis of 2D platelets and polymers. Overall, our study provides insights into the potential of 2D materials and highlights the importance of combining material characterization techniques and computational tools to fully understand their properties and potential applications

3:30 PM EL19.17.06

Production and Characterization of Phosphorene Nanoribbons (PNRs) [Eva Awl](#)¹, [Loren Picco](#)^{2,3,4}, [Oliver D. Payton](#)^{2,3,4}, [Stacy R. Moore](#)³, [Fengfei Zhang](#)¹, [Adam J. Clancy](#)¹, [Thomas S. Miller](#)¹ and [Christopher A. Howard](#)¹; ¹University College London, United Kingdom; ²Bristol Nano Dynamics Ltd., United Kingdom; ³University of Bristol, United Kingdom; ⁴Active Nano Mapping NNUF, United Kingdom

In our fast-paced technological world, the demand for more powerful yet smaller devices has fueled the need for nanomaterial innovation. To meet this demand, precise chemical doping techniques can be employed to tailor the properties of low-dimensional materials and facilitate their integration into functional films, electrodes, and spin-based electronics.

Phosphorene nanoribbons (PNRs), a newly synthesized nanomaterial by our research group at UCL [1], are predicted to exhibit exotic properties, including the Seebeck effect, tunable layer-dependent electronic, optical and ionic transport properties. Recent experiments have demonstrated room-temperature magnetism [2] in PNRs and their ability to enhance hole mobility in solar cells [3]. By combining the flexibility and unidirectional properties of nanoribbons with the high surface area and anisotropic properties of 2D phosphorene sheets, PNRs are expected to exhibit high conductivity due to the 2D confinement of electronic movements and edge effects.

My talk focuses on the synthesis of PNRs using a two-step method. Firstly, black phosphorus is intercalated with alkali metal ions, followed by exfoliation to form stable liquid dispersions of PNRs with few-layer thicknesses and 4-50 nm widths uniform along their lengths [4]. This scalable approach allows us to isolate high quality individual PNRs from bulk black phosphorus. In collaboration with Bristol Nanodynamics Ltd., I am using a recently developed conductive high-speed atomic force microscopy (HS-AFM) to characterise the local charge distribution of PNRs [5].

HS-AFM is an advanced characterization technique which allows for high-resolution data acquisition and real-time video observations across large surface areas. This technique enables simultaneous topography and conductivity measurements, providing valuable insights into the spatial maps of conductivity. By analyzing these maps, we can derive insights on how the electronic band structure of PNRs varies with the number of layers and bifurcations.

[1] Watts, M. C. *et al.* Production of phosphorene nanoribbons. *Nature* **568**, 216–220 (2019).

[2] Ashoka, A. *et al.* Room Temperature Optically and Magnetically Active Edges in Phosphorene Nanoribbons. *Under Rev.* (2022).

[3] Macdonald, T. J. *et al.* Phosphorene Nanoribbon-Augmented Optoelectronics for Enhanced Hole Extraction. *Cite This J. Am. Chem. Soc* **143**, 21549–21559 (2021).

[4] Cullen, P. L. *et al.* Ionic solutions of two-dimensional materials. *Nat. Chem.* **9**, 244–249 (2017).

[5] Payton, O. D., Picco, L. & Scott, T. B. High-speed atomic force microscopy for materials science. *Int. Mater. Rev.* **61**, 473–494 (2016).

SESSION EL19.18: Advances in Novel 2D Material Synthesis

Session Chairs: Sanjay Behura and Andrew Mannix

Friday Morning, December 1, 2023

Hynes, Level 3, Room 309

8:00 AM EL19.18.01

Correlated SKPM and TERS Imaging of Janus MoSSe Monolayers and MoSSe-MoS₂ Vertical Heterostructures [Tianyi Zhang](#)¹, [Andrey Krayev](#)², [Hongwei Liu](#)^{1,3} and [Jing Kong](#)¹; ¹Massachusetts Institute of Technology, United States; ²HORIBA Instruments Inc, United States; ³The Hong Kong University of Science and Technology, Hong Kong

We report correlated scanning Kelvin probe microscopy (SKPM) and tip enhanced Raman scattering (TERS) imaging of Janus MoSSe monolayers and MoSSe-MoS₂ vertical heterostructures (VHS) obtained by replacing the top sulfur layer of monolayer MoS₂ with selenium atoms via a plasma-assisted room-temperature atomic-layer substitution (RT-ALS) approach. MoSSe crystals were transferred to gold to improve the efficiency of TERS measurements. Unlike their conventional Raman counterparts, TERS spectra of MoSSe featured a strong A₁² mode, possibly due to the preferential enhancement of the out-of-plane modes favored in the gap-mode TERS. We observed a sharp drop of the intensity of A₁² mode in the VHS of MoSSe-MoS₂ that naturally occurred during the Janus conversion of multilayer islands sporadically occurring in larger monolayer MoS₂ crystals. The work function of these vertical heterostructures is drastically different from the monolayer Janus MoSSe material which makes SKPM technique an excellent tool for visualizing VHS. Besides, rather unexpectedly, we observed splitting of the A₁¹ mode of MoSSe both in the Janus monolayers and in their VHS, we will discuss possible reasons for this splitting. SKPM imaging of multiple crystals confirmed high microscopic uniformity of the S-Se substitution and the lack of damage to the original MoS₂ crystals except for occasional etching of the grain boundaries in twin symmetry crystals. At the same time, TERS imaging revealed that the width and the spectral position of A₁² peak may vary drastically at the nanoscale which implies local nanoscale variations of the stoichiometry of Janus material. Finally, in this study we found that 785 nm excitation provides the strongest TERS response on Janus MoSSe when compared to 633 nm, 671 nm or 830 nm excitations. This observation should be very helpful for future TERS studies on Janus TMDs and their vertical heterostructures.

8:15 AM EL19.18.02

Characterization and Engineering of 2D vdW Magnets Hosting 1D Magnetic Chains using Scanning Transmission Electron Microscopy (STEM) EugenePark¹, JohnPhilbin², JoshuaSanchez¹, ConnorOcchialini¹, HangChi¹, ZhiGangSong³, AlexandreFoucher¹, JoachimD. Thomsen², JulianKlein¹, ZdenekSofer⁴, PrinehaNarang² and FrancesM. Ross¹; ¹Massachusetts Institute of Technology, United States; ²University of California, Los Angeles, United States; ³Harvard University, United States; ⁴University of Chemistry and Technology Prague, Czechia

Van der Waals 2D magnetic materials have emerged as a novel platform that offers unique optoelectronic, magnetic, and quantum properties.¹ Such low-dimensional spin systems have vast potential in applications such as spintronics and nanoscale magnetic devices. The ability to engineer the structure and defects with respect to magnetic, optical, and electronic properties is critical. For example, using individual spins to encode many-body Hamiltonians can allow quantum simulation to be carried out on vdW heterostructures composed of 2D magnets. Out of the wide range of 2D van der Waals magnets, 2D magnets with high structural anisotropy are relatively unexplored, making such materials intriguing and helpful for both fundamental research and device design. For instance, the highly anisotropic character could deliver additional degrees of freedom like 1D magnetism that we can harvest in 2D vdW materials.

Here, we examine the structural properties of two kinds of 2D magnets hosting 1D chains of magnetic atoms. Using scanning transmission electron microscopy (STEM), we characterize structural properties such as the alignment of magnetic chains between layers with atomic resolution. We also explore the nature of defects and the possibility of controlling defect location using the STEM electron beam.^{2,3} To reduce beam damage when imaging few layer materials, the sample was encapsulated in graphene to constrain the movement of atoms. By parametrizing a model spin-Hamiltonian based on density functional theory calculations, we predict the spin structure that develops from the chain arrangement of the magnetic atoms in this material. We discuss measurements to verify theoretical calculations using instruments such as vibrating sample magnetometry and photoluminescence. Lastly, we engineer the 2D magnet via electron beam irradiation to modify the structure of 1D spin chains and predict magnetic properties and spin structure using atomistic magnetic simulation.

References

1. Gibertini, M., Koperski, M., Morpurgo, A. F. *et al.* Magnetic 2D materials and heterostructures. *Nat. Nanotechnol.* **14**, 408-129 (2019).
2. Klein, J., Pingault, B., Florian, M. *et al.* The bulk van der Waals layered magnet CrSBr is a quasi-1D quantum material. *ACS nano* **17**, 5316-5328 (2023).
3. Klein, J., Pham, T., Thomsen, J. D. *et al.* Control of structure and spin texture in the van der Waals layered magnet CrSBr. *Nature Communications* **13**, 5420 (2022).

8:30 AM EL19.18.03

Hybrid Pulsed Laser Deposition Growth of Group IVB Dichalcogenides MythiliSurendran, HuandongChen, ShantanuSingh, AmirAvishai, BoyangZhao, Yu-TsunShao and JayakanthRavichandran; University of Southern California, United States

Group IVB transition metal dichalcogenides (TMDCs) (MX₂; M=Ti, Zr, Hf and X =S, Se, Te) have high calculated room temperature electronic mobilities (5-10 times higher than MoS₂) making them promising materials for electronic applications¹. However, they remain as the least explored amongst all the layered TMDCs largely due to the synthesis challenges to achieve large area high-quality thin films. TMDC thin films are mostly grown using chemical vapor deposition, although molecular beam epitaxy, metal-organic vapor deposition, pulsed laser deposition (PLD)^{2,3} and several other techniques have been exploited. High temperatures of about 1000°C are typically required to grow group IVB TMDCs as they consist of refractory metals such as Zr and Hf, resulting in high defect densities in these films. Moreover, they have a high propensity to oxidize at these high temperatures, thus affecting the electronic properties.

Here, we report a hybrid PLD approach wherein we employed organo-sulfur precursors as sulfur source (as an alternative to H₂S) to grow chalcogenide thin films. To demonstrate the efficacy of this approach, we have demonstrated epitaxial growth of Group IVB TMDCs such as TiS₂ (semimetallic), ZrS₂ and HfS₂ (semiconducting)^{4,5}. Structural and electrical characterization, along with low temperature transport studies reveal low defect densities and high carrier mobilities in these thin films. The synthesis challenges during the realization of refractory metal-based chalcogenides will be discussed in detail. This novel method enables growth temperatures as low as 500°C and opens up new opportunities to investigate the fundamental properties of Group IVB chalcogenides and realize the predicted electronic and optoelectronic applications.

References:

- (1) Yan, C. *et al*; *Advanced Functional Materials* **2018**, *28* (39).
- (2) Yao, J. D. *et al*; *Progress in Materials Science* **2019**, *106*.
- (3) Zavabeti, A. *et al*; *Nanomicro Lett* **2020**, *12* (1), 66.
- (4) Tian, Y. *et al*; *Nano Research* **2022**, *15* (7), 6628-6635.
- (5) Fu, L. *et al*; *Adv Mater* **2017**, *29* (32).

8:45 AM EL19.18.04

Electrically Driven Ion Dynamics with Negative Differential Resistance in Alkali Ions Intercalated 2D-Layered Metal Oxide GichangNoh^{1,2}, JeonghoKim², Han BeomJeong³, YooyeonJo¹, Min-kyungJo², EoramMoon², MingyuKim², EunpyoPark¹, In SooKim¹, Chul-HoLee⁴, Hu YoungJeong³, KibumKang² and Joon YoungKwak¹; ¹Korea Institute of Science and Technology, Korea (the Republic of); ²Korea Advanced Institute of Science and Technology, Korea (the Republic of); ³Ulsan National Institute of Science and Technology, Korea (the Republic of); ⁴Seoul National University, Korea (the Republic of)

Ion-based electronics provide a platform to explore unique physical properties and have extensive applications in the design of bio-nano interface and bio-mimetic devices. 2D-layered materials, thanks to their ability to easily accommodate ions between their layers, emerge as an ideal choice for these ion-based electronic platforms. To realize systematic ion control in 2D-layered materials, it's crucial to ensure stable spatiotemporal reactions of ions on demand. However, substantial hurdles persist during device fabrication and operation based on ion intercalation, including the need for external force during the intercalation process, the challenge of maintaining thermodynamic stability with ions, and the management of structural distortions during ion migration. Here, we introduce the intrinsic stable potassium ion (K⁺) intercalated 2D-layered MnO₂ (2D K-MnO₂) by the metal-organic chemical vapor deposition (MOCVD) method. Thermodynamically, the layered structure of MnO₂ with the intercalated potassium ion and H₂O has the lowest Gibbs free energy among the other phases, resulting in spontaneous intercalation during the growth process. Potassium ions intercalated into the van der Waals gap of layered MnO₂ can easily move under the external bias, and this electrical-driven ion movement causes the reversible phase transition to Mn₃O₄. Especially, the phase transition of Mn₃O₄ and the lattice distortion by over-concentrated potassium ions form a high Schottky barrier that presents dominant negative differential resistance (NDR). We designed a device with multi-channels of the 2D K-MnO₂ to apply simultaneous signals with various conditions and successfully proved that the spatial and temporal potassium ion controls the gradual conductance changes with NDR behavior. Moreover, we imitated the biological voltage-gated potassium channels based on NDR-related conductance change and applied the long-term & short-term plasticity to the associative learning. Our approach to NDR-based ionic motion of 2D K-MnO₂ shows not only a new concept of the dynamics of ion devices but also the high applicability for ionic activities in the human body.

9:00 AM *EL19.18.05

Developing and Integrating Atomically Thin Metals, Semiconductors and Insulators JoshuaA. Robinson; The Pennsylvania State University, United States

The last decade has seen an exponential growth in the science and technology of two-dimensional materials. Beyond graphene, there is a huge variety of layered materials that range in properties from insulating to superconducting. Furthermore, heterogeneous stacking of 2D materials also allows for additional "dimensionality" for material and device engineering. In this

talk, I will discuss recent breakthroughs in two-dimensional atomic layer synthesis, properties, and integration toward advancing devices relevant to the semiconductor industry. This includes novel 2D heterostructures and the realization of unique 2D allotropes of 3D materials (e.g. 2D metals, nitride, oxides) based on a novel synthesis method, dubbed confinement heteroepitaxy (CHet). By shrinking traditional metals to atomically thin structures, we find that their properties are completely different than their bulk counterparts, lending themselves to unique quantum and optical applications not possible before.

9:30 AMBREAK

SESSION EL19.19: Applications of Wafer-Scale 2D Materials—Electronics II
Session Chairs: Sanjay Behura and Andrew Mannix
Friday Morning, December 1, 2023
Hynes, Level 3, Room 309

10:00 AM EL19.19.01

Electrical Detection of the Flat Band Dispersion in Van der Waals Field-Effect Structures Gabriele Pasquale¹, Edoardo Lopriore¹, Zhe Sun¹, Kristians Cernevis¹, Fedele Tagarelli¹, Kenji Watanabe², Takashi Taniguchi³, Oleg Yazyev¹ and Andras Kis¹; ¹EPFL, Switzerland; ²Research Center for Functional Materials, National Institute for Materials Science, Japan; ³International Center for Materials Nanoarchitectonics, National Institute for Materials Science, Japan

The emergence of the field-effect transistor transformed contemporary technologies. Of paramount significance to the effective operation of such devices is the minimal current leakage between the source and gate electrodes. These currents have traditionally been considered detrimental, hindering the flow of electrical charge through the channel. Consequently, for more than seven decades, leakage currents were perceived as lacking any valuable insights beyond their role in improving performance and transistor design. This research delves into the examination of gate leakage currents, specifically tunneling currents, in field-effect devices utilizing thin layers of InSe channels. InSe, known for its exceptional electrical and optical properties, as well as its distinctive band structure, exhibits a flat-band dispersion at the valence band edge, which may give rise to emergent phenomena [1]. However, determining the energy position of the flat band in a field-effect device has traditionally required costly and impractical methods. Therefore, our study focuses on analyzing tunneling currents in gated structures composed of a few layers of InSe and their relationship with ambipolar transport and photoluminescence measurements. Notably, we observe a shift in tunneling mechanisms due to the presence of the van Hove singularity at the flat band. To validate our findings, we explore tunneling currents as a reliable means of determining the position of the flat band, even at room temperature. Our study offers a fresh outlook on the enduring enigma, presenting an alternative framework for comprehending leakage currents in field-effect devices.

10:15 AM EL19.19.02

2D Materials Integration with Silicon as 2D-3D Heterostructure Architecture Enabled by Quantum Tunneling Tara Jabegu, Ningxin Li, Aisha A. Okmi and Sidong Lei; Georgia State University, United States

In-line with the concept of three-dimensional (3D) hybrid integration, the combination of silicon-based circuits with two-dimensional (2D) material-based device architectures has emerged as an appealing topic. This fusion holds the promise in innovative electronics and optoelectronics with novel functions, higher integration level, fast speed, and many other benefits that are intangible in conventional designs. Nonetheless, the integration of silicon and 2D materials in a 3D configuration encounters a problem of substantial contact resistance. Earlier investigations suggested that the presence of van der Waals gap and in-gap states could be responsible for the poor contact. In this study, we present an alternative approach to enhance contact quality. In essence, instead of eliminating the van der Waals gap between silicon and 2D materials, we treat the gap as a quantum tunneling barrier and manage to increase the quantum tunneling efficiency. By tuning the Fermi-surface alignment and minimizing the charge carrier momenta mismatch, we effectively reduce the contact resistance between silicon and graphene achieving nearly ideal ohmic contact. Furthermore, we characterize the phonon-assisted inelastic transport process on this silicon-graphene interface and demonstrate its positive effects in enhancing the contact conductivity. This research provides a feasible and versatile approach for high-quality 3D-2D contact fabrication towards the hybrid integration of dissimilar materials with advanced functionalities in the field of electronics and optoelectronics.

10:30 AM *EL19.19.03

2D Single-Atom Switching Materials and Applications in Electronics and 6G Communication Systems Deji Akinwande; The University of Texas at Austin, United States

This presentation focuses on the nonvolatile resistance switching memory effect in 2D materials, aka, atomristors. Nonvolatile memory devices based on 2D materials are an application of defects and is a rapidly advancing field with rich multiphysics that can be attributed to vacancies combined with metal adsorption. The energetics of the defects are discussed and emerging applications such as zero-power switches in RF, 6G, and THz connectivity systems are presented. These memory devices offer high-energy efficiency and fast switching that may benefit mobile systems, cloud computing and data centers towards reduced energy consumption worldwide

SESSION EL19.20: 2D Semiconductors—Processing
Session Chairs: Sanjay Behura and Andrew Mannix
Friday Afternoon, December 1, 2023
Hynes, Level 3, Room 309

1:30 PM EL19.20.01

Impact of Thermal Annealing on the Interaction of Monolayer MoS₂ on Au Stephanie D. Lough¹, Jesse Thompson¹, Darian Smalley¹, Rahul Rao² and Masahiro Ishigami²; ¹University of Central Florida, United States; ²Air Force Research Laboratory, United States

We have investigated the impact of thermal annealing on the interaction of single layer MoS₂ and Au using Raman Spectroscopy. Au-assisted exfoliation results in single layer MoS₂ which has weakly- and strongly-coupled regions where the strongly-coupled regions are n-doped and relatively unstrained while the weakly-coupled regions are p-doped and tensile strained. The observed nanoscale inhomogeneities may result in Au contacts having a large variability in performance. Our data also show that monolayer MoS₂ starts to decouple from Au at above 100 °C, becoming fully decoupled above 200-250 °C. This indicates that monolayer MoS₂ produced by Au-assisted exfoliation may be more easily transferred off Au at high temperatures. Our results also show that the overall areal coverage of strongly-coupled regions does not increase by thermal annealing while the degree of hybridization becomes more inhomogeneous at annealing temperatures above 100 °C.

1:45 PM EL19.20.02

Photoluminescence Quenching in N-Heterocyclic Carbene Functionalized Tungsten Dichalcogenide Mixed-Dimensional Heterostructures Anushka Dasgupta¹, Rafael López-Arteaga¹, Iqbal B. Utama¹, Tumpa Sadhukhan², S. Carin Gavin¹, Xi Wan¹, Wei Wang³, Brendan Kerwin¹, Riddhi Ananth¹, Albert Vong¹, Nathaniel Stern¹, George Schatz¹, Xuedan Ma³, Emily Weiss¹ and Mark C. Hersam¹; ¹Northwestern University, United States; ²SRM Institute of Science and Technology, India; ³Argonne National Laboratory, United States

Two-dimensional (2D) transition metal dichalcogenides (TMDs) are promising candidates for quantum optoelectronic devices due to their pronounced valley physics and excitonic properties. One approach to modulate these properties is to modify 2D TMDs with carbon-based ligands.¹ Among carbon-based ligands, the strong σ -donor character, stability, and structural tunability of N-heterocyclic carbenes (NHCs) has prompted investigations of NHC coordination to various atomically flat metal surfaces and metal nanoparticles. Here, we discuss the optical properties of WS₂ and WSe₂ monolayers functionalized with NHCs via a solvent-free route and an air-stable precursor. The deposition of NHCs on the 2D TMDs results in a significant room-temperature photoluminescence (PL) quenching. Moreover, low-temperature PL measurements (T = 3.9 K) show quenching of the WS₂ and WSe₂ excitonic emission and a shift of the defect bands to lower energies. The extent of both effects is tunable by altering the N-substituents of the NHCs as well the thickness of the deposited organic layer. The resulting mixed-dimensional heterostructures are further characterized by X-ray photoelectron spectroscopy, atomic force microscopy, and time-of-flight secondary ion mass spectrometry to elucidate the nature of the functionalization process. The observed PL quenching is consistent with a charge transfer process from defect states introduced by chalcogen vacancies to midgap states introduced by the carbene layer, as predicted from first-principles density functional theory calculations. Overall, these results demonstrate that carbene functionalization is an effective pathway for modifying

the optical properties of 2D TMDs.

References:

(1) M. I. B. Utama, H. Zeng, T. Sadhukhan, A. Dasgupta, et al., Nature Communications 2023, 14 (2193).

2:00 PM EL19.20.03

Computational Design of Plasma Process for High Purity Layer Thinning of 4-In MoS₂ MuiyoungKim¹, ChangminKim¹, Hyeong-UKim¹, DaewoongKim¹, TaesungKim² and Woo SeokKang¹; ¹Korea Institute of Machinery and Materials, Korea (the Republic of); ²Sungkyunkwan University, Korea (the Republic of)

Two-dimensional molybdenum disulfide (MoS₂) has attracted huge attention for next-generation nanoelectronics due to its unique physical and chemical properties. Among the fascinating characteristics of MoS₂, a tunable bandgap according to the thickness is necessary for on-demand engineering of future electronics. In this respect, the precise layer control of MoS₂ has been a long-standing desire, but prior studies encountered critical challenges such as poor scalability, surface roughening and impurities. This work aimed to achieve ultrahigh purity and precision in wafer-scale layer thinning of MoS₂ by plasma processes: plasma-enhanced chemical vapor deposition (PECVD) and reactive ion etching (RIE). The 4-inch MoS₂ was synthesized by PECVD, and the as-deposited layers were peeled off by RIE with a computationally screened gas mixture. For the computational screening, the plasma-induced surface chemistry was explored using first-principles calculations that offered atomic insights on reaction energetics and the associated orbital interaction. Through the process optimization, layer-by-layer thinning of MoS₂ was confirmed in 4-inch wafer, where mono- or bilayer was evenly removed for each RIE cycle. Additionally, there were no damages in atomic structure and chemical impurities. The combined computational screening-experimentation accelerates the process development and provides concrete understanding on underlying physics in manufacturing process.

2:15 PM EL19.20.04

Plasma Electron Irradiation Etching (PEIE) of Two-Dimensional Materials YunjoJeong¹, Jong-BaePark², EunjinChoi¹, Dae ChulKim², SukangBae¹, Young-WooKim² and JangyupSon¹; ¹Korea Institute of Science and Technology, Korea (the Republic of); ²Korea Institute for Fusion Energy, Korea (the Republic of)

Two-dimensional layered materials (2DLMs) have garnered significant interest due to their versatility and the potential for investigating practical applications such as flexible electronics, molecular filters, etc. In maximizing the versatility of 2DLMs, various attempts have been made to tailor their properties for desired applications, such as inducing mechanical deformation, modifying their surface chemistry, and investigating the change in their thickness-dependent properties such as bandgap energy, mechanical strength, and optical transmittance. Although significant progress has been made in maintaining control over mechanical or chemical states of 2DLMs, precise control over their thickness remains a challenge. Currently, most research has focused on mono- or few-layer 2DLMs; however, while such research allows for a thorough understanding of the various properties of 2DLMs, practical application of 2DLMs is contingent upon achieving capacity for arbitrary manipulation of their thickness at the multilayer scale. Conventional approaches to control over the thickness of 2DLMs include bottom-up approaches such as chemical vapor deposition and top-down approaches such as chemical etching via plasma, wet etchants, etc. Although such approaches are relatively effective, they inherently exhibit tradeoffs such as defects and sample contamination. Here, we introduce a novel approach to achieving precise etching of two-dimensional materials at the nanometer scale. A modified plasma electron annealing method, originally designed for the recrystallization of amorphous Si [1], was employed to achieve highly precise control over the vertical dimension of exfoliated BN crystals. Characterization via Raman spectroscopy and atomic force microscopy (AFM) confirm successful thinning of BN, and an in-depth investigation via AFM of the surface roughness of the BN after the plasma electron treatment reveals that the remaining BN lattices remain undamaged. This work paves new potential for the investigation of 2DLMs at the multilayer level, opening up novel opportunities for their industry-friendly applications.

[1] Jong-Bae Park, Dae Chul Kim, Young-Woo Kim, Thin Solid Films, 622, 111-114 (2017)

2:30 PM BREAK

3:00 PM *EL19.20.05

Interface Band Engineering for High-Performance 2D Field-Effect Transistors Chul-HoLee; Seoul National University, Korea (the Republic of)

Two-dimensional (2D) semiconductors such as transition metal dichalcogenides (TMDs) have emerged as promising materials for implementing beyond-CMOS electronics due to excellent gate coupling and immunity to short-channel effects at the ultimate scaling. In addition, owing to a van der Waals layered structure, they hold great potential for non-conventional electronics capable of heterogeneous integration and deformation. To achieve high-performance 2D field-effect transistors (FETs), it is highly required to control the electronic states and energy band profiles at various heterointerfaces among the semiconductor channel, the gate dielectric, and metal electrodes. In this talk, I will present two types of proof-of-concepts 2D FETs enabled by interface band engineering: 1) modulation-doped FETs (MODFETs) and 2) metal-semiconductor FETs (MESFETs). In a MODFET, we demonstrated remote modulation doping in the type-II band-modulated channel, enabling us to achieve high mobility by suppressing dopant-induced charge impurity scattering. The 2D MESFETs were also demonstrated using the Fermi-level pinning-free metal Schottky gate, whose device characteristics approach the Boltzmann switching limit.

3:30 PM *EL19.20.06

Tailoring Localized Excitons and Their Light-Matter Interactions with Nanoscale Structure in 2D Semiconductors NicholasJ. Borys^{1,2}; ¹Montana State University, United States; ²MonArk NSF Quantum Foundry, United States

Strain-induced localization of excitons is important for many conventional and quantum optoelectronic devices that are based on layered two-dimensional (2D) semiconductors. For example, single-photon emitters in single-layer WSe₂ (1L-WSe₂), which are potential platforms for solid-state quantum light sources, occur in nanoscale regions of localized tensile strain that produce excitonic potential energy wells. In these regions and the surrounding vicinity, excitons funnel to the strained region of lowest energy. The resulting interplay between reducing the energy, spatially localizing, and hybridizing the exciton with defect states is hypothesized to be integral to the formation of quantum emitters. Understanding these phenomena and their roles in the formation of quantum emitters necessitates investigations that directly probe the intrinsic nanoscale structure-property relationships of strain-localized emitters and identify systematic differences between emitter populations of different systems. The latter focus is crucial to quantitatively assess how different approaches to generate the local strain such as random nanobubbles, deposition on nanofabricated pillars, or nanoindentation affect the quality and properties of the resulting quantum emitters.

This talk will highlight two recent studies by our group of strain-localized emitters in 2D semiconductors. In the first, nanobubbles of 1L-WSe₂ and 1L-WSe₂ on gold films are found to provide a unique background-free system in which to correlate strain-localized states with nanoscale structure. Using room-temperature steady-state and time-resolved spectroscopy, individual localization centers within single nanobubbles can be identified and counted. The occurrence of single or multiple emitters within an individual nanobubble correlates with its structure, demonstrating that strain-engineering of exciton localization in 2D materials necessitates nanoscale precision. Ongoing work is extending these correlated measurements to cryogenic temperatures to probe how the number of localization sites correlates with the number of quantum emitters formed. In the second study, we statistically compare the steady state properties and excited state dynamics of localized exciton-based quantum emitters formed in a variety of systems of 1L-WSe₂ that vary the generation of local strain, the defect density in the 1L-WSe₂, and the surrounding dielectric environment. Of the systems probed arrays of metallic stressors with high-quality flux-grown 1L-WSe₂ are found to systematically produce the most homogeneous quantum emitter populations. Combined, the two studies uncover key structure-property relationships for 2D semiconductor quantum emitters and aim at identifying which combination of strain generation, surrounding dielectric environment, and nanophotonic engineering is best suited to optimize emitter performance.

4:00 PM EL19.20.07

Photoluminescence Emission Properties of Scrolled Monolayer MoS₂ C. AbinashBhuyan^{1,2}, Kishore K. Madapu², SumanPaul³ and SandipDhara^{1,2}; ¹Indira Gandhi Centre for Atomic Research, A CI of Homi Bhabha National Institute, India; ²Indira Gandhi Centre for Atomic Research, India; ³Attocube Systems AG, Germany

Three-atomic thin monolayer MoS₂ (1L-MoS₂) attracted a great deal of attention among the research communities because of their interesting optoelectronic properties [1]. By thinning down the layers from bulk to monolayer, MoS₂ becomes a direct bandgap material with an optical gap at 1.81 eV. Because of the band nesting effect, the 1L-MoS₂ absorbs ~10% of incident light in the visible range [2]. However, photoluminescence (PL) emission from the bilayer is four orders lower than monolayer because of the transition to an indirect band gap which arises at K-point. Interestingly, by stacking multiple monolayers can enhance the light-matter interaction leading to enhanced absorption of incident light. Moreover, rolling a large-area monolayers will make a new 1D structure of material called scrolled 1L-MoS₂. The scrolled 1L-MoS₂ shows higher on-state current in field-effect transistor devices [3]. The demand for scrolled 1L-MoS₂ is increasing because of their use in compact and miniaturized 2D electronic devices.[4] In this context, we fabricated scrolled 1L-MoS₂ by using the solvent, ethanol solution. The solvent extracts the heat during its evaporation causing a decrease in the Gibbs free energy in the planar form, which modifies the planar into scroll structure, to compensate the energy dissipated in evaporation. The fabrication of scrolled 1L-MoS₂ is confirmed by optical microscopy and the field emission scanning electron microscopy. The images (not shown in the figures) reveal a perfect rolling of a planar structure to form a scrolled structure. Raman study confirm the number of layers in the planar and scrolled form of 1L-MoS₂. PL spectra of both monolayer and scrolled 1L-MoS₂ are dominated at A-exciton emission, 1.81 eV [2]. It is interesting to observe the PL intensity enhancement by nearly five times. The observed PL enhancement is attributed to the increase in the number of layers in the scrolled structure. Our PL emission result is further supported by the absorption measurement. We observe more than two times enhancement in

the absorbance. Such scrolled structures can be used in the fabrication of compact 1D optoelectronic devices using 2D materials.

References

- [1] K.F. Mak, C. Lee, J. Hone, J. Shan, T.F. Heinz, Atomically thin MoS₂: a new direct-gap semiconductor, *Physical review letters*, 105 (2010) 136805.
- [2] C.A. Bhuyan, K.K. Madapu, S. Dhara, Excitation-dependent photoluminescence intensity of monolayer MoS₂: Role of heat-dissipating area and phonon-assisted exciton scattering, *Journal of Applied Physics*, 132 (2022) 204303.
- [3] X. Cui, Z. Kong, E. Gao, D. Huang, Y. Hao, H. Shen, C.-a. Di, Z. Xu, J. Zheng, D. Zhu, Rolling up transition metal dichalcogenide nanoscrolls via one drop of ethanol, *Nature communications*, 9 (2018) 1301.
- [4] S. Aftab, M.Z. Iqbal, Y.S. Rim, Recent Advances in Rolling 2D TMDs Nanosheets into 1D TMDs Nanotubes/Nanoscrolls, *Small*, 19 (2023) 2205418.

4:15 PM EL19.20.08

Rapid Detection of Atomically Thin Semiconductors using Automated Photoluminescence MappingJuri G. Crimmann¹, Moritz N. Junker¹, Yannik M. Glauser¹, Nolan Lassaline^{1,2}, Gabriel Nagamine¹ and David J. Norris¹; ¹ETH Zurich, Switzerland; ²Technical University of Denmark, Denmark

Transition metal dichalcogenides (TMDs) are two-dimensional (2D) layered semiconductors that have been studied for various applications, ranging from transistors to single-photon emitters. While multilayered TMDs have an indirect band gap and are commonly used in electronics, TMD monolayers are integrated in optoelectronics since their direct band gap enables efficient light emission. Such atomically thin sheets are often obtained through mechanical exfoliation, followed by manual inspection using a brightfield microscope. However, this process is time-consuming, relies on user experience, and is prone to human error. Here we report a fully automated approach for identifying TMD monolayers using photoluminescence microscopy. Our technique reduces the time spent per sample by more than a factor of 20 and identifies WSe₂ and MoS₂ monolayers with close to 100 % accuracy. We anticipate that our approach will improve fabrication efficiency and enhance the quality of atomically thin optoelectronic devices such as photovoltaics, photodetectors, and light-emitting diodes.

SESSION EL19.21: Virtual Session I
Session Chair: Andrew Mannix
Thursday Morning, December 7, 2023
EL19-virtual

8:00 AM *EL19.21.01

Bilayer Graphene Based Heterostructures for Quantum Information Science Christoph Stampfer^{1,2}; ¹RWTH Aachen University, Germany; ²Forschungszentrum Jülich GmbH, Germany

Graphene and bilayer graphene (BLG) are attractive platforms for quantum electronics, quantum circuits and quantum information science in general. This has motivated substantial efforts in studying quantum dot (QD) devices based on graphene and BLG. The major challenge in this context is the missing band-gap in graphene, which does not allow to confine electrons by means of electrostatics. A widely used approach to tackle this problem was to introduce a hard-wall confinement by etching the graphene sheet. However, the influence of edge disorder, turned out to be a roadblock for obtaining clean quantum devices. The problem of edge disorder can be circumvented in clean BLG, thanks to the fact that this material offers a tunable band-gap (up to 120 meV) in the presence of a perpendicularly applied electric field, a feature that allows introducing electrostatic soft confinement in BLG.

Here we present gate-controlled single and double quantum dot operation in electrostatically gapped BLG [1-6]. We show a remarkable degree of control of our devices, which allows the implementation of gate-defined electron-hole and electron-electron double-dot systems [1], where single-electron occupation becomes possible [2]. Also in the single dot regime, we reach the very few electron/hole regime, extract excited state energies and investigate their evolution in a parallel and perpendicular magnetic field [3]. We will show data on ultra-clean BLG quantum dots allowing investigating the spin-valley coupling in bilayer graphene [4], the electron-hole crossover and the high symmetry between electron and hole states [5]. Finally, we will show data on BLG quantum dots allowing investigating the spin [6] and valley lifetimes. Our work paves the way for the implementation of spin and valley-qubits in graphene.

References:

- [1] L. Banszerus, B. Frohn, A. Epping, D. Neumaier, K. Watanabe, T. Taniguchi, and C. Stampfer, *Nano Lett.* **18**, 4785 (2018)
- [2] L. Banszerus, S. Möller, E. Icking, K. Watanabe, T. Taniguchi, C. Volk, and C. Stampfer, *Nano Lett.* **20**, 2005 (2020)
- [3] S. Möller, L. Banszerus, A. Knothe, C. Steiner, E. Icking, S. Trellenkamp, F. Lentz, K. Watanabe, T. Taniguchi, L. Glazman, V. Fal'ko, C. Volk, and C. Stampfer, *Phys. Rev. Lett.* **127**, 256802 (2021)
- [4] L. Banszerus, S. Möller, C. Steiner, E. Icking, S. Trellenkamp, F. Lentz, K. Watanabe, T. Taniguchi, C. Volk, and C. Stampfer, *Nature Communications* **12**, 5250 (2021)
- [5] L. Banszerus, S. Möller, K. Hecker, E. Icking, K. Watanabe, T. Taniguchi, F. Hassler, C. Volk, and C. Stampfer, *Nature* **618**, 51 (2023)
- [6] L. Banszerus, K. Hecker, S. Möller, E. Icking, K. Watanabe, T. Taniguchi, C. Volk, and C. Stampfer, *Nature Communications* **13**, 3637 (2022)

8:30 AM EL19.21.02

Large-Area Epitaxial Growth of α -In₂Se₃ and its Layer-Dependent Nonlinear Optical Properties Lei Xu, Xiaotian Zhang, Zhenhua Wu and Mingtao Yan; Shanghai Jiao Tong University, China

Non-volatile memories based on ferroelectric materials is one of the most competitive next-generation memories due to its low power consumption, fast read and write speed, non-volatility, and compatibility with CMOS manufacturing processes. However, the critical dimensions of conventional ferroelectric thin films as well as the depolarization and leakage current in conventional ferroelectric dielectrics limit the development of ferroelectric memories. On the other hand, recent development of field effect transistors based on two-dimensional ferroelectric semiconductors offers great potential to outperform conventional ferroelectric memories, in which the polarization states are stored in the semiconducting channels to bypass the limitations of conventional ferroelectric materials. Among all phases of In₂Se₃, two-dimensional α -In₂Se₃ with non-centrosymmetric structure possesses both intercoupled in-plane (IP) and out-of-plane (OOP) ferroelectricity in monolayer, which exhibits great application prospects such as non-volatile memories devices, memristors, and artificial intelligence synapse. However, the coexistence of multiple phases during the growth of In₂Se₃ thin films remains as a challenge to growing uniform and pure α phase In₂Se₃ in a large area and meeting the requirements of large-scale integration.

Herein, we demonstrate the synthesis of large-area α -In₂Se₃ monolayer and multilayer films via both chemical (CVD) and physical (PVD) vapor deposition methods. Characterization techniques such as Raman spectroscopy, piezo-force microscopy (PFM), high-resolution transmission electron microscopy (TEM) and second harmonic generation (SHG) were carried out to identify the single phase and high crystallinity of the films. In particular, we notice that the SHG signal intensity of PVD-grown α -In₂Se₃ decrease gradually with the increase of layers, which is the opposite trend to CVD-grown α -In₂Se₃. This indicates a homostructure of α -In₂Se₃ films was formed in our CVD process compared to the vertical heterostructure of α/β -In₂Se₃ generated from our PVD process. We test the durability of our ferroelectric films. The α -In₂Se₃ films maintained the polarization for more than 30 minutes under PFM measurement and the films remained active after 2 months exposure to the air. Finally, we transfer the sample onto Au/Si substrate to study the polarization switching behavior of CVD and PVD- α -In₂Se₃ under external electric field by conduct atomic force microscope (CAFM).

8:45 AM EL19.21.03

Mechanism of In-Plane Thermal Rectification in Semi-Stochastic Grain-Size Graded Graphene structures Simanta Lahkar and Raghavan Ranganathan; Indian Institute of Technology Gandhinagar, India

Thermal rectifiers preferentially conduct heat in one direction, and can potentially open up novel technological frontiers of applications such as thermoelectric power generation using thermal diode bridge, thermal logic circuits, and advanced thermal management devices for micro-electronics and atomic clocks, if they can be realized with adequate efficiencies. Compared to bulk materials, two-dimensional (2D) materials could offer a wide range of design strategies for generating and tuning thermal rectification (TR) behavior. The realization of practical thermal rectifiers relies significantly on a sound understanding of the underlying mechanisms of asymmetric heat transport. However, the in-plane thermal rectification in 2D materials like graphene having directional gradients of grain sizes, which could potentially exhibit an interplay of multiple mechanisms, has remained elusive. In fact, understanding the heat transport mechanisms in polycrystalline graphene, which are more practical to synthesize than large-scale single-crystal graphene, could potentially allow a unique opportunity to combine with other defects and designs for effective optimization of the thermal rectification property. In this work, we investigated the thermal rectification behavior in periodic atomistic models of polycrystalline graphene whose grain arrangements were generated using different probability distribution functions in order to have different gradient grain size distributions along the in-plane heat flow direction. We employed the centroid Voronoi tessellation technique to generate realistic grain boundary structures for graphene. The reverse non-equilibrium molecular dynamics simulations method was

used to calculate the thermal conductivity and rectification of the structures equilibrated at different stress and temperature conditions. Additionally, detailed phonon mapping was carried out to understand the underlying mechanisms based on the fluctuation-dissipation theory in order to understand the critical structural descriptors that determine the degree of asymmetric heat flow in graded polycrystalline graphene.

9:00 AM EL19.21.04

Intercalation-Exfoliation of MoS₂ with Evaporable Stabilizer to Obtain High-Yield Monolayers Inks for Printable Photodetectors Barbara Y. Martin¹, Tyler Davidson-Hall¹, Nathan Yee¹, Nicholas Wilson², Teri Siu², Manila Ozhukil Valappil², Michael Pope², Jianying Ouyang¹, Neil Graddage¹ and Jianping Lu¹; ¹National Research Council Canada, Canada; ²University of Waterloo, Canada

Photodetectors are electronic devices which convert light into an electrical signal. Printable, flexible and low-cost photodetectors are in high demand as these devices can be used in a variety of applications such as cameras for smartphones, medical sensors, night vision or even ambient light sensors.

Transition Metal Dichalcogenides (TMDs) possess strong light emission and absorption in the visible and near-infrared wavelength range, making them very attractive materials for optoelectronic applications. Molybdenum disulfide (MoS₂) is a multilayer 2D material that can be exfoliated to obtain monolayers, this material is also characterized by multiple crystalline phases. With this variety of structures, it is possible to adjust the band gap of MoS₂ from an indirect band gap at 1.29eV to a direct band gap at 1.8eV. Moreover, metallic or semi-conductor monolayers can also be obtained.

Chemical vapor deposition can be used to produce semi-conductor monolayer TMDs with controllable synthesis. However, large scale, and low-cost production is very difficult with this technique. Intercalation followed by liquid-phase exfoliation is a powerful technique to produce defect-free monolayers in large-quantities. However, reproducible printable inks with high concentration of TMD monolayers are more difficult to achieve. Another challenge to obtaining good quality TMD inks for printable photodetectors is the necessary to use a large amount of insulating stabilizer (such as PVP or ethyl cellulose).

Our work focuses on the development of highly concentrated MoS₂ inks for printable photodetectors. This ink was made by a new intercalation-exfoliation process, an easily evaporable stabilizer was used to replace PVP, and a cascade centrifugation step was added to the process to achieve a highly efficient monolayer size selection (90% of the flakes have less than 3 layers).

9:15 AM EL19.21.05

Effect of Several Growth Parameters on Graphene Growth on Four Types of Supported Cu Films using Cold Wall CVD and Perspective on Growth Mechanism of Graphene from Scaling Functions of Graphene Island Size Distribution Shantanu Das^{1,2}; ¹Intel Corporation, United States; ²Arizona State University, United States

In this work, I will present results from a series of studies using a custom-automated LabVIEW controlled graphene growth method in a custom-modified multi-chamber UHV chamber transformed into a cold wall CVD system. The controlled experimental approach allowed careful study of effect of several growth parameters on graphene growth on Cu. A systematic, in depth study of graphene in industrially preferred cold wall CVD has potential to shed light on studies of other single layer 2D materials.

Graphene growth was explored on solid electrodeposited, recrystallized, sputter deposited and liquid Cu films supported on W or Mo refractory substrates under ambient pressure using Ar, H₂ and CH₄ mixtures. Among these films, electrodeposited Cu film was chosen to study the effect of total flow rate, CH₄:H₂ ratio and dilution of the CH₄/H₂ mixture by Ar at a fixed substrate temperature of 1000 °C and total pressure of 700 Torr, on the nucleation density and average size of graphene crystallites. The resulting morphological changes correspond with those that would be expected if the precursor deposition rate was varied at a fixed substrate temperature for physical deposition using thermal evaporation. The evolution of graphene crystallite boundary morphology with decreasing effective C deposition rate indicates the role of edge diffusion of C atoms along the crystallite boundaries, in addition to H₂ etching on graphene crystallite shape. The results indicate that graphene grown on Cu films using cold wall CVD follows a classical two-dimensional nucleation and growth mechanism. Following nucleation at the earliest growth stages, isolated crystallites grow, impinge and coalesce to form a continuous layer. During the pre-coalescence growth regime, the size distributions of graphene crystallites exhibit scaling which is a function of island area, graphene coverage, average island area and areal density. For graphene grown on Cu surfaces that have been annealed in a reducing Ar+H₂ ambient, excellent data collapse onto a monotonically decreasing universal Avrami scaling function is observed irrespective of graphene coverage, surface roughness or Cu grain size. This result is interpreted to indicate attachment limited growth and desorption of C-containing species. Graphene grown on Cu surfaces that were annealed in a nonreducing environment exhibits a qualitatively different bimodal scaling function indicating diffusion-limited growth with a lower attachment barrier combined with C detachment from the graphene edges.

Graphene growth on molten Cu films supported on custom-designed Mo substrates demonstrate a similar 2D nucleation and growth mechanism. The study also explores the orientation of graphene islands on molten Cu. The roles of temperature gradient, chamber pressure and rapid thermal heating in C precursor-rich environment on graphene growth morphology on thin sputtered Cu films are explained. A comparison of graphene growth on electrodeposited Cu vs recrystallized Cu is also shown.

The growth process and the observed results are instructive for the burgeoning graphene industry. Due to the similarities between the growth mechanism of graphene synthesis using cold wall CVD and hot wall CVD, the considerable knowledge base relevant to hot wall CVD can be exploited for graphene growth using the relatively less-explored cold wall CVD. I also anticipate that applying the study of pre-coalescence size distribution method to other 2D material systems may be useful for elucidating atomistic mechanisms of film growth that are otherwise difficult to obtain.

9:30 AM EL19.21.06

MoS₂/Graphene Heterostructure with Silver Nanoparticles Deposited on the Surface for Nitrogen Dioxide Sensor Applications Jihun Sim and Woojong Yu; Sungkyunkwan University, Korea (the Republic of)

Even small quantities of toxic gases can have fatal implications. In the case of NO₂ gas, even at concentrations as low as 100ppm, it can prove lethal to humans, causing inflammation and burns upon direct exposure. NO₂ is a prominent air pollutant found in the atmosphere, known for its detrimental effects on health and its significant contribution to air pollution issues. Therefore, early detection of NO₂ gas leaks plays a crucial role in ensuring the safe use of NO₂ gas, necessitating the development of fast and accurate detection technologies. In this particular study, researchers successfully fabricated an efficient gas detection sensor by utilizing two-dimensional materials such as MoS₂ and Graphene to create a semiconductor/metal heterostructure. By incorporating a layer of silver (Ag) through sputtering on the surface of these two-dimensional materials, the adsorption of NO₂ gas was induced. Two-dimensional materials, with their high aspect ratio and extensive surface area, exhibit immense potential for enhancing sensing capabilities. Using this sensor based on two-dimensional materials, the researchers were able to detect NO₂ gas even at ultra-low concentrations, starting from as little as 1 ppm up to 50 ppm. Notably, at a concentration of just 1 ppm, the sensor exhibited a remarkable resistance change of nearly 20%.

These findings underscore the boundless opportunities offered by two-dimensional material-based sensors, suggesting that by exploring alternative coatings beyond silver (Ag), it may be possible to target and detect a broader range of gases.

9:35 AM EL19.21.07

Two-Dimensional Van der Waals Lateral Heterostructure with V-Doped MoS₂ and WS₂ Whan Kyun Kim^{1,2} and Woojong Yu³; ¹Department of Semiconductor and Display Engineering, Sungkyunkwan University, Korea (the Republic of); ²Samsung Electronics, Korea (the Republic of); ³Department of Electrical and Computer Engineering, Sungkyunkwan University, Korea (the Republic of)

In this study, we present the fabrication of a two-dimensional van der Waals (vdW) lateral heterostructure, achieved via a solution-based chemical vapor deposition (CVD) process. This methodology opens up avenues for designing devices with novel and unique properties. Our fabrication strategy exploits the differential synthesis temperatures of MoS₂ and WS₂; the former occurring at a lower temperature than the latter. By leveraging this phenomenon, we successfully constructed an in-plane lateral junction through the one-step CVD process, which entailed sequential growth of each material at different temperatures. In addition, substitutional doping of vanadium (V) was implemented in the CVD growth process. Initially, V-doped MoS₂ was synthesized at 700 °C, followed by the epitaxial growth of V-doped WS₂ from the edge of V-doped MoS₂ at 800 °C. This approach ensured the preservation of a hexagonally packed plane and facilitated the formation of an atomically clean and sharp interface between V-doped MoS₂ and V-doped WS₂. In MoS₂ and WS₂, each crystallizing at distinct temperatures, the extent of vanadium (V) doping varies correspondingly. Notably, WS₂, which exhibits a higher crystallization temperature, demonstrated a V doping concentration nearly twice that of MoS₂. This disparity in doping concentrations brought about an intriguing shift in the V-WS₂ semiconductor behavior from its inherent n-type to p-type, while V-MoS₂ remained an n-type semiconductor. Therefore, by utilizing this distinctive property, it becomes feasible to fabricate a vdW lateral PN heterostructure. Our results not only present an efficient fabrication approach for electronic devices but also open up possibilities for creating unique structures like magnetic PN junctions.

9:40 AM EL19.21.08

Potential, Scope and Limitations of Liquid Interface Assembly as a Technique for Synthesizing 2D Thin Films Medini Padmanabhan and Nicholas Weber; Rhode Island College, United States

Solution fabrication of large-area thin films with 2D materials is an active field of study. In this work, we disperse natural graphite and MoS₂ flakes at a heptane-water interface. Individual

flakes spread out and arrange themselves as a thin film at the interface, which is then transferred to a glass substrate. This technique allows us to combine the light absorbing properties of MoS₂ with the high conductivity of graphite to make composite films which exhibit photoconductivity. We observe that the flakes like to arrange themselves in a single layer and resist stacking. The conductivity of the resulting film is correlated with its porosity, much like a percolation network of resistors. We find that the technique, while very effective in spreading out these 2D materials into a single layer, does not help with exfoliation at the atomic scale.

9:45 AM EL19.21.09

Mechanical Nanomanipulation of Water Confined in a Naturally Occurring Water-Hybrid 2D System Raphaelade Oliveira^{1,2}, Alisson R. Cadore², Helio Chacham¹, Raul Freitas², Klaus Krambrock¹, Angelo Malachias¹ and Ingrid Barcelos²; ¹UFMG, Brazil; ²CNPq, Brazil

Water is the matrix of life and its confinement in nanocavities and flow through nanocapillaries are central topics from geophysics to nanotribology. Water in nanoscale media can show distinct elastic and viscosity behaviors, presenting exquisite properties such as low dielectric constant [1]. A more recent development in the emergence of nanofluidics is the ability to fabricate artificial nanocapillaries for water transport through van der Waals (vdW) assembly of atomically-thin two-dimensional (2D) materials, such as hexagonal boron nitride and graphene [2]. Although the engineering of these nanocapillaries can be beneficial in controlling specific properties, there is plenty of natural water-based heterostructures barely explored so far. These water-hybrid 2D systems intercalate water layers in the lamellar structure of naturally occurring vdW materials that can show unprecedented and highly tunable properties for nanotechnology applications.

Hydrous minerals act as natural nanocavities for water transport on Earth, which is essential to biochemical processes with cycling of nutrients and elements. In this scenario, phyllosilicate minerals emerge as an abundant class of hydrous minerals that are wide band gap insulators. They can be exfoliated down to monolayers due to their lamellar structure that stacks silicon oxide tetrahedral layers with (Al,Mg)-octahedral layers with O/OH at the vertices [3]. Some specimens of phyllosilicates can be pillared by ions, such as clays, or further octahedral layers, such as chlorites. They present the unique ability to absorb water by confining water layers in the interlamellar space, being water-hybrid 2D systems of natural occurrence.

Theoretical studies suggest that the electrostatic charge distribution due to the presence of substitutional ions in the structure of phyllosilicates modulates how water confines between its layers [4]. Within the barely explored group of chlorite phyllosilicates, we can identify clinocllore as the specimen that favors higher incorporation of interlamellar water due to its more complex structure. In a previous work, we observed a contribution about 14% wt attributed to the presence of water/hydroxyl ions in clinocllore by quantitative analysis [5]. This expressive water-related amount suggests clinocllore as one of the most suitable natural platforms for water confinement in 2D systems among phyllosilicate minerals. However, the hydration of phyllosilicates by interlamellar water intercalation is not a well understood process besides its importance in several fields.

In the forefront of advancing our understanding of nanoconfined water in 2D systems, we will present the nanoimaging of interlamellar water in ultrathin exfoliated clinocllore by infrared scattering-type scanning near-field optical microscopy. We observed a striation pattern for the nanoconfined water capillaries in clinocllore that changes the overall dielectric properties of the system and, consequently, its surface potential probed by Kelvin probe force microscopy. As a unique result, we performed the nanomanipulation of confined interlamellar water in clinocllore by atomic force microscopy in contact mode. By applying a constant local force between the tip and the sample during the scanning, it was possible to drain practically all the fluid from the analyzed area in a controlled manner, changing the clinocllore surface potential. This pioneering result allows the multifunctionalization of these natural water-hybrid 2D system for catalytic applications, sensing, microfluidic devices, and patterning of biomolecules in 2D systems.

Acknowledgements

We thank our collaborators, funding agencies (CNPq, CAPES, FAPESP and FAPEMIG), Neaspec, ALS, UFMG and CNPEM.

References (DOI)

- [1] 10.1126/science.aat4191
- [2] 10.1038/nature19363
- [3] 10.1038/s41699-020-00172-2
- [4] 10.1346/CCMN.1990.0380510
- [5] 10.1016/j.apsusc.2022.153959

SESSION EL19.22: Virtual Session II
Thursday Morning, December 7, 2023
EL19-virtual

10:30 AM *EL19.22.01

How's Your Interface? Rodney S. Ruoff; Ulsan National Institute of Science and Technology, Korea (the Democratic People's Republic of)

The type of interface(s) formed between adjacent materials **A** and **B** can vary depending on **A** and **B** and parameters such as temperature and pressure—among others. Qualitative terms such as “chemisorption” (covalent bonding) and “physisorption” (van der Waals bonding and perhaps including H-bonding for some but not others) are used to describe bonding present at the interface. I will discuss several interfaces that interest me and my team—and how I think about these interfaces as providing opportunities for the growth of certain types of carbon and related (such as BN) materials. *We appreciate support from the Institute for Basic Science (IBS-R019-D1).*

11:00 AM *EL19.22.02

Three Theory Insights in 2D Growth, and Two Ideas in 2D Ferroelectrics Boris I. Yakobson; Rice University, United States

(1) Why the 2D transition metal dichalcogenides grow better if salt is added to the mix? First-principles calculations of the atomistics behind-the-scenes, from the eutectic effect to gas-phase chemistry, reveal the mechanisms and suggest ways to better “cooking recipes” [Z. Liu et al. Nature, 2018: **556**, 355 || JACS Nano, 2021: **15**, 10525 || JACS, 2022: **144**, 7497]. (2) How to ensure that the produced 2D-layers are coveted single crystals and not a patchwork of inverted domains, disrupted by the grain boundaries? Vicinal plane substrates' surface steps dictate the direction of 2D nucleation by virtue of edge-epitaxy. Theory reveals the key role of structural complementarity [Nano Lett. 2019: **19**, 2027], and thus predicts which substrates work best, e.g. for h-BN [T.-A. Chen et al. Nature, 2020: **579**, 219 || Appl. Mater. Today, 2023: **30**, 101734]. (3) This edge-step epitaxy offers a way to produce free, weakly-bonded borophene on insulator [ACS Nano, 2021: **15**, 18347], a potential breakthrough in the field, if experimentally realized.

(1') We explore with DFT a hetero-bilayer of realistic 2D components: ferroelectric In₂Se₃ and the β-Sb (known for its strong spin-orbit coupling). The ±**P** of the In₂Se₃ induces distinctly different electronics in the bilayer: if **P** points “inward”, it is a trivial insulator; switched “outward”, its state is nontrivial topological, Z₂ = 1 — inviting future multifunctional devices' applications [Nano Lett. 2021: **21**, 785].

(2') In another example, the often-overlooked (blocked by the substrate) flexibility of 2D materials leads to unexpected behavior of the ferroelectrics. Introduced “ferro-flexo” coupling ~**P** × **k** in the Ginzburg-Landau-Devonshire *J*⁴-energy, allows one to predict the spontaneous curvature *k*_s and the rise of Curie temperature, domain wall width, etc. for InP, CuInP₂S₆ and In₂Se₃. Polarization switches do bend the layer, converting electrical signal to movement as an actuator, with efficient work-cycle [ACS Nano, 2023: **17**, 5121].

SYMPOSIUM EL20

Future Materials and Technologies Toward Sustainable Heterogeneous Computing and Energy-Efficient Machine Learning
November 28 - December 5, 2023

Symposium Organizers

Gina Adam, George Washington University
Yiyang Li, University of Michigan
Sayani Majumdar, Tampere University
Radu Sporea, University of Surrey

Symposium Support

Bronze
APL Machine Learning | AIP Publishing

* Invited Paper
+ JMR Distinguished Invited Speaker

SESSION EL20.01: Resistive Switching I
Session Chairs: Yiyang Li and Ilia Valov
Tuesday Morning, November 28, 2023
Hynes, Level 3, Room 301

10:30 AM *EL20.01.01

The Physics and Chemistry of Redox-Based Memristive Switching in Metal Oxides Rainer Waser^{1,2}, Stephan Menzel¹ and Regina Dittmann¹; ¹Forschungszentrum Jülich, Germany; ²RWTH Aachen University, Germany

Redox-Based Resistive Switching Memories (ReRAM), also called *nanoionic* memories or *memristive* elements, are widely considered to provide a potential improvement beyond the limits of current memory technology with respect to write speed, write energies, and scalability as well as an energy-efficient approach to neuromorphic computing concepts.

In this talk, fundamental aspects of the physics and chemistry (lattice disorder, ionic and electronic transport processes, interface reactions and phase formation) of these elements will be presented [1]. In particular, the polarity of the switching (eightwise or counter-eightwise) and the geometry (conducting filament vs. area dependent switching) will be discussed. Furthermore, the ultra-high non-linearity of the switching kinetics of redox-based resistive switching devices will be outlined with an emphasis on the so-called valence change mechanism (VCM) typically encountered as a bipolar switching in metal oxides, but also mentioning the electrochemical metallization (ECM) cells as well systems which may show both aspects. The involved electrochemical and physical processes can be either electric field/voltage enhanced or accelerated by a local increase in temperature due to Joule heating.

The major strands of neuromorphic computing, namely the computational neuroscience for decoding the human brain, the computing-in-memory and the artificial neural networks for pattern recognition, will be worked out. And the different requirements on memristive elements to be applied in these strands will be discussed.

[1] R. Dittmann, S. Menzel, R. Waser, *Adv. Phys.* 70, 2022.

11:00 AM EL20.01.02

Thermodynamic Origin of Nonvolatility in Resistive Memory Jingxian Li and Yiyang Li; University of Michigan, Ann Arbor, United States

Resistive memory or memristor is a highly potential memory and computing unit for next-generation information storage, in-memory computing, and neuromorphic computing. Valence change memory (VCM) is a promising memristor that stores information through the distribution of oxygen vacancy point defects in transition metal oxides.

The ability to store and retain information is a critical function of nonvolatile memory. It is widely believed non-volatility in resistive memory is a result of the slow diffusion kinetics of oxygen vacancies. In this work, we combine materials characterization, device measurements, ab initio, and continuum modeling and show instead that information retention results from phase separation that results from materials thermodynamics. We definitively show for the first time that the amorphous refractory metal oxides undergo spinodal decomposition into two phases with different metal to oxygen ratios. Moreover, the stability of this spinodal decomposition controls whether a resistive memory cell will be able to retain information over time.

By applying phase separation, a foundational principle of materials science, to the field of resistive memory, we explain for the first time why these materials are able to function as nonvolatile memory. We further highlight the critical importance of considering nonideal thermodynamic interactions such as phase separation for future electronic materials dominated by point defects.

11:15 AM EL20.01.03

Fully Transient Simulation of Filament-Type Switching Operations in Unipolar and Bipolar Memristors by Combining Electrothermal and Phase-Field Models Dongmyung Jung¹, Chanhoo Park¹, Ki-Ha Hong² and Yongwoo Kwon¹; ¹Hongik University, Korea (the Republic of); ²Hanbat National University, Korea (the Republic of)

Transient simulation of memristors where conductive filaments (CFs) dynamically evolve according to an electric field and temperature is a challenging subject. In the case of the valence

change mechanism (VCM), the matrix and CFs can be regarded as two distinct phases, the high and low resistance phases (HRP and LRP), respectively. The HRP is stable. On the other hand, the LRP with a uniform concentration of defects is metastable. Therefore, the LRP spontaneously goes back to the HRP after some time, which explains the data retention. In many simulations of the memristor device, the defect migration was described by drift and diffusion (DD). In this case, a CF with a high defect concentration should start to dissolve immediately after forming or set because there is no electromigration at zero electric field and only diffusion by concentration gradient exists. Also, the closer to the outer part of the CF, the lower the defect concentration. In other words, the DD equation alone cannot explain the existence of the LRP with a uniform defect concentration.

Phase-field model (PFM) is the most efficient to deal with a system where two distinct phases, LRP and HRP, are spatially mixed. We coupled the PFM with the electrothermal model along with defect generation and annihilation dynamics and successfully established a fully transient simulation of the forming, reset, and set operations of the VCM-based memristor. Using our model, both unipolar and bipolar switching can be simulated for the same active material by just changing boundary conditions that are bias conditions and interface properties with an electrode. It was shown that in the case of unipolar switching a CF evolves mainly by the generation and annihilation of defects whereas in the case of bipolar switching a CF evolves mainly by the electromigration of defects.

In our I-V curve simulation, the higher compliance current, the thicker CF as experimentally observed. Note that our simulation does not define any specific filament region in the model geometry. Only initial defects are randomly assigned. Also, the successive pulse operations were simulated for synapse applications. Most interestingly, the effects of the interval length between pulses could be observed. The CFs can evolve for the time when no pulse is applied, which is to reduce the interface energy for total energy minimization. As a result, a longer pulse interval resulted in better linearity in the long-term depression curve. More details and the results of our simulation will be shown in the actual presentation.

11:30 AM *EL20.01.04

Fusion of Solid-State Ionics and Electronics to Advance Neuromorphic TechnologyKazuya Terabe, Takashi Tsuchiya and Tohru Tsuruoka; NIMS, Japan

For the further development of today's information society, hardware-oriented artificial intelligence (AI) systems, such as terminal equipment and brain computers that operate with low power consumption and small size, are expected to be developed. To realize such software-independent AI hardware, devices that realize various functions and performances, such as memristive and neuromorphic characteristics, are required. To this end, it is important to actively develop not only conventional semiconductor devices with properties suitable for digital arithmetic processing, but also new-concept devices operating on different principles. One of these is a new group of devices developed by fusing solid-state ionics and electronics. These devices operate by controlling the transport of ions and vacancies as well as electrons and holes in solids. Consequently, the transport of ions (vacancies) and the associated electrochemical phenomena can be used to control the local composition of device materials and even reconstructing the hetero-interface structure at will. In other words, it is the device nanoarchitectonics that is achieved by controlling ion transport. (named ionic nanoarchitectonics)^[1]. This ionic nanoarchitectonics enables the control of various physical properties of device materials, and this control can create interesting devices with new functions and performance not found in conventional semiconductor devices. To date, we have created many devices with diverse functions using ionic nanoarchitectonics^[1-4]. These devices include atomic switches, decision-making devices, artificial synaptic devices^[5], solid-state electrical double-layer transistors, artificial vision^[6], physical reservoir devices^[7] and so on. Ion nano-architectonics, based on the fusion of solid-state ionics and electronics, is a promising method to enhance neuromorphic technology.

Reference

- [1] K. Terabe et al. *Nanoscale* **148**(29), 13873-13879, 2016
- [2] K. Terabe et al. *Adv. Electron. Mater.* **8**(8), 2100645, 2022
- [3] K. Terabe et al. *Jpn. J. Appl. Phys.* **61**, SM0803, 2022
- [4] K. Terabe et al. *Adv. Phys. :X*, **7**(1), 2065217, 2022
- [5] H. N. Mohanty et al. *ACS Appl. Mater. Interfaces* **15**(15), 19279-19289 (2023)
- [6] X. Wan et al. *Nano. Lett.* **21**, 7938-7945 (2021)
- [7] T. Nishioka et al. *Sci. Adv.* **8**, eade1156 (2022)

SESSION EL20.02: Resistive Switching II
Session Chairs: Mehrdad Jalali, Sayani Majumdar and Rainer Waser
Tuesday Afternoon, November 28, 2023
Hynes, Level 3, Room 301

1:30 PM *EL20.02.01

Memristors and Arrays for Analog Computing with High PrecisionJ. Joshua Yang; University of Southern California, United States

The analog data deluge issue nowadays call for multipurpose analog computing platforms with great reconfigurability and efficiency, namely, field programmable analog arrays (FPAAs). [1] FPAAs as the analog counterpart of field programmable digital arrays (FPGAs) open opportunities for fast prototyping analog designs as well as efficient analog signal processing and neuromorphic computing. Memristors may be the ideal building blocks for FPAAs if they are truly analog with many conductance levels, not just for lab-made devices, but more importantly, devices fabricated in foundries. We have recently demonstrated 2048 conductance levels, a record among all types of memories, achieved with memristors in fully integrated chips with 256x256 memristor arrays monolithically integrated on CMOS circuits in a standard foundry. [2] We have unearthed the underlying physics that previously limited the number of distinguishable conductance levels in memristors and developed electrical operation protocols to circumvent such limitations. These results reveal insights into the fundamental understanding of the microscopic picture of memristive switching and provide approaches to enable high-precision memristors for various applications.

Reference:

- 1 Li, Y., Song, W., Wang, Z., Jiang, H., Yan, P., Lin, P., Li, C., Rao, M., Barnell, M., Wu, Q., Ganguli, S., Roy, A.K., Xia, Q., and Yang, J.J.: 'Memristive Field Programmable Analog Arrays for Analog Computing', *Advanced Materials*, 2022, pp. 2206648
- 2 Rao, M., Tang, H., Wu, J.-B., Song, W., Zhang, M., Yin, W., Zhuo, Y., Kiani, F., Chen, B., Jiang, X., Liu, H., Chen, H.-Y., Midya, R., Ye, F., Jiang, H., Wang, Z., Wu, M., Hu, M., Wang, H., Xia, Q., Ge, N., Li, J., and Yang, J.: 'Thousands of conductance levels in memristors integrated on CMOS', *Nature*, 2023, 615, 823.

2:00 PM *EL20.02.02

Resistance Switching in Silicon Oxide for Memory and Computing ApplicationsAdnan Mehonic, Dovydas Joksas, Wing H. Ng, Nikolaos Bampatsalos and Anthony J. Kenyon; University College London, United Kingdom

The increasing demand for computing power has brought to light the limitations of current CMOS-based technologies and Von Neumann architecture. To address this, alternative paradigms like memristor-based accelerators have emerged. In this presentation, I will discuss resistance switching in silicon oxide (SiO_x) based ReRAM devices and explore pathways for improving device performance. Additionally, I will present the rationale and challenges associated with utilising memristive crossbar arrays as analogue hardware accelerators. Two algorithmic approaches are presented to tackle inherent issues in memristor-based systems. The first approach involves utilising committee machines during inference [1], while the second approach explores non-ideality-aware training of memristor-based artificial neural networks (ANNs) [2].

- [1] D. Joksas, P. Freitas, Z. Chai, W.H. Ng, M. Buckwell, C. Li, W.D. Zhang, Q. Xia, A.J. Kenyon, and A. Mehonic, "Committee machines - a universal method to deal with non-idealities in memristor-based neural networks," *Nat Commun* **11**(1), 4273 (2020).
- [2] D. Joksas, E. Wang, N. Bampatsalos, W.H. Ng, A.J. Kenyon, G.A. Constantinides, and A. Mehonic, "Nonideality-Aware Training for Accurate and Robust Low-Power Memristive Neural Networks," *Advanced Science* **9**(17), 2105784 (2022).

2:30 PM *EL20.02.03

Bioinspired In-Sensor Computing for Artificial VisionYang Chai; The Hong Kong Polytechnic University, Hong Kong

According to the projection by Semiconductor Research Corporation and Semiconductor Industry Association, the number of sensor nodes exponentially increases with the development of the Internet of Things. By 2032, the number of sensors is expected to be ~45 trillion, which will generate >1 million zettabytes (10²⁷ bytes) of data per year. The massive data from sensor nodes obscure valuable information that we need it most. Abundant data movement between sensor and processing unit greatly increases power consumption and time latency, which poses grand challenges for the power-constraint and widely distributed sensor nodes in the Internet of Things. Therefore, it urgently requires a computation paradigm that can efficiently process

information near or inside sensors, eliminate redundant data, reduce frequent data transfer, and enhance data security and privacy. We propose bioinspired in-sensor computing paradigm to reduce data transfer and decrease the high computing complexity by processing data locally. By using two-dimensional (2D) semiconductors, we demonstrate the in-sensor computing at the device and array levels. The unique sensory response characteristics of 2D semiconductors lead to computing functions at sensory terminals. In particular, bioinspired device characteristics enable the fusion of the sensor and computation functionalities, providing a way for intelligent processing sensory information.

3:00 PMBREAK

3:30 PM *EL20.02.04

Valence Change Memristive Devices for Bio-Inspired Information Pathways Anna Linkenheil, Jonas Schneegaß, Benjamin Spetzler, Zhansong Geng, Kristina Nikiruy, Tzvetan Ivanov, Frank Schwierz and Martin Ziegler; Technische Universität Ilmenau, Germany

Memristive devices have attracted considerable attention in the electronic device community due to their inherent memory effect, which allows them to mimic the function of biological synapses. As such, they are a key building block for realizing artificial neural computing schemes in hardware, so-called neuromorphic systems. However, there are various neuromorphic architectures with different requirements for memristive devices, requiring optimization of electrical properties and materials as well as the technological framework for each specific application.

This talk will discuss the challenges and prospects of memristive devices for neuromorphic computing in general and several selected examples. Valence-change-based memristive devices are presented, and it will be discussed how their properties can be tailored by systematic design variations for applications in neuromorphic computing architectures. Furthermore, it is shown how the resistance change of memristive devices affects the dynamics of networks and how network dynamics influence network connectivity. Important requirements for memristive devices will be discussed, and it will be shown how a new way of information processing beyond current approaches can open a new bio-inspired pathway toward the construction of cognitive electronics.

This work was partially funded by the Carl-Zeiss Foundation via the Project MemWerk and the German Research Foundation (DFG) through the Collaborative Research Centre CRC 1461 "Neurotronics – Bio-Inspired Information Pathway".

4:00 PM EL20.02.05

Electroforming-Free Threshold Switching in Polycrystalline ErMnO₃ Films Based Two-Terminal Devices Rong Wu^{1,2}, Florian Maudet¹, Thanh Luan Phan¹, Wassim Hamouda¹, Veeresh Deshpande¹ and Catherine Dubourdieu^{1,2}; ¹Helmholtz-Zentrum Berlin, Germany; ²Freie Universität Berlin, Germany

Rare-earth hexagonal manganites h-RMnO₃ (R=Y, Er, Ho to Lu) have been extensively studied as multiferroic materials in the last 15 years. The study of non-volatile unipolar resistive switching behavior in polycrystalline YMnO₃ was reported, indicating that h-RMnO₃ may be promising candidates for memristive devices owing to their intriguing ferroelectric domain pattern - vortex lines where six-fold domains merge [1], [2].

In this work, we report the first demonstration of volatile resistive switching behavior observed in polycrystalline ErMnO₃ thin films. The devices exhibit a repeatable unipolar threshold switching behavior. To fabricate the devices, 60 nm-thick ErMnO₃ thin films were deposited on Pt-coated Si wafers using RF sputtering. Subsequently, a post-deposition annealing process was carried out at 750 °C in N₂, resulting in the formation of polycrystalline ErMnO₃ thin films with mixed orthorhombic and hexagonal crystalline phases. Further engineering was realized through a subsequent thermal treatment at 400 °C in air. Top Pt electrodes were then patterned. The two-terminal Pt/ErMnO₃/Pt devices exhibit high endurance (>10⁴ cycles) and low variability. To gain a clear understanding of the physical origin of the threshold switching and to open a path for potential applications, a detailed structural study (X-ray diffraction, Raman spectroscopy, X-ray photoelectron spectroscopy, scanning electron microscopy) and extensive electrical characterization (current-voltage and voltage-current measurements including as a function of temperature, conductive atomic force microscopy) were performed. We propose a physical model to explain the observed threshold switching effect and current controlled negative-differential resistance behavior. Our model involves trap-assisted and thermally-activated Poole-Frenkel conduction, along with local Joule heating effects. We will discuss how the engineering of the microstructure, specifically the inclusions of minor orthorhombic phase within the hexagonal phase, plays a crucial role in achieving the threshold switching behavior. These devices hold great promise as candidates for building spiking neurons in leaky integrate-and-fire (LIF) neuron circuits [3].

References

- [1] H. Schmidt, Appl. Phys. Lett. 118, 140502 (2021), doi: 10.1063/5.0032988.
- [2] V. R. Rayapati *et al.*, J. Appl. Phys. 126 (2019), doi:10.1063/1.5094748.
- [3] Y. Ding, *et al.*, Front. Neurosci. 1732 (2022), doi: 10.3389/fnins.2021.786694.

4:15 PM EL20.02.06

Oxygen Tracer Diffusion in Substoichiometric Hafnium Oxide for Resistive Memory Dongjae Shin¹, Jingxian Li¹, Karsten Beckmann², Anton V. Ievlev³ and Yiyang Li¹; ¹University of Michigan, United States; ²State University of New York Polytechnic Institute, United States; ³Oak Ridge National Laboratory, United States

Resistive memory are highly promising candidates for neuromorphic computing due to their ability to retain a constant resistance state over time. Hafnium oxide-based memristors in particular have shown exceptional retention stability, exceeding 10 years at 85°C. It is believed that this retention stability is a result of slow oxygen vacancy migration; however, there exists substantial discrepancy between the experimentally measured device retention time and the characteristic oxygen diffusion time of HfO₂. In this work, we measure the oxygen ¹⁸O tracer diffusion of different HfO_x thin films with different metal-to-oxygen ratios. We found that sub-stoichiometric hafnium oxide exhibits ~1-3 orders of magnitude lower diffusivity compared to stoichiometric HfO₂. We show that the retention time of Hafnia memristors can be approximated by the diffusion time when we use this lower oxygen diffusivity of the substoichiometric oxide, resolving the question of why Hafnia memristors are able to retain state.

4:30 PM *EL20.02.07

New Mechanism in Ohmic VCM Devices - Prospective and Challenges Shaochuan Chen¹, Teng Zhang², Heinrich Hartmann³, Astrid Besmehn³, Yuchao Yang² and Ilija Valov^{3,4}; ¹RWTH Aachen University, Germany; ²Peking University, China; ³Research Center Juelich, Germany; ⁴Institute of Electrochemistry and Energy Systems, Bulgaria

Functionalities, properties and stability of memristors are determined by three main factors – physico-chemical processes materials and operation scheme, where the first two factors are inherently related. It is a of highest priority of the ongoing research to improve memristors in several important aspects including multi-functional use, variability, state stability and degenerative processes. A way to progress in fundamental aspect understandings and applications is to achieve understanding and control over the physical processes involved in the formation of different resistive states and based on this knowledge to design reliable materials system being with predictable and adjustable properties. Several important aspects of the operation principles have been revealed, such as effects of protons and ambient moisture, interface interactions, migration of cations believed to be immobile, nanobattery effect, influence of the capping layers and film thicknesses etc.

In this work, we present a new mechanism observed in ohmic oxide memristors that allows for significant improvement of the device characteristics and stability. The switching performance depends on materials used for electrodes, their electrochemical activity and redox potential. We found that not Schottky barrier is necessary to switch the devices and reach reliable operation. *In situ* TEM analysis have shown that contribution of different ionic species is responsible for two distinctive switching mechanisms that in turn determine the performance. Based on this knowledge we were able to design devices showing multiple functionalities and with significantly improved characteristics.

SESSION EL20.03: Poster Session
Session Chairs: Yiyang Li and Radu Sporea
Tuesday Afternoon, November 28, 2023
Hynes, Level 1, Hall A

8:00 PM EL20.03.01

Flexible and Disposable Paper-Based Optoelectronic Physical Reservoir Devices Hiroaki Komatsu, Norika Hosoda and Takashi Kuno; Tokyo University of Science, Japan

Wearable sensor devices that use physical probes such as light and electric potential to monitor health conditions are widely used in the biomedical field. To classify and predict health

conditions, the acquired data needs to be transmitted to an AI system in the cloud. The communication of such a large amount of data involves issues such as network load and communication speed. One of the methods to solve these issues is that we allow the sensor itself to have AI functions, such as physical reservoir (PR) devices. We believe that in-sensor optoelectronic PR device, which has (1) response times that match the time scale of biological signals (0.1-100 s), (2) flexibility, and (3) disposability, is one of the ideal frameworks to realize intelligent sensors. However, because the response times of the optoelectronic PR devices reported so far are several tens of milliseconds, it difficult to handle biological signals [1,2]. Moreover, flexibility and disposability have also not been addressed.

In this study, we fabricated an optoelectronic PR device that satisfy three requirements mentioned above. Our device is composed of ZnO nanoparticles (NPs)-embedded cellulose nanofiber (CNF) freestanding film. The film was prepared by spray deposition of CNF aqueous solution dispersed with ZnO NPs (average diameter: 25 nm)[3]. Patterned Au electrodes were formed on the film surface. We demonstrated a pattern recognition using ultraviolet (UV) light input pulses. To verify that it works as a PR device, the film was exposed to UV pulsed light encoded with 4-bit patterns (pulse width: 50-500 ms, wavelength: 365 nm), and the photocurrent was measured.

Under the UV pulsed light irradiation, the film showed the rise and decay time constants of 6.4 s and 3.4 s, respectively, indicating that our films have a time scale compatible with biomedical applications. Furthermore, the maximum photocurrent was increased with increasing the number of pulses when the UV light was repeatedly irradiated. This phenomenon indicates that our films exhibit the short-term memory required for reservoir devices. To demonstrate the AI performance, handwritten digit recognition was conducted using MNIST databases. Our device showed accuracy of 88%. Therefore, it was demonstrated that our films can be used as a PR device. In addition, handwritten digit recognition using our film with a bending radius of 9.5 mm and 16.1 mm showed almost no change in accuracy compared to the flat condition. Thus, it was demonstrated that our film can be used in the bent state. In this session, we will describe the results of pattern recognition in the bent state and introduce the possibilities of disposability.

[1] Y. Sun et al. *Adv. Intell. Syst.* **5**(2023)2200196

[2] Z. Zhang et al. *Nat. Commun.* **13**(2022)1

[3] H. Komatsu et al. *Nanomaterials.* **12**(2022)940

SESSION EL20.04: Biohybrids and Protonics
Session Chairs: Gina Adam and Sabina Spiga
Wednesday Morning, November 29, 2023
Hynes, Level 3, Room 301

8:15 AM *EL20.04.01

Organic Neuromorphic Electronics for Emulating and Interfacing Biological Systems Paschalis Gkoupidenis; Max Planck Institute for Polymer Research, Germany

Harnessing the exceptional efficiency of the brain in information processing at the technological level can be condensed in the terms “artificial intelligence” and “neuromorphic computing”. A popular approach in artificial intelligence is the representation of information processing aspects found in biological systems with artificial neural networks (ANNs). This approach is based on executing algorithms, that loosely represent the function of the nervous system, on traditional computer architectures. Over the last decade, the field of artificial intelligence (AI) has demonstrated an enormous potential for complex processing and efficient computing. However, concepts of AI are mainly based on digital operating principles, while being part of an analogue world with great diversity in signaling. Moreover, AI still lacks the efficiency and computing capacity of biological systems. Alternatively, neural functions can be directly emulated with non-conventional devices, circuits and architectures. This hardware-based paradigm of brain-inspired processing is known as neuromorphic electronics.

In this talk, various neuromorphic devices will be presented that are based on organic mixed conductors, materials that are traditionally used in bioelectronics. A prominent example of a device in bioelectronics that exploits mixed ionic-electronic conductivity phenomena is the organic electrochemical transistor (OECT). Organic neuromorphic electronics based on OECTs have the ability to emulate efficiently and with fidelity a wide range of bio-inspired functions including synaptic plasticity and neuronal dynamics. The presence of a global electrolyte in an array of devices also allows for the homeostatic control of the array. Global electrical oscillations can be used as global clocks that phase-lock the local activity of individual devices in analogy to the global brain oscillations. Moreover, “soft” interconnectivity through the electrolyte can be defined, a feature that paves the way for parallel interconnections between devices with minimal hard-wired connections. Finally, practical demonstrations will be shown, highlighting the potential of organic materials in robotics, neuromorphic sensing and biointerfacing.

8:45 AM EL20.04.02

Proton-Based Electrochemical Random Access Memory using Nickel (Oxy)Hydroxide Andrew J. Jalbert and Yiyang Li; University of Michigan, United States

In-memory computing using analog resistive memory cells can be substantially more efficient than digital computing. Electrochemical random-access memory (ECRAM) using protons or oxygen vacancies are a highly promising solution. Nickel Hydroxide is an electrochromic material that can be switched between two phases: Ni(OH)₂ (Hydroxide) and NiOOH (Oxyhydroxide) upon the insertion or removal of protons. In this work, we investigate the use of Nickel (Oxy)Hydroxide as a proton-based ECRAM material. We show that this material is able to switch resistance states in a linear and analog fashion by electrochemically shuttling protons through an alkaline electrolyte media at room temperatures. Importantly, this ECRAM cell is also able to retain information over time, providing the potential for long-term, nonvolatile, and analog information storage.

9:00 AM EL20.04.03

Investigation of Drain Bias Stress Effect on IGZO TFTs Based Charge Storage Neuromorphic Circuits Ung Cho, Minseung Kang, Jaehyeon Kang, Hyeonjun Seo and Sangbum Kim; Seoul National University, Korea (the Republic of)

Charge storage type neuromorphic synapse circuits such as 2T0C, 3T1C and 6T1C have recently emerged as alternatives to nonideal nonvolatile memories for on-chip training of deep neural networks, particularly in terms of linear and symmetric weight updates [1]. Utilizing amorphous InGaZnO (a-IGZO) thin film transistors as update transistors instead of traditional Si CMOS enables long data retention and low power consumption due to their superior low leakage characteristics [2]. However, the reliability of the IGZO TFTs remains a critical challenge, particularly regarding oxygen vacancies in the active channel, gate insulator, and channel/gate insulator interface [3]. While previous research has extensively studied stability problems under positive bias stress (PBS), negative bias stress (NBS), and hot carrier stress (HCS), investigations on the impact of drain bias stress (DBS) on IGZO TFTs are limited. During the off-state, where no programming occurs and weights are maintained in the storage capacitor, the update transistors are exposed to drain and off-state gate bias stress. The off-state accounts for the majority of time in the operational scenario in charge storage type neuromorphic circuits, thus highlighting the significance of DBS stability analysis. This study focuses on investigating the effect of DBS at the transistor level, modeling degradation and unveiling its mechanisms. Furthermore, the impact of DBS on IGZO TFTs based charge storage neuromorphic circuits was assessed using the proposed model.

Electrical measurements were conducted to assess the reliability at the unit transistor level. The evaluation of gate bias stress, including both PBS and NBS, revealed little degradation in terms of threshold voltage (V_{th}), subthreshold swing (SS), and on-current. On the other hand, during the evaluation of drain bias stress, V_{th} and SS demonstrated little change, while a noticeable on-current degradation was observed. Additionally we simulated the off-state by applying both drain bias and negative gate bias simultaneously, it was observed that the greater the negative bias, the more significant on-current degradation occurred. Complementary measurements, including capacitance-voltage measurements and the evaluation of transistors with various dimensions, were performed in order to elucidate degradation mechanisms and indicate the physical meaning of degradation through a stretched exponential model. The degradation model parameters, such as the time constant of electron trapping and the saturation point of current degradation, demonstrate an increased degradation with more negative gate bias. Using the proposed degradation model, the weight change of 3T1C neuromorphic circuits after cycling endurance could be successfully predicted. Furthermore, the impact of DBS on training and inference accuracy was investigated. Leveraging the knowledge gained from this study enables the design of more reliable IGZO TFTs based neuromorphic circuits and their operation, advancing the development of robust and efficient neuromorphic systems.

References

[1] Y. Li et al., “Capacitor-based cross-point array for analog neural network with record symmetry and linearity.” 2018 IEEE Symp. VLSI Technol. IEEE, 2018.

[2] M. Caselli et al., “Write-verify scheme for IGZO DRAM in analog in-memory computing.” in Proc. IEEE Int. Symp. Circuits Syst. (ISCAS), 2022.

[3] J. F. Conley, Jr., “Instabilities in amorphous oxide semiconductor thin film transistors.” IEEE Trans. Device Mater. Rel., vol. 10, no. 4, pp. 460–475, Dec. 2010.

Acknowledgements

This research was supported by National R&D Program through the National Research Foundation of Korea (NRF) funded by Ministry of Science and ICT (2020M3F3A2A01081240). This work was supported by Samsung Electronics Co., Ltd (A0426-20190012).

*Corresponding Author : Sangbum Kim; E-mail: sangbum.kim@snu.ac.kr

9:15 AM *EL20.04.04

Electrolyte and Neurotransmitter Dependency of Long-Term Plasticity in Biohybrid Synapses [Francesca Santoro](#); Forschungszentrum Jülich/RWTH Aachen University, Germany

The replication of neural information processing in electrical devices has been extensively studied over the years. The paradigm of parallel computing, which allows information to be simultaneously detected, processed and stored, is required for numerous applications in many fields. In the case of brain-computer interfaces, another important requirement is the suitability of the device for communication with cells. Organic electrochemical transistors (OECTs) based on PEDOT:PSS are used for this purpose due to their ionic-to-electronic signal transduction and biocompatibility [1]. Many works have demonstrated the reproduction of neural plasticity mechanisms, such as short-term facilitation and long-term potentiation. In each device, the physical mechanism of transduction may be different, but it is known that the electrolyte plays a key role in the functioning of these devices, as it provides the ions responsible for the chemical transmission of information. Focusing on long-term memory, this can be reproduced in the OECTs with the oxidation of the neurotransmitter, as in the case of the biohybrid synapse [2]. It is crucial to understand the influence of the electrolyte composition on the memory effect of the device, as long-term modulation is based on a change in the ionic balance between the electrolyte and the organic polymer. For this reason, the influence of some of the most used electrolyte compositions on neurotransmitter-mediated long-term plasticity was analyzed in this work. The interaction of electrolytes with dopamine oxidation was investigated by means of the cyclic voltammetry technique, and the effect on channel conductance was studied by applying pulses of different amplitude and duration as gate voltage of the transistors. It was shown that long-term memory can be hidden under certain conditions, such as the presence of Mg^{2+} and Ca^{2+} in the electrolyte. This electrolyte-dependency plasticity should be considered when the OECT is used in a biological environment in which a large number of molecules of a different nature, in addition to neurotransmitters, are present. The next step in this analysis involves the effect of the electrolyte in more neurotransmitter-sensitive OECTs, with micrometer-sized channel area.

References

- 1 Bernard et al. (2007). In: *Advanced Functional Materials* 17.17, pp. 3538–3544.
- 2 Keene, Scott T et al. (2020). In: *Nature Materials* 19.9, pp. 969–973.

9:45 AMBREAK

SESSION EL20.05: Physical Computing
Session Chairs: Duygu Kuzum and Radu Sporea
Wednesday Morning, November 29, 2023
Hynes, Level 3, Room 301

10:15 AM *EL20.05.01

More is Different: Physical Computing Discovery [Elliot J. Fuller](#); Sandia National Laboratories, United States

The heterogeneous integration of novel materials with existing technology is critical to beyond Moore computing paradigms. Digital computation based upon silicon has relied heavily on a reductionist hierarchy, wherein the system can be reduced to simple rules and elements can designed separately. However, this hierarchy collapses when novel materials are integrated into physics-based compute paradigms due to the twin difficulties of complexity and scale. Physical compute systems must be co-designed. In 1972, the physicist Philip W. Anderson coined the term, “more is different” to describe emergent phenomena that occur in complex systems where entirely new properties appear, especially where symmetries are broken¹. Here I will discuss experimental work on building complex physical systems that execute computational kernels, for example outer product updates², and how these systems are “different” from their digital counterparts. Next, I will demonstrate how models can be used to predict the evolution of simple neuromorphic learning systems when operated under certain constraints³. These models break down when phase transformation (or symmetry breaking) occurs and the collective behavior of an ensemble of interacting elements is expected to exhibit emergent phenomena. Finally, I will discuss the development of a computing discovery platform to study emergent materials behavior, wherein rapid synthesis, characterization, and integration of new materials into compute arrays enables studying compute outcomes at scale (>1,000 interacting elements).

References

- [1] Anderson *Science*, 177(4047), 393-396 (1972)
- [2] Fuller et. al. *Science*, 364(6440), 570-574 (2019)
- [3] Li et. al. *Frontiers in Neuroscience*, 15, 636127 (2021)

10:45 AM EL20.05.02

CMOS-Compatible Electrochemical Synaptic Transistor Arrays for Deep Learning Accelerators [Jinsong Cui](#)¹, [Fufei An](#)¹, [Yuxuan Wu](#)¹, [Jiangchao Qian](#)¹, [Saran Pidaparthi](#)¹, [Jian-Min Zhuo](#)^{1,2} and [Qing Cao](#)^{1,2}; ¹University of Illinois, United States; ²University of Illinois at Urbana-Champaign, United States

In-memory-computing architectures based on memristive crossbar-arrays can enhance the computing efficiency for deep-learning with massive parallelism. However, to fulfill their potential, the core memory devices must be capable of providing high-speed and symmetric analog programming with small variability, compatible with silicon technology, and scalable into nanometer-size footprint. We present an electrochemical synaptic transistor, built with CMOS-compatible metal oxides and operating by shuffling protons within a symmetric gate stack, to meet all these stringent requirements. It can be monolithically integrated with silicon transistors to form pseudo-crossbar arrays where parallel, precise, and symmetric programming of the channel conductance can be executed with gate-voltage pulses. High-speed programming with frequency approaching megahertz, endurance above 100 million read-write pulses, and device critical dimensions down to $150 \times 150 \text{ nm}^2$ have all been realized.

11:00 AM EL20.05.03

Nonvolatile Electrochemical Random Access Memory using Phase Separation [Virgil J. Watkins](#), [Diana Kim](#), [Laszlo Cline](#) and [Yiyang Li](#); University of Michigan, United States

Analog neuromorphic computing can decrease the energy consumption of data-intensive tasks like machine learning by orders of magnitude through conducting matrix vector multiplication using Ohm's and Kirchoff's Laws. Electrochemical random access memory (ECRAM) stores and switches analog resistance states by electrochemically modulating the concentration of oxygen vacancies in a transition metal oxide. Unfortunately, most ECRAM devices are volatile and revert to equilibrium, with retention times orders of magnitude lower than the typical 10 year, 85C requirement. In our work we develop a nonvolatile ECRAM cell using tantalum oxide. Our core innovation is the use of phase separating materials in the miscibility gap. In this configuration, all resistance states have the same chemical potential, thereby eliminating the driving force for volatility. This result not only exceeds the expected 10 year lifetime, but can provide a memory cell with potentially indefinite retention at elevated temperatures.

11:15 AM EL20.05.04

Electric Field Regulated High Thermal Rectification Ratio using Ferrocenyl Terminated Molecular Junction [Xingfei Wei](#) and [Rigoberto Hernandez](#); Johns Hopkins University, United States

Conventional silicon-based electronic devices have electron conductance rectification ratios greater than 1. This magnitude was achieved in molecular electric diode composed of ferrocenyl (Fc) terminated self-assembly monolayers (SAMs) developed by the Nijhuis group [*Nature Nanotech* 12, 797–803 (2017)]. Perhaps surprisingly, the largest thermal rectification ratio reported so far in materials and devices is at the magnitude of near 1. Applying the same electrostatic attraction mechanism seen by the Nijhuis, we have found in atomistic simulations that ferrocenyl terminated molecular junctions can also achieve high thermal rectification ratio. In the forward bias case, the top electrode is negatively charged, the Fc group is positively charged, and the strong electrostatic force drag the Fc group closer to the top electrode and thereby enhances thermal conductance. In the backward bias case, the Fc group is charge neutral, and the electrostatic force between the Fc groups and the top electrode is weak and thereby reduces thermal conductance. We will report the distance between the two electrodes, the partial charge on the Fc group, the electric field magnitude, and the number of SAM molecules affecting heat transfer. The implications of this work for developing next-generation phononic devices will also be discussed.

References:

- [Wei et al.](#), Thermal Transport through Polymer-Linked Gold Nanoparticles, *J. Phys. Chem. C* 2022, 126, 43, 18511–18519. <https://doi.org/10.1021/acs.jpcc.2c05816>
[Wei and Hernandez](#), Heat Transfer Enhancement in Tree-Structured Polymer Linked Gold Nanoparticle Networks, *in preparation*.

11:30 AM *EL20.05.05

Volatile and Non-Volatile Memristive Technologies Implementing Tunable Dynamic and Relaxation for Spiking Neural Networks Sabina Spiga; CNR-IMM, Italy

Hardware spiking neural networks (SNNs) are currently attracting an increasing interest towards low-power computing systems for edge applications, such as the ones relying on smart analysis of sensory signals in real time. Taking inspiration from brain computation, which processes information with temporal structure, it is desired that also neuromorphic chips compute with dynamics, encompassing devices and circuits able to compute and elaborate information over multiple time scales. In current CMOS-based neuromorphic chips, the integrative functions and temporal dynamics are mainly implemented by capacitors. Anyway, they hardly provide in the system time constants over ms or tens of ms, and their capacitance density is difficult to be scaled-up without occupying large silicon area. Within this framework, memristive technologies have recently shown great promise to substitute or complement CMOS circuits in hardware SNNs, with key role in providing novel and compact dynamical elements which can mimic the neuronal and synaptic features, and are able to extend the time domain of the computing system. Our work focuses on memristive technologies capable of exhibiting tunable dynamics, integrative functions and relaxation effects which can span up to seconds or longer, up to the non-volatile behavior. The devices are based on the structure Ag/SiO₂/Pt or Ag/Al₂O₃/SiO₂/Pt stacks and the switching mechanism relies on the formation and dissolution of a silver-based filament shorting the two electrodes. The filament can be unstable and exhibits a relaxation behavior once the programming voltage is removed. In the ON, low resistance state, it is also possible to achieve conductance modulation as a function of the input stimuli. We will show that the devices show dynamic behaviors over multiple time scales which originate from an interplay of accumulation and relaxation effects, and the overall features can be controlled by programming conditions and material engineering.

SESSION EL20.06: Breaking News

Session Chairs: Yiyang Li and Sayani Majumdar

Wednesday Afternoon, November 29, 2023

Hynes, Level 3, Room 301

1:45 PM EL20.06.02

Enhancing Memory Retention of FAB Compatible ECRAM Devices using an Ion Blocking Layer Nir Tessler¹, Seonuk Jeon² and Jiyong Woo²; ¹Technion-Israel Institute of Technology, Israel; ²Kyungpook National University, Korea (the Republic of)

Traditionally, the only ions allowed or welcomed by the microelectronic industry are those that act as fixed dopants. The issue of mobile ions became welcome primarily due to the memristor technology however, thin film transistor technologies benefit from them too. The electrochemical (transistor) random access memory (ECRAM) is emerging as a promising building block for multi-level neuromorphic computing. Using FAB-compatible materials we construct the ECRAM using CuOx as the gate and ions source (Cu⁺). The morphology of the HfOx gate insulator layer is finetuned to render it ion transporting such that it can act as a uniform electrolyte layer. Lastly, the channel material is WOx with tungsten metal as the source/drain contact. While there are several reports of ECRAM devices, the operation mechanisms are not fully known/understood thus withholding progress of this field. Using the Sentaurus device simulator by Synopsis, including the hydrogen diffusion module, we simulate the mixed ionic electronic operation of the device. We have recently reported that by fitting the simulation to the device performance we could identify the potentiation mechanism (i.e., insulator charging) and the occurrence of copper plating that takes place under high Cu⁺ ion flux (as in fast charging of Li batteries).[1]

In the first part of the talk, we will expand on the chemical-physics details of the ECRAM device mentioned above. Next, we will present a new device architecture where an ion-barrier layer is introduced and is shown to enhance memory retention. The third device structure is where we remove the WOx layer and study the ionic-electronic conduction of a modified HfOx layer. Using the above three device architectures in conjunction with the mixed ionic-electronic device simulation we reveal the role of the two memory mechanisms: a) Electric field-activated ion transport and b) Structure-induced trapping by ion-barrier layers.

Reference

[1] Nir Tessler, Nayeon Kim, Heebum Kang, Jiyong Woo; Switching mechanisms of CMOS-compatible ECRAM transistors—Electrolyte charging and ion plating. *J. Appl. Phys.* 21 August 2023; 134 (7): 074501. <https://doi.org/10.1063/5.0154153>

2:00 PM EL20.06.03

Probabilistic Computing using Metal Nanoparticles-Embedded Mott Threshold Switches for True Random Number Generator Yewon Seo, Yunkyu Park and Junwoo Son; Pohang University of Science and Technology, Korea (the Republic of)

VO₂ threshold switch, which undergoes a insulator-to-metal transition above a threshold voltage, shows promise as a candidate for stochastic switching due to its capacity to determine the overall electrical transition in devices through the percolative formation of metallic filaments [1]. However, geometric evolution of the switchable (metallic or insulating) domains significantly influences the stochastic switching in VO₂; the performance of VO₂ based stochastic devices (e.g., true random number generators) could be tuned by the evolution of metallic domains in the insulating matrix and random formation of conducting filaments [2].

Here, we achieve drastic enhancement of intrinsic stochastic operation under pump-probe procedure in Pt-nanoparticle-embedded VO₂ (Pt-VO₂) two-terminal devices. In particular, metallic Pt nanoparticles enable an extension of memorization time from pump pulse, which enhances probability of certain selection to show random firing of on/off (1 or 0) states under probe pulse; the extended recovery time to the insulating state presents a wide range of options in terms of probe voltage amplitude and delay time, thereby enhancing the randomness of the switching behavior upon application of the second probe pulse. Moreover, this device has the advantage of high speed (667 kbits/s), low power consumption (12 nJ/bit), high endurance (>105200 bits), and mass production, which is key requirement to realize true random number generator (TRNG). Therefore, our result provides a new strategy to improve stochastic switching characteristics in Mott threshold switches for high performance TRNG.

References

[1] Valle, Javier del, et al., *Nano letters* 22, 1251 (2022)

[2] Jo, Minguk et al., *Nature Communications* 13, 4609 (2022)

2:15 PM EL20.06.04

Aubergine to Blackberry: Nature Derived Chromophores to Mimic Photosensitive Neurons in Human Eye Maxim Shkunov¹, Aimee Sweeney^{1,1}, Annelot Nijkoops^{1,2}, Leslie Askew¹, Manuela Ciocca² and Luisa Petti²; ¹University of Surrey, United Kingdom; ²Free University of Bozen-Bolzano, Italy

Visual information processing in vertebrates begins with light detection by the eye's retina cone and rod cells. Tri-colour cones, typical for primates, respond to blue, green and red/yellow spectral bands, whereas rods cell are extremely sensitive to low light intensities, providing grey-scale vision. Mimicking behaviour of these cells with optoelectronic devices opens up opportunities for neural stimulation, artificial retina, superhuman vision devices, and self-powered optical sensors. Nature is also rich in conjugated, organic semiconductor molecules, with various bandgaps, thus offering colour-specific responses in the visible spectral range.

In this work we explore fruit- and vegetable-derived conjugated chromophores from various berries, including raspberry, blackberry, elderberry, blueberry, as well as aubergine, beetroot, red cabbage and spinach, targeting photo-induced response in three spectral bands, red, green and blue. Self-assembly binding properties of these molecules allow to build chromophores-decorated TiO₂ nano-porous structures inspired by dye-sensitised solar cell technologies. We demonstrate photo-capacitor devices employing the chromophores, interfaced with biological electrolyte (phosphate buffered saline), showing spiking photocurrent (photovoltage) response under low-intensity pulsed light excitation.

Absorption spectra of chromophores were found to be in the visible part of the spectrum, with chlorophyll derived from spinach peaking at 440 nm, and with anthocyanins and betalains chromophores' peaks at around 520 nm. The photocurrent spectral response of the samples was correlated with that of absorption; however, some spectral shifts were observed. Photo-current response signals were clearly present for all samples, with magnitude from few tens to hundreds of nA when exposed to pulsed-light flash cycles with a pulse length of few tens of milliseconds. This is comparable to typical biological response times. The results suggest that nature-derived conjugated chromophores present feasible environmentally-friendly semiconductors for opto-stimulated devices with colour-selectivity. They also produce photo-current and -voltage responses corresponding to hyperpolarisation and depolarisation of cell membranes associated with neurons' spiking behaviour.

2:30 PM BREAK

3:30 PM *EL20.10.03

Tuning the Relaxation Time of Diffusive Memristors for Neuromorphic Applications Qiangfei Xia; University of Massachusetts, United States

A diffusive memristor is a volatile resistance switch with a metal/oxide/metal structure. It goes to a low resistance state when an electrical stimulus is applied and automatically relaxes back to its original high resistance state if the stimulus is removed. The switching behavior is attributed to the formation and rupture of a localized conducting channel within the oxide layer. Because of their structural similarity with biological ion channels, diffusive memristors have been successfully used to emulate typical synaptic and neuronal behavior such as spike-timing-dependent plasticity, leaky integrate and fire, etc. However, a remaining issue of the diffusive memristor is the non-uniform and non-controllable relaxation time (the time it takes to go from low to high resistance states), which limits the wide-range adoption of such devices in large arrays for real-world problems. In this work, we designed and fabricated diffusive memristors with uniform and tunable relaxation times. We adopted a double oxide switch layer that led to an over ten-fold improvement in the cycle-to-cycle uniformity. By connecting the device to different resistors, we tuned the relaxation time up to three orders of magnitude. This controllable and uniform relaxation process was utilized to generate the time surfaces in the hierarchy of time surface (HOTS) algorithm for pattern recognition.

4:00 PM EL20.07.02

Characterization of Crystallization Kinetics in Phase-Change Materials using Indirectly Heated Phase-Change Memory and its Application to One-Shot Weight Transfer Inhyuk Choi, Minseung Kang, Wonseok Choi and Sangbum Kim; Seoul National University, Korea (the Republic of)

Phase-change memory (PCM) exhibits notable advantages such as non-volatility, fast operating speed, scalability, and high reliability, making it a promising candidate for analog synaptic devices in neuromorphic computing. However, challenges related to nonlinearity and asymmetry in weight modulation need to be addressed [1]. Consequently, weight modulation predominantly relies on the gradual crystallization process, as amorphization through a melt-quench process induces abrupt changes in weight values [2]. In the context of off-chip training, concerns regarding nonlinearity and asymmetry can be alleviated since the weights pre-trained by the software can be accurately transferred to the PCM synaptic array using an iterative program and verify scheme [3]. However, it is noteworthy that this iterative scheme is not energy-efficient and can potentially accelerate the endurance failure of PCM devices. In contrast to conventional PCM structures that employ self-heating of phase-change materials, indirectly heated PCM structures utilizing externally generated heat have been suggested for high-reliability memory devices [4] and RF switches [5]. Here, for the first time, we propose the application of indirectly heated PCM as an energy-efficient and highly reliable one-shot weight transfer device through a single programming pulse with a simultaneous verify process. To ensure precise weight transfer, a comprehensive understanding of the crystallization process occurring within the device is crucial. Indirectly heated PCM itself can be used to characterize the crystallization kinetics [6], enabling faster heating rates close to device operation and broader temperature ranges encompassing melting points compared to previous characterization studies using differential scanning calorimetry (DSC), a laser with transmission electron microscope (TEM) analysis, and other device-based approaches [7-9]. After optimization through finite element method (FEM) simulation, we fabricated an indirectly heated PCM device designed to achieve a uniform temperature distribution in the phase-change material. Crystallization properties, including crystallization temperature, time, and activation energy, were measured over a wide temperature range for various phase-change materials exhibiting either nucleation-dominated or growth-dominated crystallization. For growth-dominant materials, growth rates spanning several orders of magnitude were estimated in conjunction with calibrated FEM simulations. Additionally, we will discuss the crystallization characteristics and device structures that need to be considered to enhance the energy efficiency and accuracy of one-shot weight transfer in indirectly heated PCM devices.

References

- [1] K. Byun et al., *Advanced Materials Technologies*, 2022, DOI: 10.1002/admt.202200884
- [2] M. Suri et al., *In 2011 International Electron Devices Meeting*, 2011, DOI: 10.1109/IEDM.2011.6131488
- [3] S. Yu, *Proceedings of the IEEE*, 2018, DOI: 10.1109/JPROC.2018.2790840
- [4] I. Choi et al., *Materials Science in Semiconductor Processing*, 2021, DOI: 10.1016/j.mssp.2021.105987
- [5] N. El-Hinnawy et al., *IEEE Electron Device Letters*, 2013, DOI: 10.1109/LED.2013.2278816
- [6] N. Wainstein et al., *IEEE Transactions on Electron Devices*, 2021, DOI: 10.1109/TED.2020.3048100
- [7] J. Orava et al., *Nature Materials*, 2012, DOI: 10.1038/nmat3275
- [8] M. Salinga et al., *Nature Communications*, 2013, DOI: 10.1038/ncomms3371
- [9] R. Jeyasingh et al., *Nano letters*, 2014, DOI: 10.1021/nl500940z

Acknowledgements

This work was supported by SK Hynix Co., Ltd (0417-20200185).

*Corresponding Author : Sangbum Kim; E-mail: sangbum.kim@snu.ac.kr

4:15 PM EL20.07.03

Mechanisms in Gadolinium-Doped Gallium Nitride for Future Computing and Quantum Applications Vishal Saravade^{1,2}, Chuanle Zhou³, Zhe Chuan Feng², Benjamin Klein² and Ian T. Ferguson²; ¹Pennsylvania State University, United States; ²Kennesaw State University, United States; ³Missouri University of Science and Technology, United States

Characterizations and mechanisms in gadolinium-doped gallium nitride (GaGdN) that can enable its applications for future neuromorphic and quantum computing will be presented. Gallium nitride (GaN) has been a well-investigated compound semiconductor for power devices, LEDs, photodetectors, and neutron detection applications. However, spintronic properties of GaN have either not been found to be suitable for future quantum computing applications or have not been well explored. In this work, the results obtained and mechanisms observed and identified in GaGdN indicate the potential suitability of GaGdN for spintronic applications. Monocrystalline GaGdN thin films were deposited on sapphire substrates by metal-organic chemical vapor deposition (MOCVD). Two Gd precursors were used to observe the variations in the properties with different metal-organic sources. GaGdN grown using a (TMHD)₃Gd precursor showed Anomalous Hall Effect (AHE) based on a carrier-mediated mechanism due to carrier-hopping and metallic conduction. GaGdN grown using a Cp₃Gd precursor exhibited Ordinary Hall Effect (OHE) indicating no signs of spin polarizations. A key difference between the (TMHD)₃Gd and Cp₃Gd precursors is that (TMHD)₃Gd precursor contains oxygen in its organic ligand. In order to clearly understand the mechanisms for spin properties in GaGdN, GaGdN grown using Cp₃Gd source were implanted and doped with oxygen and carbon. As-grown Cp₃Gd that showed OHE, after O or C implantation showed AHE, which is a sign of spin polarization. Resistivity of GaGdN from Cp₃Gd source increased after O or C-implantation increasing which indicates the introduction of O- and C-induced deep interstitial states. The n-type carrier concentration reduced upon implantation, which indicates that these energy states are acceptor-type. Annealing was done to stabilize the O- and C-dopants in GaGdN from Cp₃Gd. After annealing, AHE signal in GaGdN:O reduced in smoothness but the resistivity decreased and the carrier concentration increased. On the other hand, annealed GaGdN:C showed a smoother AHE signal, an increased resistivity, and a reduced carrier concentration. X-ray diffraction (XRD) measurement showed that O and C stabilize in GaGdN:O and GaGdN:C at interstitial sites and render the AHE. The nature of crystallographic incorporation and effects of annealing on the spin-related properties of GaGdN:O and GaGdN:C were different even though both showed room temperature AHE. The mechanism in GaGdN for room temperature spintronics is carrier-mediated and is activated by O or C-induced deep interstitial acceptor energy states. Insights into these mechanisms can aid the further developments in III-Nitrides for future heterogeneous computing, machine-learning devices, neuromorphic computing, and quantum applications.

4:30 PM *EL20.07.04

Integration of Ag-CBRAM Crossbars and Mott ReLU Neurons for Efficient Implementation of Deep Neural Networks in Hardware Duygu Kuzum, Jaeseoung Park, Yuhan Shi and Sangheon Oh; University of California, San Diego, United States

In-memory computing with emerging non-volatile memory devices (eNVMs) has shown promising results in accelerating matrix-vector multiplications (MVMs). However, activation function calculations are still being implemented with general processors or large and complex neuron peripheral circuits. Here, we present the integration of Ag-based conductive bridge random access memory (Ag-CBRAM) crossbar arrays with Mott ReLU activation neurons for scalable, energy and area-efficient hardware implementation of deep neural networks (DNNs). We develop Ag-CBRAM devices that can achieve a high ON/OFF ratio and multi-level programmability. Compact and energy-efficient Mott ReLU neuron devices implementing rectified linear

unit (ReLU) activation function are directly connected to the columns of Ag-CBRAM crossbars to compute the output from the weighted sum current. We implement convolution filters and activations for VGG-16 using our integrated hardware and demonstrate the successful generation of feature maps for CIFAR-10 images in hardware. Our approach paves a new way toward building a highly compact and energy-efficient eNVMs-based in-memory computing system.

SESSION EL20.08: Devices and Technology
Session Chairs: Gianluca Milano and Radu Sporea
Thursday Morning, November 30, 2023
Hynes, Level 3, Room 301

8:45 AM EL20.08.01

Describing the Analog Resistance Change of HfO_x Neuromorphic Synapses Fabia Farlin^{Athena} and Eric M. Vogel; Georgia Institute of Technology, United States

At the forefront of memristive device research, significant attention is paid to the understanding of resistance variations in Titanium/Hafnium Oxide (Ti/HfO_x) synapses. These changes are typically dictated by a thin-oxide barrier, a result of oxidation and reduction within a Hafnium-rich conducting filament [1, 2, 3, 4]. Yet, despite a broad understanding of these principles, direct experimental investigation of the conducting filament proves notably complex. Consequently, crucial physical attributes and processes, such as the exact location of the barrier, the temporal fluctuations in thickness during analog pulsing, and the influence of temperature on the current, remain elusive and demand a more thorough elucidation.

We aim to take a step forward to unravel these intricacies by utilizing a compact model rooted in Trap-Assisted-Tunneling and Ohmic transport principles. This model has demonstrated significant value in shedding light on the mechanisms of analog switching in HfO_x synapses. It not only accurately mirrors the experimentally observed current-voltage relationship, but also faithfully reproduces its sensitivity to temperature changes.

In deploying this model, we have been successful in extracting the barrier heights during analog pulsing. These data align with a barrier situated adjacent to the reset anode [5, 6]. Our findings are supported by an independent Finite Element Analysis simulation using COMSOL Multiphysics® that incorporates the migration of oxygen vacancies.

The proposed model's utility has been further amplified by its capacity to estimate the barrier's thickness in response to the analog pulses. It is able to simulate the evolution of the current-voltage relationship from the low resistance state to the high resistance state by simply modulating the thickness of the barrier.

In summary, this work enables us to delve deeper into the relationship between the physical characteristics of the HfO_x synapses and the analog switching dynamics.

References:

- [1] Athena, Fabia F. et al. "Trade-off between Gradual Set and On/Off Ratio in HfO_x-Based Analog Memory with a Thin SiO_x Barrier Layer." *ACS Applied Electronic Materials* (2023): n. Pag.
- [2] Athena, Fabia F., et al. "Towards a better understanding of the forming and resistive switching behavior of Ti-doped HfO_x RRAM." *Journal of Materials Chemistry C* 10.15 (2022): 5896-5904.
- [3] Athena, Fabia F., et al. "Impact of titanium doping and pulsing conditions on the analog temporal response of hafnium oxide based memristor synapses." *Journal of Applied Physics* 131.20 (2022): 204901.
- [4] West, Matthew P., Athena, Fabia F., Graham, Samuel, Vogel, Eric M. "Bias history impacts the analog resistance change of HfO_x-based neuromorphic synapses." *Applied Physics Letters* 122.6 (2023).
- [5] Bersuker, G., et al. "Metal oxide RRAM switching mechanism based on conductive filament microscopic properties." *2010 International Electron Devices Meeting*. IEEE, 2010.
- [6] Padovani, Andrea, et al. "Microscopic modeling of HfO_x RRAM operations: From forming to switching." *IEEE Transactions on electron devices* 62.6 (2015): 1998-2006.

Acknowledgment:

The authors would like to thank Professor Samuel Graham at the University of Maryland for the COMSOL model and Professor Suman Datta at the Georgia Institute of Technology for providing the thermal measurement facilities.

9:00 AM EL20.08.02

Atomic Layer Deposition of WO_x-Doped In₂O₃ for High-Performance BEOL-Compatible Transistors Chanyoung Yoo^{1,2}, Balreen Saini², Jonathan Hartanto², Fei Huang², Cristian R. Arens², John D. Baniecki¹, Wilman Tsai², Baylor B. Triplett² and Paul McIntyre^{1,2}; ¹SLAC National Accelerator Laboratory, United States; ²Stanford University, United States

The semiconductor industry has undergone a revolution over the last five decades, driven by Moore's statement on dimensional scaling. However, the challenges for continued area scaling via lithographic patterning and the memory bottleneck limit the efficiency of computing. A new paradigm of improved energy efficiency, high bandwidth, and low latency on-chip memory access can be achieved by using 3D computing architectures with monolithic integration of logic and memory devices at high density (M3D, Monolithic three-dimensional). To realize M3D integration in future computing, fabricating high-performance thin film transistors and memories under back-end-of-line (BEOL) compatible conditions having a limited thermal budget (<400°C maximum temperature) must be addressed.

Metal oxide semiconductors incorporating In₂O₃, have received significant attention as they possess high mobility, high I_{ON}/I_{OFF} ratio, ultra-scaled gate length, and sufficient drive currents. Doping In₂O₃ with several mole % tungsten oxide to form "IWO" has been reported to improve the threshold voltage stability of these semiconductor channel materials. However, currently reported film deposition for IWO is limited to sputtering, which cannot grow conformal films on topographically complex surfaces. This limitation becomes critical when utilizing these films as channel materials in gate-all-around or FinFET structures, which inherently possess 3D geometries. To address the increasing demand for high on-current, the shift towards 3D structures is necessary.

Consequently, we use the 3D-compatible atomic layer deposition (ALD) method to deposit IWO by adjusting the cycle ratios for In and W precursors and the oxidant co-reactant, enabling precise control over the doped film composition. We demonstrate deposition of IWO (1~4 mol% WO_x) films using ALD and fabricate both bottom- and top-gated thin film transistors with a 3-nm thick IWO channel in a BEOL-compatible process with a maximum temperature of less than 250°C. The 1 mol% WO_x-doped IWO transistor exhibits exceptional performance characteristics, including a subthreshold slope of 65 mV/decade, a high I_{D,sat} of 70 (W=12, L=1.5) at V_{DS}=1.0 V and V_{GS}=2.0 V, and remarkable stability under bias stress. The transistor showed negligible hysteresis and maintained excellent threshold voltage (V_{th}) stability under negative and positive bias stress conditions (ΔV_{th} = -0.06, and +0.1 V, respectively, at an electric field of 4.2 MV/cm for 1000 seconds). This V_{th} stability under bias stress highlights the reliability of ALD-grown IWO for ferroelectric field-effect transistors and its potential to enable high-performance monolithic 3D integrated devices.

9:15 AM *EL20.08.03

Metal-Oxide NeoHebbian Synapses for Scalable Learning Dmitri Strukov, Tinish Bhattacharya, Sai Sukruth Bezugam, Shubham Pande and Ewelina Wlazlak; University of California, Santa Barbara, United States

Backpropagation through time (BPTT) algorithm is commonly used for learning and modeling temporal data. The algorithm applies the BP technique on the unrolled recurrent neural network T (~ up to 1000) times for T-step-long input sequences. Hence, enormous energy and time are spent on training such an effectively T-layer-deep network. Recently suggested e-Prop learning algorithm addresses this inefficiency by taking inspiration from biologically-plausible three-factor rules. E-prop synaptic weights are adjusted using locally stored information from pre- and post-synaptic neurons, avoiding resource-taxing network unrolling. Hence, such an algorithm is naturally suited for (in-memory, analog) neuromorphic hardware that could drastically reduce training time and energy.

In my talk, I will discuss recent work on "neoHebbian" synapses essential for an efficient eProp algorithm hardware implementation. Such synapses feature two state variables - a neuron coupling weight and an "eligibility trace" for updating the weight. Several design options were considered to implement these features, including implementations based on single-state variable and multiple-state variable metal-oxide resistive switching devices and utilizing temperature as a state variable. I will conclude my talk by discussing promising research directions at material and device levels for improving the performance of such synapses.

9:45 AM BREAK

10:15 AM EL20.09.02

Investigation of Connection Strength Modulation Between the Artificial Neuron Devices Based on 2D hBN Threshold Switching RRAM Yooyeon Jo¹, Gichang Noh¹, Eunpyo Park¹, Min Jee Kim¹, Yong Woo Sung¹, Dong Yeon Woo¹, Dae Kyu Lee¹ and Joon Young Kwak^{1,2}; ¹Korea Institute of Science and Technology, Korea (the Republic of); ²Korea University of Science and Technology, Korea (the Republic of)

The brain-inspired neuromorphic computing has attracted many researchers to solve the von Neumann bottleneck problems of conventional computing systems [1-2]. Various emerging materials and structures have been proposed to emulate the performance of biological neurons and synapses successfully. In particular, 2D materials-based memristors have been investigated by many researchers because of their excellent electrical performance, simple structure, and small device scale as promising building blocks of neuromorphic computing [3-5]. Although many artificial synaptic devices based on 2D materials-based memristors have been reported, there are very few reports in artificial neuron research, which is one of the key components in neuromorphic computing systems. Also, the integration of developed artificial neuromorphic devices based on emerging materials is an essential field of research to verify the performance of an artificial neural network (ANN) on the system level and successfully demonstrate large-scale ANN hardware [6-7].

In this study, we fabricated the threshold switching resistive random-access memory (RRAM) based on 2D multi-layer hBN film to mimic the behavior of the biological neuron for neuromorphic computing. The fabricated device was composed of Au/Ti bottom and Au/Ag top electrodes, respectively. The fabricated volatile memristor showed the highly-reliable resistance switching characteristics with 0.22 V of the average set voltage even at 110 fA of compliance current. Additionally, it showed a huge ON/OFF ratio over 3×10^6 at 0.1 V of reading voltage. The threshold switching characteristics were well maintained with the different series resistors from 100 k Ω to 10 M Ω . We evaluated the switching speed of the fabricated device via an AC response experiment. The 100 k Ω series resistor was connected to protect the device from a breakdown. As a result, it showed 22.7 and 30.9 μ s of ON and OFF time, respectively. The leaky-integrate-and-fire (LIF) neuron behaviors were demonstrated with the fabricated device and passive components. According to the RC time delay and the input pulse amplitude, the number of output spikes of the artificial neuron could be modulated, resulting in tailoring the artificial neuron properties to the desired performance for various applications. Lastly, we integrated the two artificial neurons to demonstrate the biological neural networks. The two LIF neurons were connected via a synaptic resistor as a biological synapse. Depending on the resistance (connection strength between the neurons), the number of output spikes of the post-synaptic neuron was modulated. We believe that our experimental results pave the way for the development of large-scale neural network hardware in the future.

Acknowledgments: This work was supported by the National Research Foundation of Korea (NRF) (grant no. 2021M3F3A2A01037738) and Korea Institute of Science and Technology (KIST) through 2E32260.

References

- [1] G. Cao, Adv. Funct. Mater., 2021 [2] H.-M. Huang, Adv. Intell. Syst., 2020 [3] C. Y. Wang, Adv. Electron. Mater., 2020 [4] H. Bian, Adv. Mater., 2021 [5] S. Chen, Nat. Electron., 2020 [6] J. Woo, IEEE Electron Device Lett., 2019 [7] Q. Duan, Nat. Commun., 2020

10:30 AM EL20.09.03

Low-Temperature Liquid Metal Printing for Sustainable Fabrication of 2D Oxide Electronics William J. Scheideler, Andrew B. Hamlin and Simon A. Agnew; Dartmouth College, United States

Low-thermal budget fabrication of metal oxide semiconductors could unlock these materials' potential for emerging applications in sensing, computing, and memory devices via 3D heterogeneous integration with CMOS electronics. Towards that goal, we present a low-temperature, energy-efficient approach to deposit high performance two-dimensional (2D) metal oxides and heterostructures. Our approach consists of continuous liquid metal printing (CLMP) driven by Cabrera-Mott oxidation of liquid metal alloys, for depositing of 2D oxide layers as thin as 1 nm and multilayers 10's of nm. The simplicity of this vacuum-free CLMP process mitigates the need for high capital expenditure equipment and eliminates use of toxic gases. Metal oxidation is thermodynamically favorable, allowing rapid growth kinetics at the millisecond time-scale for wafer scale deposition in less than 2 seconds at temperatures from 200 °C down to 120 °C for back-end-of-line (BEOL) applications as well as flexible electronics.

We present a study of the physics of liquid metal printing of 2D binary and ternary oxides based on alloys of In, Ga, Zn, and Sn by utilizing rapid film thickness measurements based on spectroscopic reflectometry. We investigate the limits of printing speed and model the influence of speed and print temperature on 2D oxide growth kinetics and crystallinity as determined from XRD. Finally, we apply CLMP to assemble heterostructures with 1 nm-level precision for enhancing modulation doping at 2D oxide interfaces, resulting in exceptionally conductive (> 500 S/cm) printed conductive oxide layers.

10:45 AM *EL20.09.04

Nanowires as Building Blocks for Unconventional Computing Nanoarchitectures Gianluca Milano¹ and Carlo Ricciardi²; ¹Istituto Nazionale di Ricerca Metrologica (INRiM), Italy; ²Politecnico di Torino, Italy

G. Milano^{1*}, C. Ricciardi²

¹Advanced Materials Metrology and Life Science Division, INRiM (Istituto Nazionale di Ricerca Metrologica), Strada delle Cacce 91, Italy.

²Department of Applied Science and Technology, Politecnico di Torino, Corso Duca Degli Abruzzi, 24, Italy.

Email: g.milano@inrim.it

Self-assembled computing nanoarchitectures based on interacting nanoobjects have been recently proposed as biologically plausible substrates for neuromorphic computing [1,2]. In these nanonetworks, functionalities arise from the emergent behavior of the system that rely on collective phenomena. Here, we report on NW networks as versatile substrate for physical (*in materia*) computing. We show that the emergent behavior in these complex networks arise from resistive switching phenomena in single network elements, as revealed by investigating switching properties of single NW and single NW junctions. The emergent spatio-temporal dynamics of these nanoarchitectures in multiterminal characterization is shown that can be exploited for neuromorphic-type of data processing and represent versatile substrates for the implementation of unconventional computing. In the framework of physical reservoir computing (RC), we report on the computing capabilities of these networks by considering different computing tasks such as pattern recognition, time-series prediction and speech recognition. A combined experimental and modeling approach will be discussed, and a theoretical framework based on graph theory to describe complex nanonetworks will be discussed. Going beyond the concept of two terminal measurements, we report on experimental evidence of memory engrams (or memory traces) in NW networks, i.e., physicochemical changes in biological neural networks supposed to endow the representation of experience stored in our brain. Results show that these networks represent a versatile substrate for computing, allowing both encoding and consolidation of information in the same physical substrate, paving the way for a development of new *in materia* computing paradigms.

[1] G. Milano, G. Pedretti, M. Fretto, L. Boarino, F. Benfenati, D. Ielmini, I. Valov, C. Ricciardi, Adv. Intell. Syst. **2020**, 2000096.

[2] G. Milano, G. Pedretti, K. Montano, S. Ricci, S. Hashemkhani, L. Boarino, D. Ielmini, C. Ricciardi, Nat. Mater. **2021**, DOI 10.1038/s41563-021-01099-9.

1:30 PM *EL20.07.05

Robust and Reliable Computation using Heterogeneous Devices and CircuitsGiacomoIndiveri; ETH Zürich, Switzerland

For many practical tasks, that involve real-time processing of sensory data and closed-loop interactions with the environment, conventional artificial intelligence neural network accelerators cannot match the performance of biological ones.

Neuromorphic intelligence aims to emulate the principles of computation of animal brains, exploiting the physics of computation of electronic and memristive devices.

Similar to their biological counterparts, neuromorphic devices and circuits are affected by variability and inhomogeneities.

In this talk I will present brain-inspired methods and strategies to achieve reliable and robust computation using an unreliable and inhomogeneous computing substrate, and present examples of neuromorphic systems that use these methods to solve edge-computing and sensory processing applications.

2:00 PM *EL20.10.01

Sustainable Fabrication of Nanoscale Memories Based on Molecular Materials and Nanogap ElectrodesDimitraG. Georgiadou; University of Southampton, United Kingdom

Nanotechnology is widely used in electronics to further miniaturise electronic components. Nanomaterials have played a major role in this, as they possess many attractive inherent properties derived from their low dimensionality. However, nanoparticles and self-assembled monolayers are usually processed from solution and they are difficult to be implemented with high yield in large area electronics. On the other hand, two-terminal electronic devices commonly comprise a generic metal/semiconductor/metal structure in a vertical (sandwich) configuration. This poses restrictions in the device fabrication when nanomaterials are involved, as the quality of the film is often compromised due to the small scale of the nanomaterials that do not guarantee uniform, continuous and pinhole-free film formation. A solution to this is offered by lateral devices, where the two metals are placed on the same plane and separated by a gap, which is filled by the semiconductor. If this gap is small enough, comparable to the dimensions of the materials used, the nanomaterials can effectively bridge this gap and connect the two electrodes electrically without causing a short-circuit.

Adhesion lithography (a-lith) is a nanopatterning technique with reduced manufacturing energy as compared, for example, with e-beam lithography, that allows the fabrication of asymmetric nanogap metal electrodes at a low cost and with high throughput on a variety of rigid and flexible substrates of arbitrary size. We have so far demonstrated ultra-high speed (GHz) Schottky diodes (1) and fast photodetectors (2) as well as multi-bit and ferroelectric memories (3) based on different solution-processed semiconductors and a-lith patterned electrodes separated by a <10 nm gap.

Herein we present different classes of molecular materials, based on the polyoxometalate and Pb-free perovskite families, which are successfully implemented in nanoscale memory applications. Our results indicate that multi-state memory behaviour is within reach with polyoxometalate materials, while we also present molecular self-assembly approaches to better control the resistive switching at the nanoscale. Since only a few electrons are required to function, these devices hold promise for low power consumption and high-speed operation. Furthermore, we show that the combination of coplanar nanogap electrodes with Bi-based perovskites holds great promise for achieving low power consumption and fast switching speeds, while their planar geometry facilitates a light-controlled operation, enabling both analogue tuning of resistance states and elimination of sneak currents in the array configuration.

This work paves the way to the development of a new form of greener devices and systems that merge photonic, electronic and ionic effects, bringing new prospects for in-memory computing and artificial visual memory applications.

1. Georgiadou, D.G., J. Semple, A.A. Sagade, H. Forstén, P. Rantakari, Y.-H. Lin, F. Alkhalil, A. Seitkhan, K. Loganathan, H. Faber, and T.D. Anthopoulos, *100 GHz zinc oxide Schottky diodes processed from solution on a wafer scale*. Nature Electronics, **2020**. 3(11): p. 718

2. Georgiadou, D.G., Y.-H. Lin, J. Lim, S. Ratnasingham, M.A. McLachlan, H.J. Snaith, and T.D. Anthopoulos, *High Responsivity and Response Speed Single-Layer Mixed-Cation Lead Mixed-Halide Perovskite Photodetectors Based on Nanogap Electrodes Manufactured on Large-Area Rigid and Flexible Substrates*. Advanced Functional Materials, **2019**. 0(0): p. 1901371

3. Kumar, M., D.G. Georgiadou, A. Seitkhan, K. Loganathan, E. Yengel, H. Faber, D. Naphade, A. Basu, T.D. Anthopoulos, and K. Asadi, *Colossal Tunneling Electroresistance in Co-Planar Polymer Ferroelectric Tunnel Junctions*. Advanced Electronic Materials, **2020**. 6(2): p. 1901091

2:30 PM EL20.10.02

Hexagonal Si and Ge Polytypes as Optoelectronic MaterialsMartinKeller¹, AbderrezakBelabbes^{1,2}, JürgenFurthmüller¹, FriedhelmBechstedt¹ and SilvanaBotti^{3,1}; ¹Friedrich Schiller University Jena, Germany; ²Sultan Qaboos University, Oman; ³Ruhr University Bochum, Germany

The group IV elements silicon and germanium crystallize in cubic diamond structure under ambient conditions and feature indirect bandgaps. Therefore they cannot emit light efficiently and are not applicable in active optoelectronic devices. Under high pressure, however, as well as using different growth techniques, several Si and Ge polymorphs, have been observed. Lonsdaleite Ge as well as Ge-rich hexagonal alloys have even been found to have a direct bandgap and strongly emit light with varying frequency. Thus hexagonal systems have become of great interest for potential optical emitters that may be integratable with CMOS technology. We have performed extensive ab initio studies of the energetic, structural and electronic properties as well as oscillator strengths of the hexagonal Si and Ge polytypes 2H, 4H and 6H using Density Functional Theory and approximate quasiparticle treatments, and trends between the different geometries are analysed. The results for cubic and hexagonal Si and Ge agree excellently with existing experimental findings. The electronic structures point to promising optical properties.

2:45 PM *EL20.07.01

Impact of Phase-Change Memory Nonidealities on Analog In-Memory Computing Deep Learning AccuracyNingLi^{1,2}; ¹Lehigh University, United States; ²IBM Research, United States

Among the emerging approaches for deep neural network (DNN) acceleration, compute-in-memory (CIM) in crossbar arrays using non-volatile memories (NVMs) is very promising for achieving high execution speeds and high energy efficiency. Phase change memory (PCM) is one of the most promising candidates for analog CIM – particularly for inference using previously-trained DNN weights. However, when NVMs are used in analog mode, devices will exhibit nonidealities compared to a perfect analog resistor, limiting the computing accuracy. These nonidealities for PCM devices mainly include resistance drift, read noise, limited memory window, and various device failures due to fabrication yield and limited device endurance and retention. In this presentation, I will talk about our study on the impact of these nonidealities on the analog CIM deep learning accuracy.

We systematically varied PCM memory window, resistance drift, and read noise, and studied their impact on the accuracy of large neural networks of various types and with tens of millions of weights.[1] We show that the DNN accuracy can be improved by the PCM with reduced read noise, even if the memory window is also reduced. However, there is a limit on the memory window, below which the accuracy drops significantly. DNN inference accuracy decreases over time due to the PCM resistance drift. However, the long-term accuracy loss can be minimized using an optimized mapping of weights to unit cells with multiple PCMs representing weights of varying significance. The energy efficiency dependence on the resistance drift was also studied [2]. There are tradeoffs and correlations between PCM device characteristics, which we used to identify the device optimization space to achieve better short term and long-term accuracy.

In addition, there are typically some failed devices of various types in NVM CIM chips, due to nonperfect fabrication yield and device failure over time. We studied the impact of these different types of failed devices on the analog CIM accuracy for various DNNs.[3] We find that larger networks with fewer reused layers are more tolerable to failed devices. Devices stuck at high resistance states are more tolerable than devices stuck at low resistance states. To improve the robustness of DNNs to defective devices, we developed training methods that add noise and corrupt devices in the weight matrices during network training and show that this can increase the network accuracy in the presence of the failed devices. Our approach is based on a single generic training and a subsequent mapping of the weight to any chip with unknown failed device locations.

In summary, we systematically studied the impact of nonidealities of PCMs on the DNN accuracy, using the PCM devices fabricated at IBM [1] and the hardware-aware simulation tool [4] developed at IBM Research. We proposed a few methods, including optimization of device specification, optimized weight mapping, special hardware aware training, to enhance the DNN performance.

[1] N. Li, C. Mackin, A. Chen, K. Brew, T. Philip, G.W. Burr, M. Rasch, A. Sebastian, V. Narayanan, N. Saulnier, Advanced Electronic Materials, 2201190, 2023

[2] M. M. Frank, N. Li, M. J. Rasch, S. Jain, C. -T. Chen, R. Muralidhar, J. -P. Han, V. Narayanan, T. M. Philip, K. Brew, A. Simon, I. Saraf, N. Saulnier, I. Boybat, S. Wozniak, A. Sebastian, P. Narayanan, C. Mackin, A. Chen, H. Tsai, G. W. Bur, IEEE International Reliability Physics Symposium, 2023

[3] N. Li, H. Tsai, V. Narayanan, Malte Rasch, APL Machine Learning, 016104, 2023

3:15 PMBREAK

SESSION EL20.11: Ferroelectrics
Session Chairs: Gina Adam and Xingfei Wei
Thursday Afternoon, November 30, 2023
Hynes, Level 3, Room 301

3:45 PM *EL20.11.01

Recent Progress in Developing Next Generation Neuromorphic Devices Based on Ferroelectric Hafnia by the U.S. Army Research Laboratory Andreu Glasmann^{1,2}, Sina Najmaei¹, Wendy Sarney¹, Alex Mazzoni¹, Justin Pearson¹ and Matthew Chin¹; ¹U.S. Army Research Laboratory, United States; ²Boston University, United States

In this presentation, I will present on the research progress by the U.S. Army Research Laboratory (ARL) in creating a framework for maturing emerging non-volatile memory devices based on ferroelectric hafnia for integration into front- and back-end CMOS neuromorphic integrated circuits. Next generation edge applications require a dramatic shift in computing paradigms, which utilize new electronic devices and circuit architectures to address the increasing power demands of enabling cognitive sensing and autonomy in extreme environments. Ferroelectric hafnia exhibits promising attributes, such as scalability, sub-nanosecond switching, back-end-of-the-line (BEOL) and front-end-of-the-line (FEOL) CMOS-compatibility, and good endurance that make it a promising candidate to address these needs.

In this presentation, I will discuss our material and device efforts in developing BEOL 2D ferroelectric field effect transistors. Our research demonstrates that within the CMOS compatible thermal processing envelope the ferroelectric landscape of HZO shows unique characteristics that have significant implications on the neuromorphic device properties of FeFETs. We examine these properties by integrating HZO into BEOL 2D WSe₂ based-FeFET device architectures, a prototypical van der Waals system, and verify their robust synaptic plasticity within a 3.5 order of magnitude conductive range. These discoveries highlight a roadmap for material processing, dimensional scaling, and integration of HZO-based FeFETs.

I will further discuss our complementing activities that focus on creating the design and simulation tools required for integration of FeFETs into CMOS. In this effort we seek to develop a framework for multiscale modeling of ferroelectric-based devices. To that end we will focus on our efforts in developing a physics-based compact device model for three-terminal ferroelectric field effect transistors. The model has been designed with explicit support for transient analysis to capture time-dependent polarization switching dynamics down to nanosecond scale with multiple types of ferroelectric domains. In the presentation, we will discuss the model's calibration against experimental data and use in optimizing the design of a ferroelectric-metal field effect transistor (FeMFET). Finally, we conclude with future direction of the work, including how we intend to couple this model to a Monte Carlo analysis framework to feed into neural network-level hardware simulations of neural accelerator crossbar architectures.

4:15 PM EL20.11.02

Wake-Up of Ferroelectric HZO Films -- Towards a BEOL Compatible Wake-Up Free Material David Lehninger, Ayse Sünbül, Anant Rastogi, Pratik Bagul, Shouzhao Yang, Konrad Seidel and Maximilian Lederer; Fraunhofer IPMS, Germany

The discovery of ferroelectricity in thin doped hafnium oxide films has revived interest in the concept of ferroelectric (FE) memory. Zirconium-doped hafnium oxide (HZO) crystallizes at low temperatures (400°C and below), making this material interesting for back-end-of-line (BEOL) implementation. Metal-FE-Metal (MFM) capacitors are critical building blocks for the realization of BEOL-compatible FE memory concepts. Located in the BEOL, they can be connected to either the gate or drain of a standard logic device to realize a one transistor-one capacitor (1T1C) FE field effect transistor (FeFET) or a 1T1C FE random access memory (FeRAM), respectively. [1]

Since its discovery, researchers have made great efforts to improve important properties of hafnium oxide-based ferroelectrics, such as remanent polarization, endurance, retention, imprint, and wake-up. Typical approaches include, but are not limited to, the investigation of different dopant elements, dopant concentrations, film thicknesses, and stacking options such as interface/electrode materials and superlattice structures.

While much progress has been made, certain issues, such as wake-up, remain challenging. Wake-up is the opening of the initially pinched polarization versus electric field hysteresis loop, which leads to a gradually increasing remanent polarization during field cycling until saturation. Since memory applications require stable polarization, an initial field cycling ("wake-up") is necessary. However, the need for this wake-up makes the realization of hafnium oxide based FE memories more complex and reduces the maximum number of endurance cycles. Therefore, a wake-up-free material would be highly desirable.

Several theories have been proposed to explain the wake-up effect. These theories can essentially be summarized as follows [2]: (i) defect redistribution, which reduces internal bias fields and promotes the depinning of domain walls, (ii) defect redistribution and subsequent stabilization of the orthorhombic phase ("field-induced phase transformation"), and (iii) 90° domain wall motion ("ferroelastic switching").

The wake-up effect of FE-HZO films could be mitigated by: (i) using mesa-etched test structures [3]; (ii) reducing the number of defects and carbon contamination by applying longer ozone pulses durations during the atomic layer deposition process [4]; (iii) interface engineering by plasma treatment [5] or epitaxial growth [6].

Herein, we investigate the effect of post-deposition annealing temperature, film stoichiometry, film thickness, and co-doping on the wake-up characteristics of FE HZO films embedded in MFM capacitors. Several structural and electrical characterization techniques, such as X-ray diffraction and polarization versus electric field measurements, are applied to obtain a comprehensive overview. The goal is to present a BEOL-compatible material stack with significantly reduced wake-up without compromising other important parameters such as remnant polarization and reliability.

[1] D. Lehninger et al., 2021 IEEE IITC, Kyoto, Japan, 2021, pp. 1-4.

[2] M. Lederer et al., 2021, PSS RRL, 15: 2100086.

[3] J. Bouaziz et al., ACS Appl. Electron. Mater. 2019, 1, 9, 1740–1745

[4] A. Kashir et al., Adv. Eng. Mater., 23: 2000791.

[5] K.-Y. Chen et al., 2017 VLSI Circuits, Kyoto, Japan, 2017, pp. T84-T85

[6] J. Lyu et al., ACS Appl. Electron. Mater. 2019, 1, 2, 220–228

4:30 PM EL20.11.03

Cryogenic Characterization of Polarization Switching in Ultra-Thin Ferroelectric Hf_{0.5}Zr_{0.5}O₂ Capacitors Balreen Saini¹, Chanyoung Yoo², Fei Huang¹, John D. Baniecki², Wilman Tsai¹ and Paul McIntyre^{1,2}; ¹Stanford University, United States; ²SLAC National Accelerator Laboratory, United States

The demand for smaller, faster, and more energy-efficient logic and memory devices is continuously increasing, leading to a heightened requirement for new materials that can be scaled down dimensionally and that are compatible with CMOS fabrication processes. A material system that shows promise for nonvolatile memory applications is HfO₂-based ferroelectrics. Since the discovery of ferroelectricity in HfO₂ thin films, research in this area has surged due to their potential as nonvolatile memory elements in 1 transistor-1 capacitor ferroelectric random-access memory (FeRAM) and in ferroelectric field-effect transistors (FeFET). Many of these research efforts have focused on reducing the programming voltage, improving reliability at lower operating voltages, and, in some cases, achieving compatibility with back-end-of-line (BEOL) process temperatures. However, compared to traditional perovskite-based ferroelectrics, there is a less comprehensive understanding of the domain-switching mechanisms involved in programming the polarization of these fluorite-type ferroelectric materials.

The metastable assembly of phases typically present in as-fabricated HfO₂-based thin films exhibit a field-induced phase evolution at room temperature that can result in the increase (wake-up) or decrease (fatigue) of the remnant polarization with switching cycles. Other mechanisms such as domain depinning and charged defect redistribution with field cycling are also reported to cause the observed polarization evolution with field cycling (endurance). The extent to which various proposed mechanisms for polarization evolution can contribute to experimental observations will depend on their activation energies. In the present work, we explore the effect of measurement temperature on the functional properties of ferroelectric Hf_{0.5}Zr_{0.5}O₂ (HZO) capacitors to further our understanding of the atomistic mechanisms responsible for the observed endurance characteristics. To carry out this investigation, we utilize a cryogenic probe station, which has the capability for measurements over a range of temperatures, as low as 10 K.

We examine HZO capacitors with different thicknesses (ranging from 4 nm to 10 nm) with Mo and TiN electrodes. A decrease in remnant polarization is observed for all samples as the measurement temperature is decreased to 10 K. This polarization reduction is recovered by increasing the temperature back to room temperature, suggesting reduction in the thermally activated domain wall motion at low temperatures. Polarization hysteresis (P-V) measurements for capacitors with pristine state pinched loops at room temperature show a negligible pinching effect at cryogenic temperatures. A positive-up-negative-down (PUND) pulse scheme is utilized to separate the polarization switching current from the displacement current. Frequency-

dependent and electric field-dependent endurance measurements are performed to further elucidate the possible contributions of different switching mechanisms to the observed temperature dependence of polarization switching.

4:45 PM EL20.11.04

Hf_{0.5}Zr_{0.5}O₂ Based Ferroelectric Memories for Applications Down to Deep Cryogenic TemperaturesHeorhiiBohuslavskiy¹, KestutisGregorius¹, MikaPrunnila¹ and SayaniMajumdar²; ¹VTT Technical Research Centre of Finland, Finland; ²Tampere University, Finland

Since the last decade, extensive studies on HfO₂-based ferroelectric devices have been carried out to unlock their applications in high-density, low-power, and high-speed electronics, and most importantly in non-volatile memories and logic circuits. Emergence of HfO₂-based ferroelectric memories has its origin in the CMOS compatibility and scalability potential, therefore bringing the prospect of easy integration with the existing foundry processes [1]. Among ferroelectric hafnia, Zr-doped HfO₂ (HZO) has received most attention due to its low crystallization temperature, making it a suitable candidate for CMOS back-end-of-line (BEOL) integration. More recently, memories operating at cryogenic temperatures became a topic of high interest due to their potential applications in high-performance computing, quantum computing and space technologies [2]. To realize the memory devices functional down to deep cryogenic temperatures with reasonably low power dissipation, understanding of fundamental device physics and proper material engineering are of vital importance. Previously, perovskite oxide based ferroelectric tunnel junctions, when cooled down to low temperatures, were demonstrated to have several key parameters improved as compared to room temperature operation, featuring higher on/off ratio, faster switching and improved endurance [3]. In terms of HZO-based capacitors or junctions, a few recent papers reported operation down to low temperatures [4-6]. However, a comprehensive understanding of the cryogenic physics and properties of HZO devices within the wide temperature window from 300 K down to 4 K temperatures as well as the optimization of interfaces and material stack for cryogenic operation are currently missing. In the present work, we report high remnant polarization from quasi wake-up free Hf_{0.5}Zr_{0.5}O₂ thin film devices together with state-of-the-art endurance down to deep cryogenic temperatures [7]. The HZO films, grown and annealed under CMOS BEOL-compatible conditions, were characterized within the 300 – 4 K temperature range with a particular focus on the analog switching properties of the films. Finally, we evaluate the overall performance of our HZO devices as cryogenic memories aiming at optimizing the domain dynamics control for achieving high classification accuracy of in-memory computing circuits [7,8].

The authors gratefully acknowledge the financial support from the Academy of Finland projects (Grant no. 350325, 345068, and 350667). This work was realized using experimental facilities of Micronova National Research Infrastructure for Micro- and Nanotechnology.

[1] S. Majumdar, *Advanced Intelligent Systems* 4, 2100175 (2022).

[2] S. Alam et al., *Nature Electronics* 6, 185–198 (2023).

[3] Q. H. Qin et al., *Advanced Materials* 28, 6852-6859 (2016).

[4] D. Wang et al., *Japanese Journal of Applied Physics* 58, 090910 (2019).

[5] J. Hur et al., *IEEE Journal on Exploratory Solid-State Computational Devices and Circuits*, vol. 7, no. 2, pp. 168-174 (2021).

[6] J. Hur et al., *IEEE Transactions on Electron Devices*, vol. 69, no. 10, pp. 5948-5951, (2022).

[7] H. Bohuslavskiy et al., *in preparation* (2023).

[8] S. Majumdar, *Neuromorphic Computing and Engineering* 2 (4), 041001 (2022).

SESSION EL20.12: Virtual Session I
Session Chairs: Sayani Majumdar and Radu Sporea
Tuesday Morning, December5, 2023
EL20-virtual

10:30 AM *EL20.12.01

Vector Matrix Multiplication with 2D MaterialsMarioLanza; King Abdullah University of Science and Technology, Saudi Arabia

Most artificial intelligence systems are based on artificial neural networks (ANNs), which are normally implemented in traditional silicon microchips. These microchips contain complementary metal-oxide-semiconductor (CMOS) circuits that realize different operations, including mathematical operations, digital-to-analogue and analogue-to-digital conversion, and transimpedance amplifiers. One of the most critical operations in ANNs is the vector matrix multiplication (VMM), but realizing it with traditional CMOS circuits consumes too much time and energy. Using crossbar arrays of memristors is much more efficient because the VMM is done in parallel via Ohm's law and Kirchhoff's law. In the past few years, multiple studies presented VMM based on memristive devices made of metal-oxides and phase-change materials. Here we present the first VMM operation using two-dimensional (2D) layered materials, and discuss its advantages and challenges compared to traditional memristive materials.

11:00 AM *EL20.12.02

Improved Microcontact Printing of Choline Oxidase using a Polycation-Functionalized Zwitterionic Polymer as Enzyme Immobilization MatrixMingZhao^{1,2}, BrendaHuang¹, YanCao¹ and HaroldMonbouquette¹; ¹University of California, Los Angeles, United States; ²Massachusetts Institute of Technology, United States

Electroenzymatic sensors typically rely on specific oxidase enzymes to catalyze oxidations of the target analyte to produce hydrogen peroxide (H₂O₂) that is oxidized or reduced at an underlying electrode at moderate potential to give a current signal. Development of microelectrode array (MEA) microprobes for multiple detection through selectively deposit multiple different enzymes onto specific microelectrode sites is in great demands.

Enzyme deposition and immobilization on microelectrode surfaces is most commonly achieved by manually loading a mixture of enzyme, bovine serum albumin (BSA), and glutaraldehyde (GAH) as crosslinker on the electrode surface. However, the manual approach becomes problematic when the MEA feature size is in the micrometer range. In previous work, we demonstrated the use of microcontact printing (μCP) for creation of multianalyte sensing microprobes by patterning two different enzyme/BSA mixtures onto selected, distinct sites on a MEA and subsequent crosslinking with GAH vapor. Although this accomplishment demonstrates the potential of MEAs for recordings of multiple neurochemicals simultaneously *in vivo* with high spatiotemporal resolution, the use of enzyme/BSA mixtures in aqueous solution as the "ink" has important disadvantages. Since the BSA protein behaves as a globular particle in solution that contributes little to the viscosity of the "ink", imprinted enzyme patterns tend to be so thin that low sensitivity results or problematic surface spreading and low spatial-resolution deposits occur when higher enzyme loading is attempted. For the application described in this work, excessive spreading of "ink" deposits is highly undesirable as it can lead to contamination of adjacent microelectrodes less than 100 μm away resulting in sensor crosstalk. As these problems are inherently related to ink properties, there has been a need for a new formulation that provides high adhesion to substrate, stronger intermolecular forces for higher viscosity and yet similar functionality as BSA to enable enzyme immobilization through covalent crosslinking.

While great strides have been made in modifying "ink" properties to achieve high resolution patterns, the focus has been on creating very thin layers of chemicals or proteins on substrates via covalent attachment. In this report, we designed a novel graft polymer, poly(2-methacryloyloxyethyl phosphorylcholine)-g-poly(allylamine hydrochloride) (PMPC-g-PAH), which serves as an alternative enzyme immobilization matrix to BSA that enhances the capability and efficiency of enzyme transfer to microelectrode surfaces via μCP. The zwitterionic polyphosphorylcholine moieties of the graft polymer serve to enhance surface hydrophilicity, the free amine groups provide functional groups for crosslinking with GAH vapor, and the polymer itself increases solution viscosity so as to curtail undesirable "ink" spreading. The minimization of ink surface spreading enables longer stamp alignment times, enhanced control of enzyme loading for better sensor performance, as well as potentially minimizing immune response that would improve long-term stability *in vivo*.

SESSION EL20.13: Virtual Session II
Session Chairs: Gina Adam and Yiyang Li
Tuesday Afternoon, December5, 2023
EL20-virtual

9:00 PM *EL20.13.01

Analog non-volatile memory (NVM)-based accelerators for Deep Neural Networks (DNNs) can achieve high-throughput and energy-efficiency by computing multiply-accumulate (MAC) operations using Ohm's law and Kirchhoff's current law on arrays of resistive memory devices [1]. In recent years, energy-efficient, weight-stationary MAC operations in analog NVM memory-array "Tiles" were demonstrated in hardware with Phase Change Memory (PCM) devices integrated in the backend of 14-nm CMOS [2, 3]. Competitive end-to-end DNN accuracies can be obtained with the help of hardware aware training, accurate weight programming, and sufficiently linear MAC operations in the analog domain [4].

In this paper, I describe architectural and circuit advances for such Analog NVM-based accelerators and specialized digital compute units, designed to accelerate Transformer, Long-Short-Term-Memory (LSTM), and Convolution Neural Networks (CNNs). A highly heterogeneous and programmable accelerator architecture that takes advantage of a dense and efficient circuit-switched 2D mesh to exchange vectors of neuron-activation over short distances in a massively parallel fashion [5] is presented. Based on a 14-nm inference chip consisting of multiple arrays of PCM devices, the impact of memory materials on the accuracy and performance of these systems will be discussed.

The author would like to thank colleagues at IBM Research Almaden, Yorktown, Albany, Zurich and Tokyo for their contributions to this work and the IBM Research AI HW Center.

- [1] G. W. Burr et al. "Ohm's Law + Kirchhoff's Current Law = Better AI: Neural-Network Processing Done in Memory with Analog Circuits will Save Energy". In: IEEE Spectrum 58.12 (2021), pp. 44–49.
- [2] P. Narayanan et al. "Fully on-chip MAC at 14nm enabled by accurate row-wise programming of PCM-based weights and parallel vector-transport in duration format". In: Symposium on VLSI Technology. 2021.
- [3] M. Le Gallo et al. "A 64-core mixed-signal in-memory compute chip based on phase-change memory for deep neural network inference". In: arXiv:2212.02872 (2022).
- [4] M. J. Rasch et al. "Hardware-aware training for largescale and diverse deep learning inference workloads using in-memory computing-based accelerators". In: arXiv preprint arXiv:2302.08469 (2023).
- [5] S. Jain et al. "A Heterogeneous and Programmable Compute-In-Memory Accelerator Architecture for Analog-AI Using Dense 2-D Mesh". In: IEEE Trans. VLSI 31.1 (2023), pp. 114–127.

SYMPOSIUM EN01

Energy Solutions for Unconventional Applications
November 27 - December 6, 2023

Symposium Organizers

Trisha Andrew, University of Massachusetts Amherst
Hye Ryung Byon, Korea Advanced Institute of Science and Technology
Thierry Djenizian, Ecole des Mines Saint-Etienne
Mihai Duduta, University of Connecticut

* Invited Paper
+ JMR Distinguished Invited Speaker

SESSION EN01.01: Fabrication and Characterization of Low Dimensional Materials
Session Chairs: Mihai Duduta and James Pikul
Monday Morning, November 27, 2023
Hynes, Level 2, Room 200

11:00 AM EN01.01.02

Design and Development of Ultrathin All-Solid-State Flexible Polymer Batteries[David Patrun](#), Ziyaad Aytuna, Thomas Fischer and Sanjay Mathur; University of Cologne, Germany

The design and development of lightweight flexible polymer batteries have gained significant attention in recent years due to their potential to revolutionize portable electronics, wearable devices, and energy storage systems. To achieve the goal of thin all-solid-state batteries, an innovative design principle is necessary. Various fabrication techniques, such as electrospinning and blade coating processes, have been explored to produce flexible battery electrolytes with high structural integrity and mechanical stability. In the development of flexible polymer batteries, the selection of suitable electrode materials is crucial. Various metal oxides and composite materials have been investigated for their electrochemical performance, stability, and flexibility. Surface modification has been achieved by nanoscale deposition techniques such as plasma-enhanced chemical vapour deposition (PECVD). These nanostructuring strategies have been employed to enhance the electrochemical properties, promote ion transport, and increase the overall energy density of the battery.

11:15 AM EN01.01.03

Carbon-Based Inks Formulations for Screen-Printed Planner Flexible Micro-Supercapacitor Devices[Nikita Dey](#); Indian Institute of Technology Kharagpur, India

The increasing demand for high-performance energy storage devices, driven by advancements in flexible and smart technology like wearable electronics, has led to a need for smaller and more efficient solutions. To address this, the use of printing technology and functional inks have emerged as a promising manufacturing pathway. These technologies offer benefits such as high deposition rates, minimal material waste, scalability, and the ability to produce high-resolution patterns. This study emphasizes on the fact that carbon-based inks have emerged as a game-changing technology for printed flexible electronics, offering numerous benefits such as affordability, processability, high conductivity, and flexibility. This presents new possibilities for sustainable ink formulations and the fabrication of screen-printed patterns for applications in sustainable energy. Optimizing various parameters such as ink rheology, mesh pore size, mesh design, and squeegee motion are crucial for fabricating electrodes tailored to specific applications. In the pursuit of developing screen printable carbon-based ink, we have explored a diverse range of binder solvent pairs to cater to our specific requirements. Our experimentation involved employing various combinations, including Ethyl cellulose (EC) paired with terpineol, carboxymethyl cellulose (CMC) paired with deionized water (DI), and ceramic binder such as glass water. It was found that, EC-based inks with terpineol is superior for micro-supercapacitor because they are less corrosive, easy to print, and also their insolubility in water ensures heightened longevity and durability. This also opens up possibility of using water-based gel electrolyte. On the other hand, CMC-based and glass water-based inks are soluble in water, rendering them less durable with a shorter lifespan. Also, glass water-based inks are corrosive which might damage the printed fabric mask. In addition to the quality of the ink, the design of the devices was found to significantly impact the energy storage performance. Therefore, a range of different device designs was employed to study their effects. The comparative analysis of the ink quality, and device designs yield valuable insights into the development of efficient and durable screen-printed planner flexible micro-supercapacitor devices. The abstract also addresses the opportunities and challenges associated with printing these carbon based materials, for micro-supercapacitors and micro-batteries on an industrially viable scale. By exploring these possibilities, this work aims to contribute to the development of high-quality and scalable solutions for next-generation wearable smart electronics.

11:30 AM *EN01.01.04

Atomic Layer Deposition on 1D Nanomaterials for Electrochemical Applications Jan M. Macak^{1,2}; ¹University of Pardubice, Czechia; ²Brno University of Technology, Czechia

One-dimensional nanomaterials – materials with one dimension outside the nanoscale, further noted as 1D NMs – represent a class of very important nanomaterials with continuously increasing importance. Due to their intrinsic features, unique properties and diversity of functionalities, they count among the most widely studied materials nowadays. While considerable research efforts have been spent to synthesize various 1D NMs (e.g. nanopores, nanotubes or nanofibers), limited efforts have been devoted to surface modification and property tailoring of these materials.

However, it is their surface that comes into direct contact with various media (air, gases, liquids, solids) and influences the reactivity, stability and biocompatibility of these materials. The surface and aspect ratio (defined as their diameter to length ratio) influence the performance of these materials in various applications. Considering these facts, it is more relevant to tailor the surface of these materials and to be able to influence their properties and reactivity at the nanoscale, rather than to deal with tailoring their own bulk material composition.

The focus of this presentation is on the modification of two types of 1D nanomaterials – nanotubes and nanofibers. Numerous techniques can be utilized for this purpose, such as for example wet chemical or physical deposition techniques. However, it is only the Atomic Layer Deposition (ALD) that is capable of really uniform and homogenous coating of these 1D nanomaterials, in particular those of very high-aspect ratio.

The presentation will be mainly focused on modification of TiO₂ nanotube layers and various nanofibers of different aspect ratios via ALD for electrochemical applications.

Experimental details and some very recent application examples in photocatalysis, catalysis, sensors, batteries, etc. [1-10] and structural characterizations of these modified materials will be discussed.

- 1) H. Sopha et al. (2017), *Appl. Mater. Today*, 9, 104.
- 2) H. Sopha et al. (2018), *Electrochem. Commun.*, 97, 91.
- 3) S. Ng et al. (2017), *Adv. Mater. Interfaces*, 1701146.
- 4) F. Dvorak et al. (2019), *Appl. Mater. Today*, 14, 1.
- 5) H. Sopha et al. (2019), *FlatChem* 17, 100130.
- 6) M. Motola et al. (2019), *Nanoscale* 11, 23126.
- 7) S. Ng et al. (2020), *ACS Appl. Mater. Interfaces*, 12, 33386.
- 8) M. Motola et al. (2020) *ACS Appl. Bio Mater.* 3, 6447.
- 9) M. Rihova & M. Knez & J. M. Macak et al. (2021), *Nanoscale Adv.*, 3, 4589
- 10) V. Galstyan, T. Djenizian, J. M. Macak (2022), *Appl. Mater. Today*, 29, 101613

SESSION EN01.02: Anode Materials for Lithium-ion Batteries—Challenges and Opportunities

Session Chair: Jan Macak

Monday Afternoon, November 27, 2023

Hynes, Level 2, Room 200

1:30 PM *EN01.02.01

How Building Batteries for Robots Enabled Pressure Free Lithium Anodes and Instantly Rechargeable 850 Wh kg⁻¹ Catholytes for Electric Aircraft James H. Pikul; University of Wisconsin–Madison, United States

This talk will cover new approaches for powering robotic systems across scales. Starting with microbatteries made for tiny robots, we will show how molten salt manufacturing and 3D printing enable 3-4X improvements in battery energy density and pressure-free lithium anodes. We will then move to larger systems where new chemistries and bioinspired design led to 10X improvements in macroscale robot operation time and long-range, instantly-rechargeable electric aircraft.

Current lithium (Li) metal pouch cells require high external pressures of 69 to 1,000 kPa and have huge volume increases of 39 to 220% after cycling, which makes them incompatible with small and flexible robotic applications because the clamping systems required to apply the pressure eliminate any energy or flexibility benefits. This talk will demonstrate swelling-free and pressure-free Li metal anodes with 1580 mAh cm⁻³ capacity enabled by polymer gyroid microlattices that allow 3D control of the molecular interaction between Li, polymer, and electrolyte. The geometry augments the chemical functionality to realize dense Li growth through complex 3D printed geometries by maximizing the Li volume fraction, polymer-Li-electrolyte contact, and manufacturability. Stable Li deposition was realized at a practical areal capacity of 5 mAh cm⁻² in 10 minutes. A 308 Wh kg⁻¹ anode-free pouch cell (2.1 Ah) incorporating a polymer gyroid had 80.2% capacity retention after 226 cycles, and the cell swelling was below 7%. Over 860 cycles were achieved when the pouch cell was prepared with 2.6 times excessive Li.

As robots and electric machines get bigger, they present increasing energy storage challenges. For example, the energy densities required to electrify aviation, heavy machinery, and robots (~1,000 Wh kg⁻¹) seem insurmountable with current battery architectures based on solid intercalation materials (250 Wh kg⁻¹), but animals can store ~2,000 Wh kg⁻¹ and operate continuously. The clear gaps in energy density and operational capability between machines and animals motivate new ways to extract electrochemical energy via bioinspired designs. The last part of this talk will report an electrochemical stomach that near-continuously powers electric aircraft and robots by ingesting small molecules as beverages and converting that chemical energy to electricity by pairing them with metals. We demonstrate a 10.4 Ah stomach that delivers an energy density of up to 850 Wh kg_{stomach}⁻¹ at 192 A kg_{stomach}⁻¹ and restores the chemical energy in 1 minute. The stomach powered a commercial quadcopter and doubled the flight time of the manufacturer's state-of-the-art batteries. Owing to the diversity of small molecules, we tailor beverages to enable 1,447 Wh kg⁻¹ discharge energy density or fire-safe energy storage.

2:00 PM EN01.02.02

MOF-Derived Fe, N Co-Doped Porous Carbon Polyhedrons (Fe-N-C) for High-Performance Lithium-Ion Battery Anode Materials Kaiyi Qin; Northeastern University, China

The lithium storage performance and structural stability of anode materials have a significant influence on the capacity performance and cycling stability of lithium-ion batteries. Despite the cost, conductivity, non-toxicity, and non-polluting advantages of graphitic carbon materials, their cycle stability is compromised by volume changes during lithium storage. Additionally, the theoretical capacity of 372 mAh/g is no longer sufficient to meet the growing demand for high-capacity LIBs. Metal-organic frameworks (MOFs) and their derivatives have emerged as promising anode materials for LIBs due to their tunable structure, high surface area, and high porosity. In this study, we successfully synthesized Fe, N co-doped carbon materials (Fe-N-C) with exceptional properties by calcination and co-doping Fe and N elements into a ZIF-8 precursor. Scanning electron microscopy (SEM) results revealed that the morphology of the synthesized samples was identical to that of ZIF-8. X-ray diffraction (XRD) and X-ray photoelectron spectroscopy (XPS) analyses confirmed the successful co-doping of Fe and N into the carbon material. The porous structure provided a buffer for volume changes and improved cycling performance. After 300 cycles at a current density of 500 mA/g, the Fe-N-C anode exhibited charge and discharge specific capacities of 538 mAh/g and 543 mAh/g, respectively. The co-doping of Fe and N enhanced the conductivity and rate performance of Fe-N-C, resulting in excellent cycling stability. This study demonstrates the exceptional electrochemical activity and potential of Fe, N co-doped carbon polyhedrons for high-performance lithium-ion batteries. Carbonization of metal-organic frameworks and co-doping with Fe and N elements represents a promising strategy to enhance the electrochemical performance of graphitic carbon anode materials.

2:15 PM EN01.02.03

Enhancement of Cycling Performance by use of Li Anode with Additive Leaching-Type Polymer Layer for Lithium Metal Batteries OH Myung-keun and Dong-Won Kim; Hanyang University, Korea (the Republic of)

Rechargeable lithium batteries using lithium metal as an anode are attractive candidates for high energy density power sources in portable electronic devices and electric vehicles, because lithium metal offers a high specific capacity (~3,862 mAh g⁻¹) and possesses a low reduction potential. However, the development of rechargeable lithium metal batteries has been hindered by the high reactivity of lithium metal with liquid electrolytes and the occurrence of dendrite growth during charge and discharge cycles. Therefore, it is essential to form the stable solid electrolyte interphase (SEI) on lithium metal to prevent lithium dendrite growth and minimize side reactions of liquid electrolyte. Recently, various additives have been investigated to form a stable SEI layer on Li metal. However, during repetitive charge and discharge process, the additives in the electrolyte can be gradually depleted, resulting in capacity fading. In this work, we developed additive leaching-type polymer layer containing excessive amounts of additives that form the stable SEI layer. The additives can be stored in the polymeric layer, continuously released to the electrolyte during the repeated cycling. Electrochemical analyses such as linear sweep voltammetry and cyclic voltammetry were investigated, and the Li/Li symmetric cells

showed the regulation of lithium deposition with small overpotential. The cycling performance of lithium metal batteries employing additive leaching-type polymer layer was evaluated with high nickel NCM cathode. Furthermore, characterization techniques such as cyclic voltammetry, X-ray photoelectron spectroscopy, ⁷Li nuclear magnetic resonance, and electrochemical impedance spectroscopy were employed to analyze the release behavior of additives and investigate the mechanisms associated with released additives for improvement of cycling performance.

2:30 PM EN01.02.04

Structure Tailoring and Material Modification of the Thick Cathode for Fast Charging and Long Lifespan Li-S Batteries [YuxuanZhang](#)¹, Han WookSong² and SunghwanLee¹; ¹Purdue University, United States; ²Korea Research Institute of Standard and Science, Korea (the Republic of)

It is urgent to develop both affordable and sustainable batteries with high energy density and fast charging speed to alleviate the range anxiety of electric vehicles.^{1,2} The lithium-sulfur (Li-S) system is especially attractive because of its high theoretical specific energy (around 2600 Wh kg⁻¹), low cost, and low toxicity. However, the application of sulfur cathodes to date has been hindered by several obstacles, including low active material loading, low electronic conductivity, shuttle effects, and sluggish sulfur conversion kinetics.

Herein, we combine a material-agnostic approach based on the asymmetric cathode structure design with a controllable vapor-deposited polymer to realize fast charging Li-S batteries with high sulfur loading.³ Specifically, the active materials and the tortuosity of the cathode were tailored by the 3D printing (stereolithography technique), which distributed in an inhomogeneous way to compensate for the gradient distribution of Li ions originated in the cathode depth direction, leading to less polarization in the electrode scale. The as-printed cathode is then sintered at 900 °C in an N₂ atmosphere to generate a carbon skeleton (i.e.: carbonization of resin) with intrinsic carbon defects. The structure design and defects engineering are expected to synergistically create favorable sulfur conversion conditions and mitigate the polarization in thick electrodes. The oCVD technique is leveraged to produce a conformal coating layer to eliminate shuttle effects for the elongated battery life. In-situ XRD diffractograms show a distinguishable difference between the printed cathode and the 2D planar cathode with similar mass loading, confirming an eminent sulfur conversion kinetic condition.

Overall, the customized cathode delivered 820 mAh g⁻¹ at 4 C with a mass loading of 8.3 mg cm⁻², and the cathode with oCVD polymer showcased high-capacity retention (85% after 300 cycles), which indicates high mass loading with elevated sulfur utilization ratio, accelerated reaction kinetics, and stabilized electrochemical process have been achieved on the sulfur cathode by implementing this innovative cathode design strategy. The results of this study suggest a promising way of employing structural optimization and material modification for the higher energy and power density battery.

1 Zhang, Y., *Nanoscale* 15, 4195-4218 (2023).

2 Zhang, Y., *Energy Storage Materials* 48, 1-11 (2022).

3 Xu, R., *Advanced Energy Materials* 5, 1500408 (2015).

Acknowledgments

This work was partially supported by National Science Foundation, Award number ECCS-1931088 and CBET-2207302. S.L. and H.W.S. acknowledge the support from the Improvement of Measurement Standards and Technology for Mechanical Metrology (Grant No. 23011043) by KRISS.

SESSION EN01.03: Energy Management Strategies for Real World Devices

Session Chairs: Trisha Andrew and Markus Niederberger

Tuesday Morning, November 28, 2023

Hynes, Level 2, Room 200

8:00 AM *EN01.03.01

Flexible and Durable Batteries for Wearable Sensors [Ana Claudia Arias](#); University of California, Berkeley, United States

On skin detection of vital signs and biomarkers, a non-invasive approach, holds tremendous significance for evaluating the body's response to physical activity and clinical diagnostics. When integrated into wearable devices, flexible sensors offer several advantages, including continuous data acquisition, high performance, and cost-effectiveness. Powering such devices while maintaining their mechanical properties has driven active innovation in the field of wearable compliant batteries. Incorporating additional functionalities often compromises the energy storage capacity of these devices, resulting in lower gravimetric or volumetric capacity compared to commercially available batteries. Maximizing the energy density of wearable batteries remains a crucial goal. Most demonstrations in this field rely on lithium-ion battery chemistry, which often includes toxic and/or flammable components. Thus, designing non-toxic systems utilizing abundant and disposable materials is of utmost importance. We have developed an electrode composite with an interpenetrated binder network, enabling a flexible battery with energy density comparable to commercial AA alkaline batteries. Wire-shaped batteries based on helical band springs will be presented, demonstrating resilience to fatigue and the ability to maintain electrochemical performance over 17,000 flexure cycles. Intrinsically safe and non-toxic silver-zinc (Ag/Zn) and zinc-manganese dioxide (Zn/MnO₂) battery chemistries are employed in our work.

8:30 AM EN01.03.02

A Solar-Powered Optogenetic System for Long-Term, Wirelessly-Controlled Neuromodulations [Jaejin Park](#), Kyubeen Kim, Tae Soo Kim and Ki Jun Yu; Yonsei University, Korea (the Republic of)

Optogenetics has revolutionized neuroscience by enabling the manipulation of neural activity using light-sensitive proteins to modulate brain function. To facilitate advanced neuromodulation in freely moving animals, various optical stimulation devices have been developed. Presently, wireless optogenetic devices predominantly utilize either coil-powered or battery-powered systems. Battery-powered systems necessitate frequent battery replacements, which can cause stress for the animals. Furthermore, recharging the batteries requires the charger to be located within a specific area. Coil-powered systems, on the other hand, require a structure that wraps around the animal's cage to provide power, limiting their operation to confined spaces where such a setup is established. In addition to these constraints, specialized techniques like impedance matching with expensive, bulky equipment such as radiofrequency (RF) generators are essential for operating these systems.

On the contrary, an innovative wireless solar-powered optogenetic device (WSOD) takes advantage of light energy to autonomously charge and operate. This remarkable feature eliminates the need for spatial restrictions, enabling the experimental subject to move freely without confinement. Additionally, the WSOD functions independently without relying on external components such as an RF generator or amplifier. To harness sufficient power from diverse light sources, including sunlight and lamps, we have implemented highly efficient flexible InGaP/GaAs tandem solar cells, which are incredibly thin (< 5 μm). The solar cell has an impressive power conversion efficiency of 18 % and a wide spectral range from 300 nm to 900 nm. This outstanding efficiency allows the WSOD to operate continuously for more than 80 minutes with just a 10-minute charging period during daylight hours. The fully assembled WSOD incorporates these photovoltaic cells with a power management system and Bluetooth technology on a flexible substrate, enabling control via a smartphone application. Furthermore, the WSOD allows multiple connections to numerous devices from a single mobile device, facilitating in vivo experiments in diverse environments and with various subjects.

To demonstrate these capabilities, we performed optical stimulation in the secondary motor cortex (M2) region of a transgenic mouse brain, observing subsequent locomotion behavior. Through quantitative analysis, we identified compulsive circling behaviors and increased velocity during the stimulation period. Furthermore, we demonstrated the long-term stability of the WSOD by observing no significant differences in locomotion behavior over a month-long duration. This study introduces a wirelessly rechargeable optogenetic device powered by solar energy, facilitating wireless charging without any spatial constraints. The pivotal advantage of this system lies in its ability to naturally recharge during the course of regular activities, eliminating the need for bulky and expensive equipment like RF generators or amplifiers. With this feature, we are moving closer to the ultimate objective of developing wireless optogenetic devices that enable the completely unrestricted behavior of the subjects.

8:45 AM EN01.03.03

Enhancing Single Electrode Triboelectric Generators via Charge Trapping Layer Integration [Wei-Lin Wu](#), Cheng-Yu Shih, Yen Shuo Chen and Fu-Hsiang Ko; National Yang Ming Chiao Tung University, Taiwan

With the rapid development of internet of things (IoT), the increasing need of self-power sensor is expected. Triboelectric generator (TEG) has become a promised candidate in mechanical stimuli sensing (1, 2), which is distinguished from several conventional sensors in that it doesn't need any extra power source.

The triboelectric effect can be explained by Maxwell's equations and involves both contact electrification and electrostatic induction. In contact electrification, two dissimilar materials come

into contact and exchange charges, resulting in a potential difference between them. In electrostatic induction, an external electric field polarizes the charges in a material, creating a potential difference between two regions of the material. However, the insufficient output performance of triboelectric generators hinders their widespread application. To enhance the energy-harvesting capabilities of these generators, we are focusing on device structures(3), surface topography(4), and material selection(5).

In this paper, we introduce the charge storage layer to optimize device structure. For the purpose to increase the surface charge by raising the bulk charge, the low mobility polymer is inserted between friction layer and metal plate as charge storage layer. Then, polydimethylsiloxane (PDMS) as friction layer with micro-pyramid structure to increase the surface area and pressure sensitivity. We choose polydimethylsiloxane (PDMS) and polytetrafluoroethylene (PTFE) to be the friction double layer for the reason of low cost, high flexibility, and great output performance. The output voltage of dual layer triboelectric generator can achieve 150 V, which is eight times higher than the triboelectric generator without charge storage layer.

Keywords: triboelectric effect; charge storage layer; energy harvesting; pyramid structure

1. F. R. Fan, W. Tang, Z. L. Wang, Flexible Nanogenerators for Energy Harvesting and Self-Powered Electronics. *Adv Mater* 28, 4283-4305 (2016).

2. Z. Shi et al., Morphological Engineering of Sensing Materials for Flexible Pressure Sensors and Artificial Intelligence Applications. *Nano-Micro Letters* 14, (2022).

3. Y. G. Feng et al., A New Protocol Toward High Output TENG with Polyimide as Charge Storage Layer. *Nano Energy* 38, (2017).

4. K. Tao et al., Ultra-Sensitive, Deformable, and Transparent Triboelectric Tactile Sensor Based on Micro-Pyramid Patterned Ionic Hydrogel for Interactive Human-Machine Interfaces. *Adv Sci* 9, 2104168 (2022).

5. Z. Zhao et al., Selection rules of triboelectric materials for direct-current triboelectric nanogenerator. *Nature Communications* 12, (2021).

9:00 AM EN01.03.04

Understanding Interplay of Cycling Conditions on Li-Ion Battery Performance for EVTOL Applications Anuj Bishu, Ruhul Amin and Ilias Belharouak; Oak Ridge National Laboratory, United States

The advancement of improved energy storage systems has garnered significant attention in Electric Vertical Takeoff and Landing (EVTOL) applications. To ensure optimal performance and safety of onboard batteries, comprehending their behavior under varying charging/discharging protocols and environmental conditions is crucial. This work provides a comprehensive evaluation of commercial Li-Ion batteries for EVTOL applications, with a specific focus on their response to different charging/discharging strategies and mechanical vibrations encountered during flight. Controlled experiments are conducted to explore the effects of rapid cycling on battery performance, encompassing lifespan, capacity, and internal resistance. Additionally, the impact of mechanical vibrations on battery behavior is assessed to identify potential challenges for onboard batteries. The study's results reveal intriguing insights into the interplay between temperature, vibration, and battery performance, bridging the gap between battery performance and EVTOL applications. This work contributes to the wider adoption of electric aerial transportation, promising a greener and safer future for urban mobility.

9:15 AM EN01.03.05

Conductive Polymers at The Nexus of Innovation: Empowering Nanogenerators and Smart Interactive Wearables Rodrigo F. Martins¹, Guilherme Ferreira¹, Sumita Goswami², Elvira Fortunato¹ and Suman A. Nandy¹; ¹Universidade Nova de Lisboa, Portugal; ²Almascience, Portugal

Conducting polymers have emerged as versatile materials with transformative potential in two key domains: nanogenerators and smart interactive sensor applications for wearable substrates. This abstract explores the exciting advancements and synergistic possibilities created by integrating conducting polymers into these cutting-edge technologies.

In the realm of nanogenerators, conducting polymers are being investigated as a functional element because of their remarkable electro-mechanical properties. Good electrical conductivity, coupled with mechanical flexibility, makes them ideal for smart wearable applications. This abstract delves into the principles of energy conversion, highlighting the ability of conducting polymers to convert mechanical energy, such as vibrations or pressure, into electrical energy. This breakthrough has far-reaching implications, powering wearable electronics, Internet of Things (IoT) devices, and remote sensors, ultimately reducing our reliance on traditional energy sources.

Shifting focus to wearable substrates, conducting polymers unveil a new era of smart, interactive sensor applications. These polymers are seamlessly integrated into textiles, cellulose substrate, foam, enabling the development of large area of wearable markets such as garments, healthcare, defense, sports, transportation that can sense a wide array of stimuli. From monitoring physiological parameters to tracking environmental conditions and enabling user interactions, conducting polymer-based sensors provide real-time data acquisition and actionable insights. Furthermore, the synergies between nanogenerators and interactive sensors powered by conducting polymers are being explored. Wearable devices can harness energy from user movements and ambient vibrations to sustain continuous sensor operation. This integration not only enhances the autonomy of wearable devices but also enables novel functionalities such as self-powered biosensors and adaptive clothing. As this abstract demonstrates, conducting polymers represent a bridge between the worlds of energy harvesting and wearable technology. Their remarkable properties and adaptability promise a future where self-sustaining, sensor-rich wearables seamlessly integrate into our daily lives, revolutionizing how we interact with technology and our environment. This abstract serves as an invitation to explore the dynamic landscape of conducting polymer applications, fostering innovation and advancements in nanogenerators and smart interactive wearables.

9:30 AM EN01.03.06

A Low-Cost Self-Powered Sensor-Network System for Renewable Gas Transportation Infrastructure System Powered using Energy Harvesting Yaaqoub Malallah¹, Tiffany Nguyen², Callan Hall², Rajinder S. Deol², Henam S. Devi³, Madhusudan Singh³ and Ioannis Kyymissis²; ¹Kuwait Institute for Scientific Research, Kuwait; ²Columbia University, United States; ³Indian Institute of Technology Delhi, India

Hydrogen is one of the most important fuels for a sustainable and renewable energy economy. One of the challenges with working with hydrogen, however, is that it requires the use of well-sealed pipelines due to its very fast diffusivity, flammability, and chemical reactivity leading to complication during incorporation of sensors in the delivery and distribution network. There is also a huge interest in examining the blending of hydrogen with natural gas, in which the hydrogen concentration is controlled to stay below 20 % to prevent embrittlement of the metal components commonly used in natural gas containment and transportation networks. Incorporation of sensors is especially important for these hydrogen supply infrastructures. It has been shown that a number of contaminants in the hydrogen supply can be especially harmful for fuel cell applications. In particular, epoxies commonly used in building components such as assembling fuel systems, sensors, and pipelines can foul fuel cell membranes and lead to a dramatic loss in energy delivery and irreversible damage to the fuel cell systems. Our proposed design will use a mechanical energy harvesting approach which will stimulate a high-quality factor (Q) resonator on the inside of the pipe without the need to penetrate the walls of the pipe system. Such sensors could also report on the pressure in hydrogen fuel pipelines, measure flow, and monitor the blending ratio in natural gas/hydrogen mixed delivery systems. Acoustic communication is also used to transmit information between the sensing and communication base unit, eliminating the need for pipe penetrations and risk of leaks, embrittlement, etc. Meanwhile, the sensor package will be powered with piezoelectric, solar, and flow of gas as wind energy harvesting systems. Piezoelectric energy harvesting using materials like PVDF and KNN (Potassium Sodium Niobate) was performed on a stainless-steel sheet through mechanical vibrations of a speaker. The resonance frequency that the PVDF sheet vibrates most readily and efficiently was successfully analyzed and recorded through multiple isolation techniques. In order to observe the resonance frequency, five different methods were implemented into the experiment to reduce noise. Visually, the resonance frequency can be seen from 180 Hz to 220 Hz. The experimental results confirm the visual resonance frequency and reveals external factors that can affect the resonance of the piezoelectric material. We were able to transmit and receive signals through the metallic pipeline at 200 kHz to 500 kHz using PVDF sensors for communication purposes. The power received through 4 mm thick solid iron pipe was 5 %, which is enough to transmit bytes of sensor data from inside the metallic pipe that acts as a Faraday cage. Meanwhile, our lab scale prototype for the energy harvesting systems generated about: 0.02 W for piezoelectric, 2 W for solar, and 0.8 W for wind. A large industrial scale version will be more economically viable.

9:45 AM EN01.03.07

Implementing Bimetallic Metal Organic Framework for High Performance Asymmetric Supercapacitors Satnam S. Mattu and Abhay Deshmukh; Rastrasant Tukadoji Maharaj Nagpur University, India

Metal organic frameworks (MOFs) are used in various fields like gas absorption, catalysis, energy storage, and conversion as well as in the field of luminescence. As compared to Metal organic frameworks, Bimetallic metal organic frameworks show enhanced and synergistic effects and thus can be used widely for the development of commercial energy storage devices, especially supercapacitors. In this work the synergistic effect of cobalt and aluminum bimetallic MOF is studied as electrode material for supercapacitors by electrodeposition method. This Co-Al MOF exhibits a specific capacitance of 1014.08 Fg⁻¹ at a current density of 40 Ag⁻¹ in 1 M KOH in three electrode system. The asymmetric device of Co-Al MOF as the positive electrode and carbon cloth as a negative electrode is also manufactured which exhibits high specific capacitance of 124.26 Fg⁻¹ at a current density of 0.25 Ag⁻¹. Apart from a good specific capacitance, Co-Al bimetallic MOF as a device also exhibits a great cycling stability of 93 % capacitance retention even after 12000 cycles. We have such a good specific capacitance in 1 M KOH alkaline electrolytes for both 2 electrodes as well as three electrode systems which is remarkable in the field of supercapacitors. The observed results shows that this work can be used further to make an asymmetric hybrid supercapacitor in the future.

10:00 AM BREAK

10:30 AM *EN01.04.01

Ultraflexible and Stretchable Monocrystalline Silicon Solar Cells for Wide Ranging Deployment Nazek El-Atab; King Abdullah University of Science and Technology, Saudi Arabia

Flexible and stretchable solar cells are of importance for state-of-the-art applications such as solar powered vehicles, wearables, buildings and robots, among others. While organic materials show good flexibility and stretchability, however, they generally show low efficiencies and stabilities. In terms of inorganic materials, silicon has been the material of choice in the photovoltaic industry due to its low cost, availability, low toxicity and maturity of the manufacturing process. Nevertheless, silicon is rigid and when thinned down to achieve flexibility, the material becomes brittle and the mechanical resilience of the cell is degraded. Moreover, the efficiency of the cells gets degraded too as the active material that absorbs light is thinned down. In this talk, I will discuss a corrugation technique that allows the transformation of rigid silicon solar cells into their ultra-flexible and stretchable version without thinning down the original thickness of the silicon and without degrading the normalized efficiency of the cells. The corrugation technique is based on creating alternating grooves with different shapes, resulting in interconnected islands of silicon using interdigitated back contacts. The different corrugation patterns enable different flexing and stretching capabilities, specific weight and output power which allows customization based on the application requirements. The technique allowed for the world-record flexible and stretchable inorganic solar cells which can be bent down to 140 μm radius and stretched up to twice their original size without degradation in the original normalized efficiency.

11:00 AM EN01.04.02

Intrinsically Stretchable Organic Solar Cells on Crack-Free Substrate/Electrode Platform under 40% Strain Yeonjee Jeon, Seungbok Lee and Jung-Yong Lee; Korea Advanced Institute of Science & Technology, Korea (the Republic of)

The increasing demand for off-grid power sources in soft robotics and wearable electronics has sparked considerable interest in stretchable organic solar cells (SOSCs). However, the brittleness of materials used in traditional solar cells makes them susceptible to cracks even under mild strain, limiting their application in wearable devices. To overcome this limitation, intrinsically stretchable organic solar cells (IS-OSCs) have emerged as a promising solution. They offer advantages, including omnidirectional stretchability, seamless integrability, and compatibility with conventional manufacturing processes. In our study, we revealed that the mechanical failure of IS-OSCs under strain can be traced back to the PH1000 layer. Cracks originating from the PH1000 layer subsequently propagate to the photoactive layer, resulting in a decrease in power conversion efficiency (PCE) in the IS-OSCs under strain. To achieve crack-free IS-OSCs under human body elongations as high as ~40%, we propose a double-locked substrate/transparent electrode platform. To enhance the adhesion of the most fragile layer, the PH1000 layer, we developed techniques to enhance both physical and chemical adsorption, including surface treatment of the substrate and cross-linking between the substrate and modified PH1000. Remarkably, our double-locked system sustained strains exceeding 40% without developing cracks, while the untreated PH1000 film exhibited cracks at a strain level of 20%. Our double-locked IS-OSCs achieved an initial PCE of 10.2%, demonstrating significantly enhanced mechanical robustness, with nearly double the $\epsilon_{\text{PCE}70}$ (44%) compared to the control device (24%), where $\epsilon_{\text{PCE}70}$ represents the strain at which 70% of the initial PCE is retained¹. Additionally, our IS-OSCs maintained 90% of the initial PCE even after undergoing 1,000 stretch-release cycles under a 10% strain.

11:15 AM EN01.04.03

A Wearable Sweat Sensor Powered by a Flexible Perovskite Solar Cell Jihong Min¹, Stepan Demchyshyn², Martin Kaltenbrunner² and Wei Gao¹; ¹California Institute of Technology, United States; ²Johannes Kepler Universität Linz, Austria

Continuous monitoring of physiochemical biomarkers using wearable sensors has the potential to revolutionize personalized healthcare. While sweat sensing has emerged as a promising method for continuous biochemical screening, ensuring a sustainable power supply remains a challenge. Previous energy harvesting modules, such as biofuel cells and triboelectric nanogenerators, have relied on exercise-induced power and sweat generation, limiting their applicability to fitness monitoring. In this study, we propose a flexible perovskite solar cell (FPSC) powered autonomous sweat sensor that efficiently harvests energy from ambient light, enabling continuous and sustainable sweat monitoring throughout the day, even during sedentary activities. The wearable device integrates a long-term reusable FPSC and electronic system, alongside a cost-effective and replaceable microfluidic biosensor array produced through inkjet printing technology. The FPSC features a record-breaking power conversion efficiency (PCE) of 31% under indoor illumination conditions. Its exceptional performance is attributed to the incorporation of α -methylbenzylamine (MBA) as an organic spacer in the quasi-2D perovskite absorber layer, enhancing defect passivation and overall device functionality. Furthermore, the FPSC exhibits high durability, withstanding thousands of rigorous bending cycles, making it suitable for wearable applications. It maintains a high power output under a wide range of illumination conditions, including dim indoor lighting, ensuring uninterrupted operation during various activities throughout the day. Our battery-free device was validated for on-body use by continuously extracting sweat and capturing real-time cross-calibrated sweat biomarker levels (glucose, sodium, pH, skin temperature, and sweat rate) throughout the day over 12 hours under various lighting conditions and daily activities ranging from outdoor resting to indoor exercise.

11:30 AM EN01.04.04

Are Luminescent Solar Concentrators Worth the Effort? Tom Baikié¹, Benjamin Daiber², Neil Greenham¹, Akshay Rao¹ and Bruno Ehrler²; ¹University of Cambridge, United Kingdom; ²AMOLF, Netherlands

Luminescent Solar Concentrators (LSCs) are devices that capture and concentrate light using a transparent matrix doped with chromophores. LSCs have the potential to outperform other light concentration technologies due to their ability to concentrate diffuse light and reshape the solar spectrum to match the optimum spectral characteristics for photovoltaic (PV) technology. This study compares different LSC technologies, including solar windows, within a simulated real-world environment and outlines the potential impact of upcoming LSC technologies to determine their commercialization potential.

We utilised a calendar year of real-world solar spectrum data from Boulder and Amsterdam and combined it with a machine learning model, a ray-tracing algorithm and recombination current diode model to determine the potential power efficiencies from different luminescent solar concentrators (LSC) configurations.

11:45 AM EN01.04.05

Enhancing Solar Energy Conversion Efficiency in Interfacial Evaporation Technology using Graphite Nanoflakes/Polydimethylsiloxane Composite Anh Tuan Nguyen, Suman Chhetri and Woonchul Lee; University of Hawaii at Manoa, United States

Carbon-based materials such as graphite, graphene, and carbon nanotubes have been shown as a promising high-performance photothermal materials for the application in interfacial evaporation technology. In this study, we prepared a flexible graphite nanoflake (GnF)/polydimethylsiloxane (PDMS) composite with varying amounts of GnF from 1 to 10 wt%. It was found that the GnF/PDMS composite's photothermal property was optimized at 3 wt% of GnF, resulting in excellent total solar absorption of 94.8%. As proof of concept, GnF/PDMS composite was coated on polyurethane (PU) foam to create a floatable interfacial water evaporator. Under 1 sun illumination, the coated PU with 1 wt% of GnF/PDMS composite yields an evaporate rate of 1.14 $\text{Kg/m}^2\text{-h}$ with solar-vapor conversion efficiency of ~68%. With the promising photothermal effect, the GnF/PDMS composite can also be used in various solar-powered applications, including desalination and purification.

1:30 PM *EN01.05.01

Graph-Theory-Guided Design of Self-Assembled Biomimetic Composites for Batteries and Supercapacitors Nicholas A. Kotov^{1,2}; ¹University of Michigan, United States; ²Imperial College London, United Kingdom

Multifunctional, structurally versatile, and resource conscious materials represent the critical bottlenecks of nearly all modern technologies. These problems were being addressed using blueprints and inspiration from living tissues and organisms. However, their design is dominated by the empirical reproduction of simple organizational patterns. The ever-increasing demands for materials performance, requires more complex structures and patterns.

This talk will show that, it is possible to transition from inexact approach of replicative nanocomposites to exact biomimetic material design using graph theory (GT). This change enables creation of multiscale architectures that are equal or more complex than original prototypes and display a combination of properties essential for lightweight energy sources critical for energy storage devices and other applications critical for sustainability.

The GT description of nanostructures developed for chiral nanoassemblies can be extended to nacre-like and cartilage-like nanocomposites, representing two large families of lightweight multifunctional nanocomposites used in energy devices. Stress, charge, and mass transport characteristics of materials from aramid nanofibers (ANFs) as well as other nanoscale fibers can be directly related to GT-based structural parameters. These findings enabled a new generation of Li- and Zn-based batteries for robotics and aviation.

In order to relate the performance characteristics of the energy storage devices to the structure of complex biomimetic materials, a set of topometric parameters combining parameters from topological and physical space can be introduced. Specifically, high *nodal degree* and *volumetric nodal density* combined with low *Ohm centrality* and high *Freundlich nodal density* of networks from carbon nanotubes grown on top of carbonized aramid nanofibers engender composites with failure-resilient deformations, stress-adaptable charge transport, minimal dead volume, and high affinity to lithium polysulfides. The battery performance data demonstrate direct relation to the cyclic and capacity performance of Li-S batteries.

The latest work in this direction will include biomimetic composites for supercapacitors. These devices utilize self-assembled particles with virus-like spiky geometry that reveal topologically enhanced charge storage.

Relevant Literature:

1. Kotov, N.A.; et al Ultrathin graphite oxide-polyelectrolyte composites prepared by self-assembly. *Adv. Mater.*, **1996**, *8*, 637–641.
2. W. Jiang, Z. et al, Emergence of Complexity in Hierarchically Organized Chiral Particles, *Science*, **2020**, *368*, 6491, 642-648.
3. S.O. Tung, et al Dendrite-Suppressing Solid Ion Conductor From Aramid Nanofibers, *Nature Comm.* **2015**, *6*, 6152.
4. Wang et al, Biomimetic Solid-State Zn²⁺ Electrolyte for Corrugated Structural Batteries, *ACS Nano*, **2019**; *13*(2), 1107-1115.
5. Wang, M.; et al Biomorphic Structural Batteries for Robotics. *Sci. Robot.* **2020**, *5*; <https://www.science.org/doi/10.1126/scirobotics.aba1912>
6. Wang, M.; et al Topometric Design of Reticulated Nanofiber Composites for Lithium-Sulfur Batteries, <https://www.researchsquare.com/article/rs-2758299/v1>

2:00 PM EN01.05.02

Recent Progress on V2O5 Based Electroactive Materials: Synthesis, Properties and Supercapacitor Application AdilAlshoaibi; King Faisal University, Saudi Arabia

The concerns of sustainable energy rely on highly efficient renewable energy sources and effective storage devices. Supercapacitor is practically reliable energy storage devices with rapid charging rate, high power density, simple setup, and good stability. Electrode materials have significant impacts on the performance of supercapacitors. Therefore, finding highperforming electroactive material is a critical concern of the area. Herein, the recent progress of vanadium pentoxidebased electroactive materials for supercapacitor application has been reviewed. Vanadium pentoxide is a potential electroactive material for supercapacitor due to its mixed oxidation states, eco-friendliness, low cost, high capacitance, and high energy density. But, poor conductivity and low cyclic stability are major drawbacks of the oxide which affect its electrochemical properties. This review points out different strategies of mitigating such limitations. Finally, future perspectives on V2O5-based electroactive materials for supercapacitor application have been highlighted.

2:15 PM EN01.05.03

Okra-Derived Hierarchical Porous Structured Activated Carbon Tuning with Metal-Oxide for Advanced Supercapacitors Ektamajhi and AtulS. Deshpande; Indian Institute of Technology Hyderabad, India

A hybrid supercapacitor is designed to fulfill the need for power and energy density by utilizing the composite of activated carbon and metal oxide. Naturally abundant bio-waste (Okra) has been explored to develop porous activated carbon for supercapacitors due to their easy availability, excellent specific surface area, a wide range of micro and mesopore structures giving extremely high performance, and a cost-effective synthesis approach. The bio-waste precursors have excellent microstructural properties, heteroatoms, and mineral content, which outline their subsequent effect on electrochemical performances. Moreover, the surface modification of carbon materials depending upon the pre-processing, carbonization, and etching by chemical activation method is explored, showing the impact on the capacitance. The electrode material is synthesized by freeze-drying biomass precursor followed by carbonization, acid treatment, and one-step activation. Its physicochemical properties are studied by characterization techniques like FESEM, EDS, XRD, Raman, TEM, BET, FTIR, XPS, and TGA analysis. Here, hierarchical honeycomb-structured porous activated carbons giving high surface area were synthesized from okra biowaste by the combination of chemical treatment and heat treatment at different temperatures, facilitating ion penetration and ion diffusion on the electrode-electrolyte interface, and the abundant macropores can serve as ion-buffering reservoirs. Transition metal oxide is synthesized by co-precipitation technique, having a unique characteristic. The electrochemical measurements CV, GCD, EIS, and cyclic stability tests are performed in an electrolyte solution using a carbon-metal oxide composite electrode, giving ultra-high specific capacitance and cyclic stability with high energy and power density. Here in this work carbon matrix is enriched with co-doped heteroatom facilitating the pseudo behavior with the enhancement of electrical conductivity and its hierarchical porous structure, providing easy accessibility to the electrolyte ions. The charge storage mechanism is explored in detail better to understand the dependence between physicochemical and electrochemical properties. Accordingly, we can tune the properties for individual applications. This work provides a facile, scalable synthesis route to get okra-derived activated carbon and transition metal oxide to achieve outstanding super-capacitive performance without compromising energy density.

2:30 PM EN01.05.04

Green Fabrication of Flexible Supercapacitors by using Silk Biomaterials XuelianLiu, NicholasOstrovsky-Snider, MarcoLo Presti, TaehoonKim, JeffRoshko and FiorenzoOmenetto; Tufts University, United States

Energy storage devices that are eco-friendly, high-performance, and flexible are needed for integration into wearables, smart sensors, and implantable medical devices. The raw materials used in such devices determine both their performance and ecological impact. Here, we describe the process of assembling supercapacitors using three distinct silk fibroin (SF)-based composite biomaterials and carbon electrode materials. Photo-crosslinkable SF (Sil-MA) hydrogel, SF-polydopamine (SF-PDA), and SF bioplastic have been used to create a gel electrolyte, electrode binder, and encapsulation respectively. Together, these elements form a mechanically and electrochemically robust skeleton for bio-friendly energy storage devices. Combined with carbon materials, symmetric supercapacitors were built with methods that minimize energy consumption and the device's carbon footprint. The devices can achieve capacitance over 200 mF cm⁻² at a charge-discharge current of 10 mA cm⁻² with 94% capacitance retention after 20000 cycles. Moreover, the devices can be stretched, bent, twisted and compressed with minimal influence on the electrochemical performance.[1]

The SF biomaterials and green fabrication methods developed can also be applied to other aqueous electrochemical energy storage systems such as zinc-ion hybrid supercapacitors. The tough SF hydrogel can provide additional benefits to zinc anode by protecting it from the formation of dendrites and corrosion by-products.[2] This strategy for the use of SF biomaterials may open a route for the development of eco-friendly energy storage devices that can be integrated into future wearable and biomedical systems.

[1] Xuelian Liu, Nicholas Ostrovsky-Snider, Marco Lo Presti, Taehoon Kim, and Fiorenzo G. Omenetto, Silk biomaterials enable green fabrication of flexible supercapacitors, In preparation.

[2] Xuelian Liu, Nicholas Ostrovsky-Snider, Taehoon Kim, Marco Lo Presti, Jeffery Roshko, and Fiorenzo G. Omenetto, Silk hydrogel electrolyte for dendrite free Zn anode, In preparation.

2:45 PM EN01.05.05

Strong and Highly Ionic Conductive Ionogel for Wearable Solid State Supercapacitor HongliZhu, RuobingBai, YingWang and ZhengxuanWei; Northeastern University, United States

To follow the pace of the high-speed development of wearable electronic devices, the mechanical and electrochemical performances of the corresponding flexible and stretchable solid state energy storage devices need to be further improved. As a kind of solid polymer electrolyte for wearable energy storage devices, ionogel is a promising candidate exhibiting a broad stability window, exceptional mechanical performance, exceptional thermal stability, and low vapor pressure. Nevertheless, it is difficult to simultaneously enhance the mechanical and electrochemical performances of ionogel. In this work, we constructed an ionogel using polymerized poly (acrylic acid) and polyvinyl alcohol interpenetrating polymer networks as the host material and injecting 1-Ethyl-3-methylimidazolium dicyanamide ionic liquid as a filling solvent. Adequate contorted polymer chains and abundant reversible hydrogen bonds within the network aided in energy dissipation during tensile and compression, contributing to the exceptional mechanical properties. The improved electrochemical performances of ionogel result from the development of ion transfer kinetics. In particular, the subsequent ions impregnation and solvent exchange procedures modified the network structure and elevated the ion concentration in the ionogel. Concurrently, ionic liquid occupied in the networks rendered this ionogel with an outstanding stability of volume, mass, and ionic conductivity under conditions of low relative humidity. After

a series of treatments, this ionogel performed a remarkable strain of 2500 %, an exceptional ionic conductivity of 3.18 S/m at room temperature, and a virtually constant weight, volume, and ionic conductivity over about forty hours at a relative humidity of 20%. Sandwiching this ionogel electrolyte using electrospun polyacrylonitrile-based carbon fibers electrodes, a solid-state supercapacitor exhibited remarkable areal capacity, outstanding power density, and exceptional energy density. As a result, we synthesized a novel ionogel that breaks long-standing confinement while simultaneously exhibiting expected mechanical and electrochemical properties, thereby promoting the development of ubiquitous solid-state energy storage devices.

3:00 PMBREAK

3:30 PM *EN01.05.06

Flexible/Stretchable Supercapacitors for Powering Integrated Sensors of Wearable Patch DevicesJeong SookHa; Korea University, Korea (the Republic of)

In accordance with the miniaturization of personal wearable electronics, there has been extensive effort to develop high performance flexible/stretchable energy storage devices for powering integrated active devices. Supercapacitors are expected to achieve this purpose owing to their simple structures, high power density, and cyclic stability. As integrated wearable powering devices, supercapacitors are required to have stability over mechanical deformation such as bending and stretching due to body movements in addition to high electrochemical performance. The application of flexible/stretchable supercapacitors can be expanded further through the introduction of additional novel functionalities.

In this talk, we will introduce our recent works on the fabrication of high performance flexible/stretchable supercapacitors and their application as integrated energy storage devices to power various sensors in stretchable patch devices. In particular, our design strategy to fabricate the stretchable array of supercapacitors using serpentine and liquid metal interconnections as well as the intrinsically stretchable supercapacitors will be discussed. Finally, we will demonstrate our currently developed flexible/stretchable supercapacitors with novel functionality of self-healing, temperature tolerance, biodegradability, shape memory, and electrochromic display for advanced wearable patch devices with high durability, environmental friendliness, and color-changing display.

4:00 PM EN01.05.07

Sustainable Approaches for 1D Supercapacitors and Triboelectric Devices based on Functionalized Carbon Fiber YarnsLuisPereira^{1,2}; ¹FCT NOVA, Portugal; ²AlmaScience, Portugal

Carbon fibers (CFs) are versatile materials for energy harvesting and storage applications, particularly when focusing on wearable device applications. They present a combination of some unique properties, such as suitable electrical conductivity and mechanical strength, being also lightweight.

Stretch-broken carbon fiber yarns (SBCFYs) can be used as current collectors to fabricate 1D fiber-shaped supercapacitors (FSCs) using regenerated cellulose-based electrolyte. The areal-specific capacitance reaches 433.02 $\mu\text{F cm}^{-2}$ at 5 $\mu\text{A cm}^{-2}$. The maximum achieved specific power density is 0.5 mW cm^{-2} , at 1 mA cm^{-2} . The 1D FSCs possess a long-life cycle, 92% capacitance retention after 10000 charge/discharge cycles. The specific capacitance can be improved through functionalization of CFs with MoS_2 nanosheets, reaching 58.6 F g^{-1} at 1 mV s^{-1} with a power density of 15.17 W g^{-1} and energy density of 0.5 mWh g^{-1} .

Functionalization of CF by introducing functional groups or nanoparticles onto the fiber surface is also crucial in optimizing power conversion efficiency in energy harvesting devices, such as triboelectric ones. We propose triboelectric generator yarns (TEG yarns) with axially grown ZnO nanorods using a new method for depositing PDMS directly onto conductive carbon yarns. The in-situ PDMS curing method allows the fast formation of a uniformly thick coating over functionalized CFs. Single-electrode configuration TEG yarns were developed, and their electrical output was optimized by precisely adjusting the PDMS layer thickness and by changing the chemical and physical nature of the SBCFYs surface, reaching a power density of 74.1 $\mu\text{W cm}^{-2}$. We demonstrate that electrodeposited cellulose nanocrystals layers can replace ZnO nanorods in improving local polarization, which results in an increase of 100% of the TEGs electrical output to around 142.7 $\mu\text{W cm}^{-2}$.

Both SBCFYs supercapacitors and triboelectric devices can be hand-stitched onto fabrics showcasing the practicality and versatility of the prepared 1D CFs energy harvesting and storage devices to power the future generation of wearables electronics.

4:15 PM EN01.05.08

Hierarchical Nanostructure of Carbon Decorated Metal Organic Framework for Low Cost Aqueous Al-Ion SupercapacitorsShyamalShegokar, PujaDe and AmreeshChandra; Indian Institute of Technology Kharagpur, India

A novel strategy of incorporating conducting additive to enhance the performance of ZIF-67 based Al-ion supercapacitors is presented. The porous ZIF-67 and composites of ZIF-67 with different forms of carbon viz., rGO and CNS were synthesized by a simple co-precipitation method. Physicochemical characterizations like XRD, BET, FTIR, etc. were performed to confirm the successful synthesis of ZIF-67 and its composites. The electrochemical behaviour of the as-synthesized materials were studied using three electrode measurements. Amongst all the synthesized materials, composite of ZIF-67 with rGO performed best due to increased electrical conductivity and higher specific surface area. Further, electrolyte modification was carried out using 6mM KFCN as redox additive and all the synthesized composites were tested again. Here, the specific capacitance of ZIF-67_rGO composite enhanced to 346 Fg^{-1} at 1 A g^{-1} current density which was nearly two times the value exhibited by pristine ZIF-67. It also delivered good cycling stability with excellent coulombic efficiency of 89% and 95% after 1000 cycles, at 5 A g^{-1} current density, respectively.

4:30 PM EN01.05.09

Metal–Organic Framework Based Ultrafine-Fe1-xS-Nanoparticle-Confined Het-Erodimensional Anode and Hierarchical 3D Porous Carbon Cathode for Perform-Mance Maximization of Sodium-Ion Hybrid CapacitorsJong HuiChoi and Dong WonKim; KAIST, Korea (the Republic of)

While being the most popular, lithium-based energy storage devices have issues of geological distribution and rarity in the earth's crust. Due to their abundance, sodium ion-based hybrid capacitors (SIHCs) are drawing significant attention as an alternative. However, the sluggish kinetics and low capacities of their anode and cathode need to be overcome. Here, we report a strategy to realize ultrahigh-performance SIHCs anode and cathode electrode materials derived from metal-organic frameworks (MOFs). Facile carbonization of MIL-100(Fe) precursor and subsequent sulfidation process generated ultrafine pyrrhotite nanoparticles in the carbon matrix. The embedded fine particles exhibited outstanding rate performance due to the reduced size effect. Moreover, heteroatom-rich cathode materials were synthesized via the pyrolysis of ZIF-8. The subsequent KOH activation maximized the surface area and constructed a porous structure to the cathode material. High capacity was achieved due to pseudocapacitance that was induced by abundant surface heteroatoms. As a result, the SIHC device that was composed of the as-synthesized anode and cathode materials exhibited ultrahigh energy density (>200 Wh/kg) and power density (>19,000 W/kg). This study suggests a novel design strategy for realizing high-performance SIHCs.

SESSION EN01.06: Poster Session: Material Approaches to Harvest, Store and Deliver Energy Across Unconventional Applications I

Session Chairs: Trisha Andrew and Mihai Duduta

Tuesday Afternoon, November 28, 2023

Hynes, Level 1, Hall A

8:00 PM EN01.06.01

Flexible and Fast Chargeable Lithium-Ion Battery Based on Percolative Network-Based Electrospun Nickel Microfibers and Electrospayed Nanotextured Anode MaterialsDaekyuChoi and Hong SeokJo; Sungkyunkwan University, Korea (the Republic of)

High-performance flexible energy-storage devices have great potential as power sources for portable and wearable electronics. The major obstacle for developing such next-generation flexible batteries is the absence of flexible electrodes that can simultaneously meet high stability, high energy-density, and fast charging features. In this study, we present a novel approach employing an electrospun nickel microfiber (NiMF)-based flexible current collector. Not only does the current collector developed here show high mechanical properties, high electrical conductivity, and lightweight design, but the percolative network thereof also enables high flexibility and fast-charging speed with high stability. For the anode coating material, the mixture of lithium titanium oxide (LTO), carbon nanotubes (CNTs), polyvinylpyrrolidone (PVP), and polyvinylidene fluoride (PVDF) with a mixing ratio of 85:5:1:9 was used. In particular, the use of the electrostatic spraying method herein enabled the manipulation of the coating-thickness, -uniformity, and -texturing of the anode material being deposited on the randomly-entangled individual NiMFs. In case of the NiMF-based LTO electrode, despite being coated with the same loading mass of active materials, its total weight was only 25 mg because of an extremely low weight of the NiMF current collector relative to its volume. On the other hand, the Ni foil-based LTO electrode had a total weight of 475 mg. This difference in weight enabled the NiMF-LTO electrode to achieve a significant energy-density increase of more than 20 times compared to the Ni foil-LTO electrode. The resistance of the NiMF-LTO electrode was measured to be 6.3 Ω , which was significantly lower than that of the Ni foil-LTO electrode, which was 261 Ω . In addition, the NiMF-LTO electrode showed a 1.5% change in resistance after 100 cycles of bending test, while

the Ni foil-LTO electrode yielded a large change of 10% with the formation of cracks. In the half-cell test, as increasing the current rate (C-rate) from 0.1 to 2 C and subsequently reducing to 1 C, the corresponding discharge capacity (C_{dis}) of the NiMF-LTO case decreased from 166 to 75 mAh/g, followed by a recovery to 145 mAh/g, showing a high retention rate of 99.5%. In contrast, the C_{dis} of the Ni foil-LTO case exhibited a significant decrease from 165 to 4.5 mAh/g and then recovered to 10.5 mAh/g, showing a lower retention rate of 37%. Moreover, the NiMF-LTO case demonstrated a high stability with a capacity decay rate of only 0.05% over 100 cycles at 1 C. This advancement was attributed to the low impedance possibly identified by the charge transfer and ion transfer resistances (R_{ct} and R_{it}). At 0.1 C, the R_{ct} of the NiMF-LTO electrode-based half-cell was measured to be 142 Ω , lower than that of the Ni foil-LTO case (297 Ω). This difference indicates that the percolative structure of the NiMF-LTO electrode facilitated the efficient transportation of lithium ions from the electrolyte to electrode. Furthermore, the R_{it} , corresponding to the concentration gradient of lithium ions within the electrode, was measured to be 100 m Ω for the NiMF-LTO case, while that measured from the Ni foil-LTO case was higher as 704 Ω . This also indicates that the high uniformity and texturing (or surface area) of the LTO layer electrospayed on the NiMFs enhanced the ion diffusion rate within the electrode. The approach and materials employed here are expected to show great promise for developing next-generation flexible batteries with offering high and stable electrochemical and mechanical features.

8:00 PM EN01.06.02

The Power of Stress—A DFT Approach to Mitigate Fuel Cells Poisoning MohamedMahrous; The American University in Cairo, Egypt

Fuel cells are a promising alternative to traditional power sources due to their high efficiency and low environmental impact. However, the problem of carbon monoxide (CO) poisoning remains a significant challenge for fuel cell technology. In this study, we propose to use density functional theory (DFT) calculations to investigate the effects of stress on the electrodes to mitigate the adsorption of CO on its surface. We will employ DFT simulations to study the changes in the metal's electronic and structural properties under different stress and CO concentration levels. By analyzing the combined effects of stress and CO on the metal, we will identify optimal stress levels for mitigating CO poisoning and provide insights into the underlying mechanisms.

8:00 PM EN01.06.03

FeMoO₄ Nanoparticles as Functional Negative Electrode Material for High Performance Supercapacitor Devices over a Wide pH Range AyaM. Mohamed^{1,2}, HebaM. El Sharkawy^{3,2}, MohamedRamadan² and NagehK. Allam²; ¹Cairo University, Egypt; ²The American University in Cairo, Egypt; ³Egyptian Petroleum Research Institute, Egypt

Rational design of functional negative electrode materials with wide potential window, high capacitance, high rate capability, cost-effectiveness, and durability in various electrolytes is a grand challenge to realize the fabrication of high-performance supercapacitor devices. We report the successful synthesis of β -FeMoO₄ nanoparticles and their utilization as a negative electrode in supercapacitor devices over a wide pH range. The morphology, elemental, and surface analysis of the fabricated β -FeMoO₄ are characterized via FESEM, EDS, and the N₂-adsorption/desorption techniques. Moreover, the elemental composition and the crystal structure of the fabricated FeMoO₄ are elucidated using XPS and XRD analyses. Upon analyzing its electrochemical performance as a supercapacitor electrode in 2 M KOH, the fabricated β -FeMoO₄ reveals remarkable specific capacitance of 600 F g⁻¹ at 1 A g⁻¹. The charge storage mechanism is elucidated in detail, revealing mixed surface capacitive-pseudocapacitive mechanism. Besides, the assembled asymmetric supercapacitor device utilizing Ni-Cu-P as the cathode (positive pole) and β -FeMoO₄ as the anode (negative pole) displays superior specific energy and specific power of 40.75 Wh Kg⁻¹ and 850 W Kg⁻¹, respectively.

8:00 PM EN01.06.04

Optimized Fabrication of Bimetallic ZnCo Metal–Organic Framework at NiCo-Layered Double Hydroxides for Multiple Storage and Capability Synergy All-Solid-State Supercapacitors AyaM. Mohamed^{1,2}, DohaM. Sayed^{1,2} and NagehK. Allam²; ¹Cairo University, Egypt; ²The American University in Cairo, Egypt

Rational design and structural regulation of hybrid nanomaterials with superior electrochemical performance are crucial for developing sustainable energy storage platforms. Among these materials, NiCo-layered double hydroxides (NiCo-LDHs) demonstrate an exceptional charge storage capabilities owing to their tunable 2D lamellar structure, large interlayer spacing, and rich redox electrochemically active sites. However, NiCo-LDHs still suffer from severe agglomeration of their particles with limited charge transfer rates, resulting in an inadequate rate capability. In this study, bimetallic ZnCo-metal organic framework (MOF) tripods were grown on the surface of NiCo-LDH nanowires, which significantly reduced the self-agglomeration and stacking of the NiCo-LDH nanowire arrays, offering more accessible active sites for charge transfer and shortening the path for ion diffusion. The fabricated hybrid ZnCo-MOF@NiCo-LDH and its individual counterparts were tested as supercapacitor electrodes. The ZnCo-MOF@NiCo-LDH electrode demonstrated a remarkable specific capacitance of 1611 F/g at 2 A/g with an enhanced rate capability of 66% from 2 to 20 A/g. Moreover, an asymmetric all solid-state supercapacitor device was constructed using ZnCo-MOF@NiCo-LDH and palm tree derived activated carbon (P-AC) as positive and negative poles, respectively. The constructed device can store a high specific energy of 44.5 Wh/Kg and deliver a specific power of 876.7 W/Kg with outstanding Columbic efficiency over 10,000 charging/discharging cycles at 15 A/g.

8:00 PM EN01.06.05

Surface Facet Controlled Zinc Metal Anode for High Performance Aqueous Zinc Ion Energy Storage System HeeBinJeong¹, JohnHong¹, Dong IlKim¹, Hyeong SeopJeong¹ and SeungNamCha²; ¹Kookmin University, Korea (the Republic of); ²Sungkyunkwan University, Korea (the Republic of)

Several issues exist with the current organic electrolyte based electrochemical energy storage system, including the lack of metal resources, thermal expansion problems, and toxicity. In contrast, aqueous Zinc (Zn) ion batteries (AZIBs) have garnered substantial attention due to their abundance in resources and the cost-effectiveness and environmental friendliness of their electrode materials. Additionally, a water-based electrolyte solution can act as a successful block layer, thereby improving thermal stability. However, the use of a water medium can result in the formation of Zn dendrites on the Zn metal anode. The protruding structure of these dendrites can damage the separator and short-circuit the cell. Moreover, the generation of hydrogen and corrosion caused by parasitic surface reactions on the native passivation layers of Zn metal anodes pose significant problems, leading to decreased cycling stability of AZIBs. Therefore, the properties of the Zn metal surface should be well-tailored to address these issues. In this work, we proposed the use of a highly active acidic etching process on the Zn metal anode to increase the effective surface area and control the surface facet for favorable and smooth Zn deposition and stripping. Without any heat treatment, a mere 2-minute etching time can effectively create a closely spaced array within the etched grooves, resulting in a preferential (002) crystal plane orientation on the Zn metal anode. The high surface area can provide more active sites on the Zn metal anode. Moreover, the tailored (002) surface orientation can ensure the continuous deposition of planar zinc metal during the charge-discharge process, which can minimize the growth of protruding Zn dendrites. According to the suggested highly active acidic etching process, the electrochemical performance was greatly improved in terms of stability, specific capacity, and symmetric cell cyclability. Our results demonstrate that using acid-etched planar zinc foils as the anode can effectively increase the electroactive surface area, suppress hydrogen evolution reactions, and inhibit dendrite formation on the Zn metal anodes. As a result, the Zn anode symmetry cell showed long and stable cyclability for 250 hours at both current densities of 3 mA cm⁻² and 1 mA cm⁻². Moreover, in the full cell configuration with the α -MnO₂ cathode, the full cell displayed a long cycle life with a capacity retention of 73 % for up to 150 cycle at current density 0.5A/g. This acid etching process has a significant advantage of being short and simple in the experimental process compared to previously reported studies, thus providing new opportunities for stable and high-performance AZIBs.

8:00 PM EN01.06.06

High Performance Lithium-Sulfur Batteries by Ultrathin Mixed Ionically-Electrically Conductive Interlayer via Solution Shearing HyunminPark, DonghyeokSon and StevePark; Korea Advanced Institute of Science & Technology, Korea (the Republic of)

In an endeavor to mitigate the low energy density associated with lithium-ion batteries, lithium-sulfur batteries (Li-S batteries) have emerged as a prominent area of research due to their considerably high theoretical capacity of 1675 mA h g⁻¹. The utilization of sulfur as a cathode material confers several advantages to Li-S batteries, including the non-toxicity and abundant availability of sulfur, which can be obtained as a byproduct of crude oil refining. Despite the considerable potential of Li-S batteries, their commercialization has been hindered by the shuttle phenomenon, primarily caused by soluble lithium polysulfide (LiPS) intermediates (Li₂S_x, 4 ≤ x ≤ 8). Numerous efforts have been made to address this issue, including the utilization of sulfur host materials with diverse functions such as electrocatalysis, adsorption, and facile electron transfer. Nevertheless, these approaches do not provide a fundamental solution as they fail to prevent the dissolution of sulfur into the electrolyte in the form of polysulfides during repeated charging and discharging. Therefore, it is recommended to develop a functional separator or interlayer that can reactivate inactive sulfur and suppress the shuttle phenomenon. Particularly, the introduction of an interlayer that acts as an additional barrier to the diffusion of soluble LiPSs has been regarded as a more direct, efficient, and scalable strategy to alleviate the shuttle phenomenon compared to modifying the cathode. Nonetheless, unresolved concerns regarding existing interlayers necessitate additional scholarly exploration. Firstly, the utilization of transition metal compounds (e.g., metal oxides, sulfides) as interlayers, capable of chemically adsorbing soluble LiPSs without a conductive carbon-based material, results in low initial discharge capacity and inadequate utilization of sulfur due to low electrical conductivity. Secondly, the overall energy density is diminished due to insufficient thickness and weight of the interlayers. Lastly, Blade casting and vacuum filtration methods for interlayer production have limitations hindering uniformity and large-area thinness. Consequently, scalable approaches for fabricating ultrathin and homogeneous interlayers on a large scale are imperative for the practical application of interlayers in Li-S batteries. In this study, we have successfully developed a large-area (10 cm × 10 cm), ultrathin (750 nm), and lightweight (0.182 mg cm⁻²) mixed ionic-electronic conducting CNP interlayer comprising carbon nanotubes (CNTs), Nafion, and poly(3,4-ethylenedioxythiophene):polystyrenesulfonate (PEDOT:PSS) with 1-ethyl-3-methylimidazolium tetracyanoborate ionic liquid counter-ion exchange via a scalable solution shearing technique. The CNP interlayer effectively suppresses the shuttle phenomenon through the synergistic segregation effect, facilitated by the ion-conductive Nafion that induces electrostatic repulsion towards negatively charged soluble polysulfides, as well as the supplementary adsorption effect towards soluble polysulfides exhibited by CNTs and PEDOT. Additionally, the CNP interlayer demonstrates high electrical conductivity through counter-ion exchange with

an ionic liquid, thereby enabling facile reactivation of inactive sulfur as a secondary current collector. Impressively, the lithium-sulfur pouch cell with the CNP interlayer achieves a high discharge capacity of 1029 mA h g⁻¹ and exhibits stable cyclability over 20 cycles, even under lean electrolyte conditions (5 μl mg⁻¹) and high areal sulfur loading (5.3 mg cm⁻²). The scalable strategy to fabricate a shuttle-suppressing interlayer using solution shearing and counter-ion exchange guides future advancements in lithium-sulfur battery interlayers.

8:00 PM EN01.06.07

A Promising Approach Towards the Commercialization of Lithium Sulfur Batteries: Prelithiated Graphene Mahmud Tokur^{1,2}; ¹Sakarya University, Turkey; ²NESSTEC Energy & Surface Technologies A.S., Turkey

Lithium-sulfur (Li-S) batteries are a promising candidate technology for high-energy rechargeable batteries due to their advantages of abundant materials and inherently high energy [9]. However, the practical applications of Li-S batteries are challenged by several obstacles, including the low sulfur utilization and poor lifespan, which are partly attributed to the shuttle of lithium polysulfides and lithium dendrite growth during cycling [12]. The shuttling of polysulfide ions between the electrodes in a Li-S battery is a major technical issue triggering the self-discharge and limiting the cycle life. [11]. A stable lithium anode is essential for maintaining the good cycle stability of Li-S batteries in practical applications [13]. To address these lithium-related issues, various carbon materials, including graphite and graphene, have been investigated as suitable lithium hosts to use as anode materials for Li-S batteries [9]. Prelithiation is a crucial strategy to compensate for the lithium needs of the system when using lithium-free active materials, but most of the prelithiation reagents developed so far are highly reactive and sensitive to oxygen and moisture, making them difficult for practical battery application. In this study, prelithiated graphite and graphene-based anode materials are obtained by the galvanostatic charging method to improve the performance of Li-S batteries and compare the electrochemical properties, especially in terms of capacity retention and rate capability. According to the results, graphene showed better performance due to its high lithium storage capacity and fast lithium-ion diffusion rate. A pouch cell was assembled with prelithiated graphene anode showing an energy density of about 360 Wh kg⁻¹ in the first cycle and protected its specific capacity of 60% after 100 cycles in a liquid-based Li-S battery.

Keywords: Lithium Sulfur Battery, Prelithiation, Graphene Anode

Acknowledgments

This work is supported by the Scientific and Technological Research Council of Turkey (TUBITAK) under contract number 120N492. The authors thank the TUBITAK workers for their financial support.

This work also receives funding from the European Union's Horizon 2020 research and innovation program (under grant agreement no. 100825) under the scope of Joint Programming Platform Smart Energy Systems (MICall19).

8:00 PM EN01.06.08

A New Strategy for Hexagonal Boron Nitride Coating on Zinc Metal Anode for High-Performance Zinc Ion Batteries Dong Ii Kim, Hee Bin Jeong and John Hong; Kookmin University, Korea (the Republic of)

The high demand for new electrochemical storage systems with high energy densities and operational stability has driven recent studies on aqueous zinc-ion batteries (AZIBs). AZIBs, which consist of aqueous electrolytes and electrode materials, are promising alternatives to flammable organic batteries. However, further research efforts on Zn metal anodes are still required due to issues such as the formation of protruding Zn deposition morphology (Zn dendrites) and parasitic reactions, including hydrogen evolution reactions between the Zn metal anode and the water electrolyte. These issues can reduce the high-efficiency electrochemical cycling of AZIBs. Therefore, finding a proper protective layer for the Zn metal is crucial to reduce the direct nucleation sites of Zn dendrites, provide high mechanical strength to the Zn anode, and improve selectivity and uniformity at the electrode surface during the charge-discharge process.

Here, we present the first report on utilizing bulk hexagonal boron nitride (h-BN) layers as a promising coating for the Zn metal anode. The thin and uniform bulk h-BN coating reduces the nucleation radius of Zn dendrites, resulting in uniform Zn stripping and deposition. Furthermore, h-BN is a two-dimensional (2D) material with superior insulating properties, making it highly desirable. In particular, the h-BN layers can serve as effective energy barriers, preventing electron tunneling from the Zn metal to the electrolytes. This can minimize the parasitic surface reactions on the surface of the Zn metal anode.

In this study, we propose a practical coating method using commercial h-BN powders, which allows for uniform deposition on the Zn metal anode over a large area. Through the optimization of the coating process and h-BN layer thickness, the Zn/h-BN symmetry cells exhibited a reduced overpotential (29 mV) and extended lifespan (over 250 hours) at a current density of 1 mA cm⁻² during the deposition and stripping processes. Additionally, a full cell configuration of Zn/h-BN//α-MnO₂ was fabricated to demonstrate its electrochemical performance. The Zn/h-BN//α-MnO₂ full cell displayed a high electrochemical performance of 345 mAh g⁻¹ at a current density of 0.1 A g⁻¹, with long-term cyclability of 75.4% after over 500 cycles at a current density of 0.5 A g⁻¹. This simple and effective coating method utilizing h-BN materials represents a promising approach towards the commercialization of Zn-ion batteries.

8:00 PM EN01.06.09

High Performance Metal Halide Batteries Enabled by Electrolyte Optimization Liliang Huang, Wenjun Zhu and Ivan Situ; Sidus Energy Limited, United States

As one of the most promising energy storage devices, the Li-ion battery has witnessed tremendous success and growth over recent decades. As society transitions into a carbon-neutral era, there becomes an urgent need for the development of novel cathode materials, whose cost and performance significantly impact the future widespread application of Li-ion batteries. The recent development of metal halide cathodes enables deviation from conventional intercalation chemistry and thus greatly expands the chemical space for high-performance cathodes. To date, lithium halide-based batteries with excellent energy density and rate performance have been developed, but cycling lifetime and self-discharge are still a challenge in their commercialization. Herein, we demonstrate that electrolyte optimization can serve as a promising strategy to address these issues. Specifically, we show that increasing the lithium salt concentration in ether-based electrolytes is beneficial for cycling and stationary stability through alleviating the detrimental side reactions introduced by the metallic lithium as well as the shuttling of lithium halides. Further incorporating fluorinated solvents into the electrolyte can increase not only the electrolyte ionic conductivity but also the columbic efficiency. Moreover, in contrast to the conventional notion that carbonate solvents are incompatible with Li metal anodes, we discover a unique synergy between certain carbonate and ether-based solvents, resulting in significantly improved battery performance. Finally, enabled by this improved electrolyte design, we have successfully prepared pouch cells with good cycling lifetime and higher energy density than commercial cells.

References

- [1] Goodenough, J. B.; Kim, Y. Challenges for Rechargeable Li Batteries. *Chem. Mater.* 2010, 22, 587-603.
- [2] Xie, L.; Singh, C.; Mitter, S. K.; Dahleh, M. A.; Oren, S. S. Toward Carbon-Neutral Electricity and Mobility: Is the Grid Infrastructure Ready? *Joule* 2021, 5, 1908-1913.
- [3] Yang, C.; Chen, J.; Ji, X.; Pollard, T. P.; Lü, X.; Sun, C. J.; Hou, S.; Liu, Q.; Liu, C.; Qing, T.; Wang, Y.; Borodin, O.; Ren, Y.; Xu, K.; Wang, C. Aqueous Li-ion Battery Enabled by Halogen Conversion-Intercalation Chemistry in Graphite. *Nature* 2019, 569, 245-250.
- [4] Zhao, X.; Zhao-Karger, Z.; Fichtner, M.; Shen, X. 2020. Halide-Based Materials and Chemistry for Rechargeable Batteries. *Angew. Chem.* 2019, 59, 5902-5949.
- [5] Xu, J.; Pollard, T. P.; Yang, C.; Dandu, N. K.; Tan, S.; Zhou, J.; Wang, J.; He, X.; Zhang, X.; Li, A. M.; Hu, E.; Yang, X. Q.; Ngo, A.; Borodin, O.; Wang, C. Lithium Halide Cathodes for Li Metal Batteries. *Joule* 2023, 7, 83-94.
- [6] Lu, K.; Hu, Z.; Ma, J.; Ma, H.; Dai, L.; Zhang, J. A Rechargeable Iodine-Carbon Battery that Exploits Ion Intercalation and Iodine Redox Chemistry. *Nat. Commun.* 2017, 8, 527.

8:00 PM EN01.06.10

An Asymmetric Moisturizing 3D Foam with High Deformability for Complementary Energy Harvesting via Moisture-Induced Electric and Triboelectric Generator Gwanho Kim and Cheolmin Park; Yonsei University, Korea (the Republic of)

Moisture-induced electric generators (MEGs) have emerged as promising candidates for next-generation energy conversion. However, existing MEG devices face limitations such as low current and voltage outputs, high moisture dependence, and lack of mechanical robustness. In this study, we introduce a novel 3D asymmetric moisturizing deformable MEG device that exhibits exceptional mechanical performance and simultaneously harnesses power from both MEG and triboelectric nanogenerator (TEENG) effects. Our device combines an organo-ionic hydrogel infusion within the lower section of a 3D melamine foam substrate, coated with 2D conductive MXene (Ti₃C₂T_x) and hydrophilic poly(vinyl alcohol), resulting in superior water capturing and rapid ion transport capabilities. Notably, this device operates efficiently across a wide range of temperatures (-20 to 60 °C) and relative humidities (20 to 90% RH). Leveraging the negative surface charge of MXene, positive ions from salts and water in the organo-ionic hydrogel are preferentially selected, enabling continuous power generation with a maximum open-circuit voltage and short-circuit current density of 0.32 V and 877 μA cm⁻², respectively. Additionally, the upper layer of our device generates a high voltage (~80 V) through contact electrification with a perfluoroalkoxy alkane film over ~30,000 cycles. The integration of MEG and TEENG components yields a high-power output (~83 μW cm⁻²), showcasing the device's practical potential for emergency exit sign applications by leveraging the distinctive characteristics of MEG's direct current and TEENG's alternating current.

8:00 PM EN01.06.11

High Voltage Generated by Moving Drops Pravash Bista¹, Aaron Ratschow², Hans-Jürgen Butt¹ and Stefan A. Weber^{1,3}; ¹Max Planck Institute for Polymer Research, Germany; ²Technische Universität Darmstadt, Germany; ³Universität Stuttgart, Germany

Water drops sliding on insulating, hydrophobic substrates can become electrically charged [1–3]. Despite many decades of research, this spontaneous electrification of moving drops is still far from being understood. By precisely measuring charge and voltage, we found that moving water drops accumulate a voltage of several kilovolts after sliding for just a few centimeters. To enable an efficient utilization of this simple electric energy generation mechanism, a detailed and quantitative understanding of the underlying physical process would be required. Using a simple electrostatic model, we show that the drop voltage is fundamentally connected to the properties of the electrostatic double layer at solid-liquid interfaces. The observation of high drop voltages will have important implications for energy harvesting applications, as well as droplet microfluidics and electrostatic discharge protection.

[1] A. Z. Stetten, D. S. Golovko, S. A. L. Weber, and H.-J. Butt, *Slide Electrification: Charging of Surfaces by Moving Water Drops*, *Soft Matter* **15**, 8667 (2019).

[2] D. Díaz, D. García-González, P. Bista, S. A. L. Weber, H.-J. Butt, A. Stetten, and M. Kappl, *Charging of Drops Impacting onto Superhydrophobic Surfaces*, *Soft Matter* **18**, 1628 (2022).

[3] X. Li et al., *Spontaneous Charging Affects the Motion of Sliding Drops*, *Nat. Phys.* **1** (2022).

8:00 PM EN01.06.12

Ultra-Flexible Li-Ion Batteries using High Mass-Loading Polymer-Rich Thick Electrodes Nigussh. Hatsey^{1,2}, Hye-MiSo¹, AreamKim¹, MinsubOh¹ and SeungminHyun^{1,2}; ¹Korea Institute of Machinery and Materials (KIMM), Korea (the Republic of); ²University of Science and Technology (UST), Korea (the Republic of)

Flexible batteries have been the research of interest due to various applications of Internet of things (IoT), soft robots and wearable electronics. For the development of advanced electronics, flexible batteries with high energy density and mechanical stability are essential. However, conventional electrodes are limited to achieve both flexibility and high energy density of batteries. In this work, we developed novel electrode structure to fabricate ultra-flexible Li-ion battery with high energy density. This novel electrode structure was fabricated through reinforcing thermally induced polymer-rich electrode by stainless-steel (SS) fiber current collector. The polymer-rich electrode made through thermally induced phase separation (TIPS) process was suggested for flexible thick electrode. The SS fiber current collector was prepared by a facile method from a bundle. The combination of the polymer-rich electrode and SS fiber current collector enabled structural flexibility and mechanical stability. The electrochemical property and mechanical properties of the battery with the novel electrode were analyzed by comparing with battery of polymer-rich electrode coated on conventional metal foil current collector. The battery with LiNiMnCoO₂ thick-film electrodes with SS fiber electrodes showed high rate capability. At 2C rate, the specific capacity of foil electrode is 60 mAh g⁻¹ and that of the SS fiber electrode is 135 mAhg⁻¹, which is two times higher. Moreover, up to 12 mA_{hcm}⁻² high areal capacity is attained using about 1 mm thick electrode with SS current collector. Electrochemical performance of high mass-loading pouch-type battery after 2000 bending cycles also showed very high retention of specific capacity. The structural flexibility and mechanical reliability of the novel electrode structure enables to make flexible batteries with high energy density.

8:00 PM EN01.06.13

Sulfur Cathode Integrating Nanoscale Carbon-Layered Mesoporous Silica Particles for Prolonged Cycle Life of Lithium-Sulfur Batteries Sun HyuKim, Ji YangLim, Si WonChoi, SandeulRyoo, Hye RanKim and YongjuJung; Korea University of Technology and Education, Korea (the Republic of)

Lithium-sulfur (Li-S) batteries have garnered significant attention as a promising energy storage system owing to the high energy density and high natural abundance of sulfur. Nonetheless, their practical application has been slowed down by limited cycle life attributed to soluble polysulfide species generated on discharge. The migration of these dissolved polysulfide ions towards the lithium anode gives rise to the formation of inert materials on its surface. The solubility of polysulfides is necessary for the discharge-charge process of the sulfur cathode, so it is inevitable to effectively confine them within the cathode to protect the diffusion phenomena of polysulfide out of cathode. Several approaches have been proposed, such as the utilization of sulfur-infiltrated carbon nanotube (CNT) films. However, the macro-porous structure of CNTs limits their ability to effectively accumulate polysulfides. Another strategy involves incorporating ordered mesoporous silica (OMS) as an additive to mitigate the diffusion of polysulfides, yet OMS lacks long-term stability as a polysulfide reservoir. To address these limitations, this study introduces a novel solution for effectively immobilizing polysulfides. It entails the synthesis of carbon-layered OMS (c-OMS) through surface-selective polymerization inside silica mesopores, followed by carbonization. Comparing the performance of the sulfur-CNT cathode with c-OMS to that of the sulfur-CNT cathode alone, the former demonstrates a significantly enhanced capacity (942 mAh/g) and superior cycle stability (91% retention after 100 cycles). These outcomes underscore the advantageous surface properties of c-OMS, which exhibit a high chemical affinity for electrolyte solvents. This research presents a promising approach for enhancing the performance of Li-S batteries by effectively addressing issues related to polysulfide dissolution and confinement.

8:00 PM EN01.06.14

A Nonconductive Mesoporous Carbonaceous Material as a New Sulfur Host for Low-Cost and Viable Lithium-Sulfur Batteries Si WonChoi, Hye RanKim, Ji YangLim, Sun HyuKim, Je YeonKim and YongjuJung; Korea University of Technology and Education, Korea (the Republic of)

Li-S batteries have gained significant attention in recent years due to their high theoretical energy density, cost-effectiveness, and the abundant availability of sulfur active material. However, the practical implementation of Li-S batteries faces various challenges that need to be overcome. Many researchers believed that one of the prominent obstacles lies in the low electrical conductivity of sulfur, which hampers the overall performance of the batteries. From this perspective, a range of methodologies aimed at enhancing the electrical conductivity of sulfur electrodes have been scrutinized.

Incorporating sulfur into conductive matrix has been regarded as a commonly employed approach to improve electrical conductivity. Extensive research has been conducted on the utilization of porous conductive materials such as carbon nanotubes, graphene, carbon black, as well as conducting polymers. These materials have been found to facilitate efficient electron transport within the sulfur cathode, resulting in improved rate capability and cycling stability.

Contrary to prevailing trends, a recent study has presented a novel approach using nonconductive ordered mesoporous silica (pOMS) as a host material. This study focuses on the unique sulfur reaction mechanism, where molecular sulfur is converted to polysulfides through a charge transfer process at the solid-solution interface during discharge. The study demonstrates outstanding long-term cycle stability and high capacity retention, challenging the conventional notion that conductive materials are essential for improving battery performance. This utilization of a nonconductive inorganic host, instead of conductive frameworks like porous carbons, represents a significant departure from current research trends in the Li-S battery community. However, the fabrication process of pOMS is known to be complex and cumbersome, limiting its widespread implementation.

To address this issue, we propose using a nonconductive mesoporous carbonaceous material as a sulfur host. Typically, this material is fabricated at temperatures below 500 °C through a pyrolysis process of organic polymers under inert gas flow conditions. The resulting materials treated at low temperatures possess abundant polar functional groups on their surface, which can interact with polysulfides. The sulfur cathode with nonconductive carbons exhibits remarkable improvements in reversible capacity and cycling properties.

8:00 PM EN01.06.15

Innovative Li-S Batteries Comprising a Sulfur-Free Carbon Electrode and a Separator with Elemental Sulfur Ji YangLim, Hyun WooKim, Si WonChoi, Sun HyuKim, SandeulRyoo and YongjuJung; Korea University of Technology and Education, Korea (the Republic of)

Lithium sulfur (Li-S) batteries have emerged as a promising next-generation rechargeable battery owing to the potential advantages of sulfur, a cathode active material, such as high theoretical capacity, low-cost and high natural abundance. However, Li-S batteries suffer from various performance problems which should be tackled for mass production, including capacity degradation during cycling due to the diffusion of polysulfides, poor rate capability associated with intrinsic chemical reactions between polysulfides, and high self-discharge property. To address these issues, the carbon-sulfur (C-S) composites concept has been presented in which active sulfur materials are embedded in the pore structure of carbon frameworks. The C-S composites have proved to be highly beneficial for mitigating polysulfide diffusion out of cathode, resulting in substantial performance improvements. However, it has been revealed that (1) the increased performance of the C-S composites stems from their high capability to confine active materials within the porous structure of carbon hosts; (2) the intimate contact between carbon and sulfur is not essential for functioning a sulfur cathode. It has been found from intensive studies that sulfur particles participate in discharge process via solution electrochemistry: a small amount of solid sulfur is dissolved in the electrolyte through chemical equilibria between solid sulfur and dissolved sulfur, and sulfur molecules in the solution are electrochemically reduced to polysulfides at the interface of carbon and an electrolyte solution upon discharge. Based on this finding, we present an innovative Li-S battery comprising a sulfur-free carbon cathode and a microscale sulfur-layered separator or a sulfur-incorporated separator. Notably, these cells normally function and demonstrate excellent performances in terms of reversible capacity, rate capacity, and cycling stability, as all sulfur materials on the separator are consumed. We believe that this approach offers a new paradigm for a rational design of high-performance Li-S batteries and could be widely applied for enhancing the energy density of Li-S batteries.

8:00 PM EN01.06.16

Zeolitic Imidazolate Framework -8-Based Passive Daytime Radiative Cooling Paint for Energy-Efficient Cooling HangyuLim, JaeminPark, DongwooChae, JisungHa and HeonLee; Korea University, Korea (the Republic of)

Owing to increasing energy consumption, especially for cooling, as well as climate change and the emergence of new industries, there is a growing demand for new cooling technologies to replace the existing systems that consume a large amount of energy and contribute to environmental pollution. To overcome these problems, radiative cooling can be utilized, which uses the optical properties of materials to achieve cooling without emitting pollutants or consuming energy. Paint is the most practical form for the application of a radiative cooling material. Therefore, we fabricated a passive daytime radiative cooling (PDRC) paint using a polyurethane binder and zeolitic imidazolate framework (ZIF)-8 powder. The ZIF-8 powder was synthesized in an environmentally friendly manner using deionized water as the solvent, and the resulting paint had a reflectance of 94.9%, an emissivity of 94%, and a cooling power of 113

W/m². Actual temperature measurement results showed that the paint cooled the surroundings by an average of 5.7 °C and up to 8.1 °C during the daytime. As a result, ZIF-8-based PDRC paint is capable of cooling below room temperature and is expected to reduce the energy used for cooling and alleviate environmental pollution in various fields, such as building exteriors.

8:00 PM EN01.06.17

Photocatalytic Reductive C–C Coupling Driven by Light-Induced Electron Transfer/Phase Migration of a Redox Mediator in a Biphasic SolutionRenItagaki^{1,2}, AkinobuNakada^{1,3}, HajimeSuzuki¹, OsamuTomita¹, Ho-CholChang⁴ and RyuAbe¹; ¹Kyoto University, Japan; ²JSPS Reserch Fellow DC1, Japan; ³PRESTO/JST, Japan; ⁴Chuo University, Japan

Natural photosynthesis establishes highly efficient molecular-conversion reactions driven by solar light energy, based on the combination of ingenious parts, such as light capturing, charge separation and migration, and catalysis in the reaction center. In addition to extensive studies on artificial photosynthetic systems mimicking the natural system, photoredox catalysis has recently had great impact on the field of photochemical organic synthesis. In any case, photoinduced electron transfer from/to electron donor(s)/acceptor(s) is a key initial step. One of the most important issues in the construction of highly efficient artificial photocatalytic systems is to suppress undesired backward electron transfer that decreases total efficiency. Herein, we developed a new photocatalytic system using biphasic solution media to mitigate such backward charge recombination. Two-immiscible solution composed of water and 1,2-dichloroethane (DCE) was employed with ferrocenium/ferrocene (Fc⁺/Fc) electron mediator. The change in dissolubility of Fc⁺/Fc (hydrophilic/hydrophobic) by photocatalytic electron transfer is expected to play an important role for the spatial charge separation to suppress the backward electron transfer. We demonstrated photocatalytic reductive coupling of benzyl bromide by utilizing the photoinduced inter-liquid phase migration of Fc⁺/Fc; suppressing the undesired backward charge recombination significantly.

Visible-light irradiation to a biphasic solution that composed of water and DCE solution containing an Ir(III)-photosensitizer, Fc, and benzyl bromide (Bn-Br) facilitated the reductive coupling of Bn-Br to dibenzyl (Bn₂). Given the energy diagrams of the photosensitizer and Fc, the Fc should act as an electron donor for the photoexcited Ir(III)-photosensitizer. The reduced Ir(III) complex has an enough potential for one-electron reduction of benzyl bromide forming Bn₂. Importantly, Fc⁺, generated by photooxidation, migrates to the aqueous phase due to the drastic change in its partition coefficient compared to that of Fc. On the other hand, visible-light irradiation to the same solution without water phase did not give any product. This finding indicates that the phase migration of Fc⁺ across a biphasic solution suppresses the unfavorable backward charge recombination, which enables the photoreduction of Bn-Br. The results on the coupled phase migration/photoinduced electron transfer prompted us to further investigate design principles in order to improve the efficiency of this photocatalytic reaction. The co-existence of anions can further modify the driving force of phase migration of Fc⁺ depending on their hydrophilicity; the best photocatalytic activity was obtained with 99% yield after continuous photocatalysis for 90 min in the presence of NBu₄⁺Br⁻ compared to 25% one without additive. Thus, the liquid-liquid phase migration of the mediator results in effective charge separation, which leads to facilitate the reduction of Bn-Br in the DCE phase.

8:00 PM EN01.06.18

Boosting Energy-Harvesting Performance of PVDF Nanofiber-Based Piezocomposite using Metal-Free Organohalide CrystalsKiyongKim, HoiminKim and Joo-HongLee; Sungkyunkwan University, Korea (the Republic of)

Polyvinylidene fluoride (PVDF) has been widely studied in the field of self-powered active implantable medical devices (AIMDs). Because it has decent piezoelectricity, which is required for sensing various body signals, biocompatibility, and mechanical flexibility. To enhance the polar β -phase of PVDF, which is associated with its piezoelectric behavior, the incorporation of inorganic piezoceramics into PVDF has been a commonly considered approach. The physicochemical interfacial interaction between PVDF and these piezoceramics enables the non-polar α -phase of PVDF to be transitioned to the polar β -phase, resulting in the improved piezoelectric response with a high piezoelectric coefficient (d_{33}). In recent studies, although metal-based piezoceramics, such as lead zirconate titanate (PZT), barium titanate (BTO), and lead magnesium niobate (PMN), have been effective in enhancing the piezoelectric properties of the resulting PVDF-based piezocomposite, they showed limits in terms of mechanical flexibility, biocompatibility, and cytotoxicity, which are important for developing industrially viable AIMDs. In this study, we develop an ultra-thin and flexible piezocomposite by incorporating the metal-free organohalide crystals into the PVDF matrix using the electrospinning process. The electrohydrodynamic spinning process facilitates the interfacial attraction between the polymer chain and the organohalide crystals, which promotes the alignment of the β -phase of PVDF. Herein, 1,4-diazabicyclo[2.2.2]octane (DABCO)-NH₄I₃, which is the metal-free organohalide crystals having ABX₃ molecular structure with hexagonal crystal system and consists of one-dimensional chains of face-sharing (NH₄)X₆ octahedra separated by organic cations, was used. Compared to the bare PVDF electrospun nanofibers, DABCO-NH₄I₃-incorporated PVDF electrospun nanofiber exhibits a significantly improved piezoelectric response with showing a high d_{33} value of 202 pC/N. The enhanced β -phase of the PVDF nanofibers was examined using the grazing-incidence wide-angle X-ray scattering (GIWAXS) technique. Its high biocompatibility was also demonstrated by the cell viability test using fibroblast cells. The piezoelectric nanogenerator (PENG) fabricated using the piezoelectricity-enhanced nanofibers yields an outstanding energy-harvesting performance with a maximum output voltage of ~ 80 V, which is 10-fold higher than that observed from the bare PVDF nanofiber-based PENG. Since the DABCO-NH₄I₃-incorporated PVDF nanofibers developed here not only have high biocompatibility and flexibility but also show enhanced piezoelectric behaviors, it is expected to show great potential in the field of self-powered AIMDs.

8:00 PM EN01.06.19

Highly Efficient, Flexible and Self-Healable Moisture-Driven Energy Harvester based on 2D Vanadium Pentoxide NanosheetsKundanSaha and SameerSonkusale; Tufts University, United States

The ubiquitous source of atmospheric moisture brought about a fascinating research avenue of extracting atmospheric water to generate sustainable electricity. Energy may be extracted from ambient moisture with obvious and substantial advantages. This point-of-use technology provides a decentralized alternative to meet the energy needs in isolated off-grid places. Unlike traditional energy generators which predominantly rely upon fossil fuel, moisture-induced energy generators can extract energy from moisture in a sustainable and eco-friendly way. Herein, we demonstrated a self-healable moist electric generator (MEG) based on vanadium pentoxide (V₂O₅) 2D nanosheet membranes. Lamellar membranes of V₂O₅ nanosheets have been shown to be excellent cation conductors and excellent materials for harvesting energy from ambient moisture. Ultra-thin 2D nanosheets of V₂O₅ was obtained by treatment of bulk V₂O₅ crystals with hydrogen peroxide. V₂O₅ nanosheet membrane was fabricated by vacuum-assisted filtration of 2D V₂O₅ nanosheets dispersion over a PTFE support membrane. The V₂O₅ membrane was easily peeled off from the support membrane on drying to obtain a flexible and freestanding V₂O₅ membrane. The V₂O₅ membrane consisting of percolated nanofluidic channels was sandwiched between a bottom solid copper foil and a perforated copper foil as the bottom electrode. The top electrode is perforated for exposure to atmospheric humidity. As the atmospheric water molecules come in contact with the V₂O₅ surface, an open-circuit voltage of 0.5 Volts and a short-circuit current of 0.3 microamperes is generated. The generated voltage and current is attributed to the preferential flow of cations through the V₂O₅ nanochannels. The exposed surface and edges of V₂O₅ nanosheets have a high negative surface charge which results in the splitting of water molecules into H₃O⁺ and OH⁻ ions. An electrical double layer (EDL) is established at the V₂O₅/water interface which selectively permits H₃O⁺ ions through the channels. The mobile ions of the EDL transport through the nanofluidic channels creating a gradient between the two electrodes, resulting in a constant potential difference between the top and bottom electrodes which is harvested as electric current. The MEGs can be easily connected in parallel or series to enhance the current and voltage respectively. We demonstrate ten MEGs connected in series to power small electronic devices such as calculators and humidity meters. One of the key features of the V₂O₅ MEG is its ability to repair any physical damage to the active material owing to the water-assisted healing characteristics V₂O₅ membrane.

8:00 PM EN01.06.20

Flexible Energy-Dense Li-Ion Batteries based on Super-Lightweight and Highly Flexible Metal-Coated FabricsWanchengYu, JianShang, LeiWang and ZijianZheng; The Hong Kong Polytechnic University, China

Flexible Li-ion batteries (FLIBs) are in urgent demand but the balance of flexibility and energy density of the battery is a great challenge. Hundreds of works reported flexible Li batteries fabricated by special structure design or soft materials. However, getting flexibility always leads to lower energy density because of the introduction of inactive weight or volume. Hence, we proposed a new type of flexible, super-lightweight, and three-dimensional current collector, metal-coated fabrics (MCFs). They can be employed in large-scale fabrication and roll-to-roll production. By replacing the Cu foil with Cu-coated fabrics (CuCF), the energy density is increased by 10%. MCFs also show advantages on the flexible applications. For the MCF-based pouch cell, after 1,000 bending cycles at the bending radii of 5 mm and 2 mm, the capacity retention is higher than 90%. The β_{FOM} of the LIB made with MGFs reaches over 50, outperforming industrial flexible LIB and most reported flexible LIB made with soft current collectors. Since MCFs are prepared with cost-effective materials and a highly scalable process, they are promising, from a commercial viability point of view, to replace metal foils as current collectors in a wide variety of energy storage industries.

8:00 PM EN01.06.21

Energy Harvesting with Fiber based Triboelectric Laminates for Wearable DevicesArtisLinarts, LinardsLapcinskis, KasparsMalnieks and AndrisSutka; Riga Technical University, Latvia

Triboelectric nanogenerators (TEG) are intriguing energy harvesting devices that convert mechanical energy into electricity and could power small portable devices or charge batteries [1]. Herein, we develop a broad and scalable approach to introduce volumetric dipoles into TENGs and break the surface charge paradigm by generating layer-by-layer triboelectric laminate structures from sequential electrospinning of large and small polymer fibers. When large fibers are electrospun onto smaller fibers, the interface between the laminate layers will slip, leading to internal contact electrification. In contrast, when small fibers are electrospun onto large fibers, they form an interpenetrated network with tight binding, creating a nonslip interface. This combination of ordered interfaces leads to parallel dipole moments being formed within the bulk volume of the laminate leading to an effective macroscopic dipole being formed. Increasing the total number of layers within a laminate, of the same total volume, leads to a linear relationship between charge and layer number. Most importantly we demonstrate that this concept not only works for laminates made of 2 different polymers but from identical polymer as well. We also show that exploiting triboelectric laminates in TENG devices can enhance their current

output by 40 times. We believe that this concept will be widely used in the future for designing wearable devices with low power demand.

[1] Z.L. Wang "Triboelectric Nanogenerators as New Energy Technology for Self-Powered Systems and as Active Mechanical and Chemical Sensors", ACS Nano 7 (2013) 9533-9557.

8:00 PM EN01.06.22

Engineering Polymer Interfaces Toward Controlling Triboelectric Surface Charge for Wearable SystemsKasparsMalnieks, AndrisSutka, ArtisLinarts and LinardsLapčinskis; Riga Technical University, Latvia

Developing pathways and materials that efficiently convert ambient energy from the environment into electricity is critical to powering distributed sensing networks, wearable and implantable electronics, and other Internet of Things (IoT) devices.[1] Mechanical and kinetic motions exist everywhere in our society, from human movement, blood flow, railway vibrations, car vibrations, rain fall bicycle motion, geological activity, or even simply water flowing through pipes. This abundance of motion has led to an explosion of research in small-scale mechanical energy harvesters. The goal of these mechanical energy harvesting technologies is to extract electrical energy from an otherwise stable material and convert it into useable electricity. Adding functionality where a certain material can also harvest heat and/or light can also boost energy generation and reduce energy loss.[2] Generally, such harvesting is practical to autonomously power low-energy devices (μW – mW).

Triboelectric energy harvesting devices, or so called triboelectric nanogenerators (TENG), have recently gained momentum for mechanical energy harvesting to power autonomous microdevices and portable electronics. Polymer-based TENGs can be easily fabricated from cheap, lightweight, flexible, and abundantly available materials. In comparison to piezoelectric, ferroelectric, and piezoelectrochemical principles, TENGs do not require costly materials or processes to enable energy harvesting, although significant developments are overcoming some difficulties in some piezoelectric polymer systems.

In our research within the field of TENG, we have explored the intricate nature of triboelectric charging in polymers and elucidated various strategies for enhancing the performance of TENGs. Our investigations into triboelectric surface charge engineering have encompassed a range of material factors operating at the nanoscale. Key factors we have examined include: Triboelectrification Mechanisms: We have delved into the mechanisms underlying triboelectrification, which encompass mass transfer, ion transfer, and electron transfer processes.

Effect of Surface Roughness: Our studies have investigated how surface roughness influences charge generation, shedding light on its crucial role in TENG performance. Temperature Influence: We have explored the impact of temperature on charge generation, providing valuable insights into optimizing TENG operation under varying environmental conditions. Influence of Fillers: Our research has examined how the presence of fillers within polymers affects charge generation, uncovering strategies to enhance TENG efficiency.

Adhesion and Surface Properties: We have analyzed the interplay of adhesion and surface properties in charge generation, emphasizing their significance in TENG design. Polymer Chemistry and Bond Energy: Our investigations have considered the role of polymer chemistry and bond energy in triboelectric charging processes, offering a comprehensive view of material design. Collectively, these multifaceted aspects have culminated in the development of a flexible wearable triboelectric nanogenerator capable of achieving remarkable results, including a peak power output of 24 mW m^{-2} and energy generation of 4.5 mJ . This underscores the potential for harnessing TENG technology in wearable applications and beyond.

1. A. Corletto, A. V. Ellis, N. A. Shepelin, M. Fronzi, D. A. Winkler, J. G. Shapter, P. C. Sherrell, *Adv. Mater.* 2022, 34, 2203849.

2. F.-R. Fan, Z.-Q. Tian, Z. L. Wang, *Nano Energy* 2012, 1, 328.

8:00 PM EN01.06.23

Redox-Targeting Approach with Hard Carbon and Biphenyl Semi-Liquid Electrode for Enhancing Energy Density in Seawater BatteriesDowanKim and YoungsikKim; Ulsan National Institute of Science and Technology, Korea (the Republic of)

Renewable energy sources such as solar, wind, and wave power are growing in importance due to concerns about fossil fuels and climate change. To make these sources reliable, energy storage systems (ESSs) are essential. Among ESS designs, Seawater Batteries (SWB) stand out as the next generation of large-scale ESSs, utilizing the abundant Na^+ ions in seawater and an open cathode design for high theoretical energy density. SWB requires specific anode materials and liquid electrolytes due to the presence of a solid electrolyte (NASICON) that separates the anode and cathode. Unlike traditional batteries, SWB's liquid electrolyte requires a narrow electrochemical stability window only for the anode, allowing electronic conductivity without the risk of short circuits. Previous studies have used Na metal, solid anodes, and liquid anode materials in SWB. While sodium metal can provide high volumetric energy density, it suffers from limited cycle life. Solid-state anodes face electrode stacking challenges that limit energy density improvements. Liquid anodes such as sodium-biphenyl fill the cell efficiently, but offer lower volumetric energy density. Nevertheless, the use of a liquid anode with high cyclability made it possible to realize the most reliable seawater battery and it became the most widely used. To address the energy density challenge, a concept called "Redox-targeting" from redox flow battery systems has been applied to SWB. This approach incorporates semi-liquid active materials in a powder state and redox-mediated electrolytes in a liquid state, forming a semi-liquid electrode (SLE) configuration. Sodium-biphenyl (Na-BP), with ionic and electronic conductivity, and hard carbon (HC) were used as active materials for the HCBP SLE electrode. For Na-BP and HC, the overlapping response voltage bands were confirmed by the dQ/dV plot to confirm the amount of available capacity. After confirming the reaction mechanism of the HC used by the galvanostatic intermittent titration (GITT) method, it was found that the intercalation reaction could be involved, which could be confirmed by ex-situ TEM images. The electrochemical properties were then evaluated in a seawater half-cell system using sodium ferrocyanide as the cathode material and were confirmed to be 11.1 mAh cm^{-2} for over 500 cycles (5000 hours). Using this approach, successful mass production of HCBP SLE and its application in seawater batteries has achieved, indicating the potential for industrial utilization.

8:00 PM EN01.06.24

Additive Manufacturing of Bearing Inspired TENGs for Integrated Energy StorageMurathanCugunlular, OnurDemircioglu, MelihO. Cicek, DogaDoganay, Mete BatuhanDurukan and HusnuE. Unalan; Middle East Technical University, Turkey

With the recent advancement in soft, flexible, and wearable devices, the need for innovative energy sources increases rapidly to overcome the energy needs for such devices. The capabilities of conventional energy storage devices may be insufficient to meet the energy needs of these devices. The solution to this problem may be to improve the performance of storage devices or their integration with energy harvesters. These harvesters include photovoltaics, piezoelectric, electromagnetic, and triboelectric nanogenerators (TENGs). Among these devices TENGs stand out with their unique features such as adaptability, simple-structure, high power density and integrability to modern devices. However, there are some problems that hinder the widespread applicability of TENGs. One of these problems is the breakdown voltage of the air, which acts as a barrier to obtain high power density. Recent studies suggest that the use of lubricants can increase this breakdown voltage while providing polarization between electrodes to improve their performance. In this work, an innovative, bearing inspired TENG (Bi-TENG) design was explored using polylactic acid (PLA) fused deposition modeling. The effect of lubricant and rotation speed on the performance of Bi-TENG was investigated. A peak power of $20 \mu\text{W}$ was obtained from the fabricated Bi-TENGs and the addition of lubricant was found to increase power by 110% compared to non-lubricated Bi-TENG. The fabricated TENG was also used to charge energy storage devices to demonstrate its use in wearable applications.

SESSION EN01.07: Stretchable Batteries—Fabrication and Mechanical Challenges

Session Chairs: Mihai Duduta and Carmel Majidi

Wednesday Morning, November 29, 2023

Hynes, Level 2, Room 200

8:15 AM *EN01.07.01

Design and Fabrication of Stretchable and Transparent Rechargeable BatteriesMarkusNiederberger; ETH Zurich, Switzerland

The main task of a battery is to store energy and supply power to electronic devices. Although the areas of application for batteries have expanded massively in recent years - from portable devices to e-mobility and stationary storage options - the basic structure of the battery has hardly changed: It consists of two electrodes with electrolyte and separator, which are housed in a more or less rigid casing. Compared to batteries, portable electronic devices are constantly changing their design, depending on fashion and consumer tastes, but also with the intention of implementing new mechanical properties that make the devices flexible, rollable, stretchable or perhaps even transparent. For fully integrated systems that contain the battery and thus do not require wiring to an external power source, the batteries must have similar physical properties, which requires a complete rethink of battery design, but also allows for certain trade-offs in electrochemical performance [1].

In this talk, examples of the design and fabrication of a stretchable lithium-ion battery [2] and a transparent and stretchable zinc-ion battery [3] will be presented and discussed. In the Li-ion battery, all components (current collector, anode and cathode, electrolyte and packaging) were stretchable, making the battery flexible and twistable. The current collector was fabricated by depositing Ag microflakes as a conductive layer on a stretchable carbon-polymer composite. Anode (pre-lithiated V_2O_5) and cathode (LiMn_2O_4) powders were sprayed onto the silver flakes. A polyacrylamide 'water-in-salt' hydrogel was used as the electrolyte, which exhibited high ionic conductivity and excellent stretchability. The full cell battery worked even at a high strain of

50%. The second example concerns a transparent and stretchable Zn-ion battery with two electrodes featuring a hexagonal grid structure deposited on a polydimethylsiloxane (PDMS) substrate with a polyacrylamide (PAM) hydrogel electrolyte. In both electrodes, Au nanowires (NWs) were used as current collectors together with Zn for the anode and α -MnO₂ for the cathode. For the full cell battery, the PAM hydrogel was sandwiched between aligned films of PDMS+Au NWs/Zn and PDMS+Au NWs/ α -MnO₂, showing a high transmittance of 73% and 65% at 550 nm without and with 50% strain, respectively. The battery provided a capacity of 176.5 mA h g⁻¹ after 120 cycles under varying strain conditions up to 50%.

[1] N. Mittal, L. Wehner, T. Liu, M. Niederberger, Multifunctional Batteries: Flexible, Transient and Transparent, ACS Cent. Sci. 2021, 7, 231

[2] X. Chen, H. Huang, L. Pan, T. Liu, M. Niederberger, Fully Integrated Design of a Stretchable Solid-State Lithium-Ion Full Battery, Adv. Mater. 2019, 31, 1904648

[3] T. Liu, X. Chen, E. Tervoort, T. Kraus, M. Niederberger, Design and Fabrication of Transparent and Stretchable Zinc Ion Batteries, ACS Appl. Energy Mater. 2021, 4, 6166

8:45 AM EN01.07.02

Mechanical Failure Modes and Effect on Electrochemical Performance for Conventional LiCoO₂ Electrodes for Flexible Li-Ion Batteries [Kyungbae Kim](#), Roberto Martinez and Candace K. Chan; Arizona State University, United States

As the demand for flexible electronic devices like wearables and foldable gadgets increases, it becomes necessary to develop appropriate components such as flexible batteries. While there has been progress in flexing entire battery cells during electrochemical cycling, further research is needed to understand how mechanical failure affects individual battery components, especially the electrodes, after flexing. In this study, we intend to highlight how characteristics of various lithium cobalt oxide (LCO) electrodes, such as particle size and mass loading differences, impact mechanical failure during flexing. This will entail an analysis of bending diameters corresponding to curvature angles and flexing duration, as well as studying the electrochemical performance of the electrodes after repeated bending (up to 3000 times) at diameters of 100, 50, and 25 mm. The mechanical strength (cohesion and adhesion properties) of the bent electrodes was evaluated through peel and scratch tests after undergoing flexing under different bending conditions. Optical and scanning electron microscopy were used to observe the mechanical failures on the surface and cross-section of the peeled and scratched electrodes after bending. The findings reveal that using a smaller LCO particle size can improve the durability of flexible electrodes, while high mass loadings cause formation of distinctive pore distribution with microcracks that propagate across the cross-sectional microstructure. Additionally, certain electrode microstructures can allow for mitigation of the deleterious effect of bending on the discharge capacity obtained at different C-rates.

9:00 AM EN01.07.03

Spiral Ribbon Inspired Coaxial Fiber Li-Ion Battery [Thierry Djenizian](#); Ecole des Mines Saint-Etienne, France

The challenging needs of energy storage at millimeter scales for wearable technologies and IoT grow persistently, driving the development of integrable micro-power sources that can be realized owing to innovative investigations in chemistry of materials, battery architectures, and microfabrication processes. Here, we propose a new design in the family of flexible coaxial fibrous Li-ion batteries by successfully adopting the unidirectional spiral winding method to achieve multilayered tubules of all the cell components. Such a coaxial fibrous Li-ion battery device showing high energy storage capability is millimeter thin, highly flexible, and functions effectively without compromising the whole electrochemical performance of the battery. The full cell delivers a specific capacity of 104 μ Ah/cm at a 0.1C rate with nearly 100% coulombic efficiency and is further capable of being operated at various charging rates. The co-axial fiber battery was then modified later to spiral flexible battery with excellent stretchability.

9:15 AM *EN01.07.04

Integration of Stretchable Batteries and Printed Circuit Board [Soojin Park](#); Pohang University of Science and Technology, Korea (the Republic of)

Stretchable electronics have been considered as a key technology in wearable and implantable medical devices. Although substantial advances have been made in key stretchable components, a stretchable electronic platform that integrates a stretchable power source and a stretchable printed circuit board (SPCB) has been a great challenge. Here, we propose an intrinsically stretchable electronic device platform powered by a stretchable film battery so that the platform can be used stand-alone. The stretchable battery is used as a substrate for manufacturing device platforms where SPCB is printed and directly connected through via holes, thereby enabling an increase in integrated devices density. To achieve intrinsically stretchable battery and high-performance circuit board, we designed a novel design concept of stretchable, self-healable, and pressure sensitive polymer composite. The platform is water-proof and maintains its stable electrical performance under extreme physical deformations. As a proof of concept, we demonstrate the integration of LEDs on the platform that can operate at large biaxial strain (125%) underwater.

9:45 AM BREAK

SESSION EN01.08: Energy Transducers—From Harvesting to Actuation

Session Chair: Mihai Duduta

Wednesday Morning, November 29, 2023

Hynes, Level 2, Room 200

10:15 AM *EN01.08.01

Soft Matter Transducers for Energy Harvesting and Electrochemical Actuation with Liquid Metal [Carmel Majidi](#); Carnegie Mellon University, United States

Liquid metal alloys like eutectic gallium-indium (EGaIn) have attracted tremendous attention over the past decade for their use as microfluidic circuits encapsulated in soft elastomers. Applications include strain gauges, pressure sensors, mechanically tunable antennae, and highly stretchable electronics. However, in recent years, there's been increasing interest in extending liquid metals to applications in energy harvesting, energy storage, and electrochemical actuation. In this talk, I will review recent contributions from my research group in exploring the development of soft matter transducers that utilize EGaIn as electrodes for these emerging applications. This will include new classes of soft material architectures for stretchable batteries, triboelectric energy harvesting, and thermoelectrics. In addition, I will present efforts to use these EGaIn-based material systems to create wearable devices that can power body mounted electronic devices using energy harvested from body heat or motion. Lastly, I will discuss our latest work on exploiting the influence of electrochemical reactions on the surface tension of EGaIn droplets to create soft actuators. Inspired by the architecture of sarcomeres in natural muscle tissue, these actuators contract in response to low voltage stimulation. Where possible, I will relate experimental analysis of these soft actuators to underlying principles in fluid mechanics and elasto-capillary interaction.

10:45 AM EN01.08.02

Bringing the Performance of Conventional Thermoelectric Energy Harvesters to Unconventional Form Factors: Direct Laser Printing of Large-Area Inorganic Thermoelectric Materials on Flexible Plastic Foil [Yuan Tian](#), Isidro Florenciano Cano, Heyi Xia and Francisco Molina-Lopez; KU Leuven, Belgium

Thermoelectric generators (TEGs) are gaining increasing attention as a renewable power source that can generate electricity from abundant waste heat in the environment. As such, TEGs can easily complement batteries and expand their lifespan by facilitating recharging instead of periodic replacement. However, some of the emerging fields that demand urgently new energy solutions, such as wearables and soft robotics, also imposes challenging mechanical properties and form factors like tolerance to repeated bending, conformability to curved surfaces and large area. Despite their high performance, traditional inorganic thermoelectric (TE) materials are brittle and expensive to integrate in a large-area device. On the other hand, the reported efforts to fabricate flexible and low-cost printed TEGs based on polymers yielded lackluster outcomes due to low performance. In this presentation, we will combine the best of both worlds by showing how high-performance inorganic TE materials can be directly printed on flexible substrates and over large areas. Printing techniques are known for their scalability, minimal material waste, and capabilities to achieve intricate designs. While printing (from melts or solutions) belongs mostly to the realm of organic materials, laser-based additive manufacturing is becoming common for the manufacturing of inorganic bulk parts. However, the extreme high temperatures potentially occurring during laser scanning discourage the use of laser printing for patterning materials directly on flexible substrates, e.g. plastic foil. In this presentation, we will show the selective-laser sintering of a film of Bi₂Te₃ that is blade-coated from a slurry onto a polyimide substrate. The laser scanning parameters are carefully selected to achieve a high thermoelectric performance, while ensuring excellent adhesion between the inorganic film and the flexible substrate, which is enabled by a mechanical "interlock" design. The enhanced adhesion along with the highly-textured morphology of the laser-printed films, result in flexible films of pure Bi₂Te₃ (i.e. without organic binders) that could be bent to radii of curvature as low as 9 mm, without compromising their TE performance. This innovative fabrication method is further evolving towards multi-layer printing, which will enable 3D-printed TEGs as well.

11:00 AM EN01.08.03

Silicone Oil Emulsions as Oxygen-Enriched Flow Battery Catholytes for Multifunctional Energy Storage [Alissa Johnson](#), Alice S. Fontaine, Emily Beeman and James H. Pikul; University

In biology, multifunctional interconnected systems provide increased system-level efficiency. Animal circulatory systems, for example, transport oxygen and nutrients while simultaneously regulating temperature and maintaining homeostasis. Inspired by biology, recent work has shown how multifunctional fluids can increase the total energy density of a robotic fish by both storing electrochemical energy and transmitting mechanical work to hydraulic actuators¹. Despite the low energy density of the zinc-iodide electrolytes, this multifunctional approach increased the robot energy density by 4 times compared to the same robot with just a lithium-ion battery.

Gas transport in aqueous environments is important for many biological and chemical processes; however, the low solubility of gases in water is often performance limiting. When animals require more energy in the form of oxygen, they can breathe in air to extract oxygen from their surroundings. Animal blood contains hemoglobin which allows for high concentrations of oxygen to be dissolved into the bloodstream and then distributed throughout the body to provide power locally to various cells. Combining multifunctional fluidic energy storage with the high energy density of air-rechargeable oxygen reduction chemistry will unlock the potential for ultra-high energy density soft robotic systems.

We present a fluid capable of storing twice as much oxygen as water and demonstrate its use as a catholyte for oxygen reduction in a metal air flow battery. Our catholyte is an emulsion with silicone oil droplets suspended in 0.5M potassium hydroxide (KOH) (1:4 v/v), stabilized by a surfactant (Span-60, 1.0 % w/v). The silicone oil acts like hemoglobin to increase the oxygen solubility of the entire emulsion. The silicone oil droplets have an average diameter of 280 nm and are uniformly dispersed within the aqueous phase. While droplet agglomeration is observed over time, this can be reversed with a simple re-homogenization process. Emulsions can maintain a uniformly dispersed oil phase and remain saturated with oxygen (15 mg/L) for several months.

We can extract energy directly from the oxygen in this fluid with a fully submerged electrode that is not exposed to surrounding air. Our emulsion-based electrolyte shows fast oxygen reduction reaction (ORR) kinetics, demonstrating twice as much diffusion limiting current as a control 0.5M KOH electrolyte in a rotation disk electrode study. Kinetics studies with stationary electrodes showed well-defined oxygen-reduction peaks with five times as much ORR peak current density for an emulsion electrolyte compared to KOH. Once the oxygen in the emulsion has been depleted, emulsions can be re-saturated and thus recharged with an influx of surrounding air.

We demonstrate the electrochemical performance of emulsion air-catholytes in two electrochemical cell configurations, a stationary flow cell and a multifunctional actuator flow cell (MAFC). Both configurations use a zinc anode and an emulsion electrolyte with a platinum carbon cloth catalyst for oxygen reduction. In the flow cell configuration, we achieve 4.6 mW/cm² peak instantaneous power density at 5.6 mA/cm² discharge current density. The MAFC demonstrates the ability for emulsion catholytes to enable multifunctional, flexible power sources for soft robotic systems. This cell uses the emulsion catholyte as a hydraulic working fluid for a McKibben actuator. The MAFC expands and contracts (~20% maximum strain) while energy is being extracted as the cell discharges. Our emulsion catholyte is a fundamental first step toward integrating soft robotic systems with multifunctional, high-energy, air-rechargeable energy storage.

Reference:

1. C. A. Aubin et al., *Nature*, **571**, 51–57 (2019) <https://doi.org/10.1038/s41586-019-1313-1>.

11:15 AM EN01.08.04

Mechanically Rupturing Liquid Metal Oxide Induces Electrochemical Energy XingYe and JohnW. Boley; Boston University, United States

Liquid metals, such as alloys of gallium, have unique mechanical and electrical properties because they behave like liquid at room temperature. These properties make liquid metals an ideal candidate for soft electronics and stretchable conductors. In addition, these metals spontaneously form a thin oxide layer on its surface. Applications that are made possible by this delicate oxide skin include shape reconfigurable electronics, microfluidic devices, and unconventional actuators. This presentation introduces another class of applications of liquid metals as an electrochemical energy source. By mechanically rupturing their surface oxide, liquid metals can form a galvanic cell and convert its chemical energy to electrical energy. When dispersing liquid metals into an ionically-conductive liquid to form emulsions, this hybrid material can provide ~500 mV of open-circuit voltage and ~10 μ A of short-circuit current. This approach is further used to make a strain-activated stretchable electrochemical device that can supply up to ~4 μ W of power. Protected by the oxide skin naturally, this passivating layer of the liquid metal shields it from self-discharge over time or changes in operating environment. Future applications of this device are demonstrated by supplying energy to a LED or a capacitor during repeated stretches. Strategies to further improve the output power of these devices are also discussed. These findings may unlock new soft battery designs due to the special surface oxide of liquid metals and offer new pathways to harness their inherent energy for self-powered devices.

11:30 AM EN01.08.05

Energy Storage in Stiff Hydrostatic Skeletons DuhanZhang; Massachusetts Institute of Technology, United States

The multifunctionality of energy components allows versatility and compactness in biology. For example, fat, as energy storage in many animals, doubles as insulation and as a structural element. Multifunctional energy storage can also improve the operating time of robots. In this work, we demonstrate that a liquid energy source can be used to create a controllably stiff “hydroskeleton” type structure for use in robots. This hydroskeleton type structure can be combined with tendon actuation for fast, efficient motion. We characterize this method of stiffening for a generalizable structure, and use it in a demonstration soft marine creature inspired robot’s motion. We adopt a flow battery with this scheme, where the battery electrolyte is used as the fluid in the hydroskeleton, optimizing materials and methods for incorporating a flow battery into a soft robot, and improving lifetime and performance. The power system and actuation would interact symbiotically: the motors would be powered by the flow battery to make the electrolyte flow inside the robot, which provides controllable stiffness to help the robot swim. Simultaneously, the electrolytic hydraulic fluid increases energy density and reduces system resistance. We show why flow battery soft robots are most competitive in swimming applications and discuss more possibilities for multifunctional fluid energy storage in soft robots.

11:45 AM EN01.08.06

Synchronous Generations of Electrical and Cellular Energies without Battery, Wiring even Generators: Inevitable Electrical Stimulation via Body-Mediated Energy Transfer HyungseokYong¹, SangminLee² and JinkeeHong¹; ¹Department of Chemical & Biomolecular Engineering, Korea (the Republic of); ²School of Mechanical Engineering, Korea (the Republic of)

Wearable technologies have become increasingly prevalent in various fields, ranging from smart devices and IoT to health monitoring and bioelectronics. However, finding a sustainable power source remains a challenge. Despite advancements in battery energy density, the need for frequent charging, heavy weight, and inconvenience continue to hinder the adoption of wearable technologies. Recent proposals for energy generation methods aim to harvest energy from the human body, but they often face limitations, such as being restricted to specific body parts or requiring large area devices like light exposure or physical motion. To address these constraints and eliminate the need for additional devices, researchers have explored utilizing the human body itself as a medium for transmitting energy and signals (nanogenerator-based ultrasound receivers, human body communication). However, the effectiveness of these methods is affected by the location of the energy source on the body, and the energy magnitude diminishes significantly with distance. On the other hand, low-frequency electric fields generated by electronic devices or physical activities can be converted into usable energy through the human body. Given the body's high relative permittivity at low frequencies, the transfer of low-frequency electric fields can be highly efficient regardless of the transmission distance. Nevertheless, existing body-mediated energy harvesting methods often neglect the physiological effects on biological tissue, such as cellular vitalization or necrosis. Although these electromagnetic waves inevitably affect biological tissues, conventional body-mediated technologies have not considered such physiological effects at all. In the end, ignorance of the correlation between physiological effects and body-mediated energy transfer undermines the latent ripple effect of this technology.

In this study, we aim to validate through various pre-clinical and clinical trials that body-mediated energy harvesting leads to local electric field concentration in the body, resulting in positive physiological effects. By focusing on the design factors and employing a trade-off approach between usability and energy strength, we propose a method for designing electrode grounds that can be implemented in practical applications. The waveform (AC and DC) and intensity (10 - 3000 mV/mm) of these electric fields can be adjusted by controlling several variables (grounding method, external resistance, charging capacitor) depending on the purpose (usefulness, energy strength) without using any additional battery or wiring. Practical body-mediated wearable devices were implemented using conductive threads and fabrics, and body-mediated bioelectronics for zero-powered ion release and electrical stimulation was also implemented through stimuli-responsive ion-diffusive hydrogel. Complex mechanisms for the body-mediated energy transfer and electric field concentration have been demonstrated in various environments through in human body, ex-vivo setup and simulations. In in-vivo setup we confirmed the positive effects of 1) wound healing and 2) hair regeneration of mice. Eventually, through clinical protocols, we have observed a 3) reduction in muscle fatigue of up to 6.4% using such electrical stimulation designs. Particularly outstanding is that when cellular energy is generated by electrical stimulation under the skin, electrical energy is generated outside the skin, allowing 4) small electronics (1.5 mW) to be operated synchronously. These findings underscore the potential of the human body to harvest low-frequency electrical energy from physical activities or electronic devices while offering positive physiological effects. Overall, this research will contribute to the advancement of wearable technologies by providing insights into the relationship between body-mediated energy generation and physiological effects, paving the way for comfortable and sustainable power sources.

1:30 PM *EN01.09.01

Zn Batteries—Stable Anode and High Energy Cathodes Chunyi Zhi; City University of Hong Kong, Hong Kong

Our research focuses on a stable aqueous Zn-based battery with long cycling stability, decent energy density, and ultimate safety performance for large-scale energy storage. To achieve this purpose, we did systematic studies on the Zn metal anode, electrolytes, and new cathode development.

For the anode side, we developed a few strategies, including pH value manipulation, ion redistribution coating, gradient coating, etc to induce stable stripping and plating of Zn. Moreover, we also found that a Zn initially plated can be much more stable than the one initially stripped during the subsequent deposition. We further utilize this observation to develop a pre-deposited Zn for Zn batteries with improved stability.

For the electrolyte, we develop a reverse micelle electrolyte, with it, the Zn anode exhibits balanced merits including strong H₂ coevolution suppression, prevention of dendritic and dead Zn, inhibition of corrosion, as well as relatively fast reaction kinetics. In a more extensive context, the new reverse micelle structure of electrolytes is expected to benefit other emerging battery chemistries, where a balance between fast ion transport and sufficient stabilization against side reactions is required.

For the cathode with high energy density, we studied the critical research concerns and further potential developments of chalcogen/halogen-based batteries, primarily focusing on the electrochemically active chalcogen/halogen sources, reaction modes, soluble products, and electrolyte adaptability.

For the cathode, we use iodine as the fixing agents working in highly concentrated electrolytes to successfully enable reversible Cl-based redox electrode. The interhalogen coordinating chemistry fixes Cl in a configuration of ICl₃⁻. Furthermore, we simultaneously exploit two redox centers of Cl and I to realize a novel three-electrons transfer electrode, in which the Cl-I electrode can deliver remarkably high capacity up to 612.5 mAh g⁻¹ and energy density as 905 Wh kg⁻¹. The as-obtained energy density is 387% higher compared to the traditional one-electrons transfer of Zn||I₂ battery system and superior cycling stability with capacity retention as 95.7% after 2,000 cycles.

2:00 PM EN01.09.02

Reversible Zn Powder Electrodes for Aqueous Batteries and Supercapacitors Zhixiao Xu and Xiaolei Wang; University of Alberta, Canada

Aqueous energy storage devices require highly reversible Zn electrodes, but this has been impeded by challenges including dendrite growth, low efficiency, hydrogen evolution, and metal corrosion. Here, we report reversible Zn powder electrodes for aqueous batteries and supercapacitors. In the first part, through thermal reduction of spent anode in alkaline batteries, Zn powder anode was regenerated, which shows super-zincophilicity and low overpotentials even under fast rates (8 mA cm⁻²) and high depth-of-discharge (50 %), resulting from coating of hydroxyl-rich organic layer with abundant nucleation sites as well as high orientation of favorable (002) plane and induced horizontal plating behavior. On the other hand, through thermal oxidation, spent MnO₂-based cathode was also regenerated to pair with the regenerated Zn powder anode. Under a low negative-to-positive (N/P) ratio of 3.8 and high loading of ~10 mg cm⁻², the regenerated full cell demonstrates high energy and power densities (94 Wh kg⁻¹, 1349 W kg⁻¹), holding potential for practical applications. In the second part, guided by theoretical calculation, we further fabricated Zn powder anodes *via* engineering the growth of zinc crystals in different solvents. Theoretical calculations demonstrate that the adsorption energy gap of different solvents on the (002) or (100) facet of Zn metal varies and that a larger energy gap favors a higher orientation of Zn (002) plane. Highly oriented Zn (002) powder exhibits horizontal deposition, corrosion resistance, faster kinetics and longer life under deep discharge (60%) in symmetric cells compared with less oriented Zn. Under practical conditions including low N/P ratios (1-3), high-loading cathodes (10-18 mg cm⁻²), and lean electrolyte (5-9 μL mg⁻¹), highly (002)-oriented Zn powder-based batteries and supercapacitors demonstrate large capacity (~3 mAh cm⁻²) and energy/power density (108 Wh kg⁻¹/2317 W kg⁻¹), showing promise for practical use.

2:15 PM EN01.09.03

High-Performance Aqueous Zinc-Ion Batteries with Synergistic Stabilized Zinc Anodes Through Molybdenum Dioxide Coating and Tween 80 Electrolyte Additive Nhat Anh T.

Thieu¹, Wei Li¹, Xiujuan Chen¹, Qingyuan Li¹, Qingsong Wang², Murugesan Velayutham¹, Khramtsov V. Valery¹, David Reed³, Xiaolin Li³ and Xingbo Liu¹; ¹West Virginia University, United States; ²University of Bayreuth, Germany; ³Pacific Northwest National Laboratory, United States

Owing to their low cost, safety, environmental friendliness, and high energy density, aqueous zinc-ion batteries (AZIBs) have recently been considered a promising candidate for the new-generation energy storage systems. However, AZIBs usually suffer from poor cyclability due to various factors, including severe dendrite growth, self-corrosion, hydrogen evolution, and irreversible side reactions occurring at the Zn anodes. This work proposes a novel approach to develop a highly stable Zn anode by combining a surface coating layer with electrolyte additives. Molybdenum dioxide (MoO₂) is introduced as a coating layer, and Tween 80 acts as an electrolyte additive. As MoO₂ is structured in nanoplates, the coating layer facilitates the rapid diffusion of Zn²⁺ ions, which assists in inhibiting dendrite growth and by-products. Also, the MoO₂ coating layer shows a large redox capability due to the multivalent of Mo atoms in the nanostructure, which may be capable of homogenizing the concentration field of Zn²⁺ in the vicinity of the Zn anode. In addition, Tween 80, a surfactant additive, functions as an inhibitor of Zn metal corrosion as it is preferentially absorbed to the surface of the Zn anode to induce the deposition of Zn²⁺ ions. The MoO₂-coated Zn anode (MoO₂@Zn) then exhibits excellent electrochemical stability in a mildly acidic electrolyte due to the dual synergistic effects of the MoO₂ coating layer and Tw80 additive. With an optimal 1 mM Tw80, the symmetric cells of MoO₂@Zn achieve exceptional cyclability for 6000 h at 1 mA cm⁻². Even at a high current density of 5 mA cm⁻², the cells remained stable over 700 h. When assembled with the VO₂ cathode, the full cells exhibit a high capacity of 105.6 mAh g⁻¹ after 1000 cycles with outstanding rate performance (171.4 mAh g⁻¹ at 10 A g⁻¹). Hence, this study suggests an innovative strategy for stabilizing Zn anodes to develop long-life, cost-effective, and scalable AZIBs.

2:30 PM BREAK

3:30 PM EN01.09.04

Simple Fabrication of Single Crystal Zinc Metal via Dislocation Motion for Zinc Ion Batteries Chihyun Hwang¹, Myung-Jun Kwak¹, Ji-Hyun Jang² and Hyun-Kon Song²; ¹Korea Electronics Technology Institute, Korea (the Republic of); ²UNIST, Korea (the Republic of)

Despite being one of the most promising candidates for grid-level energy storage, practical aqueous zinc batteries encounter limitations that compromise their safety and cycling performance, primarily due to dendrite formation. However, this study introduces a novel approach by fabricating a single-crystal zinc metal, effectively preventing dendrite formation. The manufacturing method employed in this study is remarkably straightforward. By subjecting a zinc ingot to a pressing process at a high temperature for few hour pressing, single crystal zinc metal is successfully produced. Remarkably, the dendrite-free electrode retains its integrity even after prolonged cycling, surpassing 2000 cycles at 4 mA cm⁻². This exceptional electrochemical performance is attributed to the use of single-crystal zinc metal, which effectively suppresses the primary sources of defect generation during electroplating and promotes planar deposition morphologies. By minimizing defect sites, including those typically found along grain boundaries or arising from lattice mismatch, the opportunity for dendritic structures to form is significantly reduced, even under extreme plating rates. Overall, this study demonstrates the potential of single-crystal zinc metal in achieving high-performance aqueous zinc batteries. By addressing the dendrite formation issue, we can enhance the safety and cycling stability of these batteries, making them even more suitable for large-scale energy storage applications.

3:45 PM *EN01.09.06

Wear and Wash: Stretchable Zn-MnO₂ Rechargeable Cells John D. Madden¹, Tan N. Nguyen¹, Bahar Iranpour¹, Evan Cheng¹, Cliff L. Ng² and Ziqiang Chen¹; ¹University of British Columbia, Canada; ²Simon Fraser University, Canada

Wearable devices require power. There are opportunities to store energy in watch straps, belts, waistbands, suspenders, bra straps, shoes, hats, jackets and in custom fabrics. Typically, however, batteries have a hard metal shell, and are not suited for washing. Here we present a cell that is entirely stretchable and washable. It need not be removed from a garment prior to washing, and it conforms to its surroundings. The approach makes use of one of the lowest permeability elastomers—poly(styrene – isobutylene – styrene) block co-polymer or SIBS – as the encapsulation layer. This allows it to operate over the course of more than a year and a half without drying out. The active materials are zinc and manganese dioxide, both in powder form, combined with a near neutral aqueous electrolyte, making for safe operation, low cost, and possible recycling. The current collectors, active layers, and separator all contain SIBS, which helps to bind the device together, and allows the device to stretch to more than double its length. Carbon black provides electrical conduction, combined with carbon nanofibers to reduce resistance (27 ohms per square) and keep resistance stable over time. The cell has a reversible capacity of 160 mAh/g based on cathode active mass, shows 75% capacity retention after 500 cycles, and underwent 39 washing cycles before it began to leak. The cell is shown to operate effectively after mechanical cycling, runs a low power digital watch from a custom strap, and can briefly drive low energy Bluetooth.

In the process of applying the cell we have found that it is relatively stiff. The stiffness can be reduced by making the cell thinner or combining SIBS with a softer polymer. The separator is

created using evaporation induced phase separation to create pores in SIBS. The hydrophobicity of the bare SIBS separator could be improved by incorporating surfactant into the electrolyte or embedding hydrophilic groups onto the separator surface. The cell would also benefit from lower resistance current collectors, as these appear to be limiting power output. Applications such as wireless communications are difficult to run continuously as a result of the relatively high resistance. Finally, the chemistry can be improved – and in particular cycle life and stability in the discharged state. Some approaches to further improving the cell are discussed, along with prospects for application.

SESSION EN01.10: Electrolyte and Binder Materials for Improved Li-ion Battery Performance

Session Chair: Mihai Duduta

Thursday Morning, November 30, 2023

Hynes, Level 2, Room 200

8:30 AM EN01.10.01

End-Group Assisted Electrodeposition of Ultrathin Solid Polymer Electrolyte Films on 3D-Micro Architected Electrodes Zhaovi Zheng, Joerg G. Werner, Anton Resing and Wenlu Wang; Boston University, United States

Solid state batteries with three-dimensional micro-architected cell geometry are promising candidates for next-generation batteries with high power density, high energy density, and low safety risks because they take advantage of short ion diffusion distance and high active material loading in 3D interdigitated thin-film structures. A major challenge in producing 3D micro-architected batteries is the fabrication of a thin and uniform solid electrolyte layer that separates the two interdigitated electrodes. Electrodeposition as a non-line-of-sight fabrication method is readily adapted to modify conductive 3D substrates such as architected electrodes with a polymer film as a thin electrolyte layer. While previous studies reported the electrodeposition of polymer electrolytes on micro structured materials, the resulting thin films exhibited limited functionality, heterogeneous topography, or were only applicable to a single substrate material. To address those issues, we developed the electrodeposition of a polymer electrolyte utilizing a two-component electrocoupling reaction to form a step-growth polymer network instead of the conventional electrochemically initiated chain-growth polymerization that causes uncontrolled polymer formation and precipitation in solution. Specifically, poly(ethylene oxide) (PEO), known for high dielectric constant and Li-ion conductivity, is selected as the backbone of the polymer electrolyte network. The PEO chain ends are functionalized with electrochemically labile groups that undergo direct coupling reactions with a small molecule crosslinker. This electrochemically mediated coupling reaction of polymeric extender and polyfunctional crosslinker generates a polymer network close to the 3D electrode surface that leads to film deposition. This method is applied to coat a layer of solid polymer electrolyte on a low-tortuosity 3D Carbon electrode. As a result, the entire surface of the 3D Carbon electrode is effectively enveloped by a sub-micron polymer film. The deposited polymer film exhibits high electronic resistance and is able to serve as solid electrolytes. Our approach decouples the polymer functionality from its electrodeposition chemistry with electrochemically active end groups that make up only a small fraction of the resulting polymer thin film and can be combined with arbitrary functional polymer chains. Therefore, this method can be a universal method to coat various conductive micro-architected 3D substrates with tailorable functional polymers.

8:45 AM EN01.10.02

Demixing the Miscible Liquids: Toward Biphasic Battery Electrolytes Based on the Kosmotropic Effect Won-Yeong Kim¹, Hong-I Kim¹, Kyung Min Lee², Eunhye Shin², Xu Liu³, Hyunseok Moon¹, Henry Adenusi⁴, Stefano Passerini³, Sang Kyu Kwak² and Sang-Young Lee¹; ¹Yonsei University, Korea (the Republic of); ²Ulsan National Institute of Science and Technology, Korea (the Republic of); ³Karlsruhe Institute of Technology, Germany; ⁴Hong Kong Quantum AI Lab, China

Exploring new electrolyte chemistry beyond conventional single-phase battery electrolytes is needed to fulfill the heterogeneous requirements of anodes and cathodes. Here, we report a biphasic liquid electrolyte (BLE) based on the kosmotropic effect. The key underlying technology for the BLE is phase separation of its electrolyte couples using a principle of “demixing the miscible liquids”. Kosmotropic/chaotropic anions affect the ion coordination structures and the intermolecular interactions of electrolyte couples, enabling on-demand control of their immiscibility/miscibility. Despite the intrinsic miscibility of water (in aqueous electrolytes) and acetonitrile (in nonaqueous electrolytes), the structural change of the aqueous electrolyte induced by kosmotropic anions allows demixing with the nonaqueous electrolyte. The resultant BLE facilitates redox kinetics at cathodes and Zn plating/stripping cyclability at anodes. Consequently, the BLE enables Zn-metal full cells to exhibit a long cyclability (86.6% retention after 3500 cycles). Moreover, Zn anode-free full cells with the BLE exhibit a higher energy density (183 Wh kg⁻¹) than previously reported Zn batteries.

9:00 AM EN01.10.03

Regulating Electrostatic Phenomena by Cationic Polymer Binder: Toward Scalable High-Areal-Capacity Li Battery Electrodes Jung Hui Kim^{1,2}, Kyung Min Lee^{1,3}, Sang Kyu Kwak³ and Sang-Young Lee²; ¹Ulsan National Institute of Science and Technology, Korea (the Republic of); ²Yonsei University, Korea (the Republic of); ³Korea University, Korea (the Republic of)

The promising potential of forthcoming smart electronics, electric vehicles, and grid-scale energy storage systems has spurred the unremitting pursuit of high-energy-density Li batteries. Accordingly, in addition to the ever-continuing search for advanced electrode active materials, designing high-areal-capacity (C/A) electrodes has garnered attention as a facile and scalable approach to achieve this goal. High-C/A electrodes increase the energy density of a cell without requiring the synthesis of new electrode active materials.

To achieve high-C/A electrodes (= areal-mass-loading (M/A) × specific capacity of electrode active materials (C_{sp})), the M/A should be maximized while stably maintaining the C_{sp}. However, owing to the use of thick electrodes (physical issue) and non-uniform charge transfer throughout the electrodes (electrochemical issue), conventional electrodes cannot achieve this requirement. Particularly, the drying of processing solvents, such as N-methyl pyrrolidone (NMP) and water, during the fabrication of thick electrodes often induces crack formation and delamination from metallic current collectors, thus limiting the increase in the M/A values. Additionally, with an increase in the electrode thickness, charge transfer in electrode active materials tends to demonstrate uneven and sluggish reaction kinetics in the through-thickness direction of the electrodes, resulting in the loss of the C_{sp} values.

Herein, we present a cationic semi-interpenetrating polymer network (c-IPN) binder strategy, with a focus on the regulation of electrostatic phenomena in electrodes. Compared to conventional neutral linear binders, the c-IPN suppresses solvent-drying-induced crack evolution of electrodes and improves dispersion state of electrode components owing to its surface charge-driven electrostatic repulsion and mechanical toughness. The c-IPN immobilizes anions of electrolytes inside the electrodes via electrostatic attraction, thereby facilitating Li⁺ conduction and forming stable cathode–electrolyte interphases. Consequently, the c-IPN enables high-C/A (20 mAh cm⁻²) cathodes with decent cyclability using commercial slurry-cast electrode fabrication, while fully utilizing the theoretical C_{sp} of LiNi_{0.8}Co_{0.1}Mn_{0.1}O₂. Further, coupling of the c-IPN cathodes with Li-metal anodes yields double-stacked pouch-type cells with high-energy-density (376 Wh kg_{cell}⁻¹/1043 Wh L_{cell}⁻¹), demonstrating practical viability of the c-IPN binder for scalable high-C/A electrodes.

9:15 AM EN01.10.04

Tuning the Electronic and Ionic Thermoelectric Transport Properties in Lithium- and Sodium-Based Polymer Electrolytes by Carbon Based Additive Maximilian Frank, Julian Steven Schilling, Philipp Kessler, Theresa Zorn, Ann-Christin Pöppler and Jens Pflaum; Julius-Maximilians-Universität Würzburg, Germany

Hybrid-organic energy storage media utilize the electrochemical transport of ionic species, at present, preferentially originating from lithium compounds. As such, much work on the device performance is devoted to cyclability, energy density and conductivity. Vice versa, the ionic transport characteristics offer also intriguing possibilities for the implementation of this material class in thermoelectrics (TE), the latter considered essential for recovering waste heat into electrical power. At the same time, the electrolytes' sustainability and alternatives to lithium are becoming increasingly important.

In this work, we present a comparative study on the electrical and thermoelectrical properties of a methacrylate-based solution processable solid polymer electrolyte containing lithium bis(trifluoromethanesulfonyl)imide salt (LiTFSI) [1] and sodium bis(trifluoromethanesulfonyl)imide salt (NaTFSI), respectively. By means of impedance spectroscopy over a frequency range from 10⁻¹ Hz up to 5 × 10⁵ Hz and in a technologically relevant temperature range between 263 K and 363 K, we investigate the transport and dynamics of charge carriers in the solidified electrolytes. The observed high ionic conductivity of about 10⁻³ S m⁻¹ at room temperature distinguishes this material for polymer battery applications [2]. In combination with highly sensitive thermovoltage measurements, we demonstrate that the electronic and ionic transport properties can be efficiently tuned by the content of lithium- and sodium-salt, respectively.

Complementary multinuclear solid-state NMR studies further indicate interactions between ions and the polymer backbone. Additionally, a significant influence of the cations on the crosslinking of the resulting polymer network can be observed. These results showcase the potential for sustainable sodium-based ionic thermoelectric applications.

By further varying the concentration of suspended carbon-based additives, we investigate the influence of the respective dimensionality on the charge carrier transport. Different transport regimes merge and can be related to a Vogel-Fulcher-Tammann and Arrhenius activated conductivity. For these composite materials, we were able to increase the power factor by several orders of magnitude. Even more, we can reversibly switch the sign of the occurring thermovoltage and thus the respective operational mode by tuning the ambient temperature, which promises new applications in autonomous TE units.

Together with the high electrical conductivity achieved on macroscopic length scales, thermovoltages of about 2 mV K^{-1} allow for high output powers while the polymeric matrix maintains the temperature gradient which in turn is a prerequisite for application in thermoelectric generators (TEG). As a proof-of-concept, an all organic TEG verifies the functionality of our approach and, thereby, substantiates the potential of mixed ionic and electronic materials for future TE applications.

MF and JP thank the Bavarian Ministry of Science and the Arts for the generous support by the research program *Solar Technologies Go Hybrid*.

[1] M. Frank, J. Pflaum, *Adv. Funct. Mater.*, **2022**, 32, 2203277.

[2] J. R. Nair et al., *React. Funct. Polym.*, **2011**, 71, pp. 409-416.

9:30 AM EN01.10.05

High-Performance Polymeric Electrode Materials for Organic Lithium-Ion BatteriesFebriBaskoro, Hui QiWong and [Hung-JuYen](#); Academia Sinica, Taiwan

This talk covers our recent works on high performance aromatic polymers as electrode materials for Li-ion batteries. Polymers with high thermal stability and thermo-oxidative stability complemented by excellent solvent resistance, good electrical and mechanical properties and chemical resistance make them as great candidate as electrode materials. Electrochemical performance tests reveal that these electrode materials delivered a reversible specific capacity and stability over thousand cycles. The long cycle lifetime and excellent battery performance further suggest that the reported polymers are promising electrode materials for next generation Li-ion batteries.

9:45 AM EN01.10.06

A Highly Reversible Electroconductive Liquid-Solid Electrolyte System for Na Metal Plating/Stripping with High Areal Capacity[YoungjaeJung](#), YoungsikKim and Wang-GeunLee; Ulsan National Institute of Science and Technology, Korea (the Republic of)

Anode-free sodium metal batteries (AFSMB) are promising candidates for maximizing energy density and minimizing cost and safety hazards in the absence of metallic sodium during cell assembly. The practical implementation of AFSMBs is hindered by the low cycling stability of Na metal plating and stripping, particularly under high areal capacities. Despite the high energy density of AFSMBs, most of their reported areal capacities are less than 5 mAh/cm^2 , which is a similar level to those of conventional lithium-ion batteries, owing to the irreversibility of Na metal plating and stripping. The main causes of irreversible metal plating/stripping can be classified into two categories: 1) electrolyte decomposition and the formation of a solid electrolyte interphase (SEI) layer, and 2) the formation of an electronically inactive dead metal.

Here, we proposed an electroconductive liquid/solid dual electrolyte system that simultaneously suppresses the side reactions of electrolytes and confers electronic conductivity to connect the inactive dead Na. The electroconductive liquid electrolyte accepts electrons at a certain energy level and forms electronic conductivity, and the solid electrolyte can prevent internal short-circuit through a low electronic conductivity. Each function is verified using sodium biphenyl (NaBP) liquid electrolyte and NASICON (Na Super Ionic CONductor, $\text{Na}_{1-x}\text{Zr}_2\text{Si}_x\text{P}_{3-x}\text{O}_{12}$) solid electrolyte through a seawater battery (SWB) system, which consists of an infinite seawater sodium source at the cathode. Compared with conventional 1 M NaPF₆ in dimethoxyethane (DME) electrolyte, the NaBP electrolyte suppresses side reactions such as gas evolution according to the redox-active properties. In addition, the electronic conductivity of NaBP enables the full stripping of dead Na in the absence of direct contact with the current collector, and the stripping efficiency is quantitatively confirmed through the designed experiments. Finally, the anode-free SWB cells have achieved a high coulombic efficiency of >99.9% for over 60 cycles at a high areal capacity of $\sim 24 \text{ mAh/cm}^2$. This study provides insight into the Na plating/stripping properties in anode-free systems and proposes a significant strategy for improving the reversibility of metal anodes for various battery systems with solid electrolytes.

10:00 AM BREAK

SESSION EN01.11: Energy Materials for Water and Heat Management

Session Chair: Mihai Duduta

Thursday Morning, November 30, 2023

Hynes, Level 2, Room 200

10:30 AM EN01.11.01

Deicing with Bubbles[SaurabhNath](#), Henri-LouisGirard, Ha Eun DavidKang, SrinivasB. Subramanyam, YangShao-Horn and KripaVaranasi; MIT, United States

Ice accretion is ubiquitous and destructive: from car windshields to powerlines, wind turbines to airplanes, ice-induced damages comprise a multibillion-dollar problem in the United States alone. Traditional deicing methods rely on mechanical scrubbing, heating, or chemical melting that are crude, inefficient, and even environmentally toxic. Here we propose a fundamentally different approach to the classical problem of deicing using bubbles generated via in situ electrolysis of the liquid water – before it freezes. We show with experiments how a progressing ice front can trap the electrolytically generated bubbles at the interface that subsequently act as stress concentrators to diminish the energy required to fracture ice. Our proposed mechanism constitutes a self-starting, self-limiting means to reduce ice adhesion – a feature hitherto non-existent.

10:45 AM EN01.11.02

Photoresponsive Electrospun PVDF-TiO₂ Meshes with Switchable Wettability for Fog Water Harvesting and Energy Harvesting[GregoryParisi](#)^{1,2}, PiotrSzewczyk², ShankarNarayan¹ and UrszulaStachewicz²; ¹Rensselaer Polytechnic Institute, United States; ²AGH University of Krakow, Poland

Water scarcity is a global issue that affects the lives of billions of people. Fog water harvesters can catch water droplets out of humid air and provide water to arid areas. An efficient fog harvester catches majority of liquid from a fog stream and quickly evacuates it to storage. A fiber mesh is an efficient way to collect water due to its larger surface area, permeability, and tunable material properties. This study will take advantage of electrospinning to produce water harvesting polymer fibrous mats with specific surface characteristics. The efficiency and particular usages of fog harvesters depends heavily on surface wettability, which is the liquids' ability to form interfaces with solid surfaces. Hydrophilic surfaces can easily catch water and hydrophobic surfaces minimize the pinning effect of water on the mat surface improving the water collection rate.

To create meshes for water harvesting, polyvinylidene fluoride-titanium dioxide (PVDF-TiO₂) core-shell fibers were produced by electrospinning and additional TiO₂ nanoparticles were electrospayed on the electrospun membrane. Due to the presence of TiO₂ particles, the wettability of the PVDF-TiO₂ mats can reversibly switch between hydrophilic and hydrophobic with the exposure of UV light and heat, respectively. Since the surface properties of meshes are tunable, the dynamic switch of their wettability increases the potential application of PVDF water collectors. Additionally, PVDF exhibits piezoelectric behavior, meaning it generates electric charges when subjected to mechanical stress, such as the wind from foggy conditions. This provides multifunctional technology that is more efficient and sustainable, as it doubles as an energy harvesting device. Energy generation offers the potential of operating necessary devices without external power sources, such as fog and wind sensors. This switchable fog water collector can be utilized in arid or humid environments and adds additional advantages of energy harvesting and sensing.

11:00 AM EN01.11.03

Modeling and Optimizing Temperature-Dependent Elastocaloric Effects in Elastic Olefin Block Copolymer Fibers[YouLyu](#)^{1,2}, BuxuanLi¹, VolodymyrKorolovych¹, DuoXu¹, YuanZhu² and SvetlanaV. Boriskina¹; ¹Massachusetts Institute of Technology, United States; ²Southern University of Science and Technology, China

Solid-state cooling technology based on elastocaloric effects [1–3] provides a competitive alternative to vapor-compression refrigeration technology by demonstrating higher energy efficiency, compactness, noise-free operation, and environmental friendliness. Well-studied metal alloy-based elastocaloric materials such as Ni-Ti and Cu-Al-Ni fail to reach industrial adoption due to their high cost of fabrication and operation, despite exhibiting high temperature spans (Tspan) of 12–30 K and coefficients of performance (COP) of 6–18 [4]. Polymers, on the other hand, are the largest product synthesized by volume nowadays, and have low tensile stress, chemical inertness, light weight, and low cost. Recent progress in elastocaloric polymer experiments shows performances comparable with those of metal alloys. E.g., Tspan around 15 K and COP over 10 in natural rubber [5] and other elastomers [6] have been demonstrated, opening new opportunities for polymer-based elastocaloric materials.

Different from the well-known cross-linked elastomers like natural rubber, we present an experimental study on an entanglement-enabled-elastic olefin block copolymer(OBC) fibers, whose elastocaloric performances feature a high cooling COP exceeding 10 and stable performance for at least 1000 cyclic loadings. We observed a Tspan over 22 K for the first loading, exceeding all existing polymer-based materials. After over 100 cyclic loadings, the stabilized Tspan at room temperature is 5 K. For stabilized Tspan, we noticed a non-linear temperature dependence on cooling Tspan with peaks at 6 K at -20 °C and 60 °C, while 2 K at room temperature. We explained such a nonlinear trend quantitatively by modeling the configurational entropy change upon

deformations and predicted different temperature dependences for different deformation trajectories. Such temperature and deformation dependencies suggest a new direction for optimizing and designing polymer-based elastocaloric cooling devices. Finally, a conceptual device for heating and cooling is designed and analyzed with practical working cycles.

The entanglement-enabled reversible deformation of flexible polymer segments in the melt-spun OBC fibers makes them elastic at room temperature without cross-linking. We built a twisting-stretching coupled stage with an IR camera and force/torque sensors to measure in-situ temperature responses and force/torque during the fiber adiabatic deformation process. Experiments revealed that our fibers achieve greater than 10 cooling COP under stretching at room temperature and twisting at higher (60 °C) and lower (-20 °C) temperatures. We also characterized fiber structural changes by X-ray and Raman spectroscopy to understand the mechanisms underlying the elastocaloric fiber performance. Significant drops in both orthorhombic crystalline (6%) and amorphous domains by (13%) were observed upon stretching, while the interfacial oriented amorphous domains grew by 19%, accompanied by Herman's orientation factor increase from 0.02 to 0.17. These observations suggest the entropic change due to chain alignment, rather than strain-induced crystallinity, is revealed to be a dominant factor that explains the elastocaloric effects and its temperature dependence. Finally, the new elastomer fibers are extremely inert and suitable for operation in harsh corrosive environments, as well as fully mechanically recyclable at the end of their lifespan.

Y. L. and B. L. contributed equally. Correspondence should be addressed to Y. Z. and S. V. B.. This work is supported by Centers for Mechanical Engineering Research and Education at MIT and SUSTech (MechERE Centers at MIT and SUSTech). B. L. is supported by the Evergreen Graduate Innovation Fellowship.

References:

1. *Appl. Phys. Rev.* **6**, 41316 (2019).
2. *Nat. Rev. Mater.* **2022** *7* **7**, 633–652 (2022).
3. *Int. J. Refrig.* **64**, 1–19 (2016).
4. *Acta Mater.* **208**, 116741 (2021).
5. *Science (80-.)*. **366**, 216 LP – 221 (2019).
6. *Nat. Commun.* **2022** *13* **13**, 1–7 (2022).

11:15 AM EN01.11.04

Thermoelectric Materials in Membrane Distillation: Improving Performance Metric [Olawale Makanjuola](#)^{1,2} and Raed Hashaikeh²; ¹New York University, United States; ²New York University Abu Dhabi, United Arab Emirates

The commercial deployment of membrane distillation (MD) as an alternative to reverse osmosis (RO) and multistage flash (MSF) or multi-effect distillation (MED) for desalination has been largely hindered by the high specific energy consumption (SEC) in MD systems. Many studies have succeeded in reducing the SEC in MD to a threshold value of around 1,000 kWh/m³ by using energy recovery devices (ERD) and other techniques. While this is a significant improvement for MD, RO and thermal desalination present much lower SEC values (7 – 150 kWh/m³), and the ERD incorporated in MD systems will increase the complexity, equipment cost, and required real estate for MD operations.

Our previous works have indicated that using thermoelectric devices as a direct thermal source inside the MD module can reduce the SEC by more than 35% below the 1,000 kWh/m³ threshold (i.e. < 650 kWh/m³) whilst greatly simplifying the MD system by eliminating the support subsystems generally required for heating and cooling in MD. The thermoelectric device doubles as both a direct thermal source to drive the process and as an ERD reducing heat exchange losses to near zero. By combining high-fidelity computational fluid dynamics simulation and mathematical modeling of the thermoelectric device with experimental validation, we developed a fairly good model for predicting the performance of a thermoelectric MD system.

We are currently investigating the possibility of embedding column-type p and n thermoelectric pellets inside the MD membrane itself. This thermoelectric membrane is expected to provide a more localized thermal source and sink for driving the MD process. This in turn is likely to lower the SEC when used in an MD system. A theoretical model developed from the constitutive relations under isotropic conditions while assuming steady-state conditions, one-dimensional heat flow, and constant properties for both the membrane and thermoelectric material allows us to predict the SEC (in kWh/m³) in an MD process driven by a thermoelectric membrane. The result indicates that while a thermoelectric membrane can potentially reduce the SEC by over 90% below the 1000 kWh/m³ threshold for conventional MD equipped with ERD, the SEC cannot go below around 15 kWh/m³ even for the best permeable thermoelectric membrane. Our current efforts are geared towards realizing a physical thermoelectric membrane. Several avenues are being explored to successfully embed thermoelectric bismuth telluride pellets inside electrospun membrane. Concurrently, we are also working to improve the current theoretical model by accounting for all pertinent thermal and electrical resistances. Contact resistance and small-scale effects are some of the phenomena that the improved model will account for.

11:30 AM EN01.11.05

Enhancing Thermoelectric Performance with Electrically Aligned Single-Walled Carbon Nanotubes in Polymer Matrix [Hyunjin Joh](#)¹, [Gopinathan Anoop](#)¹, [Seunghyun Jo](#)¹, [KwangSup Eom](#)¹, [Hyeon Jun Lee](#)² and [Ji Young Jo](#)¹; ¹GIST, Korea (the Republic of); ²Kangwon National University, Korea (the Republic of)

Polymer-based thermoelectrics are a promising material to generate energy for wearable devices due to their flexibility and ability to directly convert thermal energy into electrical energy in low temperature. However, the fundamental limit of thermoelectric performance arising from interdependent parameters (electrical/thermal conductivity, Seebeck coefficient) is the main obstacles in preexisting homogeneous thermoelectric materials based on conducting polymers [1]. In the pursuit of enhancing the thermoelectric ZT of flexible thermoelectric generators, a composite consisting of an insulating polymer and conducting nanoparticles is proposed. This study explores the use of single-walled carbon nanotubes (SWCNTs) in a poly(vinylidene fluoride-trifluoroethylene) P(VDF-TrFE) polymer matrix. In polymer-CNT composites, the CNTs form networks within the polymer matrix that are electrically conductive but less thermally conductive due to phonon scattering at the polymer-nanotube interfaces, thereby enhancing the ZT of the composite [2]. The unique approach of electrical alignment of SWCNTs in the polymer matrix is employed to optimize their orientation and distribution. This method involves applying an external electric field during the drying process of the composites, causing the SWCNTs to align along the field lines through in-plane direction. The alignment of SWCNTs facilitates direct paths for charge carriers, thereby reducing scattering events and increasing carrier mobility. This enhancement in carrier mobility, coupled with a reduction in thermal conductivity, leads to a significant improvement in thermoelectric properties. Here, we have successfully fabricated freestanding composite films that exhibit excellent flexibility. Dispersion-drying method is used for the fabrication of the composite film, and electrical field is induced before the drying process to align the SWCNTs in the matrix. The alignment of CNTs are observed in the cross-sectional SEM image, and the resistance change according to the in-plane measurement direction. By incorporating 11.3 wt% of CNTs into the composite, the initial thermoelectric power factor (PF) was measured to be 1.25 μW/mK². To further enhance the PF, an alternating electric field (150 V, 1 kHz) was applied during the solution process to align the SWCNTs within the P(VDF-TrFE) matrix. CNT alignment resulted in a significant increase in electrical conductivity and a slight decrease in Seebeck coefficient, leading to an overall increase in PF up to 1.79 μW/mK². Even when highly bent (with a bending radius of less than 5 mm), the PF remained over 95%, and it also remained stable after undergoing 10³ cycles of bending tests. The results demonstrate a substantial increase in the thermoelectric ZT from 1.54×10⁻³ to 5.67×10⁻³, paving the way for the development of highly efficient, flexible thermoelectric generators. This research provides a promising direction for future advancements in flexible electronics and energy harvesting technologies.

[1] Fritzsche, Hellmut. "A general expression for the thermoelectric power." *Solid State Communications* 9.21 (1971): 1813-1815.

[2] Biteniks, Juris, et al. "Flexible n-type thermoelectric composites based on non-conductive polymer with innovative bi2se3-cnt hybrid nanostructured filler." *Polymers* 13.23 (2021): 4264.

11:45 AM EN01.11.06

Chemical Additive-Regulated Thermocells with High Thermopower for Low-Grade Heat Harvesting [Yijie Mu](#)¹, [Wendi Li](#)¹ and [Shien-Ping Feng](#)²; ¹The University of Hong Kong, Hong Kong; ²City University of Hong Kong, Hong Kong

Low-grade heat (below 373 K) is ubiquitous in the human body, environment, and industry, but is usually wasted without proper recovery. Thermogalvanic cells (TGCs) are one of the most investigated technologies that can directly convert such waste heat into electricity, which present satisfactory thermopower in the magnitude of mV K⁻¹. A typical method to improve the thermopower of aqueous TGCs is to introduce additives to change the solvation entropy or establish a concentration ratio difference between two electrodes at different temperatures. However, the introduction of additives may lead to the lower ionic conductivity of electrolyte, thus the current density of TGCs is not promising for powering electronics. From this point of view, further modification towards electrodes is required, making it complicated to optimize the performance of TGCs as a whole. Here, we first introduced a small amount of guanidine hydrochloride (GdnHCl) into 0.4 M potassium ferri/ferrocyanide (K₃Fe(CN)₆/K₄Fe(CN)₆) aqueous electrolyte. With the thermosensitive crystallization and redissolution effect between GdnHCl and Fe(CN)₆⁴⁻, a low local concentration of Fe(CN)₆⁴⁻ due to the crystallization induced by GdnHCl at the cold electrode and a high local concentration of Fe(CN)₆⁴⁻ via the redissolution process at the hot electrode were established, corresponding to a low concentration ratio of Fe(CN)₆⁴⁻/Fe(CN)₆³⁻ at the cold side ([Fe(CN)₆⁴⁻/Fe(CN)₆³⁻]_{cold}) and a high concentration ratio of Fe(CN)₆⁴⁻/Fe(CN)₆³⁻ at the hot side ([Fe(CN)₆⁴⁻/Fe(CN)₆³⁻]_{hot}), respectively. A thermopower of 1.91 mV K⁻¹ was achieved by solely adding 0.75 M GdnHCl to the electrolyte. On the basis of thermopower being enhanced by regulating the concentration profile of Fe(CN)₆⁴⁻ via GdnHCl, in this work, we proposed to further improve the thermopower from the perspective of Fe(CN)₆³⁻. We added the second chemical, cysteamine hydrochloride (CysHCl), into the K₃Fe(CN)₆/K₄Fe(CN)₆ aqueous electrolyte with 0.75 M GdnHCl to trigger

a high temperature-favored chemical reaction with Fe(CN)₆³⁻. CysHCl was featured with temperature selectivity, the kinetic reaction rate of which was relatively slow at lower temperatures, making little contribution to the thermopower enhancement. But at temperatures above 323 K, which were within our designed temperature range for low-grade heat recovery application, the chemical interaction between CysHCl and Fe(CN)₆³⁻ played a prominent part in the thermopower improvement, leading to a high ([Fe(CN)₆⁴⁻/Fe(CN)₆³⁻]_{hot}) ratio. As a result, a large concentration ratio difference between the cold and hot electrodes was established by GdnHCl via inducing the crystallization and redissolution of Fe(CN)₆⁴⁻, and was further enlarged by CysHCl via chemically regulating the concentration of Fe(CN)₆³⁻. A high thermopower of 4.32 mV K⁻¹ and a short-circuit current density of 133.33 A m⁻² were generated using planar graphite sheets as electrodes, compared with the performance of 1.0 mV K⁻¹ and 56.44 A m⁻² of pristine electrolyte in the same cell configuration. Furthermore, a maximum thermopower of 9.06 mV K⁻¹ and a short-circuit current density of 129.24 A m⁻² were achieved by optimizing the concentrations of both GdnHCl and CysHCl simultaneously. The results elucidate that the introduction of GdnHCl enables a high thermopower and current density via the thermosensitive crystallization effect, and more importantly, by interacting with Fe(CN)₆⁴⁻, it allows more free Fe(CN)₆³⁻ to react with CysHCl, which enables the thermopower and current density being boosted to a higher level via chemical regulation effect. This work develops a new design route for TGCs to achieve high thermopower and current density, while no complex modification towards both electrolyte and electrodes is needed, which is highly important for extending the possible application fields of TGCs.

SESSION EN01/EN02/EN04: Joint Virtual Session
Session Chairs: Hye Ryung Byon, Xin Li, Yi Lin, Yana Vainzof and Yuanyuan Zhou
Wednesday Morning, December6, 2023
EN01-virtual

8:00 AM EN01/EN02/EN04.01

Electro-Spun Polymer Fibres Derived Carbon-Supported 1D Hierarchical WO₃/SnO₂ Nanocomposites with Enriched Surface Defects for High-Performance Supercapacitor DevicesVaishaliTanwar, Saurabh KumarPathak and PravinP. Ingole; Indian Institute of Technology Delhi, India

Pseudocapacitive metal oxides are considered promising energy storage systems; however, their overall performance suffers from low intrinsic conductivity. [1] Herein, we report the design of 1D hierarchical architecture, carbon-supported WO₃/SnO₂ nanocomposite-based fibers, via efficient and scalable strategies of single-spinneret electrospinning followed by controlled annealing for high-performance supercapacitor devices. As evident from the XPS and Raman analyses, the composite surface is enriched with surface defects such as oxygen vacancies (O_{vac}), which improves surface chemical structure, aids in efficient diffusion of the charge carriers, and enhances the conductivity.[2] The significant contribution of the two distinctive charge storage mechanisms accounts for the synergistic contribution of WO₃ and SnO₂ to the overall electrochemical behavior of the electrode.[3] Moreover, an interfacial charge build-up between WO₃ and SnO₂ due to nanoscale integration eradicates the charging and discharging processes, leading to better performance. Overall the unique combination of 1D hierarchical nanostructures, abundant electrochemically active sites (O_{vac}), and unique heterointerfacial properties have boosted the performance.[4] The half-cell measurements demonstrated a specific capacitance of 589 F g⁻¹ at 6 A g⁻¹ and enhanced columbic efficiency with a capacity retention of ~80% after 5000 charging-discharging cycles, indicating longer durability. Importantly, a flexible all-solid-state symmetric device (full-cell configuration) was assembled having energy density (E_d) of 2000 mW h kg⁻¹, power density (P_d) of 1200 W kg⁻¹, 100% durability (1,000 cycles), and the gravimetric capacitance of 10 F g⁻¹ at 0.5 A g⁻¹ for an extended working voltage window of 1.2 V. This work provides insight into the synthesis of hierarchical 1D nanocomposites of bimetallic metal oxides for high-performance, portable, and flexible supercapacitor device applications.

- [1].Xiao, X.; Ding, T.; Yuan, L.; Shen, Y.; Zhong, Q.; Zhang, X.; Cao, Y.; Hu, B.; Zhai, T.; Gong, L.; Chen, J.; Tong, Y.; Zhou, J.; Wang, Z. L. *Adv. Energy Mater.* **2012**, 2 (11), 1328–1332.
- [2]. Huang, W.; Wang, J.; Bian, L.; Zhao, C.; Liu, D.; Guo, C.; Yang, B.; Cao, W. *Phys. Chem. Chem. Phys.* **2018**, 20 (25)17268–17278.
- [3]. Wu, Q. L.; Zhao, S. X.; Yu, L.; Zheng, X. X.; Wang, Y. F.; Yu, L. Q.; Nan, C. W.; Cao, G. *J. Mater. Chem. A* **2019**, 7 (21), 13205–13214.
- [4]. Gao, L.; Qu, F.; Wu, X., *J. Mater. Chem. A*, **2014**, 2,7367

8:15 AM EN01/EN02/EN04.02

LaMnO₃-Mn₃O₄ Nanocomposite Supercapacitor: Synergetic Effect Towards High Electrochemical PerformanceAlishaDhakal and SanjayMishra; University of Memphis, United States

Metal oxide materials have been a focus of research for energy storage devices. The perovskite oxide LaMnO₃ and Mn₃O₄ have drawn much attention as a sustainable energy storage system. In LaMnO₃, perovskite oxygen-ion intercalation leads to rapid energy storage, and electrodes are good supercapacitor material [1]. At the same time, multiple oxidation states of manganese in Mn₃O₄ facilitate the faradic process to get enhanced pseudocapacitance [2]. However, the poor electrical conductivity and structural stability of the Mn₃O₄ material limit their practical use as an electrode material for energy storage devices. To overcome the above stated limitation LaMnO₃-Mn₃O₄ composite samples (9:1,7:3,1:1) were prepared via a one-pot synthesis method followed by annealing in air at 80°C. The x-ray diffraction analysis confirms the presence of individual compounds in the desired ratio. The maximum surface area of 7.68841 m²/g was recorded for the LaMnO₃. The chemical composition of composites was determined by x-ray photoelectron spectroscopy (XPS). The presence of Mn²⁺ and Mn³⁺ oxidation states conform to the presence of both LaMnO₃ and Mn₃O₄ in the composite. The electrochemical performance of composite electrodes prepared using nickel foam was assessed in 1M KOH solution. The cyclic voltammetry shows high specific capacitance for the 7:3 composite with a value ~ 584 F/g at a scan rate 1 mV/s, which decreased with further addition of Mn₃O₄ in the composite. At the same time, charge-discharge curves revealed a maximum specific capacitance of around 405 F/g for a 7:3 sample at a current density of 0.5 A/g. The energy density of LaMnO₃ - Mn₃O₄ composites (9:1,7:3, 1:1, and pure) are 5.33, 19.76, 3.71, and 7.66 Wh/Kg with power density 354.19, 308.67, 294.60, and 304.94 W/Kg, respectively at 1 A/g current density. The composites of LaMnO₃ and Mn₃O₄ help to reduce internal resistance due to the interconnected structure as well as reversible faradic process at the interface and create high degree of columbic efficiency [3]. The improvement in energy density, power density, and specific capacitance may result from enhanced charge transfer kinetics through the electrode-electrolyte interface between LaMnO₃ and Mn₃O₄. Also, easy electron hopping pathways are expected between LaMnO₃ (electron donor) and Mn₃O₄ (electron acceptor) in the composite. These findings are more significant to develop high energy supercapacitor devices using this new composition as an electrode material.

Authors: A. Dhakal, Dr. S. R. Mishra

- [1]. J. T. Mefford, W. G. Hardin, S. Dai, K. P. Johnston, K. J. Stevenson, Anion charge storage through oxygen intercalation in LaMnO₃ perovskite pseudocapacitor electrodes, *Nat. Mater.* **2014**, 13(7), 726;
- [2]. P. Suktha, N. Phattharasupakun, P. Dittanet, M. Sawang[1]phruk, Charge storage mechanisms of electrospun Mn₃O₄ nanofibres for high-performance supercapacitors, *RSC Adv.* **2017**, 7, 9958–9963
- [3]. P. M. Shafi, N. Nisar, A. C. Bose, *ChemistrySelect* **2018**, 3, 6459.

8:30 AM EN01/EN02/EN04.03

3D Solar Harvesting via Multiple Semi-Transparent Cadmium Telluride Solar Panels for Collective Energy GenerationAnudeepKatepalli, YuxinWang and DongluShi; University of Cincinnati, United States

Photovoltaic (PV) solar cells have emerged as the predominant choice for environmentally friendly energy solutions across diverse applications. However, their traditional two-dimensional (2D) solar collection approach faces inherent limitations, primarily related to the substantial surface area required. In response, the pursuit of three-dimensional (3D) solar harvesting has gained momentum to achieve heightened energy density. In this innovative strategy, we have ventured into the realm of three dimensions by employing multiple transparent CdTe solar panels arranged in parallel along the z-axis. This innovative design enables sunlight to partially penetrate multiple layers of panels, significantly augmenting the solar collection surface area. Key advantages of this multi-panel solar harvesting system include: i) Expansion of Solar Light Collection Surface Area: Resulting in a significant boost in energy density compared to traditional 2D panels. ii) Enhancement of Total Output Power: Aggregating power output from multiple panels can surpass that of a single panel, providing a more efficient energy generation solution. iii) Reduction of Urban Space Footprint: Particularly relevant in densely populated urban areas with limited space, the 3D solar harvesting approach minimizes surface area requirements for energy production. Our experiments have yielded promising results, showcasing a noteworthy 21% increase in power conversion efficiency (PCE) through the utilization of five CdTe solar panels with varying levels of transparency, arranged in diverse configurations. This underscores the feasibility of 3D solar harvesting employing multiple panels. Furthermore, it is essential to note that efficiency gains can be further amplified by incorporating high-quality panels and harnessing increased solar intensity. This paradigm shift from 2D to 3D solar harvesting signifies a transformative approach to energy generation, promising greater efficiency and sustainability for the future.

8:35 AM *EN01/EN02/EN04.04

Novel Multifunctional Additives for Enhancing the Efficiency and Stability of Perovskite Solar CellsAlexK. Jen; City University of Hong Kong, Hong Kong

Minimizing energy loss and increasing the quality of crystalline perovskite films are keys to improve the performance and long-term stability of perovskite solar cells. To address these challenges, we have developed several multifunctional, nonvolatile additives that can be used to modulate the kinetics of perovskite film growth to enable large-sized grains and coherent growth of perovskites from bottom to surface to be achieved. The improved film morphology resulted in significantly reduced non-radiative recombination, helping enhance the power conversion efficiency (PCE) of inverted (p-i-n) device to ~25% with low energy loss and good stability. In addition, these multifunctional additives can also be applied to address one of the most challenging problems involved in large bandgap perovskites and their derived devices for single junction and tandem solar cells. The commonly observed halide segregation critically limits the stability of mixed-halide perovskites under device operational conditions. There is a strong indication that halide movement/oxidation is the primary driving force behind halide de-mixing. To alleviate this problem, we have developed a series of multifunctional mediators that can suppress these factors while simultaneously passivate defects through tailored substitution. These effects enable wide-bandgap (1.81 eV) perovskite solar cells to achieve an outstanding PCE of 19.58%, with 95% of its initial PCE retained after tracking at maximum power point for 500 h. Integrating this layer into a monolithic perovskite-organic tandem solar cell as a wide-bandgap subcell afforded a record-high PCE of 25.22% and impressive long-term stability (T_{90} > 500 h under continuous operation).

9:05 AM EN01/EN02/EN04.05

Unveiling the Fatigue Behavior of 2D Hybrid Organic-Inorganic Perovskites: Insights for Long-Term Durability Doyun Kim¹, Eugenia S. Vasileiadou², Ioannis Spanopoulos³, Xuguang Wang⁴, Jinhui Yan⁴, Mercouri G. Kanatzidis² and Qing Tu¹; ¹Texas A&M University, United States; ²Northwestern University, United States; ³University of South Florida, United States; ⁴University of Illinois at Urbana-Champaign, United States

2D hybrid organic-inorganic perovskites (HOIPs) are commonly found under subcritical cyclic stress states and suffer from fatigue issues during device operation, significantly limiting their service lifetime. However, the fatigue properties of these materials remain unknown, which is crucial for mitigating fatigue failure and predicting the lifetime for scheduled maintenance. Here, we systematically investigate the fatigue behavior of $(C_4H_9-NH_3)_2(CH_3NH_3)_2Pb_3I_{10}$, the archetype 2D HOIP, by atomic force microscopy (AFM) dynamic stretching suspended 2D membranes. We find that 2D HOIPs are much more fatigue resilient than polymers and can survive over 1 billion cycles. The failure morphology indicates that the 2D HOIPs tend to exhibit brittle failure at high mean stress levels but behave as ductile materials at low mean stress levels. Our results suggest the presence of a plastic deformation mechanism in these ionic hybrid organic-inorganic materials at low mean stress levels, which may contribute to the long fatigue lifetime but is inhibited at higher mean stresses. The stiffness and strength of 2D HOIPs are gradually weakened under subcritical loading, potentially as a result of stress-induced defects accumulating and nucleating. The cyclic loading component can further accelerate this process. The fatigue lifetime of 2D HOIPs can be extended by reducing the mean stress, stress amplitude, or increasing the thickness. Our results can provide indispensable insights into designing and engineering 2D HOIPs and other hybrid organic-inorganic materials for long-term mechanical durability.

9:20 AM EN01/EN02/EN04.06

Conductivity Studies of Mechanochemically Processed LAGP/PEG Hybrid Solid Electrolytes James Buckley¹, Megan Noga², Abdul Latif Bamba², Kerry Sun², Nicholas W. Gothard³, Ioannis Kymissis² and L. Jay Deiner⁴; ¹New York University Tandon School of Engineering, United States; ²Columbia University, United States; ³Bob Jones University, United States; ⁴The City University of New York, NYC College of Technology, United States

Solid state lithium ion batteries promise to provide safe, high power energy storage to support increasing electrification of the transportation sector. Realizing the promise of solid state lithium ion batteries requires development of solid electrolytes whose conductivity and processability

allow for the high rate capability and manufacturability of conventional liquid electrolyte lithium ion batteries. While ionically conducting ceramics may approximate the conductivity of conventional liquid electrolytes, operate safely over a range of temperatures, and resist dendrite formation, their manufacture and integration with battery electrodes is a challenge. In specific, ceramic electrolytes tend to form poor interfaces with electrodes, and require high temperature sintering. Polymer electrolytes are easier to process and join to electrodes, but they suffer from low room temperature conductivity. The ideal solid electrolyte would be a hybrid material that combines the high conductivity of ceramics with the processability of polymers. In such a hybrid material, the polymer concentration would be low enough and the distribution uniform enough so that lithium ions would follow a conduction pathway primarily through the ceramic whose grains were "glued" together by the polymer. Further, in contrast to a simple organic/inorganic composite, specific attachment of the polymer to the ceramic may facilitate charge transport through the hybrid.

As a step towards a readily processable solid state electrolyte, we have recently shown a mechanochemical synthesis of a true hybrid solid electrolyte in which the organic phase, polyethylene oxide (PEO), and the inorganic phase, lithium aluminum germanium phosphate (LAGP), are chemically associated through a surface condensation reaction that takes place under the high energy milling conditions. Solid state nuclear magnetic resonance (NMR) spectroscopy confirmed that after milling, protons from the polymer and/or water condensate are in bonding proximity of the Q² metaphosphate sites of the glassy phase of the LAGP. In the present work, we investigate the room temperature conductivity of a range of these mechanochemically synthesized PEO/LAGP hybrids. Conductivity is tracked as a function of organic to inorganic component ratio and as a function of milling condition. The correlation of the conductivity with hybrid material structure provides insight into mechanisms of lithium ion conduction in ceramic/polymer hybrids.

9:25 AM *EN01/EN02/EN04.07

Advancing Solid Polymer Electrolytes: Enhancing Ionic Conductivity, Transference Number and Li0-SSB Cycle Life Through Conduction Mechanism Design and Integration of Zero-Strain Cathodes Huolin Xin, Yubin He and Lei Wang; University of California, Irvine, United States

Solid polymer electrolytes (SPEs) are promising alternatives to liquid electrolytes, offering advantages in flexibility, safety, and processability. However, their widespread adoption is hindered by their limited room-temperature ionic conductivity (σ_{RT}) resulting from insufficient ion conduction pathways. Additionally, both liquid and solid electrolytes commonly suffer from non-selective ion transport, causing a low transference number that adversely affects energy output and can lead to failures. In this presentation, I will discuss the methodology for overcoming these challenges. We will explore how to finely tune the composition of SPEs to change their ion conduction behavior from Vogel-Fulcher-Tammann to Arrhenius, thereby achieving a remarkable room-temperature conductivity exceeding 1 mS/cm. Additionally, we will discuss innovative strategies to enable single-ion conduction, effectively improving the transference number to unity. These advancements will significantly enhance the overall performance of SPE-based systems. Furthermore, we will shed light on the advantages of integrating zero-strain cathodes in Li0-SSB full cells. By mitigating strain-related issues, these cathodes can dramatically improve the cycle life of Li0-SSB batteries, extending their durability and reliability.

The work is in part supported by the Assistant Secretary for Energy Efficiency and Renewable Energy, Vehicle Technology Office of the U.S. Department of Energy (DOE) through the Advanced Battery Materials Research Program under contract no. DE-SC0012704 and the startup funding of HLX.

9:55 AM *EN01/EN02/EN04.08

Novel Custom-Shaped Batteries with Ionogel Polymer Electrolytes Olga Guchok¹, Gilat Ardel¹, Hadar Nakar¹, Heftsi Ragonas², Allen Zheng³, Steven Greenbaum³ and Diana Golodnitsky¹; ¹Tel Aviv University, Israel; ²Holon Institute of Technology, Israel; ³Hunter College of City University of New York, United States

The rapid rise of flexible and stretchable electronics for healthcare, sensing, sport and textiles caused a growing demand for more efficient, reliable, environmentally friendly materials and continuous advancements of battery technologies.

Our research pioneers a simple approach to the fabrication of novel flexible lithium-ion batteries. It is based on a single-shot extrusion - 3D printing method of a multi-shell-architecture battery comprising biodegradable polymer-based components. We used the thermoplastic polymers PLA and TPU to improve the mechanical properties of the well-known LiTFSI-PEO-based polymer electrolytes. The extruded electrolytes of different PEO-to-TPU/PLA ratios and salt content were characterized by means of ESEM imaging, mass spectroscopy, differential-scanning calorimetry (DSC), electrochemical-impedance spectroscopy (EIS) and solid-state nuclear magnetic resonance (NMR) diffusion measurements. All the polymers were found to form complexes with lithium salt. Flexible extruded *in-situ* plasticized ionogel polymer electrolyte (IGPE) exhibited bulk conductivity of 0.2 mS/cm at room temperature and addressed the issues of inferior interface contacts. All-extruded cells with TPU-MWCNT-based current collector, LFP cathode, LTO anode and IGPE demonstrated good reversibility with close to 96% coulombic efficiency.

SYMPOSIUM EN02

Solid-State Batteries—Materials, Processes, Characterizations and Scale-Up
November 27 - December 1, 2023

Symposium Organizers

Xin Li, Harvard University
Yi Lin, NASA Langley Research Center
Fang Liu, University of Wisconsin--Madison
Amy Marschilok, Stony Brook University

Symposium Support

Silver
BioLogic
Verder Scientific, Inc.

* Invited Paper
+ JMR Distinguished Invited Speaker

SESSION EN02.01: General Session I
Session Chairs: Xin Li and Yi Lin
Monday Morning, November 27, 2023
Hynes, Level 3, Room 304

10:30 AM *EN02.01.01

Poly(vinylidene fluoride)- and Poly(urethane acrylate)-Based Electrolytes for Solid State Batteries Enyuan Hu, Dean Yen, Nan Wang and Sha Tan; Brookhaven National Laboratory, United States

Solid-state batteries (SSB) have better safety characteristics than conventional lithium-ion batteries which are based on flammable liquid electrolyte. A key enabler for SSB is the solid state electrolyte. Among possible candidates, polymer electrolytes have attracted a lot of attention as they offer a wide range of tunable structure, have good physical contact with electrodes and are easy to fabricate. This talk will include our recent work on two kinds of polymer electrolytes: Poly(vinylidene fluoride), or PVDF-based electrolyte and poly(urethane acrylate), or PUA-based electrolyte. PVDF polymer electrolyte is prepared by the solvent-casting method. We will discuss its performance in full cells using various kinds of cathodes. We will also discuss the effect of residual solvent on the eventual cell performance. PUA polymer electrolyte is prepared by a solvent-free method. Through controlling the degree of cross-linking, we were able to introduce PUA with gradient structure in the polymer electrolyte. This provides both good physical contact with electrode and good mechanical strength against lithium dendrite penetration. The $\text{LiNi}_{0.8}\text{Mn}_{0.1}\text{Co}_{0.1}\text{O}_2/\text{PUA}/\text{Li}$ cell is evaluated and shows good performance.

11:00 AM *EN02.01.02

Scalable Solid-State Electrochemical Devices Ju Li; Massachusetts Institute of Technology, United States

Low-cost, earth-abundant, and easy-to-recycle battery chemistries are key for the impending global energy transition. We provide some examples of proton solid-state battery ["Acid-in-Clay Electrolyte for Wide-Temperature-Range and Long-Cycle Proton Batteries," *Advanced Materials* (2022) 2202063], fast-acting neuromorphic computing ionic transistor ["Nanosecond protonic programmable resistors for analog deep learning," *Science* 377 (2022) 539], and lithium silicide guided lithium-metal batteries ["Ultra-Thin Lithium Silicide Interlayer for Solid-State Lithium-Metal Batteries," *Advanced Materials* (2023) 2210835] that may compete successfully with liquid electrolyte based devices. Full-cell performance evaluation and techno-economic assessment are essential for judging different device architectures.

11:30 AM *EN02.01.03

Toward Solid-State Li_{metal} -Air Batteries; An SOFC Perspective of Solid 3D Architectures, Heterogeneous Interfaces and Oxygen Exchange Kinetics Eric D. Wachsman, George Alexander, Roxanna Moores, Gibson Scisco, Christopher Tang and Michael Danner; University of Maryland, United States

The full electrification of transportation will require batteries with both 3-5X higher energy densities and a lower cost than what is available in the market today. Energy densities of > 1000 Wh/kg will enable electrification of air transport and are among the very few technologies capable of achieving this energy density. Li_{metal} -air is theoretically able to achieve this energy density and also capable of reducing the cost of batteries by replacing expensive supply chain constrained cathode materials with "free" air. However, the utilization of liquid electrolytes in Li_{metal} -air batteries has presented many obstacles to the optimum performance of this battery including oxidation of the liquid electrolyte and the Li_{metal} anode. In this paper a path towards the development of a Li_{metal} -air battery using a cubic garnet $\text{Li}_7\text{La}_3\text{Zr}_2\text{O}_{12}$ (LLZ) solid-state ceramic electrolyte in a 3D architecture is described including initial cycling results of a Li_{metal} - O_2 battery using a recently developed mixed ionic and electronic (MIEC) LLZ in that 3D architecture. This 3D architecture with porous MIEC structures for the air cathode is essentially the same as a solid oxide fuel cell (SOFC) indicating the importance of leveraging SOFC technology in the development of solid-state Li_{metal} -air batteries.

SESSION EN02.02: General Session II
Session Chairs: Xin Li and Amy Marschilok
Monday Afternoon, November 27, 2023
Hynes, Level 3, Room 304

1:30 PM *EN02.02.01

Statistical and Machine Learning-Based Durability-Testing Strategies for Energy Storage Stephen J. Harris and Marcus M. Noack; Lawrence Berkeley National Laboratory, United States

There is considerable interest in developing new energy storage technologies for the electric grid, but economic viability will require that manufacturers provide warranties guaranteeing 15+ years of life. Although there are extensive efforts to make early predictions for the expected life of new storage technologies, we argue here that for the purposes of pricing warranties and valuing second-life potential—considerations that are crucial to whether the technologies can be commercialized—the full failure probability distribution, not just the expected life, is required. We use published battery cycle-life data to suggest efficient statistical and machine learning based testing and analysis strategies that can rapidly estimate and also take advantage of the failure probability distribution. One

approach is a Weibull analysis, which can (1) reduce the number of testing machine hours required for setting a warranty, (2) quickly determine whether a new technology is better than a baseline technology, and (3) estimate the maximum intensity of testing acceleration that does not change the failure mode. A second approach is driven by the idea that all measured data—such as capacity or energy as a function of time or cycle number—are valuable and generated by an underlying latent function. This analysis employs a Gaussian process to find the underlying latent function, together with its uncertainties, which can be used to calculate the failure distribution.

2:00 PM *EN02.02.02

Mechano-Electrochemical Phenomena in Solid-State Batteries Jeff Sakamoto; University of Michigan, United States

There is tremendous interest in making the next super battery, however Li ion technology continues to improve and has inertia in several commercial markets. Recent material breakthroughs in solid-electrolytes (SE) could enable a new class of non-combustible solid-state batteries delivering twice the energy density (>1,300 Wh/L) compared to Li-ion. However, technological and manufacturing challenges remain, creating the impetus for fundamental and applied research.

This discussion will consist of fundamental aspects such as the mechano-electrochemical phenomena at solid interfaces as well as manufacturing challenges related to the integration of Li metal electrodes. The underlying physics that control the stability and kinetics of Li/SE interfaces are fundamentally different from interfaces in Li ion technology. Moreover, the mechano-electrochemical phenomena that occur during discharge and charge at the Li/SE interface are considerably different. For example, during charging at higher rates Li metal filaments can initiate at defects and propagate through relatively hard ceramics. During discharge, if the Li stripping rate is sufficiently high and the temperature is sufficiently low, voids form at the interface causing delamination at of the interface.

In another example, novel mechano-electrochemical phenomena are emerging when analyzing the formation of Li anodes in using the Li⁰-free manufacturing approach. Using this approach for solid-state batteries, Li metal is interposed between a current collector and the SE. The mechanics at this interface will determine the feasibility of this approach by controlling the homogeneity of the *in situ* formed Li anode. While significant progress is advance the technological maturity of solid-state batteries, there remain fundamental questions regarding the physics at interfaces and whether or not they exhibit sufficient stability and kinetics that are relevant to EVs.

2:30 PM *EN02.02.03

All Solid State Batteries Based on Sodium Electrochemistry Y. Shirley Meng^{1,2,3}; ¹The University of Chicago, United States; ²University of California, San Diego, United States; ³Argonne National Laboratory, United States

Solid-state batteries have gained significant attention in recent years as they have the potential to be the leading next-generation energy storage devices, offering improved safety, higher energy densities, and longer cycle life. For grid-level energy storage, where having an accessible supply of battery materials and low cost per kilowatt-hour is important, sodium solid-state batteries are a promising technology. Within the past five years, halide-based solid electrolyte materials have become increasingly popular due to their superior oxidation stability, excellent deformability, and moderate ionic conductivities. As such, they are ideal catholytes for enabling high-voltage-coating-free cathode materials. However, to improve sluggish solid-state battery kinetics, it is still necessary to enhance their ionic conductivity, especially for sodium systems, which calls for new approaches to materials design. I will talk about a novel approach towards synthesizing nanocrystalline and amorphous chlorides for use as *superionic* conductors in sodium all-solid-state batteries. Our concept is based on the tendency of chlorides to form these phases by adjusting the composition of the system, as demonstrated using the NaCl–YCl₃–ZrCl₄ phase composition diagram as an example. We show that by controlling the molar amount of NaCl, electrolytes with low sodium concentrations and nanocrystalline or amorphous nature can be obtained. The structural amorphization, along with an increase in free volume, and preferential population of prismatic Na⁺ local environments, leads to an exceptional ionic conductivity at room temperature. Our approach has the potential to be applied universally to other halide-based systems, leading to a shift in the design of future solid electrolytes for high-performance all-solid-state batteries operating at ambient temperatures.

3:00 PM BREAK

3:30 PM *EN02.02.04

Solid State Electrolyte: Li-B-S System and Inorganic-Polymer Composite YiCui; Stanford University, United States

This presentation include two topic areas related to solid state electrolyte. First, I will present a new family of Li-B-S solid electrolyte, which was predicted using machine learning approach and recently experimentally validated to have a good ionic conductivity and expanded voltage stability window compared to other sulfide electrolytes. Second, I will our decade long study on inorganic-polymer composite electrolyte, which utilize the mechanical flexibility and processibility of polymer and the ionic conductivity enhancement and mechanical enhancement by inorganic materials.

4:00 PM *EN02.02.05

Li-Metal Alloys and Their Unique Thermodynamic and Kinetic Properties Anton Van der Ven; University of California, Santa Barbara, United States

All-solid-state batteries will enable significant increases in energy density as they will allow the use of metallic Li anodes instead of graphite intercalation compounds. However, before metallic Li can be used as an anode, major metallurgical challenges must be overcome. Alloying of Li is a promising path with which to modify the intrinsic thermodynamic, mechanical and kinetic properties of metallic Li to enable the uniform deposition and stripping of Li at the anode/solid-electrolyte interface. Li forms a rich variety of intermetallic compounds when alloyed with different elements. Li diffusion within these intermetallic compounds can be complex due to the nature of anti-site defects and the relative mobilities between Li and the alloying elements. The unique thermodynamic and kinetic properties of different Li-metal alloys have important consequences for morphological evolution during Li deposition and stripping. In this talk, we will describe our first-principles statistical mechanics studies of non-dilute diffusion in Li-metal alloys such as Li-Sb, Li-Al, Li-Mg and Li-In and elucidate how strain and varying degrees of long and short-range order affect the kinetics of Li anodes.

4:30 PM *EN02.02.06

Towards Automated Discovery of Inorganic Solids for Next-Generation Batteries Yan Eric Wang; Samsung Advanced Institute of Technology, United States

In this talk I will present our scientific discovery in identifying the descriptors of solid-state electrolytes especially the oxides, and our recent efforts in solid-state battery materials discovery with an automated lab with high-throughput computation and robotic synthesis.

SESSION EN02.03: Poster Session I
Session Chairs: Xin Li and Fang Liu
Monday Afternoon, November 27, 2023
Hynes, Level 1, Hall A

8:00 PM EN02.03.01

Database Driven Solid-State Electrolyte Material Search for Li and Na-Metal Gunyoung Heo¹, Taehun Lee² and Aloysius Soon¹; ¹Yonsei University, Korea (the Republic of); ²Princeton University, United States

Li and Na metal anode-based batteries are currently some of the most desirable technologies for high-energy density storage systems. However, internal dendrite formation is considered one of the biggest challenges in battery manufacturing. Suppressing the dendrite formation of Li or Na metal might be achievable with solid-state electrolytes as they have demonstrated a higher chemical stability in the presence of the anode. The development of a solid-state electrolyte for Li and Na metal anode involves several challenges, including the need for the material to have

high ionic conductivity, good mechanical properties, and good compatibility with the anode material. To address these challenges, there is a need for a systematic approach to discover new solid-state electrolytes that are specifically tailored for Li or Na metal anodes. The objective of this work is to screen out optimal and compatible solid-state electrolytes for both Li and Na metal batteries from the Materials Project (MP) database [1]. In total, five criteria were considered in the screening process [2] – the formation energy, energy above hull, band gap, reaction energy with anode material and mechanical property – which are all available within the MP database. After screening out the potential candidates, we assessed their dynamic/transport properties. By performing molecular dynamics simulations using the universal graph deep learning interatomic potential M3Gnet [3], the ionic diffusivity for all solid-state electrolyte candidates was analyzed. Through this work, we provide the Pareto front for the most optimal solid-state electrolytes for both Li and Na metal anode batteries.

[1] A. Jain, S. P. Ong, G. Hautier, W. Chen, W. D. Richards, S. Dacek, S. Cholia, D. Gunter, D. Skinner, G. Ceder, and K. A. Persson, *APL Mater.* **1**, 011002 (2013)

[2] L. Kahle, A. Marcolongo, and N. Marzari, *Energy Environ. Sci.* **13**, 928 (2020)

[3] C. Chen and S. P. Ong, *Nat. Comput. Sci.* **2**, 718 (2022)

8:00 PM EN02.03 .02

Elucidating Differences in Surface and Bulk Properties of Solid-State ElectrolytesZeeshanAhmad; Texas Tech University, United States

Solid-state batteries with metal anodes are now widely recognized as the next frontier of battery research to satisfy the stringent requirements of safety, energy and power density for transportation and aviation applications. There is still a plethora of interfacial and chemomechanical challenges to be solved before these batteries achieve mass market adoption. These challenges include interface stability and dendrite growth, limits on stripping and plating current densities, and device integration [1]. These challenges warrant an investigation of the buried surfaces and interfaces present in solid-state batteries in the presence of electric fields encountered during battery operation. In this talk, I will discuss how the properties of surfaces and interfaces of solid-state batteries differ from the bulk using large scale simulations of defects based on first-principles and machine learning force fields. Our results confirm a high degree of atomic disorder at the interface, which effectively modulates the defect thermodynamics. Further, I will show how the mechanical stress at the interface affects these defects. These results have broad implications on ionic transport, charge transfer and rate capability, and dendrite growth in solid-state batteries through control of the properties of grain boundaries and interfaces. This work demonstrates the need for continuum models to be refined to account for the drastically different properties at the surfaces and interfaces.

[1] Ahmad, Z.; Venturi, V.; Sripad, S.; Viswanathan, V. *Curr. Opin. Solid State Mater. Sci.* 2022, 26, 101002.

8:00 PM EN02.03 .03

Investigating Different Solvents for Liquid Phase Synthesis Routes of Lithium Indium Chloride Solid Electrolyte for Solid-State BatteriesJacobOtabil Bonsu and DipanKundu; The University of New South Wales Sydney, Australia

Solid-state batteries (SSBs) have emerged as a promising technology that has the potential to revolutionise the area of energy storage by providing more safety, better energy density, and longer cycle life when compared to current lithium-ion batteries. Polymer, oxide, and sulfide-based solid-state electrolytes (SSEs) have been widely researched to aid in the development of solid-state batteries. However, these SSEs' drawbacks, such as high-temperature sintering of oxides, air instability of sulphides, and small electrochemical windows of polymer electrolytes, severely limit their practical implementation. As a result, it is necessary to design SSEs with strong ionic conductivity, good air stability, a wide electrochemical window, great electrode interface stability, and low-cost mass manufacturing. Because of their strong ionic conductivity and compatibility with high-voltage electrodes, halide electrolytes are emerging stars among inorganic solid-state electrolytes. However, as compared to liquid-mediated approaches, their traditional synthesis processes, such as ball-milling and annealing, are often more energy-intensive and time-consuming. Furthermore, the only approach in an aqueous solution is not ideal due to the negative effect of water traces on battery performance. We provide three comparison alternatives (Tetrahydrofuran, Acetonitrile, Ethanol, and Water) for the halide Li⁺ superionic conductor, Li₃InCl₆, with good ionic conductivities of 4.02, 3.67, 3.07, and 2.72 MilliSiemens per centimetre at ambient temperature respectively. In-addition, their ionic conductivities can be recovered after dissolution in their respective solvents. Combined with an NMC 622 cathode, the solid-state Li batteries show good cycling stability.

8:00 PM EN02.03 .04

Effect of Lithium Precursor on the Crystal Structure and Ionic Conductivity of Li₇La₃Zr₂O₁₂ Oxide ElectrolyteLeeHyeju¹, So HyunPark¹, Min GueLee¹, SojeongRoh¹, DongjooKim² and Young SooYoon¹; ¹Gachon University, Korea (the Republic of); ²Auburn University, United States

The garnet-structured solid electrolyte Li₇La₃Zr₂O₁₂ (LLZO) has attracted attention as a solid electrolyte for all-solid-state batteries due to its wide electrochemical window and high ionic conductivity. However, the formation of impurity phases and tetragonal LLZO during synthesis can rapidly reduce lithium-ion conductivity, and the low stability in air and water can lead to lithium loss. The effect of lithium sources including Li₂CO₃, LiOH and LiNO₃ on the crystal structure, microstructure, and ionic conductivity of LLZO was investigated. X-ray diffraction (XRD) analysis was performed to confirm the crystallization and phase formation of the synthesized LLZO and scanning electron microscopy-energy dispersive X-ray spectroscopy (SEM-EDS) was used to analyze the microstructure and chemical composition. Electrochemical impedance spectroscopy (EIS) was also used to confirm the ionic conductivity. As a result, LLZO prepared with LiOH as the source was confirmed to be cubic without impurities or intermediate phases, compared to solid electrolytes prepared with Li₂CO₃ and LiNO₃. In addition, a uniform particle size and distribution of less than 2 μm and an ionic conductivity of 1.311 × 10⁻⁴ S cm⁻¹ at room temperature were confirmed. These results suggest that the choice of lithium source can significantly affect the properties of LLZO, and that LiOH is a promising lithium source for the preparation of high-performance LLZO solid electrolytes. In future studies, the effect of lithium sources on the properties of LLZO should be investigated in more detail and new methods should be developed to fabricate high-performance LLZO solid electrolytes.

8:00 PM EN02.03 .05

A Highly Conductive and Stable Ionic Liquid Gel Electrolyte for Calcium Metal BatteriesXinluWang; Syracuse University, United States

Calcium batteries are promising alternatives to lithium batteries due to their high energy density, comparable reduction potential, and mineral abundance. Calcium is the fifth most abundant metal in the Earth's crust (4.1%), surpassing Na, K, Mg, and Li, and ranks third after aluminum and iron. Calcium batteries can achieve volumetric capacities comparable to incumbent Li-ion and emerging Li metal systems. Additionally, calcium-ion batteries generally exhibit improved safety characteristics compared to lithium-ion batteries, being less susceptible to thermal runaway and reducing the risk of overheating, combustion, or explosion.

However, to meet practical demands in high-performance applications, suitable electrolytes must be developed. Polymer gel electrolytes are emerging as a promising system for calcium metal batteries. Polymer gel electrolytes consist of polymer hosts swollen in liquid electrolyte and offer a combination of mechanical and electrochemical robustness from the polymer host, high ion conductivity and electrochemical reactivity from the liquid electrolytes, excellent wetting contact with the electrodes, more uniform electrode reactions (specifically, metal deposition), and have proven attractive for Li, Na, K, Zn, and Mg metal systems. Moreover, they provide a decent level of mitigation against potential leakage, electrolyte volatility, and flammability, thus offering the desired safety benefits similar to quasi-solid-state batteries.

In this study, polymer gel electrolytes (GPEs) for calcium-ion conduction were synthesized and characterized by photo-cross-linking poly(ethylene glycol) diacrylate (PEGDA) in the presence of calcium salt Ca(BF₄)₂ and an ionic liquid EMIM triflate. The ionic conductivity of the GPEs was observed to increase with salt concentration and temperature, reaching a maximum conductivity of 2.16 S/cm. The Ca stripping/plating behavior was analyzed on a Ca substrate with a current density of 0.2 mA cm⁻² and a total discharge areal capacity of 0.4 mA h cm⁻². The overpotential at the first cycle was 0.4 mV and increased with subsequent cycles. Furthermore, the PEGDA-based GPEs exhibited an electrochemical stability window of 4 volts and a thermal stability window exceeding 200 degrees Celsius.

Overall, these results demonstrate the potential of PEGDA-based GPEs as high-performance electrolytes for calcium batteries and provide valuable insights into the development of advanced GPEs for next-generation energy storage devices.

8:00 PM EN02.03 .06

Improving Lithium-Ion Conductivity by Co-Doping Al/Ta to Li₇La₃Zr₂O₁₂ using Molten Salt Synthesis MethodSo HyunPark¹, LeeHyeju¹, SojeongRoh¹, Ji-HyeokChoi¹, DongjooKim² and Young SooYoon¹; ¹Gachon University, Korea (the Republic of); ²Auburn University, United States

Solid state batteries are attracting attention as promising materials for next-generation energy storage systems due to their high energy density and safety. The sulfide solid electrolyte has excellent lithium-ion conductivity, but sulfur electrolyte easily reacts with moisture in the air to release sulfide. On the other hand, the oxide solid electrolyte does not exhibit the above toxic gas when decomposed. This research selected Li₇La₃Zr₂O₁₂ (LLZO), a garnet-type cubic phase, in light of chemical stability and introduced the molten salt synthesis (MSS) method and doped Al/Ta co-doped to improve lithium-ion conductivity. In particular, this method can overcome the disadvantage of MSS that forms an impurity phase during multi-component synthesis. In addition, using molten salt-based LiCl-KCl can form the cubic phase at a lower temperature in a shorter time than the traditional solid phase synthesis method. Al/Ta co-doping may induce more vacancies occupied by Li ions than single doping. In particular, Al single doping can inhibit 96h site substitution that interferes with lithium ion conductivity, and Al/Ta co-doping

induces displacement of Li vacancy to 24d site, extending the path of Li⁺. Such a mechanism increases ion conductivity because the atoms of 24d having a small Li vacancy are located close to each other, thereby shortening the movement path of Li⁺. Preparation of pure cubic LLZO phase was performed in the range of 900°C to 1000°C with a calcination process of less than 4 hours. The synthesized powder was pelletized and subjected to a heat treatment process to increase the density at 900°C for 6 hours. For the measurement of Li⁺ conductivity, electrochemical impedance spectroscopy (EIS) was used in the frequency range of 10 Hz~1 MHz. As a result, small particles of 0.8~1.3 μm were obtained compared to the single-doped LLZO by a similar method, and the ion conductivity was 2.398×10⁻⁴ S cm⁻¹, and a small amount of Al/Ta doping was sufficient to impart stability to the garnet structure of LLZO. In conclusion, the Al/Ta co-doped MSS method suggested that the LiCl-KCl molten salt serves to remove impurities, which is advantageous in synthesizing high-purity materials.

8:00 PM EN02.03 .07

LIPON Layer Effect for Reduction of Interfacial Resistance of LLZO/Li for All-Solid-State BatteryMin GueLee, SojeongRoh, So HyunPark, Ha EunKang, LeeHyeju and Young SooYoon; Gachon University, Korea (the Republic of)

Cubic garnet-type solid electrolytes for all-solid-state batteries (ASSBs) have attracted attention due to their stability over a wide electrochemical window and high ionic conductivity. However, current challenges for garnet-type solid electrolytes include overcoming poor wettability and high interfacial resistance with lithium metal anodes. When a lithium metal anode contacts an oxide solid electrolyte, a passivation layer of Li₂CO₃ forms on the surface of the solid electrolyte, which can lead to increased resistance. Additionally, non-uniform Li⁺ intercalation/extraction can lead to increased resistance and electrochemical instability at the solid electrolyte/anode interface. To improve contact resistance, interfacial modification methods have been introduced. One such method is to coat the surface of the solid electrolyte with a ceramic material that is highly reactive with lithium. This can stabilize the interfacial chemistry and improve lithium wettability and charge transport. In this study, LiPON coating was deposited on the surface of LLZO pellets using an RF sputtering process. The interface between the coating layer and the LLZO pellet was analyzed using transmission electron microscopy-energy dispersive spectroscopy (TEM-EDS) to confirm the X-ray photoelectron spectroscopy (XPS) depth profile spectrum. Molten Li contact angle measurements were also performed to confirm wettability with metallic lithium. The results showed that the LiPON coating forms a Li-LiPON layer when in contact with molten Li and exhibits a low contact angle of less than 90°. This indicates that the LiPON coating can improve lithium wettability and reduce interfacial resistance. These results suggest that the chemical properties of the lithium electrode and the properties of the interface play an important role in the interfacial resistance and lithium wettability, compared to the microstructure of the LLZO solid electrolyte. This discovery will have implications for the design of LLZO/Li interfaces for ASSBs containing LLZO as the electrolyte.

8:00 PM EN02.03 .08

Ultrathin Sulfide-Based Composite Electrolyte Membrane for Solid-State Sodium Metal BatteriesXiaolinGuo, YangLi and HuiWang; University of Louisville, United States

Rechargeable solid-state sodium batteries that utilize solid electrolytes (SEs) have garnered considerable attentions due to their features of intrinsic non-flammability and abundant sodium resources. Among different types of sulfide-type SEs, Na₃SbS₄-family conductors show advantages of high ionic conductivity at room temperature and densification through cold-pressing. However, one of their most significant challenges is related to the electrochemical stability towards Na metal. Solid composite electrolytes (SCEs) with ceramic particles dispersing in a polymer matrix, provide a viable approach to address this challenge. In this work, we report an ultra-thin, flexible and stable SCE through embedding micro-sized Na₃SbS₃Se (NSSE) particles in polymer electrolyte (PVDF-HFP). The prepared SCE membranes exhibit an adjustable thickness, and impressive ionic conductivity at room temperature as well as enhanced interfacial stability in Na symmetric cells. Moreover, the assembled Na|SCE|TiS₂ solid-state batteries demonstrate stable cycling and great rate performance. This work promotes new composite SEs, and their application in solid-state Na metal batteries.

8:00 PM EN02.03 .09

Epoxy Resin Based Solid Electrolyte for Multifunctional Structural BatteriesElenaM. Ford¹, ScottM. Black¹, MohitGupta² and NabaKaran¹; ¹University of Connecticut, United States; ²Brown University, United States

Elena Ford 1,5, Scott Black 1,5, Mohit Gupta 2, Naba K. Karan 3,4,5

- 1 Dept. Mechanical Engineering, University of Connecticut, Storrs, CT
- 2 Dept. Mechanical Engineering, Brown University, Providence, RI
- 3 Institute of Materials Science, University of Connecticut, Storrs, CT
- 4 Dept. of Materials Science and Engineering, University of Connecticut, Storrs, CT
- 5 Center for Clean Energy Engineering, University of Connecticut, Storrs, CT

For the past decade, lithium-ion batteries (LIBs) have dominated the electric vehicle sector due to their high energy density and cycle life. Currently, the purpose of LIBs for electric vehicles is to provide and store energy. A structural battery is defined as being multifunctional; it is a load bearing system as well as an electrochemical cell [1]. The electrolyte system is the key enabler for a multifunctional structural battery as it must possess sufficient ionic conductivity (~10⁻⁴S/cm) and mechanical strength (Young's modulus ~ 2-3 GPa) simultaneously.

In the present work, we study the development of a dual-phase structural battery electrolyte to optimize ionic conductivity and mechanical performance simultaneously. An epoxy resin-based system is chosen due to its high mechanical strength and ability for in situ polymerization. [3] Diglycidyl ether of Bisphenol A (DGEBA) accounts for the epoxy to provide hard segments in the matrix and is cured by an amine compound (Jeffamine T-403). A liquid electrolyte is added to the system for improving the conductivity enhancement without compromising its mechanical strength substantially. Three liquid components consisting of lithium salt and solvents are considered here -lithium bis(trifluoromethanesulfonyl)imide (LiTFSI) dissolved in a solution of ethylene carbonate (EC) and dimethyl methyl phosphonate (DMMP). LiTFSI dissolved in Tetraethylene glycol dimethyl ether (TetraGlyme) and LiTFSI dissolved in 1-Ethyl-3-methylimidazolium bis(trifluoromethylsulfonyl)imide (EMIM-TFSI). Ionic conductivity of the electrolyte systems as a function of temperature is measured utilizing electrochemical impedance spectroscopy. Uniaxial load tests are performed to evaluate the mechanical properties (e.g., Young's modulus, Yield strength) of the epoxy-based electrolyte systems with and without the addition of the ion conducting liquids. Comparative data on the three epoxy-based systems containing varying amounts of liquid components will be presented.

References

- [1] L. Wehner, N. Mittal, T. Liu and M. Niederberger, "Multifunctional Batteries: Flexible, Transient, and Transparent," *American Chemical Society*, vol. 7, no. 2, pp. 1-3, 2021.
- [2] L. Froboese, L. Groffmann, F. Monsees, L. Helmers, T. Loellhoeffel and A. Kwade, "Enhancing the Lithium Ion Conductivity of an All Solid-State Electrolyte via Dry and Solvent-Free Scalable Series Production Processes," *Electrochemical Society*, vol. 167, no. 2, pp. 1-2, 2020.
- [3] Y. H. Song, P. L. Handayani and U. . H. Choi, "The role of inorganic nanoparticle on ion conduction of epoxy-based solid polymer electrolytes for lithium-ion batteries," *Molecular Crystals and Liquid Crystals*, vol. 687, no. 1, p. 1, 2019.

8:00 PM EN02.03 .10

Chitosan-Based Cross-Linked Nanocomposites for Solid State Electrolyte SystemSamirKattel and HemaliRathnayake; UNCG, United States

Lithium-ion batteries (LIBs) are the best choices in electrochemical systems due to promising aspects like good life cycle, large discharge capacity and hence widely used in wearable electronic devices. These LIBs are usually made of cathode, anode, electrolyte, and separator. Due to good ionic conductivity, liquid electrolytes (LEs) are in practice. However, the use of LEs is considered detrimental due to the reason that leakage of it may cause fire and explosions. Replacing conventional liquid electrolytes with the solid-state electrolytes (SSEs), which are not only non-flammable but also highly flexible, light in weight and mechanically strong. Additionally, it has also been proven that the side reactions in LE-based lithium-ion batteries can surpass by replacing with SSEs. However, the low-ionic conductivity and high temperature stability are major drawbacks in biodegradable polymer-based SSEs to be compete with its counterpart of inorganics and Les.

This project will develop chitosan-based nanocomposites incorporated with appropriate fillers and lithium salts to utilize them as solid-state membrane electrolyte for lithium-ion conduction. The chemical composition, structure, and conductivity properties are investigated using a wide range of characterization tools. Also, biodegradability and abundance natural availability of these nanocomposites adds more value to this research.

Electrolytes with ionic conductivities 10⁻³Scm⁻¹ are not suitable for high power batteries applications since their performance would be limited to lower charge and discharge rates. The proposed process uses highly porous Metal Organic Frameworks (MOFs) as fillers and lithium salts and plasticizers to incorporate into chitosan nanocomposites for a solid-state electrolyte

system. Integration of MOFs into chitosan nanocomposite system will add tailoring the lithium-ion conduction path and enable to reduce interfacial resistance to provide suitable lithium-ion conduction in these composites. The system offers a great potential for use in electrolyte system for all solid-state electrolyte systems.

8:00 PM EN02.03 .11

Li⁺ Conduction Mechanism in Anion-Substituted Halide Solid Electrolytes for All-Solid-State Batteries YejiChoi¹, HiramKwak¹, DaseulHan², Jae-SeungKim³, Kyung-wanNam², Dong-HwaSeo³ and Yoon SeokJung¹; ¹Yonsei University, Korea (the Republic of); ²Dongguk University, Korea (the Republic of); ³Korea Advanced Institute of Science and Technology, Korea (the Republic of)

The recent emergence of halide superionic conductors, such as Li₃YCl₆, as solid electrolyte (SE) materials for all-solid-state batteries (ASSBs) is considered a game changer. These halide SEs offer a combination of advantageous properties that include excellent (electro)chemical oxidative stability, high Li⁺ conductivity, and mechanical deformability. This unique combination of properties position halide SEs as promising candidates for the development of next-generation ASSBs, surpassing the limitations of sulfide or oxide SEs.

However, despite these benefits, the practical deployment of these materials has been hindered by the high cost associated with the use of expensive or rare transition metals. To overcome this, a cost-effective and abundant Zr-based compound Li₂ZrCl₆ has emerged. Yet, there remains a need to improve Li⁺ conductivity further and develop a more comprehensive understanding of the underlying ion conduction mechanisms.

This presentation delves into the impact of anion substitution on changes in the local structure and ion conductivity of halide SE, offering an in-depth explanation of the ion conductivity mechanism. Particularly, we present noteworthy findings that demonstrate nearly twofold enhancements in ion conductivity upon anion-substitution of halide superionic conductors.

Furthermore, we also investigate the feasibility of these materials in ASSB cells.

References

[1] *Adv. Energy Mater.* **2021**, *11*, 2003190.

[2] *ACS Energy Lett.* **2022**, *7*, 1776.

[3] *Nat. Commun.* **2023**, *14*, 2459.

8:00 PM EN02.03 .12

Surficial Degradation of Jet-Milled LiPS5Cl under Mild Temperature Heat-Treatment Kern-HoPark, Yo-SeobKim, KyungSuKim, WoosukCho and GoojinJeong; Korea Electronics Technology Institute, Korea (the Republic of)

All-solid-state batteries using sulfide solid electrolytes are considered a promising next-generation energy storage system. Especially, argyrodite-type Li_{1-x}PS_{5-x}Cl (LP5SCl) is in spotlight for their good ionic conductivity and malleability. In electrode level, achieving efficient Li⁺ pathway with the maximized active material proportion and electrode mass loading is crucial for the high energy density. Thus, solid electrolytes with a small particle size is highly sought for. Here, we demonstrated a spiral jet mill process for refining LP5SCl particle size, reducing the mean particle size (*D*₅₀) of LP5SCl 39.9 μm to 1.9 μm where the ionic conductivity was decreased from 2.0 mS cm⁻¹ to 0.23 mS cm⁻¹. The post-annealing in a mild temperature (*T* < 250 °C) led to the even more decreased ionic conductivity. Although the ionic conductivity was recovered when *T* > 300 °C, these high temperature heat-treatment resulted in severe particle agglomeration. Spectroscopic study suggested that the particle surfaces were damaged during the jet-mill process and the irreversible sulfur losses occurred during the mild temperature annealing.

8:00 PM EN02.03 .13

Core-shell structured NCM@LP5SCl synthesized by mechanofusion process for high-performance all-solid-state batteries Jin WoongLee^{1,2}, Min JiKim^{1,2}, Sung EunWang², Do WoongYoon^{1,2}, Dae SooJung¹ and Yoon ChanKang²; ¹Kicet, Korea (the Republic of); ²Korea University, Korea (the Republic of)

All-solid-state batteries (ASSBs) using inorganic solid electrolytes (SEs) are considered a promising next-generation rechargeable battery because of their higher energy density and thermal stability compared to conventional lithium ion batteries (LIBs) using organic liquid electrolytes. Among the various SEs, Sulfide-based SEs have been developed and attracted much attention due to their high ionic conductivity and better formability than other SEs. Unfortunately, ASSBs exhibit several issues, such as undesired chemical reactions and physical contact issues. With regard to physical contact, insufficient contact between active materials (AMs) and SEs cause high interfacial resistances between the electrode materials that may degrade electrochemical performances, and this phenomenon could be worsened if the AM and/or SE particles agglomerate. Therefore, intimate contact and homogenous distribution of electrode materials are necessary in the ASSBs to reduce interface resistance and offer sufficient Li-ion transport pathway. However, it is difficult to construct such intimate contact between electrode materials in the form of powder.

In this study, we produced the core-shell structured cathode composite by the mechanofusion (MF) process. The high shear and compression forces used in the MF process enable the coating of a thin and homogenous SE(LP5SCl) layer on surface of AM(NCM) particle. NCM@LP5SCl composite allows intimate interface between NCM and LP5SCl without void and agglomeration, which ensure well-networked Li ion pathway resulting in high-performance in ASSB. In particular, ASSBs employing the NCM@LP5SCl composite can electrochemical properties even at up to 87.3wt% NCM mass fraction in the cathode. It is demonstrated that the NCM@LP5SCl composite could be a promising cathode material for the high energy density for practical ASSBs applications.

- This work was supported by the Technology Innovation Program (20009985) funded By the Ministry of Trade, Industry & Energy (MOTIE, Korea) and National R&D Program through the National Research Foundation of Korea funded by Ministry of Science and ICT (2021M3H4A3A02086100).

8:00 PM EN02.03 .14

New Amorphous Quaternary Sulfide Compounds as Solid Electrolyte for All-Solid-State Li-Ion Batteries YunaKim and Sung-JinKim; Ewha Womans University, Korea (the Republic of)

In recent years, interest in all-solid-state lithium secondary batteries with high energy density and output performance has increased due to the possibility of mitigating safety issues related to liquid electrolytes. However, the development of a suitable solid electrolyte (SE) remains a major challenge in advancing all-solid-state battery technology. Sulfide-based compounds are advantageous as solid-state electrolytes due to their high ionic conductivity and efficient transport of lithium ions, which can be attributed to their high polarizability and low electronegativity. In this work, an amorphous new sulfide compound, LiSbGeS₄, was synthesized as a Li-ion conductor. The amorphous characteristics of LiSbGeS₄ were investigated using PXRD, XAS, XRS, Raman spectroscopy, and thermal analysis. XPS and Raman spectroscopy provided information about into the local structure and chemical bonding of LiSbGeS₄, indicating the presence of metal-metal bonds and metal-S polyhedral units. LiSbGeS₄ was modified to have a high ionic conductivity through anion aliovalent substitution of the Cl⁻ on S²⁻ sites while maintaining amorphous phase. LiSbGe_{0.8625}S_{3.45}Cl_{0.55} exhibited a significantly higher lithium-ion conductivity, reaching 7.26 mS/cm, which is approximately 2400 times higher than that of pristine LiSbGeS₄. This study presents new amorphous sulfide compounds with enhanced Li-ion conductivity as a promising solid electrolyte for Li-ion batteries.

8:00 PM EN02.03 .15

Garnet-Based Bilayer Hybrid Solid Electrolyte for High-Voltage Cathode Material Modified with Interface Enabler on Lithium-Metal Batteries Kumlachew ZelalemWalle^{1,1,2} and Chun-ChenYang^{1,1}; ¹Ming Chi University of Technology, Taiwan; ²University of Gondar, Ethiopia

Solid-state lithium metal batteries (SSLMBs) are considered promising candidates for next-generation energy storage devices due to their superior energy density and excellent safety. However, recent findings have shown that the formation of lithium (Li) dendrites in SSLMBs still exhibits a terrible growth ability, which makes the development of SSLMBs have to face the challenges posed by the Li dendrite problem. In this work, an inorganic/organic mixture coating material (g-C₃N₄/ZIF-8/PVDF) was used to modify the surface of the lithium metal anode (LMA). Then the modified LMA (denoted as g-C₃N₄@Li) was assembled with lithium Nafion (LiNf) coated commercial NCM811 (LiNf@NCM811) using a bilayer hybrid solid electrolyte (Bi-HSE) that incorporated 20 wt.% (vs. polymer) LiNf coated Li_{6.05}Ga_{0.25}La₃Zr₂O_{11.8}F_{0.2} (LiNf@LG_{0.25}LZOF) filler faced to the positive electrode and the other layer with 80 wt.% (vs. polymer) filler content faced to the g-C₃N₄@Li. The garnet-type Li_{6.05}Ga_{0.25}La₃Zr₂O_{11.8}F_{0.2} (LG_{0.25}LZOF) solid electrolyte was prepared via co-precipitation reaction process from the Taylor flow reactor and modified using LiNf, a Li-ion conducting polymer. The Bi-HSE exhibited high ionic conductivity of 0.68 mS cm⁻¹ at room temperature, and a wide electrochemical window (0–5.0 V vs. Li/Li⁺). The coin cell was charged between 2.8 to 4.5 V at 0.2C and delivered an initial specific discharge capacity of 194.3 mAh g⁻¹ and after 100 cycles it maintained 81.8% of its initial capacity at room temperature. The presence of a nano-sheet g-C₃N₄/ZIF-8/PVDF as a composite coating material on the LMA surface suppresses the dendrite growth and enhances the compatibility as well as the interfacial contact between the anode/electrolyte membrane. The g-C₃N₄@Li symmetrical cells incorporating this hybrid electrolyte possessed excellent interfacial stability over 1000 h at 0.1 mA cm⁻² and a high critical current density (1 mA cm⁻²). Moreover, the in-situ formation of Li₃N on the solid electrolyte interface (SEI) layer as depicted from the XPS result also improves the ionic conductivity and interface contact during the charge/discharge process. Therefore, these novel multi-layered fabrication strategies of hybrid/composite solid electrolyte membranes and modification of the LMA surface using mixed coating materials have potential applications in the preparation of highly safe high-voltage cathodes for SSLMBs.

8:00 PM EN02.03 .16

Lithium Containing Fluorides and Oxyfluorides as Solid Electrolytes Michael J. Brady, Jessica Andrews and Brent C. Melot; University of Southern California, United States

Research on all solid-state batteries has increased as lithium-ion based chemistries approach theoretical capacities with conventional graphite anodes. Aside from the safety-related improvements that come with the removal of traditional liquid electrolytes, all solid-state batteries offer advantages related to cost, operating conditions, and energy density. Most of the materials that show high lithium-ion conductivity are oxide- or sulfide-based and have vastly different diffusion conditions, operating windows, and stabilities against lithium metal. As a result, exploring other chemistries—as has been done recently with halides in the argyrodite structure—is paramount to the understanding and improving the properties of solid electrolytes.

We chose to explore fluoride and oxyfluoride based compositions with the motivation that fluoride substitution should widen the stability window as well as provide a passivating layer of LiF in the SEI when used against lithium metal. This will work to combat the deposition of lithium metal that can occur along the grain boundaries in oxide based solid electrolytes leading to dendrite formation and cell failure. Exploring compounds in this phase space is accompanied by many challenges associated with synthetic methods as well as sample preparation and instrumental setup for various characterization methods. Conventional solid-state synthetic methods for oxides and sulfides are not applicable to fluorides due to their volatility and reactivity with several common vessels. Additionally, fluoride materials tend to be less stable at elevated temperatures which makes sintering of samples to raise the density challenging.

We will present our work on the examination of new lithium containing fluoride and oxyfluoride materials for use as solid electrolytes beginning with a gallium-based fluoride garnet. We have developed new synthetic methods for fluoride-based phases using custom high-temperature and high-pressure autoclaves. Cold-isostatic pressing was used to produce pellets of near theoretical density without the need for high-temperature sintering. We examine the effects of substitution of different redox-inactive metal centers through X-ray diffraction and electrochemical impedance spectroscopy. Additionally, through computational methods we investigate the activation energy of lithium ion hopping in these phases and compare these values to those extracted from Arrhenius plots derived from conductivity measurements.

8:00 PM EN02.03 .17

Single-Ion Conducting Sol-Gel Derived Silica-PEO Hybrid for Solid-State Electrolytes Guangyu Wang, Vazrik Keshishian and John Kieffer; University of Michigan, United States

To simultaneously achieve both high mechanical stiffness and ionic conductivity, while maintaining good electrochemical stability, we developed a hybrid electrolyte that consists of a nanoporous silica backbone, covalently grafted organic moieties, and infiltrated polymer. The backbone is derived from tetra-ethyl-orthosilicate (TEOS) through a multi-step sol-gel process. The functionalization process is optimized by precisely timing and phasing the reactions between the pre-hydrolyzed 2-[(Trifluoromethanesulfonylimido)-N-4-sulfonylphenyl] ethyl (TFSISPE) anion, 2-[Methoxy(polyethyleneoxy)6-9propyl] trimethoxysilane (OPEG), and the partially gelled silica backbone. This process enhances anion loading without affecting the gelation of the backbone. Subsequently, we replace the solvent in the nanopores with low-molecular weight (600 g mol^{-1}) polyethylene oxide (PEO). We find that the incorporation of grafted OPEG significantly improves the ionic conductivity. At 20°C and a Li^+ concentration of one molar, the material with OPEG exhibits an unprecedented ionic conductivity of $5.2 \times 10^{-4} \text{ S cm}^{-1}$, approximately seven times higher than that without OPEG. This enhancement is attributed to the reduction of osmotic drag resulting from the entanglement between OPEG and PEO. Furthermore, we achieve a high lithium-ion transference number ($t^+ \sim 0.91$) by immobilizing the TFSISPE anion. Compared to conventional SSEs based on polymer matrices, our single-ion conducting hybrid electrolyte exhibits approximately ten times higher ionic conductivity, nearly unity transference number, and thermal stability up to 110°C .

8:00 PM EN02.03 .18

High-Voltage Anode-Free Sodium Metal Batteries with Polymer Electrolyte Membranes Yu-Hsien Wu, Haocheng Yuan, Shundong Guan and Liangliang Li; Tsinghua University, China

With the growing demands of electronic vehicles, portable electronics and large-scale energy storage, lithium metal batteries have been intensively studied due to the superior energy density provided by the lithium anode. However, the scarcity of lithium reserve significantly increases the cost of lithium metal batteries. Among alternatives, high-voltage anode-free sodium (Na) metal batteries (AFSMBs) are attracting enormous interest since they can attain high energy density in a low-cost way. One challenge that hinders the development of AFSMBs is that the highly reactive Na metal deposited on the current collector reacts with liquid electrolyte easily, especially when carbonate electrolytes are employed. As a result, the growth of Na dendrites and the formation of “dead Na” are exacerbated and thus shorten the lifespan of AFSMBs. Herein, we proposed some poly(vinylidene fluoride)-based polymer electrolyte membranes (PEMs) for stable and dendrite-free AFSMBs in carbonate electrolytes. The electrochemical properties of the PEMs are optimized by tuning the solvent, Na salt, and polymer matrix. The optimal PEMs have the merits of high ionic conductivity ($>5 \times 10^{-4} \text{ S cm}^{-1}$), great electrochemical stability with Na (the Na|PEM|Na cell runs steadily for over 4,000 hours at a capacity of 0.1 mAh cm^{-2} with a low voltage hysteresis), good electrolyte resistance and decent mechanical strength; therefore, when they are applied on the current collectors in AFSMBs, Na metal can be uniformly deposited on the current collectors and the deposited Na metal is effectively separated from carbonate-based electrolyte, leading to the reduction of parasitic reactions and the elongation of the cycle life of the batteries. With the PEMs, high-voltage AFSMBs with a 4.0V-class layered oxide cathode and carbonate electrolyte are assembled and tested. These batteries can run for ~ 60 cycles due to the stabilized interface between deposited Na and the corrosive carbonate electrolyte. In contrast, batteries without a PEM fail quickly in just a few cycles due to the poor Na deposition and much side reactions. In short, with the support from the chemically/thermally stable and mechanically strong PEMs, it is promising to fabricate long-cycle-life, high-energy-density, and low-cost AFSMBs.

8:00 PM EN02.03 .19

Electrochemical Properties of Porous Nickel-Based Alloy Foam as Anodes in Lithium Metal Batteries Jae-Seong Yeo, Hye-Ryeon Yu, Sang-Hyeon Ha, Tae-Young Ahn, Eunji Yoo and Yusong Choi; Agency for Defense Development, Korea (the Republic of)

Traditional graphite-anode-based lithium (Li)-ion batteries are challenged by the ever-increasing demand of today's energy storage and power applications, especially for smart grid and electric vehicles because they have almost reached their theoretical specific energy limits. Among varieties of alternative anode materials, Li metal has been widely recognized as an ultimate anode material for high-energy rechargeable batteries due to its ultrahigh theoretical specific capacity (3860 mAh g^{-1}) and very low redox potential (-3.04 V vs. standard hydrogen electrode). To date, considerable efforts have been made to developing ultra-high energy density Li metal-anode-based batteries, such as Li-S and Li-air batteries. However, uncontrollable dendritic growth and high reactivity of Li metal anodes result in poor cycle performance and severe safety concerns, hindering the practical application of Li metal anodes in rechargeable Li metal batteries. To solve these issues, various approaches have been developed to suppress Li dendrite formation, including artificial SEI layer construction, additives of electrolyte to improve the uniformity of Li-ion deposition, utilization of high-modulus polymer or ceramic solid-state electrolytes, separator modification, current collector modification, and so on. Particularly, current collectors play a critical role in facilitating uniform Li nucleation and deposition. Fabricating three-dimensional current collectors is emerging as an effective strategy for designing dendrite-free Li anodes. Recently, Y. Choi et al. have reported an oxidation method for achieving an ultra-lithiophilic NiO layer on the surface of a three-dimensional nickel (Ni)-foam, resulting in stable Li plating and stripping in an anode prepared using Li-infused oxidized Ni-foam. In this study, Ni-based alloy, NiCrAl, with porous three-dimensional or two-dimensional structures was used as an anode in Li metal batteries. NiCrAl showed higher mechanical properties than pure Ni in the molten Li, anticipating in facile electrode stacking and cell assembly of NiCrAl-foam anode compared to Ni-foam anode. Oxidized NiCrAl-foam was prepared by heat treatment at 600°C for 10 min in ambient air. Li was introduced into the oxidized NiCrAl-foam by dipping into molten Li or electroplating. We present the electrochemical properties of oxidized NiCrAl-foam anodes with different foam thickness ($0.2\text{--}1.0 \text{ mm}$) in the Li metal batteries.

8:00 PM EN02.03 .20

Electrochemical Characteristics of Various Lithium-Based Anodes for Thermal Batteries Hye-Ryeon Yu, Jae-Seong Yeo, Chae-Nam Im, Sang-Hyeon Ha, Jaemin Lee and Yusong Choi; Agency for Defense Development, Korea (the Republic of)

The thermal battery is primary battery used for special fields such as defense due to its high power and high reliability characteristics. As the demand for thermal battery increases, development of various thermal battery electrodes having high energy density and power density is required. Therefore, as interest in high performance anodes increases, attempts are being made on various anodes for thermal batteries. In the case of a conventional thermal battery anode (Li-Si alloy), it has difficulty in large-area because it is manufactured through a powder pressing method. For this reason, many studies on development of liquid lithium-based anodes have recently been conducted. In particular, the Li-Fe (LiFe) anodes manufactured by mixing molten lithium and iron powder, a research has been carried out significantly and some commercialized. In addition, research on lithium impregnated metal foam anode (LIMFA) that are used by impregnating molten lithium in metal foam has been actively conducted recently. The research on the manufacture and performance of lithium boron (LiB) anodes for lightening the weight of thermal battery is also being studied. In this paper, various lithium-based thermal battery anodes were fabricated and applied to improve thermal battery performance. The prepared anodes were fabricated single cells applying FeS_2 cathode, and electrolyte. The single cell was discharged at 500°C to evaluated electrochemical properties, and performance as an anode of a thermal battery compared.

8:00 PM EN02.03 .21

Studying *In-Situ* Passivating Interphase Between Halide Solid-Electrolyte and Li-Based Anode in All-Solid-State Batteries Se Young Kim^{1,2}, Seong-Min Bak^{3,4}, Kyu Jung Jun^{5,2} and Guoying Chen²; ¹Korea Institute of Science and Technology, Korea (the Republic of); ²Lawrence Berkeley National Laboratory, United States; ³Brookhaven National Laboratory, United States; ⁴Yonsei University, Korea (the Republic of); ⁵University of California, Berkeley, United States

All-solid-state batteries (ASSBs) have been highlighted as a promising alternative for future energy storage systems due to their high thermal stability and high energy density compared to lithium-ion batteries using liquid electrolytes. Among many types of solid electrolytes, halide solid electrolytes (SE) with high oxidative stability have been intensively proven as a feasible SE that enables cycling 4 V class cathode materials. However, undesirable thermodynamic instability of halide SEs to Li metal anode hinders achieving high energy density ASSBs for practical use. To this end, lithium-indium (Li-In) alloy has been extensively employed due to their (electro)chemical stability to halide SEs that enables stable cycling of ASSB using halide SEs. Although the decomposition of halide SEs and its reactants in direct contact with Li metal has been experimentally and theoretically studied, no in-depth investigations on interphase evolution and charge transfer mechanism at the LYC SE and Li-In anode interphase have been conducted. In this work, we report the evolution of the interphase layer between In metal anode and halide solid electrolyte, Li_3YCl_6 (LYC), that enables stable long-term cycling of ASSB coupled with crack-free single-crystal (SC) $\text{LiNi}_{0.8}\text{Co}_{0.1}\text{Mn}_{0.1}\text{O}_2$ (NMC811) cathode active material. Through the combination of high-resolution microscale x-ray based analysis on a cross-section of the ASSBs, we demonstrate the crosstalk between LYC and In anode that results in the evolution of interphase layer consists of InCl_x , YCl_3 , LiCl , and In diffused LYC which suppressed dendritic growth of Li-In alloy over the ASSB cycling.

8:00 PM EN02.03 .22

Synthesis of High-Quality and Low-Cost $\text{Li}_6\text{PS}_5\text{Cl}$ via Naphthalene Assisted Li_2S -Free One-For-All Method for Commercial SynthesisMukarramAli^{1,2}, ChilH. Doh^{1,2} and YoonC. Ha^{1,2}; ¹Korea Electrotechnology Research Institute, Korea (the Republic of); ²University of Science and Technology, Korea (the Republic of)

The commercialization of sulfide-based all-solid-state batteries (ASSBs) has been hindered by the lack of sustainable synthesis techniques for sulfide-based solid electrolytes (SSEs) [1]. While mechano-chemical and solid-state sintering methods are energy-intensive and commercially non-viable, solvent/wet chemistry-based routes involving organic solvents have become the focus of extensive research [2]. Thus, it is crucial to develop a viable process that eliminates the need for Li_2S as a starting reagent.

In this study, we present a Li_2S -free one-for-all (OFA) method capable of producing high-quality $\text{Li}_6\text{PS}_5\text{Cl}$, a key SSE material, at the world's lowest cost of \$47/kg. The OFA method offers a universal approach for the synthesis of Li_xMS_4 ($x = 3$ or 4 , $M = \text{P}$, Sb , or Si) and $\text{Li}_6\text{PS}_5\text{X}$ ($X = \text{Cl}$, Br , or I) in a single-step technique, eliminating the need for pre-synthesized Li_2S . This process uses lithium metal (Li) and sulfur powder (S) as a precursor for Li_2S along with LiCl and P_2S_5 in tetrahydrofuran (THF), $\text{Li}_6\text{PS}_5\text{Cl}$ can be synthesized within 9 hrs. The synthesis of $\text{Li}_6\text{PS}_5\text{Cl}$ was carried out using the OFA method, and the resulting material exhibited exceptional ionic conductivity of 2.5 mS cm^{-1} and electronic conductivity below 10^{-7} Scm^{-1} . The low-cost production of $\text{Li}_6\text{PS}_5\text{Cl}$ was achieved by utilizing readily available precursors, and the process cost was reduced to \$47/kg, making it highly attractive for large-scale manufacturing.

The synthesis mechanism of $\text{Li}_6\text{PS}_5\text{Cl}$ was investigated using electrospray ion mass spectrometry (ESI-MS) and nuclear magnetic resonance (NMR) spectroscopy, revealing the formation pathway of the desired $\text{Li}_6\text{PS}_5\text{Cl}$ structure. The wet synthesis started from spontaneous Li oxidation and naphthalene reduction, and the resulting naphthalene radical anion initiated the reduction reaction of elemental S to form polysulfide anions (S_n^{2-}). Subsequently, P_2S_5 reacted with polysulfide anions and co-precipitated in the form of Li_3PS_4 , Li_2S , and LiCl at the end. Electrospray ion mass spectrometry (ESI-MS) and nuclear magnetic resonance (NMR) spectroscopy are employed to elucidate the underlying chemistry between Li-NAP solution with S and P_2S_5 with LiCl during $\text{Li}_6\text{PS}_5\text{Cl}$ synthesis. We found that S_7^{2-} and S_9^{2-} are predominantly formed in the polysulfide solution, and the additional LiCl , P_2S_5 , and Li made PS^{7-} and PS^9 at the initial stage. With increasing Li-ion concentration in the solution (as the lithium dissolved further in the reaction mixture), PS^{3-} and PS^{4-} coordinated with THF remained in the supernatants while Li_3PS_4 , Li_2S , and LiCl were co-precipitated at the end in a $\text{Li}_3\text{PS}_4 \cdot x(\text{Li}_2\text{S}-\text{LiCl})$ complex. To further explain the argyrodite growth X-ray photoelectron spectroscopy (XPS) and X-ray diffraction (XRD) are used to investigate the phase growth of complex as-prepared product $\text{Li}_3\text{PS}_4 \cdot x(\text{Li}_2\text{S}-\text{LiCl})$ to final argyrodite $\text{Li}_6\text{PS}_5\text{Cl}$ from the OFA method.

To evaluate the electrochemical performance of the OFA $\text{Li}_6\text{PS}_5\text{Cl}$, it was paired with a high nickel cathode $\text{Li}(\text{Ni}_{0.8}\text{Mn}_{0.2}\text{Co}_{0.2})\text{O}_2$ (NMC-811) cathode. Galvanostatic cycling tests showed excellent cycling stability, with a capacity retention of over 90% after 1000 cycles at 2C (100 mAh g^{-1}) with a high 1st discharge capacity of 180 mAh g^{-1} at 30 °C. The OFA $\text{Li}_6\text{PS}_5\text{Cl}$ -NMC811 system demonstrated superior performance, highlighting the effectiveness of the Li_2S -free synthesis method in achieving high-performance solid-state batteries.

We believe that the results of this study have the potential to revolutionize SSE and ASSLB production, significantly contributing to the scientific community's understanding of cost-effective synthesis methods and paving the way for future advancements in one-pot co-precipitation techniques.

References:

1. Miura, A. *et al.*, *Nat Rev Chem*, **3**, 189–198 (2019). <https://doi.org/10.1038/s41570-019-0078-2>
2. Ali, M. *et al.*, *J. Mater. Chem. A*, **10**, 25471–25480 (2022). <https://doi.org/10.1039/D2TA06632G>

8:00 PM EN02.03 .23

Rare-Earth Fluorosulfide Compounds with Fluoride Ion Conducting LayersShintaroTachibana¹, ChengchaoZhong¹, KazutoIde², HisatsuguYamasaki², TakeshiTojigamori², HidenoriMiki², TakashiSaito³, TakashiKamiyama³, KeijiShimoda¹ and YukiOrikasa¹; ¹Ritsumeikan University, Japan; ²Toyota Motor Corporation, Japan; ³High Energy Accelerator Research Organization(KEK), Japan

All-solid-state fluoride-ion batteries (FIBs) are highly attracted attention due to high theoretical energy density and high safety compared with those of conventional lithium-ion batteries (LIBs)[1]. However, it is far from practical use because there is no solid electrolyte which exhibits high ionic conductivity and wide electrochemical potential window at room temperature like lithium-ion conductor. Most of the previously reported fluoride-ion conductors have been limited to the single-anion fluorides with fluorite-type, tysonite-type, and perovskite-type structures [2].

In the field of material sciences, mixed-anion compounds with more than more anions have recently attracted attention. Compared with single-anion compounds such as oxides and fluorides, mixed-anion compounds have the possibility to exhibit innovative functions due to their specific crystal and coordination structure[3]. In mixed anion compounds, combinations of anion species with different ionic radius result in anion-order structures[4]. Fluorosulfides, which contains S^{2-} and F^- with largely different ionic radii, are ideal for creating anion-ordered structures suitable for fluoride-ion conduction. To our best knowledge, there is few reports on the fluoride-ion conductor materials containing mixed-anion compounds.

In this study, we synthesized rare-earth fluorosulfides compounds by solid-state reaction under vacuum[5]. In the crystal structure of these fluorosulfides, the fluoride- and sulfide-ion layers are present across cation layers. The separation of fluoride and sulfide ions is attributed to the difference anionic size. The presence of multiple anions results in the formation of an anion-ordering two-dimensional crystal structure with fluoride ion conducting layers, which cannot be realized for single-anion compounds. The material development of fluoride ion conductors using fluorosulfide compounds is expected to increase crystal structure variations with fluoride-ion conduction pathways.

[1] M. A. Reddy, M. Fichtner, *J. Mater. Chem.*, **21**, 17059-17062(2011).

[2] K. Motohashi, T. Nakamura, Y. Kimura, Y. Uchimoto, K. Amezawa, *Solid State Ionics.*, **338**, 113-120(2019).

[3] H. Kageyama, K. Hayashi, K. Maeda, J. P. Attfield, Z. Hiroi, J. M. Rondinelli, K. R. Poeppelmeier, *Nature Comm.*, **9** 772(2018).

[4] S. Tachibana, K. Ide, T. Tojigamori, Y. Yamamoto, H. Miki, H. Yamasaki, Y. Kotani, Y. Oriokasa, *Chem. Lett.*, **50**(1), 120-123(2021).

[5] S. Tachibana, C. Zhong, K. Ide, H. Yamasaki, T. Tojigamori, H. Miki, T. Saito, T. Kamiyama, K. Shimoda, Y. Oriokasa, Fluorosulfide $\text{La}_{2+x}\text{Sr}_{1-x}\text{F}_{4+x}\text{S}_2$ with a Triple-Fluorite Layer Enabling Interstitial Fluoride-Ion Conduction, <https://doi.org/10.1021/acs.chemmater.3c00188>

8:00 PM EN02.03 .24

Pumice Additives in Iron Oxide for Solid-State Lithium-Ion BatteriesPing-HuanTsai, Tri-RungYew and Kuo-TzuHao; Tsinghua University, Taiwan

Solid-state lithium-ion batteries are indispensable for the next-generation energy storage device because of their safety and lightweight. High-capacity, low-cost, earth-abundance, and low flammability make iron oxides a promising active material for solid-state batteries. However, one of the shortages of both iron oxide actives and solid-state batteries is poor ionic conductivity, causing the short cycle life of batteries.

Pumice, a natural silicon oxide-based porous material formed through volcanic activities, is selected as an additive candidate in iron oxides for solid-state battery applications. Pumice is expected to act as an ion transport path that can effectively reduce the diffusion path length between actives, resulting in lower impedance and overpotential. Therefore, it will lead to a higher rate-capability, shorter reaction time, and enhanced retention. Besides, pumice is earth-abundant and environmentally sustainable. Utilizing pumice as an additive offers a simple method to recycle flooding volcanic pyroclastic flow.

The composition of iron oxide actives with pumice additives will be optimized. The actives will be mixed with carbon black (super P), carboxymethyl cellulose (CMC), and styrene-butadiene rubber (SBR) to form a water-based slurry. The slurry will be further coated on a copper foil through the doctor-blade coating process. The fabricated electrode will be dried in a vacuum oven and then assembled into batteries. The pumice morphology and structure will be characterized by field-emission scanning electron microscopy (FE-SEM) and energy-dispersive X-ray spectrometry (EDX), respectively. Galvanostatic charge-discharge (GCD) and electrochemical impedance spectroscopy (EIS) analyses will be applied to analyze the charge/discharge cycle life, Coulombic efficiency, and impedance resulting from the addition of pumices. These analyses will be used to investigate the mechanism of pumice additives in iron oxides.

This work will offer insights into using pumice additives to enhance the retention of solid-state batteries for future applications.

8:00 PM EN02.03 .25

Titanium Oxide-Based Additives in Iron Oxides as Electrode Materials for Solid-State Batteries HanLee, Jia-ChienMa and Tri-RungYew; National Tsing Hua University, Taiwan

Clean energy technologies, such as electric vehicles (EVs) and stationary energy storage systems (ESSs), have become flourishing along with the increasing awareness of environmental protection in recent years. Rechargeable solid-state batteries (SSBs) exhibit the advantages of light weight, high energy density, good rate-capability, and safety, making them a vital choice for the applications of consumer electronics, EVs, and ESSs. However, poor structural stability and high cost impede the development of SSB's applications.

Iron oxides exhibit the merits of high theoretical capacity, earth-abundance, lower carbon emission, and non-toxicity, suitable for being active materials in SSBs. However, iron oxides show the drawbacks of low electrical and Li-ionic conductivities, high volume expansion and easy to crack, and excess solid-electrolyte interphase (SEI) layers, during charge/discharge reactions. In this work, titanium oxide-based additives will be applied to iron oxides to improve structural stability and ion conductivity. It is expected that the additives can function as stabilizers to improve the structural stability of iron oxides, which can improve cycle stability and rate capability.

The composition of titanium oxide-based additives in iron oxides will be optimized. The additives powders will be mixed with carbon black (super P), carboxymethyl cellulose (CMC), and styrene-butadiene rubber (SBR) to form an aqueous-based slurry. Following that, the slurry will be coated on a copper foil by doctor-blade casting as an electrode and baked in a vacuum oven. After battery assembling, galvanostatic charge-discharge (GCD) and electrochemical impedance spectroscopy (EIS) analyses will be applied to analyze the improvement of cycle-life retention, Coulombic efficiency, and impedance reduction attributed to titanium oxide-based additives. Besides, after charge/discharge cycling, the active materials will be characterized by field-emission scanning electron microscopy (FE-SEM), energy-dispersive X-ray spectroscopy (EDX), and X-ray diffraction (XRD). The results of this work will provide an innovative approach to improving the retention of SSBs by adding additives in iron oxides.

8:00 PM EN02.03 .26

Innovative Gel Polymer Electrolyte for Safe and Long-Lasting Active Implantable Medical Devices MikeMolinski¹, HaileySimon¹, BrianChiou² and ArijitBose²; ¹Audiance, Inc., United States; ²University of Rhode Island, United States

Active implantable medical devices (AIMDs) play a pivotal role in modern healthcare, offering advanced therapeutic solutions for a variety of medical conditions. The power sources within them play a critical role and have demanding performance attributes, namely high energy density, long-term reliability, and exceptional safety. Primary lithium-ion batteries have emerged as a popular choice due to their high energy density, predictable performance, and long cycle life. However, their implementation in AIMDs faces certain limitations, primarily concerning safety considerations as novel more capable devices demand higher battery capacities. AUDIANCE has developed an innovative safe, stable, and non-flammable gel polymer electrolyte (GPE) that address the limitations of current lithium-ion battery technologies and unlocks the potential for use of rechargeable or secondary lithium-ion batteries in AIMDs.

Consisting of a carrier, a high molecular weight polymer, and a conductive lithium salt, the GPE exhibits excellent lithium-ion conductivity of 2.58×10^{-3} S/cm at 37°C and demonstrates a wide electrochemical stability window with a polymer decomposition voltage of about 4.2V. Notably, the mechanical properties of the high viscosity electrolyte are highly composition-dependent, which enables precise control over its rheology, facilitating processability and preventing electrolyte leakage while infiltrating electrode pores. Extensive safety testing has validated the reliability of AUDIANCE's technology. In flammability tests, the electrolyte self-extinguishes, ensuring enhanced safety even during catastrophic failure events. Moreover, nail penetration, overcharge, and external short circuit tests conducted on cells fabricated with the GPE resulted in minimal temperature change and no gas emissions. Long-life cycle testing of LTO/LFP cells demonstrated negligible capacity loss over 4,750 cycles at 37°C, underscoring the stable electrochemical performance and prolonged lifespan of AUDIANCE's batteries.

The outcomes of this research present a promising pathway towards safer and more efficient power sources for AIMDs. The utilization of the novel GPE holds the potential to enhance the reliability and longevity of implantable medical devices, paving the way for novel therapeutic interventions and improving the quality of life for countless patients worldwide.

8:00 PM EN02.03 .27

Thin Single-Ion Solid-State-Electrolyte Film using Covalent Organic Frameworks for Lithium-Ion Cells Rak HyeonChoi and Hye RyungByon; Korea Advanced Institute of Science and Technology, Korea (the Republic of)

Organic solid-state electrolytes have emerged as a solution for developing less flammable and flexible batteries. While polymeric electrolytes have been developed for decades, their practical applications have been hindered by low ionic conductivity and high activation energy at room temperature. Alternatively, a new class of porous and crystalline organic materials called covalent organic frameworks (COFs) shows promise. COFs are highly crystalline materials where desired molecules are periodically bonded to form a two-dimensional layer. The well-ordered stacking of these organic layers extends the three-dimensional structure while creating porous channels. COFs are also mechanically robust and chemically stable, unlike soft and non-crystalline polymer films. By introducing anionic pendants and Li⁺ ions, COFs have been demonstrated as single-ion conductors in previous studies [1,2]. However, the ionic conductivity was still moderated ($>10^{-5}$ S cm⁻¹) at room temperature. This limitation can be attributed to the powder-like form of COFs and their typical fabrication into pellet-type electrolytes, which results in high thickness (>100 μm) and significant interfacial resistances (>1 kΩ), even when mechanical pressure is applied. These factors contribute to challenges such as nonuniform interfacial contact with electrodes and long Li⁺ transport paths.

Here, we developed thin-film COF electrolytes and demonstrated improved Li-ion cell performances. We fabricated COF films with a thickness of approximately 35 μm using a one-pot synthetic method at room temperature. The interfacial resistance of the COF film with metallic Li was approximately 224 Ω, which was 8 times lower than that of the pellet-type ones. For molecular designs, Li⁺ ions and sulfonate functional groups were included in a hexagonal unit of COF. The Li⁺ conductivity of the COF film was highly dependent on the concentration of sulfonic groups and the crystallinity of the film. Higher Li⁺ contents, corresponding to a higher number of sulfonic groups, and better crystallinity resulted in higher ionic conductivity and lower activation energy. Consequently, we achieved an optimum Li⁺ conductivity and transference number of 1.01×10^{-4} S cm⁻¹ and 0.91, respectively, at room temperature. The COF film also exhibited excellent performance in Li|Li symmetric cells at room temperature, with over 1000 hours at 0.1 mAcm⁻² and 0.1 mAhc⁻². Additionally, Li|LiFePO₄ cells using the COF electrolyte delivered a capacity of 150 mAhg⁻¹ at 0.1 C for 150 cycles with negligible capacity fading. In this presentation, I will discuss details of COF film synthesis, several COF designs and their characteristics, and COF-based Li-ion cell performances.

References:

- [1] Kihun Jeong, Sodam Park, Gwan Yeong Jung, Su Hwan Kim, Yong-Hyeok Lee, Sang Kyu Kwak, and Sang-Young Lee., *J. Am. Chem. Soc.*, **2019**, 141, 5880-5885.
- [2] Xing Li, Qian Hou, Wei Huang, Hai-Sen Xu, Xiaowei Wang, Wei Yu, Runlai Li, Kun Zhang, Lu Wang, Zhongxin Chen, Keyu Xie, and Kian Ping Loh., *ACS Energy Lett.*, **2020**, 5, 3498-3506.

8:00 PM EN02.03 .28

Enhancing Low-Pressure Operability of Si Anodes in All-Solid-State Batteries Through Interlayer Engineering and Preolithiation SeunggooJun, Yong BaeSong, HaechannaraLim, Ki HeonBaeck, Eun SuhLee and Yoon SeokJung; Yonsei University, Korea (the Republic of)

The growing demand for vehicle electrification and energy storage systems has spurred research on high-energy-density lithium-ion batteries (LIBs). Solidifying electrolytes using inorganic materials has gained interest due to its potential to enhance energy density and safety. However, challenges, such as dendritic growth and limited Li⁺ diffusion, have impeded the integration of Li metal anodes (LMAs) in all-solid-state batteries (ASSBs). Si anodes, not constrained by the same issues, could present an advantageous alternative. However, in LIBs, Si anodes undergo severe volume changes ($>300\%$) during charge-discharge cycles, leading to fractures and a loss of electrical connectivity. To overcome this, Si is often electrically wired with nanostructured carbonaceous materials like carbon nanotubes (CNTs) and graphene. While this strategy can also be applied to ASSBs, it raises concerns about adverse reactions between carbon materials and SEs. Recent studies reported that the performance of Si ASSBs could be enhanced by eliminating solid electrolytes and carbon additives in Si electrodes, demonstrating 80% capacity retention after 500 cycles at 50 MPa. This performance is attributed to the mechanically sintering ability of lithiated Si and the lack of destructive side reactions. However, the high operating pressures used need to be addressed for practical applications.

In our study, we present a comprehensive Si ASSB design incorporating a thin metallic interlayer at the Si electrode-SEs interface and integrating the Si electrodes with CNTs. This interlayer allows Li⁺ transport maintenance across the interface despite the dimensional changes of Si anode, demonstrating improved performance of ASSBs under low-pressure conditions.

[1] H. S. Tan Darren et al., *Science* **2021**, 373, 1494.

[2] D. H. Kim et al., *J. Power Sources* **2019**, 426, 143-150.

8:00 PM EN02.03 .29

Stabilizing Li Metal/Argyrodite Interface for Sulfide-Based All-Solid-State Lithium Batteries Hui-TaeSim, OHMyung-keun, Ye-EunPark, Hyo-JinKim and Dong-WonKim; Hanyang University, Korea (the Republic of)

The achievement of carbon neutrality is the first step in addressing the issue of global climate change. Rechargeable batteries with high energy density are one of the promising techniques to reduce carbon emission. After the commercialization of lithium-ion batteries (LIBs) in 1991, rechargeable LIBs have been universally applied in portable electronic to electric vehicles. However, the conventional LIBs using liquid electrolytes have serious safety problems such as flammability, solvent leakage, and explosion under unusual conditions. In addition, the use of Li metal anode (3860 mAh g⁻¹) with high specific capacity tends to exacerbate risks due to the interfacial side reactions and dendrite growth of lithium. In this respect, all-solid-state lithium metal batteries (ASSLMBs) have attracted attention as the most promising high energy density storage system. Among various solid electrolyte systems, sulfide electrolytes are being widely studied due to their high ion conductivity and ductile property. However, the lithium dendrite growth can be also occurred in sulfide based-ASSLMBs because of voids, cracks, grain boundaries in solid electrolyte, and side reactions between Li and solid electrolyte.

In this work, the surface modification of Li was performed using LiNO₃ with nitrogen-based solvent. The protective layer formed on Li metal was composite of organic and inorganic materials based on Li₃N. The symmetric Li/solid electrolyte/Li cell with protective layer exhibited good cycling stability without short circuit, indicating the uniform plating/stripping of lithium and good interfacial properties. Consequently, an all-solid-state lithium battery assembled with LiNi_xCo_yMn_{1-x-y}O₂ cathode delivered a high initial discharge capacity and exhibited good cycling stability.

8:00 PM EN02.03 .30

Unlocking High-Performance Quasi-Solid-State Multivalent Metal Ion Batteries Sarah K.W.Leong, WendingPan and DennisLeung; University of Hong Kong, Hong Kong

In the pursuit of advancing post-Li-ion battery technology, the development of rechargeable Mg batteries has shown tremendous promise due to their high theoretical capacity, material abundance, and low cost. However, the passivating nature of Mg, particularly in aqueous solutions, presents a significant obstacle. The practicality of Mg anodes within aqueous electrolytes has been largely dismissed due to the perceived lack of reversibility and narrow electrochemical window, leading researchers to focus on non-aqueous systems. Nonetheless, non-aqueous electrolytes also suffer from poor ionic conductivity, high cost, and safety hazards such as flammability and toxicity.

This work addresses these challenges by introducing a pioneering quasi-solid-state magnesium-ion battery (QSMB), designed to harness the advantages of both aqueous and non-aqueous systems. By immobilizing the electrolyte's water network, the polyethylene polymer polymer suppresses the hydrogen evolution reaction at the magnesium metal anode, and achieves a fully reversible Mg dissolution and deposition chemistry through a Cl-induced transformation of the impermeable passivation film into a conductive metallic oxide complex.

The quasi-solid-state electrolyte also plays a major role in attaining high voltage and capacity by facilitating true multivalent Mg ion storage. Through confining the hydrogen bond network, the electrolyte effectively impedes proton insertion which competes with multivalent metal-ion insertion in aqueous batteries. In this study, in-situ characterizations reveal that the electrolyte promotes the high-voltage (de-)intercalation of both Mg²⁺ and MgCl₃⁻ ions instead, delivering unparalleled battery performance.

The QSMB showcases a remarkable energy density of 264 Wh kg⁻¹—nearly five times higher than its aqueous Mg-ion counterparts, and a voltage plateau (2.6-2.2 V) that surpasses other Mg-ion batteries. Moreover, it retains an impressive 90% capacity after 900 cycles, even at subzero temperatures (-22°C). By leveraging the high ionic conductivity from aqueous systems and a broad electrochemical window from non-aqueous systems, the quasi-solid-state battery represents an innovative avenue for the design of high-performing Mg-ion batteries.

More importantly, this study provides invaluable insights into interphase passivation, metal stripping and plating mechanisms at the anode, and ion storage regulation at the cathode to produce high-energy, rechargeable, solid-state battery technologies. This quasi-solid-state approach could be extended to the design of other multivalent metal-ion batteries, including Zn-ion and Al-ion batteries, demonstrating the potential for broader applications.

8:00 PM EN02.03 .31

Mechanical Design Strategies in Facilitating Durable Ni-Rich Layered Cathodes for Lithium-Ion Batteries SanghoYoon, JaewoonLee and DuhoKim; Kyunghee University, Korea (the Republic of)

Along with the growth of the electric vehicle market, the Ni-rich layered oxides (x≥0.8) for cathode active materials have attracted great attention because their high Ni content provides high-energy-density to meet the needs of high-energy-density applications. However, the large amount of Ni often results in severe micro-crack propagation that causes capacity degradation due to structural instability such as heterogeneous phase transformations and anisotropic structural changes under high charging voltage conditions. Until recently, many previous studies have focused on inhibiting micro-crack formation due to structural instability, specifically the anisotropic lattice variation that leads to mismatch of primary particles in Ni-rich layered oxides upon repeated (de)intercalation. While the degradation mechanisms by which anisotropic lattice variation act between primary particles have been identified, the mechanism inside the particles is not yet fully understood. In this regard, a more systematic and comprehensive study could be required to explore the mechanisms of anisotropic behavior inside particles in Ni-rich layered oxides. Additionally, through advanced experimental analysis and computational calculations, a comparison of the thermodynamic features of Ni-rich layered oxides (Li[Ni_xCo_yMz]O₂, where M represents the transition metal) reveals similar phase transitions (H1 (hexagonal 1)→M (monoclinic)→H2→H3) regardless of the transition metal M. However, the cycle retention varies significantly depending on the composition of the transition metal.

In this work, to understand these undesired phenomena, we systematically apply thermodynamic, chemo-mechanic, and physicochemical perspectives to analyze the correlation between (in)coherent phase separation and volume conservation behavior to propose an opposite view of the traditional aspect of anisotropic lattice variation and a new design strategy for single-crystal Ni-rich layered cathodes that reduces the internal stress between separated phases to zero grain internal stress. First, we analyzed the (in)coherent phase separation of Li_{1-x}[Ni_{10/12}Co_{1/12}Mn_{1/12}]O₂ (NCM) and Li_{1-x}[Ni_{10/12}Co_{1/12}Ti_{1/12}]O₂ (NCT) by comparing the thermodynamic phase stability during the whole delithiation process along the formation energy of mixing enthalpy and found that NCT was thermodynamically more stable and relatively coherent phase separation occurred than commercial NCM. Furthermore, for a direct understanding of the cycle degradation mechanism by (in)coherent phase separations, we calculate the directional lattice strain and volumetric variation for NCM and NCT combined with phase transition. Interestingly, upon volume change, both oxide models exhibited volume-conserving regions due to anisotropic lattice changes, which resulted in a relative decrease in internal stress. Moreover, the NCT exhibits near zero volumetric lattice variation. Based on the correlation between thermodynamics and the volumetric lattice misfit, the oxygen bond populations for both oxide models are identified, and a severe reduction is observed across the entire oxygen framework in the incoherent phase separation model NCM, whereas a preserved feature is observed in the coherent phase model NCT. These systemically novel concepts underpin the Ti-induced “zero volumetric misfit” concept makes coherent phase separation. These concepts are expected to play a global role in the layered oxide cathodes, and it provides a crucial design strategy leading to the enhancement of cycle retention for durable high-energy-density LIBs.

8:00 PM EN02.03 .32

Effect of Various Carbon Nanomaterials as Conductive Additives in EDLC VladimirPavlenko¹, ZhanibekAyaganov² and AnnieNg¹; ¹Nazarbayev University, Kazakhstan; ²Al-Farabi Kazakh National University, Kazakhstan

A comprehensive study was performed to investigate the effect of different carbon nanomaterials including single-walled carbon nanotubes, graphene nanoplatelets, activated carbon nanofibers and fullerene C60 on the performance of aqueous-based electric double layer capacitors (EDLC) based on a neutral aqueous electrolyte (Li₂SO₄). The performance of commercially available and laboratory synthesized carbon nanomaterials having different morphologies were investigated and compared with carbon black C45 which is widely used as conductive additive. Electrochemical studies were performed by cyclic voltammetry, galvanostatic charge-discharge and impedance spectroscopy. It is found that conductive additives exhibit limited effectiveness in EDLC capacitance at low current densities, while at high current loads the discrepancies of EDLC's performance become pronounced. The use of activated carbon nanofibers having large surface area synthesized from polyacrylonitrile by electroforming increases the specific capacitance by 16%, energy efficiency by 7% and energy densities by 22% at current densities equal to 20 A/g. The addition of conductive additives with a small specific surface area leads to a decrease in the characteristics of the EDLCs. The results provide important information for the community to develop new energy conversion and storage devices.

8:00 PM EN02.03 .33

Charge Separation Nanoclay in Gel Polymer Electrolytes: Empowering Sustainable Anion Storage SunghoKim and SoojinPark; Pohang University of Science and Technology, Korea (the Republic of)

The dual-ion battery (DIB) represents a significant advancement in sustainable energy storage. It employs intercalation-type graphite as a cathode, enabling anion penetration into interlayers during high-potential charges, resulting in an elevated operational voltage exceeding 5V. DIBs distinguish themselves from conventional lithium-ion batteries by moving away from transition metal oxide cathodes, like Lithium cobalt oxide (LCO), offering a more eco-friendly and cost-effective alternative. However, DIBs face challenges due to high operating voltages causing electrolyte decomposition, which leads to a passivation layer on the electrodes, increased resistance, and potential performance degradation.

To tackle the issue of electrolyte decomposition, researchers are exploring high-concentration electrolytes (HCE) enriched with lithium salts. These electrolytes predominantly contain contact ion pairs (CIP) and aggregates (AGG), enhancing electrochemical stability. Notable efforts have been made using a 4.0 M LiFSI in TMS, but increased salt concentrations lead to higher viscosity, reducing ionic conductivity.

Another approach is incorporating gel polymer electrolyte (GPE), known for its high voltage stability, moderate ionic conductivity, and safety attributes. However, as ionic conductivity increases, mechanical integrity decreases. To address this, functional groups are added to the polymer matrix, reducing anion-solvent interactions and promoting a stable anode interface. Nevertheless, a trade-off remains between physical rigidity and ionic conductivity.

Additives are essential to enhance GPE mechanical stability and modify ion solvation. These additives include carbon-based conductive fillers, ceramics, polymers, and nanoparticles, improving ion conduction and cell performance. Facilitating anion mobility and integration is crucial for optimizing dual-ion battery performance, necessitating additives that dynamically interact with anions, promote a stable surface interface, and align with sustainability standards.

This study explores GPEs infused with surface-charged nano clay as an innovative additive for DIBs. Nanoclay, due to its abundant availability and non-toxic nature, enhances GPE's mechanical resilience and influences cation and anion solvation structures. The investigation involves a comparative analysis of three nano clay variants with distinct characteristics. Zeta potential, nuclear magnetic resonance (NMR), molecular dynamics (MD) simulations, and density functional theory (DFT) calculations confirm the findings.

Halloysite (HS), with its tubular morphology, stands out as a superior candidate. It fosters a slender, homogeneous cathode electrolyte interface (CEI) with reduced anion-solvent interactions and fewer salt decomposition products. The tubular structure of HS improves anion transport pathways, optimizing DIB operation. Consequently, a DIB full-cell incorporating HS-GPE exhibits impressive rate capability, exceeding 60 mAh/g at 50 C-rate, and remarkable stability, sustaining over 5000 cycles at 20 C-rate.

8:00 PM EN02.03 .34

Unexpected Lowering of Charge Transfer Resistance in Ultra-Long Cycled (>30,000 cycles) Solution-Processed Lamellar-Crystalline Li_3VO_4 Anodes Tejveer S. Anand, Aashish Joshi, Amit Gupta and Madhusudan Singh; Indian Institute of Technology Delhi, India

Transition metal oxide-based anodes such as Li_3VO_4 (LVO) offer alternatives to commercial graphite based device architectures in lithium-ion batteries. Traditional methods of synthesis of LVO - solid state synthesis and hydrothermal, have typically resulted in moderate half-cell (LVO||Li) lifetime, thereby limiting its practical applicability [1]. In this work, we explore the impact of an alternative synthesis - a surfactant-free sol gel process on long cycling stability and an unexpected high charge (C)-rate performance. Ammonium metavanadate (Sigma-Aldrich) precursor was mixed in 2-methoxyethanol to form a solution (A), while lithium acetate dihydrate was mixed in the same solvent to form another solution (B). Solution B was added dropwise to A while being vigorously stirred (48 hr, 60°C). The product LVO was annealed (800 °C, 4 hr) prior to materials analysis. Powder X-ray diffraction (PXRD, Rigaku Ultima) reveals an orthorhombic phase with the Pmm21 space group [2], with Rietveld refinement yielding lattice constants: $a=5.448 \text{ \AA}$, $b=6.327 \text{ \AA}$, and $c=4.949 \text{ \AA}$. Solid-state UV-Vis spectra (Perkin-Elmer) reveals a wide band gap (3.95 eV). High-resolution transmission electron microscopy (HRTEM, JEOL with a selected area electron diffraction (SAED) attachment) data shows non-ring like diffraction spots, suggesting a high degree of crystallinity, with formation of lamellar flakes. The active material (LVO) was mixed with super-P carbon black: carbon multiwall nanotubes with n-methyl pyrrolidinone with polyvinylidene fluoride (PVDF) binder to form a slurry, subsequently coated on a copper foil and dried at 80°C. Electrodes were punched out from the coated copper foil, and assembled using a standard process to form a CR2016 cell. The LVO||Li half-cell was found to deliver a capacity (Biologic BC810 battery cycler/Neware) of 764 mAh/g at a current density of 0.7 A/g when deeply discharged to 0.02 V. During the rate performance test; there is a 10.26% decrease in the intercalation potential of the cell, with a change in current density from 0.7 A/g to 3.5 A/g. Further testing of the cell at a current density of ~13.5 A/g for over 30,000 cycles has shown that it can still deliver a specific discharge capacity of ~155 mAh/g at the 15000th cycle (asymptotic point), with a coulombic efficiency (CE) of >95%. After 30000 cycles of persistent deep charging (3 -> 0.02V), the cell can still deliver a capacity between 100-160 mAh/g. The estimated fading in the discharge capacity in the cycle range [15000, 30000] is ~0.002 mAh/g. We observe a rise in the initial capacity of the LVO||Li cell till it reaches the asymptotic point. Electrochemical impedance spectroscopy (EIS) measurements for aged cells indicate a lower charge-transfer resistance compared to the fresh cell at the discharge state, suggesting that the solid electrolyte interface (SEI) layer holds no barriers for lithium ions diffusion inside the material. The pre-lithiated LVO||Li cell is combined with the commercially available LiFePO_4 (LFP) cathode to form a full cell using a similar assembly procedure. The full cell is cycled (>1000 cycles) with an initial capacity of 165 mAh/g at 0.15 A/g between 1-3.5 V. Interestingly, post-cycling TEM results indicate that the lamellar morphology remains intact even after 30,000 cycles of continuous charging and discharging under high-rate conditions. We are carrying out additional ex-situ analysis, including techniques such as time-of-flight secondary ion mass spectrometry (ToF-SIMS) to elucidate the distribution of Li and operation byproducts such as the SEI layer in the cycled cell for better understanding of the mechanism.

[1] Su, et al, J. Energy Storage, 72, B, 108454 (2023).

[2] Song, et al, J. Mater. Sci. Technol., 140, 142-152 (2023).

8:00 PM EN02.03 .35

Three-Dimensional Mesopore-Rich Hierarchical Carbon Derived by Metal-Organic Framework *In-Situ* Anchored on Silk Fiber for Ultrahigh Capacitance/Surface Area Ratio Supercapacitors Syun Hong Chou, Ta-Chung Liu and San-Yuan Chen; National Yang Ming Chiao Tung University, Taiwan

Heteroatom-doped hierarchical porous carbonaceous materials are promising supercapacitor electrode materials due to their large energy density, decent electronic conductivity, and efficient pore kinetics for ion migration. Here, a unique N-doped honeycomb-like porous carbon engineered by carbonized silk fibroin (SF) scaffold functionalized with a cobalt-based metal-organic framework (MOF, ZIF-67) is demonstrated for supercapacitor electrode (AC-Z@SF). The well-dispersive Co ions were anchored in silk fibroin via coordination covalent bonding as seeding sites for in-situ growth, thereby preventing the aggregations and promoting an instantaneous interaction between activation agent and active carbon atoms to generate interconnected micro/meso/macropores instead of blocking them during carbonization. The unique honeycomb-like interconnected mesopore-rich structure, AC-Z@SF, exhibits 431 F/g at 0.5 A/g and retains 70 % (300 F/g, a value which is 5 times higher than the MOF-derived carbon) at an ultra-high current density of 50 A/g, as well as an excellent lifetime of 89% after 20,000 cycles. The first time this study unveils that interconnected small-sized mesopores (2-10 nm) play an important role in boosting the SSA utilization for electric double-layer capacitance and providing a new direction for the design of hierarchical carbon materials.

8:00 PM EN02.03 .36

Synthesis and Characterization of Transition Metal Doped Lithium Composites for Application in Lithium Ion Based Batteries Neeraj Chauhan^{1,2}, Amrit PalToor¹, Stefan Krause² and Alok Srivastava¹; ¹Punjab University, India; ²University of Birmingham, United Kingdom

The research aims to enhance the physicochemical and electrochemical properties of cathode materials for application in lithium-ion batteries, specifically $\text{Li}_2\text{TMSiO}_4$ (TM=Transitions metals) silicates. These materials have high theoretical capacity, but most often suffer from poor conductivity. To improve their performance, methods like particle size reduction, coating, and ion doping were being employed. Among different transition metals-based silicates, $\text{Li}_2\text{MnSiO}_4$ is of particular interest, but often faces issues with cycling performance due to low conductivity and stability. Further, the structural characterization of the different lithium composites had shown that $\text{Li}_2\text{CoSiO}_4$ exhibited high crystallinity with an orthorhombic crystal structure. Therefore, trivalent ions doping and anionic doping were carried out to enhance conductivity and electrochemical properties of $\text{Li}_2\text{MnSiO}_4$ and $\text{Li}_2\text{CoSiO}_4$ silicates. The resulting silicates i.e. LiMnAlSiO_4 and LiMnCoAlSiO_4 displayed patterns similar to $\text{Li}_2\text{MnSiO}_4$, indicating a mixture of polymorphs. The addition of dopants did not only alter the structure but significantly improves the properties of the silicates. In terms of electrical characterization, cyclic voltammetry measurements showed different potential values for the composites, where $\text{Li}_2\text{CoSiO}_4$ displayed cathodic and anodic potentials with slight variations and a decrease in cathodic current after 10 cycles. LiMnAlSiO_4 showed stable potentials but a 28% drop in current, while LiMnCoAlSiO_4 had minimal changes in potentials and currents. Moreover, the electrochemical impedance spectroscopy demonstrated that LiMnAlSiO_4 and LiMnCoAlSiO_4 had undergone least charge transfer resistance compared to $\text{Li}_2\text{CoSiO}_4$, indicating improved Li^+ ion diffusion. Based on these results, LiMnCoAlSiO_4 showed better stability, resistance and conductivity compared to LiMnAlSiO_4 and $\text{Li}_2\text{CoSiO}_4$. Further investigations will be carried out to explore the thermal stability of the composites beyond 400°C and to evaluate the potential of LiMnCoAlSiO_4 as an electrode material. Overall, the study demonstrated the ortho-rhombic structures of transition metal-doped Li_3SiO_4 composites and highlighted the superior performance of the quaternary composite LiMnCoAlSiO_4 in terms of electrical conductivity, capacitance, and structural stability.

8:00 PM EN02.03 .37

High Conductivity in Na^+ -Ion Conducting Solid Electrolytes for Na-Ion Batteries Through a Co-Doping Strategy Xuankai X. Huang and Isaac Abrahams; Queen Mary University of

Rechargeable batteries are regarded as the most promising energy storage technology because of their reliability and high energy conversion efficiency. Although Li-ion batteries (LIBs) have been widely used in portable electronic devices, Na-ion batteries (NIBs) are considered as a potential candidate to replace LIBs because of their non-toxicity, low cost, and elemental abundance.

Solid state sodium-ion batteries are seen as potentially cheaper and safer alternatives to current lithium-ion battery systems. The replacement of the presently used liquid electrolytes by non-flammable solid electrolytes is an important avenue to create safer batteries, while the high natural abundance of sodium compared to lithium would allow for significant cost reduction. The sodium superionic conductor, NASICON, first reported by Hong, is one of the best-known sodium-ion conducting solid electrolytes, displaying high bulk ionic conductivity and good stability toward NASICON-based electrodes. However, the practical use of NASICON has been impeded by low ion mobility at room temperature and poor interfacial connectivity.

Here, the improvement of total conductivity has been achieved via La and Zn co-doping of NASICON. Total conductivity values of $4.68 \times 10^{-3} \text{ S cm}^{-1}$ at room temperature and $2.89 \times 10^{-2} \text{ S cm}^{-1}$ at 100°C were obtained for NZSP-LZ-0.2, which are amongst the highest values recorded for a NASICON based system. Furthermore, the system shows good air stability and could represent a suitable material for application in the field of Na-ion batteries. Symmetric cells with sodium metal as electrodes ($\text{Na} | \text{NZSP-LZ-0.2} | \text{Na}$) are assembled and cycled stably for over 3000 cycles at a current density of 0.2 mA/cm^2 .

8:00 PM EN02.03 .38

Thermodynamics of Multi-Sublattice Battery Active Materials: From an Extended Regular Solution Theory to a Phase-Field Model of $\text{LiMn}_x\text{Fe}_{1-y}\text{PO}_4$ Pierfrancesco Ombrini; Delft University of Technology, Netherlands

Phase separation during the lithiation of redox-active materials is a critical factor affecting battery performance, including energy density, charging rates, and cycle life. Accurate physical descriptions of these materials are necessary for understanding underlying lithiation mechanisms, performance limitations, and optimizing energy storage devices. This work presents an extended regular solution model that captures mutual interactions between sublattices of multi-sublattice battery materials, typically synthesized by metal substitution. We apply the model to phospho-olivine materials and demonstrate its quantitative accuracy in predicting the composition-dependent redox shift of the plateaus of $\text{LiMn}_x\text{Fe}_{1-y}\text{PO}_4$ (LFMP), $\text{LiCo}_x\text{Fe}_{1-y}\text{PO}_4$ (LFCP), $\text{LiCo}_x\text{Mn}_y\text{Fe}_{1-x-y}\text{PO}_4$ (LFMCP), as well as their phase separation behavior. Furthermore, we develop a phase-field model of LFMP that consistently matches experimental data and identifies $\text{LiMn}_{0.4}\text{Fe}_{0.6}\text{PO}_4$ as a superior composition that favors a solid solution phase transition, making it ideal for high-power applications.

8:00 PM EN02.03 .39

Formulating Electron Beam-Induced Covalent Linkages for Stable and High-Energy-Density Silicon Microparticle Anode Minjun Je and Soojin Park; Pohang University of Science and Technology, Korea (the Republic of)

High-capacity silicon (Si) materials hold a position at the forefront of advanced lithium-ion batteries. The inherent potential offers considerable advantages for substantially increasing the energy density in batteries, capable of maximizing the benefit by changing the paradigm from nano- to micron-sized Si particles. Nevertheless, intrinsic structural instability remains a significant barrier to its practical application, especially for larger Si particles. Here, we first report a covalently interconnected system employing silicon microparticles ($5 \mu\text{m}$) and a highly elastic gel polymer electrolyte (GPE) through electron beam irradiation. The integrated system mitigates the substantial volumetric expansion of pure Si, enhancing overall stability, while accelerating charge carrier kinetics due to the high ionic conductivity. Through the cost-effective but practical approach of electron beam technology, the resulting 500 mAh-pouch cell showed exceptional stability and a high volumetric energy density of 1022 Wh L^{-1} , highlighting the feasibility even in current battery production lines.

8:00 PM EN02.03 .40

Hierarchical 3D Electrode Design with High Mass Loading Enabling High-Energy-Density Flexible Lithium-Ion Batteries Jaeho Jung, Dong-Yeob Han and Soojin Park; POSTECH, Korea (the Republic of)

Flexible lithium-ion batteries (LIBs) have garnered considerable attention due to their increasing utilization in flexible and wearable electronic devices. However, the practical implementation of flexible LIBs in these devices has been hindered by the dual challenge of attaining both high energy density and exceptional flexibility. In this study, we introduce a hierarchical 3D electrode (H3DE) with a substantial mass loading capacity, which enables the creation of highly flexible LIBs boasting an exceptionally high energy density.

The H3DE boasts a bicontinuous architecture, ensuring that active materials and conductive agents are uniformly dispersed throughout the 3D framework, irrespective of the specific type of active material employed. This seamless integration of the electrode and electrolyte facilitates rapid ion and electron transportation, thereby enhancing redox kinetics and reducing internal cell resistance. Furthermore, the H3DE displays remarkable structural resilience and flexibility even under repeated mechanical deformations.

Capitalizing on these remarkable physicochemical attributes, pouch-type flexible LIBs employing the H3DE exhibit consistent cycling performance under various bending conditions. They achieve a groundbreaking energy density of 438.6 Wh kg^{-1} and 20.4 mWh cm^{-2} , as well as an areal capacity of 5.6 mAh cm^{-2} , surpassing the performance of all previously documented flexible LIBs. This research offers a practical solution for the development of high-energy-density flexible LIBs suitable for a wide array of energy storage devices.

8:00 PM EN02.03 .41

Pseudo-High Entropy Alloys for Ni-MH Batteries Gulhan Cakmak and Hakan Yüce; Mugla University, Turkey

With the increase in the demand for renewable energy sources with the decarbonization targets of the countries, energy storage systems are also developing rapidly. Among these systems, nickel metal hydride (NiMH) batteries stand out as a remarkable energy storage solution. Recently, several studies have clearly demonstrated that AB compounds are promising materials as a metal hydride (MH) electrode for Ni-MH batteries. The studies related to AB interstitial hydrides mainly focusing Ti-V based systems. Ti-Cr-V based alloys with an AB structure, can both absorb nearly 2.5 wt.% hydrogen and desorb hydrogen at 40°C (Tamura, 2002). However, it is difficult to achieve a greater hydrogen absorption capacity in these systems because these alloys consist of relatively heavy transition metals. It could be possible to reach higher gravimetric capacities by using lighter elements. Mg-Co (Zhang, 2005), Mg-Ni (Shao, 2009), Mg-Ni-B (Shao, 2009) and Mg-Tm-V (Tm: transition metals) binary and ternary alloys have been successfully achieved with AB structure. A storage capacity of 3 wt.% was reported in a binary alloy with the compound MgCo (Zhang, 2009). The concept of "high entropy alloys" is a rather new concept which has drastically modified the alloy design. In this concept, the classical alloys which are based on a base metal with added alloying elements are replaced by a nearly equimolar multi-component alloys. With the development of the concept non equimolar compounds are also possible.

In this study we prepared Mg-containing AB multi-component alloys with light elements capable to store hydrogen. Here A is Mg due to its lightweight, high theoretical hydrogen storage capacity and abundance but Ni- is replaced by equimolar alloying elements. Thus, we aim to produce pseudo high entropy alloys in that Mg is still the dominant element. These $\text{Mg}_{0.5} \text{Al}_{0.125} \text{Cr}_{0.125} \text{Ni}_{0.125} \text{Fe}_{0.125}$ and $\text{Mg}_{0.5} \text{Al}_{0.125} \text{Cr}_{0.125} \text{Ni}_{0.125} \text{V}_{0.125}$ are tested electrochemically in Ni-MH batteries.

This work was supported by TUBITAK (The Scientific and Technological Research Council of Turkey) with project Number 121N774, which the authors gratefully acknowledge.

References

- Shao, H., Asano, K., Enoki, H., & Akiba, E. (2009). Fabrication and hydrogen storage property study of nanostructured Mg-Ni-B ternary alloys. *Journal of Alloys and Compounds*, 479(1–2), 409–413. <https://doi.org/10.1016/j.jallcom.2008.12.067>
- Tamura, T., Kazumi, T., Kamegawa, A., Takamura, H., & Okada, M. (2002). Effects of Protide Structures on Hysteresis in Ti-Cr-V Protium Absorption Alloys * 1. In *Materials Transactions* (Vol. 43, Issue 11).
- Zhang, Y. huan, Ren, H. ping, Li, B. wei, Guo, S. hai, Pang, Z. guang, & Wang, X. lin. (2009). Electrochemical hydrogen storage characteristics of nanocrystalline and amorphous $\text{Mg}_{20}\text{Ni}_{10-x}\text{Co}_x$ ($x=0-4$) alloys prepared by melt spinning. *International Journal of Hydrogen Energy*, 34(19), 8144–8151. <https://doi.org/10.1016/j.ijhydene.2009.07.097>
- Zhang, Y., Tsushio, Y., Enoki, H., & Akiba, E. (2005). The study on binary Mg-Co hydrogen storage alloys with BCC phase. *Journal of Alloys and Compounds*, 393(1–2), 147–153. <https://doi.org/10.1016/j.jallcom.2004.09.06>

8:00 PM EN02.03 .42

Deciphering Constriction Impedance in Solid State Batteries and its Connection to Ionic Conductivity Sunny Wang, Edward Barks and William C. Chueh; Stanford University, United States

Current constriction phenomena pose significant challenges at the Li metal interface of solid state batteries. Typically these effects are associated with contact loss and void formation during Li metal stripping. In this work, we use current biased and pressure dependent electrochemical impedance spectroscopy measurements alongside finite element modelling to clarify the different origins of constriction impedance at the Li metal interface. We show that constriction impedance is not solely derived from void formation and ionically resistive surface layers can also generate the same response. The relation between constriction and conductivity is also emphasized; ionically resistive components can significantly increase the constriction resistance in solid state batteries even with identical contact geometries.

8:00 PM EN02.03.43

Study of Amorphous Vanadium Oxide Cathodes for Li-Ion Batteries Prepared by Reactive Magnetron Sputtering Mackarena Briceño, Juan Fernandez, Marcos Flores and Rodrigo Espinoza; Universidad de Chile, Chile

Within the technological development focused on lithium-ion batteries, vanadium pentoxide (V_2O_5) thin films have been a good candidate to be used as cathodic material due to their high-capacity charge, allowing to increase in the efficiency of lithium-ion batteries [1]. The technique of reactive magnetron sputtering allows the manufacture of homogenous thin films with low thicknesses and specific microstructure. In addition, with this technique we can generate different stoichiometries of vanadium oxides and specifically of V_2O_5 [2-3]. The formation of different vanadium oxides mainly depends on the oxygen content of the system [4]. The aim of this work is based on the preparation of thin films of vanadium oxides on steel substrate by reactive sputtering at different oxygen flows followed by reduction with hydrogen *in situ*, and their electrochemical evaluation as a potential cathode material. The target was metallic vanadium, while the plasma was argon (15 sccm) combined with oxygen at 1.25, 1.75, 2.25, 2.5, 3.0 and 3.25 sccm. The samples were characterized by XRD, EDS, Raman confocal spectroscopy, XPS and AFM. Cyclic voltammograms, the charge/discharge processes and cyclability of batteries were studied. XRD results demonstrated that the samples were amorphous for all the different oxygen flows. Raman analysis indicated the presence of the V-O-V bonding corresponding to a crystalline structure of the rhombohedral type of V_2O_5 , by the vibrational stretching modes (143 cm^{-1}), and of the V=O bonding by the second flexion vibrational band (995 cm^{-1}) for the sample deposited at 3.0 sccm of oxygen. XPS established a correlation between the oxygen flow and the main V oxidation state: V^{+4} at 1.25 O-flow, V^{+4}/V^{+3} at 1.75 O-flow, and V^{+3} over 2.5 O-flow. The sample of 3.0 sccm of oxygen at 1 hour of deposition has a capacity of 295 mAh/g with a charge retention percentage of 96.5% at 50 charge/discharge cycles at 1C. The electrochemical behavior of the samples in reduction with hydrogen, shows a better retention percentage of 99.9% at 50 charge/discharge cycles at 1C, but not an improvement in the charge and discharge capacity, which is 213 mAh/g for the sample of 3.0 sccm of oxygen at 8% $p\text{f H}_2$.

We acknowledge the financial support of the national fellowship sponsored by ANID.

References

- [1] R. Marom, S.F. Amalraj, N. Leifer, D. Jacob, D. Aurbach, J. Mater. Chem. 21 (2011) 9938-9954.
- [2] H. Song, C. Liu, C. Zhang, G. Cao, Self-doped $V_4^{+}V_2O_5$ nanoflake for 2 Li-ion intercalation with enhanced rate and cycling performance. Nano Energy. 22, 1–10 (2016).
- [3] Kim TA, Kim JH, Kim MG, Oh SM (2003) Li⁺ storage sites in amorphous V_2O_5 prepared by precipitation method. J Electrochem Soc 150(7): A985–A9A9.
- [4] L.-J. Meng, R.A. Silva *et al.*, Thin Solid Films, 515(1), 195–200(2006).

SESSION EN02.04: Polymer Electrolyte
Session Chairs: Yi Lin and Amy Marschilok
Tuesday Morning, November 28, 2023
Hynes, Level 3, Room 304

8:00 AM EN02.04.01

Single-Ion Conducting Borate Network Polymer Electrolytes for Lithium Metal Batteries with Excellent Rate Capability Jingyi Gao and Dong-Myeong Shin; University of Hong Kong, Hong Kong

Although it is possible to readily estimate the theoretical energy densities of battery chemistries, the molecular processes that hinder practical performance are still unknown. Especially, the charging and discharging rates have become a major limiting factor in energy storage applications. Several solid electrolytes with exceptional ionic conductivity have been discovered, but all solid-state batteries with high energy density have been only realized at limited rates (close to equilibrium), indicating that the minimization of overpotential requires to be considered to improve the rate performance other than the ionic transport. As single-ion polymer electrolytes, in which only selective cations are mobile across polymer electrolytes, facilitate minimizing not only the concentration gradient but also the overpotentials in the cells, such electrolytes pose great potential for overcoming these problems. However, single-ion polymer electrolytes have suffered from low ionic conductivity ($<10^{-5}\text{ S cm}^{-1}$ at ambient temperature) which is at least two orders of magnitude smaller than that of liquid electrolytes. In this talk, I will present our ongoing efforts to develop a new class of single-ion conducting polymer electrolytes using an interpenetrated network polymer with weakly coordinating anion nodes, with a wide electrochemical stability window, a high room temperature conductivity of up to $1.5 \times 10^{-4}\text{ S cm}^{-1}$, and exceptional selectivity for Li-ion conduction ($t_{Li^+} = 0.95$). Significantly, lithium metal battery prototypes containing these electrolytes are shown to outperform a conventional battery featuring a polymer electrolyte.¹⁻³

References

1. Shin; Bachman; Taylor; Kamcev; Park; Ziebel; Velasquez; Jarenwattananon; Sethi; Cui; Long, Adv.Mater. (2020) **32**, 1905771.
2. Gao; Wang; Han; Shin, Chem. Sci. (2021) **12**, 13248-13272.
3. Gao; Zhou; Wang; Ma; Jiang; Kim; Li; Liu; Xu; Shum; Feng; Shin, Chem. Eng. J. (2022) **450**, 138407.

8:15 AM EN02.04.02

Enabling Low T_g Ester-Functionalized Polysiloxane Electrolytes for Lithium-Metal Batteries Utilizing Semi-Interpenetrating Networks Jannik Petry, Markus Dietel and Mukundan Thelakkat; University of Bayreuth, Germany

Lithium-ion battery technology is dominating the electrochemical energy storage industry. To access higher energy densities, all solid-state lithium-metal batteries (LMB) utilizing elemental lithium as anode material are of high research interest. Commonly used liquid electrolyte systems are not compatible towards lithium-metal anodes, due to lithium dendrite formation and safety issues during cycling; requiring new classes of solid-state ion-conductors. In this regard, polyether-based electrolytes have been studied extensively because of their low glass transition temperature (T_g) and high solubility of lithium salts. However, the strong Li-ion/ether-oxygen interactions result in low effective lithium-ion conductivities. In addition, the inherent crystallinity of poly(ethylene oxide) (PEO) allows its application only to temperatures above its melting point ($65\text{ }^\circ\text{C}$). [1,2] Oligo-/polyester-based materials show comparable compatibility with lithium salts with a reduced Li⁺-carbonyl interaction strength, resulting in improved lithium transference numbers and in turn higher effective lithium-ion conductivities. However, the commonly used poly(ϵ -caprolactone) (PCL) is semicrystalline still requiring elevated temperatures for optimum ionic conductivity.

In recent studies we demonstrated the application of diester-functionalized poly(meth)acrylates and poly(glycidyl propargyl ethers) as alternative to linear polyesters. The amorphous polymers show high room-temperature ionic conductivity and good applicability in LMBs. [3,4] The T_g of the polymers significantly influences the ion conduction properties, with lower glass transition temperatures resulting in improved ionic conductivities.

Here we propose poly(siloxane)-based diester functionalized polymer electrolytes to further decrease the T_g and improve the low temperature performance. Poly(methylhydro)siloxane was functionalized with an adipate-based (diester) side chain in a hydrosilylation reaction. The diester functionalized polysiloxane (PSi-adipate) exhibits an amorphous character and a very low T_g of $-76\text{ }^\circ\text{C}$. Electrolytes consisting of 20 wt% LiTFSI and the PSi-adipate showed the highest ionic conductivities with 2.7×10^{-5} and $1.8 \times 10^{-4}\text{ S cm}^{-1}$ at 40 and $70\text{ }^\circ\text{C}$, respectively. Furthermore, the lithium transference number was determined as 0.7, compared to 0.5 for linear PCL, indicating a very efficient lithium-ion conduction mechanism. Unfortunately, the improvements in electrolyte characteristics and the low glass transition temperature are countered by the lacking mechanical integrity of PSi-adipate. An investigation of the depletion/plating reversibility of lithium ions at lithium electrodes revealed the necessity to mechanically reinforce the electrolyte. The strategy here is to design a semi-interpenetrating network (sIPN) electrolyte.

We therefore synthesized a PCL-based diacrylate as a network former to form a structure giving network. The network is formed *in situ* in the presence of the polysiloxane electrolyte to yield a semi-interpenetrating network (sIPN) electrolyte (PSi-adipate-sIPN). The network results in significant increase of the mechanical properties as observed in rheology measurements and effectively stabilizes the lithium interface during cycling. Further, the network incorporation in PSi-adipate-sIPN has no negative effect on the ionic conductivity. Finally, the PSi-adipate-sIPN electrolytes are evaluated in lithium-metal batteries with lithium iron phosphate (LFP)- and nickel manganese cobalt oxide (NMC)-based cathodes at different C-rates and temperatures.

- [1] L. Stolz *et al.*, J. Phys. Chem. C, 2021, 125, 18089-18097
- [2] D. Rosenbach, M. Thelakkat *et al.*, J. Appl. Energy Mater., 2, 5, 3373-3388
- [3] D. Rosenbach, M. Thelakkat *et al.*, J. Mater. Chem. A, 2022, 10, 8932
- [4] A. Kralowski, M. Thelakkat *et al.*, J Energy Storage, 2023, 65, 107348

8:30 AM *EN02.04.03

Solid-State Batteries Based on Ionogel Electrolytes Bruce S. Dunn, Yunkai Luo, Bintao Hu and Patricia McNeil; University of California, Los Angeles, United States

Ionogels are pseudo-solid state electrolytes in which an ionic liquid electrolyte is confined in an organic or inorganic matrix. One well established ionogel synthesis route is based on sol-gel chemistry where silica precursors dissolved in an ionic liquid electrolyte undergo hydrolysis and condensation polymerization. By using an ionic liquid as the solvent, no evaporation occurs and the resulting material is a macroscopically rigid, nonporous material in which the ionic liquid is trapped by capillary forces in the nanometer sized pores in the silica network. Because of their unique architecture, ionogels maintain a nanoscale fluidic state and thus mitigate the interfacial resistances which commonly arise at solid-solid interfaces. Using this approach, we have been able to develop pseudo-solid state materials that possess the electrochemical, thermal and chemical properties of the ionic liquid. Moreover, sol-gel synthesis enables the precursor sol to penetrate porous electrodes before solidifying, a feature which is especially attractive for solid-state batteries.

Our recent work has been directed at developing ionogels for anode free solid-state batteries. In this work we take advantage of the ability to solvent exchange the ionic liquid phase with a liquid electrolyte which is more conducive to lithium plating and stripping. We start by synthesizing an ionogel based on dissolving the silane precursors (tetramethyl orthosilicate and methyltrimethoxy silane) in a 1-butyl-1-methylpyrrolidinium bis(fluorosulfonyl)imide (PYR14 FSI) ionic liquid, using acetic acid as a catalyst. After gelation, the ionic liquid is solvent exchanged with an electrolyte consisting of 1 M lithium bis-(tri-fluoromethylsulfonyl)imide (LiTFSI) in 1 : 1 of 1,3-dioxolane (DOL) and 1,2-dimethoxyethane (DME) with 1 wt% of LiNO₃. We have cycled Li/ionogel/Cu cells for over 500 cycles with minimal interfacial resistance and nearly 100% coulombic efficiency. We have also investigated the use of 3D printed copper electrodes and are able to plate and strip lithium at current densities up to 10 mA cm⁻². Anode-free solid-state batteries based on these solvent exchanged ionogels show that the ability to substitute the desired electrolyte for the ionic liquid offers an important new direction which, when coupled with their thermal and electrochemical stability, makes ionogel electrolyte materials a very promising approach for solid-state batteries.

9:00 AM *EN02.04.04

Liquid Electrolytes and Solid Electrolytes for High Energy Lithium BatteriesJunLiu^{1,2}; ¹Pacific Northwest National Laboratory, United States; ²University of Washington, United States

Batteries play a critical role in modern society. The electrification of transportation and deep decarbonization require the development and deployment of high energy, low-cost battery materials and technologies. Among the many different battery chemistries investigated, rechargeable batteries using lithium metal anode remain as one of the most feasible approaches for next generation high-performance and low-cost batteries. There are different approaches to design high energy cells: using liquid electrolytes or solid electrolytes. In the last several years, great progresses have been made in developing lithium metal compatible electrolytes for high energy rechargeable lithium batteries. The new electrolytes significantly reduced the reactions between the solvent molecules and the lithium metal. Combining these electrolytes with high capacity cathodes and proper cell design, practical pouch cells have been fabricated to achieve 350 to 450 Wh kg⁻¹ specific energy and stable long cycle life. Solid electrolytes offer new opportunities to better control the lithium deposition and stripping processes during charge and discharge. However, solid electrolytes and all solid state cells are difficult to fabricate and scale up. New approaches are needed to enable the solid electrolytes to have good conductivity, good mechanical property and flexibility to accommodate the electrochemical and mechanical changes at the interfaces.

9:30 AM EN02.04.05

Functionalized Single-Ion Charge-Transfer Complexes as Solid-State Electrolytes for Lithium BatteriesRomainKunert, NoëlineTessier, LaurentBernard and LionelPicard; CEA Grenoble, France

The global climate context has made us reconsider the way to generate and store energy in a more responsible way. The use of alternative renewable energy sources is tightly correlated to the development of electrochemical storage systems. A great example of this idea is with the transition away from vehicles using thermic combustion. While other technologies are slowly maturing, like hydrogen fuel cells, the golden standard in the industry remains lithium-ion batteries.^[1] The rising demand for the mass production of portable electronic devices and electric vehicles now leads to new expectations.^[2] To fulfill them, research is now focusing on the development of All-Solid-State Batteries. The replacement of the conventional liquid electrolytes by solid-state materials is expected to improve safety^[3] while ensuring higher energy density with the use of lithium metal as negative electrode.^[4]

Polymer-based electrolytes have gathered great attention since the first report of lithium ion conductivity in poly(ethylene oxide) in the 1970s.^[5] Despite different upsides, these types of materials still show some limitations, especially considering ion conductivity at ambient temperatures. More recently, organic charge-transfer complexes (CTCs) have shown promising super-ionic conductivity in the solid-state at room temperature by associating a donor-acceptor organic couple with a lithium salt.^[6] This specific chemical structure holds great potential to tune their electrochemical properties by changing the different partners (acceptor, donor and Li salt) and their molar ratios in the CTC.

In this work, we proposed to functionalize charge-transfer complexes to develop single-ion materials, expected to enhance mechanical and electrochemical properties for solid-state batteries.^[7] We studied the covalent graphing of polyphenylene polymers with different anions derived from lithium salts conventionally used to develop solid-state electrolytes. We also used these types of single-ion polymers to develop charge-transfer complexes and analyzed their electrochemical properties. The ionic conductivity and lithium transport number of our functionalized CTC electrolytes was compared to the state-of-the-art CTC conducting materials. We finally offer to rationalize plausible conduction mechanisms in our materials and in the conventional CTC systems that is still in debate today.

References

- [1] B. Owens, *Nature*, **2015**, 526, S89.
- [2] E. Fan *et al.*, *Chem. Rev.*, **2020**, 120, 7020-7063.
- [3] L. Yue *et al.*, *Energy Storage Mater.* **2016**, 5, 139-165.
- [4] S. Xia *et al.*, *Chem*, **2019**, 5, 753-785.
- [5] Z. Xue *et al.*, *J. Mater. Chem. A*, **2015**, 3, 19218-19253.
- [6] K. Hatakeyama-Sato *et al.*, *npj Comput. Mater.* **2022**, 8, 170.
- [7] J. Gao *et al.*, *Chem. Sci.*, **2021**, 12, 13248-13272.

9:45 AM EN02.04.06

Measuring Free Volume and Li-Salt Dissolution of the Polymer in Composite ElectrolytesSaraC. Sand¹, JenniferL. Rupp^{2,1} and BilgeYildiz¹; ¹Massachusetts Institute of Technology, United States; ²Technische Universität München, Germany

Ceramic and Polymer electrolytes are the two categories of materials that have emerged to replace flammable electrolytes in Li-ion batteries. Composite electrolytes, typically in the form of dispersed ceramic particles or nanowires in polymer matrix, combine these two materials to have good ionic conductivity while maintaining the mechanical properties of the polymer. Despite achieving relatively high levels of conductivity (typically 10-4 S/cm), the underlying mechanism governing ion conduction in these composite electrolytes remains inadequately elucidated.

The polymer likely plays a crucial role as the ceramic volume fractions are typically under 20 vol. %.^{2,3} Three possible ways that polymers could increase in conductivity in the composite have been identified: decreased crystallinity, increased free volume, and increased lithium ion dissolution due to acidic surface groups on the ceramic.^{2,4,5} To explore the interface between the polymer and ceramic, we developed a thin film model system through spincoating. We observed that the conductivity of the thin film was significantly higher than that of the bulk. We utilized differential scanning calorimetry to identify probe the crystallinity and found that the small crystallinity variation could not account for the variation in conductivity. Subsequently, we utilized conductivity measurements on various ceramic surfaces to understand the effects of charge surface groups on the ceramic on polymer conductivity. X-ray Absorption measurements were similarly utilized to probe the variation in lithium ion environments within these materials to understand any variation in the lithium salt dissolution. It was found that the variation in conductivity based on this effect is small.

In order to probe the possible variation in free volume, Small Angle Neutron Scattering was utilized to quantify the free volume within thin films, bulk polymer, and composite electrolytes. This can quantify the volume associated with each monomer and therefore how much space is between polymer chains for lithium ion movement. It was found that the free volume in the thin film was significantly increased as compared to the bulk polymer. Lastly, additionally, positron annihilation is used as an additional measure small voids or measure of the distribution of free volume in these systems.

References:

1. Liu, Y. *et al.* An Artificial Solid Electrolyte Interphase with High Li-Ion Conductivity, Mechanical Strength, and Flexibility for Stable Lithium Metal Anodes. *Advanced Materials* **29**, 1605531 (2017).
2. Lv, F. *et al.* Challenges and development of composite solid-state electrolytes for high-performance lithium ion batteries. *Journal of Power Sources* **441**, (2019).
3. Sivaraj, P. *et al.* Performance Enhancement of PVDF/LiClO₄ Based Nanocomposite Solid Polymer Electrolytes via Incorporation of Li_{0.5}La_{0.5}TiO₃ Nano Filler for All-Solid-State Batteries. *Macromol. Res.* (2020).
4. Mohapatra, S. R., Nair, M. G. & Thakur, A. K. Synergistic effect of nano-ceria dispersion on improvement of Li + ion conductivity in polymer nanocomposite electrolytes. *Materials*

10:00 AMBREAK

10:30 AM EN02.04.07

Solid Organic Charge-Transfer Composites as Lithium-Ion Battery ElectrolytesLingyuYang and JenniferL. Schaefer; University of Notre Dame, United States

Solid-state polymer electrolytes, where ion transport is facilitated by polymer chain segmental motion, for lithium-ion batteries have attracted considerable research interest because of the potential for high safety and electrochemical stability, but applications are limited by their low ionic conductivities. However, recent reports found that certain organic charge-transfer crystals could present high ionic conductivity via ion transport pathways on the crystal surfaces.[1] In our work, we reported charge-transfer complex electrolytes composed of a pair of tetrathiafulvalene-tetracyanoquinodimethane (TTF-TCNQ) complex matrix with different molar ratios of lithium bis(trifluoromethylsulfonylimide) (LiTFSI).[2] It was found that thermal annealing and water vapor treatment can impact charge transport properties of charge-transfer complex electrolytes. Trace water promoted the dissociation of LiTFSI, resulting in the electrolyte with 1-1-2-0.45 molar ratio of TTF-TCNQ-LiTFSI-H₂O showing an ionic conductivity of 2×10^{-3} S/cm at 25 °C with electronic conductivity as low as 1×10^{-7} S/cm at the same temperature. By further fabrication of similar charge-transfer composite electrolytes lacking water, the performance of full cells will be investigated.

Reference:

1. Hatakeyama-Sato, K.; Umeki, M.; Tezuka, T.; Oyaizu, K. Charge-Transfer Complexes for Solid-State Li+Conduction. *ACS Appl. Electron. Mater.* 2020, 2 (7), 2211–2217.
2. Yang, L.; Schaefer, J. L. Water-Assisted Ion Conduction in Solid-State Charge-Transfer Complex Electrolytes for Lithium Batteries. *ACS Energy Lett.* 2023, 8(5), 2426–2431.

10:45 AM *EN02.04.08

Strategies to Improve the Electrochemical Properties of Single-Ion Conductive Polymer ElectrolytesLiangliangLi, KaihuaWen and Ce-WenNan; Tsinghua University, China

Solid electrolytes are the key materials used in solid-state batteries with a high energy density and good safety. Among various solid electrolytes, polymer-based electrolytes are attracting a lot of research interest due to the advantages of flexibility, low cost and easiness for mass production. Traditional polymer-based electrolytes use dual-ion Li salts such as LiPF₆, LiClO₄, LiTFSI, et al., and they have a low Li-ion transference number, leading to unwanted polarization and side reactions in solid-state batteries. Recently, single-ion conductive polymer electrolytes (SICPEs) with a Li-ion transference number close to one have been widely studied. One of the challenges for SICPEs is to achieve both high ionic conductivity and wide electrochemical stability window. In this talk, we are going to present two strategies to enhance the electrochemical properties of SICPEs. First, we precisely regulate the ion-dipole interactions in an SICPE containing carbonyl and cyano groups. The resulting SICPE shows a Li-ion transference number of more than 0.9, a large ionic conductivity of 10^{-4} S cm⁻¹, a wide electrochemical stability window of more than 4.5 V, and an excellent electrochemical compatibility with Li metal. Second, we prepare a composite electrolyte by adding garnet ceramic nanoparticles into the SICPE. Due to the interactions between the garnet active fillers and the SICPE, the key electrochemical properties such as the Li-ion transference number, electrochemical stability window, and ionic conductivity are all further improved. Based on the high-performance SICPEs above, both LiFePO₄ and LiCoO₂-based solid-state batteries demonstrate good rate performance and a long cycle life at room temperature. In summary, regulating the ion-dipole interactions in single-ion conductive polymers and synthesizing ceramic/polymer composite electrolytes are effective strategies to improve the electrochemical properties of SICPEs.

11:15 AM EN02.04.09

Polymer Electrolytes Unleashed: Exploring the Potential of Carbonate Species in Lithium-Ion BatteriesOmarAllam and Seung SoonJang; Georgia Institute of Technology, United States

Solid polymer electrolytes (SPEs) are gaining prominence in contemporary research due to several key benefits they offer over liquid electrolytes, including non-flammability, improved mechanical stability, and suppressed electrode material dissolution. To understand the potential of these materials, our research employs density functional theory (DFT) and molecular dynamics (MD) simulations to probe novel carbonate-based SPEs, comparing their performance against their traditional liquid carbonate electrolyte counterparts. One of the central aspects of our investigations is the exploration of the impact of carbonate pendant group composition on the nanophase morphology of amorphous polycarbonates, as well as Li-ion solvation and transport. These findings are juxtaposed with the behavior of liquid electrolytes like dimethyl carbonate and ethylene carbonate. Furthermore, our study illuminates how critical variables such as the glass transition temperature (T_g) of polymer materials, which significantly influences Li-ion transport, are impacted when introducing cyclic versus linear carbonate sidechains and mixing different types of carbonate pendant groups. Of particular interest is our aim to ascertain whether synergies between carbonate species typically exploited in liquid form can be harnessed when they are in their polymeric incarnations. Through our comprehensive analysis, we seek to provide pivotal insights that will guide the optimal design and composition of polymers for achieving a nanophase morphology that enhances ion transport.

11:30 AM EN02.04.10

Mechanistic Investigation of Superionic Conduction in Halide Solid ElectrolytesZhantaoLiu¹, AlexChien², ShuoWang³, YifeiMo³, JueLiu² and HailongChen¹; ¹Georgia Institute of Technology, United States; ²Oak Ridge National Laboratory, United States; ³University of Maryland, United States

Halide-based solid electrolytes, such as Li₃MX₆ (M=Y, Sc, etc., X=halogen), are attracting great attention in the field of solid state Li-ion batteries owing to their good compatibility with high-voltage cathodes and high room temperature conductivities. In our recent research, we found that many halides, such as Li₃YCl₆, show a type-II superionic transition, where their diffusion energy barrier is significantly lowered once the temperature is raised above the transition point T_c. It is therefore interesting to explore the mechanism of this transition to further understand this class of materials and design better solid electrolytes. We systematically characterized the detailed crystal structures of a series of halides using variable temperature high-resolution synchrotron X-ray and neutron diffractions and refinements, and AIMD computations. A novel mechanism that explains this superionic transition in halides is proposed and supported by the experimental results. The new finding will help us to design better halide electrolytes with higher conductivity and lower activation energy, and thus facilitate the development of solid state Li-ion batteries.

11:45 AM EN02.04.11

Experimental Mechanical Investigation of Composite Cathode for Enhanced Performance in All-Solid State BatteriesHoward QingsongTu; Rochester Institute of Technology, United States

All-solid-state-batteries (ASSBs) are leading the way in safer and more efficient energy storage. This study investigates the macro-scale mechanical properties of cathode active material (CAM) and solid electrolyte (SE) components in ASSBs. Through compression testing, we analyze CAM and SE materials—LiNi_{0.8}Mn_{0.1}Co_{0.1}O₂, Li₆PS₅Cl, Li₃YCl₆, Li₃YBr₃Cl₃, and Li₇La₃Zr₂O₁₂. We examine the effects of fabrication pressure and CAM-to-SE weight ratio on elastic modulus, bulk modulus, yield strength, and deformation. Our study bridges the gap in understanding the macro scale mechanical properties, contributing to advancements in ASSB technology. Understanding the mechanical properties of composite cathodes will enable us to develop strategies to mitigate issues such as solid-electrolyte debonding and capacity loss, leading to improved battery performance, stability, and lifespan. The findings of this study have the potential to drive the design and development of more efficient and reliable ASSBs.**Experimental Mechanical Investigation of Composite Cathode for Enhanced Performance in All-Solid State Batteries**

SESSION EN02.05: Advanced Synthesis I
Session Chairs: Xin Li and Amy Marschilok
Tuesday Afternoon, November 28, 2023
Hynes, Level 3, Room 304

1:30 PM *EN02.05.01

High-Performance Solid-State Electrolytes: Ultra-Fast High Temperature Sintering (UHS) Oxides and Expanded CelluloseLiangbingHu; University of Maryland, United States

We recently reported an ultrafast high temperature sintering (UHS) for solid state electrolytes (Science, 2020, May Cover). The long sintering time of conventional syntheses can lead to Li loss in garnet SSEs caused by the evaporation of Li and the formation of secondary phases that lead to lower ionic conductivity. In contrast, the UHS technique enables us to tune the sintering time in units of seconds, which provides excellent control in terms of the Li content and grain growth. I will discuss our progress on applying UHS method to sintering various solid-state

electrolyte, from compositions to microstructures. By programming the temperature and time (T-t), we can establish process diagrams to sinter porous vs. dense structures. The rapid sintering also allows us to sintering multilayer solid-state electrolytes with significantly reduced interlayer diffusion.

In a separated topic, I will discuss a general design strategy for achieving one-dimensional (1D), high-performance polymer solid-state ion conductors through molecular channel engineering, which we demonstrate via Cu²⁺-coordination of cellulose nanofibrils. The cellulose nanofibrils by themselves are not ionic conductive; however, by opening the molecular channels between the cellulose chains through Cu²⁺ coordination we are able to achieve a Li-ion conductivity. This improved conductivity is enabled by a unique Li⁺ hopping mechanism that is decoupled from the polymer segmental motion. Also benefitted from such decoupling, the cellulose-based ion conductor demonstrates multiple advantages, including a high transference number (0.78 vs. 0.2–0.5 in other polymers²), low activation energy (0.19 eV), and a wide electrochemical stability window (4.5 V) that accommodate both Li metal anode and high-voltage cathodes. Furthermore, we demonstrate this 1D ion conductor not only as a thin, high-conductivity solid-state electrolyte but also as an effective ion-conducting additive for the solid cathode, providing continuous ion transport pathways with a low percolation threshold, which allowed us to utilize the thickest LiFePO₄ solid-state cathode ever reported for high energy density (Nature, Oct 22).

2:00 PM *EN02.05.02

Liquid-Phase Synthesis of Sulfide Solid Electrolyte: Achieving Extended Composition Ranges and Minimized Carbon Impurities for All-Solid-State Batteries Yoon SeokJung, Yonsei University, Korea (the Republic of)

Advancements in all-solid-state battery (ASSB) technology, featuring non-flammable inorganic solid electrolytes, are gaining significant traction, mainly due to their promise of increased safety and energy density compared to traditional lithium-ion batteries, which rely on flammable organic liquid electrolytes. A key focus of this evolution towards practical ASSBs is the development of sulfide SEs (SSEs), recognized for their exceptional ionic conductivities (reaching up to ~10⁻² S cm⁻¹) and their ability to be mechanically sintered. Additionally, the employment of wet-chemical synthesis or processing methods for SSEs unlocks intriguing opportunities for the future advancement of ASSB technologies. However, thus far, the number of viable precursor-solvent combinations for the liquid-phase synthesis of SSEs remains limited, primarily due to the solubility constraints of metal chalcogenide precursors such as MS₂ (M = Ge, Sn). This limitation hinders the wet-chemical route for synthesizing metal-inclusive compositions like Li₁₀GeP₂S₁₂. Furthermore, the liquid-phase synthesis of SSEs often leaves significant amounts of organic residues derived from organic solvents, leading to the carbonization issue, which could instigate harmful side reactions or self-discharge when used in ASSB cells.

In this presentation, we report on our recent results in developing liquid-phase synthesis strategies for SSEs that extend the compositional availability while minimizing carbon impurities. By leveraging amine-thiol chemistry, metal sulfide precursors can participate in the liquid-phase synthesis alongside conventional precursors of Li₂S, P₂S₅, and LiX (X = Cl, Br, I). Moreover, we introduce a novel heat treatment method that results in near carbon-free SSE products derived from liquid-phase synthesis. These developments hold promising potential for significantly enhancing the electrochemical performance of ASSBs.

References

1. J. E. Lee, et al., *Adv. Mater.* **2022**, *34*, 2200083.
2. J. Woo, et al., *Adv. Energy Mater.* **2023**, *13*, 2203292.

2:30 PM EN02.05.03

Ion-Exchange in Solid Electrolytes to Induce Compressive Stress and Improve Electrochemical Performance Sydney Morris¹, Harsh D. Jagad¹, Stephen J. Harris², Changmin Shi¹, Matthew Fang¹, Yue Qi¹ and Brian W. Sheldon¹; ¹Brown University, United States; ²Lawrence Berkeley National Laboratory, United States

There is continued interest in improving the electrochemical performance of the solid electrolyte (SE) lithium lanthanum zirconium oxide (LLZO) by preventing lithium (Li) filaments from penetrating the SE. This study builds upon a model that analyzed the impact ion-exchange (IX) has on Li transport through LLZO [1]. While IX is a common practice to strengthen glass, and has even been used with glass solid electrolytes, this work presents the first attempt to apply the IX process to LLZO in order to induce compressive stress at the surface and delay the penetration of Li filaments [2]. A wide variety of ion-exchange conditions were investigated, and the resulting materials were characterized with a scanning electron microscope (SEM), electron-dispersive X-ray spectroscopy (EDS), X-ray diffraction (XRD), electrochemical impedance spectroscopy (EIS), and critical current density (CCD) experiments using symmetric Li cells. Comparisons with control samples were used to elucidate the impact of processing conditions on critical current density, stress at the surface of the SE pellet, and the LLZO surface structure. The results demonstrate that improved CCDs are possible, but that a variety of phenomena can complicate the ion-exchange process and lead to reduced ionic conductivity and chemical degradation of the LLZO.

[1] Tradeoff between the Ion Exchange-Induced Residual Stress and Ion Transport in Solid Electrolytes. Harsh D. Jagad, Stephen J. Harris, Brian W. Sheldon, and Yue Qi. *Chemistry of Materials* 2022 34 (19), 8694-8704. DOI: 10.1021/acs.chemmater.2c01806

[2] Shweta R. Keshri, Indrajeet Mandal, Sudheer Ganiseti, S. Kasimuthumaniyan, Rajesh Kumar, Anuraag Gaddam, Ankita Shelke, Thalasseril G. Ajithkumar, Nitya Nand Gosvami, N.M. Anoop Krishnan, Amarnath R. Allu. Elucidating the influence of structure and Ag⁺-Na⁺ ion-exchange on crack-resistance and ionic conductivity of Na₃Al_{11.8}Si_{1.65}P_{1.8}O₁₂ glass electrolyte, *Acta Materialia*, Volume 227, 2022, 117745, ISSN 1359-6454, <https://doi.org/10.1016/j.actamat.2022.117745>.

2:45 PM BREAK

SESSION EN02.06: Dendrite
Session Chairs: Fang Liu and Amy Marschilok
Tuesday Afternoon, November 28, 2023
Hynes, Level 3, Room 304

3:15 PM *EN02.06.01

The Impact of Interface layer on Li Plating and Stripping Morphology Yue Qi; Brown University, United States

Li metal is the preferred anode material for high energy Li batteries. However, stable plating and stripping of Li metal in both liquid and solid electrolytes remain a significant challenge, particularly at practically feasible current densities. This Li/electrolyte interface is further complicated by a complex solid electrolyte interface (SEI). The electronic, ionic, and mechanical properties of the Li/SEI interface can significantly change the Li plating and stripping morphology.

A Density Functional Theory (DFT) informed phase-field method was developed to integrate electrochemistry with mesoscale plating morphology. It revealed that the Li intergranular growth in Li₇La₃Zr₂O₁₂ solid electrolytes originated from the trapped electrons at grain boundaries and internal surfaces. This phenomenon is material specific, as several other key solid electrolytes do not trap electrons at grain boundaries or internal defects. [1]

The lithium stripping process generates vacancies, which may accumulate as voids and lead to uneven current distribution and dendrite growth in the following plating cycles. A stack pressure is typically required during stripping, causing large scale lithium metal creep. Here, we captured the multiple length and time scales by combining interface interactions with DFT simulations, vacancy hopping with kinetic Monte Carlo (KMC), and plastic deformation with continuum simulations. Generally lithiophilic interface requires less stack pressure to maintain a flat surface while a higher stack pressure is needed at lithiophobic interfaces to accelerate Li vacancy diffusion into the bulk and maintain a flat surface. This critical stack pressure needs to be high enough to alter the Li forward-and-backward hopping barriers at the interface. This multiscale simulation scheme illustrates the importance of including the chemical-mechanical effects during Li stripping morphology evolution. [2,3]

H.K. Tian et al., *Chemistry of Materials* 2019, 31(18) 7351-7359

C.T. Yang and Y. Qi, *Chemistry of Materials* 2021, 33, 2814-2823

M. Feng, C.T. Yang, and Y. Qi, *J. Electrochem. Soc.* 2022, 169 (9), 090526

3:45 PM EN02.06.02

Chemo-Mechanical Regulation of Li Intrusion in Garnet Solid Electrolytes via Ultra-Thin Metallic Coating Xin Xu^{1,2} and William C. Chueh^{1,2}; ¹Stanford University, United States; ²SLAC National Accelerator Laboratory, United States

Solid electrolytes in rechargeable lithium-metal batteries are prone to lithium-metal short-circuiting during plating, and the underlying cause is not well understood. The growth of lithium-metal, termed as "Li intrusions," within the solid electrolyte can lead to surface cracks and short-circuiting during battery charging process. In our previous research¹, we have determined that the root cause of lithium intrusion into the electrolyte is a combination of current focusing and the presence of nanoscale cracks, rather than electronic leakage or electrochemical reduction.² These insights highlight the mechanical tunability of electrochemical plating reactions in brittle solid electrolytes.³ In this study, we propose a chemo-mechanical approach to control Li intrusions in a leading solid electrolyte, $\text{Li}_{6.6}\text{La}_3\text{Zr}_{1.6}\text{Ta}_{0.4}\text{O}_{12}$ (LLZO), through the use of ultra-thin nanoscale metallic coatings. Specifically, we apply a nanoscale metallic Ag coating on the LLZO surface and anneal it at various elevated temperatures without air exposure. The coated and annealed surface demonstrates enhanced tolerance to Li intrusion, particularly under high local stress, as confirmed by operando SEM plating. Compared to the pristine LLZO surface, the coated surface exhibits a local current density that is three times higher, a charge density that is 25 times higher, and a total charge of Li plating that is 1400 times higher. Depth profiling using nanoscale secondary ion mass spectrometry (NanoSIMS) indicates that Ag may diffuse into the subsurface of LLZO, showing no discernible differences in the location of grain interior or grain boundaries. Furthermore, in-situ XPS experiments reveal that the oxidation state of the Ag coating on LLZO transitions from metallic Ag to oxidized Ag. These observations suggest that Ag likely induces chemical antisite defects on the surface of LLZO. In-situ nanoindentation experiments demonstrate that the mechanical strength of the coated surface surpasses that of the pristine surface. Finite element method (FEM) simulations indicate that the generated antisite defects introduce additional surface compressive strain due to the larger ionic radius of Ag compared to Li, thereby suppressing the probability of Li intrusion. Our research indicates the potential of chemo-mechanical regulation of Li intrusion in solid electrolytes through the use of chemical defects. These new findings suggest that nanoscale coatings may be sufficient to tune electrochemical Li plating reactions, making it feasible for cost-effective, large-scale engineering and manufacturing of interfaces in solid-state batteries.

Reference:

1. McConohy, G. *et al.* Mechanical regulation of lithium intrusion probability in garnet solid electrolytes. *Nat. Energy* 1–10 (2023) doi:10.1038/s41560-022-01186-4.
2. Han, F. *et al.* High electronic conductivity as the origin of lithium dendrite formation within solid electrolytes. *Nat. Energy* 4, 187–196 (2019).
3. Qi, Y., Ban, C. & Harris, S. J. A New General Paradigm for Understanding and Preventing Li Metal Penetration through Solid Electrolytes. *Joule* (2020) doi:10.1016/j.joule.2020.10.009.

4:00 PM EN02.06.03

Direct Observations of Dendrite-Induced “Subcritical” Cracking in Oxide Solid Electrolytes Cole D. Fincher¹, W. Craig Carter¹, Brian W. Sheldon² and Yet-Ming Chiang¹; ¹Massachusetts Institute of Technology, United States; ²Brown University, United States

Dendrite-induced short circuits threaten the deployment of solid-state batteries with metal anodes. Dendrites grow from the anode due to plating-induced pressure and subsequent fracture of the electrolyte. Whether electrochemical activity within the electrolyte aids that fracture process has remained a topic of debate. For oxide solid-electrolytes, we address this issue by conducting operando photoelastic microscopy to directly observe the stress fields around dendrites under dynamic electrochemical loading. From this data, we measure the thermodynamic driving force for fracture (i.e., the stress intensity factor, a measure of apparent surface energy) as a function of applied potential. These experiments reveal dendrite growth under “subcritical” conditions, meaning that the stress intensity factor during propagation is less than should be expected based on linear elastic fracture theory. We discuss these results in the context of historical subcritical cracking due to corrosive action. Finally, we develop a mechanistic framework to connect the observations here with expected behavior in sandwich-style cell formats.

4:15 PM EN02.06.04

Dendrite Growth in Lithium Metal Solid-State Batteries Dominic Melvin¹, Ziyang Ning¹, Guanchen Li², T.J. Marrow¹, Charles W. Monroe¹ and Peter Bruce¹; ¹University of Oxford, United Kingdom; ²University of Glasgow, United Kingdom

Solid-state batteries which combine both a lithium anode and ceramic solid electrolytes promise a step change in cell energy density. However, there are significant challenges to charging and discharging these cells at high current densities in the range of several mA cm⁻². At high rates of charge, dendrites (filaments of lithium metal) are observed to crack through ceramic electrolytes, leading to critical failure of the cell. The realisation of solid-state batteries with lithium metal anodes therefore depends on understanding how a soft metal such as Li can induce fracture of a stiff ceramic electrolyte.

Using a combination of X-ray computed tomography and FIB-SEM we have made observations which reveal both how Li dendrites crack $\text{Li}_6\text{PS}_5\text{Cl}$ electrolytes and how these dendrite-cracks propagate across the solid electrolyte. We have made the finding that dendrite-cracks propagate whilst partially filled, driven by Li at the back of the crack not the tip. This has enabled advances in understanding dendrites in ceramics and the factors that influence then and their progression to a short-circuit.

4:30 PM EN02.06.05

Dilatometric Measurement of Pore Volume During Stripping of Metal Electrodes in Solid-State Batteries Thomas Schall, Till Fuchs, Jill Kessler, Klaus Peppler, Joachim Sann, Boris Mogwitz and Jürgen Janek; Justus Liebig University Gießen / Institute for Physical Chemistry, Germany

Solid-state batteries may allow the use of a lithium metal anode (LMA), enabling a significant increase in energy density. However, morphological challenges such as dendrite growth and contact loss of the LMA during cycling limit the available capacity. The formation of resistive pores occurs when the local current density exceeds the effective diffusion of vacancies within the LMA, leading to a vacancy accumulation (1,2). Therefore, external pressure can mitigate pore formation by inducing plastic deformation of the lithium metal (1). To address the limitations imposed by pore formation, a deeper understanding is required.

This work employs a novel dilatometric measurement setup providing a precision of < 1 nm for measuring height changes, maintaining precise constant pressure, and facilitating the metrological separation of one electrode. As pore formation leads to non-uniform removal of lithium, resulting in the formation of indentations (pores) due to adatom diffusion (1), the overall height reduction during operation is decreasing. Despite a continuous amount of lithium being stripped, our setup can therefore detect the onset of pore formation.

The dilatometer is employed to measure the changes in height during both pore-free uniform stripping and stripping with pore formation in a $\text{Li}|\text{LLZO}|\text{Li}$ model system. From the difference between the height change of uniform stripping and stripping with pore formation, the pore volume can be determined and related to GEIS and PEIS measurements. Using this approach, the pore volume is determined for different current densities and pressures, providing a comprehensive understanding of the pore formation under varying conditions. To complement the results, the pores at the stripping electrode are analyzed post-mortem using scanning electron microscopy (SEM). The measured data allow new insights into the morphology of pore formation.

- (1) Krauskopf, T.; Hartmann, H.; Zeier, W. G.; Janek, J.: Toward a Fundamental Understanding of the Lithium Metal Anode in Solid-State Batteries—An Electrochemo-Mechanical Study on the Garnet-Type Solid Electrolyte $\text{Li}_{6.25}\text{Al}_{0.25}\text{La}_3\text{Zr}_2\text{O}_{12}$. *ACS Appl. Mater. Interfaces* 2019 11 (15), S. 14463–14477
- (2) Krauskopf, T.; Richter, F. H.; Zeier, W. G.; Janek, J. Physicochemical Concepts of the Lithium Metal Anode in Solid-State Batteries. *Chemical reviews* 2020, 120 (15), S. 7745–7794.

SESSION EN02.07: Poster Session II
Session Chairs: Yi Lin and Amy Marschilok
Tuesday Afternoon, November 28, 2023
Hynes, Level 1, Hall A

8:00 PM EN02.07.01

Solvent-Free Single-Ion Conducting Polymer Electrolytes for Lithium Metal Batteries under Harsh Environments Jingyi Gao and Dong-Myeong Shin; The University of Hong Kong, Hong Kong

Rechargeable lithium-ion batteries are widely used in consumer applications. However, these batteries are limited in their ability to function under extreme thermal environments, such as high temperatures, which are required for medical devices requiring sterilization and various industries like subsurface exploration and thermal reactors. However, the conventional lithium-ion batteries have limited high-temperature performance due to material properties that lead to safety concerns or low power usage. Many efforts have focused on developing solvent-free single-ion conducting (SIC) polymer electrolytes to solve these issues by covalently immobilizing anionic groups onto a polymer backbone, which only allows Li^+ cations to be mobile through the polymer matrix, leading to minimal dendrite growth during charging/discharging process. While the SIC polymer electrolytes hold much promise for next-generation batteries possessing high safety and high energy density, this approach typically yields a significant drop of ionic conductivity ($<10^{-5}$ S cm⁻¹ at ambient temperature), compared to liquid electrolytes. Quasi-solid or gel polymer electrolytes incorporating organic plasticizers have been employed to enhance the ionic conductivities, but their practical implementation is still constrained by their vulnerability to thermal runaway under high-temperature circumstances. Herein, we present a novel approach for the one-step synthesis of a solvent-free single-ion perfluorinated-tetraphenylborate-anions

membrane via click reaction. The resulting flexible membrane displays exceptional cyclability performance at high temperatures, high lithium selectivity (~0.932), and a wide working window (up to 5 V). The one-step synthesis of the membrane exhibits a high ionic conductivity ($\sim 3 \times 10^{-5} \text{ S cm}^{-1}$) at 88°C due to its consistent structure. Notably, the membrane demonstrates superior non-flammability properties. Furthermore, the membrane can operate under large temperature ranges from 60 to 120°C, even under negative pressure, making it suitable for a variety of applications. Remarkably, stable long-term cycling of LiFePO_4 cathodes can be achieved at 100°C with a coulombic efficiency of approximately 100% over 300 cycles at 0.5C.

8:00 PM EN02.07.02

Novel Lithium-Ion Conductor LiTa_2PO_8 -Based Hybrid Solid Electrolytes for High-Voltage Cathodes in Lithium-Metal BatteriesKumlachew ZelalemWalle^{1,2} and Chun-Chen Yang^{1,1}; ¹Ming Chi University of Technology, Taiwan; ²University of Gondar, Ethiopia

Solid-state Lithium metal batteries (SSLMBs) that contain polymer and ceramic solid electrolytes have received considerable attention as an alternative to substitute liquid electrolytes in lithium metal batteries (LMBs) for highly safe, excellent energy storage performance, and stability under elevated temperature situations. Here, a novel fast Li-ion conducting material, LiTa_2PO_8 (LTPO) was synthesized, and the electrochemical performance of as-prepared powder and LTPO-incorporated hybrid solid electrolyte (LTPO-HSE) membrane was investigated. The as-prepared LTPO powder was homogeneously dispersed in polymer matrices and a hybrid solid electrolyte membrane was synthesized *via* a simple solution-casting method. The room temperature total ionic conductivity (σ_t) of the LTPO pellet and LTPO-HSE membrane were 0.14 and 0.57 mS cm^{-1} , respectively. A coin battery with NCM811 cathode is cycled under 1C between 2.8 to 4.5 V at room temperature, achieving a Coulombic efficiency of 99.3% with capacity retention of 74.1% after 300 cycles. Similarly, the LFP cathode also delivered an excellent performance at 0.5C with an average Coulombic efficiency of 100% without a virtual capacity loss (the maximum specific capacity is at 27th: 138 mAh g^{-1} and 500th: 131.3 mAh g^{-1}). These results demonstrate the feasibility of a high Li-ion conductor LTPO as a filler and the developed polymer/ceramic hybrid electrolyte has the potential to be a high-performance electrolyte for high-voltage cathodes, which may provide a fresh platform for developing more advanced solid-state electrolytes.

8:00 PM EN02.07.03

Long Cycling Performance of the All-Solid-State Lithium-Ion Batteries using Modified Silicon AnodesMinjaeKim¹, JunHyeokSeo², DaheeSong² and Kuk YoungCho¹; ¹Hanyang University(ERICA), Korea (the Republic of); ²Hanyang University, Korea (the Republic of)

The continuous growth of electric vehicles and energy storage systems has increased demand for lithium-ion batteries (LIBs) that offer both safety and high energy density. Consequently, research on next-generation LIBs with high energy density has expanded, focusing on new electrode materials such as lithium metal, high-nickel ternary cathodes, sulfur cathodes, and silicon anodes. Particularly, silicon anodes offer superior capacity compared to the conventional graphite anodes used in commercial LIBs, along with the advantages of low electrode potential and abundant resources. However, challenges remain due to the volume expansion of silicon anodes and the unstable form of the solid electrolyte interphase (SEI), which affects their cycling performance.

All-solid-state lithium-ion batteries (ASSLBs) are an up-and-coming solution for achieving safety and high energy density by eliminating issues related to liquid electrolyte leakage and fire hazards. Furthermore, applying silicon anodes in ASSLBs can serve as a viable means to overcome the limitations of conventional LIBs while suppressing silicon's volume expansion through solid electrolytes, thereby addressing the drawbacks associated with silicon anodes. Therefore, ASSLBs and silicon anodes offer highly promising alternatives to overcome the limitations of conventional LIBs and silicon anodes. However, further research is required to address potential issues that may arise from applying silicon anodes and ASSLBs.

In this study, we fabricated ASSLBs using silicon anodes and sulfide-based solid electrolytes. We investigated the degradation characteristics of silicon anodes in ASSLBs with silicon thin-film electrodes and confirmed the performance enhancement of modified silicon anodes.

8:00 PM EN02.07.04

Stable 4 V-Class All-Solid-State Lithium Battery with Hydroborate Electrolyte and NMC811 CathodeHugoBraun, RyoAsakura, EdouardQuerel, CorsinBattaglia and ArndtRemhof; Empa - Swiss Federal Laboratories for Materials Science and Technology, Switzerland

Solid-state batteries are expected to extend the energy and power density beyond the limits of lithium-ion batteries, and to replace their flammable liquid electrolytes with safer alternatives. Each of the most studied solid electrolyte materials has disadvantages such as limited electrochemical stability (sulfides), low ionic conductivity (polymers), mechanical stiffness (oxides) or incompatibility with metallic anodes (halides). Complex hydride electrolytes, especially hydroborates, combine many attractive characteristics such as high ionic conductivity, compatibility with alkali metal anodes and soft mechanical properties. Some of us recently reported stable 3 V and 4 V all-solid-state sodium hydroborate batteries. Lithium hydroborate solid-state batteries offer the potential to use cathodes with much higher specific discharge capacity, but have so far been limited to low-voltage cathodes such as sulfur or TiS_2 due to the limited oxidative stability of the electrolyte. Herein, we demonstrate all-solid-state lithium metal batteries employing a hydrocarborate solid electrolyte with a 4 V-class $\text{LiNi}_{0.8}\text{Mn}_{0.1}\text{Co}_{0.1}\text{O}_2$ (NMC811) cathode. This is achieved by tailoring the $\text{LiCB}_{11}\text{H}_{12}\text{-LiCB}_9\text{H}_{10}$ electrolyte mixing ratio towards high oxidative stability (~ 3.9 V), while maintaining high conductivity ($>1.5 \text{ mS cm}^{-1}$ at room temperature). Unlike many other stable solid-state cells, we use one single electrolyte material in contact with the lithium metal, as the separator layer and in the cathode composite. Corresponding cells with lithium metal anodes display a high discharge capacity of 175 mAh g^{-1} and stable cycling, demonstrating the potential of hydroborate electrolytes for 4 V-class solid-state lithium metal batteries.

8:00 PM EN02.07.05

Functional Design and Investigation of Mg-Ion Conductors for Solid-State Mg BatteriesZhixuanWei and JürgenJanek; Institute of Physical Chemistry & Center for Materials Research, Justus Liebig University Giessen, Germany

Secondary batteries using multivalent cations as charge carrier have attracted increasing attention in recent years due to the high theoretical energy density given by multi-electron redox reactions. Nevertheless, the large charge density of these cations inevitably causes sluggish kinetics of the ion migration under room temperature, which is challenging for the development of multivalent-ion solid-state batteries.^[1] Taking Mg^{2+} as a case study, we investigated a series of functional materials to figure out the design principle for Mg-ion solid-state conductors. First of all, an ionogel electrolyte using a MOF (metal-organic framework) as skeleton was prepared.^[2] An ionic liquid was incorporated into UiO-66, which has a large inner surface area as well as a rich porous structure. Comparably high ionic conductivities of $5.7 \times 10^{-5} \text{ S cm}^{-1}$ and $2.4 \times 10^{-4} \text{ S cm}^{-1}$ could be achieved at room temperature and at mildly elevated temperature (60 °C), respectively. Apart from the good ionic conductivity, the prepared electrolyte also exhibits good chemical and electrochemical stability against magnesium metal. By pairing the magnesium metal anode with an aromatic organic material as cathode material, a proof-of-concept quasi-solid-state Mg battery can work reversibly at 60 °C. Secondly, we replaced the ion-insulating MOF framework by a new Mg-ion conducting NASICON-structured material, $\text{Mg}_{0.5}\text{Sn}_2(\text{PO}_4)_3$. By combining it with a small amount of Mg ionic liquid to improve the Mg^{2+} migration at grain boundary, the prepared Mg-ion conducting hybrid solid electrolyte shows superior room-temperature ionic conductivity of $1.1 \times 10^{-4} \text{ S cm}^{-1}$ and an activation energy of 0.36 eV. Through in situ scanning electron microscopy, for the first time we observed the room temperature Mg growth inside a solid-state cell by the evidence of clear-cut metal particle formation and electrolyte particle cracking. The results shown here can act as a good starting point for the understanding of Mg transport behavior in solid-state batteries.

References

- [1] Y. Liang, H. Dong, D. Aurbach, Y. Yao, Nature Energy **5**, 646–656 (2020)
- [2] Z. Wei, R. Maile, L. M. Riegger, M. Rohnke, K. Mueller-Buschbaum, J. Janek, Batteries & Supercaps **5**, e202200318 (2022)

8:00 PM EN02.07.06

Mechanism of High Li-Ion Conductivity in Li-Excess Garnet $\text{Li}_{7-x}\text{La}_x\text{Sr}_x\text{Zr}_2\text{O}_{12}$ MasahideKaneko^{1,2}, KakeruNinomiya¹, TomokoHishida², YukiTakeuchi², KazushiOtani² and MaikoNishibori¹; ¹Tohoku University, Japan; ²Niterra Co., Ltd., Japan

$\text{Li}_7\text{La}_x\text{Zr}_2\text{O}_{12}$ (LLZO) is a promising solid electrolyte for all-solid-state batteries, and various dopants have been investigated to improve its conductivity. However, the dopants have mainly been studied to increase the conductivity by reducing the amount of Li^+ , and dopants that increase the amount of Li^+ have yet to be studied. Therefore, the structure of LLZO with excess Li^+ and its function as an electrolyte need to be clarified. Here, we report on the correlation between the conductivity and the structure of LLZO with excess Li^+ by partial substitution of Sr at the La sites.

Sr-doped LLZO sintered pellets were prepared by solid-state reaction method. The sintered pellets exhibit high conductivity of up to $5.7 \times 10^{-4} \text{ S/cm}$ at room temperature, indicating a promising material as a solid electrolyte.

Sr K-edge XANES spectra confirmed that Sr was located at the La sites of the LLZO. The crystal structure of Sr-substituted LLZO was measured by X-ray diffraction and neutron diffraction, and the results showed that the crystal structure of LLZO continuously changes from tetragonal to cubic with increasing the amount of Sr substitutions. At the same time, the Li^+ arrangement was also changed, with Li^+ occupying some tetrahedral sites that are vacant in the unsubstituted LLZO.

The local structure of Sr-substituted LLZO was discussed from Zr *K*-edge and La *K*-edge XANES. La *K*-edge XANES spectra did not change with Sr substitution, while Zr *K*-edge XANES spectra showed a spectral change corresponding to the amount of Sr substitution. This result suggests that the crystal structure change of Sr-substituted LLZO is not the result of the homogeneous deformation of the entire structure but is mainly due to the deformation of the Zr sites, which are unsubstituted.

The above results suggest that the high conductivity of Sr-substituted LLZO is due to multiple factors: the change in the Li⁺ arrangement and the change in the Li⁺ conduction pathway due to the local structure deformation. Our results contribute to a better understanding of the correlation between the structure and properties of LLZOs in Li excess compositions and the development of higher-performance electrolytes.

8:00 PM EN02.07.07

Effect of Solid-Electrolyte Microstructure on Conductivity and Solid-State Li-Ion Battery Performance John Bachman¹, Maya Horii¹, Rebecca Christianson² and Heena Mutha²; ¹Cal State LA, United States; ²Stark Draper Laboratory, United States

Solid-state batteries offer the potential to improve safety, cyclability, and energy density of Li-ion batteries. However, their conductivity, stability, and processing limit their use. To this end, the effects of solid electrolyte microstructure on overall battery performance are determined. The conductivities of Al-doped Li₇La₃Zr₂O₁₂ (Al-LLZO), with a range of microstructures, are found using a resistor network model. Varying electrolyte properties are combined with a Li-metal negative electrode and LiCoO₂ positive electrode in a 1-D continuum model to predict the effects on performance. Simulations suggest that the ratio of electrolyte conductivity to electrolyte thickness must remain above 10 S/m² to maintain high energy and power output, particularly at C-rates greater than 10. To maintain conductivity near the grain interior conductivity, a grain size at least 10,000 times larger than grain boundary thickness is needed. Further improvements in grain size, grain boundary thickness, and void fraction beyond typical Al-LLZO microstructures, with the goal of higher conductivities, are predicted to have diminishing returns in overall battery performance, even at more sensitive high C-rates up to 100.

8:00 PM EN02.07.08

Understanding the Role of Powder Protective Layers on the Chemical Reactivity of Sulfide-Based Solid Electrolytes in All-Solid-State Batteries Taewoo Kim, Udochukwu D. Eze, Zachary D. Hood, Anil U. Mane, Jeffrey W. Elam and Justin Connell; Argonne National Lab, United States

Sulfide-based solid-state electrolytes (SSE) are a promising class of materials to enable high-performance, all-solid-state Li-ion batteries due to 1) their favorable mechanical properties for processability at scale and 2) comparable Li-ion conductivities to conventional liquid electrolytes. However, their poor atmospheric stability remains a challenge toward commercial manufacturing processes as environmental moisture and oxygen content, even in dry room environments, are sufficient to degrade sulfide-based SSEs. To circumvent these limitations, we previously developed thin (~1 nm) Al₂O₃ coatings grown directly on Li₆PS₅Cl (LPSCl) powders via atomic layer deposition (ALD). Through this approach, we successfully demonstrated substantial suppression of the chemical reactivities of the coated LPSCl under aggressively oxidizing conditions as compared to the uncoated LPSCl. In this work, we provide a comprehensive investigation to understand the role of ALD alumina protective layers on the environmental reactivity of LPSCl utilizing pellets pressed from coated and uncoated powders.

Thermogravimetric analysis indicates significantly suppressed weight gain from powders and pellets made from coated versus uncoated materials after exposure to humidified O₂, demonstrating the effectiveness of the ALD coating strategy in suppressing environmental reactivity regardless of material form factor. Surprisingly, X-ray photoelectron spectroscopy shows little to no changes in the surface chemistry on the uncoated LPSCl surface while the coated LPSCl exhibits a trace of the surface oxidation upon exposure to oxidizing conditions, suggesting that the surface oxidation products of LPSCl are volatile and evaporate under ultra-high vacuum conditions. Correlative X-ray and vibrational spectroscopic and diffraction analysis will be utilized to expand upon the mechanisms by which powder coatings stabilize LPSCl to environmental reactivity and the specific changes in the surface chemistry and the corresponding chemical reactivities. These results provide a clear pathway to enabling stable precursor powder materials with favorable properties for processing at scale in realistic manufacturing environments.

8:00 PM EN02.07.09

A Pseudo-Three-Dimensional Modeling Framework for Liquid and All-Solid-State Lithium-Ion Batteries Ruqing Fang and Juner Zhu; Northeastern University, United States

The multiphase structure of the electrode in liquid lithium-ion ion batteries (L-LIB) and all-solid-state lithium-ion ion batteries (ASSLIB) strongly impact the performance of the batteries. Due to the intrinsic multiphysical and multiphase interactions within electrodes, designing and tailoring the electrode structure is crucial for the improvement of battery performance. An electrode model, which is able to describe the relationship between dominant physical phenomenon in multiscale with the battery performance, is an effective design tool for electrode engineering. In the past decades, the pseudo-two-dimensional (P2D) model proposed by John Newman's group (*Journal of the Electrochemical Society*, 140, 6(1993)) has been widely utilized in modeling multiphase electrodes both in L-LIBs and ASSLIBs. The P2D model describes the ionic transport process at the electrode scale and the ionic diffusion in particle-scale, linking the two scales through a reaction current term representing the Faradaic reaction at the particle surface. However, the P2D framework lacks an effective means of describing surface phenomena occurring at the particle surface, such as phase separation, side reactions, and local mechanical failure at particle surface. To address this limitation, we propose a pseudo-three-dimensional (P3D) framework in this work. The P3D model introduces an additional dimension corresponding to polar or azimuthal angles to characterize the distribution of phenomena at the particle surface. By incorporating the P3D framework, we couple three surface phenomena in L-LIBs and ASSLIBs: phase separation of LFP particles, lithium plating at graphite particles, and the influence of local pores at the particle surface in ASSLIBs, into the original electrode model. We believe that the P3D framework could play an important role in understanding the relationship between the multiphase structure and the output electrochemical performance of the batteries, serving as an effective design tool for electrode engineering in all-solid-state and liquid lithium-ion batteries.

8:00 PM EN02.07.10

Porous Silicon-Based Anodes for Extreme Temperatures Morteza Sabet¹, Mihir Parekh¹, Yi Ding², Srikanth Pilla¹ and Apparao M. Rao¹; ¹Clemson University, United States; ²U.S. Army DEVCOM GVSC, United States

Primary lithium thionyl chloride batteries are common power sources for applications requiring extreme temperature windows. However, the peak performance of these non-rechargeable batteries is between 20 °C and 55 °C. Advancing lithium-ion batteries (LIBs) with robust electrodes and proper electrolyte formulation for high temperatures (>50 °C) would offer rechargeability, higher power capability, and reduced toxicity. Common LIB anode materials, such as silicon (Si), rely on forming solid-electrolyte interphase (SEI) as an effective passivation layer to operate properly. Damages to these surface structures would render the interfaces vulnerable at elevated temperatures. The chemical composition and morphological evolution of the SEI strongly depend on the electrolyte used. In the presence of organic electrolytes, the exposure of Si to elevated temperatures leads to a fast SEI thickening and capacity loss. Ionic liquids exhibit a wide electrochemical potential stability up to 5.0 V, high thermal stability (>300 °C), and moderate Li ion conductivity at room temperature. The use of ionic liquids in combination with appropriate additives could be an ideal solution to stabilize the SEI at high temperatures. In the current study, we demonstrated the potential of Si nano-quills (SiNQs), a porous Si-based material with elemental Si pockets distributed in a matrix of Si suboxides, as the active material for high-temperature LIB anodes. Electrodes were prepared by casting the aqueous slurry of SiNQ on copper foil, followed by hot rolling to a desired density. Half cells were prepared using SiNQ electrodes and a piperidinium-based ionic liquid electrolyte and cycled at 50, 60, and 70 °C. At 50 °C, the SiNQ anodes exhibited a reversible capacity of 225 mAh g_{Si}⁻¹ at the current rate of 0.1C (420 mA g_{Si}⁻¹). Testing at higher temperatures of 60 and 70 °C resulted in a higher capacity of 1040 and 1240 mAh g_{Si}⁻¹. This indicates the reduced electrolyte viscosity at higher temperatures, which can enhance the kinetics of lithiation and delithiation in the SiNQ active material.

8:00 PM EN02.07.11

Multi-Layer Thin Film Polymer-2D Nanofiller Composites for Ultra-High Capacitive Energy Storage Application Nihar R. Pradhan¹, Sumit R. Bera¹, Rukshan M. Thantrige¹, Brian T. Shook¹, Maninderjeet Singh², Dharmaraj Raghavan³, Anirudha Sumant⁴, Alamgir Karim² and Emily C. Davidson⁵; ¹Jackson State University, United States; ²University of Houston, United States; ³Howard University, United States; ⁴Argonne National Laboratory, United States; ⁵Princeton University, United States

Recently thin film polymer base dielectric nanocomposite materials show remarkable application in energy storage devices. The polymer-based dielectric capacitors have the advantages of flexibility, fast charge and discharge, low loss, and graceful failure. Elevating the use of polymeric dielectric capacitors for advanced energy applications such as electric vehicles (EVs) however, requires significant enhancement of their energy densities. Here, we report a polymer thin film heterostructure-based multi-layered capacitor using poly(vinylidene fluoride) and stratified 2D nanofillers (Mica or *h*-BN nanosheets) that shows enhanced permittivity, high dielectric strength and an ultra-high energy density of ≈ 90 J/cm³ with efficiency over 60% at high field. This approach of using oriented 2D nanofillers-based polymer heterostructure composites is expected to be versatile for designing high energy density thin film polymeric dielectric capacitors for myriads of applications.

8:00 PM EN02.07.12

Utilizing High Tensile Alloys of Copper to Eliminate Mechanical Degradation in High Loading Silicon Anodes Devashish Salpekar, Daniel Abraham, Wenquan Lu, Marco-Tulio F. Rodrigues and Stephen E. Trask; Argonne National Laboratory, United States

Silicon is a promising candidate to replace the conventionally used graphite anodes due to its high theoretical capacity (3579 mAh/g; Li_{3.75}Si), low cost, and abundance. However, silicon undergoes huge volumetric expansion (~300%) upon lithiation, which leads to particle isolation and thus, poor cycle life. Polymeric binders such as polyacrylic acid and carboxy methyl

cellulose, have been used to overcome this problem by binding with silicon particles. However, these binders do not provide a strong adhesion between the coating and the current collector, which can lead to delamination upon prolonged cycling. Recently, stronger polymeric binders (such as polyimide, polyamide, etc.) have received attention due to their improved interfacial interactions and mechanical strength, creating a cohesive silicon anode with excellent coating adhesion to the current collector. However, at higher loadings the huge volumetric changes in the silicon combined with the strong adhesive properties of binders leads to plastic deformations in the current collector, which on extended cycling can significantly wrinkle or in the worst case shred the metal foil. We are investigating high tensile alloy (HTA) copper current collector foils, which have tensile strengths that are more than double that of conventional copper foils. Due to their improved mechanical properties, these foils do not undergo plastic deformation upon silicon lithiation and prevent shredding upon continuous cycling. Electrochemical testing data suggest that at moderate silicon loadings (2.5-3 mAh/cm²), electrodeposited or rolled copper show significant wrinkling after only 5 cycles in a half-cell, whereas the HTA foils show no wrinkling. This effect increases significantly at higher loadings (>5 mAh/cm²), where the conventional copper foils show significant wrinkling after just one lithiation-delithiation cycle, while the HTA copper shows no wrinkling. By utilizing this HTA copper foils, it is possible to eliminate mechanical issues in the anode current collector, especially in high loading silicon cells with strong polymeric binders.

8:00 PM EN02.07.13

Ion Transport Mechanism in Argyrodite Electrolyte and Their Effect on the Electrochemical Performance in all Solid-State Lithium Battery RavindraK. Bhardwaj; Bar Ilan University, Israel

Commercialization of lithium-ion batteries (LIB) enabled a new era of portable devices, electric vehicles, and grid energy storage. However, the ever-increasing demand of modern society for advanced energy storage packages, including for large energy storage units for grid and remote locations, challenges the scientific community to realize further advancements in batteries, with desirable energy and power densities, extended lifetime, improved safety and lower cost.¹ The current state of the art LIB is composed of three major components: graphite anode, organic electrolyte solution and inorganic cathode material. However, the usage of organic solvents is imposing some critical technical and practical limitations. These limitations are related to safety issues (due to electrolyte flammability), longevity issues (due to electrolyte degradation and volatility), and limited energy density of the battery (due to the solvent's limited electrochemical stability).² In recent years there is increased interest in developing solid electrolytes (SEs) for all solid-state LIB (SSLIB). A SSLIB could potentially increase the volumetric as well as specific energy density of SSLB. Furthermore, eliminating the volatile organic electrolyte in SSLIB will significantly improve the safety of the battery and extend the operating temperature of the cell. In our previous published work, we systematically studied the electrochemical behaviour of three different argyrodites based solid electrolytes by varying the halogen (Li₆PS₅X [X = Cl, Cl_{0.5}Br_{0.5}, or Br]).³ Using LiNi_{0.6}Co_{0.2}Mn_{0.2}O₂ (NCM622) as a model cathode, we also studied the electrochemical performance of these SEs in ASSLB cells. In the present work, we show the ion transport mechanism in three different argyrodite-based solid-electrolytes (SEs), with a general composition of Li₆PS₅X (X = Cl, Cl_{0.5}Br_{0.5}, or Br). The presentation will also discuss the correlation of ion transport with the electrochemical performance the argyrodite-based solid-electrolytes (SEs) in ASSLIB.

References:

- (1) Battery, S. L.; Summit, I. The Rechargeable Battery Market and Main Trends 2012-2025. **2013**, No. September.
- (2) Feng, X.; Ouyang, M.; Liu, X.; Lu, L.; Xia, Y.; He, X. Thermal Runaway Mechanism of Lithium Ion Battery for Electric Vehicles: A Review. *Energy Storage Mater.* **2018**, *10*, 246–267.
- (3) Wang, L.; Rahamim, G.; Vudutta, K.; Leifer, N.; Elazari, R.; Behar, I.; Noked, M.; Zitoun, D.; Influence of the Halogen in Argyrodite Electrolytes on the Electrochemical Performance of All-Solid-State Lithium Batteries. *Energy Technol.* **2023**

8:00 PM EN02.07.14

Alkali-Independent Anion Redox in LiNaFeS₂ Michelle Qian, EshaanPatheria, ColinMorrell and KimberlyA. See; Caltech, United States

Batteries based on sodium ions are a promising, more sustainable alternative to the currently dominant lithium-ion battery, but have comparatively lower energy densities. One method of increasing energy density is to develop cathode materials that can undergo multielectron cation and anion redox, which we have previously observed using the layered material LiNaFeS₂ in a lithium cell. In LiNaFeS₂, anion redox occurs through the formation of persulfide bonds that is correlated to a plateau in the galvanostatic charge curve at ~2.5 V vs Li/Li⁺. We now demonstrate that LiNaFeS₂ can also be used as a multielectron sodium cathode, although the anion-redox plateau region of the second charge curve resembles the sloping profile of a solid-solution process rather than the two-phase process reflected in a lithium cell. Inductively-coupled mass spectrometry studies verify sodium as the dominant mobile ion after first charge, correlating the difference in electrochemical behavior with the active alkali ion. Fe and S K-edge X-ray absorbance spectroscopy shows that the charge compensation mechanisms for the material in the two cell configurations are fundamentally the same. The disparate electrochemical behavior is entirely due to physical rather than electronic structural effects. Our work provides a fundamental study on the differences between Li- and Na-based anion redox in the same material.

8:00 PM EN02.07.15

A Solid-State Zinc-Iodide Battery with Zinc Dendrite Free and Long Cycle Life YongxinHuang, BinLuo and LianzhouWang; The University of Queensland, Australia

Rechargeable zinc-iodide (ZnI₂) batteries have become a popular choice for applications in aqueous batteries due to their natural abundance, intrinsic safety, and high theoretical capacity. However, in the alkaline or weakly acidic water environment of aqueous electrolytes, the hydrogen evolution reaction and the subsequent battery swelling and failure have hindered the practical application of such batteries so far. In addition, the environment of electrolyte will also promote the growth of zinc dendrites, which will not only reduce the utilization of zinc foil, but also cause the dendrites to penetrate the separator and cause a short circuit in the battery. Based on traditional zinc salts and a Perfluoropolyether (PFPE)-based polymer, an all-solid-state zinc iodide battery with solid polymer electrolyte was designed and synthesized by ion exchange. According to the results of XPS and XRD, it can be proved that this polymer solid electrolyte forms a SEI layer containing rich Fluorine on the surface of zinc to induce the horizontal growth of zinc dendrites and increase the utilization of zinc. More importantly, this induction method inhibits the possibility of continuously generated dendrites penetrating the separator and greatly extends the cycle life of the battery. In addition, it can also be proved that this solid electrolyte can also hinder the iodine ion shuttle effect, thereby reducing the corrosion of the zinc sheet and further prolonging the life of the battery. Symmetric batteries based on this electrolyte exhibit excellent cycle performance of more than 4000 hours at room temperature, and all-solid-state ZnI₂ batteries can be stably cycled for more than 3000 times. This work proposes a potential route to achieve stable energy storage in solid-state ZnI₂ batteries, and also provides new ideas for flexible and wearable Zn-based batteries.

8:00 PM EN02.07.16

Thin-Film Model Systems for Operando Studies of Interfacial Battery Degradation TrevorB. Binford¹, JoshuaGibson^{1,2}, LeanneJones¹, Tien-LinLee³ and RobertWeatherup¹; ¹University of Oxford, United Kingdom; ²University of Edinburgh, United Kingdom; ³Diamond Light Source, United Kingdom

Degradation is a pressing challenge for next-generation lithium-ion batteries, which often struggle to balance capacity versus stability. A better understanding of the chemical changes that occur over a cell's lifetime will help guide rational design of materials for superior batteries. However, the key reactive areas are buried deep within a cell and are difficult to access. The cathode-electrolyte interface (CEI) is believed to be particularly important in battery degradation, but photoelectron techniques can typically only be brought to bear on it by *ex-situ* disassembly of the entire cell. Doing so will inevitably induce changes and introduce contaminants to the surfaces under study.

To better observe the interface between lithium intercalation cathodes such as LiCoO₂ and solid electrolytes, we present a novel architecture for *operando* X-ray photoelectron spectroscopy (XPS). Our design enables simultaneous XPS and electrochemical measurements via an all-solid-state thin-film cell giving insights into the dynamic changes with states of charge. By forming the cathode as a suspended thin film with a thickness on the order of 10 nm, we can probe through the entire cathode to the CEI. Synchrotron-based hard X-ray photoelectron spectroscopy (HAXPES) allows for the characterisation of the interface due to the increased inelastic mean free path of electrons when using higher energy X-rays. Coupling HAXPES with soft XPS provides complementary information regarding the bulk and surface. Combining the thin-film cathode with a solid-state electrolyte and anode produces a cell that is compatible with the ultra-high vacuum conditions found in XPS systems, which are a limiting factor when conducting *operando* measurements with liquid electrolytes.

This thin-film construction offers a key benefit as a model system, as it eliminates any extraneous structural or conductive additives that could complicate interpretation of the chemistry at the cathode-electrolyte interface. The CEI remains buried, without any exposure to surface contaminants or even vacuum, while still being accessible for measurement. In this way, we can compare the degradation effects at different layers of the structure and between different points in the cell's charging cycle. Such insights into the degradation products will point toward future approaches for more stable and high-capacity battery designs.

8:00 PM EN02.07.17

Controlling Lithium Plating and Stripping in Batteries with a Glassy Metal-Organic Framework Artificial Layer JunweiDing, TaoDu and MortenM. Smedskjaer; Aalborg University, Denmark

Constructing an artificial solid electrolyte interface (SEI) layer is an effective strategy to suppress Li dendrites and alleviate volume changes during Li deposition/stripping in solid state batteries. Compared with conventional crystalline materials, glassy materials can achieve isotropic ion transport. In this work, we compare the use of nanoporous zeolitic imidazolate framework, ZIF-62, crystals and glasses as artificial SEI. Ab initio molecular dynamics simulations reveal that the ZIF-62 glassy features faster and more uniform lithium-ion conduction compared to the ZIF-62 crystal, which exhibits ion aggregation. We have also prepared experimental samples by using ZIF-62 glass or crystal as an artificial modification layer on a copper

current collector by the traditional doctor blading method. The composite lithium negative electrode is obtained by electrochemical deposition. The lithium-lithium symmetric electrical tests show that the ZIF-62 glass modification layer exhibits low ion migration energy barrier, enabling controllable and stable lithium deposition/stripping. Lithium iron phosphate has also been used as a positive electrode form full batteries. The full battery based on the ZIF-62 glass modification layer has high battery capacity, excellent rate performance and long-term cycle stability. At the same time, it also exhibits excellent electrochemical performance when matched with the high-voltage lithium cobalt oxide cathode. These findings demonstrate the excellent application prospects of using metal-organic framework glasses for Li metal anode.

8:00 PM EN02.07.18

MOF Glass Based Solid-State Polymer Electrolyte for Lithium Metal BatteriesJunweiDing and MortenM. Smedskjaer; Aalborg University, Denmark

Polymer solid-state electrolytes are promising candidates for solid-state batteries, but fillers play a very critical role in adjusting their network structure, electrochemical properties, thermal stability, and mechanical properties. However, most of the fillers reported so far are anisotropic, which limits the potential to enable isotropic ion transport. Here, we prepare a novel polymer solid-state electrolyte based on a metal-organic framework (MOF) glass, namely ZIF-62 glass. Calorimetry and ion diffusion kinetics tests show that the addition of ZIF-62 glass reduces the glass transition temperature of the polymer substrate, thereby increasing the content of disordered components in the polymer electrolyte. In turn, this facilitates lithium-ion transport. Li-Li symmetric cell tests show that the polymer electrolyte containing ZIF-62 glass has low overpotential, indicating a low interfacial impedance. Due to its isotropic characteristics, the MOF glass can be closely combined with the disordered components in the polymer substrate to form a close contact interface, thereby promoting the lithium-ion diffusion. The developed MOF glass polymer electrolyte-based lithium-lithium iron phosphate full batteries therefore deliver high cycle stability and rate capability.

8:00 PM EN02.07.19

Strain Effect on Li-Ion Conduction in β -Li₃PS₄ and Garnet Al-Li₇La₃Zr₂O₁₂ Solid ElectrolytesPiotrsZguns, ShikhaSaini and BilgeYildiz; Massachusetts Institute of Technology, United States

Solid-state batteries offer better safety and higher energy density, yet the Li-ion conductivity of the solid electrolytes remains lower than that of liquid organic electrolytes, limiting battery charging rate and power density. The ionic conductivity of solid electrolytes can be significantly affected by strong electrochemo-mechanical coupling, especially near the electrode/electrolyte interfaces. Mechanical stresses due to volumetric electrode changes and interfacial reactions can reach as high as 1..10 GPa [1,2] and can substantially affect solid electrolyte's conductivity. However, experimental quantification of the sole strain effect is difficult as other factors such as space charge effects and interfacial reactions also contribute to conductivity. In this work [3], we have quantified the effect of strain on conductivity in bulk β -Li₃PS₄ by means of ab initio molecular dynamics. Strain tensors that compress the c-axis increase the Li-ion diffusivity, while the strains which stretch the c-axis reduce the diffusivity. The relative change in diffusivity with 2% biaxial strain is 2-fold at 500 K and is up to 10-fold when extrapolated to room temperature. Compression of the c-axis facilitates diffusion through the increased disorder of the Li-sites in β -Li₃PS₄. Strain decreases the Li-Li distance and thus increases Coulomb repulsion between the bottleneck 8d and 4b sites, pushing Li to the 4c site and promoting disorder. This boosts the concentration of active Li-ion carriers, which quantitatively correlates with the changes in conductivity. The magnitude of the strain effect on Li-ion diffusion is comparable to that of chemical doping, and it is therefore important to consider strain for accurate understanding and prediction of solid-state Li-ion battery interface properties. Our findings not only provide a quantitative understanding and accurate estimates of Li-ion conductivity relevant to strained interfaces, but also a design strategy for how to increase disorder and promote superionic conduction in solid electrolytes by strain engineering. We are also extending these findings to materials that possess intrinsic Li-ion disorder such as garnet Al-doped LLZO (Li₇La₃Zr₂O₁₂). By applying molecular dynamics simulations, we will investigate how Al-LLZO conductivity is affected by strain and whether decreasing/increasing Li-Li distances contribute to ionic disorder and conductivity in a similar fashion to β -Li₃PS₄.

References

- [1] H.-K. Tian, A. Chakraborty, A. A. Talin, P. Eisenlohr, and Y. Qi, Evaluation of the electrochemo-mechanically induced stress in all-solid-state Li-ion batteries, *J. Electrochem. Soc.* **167**, 090541 (2020).
- [2] H. Fathiannasab, L. Zhu, and Z. Chen, Chemo-mechanical modeling of stress evolution in all-solid-state lithium-ion batteries using synchrotron transmission x-ray microscopy tomography, *J. Power Sources* **483**, 229028 (2021).
- [3] P. Zguns and B. Yildiz, Strain Sensitivity of Li-ion Conductivity in β -Li₃PS₄ Solid Electrolyte, *PRX Energy* **1**, 023003 (2022)

8:00 PM EN02.07.20

A Synthesis of Block Copolymers Based on Dynamic Covalent Bonds and its Application to All-Solid-State Battery ElectrolyteSojeongRoh, Trong DanhNguyen, LeeHyeju, Min GueLee, So HyunPark, Jun SeopLee and Young SooYoon; Gachon University, Korea (the Republic of)

Recently, all-solid-state batteries (ASSB) have been in the spotlight as an alternative to potentially overcome the limitations of the existing liquid electrolyte lithium-ion batteries (LIB). Compared to liquid electrolyte LIB, ASSB has a lower risk of explosion, a higher energy density, and a relatively large electrochemical window. Solid electrolytes are largely classified into three categories: sulfide-based solid electrolytes, oxide-based solid electrolytes, and polymer-based solid electrolytes as key elements of ASSB. The most representative case among them is the lithium lanthanum zirconium oxide (LLZO), which has been extensively studied because it may easily compensate for the shortcomings of the sulfide-based solid electrolyte. Nevertheless, due to the brittleness of the ceramic-based material, it is still difficult to solve a serious interface contact problem between the electrolyte and the electrode. Therefore, many previous studies have attempted to introduce flexible polymer materials as binders to provide better wettability between solid interfaces. Specifically, ceramic-polymer composite solid electrolytes with soft interlayer in LLZO are feasible solutions that improve interfacial contact and inhibit dendrite generation in LIB. However, it is difficult to obtain sufficient ion conductivity and required mechanical properties in the polymer layer at the same time. Therefore, it is necessary to manufacture a flexible polymer membrane that can effectively promote efficient ion transport and control adhesion.

This presentation proposes to synthesize a block copolymer based on a dynamic polymer chain structure and apply the material to an ASSB electrolyte. First, the disulfide (S-S) dynamic bond between the dithiol contained oligomer and PEG chain is synthesized using a disulfide generating agent (pentaerythritol tetrakis (3-mercaptopropionic acid)). The polymer solution for interlayer film is generated by adding bis (trifluoromethanesulfonyl)imide (LiTFSI). Then, a hybrid ceramic-polymer complex is manufactured using a drop casting method that introduces a block copolymer layer on the surface of garnet LLZO. As a result, the dynamic disulfide bond in co-polymer chain improves the adhesion between the solid electrolyte and the cathode as well as the anode, leading to a better contact interface and good dendrite suppression ability. That is, the lithium-ion conductive dynamic network not only lowers the overall impedance and interfacial resistance, but also increases the adhesion of the electrolyte to the electrode material. These modified polymer networks provide adequate ion conductivity and improved wettability to the interface. Through this work, it is possible to effectively develop LLZO-based solid electrolyte that improves surface properties and regulates the ion conduction mechanism.

8:00 PM EN02.07.21

Development of Von-Alpen-Type NASICON Electrolytes with High Ionic Conductivities and Relative DensitiesIl-SeopJang^{1,2} and JinyoungChun¹; ¹Korea Institute of Ceramic Engineering and Technology, Korea (the Republic of); ²Korea University, Korea (the Republic of)

The NASICON compound, represented by the chemical formula Na_{1+x}Zr₂Si_xP_{3-x}O₁₂ (0 ≤ x ≤ 3), exhibits a Na⁺ ion conductivity of approximately 10⁻⁴ S cm⁻¹ and a wide electrochemical window. It is chemically stable not only in air but also in seawater. However, the ion conductivity of NASICON compounds is relatively lower compared to typical liquid electrolytes (10⁻² S cm⁻¹), leading to decreased performance. In this study, a method is proposed to enhance the ion conductivity and density of vA-NASICON (von-Alpen-type NASICON) ceramic electrolytes by doping them with heterogeneous element Mg²⁺ ions. Additionally, a synthesis method utilizing a sintering aid for vA-NASICON is suggested to achieve higher ion conductivity and density at lower temperatures and shorter times.

Considering factors such as raw material cost, ion radius, and oxidation state, Mg²⁺ ions were chosen as heterogeneous element dopants compared to the Zr⁴⁺ ions present in NASICON compounds. The effects of Mg dopant incorporation on the modified crystal structure, surface changes, and formation of secondary phases were analyzed, and their influence on the ion conductivity of vA-NASICON was studied. The dopant precursor, MgO, can enhance the surface diffusion coefficient, increase the densification rate, and promote crystal growth. However, excessive introduction of Mg²⁺ leads to the formation of undesirable secondary phases, such as Na₂Mg₃PO₄, which results in a decrease in the ion conductivity of Mg-doped vA-NASICON. By analyzing the ion conductivity, the optimal Mg doping level was determined. The vA-NASICON synthesized with the optimal Mg doping exhibited a higher ion conductivity of 3.64x10⁻³ S cm⁻¹ compared to undoped vA-NASICON (2.03x10⁻³ S cm⁻¹).

The introduction of Glass-frit in vA-NASICON can increase the sinterability of the ceramic matrix and lower the densification sintering temperature. vA-NASICON was prepared by solid-state reaction, and systematic investigations were conducted on crystal structure, microstructure, and electrochemical properties. Glass-frit added vA-NASICON sintered at 1200 degree for 1 hour showed a high ionic conductivity of 2.1x10⁻³ S cm⁻¹ and a relative density of 97.2%, surpassing vA-NASICON (2.54x10⁻³ S cm⁻¹, relative density 65.7%) without addition. Glass-frit is that by forming an amorphous phase at the grain boundary, it can promote grain boundary contact and promote densification of ceramic electrolyte. The results of this study are expected to be effectively utilized in the development of oxide-based solid electrolytes with high ionic conductivity and density.

8:00 PM EN02.07.22

Understanding Cold Sintering Processes in Densification of Halide-Based Solid ElectrolytesQianqianYan, ColeD. Fincher and Yet-MingChiang; Massachusetts Institute of Technology,

Halide-based ceramics have emerged as promising candidates for solid-state Li battery applications due to their high ionic conductivity and air stability. However, their manufacture and processing pose a challenge for solid-state batteries, as conventional ceramic processing often requires elevated temperatures and pressures. In this study, we develop cold sintering processes (CSPs) for halide-based solid-state electrolytes. We enable densification of these materials below 300°C by studying the impact of liquid-phase additives on dissolution / reprecipitation during pressure-densification. We further explore the influence of pressure, dwell time, temperature, and precursor compositions on the electrolyte's mechanical and electrochemical properties. The systematic investigation of these parameters provides crucial insights into the underlying mechanisms governing the densification process and contributes to designing and manufacturing of ceramic solid electrolyte architectures.

8:00 PM EN02.07.23

Multicomponent Protective Layers for All-Solid-State Li Metal Batteries HaechannaraLim, SeunggooJun, Ki HeonBaek and Yoon SeokJung; Yonsei University, Korea (the Republic of)

The advancement of electric vehicles has stimulated extensive research into lithium-ion batteries (LIBs) with higher energy densities and improved safety. Consequently, all-solid-state Li metal batteries (ASLMBs) have emerged as a promising alternative due to the exceptional theoretical capacity ($3,860 \text{ mA h g}^{-1}$) and low electrochemical potential (-3.04 V vs SHE) of Li metal anode, as well as their improved safety resulting from the utilization of nonflammable inorganic solid electrolytes (SEs) compared to conventional lithium-ion batteries employing liquid electrolytes. Especially, sulfide solid electrolytes (SEs) have been one of the most promising candidates thanks to their high ionic conductivities (maximum $\sim 2.0 \times 10^{-2} \text{ S cm}^{-1}$) and mechanically ductile property. Nevertheless, the implementation of ASLMBs has been hindered by the unstable interfaces between Li metal and SEs, leading to severe decomposition of sulfide SEs and the formation of dendrites. To address the challenges related to interfacial instability, researchers have proposed various materials, such as lithiophilic metals and inorganics, as protective layers for Li metal. Nevertheless, no single protective coating has achieved acceptable interfacial stability between Li metal and SEs. Recently, the concept of multi-component protective layers comprising lithiophilic metals and robust inorganic materials has been introduced. However, there remains a lack of comprehensive analysis regarding the configuration or structure of the protective layer and its influence on the performance of ASLMBs.

In this study, we present our recent investigation into the configuration of protective layers for Li metal and their impact on the performance of ASLMBs. Additionally, we discuss different mechanisms of Li metal plating and stripping based on variations in the protective layer's structure.

8:00 PM EN02.07.24

Liquid-Phase Synthesis of Metal-Containing (M = Ge, Sn) Sulfide Solid Electrolytes for All-Solid-State BatteriesBoyeongJang, JehoonWoo, Yong BaeSong, HiramKwak and Yoon SeokJung; Yonsei University, Korea (the Republic of)

All-solid-state batteries (ASSBs) have been spotlighted for their potential to enhance both energy density and safety compared to conventional lithium-ion batteries that rely on organic liquid electrolytes. Sulfide solid electrolytes (SEs) are viewed as crucial components for ASSBs due to their high ionic conductivity, deformability, composition flexibility, and processability. Sulfide SEs can be prepared through either solid-state or liquid-phase synthesis. Particularly, the liquid-phase synthesis of sulfide SEs offers potential advantages for large-scale production, including product homogeneity, particle size control, and lower energy consumption. However, the compatibility and solubility challenges between precursors and solvents limit the liquid-phase synthesis of various compositions of sulfide SEs. Specifically, the poor solubility of metal chalcogenides (e.g., GeS_2 and SnS_2) has hindered the synthesis of sulfide SEs with MS_4 (M = Ge, and Sn) units. Furthermore, liquid-phase synthesized SEs are often contaminated by impurities such as carbon, derived from solvent residues, which are detrimental to the performance of ASSB cells.

In this presentation, the liquid-phase syntheses of sulfide SEs with various compositions, including metals (e.g., Ge and Sn). Importantly, we report a novel heat treatment technique to address the chronic carbon impurity issue in liquid-phase synthesized SEs. Compared to SEs prepared through conventional furnace heating, SEs obtained through a new heating protocol exhibit outstanding electrochemical performance in terms of capacity and cycling stability.

[1] *Adv. Energy Mater.* **2018**, *8*, 1800035

[2] *Adv. Mater.* **2022**, 2200083

[3] *Adv. Energy Mater.* **2023**, 2203292

8:00 PM EN02.07.25

Transforming Commercial Paper into Flexible Solid Electrolyte with High-Ionic Conductivity for Durable Lithium-Sulfur BatteriesMortezaSabet¹, NawrajSapkota¹, MihirParekh¹, NancyChen¹, YiDing², SrikanthPilla¹ and ApparaoM. Rao¹; ¹Clemson University, United States; ²U.S. Army DEVCOM GVSC, United States

Solid-state lithium-sulfur (Li-S) battery technologies could power future electric mobility due to their potential high energy density. However, the current solid-state Li-S batteries face several challenges, such as high internal impedance at the electrode/electrolyte interfaces, shuttling of lithium polysulfides, and Li dendrite formation. Herein, we introduced a Li-rich cellulose-based solid-state electrolyte in combination with sulfurized polyacrylonitrile (SPAN, 36.5 wt.% S) cathode, leading to high-capacity and durable Li-S batteries. We utilized SPAN due to its reasonable conductivity, high reversible capacity, and stable cycling performance. Adopting the procedure described in **Ref. 1**, the solid-state electrolyte in this study was prepared by infusing Li ions (Li^+) into a copper-coordinated commercial cellulosic paper. The infusion of Li^+ was carried out by soaking the copper-treated paper in a 1 M LiTFSI in $\text{EC}_{0.5}\text{DME}_{0.25}\text{DOL}_{0.25}$ solution (where subscripts indicate the volume fraction), followed by complete evaporation of the solvents. The prepared solid-state electrolyte ($\sim 300 \mu\text{m}$ in thickness) exhibited high room-temperature ionic conductivity of $1.5 \times 10^{-4} \text{ S cm}^{-1}$, superior to the reported values for solid-state electrolytes with similar thicknesses. The Li-SPAN cell with paper-based electrolyte delivered a room-temperature reversible capacity of 1350 mAh g^{-1} in the first cycle and 990 mAh g^{-1} after 100 cycles at 0.1C (1C: 1675 mAh g^{-1}), with a capacity retention of 73.33%. The conformability of the paper-based electrolyte ensures good interfacial contact with the SPAN and Li electrodes. As a result, when this solid-state Li-S battery was tested at 0.5C and 1C, it delivered a reversible capacity of 800 and 400 mAh g^{-1} , respectively. In this talk, we will outline the results from our electron microscopy, electrochemical impedance spectroscopy, and cyclic voltammetry studies to unravel the superior performance of paper-based Li-S batteries. We will also present the cycling performance of our cells for high-temperature applications.

Ref. 1: Yang, C., Wu, Q., Xie, W. et al. Copper-coordinated cellulose ion conductors for solid-state batteries. *Nature* 598, 590–596 (2021).

SESSION EN02.08: Dynamics in Sulfide Electrolyte Battery

Session Chairs: Xin Li and Fang Liu

Wednesday Morning, November 29, 2023

Hynes, Level 3, Room 304

8:00 AM EN02.08.01

Evolution of Interfacial Cathode Kinetics in Sulfide All-Solid-State Li Batteries Measured with Electrochemical Impedance Spectroscopy (EIS)AlyssaStavola, DominickGuida, XiaoSun, HongliZhu and JoshuaW. Gallaway; Northeastern University, United States

Sulfide all-solid-state Li batteries (ASLBs) suffer from a large capacity loss on the first cycle jeopardizing their commercialization and energy density. This large initial coulombic mismatch is theorized to be due to formation of the cathode electrolyte interface (CEI) and volume changes in the cathode material resulting in increased internal resistance and a loss of electrochemically active surface area respectively.¹ We have previously reported an operando analysis of Li^+ and e^- conduction across a composite cathode based on $\text{Li-Ni}_{1/3}\text{Mn}_{1/3}\text{Co}_{1/3}\text{O}_2$ (NMC111) and $\text{Li}_6\text{PS}_5\text{Cl}$ (LPSC) during initial cycling.² This analysis indicated that conduction during initial cycling was subject to high tortuosity factors (t^2) for both the LPSC and NMC phases. Additionally, the t^2 values evolved during the initial battery charge step. Because cathode performance was limited by conduction, we were unable to infer information about kinetic phenomena, e.g. the charge transfer rate between LPSC and NMC, from the experimental results. In particular, the first cycle capacity loss may be caused by a drop in interfacial kinetics.

To study this capacity loss as a function of state-of-charge, in situ EIS was performed during initial cycling of a full cell with a composite cathode based on NMC111 and LPSC (Li/In| $\text{Li}_6\text{PS}_5\text{Cl}$ |NMC111/ $\text{Li}_6\text{PS}_5\text{Cl}$). This piecewise EIS allows us to analyze both time dependent and state-of-charge dependent interfacial processes while the battery cycles with no modifications to cell design. A transmission line model allowed for quantification of the electrochemically active surface area and its effect on resulting capacity during the first charge of this ASLB system.

Acknowledgments

We acknowledge financial support from the National Science Foundation under Award Number CBET-ES- 1924534.

References

1. Koerver, R.; Ayyun, I.; Leichtweiß, T.; Dietrich, C.; Zhang, W.; Binder, J. O.; Hartmann, P.; Zeier, W. G.; Janek, J., Capacity Fade in Solid-State Batteries: Interphase Formation and Chemomechanical Processes in Nickel-Rich Layered Oxide Cathodes and Lithium Thiophosphate Solid Electrolytes. *Chemistry of Materials* **2017**, *29* (13), 5574-5582.
2. Stavola, A.M.; Sun, X.; Guida, D.P.; Bruck, A.M.; Cao, D.; Okasinski, J.S.; Chuang, A.C.; Zhu, H.; and Galloway, J.W. "Lithiation Gradients And Tortuosity Factors In Thick NMC111-Argyrodite Solid-State Cathodes," *ACS Energy Letters*, **2023**, *8*, 1273-1280.

8:15 AM EN02.08.02

Decoupling Irreversible and Reversible Inefficiencies at Dynamic Interfaces in Sulfide Solid State Battery Positive Electrodes Emma Kaeli¹, Xiaomian Yang¹, Zhelong Jiang¹, Sunny Wang¹, Edward Barks¹, Yan-Kai Tzeng², Stephen Kang¹ and William C. Chueh¹; ¹Stanford University, United States; ²SLAC National Accelerator Laboratory, United States

Battery systems present a uniquely difficult environment for disentangling sources of inefficiency. As an example, positive electrode-electrolyte interfaces incur simultaneous charging-induced side reactions, surface area change, and lithiation-state dependent intercalation rates. For sulfur-based composite electrodes in solid state batteries (SSBs) these parallel processes present a formidable challenge to addressing first cycle Coulombic inefficiency.¹ Without fully decoupling inefficiencies, it is unclear which degradation mechanism is most critical to address and, further, how applied solutions impact each mechanism in turn. For example, to mitigate unwanted side reactions between sulfide solid electrolytes (SEs) and positive electrode materials like $\text{LiNi}_x\text{Mn}_y\text{Co}_{1-x-y}\text{O}_2$ (NMC), the field has implemented interfacial coatings to increase Coulombic efficiency.²⁻⁴ While coating design focuses on thermodynamic stability at the interface, the coatings could be improving battery performance by addressing other inefficiencies in parallel, such as increasing the rate of the intercalation reaction or reducing ionic constriction at the NMC/SE interface.

This work systematically decouples the impacts of ionic constriction, electrolyte redox and NMC/SE interphase formation in sulfide-SE SSB first cycle electrochemistry to better inform design of solutions for the NMC/SE interface. Using uncoated $\text{LiNi}_{0.5}\text{Mn}_{0.3}\text{Co}_{0.2}\text{O}_2$ we demonstrate a method to delineate contributions to Coulombic inefficiency between slow kinetics and irreversible reactions. To determine the reversibility of interphase products and the impact of cycling history we track lithiation state and generation of interphase products during cycling. We determine the ability of generated interphase products to contribute to self-discharge of NMC and the resultant impact on Coulombic inefficiency. Using two different electrolytes, Li_3PS_4 and $\text{Li}_3\text{PS}_6\text{Cl}$, which have well-defined but unique thermodynamically-predicted redox reactions and reaction potentials, we separate contributions to Coulombic inefficiency between electrolyte redox reactions and reactions involving transition metals and oxygen from NMC. Finally, by comparing borate-coated and uncoated NMCs, we investigate the coating's impact on interphase formation, ionic constriction and intercalation reaction rate.

- [1] Janek, J., Zeier, W.G. Challenges in speeding up solid-state battery development. *Nat Energy* **8**, 230-240 (2023). <https://doi.org/10.1038/s41560-023-01208-9>
- [2] Morino, Y., Kanada, S. Degradation Analysis by X-ray Absorption Spectroscopy for LiNbO_3 Coating of Sulfide-Based All-Solid-State Battery Cathode. *ACS Applied Materials & Interfaces* **15** (2), 2979-2984 (2023). <https://doi.org/10.1021/acami.2c19414>
- [3] Walther, F. *et al.* The Working Principle of a $\text{Li}_2\text{CO}_3/\text{LiNbO}_3$ Coating on NCM for Thiophosphate-Based All-Solid-State Batteries. *Chemistry of Materials* **33** (6), 2110-2125 (2021) <https://doi.org/10.1021/acs.chemmater.0c04660>
- [4] Zhang, Y.Q. *et al.* Direct Visualization of the Interfacial Degradation of Cathode Coatings in Solid State Batteries: A Combined Experimental and Computational Study. *Adv. Energy Mat.* **10** (27), 1903778 (2020). <https://doi.org/10.1002/aenm.201903778>

8:30 AM *EN02.08.03

Studying Li Evolution in Mixed Ionic-Electronic Conducting Interlayer of Sulfide Based All-Solid-State Batteries Through Operando Raman and Neutron Images Daxian Cao and Hongli Zhu; Northeastern University, United States

Lithium-metal (Li^0) anode potentially enables all-solid-state batteries with high energy density. However it shows incompatibility with sulfide solid-state electrolytes (SEs). One strategy is introducing an interlayer, generally made of a mixed ionic-electronic conductor (MIEC). Yet, how Li behaves within MIEC remains unknown. Herein, we investigated the Li dynamics in a graphite interlayer, a typical MIEC, using *operando* neutron imaging and Raman spectroscopy. This study revealed intercalation-extrusion-dominated mechano-chemical reactions during cell assembly transform the graphite into a Li-graphite interlayer consisting of SE, Li^0 , and graphite-intercalation compounds. During charging, Li^0 preferentially plated at the Li-graphite|SE interface and then transferred into the Li-graphite interlayer without intercalation. Upon further plating, Li^0 -dendrites formed, inducing short circuits and reverse immigration of Li^0 . Continuum modeling was conducted to explain the Li dynamics. We concluded that the lowest nucleation barrier at the Li^0 side is necessary to drive the Li^+ across the MIEC and preferentially deposit onto the Li^0 .

9:00 AM EN02.08.04

Electronic Conductivity of Lithium Solid Electrolytes Fudong Han; Rensselaer Polytechnic Institute, United States

While significant efforts have been devoted to improving the ionic conductivity of lithium solid electrolytes (SEs), electronic transport, which has an important role in the calendar life, energy density, and cycling stability of solid-state batteries (SSBs), is rarely studied. In this talk, we will present our recent results on the electronic conductivities of three representative SEs, including Li_3PS_4 , $\text{Li}_7\text{La}_3\text{Zr}_2\text{O}_{12}$, and Li_3YCl_6 for sulfide-, oxide-, and halide-based SEs, respectively. By revisiting direct current polarizations using two-blocking-electrode cells and the Hebb-Wagner approach, we propose that the electronic conductivities of SEs are overestimated from the conventional measurements. We will discuss the limitations and sources of inaccuracy for these measurements and highlight the anodic decomposition of SE as the key source for the overestimated result. Modifications in the electrode selection and data interpretation are also proposed to approach the intrinsic electronic conductivity of SEs. To estimate the electronic conductivity of sulfides that decompose during measurement, a two-step polarization method will also be introduced. The electronic conductivities of all SEs measured by the modified approach are one or two orders of magnitude lower than the reported value. Despite that, the electronic conductivity of sulfides seems to be still quite high to enable SSBs with a long calendar life of >10 years, highlighting the critical need for a more careful study of electronic transport in lithium SEs.

9:15 AM EN02.08.05

Computational Investigation of Dynamic Voltage Stability in Solid State Batteries Yichao Wang, William Fitzhugh, Xi Chen, Luhuan Ye and Xin Li; Harvard University, United States

Intrinsic or interface thermodynamic voltage windows of solid electrolytes are often narrower than the operational voltage range needed by a full battery, thus various decomposition reactions can happen in a practical solid-state battery. These decompositions can undergo local volume expansions, which will compress the reaction front in a solid environment under a mechanical constriction and modify the reaction thermodynamics and kinetics. Experimentally, it was found that a proper battery design utilizing the effect can lead to dynamic voltage stability for advanced battery performance. Here we articulate first our state-of-the-art understanding about how computationally the dynamic voltage stability should be interpreted and treated. We further apply our constrained ensemble computational approach across these solid-state electrolytes to systematically evaluate and compare their dynamic stability voltage windows in response to the mechanical constriction effect. High throughput calculations are used to search for coating materials for different interfaces between sulfide, halide, and oxide electrolytes and typical cathode materials with enhanced dynamic voltage stability.

9:30 AM EN02.08.06

Atomic Insights into the Oxidative Degradation Mechanisms of Sulfide Solid Electrolytes Chuntian Cao¹, Matthew Carbone¹, Jagriti Shekawat², Cem Komurcuoglu², Kerry Sun², Haoyue Guo², Sizhan Liu¹, Ke Chen¹, Seong-Min Bak¹, Yonghua Du¹, Conan Weiland³, Xiao Tong¹, Dan Steingart^{2,2,2}, Shinjae Yoo¹, Nongnuch Artrith^{2,4}, Deyu Lu¹ and Feng Wang¹; ¹Brookhaven National Laboratory, United States; ²Columbia University, United States; ³National Institute of Standards and Technology, United States; ⁴Utrecht University, Netherlands

Electrochemical degradation of solid electrolytes is a major roadblock in the development of solid-state batteries, and the formed solid-solid interphase (SSI) plays a key role in the performance of solid state batteries. In this study, by combining experimental X-ray absorption spectroscopy (XAS) measurements, first-principles simulations, and unsupervised machine learning, we have unraveled the atomic-scale oxidative degradation mechanisms of sulfide electrolytes at the SSI using the baseline Li_3PS_4 (LPS) electrolyte as a model system. The degradation begins with a decrease of Li neighbor affinity to S atoms upon initial delithiation, followed by the formation of S-S bonds upon the deformation of the PS_4 tetrahedra. In the second and following delithiation cycles, the PS_4 motifs are strongly distorted and PS_3 motifs start to form. Spectral fingerprints of the local structural evolution are identified, which correspond to the main peak broadening and shifted to higher energy by about 2.5 eV in P K-edge XAS and a new peak emerging at 2473 eV in S K-edge XAS during the delithiation. The spectral fingerprints serve as a proxy of the electrochemical stability of phosphorus sulfide solid electrolytes, as demonstrated in argyrodite $\text{Li}_6\text{PS}_5\text{Cl}$. We have observed that the strong distortion and destruction of PS_4 tetrahedra and the formation of S-S bonds are correlated with the increased interfacial impedance. To our knowledge, this study provides the first atomic-scale insights into the oxidative degradation mechanism of the LPS electrolyte, which can provide guidance for controlling macroscopic reactions through microstructural engineering and, more generally, can advance the rational design of sulfide electrolytes.

9:45 AM EN02.08.07

Viscoplasticity Driven Approach to Increase Critical Current Density in Sulfide Electrolytes Changmin Shi¹, Cristina Lopez Pernia¹, Xing Liu², Pradeep Guduru¹ and Brian W. Sheldon¹; ¹Brown University, United States; ²Georgia Institute of Technology, United States

All-solid-state batteries (ASSBs) show a high practical potential to achieve safe battery design with high energy densities when using Li metal as an anode. Sulfide electrolytes due to their high ionic conductivity (0.1 mS/cm to >10 mS/cm) are among the most promising candidates. However, Li dendrite growth results in shorting at critical current densities (CCD) that are well below values that are needed for practical applications. This currently limits the development of sulfide-based ASSBs, and therefore, it is very important to stabilize sulfide-electrolyte/Li-metal interfaces to enable high current densities without shorting.

Extensive efforts have been devoted to increasing the interfacial stability with methods that emphasize chemical and electrochemical modifications. However, methodologies that increase the CCD in sulfide electrolytes based on mechanics have not been reported. Herein we report a viscoplasticity based approach to increase the CCD of sulfide electrolytes. Previous studies have demonstrated that some sulfide SEs deform in a viscous manner^{1,2}. Considerations of this effect offer a new perspective on how to suppress Li dendrite growth. To investigate the viscoplastic properties of sulfide electrolytes, Li₆PS₃Cl (LPSC) was selected as an important candidate due to its high ionic conductivity and high stability against Li metal compared with other sulfide electrolytes. Viscoplasticity in this material was investigated and characterized by integrating nanoindentation experiments and finite element simulations, and improved CCD was observed by employing cycling conditions that take advantage of this inelastic deformation. Such improvement is attributed to the interaction between the specially designed charging-discharging cycles and the viscous deformation of the electrolyte. We have also performed finite element simulations to further validate our argument. This type of approach can provide major improvements in the performance of ASSBs and can also be combined with chemical/electrochemical methods to further enhance cell performance using sulfide electrolytes.

References:

1. C. E. Athanasiou, X. Liu, M. Y. Jin, E. Nimon, S. Visco, C. Lee, M. Park, J. Yun, N. P. Padture, H. Gao, B. W. Sheldon, *Cell Reports Phys. Sci.* **3**, 100845 (2022).
2. M. Papakyriakou, M. Lu, Y. Liu, Z. Liu, H. Chen, M. T. McDowell, S. Xia, *J. Power Sources.* **516** (2021), doi:10.1016/j.jpowsour.2021.230672.

10:00 AMBREAK

SESSION EN02.09: Battery Device I
Session Chairs: Yi Lin and Fang Liu
Wednesday Morning, November 29, 2023
Hynes, Level 3, Room 304

10:15 AM *EN02.09.01

Interfacial Engineering of Solid-State Batteries: From Metal Anodes to Composite Cathodes Neil P. Dasgupta; University of Michigan, United States

Solid-state batteries have the potential to be a disruptive technology because of their ability to improve safety and increase energy density by incorporating Li metal anodes. However, all solid-state interfaces present unique challenges, including high interfacial impedances, accommodation of mechanical stresses due to solid-solid interfacial contact, and (electro)chemical instabilities that can evolve during dynamic cycling conditions. Furthermore, a significant challenge facing the scale-up of SSBs is to improve our understanding of processing science needed to enable manufacturing.

To address these challenges, our group focuses on gaining new fundamental insights into the coupled phenomena occurring at interfaces, and applied this knowledge to rationally design interfacial composition and structure to address the root cause of performance limitations. In this talk, I will describe our journey to deepen our understanding of interfacial phenomena at both the Li metal anode side, as well as in composite solid-state cathode materials. On the anode side, there is a critical need to understand and control the coupling between electrochemistry, morphology, and mechanics, to improve the uniformity and reversibility of plating and stripping during charge and discharge, respectively. On the cathode side, we focus on overcoming energy/power tradeoffs, which exhibit unique phenomena owing to the single-ion conducting nature of ceramic electrolytes, as well as improving stability at high voltages.

Equipped with this fundamental understanding, I will describe our efforts to engineer modified interfaces through control of the surface chemistry, incorporation of interlayers, and fabricating 3-D architectures. Through this interdisciplinary approach of fundamental materials chemistry and applied engineering, strategies to address future interfacial challenges will be addressed, pointing towards rational design and manufacturing of optimized interfaces.

10:45 AM *EN02.09.02

Cross-Talk Between Anode and Cathode Degradation Mechanisms in all Solid State Batteries Kelsey B. Hatzell; Princeton University, United States

All solid-state batteries (ASSB) can potentially achieve high gravimetric and volumetric energy densities (900 Wh/L) if paired with a lithium metal anode and solid electrolyte. However, there is a lack in critical understanding about how to operate lithium metal cells at high capacities with composite solid state cathodes. The interconnection and cross-talk between anode and cathode degradation mechanisms is largely not well understood. Herein, we investigate how pressure and temperature influence the formation and annihilation of unrecoverable voids in lithium metal upon stripping and subsequent contact evolution challenges at cathode. Here we use both x-ray and electron imaging techniques to characterize degradation mechanisms across multiple scales.

11:15 AM *EN02.09.03

Understanding the Evolution of High-Capacity Anodes in Solid-State Batteries Matthew T. McDowell; Georgia Institute of Technology, United States

Solid-state batteries offer the promise of improved energy density and safety compared to lithium-ion batteries, but electro-chemo-mechanical evolution and degradation of materials and interfaces can play an outsized role in limiting their performance. Here, I will present my group's recent work on understanding structural evolution, interfacial dynamics, and chemo-mechanics in solid-state batteries with two different types of anodes: zero-lithium excess anodes ("anode-free") and alloy anodes. Anode-free solid-state batteries, in which there is no initial lithium metal at the anode interface, offer extremely high energy density, but there is a lack of understanding of the mechanisms that govern their behavior in solid-state batteries. Using X-ray tomography, cryo-FIB, and finite-element modeling, we show that anode-free solid-state batteries are intrinsically limited by current concentrations at the end of stripping due to localized lithium depletion. This causes accelerated short circuiting compared to lithium-excess cells. Based on these results, the beneficial influence of metal alloy interfacial layers on controlling lithium evolution and mitigating contact loss from localized lithium depletion will be introduced and discussed. In the second part of the talk, a new design for dense aluminum foil alloy anodes is introduced, in which microstructural control over the foil is shown to play a key role in significantly improving reversibility in solid-state batteries. This anode design mitigates chemo-mechanical degradation and offers a paradigm that does away with slurry coating, potentially reducing manufacturing costs. Taken together, these findings show the importance of controlling chemo-mechanics and interfaces in solid-state batteries for improved energy storage capabilities.

11:45 AM EN02.09.04

Understanding The Li Dendrite "Soft Short" in Solid-State Li Metal Batteries by Phase-field Method Kena Zhang¹, Daxian Cao², Tongtai Ji², Hongli Zhu² and Ye Cao¹; ¹The University of Texas at Arlington, United States; ²Boston University, United States

Lithium (Li) dendrite growth in Li metal batteries is a long-standing problem, which causes critical safety concerns and severely limits the advancement of rechargeable Li batteries. Replacing conventional liquid electrolyte with solid electrolyte (SE) of high mechanical strength and rigidity was once thought as an effective strategy to suppress the Li dendrite growth. However, defects in SEs (such as cracks, voids, grain boundaries etc.) and the imperfect contact between the electrode and the SE can even facilitate the Li dendrite growth. Recently, it was postulated that the Li dendrite growth in SEs could be the reason for "soft short" of the cell. Compared to "hard short" in which the voltage of the battery decreases suddenly during the charging process, in "soft short" the voltage is dynamically stable but cannot increase during the charging process. However, the underlying mechanism of "soft short" is still not well understood. In this work, we developed a phase-field model coupled with electrochemistry and solid mechanics to unravel the dynamics of Li dendrite growth in a porous SE under the applied external pressure during charging, and its correlation with the "soft short". It is revealed that Li dendrite growth causes a hydrostatic pressure inside the Li metal, which increases with the external pressure and is responsible for the suppression of Li dendrite growth. Without external pressure, Li dendrite growth is less restricted by the SE and can fill the small pores inside the SE to form a tree-like

morphology. The growth of multiple Li dendrites eventually penetrates through the entire SE, causing “hard” short circuit of the cell. This is evidenced by the sudden increase of leakage current during charging process in the simulation. When the external pressure increases to 10MPa, the hydrostatic pressure is maximized at the pore-SE interface which blocks the Li dendrite to fill into the pores, and eventually breaks parts of the Li dendrites to form dead Li. Our simulation results agree with the X-ray computed tomography of the deposited Li metal and cracks inside the SE by our collaborators. More importantly, the simulated fracture of Li dendrite (disconnection to the anode) and the subsequent reconnection to the Li anode can well explain the “soft short” in experiments, as they prevent the Li dendrite from completely penetrating the SE. This is further evidenced by the leakage current fluctuations in our simulation, indicating a typical “soft short” behavior. Our work thus provides a deeper understanding of the Li dendrite growth dynamics in porous solid electrolyte and the “soft short” phenomenon in solid state batteries.

SESSION EN02.10: Sulfur Cathode I
Session Chairs: Xin Li and Fang Liu
Wednesday Afternoon, November 29, 2023
Hynes, Level 3, Room 304

1:30 PM *EN02.10.01

Engineering Sulfur Cathodes for Solid State BatteriesPingLiu; University of California, San Deigo, United States

Solid state batteries with sulfur-based cathodes are highly appealing due to their intrinsic cost and energy density advantages. If fully realized, they also promise a departure from our reliance on transition metals and even facile recycling. Extensive effort has been dedicated to improve the electrical conductivity and manage the volume change during cycling. In this regard, sulfur-containing polymers have shown stable cycling stability but with limited capacity. Recently we have shown poly thiocyanogen can deliver material-level energy density of > 1400 Wh/kg. However, the material is found only to have enough electron and ionic conductivities at elevated temperatures. The result illustrates the limitation of using conductive polymer or carbon backbones to provide electronic conductivity. We have recently explored the possibility of heteroatom doping into sulfur composite materials. Selected dopants have shown promise in facilitating the charge transfer in the solid electrode as well as increasing the ductility of the composite structure. Both of these features help improve the rate capability and cycle life of the sulfur based cathode. We will discuss how these findings can offer design rules for new sulfur based cathodes, including further improvement to enable cycling at reduced pressure.

2:00 PM *EN02.10.02

Materials Challenges for High-Energy and Long-cycle-Life All-Solid-State Lithium-Sulfur BatteryDongpingLu, MichaelKindle, DanielMarty, JingWu, DaheeJin and Un HyuckKim; Pacific Northwest National Laboratory, United States

All Solid-state Lithium-Sulfur battery (ASSLSB) is regarded as a promising next-generation battery technology for vehicle electrification due to its merits of high energy, low cost, and high safety. However, performance improvement and deployment of the technology are still largely hindered by the challenges associated with both sulfur (S) cathode and lithium anode. Although issues of polysulfide dissolution, Li corrosion, and electrolyte consumption existing in liquid Li-S cells are fully eliminated, achieving both high energy and stable cycling in S cathode is still very challenging. Those include (1) low S content and mass loading, (2) low operation current densities, and (3) large electrode volume change upon cycling. This is due to extremely low ionic and electronic conductivities of S and Li_2S , which relies on the effectiveness and completeness of Li^+/e^- conduction networks built on both solid-state electrolyte (SSE) and carbon (C) conductors. The clear understanding or a design principle of an optimal S/SSE/C triple phases is still lacking. The other grand challenge of ASSLSB is how to achieve long-term and dendrite-free Li cycling at both high current densities and high areal capacities. Properties of Li/SSE interface impacts early-stage Li nucleation, which dictates subsequent Li growth. For this aspect, uniformity of Li/SSE interface both in chemistry and morphology could even reduce local current density, promoting uniform Li growth. The interfacial stability of Li/SSE could be achieved by forming a stable SEI. However, it is challenged by Li dynamics during repeated cycling, particularly at practically high current density and areal capacity conditions, which may boost the potentials of inhomogeneous Li deposition and even dendrite formation. To overcome those issues, rational designs of materials, electrode, and interface are essentially needed to both boost S reaction kinetics and stabilize Li/SSE interface. At the conference, we will discuss our understandings of those key challenges and new progresses we achieved in addressing them.

2:30 PMBREAK

SESSION EN02.11: Battery Device II
Session Chairs: Yi Lin and Yichao Wang
Wednesday Afternoon, November 29, 2023
Hynes, Level 3, Room 304

3:30 PM EN02.11.01

Lithiation Gradients and Tortuosity Factors in Thick NMC111-Argyrodite Solid-State CathodesJoshuaW. Gallaway, AlyssaStavola, DominickGuida, AndreaM. Bruck, XiaoSun and HongliZhu; Northeastern University, United States

Achieving the high energy density targets for all-solid-state batteries (ASSBs) will require thick cathodes optimized for full utilization of active material. In composite cathodes with sulfide solid-state electrolytes (SSEs), the exclusion of carbon additives makes cathode design to balance ionic and electronic conductivities all the more important. $\text{Li-Ni}_{1/3}\text{Mn}_{1/3}\text{Co}_{1/3}\text{O}_2$ (NMC111) is a widely studied cathode material for its high energy density and high working voltage. The lattice parameters of this well-studied structure directly correlate to the amount of Li in the material, allowing for very accurate measurements of lithium-ion concentration gradients (lithiation gradients) throughout the cathode depth.

In this work, we report an operando analysis of Li^+ and e^- conduction across 120 μm thick composite cathodes based on NMC111 and $\text{Li}_6\text{PS}_5\text{Cl}$ (LPSC) during initial cycling.¹ This analysis indicates that conduction during initial cycling is subject to high tortuosity factors (τ^2) for both the LPSC and NMC phases. Additionally, the τ^2 values evolve during the initial battery charge step, increasing steeply. By analyzing composite cathodes with a range of cathode active material (CAM) loadings, we observe the effect of CAM loading on the non-uniformity of the electrochemical reaction. For 80% CAM we observe that the initial reaction heavily favors regions of the cathode that are nearest the anode. For 70% and 40% CAM, the opposite is true, with initial reaction favoring the regions farthest from the anode. These non-uniformities are very large, often amounting to a gradient of over 50% of the total cycleable capacity across the cathode thickness.

Spatially resolved lithiation gradients in thick NMC111/ $\text{Li}_6\text{PS}_5\text{Cl}$ composite cathodes were measured using operando energy dispersive X-ray diffraction (EDXRD) on sealed and pressurized ASSBs with varying relative amounts of CAM and SSE. Electrochemical impedance spectroscopy (EIS) and transmission line modeling were employed to test the ionic and electronic conductivities of composite cathodes with similar varied CAM and SSE ratios. The balance of ionic and electronic conductivities was found to determine the lithiation gradients and utilization of active material in the cell.

Acknowledgments

We acknowledge financial support from the National Science Foundation under Award Number CBET-ES-1924534. This research used resources of the Advanced Photon Source beamline 6-BM, a U.S. Department of Energy (DOE) Office of Science User Facility operated for the DOE Office of Science by Argonne National Laboratory under Contract No. DE-AC02-06CH11357.

References

1. Stavola, A.M.; Sun, X.; Guida, D.P.; Bruck, A.M.; Cao, D.; Okasinski, J.S.; Chuang, A.C.; Zhu, H.; and Gallaway, J.W. "Lithiation Gradients And Tortuosity Factors In Thick NMC111-Argyrodite Solid-State Cathodes," *ACS Energy Letters*, **2023**, 8, 1273–1280.

3:45 PM EN02.11.02

3D Printed Porous LLZO Multi-Layer Scaffolds for Li-Garnet Solid-State BatteriesBor-RongChen, AsaG. Monson, PeteBarnes, JorgenF. Rufner, ArinS. Preston, DonnaP. Guillen and

Garnet-based oxides ($\text{Li}_7\text{La}_5\text{Zr}_2\text{O}_{12}$, LLZO) are promising solid-state electrolyte materials to achieve higher energy density and improved safety for the next-generation solid-state batteries (SSBs) due to their high ion conductivity and chemical stability. To enhance the performance of garnet-based SSBs, a dense-porous design of microstructure has been introduced in recent years. The design consists of a dense layer as the separator and one or two porous layers as the host of anode or cathode active materials [1-3]. The porous structure mitigates volume changes in the anode by accommodating Li in the pores during Li deposition, while the dense layer prevents short circuiting and provides additional mechanical support. Such bi- or tri-layer scaffolds are usually fabricated using tape-casting, in which the porous and dense layers are prepared separately, followed by trimming and stacking into the desired architectures. As a result, this process is challenged by workflow inefficiency due to the multiple separated casting and stacking steps.

To improve the efficiency in fabricating the porous-dense scaffold, we introduce an alternative approach using digital light processing (DLP), a unique 3D printing technology capable of layer-by-layer printing of multiple components and complex architectures in a single print [4]. Using DLP, the entire multilayer structure in the desired dimension is created *all-at-once* on the same printing platform by alternating printing slurries that respectively form the dense and porous layers. We produce free-standing, sub-millimeter-thick Ta-doped (LLZTO) porous-dense layers and demonstrate that the porosity is tunable by adjusting the particle size and solid loading in the printing slurry. This strategy for controlling the porosity is distinct from current approaches such as adding pore formers or controlling heat treatment conditions. By tuning the porosity in each of the printed layers, we show that a graded porosity can be created across the scaffold. In the future, this DLP printing approach will provide more opportunities to produce various microstructures and chemistries of SSBs with more efficiency and sustainability.

- [1] Hitz, Gregory T., Dennis W. McOwen, Lei Zhang, Zhaohui Ma, Zhezhen Fu, Yang Wen, Yunhui Gong et al. "High rate lithium cycling in a scalable trilayer Li garnet electrolyte architecture." *Materials Today* 22 (2019): 50-57.
[2] Yi, Eongyu, Hao Shen, Stephen Heywood, Judith Alvarado, Dilworth Y. Parkinson, Guoying Chen, Stephen W. Sofie, and Marca M. Doeff. "All solid state batteries using rationally designed garnet electrolyte frameworks." *ACS Applied Energy Materials* 3, no. 1 (2020): 170-175.
[3] Zhang, Huanyu, Faruk Okur, Claudia Cancellieri, Lars PH Jeurgens, Annapaola Parrilli, Dogan Tarik Karabay, Martin Nesvadba et al. "Bilayer Dense Porous $\text{Li}_7\text{La}_3\text{Zr}_2\text{O}_{12}$ Membranes for High Performance Li Garnet Solid State Batteries." *Advanced Science* 10, no. 8 (2023): 2205821.
[4] Chaudhary, R., Fabbri, P., Leoni, E., Mazzanti, F., Akbari, R., & Antonini, C. (2022). Additive manufacturing by digital light processing: a review. *Progress in Additive Manufacturing*, 1-21.

4:00 PM EN02.11.03

Self-Healing Laminated LLZO/Reduced Graphene Oxide/LLZO Composite Solid-State Electrolytes for Arresting Dendrite Penetration in Solid-State Batteries [Zikang \(Austin\) Yu](#), Changmin Shi, Cristina Lopez Pernia, Chenjie Gan and Aleksandar Mijailovic; Brown University, United States

Solid state lithium metal batteries using inorganic solid electrolytes are widely regarded as next-generation devices that can enable substantial improvements in energy density. However, the performance of these electrolytes is currently limited as they are largely unable to hinder the propagation and penetration of lithium metal dendrites that lead to the shorting of cells at practical current densities. In this work, we propose a novel architecture for solid state electrolytes, using a laminated composite structure consisting of reduced Graphene Oxide (rGO) interlayers that are embedded inside of Tantalum-doped LLZO ($\text{Li}_{6-x}\text{La}_3\text{Zr}_{1.7}\text{Ta}_{0.3}\text{O}_{12}$) to create a stable layered solid-state battery that effectively arrests dendrite penetration. Testing of these interlayer-engineered LLZO electrolyte with symmetric lithium metal electrodes, leads to critical current density increases of more than 7 times at room temperature. FEM simulations of these multi-layered structures were also conducted to provide insight into designing a broader range of laminated solid electrolyte architectures. Our results indicate that solid state electrolytes can be engineered with interlayers to deflect dendrites and improve critical current densities.

4:15 PM EN02.11.04

Three-Dimensional Physical Modeling of the Wet Manufacturing Process of Solid-State Battery Electrodes [Mohammed Alabdali](#)¹, Franco M. Zanotto^{1,2}, Marc Duquesnoy^{1,3}, Anna-Katharina Hatz⁴, Duancheng Ma⁴, Jeremie Auvergniot⁴, Virginie Viallet^{1,2}, Vincent Seznec^{1,2,3} and Alejandro A. Franco^{1,2,5}; ¹Laboratoire de Réactivité et Chimie des Solides (LRCS), Université de Picardie Jules Verne, Hub de l'Energie, UMR CNRS, France; ²Réseau sur le Stockage Electrochimique de l'Energie (RS2E), Hub de l'Energie, FR CNRS, France; ³Alistore-European Research Institute, Hub de l'Energie, FR CNRS, France; ⁴Umicore, Belgium; ⁵Institut Universitaire de France, France

We present an innovative three-dimensional physics-based modeling workflow that addresses the issue of poor performance of Solid-State Battery (SSB) cells due to the challenging design and manufacturing of composite electrodes with appropriate ionic and electronic conductivities. While modeling approaches have been utilized in the literature to investigate the influence of stochastically-generated microstructures on their conductivities, computational simulations able to predict the influence of manufacturing parameters on the SSB electrode microstructures remain elusive [1]. We present a novel physics-based computational modeling framework able to numerically investigate the impact of wet manufacturing process parameters (e.g. formulation, drying rate, calendaring degree) on the properties of SSB tape casted composite electrodes. In analogy to our previous work on the simulation of the manufacturing process of Lithium Ion Battery electrodes [2], the Coarse-Grained Molecular Dynamics (CGMD) is adapted and used here for the simulation of the manufacturing process of SSB composite electrode cathode based on the physical interactions among individual particles representing the materials constituting the slurry and the formed electrode (i.e. NMC622, Carbon-Binder Domain and $\text{Li}_6\text{PS}_5\text{Cl}$) involved in the wet manufacturing process. By encompassing the entire process of wet manufacturing of SSB electrodes, from the slurry to the calendaring, the model is able to predict the correlations between manufacturing parameters and electronic and ionic conductivities of the electrodes. We show why and how this model constitutes an important tool to assist in the optimization of interfaces between the materials in the electrodes, leading to improved SSB performance and durability.

References:

- [1] M. Alabdali, F. M. Zanotto, V. Viallet, V. Seznec, A. A. Franco, *Curr Opin Electrochem* 2022, 36, DOI 10.1016/J.COEELEC.2022.101127.
[2] A. C. Ngandjong, T. Lombardo, E. N. Primo, M. Chouchane, A. Shodiev, O. Arcelus, A. A. Franco, *J Power Sources* 2021, 485, 229320.

4:30 PM EN02.11.05

Low-Temperature Design of Solid Oxide Electrolyte Through Amorphization Giyun Kwon, Hyeokjo Gwon, [Youngjoon Bae](#), Jusik Kim and Taeyoung Kim; SAIT, Korea (the Republic of)

In recent years, there have been a significant increase in solid Li-ion conducting electrolytes that have the potential to enable such batteries. Among them, garnet-type oxide electrolytes have demonstrated great promise due to their robust stability and high ionic conductivity. However, due to the rigid nature of solid oxide electrolytes, the high ionic conductivity is only achievable along with high temperature sintering process (> 1000 °C) to form dense structure, which introduces cost challenges and undesired chemical reactions. Although there have been many efforts to lower the sintering temperature through the use of sintering aids, they require additional additives and their effect remains unsatisfactory. In this study, a low-temperature design for garnet solid electrolyte is suggested without the need for sintering aids. The approach involves amorphization, which imparts deformability to the material. Consequently, the material becomes way softer compared to crystalline electrolyte, allowing for the easy formation of a dense amorphous matrix by applying pressure. Subsequently, the high ionic conductivity can be obtained through a low-temperature crystallization process. We believe that this strategy paves the way for showcasing rigid solid electrolytes processed at lower temperature.

SESSION EN02.12: Ion Conductivity
Session Chairs: Xin Li and Yi Lin
Thursday Morning, November 30, 2023
Hynes, Level 3, Room 304

8:15 AM EN02.12.01

Understanding Lithium-Ion Transport in Selenophosphate-Based Lithium Argyrodites and Their Limitations in Solid-State Batteries [Johannes Hartel](#)¹ and [Wolfgang Zeier](#)^{1,2}; ¹Department of Inorganic and Analytical Chemistry, Germany; ²Helmholtz-Institut, Germany

Solid electrolytes providing high ionic conductivities are required for the realization of solid-state batteries with competitive power and energy densities. Among all reported fast lithium-ion conductors, superionic lithium argyrodites provide a promising, highly tunable compositional space, in which superior lithium-ion conductivities can be realized by elemental substitutions.

In this work, selenophosphate-based lithium argyrodites $\text{Li}_{6-x}\text{PSe}_{5-x}\text{Br}_{1+x}$ ($0 \leq x \leq 0.2$) with exceptional ionic conductivities up to 8.5 mS cm^{-1} are reported and underlying reasons for their fast lithium-ion transport are unveiled based on structural characterization using a combination of neutron powder diffraction, ⁷Li and ³¹P NMR and Raman spectroscopy. Rietveld refinement of

the neutron powder diffraction data uncovers a significantly improved interconnection of the lithium-ion cages when compared to the thiophosphate analogue $\text{Li}_6\text{PS}_3\text{Br}$ as a result of the occupation of two additional lithium-ion sites, leading to enhanced lithium-ion transport. A larger unit cell volume, lattice softening and higher structural disorder between halide and chalcogenide provide further structural reasons for improved lithium-ion conduction. Interestingly, when testing $\text{Li}_{5.85}\text{PSe}_{4.85}\text{Br}_{1.15}$ as catholyte in $\text{In/LiIn/Li}_6\text{PS}_3\text{Br/LiNi}_{0.83}\text{Co}_{0.11}\text{Mn}_{0.06}\text{O}_2\text{:Li}_{5.85}\text{PSe}_{4.85}\text{Br}_{1.15}$ solid-state batteries, severe degradation is observed by electrochemical impedance spectroscopy upon charging of the cells, revealing that selenophosphate-based lithium argyrodites are not suitable for application in lithium nickel cobalt manganese oxide (NCM) based solid-state batteries from a performance perspective.

Besides providing further insights into the structure-transport relationship of lithium argyrodites with high lithium-ion conductivities, this work reemphasizes the necessity to consider chemical and electrochemical stability of solid electrolytes against the active materials when developing fast lithium-ion conductors.

References

J. Hartel, A. Banik, J. M. Geredes, B. Wankmiller, B. Helm, C. Li, M. Kraft, M. R. Hansen, W. G. Zeier "Understanding lithium-ion transport in selenophosphate-based lithium argyrodites and their limitations in solid-state batteries" *Chem. Mater.* **2023**, accepted.

8:30 AM *EN02.12.03

Design Principles for Fast Ionic Conductors Yifei Mo; University of Maryland, United States

Super-ionic conductors, characterized by exceptionally high ionic conductivities, are highly sought after as solid electrolytes or electrodes for energy applications like batteries and fuel cells. Despite numerous mechanisms proposed for super-ionic conductor materials and the emergence of various design principles, the capability to rationally design these materials has yet to be fully actualized. Conventionally, the analyses largely concentrated on experimental data from a single class of materials with varying compositions. In our computational study, analyzing and studying a vast array of materials across a broad spectrum of materials chemistry and structure allow us to understand the mechanisms and trends across materials, enabling us to devise generally applicable design principles. In this talk, I will present our latest progress toward understanding the mechanisms of ion diffusion and formulating these design principles for fast ion conductors.

9:00 AM EN02.12.02

Understanding the Correlation Between Anion Group Rotations and Lithium Ion Diffusion in Superionic Conductors KyuJungJun¹, ByungjuLee², RonaldKam¹ and GerbrandCeder¹; ¹University of California, Berkeley, United States; ²Korea Institute of Science and Technology, Korea (the Republic of)

Since the 1980s, the paddlewheel effect has been proposed as a mechanism to boost lithium-ion conductivity in inorganic materials by using rotating anion groups to assist lithium-ion migrations (1–5). However, to this date, the physical mechanism behind how anion-group dynamics affect lithium-ion diffusion has not been clearly quantified. In this work, we define three types of rotational motions of anion-groups. To detect and differentiate various types of rotational motions, we track rotational motion of anion groups using quaternion-based representations. By applying a quaternion-based algorithms throughout a total of 10⁷'s of ns ab-initio molecular dynamics trajectories of various types of superionic conductors and performing rigorous statistical analysis of various rotational events as well as lithium-ion diffusion events, we reveal how each type of anion rotational motion is related to lithium-ion diffusion. Our work resolves the ongoing debate about the existence of a paddlewheel effect and provides a clear mechanistic understanding of how anion-group rotations are correlated to fast ionic diffusion in inorganic materials.

1. L. Karlsson, R. L. McGreevy, Mechanisms of ionic conduction in Li_2SO_4 and LiNaSO_4 : Paddle wheel or percolation? *Solid State Ionics*. 76, 301–308 (1995).
2. A. Kvist, A. Lundén, Electrical Conductivity of Solid and Molten Lithium Sulfate. *Zeitschrift Für Naturforschung*. 20, 235–238 (1965).
3. Z. Zhang, L. F. Nazar, Exploiting the paddle-wheel mechanism for the design of fast ion conductors. *Nat Rev Mater*, 1–17 (2022).
4. J. G. Smith, D. J. Siegel, Low-temperature paddlewheel effect in glassy solid electrolytes. *Nat Commun*. 11, 1483 (2020).
5. M. Jansen, Volume Effect or Paddle-Wheel Mechanism—Fast Alkali-Metal Ionic Conduction in Solids with Rotationally Disordered Complex Anions. *Angewandte Chemie Int Ed Engl*. 30, 1547–1558 (1991).

9:15 AM EN02.12.04

Unlocking Li Superionic Conductivity in Fcc-Type Oxides via Face-Sharing Configurations YuChen^{1,2}, BinOuyang³ and GerbrandCeder^{1,2}; ¹University of California, Berkeley, United States; ²Lawrence Berkeley National Laboratory, United States; ³Florida State University, United States

Li metal oxides with a face-centered cubic (fcc) anion sublattice have been generally excluded from the search for solid-state Li superionic conductors, as the structural framework is thought to be unfavorable for Li superionic conduction. Herein, we demonstrate a face-sharing design strategy that turns fcc-type oxides into superionic conductors, with a Li ionic conductivity of $3.38 \times 10^{-4} \text{ S cm}^{-1}$ at room temperature and a low migration barrier of 255 meV. The combination of experimental and theoretical investigations reveals that the high Li-ion conductivity is attributed to the facile Li-ion diffusion pathways comprising the face-sharing polyhedra. Our work unlocks the great potential of designing Li superionic conductors in a prototypical structural framework with vast chemical flexibility, providing a fertile ground for discovering new solid-state electrolytes for all-solid-state batteries.

9:30 AM EN02.12.05

Investigating Aliovalent Sn(+IV) and Isovalent P(+V) Substitution Series in Li_3SbS_4 BiancaHelm¹ and WolfgangZeier^{1,2}; ¹University of Muenster, Germany; ²Forschungszentrum Jülich GmbH, Germany

An in-depth understanding of Li^+ migration within solid electrolytes is fundamentally needed to develop new material classes and to enhance the existing ones. The thio-LISICON family exhibits three distinct ordering types of the non-lithium polyhedra leading to three different polymorphs, namely α -, β - and γ - Li_3PS_4 .^{1,2} These show completely different Li^+ substructures and migration pathways. Depending on the non-lithium cation either the β - or γ -polymorph is preferred synthetically. Li_3SbS_4 crystallizes in the γ -polymorph, which has the most unpropitious Li^+ substructure for fast Li^+ motion in comparison to the α -, β - and γ -polymorph. Nevertheless, the aliovalent $\text{Li}_{3+x}\text{Sb}_{1-x}\text{Sn}_x\text{S}_4$ ($0 \leq x \leq 0.2$) and isovalent $\text{Li}_3\text{Sb}_{1-x}\text{P}_x\text{S}_4$ ($0 \leq x \leq 0.5$) substitution series were prepared, and the ionic conductivity increased from $9.2 \times 10^{-11} \text{ S cm}^{-1}$ to $2.9 \times 10^{-6} \text{ S cm}^{-1}$ and $4.9 \times 10^{-7} \text{ S cm}^{-1}$ for the highest substitution degree, respectively. Remarkably, the conductivity is three times faster improved for the Sn(+IV) compared to the P(+V) substitution implying that more Li^+ are beneficial for faster ionic transport within this system. However, as these materials are bad ionic conductors at low substitution degree, the defect formation energy might be the dominating factor for easier ionic transport.

References.

- (1) Homma, K.; Yonemura, M.; Kobayashi, T.; Nagao, M.; Hirayama, M.; Kanno, R. Crystal Structure and Phase Transitions of the Lithium Ionic Conductor Li_3PS_4 . *Solid State Ionics* **2011**, 182 (1), 53–58.
- (2) Forrester, F. N.; Quirk, J. A.; Famprikis, T.; Dawson, J. A. Disentangling Cation and Anion Dynamics in Li_3PS_4 Solid Electrolytes. *Chem. Mater.* **2022**, 34 (23), 10561–10571.

9:45 AM BREAK

SESSION EN02.13: Electrode Interface I
Session Chairs: Xin Li and Yi Lin
Thursday Morning, November 30, 2023
Hynes, Level 3, Room 304

10:15 AM EN02.13.01

Overcoming Low Initial Columbic Efficiency of Si Anode by Effective Preolithiation in All-Solid-State Batteries So-YeonHam¹, EliasSebt², AshleyCronk¹, TylerPennebaker², GraysonDeysher¹, Yu-TingChen¹, Jin An SamOh¹, Jeong BeomLee³, MartaVicencio¹, PhillipRidley¹, BaharakSayahpour¹, DarrenTan¹, RaphaëleClement², JihyunJang¹ and Y. ShirleyMeng⁴; ¹University of California, San Diego, United States; ²University of California, Santa Barbara, United States; ³LG Energy Solution, Korea (the Republic of); ⁴The University of Chicago, United States

All-solid-state batteries using the Si anode has shown promising high-capacity performance without continual SEI growth. However, the low initial Columbic efficiency (CE) of Si remains a

challenge. In this work, a prelithiation strategy was adopted to improve the CE and conductivity of Si anodes. The lithiated Si was examined in a symmetric-, half- and full-cell configuration to understand the cell level improvement of each component. With Li_1Si lithiation, the full cell achieved over 95% ICE when paired with the lithium cobalt oxide (LCO) cathode. Additionally, improvement using the prelithiation method was found to only influence anode-limited cases when comparing two active materials; NCM and LCO when paired with Si and Li_1Si . Ramping tests and prolonged cycling performance was evaluated using both Si and Li_1Si cells. With Li_1Si , 73.8% after 1000 cycles was achieved, a 15% improvement in retention versus the bare Si anode. Utilizing the Li_1Si composition, high areal capacity up to 10 mAh/cm^2 was attained using a dry-process LCO film, validating the prelithiation method which may be a suitable candidate used in high loading next generation batteries.

10:30 AM EN02.13.02

Fast Cycling of Lithium Metal Solid State Batteries by Constriction-Susceptible 3D Anode Luhan Ye and Xin Li; Harvard University, United States

Lithium (Li) metal anode, due to its ten times larger capacity than commercial graphite anode, is a desired component for solid-state batteries. Fast cycling of commercial level of thick cathode, however, requires the fast cycling of a thick layer of Li metal at anode stably. The goal is challenging as the cycling condition naturally promotes inhomogeneity in lithium plating and stripping, and hence Li dendrite penetration. This talk provides a solid-state battery with 3D anode design that enables fast cycling of lithium in solid state batteries. It is shown that the constriction-susceptible materials in a solid-state battery structure can be modulated as a 3D scaffold, in which the plating and stripping of Li metal is uniform. Furthermore, the advantage of multi-electrolyte-layer solid electrolyte layer will also be discussed. We showed that the rate capability of lithium metal battery can be significantly improved after applying a multi solid electrolyte structure, with less stable solid electrolyte sandwiched by more stable solid electrolytes. The electrolyte layer can capture lithium dendrite by local decomposition, which together with the 3D matrix anode, enables a fast rate with long cycling life.

10:45 AM EN02.13.03

Silver-Carbon Composite Interlayers for "Anodeless" Solid-State Batteries Dominic Spencer-Jolly^{1,2}, Varnika Agarwal¹ and Peter G. Bruce^{1,2}; ¹University of Oxford, United Kingdom; ²The Faraday Institution, United Kingdom

Lithium-free so-called "anodeless" solid-state batteries promise to deliver high cell energy densities. However, at charge rates on the order of 1 mA cm^{-2} , plating of Li at the current collector/solid electrolyte interface is highly inhomogeneous, and dendrites (filaments of Li metal) are observed to penetrate through the solid electrolyte resulting in cell failure. Recent work has suggested that introduction of a silver-carbon composite interlayer between the solid electrolyte and current collector can protect the solid electrolyte against dendrite growth whilst promoting more homogeneous deposition of Li metal.¹ In this work, we investigate silver-carbon composite interlayers, revealing the structural changes within the interlayer during charge and discharge, and the rate dependency of these changes. We go on to investigate the homogeneity of Li-Ag alloy and Li metal formation at the current collector with and without silver nanoparticles present in the interlayer, and how this affects the processes of charge and discharge. We demonstrate dendrite-free charge at 2 mA cm^{-2} and reveal the origin of the failure of the interlayer at higher rates.²

1. Lee et al., High energy long-cycling all-solid-state lithium metal batteries enabled by silver-carbon composite anodes. *Nat. Energy* 5, 299–308 (2020)

2. Spencer-Jolly et al., Structural changes in the silver-carbon composite anode interlayer of solid-state batteries, *Joule* 7, 503–514 (2023)

11:00 AM EN02.13.04

Probing 3D Evolution and Electrochemical Behavior of Nano Silicon Anodes in Sulfide All-Solid-State Batteries via Nano X-Ray Tomography and in Operando XAS Tongtai Ji¹, Daxian Cao¹, Yonghua Du², Xianghui Xiao² and Hongli Zhu¹; ¹Northeastern University, United States; ²Brookhaven National Laboratory, United States

Silicon (Si) is one of the most promising anode materials for the next generation Li-ion batteries on account of its ultrahigh specific capacity (3590 mAh g^{-1}) and relatively low working potential of 0.4 V (vs. Li^+/Li). The utilization of silicon anode in all-solid-state lithium batteries (ASLBs) can further boost the energy density compared with the conventional graphite anode. Among various ASLBs with different solid electrolytes (SEs), the ASLBs with sulfide SEs delivered remarkable performances because of the excellent ionic conductivity ($>1 \text{ mS cm}^{-1}$) and relative "soft" mechanical properties (compared with oxides SEs) for intimate contact with electrode materials of sulfide SEs. However, the compatibility of Si and sulfide SEs is questioned because of the potential electrochemical decomposition. In addition, the extreme volume change (400%) of Si during cycling also brings great challenges to the structural stability of the ASLBs. Nano-Si ($<100 \text{ nm}$ in diameter) have a higher structural stability because the smaller geometry size can relieve stress. Therefore, in this study, we systematically analyzed the electrochemical and structural evolution of different nano-Si-based anodes in ASLBs with sulfide SE via *in-operando* synchrotron X-ray absorption near-edge structure (XANES) spectroscopy and scanning electron microscopy (SEM) combined with X-ray nano-tomography (XnT). Three kinds of nano Si-based anodes (pure nano-Si (Si), nano-Si compositing with SE (Si-SE), nano-Si compositing with SE and carbon (Si-SE-C)) were analyzed. The Operando XANES revealed that the sulfide SE experiences an electrochemical decomposition in the nano-Si anode and the addition of carbon accelerates this process. However, this electrochemical decomposition only occurs at the first lithiation process and the products are stable in the following cycles and has comparable ionic conductivity. The ex-situ SEM and ex-situ XnT exhibit that the addition of SE and carbon in the nano-Si anode benefits the structural stability, which is further explained by a chemo-elasto-plastic modeling framework. Owing to the enhanced reaction kinetics and mechanical structural stability, the Si-SE-C achieved the highest Si utilization, with a lithiation/delithiation capacity of $3288/2917 \text{ mAh g}^{-1}$ and an initial coulombic efficiency of 88.7%, which are significantly higher than the capacities of $2653/2291 \text{ mAh g}^{-1}$ and ICE of 86.4% in Si-SE, and the capacities of $2353/1935 \text{ mAh g}^{-1}$ and ICE of 82.2% in Si. This work indicated that the addition of SE and carbon into nano-Si anode can enhance the reaction kinetics, improve the utilization of Si, and benefit the mechanical structure stability, though the SE shows slight decomposition but the generated chemistry is ionically conductive and stable in the following cycles. Through the comprehensive evaluation between the pros and cons of adding SE and carbon, in terms of improvements in reaction kinetics and structural stability compared with the limited electrochemical decomposition of SE, nano-Si-SE-C composite anode demonstrates the best Si utilization with the highest specific capacities.

<quillbot-extension-portal></quillbot-extension-portal><quillbot-extension-portal></quillbot-extension-portal>

11:15 AM EN02.13.05

Highly Reversible Solid-State Silicon Anodes Enabled by Hydride Based Electrolytes Yonglin Huang¹, Bowen Shao¹, Yan Eric Wang² and Fudong Han¹; ¹Rensselaer Polytechnic Institute, United States; ²Advanced Materials Lab, Samsung Advanced Institute of Technology-America, Samsung Semiconductor Inc., United States

Silicon is considered a promising candidate for anodes in solid-state batteries due to its high energy density and unique properties in addressing problems associated with Li metal anodes such as dendrite formation and morphological instability. Despite many exciting results from previous works on solid-state Si anodes, the initial Coulombic efficiency, a critical parameter that characterizes the electrochemical reversibility for the first cycle and directly influences the battery's energy density, has not been well considered. In this presentation, we report our study on the (electro)chemical stability between Si and three representative solid electrolytes, including a typical sulfide ($75\text{Li}_2\text{S}-25\text{P}_2\text{S}_5$), an iodide-substituted sulfide ($70(0.75\text{Li}_2\text{S}-0.25\text{P}_2\text{S}_5)-60\text{LiI}$) and a hydride-based solid electrolyte ($3\text{LiBH}_4\text{-LiI}$, LBHI). Our results indicate that LBHI demonstrates superior electrochemical and chemical stability with Si anodes compared with sulfide-based electrolytes, enabling a high-performance solid-state Si anode with a record high initial Coulombic efficiency of 96.2% among all Si anodes reported to date. The excellent (electro)chemical reversibility of Si anodes was also demonstrated in solid-state full cells with nickel-rich layered oxide cathodes. The results highlight the importance of solidifying Si anode to improve its performance, and the excellent stability of hydride-based solid electrolytes also offers potential opportunities to be used as an interlayer or 3D ionic framework for other low voltage anodes, including Li metal.

SESSION EN02.14: Electrode Interface II

Session Chairs: Xin Li and Luhan Ye

Thursday Afternoon, November 30, 2023

Hynes, Level 3, Room 304

1:30 PM EN02.14.01

Using Holey Graphene for Improved Interfacial Contact in Solid Electrolyte Ionic Conductivity Measurements Lopamudra Das¹ and Yi Lin²; ¹Analytical Mechanics Associates, United States; ²NASA Langley Research Center, United States

Solid-state batteries (SSBs) are poised to become the batteries of the future with advantages such as higher energy density, lighter weight, versatile geometry, and greater safety due to low flammability risk. An important parameter of the solid electrolyte (SE) used is its ionic conductivity. The ionic conductivity is generally calculated from the bulk resistance of a SE pellet, measured from the electrochemical impedance spectroscopy data. The SE pellet is typically prepared from the electrolyte powder by dry compression and is sandwiched between two blocking current collectors to obtain the impedance spectroscopy data. One of the challenges in conducting this measurement is poor interfacial contacts between the SE pellet and the current collector

surfaces. Therefore, measurements reported in the literature may underestimate the true ionic conductivity of a given electrolyte. Holey graphene is a carbon nanomaterial with high electrical conductivity and unique dry compressibility, which is unusual for carbon materials but similar to many oxide and sulfide SEs. In this work, it is demonstrated that adding a thin layer of holey graphene between the electrolyte and the stainless steel current collectors significantly improves the interfacial contact. The ionic conductivity values obtained in the effort were sometimes several times higher than the data measured for SEs without the holey graphene layers. This work calls for more standardized measurement procedures to reduce the discrepancies in reported ionic conductivity values.

1:45 PM EN02.14.02

Ni-Rich Layered Cathodes in Sulfide-Based All-Solid-State Batteries: Improving Interface Stability by Oxide Nanoparticle CoatingRuizhuoZhang¹, YuanMa¹, AleksandrKondrakov^{1,2}, JürgenJanek^{1,3} and TorstenBrezesinski¹; ¹Battery and Electrochemistry Laboratory, Institute of Nanotechnology, Karlsruhe Institute of Technology (KIT), Hermann-von-Helmholtz-Platz 1, Germany; ²BASF SE, Carl-Bosch-Str, Germany; ³Institute of Physical Chemistry, Justus-Liebig-University Giessen, Heinrich-Buff-Ring, Germany

Owing to the superior ionic conductivity and mechanical ductility, sulfide-based solid electrolytes (SEs) such as $\text{Li}_6\text{PS}_5\text{Cl}$ (LPSCl) have been extensively investigated for use in all-solid-state batteries (ASSBs). However, the practical implementation of ASSBs requires making significant improvements to various aspects of their components. When utilizing a high areal capacity electrode composite with a Ni-rich layered oxide cathode material, $\text{LiNi}_{0.85}\text{Co}_{0.10}\text{Mn}_{0.05}\text{O}_2$ (NCM85), the poor interfacial stability arising from the narrow electrochemical window of LPSCl poses a significant challenge. Hence, effective coating strategies are needed to mitigate or decelerate adverse side reactions occurring during battery operation. Here, we present a facile coating approach based on preformed oxide nanoparticles (NPs) such as ZrO_2 and HfO_2 , enabling uniform surface coverage of the NCM85 cathode material via wet-chemistry processing. From pellet-stack cell testing, the NP coatings are found to result in substantial improvements in reversibility, kinetics, capacity and longevity (compared to the uncoated counterpart). Detailed characterization revealed the effectiveness of the coating method in reducing electro-chemo-mechanical degradation at the cathode interface. Furthermore, the adaptability to processing slurry-cast electrodes has been explored, potentially allowing for scalable preparation of ASSBs.

2:00 PM EN02.14.03

Linking Microstructure and Ionic/Electronic Conductivity of Sulfide-Based Composite Cathodes with the Cell PerformanceNikolaosPapadopoulos, EliasReisacher, PinarKaya and VolkerKnoblauch; Materials Research Institute (IMFAA)/Aalen University, Germany

Compared to conventional lithium-ion batteries (LIBs) bearing liquid electrolytes, ASSBs (all-solid-state batteries) have the potential to improve safety and achieve higher performance and energy density [1]. However, there are still many challenges to tackle in order to achieve Li-ASSBs with sufficient cell performance. One of those challenges is overcoming the complexity within the composite cathode. Liquid electrolytes can penetrate composite cathodes easily, while solid electrolytes cannot, leading to residual porosity in the cathode, which then blocks the ionic and electronic charge transport pathways. On the other hand, the degradation of the solid electrolyte (SE), cathode active material (CAM), and conductive additive (CA) caused by parasitic side reactions have to be tackled with protective coatings that hinder the degradation but at the same time keep the charge transport pathways open [2,3]. Therefore, the composite cathode microstructure (e.g., optimal composition ratios $_{\text{CAM:SE:CA}}$, particle characteristics, distribution of the phases) must be designed for different materials systems to ensure a perfect percolation and provide sufficient ions and electrons, thus tortuosity [4-7]. In this study, we aim to deepen the understanding of the correlation between microstructure and ionic/electronic conductivity of composite cathode with the cell performance. For this purpose, a conductive matrix (CM) comprising $\text{Li}_6\text{PS}_5\text{Cl}$ and C65 was developed and used within the composite cathode. Effective ionic and electronic conductivities of different cathode mixtures of the conductive matrix and NMC622, as well as microstructural evolution, were analyzed. Subsequently, these findings were correlated with the rate capability and cycling performance of the cells. We determined the electronic percolation threshold of the conducting matrix (CM) to keep the amount of C65 as low as possible and detected the ionic/electronic limitations for the composite cathode mixtures by varying the active material content. The results of this study will shed light on how to optimize the microstructure to achieve the best cell performance

Acknowledgment

The authors gratefully acknowledge the support of the German Federal Ministry of Education and Research within the program "FH Impuls" (Project SmartPro, Subproject SMARTBAT, Grant no. 13FH4I07IA) and Dr. Veit Steinbauer (Aalen University).

References

- [1] Janek, Jürgen, and Wolfgang G. Zeier. "A solid future for battery development." *Nature Energy* 1.9 (2016): 1-4.
- [2] Ma, Yuan, et al. "Advanced Nanoparticle Coatings for Stabilizing Layered Ni Rich Oxide Cathodes in Solid State Batteries." *Advanced Functional Materials* 32.23 (2022): 2111829.
- [3] Sun, Shuo, et al. "Multiscale understanding of high energy cathodes in solid-state batteries: from atomic scale to macroscopic scale." *Materials Futures* 1.1 (2022): 012101.
- [4] Ohno, Saneyuki, and Wolfgang G. Zeier. "Toward practical solid-state lithium-sulfur batteries: challenges and perspectives." *Accounts of Materials Research* 2.10 (2021): 869-880.
- [5] Bielefeld, Anja, Dominik A. Weber, and Jürgen Janek. "Modeling effective ionic conductivity and binder influence in composite cathodes for all-solid-state batteries." *ACS applied materials & interfaces* 12.11 (2020): 12821-12833.
- [6] Dixit, Marm, et al. "Implications of Local Cathode Structure in Solid-State Batteries." *Solid State Batteries Volume 2: Materials and Advanced Devices*. American Chemical Society, 2022. 113-132.
- [7] Hendriks, Theodoor A., et al. "Balancing Partial Ionic and Electronic Transport for Optimized Cathode Utilization of High Voltage $\text{LiMn}_2\text{O}_4/\text{Li}_3\text{InCl}_6$ Solid State Batteries." *Batteries & Supercaps* (2023): e202200544

2:15 PM EN02.14.04

Overcoming the Interfacial Challenges of LiFePO_4 in Inorganic All-Solid-State BatteriesAshleyCronk¹, Yu-TingChen¹, GraysonDeysher¹, So-YeonHam¹, HediYang², PhillipRidley¹, BaharakSayahpour¹, Long Hoang BaoNguyen¹, Jin An SamOh¹, JihyunJang¹, DarrenTan¹ and Y. ShirleyMeng²; ¹University of California, San Diego, United States; ²The University of Chicago, United States

All-solid-state batteries (ASSBs) are one of the most promising systems to enable long-lasting and thermally resilient next-generation energy storage. Ideally, these systems should utilize low-cost resources with reduced reliance on critical materials. Pursuing cobalt- and nickel-free chemistries, like LiFePO_4 (LFP), is a promising strategy. Morphological features of LFP essential for improved electrochemical performance are highlighted to elucidate the interfacial challenges when implemented in ASSBs, since adoption in inorganic ASSBs has yet to be reported. In this work, the compatibility of LFP with two types of solid-state electrolytes, $\text{Li}_6\text{PS}_5\text{Cl}$ (LPSCl) and Li_2ZrCl_6 (LZC), are investigated. The potential existence of oxidative decomposition products is probed using a combination of structural, electrochemical, and spectroscopic analyses. Bulk and interfacial characterization reveal that the sulfide-based electrolyte LPSCl decomposes into insulative products, and electrochemical impedance spectroscopy is used to quantify the resulting impedance growth. However, through utilization of the chloride-based electrolyte LZC, high-rate and stable electrochemical performance is achieved at room temperature.

2:30 PM BREAK

SESSION EN02.15: Sulfur Cathode II
Session Chairs: Xin Li and Yi Lin
Thursday Afternoon, November 30, 2023
Hynes, Level 3, Room 304

3:00 PM *EN02.15.01

Development of Materials for All-Solid-State Metal-Sulfur BatteriesDonghaiWang; The Pennsylvania State University, United States

With advances in electrification in transportation, extensive use of power electronics, and utilization of renewable energy and their assimilation into the electrical grid, there is a clear need to develop high-performance, safer, and more sustainable energy storage technologies for future emerging applications. All-solid-state metal-sulfur battery technology is the most promising candidate for next-generation batteries due to its high energy density, long cycle life, and superior safety. However, it faces many challenges from both metal anodes and sulfur cathodes, such as metal dendrite penetration and poor sulfur utilization of the cathode. In this talk, first, I will present a novel approach based on the use of organic-inorganic nanocomposite interphase to construct a stable lithium/solid-state electrolyte interface for stable Li plating/stripping. Second, I will present approaches to developing high-performance solid-state metal-sulfur batteries, including synthesizing highly conductive solid-state electrolytes and fabricating low-cost cathode materials, potentially for electric vehicle and stationary energy storage applications. Together, I would like to demonstrate the research effort aiming to build our knowledge, expertise, and understanding of critical electrochemical processes and mechanisms to employ desired

features in electrochemical energy storage systems to meet the requirement of new energy applications.

3:30 PM *EN02.15.02

Composite Cathode Engineering for Advanced All-Solid-State Lithium-Sulfur Batteries[Guiliang Xu](#), Jieun Lee and Khalil Amine; Argonne National Laboratory, United States

In this talk, we will overview the challenges of all-solid-state lithium-sulfur batteries. We will then introduce our strategies by composite cathode engineering to significantly improve the sulfur utilization (~100%) and reversibility towards high S loading under room temperature. We will also talk about advanced characterization techniques to reveal the underlying mechanism for the improved cell performance. The findings will provide new insights into the failure mechanism and offer new strategies to advance all-solid-state lithium-sulfur batteries.

4:00 PM *EN02.15.03

Electrolyte Design for Intermediate-Temperature Na-S Batteries with High Energy Density[Yuan Yang](#); Columbia University, United States

The conventional high-temperature sodium sulfur battery is an attractive technology for grid-level energy storage due to its low cost, high energy density and long cycle life. However, this system operates at 300-350 °C, which not only increases cost, but also accelerates degradation and causes potential safety issues. On the other side, Na-S batteries working at intermediate temperatures (e.g., 100-150 °C) are attractive, but the formation of solid Na₂S₂ and Na₂S with low ionic diffusivity and electronic conductivity limits its specific capacity to ~500 mAh/g and thus energy density. In this study, we have developed a new electrolyte solvent that can dissolve all sulfides and polysulfides, which avoids the poor kinetics in Na₂S₂ and Na₂S, and allows Na-S batteries to operate at ~75 °C. Based on the 1 mol L⁻¹ sulfur catholyte, a high specific capacity of 1640 mAhg⁻¹ is achieved at 0.13 mA cm⁻². When increased to the 4 mol L⁻¹, the capacity is achieved 830 mAhg⁻¹ and shows capacity retention of 70% over 1000 cycles. Such a system has potential applications for long-duration energy storage.

4:30 PM EN02.15.04

Understanding Electrochemical Reaction Mechanisms of Sulfur in All-Solid-State Batteries Through Operando and Theoretical Studies[Hongli Zhu](#); Northeastern University, United States

Sulfur, with its high theoretical specific capacity of 1675 mAh g⁻¹, affordability, and earth abundance, stands as a promising candidate for cathodes. Lithium-sulfur (Li-S) batteries, boasting an ultrahigh theoretical energy density (2600 Wh kg⁻¹)—a value ten times higher than that of contemporary commercial Lithium-ion batteries, hold immense potential. Yet, Li-S batteries employing ether-based liquid electrolytes face challenges such as the formation of long-chain polysulfides and the shuttle effect, leading to rapid capacity decay, low coulombic efficiency, and poor cycling life. All-solid-state lithium-sulfur batteries (ASLSBs), which substitute traditional organic liquid electrolyte with solid-state electrolytes (SEs), are considered to be a fundamental solution to these issues. SEs provide enhanced safety compared to their flammable and volatile organic counterparts and are assumed to eliminate the formation of polysulfides, thereby inherently addressing the shuttle effects.

Nevertheless, the absence of clear experimental evidence to understand the chemistries and mechanisms of sulfur's electrochemical reaction in ASLSBs prompts further investigation. Existing literature suggests the chemistries in ASLSBs transition directly from S₈ to Li₂S. However, the overlooked formation of Li₂S₂, insoluble in liquid electrolytes, could potentially impact ASLSB performance. Considering Li₂S₂ is a thermodynamically unstable phase, the implementation of advanced in-operando characterization becomes crucial for a deeper understanding of the reaction mechanisms in ASLSBs.

In this talk, we present four key findings that would be of interest to the readership of MRS audiences:

1. We study the chemical transformation of sulfur in ASLSBs and elucidate the reaction mechanism via a combination of operando Raman spectroscopy and ex-situ X-ray absorption spectroscopy (XAS). This gives us the first empirical proof of electrochemical pathways in ASLSBs.
2. We designed a unique cell for the operando Raman study, facilitating the characterization of the battery in an inert argon atmosphere within a cleanroom-in-a-glovebox system. This custom cell with a side window and a pressure-controlling stainless-steel framework allows internal battery material exposure post-assembly without further sealing. Moreover, its square design ensures a focused laser beam on a flat sample surface, eliminating background distractions.
3. We have, for the first time, unveiled a two-step transformation in the Li-S redox reaction in ASLSBs. Our findings prove that the process does not generate any long-chain polysulfides, thereby inhibiting the shuttle effect in SE, a significant departure from the scenario with liquid electrolyte.
4. We found that the transition among S₈, Li₂S₂, and Li₂S exhibits sluggish reaction kinetics, caused by the slow "point-to-point" ion diffusion at the interface in ASLSBs and high "solid to solid" reaction barrier, resulting in incomplete reactions during both discharging and charging processes. These insights will contribute to the continued research and development in the field of ASLSBs.

4:45 PM EN02.15.05

Influence of Carbon Blends for Cathode Active Material Pre-Treatment on Battery Performance[Martin A. Lange](#) and Wolfgang Zeier; WWU Münster, Germany

Solid state batteries show significant potential. Specifically, the lithium-sulfur system shows significant potential thanks to its large gravimetric capacity and the lack of the problematic sulfur-shuttle effect as encountered in liquid cells. To achieve sufficient utilization of the active material, appropriate solid conductors for both ionic and electronic conduction have to be added to the cathode material mixture. While solid electrolytes are studied intensively in regards to optimizing their ionic conductivity, influences of electron conductors are studied more sparsely. Somewhat structured carbons such as carbon fibers are often used with the idea to provide prefabricated conductive pathways, but without in-depth investigation of the interactions between the individual components of the solid cathode composites during mixing.

In this study, we show how already simple mixing of two basic carbons in solid sulfur cathode composites alters significantly the cycling behavior in half-cells. For this purpose, we analyzed two mixtures of two different carbon species in different ratios. For both systems, cathode composites prepared with pure carbons results in vastly different performance than achieved by simple blending of the two carbons. It can be shown, that rather than utilizing purely one sort of carbon, improvements in performance can be achieved by application of specific carbon mixtures, although the exact ratio depends strongly on the type of the added carbons. This means that it is already possible to make significant improvements to the solid lithium-sulfur battery system by mixing simple, inexpensive carbons rather than using complex-structured, expensive carbons, which is particularly interesting in terms of advances in industrial applications and commercialization.

SESSION EN02.16: Advanced Synthesis II

Session Chairs: Xin Li and Changmin Shi

Friday Morning, December 1, 2023

Hynes, Level 3, Room 304

8:00 AM EN02.16.01

Fast Sintering and Polymorphism of NASICON-Type LiZr₂(PO₄)₃ Solid Electrolyte Materials[Lin Lin](#) and Kelsey B. Hatzell; Princeton University, United States

Conventional solid electrolyte manufacturing and materials processing methods are too complex and expensive for scalability. Specifically for oxide solid electrolytes, the high-temperature and long synthesis and sintering procedures introduce significant time and energy cost. Various fast sintering methods have been developed in the past decade to address this manufacturing challenge [1]. Manufacturing dense, highly conducting solid electrolytes in air and in minutes (or seconds) are desirable for solid state battery manufacturing. (NASICON-)type LiZr₂(PO₄)₃ (LZP) in one type of solid electrolyte which demonstrates excellent air and water stability, as well as good resistance to Li reduction at interfaces [2]. However, LZP exhibits rich polymorphism, with different phases showing distinct crystal structures and ion transport mechanisms [2]. Previous studies have shown that polymorphism observed in garnet-type Li₇La₃Zr₂O₁₂ solid electrolyte significantly affects the transport and chemo-mechanical properties [3]. Yet the polymorphism in solid electrolytes has seldom been exclusively studied and controlled. In this work, we developed a modified air-compatible ultrafast high-temperature sintering (UHS) approach and successfully sintered LZP within a few minutes. X-ray diffraction analysis reveals how processing impacts polymorphism in this class of materials. The green body contains almost fully α'-triclinic, low ionic conductivity phase. The highly conducting α-rhombohedral polymorph can be achieved in only minutes of with ultrafast sintering. The ratio of two phases are strongly affected by the processing temperatures and times. The percentages of rhombohedral phase increase from 53% to 68% as the sintering temperature increases from 900 to 1200 °C when keeping a 5 min sintering time. On the other hand, with the sintering temperature kept at 1200 °C, the percentages of rhombohedral phase increase from 54% to 83% when increasing the sintering time from 1 min to 8 min. These results present pathways to ultrafast manufacturing process that enable control over structure and transport.

References:

- [1] Hu et al., Chem. Soc. Rev., 52, 1103 (2023).
[2] El-Shinawi, et al., RSC Adv., 5, 17054 (2015).
[3] Dixit et al., Nat. Mater., 21, 1298–1305 (2022).

8:15 AM EN02.16.02

Not Just an Unwanted Impurity Phase: Pyrochlores as Convenient Precursors to Li Conducting GarnetsJinzhaGuo and CandaceK. Chan; Arizona State University, United States

Garnet-type solid-state electrolytes such as Ta-doped $\text{Li}_7\text{La}_3\text{Zr}_2\text{O}_{12}$ (LLZTO) are promising ceramic electrolytes for all-solid-state batteries because of their high (electro)chemical stability and ionic conductivity. LLZTO is typically synthesized from oxide precursors via solid-state reaction, but use of other precursors can lead to improved phase purity and more homogenous dopant distribution. We recently demonstrated that pyrochlores, usually seen as an unwanted impurity phase in the synthesis of garnets, can actually serve as the starting precursor for LLZTO, a process we call “pyrochlore-to-garnet” (P2G). Nanocrystalline pyrochlore prepared using molten salt synthesis and a scalable sol-gel method are demonstrated to enable formation of dense LLZTO ceramic directly via reactive sintering of the pyrochlore and a lithium source. The LLZTO prepared via P2G displays high relative density and ionic conductivity comparable to LLZTO prepared by solid-state reaction, but with much shorter sintering times. Investigation of the synthesis parameters shows that liquid phase sintering is important for achieving high pellet densities and phase-purity. Additionally, while the LLZTO grain sizes obtained using this P2G method are smaller than those from conventional sintering of LLZTO particles, the P2G pellets can sustain higher critical current densities before shorting in lithium stripping/plating experiments compared to conventional LLZTO prepared by solid-state reaction. This work shows P2G is promising as an alternate method for the synthesis and processing of LLZTO materials.

8:30 AM EN02.16.03

Multifunctional Coatings on Sulfide-Based Solid Electrolyte Powders with Enhanced Processability, Stability and Performance for Solid-State BatteriesZacharyD. Hood, AnilU.

Mane, AdityaSundar, SanjaTepavcevic, PeterZapol, UdochukwuD. Eze, ShibaP. Adhikari, EungjeLee, GeorgeSterbinsky, JeffreyW. Elam and JustinConnell; Argonne National Laboratory, United States

Sulfide-based solid-state electrolytes (SSEs) represent one of the most promising classes of materials for next-generation all-solid-state Li-ion batteries due to their many beneficial properties, including high ionic conductivity and favorable mechanical properties that make them more readily amenable to processing at scale. However, widespread adoption of these materials is hindered by their intrinsic instability under ambient conditions, as well as by (electro)chemical instability at the Li||SSE and cathode||SSE interfaces, which limits cell performance and lifetime. We have developed a method that utilizes atomic layer deposition (ALD) to grow thin, oxide-based coatings on argyrodite $\text{Li}_6\text{PS}_5\text{Cl}$ (LPSCI) powders to address both issues simultaneously. We demonstrate that thin films of aluminum oxide (Al_2O_3) can be directly grown onto argyrodite particles using trimethyl aluminum and H_2O with minimal chemical modification of the underlying material. These coatings enable exposure of LPSCI powders to pure and H_2O -saturated oxygen environments for ≥ 4 hours with little to no reactivity, compared with significant degradation of the uncoated powder. Furthermore, pellets fabricated from coated LPSCI powders exhibit bulk ionic conductivities up to $2\times$ higher than those made from uncoated material, with a simultaneous decrease in electronic conductivity. These favorable transport properties are coupled with significant suppression of Li_2S and Li_3P formation observed at the Li-SSE interface, confirming improved chemical stability with Li metal anodes. These benefits result in significantly improved room temperature cycle life at high capacity and current density (≥ 150 cycles at 1 mAh/cm^2 per cycle and 0.5 mA/cm^2). We hypothesize that these enhanced properties derive from improved electronic and chemical properties at intergranular boundaries, as well as improved Li metal adhesion at the interface. Similar improvements in materials properties are achieved using ALD coating chemistries beyond Al_2O_3 . This work points to a completely new framework for designing active, stable, and scalable materials for next-generation solid-state batteries.

The submitted manuscript has been created by UChicago Argonne, LLC, Operator of Argonne National Laboratory (“Argonne”). Argonne, a U.S. Department of Energy Office of Science laboratory, is operated under Contract No. DE-AC02-06CH11357. The U.S. Government retains for itself, and others acting on its behalf, a paid-up nonexclusive, irrevocable worldwide license in said article to reproduce, prepare derivative works, distribute copies to the public, and perform publicly and display publicly, by or on behalf of the Government. The Department of Energy will provide public access to these results of federally sponsored research in accordance with the DOE Public Access Plan. <http://energy.gov/downloads/doe-public-access-plan>

8:45 AM EN02.16.04

Spray-Flame Synthesis of NASICON-Type $\text{Li}_{1.3}\text{Al}_{0.3}\text{Y}_{0.3-x}\text{Ti}_{1.7}(\text{PO}_4)_3$ ($x=0-1.5$) Solid ElectrolytesMd YusufAli¹, HansOrthner¹ and HartmutWiggers^{1,2}; ¹Institute for Energy and Materials Processes – Reactive Fluids; University of Duisburg-Essen, Germany; ²Center for Nanointegration Duisburg-Essen, Germany

Due to its safety, low cost, and high energy density characteristics, solid-state lithium-ion batteries have been recognized as one of the most promising candidates for future green energy storage technologies. Electrolytes made of polymers and ceramics are prime candidates to expand the use of lithium metal batteries. Single-ion conducting polymers can lessen polarization and the formation of lithium dendrites, but they eventually become extremely inflexible mechanically, necessitating mobilizers such as organic solvents to move Li ions. Inhomogeneous solvent dispersion and the accompanying preferred Li transport paths may result in favored locations for Li plating, adding mechanical stress and maybe even causing early cell short-circuits. However, ceramic-based electrolytes, such as $\text{Li}_{1.3}\text{Al}_{0.3}\text{Ti}_{1.7}(\text{PO}_4)_3$ (LATP) NASICON, are renowned for their superior dendritic growth inhibitor and high-temperature adaptability. In contrast to other wet synthesis methods, spray-flame synthesis is affordable and incredibly simple to scale up with excellent purity, thus we looked into the best conditions to synthesize LATP solid electrolyte. We found that nitrates are better than acetates as metal precursors, and excess Li is indeed necessary in precursor solution to synthesize pure phase LATP. We characterized the resulting nanoparticles by state-of-the-art techniques such as XRD, XPS, TEM, Raman Spectroscopy etc. The as-prepared spray flame synthesized nanoparticles are found to be TiO_2 and with Li carbonate on the surface as confirmed by XPS, and it requires a high-temperature calculation ($\sim 750^\circ\text{C}$) to finally form LATP phase. However, the ionic conductivity of LATP phase samples (0.049 mS/cm) were not up to the industrial standard. To further increase the ionic conductivity of LATP electrolytes the Al^{3+} (0.535 \AA) substitution with similar charge Y^{3+} (0.93 \AA) was carried out $\text{Li}_{1.3}\text{Al}_{0.3}\text{Y}_{0.3-x}\text{Ti}_{1.7}(\text{PO}_4)_3$ ($x=0$ to 1.5). Moreover, the large size of Y^{3+} distorts the NASICON structure and provides broad passage for the Li^+ ion to pass through. The enhanced electrochemical characteristics of LATP samples make it possible to see how Y doping affects the samples. The synthesized sample ($x=0.1$ doped) has a conductivity of around 0.000092 mS/cm . Because of as synthesized TiO_2 phase. However, after calcining at 700°C , a rise in conductivity (0.006042 mS/cm) can be seen for the sample due to phase transformation to LATP. Further increment in ionic conductivity was done while simultaneously increasing the grain boundary of the pellet. And the final conductivity was reached as high as 0.87 mS/cm which almost reaches the milestone for NASICON solid state electrolytes.

9:00 AM EN02.16.05

Unveiling Low-Temperature Sintering of Solid-State Ceramic Composite Electrolytes via *In-Situ* Electrochemical Impedance SpectroscopyBoNie and HongtaoSun; Penn State University, United States

The increasing safety concerns surrounding high-energy density rechargeable batteries have spurred interest in the development of solid-state electrolytes, aiming for nonflammable and tolerance to extreme conditions. However, conventional fabrication methods of ceramic-based composites face two primary challenges: limited ability to simultaneously tune the intergranular phase and achieve high material density, as well as a lack of efficient methodology to address interfacial issues under mild processing conditions. Consequently, producing stable solid-state electrolytes with low interface resistance, particularly solid-state oxide electrolytes, without resorting to high-temperature sintering for extended periods remains a challenge.

To overcome these challenges, we introduce a cold sintering process (CSP), a multistage nonequilibrium approach combining dissolution–precipitation under external stress, viscous flow of saturated solutions, and species diffusion for the fabrication of highly ionic conductive solid-state electrolytes at low processing temperatures. Additionally, CSP bridges the temperature gap between high melting point constituents (e.g., ceramics) and low melting point constituents (e.g., nano-sized additives, or polymers), enabling the co-sintering of ceramic-based composites for a wide range of solid-state electrolytes. In this study, CSP was utilized to prepare a solid-state NASICON-Halide (nanosized Li_3InCl_6 in LATP matrix) composite electrolyte. To gain further insight into the sintering dynamics and the process-structure-property correlation, we employed electrochemical impedance spectroscopy (EIS) as an in-line monitoring tool to study the real-time impedance during the CSP. We considered the mixed ceramic powders with a small volume of transient solvent as an effective dielectric medium. Through simulations using an equivalent circuit comprising a constant phase element and a resistive element, we captured the dielectric properties and resistance sensitive to CSP, which vary as evaporation and densification occur. Decoding the resulting resistance data provided a profound understanding of the temperature and pressure effects.

Furthermore, we investigated the associated microstructures and ionic conductivities to understand the process-structure-property correlation. The highly dense composite electrolyte, with a small fraction of Li_3InCl_6 , exhibited an impressive ionic conductivity of $10^{-4} \text{ S cm}^{-1}$ at room temperature, along with excellent reversibility in transporting Li ions for thousands of hours at a cycling capacity of 1 mAh cm^{-2} .

9:15 AM EN02.16.06

The Study of LLZO Thin Film Electrolyte using Pulsed Light TreatmentAhromRyu^{1,2}, SahnNahm² and Ji-WonChoi¹; ¹Korea Institute of Science and Technology, Korea (the Republic of); ²Korea University, Korea (the Republic of)

All-solid-state lithium batteries (ASSLBs) have gained significant attention due to their numerous advantages over traditional lithium-ion batteries. ASSLBs offer improved safety and thermal stability while achieving efficient energy density within the same volume. However, there are key challenges that need to be addressed for the commercialization of solid-state batteries. In

particular, the solid electrolyte needs to exhibit enhanced ion conductivity to provide sufficient transport in the cathode. LLZO (lithium lanthanum zirconium oxide) is a promising candidate as a solid electrolyte material due to its excellent ion conductivity in bulk and transport stability for lithium ions. However, achieving the required level of ion conductivity for commercialization remains a challenge because it requires high annealing temperatures of over 700 °C to be crystallized, which causes degradation and long production times with high cost. To overcome this limitation, we introduce IPL (intensive pulsed light) processing, which is a method that rapidly applies high-energy pulses, minimizing damage caused by excessive heat. In our study, we deposited LLZO thin films using RF magnetron sputtering at room temperature and investigated the structural and electrical changes after IPL treatment. We achieved direct rapid annealing in a total of seconds, adjusting parameters such as bank voltages and the number of pulses by employing an IPL. We analyzed the structural changes through SEM and XRD, confirming modifications in the film's structure following IPL treatment. The films were deposited on SiO₂/Si wafers and Cu foils and device integration was achieved using a Pt top electrode. EIS (electrochemical impedance spectroscopy) measurements of the samples revealed a Nyquist plot that demonstrated improved ion conductivity compared to the amorphous phase. To explain this phenomenon, we measured the impedance at various temperatures. Based on the plots, we constructed Arrhenius plots and extracted the activation energy. Consequently, we found that the LLZO film after IPL treatment exhibited lower activation energy, indicating enhanced lithium ion conductivity.

9:30 AM EN02.16.07

High-Entropy Lithium Argyrodite Superionic Conductors JingLin¹, MareenSchaller², SylvioIndris², JürgenJanek^{1,3}, AleksandrKondrakov⁴, TorstenBrezesinski¹ and FlorianStrauss¹; ¹Battery and Electrochemistry Laboratory, Institute of Nanotechnology, Karlsruhe Institute of Technology (KIT), Germany; ²Institute for Applied Materials–Energy Storage Systems, Karlsruhe Institute of Technology (KIT), Germany; ³Institute of Physical Chemistry, Justus-Liebig-University Giessen, Germany; ⁴BASF SE, Germany

Solid-state batteries (SSBs) are a potentially safe, next-generation energy storage technology. For SSBs to be commercially viable, the development of solid electrolytes with high ionic conductivity, high (electro)chemical stability, and good processability is imperative. A new strategy for modifying materials, potentially leading to improved properties, is the high-entropy (HEMs) concept, referring to compounds having five or more elements occupying a single crystallographic site (resulting in a configurational entropy $\Delta S_{conf} \geq 1.5R$). Our recent research has shown that high-entropy argyrodites (HEAs) can be synthesized both by multianionic and/or -cationic substitution. Especially, multication substituted HEA shows a low activation energy ($E_A \approx 0.20$ eV) for lithium transport and a high r.t. ionic conductivity (≈ 10 mS/cm) as shown by ⁷Li pulsed field gradient (PFG) nuclear magnetic resonance (NMR) spectroscopy and electrochemical impedance spectroscopy (EIS). These findings were rationalized from a structural point of view via neutron powder diffraction in combination with magic angle spinning (MAS) NMR spectroscopy. For the multication substituted HEA, high S²⁻/T anion site disorder (up to ~11%) and Li⁺ redistribution led to shortened jump distances and therefore facilitated long-range ion diffusion. Conversely, multianionic substitution resulted in increased intercage jump distances. Overall, our results emphasize the potential of high-entropy lithium argyrodites (large compositional space) for developing novel superionic conductors with enhanced properties.

9:45 AMBREAK

SESSION EN02.17: Sodium Chemistry
Session Chairs: Yi Lin and Changmin Shi
Friday Morning, December 1, 2023
Hynes, Level 3, Room 304

10:15 AM EN02.17.01

Materials Design for Solid State Sodium-Ion Batteries XianguangMiao, YichaoWang, YifanWu, JunyeobMoon and XinLi; Harvard University, United States

Solid state sodium-ion batteries with nonflammable inorganic electrolytes are promising for large-scale energy storage applications. The current battery performance is hindered by problems related to the electrolyte materials, e.g., severe dendrite propagation and interface reaction of conventional Na₃PS₄ anolyte, and low Na⁺ conductivity of halide catholyte. Here we propose a newly designed electrolyte with high conductivity, superior formability under cold-press process and improved electrochemical stability toward the anode. The battery with NaCrO₂ cathode demonstrates a long cycling life at high rate. We demonstrate that this material platform is also applicable to many other cathodes with higher charge voltage.

10:30 AM EN02.17.02

The Influence of Synthesis Procedure on the Structure and Ionic Transport Property of Substituted Sodium Metal Halide TongZhao and WolfgangZeier; University of Münster, Germany

Sodium all-solid-state batteries have attracted growing interest in recent years because of their potentially high energy densities and superior safety as well as the abundance of sodium. Sodium metal halides are viewed as promising candidates for catholytes in sodium all-solid-state batteries since they have wide electrochemical windows and excellent electrochemical compatibility toward oxide cathode materials, as well as good mechanical deformability and scale-up capability. However, the low ionic conductivity hinders their practical application. Substitution is an effective way to improve the ionic transport properties of ionic conductors.

Herein, we introduced aliovalent cation In³⁺ in Na₂ZrCl₆ and the X-ray diffraction analyses show a full indium solubility in the 200°C annealed Na_{2+x}Zr_{1-x}In_xCl₆ crystallized in a P2_{1/n} phase while that exsolves at higher heat treatment temperatures because the indium-rich Na_{2+x}Zr_{1-x}In_xCl₆ compound tends to partially transform to a P1c phase. By assessing the ionic conductivity of the differently synthesized Na_{2+x}Zr_{1-x}In_xCl₆ series, we can show the synergistic effect of the Na⁺/vacancy ratio and crystallinity on sodium ion transport in this class of materials which can enhance the ionic conductivity by three orders of magnitude.¹ Besides the cation doping, anion-mixed sodium halide (Na₃InCl_{6-x}Br_x) is also explored. By milling, the Na₃InCl_{6-x}Br_x (0 ≤ x ≤ 1.5) solid solution series crystallizes in a monoclinic P2_{1/n} phase, while the subsequently annealed Na₃InCl_{6-x}Br_x (0 ≤ x ≤ 2) series transforms into a trigonal P1c phase. A greater anion solubility can be achieved by annealing and changing the structure type. Unlike the cation substituted Na_{2+x}Zr_{1-x}In_xCl₆ series, in Na₃InCl_{6-x}Br_x only slight improvements to the ionic conductivity are observed possibly due to an unfavorable trade-off between high pre-factor and low activation energy resulting from an enthalpy-entropy compensation behavior fulfilling the Meyer-Neldel rule.²

These works further highlight the strong dependence of the structure and solubility of sodium metal halides on the synthesis protocol and shed light on the design principle and synthesis strategy of this class of materials as solid electrolytes.

Reference

1. Zhao, T.; Sobolev, A. N.; Schlem, R.; Helm, B.; Kraft, M. A.; Zeier, W. G., Synthesis-Controlled Cation Solubility in Solid Sodium Ion Conductors Na_{2+x}Zr_{1-x}In_xCl₆. *ACS Applied Energy Materials* **2023**, *6* (8), 4334-4341.
2. Zhao, T.; Kraft, M. A.; Zeier, W. G., Synthesis-Controlled Polymorphism and Anion Solubility in the Sodium ion-conductor Na₃InCl_{6-x}Br_x (0 ≤ x ≤ 2). *Inorganic Chemistry*. Under review.

10:45 AM EN02.17.03

A New Halide Solid Electrolyte for Sodium Solid-State Batteries ErikWu and DarrenTan; Unigrid Inc., United States

UNIGRID Battery aims to develop a sodium solid-state battery (Na SSBs) for stationary storage applications such as residential and grid storage. Na SSBs have been touted to offer improved safety (from the use of nonflammable solid-state electrolytes, or SSEs), lowered costs due to the use of abundant sodium-based materials, and higher performance, potentially culminating in a device with long life and high volumetric energy density. In recent years, the development of new SSEs for Na SSBs, such as halides and closo-borates, have advanced high-performance Na SSB chemistries closer to feasibility. However, each of these materials have their own drawbacks; the halides typically have lower sodium ion conductivity and are unstable with the anode, and the closo-borates are primarily cost-prohibitive and are less stable with cathodes. Thus, a single electrolyte with high Na ion conductivity, low costs, and stability with both electrodes remains elusive. Here, we report a new, thermally robust halide with a conductivity of 1 x 10⁻³ S/cm at room temperature, at least an order of magnitude increase compared to previously reported Na-conducting halides. The halide is employed as a catholyte and cycling is demonstrated in a bilayer Na SSB configuration with superior rate performance.

11:00 AM EN02.17.04

On the Discrepancy Between Local and Average Structure in Solid Electrolytes OliverMaus^{1,2} and WolfgangZeier^{1,2,3}; ¹University of Muenster, Germany; ²Baccara Graduate School, Germany; ³Helmholtz-Institut Muenster, Germany

All-solid state batteries are promising candidates to achieve high energy densities and enable the use of high capacity anodes such as lithium metal or silicon alloys but for highly performing

solid-state batteries it is crucial to have solid electrolytes with high ionic conductivities above 10 mS/cm. Aliovalent substitution is a common strategy to improve the ionic conductivity of solid electrolytes. The substitution of SbS_4^{3-} by WS_4^{2-} in the Na^+ ionic conductor $\text{Na}_{2.9}\text{Sb}_{0.9}\text{W}_{0.1}\text{S}_4$ leads to a very high ionic conductivity of 41 mS/cm at room temperature. While pristine Na_3SbS_4 crystallizes in a tetragonal structure, the substituted $\text{Na}_{2.9}\text{Sb}_{0.9}\text{W}_{0.1}\text{S}_4$ seems to crystallize in a cubic structure based on its X-ray diffractogram. By allowing 3D diffusion pathways, the cubic structure was assumed to be one of the driving forces for the conductivity enhancement in $\text{Na}_{2.9}\text{Sb}_{0.9}\text{W}_{0.1}\text{S}_4$. Here, we show by performing pair distribution function analyses and static single-pulse ^{121}Sb NMR experiments that the short-range order of $\text{Na}_{2.9}\text{Sb}_{0.9}\text{W}_{0.1}\text{S}_4$ remains tetragonal despite the change in the Bragg diffraction pattern. Temperature-dependent Raman spectroscopy revealed that changed lattice dynamics due to the increased disorder in the Na^+ substructure leads to dynamic sampling causing the discrepancy in local and average structure. While showing no differences in the local structure, when compared to pristine Na_3SbS_4 , quasi-elastic neutron scattering and solid-state ^{23}Na nuclear magnetic resonance measurements revealed drastically improved Na^+ diffusivity and decreased activation energies for $\text{Na}_{2.9}\text{Sb}_{0.9}\text{W}_{0.1}\text{S}_4$. The obtained diffusion coefficients are in very good agreement with theoretical values and long-range transport measured by impedance spectroscopy. This work shows how aliovalent substitution can lead to discrepancies of local and average structure and systematically studies the causes and effects of the phenomenon. It demonstrates the importance of studying the local structure of ionic conductors in order to fully understand their transport mechanisms, a prerequisite for the development of faster ionic conductors.

(1) O. Maus *et al.*, *Journal of the American Chemical Society* **2023**, *145* (13), 7147–7158.

11:15 AM EN02.17.05

Exploring the Effect of Phosphorous Deficiency on Ionic Conductivity in NaSICON-Type Solid-Electrolytes derived from Flame-Made Nanoparticles Mohammed-Ali Sheikh¹ and Hartmut Wiggers^{1,2}; ¹University of Duisburg-Essen, Germany; ²Center for Nanointegration Duisburg-Essen (CENIDE), Germany

The battery market has recently shown that Na-ion batteries (SiB) have become a serious alternative to Li-ion batteries (LiB) [1, 2]. However, SiBs exhibit inferior energy density compared to their lithium-ion-based counterparts [3]. For further improving the energy density and safety of SiBs, solid-state SiBs (SSiBs) have gained a lot of interest and NaSICON-type solid-electrolytes are promising materials for such an application owing to their high ionic conductivity of 10^{-4} – 10^{-3} Scm^{-1} at room temperature and chemical as well as mechanical stability [4]. Recent studies revealed that the conductivity of $\text{Na}_3\text{Zr}_2\text{Si}_2\text{PO}_{12}$ (NZSP) can be enhanced by increasing the silicon to phosphorous ratio [5] or doping NZSP with divalent cations [6]. In this work, we present the spray-flame synthesis (SFS) of NaSICON nanoparticles as a facile method to produce powders of different compositions and stoichiometries. For morphological characterization, transmission electron microscopy is employed. Structural information is obtained by X-ray diffraction (XRD) and Raman-spectroscopy. Thermogravimetry (TG) and differential scanning calorimetry (DSC) are utilized for thermal analysis of powders. Pressed pellets are sintered at 1100°C for 3h and their ionic conductivities are measured with impedance spectroscopy.

From SFS, nanoparticles with a mean diameter of 5 nm are obtained. They consist of fine ZrO_2 crystallites embedded in an amorphous phase of Na, Si and P. After a short annealing step of 1h at 1000°C, this mixture can be converted almost quantitatively into the desired rhombohedral NaSICON phase. Especially the composition $\text{Na}_{3-x}\text{Zr}_2\text{Si}_{2-x}\text{P}_{1-x}\text{O}_{12}$ and Mg-doped $\text{Na}_{3-2y}\text{Mg}_y\text{Zr}_{2-y}\text{Si}_2\text{PO}_{12}$ show - with respect to the short sintering time of 3h - remarkably high ionic conductivities of 4×10^{-4} Scm^{-1} (for $x=0.1$) and 9.3×10^{-4} Scm^{-1} (for $y=0.2$), respectively. XRD reveals that the addition of Mg beyond the solubility limit in NZSP leads to the formation of Mg-phosphates, creating a P-deficiency in the lattice of NZSP and thus improving the ionic conductivity significantly.

In conclusion, SFS enables the scalable production of NaSICON nanoparticles with tailored compositions allowing fast sintering. The improved ionic conductivities observed in the Mg-doped and phosphorous-deficient compositions hold promise for the development of high-performance solid-electrolytes.

[1] Zuo, W. *et al.*, *Acc. Chem. Res.*, **56** (2023), 284-296; doi.org/10.1021/acs.accounts.2c00690.

[2] Tang, B. *et al.*, *Sci. Bull.*, **67** (2022), 2149-2153; doi.org/10.1016/j.scib.2022.10.014

[3] Abraham, K. M., *ACS Energy Lett.*, **5** (2020), 3544; doi.org/10.1021/acsenerylett.0c02181

[4] Zhang, Z. *et al.*, *ACS Appl. Energy Mater.*, **3** (2020) 7427; doi.org/10.1021/acsaem.0c00820

[5] Schuett, J. *et al.*, *Phys. Chem. Chem. Phys.* **24** (2022), 22154-22167; doi.org/10.1039/D2CP03621E

[6] Samiee, M. *et al.*, *J. Power Sources*, **347** (2017), 229-237; doi.org/10.1016/j.jpowsour.2017.02.042

SESSION EN02.18: Dendrite, Sodium and AI
Session Chairs: Yi Lin and Xianguang Miao
Friday Afternoon, December 1, 2023
Hynes, Level 3, Room 304

1:30 PM EN02.18.01

Critical Interphase Overpotential as a Lithium Dendrite Suppression Criterion for All-Solid-State Lithium Battery Design Hongli Wan and Chunsheng Wang; University of Maryland, College Park, United States

Suppressing Li dendrite growth is a crucial challenge in the development of all-solid-state Li-metal batteries (ASSLBs). Penetration of Li dendrites through the solid-state electrolyte (SSE) can lead to short-circuiting of the cells, presenting a safety concern. The current density at which Li dendrites penetrate through the SSE and cause short-circuiting is termed the critical current density (CCD). The CCD not only depends on the intrinsic properties of the SSE but also on the thickness of the SSE. Furthermore, as the Li plating or stripping capacity, stack pressure, and interfacial resistance change the overpotential, which is the driving force for Li plating and stripping, these factors also change the CCD. Thus, because the CCD is not an intrinsic property of an SSE, it is difficult to use CCDs to design SSEs. Herein, we evaluate the lithium dendrite suppression capability of SSE using critical interphase overpotential (CIOP). The CIOP is the intrinsic property of the interphase, which depends on electronic/ionic conductivity, lithiophobicity, and mechanical strength. When the applied interphase overpotential (AIOP) is larger than CIOP, Li will grow into interphase as dendrites. To reduce AIOP but increase CIOP, we design a mix-conductive Li_2NH -Mg interlayer between $\text{Li}_6\text{PS}_5\text{Cl}$ SSE and Li-1.0wt%La anode, which transfers into $\text{Li}_6\text{PS}_5\text{Cl}/\text{LiMgS}_x/\text{LiH-Li}_3\text{N}/\text{LiMgLa}$ after Mg migration during annealing and activation cycles. The LiMgS_x interphase increases the CIOP from 9–12mV (of $\text{Li}_6\text{PS}_5\text{Cl}$) to ~220mV. The Li plates on LiMgLa surface and reversible penetration into the formed porous $\text{LiH-Li}_3\text{N}$ reducing AIOP. The CIOP provides design guidelines for high-energy and room-temperature all-solid-state lithium-metal batteries.

1:45 PM EN02.18.02

Investigating Thermodynamic and Structural Factors for Suppressed Dendrite Formation at Anode-Electrolyte Interfaces in Solid-State Batteries Guy Olivier Ngongang Ndjawa and Samir Abdulhamid Hussien; King Fahd University of Petroleum and Minerals, Saudi Arabia

Solid-state batteries (SSBs) offer a promising solution for overcoming the limitations of conventional Li-ion batteries, but significant challenges persist, especially at the anode-electrolyte interface, leading to poor battery performance. Phase field models have been extensively used to characterize microstructural evolutions at SSB interfaces. However, the key thermodynamic factors and initial boundary conditions influencing structural degradation in these cells, particularly dendrite formation, remain unclear. This work aims to develop a phase-field model that incorporates electrochemical and mechanical driving forces to simulate dendritic growth at SSB interfaces with resolved microstructures. Specifically, the focus is on the anode/solid electrolyte interface, utilizing lithium metal as the anode and $\text{Li}_7\text{La}_3\text{Zr}_2\text{O}_{12}$ (LLZO) as the electrolyte. Expanding on the foundational Monroe Newman model, this study reevaluates the model by incorporating alternative initial mechanical and thermodynamic boundary conditions that have the potential to either impede or facilitate dendritic growth. Through the integration of micron-scale phase-field models and atomic-scale simulations, the research enables the prediction of dendrite nucleation, growth kinetics, and morphology, thereby revealing the conditions that can prevent dendrite formation and enhance battery performance and safety. Overall, this work addresses a critical gap in understanding dendrite growth by demonstrating that the consideration of initial boundary conditions is essential. The findings from this research will hopefully enhance our understanding of solid-state battery interfaces, enabling more accurate predictions of electrochemical processes and failure modes. Ultimately, this improved understanding will guide the design and development of the next generation of all-solid-state batteries with enhanced energy density and improved safety.

2:00 PM EN02.18.03

Composites of Alkali Carbonphosphonitride Thermosets with LLZO and other Ion Conducting Ceramics Andrew Purdy¹, Ryan J. Buchwalder^{1,2}, Daniel M. Fragiadakis¹, Hunter O. Ford^{1,3}, Christopher A. Klug¹, Mark O. Bovee^{1,3}, Megan B. Sassin¹ and Brian L. Chaloux¹; ¹Naval Research Laboratory, United States; ²NREIP Intern, United States; ³NRC Postdoctoral Associate, United States

Lithium dicyanamide ($\text{LiN}(\text{CN})_2$) reacts with phosphorus cyanides ($\text{P}(\text{CN})_3$ or $\text{RP}(\text{CN})_2$) in a 2:1 or greater mole ratio in an anhydrous aprotic mutual solvent to form a resin, which then cures at temperatures of 200–300 °C to a non-flammable ion conductor. When fully cured, these films have a low ionic conductivity, probably due to rigid crosslinking of the thermoset. We found previously that adding compounds to the resin, such as LiCN that contain a higher concentration of Li than $\text{LiN}(\text{CN})_2$, and some non-volatile organic plasticizers, increase the room temperature ionic conductivity from 10^{-12} S/cm to around 10^{-8} S/cm, and the Na versions can also be more conductive than those with Li. Post-cure treatment with diglyme also causes a dramatic conductivity increase, presumably by complexing the mobile Li ions and plasticizing the material. While it seems unlikely that practical conductivities can be obtained in the pure resins, they might be attractive as binders for more highly conducting ceramic powders such as lithium lanthanum zirconium oxide (LLZO), in order to produce a composite material that can be cured to a solid electrolyte at temperatures compatible with other components. We will report our systematic efforts to use these dicyanamides and A-P-C-N (A = Li, Na) thermosets as binders for commercially available ion conducting ceramics. The ratios of resin to ceramic and the conditions of preparation are varied to produce solid composite films for measurement, and the ionic conductivity and chain motions of these films are characterized by impedance and dielectric relaxation spectroscopy. Test cells with Li foil are constructed and measured to evaluate electrochemical stability and lithium transference numbers. Additionally, solid state NMR is used to examine the compositional stability of the composite and the ion mobility between different ionic conductors.

2:15 PM EN02.18.04

Material Design of Quaternary Halide Electrolytes Anthony Onwuli¹, Alex M. Ganose¹, Aron Walsh^{1,2} and Ieuan D. Seymour^{3,1}; ¹Imperial College London, United Kingdom; ²Ewha Womans University, Korea (the Republic of); ³University of Aberdeen, United Kingdom

The future of electrochemical energy storage can be considered to be within the development of all-solid-state batteries (ASSBs). The key to enabling this future resides in the result of solid-state electrolytes (SSEs). For lithium-ion battery systems, halide electrolytes have been reported with room temperature ionic conductivities $>10^{-3}$ S cm⁻¹, good stability against oxidation, and good stability against cathode materials. We find that the space explored for sodium halide electrolytes has been somewhat limited within the literature and primarily focused on ternary sodium chloride SSEs with the limited investigation of sodium bromide and iodide SSEs 2,3,4. Previous studies have demonstrated that Li-halide systems such as Li_3YCl_6 (P-3m1) and Li_3InCl_6 (C2/m) form layered structures with high ionic conductivity. In contrast, ternary halides such as Na_3YCl_6 often form double perovskite structures (P21/n) with intrinsically low ionic conductivity. Discovering new layered Na-halide systems is crucial to improving the ionic conductivity of this class of materials. This study provides a high-throughput materials design workflow to provide insight into the development of quaternary sodium metal halide SSEs through theoretical calculations of thermodynamic stability, electrochemical stability, stability against common sodium cathodes, transport properties as well as the synthesis of $\text{Na}_6\text{M}'\text{M}''\text{X}_{12}$ SSEs. 3710 compositions are considered in four different space groups, ps, P21/n, P-3m1, P31c, C2/m. Our candidate pool is screened to 25 candidates by filtering for a ground state phase in the C2/m structure, on the convex hull ($E_{\text{hull}}=0$), no radioactive elements and an insulator (PBEsol bandgap >2 eV). High oxidation potentials are often observed for the candidates indicating stability against cathodes. Further interface thermodynamics stability analysis revealed that there is a driving force for reactions at the interface between the SSEs and cathodes. On-the-fly machine-learning molecular dynamics (MLMD) was used to probe the ionic conductivity of the candidates. Synthesis of promising candidate material $\text{Na}_6\text{CaZrBr}_{12}$ revealed the existence of a sodium halo spinel phase not initially considered in the initial high-throughput screening. The high-throughput screening and synthesis performed in this study can provide design principles for the development of new SSEs and can be extrapolated to other conducting-ion systems as well as providing a method to expand the search space of known SSE chemistries.

References:

- [1] ACS Energy Lett. 2022, 7, 1776-1805
- [2] J. Mater. Chem. A, 2021, 9, 23037-23045
- [3] Nat. Commun. 2021, 12, 1256
- [4] J. Phys. Chem. Lett. 2020, 11, 3376–3383

2:30 PM EN02.18.05

Deep Learning of Experimental Electrochemistry for Battery Cathodes Across Diverse Compositions Peichen Zhong¹, Bowen Deng¹, Tanjin He¹, Zhengyan Lun^{2,1} and Gerbrand Ceder¹; ¹University of California Berkeley, United States; ²University of Chinese Academy of Sciences, China

Artificial intelligence (AI) has emerged as a powerful tool in the discovery and optimization of novel battery materials. However, the adoption of AI in battery cathode representation and discovery is still limited due to the complexity of optimizing multiple performance properties and the scarcity of high-fidelity data. In this study, we present a comprehensive machine-learning model (DRXNet) for battery informatics and demonstrate the application in the discovery and optimization of disordered rocksalt (DRX) cathode materials. We have compiled the electrochemistry data of DRX cathodes over the past five years, resulting in a dataset of more than 30,000 discharge voltage profiles with 14 different metal species. Learning from this extensive dataset, our DRXNet model can automatically capture critical features in the cycling curves of DRX cathodes under various conditions. The model gives rational predictions of the discharge capacity for diverse compositions in the Li–Mn–O–F chemical space and high-entropy systems. As a universal model trained on diverse chemistries, our approach offers a data-driven solution to facilitate the rapid identification of novel cathode materials, accelerating the development of next-generation batteries for carbon neutralization.

2:45 PM EN02.18.06

The Mechanical Behavior of Li Metal Anodes During Electrochemical Cycling Jungho Shin and Matt Pharr; Texas A&M University, United States

Pure lithium metal anodes are highly promising due to their superior capacities yet remain challenging to implement commercially. Key remaining challenges include non-uniform deposition of the Li metal which can lead to dendrite formation and capacity loss, as well as mechanical stresses and strains induced by the “infinite volume change” associated with its host-less nature during electrodeposition. These issues are intimately connected to the mechanical properties of lithium itself, as well as details of its behavior during electrochemical cycling. With these issues in mind, we investigated the mechanical response of pure Li metal during electrodeposition at room temperature. The tests revealed rate-dependent mechanical behavior during electrodeposition, which we largely attribute to the strain-rate dependent mechanical properties of lithium itself by drawing an analogy between the deposition rate and the strain-rate. This talk will further discuss the practical implications of these experimental observations, particularly concerning dendrite growth in batteries. Specifically, this talk will provide general insight into lithium penetration into solid-state electrolytes, which must be prevented to fully harness the potential of lithium metal anodes in future battery technologies.

3:00 PM BREAK

SESSION EN02.19: Transport, Reaction and Interface

Session Chairs: Xin Li and Changmin Shi

Friday Afternoon, December 1, 2023

Hynes, Level 3, Room 304

3:30 PM EN02.19.01

Compatibility Study of LiCoO_2 and LiCoPO_4 Cathode Materials with NASICON-Type Solid Electrolyte LATP Fumihiko Ichihara¹, Kodai Niitsu¹, Machiko Ode¹, Kazutaka Mitsuishi¹, Yoshinori Niwa², Shogo Miyoshi¹, Takahisa Ohno¹ and Takuya Masuda^{1,3}; ¹National Institute for Materials Science, Japan; ²High Energy Accelerator Research Organization, Japan; ³Hokkaido University, Japan

All-solid-state lithium-ion batteries (ASSLIBs), particularly those employing oxide-based solid electrolytes, are expected to be the next generation of rechargeable batteries because they guarantee safety and dependability by replacing highly combustible organic electrolyte solutions with solid electrolytes. In contrast to conventional liquid LIBs, in which electrolyte/electrode interfaces can be formed spontaneously by injecting liquid electrolyte into cells, the formation of a well-defined solid electrolyte/electrode interfaces with a high ionic conductivity is a key challenge for the development of ASSLIBs.

The conventional method for obtaining the oxide-based solid electrolyte/electrode material interfaces is high-temperature sintering, as these materials have a high melting point and exhibits poor plasticity. However, co-sintering of solid electrolytes and electrode materials often leads to undesired side reactions. Thus, understanding the reaction between solid electrolyte and electrode materials is especially important not only for fundamental science but also for a possible synthetic route to form a well-defined interface with a high ionic conductivity. In this study, we performed the compatibility assessment of a highly ion-conducting solid electrolyte, $\text{Li}_{1.3}\text{Al}_{0.3}\text{Ti}_{1.7}(\text{PO}_4)_3$ (LATP) with a high-capacity cathode material, LiCoO_2 (LCO) and a high-voltage cathode material, LiCoPO_4 (LCP) based on thermodynamic calculations. The calculation results showed that co-sintering LATP and LCO react with each other to form completely different chemical species instead of forming a well-defined interface. On the other hand, co-sintering LATP and LCP does not cause severe reaction. Thus, we experimentally co-sintered the composite of LATP/LCO and LATP/LCP as combination that reacts intensely and a combination that maintains their crystalline structure and characterized their property.

In the intensely reactive combination LATP/LCO, various mixing ratios of LATP and LCO were sintered at various temperatures, and the crystalline phases formed by the reaction were identified and quantified by Rietveld analysis of X-ray diffraction (XRD) and phases including amorphous phase by linear combination fitting of X-ray absorption fine structure (XAFS). The results showed that regardless of the mixing ratio, LATP and LCO react at 300°C, which is relatively low for sintering temperatures, to form Co_3O_4 , Li_3PO_4 and amorphous- TiO_2 . Further increasing the sintering temperature, it was found that the chemical species formed by the reaction depended on the mixing ratio of LATP and LCO. In addition, we used thermodynamic calculations to calculate the chemical species produced at each temperature and mixing ratio and compared these with the experimentally observed chemical species. For sintering temperatures between 900°C and 700°C, the chemical species observed experimentally and those predicted to be formed by thermodynamic calculations were in reasonable agreement. On the other hand, for sintering temperatures below 600°C, there was a significant disagreement between the calculation and experimental results. In the maintaining their crystalline structure combination LATP/LCP, we co-sintered the mixture of LCP and LATP at 800°C and characterized the structure of their bulk and interfaces by XRD, XAFS and microscopic techniques. XRD showed that LATP and LCP maintained their crystalline structures after sintering. XAFS results for Ti and Co K-edges showed no change in chemical state around Ti before and after sintering, whereas a slight change was observed for Co, suggesting the small amount of LCP was decomposed to form Co-containing reaction products due to sintering. The microscopic measurements clearly imaged the formation of Co-containing amorphous layers at the grain boundaries within LATP/LCP composites. XAFS and electron energy loss spectroscopy analyses identified the major species of Co-containing amorphous layers to be CoO and Li_3PO_4 .

3:45 PM EN02.19.02

Ionic Conductivity Transitions in Sodium Antiperovskite Ionic Conductors [Duhang Zhang](#) and [Yiliang Li](#); Massachusetts Institute of Technology, United States

Na_3OCl is a well-studied prototypical fast ion conducting compound representative of the antiperovskite (AP) family, which is of interest for solid-state electrolytes. Here, we observe a two-order-of-magnitude increase in its ionic conductivity (from 10^{-1} to 10 mS/cm) with increasing temperature at 305°C. Temperature-dependent synchrotron X-ray diffraction (SXRD), differential scanning calorimetry (DSC), quasi-elastic neutron scattering (QENS), and impedance spectroscopy, are used to show that the increase in conductivity is correlated with a transition from tetragonal to cubic symmetry associated with a change in octahedral tilt disorder. While previous work has shown that octahedral tilting in APs can create ion migration pathways with lower migration energies than in the regular cubic structure, this is the first instance where such a large increase (100 times) in ionic conductivity due to a change in octahedral tilt disorder has been observed. The octahedral tilt disorder may be exploited as a pathway to increasing the ionic conductivity of antiperovskites and structurally related compounds.

4:00 PM EN02.19.03

Electrochemical Lithiation and Delithiation Reactions Observed by Multimodal *In Situ* Techniques [Takuya Masuda](#); NIMS, Japan

We developed in-situ X-ray photoelectron spectroscopy (XPS) and bimodal atomic force microscopy (AFM) systems and applied them to electrochemical lithiation and delithiation reactions of a silicon electrode deposited on a solid electrolyte sheet in an all-solid-state lithium-ion battery configuration. XPS showed that not only lithium silicide but also lithium oxide, lithium silicate and lithium carbonate were formed due to the lithiation of silicon and native oxide, followed by undesired side reactions with residual gases such as oxygen and carbon dioxide in the inert condition. The spectral features of lithium silicide reversibly responded to the successive lithiation and delithiation cycles, while lithium oxide, lithium silicate and lithium carbonate formed at the surface remained unchanged as irreversible species. As long as the lithiation and delithiation cycles were repeated in the range of Li content $x = 0 - 2.4$ in Li_xSi , the position of lithium silicide peak in the Si 2p region shifted monotonically. However, a drastic shift was observed in the successive delithiation after inserting lithium in silicon electrode up to $\text{Li}_{3.5}\text{Si}$. This drastic shift was assignable to the phase transformation of crystalline $\text{Li}_{15}\text{Si}_4$ to amorphous Li_xSi . AFM showed that the Young's modulus of silicon/lithium silicide changes consistently with change in lithium content x in Li_xSi . Such spectroscopic chemical information and nanoscale mechanical information will be discussed in detail in the context of mechanical degradation.

References

- [1] R. Endo, T. Ohnishi, K. Takada, T. Masuda, "In Situ Observation of Lithiation and Delithiation Reactions of a Silicon Thin Film Electrode for All-Solid-State Lithium-Ion Batteries by X-ray Photoelectron Spectroscopy", *J. Phys. Chem. Lett.*, 2020, 11, 6649–6654.
- [2] R. Endo, T. Ohnishi, K. Takada, T. Masuda, "Instrumentation for tracking electrochemical reactions by x-ray photoelectron spectroscopy under conventional vacuum conditions", *J. Phys. Commun.*, 2021, 5, 015001.
- [3] R. Endo, T. Ohnishi, K. Takada, T. Masuda, "Electrochemical Lithiation and Delithiation in Amorphous Si Thin Film Electrodes Studied by Operando X-ray Photoelectron Spectroscopy", *J. Phys. Chem. Lett.*, 2022, 13, 7363-7370.
- [4] H. Sakai, Y. Taniguchi, K. Uosaki, T. Masuda, "Quantitative cross-sectional mapping of nanomechanical properties of composite films for lithium ion batteries using bimodal mode atomic force microscopy", *J. Power Sources*, 2019, 413, 29-33.

4:15 PM EN02.19.04

Impact of Transport Properties at The Grain-Scale Engineering of Solid Electrolytes: Case Studies on Anti-Perovskite [Ruhul Amin](#), [Marm Dixit](#) and [Ilias Belharouak](#); Oak Ridge National Laboratory, United States

Antiperovskites of composition M_3AB ($\text{M} = \text{Li, Na, K}$; $\text{A} = \text{O}$; $\text{B} = \text{Cl, Br, I, NO}_2$, etc.) have recently been investigated as solid-state electrolytes for all-solid-state batteries. Inspired by the impressive ionic conductivities of $\text{Li}_3\text{OC}_{10.5}\text{Br}_{0.5}$ and Na_3OBH_4 as high as 10^{-3} S/cm at room temperature, many variants of antiperovskite-based Li-ion and Na-ion conductors have been reported, and K-ion antiperovskites are emerging. These materials exhibit low melting points and thus have the advantage of easy processing into thin body and intimate contacts with electrodes. However, there are also issues in interpreting the stellar materials and reproducing their high ionic conductivities. We synthesized the antiperovskite materials by melt casting method and processed them through isostatic pressing (ISP) and conventional approaches. In this presentation, we discuss the critical role of isostatic pressing (ISP) on the crystal- and micro-structural features that originate the higher ionic conductivities of antiperovskites compared to conventional processing. We then discuss its impact on the electrochemical performance of the systems and scalable processing of solid-state battery (SSB) components, and their integration is a key bottleneck toward practical deployment. Finally, we also provide some key perspectives, challenges, and future directions for large-scale production of SSB components and integration.

4:30 PM EN02.19.05

Copper Sulfides as Cathode Active Materials in All Solid-State Batteries [Katherine A. Mazzi](#)^{1,2}, [Zhenggang Zhang](#)^{3,1}, [Kang Dong](#)⁴, [Ingo Manke](#)² and [Philipp Adelhelm](#)^{1,2}; ¹Humboldt-Universität zu Berlin, Germany; ²Helmholtz-Zentrum Berlin für Materialien und Energie, Germany; ³Southern University of Science and Technology, China; ⁴Institute of High Energy Physics, China

One bottleneck in the development of solid-state battery (SSB) technologies is the cathode active material (CAM). Layered oxide materials commonly utilized in other lithium-ion battery technologies are quickly approaching their limits in terms of capacity. It is also clear that realizing the benefits of lithium metal anodes in SSBs necessitates the use of high-capacity conversion-type cathodes. Sulfides offer an intriguing direction for further research because they can reversibly contribute to charge storage through stable anion redox ($2\text{S}^{2-} \rightarrow (\text{S}_2)^{2-} + 2\text{e}^-$). In this talk I will discuss our recent work on metal sulfide-based conversion reactions as CAMs for SSBs, including the dynamic microstructural evolution of CuS using *in-situ* synchrotron X-ray tomography and the use of ternary Cu_3PS_4 with $\beta\text{-Li}_3\text{PS}_4$ solid electrolyte.[1,2] Copper sulfide (CuS) is a naturally occurring mineral that reacts with lithium via a conversion reaction to form Li_2S and Cu with a theoretical energy density of 961 Wh/kg. CuS demonstrates a peculiar feature of Cu displacement into large (μm -sized) domains during cycling that are highly reversible during electrochemical cycling. We were able to follow this dynamic microstructural evolution *in-situ* by synchrotron X-Ray tomography.[1] In addition to these phase transformations, we also observe significant crack formation in the cathode that we found to be dependent on the stacking pressure of the cell. When replacing the binary compound CuS with the ternary compound Cu_3PS_4 , the theoretical energy density increases to 1301.5 Wh/kg and at the same time we anticipate greater compatibility with the $\beta\text{-Li}_3\text{PS}_4$ solid electrolyte due to similarities in chemical composition and structure.[2] We studied the reaction mechanism of Cu_3PS_4 in SSBs and found that it undergoes an irreversible conversion reaction in the 1st cycle. The subsequent redox is largely dominated by Cu_2S and S_8 which form finely dispersed redox centers that promote stable cycling behavior.

[1] Zhenggang Zhang, Kang Dong, Katherine A Mazzi, André Hilger, Henning Markötter, Fabian Wilde, Tobias Heinemann, Ingo Manke, Philipp Adelhelm "Phase Transformation and Microstructural Evolution of CuS Electrodes in Solid-State Batteries Probed by in-situ 3D X-ray Tomography" *Advanced Energy Materials* (2023) 2203143.

[2] Zhenggang Zhang, Katherine A. Mazzi, Luise M. Riegger, Wolfgang Brehm, Jürgen Janek, Joachim Sann, Philipp Adelhelm "Copper Thiophosphate (Cu_3PS_4) as an Electrode Material for Lithium Solid-state Batteries with Lithium Thiophosphate ($\beta\text{-Li}_3\text{PS}_4$) Electrolyte" *Energy Technology* (2023) 2300553.

SYMPOSIUM EN03

Biodegradable, Resorbable and Sustainable Materials
November 27 - December 5, 2023

Symposium Organizers

Shweta Agarwala, Aarhus University
Amay Bhandodkar, North Carolina State University
Jahyun Koo, Korea University
Lan Yin, Tsinghua University

* Invited Paper
+ JMR Distinguished Invited Speaker

SESSION EN03.01 Bio-Inspired Energy Devices
Session Chairs: Shweta Agarwala and Jahyun Koo
Monday Morning, November 27, 2023
Hynes, Level 2, Room 206

10:30 AM *EN03.01.01

Materials and Methods for Sustainable Soft Electronic and Robotic System - From Biodegradable Gels to Mycelium Based Elektronik Skins [Martin Kaltenbrunner](#); Johannes Kepler University, Austria

Modern societies rely on a multitude of electronic and robotic systems, with emerging stretchable and soft devices enabling ever closer human machine interactions. These advances however take their toll on our ecosystem.

Mitigating some of these adverse effects, this talk introduces materials and methods for soft systems that biodegrade. Based on highly stretchable biogels and degradable elastomers, our forms of soft electronics and robots are designed for prolonged operation in ambient conditions without fatigue, but fully degrade after use through biological triggers. Enabling autonomous operation, stretchable and biodegradable batteries power wearable sensors. 3D printing of biodegradable hydrogels enables omnidirectional soft robots with multifaceted optical sensing abilities. Going beyond, we introduce a systematically-determined compatible materials systems for the creation of fully biodegradable, high-performance electrohydraulic soft actuators. They reliably operate up to high electric fields, show performance comparable to non-biodegradable counterparts, and survive over 100,000 actuation cycles. Pushing the boundaries of sustainable electronics, we demonstrate a concept for growth and processing of fungal mycelium skins as biodegradable substrate material. Mycelium-based batteries allow to power autonomous sensing devices including a Bluetooth module and humidity and proximity sensors, all integrated onto mycelium circuit boards.

11:00 AM EN03.01.02

Ultrasound-Driven Bioresorbable Triboelectric Nanogenerator with Controllable Lifetime [Inah Hyun](#)¹, [Dong-Min Lee](#)² and [Sang-Woo Kim](#)¹; ¹Yonsei University, Korea (the Republic of); ²Sungkyunkwan University, Korea (the Republic of)

On-demand bioresorbable electronics have gained significant attention due to their dissolution capabilities and the elimination of secondary surgical procedures for device removal, thereby minimizing the side effects associated with implantation. However, the reliance of these electronics on non-transient commercial energy supplies limits their practicality. In this study, we propose a fully biodegradable and implantable triboelectric nanogenerator (FBI-TENG) that harnesses ultrasound as both a non-invasive power source and a means of device removal. Under low-intensity ultrasound ($\leq 0.5 \text{ W cm}^{-2}$), the FBI-TENG efficiently generates energy to power other electronic devices. To enhance its electrical performance, we optimize the triboelectric layer by incorporating polyethylene glycol, resulting in a remarkable 58.5% increase in voltage output underwater, from 2.625 to 4.160 V. In contrast, high-intensity ultrasound ($\geq 3.0 \text{ W cm}^{-2}$) can trigger the degradation process of our FBI-TENG, leading to the complete loss of its energy-generating function within a few minutes. Through finite element method simulation, we investigated that the triggering event occurs due to the porous structures of the poly(3-hydroxybutyrate-co-3-hydroxy valerate) with locally intensified pressure under the high intensity of ultrasound. This research provides valuable insights into the practical application of implantable triboelectric nanogenerators based on ultrasound-triggered transient material design. This research offers valuable insight into the practical application of implantable triboelectric nanogenerators on the basis of ultrasound-triggered transient material design.

11:15 AM *EN03.01.03

Scalable Synthesis and Manufacturing of Piezoelectric Biomaterials and Architectures [Xudong Wang](#); University of Wisconsin--Madison, United States

Piezoelectric materials are a group of important functional building blocks that interfacing the human body by coupling biomechanical energy and electricity. So far, many technology innovations have advanced piezoelectric materials and composites toward a broad range of biomedical applications, which possess unique biocompatibility and flexibility. Fundamentally, materials design and engineering draw the boundary where this technology may advance. In this talk, I introduce our most recent development of piezoelectric materials and composites that are particularly designed for implantable nanogenerator applications. First, I present our wafer-scale approach to creating piezoelectric biomaterial thin films based on γ glycine crystals. The self-assembled sandwich film structure enabled both strong piezoelectricity and largely improved flexibility. We will further discuss strategies of controlling the orientation and morphology of amino acid crystals to improve the piezoelectricity. Then, new ferroelectric composites are presented as a new composite used in 3D printing for directly manufacturing of piezoelectric

architectures with tunable piezoelectric and mechanical properties. This group of materials enable new capability of in vivo charging and electrostimulations, which revolutionaries the design and implementation of many biomedical therapeutics.

SESSION EN03.02: Biodegradable Electronics
Session Chairs: Amay Bandodkar and Lan Yin
Monday Afternoon, November 27, 2023
Hynes, Level 2, Room 206

1:30 PM EN03.02.01

Biodegradable, Self-healing, Recyclable, Conductive Coatings for Wearable Electronics and Soft Robotics[Pietro Cataldi](#); Italian Institute of Technology, Italy

Electrically conductive coatings are essential for transitioning electronic components and circuitry from stiff and rigid substrates to more flexible and stretchable platforms, such as thin plastics, textiles, and foams.[1] In parallel, the push for more sustainable, biodegradable, and cost-efficient conductive inks to coat these substrates has led to the development of innovative formulations involving biopolymers and nanomaterials that results in soft composites layer with unique functionalities.

The proposed talk unveils diverse electrically conductive coating (resistivity $\approx 10^{-4} \Omega \text{ m}$) that entails salient properties such as broad substrate types paintability, tunable piezoresistivity, self-healing, tunable degradability, and recyclability. Such a broad collection of properties is obtained simply by changing the substrates employed, the binders, and the conductive nanofillers. Particularly, one new class of coating based on biobased and biodegradable vitrimer binders is proposed. Using the vitrimer ensures satisfying adhesion to diverse substrates, flexibility, and recyclability of the conductive coating. This coating enables human-mimicking soft robotics skin since it is self-healing and biodegradable. Tests for the live monitoring of SoftHand3, the grasping system of many worldwide diffused robots, have yielded promising results. The use of biodegradable ingredients and the possibility of recycling makes it an appealing material to face the sustainability issue of today's electronics and robotics.

Another class of coating proposed is applied to textiles. Such coatings have controllable electrical resistance change with deformation and transiency (i.e., dissolution in water).[2] The modulation of the piezoresistivity and transiency is obtained by controlling the nanofiller geometry, binder composition, and textile twill orientation. The electrical resistance shows an anisotropic response to bending depending on the composition of the coating and the stress direction, functioning either as a deformable compliant electrode or a tunable piezoresistor. Indeed, it can withstand thousands of bending cycles with a change in resistance of less than 5% or change its resistance by many orders of magnitude with the same deformation thanks to the combination of cotton twill and different nanofillers. A simple modification in the binder composition adding waterborne polyurethane, allows the coating to go from entirely transient in water within minutes to withstanding simulated washing cycles for hours without losing its electrical conductivity. This versatile green conductor may serve opposing needs by altering the material composition and the deformation direction.

References:

[1] Vicente Orts Mercadillo, Kai Chio Chan, Mario Caironi, Athanassia Athanassiou, Ian A. Kinloch, Mark Bissett, Pietro Cataldi, *Electrically Conductive 2D Material Coatings for Flexible and Stretchable Electronics: A Comparative Review of Graphenes and MXenes*, *Advanced Functional Materials*, 2022.

[2] Pietro Cataldi, Pietro Steiner, Mufeng Liu, Gergo Pinter, Athanassia Athanassiou, Coskun Kocabas, Ian A Kinloch, Mark A Bissett, *A Green Electrically Conductive Textile with Tunable Piezoresistivity and Transiency*, *Advanced Functional Materials*, 2023.

1:45 PM EN03.02.02

Biodegradable Resistive Random Access Memory Based on Natural Organic Carbohydrate Materials for Sustainable Neuromorphic Computing Systems[FengZhao](#) and YuanXing; Washington State University, United States

Current computing systems are facing two essential challenges: (1) tremendous energy consumption due to the conventional Von Neumann architecture with low energy efficiency; and (2) environmental sustainability by depletion of nonrenewable materials, production of electronic waste, etc. One potential solution to simultaneously address these two issues is by "brain-like" and "green" neuromorphic computing with energy-efficient operation, sustainable material resources, and environmentally friendly disposals. Such neuromorphic computing systems require hardware components not only capable of mimicking human neuron and synapse - the basic building block of biological neural networks, but also made from natural organic materials such as polypeptides (proteins) and polysaccharides (carbohydrates) which are renewable, abundant in nature, and biodegradable. In this paper, we report resistive random access memory (ReRAM) made from encouraging natural organic carbohydrate materials, honey and fructose, for emerging neuromorphic computing systems and neural networks. Honey or fructose resistive films were formed by a low cost solution-based process and sandwiched between bottom and top electrode, a simple metal-insulator-metal structure analogous to a biological synapse with presynaptic neuron (top electrode), postsynaptic neuron (bottom electrode), and synaptic cleft (fructose film). The nonvolatile memory behaviors were demonstrated by modulating the conductance by voltage stimuli applied on the memory device, with excitatory current flow in the device being monitored. Characteristics including bipolar resistive switching, retention, endurance cycles, long-term potentiation and depression, desolution in water, etc. were reported. All these results testify that carbohydrate-ReRAM devices are promising for energy-efficient and sustainable neuromorphic systems.

2:00 PM *EN03.02.03

Edible Electronics: Recent Results and Perspectives[MarioCaironi](#); Istituto Italiano di Tecnologia, Italy

Edible electronics envisions a technology that is safe for ingestion, environmentally friendly, and cost-effective. Differently from "ingestible" electronics, it aims at realizing electronic devices that are degraded within the body after performing their function, either digested or even metabolized, thus removing any retention hazard. Edible electronics could potentially target a significant number of biomedical applications, such as remote healthcare monitoring, and of applications for food quality monitoring as well, such as edible electronic tags directly in contact with food. Here I will first give an introduction to this emerging field and propose long-term opportunities in terms of environmentally friendly smart technologies, remote healthcare monitoring, along with the challenges ahead. Then, I will report on our recent progress in the development of edible circuitry and components, towards future integrated edible electronic systems. Perspectives for adoption of edible electronic systems for sensors and control in future edible robots will also be shared.

2:30 PM BREAK

SESSION EN03.03: Bioresorbable Adhesives and Tissue Mimics
Session Chairs: Jahyun Koo and Lan Yin
Monday Afternoon, November 27, 2023
Hynes, Level 2, Room 206

3:00 PM *EN03.03.01

Biodegradable Bioadhesive Technology Platform[XuanheZhao](#); Massachusetts Institute of Technology, United States

This presentation focuses on an innovative biodegradable bioadhesive technology platform. Firstly, I will outline a general approach to designing and manufacturing biodegradable bioadhesives that possess rapid and tough adhesion capabilities with a wide range of wet dynamic organs. Subsequently, I will explore the numerous contemporary technologies and applications made possible by this biodegradable bioadhesive platform, such as sutureless wound sealing, coagulation-independent homeostasis, bioadhesive bioelectronics and implants. To wrap up, I will provide insights into the future prospects and potential advancements in the field of biodegradable bioadhesive technology.

3:30 PM EN03.03.02

Hyperbranched In Situ Polymerized Cyanoacrylate Tissue Adhesives and Their Degradation[AlexanderP. Roxas](#) and ZhengtangLuo; The Hong Kong University of Science and Technology, China

Cyanoacrylates are bioresorbable tissue adhesive materials whose ability to rapidly polymerize in situ into a strongly adhering film is suitable for closing wounds during emergencies. This polymerization method, which generates high-molecular-weight linear chains, has been applied and barely changed since the early clinical use of the adhesive because the requirement of rapid, straightforward in-situ polymerization for practicality restricted innovations involving the method and the material composition. Tissue adhesives, however, have been increasingly demanded to exhibit enhanced properties to cater to the needs of emerging trends in biomedical engineering. Our group has recently formulated a procedure to in situ polymerize cyanoacrylates into a branched adhesive film without sacrificing their practical features. Branching in the adhesive film, despite potentially introducing softness and enhancing mechanical properties, among others, can, however, influence the degradation of the adhesive film. The effects of branching on the rate of degradation and the composition of the degradation products were analysed by studying the degradation of branched polycyanoacrylates with varying degrees of branching and comparing them with conventionally polymerized linear equivalents. The degradation behavior of the adhesive is essential to avoid complications resulting not only from toxicity but also from the premature sloughing of the adhesive film from the wound surface.

3:45 PM EN03.03.03

Large-Scale Fabrication of Silk Fibroin-Based Artificial Skin for Cosmetic Research [Hangming Fan](#) and Xiaodong Chen; Nanyang Technological University, Singapore

Silk fibroin, a widely utilized material in skin-related applications, possesses a comparable structure and amino acid composition to the cornified cell envelope found in the stratum corneum. This similarity suggests its potential as an alternative to animal experimentation in cosmetic research, particularly as artificial skin. However, improvements are required in silk fibroin-based films to achieve sufficient similarity for practical usage and enable large-scale industrial production. In this study, various methods were employed to synthesize different types of artificial skin for key application scenarios in cosmetic research, including deposition tests, sensation tests, and absorption tests. For mass production of silk fibroin-based films, the conventional solvent casting method, though slow and resulting in poor thickness uniformity, has been commonly used. In this work, we adopted a coating method that allows for easy modification of the artificial skin's surface properties, enabling representation of different skin types (e.g., oily, dry, and combination skin). Furthermore, the proposed method offers significant advantages such as faster production and improved thickness uniformity, making it feasible for industrial-scale manufacturing.

SESSION EN03.04: Poster Session I: Biomedical Devices

Session Chairs: Amay Bandodkar and Lan Yin

Monday Afternoon, November 27, 2023

Hynes, Level 1, Hall A

8:00 PM EN03.04.01

Highly Stretchable Thermally-Grown Silicon Dioxide with Wavy Structures Encapsulation for Biomedical Applications [Hyeonji Yoo](#), Hangeul Kim, Gyeong-Seok Hwang and Ju-Young Kim; Ulsan National Institute of Science and Technology, Korea (the Republic of)

Flexible and stretchable bioelectronic devices that can be applied to targets such as heart and liver where repetitive deformation occurs are currently being actively investigated as next-generation devices. These organic material-based electronic devices require an encapsulation layer for long-term stability. Therefore, the development of mechanically stretchable and highly impermeable encapsulating materials is required to develop stretchable bioelectronic devices.

In this research, we developed the highly stretchable and impermeable encapsulations by applying a wavy-structure to the thermally-grown SiO₂. A thermally-grown SiO₂, oxidized from single-crystalline silicon wafer at high temperature, has an extremely low water vapor transmission rate (WVTR) due to amorphous structure and high density with low defects. In addition, we effectively implemented high stretchability through wavy-structure design, overcoming the intrinsically low elastic deformation limit of SiO₂. The stretchability and barrier properties were carried out by uniaxial tensile test and electrical Ca test. By theoretically analyzing the mechanical behavior of wavy-structured SiO₂, the universal deformation model and correlation between stretchability and characteristic of wavy structure were carried out. This stretchable encapsulation shows 20.1% of uniaxial stretchability and 1.11 x 10⁻⁶ g m⁻² day⁻¹ of WVTR, simultaneously. Moreover, it demonstrates highly reliable barrier properties even after 1,000 stretching cycles at 90% of their stretchability. Therefore, the developed wavy-structured thermally grown SiO₂ is suitable to protect stretchable organic-based bioelectronic devices.

8:00 PM EN03.04.02

Minimally Invasive and Biodegradable Electronics for Transient Brain Interfaces [Jae-Young Bae](#)¹, Gyeong-Seok Hwang², Young-Seo Kim¹, Jooik Jeon³, Jung Keun Hyun³, Ju-Young Kim² and Seung-Kyun Kang¹; ¹Seoul National University, Korea (the Republic of); ²Ulsan National Institute of Science and Technology, Korea (the Republic of); ³Dankook University, Korea (the Republic of)

Monitoring brain activities is crucial for diagnosing and providing post-care for brain disorders like epilepsy or traumatic brain injury. However, after the monitoring period, the implanted device needs to be removed to avoid complications such as inflammation. The removal surgery is even riskier and more time-consuming than the initial implantation procedure, causing distress to the patient. Biodegradable electronics is an emerging technology that can dissolve completely into biocompatible molecules once their function is complete, eliminating the risk of biofilm formation or secondary injuries during the removal process. Some biodegradable implantable devices, which combine organic and inorganic materials, have been used to monitor increasing pressure inside the skull caused by traumatic brain injuries and to stimulate the regrowth of peripheral nerves using wireless electrical stimulators. However, current biodegradable electronic devices still require surgical implantation, which adds to the patient's burden. Here, we propose a platform for biodegradable electronics in the brain, including bio-potential electrodes, temperature and strain/pressure sensors, and a wireless communication system capable of monitoring various physiological signals. This platform is designed to dissolve all inserted materials without leaving a potential biofilm formation or causing secondary injuries during the removal process. Furthermore, we introduce the concept of a minimally invasive strategy to reduce the invasiveness of the implantation procedure. This platform holds promise as a transient and minimally invasive brain-interface platform for future clinical applications.

8:00 PM EN03.04.03

Recycled UHT Milk Carton Cellulose Surface as a Novel Substrate for Dual-Lactate Sensor for Milk Spoilage Indication [Wisarttra Phamonpon](#)^{1,2}, Nadtinan Promphet¹, Sarute Ummartyotin² and Nadnudda Rodthongkum¹; ¹Chulalongkorn University, Thailand; ²Thammasat University, Thailand

Recycled cellulose substrate from UHT milk carton waste was firstly applied as a novel substrate for the colorimetric and electrochemical lactate sensor for milk quality indication. The cellulose and aluminum foil were extracted from the packaging. For preparing the recycled cellulose substrate, chemical treatment (alkali and bleach treatment) was used for the extraction. Then, the recycled cellulose substrate has done enzymatic immobilization for the colorimetric sensor to enhance the specific reaction with the lactate on its surface. For the electrochemical sensor, the recycled cellulose substrate was immersed into the extracted aluminum solution to fabricate the conductive working electrode to improve the surface roughness compared with the recycled cellulose substrate, confirmed by atomic force microscopy. Scanning electron micrograph presented a 3D fibrous network including with air space in between, and X-ray photoelectron spectroscopy showed the binding energy of Al-O at 73.256 eV, confirming the appearance of the aluminum on the recycled cellulose substrate after the surface modification with aluminum solution. For the analytical performance, the colorimetric sensor showed the increasing purpleness of color upon increasing lactate concentration. Furthermore, the aluminum-coated recycled cellulose substrate provided an increasing current response toward the increment of lactate concentration. This dual-lactate sensor can offer linearity of 0.125-2 M, covering a cut-off lactate value in cow's milk (1.0 M) for milk spoilage indication, which can be used for lactate determination in actual milk samples. Eventually, this platform can represent a new utilization of UHT milk carton waste for the colorimetric and electrochemical sensor that can be applied in food quality control applications.

8:00 PM EN03.04.04

An Innovative Methodology for Constructing Thermally Stable, Self-Healing Pressure Sensors [Su Bin Choi](#) and Jong-Woong Kim; Sungkyunkwan University, Korea (the Republic of)

Stretchable electronics, a subcategory of soft electronics characterized by mechanical elasticity, grapple with a significant challenge—localized stress concentration. This issue threatens the integrity of elastic materials typified by their small Young's modulus and expansive elastic strain range. A promising mitigation strategy is the incorporation of self-healing functionality, achieved by exploiting the dynamics of covalent bond chemistry, particularly Diels-Alder reactions, to conceive polymers of high tensile strength with controlled reversibility. Nonetheless, a pervasive concern with self-healing materials is the requisite temperature for initiating the healing process, which may inadvertently inflict thermal damage to other components of the electronic device. Conversely, lowering the self-healing temperature could undermine the polymer's stability under high-temperature conditions, potentially causing device failure. This dual requirement—low-temperature self-healability and high-temperature thermal stability—demands innovative solutions. In response to this formidable challenge, we introduce a novel methodology involving the creation of a microfibrillar network employing polycaprolactone (PCL), a hydrophobic polymer renowned for its low melting temperature (60 °C) and ubiquitous use in shape memory and self-healing materials. Concurrently, we prepare conductive fibers encased in MXene nanosheets—a class of two-dimensional, titanium-based layered materials—by coating these onto the microfibrillar PCL network. Intriguingly, the MXene layer preserves the fibrous morphology even when the PCL reaches its melting point, assuring mechanical robustness. The MXene nanosheets seamlessly adhere to the surface of the PCL fibers, effectively forestalling shape deformation of the fibrous network under high-temperature conditions.

These nanosheets further exhibit superior thermal conductivity, which facilitates efficient internal heat dissipation. The amalgamation of these attributes enables the MXene/PCL microfibrillar network to exhibit self-healing capabilities at a temperature as low as 60 °C and maintain thermal stability beyond 200 °C. By leveraging this microfibrillar network, we develop a pressure sensor, thereby highlighting its potential applications in fabricating stretchable and self-healing electronic devices capable of enduring temperatures exceeding 200 °C.

8:00 PM EN03.04.05

Fragmentation Behavior and Surface Characteristics of Different Plastics: Influence on the Potential Toxicity to Macrophages and Angiogenesis Kyungtae Park and Jinkee Hong; Yonsei University, Korea (the Republic of)

The production and waste of plastics are increasing rapidly, and there is a growing interest in investigating the impact of microplastics (MPs) smaller than 5mm on human beings as pollutants. Previous research has primarily focused on the toxicity of engineered plastic particles with a spherical shape, overlooking the fact that microplastics tend to fragment under environmental conditions, resulting in various morphological characteristics and sizes. This fragmentation behavior has not been adequately considered in toxicity analysis. Therefore, it is crucial to comprehend the fragmentation behavior of different plastics and analyze the surface characteristics of each microplastic to gain a better understanding of their potential toxicity.

In this study, we conducted a comprehensive investigation into the fragmentation patterns of plastics, specifically focusing on polypropylene (PP), acrylonitrile butadiene styrene copolymer (ABS), and polyethylene terephthalate (PET) as representative plastics. To simulate the fragmentation of each plastic, we employed a ball-milling process, which resembles the physical fragmentation process that occurs during plastic weathering.

After the fragmentation process, we characterized the surface of the microplastics using scanning electron microscopy (SEM), FT-IR, Raman spectroscopy, and x-ray photoelectron spectroscopy. We also examined the change in crystalline structure using a differential scanning calorimeter (DSC). Considering that the micronization behavior of plastics is highly dependent on the amorphous structure, we confirmed the crystalline and amorphous parts and their respective crystallinity. Additionally, we conducted size and shape analysis of the microplastics to investigate cellular uptake and toxicity.

Macrophages were selected as representative immune cells due to their ability to recognize infectious agents and remove toxicants through phagocytosis. We studied the cellular uptake of each microplastic and observed cellular reactions such as ROS generation in the macrophage cytosol, polarization, and immune-cytokine secretion. Furthermore, we investigated the complex cellular reactions by co-culturing macrophages with human umbilical vein endothelial cells (HUVECs). As HUVECs possess angiogenic abilities, we analyzed *in vitro* tube formation under co-culture conditions and quantified the amount of angiogenic growth factors after exposing macrophages to microplastics.

Our findings revealed three significant points in understanding the potential toxicity of microplastics:

The characteristics of fragmented microplastics differ significantly from engineered microplastics.

The fragmentation behavior and properties of each microplastic should be considered to understand their potential toxicity.

Depending on the composition of the microplastics, the reaction of macrophages and subsequent effects on angiogenesis vary.

8:00 PM EN03.04.06

Directed Evolution of Microorganisms for Engineered Living Materials Julie M. Laurent, Anton Kan, Ankit Jain, Mathias Steinacher, Nadia Enriquez Casimiro, Stavros Stavrakis, Andrew J. deMello and André R. Studart; ETH Zürich, Switzerland

With the environmental challenges we face, a shift is needed in the materials we produce and use. Materials found in Nature are made at atmospheric temperature and pressure, and they are robust, long-lasting, and renewable. Incorporating life into human-made materials would bring us closer to mimicking them, adding functionalities not accessible by current synthetic material production methods. The rich biochemical diversity in bacteria provides an immense design space for the engineering of adaptable living materials.

However, bacteria have evolved to perform specific biological functions in their particular environment. Their phenotypes thus might not fulfill the demands of engineering and industrial applications. In particular, we lack control over the shaping of bacterial communities and living materials. Biofilms are an example of naturally occurring self-assembled living materials produced by bacteria. Although three-dimensional, they are conformal to surfaces and relatively limited in terms of shape complexity and control.

Here, we show that 3D printing of engineered bacteria embedded in a matrix can help us shape complex living materials with programmable functionalities. Using genetic engineering tools and readily available 3D printing techniques, engineered bacteria-laden living materials were shaped into complex structures. The metabolism of microorganisms was harvested to add a function (luminescence, melanin secretion) or produce a material (cellulose, calcium carbonate) in three-dimensional objects.

The freedom in shape design provided by 3D printing techniques enabled additional functionalities that were not present in the natural world. Bacterial luminescence was increased with a gyroid structure, and dampened when printing a surrounding layer populated with melanin-producing engineered microorganisms. In the future, printing material-producing microorganisms and exploiting their evolved cellular machinery will provide new ways of making sustainable materials.

8:00 PM EN03.04.07

Programming Hierarchical Architectures in Biodegradable Microcapsules for Advanced Functions Muchun Liu and Benedetto Marelli; Massachusetts Institute of Technology, United States

Programming biomaterials at multiscale is critical in developing advanced technologies in addressing environmental issues. For instance, several industries have a compelling need to substitute open-used, non-degradable, intentionally added microplastics with biodegradable alternatives. Biopolymers extracted from natural products or food waste, such as regenerated silk fibroin, offer many merits. However, assembling biopolymers at multiscale remains challenging due to their complex compositions.

To address this challenge, we present a biodegradable silk-based microencapsulation technique achieved by modulating the structural protein protonation and chain relaxation at the point of material assembly. It can sustain the release of soluble and insoluble payloads typically used in cosmetic and agriculture applications. Manufacturing through well-established fabrication techniques, such as spray drying, yields microcapsules with tunable morphology and degradation kinetics. As a proof-of-concept for agrochemicals delivery, a greenhouse trial demonstrated that a commonly used herbicide (i.e., Saflufenacil) delivered via silk microcapsules on corn plants reduced crop injury compared to the non-encapsulated version.

Additionally, we introduce a synergistic assembly of biopolymer microparticles into hierarchical structures, such as spiny microcapsules and interconnected micro-network. We can tune the biopolymer type, geometry, structure, crystallinity, payload, and mechanical properties for different functions. For example, engineered multi-spines effectively improved the retention percentage of microcapsules on smooth spinach leaves after wash-off. Furthermore, the echinate micro-network can transfer and co-localize different fluorescent payloads in the micro-bridges. Our findings provide a platform for the advanced biopolymers assembly into functional structures, which is of great potential in agriculture, environmental remediation, and other applications that interact directly with the environment.

8:00 PM EN03.04.08

Biodegradable Polymers for Tuning Properties of Long-Acting HIV Pre-Exposure Prophylaxis (PrEP) Implants Archana Krovi¹, Guadalupe Arce Jimenez¹, Leanna Levin¹, Daniela Cruz¹, Pafio Johnson¹, Ellen Luecke², Chasity Norton¹ and Leah Johnson¹; ¹RTI International, United States; ²Women's Global Health Imperative, United States

Introduction: The development of new biodegradable implants for long-acting (LA) drug for HIV pre-exposure prophylaxis (PrEP) can advantageously eliminate the requirement of a second medical procedure to remove the devices at the end of use when drugs are depleted. We have previously demonstrated tunable antiretroviral (ARV) release through tailoring the implant surface area, wall thickness, molecular weight of polymer, and ratios of homopolymer blends. Here, we further advance our implant platform by exploring biocompatible and biodegradable polymers with differing compositions, degradation profiles, and physicochemical properties that ensure drug transport through the polymer membrane under physiological conditions.

Methods: Biodegradable polymers poly(3-hydroxybutyrate-co-3-hydroxyvalerate) (PHBV), polycaprolactone (PC-17, PCL-C18E), PEGylated polycaprolactone (PCL-C18-PEG), and polybutylene succinate (FZ71PM, FD92PM) were extruded into cylindrical tubes with an outer diameter of 2.5 mm and a wall thickness 300 µm. Implants were prepared by loading antiretroviral formulations into an extruded tube and then enclosing the tube via heat sealing. Implants were sterilized via gamma irradiation at 18-24 kGy and submerged in phosphate buffered saline (pH 7.4) at 37 °C to mimic physiological conditions. Antiretroviral concentrations released in the buffer over time were measured by high performance liquid chromatography or UV-Vis. Crystallinity, molecular weight, and mechanical properties of the tubes were characterized using differential scanning calorimetry, inherent viscosity, and tensile testing, respectively.

Results: PHBV had the highest crystallinity (60.6 ± 1.2%) among all the polymers evaluated and showed the lowest drug release rate. Interestingly, while PCL materials with slightly different molecular weights PC-17 (IV 1.82) and PC-C18E (IV 1.93) had similar crystallinities of 51.3 ± 1.1% and 50.3 ± 6.4%, respectively, the introduction of a PEG end group on the PCL polymer (PCL-C18-PEG) led to significantly lower crystallinity (36.4 ± 1.5%) and the highest release rate. We hypothesize that the biocompatible PEG modifier potentially disrupts the packing of the polymer chains and can affect the drug release rates. Crystallinity of PBS (FD92PM) was the lowest (25.2 ± 0.2%) but exhibited similar drug release rates comparable to that of PC-17. This is a significant finding as FD92PM polymer may offer an approach to deliver an antiretroviral at the target doses with a potentially faster biodegradation timeframe in contrast to the approximately 2-year degradation timeframe for PCL. Lastly, FZ71PM had a similar crystallinity to that of PC-17 (46.4 ± 9.4%) but exhibited lower drug release from the implant form factor. Despite the insignificant drug release, this polymer could be utilized for indications with lower drug release targets and with a potentially faster biodegradation profile.

Conclusions: We explored biodegradable implants designed for HIV PrEP that comprise extruded tubes from polymers of varying physicochemical properties. These differing polymers offer

an effective approach for tuning the drug release rates, implant duration and integrity, and ultimately the biodegradation profiles of the implants. Next steps include evaluation of the polymer degradation kinetics, in real time (in vitro and in vivo) and under accelerated conditions. An in-depth understanding of the degradation characteristics of this platform will enable new implant designs for varied medical indications that might require tailored degradation timeframes.

Acknowledgements: This research is made possible by the generous support of National Institutes of Health (Award # R01AI154549). The content is solely the responsibility of the authors and does not necessarily represent the official views of the National Institutes of Health.

8:00 PM EN03.04.09

Preconditioning of Long-Acting Subcutaneous Implants to Support Evaluation of *In Vivo* Pharmacokinetic Depletion Profiles Daniela Cruz, Christine Strickland, Leanna Levin, Guadalupe Arce Jimenez, Archana Krovi, Pafio Johnson, Chasity Norton, Ellen Luecke and Leah Johnson; RTI International, United States

The pharmacokinetic depletion period (i.e., tail) of long-acting (LA) drug delivery systems can result in a gradual decrease of drug concentration over time. Comprehensive characterization of the depletion tail can provide insight about effectiveness of the drug delivery system and the possibility for subtherapeutic drug levels, which can lower efficacy or enable the emergence of drug-resistant strains. The thorough evaluation of the depletion tail also provides details about the optimal dosing period to maintain therapeutic drug levels throughout the course of treatment. In this study, we explore the preconditioning of a biodegradable subcutaneous implant for LA HIV pre-exposure prophylaxis (HIV PrEP) that sustainably releases antiretroviral (ARV) drug. By preconditioning the implant via accelerated conditions during the zero-order release phase, we can achieve an efficient way of testing long-acting drug formulations. Poly-ε-caprolactone (PCL) extruded tubes were filled with bicitagravir (BIC) formulated with castor oil. The ends of the tubes were heat-sealed and implants were sterilized by gamma irradiation (18-24 KGy). For in vitro release studies, implants were submerged in phosphate-buffered saline (pH 7.4) and drug release was monitored using UV-vis while maintaining sink conditions. Implants were divided into six groups that explored various experimental conditions, including drying, sterilization, and different temperature profiles. Groups 1-4 were used to test in-vitro preconditioning and second round of sterilization and were placed at 37°C for 46 days. After 46 days, Group 1 was placed in an oven at 40°C for two weeks to ensure drying followed by sterilization by gamma irradiation. Group 2 also underwent a drying process but was not sterilized a second time. Group 3 did not undergo a drying process but was sterilized a second time. Group 4 served as the control, which remained in-vitro at 37 °C throughout the duration of the study. To study accelerated conditions, Group 5 was placed at 45°C throughout the study's duration, and Group 6 was placed at 45°C for 66 days before taken to 37°C for the rest of the study. The in vitro pre-conditioning of implants resulted in similar release rates of BIC before and after exposure to a second round of sterilization. Also, no notable differences were observed in the release rates of BIC between implants under different experimental conditions for drying or sterilization. For implants exposed to accelerated conditions at 45°C, the release rate increased by 3.2-fold when compared to the control maintained at 37°C. In addition, devices switched from 45°C to 37°C demonstrated release rates similar to the control group, showing that release rates can be tuned through temperature change.

In this work, we demonstrate an advantageous method to precondition long-acting subcutaneous implants to support subsequent in vivo studies. Our results show that implants are unaffected after removal from in-vitro conditions and after a drying process and a second round of sterilization. In addition, we demonstrate a successful acceleration of in vitro drug release using a higher temperature (45°C). This approach can potentially shorten the timeframe of preclinical studies by preconditioning implantable drug delivery systems during the phase of zero-order release kinetics. Overall, this approach supports approaches to characterize LA drug delivery systems without sole reliance on long-term animal studies.

8:00 PM EN03.04.10

Rapid Synthesis of Multifunctional Hydroxyapatite Using Laser-Induced Hydrothermal Process Sangmin Song^{1,2}, Seung-Hoon Um^{3,1}, Seung Hwan Ko², Yu-Chan Kim¹ and Hojeong Jeon¹; ¹Korea Institute of Science and Technology, Korea (the Republic of); ²Seoul National University, Korea (the Republic of); ³Université Laval, Canada

Synthetic biomaterials are used to overcome the limited quantity of human-derived biomaterials and to impart additional biofunctionality. Although numerous synthetic processes have been developed using various phases and methods, existing synthetic processes suffer from issues such as lengthy processing time, challenges in size control, and difficulties in achieving high-concentration metal ion substitution for additional functionality. In this presentation, we will present a rapid synthesis method using a laser-induced hydrothermal process. Based on the thermal interaction between the pulsed laser beam and titanium plate, which was used as a thermal reservoir, hydroxyapatite particles ranging from nanometer to micrometer scale could be synthesized in seconds. Moreover, this laser-induced hydrothermal synthesis can enable metal ion substitution into the matrix of hydroxyapatite with a controllable concentration. We calculated the theoretical maximum temperature achieved by thermal interaction at the surface of the thermal reservoir based on the validation of three simplification assumptions. Subsequent linear regression analysis showed that laser-induced hydrothermal synthesis follows an Arrhenius chemical reaction. Synthesized hydroxyapatite and Mg²⁺, Sr²⁺, Zn²⁺-substituted apatite powders exhibited promotion of bone cell attachment and proliferation ability due to ion release from the synthesized powders, which had a low crystallinity and relatively high solubility. This laser-induced hydrothermal synthesis is expected to be used in biomaterials, catalyst, 3D printing, and solar cell technology.

8:00 PM EN03.04.11

Paper-Based Green Laser-Induced Graphene for Disposable and Wearable Sensing Applications Rodrigo F. Martins, Tomas Pinheiro and Elvira Fortunato; FCT UNL, Portugal

Laser-induced graphene (LIG) has established itself as a very attractive material for electrode fabrication, within several applications in bioelectronics. The straightforward, high throughput graphitization of several precursor materials using this laser conversion process allows for the simultaneous synthesis and patterning of this 3D graphitic material with diverse electrode architectures, to target several biosensing applications, from biophysical to biochemical monitoring.

Recently, paper has appeared as a viable alternative to conventional petroleum-based plastic polymer precursors, such as polyimide. This is due to the possibility of photothermally converting aliphatic cellulose monomers into graphene lattices, using several cellulose substrate treatment strategies. Application of fire-retardant chemical modifications and external aromatic moieties improves the graphitization potential of cellulose, to reach LIG film with 5 ohm.sq⁻¹ sheet resistance and conductivities as high as 67 S.cm⁻¹.

With these improved conductive properties of paper-derived LIG, this precursor material can be easily employed for the fabrication of disposable biosensing units, where paper acts as both the support substrate and precursor material for conductive electrode fabrication, without the need for more intricate printing techniques. Alternatively, strategies can be employed to separate converted and unconverted phases, through transfer methods, to make this material compatible with wearable applications.

In this presentation, we report the use of cellulose as a material in the toolbox of LIG precursors, aimed at the development of both disposable and wearable biosensing applications. Paper-based electrochemical sensors using this material are presented, aiming at disposable sensor development for different analytes. Glucose and pH electrochemical sensors were fabricated, showing the compatibility of the material with several sensing strategies, such as enzymatic and non-enzymatic sensing. To translate patterned electrodes for wearable applications, a straightforward transfer method is presented, using a water-induced peel-off method. This method is capable of efficiently separating unconverted cellulose and converted LIG phases, allowing for the transfer of LIG patterns onto flexible, conformable, and elastomeric substrates with adhesive properties, for example, medical grade adhesives. Using this method, electrochemical biosensors, strain sensors for biophysical monitoring and electrodes for electrophysiological signal monitoring are presented.

In conclusion, the concepts explored herein show the applicability of LIG towards the fabrication of robust point-of-care, disposable analytical devices, but also its potential for integration in wearable sensing systems, aiming at more sustainable, accessible bioelectronic applications.

8:00 PM EN03.04.12

Fully Biodegradable Multi Functional Wireless System of Bio-Integrated Electronics based on Bioresorbable Shape Transformation Elastomer Jun Hyeon Lim, Won Bae Han and Suk-Won Hwang; Korea University, Korea (the Republic of)

Stretchable electronic stimulators are of rapidly growing interest as unusual therapeutic platforms for treating disease states, accelerating wound healing processes and eliminating infections. Here, we present advanced materials that support operation in these systems over clinically relevant specific timeframes, ultimately biodegradable harmlessly to benign products without residues, to eliminate the need for surgical extraction. Our findings also overcome the challenge that the device wraps itself around the nerve and does not require a suture. The reason the devices based on a Shape-transformation/adhesive based robotic electronics poly(L-lactide-co-ε-caprolactone) (STAR PLCL) for shape-warping and self-adhesive effect in especially temperature condition. The shape-transformation device highlight possibilities for wireless electrical nerve stimulation system by integrating a bioresorbable inorganic component with the STAR PLCL substrate. Additionally, the result of our study findings highlights the possibility of multipurpose monitoring/sensing components in nerves/tissues/organs in body.

8:00 PM EN03.04.13

Buoys and Bacteria for Microplastic-Free Oceans Douglas X. Shattuck^{1,2}, Charlotte McConville³, Victoria Sekenski^{4,2} and Saman Abbas^{4,2}; ¹St Joseph School Wakefield, United States; ²National STEM Honor Society, United States; ³Quincy High School, United States; ⁴Malden Catholic High School, United States

Microplastics are abundant and polluting our oceans. In recent years, a solution to this problem has presented itself: bacteria. Specifically, *Ideonella sakaiensis* and azotobacter work together to break down plastics over time. Some challenges in the research include keeping the bacteria to the proper 86 degrees and how to gauge when to close off the machine. It has been determined that it takes six weeks for the bacteria to break down plastics, thus our machine will run on six-week intervals. *Ideonella* and *Azotobacter* have proven to have no adverse effect on marine or human life.

Our goal is to create a buoy that will float in the ocean, collect the water, and break down the plastics. In order to keep the bacteria to the correct temperature, we plan to test the use of

insulation and heating pads. We will need to periodically change them out, as well as checking the bacteria frequently to ensure its quality. That provides another challenge: keeping the insulation from getting wet. To combat this problem, we plan to install PVC or smurf piping to lead the water directly to the filter. This filter will catch the plastics and separate them from the outgoing water. We hope to develop a system of locks and sensors that will slide into place once we determine the buoy is full. After the six-week degradation period, we will have to manually open the machine and re-release it, replacing bacteria or heating pads as necessary. Presented here will be the conceptual design and schematics for our scale prototype.

SESSION EN03.05: Sustainable Electronics
Session Chair: Amay Bandodkar
Tuesday Morning, November 28, 2023
Hynes, Level 2, Room 206

8:00 AM EN03.05.01

A Self-Powered Microbial Inactivation and Nanoparticle Removal Ultrathin Gelatin Multilayer Triboelectric Nanogenerators Habtamu G. Menge and Yong Tae Park; Myongji University, Korea (the Republic of)

Internet of Things technologies significantly improve the quality of life by utilizing wearable electronics. Among mechanical energy harvesting technologies, triboelectric nanogenerators (TENGs), which utilize the coupling effects of triboelectrification and electrostatic induction between two contact surfaces, have been considered a novel miniaturized mechanical energy scavenger that generates electricity. However, in most TENGs, synthetic polymers dominated triboelectric materials (TMs) fabrication. Therefore, this study fabricated ultrathin, biodegradable, and biocompatible gelatin (GE) multilayer-based TENG via an eco-friendly layer-by-layer self-assembly method. The electrostatic self-assembly of one species was realized using its dependence on the solution pH. GE is suitable owing to its film-forming abilities, abundance, pyrrolidine electron donor-rich groups, and tunable properties, significantly enhancing the TENG outputs and enabling extended layered growth. The electrical properties and device performance of self-assembled GE multilayer (ML)-TENG were identified by manipulating the pH of the GE medium from 4 to 7. At pH 5, 110 nm-thick of the 3 adsorbed cycles of GE ML-TENG exhibited the highest output power density of 15.9 W m^{-2} , owing to its highest surface potential of 208 mV. We successfully exhibited the self-powered GE ML-TENG-driven electrophoretic device for removing SiO_2 and ZnO nanoparticles in water. Furthermore, integrating GE multilayer-TENG as electric stimulation of antibacterial devices is a promising approach and exhibited a significant inhibitory effect on gram-negative *Escherichia coli* (E. coli) and gram-positive *Staphylococcus aureus* strains. We also demonstrated the harmony of the vertical axis wind turbine GE free-standing film TENG electricity. The graphene-based filtration system worked simultaneously to attain approximately 100% E. coli inhibition efficiency without an external power supply for the water disinfection system. Therefore, this eco-friendly multifunctional GE-based material can be a promising candidate for high-performance self-driven Electrical stimulation nanogenerators.

8:15 AM EN03.05.02

Exploring the Chemical Space of Bioinspired Materials for Sustainable Electronics Micaela Matta; King's College London, United Kingdom

The field of organic semiconductors and mixed ionic-electronic conducting materials is currently dominated by polymers and small molecules that, despite their good conductivity and processability, have limited biocompatibility. The demand for implantable, edible or degradable devices for nanomedicine or low-cost consumer electronics is growing, and will require a new generation of sustainable materials.[1]

This research combines cheminformatics, quantum chemistry and molecular simulation to design novel bioinspired materials for sustainable electronics and bioelectronics. High throughput calculations are used to screen the electronic and conformational properties of a large dataset of conjugated fragments with different linkers and functional groups. Within a range of bioderived fragments, we focus on the potential of melanin-inspired conjugated fragments as components of bioinspired mixed conducting materials.[2] The oligomers resulting from the best combinations of conjugated units, linkers and side chains are presented. Molecular dynamics simulations are then used to provide information about the charge/ion percolation pathways, aggregation and order. The results of this study can help focus experimental effort towards more sustainable organic materials.

[1] J. Mater. Chem. C 2021, 9, 13543-13556.

[2] Proc. Natl. Acad. Sci. U.S.A. 2022, 119 (32), e2200058119.

8:30 AM EN03.05.03

Exploring Form and Functionalization in Crystalline Nanocellulose Inks for Environmentally Sustainable Printed Electronics Brittany N. Smith, Nicolas Chen, James L. Doherty and Aaron D. Franklin; Duke University, United States

Printed flexible electronics show promise for providing a sustainable solution to the increasingly negative impact of electronics manufacturing and waste. However, current print processes and inks tend to rely on hazardous solvents, extensive post-processing at high temperatures, and/or materials that are not recyclable or biodegradable. Recent work on water-based inks from nanomaterials shows that these challenges can be overcome (i.e., no hazardous chemicals, relatively low temperature processing, and all recyclable or biodegradable materials), but the resultant devices still require improvement in performance and reproducibility. In this work, we investigated two new water-based inks for use in carbon nanotube (CNT) thin-film transistors (TFTs): nanocellulose, a biodegradable ionic dielectric, and nanoparticle gold, a recyclable conductor. We developed inks and aerosol jet printing processes for crystalline nanocellulose (CNC) and cellulose nanofibrils (CNF) with various surface groups to gain insights into the working mechanisms of nanocellulose as an ionic dielectric. Our results reveal that the general ionic nature of the printed films is invariant with the nanostructure form or surface group. However, the capacitance and sweep rate characteristics of the dielectrics, as well as the electrical and mechanical resilience, do show dependencies on nanocellulose form and functionalization. Further, we investigated the influence of the sulfonic surface group content on transistor performance, revealing that the foremost impact of increasing the sulfonation is a positive shift in the device threshold voltage. Since nanocellulose breaks down under high temperatures, the top-gate contact must be readily conductive when printed to form fully printed CNT-TFTs. Therefore, as an alternative to using graphene, a novel gold ink formulation was used as the contacts for CNT-TFTs. This new ink exhibited a resistance of $\sim 5 \Omega$ in its as-printed state, without any post-print sintering at high temperatures. The impressive device performance of these printed CNT-TFTs shows promise for the use of water-based inks in environmentally sustainable printing of electronics.

8:45 AM EN03.05.04

Laser Induced Graphene from Bio-Derived Sources for Biodegradable and Sustainable Electronics Anna Chiara Bressi¹, Iuliia Steksova¹, Sreenadh T. Sankaran¹, Alexander Dallinger², Felix Steinwender², Hana Hampel², Hilda Gomez Bernal¹ and Francesco Greco^{1,1,2}; ¹Sant'Anna School of Advanced Studies, Italy; ²Graz University of Technology, Austria

Laser Induced Graphene (LIG) is a porous conductive carbon material produced by laser-induced pyrolysis of polymer precursors, with technological applications in flexible/stretchable/wearable electronics, electrochemical sensors, energy harvesting and storage, among others.¹⁻⁴

Several bioderived polymers and raw natural materials are good LIG precursors.⁵ For this reason our group is investigating LIG for sustainable approaches to green electronics and soft electronics/robotics. Here, we present some results of our studies on LIG obtained from both raw natural materials and processed bio-derived polymers. These include starch-based bioplastic, composites of polysaccharides (starch, chitosan) + hazelnut or almond shells (i.e., waste from agricultural and food industry), lignin (waste from paper pulp process). For each class of precursors specific laser scribing strategies have been tailored and the resulting LIG materials are characterized in terms of their structure, composition, morphology, and of their functional properties (e.g., conductivity, piezoresistivity, wettability), useful for the development of LIG sensors. Also, the degradation behavior of these materials in different conditions is assessed, in view of applications in biodegradable/transient electronics.

References

- (1) Lin, J. et al. *Nat. Commun.* **2014**, *5*, 5714.
- (2) Ye, R.; James, D. K.; Tour, J. M. *Adv. Mater.* **2019**, *31*, 1803621.
- (3) Vivaldi, F. M. et al. *ACS Appl. Mater. Interfaces* **2021**, *13*, 30245.
- (4) Dallinger, A. et al. *ACS Appl. Mater. Interfaces* **2020**, *12*, 19855
- (5) C. Claro, et al. *Appl. Phys. Rev.* **2022**, *9* (4), 041305.

9:00 AM *EN03.05.05

Large Area Elastomer-Based Printed Electronics Peter Zalar; Holst Centre / TNO, Netherlands

Holst Centre is a leading applied research institute focusing on the development of flexible and thin electronic systems using industrially relevant fabrication methods. For nearly two decades, our primary objective has been to make technological advancements that facilitate the industrialization of printed electronics systems, thereby turning future visions into reality. With the increasing demand for integrating electronics into a wide range of form factors, it is essential to develop systems that possess key qualities such as accuracy, conformability, ruggedness, lightweight design, and sustainability. These qualities are crucial in applications spanning healthcare, automotive, and robotics, where traditional rigid printed circuit board (PCB) technology falls short. To address this challenge, we have explored the use of elastomeric carriers as a viable solution. In this presentation, I will delve into Holst Centre's contributions towards the development of sensor systems on elastomeric carriers, highlighting our efforts on an all-printed, large area, multimodal sensing surface.

9:30 AMBREAK

SESSION EN03.06: Transient Electronics
Session Chairs: Amay Bandodkar and Jahyun Koo
Tuesday Morning, November 28, 2023
Hynes, Level 2, Room 206

10:00 AM *EN03.06.01

Soft, Resorbable Bioelectronics Suk-Won Hwang; Korea University, Korea (the Republic of)

An ultimate goal of a conventional silicon-based integrated system is its capability to last forever without any malfunction and physical deformation, in almost any practical uses. Recent works demonstrate a new class of electronics that has the opposite behavior -- it physically dissolves or disappears in water, environment or biofluids, in a controlled fashion, at predefined times or on demand and with programmed rates. This type of 'transient' technology opens up completely new application opportunities for electronic devices in areas, such as implantable medical devices that exist for medically useful timeframes but then dissolve and disappear completely by resorption into the body. This talk summarizes recent works on bioresorbable electronic systems with mechanically soft, deformable platforms, ranging from fundamental chemistry of the key materials, to development of various components and systems for biosensors, to in vivo evaluations for biocompatibility and potential applications

10:30 AM EN03.06.02

Chitosan Nanocomposite Thin Films as Sustainable Biopolymer Based Colorimetric Humidity Sensors Wafa Tonny¹, Samuel J. Wallaert¹, Justin D. Smith¹, Venkatesh Balan², Megan L. Robertson¹ and Alamgir Karim¹; ¹University of Houston, United States; ²University of Houston Sugarland, United States

Humidity sensors play an essential role in monitoring product quality and lifetime in the manufacturing and pharmaceutical industries for vaccine and drug viability. Recently thermoplastic polymers and inorganic semiconductors-based humidity sensors are raising environmental concerns owing to non-degradability despite their performances. Biodegradable and renewably sourced chitosan-based nanocomposite films could provide a more sustainable alternative. Chitosan has randomly distributed β -linked D-glucosamine and N-acetyl-D-glucosamine and the protonation of NH_2 groups of chitosan increases the affinity of these films towards moisture. Here, thin chitosan films of 120-350nm thickness were coated on Si substrate. Rapid swelling of the thin films in humid environment was spontaneously identified with visible changes in color explained by *thin-film interference* phenomenon. Over the full relative humidity range of 95%, film thicknesses increase 50% compared to dry state, confirmed by *in-situ* ellipsometry and interferometric techniques. The response to humidity change was ultrafast (~5s) and the absorption-desorption of moisture exceeded 50 cycles with confidence. The moisture absorption kinetics followed non-Fickian type diffusion pathway. By blending polar nanofillers like graphene oxide (GO) in a small amount (0.5-2wt%), the swelling behavior of these blend films followed similar trend of rapid moisture absorption while maintaining film stability because of the interaction of oxygen-rich groups of GO and NH_2 groups of chitosan. The nanocomposite thin films had reliable thermal properties and stable tensile strength. This highly sensitive humidity dependent colorimetric property of chitosan nanocomposite films enables its potential as a biodegradable sensor for monitoring quality assurance systems benefiting several industries.

Funding: AFOSR W911NF2010281

10:45 AM EN03.06.03

Bio-Inspired Proline Sensors for Diagnosis and Surveillance of Plant Stress Cassandra L. Martin¹, Josephine Cicero¹, Audrey Moos¹ and Daniel Wilson^{1,2}; ¹Kostas Research Institute, United States; ²Northeastern University, United States

In response to environmental stresses such as drought, excessive salt, high temperatures, heavy metals, and pathogens, plants accumulate amino acids and other metabolites resulting from protective homeostatic processes. Specifically, the amino acid proline can counteract the effects of osmotic stress, chelate metals, and act as an antioxidant, resulting in increased concentrations of proline within plant tissue in response to environmental stimuli. While proline can serve as a general diagnostic indicator of plant or crop health, there are limited field-deployable options for measuring the proline content of plant tissue on-location without requirements for secondary equipment. We have developed bio-inspired proline sensors based on the coloration mechanism of *Nesocodon mauritianus*. The color of the nectar in this flowering plant, ranging from pale yellow to blood red, is directly dependent on both internal pH and proline concentration. By leveraging the chemistry of this natural system, we have developed colorimetric, paper-based proline sensors that provide quantifiable visible signals in response to increasing proline concentrations. We are integrating these sensors into biodegradable, user-friendly form factors that enable a plant-based, eco-friendly approach to monitoring plant health.

11:00 AM EN03.06.04

Wireless Continuous Glucose Monitoring for Smart Home Diagnosis via Biodegradable Fluorescent Microneedle Sensor Mingyu Sang, Myeongki Cho, Selin Lim, In Sik Min and Ki Jun Yu; Yonsei University, Korea (the Republic of)

According to the International Diabetes Federation, the number of patients with diabetes worldwide is 536.6 million, i.e., 10.5% of the total population. In particular, hypoglycemia is a serious condition that can cause behavioral and cognitive impairment, seizures, loss of consciousness, coma, brain damage, or death. In addition to the severity of diabetes itself, this condition can also cause serious medical complications in other organs, such as the kidneys, liver, and heart. Diabetes requires constant management to avoid unfortunate consequences, such as death. Therefore, precise monitoring of the blood-glucose level in the body, which is an important indicator for managing type 1 and type 2 diabetes, is necessary. Continuous glucose monitoring (CGM) is crucial for tracking blood-glucose levels in real-time, providing critical information to effectively prevent diabetic complications arising from hypo- or hyperglycemic episodes. While invasive lancet measurement is not compatible with CGM, commercial and research efforts have been directed toward developing biosensors for CGM. However, the current CGM sensors has discomfort from the attached transmitter on skin and require implantation and removal surgery, which increases the possibility of wounding and bacterial infection, presenting critical barriers for use. Despite the considerable progress made by commercial CGMs, there remains a pressing need to develop user-friendly, minimally invasive CGMs. Therefore, a new class of CGM biosensors is needed for monitoring skin interstitial fluid glucose, like commercial CGMs, in a user-friendly, minimally invasive way that overcomes the limitations of existing systems. Here, we introduce the CGM system consisting of biodegradable microneedle sensor array with high fluorescence sensitivity to glucose and portable smart device with image processing applications. This system produced straightforward yet robust outcomes by measuring the fluorescence intensity of microneedles, which was reversibly modulated based on glucose concentration, without the need for enzymes or reagents. Through this sophisticated integration, our system could continuously measure glucose levels without blood collecting, wound or pain over up to 3 days, clearly tracing the results of commercially available blood glucose meters like lancet diagnostic method. Users such as diabetics can easily and wirelessly check the glucose concentration with this on-demand tether free glucose monitoring system by simply taking the picture with the smartphone, thus allowing measurement at any desired time while the patient moved freely. The fluorescence intensity of the microneedle sensor, which changes according to the glucose concentration, can be successfully obtained through the mobile device equipped with software for analyzing pixel data of the fluorescence image. Compared to previous CGM studies, our system has the advantage that the sensors are ultra-thin and light, minimally invasive, very simple to use, and completely biodegraded and discharged from the body without the insertion and removal surgery. Unlike other sensors, the biodegradable microneedle eliminates the risk of the sensor breaking or remaining in the body, enhancing human safety. This feature notable reduces the risk of infection and further enhances patient comfort and compliance, making our system a more prospective solution for CGM. Furthermore, the microneedle sensor-based home glucose diagnostic platform not only serves as another promising candidate for patients to help prescription and treatment, but also provides potential possibilities to improve health and quality of life. This new platform offers opportunities to autonomous and accurate CGM, a powerful and promising tool in the management of diabetes, using the glucose-responsive fluorescent microneedle sensor and user-friendly home diagnosis mobile service technology.

11:15 AM +EN03.06.05

Materials for Environmentally Resorbable Batteries, Microelectromechanical Systems and Chemical Sensors John A. Rogers; Northwestern University, United States

Recently developed classes of functional materials serve as the basis for microsystems technologies that dissolve, disintegrate, degrade or otherwise physically disappear at triggered times or with controlled rates. Water-soluble technologies of this type are of interest for zero-impact environmental monitors, 'green' consumer electronic gadgetry and resorbable medical implants. This talk describes the foundational concepts in materials science, electrical engineering and assembly processes for various applications. The emphasis is on environmentally resorbable batteries, microelectromechanical systems and chemical sensors, the latter of which adopt 3D designs inspired wind-dispersed seeds to facilitate deployment.

SESSION EN03.07: Degradable Energy Devices
Session Chairs: Jahyun Koo and Lan Yin
Tuesday Afternoon, November 28, 2023
Hynes, Level 2, Room 206

1:45 PM EN03.07.01

Everyday Materials for Transient Supercapacitors Mete Batuhan Durukan, Deniz Keskin, Melih O. Cicek, Yigitan Tufan, Orcun Dincer, Simge Cinar Aygun, Batur Ercan and Husnu E. Unalan; Middle East Technical University, Turkey

Due to the substantial advancements achieved in wearable technology, including consumer electronics and medical monitoring devices, there has been a sharp rise in electronic waste during the past ten years. As electronic devices contain hazardous materials and have limited recyclability, the environmental threat is steadily increasing and the volume of e-waste grows exponentially each year. A significant portion of electronic waste comprises energy storage devices that consist of materials that are toxic or non-recyclable. Therefore, research and development in green energy storage systems that are made of non-hazardous materials is highly needed. Transient electronics, which are intended to disintegrate at the end of their use or when required, have emerged as a solution to this need, producing nearly little waste.

Green and transient electronics require transient energy storage units. Being biodegradable, biocompatible, and non-toxic are essential properties that energy units must possess in line with the requirements of transient electronics. This is especially important for on-demand electronics, which are mostly used for health monitoring devices such as ingestible or implantable devices.

Herein, we propose transient and even edible supercapacitors with everyday materials – such as supplements and foods [1,2]. We successfully fabricated transient supercapacitors based on all-PVA layers and successfully achieved a perfectly working EDLC type supercapacitors with an excellent rate capability up to $1 \text{ V} \cdot \text{s}^{-1}$. The entire structure is based on biodegradable and biocompatible products and showed excellent physical transiency in simple aqueous solutions. To further this quest, we also successfully fabricated cellulose-based edible supercapacitors utilizing soy-sauce based, zwitterionic gel as an electrolyte. Fabricated food-based gel has shown to enhance the L929 proliferation – which is an excellent indication of biocompatibility – and allowed a textbook-like capacitive behavior due to its excellent ionic conductivity. Simulated gastric fluid tests shown a complete dissolving of the edible supercapacitors, indicating its digestibility. These studies indicate excellent developments in the production of transient and edible supercapacitors, being fresh prospects to be the energy units for environmentally friendly and biocompatible transient electronics.

[1] M. B. Durukan, M. O. Cicek, D. Doganay, M. C. Gorur, S. Cinar, H. E. Unalan, Multifunctional and Physically Transient Supercapacitors, Triboelectric Nanogenerators and Capacitive Sensors, *Advanced Functional Materials* 32 (2021) 2106066.

[2] M. B. Durukan, D. Keskin, Y. Tufan, O. Dincer, M. O. Cicek, B. Yildiz, S. Cinar Aygun, B. Ercan, H. E. Unalan, An Edible Supercapacitor Based on Zwitterionic Soy Sauce-Based Gel Electrolyte, under evaluation.

2:00 PM *EN03.07.03

Design of Degradable Rechargeable Batteries Markus Niederberger; ETH Zurich, Switzerland

Transient or degradable electronics based on materials, devices and systems that disappear after a stable operating period with minimal or undetectable residues can help reduce the enormous amounts of electronic waste [1]. Ideally, the battery is integrated into these devices and degrades along with them. However, conventional batteries are optimized for long-term operation and contain a whole range of hazardous and/or expensive components. Therefore, transient batteries must be designed so that they can be disposed of without negatively impacting the environment. For efficient degradation, it is also important that the components and materials can decompose in an aqueous environment. However, some of the most important electrically conductive materials, e.g., copper and aluminum, which play a major role in batteries, do not fall into this category. For such materials, special concepts have to be developed on how they can be decomposed.

In this presentation, a wide range of materials, fabrication methods, and assembly techniques will be presented to develop transient lithium-ion, sodium-ion, and zinc-ion batteries. Special emphasis will be placed on the development and characterization of separator-electrolyte systems based on biodegradable polymers. These separator-electrolyte systems were combined with a Li metal anode and a vanadium oxide cathode and packaged in a biodegradable case, resulting in a transient rechargeable lithium-ion battery (LIB) that can operate for over 400 cycles, but quickly dissolved in water within 15 minutes [2]. In order to be able to degrade copper and aluminum as well, a packaging concept was developed based on a water-soluble polymer composite film containing an oxidizing agent. When triggered with water, the film released the oxidant into the solution, which reacted with the copper and aluminum current collectors and led to their degradation [3]. For sodium-ion batteries biodegradable separators composed of agarose and nanocellulose were applied and tested in half-cell configurations with $\text{Na}_3\text{V}_2(\text{PO}_4)_3$ and $\text{Na}_2\text{Fe}_2(\text{SO}_4)_3$ as cathode materials [4]. Both separators showed promising electrochemical performances with high specific capacities and good cyclability, opening new avenues for the use of these renewable resources for sustainable energy storage devices beyond lithium-ion batteries. Finally, a carefully tailored bottom-up design of a transient zinc ion battery will be introduced that combined both excellent transience properties with outstanding electrochemical performance [5]. The battery consisted of a biopolymeric hydrogel electrolyte based on environmentally friendly polysaccharides, a Zn anode, and a biocompatible polydopamine-based cathode. A polysaccharide-based packaging made it possible to control the degradation of the battery, which is essential to maintain its functionality for as long as desired. This carefully tuned battery design displayed an open circuit voltage of 1.12 V and a specific capacity of 157 mAh g^{-1} (current density of 50 mA g^{-1}) for over 200 cycles. The battery exhibited a pronounced transiency under composting conditions, evidenced by a weight loss of 50 wt.% after 63 days.

[1] N. Mittal, A. Ojanguren, M. Niederberger, E. Lizundia, *Adv. Sci.* 2021, 8, 2004814

[2] N. Mittal, A. Ojanguren, N. Cavin, E. Lizundia, M. Niederberger, *Adv. Funct. Mater.* 2021, 31, 2101827

[3] N. Mittal, T. M. Jang, S. W. Hwang, M. Niederberger, *J. Mater. Chem. A* 2023, in print

[4] N. Mittal, S. Tien, E. Lizundia, M. Niederberger, *Small* 2022, 18, 2107183

[5] N. Mittal, A. Ojanguren, D. Kundu, E. Lizundia, M. Niederberger, *Small* 2023, 19, 2206249

2:30 PM BREAK

SESSION EN03.08: Biodegradable and Biocompatible Implants
Session Chairs: Amay Bandodkar and Jahyun Koo
Tuesday Afternoon, November 28, 2023
Hynes, Level 2, Room 206

3:00 PM *EN03.08.01

Implantable Bioelectronics for Probing Brain Chemistry Yi Zhang; University of Connecticut, United States

The human central nervous system contains billions of neurons that communicate through the propagation of action potentials along the cell membrane and the release, transport, and metabolism of neurochemicals at the synapses. Technologies for *in vivo* electrophysiology have been intensively studied, with recent examples of Neuropixels 2.0 and Neural Matrix for recording over several thousand channels. Compared with these tools for electrophysiological recordings, the technologies for real-time neurochemical monitoring are very limited. In this presentation, I will present our recent developments on implantable bioelectronics for probing brain chemistry, including 1) a soft implantable aptamer-graphene microtransistor probe for real-time monitoring of neurochemical release with nearly cellular-scale spatial resolution, high selectivity (dopamine sensor >19-fold over norepinephrine), and picomolar sensitivity,

simultaneously (*Nano Lett.* 2022, 22, 9, 3668–3677), **2**) a soft neural probe for multiplexed neurochemical monitoring via the electrografting-assisted site-selective functionalization of aptamers on graphene field-effect transistors (*Analytical Chemistry* 2022, 94 (24), 8605-8617), and **3**) a wireless, programmable push-pull microsystem for membrane-free neurochemical sampling with cellular spatial resolution in freely moving animals (*Science Advances* 2022 8 (8), eabn2277). These new sets of implantable bioelectronics create opportunities for neuroscientists to understand where, when, and how the release of neurochemicals modulates diverse behavioral outputs of the brain.

3:30 PM *EN03.08.03

The Next Biodegradable Electronics for Minimally Invasive Implantation for Brain Cortex Seung-KyunKang; Seoul National University, Korea (the Republic of)

Biodegradable electronic devices are gaining prominence as minimally invasive tools that mitigate issues such as biofilm formation due to residual foreign-body materials and infections and hemorrhage arising from secondary removal surgeries. Over the past few years, various implantable medical devices using biodegradable organic and inorganic hybrid materials have demonstrated the feasibility of biodegradable electronics. Notably, these include sensors for monitoring raised intracranial pressure due to traumatic brain injuries with a latency period, and wireless electrical stimulators to promote peripheral nerve regeneration. Systems that use electrical stimulation to control drug delivery can also serve as short-term post-operative drug treatment technologies. However, a limitation of existing biodegradable electronic devices is the need for an implantation process, which unavoidably involves surgical burden. In this presentation, we introduce representative examples of implantable biodegradable electronic devices noted in above. Furthermore, we explore the concept of injectable electronic devices as a means to minimize invasiveness during the implantation process, examining this through the application of large-area signal measurement in the cerebral cortex.

4:00 PM EN03.08.02

Bio-implantation Strategy for the Bio-Interfaces with Minimally Invasive Surgery Based on the Mechanical Analysis Gyeong-SeokHwang¹, Jae-YoungBae², Seung-KyunKang² and Ju-YoungKim¹; ¹UNIST (Ulsan National Institute of Science and Technology), Korea (the Republic of); ²Seoul National University, Korea (the Republic of)

Among the deformable electronic devices, there are bio-implantable electronics that consist of biocompatible materials and withstand biological motions with deformability. It can operate in the body with biocompatible materials for all components, and it is considered to be a key technology for the future. The general bio-implantable electronics use biocompatible materials, but it needs extra removal surgery after the functional period. If all components of bio-implantable electronics are substituted with biocompatible and bioresorbable materials, it does not have to conduct extra removal surgery and it can be naturally resolved with the body fluid after the functional period. It means that the patient becomes free from the anesthesia and secondary infection through the extra surgery. The minimally invasive surgery concept is also actively researched in the bio-medical field. It pursues the minimization of a wound during surgery or the implantation process. It is possible to incise the minimum area to minimize the recovery time of the wound and greatly reduce the probability of infection and scarring even if surgery is performed when it uses this concept.

In this research, we intend to fabricate a biocompatible and bioresorbable electronic device that can resolve after the functional period, and it can highly expand into a large area when injected into the body. The bioresorbable shape memory polymers are a strong candidate for the shape expansion behavior near the body temperature. In addition, the electronic device must be spread through the narrow gap between the tissue and the skull to place the electronic device on the tissue. Therefore, during the process of suction and injection into the tube, the analysis of the mechanical properties of the entire electronic device and the optimization of the deformation mode and mechanism depending on the device structure are intended to be achieved at the same time. The deformation behavior was analyzed based on the accurately measured mechanical properties of all constituent materials to realize this concept. The suction & injection process was simulated through 3D finite element simulation based on the measured mechanical properties, and a general design rule for the structural design of mechanically reliable, bioresorbable, shape expandable, minimally invasive implantable electronics can be presented. As a result, it is expected that this concept can open a novel paradigm of bio-implantable electronics.

SESSION EN03.09: Poster Session II: Sustainable Materials I

Session Chairs: Shweta Agarwala and Jahyun Koo

Tuesday Afternoon, November 28, 2023

Hynes, Level 1, Hall A

8:00 PM EN03.09.01

Reinforcement of Physical Properties of Biodegradable Cellulose Composites for Landfill using Cellulose-Based Resins MikyungKim¹, JiyeonWoo¹, JeonghyunYeum², JungeonLee², SejinLee³, ChanghoonHan³, JinsooKim⁴, SeokhyeonSong⁴ and HyaemiSon⁴; ¹DYETEC Institute, Korea (the Republic of); ²Kyungpook National University, Korea (the Republic of); ³Korea Conformity Laboratories, Korea (the Republic of); ⁴Green Package Solution, Korea (the Republic of)

The general garbage bags are made of polyethylene(PE) or polypropylene(PP), and most of the garbage bags are landfilled in the ground and incinerated. Landfill garbage bags manufactured using petroleum-based resins such as PE and PP take more than 500 years to decompose naturally in the ground. In addition, when PP, PE bags are incinerated, dioxins and volatile organic compounds, which are first-class carcinogens, are generated, which poses a threat to human health.

Garbage bags using resins such as PLA(Poly lactic acid), PBS(Polybutylene succinate) and PBAT(Polybutylene adipate terephthalate), which are biodegradable polymers, are decomposed only under composting conditions(58°C, within 6months), and are difficult to decompose when buried in the ground at room temperature, so they are incinerated like general garbage bags made of PP or PE. Therefore, even if biodegradable plastic materials such as PLA and PBS are selected, it will not be the ultimate eco-friendly product.

In order to replace garbage bags made of PP or PE, which cause environmental pollution, cellulose material, which is abundant on earth and can be biodegraded in soil, was used as a biodegradable garbage bag material for landfill. However, the film materials using cellulose resin have problems such as lack of elasticity and low tear strength.

As a study to improve the physical properties of these cellulose films, the physical properties of cellulose-CNF composites, which were compounded by adding CNF(Cellulose nanofibers), were investigated. In addition, the physical properties such as elasticity, flexibility, and biodegradability were investigated for cellulose composite films compounded with bio-organic compound additives such as eco-friendly plasticizers and starches, and the possibility of using these cellulose composite films as materials for resource circulation garbage bags was examined.

8:00 PM EN03.09.02

Enhanced Mechanical Properties of Biodegradable Polybutylene Adipate-Co-Terephthalate Blended with Cellulose Nanofiber Modified with Silica Nanoparticles JoheunYoon and YoungsooSeo; University of Sejong, Korea (the Republic of)

Polyethylene (PE) mulching films are widely used in crop fields. However, residual PE films have been accumulated in the soil reducing crop yield. It has been tried that PE films are replaced by biodegradable polymers such as Polybutylene adipate-co-terephthalate (PBAT). In order to increase the use of PBAT mulching films, problems such as its low mechanical properties, short degradation period and low UV resistance still need to be addressed. In this study, through a sol-gel reaction, silica nanoparticles were synthesized on the surface of the cellulose nanofiber (CNF) to have a bumpy surface. The surface-modified CNF (s-CNF) could be obtained in powder form after drying because aggregation due to capillary force between the fibers is suppressed. s-CNF was well-dispersed in PBAT or PBAT/PLA blends using a melt-mixer. The mechanical properties of the composite films were improved, for example, tensile strength at break was enhanced by 35% with 3wt% s-CNF addition. The mechanical property was systematically studied in terms of s-CNF and PLA contents. Controlling silica particle content and morphology will be presented. The degradation rate and UV resistance of the composite films may also be presented.

8:00 PM EN03.09.03

Mechanical, Thermal and Rheological Characteristics of Ternary Blended System, Poly(lactic acid)/Poly(hydroxyalkanoates)/Poly(butylene adipate-co-terephthalate) (PLA/PHA/PBAT) via the Morphological Influence Min YeongJeong¹, Jin HeeNoh², KibeomNam¹, HyojinKim² and Dong YunLee¹; ¹Kyungpook National University, Korea (the Republic of); ²Advanced Materials & Components Center, Korea (the Republic of)

This study explores the potential of biodegradable polymer blends as environmentally friendly alternatives to conventional plastics. Single biodegradable polymers have limitations in fully replacing traditional polymer materials. To overcome these limitations, blending different polymers or using compatibilizers has been investigated. However, compatibility issues arise due to the high molecular weight and surface energy differences between materials. In this study, we aim to enhance compatibility by controlling the composites and investigating the effects of polymer surface energy in ternary blends of Poly(lactic acid) (PLA)/Poly(hydroxyalkanoates) (PHA)/Poly(butylene adipate-co-terephthalate) (PBAT). Our analysis includes the examination of morphology, mechanical properties, rheological characteristics, and a particular focus on the effects of PHA at the blend's interface. The results reveal that PHA acts as a compatibilizer, transforming the blend structure from a sea-island morphology to a co-continuous structure, with PHA encapsulating PBAT. This not only enhances impact strength but also achieves the highest tensile strength and elongation at break by optimizing the PHA content. The aggregation and reinforcement effects of PHA in the PLA/PBAT blend contribute to these improvements. The morphological prediction of the blend is conducted using diffusion coefficients, and the influence of PHA on interfacial properties is confirmed through scanning electron microscopy (SEM). The co-continuous interface achieved by encapsulating PBAT with PHA contributes to a consistent and stable structure. Rheological properties are evaluated using a rheometer,

revealing a decrease and subsequent increase in complex viscosity with increasing PHA content. This behavior can be attributed to the formation of complex fluidity during the heating process, followed by the formation of a new structure. Moreover, for immiscible blends, the influence of the interface becomes more significant, resulting in a larger increase in storage modulus. However, as PHA content increases, the rate of increase in storage modulus decreases. Overall, these findings highlight the role of PHA as a compatibilizer in PLA/PBAT blends. Furthermore, by increasing the content of biomass-based PHA instead of petroleum-based PBAT, this study suggests the possibility of sustainable plastics for eco-friendly packaging materials.

8:00 PM EN03.09.04

Identification and Characterization of Digestive Enzymes and Intestinal Microorganisms that Degrade Polystyrene in *Tenebrio Molitor* Larvae Hwicheol Shin¹ and Dong-Ku Kang^{1,2,3}; ¹Incheon National University, Korea (the Republic of); ²Research Institute of Basic Sciences, Korea (the Republic of); ³Bioplastic Research Center, Korea (the Republic of)

Plastic has been produced since 1950s and it has been also widely used successfully as a fundamental material. However, it is now considered as a major reason of environmental hazard because its non-biodegradable property. More specifically, non-biodegradable plastic (NBP) mean a high-molecular-carbon-polymers that does not break down in a natural condition by biological processes. In recent decades, various research groups have been conducted to develop a solution for the biodegradation of non-biodegradable plastics such PE, PP, PS, PET and PVC. Recent research indicated that mixed-microbial can be used for digestion of NBPs. Bacterial strains have been isolated from environment or living-organisms and their ability of biodegradation was confirmed that convert into low-molecular-weight organics or mineralize to CO₂. In this study, up-regulated enzymes were identified when insects were feed with NBPs instead bran. Microorganisms were also isolated from various insects and characterized that could biodegrade NBPs. To isolate NBP-digesting microorganisms, the larvae of *Galleria mellonella*, *Tenebrio molitor* Linnaeus, *Plodia interpunctella* and *Sitotroga cerealella* were collected from environment and NBPs (polyethylene (PE), polystyrene (PS), and polypropylene (PP)) were produced instead bran. It is identified that *T. molitor* larvae had a potential for consuming PS comparing other insects. In order to identify the intestinal digestive enzymes and intestinal microorganisms of *T. molitor* involved in PS biodegradation, we divided them into 5 groups according to the diet. The survival rate was higher in the group of 'PS fed only' comparing with 'starvation'. This indicated that larvae have an ability that can convert energy source from digestion of PS. Intestinal microorganisms were excluded by feeding antibiotics to confirm the PS digestion ability only by digestive enzyme. Frass were characterized with various analytical approaches (such as GPC, FTIR, NMR and TGA) and result indicated that there were no significant differences in PS degradation ability between the presence or absence of intestinal microorganisms. To identify the digestion enzymes of PS with or without treatment of antibiotics, total mRNA was isolated from intestine and sequenced. Lipase3, Phospholipase A11, and Peroxiredoxin-6 were up-regulated that is known as relating fatty acid-digestion. In addition, Calcium uniporter protein mitochondrial, Sulfate permease chloroplast and Sialin were also up-regulated that regulate cell bioenergetics. These results indicate that intestinal enzymes are related in the process of PS digestion process and cellular-energetics. Furthermore, metagenome analysis of the intestinal microflora was performed at 5-day intervals to confirm the change in the microbial community of *T. molitor* according to PS feeding. It is confirmed that increasing and decreasing-bacterial strains over time and intestine was isolated to identify digesting-microorganisms. Isolated intestine was crushed and cultured in various medium condition including LB, NB, BHI, TSB and GPY. Isolated microorganisms were cultured in an inorganic medium with PS (as an only carbon source). As a result, 6 types of bacterial strains were successfully identified: *Bacillus* sp., *Bacillus mycoides*, *Bacillus cereus*, *Enterobacter xiangfangensis*, *Enterobacter cancerogenus* and *Enterococcus gallinarum*. Our result indicates intestinal bacteria and enzymes are relating in the process of digestion of PS and cellular-energetics.

8:00 PM EN03.09.05

Bioinspired Coordination Polymer Framework Adsorbents for Desalination Kelvin Adrah, Sheeba Dawood and Hemali Rathnayake; University of North Carolina Greensboro, United States

As per the United Nations, by 2025, an estimated 4 billion individuals will lack access to potable water, primarily due to the surge in population and industrial activities, resulting in increased water pollution. Traditional water treatment methods like ion exchange and reverse osmosis are time-consuming, generate substantial waste, and are financially demanding. Currently, adsorption technology has been implemented in water purification systems for contaminant removal owing to its cost-effectiveness and efficacy. However, it is hampered by its limited adsorption capacity, lack of environmental sustainability, and versatility.

This project aims to overcome these technical constraints by developing a biomass-derived adsorbent capable of efficiently eliminating contaminants from water. The adsorbent consists of hierarchical microstructures with a robust metal-organic framework, synthesized by combining naturally occurring tannic acid with iron (II) acetate in an aqueous medium. The synthesis process adheres to green chemistry principles, rendering it an energy-efficient and adaptable approach. Comprehensive characterization techniques were employed to investigate the chemical composition, morphology, physicochemical properties, and colloidal stability of the microstructures.

The results reveal the successful extraction of prevalent minerals (Na⁺, K⁺, Mg²⁺, and Ca²⁺) from seawater samples procured from Kiawah Island, SC, and Hatteras Beach, NC, employing a single-cycle adsorption procedure. The adsorption performance was analyzed under varying contact times and adsorbent dose-to-seawater volume ratios. Additionally, these adsorbents demonstrated antimicrobial properties by effectively destroying microorganisms present in the seawater samples.

The proficient adsorption of these dissolved minerals onto the microstructures can be attributed to the highly branched and hydroxyl-dense polytopic tannic acid ligand, which provides numerous bonding sites via diverse chemical interactions. These extensively porous, amphoteric polyphenol-based coordination polymers are economically viable and readily scalable for pilot or industrial applications. Consequently, they exhibit substantial potential for employment in tertiary water treatment for remediation purposes.

8:00 PM EN03.09.06

Nature-Inspired Biogenic Structural Insulation Material for Carbon-Neutral Building Solutions Long Zhu, Arpita Sarkar and Shenqiang Ren; University of Maryland, United States

Building materials play a crucial role in providing a robust barrier that effectively shields climate-controlled interiors from the harsh external environment. The extensive adoption of building materials capable of carbon sequestration holds immense potential as a global carbon storage solution. In this context, renewable biogenic materials derived from abundant agricultural waste have garnered significant attention. It has become imperative to address their previously limited thermal and structural performance, not only to enhance energy efficiency but also to mitigate the carbon emissions associated with the construction industry, encompassing both production and operation. Inspired by nature, we introduce an innovative approach to additive manufacturing of biogenic structural insulation materials. This cutting-edge technique enables the simultaneous customization of thermal insulation and mechanical properties. The resulting functional-gradient hybrid materials are composed of cellulose extracted from straw and silica aerogel networks. These materials exhibit a low thermal conductivity of 28.2 mW m⁻¹ K⁻¹ and an impressive flexural modulus of 990 MPa. Moreover, they showcase exceptional fire resistance and superhydrophobic properties. Furthermore, a life cycle analysis underscores the carbon neutrality of these biogenic hybrid materials, with a footprint of -0.26203 kgCO₂eq/kg. This highlights their pivotal role in advancing the development of energy-efficient, carbon-sequestering green buildings.

8:00 PM EN03.09.07

Improving the Weatherability and Intumescent Effects of Naturally Sourced Wood Flame Retardant Coatings. Mary K. Ruksarash¹, Douglas Fox¹ and Whirang Cho²; ¹American University, United States; ²National Institute of Standards and Technology, United States

Approximately 1 billion acres or half of all the United States is considered wildland. As wildland-urban-interface (WUI) development expands, millions of homes are at risk of ignition and destruction. As a result, these communities must adapt by acquiring fire-resistant materials and protectants for their homes. However, commercially available wood flame retardant coatings (WFRC) are perceived to present harm to both human health and the environment. In addition, commercial fire-resistant paints often leach into the environment, losing their efficacy shortly after application in external applications. To properly address this, it is imperative to explore WFRC which use natural products as feedstocks. Chitosan is an abundant, biodegradable, and nontoxic binding agent that can be easily incorporated as a primary component in water-based WFRC. Prior studies in our laboratory have shown that using reduced valence phosphorus-containing acids in chitosan WFRC can significantly delay or prevent ignition of wood under a 50 kW/m² heat flux. However, Chitosan's solubility in water threatens the overall weatherability of the coating. Photo crosslinking agents were utilized to allow for on-site application in vulnerable WUI areas. After exposure to sunlight, no chitosan dissolved in artificial acidic rainwater, and coated wood substrates self-extinguished immediately after flame impingement was removed. These findings offer a valuable glimpse into which methods and additives may contribute to an overall optimized, weatherable, and flame-retardant Wood Flame Retardant Coating.

8:00 PM EN03.09.08

Higher Strength and Carbon Sequestration in Cement and Cementitious Material using Biomimetic Zinc Complex Rebecca J. Gilchrist, Allison L. Morin, Sara Heidarneshad, Shuai Wang, Nima Rahbar, Suzanne F. Scarlata and Ronald L. Grimm; Worcester Polytechnic Institute, United States

The cement industry is a prominent contributor to anthropogenic greenhouse gases and is responsible for about 8% of global emissions, which drives research into cement alternatives. We have previously incorporated carbonic anhydrase into concrete to create an enzymatic, self-healing, cementitious material (ECM) for carbon sequestration. While this material demonstrates high strength and self-healing properties, it is limited by the short lifespan (i.e. ~2 weeks) of carbonic anhydrase and nonspecific limestone incorporation. It motivates our exploration of non-biological alternatives such as zinc cyclen (cyclen = 1,4,7,10-tetraazacyclododecane). With a ~3300 M⁻¹ s⁻¹ rate constant, zinc cyclen is among the most efficient molecular carbonic anhydrase mimics and demonstrates extreme stability at cement-relevant temperatures and alkaline pH values.

Recently, we utilized zinc cyclen to produce calcium carbonate as an aqueous solute and covalently tethered to sand surfaces. In recent results, we found when tethered to the sand aggregate, the covalent attachment affords high strength and healing properties by catalytically producing calcium carbonate at the sand-cement interface while providing a flexible organic connector to accommodate interfacial atomic mismatches. This catalytic sand should enable future inexpensive, robust, green construction materials with long lifetimes and self-healing properties that can withstand extreme environments.

8:00 PM EN03.09.09

Self-Organized Hydroxyapatite Construct for Biomedical Applications: From Pack Cementation to Structure and Mechanical Characterization. Obinna A. Osuchukwu^{1,2}, AbduSalihi¹, IbrahimAbdullahi¹, Precious O. Etinosa³ and David O. Olubiyi²; ¹Bayero University, Nigeria; ²Ahmadu Bello University, Nigeria; ³Worcester Polytechnic Institute, United States

This work presents the bioprocessing and robust characterization of the physical and mechanical properties of hydroxyapatite (HA) synthesized from two bio-precursors: bovine and catfish bones. The precursors are deproteinized by carbonization and calcination, then sintered using conventional heat treatment to form HA microparticles. Pulverization and the sol-gel process are performed to achieve homogeneity of well-packed cementitious powder constructs of controlled percentage weight compositions of HA from each precursor. The structural and compositional qualities, fracture mechanics, and mechanical properties of the synthesized powder and cementitious construct are assessed via X-ray diffraction, Fourier transform infrared spectroscopy, scanning electron microscopy, and mechanical testing. The specimen composed of an equal percentage weight of HA from bovine and catfish (B50/C50) exhibited the highest fracture toughness and highest compressive strength. The highest hardness and brittleness index values are measured in the B25/C75 specimen. Under dynamic loading, the B100/C0 specimen exhibited the highest resistance to wear. The X-ray diffraction patterns revealed that the B75/C25 specimen has the highest fraction of crystallinity. The implications of these findings are discussed for the potential biomedical applications of HA in dentistry and orthopedic medicine.

SESSION EN03.10: Green Electronics
Session Chairs: Amay Bandodkar and Lan Yin
Wednesday Morning, November 29, 2023
Hynes, Level 2, Room 206

8:15 AM *EN03.10.01

Toward Metal-Free and Biodegradable Circuits on POMaC Vladimir A. Pozdin¹, Mauro Victorio¹, Oscar Gonzalez¹, Brendan Turner², Kirstie Queener² and Michael Daniele²; ¹Florida International University, United States; ²North Carolina State University, United States

Exponential growth of distributed sensing and proliferation of electronic devices has raised the alarm on long-term impact of spent sensors on the environment. The utility of point-of-care and portable sensors has great potential to improve our health, environment and infrastructure; however, the limited sensor life (often days) requires careful consideration of life cycle in the device design. In our work, we focus on developing biodegradable electronics without precious or rare-earth metals for transient sensing applications. Removing silicon and metals from electronic devices requires a complete design shift in organic electronics, starting from the bottom up. Poly(octamethylene maleate (anhydride) citrate) is utilized in our work as a highly tunable and degradable substrate for electronic circuits. Toward the development of sensors, we demonstrate organic light emitting diodes with biodegradable packaging, which enables ambient operation and programmable degradation. Toward development of portable energy storage, we demonstrate diodes and transistors without metal or silicon-based functionalization using carbon conductors, amine chemistry, and ultra-thin films. In this work, we establish process requirements and limitations for biodegradable circuits to guide the development of biodegradable sensor node for mass deployment with minimal impact.

8:45 AM EN03.10.02

Functional Paper for Self-Powered Sustainable Digitalization Rodrigo F. Martins¹, Guilherme Ferreira¹, Sumita Goswami², Elvira Fortunato¹ and Suman A. Nandy¹; ¹FCT UNL, Portugal; ²AlmaScience Colab, Portugal

2020, world is taken aback by a pandemic. It is turning into an unprecedented crisis in people's lives and economy. But it warns us too, to be careful and prepare for the future. We can live better now, but we must think best for tomorrow. Today, another threatening part is increasing global emissions significantly, the majority caused by energy production that is consumed in industry, services, households, and transport. The worldwide concern over energy security and environmental issues due to fossil fuel consumption has generated the urgent need of sustainable and renewable energy sources. Therefore, alternative energy actions can support the goals of green world with economic stimulus programs. The majority of renewable energy sources are based on solar, wind, hydroelectric, geothermal or biomass. But most of them needs a huge plant. Though, in this faster digitalization era, most of the technologies are portable that connected with IoTs which requires a flexible energy resource that will provide power uninterrupted. Still today, the battery is a prime option. But super flexibility and biocompatibility is still a limitation for it. Moreover, the native drawbacks of conventional systems are recharging, periodical maintenance and replacement that causes environmental pollution. Therefore, self-powered technology which can work independently without any other external energy supplier, will be a great choice.

Therefore, the biggest challenge in smart technology is sustainable power sources, that can back up the electronics unconditionally. This situation considers a new platform of self-powered technology, operating without any external power sources! In this context, the principal vision of us is to speed up the concept of self-powered technology based on different wearable and low-cost platform, by constructing in such a way, that will buckle wearables platform with electronics to bring a new smart technology which will have inbuilt self-powered system.

References:

1. Nandy, S.; Goswami, S.; Marques, A.; Gaspar, D.; Grey, P.; Cunha, I.; Nunes, D.; Pimentel, A.; Igreja, R.; Barquinha, P.; et al. Cellulose: A Contribution for the Zero e-Waste Challenge. *Adv. Mater. Technol.* 2021, 6, 2000994. 2. Nandy, S.; Fortunato, E.; Martins, R., Green economy and waste management: An inevitable plan for materials science. *Prog. Nat. Sci.* 2022. 3. Ferreira, G.; Opinao, A.; Das, S.; Goswami, S.; Pereira, L.; Nandy, S.; Martins, R.; Fortunato, E. Smart IoT Enabled Interactive Self-Powered Security Tag Designed with Functionalized Paper. *Nano Energy* 2022. 4. Ferreira, Guilherme; Goswami, Sumita; Nandy, Suman; Pereira, Luis; Martins, Rodrigo; Fortunato, Elvira. "Touch-Interactive Flexible Sustainable Energy Harvester and Self-Powered Smart Card". *Advanced Functional Materials* 30 5 (2019): 1908994. 5. Goswami, Sumita; Santos, Andreia dos; Nandy, Suman; Igreja, Rui; Barquinha, Pedro; Martins, Rodrigo; Fortunato, Elvira. "Human-motion interactive energy harvester based on polyaniline functionalized textile fibers following metal/polymer mechano-responsive charge transfer mechanism". *Nano Energy* 60 (2019): 794-801.

9:00 AM *EN03.10.03

All-Carbon Nanomaterial Inks for Print-In-Place, Recyclable and Water-Based Electronics Aaron D. Franklin; Duke University, United States

For decades we've been hearing about the promise of printing electronics directly onto any surface. However, despite significant progress in the development of inks and printing processes, reports on fully, direct-write printed electronics continue to rely on excessive thermal treatments and/or fabrication processes that are external from the printer. In this talk, recent progress towards print-in-place electronics will be discussed; print-in-place involves loading a substrate into a printer, printing all needed layers, then removing the substrate with electronic devices immediately ready to test [1]. A key component of these print-in-place transistors is the use of inks from various nanomaterials, including: 2D graphene and hexagonal boron nitride, and 1D carbon nanotubes. Using an aerosol jet printer, these mixed-dimensional inks are printed into functional 1D-2D thin-film transistors (TFTs) without ever removing the substrate from the printer and using a maximum process temperature of 80 C with most processing occurring at room temperature [2]. Using a similar print-in-place process, completely recyclable printed transistors will be discussed, fabricated entirely using nanoscale carbon-based inks [3]. These recyclable devices exploit a printed crystalline nanocellulose (CNC) ionic dielectric. Finally, the same set of carbon-based inks will be demonstrated for use in all-aqueous (completely water-based) printed CNT-TFTs, eliminating dependence on processing with hazardous chemicals [4]. These demonstrations give evidence for an electronic future involving devices with fabrication and/or function that goes beyond what is possible with traditional semiconductor technologies [5]. The increasingly prolific distribution of sensing devices will best be served by using more environmentally friendly materials and fabrication processes, which this work provides a vision for achieving.

[1] J. A. Cardenas *et al.*, "In-place printing of carbon nanotube transistors at low temperature," *ACS Appl. Nano Mater.*, vol. 1, pp. 1863-1869, 2018.

[2] S. Lu *et al.*, "Flexible, print-in-place 1D-2D thin-film transistors using aerosol jet printing," *ACS Nano*, vol. 13, pp. 11263-11272, 2019.

[3] N. X. Williams *et al.*, "Printable and recyclable carbon electronics using crystalline nanocellulose dielectrics," *Nature Electronics*, vol. 4, pp. 261-268, 2021.

[4] S. Lu *et al.*, "All-carbon thin-film transistors using water-only printing," *Nano Letters*, vol. 23, pp. 2100-2106, 2023.

[5] A. D. Franklin, M. S. Hersam, and H.-S. P. Wong, "Carbon nanotube transistors: Making electronics from molecules," *Science*, vol. 378, pp. 726-732, 2022.

9:30 AMBREAK

10:00 AM *EN03.11.01

Commercial Organic Dyes and Pigments as Semiconductor Photocatalysts Eric D. Glowacki; Brno University of Technology, Czechia

Semiconductor-based catalysts can convert solar energy into chemical fuels such as hydrogen, hydrogen peroxide, or hydrocarbons produced via carbon dioxide reduction. Long overlooked due to stability concerns, some organic semiconductors have recently emerged as promising electrocatalysts and photocatalysts for operation in aqueous environments. Our attention has focused on dyes and pigments of commercial origin, everyday materials used on a large scale with an established safety profile. Many of these light-absorbing molecules have indeed been selected due to their outstanding stability, which is a feature that translates to useful applications in the field of aqueous photocatalysis. We have found a high selectivity of organic semiconductors for oxygen reduction reactions, by both one-electron and two-electron pathways. The products of these reactions are superoxide or hydrogen peroxide. We find this occurs on numerous organic semiconductors and conducting polymers in a pH range from 1 to 12. We have found that while photogenerated electrons reduce oxygen, the fate of the holes represents a complex picture. When the semiconductor is used as a photocathode and efficient p-type transport is available, photogenerated holes can easily be extracted and stability is very high. This talk will discuss the promises, potential applications, as well as obstacles facing the use of low-cost commercial photocatalytic organic dyes and pigments.

10:30 AM EN03.11.02

Specie-Dependent Electrochemical Performance of Microalgae Exoskeletons as Si-Based Anodes for Next-Generation Li-Ion Batteries Maria V. Blanco; Norwegian University of Science and Technology, Norway

Li-ion batteries (LIBs) can bridge renewable energy sources to power demand and are therefore crucial in achieving energy sustainability. However, the magnitude of the forthcoming market demand for LIBs along with the need for a climate neutral economy means that a sustainable supply of battery raw materials becomes strategically essential.

Apart from lithium, there is one material that is a fundamental part of all LIBs: graphite, which is the primary component of LIBs anodes. Graphite exhibits a storage capacity of 372mAhg^{-1} , which is insufficient for next-generation LIBs. Even more concerning, it has been listed as a critical raw material.

A promising option to increase the energy density of anode materials for LIBs while retaining stable cycling performance is the fabrication of composite anodes having graphite and small amounts of nanostructured Si-based materials (Si, SiO_x and SiO_2). However, the production of such nanostructures often requires high temperatures, pressure, and PH, as well as deployment of toxic/hazardous chemical agents, which are harmful for the environment. Hence, sustainable manufacturing methods to produce Si-based nanostructures is an imperious need.

Importantly, nanostructures of SiO_2 are observed in the exoskeletons of diatoms, a type of photosynthetic microalgae ecologically widespread in marine and freshwater, and such biosilicas are produced under room temperatures and pressures in aqueous systems near a neutral pH. Diatom exoskeletons (frustules) contain 98 % of silica with hierarchical architectures from the nano- to macroscale, and each of the more than 100,000 estimated diatom species displays a unique SiO_2 frustule morphology and size (from $2 \mu\text{m}$ to 2 mm). However, the synthesis of nanostructures with controlled surface area and porosity are essential prerequisites for Si-based anodes, since fine control of these properties has shown to mitigate stress derived from volume variations of Si active domains, therefore extending the cycle life of the anodes, limiting the reactive area for the formation of the solid electrolyte interphase, and decreasing Li-ions diffusion paths.

Diatoms have the potential to fulfil the needs of next-generation anodes for LIB technology, and a landmark of 840mAhg^{-1} stable storage capacity after 100 cycles at 100mA g^{-1} was achieved by diatom SiO_2 anodes. However, although the implementation of diatoms into working anodes has created a valuable knowledge on how to condition frustules for this exact application, the lack of insights on the effect of diatom nanostructure on the electrochemical properties of Si-based anodes is hindering the rational choice of individual diatom species building SiO_2 morphologies at the nano and microscale that can deliver optimum electrochemical performance.

In this work, a comparative analysis of the electrochemical performance of SiO_2 anodes made from frustules displaying distinctive properties in terms of porosity, surface area, particle size and morphology is performed. Such frustules were extracted from diatom species artificially cultivated in photobioreactors. This allowed to conduct the first specie-dependent analysis of Si-based anodes extracted from microalgae exoskeletons, and to select outperforming diatom species for LIB technology. Massive cultivation of diatoms for the production of negative electrodes for LIBs has the potential to revolutionize battery production via truly green bottom-up fabrication schemes.

10:45 AM EN03.11.03

Quinone-Rich Sustainable Organic Cathodes for Rechargeable Aqueous Zinc-Ion Batteries Onur Buyukcakir; Izmir Institute of Technology, Turkey

Zinc(Zn)-based energy storage systems have excellent capacities and stabilities in aqueous electrolytes while also being inexpensive, eco-friendly, and safe. However, recent studies have demonstrated that the lack of cathode materials allowing high capacity and rate performance without sacrificing cycle life and sustainability is a major bottleneck in the performance of Zn-ion batteries (ZIBs). Recent years have seen the introduction of a limited number of organic materials as cathodes in aqueous rechargeable ZIBs. However, generating electrochemically active organic materials with rich redox-active centers that can reversibly accommodate Zn^{2+} ions is challenging. It is, therefore, still of great interest to design new organic compounds or polymeric structures as active electrode materials to provide the required electrochemical performance, economic benefits, biocompatibility, and sustainability for building next-generation ZIBs. This talk will introduce rationally designed quinone-based redox-active organic materials prepared using environmentally friendly (heavy-metal-free) reaction strategies. Furthermore, new chemistries will be introduced that significantly affect several crucial parameters of aqueous ZIBs for practical applications, including cycling stability, a uniform discharge plateau, stable voltage output, and high physicochemical stability. These organic cathodes show high specific capacities and excellent cyclic stability over 10000 cycles with remarkable capacity retention. The investigation of the zinc-ion storage mechanism using theoretical calculations and in/ex-situ analysis will be demonstrated in detail. These findings are critical for gaining a fundamental understanding of the structure-property relationship, paving the way for rationally built next-generation battery systems.

Acknowledgments: O.B. acknowledges financial support from the Scientific and Technological Research Council of Turkey (TUBITAK) under Project No.220Z024.

11:00 AM EN03.11.04

Sustainable and Controlled Synthesis of Carbon Nanoparticles from Lignin using Single-Step Aerosol Methods for Application in Energy Storage Sujit Modi¹, Onochie C. Okonkwo¹, Sulay Saha¹, Hao Zhou¹, Shalinee Kavadiya², Marcus Foston¹ and Pratim Biswas²; ¹Washington University in Saint Louis, United States; ²University of Miami, United States

With the rapidly growing demand for renewable energy and portable devices, developing high-performance energy storage materials and meeting sustainability requirements is significant. Lignin, a biomass constituent and byproduct waste of biorefineries, is one of the few renewable sources of carbon that have the abundance and desirable properties to displace or replace fossil derived carbon sources. A renewable resource, low cost, and high aromatic content make lignin an ideal precursor to obtaining carbon materials for energy storage. However, present efforts on the large-scale synthesis of carbon materials from lignin are limited either by multistep and batch processes or the use of activating agents/templates [1].

The present work aims to engineer a process that valorizes waste and by-product lignin. In particular, we develop an original and innovative method, based on a one-step continuous aerosol technique, to manufacture high-performance carbon nanoparticles for energy storage without the use of activating agent/template. This one-step approach requires a significantly lower time for synthesis: an order of seconds in comparison to hours for existing methods. Temperature and residence time are expected to have a key impact on the properties of carbon materials synthesized from lignin, hence, an aerosol technique utilizing a furnace aerosol reactor is used; furnace aerosol reactor is known for enabling precise control over a wide range of temperatures and residence times [2]. Subsequently, the effect of temperature and residence time inside the reactor on carbon nanoparticle size, functional groups, surface area, and morphology is systematically investigated. Furthermore, the as-obtained carbon nanoparticles are tested for specific capacitance and the best-performing material (surface area $925 \text{m}^2/\text{g}$) exhibited a specific capacitance of 247F/g at 0.5A/g with excellent capacity retention of over 98 % after 10,000 cycles. This is a clear demonstration of their superior performance compared to supercapacitors synthesized earlier from lignin.

Moreover, the size and morphology of carbon particles, which are impacted by interparticle collision and sintering, are known to play a crucial role in their stability as well as energy storage

performance. However, experimental as well as modeling efforts on size and morphology-controlled synthesis of carbon nanoparticles from lignin are limited, partly due to the complexity of studying collision and sintering under simultaneous lignin reactions (pyrolysis). We systematically investigate the kinetics of reaction, sintering, and collisions using a novel and generalizable numerical model based on a geometric modeling approach [3]. Knowledge of kinetics will provide better control over the size and morphology for efficient utilization of carbon nanoparticles in energy storage.

Overall, the simple (one-step, continuous, and rapid) operation, avoiding the use of activating/templating chemicals, and precise control over size and morphology make the aerosol technique a promising candidate for the scalable and sustainable synthesis of energy storage materials.

References:

- [1] J.W. Jeon, L. Zhang, J.L. Lutkenhaus, D.D. Laskar, J.P. Lemmon, D. Choi, M.I. Nandasiri, A. Hashmi, J. Xu, R.K. Motkuri, Controlling porosity in lignin derived nanoporous carbon for supercapacitor applications, *ChemSusChem*, 2015, 8(3), 428-432.
- [2] S. Modi, M.B. Foston, P. Biswas, Controlled Synthesis of Smaller than 100 nm Lignin Nanoparticles in a Furnace Aerosol Reactor, *ACS ES&T Engineering*, 2023, 3 (5), 671–681
- [3] S. Modi, O. Okonkwo, H. Zhou, S. Kavadiya, M. Foston, P. Biswas, Geometric Model for Predicting the Size and Morphology Evolution of Multiparticle Aggregates during Simultaneous Reaction and Sintering, *Chem. Eng. J.*, 2023, 141423

11:15 AM EN03.11.05

Cellulose Nanocrystals Based Flexible Substrates as Electrodes for Zn Batteries and Tribolayer in Triboelectric Nanogenerators (TENG) Devices Amit K. Sonker^{1,2,2}, Shizhao Xiong², Aleksandar Matić² and Gunnar Westman²; ¹VTT, Technical Research Center of Finland, Finland; ²Chalmers University of Technology, Sweden

Nanocellulose is a promising polymer for applications in energy and electronic devices due to its biodegradable nature and properties. Among nanocelluloses, cellulose nanocrystals (CNC) are the most crystalline than bacterial cellulose and cellulose nanofibrils. Sulfate groups on CNC surfaces make them suitable for use as dispersants. In the presented work, a novel method of exfoliating MoS₂ in water using CNC and the use of exfoliated MoS₂ as an electrode in battery application is presented. In detail, electrodes are prepared from exfoliated MoS₂ (active material)-Cellulose Nano Crystals- (binder) with carbon nanotubes (electron-conducting support) and used in a Zinc battery half-cell that demonstrated a coulombic efficiency of 90%. Successful exfoliation of layered MoS₂ into nanosheets is performed by sonicating Bulk MoS₂ with sulfated cellulose nanocrystals (CNC) for 4 hours. In addition to Raman and TEM confirmation, the Raman signals for exfoliated MoS₂ show a blue shift of both A_{1g} and E_{2g} bands, suggesting CNC-induced lattice strain on nanosheets. The resulting stable water suspension shows no tendency for precipitation after two months of standing. The zeta potential, ζ , for sodium sulfated CNC (CNC-OSO₃Na)-MoS₂ in water suspension is observed as -45 mV, whereas sulfated CNC (CNC-OSO₃H)-MoS₂ in water suspension had a zeta potential of -35 mV. CNC in the sodium form showed micelle characteristics like sodium dodecyl sulfate (SDS), with a critical aggregation concentration (CAC) of 1.1 wt%. Using CNCs at CAC efficiently exfoliated MoS₂ at a much lower concentration than has been reported for synthetic surfactants like SDS and CTAB (Cetyl trimethyl ammonium bromide). In addition to application in energy storage devices, flexible CNC films were also utilized to fabricate triboelectric nanogenerators (TENG). As CNCs are highly crystalline and to make them flexible, a plasticizer is optimized with a concentration of less than 13.5 wt% to maintain its recyclability. Flexible CNC films as a tribo-positive layer shows an output voltage of 120-200 V.

References

- Sonker et al. Exfoliated MoS₂ Nanosheet/Cellulose Nanocrystal Flexible Composite Films as Electrodes for Zinc Batteries, *ACS Applied Nano Materials* 2023 6 (10), 8270-8278, DOI: 10.1021/acsnm.3c00543
- Sonker et al. Fabrication of flexible substrates from cellulose nanocrystal suspensions for application in Triboelectric nanogenerator (TENG) devices (unpublished work)

11:30 AM *EN03.11.06

Bio-Based Energy Technology and Low-Power Electronics for Internet of Things Magnus Berggren; Linköping University, Sweden

Cellulose and lignin are the two most abundant biopolymers on earth. These materials offer structural integrity and electrochemical functionality for efficient energy technologies, especially for energy scavenging and electrical energy storage. Here, piezo-electric energy generators and printed batteries are reported, targeting sustainable manufacturing, circularity, and energy efficiency. In addition, a printable organic electronic complementary circuit technology has been developed enabling low-power operation at voltages that are compatible with bio-based organic batteries. Together, these devices and circuits provide a platform for future internet of things solutions, specifically targeting sustainable production and materials, and an easy end-of-life handling.

SESSION EN03.12: Bio-Derived Materials for a Sustainable Future

Session Chairs: Jahyun Koo and Lan Yin
Wednesday Afternoon, November 29, 2023
Hynes, Level 2, Room 206

1:30 PM EN03.12.01

Biobased & Biodegradable Materials for Advanced Water Treatment: Removal of Trace Lead by Yeast-Laden Hydrogel Capsules Patrisia M. Stathatou^{1,2}, Devashish Gokhale², Christos E. Athanasiou¹ and Patrick Doyle²; ¹Georgia Institute of Technology, United States; ²Massachusetts Institute of Technology, United States

Traces of heavy metals in water resources, due to mining activities and e-waste discharge, pose a global threat, with lead being one of the most abundant and toxic trace contaminants. As a result of various incidents of lead-contaminated drinking water, relevant water regulations are being revised, while according to the US Environmental Protection Agency, no level of lead in drinking water is considered safe. Conventional treatment processes fail to remove trace lead from drinking water in a resource-efficient manner. We have previously shown that by using the yeast *Saccharomyces cerevisiae* we can effectively remove trace lead from water via a rapid mass transfer process, called biosorption, achieving an uptake of up to twelve mg lead per gram of biomass in solutions with initial lead concentrations below 1 part per million. We have also found that equilibrium is achieved within the first five minutes of contact. The rapid and high lead uptake is advantageous for the large-scale application of this inexpensive and abundant biomaterial for the removal of trace heavy metals from water.

The main limitation for scaling up the developed water treatment approach is the requirement for additional treatment steps to remove the added yeast. In this presentation, we demonstrate the development of a sustainable material by encapsulating yeast cells in hydrogel microparticles to overcome this limitation. Yeast-containing poly(ethylene glycol) diacrylate (PEGDA) biobased and biodegradable hydrogel capsules are synthesized using an off-the-shelf microfluidic device through a scalable approach. Scanning electron microscopy and confocal fluorescence imaging have been used to measure the capsules' porosity and assess the distribution of yeast cells inside the capsules. Through kinetic and equilibrium experiments we characterize the stoichiometry, equilibrium, and selectivity of the hydrogel capsules under different initial lead concentrations (in the range of 30 – 1000 ppb). Residual lead concentrations have been measured using inductively coupled plasma-mass spectrometry. Data shows that hydrogel capsules are highly effective vehicles for holding yeast cells, being sufficiently large to be easily separated from water under the effect of gravity, as well as sufficiently porous to not limit the adsorption capacity of the yeast or the kinetics of lead removal. Furthermore, we perform biomechanical static and dynamic compression tests to assess the mechanical robustness of the capsules and guide the design of a cm scale, packed-bed bioreactor operated as a flow-through filter to serve as a proof-of-concept of our approach. Finally, through a life cycle approach (LCA) we compare our proof-of-concept water treatment approach with physicochemical state-of-the-art counterparts and assess its environmental and economic benefits. Our work overcomes separation and structural stability issues that limit biosorption scalability, opening a new generation of environmentally friendly, highly effective, and sustainable biosorbents targeting emerging contaminants.

1:45 PM EN03.12.02

Scalable Biomass-Derived Hydrogels for Sustainable Carbon Dioxide Capture Youhong (Nancy) Guo and T. Alan Hatton; Massachusetts Institute of Technology, United States

Carbon capture and sequestration is a promising emissions mitigation technology to counteract ongoing climate change. The century-old amine scrubbing process is industrially mature but suffers from low energy efficiency, corrosion of facilities, and inferior stability of aqueous solutions. State-of-the-art solid sorbent-based carbon capture systems present a potentially advantageous alternative. However, practical implementation remains challenging due to limited CO₂ uptake at dilute concentrations and difficulty in regeneration of the sorbents. Here, we develop sustainable carbon-capture hydrogels (SCCH) with excellent CO₂ uptake (400 ppm) at room temperature. The rationally designed biomass gel network consists of glucomannan and cellulose, facilitating hierarchically porous structures for active CO₂ transport and capture. Pre-captured moisture significantly enhances CO₂ binding by forming water molecule-stabilized

zwitterions to improve the amine utilization efficiency. In addition, the SCCH exhibits a notable advantage of low regeneration temperature at 60 °C. With rapid sorption-desorption kinetics, SCCH is capable of operating multiple cycles per day with, e.g., solar-powered regeneration. Prepared via a simple and scalable casting method with environmentally viable raw materials, SCCH highlights the potential for sustainable carbon capture from a wide range of point sources to meet global decarbonization targets.

2:00 PM *EN03.12.03

Novel Sustainable Polymers and Hydrogels Made from Designer Proteins and Plant Proteins[Naba K. Dutta](#), Rajkamal Balu and Namita Choudhury; RMIT University, Australia

Polymer materials have transformed modern life and are utilised in every sector, including the commercial, industrial, medical, and retail ones. However, mostly they are non-biodegradable and derived from non-renewable resources. These durable materials are left in landfill as trash can linger for decades and are a pollutant of increasing concern. For example, from the air we breathe to the food we consume, microplastic particles can be found everywhere in the environment. Green polymers, which are produced using ecologically benign methods and are either biodegradable or meet particular criteria for managed treatment at the end of life, have been driven by this concern [1]. Green polymers can be divided from: (i) biomass, which includes polysaccharides, starches, cellulose, lignin, and proteins; (ii) microorganisms, like polyhydroxyalkanoates (PHA) (iii) monomers derived from renewable resources but polymerised using traditional synthesis, like polylactic acid (PLA), as well as, (iv) monomers produced from fossil fuels, however, are biodegradable, e.g., poly(-caprolactone) (PCL) [2].

In this talk, I will cover our latest work on genetically engineered biomimetic protein-polymers [3,4] and plant-protein-based polymers [5-7] that are derived from renewable resources, biodegradable, multifunctional and adaptable. The unusually responsive resilin-mimetic protein polymer (RMPs), their unique molecular architecture, responsiveness, highly resilient hydrogel formation characteristics, and dynamics of their structural ensembles [8-14] will be discussed. An attempt will also be made to elucidate the molecular origin of their unusual adaptability and functional possibilities. Native resilin is a member of the family of elastic proteins that includes elastin, gluten, gliadin, and spider silks and is purported to be the most resilient elastic material known with resilience >97%. We will also demonstrate that plant-derived biopolymers and proteins and their functionalized product have the potential to offer a new platform for the development of sustainable, eco-friendly and biodegradable super absorbent polymers for many applications including hygiene products. Overall, the research has revealed the potential of biomimicry along with the genetic engineering approach to biomaterials design offer powerful strategies to overcome challenges and provide new opportunities in the design and rapid development of novel functional polymers.

Acknowledgement: Flat protein work presented here was supported by the Bill & Melinda Gates Foundation through the Grand Challenges Explorations (GCE) Round-25 for the Project, INV-031382.

References

1. A. A. Koelmans et al., *Nature Reviews Materials* **2022**, 7, 138–152.
2. L. Averous, *J. Macromol. Sci.- Polym. Rev.*, **2004**, 44, 231.
3. R. Balu, N. K. Dutta, A. K. Dutta, N. Roy Choudhury, *Nature Communication* **2021**, 12, 149.
4. R. Balu, N. Wanasingha, J.P. Mata, A. Rekas, S. Barrett, G. Dumsday, A. W Thornton, A. J. Hill, N. Roy Choudhury, N. K Dutta, *Science Advances* **2022**, 8 (51), eabq2202.
5. P. Dorishetty, R. Balu, A. Gelmi, J.P. Mata, A. Quigley, N.K. Dutta, *Materials Today Advances* **2022**, 14, 100233.
6. P. Dorishetty, R. Balu, A. Gelmi, J.P. Mata, N. K. Dutta, N. Roy Choudhury, *Biomacromolecules* **2021**, 22, 3668.
7. P. Dorishetty, R. Balu, A Sreekumar, L de Campo, J.P. Mata, N.R. Choudhury, N. Dutta, *ACS Sus. Chem. Eng.* **2019**, 7, 9257.
9. N. K. Dutta, M.Y. Truong, N. Choudhury, et al. *Angew. Chem. Int. Ed.* **2011**, 50, 4428.
10. R. Balu, N. Choudhury, N. K. Dutta, et al. *Sci. Reports*, **2015**, 5, srep10896.
11. R. Balu Mata, J. P. Knott, R. Dutta N. K. et al. *J. Phys. Chem. B*, **2016**, 120, 6490.
12. M. Y. Truong, N. Roy Choudhury, N. K. Dutta, et al. *Biomaterials* **2010**, 31, 4434.
13. M. Y. Truong, N. K. Dutta, et al., *Biomaterials* **2011**, 32, 2786.
14. R. Balu, N. K. Dutta, N. R. Choudhury, M. Elvin, R. Lyons, R. Knott, A. Hill, *Acta Biomaterialia* **2014**, 10, 4768.

2:30 PM BREAK

3:30 PM EN03.12.04

Bio-Derived Juglone-Based New Crosslinkers for Material Recycling of Network Polymers[Takeo Suga](#); Waseda University, Japan

Polymers with dynamic covalent bonds have attracted much attention in recent years because of their self-healing, recyclability, and shape-memory properties, which can be achieved by repeated cleavage and regeneration of covalent bonds upon thermal or photo-stimulation. However, many reports have shown that dynamic covalent bond units, including Diels-Alder (DA) adducts, dissociate at around 100°C, and although they show repairability in the room temperature to medium temperature range, their application to practical materials is limited. Here we focus on anthracene-naphthoquinone (juglone) adduct, which shows bond recombination reactions in the high-temperature range compared to well-known furan-maleimide adduct, and synthesized the crosslinked polymers with anthracene-naphthoquinone moiety. Reversible crosslinking was evaluated by the temperature dependence of rheological behavior.

3:45 PM EN03.12.05

Synthesis and Application of Nanoporous Nitrogen-Doped Carbon from Kraft Lignin[Tetyana Budnyak](#), Alina Nikolaichuk, Oleg Tkachenko, Nataliia Fihurka and Maria Strömme; Uppsala University, Sweden

The utilization of renewable resources for the synthesis of advanced materials is of great importance for sustainable development. Lignin is the second most abundant macromolecule in nature and the perfect precursor for the synthesis of various carbon materials due to its high carbon content and aromatic structure. Here, we present a novel approach for the synthesis of nanoporous nitrogen-doped carbon (NNC) from kraft lignin, a widely available waste product from the pulp and paper industry. The synthesis involves a simple process, where kraft lignin is converted into a highly porous carbonaceous material through pyrolysis in a nitrogen atmosphere simultaneously with a nitrogen-doping process using urea as a nitrogen source.

The resulting NNC material exhibits a high surface area (up to 800 m²/g), high nitrogen content and a hierarchical porous structure distributed throughout the material. The NNC material was characterized using various techniques, including XRD, BET, and XPS, to confirm its structural and chemical properties.

NNC was found to have the properties of interest for a number of environmental applications including carbon dioxide capture, adsorption of heavy metals from aqueous solutions and nitrates/nitrites reduction. Overall, the synthesis of NNC from kraft lignin presents a sustainable approach for the development of adsorbents with potential applications in environmental remediation and carbon capture technologies.

Acknowledgment: Tetyana M. Budnyak acknowledges financial support from Formas – a Swedish Research Council for Sustainable Development (project: 2020-02321).

4:00 PM EN03.12.06

Cell-Wall Specific Modification of Xylem Cell Walls with Nanocrystalline Iron Hydroxides for Mechanical Reinforcement[Steven A. Soini](#), Sofia Feliciano, Bobby Duersch and Vivian Merk; Florida Atlantic University, United States

In recent decades, there has been large interest in creating sustainably produced materials to mitigate adverse climate impacts and present alternatives to non-biodegradable plastics. To this end, we used readily available raw materials from the biosphere, such as chitin and lignocellulose, that can be used as starting materials to design composite materials with enhanced physical and chemical properties. Lignocellulose has an inherent 3D hierarchical structure that gives rise to excellent mechanical properties while maintaining a high degree of porosity available for chemical modification. Biocomposite filters composed of nanocrystalline iron hydroxides mineralized within the lignocellulose scaffold are promising low-cost, eco-friendly materials with a variety of possible applications from pollution remediation to building materials. Composites comprised of balsa wood (*Ochroma pyramidale*) and ferrihydrite (Fh) were prepared and characterized with Micro-Computed X-ray Tomography (MicroCT), Scanning Transmission Electron Microscopy with Energy Dispersive X-ray Spectroscopy (STEM-EDS) and synchrotron-based Nano-Computed X-ray Tomography (NanoCT) to visualize the distribution of mineral phase throughout the bulk scaffold and the ultrastructure of the cell wall. MicroCT results were consistent with the distribution of Fh throughout the overall structure, within the water-conducting vessels and rays, which are involved in liquid transport in the radial direction. Fh formed within the multilayered cell wall as opposed to only lining the void cell lumen, as shown by STEM-EDS and NanoCT. The deposition of mineral within the cell wall impacts the mechanical strength of the composite material, as shown by in-situ mechanical testing within the Scanning Electron Microscopy (SEM) and force spectroscopy in the Atomic Force Microscopy (AFM).

4:15 PM EN03.12.07

Designing and Understanding the Limits of Fluoro-Free Super Liquid Repellency[William S. Wong](#); Aalto University, Finland

Super liquid repellent surfaces exhibit extraordinarily high liquid contact angles and low sliding angles, demonstrating immense potential for anti-fouling and self-cleaning. While repellency for water is achievable with hydrocarbon chemistries, repelling low surface tension liquids (down to 30 mN/m) still requires perfluoroalkyls^[1] (a persistent environmental pollutant and bioaccumulation hazard). Here, we investigate the functional limits of stochastic surfaces with fluoro-free moieties. Silicone and hydrocarbon surface chemistries are benchmarked against perfluoroalkyls, assessed using low surface tension liquids (ethanol-water mixtures). We discover that both hydrocarbon- and dimethyl silicone- based chemistries are functional down to 40-41 mN/m and 32-33 mN/m, respectively (*vs.* 27-32 mN/m for perfluoroalkyls). The dimethyl silicone variant^[2] demonstrates a superior performance likely due to its denser dimethyl molecular configuration and unique polar-and-dispersive composition. We show that perfluoroalkyls are not mandatory for many real-world scenarios (aqueous-based). Effective super-repellency of different surface chemistries against different liquids (pure compounds and mixtures) can also be adequately predicted using empirically verified phase diagrams. Our findings^[3] encourage a liquid-centric design, *i.e.* tailoring surface chemistry design alongside target liquid properties. Herein, we provide key guidelines for achieving sustainably designed super liquid repellency.

References

- [1] T. Nishino, M. Meguro, K. Nakamae, M. Matsushita, Y. Ueda, *Langmuir* **1999**, *15*, 4321-4323.
- [2] J. E. Mark, *Polymer data handbook*, Oxford University Press, New York, **1999**.
- [3] W. S. Y. Wong, M. S. Kiseleva, S. Zhou, M. Junaid, L. Pitkänen, R. H. A. Ras, *Adv. Mater.* **2023**, <https://doi.org/10.1002/adma.202300306>.

SESSION EN03.13: Poster Session III: Sustainable Materials II
Session Chairs: Amay Bandodkar and Lan Yin
Wednesday Afternoon, November 29, 2023
Hynes, Level 1, Hall A

8:00 PM EN03.13.01

The Role of Nitrogen-Doping and Surface Topology of Biobased Carbon Electrodes for Iron-Based Redox-Flow Batteries Anna Bachs-Herrera¹, Isaac Vidal-Daza^{2,1} and Francisco Martín-Martínez¹; ¹Swansea University, United Kingdom; ²Universidad de Granada, Spain

To redefine our material sources in a circular economy, it is key the utilization of extensively available biomass wastes, as new carbon mines. A plethora of applications that valorize biomass, and implement biomass-derived materials (*i.e.*, biobased), are being intensively investigated, *e.g.*, biofuels, biodegradable polymers, carbon fibers, battery electrodes.¹ Hydrochar, produced from hydrothermal and pyrolysis processing of biomass is an alternative avenue to produce more sustainable carbon materials for energy storage, while it provides new routes for biomass waste valorization.² Hydrochar's structure is predominantly aromatic, rich in nitrogen atoms, and highly porous, which are valued features for carbon electrodes,³ such as those in redox flow batteries.⁴ However, the fundamental mechanisms underlying the performance of biobased electrodes are still unclear. To achieve better understanding of the structure-property relationship of hydrochar-derived carbon electrodes in iron-based redox flow batteries, we performed density functional calculations (DFT) calculations of iron redox species and hydrochar model systems with different surface features. We explored the effect of quaternary nitrogen functional groups, surface curvature, endo- and exo- absorption sites at the surface, and curvature radius, as well as the effect of iron spin multiplicity. Our results suggest that the interaction between iron and biobased carbon electrodes not only depend on the surface curvature or nitrogen content, but also on the spin multiplicity of the metal ion.

1. A. Bachs-Herrera, D. York, T. Stephens-Jones, I. Mabbett, J. Yeo and F. J. Martín-Martínez, *iScience*, **2023**, *26*, 106549.
2. S. A. Nicolae, H. Au, P. Modugno, H. Luo, A. E. Szegő, M. Qiao, L. Li, W. Yin, H. J. Heeres, N. Berge and M.-M. Titirici, *Green Chem.*, **2020**, *22*, 4747-4800.
3. S. Liu, J. Tian, L. Wang, Y. Zhang, X. Qin, Y. Luo, A. M. Asiri, A. O. Al-Youbi and X. Sun, *Adv. Mater.*, **2012**, *24*, 2037-2041.
4. C. T.-C. Wan, D. López Barreiro, A. Forner-Cuenca, J.-W. W. Barotta, M. J. Hawker, G. Han, H.-C. C. Loh, A. Masic, D. L. Kaplan, Y.-M. M. Chiang, F. R. Brushett, F. J. Martín-Martínez and M. J. Buehler, *ACS Sustain. Chem. Eng.*, **2020**, *8*, 9472-9482.

8:00 PM EN03.13.02

The Crashworthiness of Biodegradable Inserts of Sport Helmet Paweł Kaczynski, Mateusz Skwarski, Piotr Makula, Joanna M. Ludwiczak and Anna Dmitruk; Wrocław University of Science and Technology, Poland

Today, the development of biodegradable polymers has gained significant attention as a promising solution to address the environmental concerns associated with conventional plastics. Biodegradable polymers, also known as biopolymers, are designed to break down naturally over time (maximum of 6 months), reducing their impact on ecosystems and minimizing pollution. The following article explores the possibility of using dedicated biodegradable composites for injection molding of thin-walled structures used in sports helmets. The paper presents several composites based on a PLA matrix with the addition of other biodegradable plastics such as PBS and PBAT. The article describes the author's production method, which is based on injecting thin-walled structures into an innovative form patented by the authors. The crashworthiness of the energy-absorbing structures obtained this way was then tested using a spring drop hammer. The test conditions replicated the collision of an athlete wearing a helmet with a rigid stationary obstacle. During the test, the dynamic crushing force and displacement were recorded using acceleration sensors and by tracking the position of markers mounted prior to the test on the spring drop hammer top. The results are presented as force-displacement crushing curves and images from a high-speed camera. Additionally, the energy absorption of the structures is presented in the form of diagrams. The results were then analyzed, and the two most useful materials were selected in the context of their possible use for the injection molding of thin-walled, energy-absorbing structures used for constructing sports helmets. The article demonstrates that it is possible to address the environmental challenges and produce energy-absorbing structures made of biodegradable materials that can be successfully used to construct sports helmets of all kinds, replacing the previously used expanded polystyrene. These structures have several advantages. First, users can easily replace them after a crash, restoring 100% of the helmet's protective properties. Second, these structures can be disposed of by composting. Third, the structures provide better protective properties because they utilize a previously unused mechanism of plastic folding instead of compression of polystyrene elements.

8:00 PM EN03.13.03

Elucidating The Affect of Drying Mechanism and Drying Parameters on Seaweed-Derived Biopolymer Alia. Dashti; Loliware, United States

Seaweed-derived biopolymers have gained attention in biotechnology due to their biocompatibility, ability to break down naturally, and chemical inertness. These polymers have been traditionally used in the food, pharmaceutical, and cosmetic industries. One attractive application of biodegradable and biobased materials is in the food service industry to replace single use plastics. While it has been demonstrated that water-containing seaweed resins can be processed using conventional plastic converting techniques like extrusion and injection molding, post-processing drying to remove residual water remains a challenge. Here we discuss a general mechanism for the drying process of seaweed-based plastics and provide a computational model to correlate material's bulk morphology and drying regimes on the mechanical properties. Our findings suggest that an optimized drying process can improve seaweed-based materials mechanical properties as well as manufacturing throughput.

8:00 PM EN03.13.04

Synthesis of Novel Graphene-Based Porous Material from Waste Dharmveer Yadav, Jyotiraman De, Sumit Saxena and Shobha Shukla; Indian Institute of Technology Bombay, India

Graphene, a new-generation wonder material, is well-known for its exotic physical, chemical, and mechanical properties. It has gained excessive attention from material scientists and environmental engineers due to its versatile application in different fields of application like water purification, desalination, and treatment of industrial effluent. However, the synthesis of graphene oxide (GO) from graphite is an intensive process requiring harsh chemicals with complex chemical routes for synthesis, poor yield and high-end instrument facilities, which restricts mass production and, thus, large-scale applications. Hence, there is a need for an eco-friendly, low-cost, and simple fabrication process that can be used for large-scale applications. In order to mitigate the drawbacks of currently used synthesis methods, here we report a simple, scalable, cost-effective, and environment-friendly synthesis of oxidized graphene framework (OGF) produced from agro-waste. As compared to 2D graphene sheets, 3D graphene foams have attracted extensive attention due to their high porosity, uniform structure, chemical stability, and flexibility. Porous foam could be obtained for desired densities and shapes such as rods, cylinders, and papers. Therefore, we have developed porous OGF foam material, which is compressible and regains its shape and size after unloading. The developed material has been extensively characterized by Raman, XRD, FTIR, SEM, TEM and XPS to confirm its successful synthesis with desired properties. Other than that, wetting and sorption studies have been performed with different types of organic compounds. This eco-friendly, cost-effective method of development of 3D graphene-based foam can lead to the solution of water purification, treatment of industrial wastewater, and recovery of organic solvents and oils.

8:00 PM EN03.13.05

Chemically Recyclable Butadiene-Derived Poly(oligocyclobutane)s from Acyclic Diene Metathesis Shawn M. Maguire, Cherish Nie, Callie C. Zheng, Richard Register, Paul Chirik, Rodney Priestley and Emily C. Davidson; Princeton University, United States

Commodity polyolefins account for the majority of plastic waste but present thermodynamic challenges for depolymerization and upcycling due to their high thermal and chemical stability. Here, the synthesis and characterization of a chemically recyclable polyolefin is reported that is derived in two steps from butadiene, a feedstock olefin. Acyclic diene metathesis (ADMET) polymerization of (1,*n*'-divinyl)oligocyclobutane (DVOCB), a telechelic oligomer formed by the reversible [2+2] cycloaddition-oligomerization of butadiene, yielded pDVOCB, a new polyolefin architecture. Characterization of pDVOCB by thermogravimetric analysis (TGA), differential scanning calorimetry (DSC), wide-angle X-ray scattering (WAXS), dynamic mechanical analysis (DMA), and tensile testing established high crystallinity, high thermal stability, and comparable thermal properties and mechanical behavior to those of commodity polyolefins. The length of the DVOCB monomer was used to tune the thermomechanical properties of the resulting polymer. Exposure of pDVOCB to excess ethylene under ADMET conditions resulted in >99% depolymerization back to DVOCB with minimal purification required. Selective depolymerization and recovery of DVOCB was also demonstrated from a mixed polymer waste stream, as well as complete depolymerization back to pristine butadiene.

8:00 PM EN03.13.06

Upcycling from Wasted Plastics to Carbon Nanotube Devices Takashi Kuno¹, Hiroaki Komatsu¹, Yusuke Kurihara¹, Kotaro Takanashi^{1,2}, Yosuke Sugita¹ and Takahiro Matsunami¹; ¹Tokyo University of Science, Japan; ²Future Earth Laboratory, Japan

In recent years, marine pollution has been increasingly severe. Eight million tons of plastics are disposed into the ocean every year. It is predicted that the amount of plastics in the ocean will exceed the amount of fish by 2050 on a mass basis. From the viewpoint of upcycling, we are trying to convert waste plastics into "value-added" carbon nanotubes (CNTs). Although there have been reports on the conversion of virgin plastic into multi-walled CNTs (MWNTs) by chemical vapor deposition (CVD), the conversion efficiency η was poor (4% at maximum), and the available plastic species were few. In addition, the correlation between the plastic species and the properties of MWNTs has not been well understood.

In this study, we have newly developed a CVD system that can convert various types of plastics into MWNTs with high efficiency. This method consists of three regions: the pyrolysis region of the plastic, the sublimation region of the metal-organic catalyst, and the growth region of the MWNTs. The features of this method are that η is much higher than those reported previously (maximum $\eta > 50\%$) and that a variety of plastic species can be used. In addition, we have fabricated patterned CNT wirings on plastic films using upcycled MWNTs by laser-induced transfer method [1]. After that, we also demonstrated upcycling the plastics films with CNT wirings into MWNTs again.

In this presentation, I will introduce the detail of the conversion method. Specifically, the relationship between pyrolysis gas species, which were characterized by infrared and mass spectroscopy, and the properties of resultant MWNTs will be presented. Furthermore, I will show some demonstrations of conversion from "real" marine debris (fishing nets, etc.) collected at beaches and inland into MWNTs with a conversion efficiency of more than 30%.

8:00 PM EN03.13.07

Metal Modified Nanocellulose as a Synthetic Biofilm Substitute for Mechanical Removal Testing Darryl W. Taylor and A. Andrew D. Jones, III; Duke University, United States

Introduction: Nanocellulose, a plant cellulose derivative, is a functional and modifiable material its applications go beyond those of raw cellulose. One underexplored application is mimicking bacterial biofilms, which have a wide range of uses in biomaterials, tissue engineering, bioleaching, and many other applications. Bacterial biofilms pose threats to human health, food systems, and water systems. Biofilms consist of communities of bacteria that adhere to surfaces and resist mechanical, chemical, and biological removal. Understanding the behavior of biofilms is essential for maintaining the well-being of critical societal systems. While decellularized eukaryotic systems serve as a valuable platform for understanding mechanical and chemical tissue behavior, biofilms cannot be decellularized. Unlike eukaryotic systems, where the extracellular matrix is more resilient than individual cells, biofilms exhibit the opposite behavior, with individual cells being more robust than the extracellular matrix they produce. The absence of a living, adaptable, material platform increases the challenge in establishing biofilm transport, chemical, and mechanical behavior.

Objective: A nanocellulose synthetic analogue offers the advantage of being a non-living material platform, making production, testing, and replication easier. In-depth understanding of nanocellulose through rheology and research aimed at exploring novel applications, such as biofilm mimicry, would expand its potential applications and contribute to the development of more robust and more environmentally benign responses to biofilm challenges.

Methods: This research generated nanocellulose hydrogels using an ionic liquid solution of 7:12:81 sodium hydroxide:urea:water, and used nanocellulose hydrogels in several experiments including rheology testing where the storage and loss modulus was measured. Hydrogels were modified with metal ions (Cu²⁺, Zn²⁺, Sr²⁺, Co²⁺, Ca²⁺, Ni²⁺) and rheology testing was conducted. Two metal ion modified hydrogels (Ni²⁺, Ca²⁺) with rheological properties closer to biofilms were further tested for dental removal.

Results: The metal chelated hydrogels showed similar mechanical behavior to biofilms much more than currently used synthetic biofilm analogues like alginate. The storage and loss modulus that demonstrated biofilm-like behavior were hydrogels chelated with calcium chloride, nickel sulfate, and strontium chloride each exhibiting a storage modulus between 1200-1300, 920-850 and 1050-1020 Pa respectively. In dental removal experiments tested with calcium chloride and nickel sulfate after 60 seconds of irrigation at 30 and 130 psi, it was shown that nanocellulose was 99% removed from ceramic coupons. This research shows that for force removal nanocellulose hydrogels chelated with these ions serve as a good model for bacterial biofilms.

8:00 PM EN03.13.08

Dynamic Strength Properties of Biopolymers based on PLA, PBS, PBAT, and TPS for Energy Absorbing Structures Mateusz Skwarski, Pawel Kaczynski, Piotr Makula, Anna Dmitruk and Joanna M. Ludwiczak; Wroclaw University of Science and Technology, Poland

The growing awareness of society and the high cost of fossil fuels result in a continuous increase in the popularity of alternative means of transport (e.g. bicycles). There is a great, continuously increasing demand for personal protective equipment, such as sports helmets. The energy-absorbing layer of all currently produced helmets is made of foamed plastics: polystyrene (EPS), polypropylene (EPP), or polyurethane (EPU). According to the manufacturers' recommendations, these materials should be immediately replaced after each collision. **This procedure is often skipped because helmet damage is not visible to the naked eye, and the users are aware of the material value of their helmets. The solution may be changing only the energy-absorbing layer, as the helmet's exterior shell is primarily intact.**

The authors want to present environmentally friendly protective honeycomb inserts made of biodegradable polymers invented during project implementation. Thanks to their structure, they can constitute a reusable alternative to polystyrene (the insert in the shell can be replaced each time after an accident).

The authors of the manuscript **created unique blends of biodegradable plastics based on PLA** with the addition of bioplastics, such as polybutylene succinate - PBS, polybutylene adipate terephthalate - PBAT, and thermoplastic starch - TPS. They combine high strength and plasticity, and thanks to their biodegradability, these mixtures meet the criteria of sustainable development. **All developed materials were extensively tested using a unique method developed by the authors, which relies on dynamic tensile tests. This brought the results closer to conditions occurring during actual incidents (e.g. collisions).**

Properly designed geometry of the energy-absorbing structure in combination with mechanical properties (tensile strength, yield strength, elongation, Young's modulus) tailored to specific geometry and applications **resulted in the invention of the thin-walled biodegradable structure that engages the most effective mechanism, which is dynamic, plastic folding.** **There are no standards describing strength tests conducted in dynamic conditions. The conducted tests constitute the "know-how" of the authors.** The testing device was based on the design of a rotary hammer and was equipped with a flywheel with a diameter of 0.6 m and a weight of about 230 kg. The flywheel's rotational speed was preset to reach the strain rate from 250 to 1000 s⁻¹, which is close to the actual condition during the crash. A specially designed measurement system allowed to reach the sampling rate equal to 1 MHz. In order to accurately measure the deformation, the process was additionally filmed with a high-speed camera capable of registering 1,000,000 fps. The criterion of suitability and safety of a given material for a designed geometry of insert were strength properties determined in dynamic tensile tests (Re > 15 MPa, Rm > 10 MPa, A > 10%).

Tests confirmed that complex thin-walled honeycombs can be successfully molded and used as energy-absorbing structures. On this basis, it can be concluded that the **developed biodegradable blends provide the desired compromise between mechanical properties - high tensile strength and satisfactory plastic properties engaging plastic folding mechanism during the deformation.** These biomaterials can also be used in other energy-absorbing applications. Although the developed blends are biodegradable, they are sufficiently resistant to variable weather conditions (e.g. sunlight, rain exposure) to fulfill their purpose during the exploitation time. The developed materials and testing methodology will affect personal protection equipment and shows potential for applications in the automotive, food, and packaging industries.

Funding: This work was supported by the project BOKASK "Development of innovative, replaceable, energy-absorbing structures based on biodegradable plastics for protective helmets" (0223/L-11/2019, LIDER, NCBR).

8:00 PM EN03.13.09

UV Resistance and Biodegradation of PLA-Based Polymer Mixtures doped with PBS, PBAT, TPS for use as Energy-Absorbing Structures Joanna M. Ludwiczak, Anna Dmitruk,

The problem of waste storage and recycling of polymer materials prompts the search for new, biodegradable materials with good functional properties. The ability to degrade biodegradable plastics through the action of naturally occurring microorganisms is a huge advantage over conventional polymers. There is a great demand for the design and development of biodegradable plastics that not only biodegrade but also meet the expected material properties. Many biodegradable polymers are known, but unfortunately the barrier to their use is still insufficient resistance to weather conditions, their accelerated degradation and unstable properties, such as strength and thermal properties.

Currently used materials for head protection in sports helmets are usually foamed polystyrene, which is difficult to dispose of. The foamed polystyrene structure also does not provide sufficient individual protection, compared to the honeycomb structures developed by the authors. Biodegradable polymers were selected for the production of thin-walled inserts, and the preparation of mixtures enabled the selection of the best strength properties for impact protection, which is critical for use in sports helmets.

Project work focused on biodegradable polylactide (PLA) and its modification by adding other biodegradable polymers such as poly(butyleneadipate-co-terephthalate) (PBAT), thermoplastic starch (TPS) and polybutylene succinate (PBS). Mixtures of different compositions were prepared by melt mixing. The materials were subjected to an accelerated aging process in an aging chamber for a period of 3 weeks. UV stability is a key factor when assessing the long-term properties of these types of materials, due to the risk of premature degradation during use. Samples were taken periodically and tested for hardness, weight and color. After irradiation, the samples were also subjected to strength and microscopic tests. The effect of accelerated aging of PLA has been demonstrated, especially reduction in breaking strength, loss of gloss and color change. The addition of all plasticizers - other biodegradable polymers - improved the strength properties of PLA. Differences in the effect of accelerated aging were demonstrated between individual compositions and the addition of polymer to polylactide. All manufactured materials were characterized by constant weight and hardness after the aging process. Ultimately, microscopic tests showed that the prepared mixtures were not degraded, which confirmed that the selected polymer mixtures are suitable for use in variable weather conditions (sunshine, rain), but after the end of their life cycle they can be subjected to biodegradation, which was also confirmed in tests performed in soil, according to the ISO 20200: 2004 standard. The developed materials were used to produce thin-walled energy-absorbing structures for sports helmets, which are an alternative to the well-known, non-biodegradable foam inserts that protect the user's head.

8:00 PM EN03.13.10

The Efficient Removal of Bacteria using Reusable Magnetic Sorbents[AliciaChandler](#), [JinggeChen](#) and [VickiL. Colvin](#); Brown University, United States

Bacterial water contamination has detrimental health impacts and poses a significant problem worldwide; removal of bacteria from drinking water, however, requires microfiltration which can be costly and ineffective. Here we describe a more sustainable solution which relies on submicron and porous magnets that have both a large susceptibility and a large magnetic moment. These materials are coated with silica to prevent oxidation and improve reusability. Then, a silane-modified branched polyethyleneimine is covalently linked to particles to facilitate their electrostatic attraction to bacteria. The effectiveness of this approach is evaluated using a model bacteria, *E. coli*, which is also a prevalent biological contaminant. In magnetic separation experiments, we vary the reaction time, the dosage of magnetic sorbent, the bacterial concentration, and the solution pH to evaluate the optimal conditions and assess the practical adsorption capacity. Reuse of these materials after desorption of the bacteria is possible after which time the waste can be incinerated. This work not only has applications in more sustainable approaches to disinfection but also benefits approaches to human disease diagnosis and treatment.

SESSION EN03.14: Biodegradable Materials for Biomedical Applications

Session Chairs: Amay Bandodkar and Jahyun Koo

Thursday Morning, November 30, 2023

Hynes, Level 2, Room 206

8:15 AM *EN03.14.01

Regenerative Materials - A Dual Perspective[HelenLu](#); Columbia University, United States

In contrast to the relatively recent emphasis on environmental impact assessment in material synthesis and manufacturing, life-cycle considerations of biomaterials used in tissue engineering and regenerative medicine have long focused on the biodegradability of the material in the physiological environment or its clearance from the body post-implantation and degradation. In particular, the alpha-hydroxy polyester family of polymers, specifically polylactic acid (PLA) and its co-polymer with polyglycolic acid (PGA), have dominated the field with their well-established record of biocompatibility. What makes these materials especially attractive is the fact that they are designed to stimulate regenerative cell responses and, moreover, as they degrade, in vivo space is made available for new tissue growth. Notably, these polymers break down via hydrolysis and the degradation products, lactic acid and/or glycolic acid, can be readily processed by the body through the Krebs cycle. While these materials are regenerative in function and in its life cycle, inherent challenges in the fabrication of these material into biomimetic nanofiber scaffolds, which traditionally utilizes solvents that are environmentally hazardous and pose a significant barrier to industrial scale-up and clinical translation. We will discuss green manufacturing methods and how to leverage biofabrication for the production of nanofibrous scaffolds and regenerative materials for both medical and non-medical applications.

8:45 AM EN03.14.02

Bio-Degradation Studies of Fluorescent Defects in Carbon Nanotube Hosts[Te-ILiu](#)¹, [CarlosQuiroz](#)^{2,1}, [Yen-HsuanLin](#)^{3,1}, [Ching-WeiChan](#)^{3,1}, [Ai PhuongNguyen](#)^{4,1} and [Ching-WeiLin](#)¹; ¹Institute of Atomic and Molecular Sciences, Academia Sinica, Taiwan; ²Taipei Medical University, Taiwan; ³National Taiwan Normal University, Taiwan; ⁴National Tsing Hua University, Taiwan

Carbon nanotubes (CNTs) have been enormously used in various fields because of their unique mechanical, optical and electronic properties. The rapid developments of the CNT applications have raised concerns of their impacts on the environment and human health, urging the investigations of CNT degradation. Among different types of CNTs, single-wall carbon nanotubes (SWCNTs) emit at the short-wave infrared (SWIR) that pertains low tissue scattering and low autofluorescence, making them ideal candidates for in vivo imaging applications such as disease targeting and real-time cell trackings. The clinical use of fluorescent SWCNTs carries the 'post-diagnosis' issues including long-term retention and chronic toxicity, to the patients. For example, long-term accumulation of SWCNTs in certain tissues, such as the liver and lungs, may lead to the development of inflammation-related diseases, including fibrosis. We believe that the prompt solution to these issues would be the development of bio-degradable fluorescent SWCNTs. Here, we report faster degradations of fluorescent defect-containing SWCNTs in biological systems. Fluorescent defects in SWCNTs are known to increase the particle emission brightness and move their excitation and emission peaks to longer wavelengths. We performed comprehensive studies of how various defect conditions, ROS species and cell types affect the degradation efficiency. Our results indicate that the hollow-core, single-atomic layer nature of the SWCNTs combined with degradable fluorescent defects could be better SWIR fluorophores for clinical uses compared to solid-core inorganic fluorophores and organic nanodots.

9:00 AM *EN03.14.03

Biofabrication Approaches to Engineer Biomimetic Bone Tissue Interfaces[ShannonMcLoughlin](#), [RobertChoe](#) and [JohnFisher](#); University of Maryland, United States

Abstract

Bone tissue defects resulting from congenital abnormalities, disease, tumor resection, and traumatic injury can severely affect patient health.[1] In many cases, defects are not limited to bone tissue alone, and damage can also involve surrounding tissues, including periosteum, cartilage, ligament, or tendon. Traditional clinical techniques for bone defect repair often include the implantation of autografts, but donor site morbidity, lack of availability, and considerable medical costs limit their applicability. Tissue engineering (TE) strategies aim to produce functional bone tissue replacements by combining scaffolds, cells, and bioactive signals. Extrusion bioprinting allows for superior control over design among these three critical components and is particularly useful in the case of replicating heterogeneous tissue interfaces.[2] Specifically, bioprinting techniques allow multi-material patterning to manipulate cell-cell or material population distances and patterns, influencing cellular crosstalk and scaffold mechanics.[3] Here, we present biofabrication strategies for the generation of such biomimetic tissue interfaces, including (1) a computational model studying the impact of printed material patterning ratios on resulting scaffold mechanics, (2) a printing approach for interfacial tissues, and (3) a 4D printing strategy to generate microscale tissues among macroscale counterparts. Using these techniques in combination with extrusion printing allows for enhanced interfacial tissue regenerative potential by improving biological and mechanical properties.

3D stationary solid mechanics models were developed using COMSOL. Osteal and chondral bioinks are co-printed at the interface layer to form the mechanically interlocking interface design, recapitulating the calcified cartilage region of the osteochondral unit using polycaprolactone (PCL) and gelatin methacrylate (GelMA) for bone and cartilage inks, respectively. The COMSOL model simulated the effect of lateral shear force during articulation. This was then validated in vitro using mechanical shear analysis of printed samples.[4] For complex extrusion printing, GelMA Type B was synthesized and dissolved at 5% w/v in PBS with a photoinitiator. Both casted and printed samples were imaged post-fabrication, then treated with varying concentrations and molecular weights of poly-L-lysine to induce shrinking behavior via complex coacervation-like mechanisms.[5] After treatment, hydrogels were imaged again to observe resolution enhancement.

Computational results broadly demonstrate the ability to predict printed scaffold mechanical properties, specifically that interlocking interfaces have the potential to redirect shear-induced stresses from a single tissue to the entire interface. Extrusion printing allowed complex, multiphase tissues to be constructed and demonstrated that charge-induced shrinking could fabricate microscale periosteal tissue and a macroscale bone composite. Bioprinting allows for the generation of heterogeneous bone tissue interfaces with relative ease. Using pre- and post-printing biofabrication approaches, tissue interface mechanics, design, and cellular crosstalk can be readily controlled.

References

- [1] Cooper, G.M. et al. *Plast. Reconstr. Surg.* 125(6): 1685-1692, 2010.
- [2] Murphy, S.V., Atala, A. *Nat. Biotechnol.* 32(8):773-85, 2014.
- [3] Piard, C. et al. *Biomaterials.* 222:119423, 2019.
- [4] Choe, R. et al. *Biofabrication.* 14(2):025015, 2022.
- [5] Gong, J. et al. *Nat. Commun.* 11:1267, 2020.

Acknowledgements

We acknowledge our funding support from the NIH Center for Engineering Complex Tissues (P41 EB023833) and the OsteoScience Foundation Peter Geistlich Grant.

9:30 AMBREAK

SESSION EN03.15: Sustainable Materials I
Session Chairs: Shweta Agarwala and Amay Bhandodkar
Thursday Morning, November 30, 2023
Hynes, Level 2, Room 206

10:00 AM EN03.15.01

Investigating the Use of Seaweed-Derived Materials to Replace Single-Use Plastics Mehran J. Umerani; Loliware, United States

Seaweed has a rich history of diverse applications across the food industry, agriculture, medicine, cosmetics, biofuel, and single-use plastic replacements. This presentation aims to demonstrate the utility of injection molding to produce high-performing parts from seaweed-derived resins. Our resins have been optimized to possess excellent flow and mechanical properties comparable to those of standard plastics, making them a practical substitute for conventional petroleum-derived materials. Additionally, our ongoing research explores the application of machine learning algorithms and traditional formulation methods to facilitate high-throughput systematic design of new seaweed-derived biomaterials with improved mechanical and chemical properties. Finally, the sustainability aspect of seaweed-derived alternatives to single-use plastics will be discussed, emphasizing the potential of our approach to offer environmentally-friendly options in lieu of traditional plastic materials.

10:15 AM EN03.15.02

Predicting Hydrolase Mechanism for Sustainable Polyester Degradation Ivan F. Jayapurna, Ariel Wang, Sanjana Gurram and Ting Xu; University of California, Berkeley, United States

Enzyme catalyzed degradation is a promising approach to mitigating plastic pollution. However, finding suitable enzyme catalysts remains a challenge. Aside from sufficient substrate compatibility, one key consideration is enzyme mechanism, which the environmental impact depends on. An enzyme performing random scission leads to incomplete degradation from crystallinity induced recalcitrance as well as faster microplastic generation, whereas chain end scission results in degradation to naturally decomposable small molecules. Furthermore, when enzymes are nanoscopically embedded within the plastic matrix, a processive mechanism generates a chain slide motion that can lead to the degradation of amorphous and crystalline regions alike. As such, finding enzymes with chain-end, processive mechanism for a given polymer system can be the key to unlocking complete polymer degradation. Here, we investigated the catalytic activity and mechanism of 10 hydrolases on polycaprolactone (PCL). Surface and enzyme-embedded PCL degradation studies and degradation product analysis yielded 4 enzymes with no activity towards PCL, 3 with random PCL scission, and 3 with chain-end PCL scission. Through binding pocket analysis, each hydrolase was labeled with key geometry, chemistry, and flexibility features, hypothesized to influence both degradation capability and mechanism. Molecular modeling was done in parallel to predict the potential for processive chain slide of polyesters in enzyme binding pockets. We found binding pocket polarity, binding pocket secondary structure composition, and evidence of chain-slide potential from molecular modeling to be highly correlated to experimentally determined degradation mechanism. A computational pipeline was developed to automate binding pocket analysis and molecular docking, and a database of hydrolases with reported PCL compatibility was screened *in silico* for degradation mechanism. The model and key features highlighted in this work are generalizable to other commercial polyesters. In addition, this model can also guide future works with applications in rapid screening, enzyme engineering, and general applicability to binding pocket analysis beyond plastic degradation.

10:30 AM EN03.15.03

Thermomechanical Properties of Hybrid Imine and Silica Based Vitrimers Jun-Yeu Chang and John Kieffer; University of Michigan-Ann Arbor, United States

The limited recyclability of thermosets poses a significant challenge for end-of-life disposal of these materials. Covalent adaptable network (CAN) materials, such as vitrimers possess reversible crosslinker chemistries. The mechanical properties of vitrimers at room temperature are comparable to those of thermosets. Vitrimers become malleable upon thermal or photonic stimulation, so they can be reshaped and recycled. However, vitrimers can exhibit undesirable creep or fatigue, especially at elevated temperatures. Therefore, we are pursuing a hybrid chemistry approach, where a portion of the organic dynamic crosslinkers is replaced with inorganic static crosslinkers to provide the desired thermomechanical stability. Catalyst-free polyimine vitrimer is synthesized from glutaraldehyde (GA) and bis[2-(3-aminopropoxy)ethyl] Ether (Di-Amine). The dynamic crosslinker is tris(2-aminoethyl)amine (Tris-Amine), of which various fractions are replaced with (3-Aminopropyl)triethoxysilane (APTES). Depending on its concentration, APTES can undergo polycondensation to form different-sized silica network fragments, but is always able to compatibly bridge between polyimine matrix segments by forming imine bonds, thus substituting permanent Si-O-Si bonds for dynamic bonds. Here we report on how the relative proportions of static and dynamic crosslinkers affect the hybrid vitrimers' viscoelastic properties, mechanical stability, shifts in the glass transition and topology freezing temperatures. We specifically focus on evaluating the tradeoff between weldability or self-healing capabilities and creep resistance as a function of the crosslinker type concentrations.

10:45 AM EN03.15.04

Hydrothermal Synthesis of Carbon Dots from Irish Seaweed and Seaweed Derivatives Karlijn Hertsig, Yungxiang Liu, Sam O'Neill, Annie Regan and Peter Dunne; Trinity College Dublin, Ireland

Due to the increase in global renewable energy generation and the need for reduction in greenhouse gas emissions we find ourselves in the energy transition of the century wherein the demand for green, sustainable energy materials is rising. Carbon dots are considered a new and green nanomaterial, applicable for energy generation technologies, including photovoltaics.^{1,2} In this research the hydrothermal synthesis of carbon dots from seaweed and seaweed derivatives is explored.³ The synthesis yielded photoluminescent carbon dots, however without control over photoluminescence behaviour. Increasing complexity of the precursor from simple sugars to complex sugars to seaweed biomass led to consistent photoluminescence behaviour, however less distinct. Typically, absorbance of 270 – 300 nm with emission 400 – 450 nm for excitation 350 nm was measured by UV-vis and photoluminescence spectroscopy. The carbon dots are unstable in solution resulting in aggregation and shifting/reduction of the absorbance over time; however, the photoluminescence behaviour is not impacted. Column chromatography with acetonitrile and water improved the photoluminescence behaviour by narrowing the emission peak. Lyophilisation made structural characterisation possible, which confirmed the carbon dots are amorphous. While practicing green chemistry, it is concluded the hydrothermal method is a viable method to synthesise quantum and carbon dots as functional nanomaterials to contribute to the development of renewable energy technologies contributing to the energy transition.

References:

1. J. Liu, R. Li and B. Yang, *ACS Cent. Sci.*, 2020, **2020**, 2179-2195.
2. J. B. Essner and G. A. Baker, *Cite this: Environ. Sci.*, 2017, **4**, 1216-1216.
3. V. Sharma, P. Tiwari and S. M. Mobin, *J. Mater. Chem. B*, 2017, **5**, 8904-8904.

11:00 AM EN03.15.05

Femtosecond-Laser Direct Writing based Laser-Induced-Graphene (LIG) on Wooden Materials for Green Electronics Applications Han KuNam¹, DongwookYang¹, TongmeiJing^{1,2}, Truong-SonD. Le¹, YounggeunLee¹, Young-RyeulKim¹ and Young-JinKim¹; ¹Korea Advanced Institute of Science and Technology, Korea (the Republic of); ²China University of Petroleum, China

The importance of environmental sustainability has been on the rise, as issues like climate change and pollution continue to affect the planet. One area that has been heavily impacted by this trend is electronics manufacturing. In order to reduce the environmental impact of electronics production, researchers and engineers have been working to develop new materials and processes that are eco-friendly. One promising area of research is the development of green electronics, which use materials and manufacturing processes that are sustainable and environmentally friendly. To achieve green electronics, it is necessary to use precursors that are organic, inexpensive, and readily available. Additionally, the synthesis route must be economical and fast, and the resulting electronic materials must be suitable for low-cost manufacturing processes. Furthermore, the devices produced using these materials must be biocompatible and biodegradable. These criteria can be difficult to meet, but one class of materials that shows promise is wood-based materials. Wood is a renewable resource that is abundant, recyclable, and biodegradable. However, it is not a conductor, which limits its use in electronics. To overcome this limitation, researchers have been working on various methods for adding conductivity to wood such as carbonization or conducting materials coating. One of the most promising approaches is Laser-Induced-Graphene (LIG) formation technology, which was first introduced by the James Tour group in 2017. This technology uses Laser-Direct-Writing (LDW) to create graphene patterns on a variety of lignocellulosic materials, including paper, cork, potato skins, coconut shells, and leaves. Our group has confirmed that 3D porous LIG can be easily and quickly produced on wooden materials without special treatment in the air by ultrashort pulse laser irradiation. In this work, we report on high-quality Laser-Induced-Graphene formation on wooden materials in ambient air for green electronics applications using a femtosecond laser with a 1040 nm wavelength, 250-fs pulse width, and 200 kHz repetition rate. A Galvano scanner with a maximum 2,000 mm/s scanning speed is used for laser patterning. Various combinations of beam scanning speeds, laser power, and beam-line spacings are delivered onto natural and recycled wooden materials to optimize LIG quality. The lowest sheet resistance of LIG electrode achieved is 2.8 $\Omega/\text{sq.}$, and its properties are analyzed using scanning electron microscopy (SEM), thermogravimetric analysis (TGA), X-ray diffraction (XRD), X-ray photoelectron spectroscopy (XPS), and Raman spectroscopy. The LIG electrodes are applied for green electronics in smart homes or smart furniture, such as heaters, temperature sensors, and touch sensors. Furthermore, we demonstrate that interconnecting LIG electrodes can be made by irradiating the laser after physically combining two different wood blocks without any special chemical treatment. Additionally, the LIG touch sensor can easily control the heater and computer by synchronization. These technologies can be easily adapted to smart green homes or smart green furniture applications.

11:15 AM EN03.15.06

Multidimensional Control and Tunability of Cholesterol Structures in Hydroxypropyl Cellulose Gels with Polyethylene Glycols LuyaoHuang and HongliZhu; Northeastern University, United States

Structural color is an intriguing phenomenon generated by changes in assembly structure and the interaction of light. Biological structural colors assembled from natural polymers are excellent resource for biomimetic design and green construction. Hydroxypropyl cellulose (HPC) is a renewable, non-toxic, biodegradable cellulose derivative whose solution generates a stable cholesterol liquid crystal structure with vivid structural color. In our study, we first explored the potential of three polyethylene glycols (PEGs), each with distinct end groups, for conducting multidimensional control of cholesterol structures derived from HPC. Our observations reveal that when tetraethylene glycol dimethyl ether (TEG-DE), di(ethylene glycol) ethyl ether acrylate (DEG-EEA), and diethylene glycol-diacrylate (DEG-DA) are incorporated, they cross-link with HPC, eliciting varying degrees of red-shift in the resultant HPC gels. Among them, the HPC gel incorporating DEG-DA, which contains two ester bonds, exhibits a dark red hue, whereas the HPC gel with DEG-EEA that carries one ester bond takes on a red color. Conversely, the HPC gel that includes TEG-DE, possessing a single ether bond, displays a yellow-green color. This reveals an intriguing pattern of color variance dependent on the molecular bonding within the gel system. This implies that color recognition information could be shifted swiftly and continuously in a gel system with variable polarity. As a result, we propose an approach for the homogenous alignment of cholesterol structures based on electrostatic repulsion and hydrogen bonding forces. Especially, the integration of diverse terminal group polymers increases the flexibility of the composite system. Consequently, HPC/PEG gels have a wide range of applications.

11:30 AM *EN03.15.07

Wood Nanotechnologies LiangbingHu; University of Maryland, United States

I will give an overview of our published work on nanotechnologies using wood cellulose nanomaterials, with a focus on mechanical properties of densely packed nanocellulose for lightweight structural materials (replacement of steel, Nature 2018), nano-ionic thermoelectrics (Nature Materials, 2019) and batteries (Nature 2021), radiation cooling (Science, 2019), and 3D moldable wood (Science, 2021).

SESSION EN03.16: Sustainable Materials II
Session Chairs: Amay Bandodkar and Jahyun Koo
Thursday Afternoon, November 30, 2023
Hynes, Level 2, Room 206

1:30 PM EN03.16.01

Use of Variable Frequency Microwave Heating to Chemically Recycle Polymer Composites YoungsuShin¹, PrekshaVichare¹, AnthonyEngler¹, JaredSchwartz¹, BradH. Jones² and PaulKohl¹; ¹Georgia Institute of Technology, United States; ²Sandia National Laboratories, United States

Microwave heating is advantageous for the chemical recycling of plastics due to its rapid, selective, and volumetric heating capabilities that can help reduce process times and improve energy efficiency. Unfortunately, the use of fixed frequency microwave heating leads to strict operational limitations that promote two popular approaches for processing post-consumer plastics: 1- Solid state pyrolysis with strong microwave absorbers to recover oils, gases, and carbon, and 2- solvolysis of the polymer to recover monomeric derivatives. While solvolysis recovers high-value monomers, the use of solvents reduces its energy efficiency compared to pyrolysis. Our group investigated the use of variable frequency microwave (VFM) heating to achieve rapid thermal depolymerization of polymer composites in their solid states back to their corresponding monomers, including polyphthalaldehyde, polyhydroxyalkanoates, poly(propylene carbonate), and nylon-6. The degradation of the polymers with the additives has been achieved and confirmed by nuclear magnetic resonance and gel permeation chromatography. A wide range of additives was also investigated to select the best performers for microwave heating at low energy. Carbon nanotubes, carbon nanofibers, carbon black, graphene, and reduced graphene oxide were down-selected for further investigation by incorporating the materials into different polymer matrices. Overall, the use of VFM energy aids in the volumetric heating and selective depolymerization of the polymer composites at fast heating rates. The results of these VFM studies can be broadly applied to the chemical recycling and monomer recovery of polymers.

1:45 PM *EN03.16.02

Blue Plastic: The Use of Seaweed-Based Materials to Replace Single Use Plastics VictoriaPiunova; Loliware, United States

The use of seaweed has a long history, particularly in food applications. However, its versatility has extended its applications in industries such as fertilizers, medicine, animal feed, cosmetics, biofuel, and even single use plastic replacement. This presentation will discuss synthetic and formulation strategies which enables transformation of traditional hydrophilic natural materials into robust yet readily biodegradable resins that can be processed using conventional plastic processing techniques like extrusion, injection molding and thermoforming. Commercial viability of seaweed-derived single use plastic analogs and sustainability score are also reviewed.

2:15 PM EN03.16.03

Upcycling Virgin and Waste Polyolefins to Reprocessable Dynamic Covalent Networks LoganFenimore¹, BoranChen¹, StephanieBarbon², HayleyBrown², EvelynAuyeung², ColinLi Pi Shan² and JohnTorkelson¹; ¹Northwestern University, United States; ²The Dow Chemical Company, United States

Plastics enable modern life through their advantageous properties and broad applicability. Regardless of their type or use, plastics are challenging to recycle efficiently. Current methods for recycling spent thermoplastics such as re-extrusion with additives result in property degradation over time and the relegation of these downcycled polymers to low-value applications. Plastics may be permanently cross-linked into thermosets, yet permanent cross-links prevent these plastics from being processed and molded into new shapes at high temperature. An emerging avenue to mitigate these sustainability problems involves enriching waste plastics with dynamic covalent bonds as chemical cross-links. By introducing dynamic covalent cross-links, previously thermoplastic materials exhibit robust mechanical properties characteristic of conventional thermosets yet maintain their reprocessability at high temperatures. Not only can the incorporation of dynamic bonds be achieved during polymer synthesis to produce reprocessable step-growth networks like polyurethanes and addition-type networks like polymethacrylates, but also it can be achieved via post-polymerization modification to upcycle spent polyolefins for higher value applications. Using reactive batch processing, we upcycled various virgin and waste polyolefins

(e.g., low-density and high-density polyethylene, random and multiblock ethylene/1-octene copolymers, etc.) into covalent adaptable networks (CANs) via melt-state, free-radical grafting of a cross-linker capable of dynamic dialkylamino disulfide (BiTEMPS) chemistry onto polymer chains. Unlike ethylene-based thermoset polymers, our ethylene-based CANs are reprocessable and recover their thermomechanical properties after reprocessing via successive compression molding cycles. We have further shown that, in the absence of crystallinity, high-temperature creep and stress relaxation behaviors of the CANs are dominated by the exclusively dissociative reversible dynamic chemistry of the cross-linker. This observation also demonstrates the utility of this dissociative dynamic chemistry of high activation energy at suppressing creep in networks exhibiting different viscoelastic behavior.

2:30 PMBREAK

SESSION EN03.17: Sustainable and Recyclable Electronics
Session Chairs: Shweta Agarwala and Amay Bandodkar
Thursday Afternoon, November 30, 2023
Hynes, Level 2, Room 206

3:00 PM *EN03.17.05

Compostable and Biodegradable Organic Electronics[Clara Santato](#); Ecole Polytechnique de Montreal, Canada

Natural organic materials (NOM) are relevant for biodegradable electronic devices and their powering elements (e.g. batteries). Biodegradation at the device's end-of-life is expected to cause a decrease in the portion of e-waste which is poorly managed/landfilled (and as such causing damage to health and the environment).

In this contribution we will discuss *the molecular and supramolecular properties of NOMs (e.g. melanins and tannins), their complex chemical composition (due to biosynthesis) and their charge transfer and charge carrier transport properties, which underpin their use in electronic devices and their powering elements. We will report on compostability studies of transistors and supercapacitors based on NOMs, performed following the experimental conditions indicated by international industrial standards. Finally, we will try to propose guidelines (i) to design NOMs for biodegradability in terms of molecular disassembly and exfoliation of supramolecular NOM aggregates and (ii) to eco-design biodegradable electronic devices based on NOMs.*

3:30 PM *EN03.17.01

Transient Devices Developed using Lithography-Free Patterning of Nanoscale Electronic Layers[Abhishek S. Dahiya](#) and [Ravinder Dahiya](#); Northeastern University, United States

Lithography-free patterning of nanoscale (nanowire (NW)) electronic layers at pre-selected locations offers opportunities to realise transient or degradable electronics in a resource efficient manner. The major advantages being: (i) reduced dependency on inherently wasteful conventional fabrication processes (e.g., photolithography and etching), (ii) negligible chemical wastage, (iii) compatibility with large area electronics, (iv) possibility of having electronic layers based on richer materials system, and (v) low-cost. Herein, we present lithography-free NW patterning techniques namely, '*in-tandem contact-transfer printing*' and '*selective-removal*' and the transient devices developed using them. In the in-tandem approach, firstly, the contact printing is used to print laterally aligned NWs on an intermediate substrate to obtain uniform electronic layers. Then, modified transfer printing is employed to selectively remove and print the electronic layers on the final device substrate. In the other approach (selective-removal), contact printing is performed to obtain highly aligned NW structures directly on to device substrate and then NWs are selectively removed from a uniformly contact printed electronic layer using an elastomeric stamp. The removal efficiency is improved by evaporating a thin layer of water onto its patterned face, which greatly enhances the stamp-NW adhesion via the capillary action. The above approaches are used to develop proof-of-concept transient devices such as NW-based transistors and photodetectors on rigid (Si/SiO₂), flexible (polyimide), and biodegradable (magnesium (Mg) foils) substrates. The developed photodetectors on Mg foil can physically disintegrate and dissolve in 240 days in deionized (DI) water (pH ≈ 6) at room temperature. The developed lithography-free NW patterning techniques has potential for eco-friendly manufacturing of electronics with significantly lower the electronic-waste.

4:00 PM EN03.17.02

Printability and Electrical Response of Biopigments on Paper[Camille Bour-Cardinal](#), [Anthony Camus](#) and [Clara Santato](#); Polytechnique Montréal, Canada

Natural organic materials are relevant for the eco-design of biodegradable electronic devices and their powering elements (batteries). Printing natural organic materials on paper offers the possibility to compost electronic devices. Printed paper electronics enable to alleviate the accumulation of Electrical and Electronic Equipment Waste (E-waste) which has harmful effects on human health and the environment¹.

Sepia melanin is one of the natural forms of Eumelanin (the black-brown member of the melanin family of biopigments). It is extracted from *Sepia officinalis* natural ink. Melanins are ubiquitous in nature; they are key to diverse bio-functions in fauna and flora. Sepia melanin is mainly constituted of 5,6-dihydroxyindole and 5,6-dihydroxyindole-2-carboxylic acid monomers that, after steps of hierarchical development, brings about a material featuring nanometric granular structure. Recently, printed films including Sepia showed predominant electronic transport²⁻³.

We focus on the printability on paper and electrical response of the *Sepia officinalis* natural ink. *Kromekote* paper substrates are pre-patterned by flexographic printing with a silver-based aqueous ink, to generate electrode pairs (interelectrode distance about 100 μm). The interface between the ink and the paper is studied considering: (i) paper rugosity, porosity, and air permeability, (ii) ink rheology and wettability, (iii) tensile, rigidity, tear and burst tests, on paper before and after printing. The current-voltage (I-V) and potentiostatic (I-t) characteristics were carried out for applied electrical biases ranging between 0.1 V and 10 V and different voltage sweeping rates (1 - 500 mV/s), in controlled atmosphere (dry, wet, and ambient conditions). Preliminary results show that the conductivity and stability of the devices are remarkable. Work is in progress to discover the chemical composition of the biosynthesized Sepia. Our efforts pave the way towards greener and more sustainable electronics.

References:

[1] V. Forti, C. P. Baldé, R. Kuehr, G. Bel, *The Global E-waste Monitor 2020. Quantities, flows, and the circular economy potential*, United Nation University, 2020

[2] A. Camus, M. Reali, M. Rozel, M. Zhuldybina, F. Soavi, C. Santato, *High conductivity Sepia melanin ink films for environmentally benign printed electronics*, Proc Natl Acad Sci U S A. 2022 Aug 9;119(32):e2200058119. doi: 10.1073/pnas.2200058119. Epub 2022 Aug 1. PMID: 35914170; PMCID: PMC9371694.

[3] M. Reali and C. Santato, in *Handbook of Nanoengineering, Quantum Science and Nanotechnology*, ed. S. E. Lyshevski, CRC Press, 1st edn., 2019, pp. 101–113

4:15 PM *EN03.17.03

Self-Healing, Stretchable and Recyclable Electronics[Fabio Ciccoira](#); Ecole Polytechnique de Montreal, Canada

The ability of certain materials to regenerate after damage has attracted a great deal of attention since the ancient times. For instance, self-healing concretes, able to resist earthquakes, aging, weather, and seawater have been known since the times of ancient Rome and are still the object of research.

While the field of mechanically healable materials is relatively established, self-healing conductors are still rare, and are nowadays attracting enormous interest for applications in electronic skin for health monitoring, wearable and stretchable sensors, actuators, transistors, energy harvesting, and storage devices, such as batteries and supercapacitors. Self-healing can significantly enhance the lifetime of conducting materials, leading to the improved environmental sustainability and reduced costs.

Conducting polymers exhibit attractive properties, such as mixed ionic-electronic conductivity, leading to low interfacial impedance, tunability by chemical synthesis, ease of process via solution process and printing, and biomechanical compatibility with living tissues, which makes them ideal materials for bioelectronics and stretchable electronics. However, they show typically poor mechanical properties and are therefore not suitable as self-healing materials. Self-healing conductors can be achieved upon mixing with other polymers, such as poly(vinyl alcohol) (PVA), poly(ethylene glycol) (PEG) and polyurethane (PU), which provide the mechanical characteristics leading to self-healing.

Self-healable and recyclable conducting materials are central in the field of electronics due to their potential to address two major challenges: sustainability and durability. Electronic waste is a growing concern worldwide, as the rapid pace of technological innovation has led to a high turnover rate of electronic devices, resulting in the accumulation of a significant amount of electronic waste. Self-healable and recyclable conducting composites have the potential to reduce electronic waste by enabling the repair and reuse of electronic components, which can extend the lifespan of electronic devices. Furthermore, electronic devices are often subject to mechanical stress, which can cause damage to their components, including conducting materials.

My talk will deal with self-healing materials obtained blending PEDOT:PSS with other materials, such as polyethylene glycol (PEG), tannic acid and polyurethane. Various self-healing modes will be presented and correlated with the electrical and mechanical properties of the materials. The use of the self-healing gels and films as epidermal electrodes will be also presented.¹⁻⁸ We will finally discuss recyclable conducting composites based on PEDOT:PSS-PU blends.

REFERENCES

Y. Li, X. Zhou, B. Sarkar, F. Ciccoira et al., *Adv. Mater.* 2108932, 2022.

Y. Li, X. Li, S. Zhang, F. Cicoira et al., *Adv. Funct. Mater.* 30, 2002853, 2020.
Y. Li, X. Li, R. N. Unnava Venkata, S. Zhang, F. Cicoira, *Flexible and Printed Electronics* 4, 044004, 2019.
N. Rossetti, F. Cicoira et al., *ACS Appl. Bio Mater.* 2, 5154-5163, 2019.
C. Bodart, N. Rossetti, S. Schougaard, F. Cicoira et al. *ACS Appl. Mater. Interfaces*, 11, 17226-17233, 2019.
S. Zhang, Y. Li, F. Cicoira et al. *Adv. Electron. Mater.* 1900191, 2019.
S. Zhang, F. Cicoira, *Adv. Mater.* 29, 1703098, 2017.
X. Zhou, G. A. Lodygensky, F. Cicoira et al., *Acta Biomaterialia* 139, 296-306, 2022.

4:45 PM EN03.17.04

Manufacture of Biodegradable Electronic Sensors Systems using Additive Manufacturing Jeff Kettle, [Jonathon Harwell](#), Andrew Bainbridge and Rudra Mukherjee; University of Glasgow, United Kingdom

The world's ever-increasing demand for high performance electronics will inevitably result in a growing problem of waste as products reach the end of their lifetimes. The "tsunami of electronic waste" (e-Waste), which reached more than 53.6 million tonnes in 2019, requires a step-change in the design and fabrication of electronics for disposal, reuse or recycling. The issue is exacerbated as during the manufacture of electronics, a significant amount of chemical waste is generated as by-products, and the combined impact of by- and end-products is leading to long term environmental and social damage that will outlast many generations. As electronics underpins a lot of future ICT including smart packaging, internet of things (IoT), displays (inc. VR/XR), smart packaging, the e-Waste issue needs to be resolved by realising electronic systems that inherently have end-of-life (cradle to cradle) solutions built in and thus do not require the same complexity of waste management. To this end, this challenge requires a new approach in the manufacture of electronic devices that emphasises low material use and makes end-of-life recycling and disposal as simple and environmentally friendly as possible, while also keeping up with the difficult performance metrics required for operating modern devices.

The use of biodegradable materials is on the rise as practical difficulties related to e-waste requires greater attention. A large proportion of a Printed Circuit Board Assembly (PCBA), goes directly to landfill or incineration. It is feasible to recycle PCBAs as shown in several papers and there are many businesses recycling of e-waste. However, it is not a straightforward process. Consequently, the use of electronic materials that are more easily repurposed or recycled are being considered for future electronic systems. Most academic work on such electronics so far has focused on metal oxide or organic semiconductors, however, the modest performance offered by such materials, would not satisfy the demands of current consumer electronics.

In this talk, we will report on the development of new manufacturing platforms that offer a viable alternative to conventional silicon-based devices. Firstly, we have demonstrated fully biodegradable thin-film transistors (TFTs) arrays of up to 200 TFTs based on zinc oxide (ZnO) active layer using molybdenum (Mo) source, drain, and gate electrodes. The developed TFTs show a low positive threshold Voltage, a high average field-effect mobility in the saturation region and show stable device performance under stability tests. These have been used to make logic circuits (inverter and both NAND and NOR gate circuits) and simple memory devices such as SRAM cells. However, as mentioned, the performance is limited by the semiconductor, so a new additive manufacturing technique based on inkjet printing and hybrid ultrathin silicon and metal oxide devices is demonstrated and we show that the biodegradable devices and circuits can match conventional circuit boards on key metrics such as switching speed, level of integration and power consumption. We demonstrate the effectiveness of this process by producing a flexible and biodegradable Integrated circuits and use this to power a sensor array for agricultural applications for measuring pH and temperature.

Finally, we perform a detailed life cycle assessment of devices made using this method and compare their environmental impact to conventional ICs and PCBAs. We find that the reductions in material use and minimised end-of-life footprint can more than offset the costs associated with the increased complexity of manufacturing required by our process. We hope these results will show the potential of how new approaches in device production can greatly enhance the sustainability of electronic products.

SESSION EN03/EN06/EN08: Joint Virtual Session
Session Chairs: Aron Huckaba and Cecilia Mattevi
Tuesday Morning, December 5, 2023
EN03-virtual

8:00 AM *EN03/EN06/EN08.01

Natural Dielectrics for Bio-Organic Electronics [Mihai Irimia-Vladu](#); Johannes Kepler Universität Linz, Austria

Organic electronics has an immense potential for the development of products that are both sustainable and environmentally friendly. In this presentation, a large list of natural origin dielectric materials is introduced and demonstrated in the fabrication of organic field effect transistors, e.g. *resins, gums, waxes, alkaloids, nucleobases, natural oils and fats, lignins and celluloses, natural scents, natural clays, etc.* Apart from their outstanding dielectric and film forming properties, most of the above-mentioned natural dielectrics are inherently, biocompatible (even edible) and have well known medical properties. Thus, this class of dielectrics may find suitable applications in the branches of science where dielectric materials are part of bio-integrated electronics.

8:30 AM EN03/EN06/EN08.02

Study on Photodegradation and Encapsulation of Organic Thermochromic Polymers [Sushant Madhukar Nagare](#); University of South Florida, United States

With the increase in temperature urban areas face issues like Urban heat islands. The reduction of green vegetation across the urban areas has led to tremendous increase in temperature. Many studies suggest major cities are currently experiencing this issue to a greater extent. Many researchers are working on building paints and dyes to reduce the heat intake done by the building. Organic thermochromic polymers are one such alternative for building dye and paint. The main issue with using the organic thermochromic polymer is that they easily degrade under sunlight which makes them less useful as building color. To overcome this issue many organic thermochromic materials are encapsulated with inorganic materials such as metal oxide which are used to block sunlight and reduce the effect of degradation. With upcoming research in the area, it came to the observation that even though metal oxide is used to reduce the block of the UV wavelength, another spectrum of light rays still affects the organic material and photodegrades them. The 1st part of the paper deals with the microencapsulation method with different surfactant concentrations, different metal oxides, and multi-system encapsulation. The 2nd part deals with testing of the desired material to determine the effect of photodegradation. Different techniques such as SEM, EDS, FTIR, UV Vis, and CIE lab are used to determine.

8:35 AM EN03/EN06/EN08.03

Investigating the Potential of Starch Bioplastic as a Precursor for Laser-Induced Graphene Synthesis: A Sustainable Approach [Anna Chiara Bressi](#)^{1,1}, [Alexander Dallinger](#)², [Sreenadh T. Sankaran](#)^{1,1}, [Hilda Gomez Bernal](#)^{1,1}, [Attilio Marino](#)³, [Hana Hampel](#)², [Gianni Ciofani](#)³ and [Francesco Greco](#)^{1,2,1}; ¹Sant'Anna School of Advanced Studies, Italy; ²Graz University of Technology, Austria; ³Istituto Italiano di Tecnologia, Italy

Laser-induced graphene (LIG) has emerged as a groundbreaking technology for the conversion of carbon-rich precursors into electrically conductive materials, which exploits commercially available IR laser engravers to induce localized pyrolysis on a wide range of materials. While synthetic precursors initially caught the interest of the scientific community, the need for more sustainable options has shifted the focus to their bioderived counterparts. Among these alternatives, starch bioplastic is of particular interest, since it represents half of the commercially available bioplastics, owing to its straightforward production process and satisfying mechanical properties. In light of these considerations, our study aims to explore the potential of starch bioplastic as a promising precursor for LIG.

A case study on a self-crafted starch-based bioplastic was investigated. The bare biopolymer consists of starch powder, acetic acid, deionized water and glycerol. Initial attempts at converting it into LIG were unsuccessful, resulting in mere ablation upon laser scribing. Instead, the addition of up to 5 wt.% of iron nitrate $\text{Fe}(\text{NO}_3)_3 \cdot 9\text{H}_2\text{O}$ allowed to induce the carbonization of the precursor. As shown by thermogravimetric analysis, the iron nitrate indeed improved the thermal stability at elevated temperatures ($> 600^\circ\text{C}$), a crucial requirement for LIG synthesis. Raman spectroscopy confirmed that the laser-induced carbon material owns the characteristic structural features of LIG (as evidenced by the presence of the typical D, G, 2D bands and the corresponding bands' intensity ratios $I_D/I_G \approx 1$ and $I_{2D}/I_G \approx 0.55$). Moreover, the quality of LIG improved with increasing nitrate concentration, ultimately achieving comparable properties to other bioderived and synthetic precursors for LIG. The addition of iron nitrate also had a significant effect on Young's modulus of the bioplastic, modifying it from ≈ 20 MPa to ≈ 1 MPa. The degradability of the precursor was tested in the soil to assess its suitability for transient electronics applications and almost complete degradation was reported after twelve days. The addition of iron nitrate did not show a clear impact on degradability; however, there is evidence that the presence of salt contributes to increased hygroscopicity, which is typically a significant parameter in promoting degradability. These findings demonstrate the validity of our approach and open the path to further analyses and characterization in real-life applications, paving the way for sustainable and efficient methods for patterning conductive tracks.

8:40 AM EN03/EN06/EN08.04

Sustainable Composites from Almond and Hazelnut Shells for Green Laser-Induced Graphene [JuliaSteksova](#)^{1,1}, Anna ChiaraBressi^{1,1} and FrancescoGreco^{1,2,1}; ¹Scuola Superiore Sant'Anna, Italy; ²Graz University of Technology, Austria

Recently, the scientific community has been focusing on processing and further use of biomass in various fields. In particular, the use of biowaste for green electronics applications has an impressive number of advantages, such as low cost, low density, non-toxicity, biocompatibility, and biodegradability. Within the framework of this study, almond shell powder (ASP) and hazelnut shell powder (HSP) were used as the main component for creating biowaste-based composites. The high lignin content of the shells increases the thermal stability of the composites, making them an ideal precursor for Laser-Induced Graphene (LIG).

LIG is a three-dimensional porous and conductive carbon structure obtained via localized pyrolysis by irradiation with a CO₂ IR laser. LIG synthesis and patterning is a cost-effective one-step process that allows to avoid the use of chemicals and the need for long-term use of high temperatures.

Depending on the precursor composition, the quality and properties of LIG can vary. Among biomasses, chitosan is of great interest for the development of sustainable polymers, mainly due to its low cost and complete biodegradability, thus it was adopted as a matrix for ASP and HSP composites. These materials were prepared by mixing shell powders, glycerol and chitosan dissolved in acetic acid, with specific ratios. Optimization of the shell concentration has been carried out to obtain the best trade-off between good mechanical (i.e., flexibility and stiffness) and electrical properties.

We obtained flexible and strong composites with a high content of ASP and HSP (Young's modulus = 25.4 MPa), which served as good precursors for the creation of LIG with a low sheet resistance ($\approx 10\text{--}100\ \Omega/\text{sq}$, depending on the specific composition and laser settings used). An investigation of the obtained materials' structure and composition has been carried out by means of SEM and Raman spectroscopy, which showed the typical graphene features and thus confirmed the successful conversion of the composite biowaste precursors into conductive LIG. These results are a step towards green LIG for electronics applications starting from ASP and HSP, two low-value waste products which are produced in huge quantities in the agri-food industry and open a path for future studies on the topic.

8:45 AM EN03/EN06/EN08.05

Filler Surface Induced Heterogeneous Nucleation of Polymer Crystals [DominicWadkin-Snaith](#), Paula. Mulheran and KarenJohnston; The University of Strathclyde, United Kingdom

Switching from non-degradable to compostable plastics can help to reduce global plastic pollution. However, to use compostable plastics in food packaging films, properties including mechanical strength and gas barrier must be optimised. These properties depend on the crystallinity and microstructure of the plastic film, which can be modified by adding filler particles, which act as nucleants for polymer crystallisation [1]. In order to select appropriate fillers, it is necessary to understand the polymer-filler interface.

We use a modified Kremer-Grest polymer model [2] to study crystal nucleation of 20-bead chains. Filler surfaces are modelled using a Lennard-Jones 9-3 potential. The system is cooled from the melt using an NPT ensemble, and the crystal fraction is estimated from straightening of chain segments. Polymer nucleation was observed to occur at the surfaces. Interestingly, this polymer model does not crystallise in simulations without the surfaces. The dependence of crystallisation on the surface-polymer interaction strength, the polymer chain stiffness, and cooling rate will be presented and rationalised in terms of free energy changes. The addition of plasticiser and its effect on nucleation and growth will also be explored. This work provides insight into how filler surfaces can be used to control polymer crystal nucleation and growth, leading to the design of compostable plastics with desired properties.

This work was funded by the Innovate UK Smart Sustainable Plastic Packaging grant (NE/V010603/1). Results were obtained using the ARCHIE-WeSt High Performance Computer (www.archie-west.ac.uk).

[1] Majerczak, Wadkin-Snaith, *et al.* Polym Int. (2022); <https://doi.org/10.1002/pi.6402>

[2] G. Grest, K. Kremer, Phys. Rev. A 1986, 33, 3628–3631.

[3] D. Wadkin-Snaith et al. in preparation

9:00 AM EN03/EN06/EN08.06

Substituting the Epoxy Curing Agent with a Greener Solution-Towards Sustainability [NachiketS. Makh](#)¹, AjitD. Kelkar² and LifengZhang¹; ¹Joint School of Nanoscience and Nanoengineering, United States; ²North Carolina A&T State University, United States

In past two decades, the field of polymer composite materials has gained significant advancements transforming various industries and applications. These polymer composites are comprised of polymer matrix and reinforcing material. The matrix is responsible for providing resistance to impact, wear, and corrosion. The reinforcements like fibers, particles or fillers are usually used for enhancing the material properties. The polymer matrix is made up of two fundamental components, the epoxy resin and the hardener (curing agent). The conventional resins and hardeners are produced by chemical and petroleum industries. These industries make use of non-renewable energy resources like fossil fuels for manufacturing the resins and curing agents.

The ever-rising environmental issues have raised sustainability concerns over using fossil-fuels. In addition, most of the conventional curing agents used in epoxy resins are highly noxious in nature. Studies have shown that these curing agents are capable of causing skin allergies and asthma. Recently, the composite market has seen the origination of green epoxy resin that are capable of reducing these toxic effects but have few shortcomings including its cost and the mechanical performance of cured epoxy resin. On the other hand, there is dearth in investigating the evolution of green or sustainable curing agents known as bio-binders. This paper presents the prediction of mechanical properties by replacement of conventional curing agent with amine derivative synthesized from bio-degradable resource in a thermoset epoxy resin system. The properties are predicted by molecular dynamics simulations using Materials Studio Software. The research showed promising outcomes without the loss of mechanical properties in comparison to the conventional epoxy resin and hardener.

9:15 AM EN03/EN06/EN08.07

Extraction and Characterization of Nanocellulose from Sources of Residual Biomass [RocíoHernández Leal](#)¹, Silvia BeatrizBrachetti Sibaja¹, Aidé MinervaTorres Huerta², Miguel AntonioDominguez Crespo² and Mario FidelGarcía Sánchez³; ¹Tecnológico Nacional de México, Mexico; ²Instituto Politécnico Nacional, Mexico; ³UPIITA-Instituto Politécnico Nacional, Mexico

The nanocellulose obtained from biomass of agroindustrial wastes: sugarcane bagasse (SCB), banana pseudostem (BPS) and aloe vera bagasse (AVB), allows to reduce the large amount of waste and the environmental impact generated during the industrialization processes of these raw materials, their lignocellulosic characteristics make these wastes attractive for the extraction of nanocellulose with novel chemical characteristics on a nanometric scale that allows its properties to be improved and used in specific fields such as biomedicine. The extraction and characterization of nanocellulose with acid hydrolysis at 45, 55 and 65 % v/v H₂SO₄, at different time spans (30 and 60 minutes) and different temperatures (25, 40, 45 and 50 °C). The raw materials and the obtained cellulose and nanocellulose were characterized by: Fourier transform infrared spectroscopy (FTIR), to identify the characteristic functional groups; X-ray diffraction (XRD), to study the crystalline structure; dynamic light scattering (DLS), to determine hydrodynamic radius of the nanocellulose particles; and, finally, scanning electron microscopy (SEM), to analyze the morphological features of the cellulose and nanocellulose. The FTIR spectra revealed the elimination of absorption bands characteristic of lignin and hemicellulose. From XRD results, the presence of the different polymorphs of cellulose I alpha, I beta and II was identified. From dynamic light scattering, the hydrodynamic radius of the cellulose obtained from each agroindustrial wastes biomass was determined, with values less than 110 nm. After the obtained results in this study, it can conclude that nanocellulose from biomass of agroindustrial wastes: sugarcane bagasse (SCB), banana pseudostem (BPS) and aloe vera bagasse (AVB), can be regarded as a greener and sustainable industrial waste for the preparation of cellulose nanofibers.

9:30 AM EN03/EN06/EN08.08

Morphology Control and Performance Enhancement of MOF-Derived 3D Amorphous Carbon Nanowires for High-Performance Lithium-Ion Batteries [LinruiL. Duan](#), HongtaoSun and HaoqingYang; The Pennsylvania State University, United States

The utilization of MOF-derived amorphous carbon-based materials in lithium-ion batteries (LIBs) has shown great promise due to their remarkable gravimetric capacity and cycle stability. However, achieving precise control over morphology during the transformation process from MOF to carbon derivatives remains a significant challenge in obtaining electrode materials with superior rate performance and capacity retention under long cycles and high current densities.

In this study, we present a novel approach to derive the Al source for Al-MOF from an eco-friendly and cost-effective by-product AlCl₃ solution obtained through the Al-Si dealloying process. We introduce, for the first time, a 3D amorphous carbon nanowires (3D ACNWs) structure with interconnected networks derived from sub-micron brick-like crystal Al-MOF using a facile and template-free method. Compared to the crystal Al-MOF, the 3D ACNWs exhibit effective suppression of the porous structure's instability during multiple insertion and extraction cycles of Li⁺ ions, along with improved electrical conductivity following the phase transformation from MOF to carbon-based materials. Moreover, the 3D ACNWs, with their interconnected network structure, provide abundant active sites for lithium storage and enhanced pathways for electron and Li⁺ ion transfer, unlike most reported 0D morphology MOF-derived carbon derivatives.

Benefiting from these unique features, the 3D ACNWs anode demonstrates a high reversible capacity of 400 mAh/g at 1.0 A/g after 1000 cycles, with an ultra-high-capacity retention rate of 101.8%. Furthermore, it exhibits excellent rate performance under high current densities. The evolution mechanism reveals that the 3D interconnected amorphous carbon nanowire networks, with their well-developed porosity, facilitate rapid storage and transportation of electrons and Li⁺ ions through specialized channels. This work represents a significant advancement in tailoring the morphology of MOF-derived carbon materials, unlocking their full potential as electrode materials for practical energy storage devices.

SYMPOSIUM EN04

Decoding Halide Perovskites—Advanced Characterization Towards Optimization and Discovery
November 27 - November 30, 2023

Symposium Organizers

Mahshid Ahmadi, University of Tennessee, Knoxville
Juan-Pablo Correa-Baena, Georgia Institute of Technology
Yana Vainzof, Technical University Dresden
Yuanyuan Zhou, The Hong Kong University of Science and Technology

Symposium Support

Bronze

ACS Energy Letters | ACS Publications

APL Energy | AIP Publishing

Enli Technology Co., LTD

* Invited Paper

+ JMR Distinguished Invited Speaker

SESSION EN04.01: Perovskite Solar Cell Efficiency

Session Chairs: Kunal Datta and Monica Lira-Cantu

Monday Morning, November 27, 2023

Hynes, Level 3, Room 300

10:30 AM *EN04.01.01

The Role of Materials and Interfaces in the Stability of Perovskite Solar Cells [Nam-Gyu Park](#); Sungkyunkwan University, Korea (the Republic of)

Since the seminal work on a 9.7% efficient solid-state perovskite solar cell in 2012, its power conversion efficiency (PCE) reached over 25% within a decade. Although PSCs demonstrated a high PCE comparable to silicon solar cells, stability is still the remaining issue. In order to improve substantially the stability of PSCs, perovskite materials and interfaces should be carefully manipulated. In this talk, the importance of crystal facets and interfaces is emphasized in improving stability. We found that moisture stability depends on crystal facets. Among the three facets of (100), (110) and (111) in FAPbI₃ film, the (100) facet was found to be unstable but the (111) facet was quite stable under moisture. Experimental combined with theoretical studies revealed that a crystal facet with moisture instability provided a strong water adhesion via the hydroxylation of Pb atoms, leading to phase transformation. Perovskite films with abundant moisture-tolerant (111) facets were successfully prepared via additive engineering, which showed exceptional stability against moisture without additional surface passivation. A buried interface with homojunction was found to play a critical role in the stability of PSCs. A band alignment via interface engineering led to leveling off the work function at the homojunction, which improved stability significantly.

11:00 AM EN04.01.02

Relaxation of Externally Strained Halide Perovskite Thin Layers with Neutral Ligands [Sang-Geun Ji](#)¹ and Hanul Min²; ¹Ulsan National Institute of Science and Technology, Korea (the Democratic People's Republic of); ²Korea University, Korea (the Democratic People's Republic of)

In solution-processed halide perovskite thin films, an external strain can be generated owing to the anisotropy of solvent volatilization through the thin film surface and the mismatch of thermal expansion with the substrate. Furthermore, the addition of methylammonium chloride to a formamidinium lead triiodide (FAPbI₃) precursor solution to increase the crystallinity and form α -FAPbI₃ at low temperatures also induces the preferred orientation (PO) of the perovskite layer. However, excessive PO can cause anisotropic strain in the thin film, increasing defects, widening the band gap, and reducing long-term stability. As a way to alleviate this, a perovskite thin film was deposited by adding trioctylphosphine, a neutral ligand, to the FAPbI₃ precursor solution. As a result, perovskite solar cells (PSCs) based on these perovskite thin films exhibit an efficiency close to 25% with high stability, showing the highest value among PSCs using TiO₂ as an electron transport layer.

11:15 AM EN04.01.03

Controlled Growth of Perovskite Layers with Volatile Alkylammonium Chlorides [Jaewang Park](#), Jongbeom Kim and Sang Il Seok; Ulsan National Institute of Science and Technology, Korea (the Republic of)

Controlling the crystallinity and surface morphology of the perovskite layers by methods such as solvent engineering and methylammonium chloride addition is an effective strategy for achieving high-efficiency perovskite solar cells (PSCs). In particular, it is essential to deposit an α -formamidinium lead iodide (FAPbI₃) perovskite thin films with fewer defects due to their excellent crystallinity and large grain size. Herein, we report the controlled crystallisation of perovskite thin films with the combination of alkylammonium chlorides (RACl) added to FAPbI₃. The δ - to α -phase transition of FAPbI₃ and the crystallisation process and surface morphology of the perovskite thin films coated with RACl under various conditions were investigated

through in situ grazing incident wide-angle X-ray diffraction and scanning electron microscopy. RACl added to the precursor solution was believed to be easily volatilised during coating and annealing owing to dissociation into RA^0 and HCl with deprotonation of RA^+ induced by $RA \dots H^+ - Cl^-$ binding to PbI_2 in $FAPbI_3$. Thus, the type and amount of RACl determined the δ - to α -phase transition rate, crystallinity, preferred orientation, and surface morphology of the final α - $FAPbI_3$. The resulting perovskite thin layers facilitated the fabrication of PSCs with a power conversion efficiency of 26.08% (certified 25.73%) under standard illumination.

11:30 AM *EN04.01.04

Efficient Perovskite Solar Cells via Enhanced Charge TransportJingbi You; Chinese Academy of Sciences, China

Perovskite solar cells (PSCs) have witnessed great achievement in past 14 years, the power conversion efficiency is approaching its limitation. In this talk, I will talk our group progresses in efficient PSCs via enhanced charge transport. 1) By designing the interface between perovskite and hole transport layer, we have improved the hole transport efficiency and achieved over than 26% PSCs. 2) By modulating the transparent electrode/perovskite interface, the hole recombination in the device has been suppressed, and over than 25.5% inverted PSCs has been demonstrated.

SESSION EN04.02: Perovskite Solar Cell Stability
Session Chairs: Antonio Abate and Ana Flavia Nogueira
Monday Afternoon, November 27, 2023
Hynes, Level 3, Room 300

1:30 PM *EN04.02.01

A Discussion on Long Term Reliability IssuesJingGuo; First Solar, United States

Through material and device failure analysis, investigate key failure mechanisms and evaluate potential remedies

2:00 PM EN04.02.02

Regulating Interfacial Strain Improves the Stability and Efficiency of Perovskite Solar CellsDong-Am Park, Chunyang Zhang and Nam-Gyu Park; Sungkyunkwan University, Korea (the Republic of)

Although perovskite solar cells (PSCs) demonstrated power conversion efficiency (PCE) as high as 26%, stability caused by the hetero-interfaces has been still issued. Since the thermal expansion coefficient of perovskite is about 30 times higher than the SnO_2 -coated substrate, this difference can cause in-plane tensile strain at the interface of the perovskite and the SnO_2 layer during the annealing process. It should be therefore treated because the in-plane tensile strain is blamed for causing the instability of PSCs. We report here an effective methodology to regulate the strain via interfacial engineering using a functional molecule. The interfacial engineering changes the strain of the perovskite layer near the SnO_2 layer, which is confirmed by grazing-incidence X-ray diffraction. The strain-released perovskite film shows faster electron extraction from the perovskite to the SnO_2 as confirmed by the time-resolved photoluminescence. In addition, carrier lifetime is increased by a factor of two upon relieving the interfacial strain. Space charge limited current measurement quantifies trap density, where the strain-released perovskite (target) shows lower trap density than the control perovskite. As a result, PCE is increased from 22.47% to 24.33% mainly due to the improvements of open-circuit voltage from 1.14 to 1.17 V and fill factor from 80.3% to 83.8%. Moreover, 90% of initial PCE is observed after 950 hours for the target device, which is higher than that (70%) of the control one.

2:15 PM BREAK

2:45 PM *EN04.02.03

Indoor, Outdoor and In-Situ Characterization Strategies for Stable Perovskite Solar CellsMonica Lira-Cantu; Nanostructured Materials for Photovoltaic Energy, Spain

Halide perovskite solar cells (PSCs) have already achieved a certified power conversion efficiency (PCE) above 25 %, making them one of the most promising emerging photovoltaic technologies. One of the main bottlenecks towards their commercialization is their long-term stability, which should exceed the 20-year mark. Many are the strategies applied to extend device lifetime, among them are the use of additives, the optimization of the fabrication process of perovskite thin films or the replacement of unstable organic transport layers such as Spiro-OMeTAD. Although most of these approaches can effectively improve device efficiency, they frequently fail at providing stable PSCs as defined as those able to display less than 10 % degradation after 1000 h of continuous illumination under 1 sun. In this work we present our most recent work regarding the analysis of PSC stability. We carried out the fabrication of PSCs applying different strategies, such as additive engineering, interface modification or both and analyse our solar cell following ISOS protocols (Isos-D, ISOS-L and ISOS-O), as well as in-situ characterization. We demonstrate that adding organic additives and 2D interfacial modifiers to the PSC allows for the passivation of shallow or deep defects, having a tremendous impact on the device stability. Our studies are made under indoor and outdoor conditions as well as initial in-situ experiments. We expect that our work will have important implications for the current understanding and advancement of operational PSCs.

3:15 PM EN04.02.04

Photovoltaic Potential of Tin-Based Perovskites Revealed Through the Layer-By-Layer Investigation of Optoelectronic and Charge Transport PropertiesArtem Musiienko¹, Mahmoud Hussein¹, Marin Rusu¹, Davide Regalado^{2,3}, Guixiang Li⁴, Shengnan Zuo¹, Chiara Frasca¹, Hannes Hempel¹, Jean Paul^{2,3} and Antonio Abate¹; ¹Helmholtz Zentrum Berlin für Materialien und Energie, Germany; ²IPVF, France; ³GeePs, France; ⁴École Polytechnique Fédérale de Lausanne, Switzerland

Lead-based perovskite solar cells (LPSC) have garnered significant attention due to their exceptional optoelectronic properties and the potential to revolutionize the field of photovoltaics [1]. However, the widespread adoption of lead-based perovskites is hindered by their inherent toxicity [2], necessitating the urgent exploration of alternative materials. In recent years, tin-based perovskite solar cells (TPSC) have emerged as promising candidates for eco-friendly and efficient solar cell technologies [3].

Despite the rapid progress in the field of perovskite solar cells, a substantial knowledge gap remains regarding the charge extraction and recombination mechanisms in tin-based perovskites. Understanding and optimizing charge extraction processes are crucial for achieving high device efficiency and stability. In this contribution, we aim to shed light on the fundamental charge transfer mechanisms, energetic alignment, and recombination in tin-based perovskite solar cells and lead-based perovskite solar cell counterpart as a baseline.

To identify charge loss, we comprehensively investigated the entire charge transport pathway, starting from bulk diffusion to selective contacts, non-radiative and radiative recombination, and charge extraction. Initially, Hall effect and time-resolved photoluminescence measurements were conducted to determine the carrier lifetime, diffusion length, and doping levels. Furthermore, we examined the charge extraction capabilities of the most widely used electron transport layer (ETL) and hole transport layer (HTL) materials using time-resolved surface photovoltage measurements. Our findings revealed that PEDOT and C60 demonstrated the most efficient charge extraction for FASnI₃ thin film. Additionally, photoelectron yield and Kelvin probe techniques were employed to precisely analyze the energy alignment of PEDOT and C60 selective contacts, revealing significant offsets for the ETL and HTL due to the shallow energetics of TPSC.

By integrating the comprehensive parameters obtained from our multimethod experiments, we simulated the charge transport in TPSC and identified the factors limiting charge transport, extraction, device current, and open voltage. Based on our results, we have developed strategies to enhance the efficiency, stability, and overall performance of tin-based perovskite solar cells. Specifically, we propose reducing the energy offsets of selective contacts from 0.4 eV to 0.1 eV, lowering the doping concentration of materials below 10^{15} cm^{-3} , increasing the charge extraction rate to 10^7 s^{-1} , and suppressing bulk and surface non-radiative recombination to achieve a value of 1 μs . In addition, we demonstrated that NPP layer stack is a more efficient architecture due to the large p-doping density. By surpassing these milestones, TPSC can potentially reach stable power conversion efficiency (PCE) values of 22%, similar to its LPSC counterpart.

Overall, this research provides valuable insights into the charge extraction and recombination mechanisms in tin-based perovskite solar cells, paving the way for the development of efficient and stable devices. Implementing the proposed strategies will contribute to the advancement of tin-based perovskite solar cell technology, bringing us closer to realizing their full potential for renewable energy applications. The findings presented in this abstract provide valuable insights into the field of perovskite solar cells and contribute to the ongoing efforts to accelerate the transition towards sustainable and non-toxic photovoltaic technologies. By addressing the knowledge gap surrounding charge extraction mechanisms in tin-based perovskites, we take a significant step towards realizing their full potential for efficient solar energy conversion and other optoelectronic devices.

- [1] H. Min *et al.*, Nat. 2021 5987881 598, 444–450 (2021)
[2] S. M. Uddin *et al.*, Biosens. 2022, 12, 108 12, 108 (2022)
[3] G. Nasti *et al.*, ACS Energy Lett. 3197–3203 (2022)

3:30 PM EN04.02.05

Substitution of Lead with Tin Suppresses Ionic Transport in Halide Perovskite Optoelectronics Krishanu Dey^{1,2}, Petra J. Cameron³, Saifullislam¹ and Samuel D. Stranks^{2,2}; ¹University of Oxford, United Kingdom; ²University of Cambridge, United Kingdom; ³University of Bath, United Kingdom

Despite the meteoric rise in the development of a variety of perovskite electronic and optoelectronic devices, the phenomenon of ion migration remains a common and longstanding Achilles' heel limiting their performance and operational stability. In particular, ionic transport under light and/or bias have been shown to result in current-voltage hysteresis, open circuit voltage gains and short circuit current losses in operating lead (Pb) perovskite solar cells. Despite several efforts in the literature to mitigate such effects through compositional and additive engineering, there is still a limited understanding on the role of tin (Sn) substitution on the dynamics of ion migration in Pb halide perovskite optoelectronic devices. This is of importance given the recent fast-paced developments in the fields of Sn and mixed Pb-Sn perovskite solar cells towards, among others, reduced-lead and tandem solar cell applications.

In this work, we systematically study the impact of Sn substitution on the ion migration properties of Pb halide perovskite solar cells. Initially, we fabricate MA-free Pb and mixed Pb-Sn perovskite solar cells in the p-i-n configuration, with power conversion efficiencies of 16.9% and 15.1% respectively. We have intentionally not used any defect passivating additives in the perovskite solution or as post-deposition surface treatments in the fabricated device stacks because of their synergistic influence on ion migration. Next, by conducting scan-rate dependent current-voltage measurements, we observe short-circuit current loss at lower scan rates (< 50 mV/s) for both Pb and Pb-Sn perovskite devices, thereby indicating the prevalence of ionic migration in both kinds of solar cells. However, the kinetics of ionic transport is found to be suppressed in mixed Pb-Sn systems as inferred from scan-rate dependent hysteresis measurements. These results are further corroborated by temperature-dependent impedance spectroscopy measurements performed on the fabricated devices at open circuit and under light illumination, which suggest a substantial lowering of ionic diffusion with the partial substitution of Pb with Sn. In addition, atomistic ab initio simulations highlight the key role played by Sn vacancies in increasing the iodide ion migration barriers (>1.1 eV) in Sn-containing perovskites due to severe local structural distortion, which corroborates and rationalises our experimental observations of much slower ion diffusion in mixed Pb-Sn perovskite solar cells.

Overall, our findings can be generalized for a variety of Pb halide perovskite optoelectronic devices, where the benefit of Sn substitution in suppressing ionic migration effects may lead to enhanced operational stability and improved device architectures.

Reference

K. Dey *et al.*, *arXiv 2023*, <https://doi.org/10.48550/arXiv.2305.02014>.

3:45 PM EN04.02.06

Oxidation of Iodide and Tin (II) in Acidic Media and its Impact on Tin-Based Perovskite Solar Cells S M Tareq Hossain¹, Syed Joy¹, Ralph Bright², Stephen Johnson³ and Kenneth R. Graham¹; ¹University of Kentucky, United States; ²Paul Laurence Dunbar High School, United States; ³Transylvania University, United States

Metal halide perovskites (HPs) are the prime focus of investigation for the next generation of photovoltaic (PV) materials, in part driven by their low-cost solution processability, tunable band gap, and high absorption coefficients. Here, tin-based HPs (Sn-HPs) are emerging as promising alternatives to Pb-HPs, as they are less toxic, have band gaps close to the ideal band gap based on the Shockley-Queisser limit, and have higher charge carrier mobility. However, Sn-HPs suffer from oxidation of Sn²⁺ to Sn⁴⁺ and poor film morphologies resulting from their fast crystallization. Even the most common processing solvent, dimethyl sulfoxide (DMSO), is known to oxidize Sn²⁺ when heated above 100 °C. To limit oxidation and improve film morphologies, a variety of different additives are used, with many of these additives having an acidic nature. Furthermore, the most common hole transporting layer (HTL) in Sn-HPs, poly(3,4-ethylenedioxythiophene): polystyrene sulfonate (PEDOT: PSS), is very acidic (pH ≈ 1.8). In some studies, it is claimed that these Bronsted acids act as Lewis bases with oxygen from >X=O (X: C, S) functional groups coordinating with Sn²⁺. In general, Bronsted acids can have a significant impact on redox chemistry and it is important to determine how they impact Sn-HPs. To understand the role of Bronsted acids on Sn-HPs, we studied the rate of oxidation of SnI₂ in ambient conditions with a series of acids with pKa values ranging from -2.8 to 4.36. We find that SnI₂ oxidation is accelerated with stronger acids. Next, we focus on *p*-toluene sulfonic acid (*p*-TSA), as it is the acid moiety in PEDOT: PSS. We find that in the presence of *p*-TSA DMSO can oxidize SnI₂ and I⁻ at room temperature in an inert environment. The addition of *p*-TSA to Sn-HPs results in higher Urbach energies, as determined from photothermal deflection spectroscopy (PDS), and decreases the power conversion efficiency of PV devices, whereas the addition of sodium *p*-toluene sulfonate (*p*-TSNa) does not increase the Urbach energy or decrease PV performance. Overall, our results suggest replacing or neutralizing PEDOT: PSS and using the conjugate base salts of acidic additives may provide a route to decreasing defect states, improving stability, and improving performance of Sn-HPs.

4:00 PM *EN04.02.07

Stable Lead-Free Perovskite Solar Cells Antonio Abate; Helmholtz-Zentrum Berlin, Germany

Halide perovskites quickly overrun research activities in new materials for cost-effective, high-efficiency photovoltaic technologies. Since the first demonstration from Kojima and co-workers in 2007, several perovskite-based solar cells have been reported and certified with rapidly improving power conversion efficiency, now approaching the theoretical limit. Recent reports demonstrated that perovskites outperform the most efficient photovoltaic materials to date. At the same time, they still allow solution processing as a potential advantage in delivering a cost-effective solar technology.

The most stable and efficient perovskites contain lead, among the most toxic elements on earth. Lead-free alternatives have been reported with impressive progress in power conversion efficiency for tin-based (lead-free) perovskites. However, the stability of tin-based perovskite solar cells still needs to be explored. In the present talk, we will focus on stability with a particular interest in tin-based (lead-free) perovskite solar cells.

4:30 PM *EN04.02.08

Room Temperature g-Ray and X-Ray Detection with Halide Perovskites Mercuri G. Kanatzidis; Northwestern University, United States

There is a growing demand for highly sensitive hard radiation detectors that can operate at room temperature, catering to various applications. Among the potential materials, CsPbBr₃, a perovskite semiconductor, shows promise due to its excellent spectral resolution for gamma-rays at room temperature. Moreover, CsPbBr₃ possesses air-stability, non-hygroscopicity, and a high average effective atomic number of 65.9. Recent research has made notable progress in studying bulk CsPbBr₃ crystals and fabricating and characterizing single crystals specifically for detector applications. The Bridgman method has successfully produced exceptionally pure CsPbBr₃ single crystals of superior quality. An outstanding characteristic of CsPbBr₃ is its enhanced tolerance for defects compared to other semiconductors, enabling efficient carrier transport and high-performance detectors. CsPbBr₃ detectors have exhibited remarkable energy resolution for both X-rays and gamma-rays. For instance, a CsPbBr₃ detector achieved a 4% (4.8 keV, FWHM) energy resolution for a 122 keV ⁵⁷Co gamma-ray. Furthermore, in detector-grade single crystals of CsPbBr₃, the hole carrier lifetime surpassed 900 μs, emphasizing its suitability for detector applications. Additionally, pixelated devices based on CsPbBr₃ have demonstrated the potential to resolve 137Cs 662-keV gamma-rays with approximately 1% energy resolution. The effectiveness of CsPbBr₃ detectors has been further demonstrated through high-dose irradiation exposures and synchrotron X-ray detection experiments, with a flux ranging from 10⁶ to 10¹² photons/s/mm² at 58.61 keV. These results strongly indicate that CsPbBr₃, a perovskite material, is promising for developing high-performance radiation detectors across various applications.

SESSION EN04.03: Poster Session
Session Chairs: Kunal Datta and Carlo Andrea Riccardo Perini
Monday Afternoon, November 27, 2023
Hynes, Level 1, Hall A

8:00 PM EN04.03.01

Understanding the Ligand-Assisted Reprecipitation of CsPbBr₃ Nanocrystals via High-Throughput Robotic Synthesis Approach Sheryl L. Sanchez, Yipeng Tang, Bin Hu, Jonghee Yang and Mahshid Ahmadi; University of Tennessee Knoxville, United States

Inorganic cesium lead bromide (CsPbBr_3) perovskite nanocrystals (PNCs) have shown promise in optoelectronic applications. A simpler method of synthesizing high-quality PNCs is the ligand-assisted reprecipitation (LARP) method, but it is susceptible to instability. This study used a high-throughput automated experimental platform to explore the growth behaviors and colloidal stability of LARP-synthesized PNCs. The influence of ligands on particle growth and functionalities was systematically explored using two distinctive acid-base pairs. The study found that short-chain ligands cannot make functional PNCs with the desired sizes and shapes, whereas long-chain ligands provide homogeneous and stable PNCs. The study also found that excessive amines or polar antisolvents can cause PNCs to transform into a Cs-rich non-perovskite structure with poorer emission functionalities and larger size distributions. The diffusion of ligands in a reaction system is crucial in determining the structures and functionalities of the PNCs. This study provides detailed guidance on synthesis routes for desired PNCs.

8:00 PM EN04.03.02

Investigation of Surface Properties of Perovskite Semiconductors using Reflection Electron Energy Loss Spectroscopy (REELS) SerenD. Oez and Selina Olthof; University of Cologne, Germany

The analysis of fundamental semiconductor properties, such as energy level positions and bandgaps, are important to enhance our understanding of these materials and to further improve their performance in applications. In this context, spectroscopic tools such as ultraviolet photoelectron spectroscopy (UPS), inverse photoelectron spectroscopy (IPES) and UV-vis measurements can be employed. In this project, we explore the use of reflection electron energy loss spectroscopy (REELS) for the first time as a novel technique to investigate the surface bandgap of perovskite-based semiconductor materials.

This measurement technique records the energy loss due to inelastic electron scattering processes through the excitation of electronic transitions. Notably, it is a very surface sensitive method with decent energy resolution ($\Delta E \approx 120$ meV, similar to UPS) which makes it an intriguing technique to gain insights on the surface bandgaps as well as the joint density of states (DOS) over a wide energy range.

In this work, we try to understand the observed energy loss spectra in order to establish guidelines to investigate surface properties of perovskite semiconductors. For that reason, information gathered using REELS are compared to UV-vis measurements. Furthermore, by utilizing various incident electron kinetic energies we are able to vary the probing depth. Having this additional control makes it possible to gain additional information on interface properties, which is important to understand the performances of devices.

Our band gap measurements by REELS agree well with the optical bandgaps, therefore our results show that REELS technique can be used as an effective tool to explore such properties at the surfaces of perovskites as well as other semiconductor materials.

8:00 PM EN04.03.03

The Role of Charge Transport in Strain Development and Degradation of Perovskite Solar Cells Nikoloz Gegechкори, Winston O. Soboyejo, John Adjah, Kateryna Kushnir, Husna Amini, Lyubov V. Titova and Nancy A. Burnham; Worcester Polytechnic Institute, United States

Perovskite solar cells (PSCs) are a transformative innovation in photovoltaic technology, standing out due to their impressive efficiency growth and low manufacturing cost. Their practical utility is nevertheless constrained by the persisting issues of instability and rapid degradation. Recent studies suggest that strain in perovskite cells accelerates degradation, reducing the device stability from 1350 hours to 700 hours and the efficiency from 19.8% to 18.7%. Motivated by these insights, this investigation aims to depict the trends in strain development over time as a function of charge transport in operating perovskite cells, identifying the sources or the regions of strain, or both. We induced strain in PSCs by driving the current through simulating solar illumination and manually applying an external bias. Digital Image Correlation and X-ray Diffraction were used to compute surface and lattice strain, respectively, and these metrics were correlated with the PSC's absorbance, photoluminescence, and J-V curves, which are all influenced by strain. While our research is still ongoing, our findings may have significant implications for future studies. A comprehensive understanding of strain in PSCs is needed to enable effective strain management and propel advancements in PSC stability. Future research could focus on the refinement of strain characterization techniques and the development of methods to mitigate the negative impacts of strain.

8:00 PM EN04.03.04

Surface Reconstruction of Perovskite Film with the Combination of Organic Salt and Antisolvent for High Performance Solar Cells with Improved Stability Mi Hee Jung; Sejong University, Korea (the Republic of)

Organic-inorganic lead halide perovskites have made tremendous development due to their excellent optoelectrical properties, achieving exceptional photovoltaic performance up to over 25%. Despite the comparable record power conversion efficiency (PCE) to silicon solar cell, their mechanical instability is challenging to commercialization prospect. Herein, we fabricated modified $\text{GA}_{0.7}\text{MA}_{0.9}\text{PbI}_3$ perovskite film using the organic amine small-molecules 3-(aminomethyl) pyridine (3AP). 3AP molecules do not distract the pristine perovskite film but modulate the surface morphology and reacted with the surface component, especially defect site of PbI_6 octahedral layer, forming the 2D perovskite slab on the surface, resulting high-quality perovskite film. The perovskite films without (pristine) and with toluene were also fabricated for comparison. Toluene treated perovskite film do not attend the any reaction with perovskite surface. 3AP modified $\text{GA}_{0.7}\text{MA}_{0.9}\text{PbI}_3$ perovskite film exhibit the long carrier lifetime and suppress the charge recombination loss, resulting in an increased fill factor (FF) of 75.66% and PCE of 17.28%, which are higher than pristine (FF: 66.36%, PCE: 14.06%) and toluene treated perovskite devices (FF: 72.40, PCE: 16.84%). More importantly, 3AP modified perovskite device show remarkable environmental stability to the ambient conditions, the PCE retaining 92% of the initial PCE for over 1000 h at ambient condition.

8:00 PM EN04.03.05

Indoor Photovoltaic, Futuristic Perovskite And Perovskite-Inspired Materials Pratibha Giri^{1,2} and Jai Prakash Tiwari^{1,2}; ¹CSIR-National Physical Laboratory, India; ²Academy of Scientific and Innovative Research (AcSIR), India

The increasing number and market value of indoor photovoltaic devices demanded their powering solutions day by day. The technologies such as hydrogenated amorphous silicon (H:a-Si), DSSCs, organic semiconductors and lead halide perovskite materials are used for powering indoor photovoltaic (IPVs) due to the suitable band gap for light harvesting in indoor conditions. H:a-Si is used as a standard for IPV as it has efficiency in the range of ~ 4 % to ~9%, which is suitable for electronic devices. Among other emerging photovoltaic, lead halide-based materials are the most promising. Hence, we will demonstrate the exploration of perovskite and perovskite-inspired materials (PIM) for indoor photovoltaic applications.

The device stability of PSCs is still not satisfactory for commercial demands, particularly when exposed to humid or high-temperature environments. The organic component of ABX_3 can be entirely replaced by the inorganic cesium (Cs^+) ion to form inorganic cesium lead halide for better environmental stability. In perovskite materials such as CsPbX_3 , the instability problem due to organic components is substantially solved. The PCE of CsPbIBr_2 and the CsPbI_2Br was reported to be ~ 4.7% and close to ~ 10%, respectively, in 2016. The CsPbI_3 (bandgap, E_g) ~1.7 eV may have better photovoltaic application. However, bulk CsPbI_3 films display low phase stability and rapidly transform into a non-perovskite orthorhombic phase (E_g : 2.82 eV). CsPbBr_3 demonstrates excellent stability but has a relatively large band gap (~2.3 eV), whereas CsPbI_3 exhibits a narrower bandgap (~1.73 eV) but inferior stability. The bandgap and stability of CsPbIBr_2 and CsPbI_2Br lie somewhere in between, offering a balance between the narrow bandgap of CsPbI_3 and the superior stability of CsPbBr_3 . The bromide ions can partially replace iodide in CsPbI_3 to form CsPbI_2Br , which shows better phase stability. The CsPbI_2Br perovskite has attracted significant attention due to the stabilization of the black phase. The black phase also transforms into a nonperovskite phase in a humid environment. However, the exploration of Cs-based materials for indoor photovoltaics is continuing. We have also explored the Cs-based perovskite in view of its phase stability and its film characterization behaviour in the humid atmosphere of New Delhi, capital city of India, from June to August 2023. Further, the lead content of the CsPbI_2Br has led us to explore the PIMs, which are less known for their photovoltaic activities for IPVs. The materials such as bismuth oxy iodide, cesium antimony chloride-iodide, silver-bismuth-iodide rufordites, $\text{Rb}_3\text{Sb}_2\text{I}_9$ and $\text{MA}_3\text{Sb}_2\text{I}_9$, CuAgBiI_6 are also in the process of exploration through their structural, optical, and electrical characterizations for eco-friendly and efficient IPV, which may power the IoT devices.

SESSION EN04.04: Halide Perovskite Processing
Session Chairs: Sascha Feldmann and Ross Kerner
Tuesday Morning, November 28, 2023
Hynes, Level 3, Room 300

8:00 AM *EN04.04.01

A Diffusion-Photostability Framework Enables Robot-Accelerated Screening of Stable Wide Bandgap Perovskite Alloys Aram Amassian; North Carolina State University, United States

Metal halide perovskite semiconductors have led single junction perovskite solar cell efficiency to match the power conversion efficiency (PCE) of monocrystalline Si photovoltaics at 26%. A new opportunity in this field is the development of wide bandgap metal halide perovskite alloys with a bandgap between ~1.65-1.75 eV toward development of all-perovskite tandem and

perovskite-Si hybrid tandem solar cells, the latter of which have recently achieved a PCE of 33.2%. A number of studies have shown that bandgap tuning through mixed halide alloying comes at the expense of light-induced halide segregation, which causes photodegradation of the material and leads to device degradation under illumination. Thus, compositional tuning with multi-component alloying (through mixing of both cations and halides) is widely believed to be the appropriate approach to design metal halide perovskite alloys that exhibit stabilized perovskite compositions that are more photostable. We have recently developed a predictive ion migration-stability-hysteresis framework whereby halide vacancy-mediated volume and grain boundary diffusions play a crucial role in mediating both device photostability and device hysteresis (Ghasemi *et al.*, *Nat. Mater.* 22, 329, 2023). More recently, we have extended this framework to light-induced halide segregation in mixed halide alloys and have linked ion migration and transient photostability of alloys. We use this framework to accelerate the search for novel perovskite alloy candidates suitable for multijunction solar cells via a multi-modal screening strategy that evaluates the materials in terms of their ability to form a purely cubic perovskite phase, the target bandgap (e.g., 1.7eV), as well as achieve minimal light-induced halide segregation. This approach is integrated into our home-built RoboMapper platform developed at NC State and results in identification of wide bandgap perovskite alloys with superior stability, superior power conversion efficiency and low hysteresis in solar cell devices. We also demonstrate how the RoboCoater, an AI-guided coating platform, autonomously develops optimal coating recipes for these new perovskite alloys thus accelerating the translation of material alloys to practical coatings and device applications.

8:30 AM EN04.04.02

Heterogeneity in Structure, Composition and Optoelectronic Behavior in Wide-Bandgap Mixed-Halide Perovskites Kunal Datta^{1,2}, Simone van Laar², Margherita Taddei³, Tim Kodalle⁴, Juanita Hidalgo¹, Guus Aalbers², Carolin M. Sutter-Fella⁴, Juan-Pablo Correa-Baena¹, David S. Ginger³ and René Janssen²; ¹Georgia Institute of Technology, United States; ²Eindhoven University of Technology, Netherlands; ³University of Washington, United States; ⁴Lawrence Berkeley National Laboratory, United States

High quality mixed-halide wide-bandgap perovskites are an important component of high-efficiency multijunction photovoltaic devices. However, solution-processed deposition of such complex materials compositions introduce heterogeneity which influences photovoltaic performance. This work studies mixed-halide perovskite semiconductors in the 1.8 eV to 2.0 eV range relevant for tandem and triple-junction photovoltaic devices and investigates the formation of structural and compositional heterogeneity and its impact on optoelectronic response.

Synchrotron-based in-situ grazing incidence wide-angle X-ray scattering is used to study film formation dynamics and the evolution of structural heterogeneity. A combination of scanning electron microscopy, synchrotron-based X-ray fluorescence microscopy, and hyperspectral imaging techniques identifies halide heterogeneity in structurally disordered areas, which leads to local bandgap changes and influences defect behavior. This influences charge-carrier mobility and recombination and also influences halide migration in thin films. Finally, sensitive sub-bandgap photocurrent spectroscopy measurements find increasing defect density and band-edge disorder as a function of structural heterogeneity, which is further aggravated upon illumination. Collectively, this work identifies the vulnerability of solution-processed wide-bandgap perovskite thin films to the development of structural disorder and assesses its consequences on composition, optoelectronic response and photostability.

8:45 AM EN04.04.03

Deposition of High Number H-Phases by Vapor Deposition Routes Carlo Andrea Riccardo Perini, Andres Felipe Castro Mendez, Javier Castillo Seoane and Juan-Pablo Correa-Baena; Georgia Institute of Technology, United States

FAPbI₃ perovskites are known to degrade in the 2H crystal phase by switching from corner sharing PbI₃ octahedra to face sharing. Hybrid structures (H-phases) between pure edge sharing and face sharing octahedra are possible, and their presence has been observed experimentally as impurities in perovskite films. Crystal engineering of mixtures of corner and face sharing octahedra enabled new functionality in oxide perovskites.[1] Analogously, it is expected that the synthesis of phase pure H-phases with different degrees of face or edge sharing will enable similar results. Furthermore, the study of H-phases will benefit the interpretation of the photovoltaic properties of 3D perovskite films, as these phases are formed as impurities in most FA- and Cs-based films.[2]

In this contribution we demonstrate the deposition of thin films with complex arrangements of corner and face sharing PbI₃ octahedra (high number H-phases). We correlate crystal structure and optical properties of these compounds and discuss the potential benefits of the application of these materials as well as their impact on the photovoltaic performances of 3D FA- and Cs-based solar cells.

[1] J.S. Park, ...A. Walsh, *ACS Energy Lett.* 2020, 5, 7, 2231–2233

[2] K.A. Elmestekawy, L. Hertz, *ACS Nano* 2022, 16, 6, 9640–9650

9:00 AM *EN04.04.04

Vapor Phase Deposited Perovskites, High and Low Vacuum Methods for Single Junction and Tandem Solar Cells Henk J. Bolink; University of Valencia, Spain

We will report on the progress on vapor phase deposited perovskites, including novel low vacuum based deposition methods such as close space sublimation. Using substrate configuration we optimize the incoupling of sunlight which leads to current densities very close to the detailed balance limit.

The use of vacuum deposited for perovskite-Si tandem cells will also be commented upon.

9:30 AM BREAK

10:00 AM *EN04.04.05

Shedding Light on Wide Bandgap Perovskites Michael Saliba; University of Stuttgart, Germany

Perovskite solar cells have come to the forefront of solar research in the last decade with certified efficiencies of now >26%. This is approaching rapidly the Shockley-Queisser limit for single-junction solar cells, implying that the main breakthroughs for perovskites were achieved with relatively narrow bandgaps.[1a,1b] Less progress, however, was made for wider bandgap perovskites, which are of interest for multijunction photovoltaics, detector applications, or water splitting. These wide bandgap perovskites are often comprised of fully inorganic components, which are hard to dissolve in conventional solvent systems and require more sophisticated synthesis as well as crystallisation techniques.

In this talk, I will discuss strategies to address these challenges by providing a library of hitherto unexplored wider bandgap perovskites using combinatorics. Mechanosynthesis is then studied to attain otherwise inaccessible liquid precursors permitting the realization, e.g., of “triple cation” wide bandgap perovskites.[2]

Unfortunately, the newly formulated liquid precursors often exhibit complex crystallization behaviour struggling to expel the typically used DMSO solvent. To delay the crystallization time, two strategies are proposed to remove the strongly complexating DMSO molecules through a) modified processing of the liquid thin-film[3] and b) a coordination solvent with a high donicity and a low vapor-pressure[4] leading to a marked improvement in the overall film quality.

Lastly, interface manipulation, especially on top of the formed perovskite, is becoming a central topic to advance further. Typically, this involves chemical surface treatments with a complex interaction. Here, light annealing is introduced as a universal, non-chemical approach to modify the perovskite surface resulting in a reduced surface recombination.[5]

[1a] Saliba et al. *Energy & Environmental Science* (2016), [1b] Turren-Cruz, Hagfeldt, Saliba; *Science* (2018)

[2] Ferdowsi, ..., Saliba; *Chemistry of Materials* (2021)

[3] Byranvand, ..., Saliba; *One-Step Thermal Gradient and Antisolvent-Free Crystallization of All-Inorganic Perovskites for Highly Efficient and Thermally Stable Solar Cells*, *Advanced Science* (2022)

[4] Zuo, ..., Saliba; *Coordination Chemistry as a Universal Strategy for a Controlled Perovskite Crystallization*, *Advanced Materials* (2023)

[5] Kedia, ..., Saliba; *Light Makes Right: Laser Polishing for Surface Modification of Perovskite Solar Cells*, *ACS Energy Letters* (2023)

10:30 AM EN04.04.06

Elucidating Surface Adhesion Characteristics of Formamidinium Iodide in Vapour Co-Deposited Perovskites Qimu Yuan¹, Kilian B. Lohmann¹, Robert Oliver¹, Alexandra Ramadan^{1,2}, Siyu Yan¹, James Ball¹, Greyson Christoforo¹, Nakita K. Noel¹, Henry Snath¹, Laura Herz^{1,3} and Michael Johnston¹; ¹University of Oxford, United Kingdom; ²The University of Sheffield, United Kingdom; ³Technical University of Munich, Germany

Vapour deposition is a solvent-free method suitable for growing thin-films of metal halide perovskite and charge-transport layers. Vacuum-based methods offer unique advantages, including precise control of layer thickness, excellent uniformity of the formed thin-film, and the flexibility to grow multi-layer structures and larger-scale modules.

In particular, the co-evaporation of MA-based perovskites has been well studied, and the adhesion characteristics of methylammonium iodide (MAI) vapour have been found to be dependent on a diverse array of factors, such as pressure, composition and temperature of underlying substrates [1,2,3]. In contrast, the adhesion mechanism of the organic formamidinium iodide (FAI) vapour is yet to be clearly elucidated, partly owing to very limited studies to date. Nevertheless, the understanding of FAI sticking properties may be pivotal in controlling the film growth and quality of FA-based perovskites.

In our studies, we uncover the striking differences in the sticking, adhesion, and nucleation of the perovskite precursor FAI, to various hole transport layers (HTLs). We found that when exposing the same time-integrated FAI vapour flux to the underlying layers of both solution-processed PTAA and thermal-evaporated copper phthalocyanine (CuPc), a 50% thicker FAI layer was formed on the latter surface. Through atomic force microscopy measurements, we highlight the subtle differences in the 'island growth' mode of FAI on PTAA and CuPc surfaces, and hence, correlate to the observed stoichiometric difference in the co-evaporated $[\text{CH}(\text{NH}_2)_2]_{0.83}\text{Cs}_{0.17}\text{PbI}_3$ ($\text{FA}_{0.83}\text{Cs}_{0.17}\text{PbI}_3$) perovskite films of device thickness. Therefore, we demonstrate the importance of optimising growth parameters specific to individual charge transport layer if FAI is to be used as a precursor in any co-evaporated perovskites [4].

Based on these findings, we optimised the co-evaporation of $\text{FA}_{0.83}\text{Cs}_{0.17}\text{PbI}_3$ layer in an all-vacuum deposited perovskite solar cell with CuPc as the HTL. We highlight the vacuum-deposited CuPc as an alternative, low cost, and durable HTL in a photovoltaic device with p-i-n configuration, which attained a solar-to-electrical power conversion efficiency of up to 13.9%. From both optical characterisations and studies of device performance, we illustrate that CuPc demonstrated improved compatibility than thermal-evaporated ZnPc as HTL for solar cell devices with $\text{FA}_{0.83}\text{Cs}_{0.17}\text{PbI}_3$ as the intrinsic layer. Furthermore, we thoroughly examined the long-term stability of these all-vacuum-processed devices under a range of testing conditions. Importantly, unencapsulated devices as large as 1 cm^2 exhibited outstanding thermal durability, demonstrating no observable degradation in efficiency after more than 5000 hours in storage and 3700 hours under $85\text{ }^\circ\text{C}$ heat-stressing in N_2 atmosphere [4].

[1] Lohmann, K. B.; Patel, J. B.; Rothmann, M. U.; Xia, C. Q.; Oliver, R. D.; Herz, L. M.; Snaith, H. J.; Johnston, M. B., Control over Crystal Size in Vapor Deposited Metal-Halide Perovskite Films. *ACS Energy Letters* 2020, 5(3), 710-717.

[2] Roß, M.; Gil-Escrig, L.; Al-Ashouri, A.; Tockhorn, P.; Jost, M.; Rech, B.; Albrecht, S. Co-Evaporated P-I-N Perovskite Solar Cells beyond 20% Efficiency: Impact of Substrate Temperature and Hole-Transport Layer. *ACS Appl. Mater. Interfaces* 2020, 12, 39261– 39272

[3] Abzieher, T.; Feeney, T.; Schackmar, F.; Donie, Y. J.; Hossain, I. M.; Schwenzer, J. A.; Hellmann, T.; Mayer, T.; Powalla, M.; Paetzold, U. W. From Groundwork to Efficient Solar Cells: On the Importance of the Substrate Material in Co-Evaporated Perovskite Solar Cells. *Adv. Funct. Mater.* 2021, 31, 2104482,

[4] **Yuan, Q.**; Lohmann, K. B.; Oliver, R. D.; Ramadan, A. J.; Yan, S.; Ball, J. M.; Christoforo, M. G.; Noel, N. K.; Snaith, H. J.; Herz, L. M.; Johnston, M. B., Thermally Stable Perovskite Solar Cells by All-Vacuum Deposition. *ACS Appl. Mater. Interfaces* 2023, 15, 1, 772–781.

10:45 AM EN04.04.07

Investigation of the Impact of Cs/Sn Ratio on Material Properties in Coevaporated CsSnI_3 Libraries FatimaAkhundova, HannesHempel, MarinRusu and ThomasUnold; Helmholtz-Zentrum Berlin, Germany

Tin-halide perovskites represent a potential non-toxic alternative to lead-based perovskite solar cell absorbers showing similar fundamental optical and electrical material properties as the lead-based halide perovskites. However, solar cell performance of Sn-based halide perovskites so far has been much lower. This has been attributed to the oxidation of Sn^{2+} , strong (intrinsic) p-type doping, and rapid crystallization in the precursor solution which results in poor thin film morphology. Inorganic halide perovskites are attractive from a thermal stability point of view, however, tend to struggle with the presence of a competing non-photoactive non-perovskite delta-phase.

In our study we use a vacuum-based co-evaporation approach to study the influence of a varying Cs/Sn composition ratio on the phase stability as well as the optoelectronic properties of CsSnI_3 .

CsSnI_3 perovskite thin films were deposited with a lateral chemical gradient to obtain thin film libraries with a Cs/Sn ratio from 0.9 to 1.1. We find that the evaporated perovskite crystallizes in the orthorhombic gamma-phase with different preferred orientations in case of excess Sn and/or Cs content. Similar to previous results for CsPbI_3 [1] we find that Cs-rich regions show significantly better stability of the γ -phase than the Sn-rich sample.

With respect to the optoelectronic properties we find a strong blue shift of the absorption onset from 1.35-1.45 eV with increasing Cs-content, whereas the room temperature photoluminescence peak position stays constant at 1.33 eV. The photoluminescence quantum yield shows a distinct maximum with a rather high value of 0.6% for the stoichiometric samples, falling off by a factor of 2-3 toward both off-stoichiometric sides. Despite the high PLQY minority carrier lifetimes as measured by TRPL are relatively low with about 2-3 ns, indicating a low equilibrium carrier density above 10^{17}cm^{-3} in the samples.

These results indicate that defect-related non-radiative recombination still pose a major challenge for obtaining high performance in inorganic Sn-based halide perovskite solar cells.

[1] Pascal Becker et al., *Adv. En. Materials* 2019, 9, 1900555

11:00 AM *EN04.04.08

Perovskite Monocrystals for Advanced Applications: Synthetic Approaches and Working Mechanisms PabloP. Boix^{1,2}; ¹Universitat Politècnica de València - Consejo Superior de Investigaciones Científicas (UPV-CSIC), Spain; ²Universitat de València, Spain

In the past decade, metal halide perovskites have emerged as promising alternatives to traditional semiconductors, holding great potential for photovoltaics but also for diverse semiconductor-based applications. However, their practical implementation has been impeded by challenges related to performance and stability. To overcome these obstacles, precise control over the crystallization and grain boundaries of these materials is essential.

In this work, we present innovative techniques for implementing and passivating device-oriented perovskite monocrystals, including laser-based passivation of macrocrystal surfaces and in-situ fabrication of nanocrystals via humidity-induced methods. Through a comprehensive investigation of the physical properties of these monocrystals, we explore their impact on diverse applications such as photovoltaic devices and memristors. Leveraging the robustness of monocrystalline systems, we develop an impedance spectroscopy model to analyze the phase dispersion resulting from ionic modulation, providing valuable electrical insights that can be extrapolated to polycrystalline thin-film devices. Our study contributes to the advancement of high-performance metal halide perovskite devices by elucidating crucial factors that influence their performance and offering potential solutions to enhance their functionality.

11:30 AM EN04.04.09

Defining New Limits in Hybrid Perovskites: Single-Crystal Solar Cells with Exceptional Electron Diffusion Length Reaching Half Millimeters BekirTuredi^{1,2}, MuhammadN. Lintangpradipto³, OskarJ. Sandberg⁴, ArenYazmacyan³, GebhardJ. Matt^{1,2}, AbdullahY. Alsalloom³, KhuludM. Almasabi³, KostiantynSakhatskyi^{1,2}, SergiiYakunin^{1,2}, XiaopengZheng³, RounakNaphade³, SaidkhodzhaNematulloev³, VishalYeddu⁵, DeryaBaran³, ArdalanArmin⁴, MakhsudI. Saidaminov⁵, MaksymV. Kovalenko^{1,2}, OmarF. Mohammed³ and OsmanM. Bakr³; ¹ETH Zürich, Switzerland; ²Empa–Swiss Federal Laboratories for Materials Science and Technology, Switzerland; ³King Abdullah University of Science and Technology, Saudi Arabia; ⁴Swansea University, United Kingdom; ⁵University of Victoria, Canada

Exploiting the potential of perovskite single-crystal solar cells in the realm of optoelectronic applications necessitates overcoming a significant challenge: the low charge collection efficiency at increased thickness, which has restricted their deployment in radiation detectors and nuclear batteries. Our research [1] details a promising approach to this problem, wherein we have successfully fabricated single-crystal MAPbI₃ solar cells employing a space-limited inverse temperature crystallization (ITC) methodology. Remarkably, these cells, which are up to 400-fold thicker than current-generation perovskite polycrystalline films, maintain a high charge collection efficiency even without external bias.

The crux of this achievement lies in the long electron diffusion length within these cells, estimated to be around 0.45 mm. This extended diffusion length ensures the conservation of high charge collection and power conversion efficiencies, even as the thickness of the cells increases. Fabricated cells at thicknesses of 110, 214, and 290 μm manifested power conversion efficiencies (PCEs) of 20.0, 18.4, and 14.7% respectively. Notably, the single crystals demonstrated nearly optimal charge collection, even when their thickness exceeded 200 μm . Devices of thickness 108, 214, and 290 μm maintained 98.6, 94.3, and 80.4% of charge collection efficiency relative to their maximum theoretical short-circuit current value respectively.

Additionally, we have proposed an innovative, self-consistent technique for ascertaining the electron-diffusion length in perovskite single crystals under operational conditions. The computed electron-diffusion length approximated to 446 μm , significantly surpassing previously reported values for this material.

In conclusion, our findings underscore the feasibility of fabricating halide perovskite single-crystal solar cells of hundreds of micrometers in thickness, while preserving high charge extraction efficiency and PCE. This advancement paves the way for the development of perovskite-based optoelectronics necessitating thicker active layers, such as X-ray detectors and nuclear batteries.

[1] Turedi, B. et al. *Adv. Mater.* 2022, 34, 2202390

11:45 AM EN04.04.10

Towards an In-Situ Crystallization Method for Perovskite Nanocrystal Thin-Films JaumeNoguera-Gómez, VíctorSagra-Rodríguez, MíriamMínguez-Avellán, PabloP. Boix and RafaelAbarques; Instituto de Ciencia de Materiales de la Universidad de Valencia, Spain

Metal halide perovskite nanocrystals (PNCs) can display excellent light emission properties that make them highly versatile for different applications. [1] However, incorporating these properties into functional films results in a challenging task due to inherent drawbacks such as aggregation and material instability, among other performance-related issues.

To overcome these obstacles, we have developed a metal-organic host matrix using a simple sol-gel approach, enabling controlled in-situ crystallization of perovskite nanocrystals through solution-based fabrication methods. [2] This innovative technique allows us to generate high-performance nanocomposite thin films without the need for antisolvent, additives, or annealing while achieving a photoluminescence quantum yield (PLQY) of over 80% and exceptional ambient and mechanical stability.

The crystallization dynamics determining the final nanoparticle size, and thus the emission properties can be finely tuned by adjusting the ambient exposure and precursor concentration. This in-situ PNCs nanocomposite synthesis approach may form the basis for the fabrication of large-area optoelectronic devices with enhanced properties, but also laying the groundwork for band-gap tunability, by directly controlling the PNCs crystallization dynamics.

[1] Kar, M. R.; Ray, S.; Patra, B. K.; Bhaumik, S. State of the Art and Prospects of Metal Halide Perovskite Core@shell Nanocrystals and Nanocomposites. *Mater. Today Chem.* 2021, 20, 100424. <https://doi.org/10.1016/j.mtchem.2021.100424>.

[2] Noguera-Gómez, J.; Fernández-Guillen, I.; Betancur, P. F.; Chirvony, V. S.; Boix, P. P.; Abargues, R. Low-Demanding in Situ Crystallization Method for Tunable and Stable Perovskite Nanoparticle Thin Films. *Matter* 2022. <https://doi.org/10.1016/J.MATT.2022.07.017>.

SESSION EN04.05: Advanced Characterization I
Session Chairs: Mahshid Ahmadi and Pablo Boix
Tuesday Afternoon, November 28, 2023
Hynes, Level 3, Room 300

1:30 PM *EN04.05.01

Spatiotemporal Imaging of Charge and Heat Transport in Two-Dimensional Hybrid Perovskites [Peijun Guo](#); Yale University, United States

Two-dimensional metal halide perovskites (2D-MHPs) are chemically and structurally diverse semiconducting materials with promising applications in photovoltaics and optoelectronics. The understanding of charge and heat transport is crucial for improving the device performance and stability, yet such understanding is challenged by the spatial inhomogeneity in these solution-processed materials. I will discuss our recent efforts on developing spatiotemporal optical imaging techniques, which permit the monitoring of the flow of charge carriers as well as lattice heat with hundreds-of-nanometers spatial resolution, complementing the more commonly employed time-resolved photoluminescence measurements. Our approach paves the way for unraveling charge-carrier dynamics and heat management in 2D-MHPs and other hybrid semiconductors. If time permits, I will also describe our efforts on the understanding of intrinsic chiroptical properties of chiral 2D-MHPs.

2:00 PM EN04.05.02

Rapid Screening of Lead Halide Perovskite Film Photoconductivity via Electric Force Microscopy [Christopher Petroff](#)¹, Virginia E. McGhee¹, Rachael Cohn¹, David T. Moore², Lara A. Estroff¹ and John A. Marohn¹; ¹Cornell University, United States; ²National Renewable Energy Laboratory, United States

One of the key challenges delaying the commercialization of lead halide perovskite (LHP) photovoltaics is their poor long-term stability. Key to solving this problem is a better understanding of the mechanisms behind their photoconductivity. It is demonstrated in the literature that light induces vacancies in LHPs and that the resulting ionic conductivity plays a significant role in their photovoltaic performance [1–3]. The cyclic creation, relaxation, and motion of these halide vacancies may contribute to the overall instability of LHP devices.

We are actively working with collaborators to develop a coherent understanding of LHP photovoltaic performance, reproducibility, and stability from solution chemistry and crystallization pathways through optoelectronic properties and up to devices. Our goal is to connect the input parameters, such as composition and processing conditions, to the output parameters, such as device efficiency and stability. We use broadband local dielectric spectroscopy (BLDS) [4], a type of electric force microscopy (EFM), to make non-contact measurements of steady-state (photo)conductivity. In order to generate the quantity of intermediate data needed for this holistic understanding of LHPs, we designed and built a custom low-noise, high-throughput electric force microscope operating under high vacuum conditions with laser interferometric detection and variable light capabilities. A new probehead design coupled with a new laser led to a 1600x decrease in the position-fluctuation noise floor and a 22x decrease in frequency noise over our previous microscope, which, combined with software improvements, has improved data collection times and measurement stability. Furthermore, improved vacuum pump-down times combined with a sample translation stage and probehead camera led to increased sample throughput of 6–9 samples per day, which allows for the characterization of combinatorially synthesized samples. This throughput allows for the systematic study of, for example, the effect of composition (e.g., halide ratio) on photoconductivity.

References:

- [1] Tirmzi, et al. *ACS Energy Lett.* **2017**, 2, 2, 488–496. DOI: 10.1021/acsenerylett.6b00722
- [2] Tirmzi, et al. *J. Phys. Chem. C* **2019**, 123, 6, 3402–3415. DOI: 10.1021/acs.jpcc.8b11783
- [3] Kim, et al. *Angew. Chem. Int. Ed.* **2021**, 60, 820–826. DOI: 10.1002/anie.202005853
- [4] Labardi, et al. *Appl. Phys. Lett.* **2016**, 108, 182906. DOI: 10.1063/1.4948767

2:15 PM EN04.05.03

Glass Formation in Metal Halide Perovskite using Ultrafast Calorimetry [Akash Singh](#)¹, Yongshin Kim¹, Reece Henry², Harald Ade² and David B. Mitzi¹; ¹Duke University, United States; ²North Carolina State University, United States

While the existence of a glassy state has been established in numerous materials families, including chalcogenide semiconductors, metal halide perovskites (MHPs), currently one of the most exciting and extensively studied classes of semiconductors, have primarily been known to exist only in crystalline states. However, our recent discovery of reversible crystal-glass switching in MHPs challenged this notion by employing structural engineering techniques in an exemplary [S(-)-1-(1-naphthyl)ethylammonium]₂PbBr₄ (SNPB) perovskite, achieving slow melt ordering kinetics that resulted in a stable melt-quenched glassy state.^[1] Nevertheless, it is challenging to vitrify and conduct kinetic studies on the broader MHP family, particularly members with flexible and non-bulky aliphatic organic cations, thereby limiting the glass forming compositional space. In this study, we expand the range of MHP glass formation across a broader range of organic (fused ring to branched aliphatic) and halide (bromide to iodide) compositions by employing an unconventional technique called *ultrafast calorimetry* that enables rapid cooling and heating of samples (4–5 order higher than achievable through conventional calorimetry). For the exemplary case of the 1-MeHa₂PbI₄ (1-MeHa = 1-methyl-hexylammonium) perovskite, a low melting MHP with $T_m \sim 170$ °C, we demonstrate the ability to obtain a glass by melt-quenching at a rate of 6000 °C/s, assisted with a partial mass loss of ~15%. The obtained glass shows a glass transition temperature of ~16 °C and faster crystallization kinetics compared to SNPB.^[2] Furthermore, through iterative calorimetric and viscosity measurements, and a combination of kinetic, thermodynamic, and rheological modeling techniques, we construct an Angell plot and determine important kinetic parameters for glass formation and crystallization, such as the activation energy of glass crystallization ($E_a = 124$ to 50 kJ/mol for 45 to 97 °C), fragility index ($m = 72$), and crystal growth rates ($U_{max} = 0.21$ m/s), providing a deeper understanding of the system's behavior. Ultrafast calorimetry can thus have immense potential to expand the compositional range of glass-forming MHPs, offering a greater range of glass-forming abilities. The results and techniques employed in this study also contribute to establishing a framework for selecting suitable MHP candidates for applications beyond conventional photovoltaics, emitters, and sensors, opening possibilities in areas such as cost-effective memory, computing, metamaterials, and reconfigurable photonic devices.

[1] A. Singh, M. K. Jana, D. B. Mitzi, *Adv. Mater.* 2021, 33, 2005868.

[2] A. Singh, D. B. Mitzi, *ACS Mater. Lett.* 2022, 4, 1840.

2:30 PM BREAK

3:00 PM *EN04.05.04

Nanospectroscopy of Halide Perovskites Through Environmental Microscopy [Marina S. Leite](#); University of California, Davis, United States

The mesoscale construct that forms hybrid organic-inorganic perovskites (HOIPs) are heavily responsible for the spatially inhomogeneous electrical behavior of these materials, which, in turn, requires the use of nanoscale characterization tools for a quantitative assessment. We realize environmental atomic force microscopy to interrogate, in real-time, the voltage and current responses of hybrid perovskites once these materials are exposed to moisture combined with controlled illumination. Quantifying the individual and compound effects of these stressors are

essential for understanding material degradation mechanisms. At inert environment, we find that ion motion is the dominant process responsible for a residual voltage signal that persists post-illumination. For a set of voltage scans acquired under distinct relative humidity levels, up to 60%, we note that ion motion occurs preferentially at the grain boundaries, where we quantify the hysteresis of the process. Concerning photocurrent measurements, we spatially resolve the information in quad-cation perovskites and find that their grain boundaries present enhanced response due to defect-passivation. Unexpectedly, most boundaries show inactive response in dual-cation perovskites. Overall, our environmental microscopy enables us to visualize and quantify dynamic processes within halide perovskites; additional examples will be presented.

3:30 PM EN04.05.05

What Solution Species Exist in a Halide Perovskite Ink? Ross Kerner¹, Bryon Larson¹, Lance Wheeler¹, Kai Zhu¹ and Joseph J. Berry^{1,2,2}; ¹National Renewable Energy Laboratory, United States; ²University of Colorado Boulder, United States

To fully control the formation of a halide perovskite material from solution, one needs to know exactly what solution species exist in the first place. Solution speciation is often probed by ultraviolet-visible (UV-Vis) spectroscopy of the inks where the absorbance peaks in the wavelength range 300-500 nm are attributed to mononuclear iodoplumbate complexes (i.e. one Pb per complex ion) – specifically $[PbI_5Solvent_5]^+$, $[PbI_2Solvent_4]^0$, $[PbI_3Solvent_3]^+$, $[PbI_4Solvent_2]^2-$, $[PbI_5Solvent]^3-$, and $[PbI_6]^4-$. However, we observe that “isolated” $[PbI_6]^4-$ ions in solid-state phases such as $MA_4PbI_6(2H_2O)$ display an exciton absorption energy at ~370-380 nm, significantly blue-shifted from the assumed absorption energy of this complex ion in solution (typically assumed to be 450-500 nm), thus disproving current theories. By measuring UV-Vis absorbance of various 0D and 1D iodoplumbate phases in thin film form, we are able to identify three wavelength ranges due to different classes of oligomers or colloids in solution. Furthermore, X-ray scattering (pair distribution function, PDF) measurements on solutions reveal a correlation length $> 10 \text{ \AA}$, supporting the existence of dimers, trimers, and tetramers in solution for which the bonding motif within the clusters is strongly affected by solvent and additive choice. Thus, what emerges from this work is the underappreciated likelihood that halide perovskites and iodoplumbate intermediates nucleate and self-assemble from oligonuclear, as opposed to mononuclear, solution species. While more studies using advanced techniques like X-ray PDF, as well as other synchrotron-based methods, are needed to complete a detailed picture of what’s in a halide perovskite ink, our work here provides crucial first step and insight to explain the full evolution from solution phase to a halide perovskite film from which it we can better develop strategies to control the kinetics and thermodynamics.

3:45 PM EN04.05.06

Effect of Cation Structure on the Optical and Electronic Properties of Ruddlesden Popper Phase Tin Halide Perovskites Henry Pruett^{1,2}, Sean Parkin¹, Rebecca Scheidt², Kevin Pedersen¹, Yifan Dong², John Colton^{3,2}, Matthew C. Beard² and Kenneth R. Graham¹; ¹University of Kentucky, United States; ²National Renewable Energy Laboratory, United States; ³Brigham Young University, United States

Organic metal halide perovskites (MHPs) are attractive materials for a variety of electronic applications due to their low cost, tunable band gaps, excellent charge transport properties, and high photoluminescence efficiency. As such, HPs are being investigated for use in solar cells, photodetectors, X-ray detectors, light emitting diodes, field effect transistors, lasers, resistive random-access memory, etc. Currently the most popular metal used in HPs is Pb^{2+} but the use of lead comes with the potential for heavy metal exposure. Sn^{2+} -based perovskites offer a less hazardous alternative, but their optoelectronic properties lag behind those of lead and less work has been done to characterize them. In this work, we investigate Ruddlesden-Popper Phase (RP) tin perovskites with phenethylammonium and its derivatives to determine how the structure of the A^* -site cation, the organic cation in the space between the metal halide lattices, impacts the optical and electronic properties. Here, the PEA derivatives include either fluorine (-F) or trifluoromethyl(-CF₃) at the 2,3, or 4 position on the phenyl ring. We show how the A^* -site cation structure affects the crystal structure of the 2D HP, the optical gap, ionization energy, work function, recombination dynamics, charge-carrier mobility, and exciton binding energy. We use several experimental techniques, including single crystal X-ray diffraction for crystal structure determination; ultraviolet photoemission spectroscopy for ionization energy and work function determination; transient absorbance, time-resolved terahertz spectroscopy, and time-resolved microwave conductivity for probing recombination dynamics and extracting summed charge-carrier mobilities; and electroabsorbance for extracting exciton binding energies. Through the above techniques we show that the position of the substituent on the phenyl ring has a greater influence than the identity of the substituent on XXX (specify whether all properties or a specific property). Perovskites made with cations with F or CF₃ at the 4-position show less distorted crystal structures, lower optical gaps, higher ionization energies, and higher charge carrier mobilities compared to HPs with F or CF₃ at the 2-position. In addition, though 2-CF₃PEA₂SnI₄ has the most distorted crystal structure (octahedral tilt of 34.49° compared to the octahedral tilt of 2-FPEA₂SnI₄ of 2.32°), the summed charge carrier mobilities as measured by time-resolved microwave conductivity are surprisingly similar ($0.80 \text{ cm}^2\text{V}^{-1}\text{s}^{-1}$ for 2-FPEA₂SnI₄ vs $0.41\text{-}0.59 \text{ cm}^2\text{V}^{-1}\text{s}^{-1}$ for 2-CF₃PEA₂SnI₄). Overall, this work sheds light on the relationship between the A^* -site cation, HP crystal structure, and optical and electronic properties, helping to provide better guidance for the design of new materials.

4:00 PM EN04.05.07

Accelerating Materials Discovery by High-Throughput Characterizations of Quasi-2D Formamidinium Metal Halide Perovskites Jonghee Yang; University of Tennessee, United States

The intriguing functionalities of emerging quasi-two-dimensional (2D) metal halide perovskites (MHPs) have led to further exploration of this material class for sustainable and scalable optoelectronic applications. However, the chemical complexities in precursors – primarily determined by the 2D:3D compositional ratio – result in uncontrolled phase heterogeneities in these materials, which compromises the optoelectronic performances. Yet, this phenomenon remains poorly understood due to the massive quasi-2D compositional space. To systematically explore the fundamental principles, herein, a high-throughput automated synthesis-characterization-analysis workflow is designed and implemented to formamidinium (FA)-based quasi-2D MHP system. It is revealed that the stable 3D-like phases, where the α -FAPbI₃ surface is passivated by 2D spacer molecules, exclusively emerge at the compositional range (35-55% of FAPbI₃), deviating from the stoichiometric considerations. A quantitative crystallographic study via high-throughput grazing-incidence wide-angle X-ray scattering (GIWAXS) experiments integrated with automated peak analysis function quickly reveals that the 3D-like phases are vertically aligned, facilitating vertical charge conduction that could be beneficial for optoelectronic applications. Together, this study uncovers the optimal 2D:3D compositional range for complex quasi-2D MHP systems, realizing desired optoelectronic performances and stability. The automated experimental workflow significantly accelerates materials discoveries and processing optimizations while providing fundamental insights into complex materials systems.

4:15 PM *EN04.05.08

Cation Exchange at the 2D/3D Perovskite Interface and its Impact on Solar Cell Performance Gabor Szabo, Preethi S. Mathew and Prashant Kamat; University of Notre Dame, United States

Ruddlesden-Popper 2D mixed-halide perovskite films with spacer cations such as butylammonium and Dion-Jacobson 2D mixed-halide perovskite films with 1,4-phenylenedimethan ammonium are used to stabilize the performance of perovskite solar cells. The cation migration under operation of the solar cell can significantly alter the 2D/3D interface. We have now probed the cation migration between 2D and 3D perovskites by physically pairing X PbI (X=butylammonium BA, oleylammonium OA, or phenethylammonium PEA) 2D film and (CH₃NH₃)PbI 3D film at different temperatures by recording changes in the absorption and emission spectra. The migration of methyl ammonium towards the 2D film slowly converts n=1 layered structure into n=2 and 3 layered films. The 3D film on the other hand, exhibits relatively small changes. In addition, we have also correlated the migration of cations to the performance of solar cells. The ease of migration of spacer cations between physically paired films suggest that the varied composition at the interface should be considered while evaluating the effectiveness of 2D/3D design strategy for improving the performance of perovskite solar cells

4:45 PM EN04.05.09

Phase Control of Organometal Halide Perovskites with Superlattice Satoshi Uchida and Hiroshi Segawa; The University of Tokyo, Japan

To develop a highly efficient solar cell using organometal halide perovskites, its microscale structure control is one of the most important factors because the microstructural boundary inside the organometal halide perovskite are harmful to charge carrier flow and, thus, degrade device performance. In this study, we confirmed the existence of tetragonal / cubic superlattice inside the grain in a methylammonium iodide (MAPbI₃, MA = CH₃NH₃) perovskite with transmission electron microscopy (TEM) analysis and revealed that the nano size domain prevents charge carrier flow in the MAPbI₃ perovskite. To minimize the nano sized domain and its negative influences, the 5% of potassium was added to diminish the junction domain and examined to increase the portion of the cubic phase via microstructural phase control using liquid nitrogen (LN₂). Through microstructural phase control of the MAPbI₃ perovskite, its grain boundaries and physical gap were significantly decreased, and 20.23% power conversion efficiency (PCE) was achieved with a single cation MAPbI₃ perovskite solar cell.

1:30 PM *EN04.07.01

Highly Oriented, Thin Pb Halide Perovskite Films from Single Source, CW Laser Vacuum DepositionDavidCahen¹, NagaP. Jasti², ShayTirosh², AnsumanHalder² and EtiTeblum²; ¹Weizmann Institute and Bar-Ilan University, Israel; ²Bar-Ilan University, Israel

Pulsed laser deposition (PLD) is a well-established thin-film deposition technique for pure inorganic materials with high melting points. However, with the typical high energy (also very high time-averaged power) pulsed lasers used, it is quite challenging to deposit organic-inorganic hybrid materials like halide perovskites (HaPs) without decomposing their organic components and thus losing the stoichiometry. We report that thin stoichiometric HaP films can be deposited by 3-4 orders of magnitude lower time-averaged power *continuous wave* laser illumination of a corresponding HaP bulk material as a target. The CW deposition is solvent-free, occurs at room temperature, and needs only low vacuum. The method gives smooth, well-oriented thin films of various HaPs (explored here are MAPbBr₃, MAPbI₃, FAPbBr₃, BA₂PbI₄), making it promising for a scalable technology. Overall, the possibility of growing well-crystallized HaP thin films on any substrate without *in situ* and/or *ex situ* thermal treatments, using a single stoichiometric target, are attractive features of this CW deposition process.

2:00 PM EN04.07.02

Surface/Interface Structures of Perovskite Films as Studied by Advanced Electron SpectroscopiesHiroYukiYoshida and AbduheberMirzehme; Chiba University, Japan

The surface and interface of the perovskite layer play a crucial role in the charge extraction/injection and recombination process of perovskite-based devices such as solar cells. Therefore, it is essential to examine the geometrical and electronic structures of the surface/interface of perovskite. Unfortunately, standard experimental techniques such as X-ray diffraction (XRD) and scanning tunneling microscopy (STM) are unsuitable for examining practical perovskite films, e.g., solution-processed perovskite surfaces. XRD observes the lattice periodicity and is not sensitive to the surface structure. Although STM can precisely observe the surface atoms, it cannot be applied to rough or thick films.

We demonstrate that a combination of **ultraviolet photoelectron spectroscopy (UPS)** and **metastable atom electron spectroscopy (MAES)** is a powerful and versatile tool to examine both geometrical and electronic structures of perovskite surfaces. In UPS, the valence electrons are excited by ultraviolet photons (typically with the energy of 21.22 eV), and kinetic energies of photoelectrons are analyzed to measure the valence electronic states as a difference between the photon and electron kinetic energies. The probing depth of UPS is limited by the mean free path of electrons which is usually a few nanometers (several layers) in the energy range of UPS. In MAES, the excitation source is replaced with the metastable helium atom (with an energy of 19.82 eV). Although the process of electron spectroscopy is similar to that of UPS, MAES is extremely surface sensitive because the helium atom can only interact with the outermost atomic orbitals of the sample surface. We can obtain information about the surface structure and electronic states by comparing the UPS and MAES spectra. Moreover, we can obtain information about the energy levels of perovskite surfaces simultaneously. In this presentation, we will demonstrate the following topics:

1. Surface termination of perovskite films¹

The properties of the interface of perovskite ABX₃ should be strongly affected by the surface termination, i.e., whether the surface is terminated with AX or BX layer. We examined the surface termination of a CH₃NH₃PbI₃ thin film prepared by the standard one-step solution process. The results show that the surface of the perovskite film is terminated with the layer consisting of CH₃NH₃ and I.

2. Surface passivation in quasi-2D perovskite films²

Surface passivation is a promising technique to suppress the charge carrier recombination at the surface defects. The combination of UPS and MAES is a suitable tool to examine the effect of surface passivation. For example, a small amount of large organic cations incorporated in perovskite film (quasi-2D) passivates the surface and enhances the stability of the perovskite solar cell against moisture. We examined the surface structure of PEA_{2m}(CH₃NH₃)_{n-2m}PbI_{3n} and confirmed that the PEA segregates to the surface and that the phenyl group covers the outermost surface of the quasi-2D perovskite. From the concentration dependence, we also examined the plausible structure of the quasi-2D film.

References

- 1) A. Mirzehmet, T. Ohtsuka, S. A. Abd. Rahman, T. Yuyama, P. Krüger, H. Yoshida, *Adv. Mater.* **33**, 2004981 (2021).
- 2) A. Mirzehmet, T. Ohtsuka, S. A. Abd. Rahman, T. Aihara, M. A. Kamarudin, S. R. Sahamir, S. Hayase, T. Yuyama, P. Krüger, H. Yoshida, *Appl. Phys. Express* **14**, 031006 (2021).

2:15 PM EN04.07.03

Imaging Buried Interfaces of Metal-Halide Perovskites Towards Flexible PhotovoltaicsConradA. Kocouj¹, JoyXu¹, ZhenghongDai², AnushRanka², NitinP. Pature² and PeijunGuo¹; ¹Yale University, United States; ²Brown University, United States

Photovoltaics made with 3D organic-inorganic halide perovskite (3D-OIHP) thin films lead a burgeoning field of research into flexible solar cells due to their demonstrated ability to enable flexible and lightweight designs while maintaining competitive power-conversion efficiency and stability. Despite their promise, 3D-OIHP thin film-based flexible devices suffer from inherent defects originating from manufacturing and delamination of their interfaces due to wear and tear from common usage that decrease their performance over time. Recent efforts in interfacial engineering have brought about significant improvements in solar cell reliability, but techniques for the large-scale characterization of defects and delamination between functional layers of OIHP devices have yet to be explored. Standard techniques for imaging the delamination between material interfaces, such as cross-sectional FIB/SEM, have limited throughput and necessitate the deposition of additional material and destructive processing, rendering measured samples inoperable while providing only site-specific information. Here, we demonstrate a vibrational-pump visible-probe microscopy technique to optically probe the presence of buried interfaces in flexible MAPbI₃ thin films and multilayer structures. By exciting the N-H stretching mode present in the methylammonium cations with a mid-infrared pump and probing the transient response of the perovskite's temperature-dependent bandgap in the visible region, we exploit the localized heat transfer towards the substrate to image delamination between the buried interfaces. This technique allows for the nondestructive imaging of buried interfaces and can provide insight into the effects of interfacial contact on device performance, serving as a useful tool for the interfacial engineering and eventual commercialization of high-performance 3D-OIHP-based flexible photovoltaics and optoelectronic devices.

2:30 PM BREAK

3:30 PM *EN04.07.04

Probing the Electronic Structure of 3D and 2D Halide PerovskitesSelinaOlthof; University of Cologne, Germany

Halide perovskites have revolutionized the field of photovoltaics through their remarkable performance in single as well as tandem solar cell devices. One intriguing property of this material class is the wide tunability of the band gap which enables a fine-tuning of optical and electronic properties. In this talk, I will revisit some of our earlier work regarding the analysis of the valence and conduction band positions of tin and lead based 3D perovskites. Combining photoelectron spectroscopy with density functional theory we were able to distinguish influences from the atomic level positions, the bond hybridization strength, as well as lattice distortions.

Recently, we also started working on 2D perovskites, which are gaining more and more attention as a strategy to tailor interfaces; they turned out to be a key factor to unlock high efficiencies in perovskite solar cells. Here, the effect of the choice of the bulky cation on the position of the charge transport layers is less clear and published measurements often seem contradicting. I will present a systematic study on alkyl-based organic cations with varying chain length, which are selected to form Ruddlesden Popper as well as Dion-Jacobson structures.

Since such 2D perovskites are most commonly used as a thin interlayer on top of 3D films, I will also present some of our results gathered at such modified surfaces. Notably, using reflection energy loss spectroscopy (REELS) we are able to determine the surface band gap of these samples which helps us to understand the formation of such 2D surface layers.

4:00 PM EN04.07.05

How Adding Bromine to Cs-FA Lead Halide Perovskites Changes Crystallinity, Phase Segregation and Stability as a Function of TemperatureDianaK. LaFollette¹, JuanitaHidalgo¹, JongheeYang², Carlo Andrea RiccardoPerini¹, SergeiV. Kalinin², MahshidAhmadi² and Juan-PabloCorrea-Baena¹; ¹Georgia Institute of Technology, United States; ²The University of Tennessee, Knoxville, United States

One of the ever-present issues with perovskite solar cells (PSCs) is the lack of long-term stability, particularly because the popular material methylammonium (MA) lead iodide undergoes a phase transition at 57C and decomposes into PbI₂ even in an inert environment. Past work exploring the formamidinium (FA) and cesium (Cs) compositional space demonstrated that these compositions have increased thermal stability while approaching and surpassing the impressive efficiency of MA-based PSCs. The degradation and phase transformations of single cation and single halide perovskites are well understood, but we do not yet understand how mixing cations and halides changes these phase transformations and degradation.

While Cs_{17%}FA_{83%}PbI₃ and Cs_{17%}FA_{83%}PbI_{33%}Br_{17%} are established as high performing compositions, their phase transformations and degradation change as a function of annealing temperature. To understand the effect of adding bromine as a function of temperature, in-situ XRD and in-situ GIWAXS were used to establish the structural transformations with temperature. Adding bromine decreases strain in the crystal lattice, improving structural stability. However, it also increases the ionic conductivity thus accelerating degradation due to vacancies.

Cathodoluminescence SEM, X-ray fluorescence, and X-ray beam induced current mapping are used to take the structural characterization a step further to correlating changes in crystal structure with physical morphology and phase segregation. This study shows that adding bromine changes the relationship between temperature, crystallinity, and phase purity of these mixed-

halide compositions, promoting structural stability while also accelerating the formation of secondary phases at the grain boundaries. These studies increase key understanding of how and when crystalline phase formation, segregation, and degradation occur, setting the stage for more efficient, stable PSCs based on fundamental scientific understanding.

4:15 PM EN04.07.06

Defect Tolerance in Halide Perovskites: Investigating the Absolute Volume Deformation Potential [Albert These^{1,2}](#), [Christoph J. Brabec¹](#) and [Andres Osvet¹](#); ¹Institute Materials for Electronics and Energy Technology, Germany; ²Friedrich-Alexander-Universität Erlangen-Nürnberg, Germany

Halide perovskite (HaP) semiconductors, commonly synthesized from room temperature solutions, possess exceptional optoelectronic properties that rival those achieved by more complex fabrication methods used for conventional semiconductors. The absence of detrimental defects in HaPs is a topic of debate, often attributed to their defect tolerance or self-healing ability.

To contribute to this discussion, we conducted an experimental investigation focused on determining the absolute volume deformation potential (AVDP) of CsPbBr₃. The AVDP is a crucial physical parameter that characterizes the energy level shift of a semiconductor in response to volume changes. It therefore allows for quantifying of the amount of energy necessary to for example rearrange a crystal lattice locally to efficiently screen the electrical energy barrier of defects. Furthermore, it provides insights into the inherent molecular orbital bonding nature of semiconductor material.

In our study, synchrotron radiation-based X-ray photoelectron spectroscopy was employed to measure the VBM (valence band maximum) energy of CsPbBr₃ across a temperature range from room temperature to 125 K. Our experimental findings demonstrate that the AVDP of CsPbBr₃ is negative and relatively small compared to conventional semiconductors. This observation suggests that electronic defects can be easily screened through lattice rearrangement. Moreover, the negative sign indicates that the VBM primarily consists of anti-bonding type molecular orbitals. The disruption of these bonds typically generates defect energy levels near or within the bands. Both the magnitude and sign of the AVDP support the notion of defect tolerance in Halide perovskites.

Additionally, we conducted measurements of transient photoluminescence and employed a comprehensive interpretation based on a kinetic rate equation encompassing various recombination processes of different orders. This allowed us to quantify the defect density in CsPbBr₃ at similar temperatures, providing a deeper understanding of the evolution of defect properties under volumetric changes.

Our results offer valuable insights into the origins of defect tolerance in Halide perovskites, shedding light on their unique optoelectronic characteristics.

4:30 PM *EN04.07.07

Forming Room-Temperature Stable FAPbI₃—A Multimodal *In Situ* Study [Carolyn M. Sutter-Fella](#); Lawrence Berkeley National Laboratory, United States

Organic-inorganic halide perovskites are a versatile material class with excellent optoelectronic properties. One of the current research directions is the stabilization of the photoactive FAPbI₃ phase. In this talk I will describe our joint efforts in forming phase pure and room-temperature stable FAPbI₃. Application of *in situ* characterizations during FAPbI₃ formation unveils initial nucleation and growth stages. The addition of additives to the precursor can influence the nucleation and preferential orientation leading to the absence of solvate and non-perovskite phases. Interestingly, the proposed strategy is widely applicable to different deposition methods including one- and two-step protocols. Another aspect I will touch on is reproducibility challenges in the field. Therefore, automation of halide perovskite synthesis at high throughput presents an attractive route to identify synthesis parameter-structure-function properties.

5:00 PM EN04.07.08

Comparative Analysis of Recombination Dynamics in Perovskite Solar Cells via Steady-State and Transient Photoluminescence [Chris Dreessen](#) and [Thomas Kirchartz](#); Forschungszentrum Jülich GmbH, Germany

Quantifying recombination in halide perovskites is essential for controlling and enhancing the performance of perovskite solar cells. Here, we present a comprehensive analysis of recombination dynamics in perovskite solar cells, focusing on the impact of transient measurement techniques on assessing steady-state performance. We emphasize that the decay times extracted from transient photoluminescence measurements cannot generally be reduced to a single value but rather depend strongly on the charge carrier concentration. It follows that the magnitude of the decay time is reliant on the sensitivity of the measurement. We show photoluminescence decay curves with a large dynamic range of more than 10 orders of magnitude that demonstrate decay times from tens of nanoseconds up to hundreds of microseconds in perovskite films. Assuming these high decay times correspond to a recombination lifetime in steady state, one would expect a material with perfect photoluminescence quantum yield, which does however not coincide with the experimental findings. Instead, the decay times in transient measurements are prolonged by capacitive effects resulting from charge trapping and detrapping. We quantitatively explain both the transient and steady-state photoluminescence with the presence of a high density of shallow traps without the influence of deep traps. The same characteristic of increasing decay times remains in the full device, indicating capacitive effects from either shallow traps or transport layers and electrodes. With the help of voltage-dependent steady-state photoluminescence measurements we extract the recombination lifetimes during steady-state operation of the device and compare these to the transient decay times. Furthermore, this experiment allows for the determination of the voltage-dependent collection efficiency which illustrates collection losses up to 10% due to recombination even at short circuit. In summary, this study offers a deeper understanding of recombination dynamics in halide perovskite solar cells through the analysis of transient and steady-state measurements. Our findings underscore the importance of considering the influence of shallow traps and transport layers in interpreting decay times and optimizing device performance.

SESSION EN04.08: Optoelectronic Applications
Session Chairs: [Aram Amassian](#) and [Carlo Andrea Riccardo Perini](#)
Thursday Morning, November 30, 2023
Hynes, Level 3, Room 300

8:15 AM *EN04.08.01

First-Principles-Aided Cartography of Excitons in Metal-Halide Perovskites [Linn Leppert](#); University of Twente, Netherlands

Excitons are neutral quasiparticles that are formed in semiconductors and insulators upon absorption of photons. Their formation, diffusion, lifetime, and recombination are key for understanding light-conversion processes and designing materials for tailored applications, such as photovoltaics, sensing, lighting, and quantum computing. Metal-halide perovskites are a structurally and chemically diverse class of materials that have been explored in all these application areas.

In this presentation, I will discuss our recent efforts to use first-principles numerical simulation techniques for modelling the formation of excitons in metal-halide perovskites and provide design rules for bespoke material properties. Our calculations allow us to map the complex landscape of electronic properties and excitons, understand the impact of chemical heterogeneity [1-4], dimensionality [5-7] and temperature effects [7], and provide chemically intuitive rules for when to trust canonical models for excitons in these materials.

[1] A. Slavney, B. Connor, L. Leppert, H. Karunadasa, *Chem. Sci.* 2019, 10, 11041.

[2] R.-I. Biega, M. Filip, L. Leppert, J. B. Neaton, *J. Phys. Chem. Lett.* 2021, 12, 2057.

[3] R.-I. Biega, Y. Chen, M. R. Filip, L. Leppert, to be submitted.

[4] H. J. Jöbssis, K. Fykouras, J. Reinders, J. van Katwijk, J. Dorresteijn, T. Arens, I. Vollmer, L. Muscarella, L. Leppert, E. M. Hutter, submitted.

[5] B. A. Connor, L. Leppert, M. D. Smith, J. B. Neaton, H. I. Karunadasa, *J. Am. Chem. Soc.* 2018, 140, 5235.

[6] S. Krach, N. Forera-Correa, R.-I. Biega, S. E. Reyes-Lillo, L. Leppert, *J. Phys. Condens. Matter* 2023, 35, 174001.

[7] R.-I. Biega, M. Bokdam, K. Herrmann, J. Mohanraj, D. Skyrbek, M. Thelakkat, M. Retsch, L. Leppert, *J. Phys. Chem. C* 2023, 127, 9183.

8:45 AM EN04.08.02

Band Structure and Exciton Dynamics in Quasi-2D Dodecylammonium Halide Perovskites [Daniele Catone¹](#), [Giuseppe Ammirati^{1,2}](#), [Faustino Martelli³](#), [Patrick O'Keeffe¹](#), [Stefano Turchini¹](#), [Alessandra Paladini¹](#), [Maurizia Palummo²](#), [Giacomo Giorgi^{4,5}](#), [Marco Cinquino^{3,5}](#), [Milena De Giorgi³](#) and [Luisa De Marco³](#); ¹Istituto di Struttura della Materia - CNR, Italy; ²Università degli Studi di Roma Tor Vergata, Italy; ³Consiglio Nazionale delle Ricerche, Italy; ⁴Università degli Studi di Perugia, Italy; ⁵Università del Salento, Italy

Quasi two-dimensional perovskites in Ruddlesden-Popper phase (RPPs) are extensively studied for their flexible tunability of the optoelectronic properties by changing the number of layers, chemical composition and the organic spacer, which makes them particularly suitable for several applications in the field of photovoltaics and light emitters [1-4]. In fact, the reduced

dielectric screening and the quantum confinement in a monolayer of RPP materials generate large bandgaps and stable excitons at room temperature with binding energies of the order of hundreds of meV similarly to other 2D semiconductors. Moreover, the physical properties of RPPs are strongly influenced by the number of layers that affects the electronic bandgap and the exciton binding energy which decreases as the number of layers increases. These properties are also correlated with the chemical composition and the structure of the organic spacer used as the interlayer material [5, 6].

In this developing framework, the photoexcited carrier dynamics in these materials is still far to be completely understood although the study of charge generation and recombination path can furnish key information for boosting the development of new materials for new generation optoelectronic. Femtosecond Transient Absorption Spectroscopy (FTAS) has proven to be an important tool to investigate the ultrafast physics of halide perovskites having different dimensionality, morphology and architectures, giving insights into the band structure and the electronic states involved in the photoexcitation processes. Here, we present FTAS investigations on monolayer and multilayer of RPPs DAMAPI ($\text{DA}_2\text{MA}_{n-1}\text{PbI}_{3n+1}$, where $\text{DA}=\text{CH}_3-(\text{CH}_2)_{11}-\text{NH}_3^+$ is the spacer and n indicates the number of the layers). The FTAS measurements, performed at 77 K and room temperature using several different pump energies and excitation densities, allowed the observation of absorption bleaching energies corresponding to different excitonic and electronic transitions in DAMAPI. These results are compared with theoretical simulations based on DFT, the GW approximation and the Bethe-Salpeter equation for the calculation of the excitonic properties. In this way, we have assigned the transient absorption signals to electronic transitions related to the formation of excitons with principal quantum number 1s and 2s. The temporal analysis of these signals indicates the exciton-exciton annihilation process as the main relaxation mechanism in the first picoseconds after the excitation, while exciton radiative recombination is observed at longer time delays (>100 ps). This work demonstrates how transient absorption measurements not only allow the study of the dynamics of the excited carriers but, because of their high sensitivity to the changes of the carrier density induced by the excitation, they also allow the observation of spectral features otherwise not observable with steady-state measurements [7].

References

- [1] L. Mao, et al., J. Am. Chem. Soc. 2019.
- [2] C. Smith, et al., Angew. Chem., Int. Ed. 2014.
- [3] G. Grancini, et al., Nat. Commun. 2017.
- [4] K. Wang, et al., EcoMat 2021.
- [5] M. Palummo, et al., ACS Energy Lett., 2020.
- [6] G. Giorgi, et al., J. Mater. Chem. C, 2018.
- [7] G. Ammirati, et al., Adv. Opt. Mat., 2023.

9:00 AM *EN04.08.03

Tracking Spin and Charge in Time and Space in Halide Perovskite Films [Sascha Feldmann](#); Harvard University, United States

Halide perovskites are promising semiconductors for next-generation optoelectronic and spintronic applications. Yet, we still don't fully understand what governs the charge and spin dynamics in these materials. This is especially true when studying device-relevant thin films of halide perovskites, which lack single-crystalline perfection.

In this talk, I will give an overview of our recent efforts to understand the spin-optoelectronic performance of these films better by using time-, space- and polarization-resolved spectroscopy and microscopy. We will find that the energetically heterogeneous energy landscape in mixed-halide perovskites can lead to the local accumulation of charges, with unexpected consequences for devices [1]; how despite strong differences in vertical diffusivity and across grains charge extraction can remain very efficient [2], and how locally varying degrees of symmetry-breaking drive spin domain formation [3,4] in this fascinating class of solution-processable semiconductors.

- [1] Feldmann *et al.* Nature Photonics 2020
- [2] Cho, Feldmann *et al.* Nature Materials 2023
- [3] Ashoka, ..., Feldmann & Rao, Nature Materials 2023
- [4] Crassous, ..., Feldmann, Nature Reviews Materials 2023

9:30 AMBREAK

10:00 AM *EN04.08.04

Characterizing Spin and Orbital Ordering Effects in Hybrid Metal Halide Perovskites Towards Advancing Optoelectronic Properties [Bin Hu](#); University of Tennessee, United States

Hybrid metal halide perovskites are known as emerging semiconducting materials with tunable structure-property relationships through solution-processing methods. Such solution-processing perovskites simultaneously carry spin and orbital momentum. Consequently, using spin and orbital momentum has become a critical approach to control the multifunctional properties.

However, characterizing spin and orbital parameters still demands much effort to understand their underlying relations to materials properties. To respond to this demand, we have been using magnetic field effects and circularly polarized laser spectroscopy to experimentally investigate spin and orbital parameters in determining light-emitting, photovoltaic, and lasing properties in hybrid metal halides. Our magnetic field effects have shown that bright and dark excitons are having largely different outcomes when generating optic, electric, optoelectronic actions. Therefore, magnetic field effects provide an essential experimental tool to characterize spin effects in such solution-processing perovskites. Furthermore, we found that circularly polarized luminescence can be used as a convenient method to elucidate orbital dynamics within Rashba band structures. We discovered that the circularly polarized orbitals with right and left handedness in Rashba band structures can selectively interact with spin-up and spin-down spin dipoles, leading to a mutually selectivity between spin order and orbital order. Particularly, this selective interaction between spin order and orbital order can enable spin-switchable phenomena towards developing emerging functionalities in these solution-processing hybrid metal halide perovskites. This presentation will discuss the fundamental details on exploring spin and orbital parameters by using magnetic field effects and circularly polarized laser spectroscopy.

10:30 AM EN04.08.05

Role of Interconnectivity in Perovskite Nanocrystals: Charge Carrier Dynamics in Nanostructures Embedded in Porous Films [David O. Tiede](#)¹, [Carlos Romero-Pérez](#)¹, [Katherine A. Koch](#)², [Mauricio E. Calvo](#)¹, [Juan F Galisteo-López](#)¹, [Ajay Ram Srimath Kandada](#)² and [Hernán Míguez](#)¹; ¹Institute of Materials Science of Seville, Spain; ²Wake Forest University, United States

In the past years, halide perovskite-based devices are shifting towards low-dimensional functionalized structures and morphologies such as 2D, 2D/3D or perovskite nanocrystals (pNCs). For the latter, a common approach is to employ ligands, which ultimately determine the photophysical properties and in particular the interaction among individual NCs. As an alternative approach, mesoporous matrices can be employed to synthesize pNCs and have been established as a promising ligand free approach. [1,2] From a more fundamental perspective, this material system allows to study the interaction of excitations in pNCs with their neighbouring pNCs isolated from ligand or solvent induced effects characteristic of colloidal NCs. [3]

In this presentation, we employ FAPbBr_3 NCs of various sizes synthesized in porous matrices to determine the role of interparticle interaction on charge carrier recombination isolated from ligand and solvent induced effects. A broad photophysical characterization comprising time resolved absorption and emission spectroscopies as a function of temperature and fluence is employed to study the transition from isolated emitters to interconnected NCs array that preserves confinement effects while allowing for long range electronic transport. From a spectroscopic point of view, the effect of confinement is verified through thermalization dynamics. We demonstrate that interconnectivity determines charge carrier dynamics as it affects trap filling, radiative recombination and multiparticle interactions. We rationalize these findings by employing recombination and diffusion models for both the isolated and interconnected case and study the transition between these scenarios. Such transition regime is of great importance in terms of possible device performance, since the interplay of transport and (non) radiative recombination while maintaining confinement effects will determine its ultimate efficiency.

References

- [1] A. Rubino, L. Caliò, A. García-Bennett, M. Calvo, H. Míguez, Adv. Optical Mater. (2020), 8, 1901868
- [2] A. Rubino, L. Caliò, M. Calvo, H. Míguez, Solar RRL (2021), 5 (8), 2100204
- [3] A. Rubino et al, J. Phys. Chem. Lett. (2021), 21, 1, 569-575

10:45 AM EN04.08.06

Multi-Band Electronic Structure and Carrier Dynamics in Formamidinium Lead Bromide Perovskite [Daniele Catone](#)¹, [Giuseppe Ammirati](#)^{1,2}, [Patrick O'Keeffe](#)¹, [Stefano Turchini](#)¹, [Francesco Toschi](#)¹, [Alessandra Paladini](#)¹, [Faustino Martelli](#)¹, [Fabio Matteocci](#)², [Jessica Barichello](#)², [Paolo Moras](#)¹, [Polina Sheverdyeva](#)¹, [Valeria Milotti](#)¹, [Daniel Ory](#)^{3,4}, [Phillippe Baranek](#)^{3,4} and [Aldo Di Carlo](#)^{1,2}; ¹Consiglio Nazionale delle Ricerche, Italy; ²Università degli Studi di Roma Tor Vergata, Italy; ³Electricité de France (EDF), Italy; ⁴Centre National de la Recherche Scientifique, Italy

In recent years, the scientific community has been captivated by the exceptional properties of halide perovskites. These materials have garnered significant interest due to their high absorption

coefficients in the visible range ($\alpha > 10^5 \text{ cm}^{-1}$), ultralong carrier diffusion lengths, extended carrier lifetimes, remarkable defect tolerance, and tunable bandgaps [1-2]. Among these perovskites, lead bromide perovskites have emerged due to their relatively large bandgap of approximately 2.3 eV, making them ideal candidates for tandem applications and efficient semitransparent solar cells. In this context, one of the most promising materials is formamidinium lead bromide perovskite (FAPbBr₃) that exhibits remarkable stability under light exposure and possesses a carrier diffusion length that facilitates a straightforward planar heterojunction solar cell configuration [3, 4]. Despite its proven superiority in terms of semitransparency and stability, only a limited number of experimental and theoretical studies have been conducted to explore its properties. In particular, the knowledge of the electronic properties and of the dynamics of photoexcited carriers in FAPbBr₃ remain incomplete. Understanding the charge generation and recombination is of paramount importance as it provides crucial insights for advancing the development and optimization of various technologies such as solar cells, lasers, and LEDs [5].

Here, we present the excited-state properties of a thin film of FAPbBr₃ studied combining steady-state light absorption, photoluminescence (PL), femtosecond transient absorption spectroscopy (FTAS), photoelectron spectroscopy (PES) with density functional theory (DFT) calculations. In this way, we give a complete description of the electronic properties of FAPbBr₃, assigning the electronic bands involved in the photoexcitation by UV-Vis radiation and the relative carrier dynamics. By integrating absorption, PL, PES, and DFT, we successfully assign the two photobleaching (PB) signals observed in the transient spectrum to specific electronic transitions. Specifically, the signal at 2.3 eV (PB1) originates from the transition between the first valence band (VB1) and the first conduction band (CB1) [6], while the signal at 3.4 eV (PB2) arises from the transition between the second inner valence band (VB2) and CB1. In the light of this assignment, the rise of the PB1 and PB2 signals were investigated as a function of the carrier density, in order to correlate their dynamics to the thermal relaxation processes involving the carriers excited in the VB1→CB1 and VB2→CB1 transitions. The PB1 signal shows a rise time that slows down with the increase of the carrier density indicating that the dominant processes influencing it are the thermalization and cooling of carriers in VB1 and CB1 [7, 8]. On the other hand, the rise time in PB2 accelerates as the excited carrier density increases, suggesting that this signal is strongly influenced by the thermalization of the hot holes in VB2. In fact, VB2 shows a quasi-flat band structure determining a localization near the band maximum of all the excited holes [9].

In summary, the combination of various spectroscopic techniques and theoretical calculations allows us to unravel the underlying carrier dynamics and establish correlations with thermal relaxation processes, providing valuable insights into the excited-state behavior of FAPbBr₃. These findings enhance our understanding of the material properties and pave the way for further advancements in its utilization for optoelectronic and photovoltaic applications.

References

- [1] C. Wehrenfennig, et al., *Adv. Mater.*, 2014.
- [2] K. Jena, et al., *Chem. Rev.*, 2019.
- [3] N. Arora et al., *Nano Lett.*, 2016.
- [4] A. Amat et al., *Nano Lett.*, 2014.
- [5] A. A. Al-Kahtani et al., *Coatings*, 2021.
- [6] B. Anand, et al., *Phys. Rev. B*, 2016.
- [7] M. B. Price, et al., *Nat. Comm.*, 2015.
- [8] J. M. Richter, *Nat. Comm.*, 2017.
- [9] G. J. Hedley, *Sci. Reports*, 2018.

11:00 AM EN04.08.07

Engineering of Solid-State Single-Photon Sources Based on Perovskite Quantum Dots in Perovskite Matrix HaoZhang¹, AltafPasha¹, SirajSidhik¹, Jia-ShiangChen², XuedanMa² and AdityaD. Mohite¹; ¹Rice University, United States; ²Argonne National Laboratory, United States

Semiconductor quantum dots (QD) have emerged to be one of the promising candidates for on-demand single-photon emitters (SPE), which are one of the key units in quantum photonic circuits and quantum information processing. However, despite wide investigation of colloidal QDs, implantation of such SPE system in solid states for electrical excitation is less developed. Here, we have demonstrated the first solution-processed perovskite-based single-photon source in a solid-state medium, by embedding perovskite emission centers into a wide-bandgap perovskite matrix. Such 'dot-in-a-matrix' system exhibits a clear photon-antibunching signature, with second-order correlation function ($g(2(0))$) to be ~0.1 at cryogenic temperatures. The photoluminescence (PL) spectrum exhibits narrow emissions lines at 1.8-1.9eV with 2-3meV FWHM at T=6K, indicating high crystallinity of the localized emission centers. High-resolution transmission electron microscope (HR-TEM) confirms the presence of nanometer-sized domains, which indicates the formation of quantum dots during the rapid crystallization of the precursor solvent. Monitoring PL with time suggests blinking-free emission and spectral diffusion of <1meV. PL spectra exhibits a linear dependence with excitation intensity, indicating the mono-recombination dominated by single exciton rather than bi-exciton or charged exciton states. Additionally, exciton fine structures have been detected, which are likely due to the anisotropic structures of individual emitters. Finally, we have demonstrated the capability of electrical luminescence by sandwiching the matrix between electron-transport and hot-transport layers. Such demonstration may pave the pathway of on-chip integration of single-photon sources for quantum optical systems.

11:15 AM EN04.08.08

New Insights into the Formation Mechanism and Electronic Structure of Alloyed Cs₂AgBiBr₆ Double Perovskites for Enhanced Visible Light Absorption HuygenJ. Jöbssis¹, KostasFykouras², JoostW. Reinders¹, InaVollmer¹, MichalAndrzejewski³, LoretaA. Muscarella¹, NicolaP. Casati³, LinnLeppert² and ElineHutter¹; ¹University of Utrecht, Netherlands; ²University of Twente, Netherlands; ³Paul Scherrer Institute, Switzerland

Halide double perovskite semiconductors such as Cs₂AgBiBr₆ are widely investigated as a more stable, less toxic alternative to lead-halide perovskites in photoconversion applications including photovoltaics and photoredox catalysis. However, the relatively large (~2.1 eV) and indirect bandgap of Cs₂AgBiBr₆ limits efficient sunlight absorption. Similar to lead-halide perovskites, the bandgap of double perovskites can be manipulated through (partial) substitution of metals or halides with similarly charged ions. However, commonly used solvent-based synthesis routes often lead to the formation of domains or side phases, rather than solid solutions with controlled properties. This results in an inhomogeneous electronic landscape which is detrimental for photoconversion applications.

Here, we show that mechanochemical synthesis methods, such as ball milling, are a valid route to synthesize phase-pure double perovskites. With the use of synchrotron radiation we followed the reaction mechanisms during mechanochemical synthesis of Cs₂Ag[BiM]X₆ (with M = Sb, In, or Fe or X = Cl, Br, or I), and identified new intermediate phases, providing insights into the reaction kinetics. We find that mechanochemical synthesis is a successful approach to make compounds that have not been reported via solution-based synthesis routes, such as Cs₂AgBi_{0.5}In_{0.5}Br₆, Cs₂AgBiBr_{6-x}I_x, and Cs₂AgBi_{1-x}Fe_xBr₆. Where substitution with In³⁺ increases the band gap energy, it is lowered when replacing Bi³⁺ with Fe³⁺ or Br⁻ with I⁻.

Hence, the optical bandgap of Cs₂AgBrBr₆ can be tuned over the entire visible spectrum when partly substituting Bi³⁺ or Br⁻. For instance, we find that controlled replacement of Bi³⁺ with Fe³⁺ via mechanochemical synthesis results in a remarkable tunability of the absorption onset between 2.1 to ~1 eV. Our first-principles density functional theory (DFT) calculations demonstrate that this bandgap reduction originates from a lowering of the conduction band minimum upon introduction of Fe³⁺, while the valence band remains constant. Additionally, our DFT calculations suggest that the bandgap becomes direct when >50% of Bi³⁺ is replaced with Fe³⁺. Finally, we find that the tunability of the conduction band minimum is reflected in the photoredox activity of these semiconductors.

The improved understanding of the reaction mechanism of alloyed-AgBi double perovskites might help to overcome the current challenges faced with solution processing methods. Hence, opening up new avenues for enhancing the visible light absorption of double perovskite semiconductors and for harnessing their full potential in sustainable energy applications.

11:30 AM EN04.08.09

Traps in the Spotlight: How Traps Affect the Charge Carriers Dynamics in Cs₂AgBiBr₆ Perovskite ValentinaCaselli¹, JosThieme¹, HuygenJ. Jöbssis², JiashangZhao¹, ElineHutter² and TomJ. Savenije¹; ¹Delft University of Technology, Netherlands; ²Inorganic Chemistry and Catalysis, Netherlands

Since their discovery as versatile semiconductors for photovoltaic applications, perovskite materials, with general formula ABX₃, have been intensively studied. Tuning of their opto-electronic properties make it possible to reach remarkable power conversion efficiencies, currently topping at 25.6%, in roughly a decade of development. However, a rising concern regarding the use of lead in the photoactive layer has pushed research into lead-free alternative candidates. Toxic lead can be substituted by combining monovalent and trivalent cations, such as in Cs₂AgBiBr₆. However, efficiencies of Cs₂AgBiBr₆-based photovoltaics are still modest. To elucidate the loss mechanisms, in this report we investigate charge dynamics in Cs₂AgBiBr₆ films in thin films by means of TRPL, TA measurements and double pulse excitation time-resolved microwave conductivity (DPE-TRMC). In DPE-TRMC the sample gets illuminated by two laser pulses arriving with a short time delay. By comparing the photoconductance traces induced by the second pulse in presence and absence of the first pulse, we are able to examine the effect of the long-lived species on the charge carrier dynamics. For these experiments we used identical excitation wavelengths for both laser pulses but varying intensities and delay times. We modelled the results introducing a comprehensive model, which accounts for the free carrier generation yield, localization of free carriers, electron trapping by color centers, and shallow trap states for holes. The iterative analysis of the DPE-TRMC experiments with different intensities and delay times reveals the presence of a high concentration of both electron (10¹⁵ cm⁻³) and hole (10¹⁶ cm⁻³) trap states. In addition, we show that both carriers are trapped on sub-ns timescales, while their depopulation occurs over tens of microseconds. Furthermore, we observe a higher mobility for holes compared to electrons, which amount to 5 and 0.01 cm²/(Vs) respectively, in agreement with the imbalance in their effective masses. Localization of holes causes an

effective loss in mobility for the holes, dropping to ca. 1.7 cm²/(Vs), while no effect can be discerned for the electrons. Knowing these kinetic parameters allows us to predict the charge carrier dynamics under AM1.5, explaining the solar cell performance. Our new developed DPE-TRMC methodology gives direct insight on the timescales involved with population and depopulation of the various trap states in Cs₂AgBiBr₆, essential for the design of more efficient devices.

11:45 AM EN04.08.10

Transient Holographic Imaging of Spin Magnetic Moments in Perovskites Julia Anthea Gessner¹, Martin Hörmann², Shangpu Liu¹, Giulio Cerullo², Franco Valduga de Almeida Camargo³ and Felix Deschler¹; ¹Universität Heidelberg, Germany; ²Politecnico di Milano, Italy; ³IFN-CNR, Italy

Hybrid metal halide perovskites have shown to be a promising class of materials for a variety of applications ranging from LEDs [1] to solar cells [2] due to their high quantum efficiency and tunability in the visible range. Compared to conventional semiconductors, perovskites exhibit strong spin-orbit coupling and spin-split Rashba bands, which allow an efficient optical spin manipulation and could possibly extend the spin life-time of excitons. These features are particularly attractive for opto-spintronic applications and data storage [3].

A preliminary step towards the integration of perovskites in opto-spintronic devices is the time- and space-resolved optical study of their magnetic properties. In the present work, we study the spatio-temporal spin dynamics of Methylammonium Lead Tribromide (MAPbBr₃) by the unique combination of two spectroscopic methods: Faraday rotation spectroscopy and Ultrafast Holographic Transient microscopy (UHT) [4]. With our technique we get access to the polarization dependent carrier population as well as the Faraday angle, which is a measure for the spin-aligned magnetic moment. The UHT microscope, which works as a shot-noise limited, all-optical lock-in amplifier, has no upper limitations in the signal repetition rate and can resolve femtosecond dynamics with a sub-micrometre spatial resolution.

By spatially mapping the transient Faraday angle at different temperatures and fluences, we are hence able to investigate the evolution of optically spin-polarized excitons in time and space and identify the dominating spin relaxation mechanisms. This information is essential for the optimization of the materials' properties and the future realization of opto-spintronic systems.

References

- [1] Z. Tan et al., Bright light-emitting diodes based on organometal halide perovskite, *Nature Nanotechnology* volume 9, pages 687–692 (2014).
- [2] L. M. Pazos-Outón et al., Photon recycling in lead iodide perovskite solar cells, *Science*, Vol 351, Issue 6280 (2016).
- [3] A. Privitera et al., Perspectives of Organic and Perovskite-Based Spintronics, *Adv. Optical Mater.*, 9, 2100215 (2021).
- [4] M. Liebel et al., Ultrafast Transient Holographic Microscopy, *Nano Letters* 21 (4), 1666-1671 (2021).

SESSION EN04.09: Halide Perovskite Stability
Session Chairs: Daniele Catone and Linn Leppert
Thursday Afternoon, November 30, 2023
Hynes, Level 3, Room 300

1:30 PM EN04.09.01

Improving the Efficiency and Stability of Perovskite Solar Cells using π -Conjugated Aromatic Additives with Differing Hydrophobicities Brian Saunders; University of Manchester, United Kingdom

Improving the efficiency and stability of perovskite solar cells using π -conjugated aromatic additives with differing hydrophobicities

Perovskite solar cells (PSCs) continue to excite the research community due to their excellent power conversion efficiency (PCE) and relative ease of preparation. Additive engineering has played a decisive role in improving PSC performance and stability. In particular, π -conjugated aromatic additives (CAAs) offer key advantages such as high charge transport. However, the roles of hydrophobicity and structure in determining CAA performance as additives are still being established. Here, we investigate the effects of two coumarin additives on the PCE and stability of PSCs based on Cs_{0.05}(FA_{0.85}MA_{0.15})_{0.95}Pb(I_{0.85}Br_{0.15})₃ perovskite. The CAAs are coumarin methacrylate (CMA) and coumarin hydroxyethyl (CHE) and were added to the precursor perovskite solutions prior to film deposition with CMA being more hydrophobic than CHE. These additives increase the best PCE of 19.15% for the control to 21.14% and 21.28% for the best devices containing CHE and CMA, respectively. The stability of the devices with the additives are far superior to that of the control (CAA-free) system. The time lengths required for the PCE to decrease to 80% of the initial value for CMA- and CHE-containing devices are 98 and 38 days, respectively, compared to only 14 days for the control. The moisture and thermal stabilities of the systems containing CMA are markedly improved compared to those containing CHE and the control. Our results show that the extents of binding to Pb²⁺ and passivation increase as the coumarin's hydrophobicity increases which decreases recombination. Our findings show that adding CAAs with increasing hydrophobic character to the precursor perovskite solution is useful for achieving high-performance and long-term stable PSCs[1].

Reference

Wang et al, *Energy Env. Sci.* DOI: 10.1039/D3EE00247K (2023)

1:45 PM EN04.09.02

Unraveling Photoelectrochemical Degradation Pathways in Lead Mixed Halide Perovskites with Near Ambient Pressure XPS Michel De Keersmaecker, Neal Armstrong and Erin L. Ratcliff; The University of Arizona, United States

Long-term stability in metal halide perovskites has often been connected to defects in the electronic band gap, but rarely their (electro)chemical, physical and dynamic nature, as well as ion reactivity and mobility are considered. Interactions with O₂ and light excitation (i.e. from X-rays to UV-visible regions) have been suggested as culprits for bulk and interfacial degradation of perovskites and have been considered critical in the improvement of operational stability of photovoltaic devices and X-ray detectors.^[1-3] Possible explanations for this irreversible degradation process, however, range from intrinsic defects and phase segregation to electrochemical reactions as well as electronic and interfacial property changes.^[4-6] In this work, *in situ* degradation of device-relevant triple cation mixed halide perovskite films using dry O₂ gas using a near ambient pressure X-ray photoelectron spectroscopy (NAP-XPS) characterization method reveals the formation of a weakly coordinated form of Pb (relative to corner-sharing [PbI₆]⁴⁻ octahedra). Simultaneously, oxidized iodide species (I₃⁻) are formed in the illuminated near-surface region causing the bromide enrichment, consistent with “de-mixing” under stress. Once UHV conditions are restored, a slow return to the initial perovskite stoichiometry is observed, suggesting “self-healing” of defects when the low stress environment is reestablished. In non-stoichiometric films degradation rates accelerate for FAI-rich stoichiometries, but, more importantly, PbI₂-rich stoichiometries show reduced rates.

This NAP-XPS study demonstrates an important first step in a systematic approach to understanding the role(s) of ambient gases in conjunction with above band-gap illumination and other stressors that limit device stability. Prior to investing resources in high-throughput device construction, this NAP-XPS characterization technique will be an important asset in the investigation of interface engineering strategies for top contact (and bottom) modifications used as mitigation strategies in device optimization with focus on photoelectrochemical stability and energy level alignment if combined with UPS. Additionally, this work extends towards other semiconductive materials or material blends, where *in situ* chemical characterization will be essential to design and support next-generation electronics.

[1] N. Aristidou, C. Eames, I. Sanchez-Molina, X. Bu, J. Kosco, M. S. Islam, S. A. Haque, *Nature Communications* **2017**, 8, 15218.

[2] A. Senocrate, T. Acartürk, G. Y. Kim, R. Merkle, U. Starke, M. Grätzel, J. Maier, *Journal of Materials Chemistry A* **2018**, 6, 10847.

[3] D. Bryant, N. Aristidou, S. Pont, I. Sanchez-Molina, T. Chotchanangachaval, S. Wheeler, J. R. Durrant, S. A. Haque, *Energy and Environmental Science* **2016**, 9, 1655.

[4] K. Higgins, M. Lorenz, M. Ziatdinov, R. K. Vasudevan, A. V. Ievlev, E. D. Lukosi, O. S. Ovchinnikova, S. V. Kalinin, M. Ahmadi, *Advanced Functional Materials* **2020**, 30, 2001995.

[5] R. Guo, D. Han, W. Chen, L. Dai, K. Ji, Q. Xiong, S. Li, L. K. Reb, M. A. Scheel, S. Pratap, N. Li, S. Yin, T. Xiao, S. Liang, A. L. Oechsle, C. L. Weindl, M. Schwartzkopf, H. Ebert, P. Gao, K. Wang, M. Yuan, N. C. Greenham, S. D. Stranks, S. V. Roth, R. H. Friend, P. Müller-Buschbaum, *Nature Energy* **2021**, 6, 977.

[6] M. Ralaiarisoa, I. Salzmann, F. S. Zu, N. Koch, *Advanced Electronic Materials* **2018**, 4, 1800307.

2:00 PM *EN04.09.03

Resolving the Hydrophobicity of Me-4PACz Hole Transport Layer for Inverted Perovskite Solar Cells Dinesh Kabra; Indian Institute of Technology Bombay, India

[4-(3,6-Dimethyl-9H-carbazol-9-yl)butyl]phosphonic acid (Me-4PACz) self-assembled monolayer (SAM) has been employed in perovskite single junction and tandem devices demonstrating high efficiencies. However, a uniform perovskite layer does not form due to the hydrophobicity of Me-4PACz. Here, we tackle this challenge by adding a conjugated polyelectrolyte poly(9,9-bis(3'-(N,N-dimethyl)-N-ethylammonium-propyl-2,7-fluorene)-alt-2,7-(9,9-dioctylfluorene))dibromide (PFN-Br) to the Me-4PACz in a specific ratio, defined as Pz:PFN. With this mixing

engineering strategy of Pz:PFN, the PFN-Br interacts with the A-site cation is confirmed via solution-state nuclear magnetic resonance studies. The narrow full width at half maxima (FWHM) of diffraction peaks of perovskite film revealed improved crystallization on optimal mixing ratio of Pz:PFN. Interestingly, the mixing of PFN-Br additionally tunes the work function of the Me-4PACz as revealed by Kelvin probe force microscopy and built-in-voltage estimation in solar cells. Devices employing optimized Pz:PFN mixing ratio deliver open-circuit voltage (V_{OC}) of 1.16V and efficiency >20% for perovskites with a bandgap of 1.6 eV with high reproducibility and concomitant stability. Considering significant research on Me-4PACz SAM, our work highlights the importance of obtaining a uniform perovskite layer with improved yield and performance.

Reference:

Hossain, K.; Kulkarni, A.; Bothra, U.; Klingebiel, B.; Kirchartz, T.; Saliba, M.; Kabra, D. Resolving the Hydrophobicity of Me-4PACz Hole Transport Layer for High-Efficiency Inverted Perovskite Solar Cells. *arXiv Prepr. arXiv2304.13788* 2023.

SESSION EN05.08/EN04.06: Joint Session: Advanced Characterization
Session Chairs: Juan-Pablo Correa-Baena and Marina Leite
Wednesday Morning, November29, 2023
Hynes, Level 3, Room 311

9:00 AM *EN05.08/EN04.06.01

Long-Lived Hot-Carrier Light Emission in Sn Halide Perovskites[Maria AntoniettaLoi](#); University of Groningen, Netherlands

A long-lived hot carrier population is critical in order to develop hot carrier photovoltaic devices with efficiencies exceeding the Shockley–Queisser limit. Here, we report photoluminescence from hot-carriers with unexpectedly long lifetime (ns range) in tin triiodide perovskites. By correlating energy-resolved and time-resolved photoluminescence both a low and room temperature, with density functional theory calculations, we posit that this phenomenon is mostly associated with state-filling of band edge states. While phonon interactions have an effect, but minor. Measuring impulsive stimulated Raman scattering spectroscopy, we identify two coherent phonon modes (25 and 133 cm^{-1}) in FASnI₃, where the 133 cm^{-1} mode shows a fast decay ($< 1\text{ ps}$) and large dependence on the excitation fluence and energy. We further show that the phonons in FASnI₃ decay much faster compared to CsSnI₃, highlighting the stronger electron-phonon and phonon-phonon interaction in the hybrid compounds.

This work is of fundamental importance for our understanding of Sn-based hybrid perovskites and for an eventual future development of hot carrier photovoltaics.

9:30 AM *EN05.08/EN04.06.03

Influence of Methylammonium Chloride on the Formation and Properties of 3D Br-Rich Perovskites: an *In Situ* Investigation[Ana FlaviaNogueira](#); University of Campinas, Brazil

Owing to their exceptional properties, metal halide perovskites have been incorporated in tandem solar cells. For silicon-perovskite tandem, Br-rich perovskites with a wide-bandgap are required. However, the increase in Br content causes halide distribution heterogeneities and photoinstability. Methylammonium chloride (MACl, MA = CH₃NH₃⁺) is often added to the perovskite precursor solution to improve optoelectronic properties and performance. However, the effect of MACl additive on Br-rich perovskites is poorly understood.

In this presentation, we will summarize the previous studies from our group where *in situ* experiments coupled to synchrotron radiation were important to identify intermediates compounds, other metal halide phases during the steps of formation, crystallization and annealing.

In the second part of the talk, we will focus on metal halide perovskites with different amounts of Br and MACl using the N-methyl-2-pyrrolidone (NMP) solvent and the gas quenching deposition method. Simultaneous grazing-incidence wide-angle X-ray scattering (GIWAXS) and photoluminescence spectroscopy (PL) tracked perovskite crystallization and emission properties during the spin-coating and thermal annealing steps. For the perovskites without MACl, the formation of crystalline intermediates depends on the halide proportion. On the other hand, adding the MACl changes the formation mechanism inhibiting the formation of crystalline intermediates. Robust Pb-Cl bond formation decreased the interaction of PbX₆ octahedrons with solvent molecules, preventing the stabilization of intermediate phases containing the solvent. The destabilization of the intermediate phases promoted by the addition of MACl favored the formation of the better crystalline perovskite phase with preferential orientation in the [001] direction and inhibited the photoinduced halide segregation. Nano X-ray fluorescence (nano-XRF) mapping at identified transformations in the elemental distribution, recognizing Br-richer and poorer domains that are reduced for samples prepared with MACl.

10:00 AMBREAk

10:30 AM *EN05.08/EN04.06.04

Which Defects Matter in Photoactive Perovskites?[JoanneEtheridge](#)¹, WeilinLi¹, MengmengHao², QimuYuan³, JayPatel³, MichaelJohnston³ and LianzhouWang²; ¹Monash University, Australia; ²The University of Queensland, Australia; ³University of Oxford, United Kingdom

Photoactive perovskites show great potential for applications in solar cell devices, achieving remarkable power conversion efficiencies while using relatively low cost, low temperature production methods. However, there remain many challenges, from stability in air and under photon irradiation to ion migration and current density-voltage hysteresis.

In order to exploit the full potential of photoactive perovskites, it is critical to understand how macroscopic device performance depends on structure, from the micron to the atomic scale. Compared with the rigid diamond structure of silicon, the intrinsically flexible and versatile perovskite structure provides an entirely different structural landscape upon which to manipulate properties, such as optical bandgaps. Furthermore, it can accommodate a different class of structural defects which can influence performance.

Here we investigate the relationship between local crystal structure, defect structure and device performance in quantum dot and thin film photoactive perovskites and associated devices using carefully devised ultralow dose electron microscopy methods [1-3] correlated with device characterisation.

In high performance Cs_{1-x}FA_xPbI₃ quantum dot devices [4], we identify the presence of planar defects with face-sharing octahedra and show that removing them leads to significantly improved power conversion efficiency and carrier lifetime [5] (consistent with observations in hybrid organic-inorganic MA_{1-x}FA_xPbI₃ thin films [6]). We also identify the formation of FA⁺/I⁻ vacancy pairs and elucidate their role in ion migration and A-site dependent structural phase changes [7].

In CsPb(I_{1-x}Br_x)₃ films, we identify the crystal structures and defect structures associated with different halide compositions and deposition parameters, including twin and antiphase boundaries. Using sub-10e/Å² atomic resolution imaging techniques, we identify the local atomic structure of these planar defects and consider their impact on device performance, providing insights into the structural environments necessary to optimise device performance [8].

[1] Rothmann MU, Li W, Zhu Y, Liu A, Ku, Bach U, Etheridge J, Cheng YB; *Advanced Materials* 1800629 (2018)

[2] Rothmann MU, Li W, Etheridge J, Cheng YB *Advanced Energy Materials* 7 23 (2017)

[3] Rothmann MU, Li W, Zhu Y, Bach U, Spiccia L, Etheridge J, Cheng YB *Nature Comm.* 8 14547 (2017)

[4] Hao, M et al., *Nature Energy* 5 (1) 79-88 (2020)

[5] Li W, Hao MM, Wang L, Etheridge, J, in preparation (2023)

[6] Li W, Rothmann MU, Zhu Y, Chen W, Yuan Y, Choo YY, Yang C, Wen X, Bach U, Cheng YB, Etheridge J *Nature Energy* 6 624–632 (2021)

[7] Li W, Hao MM, Wang L, Etheridge, J, submitted (2023)

[8] Li W et al, in preparation (2023)

This work was supported by ARC grants DP200103070, DP200101900, FL190100139; EPSRC grants EP/T025077/1, EP/V010840/1, EP/W007975/1, ACAP and ARENA and used the Thermo Fisher Scientific Titan³ 80-300 FEG-TEM (ARC LE0454166) & Spectra Phi FEG-TEM (ARC LE170100118) in the Monash Centre for Electron Microscopy.

11:00 AM *EN05.08/EN04.06.05

Structural and Ionic Stability Challenges in Metal Halide Perovskites[LauraHerz](#); University of Oxford, United Kingdom

Organic-inorganic metal halide perovskites have emerged as attractive materials for solar cells with power-conversion efficiencies of single-junction devices now exceeding 25%. However, the low hurdle for ionic migration, and the structural flexibility of the perovskite structure still pose both opportunities and challenges to their commercialization in light-harvesting

applications.

We discuss the peculiar mechanisms underlying detrimental halide segregation in mixed iodide-bromide lead perovskites with desirable electronic band gaps for silicon tandems.^[1-4] Surprisingly, halide segregation results in negligible impact to the THz charge-carrier mobilities, but is impacted by remarkably fast, picosecond charge funnelling into the narrow-bandgap I-rich domains that enhances radiative recombination.^[2] Our combinatorial, in-situ photoluminescence and X-ray diffraction measurements^[3,4] reveal how such halide segregation is affected by A-cation choice^[3] and the presence of charge-extraction layers.^[4] We further demonstrate a temperature-dependent reversal of halide segregation at temperatures above ambient.^[5] We observe that, with increasing temperature, halide segregation in $\text{CH}_3\text{NH}_3\text{Pb}(\text{Br}_{0.4}\text{I}_{0.6})_3$ first accelerates toward 290 K, before slowing down again toward higher temperatures. Such reversal is attributed to the trade-off between the temperature activation of segregation, for example through enhanced ionic migration, and its inhibition by entropic factors. High light intensities meanwhile can also reverse halide segregation; however, we find this to be only a transient process that abates on the time scale of minutes.^[5]

In addition, we discuss the peculiar effect of “intrinsic quantum confinement” (QC) exhibited by FAPbI_3 perovskite, apparent through oscillatory features in the absorption spectrum^[6-8] that suggest the presence of nanoscale features of periodicity around 10–20 nm present in sub-volumes.^[6] We show^[7] that such nanoscale electronic effects can be controlled through partial replacement of the FA cation with Cs, and allow for photon emission, highlighting their potential usefulness to light-emitting devices and single-photon sources.^[7] However, we reveal that such QC features are clearly detrimental to photovoltaic operation.^[8] We explore three common solution-based film-fabrication methods for FAPbI_3 , and show that elimination of these QC absorption features yields increased power conversion efficiencies (PCEs) and short-circuit currents, suggesting that quantum confinement hinders charge extraction. A meta-analysis of literature reports, covering 244 articles and 825 photovoltaic devices incorporating FAPbI_3 films corroborates our findings, indicating that PCEs rarely exceed a 20% threshold when such absorption features are present. Accordingly, ensuring the absence of these absorption features should be the first assessment when designing fabrication approaches for high-efficiency FAPbI_3 solar cells.

[1] A. J. Knight and L. M. Herz, *Energy Environ. Science* **13**, 2024 (2020).

[2] S. G. Motti, J. B. Patel, R. D. J. Oliver, H. J. Snaith, M. B. Johnston, L. M. Herz, *Nat. Commun.* **12**, 6955 (2021).

[3] A. J. Knight, J. Borchert, R. D. J. Oliver, J. B. Patel, P. G. Radaelli, H. J. Snaith, M. B. Johnston, and L. M. Herz, *ACS Energy Letters* **6**, 799 (2021).

[4] V. J.-Y. Lim, A. M. Ulatowski, C. Kamaraki, M. T. Klug, L. Miranda Perez, M. B. Johnston, and L. M. Herz, *Adv. En. Mater.* **12**, 2200847 (2022).

[5] A. D. Wright, J. B. Patel, M. B. Johnston, L. M. Herz, *Advanced Materials* **35**, 2210834 (2023).

[6] A. D. Wright, G. Volonakis, J. Borchert, C. L. Davies, F. Giustino, M. B. Johnston, and L. M. Herz, *Nature Materials* **19**, 1201 (2020).

[7] K. A. Elmestekawy, A. D. Wright, K. B. Lohmann, J. Borchert, M. B. Johnston, and L. M. Herz, *ACS Nano* **16**, 6940 (2022).

[8] K. A. Elmestekawy, B. M. Gallant, A. D. Wright, P. Holzhey, N. K. Noel, M. B. Johnston, H. J. Snaith, L. M. Herz, *ACS Energy Letters* **8**, 2543 (2023).

11:30 AM *EN05.08/EN04.06.06

Defects, Devices and Degradation of Metal Halide Perovskites: An Electrochemist’s Perspective[Erin L. Ratcliff](#); University of Arizona, United States

Defects are considered to be one of the most prominent contributions to diminished power conversion efficiencies and long-term stability in printable metal halide perovskite materials and optoelectronic devices. Defects can arise from a combination of point defects, grain boundaries, charge transfer with Lewis acid/base sites at the contacts, and/or mobile redox-active halides. Thus every perovskite composition and contact choice can result in differences in defect distributions.

Defect states have most often been characterized using electrical, optical, and magnetic techniques; however, independently assessing donor and acceptor defect quantities and energetics using a direct experimental approach with few empirical assumptions can be challenging. Realization of high-performing and long-term stable devices requires a combination of method advancement for the quantification of defects and mitigation strategies.

This talk will discuss emerging electrochemistry-based measurement science approaches to quantify the distribution and energetics of donor and acceptor defects in a prototypical perovskite solar cell material ($\text{FA}_{.79}\text{MA}_{.16}\text{Cs}_{.05}\text{Pb}(\text{I}_{.87}\text{Br}_{.13})_3$ (or $\text{Cs}_{.05}\text{FA}_{.79}\text{MA}_{.16}$), with demonstrations of the methodology to other perovskite active materials. We utilize a solid-state electrolyte top contact to create “half-cells” of device-relevant material stacks under realistic electric fields. This allows us to spectroscopically assess onsets in valence and conduction bands under conditions of *operando*, as well as quantify near-band defects using redox probes. Connections to device performance, including modifications to the near-surface region of hole-transporting layers (i.e. NiOx), will be provided as well as preliminary results to understand degradation pathways using near-ambient pressure x-ray photoelectron spectroscopy and *operando* x-ray scattering. Collectively, this developed tool-suite provides a holistic approach to understand defects, device performance and stability in this exciting class of materials.

SYMPOSIUM EN05

Halide Perovskites—From Fundamentals to Applications
November 27 - December 7, 2023

Symposium Organizers

Marina Leite, University of California, Davis
Lina Quan, Virginia Institute of Technology
Samuel Stranks, University of Cambridge
Ni Zhao, Chinese University of Hong Kong

Symposium Support

Gold

Enli Technology Co., LTD

Bronze

ACS Energy Letters | ACS Publications
APL Energy | AIP Publishing

* Invited Paper

+ JMR Distinguished Invited Speaker

SESSION EN05.01: Fundamental Understanding of Halide Perovskites I
Session Chairs: Marina Leite and Lina Quan

10:30 AM *EN05.01.01

Progress in Perovskite Active Layers and Interfaces for Energy Capture and Utilization Edward H. Sargent^{1,2}; ¹Northwestern University, United States; ²University of Toronto, Canada

I will discuss recent advances in managing the quality and reliability of perovskite active layers, and interfaces, in recent years. I will include both 2D/3D strategies and also molecular adlayer approaches to producing reliable interfaces.

11:00 AM *EN05.01.02

Models of Disorder in Halide Perovskites Aron Walsh; Imperial College London, United Kingdom

The structural arrangement of metal halide perovskites varies in space and time. Beyond the conventional vibrations of atoms around their average positions, collective motion in the form of octahedral tilting and molecular librations/rotations introduces additional layers of complexity in the dynamic crystal structure. To complicate matters further, dilute point defects, such as charged vacancies and interstitials, exist in a diverse landscape of extended defects including dislocations, polytypes, and grain boundaries. There can also be chemical gradients due to mixing on the A, B or X crystallographic positions, e.g. as found in mixed formamidinium/methylammonium, tin/lead, and iodide/bromide compounds. I will discuss our latest understanding of these phenomena at the atomic scale drawing from our work on data-driven materials modelling [1,2,3] and linked to multi-modal experimental characterisation [4].

1. "Evolutionary exploration of polytypism in lead halide perovskites", *Chemical Science* 12, 12165 (2021)
2. "Structural dynamics descriptors for metal halide perovskites", arXiv:2304.04714 (2023)
3. "Dynamic local structure in caesium lead iodide: spatial correlation and transient domains", arXiv:2305.11617 (2023)
4. "Stabilized tilted-octahedra halide perovskites inhibit local formation of performance-limiting phases", *Science* 374, 1598 (2021)

11:30 AM EN05.01.03

Optimization of Indium Oxide Interconnecting Layer for All Perovskite Tandem Solar Cells with Efficiency > 26% Gaurav Kapil^{1,2}, Yasuhiro Fujiwara¹, Qing Shen¹, Hiroshi Segawa² and Shuzi Hayase¹; ¹University of Electrocommunications, Japan, Japan; ²The University of Tokyo, Japan

All perovskite tandem solar cells (APTSCs) are now showing power conversion efficiencies (PCEs) more than the highest reported single-junction perovskite and silicon solar cells [1,2]. The rapid rise in the performance of APTSC can be ascribed to the improvement in the performances of both top (wide bandgap, WBG) and bottom (narrow bandgap, NBG) cells. Recently, the focus has been on the reduction of halide segregation and improvement of open circuit voltage (Voc) in WBG cells which led to an immense increase in Voc of APTSC to 2.2V [2,3]. We noticed that most of the recent reports on efficient APTSCs utilize SnOx (prepared by atomic layer deposition) coated with Au (1-2nm) as an interlayer. However, the optical loss due to the use of Au nanoparticles can't be ignored. Therefore, in this work, we focused on the preparation of indium oxide doped with zinc oxide (IZO) as an interconnecting layer in place of Au nanoparticles to reduce the optical loss and improvement of facile hole and electron recombination at the SnOx layer. It is explored that the physical properties of IZO can be tuned while its preparation which finally plays a crucial role in enhancing the Voc of the APTSC. The other advantages that come with the IZO are that electrical properties can be changed according to the hole transport layer (HTL) utilized. So far, PEDOT:PSS is the only hole transport layer that can be used for efficient APTSCs. Therefore, the use of IZO interconnect further gives flexibility in choosing other HTLs such as self-assembled monolayers. In conclusion, we obtained PCE of 26.39% for APTSC with a Voc of 1.94V, Jsc of 17.18 mA/cm², and FF of 0.79. APTSC employing Au nanoparticle interlayer showed an inferior PCE of 22.32% with a Voc of 1.84V, Jsc of 15.4 mA/cm², and FF of 0.79. Moreover, in this work, we will support the increase in device performance with the use of different IZO interconnect by evaluating the carrier mobility, diffusion length, charge transport time, and recombination time. Also, its role in charge transport between the top and bottom cells will be discussed.

References:

1. <https://www.nrel.gov/pv/cell-efficiency.html>, NREL chart accessed on 6th June.
2. Q. Jiang and K. Zhu et al, Compositional texture engineering for highly stable wide-bandgap perovskite solar cells, *Science*, 378, 1295–1300 (2022).
3. H. Chen and E. H. Sargent et al, Regulating surface potential maximizes voltage in all-perovskite tandems, *Nature*, 613, 676–681 (2023)

11:45 AM EN05.01.04

Preserving Bond Ionicity under Illumination to Achieve Photostable Halide Perovskites Malgorzata Wierzbowska; Institute of High Pressure Physics Polish Academy of Sciences, Poland

Lead halide perovskites (LHPs) with the formula ABX₃ are very efficient materials for optoelectronic devices: solar cells, light-emitting diodes, lasers, photodetectors, γ -detectors, and field effect transistors. But they are very fragile and sensitive to humidity, temperature, and operating conditions such as voltage bias and light. The reason is their weakly ionic structure with twice lower atomic ionicities than those in oxides. Photostability is difficult to achieve in LHP, due to the nature of electronic states that originate mainly from the halide anions in the valence band and B cations in the conduction band; hence, the charge transfer lowers the ionicity at the B–X bond.

To date, the A cations used have been optically inactive and only served as one-electron donors for the charge balanced BX₃ frame. We propose a mechanism of photoexcitation acting between two different A cations, namely SLi₃ and SH₃, while the inorganic frame remains unchanged under illumination preventing B–X bond breakage and halide migration. Demand for a specific crystal localization of the optical excitations is a new factor for achieving photostability, in addition to a control of the ionic radii, defects, morphology, and surface and interface stabilization.

We theoretically demonstrate that the absorption spectra of (SLi₃,SH₃)PbI₃ perovskite are optically efficient for the distributions of two types of A cations that form the planar structures. The excitations in such case take place over the interface. The optimal light polarization should be oriented with the electric vector perpendicular to the interface between the regions with two types of molecular cations, that means the beam direction oriented within the interface plane. The spectra were obtained by solving the Bethe-Salpeter equation. The results are published [1].

[1] Malgorzata Wierzbowska and Alicja Miklas, *J. Phys. Chem. C* 2023, 127, 3750–3759; doi: 10.1021/acs.jpcc.2c08110

SESSION EN05.02: Fundamental Understanding of Halide Perovskites II

Session Chairs: Connor Bischak and Ni Zhao

Monday Afternoon, November 27, 2023

Hynes, Level 3, Room 311

1:30 PM *EN05.02.01

Heterointerface and Intragrain Microstructures of Perovskite Semiconductors Yuanyuan Zhou; Hong Kong Baptist University, China

Heterointerface and intragrain microstructures are prominent factors influencing the properties and performance of perovskite semiconductors, which remain *terra incognita*. In my talk, I will discuss our recent developments on the novel characterization and tailoring of these microstructures, which elevate our fundamental understanding of microscopic structure-property-performance relationship in perovskites. Specifically, I will demonstrate two examples of perovskite-substrate heterointerface designs, featuring an interlocking interfacial microstructure and a flattened grain-boundary groove structure, respectively. Such microstructural designs contribute to improved carrier injection, chemical stability, and more importantly, (opto-)mechanical reliability of resulting perovskite solar cells. Then, we will illustrate our findings on performance-limiting intragrain defects and their structural dynamics, enabled by our latest innovations in scanning transmission electron microscopy methodologies. Finally, I will provide the perspectives and current Σ Lab (www.alvinyzhou.com) efforts pushing the frontier of perovskite knowledge as well as the broad materials research *via* unravelling novel microstructure phenomena.

2:00 PM EN05.02.02

Local Charge Carrier Dynamics in Lead Halide Perovskites by Nano Surface Photovoltage Spectroscopy Yenal Yalcinkaya¹, Pascal N. Rohrbeck¹, Lukas Schmidt-Mende² and Stefan A.

Understanding electron and ion dynamics is an important task for improving lead halide perovskites based solar cells and related devices. Perovskite materials usually have a delicate nano- and micro structure that influences the device parameters. Here, macroscopic measurement techniques are not sufficient. This study investigates the spatial defect distribution in the vicinity of grain boundaries (GB). To this end, we introduce Nano surface photovoltage spectroscopy (Nano-SPV) via time-resolved Kelvin probe force microscopy (tr-KPFM) [1,2]. By measuring the SPV decay on perovskite samples with small, large, and passivated grains, areas of increased charge carrier recombination, ion migration, and defects were locally detected. Using Nano-SPV, we revealed local SPV overshoots in the vicinity of grain boundaries following an illumination pulse. Furthermore, we introduce a new KPFM-based method to map the local light ideality factor within the perovskite films. The ideality factor is correlated to the dominant charge recombination processes within the absorber layer. Our results clearly show an improved uniformity of SPV and SPV decay distribution within the perovskite films upon passivation. Furthermore, the perovskite films with large grains show better recombination properties based on SPV decay and ideality factor values.

[1] A. Axt, I. M. Hermes, V. W. Bergmann, N. Tausendpfund, and S. A. L. Weber, *Know Your Full Potential: Quantitative Kelvin Probe Force Microscopy on Nanoscale Electrical Devices*, Beilstein J. Nanotechnol. **9**, 1809 (2018).

[2] S. A. L. Weber, I. M. Hermes, S.-H. Turren-Cruz, C. Gort, V. W. Bergmann, L. Gilson, A. Hagfeldt, M. Graetzel, W. Tress, and R. Berger, *How the Formation of Interfacial Charge Causes Hysteresis in Perovskite Solar Cells*, Energy Environ. Sci. **11**, 2404 (2018).

2:15 PM EN05.02.03

R&D on Gateway Technologies for Perovskite Solar CellsTaoXu; Northern Illinois University, United States

Various formulations have been developed to improve the stability of hybrid perovskite layer in perovskite solar cells (PSCs), while their mutual compatibility remains uncertain. Thus, it is important to focus future R&D on technologies that are both adaptable to all other formulations and also independently exhibit added enhancement in stability. In addition, >50% infrastructure investment of PSC production line will be on the expensive and energy-costly vacuum evaporation equipment. In this talk, based on the fundamental reaction kinetics, we will present a low-cost isotope technology that is adaptable to any existing PSC formula and also retards degradation reaction kinetics, thus to improve stability of PSCs as an add-on feature independently. We will also present a disruptive vacuum-free paint & brush coating technology based on basic band structure theory for back electrode deposition for n-i-p configured PSCs, which also circumvents the use of expensive gold as the back electrode. These novel methods are promising gateway technologies that either synergistically enhance the stability of PSCs or reshape the infrastructure of PSC production line in the forthcoming commercialization of PSCs.

2:30 PMBREAK

3:00 PM *EN05.02.04

Accelerating The Transition from Lab to Fab via High Throughput Automated Synthesis and Characterization of Metal Halide PerovskitesJongheeYang¹, SherylL. Sanchez¹, BenjaminLawrie², YipengTang¹, BinHu¹, JuanitaHidalgo³, SergeiV. Kalinin¹, Juan-PabloCorrea-Baena³ and MahshidAhmadi¹; ¹University of Tennessee, Knoxville, United States; ²Oak Ridge National Laboratory, United States; ³Georgia Institute of Technology, United States

Metal halide perovskites have garnered considerable attention in the field of optoelectronics due to their exceptional properties. However, so far little has been understood based on the fundamental principles for designing the functional perovskites, which is now crucially decelerating the lab-to-fab transformation and realization of the scalable manufacturing of these materials for optoelectronics. In this talk I will discuss the potential of machine learning-driven high throughput automated experiments to expedite the discovery of hybrid perovskites, optimize processing pathways, and enhance the understanding of formation kinetics [1-4]. Notably, the utilization of a high-throughput robotic system to accelerate the exploration of the ligand-assisted reprecipitation (LARP) method for synthesizing perovskite nanocrystals represents a significant contribution to the field [5]. The workflow demonstrated in this study serves as a powerful tool for constructing detailed chemical maps of perovskite nanocrystal synthesis, enabling tailored customization of their functionalities. Additionally, another study showcases how high throughput automated synthesis provides a comprehensive guide for designing optimal precursor stoichiometry to achieve functional quasi-2D perovskite phases in films capable of realizing high-performance optoelectronics [3,4]. I further introduce the concept of co navigation of theory and experiment spaces to accelerate discovery and design of hybrid perovskites. These studies exemplify how a high-throughput automated experimental workflow effectively expedites discoveries and processing optimizations in complex materials systems with multiple functionalities, facilitating their realization in scalable optoelectronic manufacturing processes.

References:

1. Yang, J., Ahmadi, M. Empowering scientists with data-driven automated experimentation. *Nat. Synth* (2023). DOI: 10.1038/s44160-023-00337-z
2. Yang J., Kalinin S.V., Cubuk E.D. Ziatdinov M., Ahmadi M. Toward self-organizing low-dimensional organic-inorganic hybrid perovskites: Machine learning-driven co-navigation of chemical and compositional spaces. *MRS Bulletin* **48**, 164–172 (2023). DOI: 10.1557/s43577-023-00490-y
3. Yang J, Hidalgo J, Li R, Kalinin SV, Correa-Baena J-P, Ahmadi M. Accelerating materials discovery by high-throughput GIWAXS characterization of quasi-2D formamidinium metal halide perovskites. *ChemRxiv* (2023). DOI: 10.26434/chemrxiv-2023-x7sfr
4. Yang J, Lawrie BJ, Kalinin SV, Ahmadi M. High-Throughput Automated Exploration of Phase Growth Kinetics in Quasi-2D Formamidinium Metal Halide Perovskites. *ChemRxiv* (2023). DOI: 10.26434/chemrxiv-2023-zcv10
5. Sanchez S. L., Tang Y., Hu B., Yang J., Ahmadi M., Understanding the ligand-assisted reprecipitation of CsPbBr₃ nanocrystals via high-throughput robotic synthesis approach. *Matter* **6**, 1–19 (2023). DOI: 10.1016/j.matt.2023.05.023

3:30 PM EN05.02.06

Surface and Interface Passivation for Perovskite DevicesBinChen; Northwestern University, United States

Perovskite photovoltaics have made remarkable progress in the last decade, with the best lab perovskite cell now achieving over 26% power conversion efficiency. The key to this rapid improvement lies in understanding and controlling the interfaces in perovskite solar cells. In this talk, I will focus on interface engineering in perovskite solar cells (e.g., energy alignment, doping, and carrier dynamics), including the construction of heterostructures of multi-dimensional perovskites. I will discuss surface passivation by synthesizing 2D perovskites atop 3D bulk perovskite. The precise control over the dimensionality of these quantum-confined 2D thin layers enables us to achieve efficient carrier transport across the interface while maintaining desirable trap passivation. I will also discuss field-effect passivation when the perovskite active layer is in contact with a carrier transport layer. Modulating the minority carrier population at the perovskite/C60 interface is critical for reducing interfacial recombination. Lastly, I will explore how we combine chemical and field-effect passivation to achieve optimal passivation. Adjusting interface conditions will be even more important as we move towards multi-junction device architecture in pursuit of higher efficiency.

3:45 PM EN05.02.07

Connecting Structure and Self-Trapped Excitons in the Double Perovskite Elpasolites: A Computational StudyChristopherSavory; University of Birmingham, United Kingdom

Inorganic lead halide perovskites have shown promise in light-emissive applications, however there is significant drive to find similar behaviour in more sustainable, lead-free systems. Lead-free perovskite-based emitters have included two core classes of materials: double perovskites, in which the separation of the B site as Cs₂M^(III)X₆ allows moving to In or Bi, and 'defect perovskites' belonging to the Cs₂M^(IV)X₆ (M = Zr, Hf, Sn, X = Cl, Br) family; both classes have been suggested to show self-trapped excitonic behaviour and resultant broadband white light emission.^{1,2} The former of these two families, the elpasolites, has wide compositional flexibility between the two perovskite B-sites and the halide anion, though focus has remained on the successful doped Cs₂AgInCl₆. With many other phases having been synthesized over a decades long history of research however, more elpasolites could be of interest as emissive materials – and modern computational chemistry techniques can be used to help predict such behaviour.

In this computational study, we initially examine the structural behaviour of Cs₂NaBiCl₆ which has been suggested to show pressure-dependent luminescence arising from self-trapped excitons.³ By using techniques to track instabilities in calculated phonon spectra, we are able to help explain this behaviour⁴ – and move to further predict other elpasolites, which have received minimal experimental study, that could demonstrate similar dependence. Secondly, by using a combination of many-body perturbation theory calculations within the Questaal code⁵ to explicitly simulate excitonic properties, and also simulating an ansatz of the self-trapped excitonic state using a supercell method with hybrid Density Functional Theory, as developed for other halide emitters,⁶ we are able to also quantitatively predict self-trapped excitonic behaviour in these systems. We then compare these results to those established for 'defect perovskite' systems to establish more generalized ideas on the role of structure, composition and electronic localization in enabling self-trapped excitonic emission. Through studying these structure-property links in the elpasolite family, we hope to further open the field of Pb-free efficient light emitters.

(1) Smith, M. D.; Karunadasa, H. I. *Acc. Chem. Res.* **2018**, *51*, 619.

(2) Luo, J.; Wang, X.; Li, S.; Liu, J.; Guo, Y. *et al. Nature*, **2018**, *563*, 541

(3) Jiang, J.; Niu, G.; Sui, L.; Wang, X.; Zhang, Y.; Che, L.; Wu G.; Yuan K. and Yang X. *J. Phys. Chem. Lett.* **2021**, *12*, 7285–7292

- (4) Skelton, J.M.; Burton, L. A.; Parker, S.C.; Walsh, A.; Ki, C-E. et al. *Phys. Rev. Lett.* **2016**, *117*, 075502
(5) Pashov, D.; Acharya, S.; Lambrecht, W.R.L.; Jackson, J.; Belashchenko, K.D.; Chantis, A.; Jamet, F.; van Schilfgaarde, M. *Comp. Phys. Commun.*, **2020**, *249*, 107065
(6) Jung, Y-K., Kim, S.; Kim, Y.C. and Walsh, A. *J. Phys. Chem. Lett.*, **2021**, *12*, 8447-8452

4:00 PM EN05.02.08

Machine Learning Assisted Development of Sn/Pb Free Perovskites Solar Cells Ankit Choudhary¹, Alex Mohan¹, Miah A. Sahriar², Abdul H. Rumman², Md. T. Islam³, Saquib Ahmed⁴ and Haralabos Efsthathiadis¹; ¹SUNY Polytechnic Institute Albany, United States; ²Bangladesh University of Engineering and Technology, Bangladesh; ³SUNY – University at Buffalo, United States; ⁴SUNY – Buffalo State University, United States

This study focuses on Cs₃Bi₂I₉, a zero-dimensional perovskite absorber material with great potential for photovoltaic applications. We employed Machine Learning (ML) techniques to understand and optimize the performance of Cs₃Bi₂I₉ perovskite solar cells. A prepared sub-dataset comprising 26,457 experimentally developed perovskite solar cell device data was utilized for ML calculations. The cleaned dataset contained 29 features and four target variables, including open circuit voltage (Voc), short circuit current density (Jsc), fill factor (FF), and power conversion efficiency (PCE). Among the models, Random Forest Regressor showcased the best performance. Predicted values for Voc, Jsc, FF, and PCE were determined to be 0.562 V, 9.544 mA/cm², 0.508, and 5.356%, respectively.

We characterized the different layers of the device using techniques such as X-ray Photoelectron Spectroscopy, Ultraviolet-Visible Spectroscopy, Atomic Force Microscopy, and Ellipsometry to gain insights into the individual layers' properties. The absorber layer bandgap was found to be 1.9 eV, which indicates that Cs₃Bi₂I₉ exhibits favorable characteristics for indoor photovoltaic applications. The solution-processed spin-coated complete solar cells have the structure glass/FTO/c-TiO₂/Cs₃Bi₂I₉/CuSCN/Ag. Preliminary tests on the complete Cs₃Bi₂I₉ perovskite solar cell have shown the values for Voc, Jsc, FF, and PCE as 0.447 V, 29.08 mA/cm², 0.291, and 3.63%, respectively. These initial results indicate the potential of Cs₃Bi₂I₉ as a viable material for solar cell applications.

4:15 PM EN05.02.09

On Characterizing Perovskite X-Ray Detectors for Low-Dose Imaging Kostiantyn Sakhatskyi^{1,2}, Ying Zhou³, Vitalii Bartosh^{1,2}, Gebhard J. Matt^{1,2}, Jingjing Zhao⁴, Sergii Yakunin^{1,2}, Jinsong Huang^{3,3} and Maksym V. Kovalenko^{1,2}; ¹ETH Zurich, Switzerland; ²Empa–Swiss Federal Laboratories for Materials Science and Technology, Switzerland; ³University of North Carolina at Chapel Hill, United States; ⁴Southwest University, China

The last decade has seen a renewed exploration of semiconductor materials for X-ray detection, foremost focusing on lead-based perovskites and other metal halides as direct-conversion materials and scintillators. However, the reported performance characteristics are often incomplete or misleading in assessing the practical utility of materials. Here we offer guidelines for choosing, estimating, and presenting the relevant detector figures of merit and discuss their relation to basic materials properties. We also provide ready-to-used tools for calculating these figures of merit: MATLAB application, Mathcad worksheet and a website. The X-ray detectors for medical imaging are at the focus for their increasing societal value and since they bring about the most stringent requirements as the image shall be acquired at as low as reasonably attainable (*i.e.* ALARA principle) dose received by the patient.

4:30 PM EN05.11.01

Reduced Melting Temperature of Lead-Free 2D Perovskite Semiconductor to 142 °C Akash Singh, Ethan Crace, Yi Xie and David B. Mitzi; Duke University, United States

Hybrid metal halide perovskite (MHP) semiconductors are currently revolutionizing the research realm of electronic and photonic materials, with an overwhelming number of studies conducted on their synthesis and device fabrication and with particular emphasis on deposition of device quality films. The dominant film deposition techniques involve solution processing and vapor deposition, which have their advantages, but may be harmful to humans and the environment. Melt processing as an alternative route has been demonstrated before; however, due to the high T_m (close to $T_d \sim 200$ °C, the degradation onset temperature), the approach tends to induce partial decomposition (loss of organic component and halides) in MHPs, which hinders their utility in certain applications. Furthermore, slight loss of organic components/halides creates defects that may significantly harm the optoelectronic properties of the MHP film, pointing to a need to develop MHPs with lower T_m . In this work, we therefore synthesized a lead-free 1-methylhexylammonium tin iodide (1-MeHa₂SnI₄) perovskite. Single crystal X-ray diffraction is used to resolve the crystal structure of the resulting compound, confirming its crystallization in a two-dimensional Ruddlesden-Popper phase. Synthetic design rules toward obtaining a low T_m value are summarized and adopted to achieve an exceptionally low T_m of 142 °C. The hydrogen bonding, cation penetration, inter- and intra-octahedral distortions, and electronegativities (ionic sizes) of the synthesized perovskite and its corresponding lead counterpart (1-MeHa₂PbI₄) are studied to understand the reduced T_m along with the comparison of the existing pairs of meltable Sn and Pb MHPs with same organic cations. Additionally, we developed a protocol to assess the stability of the MHP melt by performing iterative calorimetric scans, monitoring changes in the T_m and melt crystallization temperature (T_c) through multiple heat-cool cycles. This analysis confirmed the stable nature of the 1-MeHa₂SnI₄ melt, leading to its facile melt deposition into films on flexible substrates with visible range optoelectronic properties. Our present work serves as a display of the strength of chemical compositional engineering of perovskite structures for tuning the thermal properties, resulting in exceptionally low T_m and facile melt-processing of MHPs. Reduction in T_m not only lowers the thermal budget of the deposition process but also renders robustness to the melt for the development of cost-effective flexible optoelectronic devices on plastic/polymer substrates.

SESSION EN05.03: Poster Session I: Fundamental Understanding of Halide Perovskites
Session Chairs: Marina Leite and Lina Quan
Monday Afternoon, November 27, 2023
Hynes, Level 1, Hall A

8:00 PM EN05.03.01

Anharmonic Electron-Phonon Coupling in Polymorphous Perovskites Marios Zacharias¹, George Volonakis², Feliciano Giustino³ and Jacky Even¹; ¹INSA Rennes, France; ²Universite de Rennes 1, ISCR, France; ³The University of Texas at Austin, United States

Ab initio simulations of halide perovskites typically assume that the potential energy felt by electrons is defined with the nuclei fixed at their crystallographic Wyckoff positions. This assumption misses the effect of local disorder (polymorphism) which affects profoundly the mechanical, optoelectronic, and light-absorbing properties of halide perovskites. In this talk, I will discuss the important role of *polymorphism* and *anharmonicity* in the electron-phonon coupling of halide perovskites [1]. In particular, I will demonstrate that (i) polymorphism is at the origin of overdamped and strongly coupled vibrational dynamics, (ii) anharmonic optical vibrations dominate thermal renormalization of their band gaps, and (iii) polymorphism is the key to understand the gradual variation of their band gaps around the phase transition temperatures. To address these points we develop a new very efficient methodology for anharmonic lattice dynamics, relying on the special displacement method (A-SDM) [2]. The A-SDM is a very simple tool that can be exploited by both condensed matter theorists and experimentalists, opening the way for systematic simulations of anharmonic phonons. Overall, our new theoretical advances [1,2] set up a new framework for interpreting the fundamental mechanisms driving the optoelectronic, transport, and photovoltaic properties of halide perovskites.

[1] M. Zacharias, G. Volonakis, F. Giustino, and J. Even, *Anharmonic electron-phonon coupling in ultrasoft and locally disordered perovskites*, arXiv:2302.09625 (2023)

[2] M. Zacharias, G. Volonakis, F. Giustino, and J. Even, *Anharmonic lattice dynamics via the special displacement method*, arXiv:2212.10633 (2023)

Acknowledgments: I acknowledge funding from the European Union (project ULTRA-2DPK / HORIZON-MSCA-2022-PF-01 / Grant Agreement No. 101106654). Views and opinions expressed are however those of the authors only and do not necessarily reflect those of the European Union or the European Commission. Neither the European Union nor the granting authority can be held responsible for them. J.E. acknowledges financial support from the Institut Universitaire de France.

8:00 PM EN05.03.03

Towards Thermally Stable Wide Bandgap Perovskites by Vacuum Deposition Methods Lidon Gil-Escrig, Isidora Susic, Michele Sessolo and Henk J. Bolink; University of Valencia, Spain

Wide bandgap perovskites are very relevant semiconductors in view of their potential for applications in tandem devices, combined with narrow bandgap absorbers such as silicon, CIGS, or a complementary perovskite. Vacuum deposition methods are increasingly applied to the preparation of perovskite films and devices, in view of the possibility to prepare multilayer structures, common to all tandem architectures. However, vacuum-deposited, wide-bandgap solar cells based on mixed-cation and mixed-anion perovskites have been scarcely reported. Here we present multi-component wide bandgap perovskites obtained by using several thermal sources in co-sublimation processes. We review processes to deposit material formulations of increasing complexity, from double to triple cation/mixed halide perovskites. Homogeneous films with bandgap up to 1.8 eV can be readily obtained, with performance on par with similar solution-

processed materials. Apart from efficiency, we focus on the development of thermally stable perovskite films and devices, that can be obtained using even more complex stoichiometry. By adding guanidinium (GA) to the material formulation, we develop CsMAFAGA quadruple-cation perovskite solar cells with enhanced thermal stability. In spite of the benefit (efficiency, thermal stability) of such complex formulations, their vacuum processing can be challenging, because one needs to simultaneously control several thermal sources during the deposition. Hence we show a simplified dual-source vacuum deposition method to obtain wide bandgap perovskite film and solar cells, with similar or even larger efficiency as those including multiple A-cations. Vacuum deposited MA-based perovskites are highly thermally stable, with lifetime up to 3500 hours at 85 °C, and record efficiency >19% for bandgap of 1.64 eV.

8:00 PM EN05.03.04

Interfacial Toughening with Self-Assembled Monolayers for Mechanical Reliability in Inverted Perovskite Solar Cells [Zhenghong Dai](#) and Nitin P. Padture; Brown University, United States

Metal halide perovskites (MHPs) have emerged as the most promising light-absorber materials in the photovoltaic community due to their near-ideal bandgaps and extraordinary optoelectronic properties. However, MHPs have extremely poor mechanical properties. They are inherently compliant, soft, and brittle. While significant progress has been made in improving the stability of MHPs, perovskite solar cells (PSCs) will also need to be mechanically reliable if they are to operate efficiently for decades. In this context, we study the mechanical integrity of PSCs by measuring their cohesion/adhesion energies (G_c) using double cantilever beam method. We will then report a novel approach to strategically enhance the interfacial adhesion and performance of p-i-n structure PSCs using carefully designed hole transporting self-assembled monolayers (SAMs), where we find that the perovskite solar cell stability is closely intertwined with its mechanical reliability. This work points to a new route for designing mechanically robust PSCs with long-term durability.

8:00 PM EN05.03.05

Triiodide Attacks The Organic Cation in Hybrid Lead Halide Perovskites: Mechanism and Suppression [Junnan Hu](#), [Zhaojian Xu](#), [Tucker L. Murrey](#), [Istvan Pelczar](#), [Antoine Kahn](#), [Jeffrey Schwartz](#) and [Barry P. Rand](#); Princeton University, United States

Molecular I_2 can be produced from iodide-based lead perovskites under thermal stress; triiodide, I_3^- , is formed from this I_2 and I^- . Triiodide attacks protic cation MA^+ - or FA^+ -based PbI_3^- perovskites as explicated through solution-based NMR studies: Triiodide has strong hydrogen-bonding affinity for MA^+ or FA^+ , which leads to their deprotonation and perovskite decomposition. Triiodide is a catalyst for this decomposition which can be obviated through perovskite surface treatment with thiol reducing agents. In contrast to methods using thiol incorporation into perovskite precursor solutions, no penetration of the thiol into the bulk perovskite is observed, yet its surface application stabilizes the perovskite against triiodide-mediated thermal stress. Thiol applied to the interface between $FAPbI_3$ and Spiro-OMeTAD ("Spiro") prevents oxidized iodine species penetration into Spiro and thus preserves its hole transport efficacy. Surface-applied thiol affects the perovskite work function; it ameliorates hole injection into the Spiro overlayer, thus improving device performance. It helps to increase interfacial adhesion ("wetting"): Fewer voids are observed at the Spiro-perovskite interface if thiols are applied. Perovskite solar cells (PSCs) incorporating interfacial thiol treatment maintain over 80% of their initial PCE after 300 h of 85 °C thermal stress.

8:00 PM EN05.03.06

Room-Temperature Amplified Spontaneous Emission and Lasing in Recrystallized Cesium Tin Bromide Perovskite Thin Films [Manuel Runkel](#)^{1,2}, [Timo Kraus](#)^{1,2}, [Timo Maschwitz](#)^{1,2}, [Cedric Kreusel](#)^{1,2}, [Kai O. Brinkmann](#)^{1,2}, [Maximilian Buchmüller](#)^{1,2}, [Patrick Görrn](#)^{1,2}, [Selina Olthoff](#)³ and [Thomas Riedl](#)^{1,2}; ¹University of Wuppertal, Germany; ²Wuppertal Center for Smart Materials & Systems, Germany; ³University of Cologne, Germany

Metal halide perovskites are of great interest for optoelectronic devices such as solar cells, LEDs and lasers, whereas by now in most of the studies lead based perovskites are used to achieve the champion devices [1]. Another promising group is tin based perovskites that offer a less toxic alternative to lead based [2]. Nevertheless the preparation and handling of Sn-based perovskites comes with its own difficulties, due to the possible oxidation of the Sn^{2+} to Sn^{4+} , either by the solvents used for film deposition or by contact with air, which can lead to the formation of defects in the perovskite.

Thermal imprint at moderate pressure and temperature has previously been shown to be a powerful method to re-crystallize perovskite thin films [3]. While the process is well explored for Pb-based perovskites, thermal imprint of Sn-based materials has not been studied as of yet. Here, we investigate the thermal imprint of $CsSnBr_3$ thin films in comparison to its Pb-based counterpart $CsPbBr_3$. To achieve homogeneous pristine $CsSnBr_3$ films as starting material, we initially established a new deposition method using the gas quenching technique, which has not been used for Sn-based perovskites before. By adding SnF_2 we can further protect the tin from oxidation and achieve pinhole free films, which show an intense photoluminescence at 677 nm with a line width of 42 nm (FWHM). In addition, we used X-ray diffractometry to confirm the formation of $CsSnBr_3$ and absence of Sn^{4+} .

In the next step we use the $CsSnBr_3$ films to examine the effect of the planar hot pressing (PHP) process using a flat stamp at different imprint temperatures. We constructed a dedicated imprint fixture that allows the imprint under controlled ambient conditions, such as vacuum or inert atmosphere. We evidence that a significantly higher temperature of >180°C is needed for the flattening and recrystallization of the layers compared to the Pb-based analogues, where imprint at temperatures as low as 80°C can be performed. The higher binding energy of the Sn-Br bond of 273 kJ/mol in comparison to that of the Pb-Br bond (201 kJ/mol) might be a possible explanation. Comparable to the before described case of Pb-based perovskites, we observe a significantly lowered ASE threshold in the $CsSnBr_3$ after the PHP-process of about 150 $\mu J/cm^2$ compared to 400 $\mu J/cm^2$ in the pristine films. The results for the PHP provided the relevant process parameters to imprint distributed feedback (DFB) gratings into the perovskite layers and to demonstrate the first $CsSnBr_3$ DFB lasers. Our results state an important milestone for Pb-free perovskite lasers.

1. Brinkmann K.O., et al., Nature **604**, 280-286 (2022), DOI: 10.1038/s41586-022-04455-0
2. Schwartz H. A., et al. ACS Appl. Mater. Interfaces **13**, 3, 4203-4210, DOI: 10.1021/acsmi.0c20285
3. Pourdavoud N., et al., Adv. Mater. **31**, 1903717 (2019), DOI: 10.1002/adma.201903717

8:00 PM EN05.03.07

Perovskite-Based Near-Infrared Quantum Emitters [Ashutosh Mohanty](#) and Jennifer Hollingsworth; Los Alamos National Laboratory, United States

The ongoing research on hybrid organic inorganic halide perovskite (HOIP) photovoltaic (PV) materials has led to an era of optoelectronics extensively using HP-based materials. As far as photophysical properties and device efficiencies are concerned, HOIP PVs have surpassed many other semiconductor technologies and at present it competes with the Si-based solar cells. In addition to this, HOIP-based quantum dots (QDs) are new building blocks for light-emitting devices. The majority of the perovskite-QDs are focused on visible-range functionalities, with only a few reports on near-infrared (NIR)-emitting nanocrystalline perovskite materials. We have employed different metal ion doping strategies to develop all-inorganic lead halide QDs, particularly doped and heterostructured $CsPbX_3$ ($X = Cl, Br, I$) QDs for NIR applications. We have grown monodisperse, high quality, defect-free perovskite QDs with emission across the telecommunications wavelengths.

8:00 PM EN05.03.08

Highly Stable and Efficient Perovskite Solar Cells by Enhanced Interface Toughening via Iodine-Terminated Self-Assembled Monolayer [Inseok Yang](#), [Anush Ranka](#) and Nitin P. Padture; Brown University, United States

The mechanical reliability of lead halide perovskite solar cells is a key factor to determine device stability. We applied iodine-terminated self-assembled monolayers (I-SAM) on the mesoporous TiO_2 layer of the perovskite solar cells. We achieve a 40% increase of adhesion toughness at the interface between the electron transporting layer (ETL) and the perovskite layer to enhance mechanical reliability. I-SAM treatment on the mesoporous TiO_2 layer leads to enhanced photovoltaic performance including power conversion efficiency (PCE) and stability of the device. The device working stability with a projected T80 (time to 80% initial PCE retained) increasing from ~792 hours for the control device to ~6,670 hours for the I-SAM device for 0.1 cm^2 sized active area device and ~2,822 hours to 6,333 hours for 1.0 cm^2 sized active area device under 1-sun illumination. The champion power conversion efficiency (PCE) is 24.12% with 25.89 mA/cm^2 , 1.131 V, and 82.35% of FF with a 0.1 cm^2 sized active area device. This device performance enhancement is derived from superior interface properties through the I-SAM layer on the mesoporous TiO_2 layer. The I-SAM layer contributes interfacial toughness between the TiO_2 layer and perovskite layer and this increased interfacial toughness property leads to performance enhancement.

8:00 PM EN05.03.09

Quartic Anharmonicity Triggers Conversion of Dominant Thermal Transport Channels in Lead-Free Halide Double Perovskite $Cs_2AgBiBr_6$ [JiongZhi Zheng](#)^{1,2}, [Changpeng Lin](#)^{3,3}, [Chongjia Lin](#)², [Ruiqiang Guo](#)⁴, [Baoling Huang](#)^{2,5,6} and [Geoffroy Hautier](#)¹; ¹Dartmouth College, United States; ²The Hong Kong University of Science and Technology, Hong Kong; ³Ecole Polytechnique Federale de Lausanne, Switzerland; ⁴Shandong Institute of Advanced Technology, China; ⁵Hong Kong University of Science and Technology, Hong Kong; ⁶HKUST Shenzhen-Hong Kong Collaborative Innovation Research Institute, China

Efficient manipulation of thermal energy in halide perovskites is crucial for their opto-electronic, photovoltaic and thermoelectric applications. However, understanding the lattice dynamics and heat transport physics in the lead-free halide double perovskites remains an outstanding challenge due to their lattice dynamical instability and strong anharmonicity. In this work, we investigate the microscopic mechanisms of anharmonic lattice dynamics and thermal transport in lead-free halide double perovskite $Cs_2AgBiBr_6$ from first principles. We combine self-

consistent phonon calculations with bubble diagram correction and a unified theory of lattice thermal transport that considers both the particle-like phonon propagation and wave-like tunnelling of phonons. An ultra-low thermal conductivity at room temperature ($\sim 0.21 \text{ W m}^{-1} \text{ K}^{-1}$) is predicted with a weak temperature dependence ($\sim T^{0.45}$), in sharp contrast to the conventional $\sim T^{-1}$ dependence. Particularly, the vibrational properties of $\text{Cs}_2\text{AgBiBr}_6$ are featured by strong anharmonicity and wave-like tunnelling of phonons. Anharmonic phonon renormalization from both the cubic and quartic anharmonicities are found essential in precisely predicting the phase transition temperature in $\text{Cs}_2\text{AgBiBr}_6$ while the negative phonon energy shifts induced by cubic anharmonicity has a significant influence on particle-like phonon propagation. Further, the contribution of the wave-like tunnelling to the total thermal conductivity surpasses that of the particle-like propagation above around 340 K, indicating the breakdown of the phonon gas picture conventionally used in the Peierls-Boltzmann Transport Equation. Importantly, when considering only three-phonon scatterings, the particle-like propagation channel dominates the thermal transport in $\text{Cs}_2\text{AgBiBr}_6$. However, further including four-phonon scatterings induced by quartic anharmonicity results in the dominance of wave-like tunnelling channel. Our work highlights the importance of lattice anharmonicity and wave-like tunnelling of phonons in the thermal transport in lead-free halide double perovskites.

8:00 PM EN05.03.10

Interface Engineering and Perovskite Thin-Film Optimization Towards Efficient Light-Emitting Diodes Muhammad Umair Ali¹, Jingsheng Miao², Hong Meng² and Aleksandra B. Djurić¹; ¹The University of Hong Kong, Hong Kong; ²Peking University, China

Organic-inorganic metal halide perovskite materials have attracted lots of attention as next-generation light-emitting candidates owing to their exciting optoelectronic features, such as high color-purity, broadly tunable emission, high photoluminescence quantum yields and low-cost fabrication. While significant progress has been made in enhancing external quantum efficiencies (EQEs) of perovskite-based light-emitting diodes (PeLEDs), there remain several technical bottlenecks, such as severe efficiency roll-off, low operational lifetime and poor reproducibility, which hinder the practicality of these emerging light sources. In this study, a comprehensive investigation is conducted to understand the underlying processes and realize efficient and stable quasi-2D perovskite light emitters with emphasis on three aspects: (i) optimizing the device structure to achieve well-controlled charge injection and consequent exciton formation in the perovskite layer for effective light emission; (ii) probing the role of various underlying organic hole transport layers (HTLs) in the growth of solution-processed perovskite thin-films and subsequent impact on the overall device performance; and (iii) exploring effective solution-processing protocols to develop perovskite thin-films with desired features and reproducible results towards the reliable development of PeLEDs. Firstly, based on an in-depth analysis of charge carrier injection and transport towards the perovskite emissive layer, interface engineering is performed and an optimized device architecture with suitable functional layers and a new cathode configuration is proposed which rendered significantly improved device performance. Secondly, research on various HTLs unveiled that apart from the role of hole-carrier mobility and energy-levels alignment with neighboring functional layers in the stack, the chemical nature and surface features of the HTL as substrate significantly impacts the crystallization kinetics of atop perovskite layer which has a substantial influence on the resulting PeLED performance. Thirdly, a solution-based vapor-assisted growth method is developed via creating an easily controllable spin-coating environment to fabricate high-quality quasi-2D perovskite thin-films with graded domain distribution for cascade energy transfer, which results in high reproducibility. Consequently, a thoroughly optimized fabrication approach enabled effective PeLEDs with high EQE, suppressed roll-off, prolonged operational lifetime and improved reproducibility. This research facilitates expanding our current understanding of constructing perovskite-based solution-processed photonic sources for solid-state lighting and display applications.

8:00 PM EN05.03.11

Mechanically-Stacked Four Terminal Perovskite/InGaAsP Tandem Solar Cell Achieving 27.7% Efficiency Bikesh Gupta, The Duong, Tuomas Hagren, Julie Tournet, Chennupati Jagadish, Hark Hoe Tan and Siva Karuturi; Australian National University, Australia

III-V semiconductor photovoltaic (PV) cells have been widely investigated owing to their numerous advantages such as thin-film feasibility, flexibility, high efficiency and adaptability in multijunction architectures. However, their application has been limited to niche areas, such as powering satellites, owing to their high costs primarily driven by high material costs and usage of capital-intensive equipment for fabrication. For widespread adoption of III-V semiconductor based solar cells, it is critical to develop low cost and high efficiency solar cells. In the present study, we address these issues by fabricating InGaAsP heterojunction solar cell reaching efficiencies close to those demonstrated by the state-of-art InGaAsP homojunction solar cells. The InGaAsP (Eg = 1.04 eV) solar cell employing a TiO₂ electron selective contact resulted in efficiencies exceeding 19% with an open circuit voltage of 650 mV. The high efficiency and open circuit voltage were achieved by synergistic coupling of the excellent passivation by thin InP layer and superior carrier selectivity by the TiO₂ layer. Furthermore, 1.55 eV perovskite semitransparent top cell was fabricated with an efficiency exceeding 22%. When mechanically stacked over InGaAsP bottom cell, a tandem efficiency of 27.7% was achieved. The current work paves the way for high-efficiency and low-cost III-V semiconductor tandem solar cell while avoiding the use of capital-intensive fabrication tools.

8:00 PM EN05.03.12

Low Temperature Sintering of Polycrystalline Hybrid Organic-Inorganic Perovskites Michael C. Brennan^{1,2}, Christopher McCleese^{1,3}, Lauren Loftus^{1,3}, Douglas Krein^{1,3} and Tod Grusenmeyer¹; ¹Air Force Research Laboratory, United States; ²Azimuth Corporation, United States; ³General Dynamics Information Technology, United States

Hybrid organic-inorganic perovskites (HOIPs) (ABX_3 ; A = CH_3NH_3 , $\text{CH}(\text{NH}_2)_2$, Cs; B = Pb, Sn; X = Cl, Br, I) embody intriguing optoelectronic properties (e.g. tunable bandgaps, high absorption coefficients, and large charge carrier mobilities). However, many target applications for these semiconducting materials (e.g., scintillators, lasers, and photodetectors) require large area, millimeter thick perovskite single crystals with high optical transparency. Unfortunately, single crystals grown by melt-based approaches are limited to all-inorganic perovskites due to organic cation volatility, and solution-based methods are inundated with scalability and reproducibility issues. Sintering HOIP powders into high relative density (>0.999) polycrystalline wafers under an applied uniaxial pressure is a promising route towards overcoming the current limitations of melt and solvothermal single crystal growth. We demonstrate low temperature ($\sim 20^\circ\text{C}$) sintering methods under an applied uniaxial pressure to compress high purity HOIP powders into high density, polycrystalline wafers with optical transparency and charge transport properties akin to their ideal single crystal counterparts. Structural, optical, and electrical properties of HOIP wafers are benchmarked against single crystals analogues. Fully understanding the tradeoff between manufacturability of polycrystalline wafers versus the performance of single crystals could enable key advancements in perovskite technologies.

8:00 PM EN05.03.13

Exploring the Diversity of Two-Dimensional Perovskite Structures by a Comprehensive Database for Advancing Solar Cell Research and Development Ayman Maqsood and T. Jesper Jacobsson; Nankai University, China

An important property of hybrid perovskites is the possibility to reduce the dimensionality to provide wider band gaps and better stability. Of special interest is two-dimensional perovskites which have emerged as a promising alternative to their three-dimensional counterparts due to their unique structural and optoelectronic properties. This project analyzes the recent advancements and key features of two-dimensional perovskite solar cells based on a comprehensive database of possible two-dimensional perovskite structures utilized in PV-devices that we have assembled. This database includes both experimentally reported structures and computationally designed ones and covers a wide range of compositions and variations, and provides a valuable resource for understanding and exploring the diverse range of two-dimensional perovskite materials employed in solar energy conversion. The database ontology outlines the criteria and parameters used to identify and classify two-dimensional perovskite structures, such as composition, layer thickness, and organic and inorganic components, and covers structures ranging from simple bilayers to more complex multilayer structures. In this talk, I will demonstrate how this resource can be used to provide insights into the structure-property relationships of 2D-perovskites, and how it can aid in the rational design of new 2D-perovskites with targeted properties suitable for specific device requirements.

8:00 PM EN05.03.14

Designing Efficient and Aesthetically Pleasing Semitransparent Perovskite Solar Cells for Building-Integrated Photovoltaics: A Biomimetic Approach Yiyi Zhu, Lei Shu, Qianpeng Zhang, Swapnadeep Poddar, Chen Wang and Zhiyong Fan; The Hong Kong University of Science and Technology, Hong Kong

The emergence of semitransparent perovskite solar cells (ST-PSCs) has made them an attractive option for building-integrated photovoltaics, especially for power generation windows that must convert sunlight into electricity while transmitting daylight to illuminate indoor spaces. In addition to power conversion efficiency (PCE), attributes such as average visible transmittance (AVT), color, and longevity are critical for ST-PSCs. Tuning the perovskite thickness or surface coverage can adjust AVT, with an AVT of 20%–30% typically sufficient for power-generating windows. However, the conventional structure of ST-PSCs, consisting of continuous ultrathin perovskites, often results in an undesired reddish-brown hue.

To address this challenge, we present a highly efficient, robust, and neutral-colored ST-PSC inspired by the moth's eye surface architecture. The moth eye-inspired structure (MEIS) uses hexagonally arranged microcavity structures to trap photons in the wavelength range where the human eye is less sensitive, resulting in a record-high figure-of-merit for ST-PSCs.

To create the structure, we used the Langmuir-Blodgett technique to assemble polystyrene spheres on planar-ITO as a mask for patterning, which we then covered with sputtering deposition of ITO. We subsequently removed the spheres to obtain a biomimetic structure. Next, we deposited SnO₂ using atomic layer deposition to achieve uniform and full coverage of the as-fabricated structure. We then applied spin-coating deposition to add the perovskites, followed by a layer of spiro-OMeTAD. Finally, we added a buffer layer of MoO₃ and 100 nm IZO sputtering to serve as a transparent electrode.

We characterized the optical and electrical properties of our moth eye-inspired perovskite solar cells using various techniques, including scanning electron microscopy, X-ray diffraction, UV-Vis spectroscopy, and current-voltage measurements. Our results showed that the MEIS modification provided a AVT of 33%, which is important for maintaining aesthetics in BIPV applications. Our perovskite solar cells exhibited a high power conversion efficiency of over 10%, comparable to that of conventional opaque perovskite solar cells. We compared the performance of our moth eye-inspired perovskite solar cells to that of other semitransparent solar cells reported in the literature and demonstrated that our devices outperform them in terms of

efficiency, AVT, and color neutrality.

We also tested the long-term stability of our perovskite solar cells and found that they exhibited excellent performance over a period of 224 days, indicating that they can withstand harsh environmental conditions. This study demonstrates the potential of using biomimetic approaches to design novel perovskite solar cells with improved optical and electrical properties and highlights the importance of developing solar cells that are both efficient and aesthetically pleasing for building-integrated photovoltaic applications. Our moth eye-inspired perovskite solar cells have the potential to revolutionize the field of building-integrated photovoltaics and accelerate the adoption of renewable energy sources in urban environments.

8:00 PM EN05.03.15

Improving Photovoltaic Performance of CuSCN-Based Perovskite Solar Cells by Aging in Humid Air [Atsushi Kogo](#) and Takuro N. Murakami; National Institute of Advanced Industrial Science and Technology, Japan

Development of inexpensive and robust hole-transport material for organohalide perovskite solar cells (PSC) is one of the most important topics for industrial application. Copper thiocyanate (CuSCN) is an inorganic p-type material, which can be used as a robust hole-transport material of PSCs. However, the CuSCN-based PSCs tend to give poor power conversion efficiency (PCE) than conventional spiro-OMeTAD-based PSCs because of low conductivity and high charge carrier trap density of CuSCN. To improve hole extraction of CuSCN from perovskite materials, we investigated an effect of atmospheric parameters during the aging process of CuSCN layers.

CuSCN was formed by spin-coating a precursor solution on glass substrates and dried at 80 °C for 5 min. Then the substrates were aged in different humidity (RH 2%, 25%, 40%, 70%) overnight. To characterize crystallinity of CuSCN layers, we performed X-ray diffraction measurement. CuSCN layers aged in 70% RH exhibited larger crystal size (29.9 nm) than those aged in dry air (2% RH, 26.6 nm). Small grains were observed in CuSCN layers aged in 2% RH by atomic force microscope observation. However, the grains were disappeared, and flat morphology was observed in the layers aged at 70% RH. This indicates that crystal growth of CuSCN was promoted by humid moisture. We measured resistance of CuSCN layers by current voltage scan using indium tin oxide (ITO)/CuSCN/Au substrates. Owing to its improved crystallinity, CuSCN aged at 70% RH exhibited smaller resistance than those aged at lower humidity. We fabricated PSCs (ITO/SnO₂/perovskite/CuSCN/Au structure) and measured photovoltaic performance under 1 sun illumination. As the aging humidity increased, PCE was improved owing to improved fill factor. Further, solar cells aged at 70% RH gave larger open circuit voltage than those aged in lower RH. The dark current analysis revealed that the solar cells aged at 70% RH contains less trap density and less resistance than those aged in lower RH. We can conclude that improved CuSCN crystallinity increased conductivity and decreased trap density and enhanced photovoltaic performance of perovskite solar cells.

8:00 PM EN05.03.16

CsCl Induced Grain Size Control and Performance Enhancement of MA-Based Perovskites Film for High-Performance Memristive Devices [Yen Shuo Chen](#)¹, Ching Chang Lin² and Fu-Hsiang Ko¹; ¹National Yang Ming Chiao Tung University, Taiwan; ²The University of Tokyo, Japan

Recently, a new class of organic-inorganic hybridized perovskites (OIHPs) materials with various functionalities such as dielectric, semiconducting, and photosensitive properties have proven to be very promising for resistance switching (RS) memory applications. Due to the atmospheric instability of OIHPs materials, defects or pinholes can appear on the film surface during the manufacturing process. Some literature discusses the posttreatment process for improving defects. In this study, we propose that the CsCl of the double-site repair mechanism not only passivates defects but also improves the electrical properties of the RS memory device due to the reduction of grain boundaries and grain size enlargement. The MAPbI₃ perovskite precursor was prepared by dissolving MAI and PbI₂ powder into the mixed solvent of GBL and DMSO. The CsCl solutions were prepared in methanol and ethanol; the concentrations were 0.5, 1 and 1.5 mg mL⁻¹, labeled as CsCl-0.5, CsCl-1 and CsCl-1.5, respectively. The untreated film is labeled as CsCl-0.

The pristine OIHPs films and the film with CsCl posttreatment both exhibit intense diffraction peaks at 13.9°, 20.2°, 21.4°, 28.5°, and 31.9°, corresponding to the (110), (200), (211), (220), and (310) MAPbI₃ tetragonal crystal planes. The XRD patterns result indicated that there is no significant peak shift. The UV-Vis absorption spectra showed a blue shift in the absorption edge after the addition of CsCl doping, indicating that some Cs substitution occurred on the OIHPs surface and most of MAPbI₃ was retained. The PL response spectra showed the same trend, with the highest intensity for the CsCl-1.5 film. It indicated a reduction of defects and pinholes in the film, which can be attributed to the higher concentration, resulting in more surface replacement effects. In addition, the average grain size of the OIHPs films was increased from ~339.2 nm (CsCl-0) to ~658.1 nm (CsCl-1.5) by raising the amount of CsCl doping. The MAPbI₃ films treated with CsCl exhibited signs of remodeling, resulting in grain size increase and grain boundary reduction. Control and moderate increases in grain size can affect the electrical characteristics of OIHPs memory devices. Thus, to achieve high-performance memory devices using OIHPs film, we realize the control of grain size in the film by CsCl facial treatment.

Herein, we reported the bipolar RS behavior of the organic-inorganic hybrid Cs_xMA_{1-x}PbI_{3-y}Cl_y perovskite memory device. The switching behavior of the OIHPs RS device in Al/PMMA/Cs_xMA_{1-x}PbI_{3-y}Cl_y/ITO configuration was studied under a direct current (DC) at ambient air conditions with high humidity between 50% and 70%. The top electrode (TE) Al is biased, and the bottom electrode (BE) ITO is grounded using a typical linear I-V sweep in the order 0V→-3V→0V→3V→0V at the bias voltage. To ensure the RS behavior and conductive filament were from the OIHPs layer, no significant switching behavior was observed for Al/PMMA/ITO. All the RS memory devices exhibited stable hysteresis I-V curves with bipolar resistive switching behavior. To prevent the RS memory device from being damaged during the measurement, a compliance current of 1 mA was applied. When an external voltage is swept from -3 to 0 V, the resistance transition from a high-resistance state (HRS) to a low-resistance state (LRS) was observed at 1.1 V, which means the set process occurs. The Al/PMMA/Cs_xMA_{1-x}PbI_{3-y}Cl_y/ITO device was maintained at LRS state when voltage was reversed from 3 to 0 V, corresponding to the reset process. The on/off current ratio of the CsCl-0 device reached about 10², 10³ for CsCl-0.5, 10³ for CsCl-1, and 10⁴ for the CsCl-1.5 device, respectively. Compared to untreated OIHPs devices, RSM devices with MAPbI₃ treated with CsCl-1.5 device are improved by two orders of magnitude. The results demonstrated the high-performance electronic applications of CsCl-induced OIHPs in resistive switching memories.

8:00 PM EN05.03.17

Introducing Ionic Liquid Dopant to Spiro-OMeTAD for Improving Thermal Stability in Perovskite Solar Cells [Kohei Yamamoto](#) and Takuro N. Murakami; National Institute of Advanced Industrial Science and Technology, Japan

Perovskite solar cells (PSCs) are attracting attention as next-generation solar cells because of their high-power conversion efficiencies (PCEs) and lightweight. Lightweight PSCs can be installed on roofs with weight limitations, further increasing the potential for renewable energy. In practical out-door use, PSCs require measures for environmental stability such as heat and light. It is well known that there are issues regarding the thermal stability of PSCs. There are issues with thermal stability in the perovskite itself and in the components such as carrier transport layer in PSCs. Thermal stability of PSCs with conventional structure has present a challenge in doping materials of hole transport layer (HTL). In conventional PSCs, LiTFSI is widely used as a doping material for Spiro-OMeTAD of HTL. However, LiTFSI is known to change to Li₂O₂ or become Li⁺ and diffuse inside PSCs. To improve the thermal stability of PSCs, it is important to avoid diffusion into the device by fixation Li⁺ at HTL. We focused on the doping method of HTL in conventional PSCs for improving thermal stability. For immobilization of the dopant in the HTL, bulky organic cations were investigated introducing PSCs. Since TFSI is an effective doping for Spiro-OMeTAD, a combination of TFSI and organic cations were selected as dopants for spiro-OMeTAD. Our PSCs structure is FTO/SnO₂/Cs_{0.05}FA_{0.95}PbI₃/Spiro-OMeTAD/Au. N-Ethyl-N-(2-methoxyethyl)-N,N-dimethylammonium TFSI (EMe-TFSI) and LiTFSI were used as dopants for HTL and compared, respectively. Optimized PSCs have PCE of 18.1% with LiTFSI and 18.2% with EMe-TFSI. The solar cell performance with EMe-TFSI was found to be equivalent to LiTFSI, and it was found that EMe-TFSI can function as a dopant. We evaluated thermal stability of both PSCs at 85°C and 30% RH. The PSC with EMe-TFSI exhibited 50% of its initial properties after 300 hours at thermal stability test. On the other hand, the PSC with LiTFSI reduced to 10% of its initial characteristics in just 24 hours. These results suggest that the thermal stability of PSCs can be improved by using bulky organic ions rather than small and easy to diffuse ions such as Li.

8:00 PM EN05.03.18

Insights from the Additive Engineering Perovskite Database. Can We Design Functional Molecules More Intelligently? [Chen Chen](#) and T. Jesper Jacobsson; Institute of Photoelectronic Thin Film Devices and Technology, Key Laboratory of Photoelectronic Thin Film Devices and Technology of Tianjin, College of Electronic Information and Optical Engineering, Nankai University, China

Additive engineering has been widely used to improve the properties of perovskite solar cells. By carefully selecting the right additive, it is possible to for example improve film uniformity, morphology, and crystallinity, alter the electronic properties and improve stability. Specifically, some of additives are used to modulate grain size and orientation, passivate defects, shift the Fermi-level, enhance charge carrier extraction, suppress recombination and ion migration, increase carrier lifetimes, etc. A large number of molecular additives have been explored in the literature. The understanding of the underlying interaction mechanisms of additives and perovskite is, however, still limited, and positive results are often the result of a trial-and-error approach based on a few simplistic heuristic rules. For more efficient additive engineering we would need to go beyond this and develop more general principles for perovskite additive interactions based on their respective molecular and crystal structure. As a step towards addressing those challenges, and to enable more rational selection and design of functional additives for specific targeted purposes, we have started to establish a database of perovskite additives and their effects. With the help of this database, we aim to leverage machine learning for intelligent screening and identification of new functionalized molecular additives. In this talk, we will give a brief overview of the historic additive landscape and discuss what new insights applicable to additive engineering that have been achieved by analyzing the historical data.

8:00 PM EN05.03.19

Nano Structural Analysis of Various Metal Halide Perovskite Films for Solar Cells using Synchrotron X-Ray [Seungyeon Hong](#) and Hyo Jung Kim; Pusan National University,

The metal halide perovskite materials were intensively researched for solar cells because of their outstanding photoelectronic properties. There are numerous methods to achieve high performance, high quality, and highly stable perovskite films, for example, formula combination, solution engineering, additive manufacturing, dimension control and etc. Most of those strategies pursue to obtain high-quality and well-aligned perovskite crystal structures. In this work, we adopt solvent and additive engineering and analyzed their effect on nano crystal structure of metal halide perovskite.

First, we obtained high quality perovskite grains in slow crystallization process by antisolvent and the ratio of DMSO in solution in the ambient air condition at RH 20-30%. The amount and state of the intermediate phase, which is consist of PbI_2 -MAI-DMSO, inside the as-deposited film were analyzed from GIWAXS analysis. The deposited perovskite layer with the pure intermediate with extremely slow crystallization showed highest absorption, few grain boundaries and suppressed defect recombination losses than fast crystallized perovskite phase. Furthermore, the water resistance of perovskite film was enhanced and as a result, the long-term stability was extremely increased.

And then, we employed the oleylamine(OAm) additive as defect the passivation and crystal cross-linker material. Generally, the defect the passivation and crystal cross-linker effect appeared simultaneously, and it is hard to separate the single effect of them. We could separately analyze the passivation and crystal cross-linker effect of OAm just by adopting a simple drying process during perovskite structure formation. Without the drying process, the OAm affected the orientation of the crystal structure from the surface to the bulk of the perovskite film and also exhibited the passivation effect. However, when the drying process was performed, the OAm only affected on the surface of the perovskite film. We could confirm this tendency from GIWAXS and XPS analysis.

8:00 PM EN05.03.20

Accelerating Perovskite Solar Cells Development: A Pathway to Accelerate Carbon Neutrality Targets and Reduce Renewable Energy Transition Costs [JieLiu](#) and XiaoShen; Bo-Zhi Digital Labs, China

The transition to renewable energy sources, including photovoltaics (PV) and wind power, is crucial for achieving carbon neutrality and addressing the challenges of climate change. To expedite the progress towards these goals, it is essential to explore technological advancements that can lower costs and reduce energy consumption and carbon emissions. Different PV technology pathways, including multi-crystalline silicon, mono-crystalline silicon, and perovskite solar cells, are evaluated using a life cycle assessment approach and learning rate analysis. By quantifying key metrics such as costs, energy consumption, carbon emissions, and material utilization, this research provides valuable insights into the comparative advantages and potential benefits of these technologies for global PV development. Utilizing data from papers, public reports, open-source databases and industry sources, this study presents a quantitative assessment of the potential impact of perovskite solar cell penetration from 2023 to 2050 under various scenarios defined by the International Energy Agency (IEA). The results underscore the importance of accelerating the development of perovskite solar cells, which have demonstrated significant potential for achieving higher cost reductions, energy savings, and greenhouse gas emissions avoidance compared to conventional silicon-based solar cells. These outcomes provide a robust foundation for policymakers, researchers, and industry professionals to prioritize and guide the accelerated development and deployment of perovskite solar cells within the global PV market. Furthermore, this study sets a precedent for future investigations into PV technology development and offers a pathway for sustainable and cost-effective global energy transformation.

8:00 PM EN05.03.21

Computer Modeling and Comparative Performance Analysis of Perovskite Solar Cells with Planar and Nanorod-Based SnO_2 Electron-Transport Layers [AskhatN. Jumabekov](#)¹, AssylanAkhanuly¹, Iliyassosyaev¹, ErikShalenov^{1,2,3}, ConstantinosValagiannopoulos¹, KarlygashDzhumagulova^{3,1} and AnnieNg¹; ¹Nazarbayev University, Kazakhstan; ²Satbayev University, Kazakhstan; ³Al-Farabi Kazakh National University, Kazakhstan

Nanorods of metal oxides such as TiO_2 , ZnO , and SnO_2 have been actively investigated for their application in perovskite solar cells (PSCs) as the electron transport layer (ETL). This is due to their remarkable optical and electronic properties, which makes them suitable for extracting charge carriers from the perovskite layer in PSCs. Among them, SnO_2 -based ETLs have attracted a significant attention in recent years due to its advantageous properties such as high carrier conductivity, good chemical stability, and desirable band alignment with the perovskite layer for charge extraction [1]. Comparative performance analysis of PSCs with planar and nanorod-based SnO_2 ETLs indicate that PSCs with the latter type of ETLs can have improved performance, owing to accelerated electron transport in SnO_2 and decreased recombination rate at the SnO_2 /perovskite interface [2,3]. Additionally, employing nanorod-based SnO_2 ETLs can enhance the long-term stability of PSCs [4].

Surveying the literature for the best performing PSCs with SnO_2 ETLs show that high-performance PSCs are usually obtained using planar ETLs [5]. This suggests that the use of nanorod-based SnO_2 ETLs for boosting the power conversion efficiency (PCE) of devices requires further investigation. Therefore, we used computer simulation methods to investigate and analyze the properties and behavior of PSCs with SnO_2 nanorod-based ETLs by varying the aspect ratio and density of SnO_2 nanorods [6]. We found that the light harvesting ability of PSCs improves with the implementation of SnO_2 nanorod-based ETLs. However, we revealed that under optimum conditions, PSCs with thin planar SnO_2 ETLs is sufficient to outperform those with nanorod-based SnO_2 ETLs. The underlying reason for this is explained through a detailed analysis of electric field, current density, and carrier recombination in devices. The results of this work provides with an insight into the device physics of PSCs with planar and nanorod-based SnO_2 ETLs and can be useful in designing ETLs for high-performance PSCs.

References:

- [1] Chen, Y.; Meng, Q.; Zhang, L.; Han, C.; Gao, H.; Zhang, Y.; Yan, H. SnO_2 -based electron transporting layer materials for perovskite solar cells: A review of recent progress. *J. Energy Chem.* **35**, 144-167 (2019).
- [2] Zhang, X.; Rui, Y.; Wang, Y.; Xu, J.; Wang, H.; Zhang, Q.; Müller-Buschbaum, P.; SnO_2 nanorod arrays with tailored area density as efficient electron transport layers for perovskite solar cells. *J. Power Sources* **402**, 460-467 (2018).
- [3] Xu, Y.; Rui, Y.; Wang, X.; Li, B.; Jin, Z.; Wang, Y.; Zhang, Q. Boosted charge extraction of SnO_2 nanorod arrays via nanostructural and surface chemical engineering for efficient and stable perovskite solar cells. *Appl. Surface Sci.* **607**, 154986 (2023).
- [4] Zhang, C.; Deng, X.; Zheng, J.; Zhou, X.; Shi, J.; Chen, X.; Sun, Z.; Huang, S. Solution-synthesized SnO_2 nanorod arrays for highly stable and efficient perovskite solar cells. *Electrochim. Acta.* **283**, 1134-1145 (2018).
- [5] Yoo, J.J.; Seo, G.; Chua, M.R.; Park, T.G.; Lu, Y.; Rotermund, F.; Kim, Y.-K.; Moon, C.S.; Jeon, N. J.; Correa-Baena, J.-P.; Bulović, V.; Shin, S.S.; Bawendi, M.G.; Seo, J. Efficient perovskite solar cells via improved carrier management. *Nature* **590**, 587-593 (2021).
- [6] Akhanuly, A.; Dossyaev, I.T.; Shalenov, E.O.; Valagiannopoulos, C.; Dzhumagulova, K.N.; Ng, A.; Jumabekov, A.N. Modeling and comparative performance analysis of perovskite solar cells with planar or nanorod SnO_2 electron-transport layers. *Phys. Rev. Appl.* **19**, 054039 (2023).

8:00 PM EN05.03.22

Electron-Hole Liquid in FAPbBr_3 Metal Halide Perovskite [GiuseppeAmmirati](#)^{1,2}, FaustinoMartelli¹, DanieleCatone¹, PatrickO'Keeffe¹, FrancescoToschi¹, StefanoTurchini¹, JessicaBarichello², FabioMatteocci² and AldoDi Carlo^{1,2}; ¹Consiglio Nazionale delle Ricerche, Italy; ²Università degli Studi di Roma Tor Vergata, Italy

In semiconductors, the optical excitation of electron-hole pairs usually results in a non-interacting gas of excitons, called free-excitons (FE). For increasing optical density of the excitation, because of the increasing dielectric screening of the Coulomb potential, excitons will tend not to form in favor of a gas of free electrons and holes, the electron-hole plasma (EHP). This paradigm is the essence of the Mott transition [1], which predicts the existence of an insulator-metal transition at the so-called Mott density. Experimental evidence for the exciton-plasma Mott transition was given for the first time in silicon by Shah et al. in 1977 [2]. Furthermore, the renormalization effect of the electronic eigenstate in the EHP results in the formation of an electron-hole liquid (EHL) state below some critical temperature [3] Unlike EHP, EHL shows incompressibility, surface tension, and short-range order similarly to classical liquid. EHL has been observed at high optical excitations in materials having long carrier lifetime as silicon [4] germanium [5] and GaP [6], as well as in 2D metal dichalcogenides [7]

The physics of electron-hole plasmas and electron-hole liquids are fascinating from a fundamental point of view but their study also helps understand the relevant properties of materials that could be used for applications, in particular as light emitters [8]. In this context, metal halide perovskites (MHPs), used in photovoltaic applications also thanks to the long lifetime of photoexcited carriers (tens to hundreds of ns) can be a novel class of materials where the observation of electron-hole condensation could be expected. For our study we have chosen a material that finds applications in transparent photovoltaics and light emitters, namely formamidinium lead bromide (FAPbBr_3).

In this work, we present photoluminescence (PL) measurements on thin films of pure FAPbBr_3 as a function of temperature and excitation intensity and provide evidence for the formation of an electron-hole liquid up to temperatures of about 100 K. At low excitation intensity and low T (12 K), the PL line shape only shows the FE recombination. As the excitation intensity is increased two further signals emerge, first a new band attributed to the recombination of electron-hole pairs in an EHP and then a third PL band appears attributed to e-h recombination in an EHL. For both the FE-EHP Mott transition and the EHP-EHL phase transition a critical carrier density has been established following the method proposed by Shah and coworkers [2]. A phase diagram that includes the exciton-plasma Mott transition and the formation of the EHL will be also presented, which allows a clearer insight on the properties of photoexcited carriers in this technologically relevant class of materials.

[1] N.F. Mott, Rev. of Mod. Phys. **40**, 677 (1968).

[2] J. Shah, M. Combescot, and A.H. Dayem, Phys. Rev. Lett. **38**, 1497 (1977).

[3] W.F. Brinkman et al., Phys. Rev. Lett., **15**, 961 (1972); M. Combescot and P. Nozières, J. Phys. C: Solid State Phys. **5**, 2369 (1972).

- [4] J.R. Haynes, Phys. Rev. Lett. **17**, 860 (1966); Jagdeep Shah et al., Phys. Rev. Lett. **38**, 1497 (1977)
 [5] C. Benoit a la Guillaume and M. Voos, Phys. Rev. B **7**, 1723 (1973); G. A. Thomas et al., Phys. Rev. Lett. **31**, 386 (1973)
 [6] J. Shah et al., Phys. Rev. Lett. **38**, 1164 (1977).
 [7] Y. Yu, et al., ACS Nano **13**, 10351 (2019); T. B. Arp et al., Nature Phot. **13**, 245 (2019).
 [8] Z. Wang, et al., Light: Science & Applications **9**, 39 (2020)

8:00 PM EN05.03.23

Enhanced Stability of Alpha-Phase FAPbI₃ Perovskite for Photovoltaics using Aerosol-Assisted Crystallisation with MASCN Additive Madsar Hameed^{1,2}, Xuan Li¹, Yuan Zhang¹, Lokeshwari Mohan¹ and Joe Briscoe¹; ¹Queen Mary University of London, United Kingdom; ²University of Engineering and Technology Lahore, Pakistan

Perovskite solar cells (PSCs) have revolutionised the photovoltaic research field with rapid increase in efficiency, from about 3% in 2009 to over 25% in short time span. However, various challenges still remain before they can become a competitive commercial technology. Hence there is a dire need to improve PSC stability and efficiency by enhancement of thin film homogeneity, grain size (eliminating grain boundaries) and by morphological and compositional modification. Methyl ammonium lead iodide (MAPbI₃) has been widely used to fabricate PSCs but its lower thermal and chemical stability limits their application towards commercialization. Hence, formamidineum lead iodide (FAPbI₃)-based perovskites have emerged as one of the most promising candidate materials for high efficiency and stable perovskite solar cells due to their high thermal stability and ideal bandgap energy near the optimum for the Shockley-Queisser limit^[1].

However, the phase degradation of 'black phase' α -FAPbI₃ perovskite to yellow, non-perovskite δ -phase FAPbI₃ in ambient conditions restricts the long-term stability of FAPbI₃ perovskite solar cells. Previously, we have demonstrated a method for performance and stability improvements in FAPbI₃-based perovskites by crystallisation in the presence of a solvent aerosol^[2]. Here, we develop this method further by adding methylammonium thiocyanate (MASCN) to the solvent aerosol for crystallisation of FAPbI₃ perovskite films, following our previous work demonstrating additive-enhanced post-treatment of perovskite films^[3]. Adding MASCN to the aerosol improved the thin film crystallinity and grain size compared to solvent-only treated films^[4]. These changes lead to prolonged charge-carrier lifetimes, enhanced stability, and ultimately improved device efficiencies. By demonstrating the benefit of additives in this aerosol-assisted crystallisation process, this work opens wider processing options to enhance the crystallinity, grain size, film homogeneity and efficiency of perovskites.

8:00 PM EN05.03.24

Strategies to Boost the Photocatalytic Activity in Halide Perovskite Nanocrystals Tae Hyung Kim and Young Hoon Kim; Hanyang University, Korea (the Republic of)

Colloidal halide perovskite nanocrystals (PNCs) are an ideal material for high photocatalytic activity, in addition to the tremendous attention already focused on optoelectronics such as light-emitting diodes and photovoltaics due to long charge carrier lifetime, narrow bandgap and facile wavelength tunability. Here, we report two strategies to improve photocatalytic activity based on colloidal CsPbBr₃ PNCs. First, we prepared CsPbBr₃ PNC/amorphous TiO₂ composites using hydrolysis of titanium butoxide in PNC dispersion under air ambient. High absorption coefficient and narrow bandgap of CsPbBr₃ can generate and transfer photo-excited electrons to the amorphous TiO₂, which performed 4.1 times higher photocatalytic CO₂ reduction efficiency (30.43 $\mu\text{mol g}^{-1} \text{h}^{-1}$) than pristine CsPbBr₃ PNCs under outdoor sunlight (7.44 $\mu\text{mol g}^{-1} \text{h}^{-1}$). Second, we doped Fe into CsPbBr₃ PNC via post-synthetic ion exchange method. Fe dopants induce dissociation of charge carriers while suppressing the recombination of them in the presence of external magnetic fields which prolong the lifetime of spin-polarized charge carriers. By application of both Fe dopants and external magnetic fields on the CsPbBr₃ PNCs, we achieved photocatalytic CO₂ reduction of 45.48 $\mu\text{mol g}^{-1} \text{h}^{-1}$ in visible region which is 1.48 times higher than that of pristine CsPbBr₃ PNCs. These results provide simple paths toward efficient photocatalytic reaction in metal halide perovskite nanocrystals for CO₂ reduction.

8:00 PM EN05.03.25

Effects of a site Cation on Perovskite Quantum Dot for Emission Wavelength and Photoluminescence Quantum Yield Ryota Sato¹, Yusaku Morikawa¹, Satoshi Asakura², Motofumi Kashiwagi³, Takayuki Chiba^{1,4} and Akito Masuhara^{1,4}; ¹Yamagata University, Japan; ²ISE Chemicals Corporation, Japan; ³ZEON Corporation, Japan

ABX₃ type (A site: Cs, Methylammonium (MA), Formamidineum (FA) etc., B site: Pb, and X site: halogen such as Cl, Br, I) perovskite quantum dot (PeQD) has attracted attention as a next generation material for the optoelectrical device such as light emitting diode (LED) due to its excellent optical properties. In general, it is known that the optical properties, in other words, the energy band gap of PeQD are composed of the hybrid orbital of the B and X site (B-X hybrid orbital). The state of the energy band gap directly depends on the PeQD optical properties such as the emission wavelength and photoluminescence quantum yield (PLQY). For instance, the emission wavelength of PeQD is controlled by inserting another X site materials (= X' site). In detail, the new hybrid orbital composed of the B site, X site, and X' site (B-X/X' hybrid orbital) was generated by inserting the X' site material, resulting in controlling the energy band gap. Therefore, controlling the emission wavelength in the entire visible range by only adjusting the halide components. On the other hand, surface defects of PeQD generate new trap levels that prevent the electron transition within the energy band gap, so excess B and X site materials are used to passivate the surface defects. As a result, it is possible to achieve a high PLQY. Based on these facts, the state of the energy band gap on PeQD was controlled by mainly using the B and X site materials composed of the energy band gap in the previous research. In this work, we proposed the strategies for "Controlling the emission wavelength" and "Improving the PLQY" by using the A site mixture on PeQD. The A site does not directly affect the B-X hybrid orbital. On the other hand, we also found the indirect effects of the A site against the emission wavelength and PLQY of PeQD. About the emission wavelength, it was successfully achieved to control the emission wavelength by inserting another A site material into the PeQD structure. In detail, the PeQD structure was distorted by using two type of the A site materials with different ionic radii. This distortion indirectly changed the distance between the B and X site. This distance is strongly related to the B-X hybrid orbital. Finally, successful control over the emission wavelength was accomplished through the indirect manipulation of the B-X hybridized orbital linked to the energy bandgap. From the results such as FT-IR, XRD, and TEM measurement, it was revealed that the PeQD structure is distorted. In addition, by effectively regulating the energy band gap, it was successfully precise controlled of the emission wavelength with a precision of 1 nm.

On the other hand, we successfully achieved to prepare PeQD with high PLQY over 80% by inserting the alkali metal on the surface of PeQD. In detail, by inserting the alkali metal with a smaller ionic radius than the A site material composed of PeQD on the A site position of the PeQD surface, it was successfully suppressed the detachment of the X site adjacent to alkali metals. This means the generation of the trap level in the energy band structure was suppressed. In fact, PL lifetime measurement supported the proof of decreasing the trap level. In addition, PLQY values of PeQD with alkali metal was improved about 2 - 3 times compared with untreated PeQD.

In summary, we proved the effect of the A site on the PeQD optical properties, notably, the emission wavelength and PLQY. By using this finding, it is possible to expand the application range not only to LED, but also to color conversion material, quantum dot laser, and so on.

8:00 PM EN05.03.26

Modification of Two-Dimensional Tin-Based Perovskites by Pentanoic Acid for Improved Performance of Field-Effect Transistors Tomasz Marszalek; Max Planck Institute for Polymer Research, Germany

Understanding and controlling the nucleation and crystallization in solution-processed perovskite thin films are critical to achieve high in-plane charge carrier transport in field-effect transistors (FETs). This work demonstrates a simple and effective additive engineering strategy using pentanoic acid (PA). Here, PA is introduced to both modulate the crystallization process and improve the charge carrier transport in two-dimensional 2-thiopheneethylammonium tin iodide ((TEA)₂SnI₄) perovskite FETs. It is revealed that the carboxylic group of PA is strongly coordinated to the spacer cation TEAI and [SnI₆]⁴⁻ framework in the perovskite precursor solution, inducing heterogeneous nucleation and lowering undesired oxidation of Sn²⁺ during the film formation. These factors contribute to a reduced defect density, improved film morphology including lower surface roughness and larger grain size resulting in an overall enhanced transistor performance. The reduced defect density and decreased ion migration lead to a higher p-channel charge carrier mobility of 0.7 cm²V⁻¹s⁻¹, which is a more than threefold increase compared with the control device. Temperature-dependent charge transport studies demonstrate a mobility of 2.3 cm²V⁻¹s⁻¹ at 100 K due to the diminished ion mobility at low temperatures. This result illustrates that the additive strategy bears great potential to realize high-performance Sn-based perovskite FETs.

8:00 PM EN05.03.27

Impact of A-site Cation Substitution on Charge Carrier Mobilities in ASnBr₃ Perovskites Adair Nicolson¹, Seán R. Kavanagh^{1,2}, Obadiah Reid³, Eve Mozur⁴, Dominic K. Asebiah⁵, James R. Neilson⁵ and David O. Scanlon¹; ¹University College London, United Kingdom; ²Imperial College London, United Kingdom; ³University of Colorado Boulder, United States; ⁴Colorado School of Mines, United States; ⁵Colorado State University, United States

Halide perovskites have been intensely studied over the last decade due to their optoelectronic properties, with applications ranging from solar cells to LEDs. However, the majority of the best performing devices contain Pb(II), raising concerns over their toxicity. A standard solution to this problem is to perform chemical substitution, swapping Sn(II) for Pb(II) in order to retain the beneficial perovskite structure.^[1] Using this technique, solar cells manufactured using CsSnBr₃ have to date achieved a record power conversion efficiency of 10.6%.^[2]

To improve devices further, a detailed understanding of the factors controlling charge carrier mobility is required. Substituting the A-site cation Cs, with methylammonium (MA) in ASnBr₃ has been shown to reduce both hole and electron mobilities.^[1] To investigate the origin of this trend, we use AMSET,^[3] a package for calculating scattering rates from first principles, to determine the band-like transport properties. As excess charge has been found to localize to form bipolarons in Sn halide perovskites,^[4] we extend our study to model small polaron transport using semiclassical Marcus theory.^[5] These results will provide a picture of the factors affecting carrier mobilities in the band-like and hopping limits of ASnBr₃ (A = Cs, MA) perovskites.

- [1] Y.-T. Huang, et al., *Nanotechnology*, 2021, 32, 132004
 [2] O. Almora et al., *Adv. Energy Mater.*, 2023, 13, 2203313
 [3] A. M. Ganose, et al, *Nat. Commun.*, 2021, 12, 2222
 [4] H. Ouhbi., *J. Phys. Chem. Lett.* 2021, 12, 22
 [5] K. Morita, et al., *Chem. Mater.* 2023, 35, 9, 3652–3659

8:00 PM EN05.03.28

Molecular Orientations and Hole-Collection Efficiency of Monolayer Materials for Hole-Transport Layer of Inverted Perovskite Solar Cells Aruto Akatsuka¹, Minh Anh Truong², Atushi Wakamiya², Gaurav Kapil³, Shuzhi Hayase³ and Hiroyuki Yoshida^{1,4}; ¹Chiba University, Japan; ²Kyoto University, Japan; ³Electro-Communications University, Japan; ⁴Chiba University MCRC, Japan

For the hole collection layer of inverted structure perovskite solar cells, recently monolayers of carbazole derivatives [1] have been proposed to replace the polymer hole transport layer materials such as PTAA and PEDOT: PSS. The monolayers have the advantages of thin film, high transparency, and stability. Large orbital overlap and good interfacial energy alignment at the perovskite/hole collection layer interface are essential to obtain high hole transfer constants. To achieve the sizable orbital overlap, the π -conjugated backbone of the monolayer materials should be aligned face-on to the conductive metal oxide electrode (ITO). However, measuring the molecular orientation is usually difficult owing to the large surface roughness of ITO. For example, polarization-dependence of optical measurements such as ellipsometry gives averaged orientation.

In this study, we employ ultraviolet photoelectron spectroscopy (UPS) and metastable atom electron spectroscopy (MAES) to examine the molecular orientation of monolayers. In UPS, the photoelectron is generated by the excitation of UV light which can penetrate the sample. On the other hand, MAES uses metastable excited atoms (He*) as the excitation source, which only interact with the outermost molecular orbital of the sample material. For example, for a molecule whose π -conjugated backbone is aligned face-on to the ITO surface, only the π orbitals are observed in the MAES spectrum while both pi and sigma orbitals are detected by UPS. The molecular orientation can be evaluated by comparing the UPS and MAES spectra. We chose 2PACz and MeO-2PACz, which have one anchor group to bind to the ITO substrate, and 3PATAT-C3, which has three anchor groups. The monolayers were prepared by spin-coating on ITO substrates, and the UPS and MAES spectra were measured. We used molecular orbital calculations (B3LYP/6-31G(d)) for the isolated molecules to assign features of UPS and MAES spectra. Comparing UPS and MAES spectra of 3PATAT-C3, the intensity of the σ orbital is weaker in MAES spectra than UPS spectra, whereas the π orbital is stronger in both. Therefore, the π -conjugated backbone of 3PATAT-C3 is aligned face-on to the ITO surface. The results of 2PACz and MeO-2PACz show that the π -conjugated backbone is tilted in 2PACz and edge-on alignment to the ITO surface in MeO-2PACz. The results are consistent with the higher hole transfer rate constant in 2PACz than MeO-2PACz obtained by time-resolved surface photovoltage [3]. To further discuss the hole-collection efficiency, we will report the energy level alignments at the perovskite-monolayer-ITO interfaces.

- [1] V. Getautis, S. Albrecht, et al, *Adv. Energy Mater.* 2018, 8, 1801892.
 [2] Minh Anh Truong, Aruto Akatsuka, Hiroyuki Yoshida, Atsushi Wakamiya, et al, *J. Am. Chem. Soc.* 2023, 145, 7528-7539.
 [3] Levine et al., *Joule*. 2021, 5, 2915–2933.

SESSION EN05.04: Poster Session II: Perovskites Photovoltaics and Stability I
 Monday Afternoon, November 27, 2023
 Hynes, Level 1, Hall A

8:00 PM EN05.04.01

Co-Deposition of Hole-Selective Contact and Absorber for Improving The Processability of Perovskite Solar Cells Xiaopeng Zheng¹ and Joseph Luther²; ¹University of Chinese Academy of Science, China; ²National Renewable Energy Laboratory, United States

Simplifying the manufacturing processes of renewable energy technologies is crucial to lowering the barriers to commercialization. In this context, to improve the manufacturability of perovskite solar cells (PSCs), we have developed a one-step solution-coating procedure in which the hole-selective contact and perovskite light absorber spontaneously form, resulting in efficient inverted PSCs. We observed that phosphonic or carboxylic acids, incorporated into perovskite precursor solutions, self-assemble on the indium tin oxide substrate during perovskite film processing. They form a robust self-assembled monolayer as an excellent hole-selective contact while the perovskite crystallizes. Our approach solves wettability issues and simplifies device fabrication, advancing the manufacturability of PSCs. Our PSC devices with positive-intrinsic-negative (p-i-n) geometry show a power conversion efficiency of 24.5% and retain >90% of their initial efficiency after 1200 h of operating at the maximum power point under continuous illumination. The approach shows good generality as it is compatible with different self-assembled monolayer molecular systems, perovskites, solvents and processing methods.

8:00 PM EN05.04.02

Ultimate 2D Perovskite-FA DJ 2D Perovskites with Maximum Symmetry Jin Hou¹, Jared Fletcher², Hao Zhang¹, George Volonakis³, Claudine Katan³, Jacky Even³, Mercuri G. Kanatzidis² and Aditya D. Mohite¹; ¹Rice University, United States; ²Northwestern University, United States; ³Université de Rennes, France

Two-dimensional halide perovskites (2D-HaP) have emerged as a class of highly durable solution-processed organic-inorganic (hybrid) low-dimensional semiconductors. They exhibit a combination of properties derived from four classes of materials - quantum wells, atomically thin 2D materials, organic semiconductors, and three-dimensional (3D)-HaP perovskites. The general formula of 2D-HaP is (A')_m(A)_{n-1}M_nX_{3n+1}, where A' is a bulky organic cation, A is a small organic cation, M is a divalent metal, and X is a halide, with m=2 in Ruddlesden-Popper (RP) phases and m=1 in Dion-Jacobson (DJ) phases. The number n determines the thickness of the perovskite layer, which consists of alternate organics (A')_m and hybrid (A)_{n-1}M_nX_{3n+1} layers, making 2D-HaP a platform to engineer hybrid composites with attractive optoelectronic properties. Currently, similar to 3D-HaP, most of the 2D-HaP takes Methylammonium (MA) as the A site cation. While the MA⁺ cation has the most suitable effective radius of any monovalent cation (either organic or inorganic) for forming a stable perovskite structure in a strain-stress perspective, the chemical instability of MA had motivated the use of less suitably sized but more chemically stable cations, such as formamidinium (FA).¹ Different from 3D-HaP which already has some successful demonstrations using FA as A site cation,² FA based 2D-HaP remains underexplored, with only a few reports achieving an “n” equal to 1 or 2.³ We propose that the difficulty of synthesizing FA based 2D perovskite coming from the larger size of FA compared to MA, which will increase lattice mismatch between the organic parts and the inorganic parts in the 2D perovskites.⁴ Therefore, the key to synthesizing a multi-layer FA based 2D perovskite is to find the appropriate organic spacer which has a small lattice mismatch with the inorganic part. Here, we demonstrate a synthesis of FA based 2D DJ perovskites crystals, from n=1 to n=4 after screening a series of different organic spacers. This new series of 2D perovskites shows a surprisingly zero distortion along both in-plane and out-of-plane (Pb-I-Pb angle is equal to 180 degrees for both directions), which is never observed before in any multi-layer 2D perovskites. They are all tetragonal phase and with P4/mmm as the space group, which is the maximum symmetry a 2D perovskite can theoretically have.⁵ The interlayer distance (below 4 Å) of the FA DJ 2D perovskite is also one of the smallest among all reported 2D perovskite, and this could allow for better interlayer electronic coupling. As the consequence of zero distortion and short interlayer distance, this new 2D perovskite series exhibits systematically lower band gap, probably the smallest bandgap among all the 2D perovskite to our best knowledge. Preliminary stability test shows this new FA DJ maintained 75% of the perovskite phase under 1.2 suns plus 100% RH (relative humidity) over 2.5 hours.

1. Metcalf, I. et al. Synergy of 3D and 2D Perovskites for Durable, Efficient Solar Cells and Beyond. *Chemical Reviews* **123**, 9565–9652 (2023).
2. Park, J. et al. Controlled growth of perovskite layers with volatile alkylammonium chlorides. *Nature* **616**, 724–730 (2023).
3. Gélvez-Rueda, M. C. et al. Formamidinium-Based Dion-Jacobson Layered Hybrid Perovskites: Structural Complexity and Optoelectronic Properties. *Advanced Functional Materials* **30**, 2003428 (2020).
4. Kepenekian, M. et al. Concept of lattice mismatch and emergence of surface states in two-dimensional hybrid perovskite quantum wells. *Nano letters* **18**, 5603–5609 (2018).
5. Quarti, C., Katan, C. & Even, J. Physical properties of bulk, defective, 2D and 0D metal halide perovskite semiconductors from a symmetry perspective. *Journal of Physics: Materials* **3**, 042001 (2020).

8:00 PM EN05.04.03

On-Site Wettability-Induced Growth of Perovskite Nano-Structure Arrays Guannan Zhang, Zhao Sun, Chuwei Liang, Zhuofei Gan, Liyang Chen and Wendi Li; The University of Hong Kong, Hong Kong

Due to their unique properties including tuneable band gaps, superior carrier mobility, high color purity, high absorption and emission efficiency, halide perovskites have been widely used in various kinds of optoelectronic applications such as photodetectors, PeLED, laser, etc [1-2]. Specifically, low-dimensional perovskite nanostructures have attracted extensive attention due to their excellent optical, electrical, and stability characteristics, as compared to continuous film materials [3]. Ensuring the size uniformity and controllability of perovskite nanostructures is a prerequisite for their adoption in practical device applications. Diverse methods, such as inkjet printing, spin coating, vapor phase growth, blade coating, and slot-die coating, have been applied to fabricate low-dimensional perovskite nanostructures. However, these methods are usually achieved by utilizing nano-templates, which increases the complexity and cost of the fabricating process. Besides, ensuring uniform morphology and good crystallization is also very challenging to achieve high-performance perovskite nanostructures.

Herein, a template-free fabrication method to realize the controllable growth of perovskite nano-structure arrays including nanowires and nanodot arrays via the inducement of patterned wettability is demonstrated. Take nanowires as an example, figure 1 shows the schematics of perovskite nano-structure fabrication strategy. The hydrophilic-hydrophobic nanograting structure is constructed by interference lithography and trichloro(1H,1H,2H,2H-perfluorooctyl)silane (FOTS) treatment. Figure 2 shows the photoresist patterns prepared by interference lithography, including nanogratings and nanopillar arrays. Then, perovskite nanowires can be fabricated by high-throughput blade coating system consisting of a blade, hot plate, and control system as well as other auxiliary equipment.

Furthermore, in order to avoid obtaining perovskite structures with discontinuous morphology and low crystallinity, we adjust blade coating parameters (i.e., blade gap, velocity, and temperature) and the solvent properties, particularly the viscosity. We found that when the blade speed is too fast, the liquid film is very discontinuous, while if the blade speed is too slow, the perovskite film is too thick so that the separate nanowire structure cannot form. The optimized coating speed is 160 $\mu\text{m/s}$, at which a continuous perovskite nanowire array with excellent morphology can be obtained. In addition to good morphology, crystallization plays a crucial role in the performance of subsequent perovskite devices. Substrate temperature is another key factor affecting the morphology and crystallization of perovskite nanowires. When the substrate temperature was higher, the deposition front was overly close to the meniscus edge, leading to the formation of the widened nanowires. At high temperature, the solvent can evaporate in a short time, and the grain grows rapidly, resulting in a larger grain size. On the other hand, when the substrate temperature was rather low, the liquid filament was found to easily dewet into segmented perovskite nanowires. And solvent evaporation rate and crystal growth rate are slower at low temperature, resulting in dendritic structure or small-sized grains.

By utilizing the optimized process parameters obtained, MAPbI_3 perovskite nanowire structure with uniform dimension and excellent crystallization can be obtained, as shown in Figure 3. In addition, this method can be used to prepare diverse perovskite nanowire arrays, such as CsPbBr_3 nanowires. Using the same approach, diverse types of perovskite nanodot arrays can also be generated, as shown in Figure 4. The strategy shows a facile method to fabricate perovskite nano-structure arrays, paving the way to low-cost, large-area, and rapid fabrication of high-performance perovskite optoelectronic devices.

8:00 PM EN05.04.04

Illuminating the Devolution of Perovskite Passivation Layers [Marcin Giza](#)¹, [Aleksy Kozikov](#)², [Paula Lalaguna](#)¹, [Jake Hutchinson](#)³, [Vaibhav Verma](#)², [Benjamin Vella](#)¹, [Rahul Kumar](#)¹, [Nathan Hill](#)², [Rebecca L. Milot](#)³, [Malcolm Kadodwala](#)¹ and [Pablo Docampo](#)¹; ¹University of Glasgow, United Kingdom; ²The University of Newcastle, United Kingdom; ³University of Warwick, United Kingdom

Surface treatment of 3D perovskite materials with their layered counterparts has become the most utilised strategy against air- and moisture-induced degradation. Whilst layered materials confer great benefits to the longevity and long-term efficiency of the resulting device stack via passivation of defects and surface traps, numerous reports have previously demonstrated that these materials evolve under exposure to light and humidity, suggesting they are not fully stable. Therefore, it is crucial to study the behaviour of these materials in isolation and as part of a device stack. Herein, it is demonstrated via optical, PL, AFM, XRD, and TAS studies that these “stable” capping layers undergo numerous changes in conditions commonly found during perovskite fabrication, such as exposure to light, solvent, and moisture. A pinhole-mediated degradation mechanism is identified as the cause of the degradation of exfoliated flakes of PEA_2PbI_4 , an $n = 1$ material. This results in the loss of whole perovskite sheets, from a few monolayers to tens of nanometres of material. We discuss important steps to take to slow down their degradation. Additionally, we show high- n PEA-based perovskite capping layers on top of MAPI undergo uncontrolled rearrangements to form lower- n phases, which can severely impact band alignment within devices, or degrade completely. Crucially, they do not act as perfect barrier layers, with the underlying 3D perovskite also demonstrating signs of degradation.

8:00 PM EN05.04.05

Antisolvent Engineering for Microstructural Improvement of Lead Free Solar Absorber Material [Memoona Qammar](#), [Bosen Zou](#) and [Jonathan Halpert](#); Hong Kong University of Science and Technology, Hong Kong

Lead free halide materials are seeking attention owing to their astonishing optoelectronic properties accompanied with better stability and less toxicity. Silver bismuth halides being ecofriendly and seen as potential candidates for photovoltaic applications but they are still struggling with power conversion. To address this issue here we have used antisolvent engineering to improve film morphology and tested the absorber material in an inverted solar cell for the first time with device architecture: $\text{ITO}/\text{NiO}/\text{AgBiI}_4/\text{C}_60/\text{BCP}/\text{Ag}$. The efficiency was improved from 0.5% to 1.3% for the solar cell based on absorber layer fabricated via chloroform assisted antisolvent solvent spin casting method. The microstructural improvement was proven by a thorough analysis with SEM and AFM. This study has demonstrated that low boiling antisolvent can assist less polar antisolvent to improve the microstructure of the thin films which ultimately resulted in enhancement of PCE in AgBiI_4 inverted solar cell.

8:00 PM EN05.04.06

Understanding The Impact of Ions on Open Circuit Voltage in Perovskite Solar Cells [Fraser J. Angus](#)¹, [Lucy J. Hart](#)², [Piers R. B. Barnes](#)² and [Pablo Docampo](#)¹; ¹University of Glasgow, United Kingdom; ²Imperial College London, United Kingdom

Metal halide perovskites are a nascent class of materials that combine competitive power conversion efficiencies with low-cost materials and manufacturing processes for use in next-gen solar cells. These materials, uniquely amongst PV materials, are capable of conducting both ionic and electronic charge. However, the presence of mobile ions can lead to extraction losses and carrier accumulation, as a function of the applied bias history of the device which can lead to unreliable performance. However, mobile ions can also reduce recombination currents at the perovskite/transport layer interfaces, increasing open-circuit voltage (V_{oc}). Employing Stabilise-and-Pulse (SaP) measurements, we show that ion accumulation can increase V_{oc} by 0.1 V, which decreases as the flat-ion potential of the PSC becomes larger. We validate these results with drift-diffusion simulations and confirm that under poor energetic alignment conditions, ions can provide a significant boost to the device performance.

8:00 PM EN05.04.07

Exploring The Correlation Between The Built-In Potential of Perovskite Solar Cells and The Thickness of Passivating Layered Perovskites. [Fraser J. Angus](#) and [Pablo Docampo](#); University of Glasgow, United Kingdom

Perovskite solar cells have shown significant improvement in recent years, with the power conversion efficiency exceeding 25%. The integration of layered perovskites into a perovskite heterojunction is a promising approach for further enhancing their performance and providing long-term device stability. However, the effects of increasing the thickness of the layered perovskite on device physics and the role of the built-in potential (V_{bi}) in charge extraction are not well understood. Herein, we discuss the intricate physics that come into play when the thickness of the layered perovskite is increased, resulting in a dynamic change in band bending and a consequent effect on the built-in potential. This work elucidates the mechanisms behind the well-known performance enhancement resulting not just from the layered perovskites' role in surface passivation, but also from their effect on the built-in potential.

8:00 PM EN05.04.08

Search for Ferromagnetism in Mn-Doped Lead Halide Perovskites [Maryam Sajedi](#), [Maxim Krivenkov](#) and [Oliver Rader](#); Helmholtz Zentrum Berlin, Germany

Lead halide perovskites are new key materials in various application areas such as high efficiency photovoltaics, lighting, and photodetectors. Doping with Mn, which is known to enhance the stability, has recently been reported to lead to ferromagnetism below 25 K in methylammonium lead iodide (MAPbI_3) mediated by superexchange. Two most recent reports confirm ferromagnetism up to room temperature but mediated by double exchange between Mn^{2+} and Mn^{3+} ions. Here we investigate a wide concentration range of $\text{MAMn}_x\text{Pb}_{1-x}\text{I}_3$ and Mn-doped triple-cation thin films by soft X-ray absorption, X-ray magnetic circular dichroism, and quantum interference device magnetometry. The X-ray absorption lineshape shows clearly an almost pure Mn^{2+} configuration, confirmed by a sum-rule analysis of the dichroism spectra. A remanent magnetization is not observed down to 2 K. Curie-Weiss fits to the magnetization yield negative Curie temperatures. All data show consistently that significant double exchange and ferromagnetism do not occur. Our results show that Mn is not suitable for creating ferromagnetism in lead halide perovskites.

8:00 PM EN05.04.09

Influence of Interface Configuration on Carrier Transport at 2D/3D Halide Perovskite Heterojunctions [Young-Kwang Jung](#) and [Samuel D. Stranks](#); University of Cambridge, United Kingdom

Halide perovskite photovoltaics have shown significant advancements, with power conversion efficiencies (PCEs) increasing to commercially viable levels. However, device stability remains a significant hurdle for the success of the technology and requires further improvement. The introduction of Ruddlesden-Popper (RP) two-dimensional (2D) perovskite overlayers on top of three-dimensional (3D) perovskite active layers has emerged as a promising strategy for enhancing the stability of perovskite solar cells (PSCs) [1-2]. While many successful cases of efficient and stable PSC fabrication via the inclusion of 2D/3D heterojunctions have been reported [3-4], a fundamental understanding of the interaction between 2D and 3D perovskites at their interfaces remains elusive. Therefore, uncovering the relationship between the atomic configuration of the interface and the behavior of electrons at this interface is crucial.

In this work, we performed first-principles density-functional theory (DFT) calculations to explore how the atomic configurations of interfaces influence the properties of 2D/3D halide perovskite heterojunctions. We adopted $\text{PEA}_2\text{PbX}_4/\text{CsPbX}_3$ ($X = \text{Br}, \text{I}$) heterojunctions as model systems, optimizing their interface geometries and calculating electronic structures. Our results show that both the thermodynamic stability and band alignment of 2D/3D halide perovskite heterojunctions are highly dependent on the configurations of Cs/PEA cations at their interfaces.

[1] G. Grancini, C. Roldán-Carmona, I. Zimmermann, E. Mosconi, X. Lee, D. Martineau, S. Narbey, F. Oswald, F. De Angelis, M. Graetzel, and M. K. Nazeeruddin, *Nat. Commun.* **8**, 15684 (2017)

[2] D. Yu, F. Cao, C. Su, and G. Xing, *Acc. Chem. Res.* **56**, 959–970 (2023)

[3] K. Ma, J. Sun, H. R. Atapattu, B. W. Larson, H. Yang, D. Sun, K. Chen, K. Wang, Y. Lee, Y. Tang, A. Bhoopalam, L. Huang, K. R. Graham, J. Mei, and L. Dou, *Sci. Adv.* **9**, eadg0032 (2023)

[4] Y.-W. Jang, S. Lee, K. M. Yeom, K. Jeong, K. Choi, M. Choi, and J. H. Noh, *Nat. Energy* **6**, 63–71 (2021)

8:00 PM EN05.04.10

The Role of Ligand Capping in Achieving High-Efficiency Perovskite Solar Cells and QD LEDs FarzanehJahanbakhshi¹, Andres FelipeCastro Mendez², ShaunGallagher³, JessicaKline³, DavidS. Ginger³, Juan-PabloCorrea-Baena² and AndrewRappe¹; ¹University of Pennsylvania, United States; ²Georgia Institute of Technology, United States; ³University of Washington, United States

Formamidinium lead iodide (FAPbI) has gained prominence in photovoltaic (PV) applications due to its notable thermal and chemical stability compared to methylammonium lead iodide (MAPI). However, a significant challenge arises from its inherent tendency to spontaneously transform from the cubic (alpha) phase to the non-perovskite yellow (delta) phase under ambient conditions, posing obstacles for practical utilization. We introduce a novel technique involving the evaporation deposition of FAPI onto the substrate that is functionalized with specific acid ligands. This method is designed to exert precise control over the preferential formation and growth of the alpha phase, thereby mitigating the unfavorable transformation to delta-FAPbI. Additionally, we investigate the impact of ligand capping on modulating photoluminescence intermittency in CsPbBr₃ Quantum Dots (QDs). Specifically, we compare the efficiency of CsPbBr₃ QDs capped with a zwitterionic ligand against the traditional approach employing oleic acid and oleylamine. Our findings demonstrate that tight-binding ligands hold promise for reducing blinking phenomena in perovskite QDs, particularly in single-particle and quantum light experiments. These strategies are elucidated through rigorously analyzing the formation and surface chemistry of these systems at the Density Functional Theory (DFT) level.

8:00 PM EN05.04.11

Efficient and Stable Inverted Perovskite Solar Cell via Incorporation of Halogenated Polystyrene SaikiranS. Khamgaonkar and VivekMaheshwari; University of Waterloo, Canada

Rationale design and use of additives to enhance the stability of Metal halide perovskite (MHP) is a key challenge that needs to be addressed for their commercial adoption in photovoltaics. Although high efficiency has been achieved, long term operational stability under daily temperature variation remains an unsolved issue for their large-scale deployment. In this work we use halogenated polystyrene as an additive to improve the long term operational and thermal stability, as well as the efficiency of perovskite solar cells. The incorporation of optimized amount halogenated polystyrene (PS) namely PS-X ($X = \text{F}, \text{Cl}, \text{Br}$) into perovskite precursor solution along with its direct interaction with PbI₂ through Lewis acid base interaction leads to the formation of enlarged, cross-linked perovskite grains. Similarly, the hydrophobic and insulating nature of PS leads to reduced ion migration effects, lower dark and enhanced stability. As a result, halogenated PS (PS-X) p-i-n inverted solar cell showed enhanced efficiency and reduced hysteresis effect when compared to pristine perovskite. A major improvement was seen in the short circuit density (J_{sc}) and fill factor (FF) of the halogenated PS cells due to effective defect passivation caused by the addition of the polymer. In addition to the improvement in performance, halogenated PS cells showed enhanced thermal stability when compared to pristine perovskite cells, which is attributed to the properties and structure of the PS-X additive.

8:00 PM EN05.04.12

Potential of Perovskite Doping Unlocked: Shaping The Future of Energy and Electronics ZuzannaMolenda¹, BastienPoliti², RaphaëlClerc², DarioBassani³ and LionelHirsch¹; ¹Laboratoire de l'Intégration du Matériau au Système (IMS), University of Bordeaux, France; ²Université de Lyon, Université Jean Monnet-Saint-Étienne, CNRS, Institut d'Optique Graduate School, Laboratoire Hubert Curien, UMR, France; ³Institut des Sciences Moléculaires, University of Bordeaux, France

Doping of metal halide perovskites (MHPs) is the next, essential step towards the implementation of perovskite semiconductor technology for electronic devices. Nonetheless, only a limited number of successful doping instances have been documented, and it is frequently mistaken for additives, grain passivation, or surface functionalization, none of which affect the semiconductor's charge carrier density. Due to the ionic character of the perovskite crystal, the introduction of heterovalent ions is accompanied by the counter ions that balance out the potential doping effect. Here we present a use of homovalent yet metastable ions, in particular Sm²⁺, to substitute Pb²⁺ in MAPbI₃ (MA = methylammonium). Sm²⁺ ions spontaneously oxidize to Sm³⁺, once incorporated into the crystal lattice and each of them releases one electron to the conduction band. The oxidation of samarium ions is confirmed by the analysis of the Sm 3d core level in the X-ray photoelectron spectrum (XPS). Residual content of the oxidized form of Sm³⁺ present in the doping solution allows to observe a slight shift of the Sm 3d peak towards higher binding energy, suggesting the environment change of the Sm³⁺ ion, once introduced inside the perovskite film. Together with the shift of the XRD pattern upon doping, this supports the hypothesis that the dopant ion is incorporated and stabilized in the crystal lattice. At the same time, the crystal structure of the doped perovskite layer is conserved and no phase separation is observed from the XRD patterns. Ultraviolet photoelectron spectroscopy (UPS) shows a shift of the Fermi level (E_F) by around 0.5 eV towards the conduction band, proving the doping to be n-type. The increase of the free electron density in the conduction band is the direct reason for the conductivity increase for the doped films by 3 orders of magnitude. Using the Mott-Schottky method, the ionized charge carrier density is estimated to be 10^{17} cm^{-3} for the sample showing the highest conductivity increase, which suggests the ionized dopant concentration in the doped perovskite film to be around 0.01% (Pb density in MAPbI₃ $\approx 20^{21} \text{ cm}^{-3}$). The discrepancy between this result and the doping concentration stemming from the XPS measurement, which is calculated to be around 20%, leads to two possible explanations. Either the majority of the Sm²⁺ introduced to the perovskite polycrystalline film resides at grain boundaries and therefore does not act as a dopant or the dopant is only partially oxidized in normal conditions, exhibiting the freeze-out effect. The dopant activation energy (the energy necessary to oxidize all the Sm²⁺ ions to Sm³⁺) of around 350 meV seems to support the latter hypothesis and is in agreement with the energy between the E_F and conduction energy (E_C). The presented method allows to reach the highest to-date conductivity increase for the n-type and may become a protocol for the efficient n-type doping of MHPs. To illustrate one of its applications, we fabricated perovskite solar cells (PSC) with poly(triaryl amine) (PTAA) as a hole transporting layer (HTL) (p-side) and Sm-doped MAPbI₃ (n-side), without the electron transporting layer (ETL). Additionally, we used gold as an electron collecting electrode ($W_{Au} = 5.22 \text{ eV}$). The strain-induced ohmic contact between highly doped perovskite and Au allows to minimize the series resistance at this interface and an efficient electron collection. This shows the potential of flexible electrode selection for the doped PSC. Therefore, the ETL-free n-doped PSC retains the same PCE as the reference sample (with PCBM as an ETL), in spite of the simplified architecture that decreases the fabrication cost and the number of interfaces.

8:00 PM EN05.04.13

Cesium Lead Halide Perovskite Ozone Gas Sensors based on Reflectivity Measurements JacobD. Wolfman, SamitaMishra and YaacovR. Tischler; Bar-Ilan University, Israel

Metal-halide perovskite (MHP) materials have been developed into high performance semiconductors primarily for photovoltaic devices, and for a variety of other applications. Recently, MHP's were used to detect ozone and other volatile gases by detecting changes in electrical conductivity, in a reversible manner. However, the fundamental problem with such films, namely that they are typically rough and inhomogeneous, has hindered photonics-based sensor development. Following the work of Bo Li et al. [*Nat. Comm.* **9**, 1076 (2018)], here we show that smooth thin films (rms roughness < 4 nm) of MHP based on CsPbBr_{3-x}I_x ($x = 0, 1, 2$ or 3) could be prepared, by incorporating 5% polymer into the precursor solutions. The MHP+polymer compounds were spin-coated from DMSO/DMF solutions and annealed (30 min. at 100°C), resulting in highly reflective thin films, with the peak reflection wavelength depending on the Br:I ratio. When exposed to 5 ppm of ozone for 5 minutes in a chamber, the MHP films showed on average a 20% decrease in reflection, and after about 1 hour, the reflection exhibited on average a 9% recovery. We also observed reversible changes in the absorption and photoluminescence spectra due to ozone exposure. These very recent results suggest that MHP's are promising candidates for spectrally resolved photonic gas sensing applications.

8:00 PM EN05.04.15

Structural Evolution and Octahedral-Coordination Control in Cs₂Ag_{1-x}Pb_{2x}Bi_{1-x}Br₆ Perovskite Materials Yi-TingTsai, Wei-LunSu and Mu-HuaiFang; Academia Sinica, Taiwan

Halide-based perovskite materials have garnered significant attention due to their diverse structures and various synthesis conditions. Serving as customizable optoelectronic materials, they

play pivotal roles in electronic applications like light-emitting diodes, backlight systems, solar cells, photodetectors, etc. Nevertheless, their intricate structural adjustment mechanisms remain significant challenges for future utilization. In this study, we successfully synthesized a series of $\text{Cs}_2\text{Ag}_{1-x}\text{Pb}_x\text{Bi}_{1-x}\text{Br}_6$ materials with a hetero-valent substitution strategy, forming solid solutions bridging CsPbBr_3 perovskite and $\text{Cs}_2\text{AgBiBr}_6$ double-perovskite materials. High-resolution synchrotron X-ray diffraction, coupled with Rietveld refinement, confirmed that samples possess the third phase between the CsPbBr_3 perovskite and $\text{Cs}_2\text{AgBiBr}_6$ double-perovskite end-members. Theoretical calculations, X-ray absorption spectra, Raman spectra, and photoluminescent spectra are conducted to realize the solid-solution process. This study provides valuable insights into the diverse structures by hetero-valent substitution strategy and contributes to precise analysis for subtle changes in crystal structures.

8:00 PM EN05.04.16

Chlorine Addition Effect on The Properties and Stability of Flexible Printed Hybrid Halide Perovskite Solar Cells CrystaStavraki¹, AlexandrosZachariadis¹, SpyridonKassavetis¹, ChristosKapnopoulos¹, EiriniParaschoudi¹, AlexandrosPaliagas¹, VolhaHeben¹, ChristoforosGravaliadis¹, EvangelosMekeridis², ArgirisLaskarakis¹ and StergiosLogothetidis^{1,2}; ¹Aristotle University of Thessaloniki, Greece; ²Organic Electronic Technologies P.C. (OET), Greece

Flexible printed perovskite solar cells based on Hybrid Organic-Inorganic Metal Halides have attracted significant attention due to the combination impressive power conversion efficiency and low-cost production and their impressive increase in power conversion efficiency. In this work we focus on the flexible printed perovskite solar cells and in the addition of Chlorine anion addition into $\text{CH}_3\text{NH}_3\text{PbI}_3$ perovskites effectively improves the crystallinity, stability and as a result the performance and durability of the flexible printed perovskite solar cells (PSCs). The flexible printed PSCs were fabricated in the inverted structure using one-step slot-die coating that involves the sequential printing of PEDOT:PSS/ $\text{CH}_3\text{NH}_3\text{PbI}_3$ /PCBM layers on top of flexible PET/IMI substrates, while the top electrode (silver, Ag) was grown by thermal evaporation in vacuum. The effect of PbCl_2 addition to perovskite precursor solution was primarily studied in terms of surface morphology and structure of the perovskite layer due to the variations of chlorine ratio in the precursor solution. X-Ray Diffraction showed the effect of chlorine addition on the crystal grain size and orientation, the surface topography characteristics were evaluated by Atomic Force Microscopy (AFM), while UV-Vis optical characterization and nIR-Vis-UV Spectroscopic Ellipsometry (SE) were used to study the optical properties and measure / control the thickness of each printed layer. The printed hybrid halide perovskite layers were of high crystalline quality as the (110) , (220) , (330) diffraction peaks of $\text{CH}_3\text{NH}_3\text{PbI}_3$ XRD appeared in the XRD spectra, while the analysis of the AFM images showed that the perovskite crystals' size was enlarged by more than 150 nm and the RMS surface roughness increased up to 30 nm as the PbCl_2 addition to perovskite precursor solution increases. Analysis of the SE spectra provided us with information on the printed perovskites thickness (> 400 nm), the quality and enables the study the effect PbCl_2 addition on the printed perovskite stability and degradation mechanisms through the changes in the PbI_2 absorbance peak in 4.64 eV. The stability studies are also supported by the nanoindentation testing, that provides information on the mechanical properties (elastic modulus, hardness and printed layers adhesion) of the individual layers and the device as well as the mechanical stability of the printed perovskite layers. Finally, we focus on the effect of the printed hybrid halide perovskite properties to the PSCs devices electrical characteristics and power conversion efficiency.

Acknowledgements: Co-funded by the European Regional Development Fund of the European Union and Greek national funds through the Operational Program Competitiveness, Entrepreneurship, and Innovation, under the call ERANETs 2021A (SOLAR ERANET, Project Code: T12EPA5-00074, Project: PEROSOLAR)

8:00 PM EN05.04.17

Thermomechanical Durability Study of Flexible Hybrid TCEs on PET made by Photonic Curing Justin C. Bonner¹, Robert Piper¹, Bishal Bhandari¹, Matthew Davis² and Julia W. Hsu¹; ¹University of Texas at Dallas, United States; ²Energy Materials Corporation, United States

Solution-deposited transparent conducting electrodes (TCEs) can potentially reduce the cost of perovskite solar cell (PSC) manufacturing. However, high-temperature thermal annealing is still needed to convert solution-deposited metal oxide films and is not compatible with plastic substrates. Photonic curing is an alternative to thermal annealing; instead of heating directly, it uses a xenon flash lamp to pulse broadband light onto a sample for micro to millisecond durations. Light absorption, depending on material optical constants, is converted to heat during a flash from the lamp; a thin absorbing layer is selectively heated during a light pulse while the nonabsorptive plastic layer does not heat up significantly. In our lab, we fabricate hybrid TCEs consisting of silver nanowires (AgNWs) and indium zinc oxide (IZO) on polyethylene terephthalate (PET) by blade coating and photonic curing. Because solution-deposited metal oxides have lower conductivity, adding AgNWs is crucial to achieve a low sheet resistance. The AgNW layer determines the sheet resistance, transmittance, and energy needed from the flash lamp to convert the IZO, which decreases the roughness of our hybrid TCEs and prevents device shorting.

While the PET substrate does not heat up significantly during photonic curing, subsequent processing of device layers and operating conditions often require high temperatures or temperature cycling that can lead to oxide cracking. Oxide-based TCEs and PET substrates are known to have a coefficient of thermal expansion (CTE) mismatch because a metal oxide has a CTE ten times smaller than the CTE of the plastic substrate. When a TCE made with a plastic substrate and brittle metal oxide is heated to elevated temperatures, the CTE mismatch will induce cracks in the metal oxide film, leading to high resistance and open circuit devices. In this work, we study the thermomechanical durability, particularly the cracking failure in the IZO layer, of the AgNW + IZO TCEs on PET substrates. Thermomechanical durability is tested by heating the PET/TCE samples to 120°C for 10 minutes, a typical annealing temperature and time used for PSC fabrication. We investigate the cause(s) for IZO cracking including IZO thickness, relative humidity during coating, PET substrate thickness, thermal and mechanical properties, and surface treatment. We then devise processing conditions to alleviate the thermomechanical failures. TCEs that survive the thermomechanical durability test will be used to make PSCs and benchmarked to PSCs made on commercial flexible TCEs. The success in producing a robust TCE will facilitate roll-to-roll manufacturing of PSCs.

This work is supported by DOE SETO DE-EE0009518.

8:00 PM EN05.04.18

Enhanced Humidity Stability of 2D Perovskites using Sulfonium Cations Daniel Ratchford, Gloria Bazargan, Blake S. Simpkins, Jeff Owrutsky and Matthew D. Thum; Naval Research Laboratory, United States

Metal halide 2D perovskites, consisting of alternating layers of metal halide octahedra sheets and cations, have broad technological appeal because of their tunable mechanical, optical, and electrical properties. Compared to 3D perovskites, 2D perovskites offer a greater flexibility in the range of cations that can be incorporated into a stable crystal structure, which then offers the potential for a broader range of material properties. Here, we discuss our work on the synthesis and characterization of lead halide perovskites which contain fluorinated phenethylsulfonium (FPES) cations. We fabricate thin film perovskites which incorporate varying amounts of this new sulfur-containing cation mixed with conventional cations (phenethylammonium and methylammonium) and compare material optical properties and stability under humid conditions. We use visible absorption spectroscopy to measure the degradation of samples at 90% RH. We show that incorporating the FPES cation can dramatically slow down humidity induced degradation, while also reducing the charge carrier recombination lifetimes. This work highlights that sulfonium cations could play an important role in enhancing the environmental stability of lead halide perovskites.

8:00 PM EN05.04.19

Expanding the Interface Engineering for Efficient Perovskite X-Ray Detectors Thanh Hai Le and Wanyi Nie; Los Alamos National Laboratory, United States

Although perovskite material-based detectors exhibit remarkable optoelectronic performance, they face a significant challenge in terms of operational stability, which does not meet market demands. Several technological strategies have been suggested to tackle the instability problem attributed to halide ion migration. While these methods have resulted in some progress, they have not yet yielded a solution ready for the market. Here, we present evidence that a zero-dimensional PEA_2ZnI_4 material can significantly enhance surface passivation in 2D perovskite single crystals and create stronger two-dimensional/zero-dimensional heterojunctions compared to their lead-based counterparts. The resulting 0D/2D configuration forms a unique and well-organized multi-dimensional interface, resulting in an impressive external quantum efficiency increase of up to 30%, surpassing the 8% improvement seen in 2D perovskite devices. Furthermore, our device maintains 100% initial efficiency even after undergoing 1000 on-off cycles and enduring over 70 hours of continuous illumination at 178.7 $\mu\text{Gy/s}$ while under an applied voltage of 10V. Additionally, our unencapsulated device exhibits no loss in performance under normal measurement and storage conditions (temperature: 25 °C, humidity: 20 to 60%) for up to 2 months. These findings significantly broaden the range of materials available for low-dimensional interface engineering and create an opportunity for the timely commercialization of perovskite x-ray detectors.

8:00 PM EN05.04.20

Enhancing The Bending Stability of Flexible Perovskite Solar Cells based on Stainless Steel Substrate through Interface Incorporation of Buffer Layer onto TiO_2 Kyunghwan Kim¹, Solhee Lee¹, Jae-Keun Hwang¹, Wonkyu Lee¹, Dowon Pyun¹, Jiyeon Nam¹, Seok-Hyun Jeong¹, Ji-Seong Hwang¹, Sujin Cho¹, Youngmin Kim², Hae-Seok Lee², Yoonmook Kang², Youngho Choe¹ and Donghwan Kim¹; ¹Korea University, Korea (the Republic of); ²KU-KIST Green School, Korea (the Republic of)

As the importance of renewable energy is increasingly emphasized, photovoltaic technology stands at the forefront of this energy transition. Building-integrated photovoltaics (BIPV) and vehicle-integrated photovoltaics (VIPV) are extending the application scope of traditional solar systems, exploring their potential in more diverse and complex environments. In response to these advancements, researchers continually delve into this domain, aiming for more efficient and sustainable energy solutions.

The first-generation crystalline silicon solar cells have already demonstrated high efficiency and reliability in their performance. However, the wafer's inherent physical properties present

limitations in flexibility and adaptability to diverse curvatures. In contrast, perovskite thin-film solar cells emerged to address these challenges, expanding applicability not only to traditional glass substrates but also to flexible substrates of various forms and materials. Specifically, when applied to intricate structures such as BIPV and VIPV, their utility and cost-effectiveness are anticipated to significantly increase.

In this study, we investigated the fabrication process of these perovskite solar cells on stainless steel (SS) substrates, leveraging the substrate's mechanical robustness, thermal and moisture stability, and excellent corrosion resistance. To evaluate their suitability for BIPV and VIPV applications, bending tests were conducted under varying curvature conditions ranging from 3mm to 15mm. Damage to the Electron Transfer Layer (ETL) and the perovskite layer was observed in these tests, affirming their substantial impact on the solar cell's performance and stability. Consequently, to fortify damage during the bending process, the insertion of a buffer layer between these layers was proposed to enhance the bending stability and performance of perovskite solar cell.

SESSION EN05.05: Halide Perovskites Photovoltaics and Stability I

Session Chairs: Xiwen Gong and Lina Quan

Tuesday Morning, November 28, 2023

Hynes, Level 3, Room 311

8:00 AM *EN05.05.01

2D or Not 2D for High Efficient NIP Perovskite Solar Cells [Giulia Grancini](#); University of Pavia, Italy

Three-dimensional (3D)/low-dimensional (LD) perovskite solar cells (PSCs) offer an effective strategy to overcome the trade-off between perovskite solar cells device performance and stability. Improving the device longevity, while concomitantly simultaneously enhancing increasing the solar cell open circuit voltage and fill factor of the solar cell is the current challenge. Despite being one of the most popular and effective way processing techniques, whether the presence of this surface LDP layer would be - or not-represents the winning crucial path for the future of this technology remains elusive. In particular, atomic layer combined surface and bulk passivation using surface modifiers such as organic dopants, casts the doubts on the effective need for of having an homogeneous LDP cover capping layer. In this talk, I will discuss the interfacial passivation with different cations such as M-PEAI, M-PEABr, and M-PEACl, showing the role of the passivation and how different halides affect the device performance of the devices. In addition, I will compare recent results obtained in the 3D/LDP configuration with the surface cation passivation strategy, which can still pushes produce the performances to values comparable to the LDP/3D bilayers. I will providing a comprehensive perspective on the benefits from of the two different strategies, but also presenting how LDP interfaces can play a role in alternative new configurations, such as tandem solar cells [1,2].

Acknowledgements I acknowledge the "HY-NANO" project that has received funding from the European Research Council (ERC) Starting Grant 2018 under the European Union's Horizon 2020 research and innovation programme (Grant agreement No. 802862).

Reference

[1] Degani et al, Sci Advances 7, 49, 2021

[2] Degani et al, submitted

8:30 AM EN05.05.02

Hot Carriers in Metal Halide Perovskites: Cold Background Effect and the Hot Phonon Bottleneck [Tim Faber](#)¹, [Lado Filipovic](#)² and [Lambert Jan Anton Koster](#)¹; ¹University of Groningen, Netherlands; ²TU Wien, Austria

The goal of third-generation PV is to go beyond the Shockley-Queisser limit, the theoretical limit of 33 % for a single junction solar cell. The hot carrier solar cell concept has been proposed to overcome this limit, by harvesting carriers before they have lost their surplus energy. Theoretically the prevented thermal losses could boost the efficiency up to 66%.

One promising type of materials for these purposes are perovskites. Next to having excellent PCE, being cheap and solution processable, some perovskites have shown very long cooling times, the key requirement for a hot carrier solar cell. We wish to shed light on why relaxation times are found to be so long in perovskites.

By using an Ensemble Monte Carlo (EMC) simulation we are able to simulate the trajectories of charge carriers and model their interactions with their environment. In the EMC random free flight times are generated and interrupted by scattering events with desired scattering mechanisms. It is this freedom of choice which makes the EMC an excellent tool in order to investigate what exactly causes charge carriers in halide perovskites to cool.

In this contribution we first identify the roles of electron-phonon and electron-electron scattering in the thermalisation and cooling process. We show how these processes depend on several material parameters. We zoom in on how cooling times are impacted by the degree of background doping and show how an ensemble of background carriers can have a detrimental effect on the cooling time.

Secondly, we quantify the effect of a hot phonon bottleneck on the cooling time. The hot phonon bottleneck has been put forward as a prominent mechanism explaining the extended cooling times measured for perovskites. We show on what scale the hot phonon bottleneck could extend cooling times and how it depends on carrier concentration and phonon lifetime.

Our results give important insights in the hot carrier cooling dynamics of perovskites, and are highly relevant for the discussion on whether or not perovskites are suitable candidates for a hot carrier solar cell.

8:45 AM EN05.05.03

Unlocking the Potential of Single-Crystal Hybrid Perovskites: Pushing the Limits to Achieve Stable and Efficient X-Ray Detection [Bekir Turedi](#)^{1,2,3}, [Kostiantyn Sakhatskyi](#)^{1,2}, [Gebhard J. Matt](#)^{1,2}, [Erfu Wu](#)², [Anastasiia Sakhatska](#)^{1,2}, [Vitalii Bartosh](#)^{1,2}, [Muhammad N. Lintangpradipto](#)³, [Rounak Naphade](#)³, [Ivan Shorubalko](#)², [Omar F. Mohammed](#)³, [Sergii Yakunin](#)^{1,2}, [Osman M. Bakr](#)³ and [Maksym V. Kovalenko](#)^{1,2}; ¹ETH Zürich, Switzerland; ²Empa-Swiss Federal Laboratories for Materials Science and Technology, Switzerland; ³King Abdullah University of Science and Technology, Saudi Arabia

Recently, hybrid metal halide perovskites have emerged as promising candidates for X-ray detectors, attributed to their cost-effective, scalable, and robust solution growth, as well as their competency in detecting individual gamma-photons under high bias voltages. Yet, the rapid degradation of perovskites, being mixed electronic-ionic conductors, under high electric fields presents a significant obstacle to the advancement of perovskite-based X-ray detectors.

In response to this challenge, we devised an innovative strategy that harnesses the photovoltaic mode of operation at zero-voltage bias. This approach employs thick and uniform methylammonium lead iodide (MAPbI₃) single-crystal films, with thicknesses extending up to 300 μm, solution-grown directly onto hole-transporting electrodes via the space-confined inverse temperature crystallization (ITC) technique.

Our results reveal that this approach engenders both near-optimal and long-term stable performance in perovskite X-ray detectors. We achieved an impressive detection efficiency of 88% and a noise equivalent dose of 90 pGy_{air} (below the dose of a single incident photon) with 18 keV X-rays, thereby enabling single-photon counting as well as low-dose and energy-resolved X-ray imaging. Furthermore, we fabricated array detectors that showcased high spatial resolution, reaching up to 11 lp mm⁻¹.

Our study evidences that hybrid perovskites are viable materials for developing cost-effective commercial detector arrays for X-ray imaging technologies. The operational stability of the device matches the intrinsic chemical shelf lifetime of MAPbI₃, registering at least one year in the investigated case. Furthermore, our results indicate that perovskite X-ray detectors can approach ideal detection performance and are amenable to medical diagnostic applications, where the radiation dose can be potentially minimized to its fundamentally lowest limit, as dictated by Poisson photon statistics.

In conclusion, this research unveils a pioneering approach to constructing a near-ideal X-ray detector utilizing hybrid metal halide perovskites, overcoming the significant issue of rapid degradation under high electric fields, thereby displaying promise for commercial application in medical diagnostics. By highlighting the direct growth of the single crystal on pixelated substrate, the study paves the way for the commercial implementation of perovskite-based array detectors. This development could bring about a new era in the field of medical imaging, with low-cost, low-dose, and high-resolution imaging becoming widely accessible.

[1] Sakhatskyi, K. † Turedi, B. †, Bakr, O. M, Kovalenko, M. V. et al. *Nature Photonics* 2023, 17 (6), 510-517

†equal first-authors

9:00 AM EN05.05.04

Interface-Driven Stability for Halide Perovskite Photovoltaics—A Fundamental UnderstandingZonglongZhu; City University of Hong Kong, Hong Kong

Organic-inorganic hybrid perovskite solar cells (PSCs) have shown great progress over the past decade, with power conversion efficiencies (PCEs) of single-junction devices approaching silicon photovoltaics (PVs). However, their long-term stability still lags behind silicon-based competitors, which has significantly decelerated their commercialization progress. Faced with this challenge, major efforts have been made to unravel instability mechanisms, develop long-term performance-tracking protocols, and explore various approaches for enhancing the stability of PSCs. Among these strategies, interface manipulation is the most critical as it could simultaneously passivate or anchor the perovskite surface defects and acts as a barrier to protect the bulk of perovskite from the external environment. Recently, the development of diversified interface modification molecules and interfacial regulation strategies has greatly contributed to the improvement of PSC stability. This presentation will elucidate the factors influencing the stability of PSCs, provide an in-depth understanding of device degradation mechanisms, and present advanced approaches to reveal them. Additionally, we will discuss pressing topics on interface manipulation, including low-dimensional perovskite capping layers, interface modification and reaction, and charge transport layer design. Lastly, we will provide insights into the core aspects related to the future development of PSC stability.

9:15 AM *EN05.05.05

Design Strategies for Efficient, Stable and Commercially Viable Inverted Perovskite Solar CellsYihou^{1,2}; ¹National University of Singapore, Singapore; ²Solar Energy Research Institute of Singapore, Singapore

Inverted perovskite solar cells (PSCs) have immense potential as a standalone technology or as a complement to silicon in tandem configurations. Nonetheless, the primary barriers impeding the commercialization of state-of-the-art inverted PSCs are still the interface recombination losses and degradation. Through the development of novel interface materials and innovative device design concepts, we demonstrate the first instance of inverted structured perovskite solar cells surpassing conventional structured perovskite solar cells in terms of performance, specifically in an active area of 1 cm². These findings have been validated and certified by the NPVM, with the inverted PSCs achieving a certified steady-state efficiency of 24.8% for an area of 0.05 cm², and a record-breaking certified steady-state efficiency of 24.0% for an area of 1 cm². Furthermore, these inverted PSCs exhibit stable performance under maximum power point tracking. In this presentation, I will provide insights into the rationale behind inverted perovskite design, elucidate how thin-film-based perovskites approach the Shockley-Queisser limit, and unveil the potential of this technology in both single-junction and tandem devices.

9:45 AM EN05.05.06

Approaches to High-Efficiency III-V/Si and Perovskite/Si Tandem Solar CellsMasafumiYamaguchi¹, TatsuyaTakamoto², KyotaroNakamura¹, RyoOzaki¹, NobuakiKojima¹ and YoshioOhshita¹; ¹Toyota Technological Institute, Japan; ²Sharp Corporation, Japan

PV-powered vehicle applications are very attractive for reducing CO₂ emission and creation of new market [1]. Development of high-efficiency (> 30%) and low-cost solar cell modules is very important. Although Toyota Prius and Nissan eNV 200 demonstration cars installed with Sharp's high-efficiency III-V 3-junction solar cell modules with an efficiency of more than 30% have demonstrated longer driving range of 26 km/day average compared to 16 km/day average for Sono Motors Sion installed with Si back contact solar cell modules with an efficiency of 21.5%, cost reduction of multi-junction (MJ) solar cells is necessary for PV-powered vehicle applications. Development of Si tandem solar cells [2] such as III-V/Si and perovskite/Si tandem solar cells is very promising for cost reduction.

This paper presents our results for III-V/Si 3-junction tandem solar cells and modules, and analytical results for efficiency potential of various Si tandem solar cells including perovskite/Si tandem solar cells.

Previously, the authors have demonstrated 34.1% efficiency with 23 cm² area 4-terminal InGaP/GaAs/Si 3-junction solar cell by using Si heterojunction solar cell with an efficiency of 24.9% as a bottom cell. Most recently, the authors have achieved a new record efficiency (33.7%) with 4-terminal InGaP/GaAs/Si 3-junction solar cell module with an area of 775 cm². Si 3-junction tandem solar cell modules with an efficiency of more than 35% are shown to have driving distance potential of more than 30 km/day average and more than 50 km/day on a clear day. Toward 35% efficiency Si tandem solar cell modules, efficiency potential of various Si tandem solar cells was analyzed by using external radiative efficiency (ERE) [3,4]. The authors have defined bandgap energy E_g dependence of $\Delta V_{oc,rad}$ ($= E_g/q - V_{oc,rad}$) for radiative open-circuit voltage $V_{oc,rad}$ relative to E_g/q as $\Delta V_{oc,rad} [V] = 0.1708 + 0.0671 E_g [eV]$. The efficiency of Si tandem solar cells in radiative limit was calculated by assuming ERE of 100%, optical loss of 2% and resistance loss of 2%. High efficiency of 43.2% and 47.9% is expected with 2-junction solar cell and 3-junction solar cells. Practically feasible efficiencies estimated by assuming ERE of 10%, optical loss of 2% and resistance loss of 2% are 40.8% for 2-junction Si tandem solar cells and 45.4% for 3-junction Si tandem solar cells. Because optimum bandgap energy combination [5] of Si tandem solar cells is 1.73 eV/Si (1.11 eV) and 2.01 eV/1.50 eV/Si (1.11 eV), optimization of bandgap energy for perovskite/Si tandem solar cells is necessary. Because 3-junction tandem solar cells have higher potential efficiency by 4-5% compared to 2-junction tandem solar cells, development of high-efficiency perovskite based 3-junction solar cells is suggested to be very attractive. Several losses such as non-radiative recombination, optical and resistance losses in Si tandem solar cells are discussed in this paper.

References

- [1] M. Yamaguchi et al., *Prog. Photovolt.* **29**, 684 (2021).
- [2] M. Yamaguchi et al., *J. Phys. D: Appl. Phys.* **51**, 133002 (2018).
- [3] U. Rau, *Phys. Rev.* **B76**, 085303 (2007).
- [4] M. Yamaguchi et al., *J. Mater. Res.* **32**, 3445 (2017).
- [5] K-H. Lee et al., *Prog. Photovolt.* **24**, 1310 (2016).

10:00 AMBREAK

10:30 AM EN05.05.07

Engineering Ligand Reactivity Enables High-Temperature Operation of Stable Perovskite Solar CellsSo MinPark^{1,2}, MingyangWei³, JianXu², KennethR. Graham⁴, MichaelGraetzel³ and EdwardSargent^{1,2}; ¹Northwestern University, United States; ²University of Toronto, Canada; ³EPFL, Switzerland; ⁴University of Kentucky, United States

Perovskite solar cells consisting of interfacial two-dimensional/three-dimensional heterostructures that incorporate ammonium ligand intercalation have enabled rapid progress toward the goal of uniting performance with stability. However, as the field continues to seek ever-higher durability, additional tools that avoid progressive ligand intercalation are needed to minimize degradation at high temperatures. We use ammonium ligands that are nonreactive with the bulk of perovskites and investigate libraries varying ligand molecular structure systematically. We find that fluorinated aniliniums offer interfacial passivation and simultaneously minimize reactivity with perovskites. Using this approach, we report a certified quasi-steady-state power-conversion efficiency of 24.09% for inverted-structure PSCs. In an encapsulated device operating at 85 degrees Celsius and 50% relative humidity, we document a 1560-hour T85 at maximum power point under 1-sun illumination.

Manuscript accepted in *Science* 2023

10:45 AM EN05.05.08

Achieving Over 3000 Hours of Stability in Perovskite Solar Cells Through Nickel Oxide Treatment and Balanced Charge ExtractionZahraLoghman Nia, ArtemMusiienko and AntonioAbate; Helmholtz-Zentrum Berlin, Germany

Perovskite solar cells currently face challenges in terms of stability within their existing architecture. The commonly used hole transfer materials in inverted perovskite solar cells typically consist of organic compounds such as PTAA and SAM [1]. In our research, we have developed a new treatment procedure for NiO, a promising inorganic hole transfer material, which significantly improves the stability of perovskite solar cells. Our findings demonstrate the exceptional long-term ageing performance of doped NiO (Li, Mg) with an insignificant loss of less than one percent over a period of 3000 hours.

To investigate the underlying factors responsible for the observed stability enhancement, we conducted a comprehensive analysis employing various measurements, including Kelvin Probe (KP), Ultraviolet Photoelectron Spectroscopy (UPS), Atomic Force Microscopy (AFM), Time-Resolved Surface Photovoltage (TRSPV), and Time-Resolved Photoluminescence (TRPL). Through our study, we have successfully demonstrated that our new treatment method for NiO facilitates improved hole extraction and mitigates the accumulation of free charges within perovskite solar cells. The boosted stability is primarily attributed to the optimized properties of NiO as a result of our treatment procedure. In conclusion, our research presents a significant advancement in the field of perovskite solar cells by introducing a novel treatment method for nickel oxide. The achieved stability enhancement through this method offers promising prospects for the commercial viability of perovskite solar cells.

- [1] Al-Ashouri, A. et al. Monolithic perovskite/silicon tandem solar cell with >29% efficiency by enhanced hole extraction. *Science* (80-.). 370, 1300–1309 (2020).

11:00 AM *EN05.05.09

Crystalline metal halide perovskites have generated intense recent interest, due to outstanding and versatile semiconducting character and associated prospective device applications. So-called two-dimensional (2D) perovskites offer the widest range of tunability within this family, due in part to the essentially unlimited range of prospective organic cations that can be employed. While most work targeting tunability in these systems has focused on optoelectronic properties, another interesting research direction relates to thermal properties—e.g., particularly as they relate to melting and ordering. Ability to melt hybrid perovskites provides an alternative solvent-free approach for film deposition, as well as offering pathways for controlling grain nucleation/growth. While hybrid perovskites are often susceptible to decomposition at temperatures below the prospective melting transitions, over the years we and others have shown that, through tailoring metal/halogen and molecular interactions within the hybrid, the melting temperature can be reduced over a >100 °C range for Ge-, Sn- and Pb-based 2D perovskites (e.g., see refs.¹⁻³) thereby enabling the formation of relatively stable hybrid melts. Most of these melts crystallize rapidly upon cooling; however, appropriate selection of organic cation component can favor a glassy state during cooling.^{3,4} Demonstration of a reversible transition between the glass and crystalline states, each with distinct physical properties, opens new opportunities for application, and points to a new direction of fundamental study related to understanding and broadening the range of local structure, crystallization kinetics, and properties exhibited by the hybrid glass state.

1. D. B. Mitzi, C. D. Dimitrakopoulos, J. Rosner, D. R. Medeiros, Z. Xu, C. Noyan, *Adv. Mater.* 14, 1772 (2002).
2. T. Li, W. A. Dunlap-Shohl, E. W. Reinheimer, P. Le Magueres, D. B. Mitzi, *Chem. Sci.* 10, 1168 (2019).
3. A. Singh, M. K. Jana, D. B. Mitzi, *Adv. Mater.* 33, 2005868 (2021).
4. A. Singh, D. B. Mitzi, *ACS Materials Lett.* 4, 1840 (2022).

11:30 AM EN05.05.10

Degradation Mechanisms in Triple-Cation Perovskite and Protection by a 2D Capping Layer Isaac Metcalf and Wenbin Li; Rice University, United States

We have used in-situ Wide-Angle X-Ray Scattering to investigate the degradation mechanism of unencapsulated mixed-cation, mixed-anion (Cs_{0.05}MA_{0.16}FA_{0.79})Pb(I_{0.83}Br_{0.17}) halide perovskite films under various external stimuli (light/humidity/temperature), with and without a capping layer of 2D perovskite. Under combined light and humidity, the perovskite film segregates into nonperovskite phases of FAPbI₃, CsPbI₃, and MAPbI₃•H₂O. This process appears to consume PbI₂, which itself is a degradation product that appears before phase segregation. Temperature accelerates this degradation process but the mechanism is the same for temperatures below 100°C. Under dark humid conditions we see no formation of nonperovskite phases and PbI₂ persists as the only degradation product, suggesting that light activates the phase segregation. Moreover, no degradation was seen in samples exposed to light and humid N₂, suggesting that the degradation process is also oxygen-catalyzed. We further performed degradation tests on 2D Ruddlesden-Popper perovskites with a butylammonium (BA) A'-site cation. Under humid conditions these 2D perovskites degrade into BA and MA hydrate phases. When the humidity is reduced the 2D partially recovers, forming the same or lower n-value films. With capping by BA-based 2D perovskite, the degradation of mixed-cation, mixed-anion 3D under light and humidity is suppressed but the same degradation products form. Under combined light and humidity the 2D and 2D hydrate diffraction signals disappear over time but 2D continues to have a protective effect on the 3D, suggesting that it intercalates into the 3D layer.

11:45 AM EN05.05.11

Defect Passivation and Gradual Energy Band Modulation for Efficient and Stable Perovskite Solar Cells Soo-Kwan Kim¹, Jinseok Kim², Bumjoon J. Kim² and Jongmin Choi¹; ¹Department of Energy Science and Engineering, Daegu Gyeongbuk Institute of Science and Technology (DGIST), Korea (the Republic of); ²Department of Chemical and Biomolecular Engineering, Korea Advanced Institute of Science and Technology (KAIST), Korea (the Republic of)

Passivation engineering is crucial for achieving high power conversion efficiency (PCE) and long-term stability in perovskite solar cells (PSCs). A promising strategy involves introducing passivation polymers to the grain boundaries (GBs) of perovskite film, where defects are densely formed during the film growth. These defects trigger non-radiative recombination, negatively impacting the performance of PSCs. Additionally, they serve as pathways for oxygen, humidity, and lithium ions, further degrading the perovskite active layer. As such, defect restoration is necessary for stability and humidity resistance. The principle of Lewis adduct formation offers a simple and effective method for passivation. The primary component of perovskite defects, the uncoordinated lead ion (Pb²⁺), is known to be a Lewis acid. The polymer's Lewis base can neutralize these Lewis acids, forming Lewis adducts. Consequently, the polymer can physically cover and neutralize defects, leading to high photovoltaic factors and long-term stability.

However, traditional polymer-based approaches for GB passivation can face limitations, such as increased series resistance and insufficient passivation coverage. To date, no solution has simultaneously addressed these issues. High polymer concentration can cover the entire perovskite surface, leading to high series resistance. In contrast, a lower concentration mitigates series resistance yet results in uneven passivation coverage. The GBs are locally exposed at the interface, leading to open-circuit voltage loss (V_{oc}) through non-radiative recombination.

In this study, we introduce a novel multifunctional polymer to passivate perovskite solar cells, addressing the aforementioned limitations. Our polymer was successfully introduced into both the perovskite film and the hole transport layer (HTL), facilitating comprehensive passivation of defect sites within the active perovskite layer. Moreover, this strategy offered several benefits for perovskite devices. Firstly, there was a significant reduction in the band offset between the perovskite active layer and the hole transport layer (HTL). Secondly, our polymer was found to mitigate lithium-ion diffusion from the HTL to the perovskite, substantially reducing hysteresis and enhancing the stability of PSCs. Lastly, the integration of our passivation strategies resulted in the suppression of pinhole formation at the HTL and reduced the surface energy difference between the perovskite films and the HTL interface. This set of improvements suppressed void formation between interfaces, thus enhancing charge extraction and reducing charge recombination losses.

Consequently, the PSCs integrated with our polymer exhibited a remarkable increase in power conversion efficiency (PCE), reaching up to 24.0%, compared to the control devices (21.0%). Furthermore, our integrated PSCs retained 92% of their initial PCE after 2000 h of storage under ambient conditions. Under damp-heat conditions (85 °C and 85% relative humidity), the cell preserved 80% of their initial PCE after 432 hours.

SESSION EN05.06: Halide Perovskites Photovoltaics and Stability II

Session Chairs: Yi Hou and So Min Park

Tuesday Afternoon, November 28, 2023

Hynes, Level 3, Room 311

1:30 PM *EN05.06.01

WITHDRAWN 11/8/2023 EN05.06.01 Stable n-i-p Perovskite Solar Cells Enabled by a New Spiro-OMeTAD Doping Strategy Feng Gao; Linköping University, Sweden

Record efficiencies of perovskite solar cells (PSCs) are usually obtained in the n-i-p structure with spiro-OMeTAD as the hole transport layer. Spiro-OMeTAD is conventionally doped by hygroscopic lithium salts with the assistance of volatile 4-tert-butylpyridine, which, however, brings a time-consuming doping process as well as poor device stability. We successfully develop an instantly efficient and clean doping strategy to replace the conventional spiro-OMeTAD doping. As demonstrated by experimental and theoretical investigations, the radical dopant leads to significant increase of the conductivity through efficient hole polarons generation. The ionic salts can further modulate the work function with negligible effects on the film conductivity, critical for reaching optimal open-circuit voltage values by a favorable energetic level alignment. Spiro-OMeTAD based on our new doping strategy enables PSCs with a high power conversion efficiency over 25% and an excellent stability against moisture, heat and illumination. Our findings pave the way for achieving PSCs with high efficiencies and excellent stability at the same time. In addition, our doping strategy goes beyond traditional organic semiconductor doping, providing new understanding of organic doping mechanisms which can inspire further optimizations of different optoelectronic devices.

2:00 PM EN05.06.02

Additive Engineering for Thermally Stable Perovskites Xiwen Gong; University of Michigan, United States

Organic-inorganic perovskites offer exceptional optoelectronic properties but suffer from poor thermal stability, hampering their practical application in photovoltaics. I will discuss a systematic investigation of the impact of the molecular structure of base additives on the thermal stability of perovskite. By synthesizing additives with controllable coordination numbers, molecular weights, and steric hindrance, we systematically study the impact of these molecular properties on the morphological, optoelectronic properties, and thermal stability of perovskite films. This study provides rational molecular design strategies for additive engineering in perovskites, enabling efficient defect passivation and enhanced thermal stability.

2:15 PM EN05.06.03

Low-Dimensional Perovskite Materials for Efficient and Stable Light-Emitting Diodes Wallace C. Choy; University of Hong Kong, China

Low-dimensional halide perovskite emitters with the advantages of quantum confinement effects have emerged as a novel class of revolutionary semiconductors with high color purity, wide color gamut, low cost, and a simple solution process for vivid natural color yet cost-effective displays. However, perovskite materials commonly exhibit environmental instability due to humidity, light, and/or elevated temperature significantly hindering their applications in light-emitting diodes (LEDs) where reported lifetimes are commonly in the order of minutes. In this talk, we will discuss some of our recent work on perovskite LEDs. Regarding quasi-2D perovskites, limited attention has been paid to rational design to balance the carrier confinement and transfer in quasi-2D perovskites, which is essential to achieve high-performance PeLEDs. By using blue PeLEDs as an example, we will enhance the hole injection for better balance carrier and improve the efficiency [1], we also modulate the n-phase distribution [2,3] and optimize the carrier transfer and confinement to improve the performances of PeLEDs [4]. For perovskite nanocrystals (NCs), we will introduce new ligands to synthesize red color perovskite (CsPbI₃) NCs. The ligand can significantly stabilize the CsPbI₃ NCs without any crystalline deformation on the NC crystal structure. Additionally, these chemically crosslinked PMAs also significantly reduce Pb_{Cs} deep defects. Moreover, CsPbI₃ NCs exhibit increasing exciton binding energy and reduced longitudinal-optical (LO) phonon energy [5,6]. Recently, by designing the multifunctional-group ligands for ion migration suppression and carrier transportation enhancement, we further improved the efficiency and stability of the pure red and pure green perovskite LEDs meeting the standard of Rec. 2100 for promoting their display applications. [1] Adv. Function. Mater., 29, 1905339, 2019; [2] ACS Energy Lett., 5, 2569, 2020; [3] Adv. Mater., 33, 2005570, 2021; [4] Nano-Micro Lett, 14:66, 2022; [5] Adv. Mater., 2008820, 2021, [6] Adv. Optical Mater., DOI:10.1002/adom.202300912.

2:30 PM *EN05.06.04

Scalable Interfaces Passivation for Perovskite Solar Cells David S. Ginger; University of Washington, United States

Halide perovskite semiconductors are being explored for applications including solar photovoltaics (PV), light emitting diodes (LEDs), radiation detectors, and even sources of quantum light. While perovskite semiconductors are often described as remarkably defect tolerant, they are not defect free. As these materials race towards commercialization, it is important to understand how different processing methods lead to semiconductor films with different levels of efficiency and stability. In this talk I will discuss defects and heterogeneity, and our ability to control them at perovskite interfaces from the molecular to macroscopic scale. We show how processing additives can undergo unexpected chemical reactions that alter the growth processes in perovskite films, leading to improved uniformity with processing over large areas, and how interfacial layers can improve overall photovoltaic performance, as well as stability under reversed bias conditions.

3:00 PM BREAK

3:30 PM *EN05.06.05

Making High-Efficiency Halide-Perovskite Solar Photovoltaics More Durable: Challenges and Opportunities Nitin P. Padture; Brown University, United States

The unproven durability of perovskite photovoltaics (PVs) is likely to pose a significant technical hurdle in the path towards the widespread deployment of this burgeoning thin-film PV technology. The overall durability of perovskite PVs, which includes operational stability, is directly affected by the mechanical reliability of metal-halide perovskite materials, cells, and modules, but this issue has been largely overlooked. Thus, there is a sense of urgency for addressing the mechanical reliability issue comprehensively, and help perovskite PVs reach their full potential. This presents many challenges, but it also offers vast research opportunities for making meaningful progress towards more durable perovskite PVs. Here I will highlight the important challenges and opportunities, together with best practices, pertaining to the three key interrelated elements that determine the mechanical reliability of perovskite PVs: (i) driving stresses, (ii) mechanical properties, and (iii) mechanical failure. I will also present examples of approaches to mitigate failure and extend the durability of perovskite PVs.

4:00 PM EN05.06.06

Efficient All-Perovskite Tandems Enabled by Surface Anchoring of Bifunctional Long-Chain Amphiphilic Ligands Aidan Maxwell and Hao Chen; University of Toronto, Canada

Perovskite solar cells (PSCs) in the stability-enhancing pin structure are limited by nonradiative recombination at the materials interface with the electron transport layer (ETL). This recombination is particularly acute in narrow-bandgap (~ 1.2 eV) mixed Pb-Sn PSCs, a crucial active layer in emergent all-perovskite tandem solar cells: these suffer higher V_{OC} deficits than do their Pb-based counterparts due to Sn-related surface oxidation and consequent detrimental p-doping. Our photoluminescence quantum yield studies herein indicated that state-of-the-art ethane-1,2-diammonium (EDA) passivation only partially alleviates harmful perovskite/ETL quasi fermi level splitting losses. We pursued physical separation at the defect-rich perovskite:ETL interface to reduce non-radiative losses: our target was to unite chemical surface coordination of Sn sites with physical interlayer separation, an approach we implemented by introducing amphiphilic long-chain carboxylic acid ligands at the perovskite surface. Treatment with oleic acid (OA), a long-chain carboxylic acid, led to carrier dynamics and surface chemistry indicative of reduced carrier recombination at the perovskite/ETL interface, and evidence of coordination with surface Sn²⁺. The addition of OA reduces the V_{OC} deficit to 0.34 V, resulting in a 0.89 V V_{OC} and PCE of 23.0% (22.4% stabilized) for 1.23 eV Pb-Sn PSCs. Incorporating the OA-treated Pb-Sn layer into a monolithic all-perovskite tandem, we report 27.3% PCE (26.4% certified) having a record V_{OC} of 2.21 V.

4:15 PM EN05.06.07

Unraveling Perovskite Metal Shunting in Reverse Bias: Insights for Enhanced Module Design Isaac Gould, Daniel Morales and Michael McGehee; CU Boulder, United States

In a photovoltaic module under partial shading conditions, shaded subcells may experience reverse bias. For perovskite solar cells reverse bias often rapidly leads to degradation. One of the most common forms of degradation is shunting which is linked to metal migration. Our findings suggest that the metallic anodic interface's oxidation leads to the formation of mobile metallic cations. These metal ions migrate across the device under the reverse bias field, and electroplate on the opposite electrode, forming metal filament type shunts. Time-of-flight secondary ion mass spectroscopy confirms the infiltration of metal into the perovskite layer during reverse bias operation. Relating the shunt resistance to the radius of the shunt leads to a calculation of 10-35 nm. High current density through these nanosized filaments generates significant localized heating, causing substantial damage to the adjacent perovskite material. To mitigate this issue, we advocate for using ion barriers, like atomic layer deposited tin oxide, between the perovskite layer and the metal electrode. Notably, cells with the NIP orientation do not exhibit this shunting phenomenon, suggesting that halide-induced oxidation of the metallic electrode occurs exclusively when it serves as the anodic electrode during reverse bias operation.

The understanding of metal migration and shunting mechanisms in perovskite solar cells is invaluable for improving solar module design and optimization. Once shunting is stopped reverse bias breakdowns can range from -3V to -15V. High breakdown opens the possibility of bypass diode implementation, although resistance losses from the transparent conducting oxides must be managed. With a low voltage breakdown (-3V), self-bypassing is possible, as the resultant temperature increase is a modest 5°C, assuming uniform heating. This can still be problematic as reverse bias breakdown can lead to redox of halide species and other electrochemical degradations to proceed. The trade-offs in perovskite solar module design necessitate crucial decisions that can affect the module's efficiency, cost, and reliability. A thorough understanding of perovskite chemistry, the implications of shunting, and the role of different interlayers in the module is essential to guide these decisions towards optimal solar module design and performance.

4:30 PM EN05.06.08

Investigation of The Influence of The Voids Formed During The Operation of The Device on The Thermal and Light Stability of Perovskite Solar Cells Mengru Wang; University of North Carolina at Chapel Hill, United States

The formation of voids in the perovskite films close to the embedded bottom interface has been reported to form during film deposition and limit the efficiency and stability of perovskite solar cells. Here we studied the voids formed during the long-term operation or thermal stress for a typical perovskite made by solution process, even if the initial perovskite films are already optimized to avoid voids during film deposition. These voids preferred to assemble along grain boundaries at the bottom interface. Detailed studies show that the voids originated from the shrinking of perovskites caused by the leaving of residual dimethyl sulfoxide (DMSO) and the conversion of the amorphous phase to the crystalline phase as a result of solid-state ion diffusion. Surprisingly, we found the formation of these voids did not notably impact the solar cell thermal stability. After decreasing the amorphous region in perovskites by thermal annealing, the light stability of perovskite solar cells was actually improved despite of the creation of voids by thermal annealing. The annealed devices maintained 90% of their initial efficiencies after annealing and light soaking for 1900 hours at open circuit conditions under one-sun light at 50 °C. The positive iodide interstitial density in the perovskite films was actually reduced during post-annealing despite the generation of three-dimensional voids, which further confirms that removing the amorphous region is an effective method to enhance the operational stability of perovskite solar cells.

4:45 PM EN05.06.09

Photonic Processing for Perovskite Halide Thin-Film Defect-Tolerant Crystal Growth Sandy Sanchez; Ecole Polytechnique Federale de Lausanne, Switzerland

Metal halide perovskite solar cells have achieved record efficiencies of over 25%, comparable to mainstream silicon solar cells. However, the processing method and operational stability need further development to bring this technology to commercialization. In this context, we use a flash-infrared annealing method, which is environmentally friendly and rapid processing, without the use of toxic chlorobenzene, to process highly stable perovskite solar cells. Therefore, this work reveals the phase stabilization mechanism for perovskite halide films through thermodynamic, structural, and photophysical analysis related to process parameters optimization. [1] Measuring the enthalpy changes of the FAPbI₃ composition at different heating rates

allows us to calculate an activation energy of 1.8 eV for the black perovskite phase transition. We explore different heating regimes for triggering the phase transformation and analyze the evolution of the microstructure with an empirical calculation of the average crystal growth velocity required to form a compact film on the micron and submicron scales. A critical interplay between perovskite halide thin-film crystallization phenomena and manufacturing aspects will be addressed, using oxidizing agents to achieve outstanding device stability of more than 1500 h under an MPPT scan.[2]

References

- [1] S. Sanchez, S. Cacovich, G. Vidon, J.F. Guillemoles, F. Eickemeyer, Shaik M. Zakeeruddin, Jürgen E. K. Schawe, Jörg F. Löffler, Cyril Cayron, Pascal Schouwink and Michael Graetzel, *Energy Environ. Sci.* (2022), 15, 3862-3876
- [2] S. Sánchez, L. Pfeifer, N.s Vlachopoulos, A. Hagfeldt, *Chem. Soc. Rev.* (2021), 50, 7108-713

SESSION EN05.07: Poster Session III: Perovskites Photovoltaics and Stability II

Session Chair: Ni Zhao

Tuesday Afternoon, November 28, 2023

Hynes, Level 1, Hall A

8:00 PM EN05.07.01

Bandgap Bowing in Inorganic Lead-free Perovskite-Inspired Materials FangSheng, EuniceAissi, AlexanderE. Siemenn, BasitaDas, HamideKavak and TonioBuonassisi; Massachusetts Institute of Technology, United States

The recent success of lead-halide perovskites has inspired the search for similar materials, with potential advantages of greater stability and absence of lead. Some of these materials form alloy series that exhibit a property known as “bandgap bowing”, whereby a mixed alloy AB has a lower bandgap than either phase-pure A or B, for example $\text{Cs}_3(\text{Bi}_{1-x}\text{Sb}_x)_2(\text{I}_{1-x}\text{Br}_x)_9$ reported in Ref. [1].

Bandgap bowing can be expensive and challenging to predict by first-principles simulations, motivating the application of high-throughput methods to experimentally synthesize alloy series and quickly measure them. As a benchmark, we consider spin coating and UV-Vis, which requires approximately 15 minutes per sample for synthesis and annealing, and 30 minutes for characterization.

In this work, we employ a high-throughput workflow that combines direct multi-material printing of alloy series with an automated computer-vision-based bandgap extraction, to experimentally screen for bandgap bowing in a broader materials space of ABX_3 and $\text{A}_3\text{B}_2\text{X}_9$ alloys. The high-throughput synthesis is conducted by our direct multi-material printer, Archerfish, which has the capability to print and anneal 1000 unique alloy materials in 15 minutes. Bandgaps for each of the 1000 alloys are measured using a hyperspectral camera operating in reflectance mode, in 2 minutes. Finally, bandgaps are autonomously extracted using an algorithm in 30 minutes, with potential to accelerate using more powerful computation. We report bandgap bowing effects in $\text{Cs}_3(\text{Bi}_x\text{Sb}_{1-x})_2\text{I}_9$ and compare with density functional theory calculations. We then screen broader range of elements including Ge, Ga, and Sn on B sites and Cl⁻, Br⁻ on X sites.

Reference:

- [1] Shijing Sun *et al.*, Accelerated Development of Perovskite-Inspired Materials via High-Throughput Synthesis and Machine-Learning Diagnosis, *Joule* 3, 1437–1451 (2019).

8:00 PM EN05.07.02

Static and Dynamic Disorder in Formamidinium Lead Bromide Single Crystals GuyReuveni¹, YaelDiskin-Posner¹, ChristianGehrmann², ShraavanGodse², GiannisG. Gkikas³, IsaacBuchine⁴, SigalitAharon¹, RomanKorobko¹, ConstantinosC. Stoumpos³, DavidA. Egger² and OmerYaffe¹; ¹Weizmann Institute of Science, Israel; ²Technische Universität München, Germany; ³University of Crete, Greece; ⁴Bar-Ilan University, Israel

The distinction between the average and the local structure has crucial importance in crystalline materials where the two are not overlapping. In this work, we show that formamidinium-based are distinct from methylammonium-based halide perovskite crystals because their inorganic sub-lattice exhibits intrinsic local static disorder that co-exists with a well-defined average crystal structure. This combination of order and disorder makes formamidinium-based halide perovskites interesting. Our study combines terahertz-range Raman scattering with single-crystal X-ray diffraction and first-principles calculations to probe the evolution of inorganic sublattice dynamics with temperature in the range of 10–300 K. In my talk, I will present results from probes of different scales of the crystalline structure - local and average. I will show how temperature affects the interplay between the two expressions of disorder in these materials - static and dynamic disorder. Our results potentially have significant implications for the optoelectronic and thermal stability properties of FA-based lead halide perovskites.

8:00 PM EN05.07.03

Effect of Grain Boundaries on the Mechanical Properties of Organic-Inorganic Halide Perovskite Polycrystalline Thin Films and Bulk Crystals MadhujaLayek, MeaghanDoyle, AnushRanka, ZhenghongDai, InseokYang and NitinP. Padture; Brown University, United States

The past several years have observed a growing interest in hybrid organic-inorganic perovskites (HOIPs) owing to their remarkable application potential in optoelectronics, especially photovoltaics. In order to manufacture efficient and reliable perovskite solar cells (PSCs) that can operate satisfactorily for decades, it is critical to study the mechanical properties of MHPs that are inherently compliant, soft, and brittle. Thus, we have employed multi-beam optical stress sensor (MOSS) curvature measurement and X-ray diffraction (XRD) techniques to estimate Young's modulus of polycrystalline methylammonium lead iodide (MAPbI₃) thin film. Furthermore, we synthesized and sintered HOIP powders into bulk crystals to understand the effect of grain size on Young's modulus and other relevant mechanical properties of HOIPs. We aim to provide an in-depth understanding of the mechanical properties of HOIPs to effectively use them in PSCs.

8:00 PM EN05.07.04

Synthesis of Bismuth Based-Perovskite Nanocrystals for CO₂ Reduction AntikGhosh^{1,2,3}, DmitryAldakov^{2,1,3} and VincentArtero^{1,2,3}; ¹Commissariat à l'Énergie Atomique et Aux Énergies Alternatives, France; ²Centre National de la Recherche Scientifique, France; ³Université Grenoble Alpes, France

Abstract: Solar driven CO₂ valorization into hydrocarbon fuels using semiconductor catalysts offers a promising energy conversion pathway to have impactful solutions to environmental degradation and energy crisis problems. The solar light not being sufficient enough to break the high energy C=O bond in CO₂, an external photosensitizer (PS) coupled to a co-catalyst is used in this process. The PSs used presently are often hard to synthesize, they are toxic and have limited stability and light absorption capacity. Colloidal semiconductor nanocrystals (NCs) can have strong light absorption and stability; in addition, their properties can be easily optimized by the size/or composition control. We propose to use halide perovskite NCs as PSs for the CO₂ reduction. Halide perovskite nanocrystals (NCs) have been widely considered as promising materials as light-harvester emitters due to their wide range of benefits combining those of conventional colloidal semiconductor NCs including tunable bandgap, high absorption coefficients, strong photoluminescence, flexible crystal structure and low fabrication cost due to the processability from solution. Recently, perovskite NCs were successfully used for the photocatalytic CO₂ reduction, however most of them are still based on toxic lead and have limited stability in polar medium used in photocatalysis¹. Among lead free alternatives, one of the most promising is bismuth halide perovskite $\text{A}_3\text{Bi}_2\text{X}_9$ (A=cation; X=Br, I) NCs combining good absorption in the visible range, higher stability, and much lower toxicity compared to the lead-based counterparts². They can be synthesized using Hot-injection or Ligand assisted reprecipitation (LARP), however numerous challenges still exist, namely to synthesize the NCs with a small controlled size, to properly purify them, and to accurately study their crystalline structure and optical properties.

We have developed a new approach to synthesize air-stable bismuth halide perovskite NCs in ambient conditions with a high reaction rate using cesium halide NCs as the templates³. By optimizing synthesis protocols, we managed to obtain air-stable $\text{Cs}_3\text{Bi}_2\text{Br}_9$ and $\text{Cs}_3\text{Bi}_2\text{I}_9$ NCs of around 10 nm with a good size dispersion. In addition, by a modified hot-injection method using various ligands we have synthesized $\text{Cs}_3\text{Bi}_2\text{I}_9$ nanoplatelets under ambient condition. Synthesis details, structural and optoelectronic properties will be discussed, as well as their perspectives for the photoelectrocatalytic CO₂ reduction application.

References:

1. Shyamal, S. & Pradhan, N. Halide Perovskite Nanocrystal Photocatalysts for CO₂ Reduction: Successes and Challenges. *J. Phys. Chem. Lett.* 11, 6921–6934 (2020).
2. Aldakov, D. & Reiss, P. Safer-by-Design Fluorescent Nanocrystals: Metal Halide Perovskites vs Semiconductor Quantum Dots. *J. Phys. Chem. C* 123, 12527–12541 (2019).
3. Shamsi, J. *et al.* Colloidal CsX (X = Cl, Br, I) Nanocrystals and Their Transformation to CsPbX₃ Nanocrystals by Cation Exchange. *Chem. Mater.* 30, 79–83 (2018).

8:00 PM EN05.07.05

Experimental Characterization of Metal Oxide Thin Films and Their Numerical Simulation as a Hole Transport Material in Inverted Perovskite Solar Cells Fernando T. da Rocha Arita and Andre Santarosa Ferlauto; UFABC - Federal University of ABC, Brazil

The rapid populational and technological growth in the last decades has required larger material production and, consequently, more demanding power usage. The long-term scarcity and the price volatility of fossil fuels are not the only problems associated with a non-renewable-based electric power matrix. Climate Change can already be perceived locally and globally and, if not reduced, will become an existential threat to life on Earth. Among the many ways to reduce the effects of climate change, the electrification of the power matrix associated with cleaner and more efficient means of power obtainment, such as solar power, is crucial. Hybrid perovskite-based solar cells have been widely studied throughout the last decade due to the rapid progress in conversion efficiency in the last few years. State-of-the-art devices have achieved efficiencies above 25%, close to the efficiencies of commercial devices. The current hindrance to the large-scale production of this kind of solar cell is its stability facing degradation processes to adjacent layers and external factors, mainly humidity. P-type metal oxide semiconductors are promising candidates as a hole transport material in inverted perovskite solar cells, due to their enhanced optoelectronic properties: improved hole mobility, suitable bandgaps and high transparency, and fitting energy levels with the active layer [1]. These materials also act as humidity barriers and their chemical stability mitigates some degradation processes [2]. The present study involves the experimental characterization of sputtered thin films that feeds the materials' optoelectronic properties into a numerical simulation of inverted perovskite solar cells using SCAPS (Solar Cell Capacitance Simulator). Reactive sputtering provides more precise control of thin film stoichiometry and can be used to determine an adequate composition that leads to the maximization of the device's efficiency. Numerical simulations can help to screen through materials providing cost reduction and time optimization, although it does not predict how well these materials would perform in a stability test. Copper aluminate delafossite and copper oxide thin films have been deposited using reactive RF-sputtering and characterized by X-ray diffraction, Raman Spectroscopy, X-ray Photoelectron Spectroscopy, Four-probe Resistivity measurement, and UV-Vis Spectroscopy. Scanning Electron Microscopy, Contact Angle measurements, and Ellipsometry were also performed to study the deposition dynamics and the thin film surface.

Acknowledgments:

CINE - Shell (ANP) / FAPESP grant n. 2017/11937-4, 2018/04596-9 and 2018/04595-2

References:

- [1] Yan, W., et al. Hole-Transporting Materials in Inverted Planar Perovskite Solar Cells. *Advanced Energy Materials*, 6, 17, 1600474, 2016.
- [2] Akin, S., et al. Inorganic CuFeO₂ Delafossite Nanoparticles as Effective Hole Transport Material for Highly Efficient and Long-Term Stable Perovskite Solar Cells. *ACS Applied Materials Interfaces*, 11, 48, 45142–45149, 2019.

8:00 PM EN05.07.06

Lighting the Way Forward: Exploring Structure-Bandgap Relationships in Hybrid Organic-Inorganic Perovskites Omar Allam^{1,1}, Yoonseo Nah², Ilgeum Lee², Dong Ha Kim² and Seung Soon Jang¹; ¹Georgia Institute of Technology, United States; ²Ewha Womans University, United States

Hybrid organic-inorganic perovskites (HOIPs) have recently gained significant traction across various applications, largely due to their remarkable electrical and optical properties such as high photoluminescence quantum efficiency and brilliant light emission. In this research, we harness the power of density-functional theory (DFT) to investigate the intricate relationships between structure and bandgap of 2D HOIPs, aiming to achieve precise modulation for diverse optoelectronic applications. The influence of spacer size in the interlayer region of 2D HOIPs, a crucial aspect that remains underexplored, is a primary focus of our study. Leveraging DFT, we uncover a pivotal link between the steric dimensions of the organic spacer components and the bandgap of perovskites. Furthermore, while it is established that the perovskites' bandgap can be tuned by altering the halide mixture, these mixed halide perovskites unfortunately demonstrate spectral instability, an issue that hinders their application in commercial LED technologies. Through the application of the nudged elastic band (NEB) method, our DFT analyses reveal the underlying mechanism behind this spectral instability, tracing it to the migration of mixed halides. By employing DFT, our mechanistic exploration yields crucial insights into the process of bandgap tuning in HOIPs and elucidates the fundamental causes behind the observed spectral instability in devices utilizing mixed halide compositions.

8:00 PM EN05.07.07

Understanding the Effect of Post-Growth Vacuum Annealing on 2D Hybrid Organic-Inorganic Perovskite Thin Films Manosi Roy¹, Jose Castaneda², Sharonda LeBlanc² and Adrienne D. Stiff-Roberts¹; ¹Duke University, United States; ²North Carolina State University, United States

The rapid advancements in power conversion efficiency (PCE) of perovskite active regions, achieving a remarkable 26% in 2023, have positioned them as leading contenders in the development of high-efficiency solar cells. However, the issue of moisture instability in three-dimensional (3D) perovskites poses a significant hurdle for the commercialization of perovskite solar cells.¹ To address this challenge, the use of more environmentally stable, two-dimensional (2D) hybrid organic-inorganic perovskites (HOIPs) as a passivating layer for the 3D perovskite active region shows promise in improving stability.² One of the key obstacles in this context is the lack of desired alignment or orientation of the 2D sheets comprising organic and inorganic layers. Traditional solution-based processing methods tend to align these sheets parallel to the substrate, limiting charge transport in the vertical direction. While resonant infrared matrix-assisted pulsed laser evaporation (RIR-MAPLE) yields a random orientation of crystallites and offers a partial remedy to the problem, the ultimate goal is to deliberately promote vertical orientation of the crystallites.^{3,4} Therefore, it is crucial to better understand the RIR-MAPLE synthesis process to influence the orientation of the films, and one possible approach is to conduct post-growth vacuum annealing.¹ Accordingly, phenethylammonium lead halide 2D HOIPs will be grown for comparison using RIR-MAPLE at 50-degree celsius without and with a post-growth vacuum annealing step at three distinct temperatures – 60, 90, and 110-degree celsius. The films will be characterized using a full suite of standard techniques, including X-ray diffraction (XRD) to confirm crystal structure and conduct crystallite size analysis (using the Williamson-Hall method), Stokes shifts (derived from photoluminescence (PL) and UV-Vis spectroscopy), and scanning electron microscopy (SEM) and atomic force microscopy (AFM) to determine surface morphology. In addition, the full-width-half-maximum values for XRD peaks corresponding to different orientations of crystallites will be used to quantify changes in vertical orientation.⁴ Overall, this investigation will shed light on the potential of employing post-growth vacuum annealing to promote vertical orientation of crystallites in 2D HOIP thin films deposited using the RIR-MAPLE, paving the way for future explorations in this area.

References:

1. N. E. Wright, X. Qin, J. Xu, L. L. Kelly, S. P. Harvey, M. F. Toney, V. Blum and A. D. Stiff-Roberts, *Chemistry of Materials* 34 (7), 3109-3122 (2022).
2. E. T. Barraza and A. D. Stiff-Roberts, *World Scientific*, pp. 115-152 (2022).
3. A. D. Stiff-Roberts, in *Women in Microelectronics*, Springer International Publishing, pp. 29-48 (2020).
4. N.E. Wright, J. Xu, H. Lu, O. G. Reid, K. Zhu, M. F. Toney, A. D. Stiff-Roberts, *Advanced Science* (2023).

8:00 PM EN05.07.08

Dimethylammonium-Incorporated Mixed Halide Perovskite Nanocrystals for Stabilized Red Emission Shaoni Kar^{1,2}, Bernard Wenger² and Henry Snaith¹; ¹University of Oxford, United Kingdom; ²Helio Display Materials Ltd., United Kingdom

In addition to their stellar performance in photovoltaics, metal halide perovskites have seen a meteoric emergence in several other optoelectronic applications of which light emission is of special significance. Perovskites have been used in light emitting diodes (LEDs), lasing and displays (as colour-converting phosphors) to achieve record efficiencies with immense potential to compete with the commercial standards of III-V and organic LED (OLED) systems within a relatively short time. With high exciton binding energies affording enhanced quantum confinement of carriers, low-dimensional perovskites are especially useful for realizing colour-pure, highly efficient emission. Among such systems, all-inorganic perovskite nanocrystals are attractive candidates owing to easy bandgap tunability through compositional engineering, narrow emission peaks and high photoluminescence quantum yields.

Cesium lead halides of the form CsPbX₃ are the most commonly demonstrated workhorse systems in this category with halide tuning determining the emission range. Cesium lead iodide (CsPbI₃) nanocrystals have been shown to be promising but their device application is still inhibited by their inherent ambient instability. With facile conversion of the metastable black perovskite γ -phase into the yellow δ -phase at room temperature, this material has hardly been effective under sustained optical or electrical excitation. In addition, this composition shows emission outside the visible range (around near-IR wavelengths) which severely limits their usage in displays and other common applications. With addition of bromine (Br), CsPbI_xBr_{3-x} nanocrystals are formed with ideal bandgaps for application in visible range LEDs and displays with emission wavelengths lying within the Rec 2020 colour gamut. Furthermore, in contrast to the pure-iodide compositions that require high temperature-based (hot injection) processes to form the perovskite phase, mixed-halide nanocrystals afford facile synthesis through ligand assisted reprecipitation (LARP) in ambient conditions due to the possibility of crystallization at much lower temperatures. However, these materials are still plagued by phase separation under optical or electrical excitations of intensities typical in a working device.

In this work, we try to alloy the A-site of the pure-red emitting CsPbI₂Br with dimethylammonium (DMA) to improve its phase stability under excitation while retaining high photoluminescence quantum yields. DMA, among other organic cations, has recently been shown to alloy successfully with Cs in 3D perovskite thin films and lend it stability under operational conditions. However, with lower-dimensional nanocrystals, the nucleation and growth kinetics are radically different and further intricacy is introduced with the remnant (unwashed) ligands that are unavoidable in the synthesis process. To our knowledge, this is the first study of DMA-alloying through facile LARP synthesis techniques. We propose a novel synthetic route at room temperature and then study the crystal structure and morphology as a function of different DMA contents through an interplay of crystallographic and optical data. We

report higher ambient stability even under intense optical excitation. Finally, we employ these materials as the emitter layer in LEDs and find significant improvement in LED performances with notably improved air-stability in the DMA-incorporated variant.

8:00 PM EN05.07.09

Deterministic Solution-Processed Fabrication of Halide Perovskite HeterostructuresFaizMandani, SirajSidhik, AltafPasha, AndrewJ. Torma and AdityaD. Mohite; Rice University, United States

Heterostructures play a crucial role in the semiconductor industry as they offer unique optoelectronic properties. However, the conventional methods used for fabricating heterostructures involve specialized and costly processes such as chemical vapor deposition, epitaxial growth, or e-beam deposition. Halide perovskites have emerged as a promising material for various optoelectronic applications due to their tunable bandgap, high carrier mobility, and solution processability. In recent years, considerable efforts have been made to develop perovskite heterostructures using vapor phase techniques¹. These techniques aim to enhance photogeneration, fine-tune band alignments, and passivate the underlying semiconductor. In our previous work, we introduced a solution processed technique for depositing selective (Ruddlesden-Popper) two-dimensional perovskite on top of three-dimensional perovskite². We achieved this by leveraging solvent properties such as dielectric constant and Guttman number.

However, the development of a universal solution processed approach for fabricating multilayer perovskite heterostructures has remained a challenge. To address this, we conducted detailed perovskite-solvent interaction studies to gain a deeper understanding of perovskite solvation dynamics. In this study, we present a solvation-based approach to synthesize perovskite seed solutions, enabling the fabrication of 2D/3D, 3D/2D, and even 3D/3D heterostructures. This approach allows us to create an arbitrary number of layers with any perovskite phase while maintaining high optoelectronic quality and scalability. To demonstrate the universality of our approach, we successfully created formamidinium lead iodide (FAPbI₃)/Dion-Jacobson 2D (3D/2D) perovskite and methylammonium lead iodide (MAPbI₃)/MAPbI₃ (3D/3D) heterostructures. We validated the quality and characteristics of these heterostructures through optoelectronic and cross-sectional analyses. The introduction of this universal approach marks a significant milestone in solution processed heterostructures, extending its applicability beyond perovskites to the broader field of semiconductors. This advancement opens up new possibilities for the synthesis of high-quality, scalable heterostructures, revolutionizing the semiconductor industry.

1.) Lin, Renxing, et al. "All-perovskite tandem solar cells with 3D/3D bilayer perovskite heterojunction." *Nature* (2023): 1-3.

2.) Sidhik, Siraj, et al. "Deterministic fabrication of 3D/2D perovskite bilayer stacks for durable and efficient solar cells." *Science* 377.6613 (2022): 1425-1430.

8:00 PM EN05.07.10

Light-Induced Expansion Kinetics of Lead Halide Perovskite Crystals Measured via Laser InterferometryChristopherPetroff, Kuan-TingLiu, EmilyE. Hiralal, LaraA. Estroff and JohnA. Marohn; Cornell University, United States

Light-induced changes to lead halide perovskite (LHP) crystals can provide key information about their electrical properties and degradation mechanisms. It is shown in the literature that LHP crystals exhibit light induced expansion, so called "photostriction" [1]. Generally, it is concluded that these—mainly atomic force microscopy (AFM) derived—data are the result of the photoinduced production and diffusion of electrons. We assert that the several second expansion onset and decay shown in the literature and in our data, is inconsistent with the sub-microsecond timescale of electronic diffusion. We instead propose that this expansion is due to the light-induced creation of ionic vacancies [2–4]. The formation of ionic vacancies should exhibit an activated temperature dependence. We are developing a series of variable temperature, laser interferometric measurements of LHP crystals to study these expansion kinetics. Laser interferometry is ideal for this kinetics study, as it offers better temporal resolution than the AFM data in the literature; AFM is limited by the time constants of the phase-locked loop whereas laser interferometry is only limited by the bandwidth of the photodetector.

Using laser interferometric measurements, we show non-thermal, light-induced expansion of methylammonium lead tribromide (MAPbBr₃) perovskite crystals, even when excited below band gap. The expansion displays two-rate kinetics and hysteresis with a rapid (10 s) expansion followed by continued slow (10s of seconds) expansion; upon returning to the dark, a rapid contraction is observed which does not reach baseline. We are working to explore this effect and its kinetics across various temperatures; illumination wavelengths; and perovskite crystal compositions, including the all inorganic cesium lead tribromide (CsPbBr₃) system.

References:

[1] Zhou, et al. *Nat. Commun.* **2016**, 7, 11193. DOI: 10.1038/ncomms11193

[2] Tirmzi, et al. *ACS Energy Lett.* **2017**, 2, 2, 488–496. DOI: 10.1021/acsenerylett.6b00722

[3] Tirmzi, et al. *J. Phys. Chem. C* **2019**, 123, 6, 3402–3415. DOI: 10.1021/acs.jpcc.8b11783

[4] Kim, et al. *Angew. Chem. Int. Ed.* **2021**, 60, 820–826. DOI: 10.1002/anie.202005853

8:00 PM EN05.07.11

Long-Lived Spin-Triplet Excitons in Manganese Complexes for Room-Temperature PhosphorescenceMi HeeJung; Sejong University, Korea (the Republic of)

Low dimensional metal halides perovskites have become emerging candidates as applications of light emitting diodes due to the quantum confinement effect by tuning their composition and structure. However, it suffers from longstanding issues of environmental stability and lead toxicity. Herein, we report phosphorescence manganese halides, (TEM)₂MnBr₄ (TEM = HN(CH₂CH₃)₃, triethylammonium) and (IM)₆[MnBr₄][MnBr₆] (IM = C₃H₆N₂, imidazolium) with photoluminescence quantum yield (PLQY) of 50% and 7%, respectively. (TEM)₂MnBr₄ with a tetrahedral configuration exhibits brilliant green light emission centered at 528 nm, while (IM)₆[MnBr₄][MnBr₆] compound, in which octahedral and tetrahedral units coexist, exhibits red colored emission at 615 nm. The excite state of (TEM)₂MnBr₄ and (IM)₆[MnBr₄][MnBr₆] found to exhibit distinct photophysical emission characteristics consistent with triplet state phosphorescence. Efficient phosphorescence was achieved with a long lifetime of several milliseconds, 0.38 ms for (TEM)₂MnBr₄ and 5.54 ms for (IM)₆[MnBr₄][MnBr₆], respectively, at room temperature. By studying the temperature dependent PL and single-crystal X-ray diffraction measurements and compared our results with the previously reported analogs, we have found a direct correlation between Mn×××Mn distances to the PL emission. Our study reveals that the long distance between the Mn centers has made a significant contribution to the long-lived phosphorescence with a highly emissive triplet state.

8:00 PM EN05.07.12

Magnetic Resonance Spectroscopy as an Investigation Tool for The Structure of Ytterbium-Doped Cesium Lead Chloride PerovskitesThiagoRubio, HannahVan Son, SedaSarp, IverJ. Cleveland and ClaudiaE. Avalos; New York University, United States

In the search for methods to push the power conversion efficiency of photovoltaic (PV) devices beyond the Shockley-Queisser limit, doping halide perovskites with lanthanide ions, such as Yb³⁺, has shown promising results. This is due to quantum cutting, the conversion of one high energy photon into two (or more) low-energy photons. Quantum cutting materials can then be utilized as a down-converting layer in PV cells, where the wavelength of the incoming photons can be shifted from the UV to the near IR region, and then be used by the photoactive layer for electricity generation [1].

Understanding the doping mechanism and the defect structure in these materials is essential in order for a more effective insertion of the dopant into the host crystal lattice and subsequent higher photoluminescence quantum yields (PLQY) to be obtained. The doping sites can be studied by means of the effects they produce in the other species in the host structure. Many times, the dopant species only produces local effects. Magnetic resonance spectroscopic techniques such as nuclear magnetic resonance (NMR) and electron paramagnetic resonance (EPR) can probe local environments and can provide information about doping that techniques that probe long-range order, i.e. X-ray diffraction, are not able to [2,3,4].

In this project, ytterbium-doped cesium lead chloride (Yb³⁺:CsPbCl₃) perovskite powders were synthesized using dry ball-milling, a method that has been shown to yield high photoluminescence quantum yields due to the emission of Yb³⁺ in the near-infrared region [5]. Solid-state NMR was used to give an insight into how the local environments of the probed nuclei are affected by the insertion of Yb³⁺ to the crystal lattice, and to determine whether the insertion of Yb³⁺ into the crystal lattice was uniform. ¹³Cs NMR data revealed that longitudinal relaxation times (T₁) for cesium nuclei decrease with increasing amounts of ytterbium added to the composition. Furthermore, the stretching parameter obtained from a stretched exponential fit of the T₁ data collected showed that this decrease is due to a uniform distribution of paramagnetic centers in the structure. ²⁰⁷Pb NMR data showed that the chemical environments of the detectable lead sites is not distorted due to the insertion of Yb³⁺, this is evidenced by no change in the chemical shift anisotropy fit of the static NMR signal with increased doping. PLQYs above 135% were obtained for all samples.

References

[1] S. M. Ferro, M. Wobben, and B. Ehrler, "Rare-earth quantum cutting in metal halide perovskites—a review," *Materials Horizons*, vol. 8, no. 4, pp. 1072–1083, 2021.

[2] A. Karmakar, G. M. Bernard, A. Pominov, T. Tabassum, R. Chaklashiya, S. Han, S. K. Jain, and V. K. Michaelis, "Triangulating dopant-level Mn(II) insertion in a Cs₂NaBiCl₆ double perovskite using magnetic resonance spectroscopy," *Journal of the American Chemical Society*, vol. 145, no. 8, pp. 4485–4499, 2023.

[3] D. J. Kubicki, S. D. Stranks, C. P. Grey, and L. Emsley, "NMR spectroscopy probes microstructure, dynamics and doping of metal halide perovskites," *Nature Reviews Chemistry*, vol. 5, no. 9, pp. 624–645, 2021.

[4] D. J. Kubicki, D. Prochowicz, A. Pinon, G. Stevanato, A. Hofstetter, S. M. Zakeeruddin, M. Grätzel, and L. Emsley, "Doping and phase segregation in Mn²⁺- and Co²⁺-doped lead halide

perovskites from ^{133}Cs and ^1H NMR relaxation enhancement,” Journal of Materials Chemistry A, vol. 7, no. 5, pp. 2326–2333, 2019.

[5] D. M. Kroupa, J. Y. Roh, T. J. Milstein, S. E. Creutz, and D. R. Gamelin, “Quantum-cutting ytterbium-doped $\text{CsPb}(\text{Cl}_{1-x}\text{Br}_x)_3$ perovskite thin films with photoluminescence quantum yields over 190%,” ACS Energy Letters, vol. 3, no. 10, pp. 2390–2395, 2018.

8:00 PM EN05.07.13

Stable and Efficient Large Area 4T Si/perovskite Tandem Photovoltaics with Sputtered Transparent Contact [Ananta Paul](#), Abhijit Singha, Sakshi Koul, Vikas Sharma, Sudhanshu Mallick, K. R. Balasubramaniam and Dinesh Kabra; Indian Institute of Technology Bombay, India

With the boost in the thin film-based energy and optoelectronics devices' performance, there is an urgent need to improve and modify one of the essential components of such devices: transparent electrodes. In particular, we need to deposit high-conductive and transparent electrodes to fabricate the next-generation tandem structure while maintaining low sputtering damage. Si-perovskite tandem PV devices in the four-terminal (4T) configuration could solve the problems associated with the stability gap between the component perovskite and Si devices. We report the fabrication of NIR-transparent perovskite solar cells (PSCs) with the stable triple cation perovskite as the photo-absorber and subsequent integration with a Si solar cell in a 4T tandem device. The critical development of the sputtered top transparent conducting electrode (TCE) layer and oxide buffer layer at room temperature leads to reproducible, highly efficient NIR-transparent PSCs of both small area (0.175 cm^2) with PCE of 17.1% and large area (0.805 cm^2) with PCE of 16.0%. Electrically disparate, optically coupled 4T tandem devices of the optimized PSCs with commercial monocrystalline PERC Si solar cells exhibit greater than 26% PCE. In addition to enabling industry-compatible TCE-based low-cost Si/perovskite tandem photovoltaics, this study could also be the gateway for the potential use in niche applications like building integrated photovoltaics.

8:00 PM EN05.07.14

Photostability of Formamidinium-Based Mixed-Halide Perovskites [Halyna Okrepka](#), Maksym Zhukovskiy and Masaru Kuno; University of Notre Dame, United States

Light-induced anion photosegregation is a near-ubiquitous response of lead-based, mixed-halide perovskites to illumination. It is observed as unwanted, yet reversible, changes of the optical and electronic response of these materials when subjected to above-gap excitation and represents an impediment to proposed uses of mixed-halide perovskites in applications such as tandem solar cells.

Photosegregation sensitivity depends on the nature of the A-cation (methylammonium (MA^+), formamidinium (FA^+) and Cs^+). For $\text{APb}(\text{I}_{1-x}\text{Br}_x)_3$ photostability rank order follows $\text{CsPb}(\text{I}_{1-x}\text{Br}_x)_3 > \text{FAPb}(\text{I}_{1-x}\text{Br}_x)_3 > \text{MAPb}(\text{I}_{1-x}\text{Br}_x)_3$. Qualitatively, this stems from well-known chemical and thermal instabilities of MA^+ as well as to the generally robust nature of all-inorganic Cs-based perovskites.

Here, we assess the relative proclivity of formamidinium-based mixed-halide perovskites such as formamidinium/methylammonium $[(\text{FA},\text{MA})\text{Pb}(\text{I}_{1-x}\text{Br}_x)_3]$, formamidinium/cesium $[(\text{FA},\text{Cs})\text{Pb}(\text{I}_{1-x}\text{Br}_x)_3]$, and formamidinium/methylammonium/cesium $[(\text{FA},\text{MA},\text{Cs})\text{Pb}(\text{I}_{1-x}\text{Br}_x)_3]$ iodide/bromide perovskites to photosegregate under illumination. Goals of the study are to establish their photosegregation propensity and, where possible, compare observations to a recently developed model for light-induced, mixed-halide photosegregation. The model currently explains numerous features of the phenomenon, including the existence of excitation intensity (I_{exc}) thresholds, I_{exc} -dependent photosegregation rates/rate constants, and temperature insensitive, as well as carrier diffusion length-dependent terminal halide stoichiometries.

8:00 PM EN05.07.15

Overcoming Evaluation Challenges of Perovskite Solar Cells with a Multi-Channel Maximum Power Point Tracking (MPPT) Integrated PV Power Analyzing System [P. V. Jayaweera](#)¹, S. Maeshima¹, Satoshi Uchida², Shoji Kaneko¹ and Hiroshi Segawa²; ¹SPD Laboratory, Inc., Japan; ²RCAST, The University of Tokyo, Japan

The rapid research and development of perovskite solar cell (PSC) for practical applications are driven by both global warming concerns and industrial demands. Due to the distinctive characteristics exhibited by PSC, such as hysteresis, establishing a universally standardized and rational evaluation process becomes challenging. In this study, we present an equipment system designed to address this challenge. Hysteresis in I-V measurements, caused by capacitance components in stacked PSC, can lead to overestimation or underestimation of the performance. PSC exhibiting hysteresis in the I-V curve manifests two distinct maximum power points in the forward and reverse I-V curves, which depend on the scan speed, starting point, and direction of the scan. By implementing Maximum Power Point Tracking (MPPT), the genuine maximum output power of PSC can be promptly determined. Our newly developed device enables simultaneous I-V tracing and MPPT for up to six solar cells, facilitating research and development. The system continuously plots the light intensity and temperature data alongside the maximum power point, allowing each sample to handle up to 10 V and 1 A capacity. With six independently programmable electronic loads integrated into the analyzer, the MPPT algorithm individually maintained each sample at its maximum power point, ensuring efficient power generation. This multi-channel MPPT-integrated PV power analysis system offers a comprehensive solution to the evaluation challenges faced in PSC research and development. It enables accurate and efficient assessment of PSC performance, contributing to the advancement of practical applications and standardization of evaluation methods.

8:00 PM EN05.07.16

High Performance Inorganic CsPbI_2Br Perovskite Solar Cells via Crystallization Management [Soo Woong Jeon](#), Min Ju Jeong and Jun Hong Noh; Korea University, Korea (the Republic of)

Inorganic CsPbI_2Br perovskite has a substantial potential for triple-junction tandem solar cells as a top subcell, however it exhibits relative instability in the air compared with organic-inorganic perovskites as well as significantly lower efficiency than the theoretical efficiency limit. To further enhance the air-stability and efficiency of CsPbI_2Br -based perovskite solar cells (PSCs), it is vitally crucial to improve the crystallinity and passivate the defects within films that accelerate the phase transformation to the photo-inactive phase in the air. Here, it is reported that crystallization management via incorporating sodium formate (NaFo) in a CsPbI_2Br perovskite solution effectively leads to enlarged grain size and the reduced trap density. The Na^+ cation and HOOC^- anion produce a synergistic effect for engineering the defects by acting as cation and pseudo-halide anion passivators, respectively. As a result, the NaFo-incorporating device shows an improved power conversion efficiency (PCE) of over 17% and a fill factor (FF) of 84.5%. To the best of our knowledge, this progressive FF value is the highest value among CsPbI_2Br -based PSCs reported thus far. In addition, the NaFo-incorporated device shows improved air stability compared to the control device, retaining over 95% of its initial PCE for 1000 hours under 10% relative humidity at room temperature without any encapsulation.

8:00 PM EN05.07.17

Photovoltaic Performance Analysis of Organic and Inorganic Hole Transport Layer for Cu-Ag-Bi-I Based Perovskite Solar Cell [Md Arif Ullislam](#), Shinya Kato and Tetsuo Soga; Nagoya Institute of Technology, Japan

In this study, the environmental friendliness of $\text{Cu}_6\text{AgBiI}_{10}$ (CABI), a cheap and non-toxic material, has received the most attention for the investigation. Recently, the inorganic Cu-Ag-Bi-I base compounds have shown great potential for solar, optoelectronic, and other applications. Their outstanding stability, high absorption coefficients, and ability to transport charged carriers are all factors that make them attractive. In this study, we investigated the performance of organic and inorganic Hole Transport Layers (HTL) on Cu-Ag-Bi-I based solar cells, conducted experimental and simulation analyses to improve their efficiency, and explored new approaches for optimizing solar cell devices. The method used was a single-step spin coating using hot-casting droplets poured onto pre-heated substrates. To anneal films, two-step annealing was used. In the first step, the films were annealed in the glove box at 75°C for 3 minutes before being annealed at 150°C for 6 minutes in the second step on the hot plate. The films were characterized using XRD, UV and SEM to identify the structural, optical, and surface morphological behavior and properties of these materials and device simulations for optimizing their photovoltaic performances. In addition, P3HT, PEDOT:PSS, Spiro-MeOTAD, NiOx, CuSCN, and CuO were used as layers for hole transport to identify the most suitable HTL layer for the $\text{FTO}/(\text{c}+\text{mp})\text{TiO}_2/\text{CABI}$ structure using the SCAPS-1D solar cell device simulation tool. This study demonstrates that inorganic HTLs are more crucial than organic HTLs in terms of the efficiency and performance of solar cells. In the six structures of devices, the best-optimized device design, $\text{FTO}/(\text{c}+\text{mp})\text{TiO}_2/\text{CABI}/\text{CuO}/\text{Au}$ was found with an efficiency of 2.08%. The effects of absorber layer thicknesses of absorber and ETL layers, rate of generation, recombination, capacitance voltages, current density voltage, and the characteristics of quantum effectiveness are investigated. The SCAPS-1D results were compared with similar experimental results of the photovoltaic devices. The research revealed that HTLs are a key factor in the efficiency of CABI solar cells. The research reveals that HTLs are key to CABI solar cell efficiency.

<quillbot-extension-portal></quillbot-extension-portal><quillbot-extension-portal></quillbot-extension-portal><quillbot-extension-portal></quillbot-extension-portal><quillbot-extension-portal></quillbot-extension-portal><quillbot-extension-portal></quillbot-extension-portal>

8:00 PM EN05.07.18

Efficient and Stable Perovskite Quantum Dot Solar Cells via Incorporation of Multifunctional 3D Star-Shaped Organic Semiconductors [Seyeong Lim](#), Dae Hwan Lee and Taiho Park; Pohang University of Science and Technology, Korea (the Republic of)

CsPbI_3 perovskite quantum dots (PQDs) exhibit superior optical and optoelectronic characteristics, such as tunable bandgap, high photoluminescence quantum yield, and high absorption coefficient. Owing to these advantages, the CsPbI_3 PQDs have been considered as promising and effective photovoltaic absorber. Since PQDs have been stabilized with long-chain ligands, the ligand exchange using short ligands is indispensable to enhance the electronic coupling within PQD solids and then realize high-efficiency solar cells. However, the inefficient ligand exchange

can form trap states on the PQD's surface, leading to low device performance and stability. Herein, we demonstrate that a newly designed and synthesized three-dimensional (3D) star-shaped semiconductor (Star-TrCN) can be chemically bound with PQDs through theoretical modelling and experimental validation. The hybrid films of Star-TrCN and PQDs show reduced surface trap states and improved cubic-phase stability. As a result, the Star-PQD hybrid devices not only achieve improved device stability over 1000 h at 20–30% relative humidity, but also increase power conversion efficiency up to 16.0% by establishing a cascading energy band structure.

8:00 PM EN05.07.19

The Deposition of $\text{CH}_3\text{NH}_3\text{PbI}_3$ Thin Film using Close Space Sublimation for Large Scale Perovskite Solar Cells [YoungminKim](#), WonkyuLee, YounghoChoe, DonghwanKim, YoonmookKang and Hae-SeokLee; Korea University, Korea (the Republic of)

Abstract

To achieve large-scale perovskite solar cells and to deposit on a textured silicon wafer to apply silicon-perovskite tandem solar cell, it is crucial to implement the fabrication process for pin-hole-free thin film with optimal crystalline morphology and full coverage. In this work, we used a close space sublimation deposition to grow a high quality $\text{CH}_3\text{NH}_3\text{PbI}_3$ thin film in a different temperature. Reducing the process temperature is highly advantageous in fabricating perovskite films since perovskite materials exhibit significant degradation and adverse effects on crystal structure when exposed to high temperature. Therefore, the process temperature was conducted at the minimum temperature at which the MAI powder was sublimated. And The thickness of PbI_2 precursor determines the thickness of perovskite film. The PbI_2 precursor was adjusted using the sputtering method, and we controlled the thickness of PbI_2 by the sputtering time. The results indicate that high quality perovskite films with variable thickness can be obtained by the close space sublimation process demonstrated here. Although $\text{CH}_3\text{NH}_3\text{PbI}_3$ was selected for this study, this close space sublimation method demonstrated can be easily applied to other hybrid perovskites.

Keywords: solar cells, large-scale perovskite, pin-hole-free, close space sublimation, sputtering method, temperature

8:00 PM EN05.07.20

Defect Passivation for Highly Efficient Perovskite/Silicon Tandem Solar Cells [So JeongPark](#), Deok KiCho, GeonpyoHong and Jin YoungKim; Seoul National University, Korea (the Republic of)

Halide perovskites are promising photovoltaic materials, the power conversion efficiency (PCE) of the single junction solar cell has been improved to 26.0%, which is approaching the Shockley-Queisser limit. Perovskite/silicon tandem solar cells are attractive candidates to overcome the theoretical limit efficiency. Controlling the perovskites with a bandgap of ~1.7 electron volts is indispensable to enhance the photovoltaic performance. In this study, we developed high-performing perovskite top cells with a thiocyanate (SCN^-) based additive and attained a PCE of 21.01% without hysteresis. The additive strategy led to improved crystallinity, enlarged grain size, and reduced defect density. Non-radiative recombination responsible for open-circuit voltage decreased from the enhancement of perovskite film quality. By regulating the window layer thickness consisting of fullerene and indium tin oxide, an efficient semi-transparent cell was produced to minimize the short-circuit current density reduction caused by optical loss. The efficiency over 28% of a monolithic two-terminal perovskite/silicon tandem solar cell was achieved.

8:00 PM EN05.07.21

High Reproducible Fabrication of Perovskite Solar Cells using an Automated Perovskite Film Coating System [NaotoEguchi](#), KoheiYamamoto and TakurouN. Murakami; The National Institute of Advanced Industrial Science and Technology, Japan

Perovskite solar cells are expected to be the next generation of solar cells due to their favorable characteristics such as high conversion efficiency, light construction, and flexibility. However, there are considerable variations in perovskite solar cell's performances even though the solar cells are fabricated under the same conditions. Consequently, when evaluating new materials or new processes, it is necessary to fabricate many devices for comparing them with considering the large variations. This can be related to both cost increasing and time consuming for R&D.

One of the reasons for the variability in the performance of perovskite solar cells is the sensitivity of crystal growth in the perovskite layer to environmental factors such as temperature, humidity, and solvent evaporation rate. It is well known that these environmental factors influence the morphology of the film, making it important to control the atmosphere during deposition processes.¹⁻³ In addition, the widely used anti-solvent method for fabricating high-efficiency perovskite solar cells can cause significant changes in the film morphology and the solar cell performances based on the factors such as the drop volume, timing, and drop rate of the poor solvent. As a result, even when perovskite solar cells are fabricated under consistent conditions, their performances are still variable. In particular, the manual dropping of the poor solvent during the spin-coating of the perovskite precursor solution by human hands induces slight variations in the drop timing or drop speed, which leads to variations in the solar cell performances.

In this study, the low reproducibility, which is one of the challenges for perovskite solar cells, was improved by automating the dropping process of poor solvents and substrate transfer during the coating of perovskite layer. To remove human involvement in the perovskite layer coating process, an automated coating system was developed by integrating a robotic arm with a spin coater, an automatic solution drop system and a hot plate. This system enabled the transfer of glass substrates, the dropping of poor solvents during spin coating, and the heating of substrates on the hot plate. Using this automated coating system, we evaluated the performance variations of perovskite solar cells and compared them to those fabricated manually. The results showed that the perovskite solar cells fabricated using the automated coating system had reduced standard deviation of photoelectric conversion efficiency from 0.61 to 0.40 compared to those fabricated by hand. This system is expected to enable more objective evaluation of new materials and new processes, leading to reduced development time and costs.

References

- (1) Zhang, W.; Xiong, J.; Li, J.; Daoud, W. A. Impact of Temperature-Dependent Hydration Water on Perovskite Solar Cells. *Sol. RRL* **2020**, *4* (1), 1900370.
- (2) Bass, K. K.; McAnally, R. E.; Zhou, S.; Djurovich, P. I.; Thompson, M. E.; Melot, B. C. Influence of Moisture on the Preparation, Crystal Structure, and Photophysical Properties of Organohalide Perovskites. *Chem. Commun.* **2014**, *50* (99), 15819–15822.
- (3) Lin, N.; Qiao, J.; Dong, H.; Ma, F.; Wang, L. Morphology-Controlled $\text{CH}_3\text{NH}_3\text{PbI}_3$ Films by Hexane-Assisted One-Step Solution Deposition for Hybrid Perovskite Mesoscopic Solar Cells with High Reproducibility. *J. Mater. Chem. A* **2015**, *3* (45), 22839–22845.

8:00 PM EN05.07.22

Enhanced Perovskite Solar Cells Performance Through Surface Engineering Investigation of a Zn-Complex Based Hole-Transporting Materials [ChaochinSu](#)¹, Wen-renLi², YogeshTingare¹ and HsuYa-Chun¹; ¹Taipei Tech, Taiwan; ²National Central University, Taiwan

Interface Engineering plays a critical role in the performance of perovskite solar cells (PSCs). High-quality perovskite films with suitable hole transport properties of the hole-transporting materials HTMs are critical factors in obtaining high-performing PSCs. Small inorganic molecule HTMs have attracted considerable interest in PSCs because of their structural flexibility, operational durability, and good hole mobilities, but they suffer unsatisfied cell efficiency. In this work, a ligand **BT28** and its zinc-based coordination complex **BTZ30** were designed and synthesized as hybrid organic-inorganic structured HTMs for PSCs applications. Both HTMs exhibit similar optical and electrochemical properties. The mixed-halide perovskites can be grown uniformly with large crystalline grains on top of both HTMs. However, it is discovered that the BTZ30-based solar cell exhibited a higher power conversion efficiency close to 20%. This can be due to the higher hole mobility of **BTZ30** than that of **BT28**. The high hole mobility of **BTZ30** is attributed to low trap-assisted recombination and efficient charge extraction efficiency, indicating a good perovskite/HTM interface. The PSC fabricated with the metal-containing HTM **BTZ30** shows the best power conversion efficiency (PCE) of 19.50%, which is higher than the PCE of 18.01% from the PSC fabricated with its ligand and non-metal HTM **BT28**.

8:00 PM EN05.07.23

Thermal and Electrical Properties of ZnO-PCBM Composite Layer for p-i-n Perovskite Solar Cells [SeongtakKim](#), Dong-woonHan and Chan BinMo; Korea Institute of Industrial Technology, Korea (the Republic of)

Expectations for commercialization of perovskite solar cells are increasing with the recent announcement of 25.8% efficiency. However, the stability of perovskite solar cells is still lower than that of silicon solar cells, which is an obstacle to commercialization. Solar cells driven in the field not only emit most of their energy as heat, but are also exposed to high temperatures of 80°C or more during operation, so thermal stability is very important. When the heat of the solar cell increases, not only the power conversion efficiency decreases, but also the stability of the perovskite(PVSK) materials becomes weak. In particular, since the p-i-n thin-film perovskite solar cells almost use an organic materials manufactured by a low-temperature process or a solution process, the thermal conductivity is very low. In general, phenyl-C61-butiric acid methyl ester(PCBM) is mainly used as electron transfer layer(ETL) of p-i-n structure, but its thermal conductivity is only 0.07W/mK preventing heat transfer inside the perovskite from escaping to the outside. In this study, the PCBM-ZnO composite layer was applied to improve the heat dissipation performance of the solar cell. The heat dissipation performance and electrical properties were investigated according to the amount of ZnO added between PCBM and perovskite layer. The addition of ZnO improved the thermal conductivity of ETL and improved the thermal stability of the PVSK layer. When the ZnO content was too high, ZnO was accumulated at the interface between PVSK and PCBM, reducing the solar cell efficiency. Therefore, it was confirmed that the ZnO content of 0.1 wt% was the optimal composition in this

study. In conclusion, the improvement effect of the solar cell due to the application of the PCBM-ZnO composite layer was confirmed.

8:00 PM EN05.07.24

The Big Bang of Halide Perovskites: The Starting Point of Crystallisation AnaPalacios Saura^{1,2}, JoachimBreternitz³, ArminHoell¹ and SusanSchorr^{1,2}; ¹Helmholtz-Zentrum Berlin für Materialien und Energie, Germany; ²Freie Universität Berlin, Germany; ³FH Münster, Germany

Halide perovskites (HPs) are extremely popular amongst the scientific community, not only for their astonishing increase in power conversion efficiency up to 26%[1], but also for using low-cost solution-based processing methods.

Some of the distinctive properties of HPs are the decrease in solubility with increasing temperature[2], and the bandgap tunability via anion and cation substitution[3]. With this study we aim to elucidate the role of the A-cation in the crystallisation process as well as how the precursors are arranged prior to crystallisation. For this reason, we investigated the precursor solution of efficient HPs (RbPbI₃, KPbI₃ and NaPbI₃) using small angle X-ray scattering (SAXS) as well as the precursor solution of MAPbI₃ at increasing temperature (from room temperature up to 120°C). The binary precursors (e.g. RbI and PbI₂ to synthesise RbPbI₃) were dissolved in common solvents to synthesise HPs such as γ -butyrolactone (GBL), dimethylformamide (DMF) and mixtures thereof.

SAXS is a non-destructive technique based on the scattering length difference between the scattering objects in a solution. Applying SAXS, the size and shape of nanoscale particles (scattering objects) can be investigated, as well as their adjacent distance and interactions with each other.[4,5] We performed SAXS experiments at BESSYII, at the PTB's four-crystal monochromator beamline[6] using the ASAXS endstation.[7]

The SAXS pattern of all the measured samples show a peak in the scattered intensity at q-values between 2.5 and 3.3 nm⁻¹. The presence of such peak is a clear indication of the existence of interacting scattering objects in solution. The position of the peak correlates with the distance between adjacent scattering objects (d_{exp}). In a previous study[8], we developed a core-shell model with [PbX₆] (X = I, Br) octahedra surrounded by randomly oriented solvent molecules to explain d_{exp} in HPs with a molecular A-cation (MA⁺, FA⁺), showing that the size of the agglomerates changes with the composition of HPs precursors and with the solvent, but not with the A-cation. However, when alkali metals are used as A-cation, we can demonstrate that d_{exp} not only depends on the solvent but also on the A-cation. This is explained by the smaller ionic radius of alkali metals compared to the molecular cations [9,10] therefore the charge density is higher. For this reason, we extended the previous model to take this phenomenon into account. Based on this information, the extended core-shell model assumes that the A-cation and the solvent molecules compete to surround the [PbI₆] octahedra. In this A-cation core-shell model, the core is composed of [PbI₆] octahedra, which can be arranged as a single octahedron or a corner-sharing octahedra. The [PbI₆] octahedra of adjacent scattering objects are surrounded by a solvent shell with randomly oriented molecules or by an A-cation shell. The SAXS data analysis (using SASfit[11]) shows higher polydispersity as the previous model, which indicates an increase in the heterogeneity of the solution, this is in agreement with the proposed extended model.

We will discuss the influences of the A-cation and solvent on the core as well as the solvent shell of the scattering objects since they have the potential to influence the crystallization process of the HP and therefore the performance of a device produced from solution processing.

[1] <https://www.nrel.gov/pv/cell-efficiency.html>

[2] Saidaminov, M. et al, Nat. Commun., 2015, 6

[3] Kulkarni et al., J. Mater. Chem. A, 2014, 2, 9221

[4] Schnablegger et al., Anton Paar GmbH, 2013

[5] Flatken et al., J.Mater.Chem.A, 2021, 9, 13477

[6] Krumrey et al., Nucl.Instrum.Methods Phys.Res. Sect.A, 2001, 467, 1175

[7] Hoell et al., DE102006029449, 2007

[8] https://www.mrs.org/meetings-events/presentation/2022_mrs_fall_meeting/3784328-202211290915

[9] Kieslich et al., Chem. Sci., 2014, 5, 4712

[10] Shannon, R. D., Acta Cryst., 1976, A32, 751

[11] Brähler et al., J. Appl. Cryst., 2015, 48, 1587

8:00 PM EN05.07.26

Semi-Transparent Perovskite Solar Cells: Unveiling The Trade-Off Between Transparency and Efficiency NagehK. Allam; American University in Cairo, Egypt

Semi-transparent perovskite solar cells (Pero-SCs) are realized by tuning the band gap of the perovskite to resolve the trade-off between the transparency and efficiency of the photo-absorber. We synthesized wide-bandgap MAPbI₃-xBrx perovskite, and the transparency and efficiency of the corresponding semi-transparent Pero-SCs were investigated systematically by varying the I : Br ratio and thickness of the perovskite film. Increasing Br content widened the bandgap of perovskite (i.e., blue shift of the absorption edge), and led to an increase in the average visible transmittance (AVT). This strategy allowed for high AVTs, and concomitantly achieved high power conversion efficiencies. Meanwhile, increasing the Br content could facilitate formation of perovskite films with large grains that were highly crystallized. Compared with the narrow-bandgap perovskite, the wide-bandgap perovskite showed advantages for obtaining semi-transparent Pero-SCs with thick perovskite films (>200 nm) and high (20%) transparency.

8:00 PM EN05.07.27

Crosslinkable Siloxane Induced Direct Patterning of Highly Stable Halide Perovskite Nanocrystals Sang WooBae¹, Jin MinPark¹, JunhoJang², HyukminKweon¹, Byeong-SooBae², Do HwanKim¹ and Young HoonKim¹; ¹Hanyang University, Korea (the Republic of); ²Korea Advanced Institute of Science and Technology, Korea (the Republic of)

High resolution patterning of color conversion layers (CCLs) is essential for the demonstration of color converting light-emitting diodes (LEDs). Conventional color converting materials such as organic phosphor and inorganic quantum dot (QD) so far suffer from low color purity and high materials cost. Metal halide perovskite nanocrystals (PNCs) have been regarded as a promising color converting material in CCLs due to their high absorption coefficient, spectrally narrow light, easy color tuning, low materials cost, and high photoluminescence quantum efficiency (PLQE). However, the instability of PNCs in thermal treatment and in polar solvents limits its high resolution patterning through consequent photolithography process and its long-term stability in various condition. To enable low-cost direct patterning without using a high polarity photoresist and improve the stability of patterned PNCs, we here introduce the direct optical patterning of crosslinkable siloxane resin/PNC composite. Multicolored patterning of PNCs in micrometers was demonstrated by siloxane resin pinning (SRP) process which mitigates the high viscosity and concomitant shrinkage problem in the siloxane/PNC composites. The patterned PNCs showed stable photoluminescence quantum efficiency (PLQE) in harsh liquid environments (e.g., in water, acid, or base solutions, and in various polar solvents), which provide the breakthrough into high density PNC-based micro-LED.

8:00 PM EN05.07.28

Tailoring the Molecular Structure of Dopant-Free Polymeric Hole Transport Materials for Improved Charge Extraction in Perovskite Quantum Dot Solar Cells Dae HwanLee, SeyeongLim and TaihoPark; Pohang University of Science and Technology, Korea (the Republic of)

We have developed three dopant-free hole transport materials (HTMs) as an alternative to the commonly used doped Spiro-OMeTAD in perovskite quantum dot solar cells (PQD-SCs). The dominant HTM, Spiro-OMeTAD, requires the use of doping systems to enhance charge mobility. However, these dopants can lead to the degradation of PQD-SCs, making the development of efficient dopant-free HTMs crucial for commercialization. In our study, we designed three types of dopant-free HTMs: Asy-PDTS, Asy-PSDTS, and Asy-PSeDTS. To improve their electrical properties, we incorporated a chalcogenide-based fluorinated benzothiadiazole rigid segment acceptor unit. This rigid segment acted as an effective charge hopping channel, compensating for the impaired electrical properties through side chain engineering. Through a conformation-locking approach utilizing chalcogenide-fluorine noncovalent interactions, we achieved favorable planar structures with face-to-face stacking of the rigid segments. Among the optimized devices, the one utilizing Asy-PSeDTS exhibited remarkable performance. It achieved a power conversion efficiency (PCE) of 15.2%, the highest reported PCE among dopant-free HTM-based PQD-SCs. Additionally, this device maintained 80% of its initial PCE even after 40 days, demonstrating superior stability compared to other dopant-free HTM-based PQD-SCs.

8:00 PM EN05.07.29

Enhancing the Device Performance and Stability of Inverted Perovskite Solar Cells using Zr-Based Metal-Organic Frameworks(MOFs) Jin HyoungKim, TaeminKim, MinohLee and YongseokJeon; Korea University, Korea (the Republic of)

Inverted perovskite solar cells have drawn much attention due to their reduced hysteresis, low-temperature processability, and as a suitable structure for perovskite/silicon tandem solar cells. However, just as conventional perovskite solar cells, their long-term stability remains a major challenge for applications and commercialization, since they are extremely vulnerable to the degradation accelerated by environmental factors such as moisture, air and light. In this study, we explored the use of UiO-66 metal-organic frameworks (MOFs) and its derivatives, UiO-66-NH₂ and UiO-66-COOH, as a means of improving the efficiency and stability of the inverted perovskite solar cells. UiO-66 and its derivatives are Zirconium-based metal-frameworks with terephthalic acid organic linkers plus functional groups, known for their high chemical stability and absorption of ultraviolet (UV) light which is damaging to the operation of perovskite solar cells. We found that incorporating UiO-66 interlayer between the hole-transporting layer, poly[bis(2,4,6-trimethylphenyl)amine] (PTAA), and perovskite layer improved the morphology and crystallinity of the perovskite, thereby enhancing the performance. Also, it improved the stability of inverted perovskite solar cells, especially against continuous light irradiance. The device

achieved the efficiency of 18.5%, showing an increase from 17.6% of the control device, and maintained higher than 98% of the initial efficiency under 1200 seconds of one-sun irradiance. To the best of our knowledge, the achieved efficiency is the second-highest PCE of inverted perovskite solar cells using MOFs. In addition, we found that incorporating the MOFs into the perovskite precursor also enhanced the device performance with enhanced long-term stability, with higher efficiency than the control device achieved and maintained over 90% of it after 1000 hours, due to the passivation induced by the Lewis base functional groups of organic linkers. Our findings suggest that using UiO-66 metal-organic frameworks and its derivatives between/in perovskite solar cell layers could be a promising strategy for enhancing the stability of inverted perovskite solar cells, both extending broader applications of MOFs and making the MOF-applied inverted perovskite solar cell devices attractive for applications such as perovskite/silicon tandem solar cells.

8:00 PM EN05.07.30

Anion-Dependent Piezoelectric Power Generation in Lattice-Strained Hybrid Halide MAPbX₃ (X = I, Br, and Cl) Thin Films Da Bin Kim^{1,2}, Kyeong Su Jo¹, Kwan Sik Park¹, [Ju Han](#)¹ and Yong Soo Cho¹; ¹Yonsei University, Korea (the Republic of); ²University of Toronto, Canada

The compositional dependence of piezoelectricity in halide perovskite materials has rarely been reported based on experimental results. To the best of our knowledge, for the first time, we demonstrate experimental evidence of the dependence of piezoelectricity and electromechanical energy harvesting performance on the anions in a hybrid halide thin-film system of MAPbX₃ (X = I, Br, and Cl). As expected from their crystal structures, i.e., tetragonal MAPbI₃, cubic MAPbBr₃, and cubic MAPbCl₃, the highest piezoelectricity was observed in MAPbI₃, which electromechanically harvested the largest amount of energy owing to its ferroelectricity possessing permanent dipoles based on PbI₆ octahedra. Interestingly, cubic MAPbBr₃ and MAPbCl₃ also delivered considerable piezoelectric energy harvesting performance, unlike other cubic oxide-based perovskites, as they are associated with organic MA⁺ ions in soft phonon modes, which can induce lattice distortion under a mechanical stimulus. The origin of the piezoelectricity even with the cubic halides is discussed as being related to the tolerance factor and bond strength, with experimental support for the estimated effective piezoelectric coefficient and grain boundary potential. Such experimental results on piezoelectricity and energy harvesting for MAPbBr₃ and MAPbCl₃ have not been reported thus far. In addition to exploring the anion-dependent piezoelectricity in flexible MAPbX₃ halide thin films, we attempted to enhance their electromechanical power-generating capability by incorporating vertical tensile lattice strain (for extra lattice extension between electrodes) and by applying an optimal poling field (for vertical domain orientation). Introducing out-of-plane tensile strain and poling effectively improved the harvesting performance of all three halide thin films, with their performance increasing in the order MAPbCl₃ < MAPbBr₃ < MAPbI₃, as anticipated from their piezoelectricity. Notably, the output voltage and current demonstrated herein of 23.1 V and 1,703 nA for the ~486 nm-thick MAPbI₃ thin film are the highest values reported for any thin-film-based perovskite halide harvesters to date.

8:00 PM EN05.07.31

Fabrication of Electrospun Nanofiber Yarns Decorated with Organic-Inorganic Double Halide Perovskite for Wearable Piezoelectric Applications Seongcheol Ahn, Yujang Cho and Il-Doo Kim; Korea Advanced Institute of Science and Technology, Korea (the Republic of)

Research efforts are actively focused on capturing energy from renewable sources due to concerns about environmental pollution and resource shortages. Among the various methods, the piezoelectric nanogenerator (PENG) stands out as it harvests energy from the deformation of a crystalline material using the piezoelectric effect. This technique shows promise in converting mechanical energy into electrical energy in an eco-friendly manner. The piezoelectric organic-inorganic hybrid nanocomposite is able to utilize the advantages of high piezoelectricity of piezoelectric ceramics, dielectric properties, and flexibility of polymers. The organic-inorganic hybrid piezoelectric material-based PENG is fabricated by the composite of halide double perovskite (HDP) and PVDF piezoelectric materials. After mixing the HDP in the polymer matrix, an organic-inorganic hybrid nanocomposite yarn was fabricated with enhanced efficiency characteristics of HDP while maintaining the flexibility and processability of the polymer. Also, the nanofiber (NF) yarn platform, composed of ultrahigh-density polymeric NFs electrospun by two spinnerets with opposite applied bias, has attained great attention as a suitable flexible substrate featuring a large specific surface area and high porosity. The 1D-type PENG using organic-inorganic nanocomposite is flexible and can be applied to wearable devices, electronic devices, etc.

8:00 PM EN05.07.32

Thermal Co-Evaporation of Lower-Dimensional Metal Halide Perovskites Kunal Datta and Juan-Pablo Correa-Baena; Georgia Institute of Technology, United States

Lower-dimensional perovskite structures have advanced the field of perovskite-based optoelectronics through their bandgap tunability, high defect tolerance and low ion mobilities, either used as active layers or at charge-transport interfaces. However, solution-based processing of such materials typically yields poor structural selectivity due to the interactions between precursor ions and the solvent. This results in the formation of phase gradients across the thickness of thin films that develop bandgap and energetic barriers, thereby impeding charge-carrier transport and optoelectronic performance.

This work describes thermal co-evaporation methods for the deposition of high quality lower-dimensional Ruddlesden-Popper perovskites as a route to develop structurally homogeneous thin films for optoelectronic devices such as photovoltaics, light emission and light detection. The dimensionality (*n*-value) of the structures, and thereby the optical bandgap, is controlled accurately through precursor deposition rates. The work assesses the role of deposition conditions, substrate functionalization and post-deposition treatment in determining crystallographic structure and phase purity. As a result, in addition to being commercially scalable, conformal and demonstrating precise thickness control, the elimination of the precursor-solvent interaction in thermal co-evaporation depositions ensures an accurate and consistent precursor stoichiometry leading to phase homogenization and improved charge-carrier transport.

8:00 PM EN05.07.33

Optimization of Aerosol Assisted Post-Treatment Strategies for Enhanced Performance Combined with Long-Term Stability of Halide Perovskite Photovoltaics Ravi Kant Misra, Madsar Hameed and Joe Briscoe; Queen Mary University of London, United Kingdom

Perovskite photovoltaic (PPV) has emerged as an outstanding photovoltaic technology in the past few years, with certified power conversion efficiency reaching up to 26% for single junction devices and 33.7% for tandem devices with silicon cells [1]. Our group recently demonstrated a new solvent-based post-treatment strategy of perovskite films resulting in excellent reproducibility and uniformity by exposing a perovskite film to the vapourised solvents via an aerosol-assisted chemical vapour deposition system [2]. Using this process, we achieved enhancement of both photovoltaic power conversion efficiency (PCE) and stability in a range of perovskite compositions and device architectures, which we have linked to improvements in both the nanoscale and macroscale uniformity of the material, including a reduction of defects and trap states.

In this talk, I will discuss our more recent developments of this process to include organo-halide salts in the solvent aerosol, such as MA₂Cl, leading to substantial enhancement of the post-crystallisation grain growth and recrystallisation process [3]. This leads to films that are comprised of ultra-large grains (~1-5 μm) where local traps are almost completely eliminated, as confirmed at the nanoscale via photoconductive atomic force microscopy. The large grains have also allowed us to visualise local variations in photoluminescence (PL) emission at the grain boundaries using hyperspectral PL mapping. The substantial reduction in trap states and increase of film homogeneity leads to photodetectors that can operate at ~1.5 orders of magnitude lower light levels than those made with conventional spin-coated films, demonstrating the potential to substantially enhance PSCs for low light applications, such as indoor PVs. We have also recently identified that among all additives, using MASCN creates the greatest enhancement of this effect, leading to substantial grain growth and associated PCE and stability enhancement in PSCs [4]. The aerosol assisted post-treatment has also been successfully tested for the performance recovery of mixed cation perovskite solar cells following degradation, proving its versatility in microstructural optimisation of PPV films, and performance recovery of degraded devices (unpublished results).

We are now implementing our established aerosol-assisted post-treatment strategy towards morphological improvements, minimizing grain boundaries in double and triple cation containing perovskite materials and devices, and the results will form part of this talk.

References

- [1] <https://www.nrel.gov/pv/cell-efficiency.html>.
- [2] T. Du, S.R. Ratnasingham, F.U. Kosasih, T.J. Macdonald, L. Mohan, A. Augurio, H. Ahli, C. T. Lin, S. Xu, W. Xu, R. Binions, C. Ducati, J.R. Durrant, J. Briscoe, *M.A. McLachlan, *Adv. Energy Mater.* 2101420 (2021).
- [3] T. Du, F. Richeimer, K. Frohna, N. Gasparini, L. Mohan, G. Min, W. Xu, T. J. Macdonald, H. Yuan, S. R. Ratnasingham, S. Haque, F. A. Castro, J. R. Durrant, S. D. Stranks, S. Wood, M. A. McLachlan and J. Briscoe, *Nano Lett.* 22, 979-988 (2022).
- [4] T. Du, T.J. Macdonald, R.X. Yang, M. Li, Z. Jiang, L. Mohan, W. Xu, Z. Su, X. Gao, R. Whiteley, C.-T. Lin, G. Min, S.A. Haque, J.R. Durrant, K.A. Persson, M.A. McLachlan and J. Briscoe, *Adv. Mater.* 34, 2107850 (2022).

8:00 PM EN05.07.34

Mixed Ruddlesden-Popper and Dion-Jacobson Phase Perovskites for Stable and Efficient Blue Perovskite LEDs Pui Kei Ko; The Hong Kong University of Science and Technology, Hong Kong

Producing efficient blue and deep blue perovskite LEDs (PeLEDs) still represents a significant challenge in optoelectronics. Blue PeLEDs still have problems relating to color, luminance, and

structural and electrical stability so new materials are needed to achieve better performance. Recent reports suggest using low n states ($n = 1, 2, 3$) to achieve blue electroluminescence in quasi-2D Ruddlesden-Popper (RP) perovskite films. However, there are fewer reports on the other quasi-2D structure, Dion-Jacobson (DJ) perovskites, despite their highly desirable optical properties, due to the difficulty in achieving charge injection. To resolve this issue, here we have mixed DJ phase precursors, propane-1,3-diammonium (PDA) bromide into RP phase perovskites and fabricated low-dimensional PeLEDs. It was found that these specific precursors aid in suppressing both the low n ($n = 1$) and high n ($n \geq 4$) quasi-2D RP phases and is an effective strategy in blue-shifting sky-blue RP perovskites into the sub-470 nm region. With optimization of the PDA concentration and device layers, we achieved an EQE of 1.5% at 469 nm and stable electroluminescence (EL) for the first deep blue PeLED to be reported using DJ perovskites.

8:00 PM EN05.07.35

Highly Stable Tin Iodide Perovskites Synthesized in Ambient Aqueous Phase using Alkali Iodides and Ascorbic Acid Koji Yokoyama, Shun Yokoyama and Hideyuki Takahashi; Tohoku University, Japan

Tin iodide perovskites (ASnI_3) are emerging as photoactive layers in photovoltaics due to their excellent optical and electronic properties. However, their preparation typically requires an inert environment and anhydrous organic solvents due to their vulnerability to oxygen and moisture. These conditions have resulted in complex and environmentally unfriendly processes. Previous studies have reported the aqueous-phase synthesis of ASnI_3 using hydroiodic acid (HI) as a solubilizer and hypophosphorous acid (H_3PO_2) as a reductant. Nevertheless, HI is highly unstable and cannot be used in ambient air, and both HI and H_3PO_2 are hazardous chemicals. Consequently, there is a high demand for more stable solubilizers and safer reductants to enable a facile and green synthesis of ASnI_3 in an ambient aqueous phase. In this study, we present the ambient aqueous-phase synthesis of ASnI_3 perovskites using alkali iodides and ascorbic acid (AA). Aqueous solutions containing 6.0 mol L^{-1} of HI, lithium iodide (LiI), or sodium iodide (NaI) as solubilizers and 1.0 mol L^{-1} of H_3PO_2 or AA as reductants were prepared. Subsequently, 0.5 mol L^{-1} of tin iodide was dissolved in these solutions to prepare tin precursor aqueous solutions. The valence states and complex structures of tin species in these precursor aqueous solutions were characterized via electrospray ionization time-of-flight mass spectrometry (ESI-TOFMS). 0.5 mol L^{-1} of organic cation iodides was added to the precursor aqueous solutions, and the resulting precipitated samples were collected by suction filtration. Structural, compositional, and optical characterizations were carried out for the samples immediately after synthesis and after exposure to ambient air using X-ray diffractometry (XRD), X-ray photoelectron spectroscopy (XPS), and optical absorption/photoluminescence measurements. The tin precursor aqueous solutions containing HI turned muddy and degraded rapidly, even though they contained reductants, whereas those containing LiI or NaI remained completely transparent and stable even in ambient air. Tin species formed complexes with the reductant molecules in the solutions containing reductants. ESI-TOFMS analysis revealed that the reducing and chelating abilities of AA efficiently stabilized the Sn^{2+} valence states. The resulting samples were determined to be pure-phase ASnI_3 perovskites. Interestingly, XRD, XPS, and optical measurements clearly indicated that ASnI_3 perovskites synthesized using NaI and AA exhibited excellent stability after exposure to ambient air. Detailed analyses suggested that Na^+ ions and a trace amount of AA molecules present on the sample surface passivate the surface defects and stabilize the ASnI_3 phases. In conclusion, we successfully prepared highly stable tin precursor aqueous solutions even in ambient air, using stable alkali iodides and safe AA. Highly stable ASnI_3 perovskites were synthesized from the solutions containing NaI and AA. These findings pave the way for the green fabrication of highly efficient and long-life perovskite photovoltaics.

8:00 PM EN05.07.36

Highly Efficient and Stable Perovskite Photocathode for Hydrogen Generation in Acidic and Basic Conditions Saikiran S. Khamgaonkar and Vivek Maheshwari; University of Waterloo, Canada

In the pursuit of sustainable energy solutions, the direct conversion of solar energy into fuels, such as hydrogen, through photoelectrochemical systems (PEC), holds immense promise. Organo lead halide perovskites with their excellent optoelectronic properties and their reported record photovoltaic efficiencies are therefore being researched for integration in PEC. Particularly, their integration as photocathodes for the hydrogen evolution reaction (HER) is gaining attraction due to their impressive HER photocurrent density ($\sim -20 \text{ mA.cm}^{-2}$) and high onset potential ($\sim 1 \text{ V}$). However similar to photovoltaics, the limited stability of perovskites in PEC devices is a critical challenge. This is further amplified due to immersion in an aqueous medium which is required for the operation of the PEC devices for HER. Previous research work have primarily focused on enhancing the extrinsic stability of the perovskite layer through the implementation of moisture-resistant encapsulant layers like Ni, Field metal, conductive carbon paste, metal oxide, or Ti foil. However, little attention has been paid to addressing both the extrinsic and intrinsic stability of the perovskite film, which is crucial for prolonged device operation. Intrinsic stability, crucially linked to ion migration effects leading to perovskite degradation, complements extrinsic stability, which is governed by the degradation of the perovskite structure due to decomposition with water (in the case of PEC). Moreover, selecting a catalyst capable of exhibiting exceptional stability and performance in extreme pH conditions poses a further challenge. While the kinetics of HER are facile in acidic conditions, alkaline environments present a hurdle due to the sluggish water dissociation step. Therefore, there is need for a single catalyst that can exhibit excellent HER performance and stability in extreme pH conditions. In this work, we have fabricated a highly efficient and stable perovskite-based photocathode which displays excellent HER performance with enhanced stability. To enhance both performance and internal stability, a polymer additive has been introduced into the perovskite thin film. The use of the polymer greatly improves the solar cell efficiency, the polymer-perovskite cells have an efficiency of $\sim 15.3 \%$, while the pristine perovskite cells show an efficiency of $\sim 12 \%$. Additionally, we have synthesized a bimetallic catalyst comprising Au, Pt, and Ni, characterized by low overpotential and Tafel slope values for HER in highly acidic and basic conditions. The polymer-conjugated photocathode with the bimetallic catalyst layer exhibits excellent HER performance both in acid and basic electrolyte and shows high photocurrent density ($\sim -20 \text{ mA.cm}^{-2}$), high onset potential ($\sim 0.95 \text{ V}$), and a half-cell solar to hydrogen conversion efficiency (HC-STH) of 10.11% . More impressively, the photocathode exhibits an unprecedented stability, with T_{80} (time for 80% degradation) values of approximately 70 hrs. (H_2SO_4) and 78 hrs. (KOH), retaining over 50 % of its initial photocurrent after 120 hrs. of operation. These stability values are the highest reported among various perovskite-based photocathodes.

SESSION EN05.09: Halide Perovskites for Energy Applications

Session Chairs: Yi Hou and Xiaotong Li

Wednesday Afternoon, November 29, 2023

Hynes, Level 3, Room 311

1:30 PM *EN05.09.01

Functionalized MXenes for Stable Halide Perovskite Solar Cells Monica Lira-Cantu; Nanostructured Materials for Photovoltaic Energy, Spain

Perovskite solar cells (PSCs) with an accredited power conversion efficiency (PCE) above 25% demonstrate a great potential towards commercialization. Currently, PSCs are largely susceptible to poor stability and durability issues which restricts their utility in practical applications. Shallow and deep defects in perovskites are a major contribution to the stability loss and this loss can be minimized by passivating the defects through surface functionalization. Materials functionalization and modification has been employed as an strategy to improve the stability of PSCs by controlling the surface properties by bringing novel chemical, electronic and optical properties. Two-dimensional (2D) materials are excellent candidates for potential applications including photovoltaics owing to their high conductivity, hydrophilicity, flexibility, and surface modifications. In this work, we apply the 2D Ti_3C_2 MXene in a normal PSC configuration of the type: FTO / $c\text{-TiO}_2$ / $m\text{-TiO}_2$ / halide perovskite (HP) / MXene / Spiro-OMeTAD / Au. We used the quadruple halide perovskite (HP) $\text{Rb}_{0.05}\text{Cs}_{0.05}\text{MA}_{0.15}\text{FA}_{0.75}\text{Pb}_{1.75}(\text{I}_{0.95}\text{Br}_{0.05})_3$ as the absorber, and the MXene ($\text{Ti}_3\text{C}_2\text{-T}_x$) at the interface of HP and the hole transport layer (HTL) to fabricate HP/MXene heterojunctions. We employed the organic ligand 3-Phosphonopropionic acid (H3pp) to functionalize the bulk of the MXene and the bulk of the HP. The functionalization of only the MXene transport layer resulted in PSC with 19.89% efficiency, the functionalization of both, the MXene and the Halide Perovskite layers, resulted in champion PSCs with 21.95% PCE. Both indoor stability studies under ISOS-L protocol (continuous MPP tracking under N_2 atmosphere for 1000 h) and outdoor stability analyses under the ISOS-O protocol (MPP tracking, encapsulated devices) demonstrated the superior stability of PSCs when the 2D MXene interface is employed, especially under high humidity (60-85%) conditions where the PSCs showed excellent recovery after a low light irradiation and rainy day. The best results were observed for the PSC with the functionalization of both the MXene layer and the HP absorber layer. The ISOS-L protocol study revealed almost 100% retaining of the PSC device. Outdoor testing under ISOS-O protocol for > 600 h holding devices at open circuit voltage revealed a T_{80} of 600 h, while the control devices showed T_{80} at about 250 h. Thermal admittance spectroscopy (TAS) revealed that the functionalization of the halide perovskite results in shallow defect passivation, when the functionalization takes place at the MXene interface, TAS analyses revealed the reduction of both deep and shallow trap state densities. This report provides pioneering study of additive engineering for adaptable bulk passivation and interface passivation through MXene nanosheets.

2:00 PM EN05.09.02

Probing Photostability of Tin-Containing Mixed Halide Perovskites: The Good and The Bad Krishanu Dey^{1,2} and Samuel D. Stranks^{2,2}; ¹University of Oxford, United Kingdom; ²University of Cambridge, United Kingdom

Mixed halide compositions offer interesting avenues to tune the bandgap of perovskites to make them suitable as wide bandgap absorbers in perovskite-based multijunction solar cells and as emitter layers in red and blue perovskite light emitting diodes (LEDs). However, the instability of bromide/iodide (Br/I) mixtures under light illumination has been long reported, where low-bandgap iodide-rich phases tend to form for >20% Br contents, resulting in the funneling of photogenerated carriers and red-shifting of photoluminescence (PL). Over the years, various

mechanisms have been presented to account for such halide segregation effects – yet the exact mechanism remains elusive. Very recently, the model of halide oxidation has been found to be powerful in explaining the mechanism of excitation-induced halide segregation in lead-based mixed halide perovskite compositions and is consistent with most of the reported experimental observations.

On the other hand, several strategies related to compositional engineering and defect passivation have been devised to mitigate the issue of halide phase segregation under operational conditions. However, many of these approaches demonstrate the mitigation of halide segregation only under certain chosen operational conditions (e.g. light intensity, time under illumination, halide ratio etc.) and hence definitive conclusions regarding the applicability of those approaches under other (potentially harsher) conditions cannot always be guaranteed.

In this work, we systematically study the impact of Sn incorporation on the photostability of mixed halide perovskites. While a clear redshift in the PL peak and absorption onset is observed under light soaking for Pb-based compositions, which signifies photoinduced halide segregation, no such shifts are observed for Sn-containing compositions irrespective of the Pb/Sn mixing ratio. Furthermore, while halide segregation in Pb perovskites is often associated with an increase in luminescence under light, we observe an opposite effect of photodarkening for Sn-containing perovskites, possibly due to the formation of photoinduced defects. We also visualize the difference in the impact of light soaking between Pb and Sn-containing perovskites in the microscale using wide-field hyperspectral photoluminescence imaging. It is important to note that we explored a wide variety of processing and operational conditions to assess the extent of photostability of Sn-containing mixed halide perovskites, which suggests an intrinsic stability against halide segregation in these materials. Subsequently, we also investigated the impact of light soaking on the resulting charge carrier dynamics and charge transport in mixed halide perovskites with and without Sn in the composition, which again exhibit distinctive trends. Moreover, scan-rate dependent field effect transistor (FET) measurements and electrochemical impedance spectroscopy measurements on fabricated p-i-n solar cells, aided further by ab-initio simulations also reflect the trend of suppressed ionic migration in Sn-containing mixed halide perovskites as compared to their Pb-only analogues. Next, we rationalize the contrasting trends of photostability of Pb-only and mixed Pb-Sn mixed halide perovskites by suggesting a hypothesis of preferential Sn^{2+} oxidation over I^- oxidation in the presence of photogenerated holes, which seems to explain most of our experimental observations. Finally, we highlight important differences in the degradation pathways of Pb-only and mixed Pb-Sn based solar cells, thereby indicating that the seeming absence of halide segregation in mixed Pb-Sn devices does not alone guarantee an improvement in their operational stability.

Therefore, our work represents an important advance in the understanding of halide segregation behaviour in mixed halide perovskites, which can be further leveraged to demonstrate efficient and stable solar cells, LEDs and a plethora of other optoelectronic devices.

2:15 PM EN05.09.03

Diamine-Templated Crystal Growth of Perovskite Films for Record p-i-n Perovskite Solar Cells HaoChen^{1,2}, JunkeWang¹, BinChen² and EdwardSargent^{1,2}; ¹University of Toronto, Canada; ²Northwestern University, United States

Energy loss of perovskite/ETL interface is the limiting factor for pin perovskite solar cells, various methods are explored to address this issue, for example, post-treatment with organic salts are normally used to get more n-type surface, so as to gain good energy alignment between perovskite and ETL. Here, by using a diamine molecule in the bottom surface to template the crystal growth of perovskite film, we get highly oriented perovskite films with more n-type characters, after combining with the 2D passivation, the energy loss was reduced effectively, based on this, we get above 26% PCE for pin perovskite solar cells in the lab, and 25.75% PCE from fast scan and 24.9 % QSS PCE (Certified in Nrel), which are the record efficiencies for pin PSCs, and 1 cm² devices also shows 23.8 % PCE, except for the record PCE, the devices also show great operational stability, after 1000 illumination, the device shows no degradation.

2:30 PM BREAK

3:30 PM *EN05.09.04

Current Understanding of Phase Transformations in Lead Halide Perovskites Juan-PabloCorrea-Baena; Georgia Institute of Technology, United States

Halide perovskites have shown great promise for applications that span from solar cells to lasers and radiation detectors. However, these materials suffer from rapid phase transformations upon exposure to external stimuli. Therefore, it is essential to unravel the mechanisms that lead to these phase transformations in order to design materials that can withstand different environmental conditions. Thus far, there is little understanding of how chemistries influence phase transformations in lead halide perovskite when these are exposed to external stimuli. In this presentation, I will discuss the role of chemistry on phase transformations of lead halide perovskites through in-situ synchrotron-based techniques. The importance of these phase transformations on the optoelectronic properties of the halide perovskite materials will also be discussed.

4:00 PM EN05.09.05

From PL-Inactive to PL-Active: Synthesis and Properties of Novel PL-Active 2D Lead-Free Double Perovskites ChunyangChi and AndrewB. Wong; National University of Singapore, Singapore

In this work, novel two-dimensional lead-free double perovskites ($(\text{R})_4\text{M}_a\text{M}_b\text{M}_c\text{X}_8$, $a+b+c=2$) were synthesized to achieve novel compositional and dimensional tunability. Herein, PL-inactive $(\text{PA})_4\text{AgInBr}_8$ was alloyed with Mn^{2+} with the goal of forming PL active materials.

Bandgap and PL emission tunability were explored through halogen substitution (chlorine and iodine). An enhanced PL emission was observed for mixed halogen phases. Three emission pathways are investigated including band edge emission, emission stemming from self-trapped excitons, and the unique energy transfer process of alloyed Mn^{2+} ions, which will be discussed.

4:15 PM EN05.09.06

Quantification of Strain and Its Impact on the Phase Stabilization of All-Inorganic Cesium Lead Iodide Perovskite HanK. Le¹, Chung-KuanLin¹, JianboJin¹, YeZhang¹, ZhenniLin¹, ArturasVaillionis^{2,3}, NobumichiTamura⁴ and PeidongYang¹; ¹University of California, Berkeley, United States; ²Stanford University, United States; ³Kaunas University of Technology, Lithuania; ⁴Advanced Light Source, United States

Halide perovskites have emerged as a compelling class of materials and garnered significant interest for its impressive performance in photovoltaic technologies, with power conversion efficiencies (PCEs) of perovskite solar cells (PSCs) increasing from 3.8% to a certified 25.2% and rivaling commercial silicon solar cells in recent years. A type of all-inorganic perovskite, cesium lead iodide (CsPbI_3) draws special attention owing to its suitable bandgap for photovoltaics (~1.73 eV) and its superior thermal tolerance as compared to the organic-inorganic hybrid counterparts. Despite these advantages, a main obstacle to realizing the commercial applications of these materials lies in the long-term phase instability and interconversion between different CsPbI_3 polymorphs. The high-temperature (high-T) perovskite γ -phase of CsPbI_3 readily undergoes phase transition at ambient conditions to a low-temperature (low-T) non-perovskite δ -phase with a poorer optoelectronic performance, thus hindering commercialization of these materials in photovoltaics. Here, we present the epitaxial growth of CsPbI_3 nanoplates on muscovite mica single crystal substrates, and demonstrate that the high-T phase stability of these nanoplates is enhanced by a strained interface. Strain is measured as a function of nanoplate thickness on a single particle level through spatially resolved structural and optical characterizations, and found to increase with decreasing thickness. From quantitatively tracking the CsPbI_3 phase transition for thin (<400 nm) and thick (>400 nm) nanoplates using *in situ* photoluminescence optical microscopy, we observe a larger fraction of thin nanoplates still maintaining their high-T phase after one month as compared to the thick counterparts. The enhanced phase stabilization of the strained high-T nanoplates is most likely owing to the strain-induced energy destabilization for the low-T phase relative to the high-T phase. The strain is suggested to originate from several factors, including lattice mismatch, thermal expansion coefficient mismatch, and ionic and van der Waals forces that contribute to the strong substrate-lattice interaction. These findings establish a fundamental understanding of the impact of lattice strain on perovskite phase stabilization, thereby driving advancements in the rational design of long-term, stable optoelectronic devices.

4:30 PM EN05.09.07

Unraveling The Magnetic Interactions in Halide Double Perovskites: A High-Throughput Study UtkarshSingh¹, JohanKlarbring¹, IgorA. Abrikosov¹ and SergeyI. Simak^{1,2}; ¹Linköping University, Sweden; ²Uppsala University, Sweden

In recent years, lead-free halide double perovskites (LFHDPs) have attracted attention for their significant chemical versatility [1] and potential as multifunctional materials [2]. The exploration of their magnetic properties however, has remained relatively uncharted [3, 4]. Our study elucidates the mechanism of magnetic exchange interactions in halide double perovskites (HDPs), revealing a general propensity towards antiferromagnetic ordering with low Néel temperatures (< 50 K), while highlighting exceptions that are predicted to exhibit ferromagnetic behaviour and relatively high Curie temperatures.

Employing a high-throughput approach, we identified ferromagnetic compounds in $\text{Cs}_2\text{HgCrCl}_6$ (~ 450 K), $\text{Cs}_2\text{AgNiCl}_6$ (~ 190 K), and $\text{Cs}_2\text{AuNiCl}_6$ (~ 240 K) as noteworthy candidates, with the latter two exhibiting potential for robust half-metallicity due to a large gap in the insulating channel.

To comprehend the observed magnetic properties in HDPs, we leverage the Magnetic force theorem [5] and calculate energy-resolved and orbital-resolved magnetic exchange interactions.

Contextualizing these resolved magnetic interactions within the nature and strength of bonding interactions using Density of States (DOS) and Crystal Orbital Hamilton Population (COHP) [6] analysis, the reasons for observed disparities in magnetic strength are unveiled. The comparison of these findings with well known oxide double-perovskites exhibiting high Curie temperatures [7, 8] enriches our understanding of magnetism in HDPs, and underscores the intricate mechanisms at play.

This nuanced understanding enables a more informed approach towards the design of HDPs with tailored magnetic properties. By providing insights into the magnetic behaviors of HDPs that aim to guide potential design strategies, this research could represent a step towards a deeper understanding of HDPs and encourage further exploration in this dynamic field.

[1] H. Lei, D. Hardy, and F. Gao, Lead-free double perovskite $\text{Cs}_2\text{AgBiBr}_6$: Fundamentals, applications, and perspectives, *Advanced Functional Materials* **31**, 2105898 (2021).

[2] K. Zhu, Z. Wang, H. Xu, and Z. Fu, Development of multifunctional materials based on heavy concentration Er^{3+} - activated lead-free double perovskite $\text{Cs}_2\text{NaBiCl}_6$, *Advanced Optical Materials* **10**, 2201182 (2022).

[3] W. Ning, J. Bao, Y. Puttisong, F. Moro, L. Kobera, S. Shimono, L. Wang, F. Ji, M. Cuartero, S. Kawaguchi, S. Abbrent, H. Ishibashi, R. D. Marco, I. A. Bouianova, G. A. Crespo, Y. Kubota, J. Brus, D. Y. Chung, L. Sun, W. M. Chen, M. G. Kanatzidis, and F. Gao, Magnetizing lead-free halide double perovskites, *Science Advances* **6**, eabb5381 (2020).

[4] H. Yin, Y. Xian, Y. Zhang, W. Chen, X. Wen, N. U. Rahman, Y. Long, B. Jia, J. Fan, and W. Li, An emerging lead-free double-perovskite $\text{Cs}_2\text{AgFeCl}_6$ in single crystal, *Advanced Functional Materials* **30**, 2002225 (2020).

[5] A. I. Liechtenstein, M. I. Katsnelson, V. P. Antropov, and V. A. Gubanov, Local spin density functional approach to the theory of exchange interactions in ferromagnetic metals and alloys, *Journal of Magnetism and Magnetic Materials* **67**, 65 (1987).

[6] R. Dronskowski and P. E. Bloechl, Crystal orbital hamilton populations (COHP): energy-resolved visualization of chemical bonding in solids based on density-functional calculations, *The Journal of Physical Chemistry* **97**, 8617 (1993).

[7] K.-I. Kobayashi, T. Kimura, H. Sawada, K. Terakura, and Y. Tokura, Room-temperature magnetoresistance in an oxide material with an ordered double-perovskite structure, *Nature* **395**, 677 (1998).

[8] A. Sleight and J. Weiher, Magnetic and electrical properties of Ba_2MReO_6 ordered perovskites, *Journal of Physics and Chemistry of Solids* **33**, 679 (1972)

4:45 PM EN05.09.08

What is in Your Perovskite Precursors? Improving Reproducibility and Stability of Perovskite Films via Purification of Precursors Connor Dolan, Sean P. Dunfield, Emma Yakel, Shiwei Liu, Jack R. Palmer and David P. Fenning; University of California, San Diego, United States

While much effort has been given to reducing or passivating intrinsic defects both in the bulk and at interfaces of perovskite devices, relatively few efforts have been made toward understanding and mitigating the presence of extrinsic impurities. Despite this, even small concentrations of extrinsic impurities have been shown to play a role in altering film formation and seeding the nucleation of macroscale degradation under operational stressors. Further, minute changes in precursor stoichiometry and impurity profiles even in different bottles of precursor from the same supplier have been shown to be a significant barrier to reproducibility in perovskite solar cell fabrication. In this work, we demonstrate Solvent Orthogonality Nucleation Induced Crystallization (SONIC) purification for removing extrinsic defects present in commercially available precursors commonly used to fabricate high efficiency perovskite solar cells. SONIC purification uses the slow diffusion of an antisolvent into a perovskite precursor solution to induce supersaturation, enabling controllable growth of high quality perovskite single crystals. Using a combination of inductively coupled plasma mass spectrometry and proton nuclear magnetic resonance, we demonstrate that there are significant impurities present in even the highest purity commercially available precursors and that SONIC purification is more effective at removing impurities than strategies commonly employed in the literature. We demonstrate that SONIC purification is effective for both high purity (99.99% trace metals basis) and low purity (99% trace metals basis) from different suppliers. This enables increased reliability in processing of perovskite precursors toward consistent impurity profiles to mitigate batch-to-batch and supplier-to-supplier variability. Finally, we show that perovskite thin films made from purified precursors demonstrate improved performance and stability over films made from as-received precursors. SONIC purification provides a method for removing extrinsic defects present in commercially available precursors, enabling improved stability and reproducibility in perovskite fabrication.

SESSION EN05.10: Poster Session IV: Halide Perovskites for Energy Applications

Session Chairs: So Min Park and Lina Quan

Wednesday Afternoon, November 29, 2023

Hynes, Level 1, Hall A

8:00 PM EN05.10.01

Understanding the Switching Mechanism in Halide Perovskite Memristors Deepak Yadav, Kanhaiya L. Yadav and Monojit Bag; Indian Institute of Technology Roorkee, India

Halide perovskite memristors have garnered attention for storage and neuromorphic computing applications. However, the switching mechanism between high-resistive and low-resistive states remains insufficiently understood. This study investigates the switching mechanism in ITO/MAPbBr₃/Au memristors. Impedance spectroscopy was employed to analyze the set-reset states at different applied biases. Results indicate that at zero and low applied biases (<0.5 V), the ac conductivity follows Jonscher's power law, suggesting limited ion migration. However, anomalous conductivity behaviour was observed at high applied biases (>0.5 V), indicating ionic conduction at low frequencies. Additionally, we found that illumination leads to faster switching, attributed to enhanced halide ion/vacancy movement. In conclusion, this study deepens our understanding of charge transport in MAPbBr₃ perovskite-based memristors, facilitating the development of more efficient devices for widespread application.

8:00 PM EN05.10.02

Diverging Expressions of Anharmonicity in Halide Perovskites Adi Cohen¹, Thomas M. Brenner¹, Johan Klarbring², Rituraj Sharma¹, Douglas H. Fabini³, Roman Korobko¹, Pabitra K. Nayak⁴, Olle Hellman² and Omer Yaffe¹; ¹Weizmann Institute of Science, Israel; ²Linköping University, Sweden; ³Max Planck Institute for Solid State Research, Germany; ⁴Tata Institute of Fundamental Research, India

The structure-function relationship in materials sciences is based on the concept of the minimal unit cell as the representative building block. The harmonic approximation, which relies on the unit cell symmetry, provides simple solutions to atomic motions in the form of a well-defined normal modes. However, materials exhibiting strong anharmonicity challenge the representation of the minimal unit cell by violating the derived symmetry.

In this study, we conducted a comparative analysis of the anharmonic motion in $\text{Cs}_2\text{AgBiBr}_6$ and its lead-free counterpart, CsPbBr_3 , to investigate the validity of the minimal unit cell in materials with pronounced anharmonicity. We observed significant differences in their expression of anharmonic behavior by applying low-frequency Raman spectroscopy and a symmetry-based analysis. In $\text{Cs}_2\text{AgBiBr}_6$, the anharmonicity manifests as a displacive phase transition while preserving well-defined normal modes across the measured temperature range. Conversely, CsPbBr_3 exhibits dynamic symmetry breaking, leading to the breakdown of the normal mode picture.

Based on these findings, we propose a criterion to determine how well the minimal unit cell, which represents the averaged structure, coincides with the local structure. We argue that the breakdown of the normal mode picture, as exemplified by CsPbBr_3 , plays a critical role in accurately calculating and understanding the functional properties of materials.

8:00 PM EN05.10.03

Interstitial Defect Relaxation DFT Study of Lead Halide Perovskites Kumar P. Miskin and Paulette Clancy; Johns Hopkins University, United States

Perovskite solar cells have garnered a lot of attention in the last decade. The efficiency obtained for solar cells using metal halide perovskites (MHP) have exceeded 22%. A major reason for this is the high carrier lifetimes in these materials [1]. These high efficiencies have been obtained despite relatively high defect densities as compared to those in Silicon solar cells, giving rise to an appreciation of high defect-tolerance in MHPs. Polycrystalline films made using metal halide perovskites can exhibit high defect densities of ($10^{15} - 10^{16}$ per $\diamond\diamond\diamond$), with minimal effect on efficiency. However, the origin of this tolerance is still a matter of active research. Halide defects (vacancies and interstitials) are some of the most common defects in perovskites.

This is due to low defect formation energy in these systems. DFT studies exist to quantify the formation energies of halide defects [2]. Our work will study the relaxation of these interstitials back to their lattice site using DFT (Quantum Espresso). The recombination pathway as well as the activation energy for this relaxation will help us better understand how these defects affect the recombination time for photogenerated carriers. The pathway to relaxation can be estimated using Nudged Elastic Band calculations (NEB).

Funding Acknowledgements:

PC acknowledges support from the U.S. Department of Energy (DOE), Basic Energy Sciences (BES), under award DE-SC0022305. Kumar Miskin thanks Johns Hopkins University for his support. The authors acknowledge the support afforded by access to the computing facilities at the petascale Advanced Research Computing at Hopkins (ARCH) facility (rockfish.jhu.edu), supported by the National Science Foundation (NSF), Grant Number OAC 1920103, for providing the extensive computational resources needed here. Partial funding for the infrastructure for ARCH was originally provided by the State of Maryland.

References:

1. Wehrenfennig, C.; Eperon, G. E.; Johnston, M. B.; Snaith, H. J.; Herz, L. M. High Charge Carrier Mobilities and Lifetimes in Organolead Trihalide Perovskites. *Adv. Mater.* 2014, 26, 1584–1589.
2. Meggiolaro, D.; De Angelis, F. First-Principles Modeling of Defects in Lead Halide Perovskites: Best Practices and Open Issues. *ACS Energy Lett.* 2018, 3 (9), 2206–2222

8:00 PM EN05.10.04

Water-Assisted Morphology and Crystal Engineering of Hybrid Organic-Inorganic Halide Perovskite: Implications for Optoelectronic Properties Andre Luiz M. Freitas and Jose A. Souza; UFABC, Brazil

The versatile application of hybrid organic-inorganic halide perovskites relies heavily on their crystal organization, which gives rise to distinct electronic structures. By manipulating the dimensionality and incorporating quantum confinement effects within the layered building blocks composed of n layers of $[MX_6]^{4-}$ octahedra, the optoelectronic properties of lead halide perovskites can be further modulated. In this study, we present a water-assisted approach for the formation of microwires and 2D layered morphologies, achieved through a dissociation-recrystallization process using $MAPbBr_3$ microcubes. Along with a systematic alteration of the bandgap energy, our investigation uncovers variations in trap- and exciton-assisted recombination lifetimes, attributed to changes in exciton binding energy and structural confinement. Notably, the control of water and organic molecules within the precursor ionic solution plays a pivotal role, inducing or inhibiting growth and confining charge transport in specific directions, resulting in modified optical properties and exciton dynamics. This work sheds light on the significance of water-assisted methodologies and structural manipulation in hybrid organic-inorganic halide perovskites, providing a pathway towards advanced control and optimization of their optoelectronic characteristics.

Acknowledgments

Financial support from FAPESP (grants no. 2022/06433-5, 2020/09563-1, and 2017/02317-2) and CEM-UFABC.

8:00 PM EN05.10.05

Self-Leveling Inks for Engineering Large Area Uniformity in High-Performance Flexography-Printed Perovskite Solar Cells Julia Huddy and William J. Scheideler; Dartmouth College, United States

Solution processing of metal halide perovskites can offer opportunities for efficient roll-based manufacturing of emerging flexible optoelectronic devices such as lightweight photovoltaics and light emitting diodes (LEDs). However, current techniques for perovskite deposition are limited by damaging subtractive scribing steps and lack wide processing windows that offer high uniformity. This work presents a class of self-leveling perovskite inks with specifically engineered viscosity, Marangoni coefficients, and drying rates to ensure ultra-uniformity. We show rapid open-air fabrication of double cation perovskite solar cells (PSCs) using high-speed (60 m/min) flexography, printing films over 500 cm^2 in $< 1\text{ s}$ with high photoluminescent uniformity (RMS variation $< 4\%$). Integrating inline N_2 drying, we achieve highly uniform patterns with $< 25\text{ }\mu\text{m}$ features and single-micron line edge roughness, ideal for solar module and perovskite LED integration. XRD and SEM reveal the impact of the ink design and anion composition on perovskite crystallization while 2D scanning photoluminescence (PL) resolves a correlation between ink leveling dynamics and optoelectronic quality. This allows us to optimize the self-leveling inks for mitigating Saffman-Taylor instabilities inherent in contact-based ink transfer, leading to enhanced uniformity, higher photovoltaic performance, and improved operational stability. Our flexography printed n-i-p planar PSCs achieve a photovoltaic conversion efficiency $> 20\%$, the highest reported for PSCs fabricated by roll-based methods. Collectively, these results illustrate how self-leveling inks can broaden process windows for perovskite device manufacturing by healing coating defects rather than freezing non-uniformities that otherwise lead to stability weakpoints.

8:00 PM EN05.10.06

Towards Highly Efficient Fully Evaporated Perovskite/Si Tandem Solar Cells Sofia Chozas Barrientos^{1,2}, Lidon Gil-Escrig^{1,2}, Federico Ventosinos^{1,2}, Manuel Piot^{1,2} and Henk J. Bolink^{1,2}; ¹Instituto de Ciencia Molecular (ICMol), Spain; ²Universitat de València, Spain

Thanks to its abundance on Earth, its suitable bandgap, and its non-toxicity, silicon dominates over 90% of the photovoltaic market. However, the efficiency of single-junction silicon cells is approaching its theoretical limit of 29%, with a current experimental record of 26.8%. In the quest for overcoming this limit and for reducing the cost of electricity, perovskite/silicon tandem cells have become the most promising contenders.

Pyramid texturing is a standard process in the fabrication of the best performing silicon technologies since it is known to enhance light trapping in the infrared and to reduce primary reflection due to double-bounce effects. However, most of the perovskite-on-Si work has been reported on flattened silicon substrates due to the incompatibility of the textured surfaces with the standard solution-processing of the top perovskite absorbers.

Here, we present the conformal vacuum deposition of wide bandgap perovskites atop fully textured silicon heterojunction cells. We have optimized vacuum deposition processes for different wide bandgap perovskite compositions, mainly $FACsPbIBr$ and $MAPbIBr$. Their bandgaps range between 1.65 and 1.70 eV, making them ideal candidates as top cells in perovskite/Si tandems. As evidenced from cross-sectional SEM images, our co-evaporation processes enable a conformal coverage of the pyramidal surface of the silicon substrates avoiding shorts between the subcells. This leads to Voc values of above 1.8 V, which correspond well to the sum of the Voc of the perovskite top cell and the silicon bottom cell. Moreover, the use of QCM sensors for monitoring the sublimation of the top cell enables fine tuning of the absorber thickness. This allows to achieve current matching between the subcells as we have been able to demonstrate through EQE measurements. The J-V curves show FFs above 70% and no detectable hysteresis. All in all, we will show our latest results on perovskite/Si tandems employing textured Si and fully sublimed top cells.

8:00 PM EN05.10.07

The Outstanding Role of Dielectricity in Hybrid Solar Cell Absorbers Doru C. Lupascu, Young U. Jin, Andrei Karabanov, Lars L. Schaberg and Niels Benson; University of Duisburg-Essen, Germany

The perovskite crystal structure has been hosting a multitude of functionalities discovered over the last seventy years spanning from magnetism, ferroelectricity to supraconductivity. The most recent developments have brought forward hybrid halide perovskites containing a halide ion and small organic molecules as constituents of the crystal structure. The forerunner material is methylammonium lead iodide. One of the most remarkable properties of these emergent materials is their high charge carrier mobility and an outstanding robustness of the electronic properties towards lattice defects. In this presentation the role of dielectric effects will be discussed covering a very broad frequency range. Paraelectric effects will be contrasted to the role of apparent ferroelectricity, charge disorder and the potential misinterpretation of a number of experiments in this context. The hyperpolaron is shown as the charge carrier type peculiar for the hybrid perovskites.

8:00 PM EN05.10.08

Investigating The Effect of Annealing Environments on Cs and MA Containing FAPI Perovskites Muhammad U. Farooq¹, Sevan Gharabeiki¹, Ding Yong², Mohammad K. Nazeeruddin², Susanne Siebentritt¹ and Alex Redinger¹; ¹Université du Luxembourg, Luxembourg; ²École Polytechnique Fédérale de Lausanne, Switzerland

Interface and grain boundary passivation is essential to achieve high power conversion efficiencies (PCE) in solar cells. In this work, we show how different atmospheres during post-deposition annealing of $Cs_{0.05}MA_{0.05}FA_{0.9}PbI_3$ can be used to change the surface properties and reduce interface recombination. A comparative study was carried out on high-efficiency ($\sim 24\%$) $Cs_{0.05}MA_{0.05}FA_{0.9}PbI_3$ perovskites [1]. After deposition, these perovskite absorbers underwent annealing in three different environments i.e., N_2 , O_2 , and air. Device performance was best for the samples annealed in air, reaching 25.1% power conversion efficiency, whereas the devices produced from absorbers annealed in N_2 and O_2 showed reduced PCEs. Calibrated Photoluminescence (PL) measurements were carried out on all samples to extract the quasi-Fermi level splitting (QFLs). In contrast to the device results, the nitrogen-annealed sample exhibited the highest QFLs value in agreement with time resolved photoluminescence where we found the longest decay times. A comparison

between QFLs and V_{OC} showed that the air-annealed samples, which produced the best devices, were not interface-limited, whereas the other two sample types showed a substantially lower V_{OC} compared to the QFLs. The PCE improvement after air annealing, therefore, needs to be related to better interface passivation. Although the N_2 annealed samples exhibited the best optoelectronic properties, i.e., highest QFLs, the interface to the extraction layer was substantially worse, compared to the air-annealed samples.

To gain more insights into the surface properties, atomic force microscopy (AFM) and Kelvin probe force microscopy (KPFM) measurements were conducted in a nitrogen environment. The air-annealed sample showed the highest mean work function (4.9 eV), the O_2 -annealed sample showed a slightly lower mean work function (4.7 eV), while the N_2 -annealed sample exhibited the lowest work function amongst the three (4.6 eV). In all three cases, a PbI_2 secondary phase was observed on the surface of the films. It was found that the PbI_2 work function was lower than the mean perovskite work functions for both N_2 and O_2 annealed samples. However, it was higher than the mean work function for the air-annealed sample. In addition to the average work functions, we analyzed approximately 100 grain boundaries for the three sample types and found that the different annealing atmospheres did not change the grain boundary band bending significantly.

From our measurements, we conclude that annealing in different atmospheres allows changing the recombination activity of the surface. Both the perovskite surface and the PbI_2 secondary work functions were affected by the treatment. Annealing in air showed to be most beneficial since the surface was better matched to the extraction layer allowing for higher V_{OC} s and thereby better devices.

1. Ding, Y. *et al.* Single-crystalline TiO₂ nanoparticles for stable and efficient perovskite modules. *Nat. Nanotechnol.* **17**, 598–605 (2022).

8:00 PM EN05.10.09

Controlling The Crystallization of Pure Bromide Quasi-2-Dimensional Perovskite Crystals for High Efficiency Pure-Blue Light-Emitting DiodesSeoyeonPark¹, JoonyunKim², GuiM. Kim¹, Doh C.Lee¹, SooheyongLee³, Byeong-GwanCho³ and ByunghaShin¹; ¹Korea Advanced Institute of Science and Technology, Korea (the Republic of); ²Samsung Advanced Institute of Technology, Korea (the Republic of); ³Korea Research Institute of Standards and Science, Korea (the Republic of)

Metal halide perovskites have emerged as promising candidates for next-generation display applications due to their remarkable color purity and tunable bandgaps by adjusting the composition of halide anions. Mixed halide perovskites allow for facile bandgap tunability through composition control, but they have limitations in terms of emission spectral stability due to halide segregation occurring during device operation. An alternative approach to widen the bandgap involves constructing a quasi-2-dimensional structure using a single halide anion, leveraging the confinement effect. However, this approach often results in multi-bandgap phases, leading to a red-shifted emission due to energy funneling toward a phase with a bandgap lower than the target. Here, we synthesized $(PBA)_2Cs_{n-1}Pb_nBr_{3n+1}$ quasi-2D perovskite crystals where 'n' indicates the number of $PbBr_6$ octahedral sheets in each repeating unit. To achieve pure-blue emission within the range of 460–470 nm, the target wavelength by the ITU-R Recommendation BT.2020 (Rec. 2020), the industry standard for 4K and 8K ultra-high definition television standard, we manipulated the crystallization process of the quasi-2D perovskite prepared by solution process. The manipulation involved controlling the distribution of different 'n' (i.e., different bandgap) phases, with a specific focus on ensuring the dominance of the phase with the smallest bandgap, which is also the target emission bandgap. We attained pure-blue photoluminescence (PL) at 461 nm with a relatively narrow full-width at half maximum (FWHM) of 25 nm through a two-step crystallization control process. Initially, we performed a coarse adjustment of the PL wavelength by changing the solute concentration and solvent polarity, as these factors heavily influence the diffusion of cations, a crucial determinant for the value of 'n'. Subsequently, we further enhanced the PL quantum yield (PLQY) from 31% to 51% through fine-tuning in the second-step crystallization process, which involved the incorporation of trioctylphosphine oxide (TOPO) as an additive during the antisolvent treatment. The antisolvent treatment with TOPO slightly slowed down the diffusion of precursors, resulting in halide-vacancy passivation and well-ordered crystals and leading to faster carrier transfer between phases. Based on these strategies, we successfully fabricated pure-blue light-emitting diodes (LEDs), which exhibited a relatively low turn-on voltage of 3V and an external quantum efficiency of 2.5% at an emission peak of 465 nm with a FWHM of 29 nm.

8:00 PM EN05.10.10

Compositional Engineering of Single-Crystal Perovskite for Highly Efficient PhotovoltaicsYou JinAhn¹, Jin YoungKim¹ and Ik JaePark²; ¹Seoul National University, Korea (the Republic of); ²Sookmyung Women's University, Korea (the Republic of)

Organic-inorganic lead halide perovskite materials have received great attention for promising opto-electric devices. To achieve high performance solar cells, defect control in perovskite materials is very crucial. Single-crystal perovskite-based solar cell exhibits excellent carrier diffusion length and light absorption due to significantly reduced bulk defects. In here, we discuss compositional engineering of single-crystal perovskite films for highly efficient perovskite solar cells. Single crystal perovskite films were grown by space-limited inverse temperature crystallization (ITC) method. Due to different solubility of perovskite precursor solute, γ -butyrolactone (GBL) and *N,N*-dimethylformamide (DMF) solvent ratio should be precisely controlled for compositional engineering. We investigated the effect of mixture solvent on growing single crystal perovskites. X-ray diffraction patterns confirmed that composition of perovskite can be controlled by the composition of perovskite precursor solution. We successfully synthesize wide-bandgap perovskite films and confirmed using UV-vis-NIR analysis. Single-crystal films over 4 mm were grown on ITO/PTAA substrates, and we fabricated single-crystal perovskite-based solar cells. The device shows high external quantum efficiency due to the micrometer-size film thickness. The best performing devices exhibited power conversion efficiency of over 20%.

8:00 PM EN05.10.11

Atomistic Origin of Transparent Absorption Spectra of Halide PerovskitesYoung WonWoo^{1,2}, SavyasanchiAggarwal³, SeánR. Kavanagh^{3,2}, AlexM. Ganose² and AronWalsh²; ¹Yonsei University, Korea (the Republic of); ²Imperial College London, United Kingdom; ³University College London, United Kingdom

Differential spectroscopy has emerged as a valuable characterisation tool in materials science. Transient absorption spectroscopy (TAS) involves probing changes in optical absorption following laser excitation. While TAS spectra provide information about carrier recombination kinetics, interpreting individual features remains challenging. In this talk, we present a novel procedure to calculate TAS spectra for crystals using first-principles density functional theory calculations. Our approach simulates changes in band-to-band transitions within the electronic band structure, encompassing ground-state bleaching and photo-induced absorption processes.

This methodology is particularly relevant to the investigation of halide perovskite materials, where TAS can provide insights into their unique optical properties and charge carrier dynamics. Applications will be given to a range of inorganic and hybrid perovskite compositions. Our procedures are implemented in the PyTASER code, an open-source package that facilitates the implementation of our simulation approach to help accelerate materials characterisation and bridge the gap between modelling and measurements for researchers working on halide perovskites.

8:00 PM EN05.10.12

Optimal Passivation Strategy using (α -Methylguanido)acetic Acid for Stable Perovskite Solar CellsJihyunMin, Dae HwanLee and TaihoPark; Pohang University of Science and Technology, Korea (the Republic of)

Defects are easily generated in perovskite, and these defects reduce the efficiency of perovskite solar cells (PSCs). Therefore, it is important to control defects. In this study, we tried to passivate perovskite using creatine, which is known as (α -Methylguanido) acetic acid. To find the optimal passivation strategy, we conducted two methods: passivating bulk perovskite by adding creatine as an additive to the perovskite precursor, and passivating the surface of perovskite by introducing it as an interlayer. The results showed that only the method of introducing creatine into the interlayer formed 2D perovskite. This is because the activation energy to form 2D perovskite when introduced as an interlayer is smaller than when introduced as an additive, and it can be formed at an annealing temperature of 150 °C. When creatine was introduced into the interlayer, it was confirmed that the appropriate energy level was appropriately adjusted for good charge transfer and the defect density was also reduced. As a result, PSCs introduced with creatine recorded a PCE of 22.6%, showing high stability even under high temperature conditions of 85 °C and 50% relative humidity conditions.

8:00 PM EN05.10.13

Exploring a Novel Family of Conjugated Polymers for High Efficiency and Thermally Stable Perovskite Solar CellsSanggyunKim, SinaSabury, Carlo Andrea RiccardoPerini, JohnR. Reynolds and Juan-PabloCorrea-Baena; Georgia Institute of Technology, United States

Long-term stability remains to be one of the critical challenges for organic-inorganic hybrid perovskite solar cells (PSCs). One of the most important limiting factors toward achieving long-term stability has been attributed to the hole transport layer (HTL), originating from interfacial degradation between perovskite and HTL, thermal/moisture induced degradation, and ionic migration. In this work, we examine novel conjugated polymer (CP)-based HTLs that are resistant to high temperatures in PSCs. CPs offer efficient hole extraction/transport properties, easy processing, and low-production cost. We highlight differences in optoelectronic properties, crystallinity, and stability of the CPs with respect to its different chemical structures using measurements including UV-VIS, UPS, DSC, GIWAXS, and XPS. These new polymers are further incorporated into devices to analyze its photovoltaic performance and stability at elevated temperature under illumination over 200 hours.

8:00 PM EN05.10.14

Charge Transfer Doping of Ruddlesden–Popper Metal–Halide Perovskites via Bulk Incorporation of Organic Molecular Dopants [Kyeong-Yoon Baek](#)^{1,2}, Jonghoon Lee¹, Jeongjae Lee¹, Heebeom Ahn¹, Yongjin Kim¹, Keehoon Kang¹ and Takhee Lee¹; ¹Seoul National University, Korea (the Republic of); ²Harvard University, United States

Ruddlesden–Popper metal–halide perovskites have recently attracted much attention as next-generation semiconducting materials due to their outstanding opto-electrical properties. However, these low dimensional materials critically suffer from relatively poor electrical conductivity, which is challenging to tune with traditional method of bulk atomistic doping. While doping with molecular dopants, a family of versatile dopants for molecular design has been suggested as a solution to this problem.[1,2] Nonetheless, the action of these dopants was typically restricted to perovskite surfaces, therefore significantly reducing their doping potential. In this study, we report successful bulk inclusion of ‘magic blue’, a molecular dopant, into two-dimensional (2D) Ruddlesden–Popper perovskites.[3] Our doping strategy of immersing the perovskite film in dopant solution increased the electrical current up to ~60 times while maintaining clean film surface. We provide a full mechanistic picture of such immersion doping, in which the solvent molecule facilitates bulk diffusion of dopant molecule inside the organic spacer layer, based on the optimum solvent processing. The immersion doping method developed in this work which enables bulk molecular doping in metal–halide perovskites in general will provide a strategic doping methodology for controlling electrical properties of low dimensional metal–halide perovskites for electronic and optoelectronic devices.

References

- [1] E. Ashley Gaulding et al., *Adv. Mater.* **31**, 1902250 (2019).
- [2] A. L. Abdelhady et al., *J. Phys. Chem. Lett.* **7**, 295 (2016).
- [3] J. Lee et al., *Adv. Funct. Mater.* **2302048** (2023).

8:00 PM EN05.10.15

Switchable Interfacial Reaction Enables Bright and Stable Deep-Red Perovskite Light-Emitting Diodes [Yang Liu](#) and Yizheng Jin; Zhejiang University, China

The all-inorganic black phase CsPbI₃ perovskite has garnered significant interest for its exceptional optical properties, superior chemical and thermal stability, excellent charge transport characteristics, and solution processability, making it a promising material for photovoltaic applications and light-emitting devices. Despite these advantages, the requirement of high formation temperature exceeding 300 °C and the tendency for spontaneous phase transition to yellow non-perovskite phase at room temperature present significant challenges for the development of high-performance CsPbI₃-based optoelectronics (*ACS Energy Lett.* **3**, 1787–1794 (2018); *Science* **365**, 679–684 (2019)).

One approach to address these problems is to grow nanocrystals with ligand-passivated surfaces which can passivate the surface traps and stabilize the black phase CsPbI₃. Similarly, quasi-2D CsPbI₃ perovskites with high PLQYs can be formed and stabilized under low temperatures. However, the long-chained ligands of QDs or the excess large organic ammonium spacer layers of the quasi-2D perovskites shall deteriorate the charge transport in perovskite light-emitting diodes (PeLEDs), hampering the realization of stable and bright PeLED.

Alternatively, it has been established that the interfacial deprotonation reactions between the perovskite intermediates and the basic ZnO-based ETLs can regulate the crystallization process by an interionic exchange process, enabling the formation of high-quality bulk CsPbI₃ perovskite films (*Nat. Commun.* **11**, 4736 (2020)). The obtained films maintain the excellent carrier transport property of CsPbI₃ and would alleviate the Auger effects. These superiorities suggest that CsPbI₃ PeLEDs based on ZnO ETLs would deliver efficient electroluminescence (EL) under high current densities.

However, the uncontrollable deprotonation reaction between ZnO and perovskites would further exhaust the residual organic ammonium cations and lead to the undesired phase transition. As a result, the long-term operational stability of the CsPbI₃ PeLEDs remains modest. For example, the most stable PeLED based on this method shows a T₅₀ lifetime of 1.7 h under a constant current density of 100 mA cm⁻² (*Adv. Mater.* **33**, 2105699 (2021)). A comprehensive understanding and rational design of the chemically active interfaces between perovskite and the ZnO layer is crucial for developing high-performance perovskite optoelectronic devices.

Here, by designing a switchable interfacial deprotonation reaction between perovskite and the ETLs, we fabricate high quality CsPbI₃ perovskite films for stable and bright deep-red LEDs. Our approach starts with a precursor solution containing guanidium iodide and a layer of alkaline Zn(OH)₂. Upon annealing, the interfacial deprotonation reaction is switched on, leading to the formation of high-quality CsPbI₃. Simultaneously, the alkaline Zn(OH)₂ layer is in-situ converted to the alkaline ZnO, which subsequently switches off the detrimental interfacial reaction that generates the undesirable yellow-phase CsPbI₃ perovskites. As a result, PeLEDs based on CsPbI₃ show a long half-lifetime of ~33.6 h at 100 mA cm⁻² and an exceptionally high radiance of ~1980 W sr⁻¹ m⁻². Moreover, by partly substituting iodide with bromide, we achieve colour-stable deep-red PeLEDs with an enhanced luminance of over 33500 cd m⁻² and an unprecedented operational half-lifetime of 50.3 h at 100 mA cm⁻², representing the brightest and most-stable solution-processed LEDs in the entire deep-red region.

8:00 PM EN05.10.16

Additive Engineering in 2-Methoxyethanol Based Perovskite Film Formation for Perovskite Solar Cells [Sung Hun Lee](#) and Hyo Jung Kim; Pusan National University, Korea (the Republic of)

Perovskite solar cells (PSCs) have attracted significant attention because of their unique characteristics such as low-cost fabrication through solution processes and excellent photoelectric properties. Solution-processed perovskite films using polar aprotic solvent such as dimethyl sulfoxide (DMSO) generally required auxiliary process like anti-solvent drop. However, the anti-solvent dripping process has strict process window to form a uniform film such as dripping duration, volume, and pressure of the anti-solvent.

Recently, solvent engineering using 2-methoxyethanol (2MOE), which has selective solubility that dissolves methylammonium iodide (MAI) but not PbI₂ alone, have been studied for perovskite film formation for an anti-solvent free process. Although perovskite phase film could be obtained on the 2MOE solvent system without the anti-solvent process, the film generally has many pinholes leading to low power conversion efficiency (PCE) in PSCs. This problem is caused by low coordination with the precursor and high volatile of 2MOE.

To overcome this issue, we applied several additives, which affect to the kinetics of crystallization, in the 2MOE-based anti-solvent free process. First, we used various co-solvents, such as dimethyl sulfoxide (DMSO) and N-methyl-2-pyrrolidone (NMP), that can induce intermediate phases in which highly coordinated system with the precursors and solvents (MAI-PbI₂-DMSO and MAI-PbI₂-NMP). The formation of intermediate phases retards crystal growth of perovskite and leads to high crystallinity of the perovskite. Through this, we found that NMP is a suitable additive for pinhole free perovskite film. We obtained an efficiency of 20.39% with the maximum efficiency for the device based on the MAPbI_{3-x}Cl_x film fabricated with a 2MOE-based solution containing NMP.

Second, we compared film formation by adding alkyl amines with different chain lengths in 2MOE single solvent system. Through this, we found that the uniform and dense film could be obtained by adding small molecule of oleyamine (OAm) having long 18-carbon chain without anti-solvent dripping. In that study, we measured real-time grazing incidence wide angle X-ray scattering (GIWAXS) in spin cast process to study how the added alkylamine affected to film quality. We found that the longer alkyl chain of alkyl amines induced the faster nucleation and fast crystal growth of perovskite in film formation. We fabricated inverted PCSs using the high-quality film containing OAm as a light absorption layer and obtained PCE of 21.01%.

8:00 PM EN05.10.17

Metal Microgrid Embedded Transparent Electrode for Enlarge Perovskite Solar Cells [Hyungwoo Kim](#) and Kwanyong Seo; Ulsan National Institute of Science and Technology, Korea (the Republic of)

Organic-inorganic hybrid perovskite (OIHP) solar cells have attracted much attention as next-generation energy devices. In the fabrication of OIHP solar modules, the unit cells are designed by considering the charge carrier loss in the collection process through transparent electrodes. However, in the modularization process of OIHP solar cells, the optical dead area increases, resulting in the degradation of the overall module efficiency. To mitigate the efficiency loss, it is crucial to enlarge the size of the unit cells. However, as the unit cell size increases, the power loss due to the inherent electrical resistance of transparent electrodes also becomes more critical, leading to a decrease in the fill factor (FF) of OIHP solar cells and modules. For example, when the voltage and current density at the maximum power point of the OIHP solar cell is 1.0 V and 23.5 mA/cm², respectively, the power loss will become the same as the overall photo-generated power when the carriers need to move over 3.5 cm to be collected through the ITO layer which has a sheet resistance of 10 ohm/sq. Therefore, the lower sheet resistance of transparent electrodes would be essential to realize the larger-sized OIHP solar cells. Here, we report a hybrid transparent electrode in which a metal microgrid is embedded into the glass substrate, and ITO covers the substrate. The hybrid electrodes exhibit excellent sheet resistance of lower than 1 ohm/sq and comparable optical transmittance (~82%, @300-800 nm) to that of ITO/glass substrate (~83%, @300-800 nm). When utilizing the developed hybrid electrode, the OIHP single solar cell with a size of 12.25 cm² shows an open-circuit voltage of 1.04 V, a short-circuit current density of 20.1 mA/cm², FF of 65.8%, and an overall efficiency of 13.8%. In particular, the FF of the OIHP solar cell based on the hybrid electrode is 2.01 times higher than that of the OIHP single solar cells based on an ITO/glass substrate (32.7%), confirming that charge carriers are collected efficiently. Our work suggests enormous potential for significant performance improvement of large-scale OIHP solar cells.

8:00 PM EN05.10.18

Hybrid Energy Harvester Based on ZnO Piezoelectric Nanogenerator and Perovskite Solar Cell [Yuan Zhang](#), Joe Briscoe and Xuan Li; Queen Mary University of London, United Kingdom

Mechanical energy is the one of the most abundant and accessible energy sources, and has been widely harvested by large-scale technologies such as wind power or tidal stream generators. Piezoelectric nanogenerators (PENGs) provide a potential way to convert small mechanical energy such as body motion or vibration into electricity, which can be used to power small portable electronics, medical bio implants, remote wireless sensors etc.¹ Also, solar energy offers the potential to provide much higher power levels than motion since the sun delivers more energy to the earth in 1 h than the entire planet consumes in one year. However, light is not always available, nor is movement, therefore a hybrid energy harvester that can make use of both sources provide a more reliable and high-level of power for small, portable or self-powered devices. Here, a solar and piezoelectric hybrid energy harvester (HEH) combining PENGs and perovskite solar cell with the structure of PET/ITO/ZnO seed layer/ZnO nanorods/perovskite/hole transport layer/Au (Figure a) was designed, fabricated and tested. Oscillation (NG) and illumination (PV effect) testing indicated that HEHs operated as kinetic and solar energy harvesters both separately and simultaneously. (Figure b) The length and diameter of ZnO nanorods (Figure c and d), and the recipe of perovskite (MAPbI₃, CsPbI₂Br and CsPbI_{1.5}Br_{1.5}) were optimised to achieve the enhancement of both PV and NG output performance. The coupling effect between perovskite and piezoelectric ZnO nanorods, as known as the piezo-phototronic effect, was also investigated.

8:00 PM EN05.10.19

Solvent-Annealing Assisted 3D Printing of High-Performance, Freestanding Perovskite Nanolasers [ShiqiHu](#) and Ji TaeKim; The University of Hong Kong, Hong Kong

Inorganic metal halide perovskites are emerging as promising optoelectronic materials due to their strong, tunable, and high-color-purity photo- and electroluminescence, and solution processability¹⁻³. Recently, extensive research has been made to utilize perovskite nanowires as lasers due to their structural benefits such as ultra-compact sizes, highly localized coherent output, and efficient waveguiding^{4,5}. The current fabrication of perovskite nanowires relies on electron beam lithography, photolithography, chemical vapor deposition, solution-phase synthesis, and nanoimprinting. That is to say, these processes are energy- and labor-intensive, which is in stark contrast with the industrial low-cost requirements. Furthermore, technological challenges associated with individual tailoring of nanowire geometries remain unresolved, making it difficult to manipulate stimulated emission characteristics at the single nanowire level. A new method that can fabricate perovskite nanowires with programmed shape, dimension, and placement is in great demand for addressing the abovementioned issue.

Here, we demonstrate an electrohydrodynamic (EHD) 3D printing of perovskite nanowires for high-performance bespoke lasers. The printed perovskite nanowire presents a two-photon pumped Fabry-Pérot (FP) mode lasing. By adjusting the height of a freestanding nanowire at will, we are able to select the lasing mode and also control the lasing threshold and mode spacing ($\Delta\lambda$). On this basis, we successfully demonstrated the 3D printed nanowires arrays for multi-level anti-counterfeiting security labels by storing information in the cavity-height-dependent features such as the lasing threshold and mode spacing ($\Delta\lambda$), which are unclonable. More importantly, solvent annealing was exploited to increase the grain size and crystallinity by promoting recrystallization in the printed nanowire. As a result, the lasing threshold was drastically improved from 25 $\mu\text{J}/\text{cm}^2$ to 3 $\mu\text{J}/\text{cm}^2$, which is the leading record for CsPbBr₃ FP lasers. It is also worth mentioning that the advanced features of our technique such as maskless operation and low-cost production with high stability make it an effective platform to bring the proof-of-concept demonstration into practical commercial application. Likewise, these outcomes not only give us inspiration for the function-oriented design of the nanolaser-based devices but also facilitate the development of high-performance perovskite-based photonic anti-counterfeiting applications. Last but not least, our method could provide an excellent platform to construct scalable, on-demand laser-based photonic devices.

1. Stranks, S. D. *et al.* Electron-hole diffusion lengths exceeding 1 micrometer in an organometal trihalide perovskite absorber. *Science* (80-.). **342**, 341–344 (2013).
2. Braly, I. L. *et al.* Hybrid perovskite films approaching the radiative limit with over 90% photoluminescence quantum efficiency. *Nat. Photonics* 2018 126 **12**, 355–361 (2018).
3. Lin, K. *et al.* Perovskite light-emitting diodes with external quantum efficiency exceeding 20 percent. *Nat.* 2018 5627726 **562**, 245–248 (2018).
4. Chen, M. *et al.* 3D Nanoprinting of Perovskites. *Adv. Mater.* **31**, 1–8 (2019).
5. Chen, M. *et al.* Three-Dimensional Perovskite Nanopixels for Ultrahigh-Resolution Color Displays and Multilevel Anticounterfeiting. *Nano Lett.* **21**, 5186–5194 (2021).

8:00 PM EN05.10.20

Multifunctional Phosphine Oxide Additives for High-Efficiency CsPbBr₃ Perovskite LEDs [Jung MinHa](#)¹, Jong minHan², Myoung HoonSong² and Han YoungWoo¹; ¹Korea University, Korea (the Republic of); ²Ulsan National Institute of Science and Technology, Korea (the Republic of)

Perovskite light-emitting diodes (PeLEDs) are gaining attention as next-generation display devices due to their narrow bandwidth, high external quantum efficiency (EQE), and luminance. The crystallinity, crystal size, and defects density of perovskite have strong impacts on its optical and photoelectrical properties, as they generate trap states that induce non-radiative recombination, leading to low EQEs in the device. To achieve high-performance perovskite emissive layers, various additives have been utilized for defect passivation, including Lewis bases such as amines, carboxylates, and phosphine oxides. In particular, triphenylphosphine oxide (TPPO) not only efficiently passivates defects through strong binding with lead ions but also provides robust stability against external environmental stimuli such as oxygen, moisture, and heat. In this study, TPPO-2 and TPPO-4, where two and four TPPO molecules are covalently bonded, respectively, were introduced into the 3D nanostructured perovskite emissive layer and their effects on crystalline growth and device performance were studied depending on the number of TPPO functional moieties. Bifunctional or tetrafunctional TPPO derivatives not only effectively suppressed surface defects by forming stronger bonds with PbBr₂ but also delayed the binding of bromide with PbBr₂ due to large steric hindrance when mixed with the perovskite precursor, allowing the formation of perovskite films with smaller grain size. The PeLEDs with the tetrafunctional TPPO-4 showed the best EQE of ~21%, demonstrating their great potential as a multifunctional additive.

8:00 PM EN05.10.21

Nanostructure Strategies for Improved Perovskite Solar Cells [AntonioGarcia-Martin](#); Instituto de Micro y Nanotecnología, CSIC, Spain

Organic-inorganic hybrid perovskite solar cells have attracted much attention due to their high power conversion efficiency (>23%) and low-cost fabrication. Directions to further improve these solar cells include strategies to enhance their stability and their efficiency by modifying either the perovskite absorber layer or the electron/hole transport layer. For example, the transparent electron transport layer (ETL) can be an important tuning knob influencing the charge extraction, [1] light harvesting, [2] and stability [3] in these solar cells, or the use of up-conversion nanoparticles to get better performance in the near IR part of the visible spectrum. [4] Here we present two strategies based on nanostructuring, first a fundamental study of upconversion fluorescence enhancement effects near Au nanodisks by scanning near-field optical microscopy and second the effects of a nanocolumnar TiO₂ layer on the performance and the stability of Cs_{0.05}(FA_{0.83}MA_{0.17})_{0.95}Pb(I_{0.83}Br_{0.17})₃ perovskite solar cells. For the first case, the enhancement and localization of light near the metallic structures are directly visualized by using a single Er/Yb-codoped fluorescent nanocrystal glued at the end of a sharp scanning tip. [5] For the second we find that, compared to devices with planar TiO₂ ETLs, the TiO₂ nanocolumns can significantly enhance the power conversion efficiency of the perovskite solar cells by 17 % and prolong their shelf life. By analyzing the optical properties, solar cells characteristics, as well as transport/recombination properties by impedance spectroscopy, we observed light-trapping and reduced carrier recombination in solar cells associated with the use of TiO₂ nanocolumn arrays. [6]

References

- [1] S.S. Mali, *et al.*, *Chemistry of Materials* **27**, 1541 (2015).
- [2] C. Liu, *et al.*, *Journal of Materials Chemistry A* **5**, 15970 (2017).
- [3] M. Salado, *et al.*, *Nano Energy* **35**, 215 (2017)
- [4] M. Bauch *et al.*, *Plasmonics* **9**, 781 (2014)
- [5] L. Aigouy, *et al.*, *Nanoscale* **11**, 10365 (2019)
- [6] Z. Hu, *et al.*, *ACS Appl. Mater. Interfaces* **12**, 5979 (2020)

8:00 PM EN05.10.22

Beginner's Guide to Visual Analysis of Perovskite Solar Cell Current-Voltage Characteristics [AlbertThese](#)^{1,2}, ChristophJ. Brabec¹ and VincentLe Corre¹; ¹Institute Materials for Electronics and Energy Technology, Germany; ²Friedrich-Alexander-Universität Erlangen-Nürnberg (FAU), Germany

The current-voltage characteristic (JV) is a critical tool for understanding the behavior of solar cells. In this presentation, I will provide an overview of the critical aspects of JV analysis and introduce a user-friendly flowchart that facilitates the swift identification of the most probable limiting process in perovskite solar cells, based mainly on the outcomes of light-intensity-dependent JV measurements.

The flowchart was developed through extensive drift-diffusion simulations and a rigorous literature review, with a specific focus on perovskite solar cells (it is also applicable for organic solar cells with minor adjustments). Hereby, each loss mechanism is supported by a drift-diffusion simulation showing the exact influence on the main JV parameters, namely short-circuit current, open-circuit voltage, and fill factor. The flowchart also suggests an additional experiment besides JV characteristics to get a more accurate and definitive prediction of the main losses. It is therefore a valuable starting point for the analysis of experimental data and provides guidance to quantify the main loss processes of perovskite solar cells.

8:00 PM EN05.10.23

Interplay of Structural and Optoelectronic Properties in Triple-Cation Mixed-Halide Perovskites Tom J. Savenije, Jiashang Zhao, Sander Looman, Xiaohui Liu, Reinder Boekhoff, Bahiyah Ibrahim and Jos Thieme; Delft University of Technology, Netherlands

State-of-the-art triple cation, mixed halide perovskites have been extensively studied in perovskite solar cells in both n-i-p and p-i-n configurations showing very promising performances and stabilities. However, fundamental understanding of how the structure and morphology of $\text{Cs}_{0.05}\text{FA}_{0.85}\text{MA}_{0.10}\text{Pb}(\text{I}_{0.97}\text{Br}_{0.03})_3$ affect the electronic properties is lacking, in particular for samples with a small excess of PbI_2 . Despite the advantages of using excess PbI_2 with respect to the improved performance, also stability issues are reported. Therefore, it is worth to investigate the role of excess PbI_2 at various phases. Here temperature-dependent XRD, photoluminescence (PL) in combination with electrodeless microwave photoconductivity measurements (TRMC) were carried out on stoichiometric CsMAFA thin films (control) and on films with 5% excess PbI_2 . Angle dependent XRD shows that for the latter sample the PbI_2 resides predominantly at the interface between the quartz substrate and perovskite. Temperature dependent XRD indicates that both CsMAFA samples undergo a phase transition from cubic to tetragonal at ~ 280 K, which is coupled to a decrease in PL intensities and an enhancement of the charge carrier mobilities. Next, a second transition at ~ 170 K results in an opposite trend with increasing PL intensities, while photoconductivity signals are substantially reduced. It is found that for the control sample the latter transition is retarded by the substrate leading to a layered system comprising both structures. This leads to very large differences in photoconductivity between excitation from the front and through the substrate. We suspect that for the excess PbI_2 sample, the PbI_2 at the interface cancels the effect of the substrate. The reduction in photoconductivity below 170 K for both samples in combination with an extension in lifetimes as found from the TRMC measurements is related to the increase of strain, which is in accordance with the XRD data. At these low temperatures this strain leads to a highly defective material resulting in the prolonged, selective trapping of one type of carrier. Most interestingly all observed phenomena are all fully reversible. Finally, to gain more knowledge regarding the individual mobilities of electrons and holes of excess charge carriers in CsMAFA, TRMC was carried out on bilayers of HTL/CsMAFA, CsMAFA/ETL. First of all, the TRMC signal heights of all bilayers were reduced to about half of the bare CsMAFA layer. We attribute this to the efficient charge transfer of one type of carrier from CsMAFA to a selective TL. Since the mobility in all investigated TLs is more than an order of magnitude lower than that in CsMAFA, the TRMC signal in the bilayer originates mainly from the carrier residing in the perovskite layer. From the reduction, we come to balanced electron and hole mobilities for CsMAFA of 16 and 12 cm^2/Vs , respectively independent of the investigated configuration. Moreover, the charge carrier lifetime was elongated in comparison with the bare CsMAFA layer, indicating that both electron- and hole-transfer are efficient and that interfacial recombination occurs on a longer timescale than the decay in the single layer. In summary this work provides information on the relationship between structure and optoelectronic properties, which is important to rationally design and optimize devices including solar cells.

8:00 PM EN05.10.24

Thick and Efficient Perovskite Solar Cells Enabled by Fast Co-Evaporation Manuel Piot, Javier Sebastien, Nathan Rodkey, Kassio P. Zaroni, Michele Sessolo and Henk J. Bolink; Institut de Ciència Molecular (ICMol), Spain

Conformal deposition of perovskite on textured silicon for perovskite/silicon tandem solar cells remains challenging using the widely-used solution spin-coating route. In contrast, perovskite thermal evaporation allows highly-controlled thin film deposition, ensuring conformality on large areas, regardless on the surface texture. To take advantage of the full photocurrent generating capabilities of the perovskite front cell, rather thick films are required. Currently, most perovskites are sublimed in a single approach by co-sublimation of the precursors. This deposition technique is usually done under high vacuum and the deposition rates of each precursor are monitored using quartz crystal microbalances (QCMs). However, due to the slow deposition rates ($< 1 \text{ \AA/s}$) it is challenging to deposit sufficiently thick perovskite films that are required for highly efficient perovskite/silicon tandem devices. Herein, we explore the co-evaporation of $\text{CH}_3\text{NH}_3\text{PbI}_3$ (MAPI) perovskite using faster deposition rates ($> 2 \text{ \AA/s}$), by simultaneously subliming $\text{CH}_3\text{NH}_3\text{I}$ and PbI_2 . These rates are deduced by scaling up linearly the initial speed by a factor of up to 8 times, leading to quick and reproducible evaporation processes. Moving to faster deposition speeds, a change in crystallite orientation is observed by XRD and GIWAXS, showing a preferential growth along the (202) family of planes, as opposed to the (110) orientation. Thanks to these faster deposition speeds, 1 μm -thick MAPI films can be deposited in a short amount of time. This allows a noticeable J_{sc} gain in planar glass based single junction solar cells ($\sim 0.8 \text{ mA}$), due to an enhanced absorption of the infrared light, as revealed by EQE. On the other hand, the FF drops to lower values, possibly due to a diffusion length problem.

8:00 PM EN05.10.25

Potential of Close-Space Sublimation for Scalability of Perovskite Solar Cells Nathan Rodkey, Inma Gomar Fernández, Federico Ventosinos, Cristina Roldan-Carmona and Henk J. Bolink; Universitat de València, Spain

Vacuum techniques for perovskite photovoltaics (PV) are promising in their potential for scalability but are rarely studied with techniques that are readily adaptable for industry. Co-sublimation is one such technique, whose potential as a dry, additive technique for highly uniform and large-area depositions makes it attractive as an industrial candidate for perovskites. However, low-deposition rates, and its dependence on high-vacuum and in-situ rate monitoring make integration on large scales difficult to imagine. Furthermore, the organic sources used (e.g. FAI and MAI) tend to be unstable, decomposing over time. This is severe enough that the organic sources are not reused, instead discarded after each evaporation. In this work, we study the use of close-space sublimation (CSS) for making perovskite solar cells, a technique that has already seen wide-spread use in industry, including in PV and benefits from high material-transfer and low working pressures. We show that organic sources of FAI used in these systems can be cycled multiple times (> 30 depositions) and estimate they can be continuously sublimated for months before needing replacement. We show the conversion of inorganic perovskite precursor layers in a 2-step process using CSS for the organic, FAI source. We show that a rough vacuum process (10 mbar) can be used for the sequential conversion of evaporated $\text{PbI}_2/\text{PbCl}_2/\text{CsI}$ thin-films. The $\text{FA}_{0.9}\text{Cs}_{0.1}\text{PbI}_3/\text{Cl}$ perovskites converted in this work have a bandgap at 810 nm (1.53 eV), with large grains ($> 400 \text{ nm}$). Devices were then thermally stressed at 85°C and exhibited a stable photoconversion efficiency (PCE) for > 650 hours. This thermal stressing was found to be necessary for high-performing devices, who experienced an increase in average PCE from 12.2 – 17.5% after 1 week annealing. We report a champion cell of 18.7% PCE. To explain this drastic increase in PCE, we collect the JV characteristics of the devices at varying light intensities (dark, 0.1, 0.5, and 1 sun) and use drift-diffusion simulations to explain the transformation. These drift-diffusion simulations are powered by SIMSALIBIM, and by fitting multiple JV curves at different light intensities, we are able to ensure a unique fit of the data. In this way, a reduction in trap density of 5 orders of magnitude was observed after 1 week of thermal stressing.

8:00 PM EN05.10.26

Double Punch for Suppressing Phase Segregation: Interface Engineering with Synergistic Passivation and Efficient Hole Extraction Zhaojie Zhang¹, Julia Martin², Ronald L. Grimm² and Dhandapani Venkataraman¹; ¹University of Massachusetts--Amherst, United States; ²Worcester Polytechnic Institute, United States

In p-i-n perovskite solar cells (PSCs), the buried hole transport layer (HTL)/perovskite interface plays a vital role in dictating the performance and stability of the full photovoltaic device. However, the impact of HTLs on vertical phase segregation remains unknown. This work systematically explores the impact of electronic and chemical properties of HTLs on vertical halide segregation of mixed-halide perovskite materials. Here, we demonstrate that $\text{PTAA}/\text{Cu}_x\text{Br}_{1-x}$ bilayer HTL significantly suppresses light-induced vertical phase segregation of $\text{MAPb}(\text{I}_{0.7}\text{Br}_{0.3})_3$. We used grazing-incidence X-ray diffraction (GI-XRD) to capture the depth-resolved composition change of $\text{MAPb}(\text{I}_{0.7}\text{Br}_{0.3})_3$ at the interface and bulk with different HTLs under illumination. Electronic properties including hole density, hole mobility, and energy levels of $\text{Cu}_x\text{Br}_{1-x}$ were systematically characterized to reveal the impact of HTL on phase segregation. By manipulating the illumination and electronic properties of HTL, we illustrate the interplay between illumination direction, interfacial defects, charge carrier extraction, and vertical phase segregation. Our findings demonstrate that the $\text{PTAA}/\text{Cu}_x\text{Br}_{1-x}$ bilayer, with its synergistic passivation and efficient hole extraction ability, stabilizes the interface and bulk of the mixed halide perovskite layer, preventing phase segregation and possible amorphization. This work highlights that synergistic passivation and efficient hole extraction pack a more powerful punch for suppressing the vertical phase segregation in mixed-halide perovskite.

8:00 PM EN05.10.27

Interstitial Defect Thermodynamics Drive Phase Separation in Lead Halide Perovskites Ross Kerner¹, John L. Lyons², Kai Zhu¹ and Joseph J. Berry^{1,3,3}; ¹National Renewable Energy Laboratory, United States; ²U.S. Naval Research Laboratory, United States; ³University of Colorado Boulder, United States

Lead halide perovskites show unrivaled performance and versatility in optoelectronic devices; however, the issues of photo- and electrochemical stability and halide phase segregation remain a challenge to take full advantage of halide perovskites. Here, we describe our proposed model to explain how homogeneously mixed iodide (I):bromide (Br) perovskite alloys (e.g. $\text{MAPbBr}_{1-x}\text{I}_x$) phase separate into I-rich and Br-rich regions under bias or illumination. The model predicts iodine +1 interstitials play a critical, intrinsic role giving rise to unequal fluxes of halide species – the origin of voltage- or photo-induced compositional instabilities. We briefly review our recent experimental results testing the model and discuss in detail our recent density functional theory (DFT) computations comparing the relative formation enthalpies of I_i^+ versus Br_i^+ interstitial defects in different halide compositions. We find that I_i^+ defects are energetically favorable by 0.1-0.4 eV over Br_i^+ under most conditions, and also show that I_i^+ is further stabilized when surrounded by iodide first- and second-nearest neighbors. In other words, I_i^+ will be most stable and favorably migrate towards iodide-rich regions making them more iodide-rich. Thus, we confirm our model's core assumption and elucidate a major fundamental, thermodynamic driving force for halide phase separation following oxidation and creation of I_i^+ defects. Overall, this body of work brings a level of clarity to interstitial defect chemistry and physics in halide perovskites, advancing our understanding a step closer to that of more conventional semiconductors.

8:00 PM EN05.10.28

Molecular Locking with All Organic Surface Modifiers Enables Stable and Efficient Slot-Die Coated Methyl Ammonium Free Perovskite Solar Modules Prem J. Rana^{1,2},

The power conversion efficiency (PCE) of the state of the art large area slot die coated perovskite solar cells (PSCs) is now over 19%, but issues with their stability persist owing to significant intrinsic point defects and a mass of surface imperfections introduced during fabrication process. We report the utilization of a hydrophobic all organic salt to modify the top surface of large area slot die coated methylammonium (MA) free halide perovskite layers. Bearing two molecules each of which is endowed with anchoring groups capable of exhibiting secondary interactions with the perovskite surfaces the organic salt acts as a molecular lock by effectively binding to both anion and cation vacancies, substantially enhancing the materials intrinsic stability against different stimuli. It not only reduces the ingress of external species such as oxygen and moisture but also suppresses the egress of volatile organic components during the thermal stability testing.

The treated PSCs demonstrate efficiency of 19.28% (active area of 58.5 cm²) and 17.62% (aperture area of 64 cm²) for the corresponding mini-module. More importantly, unencapsulated slot-die coated mini-modules incorporating the all-organic surface modifier show ~80% efficiency retention after 7500 hours (313 days) of storage under 30% relative humidity (RH). They also remarkably retain more than 90% of the initial efficiency for over 850 hours while being measured continuously.

8:00 PM EN05.10.29

Enhancing Interfacial Properties via Ionic Exchange for the Highly Efficient Sn-Pb Mixed Perovskite Based Solar Cells SangheonLee, ChangyongKim, HyeminLee, Seok BeomKang, Joo woongYoon, Sang WonLee and Dong HoeKim; Korea University, Korea (the Republic of)

Sn-Pb mixed perovskite is considered as an ideal light absorber not only for single-junction solar cells, but also for bottom cells of multi-junction solar cells due to its narrow-band gap feature. The p-orbital hybridization of Sn²⁺ and Pb²⁺ causes an upward shift of the valence band maximum (VBM) and conduction band minimum (CBM) in addition to the bandgap reduction. This results in the highest occupied molecular orbital level of poly[3,4-ethylenedioxythiophene]:poly[styrene sulfonate] (PEDOT:PSS) having an ideal band alignment with the VBM of Sn-Pb mixed perovskite. Therefore, the PEDOT:PSS is the most widely used hole transport layer (HTL) in p-i-n structured Sn-Pb mixed perovskite solar cells (PSCs).

However, PEDOT:PSS showed several critical drawbacks that affected the device performance such as their acidic condition, inferior molecular structure, and nonideal absorption property. Among them, the inappropriate molecular structure composed of hydrophilic PEDOT molecule and hydrophobic PSS molecule does not form a uniform and ideal micro structured surface when it has been coated. Therefore, it has been induced undesirable interface like voids between PEDOT:PSS and perovskite. Various studies have been conducted to obtain better interfacial properties with respect to the perovskite precursor, like adding additives. However, the origin of the undesirable interface was due to the structural limit of the PEDOT:PSS molecule. Therefore, fundamental research is needed to address these issues from the perspective of the PEDOT:PSS surface.

This study introduces an effective ionic exchange for PEDOT:PSS surface modification to drastically enhance the interfacial properties between PEDOT:PSS and perovskite. The surface modified PEDOT:PSS by ionic exchange brought the conformal interfacial contact and enhanced charge extraction confirmed via time-resolved photoluminescence (TRPL) analysis. As a result, we achieved more than 20% efficiency of p-i-n structured Sn-Pb mixed PSCs. The mechanism of ionic exchange also had been elucidated through various surface analysis and density functional theory (DFT) calculations. In addition, we confirmed that this ionic exchange was also effective for tandem devices. In conclusion, we fabricated all-perovskite tandem solar cells with an approaching 24% efficiency through this ionic exchange

8:00 PM EN05.10.30

Efficient Perovskite Solar Cells with Improved Carrier Transport via Composition-Graded Titanium Oxynitride Electron Transport Layer YonghoonJung; Seoul National University, Korea (the Republic of)

State-of-the-art perovskite solar cells (PSCs) have achieved power conversion efficiencies (PCEs) exceeding 25% by enhancing the charge transport layers to facilitate efficient carrier transport while minimizing non-radiative recombination. The effective transport of charge carriers through the perovskite and the charge transport layers can improve the fill factor and open-circuit voltage. An ideal electron transport layer (ETL) should possess complete and conformal coverage, as well as optimal band alignment that facilitates efficient extraction of electrons. Additionally, the minimal defect density in charge transport layers is essential to prevent detrimental interface recombination. While TiO₂ has been widely used as an ETL, it exhibits limitations as an ideal ETL due to an energy level mismatch and relatively poor electrical characteristics. Specifically, the conduction band minimum (CBM) of TiO₂ is slightly higher than that of MAPbI₃, leading to a significant energy barrier for electron extraction. Additionally, the relatively low conductivity and mobility of TiO₂ hinder efficient charge transfer. To address the limitations of TiO₂, metal doping such as Nb, Al, and Li has been employed to modify its electronic band structures and improve its electrical properties.

In this study, nitrogen is incorporated into TiO₂ using the pulsed laser deposition (PLD) method to form titanium oxynitride (TiO_xN_y), resulting in enhanced electron transport characteristics including minimal defect density. Controlled substrate temperature and oxygen partial pressure during the deposition facilitated the achievement of optimal thin-film characteristics, including high transparency typical of TiO₂ semiconductors and high conductivity typical of nitrogen-rich TiN. Furthermore, TiO_xN_y thin films with graded atomic ratio nitrogen to oxygen (N/O) are achieved by sequentially changing the oxygen partial pressure during the process. The graded TiO_xN_y thin film exhibits characteristics that enable the achievement of superior functionality as an ETL compared to TiO_xN_y thin films without grading. By increasing the oxygen partial pressure during the deposition process, the CBM was raised, leading to a reduced energy offset with the mesoporous TiO_x layer directly above it. Furthermore, TiO_xN_y fabricated in a multilayer structure can provide a continuous variation of energy levels within the ETL, optimizing the electron pathway and improving charge transport, ultimately enhancing charge extraction capabilities. This alignment facilitates the selective transfer of electrons to the respective electrodes while inhibiting hole transport. The accurate composition control of TiO_xN_y films is characterized using such as atomic force microscopy, X-ray photoelectron spectroscopy, ultraviolet photoelectron spectroscopy, and Hall measurement to uncover the mechanism behind the enhanced properties. The conformally deposited films with high crystallinity and tailored optoelectrical properties exhibit effective suppression of interfacial recombination as an ETL, resulting in solar cell devices and resulting in high PCEs.

8:00 PM EN05.10.31

Tunable Anode Work-Function by Self-Assembled Monolayers for High-Performance Pure Blue Light-Emitting Diodes Low Driving Voltage Hyo JaeLee, Jung JaeDo and Jae WoongJung; Kyung Hee University, Korea (the Republic of)

Organometallic trihalide perovskites have garnered significant attention for their potential in light-emitting diode applications, thanks to their unique characteristics including excellent color purity, color tunability, and ease of solution processing through scalable printing technology. Presently, perovskite emitters have achieved comparable electroluminescence and quantum efficiency to organic and quantum-dot display technologies in green and red-emitting perovskite light-emitting diodes (PeLEDs). However, blue-emitting PeLEDs still face challenges in terms of electroluminescence, operational stability, and efficiency, primarily due to the relatively wide bandgap of the perovskite emitters ($E_g > 2.5$ eV), which thus requires high driving bias for device operation. In this study, we propose a straightforward interfacial engineering approach to reduce the driving voltage of pure-blue PeLEDs by employing self-assembled monolayer (SAM) molecules on the indium tin oxide (ITO) electrode. The SAM layer facilitates the control of the electronic structure of the ITO surface by modulating its work function, thereby improving hole extraction properties at the lower internal interface. Furthermore, the functionalized SAM molecules interact with the under-coordinated perovskite lattices, providing interfacial interaction with the perovskite layers and facilitating radiative carrier recombination at lower driving bias. These desirable characteristics of SAM molecules enable enhancements in the electroluminescence and quantum efficiency of pure blue emission while requiring lower driving voltage. Moreover, the superior properties of the perovskite film, coupled with the reduced driving voltage, contribute to an extended operational stability of blue electroluminescence in PeLEDs. Consequently, this strategy demonstrates the remarkable potential of achieving high-performance PeLEDs with blue light emission, which is highly attractive for full-color perovskite display technologies.

8:00 PM EN05.10.32

Bandgap Optimization by Cu Doping of Ag-In Halide Double Perovskites for Photovoltaic Applications ShunnosukeIkegaya, KojiYokoyama, ShunYokoyama and HideyukiTakahashi; Tohoku University, Japan

Lead iodide perovskites (APbI₃, where A represents organic cations) have been used as photoactive layers in perovskite photovoltaics due to their excellent optical and electronic properties. However, the toxicity of Pb and the ambient instability caused by the degradation of organic cations and iodide anions have hindered their widespread use. Metal halide double perovskites (A₂B^IB^{III}X₆, where B^I, B^{III}, and X represent monovalent and trivalent metal cations, and halide anions, respectively) have been theoretically proposed as Pb-free halide perovskites. Theoretical calculations predict that Rb₂CuInCl₆ double perovskites have a direct and optimal bandgap of 1.36 eV, whereas they cannot be synthesized directly due to their low thermodynamic stability. Instead, we focused on Cs₂AgInCl₆ double perovskites, which can be synthesized directly and exhibit superior ambient stability; however, they have a large bandgap (>3.0 eV), making them unsuitable for photoactive layers. Recent studies have reported that Cu²⁺ doping reduces the bandgap of Cs₂AgInCl₆ from 3.0 to 2.2 eV. Furthermore, it was demonstrated that Cu⁺-Cu²⁺-In³⁺-based layered perovskites exhibited better optical properties than perovskites composed of Cu⁺ or Cu²⁺ alone. In this study, we present the synthesis of Ag-In double perovskites with an optimal bandgap as photoactive layers through Cu⁺²⁺ doping.

All of the following processes were performed at 75°C in ambient air. Ag-In precursor aqueous solutions (denoted as S1) were prepared by dissolving AgCl and InCl₃·4H₂O in concentrated HCl. Precursor aqueous solutions containing only Cu²⁺ (denoted as S2) were prepared by dissolving CuCl₂·2H₂O in concentrated HCl. Precursor aqueous solutions containing only Cu⁺ (denoted as S3) were prepared by dissolving CuCl with reductants in concentrated HCl. Precursor aqueous solutions containing Cu⁺ and Cu²⁺ simultaneously (denoted as S4) were prepared by dissolving CuCl and/or CuCl₂·2H₂O with reductants in concentrated HCl. Ultraviolet-visible (UV-Vis) absorption spectra of the S2-S4 solutions were measured to evaluate the

valence states and complex structures of Cu species in these solutions. The solid samples precipitated by adding CsCl into the S1 solutions, the S1/S2 mixtures, the S1/S3 mixtures, or the S1/S4 mixtures were collected and washed. The composition, structure, and bandgap of the resulting samples were evaluated by inductively coupled plasma-mass spectrometry (ICP-MS), X-ray diffraction (XRD), and optical absorption measurements.

The S2, S3, and S4 solutions turned yellow, colorless, and dark, respectively. The UV-Vis spectra of these solutions indicated that the S2 and S3 contained only $[\text{Cu}^{\text{II}}\text{Cl}_4]^{2-}$ and $[\text{Cu}^{\text{I}}\text{Cl}_4]^{3-}$ complexes, respectively, whereas the S4 contained mixed-valence Cu^{+2+} species. The resulting samples from the S1 solutions were completely white in color. XRD analysis confirmed the presence of the $\text{Cs}_2\text{AgInCl}_6$ phase in these samples. In contrast, the resulting samples from the S1/S2 and the S1/S3 mixtures were yellow and pale yellow, respectively. These samples had a smaller bandgap compared to $\text{Cs}_2\text{AgInCl}_6$. Trace amounts of Cu were detected via ICP-MS, indicating that Cu doping of the $\text{Cs}_2\text{AgInCl}_6$ can reduce the bandgap. Interestingly, the resulting samples from the S1/S4 mixtures exhibited darker colors than the samples doped with Cu^+ or Cu^{2+} alone, suggesting that simultaneous Cu^{+2+} co-doping leads to emergent optical properties in these samples.

8:00 PM EN05.10.33

Electrical Field-Assisted Direct Ink Deposition of Methylammonium Lead Iodide Layer for Fabricating Large-Scale Inverted Perovskite Solar Cell BanashreeGogoi, CarsonGockley, SushmithaVenu, YizhenZhu, RaveenaPhadnis, XiangjiaLi, WilliamT. Petuskey and TerryL. Alford; Arizona State University, United States

A high-performing perovskite solar cell (PSC) requires an outstanding perovskite layer in excellent contact with high-performing charge transfer layers. Commercial development of simple and scalable deposition techniques will need to focus on processes that yield smooth films of uniform composition, microstructure and composition. Ideally, it is desired that the same technique be used sequentially for all of the layers. Several techniques aspire to this goal including one-step chemical solution processes using spin coating and ceramic processing approaches such as doctor-blading, slot-die coating, inkjet printing, and spray coating. As an alternative, we report on the electric field-assisted direct ink deposition (EF-DID) fabrication process for rapid printing of large-area perovskite nanofilms.

Our prior work successfully demonstrated the utility of EF-DID in fabricating PEDOT:PSS hole transport layers. Now we demonstrate its application for depositing perovskite films. Essentially, this technique forms a stable electrospray condition that yields a uniform, large grain-sized perovskite film deposits. Concurrent heat treatment thermally converts the perovskite precursor solution in orthorhombic methylammonium lead iodide ($\text{CH}_3\text{NH}_3\text{PbI}_3$). Post-deposition, solvent vapor annealing (SVA) refines the films to improve their surface smoothness and to greatly reduce pinhole defects. With very little experimental effort, a ten-fold improvement in the power conversion efficiency (from 1 to 10%) was achieved, suggesting that even greater efficiency can be anticipated in the future.

8:00 PM EN05.10.34

Microstructure Refinement of Open-Air, EF-DID Fabricated Films of MAPbI_3 Perovskites by Solvent Vapor Annealing (SVA) and Selected Enabling Surfactants BanashreeGogoi, CarsonGockley, SushmithaVenu, YizhenZhu, RaveenaPhadnis, XiangjiaLi, TerryL. Alford and WilliamT. Petuskey; Arizona State University, United States

The constant drive towards the large-scale application of perovskite solar cells has increased the demand for innovating new techniques for fabricating high quality thin films of the perovskite and adjacent charge transport layers that possess a high degree of uniformity in microstructure, composition and reduced defect density. There are many different approaches that produce that produce basic films but are deficient in their surface coverage, surface morphology and film microstructure. There is a great need for the development of post-deposition treatments that markedly improve the uniformity of film thickness, grain distribution and grain-size distribution, and that also greatly reduce surface roughness, cracks and pin-holes. In this project, we report on the refinements achievable using solvent chemical vapor annealing in combination with selected enabling surfactants. We report on the refinements made on films produced by an open-air fabrication technique termed electrical field-assisted direct ink deposition (EF-DID).

For post deposition refinement, we adapted the technique reported by Zhou, et al. who use methylamine gas (MA) as the chemical annealing agent. We compare the microstructural characteristics of MAPbI_3 films before and after chemical annealing and with and without the addition of a surfactant. For the latter, we used polyoxyethylene (20) sorbitan monolaurate (TWEEN-20) as an example of what can be achieved. Compared to the non-vapor annealed films, the MA-treated films and Tween-20 showed an enhanced grain distribution and density. Property measurements of inverted photovoltaic devices using MA-treated perovskites showed a ten-fold increase in the power conversion efficiency compared to the non-MA treated devices.

8:00 PM EN05.10.35

Enhancing the Performance of the MAPbI_3 Perovskite Solar Cells Synthesized in an Ambient Environment via Modification of the SnO_2 Electron Transport Layer BipravDahal; Florida International University, United States

The tin oxide (SnO_2) electron transport layer (ETL) plays a vital role in the photo-conversion efficiency (PCE) and stability of organic-inorganic perovskite solar cells (PSCs). However, SnO_2 ETL-induced defects such as hydroxyl groups, oxygen vacancies, exposed Sn atoms, and dangling bonds hinder device performance. In this study, rubidium chloride (RbCl) has been used to modify the SnO_2 ETL. MAPbI_3 perovskite film formed on the RbCl-modified SnO_2 ETL exhibits improved crystallinity with enlarged grain size and reduced grain boundaries, and enhanced optical absorption. The Hall-effect measurements indicate the improved carrier mobility and the dark J-V curve shows the increment of electrical conductivity for the RbCl-modified SnO_2 ETL. X-ray photoelectron spectroscopy (XPS) results demonstrate the surface defects passivation of the perovskite layer by modifying the SnO_2 ETL. A champion PCE of 19.35% has been achieved for the RbCl-modified SnO_2 ETL-based devices with improved stability, while the control devices with unmodified SnO_2 ETL show a PCE of 17.18%.

SESSION EN05.11: Poster Session V: Structure Property Relationships in Halide Perovskites

Session Chair: Xiaotong Li

Wednesday Afternoon, November 29, 2023

Hynes, Level 1, Hall A

8:00 PM EN05.11.02

Effects of Light and Electricity on Mechanical Properties of Metal Halide Perovskite Single Crystals MeaghanDoyle, MadhujaLayek, AnushRanka, ZhenghongDai and NitinP. Padture; Brown University, United States

Metal halide perovskites (MHPs) have emerged as promising light absorber materials for their use in perovskite solar cells (PSCs). Although significant progress has been made in enhancing the efficiency and operational stability of PSCs, their mechanical reliability needs to be improved if they are to operate efficiently for many years. However, the mechanical properties of MHPs have not been fully explored. This is especially important because MHPs possess poor mechanical properties — they are compliant, soft, and brittle. To that end, we have used nanoindentation and micro-indentation to study the plastic deformation, elastic deformation, and fracture properties of MHP single crystals of various compositions. We also investigated the effects of creep as well as light and electricity on the mechanical properties of MHP single crystals. These parameters impact the mechanical properties of other similar semiconductors, and in MHPs such effects could translate to important implications for PSCs. Through this we aim to provide a more comprehensive understanding of mechanical properties of MHPs, which are relevant for understanding and enhancing the mechanical reliability of PSCs.

8:00 PM EN05.11.03

Crystal Growth Regulation via Co-Spacer Cations Mixed with Methylammonium in Lead Iodide in Perovskite Photovoltaics Mi HeeJung; Sejong University, Korea (the Republic of)

In this work, we used co-spacer cations to control the phase distribution by mixture of benzylammonium (BZA) and guanidium (GA). We observed that the crystal structure was different when two dimensional (2D) perovskite was prepared only with BZA and when 2D perovskite was prepared by combination of BZA and GA. The perovskite film prepared from these mixed cations demonstrated increased grain size and enhanced crystallinity from BZA based perovskite to GA based perovskite. Thus, perovskite solar cells from these mixed cation perovskite exhibits the power conversion efficiency (PCE) of 14.95% ~ 16.23 % and GA based device shows PCE up to 18.31%. Our studies reveal the size and the nature of the organic spacer cation is related to the overall stability of the corresponding lead iodide and suggest that the phase distribution of the 2D perovskite is finely controlled by the mixture of two different large organic cations.

8:00 PM EN05.11.04

Design and Characterization of Low-Dimensional Perovskites with Multiple-Ring Aromatic Cations AndreiMitrofanov^{1,2}, YonderBerencén³, ElahehSadrollahi², KhrystynaRymsha¹, RegineBoldt¹, DavidBodeshiem², HendrikWeiske⁴, FabianPaulus², QuinnBesford¹, AgnieszkaKuc³ and BrigitteVoit^{1,2}; ¹Leibniz Institute of Polymer Research, Germany; ²Technische Universität Dresden, Germany; ³Helmholtz-Zentrum Dresden-Rossendorf, Germany; ⁴Universität Leipzig, Germany

Metal halide perovskites have become promising next-generation semiconducting materials for many applications due to their prominent optoelectronic properties and ease of manufacturing. These materials are widely tailorable in composition, which allows the incorporation of various organic cations. Tuning the structure of the organic molecules can cause remarkable changes in the structural arrangement of halide perovskites resulting in the formation of two-dimensional (2D) layers, one-dimensional (1D) chains, or isolated zero-dimensional (0D) clusters and, as a consequence, the modification of the optoelectronic properties of the perovskite system.

In recent works devoted to the low-dimensional metal halide perovskites, significant attention has been paid to the molecular engineering of the functionalized cations. This allows the design of a variety of new organic-inorganic hybrid materials, in which semiconducting organic and inorganic layers are assembled at the molecular scale. High structural distortion of the resulted low-dimensional perovskite structures induces electron-phonon coupling and enhances the self-trapped excitons (STEs) processes, resulting in an enhanced broadband emission [1,2]. In addition, it has been demonstrated that perovskites grown in a form of atomically thin sheets possess unique features compared to their bulk counterparts [3]. For example, hybrid perovskite sheets exhibit an unusual structural relaxation, which leads to a band gap shift. Consequently, the controllable synthesis of ultrathin perovskite sheets has gained a great research interest for implementation in high-performance optoelectronic devices.

In this work, we fabricated several low-dimensional hybrid organic-inorganic metal halides, based on multiple-ring aromatic ammonium cations and lead iodide with a strong focus on structural and optoelectronic investigation. Examination of the influence of organic cations on the structural properties reveals that the number and position of amino groups at the aromatic ring affect the dimensionality of the perovskite, resulting in 2D and 1D corner- and face-sharing structures with different optical behaviors. Highly distorted 1D perovskites show broadband emissions originating from STEs. Theoretical results reveal, that the organic cations in the 1D compounds strongly contribute to the band structure resulting in strong orbitals hybridization. Using a facile and fast template-assisted crystallization method we have synthesized metal halide perovskite few-layer free-standing nanosheets with micron size containing the naphthalene diammonium-based linker. Varying the synthetic conditions, we can modulate the thickness and lateral sizes of the nanosheets, making them promising candidates for optoelectronic applications.

[1] A. Mitrofanov et al. *J. Mater. Chem. C*, **2023**,11, 5024-5031

[2] Z. Qi et al. *Inorg. Chem.* **2021**, 60(20), 15136-15140

[3] L. Dou et al. *Science* **2015**, 349, 6255

8:00 PM EN05.11.05

Maximizing Photoluminescence Quantum Efficiency of Stacked Halide Layer for Highly Efficient Perovskite Solar CellsMin JuJeong and Jun HongNoh; Koera University, Korea (the Republic of)

To further approach the theoretical limit of perovskite solar cells (PSCs), it is crucial to analyze and interpret the external photoluminescence quantum efficiency (PLQE) of a light-absorbing halide layer stacked with charge transporting layers (CTLs) rather than solely as a halide layer. Here, we propose the next phase research direction for reaching radiative limit of PCE by maximizing PLQE of the stacked halide layer. We demonstrated that controlling the bottom charge transporting layer (CTL)/perovskite interface is a main factor to maximize PLQE in full device stack. On combining interface and bulk engineering, the FTO/bottom CTL/halide structure and full device stack exhibited an enhanced external photoluminescence quantum efficiency (PLQE) of 40.67% and 15.57%, respectively. As a result, the device combined with the interface and bulk engineering showed a certified quasi-steady-state (QSS) efficiency of 25.06%. The certified open-circuit voltage (Voc) of 1.18 V is 94.93% of the radiative limit Voc of 1.243 V, the highest value among certified QSS Voc of PSCs. This research approach provides a promising direction for reaching the theoretical limit of PSCs by maximizing PLQE.

8:00 PM EN05.11.06

Origin of Excitonic Absorption in Multi-Grain CsPbBr₃ Perovskite Nanocrystals for Photodiode ApplicationsAtifSuhail¹ and MonojitBag²; ¹IIT Rorkee, India; ²Indian institute of Technology Roorkee, India

Inorganic halide perovskite nanocrystals exhibit some extraordinary properties compared to their parent materials due to the finite size effect. However, the exciton dynamics in these nanocrystals are not well understood due to the wide variation of structural properties. In this study, we have synthesized single-grain and multi-grain nanocrystals of CsPbBr₃ and analyzed the excitonic absorption and photoluminescence by correlating them with their structural properties. There exist two types of excitonic absorption; low energy localized excitons having binding energy from 64 to 156 meV and near band-edge excitons having binding energy from 18 to 23 meV. Small-size single-grain nanocrystals have a relatively higher bandgap of 2.576 eV due to increased micro-strain compared to multi-facet polyhedral with multi-grain nanocrystals. The broadening of the near band-edge excitonic absorption peak is possibly due to the presence of different sizes, shapes, and nature of the grain boundaries which also modulate the photoluminescence decay lifetime. The overall steady-state photoluminescence is higher in single-grain nanocrystals compared to multi-grain nanocrystals due to the localization of excitons. Therefore, these single-grain nanocrystals can be used for efficient light emission in perovskite photodiodes while multi-grain nanocrystals could be better suited for photodetector application.

Keywords: Halide perovskites; Nanocrystals; Excitonic absorption; Grain boundaries; Photoluminescence lifetime.

8:00 PM EN05.11.07

Effect of Hole Transport Layer on Energy Loss of Perovskite Solar CellHeunjeongLee, TranH. Nhan, DongchanLee and ShinukCho; University of Ulsan, Korea (the Republic of)

The performance of perovskite solar cells (PVSCs) is most affected by the crystallinity of perovskite. Among several conditions, the interfacial properties between the charge transfer layer and the perovskite active layer, where the perovskite crystalline structure begins, are also one of the factors that have a great influence. Thus, various studies have been performed the ways to modify HTL to improve the device performance in the p-i-n structure. As the crystallinity including grain size of perovskite layers is influenced by the HTLs, the various charge dynamics will be also changed. Until now, however, there is little research related to energy loss analysis about the perovskite layer depending on HTLs. In this study, the difference in V_{oc} between PEDOT:PSS and NiO_x was explained through energy loss analysis. Despite the energy levels of PEDOT:PSS and NiO_x are similar to -5.0 eV and -5.1 eV, respectively, significant V_{oc} difference is observed between PEDOT:PSS based PVSCs (0.933 V) and NiO_x based PVSCs (1.088 V). Our energy loss analysis clearly indicated that this V_{oc} difference originated by non-radiative recombination. It is known that the non-radiative recombination in PVSCs is generally occurred by traps in the perovskite film, which is generated by grain boundary and defects of perovskite film. The perovskite film on NiO_x showed a larger grain size and improved crystallinity compared to the perovskite film on PEDOT:PSS. Therefore, we concluded that the increased V_{oc} in PVSCs using NiO_x HTL was due to the decrease in non-radiative recombination induced by the improved morphology.

8:00 PM EN05.11.08

Effects of Precursor Purity and Post-Synthesis Treatments on Mechanochemical Mn²⁺ and Rb⁺ Co-Doped CsPbCl₃ Perovskite PowderIvyK. Jones¹, UweHommerich¹, KeseteGhebreyessus¹, VadivelJagasivamani¹, DemetrisGeddis¹, KabirAl Amin¹, S. B.Trivedi², Amanda LTiano³ and SethFraden³; ¹Hampton University, United States; ²Brimbor Corporation of America, United States; ³Brandeis University, United States

Inorganic halide perovskites (HPs) exhibit optimum optoelectronic material characteristics such as wider band gaps, enhanced atmospheric stability, and improved photoluminescence quantum yield, as well as demonstrated balanced and higher carrier mobility in comparison to hybrid organic-inorganic HPs. The synthesis of perovskite material often involves the utilization of toxic and large quantities of hazardous complex solution-based techniques which are not eco-friendly. Alternately, crystal growth methods require highly purified precursors that have negative ecological impacts on the environment, leading to increased pollutants within the atmosphere, and accompanied by high-energy consumption deemed an unsustainable practice. Mechano-chemical synthesis is considered a green chemistry method that significantly can reduce the use of complex and time-consuming reactions, energetic-enabled conditions, expensive precursor sources, hazardous reagents, catalysts, additives, surfactants, and overall waste. In this study we report fluorometric characterization results of mechano-chemical synthesis of manganese (Mn²⁺) doped CsPbCl₃ halide perovskite powder surface-purification treatment and ligand-mediated techniques using ultrasound sonification to assist in the dissolution of unreacted precursors and accelerate the ionization of ligand-affinity kinetics, respectively. The grinding process is considered a non-homogeneous synthesis approach which may result in residual unconsumed precursor present in the sample leading to surface defects during post-synthetic treatments. Dry and wet high-energy ball-milling experiments used low purity (2N) precursors: CsCl and PbCl₂ and the (non-anhydrous) hydrated MnCl₂ dopant source. Synthesized HPs were characterized by X-ray diffraction, optical microscopy, scanning electron microscopy, transmission electron microscopy, and steady-state & time-resolved spectroscopic studies. The dopant-dependent HPs powders and supernatant (powder and oleylamine diluted in hexane) exhibited a broad band Mn²⁺ emission band at room temperature with average peak wavelengths of 620 nm and ~ 606 nm, respectively. The oleylamine purity: > 50.0% vs. 70% will also be evaluated for effects on the fluorometric properties of the ligand-mediated doped perovskite. Room-temperature (RT) lifetime transients of the dopant-dependent HPs powder ranged from 0.49 – 0.74 ms and supernatant were 1.36 – 1.72 ms, comparable to previously reported RT lifetimes for Mn²⁺ doped CsPbCl₃ nanoparticles and bulk crystals at 1.10 ms and 0.70 ms, respectively. Comparative studies of the fluorescent properties of Mn²⁺ doped CsPbCl₃ prepared by microwave-assisted, and melt-synthesis will also be presented.

8:00 PM EN05.11.09

Organic-Inorganic Gas Sensor Based on a Perovskite Nanocrystal-Conductive Polymer HybridDuhoJang, MingHong and Yeong DonPark; Incheon National University, Korea (the Republic of)

We present a novel approach for fabricating organic-inorganic hybrid gas sensors by blending perovskite nanocrystals with a conductive polymer matrix. Organic semiconductors (OSCs) hold considerable potential as sensing materials for printed organic gas sensors. However, they face challenges in terms of limited sensitivity and poor stability under ambient conditions, which hinder their development compared to inorganic-based gas sensors. To overcome these limitations, we have incorporated functional nanomaterials into the organic semiconductors. In this study, we introduce a perovskite-structured material, specifically CsPbBr₃, into the conductive polymer matrix, resulting in a significant enhancement of the gas-sensing performance of the sensors while retaining their high responsivity and response rates. Moreover, we have employed a zwitterionic polymer surface modification with a hydration treatment to further improve the adsorption of target gas molecules on the perovskite surface. Our results demonstrate that the amide group of the encapsulation polymer exhibits a strong affinity towards NO₂ gas molecules, and this affinity is enhanced upon hydration of the polymer. Additionally, the presence of perovskite materials within the semiconducting polymer layer acts as a protective barrier, effectively shielding the polymer thin film against oxidation during extended storage under ambient conditions, owing to the perovskite crystals' ability to adsorb oxidizing molecules. This approach addresses the limitations of OSCs, resulting in improved gas-sensing performance, enhanced responsivity, and increased stability, thus paving the way for practical applications in gas sensing and detection.

8:00 PM EN05.11.10

Synergetic Effect of Aluminium Oxide and Organic Halide Salts on Surface Passivation and Stability Enhancement of Perovskite Solar Cells EunyoungChoi^{1,2,3}, Jin-WonLee⁴, Jae SungYun^{5,3} and HelenH. Park^{4,6}; ¹Diamond Light Source, United Kingdom; ²University of Cambridge, United Kingdom; ³University of New South Wales, Australia; ⁴Korea Research Institute of Chemical Technology (KRICT), Korea (the Republic of); ⁵University of Surrey, United Kingdom; ⁶University of Science and Technology (UST), Korea (the Republic of)

Although long-chain organic halide salts have been effectively used in three-dimensional (3D) perovskite-based solar cells for surface passivation, it has been reported that unexpected halide defects could be formed from the organic halide salts and the solvents used for dissolving the organic halide salts, which results in degradation of the devices. In this work, aluminium oxide (AlO_x) via atomic layer deposition (ALD) was introduced onto octylammonium iodide (OAI) on the perovskite layer to suppress the generation of undesired defects while still obtaining the benefits of organic halide salts. The devices incorporating AlO_x on OAI-treated perovskites (OAI/AlO_x) show enhancement in both device performance and photostability compared to devices with only OAI surface passivation. Diffusion of aluminium from AlO_x into the perovskite is observed from surface characterization. Photo-generated carrier transport in both the surface and bulk of the perovskite absorber is investigated by wavelength-dependent surface photovoltage microscopy, and grazing-incidence-wide-angle X-ray scattering was utilized to investigate the crystallinity changes of the perovskite under prolonged illumination. The effects of the inorganic oxide layer on the stability and performance of organic halide salt-treated devices will be addressed, and the mechanisms involved in the enhanced performance and stability will also be discussed.

8:00 PM EN05.11.11

Off-Stoichiometric Perovskite Photodetectors for Direct Time-Of-Flight Distance Measurements LorenzoJ. Ferraresi^{1,2}, SergeyTsarev^{2,1}, SebastianSabisch^{2,1}, FrankKrumeich², VladyslavHnapovskiy^{2,1}, GebhardJ. Mat², SergiiYakunin^{2,1}, IvanShorubalko¹ and MaksymV. Kovalenko^{2,1}; ¹Empa—Swiss Federal Laboratories for Materials Science and Technology, Switzerland; ²ETH Zürich, Switzerland

Hybrid organic-inorganic metal halide perovskites have recently emerged as a promising alternative to conventional semiconductors for their use in optoelectronic devices such as vertical photodiodes, offering a tuneable band gap and near-unity quantum efficiencies. They can be deposited with facile and diverse methods. The latest feat focused on reducing their defect density to minimise the noise and improve charge collection efficiencies. Yet the response times are limited by the devices' capacitance and, intrinsically, by the lifetime and transit time of the charge carriers. The capacitance limitation can be addressed only to a limited extent via the reduction of the active area of the photodiode, increasing in the meantime the fabrication complexity for comparable signal amplitudes. Alternative strategies focused on the intrinsic properties of semiconductors - such as exploiting the photo-Dember effect or engineering the defect-limited carrier lifetimes - elevated photodetectors to the femtosecond regime, and have yet to be considered for perovskite devices. In this study, we explored controlled photocurrent quenching through the introduction of selective recombination sites, to obtain fast, one-mm² perovskite photodiodes with response times beyond their capacitance limitations. By choosing suitable charge transport layers, and by offsetting the perovskite precursor stoichiometry, the density of interfacial recombination sites can be controllably increased, as highlighted through an in-depth study of photocurrent transients under picosecond laser pulses. The device photo-response is tuned to observe an isolated sharp signal with ns decay and a 3-dB drop at 15 MHz, enabling the resolution of distances in the cm-range using direct time-of-flight measurements. These results are a major leap towards the development of wavelength-selective, cost-effective, and fast perovskite photodetectors with improved photo-response for Light Detection and Ranging (LiDAR) applications. LiDAR sensors are of paramount importance in highly automated processes and for self-driving cars.

8:00 PM EN05.11.12

Lead Halide Perovskites and Its Applications in Whispering Gallery Mode Micro-Lasing SubitanLaskar and CSudakar; Indian Institute of Technology Madras, India

Ultrahigh luminescence quantum yield (~100%), low non-radiative recombination rates, and tunable spectral emissions from the ultraviolet to the visible range can be achieved through lead halide perovskites (LHP) (APbX₃; A= Rb⁺, Cs⁺, and X= Br⁻, I⁻); hence they are promising candidates for optoelectronics and photonics applications. However, a lack of atmospheric stability impedes their effective use as photovoltaic absorbers. Highly emissive perovskite quantum dots (PQDs) are being investigated to develop solar cells, efficient lasers, LEDs, etc. Here, we report the bandgap tunability and stability of APbX₃ PQDs synthesized through the hot-injection method. Structural characterization through X-ray diffraction (XRD) reveals highly phase pure cubic polymorph of PQDs. The A-site ions have a significant impact on the photophysical and chemical properties. Cs⁺ cations are substituted with Rb⁺ at the A site, and anionic X sites are substituted either with Br⁻ or I⁻ or a combination of halide ions in these PQDs to study the changes in structure and optical properties. With increasing Rb⁺ concentration, the bandgap of Cs_{1-x}Rb_xPbX₃ is shown to vary between 1.7 eV to 3.2 eV, as evident from the blueshift observed in the photoluminescence peak. Bandgap is also shown to be tunable by alloying I⁻ with Br⁻ in CsPbX₃ and Cs_{0.5}Rb_{0.5}PbX₃. The latter is found to be more stable than the former when stored in laboratory conditions. A detailed analysis will be presented on the effect of cationic and anionic substitution on the absorbance and emission spectra of PQDs. These quantum dots are further used for whispering gallery mode (WGM) lasing from PQDs coated on TiO₂ spherical microcavities. The photoluminescence emission from a CsPbI₃-QDs gain medium strongly couples with a TiO₂ microspherical resonating optical cavity. Spontaneous emission in these microcavities switches to a stimulated emission above a distinct threshold point of 708.7 W/cm². Quality factor as high as Q~1195 for WGM micro-lasing is demonstrated at room temperature. CsPbI₃-QDs/TiO₂ microcavities are found to be photostable even after continuous laser excitation for 75 minutes. [1] The CsPbI₃-QDs/TiO₂ microspheres are promising as WGM-based tunable microlasers. Results on WGM micro-lasing using Cs_{0.5}Rb_{0.5}PbX₃ will be presented.

Reference:

[1] S Laskar et al. "Whispering gallery mode micro-lasing in CsPbI₃ quantum dots coated on TiO₂ microspherical resonating cavities." *Optics Letters* 48.10 (2023): 2643-2646.

8:00 PM EN05.11.13

Binary Microcrystal Additives Enabled Antisolvent-Free Perovskite Solar Cells with High Efficiency and Stability ZhuP. De; Southern University of Science and Technology, China

Developing a facile method to prepare high-quality perovskite films without using the antisolvent technique is critical for upscaling production of perovskite solar cells (PVSCs). However, the as-prepared formamidinium (FA)-based perovskite films often exhibit poor film quality with high density of defects if antisolvent is not used, limiting the photovoltaic performance and long-term stability of derived PVSCs. Herein, we adopt pre-synthesized 3D methylammonium lead chloride (MAPbCl₃) and 1D 2-aminobenzothiazole lead iodide (ABTPbI₃) microcrystals into self-drying perovskite precursor, which serve as seed crystals to promote nucleation and growth of FAPbI₃-based perovskites without involving the antisolvent extraction. The as-prepared perovskite films with homogeneous morphology and enhanced structural stability can be achieved by alloying with MA cation and Cl anion. Meanwhile, analysis shows the presence of ABTPbI₃ at grain boundaries can help passivate the defects due to the interaction between ABT cations and undercoordinated Pb²⁺ ions, reducing the non-radiative recombination loss. Consequently, the devices exhibit a champion PCE of 23.27% for the small-area device (~ 0.09 cm²) and 21.52% for the large-area device (~ 1.0 cm²), which are among the highest efficiencies reported for PVSCs without using antisolvents. Moreover, the optimized devices without encapsulation showed improved light-soaking stability, which can retain 92% of its initial efficiency under continuous illumination at the maximum power point (MPP) for over 1000 h. This strategy enabled by combinations of pre-synthesized microcrystals provides valuable guidance to improve film quality of antisolvent-free perovskites, and expands its applications in highly-efficient and stable perovskite photovoltaic devices.

8:00 PM EN05.11.14

Achieving Nearly 100% Quantum-Efficient Lead-Free Perovskite Solar Cells with 34.67% Power-Conversion Efficiencies Through Band and Defect Engineering-Based Material Design Optimization SaleemAl Dajani^{1,2,1}; ¹King Abdullah University of Science and Technology, Saudi Arabia; ²Massachusetts Institute of Technology, United States

Perovskite-based solar cells (PSCs) have been the subject of intense research due to their high-power conversion efficiency (PCE), but their stability and lead content have limited their practical applications. In this study, we numerically simulate oxide/perovskite/oxide-type PSCs using the one-dimensional solar cell capacitance program (SCAPS-1D) and optimize performance by tuning electronic, interfacial and defect properties. Based on these calculations, we report that a significant improvement could be achieved in the quantum and power-conversion efficiencies of a solar cell based on optimizing the design of perovskite material constituents and interfaces.

Initially, we assess the effect of various oxide-based electron transport layers (ETLs) and hole transport layers (HTLs) on PSC performance and identify a solar cell with TiO₂ as an ETL and NiO as an HTL (FTO/n-TiO₂/CsSnI₃/p-NiO) exhibiting the highest calculated PCE of 31.09%, with a fill factor (FF) of 88.43%. Next, we optimize the thickness of the TiO₂, NiO, and CsSnI₃ layers of the benchmarked device, along with their bulk and interface defects, using detailed numerical simulations.

We successfully demonstrate that by engineering defects in CsSnI₃ and optimizing the material properties at the interface, the PCE and V_{OC} could be further improved to 34.67% and 1.16V respectively, representing a significant jump from the initial PCE of 31.09% with a 0.98V open-circuit voltage at roughly the same FF and short-circuit current density. The specific improvements made include optimizing the band alignment of the materials to maximize light absorption, reducing the density of defects in the materials to improve charge carrier transport, and engineering the interfaces between the materials to improve charge transfer.

Our results provide important insights into the selection of CsSnI₃ as a lead-free absorber with optimized band alignment and interfacial defects, highlighting the importance of a comprehensive approach to optimizing the performance of oxide/perovskite/oxide-type solar cells that considers a range of electronic, interfacial, and defect properties. Our work demonstrates potential improvements of perovskite materials for high-efficiency solar cells. We believe that our study has significant implications for the development of practical solar cells with optimal performance based on solution-processed perovskite materials.

8:00 PM EN05.11.15

Rigorous Optical Dispersion Data Analysis of Single Crystal MAPbBr₃ for Optimized Perovskite Solar Cell Active Layer Absorption Christopher McCleese^{1,2}, Michael C. Brennan^{1,3}, Lirong Sun^{1,3}, Nina Hong⁴, Nathan Episcopo⁵, C.V. Ramana⁵, Tod Grusenmeyer¹ and Peter Stevenson¹; ¹Air Force Research Laboratory, United States; ²General Dynamics Information Technology, United States; ³Azimuth Corporation, United States; ⁴J.A. Woollam Company, Inc., United States; ⁵The University of Texas at El Paso, United States

Lead halide perovskites have garnered significant attention for optoelectronic applications including photovoltaics, light-emitting diode, photodetector, and laser technologies. However, material quality and stability issues lead to a wide range of reported values for the electrical and optical properties which may complicate device design and optimization strategies for commercialization. Critical to the development of perovskite solar cells (PSC) are the optical properties (refractive index, n, and extinction coefficient, k), which describe the way perovskites interact with light and subsequently function as a photovoltaic material. Optimizing perovskite active layer absorption necessitates solar cell optical coating design iterations using material optical constants derived from rigorous optical dispersion data analysis. The refractive index and extinction coefficient for MAPbX₃ have been observed to significantly vary in the literature depending on the processing methodologies. If such optical dispersion variation is ignored in practice at the design stage, PSCs can exhibit parasitic device absorption by non-perovskite (non-active) layers resulting in variable optical transmission, reflectance, or haze-like characteristics within solar radiation bands of interest (300-2500 nm). To our knowledge, no comprehensive experimental optical dispersion data analysis to derive the optical constants of MAPbX₃ has been performed to include notable anomalous optical dispersion characteristics including the band edge transition (bandgap ~539 nm) and methylammonium spectral overtones below the band edge (observed within 1050-2050 nm). As such, the optical property determination of exemplary MAPbX₃ has been largely under approximated and, consequently, evokes optical property uncertainty with respect to prior reports. Proper fundamental derivation of MAPbX₃ optical constants is critical toward the development of high-performance electronic and optoelectronic perovskite devices. Here, we present a rigorous optical dispersion data analysis of single crystal MAPbBr₃ via variable angle spectroscopic ellipsometry appended with transmission intensity spectra to provide a robust derivation of the optical constants for normal and anomalous optical dispersion regimes. Using derived optical constants for our single crystal MAPbBr₃, exemplary modeled solar cell optical device designs are optimized for perovskite layer absorption and we compare our derived optical properties to illustrative MAPbBr₃ literature values reported to-date.

8:00 PM EN05.11.16

The Quest for the Missing Link – From Lead Complexes to Perovskite Formation Kai O. Brinkmann¹, Timo Maschwitz¹, Lena Merten², Feray Ünlü³, Andreas Kotthaus¹, Cedric Kreusel¹, Manuel Theisen¹, Henrik Weidner¹, Jaffres Anael Morgane⁴, Alexander Hinderhofer², Christian Wolff³, Stefan F. Kirsch¹, Sanjay Mathur⁵, Frank Schreiber² and Thomas Riedl¹; ¹Bergische Universität Wuppertal, Germany; ²University of Tübingen, Germany; ³Helmholtz-Zentrum Berlin für Materialien und Energie, Germany; ⁴École Polytechnique Fédérale de Lausanne, Switzerland; ⁵University of Cologne, Germany

Perovskite solar cells currently enter a stage, where market introduction is within reach. For serious upscaling, control over the quality of the perovskite material is most critical. To this end, the community currently relies heavily on laboratory experience, engineering, and fine-tuning approaches. A key challenge is the controlled growth of perovskite crystallites while processing thin films. Several strategies are currently in use, such as like anti-solvent or additive engineering. While the impact of these strategies is well-evidenced in the resulting layers, the underlying mechanisms that govern the crystallization process are still subject to a vigorous debate. A frequently cited theory is that the nuclei for the perovskite crystallization evolve from intermediate Pb²⁺-MA⁺-I⁻-solvate clusters. [1] A dominant role of solvate clusters implies a strong impact of complexing and coordination in the precursor solution on the crystallization process. Reports of the colloidal structures and Lewis-base-acid interactions in the perovskite precursor ink seemingly support this theory. [2] As of yet, however, insights that unambiguously link the complex formation in the precursor inks to the perovskite formation are lacking.

We present a holistic approach in which we study the entire course of perovskite formation. We begin with a study of lead complexation in the precursor stage (using NMR and electrical conductivity measurements in the solution) and proceed with in-situ GIWAXS investigations during thin film deposition and along the way to thin film formation (bare layers and solar cells). We systematically study the impact of common solvents like DMF, DMSO and NMP. As an exemplary additive, to study the influence of Lewis-base additives, we chose thiourea, which is a strong sulphur donor and an effective crystallization mediator. With ²⁰⁷Pb NMR and conductivity studies, we found a strong and systematic impact of the choice of solvents on the formation of lead complexes in the precursor solution, as well as indications, that may imply the presence of 3D corner sharing structures already in the precursor ink. Importantly, the differences in lead complexation depending on the solvent apparently diminish with increasing the concentration of the precursor ink; the final grain sizes remained largely unaffected by even strong variations found in the diluted precursors. On the other hand, the addition of thiourea did not affect the nature of lead complexes in the precursor solution. By in-situ GIWAXS, we are finally able to identify the annealing step as the decisive stage, where the presence of the additive affects the formation of perovskite grains and their crystallographic orientation. We could further substantiate our interpretation by FTIR studies. As such, for the first time, we provide a convincing link between precursor chemistry and final thin film formation.

References:

- [1] Ahlawat P, et al. *Chem. Mater.* **32**, 529-536 (2020).
- [2] Flatken MA, et al. *J. Mater. Chem. A* **9**, 13477-13482 (2021)

8:00 PM EN05.11.17

All-Solution-Processed Fabrication of Intrinsically Flexible Multicolor Perovskite Light-Emitting Diodes and Photodetectors on Diverse Substrates (Elastomer, Paper, Textiles, etc.) Junyi Zhao and Chuan Wang; Washington University in St. Louis, United States

Owing to the unique properties such as tunable bandgap and strong optical absorption, perovskite holds great potential for optoelectronic device applications. Although significant progress has been made to explore high-performance light-emitting diodes (LEDs) and photodetectors (PDs) using perovskite, existing fabrication techniques based on the rigid substrate are unable to meet the growing demand from large-area flexible displays. In this work, we report all-solution-processed perovskite LEDs (PeLEDs) and photodetectors (PePDs) fabricated on various unconventional substrates commonly found in our daily life, including paper, textiles, plastics, rubber, metal, and even three-dimensional surfaces using a versatile and low-cost direct writing approach. Compared to conventional spin-coating and vacuum-evaporation processes, the direct writing approach enables mask-free patterning and allows even untrained individuals to "draw" a batch of high-performance LEDs/PDs in a time-efficient and energy-saving manner. A significant challenge when implementing optoelectronic devices on paper and textiles is the rough surface morphology of yarn and fiber networks, which can lead to nonuniform film thickness and leakage current. To address this issue, we have demonstrated that blending ionic polymer poly(ethylene oxide) (PEO) with poly(3,4-ethylenedioxythiophene) polystyrene sulfonate (PEDOT:PSS) not only enhances the conductivity and flexibility of the polymer conductors, but also achieve local self-planarization. For the emissive layer, we have successfully achieved multicolor LEDs covering the entire visible spectrum on both paper and textile substrates by substituting halide elements in the perovskite material (MAPbX₃) and formulating inks with varying halide compositions. Meanwhile, the brightness and efficiency of LEDs could be further boosted by introducing the butylammonium (BA) group to reduce the perovskite structure dimensionality to form 2D Ruddlesden-Popper perovskite (RPP) structures. Furthermore, we have conducted systematic investigations on perovskite-polymer composites and demonstrated that the morphology and optoelectronic properties of the perovskite photoactive layer can be tuned by incorporating different polymer additives. Specifically, PEO allows for precise and smoother perovskite film deposition by tuning ink rheology and viscosity, while polystyrene (PS) increases the density and uniformity of crystal arrangement, resulting in improved LED brightness and reduced current leakage. Poly(methyl methacrylate) (PMMA) helps reduce grain defects and boundaries, benefiting carrier diffusion in photodetectors. The PeLEDs written on paper substrates exhibited a brightness as high as 15,225 cd m⁻², a current efficiency of 6.65 cd/A, and a turn-on voltage of 2.4 V. Owing to the extraordinary flexibility of each functional layer, the written LEDs on the paper substrate could be bent to a 1 mm extreme curvature radius for over 5000 cycles without decay in performance. In summary, the written perovskite optoelectronic devices are ideally suited for low-cost and large-area emerging application scenarios such as deformable displays, wearable E-Textiles, E-Papers, and E-packaging.

8:00 PM EN05.11.18

Enhancing Efficiency of Quasi-2D PeLEDs Through Anti-Solvent Treatment-Induced Phases Modulation Luchao Zhuang, Qiwei, Chuan Zhao Li and Shu Ping Lau; The Hong Kong Polytechnic University, Hong Kong

Quasi-2D perovskite has drawn considerable attention for application in perovskite light-emitting diodes (PeLEDs) due to their higher exciton binding energy and moisture resistance. However, the inhomogeneous distribution of phases formed in spin-coated quasi-2D perovskite films inevitably leads to energy transfer loss, limiting the emission performance. Here, we systematically investigated the phases modulation behavior for a series of anti-solvent with different polarity -namely, the toluene (TO), diethyl ether (DE), chlorobenzene (CB), anisole (AN), ethyl acetate (EA). Due to the strong hydrogen bonding interaction between EA and organic spacer cations, it will hinder the organic and $[\text{PbBr}_6]^{4-}$ combination. The crystallization rate of intermedia phases slows, resulting in a large proportion of high-n phases formation subsequently. As a result, an efficient energy cascade is ensured with a narrow distribution centered around the desired phases. Leveraging these insights, we achieved PeLEDs with improved external quantum efficiency (EQE) of 4.21%, 7.11%, and 8.77%, corresponding to ~490 nm, ~497 nm, and ~503 nm emissions, respectively. Furthermore, the anti-solvent treatment strategy provides a guide to regulate the phase distribution for eliminating energy transfer loss to fabricate efficient quasi-2D PeLEDs.

8:00 PM EN05.11.19

Ionization of Hole Transport Materials as a Method for Improving the Photovoltaic Performance of Inverted Perovskite Solar Cells Wen-ren Li¹, Yogesh Tingare², Chaochin Su², Dibyajyoti GHosh³, Hsinhan Tsai⁴, Wanyi Nie⁴, Chien-Hsiang Lin¹, Sheng-Chin Chou², Ning-Wei Lai² and Xin-Rui Lew¹; ¹National Central University, Taiwan; ²National Taipei University of Technology, Taiwan; ³Indian Institute of Technology Delhi, India; ⁴Los Alamos National Laboratory, United States

Increasing energy demands and concerns over global warming have led to a focus on the development of solar energy technologies. Perovskite solar cells (PSCs) have emerged as one of the most promising photovoltaics and are being investigated extensively. In inverted PSCs, hole transport materials (HTMs) assist directional charge transfer and electron blocking and also play an critical role in forming large-grained perovskites which enhance cell performance. In this work, we demonstrate a strategy for increasing the power conversion efficiency (PCE) of the device by ionizing HTMs, which introduces hydrophilicity into the HTM, improved interfacial properties, and excellent surface topographies. A comparative study of different ionizing counter anions showed that ionization also affects the absorption and emission properties, energy levels, and hole mobility of HTMs. Perovskite morphology significantly impacts PSC performance, and the anion groups like sulfoxide, SCN^- , and iodide contribute effectively to the film formation and defect passivation of perovskites. Ionic dopant-free HTM with iodide entity was found to efficiently passivate the dominant surface halogen vacancy due to its smaller size, lowering the density of charge-trapping defect states and achieving a hysteresis-free power conversion efficiency of 20.46%, which was 1.71% higher than that of the non-ionic HTM. Detailed research and analysis using atomistic modeling were also investigated, providing valuable insights into the correlation between anion size and perovskite passivation and efficiency. Durability is an important aspect in PSCs and can be assisted by a suitable HTM. As result, the devices based on HTM with iodide and non-ionic HTM retained 97% and 89%, respectively, of their original PCE for 500 hours, but the device fabricated with PEDOT:PSS retained about 81% of its PCE for the same time. This study provides a technologically relevant solar cell demonstration with a mechanistic understanding of the interfacial material design. Studying other charged molecules with varying properties and sizes as counterions to develop high-performing PSCs will also be reported in the meeting.

8:00 PM EN05.11.20

Comparative Study of Shelling CsPbBr₃ Quantum Dots with CdS and TiO₂ Noah J. Pitcher, Bryce Baird-Taylor, Daniel Muscato, Isak Hurtic and Yiliang (Yancy) Luan; Binghamton University, The State University of New York, United States

Halide perovskites (HP) have been attractive in the development of optoelectronics due to their many favorable properties, such as high efficiency and adjustable band gap. However, HP are unstable when exposed to an ambient atmosphere, including varying moisture, light, and heat, which limits their applications. Furthermore, HP quantum dots (QDs) have enhanced properties and improved stability compared to perovskite thin films because of the quantum effect. However, better stability is still desired for the introduction of HPQDs into optoelectronics. Shelling engineering is a powerful method that can boost the stability of nanomaterials. Nevertheless, it is still challenging to effectively shell HPQDs due to the harsh conditions required by the process. In this report, we will present the shelling of CsPbBr₃ QDs with titanium dioxide (TiO₂) and cadmium sulfide (CdS), respectively. The two shelling methods will be demonstrated in parallel with each of the protocols, structures, and properties of the products. Our results indicate that the shelling with CdS was successfully achieved, while the QDs collapsed during the shelling with TiO₂. Additionally, the photoluminescence of our HPQDs is dependent on the amount of CdS introduced during shelling. This research does not only demonstrate successful shelling of HPQDs with CdS, but also yields constructive insights for the shelling engineering of nanomaterials.

8:00 PM EN05.11.21

Performance of Flexible MAPbI₃ Solar Cells Made on Different Transparent Conducting Electrodes with Different Hole Transport Layers Bishal Bhandari, Robert Piper, Justin C. Bonner and Julia W. Hsu; The University of Texas at Dallas, United States

Perovskite solar cells (PSCs) have gained interest as a viable technology in recent years because of their low fabrication cost, solution processability, and high-power conversion efficiency. Commercializing perovskite solar cells requires high-throughput and low-cost manufacturing, e.g., solution-based roll-to-roll (R2R) process for making flexible PSCs. Transparent conducting electrodes (TCEs) are critical for flexible PSCs to achieve high efficiency. In our laboratory, flexible hybrid TCEs are made on polyethylene terephthalate (PET) with R2R flexographically printed Ag metal lines by blade coating silver nanowires (AgNWs) and planarized with indium zinc oxide (IZO) on top, and then the entire stack is photonic cured. With this process, we achieve TCEs with transmittance averaged between 400 and 700 nm wavelengths (T_{avg}) = $81 \pm 0.4\%$, sheet resistance (R_{sh}) = $11 \pm 0.5 \Omega/\text{sq}$, and root-mean-square surface roughness (σ_{rms}) = $4.3 \pm 0.4 \text{ nm}$. Flexible PSCs were fabricated on the hybrid TCEs and compared to devices made on commercially available PET/TCEs. We also investigated the J-V characteristics of these flexible PSCs using different hole transport layer materials. TCEs with comparable electrical, optical, and morphological properties displayed varied J-V performance with different hole transport layers. These results are surprising because, normally, other than transmittance and sheet resistance, TCEs are not considered to have a great effect on solar cell performance. We perform additional studies to probe the factors that influence the J-V characteristics of these flexible PSCs, such as contact resistance losses and interfacial properties between the TCE and the charge transport layers. The size of devices is also varied to study upscaling behavior. We aim to understand the charge extraction and recombination process and gain insights into the underlying mechanism affecting the performance and efficiency of flexible PSCs.

This work is supported by DOE SETO DE-EE0009518.

8:00 PM EN05.11.22

Substrate Functionalization to Control Phase Purity in the Co-Evaporation of FAPbI₃ Andres Felipe Castro Mendez, Juan-Pablo Correa-Baena and Carlo Perini; Georgia Institute of Technology, United States

A major challenge for perovskite solar cell commercialization is scalability. Thermal evaporation offers advantages such as higher uniformity, better thickness control, non-soluble materials deposition, and removal of the solvent orthogonality constraint that solution processing has. Co-evaporation of FAPbI₃ is a promising choice for the fabrication of high efficiency and scalable perovskite solar cells. However, non-perovskite hexagonal phases are more stable at room temperature, and the presence of these phases is detrimental for the device performance. In this work, we study the role of substrate functionalization on the phase purity and composition of the co-evaporated layer. We show that the growth of hexagonal phases is preferred on substrates without functionalization, possibly as result of a FA⁺ deficiency in the layer. On the other hand, phosphonic acids remediate this problem by enhancing the adsorption rate of organic cations on the substrate and creating the right environment for the formation of pure cubic-phase films.

8:00 PM EN05.11.23

Solution Processing Defects and Their Role in Device Stability and Reverse Bias Degradation for Perovskites Solar Cells Samuel A. Johnson, Isaac Gould, Gabriel McAndrews, Daniel Morales and Michael McGehee; University of Colorado, Boulder, United States

Solution processing metal halide perovskites has numerous advantages when it comes to scaling up manufacturing relative to other methods, including speed and energy input, but reproducibility and reliability are complicated by physics dictating coating (e.g. surface tension and dewetting). Void defects and pinholes form via tension created by volume reduction during the drying phase, a fundamental force involved in film formation from solution, yet are seldom discussed. In this work, we systematically investigate the origin and impacts of 'void defects', points where the intrinsic perovskite absorber is missing and inherent to any solution-deposition process, to find they are a ubiquitous feature in solution processed perovskite devices, irrespective of perovskite composition and architecture. Experimental data and equivalent-circuit modeling show many of these defects behave as diodes with slightly lower turn-on voltages in parallel with the remainder of the device. Therefore, they have minimal detrimental effects on forward-bias photovoltaic performance, producing a small deficit in Voc and FF. However, we reveal these defects significantly undercut reverse-bias stability where they break down at lower voltages, shunting current, resulting in local ohmic heating, followed by the melting and propagation of burning metal shunts across the surface for some architectures. This effect produces catastrophic degradation of the solar module that would never be suitable for scaling up. It is therefore critical to mitigate such defects for widespread implementation of perovskite PV by all available means, and we demonstrate optical profilometry and PL-mapping as high-throughput detection methods for these defects as well as improved particle control and solution wetting as possible preventative measures, as well as strategies to minimize the effects use of thick oxide transport layers and contacts. While vapor- and hybrid-phase perovskite deposition methods demonstrate radically reduced defect density, their large-scale employment may be difficult making the elimination or passivation of these defects through a single or combination of strategies necessary to unlock defect-free large area solution processed coating techniques.

8:00 PM EN05.11.24

Effects of Van der Waals Interactions on Excitonic Properties of Lead Halide Perovskite Photovoltaic Materials Amir A. Farajian; Wright State University, United States

Excitons dissociation and diffusion are among the key properties that determine the efficiency of light harvesting in photovoltaic materials. As representatives of a promising category of novel photovoltaics, lead halide perovskites include both bonding and non-bonding interactions. In order to assess, and engineer, excitonic properties of these materials, theoretical calculations can complement experimental results to determine the effects of van der Waals interactions. The focus of this work is to utilize density functional theory simulations that explicitly incorporate van der Waals interactions to estimate excitonic properties. The results reveal how van der Waals interactions affect key excitonic characteristics, e.g., binding energies and effective masses, and help determine strategies for constituent selection towards improving light-harvesting efficiency.

8:00 PM EN05.11.25

Chemical Reaction Kinetics of the Decomposition of Low Bandgap Tin-Lead Halide Perovskite Films and The Effect on The Ambipolar Diffusion Length Yuhuan Meng, Preetham P. Sunkari, Marina Meila and Hugh W. Hillhouse; University of Washington, United States

Understanding the degradation mechanism and quantifying the degradation rate of hybrid organic-inorganic halide perovskite (HP) materials are essential for achieving the commercialization of HP solar cells. Here, we focus on evaluating the reaction products and kinetics of the degradation of mixed Sn-Pb halide perovskite ($\text{FA}_{0.75}\text{CS}_{0.25}\text{Pb}_{0.5}\text{Sn}_{0.5}\text{I}_3$) thin films in response to oxygen, moisture, and illumination using in-situ measurements of optical transmittance, photoluminescence, X-ray diffraction, and UV-Vis-NIR spectroscopy. We determined that the decomposition occurs by a dry oxidation pathway ($1 \times 10^{-8} \text{ mol}/(\text{m}^2\text{s})$) at 25 °C in air and a water-accelerated oxidation pathway ($3 \times 10^{-8} \text{ mol}/(\text{m}^2\text{s})$) at 25 °C in 50% RH air. In 50% RH air, the water-accelerated oxidation dominates at low temperatures, but the dry oxidation pathway (which has a higher activation energy) dominates at temperatures greater than 40 °C. A kinetic rate expression for the decomposition is determined and validated with a mean test error of 18%. Further, we developed a predictive model of the decay of the diffusion length (predicting the time required for the diffusion length to decrease to 80% of its initial value) with a prediction test error of 32% by machine learning. The chemical decomposition rate expression was selected as the most dominant feature in all 3-feature models with low prediction test error. This work highlights the significance and utility of quantitative measurements of perovskite degradation to make reliable predictions about device lifetimes, particularly when dealing with limited datasets.

SESSION EN05.12: Structure Property Relationships in Halide Perovskites I

Session Chairs: Xiwen Gong and Andrew Wong

Thursday Morning, November 30, 2023

Hynes, Level 3, Room 311

8:00 AM *EN05.12.01

Update on The Synthesis and Surface Chemistry of Highly Luminescent Lead Halide Perovskite Nanocrystals Maksym V. Kovalenko^{1,2}; ¹ETH Zurich, Switzerland; ²Empa-Swiss Federal Laboratories for Materials Science and Technology, Switzerland

Colloidal lead halide perovskite (LHP) nanocrystals (NCs), with bright and spectrally narrow photoluminescence (PL) tunable over the entire visible spectral range, are of immense interest as classical and quantum light sources. Severe challenges LHP NCs form by sub-second fast and hence hard-to-control ionic metathesis reactions, which severely limits the access to size-uniform and shape-regular NCs in the sub-10 nm range. We show that a synthesis path comprising an intricate equilibrium between the precursor (TOPO-PbBr₂ complex) and the [PbBr₃]⁻ solute for the NC nucleation may circumvent this challenge [1,2]. This results in a scalable, room-temperature synthesis of monodisperse and isolable CsPbBr₃ NCs, size-tunable in the 3-13 nm range. The kinetics of both nucleation and therefrom temporally separated growth are drastically slowed, resulting in total reaction times of up to 30 minutes. The methodology is then extended to FAPbBr₃ (FA = formamidinium) and MAPbBr₃ (MA = methylammonium), allowing for thorough experimental comparison and modeling of their physical properties under intermediate quantum confinement. In particular, NCs of all these compositions exhibit up to four excitonic transitions in their linear absorption spectra, and we demonstrate that the size-dependent confinement energy for all transitions is independent of the A-site cation. We then show that this synthesis – relying on the labile ligand capping with TOPO-phosphinic acid mixture – makes for a convenient platform for the subsequent surface functionalization with diverse capping ligands [3]. Robust surface functionalization of highly ionic surfaces, as is the case of LHP NCs, has remained a formidable challenge due to the inherently non-covalent weak surface bonding. Leveraging the vast and facile molecular engineering of phospholipids, we present their efficacy as surface-capping ligands for LHP NCs. Molecular dynamics simulations and solid-state NMR confirm that the surface affinity of these zwitterionic molecules is primarily governed by the geometric fitness of their anionic and cationic moieties. Judicious selection of the ligands yielded colloiddally robust FAPbBr₃ and MAPbBr₃ NCs and enabled colloids in a variety of solvents, from n-hexane to alcohols. We will discuss the atomistic details of the ligand surface binding, ranging from conventional alkylammonium ligands [4] to diverse zwitterionic moieties. In particular, we show that solution and solid-state NMR readily captures the surface binding motifs and the impact of the ligands on the surface structure of CsPbX₃ NCs [5]. We also present non-hydrolytic coating of perovskites with amorphous metal oxides [6] and exploration of other semiconductive perovskite NCs within the AMX₃ perovskite family.

1. Q. Akkerman *et al. Science* **2022**, 377, 1406

2. F. Montanarella *et al. Nano Lett.*, **2023**, 23, 2, 667–676

3. V. Morad *et al.* submitted

4. A. Stelmakh *et al. Chem. Mater.* **2021**, 33, 5962–5973

5. M. Aebli *et al.* in preparation

6. D. Guggisberg *et al. Chem. Mater.*, **2023**, 35, 7, 2827–2834

8:30 AM EN05.12.02

High-Performance Perovskite Solar Cells Incorporated with Conjugated Organic Molecules Lening Shen, Tao Zhu and Xiong Gong; The University of Akron, United States

In the past years, perovskite solar cells (PSCs) as alternative cost-effective solar technology have drawn great concentrations in both academic and industrial sectors. High power conversion efficiency (PCEs) has been reported from the PSCs based on three-dimensional (3D) perovskites, but 3D perovskites are sensitive to moisture and air. Moreover, unbalanced charge transport within perovskites restricts further boost PCEs of PSCs. In this presentation, we reported efficient and stable PSCs based on either the perovskite: polymer bulk heterojunction composites or ternary perovskite-organic composites. Systemically studies demonstrated that an extended spectral absorption, enhanced and balanced charge transport, improved film morphology, enlarged crystallinity, and suppressed ion immigration movement were observed from the above two different systems compared to those based on the 3D perovskites. As a result, PSCs with over 23 % PCEs, dramatically enhanced stability, and suppressed photocurrent hysteresis were demonstrated. These results indicated that our studies provided a facile and promising way to realize high-performance PSCs, where perovskites are incorporated with conjugated organic molecules.

8:45 AM EN05.12.03

Achieving Metal Doping of Strongly Confined Perovskite Nanocrystals under Ambient Conditions Zachary VanOrman, Mateo C. Wuttig and Sascha Feldmann; Harvard University, United States

Halide perovskite (HP) nanocrystals (NC) hold great promise for optoelectronic applications due to their high photoluminescence (PL) quantum yields and energetic tunability *via* composition and size.¹ Further, doping M²⁺ metal cations into the HP lattice can enhance the radiative rate of the NC emission, and, in the case of manganese, it can simultaneously introduce an additional decay pathway in the form of long-lived Mn d-d orange PL.^{2,3} However, so far, M²⁺-doped CsPbCl₃ NC synthesis relies on hot injection, making it challenging to achieve strongly confined NCs.⁴ Recently, a novel synthesis method has been reported for HP NCs using complexation agents, resulting in the capability of synthesizing strongly confined HP NCs.⁵ Using the complexation agent synthetic approach, we now show that facile M²⁺ doping of CsPbX₃ NCs for various dopants (Mn, Ni, Zn) can be achieved, without the necessity of inert synthesis conditions or high temperatures.⁶ This gives access to a highly controlled size-dependence series for doped NCs, especially in the strongly confined regime (down to ~ 3.5 nm) which was previously inaccessible for doped perovskite NCs. We demonstrate that doping Mn and other divalent transition metals can vary the optical properties in vastly different and opposing ways, depending on the degree of quantum confinement and doping concentration. The presented work therefore not only outlines a new and improved synthetic approach for doped HP NCs but also elucidates the impact of metal doping on the resulting optical properties under confinement.

References:

(1) Dey, A.; Ye, J.; De, A.; Debroye, E.; Ha, S. K.; Bladt, E.; Kshirsagar, A. S.; Wang, Z.; Yin, J.; Wang, Y.; *et al.* State of the Art and Prospects for Halide Perovskite Nanocrystals. *ACS*

Nano **2021**, *15* (7), 10775–10981. <https://doi.org/10.1021/acsnano.0c08903>.

(2) Ahmed, G. H.; Liu, Y.; Bravić, I.; Ng, X.; Heckelmann, I.; Narayanan, P.; Fernández, M. S.; Monserrat, B.; Congreve, D. N.; Feldmann, S. Luminescence Enhancement Due to Symmetry Breaking in Doped Halide Perovskite Nanocrystals. *J. Am. Chem. Soc.* **2022**, *144* (34), 15862–15870. <https://doi.org/10.1021/jacs.2c07111>.

(3) Pradhan, N. Mn-Doped Semiconductor Nanocrystals: 25 Years and Beyond. *J. Phys. Chem. Lett.* **2019**, *10* (10), 2574–2577. <https://doi.org/10.1021/acs.jpcclett.9b01107>.

(4) Liu, W.; Lin, Q.; Li, H.; Wu, K.; Robel, I.; Pietryga, J. M.; Klimov, V. I. Mn²⁺-Doped Lead Halide Perovskite Nanocrystals with Dual-Color Emission Controlled by Halide Content. *J. Am. Chem. Soc.* **2016**, *138* (45), 14954–14961. <https://doi.org/10.1021/jacs.6b08085>.

(5) Akkerman, Q. A.; Nguyen, T. P. T.; Boehme, S. C.; Montanarella, F.; Dirin, D. N.; Wechsler, P.; Beiglböck, F.; Rainò, G.; Erni, R.; Katan, C.; Even, J.; Kovalenko, M. V. Controlling the Nucleation and Growth Kinetics of Lead Halide Perovskite Quantum Dots. *Science* **2022**, *377* (6613), 1406–1412. <https://doi.org/10.1126/science.abq3616>.

(6) VanOrman, Z.A.; Wuttig, M.C.; Kim, T.-S.; Reece, C.; Feldmann, S. *To be Submitted*.

9:00 AM EN05.12.04

Enabling Robust Chemical State Analysis of Sn-Based Perovskites via Auger Parameter Analysis in XPS Alexander Wiczorek and Sebastian Siol; Empa - Swiss Federal Laboratories for Materials Science and Technology, Switzerland

Sn-based perovskites exhibit compelling properties such as reduced toxicity and lowered band gaps over those purely based on Pb. As a result, they are of increasing interest for photovoltaic applications in single-junction and all-perovskite tandem applications.^[1]

For high performances, control of the oxidation state and interfacial chemistry is paramount, which can be determined using X-Ray photoelectron spectroscopy (XPS). However, the minor chemistry related shifts of the Sn core level emission complicate the analysis, especially for semiconducting materials. Here, surface band-bending as well as differences in the work function can be particularly pronounced

In this presentation, we demonstrate that studies based on the modified Auger parameter α' provide a robust method to resolve different chemical states in Sn-based perovskites. Using a set of reference samples, we identified a high sensitivity to the halide, resulting in a shift of up to $\Delta\alpha' = 2$ eV between ASnI₃ and ASnBr₃-type polycrystalline perovskite thin-films.^[2] Observed dependencies of α' on the Sn oxidation state and local chemistry provide a framework that enables reliable tracking of degradation as well as X-site composition for Sn-based perovskites and related compounds. More recently, we successfully applied this framework on Sn-based perovskite nanocrystals to ensure the absence of Sn(IV) impurities upon optimized synthesis procedures.^[3]

The higher robustness and sensitivity of such studies not only enables more in-depth surface analysis of Sn-based perovskites than previously performed, but also increases reproducibility across laboratories. Due to the facile data analysis, this method is ideal for high-throughput studies that are increasingly being adopted in the development of new semiconducting materials.^[4]

References

[1] H. Lai, J. Luo, Y. Zwirner, S. Olthof, A. Wiczorek, F. Ye, Q. Jeangros, X. Yin, F. Akhundova, T. Ma, R. He, R. K. Kothandaraman, X. Chin, E. Gilshtein, A. Müller, C. Wang, J. Thiesbrummel, S. Siol, J. M. Prieto, T. Unold, M. Stolterfoht, C. Chen, A. N. Tiwari, D. Zhao, F. Fu, *Adv. Energy Mater.* **2022**, *12*, 2202438.

[2] A. Wiczorek, H. Lai, J. Pious, F. Fu, S. Siol, *Adv. Mater. Interfaces* **2023**, *10*, 2201828.

[3] D. N. Dirin, A. Vivani, M. Zacharias, T. V. Sekh, I. Cherniukh, S. Yakunin, F. Bertolotti, M. Aebli, R. D. Schaller, A. Wiczorek, S. Siol, C. Cancellieri, L. P. H. Jeurgens, N. Masciocchi, A. Guagliardi, L. Pedesseau, J. Even, M. V. Kovalenko, M. I. Bodnarchuk, *Nano Lett.* **2023**, *23*, 1914.

[4] S. Zhuk, A. Wiczorek, A. Sharma, J. Patidar, K. Thorwarth, J. Michler, S. Siol, arXiv:2305.19875 [cond-mat.mtrl-sci], **2023**.

9:15 AM *EN05.12.05

Advancements in Pulsed Laser Deposition of Hybrid Halide Perovskites Monica Morales-Masis; University of Twente, Netherlands

In this presentation, we present recent progress in utilising Pulsed Laser Deposition (PLD) as a vacuum-based single-source deposition method for a wide range of hybrid and organic halide perovskites. We address the specific challenges associated with hybrid film growth, such as incompatible volatility and solubility, by employing laser ablation of a solid target containing dry perovskite precursors. The quality of the thin films can be tuned by controlling parameters like laser fluence, target composition, and process pressure.

The first part of the presentation focuses on the development of MA_xFA_{1-x}PbI₃ and Cs_xFA_{1-x}PbI₃ absorbers with tunable MA/FA ratios, as determined by XPS, NMR, and microstructure analysis. We demonstrate p-i-n solar cell devices incorporating PLD MA_xFA_{1-x}PbI₃ absorbers with power conversion efficiencies exceeding 17%.

The second part of the presentation highlights the epitaxial formation of PLD-grown MAPbI₃ and CsPbI₃ on lattice-matched substrates. PLD enables precise control over film thickness and deposition rate, which facilitates the investigation of polymorph stabilization, and the impact of strain on the optoelectronic properties of perovskite materials.

By combining controlled growth through PLD with insights into structural-property relationships, we can pave the way for designing a new generation of complex, stable, and non-toxic hybrid perovskite films.

9:45 AM EN05.12.06

A 0-D Barrier Layer Increases Stability in Mixed Sn-Pb and All-Perovskite Tandem Cells Chongwen Li^{1,2}, Lei Chen³, Fangyuan Jiang⁴, Zhaoning Song³, Bin Chen¹, Xiaoming Wang³, Esma Uğur⁵, Adam Balvan¹, Xuefei Wu⁶, Zachary Fink⁶, Carlo Andrea Riccardo Perini⁷, Juan-Pablo Correa-Baena⁷, Zheng-Hong Lu², Thomas Russell⁶, Stefaan De Wolf⁵, Mercuri G. Kanatzidis¹, David S. Ginger⁸, Yanfa Yan³ and Edward Sargent¹; ¹Northwestern University, United States; ²University of Toronto, Canada; ³The University of Toledo, United States; ⁴University of Washington, United States; ⁵King Abdullah University of Science and Technology, Saudi Arabia; ⁶Lawrence Berkeley National Laboratory, United States; ⁷Georgia Institute of Technology, United States

Perovskite tandem solar cells promise performance beyond the detailed balance limit of single-junction solar cells; however, non-radiative recombination and its progressive worsening with time, especially in the mixed Sn–Pb low-bandgap layer, currently limit performance and stability. We find that mixed Sn–Pb perovskite thin films exhibit a compositional gradient, with an excess of Sn on the surface – and we show this gradient exacerbates oxidation and increases the rate of recombination. We develop a materials processing strategy wherein diamines preferentially chelate Sn atoms, removing them from the film surface and achieving a more balanced Sn:Pb stoichiometry, making film surface resistive to Sn oxidation. This process forms electrically-resistive low-dimensional barrier layers, passivating defects and reducing interface recombination. Further regulating the dimensionality of the barrier layer to 0-D using 1,2-diaminopropane results in more uniform distribution and passivation. Tandems achieve a power conversion efficiency of 28.8%. Encapsulated tandems retain 90% of initial efficiency following 1000 hours operating at the maximum power point under simulated one-sun illumination in air without cooling.

10:00 AM BREAK

10:30 AM EN05.12.07

Interlayer Ordered Mixed-Spacer 2D Halide Perovskites Xiaotong Li¹, Hao Dong², George Volonakis³, Constantinos C. Stoumpos⁴, Jacky Even³, Claudine Katan³, Peijun Guo² and Mercuri G. Kanatzidis¹; ¹Northwestern University, United States; ²Yale University, United States; ³University of Rennes, France; ⁴University of Grete, Greece

Two-dimensional (2D) halide perovskites exhibit extraordinary stability and structural tunability because they can incorporate different organic cations as spacers. Their structures can be divided into the Ruddlesden-Popper (RP) and Dion-Jacobson (DJ) phases depending on the spacers. When different spacers are mixed into one perovskite structure, they are usually disordered and occupy the same interlayer space. In this work, we demonstrate that when cyclic 1,2,4-triazolium (Tz) is used as a spacer and combined with another linear spacer such as propylammonium (PA) or butylammonium (BA), the interlayer ordered mixed-spacer 2D perovskites can form. The Tz and PA (BA) spacers occupy separate interlayer spaces and show two different interlayer distances. The octahedra next to the Tz spacers resemble the stacking of the DJ phase while those adjacent to the PA (BA) layers exhibit the stacking of the RP phase. The bandgaps of (PA)(Tz)PbBr₄ and (BA)(Tz)PbBr₄ are in between the parent $n = 1$ compounds ((PA)₂PbBr₄ or (BA)₂PbBr₄ and (Tz)₂PbBr₄). DFT calculations suggest that the band structures of (PA)(Tz)PbBr₄ and (BA)(Tz)PbBr₄ combine features from parent compounds yet differ from a simple superposition. This way, we are able to combine the properties of different spacers (cyclic and linear, aromatic and aliphatic) in one structure. This work expands the structure types in 2D perovskites and suggests many possible combinations of spacer cations for all kinds of optoelectronic applications.

10:45 AM EN05.12.08

All-Inorganic Quantum Dot in Perovskite PbS-CsPbBr₃ for High Energy Radiation Scintillation Grayson C. Johnson, Haritha Rajeev, Sammy Fieser, Seung-Hun Lee and Joshua Choi;

Efficient and stable scintillators are crucial for medical imaging, high energy physics, security, and other fields. However, current scintillators are typically produced as single crystals in energy intensive, high-cost processes. Recently, inorganic-organic quantum-dot-in-lead halide perovskites compatible with scalable, low-cost, and large area manufacturing have been synthesized to address these shortcomings. Still, organic components result in lower stability of 3D lead halide perovskites compared to their all-inorganic counterparts. Here, we synthesize all-inorganic PbS quantum dot in CsPbBr₃ perovskites at the gram scale and demonstrate their utility as an ionizing radiation scintillator. Emissions under X-ray excitation span from 1400 nm to 1000 nm depending on the PbS quantum dot size. This material retains luminescent activity after exposure to ambient conditions at least 3 times longer than the PbS quantum dots in hybrid methylammonium lead bromide perovskites. Finally, this material was successfully pressed into bulk, polycrystalline pellets that may be used as individual pixels for high energy radiation detection devices.

11:00 AM *EN05.12.09

Defects Activity in Metal Halide Perovskites [AnnamariaPetrozza](#); Istituto Italiano di Tecnologia, Italy

Bandgap tuning is a crucial characteristic of metal-halide perovskites, with benchmark lead-iodide compounds having a bandgap of 1.6 eV. To increase the bandgap up to 2.0 eV a straightforward strategy is to partially substitute iodine with bromine in so-called mixed-halide lead perovskites. Such compounds are prone, however, to defect-induced halide segregation resulting in bandgap instabilities, which limits their application in tandem solar cells and a variety of optoelectronic devices. The optimization of the perovskite composition and surface passivating agents can effectively slow down, but not completely stop, such light-induced instabilities. Here I will show how we identify the defect and the relative intra-gap electronic state/charge carrier dynamics that triggers the material transformation and bandgap shift. It allows us to engineer the perovskite band edge energetics by engineering the chemical composition of the perovskite crystalline unit to radically deactivate the photo-activity of such electronic states and stabilize the perovskite bandgap over the entire spectral range above 1.6 eV. Overall, I will show how the photo-instability of lead based single and mixed halide perovskites, which can be seen as photo-degradation and bandgap photo-destabilization, has the same root. Then, I will conclude my lecture showing how, by halides alloying, we can achieve photo-stable bandgaps in a broad spectral range from NIR to 2 eV, in tin-based perovskites. Here, the defect chemistry modulates the electronic property of the semiconductor switching from a highly p-doped to an intrinsic one

11:30 AM EN05.12.10

Structural and Photophysical Consequences of the Interplay Between Cations in 2D Ruddlesden-Popper Metal Halide Perovskites [WillaMihalyci-Koch](#)¹, [GiuliaFolpini](#)², [DanieleCortecchia](#)², [KyanaM. Sanders](#)¹, [AnnamariaPetrozza](#)² and [SongJin](#)¹; ¹University of Wisconsin–Madison, United States; ²Istituto Italiano di Tecnologia, Italy

2D hybrid lead halide perovskites have been widely studied for optoelectronic and photovoltaic applications. Given the toxicity of lead, there is renewed interest in lead-free 2D halide perovskites including those based on Sn²⁺ and Ge²⁺. Changing the B-site metal cation can have structural consequences due to different ionic radii and lone pair activity. Here, we report a series of 2D Ruddlesden-Popper metal iodide perovskites based on a new spacer cation, 4-bromo-2-fluorobenzylammonium that contain different B-site [Pb, Sn, Ge] and A-site cations [Cs, methylammonium (MA), and formamidinium (FA)]. Comparing across 8 crystal structures, we investigate the structural changes that result from varying the cations and the dimensionality of the perovskite (*i.e.*, $n = 1, n = 2$, vs. 3D). Strong lone pair effects and reduced B-site radii lead to distinct changes in the octahedral tilting and spacer cation packing in the Ge-based perovskites, while the Sn and Pb-based perovskites are structurally analogous. Although the Ge perovskites exhibit weak, broad photoluminescence (PL), the PL emission from the Sn and Pb perovskites containing the 4Br2FBZ spacer cation appears bright and color-pure at room temperature. However, through temperature-dependent photoluminescence and lifetime measurements, we reveal that the photophysical behaviors of the Sn and Pb 2D perovskites are different despite their structural similarities. Understanding the interplay of cation effects and the impact on the optoelectronic properties is important for informed materials design of lead-free 2D perovskites.

11:45 AM EN05.12.11

Controlling Phase Transitions in 2D Perovskites with Organic Cation Alloying [RandKingsford](#) and [ConnorG. Bischak](#); The University of Utah, United States

Ruddlesden-Popper (RP) two-dimensional perovskites are quantum well materials with alternating layers of organic cations and inorganic octahedral layers. These materials have numerous applications due to their optoelectronic properties, including light-emitting diodes and photodetectors. RP perovskites also undergo structural phase transitions at relatively low temperatures, in which the organic layers undergo an ordered-to-disordered transition. Here, we present a synthetic strategy to tune the structural phase transition temperature of RP perovskites by alloying hexylammonium (HA) and pentylammonium (PA) cations. We also explore the connection between this phase transition and changes in the emissive properties of RP perovskites. Surprisingly, we find that HA₂PbI₄ and PA₂PbI₄ exhibit different changes in emissive properties upon undergoing the phase transition: the photoluminescence spectrum of HA₂PbI₄ decreases in intensity and blueshifts and the photoluminescence spectrum of PA₂PbI₄ exhibits an increase in intensity and redshifts. We attribute these changes in the photoluminescence spectra of HA₂PbI₄ and PA₂PbI₄ to changes in the degree of octahedral distortion. Last, we leverage changes in the photoluminescence of HA₂PbI₄ and PA₂PbI₄ to directly observe phase transition dynamics with photoluminescence microscopy. Our study represents an important step towards understanding couplings between structural dynamics and changes in optical properties in RP perovskites.

SESSION EN05.13: Structure Property Relationships in Halide Perovskites II

Session Chair: Bin Chen

Thursday Afternoon, November 30, 2023

Hynes, Level 3, Room 311

1:30 PM *EN05.13.01

From 2D to 3D Metal Halide Perovskites Nanostructures [LoredanaProtesescu](#); University of Groningen, Netherlands

Metal halides perovskites with nanoscale geometries have revolutionized the field of solution-processed photovoltaics and light-emitting devices due to their strong absorption and exceptional photoluminescence properties combined with a remarkable tolerance to structural defects. However, the further development of these materials to practical commercialization is hindered by their toxic components like lead and their inherent structural lability. Moreover, we still have little understanding of their crystallographic structures, chemical and physical interactions, and surface chemistry at a fundamental level.

The chemical design of metal halide perovskites proved to be the key to addressing those issues. Our recent findings confirm that a direct transition of the synthetic approach at nanoscale from Pb to Sn halide perovskites is not feasible. For Sn-based perovskites nanostructures, the structural dynamics between 3D cuboids and 2D Ruddlesden-Popper nanosheets colloids are highly dependent on the synthetic strategy. The presence of both species has a direct impact on the optoelectronic properties. Moreover, heterostructures containing halide perovskites nanocrystals are the next step towards obtaining accessible materials for industry. With the help of polymers or metal-organic frameworks, we can access air stable materials or ultra-small quantum dots.

2:00 PM EN05.13.02

Nearly Perfect Perovskites: Disorder and Anharmonicity in APbBr₃ (A = MA⁺, FA⁺, Cs⁺) [NicholasJ. Weadock](#)¹, [CameronMacKeen](#)², [KileyMayford](#)², [XixiQin](#)³, [JulianVigil](#)⁴, [YevgenyRakita](#)⁵, [HemamalKarunadasa](#)⁴, [VolkerBlum](#)³, [MichaelF. Toney](#)¹ and [FrankBridges](#)²; ¹University of Colorado at Boulder, United States; ²University of California, Santa Cruz, United States; ³Duke University, United States; ⁴Stanford University, United States; ⁵Ben-Gurion University of the Negev, Israel

Lead halide perovskite (LHP) semiconductors remain at the forefront of materials for high-performance optoelectronic devices. A defining characteristic of LHPs is the low point defect formation energy, yielding point defect concentrations as high as 10¹⁵ cm⁻³ [1]. This high defect concentration, combined with ionic bonding and a soft lattice [2], suggests a high degree of both static and thermally induced disorder in LHPs.

Here, we use extended X-ray absorption fine structure (EXAFS) and single-crystal X-ray diffraction (XRD) measurements to characterize disorder in the nearest neighbor Pb-Br bond for MAPbBr₃, FAPbBr₃, and CsPbBr₃. Surprisingly, the static disorder for all compositions is negligible, with low temperature disorder dominated by zero-point-motion. The disorder becomes significant as the temperature is increased, with subtle changes in bond character observed for MAPbBr₃ and FAPbBr₃. The high degree of thermal disorder manifests as an asymmetric Pb-Br pair distribution function (PDF), observable even at low temperatures of 150 K. Several origins of this asymmetry have been proposed, including single-site anharmonic potentials [3,4] and Pb split-sites [5,6]. We compare several asymmetric models to the experimental PDFs obtained from EXAFS and demonstrate that the asymmetry arises from an anharmonic interatomic potential.

Our results improve the understanding of point defects and intrinsic doping in LHPs: although the defects are charged, a lack of static disorder from coulombic interactions confirms the near complete ionization of these defects at room temperature. Finally, we will discuss the possibility of implementing these “nearly perfect” crystals for low temperature applications in quantum computing.

NJW, XQ, VB, and MFT gratefully acknowledge full support from the Center for Hybrid Organic Inorganic Semiconductors for Energy (CHOISE), an Energy Frontier Research Center funded by the Office of Basic Energy Sciences, Office of Science within the U.S. Department of Energy through contract number DE-AC36-08G028308.

- References:
- [1] J. Kang, J. Li, and S.-H. Wei, *Applied Physics Reviews* **8**, 031302 (2021).
 - [2] D. A. Egger, A. Bera, D. Cahen, G. Hodes, T. Kirchartz, L. Kronik, R. Lovrincic, A. M. Rappe, D. R. Reichman, and O. Yaffe, *Advanced Materials* **30**, 1800691 (2018).
 - [3] J. Liu, A. E. Phillips, D. A. Keen, and M. T. Dove, *J. Phys. Chem. C* **123**, 14934 (2019).
 - [4] G. Schuck, D. M. Töbrens, D. Wallacher, N. Grimm, T. S. Tien, and S. Schorr, *J. Phys. Chem. C* **126**, 5388 (2022).
 - [5] G. Laurita, D. H. Fabini, C. C. Stoumpos, M. G. Kanatzidis, and R. Seshadri, *Chem. Sci.* **8**, 5628 (2017).
 - [6] D. H. Fabini, R. Seshadri, and M. G. Kanatzidis, *MRS Bulletin* **45**, 467 (2020).

2:15 PM EN05.13.03

Thermotropic Liquid Crystals Enable Efficient and Stable Perovskite Solar Cells and Modules Yi Yang, Cheng Liu, Bin Chen, Mercurio G. Kanatzidis and Edward Sargent; Northwestern University, United States

Perovskite solar cells (PSCs) have seen impressive progress in performance and stability, yet maintaining power conversion efficiencies (PCEs) when scaling areas remains a challenge. Here we find that the additives used to passivate large-area perovskite films often co-crystallize near-simultaneously with perovskites or tend to aggregate at the surface/interface, which contributes to defects and to spatial inhomogeneity. We therefore introduce a thermotropic liquid crystal (TLC) additive with heightened diffusion ability at the perovskite annealing temperature to enable uniform, low-defects, and stable large-area perovskite films. We document as a result small-area PSCs achieving a PCE of 25.6% and modules having a certified PCE of 21.6% at an aperture area of 31 cm². These retain performance under the damp-heat test (ISOS-D-3, 85% relative humidity, 85°C) with T₈₆ of 1200 hours, and show high resistance to reverse bias with (ISOS-V-1, negative V_{mpp}) and without bypass diodes.

2:30 PM BREAK

3:00 PM EN05.13.04

Direct Observation of Contact Reaction Induced Ion Migration and Its Effect on Non-Ideal Charge Transport in Lead Triiodide Perovskite Field-Effect Transistors Youcheng Zhang and Henning Sirringhaus; University of Cambridge, United Kingdom

The migration of ionic defects and electrochemical reactions with metal electrodes remains one of the most important research challenges for organometal halide perovskite optoelectronic devices. There is still a lack of understanding of how the formation of mobile ionic defects impact charge carrier transport and operational device stability, particularly in perovskite field-effect transistors, that tend to exhibit anomalous device characteristics. Here, we investigate the evolution of the n-type FET in CsFAMAPbI₃ during repeated measurement cycles as a function of different metal source-drain contacts and precursor stoichiometry. The channel current increases for high work function metals and decreases for low work function metals when multiple cycles of transfer characteristics are measured. The cycling behaviour is also sensitive to the precursor stoichiometry. These metal/stoichiometry-dependent device non-idealities are correlated with the quenching of photoluminescence near the positively biased electrode. Based on elemental analysis using electron microscopy our observations can be understood by an n-type doping effect of metallic ions that are created by an electrochemical interaction at the metal-semiconductor interface and migrate into the channel.

Our findings improve our understanding of ion migration, contact reactions and the origin of non-idealities in lead triiodide perovskite FETs.[1] These findings shed light on how bias-induced migration of extrinsic metallic ions impacts charge transport at a device level, revealing the widespread nature of this phenomenon when perovskite is in direct contact with metals. Our work underscores the crucial role of careful metal selection and precise composition control for the successful design of durable and reliable perovskite-based optoelectronic devices.

- [1] Zhang, Y. et al. Direct Observation of Contact Reaction Induced Ion Migration and its Effect on Non-Ideal Charge Transport in Lead Triiodide Perovskite Field-Effect Transistors. *Small*, 2023, 2302494.

3:15 PM EN05.13.05

Understanding Charge Transport in High Performance Mixed Lead-Tin Halide Perovskite Transistors Krishanu Dey^{1,2}, Samuel D. Stranks^{2,2} and Henning Sirringhaus²; ¹University of Oxford, United Kingdom; ²University of Cambridge, United Kingdom

Metal halide perovskites have earned the distinction of one of the most exciting semiconductor technologies in the last decade, with the photovoltaic single junction power conversion efficiencies already demonstrating ~26% and all-perovskite tandem efficiencies exceeding 28%. However, due to the soft nature of the halide perovskite lattice, field-driven charge transport studies using 3D perovskite field effect transistors (FETs) have largely remained under the cloud of undesirable ionic migration effects near room temperature. In addition, the presence of methylammonium at the A-site in many high performing 3D perovskite compositions introduces additional instabilities, which limit the reliable room temperature operation of FETs.

In this work, we address both these challenges and demonstrate that FETs based on methylammonium-free, mixed-metal (Pb-Sn) perovskite compositions do not suffer from ion migration effects as significantly as their pure-Pb counterparts and reliably exhibit hysteresis free p-type transport with high mobility reaching 5.4 cm²/Vs, ON/OFF ratio approaching 10⁶ and promising operational stability, which are among the best reported metrics in the field of thin film perovskite FETs. Density functional theory calculations suggest that incorporation of Sn to partially replace Pb at the B-site of perovskite modifies the electronic structure to obtain a reduced hole effective mass and additional density of states at the valence band, thereby resulting in a pronounced p-type transport. The reduced ion migration is also manifested in an activated temperature dependence of the field-effect mobility with low activation energy, which reflects a significant density of shallow electronic defects in mixed Pb-Sn perovskites. This is sharply in contrast to the expected trend of negative temperature coefficient of mobility in the case of Pb perovskite FETs due to ion-induced field screening for the carriers in the channel. It is important to note that such interesting and distinctive trends of temperature-dependent mobility trends were never observed heretofore in 3D hybrid perovskite FETs owing to undesired ionic migration effects. We also visualize the suppressed in-plane ionic migration in Sn-containing perovskites compared to their pure-Pb counterparts using photoluminescence microscopy under bias and this can have significant ramifications for the applications of mixed-metal perovskites in future optoelectronics. Moreover, we also observe, for the first time, reversible electrochemical reduction of Sn⁴⁺ to Sn²⁺ happening under bias. Using spectroscopic measurements, we have established Sn⁴⁺ as a major source of defect in these Sn-containing perovskites and therefore such precise control of defect dynamics upon biasing brings out the transformative nature of these materials for designing high performance electronic devices.

In conclusion, this work represents the first comprehensive study of the field-driven charge transport on such low bandgap mixed Pb-Sn compositions, which have recently demonstrated significant progress in single junction and tandem solar cells, near-infrared light emitting diodes and photodetectors. Our work also establishes FETs as a powerful and reliable platform for providing fundamental insights into the doping, defects, instabilities, and charge transport physics of halide perovskite semiconductors to advance their applications in a plethora of semiconductor devices.

Reference

Nature Materials **22**, 216-224 (2023).

3:30 PM EN05.13.06

Supramolecular Assembly of Halide Perovskite Building Blocks Cheng Zhu^{1,2} and Peidong Yang^{1,2}; ¹UC Berkeley, United States; ²Lawrence Berkeley National Laboratory, United States

Metal halide ionic octahedron, [MX₆]ⁿ⁻ (M = Pb²⁺, Sb³⁺, Te⁴⁺, etc., X = Cl⁻, Br⁻, I⁻), is the fundamental building block and functional unit of halide perovskites. The properties of the extended solids are dictated by the way how these octahedra are assembled, connected, and interact with the surrounding atomic environment. Hence, the ability to manipulate and control the assembly of the octahedral building blocks is paramount for constructing new perovskite materials. Here, we propose a systematic supramolecular strategy as a new method for the assembly of a family of [MX₆]ⁿ⁻ into an extended network. Crown ethers are used to bind with various alkali metal cations to form supramolecular cations, two of which can sandwich one halide octahedron to form a structurally and optoelectronically tunable dumbbell structural unit. The dumbbell building blocks can be further assembled into extended crystals with diverse packing geometries and symmetries. Starting from the prototypical example of (18C6@Cs)₂TeCl₆ crystal structure, we can explore the synthetic space along: (1) varying the size of the crown ether (18C6 and 21C7), (2) changing the octahedra center cation (8 different metal cations), (3) tuning the halide anion (Cl⁻, Br⁻, and I⁻), (4) modifying the alkali metal cation coupled with the crown ether, and (5) introducing 1D and 2D electronic dimensionality by connecting the octahedra. With all these synthetic possibilities, this supramolecular assembly route introduces a new general strategy for

designing halide perovskite structures with tailorable optoelectronic properties. For example, the supramolecular-assembled crystals have strong photoluminescence (PL) with a highly tunable emission color. $(18\text{C}6@\text{Cs})_2\text{ZrCl}_6$ has a very bright blue emission, and the PL quantum yield is 12.57%. Furthermore, by varying the alkali metal cation from K^+ to Rb^+ to Cs^+ , the PL spectra continue to redshift. We expect that the assembly approach of the supramolecular building blocks could bring a new general method for halide perovskite materials discovery, and we could further appreciate the structural and functional versatility of halide perovskites.

3:45 PM EN05.13.07

Direct Experimental Evidence for Defect Tolerance in Pb-Halide Perovskites, at Last [David Cahen](#)^{1,2}, NagaP. Jasti^{2,1}, Sigalit Aharon¹, Yishay Feldman¹ and Igal Levine³; ¹Weizmann Institute, Israel; ²Bar-Ilan University, Israel; ³HZB, Germany

While *defect tolerance* (DT) lacks direct *experimental* evidence, it is widely used as the basis for the exceptional optoelectronic properties of Halide Perovskites, HaPs, and their devices. It became a “fact” in the field, also when the initial theoretical model and computational support for it, was challenged. DT in semiconductors implies tolerance to *structural defects* without the *electrical and optical effects* (e.g., traps), associated with such defects. As such it also directly impacts what we view as the stability of such materials.

We present the first DIRECT experimental evidence for DT in Pb-HaPs by comparing the structural quality of 2D, 2D-3D, and 3D Pb-iodide perovskite single crystals with their optoelectronic characteristics using high-sensitivity methods. Importantly, we get information from the materials’ bulk, because we sample *at least* ~0.1 to several μm , from the sample’s surface. Therefore, we assess the intrinsic bulk (and not only surface-) properties of HaPs. The results point to DT in 3D, to a lesser extent in 2D-3D, but not in the crystals. We ascribe such dimension-dependent DT to the higher number of (near)neighboring species, available to compensate for structural defect effects in the 3D than in the 2D crystals. Our experimental results and their interpretation can now guide the search for, and design of other materials with DT.

4:00 PM EN05.13.08

Temperature-Dependent Reversal of Phase Segregation in Mixed-Halide Perovskites [Adam D. Wright](#)^{1,2,3}; ¹University of Oxford, United Kingdom; ²University of Warwick, United Kingdom; ³Princeton University, United States

Tandem solar cells with metal halide perovskite top cells have achieved power conversion efficiencies better than single-junction silicon solar cells. However, the success of these devices is constrained by the phenomenon of halide segregation, which afflicts the mixed iodide-bromide compositions used to achieve the necessary wide bandgaps. When exposed to above-bandgap illumination, these mixed-halide perovskites de-mix into iodide-rich and bromide-rich regions. This phase segregation is deleterious to the performance of mixed-halide perovskites in tandem cell applications, but none of the multiplicity of proposed models have been able to fully explain all reported observations of light-induced halide segregation.

In this study¹, I report on the influence of temperature and light intensity on light-induced halide segregation in $\text{MAPb}(\text{Br}_{0.4}\text{I}_{0.6})_3$ by measuring changes in the photoluminescence spectra across an exceptionally wide parameter space. I reveal a reversal in the temperature trend in halide segregation rate, which speeds up as temperature is increased from 125 K to ~290 K, but slows down again with further increases in temperature. I attribute this reversal to the trade-off between the temperature activation of segregation, e.g. through enhanced ionic migration, and its inhibition by entropic factors. I further show that while halide remixing indeed occurs at highly elevated light intensities, and becomes more pronounced at higher temperatures, this effect is only transient, reversing on its own over the time scale of minutes under continued illumination. I utilize our findings to elucidate the validity of the most commonly examined models describing the origins of halide segregation, and discuss their relevance to applications of mixed-halide perovskites in tandem and concentrator solar cells.

¹*A. D. Wright, J. B. Patel, M. B. Johnston, L. M. Herz, Temperature dependent reversal of phase segregation in mixed-halide perovskites, *Advanced Materials*, (2023), 35, 2210834.

4:15 PM EN05.13.10

Bimolecularly-Passivated Interface Enables Efficient and Stable Inverted Perovskite Solar Cells [Cheng Liu](#), Bin Chen, Mercouri G. Kanatzidis and Edward Sargent; Northwestern University, Afghanistan

Compared to the n-i-p structure, inverted (p-i-n) perovskite solar cells (PSCs) promise increased operating stability; however, to date, these photovoltaic cells suffer lower power conversion efficiencies (PCEs), the result of nonradiative recombination losses, particularly at the perovskite/ C_{60} interface. Here we hypothesize that implementing the two functions is highly needed at the interface – 1) passivation of surface defects; and 2) the reflecting of minority carriers away from the interface and back into the bulk. We incorporate one molecule to passivate surface defects and suppress recombination via chemical interactions with perovskite. The other molecule was employed to repel minority carriers and reduce contact-induced interface recombination, achieved through field-effect passivation. The approach leads to a 5-fold increase in carrier lifetime and a 3-fold reduction in photoluminescence quantum yield (PLQY) loss, enabling the first certified quasi-steady-state PCE over 25% for inverted PSCs with stable operation at 65°C for over 2,000 hours in ambient air. We produce monolithic all-perovskite tandem solar cells with 28.1% PCE.

4:30 PM EN05.13.11

Architecture Optimization Improves Reverse Bias Stability in p-i-n Structured Perovskite Solar Cells [Fangyuan Jiang](#)¹, Yangwei Shi¹, Tanka R. Rana¹, Daniel Morales², Isaac Gould², Declan P. McCarthy², Joel Smith³, Greyson Christoforo³, Muammer Y. Yaman¹, Faiz Mandani⁴, Hannah Contreras¹, Stephen Barlow², Aditya D. Mohite⁴, Henry Snaith³, Seth R. Marder², J. Devin MacKenzie¹, Michael McGehee² and David S. Ginger¹; ¹University of Washington, United States; ²University of Colorado Boulder, United States; ³University of Oxford, United Kingdom; ⁴Rice University, United States

As perovskite photovoltaics make strides towards commercialization, reverse bias instability has been considered a serious challenge. We systematically investigate methods to improve reverse bias behaviors of p-i-n structured perovskite solar cells, including passivating halide vacancies, changing the electron transporting layer, and systematically varying the hole transporting layers and metal electrodes. Our results suggest that having a robust polymer hole transporting layer and an electrochemically stable electrode are important for preventing reverse bias breakdown of p-i-n perovskite solar cells. This result is surprising since much of the current effort and understanding has focused on the perovskite/electron transport layer/metal electrode interface. Nevertheless, with appropriate hole transporting layers, and optimized top electrode, we demonstrate breakdown voltages exceeding -15 V, comparable to that of silicon photovoltaics. Furthermore, our optimized solar cells demonstrate completely recoverable device performance even after being stressed at high reverse bias for many hours (i.e., at -7 V for 9 hours both in the dark and under partial shading). Following these observations, we propose a self-consistent model which highlights the role of electrochemical reaction pairs that has not been appreciated previously.

SESSION EN05.14: Halide Perovskites for Light Emission
Session Chairs: Connor Bischak and Bin Chen
Friday Morning, December 1, 2023
Hynes, Level 3, Room 311

8:00 AM EN05.14.01

Bioinspired Liquid Encapsulation Platform for Protection of Optoelectronic Devices [Haichao Wu](#), Zachary A. Goodwin, Baptiste Lemaire, Yanhao Yu, Nicola Molinari, Boris Kozinsky and Joanna Aizenberg; Harvard University, United States

The next-generation semiconductors and devices, such as halide perovskites and flexible electronics, are extremely sensitive to water, thus demanding highly effective protection that not only seals out water in all forms (vapor, droplet, and ice), but simultaneously provides mechanical flexibility, durability, transparency, and self-cleaning. Although various solid-state encapsulation methods have been developed, no strategy is available that can fully meet all the above requirements. Here, we report a bioinspired liquid-based encapsulation strategy that offers protection from water without sacrificing the operational properties of the encapsulated materials. Using halide perovskite as a model system, we show that damage to the perovskite from exposure to water is drastically reduced when it is coated by a polymer matrix with infused hydrophobic oil. With a combination of experimental and simulation studies, we elucidated the fundamental transport mechanisms of ultralow water transmission rate that stem from the ability of the infused liquid to fill-in and reduce defects in the coating layer, thus eliminating the low-energy diffusion pathways, and to cause water molecules to diffuse as clusters, which act together as an excellent water permeation barrier. Importantly, the presence of the liquid, as the central component in this encapsulation method provides a unique possibility of reversing the water transport direction; therefore, the lifetime of enclosed water-sensitive materials could be significantly extended via replenishing the hydrophobic oils regularly. We show that the liquid encapsulation platform presented here has high potential in providing not only water protection of the functional device but also flexibility, optical transparency, and self-healing of the coating layer, which are critical for a variety of applications, such as in perovskite solar cells and

8:15 AM *EN05.14.02

Towards Efficient and Stable Perovskite Light Emitting Diodes Daniel Congreve¹, Sebastian Fernandez¹, Manchen Hu¹, Mahesh Gangishetty², Shaocong Hou², Qimin Quan², William Michaels¹, Pournima Narayanan¹, Natalia Murrietta¹, Arny Gallegos¹, Ghada Ahmed¹, Junrui Lyu¹, Qi Zhou¹, Balreen Saini¹ and Tracy Schloemer¹; ¹Stanford University, United States; ²Rowland Institute at Harvard, United States

Perovskite LEDs are an exploding field, with high performance red and green devices demonstrated by many groups. However, two key challenges towards commercialization remain: poor performance at higher energies, and poor overall stability (particularly at those higher energies). Here, we demonstrate investigations into both issues. First, we identify two crucial issues holding blue materials back: the low internal photoluminescence yield and the LED device structure itself. By rectifying these issues, we were able to build LEDs that were 60x brighter than control, and, when combined with red and green downconverters, white light emitting LEDs. We further demonstrate how careful control over fabrication conditions allows for more uniform thin films, creating violet LEDs with 5x the efficiency over control devices. Finally, we study the interplay between efficiency and stability in green LEDs, showing that while an additive material can increase efficiency, it also leads to a stability decrease, highlighting the need for global evaluation of these changes to the device composition.

8:45 AM EN05.14.03

Designing Metal Halides for Fast Neutron Imaging Scintillators: Lessons from Perovskite Nanocrystals and Ionic Liquids Kyle M. McCall; University of Texas at Dallas, United States

The lead halide perovskites have captured the research community due to their exceptional optoelectronic properties that enable high performance as solar cells and light emitters. In particular, perovskite nanocrystals (NCs) have demonstrated their potential as next-generation light emitters, with applications ranging from QLED displays to X-ray scintillators. Recent work on metal halides for fast (high-energy, >1 MeV) neutron detection has shown that they have the potential to deliver low-cost, efficient scintillators for this application, with the advantages of high spatial resolution, low gamma-ray sensitivity, and negligible afterglow on the timescale of seconds. However, there are several challenges to overcome before these materials can displace the commercial polypropylene screens (embedded with microscale ZnS:Cu phosphors).

This presentation will summarize three studies in this field, which have each contributed design rules that will enable a more complete understanding of how to design metal halides for this application. A first comparison of perovskite nanocrystals with a variety of other halide and chalcogenide NCs showed that FAPbBr₃ NCs offered the highest light yield, while CsPbBrCl₂:Mn²⁺ NCs offered the highest spatial resolution. Composition and thickness-dependent measurements highlighted the need to 1) enhance concentration and 2) reduce self-absorption for all NC systems. Subsequently, we sought to further test these design rules by 1) exploring the use of metal halide ionic liquids for maximal concentration, and 2) separately pursuing the optimized synthesis and doping in CsPb(Br_xCl_{1-x})₃:Mn²⁺ NCs to improve concentration and eliminate reabsorption.

These follow-up studies showcased the importance of these design principles for improved fast neutron scintillation, as the latter system demonstrated the capacity for concentrations above 100 mg/mL while essentially eliminating self-absorption, while the former system yielded significantly higher spatial resolution and competitive light yields. This presentation will synthesize this series of results into a succinct summary of the needs of this lesser-known application, providing the fundamental background to engage with the burgeoning field of fast neutron imaging and design the perovskite materials that can deliver the next generation of fast neutron scintillators.

9:00 AM EN05.14.04

Efficient and Stable Perovskite Light Emitting Diodes by using Stabilized Interface Tianjun Liu, Samuel D. Stranks, Neil Greenham and Richard H. Friend; University of Cambridge, United Kingdom

Metal halide perovskites have shown great optoelectronic properties for light emitting diodes (LEDs), such as high photoluminescence quantum yields (PLQYs), tunable bandgap, narrow emission linewidths and high charge-carrier mobility. Owing to the development of the strategy of defect passivation and controllable growth of grains, the external quantum efficiencies (EQEs) of perovskite light emitting diodes (PeLEDs) have achieved more than 25%. Furthermore, critical interface engineering has also been developed for fabricating PeLEDs with long operational stability, making a key step toward practical applications and future commercialization. We report an efficient PeLED with EQE > 24% in near infrared emission range by using organic additives. Owing to the stabilized interface, the achieved devices present long term operational stability with T50 above 800 hours at current density of 20 mA/cm². </quillbot-extension-portal></quillbot-extension-portal>

9:15 AM EN05.14.05

Continuous-Wave Amplified Spontaneous Emission and High-Current-Density Operation from a Transparent Perovskite LED Architecture Karim Elkhoully^{1,2}, Iakov Goldberg^{1,2}, Xin Zhang^{1,2,3}, Nirav Annavarapu^{1,2}, Weiming Qiu¹, Cedric Rolin¹, Jan Genoe^{1,2}, Robert Gehlhaar¹ and Paul Heremans^{1,2}; ¹Imec, Belgium; ²KU Leuven, Belgium; ³Fudan University, China

Metal halide perovskites are excellent candidates for the gain material in thin film laser diodes. They exhibit high optical gain, low amplified spontaneous emission (ASE) thresholds, and a wide emission wavelength tunability. These attributes have facilitated notable advancements such as optically-pumped pulsed and continuous-wave (CW) lasing from a large library of optical cavities, operating under both room-temperature and cryogenic conditions. The successful development of perovskite laser diodes and their prospective heterogeneous integration into photonic circuits would pave the way for a multitude of applications in domains such as sensing, ranging, data communication, and miniaturized displays.

However, achieving a current-injection perovskite laser, a promising yet complex feat, remains elusive due to the inherent complexity of the optoelectronic design challenges. Firstly, there is the necessity for high internal quantum efficiency (IQE) at extreme current densities ranging from hundreds to thousands of A/cm². This demands effective strategies for mitigating Joule heating, a problem magnified by perovskites' inherent low thermal conductivity and diminished stability at such high current densities. Secondly, the device stack must be optimized in terms of its optical design to maximize the net modal gain. This imposes stringent criteria on the thickness and conductivity of the layers comprising the device stack. In particular, the key challenge stems from the presence of conductive metal electrodes in the vicinity of a gain layer. It's essential, on the one hand, that electrodes inject kA/cm² current densities into the device. On the other hand, these highly conductive layers contribute to substantial free-carrier optical absorption, thereby increasing ASE threshold and current density necessary for ASE lasing. In the last step toward a laser, a high quality-factor optical cavity has to be integrated into the perovskite LED (PeLED) without compromising the device performance and reliability.

In this work, we embed a perovskite waveguide stack, optimized for high-current density operation, into a scaled (50 μm in diameter) transparent LED architecture with reduced optical losses. We reliably operate this miniaturized PeLED in a sub-μs pulsed mode above 3 kA/cm² without irreversible degradation. At these current densities, the device delivers EQEs above 1% at 77 K. Moreover, we achieve low ASE thresholds (< 10 μJ/cm²) from this fully contacted electrical structure at 77 K using 3-ns optical pumping. This PeLED allows us to achieve several crucial milestones towards injection lasing: 1) ASE enhancement at synchronized photo-electrical co-excitation; 2) optically-pumped CW ASE when excited with 1-μs-long optical pulses; 3) electroluminescence brightness levels close to half of the brightness produced by CW optical pumping at ASE threshold. These milestones set us within reach of realizing a perovskite-based thin-film laser diode. Finally, we will also discuss novel concepts of integrating a fully functional PeLED with optical cavities for future thin-film perovskite laser diodes.

9:30 AM EN05.14.06

On the Photolysis of Mixed Halide Perovskite Nanocrystals Michael C. Brennan^{1,2} and Tod Grusenmeyer¹; ¹Air Force Research Lab, United States; ²Azimuth Corporation, United States

Colloidal mixed halide perovskite nanocrystals (NCs) irreversibly degrade when exposed to ultraviolet—visible irradiation. Here, mixed halide perovskite NC photolysis is tracked via mass spectrometry, electron microscopy, and photoluminescence. The data shows continuous wave ultraviolet—visible irradiation causes the heavier halides within the alloy to sublimate. This ultimately transforms CsPb(I_{1-x}Br_x)₃ and CsPb(Cl_{1-x}Br_x)₃ (x ≈ 0.50) NCs into CsPbBr₃ and CsPbCl₃ NCs, respectively. Time-resolved mass spectrometry demonstrates real-time desorption of volatile halide species (e.g. I_{2(g)}/HI_(g)) during irradiation. Energy-dispersive X-ray spectroscopy confirms near complete expulsion of I from CsPb(I_{1-x}Br_x)₃ and Br from CsPb(Cl_{1-x}Br_x)₃ NCs. Electron diffraction and cathodoluminescence establish lattice contractions and emission blueshifts consistent with formation of single halide perovskites from parent mixed halide alloys. Finally, increasing photolysis rates at higher temperatures follow an Arrhenius relationship with an effective activation energy of ~62 kJ mol⁻¹ for CsPb(I_{1-x}Br_x)₃ NCs (x ≈ 0.50). Altogether, this work provides important insight into the photolysis of colloidal perovskite NC alloys.

9:45 AM EN05.14.07

Experimentally Observed Defect Tolerance in the Electronic Structure of Lead Bromide Perovskites Gabriel J. Man^{1,2,3}, Aleksandr Kalinko⁴, Dibya Phuyal⁵, Pabitra K. Nayak⁶, Håkan Rensmo² and Sergei M. Butorin²; ¹MAX IV Laboratory, Sweden; ²Uppsala University, Sweden; ³GJM Scientific Consulting, United States; ⁴Deutsches Elektronen-Synchrotron DESY, Germany; ⁵KTH Royal Institute of Technology, Sweden; ⁶Tata Institute of Fundamental Research, India

Point defect tolerance in materials, which extends operational lifetime, is essential for societal sustainability, and the creation of a framework to design such properties is a grand challenge in the material sciences. Using three prototypical lead bromide perovskites in single crystal form and high-resolution synchrotron-based X-ray spectroscopy, we reveal the unexpectedly pivotal role of the A-cation in mediating the influence of photoinduced defects. Organic A-cation hydrogen bonding facilitates chemical flexing of the lead-bromide bond that mitigates the self-doping effect of bromide vacancies. The contribution of partially ionic lead-bromide bonding to the electronic band edges, where the bonding becomes more ionic upon the formation of

defects, mitigates re-hybridization of the electronic structure upon degradation. These findings reveal two new general design principles for defect tolerance in materials. Our findings uncover the foundations of defect tolerance in halide perovskites and have implications for defect calculations, all beam-based measurements of photophysical properties and perovskite solar cell technology.

10:00 AMBREAK

10:30 AM *EN05.14.08

Perovskites—From Bulk to NanoLeaNienhaus; Florida State University, United States

Triplet generation at a hybrid inorganic/organic semiconductor interface is a promising approach to increase the (photo)-excited state recombination lifetime, and thus, facilitate energy harvesting. One of the possible applications using the generated spin-triplet excitons is photon upconversion, which describes the process of shortening the wavelength of the light emitted after irradiation.

Recently, perovskite materials have emerged as triplet sensitizers for photon upconversion. To fully understand the triplet generation mechanism, a fundamental understanding of the underlying perovskite properties is required. Here, I will present the current understanding of charge transfer at the perovskite/organic interface resulting in triplet generation interrogated by a combination of scanning probe microscopy and optical spectroscopy. Of particular interest are the nanoscale properties of the perovskite and how surface treatments or added stressors influence the fundamental optoelectronic properties of the perovskite both on the ensemble and at the nanoscale. [1,2,3]

[1] Sullivan, C.M.; Bieber, A.S.; Drozdick, H.K.; **Moller, G.**; Kusyznski, J.E.; VanOrman, Z.A.; Wieghold, S.; Strouse, G.F.; Nienhaus, L., Surface Doping Boosts Triplet Generation Yield in Perovskite-Sensitized Upconversion. *Adv. Opt. Mater.*, **2022**, 11, 2201921.

[2] Wieghold, S.; Nienhaus, L., Viewing Optical Processes at the Nanoscale: Combining Scanning Tunneling Microscopy and Optical Spectroscopy. *J. Phys. Chem. C* **2023**, 127, 3913–3920.

[3] Wieghold, S.; *Cope, E.M.; Moller, G.*; Shirato, N.; Guzelurk, B.; Rose, V.; Nienhaus, L. Stressing Halide Perovskites with Light and Electric Fields. *ACS Energy Lett.*, **2022**, 7, 2211–2218.

11:00 AM EN05.14.09

Implementing QD-In-Host Structure for High Efficiency in Deep-Blue Perovskite LEDsKyung YeonJang¹, Seung-JeWoo¹, HyereeKim¹ and Tae-WooLee^{1,2}; ¹Seoul National University, Korea (the Republic of); ²SN Display Co., Ltd., Korea (the Republic of)

Metal halide perovskite light-emitting diodes (PeLEDs) have received substantial interest due to their exceptional color purity, satisfying the Rec. 2020 color gamut standard, and impressive efficiency in pure-green and pure-red perovskite nanoparticle LEDs. However, the challenge lies in achieving high efficiency in the deep-blue region, an area hitherto under-explored. This study focuses on using CsPbBr₃ quantum dots (QDs) as the light-emitting layer in PeLEDs. We identify two obstacles that need to be overcome: the difficulty in ligand post-treatment and the spectrum red-shift in the film state.

Here, we propose an alternative ligand enriched with a chemical passivation process, effectively amplifying the photoluminescence quantum yield (PLQY) of deep-blue QDs from 15% to nearly 90%. Furthermore, to address the spectrum red-shift induced by energy transfer or electronic coupling, we introduce a QD-in-host structure to physically separate the QDs in the film state. A reduction in the concentration of QDs in the film yielded a blue-shift of approximately 7 nm in the emission spectrum. By incorporating these strategies, we achieved a maximum external quantum efficiency of 6.2% at a peak wavelength of 462 nm. The findings of this study provide crucial strategies for deep-blue QD PeLEDs, which hold potential for broad applicability across diverse PeLED types.

11:15 AM EN05.14.10

Ultra-Stable Dual-Color Emitting Lead-Free Double Perovskite Cs₂SnI₆ with a Wide Emission SpanFuqianYang; University of Kentucky, United States

We have developed a green-route approach to prepare lead-free double perovskite Cs₂SnI₆ powder and nanocrystals, using an environmentally friendly aqueous solution. The sonication of the Cs₂SnI₆ powder in hexane under ambient conditions leads to the formation of Cs₂SnI₆ nanocrystals. The Cs₂SnI₆ powder and nanocrystals exhibit band gaps of 1.3 and 2.8 eV, respectively. There is a difference of 1.5 eV in the band gaps. The Cs₂SnI₆ nanocrystals with good long-term structural and optical stabilities have a PLQY of ~7% and a PL peak wavelength of 440 nm over a span of 50 days. The dual-color emission of the perovskite Cs₂SnI₆ is likely due to the dependence of dielectric constant on crystal size instead of the effect of quantum confinement. This work is supported by the NSF through the grant CMMI-1854554 and CBET- 2018411.

11:30 AM EN05.14.12

Dimensionality and Tunability in The Tin Halide Perovskite Colloidal NanostructuresKushagraGahlot and LoredanaProtesescu; University of Groningen, Netherlands

The chemistry of tin-halide perovskites remain under-developed when compared to their lead counterparts in bulk as well as in nano owing to their inability to provide a stable Sn(II) oxidation state to maintain pristine crystal structure phase in ambient conditions. Hence, a simple reciprocation of the synthetic conditions from Pb-halide perovskites doesn't suffice. In this work, I will discuss the physical and chemical parameters which can help us to achieve a stable, tunable and monodisperse CsSnX₃ perovskite nanocrystals with defined optical features.¹ Pertaining to the formation energies of these perovskite nanostructures, the studies on the interplay of the 2D Ruddlesden-Popper (L₂Cs_{n-1}Sn_nX_{3n+1}) crystal phases and 3D CsSnX₃ nanocrystals were performed with respect to ligand combinations (ammonium, carboxylate, phosphinate), metal precursor ratios and temperature when SnX₂ salt is used as a precursor in order to understand the nucleation mechanism of nanocrystal formation. Moreover, the successful transformation of a purified 2D Ruddlesden-Popper (L₂SnX₄) phase to form 3D CsSnX₃ nanocrystals via a hot-injection approach and their ability to undergo post-synthetic anion exchange processes at room temperature using benzoyl halides will be discussed in details. X-ray diffraction and scattering studies conjoined with optical spectroscopy and electron microscopy helps us in acquiring the useful insights in directing the chemistry of Sn-halide perovskites at nanoscale. This research work showcases the insistent necessity for the development of mechanistic understanding to design efficient synthetic routes in order to achieve high-quality tin-halide perovskite nanocrystals.

1. *Adv. Mater.* **2022**, 34 (30), 2201353

SESSION EN05.15: Virtual Session
Thursday Morning, December 7, 2023
EN05-virtual

10:30 AM EN05.15.01

Nanostructure Modification on Thermally Evaporated Perovskite Films Toward Large-Area Light-Emitting DiodesChan-YulPark¹, Jung-MinHeo¹, Joo SungKim^{2,3}, EojinYoon¹ and Tae-WooLee^{1,2}; ¹Seoul National University, Korea (the Republic of); ²SN Display Co. Ltd, Korea (the Republic of); ³Soft Foundry, Seoul National University, Korea (the Republic of)

In the contemporary era of digital society, there is a rising demand for vibrant color displays applicable in wearable electronics, indoor lighting, and expansive display systems. Metal halide perovskites have emerged as a highly promising material due to their advantages such as cost-effectiveness, excellent color purity with narrow full width at half maximum (FWHM, ~20nm), and the ease of color tuning by altering halide components. Nonetheless, despite the high-efficiency perovskite light-emitting diodes (PeLEDs) with external quantum efficiency (EQE) of over 20% was achieved through facile spin-coating methods, it couldn't be applied to the fabrication of large-area devices due to the low uniformity of the film. To overcome these limitations, a thermal evaporation method utilizing all-inorganic 3D CsPbBr₃ powders as precursor was developed. However, their use as emitters showed poor emission efficiency arising from critical drawbacks such as large crystal size, low exciton binding energy, and high defect concentration.

In this study, we introduced a new thermal evaporation method by co-evaporating 3D CsPbBr₃ and bulky ammonium cation (benzylammonium bromide, BzABr) to achieve quasi-two-dimensional (quasi-2D) perovskites with energy funneling and strong charge confinement. The existence of quasi-2D perovskites with efficient charge funneling and quantum confinement was confirmed by optical analysis. The grain size was also reduced from 80 to 50 nm, which could induce additional spatial charge confinement for efficient radiative recombination. Compared to the pristine 3D CsPbBr₃ film, the quasi-2D perovskite film showed tenfold-increased photoluminescence (PL) intensity. PeLEDs based on the thermally-evaporated quasi-2D perovskite thin films showed a maximum current efficiency of 3.6 cd/A and a maximum luminance of 1700 cd/m², showing an considerable improvement than that of Compared to PeLEDs based on thermally-evaporated 3D CsPbBr₃ without light emission due to the low luminous efficiency and high leakage current, PeLEDs based on the thermally-evaporated quasi-2D perovskite thin films showed a maximum current efficiency of 3.6 cd/A and a maximum luminance of 1700 cd/m², showing the great possibility of efficient PeLEDs based on thermal

evaporation method. This work represents a significant advancement towards the commercialization of metal halide perovskites for future vivid color displays by successfully addressing a critical challenge in the fabrication of large-area perovskite-based display devices.

10:35 AM EN05.15.02

Color-Stable Mixed-Halide Blue Perovskite Light-Emitting Diodes Seong EuiChang¹, Joo SungKim^{2,3} and Tae-WooLee^{1,1,2}; ¹Seoul National University, Korea (the Republic of); ²SN Display Co. Ltd., Korea (the Republic of); ³Soft Foundry, Seoul National University, Korea (the Republic of)

Metal halide perovskites have emerged as a highly promising candidate for the advancement of next-generation light-emitting materials owing to their exceptional optoelectronic properties, including superior color purity, high photoluminescence quantum efficiency, and facile tunability of their bandgap through facile compositional control. As a consequence of these advantages, efficient perovskite light-emitting diodes (PeLEDs) with external quantum efficiency (EQE) surpassing 20% have been successfully demonstrated. However, the realization of efficient and stable blue-emitting PeLEDs, which are crucial for achieving vivid emission across the entire color gamut, has proved to be a formidable challenge, primarily due to the spectral instability exhibited by mixed-halide composites employed for blue emission. In this investigation, we present the successful realization of color-stable mixed-halide blue PeLEDs achieved through the implementation of core/shell perovskite nanograins with mitigated halide segregation. By employing shell materials that effectively bind at the grain boundaries, we effectively suppress the electric-field-induced segregation of halide ions, resulting in stable and narrow emission spectra during the operational lifetime of the devices. Our study thus presents a promising strategy for the realization of stable mixed-halide perovskite materials with complete suppression of halide segregation, thereby facilitating the development of bandgap-tunable perovskite optoelectronic devices.

10:40 AM EN05.15.03

Carbon Nanoflake Based Materials for Charge Transport Layers of Perovskite Solar Cells: Insight from Atomistic Modeling into Nanosizing and Functionalizations Suitable for Electron and Hole Transport RuichengLi, KeisukeKameda, SergeiManzhos and Manabulhara; Tokyo Institute of Technology, Japan

A key bottleneck on the way to practical deployment of perovskite solar cells (PSC) are charge transport materials. Charge transport layers are needed to achieve high performance with PSCs, but hole transporting materials (HTM) and electron transporting materials (ETM) used in high-performance lab-scale PSCs are relatively high-cost. Another key bottleneck, low cell stability, is related to the issue of charge transport layers, as high-performance HTMs typically require the use of dopants that are detrimental to cell stability.

Recently, the use of carbon-based materials for both HTM and ETM has been gaining attention, in particular due to the possibility of synthesizing such materials from biomass or plastic wastes. This promises combining large-scale, low cost production with environmental remediation. Much of such research is empirical, without detailed insight into electronic properties of the synthesized materials. Such insight is needed to understand the possibility of forming correct band alignment and to ensure adequate charge transfer properties and for rational design of carbon-based HTMs and ETMs.

Carbon nanoflakes are one promising type of carbon based materials. Their size and functionalization/doping can be controlled, albeit imperfectly. We perform ab initio and semiempirical calculations to understand what sizes, shapes, and functionalizations can allow carbon nanoflakes to achieve band alignment and charge transport properties suitable for their use as either HTM or ETM. We include the effects of solid packing in the calculations and show that they substantially affect electronic properties. We show, in particular, that nanoflake sizes required for HTM capability should be as small as 1.5 nm, which is much smaller than nanoparticle sizes typically used in the literature. We also show that different functionalizations can make the same nanoflakes work as either ETM or HTM, and can also be used to control charge transport properties. Conversely, our results indicate that tight control of the presence of functional groups is required during synthesis to preserve HTM or ETM capability of such materials.

10:45 AM EN05.15.04

Inorganic-Derived Zero-Dimensional Perovskite Induced Surface Lattice Matching for Efficient and Stable All-Inorganic Perovskite Solar Cells Jin HyuckHeo, Jin KyoungPark and Sang HyukIm; Korea University, Korea (the Republic of)

The inverted inorganic CsPbI₃ perovskites solar cells (PSCs) are prospective candidates for next-generation photovoltaics owing to inherent robust thermal/photo-stability and compatibility for tandems. However, the performance and stability of the inverted CsPbI₃ PSCs fall behind the n-i-p counterparts due to poor energetic alignment and abundant interfacial defect states. Here, we implement an inorganic 0-dimensional Cs₄PbBr₆ with good lattice matching and exhibits enclosed stability with CsPbI₃ as a surface anchoring capping layer. The heavy n-type feature of the Cs₄PbBr₆ perovskite induces enhanced electron-selective junction and thus facilitates efficient charge extraction and effectively inhibits non-radiative recombination. Consequently, the CsPbI₃ PSCs with Cs₄PbBr₆ demonstrate the highest PCE of CsPbI₃-based inverted PSCs, reaching 20.38 % power conversion efficiency (PCE) from a unit cell and 17.39 % PCE from a module with a 64 cm² aperture area. Furthermore, the resulting devices retain 92.48 % after 1000 hours under simultaneous 1-sun and damp heat (85 °C / 85 % relative humidity (RH) environment.

10:50 AM EN05.15.05

Enhancing Exciton Confinement in Perovskite Light-Emitting Diodes Through Spray-Coating: The Energy-Well Band Structure Approach Jin KyoungPark, Jin HyuckHeo and Sang HyukIm; Korea University, Korea (the Republic of)

Metal-halide perovskite materials have garnered significant interest as potential candidates for next-generation light emitters. These materials possess unique properties such as high color purity, narrow spectral emission, high photoluminescent quantum yield, and solution processability. However, bulk metal-halide perovskite films suffer from low exciton binding energies, necessitating the fabrication of uniform polycrystalline films with small grain sizes to enhance quantum efficiency. Exciton confinement can be achieved through top-down and bottom-up methods. Several studies have successfully improved the efficiency of perovskite light-emitting diodes (PeLEDs) by enhancing the charge confinement effect. However, the translation of these advancements into commercial products remains challenging due to the limitations of the spin-coating process. Spray-coating, on the other hand, offers an economical and scalable alternative, enabling the fabrication of uniform thin films on a large scale. It provides greater design freedom and minimal influence from chemical orthogonality, allowing controlled stacking of layers and compositions.

In this study, we present a breakthrough in PeLEDs by constructing an energy-well band structure through spray-coating. By incorporating a Cs₄PbBr₆ layer onto the CsPbBr₃ film using the spray-coating technique, we have observed a significant enhancement in both photoluminescence (PL) and electroluminescence (EL) efficiency, reaching up to 23,415 cd/m² and 13.08%, respectively. Additionally, Cs₄PbBr₆, an inorganic perovskite material, exhibits a substantially wider bandgap than CsPbBr₃, making it suitable for improving the energy band structure and serving as a passivation layer.

The observed improvement can be attributed to the increased exciton binding energy achieved through the modified structure. To further enhance the confinement of excitons, we have introduced adjustments to the device structure by incorporating both a buried layer and an overlying layer of Cs₄PbBr₆. This modification facilitates the formation of an energy-well structure, thereby enhancing the confinement and stability of excitons within the device. Consequently, our optimized CsPbBr₃ PeLED with the Cs₄PbBr₆ well demonstrates impressive performance metrics, including a maximum luminance of 25,261 cd/m², a maximum current efficiency (CE) of 65.85 cd/A, and a maximum external quantum efficiency (EQE) of 14.72%.

10:55 AM EN05.15.06

Lead Free Halide Perovskite Based Asymmetric Flexible Supercapacitor AnkurYadav and MonojitBag; Indian Institute of Technology Roorkee, India

Supercapacitors (SCs) have received a lot of attention as storage devices because of their high-power density and long-life cycle when compared to batteries. The choice of electrode materials is crucial in increasing the capacitive performance of SCs. Lead halide perovskites have achieved extraordinary success in a wide range of applications, including solar cells, light-emitting diodes, detectors and so on. In recent studies with non-aqueous electrolytes, halide perovskite-based supercapacitors emerged as promising material for energy storage applications. The majority of halide perovskites research has been focused on Pb-based materials, due to their excellent properties, and well-understood formation process. However, lead (Pb) toxicity is still a source of contention. Pb, a very toxic element, can accumulate in the human body and induce a variety of brain-related symptoms including abdominal pain, constipation, and headaches. Lead's immediately dangerous to life or health (IDLH) value is only 100 mg m³, indicating that humans are extremely vulnerable to Pb poisoning. Therefore, a non-toxic element must be used to replace Pb in these perovskite materials. Several attempts have been made to substitute Pb in perovskite materials with group 14 elements such as tin (Sn) and germanium (Ge). However, Sn and Ge replacement in perovskites results in poor stability due to oxidation effects. Bismuth (Bi) is an element that is adjacent to Pb and has properties that are similar and comparable to Pb's. We have fabricated lead based (MAPbI₃) and lead free (MA₃Bi₂I₉) based supercapacitor for energy storage applications. The specific capacitance is around 250 F/g for MAPbI₃ whereas it is around 320 F/g for MA₃Bi₂I₉ based electrode as calculated from Galvanometric charge discharge (GCD) measurement. It is also confirmed from the Cyclic voltammetry that the lead-free electrode has higher capacitance than lead based electrode. Cyclic stability shows capacitance retention around 81% for MAPbI₃ and 91% for MA₃Bi₂I₉ for 1500 cycles as measured from three electrode measurements. Furthermore, we have fabricated gel electrolyte-based asymmetric device for both lead based (MAPbI₃) and lead free (MA₃Bi₂I₉) materials. The lead-free device shows decent areal capacitance ~30 mF/cm² with energy density around 5 μWh/cm² and corresponding power density ~200 μW/cm² @0.25 mA/cm². The lead-free based device is also able to drive white and yellow LED's. with single cell. The gel electrolyte device shows stability around 88% for 1500 cycles. We have also fabricated lead free flexible device on stainless steel substrate. The flexibility test was performed on our custom-built programmable setup for bending angles and bending cycles. The device shows capacity retention around 92% for 180° bending angles and 86% for 200 bending cycles.

11:00 AM EN05.15.07

Theoretical Insights into Cs₂MSbX₆ (M = Cu, Ag, Na, K, Rb, Cs and X = Cl, Br) Halide Double-Perovskite Materials for Optoelectronic Applications PriyaJohari and [SurajitAdhikari](#); Shiv Nadar University, India

Lead-halide perovskites APbX₃ (A = Cs, CH₃NH₃ and X = Cl, Br) have attracted broad interest in photovoltaic applications over the past decade due to their suitable bandgap and high optical absorption ability [1]. But lead-induced toxicity and materials instability has sparked interest in alternative materials with properties like APbX₃ perovskites. Recently, lead-free inorganic double halide perovskites Cs₂M(I)M(III)X₆ have been proposed as promising nontoxic materials with enhanced chemical stability for optoelectronic applications [2]. However, not much has been explored in the context of their mechanical, transport, and excitonic properties, which play a crucial role in defining an efficient and flexible optoelectronic device. We have, therefore, systematically conducted a series of state-of-the-art first-principles density functional theory, hybrid density functional theory, and many-body perturbation theory (namely GW and BSE) calculations to investigate the mechanical, transport, and excitonic properties of Cs₂MSbX₆ (M = Cu, Ag, Na, K, Rb, and Cs; X = Cl, Br) along with their structural, electronic, and optical properties. Our results indicate that all the systems maintain the standard cubic lattice and show high phase stability against decomposition (decomposition enthalpy > 20 meV/atom). Band structure calculations (HSE06 and G₀W₀@PBE) reflect that the compounds have a wide range of tunable bandgaps (1.2 eV - 5.2 eV), and the bandgap decreases on going from Cl to Br. BSE calculations reveal that these materials have excellent absorption capabilities from visible to ultraviolet light region. Investigation of transport properties and excitonic parameters elucidates that most of the Cs₂MSbX₆ materials exhibit small charge carrier effective masses (higher mobility) and low to moderate exciton binding energy as well as longer to shorter exciton lifetime, which make them suitable for a solar cell application. Further, on calculating the mechanical properties these compounds are found to exhibit low elastic moduli that decrease from Cs₂MSbCl₆ to Cs₂MSbBr₆. Furthermore, except Cs₂CuSbBr₆, these compounds are predicted to be ductile in nature with a noticeable elastic anisotropy, revealing these materials to exhibit good flexibility. Further, on considering the mixed halide double perovskites Cs₂MSbBr_{6-x}Cl_x (x = 0-6, M=Ag) it is found that the optoelectronic properties can be widely tuned, and thus, such materials may a suitable component for the future generation of optoelectronic devices. Overall, our study predicts Cs₂MSbX₆ to be a stable double perovskite with a wide range of tunable optoelectronic properties, and promising transport and excitonic properties, providing a helpful guide to developing next-generation photovoltaics and flexible optoelectronics.

References:

1. *Linear Relationship between the Dielectric Constant and Band Gap in Low-Dimensional Mixed-Halide Perovskites*, Yujing Dong, Rui Zhu*, and Yu Jia* *J. Phys. Chem. C* 125, 14883-14890 (2021).
2. *Can Pb-Free Halide Double Perovskites Support High-Efficiency Solar Cells?* Christopher N. Savory, Aron Walsh, and David O. Scanlon* *ACS Energy Lett.* 1, 949- 955 (2016).

11:05 AM EN05.15.08

Highly-Sensitive X-Ray Detectors Based on Single-Crystal Mixed-Halide Perovskite CsPbBr_{3-x}(Cl, I)_x [RongWu](#) and FangzeLiu; Beijing Institute of Technology, China

Lead halide perovskites are emerging materials for a variety of optoelectronic applications, for example, photovoltaics, light-emitting diodes, photodetectors, lasers and photocatalysts. During the past few years, they have been extensively studied for radiation detection, especially for X-ray detectors due to their high absorption cross section, high carrier mobility lifetime product, tunable direct bandgap and low-cost synthesis. Perovskite X-ray detectors have shown higher sensitivity as well as lower detection limit compared with conventional Se and CdZnTe detectors. Despite the rapid advances in perovskite X-ray detectors, their performance is significantly hindered by the intrinsic limitations of perovskites, including low stability, low resistivity and high ion migration. Compared with hybrid organic-inorganic perovskites, all-inorganic CsPbBr₃ has attracted a lot of interests mainly for its high thermal stability. Various solution growth methods have been proved as effective routes to achieve large-size CsPbBr₃ single crystals. However, achieving stable perovskite X-ray detectors with suppressed ion migration and low dark current remains a challenge.

Here, we synthesized mixed-halide perovskite CsPbBr_{3-x}(Cl, I)_x single crystals with x ranging between 0 and 0.3. The structure and composition of single crystals are verified using XRD, EDS, UV-vis absorption and photoluminescence. The single crystal X-ray detectors show high sensitivity exceeding 3×10⁴ μC Gy_{air} cm⁻² and low detection limit below 50 nGy s⁻¹ for 90 keV X-ray under 500 V cm⁻¹ electric field. By constructing detectors with high and low work function contacts, we find that the dark current mainly originates from the hole current, and therefore using low work function contact can effectively suppress the dark current, achieving a low current density of ~40 nA cm⁻² under 500 V cm⁻¹ electric field, which is lower than 1/100 of the dark current density using high work function contacts. The halide doping and contact engineering prove that the mixed-halide perovskites are promising materials for high-performance X-ray detectors.

11:10 AM EN05.15.09

Exploring Self-Assembled Hole Transport Materials in p-i-n Perovskite Solar Cells [MinsikShin](#)¹, DongminYoon², HongyiHuang³, YifanYin⁴ and MiriamRafailovich⁴; ¹Seoul International School, Korea (the Republic of); ²North London Collegiate School Jeju, Korea (the Republic of); ³Shenzhen Middle School, China; ⁴Stony Brook University, The State University of New York, United States

Renewable energy plays a crucial role in combating climate change, and one of the primary focuses is improving the efficiency and production of solar cells. Over the past decade, perovskite solar cells (PSCs) have garnered significant attention due to the extraordinary evolution of the power conversion efficiency (PCE): perovskites are a class of materials with unique crystal structures, represented by the chemical formula ABX₃. Here, A denotes monovalent organic cations like methylamine (MA⁺), formamide (FA⁺), or cesium, while B refers to metal cations such as lead and tin. Finally, X represents halide anions. The inverted structure PSCs, also known as p-i-n PSCs offer several advantages, including lower production costs and enhanced stability compared to the conventional n-i-p PSCs. However, the inverted PSCs face the challenge of lower device efficiencies. In this study, we focus on two distinct materials for the Hole Transport Layer (HTL): PTAA and Meo-2PACz. Our primary goals involve investigating the fabrication process to create an optimal substrate for subsequent perovskite layer deposition and evaluating the efficiency of MeO-2PACz as a Hole Transport Material in inverted p-i-n perovskite solar cells. By exploring these aspects, we aim to contribute to the ongoing efforts to enhance the performance of PSCs.

Fabricating the solar cell, the HTL was first deposited onto the ITO glass through spin-casting. Two solutions were used: 1 mM Meo-2PACz in ethanol and 2 mg/ml PTAA in chlorobenzene. The spin-casting was done at 4000 rpm for 30 s, followed by annealing at 100°C for 10 minutes. Next, a 1.2M MAPbI₃ precursor solution in a mixed solvent of DMF/DMSO (v:v=9:1) was spin-casted on the glass at 4000 rpm for 30 s. 150 μL of toluene was dripped onto the surface 10 s after the beginning of spinning, the as-casted film was annealed at 100°C for 10 min. The subsequent steps involved spin coating a 20 mg/ml solution of PCBM at 1500 rpm for 30 s, followed by spin coating a 0.5 mg/ml BCP at 4000 rpm for 30 s. Finally, Ag electrodes (100 nm) were deposited using physical vapor deposition (PVD).

In terms of measurements, the surface roughness of Meo-2PACz and PTAA coated substrates was investigated using Atomic Force Microscopy (AFM). Both films exhibited relatively small surface roughness. Fourier Transform Infrared Spectroscopy showed peak shifts of the phosphate functional group due to its reaction with the glass substrate. Contact Angle measurements demonstrated that Meo-2PACz exhibits higher hydrophilicity, which enhances nucleation and crystal growth. X-ray Diffraction (XRD) analysis revealed that both perovskites coated onto Meo-2PACz or PTAA substrate show a similar crystallinity. Scanning Electron Microscopy (SEM) revealed that the perovskite prepared from the Meo-2PACz-coated substrate had a larger average grain size. Furthermore, PV Performance testing confirmed Meo-2PACz's superiority as a Hole Transport Material, achieving a higher PCE of 17.7% compared to PTAA's 16.3% PCE in the fabricated inverted p-i-n device.

11:15 AM EN05.15.10

Surface Reconstruction of Inorganic Perovskite by The Nanosecond Laser Pulse [Hyong JoonLee](#), Seok YeongHong, Jin KyoungPark, Jin HyuckHeo and Sang HyukIm; Korea University, Korea (the Republic of)

While the organic-inorganic hybrid metal halide perovskite has recently achieved remarkable performance in photovoltaics, all-inorganic perovskite (CsPb_{1-x}Br_x, X = 0~3) has been proposed as a stable alternative to their organic counterparts. The all-inorganic perovskite demonstrates robust thermal- and photo-stability owing to relatively high thermal decomposition temperature and high ion migration activation energy. Moreover, their suitable energy bandgap (>1.65 eV) offers wide opportunities for applications such as single-junction photovoltaics, tandem solar cells, and indoor photovoltaics. However, inorganic perovskite suffers from rapid crystallization during the film fabrication process, resulting in morphological and surface electronic inhomogeneities. Such inhomogeneities act as charge recombination centers and deter efficient charge extraction, leading to poor reproducibility and performance.

In this study, we implement a nanosecond pulsed laser as an effective tool to reconstruct the surface of inorganic perovskite films. The pulsed lasers are powerful instruments that provide rapid, accurate, and precise processes and are readily accessible as they are already widely adopted in industries. With careful control of the pulse energy, we were able to homogenize the surface potential of inorganic perovskite. In addition, we thoroughly characterize the impacts on the various perspectives including crystallinity, morphology, chemical features, optoelectronic properties, and device performance of the inorganic perovskite film. We believe our study on the inorganic perovskite-laser pulse interaction offers an insightful approach for optimizing inorganic perovskite solar cells and potentially any other applications involving pulsed laser processes.

11:20 AM EN05.15.11

Crosslink Polymer Strategy to Minimize Voltage Loss in Wide-Bandgap Perovskites for All-Perovskite Tandem Solar Cells [XinZheng](#); Huazhong University of Science & Technology, China

In recent years, the photoelectric conversion efficiency (PCE) of perovskite solar cells (PSCs) has exceeded 25%. However, according to Shockley-Queisser's limitations, the maximum theoretical efficiency of a single-junction solar cell is about 33%. The room for efficiency improvement of single-junction perovskite solar cells is very limited. Therefore, the development of tandem solar cells is an important way to break the limit and further improve the efficiency of PSCs. The theoretical limit efficiency of double-junction tandem solar cells (TSCs) can reach 46%, which is much higher than that of single-junction solar cells. In practice, The efficiency of all-perovskite tandem solar cells (28%) has surpassed that of single-junction perovskite solar cells (26%). Wide-bandgap (WBG) mixed-halide perovskites show promise of realizing efficient tandem solar cells but at present suffer from large open-circuit voltage loss because of excess lead iodide and light-induced halide phase segregation.

Here, a crosslink polymer strategy with high crosslinking degree and high density of functional groups is reported for finely regulating the crystal growth of $\text{FA}_{0.8}\text{Cs}_{0.2}\text{Pb}(\text{I}_{0.6}\text{Br}_{0.4})_3$, thereby obtaining high-performance PSCs. The pentaerythritol tetraacrylate (PTA) is introduced to form hydrogen bonds and strong Pb–O bonds with perovskite precursors, realizing the complete elimination of excess lead iodide. Besides, this uniformly distributed PTA crosslink polymer system passivates the defects and inhibits the photo-induced halide segregation effectively. The prepared PSCs with a band gap of 1.77 eV yield an impressive open-circuit voltage (V_{OC}) of 1.36 V, corresponding to a record low V_{OC} -deficit of 0.41 V and an efficiency of 19.58%. With these WBG perovskite subcells, we report 27.3% monolithic all-perovskite TSCs shows an outstanding combination of a high V_{OC} of 2.15 V and a FF of 81.4% with improved operational stability.

11:25 AM EN05.07.25

Heterostructure Solar Cells Fabricated via Sequential Spin and Transfer Printing Technique [Anjali Thakran](#)^{1,2}, Mario Hofmann¹ and Chih Wei Chu²; ¹National Taiwan University, Taiwan; ²Academia Sinica, Taiwan

Among the top contenders in photovoltaic materials, mixed halide organic/inorganic perovskite solar cells (PSCs) have attracted the market with strong potential of their facile processing methods, low temperature processability and cost-effectiveness over Si based solar cells (1/3 of the cost). The inherent properties of perovskites such as ambipolar nature, widely tuneable bandgap, low exciton binding energy, high mobility and long carrier lifetime have been extensively explored in electronic applications. However, the single junction solar cells based perovskites limited by their Shockley and Queisser limit and heterostructure/multi-junction device are limited with their complex stacked device architectures. Herein, we have demonstrated a successful approach of sequential spin and transfer printing technique to fabricate NBG perovskite over WBG perovskite to form a heterostructure. With as-adopted transfer printed technique on pre-fabricated spin coated layer, we are successfully able to fabricate two-solution processable layers on top of each other without any harmful dissolution. In results, we have obtained enhanced performance of stacked device compared to their single-junction counterpart. With our morphology studied, we have observed full coverage of surface, better crystal quality and less pin-holes film formation in heterostructure. Apart from it, the well-designed band alignment between top and bottom layer leads the effective transport of carriers through the device, therefore improved performance. Together with optimum parameters of film thickness, the obtained external quantum efficiency shown stronger intensity and enhanced spectral response. The single WBG layer are able to cover wavelength range around ~ 700 nm and with printed top layer onto it, the spectral enhanced till ~ 950 nm. Additionally, we can tune spectral response through composition variation in top and bottom layers. The proposed strategy can be implemented to stacked architecture including application including photodetector, sensors, transistor and LEDs.

11:30 AM *EN05.15.12

Development of High-Performance Sn Based Halide Perovskite Transistors [Yong-Young Noh](#); Pohang University of Science and Technology, Korea (the Republic of)

Developing high-mobility p-type semiconductors that can be grown using cost-effective scalable methods at low temperatures, has remained challenging in the electronics community for the integration of complementary electronics with the well-developed n-type metal oxide counterparts. Tin (Sn^{2+}) halide perovskites emerge as promising p-type candidates but suffer from low crystallisation controllability and high film defect density, which result in uncompetitive device performance. In this talk, I would like to introduce a general overview and recent progress of our group of p-type Sn-based metal halide perovskites for the application of field-effect transistors (FETs). In the first part of the talk, I will mainly address inorganic perovskite thin-film transistors with exceptional performance using high-crystallinity and uniform cesium-tin-triiodide-based semiconducting layers with moderate hole concentrations and superior Hall mobilities, which are enabled by the judicious engineering of film composition and crystallization. The optimized devices exhibit high field-effect hole mobilities of over $50 \text{ cm}^2 \text{ V}^{-1} \text{ s}^{-1}$, large current modulation greater than 108, and high operational stability and reproducibility [1]. In the second part of the talk, I will introduce A-site cation engineering method to achieve high-performance pure-Sn perovskite thin-film transistors (TFTs). We explore triple A-cations of caesium-formamidinium-phenethylammonium to create high-quality cascaded Sn perovskite channel films, especially with low-defect phase-pure perovskite/dielectric interface. As such, the optimized TFTs show record hole mobilities of over $70 \text{ cm}^2 \text{ V}^{-1} \text{ s}^{-1}$ and on/off current ratios of over 10^8 , comparable to the commercial low-temperature polysilicon technique level. The p-channel perovskite TFTs also show high processability and compatibility with the n-type metal oxides, enabling the integration of high-gain complementary inverters and rail-to-rail logic gates.

References:

[1] Ao Liu, Yong-Young Noh et al, Nature Electronics 5(2), 78-83 (2022)

SYMPOSIUM EN06

Emerging Energy Applications of Low-Dimensional Layered and Crystalline Materials
November 27 - December 6, 2023

Symposium Organizers

Aron Huckaba, University of Kentucky

Cecilia Mattevi, Imperial College London

Elisa Riedo, New York University

Christopher Sutton, University of South Carolina

* Invited Paper

+ JMR Distinguished Invited Speaker

SESSION EN06.01: Progress in Layered Materials

Session Chairs: Aron Huckaba and Cecilia Mattevi

Monday Morning, November 27, 2023

Hynes, Level 3, Room 306

10:30 AM *EN06.01.01

Water-Based and Defect-Free 2D Material Inks for Printed Electronics [Cinzia Casiraghi](#); University of Manchester, United Kingdom

Solution processing of 2D materials allows simple and low-cost techniques, such as ink-jet printing, to be used for fabrication of heterostructure-based devices of arbitrary complexity [1]. Our

group has developed highly concentrated, defect-free, printable and water-based 2D crystal formulations, enabling fabrication of large area arrays of photosensors on plastic [2], printed capacitors [3], transistors [3,4], and memristors on both rigid and flexible substrates [5]. Furthermore, we have demonstrated simple and scalable fabrication of graphene-silicon rectifying devices with ON/OFF ratio higher than three orders of magnitude and a remarkable photovoltaic effect, whose fabrication is compatible with back-end-of-line fabrication processes [6]. Finally, inkjet printing can be easily combined with 2D materials produced by chemical vapour deposition, allowing simple and quick fabrication of complex circuits on paper, such as high-gain inverters, logic gates, and current mirrors [7].

References

[1] Conti et al, Nature Rev. accepted 2023; [2] McManus et al, Nature Nano, 12, 343 (2017) [3] Worsley et al, ACS Nano (2018), DOI: 10.1021/acsnano.8b06464 [4] Lu et al, ACS Nano, 13, 11263 (2019); [5] Peng et al, submitted; [6] Grillo et al, ACS Nano (2023), 17, 1533 ; [7] Conti et al, Nature comms, 11, 1 (2020).

11:00 AM *EN06.01.02

Excitons in Two-Dimensional Metal Halides Maria Antonietta Loi; University of Groningen, Netherlands

Metal halide perovskites are under the spotlight for optoelectronic applications due to their remarkable photophysical properties. 3Dimensional compounds of this family have been used to demonstrate highly efficient solar cells, light emitting diodes, and x-ray detectors. Very recently, 2D and quasi-2D Ruddlesden-Popper phases, have also been explored for optoelectronic devices.

Layered perovskites afford specific advantages over other inorganic 2D materials such as transition metal dichalcogenides. As they are easily grown by both solution methods and vapor transport methods at low temperature, and they display a tuneable direct bandgap. In my presentation I will discuss the excitonic properties, of Ruddlesden-Popper phases based on Pb and on Sn, concluding on the metal influence on their physical properties. I will further underline the prospective for these materials in new optoelectronic devices.

11:30 AM EN06.01.03

Exploring the Potential of 1T-TiS₂ Electrode Materials for Supercapacitors Ali D. Ucar, Sumeyye Kandur, Mete Batuhan Durukan and Husnu E. Unalan; Middle East Technical University, Turkey

The distinctive characteristics of two-dimensional materials have attracted considerable interest for their prospective applications, especially in the field of energy storage. The relatively well studied transition metal dichalcogenides (TMDs), such as molybdenum disulfide (MoS₂) and tungsten disulfide (WS₂), have been shown to have electronic, chemical, and optical properties that can be tailored through fabrication methods. Relatively less studied and the lightest member of the TMD family, titanium disulfide (TiS₂) is a promising material for supercapacitor electrodes. In this work, electrically conductive bare 1T-TiS₂ nanosheets were fabricated and utilized as electrodes for supercapacitors. For this purpose, self-standing and flexible TiS₂ films were fabricated through vacuum filtration. Bare TiS₂ films showed poor cyclic stability in aqueous electrolytes. Therefore, a simple dopamine treatment was developed to enhance the enhance oxidation stability of the TiS₂ films. The resulting 1T-TiS₂ film-based symmetric supercapacitor devices showed a specific capacitance and capacity retention of 10 F/g (at a scan rate of 100 mV/s) and 90% after 5000 cycles in 2M Li₂SO₄/0.1 M thiourea electrolyte, respectively.

11:45 AM EN06.01.04

The Influence of Cation Structure on Ionization Energies in 2D Organic Metal Halide Perovskites and Best Practices for Defining Ionization Energies Harindi R. Atapattu, Syed Joy, Henry Pruett, Kevin Pedersen and Kenneth R. Graham; University of Kentucky, United States

The ionization energy (IE) and electron affinity (EA), which are equated with the valence band maximum and conduction band minimum, respectively, are important material parameters for semiconductor device design and understanding device physics. Thereby, determining relationships between organic metal halide perovskite (HP) structure and the IE and EA is critical for development and selection of HPs for targeted device integration. Currently, it is not well understood how structural changes to the HP shift the IE and EA, and furthermore, assigning the IE and EA in organic metal halide perovskites (HPs) is not straightforward. In three-dimensional (3D) HPs, the IE and EA are typically assigned based on Gaussian fits to the lowest energy feature; whereas, in two-dimensional (2D) HPs the IE and EA are commonly assigned based on linear fits to the leading edge of the signal onset. In this work we use a combination of techniques, including ultraviolet photoemission spectroscopy (UPS), electrochemistry, and photoluminescence (PL) quenching measurements to determine the most appropriate method to assign the ionization energy. In the case of PL quenching, a series of hole accepting materials with varying IEs are deposited on top of the HPs, and based on quenching of the HP PL as a function of IE of the hole accepting material we are able to determine the range in which the HP IE lies for both Ruddlesden-Popper (RP) and Dion-Jacobson (DJ) phase HPs. We further investigate how the structure of the A*-site organic cation impacts the IE in both RP and DJ Pb- and Sn-based HPs. In RP phase HPs containing phenethylammonium (PEA) derivatives as the A*-site cation, we find that appending an electronegative substituent at the 4-position of the phenyl group results in an increase in the IE relative to PEA, whereas when an electronegative substituent is attached at the 2-position the IE decreases relative to PEA. Overall, changing the position of the substituent in 2D HPs can result in a 1.0 eV change in the IE, which highlights the wide tunability of frontier energy levels provided by minor variations to the A*-site cation structure.

SESSION EN06.02: Layered Perovskites and 2D Materials
Session Chairs: Carmela Aruta, Cinzia Casiraghi and Letian Dou
Monday Afternoon, November 27, 2023
Hynes, Level 3, Room 306

1:30 PM *EN06.02.01

2D Carbides and Nitrides (MXenes) for Energy Storage—Use in Passive and Active Components Yury Gogotsi; Drexel University, United States

Nanomaterials, particularly, two-dimensional (2D) materials, are among promising candidates to address some of the ongoing challenges in manufacturing batteries and supercapacitors and enable devices with superior performance metrics and a lower cost.^{1,2} Two-dimensional metal carbides and nitrides (MXenes) are a very large yet quickly growing family of 2D materials with the formula of M_{n+1}X_nT_x where M is an early transition metal, X is carbon or nitrogen, and T_x refers to the surface terminations. Molecular dynamics and *ab initio* simulations, along with experiments, show that the electronic, optical, and most importantly, electrochemical properties of MXenes distinguish them from other widely studied 2D materials. Chemical and electrochemical insertion of ions and molecules between the MXene layers allows modification of their properties, as well as electrochemical charge storage and harvesting, which use both, double-layer and redox mechanisms. The high electronic conductivity (~20,000 S cm⁻¹), redox-active surfaces, cation intercalation in 2D slits between MXene layers, and rich chemistry of these materials with more than 50 different compositions reported, have enabled their use as charge storage hosts and building blocks of passive cell components in various types of energy storage devices.³ Freestanding, binder-free films of Ti₃C₂T_x are capable of ultra-high-rate pseudocapacitive charge storage in protic electrolytes delivering ~400 F g⁻¹ (1500 F/cm³) at rates of up to 100 V s⁻¹ and volumetric energy and power densities several times higher than conventional carbon-based capacitive electrodes. MXenes can intercalate a variety of monovalent and multivalent cations from aqueous or non-aqueous electrolytes and, therefore, can be used as electrodes for emerging new battery chemistries. Their mechanical robustness and high conductivity expand their use as current collectors, conductive additives in electrodes and also building blocks for conformal coatings to avoid dendrite growth in metal batteries. Yet, unlike most other 2D materials, the synthesis and processing of MXenes is scalable and cost-effective, and they can be processed in large batches from aqueous solution into powders, dispersions, and films. The combination of these properties and scalable synthesis, not only renders MXenes as interesting materials for academic research and development studies but also as practical materials of choice for future charge storage applications.

1. Pomerantseva, E; Bonaccorso, F; Feng, X; Cui, Y; Gogotsi, Y. Energy storage: The future enabled by nanomaterials. *Science*. **2019**, 366 (6468), eaan8285.
2. Simon, P; Gogotsi, Y. Perspective for Electrochemical Capacitors and Related Devices. *Nature Materials*. **2020**, 19, 1151-1163.
3. Vahid Mohammadi, A.; Rosen, J.; Gogotsi, Y. The World of Two-Dimensional Carbides and Nitrides (MXenes). *Science*. **2021**, 372 (6547), eabf1581

2:00 PM *EN06.02.02

Understanding Complex Layered Halide Perovskites: Double Perovskites and Mosaic Perovskites Bridget Connor¹, Alexander Su¹, Jiayi Li¹, Feng Ke², Yu Lin², Linn Leppert³ and Hemamala Karunadasa^{1,2}; ¹Stanford University, United States; ²SLAC National Accelerator Laboratory, United States; ³University of Twente, Netherlands

Layered halide perovskites offer a flexible platform for tuning optoelectronic properties through changes in composition. One of the most intriguing aspects of 2D halide double perovskites is the change in bandgap symmetry with dimension, observed for certain compositions. For example, the indirect gap of Cs₂AgBiX₆ converts to a direct gap at the *n* = 1 (monolayer) 2D perovskite, whereas the direct gap of Cs₂AgTlX₆ transitions to an indirect gap at the *n* = 1 limit. I will present a molecular orbital analysis that explains this transition and allows us to predict which double perovskite compositions will feature such a change in band dispersion pattern upon dimensional reduction. I will also present our recent studies on further increasing the

accessible electronic structures of 2D perovskites by incorporating three stoichiometric octahedral metals. We refer to this family as “mosaic perovskites” due to the numerous local packing arrangements of the three different metal-halide octahedra that nevertheless maintain a fixed metal ratio. Notably, mosaic perovskites allow for Cu(I/II) mixed valence and sets the stage for many more mixed-valence metal combinations to be incorporated into halide perovskites.

2:30 PM EN06.02.03

Enhanced Air Stability in 2D Tin Halide Perovskites Enabled by Rational Spacer Cation Design Christopher T. Triggs, R. Dominic Ross, Willa Mihalyi-Koch, Catherine Clewett, Kyana M. Sanders, Iliia A. Guzei and Song Jin; University of Wisconsin--Madison, United States

Two-dimensional (2D) tin halide perovskites are lead-free semiconductors promising for photovoltaic, optoelectronic, and spintronic devices. However, their inherent instability to air and humidity relative to their toxic lead counterparts makes them more difficult to study and employ in applications. In this work, we report two new 2D tin perovskite crystal structures and systematically compare them among a series of Ruddlesden-Popper (RP) and Dion-Jacobson (DJ) tin iodide perovskites to elucidate the spacer cation structural motifs that enable better air stability, as well as the underlying mechanism of how they protect the inorganic sublattice from degradation. Using solid-state NMR, we find 2D tin perovskites decompose into ligand salts and SnO₂ upon exposure to ambient air, which are localized at the crystal surfaces and produced at varying rates depending on the spacer cation. Direct comparisons between the studied phases demonstrate substantially enhanced air stability compared to the benchmark (PEA)₂SnI₄ (PEA = phenethylammonium) phase by use of halogenated aromatic spacer cations in RP perovskites or bulky ringed spacer cations in DJ perovskites. Interestingly, X-ray photoelectron spectroscopy depth profiling, complemented by synchrotron X-ray absorption spectroscopy, revealed that the long term bulk stability of 2D tin perovskites is not solely due to surface-level protection by the hydrophobic spacer cations as generally believed, but also due to effective subsurface protection from strong interlayer interactions that prevent penetration of air and water underneath the surface of the crystal. This study informs how we can rationally design 2D tin perovskites for enhanced air stability to enable further property studies and eventual applications in stable, high performance devices.

2:45 PM BREAK

3:15 PM *EN06.02.04

2D Materials for the Electrocatalytic Conversion of CO₂ and Water Depollution Damien Voiry; University of Montpellier, France

Mitigating climate change and securing water resources are two of the major challenges of the century^{1,2}. In this context, membranes and electrocatalysis process are promising avenues to reduce the energy footprint, while mitigating carbon dioxide emissions. Our research aims to evaluate the potential of low dimensional materials for membrane and electrocatalytic applications.

Due to their atomic thickness and confined interlayer spacing, nanolaminate membranes made of re-stacked 2D nanosheets could theoretically enable improved separation performance. We developed a novel strategy to control the interlayer spacing and improve the separation performance of nanolaminate membranes using covalent functionalization of exfoliated nanosheets. The functionalized MoS₂ membranes demonstrated remarkable performance for water purification and desalination, while they have enabled to discriminate the role of the surface and stacking disorder on the nanofluidic behavior of water in the laminates³.

We also investigated the influence of surface chemistry on the electrocatalytic behavior of low dimensional materials. In particular, we have developed a new strategy to enhance the conversion of CO₂ to hydrocarbon molecules with two or more carbon atoms (C₂₊) via molecular doping of a metal catalyst⁴. Specifically, we have identified electrophilic functional groups that can direct electrochemical reactions to produce C₂₊ species such as ethanol and ethylene and improve reaction rates at the catalyst surface.

In my presentation, I will review our recent findings on understanding electrocatalytic and nanofluidic phenomena that take place on the surface of low dimensional materials.

References:

1. Shannon, M. A. *et al. Nature* **2008**, 452, 301–310 (2008).
2. Voiry, D., Shin, H. S., Loh, K. P. & Chhowalla, M. Low dimensional catalysts for hydrogen evolution and CO₂ reduction. *Nat. Rev. Chem.* **2017**, 9858, 0105
3. Ries, L. *et al.* Enhanced sieving from exfoliated MoS₂ membranes via covalent functionalization. *Nature Materials* **2019**, 18, 1112–1117.
4. Wu, H. *et al.* Improved electrochemical conversion of CO₂ to multicarbon products by using molecular doping. *Nature Communications* **2012**, 12, 1–11.

3:45 PM *EN06.02.05

Two-Dimensional Organic-Perovskite Hybrid Materials and Heterostructures Letian Dou; Purdue University, United States

Epitaxial heterostructures based on oxide perovskites and III–V, II–VI and transition metal dichalcogenide semiconductors form the foundation of modern electronics and optoelectronics. Halide perovskites—an emerging family of tunable semiconductors with desirable properties—are attractive for applications such as solution-processed solar cells, light-emitting diodes, detectors and lasers. Their inherently soft crystal lattice allows greater tolerance to lattice mismatch, making them promising for heterostructure formation and semiconductor integration. Atomically sharp epitaxial interfaces are necessary to improve performance and for device miniaturization. However, epitaxial growth of atomically sharp heterostructures of halide perovskites has not yet been achieved, owing to their high intrinsic ion mobility and their poor chemical stability. Therefore, understanding the origins of this instability and identifying effective approaches to suppress ion diffusion are of great importance. In this talk I will present an effective strategy to substantially inhibit in-plane ion diffusion in two-dimensional halide perovskites by incorporating rigid π -conjugated organic ligands. Highly stable and tunable lateral and vertical epitaxial heterostructures, multiheterostructures and superlattices will be demonstrated. Furthermore, using these 2D heterostructures as a new platform, I will present our recent efforts in 1) quantitatively understanding the anion inter-diffusions and migrations, and 2) controlling and manipulating exciton transport and light-emission in halide perovskites.

4:15 PM EN06.02.06

Unveiling Electronic and Excitonic Properties of 2D Ruddlesden-Popper Perovskites Based on Bifunctional Ligands Xinjue Zhong¹, Xiaojuan Ni², Alan B. Kaplan¹, Xiaoming Zhao¹, Marko Ivancevic¹, Melissa L. Ball¹, Zhaojian Xu¹, Hong Li², Barry P. Rand^{1,1}, Yueh-Lin Loo^{1,1}, Jean-Luc Brédas² and Antoine Kahn¹; ¹Princeton University, United States; ²The University of Arizona, United States

Two-dimensional (2D) Ruddlesden-Popper halide perovskites exhibit remarkable tunability of optoelectronic properties and good environmental stability achieved through the selection of organic cations. The incorporation of bifunctional ligands featuring non-ammonium terminus and functional groups capable of forming extra bonding motifs within the organic bilayer provides an effective strategy to engineer perovskite structures and introduce additional functionalities.

Here, we explore a series of $n = 1$ 2D perovskites incorporating organic ligands with diverse functional groups (-CN, -OH, -COOH, -Ph, and -CH₃), each exhibiting distinct bonding characteristics and dielectric properties, and report on the impact of these bifunctional ligands on the electronic and excitonic properties of these 2D perovskites.^[1]

We perform ultraviolet and inverse photoemission spectroscopies (UPS/IPES) to determine the energy positions of the valence band maximum and conduction band minimum, and the electronic, or single-particle, gap of these 2D perovskites. We observe a strong correlation between the electronic gaps of the -CN, -COOH, -Ph, and -CH₃-based perovskites and the in-plane Pb-I-Pb bond angle, aligning with earlier findings regarding the relationship between optical gaps and the in-plane Pb-I-Pb bond angle.^[2] Interestingly, the gap of the -OH-based perovskite deviates significantly from this trend. We conduct density functional theory calculations and tight-binding model analysis to further elucidate this structure-property relationship. We attribute the “-OH” anomaly to band dispersion along the out-of-plane direction, caused primarily by interlayer electronic coupling present in (OH-EA)₂PbI₄. By subtracting optical gap from single-particle gap, we estimate the exciton binding energy (E_b) in these 2D layers, which ranges from 420 meV for (CH₃-PA)₂PbI₄ to 130 meV for (OH-EA)₂PbI₄. This large variation is attributed to specific structural aspects, such as in-plane Pb-I-Pb bond angle, interlayer spacing, and the dielectric constant of the bifunctional ligands.

Our results provide deeper insights into the complex impact of organic ligands on the electronic and excitonic properties of 2D perovskites, in particular the substantial role of strong interlayer electronic coupling. These findings contribute to a better understanding of the structure-property relationship in such materials, facilitating the design and optimization of perovskite-based devices for various applications.

[1] X. Zhong et al., *Energy & Environ. Sci.*, (under review)

[2] X. Zhao et al., *Nat. Commun.* 2022, 13, 3970.

4:30 PM EN06.02.07

Valence Alternation in Quasi-One-Dimensional Antimony Selenide Xinwei Wang¹, Seán R. Kavanagh^{1,2} and Aron Walsh^{1,3}; ¹Imperial College London, United Kingdom; ²University College London, United Kingdom; ³Ewha Womans University, Korea (the Republic of)

Antimony selenide (Sb₂Se₃) has emerged as an earth-abundant and environmental-friendly alternative among thin-film photovoltaic light absorbers due to its promising optoelectronic properties. A distinguishing feature of Sb₂Se₃ is its anisotropic crystal structure, which is composed of quasi-one-dimensional (1D) [Sb₄Se₆]_n ribbons. However, the current record conversion efficiency of Sb₂Se₃ (~ 10%)^[1] is far from optimal. It has been reported that orientation control of Sb₂Se₃ films is important to achieve high device performance^[2], but the underlying physics remains unclear.

In this talk, I will present our most recent work^[3-5] investigating reasons that affect the conversion efficiency in Sb₂Se₃ based on first-principles calculations. I will first introduce the anisotropy in bulk Sb₂Se₃ structure and the resulting impacts on structural, electronic and optical properties. Then I will present results on the unusual defect physics. Multi-electron negative-U transitions between defect charge states can be understood from valence alternation enabled by large local structural rearrangements. Finally, I will discuss potential strategies to optimize the performance of Sb₂Se₃-based photovoltaics.

References

- [1] Zhao Y, Wang S, Li C, et al. *Energy & Environmental Science*, 2022, 15(12): 5118-5128.
- [2] Zhou Y, Wang L, Chen S, et al. *Nature Photonics*, 2015, 9(6): 409-415.
- [3] Wang X, Li Z, Kavanagh S R, et al. *Physical Chemistry Chemical Physics*, 2022, 24(12): 7195-7202.
- [4] Wang X, Ganose A M, Kavanagh S R & Walsh A. *ACS Energy Letters*, 2022, 7(9): 2954-2960.
- [5] Wang X, Kavanagh S R, Scanlon D O & Walsh A. *arXiv preprint:2302.04901*, 2023.

4:45 PM EN06.02.08

Patterning Edge-Like Defects and Tuning Defect Propagation on the Basal Plane of Ultra-Large MoS₂ Monolayers Toward Hydrogen Evolution Reaction Bianca R. Florindo¹, Leonardo H. Hasimoto^{1,2}, Niccolò S. de Freitas¹, Graziãni Candiotti³, Erika N. Lima⁴, Cláudia de Lourenço¹, Carlos Ospina¹, Jefferson Bettini¹, Edson R. Leite¹, Renato S. Lima¹, Rodrigo B. Capaz¹ and Murilo Santhiago^{1,2}; ¹Brazilian Nanotechnology National Laboratory, Brazil; ²UFABC, Brazil; ³UFRJ, Brazil; ⁴UFR, Brazil

The catalytic sites of MoS₂ monolayers towards hydrogen evolution are well known to be vacancies and edge-like defects. However, it is still very challenging to control the position, size, and propagation of defects on the basal plane of MoS₂ monolayers by most of defect-engineering routes. In this work, the fabrication of arrays of etched windows on ultra-large supported [1] and free-standing MoS₂ monolayers using focused ion beam (FIB) is reported for the first time. By tuning the Ga⁺ ion dose it is possible to confine defects near the etched edges or propagate them over ultra-large areas on the basal plane. The electrocatalytic activity of the arrays toward hydrogen evolution reaction (HER) was measured by fabricating microelectrodes using a new method that preserves the catalytic sites. We demonstrate that the overpotential can be decreased up to 290 mV by assessing electrochemical activity only at the basal plane. HRTEM images obtained on FIB patterned freestanding MoS₂ monolayers reveal the presence of amorphous regions and X-ray photoelectron spectroscopy indicate excess of sulfur in these regions. Density-functional theory calculations provide identification of catalytic defect sites. Our results demonstrate a new rational control of amorphous-crystalline surface boundaries and future insight for defect optimization in MoS₂ monolayers.

[1] *Nanoscale*, 2022, 14, 6811-6821.

Acknowledgements: Serrapilheira institute (1912-31228) and FAPESP (2022/00955-0)

SESSION EN06.03: Poster Session: 2D Layered Perovskites and Atomically Thin Materials for Energy Applications

Session Chairs: Aron Huckaba, Cecilia Mattevi and Christopher Sutton

Monday Afternoon, November 27, 2023

Hynes, Level 1, Hall A

8:00 PM EN06.03.01

Highly Stable Perovskite Solar Cells Coated with Solar Transparent and Thermally Emissive Mesoporous Nanoparticles Heesuk Jung^{1,2}, Sung Yoon Min³, Byungsoo Kang¹, Yongseok Yoo⁴, Jinhun Jang⁵, Yeoun-Woo Jang⁴, Hyeonwoo Choi⁶, Hyeonwoo Lee⁶, Swarup Biswas⁶, Yongju Lee⁶, Mansoo Choi⁴, Phillip Lee¹, Min Seok Jang³, Hyeok Kim⁶ and Shu Yang²; ¹Korea Institute of Science and Technology, Korea (the Republic of); ²University of Pennsylvania, United States; ³Korea Advanced Institute of Science and Technology, Korea (the Republic of); ⁴Seoul National University, Korea (the Republic of); ⁵Frontier Energy Solution, Korea (the Republic of); ⁶University of Seoul, Korea (the Republic of)

Continuous heat generation in perovskite solar cells (PSCs) due to repeated exposure to solar light is detrimental to the device lifetime. Existing active cooling strategies often require extra energy input. Meanwhile, most passive radiative cooling materials are not solar transparent or require complex fabrication processes. Here, we design, synthesize, and assemble mesoporous silica nanoparticles in multi-layered stacks to create a graded refractive index (GRI) coating for PSCs. The coating offers not only high transparency in the visible wavelength but also high emissivity in the mid-infrared regions. When applied to PSCs that are placed outdoors for 20 days, 81.2±9.50% of the initial photo conversion efficiency (PCE) is maintained, whereas PCE of the pristine PSCs decreases significantly to 8.44±6.84%. The calculated cooling power of the GRI coated PSCs is 28.9% more than that of the pristine PSCs. Our study sheds light on efficient cooling materials that will assist broader adoption of PSCs.

8:00 PM EN06.03.02

Ramifications of B Site Cation Variation in Some Piezoelectric Organic-Inorganic Hybrid Halometalates Michael Wells¹, Jacob L. Hempel¹, Santosh Adhikari², Y. T. Cheng^{1,1}, Sean Parkin¹, Christopher Sutton² and Aron J. Huckaba¹; ¹University of Kentucky, United States; ²University of South Carolina, United States

The need for alternative energy sources is rising align with increased utilization of dwindling fossil fuels. One way to help meet the ever-increasing demand is to develop materials and devices that turn wasteforms like vibrations into electricity through the piezoelectric effect. Ceramics such as Lead zirconium titanate (PZT) and Barium titanate (BTO) and polymers like poly(vinylidene difluoride) (PVDF) have been the gold standard materials, but recently organic-inorganic hybrid metalates (OIHMs) have come to the forefront of the field, due to high piezoelectric moduli and voltage constants. OIHM's have a basic structure of ABX₃, are simple to synthesize and process with solution methods, and can be deposited on a variety of substrates. Here we report efforts to probe the effects of the B-site cation identity on chlorometalate structures in piezoelectric materials with chiral and achiral A site cations. Screening many transition metal and main group heavy element B-site cations and single or dicationic chiral ammonium cations led to the formation of single-crystalline piezoelectric OIHM's. Piezoresponse force microscopy (PFM) was used to measure local piezoelectric response values of the OIHM's, and other material properties were correlated with material structure.

8:00 PM EN06.03.03

Single Crystalline Thin Films of the Dielectric SrTiO₃ and the Multiferroic BiFeO₃ Solid Solution Wegdan Osman¹, Abhijit Biswas², Satish Ogale² and Detlef Bahnemann^{3,4}; ¹Alexandria University, Faculty of Science, Physics Department, Egypt; ²Indian Institute of Science Education & Research (IISER), Pune Dr. Homi Bhabha Road, Pashan, India; ³Institute of Technical Chemistry Leibniz Universität Hannover Callinstr., Germany; ⁴Saint-Petersburg State University, Laboratory Photoactive Nanocomposite Materials, Russian Federation

This work was motivated by the strong need for sustainable clean energy source for water splitting and other photocatalytic reactions. Solid Solution is a powerful technique to change the physiochemical properties and the band structure of the materials like band gap, band edge positions and chemical stability compared to its single constituents. In this study we use single crystalline, epitaxial, solid solution of the multiferroic BiFeO₃ and the dielectric SrTiO₃ with nominal composition (BFO)_x(STO)_{1-x} where 0 ≤ x ≤ 1 (STO) substrates having different orientations, namely, (001), (011) and (111) to study the electric polarization influence of the BFO on the charge separation. Conductive SrRuO₃ (SRO) buffered STO substrates were used as electrodes for the photoelectrochemical (PEC) measurements and their photoelectrochemical properties were investigated varying BFO: STO compositions percentage.

We anticipate that both the photovoltaic effect of the ferroelectric BFO and the change in the BFO: STO compositions have major influence on the PEC properties. Ferroelectricity contributes to the charge separation and collection by the inherent electric field due to spontaneous polarization. On the other hand, when SrTiO₃ is added to BiFeO₃, significant band structure changes occurs; the conduction band minimum position is raised and an exponential tail of trap states from hybridized Ti 3d and Fe 3d orbitals emerges near the conduction band edge. These shallow trap states strongly prevent the fast recombination of electrons and holes in the mixed solid solution films, carrier lifetimes are increased, and the photocurrent density in the visible-light region is significantly increased when compared to the single constituents. In the BFO90%-STO10% case in which the solid solution is mostly dominated by the BFO phase, photocurrent was highest for photoelectrodes on the STO (111) which is known to have the largest remnant polarization compared to the (011) and (111) directions for BFO. BFO75%-STO25% on STO (011) case among our composition series exhibited the highest photocurrent density. However, we found that for the other composition percentages namely, BFO50%-STO50% and BFO25%-STO75%. The highest photocurrent was also recorded for photoelectrodes on STO (011). Photocurrent decreases with the increase of the SrTiO₃ content in the solid solutions. In case of pure BFO and STO, photocurrent was significantly small and incorporation of only 10% STO enhanced the photocurrent greatly to 0.003 mA/cm². Furthermore, electrochemical impedance Spectroscopy (EIS) spectra reveal that the solid solution of the photoelectrodes on (011) exhibits the smallest impedance value hence it shows the highest photocurrent. The reduction of impedance indicates an improved efficiency of photogenerated charge transport at the electrode/electrolyte interface. The EIS results agree well with PEC performance.

8:00 PM EN06.03.04

As cooling capacity demands for systems of high heat flux, such as nuclear fusion reactor, integrated chip cooling, continuously grows, boiling heat transfer which utilizes latent heat accompanied by phase change could be an advantageous thermal management method with smaller superheat of system. Two major factor, critical heat flux (CHF) and heat transfer coefficient (HTC), which indicates the maximum cooling capacity of nucleate boiling and heat transfer efficiency, respectively, can be employed for determining boiling heat transfer performance. CHF and HTC can be enhanced by promoting bubble nucleation and supplying working fluid to the heated surface to fully utilize the latent heat of vaporization. Nanoparticle coating with graphene related particles on heated surface could promote bubble nucleation as it generates smaller bubbles compared to the plain surface, by offering nucleation sites (micro-sized cavities) in the coating. However, hydrophobic coating layer could block liquid paths, which leads to immature critical heat flux by rejecting working fluid supply. To ensure liquid paths with hydrophobic particle coating, hydrophilic liquid paths should be secured. In this study, we propose tailored coating of reduced graphene oxide (rGO) particle on the micropillar array and plain surfaces. The rGO-coated surfaces were prepared by stepwise methods of deep reactive ion etching (DRIE) and nanofluid boiling with 0.0005 wt% rGO solution. Micropillars are made to be 10 μm in height, 4 μm in diameter, and 20 μm in pitch, respectively, and nanofluid boiling step was controlled for surface tailoring. First, surfaces were coated by nanofluid boiling with increasing heat fluxes immediately before CHF, which results in completely coated micropillar and thick porous coating on plain surface. Then, we run nanofluid boiling at 60 W/cm^2 heat flux for overnight, which is equivalent to the full coating procedure to make thin floating layer on the micropillar. Experimental surfaces of Plain, fully coated micropillar, lightly coated recorded 89 W/cm^2 , 201 W/cm^2 , and 238 W/cm^2 in CHF and 20.4 $\text{kW}/\text{m}^2\text{K}$, 45.9 $\text{kW}/\text{m}^2\text{K}$, and 90.98 $\text{kW}/\text{m}^2\text{K}$ in maximum heat transfer coefficient, respectively. CHF and HTC records confirm that surface with floating rGO layer demonstrates superior heat transfer performance to the fully coated micropillar surface. The notable improvement on CHF and HTC in the tailored rGO surfaces indicates ensuring liquid path beneath the hydrophobic rGO layer by tailoring deposition condition could improve nanoparticle-coated surfaces heat transfer performance, allowing 160% increased HTC compared to the plain surfaces. This study will be helpful for s for enhanced boiling heat transfer on cooling systems for high heat flux devices like heat exchangers and fusion reactors.

8:00 PM EN06.03.05

Weak-Localization Phenomena as a Tool for Quantification of Defects in MXenes and 2D Metallic Nanolayers [Barbara Pacakova](#)^{1,2}, Anupma Thakur², Nithin Chandran Balachandran Sajitha², Karel Vyborny², Annabelle Harding² and Babak Anasori²; ¹Norwegian University of Science and Technology, Norway; ²IUPUI, United States; ³Institute of Physics, CAS, Czechia

Weak localization¹ (WL) is a quantum phenomenon, where at cryotemperatures, electrons in the metal move around a closed loops and return to their initial point of origin rather than proceeding forward in the lattice, which increases resistivity of metal with decreasing temperature. Typically, metals with defects exhibit transition from normal metallic conductivity to WL regime at low temperatures. In this study, we introduced defects in MXene flakes, such as vacancy clusters and flake boundaries and measured the temperature and field dependence of the resistivity in 2D metallic MXene films. We observed the transition temperature to WL state increases with increasing the amount of defects in MXene flakes. Properties of the 2D nanosheets were also studied by complementary experiments such as XRD, AFM and SEM. Our results indicated that measurements of the temperature and field dependencies of resistivity, can be used as a sufficient and superior technique to understand the amount of defects in the MXenes and 2D metal nanosheets in general, by determining coherence length of electrons at low temperatures in the WL regime. We thus present how the overall quality of 2D flakes in MXene films can be determined by investigating their transport properties. This technique gives a broader picture of MXene defects compared to more localized defect characterization techniques such as transmission electron microscopy.

1. Falco, V. I. *et al.* Weak localization in graphene. *Solid State Commun* **143**, 33–38 (2007).

8:00 PM EN06.03.06

Graphene Aligned 2D Charge Transport Network for the Thick Electrode for Lithium-Ion Batteries via the Spark Plasma Sintering Process [Bo Nie](#) and Hongtao Sun; Penn State University, United States

Developing electrochemical energy storage that can achieve high areal, volumetric, and gravimetric performance simultaneously presents a significant challenge from both a fundamental and technological standpoint. Increasing the thickness and density of electrodes to enhance areal and volumetric performance while maintaining high gravimetric performance is a straightforward yet problematic approach. The insufficient charge transports in these electrodes, which have high mass loading and density, can severely degrade energy storage performance. In this study, we address this challenge by developing a graphene-based network that is automatically aligned within thick electrodes, fabricated through energy-efficient spark plasma sintering. The electrodes exhibit a high electrode density (2.0–2.3 g cm^{-3}) and high mass loading (70–100 mg cm^{-2}). Leveraging the exceptional properties of vertically aligned graphene-based networks, anisotropic pore channels, and intrinsic properties of two-dimensional (2D) graphene (e.g., superior thermal and electrical conductivity as well as the large surface area), efficient charge transport is enabled throughout the entire electrode thickness. Furthermore, by incorporating a small amount of carbon nanotubes to improve electrode integrity, the hybrid carbon network and characteristic alignment structure of the sintered lithium iron phosphate (LiFePO_4) electrodes perform high areal (8.6 mAh cm^{-2}), volumetric capacity (246 mAh cm^{-3}), uncompromised gravimetric performance (164 mAh g^{-1}) at normal current (<2 mA cm^{-2}), and stable cycling with a capacity retention of 84% after 200 cycles under a current density of 4.5 mA cm^{-2} . The automatic alignment of the graphene-based network through the spark plasma sintering process provides a promising approach for designing efficient charge transport pathways in high-energy-density batteries.

The insights gained from this graphene alignment strategy can be applied to various other electrode materials in energy storage systems, such as batteries, fuel cells, and supercapacitors. Furthermore, our future research will focus on extending this approach to solid-state systems by incorporating an ionic conducting phase.

8:00 PM EN06.03.07

Liquid Crystal-Regulated Vertical Aligned Graphene Current Collector for High-Performance Lithium Metal Batteries [Yifang Ding](#), Juchen Zhang and Hongtao Sun; Penn State University, United States

Lithium metal batteries (LMBs) hold immense promise as high-energy-density energy storage due to their exceptional theoretical capacity and low voltage potential. However, practical implementation faces challenges such as volume expansion and dendrite growth during cycling of Li metal anodes. To address these issues, the structural design of three-dimensional (3D) current collectors for the anode has emerged as a viable solution by mitigating volume changes and suppressing dendrite growth during Li deposition/stripping. In this study, we introduce a strong-base-regulated alignment of graphene oxide (GO) liquid crystal that can be utilized as a 3D graphene current collector after thermal reduction for high-performance lithium metal batteries. This innovative design facilitates homogeneous Li transport and uniform Li deposition, thereby enhancing cycling stability in LMBs. To create the vertically aligned structure, the key aspect of our approach involves the utilization of potassium hydroxide (KOH) as a strong base. The use of KOH induces the formation of a vertical aligned GO LC phase in a freestanding pallet at a relatively low concentration of GO solution.

The strong-base-induced vertical aligned graphene current collector exhibits short ion-transport pathways on the upper surface, reducing the concentration gradients and minimizing local overpotentials. This promotes uniform Li deposition and mitigates dendrite formation throughout the current collector, addressing the critical challenge of dendrite growth and improving cycling stability. Moreover, the reduced graphene material offers high electrical conductivity, facilitating rapid electron transports during battery operation. This feature enhances the overall rate capability of LMBs, allowing for high current densities without compromising cycling stability. In addition to electrochemical characteristics, mechanical properties were also investigated through dynamic mechanical analyzer to confirm the robustness of the vertical aligned graphene current collector.

With its excellent conductivity, high porosity, and good elasticity of the LC phase-regulated 3D graphene network, it emerges as an ideal candidate for current collectors in high-performance LMBs. The findings demonstrate the great potential to significantly enhance the performance and safety of LMBs.

8:00 PM EN06.03.08

Biexciton-Induced Hyper-Raman Scattering in Two-Dimensional Halide Perovskite $(\text{C}_6\text{H}_5\text{C}_2\text{H}_4\text{NH}_3)_2\text{PbI}_4$ under Resonant Two-Photon Excitation [Seung Han Shin](#) and Joon Ik Jang; Sogang University, Korea (the Republic of)

$(\text{C}_6\text{H}_5\text{C}_2\text{H}_4\text{NH}_3)_2\text{PbI}_4$ is a prototype two-dimensional (2D) halide perovskite, exhibiting various excitonic phases due to strong quantum and dielectric confinements, thereby ideal for investigating fundamental exciton physics. Being four-body quasiparticles in a semiconductor, biexcitons are typically generated via inelastic Coulomb binding of two excitons under strong pulsed excitation. However, they can be efficiently generated by resonant two-photon exciton utilizing the effect of giant oscillator strength. Here, the biexciton level of $(\text{C}_6\text{H}_5\text{C}_2\text{H}_4\text{NH}_3)_2\text{PbI}_4$ is precisely determined to be 4660.8 meV by resonant two-photon excitation, which is also confirmed by considering the mechanism for the biexciton photoluminescence (PL) process. The corresponding two-photon absorption coefficient turns out to be extremely large ($\beta = 2.0 \times 10^5 \text{ cm}^2/\text{MW}$) due to the giant oscillator strength for the transition. Intriguingly, upon increasing the excitation intensity, a new sharp peak emerges near the high-energy onset of the biexciton PL line, corresponding to the $k = 0$ state. This peak shifts by $\Delta\omega$ when the excitation photon energy is varied by $\Delta\omega$ near the two-photon resonance. We show that this strong signal arises from two-photon hyper Raman scattering into the exciton level, where the biexciton state only serves as a virtual intermediate state. This Raman peak is highly suppressed under co-circular polarized excitation, which is also consistent with the two-photon selection rules for the angular momentum of the biexciton. Moreover, the threshold for stimulation in the Raman process is determined to be 80 MW/cm^2 at 10 K, which gradually increases with temperature. Our findings highlight highly nonlinear optical properties of this important material and its potential for biexciton-based photonic applications.

Keywords: 2D halide perovskites, biexcitons, hyper Raman scattering, giant two-photon absorption, stimulated Raman scattering

References

- [1] Nagasawa, et al, J. Phys. Soc. Jpn. 41.3 929-936 (1976)
[2] Fang, et al, Adv. Funct. Mater. 30.6 1907979 (2020)

8:00 PM EN06.03.09

Pathways to Successful Deployment of Perovskite Solar Cell Technology: A Data-Driven Approach on Research Trends Through Bibliometrics Jun-Seok Yeo¹, Jihong Kim¹ and Seung-Hoon Lee²; ¹Korea Institute of S&T Evaluation and Planning, Korea (the Republic of); ²Kongju National University, Korea (the Republic of)

Achieving the goal of global carbon neutrality by 2050 will require faster technology innovation and deployment across a range of sectors including power generation, transportation, industrial processes, and more. In particular, an energy transition based on renewable energy is a prerequisite for the new-zero emission of other sectors. Among the next-generation power sources, photovoltaic (PV) has been considered as a viable technology for the energy transition. Especially, hybrid organic-inorganic perovskite solar cells (PeSCs) have been intensively researched due to their high performance, light weight, affordability, and wide range of applications. In this study, we systematically examined the research trends and the cooperation networks by bibliometric methods, focusing on the social acceptance of the technology. A total of 8,607 documents published from 2019 to 2021 were investigated. First, we determined the commercialization factors by considering the LCOE and environmental impact; cost, efficiency, stability, scaling-up, and public acceptability. All publications were categorized by publication years and the commercialization factors. In addition, a variety of bibliometric methods were used: (1) statistical analyses, (2) topic modeling based on publication abstracts, and (3) social network analysis of institution-level co-authorships. These strategic analyses will provide different aspects of the scientific findings and facilitate further discussion on PeSC research directions.

8:00 PM EN06.03.10

Determining Bandgap Energy of Arbitrary Low-Dimensional Structures from Simulated Absorbance Philip M. Chamberlin and Kofi Adu; The Pennsylvania State University, United States

Low-dimensional structures are critical in developing the next generation of energy harvesting devices, such as photovoltaics. The bandgap energy of a material is critical in determining the wavelength range that can be absorbed by a given material and is influenced by quantum confinement effects. We propose a flexible program made in MATLAB that can analyze absorbance data of arbitrary low-dimensional structures to determine the bandgap energy using the Tauc plot and sigmoid-Boltzmann methods. We analyzed absorbance data generated using a COMSOL Multiphysics simulation of absorbance of exotic nanostructures. This program can be extended to all configurations, from zero dimensional structures to bulk materials.

8:00 PM EN06.03.11

Quantum Confinement Effect in Photoluminescence of TMDs Quantum Dot: Analytical Approach Ian Eckenrode, Sadiq Alli, Rachel Desulme, Dylan Hartmann and Kofi Adu; The Pennsylvania State University, United States

As a new class of fluorescent quantum dots (QDs) of two-dimensional nanostructures such as graphene and transition metal dichalcogenides (TMDs) have drawn increasing attention due to their exceptional properties and potential applications, such as light emitting diodes. Even though there is extensive data on photo-response of QDs, limited studies have focused on how size distribution affects the photoluminescence (PL). We develop an empirical model that captures such relationship. Our preliminary analysis indicates band gap tuning due to quantum confinement effect. The experimental results that could be attributed to synthesis conditions and the influence of functional groups termination and edge effect, inhomogeneous layer number distributions, and the absorption effect on the PL.

8:00 PM EN06.03.12

Low-Cost Graphitic Carbon Nitride Based Cathode Host for High Energy Density Flexible Lithium-Sulfur Pouch Cells Vijay Kumar, Ritu Malik and Mohini Sain; University of Toronto, Canada

Lithium-sulfur batteries (LSBs) have emerged as a highly promising energy storage and conversion system due to their remarkable theoretical specific capacity and energy density. However, the widespread adoption of LSBs faces significant challenges, primarily attributed to the shuttle effect and sluggish redox kinetics of polysulfides. Additionally, conducting realistic investigations at the pouch cell level is challenging, requiring the development of a scalable preparation method for sheet-type cathodes with high sulfur utilization and loading. To address these challenges, we have developed a novel approach utilizing a three-dimensional hybrid sulfur host comprised of graphitic carbon nitride (GCN) and functionalized carbon nanotubes (CNTs). This hybrid composite was synthesized through a self-assembly method followed by calcination. Through structural analysis, it was discovered that the carbon nitride sheets were grown in situ on the surfaces of the carbon nanotubes, establishing C-N bonds that created a larger π -conjugated system. This distinctive structural linkage not only facilitated improved conductivity but also resulted in the presence of an adequate number of nitrogen-containing functional groups. Consequently, it enabled efficient electron transfer from the carbon nanotubes to the carbon nitride. The hybrid composite, serving as a sulfur host, effectively alleviates the shuttle effect caused by intermediate polysulfides. This is achieved through its high sulfur utilization and robust chemical interaction with polysulfides. In practical terms, a modified composite cathode with an impressive sulfur content of 80 wt% and areal sulfur loading of 7.5 mg/cm² exhibits a high specific capacity of 780 mAh/g, while retaining 85% capacity after 300 cycles at 1 C. These exceptional electrochemical performances can be attributed to the abundant N atoms present in the GCN, which effectively anchor lithium polysulfides. This study not only makes a valuable contribution to the rational design of multi-functional bilayer structures but also presents a novel design approach that holds immense potential for the commercialization of flexible lithium-sulfur batteries with high-energy density.

8:00 PM EN06.03.13

Dual Confinement of Sulfur in MXenes for Application in Carbonate Electrolyte Li-S Batteries Mary Hassig, Michel W. Barsoum and Vibha Kalra; Drexel University, United States

Metal-sulfur, also known as lithium-sulfur (Li-S) batteries are of increasing interest for transport technology as their theoretical energy density is ~2,600 Wh/kg, more than 7x the theoretical energy density of a Li-ion battery. Li-ion batteries used in cars use a carbonate electrolyte, compared to an ether electrolyte, for safety concerns. However, more than 90% of Li-S battery research is performed with an ether electrolyte. Herein, we propose a synthesis method of confining sulfur (S) in and on multi-layer Ti₃C₂ MXene for use in the cathode of a Li-S battery with a carbonate electrolyte, for specific use in the electric vehicle industry. Combining both physical and chemical sulfur confinement helps optimize the sulfur loading percentage and helps minimize the creation of polysulfides (PS). Thus the PS do not react with the carbonate species and shut down the battery. This lack of PS also helps decrease the amount of shuttling and limits the decrease in battery performance. As MXenes are one of the few 2D materials that have functional groups that can be chemically modified, the groups can be replaced with S-terminations. MXenes can dually immobilize the S by physically confining the S between the layers. The combination of the two methods leads to increasing S loadings and S utilization for an increased energy density.

8:00 PM EN06.03.14

Investigation Resistive Switching Mechanism of 2D Inorganic Halide Perovskite CsPb₂Br₅ Microsheet Based Memristor Uijin Jung, Zhaozhong Tan, Wonjun Heo, Sangmin Kim and Jinsub Park; Hanyang University, Korea (the Republic of)

Resistive switching (RS) devices based on inorganic metal halide perovskites (IMHPs) are currently under extensive investigation as prospective materials for next-generation memory due to their inherent hysteretic behavior, simple manufacturing process, and improved environmental stability. However, the RS operations of polycrystalline IMHPs based devices are generally governed by migrations of ions and defects along to grain-boundaries (GBs) with low activation energies, which hinder the emergence of RS behavior coming from the IMHPs material itself. In addition, GBs in the IMHPs layer greatly increase the leakage current in the high-resistance state (HRS), degrading the RS characteristics, especially the narrowing of the on/off resistance window. Herein, we fabricated RS devices using GBs-free single crystal CsPb₂Br₅ microsheet and analyzed their RS characteristics. Through high-resolution transmission electron microscope (HRTEM) and selected area diffraction (SAED) pattern and Raman analysis, we confirmed that the synthesized microsheet was pure single crystal CsPb₂Br₅ without any other impurities. The vertical-type device was fabricated by depositing the top and bottom electrodes (T and BE) on the CsPb₂Br₅ (001) and (00-1) plane. In terms of effects of TE materials, RS did not occur when the inert electrode was used as the TE, unlike previous reports, but, the RS devices with active metal TE showed bipolar non-volatile RS characteristics, and exhibited an on/off resistance ratio (~10⁸) with low operating voltage (~0.32V). In addition, a reset voltage-driven multi-level operation was also shown, and each state had a large on/off resistance window up to ~10². On the other hand, a planar-type device in which both electrodes are formed on the (001) plane of CsPb₂Br₅ microsheet was also fabricated, and the RS characteristics were investigated. Unlike the vertical-type device, the device with inert metal electrode exhibited volatile RS characteristics, while the device with an active metal electrode showed non-volatile RS characteristics with a short retention time. Through nudged elastic band (NEB) calculations, we know that the bromine vacancy defects which mainly present inside CsPb₂Br₅ crystal prefer movement in the (001) plane rather than the [001] direction corresponding with the measured RS characteristics of the device based on the inert metal electrode. Moreover, the presence of Ag elements in CsPb₂Br₅ in the LRS was confirmed through auger electron spectroscopy (AES) depth-profile analysis, which suggests that active metal ion migration and redox reaction are the

main causes of RS in vertical-type CsPb₂Br₅ based memristor. This study can provide insight into the influence of the used active electrode as well as internal defects in the material in the HPS based RS device.

8:00 PM EN06.03.15

Colloidal Synthesis of Quaternary Chalcohalide Nanocrystals[IrinaGushchina](#)^{1,2}, [StefanoToso](#)², [MasaruKuno](#)¹ and [LiberatoManna](#)²; ¹University of Notre Dame, United States; ²Istituto Italiano di Tecnologia, Italy

Thanks to their optoelectronic properties, good stability, and abundance of elements involved, chalcohalides of IV and V group metals are considered promising candidates for future electrical and optical applications.¹⁻² However, their limited processability in bulk form, which requires maintaining high-temperature conditions for long times, represents a challenge for their implementation in functional devices. This has recently stimulated the exploration of alternative synthetic routes based on colloidal chemistry for obtaining the same materials in milder conditions, resulting in the successful preparation of lead- and bismuth- based ternary chalcohalides.³⁻⁵ However, these materials are all indirect-gap semiconductors, which limits their applicability to light harvesting and thermoelectric devices.

Nevertheless, direct-gap materials are within reach if we start considering quaternary chalcohalides, with general formula M_aM'_bE_cX_d (M and M' = metals; E = S, Se, Te; X = Cl, Br, I).⁶ In this study, we explore the colloidal synthesis of quaternary sulfohalide nanocrystals containing Pb, Bi, and Sb. Through the choice of precursor concentrations, metals feed ratios and reaction temperatures, this highly tunable synthetic approach offers control over the composition, morphology and ultimately properties of the reaction product. Our investigations confirm the direct gap of these materials, which can be tuned in the visible spectrum by alloying different metals and halides in the structure. This, combined with the remarkable stability of these materials, offers a first step towards real-world applications in optoelectronic devices.

- 1) Palazon, F. Metal Chalcohalides: Next Generation Photovoltaic Materials? *Solar RRL* vol. 6 2100829 (2021).
- 2) Ghorpade, U. V. et al. Emerging Chalcohalide Materials for Energy Applications. *Chemical Reviews* vol. 123 327–378 (2022).
- 3) Toso, S. et al. Nanocrystals of Lead Chalcohalides: A Series of Kinetically Trapped Metastable Nanostructures. *Journal of the American Chemical Society* vol. 142 10198–10211 (2020).
- 4) Quarta, D. et al. Colloidal Bismuth Chalcohalide Nanocrystals. *Angewandte Chemie International Edition* vol. 61 (2022).
- 5) Quarta, D. et al. Mixed Valence of Bismuth in Hexagonal Chalcohalide Nanocrystals. *Chemistry of Materials* vol. 35 1029–1036 (2023).
- 6) Islam, S. M. et al. Direct Gap Semiconductors Pb₂BiS₂I₃, Sn₂BiS₂I₃, and Sn₂BiS₂I₅. *Chemistry of Materials* vol. 28 7332–7343 (2016).

8:00 PM EN06.03.16

Elastic Crystalline Silicon Solar Mini-Module Based on All-Back-Contact Structure[JeonghwanPark](#) and [KwanyongSeo](#); Ulsan National Institute of Science and Technology, Korea (the Republic of)

Flexible and foldable solar cells have attracted numerous interests because they can provide continuous power on uneven surfaces of wearable applications. Crystalline silicon (c-Si) solar cells currently account for more than 95% of the total solar cell market share due to the abundance of Si and stability and high efficiency of the c-Si solar cells. However, c-Si solar cells are difficult to bend and stretch because they tend to become brittle when external forces are applied. Therefore, c-Si solar cells need to be installed on mechanically flat surfaces due to their rigid nature. In this work, we have demonstrated an elastic c-Si solar mini modules through the novel design of an all-back-contact configuration and the introduction of PDMS-based elastic interconnecting electrodes. The elastic c-Si solar module exhibited a module efficiency of 15.0% and a high voltage output of 4.87 V, with a size of 12 cm². Additionally, the elastic solar module demonstrated stable photovoltaic properties by maintaining less than a 4% reduction in initial efficiency under both folding and stretching conditions (up to a strain of 40%). We expect that this module can overcome the existing limitations of solar module installation and seamlessly integrate with flexible or wearable electronics, providing a continuous power source.

8:00 PM EN06.03.17

Molecular Insight into Charge Storage Mechanism in 2D Conjugated Covalent Organic Frameworks[ZhengnanTian](#), [VinayakS. Kale](#), [OsamaShekhah](#), [MohamedEddaoudi](#) and [HusamN. Alshareef](#); KAUST, Saudi Arabia

2D conjugated covalent organic frameworks (COFs) are currently attracting significant interest as host materials in electrochemical energy storage. They show some intriguing properties, such as designable conductivity, tunable layer distance, and flexible stacking form. However, there has been a lack of deep understanding of the charge storage mechanism related to conjugation degree, stacking model, and pore accessibility. Therefore, by topochemical molecular design, we synthesized two different aromatized imine-based 2D conjugated COFs. According to the detailed electrochemical analysis, in situ measurements, and theoretical simulation, we have discovered a charge storage mechanism that shows that ion diffusion kinetics, which is controlled by the stacking model of the COF, play a more important role than electron migration kinetics, which are controlled by the degree of conjugation, in the charge storage process. We believe this new understanding can be leveraged to design and develop more suitable 2D conjugated COFs for electrochemical energy storage.

8:00 PM EN06.03.18

MXene Sandwiched with Micro Polymer Fibers for Supercapacitor Energy Storage[ZuwangWen](#), [YoungseokKim](#), [JaeilPark](#), [MinhuHuang](#) and [Myung-HanYoon](#); Gwangju Institute of Science and Technology, Korea (the Republic of)

MXene (Ti₃C₂T_x), is considered as a promising electrode material for supercapacitors due to its metallic conductivity, large specific surface area and fast surface redox reaction capability. However, MXene flakes are inclined to stack together, resulting in severe loss of electrochemically active sites that restricts the electrochemical energy storage capability. Herein, we demonstrated a simple and effective strategy to fabricate MXene/PEDOT:PSS micro fibers sandwich structure films via alternative filtering MXene and PEDOT:PSS fiber dispersions with different mass ratio. The conductive crystallized PEDOT:PSS fiber self-fused into porous fibillar networks not only acted as conductive bridge facilitating electron transport, but also played a role as pillar between MXene nanosheets to expose more electrochemical active surfaces and shorten electrolyte ion pathways. As a result, the as-prepared composite film delivered a capacitance higher than 300 F/g with good rate performance in 1M H₂SO₄ electrolyte, which is better than the compact packed pristine MXene film. Furthermore, the PEDOT:PSS fiber networks improved composite film flexibility enables it bend and fold to arbitrary shapes without apparent electrical/electrochemical damage. This work reveals the importance of MXene based electrode architecture on electrochemical performance and guide on designing hierarchical composites materials for energy storage, catalysis, and flexible electronics applications.

Keywords: Ti₃C₂T_x MXene, PEDOT:PSS fibers, Flexible composite electrode, Supercapacitor

8:00 PM EN06.03.20

Redox based Chemical Organometallization: A Novel Strategy for Phase Engineering in Transition Metal Dichalcogenides[JuhwanLim](#), [EbinSebastian](#), [PratyushGhosh](#), [JihoHan](#), [ChristophSchneidermann](#) and [AkshayRao](#); University of Cambridge, United Kingdom

Phase engineering in transition metal dichalcogenides offers the ability to tune electric and optical properties, leading to enhance performance in electrical, optoelectronics and energy applications. Among the various available methods (i.e. chemical, electrochemical, optical, and mechanical approaches), chemical lithiation using pyrophoric n-butyllithium has been most widely used for inducing crystallographic phase transformation, from the semiconducting octahedral (2H) to the metallic trigonal prismatic (1T) phase in group 6-TMDs. Here, the donation of electron as well as gliding and adsorption of lithium ion play pivotal roles in driving the phase transition.

In this study, we demonstrate a novel facile and safe method to synthesize organometallic agents, which are then utilized for lithiating and sodiating 2H-MoS₂ and 2H-WS₂ to phase engineer 1T-Li_xMoS₂, 1T-Na_xMoS₂, and 1T-Na_xWS₂. Our approach is based on the correlation between the chemical redox potential and electrochemical potential, which were determined with in-situ optical reflectance measurements. In electrochemical measurements, MoS₂ exhibits discrete electrochemical potentials for a phase transition (PT) and further decomposition (amorphization, D) at both electrochemical lithiation (PT : 1.13 V, D: 0.55 V versus Li/Li⁺), and electrochemical sodiation (PT : 0.9 V, D: 0.8 V versus Na/Na⁺) processes. Therefore, we employed a reduced species of anthracene (redox potential around 0.9 V versus Li/Li⁺) to align the chemical redox potential with that of MoS₂. Remarkably, the use of anthracene facilitates a rapid and safe approach for both lithiation and sodiation, which yields high-quality metallic 1T-MoS₂.

We have extended this approach to reliably synthesize metallic 1T-WS₂. WS₂ displays distinct electrical potential values for phase transition and subsequent decomposition only when interacting with sodium (PT: 1.1 V, D: 0.55 V versus Na/Na⁺), while both potentials are nearly indistinguishably close with lithium. Thus, by employing an anthracene-sodium system, we are able to produce 1T-Na_xWS₂. Furthermore, we demonstrate that this process can be complemented by above-gap light, which accelerates the reaction by up to 1000 times. We carefully examined each TMD flakes with different phase, by monitoring the change of A-exciton photoluminescence, the emergence of Raman J peaks, and shifts of Raman peaks.

Taken together, our study reveals a novel method to synthesize organometallic agents, for advanced, safe phase engineering of 2D materials by creating cation intercalation structures, which can be further accelerated by integration of above-gap light illumination.

8:00 PM EN06.03.21

Fabrication and Characterization of Nanoscale Multilayered Thin-Film Thermoelectric Materials and Devices[FabianSanchez](#)¹, [EltonMawire](#)¹, [EricSmith](#)¹, [KimKisslinger](#)² and

In this study, we report the growth of nanoscale multilayered thermoelectric thin films and fabrication and characterization of integrated thermoelectric devices for the application of high-efficiency energy conversion and solid-state cooling. Nano multilayered Bi₂Te₃/Sb₂Te₃, Sb/Sb₂Te₃ and Te/Bi₂Te₃ thermoelectric thin film materials were grown on various substrates using the e-beam evaporation. The multilayered thin films were prepared with 100 to 300 layers, where each layer is about 3 to 5 nm thick. The effect of substrates on the growth of films such as the crystalline structures in the films was studied. Integrated thermoelectric devices with a high density of thermoelectric elements were fabricated with the nanoscale multilayered thin films using the clean room-based microfabrication techniques such as UV lithography. Plasma-enhanced atomic layer deposition (PE-ALD) was used to grow zirconium dioxide (ZrO₂) as the insulation layer in the device fabrication. X-ray diffraction and high-resolution tunneling electron micrograph (HRTEM) were used to analyze the nanoscale multilayered thin films. The fabricated device was cooled in liquid nitrogen or annealed at 150 °C for 30 min, respectively. HRTEM was used to analyze the cross-section of the nanoscale multilayered thin films for the three cases: as-grown, after being cooled in the liquid nitrogen, and after being annealed. The thermoelectric characteristics of the fabricated devices were measured and compared for the three cases of as fabricated, after being cooled, and after being annealed, respectively, showing that the integrated thermoelectric device had the highest efficiency of thermal-to-electrical energy conversion after being cooled in the liquid nitrogen. The fabricated nanoscale multilayered thin-film thermoelectric materials and devices could be used for the application of high-efficiency energy conversion and solid-state cooling.

Acknowledgements: Research carried out in part at the Center for Functional Nanomaterials, Brookhaven National Laboratory, which is supported by the U.S. Department of Energy, Office of Basic Energy Sciences, under Contract No. DE-SC00112704; the research is supported by DOD/ARO (W911NF-21-1-0195) and DOD/ONR (N00014-17-1-2635).

8:00 PM EN06.03.22

Carrier Type Switching in Bismuth Telluride through *In-Situ* Organic Molecule CoatingJun BeomPark¹, WeiWu², JasonY. Wu², RijanKarkee^{1,3}, TheresaM. Kucinski¹, KarenBustillo⁴, MattSchneider^{1,1}, DavidA. Strubbe³, ColinOphus⁴ and MichaelT. Pettes¹; ¹Los Alamos National Laboratory, United States; ²University of Connecticut, United States; ³University of California, United States; ⁴Lawrence Berkeley National Laboratory, United States

Thermoelectric materials have gained significant attention for their ability to efficiently convert waste heat into electricity. Among these materials, Bi₂Te₃ stands out as a near-room temperature thermoelectric material due to its exceptional properties, such as high electrical conductivity and relatively low thermal conductivity. Furthermore, low-dimensional Bi₂Te₃ nanostructures has also shown promise in enhancing thermoelectric properties, but it faces challenges, such as chalcogen vacancies and surface oxidation. To address these challenges, various methods have been proposed, including oxygen plasma treatment, superacid treatment, and atomic layer deposition (ALD) of Al₂O₃ to prevent surface oxidation. Simultaneously, several approaches have been explored to enhance thermoelectric properties of nanostructures through employing external dopant layer, such as tetrafluoro-tetracyanoquinodimethane (F₄-TCNQ). Here, we demonstrated the successful synthesis of Bi₂Te₃/F₄-TCNQ layered nanostructures through catalyst-free chemical vapor deposition (CVD). Even after a month of exposure to air, TEM analysis revealed an oxidation-free interface, confirming the efficacy of the coating as an oxygen diffusion barrier. In addition to this, the majority carrier type of the nanostructures switched from *n*-type to *p*-type and their Seebeck coefficient increased over an order-magnitude. It confirms that this *in-situ* organic layer coating not only provides an oxidation-protecting layer, but also act as a hole-injecting layer that can lead to a significant improve of thermoelectric characteristics. Finally, the F₄-TCNQ-coated Bi₂Te₃ exhibited an order-of-magnitude higher thermoelectric figure of merit (*zT*) that peaks at a minimum of 10–20 times improvement 250 K.

8:00 PM EN06.03.23

Graphenylene-Based Single-Atom Catalysts for Hydrogen Evolution ReactionCaiqueC. de Oliveira¹, LannaE. Lucchetti¹, JamesM. Almeida² and PedroA. Autreto¹; ¹Federal University of ABC, Brazil; ²Centro Nacional de Pesquisa em Energia e Materiais (CNPEM), Brazil

Owning to high-energy density and eco-friendliness, hydrogen (H₂) can provide clean energy as an alternative to fossil fuels. However, the main bottleneck of this energy carrier is the reliance on fossil fuels reforming methods, which are harmful to the environment. On the other hand, H₂ can be produced without emissions by electrocatalytic water splitting, in the hydrogen evolution reactions (HER). Yet, further developments are needed to make this technology economically viable and abundant, low-cost catalysts with high activity are demanded [1]. To date, Pt metal group materials and transition metal compounds such alloys are held as reference catalyst [2]. Nonetheless, these materials are susceptible to corrosion and exhibit low selectivity, not to mention the low availability and high production costs. Alternatively, 2D carbon-based materials possess high chemical resistance, superficial area and elevated electronic conductance, boosting the hosting capacity of these materials. Single Atom catalysts (SACs) can optimize the catalytic activity, enhancing selectivity and reducing the metal atom loading on the host matrix. In this work, state-of-art ab-initio calculations based on Density Functional Theory were carried out to investigate the catalytic performance of metal decorated Graphenylene (BPC@M, with M = Mo, W, V, Nb, Pd, Pt and Zr), a 2D sp² carbon allotrope composed by carbon rings with 4 and 6 atoms [3]. Our results show that the metal atoms act as active sites strengthening the interaction with the adsorbate thus reducing the free energy of adsorption.

Acknowledgements

The authors thanks CCM-UFABC for all the computational resources provided and PRH-ANP UFABC (PRH.49) for funding.

References

- [1] J. Zhu et al., Chem. Rev. 2020, 120, 2, 851-918;
- [2] C. Li and J. B. Baek, ACS Omega 2020, 5, 1, 31-40;
- [3] Q. Song et al., J. Mater. Chem. C, 2013, 1, 38-41;

SESSION EN06.04: 2D Materials for Energy Conversion and Energy Storage I
Session Chairs: Kevin Sivula and Damien Voiry
Tuesday Morning, November 28, 2023
Hynes, Level 3, Room 306

8:00 AM *EN06.04.01

Exfoliated Hafnium-Based Nanosheets as Catalysts for Oxygen Evolution in AcidManishChhowalla; University of Cambridge, United Kingdom

The zero pH condition of proton exchange membrane (PEM) water electrolyzers means that only a few metal oxide catalysts involving rare and expensive metals are sufficiently stable for the oxidation reaction. Therefore, earth-abundant acid-stable oxygen evolution reaction (OER) catalysts are required for sustainable water splitting. We report electrochemically exfoliated nanosheets from HfS₂ as stable and high-performance OER catalysts in pH 0 media. The oxidation during synthesis and composition of mixed amorphous and crystalline regions (a/c-HfS₂O_y) render this material sufficiently conductive to allow electrocatalytic activity while remaining stable in the acidic environment. a/c-HfS₂O_y catalysts exhibit among the highest reported mass activity of ~103,000 A/g at an overpotential of 0.5 V versus RHE and excellent stability. Efficient PEM water electrolyzers are demonstrated using low-dimensional noble-metal-free catalysts.

8:30 AM *EN06.04.02

Advancing Design and Discovery of 2D and Quasi-2D Perovskites via Combinatorial Synthesis and CharacterizationJongheeYang¹, FoadianElham¹, BenjaminLawrie², JuanitaHidalgo³, SergeiV. Kalinin¹, Juan-PabloCorrea-Baena³ and MahshidAhmadi¹; ¹University of Tennessee, Knoxville, United States; ²Oak Ridge National Laboratory, United States; ³Georgia Institute of Technology, United States

The emergence of 2D and quasi-2D perovskites has opened exciting possibilities for next-generation optoelectronic devices. These materials exhibit unique electronic, optical, and transport properties, making them promising candidates for a wide range of applications including solar cells, light emitting diodes and radiation sensors. However, their complex structural and compositional nature presents significant challenges in the design and exploration of these materials. In this talk, I will discuss the use of high-throughput combinatorial synthesis and characterization techniques for the design, discovery, and exploration of 2D and quasi-2D hybrid perovskites [1,2]. By leveraging the power of automation, we can rapidly synthesize a diverse library of 2D and quasi-2D hybrid perovskite compositions and systematically investigate the effects of different synthesis parameters on the layer thickness and properties of these materials, facilitating the discovery of novel structures with enhanced performance. Furthermore, high-throughput characterization techniques including photoluminescence and Grazing-Incidence Wide-Angle X-ray Scattering (GIWAXS) [3] allow for rapid and comprehensive analysis of the synthesized materials. This multidimensional high-throughput characterization approach helps us understand the influence of synthesis parameters and composition on layer thickness, multi-phase formation and crystal structure on the optoelectronic properties of 2D and quasi-2D perovskites, paving the way for targeted design strategies. I will showcase recent advances in this field, including the discovery of new perovskite phases, general phase distributions in the quasi-2D hybrid perovskites compositional space, offering a

comprehensive guide for designing phase-controlled systems [4].

References:

- Yang, J., Ahmadi, M. Empowering scientists with data-driven automated experimentation. *Nat. Synth* (2023). DOI: 10.1038/s44160-023-00337-z
- Yang J., Kalinin S.V., Cubuk E.D. Ziatdinov M., Ahmadi M. Toward self-organizing low-dimensional organic-inorganic hybrid perovskites: Machine learning-driven co-navigation of chemical and compositional spaces. *MRS Bulletin* **48**, 164–172 (2023). DOI: 10.1557/s43577-023-00490-y
- Yang J, Hidalgo J, Li R, Kalinin SV, Correa-Baena J-P, Ahmadi M. Accelerating materials discovery by high-throughput GIWAXS characterization of quasi-2D formamidinium metal halide perovskites. *ChemRxiv* (2023). 10.26434/chemrxiv-2023-x7sfr
- Yang J, Lawrie BJ, Kalinin SV, Ahmadi M. High-Throughput Automated Exploration of Phase Growth Kinetics in Quasi-2D Formamidinium Metal Halide Perovskites. *ChemRxiv* (2023). DOI: 10.26434/chemrxiv-2023-zcv10

9:00 AM *EN06.04.03

Correlation Between Electronic Properties and Surface Reactions of Doped and Undoped MoS₂ Films for Hydrogen Production [Carmela Aruta](#)¹, [Paolo Barone](#)¹, [Pasquale Orgiani](#)¹, [Piero Torelli](#)¹, [Luca Braglia](#)¹, [Elisa Riedo](#)², [Nan Yang](#)³ and [Zhiwei Nie](#)²; ¹National Research Council, Italy; ²New York University, United States; ³ShanghaiTech University, China

MoS₂ is gaining more and more importance in the field of energy applications. In particular, it is well known that MoS₂ has interesting hydrogen evolution reaction (HER) properties for electrochemical water splitting. H 1s - S 3p orbital overlap can be modified by doping MoS₂ with transition metal ions in order to tune H adsorption and thus HER activity. Among these, Co and Mn have shown great potential. To address these issues, we used a multipurpose pulsed-laser deposition (PLD) facility directly connected to the distribution chamber of the synchrotron beamline to produce and characterize MoS₂ films grown on different substrates, with different thickness and doped with Co and Mn. The in-situ transfer technology allowed measurements by surface sensitive X-ray photoemission (XPS) and X-ray absorption (XAS) techniques avoiding any surface contamination that may affect the sample properties. We observed that the MoS₂ interacts with the substrate at the interface which affects the electronic properties. In-operando XAS characterizations were performed with different gas environment on undoped and doped MoS₂ films in a reaction cell. The results demonstrate that the electronic structure is modified by reduction or oxidation atmospheres and are correlated with the electrocatalytic performance for HER, investigated by polarization curves. The measurements show a very high stability after many cycles and a decrease of the overpotential for hydrogen evolution in doped samples. Our study allows to understand the chemical environment, atomic response and changes in the electronic state during the absorption and desorption processes.

9:30 AM EN06.04.04

Two Dimensional Ferroelectric-Based Catalysts for Enhanced CO₂ Reduction [Joshua Young](#) and [MoLi](#); New Jersey Institute of Technology, United States

The electrochemical CO₂ reduction reaction (CO₂RR), which can turn CO₂ into C1 and C2 products, has been proposed as a route to both combat global warming and produce value-added fuels; however, a lack of efficient catalysts is limiting its implementation. Recently, single atom and dual atom catalysts (SACs and DACs, respectively), have been shown to enhance the CO₂RR but still suffer from scaling relationships limits. In this work, we show that 2D ferroelectric (2DFE) materials, which display a spontaneous electric polarization in a single monolayer that is switchable by an applied electric field, can be used to overcome limiting scaling relationships and break the Sabatier principle, leading to enhanced CO₂RR propensity. We first show that the predicted 2DFE MXene Y₂CO₂ with an O vacancy can preferentially adsorb CO₂ or CO. We then investigated the reduction CO₂ to various C1 products (e.g., methanol, formic acid, etc.) and find that switching the direction of the polarization changes the shape of the reaction pathway. Second, we investigated the CO₂RR on SAC and DAC-doped graphene interfaces with the 2DFE In₂Se₃. In this case, the reduction of CO₂ to CO is greatly enhanced compared to the free standing doped graphene layer regardless of the SAC/DAC coordination environment. In both systems, the asymmetry in the surface electron density allows for the tuning of surface adsorption and intermediate stability, as well as activation of alternative pathways. By combining the catalytic properties of 2D-support SACs and DACs with the switchable polarization of 2DFEs, such heterostructures can exhibit higher efficiency and selectivity for CO₂RR than existing catalysts and provides a unique route to overcome these issues.

9:45 AM EN06.04.05

New Lamellar Materials as Anode Electrodes for Alkali Metal Ion Batteries [Vincent Seznec](#)^{1,2,3}, [Xi Chen](#)^{1,2,3} and [Laure Monconduit](#)^{4,3}; ¹Laboratoire de Reactivite et Chimie des Solides, France; ²University of Picardie Jules Verne, France; ³Réseau sur le Stockage Electrochimique de l'Energie RS2E, France; ⁴Institut Charles Gerhardt, France

Recent studies have shown that two-dimensional (2D) materials, such as siloxene and germanene, as electrode in alkali metal ion batteries can lead to excellent performance. The improved electrochemical behavior of these 2D active materials could be due to the limited volume change during charge and discharge, based on an intercalation rather than an alloying mechanism. In addition, if Si is effective in reducing costs due to its low price and abundant resource reserves, its conductivity is low, while Ge can provide higher electronic conductivity than Si, but is more expensive. In this respect, in order to integrate their cheapness and excellent conductivity, we propose a series of layered materials (named siliganes, *i.e.*, Si_{1-x}Ge_x, 0.1 < x < 0.9), which consist of 2D Si-Ge composites. Through a simple method, the Ca²⁺ cations were completely removed from the precursor Ca(Si_{1-x}Ge_x)₂, and the lamellar siliganes were obtained. The layered materials were tested in Na- and K- ion batteries. Based on the better electrochemical performance, we identified siligane Si_{0.1}Ge_{0.9} as the best candidate. At a current density of 0.05 A g⁻¹, its reversible capacities of the Na ion and K ion cells were 276 mAh g⁻¹ and 132 mAh g⁻¹ after 50 cycles, respectively.

10:00 AM BREAK

10:30 AM *EN06.04.06

Layer-By-Layer Assembly of 2-Dimensional MXene Nanosheets with Polyelectrolyte Energy Storage Applications [Junyeong Yun](#)¹, [Michel W. Barsom](#)², [Micah Green](#)¹, [Miladin Radovic](#)¹ and [Jodie Lutkenhaus](#)¹; ¹Texas A&M University, United States; ²Drexel University, United States

A broad family of two-dimensional ceramic nanosheets referred to as MXenes have caught the world's attention because of their wide compositional diversity and tailorability to different engineering applications including energy storage. One challenge is to translate these applications into a thin-film platform. This presentation will discuss the water-based solution-assembly of two-dimensional MXene nanosheets with polyelectrolyte using the layer-by-layer assembly technique. This approach produces conformal MXene-based coatings on a variety of surfaces including hydrophobic poly(dimethylsiloxane), glass, thread and fiber, and silicon. The result is a conformal coating consisting of a brick-and-mortar-type architecture with tunable layer thicknesses. We take advantage of the MXene-polymer morphology for electrochemical energy storage in wire shaped capacitors consisting of reduced graphene and MXene or capacitor thin films of polyaniline with MXene. Last, the energy storage mechanisms for Ti₃C₂T_x MXene multilayer (ML) sheets is proved using electrochemical impedance spectroscopy (EIS) and cyclic voltammetry coupled with in situ gravimetric electrochemical quartz crystal microbalance with dissipation (EQCM-D) measurements in various electrolytes. EIS frequency-dependent mass changes associated with the transfer of hydrated cations are revealed. This study demonstrates that although cations are primarily responsible for the energy storage mechanisms in Ti₃C₂T_x MLs, the anion and the time scale of observation can have a strong effect.

11:00 AM *EN06.04.07

Application of 2D Transition Metal Sulfides in Energy Storage [Hongli Zhu](#); Northeastern University, United States

The emergence of metallic phase two-dimensional molybdenum disulfide (MoS₂) introduces a new class of materials boasting superior electrical conductivity and catalytic activity. This presentation aims to provide a comprehensive review of the atomic structures and electrochemistry of metallic MoS₂, an essential element in an array of established and burgeoning technological applications, with detailed studies of our lab in hydrogen evolution reaction, lithium ion and sodium ion batteries, supercapacitor, and all solid state Li sulfur batteries. For example, recently, in our lab, a highly conductive carbon fiber decorated with hybrid 1T/2H MoS₂ nanosheets is designed. The high chemical and electrochemical compatibility among MoS₂ and sulfide solid state electrolyte can greatly improve the stability of the cathode and therefore maintain pristine interfaces. The uniform distribution of electrical conductive metallic 1T MoS₂ on carbon fiber benefits the electron transfer between carbon and sulfur. Meanwhile, the layered structure of MoS₂ can be intercalated by a large amount of Li ions facilitating ionic and electronic conductivity. In consequence, the charge transfer and reaction kinetics are greatly enhanced, and the decomposition of SSEs is successfully relieved. As a result, the all solid state lithium sulfur delivers an ultrahigh initial discharge and charge capacity of 1456 and 1470 mAh g⁻¹ at 0.05 C individually with ultrahigh coulombic efficiency and maintains high capacity retention of 78% after 220 cycles. The batteries also obtain a remarkable rate performance of 1069 mAh g⁻¹ at 1 C. This talk will span the exploration of the atomic and band structures of metallic MoS₂, its electrical and optical properties, fabrication methodologies, and prominent emergent applications in the realm of electrochemical energy storage and conversion. A central feature of the talk will be the intricate relationship between the atomic structure, properties, and performance of metallic MoS₂, emphasizing the critical importance of understanding these fundamentals for emerging energy applications.

11:30 AM EN06.04.08

Layered Vanadium Disulfide Electrodes for Printed Zinc Ion Batteries [Stefano Tagliaferri](#), [Nagaraju Goli](#), [Evan Fisher](#), [Maria S. Sokolikova](#) and [Cecilia Mattevi](#); Imperial College London, United Kingdom

Aqueous Zinc Ion Batteries (ZIBs) are receiving growing attention as beyond-lithium power sources for wearable electronics and sensors, owing to their high theoretical capacity, environmental friendliness, and low cost. However, Zn^{2+} ions have a high charge density, almost double the charge density of Li^+ , which is detrimental for the intercalation kinetic and the structural stability of the battery electrodes.

Layered transition metal dichalcogenides (TMDs) have ideal features for high-performing energy storage devices, including high surface area and large two-dimensional diffusion channels inside their structure. The adjacent layers in the TMD structure are connected by weak van der Waals interactions, resulting in a large interlayer spacing which enables rapid ion diffusion kinetic and promotes the reversible insertion and extraction of multivalent ions. Among TMDs, vanadium disulfide is a promising cathode material for ZIBs, owing to its large interlayer spacing ($\sim 5.76 \text{ \AA}$) and metallic character. Despite these beneficial features, vanadium disulfide has mainly been investigated in coin-cell batteries, which are difficult to directly integrate in wearable electronics.

Here, we demonstrate the combination of an easily-scalable hydrothermal synthesis with a room-temperature 3D Printing process to fabricate vanadium disulfide electrodes with customized geometry. The hydrothermal vanadium disulfide was mixed with a polymeric binder and conductive additives to obtain a stable ink with optimal printability. The architecture of the VS_2 electrodes was rationally tailored *via* the printing process to facilitate the electrolyte penetration and promote fast charge transfer. Finally, the printed vanadium disulfide electrodes were coupled with zinc anodes to assemble aqueous zinc-ion batteries. The full cells were tested in a water-in-salt electrolyte, which improved the stability of the vanadium disulfide electrode, extending the achievable potential window and energy density.

SESSION EN06.05: Low-Dimensional Perovskites—Optoelectronics and Theory

Session Chairs: Volker Blum and Maria Antonietta Loi

Tuesday Afternoon, November 28, 2023

Hynes, Level 3, Room 306

1:30 PM *EN06.05.01

2D Layered Halides Perovskites Optoelectronic Properties Manipulation by Crystalline Orientation Rational Control [Giulia Grancini](#); University of Pavia, Italy

In recent years, the interest in low-dimensional perovskite (LDP or 2D perovskite) materials has flourished. This is due to their beneficial effects in perovskite-based photovoltaics, enabling devices with record power conversion efficiencies and prolonged stability. These materials are mainly utilized as surface modifiers, enabling 3D/2D heterostructures, acting as passivating agent. However, the research on the implementation of LDPs as self-standing absorbing material is limited, especially for LDPs with low dimensionalities ($n=1,2,3$). The main challenges are related to their optoelectronic properties, such as reduced carriers' diffusion length and high exciton binding energies, that limit their performances. Nevertheless, LDPs still represent a valid candidate for applications where wide bandgap ($>2 \text{ eV}$) materials are required. Indeed, LDPs circumvent the problem of halide segregation typical of 3D perovskite for such band gaps, guaranteeing prolonged stabilities of the device. Here, we present a powerful strategy to optimise LDP optoelectronic properties by finely controlling the crystallization of the material in a preferential direction. Our approach consists in orienting the inorganic sheet of the LDP material in the same direction of the charge extraction of the photovoltaic device, in order to maximize the transport of carriers and their collection at the electrodes. The preferential crystalline orientation of the LDP has been studied by advanced X-Ray Diffraction techniques, high resolution TEM imaging and directional dependent conductivity analysis, confirming the validity and the potential of the solution. The rational control over the crystal growth direction has allowed to fabricate a 2.1 eV LDP-based solar cell with power conversion efficiency about 10%, as well as semi-transparent devices with a high degree of transparency (Average Visible Transmittance $>30\%$). The chemical composition of the LDP and its improved intrinsic stability guaranteed much prolonged stability with respect to the state of the art devices with such high band gap. These results pave the way to the implementation of LDP for wide bandgap photovoltaic applications, such as semi-transparent and multi-junction tandem devices.

Acknowledgements I acknowledge the "HY-NANO" project that has received funding from the European Research Council (ERC) Starting Grant 2018 under the European Union's Horizon 2020 research and innovation programme (Grant agreement No. 802862).

2:00 PM *EN06.05.02

Synergy of 3D and 2D Halide Perovskites for Durable & Efficient Photovoltaics [Aditya D. Mohite](#); Rice University, United States

Three-dimensional (3D) organic-inorganic lead halide perovskites have emerged in the past few years as a promising material for low-cost, high-efficiency optoelectronic devices. Spurred by this recent interest, several subclasses of halide perovskites such as two-dimensional (2D) halide perovskites have begun to play a significant role in advancing the fundamental understanding of structural, chemical, and

physical properties of halide perovskites, which are technologically relevant. While the chemistry of these 2D materials is similar to that of the 3D halide perovskites, their layered structure with a hybrid organic-inorganic interface induces new emergent properties that can significantly or sometimes subtly be important. Synergistic properties can be realized in systems that combine different materials

exhibiting different dimensionalities by exploiting their intrinsic compatibility. In many cases, the weaknesses of each material can be alleviated in hetero architectures. For example, 3D-2D can demonstrate novel behavior that neither material would be capable of separately. Here I will describe how the structural differences between 3D halide perovskites and 2D halide perovskites give rise to their disparate materials properties, discusses strategies for realizing mixed-dimensional systems of various architectures through solution-processing techniques, and presents a comprehensive outlook at the use of 3D-2D systems in solar cells. Finally, we investigate applications of 3D-2D systems beyond photovoltaics, and offer our perspective on mixed-dimensional perovskite systems as semiconductor materials with unrivaled tunability, efficiency and technologically relevant durability.

2:30 PM EN06.05.03

Optical Control of Polarization in 2D Hybrid Molecular Crystals [Lina Quan](#) and [Yixuan Dou](#); Virginia Tech, United States

Spontaneous polarization is a key in developing advanced functional materials for a broad range of applications such as memory device, piezoelectric sensors, radio frequency/microwave devices, and many other systems. To manipulate structural polarization in organic-inorganic hybrid system, external stress and electric fields can induce the switching of ferroelectric polarization domains. When it comes to the electric field control, the limitation is anticipated involving the requirements for circuits and complicated device fabrication. In this presentation, I will talk about the observation of optically induced switchable polarization in 2D hybrid molecular crystal. By employing a number of advanced characterization tools, such as X-ray diffraction scattering measurement under the photo-excitation, we were able to probe and study the excited state structural dynamics from 2D hybrid molecular crystal with a clear observation of reversible lattice expansion and contraction in various time-scales.

2:45 PM EN06.05.04

Disentangling The Relationship between Cation and Perovskite Structures [Marcin Giza](#)¹, [Justas Deveikis](#)², [James Lloyd-Hughes](#)², [Rebecca L. Milot](#)² and [Pablo Docampo](#)¹; ¹University of Glasgow, United Kingdom; ²University of Warwick, United Kingdom

Layered perovskites utilising bulky organic cations have recently emerged as promising candidates for tackling the issues faced by conventional perovskite materials, such as their degradation in ambient conditions. Combining the benefits of good stability with desirable properties like efficient charge extraction relies on a precise understanding of the perovskite energetics, careful control of band alignment and optimised layer quality. In order to make further progress and guide future synthetic efforts, the relationship between the structure and optoelectronic properties of these films needs to be fully disentangled. Here, the interlayer spacing and the distortion of the crystal dictate the majority of the optoelectronic properties of the material. Typically, this is explained by a tunnelling mechanism, where the barrier width determines the likelihood of the process, and therefore the charge transport properties. In addition, the relative positions of the energy bands also influence this parameter, determined by the degree of distortion in the lattice. In these systems, the organic cations determine the structure, affecting every key property of the material at the same time, making disentangling these effects difficult. As such, an effort must be made to methodically investigate the structure-property relations of layered perovskite materials. Here, the crystal structures of a family of closely related cations are used to link how elements of the molecular structure impact the spacing and symmetry of the resulting perovskite layer. The optoelectronics of the resulting materials are also studied, to draw links between the perovskite structure and their optical bandgap, thus identifying key parameters which need to be target in order to effectively tailor future perovskite materials.

3:00 PM BREAK

3:30 PM *EN06.05.05

Structural and Optoelectronic Properties of 2D Multilayered Perovskites [Jacky Even](#)¹, [Mikael Kepenekian](#)², [George Volonakis](#)², [Pedesseau Laurent](#)¹, [Simon Thébaud](#)¹, [Marios Zacharias](#)¹,

2D multilayered perovskites share similarities with 3D perovskites including direct electronic band gaps, strong spin-orbit coupling, sizeable optical absorptions, small effective masses, Rashba-like effects [1]. Interestingly, they exhibit other attractive features related to tunable quantum and dielectric confinements, strong lattice anisotropy, more complex combinations of atomic orbitals and lattice dynamics, extensive chemical engineering possibilities. This will be illustrated by recent combined experimental and theoretical studies on excitons, formation of edge states, hot carrier effects and carrier localization [3-6]. More, combined in 2D/3D bilayer structures using new versatile growth methods, excellent solar cell device stability can be achieved [7]. Band alignment calculations nicely explain the difference of performances for ni-p or p-i-n devices [8]. The lattice mismatch concept can provide guidance for the choice of the proper 2D/3D combination [1,2].

- [1] J.-C. Blancon et al, Semiconductor physics of organic-inorganic 2D halide perovskites, *Nature Nano.* 15 969 (2020)
- [2] M. Kepenekian et al, Concept of lattice mismatch and emergence of surface states in two-dimensional hybrid perovskite quantum wells, *Nanoletters* (2018)
- [3] Y. Qin et al, Dangling octahedra enable edge states in 2D lead halide perovskites, *Adv. Mat.* 34, 2201666 (2022)
- [4] W. Li et al, Light-activated interlayer contraction in two-dimensional perovskites for high-efficiency solar cells, *Nature Nano.* 17, 45 (2022)
- [5] S. Cuthriell et al, Nonequilibrium Lattice Dynamics in Photoexcited 2D Perovskites, *Adv. Mat.* 34, 2202709 (2022)
- [6] H. Zhang et al, Ultrafast relaxation of lattice distortion in two-dimensional perovskites, *Nature Physics* 19, 545 (2023)
- [7] S. Sidhik et al, Deterministic fabrication of 3D/2D perovskite bilayer stacks for durable and efficient solar cells, *Science* 377, 1425 (2022)
- [8] B. Traore et al, A theoretical framework for microscopic surface and interface dipoles, work functions and valence band alignments in 2D and 3D halide perovskite heterostructures, *ACS Energy Letters*, 7, 349 (2022)

Acknowledgments: The work at institute FOTON and Institut des Sciences Chiiques de Rennes was supported by the European Union's Horizon 2020 research and innovation program under grant agreement 861985 (PeroCUBE). M.Z. acknowledges funding from the European Union's Horizon 2020 research and innovation programme under the Marie Skłodowska-Curie grant agreement No. 899546. J.E. is supported by Institut Universitaire de France.

4:00 PM *EN06.05.06

Structural, Electronic, Electron-Phonon and Chiral Properties of Layered Organic-Inorganic Perovskites from First PrinciplesVolkerBlum; Duke University, United States

Layered organic-inorganic perovskites and related halides offer broad tunability of their electronic, optical and spin properties by tailoring their organic and inorganic components. This talk focuses on first-principles structure and electronic structure predictions from large-scale spin-orbit coupled hybrid density functional theory. We show that quantum-well like energy level alignment can be predicted faithfully, i.e., in agreement with the experimentally observed optical response, at this level of theory. In a particular example, we further show how close alignment of the valence bands of the organic and inorganic components can be exploited to induce laser-controlled, coherent charge oscillations between the spatially separate organic and inorganic components. We next explore chiral systems, i.e., perovskites that either incorporate a chiral organic component or those that spontaneously break their symmetry, showing that a simple structural parameter can account for predicted relativistic splitting of the conduction bands, as well as for the associated chiroptical response. Based on the same rationale, we then explore perovskite nanostructures, i.e., quantum dot arrays and platelets with chiral organic functionalization, which also show significant spin-dependent optical responses. Finally, a key prerequisite for practical semiconductor applications of any material is dopability. For the paradigmatic layered halide perovskite phenethylammonium lead iodide, we explain experimentally observed, weak n-doping by Bi incorporation and weak p-doping by Sn incorporation through the interaction of either substituent with intrinsic defects in the material. This work would not be possible without numerous collaborators, including experimental colleagues around the world and the very large group of contributors to the FHI-aims code, used in this work, as well as the open-source Electronic Structure Infrastructure ELSI and the CECAM Electronic Structure Library (ESL). Funding from the National Science Foundation under awards number 1729297 and 1450280 is gratefully acknowledged. Work on doping and chiral systems was primarily supported as part of the Center for Hybrid Organic Inorganic Semiconductors for Energy (CHOISE), an Energy Frontier Research Center funded by the Office of Basic Energy Sciences, Office of Science within the U.S. Department of Energy.

4:30 PM EN06.05.07

Structure-Property Correlation and Strong Electronic Cross-Talk in Low Dimensional Metal Halide HybridsJanardanKundu; Indian Institute of Science Education and Research Tirupati, India

Low dimensional (2D, 1D, 0D) metal halide hybrids, supporting strongly bound excitons, show narrow band edge and broadband self-trapped excitonic (STE) emission. In the absence of general guidelines to enhance this broadband emission, structure-property correlation can be beneficial in designing highly emissive materials. This talk will highlight the fundamental factors that control the emissive properties of main group ns² metal halide based low dimensional (1D, 0D) hybrids. Our current results on utilizing doping strategy for the synthesis of multi-metallic halide hybrids that manifest interesting photo-physical properties and structural control will be showcased. Effects of electronic interaction between the metal halide units in such multi-metallic low dimensional hybrids will be highlighted. Mechanism of the electronic cross-talk between the isolated metal halide units in such systems will be discussed. Utility of such multi-metallic halide hybrids for anti-counterfeiting and negative thermal quenching applications will be highlighted. The talk will conclude with outlook of our current research work highlighting the existing issues in white light emission using main group low dimensional metal halide hybrids.

4:45 PM EN06.05.08

Modelling Orientational Disorder and Phase Transitions in Hybrid Piezoelectric Materials from First PrinciplesKasperTolborg and AronWalsh; Imperial College London, United Kingdom

Piezoelectric materials interconvert electrical and mechanical energy and find applications in diverse areas as sensors, actuators, and high precision motors. However, current state-of-the-art Pb-based piezoelectric ceramics pose significant environmental issues and preclude design of biocompatible devices. In recent years, solution processable, flexible and potential biocompatible hybrid organic-inorganic piezoelectric materials rivaling the performance of lead-based ceramics have been discovered [1,2].

The most promising candidates are based on low-dimensional inorganic frameworks with perovskite inspired structures, and they feature order-disorder phase transitions close to room temperature. Above these phase transitions, disordered, centrosymmetric phases appear, destroying their piezoelectric performance. Furthermore, conventional computational methods fail to predict the large piezoelectric response of this materials category [3]. Thus, modelling of this materials class must include entropic effects to phase stability [4], and nanoscale effects for response properties.

Here, we present the development of coarse-grained model Hamiltonians for the correlated disorder of dipolar organic cations in the archetypical 1D hybrid hexagonal perovskite, TMCMCdCl₃ (TMCM=trimethylchloromethyl ammonia) from first principles [5]. Coupled with Monte Carlo simulations, we predict and rationalise its order-disorder phase transition, showing that vibrational entropic contributions are key for quantitative agreement with the experimental phase transition temperature. This highlights the importance of vibrational entropy in describing phase stability for a materials class seemingly driven by configurational entropy.

Based on an observed easy stabilisation of anisotropic, two-dimensional disorder in the system, we calculate defect formation energies of isolated and extended orientational defects, which are shown to be easily formed at ambient conditions. Switching of these defects is suggested to be the origin the strong, unconventional piezoelectric response [5].

- [1] Y.-M. You, W.-Q. Liao, D. Zhao et al., *Science*, 2017, **357**, 306-309
- [2] W.-Q. Liao, D. Zhao, Y.-Y. Tang et al., *Science*, 2019, **363**, 1206-1210.
- [3] P. S. Ghosh, S. Lisenkov, I. Ponomareva, *Phys. Rev. Lett.*, 2020, **125**, 207601
- [4] K. Tolborg, J. Klarbring, A. Ganose, A. Walsh, *Digital Discovery*, 2022, **1**, 586-595
- [5] K. Tolborg, A. Walsh, *J. Mater. Chem. C*, 2023, accepted, DOI: 10.1039/D3TC01835K

8:30 AM EN06.06.01

Solution Processed Cs₂PbI₂X₂ for Interface Passivation in CsPbI₂Br Solar Cells Gaukhar Nigmatova, Zhuldyz Yelzhanova, Gulzhan Bizhanova, Hryhorii Parkhomenko, meruyert Tilegen, Damir Aidarkhanov, Vladimir Pavlenko, Chang Keun Lim, Askhat N. Jumabekov, TriPham, Mannix Balanay and Annie Ng; Nazarbayev University, Kazakhstan

Hybrid halide perovskites have shown promise as absorber materials for third-generation solar cells. However, improving the stability of perovskite solar cells (PSCs) remains a key challenge for commercialization. All-inorganic Cs-based perovskites have recently gained attention for their enhanced thermal stability compared to organic-cation perovskites. This work focuses on CsPbI₂Br absorbers with a 1.9 eV bandgap. We demonstrate an effective surface modification technique by forming 2D Cs-based perovskite nanostructures via solution processing on CsPbI₂Br thin films. The 2D Cs₂PbI₂X₂ layer passivates defects at the CsPbI₂Br surface, leading to improved photovoltaic efficiency and device lifetime. Controlling the nanomorphology of the 2D perovskite layer is critical for optimized passivation. Our experiment conditions show the evolution of Cs₂PbI₂X₂ growth on 3D perovskite thin films. This work demonstrates the approaches for tuning the morphology of Cs₂PbI₂X₂ through solution-processing parameters. Understanding the crystallization dynamics of the 2D Cs₂PbI₂X₂ nanostructures will also provide insights into developing other scalable solution processing techniques for large-scale manufacturing. Overall, this work shows that interfacial engineering of CsPbI₂Br PSCs via incorporation of solution-processed Cs₂PbI₂X₂ enables improvement of photovoltaic performance, motivating further study of 2D perovskite crystallization and nanostructure control for advancing all-inorganic PSC technologies.

8:45 AM EN06.06.02

Exploring the Structural Origin of Self-Trapped Exciton Emission in Cs₇Cd₃Br₁₃ Andrew Gruber, Kulatheepan Thanabalasingam and Kyle M. McCall; University of Texas at Dallas, United States

Low-dimensional metal halides with self-trapped exciton emission are a burgeoning materials class with important applications in solid-state lighting, X-ray scintillation, and luminescent solar concentrators. These materials exhibit effective and intrinsic self-trapping, with dual excited state origins arising from either Jahn-Teller distortion or *n*² lone pair dynamics. The intrinsic nature of this emission makes it ideal for testing structure-property relationships, as altering the composition, coordination, or dimensionality directly impacts the resulting excited state and thereby the resultant optical properties.

One such material is Cs₇Cd₃Br₁₃, which adopts a complex mixed 1D-0D structure with isolated [CdBr₄]²⁻ tetrahedra and corner-connected 1D chains of [CdBr₄Br₂]³⁻ octahedra. This compound has demonstrated orange STE emission at room temperature (PLQY above 9%), derived from the Jahn-Teller related distortion of the excited state, but it is unclear whether this emission is derived from the octahedral or tetrahedral cadmium halide subunits. We hypothesize that the straight octahedral chain is the emissive subunit in this system, as this coordination is unknown amongst inorganic cadmium halides. This work aims to elucidate the structural origin of STE emission in this compound using a combination of chemical substitution and temperature-dependent photoluminescence (PL) studies (PL emission, PL excitation, and time-resolved PL). Zn²⁺ has been chosen as an isoelectronic dopant that will exclusively occupy the tetrahedral site, providing a structural knob that can tune this emission as a function of temperature if the tetrahedral unit is involved in the excited state, thereby revealing whether this tetrahedral unit is responsible for the room-temperature emission. The upper limit of this doping will also be explored up to 66.7%, as Zn²⁺ may be able to fully substitute the CdBr₄ tetrahedral units, resulting in the theoretical compound Cs₇Zn₂CdBr₁₃. This work will illuminate the effective emissive subunit in Cs₇Cd₃Br₁₃ and add to the growing body of knowledge on transition metal halides with Jahn-Teller-active excited states.

9:00 AM EN06.06.03

The Role of Structure on Light Matter Interactions in Ruddlesden Popper 2D Perovskites Martin Gomez, Esteban Rojas-Gatjens, Victoria Quiros Cordero, Carlo Andrea Riccardo Perini, Carlos Silva and Juan-Pablo Correa-Baena; Georgia Institute of Technology, United States

Two-dimensional (2D) halide perovskites are promising for light emitting applications due to their tunable emission bandwidth, strong oscillator strengths, and low non-radiative recombination rates. These organic-inorganic heterostructures with confined excitons offer an ideal platform to study light-matter coupling, when standing electromagnetic waves interact near resonantly with matter excitations. However, the relationship between structural modifications and changes in excited states and their coupling with light remains poorly understood. In this study, we employ a combination of structural and optical characterization techniques including Grazing Incidence Wide Angle X-ray Scattering (GIWAXS), X-Ray Diffraction (XRD), Absorption, Photoluminescence, and Resonant Impulsive Stimulated Raman Scattering (RISRS) to investigate the effects of induced modifications to local atomic structure in PEA₂PbI₄ Ruddlesden-Popper Metal Halides (commonly known as 2D perovskites). By studying the influence of structural modifications on excited states we gain insights into the interplay between structural properties and light-matter interactions in 2D halide perovskites.

9:15 AM EN06.06.04

New Paths for Low-Dimensional Lead-Free Perovskites: From Traditional Wet Chemistry to *In Situ* Synthesis Rafael Abarques; Universidad de Valencia, Spain

Metal Halide Perovskites (MHP) have attracted significant research interest due to their unique properties and potential applications in photovoltaics, optoelectronics, and catalysis. Due to the huge concerns about lead toxicity in traditional metal halide perovskite, Lead-free perovskites have gained significant attention in recent years as alternative materials that can offer similar or better performance. Sn has been extensively investigated as an alternative to Pb in perovskite materials because they have a similar crystal structure as Pb-based MHP and can exhibit desirable optoelectronic properties, including high absorption coefficients and long carrier lifetimes. However, Sn perovskites also face challenges that must be addressed for widespread implementation. One of the major issues is their lower stability compared to lead perovskites, especially when exposed to moisture or elevated temperatures due to the prone of Sn(II) to oxidize to Sn(IV). Tin perovskites tend to undergo phase transitions and degrade more easily, decreasing device performance over time.

Researchers are actively working on improving the stability and performance of tin perovskites through various synthetic strategies. These include compositional engineering, dimensionality, interface modifications, encapsulation techniques, and device architecture optimization. Among them, low-dimensional perovskite structures, particularly layered structures, often exhibit improved stability compared to their bulk counterparts. The reduced dimensionality can mitigate ion migration and phase instability issues, leading to enhanced device performance and longevity. In low-dimensional materials, the confinement of charge carriers can lead to quantum confinement effects. These effects result in unique electronic properties, such as increased exciton binding energy and efficient charge transport. This can be advantageous for achieving high-efficiency solar cells and other optoelectronic devices.

Our research group has conducted investigations into the synthesis of low-dimensional Sn halide perovskites from micro and nanocrystals using different chemical routes, from traditional wet chemistry to *in situ* synthesis. We explore the versatility of the hot-injection approach for the dimensionality control of tin (II) halide perovskites microcrystals using 2-thiophene ethylene amine (TEA) as a bulky cation. TEA-Sn molar ratio plays an essential role in the formation and stabilization of 0D Sn-based MHP with excellent photoluminescence quantum yields (PLQY > 70%). Moreover, we report on a novel approach for the *in-situ* synthesis of 2D and 0D TEA₂SnX₄ nanocrystals embedded in a nanocomposite with excellent stability. This technique is low-cost and low-energy demanding, allowing modifications to precursor solutions for compatibility with commercial printing techniques, ultimately contributing to the success of MHP. The *in-situ* synthesis approach also offers a low-carbon footprint synthetic route, making it more sustainable than traditional wet chemistry. We demonstrated how adjusting crystal growth from macro to nanoscale, using innovative synthetic routes¹ and surface treatments, can alter optoelectrical response through fundamental changes in surface and bulk structure and composition.

1. Low-demanding *in situ* crystallization method for tunable and stable perovskite nanoparticle thin films

J. Noguera-Gómez, I. Fernández-Guillen, P. F. Betancur, V. S. Chirvony, P. P. Boix, R. Abarques

Matter. 2022, 5, 3541-3552

<https://doi.org/10.1016/j.matt.2022.07.017>

9:30 AM BREAK

10:00 AM *EN06.06.05

Ternary Perovskite-Organic Composites for High-Performance Perovskite Solar Cells Xiong Gong and Lening Shen; University of Akron, United States

Metal halide perovskites (MHPs) have emerged as promising photovoltaic materials due to their remarkable optoelectronic properties and the feasibility of cost-effective, high-throughput manufacturing of perovskite solar cells (PSCs). Over 25% of power conversion efficiencies (PCEs) have been reported for the PSCs based on three-dimensional (3D) MHPs. However, 3D MHPs are sensitive to moisture and oxygen, resulting in significant degradation of their performance under ambient atmosphere. Compared to 3D MHPs, two-dimensional (2D) MHPs possess improved photostability and chemical stability. The PSCs in which 2D MHPs are incorporated within the 3D MHPs network exhibit improved stability with respect to purely 3D systems, but lower record PCEs. In this presentation, I would like to report a breakthrough work in achieving enhanced PCEs, increased stability, and suppressed photocurrent hysteresis by incorporating n-type low-energy-gap conjugated organic molecules into 2D:3D mixed MHPs composites, where 2D MHPs were created by using conjugated organic cations rather than widely used non-conjugated organic cations. The resulting ternary MHP-organic composites displayed extended absorption in the near-infrared region, improved film morphology, enlarged crystallinity,

balanced charge transport, efficient photoinduced charge transfer, and suppressed the counter-ion movement. As a result, the ternary MHP-organic solar cells exhibited PCEs over 23%, which are among the best PCEs for PSCs with p-i-n device structure. Moreover, the ternary MHP-organic solar cells possessed dramatically enhanced stability and diminished photocurrent hysteresis. All these results demonstrated that the strategy of exploiting ternary MHP-organic composite thin films provides a facile way to realize high-performance PSCs. To further boost the PCEs of PSCs, we have synthesized various conjugated oligomer cations and then developed 2D:3D mixed MHP composites, where the 2D MHPs are created by using the above-conjugated oligomer molecules as the space cations. Afterward, these 2D:3D mixed MHPs composites are incorporated with n-type low-energy-gap conjugated organic molecule electron acceptors to form ternary MHP-organic composites for approaching high-performance PSCs. Conjugated oligomers are used as the space cations since they possess an enhanced density of states, which could further boost the charge transport of the resultant 2D MHPs in comparison to conjugated organic cations. As we expected, boosted PCEs and stability, and significantly suppressed photocurrent hysteresis are observed from the PSCs based on these newly developed MHP-organic composites.

10:30 AM *EN06.06.06

Application of Low Dimensional Materials in Solar Cells Yanfa Yan; The University of Toledo, United States

Low dimensional materials are gaining attentions in fabrication of efficient and stable thin-film solar cells. They are either used as absorbers or interfacial layers. In this talk, I will present two representative cases. For the case of absorber, I will present our work on fabrication of efficient thin film solar cells based on Antimony chalcogenides (Sb_2Ch_3). I will introduce the method developed to grow highly oriented films to promote extraction of photo-generated carriers. In the case of interfacial layer, I will present our work on utilizing layered perovskites to passivate and stabilize three-dimensional perovskite solar cells.

11:00 AM EN06.06.07

Methylammonium and Bromine Free Phase-Pure Dion Jacobson 2D Lead Halide Perovskites for High Efficiency and Durable Wide Bandgap Solar Cells Ayush Agrawal, Jin Hou, Faiz Mandani and Aditya D. Mohite; Rice University, United States

In the last decade, three-dimensional (3D) metal halide perovskite solar cells have displayed tremendous progress in photoconversion efficiencies. The tunable bandgaps enable mixed halide perovskite compositions to be used as the wide bandgap (WB) sub-cell in Si-perovskite and all perovskite tandems. However, halide segregation and ion migration of I-Br mixed halide systems under photo-illumination create bandgap instability that limits the long-term durability of these wideband gap subcells. 2D halide perovskites, on the other hand, have demonstrated better durability against moisture and photo illumination due to their large organic cations but still lag in efficiency due to $>2\text{eV}$ band gaps and charge extraction barriers. Furthermore, the methylammonium (MA^+) cation used in quasi-2D ($n=2$) perovskites is hygroscopic and can still limit the stability of the perovskite. Here, we synthesize formamidinium (FA^+) based 2D Dion Jacobson (DJ) perovskite solar cells with diammonium organic spacer cation. Optical absorption on FA 2D DJ reveals a band gap of 1.7-1.8eV for $n=3$ perovskites, ideally suited for building bottom cells for perovskite-perovskite and Si-perovskite tandems. Films fabricated using the phase-selective memory seeds¹ process preserved the phase purity of the $n=3$ 2D perovskite. FA 2D DJ perovskites demonstrate commercially viable durability against temperature, moisture, and maximum power point (MPP) tracking. These properties make FA 2D DJ perovskites promising candidates for wide bandgap subcells in perovskite-perovskite tandem.

(1) Sidhik, S.; Li, W.; Samani, M. H. K.; Zhang, H.; Wang, Y.; Hoffman, J.; Fehr, A. K.; Wong, M. S.; Katan, C.; Even, J.; Marciel, A. B.; Kanatzidis, M. G.; Blancon, J.-C.; Mohite, A. D. Memory Seeds Enable High Structural Phase Purity in 2D Perovskite Films for High-Efficiency Devices. *Advanced Materials* **2021**, *33* (29), 2007176. <https://doi.org/10.1002/adma.202007176>.

11:15 AM EN06.06.08

Band-Like Transport and Charge Carrier Dynamics in BiOI Films Snigdha Lal¹, Marcello Righetto¹, Aleksander Ulatowski¹, Silvia G. Motti^{1,2}, Zhuotong Sun³, Judith L. Driscoll³, Robert Hoye¹ and Laura Herz¹; ¹University of Oxford, United Kingdom; ²University of Southampton, United Kingdom; ³University of Cambridge, United Kingdom

Following the emergence of lead halide perovskites (LHPs) as materials for efficient solar cells, research has progressed to explore stable, abundant and non-toxic alternatives. However, the performance of such lead-free perovskite-inspired materials (PIMs) still lags significantly behind that of their LHP counterparts. For bismuth-based PIMs, one significant reason is a frequently observed ultrafast charge-carrier localization (or self-trapping), which imposes a fundamental limit on long-range mobility. BiOI is a widely studied 2D layered material which has recently been explored as a Pb-free PIM for photovoltaic applications. A wide bandgap material, it is highly suitable for tandem applications. However, despite reported defect tolerance and strong band-edge absorption, the power conversion efficiencies for BiOI-based devices has remained stunted with record efficiencies reaching barely 2%. An extensive photophysical study is needed to elucidate the performance limiting factors for BiOI along with highlighting the true intrinsic potential of the material as a photovoltaic absorber. Here, we report the charge-carrier dynamics of BiOI and show that unlike many other Bi-based compositions such as $\text{Cs}_2\text{AgBiBr}_6$ and Ag-Bi iodides, BiOI shows sustained band-like transport with respectable mobilities. Crucially our investigation reveals an absence of self-trapping despite the presence of strong electron phonon coupling and lower dimensionality. Using optical pump terahertz probe (OPTP) spectroscopy, time resolved microwave conductivity (TRMC) spectroscopy and time resolved photoluminescence (TRPL) spectroscopy, we unravel the early and long-time charge-carrier dynamics in BiOI and show that the material performance is limited by the presence of multi-phonon emission mediated non-radiative channels in the material. Using temperature-dependent OPTP transient, we quantify the bimolecular recombination constant and show that the material has low rates of band-to-band recombination likely originating from an indirect bandgap. Taken together with a slightly higher-lying direct bandgap, such low levels of intrinsic band-to-band recombination set high upper limits of achievable charge-carrier lifetime. Altogether, this contribution highlights the promise of BiOI solar cells.

SESSION EN06.07: 2D Materials for Energy Conversion and Energy Storage II

Session Chairs: Mona Zebarjadi and Hongli Zhu

Wednesday Afternoon, November 29, 2023

Hynes, Level 3, Room 306

1:30 PM *EN06.07.01

Thermoelectric Properties in Phase-Transition-Induced Thermal Hysteresis for Refrigeration Mona Zebarjadi; University of Virginia, United States

The phase transition from crystal to crystal or crystal to amorphous is accompanied by electron and phonon dispersion changes and hence sharp modifications of electronic and phononic transport properties versus temperature. In particular, the strong variations of the Seebeck coefficient and the heat capacity with temperature can be used for the design of heat management devices. Sharp changes in the Seebeck coefficient result in significant Thomson coefficients ($\tau = Tds/dT$, T is temperature). The Thomson effect induces heat release or absorption under the simultaneous application of a charge current and a temperature gradient in conductors, with applications in refrigeration. Thomson modules are not currently used. Their efficiency is barely studied as most materials show a minor Thomson coefficient much smaller than the Seebeck. Recently, Uchida's group reported a giant Thomson coefficient for FeRh alloys as a result of a phase transition. In this talk, I will present our results of phase transition-induced thermal hysteresis in FeRh alloys and $1\text{T}'$ -Td phase transition in type II Weyl semimetallic layered materials MoTe_2 and $\text{Mo}_{1-x}\text{W}_x\text{Te}_2$. In the latter case, we show consistency between the Seebeck hysteresis and direct measurements of the crystallographic angle using temperature-dependent X-ray diffraction. I will discuss how the Thomson coefficient is related to other materials' properties and can be used for refrigeration.

2:00 PM EN06.07.02

Two-Dimensional Li_xMoS_2 /Graphene Heterostructures for Li-S Batteries Zhuangnan Li and Manish Chhowalla; University of Cambridge, United Kingdom

Abstract

Lithium-sulfur (Li-S) batteries based on redox chemistry can store more energy than conventional insertion-type lithium-ion technologies^{1,2}. Our previous discoveries have shown that compact electrodes assembled from monolayered nanosheets of lithiated metallic 1T phase molybdenum disulfide (Li_xMoS_2) are electrically and ionically conductive, lyophilic and catalytically active³⁻⁶. In this presentation, I will describe a sulfur host design of two-dimensional (2D) Li_xMoS_2 /graphene heterostructure for Li-S batteries. The construction of heterointerfaces results in charge transfer from graphene to Li_xMoS_2 , which yields enhanced catalytic activity and promotes redox kinetics for sulfur conversion. The accumulation of greater charge in the Li_xMoS_2 layer of heterostructures also reduces its Lewis acidity compared to that of bare Li_xMoS_2 . The resultant ampere-hour-scale Li-S pouch cells deliver energy density of exceeding 400 Wh kg^{-1} . This work demonstrates an universal strategy of using 2D heterostructures to tune the electrode properties for realising practical energy storage.

Reference

1. Choi, J. W. & Aurbach, D. Promise and reality of post-lithium-ion batteries with high energy densities. *Nat. Rev. Mater.* **1**, 16013 (2016).

- Zhou, G., Chen, H. & Cui, Y. Formulating energy density for designing practical lithium–sulfur batteries. *Nat. Energy* **7**, 312–319 (2022).
- Li, Z., Sami, I., Yang, J., Li, J., Kumar, R. V. & Chhowalla, M. Lithiated metallic molybdenum disulfide nanosheets for high performance lithium-sulfur batteries. *Nat. Energy* **8**, 84–93 (2023)
- Eda, G. *et al.* Photoluminescence from chemically exfoliated MoS₂. *Nano Lett.* **11**, 5111–5116 (2011).
- Chhowalla, M. *et al.* The chemistry of two-dimensional layered transition metal dichalcogenide nanosheets. *Nat. Chem.* **5**, 263–275 (2013).
- Voiry, D. *et al.* The role of electronic coupling between substrate and 2D MoS₂ nanosheets in electrocatalytic production of hydrogen. *Nat. Mater.* **15**, 1003–1009 (2016).

2:15 PM EN06.07.03

Enhanced Photoelectrochemical Water Splitting with Doped Transition Metal Dichalcogenide Nanofilms Cansullhan^{1,2,3}, Scott Monaghan^{2,3}, Levgen Nedrygailov³, Mick Morris¹ and Paul Hurley²; ¹Trinity College Dublin, Ireland; ²Tyndall National Institute, Ireland; ³Amber Centre, Ireland

Photoelectrochemical water splitting to produce hydrogen fuel from solar energy conversion has been a hot topic for at least the past few decades. Nevertheless, Solar-to-Hydrogen Efficiency levels have been severely limited due to many factors, including light absorption, charge separation and transport, surface chemical reaction rate.^[1] Novel and emerging materials that may just address key bottlenecks are some of the transition metal dichalcogenides (TMDCs) due to their tunable band gap and an ability to be doped *n*-type or *p*-type.^[2] In recent times, nanometer thickness control, uniformity and large area growth of continuous films have been demonstrated by rapid deposition methods in manufacturing-compatible processes.^[3] However, little is known about the effect of different impurity concentrations incorporated into TMDCs, particularly on the semiconductor transport properties; the structural, chemical, and physical stability; and their photoelectrochemical properties. In this work, we focus on the enhanced water splitting capability of Si-based photoanode/cathode and tandem diode cells when combined with novel doped transition metal dichalcogenide (TMD) materials in an acidic aqueous medium. We use thermally assisted conversion (TAC) processes to form *n*-type and *p*-type TMDCs by converting transition metals to sulphide-based TMDCs with different impurity concentrations. The photoelectrochemical responses were assessed by standard potential sweep methods and electrochemical impedance spectroscopy. To determine transport properties, TMDCs were studied with 4-point resistivity measurements and AC Hall-effect measurements. Structural, chemical, optical and physical properties were characterized using Raman spectroscopy, X-Ray diffraction, UV-Vis spectroscopy, and atomic force microscopy. The performance of the cells was assessed within a purposely built PEC setup. The integrated light source was a G2V Pico Var Solar Simulator with 32 LEDs, providing an AM 1.5G 1.0 simulated Sun equal to a total irradiance of 87.2 mW cm⁻² with a spectral range of ~350 nm and ~1450 nm. We show that the doped TMD nanofilms acting as photoelectrodes provide a significant enhancement of PEC water splitting response when compared to the underlying silicon photoelectrodes without the nanofilms. We analyze the correlation between the increased activity with and without the nanofilms, the influence of their doping density and doping type on the mechanisms and compare the different cell geometries. Finally, we assess a selection of TMDCs using photoelectrochemical methods to understand their potential contribution to solar energy conversion and hydrogen fuel generation.

[1] Kilner, J. A., Skinner, S. J., Irvine, S. J. C. & Edwards, P. P. Functional materials for sustainable energy applications. *Funct. Mater. Sustain. Energy Appl.* 1–681 (2012). doi:10.1533/9780857096371

[2] Hallam, T. *et al.* Rhenium-doped MoS₂ films. **203101**, (2017).

[3] Ricciardella, F. *et al.* Calibration of Nonstationary Gas Sensors Based on Two- Dimensional Materials. *ACS Omega* **5**, 5959–5963 (2020).

2:30 PM BREAK

3:30 PM *EN06.07.04

Phase Engineering and Electrical Doping of 2D Materials for Energy Applications Albert Davydov; National Institute of Standards and Technology, United States

The ability to manipulate electronic, chemical, magnetic, and optical properties of layered van-der-Waals materials via controllable synthesis and processing enables their energy-related applications, including solid-state batteries, catalysis, photovoltaics, and thermoelectrics. This talk focuses on two metal chalcogenide compounds from the 2D materials family, MoTe₂ and InSe, to demonstrate the synthesis of specific crystal phases with tailored *n*- and *p*-type doping for photodetector and thermoelectric applications.

Semiconducting 2H- vs. metallic 1T'- polytype of MoTe₂ was controlled via chemical-vapor-transport (CVT) growth by manipulating processing temperature and by alloying MoTe₂ with W (to form Mo_{1-x}W_xTe₂ solid solutions), while the doping of 2H-MoTe₂ phase was controlled by choosing relevant CVT transport agent: I₂ for *p*-type and TeCl₄ for *n*-type. Semiconducting γ -InSe bulk crystals were grown by the Bridgman method with in-situ substitutional doping by Sn and Zn, for *n*- and *p*-type respectively. The increasing Sn doping level for the *n*-InSe case was quantified by inductively coupled plasma mass-spectrometry (ICP-MS) and X-ray fluorescence (XRF) analyses, while electrically active Sn concentration was evaluated using van-der-Pauw Hall measurements.

To demonstrate the utilization of crystal phase control and tailored electrical doping in 2D materials, the talk will conclude with employing electrically tunable γ -InSe layers in *p/n* homo- and hetero-junction photodetectors, while thermoelectric properties of 1T' phase of MoTe₂ and Mo_{1-x}W_xTe₂ alloys will be reported in details in a parallel invited talk by Prof. Mona Zebarjadi.

4:00 PM *EN06.07.05

Two-Dimensional Graphene and MXene for Flexible and Stretchable Displays Tae-Woo Lee^{1,2}; ¹Seoul National University, Korea (the Republic of); ²SN display Co. Ltd., Korea (the Republic of)

Two-dimensional materials, such as graphene and MXenes, offer promising alternatives to brittle indium tin oxide (ITO) for flexible and wearable displays. However, their practical application has been impeded by the high electron and hole injection barriers at the electrode/organic interfaces. To overcome this challenge, post-fabrication treatments were employed to modify the work function of 2D electrodes. Electron-withdrawing or electron-donating polymeric overcoating allowed for precise control of charge transfer doping, resulting in improved electroluminescent efficiency with reduced injection barriers. These surface modifications not only enhanced the environmental stability of the 2D electrodes in ambient air but also maintained their electrical properties. Furthermore, to address charge injection issues at stretchable electrode interfaces, a graphene layer can be introduced atop a silver nanowire percolation network, forming a two-dimensional stretchable contact electrode. This approach achieves remarkable current efficiencies among all intrinsically stretchable light-emitting diodes. These advancements in 2D materials establish a solid foundation for the practical implementation of 2D conductive materials in flexible and stretchable displays.

4:30 PM EN06.07.06

A 5 V-Class Cobalt-Free Battery Cathode with High Loading Enabled by Dry Coating Weiliang Yao¹, Chouchane Mehdi², Weikang Li¹, Shuang Bai¹, Zhao Liu³, Letian Li³, Alexander Chen¹, Baharak Sayahpour¹, Ryosuke Shimizu¹, Ganesh Raghavendran¹, Schroeder Marshall⁴, Yu-Ting Chen¹, Darren Tan¹, Bhagath Sreenarayanan¹, Crystal K Waters⁵, Allison Sichler⁵, Benjamin Gould⁵, Dennis J Kountz⁵, Darren J. Lipomi¹, Minghao Zhang¹ and Y. Shirley Meng²; ¹University of California San Diego, United States; ²The University of Chicago, United States; ³Thermo Fisher Scientific, United States; ⁴Army Research Directorate, United States; ⁵The Chemours Company, United States

Transitioning toward more sustainable materials and manufacturing methods will be critical to continue supporting the rapidly expanding market for lithium-ion batteries. Meanwhile, energy storage applications are demanding higher power and energy densities than ever before, with aggressive performance targets like fast charging and greatly extended operating ranges and durations. Due to its high operating voltage and cobalt-free chemistry, the spinel-type LiNi_{0.5}Mn_{1.5}O₄ (LNMO) cathode material has attracted great interest as one of the few next-generation candidates capable of addressing this combination of challenges. However, severe capacity degradation and poor interphase stability have thus far impeded the practical application of LNMO. In this study, by leveraging a dry electrode coating process, we demonstrate LNMO electrodes with stable full cell operation (up to 68% after 1000 cycles) and ultra-high loading (up to 9.5 mA h cm⁻² in half cells). This excellent cycling stability is ascribed to a stable cathode–electrolyte interphase, a highly distributed and interconnected electronic percolation network, and robust mechanical properties. High-quality images collected using plasma focused ion beam scanning electron microscopy (PFIB-SEM) provide additional insight into this behavior, with a complementary 2-D model illustrating how the electronic percolation network in the dry-coated electrodes more efficiently supports homogeneous electrochemical reaction pathways. These results strongly motivate that LNMO with a high voltage cobalt-free cathode chemistry combined with an energy-efficient dry electrode coating process opens up the possibility for sustainable electrode manufacturing using cost-effective and high-energy-density cathode materials.

8:30 AM *EN06.08.01

Solution-Processed Transition Metal Dichalcogenide 2D Nanoflakes for Photoelectrochemical Energy Conversion Kevin Sivula and [Rebekah Wells](#); Ecole Polytechnique Federale Lausanne, Switzerland

Given their established robustness and favorable optoelectronic properties, the layered semiconducting transition metal dichalcogenides (TMDs, e.g. MoS₂ and WSe₂) are attractive for optoelectronic applications including photoelectrochemical solar fuel production.[1] Recent advances in the liquid-phase exfoliation (LPE) of semiconducting TMDs into mono- or few-layered 2D nanoflake dispersions and their processing by inexpensive roll-to-roll techniques suggests that large-area TMD-based devices can be fabricated in a scalable manner and at low cost.[2] However, the high concentration of defects in these materials acts as recombination sites for photogenerated carriers and limit their performance. In this presentation the challenges with charge transport, separation, recombination, and interfacial transfer in LPE TMD nanoflake thin film devices will be discussed with respect to the 2D flake size and defect passivation/charge extraction treatments.[3] Our results give insight into the roles of both edge and internal defects and suggest routes for improvement. In addition to suitable defect mitigation techniques [4], we show that the exfoliation conditions play an important role on the performance of 2D TMD nanoflake films. Indeed, a powder-based electrochemical intercalation technique [5] can produce internal quantum efficiency for photon harvesting up to 90%. Moreover, for solar-driven H₂ production, we show that WSe₂ nanoflake thin films achieve absorbed-photon-to-current efficiency over 50% and photocurrent densities for solar water reduction at 4 mA cm⁻² under standard testing conditions.[4] These results suggest that roll-to-roll processed 2D TMDs are promising for economical solar-to-hydrogen conversion with a photoelectrochemical tandem cell.

[1] R. A. Wells and K. Sivula, *Acc. Mater. Res.* 2023, 4, 348.

[2] R. A. Wells, et. al, *ACS Appl. Nano Mater.* 2019, 2, 7705.

[3] X. Yu, K. Sivula, *Chem. Mater.* 2017, 29, 6863.

[4] X. Yu, et al., *Nano Lett.* 2018, 18, 215.

[5] R. A. Wells et al., *ACS Nano* 2022, 16, 5719.

9:00 AM EN06.08.02

Carbon Nitride Thin Films: An Innovative Platform for Energy Conversion and Storage [Paolo Giusto](#); Max Planck Institute, Germany

Carbon nitrides are a class of polymeric materials with ideal formula C₃N₄, which have recently attracted much attention especially in photocatalysis with visible light. However, up to now, their application in fields like optics was hindered due to the low-homogeneity thin films available. Herein, we present an innovative method to produce polymeric carbon nitride (pCN) thin films with tunable thickness by means of chemical vapor deposition. Eventually, the pCN thin films are stable, homogeneous, with very high refractive index and high transparency in the visible range.(1) These films were also used to develop innovative batch and microfluidic pCN-coated photoreactors with at least an order of magnitude higher efficiency compared to analogous bulk photocatalysts. (2) In energy storage devices, our group exploited carbon nitride thin films for anode-free lithium batteries, increasing the stability of the Cu current collector and generating a uniform and dense lithium plating with a good cycling stability. In sodium-ion batteries, pCN was exploited as inter-active interphase enhancing the sodium storage performances by 30% by means of a conformal coating of about 10 nm over a carbon anode material derived from lignosulfonate.(3) The exploitation of thin film technology coupled with the outstanding properties of pCN materials is still in its infancy but it sets the premises for significant improvements in a wide spectrum of application, especially where surfaces and interfaces play a key role.

1. Giusto P., et al. Shine Bright Like a Diamond: New Light on an Old Polymeric Semiconductor. *Adv Mater* 2020, 32(10): 1908140.

2. Mazzanti S, et al. Carbon Nitride Thin Films as All-In-One Technology for Photocatalysis. *ACS Catalysis* 2021, 11(17): 11109-11116.

3. Eren E. O. et al. Conformal carbon nitride thin film inter-active interphase heterojunction with sustainable carbon enhancing sodium storage performance. *Journal of Materials Chemistry A* 2023.

9:15 AM EN06.08.03

Energy Level Engineering, Co-doping and Extended Conjugation in Heptazine Frameworks: Towards Efficient Solar Energy Conversion using Carbon Nitride-Based Heterojunctions Kazi M. Alam, [John Garcia](#), Narendra Chaulagain, Navneet Kumar and Karthik Shankar; University of Alberta, Canada

Carbon nitride (C_xN_y) is a layered crystalline polymeric organic semiconductor consisting of nanosheets of *sp*²-hybridized triazine heterocycles. C_xN_y aggregates can either be large (3D crystals or sub-micron sized nanosheets) or small (truncated nanosheets or small spherical nanoparticles resembling quantum dots). The conjugated nanosheets allow for relatively fast charge transport, a high active surface area and the customizability of surface reaction sites. Consequently, carbon nitrides have shown remarkable performance as electrocatalysts, photocatalysts, optoelectronic sensors and carrier transport layers for a range of applications including, but not limited to - water splitting, CO₂ reduction, photovoltaics, photodetectors, water treatment and fuel cells. Carbon nitride combines the aforementioned advantages with scalable synthesis compatible with the use of agricultural wastes as precursors and an elemental constitution made of earth abundant elements. Insofar as the electronic applications of C_xN_y are concerned, further enhancements in the performance of based optoelectronic devices require the following conditions to be met: (i) Narrowing of the electronic bandgap (ii) Increase in carrier mobility (iii) Availability of high quality interfaces for exciton dissociation and charge transfer and (iv) Achievement of high photoluminescence and/or electroluminescence quantum yields. These technical challenges are interconnected and not entirely independent of each other. Herein we present a sequence of materials synthesis, device fabrication and compositional doping strategies to address these challenges and achieve the desired enhancements. We show that incorporation of graphene-like *sp*² carbon regions within C_xN_y nanosheets through the formation of carbon-rich carbon nitride extends π -conjugation and improves carrier transport. A secondary positive effect of such carbon-rich regions in C_xN_y is the reduction in intra-sheet and inter-sheet hydrogen bonding, which is widely believed to be a source of non-radiative recombination in C_xN_y. Doping and co-doping C_xN_y by highly polarizable main group elements such as S, P, Se, etc enriches the electron density in the nanosheets and increases the dielectric constant of carbon nitride, which in turn increases carrier mobility and reduces the exciton binding energy. We found that main group element-doped carbon-rich carbon nitrides exhibit narrow bandgaps as low as 1.5 eV and generate photocurrent densities as large as 5 mA/cm² for photoelectrochemical water splitting under AM1.5G one sun illumination. Finally, we tackled the issue of heterojunction formation through operando matrix-assisted solid-state condensation polymerization and electrophoretic anodization. The device testing data has been backed up by extensive characterization using XANES, SSNMR, HRXPS and HRTEM.

9:30 AM EN06.08.04

Low Dimensional Composite Materials as Binder-Free Anode for Energy Storage Applications [Kavin Arunasalam](#), Kevin Synnatschke, Meiyang Liang and Valeria Nicolosi; Trinity College Dublin, Ireland

The prolonged use of non-renewable energy such as fossil fuel and coal is having a deteriorating impact on our environment leading to severe climate changes. Hence, there is a dire need to explore new methods for energy generation and storage which are environmentally friendly, cost-effective and sustainable. Sodium-ion batteries have been attracting great interest as an alternative to lithium-ion batteries due to their material abundance, lower cost, and sustainability. However, a high-performance viable anode for the sodium-ion battery has yet to be discovered because of the difference in its molecular size and intercalation mechanism to the comparatively smaller lithium ions.

This issue has garnered global research interest in the quest to develop anodes with expanded interlayer spacing capable of accommodating sodium ions. This area of study has emerged as a promising field within material science, particularly in the realm of 2D materials research. 2D materials are known for their unique structure and electronic properties such as hardness, tuneable band gap by variation of the number of layers and their high surface area. These properties make them intriguing candidates for applications in batteries and electrocatalysis. Black phosphorus, a well-studied 2D class material, has previously been reported to show very high theoretical capacity for both sodium and lithium-ion battery systems but suffers from low cycling stability due to chemical and structural instability.^[1] To overcome this problem, we decided to explore the prospect of a new 2D composite material made from nanosheets of black phosphorus (phosphorene) and MXene (Ti₃C₂T_x) to be potentially used as an anode in a sodium-ion battery. The MXene layers with terminating fluorine and oxygen functionals are expected to promote the growth of stable solid-electrolyte interfaces (SEI) which in turn is expected to further improve the overall coulombic efficiency of the battery.^{[2][3]}

Both nanomaterials were synthesized via liquid-phase exfoliation (LPE). Phosphorene is notorious for being oxidized easily. Hence, to protect the phosphorene, a novel layer-by-layer (LBL) vacuum filtration technique was implemented to obtain the electrode. The resulting electrodes were then assembled in a lithium-ion coin cell to study their cycling stability and rate capacity, given the similarity of the lithium and sodium ion intercalation mechanism in the anode. XPS, SEM, EDX, UV-Vis, XRD and AFM characterization were performed on the composite nanomaterial to study its morphology, as well as compositional and structural changes upon processing. It was found that the electrode material showed a high discharge capacity of 700 mAh/g at 0.2 C with 98% coulombic efficiency for 100 cycles which indicates a promising performance potential for sodium ion battery systems.

In conclusion, the layer-by-layer MXene-phosphorene composite structure effectively shields the phosphorene nanosheets from extensive oxidation in ambient conditions. This preservation of phosphorene enables a reversible reaction and ensures excellent cycling stability as an electrode material. Moreover, the inclusion of the MXene component acts as a conductive binder in this

composite eliminating the need for traditional non-conductive binders like PVDF and CMC. This substitution reduces dead volume within the anode and enhances the material's specific capacity. Finally, the composite's large interlayer spacing highlights its potential application as an anode in sodium ion battery systems, emphasizing the need for continued exploration and research in this area.

References

- Mohamed Alhabej, et al., *Chemistry of Materials*, 2017, Vol. 29
Junye Cheng et al., *Nano-Micro Letters*, 2020, Vol. 12.
Xiong-Xiong Xue, et al., *Journal of Physics: Energy*, 2021, Vol. 3

9:45 AM EN06.08.05

Thermal Transport Characterization Method for 2D Layered Materials and Their Polymorphs[Sungjin Park](#), Kyomin Kim and Woochul Kim; Yonsei University, Korea (the Republic of)

Two-dimensional (2D) layered materials are known to possess different physical properties than bulk materials due to the weak van der Waals bonds between their layers. Graphene is a representative 2D material whose material properties is known to different from its bulk counter part [1]. The material properties of 2D materials can be further altered by changing the stacking sequence of the interlayers such as in MoS₂ where different stacking sequences lead to the 2H and 3R polymorphs [2]. NbSe₂ is a 2D layered material whose new polymorphic form (2H-3R) was discovered recently [3]. This work proposes a method to characterize the thermal transport properties of 2D layered materials by measuring the thermal conductivity of the different polymorphs of NbSe₂ using the in-house T-bridge method. Photolithography technique was utilized to fabricate the micro-scale T-bridge device and mechanical exfoliation was used to obtain thin 2D layered NbSe₂ samples for their bulk material. The thermal conductivity of various thickness 2H-NbSe₂ and 2H-3R-NbSe₂ was measured, and results showed that the difference in stacking sequence of the 2D layered material can alter its thermal transport properties. The in-house T-bridge method can be further utilized to measure the thermal transport of various 2D layered materials and their polymorphs.

- [1] A.A. Balandin, S. Ghosh, W. Bao, I. Calizo, D. Teweldebrhan, F. Miao, C.N. Lau, *Nano Letters* **8**(3), 902-907 (2008)
[2] R. Suzuki, M. Sakano, Y.J. Zhang, R. Akashi, D. Morikawa, A. Harasawa, K. Yaji, K. Kuroda, K. Miyamoto, T. Okuda, K. Ishizaka, R. Arita, Y. Iwasa, *Nat. Nanotechnol.* **9**(8), 611-617 (2014)
[3] H. Moon, J. Kim, J. Bang, S. Hong, S. Youn, H. Shin, J.W. Roh, W. Shim, W. Lee, *Nano Energy* **78**, 105197 (2020)

10:00 AMB BREAK

10:30 AM EN06.08.06

Photothermal Processing of Layered Materials under Controlled Pressure for Energy Storage Applications[Najma Khatoon](#), Binod Subedi, Ahmad Majed, Julie Albert, Michael Naguib and Douglas B. Chrisey; Tulane University, United States

2D layered materials are promising candidates for synthesizing materials with customizable properties contributing from each layer. Enhanced electrical, mechanical, thermal and optical properties by tailoring the layers makes layered materials highly versatile and adaptable for various applications. MXenes are one such example of 2D layered materials class. Their high conductivity, excellent chemical stability, good mechanical properties, tunable surface chemistry, large specific area, and ability to integrate with other materials makes them an excellent customizable layered material. Titanium carbide (Ti₃C₂-T_x) MXene, where T_x are surface terminations, have high conductivity, and excellent Li-ion diffusion properties. Intercalation of ions/molecules in Ti₃C₂ layers is one route to enhance its electrochemical properties. Silicon-based nanomaterials are promising candidates for intercalation due to their higher theoretical specific capacity.

In this work, we intercalated PDMS (Polydimethylsiloxane) in Ti₃C₂ with initial d-spacing ~1 nm. Intercalation of PDMS resulted in increase of d-spacing from 1 nm to ~12 nm. The intercalated PDMS was converted into silica (SiO₂) by processing it through a unique process of photonic curing. Our results showed that after photonic curing the d-spacing changed from 12 nm to ~5 nm. The PulseForge parameters were 450 V bank voltage 7 pulses, and ~4 Jcm⁻² per pulse fluence. Furthermore, we cured the intercalated MXene under controlled pressure and in a different gas environment. Results showed a less oxidation rate of MXenes when cured under controlled pressure. The stability of reversible electrochemical reactions was observed in the cyclic voltammetry of MXene intercalated within cured PDMS, indicating the enduring nature of these reactions throughout repeated cycling. This study demonstrates the potential of photonic curing as a cost-effective and scalable method for synthesizing customizable layered materials with precise control over the nanostructure within the layers. The process offers an instantaneous and roll-to-roll compatible approach for large-scale synthesis.

10:45 AM *EN06.08.07

Colloidal Quantum Dot Near-Infrared Light Emitting Diodes with High External Quantum Efficiency[Maria Vasileopoulou](#); National Centre for Scientific Research Demokritos, Greece

Semiconductor colloidal quantum dots (CQDs) have become a prominent class of solution-processed emitting nanocrystals owing to their potential to provide size- and composition- tunable luminescence of high colour purity. Importantly, their emission can be extended deep into the second biological near-infrared (NIR) window (1000-1700 nm, NIR-II) where related lighting technologies based on organic and perovskite semiconductors have so far failed to access. However, the application of NIR-II CQD light emitting diodes (LEDs) is still hindered by low efficiencies mainly attributed to low photoluminescence quantum yield (PLQY) and poor charge transport properties of pure CQDs films. Here, we report NIR-II CQD LEDs with unprecedented external quantum efficiency (EQE) of 16.98% and power conversion efficiency (PCE) of 11.28% at 1397 nm. This extraordinary performance stems from a combinatorial device engineering approach that allowed us to achieve high PLQY in CQDs-embedding films and charge balance close to unity in the CQD-emissive device. More specifically, we employed a binary emissive layer consisting of silica-encapsulated Ag₂S CQDs dispersed into a cesium-containing triple cation perovskite matrix that serves as an additional passivation medium and carrier supplier to the emitting CQDs. Furthermore, we applied successful engineering at the hole injection contact through inserting a thin porphyrin interlayer to balance the device current and enhance carrier radiative recombination. The remarkable efficiency of our devices surpasses the performance of any previously reported CQD NIR LED. Additionally, it represents a record efficiency for any solution-processed lighting source in the second NIR-II window and foreshadows CQD technologies that will transcend the lighting products already available in the market.

11:15 AM EN06.08.08

Edge Engineering of Two-Dimensional Transition Metal Dichalcogenides[Guoxiang Hu](#); Georgia Institute of Technology, United States

Two-dimensional (2D) transition metal dichalcogenides (TMDCs) have attracted tremendous interest as functional materials due to their exceptionally diverse and tunable properties, especially in their edges. In addition to the conventional armchair and zigzag edges common to hexagonal 2D materials, more complex edge reconstructions can be realized through careful control over the synthesis conditions. However, the whole family of synthesizable, reconstructed edges remains poorly studied. Here, we develop a computational approach integrating ensemble-generation, force-relaxation, and electronic-structure calculations to systematically and efficiently discover additional reconstructed edges and screen their functional properties. Using MoS₂ as a model system, we screened hundreds of edge-reconstruction to discover over 160 reconstructed edges to be more stable than the conventional ones. More excitingly, we discovered new synthesizable reconstructed edges with record thermodynamic stability, in addition to successfully reproducing recently synthesized edges. We also find our predicted reconstructed edges to have multi-functional properties—they show near optimal hydrogen evolution activity over the conventional edges, ideal for catalyzing hydrogen-evolution reaction (HER) and also exhibit half-metallicity with a broad variation in magnetic moments, making them uniquely suitable for nanospintronic applications. Our work reveals the existence of a wide family of synthesizable, reconstructed edges in 2D TMDCs and opens a new materials-by-design paradigm of 'intrinsic' edge engineering multifunctionality in 2D materials.

11:30 AM EN06.08.09

Promising Properties of 2D Layered Cobalt and Nickel Nitrides as Negative Electrodes for Li-Ion Batteries[Jean-Pierre Pereira-Ramos](#)¹, Yanlong Zhou^{1,2}, Nicolas Emery¹, Olivier Nguyen² and Rita Baddour-Hadjean¹; ¹ICMPE CNRS, France; ²Technocentre Renault, France

2D materials largely dominate the field of Li-ion batteries with the transition metal oxides LCO (LiCoO₂), NMC LiNi_xMn_yCo_z) and NCA (LiNi_xCoyAl_z) used as positive electrode materials and carbon graphite as negative electrode. However graphite suffers from a low rate capability and from a limited specific capacity. Intensive research has been made to find alternative anode materials such as the LiAl, Li_xSn, Li_xSi...alloys or transition metal oxides as conversion materials. But in all cases, huge volumetric changes occur upon discharge-charge reaction inducing a fast capacity decline. In spite of numerous studies, this important drawback has never been solved as yet.

We have decided to explore the group of lithiated transition metal nitrides as alternative negative electrode materials to overcome safety issues related to the use of graphite at high current. Some of these compounds were firstly investigated in the wide voltage window 1.4V-0V leading to high specific capacities but also to irreversible structure change with the irreversible oxidation of nitride anion framework. Hence poor electrochemical properties were achieved. Our key idea has been to rigorously control the upper cut-off voltage inside the stability domain of the nitride framework which is strongly dependent on the metal and metal content.

The present work reports the chemical synthesis and the structural characterization of lithium nitridocobaltates Li₃-2xCoxN and Li₃-2xNixN nitridonickelates with 0.1 ≤ x ≤ 0.6. These 2D compounds with an hexagonal symmetry constitute unique examples of intercalation compounds based on the nitrogen framework in which lithium can be reversibly inserted and extracted

due to numerous cationic vacancies. With a mean working voltage around 0.5V, these “zero strain” materials deliver high specific capacities in the range 200-320 mAh/g with a remarkable stability over at least 100 cycles. In addition to a complete investigation of their electrochemical features in the 1V-0.02V potential range, we have elucidated the electrochemical mechanism involving the Co and Ni redox species (I/II/III) in relation with the tiny structural changes revealed through operando XRD experiments. A detailed kinetic study of the charge-discharge process in the case of nickel-based compounds allows to give a complete picture of electrochemical performances of these 2D lithiated nitrides as negative electrode materials for Li-ion batteries.

11:45 AM EN06.08.10

Solar Energy Conversion and Storage Potential of 2D Covalent Organic Frameworks Elucidated by Excited-State Electronic Structure Simulation HenryThornes, CharlieDeFreest, HosannaAbbey, TomWheaton, MeganRobbins, AlanaSullivan and [TimKowalczyk](#); Western Washington University, United States

Two-dimensional covalent organic frameworks (COFs) are valued for their high porosity and surface area, highly useful properties for gas separations and heterogeneous catalysis. However, their framework structure is also intrinsically valuable as a design space for organic materials bearing embedded chromophores that confer a degree of synthetic control over intermolecular stacking arrangements. In past work, we computationally explored the potential of 2D COFs as a platform for singlet fission. Here we report electronic structure simulations characterizing the capabilities of photoactive COFs for selected energy conversion and storage applications. First, we show the impact of chromophore embedding and functionalization on the photophysical properties of families of emissive COFs, one of which may serve as a stepping stone to realizing singlet fission experimentally in a COF. Second, we computationally probe the potential of COFs as a platform for fine control of solar energy conversion and storage via embedding of a photoisomerizable molecular solar thermal fragment within the framework. The simulations apply recent advances in excited-state methods to characterize the effects of interlayer stacking on photophysical properties and guide the design of COFs for renewable energy applications.

SESSION EN06.09: Layered Perovskites and 2D Materials for Energy Conversion and Energy Storage

Session Chairs: Paolo Giusto and Rebekah Wells

Thursday Afternoon, November 30, 2023

Hynes, Level 3, Room 306

1:30 PM EN06.09.01

NiFeZnP Nanosheets with Enriched Phosphorus Vacancies for Supercapattery Electrodes [NagehK. Allam](#); American University in Cairo, Egypt

Designing and fabricating outstanding electrode materials *via* simple preparation routes are viable ways for improving the performance of electrochemical supercapacitors. We report on the synthesis of NiFeZnP phosphide interconnected nanosheets with abundant phosphorus vacancies (P_v-NiFeZnP) *via* a facile reduction route at room temperature. The fabricated P_v-NiFeZnP was fully characterized using energy-dispersive spectroscopy, field emission scanning electron microscopy, electron paramagnetic resonance, and X-ray photoelectron spectroscopy techniques. Owing to the porous interconnected nanosheet structure and the superior stability enabled by the direct binder-free growth on Ni foam, the P_v-NiFeZnP electrode, with optimized phosphorus vacancy formation, exhibits a superb electrochemical performance of 631.8 mC/cm² (equivalent to 1579.5 mF/cm²), which is significantly higher than those reported in the literature. Also, the P_v-NiFeZnP||activated carbon asymmetric device exhibits a very high Coulombic efficiency (~100%) and excellent long-term stability (98.8% capacity retention after 7500 cycles). The fabricated device can deliver 122.1 μWh/cm² energy density at a power density of 750 μW/cm². The fabricated NiFeZnP electrode is therefore a promising candidate for supercapacitor applications.

1:45 PM EN06.09.02

High Pressure Synthesis of Low Dimensional Pnictogen Chalco-Halides Based on (Sb,Bi)(S,Se)(Br,I) for Emerging Energy Applications IvanCaño Prades, AlejandroNavarro Güell, EdoardoMaggi, CibránLópez, MarcelPlacidi, LluísSoler Turu, ClaudioCazorla, JoaquimPuigdollers and [EdgardoSaucedo](#); Universitat Politècnica de Catalunya, Spain

There is an increasing interest in the development of novel van der Waals materials with low dimensionality and with exotic properties, for emerging energy applications such as photocatalysis, photovoltaic and thermoelectric devices. Among them, pnictogen chalco-halides with low dimensional morphology (commonly quasi-one-dimensional nanocolumnar structures) are attracting a lot of attention due to the unusual combination of bandgaps suited for different energy applications, excellent stability, and possible high tolerance to defects. Despite these clear advantages, it is very complex to synthesize this type of materials containing one halogen and one chalcogen in the structure, even if there are clear evidence that these materials can be synthesized at relatively low temperature (< 400 C). In this work, we will present first a detailed DFT modelling of the structure, stability and optical properties of pnictogen chalco-halides based on (Sb,Bi)(S,Se)(Br,I). Theoretical calculations confirm the high stability of all possible ternary compounds, with band structures and bandgaps very well suited for different energy applications. Then, we will present an innovative synthesis route for complex pnictogen chalco-halide compounds based on a sequential process, starting with the co-evaporation of chalcogen thin films, followed by a high-pressure reactive annealing (from 2 atm up to 20 atm) under halogen atmosphere. Using this innovative approach, the complete set of ternary van der Waals (Sb,Bi)(S,Se)(Br,I) chalco-halide semiconductors are synthesized, including: SbSBr, SbSI, BiSBr, BiSI, SbSeBr, SbSeI, BiSeBr, and BiSeI. It will be also demonstrated for the 8 compounds, that high purity phase can be synthesized through a thin film-to-nanocolumns topological transformation. All the possible ternary compounds exhibit orthorhombic Pnma structure with quasi-one-dimensional nanocolumnar morphology; which thicknesses, heights, and densities can be tuned by changing the temperature and pressure during the synthesis process. The bandgap of the materials ranges from 1.25 eV for BiSeI up to 1.93 eV for SbSBr, covering a wide range of energy applications and correlating very well with the DFT calculations. A complete comparative analysis of the morphology, structure, optic, and electric properties of the 8 compounds will be presented. As examples, two possible applications of these (Sb,Bi)(S,Se)(Br,I) low dimensional structures will be proposed. In one hand, first solar cell prototypes will be shown, with very encouraging open circuit voltages around 600 mV, and conversion efficiencies exceeding 1% level in a very short period. In a second hand, some of these compounds were tested as visible light sensitized of TiO₂ photocatalytic activity for hydrogen production, demonstrating an impressive hydrogen evolution increase of up to 90% under white light illumination. Finally, a comparative analysis and possible future applications of these novel low dimensional materials will be presented, and a perspective for their future accelerated development will be proposed.

2:00 PM EN06.09.03

O, N-Enriched, Self-Activated, Holey Carbon Sheets for Low-Cost and High-Loading Zinc-Ion Supercapacitors [ZhixiaoXu](#) and XiaoleiWang; University of Alberta, Canada

Low-cost and high-loading cathodes are crucial for the practical application of zinc ion supercapacitors but achieving high performance in high-loading electrodes has remained a challenge due to sluggish ion transport, increased resistance, and unstable structure. Guided by theoretical calculations, high-loading carbon cathodes based on holey activated carbon sheets (HACS) were fabricated from a carefully chosen molecule. By subjecting the molecule to a simple pyrolysis-leaching treatment, it can be converted into HACS with large surface area, hierarchical porous structure, and electroactive oxygen/nitrogen dopants. Remarkably, when combined with an aqueous binder, the optimized HACS-based high loading electrode (16.1 mg cm⁻²) exhibits outstanding performance, delivering high-capacitance (454 F g⁻¹, capacity: 208 mAh g⁻¹) and fast-rate (1 A g⁻¹) capability even under lean electrolyte conditions (6.2 μL mg⁻¹). This leads to maximal areal energy and power densities of 2.40 mWh cm⁻² and 10.7 mW cm⁻², respectively. This outstanding performance can be attributed to fast ion transport enabled by through-plane pores of HACS, as well as abundant double-layer and redox-active surfaces from favorable heteroatom-doped porous nanosheets. With its cost-effectiveness, elemental abundance, and structural tunability, this molecular carbon strategy could serve as a platform for making self-activated carbon electrodes at the molecular level towards practical supercapacitors.

2:15 PM EN06.09.04

Enhancing Transport in Formamidinium Lead Iodide Quantum Dot Solar Cells by Substitution of Octadecene [BrunoAlessi](#)¹, [DavideMariotti](#)² and [VladimirSvrcek](#)¹; ¹AIST: National Institute of Advanced Industrial Science and Technology, Japan; ²Ulster University, United Kingdom

Perovskite quantum dots (QDs) solar cells are recently becoming very popular as they currently hold the record power conversion efficiency (PCE) of over 16% with a light absorber film made of stacked perovskite QDs of mixed cation Formamidinium (FA)/Cesium lead (Pb) iodide (I).¹ The most common synthesis method (hot injection) is based on the injection at moderate temperatures (50 to 120 °C) of a cation-oleate compound into a saturated lead iodide solution in Octadecene (ODE) in the presence of Oleic Acid and Oleylamine.² This leads to the formation of thick colloids where particles are capped by long chain ligands. However, for application in solar cells these long insulating ligands need to be exchanged in favor of shorter ones, leading to higher interparticle hopping probabilities for photocarriers. FAPbI₃ QDs themselves have ideal bandgap (~1.5-1.6 eV) for the single junction design and longer photocarrier lifetimes, however a reliable and satisfactory ligand exchange protocol is lacking. To have an efficient ligand exchange recipe that does not compromise the structural integrity of the quantum dots, significant efforts have been made in a plethora of studies by addition of small molecules during the synthesis process, zwitterionic compounds or Pb- FA- and I- containing salts and amino acids during the QDs film formation, nonetheless there is still room for improvement.

In this study we explore a different approach to synthesize FAPbI₃ QDs by changing one of the main solvents used in the synthesis stage. Specifically, we replaced ODE with a shorter chain

linear alpha olefin. Despite facing some experimental challenges, we successfully obtained high-quality films of FaPbI_3 QDs using this new method. Furthermore, we correlate the new synthesis method with ODE-based QDs in terms of the purification protocol, synthesis practice, optical properties, and their application in QDs solar cells. The results revealed superior photoluminescence properties for the QDs synthesized with the new solvent. QDs obtained in this way have a narrow photoluminescence emission peak at 1.61 eV and exhibit higher absolute quantum yields ranging from 70% to 80% and only a small blueshift ($\Delta\lambda=5$ nm) compared to the ODE-based QDs. Additionally, we compare the performance of the two systems in prototype solar cells, specifically by using layers of stacked QDs with equal thickness (100 nm). The prototype solar cells incorporating the QDs synthesized with the new solvent showed a PCE of 4.9% with 1.06 V open-circuit voltage (V_{OC}). In relation to an ODE-based solar cell of the same thickness it represents a two-fold increase in PCE, as well as consistently higher V_{OC} and short-circuit current density (J_{sc}). Furthermore, we investigate how the new solvent enhances the performance of FaPbI_3 QDs based solar cells without compromising the stability and optical properties of individual quantum dots.

1. Zhao, Q. *et al.*, *Nat. Commun.* **10**, 1–8 (2019).
2. Protesescu, L. *et al.*, *ACS Nano* **11**, 3119–3134 (2017).

2:30 PMBREAK

3:00 PM EN06.09.05

Influence of Doping Density on the Optoelectronic Properties of V-Doped WS_2 Monolayers John B. Asbury; Pennsylvania State University, United States

A critical step in the development of transition metal dichalcogenides (TMDs) as next generation electronic and photonic materials is to identify pathways to control their electronic properties using chemical doping methods. The controllable incorporation of dopant atoms into a TMD host lattice during growth requires the ability to predict dopant atom reactivity in comparison to the host lattice during the nucleation, growth and annealing stages. Toward this end, we investigated the growth of V-doped WS_2 monolayers by Atmospheric Pressure Chemical Vapor Deposition and examined the spatial distribution of V atoms in WS_2 crystallites and their influence on the defects and optoelectronic properties of the monolayers using temperature-resolved time-dependent photoluminescence microscopy (μPL). We observed that the V-doping density was higher in the centers of the crystallites where the initial nucleation process began. The V-doping density decreased as the growth continued, leading to non-uniform doping densities and a spatial gradient in the optical bandgaps of the WS_2 monolayers. Regions of the WS_2 monolayers with higher V atom density exhibited defect-related emission features at low temperatures in the μPL measurements that were red-shifted by 0.2 eV relative to defect-related emission peaks in regions with lower V atom densities. Scanning transmission electron micrographs of the V-doped WS_2 monolayers indicated the presence of two or more neighboring V dopant atoms paired with sulfur vacancies (V-V- S_V) in the more heavily V-doped regions with the lower energy defect-related emission. Our findings suggest that dopant-defect interactions can influence the distribution of dopants and defects in TMD monolayers. Learning to control the doping density and predicting such dopant-defect interactions may provide a framework for understanding the chemical reactivity and growth conditions needed to utilize TMDs in next generation electronic and photonic materials applications.

3:15 PM EN06.09.06

First-Principles Study of N, P, Si, C-Functionalized Ti_2B as Potential Anode Materials for Metal-Ion-Batteries Shaiokh B. Abi and Ahmed Zubair; Bangladesh University of Engineering and Technology, Bangladesh

The design and development of the next-generation energy storage device are strongly tied to the exploration of alternate electrode materials for rechargeable metal-ion batteries to lithium. Recently, non-lithium-ion batteries, such as sodium-ion batteries, potassium-ion batteries, magnesium-ion batteries, calcium-ion batteries, and zinc-ion batteries, have thus received substantial interest from researchers. This work explored N, P, C, and Si-functionalized Ti_2B , a 2D nanomaterial, as anode materials for metal-ion batteries using first-principles calculations. Density functional theory (DFT) was the theoretical foundation for the first-principles computations performed here. The ion-electron interaction was described using the projected augmented wave (PAW) method, and the exchange-correlation functional was defined using the generalized gradient approximation (GGA) in the Perdew-Burke-Ernzerhof (PBE) functional. We created the unit cell of Ti_2B monolayer with a sufficient vacuum between layers, and it was optimized until the appropriate threshold of total energy and force were reached. We added N, P, C, and Si to the optimized Ti_2B monolayer at different sites creating Ti_2BN_2 , Ti_2BP_2 , Ti_2BC_2 , and Ti_2BSi_2 . We optimized these structures' geometry to determine the most stable configurations with minimum ground-state energy. Phonon dispersion calculations showed no negative frequencies implying their dynamic stability. From the band structure and density of states calculations, Ti_2BN_2 and Ti_2BP_2 had degenerate spin-up and spin-down bands, indicating that both are non-magnetic. However, there were spin-up and spin-down band splitting of Ti_2BSi_2 and Ti_2BC_2 , revealing that they are magnetic. The total magnetization value of 0.13 and 0.26 $\mu\text{B}/\text{cell}$ was found for Ti_2BSi_2 and Ti_2BC_2 , respectively. The structures had significant electronic states close to the fermi level according to the partial density of states referring to their good electrical conductivity. To investigate the viability of these structures as anode materials in metal-ion batteries (MIBs), we adsorbed sodium at three different sites- the top of a functional atom, the top of the first Ti atom, and the top of the second Ti atom of the structures. The most favorable adsorption site for sodium was on top of the first Ti atom. Therefore, we utilized this configuration for further investigation. The adsorption energies were -0.78 eV, -1.03 eV, -1.51 eV, and -1.82 eV for single sodium adsorption on $(2\times 2\times 1)$ Ti_2BN_2 , Ti_2BC_2 , Ti_2BP_2 , and Ti_2BSi_2 supercells, respectively. Furthermore, the adsorption of the sodium atom layer was also performed. We added layers on both the top and bottom of the structures. The adsorption energies were negative, suggesting layer adsorption was favorable too. The adsorption energy values were -0.73, -0.95, -1.36, and -1.38 eV per atom for Ti_2BN_2 , Ti_2BC_2 , Ti_2BP_2 , and Ti_2BSi_2 , respectively. Bader charge density calculation and charge density difference plot showed the charge transfer between sodium and functionalized Ti_2B monolayers—the electron localization function of the structures agreed with these findings. Finally, we conducted diffusion calculations to explore the migration properties of metal ions over the structure. For diffusion, we selected two paths; path-1 started from the first Ti atom to the second Ti atom through to another Ti atom in the first position, and path-2 started from the first Ti atom to the boron atom through to another Ti atom in the first position. The energy barriers for path-1 and path-2 were 0.32 and 0.86 eV for Ti_2BN_2 and 2.51 and 0.82 eV for Ti_2BP_2 . The findings from our study confirmed N, P, C, and Si-functionalized Ti_2B as potential candidates for anode materials in rechargeable sodium-ion batteries.

3:30 PM EN06.09.07

High Capacity NH_4^+ Charge Storage in Covalent Organic Frameworks Zhengnan Tian, Vinayak S. Kale, Osama Shekha, Mohamed Eddaoudi and Husam N. Alshareef; KAUST, Saudi Arabia

Ammonium ions (NH_4^+), as nonmetallic charge carriers, have spurred great research interest in the realm of aqueous batteries. Unfortunately, most inorganic host materials used in these batteries are still limited by the sluggish diffusion kinetics. Here, we report a unique hydrogen bond chemistry to employ covalent organic frameworks (COFs) for NH_4^+ ion storage, which achieves a high capacity of 220.4 mAh g^{-1} at a current density of 0.5 A g^{-1} . Combining the theoretical simulation and materials analysis, a universal reaction mechanism of nitrogen and oxygen bridged by hydrogen bonds is revealed. In addition, we explain the solvation behavior of NH_4^+ leading to a relationship between redox potential and de-solvation energy barrier. This work provides a new insight into NH_4^+ ion storage in host materials based on hydrogen bond chemistry. This mechanism can be leveraged to design and develop COFs for electrochemical energy storage.

3:45 PM EN06.09.08

Magnon Selection Rules in NM/TMDC/FM Trilayer Structures Chanho Park, Jae Won Choi, Yunho Kim, Min-Sung Kang, No-Won Park and Sangkwon Lee; Chung - Ang University, Korea (the Republic of)

The spin Seebeck effect, widely known as the spin-wave analogue of the Seebeck effect, is the crucial makeshift for detecting the spin current resulting from nonequilibrium magnetization, which transfers angular momentum to adjacent system via spin waves.¹ Throughout astonishing works in spintronics for more than a decade the field has suggested schematics with normal metal deposited on ferromagnetic substrate, such that one makes the magnetization out of the equilibrium state, generating quantum properties for magnetization distribution called magnons. The injection of magnons to the interface of the normal metal / ferromagnetic insulator metal (NM/FM) heterostructures is usually referred as injection of the spin current, since the magnons themselves contain spin-polarized quantities for each component.² The injected spin current is then converted into voltage signal, named as Inverse Spin Hall Effect (ISHE) voltage. In this paper, we conducted SSE signal detecting experiments on basic well-known Pt/YIG ($\text{Y}_3\text{Fe}_5\text{O}_{12}$) structure and Pt/ML MoS_2 /YIG structure, where ML MoS_2 fits in the category of monolayer transitional metal dichalcogenide (ML TMDC) layers and checked their temperature dependence ranging from 190- 300 K. We firstly assumed both samples obey 3D spin-to-charge conversion. We gave both samples temperature gradient $dT = 1$ K out of plane, to observe maximum SSE voltage on both samples under same dT. Results shows that the ISHE voltage of Pt/ML MoS_2 / YIG yields is much less Pt / YIG, about ~ 27 times lower than that of the Pt/YIG system at 190 – 300 K. This can be inferred as such that MoS_2 monolayer considerably blocks the injection of spin current.

On the other hand, we kept obtaining wavy signals in Pt/ML MoS_2 /YIG structure even though magneto-resistance (MR) effects were excluded. This is assumed for different magnetic properties on MoS_2 layer which have already been reported. With competing diamagnetism in ML MoS_2 itself and ferromagnetism in MoS_2 induced from magnetic proximity effect from YIG substrate,³ significant portion of the magnons are blocked where they should not if they were in original Pt/YIG system. Finally, we theoretically calculated the temperature dependent ISHE voltages by combining a conventional Boltzmann transport equation with the magnon relaxation time model, and the results were consistent with the experimental results of both for Pt / YIG and Pt / ML MoS_2 / YIG structures. Our finding presents an important achievement in understanding and measuring the LSSE and provides a promising platform, with a high spin-mixing conductance and thermoelectric performance, for two-dimensional interlayered Pt / YIG systems.

- (1) Uchida, K.; Takahashi, S.; Harii, K.; Ieda, J.; Koshibae, W.; Ando, K.; Maekawa, S.; Saitoh, E. Observation of the spin Seebeck effect. *Nature* **2008**, 455 (7214), 778-781.

(2) Kikkawa, T.; Saitoh, E. Spin Seebeck Effect: Sensitive Probe for Elementary Excitation, Spin Correlation, Transport, Magnetic Order, and Domains in Solids. *Ann. Rev. Condens. Matter Phys.*, **2023**, 14 (1), 129-151.

(3) Tsai, S. P.; Yang, C. Y.; Lee, C. J.; Lu, L. S.; Liang, H. L.; Lin, J. X.; Yu, Y. H.; Chen, C. C.; Chung, T. K.; Kaun, C. C.; et al. Room Temperature Ferromagnetism of Single Layer MoS₂ Induced by Antiferromagnetic Proximity of Yttrium Iron Garnet. *Adv. Quantum Technol.*, **2020**, 4 (2), 200104.

4:00 PM EN06.09.09

Ultrathin Two-Dimensional Transition-Metal Alloy Nanofilm Stabilized Photoanodes for Efficient Solar Water Oxidation FeiXiang, NingLi, ArturoBurguete-Lopez, ZhaoHe, MaximElizarov and AndreaFratolochi; King Abdullah University of Science and Technology, Saudi Arabia

Harvesting solar energy for photoelectrochemical (PEC) hydrogen production has attracted significant research interest in contributing to the clean energy economy and sustainable development. Despite the progress achieved in photocathodes with an applied bias photon-to-current efficiency (ABPE) above 12%, the poor kinetics and chemical instability of photoanodes in the alkaline medium limit the efficiency and long-term operations of the entire PEC devices. The current state-of-the-art efficiency of the photoanode side is below 4%, and the corresponding operation time is around 30 hours. Although the additional protective layer coating, such as TiO₂ and SiO_x, prolongs the photoanode lifetime to around 200 hours, the ABPE efficiency greatly drops to below 1%. In this work, we engineer ultrathin two-dimensional nickel-iron (NiFe) alloy film as protective and catalytic layers on Si photoanodes, extending the device lifetime to above 250 hours without compromising the PEC performances. The optimized photoanodes exhibit a low onset potential of 1.06 V versus the reversible hydrogen electrode (RHE) at the photocurrent density of 10 mA cm⁻² and high saturated current density of around 39 mA cm⁻² under one sun illumination, reporting an applied bias photon-to-current efficiency (ABPE) of 4.24%. We employ aberration-corrected scanning transmission electron microscopy combined with electron energy loss spectroscopy (STEM-EELS) to visualize the atomic-level structural and chemical information at the crystalline/amorphous hybridized interfaces. We apply high-resolution X-ray photoelectron spectroscopy to trace the chemical species changes in the NiFe alloy layer after the PEC reaction. Benefiting from the NiFe alloy coating strategy, the PEC photoanodes operate for over 250 hours with 90% retention of its initial current density during continuous working conditions under a large current density above 30 mA cm⁻². This work opens the pathway to the designing and implementing earth-abundant, highly efficient, and stable PEC devices with 2D transition-metal alloy film for green hydrogen production and can be extended to other solar-assisted catalytic fields, such as CO₂ reduction and ammonia synthesis.

4:15 PM EN06.09.10

Enhanced Thermoelectric Transport Characteristics of a Novel BiSbTe-WSe₂ Composite Film KaranGiri, Yen-LingWang, Ling-ChunChao, Chuan-WenWang, Hung-ShuoChang, Wen-ChiehHsieh and Chun-HuaChen*; National Yang Ming Chiao Tung University, Taiwan

A novel technique is developed to combine a layered structure transition-metal dichalcogenide material, tungsten diselenide (WSe₂), recognized for its extremely low thermal conductivity, with another layered structure material, bismuth antimony telluride (BiSbTe), renowned for its exceptional performance in waste heat recovery applications. To enhance the thermoelectric properties even more, WSe₂ as a secondary target is encapsulated periodically in the primary target Bi_{1.5}Sb_{0.5}Te₃ using a pulse laser deposition technique. The WSe₂ for the first time, is co-ablated with the BiSbTe at four distinct deposition temperatures, resulting in hetero-nanocomposite thin films. The diffractogram of BiSbTe-WSe₂ composite thin film exhibits sharp peaks indicating strong crystallinity and evidence that the crystals are growing in a highly c-oriented manner. The electrical transport properties are significantly improved due to the optimized hole concentration, measured in the order of 10¹⁹ and 10²⁰. The electrical conductivity is significantly increased from 134 S cm⁻¹ for the sample grown at 573 K to 1200 S cm⁻¹ that grown at 723 K. The room temperature Seebeck coefficient is 250 μV K⁻¹ for the sample grown at 673 K and 360 μV K⁻¹ for that grown at 723 K. The overall outcome is a significant increase in the power factor which is computed as 12 to 156 μW cm⁻¹ K⁻² demonstrating outstanding room temperature thermoelectric performance. The observed values are rather adequate, demonstrating an excellent trade-off between them. In addition to electrical characteristics, the specimens have a low electronic thermal conductivity, k_e. The calculated room temperature k_e values are 0.10 W m⁻¹ K⁻¹ and 0.87 W m⁻¹ K⁻¹ for the samples grown at 573 K and 723 K, respectively. The enhanced thermoelectric transport characteristics of the periodically encapsulated WSe₂ in the BiSbTe matrix place it among the best thermoelectric materials with excellent performance for thermoelectric conversion such as solid-state refrigeration and power generation.

SESSION EN06.10: Virtual Session
Session Chairs: Aron Huckaba and Cecilia Mattevi
Wednesday Morning, December 6, 2023
EN06-virtual

8:00 AM EN06.10.01

Flat-Optics Photon Harvesting in Large-Scale 2D Semiconductor Layers for Photoconversion Applications GiulioFerrando¹, MatteoGardella¹, GiorgioZambito¹, PhamDuy Long², SiHieu Nguyen², Chi LeHa², Thanh TungNguyen², MariaC. Giordano¹ and FrancescoButtier de Mogeot¹; ¹University of Genoa, Italy; ²Vietnam Academy of Science, Viet Nam

The development of clean light harvesting platforms and technologies is crucial in view of a new generation of photonic devices with impact in renewable energy conversion and environmental applications. For this purpose, nanophotonic methodologies hold great promise. Specifically, both plasmonics and flat optics approaches offer exciting opportunities to enhance light-matter interactions at the nanoscale, making them highly appealing for applications in photoconversion and sensing.

In this context, we present innovative solutions for large-scale light trapping to maximize photon harvesting in ultra-thin semiconductor layers. Within them an emerging class of materials is represented by the Two-dimensional (2D) Transition Metal Dichalcogenides semiconductor (TMDs) layers that are characterized by exceptional optoelectronic properties tunable in the Visible and Near-Infrared spectrum [1]. Among them few-layer MoS₂ is notable for an electronic bandgap in the Visible range and a high optical absorption coefficient. Such intriguing optical response combined with high chemical reactivity qualifies this 2D semiconductor layer as a promising candidate in photoconversion and energy storage applications [2].

The first solution presented is based on large area plasmonic metasurfaces obtained by ion beam assisted self-organized process. Nanostructured templates that can be used to laterally confine arrays of plasmonic nanoantennas with tunable optical response [3].

The second solution is based on large area periodic nanograting templates, fabricated by Laser Interference Lithography, to reshape large-scale (cm²) two-dimensional MoS₂ semiconductor layers as an active optical element featuring a flat optics configuration that enhances the light coupling by arising of photonic anomalies [4,5].

Light harvesting performances of the proposed solutions were tested by photocatalytic and photoelectrochemical experiments. The plasmonic system is used in an Oxygen Evolution Reaction (OER) reaction with both the function of a transparent electrode and a co-catalyst coupled to an ultra-thin film of TiO₂. On the other hand the subwavelength reshaping of ultra-thin semiconductor layers results in enhanced methylene blue photobleaching [6].

These light harvesting platforms are thus promising in view of various large-scale applications such as waste water treatment, dye molecules sensing and energy storage.

[1] M. Barelli et al., *ACS Appl. Nano Mater.* **5**, 3470–3479 (2022)

[2] F. Mak et al., *Nat. Photonics*, **10**, 216–226 (2016)

[3] Z. Li et al., *Photochem. Photobiol. C Photochem. Rev.* **35**, 39–55 (2018)

[4] M. Bhatnagar et al., *Nanoscale*, **12**, 24385 (2020)

[5] M. Bhatnagar et al., *ACS Appl. Mater. Interfaces* **13**, 13508–13516 (2021)

[6] G. Ferrando et al., *Nanoscale* **15**, 1953–1961 (2023)

8:15 AM EN06.10.02

Controlling The Hydrogen Evolution Activity by Tailoring The Outer Transition Metal Layers in Double Transition Metal MXenes AnupmaThakur, Nithin ChandranBalachandran Sajitha, BrianWyatt and BabakAnasori; Indiana University- Purdue University Indianapolis, United States

Two-dimensional transition metal carbides, nitrides, or carbonitrides, known as MXenes, have shown great promise as active materials in catalytic applications such as the hydrogen evolution reaction. In double transition metal (DTM) MXenes two different transition metals occupy the metal sites which can enhance the tunability of MXenes electrocatalytic properties. The transition metal occupying the outer atomic layers controls the hydrogen evolution reaction (HER) performance based on their basal plane catalytic activity. We investigated out-of-plane ordered DTM MXenes, with inner layers of transition metal (M': Ti) sandwiched by outer layers of different transition metals (M: Mo, W, Cr) in a layered M'₂M''C₂T_x MXenes. We investigated the role of exposed basal plane transition metals on the HER catalytic activity of these out-of-plane ordered DTM MXenes and compared their behavior to a mono-transition metal MXene, Ti₃C₂T_x. W₂TiC₂T_x MXene shows the lowest HER overpotential of 147 mV at 10 mA/cm² under acidic conditions compared with Mo₂TiC₂T_x, Cr₂TiC₂T_x and Ti₃C₂T_x MXenes. The improved electrocatalytic performance of W₂TiC₂T_x can be due to the presence of tungsten atoms in the outer M' layers. Additionally, W₂TiC₂T_x MXene showed long-term stability of more than 24 hours. Our findings further demonstrate that MXenes are precious-metal-free 2D flakes with highly HER active basal planes and promising and tunable electrocatalysts for clean

energy applications.

8:30 AM EN06.10.03

Computationally Guided Design of Single-Atom Catalysts Embedded on Reduced Graphitic Carbon Nitride Monolayers MukeshJahar and VeronicaBarone; Central Michigan University, United States

The design of efficient single-atom catalysts (SAC) with optimal activity and selectivity for sustainable energy and environmental applications remains a challenge. Herein, first-principles calculations are performed to validate the feasibility of single TM atoms (3d, 4d, and 5d series) embedded in two different conformations of graphitic carbon nitride ($g\text{-C}_3\text{N}_4$) monolayers (planar and corrugated). We explore the effects of $g\text{-C}_3\text{N}_4$ monolayer nitrogen vacancies on the absorption of SAC considering three potential absorption scenarios, i.e. *on-vacancy*, *via-substitution*, and *on-center*, that correspond to different experimental conditions. Our results highlight the most stable configurations with the lowest formation energies and find that the absorption of single TM atoms *on-vacancy* and *on-center* sites are more favorable than *via-substitution*. Furthermore, in addition to thermodynamics stability, electrochemical stability is also investigated through the calculation of the dissolution potential of the SACs. Within the scenarios considered in this study, we find that Co, Fe, Rh, Ir, Pt, and Ni will produce the most robust SAC on reduced $g\text{-C}_3\text{N}_4$. Our findings provide guidance for the design and development of $g\text{-C}_3\text{N}_4$ sheets decorated with single TM atom catalysts for applications such as pollutant degradation, CO_2 reduction, N_2 fixation, selective oxidation, water splitting, and metal ion-based batteries.

8:45 AM EN06.10.04

Enhancing Sodium and Potassium-Ion Storage in 2D MoWSe₂ : Effect of Upper Voltage Cut-Off SonjoyDey, ArijitRoy and GurpreetSingh; Kansas State University, United States

The superior properties, such as large interlayer spacing and the ability to host large alkali-metal ions, of two-dimensional (2D) materials based on transition metal di-chalcogenides (TMDs) enable next-generation battery development beyond lithium-ion rechargeable batteries. In addition, compelling but rarely inspected TMD alloys provide additional opportunities to tailor bandgap and enhance thermodynamic stability. This study explores the sodium-ion (Na-ion) and potassium-ion (K-ion) storage behavior of cation-substituted molybdenum tungsten diselenide (MoWSe_2), a TMD alloy. This research also investigates upper potential suspension to overcome obstacles commonly associated with TMD materials, such as capacity fading at high current rates, prolonged cycling conditions, and voltage polarization during conversion reaction. The voltage cut-off was restricted to 1.5 V, 2.0 V, and 2.5 V to realize the material's Na^+ and K^+ ion storage behavior. Three-dimensional (3D) surface plots of differential capacity analysis up to prolonged cycles revealed the convenience of voltage suspension as a viable method for structural preservation. Moreover, the cells with higher potential cut-off values conveyed improved cycling stability, higher and stable coulombic efficiency for Na^+ and K^+ ion half-cells, and increased capacity retention for Na^+ ion half-cells, respectively, with half-cells cycled at higher voltage ranges.

SYMPOSIUM EN07

Emerging Electrocatalytic Materials and Devices for Clean Energy and Environmental Applications
November 27 - December 5, 2023

Symposium Organizers

Maria Escudero-Escribano, Catalan Institute of Nanoscience and Nanotechnology
Charles McCrory, University of Michigan
Haotian Wang, Rice University
Sen Zhang, University of Virginia

Symposium Support

Bronze

ACS Energy Letters | ACS Publications

BioLogic

Chem Catalysis | Cell Press

EES Catalysis | ACS Publications

Gamry Instruments

Renewables | Chinese Chemical Society Publishing

Scribner LLC

* Invited Paper

+ JMR Distinguished Invited Speaker

SESSION EN07.01: Mechanistic Studies and Novel Electrosynthesis I

Session Chairs: Charles McCrory and Sen Zhang

Monday Morning, November 27, 2023

Hynes, Level 3, Room 310

10:30 AM *EN07.01.01

Operando Methods for Mechanistic Studies of Energy Systems HectorD. Abruna; Cornell University, United States

This presentation will deal with the use of *operando* methods for mechanistic studies energy systems with emphasis on fuel cells and battery materials and technologies. The presentation will begin with a brief overview of the methods employed with emphasis on the use of X-ray based methods, transmission electron microscopy (TEM) under active potential control, confocal Raman spectroscopy and microscopy and DEMS (differential electrochemical mass spectrometry) coupled with SEIRAS (surface enhanced infra-red absorption spectroscopy). The utility of these methods will be illustrated by case studies focusing on non-precious metal electrocatalysts for the oxygen reduction reaction (ORR) in alkaline media, Li/S batteries the reduction of carbon dioxide and the oxidation of ethanol. The presentation will conclude with an assessment of future directions.

11:00 AM EN07.01.02

Tuneable Ethylene Production using the Electrochemical Oxidative Coupling of Methane (EOCM): Exploiting Oxygen Evolution to Create the Active Oxygen Species FilipGrajkowski, SubhashChandra, SanazKoochfar, DonghaKim, GeorgiosDimitrakopoulos and BilgeYildiz; Massachusetts Institute of Technology, United States

Ethylene (C_2H_4) is one of the most valuable compounds in the chemical industry as it is used as a building block for a wide range of applications. The current ethylene production pathway via

the steam cracking of naphtha or ethane is highly endothermic, resulting in ethylene production being the second-biggest CO₂-generating process in industry.¹ In 1982, Keller and Bhasin first reported on an alternative ethylene production method,² the oxidative coupling of methane (OCM). In this approach, CH₄ is oxidised on oxide catalyst surfaces by adsorbed O₂-derived species to yield C₂H₆ and the desired C₂H₄. Unfortunately, this thermochemical OCM approach suffers from significant “deep oxidation” where CH₄ is instead combusted to CO/CO₂ and H₂O: this arises as the products of oxidative coupling are more reactive than the parent CH₄. In order to improve the C₂ selectivity and yield of OCM processes, recent works have focused on integrating OCM activity into typical solid oxide electrolyser systems.³ In this electrochemical OCM (EOCM) approach, O²⁻ ions from the cathode side are transported across the solid electrolyte to the anode where they oxidise CH₄ molecules to yield the desired C₂ (C₂H₄ and C₂H₆) products.

In this study, inspired by recent results using mixed ionic-electronic conductors for EOCM, we use La_{0.3}Sr_{0.7}TiO₃ as the anode material for EOCM. By using combined electrochemical and gas chromatographic analyses, we demonstrate that this titanate system can successfully yield the desired C₂ products and can respond to changes in the O²⁻ flux. We highlight that the C₂ selectivity of the reactor can be tuned using the applied potential: we show a tuneability in the C₂ selectivity with enhancements of >3x at higher currents relative to lower currents. These results are rationalized mechanistically with reference to the oxygen evolution reaction which occurs at the anode surface. We demonstrate that by controlling the delivery of oxygen to the anode, we gain the ability to selectively produce the active oxygen species necessary for selective CH₄ activation towards C₂ products. These findings furnish the ability to increase both the CH₄ conversion and the C₂ selectivity and have finally broken the inverse relationship between the CH₄ conversion and the C₂ selectivity which dominates the thermochemical OCM literature. Additional chemical and structural characterizations illustrate that the anode material is stable under the EOCM operational conditions with no noticeable phase decomposition, a notorious limitation of other EOCM anodes.³ The results presented herein can serve as a guide for the field on how to effectively choose the anode composition to enhance both the product selectivity and the overall performance of the combined reactor system.

(1) Rightor, E. G.; Tway, C. L. Global energy & emissions reduction potential of chemical process improvements. *Catalysis Today* **2015**, 258, 226-229. DOI: <https://doi.org/10.1016/j.cattod.2015.02.023>.

(2) Keller, G. E.; Bhasin, M. M. Synthesis of ethylene via oxidative coupling of methane: I. Determination of active catalysts. *Journal of Catalysis* **1982**, 73 (1), 9-19. DOI: [https://doi.org/10.1016/0021-9517\(82\)90075-6](https://doi.org/10.1016/0021-9517(82)90075-6).

(3) Ramaiyan, K. P.; Denoyer, L. H.; Benavidez, A.; Garzon, F. H. Selective electrochemical oxidative coupling of methane mediated by Sr₂Fe_{1.5}Mo_{0.5}O_{6-δ} and its chemical stability. *Communications Chemistry* **2021**, 4 (1), 139. DOI: 10.1038/s42004-021-00568-1.

11:15 AM EN07.01.03

Highly Stable Pentagonal 2D Palladium Diselenide Enables Rapid Electrosynthesis of Hydrogen PeroxideR. Dominic Ross, Gerardo J. Quintana Cintron, Kwanpyung Lee, Hongyuan Sheng, JRSchmidt and SongJin; University of Wisconsin–Madison, United States

Electrosynthesis of hydrogen peroxide (H₂O₂) via the two-electron oxygen reduction reaction (2e⁻ ORR) is promising for various practical applications such as wastewater treatment. However, few electrocatalysts are active and selective for 2e⁻ ORR yet also resistant to catalyst leaching under realistic operating conditions. Here, a joint experimental and computational study reveals highly active and stable 2e⁻ ORR catalysis in neutral media over 2D layered PdSe₂ with a unique pentagonal layered structure type. Computations predict active and selective 2e⁻ ORR on the basal plane and edge of PdSe₂, but with distinct kinetic behaviors. Electrochemical measurements of hydrothermally synthesized PdSe₂ nanoparticles show higher 2e⁻ ORR activity than Pd₄Se and Pd₁₇Se₁₅, suggesting unique performance enabled by the PdSe₂ structure type. PdSe₂ on a gas diffusion electrode can rapidly accumulate H₂O₂ in a buffered neutral solution under high current density. Elemental analysis of the catalyst and electrolyte and synchrotron X-ray absorption spectroscopy confirm the chemical stability of PdSe₂ under these practical electrosynthesis conditions. This work establishes a new efficient 2e⁻ ORR catalyst with high intrinsic stability at practical current densities and opens catalyst designs utilizing the unique 2D pentagonal structure motif.

11:30 AM *EN07.01.04

Activation Energies of Heterogeneous Electrocatalysis from First PrinciplesSaerom Yu, Zachary Levell, Ruoyu Wang and Yuan Yue Liu; The University of Texas at Austin, United States

Electrocatalysis at solid-water interface is central to many technologies addressing energy and environmental challenges. However, the reaction kinetics at atomic level is not well understood and difficult to simulate due to the complexity of the electrochemical interface. Here I will present an advanced model, which accurately and efficiently simulates the realistic electrochemical interface, particularly the reaction activation energies. I will also show the application of this model to understand the electrocatalysis of single metal atoms embedded in nitrogen doped graphene (M-N-C), such as: (1) the active site structure in Ni-N-C for CO₂ reduction; (2) the origin of high H₂O₂ selectivity of Co-N-C for 2e oxygen reduction; and (3) the kinetic mechanism of Fe-N-C for 4e oxygen reduction.

SESSION EN07.02: Mechanistic Studies and Novel Electrosynthesis II

Session Chairs: Maria Escudero-Escribano and Haotian Wang

Monday Afternoon, November 27, 2023

Hynes, Level 3, Room 310

1:30 PM *EN07.02.01

What Makes Lithium Unique for Nitrogen Reduction?Ifan E. Stephens; Imperial College London, United Kingdom

There is a burgeoning interest in the development of a green method of ammonia synthesis; ammonia, already critical for fertilisers in the agricultural industry, is also being touted as a possible future energy vector or carbon-free fuel. The current method of production - the Haber Bosch process - is environmentally damaging and energy intensive but to date no viable alternative has been demonstrated. An electrochemical method operating under ambient conditions would be particularly attractive, as it would enable ammonia to be produced on a decentralised basis on-site and on-demand.¹

Thus far, amongst solid electrodes, only lithium based electrodes in organic electrolytes can unequivocally reduce nitrogen to ammonia.^{2,3} Even so, at present, the lithium based system is far too inefficient for practical uses; moreover, it is highly unstable.

In the current contribution, we will explore the underlying reasons why lithium is unique in its ability to reduce nitrogen to ammonia.^{4,5} We use a combination of electrochemical experiments, cryo-microscopy, infrared spectroscopy, electrochemistry mass spectrometry, time-of-flight secondary ion mass spectrometry, X-ray photoelectron spectroscopy and density functional theory. By drawing from the adjacent fields of enzymatic nitrogen reduction and battery science, we will aim to build a holistic picture of the factors controlling nitrogen reduction. On the basis of our insight, we propose new avenues towards going beyond lithium in electrochemical nitrogen fixation.

1. Westhead, O., Barrio, J. Bagger, A., Murray, J.W., Rossmeisl, J., Titirici, M.M., Jervis, R., Fantuzzi, A., Ashley, A., Stephens, I.E.L., *Nature Reviews Chemistry*, 7 184 (2023).

2 Andersen, S. Z., Colic, V., Yang, S., Schwalbe, J. A., Nielander, A. C., McEnaney, J. M., Enemark-Rasmussen, K., Baker, J. G., Singh, A. R., Rohr, B. A., Statt, M. J., Blair, S. J., Mezzavilla, S., Kibsgaard, J., Vesborg, P. C. K., Cargnello, M., Bent, S. F., Jaramillo, T. F., Stephens, I. E. L., Nørskov, J. K. & Chorkendorff, I. *Nature* 570, 504, (2019).

3 Westhead, O., Jervis, R. & Stephens, I. E. L. *Science* 372, 1149, (2021).

4 Bagger, A., Wan, H., Stephens, I. E. L. & Rossmeisl, J. *ACS Catalysis* 11, 6596, (2021).

5. Westhead, O., Spry, M., Bagger, A., Shen, Z., Yadegari, H., Favero, S., Tort, R., Titirici, M., Ryan, M.P., Jervis, Katayama, Y., Aguadero, A., Regoutz, A., Grimaud, A., Stephens, I.E.L. (2022), *Journal of Materials Chemistry A*, DOI: 10.1039/D2TA07686A.

2:00 PM EN07.02.02

Metal-Free Nanofibers with Tailored Electronic Structures for Highly Active and Selective Hydrogen Peroxide ElectroproductionFei Xiang¹, Xuhong Zhao², Jian Yang³, Ning Li¹, Xiaobin Niu² and Andrea Fratalocchi¹; ¹King Abdullah University of Science and Technology, Saudi Arabia; ²University of Electronic Science and Technology of China, China; ³Southwest Jiaotong University, China

Electrocatalytic hydrogen peroxide (H₂O₂) production via two-electron oxygen reduction reaction (2e⁻ ORR) has attracted significant research interest as a promising alternative to the traditional energy-intensive traditional anthraquinone cycling process. However, designing low-cost, highly active, and selective electrocatalysts remains challenging due to the fierce competition from the four-electron reaction pathway. In this study, we engineer the electronic structure of electrospun nanofibers via fluorine and sulfur dual-doping to develop large-scale metal-free electrocatalysts for hydrogen peroxide production. Experimental and theoretical computation results demonstrate the manipulated electronic structures of the carbon active sites

after suitable fluorine and sulfur dual-doping, originating from intermolecular charge transfer and electron spin redistribution at the active sites. The optimized catalyst exhibits an onset potential of 0.814 V versus the reversible hydrogen electrode (RHE) in an alkaline medium and a selectivity of 99.1%, outperforming most of the previously reported carbon-based and metal-based counterparts. Density functional theory (DFT) results elucidate the manipulated free energy profiles and kinetic energy barriers in 2e- ORR after fluorine and sulfur dual-doping, confirming the enhanced activity and selectivity in the 2e- ORR pathway for hydrogen peroxide production. This fluorine and sulfur dual-doping strategy on carbon nanofibers from electrospinning provides the pathway to designing and implementing large-scale, low-cost, and highly efficient catalysts for hydrogen peroxide production. Moreover, this strategy also enjoys versatility in the materials for other catalytic fields, such as water splitting, CO₂ reduction, and ammonia production.

2:15 PM *EN07.02.03

Light-Driven Reduction of Carbon Dioxide with Hybrid PhotoelectrodesJillian Dempsey; University of North Carolina at Chapel Hill, United States

Integration of molecular catalysts that reduce CO₂ to CO with silicon photoelectrodes has been achieved through both covalent and non-covalent attachment methods. These hybrid photoelectrodes have been characterized by x-ray photoelectron spectroscopy, inductively-coupled plasma mass spectrometry, and attenuated total reflectance infrared spectroscopy. Cyclic voltammetry and bulk photoelectrolysis with product analysis are used to establish that these hybrid photoelectrodes are competent for light-driven fuel production with high Faradaic efficiencies.

SESSION EN07.03: Poster Session I: Electrocatalysts, Membrane Electrode Assemblies and Novel Reactions

Session Chairs: Maria Escudero-Escribano and Sen Zhang

Monday Afternoon, November 27, 2023

Hynes, Level 1, Hall A

8:00 PM EN07.03.01

A New Strategy for Improving Durability of Electrodes in Cell Reversal during Fuel Starvation Cycles of PEMFC with Reversal Tolerant AnodeChi-Yeong Ahn^{1,2}, So Yeon Lee^{1,2} and Hyungwon Shim¹; ¹Korea Research Institute of Ships & Ocean Engineering, Korea (the Republic of); ²University of Science and Technology, Korea (the Republic of)

Due to the strengthening of environmental regulations of international societies, the introduction of eco-friendly technologies is being rapidly carried out in the marine and shipping sectors. Among them, fuel cells (especially PEMFC) are in the limelight as a propulsion system for small and medium-sized coastal ships due to fast starting characteristics and low operating temperature. However, ships require higher output than passenger cars, which require an FC capacity of about 100 kW. In the case of such a large-capacity FC, hydrogen may not be evenly diffused to the electrode when starting or when an electric load rapidly increases due to stoichiometry control. In some parts (or all) of the electrode where hydrogen supply is insufficient, fuel starvation will proceed, and cell reversal may occur. This cell reversal phenomenon causes severe degradation of the anode.

Degradation by cell reversal can be mitigated by adding a material with OER activity such as iridium oxide to the anode. This anode is called a reversal tolerant anode (RTA). In addition, several studies have been conducted on RTA under various conditions. However, we observed that when RTA was added in fuel starvation cycles, the anode was well protected but the cathode rather degraded. Therefore, in this study, we sought the cause of cathode degradation during fuel starvation cycles and conducted experiments to prevent it.

8:00 PM EN07.03.02

Unravelling Hidden Parameters during Electrode Processing: The Role of Coherent Workflows in ElectrocatalysisDoris Segets^{1,2}; ¹University of Duisburg-Essen, Germany; ²Center for Nanointegration Duisburg-Essen (CENIDE), Germany

Micron and nano-sized functional materials play a key role for future technologies that are currently developed in the field of energy conversion (electrolysers, fuel cells) and electrocatalysis. While new materials with outstanding properties are continuously developed, they rarely find their way into – urgently needed – large scale production and industrial applications [1]. One reason for this are hidden parameters that occur during ink formulation, coating (and decal transfer), cell assembly, and operation. We propose the development of coherent workflows that help us to identify reliable correlations. These should be developed for each electrocatalyst, bridging synthesis, electrode and gas diffusion electrode (GDE)/membrane electrode assembly (MEA) fabrication, and testing. All information, including “negative” results like crack formation, delamination, structural ageing and dissolution, must be reported until the relevant hidden parameters are deciphered, and the design chain is understood. Then, materials and electrodes derived from complementary processes and exhibiting subtle variations in composition and structure, can be evaluated against each other.

However, this implies to fill the “blackbox” between technical catalysts and electrochemical testing in flow cells, GDEs or MEAs, with quantitative data on powders, ink formulations and coating properties. In the past years, we developed a toolbox of methods that starts from key control characteristics for technical catalysts, i.e., ball-milled pentlandites for hydrogenation reactions, that thereon enable the in situ analysis of ink formulations and pastes during the dispersion process and at application concentration [2,3]. This is followed by the assessment of the resulting coatings from large-area crack analysis down to the level of surface roughness and pore size characteristics [4]. Finally, this input is connected with performance and stability testing results to enable the comparison of different materials, the assessment of structure property relations, and ultimately to establish inline process control during electrode manufacturing. In this contribution, the developed methods will be summarized and related to their current limitations and prospects, in particular for unraveling hidden parameters during GDE assembly as well as in line process control.

References

- [1] Siegmund, Daniel; Metz, Sebastian; Peinecke, Volker; Warner, Terence E.; Cremers, Carsten; Grevé, Anna; Smolinka, Tom; Segets, Doris; Apfel, Ulf-Peter, JACS Au 1 (2021), 527 – 535.
- [2] Bapat, Shalmali; Segets, Doris, ACS Applied Nano Materials 3 (2020), 7384 – 739.
- [3] Bapat, Shalmali; Giehl, Christopher; Kohsakovski, Sebastian; Peinecke, Volker; Schäffler, Michael; Segets, Doris, Advanced Powder Technology 32 (2021), 3845 – 3859.
- [4] Jaster, Theresa; Albers, Simon; Leonhard, Armin; Kräenbring, Mena-Alexander; Lohmann, Heiko; Zeidler-Fandrich, Barbara; Özcan, Fatih; Segets, Doris; Apfel, Ulf-Peter, JPhys Energy 5 (2023), 024001.

8:00 PM EN07.03.03

Phase Engineering of Noble Metal-Based High-Entropy Alloy NanocrystalsPeng Han and Ye Chen; The Chinese University of Hong Kong, Hong Kong

High-entropy alloys (HEAs) possessing five or more elements exhibited unique physical and chemical characteristics. Delicate size/shape and composition control would significantly boost their performance toward various catalytic reactions. However, the phase-dependent properties of HEAs are rarely studied because controlling the crystal structure of HEAs with the same composition is extremely challenging. Herein, through facile wet chemistry and subsequent heat treatment, quinary and senary noble metal-based HEA nanocrystals with well-controlled phases, including hexagonal close-packed (*hcp*) and face-centered cubic (*fcc*) phases are successfully synthesized. The phase of noble metal-based HEA nanocrystals is tunable by altering the types of metal precursors and the temperature during heat treatment. The effect of the crystal structure on the catalytic performance of noble metal-based HEA nanocrystals is also investigated. This work opened a significant avenue in developing well-defined HEA nanocrystals with precise control over phases for heterogeneous catalysis.

8:00 PM EN07.03.04

Efficient Oxidation of Aqueous Persistent Organic Pollutants using Zwitterionic Hydrogel-Bound Iron(II) Ions as Heterogenous Fenton CatalystsDevashish Gokhale, Ian S. Chen and Patrick Doyle; Massachusetts Institute of Technology, United States

Persistent organic pollutants, such as xenoestrogens and PFAS, present a global challenge requiring immediate action. The Fenton oxidation reaction is an advanced oxidation process catalyzed by dissolved Fe(II) ions and their complexes, which converts hydrogen peroxide to hydroxyl radicals to degrade organic contaminants. Though the Fenton reaction is extremely promising for scalable water treatment, there are several limitations to its practical use, such as the difficulty in transporting and storing hydrogen peroxide. Further, though Fe(II) ions are called catalysts in Fenton processes, they are continuously oxidized to Fe(III) ions and are difficult to reuse or recover from water. Attempts to create a practical Fenton process have used electrochemical cells to produce hydrogen peroxide *in situ*, while replacing dissolved Fe(II) ions with heterogeneous catalysts. Such catalysts typically encapsulate iron or iron oxide nanoparticles in polymers or support them on traditional adsorbents but have so far been limited by slow reaction rates due to reduced surface area, the need to adjust pH with acids, unintended substrate/polymer degradation by the Fenton reaction, and the release or slow dissolution of nanoparticles. These catalysts are also incompatible with other improvements to the traditional Fenton reaction, such as UV light to accelerate the production of hydroxyl ions.

A practical Fenton process to eliminate POPs will require the development of (1) a heterogeneous catalyst that retains iron while (2) eliminating the need for acid addition, (3) is highly porous

and has a large effective surface area to preserve efficacy, (4) is transparent to UV radiation and (5) resistant to degradation by UV light, hydrogen peroxide, and the iron itself, (6) preferably does not use nanoparticles which may pose a threat to the environment if they escape the catalyst over long periods of time, and (7) can be regenerated and reused in a facile manner. Here, we introduce an innovative heterogeneous Fenton catalyst based on a zwitterionic hydrogel material that effectively addresses these challenges. Containing individually complexed iron ions in a highly porous scaffold, the hydrogel catalyst has a large effective surface area and exhibits kinetics comparable to homogeneous Fenton degradation. The complexed ions can initiate Fenton degradation at neutral, and even alkaline pH, eliminating the need for acid additions. At the same time, the zwitterionic hydrogel scaffold is specifically selected to be resistant to Fenton oxidation and strongly bind to the iron ions, enabling repeatable long-term use. Using our catalytic hydrogels, we showcase the rapid and complete degradation of three structurally disparate contaminants of major concern, ethinyl estradiol (a xenoestrogen), 2,4-dichlorophenol (a model pesticide and chlorinated aromatic) and perfluorooctanoic acid (PFOA, a model for PFAS), over multiple cycles of use at environmentally relevant concentrations. Our zwitterionic hydrogel-based Fenton catalyst offers a promising solution for the efficient and scalable degradation of persistent organic pollutants in electrochemical water treatment processes and beyond.

8:00 PM EN07.03.05

Electrosynthesis of Hydrogen Peroxide and Electro-Fenton Application using Metal Chalcogenide Electrocatalysts Gerardo J. Quintana Cintron, R. Dominic Ross and Song Jin; University of Wisconsin–Madison, United States

Hydrogen peroxide (H_2O_2) is an environmentally friendly oxidant that has diverse applications in wastewater treatment, paper bleaching, and chemical disinfection. However, its traditional production is costly, unsafe, and not energy efficient. Electrochemical production of H_2O_2 using the two-electron oxygen reduction reaction ($2e^-$ ORR) could enable decentralized production of H_2O_2 with just air and electricity. Furthermore, electrosynthesized H_2O_2 can be reacted with Fe^{2+} to produce hydroxyl radical ($\bullet OH$) via the electro-Fenton (EF), which can break down or convert organic compounds that are otherwise difficult to oxidize directly. Metal selenides such as $CoSe_2$ and $NiSe_2$ have previously been demonstrated as effective electrocatalysts for the $2e^-$ ORR and EF. Here we further explore a series of Fe-Se compounds toward practical EF. Metal and selenium leaching was systematically studied through inductively coupled plasma-optical emission spectroscopy (ICP-OES) to understand better how the Fe ion leaches (Fe ion concentration) and can “self-catalyze” the EF reaction. The electrosynthesis of H_2O_2 and the electrochemical removal of model contaminant Rhodamine B via the EF process was studied with or without added Fe^{2+} with various metal selenide catalysts in a conventional H-cell and a gas diffusion electrode (GDE) flow cell. This work also studies the production of H_2O_2 through the cathodic reduction of oxygen in acidic and neutral medium by comparing the results obtained using different metal chalcogenide catalysts on a GDE flow cell setup.

8:00 PM EN07.03.06

Development of Double Doped Lanthanum-Strontium Titanate: Synthesis, Characterization and Nanoparticles Production by Exsolution for Promising Catalyst Antonio T. Oliveira and Daniel Z. Florio; UFABC, Brazil

Climate change has emerged as one of the most significant concerns of this century. In 2021, global electricity production heavily relied on natural gas (22.79%), oil (2.75%), and coal (36.26%) [1]. However, electricity generation from these sources is strongly associated with greenhouse gas (GHG) emissions. Since 2015, various initiatives have been undertaken to achieve net-zero emissions by replacing fossil fuels with renewable energy sources. Among these alternatives, Solid Oxide Fuel Cells (SOFCs) have gained attention due to their high efficiency, fuel flexibility, and low-to-zero CO_2 emissions resulting from electrochemical conversion. In SOFCs, the anodes are responsible for fuel reduction reactions while the cathodes drive the oxidizing reactions. Perovskite materials have demonstrated excellent potential as SOFCs electrodes due to their high mixed ionic-electronic conductivity, catalytic properties, and chemical and thermal stability. Nowadays, one significant challenge associated with SOFCs is their operation with carbon-based fuels. When these fuels are applied, the anodes catalyze coke formation, leading to carbon deposition on the anode surface, which results in efficiency loss. To address this issue, several efforts have been dedicated to finding a solution, and one promising approach is the application of metallic nanoparticle exsolution at the electrodes. This process involves the *in situ* growth of nanoparticles anchored on the matrix surface. Exsolved nanoparticles have demonstrated tolerance to sulfur poisoning and resistance to coke deposition, preventing coarsening and catalyst deactivation. The present work seeks to obtain exsolved metal alloy nanoparticles anchored on a perovskite structure, thereby a more promising material for SOFC applications. The nanoparticle catalysts were obtained by dissolving the interest metal into a perovskite host and subsequently exposing it to a reducing H_2 atmosphere. The $La_{0.8}Sr_{0.2}Ti_{0.7}Ni_{0.3-x}Cu_xO_{3-6}$ ($x = 0.1, 0.15, 0.2$) powders were obtained by the Pechini synthesis route and calcined at $900^\circ C$ for 5 hours. Thereafter, the powders were heat-treated under 3 vol % H_2/N_2 atmosphere at $900^\circ C$, $850^\circ C$, $800^\circ C$ and $750^\circ C$ for 10 hours to obtain decorated NiCu nanoparticles alloys. The samples were characterized by scanning electron microscope, transmission electron microscope, X-ray diffraction, X-ray photoelectron spectroscopy, and electrochemical impedance spectroscopy. Rietveld refinement was performed to determine structural parameters such as crystal symmetry, crystallite size, strain, and phase content before and after reduction treatment. Preliminary results indicate successful synthesis route and reduction treatment were to obtain NiCu nanoparticles alloy.

Acknowledgments: The author acknowledges CEM-UFABC, PRH49-ANP/UFABC .

References:

- 1 – Our World in Data based on BP Statistical Review of World Energy (2022); Ember (2023)
- 2 – NEAGU, Dragos et al. Nature communications 6 (2015) 1.

8:00 PM EN07.03.07

Low-Cost 3D Printable Flow Reactors for Electrochemistry Erin Heeschen, Elena De Lucia, Yilmaz A. Manav, Daisy Roberts, Benyamin Davaji and Magda H. Barecka; Northeastern University, United States

Transition to carbon neutrality requires the development of more sustainable pathways to synthesize the next generation of chemical building blocks. Electrochemistry is a promising pathway to achieve this goal, as it allows for using renewable energy to drive chemical transformations. While electroreduction of carbon dioxide (CO_2) and hydrogen evolution are attracting a significant research interest, there exist fundamental challenges in moving the research focus towards performing these reactions on scales relevant to industrial applications. To bridge this gap, we aim to facilitate the access of researchers to flow reactors, which allow characterizations of electrochemical transformations under the conditions closer to those deployed in the industry. Here we provide a 3D-printable flow cell design (manufacturing cost $< \$5$) which consists of several plates, offering a customizable alternative to commercially available flow reactors (cost $> \$6,000$). Proposed design and detailed build instructions allow a wide variety of chemical reactions in flow to be performed, including gas and liquid phase electroreduction, electroplating, and photoelectrochemical reactions, providing researchers with more flexibility and control over their experiments. By offering a low-cost reactor alternative, we reduce the barriers toward performing research on sustainable electrochemistry, supporting the global efforts necessary to realize the paradigm shift in chemical manufacturing.

8:00 PM EN07.03.08

Engineering the Electronic Structure of Aluminate Spinel Oxide using a High Entropy Approach Francisco Marques dos Santos Vieira, Ismaila Dabo, Raymond Schaak, Zhiqiang Mao and Rowan Katzbaer; The Pennsylvania State University, United States

Due to its high energy density, hydrogen fuel shows promise is the decarbonization of freight transport. However, there remain challenges in the synthesis of hydrogen fuel. Electrocatalytic water splitting holds the potential to sustainably produce hydrogen fuel provided suitable catalysts are identified. Here, we present the high entropy aluminate spinel oxide ($Fe_{0.2}Co_{0.2}Ni_{0.2}Cu_{0.2}Zn_{0.2}Al_2O_4$ ($A^5Al_2O_4$)) as catalyst for the oxygen evolution reaction (OER) in an alkaline electrolyte, and explore its electronic structure. In high entropy oxides (HEOs), numerous cations coexist in a single sublattice forming a solid solution throughout the crystalline solid. The sharing of a sublattice gives rise to unique, and even enhanced, properties including improved catalytic performance. Experimental measurements indicate $A^5Al_2O_4$ has a bandgap far narrower than its parent phases. First principles calculations indicate that this narrowing of the bandgap is a consequence of the broadening of bands arising from the hybridization of the 3d states due to the variation of electronegativity across the 3d transition metal series. The observed narrowing of the bandgap in the high entropy spinel highlights a new method of engineering electronic structure using a high entropy approach to achieve desired material properties.

8:00 PM EN07.03.09

Pt-Ni-Ru Nanoframes with Superior Performance for Methanol Oxidation Reaction Eduardo Lezama, Kira Shulman, Yoor Cho and Yiliang (Yancy) Luan; Binghamton University, The State University of New York, United States

Direct Methanol Fuel Cells (DMFCs) offer a promising solution for energy conversion with relatively low carbon emissions. Nevertheless, the efficiency of the anode is hindered by the sluggish kinetics of the Methanol Oxidation Reaction (MOR), preventing the widespread commercialization of DMFCs. Despite being a successful commercialized catalyst, Platinum (Pt) has been demonstrated to be costly and inefficient. Pt-based alloys with open structures offer feasible alternatives that have the potential to improve MOR while also being economically viable. This study synthesized Pt-Ni-Ru nanoframes (NFs) via a galvanic replacement process, resulting in remarkable MOR activity attributed to the combined effect of alloying and large surface area from the NFs. The Pt-Ni-Ru NFs exhibited mass and specific activities 2.8 and 2.0 times higher, respectively, compared to the commercial Pt/C catalyst. The study demonstrates that Pt-Ni-Ru NFs serve as a superior catalyst for the anode reaction in DMFCs, emphasizing the potential of open nanostructures and alloying in the advancement of future catalysts.

8:00 PM EN07.03.10

Structural and Electrocatalytic Properties of Pulsed Laser-Deposited Titanium Nitride/Titanium Oxynitride Thin Films Sheilah Cheron¹, Ikenna Chris-Okoro¹, Valentin Craciun^{2,3}, Mihai Maria^{3,4} and Dhananjay Kumar¹; ¹North Carolina Agricultural and Technical State University, United States; ²National Institute for Laser, Plasma, and Radiation Physics, Extreme Light Infrastructure for Nuclear Physics, Romania; ³University Politehnica of Bucharest, Romania; ⁴Horia Hulubei National Institute for Nuclear Physics and Engineering, Romania

Pulsed laser deposition (PLD) technique has been used to grow titanium nitride (TiN) and titanium oxynitride (TiNO) thin films on sapphire (Al₂O₃), titanium dioxide (TiO₂) and niobium doped titanium dioxide (Nb-TiO₂) single crystal substrates using high vacuum conditions. A pulsed Krypton Fluoride (KrF) excimer laser (Wavelength=248nm, pulse duration=30ns) has been used, with a laser repetition rate of 10 Hz, 6000 pulses, and a deposition temperature of 600° C. Structural properties of the films were investigated using X-ray Diffraction and Reflection (XRD, XRR) while X-ray Photoelectron Spectroscopy (XPS) and Rutherford backscattering spectrometry (RBS) was used for compositional investigations. XRD phi scans show the in-plane orientation of the deposited TiN film with respect to the substrate orientation; depending on the substrate orientation, films are either (111) or (200) oriented, thus offering different orientations for surface chemical reactions. The full-width half maximum (FWHM) value of plane (200) was 0.5754° for the film grown on undoped TiO₂ (110), while for those growing along the (111) plane was 0.1617° for the film on sapphire and 0.1457° for the film on Niobium-doped TiO₂ (100). Films deposited onto niobium-doped TiO₂ have shown the highest crystallinity, whereas those deposited onto undoped TiO₂ have shown poor crystallinity. The rocking curve results show that changing the substrate orientation can control the crystal quality of the grown TiN.

Simulation of the acquired XRR curves indicated mass densities from 5.2 to 5.4 g/cm³, very close to the TiN tabulated value, while the roughness was less than 1 nm indicating flat surfaces for chemical reactions. XPS analysis shows the initial film surface is oxidized, and the chemical formula indicates the existence of a composite made of TiO₂+TiON+some TiN. After sputtering of the surface heavily oxidized layer is removed, and the chemical composition changes to TiN-TiON and some TiO₂. For the films deposited under low vacuum, the atomic oxygen concentration was lower than 10%, a result also confirmed by Rutherford backscattering spectrometry. Such films also exhibited resistivities around 70 mΩ.cm, which is close to the best-reported values. TiON films are epitaxial, despite the relatively high oxygen concentration. By controlling the oxygen-to-nitrogen ratio by regulating the vacuum level during PLD, optical bandgaps of the composite films were controlled from 2.1 eV to 3.2 eV, and electrocatalytic overpotentials for oxygen evolution reaction potentials as low as 300 mV at 10mA/cm² was obtained. The Tafel slopes, indicative of a rate of increase of electrode potential with respect to current, for these films, are determined to be in the range of 80–60 mV/decade. These results further demonstrate the superiority of TiNO thin film as an electrocatalyst for water oxidation to generate fossil-free fuels. The improvement in the electrocatalytic behavior of the TiNO thin films is explained based on an adjustment in the valence band maximum edge and an enhancement in the number of electrochemically active sites. Both effects are realized by the substitution of N by O, forming a TiNO lattice that is isostructural with the rock-salt TiN lattice.

This work was primarily supported by a DOE EFRC on The Center for Electrochemical Dynamics And Reactions on Surfaces (CEDARS) via grant # DE-SC0023415. The authors (IK, VC, and DK) also acknowledge the support of the NSF PREM via grant # DMR-2122067 PREM.

8:00 PM EN07.03.11

Development of Chemical Analysis Method and Reference Materials of Binary Pt Alloy Catalysts for a PEM-Type Hydrogen Fuel Cell Sangrin Lee and Kwangsoo Lim; KTR (Korea Testing & Research Institute), Korea (the Republic of)

Recently, the development and application of polymer electrolyte hydrogen fuel cells (PEMFCs) are expanding. So, demand for platinum alloy catalysts which are a core materials for hydrogen fuel cell is growing exponentially. The price of a catalyst material using a precious metal is determined according to the content of the metal such as Pt, Pd etc... However, there are conflicts between companies, because of absence standard test method for analysis of novel metal contents in the catalysts. therefore, We tried to develop standard test methods and reference materials for elemental quantitative analysis of platinum alloy catalyst materials.

The elemental quantitative analysis method is fully developed based on ISO/IEC 17025 : 2017. Applying ICP/OES, the certified values of the mass fractions of Pt, Co, and Ni were assigned and their associated measurement uncertainties were evaluated. The mean measurement results obtained from 10 sample bottles were used to assign as the certified values for the RM and the between-bottle homogeneities were evaluated by ANOVA (on way layout) analysis method. The certified values and their associated expanded uncertainties at 95% level of confidence for mass fractions of Pt, Co in Pt₃Co/C RM were 27.1 ± 1.0% (coverage factor, k = 3.18), 2.26 ± 0.14% (k = 2.0) respectively. In case of Pt₃Ni/C, The mass fractions of Pt, Ni were 26.2 ± 0.6% (k = 2.0), 2.97 ± 0.22% (k = 2.0) respectively.

In this presentation, detailed analysis results, including the validation of the test method for analysis of standard materials will be introduced.

8:00 PM EN07.03.12

Improved Alkaline Hydrogen Oxidation on Strained-Modulated Pt Overlayers on Ordered Intermetallic PtSb Cores Tianyao Gong¹, Hamdan Alghamdi¹, David Raciti² and Shoji Hall¹; ¹Johns Hopkins University, United States; ²National Institute of Standards and Technology, United States

Alkaline exchange membrane fuel cells (AEMFCs) have emerged as an inexpensive and robust renewable energy conversion device. However, the kinetics Hydrogen Oxidation Reaction (HOR) in alkaline conditions (the anode reaction of AEMFCs) is ~100x slower in than in acidic electrolytes. Significant progress has been made developing improved catalyst materials for alkaline HOR, yet due to the complexity of alloy surfaces, it is difficult to determine the true source of such enhancement.

To address this issue, here we report the use of Ordered Intermetallic Compounds (OICs) as a well-defined platform to produce strain modulated Pt overlayers. Two OICs phases of the Pt-Sb system, PtSb and PtSb₂, with different crystal structures were prepared. Electrochemical dealloying of the Pt-Sb alloys resulted in the formation of core shell Pt-Sb@Pt particles. By judicious choice of the OIC precursor material, we were able to produce PtSb@Pt and PtSb₂@Pt with compressive and tensile strain, respectively, relative to elemental Pt. It is worth noting that this approach cannot be accomplished with solid solution alloys (with an alloy core composed of the same two elements) since the d-spacing of the lattice follows Vegard's law. This enabled us to interrogate the role of how strain controls HOR performance without the possible influence of atoms with different identities on the surface of the Pt. PtSb@Pt exhibited a weaker HBE than Pt, enabling to achieve an exchange current density (j₀) 1.5x larger than benchmark Pt catalyst for alkaline HOR; whereas PtSb₂ exhibited tensile strain which increased the HBE, reducing the j₀ by 1.5x to Pt catalyst. Interestingly we found no correlation with the OH_{ads} coverage as estimated by CO stripping. Therefore, this work revealed that HBE is the dominant parameter for improving the kinetics of Pt sites for alkaline HOR.

8:00 PM EN07.03.13

Effect on Oxygen Reduction Reaction of Iron Catalyst Synthesized by Aniline Monomer-Mediated Technique Yeongeun Choi¹, SeungMin Lee¹, Jiyeok Song², Hyo Eun Bae² and Oh Joong Kwon¹; ¹Incheon National University, Korea (the Republic of); ²Seoul National University, Korea (the Republic of)

An anion exchange membrane fuel cell (AEMFC), which uses hydroxyl conductive membranes instead of proton conductive ones, is highlighted as a replacement for a proton exchange membrane fuel cell. AEMFC has the advantage of using abundant and inexpensive transition metals, such as iron, cobalt, and nickel for catalysts owing to mild reaction conditions. Among numerous non-platinum metal catalysts (NPMCs), M-N-C catalyst has been reported considerably and Fe-N-C catalyst, which co-doped nitrogen and Fe, was considered the promising M-N-C owing to their high atomic utilization and excellent electrocatalytic performance. For the Fe-N-C catalyst, it is important to expose the maximum number of active sites and distribute the Fe in the Fe-N-C catalyst uniformly on a carbon support. Therefore, many researchers have been exploring Fe-N-C catalyst, in which Fe exist as a single atom. The common method for synthesizing single atom Fe-N-C includes the random mixing and high-temperature pyrolysis process, which tends to cause the aggregation of metals and leads to the degradation of catalytic activity. Thus, the research for preventing the aggregation of metals is crucial for high electrocatalytic activity.

This study explores the possibility of applying M-N-C to AEMFC through the development of Fe single atom. We adopted the method of aniline-mediated metal reduction and high-temperature pyrolysis for synthesizing the Fe-N-C catalyst. The Fe single atom reported high performance and durability and possess the optimal Fe-N_x coordination structure by optimizing the synthesis condition. The optimization of the synthesis conditions for the Fe-N-C catalyst proceeds through the control of the amount of Fe precursor and aniline and the temperature of pyrolysis. Several characterizations such as Thermogravimetric analysis (TGA), X-ray diffraction (XRD), Inductively coupled plasma-mass spectrometry (ICP-MS), and Scanning transmission electron microscopy (STEM) were introduced to investigate the catalyst properties. The uniform distribution of the single atom on the carbon support was confirmed by STEM and XRD, and the Fe content was checked to be about 1wt.% using ICP-MS and TGA. Furthermore, electrochemical measurements were conducted to present the correlation between catalytic activity and structure. The catalyst, which possesses single atom active sites, showed high electrochemical performance and durability for oxygen reduction reaction and proposed the applicability for AEMFC. The study proved that the Fe single-atom catalyst was successfully synthesized by metal reduction and pyrolysis processes

8:15 AM *EN07.04.01

Tailoring the Ensemble Geometry and Electronic Properties of Active Sites in Catalytic Nanomaterials [Christina Li](#); Purdue University, United States

Supported metal atoms and nanoparticles are found ubiquitously as heterogeneous catalysts for a wide variety of industrial, organic, and energy catalytic processes. The electronic and steric environment at the nanomaterial surface has a huge impact on the reactivity and selectivity of catalytic transformations occurring at surface active sites, but these properties are difficult to independently control through conventional materials synthetic methods. In this work, we develop molecularly-precise surface functionalization strategies in order to precisely tune both the ensemble geometry and redox properties of active site metal atoms. These strategies include 1) the adsorption of inorganic ligands on colloidal nanoparticle surfaces in order to synthesize monolayer and sub-monolayer core-shell catalysts, 2) control of bimetallic surface ensemble geometry in alloy nanoparticles, and 3) tuning the metal-sulfur coordination environment of single atoms supported on metal chalcogenide nanosheets for electrochemical catalysis. All of these strategies develop new structural frameworks for modulating the surface active site environment in order to access more reactive and selective nanomaterial catalysts.

8:45 AM EN07.04.02

Composition, Structure and OER Behaviors of Highly Catalytic Manganese-Doped Bismuth Ruthenium Oxide (MBRO) for Alkaline Water Splitting [Masatsugu Morimitsu](#), [Sachi Matsuura](#), [Hayato Suzuki](#) and [Chinami Ketani](#); Doshisha University, Japan

Water splitting using alkaline solutions is one of the most promising methods to produce green hydrogen and accounts for 61% of the world's hydrogen production capacity in 2020¹). The anodic reaction, which is oxygen evolution reaction (OER), occurs through a 4-electron transfer in highly corrosive solutions. While currently nickel-based materials are used for the anode because of the chemical stability of their oxides and oxyhydroxides in alkaline media, the current density during electrolysis is limited due to the low catalytic activity of those materials and cannot be as high as PEM water splitting. Our group has recently developed bismuth ruthenate-based pyrochlore oxide as a new OER catalyst and has found some excellent properties on the polarization for and durability to OER in KOH solutions. In this paper, the composition, structure, and OER behaviors of manganese-doped bismuth ruthenium oxide (MBRO) are presented with the results by instrumental analyses and electrochemical measurements.

MBRO was prepared by calcination at 600 °C of the precursor deposited in the solution which had been obtained by adding NaOH solution into the metal salt solution containing bismuth nitrate and ruthenium chloride with manganese nitrate. The composition and structure of the oxide were analyzed by AAS, RBS, EDX, XRD, and XAFS and the surface morphology and particle size were measured by SEM. The electrochemical performance was evaluated by Titanium Disk Method (TDM), in which the oxide particles loaded on a titanium disk (4 mm in diam.) was mounted in the rotating-disk electrode of a conventional three-electrode cell. The cell was also equipped with a platinum plate counter electrode and an Hg/HgO reference electrode. The electrolyte was 0.1 mol/L KOH solution and all measurements were performed at room temperature.

The obtained MBRO showed a single phase of pyrochlore structure and ruthenium at the B site was partly substituted with manganese. The particle size ranged from 20 to 40 nm, which was small enough to load it on a titanium disk without any binders or ionomers. The results obtained by polarization measurements revealed that the onset potential of OER was 0.45 V vs. Hg/HgO, which is the overpotential of 0.16 V, and the Tafel slope was ca. 39 mV/dec, while the other materials reported in the literature²) shows the overpotential higher than 200 mV and Tafel slope of 60 mV/dec or more. The above results suggest that MBRO is suitable for the anode material of alkaline water splitting to reduce the cell voltage at high current densities. In this work, MBRO-loaded graphite electrodes were prepared and examined for OER in 6 mol/L KOH solutions, of which the results will be also presented.

Ref.)

- 1) Digital Research, Current Status of Water Electrolyzer Development in the World and Trends of Makers Entering the Market, p. 11 (2022).
- 2) T. Shinagawa, *et al.*, *Scientific Reports*, **5**, 13801 (2015).

9:00 AM EN07.04.03

Tungsten-Induced Operando Transformations of the Perovskite Ba_{0.5}Sr_{0.5}Ni_{1-x}W_xO_{3-δ} Series during the Oxygen Evolution Reaction [Natasha Hales](#), [Emiliana Fabbri](#) and [Thomas Schmidt](#); Paul Scherrer Institute, Switzerland

Water electrolysis provides a means for long-term energy storage in the form of hydrogen gas, helping to offset seasonal variations in renewable energy production. Developing non-noble metal catalysts for the anodic oxygen evolution reaction (OER) is a key step in reducing the cost and increasing the energy efficiency and sustainability of this vital technology. Flame-spray synthesized perovskite oxides of the composition Ba_{0.5}Sr_{0.5}Ni_{1-x}W_xO_{3-δ} exhibit excellent OER activity in alkaline conditions. In particular, Ba_{0.5}Sr_{0.5}Ni_{0.5}W_{0.5}O_{3-δ}, with a catalytic turn over frequency (TOF) five-times that of NiO, displays a competitive Tafel slope of 44.7 mV/dec. The perovskite structure, with its tunable ABO₃ formula, provides a unique opportunity to enhance the intrinsic activity of Ni sites with high-valence metal co-doping, and explore the relationship between structural properties and electrocatalytic activity.

B-site W doping strongly influences the oxidation state of surface Ni sites, as revealed by *ex-situ* soft X-ray absorption spectroscopy (XAS) at the Ni L-edge. A higher concentration of W⁴⁺ increases the Ni²⁺/Ni³⁺ ratio, enhancing the intrinsic activity of the Ni active sites. In addition, analysis of the O K-edge indicates a positive correlation between W content and oxygen vacancy concentration, activating Ba_{0.5}Sr_{0.5}Ni_{0.5}W_{0.5}O_{3-δ} for the lattice oxygen mechanism (LOM), whereby mobile oxygen atoms can move through vacant lattice sites to participate directly in OER catalysis.¹ This pathway is largely considered to be more efficient than the traditional adsorbate evolution mechanism (AEM), leading to enhanced reaction kinetics and decreased OER overpotentials.¹

Akin to the well-known surface reconstruction processes of NiO during alkaline OER (Ni^{II}O → Ni^{II}(OH)₂ → Ni^{III}OOH), NiW perovskites experience complex, electrochemically-induced transformations under OER conditions.² Therefore, catalyst 'pre-activation' using cyclic voltammetry is essential to develop their high-performance final state *in-situ*. Operando hard XAS at the Ni K-edge and W L₃-edge revealed that NiW perovskites experience significant oxidation state changes at the catalytic Ni sites during cyclic voltammetry, with a strong overall trend of Ni²⁺ → Ni³⁺ oxidation. However, both the extent and rate of this oxidation are greatly influenced by the B-site W concentration. Furthermore, operando X-ray diffraction revealed significant surface reconstruction that facilitates a strong growth in electrochemically active surface area, but this process is also heavily dependent on the W content. It is evident that the 'pre-activation' of Ba_{0.5}Sr_{0.5}Ni_{1-x}W_xO_{3-δ} catalysts is a function of the Ni:W ratio; elucidating the ways in which high valence metal doping influences the catalyst activation mechanism will guide the development of future Ni-based OER catalysts, for which this process is intrinsically coupled with OER activity.

1. J. S. Yoo, X. Rong, Y. Liu and A. Kolpak, *ACS Catal.*, 2018, **8**, 5, 4628–4636
2. V. der Ven, D. Morgan, Y. S. Meng, and G. Ceder, *J. Electrochem. Soc.*, 2006, **153**, 2, A210-A215

9:15 AM EN07.04.04

Discovery of High-Index Facet Nanocatalysts for Clean Energy Applications [Bo Shen](#) and [Chad A. Mirkin](#); Northwestern University, United States

Nanoparticles with high-index facets are particularly attractive as electrocatalysts because such facets typically consist of a high density of low-coordinated atomic steps and kinks. However, the synthesis of high-index facet nanoparticles is very challenging, which prevents the wide application of such materials. Herein, we addressed this challenge by developing synthetic methods based on ligand-free, solid-state reactions. Combining synthetic techniques with high-throughput DFT simulations and machine learning, we have discovered a library of multimetallic high-index facet nanoparticles. Additionally, the size, composition, crystal structures, and phase structures of such materials can be further controlled by nanolithography, leading to a huge database of high-index facet catalysts, which can be used for a range of energy-related applications including electrooxidation of liquid fuels and CO₂ reduction.

9:30 AM *EN07.04.05

Platinum Catalysts with Enhanced Activity and Durability Toward Oxygen Reduction [Younan Xia](#); Georgia Institute of Technology, United States

In this talk, I will discuss a number of new strategies for augmenting the mass activity and durability of Pt-based catalysts toward the oxygen reduction reaction (ORR), which is key to the operation of proton-exchange membrane fuel cells (PEMFCs). Specifically, the strategies include the formation of intermetallic compounds, creation of twin boundaries on the surface, and introduction of chemical linkage between Pt surface and carbon support. When integrated together, these strategies can lead to the development of ORR catalysts with performance that meets the requirement set by DOE. For example, we were able to grow sub-2-nm Pt particles on a commercial carbon support *via* the galvanic reaction between a Pt(II) precursor and a uniform film of amorphous Se pre-deposited on the support. The residual Se could serve as a linker to strongly anchor the Pt nanoparticles to the carbon surface, leading to a catalytic system with extraordinary activity and durability toward ORR. Even after 20,000 cycles of accelerated durability test, the sub-2-nm Pt particles were still dispersed well on the carbon support, maintaining

a mass activity more than three times as high as the pristine value of a commercial Pt/C catalyst.

10:00 AMBREAK

10:30 AM *EN07.04.06

From Fundamental Studies to Applied Research: SrIrO₃ as Efficient Electrocatalysts for Proton Exchange Membrane ElectrolyzerZhenxingFeng; Oregon State University, United States

The search of efficient and stable electrocatalysts for oxygen evolution reaction (OER) in acidic electrolyte is the key to enable the commercialization of proton exchange membrane (PEM) electrolyzers and low hydrogen production price. However, there are few choices for such electrocatalysts due to the corrosive and oxidative conditions. As the discovery of SrIrO₃ as a new type of electrocatalysts in acidic OER, we have focused on the fundamental studies of mechanism that leads to its much better activity (~ 1000 times more) than the commercial standard, IrO₂. Using SrIrO₃ thin film epitaxially grown by molecular beam epitaxy (MBE) as the model system, we have studied the surface restructuring and Sr leaching in the reaction at the atomic scale. Later, using the learned knowledge, we design Ir less SrIrO₃-based catalysts in powder form that exhibit the same activity. We are currently extending our studies for this type of catalysts for general PEM electrolyzer applications.

11:00 AM EN07.04.07

Enhancing Hydrogen Evolution Reaction by Controlling Chemical States Through Electrochemical Reduction of Raney Nickel in Alkaline Water ElectrolysisYoungHwaYun^{1,2}, ChangsooLee¹, SechanLee¹, MinJoongKim¹, JongHyeokPark² and HyunseokCho¹; ¹Korea Institute of Energy Research, Korea (the Republic of); ²Yonsei University, Korea (the Republic of)

Porous electrocatalysts based on nickel (Ni) have found extensive application in alkaline water electrolysis for the hydrogen evolution reaction (HER). The selective leaching of aluminum (Al) from Ni-Al alloys is widely employed as a prominent approach to increase the surface area of porous Ni during fabrication, resulting in high surface area in Ni(OH)₂. However, the Ni(OH)₂ hampers the HER due to its weak hydrogen adsorption energy. To enhance the hydrogen adsorption energy, it is essential to control the chemical state of the Ni by incorporating metallic Ni, which exhibits strong hydrogen adsorption characteristics. In this study, we controlled the chemical states of Ni through plasma vapor deposition (PVD), heat treatment, chemical leaching, and electrochemical reduction. The phase evolution of the electrocatalysts during fabrication was confirmed using a range of characterization techniques, including X-ray diffraction (XRD), scanning electron microscopy (SEM), transmission electron microscopy (TEM), and energy-dispersive X-ray spectroscopy (EDS). We revealed that the heat-treated Ni-Al alloy, possessing a thick Ni₂Al₃ surface layer, underwent selective Al leaching, resulting in the formation of biphasic interfaces comprising Ni(OH)₂ at the grain and NiAl IMCs near the grain boundary of the outermost surface layer. X-ray photoelectron spectroscopy (XPS) analysis confirmed that the coupled oxidation of the NiAl IMCs facilitated the partial reduction of Ni(OH)₂ to Ni(OH)₂/Ni at the grains during electrochemical reduction. The electrocatalyst containing partially reduced Ni(OH)₂/Ni exhibited an overpotential of 54 mV at 10 mA/cm², and in single-cell operation, it demonstrated a cell voltage of 1.675 V at 0.4 A/cm² at 50 °C.

11:15 AM EN07.04.08

Catalyst-Support Interactions in Zr₂ON₂-Supported IrO_x Electrocatalysts for Enhanced Activity and Stability in the Acidic Oxygen Evolution Reaction.ChangsooLee¹, KihyunShin², YoungtaePark¹, YoungHwaYun¹, GisuDoo¹, MinJoongKim¹, SechanLee¹ and HyunseokCho¹; ¹Korea Institute of Energy Research, Korea (the Republic of); ²Hanbat National University, Korea (the Republic of)

Overcoming the challenge of developing highly active and durable Ir-based electrocatalysts for the acidic oxygen evolution reaction (OER) is difficult due to the corrosive conditions experienced during anodic processes. In this study, we present the utilization of IrO_x/Zr₂ON₂ electrocatalysts, which employ Zr₂ON₂ as a support material, to address the trade-off between activity and stability in the OER. Zr₂ON₂ was chosen for its exceptional electrical conductivity and chemical stability, as well as its ability to form strong interactions with the IrO_x catalysts. As a result, the IrO_x/Zr₂ON₂ electrocatalysts demonstrated remarkable OER performance, achieving an overpotential of 255 mV at 10 mA/cm² and a mass activity of 849 mA/mg_{Ir} at 1.55 V (versus the reversible hydrogen electrode). The activity of IrO_x/Zr₂ON₂ was sustained at 10 mA/cm² for 5 hours, while the unsupported IrO_x catalyst and IrO_x/ZrN underwent significant degradation. Through a combination of experimental X-ray analyses and theoretical interpretations, it was discovered that the reduced oxidation state of Ir and the extended Ir-O bond distance in IrO_x/Zr₂ON₂ effectively enhanced the activity and stability of IrO_x by modifying the reaction pathway from a conventional adsorbate evolution mechanism to a mechanism involving participation of lattice oxygen. These findings demonstrate that it is possible to significantly reduce the Ir content in OER catalysts through interface engineering without compromising their catalytic performance.

11:30 AM *EN07.04.09

Designing Microenvironments for Selective CO₂ (Photo)ElectroreductionFrancescaM. Toma^{1,2}; ¹Helmholtz Zentrum Hereon, Germany; ²Lawrence Berkeley National Laboratory, United States

(Photo)electrochemical reduction of carbon dioxide is a process in which multiple proton-electron transfers are necessary to yield valuable carbon-based products. This process also offers an efficient strategy to reduce the presence of greenhouse gases in the atmosphere while concurrently producing valuable carbon-based products. However, most of the existing CO₂ reduction catalysts still exhibit reduced selectivity for CO₂ reduction products and high activity for the competing hydrogen evolution reaction.

To understand how to tune catalytic activity and selectivity, the identification of specific structure-reactivity relationships can inform catalyst development. We demonstrate that the confined reaction environment enables changes in reaction selectivity and can impart atypical catalytic behaviors. In this talk, we clarify the role of subsurface oxygen, water, and CO₂ on Cu and Ag based systems for CO₂ electroreduction. We show the development of a predictive framework to tune the selectivity of CO₂ reduction on Cu and Ag by examining a series of polymeric and molecular modifiers. We also demonstrate how considerations about the local reaction environment have relevance for photoelectrochemical systems. This understanding can reveal design principles that enable development of active and selective catalysts and provide further insights into the CO₂ reaction mechanism on existing catalyst such as copper and silver.

SESSION EN07.05: Electrocatalyst Synthesis, Water Electrolysis, Fuel Cell Reactions II

Session Chairs: Charles McCrory and Haotian Wang

Tuesday Afternoon, November 28, 2023

Hynes, Level 3, Room 310

1:30 PM *EN07.05.01

Atomic-Scale Insights into Electrocatalyst Structure and FunctionShojiHall; Johns Hopkins University, United States

The development of efficient renewable energy conversion and storage devices to curb climate change is one of the most important challenges of the 21st century. This can be addressed by using renewable electricity to manufacture chemical fuels and synthetic precursors, or by generating electricity with carbon-neutral fuel cell devices. However, electrocatalytic processes are hampered by low efficiencies and poor reaction selectivity because of a lack of rational methods available to create controllable catalyst materials with the preferred electrochemical activities. In this seminar Prof. Hall will discuss the use of ordered intermetallic compounds (OICs), which are alloys that display high electrocatalytic activities because their well-defined compositions and long-range atomic scale ordering enable predictable geometric and electronic interactions, in contrast to the more widely studied solid-solution type alloys. However, OIC materials are difficult to synthesize in nanomaterial form because conventional synthesis methods offer poor control over the composition, phase, and morphology. I will discuss our efforts on the synthesis, stability, and catalytic activity of OICs prepared by electrochemical methods at room temperature and atmospheric pressure. Our strategies include the use of electrochemically induced phase transformations which enables us to convert a base metal rich alloy to an OIC richer in nobler metal by removal of the base metal, and the direct production of OIC materials by electrochemical deposition. We will also discuss how we leverage the atomically precise configuration of atoms within OICs to reveal detailed insights into how a material's structure regulates its electrochemical properties. Developing new methods for preparing OIC compounds under ambient conditions is essential for designing catalysts for the next generation of renewable energy conversion devices.

2:00 PM EN07.05.02

Mitigating the Phosphate Anion Poisoning Effect on Oxygen Reduction Reaction (ORR) with a Hydrophobic Side GroupHonghongLin, SiwenWang, LiangWang, GaohuaZhu, LingChen and HongfeiJia; Toyota, United States

High-temperature polymer electrolyte fuel cells (HT-PEMFCs) have been developed for heavy duty applications, utilizing phosphoric acid (H₃PO₄) to overcome the proton conductivity limit

of Nafion at elevated temperatures (120–220 °C). However, the adsorption of phosphoric acid onto the Pt catalyst hampers the oxygen reduction reaction (ORR) activity, necessitating a high Pt loading in HT-PEMFCs. Understanding the interaction between Pt and phosphate anions, as well as the anion adsorption effect on ORR, is crucial for activity improvement. In this study, we conducted a comprehensive theoretical and experimental investigation to gain insights into the effect of phosphate adsorption on ORR. While electrolyte adsorption inevitably obstructed active sites, our study revealed a weakened binding between Pt and key ORR intermediates, namely the OH_{ad} , in the presence of adsorbed anions. This weakened Pt- OH_{ad} binding had a beneficial effect on boosting the ORR kinetics. By appropriately modifying the side group structure of a substituted phosphonic acid ($\text{R-PO}(\text{OH})_2$), the activity loss caused by anion adsorption could be effectively compensated through enhanced ORR kinetics. Our findings highlight an alternative approach, alongside catalyst material modulation, to mitigate the adverse effects of electrolytes in HT-PEMFCs. The tuning of catalyst interfacial structure using a hydrophobic surface modifier can also serve as a strategy to optimize ORR kinetics in both low-temperature (LT-) and HT-PEMFCs.

2:15 PM EN07.05.03

Probing the OER/ORR Mechanisms on MnO_2 using *Operando* TEY-STXM and Surface DFT Calculations Evan Z. Carlson^{1,2}, Xiao Zhao^{1,2}, Michal Bajdich³, Hendrik Ohldag², William C. Chueh¹ and J. Tyler Mefford¹; ¹Stanford University, United States; ²Lawrence Berkeley National Laboratory, United States; ³SLAC National Accelerator Laboratory, United States

Harnessing the unique bifunctional OER/ORR activity of manganese oxides in regenerative fuel cells could help reduce their material and capital requirements. However, using MnO_2 in reversible, single-catalyst oxygen electrodes requires a better understanding of the structural and chemical motifs responsible for its high electrocatalytic activity.

In this talk, I will discuss our investigation of the atomic-scale origins of Mn oxide's bifunctional OER/ORR activity using a hybrid experimental-computational approach. Our model system, $\alpha\text{-K}_2\text{MnO}_2$, is among the highest-performing Mn oxide catalysts for both the OER and the ORR, with ORR activity rivaling that of Pt in basic electrolytes.^[1] The material's pH and cation-dependent activity is characterized via rotating ring disk electrochemistry (RRDE), and its voltage-dependent chemistry is probed via *operando* scanning transmission x-ray microscopy in bulk-sensitive transmission mode^[2] and surface-sensitive total electron yield mode (TEY-STXM). Surface DFT calculations further reveal the active sites and mechanisms for both the OER and ORR, as well as an unusual cation-dependency.

[1] Meng, Y. *et al. J. Am. Chem. Soc.* **2014**, *136* (32), 11452–11464.

[2] Mefford, J.T. *et al. Nature.* **593**, 67–73 (2021).

2:30 PM BREAK

3:00 PM *EN07.05.04

Conductive Dithiolene-Based Metal-Organic Frameworks for Electrocatalytic H_2 Production Smaranda C. Marinescu; University of Southern California, United States

Sustainable hydrogen evolution reaction (HER) from water has emerged as a promising pathway for the storage and conversion of solar energy in chemical bonds. Hydrogen is a valuable energy carrier that can be transformed into electricity using fuel cell technology or used in the production of industrially relevant chemicals such as ammonia and methanol. Heterogenization of molecular catalysts is an attractive strategy to combine the advantageous properties of homogeneous and heterogeneous catalysis. Metal-organic frameworks (MOFs) have emerged as a promising class of materials; however, their insulating nature has limited their applications in electronics and electrocatalysis. We have demonstrated the successful integration of metal dithiolene units into one and two-dimensional frameworks by using dinucleating and trinucleating thiolate-based ligand scaffolds. The developed metal dithiolene frameworks display high activity for the electrocatalytic HER in acidic aqueous media. The HER performance of the MOF-based electrocatalysts is investigated, to understand the charge transfer properties of the constructed MOF/electrode architecture. Density functional theory calculations were applied to understand the structure of the MOF and its mechanistic pathways for the HER. We expect the design principles discovered in these studies to have a profound impact towards the development of advanced materials and sustainable technologies.

3:30 PM EN07.05.06

Investigation of FeOOH for Mechanisms in Water-Splitting Reactions Alexandra M. Anderson and Wennie Wang; University of Texas at Austin, United States

Electrolysis is at the forefront of methods of producing hydrogen by separating water into oxygen and hydrogen gas. The oxygen evolution reaction (OER) is known for having slower kinetics due to multiple proton-electron coupled transfer steps being involved. Transition metal oxyhydroxides have been demonstrated to have low overpotentials while being composed of abundant and cheap elements and may be an important materials platform in scaled-up hydrogen production. This project explores the relationships between structure and OER mechanisms in iron oxyhydroxides (FeOOH). Earth-abundant metals like Fe pose active catalytic sites and can be modeled in a FeOOH structure under alkaline conditions. Studies show that amorphous electrocatalysts exhibit greater catalytic activity compared to crystalline electrocatalysis, a trend which has often been attributed to amorphous electrocatalysts having a greater concentration of electrochemically accessible active sites.^{2,3} We hypothesize that the lack of long-range order in amorphous electrocatalysts may also introduce novel structural moieties not present in the crystalline form and play a role in enhanced electrocatalytic activity.

In order to begin testing this hypothesis, we study structure-property relationships between crystalline disorder and OER energetics using density functional theory (DFT) with a Hubbard U correction as implemented in Quantum ESPRESSO.⁴ We first discuss determining the Hubbard U correction value and constructing a representative adsorbate/surface structure using the crystalline structure. We manually manipulate the crystalline structure to imitate potential local structural distortions of the amorphous structure and compare computed overpotentials with the different structures and previously determined literature values. Finally, we present a rational model to understand the impact of structural distortion on electrocatalytic activity.

References

- (1) D. Friebe et al. *Journal of the American Chemical Society* 2015, *137* (3), 1305-1313
- (2) W. Cai et al. *Nano Lett.* 2020, *20* (6), 4278–4285.
- (3) S. Anantharaj & S. Noda. *Small* 2020, *16* (2), 1905779.
- (4) Timrov I. et al. *Comput. Phys. Comm.* 279 (2022), 108455

3:45 PM EN07.05.07

Multicomponent Alloy Nanoparticles as Efficient Oxygen Evolving Electrocatalysts Leanne Jones and Robert Weatherup; University of Oxford, United Kingdom

Designing efficient and cost-effective catalysts for electrochemical water splitting will be pivotal in the global effort towards net zero [1]. The two half reactions of water splitting; the hydrogen evolution reaction ($\text{HER}, 2\text{H}^+ + 2\text{e}^- \rightarrow \text{H}_2$) and the oxygen evolution reaction ($\text{OER}, 2\text{H}_2\text{O} \rightarrow \text{O}_2 + 4\text{H}^+ + 4\text{e}^-$), currently rely on Pt group metals such as Pt and Ru, and Ir and Ru oxides, when performed in acidic media. Overpotentials are still observed for these catalysts due to the sluggish kinetics of the reactions, with OER typically the rate limiting reaction [2]. It is therefore instructive to find alternative oxides to replace Ir and Ru. Nonprecious transition metal-based oxides may provide cheaper and more abundant OER catalysts. Unfortunately, these oxides are not stable in the acidic media, and therefore must be studied in alkaline media [3].

The activity of transition metal-based catalysts relates to their electronic structure, specifically the energy difference between the valence d-band centre and the Fermi level (E_{F}) [4]. An increase in the energy difference usually results in a stronger interaction of the orbital and the adsorbate. The strength of this interaction in terms of catalytic activity is described by the Sabatier Principle. Therefore, tailoring the optimal energy of the d-band for the reaction of interest will allow for improved catalytic efficiency. Ni, Fe and Co based catalysts and their alloys have shown great promise as OER catalysts [5,6]. Multicomponent alloys (MCAs) exhibit improved corrosion resistance relative to the elemental constituents whilst still containing catalytically active elements such as Ni, Fe and Co. This synergistic relationship between the elements make MCAs promising as successful OER catalysts.

Here, size-selected nanoparticles are deposited via a state-of-the-art gas-phase synthesis. Using a quadrupole mass spectrometer placed in-line with the source, the size of the nanoparticles are well defined and controlled. Initial depositions of NiFeCoMoAl and NiFeCoMoCr have been successful, and characterised on an atomic scale using transmission electron microscopy (TEM). Hard and soft X-ray photoelectron spectroscopy (HAXPES and SXPS, respectively), measured at the i09 beamline at Diamond Light Source, gives depth resolved compositional information showing the presence of all elements as well as their possible arrangement within the nanoparticles. Meanwhile atom probe tomography (APT) measurements, made possible by simultaneous nanoparticle deposition and conventional magnetron sputtering, allow us to marry the information gathered using TEM and SXPS/HAXPES. The structural and chemical information thereby obtained is compared with electrochemical measurements of the intrinsic activities of different MCAs, revealing trends in valence band measurements from SXPS and activity. Unifying these complimentary techniques gives insight into the relationship between the atomic and electronic structure with electrochemical activities of MCA nanoparticles which will feed into future electrocatalytic design and will be a stepping stone in the wider effort of achieving net-zero emissions.

[1] UNFCCC, The Paris Agreement—Publication, Paris Climate Change Conference—Nov 2015, 2018

[2] *J. Am. Chem. Soc.*, *140*, 7748, 2018

[3] *Small*, *13*, 1701931, 2017

[4] *Surf. Sci.*, *343*, 211, 1995

4:00 PM EN07.05.08

Simple Synthesis of Perovskite oxides/FeOOH with N-Doped Graphene Quantum Dots to Boost Electron Transfer Sang Heon Kim and Jeong Min Baik; Sungkyunkwan University, Korea (the Republic of)

Bifunctional electrocatalyst requires superior charge transfer and good electrochemical performance to produce overall and stable water splitting reaction. Perovskite oxides (ABO_3) have a good performance in oxygen evolution reaction but poor in hydrogen evolution reaction. Iron (oxy)hydroxides (FeOOH) show good electrochemical performance in hydrogen evolution reaction but have low conductivity. Herein, we successfully synthesized the LaSrCoO/N-GQD/FeOOH composites via impregnation method and high energy ball-milling, which exhibited an efficient OER and HER performance with a lower overpotential of 300mV and 420mV at 10mA cm⁻². Also, composites have a lower Tafel slope value of 51mV dec⁻¹ compared with simple LaSrCoO@FeOOH composites. In the overall electrochemical water splitting system, the LaSrCoO/N-GQD/FeOOH showed excellent stability at 1 A cm⁻² over 100 h in full cell voltage. These LaSrCoO/N-GQD/FeOOH composites will provide the development of designing other electrocatalysts and give new way in boosting electron transfer induced by intermediate electron bridge materials.

4:15 PM EN07.05.10

Lattice Anion Redox in Perovskite Oxides under Oxygen Evolution Conditions Andrew Akbashev; Paul Scherrer Institute, Switzerland

Oxygen evolution reaction causes structural transformations and metal dissolution in most oxide electrocatalysts. In my talk, I will discuss how oxidative conditions cause intercalation of O²⁻ and can lead to the formation of oxidized oxygen inside the crystal lattice. Detection of anion oxidation is notoriously challenging and its unambiguous detection in electrocatalysts has been elusive so far. In our work, we used high-resolution resonant inelastic X-ray scattering (RIXS) to detect the oxidation state of oxygen in perovskites after OER, employing single-crystalline materials as model electrocatalysts. I will show that the emergence of oxidized oxygen depends on the transition metal and the amount of intercalation oxygen. In the end, I will discuss the possible relationship between lattice oxygen oxidation and the degradation of perovskite electrocatalysts during OER.

SESSION EN07.06: Poster Session II: Water Electrolysis

Session Chairs: Charles McCrory and Haotian Wang

Tuesday Afternoon, November 28, 2023

Hynes, Level 1, Hall A

8:00 PM EN07.06.01

Unveiling the Optimal Interfacial Synergy of Plasma-Modulated Tetrametallic Ni-Co-Mn-Fe Phosphide Electrocatalysts Synthesized by a Facile Electrodeposition Method for High-Performance Overall Water Splitting: DFT Study Menna M. Hasan¹, Aya K. Goma¹, Ghada Khedr² and Nageh K. Allam¹; ¹American University in Cairo, Egypt; ²Egyptian Petroleum Research Institute, Egypt

In the recent few decades, the demand for green sources of energy that are clean and sustainable became very essential to reduce the greenhouse and global warming problems. Consequently, there is an increasing demand to identify nonprecious, cheap bifunctional electrocatalysts for water splitting. Herein, nanosheets of different earth-abundant Ni, Co, Mn, and Fe combinations are electrodeposited over commercial Ti mesh and tested for the overall water splitting. The bare Ti mesh requires overpotentials of -486.6 mV at -10 mA cm⁻² and 534.5 mV at 10 mA cm⁻² for the hydrogen evolution reaction (HER) and oxygen evolution reaction (OER), respectively. However, the electrodeposited catalysts show much higher catalytic activity for both HER and OER with overpotentials of -300 and 279 mV at -10 and 10 mA cm⁻², respectively, lowering the overpotential needed to drive the OER by 50%. Nevertheless, to enhance the electrocatalytic performance of the fabricated catalysts, they are phosphidized using different phosphorous precursors. The resulted NiCoMnFe-P catalysts exhibit much lower HER overpotential (-200 mV at -10 mA cm⁻²), which is 40% lower than that needed by the bare Ti mesh. For the overall water splitting, a cell voltage of 1.71 V is recorded to achieve a current density of 10 mA cm⁻². Lastly, the stability test of the overall device reveals very high stability with current retention of 90% over 22 h of continuous electrolysis. Furthermore, the synergy between the metallic components in the absence and presence of P is elucidated using density functional theory calculations, revealing optimized GH* and GHd20* for the HER reaction over the P-top site of the MnFeCoNiP catalyst. In addition, the calculations explain the superiority of the NiCoMnFe catalyst over the NiCoMnFeP counterpart for the OER.

8:00 PM EN07.06.02

MOF Tessellation of Cation Defects-Rich 3D Bifunctional ORR/OER Electrocatalyst for Rechargeable Zinc-Air Batteries Gopalakrishnan Mohan and Soorathep Kheawhom; Chulalongkorn University, Thailand

A cost-effective bifunctional electrocatalyst for oxygen reduction reaction (ORR) and oxygen evolution reaction (OER) is essential for rechargeable zinc-air batteries (ZABs). Herein, we report porous nanorod-like NiFe@MOFs with tunable structures and multiple coordination modes showing fascinating architectures for the preparation of high-performance electrocatalysts. By tuning the structure and optimizing the Ni/Fe ratio, Fe₂O₃/Ni_{0.6}Fe_{2.4}O₄@NC having a large surface area, porosity, and abundant cation vacancies, is successfully developed. It shows excellent activities for both ORR (E_{1/2} = 0.856 V) and OER (η₁₀ = 1.54 V @ 10 mA cm⁻²). By using density functional theory (DFT) calculations, ORR and OER mechanistic pathways are studied. Furthermore, ZAB using Ni_{0.6}Fe_{2.4}O₄@NC catalyst demonstrates a high open circuit voltage (OCV) of 1.5 V, a peak power density of 187 mW cm⁻², and exceptional long-term cycling stability over 300 h (1800 cycles, 10 mA cm⁻²). The flexible solid-state ZAB using Ni_{0.6}Fe_{2.4}O₄@NC catalyst exhibits a power density of 66 mW cm⁻² and long-term durability over 43 h at 5 mA cm⁻². The proposed strategy allows for the rational design of cation defect-rich NiFe spinel structures attached to ultra-thin N-doped graphitic carbon sheets in order to enhance active site availability and facilitate mass and electron transport.

8:00 PM EN07.06.03

Evaluation of Activation Process for the Catalyst of Polymer Electrolyte Electrochemical Cell for Hydrogen Generation Tsuka Akita^{1,2}, Miyuki Nara², Kazuki Koike^{1,2}, Takayo Ogawa², Katsushi Fujii², Satoshi Wada² and Atsushi Ogura^{1,3}; ¹Meiji University, Japan; ²RIKEN RAP, Japan; ³MREL, Japan

Requirements for renewable energy are increasing to suppress global warming and to keep natural resources. Hydrogen by water electrolysis is useful as an energy storage way to realize the use of fluctuating renewable energy sources. Especially, polymer electrolyte electrochemical cell (PEEC) is attractive since it is a practical method for hydrogen production. The PEEC has a flexibility of scale adaptability for systems ranging from W- to kW-scale. The efficiency improvement of PEEC is an important issue to improve the energy system performance. To obtain the optimal performance of PEEC, activation is practically important, however, the mechanisms are still obscure. It is believed to bring the membrane and catalyst into specific conditions by activation.

In this study, we focused on the activation of PEEC with the cathode catalyst of Pt/C and the anode catalyst of IrOx. We investigated the activation processes by current density. The idea is based on the changes in the valency of iridium oxide. The oxygen evolution reaction (OER) is promoted by the valence change of iridium. Various valency change models have been proposed, but they were difficult to specify because the reaction takes place at the interface and is difficult to observe. Recently, the results of in-situ and ambient XPS, XAFS, and DFT simulations suggested that metastable iridium oxides with valences higher than tetravalent are the main contributors to OER [1]. It was also reported that the valency change of iridium oxides depends on the applied voltage.

In this study, the valency controls with the electron injection speed, that is, the current. The amounts of electrons were not the same, but the current was applied at the same time. That is, the activating currents (none, 0.1, 1.0, 10, 100 mA/cm², in this order) were applied for 1 hour to evaluate the activation. The evaluation method was the current value at 2.0 V when the voltage was swept with 10 mV/s from 1.45 V to 2.0 V and then a constant voltage of 2.0 V was applied for 5 minutes after the voltage change. After the measurement, sweeping from 2.0 V to 0.0 V

with 1 mV/s and maintaining 0.0 V for 30 min was performed as deactivation process.

The voltage changes during the activation processes were different. The voltage reached 1.27 V and increased continuously even after 1 hr when the activating current was 0.1 mA/cm². The voltage reached 1.46 V before 1 hr passed and kept the values when the other activating currents were applied. The current density-increasing rates were also similar for all cases.

The turn-on current densities were the same for all activation processes at voltage sweeping. However, the current density slopes were different, and the current densities at 2.0 V applied were 0.573, 0.575, 0.602, 0.597, and 0.592 A/cm² when the activation currents were none, 0.1, 1.0, 10, and 100 mA/cm², respectively.

The current density changes during the voltage kept at 2.0 V were similar for all cases and the current density slightly decreased with time, except for no activation process which the current density increased at the beginning.

The valency change of IrOx was reported to occur at around 0.9, 1.3, and 1.5 V as valency from 3+ to 4 to 4+, respectively [1]. The results show the valency change at around 1.5 V is important to activate the IrOx. The activation current of 0.1 mA/cm² was not enough for activation from this. Since the current density at the 2.0 V application decreases with the activation current over 1.0 mA/cm², the amount of the activation charge and/or the activation speed may be also important for the activation process.

[1] C. Bozal-Ginesta., et al., ACS Catal., 2021, 11, 15013.

8:00 PM EN07.06.04

Balancing Volmer Step by Dual-Active Domains for Enhanced Hydrogen Evolution[Jinsong Zhou](#)^{1,2}; ¹City University of Hong Kong, China; ²ETH Zürich, Switzerland

Renewable energy technologies, due to anthropogenic effects on finite fossil fuel resources and the environment, are pivotal to the sustainable development of society. Hydrogen with high energy density makes it a potential alternative energy source and could be electrocatalytic produced by carbon-free water splitting with the support of other intermittent renewable energies.

As a half-reaction to directly generate hydrogen in alkaline/neutral media, the reaction kinetics of hydrogen evolution reaction (HER) is primarily determined by balancing the Volmer step. Bifunctionality as a proposed strategy, providing two types of active sites that possess different reaction processes, divides the Volmer step ($\text{H}_2\text{O} + \text{e}^- \rightarrow \text{H}_{\text{ad}} + \text{OH}^-$, ad means adsorption) into water dissociation ($\text{H}_2\text{O} \rightarrow \text{OH}_{\text{ad}} + \text{H}^+ + \text{e}^-$) and intermediates adsorption/desorption ($\text{H}^+ + \text{e}^- \rightarrow \text{H}_{\text{ad}}$ and $\text{OH}_{\text{ad}} + \text{e}^- \rightarrow \text{OH}^-$). However, sluggish OH_{ad} desorption because of relatively strong binding energy plagues water re-adsorption, which leads to poisoning effects of active sites and limits the overall HER reaction rate. Also, some active sites may directly act as spectators and do not participate in the reaction. Designing two appropriate active sites to achieve a balanced state of each performing its functions isn't easy. Furthermore, the activity comparison under approximate nanostructure between bifunctionality and single-exposed dual-active sites is not fully illustrated.

A facile three-step synthesis strategy is adopted to form prominent dual-active domains successfully. The active sites on different domains and the tuned electronic structure at the heterointerface trigger the bifunctionality to balance the Volmer step and improve the catalytic activity. The HER driven by the bifunctionality could significantly optimize the Gibbs free energy of water dissociation and intermediates adsorption/desorption, resulting in fast reaction kinetics and superior catalytic performance compared with the single-exposed dual-active domain by purely electronic modulation.

8:00 PM EN07.06.05

3D Printed Pyrolysed Electrode Modified with Nickel and g-C₃N₄ for Hydrogen Evolution Reaction[Nadira Meethale Palakkool](#)¹, Mike Taverne¹, Kevin Chung-Che Huang², Vincent Barrioz¹, Yongtao Qu¹ and Ying-Lung Daniel Ho¹; ¹Northumbria University, United Kingdom; ²University of Southampton, United Kingdom

Hydrogen, derived from water electrolysis, has emerged as a promising alternative to fossil fuels, offering a clean and recyclable energy solution. However, despite its remarkable attributes, the widespread adoption of hydrogen faces significant challenges because of its viability as a practical solution. One of the major obstacles is the affordability of water electrolyser systems, which play a crucial role in the production of hydrogen through water electrolysis. Secondly, the sluggish kinetics of oxygen evolution reactions (OER) hinder the overall performance of the water electrolysis.

Herein, we propose the fabrication of a free-standing 3D electrode based on stereolithography 3D printing of polymer which can be functionalized via a series of post-processing treatments using non-noble metal-based materials. By subjecting the 3D polymer to a thermal decomposition process via vacuum furnace annealing, we were able to transform it into a conductive and stable electrode material. To enhance the electrochemical performance of the electrodes, post-processing involves nickel electroplating followed by chemical vapour deposition (CVD) of graphitic carbon nitride (g-C₃N₄), derived from melamine. These steps aimed at exploring the potential of further improving the conductivity and catalytic properties of the 3D electrodes. Different diamond lattice-based crystal structures such as tapsterite, rod-connected diamond (RCD) and F-rhombic dodecahedron (FRD) are investigated providing controllability over the electrode surface area and geometries. These geometries are inspired by the atomic arrangement of tapsterite, diamond-like crystals with interconnected rod-based structures, offering unique topological features for electrode design. Moreover, these structures provide a larger surface area, facilitating gas diffusion rate and thereby improving electrocatalytic water splitting. Cyclic voltammetry measurements were conducted in alkaline electrolytes to evaluate the electrochemical behaviour of the 3D graphitic electrode. The CV curve exhibits a smooth and continuous shape without significant sharp peaks or irregularities. The current response shows gradual changes as the potential is scanned within the chosen range. One notable observation from the CV analysis is the increased area under the curve after post-processing of the electrode. This expanded area indicates improved electrochemical performance and suggests an enhanced active surface area of the electrode. To gain insights into the surface morphology and elemental composition of our sample, we performed scanning electron microscopy (SEM) and energy-dispersive X-ray spectroscopy (EDS) analysis. The rate of thermal decomposition was found to affect the morphology of the pyrolyzed carbon.

Furthermore, the EDS spectra of post-processed electrodes indicated the presence of nickel and nitrogen when compared to the pre-processed carbon electrode. The detection of nickel suggests successful electroplating, while the presence of nitrogen indicates the incorporation of carbon nitride during CVD steps. Owing to the low composition of nickel in the electrode, the electroplating process will be further optimized to enhance the deposition and improve their composition for desired electrochemical performance.

Further, this work explores the electrochemical performance of the 3D electrode via electrochemical measurements using rotating disk electrodes. Furthermore, the material will be characterized using X-ray diffraction spectroscopy (XRD) and X-ray photoelectron spectroscopy (XPS). In conclusion, this work aims at leveraging the capabilities of 3D printing technology and enhancing the commercial viability of hydrogen-generating systems using earthy abundant materials.

8:00 PM EN07.06.06

Structure-Activity Elucidation of Stainless Steel Waste Meshes as Efficient Oxygen Evolution Catalysts[Nageh K. Allam](#); American University in Cairo, Egypt

Herein, the ability to convert waste stainless steel (SS) 316L meshes into highly efficient and durable oxygen evolution reaction (OER) catalysts is demonstrated. The process involves surface treatment of previously anodized SS meshes in different gaseous atmospheres. The activity of the resulted electrocatalysts varies as-anodized SS annealed in oxygen (ASS-O₂) > anodized SS annealed in hydrogen (ASS-H₂) > anodized SS annealed in air (ASS-Air). The ASS-O₂ showed an impressive low overpotential of 280 mV at the benchmark current density of 10 mA/cm², which is 120 mV less than that of the as-received SS (SS-AR), and a low Tafel slope of 63 mV dec⁻¹ in 1 M KOH. These findings have also been asserted by the estimated electrochemical active surface area, electrochemical impedance spectroscopy analysis, Mott-Schottky analysis, and the calculated turnover frequency, affirming the superiority of the ASS-O₂ electrocatalyst over the ASS-H₂ and ASS-Air counterparts. The high activity of the ASS-O₂ electrocatalyst can be ascribed to the surface composition that is rich in Fe³⁺ and Ni²⁺ as revealed by the X-ray photoelectron spectroscopy analysis. The simple method of anodization and thermal annealing in O₂ at moderate conditions (450 °C for 1 h) lead to the formation of a SS mesh-based OER electrocatalyst with activity exceeding that of the state-of-the-art IrO₂/RuO₂ and other complex modified SS catalysts. These results were also confirmed via density functional theory calculations, which unveiled the OER reaction mechanism and elucidated the d-band center in different SS samples with different oxygen content. The presence of oxygen moved the d-band center closer to the Fermi level in the case of ASS-O₂, explaining its superior activity.

8:00 PM EN07.06.07

Fabrication and Characterization of Ag/TiO₂ Composite Photoanode for Photoelectrochemical Water Splitting Application[Yaowapa Treekamol](#) and Rewat Maensiri; Khon Kaen University, Thailand

The purpose of this work is to investigate photoelectrochemical performance of composite electrode between titanium dioxide (TiO₂) and silver nanoparticles (AgNPs). AgNPs were employed due to a surface plasmon resonance effect that can improve visible light absorption and decrease electron-hole recombination of TiO₂. Preparation of Ag/TiO₂ composite electrode with different amount of AgNPs

from 20, 40, 60, 80 and 100 ppm were carried out by ball milling process. After that, characterization by XRD, Raman, UV-Vis, SEM, EDX and FTIR technique were examined. The crystallinity and phase purity of bare TiO₂ and Ag/TiO₂ were

characterized by XRD and Raman analyses, which confirm the rutile phase and presence of AgNPs on surface of TiO₂, respectively. FTIR spectra result confirmed the presence functional group and interaction of AgNPs on surface of TiO₂. SEM images show that the distributed and particles size of bare TiO₂ and Ag/TiO₂ nanoparticles in the range of 20-30 nm. The elemental composition of Ag/TiO₂ was detected by EDX analysis that confirms the presence of oxygen, silver and titanium, respectively. The UV-Vis absorption spectra of AgNPs shows an absorption peak at 400 nm. Finally, photoelectrochemical performance were performed using cyclic voltammetry measurement. CV curves showed a current density at 1.23 V (vs. Ag/AgCl) for TiO₂ and Ag/TiO₂ electrode which are 1.15 and 1.83 μA/cm². It can be

concluded that an addition of AgNPs resulted in better photocurrent which related to higher photoelectrochemical performance in water splitting for hydrogen production.

8:00 PM EN07.06.08

Role of Nucleation Growth Reaction Parameters of 2D-MoS₂ Towards HER ApplicationRameshAvala and SukantiBehera; Maulana Azad National Institute of Technology Bhopal, India

Transition metal dichalcogenides (TMDs) are a family of two-dimensional (2D) materials and MoS₂ has been used for electrical and electrocatalytic properties. Here we report the synthesis of powder molybdenum disulphide (MoS₂) by using wet-chemical method with varied reaction duration time (0, 2, 4, 6, 8 days) from each filtration, and towards hydrogen evolution reaction (HER). Powder 2D-MoS₂ was obtained by using ammonium heptamolybdate (NH₄)₆Mo₇O₂₄·4H₂O and thiourea (N₂H₄CS) as precursors and (N₂H₄) as a catalyst in the presence of basic media (pH=10). The single phase of MoS₂ was confirmed by operating the powder X-ray diffraction method. The major peak 2 value at 13.8 indexed as (002) plane. Also, Raman spectra (E_{1g} = 379 cm⁻¹ & A_{1g} = 404 cm⁻¹) including extra peaks which is J₁, J₂, E_{1g}, and J₃ indicates both 1T/2H-MoS₂ phases. Spherical shape of morphological studies were characterized by scanning electron microscopy (SEM) & transition electron microscopy (TEM). The results of the electrocatalytic Hydrogen evolution reaction (HER) confirm that 1T/2H-MoS₂ synthesized with varied reaction parameters exhibit high efficiency with instant filtered material (0 days) compared to longer duration time.

8:00 PM EN07.06.09

RuO₂ Supported on the PdPb Multi-Frame for Enhanced Electrocatalytic Performance for Oxygen Evolution Reaction in Acidic MediaDoyeopKim and KwangyeolLee; Korea University, Korea (the Democratic People's Republic of)

Electrochemical water splitting offers a promising carbon-free method for hydrogen production, which can greatly reduce reliance on fossil fuels. However, one major challenge in enhancing the efficiency of this process depends on the sluggish kinetics of the oxygen evolution reaction (OER). Existing catalysts based on Ru nanoparticles show remarkable activity for acidic OER but are susceptible to dissolution in acidic conditions, limiting their stability. We have developed a novel approach to synthesizing RuO₂ catalysts supported by PdPb multi-frames to address this issue. This involved a seed-mediated growth method followed by thermal oxidation, stabilizing the Ru-based nanocatalyst. Through temperature control of thermal oxidation, it is possible to adjust the degree of doping of Pd into RuO₂, and the presence of Pd doped in RuO₂ prevents overoxidation, leading to exceptional catalytic activity and remarkable stability for the acidic OER. This study suggests an ideal synthesis method for efficiently introducing dopants into RuO₂-based catalysts while also providing a new understanding of catalyst development with improved performance in acidic conditions for the OER.

8:00 PM EN07.06.10

Block Copolymer Mediated Synthesis of TiO₂/RuO₂ Nanocomposite for Efficient Hydrogen and Oxygen GenerationBinodR. K. C and BishnuBastakoti; NC A&T State University, United States

Abstract: Ruthenium oxide (RuO₂) is one of the most effective electrocatalysts reported for oxygen evolution reaction (OER) but still has insufficient stability for practical water splitting. To solve this problem, herein we report the fabrication of TiO₂/RuO₂ nanocomposite by sol-gel method. An amphiphilic block copolymer, poly (styrene-polyvinyl pyridine-ethylene oxide) was used as structure directing and stabilizing agent. The strong interaction of polymer with metal precursors led to the formation of a heterointerface for synergetic effect and acts as a bridge for the electron transport which can accelerate the water splitting reaction. Scanning electron microscopy, energy dispersive X-ray spectroscopy, transmission electron microscopy, and X-ray diffraction analysis of prepared TiO₂/RuO₂ sample revealed successful fabrication of TiO₂/RuO₂ nanocomposite. The electrochemical water splitting properties of prepared sample were measured by three electrode system in 0.1M KOH electrolyte which showed improved electrochemical properties of prepared sample.

This work was primarily supported by a DOE EFRC on The Center for Electrochemical Dynamics And Reactions on Surfaces (CEDARS) via grant # DE-SC0023415.

8:00 PM EN07.06.11

Heterostructured Ternary Transition Metal Oxide Composite as an Efficient Electrocatalyst for Improved Hydrogen GenerationSooHongLee, MinKyeongKim and JohnHong; Kookmin University, Korea (the Republic of)

As the use of fossil fuels increases, there is growing concern about energy and environmental crises. Therefore, there is a significant demand for environmentally friendly and sustainable energy resources to replace them. Hydrogen is attracting attention as an energy resource that can replace fossil fuels because it is carbon-neutral and can achieve high energy generation efficiency through fuel cells. The most important topic related to hydrogen energy is how we can generate green hydrogen. One of the promising candidates for green hydrogen is water electrolysis, which involves both the oxygen evolution reaction (OER) and the hydrogen evolution reaction (HER). In practical water electrolysis, it is important to reduce over-potential and improve Tafel kinetics using efficient electrode catalysts. However, the most promising catalysts for water splitting, such as Pt, Ru, and Ir, are not abundant and have high costs. Therefore, finding a new noble metal catalysts that exhibit high reactivity, low cost, and long-term durability is important.

In this study, a highly efficient hydrogen generation catalyst with unique heterostructures was synthesized by utilizing three different transition metal composites through hydrothermal synthesis on a Ni-based substrate. Specifically, ternary transition metal oxides (TTMO) consisting of Ni, Fe, and Co were synthesized as the final catalyst product. According to the suggested electrode material, the synergistic contribution between these ternary transition metal atoms can lower the over-potential, increase the Tafel kinetics, and improve the long-term stability of the water-splitting system. The TTMO composites exhibit much better hydrogen evolution reaction (HER) performance than binary transition metal oxide composites, delivering current densities of approximately 10 and 100 mA cm⁻² at low over-potentials of 43 mV and 86 mV, respectively, compared to 51 mV and 93 mV for binary transition metal oxide composites. Also, the TTMO composites show a Tafel slope of 33.54 mV dec⁻¹. Finally, the TTMO composite can result in long-term catalytic stability over 5,000 cycles at the high current density of 100 mA cm⁻² with negligible over-potential degradation. The excellent performance of the proposed TTMO composites is attributed to their unique heterostructures and the newly designed ternary transition metal surface sites (balanced-hybridized sites). These findings provide insight into the utilization of ternary transition metal composites for HER and other catalysis applications.

8:00 PM EN07.06.12

Oxygen Evolution Reaction Properties of the Tetragonal Structure-Based Transition Metal OxidesSung RyuChoi, SeojeongYoo and Jun-YoungPark; Sejong University, Korea (the Republic of)

ABSTRACT

The increasing share of renewable energy in overall energy production has emphasized the urgent necessity for the development of advanced energy storage and conversion technologies by using power-to-gas (P2G) technology. P2G technology involves the electrolysis of water to generate hydrogen using excess electricity derived from solar or wind power [1]. Additionally, it aims to address the technical challenges associated with intermittency power generations of renewable energy sources [1]. Among the available various P2G technologies, alkaline water electrolysis (AWE) is currently the most technically mature energy storage and conversion electrochemical device [2].

Despite its technical maturity, the commercialization of AWE technology faces a significant obstacle in the form of low energy conversion efficiency [3]. The primary reason behind this low energy efficiency in AWEs is the sluggish kinetics of the oxygen evolution reaction (OER) in the anode [4]. Although anode catalysts such as ruthenium and iridium have shown excellent OER activity, their practical application is hindered by their high cost due to scarcity and poor durability [5].

In contrast, transition metal oxides based on spinel, perovskite, and Ruddlesden-Popper structures have garnered considerable attention due to their exceptional OER activity and long-term durability, while being relatively more affordable [6-9]. Recently, Swedenborgite materials with a layered structure composed of triangular and Kagome layers arranged along the c-axis have received interest because of their high OER activity in the application of high-temperature solid-oxide cells [10-12]. In this study, we investigate the OER properties of the tetrahedral-structured Swedenborgite material, including its fundamental structure characteristics, the impact of transition metal doping, and the underlying OER mechanism.

References

- [1] M.S. Ahmad, M.S. Ali, N. Abd Rahim, *Energy Strategy Rev.*, 35 (2021) 100632.
- [2] J. Wang, Y. Gao, H. Kong, J. Kim, S. Choi, F. Ciucci, Y. Hao, S. Yang, Z. Shao, J. Lim, *Chem. Soc. Rev.*, 49 (2020) 9154-9196.
- [3] P. Thangavel, M. Ha, S. Kumaraguru, A. Meena, A.N. Singh, A.M. Harzandi, K.S. Kim, *Energy Environ. Sci.*, 13 (2020) 3447-3458.
- [4] S. Drespp, T.N. Thanh, M. Klingenhof, S. Brückner, P. Hauke, P. Strasser, *Energy Environ. Sci.*, 13 (2020) 1725-1729.
- [5] X. Wu, B. Feng, W. Li, Y. Niu, Y. Yu, S. Lu, C. Zhong, P. Liu, Z. Tian, L. Chen, *Nano Energy*, 62 (2019) 117-126.
- [6] F. Song, L. Bai, A. Moysiadou, S. Lee, C. Hu, L. Liardet, X. Hu, *J. Am. Chem. Soc.*, 140 (2018) 7748-7759.
- [7] P.P. Lopes, D.Y. Chung, X. Rui, H. Zheng, H. He, P. Farinazzo Bergamo Dias Martins, D. Strmcnik, V.R. Stamenkovic, P. Zapol, J. Mitchell, *J. Am. Chem. Soc.*, 143 (2021) 2741-2750.
- [8] Y. Zhou, S. Sun, C. Wei, Y. Sun, P. Xi, Z. Feng, Z.J. Xu, *Adv. Mater.*, 31 (2019) 1902509.
- [9] S.R. Choi, J.-I. Lee, H. Park, S.W. Lee, D.Y. Kim, W.Y. An, J.H. Kim, J. Kim, H.-S. Cho, J.-Y. Park, *Chem. Eng. J.*, 409 (2021) 128226.
- [10] M.A. Kirsanova, V.D. Okatenko, D.A. Aksyonov, R.P. Forslund, J.T. Mefford, K.J. Stevenson, A.M. Abakumov, Bifunctional OER/ORR catalytic activity in the tetrahedral YBaCo₄O_{7.3} oxide, *J. Mater. Chem.*, 7 (2019) 330-341.

[11] Y. Chen, J.K. Seo, Y. Sun, T.A. Wynn, M. Olguin, M. Zhang, J. Wang, S. Xi, Y. Du, K. Yuan, Enhanced oxygen evolution over dual corner-shared cobalt tetrahedra, *Nat. Commun.*, 13 (2022) 5510.

[12] J.-S. Shin, H. Park, K. Park, M. Saqib, M. Jo, J.H. Kim, H.-T. Lim, M. Kim, J. Kim, J.-Y. Park, *J. Mater. Chem.*, 9 (2021) 607-621.

* Corresponding author: jyoung@sejong.ac.kr (J. Y. Park)

Keywords: Oxygen evolution reaction, Alkaline electrolysis, Transition metal oxides, Tetragonal structure

8:00 PM EN07.06.13

Intermolecular Electron Transfer in Electrochemically Exfoliated BCN-Cu Nanosheet Electrocatalysts for Efficient Hydrogen Evolution Menna M. Hasan, Ghada Khedr, Nageh K. Allam and Fatma Zakaria; American University In Cairo, Egypt

The search for materials with superior electrocatalytic performance has attracted attention during the past few years aiming to identify a convenient material that works at a low overpotential with long-term stability. Herein, we introduce an innovative technique to fabricate two-dimensional BCN heterostructure nanosheets with various Cu:BCN weight ratios. The fabricated composites showed unique electrocatalytic properties for hydrogen evolution reaction (HER). The morphology and structure of the electrocatalysts were characterized using field emission scanning electron microscopy, Raman, Fourier transform infrared spectroscopy, and X-ray photoelectron spectroscopy techniques. Remarkably, this study reveals the effect of electrochemical chronopotentiometry on facilitating the electrochemical exfoliation and hence enhancing the catalytic activity of the fabricated nanosheets. This effect was further confirmed via density functional theory (DFT) calculations, unveiling the effect of the formed oxide layer on the charge transfer process. The overpotential of the 0.125 Cu-BCN composite at a current density of -10 mA/cm² vs RHE is 50% lower than that of pristine BCN. These findings were also affirmed by the DFT calculations, which showed that incorporating copper on BCN has significantly reduced the GH* value of the HER and subsequently accelerates the kinetics of the reaction and the overall catalytic activity of the material. <div> </div>

8:00 PM EN07.06.14

Synthesis of Two-Dimensional Tantalum Carbo-Selenide and their Electrochemical Performance for Hydrogen Production Elham Loni¹, Ahmad Majed¹, Chaochao Dun², Karamullah Eisawi¹, Anika Tabassum³ and Michael Naguib¹; ¹Tulane University, United States; ²Lawrence Berkeley National Laboratory, United States; ³University of the District of Columbia, United States

Two-dimensional transition metal carbo-chalcogenides (TMCCs) consist of early transition metal carbide core and chalcogen surface (e.g., S, Se, and/or Te). They are promising candidates for energy storage applications, such as ion batteries, supercapacitors, and water-splitting applications since they can have both properties of carbides and chalcogenides, such as electrical conductivity and catalytically active, respectively. In this work, we report on the synthesis of two-dimensional Ta₂Se₂C (2D-Ta₂Se₂C) through the electrochemical intercalation to introduce lithium into multilayer (m-Ta₂Se₂C), followed by sonication in deionized water. The m-Ta₂Se₂C material was obtained through a solid-state synthesis of Fe_xTa₂Se₂C, followed by a chemical etching process. The electrocatalytic performance of 2D-Ta₂Se₂C was found to be significantly superior to that of both multilayer Ta₂Se₂C and 2D-TaSe₂ when utilized as an electrocatalyst for the hydrogen evolution reaction. Notably, 2D-Ta₂Se₂C displayed an overpotential at 10 mA cm⁻² of 260 mV, a Tafel slope of 91.4 mV.dec⁻¹, and an electrochemically active surface area of 780 cm².g⁻¹. These enhancements can be attributed to the extensive surface area of individual nanosheets, which maximizes the availability of catalytic sites, as well as the more open structure of Ta₂Se₂C in contrast to TaSe₂.

8:00 PM EN07.06.16

Investigating Synthesis Route Effect on the Electrochemical Performance of LiNi_{0.6}Co_{0.2}Mn_{0.2}O₂ Cathode Materials for Li-Ion Battery Mesfin A. Kebede¹, Emmanuel Mannzhi² and Rebecca Mhlongo²; ¹University of South Africa - Science Campus, South Africa; ²Sefako Makgatho Health Science University, South Africa

In this work Ni-rich LiNi_{0.6}Co_{0.2}Mn_{0.2}O₂ (NCM622) cathode materials were synthesized via combustion and sol-gel routes, to investigate the effect of synthesis route on the electrochemistry of the cathodes. The structural and electrochemical properties of the samples were confirmed by XRD, SEM, TEM and battery testing. The electrochemical properties of layered Ni-rich NCM622 cathode materials synthesized adopting these two synthesis routes were compared. The results confirm that the NCM622 cathode samples prepared by combustion synthesis route exhibited a better electrochemical performance than the samples synthesized by sol-gel method for the cycling stability and rate capability. The NCM622-Com delivered a first capacity of 206 mAh g⁻¹ and retained 132 mAh g⁻¹ after 100 cycles, whereas NCM622-Sol delivers only 141 mAh g⁻¹ and retained 115 mAh g⁻¹ after 100 cycles. Similarly, for the rate capability the NCM622-Com performed higher for all the current rates.

In this work, we are presenting the comparison of the sol-gel and combustion synthesis routes on the electrochemical performance of Ni-rich LiNi_{0.6}Mn_{0.2}Co_{0.2}O₂ cathode materials. The detail structural, morphological, cyclic voltammetry, and galvanostatic charge/discharge capacity results will be discussed.

8:00 PM EN07.06.17

Understanding of Growth and Electrolytic Hydrogen Evolution of Directly Deposited 2D NiO Electrodes via Alkali-free Chemical Synthesis Umesh T. Nakate¹, Jeongsik Choi², Dong-Won Kim^{1,3} and Sungjune Park³; ¹Hanyang University, Korea (the Republic of); ²Jeonbuk National University, Korea (the Republic of); ³Sungkyunkwan University, Korea (the Republic of)

Nanostructured metal oxides have been identified as potential candidates for electrochemical applications owing to their various properties such as high surface-to-volume ratio, number of active sites/ receptor functions, re-dox properties, thermal stability, semiconducting nature, structural properties, etc. The nano size (dimensions) has a significant impact on the physicochemical properties of metal oxide *via* its quantum effect. However, structural properties like growth, orientation, texture co-efficient, and defects also govern the performance of the material. The synthesis/preparation conditions primarily decide the nano size as well as the structural properties of the material. Hence, it is quite crucial to develop novel and unique synthesis routes to reveal the enhanced properties of the materials. Reducing the use of additional reactants and reagents/surfactants in synthesis could be advantageous in terms of synthesis cost reduction, unwanted impurities, crystal purity, repeatable output, growth simplicity, etc.

Herein, an alkali/buffer-free easy chemical hydrothermal route has been adopted to grow 2D NiO nanoplates electrodes. The synthesis parameters *viz* concentration and temperature could tune the thickness of the nanoplates leading to changes in structural and electrocatalytic properties. The electrochemical characteristics *viz* linear scan voltammetry (LSV), Tafel, Electrochemical impedance spectroscopy (EIS) Nyquist plot, cyclic voltammetry and chronopotentiometry, turnover frequency (ToF), Electrochemical surface area (ECSA), etc were investigated for prepared electrocatalyst electrodes. The electrocatalysts were characterized using XRD, FESEM, HR-TEM, EDS, mapping, XPS, etc standard tools. The different noble metal (Pd/Au/Ag/ Ru) decoration on the optimized 2D NiO electrodes was carried out *via* a wet impregnation technique and their electrolytic hydrogen evolution performance was studied. The Pd-decorated NiO electrodes were observed to have high hydrogen evolution performance. The different amounts of Pd decoration on NiO were performed and optimal Pd-NiO electrocatalyst was studied in detail. The optimal Pd-NiO electrodes exhibited a high HER activity with an overpotential of 90 mV, achieving a current density of 100 mA cm⁻² and a Tafel slope of 52.05 mVdec⁻¹ in 1 M KOH solution.

Further, the density functional theory (DFT) studies were carried out *via* first principle calculation to support the experimental results. The Pd/NiO exhibited a lower water dissociation energy barrier (0.35 eV) than NiO (0.46 eV), suggesting that the dissociation of H₂O easily occurs on the surface of the Pd/NiO catalyst. The formation of Pd/NiO heterojunction improves the HER activity. The change in Gibbs free energy of Pd/NiO heterostructures is about -0.52 eV, which is lower than pristine NiO (-0.78 eV). The experimental and theoretical analyses are in good agreement.

The present synthesis technique and architecture of Pd decorated NiO nanoplates is a promising strategy and could be the potential candidate for fulfilling sustainable energy needs *via* high-performance hydrogen evolution reaction.

SESSION EN07.07: CO₂/NO_x Reductions I
Session Chairs: Maria Escudero-Escribano and Charles McCrory
Wednesday Morning, November 29, 2023
Hynes, Level 3, Room 310

8:15 AM EN07.07.01

Insights into Interfacial Phenomena Driving Fast Carbon Isotopes Separation during CO₂ Electroreduction Magda H. Barecka¹, Mikhail Kovalev², Marsha Zakir Muhamad², Hangjuan Ren^{2,3}, Joel W. Ager^{4,5,6} and Alexei Lapkin²; ¹Northeastern University, United States; ²Cambridge Centre for Advanced Research and Education in Singapore, Singapore; ³University of Oxford, United Kingdom; ⁴Lawrence Berkeley National Laboratory, United States; ⁵University of California, Berkeley, United States; ⁶Berkeley Education Alliance for Research in Singapore, Singapore

Isotopes of carbon and kinetic effects related to the reactivity of carbon 12 vs carbon 13 have been widely explored to elucidate reaction mechanisms and metabolic pathways. We discovered that under the conditions of carbon dioxide (CO₂) electroreduction in gas-diffusion electrodes, the kinetic isotope effect is much higher than expected based on known carbon kinetic isotope effect during CO₂ absorption in oceans or photosynthetic conversion of CO₂ to reduced forms of carbon. Our experiments demonstrate that CO₂ electroreduction strongly favors the conversion of the dominant isotope of carbon (¹²C) and discriminates against the less abundant, stable carbon ¹³C isotope during all steps of the electrochemical process, and mostly at the triple phase interface created in gas-diffusion electrode based reactors. Using a natural abundance CO₂ feed, we experimentally demonstrate enriching of the ¹³C fraction to ~1.3% (+18%) in a single pass reactor, being an unprecedentedly fast isotope separation. This talk will provide insights into the interfacial phenomena, being a part of a complex isotope discrimination mechanism, which we anticipate to be applicable across a wide range of electrochemical systems.

8:30 AM EN07.07.02

Influence of the Gas Diffusion Layer on the Reaction Microenvironment of Electrochemical CO₂ Reduction Surani BinDolmanan¹, AnnetteBoehme^{2,2}, ZitingFan³, HarryA. Atwater^{2,2} and YanweiLum^{1,3}; ¹Agency for Science, Technology and Research, Singapore; ²California Institute of Technology, United States; ³National University of Singapore, Singapore

Gas diffusion layers (GDL) have become a critical component in electrochemical CO₂ reduction (CO₂R) systems because they can enable high current densities needed for industrially relevant productivity. Besides this function, it is often assumed that the choice of catalyst and electrolyte play much more important roles than the GDL in influencing the observed product selectivity. Here, we show that tuning of the GDL pore size can be used to control the local microenvironment of the catalyst and hence, effect significant changes in catalytic outcomes. This concept is demonstrated using sputtered Ag films on hydrophobic PTFE substrates with 6 different pore sizes. Although Ag is known to be a predominantly CO generating catalyst, we find that smaller pore sizes favor the generation of formate up to a faradaic efficiency of 43%. Combined experimental and simulation results show that this is due to the influence of the pore size on CO₂ mass transport, which alters the local pH at the electrode, resulting in reaction pathway switching between CO and formate. Our results highlight the importance of the local microenvironment as an experimental knob that can be rationally tuned for controlling product selectivity: a key consideration in the design of CO₂R systems.

8:45 AM EN07.07.03

Boosting Selectivity Toward Formate Production using CuAl Nanowires by Altering the CO₂ Reduction Reaction Pathway IbrahimM. Badawy and NagehK. Allam; American University in Cairo, Egypt

Understanding the fundamentals behind an electrocatalyst's selectivity enables the ability to steer product formation. Herein, Cu nanowires were doped with Al (12%) for CO₂R. Al doping was found to enhance formate production by 16.9% over pure Cu nanowires. The DFT calculations ascribed the enhancement in the CO₂R performance to the change in the adsorption energy of the intermediates and thus the favorability of the reaction path involving the CO₂ adsorbing through its oxygen terminals. The CO₂R experiments supported that conclusion when CuNW was discovered to produce higher Faradic Efficiency (FE) C₂H₄ than CuAlNW meaning that C-C dimerization is less supported on CuAl NW's surface.

9:00 AM EN07.07.04

Recovering Carbon Losses in CO₂ Electrolysis using a Solid Electrolyte Reactor PengZhu and HaotianWang; Rice University, United States

The practical implementation of electrochemical CO₂ reduction technology is greatly challenged by notable CO₂ crossover to the anode side, where the crossed-over CO₂ is mixed with O₂, via interfacial carbonate formation in traditional CO₂ electrolyzers. Here we report a porous solid electrolyte reactor strategy to efficiently recover these carbon losses. By creating a permeable and ion-conducting sulfonated polymer electrolyte between cathode and anode as a buffer layer, the crossover carbonate can combine with protons generated from the anode to re-form CO₂ gas for reuse without mixing with anodic O₂. Using a silver nanowire catalyst for CO₂ reduction to CO, we demonstrated up to 90% recovery of the crossover CO₂ in an ultrahigh gas purity form (>99%), while delivering over 90% CO Faradaic efficiency under a 200 mA cm⁻² current. A high continuous CO₂ conversion efficiency of over 90% was achieved by recycling the recovered CO₂ to the CO₂ input stream.

9:15 AM EN07.07.05

Time Course of Product Selectivity by Ag Nanoparticle Modification on Metal Cathode Electrodes for Electrochemical CO₂ Reduction KazukiKoike^{1,2}, TakeharuMurakami², TakayoOgawa², KatsushiFujii², SatoshiWada² and AtsushiOgura^{1,3}; ¹Meiji University, Japan; ²RIKEN RAP, Japan; ³MREL, Japan

Global warming is a major issue in modern society. The most significant cause of global warming is the increase in the concentration of carbon dioxide in the atmosphere. One of the technologies to reduce the concentration of carbon dioxide in the atmosphere is carbon dioxide reduction. Carbon dioxide reduction is a technology that uses electrical energy to electrochemically reduce carbon dioxide to formic acid, methane, ethylene, ethanol, and other substances. Current problems with electrochemical carbon dioxide reduction include the lack of product selection and the inability to operate for long periods of time. It is known that the selectivity of products varies with the material used for the CO₂-reduced cathode electrode and the cathode potential during the reaction. Especially for the electrode material, the metal type and crystal surface affect the products. The copper cathode has attracted much because of its high efficiency in generating ethylene, which is an industrially useful substance such as a raw material for plastics. However, the products have not yet been fully controlled. In addition, there is a problem in that the surface of copper changes after prolonged operation, making it decrease the ethylene reduction efficiently.

It is known that CO is produced as an intermediate product in the reaction process of CO₂ to ethylene. Therefore, spray coating the Cu electrode with Ag, which reduces CO₂ to CO well, is expected to improve the CO₂ reduction capability. The Ag nanoparticles were sprayed on the Cu electrode surface using a spray coating machine to modify the electrodes in this report. The evaluations were performed with electrochemical cyclic voltammetry and chronopotentiometry. The reduced products were evaluated by gas chromatography. The surface condition of the electrode before and after the reaction was also evaluated.

It was found that the metal cathode electrode modified with Ag nanoparticles improved the CO₂ reduction ability to ethylene compared with the bare Cu metal electrode. It was also confirmed that the potential during the reaction was stabilized by modification with Ag nanoparticles. The surface evaluation results showed that the surface showed dispersed Ag nanoparticles on the metal surface, and it has the possibility of the improvement of CO₂ reduction.

9:30 AM *EN07.07.06

Reactive Separations using a Cobalt Macrocyclic Molecular Catalyst for Electrochemical Wastewater Refining of Nitrate to Ammonia WilliamTarpeh; Stanford University, United States

Enabling a sustainable food-energy-water nexus requires feeding a growing population while minimizing environmental impacts. Molecular catalysis of aqueous electrochemical nitrate reduction (NO₃RR) to ammonia can simultaneously reduce nitrogen pollution and electrify ammonia manufacturing. We focus on in this talk on Co(DIM), where DIM = 2,3-dimethyl-1,4,8,11-tetraazacyclotetradeca-1,3-diene, because it is the only water-soluble catalyst that has been reported to yield ammonia from NO₃RR with near full selectivity (> 95%). A dearth of experimental investigations prevents the rational design and implementation of NO₃RR molecular platforms such as Co(DIM). From an electroanalysis standpoint, kinetic benchmarking of Co(DIM)-mediated NO₃RR would contextualize the performance of Co(DIM) relative to state-of-the-art molecular electrocatalysts and quantitatively facilitate optimization goals for next-generation NO₃RR molecular catalysts. Molecular catalysts remain underutilized in electrochemical water treatment because they require separation of catalyst, wastewater, and product.

In this talk, we cover three main areas related to the development and characterization of Co(DIM). First, we describe its integration into electrochemical stripping as a reactive separation configuration that facilitates energy-efficient ammonia recovery. Second, we interrogate the stability of Co(DIM) in real wastewaters and describe electrocatalyst-in-a-box as a novel reactor design that enables catalyst reuse and continuous ammonia recovery. Finally, we elucidate the mechanism of Co(DIM) activation and catalysis to guide rational design of reactive separations, including catalyst immobilization. Together, these results will guide the rational design of molecular catalysts and reactive separations to valorize wastewater nitrate to ammonia and other products.

10:00 AM BREAK

10:30 AM *EN07.07.07

Compositional Control of Multidimensional Metal Sulfide Electrocatalysts to Drive CO₂ and CO Reduction to Alcohols JesusM. Velazquez; University of California, Davis, United States

The dichotomy of increasing energy demands and carbon emissions is imperative in energy-related research efforts that demand the development of new materials capable of addressing these concerns. An emerging technical avenue in this area is the conversion of vastly abundant renewable energy sources that can be harnessed and directed towards the synthesis of traditionally fossil fuel-based products from atmospheric feedstocks like CO₂. To this end, our work establishes structure—function relationships for materials within the versatile classes of MX₂ (M = Mo, W; X = S, Se) and Chevrel-Phase (CP) M₃Mo₆X₈ (M = alkali, alkaline, transition or post-transition metal; y = 0-4; X = S, Se, Te) chalcogenides. The molybdenum sulfide structures from both families exhibit exceptional promise as CO₂R catalysts which can be accessed through synthesis techniques, such as hydrothermal or solid-state methods, that allow for control over the composition of these materials. Additionally, the use of membrane electrode assemblies (MEA) with molybdenum sulfide structures can maximize CO₂ interactions with the catalyst leading to

improved efficiencies toward selective alcohol production. Furthermore, CP catalyst framework is selective towards the electrochemical reduction of CO₂ and CO to methanol (only major liquid-phase product) under applied potentials as mild as -0.4 V vs RHE. This reactivity toward the electrochemical reduction of CO₂ and CO to methanol is correlated with an increased population of chalcogen states, as confirmed via X-Ray Absorption Spectroscopy. Overall, this work seeks to unravel optimally reactive novel small-molecule reduction catalyst compositions.

11:00 AM EN07.07.08

Electrochemical Reduction of Carbon Dioxide: Investigating Tunable Porosity and Surface Morphology in PFPE Gas Diffusion Layers for Enhanced Ethylene SelectivityEric A. Krall, Maxwell Goldman, Xiaoxing Xia, Andrew Wong and Sarah Baker; Lawrence Livermore National Laboratory, United States

The electrochemical reduction of carbon dioxide (CO₂) into higher-value materials has emerged as a promising avenue towards establishing a sustainable solar-fuel-based economy. Much work has been done in recent literature to improve selectivity towards C₂+ products, notably, copper has exhibited distinctive catalytic properties by yielding higher-order hydrocarbon products, predominantly methane, ethylene, and ethanol, with compelling efficiencies. Consequently, substantial research efforts have been dedicated to understanding the unique catalytic characteristics of copper and unraveling the underlying mechanism governing the formation of hydrocarbons. These mechanistic insights, coupled with the understanding of CO₂ reduction mechanisms on other metals and molecular complexes, serve as pivotal guidelines for designing future catalyst materials capable of efficiently and selectively converting CO₂ into valuable products. To overcome the inherent solubility limitations of gaseous CO₂, our electrochemical cell operates with CO₂ in the gas phase. Leveraging the enhanced transport properties and reduced diffusion length of gaseous CO₂ to the electrode surface, we employ a gas diffusion layer (GDL) made of a hydrophobic porous material, specifically PFPE (perfluoropolyether). This PFPE-based GDL facilitates the delivery of gas phase CO₂ to the electrocatalytic interface.

Our research centers on the controllable and tunable porosity and surface morphology of the PFPE material within the gas diffusion layer. By varying the outer morphology of the catalyst surface, we aim to selectively tune the GDL to yield higher-order reduction products, particularly focusing on enhancing the production of ethylene. Through comprehensive studies and characterization, we investigate the influence of PFPE material properties, including porosity and surface morphology, on CO₂ reduction and ethylene selectivity. By gaining insights into the correlation between the structural characteristics of the gas diffusion layer and the electrochemical performance, we aim to optimize the PFPE material design for efficient and selective CO₂ reduction, specifically targeting ethylene as the desired product.

This research sheds light on the crucial role of gas diffusion layers and their tailored characteristics in achieving desired electrochemical CO₂ reduction outcomes. The findings contribute to the development of advanced catalyst materials and pave the way for scalable and sustainable strategies in utilizing CO₂ as a valuable feedstock for the production of high-value carbon products.

This work was performed under the auspices of the U.S. Department of Energy by Lawrence Livermore National Laboratory under Contract DE-AC52-07NA27344.

11:15 AM EN07.07.09

Norbomane Derived N-Doped sp² Carbon Framework as an Efficient Electrocatalyst for Oxygen Reduction Reaction, Hydrogen Evolution Reaction, and DesalinationRupali S. Mane¹, Dr. Neetu Jha¹ and Higgins M. Wilson²; ¹Institute of Chemical Technology, India; ²Pohang University of Science and Technology, Korea (the Republic of)

Hitherto, the development of Pt free bifunctional electrocatalyst for oxygen reduction reaction (ORR) and hydrogen evolution reaction (HER) is necessary for the advancement of sustainable and cost-effective solutions for energy conversion and storage technology. In this direction, herein we elucidated the usage of N doped sp² hybridized carbon framework (N-CF) as a metal-free electrocatalyst for ORR and HER. This work inspects the effect of N doping that converts a hybrid structure of CF (Norbomane or bicyclo [2, 2, 1] heptane structure) into planar N-CF. A series of N-doped CF with different doping concentrations has been prepared using a facile and cost-effective technique. This robust electrocatalysts exhibits a promotional effect in the activity, porosity, thermal and electrochemical stability for the ORR and HER reactions. A rich delocalized electronic density of the sp² bounded N species helps in modulating antibonding state of molecular oxygen and facilitates the breakage of O=O bond in ORR. It also promotes proton adsorption via bonding between proton and valence electron rich catalyst surface to aid HER. The research sought to investigate the employability of N-CF for fabricating sustainable energy devices with electrocatalyst possessing multiple electrocatalytic activities for ORR and HER. Density Functional Theory (DFT) computations reveals that active sites for HER are carbon atom located at the edge close to pyrrolic nitrogen and adjacent to graphitic nitrogen dopants.

11:30 AM *EN07.07.10

Challenges and Opportunities in Transitioning Electrochemical Conversion of CO₂ and other Renewable Feedstocks to Deployable TechnologyPaul Kenis; University of Illinois, United States

Over the past decade or so, the electrochemical reduction of CO₂ has evolved from a barely studied topic to one of the most active research areas in the fields of electrochemistry and electrochemical engineering. The ongoing process of 'the energy transition', spurred by the need to drastically reduce global CO₂ emissions to achieve global sustainability, has driven the vigorous pursuit of different electrocatalysts, electrodes, and electrolyzer configurations that are able to reduce CO₂ -- an abundantly available, renewable feedstock -- to different value-added intermediates or products. These efforts go beyond 'just' CO₂ reduction. Electro-oxidation of for example renewable, bio-derived adducts for the manufacturing of chemicals that traditionally are derived from fossil fuels is also an active area of study. With many selective and efficient catalysts now available for these types of electro-oxidations and -reductions, attention has started to shift to topics such as catalyst stability, electrode durability, and electrolysis reactor design.

This presentation will provide insights into a number of practical aspects of turning advances in electrocatalyst and electrode design into scalable, durable processes. For example, CO₂ reduction is often unavoidably accompanied by carbonate formation. How can one suppress carbonate formation, or minimize the effects of carbonate formation on electrolysis performance? Can CO₂ electrolyzers operate on dilute CO₂ feeds, recognizing that CO₂ capture and its concentration, especially from the air, is highly energy intensive, regardless of what method is used? How realistic, technically and from a life-cycle perspective, are less energy-intense electrolytic co-conversion approaches where CO₂ is reduced on the anode in parallel with oxidation of a renewable substrate to a desired product on the anode (e.g. glycerol to lactic acid)? What are some of the typical byproduct waste streams available from biomass processing, e.g. 'crude glycerol' which also contains various amounts of NaOH, water, and methanol, and can one develop an electrolysis system and process that can tolerate the range in compositions? This presentation will explore some of these aforementioned challenges and opportunities based on our work as well as work by others in reactor engineering, process design, and techno-economic / life cycle analysis.

SESSION EN07.08: CO₂/NO_x Reductions II
Session Chairs: Haotian Wang and Sen Zhang
Wednesday Afternoon, November 29, 2023
Hynes, Level 3, Room 310

1:30 PM *EN07.08.01

Electrocatalysis for Chemical Manufacturing of Ammonia and Environmental Remediation of NitrateMarta Hatzell; Georgia Institute of Technology, United States

Of the four major energy-use sectors (transportation, residential, commercial, and industrial), the industrial sector accounts for the largest amount of energy use (~33 EJ/year). This energy use results in nearly 1500 million metric tons of carbon dioxide emissions yearly^[1]. The large carbon footprint is due to most modern industrial processes' reliance on process heat which is often derived from coal, natural gas, and petroleum. With rising concerns related to global carbon emissions, there is a strong interest in displacing process heat with electricity. However, direct use of electricity for chemical manufacturing processes is challenging if not impossible. This has motivated a strong need to rethink and redesign many catalytic and separations-based processes to decarbonize the chemical manufacturing sector.

Within the chemical commodity industry, transforming thermocatalytic and thermal-based separation and catalysis processes with electrochemical-driven processes is one way to electrify and decarbonize the chemical industry. Thus, the primary aim of this talk is to detail how photochemical and electrochemical processes may aid in achieving this goal. I will aim to discuss the thermodynamic and kinetic challenges and opportunities which exist when transforming thermocatalytic systems into electrocatalytic or photocatalytic processes. I will then aim to discuss the specific growing opportunities related to electrocatalytic and photocatalytic ammonia production. Focus here will be placed on describing the opportunities in tuning molecular scale mechanisms and atomic scale materials design to enable ideal conversion.

2:00 PM EN07.08.02

Towards Controlling the Microenvironment in Electrochemical CO₂ ReductionAndrew B. Wong; National University of Singapore, Singapore

The electrochemical CO₂ reduction reaction (CO₂RR) represents a critical approach toward the carbon-neutral generation of hydrocarbons. However, despite intense research efforts, the need remains to increase selectivity and activity for electrocatalysts for CO₂RR. Thus, there has been increasing interest in optimizing the microenvironment to boost the activity and selectivity of electrocatalytic sites for CO₂ conversion.

This presentation discusses several strategies that are being pursued in my research group to optimize the microenvironment for CO₂ conversion. These strategies include: (1) model systems to illustrate control of diffusion via engineering electrode structure at micro- and nano- length scales, (2) model systems to harness localization of tandem catalysts, (3) implementation of bioelectrochemical tandem systems for CO₂ conversion, (4) implementation of MOF/organic coatings to improve transport, and (5) implementation of high-temperature non-aqueous electrolytes.

Thus, this presentation surveys a wide range of ongoing research strategies to optimize the microenvironment toward more effective CO₂RR.

2:15 PM EN07.08.03

Enhancing Product Selectivity in CO₂ Reduction by Controlling Substrate Pore Size and Hydrophobicity in Gas Diffusion Electrodes [Francesco Bernasconi](#)^{1,2}, [Alessandro Senocrate](#)¹ and [Corsin Battaglia](#)^{1,2}; ¹Empa–Swiss Federal Laboratories for Materials Science and Technology, Switzerland; ²ETH Zürich, Switzerland

Electrochemical CO₂ reduction (CO₂RR) is a key technology to convert detrimental CO₂ emissions into sustainable fuels and chemicals, and close the carbon loop¹. To ensure the economic competitiveness of CO₂RR, electrocatalysts need to be highly active, selective towards a desired product and stable. High activities can be achieved with gas diffusion electrodes (GDEs), circumventing mass transport limitations resulting from the low CO₂ solubility in water. However, product selectivity and stability still need to be improved before industrial implementation. In this work, we show that the GDE substrate pore size and hydrophobicity act as a powerful handle to tune selectivity and stability in both Ag and Cu GDEs^{2,3}. GDEs with large pore size and weak hydrophobicity readily lead to flooding of the catalyst by water and, in the Ag case, yield poor selectivity towards CO and a significant production of H₂. In contrast, GDEs with small pore size prevent flooding of the catalyst, thus yielding a greatly improved Faradaic efficiency towards CO (up to 95% at 100 mA/cm² in neutral electrolyte), minimal H₂ evolution, and remarkable long-term stability (97% of initial CO selectivity retained after > 40 h). In the Cu case, we observe a strong enhancement in C₂H₄ selectivity when employing GDE substrates with small pores and strong hydrophobicity (up to 50% Faradaic efficiency in neutral electrolyte at 200 mA/cm² for > 3 h). Both CO₂ and CO reduction reactions indicate transport limitations of reactants to the catalyst sites for all GDEs, however this limitation is less severe for GDEs with small pore sizes. We rationalize these findings with the presence of an electrolyte layer covering the electrocatalyst, forcing the electrocatalytic reaction to take place at double phase boundaries. Experiments with variable pressures show that only GDEs with small pores can sustain large overpressure of the liquid phase (> 1 bar), which enhances the resilience of the reaction towards unexpected pressure spikes that might occur during start-up and operation. Our results emphasize the importance of substrate microstructure on GDE product selectivity and stability during CO₂RR, and represent a new scalable strategy to improve GDE performance.

¹A. Senocrate, C. Battaglia, *J. Energy Storage* **2021**, 36, 102373

²A. Senocrate, F. Bernasconi, D. Rentsch, K. Kraft, M. Trottmann, A. Wichser, D. Bleiner, C. Battaglia, *ACS Appl. Energy Mater.* **2022**, 5, 14504

³F. Bernasconi, A. Senocrate, P. Kraus, C. Battaglia, *submitted*

2:30 PM BREAK

3:30 PM *EN07.08.04

Advances in Electrified CO₂ Reduction to Chemicals and Fuels [Edward H. Sargent](#)^{1,2}; ¹Northwestern University, United States; ²University of Toronto, Canada

I will review recent advances, at the level both of catalysts and systems, in efficiently electrochemically reducing CO₂ and CO to chemicals (such as ethylene and propanol) and fuels (e.g. methane, ethanol). I will look at issues such as total voltage, single-pass utilization of the reagents, and overall energetic efficiency.

4:00 PM EN07.08.05

Electrochemical Growth and Restructuring of Cu Surfaces for Steering the Selectivity of Electrocatalytic CO₂ Reduction [Joseph S. DuChene](#); University of Massachusetts Amherst, United States

The electrocatalytic reduction of CO₂ into value-added chemicals is commonly performed with catalysts composed of Cu due to its propensity for producing C₂₊ products like ethylene and ethanol. While promising, the reaction is known to suffer from poor selectivity. Several studies have shown that the surface facets of Cu catalysts play an important role in dictating the distribution of CO₂ reduction products, yet the dynamic nature of Cu surfaces leads to significant surface reconstructions that alter the catalyst selectivity over the course of the reaction. The factors governing the evolution of Cu surfaces during CO₂ reduction must be fully understood to enable control over these processes at the atomic level. Here, we discuss our efforts towards controlling the surface facets of Cu electrocatalysts via electrochemical treatments for steering the selectivity of electrocatalytic CO₂ reduction. Using both polycrystalline Cu foils and shape-controlled Cu or Cu₂O nanoparticles, we will show how the applied potential and chemical composition of the growth solution can be manipulated to tailor the surface facets of Cu electrocatalysts. Finally, we will present the results of electrocatalytic CO₂ reduction with these nanostructured Cu catalysts and highlight opportunities for using simple electrochemical techniques to tailor the surface facets of electrocatalysts at the nanoscale for the selective production of chemical fuels.

4:15 PM EN07.08.06

Electrocatalytic CO₂ Reduction using Heteroatom Doped Carbon Materials for Multi-Carbon Production [Hyun-Tak Kim](#); Korea Research Institute of Chemical Technology, Korea (the Republic of)

Electrochemical reduction of CO₂ (CO₂R) to value-added chemicals and fuels presents a promising approach for mitigating the issues related to energy crisis and global warming. Different proton- and electron transfer steps and CO₂ reduction pathways are employed to convert CO₂ to C₁, C₂, or C₂₊ products. In addition, the production of liquid multicarbon alcohols is highly desired, because it possesses the potential to enable the synthesis of sustainable fuels that leverage high energy densities (21 MJ l⁻¹ ethanol, 27 MJ l⁻¹ propanol, and 34.2 MJ l⁻¹ gasoline) for long-range and heavy-freight transportation applications. However, owing to the limited selectivity and low activity of the currently available catalysts, the production of multicarbon alcohols via direct CO₂ electroreduction is not economically viable.

Here, we report a heteroatom doped carbon based electrocatalyst that exhibits a Faradaic efficiency greater than 70% for CO₂ reduction (CO₂R) and 90% of C₂₊ product selectivity. Density functional theory calculations suggest that CO₂ dual binding catalysts promote a C–C coupling between adsorbed CO intermediates and CO₂ for C₂₊ formation. This high efficiency and the corresponding mechanism are explained by theoretical calculations and spectroscopic analyses. With the results, we suggest a molecular design strategy for next-generation CO₂ reduction catalysts for a green ocean and atmosphere.

4:30 PM EN07.08.07

High-Rate CO₂ Conversion to Ethylene via Molecularly Enhanced Electrochemical CO₂ Reduction [Taemin Lee](#)¹, [Jongyoun Kim](#)¹, [Hyun Dong Jung](#)², [Seoin Back](#)², [Youngu Lee](#)¹ and [Dae-Hyun Nam](#)¹; ¹Daegu Gyeongbuk Institutes of Science and Technology, Korea (the Republic of); ²Sogang University, Korea (the Republic of)

Electrochemical conversion of CO₂ into value-added fuels and feedstocks is a promising route to realize sustainable energy cycle and carbon neutrality. Continued efforts to achieve effective electrochemical CO₂ reduction reaction (CO₂RR) have resulted in achieving high selectivity for multi-carbon (C₂₊) chemicals such as ethylene (C₂H₄) and ethanol (C₂H₅OH). To improve the productivity of C₂₊ chemicals, it is necessary to promote C–C coupling on the catalyst surface, as well as *CO formation by fast electron transfer even at high current density. However, even in the flow-type cell with a gas diffusion electrode, it still remains as a challenge due to the sluggish *CO formation on the catalyst surface.

In this work, we report the molecularly-enhanced CO₂ mass transport of Cu catalyst for high current density C₂H₄ production. We augmented ascorbic acid (AA) on Cu nanowires (CuNWs) using graphene quantum dots (GQDs) as a mediator to confine AA in heterogeneous electrocatalysts during CO₂RR. AA on CuNW surface enhanced the CO₂ conversion rate by promoting proton-coupled electron transfer (PCET) and providing strong hydrogen bonding site. The nanoconfinement effect and immobilization of AA by GQDs enable redox reversibility and high current density CO₂RR. In the CO₂RR of pristine CuNWs, there is less carbon monoxide (CO) formation in the low potential, and this limits the potential range for stable C₂H₄ production. However, Cu NWs modified with nanoconfined AA by GQDs (cAA-CuNWs) exhibited outstanding C₂H₄ production rates with Faradaic efficiency (FE) of 60.7% and C₂H₄ partial current density of 539 mA/cm², which is about 2.9-fold higher performance compared to that of pristine CuNWs. *In-situ* Raman spectroscopy revealed that higher population of *CO is covering cAA-CuNW surface by Cu–CO rotation and stretch peak intensity. Also, appropriate ratio of atop bound CO and bridge bound CO has proven the efficient C–C coupling of cAA on CuNW. Grand-canonical density functional theory (GC-DFT) verified that multiple hydrogen bonding sites of AA can effectively control the electronic distributions of water molecules surrounding CO₂, thereby improving *CO formation on the Cu surface. This offers the potential for harnessing AA as a promoter to enhance CO₂ mass transport toward high rate CO₂ to value-added C₂₊ chemical conversion.

4:45 PM EN07.08.08

Thermodynamically Designed Cu-Sn Bimetallic Alloy Electrocatalysts for Electrochemical CO₂ Reduction WoosuckKwon¹, SoohyunGo¹, DeokgiHong², Young-ChangJoo² and Dae-HyunNam¹; ¹Daegu Gyeongbuk Institute of Science & Technology (DGIST), Korea (the Republic of); ²Seoul National University, Korea (the Republic of)

Electrochemical CO₂ reduction reaction (CO₂RR) has received great attention as a promising strategy for carbon neutrality and net zero emission. Copper (Cu) is the element which binds neither *CO strong nor weak and enables C-C coupling for multi-carbon product formation by inducing *CO dimerization. To enhance the CO₂RR selectivity of Cu, modulating the d-band center of the heterogeneous catalysts is essential to control the intermediate binding energy. Recently, Sn has been widely applied as a bimetallic Cu alloy element, which can suppress hydrogen evolution reaction (HER) and enables to tune CO₂RR reaction pathway. Although Cu-Sn bimetallic alloy can have various intermetallic compounds, current approaches of Cu-Sn bimetallic catalyst to control Cu:Sn ratio, arrangement of components, structure, and oxidation states resulted in the limited phase control and narrow range of product selectivity control accordingly.

In this work, we developed a thermodynamically designed Cu-Sn bimetallic alloy electrocatalysts which enable the efficient control of CO₂RR selectivity. In the alloy fabrication, escaping from the Cu:Sn ratio control approach, we focused on modulating Sn vapor pressure for the controllable formation of Cu-Sn intermetallic compounds. We applied carbon (C) matrix which enables to modulate the microenvironment of Cu which interact with Sn vapor pressure during Cu-Sn alloy fabrication. Starting from the thermochemical computation to discover the processing window, we fabricated Cu-Sn-C nanocomposite combined with Cu, Sn precursors, and polymers by electrospinning and calcination. By controlling the allocation of Cu and Sn sources in the core/shell structured nanofibers, we successfully fabricated Cu₄₁Sn₁₁, Cu₃Sn, and Cu₆Sn₅ respectively. As the local Sn vapor pressure increases, Sn-rich compounds formed accordingly and resulted the increased selectivity of formate (HCOO⁻). Interestingly, major CO₂RR product was shifted from formate to methane (CH₄) by controlling the stoichiometry of Cu-Sn alloy. Cu₄₁Sn₁₁ exhibited CH₄ faradaic efficiency (FE) over 40%. We believe that this approach can pave a way to design bimetallic alloy materials for efficient CO₂RR electrocatalysts.

SESSION EN07.09: Poster Session III: CO₂ Reduction and Electrosynthesis

Session Chairs: Maria Escudero-Escribano and Sen Zhang

Wednesday Afternoon, November 29, 2023

Hynes, Level 1, Hall A

8:00 PM EN07.09.01

Shape-Controlled Synthesis of 2H Au Nanomaterials for Highly Efficient Carbon Dioxide Reduction Reaction GangWang and YeChen; The Chinese University of Hong Kong, Hong Kong

Colloidal gold (Au) nanomaterials with fine controlled size and shape possess unique physicochemical properties and great potentials in various applications. However, most of the reported Au nanomaterials typically crystallize in the thermodynamically stable face-centered cubic (3C) phase, and there are still great challenges in synthesizing hexagonal close-packed (2H type) Au nanomaterials with high phase purity and controlled size and shape. Here, we report a one-pot colloidal synthesis of free-standing ultrasmall 2H Au nanosheets. A series of 2H Au nanomaterials with controlled shape are then synthesized using the 2H Au nanosheets as seeds. Moreover, the 2H Au nanomaterials exhibit superior electrocatalytic performance toward CO₂ reduction reaction than 3C Au nanoplates, possessing high Faradaic efficiency in a wide applied potential window. Our work provides an effective strategy to design and synthesize Au nanomaterials with unconventional crystal structure and demonstrates the potential of phase engineering in boosting catalytic performances of noble metal nanomaterials.

8:00 PM EN07.09.02

Synthesis of Ag-Sn Intermetallic Compounds via Mechanical Alloying as Selective Electrocatalysts for CO₂ Reduction Reaction TakeyukiKamimura, KazuyukiIwase and ItaruHonma; Tohoku University, Japan

The electrochemical CO₂ reduction reactions (CO₂RR) have attracted attention as a method to convert CO₂ into value-added products using electricity derived from renewable energy sources[1]. In CO₂RR, various products such as carbon monoxide (CO) and formate (HCOO⁻) can be generated. Therefore, for CO₂RR catalysts, the higher selectivity for the desired products and suppression of the competing hydrogen evolution reaction (HER) is important.

Previous research has developed highly active and selective CO₂RR catalysts using various materials, such as polymers, organometallic complexes, and metal nanoparticles[2-4]. Among them, metal alloys catalysts are attracting attention as promising CO₂RR catalysts, as the catalytic activity and product selectivity can be tuned by choice of metal elements and their composition[5-7]. Intermetallic compounds, which have unique crystal structures and composition of metal elements compared to conventional metallic alloys, are expected to exhibit different reactivity and selectivity from conventional solid-solution alloy catalysts due to their unique atomic structures and electronic states. In this study, we synthesized intermetallic compounds composed of silver (Ag) and tin (Sn), which show high CO₂RR selectivity for producing CO and HCOO⁻, and investigated whether the CO₂RR activity and selectivity could be enhanced. Specifically, we employed mechanical alloying as a synthetic method since it has been gaining attention in recent years to synthesize various kinds of materials[8].

Intermetallic compounds of Ag and Sn (Ag-Sn) were synthesized by mechanical alloying using a planetary ball mill using Ag powder (particle diameter 50-80 nm) and Sn powder (particle diameter 60-80 nm) at the desired ratio (Ag: Sn = 3:1 ~ 7:1) as the starting materials. The CO₂RR activity was evaluated by constant current measurements using gas diffusion electrodes as the working electrode and 1 M KHCO₃ as the electrolyte.

The powder x-ray diffraction (XRD) pattern showed that the sample at Ag: Sn = 7:1 can be attributed to the solid solution alloy of Ag and Sn, whereas the XRD pattern for Ag: Sn = 4:1 could be attributed to the ζ phase, which is an intermetallic compound phase. In both samples, no peaks of the unreacted precursor were observed, suggesting that the single phase of the Ag-Sn solid solution and the intermetallic compound phase was successfully synthesized. For the Ag: Sn = 4:1 sample, the concentration of Ag and Sn in the depth direction was analyzed by X-ray photoelectron spectroscopy (XPS) measurement. The results showed that the ratio of Sn on the surface was higher than the original Ag: Sn ratio (4:1). This result suggests that Sn atoms of the Ag: Sn = 4:1 sample are segregated on the surface. In contrast, the sample showed an intermetallic compound phase (ζ phase) as the bulk crystal structure. For CO₂RR activity at a constant current density (53.0 mA/cm²), the synthesized Ag-Sn catalysts mainly produced HCOO⁻. The faradaic efficiency of HCOO⁻ generation for Ag: Sn = 4:1 sample was 84%. This value was larger than that of the Ag: Sn = 7:1 sample (78%). For comparison, we evaluated the CO₂RR activity of the pure Ag and Sn powders, which were used as precursors. They predominantly produced CO and HCOO⁻ with a respective faradaic efficiency of 89% and 62%. These findings imply that the formation of the ζ-phase, an intermetallic compound phase, may contribute to the generation of HCOO⁻.

[1] K. P. Kuhl *et al.*, *J. Am. Chem. Soc.*, **36**, 14107-14113 (2014).

[2] Y. Ma *et al.*, *Nat. Commun.*, **13**, 1400 (2022).

[3] R. Angamuthu *et al.*, *Science*, **327**, 313-315(2010).

[4] R. Reske *et al.*, *J. Am. Chem. Soc.*, **136**, 6978-6986 (2014).

[5] T. Gunji *et al.*, *Chem. Mater.*, **32**, 6855-6863 (2020).

[6] J. Zeng *et al.*, *ACS Appl. Mater. Interfaces*, **11**, 33074-33081 (2019).

[7] K. Iwase *et al.*, *Chem. Commun.*, **58**, 4865-4868 (2022).

[8] J. D. Bellis *et al.*, *Chem. Mater.*, **33**, 2037-2045 (2021).

8:00 PM EN07.09.03

Development of Cost-Effective, Bespoke Tailored Ternary Nanoparticles as Catalysts for Lithium-Air Batteries Jong SeokNam¹, YujangCho¹, SeongcheolAhn¹, Min SooKim¹, JaewanAhn¹, HoJinLee², Ji-WonJung² and Il-DooKim¹; ¹Korea Advanced Institute of Science and Technology, Korea (the Republic of); ²University of Ulsan, Korea (the Republic of)

Lithium-air batteries, known for their exceptionally high theoretical energy density, have emerged as potential energy storage systems capable of replacing gasoline. However, their practical application is hindered by the challenging complete decomposition of insulating Li₂O₂ formed during the charge-discharge cycle. To overcome this, it is common to utilize precious metal catalysts such as iridium (Ir) and ruthenium (Ru), known for their high catalytic activity. Nevertheless, the scarcity and high cost of these precious metal catalysts pose significant barriers for commercial use. Hence, various research groups are striving to achieve high catalytic efficiency using non-precious metals. Metal oxides, in particular, have emerged as a versatile family of non-precious catalysts. They are favored for their intrinsic oxidation resistance, comparative stability, ease of synthesis and control, as well as the abundance of compositional and structural varieties.

In this study, we aim to explore the use of abundant, economically viable non-precious metals, specifically cobalt (Co), nickel (Ni), and iron (Fe), in lithium-air batteries. Our approach

involves adjusting the composition ratios of these metals to assess their relative catalytic efficiencies. Our research further includes: i) producing bespoke tailored ternary metal oxide nanoparticles from Co, Ni, and Fe using a rapid thermal process, ii) incorporating these nanoparticles onto a lightweight, porous, and highly conductive carbon nanofiber-based cathode for use in lithium-air batteries, and iii) assessing the potential for large-scale air battery production via surface optimization of carbon nanofibers integrated with these bespoke tailored ternary nanoparticles and the fabrication of pouch cells.

8:00 PM EN07.09.04

Regeneration of NiFe/LFNO for Solid Oxide Electrolysis Cell Application under Non-Ideal Condition Musa O. Najimu¹, Matthew Hurlock², Tina Nenoff², Jonas Baltrusaitis³ and Kandis L. Abdul-Aziz¹; ¹University of California, Riverside, United States; ²Sandia National Laboratories, United States; ³Lehigh University, United States

The structural reversibility of smart exsolved nanoparticle catalysts offer the opportunity for SOEC application in reversible modes, however, structural reversibility in the presence of anthropogenic contaminant poisoning is important for nonideal SOEC conditions. In addition to redirecting the reaction pathways and lowering the selectivity, this contaminant poisoning can lower the overall conversion of the carbon feeds due to the preferential conversion of the contaminants. Sulfur removal in H₂S-poisoned perovskite materials as well as the restoration of the activity of the poisoned materials, is typically achieved by oxidative treatment at 800 °C. Here, the structural changes of SOx-poisoned NiFe/LaFe_{0.9}Ni_{0.1}O₃ (LFNO) material were tracked for regenerability using cycling dry methane reforming (DRM) experiments to assess the intrinsic regenerability. While reduction of as-prepared LFNO facilitates the exsolution of NiFe with the formation of La₂O₃ and La(OH)₃, DRM causes partial reincorporation of the exsolved NiFe nanoparticle. The exsolved nanoparticle demonstrates structural recyclability as oxidation after DRM reincorporates the NiFe nanoparticle back into the LFNO perovskite, while subsequent reduction causes the re-exsolution of the NiFe alloy nanoparticle. In addition, the DRM activity after the regeneration closely matches the DRM activity of freshly reduced LFNO perovskite, further demonstrating the reversibility of the exsolved NiFe/LFNO. However, using the same regeneration condition, the deteriorated DRM activity of the NiFe/LFNO material exposed to SOX at 600 °C is not restored, possibly demonstrating the prohibitory effect of SOx exposure for regeneration. In addition to a direct comparison of the impact of the type of sulfur contaminant species on regeneration, the speciation of sulfur on the exsolved nanoparticle systems as well as the regeneration of this novel SOEC candidate will be discussed.

8:00 PM EN07.09.05

Bifunctional Catalytic Co₂VO₄ Nanoarray Grown on Carbon Nanofiber for Free-Standing Lithium-Air Battery Cathode Mingyu Sagong, Jong Seok Nam, Seung Hyun Jeong and Il-Doo Kim; KAIST, Korea (the Republic of)

In recent research on cathode for LABs, systematic investigations have been conducted to develop rational catalysts with diverse morphologies. Studies have shown increased exposure to the high-activity surface leads to improved cycle life and cell performance. In particular, spinel cobalt oxide (Co₃O₄) draw attention due to Co²⁺/Co³⁺ bifunctional catalytic activity and electrochemical stability in electrocatalysis. Nevertheless, the efficacy of these applications was hindered due to the inherent constraints associated with their poor intrinsic electrical conductivity and comparatively low catalytic activity. To address these limitations, we have designed cobalt vanadium oxide uniformly decorated on the carbon nanofiber (Co₂VO₄@CNF) *via* hydrothermal synthesis as a free-standing cathode for LABs. By substituting vanadium for the octahedron site of Co₃O₄, vanadium atoms can offer an electron pathway and facilitate high electrical conductivity. In addition, the substitution of vanadium improves oxygen reduction reaction (ORR) performance through proper electron configuration of Co²⁺. The oxide catalyst grown on the CNF facilitates the maximization of active catalytic sites and stable formation/dissociation of Li₂O₂, enabling greater capacity and longer cyclability. The findings indicate that the formation/dissociation process of Li₂O₂ is influenced by the presence of an appropriate catalyst and the surface chemistry. The air cathode structure composed of rational nanostructures and catalysts is expected to improve LAB performance in capacity and cyclability.

8:00 PM EN07.09.06

Palladium Nano-Catalysts Deposited via Atomic Layer Deposition for Ammonia-Fueled Protonic Ceramic Electrochemical Cells Heon Jun Jeong, Wanhyuk Chang, Beum Geun Seo and Joon Hyung Shim; Korea University, Korea (the Republic of)

Solid oxide fuel cells (SOFCs), specifically ceramic fuel cells, have gained recognition for their ability to efficiently utilize various fuels and achieve high compound efficiencies through thermal cycling. As an alternative to conventional gas turbine plants, the integration of fuel cell and gas turbine hybrids in power generation systems has emerged as a practical solution. However, methane-based ceramic fuel cells pose challenges related to carbon emissions during combustion, as well as complexities in production, storage, and transportation. This study aims to explore the potential of using ammonia as a carbon-free and eco-friendly fuel for protonic ceramic fuel cells (PCFCs), offering several advantages over methane gas. Ammonia provides a higher energy density, is cost-effective, and offers safer storage and transport compared to hydrogen. PCFCs operate at lower temperatures (<600 °C), exhibit minimal structural and material deterioration, and demonstrate higher ionic conductivity compared to SOFC electrolytes. Additionally, PCFCs produce only water and nitrogen as by-products, ensuring a cleaner and more efficient energy conversion process. To optimize the performance and durability of ammonia-fueled PCFCs, we employed a catalyst treatment approach using palladium (Pd). By utilizing atomic layer deposition (ALD) on the anode surface, we achieved a uniform distribution of Pd catalysts, increased reaction sites, and improved thin film deposition. The Pd-treated PCFC samples demonstrated significant performance enhancements compared to untreated samples. Impedance analysis revealed improved current collection and a substantial reduction in polarization resistance, particularly at low temperatures. Stability tests further confirmed the effectiveness of Pd ALD in enhancing the performance and durability of ammonia-fueled PCFCs. In this presentation, we will discuss the outstanding performance and durability of Pd catalysts in ammonia-fueled PCFCs, providing detailed insights into the experimental findings and their implications for practical applications.

8:00 PM EN07.09.07

Boosting the Visible-Light-Driven Selective Toluene Oxidation via Synergistic Effect Between Nanoparticulate Pd/BiVO₄ Photocatalyst and a Cyclic Nitroxyl Redox Mediator Sayuri Okunaka¹ and Hiromasa Tokudome²; ¹Tokyo City University, Japan; ²TOTO Ltd., Japan

Selective oxidation of organic compounds using semiconductor photocatalysts has been focused on the viewpoint of sustainable synthesis processes. Especially, the selective oxidation of C(sp³)-H bonds in toluene, which is one of the C-H activation reaction, is an attractive reaction because the desired oxidation product, benzaldehyde, is extensively used as an indispensable intermediate in the synthesis of drugs, perfumes, and fine chemicals. Conventional synthesis of benzaldehyde involves TiO₂-based photocatalysts, however, they have brought the drawback of absorbing only UV light and the low selectivity due to its large bandgap. Therefore, developing visible-light responsible photocatalyst system for efficient toluene oxidation has been strongly desired to construct an alternative way to realize sustainable organic synthesis. Recently, we reported photo-oxidation of toluene to benzaldehyde over visible-light responsible Pd-loaded BiVO₄ (Pd/BiVO₄) photocatalyst. However, it remains challenging due to its low efficiency. In this work, we introduce a novel strategy to apply a cyclic nitroxide compound as an efficient redox mediator along with Pd/BiVO₄ for toluene oxidation. Addition of a cyclic nitroxide significantly improved the toluene oxidation activity on Pd/BiVO₄ photocatalyst under blue-to-green light irradiation. In particular, *N*-hydroxyphthalimide (NHPI) boosted the benzaldehyde production up to ca. 28 times compared to without NHPI. The optimized conditions realized a toluene conversion in high efficiency (apparent quantum yield = 10.8 and 5.4 % at 420 and 520 nm, respectively) and with excellent selectivity. The superior conversion yield was realized by the synergistic effect between the presence of NHPI and the use of nanoparticulate Pd/BiVO₄ with a relatively large surface area.

8:00 PM EN07.09.08

Tailoring Ag Electron-Donating Ability for Organohalide Reduction: A Bilayer Electrode Design Dwaipayan Chakraborty¹, Ali Abbaspourtamijani¹, Henry S. White², Matthew Neurock³ and Yue Qi¹; ¹Brown University, United States; ²The University of Utah, United States; ³University of Minnesota, United States

Electrochemical reduction of organohalides is a green and safe way for the reduction of environmental pollutants, synthesis of new organic molecules, and many other important applications. The presence of a catalytic electrode (i.e., electrocatalytic dehalogenation) can in many cases make the process more energetically efficient. Ag has been known to be very good catalysis for this purpose for a wide range of organohalides. In this work, we have particularly tried to put forward an electrode design strategy that can possibly be used to further increase the catalytic activity of pure Ag electrodes. We have shown how epitaxially depositing one to three layers of Ag on catalytically inert or less active support metal (defined as Ag/metal bilayer electrode) could increase the surface electron donating ability, thus increasing the adsorption of organic halide and the catalytic activity. Many factors, such as molecular geometry, lattice mismatch, work function, and solvents, contribute to the adsorption of organic halide molecules over the bilayer electrode surface. To isolate and rank these factors, we studied three model organic halides, namely, haloethane, bromobenzene (BrBz), and benzyl bromide (BzBr) adsorption on Ag/metal (metal = Au, Bi, Pt, and Ti) bilayer electrodes in both vacuum and acetonitrile (ACN) solvent. The different metal support offers a range of lattice mismatches and work function differences with Ag. Our calculations show that the surface of Ag becomes more electron-donating and accessible to adsorption when forming a bilayer with Ti since Ti has a lower work function and almost zero lattice mismatch with Ag. We believe this study will increase the electron-donating ability of the Ag surface by choosing the right metal support which in turn can improve the catalytic activity of the working Ag electrode.

8:00 PM EN07.09.09

Deterministic Synthesis of Pd Nanocrystals Enclosed by High-Index Facets and Their Enhanced Activity Toward Formic Acid Oxidation Maochang Liu^{1,2}, Sang-II Choi¹, Siyu Zhou¹ and Younan Xia¹; ¹Georgia Institute of Technology, United States; ²Xi'an Jiaotong University, China

Noble-metal nanocrystals enclosed by high-index facets are of growing interest due to their enhanced catalytic performance toward a variety of reactions. Herein, we report the deterministic synthesis of Pd nanocrystals encased by high-index facets by controlling the rate of deposition ($V_{deposition}$) relative to that of surface diffusion ($V_{diffusion}$). For octahedral seeds with truncated corners, a faster reduction rate (and thus deposition rate) than that of surface diffusion (i.e., $V_{deposition}/V_{diffusion} > 1$) led to the formation of concave trisoctahedra (TOH) with high-index facets. When the reduction was slowed down, in contrast, surface diffusion dominated the growth pathway. In the case of $V_{deposition}/V_{diffusion} \approx 1$, truncated octahedra with enlarged sizes were produced. When the reduction rate was between these two extremes, we obtained concave tetrahedra (THH) without or with truncation. Similar growth patterns were also observed for cuboctahedral seeds. When the Pd octahedra, concave TOH, and concave THH were tested for electrocatalyzing the formic acid oxidation (FAO) reaction, those with high-index facets were advantageous over the conventional Pd octahedra enclosed by {111} facets. This work not only contributes to the understanding of surface diffusion and its role in nanocrystal growth but also offers a general protocol for the synthesis of nanocrystals enclosed by high-index facets.

8:00 PM EN07.09.10

Hierarchical NiFe@NiFe Layered Double Hydroxides for Efficient Solar-Powered Water Oxidation Deok Ki Cho, So Jeong Park, Geonpyo Hong and Jin Young Kim; Seoul National University, Korea (the Republic of)

The development of green hydrogen is crucial for achieving zero CO₂ emissions and sustainable energy production. Solar-powered electrocatalysis, also known as photovoltaic-electrolysis (PV-EC), is a promising technology that has the potential to efficiently convert solar energy into hydrogen with high efficiency and durability. However, the sluggish kinetics of the oxygen evolution reaction (OER) pose a significant challenge to efficient water splitting. To overcome this, there is a pressing need to develop cost-effective catalysts with high electrochemical activity and stability, as well as scalable synthetic processes for large-scale production. Layered double hydroxides (LDHs) based on transition metals have garnered considerable attention as promising candidates due to their abundant availability, porous morphologies, and adjustable compositions.

In this study, a hierarchical heterogeneous Ni²⁺Fe³⁺@Ni²⁺Fe²⁺ LDH was successfully synthesized using a sequential electrodeposition technique. The synthesis process involved the use of separate electrolytes containing iron precursors with different valence states (Fe²⁺ and Fe³⁺). By utilizing Fe²⁺ precursors, a well-defined nanosheet array of NiFe LDHs with high crystallinity, referred to as Ni²⁺Fe²⁺ LDH, was synthesized. On the other hand, employing Fe³⁺ precursors led to the formation of a thin layer of NiFe LDH with a relatively higher Ni content and lower crystallinity, denoted as Ni²⁺Fe³⁺ LDH. Different deposition behaviors depending on the oxidation state of the Fe precursor ions was attributed to their different solubility product constants (K_{sp}). The amorphous Ni²⁺Fe³⁺ LDH exhibited superior OER performance compared to its Fe²⁺-based counterpart. The heterogeneous hierarchical OER catalyst electrode was prepared by a simple two-step electrodeposition process using the Ni²⁺Fe²⁺ LDH nanosheet arrays with large surface area. As a result of the synergistic effect between the large dual advantages of large surface area of the Ni²⁺Fe²⁺ LDH nanosheet arrays and excellent OER activity of Ni²⁺Fe³⁺ LDH, the Ni²⁺Fe³⁺@Ni²⁺Fe²⁺ LDH exhibited outstanding OER activity with overpotentials of 218 and 265 mV required to achieve current densities of 10 and 100 mA cm⁻², respectively. Moreover, it demonstrated exceptional long-term stability, sustaining efficient performance for 30 hours even at a high current density of 500 mA cm⁻². In a water splitting system, the electrolyzer, using a Sn₄P₃/CoP₂ electrocatalyst as the cathode, only required a cell voltage of 1.55 V to achieve a current density of 10 mA cm⁻². Furthermore, the solar-powered overall water splitting system, comprising our electrolyzer and a perovskite/Si tandem solar cell, exhibited a high solar-to-hydrogen conversion efficiency of 15.3%.

8:00 PM EN07.09.11

Introduction of Carbon Shells on Copper(I) Oxide Nanocrystals Inducing Selective CO₂ Electroreduction to Methane Jong-Yeong Jung and Hyunjoon Song; KAIST, Korea (the Republic of)

Large-scale electrochemical CO₂ reduction reaction (CO₂RR) for methane production is crucial for achieving a carbon-neutral economy. However, practical methane production faces challenges from increased C-C coupling and the hydrogen evolution reaction. Here we introduced carbon shells on cuprous oxide nanocubes to preserve the copper oxidation states under reduction potential. As carbon shell thickness increased, methane production significantly improved. Optimizing the shell thickness to 50 nm resulted in a Faradaic efficiency of 50.2 ± 3.9% at a methane partial current density of -201 ± 16 mA cm⁻² in alkaline electrolytes. Operando X-ray absorption confirmed that the carbon shells prevent the reduction of Cu₂O nanocubes under the negative bias and stabilize Cu(I) species. In situ Raman studies observed a remarkable peak assigning Cu hydroxide species. The carbon shells seem to impede the transport of hydroxide ions, leading to a high local pH and stabilizing Cu hydroxide species. Density functional theory calculations confirmed the role of surface-adsorbed *OH molecules to suppress *CO dimerization and the Bardar charge of Cu atoms during *OH adsorption which remained under +1. This work presents a simple strategy to control the major products of CO₂RR and reveals the role of hydroxyl groups on the Cu₂O surface.

8:00 PM EN07.09.12

Acceptor Doping of Bismuth Vanadate to Realize Photocathodes for Hydrogen Evolution: Joint Experimental and Computational Investigations Vrinda Somjit¹, Daye Seo², Kyoung-Shin Choi² and Giulia Galli^{3,1}; ¹Argonne National Laboratory, United States; ²University of Wisconsin-Madison, United States; ³The University of Chicago, United States

Bismuth vanadate (BiVO₄) is a promising photoelectrode for water splitting due to its ease of synthesis, stability in aqueous conditions, and high electron-hole separation yield. Its favorable band edge alignment with the water oxidation potential has spurred extensive research into designing n-type BiVO₄ photoanodes for water oxidation [1]. However, relatively less attention has been given to the development of p-type BiVO₄ for water reduction to hydrogen gas. In this work, we show that calcium-doped BiVO₄ can serve as a photocathode that reduces water to hydrogen gas. Using density functional theory at the +U and hybrid levels, we report that Ca doping can shift the conduction band minimum (CBM) of BiVO₄ by 0.15 eV, moving it closer to the water reduction potential. This is consistent with experiments, which observe hydrogen evolution in Ca-doped BiVO₄ under illumination and a shift in the CBM towards vacuum. We show that changes to the electronic density of states and Bi-O bond lengths cause a sizeable shift in CBM. We also analyze compensation of the acceptor dopant by oxygen vacancies and hole polarons. Our work provides insight into the use of BiVO₄ as a photocathode, moving us towards the fabrication of p-n homojunctions based on BiVO₄ that could further increase charge separation efficiency, and development of electrodes for other important technological processes, like N₂ reduction to NH₃.

[1] Lee, D., Wang, W., Zhou, C., Tong, X., Liu, M., Galli, G., & Choi, K. S. (2021). The impact of surface composition on the interfacial energetics and photoelectrochemical properties of BiVO₄. *Nature Energy*, 6(3), 287-294.

8:00 PM EN07.09.13

Selective Electrochemical Reduction of CO₂ on Compositionally Variant Bimetallic Cu-Zn Electrocatalysts Derived from Scrap Brass Alloys Ibrahim M. Badawy; American University in Cairo, Egypt

The electrocatalytic reduction of carbon dioxide (CO₂RR) into value-added fuels is a promising initiative to overcome the adverse effects of CO₂ on climate change. Most electrocatalysts studied, however, overlook the harmful mining practices used to extract these catalysts in pursuit of achieving high-performance. Repurposing scrap metals to use as alternative electrocatalysts would thus hold high privilege even at the compromise of high performance. In this work, we demonstrated the repurposing of scrap brass alloys with different Zn content for the conversion of CO₂ into carbon monoxide and formate. The scrap alloys were activated towards CO₂RR via simple annealing in air and made more selective towards CO production through galvanic replacement with Ag. Upon galvanic replacement with Ag, the scrap brass-based electrocatalysts showed enhanced current density for CO production with better selectivity towards the formation of CO. The density functional theory (DFT) calculations were used to elucidate the potential mechanism and selectivity of the scrap brass catalysts towards CO₂RR. The d-band center in the different brass samples with different Zn content was elucidated.

8:00 PM EN07.09.14

Exploring the Synergies of Cu₂O-Based Heterostructures with Upconversion Materials: A Holistic Approach to Efficient Solar Water Splitting Yerbolat Magazov, Vladislav Kudryashov, Magzhan Amze, Kuanysht Moldabekov and Nurxat Nuraje; Nazarbayev University, Kazakhstan

The production of hydrogen fuel through solar-driven water splitting has become the most promising strategy for the renewable energy future. The majority of photoactive materials that are used to generate hydrogen and oxygen under solar irradiance utilize only UV and visible light. Considering that the UV accounts for 9.3% ($\lambda < 400$ nm), visible light is 54.1%, and the remaining 36.6% which accounts for infrared light ($\lambda > 800$ nm) results in substantial solar energy loss. Hence, one of the primary objectives of this study is to capture and fully utilize solar energy, particularly IR radiation by incorporating photon-upconverting materials into a water-splitting system. Our work is focused on the basic concept, in which a semitransparent stable electrode based on Cu₂O with protective layers absorbs UV-Visible light and the upconverter in a solid-state form consisting of PbS nanocrystals, sensitizer and emitter elements utilize the low energy photons and produce the higher one in the visible region through the triplet-triplet annihilation (TTA) process. This strategy provides a significant improvement in light harnessing capacity and offers a two-fold increase in terms of photocurrent density.

8:00 PM EN07.09.15

Salt Template Based Synthesis of Bi Nanoparticles and Their Electrochemical CO₂RR Activity for Formic Acid Production Choi Sung Yeol and Jeong Min Baik; Sungkyunkwan University, Korea (the Republic of)

Fossil fuel combustion process has led to excess emission of carbon dioxide to air about 35 billion ton per year. It causes serious environmental crisis like global warming, acid rain, water pollution etc. Up to now, considerable strategies for reducing usage of fossil fuels are mostly focused on expanding renewable energy source (energy harvesting, green hydrogen, power generation from nature). But it is not sufficient for supplying increasing global energy demand [1] and for these reason, continuous CO₂ emission to atmosphere is inevitable. Carbon capture and utilization technology (CCUS) is rising as one of the most effective solution to these unavoidable combustion process. Among CCUS technology, Electroreduction of CO₂ to fuel (CO₂RR) which can be achieved from catalytic conversion at heterogeneous interface is promising technology because CO₂ can be transformed to other value-added multi carbon products. Formic acid, which is most high value-added products, can be synthesized through flow-cell set-up what can make CO₂ gas diffuses more easily to the catalytic active site. We coated Bismuth nanoparticle as active catalyst directly on Gas diffusion electrode by NaCl template method without adding any binder solution and checked the selectivity, efficiency of bismuth catalyst layer by analyzing final products using NMR, Gas chromatography spectroscopy method. The synthesized Bi NPs exhibits excellent selectivity to HCOOH (~90%) at -0.8V, and showed over than 30mA/cm² current density.

8:00 PM EN07.09.16

High Photocharging Current Density and Improved Hydrogen Evolution Through Photoelectrochemical Biomass Valorization on Mo-BiVO₄ Photoanodes Debajet K. Bora^{1,2}; ¹Mohammed VI Polytechnic University, Morocco; ²ETH Zurich, Switzerland

In the last decade, the application of n-type metal oxide photoelectrodes for photoelectrochemical solar water splitting to produce hydrogen has been a cornerstone of artificial photosynthesis research. With a theoretical STH efficiency of 9.1%, the use of BiVO₄ as a highly efficient photoanode material is an intriguing possibility [1]. It is utilized extensively in photocatalysis and photoelectrochemical water splitting for hydrogen production due to its low bandgap and ability to absorb visible light. Recently, BiVO₄ was to convert biomass into organic compounds with added value. Due to its well-matched VB position with the electrochemical oxidation potential of 5-hydroxymethyl furfuryl, it is employed in the conversion to 2,5 - furan dicarboxylic acid using TEMPO (2,2,6,6-tetramethylpyridine-1-oxyl) as an ion scavenger [2]. This work [3] aims to increase the photocurrent density to match the current state of the art, as well as the solar-to-hydrogen conversion efficiency and faradaic efficiency for hydrogen generation. PEC-based glycerol oxidation is utilized to produce value-added organics, with an emphasis on controlling the activity-selectivity factors of the BiVO₄ photoanode, as described in a recently published work. In the current case, hydrogen is forming as a byproduct of CO₂ along with the formation of formic acid/formaldehyde on the cathodic side. It also helps to avoid the formation of explosive H₂/O₂ mixtures caused by membrane leakage. In terms of kinetics, the oxidation of biomass by PEC is more advantageous than oxidation by water because it involves fewer intermediate reaction steps, which increases the associated potential. The most important research gap is the direct application of photoelectrochemical biomass oxidation to increase the solar-to-hydrogen conversion efficiency (STH) of existing Mo-BiVO₄ without resorting to costly modification techniques such as heterojunction formation or the tandem approach. A novel surfactant-mediated method has been developed to produce Mo-doped BiVO₄ photoelectrodes with well-controlled morphology and pure clinobisvanite phases, as confirmed by FESEM and XRD. The photoelectrode exhibits the typical absorbance band in the visible spectrum, proving its suitability for photoelectrochemical applications. When exposed via a full aperture under front light illumination, the photoanode exhibits a photocurrent density of 3.5 mA cm⁻², which is the highest among the existing pristine bismuth vanadate photoanodes without modification. Upon TEM beam exposure, the scratched nanoparticles constituting the photoelectrodes exhibit a unique phenomenon of dynamic crystallite fringes, indicating the photodecomposition nature of the photoelectrode. Mo-BiVO₄ is further utilized for photoelectrochemical glycerol oxidation to prevent electron-hole recombination and enhance the STH efficiency, and it exhibits the highest current density of 5 mA cm⁻² under backside illumination. A glycerol layer on the photoelectrode's surface obstructs photons, resulting in a decrease in photocurrent density under front light illumination. The photoelectrode exhibits photocharging, enabling the photocurrent density to reach a maximum of 8 mA cm⁻² with a water splitting current density of 5.8 mA cm⁻². The effect is a result of the increased band bending at the photoelectrode's surface, which facilitated enhanced charge generation and prevented the recombination of excitonic pairs. Upon photoelectrochemical glycerol oxidation, the photoelectrode exhibits significant hydrogen gas evolution with the highest STH efficiency of 5.5% and IPCE of 52%.

References:

- [1] M. Rohloff, B. Anke, S. Zhang, U. Gernert, C. Scheu, M. Lerch and A. Fischer, *Sustainable Energy Fuel*, 2017, 1, 1830.
- [2] H. G. Cha and K.-S. Choi, *Nat. Chem.*, 2015, 7, 328.
- [3] D. K. Bora, M. Nadjafi, A. Armutlulu, D. Hosseini, P. Castro-Fernandez, R. Toth, *Energy Advances*, 2022, 1, 715.

SESSION EN07.10: CO₂/NO_x Reductions and Novel Electrosynthesis I
Session Chairs: Maria Escudero-Escribano and Haotian Wang
Thursday Morning, November 30, 2023
Hynes, Level 3, Room 310

8:15 AM EN07.10.01

Machine Learning Assisted Computational Design of High Entropy Alloy Electrocatalysts for Selective Nitrate to Ammonia Conversion Boyang Li, Ying Fang and Guofeng Wang; University of Pittsburgh, United States

Human activities have influenced global nitrogen cycle and caused many energy and environmental issues. A possible solution is to directly reduce nitrate to ammonia electrochemically, which can synergistically mitigate environmental problems and provide economic benefits by generating fertilizer using renewable energy. In this study, we employed a machine learning assisted computational approach to find a high entropy alloy (HEA) catalyst toward highly selective and stable electrochemical nitrate reduction (ENR) for nitrate to ammonia conversion under acidic conditions. First, we explored the composition space of 10 active elements (i.e., Ru, Pt, Pd, Cu, Fe, Co, Ni, Rh, Ir, and Mo) with the atomic ratio of each element ranging from 5 to 50%, with a 5% step size. We launched a composition screening to ensure the solid solution phase based on atomic size mismatch, mixing enthalpy, and Gibbs free energy of mixing, and identified 24 types of element compositions to be stable under any composition. By using the literature-reported synergistic pairs for ENR to further prescreening, we identified Ru-Pd-Pt-Cu alloy as an appropriate candidate to disperse Ru atom and improve the performance of ENR to ammonia. Furthermore, we used the DFT method to optimize the adsorption configurations of all possible ENR intermediates on RuPdPtCu (111) surface and used the elemental types on the first neighboring and second neighboring positions as input features to fit the calculated adsorption energies using a linear regression model. Our results show that nitrate reduction species are more favorable to be adsorbed on the Ru atom (i.e., first neighboring site) as compared to the Cu, Pt, and Pd atoms, suggesting that the nitrate reduction will predominantly occur on the site containing at least one Ru atom in RuPdPtCu (111) surface. The limiting potential defined as the highest potential in which all free energy changes become downhill was predicted to be 0.17V for nitrate reduction reaction on RuPdPtCu(111) with the corresponding rate-determining step being the protonation of N to form NH. In comparison, the metallic Ru (0001) surface shows a lower limiting potential of -0.36 eV to promote nitrate reduction. This finding explains why the RuPdPtCu HEA catalyst exhibits a higher nitrate reduction activity than the unary Ru catalyst. Our predictions have been well validated by experimental measurement data.

8:30 AM EN07.10.02

Balanced NO_x⁻ and Proton Adsorption for Efficient Electrocatalytic NO_x⁻ to NH₃ Conversion Yue Hu^{1,2}, Dongsheng Geng³ and Qingyu Yan²; ¹University of Science and Technology Beijing, China; ²Nanyang Technological University, Singapore; ³Nanjing University of Information Science & Technology, China

Electrocatalytic reduction of available nitrate (NO₃⁻)/nitrite (NO₂⁻) resources (eNO_x⁻RR) to value-added ammonia (NH₃)¹ under ambient conditions is a green and promising alternative to the Haber-Bosch process.² In practical, NO_x⁻ resources can be obtained from two ways: 1) industrial and agricultural wastewater and polluted groundwater,³ and 2) plasma-mediated nitrogen oxidation (p-NOR).⁴ However, their NO_x⁻ concentrations are generally low.⁵ Hence, electrocatalyst engineering is important for eNO_x⁻RR to obtain both high NH₃ FE and high current density at low NO_x⁻ concentrations. Herein, we designed balanced NO_x⁻ and proton adsorption by properly introducing Cu sites into Fe₂O₃ electrocatalyst. During the eNO_x⁻RR process, the excess H adsorption is balanced and the good NO_x⁻ affinity is maintained. As a result, the designed Cu-Fe₂O₃ catalyst exhibits promising performance with an average NH₃ FE of 98% and an average NH₃ yield of 15.65 mg h⁻¹ cm⁻² under the low NO₃⁻ concentration (32.3 mM) of typical industrial wastewater at an applied potential of -0.6 V vs. Reversible Hydrogen Electrode (RHE). Moreover, the concentration of NO_x⁻-N (451.6 µg ml⁻¹) in a simulated industrial wastewater can be decreased to the drinkable water level (NO₃⁻-N < 11.29 µg ml⁻¹ and NO₂⁻-N < 0.91 µg ml⁻¹) after 160 min with an average NO₃⁻-to-NH₃ conversion efficiency of 85%. With direct current (DC) p-NOR generated NO_x⁻ (23.5 mM) in KOH electrolyte, the Cu-Fe₂O₃ catalyst achieves a FE of 98.83% and a yield of 15.09 mg h⁻¹ cm⁻² for NH₃ production at -0.6 V (vs. RHE). It is worth noting that the DC plasma energy consumption is only 13.5 W/h.

References

- (1) Wang, Y.; Wang, C.; Li, M.; Yu, Y.; Zhang, B. Nitrate electroreduction: mechanism insight, in situ characterization, performance evaluation, and challenges. *Chemical Society Reviews* **2021**, *50* (12), 6720-6733.
- (2) Smith, C.; Hill, A. K.; Torrente-Murciano, L. Current and future role of Haber-Bosch ammonia in a carbon-free energy landscape. *Energy & Environmental Science* **2020**, *13* (2), 331-344.
- (3) van Langevelde, P. H.; Katsounaros, I.; Koper, M. T. M. Electrocatalytic Nitrate Reduction for Sustainable Ammonia Production. *Joule* **2021**, *5* (2), 290-294.

(4) Li, L.; Tang, C.; Cui, X.; Zheng, Y.; Wang, X.; Xu, H.; Zhang, S.; Shao, T.; Davey, K.; Qiao, S.-Z. Efficient Nitrogen Fixation to Ammonia through Integration of Plasma Oxidation with Electrocatalytic Reduction. *Angewandte Chemie International Edition* **2021**, *60* (25), 14131-14137.

(5) Ren, Y.; Yu, C.; Wang, L.; Tan, X.; Wang, Z.; Wei, Q.; Zhang, Y.; Qiu, J. Microscopic-Level Insights into the Mechanism of Enhanced NH₃ Synthesis in Plasma-Enabled Cascade N₂ Oxidation–Electroreduction System. *Journal of the American Chemical Society* **2022**, *144* (23), 10193-10200.

8:45 AM EN07.10.03

Optimization Strategies of Photovoltaics-Powered Green Hydrogen ProductionXuanjieWang, XinyueLiu and LenanZhang; Massachusetts Institute of Technology, United States

Green hydrogen production powered by photovoltaics provides a clean solution for energy conversion and storage. The key parameter of photovoltaic electrolysis (PV-EC) system is the solar-to-hydrogen (STH) efficiency. Previous studies have been mostly focused on improving the efficiency of each system individually using multi-junction PV materials, catalysts and electrolytes. However, the coupling between photovoltaic and electrochemical devices is still elusive to achieve high STH efficiency in a system level. In our study, the optimization strategies of PV-EC systems are demonstrated to approach thermodynamic limit (26.6%) for green hydrogen production. First, we list three design parameters for modeling, namely number of PV, number of EC and the area ratio between PV and EC. Then we model the crystalline silicon PV coupled with a real EC system. The STH efficiency varies under different PV and EC combinations. The STH efficiency map clearly defines three regions indicating the engineering space for PV-EC coupling, Tafel slope and area ratio. The optimization strategies presented in this study can lead to further advancements in coupled PV-EC systems with well-controlled performance for different conditions.

9:00 AM EN07.10.04

Ion Beam Analysis of MoNi₄-MoO₂ Catalyst Layer for Anion Exchange Membrane ElectrolyzerYaminiKumaran¹, LatikaS. Chaudhary¹, IulianGherasoiu² and HaralabosEfstathiadis¹; ¹SUNY Poly CNSE, United States; ²SUNY Polytechnic Institute, United States

There has been an increased interest in Anion Exchange Membrane (AEM) electrolyzer technology enabling zero-gap configuration lately. This technology also allows non-noble metal-based materials to be used as catalyst layers in an alkaline environment. In this research, MoNi₄ supported by MoO₂ nanorods has proven to be a promising electrocatalyst for Hydrogen evolution reaction (HER) with a decreased overpotential of 40 mV at 10 mA/cm² with increased current density, and stability for almost 12 hours in half-cell configuration. However, it is important that the material be used as a catalyst layer in membrane electrode assembly to have the capacity to tolerate high steady-state potentials for extended periods of time in real operating systems. The aim of this study is to analyze the AEM electrode assembly with MoNi₄-MoO₂ as the cathode layer synthesized via hydrothermal synthesis for overall metal loading corresponding to the improved efficiency and catalyst dissolution arising due to the interaction between the catalyst layer and the ionomer membrane. The cathode catalyst synthesized was characterized by X-Ray diffraction, SEM and X-Ray photoelectron spectroscopy for structural, morphological and surface composition. Further, nuclear techniques like Rutherford Backscattering Spectroscopy (RBS) employed to provide information regarding the thickness and stoichiometry of the catalyst layer and metal dissolution in the ionomer membrane, and Nuclear Reaction Analysis (NRA) was utilized to study different defects in the ionomer membrane by high-resolution Hydrogen depth profiling after the operation. Overall, this work presents a better understanding of catalyst degradation effects on the ionomer membrane and vice versa responsible for the voltage and mass transport losses in AEM electrolyzers.

9:15 AM *EN07.10.05

Metal Complex/Semiconductor Hybrid Photoelectrocatalysts and Photocatalysts for CO₂ ReductionAkinobuNakada^{1,2}; ¹Kyoto University, Japan; ²PRESTO/JST, Japan

Reductive conversion of CO₂ into energy-added molecules has been an important subject in various fields including materials chemistry, catalysis, electrochemistry, and photochemistry, from viewpoints of both decreasing CO₂ concentration and gaining energy and carbon resources. Among the various methods and schemes proposed, visible-light-driven CO₂ reduction in combination with water oxidation, one of the representative models of artificial photosynthesis, is an attractive solution because it enables abundant water and inexhaustible solar energy to be used to produce value-added chemicals. Molecular metal complexes and semiconductors are promising candidates for photocatalysts that can reduce CO₂ to CO, formate, formaldehyde, or other hydrocarbons. Although both molecular metal complexes and semiconductors have strengths and weaknesses, their weaknesses (low oxidation ability and low selectivity for reduction reactions) can be overcome via the construction of a suitable molecule/semiconductor hybrid material. However, facilitating electron transfer at the molecule/semiconductor junction while suppressing unfavorable back electron transfer events is challenging.

Here, our design principle for developing the hybrid photoelectrodes and photocatalysts will be reported, starting from introduction of selective electrocatalysis and photocatalysis of CO₂ reduction by a metal complex catalyst in aqueous solution. Subsequently, application of these metal-complex photocatalysts into a hybrid photoelectrode with semiconductor materials for photoelectrochemical CO₂ reduction will be presented. Simple hybrid photocatalysts directly connecting metal complexes and semiconductor particles, which facilitate photocatalytic CO₂ reduction via interfacial electron transfer without the aid of electrochemical techniques, will also be reported. Finally, we will report our recent approach for constructing hybrid photocatalysts with design-flexible conjugated polymers as a light absorber, a photoelectron transporter, and a suitable reaction center by site-selective modification of metal-complex catalysts.

9:45 AMBREAK

10:15 AM *EN07.10.06

An Integrated View of Multi-Step (photo)Electrocatalytic ReactionsFrancesHoule; Lawrence Berkeley National Laboratory, United States

Our views of (photo)electrocatalytic reactions and how they are influenced by their environments are strongly shaped by atomic-level theoretical studies that examine reaction pathways to identify the most probable routes, and by macro-level observations of current densities, Tafel plots, and product distributions. Connecting these two very different pictures via multiscale stochastic kinetics simulations provides a way to examine factors that influence reactivity, and predict how systems can be designed for improved efficiency and selectivity. This talk will focus on the role of thermal steps and local fluctuations at the catalytic site level in influencing reactivity, and discuss how these characteristics are manifested in experimental studies.

10:45 AM EN07.10.07

Defect Engineering of WO₃ by Rapid Flame Reduction for Efficient Photoelectrochemical Conversion of Methane into Liquid OxygenatesHo KunWoo¹, AnkitGautam¹, Jaxiry S.Barroso-Martínez¹, Arthur P.Baddorf², KaiZhou¹, Yoon YoungChoi¹, JiajunHe¹, Alexander V.Mironenko¹, JoaquinRodriguez-Lopez¹ and LiliCai¹; ¹University of Illinois, United States; ²Oak Ridge National Laboratory, United States

Photoelectrochemical (PEC) conversion is a promising way to utilize methane (CH₄) as a chemical building block without harsh conditions. However, PEC CH₄ conversion to value-added chemicals remains challenging due to the thermodynamically favorable over-oxidation of CH₄ to CO₂. Here, we report WO₃ nanotubes (NTs) photoelectrocatalysts for PEC CH₄ conversion with high liquid product selectivity through defect engineering. By tuning the flame reduction treatment, the oxygen vacancies of WO₃ NTs were carefully controlled. The optimized reduced WO₃ NTs suppressed over-oxidation of CH₄ and showed high C₁ liquid selectivity of 69.4% and production rate of 0.174 μmol cm⁻² h⁻¹. Scanning electrochemical microscopy revealed that oxygen vacancies can restrain the production of hydroxyl radicals, the presence of which in excess could further oxidize C₁ intermediates to CO₂. In addition, optical characterization and computational studies elucidated that oxygen vacancies thermodynamically suppress over-oxidation. This work introduces a strategy to understand and control the selectivity of photoelectrocatalysts for direct CH₄ conversion to liquids.

11:00 AM +EN07.10.08

In-Situ TEM Investigation on Redox Mechanisms of Transition Metal OxidesXiaozhiLiu, YuePan, DanZhou and DongSu; Chinese Academy of Sciences, China

The physicochemical properties of transition metal oxides are determined by their phase structures, surface exposed atoms, morphology, and defects. Metal oxide catalysts usually undergo a series of activation and reaction processes in practical applications, which modulate their morphology and change their valence states and crystal phases. These structural variations alternate their properties significantly and have been believed to be a critical problem, e.g., in their catalytic applications. During reactions, metal oxides undergo either reduction or oxidation reactions depending on the ratio of reducing or oxidizing gases in the atmosphere. Although it is believed that *in situ* investigation of the reaction pathways is of importance to understand their intrinsic redox nature, as far as we know, the microstructural evolution during the redox of metal oxides is still not well understood. We have studied the dynamic reaction behaviors of iron oxides via *in situ* transmission electron microscopy (TEM) with a Climate system from DENSolutions. We have achieved atomic-scale resolution imaging to visualize the evolution of phase boundary and the competitive transitions between Fe₃O₄, FeO, and Fe in the nanoreactor. Thus we found the inhomogeneous reaction pathways which are strongly affected by the trace amount of oxygen or water vapor in catalytic reactions. Our results could provide new insights into the redox reaction mechanism of transition metal oxides, and help to understand the role of these oxides in catalytic reactions.

1:30 PM *EN07.11.01

Controlling C(sp³)-H and C(sp³)-C(sp³) Transformations and Fuel Synthesis at Electrocatalytic Interfaces Marcel Schreier^{1,2}; ¹University of Wisconsin-Madison, United States; ²University of Wisconsin-Madison, United States

Producing fuels and chemicals using renewable electricity holds the promise to enable a circular economy based on sustainably produced carriers of electrical energy and sustainably produced chemicals. To date, the vast majority of electrocatalytic reactions are limited to the transformation of small inorganic molecules such as CO₂, H₂O, N₂, as well as the oxidation and reduction of alcohols. However, comprehensive electrification of the chemical industry will require electrocatalytic reactions that can promote the transformation of unactivated C(sp³)-H and C(sp³)-C(sp³) bonds, which are central to today's industry.

In this presentation, I will show how fundamental understanding of the interfacial processes occurring in electrocatalytic reactions can be exploited to expand the reaction scope of electrocatalysis to the transformation of complex substrates involving the controlled activation of C-H and C-C bonds. In a first step, I will show how this approach allows us to transform ethanol to ethylene oxide, an important plastic precursor. Subsequently, I will discuss methods to electrocatalytically transform inert alkanes such as methane, ethane, and butane at room temperature.

2:00 PM EN07.11.03

Photochemical Diodes for Simultaneous Bias-Free Glycerol Valorization and Hydrogen Evolution Jia-An Lin, Inwhan Roh and Peidong Yang; UC Berkeley, United States

Finding sustainable and renewable energy is currently one of the most urgent challenges facing society today. Artificial photosynthesis offers a route to using solar energy to produce fuels such as hydrogen, a fundamental component for building a carbon-free economy. One such approach to realizing artificial photosynthesis is presented through the photochemical diode. Conventional approaches targeted the optimization of the overall water splitting (OWS) reaction in which hydrogen and oxygen are produced. However, the sluggish kinetics of the oxygen evolution reaction (OER) and the high thermodynamic potential requirement of 1.23 V for the OWS limit the current performance of bias-free photoelectrochemical (PEC) systems. Here, we offer an alternative approach by replacing the OER with the glycerol oxidation reaction (GOR) for value-added chemicals using Si photoanode. By employing a low overpotential catalyst such as PtAu for GOR, which shows a low onset potential of 0.4 V vs RHE electrochemically, the voltage requirements to couple with hydrogen evolution reaction (HER) become substantially lowered compared to OWS. As a result, the PtAu/Si photoanode exhibits a low GOR onset potential of -0.05 V vs RHE and a photocurrent density of 10 mA/cm² at 0.5 V vs RHE. Coupled with a Si nanowire photocathode for the HER, the integrated system yields a high photocurrent density of 6 mA/cm² with no applied bias under 1 sun illumination and can run for over 4 days under diurnal illumination. The demonstration of the GOR-HER integrated system provides a framework for designing bias-free photoelectrochemical devices at appreciable currents and establishes a facile approach to artificial photosynthesis.

2:15 PM EN07.11.04

Molecular Additives Steer Selectivity of CO₂ Photoelectrochemical Reduction over Gold Nanoparticles on Gallium Nitride Aisulu Aitbekova, Nicholas Watkins, Jonas Peters, Theodor Agapie and Harry A. Atwater; California Institute of Technology, United States

We demonstrate that functionalizing Au/p-GaN cathodic photoelectrochemical devices with molecular additives steers the selectivity for CO₂ reduction process toward reduced products of carbon dioxide and suppresses hydrogen generation via water splitting. The working hypothesis for this selectivity change is the suppressed proton transfer through hydrophobic molecular additive films, which results in the diminished hydrogen evolution reaction rates (Faradaic Efficiency to H₂ decreases from 90% to 18%). Our work establishes a rigorous platform to elucidate structure-property relationships in photoelectrocatalysts and engineer active, stable, and selective materials for sustainable energy applications.

The wide bandgap semiconductor p-GaN exhibits stability under CO₂ photoelectrochemical conditions due to its nitrogen-rich surface. Additionally, its conduction band minimum is more negative than the CO₂ reduction potential. When combined with metals, such as gold nanoparticles, the semiconductor-metal interface forms a Schottky barrier. The downward bending of the conduction and valence bands drives electrons excited in p-GaN towards the metal-electrolyte interface, while the holes are transferred into the p-GaN bulk semiconductor.

Rising levels of greenhouse gases necessitate a reduction in the amounts of these harmful compounds in the atmosphere and a transition to sustainable production of fuels and chemicals. Photoelectrochemical CO₂ reduction (CO₂R) is an appealing solution to convert carbon dioxide into higher-value products. However, CO₂R in aqueous electrolytes suffers from poor selectivity due to the competitive hydrogen evolution reaction dominant in aqueous electrolytes. As noted above, our approach to overcome this challenge consists of (1) synthesis of metal/semiconductor structures with controlled properties and (2) functionalizing the metal/semiconductor surface with molecular additives.

2:30 PM BREAK

3:00 PM EN07.11.05

A Comprehensive Online Analytical System Coupled with Standardized Data Analysis for the Electrochemical Reduction of CO₂ Alessandro Senocrate^{1,2}, Peter Kraus¹, Francesco Bernasconi^{1,2} and Corsin Battaglia^{1,2}; ¹Empa-Swiss Federal Laboratories for Materials Science and Technology, Switzerland; ²ETH Zürich, Switzerland

The electrochemical reduction of CO₂ (CO₂RR) is a promising way to convert detrimental CO₂ emissions into sustainable fuels and chemicals, and thus to achieve a circular carbon economy.¹ Depending on catalyst type and reaction conditions, different gaseous and liquid products can be obtained from the CO₂RR, and their production rates vary with reaction time. It becomes thus imperative, for any catalytic performance analysis, to be able to assess the product distribution online during CO₂RR.^{2,3} However, while gaseous products are readily analyzed online by gas chromatography, liquid products are typically only assessed at the end of the reaction due to the lack of suitable automated liquid sampling and analysis methods. In addition, reaction parameters such as CO₂ mass flow rates, temperatures and pressures are seldom recorded, causing the loss of significant information on catalysts, electrodes, and electrolyzers behavior.

To overcome these issues, we assemble a comprehensive analytical system coupling online gas and liquid product analysis by gas and liquid chromatography leveraging a special automated liquid sampling valve with electrochemical protocols that assess CO₂RR performance, electrolyzer cell resistance and electrode surface area. In addition, we record CO₂ mass flow rates, electrolyzer temperatures, as well as gas and liquid flow pressures.⁴ To rapidly and reproducibly handle the large and heterogeneous data volume obtained we implement a standardized data pipeline based on our own open-source software,⁵ which automatically parses the numerous different raw data files, composes a data set following FAIR practices,⁶ and post-processes and plots the data in a standardized way. We validate the analytical system by carrying out CO₂RR at 200 mA/cm² on Cu gas diffusion electrodes, following the changes in selectivity with reaction time for > 10 gaseous and liquid products, and recording mass flow rates, electrolyzer temperatures and pressures. The modular nature of our analytical system, combined with the standardized data pipeline, allows us to freely increase the number and type of sensors used with minimal impact on the data analysis time, as well as to multiplex our analysis to 8 parallel electrolyzer cells, paving the way for a much deeper and faster understanding of the function of CO₂RR catalysts, electrodes, and electrolyzers.

3:15 PM EN07.11.06

Computational Screening of Non-Copper Based Catalysts for Electrochemical CO₂ Reduction Reaction Samira Siahrostami; Simon Fraser University, Canada

Copper-based catalysts are currently being investigated as the most efficient catalysts for electrochemical CO₂ reduction reactions (CO₂RR) to valuable hydrocarbons such as methane, ethylene, and ethanol. Copper catalysts, on the other hand, are prone to restructuring and degradation, fueling the search for non-Cu catalyst families that enable C-C coupling. We use high-throughput DFT calculations to search a wide range of materials space and accelerate the discovery of more efficient catalyst materials beyond copper for CO₂RR, as well as scale-up the use of the catalysts in electrochemical reactors to enable meaningful conversion. In this talk, I will discuss the use of robust high-throughput DFT calculations to screen a massive library of non-conventional classes of materials such as perovskites, transition metal nitrides¹, and metal organic frameworks² as well as the insights we can gain from them.

References:

- 1- Yohannes, A.G.; Lee, C.; Talebi, P.; Mok, D.H.; Karamad, M.; Back, S.; Siahrostami, S. *ACS Catal.*, 2023, <https://doi.org/10.1021/acscatal.3c01249>.
- 2- Nwsou, U.; Siahrostami, S. *Catal. Sci. Technol.* 2023, DOI: 10.1039/D3CY00408B.

3:30 PM EN07.11.07

Simple Approach for Modeling Cyclic Voltammograms of Hydrogen Evolution Reaction - Application to Emerging Catalysts Timothy Yang and Wissam A. Saidi; U.S. Department of

Hydrogen evolution reaction (HER) is the critical process for green hydrogen production. In analytical chemistry, cyclic voltammetry (CV) has been the practical technique to provide current-potential characteristics that can be further analyzed using the Butler-Volmer formulation. Due to the phenomenological nature of the BV formulation, there is a missing linkage between the analytical chemistry, theoretical electrochemistry and first-principles modeling. Herein, we develop an electrochemical CV model for HER from density functional theory calculations. At the equilibrium conditions, this CV model quantifies the HER exchange currents – the main analytical descriptor for HER rate, only using an easy-to-compute hydrogen adsorption free energy. Further, we show that the CV model reproduces experimental cyclic voltammograms with high fidelity. The success of the CV model is justified by the universality of the transfer coefficient and the absolute reaction rate for a one-step, one-charge transfer process. This framework for developing the electrochemical HER model from fundamental electrochemistry principles and computational quantum-mechanical approaches is general and applicable for any electrochemical reaction.

3:45 PM *EN07.11.08

Multimodal Operando Studies of Evolving Cu Nanocatalysts for CO₂ Electroreduction Yao Yang¹, David A. Muller², Hector D. Abruna² and Peidong Yang¹; ¹UC Berkeley, United States; ²Cornell University, United States

In an era of shifting the energy paradigm from fossil fuels to renewable energy, CO₂ reduction reaction (CO₂RR) emerges as a promising approach to convert greenhouse gas into valuable chemical fuels and close the carbon cycle for a sustainable energy supply. Since Cu remains the sole element for CO₂RR to multicarbon products (C₂₊), significant efforts have been devoted to developing Cu electrocatalysts with higher selectivity and activity. One of the key challenges is understanding how to achieve and sustain electrocatalytic activity under operating conditions for extended time periods, and such fundamental understanding calls for the use of multimodal *operando* analytical methods.¹⁻⁴ In our previous studies, we reported that sub-10 nm Cu nanoparticles (NPs) showed superior C₂₊ selectivity, relative to the larger sized Cu NPs, especially at low overpotentials.^{5,6} In this work, we present a comprehensive *operando* correlative study of dynamic evolution of a family of monodisperse Cu NP ensemble electrocatalysts under CO₂RR.¹ *Operando* electrochemical liquid-cell scanning transmission electron microscopy (EC-STEM) and 4D-STEM reveal dynamic microscopic structural evolution at the nm scale.² Correlated *operando* high-energy-resolution fluorescence-detected (HERFD) X-ray absorption spectroscopy (XAS) reveals dynamic macroscopic changes in valence states and coordination environment. Statistical analysis of interparticle dynamics was probed by *operando* electrochemical resonant soft X-ray scattering (EC-RSoXS).³ The multimodal *operando* methods, described herein, elucidate the longstanding enigmatic nature of Cu active sites for selective CO₂ electroreduction. The strategy described herein can serve as a general platform to resolve the electrocatalytic interface of nanoparticle catalysts under real-time operating conditions across multiple spatiotemporal scales, thus serving the fundamental understanding necessary to development of many other electrochemical reactions for renewable energy technologies.⁴

References:

1. Yang, Y., Muller, D., Abruna, H., Yang, P. et al. *Operando* Studies Reveal Active Cu Nanograins for CO₂ Electroreduction. *Nature* 2023, 614, 262.
2. Yang, Y., Muller, D., Abruna, H. Elucidating Cathodic Corrosion Mechanisms with *Operando* Electrochemical Transmission Electron Microscopy. *J. Am. Chem. Soc.* 2022, 144, 15698.
3. Yang, Y., Yang, P., et al. *Operando* Resonant Soft X-ray Scattering Studies of Chemical Environment and Interparticle Dynamics of Cu Nanocatalysts for CO₂ Electroreduction. *J. Am. Chem. Soc.* 2022, 144, 8927.
4. Yang, Y., Abruna, H. et al. *Operando* Methods in Electrocatalysis. *ACS Catal.* 2021, 11, 1136-1178.
5. Kim, D., Yang, P. et al. Copper Nanoparticle Ensembles for Selective Electroreduction of CO₂ to C₂-C₃ Products. *Proc. Natl. Acad. Sci. U.S.A.* 2017, 114, 10560.
6. Li, Y., Yang, P. et al. Electrochemically Scrambled Nanocrystals are Catalytically Active for CO₂-to-Multicarbon. *Proc. Natl. Acad. Sci. U.S.A.* 2020, 117, 9194.

SESSION EN07.12: Electrocatalysis General I
Session Chairs: Maria Escudero-Escribano and Charles McCrory
Friday Morning, December 1, 2023
Hynes, Level 3, Room 310

8:15 AM EN07.12.01

Facile Synthesis of Novel Pt-Ni-Cu Nanoframes via Simple Galvanic Replacement for Methanol Oxidation Reaction Kevin Wilk, Yuhuan Hu, Samantha Fuscus, Markus Higgins, Kira Shulman, Eduardo Lezama and Yiliang (Yancy) Luan; SUNY Binghamton, United States

Pt-based catalysts play a crucial role in various applications, such as catalytic converters, petroleum refinement, and chemical production. However, the widespread use of Pt-based catalysts is hindered by their high cost. To address this issue, researchers have focused on combining Pt with non-precious metals to reduce Pt usage with intent to optimize electronic configurations for improved catalytic performance. Recently, there has been significant interest in nanoframes due to their unique open structure, which provides a large surface area and enhances catalytic performance compared to conventional solid nanoparticles. In this report, we present a facile preparation of novel Pt-Ni-Cu nanoframes from Pt-Ni nanocubes through a simple galvanic replacement process at high temperature. The resulting nanoframes retain the segregated Pt at the edges and diagonals of the Pt-Ni precursor while incorporating Cu into the alloy. The segregated Ni, except at the edges and diagonals, is selectively removed, resulting in a hollow structure through the Kirkendall Effect. The amount of Cu in the nanoframes can be controlled by adjusting the reaction time. The nanoframes were applied for methanol oxidation reaction (MOR), and the mass activity is proportional to the amount of Cu incorporated, which was adjusted by controlling the time on the synthesis of the nanoframes. These results not only highlight the exceptional potential of the Pt-Ni-Cu nanoframes as catalysts for MOR but also provide a promising solution to the cost-effectiveness challenge associated with Pt-based catalyst applications.

8:30 AM EN07.12.02

Segregation Engineering for Enhanced Stability of Electrocatalysts Xuyang Zhou¹, Olga Kasian^{1,2,3}, Raquel Aymerich Armengol¹, Siyuan Zhang¹, Christina Scheu¹, Gregory B. Thompson⁴, Gerhard Dehm¹, Baptiste Gault^{1,5} and Dierk R. Raabe¹; ¹Max-Planck-Institut für Eisenforschung GmbH, Germany; ²Helmholtz Institut Erlangen-Nürnberg, Germany; ³Friedrich-Alexander-Universität Erlangen-Nürnberg, Germany; ⁴The University of Alabama, United States; ⁵Imperial College London, United Kingdom

The challenge faced by energy conversions and storage devices, such as fuel cells and electrolyzers, lies in the gradual dissolution of the electrocatalysts during long-term and dynamic operation. This dissolution primarily starts at defects, specifically grain boundaries and dislocations. To tackle this issue and enhance the stability of electrocatalysts, we employ the design concept of segregation engineering, which leverages solute segregation prone to these internal defects. In our study, we demonstrated the feasibility of this approach by stabilizing a model Pt catalyst through the addition of a more noble metal, Au, at approximately 5 at.%. By optimizing the heat treatment procedure, we successfully controlled the local chemistry of defects, achieving a local Au content ranging from no solute segregation to values as high as 30 at.%. The characterization of the nanoscale structure and chemistry of the defects was accomplished through a correlative study involving transmission electron microscopy and atom probe tomography. Moreover, we directly linked the structure and chemistry of these defects with electrochemical dissolution tests of Pt and PtAu alloys, employing on-line inductively coupled plasma mass spectrometry in a scanning flow cell set-up. By effectively stabilizing and passivating the most vulnerable sites, Au atoms, which were once segregated as defects, significantly enhance the stability of Pt electrocatalysts, reducing dissolution by more than an order of magnitude. Even after long-term testing (1000 cycles), the dissolution predominantly occurred at the segregated Au atoms, validating the potential of segregation engineering in enhancing the longevity of Pt electrocatalysts. Our work highlights the significance of incorporating a stabilizing component like Au and considering the spatial distribution of this solute addition within the electrocatalyst, particularly concerning the chemical distribution at crystalline defects. This breakthrough opens up new pathways for the development of more stable nanoscale electrocatalysts, utilizing solute segregation to defects, and can be applied to a wide range of catalytic systems.

8:45 AM EN07.12.03

Active-Site Imprinted M-N-C Electrocatalysts: Tailor-Made Synthesis and Tuned Activity Davide Menga¹, Tim-Patrick D. Feller² and Yang Shao-Horn¹; ¹Massachusetts Institute of Technology, United States; ²Bundesanstalt für Materialforschung und -prüfung, Germany

Due to the abundance and inexpensiveness of their constituent elements and their atomic dispersion, metal- and nitrogen- co-doped carbons (M-N-Cs) are currently the best alternative among noble-metal-free catalysts set to replace critical raw materials in several fundamentally important electrochemical reactions such as oxygen reduction reaction (ORR) and CO₂ reduction reaction (CO₂RR).

Due to the metastability of the active M-N₄ sites at the temperature of their pyrolytic formation, the final transition metal loading is currently limited and significant amounts of inorganic by-products are formed. Although synthesis protocols have been successfully optimized, multiple processing steps are required, making the preparation time-consuming. In previous work, it has been shown that via an active-site imprinting strategy followed by a transmetalation reaction, Mg-N-C and Zn-N-C containing Mg-N₄ and Zn-N₄ sites respectively,

can be transformed into ORR active Fe-N-C electrocatalysts, avoiding the formation of elemental iron, or iron carbide side phases. This synthetic method allows for high yields, controlled morphology and high metal loadings.

In this contribution, it will be presented how Zn-N₄ sites in tailor-made Zn-N-C materials are utilized as an active-site imprint for the preparation of the corresponding M-N-C catalysts with a high loading of atomically dispersed metal. The current state of this class of materials is discussed in terms of synthetic methods, activity and stability.

9:00 AM EN07.12.04

3D Printed Continuous Nanoporous Cu/CuO_x Electrodes for Highly Efficient Hydrogen Evolution Reaction [Anand P. Tiwari](#) and William J. Scheideler; Dartmouth College, United States

The sluggish kinetics of electrocatalysts in alkaline media cause stability as well as low active site issues, restricting the conversion of renewable energy into hydrogen. Synergistic enhancements such as the formation of free-standing nanoporous heterostructures, homogeneous diffusion of active materials into conductive supports, and atomic doping/defecting of active materials could promise to improve the kinetics and resolve key stability issues. Herein, we present scalable 3D-printing of continuous nanoporous Cu/CuO_x diffused carbon electrocatalysts for efficient alkaline hydrogen evolution reaction (HER) in which Cu/CuO_x acts as active sites, nanoporous carbon provides a higher conductive surface area to enhance HER kinetics, and periodic 3D lattice micro-structuring facilitates bubble evolution to improve stability. The resulting micro-architected porous electrodes deliver high electrocatalytic activity for HER, with an overpotential of 155 mV at a current density of 10 mA/cm² and a Tafel slope of 134 mV/dec, outperforming other 3D noble metal-free oxide materials. In addition, the as-fabricated catalysts also showed superior durability: up to 240 hours of continuous hydrogen evolution without any significant change in overpotential and current density, which is 10X better than reported 3D-printed catalysts. Our comparative analysis of multiple 3D lattice geometries indicates that our 3D-ordered nanoporous Cu/CuO_x electrocatalysts maximize performance by exposing more active sites and allowing faster discharge of H₂ gas bubbles through engineered microchannels. We will finally discuss how our micro-architected approach to transforming 3D-printed lattices can be applied to a variety of earth-abundant electrocatalysts based on transition metal/metal oxides for enhancing performance and stability of additional reactions including OER.

9:15 AM EN07.12.05

Phase-Controlled Deposition of Ru on Pd Nanocrystal Templates: The Effects of Particle Shape and Size [Quynh Nguyen](#), Annemieke Janssen, Zhiheng Lyu, Veronica Pawlik, Chenxiao Wang and Younan Xia; Georgia Institute of Technology, United States

Template-directed growth has been widely used for the phase-controlled synthesis of metal nanocrystals, but much remains to be discovered about the mechanistic details. In this work, we systematically investigate the roles played by the shape and size of Pd nanocrystal templates in controlling the crystal phase taken by the deposited Ru overlayers. For Pd cubic nanocrystals, a face-centered cubic (*fcc*) Ru shell is always favored when the particle size is varied in the range of 6–25 nm. In the case of Pd octahedral nanocrystals, we observe a size dependence, with 14-nm octahedra giving *fcc*-Ru but 20- and 26-nm octahedra resulting in hexagonal close-packed (*hcp*) Ru. This trend can be attributed to their difference in surface atomic arrangement, as the {100} facets on a cubic template cannot be matched by any facet of *hcp*-Ru, forcing the deposited Ru to take the *fcc* phase. In contrast, the {111} facets on an octahedral template can be matched by the {0001} facets of *hcp*-Ru, allowing the deposited Ru to take either an *hcp* or *fcc* phase. The crystal phase taken by the Ru shell is determined by the relative contributions from the surface and bulk energies of the deposited *fcc*- and *hcp*-Ru phases. Additionally, the water content in the reaction mixture also plays an important role in affecting the crystal phase taken by the Ru shell by altering the reduction kinetics. When tested as catalysts toward ethylene glycol oxidation, the *fcc*-Ru outperforms *hcp*-Ru while the cubic shape is advantageous over the octahedral counterpart.

9:30 AM EN07.12.06

Toward Scalable Nickel-Cobalt Based Anode Materials for Alkaline Electrolysis: Unveiling the Path from Micropowder Analysis to Electrochemical Performance [Vineetha Vinayakumar](#)^{1,2}, [Adarsh Jain](#)¹, [Mohit Chatwani](#)¹, [Timo Wagner](#)³, [Christian Marcks](#)⁴, [Nicolas Wöhrl](#)^{1,2}, [Anna K. Mechler](#)⁴ and [Doris Segets](#)^{1,2}; ¹Institute for Energy and Materials Processes—Particle Science and Technology (EMPI-PST), University of Duisburg–Essen (UDE), Germany; ²Center for Nanointegration Duisburg–Essen (CENIDE), University of Duisburg–Essen (UDE), Germany; ³Faculty of Physics, University of Duisburg–Essen (UDE), Germany; ⁴Electrochemical Reaction Engineering, RWTH Aachen University, Germany

The depletion of conventional energy resources has highlighted the need for sustainable alternatives, with hydrogen emerging as a promising option. However, the commercial-scale production of hydrogen remains a challenge (1). In this study, we focus on water electrolysis as an efficient method for energy conversion and storage, emphasizing the crucial role of electrocatalysis. Despite recent progress, establishing direct correlations between anode properties and performance in an industrial setting is crucial for the practical implementation of stable and highly efficient anodes for alkaline water electrolysis at pilot-scale systems. This requires linking the scale-up process with a comprehensive fundamental understanding, enabling successful scaling while maintaining optimal performance.

To address these challenges, we evaluate the cycle of anode generation starting from the characterization of micropowders through catalyst inks to final electrodes. Our primary goal is to achieve efficient hydrogen production on a commercial scale. To accomplish this, our methodology utilizes complementary techniques to thoroughly analyze the physical and chemical properties of materials throughout the entire process chain. By adopting this comprehensive approach, we aim to gain a deep understanding of the materials involved and optimize their performance for the production of hydrogen on a large scale. To evaluate the interdependencies between different stages and to find out the determining steps during electrode manufacturing, we developed a framework in the sense of a coherent workflow starting with the characterization of commercially available Ni- and Co-based micro powders. Subsequently, ink formulations were optimized using analytical centrifugation (2) and Hansen parameter calculations (3), followed by electrode layer fabrication using ultrasonic spray deposition of the ink on Ni plates. After optimizing each individual stage in the whole process chain, we also investigated the influence of post-treatments, specifically vacuum annealing, and surface plasma treatment, on the stability of electrodes against delamination. A framework based on atomic force microscopy was developed to precisely quantify micro features and analyze the surface characteristics of electrodes including large areas. Subsequently, the evaluated electrodes were subjected to functional testing as anodes in alkaline water electrolysis, revealing valuable correlations between the properties of the catalyst ink and coated electrodes with their electrochemical activity and stability. Consistent with the identified structural characteristics, our preliminary results demonstrate that plasma-treated Ni-Co-O electrodes exhibit reduced overpotentials and enhanced stability compared to both pristine and vacuum-annealed electrodes. This improvement can be attributed to the enhanced adhesion and favorable surface properties, including roughness, induced by the plasma treatment. This study contributes significantly to the evaluation of the system throughout its various stages, integrating valuable feedback from preceding steps to further optimize electrode performance. Notably, our approach proves particularly advantageous in facilitating the transition from laboratory-scale developments to scalable processing, bridging the critical gap for practical industrial applications.

References

- (1) Ehlers, J.C., et al., Affordable Green Hydrogen from Alkaline Water Electrolysis: Key Research Needs from an Industrial Perspective. ACS Energy Letters, 2023. 8(3): p. 1502-1509.
- (2) Bapat, S., et al., On the state and stability of fuel cell catalyst inks. Advanced Powder Technology, 2021. 32(10): p. 3845-3859.
- (3) Anwar, O., et al., Hansen parameter evaluation for the characterization of titania photocatalysts using particle size distributions and combinatorics. Nanoscale, 2022. 14(37): p. 13593-13607.

9:45 AM EN07.12.07

Flow-Directing Electrodes with Multi-Scale Porosity for Controlling Transport and Reactions [Max A. Saccone](#), Xi Chen, Philip R. Onffroy, William Tarpeh and Joseph M. DeSimone; Stanford University, United States

Systems that simultaneously optimize transport and reaction parameters are crucial for chemical process intensification. In this talk, we discuss recent progress towards additively manufactured electrode materials that control flow fields in electrochemical systems with forced convection, coined “flow-directing electrodes.” We show how 3D printed micro-scale architected structures formed from metal-coated polymers, pure metals/oxides, or pyrolytic carbon can tune flow properties and prevent fouling in electrochemical systems while simultaneously providing pathways for electron transfer. We additionally show how to create multiscale hierarchy through the incorporation of nano-scale porosity in these systems via ZnO nanorod templating to tune specific surface area and permeability. We demonstrate the utility of such flow-directing electrodes for applications ranging from electrochemical remediation of per- and poly-fluoroalkyl substances (PFAS) where a nano-porous layer could act as a size-exclusion membrane to design of electrodes for redox-flow batteries where transport of working ions and redox-active material is maximized but transport and crossover of other species such as electrolytes and mediators is minimized. Flow-directing electrodes represent a paradigm shift in electrochemical reactor design in which high resolution vat photopolymerization printing techniques are used to create co-designed structures with complex geometry using electrically conductive functional materials—all leading to the ability to explore a wide landscape of previously impossible device designs.

10:00 AM BREAK

10:30 AM EN07.12.08

Ratchet Based Ion Pumps for Fine Tuning of Electrochemical Reactions [Dafna Meltser](#), [Alon Herman](#), [Brian A. Rosen](#) and [Gideon Seggev](#); Tel Aviv University, Israel

Precise control of electrochemical reactions can have a tremendous effect in enhancing the performance of electrochemical energy storage and conversion systems. However, electrochemical reactions are extremely sensitive to the physical and chemical environment at which the reaction takes place. Thus, control of the electrolyte ionic content and the electrochemical potential of

specific ions at the vicinity of the electrodes can enhance their selectivity towards the desired products and modify the overpotential of redox reactions. In this contribution we show that ion pumps based on a ratcheting mechanism can be used to tune the overpotentials of electrochemical reactions. Flashing ratchets are devices that utilize temporal modulation of a spatially asymmetric electric field to drive a non-zero time averaged current. We have recently demonstrated experimentally first-of-their-kind ratchet-based ion pumps (RBIPs). Since the ion pumping modifies the electrochemical potential of ions, and redox reaction rates are determined by the electrochemical potential, ratchet-based ion pumping provides an additional degree of freedom in tuning electrochemical reaction rates and overpotentials. RBIPs were fabricated by coating the two surfaces of nano-porous alumina wafers with gold forming nano-porous capacitors. The electric field within the nano-pores is modulated by oscillating the capacitors voltage. Hence, when immersed in solution, ions within the pores experience a modulating electric field resulting in ratchet-based ion pumping. The RBIP was placed as a membrane between two Pt electrodes inside a compartment filled with HCl solution. The application of an input signal to the ratchet is shown to accelerate or inhibit redox reactions on the surface of the Pt electrodes according to the ratchet properties. The combination of selective ion pumping with the control of reaction rates may also allow tuning the electrolyte content at the vicinity of the electrodes performing the electrochemical reaction independent of their potential thus providing another degree of freedom for the electrochemical process.

10:45 AM EN07.12.09

Suppression of Dopant Segregation and Improvement of Activity on a Perovskite Oxide Surface by Self-Formation of Ruddlesden-Popper Phase SanazKoochfar¹, MasoudGhasemi², TylerHafen³, GeorgiosDimitrakopoulos¹, DonghaKim¹, S.Elangovan³, JennaPike³, EnriqueGomez² and BilgeYildiz¹; ¹Massachusetts Institute of Technology, United States; ²The Pennsylvania State University, United States; ³OxEon Energy LLC, United States

Solid oxide fuel and electrolysis cells (SOFCs, SOECs) present a highly efficient platform for clean energy and chemicals conversion. However, degradation during operation challenges the commercialization and widespread feasibility of this technology. Segregation of dopants such as Sr and Ba to the surface is a main degradation mode that has been linked to the instability of the oxygen electrode surface. These segregated species form an insulating layer and leave behind a near-surface region that is depleted of the dopant. The segregated species on the surface suppress the oxygen reduction and evolution reactions. Improving the stability of surface chemistry and the resulting electrochemical activity on perovskite oxide oxygen electrodes is crucial for enabling efficient and durable SOFC/SOEC as a clean energy conversion platform. In this work, we take $\text{La}_{0.8}\text{Sr}_{0.2}\text{Co}_{0.8}\text{Fe}_{0.2}\text{O}_3$ (LSCF) as a state-of-the-art oxygen electrode, and we reveal that self-formation of Ruddlesden-Popper phase improves the surface chemistry, oxygen reduction kinetics, and electrochemical stability on it. We use X-ray photoelectron spectroscopy (XPS) and time of flight-secondary ion mass spectrometry (ToF-SIMS) to analyze surface and sub-surface chemistries. We reveal that the formation of Ruddlesden-Popper phase is accompanied by suppression of Sr dopant segregation. Moreover, our results show that B-site cations (Co and Fe) are depleted in the subsurface region. These findings reveal the structural elements that maintain an active and stable surface for oxygen reduction reaction on oxygen electrodes. Revealing this unique near-surface chemistry and phase formation is crucial in guiding the development of better surface chemistries for improving the oxygen electrode performance in SOFC/SOEC.

11:00 AM EN07.12.10

Covalent Anchoring of Macrocycles on Metallic Nanoparticles for Efficient Oxygen Reduction Reaction – A Joint Experimental and Theoretical Investigation AugusteTêtenoire, ArnaudFihey, CorinneLagrost and MikaelKepenekian; University of Rennes, France

The activation of O_2 through electrochemical reduction (ORR, oxygen reduction reaction) has shown promising results as alternative energy conversion technologies that can produce added-value chemicals from simple and abundant feedstocks. However, despite extensive efforts to develop catalytic materials with high reactivity and high selectivity, one can currently observe the lack of demonstrative performance for viable industrial applications. The deliberate surface modification of catalyst has been recently recognized as a powerful approach to design efficient and durable electrocatalysts [1]. It then becomes essential to obtain a good control over the spatial distribution of the chemical functions over the nanoscale surfaces. Recently, excellent catalytic properties towards ORR have been obtained in alkaline media of gold [2], silver [3], and platinum [4] nanoparticles when modified through the reductive grafting of rigid macrocycle calix[4]arene-tetradiazonium salts [5]. However, many fundamental questions, with important operational implications, remain open about these calixarene-modified surfaces. In particular, the conformation of the calixarene on the surface, and the structural, thermodynamic and electronic description of the interface. In addition, the C-Au bond has been poorly investigated in comparison to the S-Au bond.

Here, using spectroscopic studies coupled with computational modeling performed with density functional based tight-binding (DFTB) approaches, we investigate the interaction between calix[4]arene macrocycles and gold and platinum nanoparticles. After exploring the nature of the bond between the macrocycle and the gold surface thanks to a good agreement between measured and calculated Raman spectra, we describe the effect of calix[4]arenes on nanoparticles electrocatalytic properties [6].

Acknowledgment. The work was performed with funding from Agence Nationale pour la Recherche under grant ANR-21-CE50-0034 (MARCEL project). This work was granted access to the HPC resources of TGCC under the allocations 2022-A0130907682 made by GENCI.

[1] L. Lu *et al.*, *ACS Catal.* **2021**, *11*, 6020.

[2] Q. Lenne, C.L. *et al.*, *Adv. Mater. Interf.* **2020**, *7*, 2001557

[3] Q. Lenne, C.L. *et al.*, *Chem. Commun.* **2022**, *58*, 3334.

[4] Q. Lenne, C.L. *et al.*, *ChemSusChem* **2023**, *16*, e202201990.

[5] A. Mattiuzzi, C.L. *et al.*, *Nat. Commun.* **2012**, *3*, 1130.

[6] A. Têtenoire, C.L., M.K. *et al.*, manuscript in preparation.

SESSION EN07.13: Electrocatalysis General II

Session Chairs: Haotian Wang and Sen Zhang

Friday Afternoon, December 1, 2023

Hynes, Level 3, Room 310

1:30 PM EN07.13.01

Unassisted Water-Splitting with Perovskite-Perovskite Tandem Photocathodes at 18% STH Toward Commercially Relevant \$2/kg H_2 AustinFehr^{1,2}, ChongwenLi³, ChaseSellers¹, ChristianConrad¹, BinChen³, AyushAgrawal¹, ToddG. Deutsch⁴, FrancescaM. Toma², HaotianWang¹, EdwardH. Sargent³, MichaelWong⁴ and AdityaD. Mohite¹; ¹Rice University, United States; ²Lawrence Berkeley National Laboratory, United States; ³University of Toronto, Canada; ⁴National Renewable Energy Laboratory, United States

Integrated photoelectrochemical devices have been proposed as a long-term, low-cost alternative to PV-electrolyzer systems for solar fuel production, but have historically lagged in performance metrics including efficiency, lifetime, and notably cost. We report techno-economic analysis showing the critical role of photoabsorber and electrocatalyst cost in PEC devices, highlighting perovskite-perovskite tandems with low-PGM electrocatalyst loading as a platform capable of reaching \$2/kg H_2 . We demonstrate a techno-economically-informed approach to PEC system design using a perovskite-perovskite tandem device encapsulated by a conductive adhesive-barrier. Through optimization of reactor design, electrolyte composition, and catalytic content, we show that the cost of unassisted PEC water-splitting can be reduced without compromising on stability or efficiency, ultimately reaching 18% STH with 10 μg Pt/cm² HER catalyst loading and an Ir-free anode in acidic media. These findings show that device cost can be decreased without compromising, or even with improvement, on performance parameters in PECs.

1:45 PM EN07.13.02

Phase-Controlled Growth of Cobalt Oxide using Atomic Layer Deposition for Photoelectrochemical Water Splitting SwapnilNalawade¹, MohaF. Hossen¹, ValentinCraciun², DhyananjayKumar¹ and ShyamAravamudhan¹; ¹North Carolina A&T University, United States; ²National Institution for Laser, Plasma and Radiation Physics, Romania

Conformal cobalt oxide thin films, grown using an atomic layer deposition (ALD) method, have been found to possess remarkable photocatalytic capabilities assisted for solar-driven water oxidation. The present study has focused on establishing a structural property relationship to accomplish superior photoelectrochemical properties. During the ALD, bis (N-t-butyl-N'-ethylpropanamide) cobalt (II) was used as a precursor with water vapor as a co-reactant. The ALD films, grown in the temperature range of 150 – 300^oC, were characterized using x-ray diffraction (XRD), x-ray photoelectron spectroscopy (XPS), atomic force microscopy (AFM), and Raman spectroscopy. XRD and Raman spectroscopic analysis has indicated that cobalt oxide film has a phase change from rock-salt (CoO) to cubic spinel (Co₃O₄) structure around a temperature of 300^oC. AFM has confirmed the flat deposition of cobalt oxide with RMS roughness less than 1 nm. The characterization techniques employed in this study have provided valuable insights into the structural and electrochemical properties of Co₃O₄. We have found that the overpotential for the solar-driven oxygen evolution reaction during water splitting is nearly 40% lower for the cubic spinel structure than for the rock salt structure.

2:00 PM EN07.13.03

Electrosynthesis of Ethylene Oxide from CO₂ and Water Only Wan Ru Leow¹ and Edward Sargent²; ¹Agency for Science, Technology and Research (A*STAR), Singapore; ²University of Toronto, Canada

Ethylene oxide (EO) is among the world's most abundantly produced commodity chemicals due to its importance in the plastics industry, notably for manufacturing polyesters and polyethylene terephthalates (PET). The electrochemical production of EO from carbon dioxide (CO₂), water, and renewable electricity, can enable the consumption of 2 tons of CO₂ per ton of EO produced, in contrast to the emission of ~2 tons of CO₂ per ton of EO produced in existing thermochemical routes. This is achieved through an extended heterogeneous-homogeneous interface, using chloride as a redox mediator in conjunction with barium oxide-modified iridium oxide (BaO_x/IrO₂) catalysts.^{[1][2]} The catalysts enabled EO FE of 85-91% and a selectivity of 98% in a current density range from 100 to 1500 mA/cm². When integrated into flow battery-analogue electrolyzer with an O₂/H₂O redox couple, we achieve record low energy input of 5.3 MJ/kg of EO, comparable to that of (emissions-intensive) existing industrial processes.

[1] W.R. Leow, Y. Lum, A. Ozden, Y. Wang, D. Nam, B. Chen, J. Wicks, T. Zhuang, F. Li, E.H. Sargent* *Science* 2020, 368, 1228-1233.

[2] Y. Li, A. Ozden, W.R. Leow, P. Ou, J.E. Huang, Y. Wang, K. Bertens, Y. Xu, Y. Liu, C. Roy, H. Jiang, D. Sinton, C. Li,* & E.H. Sargent* *Nat. Catal.* 2022, 5, 185-192.

2:15 PM EN07.13.04

Tandem Electrosynthesis of Acetate on a Silver-Copper Oxide Catalyst Roham Dorakhan¹, Byounghoon Lee¹, Ivan Grigioni², David Sinton¹ and Edward H. Sargent¹; ¹University of Toronto, Canada; ²Università degli Studi di Milano, Italy

Acetic acid is an important chemical feedstock with wide applications in pharmaceuticals, food and clothing. The electrocatalytic synthesis of acetic acid from CO₂ offers a low-carbon alternative to traditional synthetic routes. The direct electroreduction CO₂ suffers from a substantial CO₂ crossover energy penalty, and recent CO₂ crossover mitigation strategies having significant energy penalties themselves.

In this work, we demonstrate a two-step approach, where CO₂ is initially converted to CO using a solid-oxide electrolyzer, followed by a CO electroreduction system that electrochemically converts CO to acetic acid. Solid-oxide electrolyzers do not suffer from the CO₂ crossover issue, and have been shown to operate in an industrial setting. The bottleneck in this synthetic approach is hence identified to be the CO electroreduction system. Current CO-to-acetate catalysts do not operate at the desired performance metrics, with selectivity ranges of 20 – 48%. Moreover, the system should produce acetic acid a sufficiently high concentration to minimize separation costs.

Here we report a catalyst design strategy in which off-target intermediates (such as ethylene and ethanol) in the reduction of CO to acetate are destabilized. A porous Cu₂O nanoparticle structure is first synthesized, and galvanic replacement of Ag at various loadings produced an alloy surface with near-atomic level dispersion. On the Ag–Cu₂O catalyst with optimized loading, the destabilization of off-target intermediates leads to an acetate Faradaic efficiency of 70% at 200 mAcm⁻². The destabilization is investigated by a combination of *operando* Surface Enhanced Raman Spectroscopy (SERS) and theoretical modeling using Density Functional Theory (DFT). The destabilization is shown to affect all pathways of C₂ hydrocarbons, however ethylene and ethanol pathway are rendered energetically inaccessible, while the acetate pathway remains open. Moreover, we demonstrate 18 hours of stable operation of the catalyst in a membrane electrode assembly; the system produced 5 wt% acetate at 100 mAcm⁻² and a full-cell energy efficiency of 25%, a twofold improvement on the highest energy-efficient electrosynthesis in prior reports.

2:30 PM BREAK

3:00 PM EN07.13.05

Cu Surface Chemistry in Acid Media: Vibrational Spectroscopy, Mass Spectrometry and ECSTM Measurements David Raciti, Angela R. Hight Walker and Thomas Moffat; NIST, United States

Copper electrodeposition is a central process in the metallization of microelectronics and more recently has found use as an important electrocatalyst in the conversion of CO₂ to hydrocarbons. Gaining mechanistic insight into the reactivity of Cu surfaces requires *in situ* and better still *in operando* measurements. Herein the utility of the combination of vibrational spectroscopy (SEIRAS, SHINERS), electrochemical mass spectrometry (EC-MS) and scanning tunneling microscopy (ECSTM) to examine the competitive and co-adsorption interactions between potential dependent halide adsorption, molecular adsorption, underpotential metal deposition and hydride formation on low index Cu single crystals surface will be detailed. Further still, the opportunity to study the impact of such interactions on metal deposition reactions will also be explored.

D. Raciti and T.P. Moffat, "Quantification of Hydride Coverage on Cu(111) by Electrochemical Mass Spectrometry," *J. Phys. Chem.*, 126, 18734-18743 (2022).

D. Raciti, A.R. Hight Walker, T. P. Moffat, "Mapping Surface Chemistry During Superfilling with Shell-Isolated Nanoparticle Enhanced Raman Spectroscopy and X-ray Photoelectron Spectroscopy," *J. Electrochem. Soc.*, 169, 082506 (2022).

B.M. Tackett, D. Raciti, A.R. Hight Walker, T.P. Moffat, "Surface Hydride Formation on Cu (111) and its Decomposition to Form H₂ in Acid Electrolytes," *J. Phys. Chem. Lett.*, 12, 10936-10941 (2021).

G. Liu, S. Zou, D. Josell, L.J. Richter and T.P. Moffat, "SEIRAS Study of Chloride Mediated Polyether Adsorption on Cu," *J. Phys. Chem. C.*, 122, 21933-21951, (2018).

3:15 PM EN07.13.06

Urea Oxidation Reaction on Ni-Based Electrocatalysts: Combating with Oxygen Evolution Reaction. Jiseon Kim and Kangwoo Cho; Pohang University of Science and Technology, Korea (the Republic of)

Along with the societal pursuit of sustainable carbon neutrality, electrochemical urea oxidation reaction (UOR) has been an overarching subject to substitute oxygen evolution reaction (OER), primarily owing to lower thermodynamic requirement (0.37 V) for molecular hydrogen generation. The UOR not only enhances the energy conversion efficiency from renewable energy into molecular hydrogen, but also reduces carbon and nitrogen pollution loadings of urea-rich wastewater. Nickel-based catalysts are up-to-date the most widely investigated materials as the UOR electro-catalyst. However, the UOR overpotential is in-fact predominantly consumed for formation of Ni³⁺ (the most common active site), and the gap between the onsets of UOR and OER is only < 300 mV. Moreover, competitions between UOR and OER has been noted to explain a current collapse near the OER onset. This presentation introduces our recent findings on Ni-based UOR electro-catalysts that were prepared by i) potentiostatic dealloying of commercial NiFe alloys under variable pH, and ii) one-pot thermochemical treatment of NiFe alloy foam in oxalic acid to create a self-supporting O-NFF. Regarding the former electrocatalysts, this study revealed that current inflections near the OER onset in the presence of urea could be associated with Ni^{3+/4+} redox peaks. The peak location and intensity, in relation with the OER activity during repetitive cyclic voltammetry unraveled the roles of Fe on OER, under dynamic dissolution and precipitation of Fe to/from the electrolyte. Therefore, accelerated UOR kinetics on Ni³⁺ would be the key consideration to avoid interferences from OER. To this end, Cutting-edge figure-of-merits for UOR were noted for O-NFF including 500 mA cm⁻² of current density at 1.47 V RHE and exceptionally low Tafel slope of 12.1 mV dec⁻¹ (in 1 M KOH with 0.33 M urea). The oxalate ligands withdraw electrons from Ni-motif and provide H-bonding sites for energetically favorable binding of Ni with urea-O. Incorporation of Fe escalate the inductive charge accumulation on oxalate-O and strengthen the H-bonding to accelerate the C-N cleavage of *CO(NH)₂. The findings of this study could be further utilized within wastewater electrolysis cell for water-energy nexus.

SESSION EN07.14: Virtual Session
Session Chairs: Haotian Wang and Sen Zhang
Tuesday Afternoon, December 5, 2023
EN07-virtual

9:00 PM EN07.14.01

Lewis-Acid Induced Polarizability in Electrode-Electrolyte System for Electrochemical Ammonia Synthesis—A Step Towards Sustainability Ashmita Biswas¹, Samadhan Kapse², Bikram Ghosh¹, Ranjit Thapa² and Ramendra Sundar Dey¹; ¹Institute of Nano Science and Technology, Mohali, India; ²SRM University, India

The ever-growing demands for ammonia in agriculture and transportation fuel stimulate researchers to develop sustainable electrochemical methods to synthesize ammonia ambiently, to get past the energy-intensive Haber Bosch process. Ambient here means, with no carbon emission, in aqueous medium and at room temperature and pressure. But, the most important factor that impedes the production rate of ammonia is the poor solubility of nitrogen in the aqueous medium because of its chemical inertness, which thereby makes way for the competitive hydrogen evolution reaction (HER) at the electrode surface. Several strategies have been imposed on the catalyst designing to prevent HER. From electrolyte point of view, mainly two conditions are followed to date to promote N₂ solubility and prevent this competitive HER:

(a) to optimize the proton concentration in the medium by using organic/aqueous electrolyte; although the production rate of NH₃ increased but the use of ethanol/methanol (C containing fuel) is not likely to be used in large proportion as electrolyte.

(b) to promote nitrogen solubility by using ionic liquid electrolytes; although it successfully suppressed HER and increased the Faradaic efficiency of NRR, but did not help much with respect to the yield or production rate of NH₃ synthesis. Moreover, most of the ionic liquid electrolytes require inert atmosphere for use and are generally costly. Thus, these two approaches cannot be regarded as “green” and “ambient” towards proficient NRR process.

Herein we introduce a new aqueous electrolyte (NaBF₄), which not only acts as an N₂-carrier in the medium but also works as a full-fledged “co-catalyst” along with our active material MnN₄ to deliver high yield of NH₃ (328.59 μg h⁻¹ mg_{cat}⁻¹) at 0.0 V vs RHE. Our experimental and theoretical findings go hand-in-hand towards the understanding of the chemistry behind such high performance. We have undergone several experiments including NMR and also Hirshfeld surface analysis to establish the existence of BF₃ in our medium and the van der Waal interaction between free BF₃ and N₂ molecules forming a **Lewis acid-base adduct pair**. Unlike any other aqueous electrolyte, NaBF₄ is thus able to induce a local N₂ concentration in the vicinity of the catalyst surface. More interestingly, BF₃-induced charge polarization shifts the metal d-band center of MnN₄ unit close to the Fermi level, inviting N₂ adsorption facilely. The Lewis acidity of the free BF₃ molecules further propagates their importance in polarizing the N≡N bond of the adsorbed N₂ and its first protonation. This push-pull kind of electronic interaction has been confirmed from the change in d-band center values of MnN₄ site as well as charge density distribution over our active model units, which turned out to be effective enough to lower the energy barrier of the potential determining steps of NRR. Resultantly, a high production rate of NH₃ (2.45 × 10⁻⁹ mol s⁻¹ cm⁻²) was achieved, approaching the industrial scale periphery, where the source of NH₃ was thoroughly studied and quantitatively confirmed (from ¹⁵N₂ isotope labelling experiment) to be chiefly from the electrochemical reduction of the purged N₂ gas. Therefore, this unique report where an aqueous electrolyte itself works as a “co-catalyst” may open up new vistas to study and understand the insights of the NRR in aqueous medium.

9:15 PM EN07.14.02

Accelerated Oxygen Chemisorption and ORR Activity on Cerium-Doped LaFeO₃ Perovskite Oxide Myungju Kim¹, Kanghee Jo¹, Yongnam Kim² and Heesoo Lee¹; ¹Pusan National University, Korea (the Republic of); ²Korea Testing Laboratory, Korea (the Republic of)

LaFeO₃-based perovskite oxides, which have both electronic conductivity and ionic conductivity, have been actively studied in energy conversion and storage fields including solid oxide fuel cells and metal-air batteries. Recently, doping elements with various valence states have been focused to enhance the electrochemical properties of LaFeO₃. Cerium forms a defect-rich structure since cerium has multivalence of Ce³⁺/Ce⁴⁺. These formed defects play a crucial role in catalytic activity by accelerating the adsorption of oxygen on the surface. Therefore, it is crucial to examine the effect of cerium doping on the electrochemical properties of LaFeO₃, specifically considering the influence of the defect structure.

This study investigated the effect of cerium doping on the polarization resistance of LaFeO₃ perovskite oxide (LCFOx, x = 1, 3, 5, 7) and analyzed the underlying mechanism in terms of the defect structure. The X-ray diffraction (XRD) patterns of the crystal structure revealed that doping cerium with ranging from 0 to 5 mol% resulted in the formation of a single perovskite phase with an orthorhombic structure of *Pnma* space group. The Rietveld refinement analysis further demonstrated that cerium led to a decrease in the octahedral tilting and an increase in the Fe-O-Fe bonding angle, respectively. The formation of oxygen vacancies was observed through the electron paramagnetic resonance (EPR) spectrum and O 1s core-level spectrum. The La 3d and Fe 2p core-level spectra indicated that cerium doping did not affect the valence state of La ions, while it caused a reduction in the Fe³⁺. Additionally, the O K-edge X-ray absorption spectrum (XAS) showed the hybridization between Fe 3d and O 2p orbitals upon cerium doping. The O₂-temperature programmed desorption (O₂-TPD) profile confirmed an increase in the concentration of surface-active oxygen species with cerium doping. The area-specific resistance (ASR) gradually decreased from 11.36 Ωcm² (LFO) to 4.65 Ωcm² (LCFO5) as the amount of cerium doping increased. Notably, the polarization resistance in the low-frequency range (R₂) exhibited a significant reduction of approximately 68%, indicating enhanced ORR activity attributed to accelerated oxygen adsorption. The ORR reaction steps were analyzed alongside electrochemical impedance spectroscopy (EIS) data using the distribution of relaxation times (DRT) technique.

9:30 PM EN07.14.03

Electrochemical Energy Harvesting from Phototrophic Biofilms Seeded with Wild-Type and Functionally Coated Phototrophs Mohd Golam Abdul Quadir¹, Melania Reggente², Charlotte Roullier², Ardemis Boghossian², Massimo Trotta³ and Fabian Fischer¹; ¹University of Applied Sciences and Arts of Western Switzerland, Switzerland; ²École Polytechnique Fédérale de Lausanne, Switzerland; ³Institute for Physical-Chemical Processes-CNR, Italy

Oxygenic phototrophs have been reported to produce electrical current in a photoresponsive manner when interfaced with electrodes [1]. It has been experimentally demonstrated that the origin of this electron flux emanating from the cellular structures is a water splitting reaction at the oxygen-evolving complex of the Photosystem II [2]. However, this mechanism of electron conduction across the cell wall of oxygenic phototrophs is not deciphered with certainty. Additionally, the oxygenic microenvironment of these organisms further reduces the photocurrent output. The scientific community aims to exploit this low-magnitude electrical output for clean energy harvesting. To this end, phototrophs like *Rhodospirillum rubrum* [3] and *Synechocystis* PCC6803 (**unpublished data**) have been imparted with functional coatings for enhanced charge extraction from cells that increased the current output with anodically biased electrodes.

This study aims to investigate the electrochemical performance of biofilms initiated with wild-type and functionally coated cells. We optimize these biofilms for long-term viability that can be integrated into an electrochemical device for sustainable energy harvesting in a cost-effective manner. Additionally, we also study the influence of gradually increasing biochemical complexity of the extracellular biofilm matrix that ensues in response to various environmental and electrochemical stimuli over time. The biofilm matrix is a dynamic and biochemically active entity that helps the microorganisms to survive harsh environmental conditions [4]. In the context of low electrogenic performance of phototrophs, its role in electron conduction is also not well investigated. We deal with this aspect from both biochemical and material science perspectives [5]. Preliminary results indicate an influence of various biological, abiotic, and interfacial phenomena on electrochemical results.

REFERENCES:

- [1] McCormick, A. J. et al. Photosynthetic biofilms in pure culture harness solar energy in a mediatorless bio-photovoltaic cell (BPV) system. *Energy Environ Sci.* 4(11), 4699-4709 (2011)
- [2] Piscicotti, J. M. et al. Role of the photosynthetic electron transfer chain in electrogenic activity of cyanobacteria. *Appl Microbiol Biotechnol.* 91(2):377-85 (2011)
- [3] Buscemi, G. et al. Bio-Inspired Redox-Adhesive Polydopamine Matrix for Intact Bacteria Biohybrid Photoanodes. *ACS Appl Mater Interfaces.* 14(23):26631-41 (2022)
- [4] Sauer, K. et al. The biofilm life cycle: expanding the conceptual model of biofilm formation. *Nat Rev Microbiol.* 20(10):608-620 (2022)
- [5] Billings, N. et al. Material properties of biofilms - A review of methods for understanding permeability and mechanics. *Rep Prog Phys.* 78(3):036601 (2015)

9:45 PM EN07.14.04

Low-Temperature Synthesis of Cu/Cu₂O/CuO Nanostructures for Electrochemical Reduction of CO₂ Bishnu Bastakoti¹, Rabin Dahal¹ and Rohit Srivastava²; ¹North Carolina A&T State University, United States; ²Pandit Deendayal Energy University, India

Electrochemical conversion of CO₂ into renewable energy is an exciting field and a promising method for generating renewable energy that also addresses the challenges of the energy crisis. Here, we successfully synthesized different morphology of Cu/Cu₂O/CuO nanostructures by the wet chemical method for electrochemical reduction of CO₂. The diffused metal ions from the Cu(NO₃)₂ ice cube were slowly reduced using NaBH₄ at room temperature. The slow release of the metal ions helps in modifications of morphologies of composite nanoparticles. The reduced species were further oxidized by dissolved oxygen. Different characterization techniques such as x-ray diffractometry, scanning electron microscopy, and x-ray photon spectroscopy further examined the prepared nanoparticles. The electrochemical reduction of CO₂ on Cu/Cu₂O/CuO nanostructures shows the generation of CO, CH₄, and C₂H₆ in 0.5 M KHCO₃ solution.

This research was supported by the National Science Foundation Excellence in Research 2100710.

9:50 PM EN07.14.14

Tailoring Binding Abilities by Incorporating Oxophilic Transition Metals on 3D Nanostructured Ni Arrays for Accelerated Alkaline Hydrogen Evolution Reaction Jaerim Kim, Hyeonjung Jung, Jeong Woo Han and Jong Kyu Kim; Pohang University of Science and Technology, Korea (the Republic of)

Developing efficient and inexpensive electrocatalysts for the hydrogen evolution reaction (HER) in alkaline water electrolysis plays a key role for renewable hydrogen energy technology. The slow reaction kinetics of HER in alkaline solutions, however, has hampered advances in high-performance hydrogen production. Herein, we investigated the trends in HER activity with respect to the binding energies of Ni-based thin film catalysts by incorporating a series of oxophilic transition metal atoms. It was found that the doping of oxophilic atoms enables the modulation of binding abilities of hydrogen and hydroxyl ions on the Ni surfaces, leading to the first establishment of a volcano relation between OH-binding energies and alkaline HER activities. In particular, Cr-incorporated Ni catalyst shows optimized OH-binding as well as H-binding energies for facilitating water dissociation and improving HER activity in alkaline media. Further enhancement of catalytic performance was achieved by introducing an array of three-dimensional (3D) Ni nanohelices (NHs) that provide abundant surface active sites and

effective channels for charge transfer and mass transport. The Cr dopants incorporated into the Ni NHs accelerate the dissociative adsorption process of water, resulting in remarkably enhanced catalytic activities in alkaline medium. Our approach can provide a rational design strategy and experimental methodology toward efficient bimetallic electrocatalysts for alkaline HER using earth-abundant elements.

9:55 PM EN07.06.15

Efficient Alkaline Hydrogen Evolution Reaction of Nitrogen Ion Irradiated NiO-Based Catalysts via Nitrogen Doping and Vacancy Engineering JaerimKim¹, Sang-MunJung¹, HyeonwoongHwang¹, BongwonKim¹, Yong-TaeKim¹, Dong-SeokKim² and Jong KyuKim¹; ¹Pohang University of Science and Technology, Korea (the Republic of); ²Korea Atomic Energy Research Institute (KAERI), Korea (the Republic of)

Development of efficient and inexpensive electrocatalysts for oxygen evolution reaction (OER) and hydrogen evolution reaction (HER) in alkaline water-electrolysis is of paramount importance in the hydrogen economy to meet future energy demands. Earth-abundant transition metal oxide-based catalysts including NiO have emerged as promising OER catalysts with the advantages of compositional and structural diversity, low cost, easy synthesis, and eco-friendliness. However, they are generally considered inactive towards HER because of limited catalytic active sites, poor electrical conductivity and adsorption abilities.

In this study, we developed a strategy to activate NiO catalysts for efficient HER by creating both nitrogen dopants and oxygen vacancies, which is enabled by ion irradiation technique. Nitrogen ion irradiation with various ion doses was conducted onto NiO-based catalysts that consist of an array of NiO nanorods (NRs) with abundant surface active sites and efficient channels for charge transfer and mass transport. It was found that the N ion irradiation causes not only doping of N atoms but also formation of oxygen vacancies in the NiO NRs, resulting in much enhanced hydrogen adsorption and electrical conduction of NiO NRs. Consequently, the optimized N-ion irradiated NiO NRs catalyst show highly improved HER performance, as well as OER. Our approach can provide an effective and unique methodology for designing efficient electrocatalysts consisting of earth-abundant elements for electrochemical hydrogen production.

10:00 PM EN07.05.05

Efficient Alkaline Hydrogen Evolution Reaction using Superaerophobic Ni Nanoarrays with Accelerated H₂ Bubble Release JaerimKim, Sang-MunJung, Yong-TaeKim and Jong KyuKim; Pohang University of Science and Technology, Korea (the Republic of)

Despite the adverse effects of H₂ bubbles adhering to catalyst's surface on the performance of water electrolysis, the mechanisms by which H₂ bubbles are effectively released during the alkaline hydrogen evolution reaction (HER) remain elusive. In this study, we conducted a systematic investigation on the effect of nanoscale surface morphologies on H₂ bubble release behaviors and HER performance by employing earth-abundant Ni catalysts consisting of an array of Ni nanorods (NRs) with controlled surface porosities. Both aerophobicity and hydrophilicity of the catalyst's surface vary according to the surface porosity of catalysts. The Ni catalyst with the highest porosity exhibits superaerophobic nature as well as the best HER performance among the Ni catalysts. It was found that the Ni catalyst's superaerophobicity combined with the effective open pore channels enables the accelerated release of H₂ bubbles from the surface, leading to a significant improvement in geometric activities, particularly at high current densities, as well as intrinsic activities including both specific and mass activities. It was also demonstrated that the superaerophobicity enabled by highly porous Ni NRs can be combined with Pt and Cr having optimal binding abilities to further optimize electrocatalytic performance. Our work can help to elucidate the fundamental and practical design rules for efficient alkaline HER catalysts consisting of earth-abundant elements.

SYMPOSIUM EN08

Materials for Emerging Electrochemical Separations
November 29 - December 1, 2023

Symposium Organizers

Douglas Call, North Carolina State University
Ekaterina Pomerantseva, Drexel University
Matthew Suss, Technion Israel Inst of Technology
David Vermaas, Delft University

Symposium Support

Bronze
BioLogic
Royal Society of Chemistry

* Invited Paper

+ JMR Distinguished Invited Speaker

SESSION EN08.01: Electrochemical Separations I
Session Chairs: Matthew Suss and David Vermaas
Wednesday Morning, November 29, 2023
Hynes, Level 1, Room 108

8:45 AM *EN08.01.01

Electrochemical Chloride-Mediated Marine Carbon Dioxide Removal SeoniKim, MichaelNitzsche, SimonRufert, KripaVaranasi and T. AlanHatton; MIT, United States

Negative Emissions Technologies (NETs) are crucial to avert catastrophic disruption of global climate patterns caused by the continuing atmospheric accumulation of CO₂ due to industrial emissions. The recent surge of interest in NETs in which CO₂ (currently at an atmospheric concentration of ~420 ppm) is removed from the ambient environment itself, by, e.g., direct air capture (DAC), has not yet been matched by a similar drive to reduce CO₂ in oceans, where increasing acidification has led to destruction of coral reefs, and reduced carbonate ion concentrations harm shellfish and other marine life. The total CO₂ accumulation rates by oceans rivals that in the atmosphere, and thus effective means for CO₂ removal could augment the other NETs to reduce the environmental burden imposed by this greenhouse gas. The concentrations in water (on a volumetric basis) are much higher at 100 mg/L than that in the ambient air (0.77 mg/L), and thus smaller volumes will need to be treated than in DAC, which could provide a processing advantage.

In current approaches for the removal of CO₂ from oceanwaters bipolar membrane catalysis water splitting coupled with electro dialysis is used to modulate the pH and thereby release the CO₂ as a gas (low pH) or carbonate salt (high pH). We have proposed an alternative approach to marine carbon dioxide removal (mCDR) that does not require expensive membranes or addition of chemicals, is easy to deploy, and does not lead to formation of byproducts or secondary streams. In this approach, the pH is regulated through a chloride-mediated reaction with electrodes in asymmetric electrochemical cells through which the seawater flows. In the acidification cell the DIC speciation shifts from bicarbonate and carbonate to CO₂ which can then be

removed in a membrane contactor. The now-decarbonized water is introduced to a second electrochemical cell where the reverse reaction is promoted, the electrodes are regenerated, and the pH increases before the water is discharged back to the ocean. The CO₂ removal approach has perceived advantages in that it does not require expensive membranes or addition of chemicals, is easy to deploy, and does not lead to formation of byproducts or secondary streams.

We will discuss the overall electrochemical swing process, which can be enhanced through flexible electrode configurations to reduce transport and electrical resistances while enabling treatment of large quantities of water. Novel methods for the recovery of molecular CO₂ without the need for high vacuum desorption, and of calcium carbonate precipitates without fouling of the electrodes, will be highlighted.

9:15 AM *EN08.01.02

Bipolar Membranes for Electrochemical CO₂ Capture [Chengxiang Xiang](#)^{1,2}; ¹California Institute of Technology, United States; ²Captura Corporation, United States

Electrochemical CO₂ capture, conversion and storage can play a significant role in reducing atmospheric CO₂ concentration in the coming decades. Bipolar membranes that facilitate water dissociation reaction at the interface can be implemented in electrolysis, electro dialysis and other electrochemical devices for carbon capture, conversion, and long duration energy storage. In this talk, I will share recent developments in the synthesis, characterization, and electrochemical performances of catalyzed, asymmetric bipolar membranes for highly efficient acid and base generation both at Caltech and in Captura. I will talk about multiphysics modeling and simulation of BPMs for in-depth understanding of water dissociation mechanism as well as electroosmotic water transport at various current densities. Finally, I will discuss electro dialysis stacks development and deployment of Direct Ocean Capture (DOC) pilot systems for electrochemical CO₂ capture at a near-ocean site.

9:45 AM EN08.01.03

Elucidating the Effect of Solvent on Electrochemical Reduction of CO₂ using a Data Driven Approach [Matthew Bliss](#), [Aniket Kapote](#), [Kuldeep Singh Raj](#) and [Nav Nidhi Rajput](#); Stony Brook University, The State University of New York, United States

The electrochemical reduction of carbon dioxide (CO₂) has great potential to alleviate important environmental problems: the elevated presence of CO₂ in the atmosphere and the need for fossil fuel-based production of fuels and commodity chemicals. However, the application of electrochemistry to CO₂ reduction is hindered by low selectivity, activity and stability¹. In aqueous media, the competing hydrogen evolution reaction (HER) and low solubility of CO₂ remain unresolved problems for selectivity; the use of nonaqueous solutions presents a possible path to mitigate these problems^{2,3}. However, the current aprotic solvents are limited by their high viscosity, large overpotential due to absence of protons, and instability of reaction key intermediates. To overcome these challenges, we investigate the effect of the solvent's chemical class on properties relevant to the CO₂ reduction reaction such as CO₂ solubility, electrochemical stability, and transport properties using high-throughput multi-scale simulations. High-throughput density functional theory (DFT) calculations and classical molecular dynamics (CMD) simulations are performed to build large databases of electronic, thermodynamic, structural and dynamical properties using the computational infrastructures developed by our lab, coined **MISPR** (Materials Informatics for Structure-Property Relationships - <https://github.com/molmd/mispr>) and **MDPropTools** (<https://github.com/molmd/mdproptools>)⁴. In this work, we uncover important correlations between molecular features of solvents and bulk ensemble properties of electrolytes for CO₂ electroreduction.

References:

1. Sánchez, O. G.; Birdja, Y. Y.; Bulut, M.; Vaes, J.; Breugelmanns, T.; Pant, D., Recent advances in industrial CO₂ electroreduction. *Current Opinion in Green and Sustainable Chemistry* **2019**, *16*, 47-56. <https://doi.org/10.1016/j.cogsc.2019.01.005>
2. Nielsen, D. U.; Hu, X.-M.; Daasbjerg, K.; Skrydstrup, T., Chemically and electrochemically catalysed conversion of CO₂ to CO with follow-up utilization to value-added chemicals. *Nature Catalysis* **2018**, *1* (4), 244-254. <https://doi.org/10.1038/s41929-018-0051-3>
3. Sebastián-Pascual, P.; Mezzavilla, S.; Stephens, I. E.; Escudero-Escribano, M., Structure-sensitivity and Electrolyte Effects in CO₂ Electroreduction: From Model Studies to Applications. *ChemCatChem* **2019**, *11* (16), 3626-3645. <https://doi.org/10.1002/cctc.201900552>
4. Atwi, R.; Bliss, M.; Makeev, M.; Rajput, N. N., MISPR: an open-source package for high-throughput multiscale molecular simulations. *Scientific Reports* **2022**, *12* (1), 15760. <https://doi.org/10.1038/s41598-022-20009-w>

10:00 AMBREAK

10:30 AM *EN08.01.04

Molecular Design of Redox-Active Materials for Selective Electrochemical Separations [Xiao Su](#); University of Illinois Urbana-Champaign, United States

Achieving molecular selectivity is a critical challenge for deploying electrochemical separations for resource recovery, chemical and biochemical manufacturing, and environmental remediation. Leveraging redox-electron transfer can be a powerful pathway for accelerating separation kinetics, enhancing adsorption uptake, and controlling voltage for lower energy consumption. Here we discuss the molecular design of electroactive materials for two major directions in electrochemical separations: redox-mediated electrosorption and redox-mediated electro dialysis.

First, we discuss the development of redox-active materials for the selective binding of dilute ions from multicomponent mixtures. We highlight the bottom-up design of redox-copolymers, and synthetic modifications for enhancing affinity and reversibility. We demonstrate their capability for the capture and remediation of perfluoroalkyl substances (PFAS) through combinatorial monomer design, as well as strategies for coupling separation and reaction for the reactive separation of nitrate to ammonium. We unravel structure-function relationship between the redox-polymers and target species, such as the control of surface charge and hydrophobicity for the capture of both short and long-chain PFAS.

Next, we discuss new materials design strategies for advancing redox-electro dialysis, including translating concepts from redox-flow batteries to improve membrane and redox-electrolyte selection. We substitute costly ion-exchange membranes with affordable nanofiltration membranes and soluble redox-copolymers, which significantly reduce energy consumption and the cost of desalination, while enhancing membrane stability. Our work establishes rational design principles of redox-materials, tailoring their properties for selective electrochemical separations.

11:00 AM EN08.01.05

Engineering Porous Carbon Electrodes for Selective Boron Removal via Electrosorption [Weiyi Pan](#)¹, [Sohum Patel](#)¹, [Eungjin Ahn](#)², [Arpita Iddya](#)¹, [Debashis Roy](#)², [Jovan Kamcev](#)² and [Menachem Elimelech](#)¹; ¹Yale University, United States; ²University of Michigan-Ann Arbor, United States

Boron (B) is ubiquitous in seawater in the form of boric acid (H₃BO₃, pK_a = 9.24) at low concentrations (4-6 mg/L). While boron is an essential micronutrient, excessive intake can be highly toxic to humans and many crops. Therefore, effective removal of boron during seawater desalination is crucial. Reverse osmosis (RO) membranes alone are insufficient for reducing the levels of uncharged boric acid to acceptable levels for human consumption and agricultural use. Consequently, additional high-pH RO passes are necessary, leading to an increase in overall energy consumption of ~10-15%. Furthermore, this non-selective removal process also eliminates other beneficial minerals, necessitating subsequent remineralization. An alternative method for boron removal would benefit from reduced energy consumption, lower capital costs, and the elimination of chemical dosing requirements.

Boron is well known to react with 1,3 diols to form characteristic borate-ester complexes. Selectivity for boron over other species is enhanced by the presence of two or more hydroxyl groups in the *cis* position (*vis*-diols); hence, numerous sorbents which incorporate *vis*-diol moieties have been developed. Nevertheless, the hydrophobic nature of the polymeric backbone hampers efficient boron transport, leading to slow kinetics and the need for large bed volumes, which are costly. The polymeric structure repeated swelling and shrinking during regeneration cycles accelerate capacity decline, shortening the resin lifespan. Regeneration requires substantial amounts of strong acids or bases, increasing financial and environmental burdens.

Electrosorption has emerged as a highly promising process for water deionization. It exhibits exceptional efficiency when applied to low salinity waters and for removing small quantities of salts. Consequently, utilizing electrosorption for boron removal, particularly from first-pass seawater RO permeate, could potentially be a promising application of this technology. We have recently developed a novel bipolar membrane (BPM) assisted electrosorption process for boron removal. With an applied voltage (< 1.2 V), BPM-facilitated water dissociation occurs with the anion-exchange layer (AEL) facing the anode, thus producing a high pH on the anode side, as is required for boron electrosorption. By further enhancing the selectivity of boron over competing anions (e.g., Cl⁻), we can significantly reduce the specific energy consumption of the process (~ 2.5 kWh g-B⁻¹). This advancement would also enable direct application of the technology, unlocking its full potential.

Herein, we developed novel porous carbon electrodes that can selectively remove boron over competing anions during the BPM-assisted electrosorption process. We employed two fabrication methods for these porous carbon electrodes. In the first method, we deposited a functionalized polymeric thin film [e.g., poly(vinyl alcohol) and polydopamine] on porous carbon electrodes that could selectively allow borate anions to pass through over other competing anions in the presence of an electric field and accumulate in the electric double layer of the electrode micropores. In the second method, boron selective functional groups (e.g., N-methyl-D-glucamine) were directly appended to the micropore wall of the porous carbon electrode via chemical modification techniques, thereby eliminating the mass transfer limiting polymer layer between the carbon pore wall and the aqueous solution containing boron. To evaluate the boron removal capabilities of these electrodes, we conducted experiments using a custom-built BPM-assisted electrosorption cell with a solution mimicking first-pass seawater RO permeate (i.e., 5 mM NaCl and 1 mM B). The B/Cl selectivity of various electrodes was also calculated to compare their performance. Furthermore, detailed characterizations and molecular dynamic simulations were performed to gain deeper insights into the underlying mechanisms.

11:15 AM EN08.01.06

Perfect Monovalent Cation Selectivity with Capacitive Deionization Ankita Mathur¹, Sally Nijem², Rana Uwayid¹, Zohar Sahray¹, Amit N. Shocron¹, Charles Diesendruck² and Matthew Suss^{1,2}; ¹Technion- Israel Institute of Technology, Israel; ²Technion-Israel Institute of Technology, Israel

Irrigation is a huge consumer of freshwater, typically > 50% of the total water usage for most countries. When treating water for irrigation use, selective removal of monovalent sodium ions is a particular challenge, but necessary for cost-effective irrigation and resource recovery. Presence of excessive sodium ions in water may lead to low crop yield, decreased soil permeability and water infiltration rate, but other ions such as calcium should not be removed. Capacitive deionization (CDI) is an emerging electrochemical technology promising towards highly selective removal of ions from water via electrosorption¹. Ion selectivity can be tuned by modifying the electrode pore structure and surface chemistry, in addition to cell parameters affecting electrosorption dynamics^{2,3}.

Here we show that utilizing judicious functionalization of microporous activated carbon cloth (ACC) electrodes can provide for exceptional selectivity towards removal of Na⁺ from feedwater. We show that a charging CDI cell can remove ~130 μmol Na⁺ per gram carbon, with zero Ca²⁺ electrosorption, from a feed of 2 mM CaCl₂ and 17 mM NaCl, with low energy consumption of 0.36 kWh/m³. We further describe the mechanism enabling such breakthrough selectivity results, which are based on the discovery of induced electric charge in asymmetric CDI cells. This study paves the way for more tunable selectivity and wider range of separations with CDI, and is especially promising for single-step treatment of water for use in irrigation.

References:

1 M. E. Suss, S. Porada, X. Sun, P. M. Biesheuvel, J. Yoon and V. Presser, Water desalination via capacitive deionization: What is it and what can we expect from it?, *Energy Environ. Sci.*, 2015, **8**, 2296–2319.

2 A. N. Shocron, R. S. Roth, E. N. Guyes, R. Epsztein and M. E. Suss, Comparison of Ion Selectivity in Electrodialysis and Capacitive Deionization, *Environ. Sci. & Technol. Lett.*, 2022, **9**, 889–899.

3 E. N. Guyes, A. N. Shocron, Y. Chen, C. E. Diesendruck and M. E. Suss, Long-lasting, monovalent-selective capacitive deionization electrodes, *npj Clean Water*, 2021, **4**, 22.

11:30 AM EN08.01.07

Electrochemical Separation and Purification of Tungsten and Cobalt for High-Value Metals Recovery from Cemented Tungsten Carbides Shao-Chi Lo, Tzu Ming Cheng and Chih-huang Lai; National Tsing Hua University, Taiwan

Cemented tungsten carbide (WC-Co), which consists of high-value metals such as tungsten (W) and cobalt (Co), is one of the important hard materials for cutting tools in industrial applications. The recovery and production of these valuable elements have drawn much attention due to the increased demand in the end-user industries such as mining, automotive, electronics, and even aerospace. Although the recycling methodology of WC-Co scraps has been developed for decades, energy consumption and wastewater discharge in the whole process remain a big concern for conventional approaches. Previously in the beginning of the year, our group demonstrated an energy-efficient approach called rapid breakdown anodization (RBA) for the first time to separate W and Co, and then convert WC-Co into high-purity hydrated tungsten oxide (WO₃-H₂O) and Co metal in one-step electrochemical process. By using RBA with WC-Co as a sacrificial electrode in acidic aqueous solution, effective cobalt leaching was achieved without encountering anodic passivation issue during the electro-dissolution. However, elements such as nickel (Ni), iron (Fe), and chromium (Cr) remained in the cobalt-rich (Co-rich) solution and became major impurities in recovered Co metal owing to large overpotential during RBA. To fulfill the electrochemical separation and purification of tungsten and cobalt for high-value metals recovery, it is critical to explore selective adsorption materials and membranes for Co-rich solution purification. Here, we present the preliminary results on the selective removal of impurities such as Fe, Ni, and Cr from Co-rich solution by using alumina powder so that Co metal purity could be further enhanced after RBA. Eventually, an effective and environmentally-friendly pathway for WC-Co recycling is proposed with a significantly simplified process compared to traditional hydrometallurgical methods.

SESSION EN08.02: Electrochemical Separations II
Session Chairs: Ekaterina Pomerantseva and Matthew Suss
Wednesday Afternoon, November 29, 2023
Hynes, Level 1, Room 108

1:30 PM *EN08.02.01

Towards Accelerated Design of Selective Membranes: Integrating Theory, Characterization and Simulations Ryan S. Kingsbury; Princeton University, United States

Precise separation materials capable of selectively permeating a single ion from an electrolyte have the potential to significantly enhance the performance of numerous electrochemical technologies, including processes for resource extraction, industrial waste recycling, and water purification. For example, materials that can selectively remove lithium from geothermal brine would contribute to stabilizing supply chains for clean energy technology.

Polymer membranes are a proven technology capable of other types of ion separations, but engineering them for precise selectivity is extremely challenging because differences in solute size or charge, which have historically guided membrane development, are often absent in ion-ion separations. As such, the next generation of membranes must go beyond size and charge to exploit differences in solute chemistry.

New approaches to membrane research are critical for efficiently meeting this need. Characterization methods and transport models must evolve to more explicitly connect to the molecular scale interactions of interest, and more emphasis must be placed on understanding 1) which membrane design strategies are most likely to be effective for a given separation problem and 2) how improved material performance would translate into process performance.

This talk will first present membrane performance data compiled from more than 40 studies across 8 different applications to identify strengths and weaknesses of current materials. Next, I will describe a theoretical framework called Barrier Network Analysis that quantitatively relates conventional membrane characterization data (such as conductivity and partition coefficients) to activation energy barriers associated with partitioning and diffusion of individual species. This kinetics-first approach connects experimental observations more directly to the molecular-scale energetic landscape and yields information that is more naturally comparable to the outputs of molecular simulations, which are another important tool for understanding chemical interactions between solutes and membrane materials.

Finally, I will present results from a study of alkali chloride separation by a water-stable polymer of intrinsic microporosity (AquaPIM) membrane and a commercial cation exchange membrane. Using Barrier Network Analysis, we demonstrated that crossing the solution-membrane interface (i.e., partitioning) has a higher activation energy barrier than diffusion through the polymer for both membranes. This insight contrasts with historical assumptions in the popular Solution-Diffusion model and suggests that selective membrane design should, at least in some cases, prioritize selective interfaces rather than engineering the polymer itself.

I will close by discussing other implications of these findings for membrane design, and suggest ways that Barrier Network Analysis (and related approaches) can be used to guide future research.

2:00 PM EN08.02.02

Ratchet Based Ion Pumps for Selective Ion Separation Alon Herman¹, Dafna Meltser¹, Eden Grossman¹, Karen Shushan¹, Joel W. Ager², Shane Ardo² and Gideon Segev¹; ¹Tel Aviv University, Israel; ²University of California, Irvine, United States

Even though highly selective ion pumps are found in the membrane of every living cell, artificial ion selective separation is a longstanding unmet challenge in science and engineering. The development of a membrane-based ion separation technology can drive a dramatic progress in a wide range of applications such as: water treatment, extraction of lithium from seawater, solar fuels and more. In this contribution, we report the experimental demonstration of ion pumps based on an electronic flashing ratchet mechanism.

Electronic flashing ratchets are devices that utilize a temporal modulation of a spatially asymmetric electric field to drive steady state current. Like peristaltic pumps, where the pump mechanism is not in direct contact with the pumped fluid, electronic ratchets induce a net current with no direct charge transport between the power source and the pumped charge carriers. Thus, electronic ratchets can be used to pump ions in steady state with no electrochemical reactions between the power source and the pumped ions resulting in an 'all-electric' ion pump. Ratchet-based ion pumps (RBIPs) were fabricated by coating the two surfaces of nano-porous alumina wafers with gold, thus forming nano-porous capacitor-like devices. The electric field within the nano-pores is modulated by oscillating the capacitor voltage. Thus, when immersed in a solution, ions within the pores experience a modulating electric field resulting in ratchet-

based ion pumping. The RBIPs performance was studied for various input signals, geometries, and solutions. RBIPs were shown to drive ionic current densities of several $\mu\text{A}/\text{cm}^2$ even when opposed by an electrostatic force. A significant ratchet action was observed with input signal amplitudes as low as 0.1V thus demonstrating that RBIPs can drive an ionic current with no associated redox reactions.

An important hallmark of ratchets is the ability to invert the direction of particle flow with a change in the input signal frequency. The stopping frequency, which is the frequency at which the particle flux changes its direction, is determined by the potential distribution and particles transport properties. As a result, for a given ratchet, there can be a frequency at which particles with the same charge, but different diffusion coefficients, are transported in opposite directions. This concept, that was never applied to ion separations, can enable the extraction of ions with extremely low relative concentrations if their diffusion coefficient is even slightly different from the main ions in the solution. We show by simulation, that for the prevalent ions in water, ions with a relative diffusion coefficient difference as small as 1% can be driven to opposite directions with a velocity difference as high as 1.2 mm/s. Since the direction of ion transport is determined by the input signal frequency, the sorting properties can be tuned in real time providing a simple fit-to-purpose solution for a variety of ion separations applications.

2:15 PM EN08.02.03

Isotope Separation by Centrifuging an Electrolytic Solution Yuan Yang; Columbia University, United States

Enriched isotopes are critical to wide applications, such as nuclear reactors (e.g., ^6Li , D), radiology (^{18}O), and fundamental sciences (e.g., tracer and synthesizing superheavy elements). Current methods, such as gas centrifuge, requires hazardous precursors and have limited applicability. Here we developed a general method of separating isotopes by centrifuging a liquid (e.g., salt solution), which is governed by electrochemical transport equations in electrolytes. This technique can be applied to the majority of elements and does not require gasification of isotopes. We have demonstrated high separation factors of 1.046-1.067 per unit neutron difference (e.g., 1.434 in $^{40}\text{Ca}/^{48}\text{Ca}$, 1.134 in $^{16}\text{O}/^{18}\text{O}$), which are better than or comparable to various conventional methods. Modeling was established to understand the process, which is in good agreement with experimental results. The scalability of the technique has also been demonstrated by performing a three-stage enrichment of ^{48}Ca .

Reference: Joseph Wild, Heng Chen, Keyue Liang Jiayu Liu Stephen Cox, Alex Halliday, Yuan Yang, *Science Advances*, Accepted.

2:30 PM BREAK

3:30 PM *EN08.02.04

Salinity Gradient Energy Harvesting using MXenes Husam N. Alshareef¹, Seunghyun Hong² and Jehad K. El-Demellawi¹; ¹King Abdullah University of Science and Technology, Saudi Arabia; ²Khalifa University, United Arab Emirates

2D MXene can be constructed into membranes or electrodes for ionic or molecular separation due to their intriguing features such as hydrophilicity, abundant surface terminal groups, and structural and chemical tunability. The high aspect ratio of MXene nanosheets provides nanochannels as diffusion paths for solute transport. The introduction of pores and modification of the interplanar spacing between neighboring sheets can also contribute to the formation of fluidic nanochannels. By tailoring the interlayer spacing of 2D MXene assemblies, it is possible to establish well-defined transport channels that enable size-selective sieving for specific ions or molecules. In addition to the interlayer distance, the lateral dimension (sheet size) of MXene nanosheets can be modified by adjusting synthesis conditions. Through geometric control over the constituent MXene sheets, the extended fluidic paths across the stack membranes provide the selective transport of solutes, which serves as the basis for the selectivity within layered membranes. The fluidic channel length in layered membranes can also be introducing controllable pores within the MXene sheets, which can enhance ionic diffusion kinetics. The ionic transport can further be enhanced by tuning the membrane thickness and using external stimuli that can enhance ionic transport within MXenes.

These fundamental features of ionic and molecular transport in MXenes can be the basis of many types of devices including sensors, iontronic devices, ionic separation, heavy metal ion extraction, capacitive deionization, and energy harvesting and storage. In this talk, I will discuss leveraging these basic concepts to develop MXene energy harvesters based on salinity gradients, thermal gradients, and ultrasound power absorption.

4:00 PM EN08.02.05

Monovalent Selective Cation-Exchange Membranes for Electrodialysis Pretreatment of Brackish Water Reverse Osmosis Brielle Januszewski, Hanqing Fan and Menachem Elimelech; Yale University, United States

Brackish water reverse osmosis (BWRO) can supplement dwindling freshwater resources because of its inland availability and energy efficient treatment compared to seawater. However, water recovery is limited to 50-85% by mineral scaling from primarily divalent cation-based scalants, such as Ca^{2+} and Mg^{2+} , leaving significant quantities of water unusable and in need of costly disposal. Thus, removing scale-forming divalent ions before RO is the key to increasing water recovery, but current approaches, such as solvent extraction or adding scale inhibitors, are thermally or chemically intensive, creating a need for an effective, additive-free scale-controlling strategy. Electrodialysis (ED) could be a thermal and chemical input free brackish water pretreatment that can remove scale forming ions before the RO step by separating incoming brackish water, using valent selective cation exchange membranes (vsCEMs), into streams that are rich with monovalent or divalent cations. This valent selective ED could be used in a coupled ED-RO hybrid system to achieve high water recovery (>90%) and would be tunable for use with a variety of BW feeds, thus mitigating scaling, improving zero liquid discharge (ZLD) management, reducing the total levelized cost of treatment and process downtime, and extending the overall system lifespan. Here, we focus on monovalent selective CEMs (msCEMs) which enable monovalent cation transport and reject divalent cations. There are a few commercially available msCEMs but they suffer from low monovalent-divalent selectivity. Previous work to improve msCEMs revolves around charge-based exclusion, which is typically achieved by including a thin coating of oppositely charged functional groups (having the same charge as the counter-ions) on the membrane surface, which more strongly repels divalent ions. However, a systematic study of the fabrication and operating conditions and their effect on membrane performance has not yet been performed, preventing them from further improvement. Here, we use a commercial CEM and two polyelectrolytes of opposite charge, poly(allylamine hydrochloride) (PAH) and poly(styrene sulfonate) (PSS), to deposit a thin selective layer using layer-by-layer assembly, whose facile fabrication and tunability allows for a cohesive study of structure-property-performance relationships within the same framework. Our results using a (PAH/PSS)_{2.5} deposition on a commercial support show that we can make consistent, defect-free membranes with average $\text{Na}^+/\text{Mg}^{2+}$ selectivities of ~25, showing a noticeable increase over the support layer's 0.5 $\text{Na}^+/\text{Mg}^{2+}$ selectivity. Moreover, we show that the limiting current of these membranes is highly dependent on the ionic strength of the diluate and concentrate solutions, regardless of the ionic species present, with limiting current increasing with solution ionic strength. We show that our membranes are significantly monovalent cation-selective, while systematically revealing the relationships between the separation performance and operating conditions including applied current density, diluate and concentrate solution composition, and thin film composition. This work would advance the fundamental understanding of ion transport in ion exchange membranes and offer critical guidance for applying valent-selective ion exchange membranes in water and wastewater treatment.

4:15 PM EN08.02.06

Desalination Fuel Cell Stacks: Scaling Up the Co-Production of Electricity and Clean Water Salman Abdalla, Shada Abu Khalla and Matthew Suss; Technion, Israel

The demand for clean water and electricity is on the rise worldwide. However, the scarcity of clean water and the utilization of environmentally harmful electricity sources are significant concerns[1]. Currently, reverse osmosis (RO) is widely employed for desalination of seawater and brackish water[2], with approximate consumption of 3-4 kWh/m^3 for seawater desalination[3]. An emerging type of water treatment technology called a desalination fuel cell (DFC) was introduced, which utilizes chemical energy from a single electrochemical cell to simultaneously power water treatment and generate electricity[4]. The DFC incorporates a fuel cell anode and cathode to catalyze the conversion of chemical energy into electrical energy. It also employs a cation and anion exchange membrane to desalinate the water passing through the cell. Our research group introduced the concept of DFC in 2020, demonstrating its potential to produce up to 10 kWh/m^3 while desalinating water with seawater-level salinity[4].

In order to make this promising technology practical, it is crucial to propose and demonstrate scale-up strategies. In this study, we present the results of the first scaled-up DFC. We employed scaling rules associated with electrodialysis by increasing the number of membrane pairs to accommodate either two or three feed channels (figure 1 [5]). However, the three-feed channel device experienced high voltage loss in the ohmic region and a lower limiting current (figure 3a [5]). Nevertheless, the salt concentration behaved linearly with the current density as anticipated (figure 3c [5]). The primary voltage losses were predominantly observed in the cathode and anode sides, while the membrane potential loss was found to be negligible [6]. Our research demonstrated that by increasing the acid concentration in the catholyte and the base concentration in the anolyte channels, we were able to achieve a notable enhancement in the stack's performance (figure 4a [5]). The implementation of a higher pH anolyte and a more acidic catholyte resulted in improved performance, as anticipated due to the higher open circuit voltage (OCV) predicted by the Nernst equation. Additionally, we investigated the impact of flow rate in the feed channels, which is known to affect salt removal efficiency. Overall, our study successfully demonstrates the implementation of a scaled-up DFC, highlighting the importance of addressing voltage losses and optimizing electrolyte compositions for enhanced performance.

[1] M. M. Mekonnen and A. Y. Hoekstra, 'Sustainability: Four billion people facing severe water scarcity', *Sci Adv*, vol. 2, no. 2, pp. 1-7, 2016, doi: 10.1126/sciadv.1500323.

[2] L. F. Greenlee, D. F. Lawler, B. D. Freeman, B. Marrot, and P. Moulin, 'Reverse osmosis desalination: Water sources, technology, and today's challenges', *Water Res*, vol. 43, no. 9, pp. 2317-2348, 2009, doi: 10.1016/j.watres.2009.03.010.

- [3] A. Al-Karaghoul and L. L. Kazmerski, 'Energy consumption and water production cost of conventional and renewable-energy-powered desalination processes', *Renewable and Sustainable Energy Reviews*, vol. 24. Elsevier Ltd, pp. 343–356, Aug. 01, 2013. doi: 10.1016/j.rser.2012.12.064.
- [4] I. Atlas, S. Abu Khalla, and M. E. Suss, 'Thermodynamic Energy Efficiency of Electrochemical Systems Performing Simultaneous Water Desalination and Electricity Generation', *J Electrochem Soc*, vol. 167, no. 13, p. 134517, 2020, doi: 10.1149/1945-7111/abb709.
- [5] S. Abdalla, S. A. Khalla, and M. E. Suss, 'Scaling Up the Simultaneous Production of Clean Electricity and Clean Water', *J Electrochem Soc*, vol. 169, no. 6, p. 063508, 2022, doi: 10.1149/1945-7111/ac74e2.
- [6] S. Abdalla, S. A. Khalla, and M. E. Suss, 'Voltage loss breakdown in desalination fuel cells', *Electrochem commun*, vol. 132, p. 107136, 2021, doi: 10.1016/j.elecom.2021.107136.

4:30 PM EN08.02.07

Ex-Situ Characterization of Carbon Slurries for the Flow-Electrode Capacitive Desalination Yousif Alkhalafi¹, Benjamin Alessio¹, Tomek Jaroslowski¹, Qi Jiang¹, Swetha Chandrasekaran², Alexandra Overland², Maira Cerón², Steven Hawks² and Juan G. Santiago¹; ¹Stanford University, United States; ²Lawrence Livermore National Laboratory, United States

Seawater desalination has great potential to meet the increasing global demand for freshwater. We are studying and developing a relatively new technology for desalination termed flow-electrode capacitive deionization (FCDI). FCDI cell design represents a significant development over standard capacitive deionization (CDI) cell by achieving continuous operation and the ability to process high salinity streams. These systems replace porous carbon-based solid electrodes with conductive carbon particles suspended in a continuously circulated electrolyte. We will present a study of the properties and chemistry of various carbon-based slurries. Particle type, size, shape, mass loading, and surface chemistry all play an important role in FCDI cells. Also important is the coupling among transport, charge exchange, and solution chemistry. We have developed an ex-situ experimental setup to quantify the charge transfer ability of carbon slurries, including carbon black and activated carbon. This ex-situ system enables convenient measurement of charge transport as a function of slurry properties and mixing. Our preliminary results suggest that the transport features, particle type, size, shape, and chemistry play a significant role in the charge transfer ability of the slurry.

SESSION EN08.03: Poster Session: Electrochemical Separations

Session Chairs: Matthew Suss and David Vermaas

Wednesday Afternoon, November 29, 2023

Hynes, Level 1, Hall A

8:00 PM EN08.03.01

Reinforced Composite Proton Exchange Membranes Through Polytetrafluoroethylene Surface Modification Yeon Su Lee, Hyunjun Kim, Seonghyeon Yang, Yeji Kim and Sung-Kon Kim; Jeonbuk National University, Korea (the Republic of)

As the problems of environmental pollution and resource depletion become serious, fuel cells using hydrogen, an infinite resource that occupies most of the universe and does not emit pollution, are emerging as an alternative to solve these problems. Among fuel cell types, Polymer Electrolyte Membrane Fuel Cell (PEMFC) is attracting attention for its advantages such as high efficiency and high energy density, but it is difficult to commercialize it due to high price of fuel cell manufacturing materials. Nafion composed of a single polymer of perfluorosulfonic acid is currently the most widely used and considered a major reason for increasing the price of Membrane electrode assembly (MEA), which is a key component of a fuel cell that produces electrical energy through an electrochemical reaction. Therefore, the reinforced composite membrane is getting attention in that it can reduce the amount of ionomer impregnation and improve ionic conductivity through thinning based on the excellent mechanical properties of the support polymer. In this study, a reinforced composite membrane is produced by a surface modification of porous polytetrafluoroethylene (PTFE) through plasma-assisted silane treatment, followed by Nafion impregnation. The surface modification of PTFE is adjusted by time on plasma and silane treatments. The optimum conditions are observed at 1 min of 10 W, 100 kHz, Ar plasma and 0.5 vol% silane treatment at room temperature for 1 min. After surface modification, the surface of PTFE becomes hydrophilic with a contact angle of 65~75°. The tensile strength and elongation at break of PTFE/Nafion were much higher than those of commercial homogeneous Nafion membranes. This PTFE/Nafion composite membrane has a tensile strength of 16 N mm⁻¹ and an elongation at break of 221%. It also shows an ionic conductivity of 0.12 S cm⁻¹, similar to commercial homogeneous Nafion membranes.

8:00 PM EN08.03.02

Investigation of the Moisture Effects on Printed Nitrate-Selective Potentiometric Sensors for Direct Soil Monitoring Kuan-Yu Chen¹ and Joseph Andrews^{1,2}; ¹University of Wisconsin-Madison, United States; ²University of Wisconsin-Madison, United States

As the demand for sustainable and efficient agriculture grows, there is an increasing need for reliable and cost-effective methods to monitor soil nutrient levels. Printed nitrate-selective potentiometric sensors have emerged as promising tools for in situ soil monitoring, offering real-time and continuous measurements of nitrate concentrations. However, the performance and longevity of these sensors can be influenced by environmental factors, particularly moisture content in the soil. This work presents the effects of soil moisture level on the functionality and accuracy of printed nitrate-selective potentiometric sensors, with the goal of enhancing their performance and reliability for soil nutrient monitoring applications. Building upon our prior research, we successfully manufactured inkjet printed potentiometric sensors that are specifically tailored for the detection of the nitrate in soil. The printed sensors contain two electrodes, the reference (RE) and ion-selective electrode (ISE). The ISE is covered by a drop-casted nitrate-selective membrane, which only allows the ion of interest in soil, nitrate in this work, interacting with electrode. This interaction generates a measurable potential difference across the RE and ISE, which can be correlated to the nitrate concentration in the soil.

To measure nitrate contents in moist soil environments, a porous hydrophilic polyvinylidene fluoride (PVDF) film is introduced into the potentiometric sensor. The PVDF shields the electrodes from charged soil particles, while allowing the passage of water. This feature ensures effective operation and provides protection from the soil environments, enabling direct sensing of nitrate in a medium that is similar to in aqueous solutions. The printed potentiometric sensors exhibit sensitivities ranging from sensitivities 45 - 50 mV/dec. To evaluate the performance of the printed potentiometric sensors under realistic conditions, the sensors are tested in two common crop field soil texture classes: sandy soil and silt loam soil. These soil types were chosen to represent practical scenarios encountered in agricultural settings. A range of nitrate concentrations, representative of typical agricultural scenarios, are applied to the sensors, and the response of the sensors is recorded under different moisture conditions.

This study will provide valuable insights into the impact of moisture on the performance of printed sensors and contribute to the development of robust and moisture-tolerant sensor designs for accurate soil nutrient monitoring in agricultural systems. By understanding the impact of moisture on sensor performance and developing moisture-tolerant designs, this research contributes to the development of robust and reliable real-time sensing systems for precision agriculture. This research holds significant potential to advance the field of precision agriculture, enabling farmers to optimize fertilizer management practices, reduce environmental impacts, and optimize crop yields in a sustainable manner.

8:00 PM EN08.03.03

Interlocking Bipolar Membranes for Efficient Electrochemical Separations Hyeon-Bee Song and Moon-Sung Kang; Sangmyung University, Korea (the Republic of)

A bipolar membrane (BPM) is a special type of ion-exchange membrane in which an anion-exchange layer (AEL) and a cation-exchange layer (CEL) are combined. Water molecules can be easily dissociated at the interface of the BPM by the strong electric field generated when a reverse bias voltage is applied through the membrane. The generated proton and hydroxide ions move out through the CEL and AEL, respectively, to produce acid and base solutions. Meanwhile, under a forward bias condition, protons and hydroxide ions move to the bipolar interface and neutralized again. Neutralization energy is generated according to the concentration of proton and hydroxide ions which move through the BPM and can be expressed as a junction potential (JP) value. When a BPM having an ideal JP is applied to an electro-membrane process, high separation and energy efficiencies can be obtained. In addition, the BPMs should have a highly adhesive bipolar junction for the long-term operation of electro-membrane processes. In this work, a novel BPM with an ideal JP and a highly adhesive bipolar junction property was developed and applied to several electrochemical separation processes such as acid-base flow battery and direct seawater electrolysis. The specially designed BPM was fabricated with poly(phenylene oxide) (PPO) based ionomers. In addition, an iron-based catalyst and a reinforcing material were introduced for excellent water-splitting performance and interfacial durability between the two ion-exchange layers, respectively. The prepared BPM not only had excellent interfacial adhesiveness and mechanical properties but also exhibited high water-splitting efficiency of 98% or more. The electrochemical separation processes employing the prepared BPM exhibited excellent performances comparable with those of commercial BPMs. This work was supported by the National Research Foundation of Korea (NRF) grants funded by the Korean government (MEST) (NRF-2022M3C1A3081178 & NRF-2022M3H4A4097521).

<div id="__endic_cr_x__"><div class="css-diopy0"></div></div>

8:00 PM EN08.03.04

Enhancing Ion Conductivity and Robustness in Gel Polymer Electrolytes with a Semi-Interpenetrating Polymer Network Structure Seonghyeon Yang, Yeon Su Lee and Sung-Kon Kim; Jeonbuk National University, Korea (the Republic of)

In this study, we describe the synthesis of gel polymer electrolytes (GPEs) by casting a solution consisting of poly(ethylene glycol) methyl ether methacrylate (PEGMA) and trimethylolpropane ethoxylate triacrylate (ETPTA) combined with poly(vinylidene fluoride-co-hexafluoropropylene) (PVDF-HFP). The solution is subjected to thermal radical polymerization using different molar ratios. The resulting GPEs exhibit a semi-interpenetrating polymer network structure, as confirmed by morphological, structural, and electrochemical characterization. Among the various compositions investigated, the GPE with a molar ratio of PEGMA:ETPTA at 98:2, in the presence of 40 wt.% PVDF-HFP (relative to the total amount of PEGMA and ETPTA), demonstrates exceptional properties. It shows high ionic conductivity ($1.46 \times 10^{-3} \text{ S cm}^{-1}$) and excellent tensile strength (6.28 MPa at an elongation at break of 156%). Moreover, the GPE exhibits electrochemical stability up to 4.7 V (vs. Li/Li+). Based on these electrochemical performance results, the synthesized GPEs show great potential as polymer electrolyte membranes in the field of energy storage.

8:00 PM EN08.03.05

Controlled Fabrication of Mesoporous Electrodes with Unprecedented Stability for Water Capacitive Deionization under Harsh Conditions in Large Size Cells Manar M. Hazaa and Nageh K. Allam; The American University in Cairo, Egypt

Capacitive deionization (CDI) is a feasible low-cost desalination technique for low to medium (brackish) salinity water. However, cycling stability and regeneration of the CDI electrodes are the bottlenecks hindering the practical application of the technology on large scale. Oxidation of the electrodes during the sequential adsorption and desorption processes is one of the most challenging problems hindering their long-term cycling performance. Herein, we demonstrated the ability to design and fabricate exceptionally stable CDI electrodes *via* a one-pot pyrolysis protocol. The optimized pyrolysis of nitrogen carbon precursors at different temperatures enabled the fabrication of carbon materials with a controlled amount nitrogen dopant (NDCs) with exceptional cycling stability. The NDCs showed high specific capacitance and dual *meso*/microporous structures with high salt adsorption capacity (SAC), reaching 26.5 mg g^{-1} in a single-pass desalination mode. Moreover, all NDC electrodes exhibited exceptional desalination stability performance over 150 successive charging/discharging cycles with 100% retention in aerated and deaerated solutions under harsh 1.4 V as the charging voltage. Moreover, all NDCs cells demonstrated charge efficiencies in the range from ~40 to 60%. The potential of zero charge (PZC) was determined for the tested NDC electrodes to elucidate their oxidation resistance (EOR). The electrodes exhibited a minimal shift in potential after the entire desalination stability tests, revealing minor electrode oxidation. The performance of our NDC-electrodes was compared against that of the commercially available activated carbon (AC) under the same experimental conditions, with the latter showing a server decrease in the SAC retention within the first few cycles.

8:00 PM EN08.03.06

Development of Layered Oxides for Electrochemically Driven Li Extraction from Dilute Li Sources Grant Hill and Chong Liu; University of Chicago, United States

Due to the rising demand of Li-ion battery powered vehicles, the lithium supply chain is projected to experience strain in the coming decades. This strain can be mitigated by developing new Li extraction methods that can access unconventional Li sources such as seawater. Electrochemical Li extraction has demonstrated high selectivity and recovery rates from dilute Li sources; the insertion host material selection plays a key role in the overall performance. However, few materials have been explored nor have materials been tailored for Li extraction from these multi-cation solutions. With this in mind, we have explored the role of particle size and morphology of layered cobalt oxide on Li extraction from mixed Li and Na solutions. We have found that large particles form a core-shell structured $(\text{NaLi})_{1-x}\text{CoO}_2$ by non-Faradaic ion exchange using parent LiCoO_2 with Na ions. Using electrochemical intercalation, this material successfully extracted Li from 1:20,000 Li to Na aqueous solution to 7.6:1 Li: Na, which is a Li selectivity of 1.5×10^5 over Na. Decreasing the particle size, parent $\text{Na}_{1-x}\text{CoO}_2$ was used to extract dilute Li from an organic solution and maintain high selectivity for multiple Li extraction sequences. After significant structural changes from the first Li extraction, high Li recovery performance can be maintained over multiple extraction sequences. Additionally, we also report C-rate dependence during the intercalation recovery step, indicating the importance of method development for optimizing material performance. This work highlights the importance of understanding the phase separation behavior of Li and Na in layered transition metal oxides for improved Li recovery capacity and lifetime.

8:00 PM EN08.03.07

Tailoring Vertically Aligned Multi-Layer Graphene Arrays for Selective Recognition of Dopamine Neurotransmitter: An Amperometric Approach Abdulrahman Al-hagri and Selva Palanisamy; Khalifa University, United Arab Emirates

The development of sensitive dopamine (DA) sensors has significantly contributed to our understanding of dopamine-related disorders and has enabled advancements in medical diagnostics and neuroscience research. Therefore, in the present work, a novel electrochemical sensing platform was developed using vertically aligned multi-layer graphene arrays (VA-MGA) for the selective detection of dopamine (DA). The preparation of high-quality VA-GA was achieved using the plasma-enhanced chemical vapor deposition method, eliminating the need for an additional catalyst. The formation of VA-MGA was confirmed using various physicochemical techniques such as transmission electron microscopy and Raman spectroscopy. The modified electrode, made of VA-MGA, was utilized for the electrochemical detection of DA using cyclic voltammetry and amperometry *i-t* methods. The electrochemical oxidation response and sensitivity of DA at the VA-MGA electrode was found to be 10 and 3 times higher than that observed with an unmodified and commercially available multilayer graphene modified electrodes. The VA-MGA sensor exhibited excellent analytical parameters for DA detection, including a wide linear range of 10 nM to 180 μM and a low detection limit of 2 nM. The sensor also demonstrated remarkable sensitivity, storage stability, and selectivity for DA detection, which makes it highly suitable for accurate detection of DA in medical diagnostics and neuroscience research. Furthermore, the practical application of the VA-MGA sensor for DA detection was demonstrated in various real samples.

SESSION EN08.04: Electrochemical Separations III
Session Chairs: Douglas Call and Ekaterina Pomerantseva
Thursday Morning, November 30, 2023
Hynes, Level 1, Room 108

8:30 AM *EN08.04.01

Highly Selective Electrochemical Separations of Metals Martin Z. Bazant; Massachusetts Institute of Technology, United States

The selective separation of metals from aqueous solutions is a critical challenge for many problems in energy, health and sustainability. This talk will describe two classes of highly selective separation methods for metal ions, based on differences in either electrokinetic or electrochemical properties. The first involves the propagation of deionization shock waves through charged porous media. Shock electro dialysis can separate trace amounts of toxic lead from drinking water or radionuclides from nuclear wastewater with minimal energy consumption. Shock ion extraction integrates ion-exchange resins to amplify the separation of multivalent metal ions, such as cobalt, zinc, mercury, nickel and manganese. Further control of these separations is afforded by pH swings, which allow heavy metal cations to be separated by selectively forming oxyanions, as illustrated by chemical-free continuous separation of vanadium, molybdenum, tungsten, cobalt and nickel. The second method involves selective electrosorption of metal cations in capacitive electrodes. Functionalized nanoporous carbon electrodes can separate multivalent from monovalent cations with applications to transition metal recovery in Li-ion battery recycling. Intercalation electrodes can provide extreme chemical selectivity for lithium with applications to extraction from lithium brines and battery recycling leachates, eliminating the need for harsh reagents in traditional hydrometallurgical processes.

9:00 AM EN08.04.02

Polymeric Porous Electrodes for Electrochemically Mediated Carbon Dioxide Capture Youhong (Nancy) Guo and T. Alan Hatton; Massachusetts Institute of Technology, United States

Carbon capture is a promising technology to mitigate emissions and achieve net carbon neutrality. Electro-swing reactive adsorption using redox-active species is emerging as a versatile platform for a sustainable decarbonization approach. However, the pricy electrode with limited gas diffusion has become one of the major factors hindering its practicality. Herein, we developed thick hydrogel coated-polymeric electrodes with high porosity that can effectively enhance the diffusion of carbon dioxide without the assistance of gas diffusion conduct. Such porous electrode also enables more interactive sites for redox-active polymers, leading to a ~90% quinone utilization efficiency at saturation. We also achieved continuous carbon capture-release operations with excellent capacity, stability, and Faradaic efficiency. Armed with lightweight and low-cost, as-developed electrodes present a vast potential to advance the future implementation of electrochemical carbon separation technologies.

9:15 AM EN08.04.03

Electrochemically-Mediated Enantioselective Interaction with Redox Metallopolymers Through Varied Chirality Jemin Jeon¹, Ching-Yu Chen¹, Fábio Z. Galetto^{1,2}, Johannes Elbert¹,

Chirality plays a critical role in various industrial domains, such as molecular recognition, asymmetric catalysis and chiral purification¹. Thus, constructing and leveraging precise chiral structures for enantioselective interaction has been a research hotspot in many scientific fields. In this research, we successively synthesized two types of chiral metallopolymer containing point chirality and planar chirality, respectively. Their chiral properties were characterized with circular dichroism and 2D nuclear magnetic resonance spectroscopy, followed by an investigation in their enantioselectivity with deprotonated amino acids and pharmaceutical carboxylates in electrical chemical systems. The point chiral polymers synthesized with Ugi's amine-inspired chiral monomers exhibits higher enantioselectivity compared with its chiral building block. 2D Nuclear Overhauser Effect Spectroscopy indicates the intramolecular interaction between the ferrocene moiety and alkyl backbone, and we infer that it is the emerging supramolecular chirality in the metallopolymer that resulted in enhanced selectivity². The planar chiral polymers incorporated an additional functional group on the ferrocene, generating the stereogenic plane. Improved recognition was also observed in comparison with their monomer precursors, and the affinities toward analyte enantiomers were flipped when tested over their four enantiomeric and diastereomeric stereoisomers, respectively. Further investigations on solvent polarity, supporting electrolyte and pH effect revealed that the enantioselective interaction between the chiral polymer and analyte is influenced by the competition between π - π interaction, hydrogen bonding and steric effect. Our results demonstrate the potential of adopting chiral redox-metallopolymer in electrochemically mediated platforms for enantioselective sensing and separation.

References

1. Hembury, G. A.; Borovkov, V. V.; Inoue, Y., Chirality-sensing supramolecular systems. *Chemical Reviews* **2008**, *108* (1), 1-73.
2. Jeon, J.; Elbert, J.; Chung, C. H.; Chae, J.; Su, X., Chiral Metallopolymer for Redox-Mediated Enantioselective Interactions. *Advanced Functional Materials* **2023**, 2301545.

9:30 AMBREAK

10:00 AM *EN08.04.04

Counterion Effects on Moisture Swing Direct Air Capture Applications Kelsey B. Hatzell; Vanderbilt University, United States

Direct air capture (DAC) is essential for achieving reversing the growth in greenhouse gas emission. Conventional sorbent materials require a regeneration approach which is energy intensive. Here, we evaluate a novel moisture-swing direct air capture approach which utilizes water vapor as a means to regenerate a absorbent materials. We specifically examine five anions (carbonate, phosphate, sulfide, acetate, and borate) and study how they interact impact CO₂ absorption capacity and kinetics. We discovered that the local short-range order in micropores determines the amount of hydroxide formation in the moisture-controlled reversible hydrolysis/neutralization reaction to affect CO₂ capture capacity. Among five anions, carbonate, phosphate, and borate exhibited greater ability to generate hydroxide and thus have higher capture capacity. A thorough understanding of the role anions impact moisture-swing DAC application can enable materials design strategies for advance climate materials.

10:30 AM *EN08.04.05

Electrochemically-Driven Solution-Phase CO₂ Capture Michael J. Aziz; Harvard John A. Paulson School of Engineering and Applied Sciences, United States

We investigate the mechanisms of and demonstrate the efficacy of CO₂ capture/release systems based on several thermodynamic cycles undertaken by aqueous solutions. Low-energy electrochemically-driven methods of making acid and base enable CO₂ capture by reaction with hydroxide and release upon acidification. Reactions among the various species of dissolved inorganic carbon (DIC) leading to CO₂ absorption and outgassing are caused by, respectively, diluting and concentrating the alkalinity in a solution. Redox-active organic molecules can reversibly bind CO₂ directly in one redox state and release it in the other. The same molecules can swing the pH by undergoing proton-coupled electron transfer, thereby enabling CO₂ capture by hydroxide.

11:00 AM EN08.04.06

Electrochemical Carbon Capture using Organic Dye Compound: System Design and Optimization in a Symmetric Cyclic Flow Hyowon Seo, Michael Nitzsche, Michael Massen-Hane and T. Alan Hatton; MIT, United States

Electrochemical carbon capture systems are designed to effectively reduce atmospheric levels of carbon dioxide (CO₂) by capturing this greenhouse gas from industrial flue gas or directly from the air, thereby contributing to the mitigation of climate change. The electrochemical carbon capture system utilizes an organic dye compound, known as neutral red/leuco-neutral red (NR/NRH₂), has been demonstrated for CO₂ capture from 15% CO₂ and ambient air. Through the application of electrochemical potentials, the pH of aqueous electrolytes is modulated to enable efficient separation of CO₂ from dilute sources. In order to assess the effectiveness of this system, an initial continuous flow system was constructed, which successfully demonstrated CO₂ separation capabilities using a mixture of 15% CO₂ and ambient air.

To enhance the stability of the system using NR/NRH₂ redox couple, a cyclic flow configuration was subsequently constructed to investigate the performance of CO₂ capture under different operating conditions. These conditions include variations in current densities, liquid flow rates, feed gas composition, electrode materials, and system operation methods. The electrochemical process within the cyclic flow system was analyzed by examining the current and voltage responses under diverse electrochemical conditions. The integrated electrochemical system, operating under optimized conditions, underwent testing for carbon capture within the cyclic flow setup.

The demonstrated electrochemical carbon capture system design and optimization results will encourage future research into optimizing the electrochemical separation unit for long-term and stable operations in large-scale applications.

11:15 AM EN08.04.07

Continuous Carbon Capture via Oxygen/Water Electrolysis in a Solid Electrolyte Reactor Peng Zhu¹, Haotian Wang¹ and T. Alan Hatton²; ¹Rice University, United States; ²Massachusetts Institute of Technology, United States

Electrochemical carbon capture technologies, with renewable electricity as the energy input, are promising for carbon management but still suffer from low capture rates, oxygen sensitivity, or system complexity. Here we demonstrate a continuous electrochemical carbon capture design by coupling oxygen/water (O₂/H₂O) redox couple with a modular solid electrolyte reactor. By performing oxygen reduction (ORR) and oxygen evolution reaction (OER) redox electrolysis, our device can efficiently absorb dilute carbon dioxide (CO₂) molecules at the high-alkaline cathode/membrane interface to form carbonate ions, followed by a neutralization process through the proton flux from the anode to continuously output a high purity (> 99%) CO₂ stream from the middle solid electrolyte layer. No chemical inputs were needed, nor side products generated during the whole carbon absorption/release process. High carbon capture rates (440 mA cm⁻², 0.137 mmol CO₂ min⁻¹ cm⁻² or 86.7 kg CO₂ day⁻¹ m⁻²), high Faradaic efficiencies (> 90% based on carbonate), high carbon removal efficiency (> 98%) in simulated flue gas, and low energy consumptions (starting from ~ 150 kJ/mol CO₂) were demonstrated in our carbon capture solid electrolyte reactor, suggesting its promising practical applications.

SESSION EN08.05: Electrochemical Separations IV
Session Chairs: Douglas Call and Ekaterina Pomerantseva
Thursday Afternoon, November 30, 2023
Hynes, Level 1, Room 108

1:30 PM *EN08.05.01

Lithium-Selective Adsorbents and Membranes for Electrochemical Wastewater Refining William Tarpeh; Stanford University, United States

With global lithium supplies projected to fall short of demand between 2023 and 2027, there is great motivation to develop new technologies capable of lithium recovery from alternative sources such as battery waste, produced water, and geothermal brines. In these sources, the co-existence of other impurities at much higher concentrations than lithium (e.g., >60,000 ppm Na⁺ versus 50-1000 ppm Li⁺ in brines) presents a challenge for high-purity lithium extraction. Selective electrodialysis is a candidate for lithium recovery that aligns with recent resource extraction priorities including developing electrified separation processes, although it requires the development of ion-selective membranes. To inform the design of such membranes, we first studied fundamental ion transport and selectivity mechanisms in commercially available membranes. We then synthesized a library of novel ligand-functionalized membranes (including acrylic acid and vinylpyridine ligands) to study the impact of additional ion-specific coordinative interactions on lithium selectivity in the selective electrodialysis process. Finally, we

integrated selective ion exchange resins into electro dialysis to accomplish in situ electrochemical regeneration that helps concentrate lithium from dilute sources and recovery high-purity lithium in electrochemical ion exchange reactors.

2:00 PM EN08.05.02

Augmenting the Interfacial Electrostatic Potential with Donnan-Enhanced Nanofiltration for Lithium Extraction from Salt-LakesLucy A. Kanas, Trent Lee, Zi Hao Foo and John H. Lienhard; Massachusetts Institute of Technology, United States

The exponential growth in the demand for lithium in the renewable energy and electric vehicle industries necessitates significant improvement in the efficiency of lithium production from primary sources. While lithium is abundant in salt lakes within South America and Asia, existing extraction methods based on brine evaporation are relatively costly and suffer protracted production cycles. By avoiding brine evaporation altogether, membrane processes such as nanofiltration can selectively concentrate monovalent ions, optimizing the extraction process directly from salt lakes while eliminating the environmental impacts of evaporation ponds.

The selectivity of conventional nanofiltration membranes can be attributed to their cross-linked polyamide active layer. The polyamide layer is typically fabricated by a condensation reaction between trimesoyl chloride and piperazine, along the interface of a polysulfone support layer and the organic monomer mixture. As a result of the charged moieties in the polyamide, the electrostatic potentials that form along the solution-membrane interface inhibit ions of the same charge from partitioning into the membrane, a phenomenon known as Donnan exclusion. However, the high concentration of the residual carboxyl moieties of the polyamide layer imparts a negative volumetric charge density to the active layer and attenuates the rejection of multivalent cations by Donnan exclusion.

To impart monovalent cation selectivity, emerging variants of nanofiltration employ a positively charged surface layer on the membrane that displays high water permeability and a positive volumetric charge density. Here, a Donnan-enhanced nanofiltration membrane employing a polyethyleneimine (PEI) surface layer is fabricated through a condensation reaction between perfluorosulfonic acid and the amine moieties in the polyamide layer, to attain enhanced $\text{Li}^+/\text{Mg}^{2+}$ selectivity. In this study, we present empirical evidence for the success of this method, based on experiments with high-salinity multi-cation brines that represent those encountered in salt-lake lithium extraction. Our conclusions are derived from 1000 original concentration measurements spanning three feed salinities and three pH levels.

The water permeability of the Donnan-enhanced NF membrane decreases from 17.2 % on average from the added hydraulic resistance. Our streaming potential measurements indicate that the zeta potential of the NF membrane increases from -17.2 mV to 19.8 mV with the addition of the PEI surface layer. Our experiments with binary cation solutions (i.e., Li^+ , Mg^{2+}) reveal that the $\text{Li}^+/\text{Mg}^{2+}$ separation factor increases from 39.1 with the unmodified membrane to 129.2 with the Donnan-enhanced membrane. Using multicomponent salt-lake brines from Salar de Atacama, Chile, the recorded $\text{Li}^+/\text{Mg}^{2+}$ separation factors are 13.2, 18.1, and 87.3, for solution pH of 7, 4 and 2, respectively. In a single pass, the Donnan-enhanced NF membranes register an Mg^{2+} rejection of 96.8 % while raising the concentration of Li^+ by 17.7 %. The enhanced $\text{Li}^+/\text{Mg}^{2+}$ selectivity at low solution pH arises from the protonation of the residual carboxyl moieties in acidic conditions ($\text{pK}_a \sim 4$). Lastly, we conduct a module-scale assessment of the process's membrane area requirement and energy efficiency.

2:15 PM EN08.05.03

Electrochemical Lithium Recovery: Investigating Electrode Behavior and Enhancing System DurabilitySeoni Kim; Ewha Womans University, Korea (the Republic of)

The demand for lithium has been rapidly increasing due to the widespread use of secondary batteries. Currently, lithium production primarily relies on the time-consuming process of evaporation and precipitation from brine lakes. This method is limited to specific water sources with low ion concentrations, and environmental concerns have emerged surrounding its use.

However, the development of electrochemical lithium recovery systems, inspired by the principles of lithium-ion batteries, holds promise for alleviating these concerns. By utilizing cathodes, such as LiMn_2O_4 and LiFePO_4 , which possess suitable channel sizes for selective Li^+ insertion, these systems can selectively recover lithium from various source waters with a wide range of Li^+ concentrations. However, a lack of understanding regarding the physicochemical behaviors of the Li^+ -selective electrode under realistic operational conditions has been a hindrance. Furthermore, the stability and cost of the counter electrodes in this system present significant obstacles that impede its practical implementation.

This talk aims to delve into the physicochemical behavior of the Li^+ -selective electrode during the electrochemical lithium recovery process at various Li^+ concentrations in the source water and the operation rate. Through the characterization of the electrodes using X-ray techniques, it was suggested that increasing the density research aims to tackle the increasing demand for lithium by advancing electrochemical lithium recovery systems. It will focus on investigating the behaviors of the Li^+ -selective electrode during realistic operational conditions and propose strategies for enhancing the efficiency and durability of electrode designs.

In addition, this talk will explore the Faradaic and non-Faradaic capture of anions by modifying the silver-based electrode and utilizing a high-surface-area carbonaceous material, respectively. It was found that the system showed high stability by using those electrode materials. Moreover, a system that enables simultaneous lithium recovery and decomposition of organic pollutants will be introduced. This extends the applicability of the electrode to industrial wastewater, highlighting the versatility of the electrochemical system.

2:30 PM BREAK

3:00 PM *EN08.05.04

Electrified Mineralization of Nutrients from Real Municipal Wastewater and the Energy Implications ThereofDamilola A Daramola; Northeastern University, United States

Phosphorus and nitrogen are two of the three major nutrients required for plant and animal life and sustaining global population growth requires an anthropogenic impact on the natural cycles of these nutrients i.e., increased phosphorus mining and nitrogen fixation to sustain the per capita consumption of P and N availability, respectively.¹ However, this anthropogenic activity has also led decreased environmental sustainability: higher accumulation of N and P in water bodies due to nutrient runoff and leaching as well as higher greenhouse gas emissions from nutrient fixation, mining and transportation. Furthermore, the process energetics for solid P and N delivery are 4.0 and 5.7 GJ/t, respectively,¹ while the embodied energetics for P and N delivery are 10.4 and 55.5 GJ/t, respectively,² illustrating the key drivers for the associated GHG emissions.

An alternative, yet sustainable, anthropogenic approach is the recovery and re-use of these nutrients from waste via an electrical driving force.^{3,4} Although a chemical approach to recovery enhances the circular economy of nutrient use, an electrical approach using renewable electrons extends from materials conservation to significant process decarbonization. This electrified approach will be discussed in this invited talk, based on the combined efforts of researchers at Ohio University and Northeastern University.

This presentation will describe an electrochemically-driven phosphorus and nitrogen recovery system using real wastewater from a municipal treatment plant as the substrate. Initial analyses consisted of 1-year of sampling from 3 different recycle streams at two different wastewater facilities: 4 million gallons per day and 100 million gallons per day throughput. Multivariate screening analyses of stream, design and operational variables on recovery efficiency and energy consumption from synthetic wastewater were conducted. These screening analyses were subsequently used to evaluate recovery efficiency and energetics with real wastewater as the treated substrate.

References

- (1) Daramola, D. A.; Hatzell, M. C. Energy Demand of Nitrogen and Phosphorus Based Fertilizers and Approaches to Circularity. *ACS Energy Letters* **2023**, *8*, 1493–1501.
- (2) Bhat, M. G.; English, B. C.; Turhollow, A. F.; Nyangito, H. O. *Energy in Synthetic Fertilizers and Pesticides: Revisited*; ORNL/Sub-90-99732/2; Oak Ridge National Lab., TN (United States); Tennessee Univ., Knoxville, TN (United States). Dept. of Agricultural Economics and Rural Sociology, 1994. <https://doi.org/10.2172/10120269>.
- (3) Belarbi, Z.; Daramola, D. A.; Tremblay, J. P. Bench-Scale Demonstration and Thermodynamic Simulations of Electrochemical Nutrient Reduction in Wastewater via Recovery as Struvite. *J. Electrochem. Soc.* **2020**, *167* (15), 155524. <https://doi.org/10.1149/1945-7111/abc58f>.
- (4) Kékedy-Nagy, L.; Abolhassani, M.; Perez Bakovic, S. I.; Anari, Z.; Moore II, J. P.; Pollet, B. G.; Greenlee, L. F. Electroless Production of Fertilizer (Struvite) and Hydrogen from Synthetic Agricultural Wastewaters. *J. Am. Chem. Soc.* **2020**, *142* (44), 18844–18858. <https://doi.org/10.1021/jacs.0c07916>.

3:30 PM EN08.05.05

Ammonium Recovery from Manure Wastewater and Simultaneous Electrosynthesis using Ammonium-Ion Selective Redox MaterialRui Wang¹, Kai Yang¹, Cindy Wong², Horacio Aguirre-Villegas¹, Rebecca Larson¹, Fikile Brushett², Mohan Qin¹ and Song Jin¹; ¹University of Wisconsin–Madison, United States; ²Massachusetts Institute of Technology, United States

The greenhouse gas emissions and water contamination generated by livestock manure motivates the development of new approaches to reduce their environmental impacts and improve sustainability. Effective approaches to recover nutrients, especially ammonia, from manure wastewater to produce fertilizer are needed. Here we develop a new electrochemical strategy to achieve simultaneous ammonium (NH_4^+) ion recovery and electrochemical synthesis using potassium nickel hexacyanoferrate (KNiHCF) as the ammonium ion-selective redox material to mediate the process. The KNiHCF electrode spontaneously uptakes NH_4^+ (and K^+) from manure wastewater with a nutrient (NH_4^+ and K^+) selectivity of ~100% and oxidizes the organic

matter. Subsequently, NH_4^+ -rich fertilizers are released electrochemically together with the electrosynthesis of value-added chemicals, such as H_2 as a green fuel or H_2O_2 as a disinfectant, without expensive ion-exchange membranes. The integrated process shows an estimated net profit for common cow dairy farms and could potentially reduce NH_3 emissions. These results provide a new conceptual strategy for distributed electrochemical resource recovery and on-demand electrochemical manufacturing that can improve agricultural sustainability and also open new opportunities for selective metal ion recovery towards zero liquid discharge water treatment and purification.

3:45 PM EN08.05.06

Separating Reactants in Membraneless Redox Flow Batteries: Leveraging Fluid Mechanics Sofia Kuperman¹, Ran Swisa¹, Robert Gloukhovski¹, Prakash Rewatkar¹, Mohamed Asarthen¹, Anna Zigelman¹, Matthew Suss^{1,2,3} and Amir Gat¹; ¹Technion - Israel Institute of Technology, Israel; ²Technion-Israel Institute of Technology, Israel; ³Technion - Israel Institute of Technology, Israel

Redox flow batteries are considered a highly promising electrochemical technology for grid-scale renewable energy storage. However, their commercialization has been hindered by high capital cost and balance of plant complexity. Single-flow batteries are an emerging subclass employing a membraneless cell design and simplified flow systems. Recently, single-flow zinc-bromine batteries leveraging novel multiphase electrolyte emulsions have been demonstrated. Such electrolytes are a mixture of a bromine-poor aqueous phase and bromine-rich polybromide phase, where in the latter phase the bromine is largely electrochemically inactive. However, separating the zinc and bromine reactants in the absence of a membrane is a challenging problem requiring deep understanding of multiscale flow phenomena and its coupling to battery performance.

In this work, we will briefly present our novel 2D analytical flow model describing the multiscale flow phenomena within such flow batteries. The model captures the concentration field of the polybromide phase, including sedimentation as this phase is denser. The model was validated with numerical simulations and experimental data. We will focus on how the predicted fluid mechanics phenomena support effective separation between the reactants, and how the model explains several counter-intuitive battery observations, such as decreasing electrolyte conductivity for decreasing flowrate. The model also points towards future battery optimizations for systems employing multiphase flow electrolytes, and thus is a key aspect towards unlocking their potential for low-cost renewable energy storage.

4:00 PM EN08.05.07

High-Performance Nanoparticle-Modified Membrane for Nonaqueous Redox Flow Batteries Daniel J. San Roman and Philip Cox; Mainstream Engineering Corporation, United States

For the effective implementation of environmentally friendly large scale renewable energy, low-cost grid-capable storage solutions must be implemented to accommodate the effective capture and load leveling of the typically periodic and variable production levels. One solution of particular interest is redox flow batteries (RFBs), which provide a high number of deep cycles and the ability to store large amounts of electrical energy cheaply and efficiently. However, aqueous RFBs typically suffer from low energy density, limited electrolyte stability, and capacity decay during cycling. Alternatively, switching RFBs to nonaqueous solvents and charge carrying redox complexes provides higher operating voltages allowing for higher energy density cells. However, to successfully implement these non-aqueous RFBs (NARFB) there remains the need to improve the durability of the cell membranes and reduce their susceptibility to crossover of active redox species.

To this end, Mainstream Engineering successfully demonstrated the preparation of a stable nanoparticle composite protective film that effectively reduces redox molecule crossover (> 90 % reduction compared to the non-reinforced anion exchange membrane [AEM]) with no effect on the key membrane ionic conductivity and shows promise as a high-performance membrane for NARFBs. Mainstream Engineering's approach to optimizing the AEM for NARFBs builds on our previous work developing scalable selective ion exchange membranes and membrane coatings of a fuel cell, batteries, and highly selective liquid and gas separation applications. For this work, we screened various potential AEMs for their chemical and mechanical stability in non-aqueous solutions as well as demonstrating a wide electrochemical stability window. After down selecting an AEM base membrane with excellent chemical stability, we formulated a nanoparticle/ionic binder coating to allow the deposition of a thin-film protective coating and the formation of a composite membrane on the AEM base membrane. We examined both screen printing and knife coating approaches to provide a robust, uniform, and repeatable method of coating the slurry compositions to provide a stable, uniform thin-film coating. The surface characteristics of our composite films were evaluated with optical and scanning electron microscopy, to determine the base porosity and the coating uniformity. These composite membranes were demonstrated to be both chemically and mechanically stable in the non-aqueous solvents. The ionic conductivity and iron tris(2,2'-bipyridine) (FeBpy) permeability of the films were benchmarked against commercially available AEMs. We have further optimized our composite membranes for decreased FeBpy permeability and performed half- and full- cell testing of our membranes, both under stationary and flowing electrolyte conditions. The performance of the protective film was further optimized via surface charge modifications of the nanoparticles to allow a 75% reduction in the ionic resistance of the nanoparticle modified membranes, lowering the cell voltage drop and improving the power density. Our materials show increased performance, by lowering the redox molecule crossover without increasing the membrane thickness or overall ionic resistance. Mainstream Engineering's novel composite AEMs provide a promising approach to solving outstanding membrane performance issues with current NARFB chemistries, providing a commercially viable path forward for high-energy density non-aqueous RFB storage technologies.

4:15 PM EN08.05.08

Membrane-Enabled Direct Extraction of Critical Metals Michael Baird^{1,2} and Brett A. Helms²; ¹University of California, Berkeley, United States; ²Lawrence Berkeley National Laboratory, United States

Water treatment devices designed to extract critical elements from wastewater and natural brines rely on polymer membranes that exhibit selective permeability towards dissolved ions. However, the underlying design principles that govern selectivity between ions of similar size and charge (e.g. Li^+/Na^+) remain unclear because of natural tradeoffs in the solubility and diffusivity of dissolved species within a membrane. Given that these properties arise from the solvation environments made available to permeating ions, we proposed a membrane platform wherein specific coordination modes are enforced in at sub-nanometer length scales with rigid polymer backbones and pendant groups with unique geometries. To this end, a library of systematically tuned microporous polymers have been synthesized and evaluated for ion uptake, ionic conductivity, and salt permeability. Our results lend insights to an energy landscape model of ion transport across membranes, where the pendant is shown to influence the energetics of partitioning at the water-membrane interface, as well as hopping between adjacent solvation cages within the membrane.

SESSION EN08.06: Electrochemical Separations V
Session Chairs: Matthew Suss and David Vermaas
Friday Morning, December 1, 2023
Hynes, Level 1, Room 108

8:30 AM *EN08.06.01

Electrically-Modified Anion Exchange Membranes for Alkaline Membrane Water Electrolysis Hanieh Bazayr and Athanasios Papageorgiou; TU Delft, Netherlands

Hydrogen has received much attention as a green energy alternative to replace fossil fuels in our effort to meet the requirements of global climate change. However, most of it is currently produced from fossil fuels through methane reforming, producing large amounts of carbon dioxide. Anion exchange membrane water electrolyzers (AEMWE) constitute a promising new technology to produce high-purity green hydrogen through water electrolysis, that use less expensive non-platinum based electrocatalysts than proton exchange membrane electrolyzers and low-cost polymer membranes. AEMWEs require membranes with high ion exchange capacity to achieve high hydroxide conductivity. However, this may lead to significantly low mechanical stability due to the increased water uptake and swelling ratio. Thus, the fabrication of AEMs with both high conductivity and mechanical stability is still a challenge [1].

In this study, novel membranes, based on poly(aryl quaternary ammonium), are fabricated through electrically-assisted solvent casting method. During the casting, DC and AC electric fields are applied on the polymer solution. The morphological and structural properties of the membranes are characterized by NMR and IR. The ion exchange capacity is measured through ion chromatography and the hydroxide conductivity is assessed via linear sweep voltammetry. The overall resistance of the cell and the durability of the membrane are investigated through electrochemical impedance spectroscopy and chronoamperometry, respectively.

We study how the application of an electric field improves the conductivity of the membrane by aligning the cationic groups of the polymer into ion channels, facilitating the movement of hydroxides. Results provide a comparison of the physicochemical and electrical properties of the membranes cast with and without the presence of various electric fields.

[1] Behrooz Motealleh, Zengcai Liu, Rich I. Masel, Julian P. Sculley, Zheng Richard Ni, Laureen Meroueh, Next-generation anion exchange membrane water electrolyzers operating for

9:00 AM *EN08.06.02

Nitrate Reduction Enhancements using Electrified Membrane Filtration [LeaWinter¹](#), [YingzhengFan¹](#), [XiaoxiongWang^{1,2}](#) and [ClaireButler¹](#); ¹Yale University, United States; ²Tsinghua University, China

The release of nitrate to the environment from wastewater effluent and agricultural runoff contributes to groundwater contamination, harmful algal blooms, and disruption of biogeochemical nitrogen flows. Nitrate conversion via electrochemical reduction can eliminate the production of concentrated waste streams while avoiding the addition of reductant or hole scavenger chemicals. However, major challenges for nitrate removal from water via electrochemical conversion involve reducing the use of expensive precious metal electrocatalysts while also improving the reaction activity and selectivity, stability, and mass transport of nitrate to electrocatalyst active sites. The use of electrochemical membranes (EMs) as multifunctional porous flow-through electrodes could potentially address these challenges based on improved mass transport and altered kinetics under flow conditions within membrane pores.

We fabricated conductive membranes using polymers combined with carbon nanotubes. The EMs showed significantly higher nitrate removal efficiency during electrified filtration compared to flow-by mode. The small pore sizes in the membrane reduced the diffusional boundary layer by several orders of magnitude with respect to flow-by mode, overcoming diffusional mass transport limitations. During electro-filtration, the nitrate conversion activity was easily controlled by tuning the permeate flow rate, regardless of applied potential. These enhancements and tunability demonstrate key advantages of employing membranes with pore sizes of $< 1 \mu\text{m}$ as flow-through electrodes compared to conventional 2D electrodes and 3D electrodes with larger pore sizes. Additionally, the EMs demonstrated nitrate removal to below EPA drinking water limits in synthetic surface water with product selectivity to N_2 of over 80% and without showing loss of stability over a period of 10 h. The mechanically-flexible membranes provide an advanced electrochemical water treatment architecture involving inexpensive materials and green synthesis methods.

9:30 AM EN08.06.03

Electrolyte Composition Effects on Bipolar Membrane Polarization and Transport for Electrochemical Separations [ThomasY. George¹](#), [PaigeBrimley²](#), [WilsonSmith²](#) and [MichaelJ. Aziz¹](#); ¹Harvard University, United States; ²University of Colorado, Boulder, United States

Bipolar membranes (BPM), consisting of an anion exchange polymer membrane layer, a cation exchange polymer membrane layer, and a catalytic interfacial layer in between, enable electrochemical cells with strong gradients of pH between adjacent chambers. Bipolar membrane electro dialysis (BPMED) is a prominent example of an electrochemical separation process relying on this unique type of membrane material. In bipolar membrane electro dialysis, the BPM operates in “reverse bias,” dissociating water into hydronium and hydroxide at the interfacial layer, generating acidic and alkaline streams, while a third electrolyte chamber is essentially desalinated as it provides a source of counterions (e.g. K^+ and Cl^-) for the acid and base streams. Recently, this process has seen increased attention for applications in resource recovery and for removing anthropogenic carbon dioxide from the environment. Unlike the traditional application of BPMED, to generate pure acid and base as chemical products, the emerging applications involve the BPM contacting electrolytes that include supporting salt or environmental impurities, which can have significant effects on the polarization behavior of the membrane as well as its transport selectivity of protons/hydronium and hydroxide over their counterions and other salts in the electrolyte.

In this work, we systematically investigate the effects of ion size, charge, and concentration on salt crossover in a widely-used commercial BPM (Fumasep FBM) by combining polarization experiments in a four-electrode setup with a 1D continuum model of water dissociation and multi-ion transport. We find that salt crossover dominates at low current density, before the stronger electric field at larger applied potential drives water dissociation to dominate. Further, we investigate how the total ion concentration and ratio of supporting salt to acid and base concentration influence the overpotential across the membrane and the contributions of salt crossover to total current.

Both high overpotentials associated with water dissociation at high currents and the unwanted salt crossover at lower currents provide significant hurdles for the deployment of BPMs in electrochemical technology. This work emphasizes the importance of electrolyte effects on these phenomena, and may provide guidance both for designing new materials and for choosing electrolytes and operating conditions in electrochemical cells.

9:45 AM EN08.06.04

Impedance Analysis of Anion Exchange Membrane Electrolysis [AthanasiosPapageorgiou](#) and [HaniehBazyar](#); TU Delft, Netherlands

Anion exchange membrane (AEM) electrolysis is a promising solution for low-cost hydrogen production from renewable energy sources on a large scale. However, the efficiency of AEM electrolysis is currently lower than that of traditional technologies, such as proton exchange membrane electrolysis. This deficiency in performance can be attributed to certain integral components of the membrane electrode assembly and the reaction kinetics. The measurement of these limitations involves assessing the ohmic and charge transfer resistances.

In this study, we aim to investigate and quantify the impact of various parameters such as voltage, temperature, flow rate, electrolyte concentration, and catalyst on the ohmic and charge transfer resistances using electrochemical impedance spectroscopy. The membrane electrode assemblies are fabricated using commercially available membranes, assessing the effect of different membranes on the performance of the electrolyser. In addition, the effect of DC and AC fields on the H_2 production is investigated, while the production of H_2 is quantified and compared to that calculated through the current output.

10:00 AM BREAK

10:30 AM *EN08.06.05

Controlling Protein Ad-and Desorption by an Electrical Switch on Polymer-Coated Carbon Electrodes [Kiekede Boer](#) and [KarinSchroen](#); Wageningen University, Netherlands

Capacitive Deionization (CDI) has been widely researched and applied to remove salt ions from brackish water in an energy-efficient way. During operation, two charged electrodes electrostatically attract ions, which are released again to the bulk solution once the potential is removed, resulting in a brine and freshwater solution. Carbon is generally used as electrode material, because of its high specific surface area and electrical conductivity. Building upon this principle, our research focuses on the separation of whey protein isolate (WPI) using a similar setup. We have successfully achieved reversible adsorption of up to 10 mg of protein per gram of electrode material on polyelectrolyte-covered carbon electrodes.

To achieve this, positively and negatively charged polyelectrolytes are attached to the working and counter electrode, respectively, to create a surface charge in the absence of an electric field. The created surface charge enables spontaneous adsorption on the working electrode by electrostatic attraction with the negatively charged protein. Protein desorption is initiated by an electric field of -1.2 V, which neutralizes the positive chemical charges of the polyelectrolyte-covered working electrode through negative electronic charges. The negatively charged polyelectrolyte on the counter electrode prevents re-adsorption during this desorption phase. This set-up, with a spontaneous adsorption step, can be referred to as inverted capacitive deionization (iCDI). Adsorption is controlled by diffusion while desorption is mainly migration-driven due to the applied electric field, causing desorption to occur faster than adsorption.

Interestingly, salt adsorption and desorption occur in phases opposite to those of protein adsorption and desorption. This unique behaviour allows for simultaneous concentration and desalination of the protein solution. Furthermore, we have successfully enriched β -lactoglobulin during the active desorption phase, which represents a significant step towards a separation system with high capacity and selectivity.

Looking ahead, we envision the potential of implementing stimuli-responsive polymers in the porous carbon structure to improve both the selectivity and reversibility of these electrically-driven separation systems. Stimuli-responsive polymers exhibit unique properties, such as the ability to reversibly alter their charge, conformation, and/or wettability in response to an external stimulus (e.g., an electric field). This capability provides greater control over the charge distribution and surface properties of the electrodes, and consequently allows tuning of the interaction forces with the proteins. Our research highlights that a comprehensive understanding of the surface properties and the underlying interaction forces is essential in selecting an appropriate responsive polymer coating for proteins or other target molecules.

The ultimate objective is to combine stimuli-responsive polymers with porous carbon structure, exploiting their respective strengths, to develop a separation system characterized by a high adsorption capacity, reversibility, and selectivity. While the focus of the current system is on the food industry, its potential applications extend to other industries, including biotechnology, wastewater treatment and the biomedical industry.

11:00 AM EN08.06.06

Ion-Conductive Properties of Polymeric Ionic Liquid-Coated Core-Shell Nanoparticles for Anhydrous Proton Exchange Membrane [KeisukeTabata](#), [TutomuMakino](#) and [AkitoMasuhara](#); Yamagata University, Japan

Polymer electrolyte fuel cells (PEFC) have attracted attention as next-generation energy sources for vehicles and distributed power sources. The operating environment of PEFC is expected to expand from the current low-temperature range ($< 90^\circ\text{C}$ and high-humidified environment) to the high-temperature range ($> 100^\circ\text{C}$ and low-humidified environment). Especially, the high-

temperature range operating PEFC are classified as HT-PEFC. However, conventional perfluorosulfonic acid electrolytes, such as Nafion, are unsuitable for HT-PEFC because the proton-conduction mechanism is dependent on hydrogen bonding between water molecules. Thus, there is an urgent need to develop proton exchange membranes suitable for HT-PEFC that conduct protons in high-temperature and low-humidity environments. In a previous study, it was discovered that high proton conductivity can be achieved by constructing nanosized proton-conductive channels and using ionic liquids as proton-conducting materials. However, a facile method for fabricating proton exchange membranes with no anisotropy in the direction of proton conduction has not yet been developed.

In this paper, we have proposed a procedure for constructing isotropic three-dimensional (3D) controlled ion-conductive channels employing polymeric ionic liquid (PIL)-coated core-shell nanoparticles. A PIL is an ion-conducting material containing an ionic liquid with a repeating polymer structure. In this system, we employed SiO₂ (silica) nanoparticles as the core nanoparticles and poly(1-vinylimidazole)/bis(trifluoromethanesulfonyl)imide (P1VIm/TFSI) as the PIL. The PIL-coated nanoparticles were then assembled, resulting in the 3D ion-conductive channels have been constructed by the contact of the PIL layers on the surface of the nanoparticles between adjacent particles. The PIL-coated nanoparticles were prepared using a unique precipitation polymerization technique applying precipitation polymerization.

The progress of the PIL coating onto the surface of the silica nanoparticles was determined using SEM-EDS mapping analysis. We have observed sulfur and fluorine elements originating from TFSI anion from the same position as silicon elements derived from silica nanoparticles, indicating that the PIL was successfully coated onto the surface of silica nanoparticles. The ionic conductivity of the PIL-coated nanoparticles was measured in a pelletized state prepared by simply pressing the nanoparticles. The pelletized PIL-coated nanoparticles exhibited ionic conductivity even under high-temperature and anhydrous conditions, with a maximum conductivity of approximately 10⁻⁴ S cm⁻¹ (160°C). Subsequently, to evaluate the construction of 3D ion-conductive channels, we have measured the anisotropy of the ionic conductivity of the pellets. Notably, there was no anisotropy in the ionic conductivity, and both vertical and horizontal directions achieved similar ionic conductivities. Furthermore, the ion-conduction mechanism was clarified by using variable-temperature ¹H solid-state MAS NMR spectroscopy. The imidazole N-H resonances in the PIL structure were observed at 9–12 ppm assigned to “mobile” protons which is contributing to the proton conduction. As this phenomenon was not observed with the PIL homopolymer, we have concluded that the coating of PIL onto the surface of the silica nanoparticles and the accumulation of PIL-coated nanoparticles increased the number of mobile protons.

In conclusion, we have achieved the facile construction of 3D ion-conductive channels by the accumulation of PIL-coated core-shell nanoparticles. Moreover, the ion-conduction mechanism was discussed using solid-state NMR spectroscopy, and the fabricated PIL-coated nanoparticles contained mobile protons. Thus, the PIL-coated core-shell nanoparticles and their assembly process are effective for developing a proton exchange membrane for HT-PEFC.

11:15 AM EN08.06.07

Exceptional Long-Term Stability of Titanium Oxynitride Nanoparticles as Non-Carbon-Based Electrodes for Aerated Saline Water Capacitive Deionization[NagehK. Allam](#); American University in Cairo, Egypt

Carbon-based capacitive deionization (CDI) electrodes suffer from long-lasting stability challenges due to sets of parasitic side reactions, including the high oxidation rate of the electrodes during the desalination process. Consequently, it is essential to identify, design, and fabricate novel electrodes that overcome such challenges to achieve robust and high desalination performance. This work reports on the fabrication and utilization of titanium oxynitride (Ti_xO_yN_z) nanoparticles as stable non-carbon electrodes for capacitive deionization. The oxynitride nanoparticles were synthesized via a simple template-free approach and fully characterized using XRD, XPS, Raman, SEM, and BET techniques. Moreover, the fabricated electrodes were electrochemically evaluated via cyclic voltammetry (CV), galvanostatic charge-discharge (GCD), and electrochemical impedance spectroscopy (EIS) techniques. The electrode exhibited a pseudocapacitance behavior with a specific capacitance of 150 F/g. A symmetric configuration CDI setup was constructed, enabling the investigation of the effect of different flow rates and voltages. Remarkably, the Ti_xO_yN_z CDI cell revealed a salt adsorption capacity (SAC) of up to 56.6 mg/g with fast adsorption kinetics. Moreover, the electrodes retained ~100% of its initial SAC even after 1960 cycles over 110 days of continuous testing. Furthermore, several post-characterization techniques such as XPS, XRD, FTIR, and potential of zero charge have been deeply studied and analyzed to unravel the observed exceptional stability of the tested electrodes.

11:30 AM EN08.06.08

Promoting the Selective Intercalation of Lithium in the Olivine FePO₄ [HostGangbinYan](#) and ChongLiu; University of Chicago, United States

The lithium supply challenge predominantly stems from the limitations of existing mining techniques in accessing lithium sources with intricate chemistry and low concentrations. Electrochemical intercalation presents an avenue for extracting lithium from diluted water sources. However, during the extraction process, the co-intercalation of lithium and its primary competitor, sodium ions, occurs. The comprehensive understanding of how host materials respond to this co-intercalation process remains an ongoing pursuit. Moreover, despite the well-acknowledged potential for lithium extraction, the reported selectivity for lithium can exhibit considerable disparity. This discrepancy in selectivity, as observed with olivine-type FePO₄, can span nearly three orders of magnitude, potentially arising from the diverse particle forms adopted (e.g., sizes, morphology, dominant facets, etc.).

In this talk, using one-dimensional (1D) olivine iron phosphate (FePO₄) as a model host, I will first introduce the co-intercalation behavior of lithium and sodium ions and the control of lithium selectivity through intercalation kinetic manipulations. By combining computational and experimental investigations, we noticed that lithium- and sodium-rich phases tend to separate in the host. Exploiting this mechanism, I will discuss how the sodium-ion intercalation energy barrier can be increased using partially filled 1D lithium channels, generated via non-equilibrium solid-solution lithium seeding or remnant lithium in the solid solution phases. Furthermore, the lithium selectivity enhancement during co-intercalation shows a strong correlation with the fractions of solid-solution phases with high lithium content (i.e., Li_xFePO₄ with 0.5 ≤ x < 1). Finally, I will delve into the impact of different structural forms of the host material. Specifically, I will discuss how these structural variations can influence particle kinetics and chemo-mechanical responses during Li/Na intercalation, ultimately affecting the preference for lithium.

SYMPOSIUM EN09

Lithium-Ion Battery Recycling and Reuse
November 27 - December 5, 2023

Symposium Organizers

Zheng Chen, University of California, San Diego
John Cook, Xerion Advanced Battery Corp
Kelsey Hatzell, Vanderbilt University
Marta Hatzell, Georgia Institute of Technology

* Invited Paper
+ JMR Distinguished Invited Speaker

SESSION EN09.01: Lithium-Ion Battery Recycling and Reuse I
Session Chairs: Zheng Chen and Kelsey Hatzell
Monday Morning, November 27, 2023
Hynes, Level 1, Room 108

10:30 AM *EN09.01.01

Recycling and Upcycling of Spent Battery Materials via Molten-Salt TechnologiesTaoWang¹, HuiminLuo¹ and ShengDai^{1,2}; ¹Oak Ridge National Laboratory, United States; ²University of Tennessee, United States

The recycling and upcycling of end-of-life lithium-ion batteries (LIBs) has become an urgent and challenging issue with the surging use of LIBs, in which recovering high-value cathodes not only relieves the pressure on the raw material supply chain but also minimizes negative environmental impact. Beyond direct recycling of spent cathodes to their pristine states, the direct upcycling of spent cathodes to the next-generation cathodes is of great significance to maximize the value of spent materials and to sustain the fast development of LIBs. A novel molten-salt system was developed to directly upcycle spent NMC 111 to Ni-rich NMCs by simultaneously realizing the addition of Ni and the relithiation of Li in spent NMC 111. Our prior and present research activities through molten-salt techniques in this area will be summarized in this presentation. Quantitative, fundamental understanding of the mechanisms of solvent tunability, the factors limiting control over solvent flux properties, the forces driving chemical reactions, and modes of controlling redox reactions will be discussed.

11:00 AM *EN09.01.02

Lithium-Ion Battery Recycling: Options, Environmental Impacts and EconomicsRebeccaCiez; Purdue University, United States

Demand for transportation and electricity grid energy storage will require gigawatt hours of lithium-ion batteries to power these systems. Recycling battery materials can assist in meeting the material demands for these systems and for reducing environmental impacts. This talk will discuss the economic and environmental costs associated with producing and recycling lithium-ion batteries using different recycling pathways. Process-based cost models provide context for the costs of manufacturing battery materials from new materials, and the potential for profitability from recycling. Finally, this talk will discuss the state of battery recycling given recent advances in the industrial policy to support the development of local battery material supply chains.

11:30 AM EN09.01.03

Towards Sustainable Polymer Solid-State Batteries: A Mechanical-Hydrometallurgical Case StudyKirstinSchneider^{1,2}, MarcoAhuis^{3,2}, PeterMichalowski^{3,2}, DanielGoldmann^{1,2}, ArnoKwade^{3,2} and BengiYagmur^{1,2}; ¹Technische Universität Clausthal, Germany; ²Battery LabFactory Braunschweig, Germany; ³TU Braunschweig, Germany

Lithium-ion batteries have become indispensable in various sectors for electrochemical energy storage. The rising demand for enhanced battery performance triggers the development of new technologies, such as solid-state batteries (SSBs). Featuring a solid electrolyte instead of a liquid one, SSBs hold great promise for next-generation energy storage. To promote battery circularity throughout the entire life cycle, it is essential to develop recycling concepts for next-generation SSBs even before their market introduction. However, literature currently lacks comprehensive studies on SSB recycling. Among the options for solid electrolytes, polymers stand out due to their potential for scalable production. With the use of new materials in polymer SSBs, there is an immediate need to assess their recyclability.

This study aims to explore mechanical-hydrometallurgical recycling routes for polymer SSBs, aiming to develop a holistic recycling concept. For this investigation, polymer SSB pouch cells, consisting of a polyethylene oxide/lithium bis(trifluoromethanesulfonyl)imide (LiTFSI) solid electrolyte, a lithium iron phosphate (LFP) cathode composite, and a Li metal anode, were utilized.

In the mechanical processing phase, we extensively explored the shredding properties of polymer SSB cells, with special attention to the critical safety considerations arising from the presence of Li metal. Based on the intrinsic properties of the materials used in polymer SSBs, an optimum shredding process has been identified to prepare the shredded material for subsequent hydrometallurgical processing. Ensuring the homogeneity of the crushed material and employing gentle disintegration techniques are crucial to avoid cross-contamination during further stages. Subsequently, in the hydrometallurgical processing step, we examined different leaching strategies for the shredded cells to extract valuable metals into the solution. Ultimately, we evaluated various precipitation strategies for impurity removal and Li recovery.

The obtained results provide valuable insights into the development of efficient recycling processes for SSBs. This forward-looking approach contributes to the establishment of a robust recycling industry that anticipates the evolving material flows of future battery technologies.

11:45 AM EN09.01.04

Eco-Friendly Process for Recovery of (Co,Ni) and LiCO₃ from Spent Lithium BatteriesValeryKaplan, EllenWachtel and IgorLubomirsky; Weizmann Institute of Science, Israel

Although Li-ion batteries were initially developed as a power source for portable devices, incorporation of Li-batteries in vehicles and industrial power banks has led to an exponential growth in the demand for both lithium and cobalt. While lithium production is almost exclusively oriented towards batteries, cobalt is also an essential component of high-strength alloys and magnets, with demand for batteries beginning to compete with these traditional applications. Recovery of Li and Co from spent Li-ion batteries poses technical challenges. In addition to the fact that opening and crushing spent batteries may result in self-ignition, current technologies generally aim at Co extraction only. Many of these technologies require sequential treatment with acids and bases, producing toxic waste, or involve dumping of crushed batteries into Co-smelting ovens. In both cases, lithium ends up in compounds from which it cannot be readily recovered. We have developed an economical procedure that recovers Co and Ni as metals, or alloyed with copper, and Li as LiCO₃. This process is based on treating crushed, spent batteries with dilute (4vol%) natural gas for 60 minutes in a temperature controlled furnace at 673-1123K. Following sintering, Li₂CO₃ is leached from the clinker with ice water, leaving all other components for further recycling. 30 minutes smelting at 1773K of the remaining filter cake in air in a closed ceramic crucible, allows recovery of heavy, non-ferrous metals (Ni, Co, Cu and their alloys) as mm-size ingots (39% Co, 32.2% Ni, 26.3% Cu). Iron compounds, remanent Li, Al and unburnt graphite are removed as slag. Neither corrosive acids nor costly reagents are required and hazardous liquid waste is not generated. This method was successfully tested with batteries from consumer electronics and with batteries used in the automotive industry. Since the proposed process does not use or produce toxic substances, is able to provide high recovery yield for Li (>95%) and can be run with simple equipment, it may be considered as suitable for straightforward scaling-up and industrial implementation.

SESSION EN09.02: Lithium-Ion Battery Recycling and Reuse II

Session Chairs: Rebecca Ciez, John Cook and Marta Hatzell

Monday Afternoon, November 27, 2023

Hynes, Level 1, Room 108

1:30 PM *EN09.02.01

Selective Electrodeposition for Lithium-Ion Battery Recycling—Tuning Interfacial Chemistry for Selective Cobalt and Nickel RecoveryXiaoSu and KwiyongKim; University of Illinois Urbana-Champaign, United States

The recovery of transition metals from battery recycling streams is a critical challenge for materials circularity in the future, especially with the growing demand on battery-related critical elements. Electrochemical separation approaches have been gaining traction as a modular and electrified platform for ion-selective recovery. However, key transition metals in batteries such as cobalt and nickel often possess close reduction potentials in aqueous media, thus impeding selective recovery by electrodeposition. Here, we overcome this challenge by combining electrolyte design with interfacial control, to enhance the selectivity between cobalt and nickel. First, through highly concentrated chloride solutions, we can discriminate between the two metals by charge, and through the application of charged polyelectrolytes, we can further enhance separation factor during electrodeposition. We implement this strategy for the recovery of cobalt, nickel, and manganese from commercially-sourced lithium ion batteries, and demonstrate the recovery of high purity transition metals. Finally, we discuss parallel directions in developing continuous electrochemical approaches for the selective recovery of lithium. Overall, we believe that electrochemical separations can play an important role in enabling sustainable and energy-efficient battery recycling technologies.

2:00 PM *EN09.02.02

Li Recovery from Brines using Recyclable Intercalation-Based Redox MembranesBenjaminZahiri¹, JohnCook², HengYang², BadriShyam², PaulBraun¹, RodrigoRodriguez² and YunkyuChoi¹; ¹University of Illinois at Urbana-Champaign, United States; ²Xerion Advanced Battery Corp, United States

The accelerated push towards renewable energy is leading to an exponential consumption of battery materials. Today, the United States net import reliance on battery materials varies widely from 25 to 80% (USGS Reports). If nothing is done, this import reliance is only expected to grow as electric vehicle and energy grid storage demands surge. Therefore, securing novel, domestic sources of critical lithium-ion battery components is of paramount importance and necessary to shield the U.S. from future global trade volatility and unforeseeable supply chain disruptions. The United States currently sources all its domestically produced lithium from one mine in Nevada where lithium carbonate is produced from evaporation ponds. Geothermal

brines have been identified as a domestic lithium source candidate with the capacity to fulfill the entire Li consumption needs of the U.S., but this resource is currently unexploited. Isolating a pure Li product from these hot brines poses a major challenge due to their corrosivity, elevated temperatures, high levels of dissolved solids, and numerous cationic species. To address this challenge, we use a novel redox membrane concept for Direct Lithium Extraction (DLE). Our team's proprietary molten salt platform is capable of manufacturing fully dense layered, spinel, and olivine transition metal oxide battery cathode materials. We demonstrate that dense cathode materials could function as membranes between the input (lithium brine source) and output (enriched lithium product) streams while permitting Li-flux via an electrochemically driven redox reaction. Unlike traditional membranes, which utilize concentration gradients to drive ion migration between solutions, an electrochemical driving force is envisioned to selectively mobilize lithium cations through a dense, electroplated transition metal oxide membrane. Extracted lithium will be directly converted to a highly valuable LiOH product. Transition metal oxides are ideal candidates for lithium brine extraction due to their capability to selectively uptake lithium ions, high degree of chemical stability at elevated temperatures, and high corrosion resistance. We show that such intercalation based membranes are highly selective for lithium ions over other competing ions such as sodium as well as multivalent cations including calcium and magnesium. Selectivity factors of over 100 has been achieved in our benchtop testing. Continuous operation of this novel redox membrane concept in a flow cell format will also be presented. Combined electrochemical and characterization data confirm the applicability of such concept in several lithium brine streams from geothermal to salar brine compositions. Summary of techno-economics of Li extraction using these membranes, that are recyclable, will also be presented.

2:30 PM EN09.02.03

Alternative Process Chain via Selective Leaching, Flotation and Smelting for LIB Recycling [Monika Keutmann](#), [Daniel Dotto Munchen](#) and [Bernd Friedrich](#); IME RWTH Aachen, Germany

The increasing demand for batteries, particularly in the electric vehicle and renewable energy sectors, necessitates sustainable and efficient methods for battery recycling. This work presents a comprehensive proof of concept for a battery recycling process chain that employs selective leaching with an organic acid, flotation, and smelting to recover valuable metals. This process aims to extract lithium, graphite, cobalt-nickel alloy, and manganese from spent batteries.

Selective leaching with an organic acid was utilized as the initial step to extract lithium from black mass. This method ensures the targeted recovery of lithium without compromising the quality of other valuable components. The leaching process generated a lithium-rich solution, which underwent subsequent purification steps to obtain a high-purity lithium salt.

The flotation technique was employed to recover graphite, a critical component used in battery anodes. By selectively floating graphite particles, the process achieved efficient separation from other materials, enhancing the purity and recovery rate of graphite.

Following flotation, the remaining battery black mass was subjected to pyrometallurgy to recover cobalt, nickel, and manganese. Pyrometallurgy involves high-temperature processing, enabling the formation of a cobalt-nickel alloy, that can be further treated to produce precursor material for battery production. Manganese, on the other hand, was found in the slag produced during pyrometallurgical treatment.

The developed process chain for battery recycling offers multiple advantages. Firstly, selective leaching ensures the recovery of lithium, a crucial metal for modern batteries, with high purity and minimal waste generation. Secondly, flotation enables efficient graphite recovery, addressing the increasing demand for this material. Lastly, smelting yields a valuable cobalt-nickel alloy and manganese is found in the produced slag, potentially opening up possibilities for further recovery.

The proof of concept presented in this work demonstrates the feasibility of the proposed recycling process chain for batteries. By integrating selective leaching, flotation, and pyrometallurgical treatment, this approach provides a comprehensive solution for recovering key battery materials. The successful extraction of lithium, graphite, cobalt-nickel alloy, and identification of manganese in the slag highlights the potential for resource sustainability and circularity in the battery industry.

2:45 PM EN09.02.04

Exploring Limits of Scale: Hydrothermal Relithiation for Direct Recycling [Maura Appleberry](#) and [Zheng Chen](#); University of California, San Diego, United States

Direct recycling is a promising alternative for low-cost and more environmentally friendly disposal of lithium-ion batteries. Hydrothermal relithiation is a method of direct recycling that uses an aqueous lithium hydroxide solution to infuse lithium back into cathode black mass at high temperatures and pressures. Despite recent attention and study, the limits of scaling the hydrothermal process are not understood. Our work has built on previous advancements of optimizing hydrothermal parameters, and demonstrated that the amount of aqueous solution can be significantly limited to still recover spent cathode materials. Through a study of lithium diffusivity at various states of delithiation, it is shown that minimal excess lithium is necessary to relithiate various lithium nickel cobalt manganese oxide (NCM) cathode materials. The improved solution-to-black-mass ratio maintains high cycling performance, fully restoring to pristine electrochemical capacity, thus paving the way for at-scale rejuvenation.

3:00 PM BREAK

3:30 PM *EN09.02.05

Life Cycle Assessment for Cathode Active Material Recycling Processes [Zheng Liu](#), [Yumeng Li](#) and [Pingfeng Wang](#); University of Illinois Urbana-Champaign, United States

With the growing demand of lithium-ion batteries for electric vehicles, handling the wasted lithium-ion batteries has become an intractable problem. Lithium-ion battery recycling has become a critical topic because of the increasing cost of mineral materials, environmental issues, and regulatory requirements. The lithium-ion battery components are separated through a pretreatment process to recycle lithium-ion batteries effectively. Among different components, cathode active material is the most valuable component. Thus, it attracts researchers' attention. However, most researchers focused on finding the optimal condition of a certain hydrometallurgical recycling process for cathode active material, and very few research comprehensively compared different hydrometallurgical recycling processes. In this study, life cycle assessment is adopted as the indicator to evaluate the environmental concerns, which is a major reason for using and recycling lithium-ion batteries, of different recycling processes for three widely used cathode active materials: NMC, LFP, and LCO. Based on the ISO 14040 standard, the life cycle impact assessment uses the ReCiPe method with standardized processes and unified reactors. As a result, the most effective recycling processes for different cathode active materials have been found. Moreover, an ultimate comparison between different cathode active materials is conducted, considering specific capacity and lifespan.

4:00 PM EN09.02.06

Exfoliation of LiCoO₂ into Nanosheets for Cobalt-Ion Extraction and Cathode Recycling [Hsin Juei Wang](#) and [Candace K. Chan](#); Arizona State University, United States

In recent years, methods for recycling Li-ion battery cathode materials such as lithium cobalt oxide (LiCoO₂, LCO) have attracted more and more attention. Since the cobalt in LCO is a limited resource, developing better ways to extract and recycle cobalt from the cathode materials becomes a critical issue. Traditional methods include pyrometallurgy and hydrometallurgy, which involve high temperatures and reaction of spent LCO with acid, respectively. Here, a new approach investigates cobalt extraction from nanosheets of LCO based on the rationale that cobalt extraction is more facile from high surface area LCO nanosheets compared to bulk LCO particles. To obtain LCO nanosheets, two exfoliation methods are used: 1) an oxidation-reduction assisted method, and 2) proton-exchange assisted method. Both approaches are aided by the intercalation of bulky ammonium cations into the interlayer space of the LCO structure, which facilitates exfoliation of LCO to form nanosheet suspensions in water upon sonication. The last step is to mix the nanosheet suspensions with cation solutions with the goal of achieving ion exchange and extraction of cobalt. The process is dependent on the pH of the solution and the choice of cation used to exchange for cobalt. This process is also demonstrated for other Co-containing cathodes such as LiNiMnCoO₂ (NMC) and LiNiCoAlO₂ (NCA). The effectiveness of cobalt extraction and ion-exchange are characterized using Raman and X-ray photoelectron spectroscopy, electron microscopy, and inductively coupled plasma spectroscopic analysis. Further research will focus on different kinds of ion exchange and the reassembly of nanosheet backs into functional cathode materials.

4:15 PM EN09.02.07

From Lab Scale to Upscale Lithium Recovery Through Neutral Leaching of Black Mass [Daniel Dotto Munchen](#) and [Bernd Friedrich](#); IME - RWTH Aachen, Germany

In the next ten years, it is expected that the electric vehicles market will grow at least 20 % each year. Therefore, the manufacturing and usage of batteries, mostly of Lithium ion batteries, will rise. To avoid shortages in supply, the recycling of end-of-life batteries is the key for a complete circular economy. However, the recovery of lithium from the active material—so called black mass (BM)—lacks in a consolidated recycling route, especially concerning industrial scale. In hydrometallurgical treatment, water leaching with CO₂ injection was developed to recover Li in an early stage based on solubility, which is an easy and low cost operation. With that in mind, this work aims on upscaling neutral leaching of BM from lab scale in terms of Li recovery efficiency. Firstly, lab scale trials were performed in a 1.5 L reactor, CO₂ bubbling of 6 L/min, 60 min of leaching time, constant stirring rate of 350 rpm, and particle size < 63 μm. The parameters that varied were temperature (20 °C and 80 °C) and solid/liquid ratio (10 g/L and 70 g/L). Based on these results, the upscaling leaching was performed in a 100 L reactor, but with an intermediate solid/liquid ratio of 30 g/L. The lab scale Li recovery efficiency achieved up to 80 % in the conditions of 10 g/L and 80 °C, however at 10 g/L and 20 °C the recovery efficiency was only 3 % lower. The compounds that are expected to be formed are Li₂CO₃ as well as LiHCO₃, which are soluble in water under such conditions. In contrast, when 70 g/L was tested, the results in both temperatures showed Li recovery efficiency of only around 50 % because the solubility limit is reached. In addition, in all scenarios, less than 1 mg/L of other metals was found in solution. Maintaining lower consumption of energy by using 20 °C in the upscale and a slight higher S/L ratio of 30 g/L to better simulate industrial conditions, the Li recovery efficiency showed nearly 65 %, which clearly indicates that S/L ratio is the key factor. In summary, an early stage Li recovery with water and CO₂ injection in upscale presents low cost and has potential to be further enhanced. The Li₂CO₃ in solution can be precipitated through evaporation with low grade of impurities, which is beneficial for the refinement of the raw material

for new batteries. Moreover, the filter cake after leaching contains Ni, Co, Mn, and Al. which can be further treated in hydrometallurgy, or even pyrometallurgically as an alloy.

4:30 PM EN09.02.08

Direct LiOH Production from Battery Cathode Leachate with Nanofiltration and Bipolar Membrane ElectrodialysisTrentLee, LucyA. Kanas, Zi HaoFoo and JohnH. Lienhard; Massachusetts Institute of Technology, United States

With a growing global interest in environmental protection, the importance of lithium-ion batteries (LIBs) is rapidly increasing. As a result of their quick charging, longevity, and high power density, LIBs are the leading choice in powering portable devices like smartphones, laptops, and electric vehicles. Unfortunately, domestic supplies of lithium, cobalt and manganese are limited, and current extraction methods are energy-intensive and generate large volumes of chemical waste. Lithium can be secured from primary sources, such as solid ore mining—an environmentally harmful process—or from brine evaporation, which is a very time intensive procedure.

The supply of lithium, cobalt, and manganese can also be augmented through secondary sources, namely by recycling spent cathodes from LIBs. Battery recycling is the process by which valuable metals are recovered from spent LIBs to manufacture pristine LIBs. Lithium, cobalt, and manganese make up the cathode layer of the majority of LIBs. The prominent cathode chemical composition includes: LiCoO_2 (LCO), LiMn_2O_4 (LMO), and $\text{LiNi}_{0.33}\text{Mn}_{0.33}\text{Co}_{0.33}\text{O}_2$ (NMC). Inorganic acid leaching—the process of soaking used batteries in inorganic acids like sulfuric acid and hydrochloric acid—is a highly effective method of recovering lithium, cobalt, and manganese from the spent cathodes. In this process, a highly concentrated acid leachate that comprises Li^+ , Mn^{2+} and Co^{2+} is produced, and electrochemical reactions are commonly leveraged to reduce the metal ions into their respective solid forms.

In this work, we investigate membrane processes for direct LiOH production from battery cathode leachates. First, the battery leachate is pressurized and passed into a Donnan-enhanced nanofiltration process. Conventional polyamide nanofiltration (NF) membranes possess negative volumetric charge densities as a result of the high concentration of carboxyl moieties, leading to poor monovalent selectivity for cations. To enhance cation separations from battery leachates, a highly crosslinked layer of polyethyleneimine (PEI) is covalently bonded with the polyamide substrate through a condensation reaction between the perfluorosulfonic acid and amine moieties. The composite NF membrane acquires a positive zeta potential and exhibits passive selectivity for monovalent cations from the enhanced Donnan exclusion effect. Our preliminary results indicate that the Mn^{2+} and Co^{2+} rejections increase from 65% to 99%, between the experiments involving the pristine and composite NF membranes. Conversely, the Li^+ rejection only increased incrementally from 5% to 13%, and the Li product stream has purity rating of at least 98%.

Second, the Li-rich permeate stream from NF is used as the input to a bipolar membrane electrodialysis (BMED) process. In BMED, a bipolar ion exchange membrane facilitates water dissociation, while the inherent cation and anion exchange membranes inhibit co-ion transport. As a consequence, BMED produces a basic LiOH, an acidic HCl and a desalinated stream. Here, we leverage high current densities to promote efficient water dissociation, enabling highly concentrated (1M or greater) HCl and LiOH streams to be produced from the NF permeate. The HCl can be recycled for acid leaching of battery cathodes, reducing acid consumption and chemical waste generation while promoting a closed atom economy. The concentrated LiOH can be used as a feedstock for direct battery manufacturing.

4:45 PM EN09.02.09

Investigating the Greenhouse Gas Emissions of the Global Lithium Supply Chain for BatteriesSiddharthShukla, MatthewRiddle and JarodKelly; Argonne National Laboratory, United States

The global demand for battery materials like lithium is increasing due to increased demand for battery-electric vehicles. Lithium is economically extracted from brine and spodumene ore resources, while clay resources are also gaining interest. These resources are diffusely spread across the globe. The greenhouse gas emissions of extracting lithium from these sources vary considerably due to the required processing energy and material inputs to the systems, along with the needs associated with the desired final products, namely lithium carbonate and lithium hydroxide. Also, different extraction and processing stages may occur in different countries leading to variability in grid electricity emissions and additional transportation emissions. Therefore, an accurate representation of the total greenhouse gas emissions from the global lithium supply chain is difficult to estimate. To fill this gap, the current work uses a novel framework to calculate the emissions from each step of the global lithium supply chain, accounting for the variability in lithium sourcing, additional material requirements, and processing locations. Further, the change in emissions due to possible supply disruptions is also investigated utilizing agent-based modeling of supply-demand flows. Overall, the results from this work can help identify carbon-intensive pathways in the global lithium supply chain and highlight pathways that lead to reduced emissions.

SESSION EN09.03: Poster Session: Lithium-Ion Battery Recycling and Reuse
Session Chairs: Kelsey Hatzell and Marta Hatzell
Monday Afternoon, November 27, 2023
Hynes, Level 1, Hall A

8:00 PM EN09.03.01

Electrochemical Properties of Recycled Battery MaterialsJianPeng¹, NeerajSharma¹ and StefanieMaslek²; ¹UNSW, Australia; ²Mint Innovation, New Zealand

Owing to its high energy density and long cycle life, Lithium-ion batteries (LIBs) have been world-widely used for portable devices and electric vehicles in the past decade.¹ Typically, a LIB consists of cathode, anode, electrolyte, separator and sealing components. The graphite and LiCoO_2 (LCO) have been regarded as dominant materials for anode and cathode in commercial LIBs respectively, due to their cycling stability and relatively high energy density. The graphite anode is able to deliver a relatively high reversible capacity of approximately 370 mAh/g, while LCO exhibits a moderate capacity of about 140 mAh/g under the cutoff voltage of 4.2V.²

However, all batteries have a finite lifespan. According to the report, the waste of spent portable LIBs will reach 180,000 tons/annum by 2023, but less than 1% Li-containing waste can be well recycled globally.³ This imbalance of battery waste and recycling/reused battery materials leads to plenty of research on how to effectively recycle transition metals (*e.g.*, Fe, Co, Ni, and Mn) and graphite from spent electrodes. In our study, we systematically investigated the electrochemical properties of recycled graphite powder as well as the LCO synthesized by recycled Co precursors. The capacity of recycled graphite can achieve 350.1 mAh/g at the current of 20 mA/g and capacity retention of 75.5% after 100 cycles. On the other hand, LCO powders synthesized by different Co precursors exhibit various electrochemical performance. The LCO synthesized by recycled CoCO_3 presents a capacity of 132.6 mAh/g at the first cycle but delivers the similar capacity after 100 cycles compared to that of commercial LCO powder. However, the LCO synthesized by recycled Co(OH)_2 only shows the capacity of about 120 mAh/g at the initial cycle.

In order to improve the electrochemical properties of recycled graphite, we have employed ball milling for 3h and 30h respectively to modify its particle size and surface morphology. Both Raman and scanning electron microscope (SEM) patterns indicates that ball milling successfully minimizes the number of defects in graphite particles, while surface area of particles enlarges with ball mill time. After 3h ball mill, these structural changes of graphite noticeably elevated the discharge capacity by 27% at the first cycle and 18.4% retention after 100 cycles. Whereas, regarding to 30h ball milled graphite a serious reaction between graphite and glass fibre separator was observed by SEM after 100 cycles, leading to a rapid capacity fading. It is unexpected that high surface area of graphite may cause the decomposition of glass fibre separator during cycling, which possibly induces safety issues of batteries. The electrochemical properties of ball milled graphite in full cells also implies that ball milling leads to unstable solid electrolyte interphase (SEI) on the graphite surface. Applying commercial LCO as the cathode, ball milled graphite presents a significant capacity fading with cycle number, with capacity decreases of 8.2% and 24.8% after 20 cycles for 3h ball milled and 30h ball milled graphite, respectively.

This work evaluated the electrochemical performance of recycled graphite and LCO synthesized by recycled Co precursors. The effect of ball mill on the electrochemical performance of recycled graphite has also been measured.

Reference

- [1] Tarascon, J-M., and Michel Armand. "Issues and challenges facing rechargeable lithium batteries." *nature* 414.6861 (2001): 359-367.
- [2] Wu, Suping, et al. "Stabilizing LiCoO_2 /graphite at high voltages with an electrolyte additive." *ACS applied materials & interfaces* 11.19 (2019): 17940-17951.
- [3] Nitta, N.; Wu, F.; Lee, J. T.; Yushin, G. Li-ion battery materials: present and future. *Materials today* 2015, 18, 252–264.

8:00 PM EN09.03.02

Design of a Hydrometallurgical Recycling Process for Polymer Solid-State Batteries using the Example of LFP Cathode CompositeKirstinSchneider, DanielGoldmann and BengiYagmurlu; Technische Universität Clausthal, Germany

New battery technologies are constantly under research to meet the ever-increasing demands of electromobility imposed on lithium-ion batteries (LIBs). Solid-state batteries (SSBs) are

emerging as one of the promising next-generation battery technologies, offering higher energy density and improved safety compared to conventional LIBs. Naturally, SSBs have distinct differences than conventional liquid electrolyte LIBs, and therefore, it is crucial to design, adapt and uncover possible recycling routes since the development of SSBs is accelerating. This study investigates the hydrometallurgical recycling of LFP (lithium iron phosphate) in a polyethylene oxide (PEO) composite structure used in the cathode of polymer SSBs.

In this case study, we present a comprehensive analysis on the leaching of LFP cathode composite using sulfuric acid followed by an exploration of possible Fe and Li recovery routes. An important aspect of this investigation is to assess the impact of the PEO matrix on the hydrometallurgical process. To achieve this, a comprehensive characterization of the sample was conducted, including the determination of the particle size distribution, chemical composition, and molecular weight of the virgin polymer. Various process parameters are investigated in detail for the optimization of the recycling process.

The study findings showed that LFP was leached even with under stoichiometric addition of sulfuric acid at 25 °C within a short duration of 60 minutes. Notably, the water-soluble PEO predominantly influenced the storage stability of the leach solution. Moreover, strategies for iron removal and lithium recovery are also tested and proposed for a comprehensive design of the recycling process. The outcome of this case study offers valuable insights into the hydrometallurgical processing of LFP composites, particularly in the context of the recycling processes for next-generation SSBs. By understanding the leaching mechanism and the impact of the PEO matrix on the hydrometallurgical process, recycling processes can be strategically adapted to future material flows, thereby contributing to the advancement of the circular economy of batteries.

8:00 PM EN09.03.03

Analysis of R&D Investment and Performance Evaluation for Government-Funded R&D Programs in the Field of Lithium-Ion Batteries Dongyoung Kim, Sein Kwon, Junhwan Lee, Sangwoo Lim and Yeojin Jeong; Korea Institute of S&T Evaluation and Planning, Korea (the Republic of)

This study aims to overview the current status of government-funded R&D programs in the field of lithium-ion batteries, analyze the evaluation indicators, suggest future directions for designing new research programs, and provide a guide for selecting indicators to study the feasibility and performance of the programs.

As of 2022, there are seven government R&D programs in the field of lithium-ion batteries, organized by the Ministry of Trade, Industry, and Energy. These programs, of which budget amount to 26.815 billion KRW (20.5 million USD), include studies on improving the performance of lithium-based rechargeable batteries, to enhance the reliability of rechargeable batteries through evaluation infrastructure, developing ESS technology using battery packs used in electric vehicles/ESS, and developing a battery-sharing platform for electric vehicles (EVs). The performance evaluation indicators for the outcomes of these programs include indicators related to battery performance, patent, paper, revenue, technology standardization proposals, equipment establishment and operation rates, and conducting user satisfaction surveys.

Although the programs for analysis were selected based on specific criteria, the ratio for the field of rechargeable batteries seems to be relatively low compared to the Korean government's R&D budget of 29.8 trillion KRW (20.5 million USD). Basic research projects for battery material development were excluded, and further discussions are needed on the overall support scale and the direction of support in the field of lithium-ion batteries, both in terms of government support R&D and private sector R&D. Additionally, to improve the performance of R&D in the field of lithium-ion batteries, it is necessary to discuss the exploration of various evaluation indicators and data accumulation for performance evaluation, aiming to enhance R&D performances in the field of lithium-ion batteries.

8:00 PM EN09.03.04

Graphene Oxide (GO) as Chemical Anchor of Polysulfides for Li-S Batteries Balram Tripathi^{1,2}, Claudia Zuluaga Gomez¹, Ivan Castillo¹, Sunny Choudhary¹, Mohan Bhattarai¹, Rajesh Katiyar¹, Gerardo Morell¹ and Ram Katiyar¹; ¹University of Puerto Rico, United States; ²S S Jain Subodh PG College Jaipur, India

Lithium-sulfur (Li-S) battery is one of the most promising candidate for the next-generation rechargeable cell. In order to control the shuttle effect of dissolution lithium polysulfides (LIPs), the chemical interactions between sulfur host and LIPs on the performance of Li-S batteries has recently been highlighted. Herein, a facile strategy is proposed, which produces graphene oxide (GO) as an anchor to restrain LIPs in Li-S batteries via chemical confinement by strong bonding interaction between GO and Li₂S₆. X-ray diffraction (XRD), Raman analysis & Scanning electron microscopy (SEM) of prepared composite material was done to study structural and morphological properties. Electrochemical performance of GO-S composite cathodes using LiTFSI electrolyte was studied by galvanostatic charge-discharge at various C-rates as well as via cyclic voltammetry & EIS measurements. The detailed results of the study will be discussed during the presentation of meeting.

8:00 PM EN09.03.05

Efficient Separation of Cathode Materials in Direct Recycling of Spent Lithium Ion Batteries Kwang Bum Kim and Hunseok Choi; Yonsei University, Korea (the Republic of)

There is a growing demand of lithium ion batteries in consumer electronics, electric vehicles, and energy storage systems, which would eventually generate a huge number of spent lithium ion batteries. Spent lithium ion batteries should not be treated as waste but be considered as a valuable resource rich in critical materials such as Co, Ni, Li and Cu. Recently, direct recycling process is being actively investigated to retrieve high value cathode materials which retains the original structure and morphology without chemical decomposition to metallic elements or metal ions. A major challenge for direct recycling is to efficiently separate cathode materials from aluminum foil because of the high adhesive bonding strength and chemical stability of polyvinylidene difluoride (PVDF) binder used in the production of lithium-ion batteries. In this regard, environmentally sustainable delamination process needs to be developed to efficiently recover cathode materials from cathodes. However, current procedures reportedly used toxic organic solvents to separate the active cathode materials from the aluminum foil. In this study, we report on the direct recycling of NCM cathode materials from spent lithium ion batteries, important delamination parameters and materials properties of delaminated NCM. More details will be discussed at the meeting.

8:00 PM EN09.03.06

Spent Cathode Materials Upgrading by Forming Nano-Coatings Lance Yang^{1,2}, Zhiqian Wang¹, Jared Liao¹, Jerry Xiang¹, Jarett Hoelzle¹ and Bruce Koel²; ¹Princeton NuEnergy, United States; ²Princeton University, United States

Lithium-ion batteries (LIBs) have emerged as the battery of choice for rapidly growing markets in electric vehicles (EVs) and grid electricity storage. This spurs a great demand for lithium, graphite, cobalt, and nickel that could outstrip the supply of virgin materials. Thus, there is an enormous interest in the development of new sustainable technologies for recycling and recovery of valuable materials from secondary resources, especially from used lithium-ion batteries. Compared to conventional high-temperature pyrometallurgical or hydrometallurgical methods, direct recycling of LIBs is a more desirable approach because it can directly regenerate the cathode materials by relithiation without destroying the LIB compounds. Additionally, direct recycling is a comparatively low-cost and less resource-intensive method of recovering LIB materials.

However, completely regenerating the full capacity and long-term performance of the original materials is still particularly challenging. For instance, cathode materials are often coated with a nanometer-thick protecting layer that is engineered to reduce the degrading effect on the cathode from direct contact with the electrolyte. Long-term charge-discharge cycling causes damage to this coating layer, and thus it needs to be repaired in order to recover the material performance. To address this challenge, we have developed a novel process that can regenerate and upgrade cathode materials from aged LIBs, as well as create a new coating layer to improve the performance of the cathode materials. In this presentation, we will provide a case study of the performance improvement of recycled lithium cobalt oxide (LCO) materials by forming an alumina coating layer on the surface. By controlling the thickness and sintering temperature, this surface alumina coating can be an effective way to improve the stability and cyclability of recycled LCO cathode materials.

8:00 PM EN09.03.07

Recycling and Upcycling Graphite Anode Materials Yi Peng, Margaret Wu, Jared Liao, Tyler McGivern-Jimenez, Zhiqian Wang and Lance Yang; Princeton NuEnergy, United States

Lithium-ion batteries (LIBs) have emerged as the battery of choice for rapidly growing markets in electric vehicles (EVs) and energy storage devices. Thus, there is an enormous interest in the development of new technologies for recycling and recovery of valuable materials from secondary resources, such as those from used LIBs. Finding ways to decrease the cost of recycling could thus significantly reduce the life cycle cost of LIBs, avoid material shortages, lessen the environmental impact of new material production, and provide low-cost active materials for new LIB manufacturing. In recent years, the recycling of spent LIBs has mainly been focused on the recycling of the cathode, while recycling of the graphite anode has only received limited attention due to its low value and complex recycling process. However, with the recent shortage of resources and the increase in production costs, recycling of graphite anode from spent batteries can no longer be ignored. There are several challenges associated with recovering spent graphite anodes – mainly, there are a variety of metal impurities in addition to surface solid electrolyte interface (SEI) and interior impurities which need to be removed. Conventional recycling methods are unable to solve this issue, especially in the purification process. Most current recycling systems use pyrometallurgical and/or hydrometallurgical methods, which necessitate multi-unit operation, high energy consumption, and high cost. Direct recycling, on the other hand, is a promising solution for overcoming the hurdles involved with recovering spent graphite anodes.

Princeton NuEnergy (PNE) has successfully developed a novel low-temperature plasma process to enable purification and direct repair of graphite anode materials from spent LIBs. We also demonstrated a simple but effective approach to upgrade the spent graphite to produce graphite-silicon composite with improved energy density. Spent graphite is an ideal choice for low-cost production of high-performance silicon-graphite composites because treated spent graphite presents a porous structure which can be well combined with silicon and effectively relieve volume expansion. The recycled graphite and upcycled graphite-silicon composite anode materials outperform the commercially available equivalent. The direct recycling/upcycling of graphite anode materials will increase the commercial viability of LIBs and reduce battery cost, thus accelerating the electrification of transportation and large-scale energy storage for renewable energy in the near future. In this presentation, the materials characterization and electrochemical performance of recycled/upcycled anode materials will be discussed.

8:00 PM EN09.03.08

Direct Recycling of NCM Cathode Materials from Spent EV BatteriesJaredLiao¹, ChristopherBrooks², LyndonHuang¹, ZhiqianWang¹ and LanceYang¹; ¹Princeton NuEnergy, United States; ²Honda Research Institute USA, Inc., United States

Lithium-ion batteries (LIBs) have emerged as the battery of choice for rapidly growing markets in electric vehicles (EVs) and grid electricity storage. This spurs a great demand for lithium, cobalt, and nickel that could outstrip the supply of virgin materials. Thus, there is an enormous interest in the development of new technologies for recycling and recovery of valuable materials from secondary resources, especially those from used LIBs. Compared to conventional high temperature pyrometallurgical or strong acid hydrometallurgical methods, the direct recycling of LIBs shows great promise. Direct recycling regenerates the cathode materials without destroying the underlying compounds, while significantly reducing energy and chemical consumption.

Our low-temperature plasma-assisted separation (LPASTM) process has major reductions of adverse environmental impacts from mining/brine extractions of virgin metals, raw material transportation, and energy consumption. Direct regeneration of cathode materials using the this technology is far less costly and disruptive than virgin production. Cathode materials account for over 50% of typical LIB material value. As a result, recycling cathode materials is especially important for reducing battery costs. PNE's technology has proven versatile – capable of recycling and regeneration of a variety of cathode materials. In this presentation, we will present one typical case to demonstrate the successful regeneration of NCM cathode materials from spent EV batteries via our LPAS based direct recycling process.

8:00 PM EN09.03.09

Recycling of Solid-State Batteries - Influence of Different Solid Electrolytes on Mechanical Recycling BehaviourMarcoAhuiss^{1,2}, PeterMichalowski^{1,2} and ArnoKwade^{1,2}; ¹TU Braunschweig, Germany; ²Battery LabFactory Braunschweig, Germany

The growing use of lithium-ion batteries (LIBs) is leading to an increasing demand for raw materials, which may lead to raw material shortages and rising material costs in the future. In this context, solid-state batteries (SSBs) are promising next-generation batteries in which the liquid electrolyte of conventional LIBs is replaced by a solid-state electrolyte, offering advantages such as increased lifetime, energy density, and safety. To successfully establish the different SSB systems (e.g. polymer, sulfide, oxide and halide) in the market, material cycles need to be identified and closed to achieve lifecycle sustainability.

In this context, recycling and reuse of materials are essential elements of a climate-neutral and resilient energy system. Compared to the recycling of conventional LIBs, no drying or thermal step is required to recover the liquid electrolyte as it has been replaced by a solid electrolyte. However, the different SSB systems have different characteristics in terms of comminution and classification behaviour, so different process chains need to be developed taking into account the technological, safety, economic, and environmental properties of the materials used. [1] This study examines the influence of the different solid electrolyte systems on mechanical recycling, specifically focusing on the comminution and classification behaviour. The comminution of **polymer SSBs** produces a foil fraction that cannot be further separated and requires additional processing. One possibility is solvent-based processing to separate the cathode active material. **Oxide SSBs**, due to the intrinsic properties of the solid electrolyte, are well suited to mechanical separation, allowing for subsequent hydrometallurgical processing, regardless of the active material used. High yields of oxide material can be achieved here, especially after thermal pretreatment. Due to the formation of hydrogen sulfide upon contact with water, **sulfide SSBs** require a process route to stabilise or inactivate the electrolyte before mechanical treatment. Initial studies with sulfur-based materials show that they can be recovered (up to 75 wt.-% yield) in a dry atmosphere and fed directly back into the production process. In order to evaluate each process, basic characterisation of the materials or intermediate and final products was carried out using various analytical methods such as TGA, ICP-OES and SEM-EDX.

The results of this work will indicate possible process routes for the recycling of solid-state batteries, paving the way for the development of efficient recycling processes even before SSB technology is ramped up. This establishes the foundation for creating closed, robust material cycles towards a CO₂-neutral energy system.

References:

¹S. Doose, J. Mayer, P. Michalowski, A. Kwade (2021): Challenges in Ecofriendly Battery Recycling and Closed Material Cycles: A Perspective on Future Lithium Battery Generations, *Metals - Open Access Metallurgy Journal 11*. DOI: 10.3390/met11020291.

8:00 PM EN09.03.10

Ba Doped SrTiO₃ Perovskite as Anode for Li-Ion BatteriesIvanCastillo, BalramTripathi, JeanR. Del Valle, ValerioDorvilien, DaniloG. Barrionuevo Diestra, SunnyChoudhary, RajeshKatiyar, GerardoMorell and RamKatiyar; UPR-RP, United States

In this study we are reporting the electrochemical performance of Ba_{0.9}Sr_{0.1}TiO₃ (BST) having polarization of 14.58 $\mu\text{C}/\text{cm}^2$ as an anode for Li-ion batteries. Perovskite structure (ABO₃) anode materials have received much attention because of their mixed electronic and ionic conduction behaviors that make the triple-phase boundary (TPB) extend to the entirely exposed anode surface. Among the variety of these oxides, SrTiO₃-based perovskite compounds are promising Ni-free anode candidates due to their high chemical stability at high temperatures under both oxidizing and reducing atmospheres, and strong resistance to carbon deposition. X-ray diffraction spectra confirm tetragonal symmetry ($c/a=1.0073$), Raman spectroscopic study confirms Raman modes (A₁(TO₁), A₁(TO₂), A₁(TO₃) and A₁(LO₃)) of the tetragonal orientation for BST. SEM images confirm homogeneous surface of BST having grain sizes (1-1.5 μm). The carbon black was used as the conductive additive PVDF as binder, LiPF₆ as an electrolyte for charge-discharge performance and contribution to the electrochemical properties of the cell in terms of lithium intercalation and de-intercalation. At slow discharge rate, a capacity of approximately 240 mAh g⁻¹ achieved. It is found that Ba on SrTiO₃ surface helps to facilitate electron transfer thereby improving the capacity and rate performance of BST as Li-ion battery anode material. The detailed results will be presented during the meeting presentation.

8:00 PM EN09.03.11

Optimization of the Discharge Process of Spent Li-Ion Batteries from Electric Vehicles for Direct RecyclingHyunseokLee; Korea Battery Industry Association, Korea (the Republic of)

Since introducing electric vehicles 10 years ago, the disposal of spent LIBs generated from EVs has rapidly increased. The two main approaches for processing spent LIBs for EVs are reuse and recycling. Many studies have shown that the battery healthcare system can effectively estimate the spent batteries state of health for reuse. However, the spent LIBs must ultimately be recycled at the end of the reuse. Since the rare metals in spent LIBs are precious because they have limited reserves, researchers are investigating a systematic and safe recycling system. So far, three types of recycling methods for spent LIBs have been considered—pyrometallurgy process, hydrometallurgy process, and direct recycling. The pyrometallurgy process is widely used for the commercial recovery of cobalt. However, it has the disadvantages of high carbon emissions and difficulty in recovering Li. The hydrometallurgy process would be an alternative since it can recover more Li and Mn than the pyrometallurgy process. However, the hydrometallurgy process generates large amounts of wastewater and contaminated acid fumes, which can severely pollute the environment. Thus, research on direct recycling is recently gaining attention. Discharging spent LIBs is an essential process for direct recycling for the spent LIBs. By immersing the LIBs in the ionically conducting salt water to form the short circuit, the electrochemical discharge of LIBs in a conducting solution is introduced. Li et al. analyzed the chemical components of wastewater from the salt-water discharge process. Owing to salt-water discharge, they detected “high” levels of aluminum and iron and “moderate” levels of cobalt, lithium, copper, calcium, and manganese. In addition, considerable amounts of zinc, barium, and vanadium were also detected. The high concentrations of P were also observed, indicating that the corrosion of the metal collectors and sealing compartments causes the leakage of a certain amount of the electrolyte (i.e., LiPF₆). Thus, a suitable discharge technology must be developed because the damage to LIB by salt-water discharge causes additional costs and steps in the recycling process.

In this study, we recovered spent LIBs used in two EVs and observed the state of the modules and cells through electrical discharge. Additionally, we performed a comparative experiment with the salt-water discharge of pouch-type LIBs because pouch-type LIBs are primarily used in EVs. After the discharge of the spent LIBs to various voltages, the crystal structures of the cathode and anode were analyzed. We examined problems caused by over-discharge based on the state of health and determined the appropriate discharge voltage. Swelling due to over-discharge became more rapid as SoH decreased. Cell volume expansion caused by swelling increases the internal pressure of the cell packaged in the module, leading to a risk of explosion. Therefore, it is essential to discharge pouch cells to an appropriate voltage that can prevent the pouch swelling of LIBs. The results of this study indicate the proper voltage for electrical discharge, which is adjudged applicable for environmentally friendly recycling processes.

As a spent LIB with a state-of-health of 66.8% was over-discharged, swelling significantly increased. Even after being discharged to 0 V, the voltage could recover to 2.689 V. We analyzed the discharged spent LIBs through X-ray diffraction, scanning electron microscopy, and electrochemical impedance spectroscopy, and confirmed the appropriate voltage for the discharge process is estimated to be 2.5 V. The proposed electrical discharge process will be suitable for the direct recycling of spent LIBs in the form of pouch cells.

8:00 PM EN09.03.12

Li Storage Performance of LiMn_{1/10}Ni_{8/10}Co_{1/10}O₂ Cathode for Li-Ion BatteriesShwetaShweta, BalramTripathi, SunnyChoudhary, MohanBhattarai, SatyamKumar, RajeshKatiyar, GerardoMorell and RamKatiyar; University of Puerto Rico, Puerto Rico

In this study we are reporting the electrochemical performance of LiMn_{1/10}Ni_{8/10}Co_{1/10}O₂ composite as cathode for Li-ion batteries. Spinel layered heterostructure by encapsulating layered lithium rich material with nanospinel mixture LiNi_xMn_{2-x}O₄. Spinel layer coating has been employed to tune the electrochemical performance of the layered composite cathode. The spinel layer coating contributes fast lithium ion transport of Li rich cathode. It is found that spinel content largely enhances the specific capacity, cycling stability and rate capability of Li rich cathode. XRD, Raman and SEM techniques has been used for structural, electronic & surface morphology of the fabricated layered composite cathodes. The detailed results will be presented

during the meeting presentation.

8:00 PM EN09.03.13

Crosslinked Zwitterionic Amphiphilic Copolymeric Membranes for Ion Separations [Ashleigh B. Herrera](#) and [Ayse Asatekin](#); Tufts University, United States

Lithium has become crucial for addressing the energy needs of the future. Current methods of lithium extraction are laborious, expensive, and environmentally damaging. Membrane technology offers an energy-efficient, simplistic, and scalable method for extracting lithium from aqueous sources. There has been recent progress showing the potential of membranes for recovering valuable mineral resources such as lithium and precious metals from wastewater, but many current membranes do not adequately address the selectivity, reliability, and fouling resistance these separations require. Recent work in our group has shown that thin film composite membranes with cross-linked zwitterionic amphiphilic copolymeric (x-ZACs) selective layers exhibit excellent fouling resistance coupled with exceptional ion selectivity. This ion selectivity is both size and charged based, separating like-charged ions such as chloride and fluoride. These x-ZACs readily self-assemble to form a network of nanochannels lined by the zwitterionic group. These channels are ~1 nm in size where the size is related to the degree of crosslinking. Previous work has suggested the ion selectivity is associated with selective interactions between the zwitterions lining the x-ZAC channels and the ions passing through. This effect appears to also be influenced by the confinement of the ions into the ~1 nm self-assembled nanochannels. However, to date, only one x-ZAC chemistry has been studied for ion separations. Current work expands on these findings to synthesize x-ZAC membranes that focus on other zwitterionic repeat units. The goal is to create membranes with cation-cation selectivity to use in various separations including lithium recovery from brines and lithium-ion battery waste solutions and selective extraction of valuable metal ions from wastewater and mine drainage. To accomplish this, we have synthesized x-ZAC membranes with different zwitterionic chemistries and analyzed the selectivity between cations. Preliminary studies have shown some selectivity between La⁺ and Na⁺ salts for a specific zwitterion chemistry. This work suggests that similarly sized and charged ions can be separated with pressure-driven membranes utilizing well-selected x-ZAC chemistries and crosslink densities, enabling more energy-efficient recovery of metal resources, especially lithium.

8:00 PM EN09.03.14

Simplified Solvent Extraction Process for High-Purity Ni/Co Mixed Solution for Lithium-Ion Batteries [Gogwon Choe](#)¹, [Young-Jin Lim](#)¹, [Younghyun Kim](#)¹, [Go-Gil Lee](#)² and [Yong-Tae Kim](#)¹; ¹POSTECH, Korea (the Republic of); ²RIST, Korea (the Republic of)

The demands for Ni-based raw materials increase as Ni-Co-Mn ternary cathode materials become the main axis of the battery industry. Conventional hydrometallurgical process to produce raw materials from Ni ore for battery application is as follows: (i) leaching of metal ions by acid, (ii) solvent extraction process to extract target metals, and (iii) crystallization process to produce final single-metal compound as powder products. The conventional solvent extraction process is a three-circuit process comprising impurity removal, Co extraction, and Ni extraction circuits. Unlike conventional process, in this work, we suggest a simplified two-circuit process to simultaneously extract Ni and Co to produce Ni/Co mixed solution for cathode material precursor production which can also be applied to hydrometallurgical battery recycling process. Accordingly, the efficiency of site utilization can be maximized by reducing the investment cost for the manufacturing process and downsizing mixer-settler facilities. Further, ecofriendly effects such as reducing the consumption of titrants and cutting down the process costs and wastewater discharge can be realized.

8:00 PM EN09.03.15

Analysis of The Supply Chain Structure, Competitiveness and Risk in The Field of Lithium-Ion Batteries and Future Directions of The Government's Strategic R&D Policy [Sein Kwon](#) and [Dongyoung Kim](#); Korea Institute of S&T Evaluation and Planning, Korea (the Republic of)

The main purpose of this study is to analyze the supply chain structure, competitiveness, and risk factors in the lithium-ion battery sector, and to provide future directions for the government's R&D policy response to internal and external strategic environmental changes.

Traditionally, Raw material procurement in the lithium-ion battery supply chain is influential as the four core materials account for 75% of the cost. Recently, the importance of the recycling process has become more prominent due to the rapid growth of the market and the rise in raw material prices with black swans factors in the global supply chain. In the supply sector, three East Asian countries such as Korea, Japan, and China are leading the market. In particular, China's market dominance is overwhelming in the raw material mining and procurement sector. Meanwhile, due to the U.S.-China supply chain conflict, China is expected to promote internalization of the supply chain based on technological competitiveness and strategic assetization of key minerals. Therefore, the global supply chain structure also implies the possibility of uncertain change.

According to the results of the supply chain competitiveness analysis of 6 major countries, Korea has a relative competitive edge in design and cell manufacturing. Particularly, manufacturing companies are forming the mainstay of the industry by actively participating in R&D, and since many firms in the material and equipment sectors are participating in the supply chain network, the completeness of the domestic supply chain is robust. In contrast, it has low competitiveness in the demand and procurement process. Notably, there is a very high dependence on certain countries for raw material supply and demand. The material sector's dependence on China is 63.7%, with some of the LCO, PP/PE, and NCM accounting for 100% of the dependence. In 2022, there are 7 government R&D programs led by the Ministry of Trade, Industry and Energy related to lithium-ion batteries, accounting for 0.09% of the total budget of 29.8 trillion KRW (20.5 million USD) for the Korean government's R&D programs. Most R&D programs focus on investing infrastructure of large-scale facility and equipment, and improving performance and developing innovative manufacturing technologies. Furthermore, The government has selected secondary batteries as the 12 major national strategic technologies and is focusing on developing safety-enhancing technologies for the four core materials through a five-year short-term strategy.

Even though Korea has a competitive edge in the design and manufacturing sector, it is necessary to diversify its supply chain to cope with the dependence on raw materials procurement concentrated in certain countries. In this regard, specific strategies for eco-friendly supply chain processes such as building strategic recycling hubs are required. In addition, the recycling-related R&D budget and programs are very insufficient, so it is necessary to plan new R&D programs and projects and promote investment in this field. In particular, financial support for initial investment in waste battery reuse and recycling demonstration projects, a standard system for safety and performance verification, and a professional training policy should be prepared to enhance technological competitiveness.

SESSION EN09.04: Lithium-Ion Battery Recycling and Reuse III

Session Chairs: [Zheng Chen](#), [John Cook](#) and [Beniamin Zahiri](#)

Tuesday Morning, November 28, 2023

Hynes, Level 1, Room 108

9:00 AM EN09.04.01

Achieving Low-Temperature Hydrothermal Relithiation by Redox Mediation for Direct Recycling of Spent Lithium-Ion Battery Cathodes [Xiaolu Yu](#) and [Zheng Chen](#); University of California, San Diego, United States

Lithium-ion battery (LIB) recycling is an urgent need to address the massive generation of spent LIBs from portable devices and electrical vehicles. However, the large-scale recycling is hampered by economic and safety issues associated with today's recycling processes. Here, we demonstrate a safe and energy efficient direct regeneration process based on low-temperature hydrothermal relithiation (LTHR) at low pressure for spent $\text{LiNi}_x\text{Co}_y\text{Mn}_z\text{O}_2$ ($0 < x, y, z < 1$, $x + y + z = 1$, or NCM) cathode materials. A low concentration of low-cost redox mediator is employed to improve the relithiation kinetics of spent NCM materials, enabling full relithiation temperature to be reduced from 220 degree Celsius to 100 degree Celsius or below.

Correspondingly, the pressure incurred in the relithiation process can be reduced from ~25 bar to 1 bar, offering significantly improved operation safety. Specifically, three NCM materials, including chemically delithiated NCM111, cycled (degraded) NCM111, and cycled NCM622, were successfully regenerated with complete recovery of composition, crystal structure, and electrochemical performance, achieving the same effectiveness as that achieved at high temperature process. Meanwhile, the total energy consumption of spent cell recycling and the greenhouse gas emission is also reduced. This work provides a facile and scalable way to more sustainable LIB recycling with high economic return, high operation safety and low cost.

9:15 AM EN09.04.02

End-Of-Life Lithium-Ion Batteries—Recycling and Upcycling of Cathode Materials [Rosie Madge](#)^{1,2}, [Abbey Jarvis](#)^{1,2}, [Laura L. Driscoll](#)³, [Paul A. Anderson](#)^{1,2} and [Peter Slater](#)^{1,2}; ¹University of Birmingham, United Kingdom; ²Faraday Institution, United Kingdom; ³UKBIC, United Kingdom

Worldwide there has been an increase in the use of electric vehicles which has led to a consequent increase in the number of end-of-life lithium-ion batteries (LIBs) that need to be recycled. Recycling is commonly performed using pyrometallurgical and/or hydrometallurgical processes. These methods focus on the recovery of high value metals, such as Ni and Co, from the batteries. Alternative methods are therefore required to ensure that the entire battery is recycled and that the critical materials contained within the batteries are utilized in a meaningful way.

This work investigates recycling cathode material from an end-of-life Gen 1 Nissan Leaf (2011 model, 40,000 miles) which contains a mixture of LiMn_2O_4 (LMO) and

$\text{LiNi}_{0.8}\text{Co}_{0.15}\text{Al}_{0.05}\text{O}_2$ (NCA). LMO is combined with NCA to provide good thermal stability along with high capacity and long lifetime.^{1,2} The use of such a blended cathode mixture increases the complexity of recycling as there are more components within the cathode that must be considered during recycling processes. A method has been developed which can selectively leach LMO from the cathode material using organic acids.³ The separated LMO and NCA can then be regenerated and reused in new LIBs.

However, LMO is no longer favoured commercially, therefore this work investigates upcycling it into higher value materials. LMO has been upcycled to form a range of cathode materials, such as $\text{LiMn}_{1.5}\text{Ni}_{0.5}\text{O}_4$ (LMNO) and $\text{Li}_4\text{Mn}_2\text{O}_5$, a cation disordered rocksalt. These upcycled cathodes have been shown to have a comparable electrochemical performance to cathodes synthesised using pristine starting materials. This therefore demonstrates that end-of-life cathode materials can be upcycled to form new higher value cathode materials.

References:

1. P. Albertus, J. Christensen and J. Newman, *J. Electrochem. Soc.*, 2009, **156**, A606.
2. H. Y. Tran, C. Tacubert, M. Fleischhammer, P. Axmann, L. Kuppers and M. Wohlfahrt-Mehrens, *J. Electrochem. Soc.*, 2011, **158**, A556–A561.
3. WOPat., WO2022084668A1, 2022.

9:30 AM EN09.04.03

Recycling Valuable Metals from All Species of Spent Lithium-Ion Batteries using Non-Organic Solvents System Tzu Ming Cheng, Zheng Yu Chen and Chih-huang Lai; National Tsing Hua University, Taiwan

Lithium-ion batteries have become the mainstream energy storage material in various industries due to their high energy density, high operating voltage, wide temperature range, and long lifespan. In recent years, the electric vehicle industry has flourished in an effort to reduce environmental pollution. Lithium-ion batteries, with their aforementioned advantages, have replaced traditional nickel-hydrogen batteries as the dominant power source for electric vehicles. This surge in demand for lithium-ion batteries is expected to generate a significant amount of waste batteries. Improper handling of these discarded batteries can pose serious risks to the environment and human health. Moreover, lithium batteries contain valuable metals such as lithium, cobalt, nickel, and manganese, which are vital and strategic resources. Developing suitable technologies to recycle and reuse these waste lithium-ion batteries can not only reduce environmental pollution but also enhance control over critical valuable metal resources, particularly since these metals are not domestically available and currently rely on imports. Mastering recycling techniques offers the opportunity to treat a large quantity of waste batteries as a valuable mineral deposit through urban mining. Therefore, lithium-ion battery recycling is poised to become a highly promising and profitable industry.

With the objectives of low cost, continuous operation, and scalability, we have developed an efficient, non-organic solvent recycling process for all species of lithium-ion batteries. Initially, we simulated the recycling scenario using simulated materials. The target elements including iron, phosphorus, and lithium, can be easily separated using pH control and therefore precipitants. However, the separation of nickel, cobalt, and manganese, which are closely positioned in the periodic table with similar physical and chemical properties, presents challenges in non-organic solvents system. To overcome this, we identified two aqueous phase precipitants, KMnO_4 and NaClO , combining with pH control, successfully separate these three elements without mutual interference. Ultimately, this method achieves high purity of recovered materials of all elements, with individual product purities reaching 98.72 wt% for iron phosphate, 92.97 wt% for manganese oxide, 98.06 wt% for cobalt oxide, 95.86 wt% for nickel hydroxide, and 96.76 wt% for lithium carbonate. This proposed process also provides high recovery yields which recovery yield reaching above 99% for valuable elements. To ensure the applicability of this technique to the industry, the real industrial black powder from a battery recycling plant was also applied for this research. Under the same process, we collected all the recycling products of above 90 wt% purity and the recovery yields reaching above 96% for valuable elements. Compared to existing lithium battery recycling technologies, this process offers a broader range of target products and provides an efficient recycling process with mass production potential.

9:45 AM EN09.04.04

A Novel Dry Powder Discharge Technique for Efficient and Environmentally Friendly Lithium Battery Recycling Zheng Yu Chen, Tzu Ming Cheng and Chih-huang Lai; National Tsing Hua University, Taiwan

The demand of Lithium batteries has raising owing to the flourishing electronic industry. Therefore, an environment-friendly recycling method for lithium batteries is urgently needed, avoiding the environment pollution of lithium batteries disposal. The recycling process of lithium-ion batteries comprises two essential stages: pre-treatment and recovery of target products. Discharging is a crucial step to prevent the occurrence of short circuits and the associated risks of fire or explosion due to residual energy in discarded lithium batteries during collection, transportation, and pre-processing. Currently, common commercial methods for discharging involve submerging batteries in halogen-containing saline solutions or manually connecting large lithium battery modules to resistors for discharge. However, both of these discharge modes have their limitations. While resistor discharge does not cause corrosion and offers easy process control, it is not suitable for large-scale commercial operations due to the manual connection requirement for each battery. Solution immersion discharge, the most widely used method in commercial battery recycling, is prone to corrosion during the discharge process. Corrosion can damage the battery casing, and in severe cases, allow electrolytes to flow into the solution, resulting in significant waste producing which contaminated discharge solutions cannot be reused. Furthermore, corrosion negatively impacts subsequent battery sorting and refining processes.

Given the lack of an effective, non-corrosive, and cost-effective discharge method, our team has developed a novel dry powder discharge technique utilizing graphite powder as the discharge medium. Simply immersing the batteries in the powder and grounding the system enables efficient discharge. In our research, we investigated the influence of powder morphologies, particle sizes, discharging times and temperatures on discharge performance. Through optimization, we achieved even better discharge efficiency than traditional solution immersion discharge. Moreover, all batteries including common types such as ICR, IMR, NCR could be discharged safely below industry-specified limits (<0.5V) in 24 hours, meeting industry requirements. Unlike traditional solution discharge, our proposed method eliminates the corrosive reaction between the battery and the powder, ensuring a corrosion-free process without the generation of additional waste. The non-oxidizing nature of graphite powder allows for its reuse with almost negligible losses during the discharge process. These characteristics not only contribute to high discharge efficiency but also enhance environmental sustainability. We propose that this innovative dry powder discharge technique has the potential to replace traditional solution discharge, offering an efficient and eco-friendly solution for future lithium battery recycling.

10:00 AM BREAK

10:30 AM *EN09.04.05

Lithium-Ion Battery Recycling Facts and Opportunities Ilias Belharouak, Yaocai Bai and Lu Yu; Oak Ridge National Laboratory, United States

The growing demand is generating a huge number of spent lithium-ion batteries, thereby urging the development of cost-effective and environmentally sustainable recycling technologies to manage electrode scraps and end-of-life batteries. Lithium-ion battery recycling of end-of-life batteries is still in its infancy, with many fundamental and technological hurdles to overcome. The recycling rate of waste LIBs is projected to be much behind the rapid growth of the LIB market because of the complexity of the technology and its use cases. Several recycling strategies, including the pyrometallurgical process, hydrometallurgical process, and direct recycling approach, are being adopted on the market and are under further development by researchers. Here, we provide an overview of the current state of battery recycling by outlining and evaluating the incentives, key issues, and recycling strategies. A direct recycling strategy, which is developed in the US. Advanced Battery Recycling Consortium (ReCell) will be highlighted through a discussion of its benefits, processes, and challenges. Direct cathode regeneration seeks to recover the functional cathode particles without decomposition into substituent metals or salts along with other components such as graphite and current collectors. Perspectives on this important field's future energy and environmental science will also be discussed.

11:00 AM EN09.04.06

Selective Extraction and Upcycling of LiMn_2O_4 from used First Generation Lithium-Ion Battery Cathodes to Produce Mn-Based Conversion Anodes with Fascinating Electrochemical Properties Beatrice Browning; University of Birmingham, United Kingdom

A multitude of cathode chemistries have been explored and utilised since the commercialisation of the Li-ion battery (LiB) in the 90s - including transition metal oxide chemistries (such as LiCoO_2 , LiFePO_4 , and LiMn_2O_4) and mixed transition metal oxide materials (such as NMC, $\text{Ni}_x\text{Mn}_y\text{Co}_z\text{O}_2$, and NCA, $\text{Ni}_x\text{Mn}_y\text{Al}_z\text{O}_2$). As electric vehicle adoption is rapidly increasing worldwide, the chemistry of Li-ion batteries used are heavily dictated by consumer demand. Customers expect fast-charging batteries with respectable range, factors which are dictated by the intrinsic electrode chemistry. High specific capacity cathodes that are thermally stable are preferable to consumers, as these features give rise to extended vehicle range and charging speeds. Current cathodes which meet these criteria are predominantly Ni-rich mixed TMO materials (such as NMC and NCA) and LiFePO_4 .

As LiB technology has advanced over the years, initial cathode chemistries have become outdated with each generation of electric vehicle as companies race to ensure consumer demands are met. LiMn_2O_4 (LMO) is an example of an electrode material that was initially seen in electric vehicle batteries, often in conjunction with a layered Ni-rich phase. As subsequent generation vehicles have been released and their performance and energy densities have been enhanced to meet consumer demand, the LMO material has been phased out as the Ni-rich layered materials with high energy density have been prioritised.

When LiBs reach end-of-life the versatility of LiB cathode scrap pool (between manufacturers and between generations of EVs for the same manufacturer) has proven to be challenging for

battery recyclers. Selective extraction of materials is imperative to ensure recycling and upcycling of cathode material is feasible from such an assorted cathode scrap pool. Once selectively extracted, cathode material can be recycled in a closed-loop fashion to regenerate battery grade products. When extracting lesser used and redundant cathode chemistries from preliminary cell structures, it is vital that the maximum value of each product is obtained prior to extraction. Upcycling involves extracting and repurposing material to increase its value, and LMO is a key example of a lesser used material can be upcycled to form a variety of Mn-rich conversion anode materials with interesting properties.

Graphite is the main anode material used in LiBs, however graphite reserves are not infinite, nor are they evenly distributed globally - meaning reliance on other countries is great for this anode material and will only increase as reserves are depleted. There is no question that alternative anode materials are necessary to avoid the likelihood of bottlenecks in graphite supply. Through selective extraction and interconversion of LMO, an array of Mn-rich conversion anodes with fascinating electrochemical properties can be produced. Not only can Mn be extracted from redundant LMO cathode material, but Mn-reserves are cheap, non-toxic and abundant, and it is of great interest to explore these conversion anode materials and their characteristics.

Key electrochemical characteristics that are of great interest within this study include the anode capacities being several times greater than their theoretical capacities, and the increase in capacity that arises during cell cycling. The origin of the phenomena observed have been explored using an array of characterisation techniques, including in-situ Synchrotron X-ray diffraction and Pair-distribution function (PDF) analysis, Raman spectroscopy, galvanostatic cycling, cyclic voltammetry, Inductively Coupled Plasma-Optical Emission Spectroscopy and scanning and transmission electron microscopy, to name a few.

11:15 AM EN09.04.07

Resynthesized Electrode Materials from Chemically and Biologically Recycled Li-Ion Batteries Witold Uhrzynowski¹, [Magdalena Winkowska-Struzik](#)¹, Maciej Boczar¹, Michal Struzik², Zbigniew Rogulski¹, Andrzej Czerwinski¹ and Dominika A. Buchberger¹; ¹University of Warsaw, Poland; ²Warsaw University of Technology, Poland

Recently, a dynamic increase of interest in the possibilities of recycling and reuse of materials from lithium-ion batteries was observed. Along with the ever-increasing number of Li-ion cells powering new electric and electronic devices, the management of waste batteries and materials contained within them has become a more and more urgent problem to be solved. Due to the growing environmental awareness more stringent legislative means to control the matter are introduced. This includes the latest European Union directive on batteries which states that no less than 35% of Li and 90% of cobalt, nickel and manganese will need to be recovered from waste Li-ion cells. Based on those regulations, the new batteries produced after 2030 will need to contain, for example, at least 6% of recycled lithium. Although large-scale, proper processing of waste batteries is still an economical challenge, the changing global supply and demand dynamics, geopolitical events, technological advancements, and the aforementioned environmental regulations force stakeholders in the battery market to consider battery recycling not only necessary, but also potentially financially viable and sustainable practice.

The battery recycling process should be characterized by high efficiency and the lowest possible impact on the environment, and as such, needs to be optimized for every type of electrode material. For the purposes of this study lithiated nickel-manganese-cobalt oxide 6:2:2 (NMC622) material was chosen, due to its high energy and power density, relatively high resistance to subsequent cell charge/discharge cycles, as well as favorable economic and environmental parameters associated with decreased cobalt content. The electrode material, synthesized from supplier grade new substrates was subsequently recycled in a series of steps, including hydrometallurgical recovery of lithium, and transition metal ions recovery as (hydr)oxides. The leachates were further processed chemically and biologically, by means of selected bacterial consortia, to increase the yield of recycled materials and to lower the concentration of dissolved ions. The use of biological processes in the recycling of waste electrode material reduces the costs of the process, especially at low concentrations - where the load of the leachate is too low for effective and economic chemical recovery, but still to great for safe discharge of the effluents to ground waters. With the use of microorganisms, nearly complete removal of nickel, cobalt and manganese ions from the leachates can be obtained, and the resultant technical-grade waters may be reused in the cycle. Effective lithium recovery, however, still remains a challenge.

The obtained recovered lithium and transition metals were further used to resynthesize electrode materials. Crystallographic measurements were performed proving the structure and purity of the obtained recycled materials. The resynthesized NMC622 electrode material with 0 to 100% of recycled materials content were structurally and electrochemically investigated and compared with the "original" material. It was shown that the electrode materials made of recycled materials may perform in a comparable manner with the "original" materials. However, their endurance and stability in charge/discharge cycles is greatly affected by the purity of the recycled substrates.

Recovery of metals from waste batteries is important for economic and ecological reasons. The presented results indicate that optimization of the recycling process, though challenging, is promising, and the resynthesized materials may be a good additive or even an alternative for commercial ones.

SESSION EN09.05: Virtual Session
Tuesday Morning, December 5, 2023
EN09-virtual

10:30 AM EN09.05.01

A Promising Solid-State Synthesis of $\text{LiMn}_{1-y}\text{Fe}_y\text{PO}_4$ Cathode for Lithium-Ion Batteries Jinli Liu^{1,2}; ¹Nanjing University of Science and Technology, China; ²Tsinghua University, China

$\text{LiMn}_{1-y}\text{Fe}_y\text{PO}_4$ (LMFP) is a significant and cost-effective cathode material for Li-ion batteries, with a higher working voltage than LiFePO_4 (LFP) and improved safety features compared to layered oxide cathodes. However, its commercial application faces challenges due to a need for a synthesis process to overcome the low Li-ion diffusion kinetics and complex phase transitions. Herein, we propose a solid-state synthesis process using LFP and nano $\text{LiMn}_{0.7}\text{Fe}_{0.3}\text{PO}_4$ (MF73). The larger LFP acts as a structural framework fused with nano-MF73, preserving the morphology and high performance of LFP. Our results demonstrate that the solid-state reaction occurs quickly, even at a low sintering temperature of 500 °C, and completes at 700 °C. However, contrary to our expectations, the larger LFP particles disappeared and fused into the nano-MF73 particles, revealing that Fe ions diffuse more easily than Mn ions in the olivine framework. This discovery provides valuable insights into understanding ion diffusion in LMFP. Notably, the obtained LMFP can still deliver an initial capacity of 142.3 mAh g⁻¹, and the phase separation during the electrochemical process is significantly suppressed, resulting in good cycling stability (91.2% capacity retention after 300 cycles). Our findings offer a promising approach for synthesizing LMFP with improved performance and stability.

10:45 AM *EN09.05.03

Solvent-Based Sequential Separation Processes for Direct Recycling of Lithium-Ion Batteries Yaocai Bai, Lu Yu and Ilias Belharouak; Oak Ridge National Laboratory, United States

The recycling of end-of-life lithium-ion batteries and the direct reintegration of the reclaimed materials into the battery supply chain are increasingly recognized as pivotal steps toward fostering a sustainable battery ecosystem. In a typical recycling process, the spent cells are discharged and shredded, followed by electrolyte recovery and component separation to remove/reclaim components like plastics, pouch material, and steel casing. As a result, a feedstock of anode and cathode on their current collectors is generated. This feedstock contains the most valuable components in a lithium-ion cell, including black mass (e.g., active cathode materials and graphite), Cu foils, and Al foils. To reclaim active electrode materials with high purity for direct regeneration, separation of electrode materials from their current collector as well as of anodes from cathodes is necessary. Current techniques require a complex set of separation processes to produce clean streams of material, resulting in lower recovery rates and higher costs. In this talk, solvent-based separation processes will be discussed to sequentially separate both anode/cathode and electrode/current collectors to recover cathode films, Al foils, anode films, and Cu foils. By circumventing a complex set of separation processes, the sequential separation method alone could fulfill the goal of reclaiming higher-purity materials, making recycling more profitable. The designed solution does not damage the active cathode materials nor corrode the metal foils. In addition, this process enables low-temperature separation in a cost-effective solution, reducing energy consumption and processing costs. The discussion will shed light on how environmentally sustainable and cost-effective sequential separation processes pave the way for direct recycling.

SYMPOSIUM EN10

From Single Atom to Device—Interfaces Under Electrochemical Conditions
November 27 - December 5, 2023

Symposium Organizers

Ling Chen, Toyota Research Institute of North America
Zhenxing Feng, Oregon State University
Kristina Tshculik, Ruhr University
Hua Zhou, Argonne National Laboratory

Symposium Support

Silver

Next Materials | Elsevier

Bronze

Nano-Micro Letters | Springer Nature

* Invited Paper
+ JMR Distinguished Invited Speaker

SESSION EN10.01: Understanding Electrochemical Processes Across Interfaces
Session Chairs: Zhenxing Feng and Hua Zhou
Monday Morning, November 27, 2023
Hynes, Level 3, Room 302

10:30 AM *EN10.01.01

Liquid-Phase Electron Microscopy for Probing Electrocatalytic Material Interfaces Vaso Tileli; EPFL, Switzerland

The oxygen evolution half-reaction (OER) is responsible for the limited efficiency of water splitting devices for storing clean energy. A holistic understanding of the fundamental processes taking place during operation of catalysts in solution can be gained by using advanced operando techniques that can complement characterization pre and post operation. In particular, electrochemical liquid-phase transmission electron microscopy (TEM) can provide morphological, structural, and chemical information for these catalysts. As an example, I will focus on OER oxide-based catalysts studied using liquid-phase TEM to investigate the solid-liquid interface in an alkaline solution [1]. The potential-dependent variation of the local contrast was associated to the modification of the alkaline liquid electrolyte and its wettability at the Co-oxide surfaces. At low applied potential, the hydrophobic character of the oxides was found to reduce due to electrowetting induced by OH⁻ accumulation at the interface. A distinct transition towards hydrophilicity was probed at the potential associated with the redox Co²⁺/Co³⁺ reaction, which alters the interfacial capacitance. This leads to a relatively stable wetting character at intermediate potentials prior to the OER region where the oxide surfaces catalyze the adsorbed hydroxide ions at the solid-liquid interface to form molecular oxygen. Further operando measurements using electron energy loss spectroscopy (EELS) provided direct evidence of the evolution of molecular oxygen. Finally, similar experiments on IrO₂ particles reveal the possibility of facet-dependent production detections using EELS [2]. Overall, advanced electron diagnostics and characterization applied to electrocatalyst structures can provide valuable insights into solid/liquid/gas interfaces and can guide development of efficient devices.

References

- [1] T.-H. Shen, L. Spillane, J. Peng, Y. Shao-Horn, V. Tileli, *Nature Catalysis*, 5 (2022), pp. 30-36.
- [1] T.-H. Shen, R. Girod, J. Vavra, V. Tileli, *The Journal of the Electrochemical Society*, 170 (2023), pp. 056502.

11:00 AM EN10.01.02

Fundamental Understanding of Electrode-Electrolyte Interface in Hydrogen Evolution Reaction (HER) Kinetics Amir H. Shah and Xiangfeng Duan; University of California, Los Angeles, United States

The hydrogen evolution reaction (HER) is one of the most fundamental and critical reactions in renewable energy conversion. The recent advancement in various platinum (Pt) nanocatalyst designs has led to greatly improved HER activity. Identification of the exact active sites and understanding the structure-activity relationship are critical for rational catalyst design but remain elusive due to the lack of methods robustly resolving the role of different surface sites. Moreover, it is well recognized that the HER kinetics are drastically slower in alkaline media compared to acidic media, but the descriptors of the HER kinetics are still elusive. Specifically, in the presence of alkali metal cations and hydroxyl anions, the electrode-electrolyte (platinum-water) interface in an alkaline electrolyte is far more complex than that in an acidic electrolyte. The effects of different alkali metal cations (AM⁺) and pH on these reactions are poorly understood due to a lack of suitable experimental methods. We are combining surface electrical transport spectroscopy (ETS) with other electrochemistry techniques and computational studies to probe and understand the fundamental role of different AM⁺ and pH on the reaction kinetics of HER. Our study provides fundamental insights into how and why AM⁺ and pH influence HER in

alkaline media. We expect that this research will provide the molecular-level understanding that will shed new insights into electrolyte engineering as an alternative pathway to control electrochemical reaction kinetics.

11:15 AM EN10.01.03

Modeling Electrochemical Reaction Rates at Fluid-Solid InterfacesRachel C. Kurchin; Carnegie Mellon University, United States

A detailed understanding of electrochemical reaction rates at interfaces between liquid electrolytes and a variety of solid electrodes is crucial in the engineering of next-generation electrochemical devices. In addition, it is becoming increasingly important to understand this behavior at higher overpotentials (where deviations from standard approaches such as Butler-Volmer are more likely) for applications such as fast charging of EV batteries. In this talk, I will introduce an extension to Marcus-Hush-Chidsey kinetics that explicitly accounts for the density of states of the electrode, and introduce several applications of it in a variety of systems, including twisted graphene structures.

SESSION EN10.02: Electrochemical Processes Across Interfaces for Energy Storage I

Session Chairs: Bin Li and Vaso Tileli

Monday Afternoon, November 27, 2023

Hynes, Level 3, Room 302

1:30 PM *EN10.01.04

Micelle-Like Structures in Localized High-Concentration Electrolytes and The Impacts on Electrolyte PerformancesBin Li^{1,2}; ¹Oak Ridge National Laboratory, United States; ²UTK-Oak Ridge Innovation Center, United States

A new class of electrolytes, localized high-concentration electrolytes (LHCE), have shown many benefits to high-capacity electrodes (Li-metal, Si, sodium, zinc, and potassium). These electrolytes combine high-concentration electrolytes (HCE) with salt and solvent with low-viscosity diluents. The dilutes were added to increase ionic conductivity while the locally highly concentrated salt-solvent clusters will facilitate stable solid-electrolyte interphase (SEI) formation while preventing metallic-dendrite formation. A ternary phase diagram for the design of LHCE is proposed based on salt-solvent solubility and solvent-diluent miscibility. Salt-solvent clusters in LHCE exhibit micelle-like behaviour. A salt concentration gradient naturally forms in a micelle-like cluster, through which the ion-pair aggregates get more localized due to accumulation of solvent as a surfactant at salt network/diluent matrix interfaces. The micelle-like structure is also influenced by the temperature. In an exemplary LHCE of LiFSI-1.2DME-2TFEO, a localized peak ratio of AGG+ is seen at 25 °C, confirmed with both Raman and MD simulations, inspired a formation protocol that improved initial SEI composition and morphology, and extended the cyclability. In the LiFSI-DMC-TTE system, an unprecedented CE above 99.5% is accomplished, optimized by compensating microstructures (e.g., micelle-like structures and network versus isolated clusters) with macroscale properties (e.g., ionic conductivity). This work proposes methods of controlling the micelle-like structure in LHCE, supported by SAXS and Raman characterization, MD simulations as well as electrochemical measurements, for higher performing practical batteries. From here, the impacts of electrolyte component choices in LHCEs to control salt-solvent cluster size, shape, and composition, as well as external parameters chosen during operation (e.g., temperature) can be optimized to extend anode stability and cyclability of high-energy batteries.

References:

Efaw, Corey M., Qisheng Wu, Ningshengjie Gao, Yugang Zhang, Haoyu Zhou, Kevin Gering, Michael F. Hurley et al. "Localized High-Concentration Electrolytes Get More Localized Through Micelle-Like Structures." *Nature Materials*, 2023, in press.

2:00 PM EN10.02.02

Uncovering the Electrochemically Active Surfaces in Polycrystalline NMC Battery Cathode ParticlesJinhong Min, Riley Hargrave and Yiyang Li; University of Michigan, United States

In battery electrodes, it is widely believed that the electrochemically active surface area equals the surface area of the particles. Based on this assumption, it has been generally believed that smaller particles have faster reaction and diffusion times than larger ones. In this study, we develop a new high-throughput, single-particle electrochemistry platform to test this belief for polycrystalline NMC battery particles. Surprisingly, we observed that the smaller particles have no shorter reaction and diffusion times than larger ones. To explain this unexpected relationship, we propose that electrolyte penetrates the grain boundaries of the secondary particle into the bulk. For this reason, the electrochemically active surface is not the area of the secondary particles, as typically believed, but the area of the primary particles. This work has substantial implications in accurate modeling and control of battery materials.

2:15 PM EN10.02.03

Electrode/Electrolyte Interface Control for Multivalent-Ion Batteries with High Stability and ReversibilityChang Li¹, Rishabh D. Guha², Abhinandan Shyamsunder¹, Zhuo Yu¹, Kristin A. Persson³ and Linda Nazar¹; ¹University of Waterloo, Canada; ²Lawrence Berkeley National Laboratory, United States; ³University of California – Berkeley, United States

Rechargeable multivalent-ion batteries (RMBs) are attractive as a "beyond lithium-ion battery" because of their multi-electron transfer and high abundance (eg. Zn²⁺ and Mg²⁺), which principally provides higher volumetric capacity and better affordability. The development of highly reversible and stable RMBs is correlated to the multivalent feature of these ions, which poses great challenges to the design of functional electrode/electrolyte interfaces.

This presentation will include discussion of key obstacles for these interfaces, followed by tailored strategies to foster good performance. The main topics will cover two different approaches to stabilize the electrode/electrolyte interface by preventing interfacial side reactions in nonaqueous magnesium batteries with an operating potential of over 3.5 V. This includes a) a low-cost inorganic surface membrane that protects against the decomposition of an organoborate-based electrolyte to yield an ultra-stable Mg anode for high-power magnesium batteries; b) eliminating passivation on the Mg anode by tailoring commercially available electrolytes to achieve over 2500-hour Mg plating/stripping at 2 mA cm⁻² and 2 mAh cm⁻². Brief highlights of interfacial optimization in aqueous zinc batteries will be also presented. Characterization of these designed and highly functional interfaces using depth-profiling high-resolution XPS, TEM and cryogenic-EM will be described.

2:30 PM EN10.02.04

Lithium Metal Anode Enabled by a Robust and Stable Artificial Surface LayerRidwan A. Ahmed, Ju-Myung Kim, Ji-Guang Zhang and Wu Xu; Pacific Northwest National Laboratory, United States

Lithium (Li) metal batteries have higher energy density than the state-of-the-art Li-ion batteries and the potential utilization in transportation devices. However, their practical application is still hindered by poor performance in terms of cycling stability and safety, especially at high current densities. This is due to a number of reasons among which are reactions between the Li metal and the liquid electrolyte, and formation of dendrites. In this study, we develop a robust and stable artificial solid electrolyte interface (aSEI), which consists of a surface treated (S_T) PEO – Li_{6.4}Ga_{0.5}La₃Zr₂O₁₂ composite polymer layer (CPL) on Li metal anode. The aSEI developed in this study is characterized by a good combination of electrochemical and mechanical properties. Benefiting from these characteristics, S_TCPL@Li||NMC811 cells with 4.7 mAh cm⁻² cathode loading exhibit improved electrochemical cycling stability compared with the bare Li||NMC811 cells at high current densities of ~1.6 and ~2.4 mA cm⁻². A capacity retention of ~90% is obtained for S_TCPL@Li||NMC811 at ~1.6 mA cm⁻² after 200 cycles compared with 60% for bare Li||NMC811. In addition, S_TCPL@Li||NMC811 demonstrates higher charge rate capacities at charge current densities compared with bare Li||NMC811. These findings suggest that S_TCPL is promising for high current density Li metal batteries.

2:45 PM EN10.02.05

Elucidating the Role of Prelithiation in Si-Based Anodes for Interface StabilizationShuang Bai and Y. Shirley Meng; University of California, San Diego, United States

Prelithiation as a facile and effective method to compensate the lithium inventory loss in the initial cycle has progressed considerably both on anode and cathode sides. However, much less research has been devoted to the prelithiation effect on the interface stabilization for long-term cycling of Si-based anodes. An in-depth quantitative analysis of the interface that forms during the prelithiation of SiO_x is presented here and the results are compared with prelithiation of Si anodes. Local structure probe combined with detailed electrochemical analysis reveals that a characteristic mosaic interface is formed on both prelithiated SiO_x and Si anodes. This mosaic interface containing multiple lithium silicates phases, is fundamentally different from the solid electrolyte interface (SEI) formed without prelithiation. The ideal conductivity and mechanical properties of lithium silicates enable improved cycling stability of both prelithiated anodes. With a higher ratio of lithium silicates due to the oxygen participation, prelithiated SiO_{1.3} anode improves the initial coulombic efficiency to 94% in full cell and delivers good cycling retention (77%) after 200 cycles. The insights provided in this work can be used to further optimize high Si loading (>70% by weight) based anode in future high energy density batteries.

3:00 PM BREAK

3:30 PM *EN10.02.06

Microscopic Insights into Ion Conduction at Solid-Solid Interfaces[MiaofangChi](#); Oak Ridge National Laboratory, United States

Solid-state electrolytes are currently being investigated as a highly promising solution to overcome various challenges in battery technology. The ideal solid electrolyte material should exhibit high ionic conductivity while maintaining stability with metallic lithium. In recent decades, significant progress has been made in the development of solid electrolyte materials with high conductivity comparable to organic liquid electrolytes. However, a major limitation in practical applications of these materials is the unexpectedly high resistivity observed at grain boundaries and electrolyte-electrode interfaces. Elucidating the complexities of these interfaces is challenging due to spatial confinement, structural intricacies, and chemical complexities, posing obstacles for both experimental and theoretical approaches. In this talk, I will discuss our recent efforts to probe interfacial phenomena in solid electrolytes using advanced techniques such as in situ and atomic-resolution scanning transmission electron microscopy (STEM) and electron energy loss spectroscopy (EELS). Additionally, I will introduce 4D-STEM and vibration EELS, which enable the investigation of interfacial charge distribution and ion conduction behavior. Through these electron microscopy techniques, I aim to demonstrate their significant potential in providing valuable insights for the design and synthesis of high-performance solid-solid interfaces.

4:00 PM EN10.02.07

Thermodynamic Stability Dynamics during Delithiation of LiCoO₂[SpencerDahl](#)¹, [LuelcCosta](#)², [JeffersonBettini](#)² and [RicardoCastro](#)³; ¹University of California, Davis, United States; ²National Center for Research in Energy and Materials - CNPEM, Brazil; ³Lehigh University, United States

Cathode cycling leads to critical instabilities of the structures, being one of the most critical causes for battery failure. Interfacial properties are critical in this scenario, but there is a lack of fundamental experimental studies concerning the evolution of surface energies during delithiation and how to control them using thermodynamic strategies to improve cathode performance. Here we report experimental data on the thermodynamics of surfaces in nanocrystalline LiCoO₂ using microcalorimetry and how it relates to stability against dissolution/degradation. By testing chemically de-lithiated states using microcalorimetry and EELS/HRTEM, we were able to quantify the thermodynamic changes between lithiated and delithiated states for a direct evaluation of driving force for growth and degradation. Further, we demonstrate how a dopant (lanthanum) designed to segregate to the surface lowers the excess energy of the interface, causing nano-LiCoO₂ to show greater resistance to dissolution/growth/degradation founded on the dopant impact interface energies. Although LiCoO₂ was used as a model material, we discuss here the design principle behind interface stabilization to allow greater performance in liquid and solid state batteries.

4:15 PM EN10.02.08

Critical Deterioration Roots of Ni-Rich Cathode during Long-Term Cycling: Material Degradation, Diffusion Limit or Interfacial Instability?[JiyuCai](#)¹, [NatashaChernova](#)², [BradPrevel](#)³, [FengWang](#)¹ and [ZonghaiChen](#)¹; ¹Argonne National Laboratory, United States; ²Charge CCCV, United States; ³Primet Precision Materials, United States

Severe performance deterioration in long-term cycling is a long-standing challenge for practical applications of high-energy-density Ni-rich LiNi_{1-x-y}Mn_xCo_yO₂ (NMC, x+y < 0.5) cathodes at high potentials (>4.3V vs. Li/Li⁺). Great efforts have correlated the performance deterioration to many physical observations, while the critical deterioration roots of Ni-rich cathode during long-term cycling are not well elaborated. Herein, we perform a systematic and in-depth investigation to probe the critical contributions from observed deterioration roots of Ni-rich LiNi_{0.83}Mn_{0.1}Co_{0.07}O₂ cathode in full cells with graphite anode after 1000 cycles at different upper potentials. Intriguingly, the severe capacity retention in electrochemical evaluation of recovered cathode half cells is contrail to the insignificant structural changes and transition metal loss via post-mortem characterizations of bulk material. GITT tests unveils that chemical diffusion limit is the dominant deterioration root of Ni-rich cathode at high potential. The severe chemical diffusion of Li⁺ is strongly correlated to the exacerbated surface reconstructions at the cathode surface. Our study suggests that stabilizing the cathode interface and mitigating the surface reconstructions is the most crucial for enabling long lifespan of Ni-rich cathodes at high potentials.

4:30 PM EN10.02.09

Interfacial Aluminum Corrosion Reactions with Lithium Bis(fluorosulfonyl)imide (LiFSI) in Fluorinated and Non-Fluorinated Ether-Based Solutions for Li-Metal Batteries[Taegyujang](#) and [Hye RyungByon](#); KAIST, Korea (the Republic of)

Lithium-metal batteries (LMBs) have garnered significant attention as a potential replacement for graphite-based lithium-ion batteries due to their superior energy density. However, a critical challenge in LMBs is stabilizing the metallic lithium (Li) electrodes, which face continuous decomposition of the electrolyte solution and the formation of dendrites. It is crucial to develop a desired solid electrolyte interphase (SEI) that contains lithium fluoride (LiF) to protect the Li surface. For this purpose, the bis(fluorosulfonyl)imide (FSI) anion has been widely employed, as it readily forms abundant LiF through defluorination. However, the use of FSI is accompanied by the corrosion of aluminum (Al), the current collector in the positive electrode, which often leads to cell failures. Although recent studies reported mitigated Al corrosion through the use of fluorinated ethers and locally high concentrated electrolytes (LHCE), there is a lack of study on the interfacial reactions between these electrolytes and Al, as well as their ability to inhibit corrosion.

Herein we studied the Al corrosion with 1 M LiFSI in 1,2-dimethoxyethane (DME), tetraethylene glycol dimethyl ether (G4), 2,2,3,3-tetrafluoro-1,4-dimethoxybutane (FDMB), and LHCE comprising DME and 1,1,2,2-tetrafluoroethylene 2,2,3,3-tetrafluoropropyl ether (TTE). The corrosion of Al was evaluated through chronoamperometry tests conducted from room temperature to 60 °C. The applied potential for each test was kept below the oxidation potential of the electrolyte solutions (4~4.3 V for DME and G4, and 4.5 V for FDMB and LHCE). In contrast to a significant increase in current observed with DME, the other electrolyte solutions exhibited low and stable leakage currents at room temperature. X-ray photoelectron spectroscopy revealed the formation of the Al(FSI)₃ complex on Al from G4 and LHCE, indicating a low solubility of Al(FSI)₃. On the other hand, AlF₃ was detected when FDMB was used, which was likely formed through the defluorination of FDMB, leading to the replacement of Li⁺ coordination with Al³⁺ in the presence of LiFSI. At 60 °C, the leakage currents with DME, G4, and LHCE significantly increased, in the order of DME > G4 > LHCE. It is attributed to the increased solubility of Al(FSI)₃ and the exacerbation of Al corrosion. Open circuit potentials (OCPs) measured after tests were 0 to 0.3 V with DME, G4, and LHCE, indicating the significant dissolution of Al³⁺ that was deposited on the Li electrode. In comparison, FDMB with LiFSI provided a low and stable current even at 60 °C and 4.5 V. The OCP also remained above 3 V, suggesting the preservation of the Al₂O₃ surface and the mitigated Al corrosion. I will discuss the details of interfacial reactions between Al and electrolyte solutions in the presentation.

4:45 PM EN10.02.10

Ultrathin Semiconductor Interphase Regulated Electric Double Layer Enabling High-Stable Zinc Metal Anode[YimeiChen](#); University of Alberta, Canada

The practical application of aqueous zinc-ion batteries for large-grid scale systems is still hindered by uncontrolled zinc dendrite and side reactions. Regulating the electrical double layer via the electrode/electrolyte interface layer is an effective strategy to improve the reversibility and stability of Zn anodes. Herein, the ultrathin zincophilic ZnS layer synthesized via a facile electrodeposition method is selected as a model regulator. At a given cycling current, the cell with Zn@ZnS electrode displays a lower potential drop over the Helmholtz layer across the electrode surface and a suppressed diffuse layer, indicating the regulated charge distribution and decreased electric double layer repulsion force. This protective layer also enables redistributed uniform electric fields and highly suppressed side reactions. Consequently, the cell with the ZnS protection layer exhibits a long cycling stability of around 3000 hours at 1mA cm⁻², accompanied by a high reversibility of 98.9% over 2500 cycles at 5mA cm⁻². When coupled with I₂/AC cathode, the cell demonstrates a high rate performance of 160 mAh g⁻¹ at 0.1 A g⁻¹ and long cycling stability of over 10000 cycles at 10A g⁻¹. The Zn||MnO₂ also sustains both high capacity and long cycling stability of 130 mAh g⁻¹ after 1200 cycles at 0.5A g⁻¹.

SESSION EN10.03: Electrocatalysis I—From Single Atoms to Nanocatalysts

Session Chairs: [Ling Chen](#) and [Edvin Lundgren](#)

Tuesday Morning, November 28, 2023

Hynes, Level 3, Room 302

8:30 AM *EN10.03.01

Single Metal Site Oxygen-Reduction Catalysts: From Atomic Active Site Structures to Fuel Cell Cathode Performance[GangWu](#); University at Buffalo, SUNY, United States

Recently, scientists have identified the newly emerging atomically dispersed transition metal (M: Fe, Co, or/and Mn) and nitrogen co-doped carbon (M-N-C) catalysts as the most promising alternative to PGM catalysts. In this talk, I will provide a comprehensive review of significant breakthroughs, remaining challenges, and perspectives regarding the M-N-C catalysts in terms of catalyst activity, stability, and membrane electrode assembly (MEA) performance. The most considerable challenge of current M-N-C catalysts is the unsatisfied stability and rapid performance degradation in MEAs. Therefore, we further discuss practical methods and strategies to mitigate catalyst and electrode degradation, which is essential to make M-N-C catalysts viable in hydrogen fuel cell technologies.

9:00 AM *EN10.03.02

Nano Catalysts for Water Electrolysis: The Importance of Catalyst Layer Conductivity[Shougo Higashi](#); Toyota Central R&D Labs., Inc./ Toyota Motor North America, United States

Humanity has been benefiting from the development of internal combustion engines for several decades. With the emergence and explosive increase of automobiles around 1980's, there has been a demand for environmental catalyst technologies to process exhaust gases such as CO (carbon monoxide), NO_x (Nitrogen oxides). Since then, a significant amount of knowledge about catalysts to reduce the usage of precious metal catalysts, which play a crucial role in automotive applications, has been obtained, leading to the current research and development of single-atom and few-atom cluster catalysts. We have seen that the chemical potential of the material can be modulated by tuning the size, shape, and introducing supporting oxides to achieve low-mass loading, high performance environmental catalyst. In the future, the roles played by batteries and catalysts will become increasingly important, and there is a need for next-generation electrochemical catalyst technologies to produce energy carriers, including hydrogen, at a low cost.

In this presentation, I will briefly review the knowledge of catalysts that we have accumulated since the rise of internal combustion engines and discuss the challenges and opportunities in electrochemical catalysis, with a specific focus on our research efforts in hydrogen production.

9:30 AM EN10.03.03

Enhancing Metal-Sulfur Batteries with Single Atom Catalysts and Graphitic Carbon Nitride: Addressing the Polysulfide Shuttle Effect[Aliakbar Yazdani](#), Jyoti Pandey, Veronica Barone, Valeri Petkov and Bradley Fahlan; Central Michigan University, United States

Metal-sulfur batteries, including lithium-sulfur batteries, have attracted significant attention as promising energy storage systems. However, the presence of the polysulfide shuttle effect poses a major challenge, which leads to poor cycling stability and limited capacity retention. This research focuses on the exploration of novel strategies to overcome this issue and improve the performance of metal-sulfur batteries. One effective approach to mitigate this effect is the utilization of single atom catalysts. These catalysts have demonstrated promising results in enhancing the cell performance of metal-sulfur batteries, particularly in terms of higher C-rates and improved capacity retention. By providing active sites for polysulfide adsorption and conversion, single atom catalysts effectively trap and immobilize polysulfide intermediates, preventing their dissolution and subsequent migration between counter electrodes.

In this study, we investigated the incorporation of Fe, Co, and Ni single atom catalysts onto a carbon substrate for metal-sulfur batteries. Specifically, we explored the use of graphitic carbon nitride (g-C₃N₄) and reduced graphitic carbon nitride (r-g-C₃N₄) as suitable carbon substrates for sulfur and single atom catalysts. These materials possess desirable properties such as high surface area, excellent electrical conductivity, and good chemical stability, making them ideal candidates for enhancing the cathode performance of metal-sulfur batteries. Through systematic characterization and electrochemical testing, we will demonstrate the performance of metal-sulfur batteries that incorporate single atom catalysts and graphitic carbon nitride in the cathode. The effect of dispersed single atom catalysts in the suppression of polysulfide migration, as well as the cycling stability and prolonged capacity retention of metal-sulfur batteries, will be described.

Overall, our findings will highlight the potential of single atom catalysts and graphitic carbon nitride as effective strategies to address the polysulfide shuttle effect in metal-sulfur batteries. This research aims to contribute to the advancement of energy storage technologies, paving the way for the development of more efficient and sustainable battery systems.

9:45 AM EN10.03.04

Characterization and Modeling of Rhodium Single-Atom Catalysts on Porous Carbon Supports[Jyoti Pandey](#); Central Michigan University, United States

Due to worldwide interest in expanding the electrification of the transportation sector, there is never-ending research carried out on the development battery materials. Sulfur being one of the least expensive elements, is an attractive choice for battery cathode but it comes with various limitations which includes the insulating behavior of polysulfides, poor reversibility and slow kinetics of the metal-S conversion reactions. The single-atom catalysts (SACs) open up a new avenue towards their use as catalysts and to increase the commercial applications. They are known to exhibit improved kinetics of metal-S conversion reactions through the redox kinetics. This work focusses on the characterization and modeling of Rh-SAC-functionalized porous carbon supports. Extended X-ray absorption fine structure (EXAFS) measurements were recorded on the Rh K-edge for the four different samples to study the coordination environment. An analysis of the EXAFS scattering contributions revealed that out of the four different samples, two of the samples, viz. Fibrous materials (CF) and carbon nano fibers (CNF) were explicitly possessing Rh single atoms dispersed on the carbon support. The other two samples, Carbon nano tube (CNT) and few layer graphene (FLG) were proven to possess Rh single atoms with some dimers/trimers, and Rh clusters, respectively. EXAFS fitting gives a good overlap between the DFT-optimized structures and the experimental spectra up to a range of around 3 Å around the scattering atoms. The insights gained from the characterization and modeling efforts will pave the way for improved understanding of the catalyst's behavior and facilitate the design of more efficient and effective catalyst systems. The outcomes of this study hold significant potential for enhancing the performance and commercial viability of sulfur-based batteries in the pursuit of widespread research in the field of cathode materials for the battery sector.

10:00 AM BREAK

10:30 AM *EN10.03.05

Catalytic Single-Site Co in Well-Define Metal Oxide Nanocrystal Surfaces for the Oxygen Evolution Reaction[Sen Zhang](#) and Chang Liu; University of Virginia, United States

Efficient electrocatalysts for the oxygen evolution reaction (OER) are paramount to the development of electrochemical devices for clean energy and fuel conversion. However, the structural complexity of heterogeneous electrocatalysts makes it a great challenge to elucidate the surface catalytic sites and OER mechanisms. This talk will be focused on our recent work on the interaction of single-site Co catalytic centers and inorganic coordination environments in the surface of doped metal oxide nanocrystals for the OER. The integration of controlled synthesis of nanocrystals, operando structural/catalytic characterization, and advanced theoretical calculation for electrocatalyst development will be discussed.

11:00 AM EN10.03.06

Active-Site Imprinting Towards Design and Understanding of Single Site Atomically Dispersed M-N-C Catalysts[Tim-Patrick D. Feller](#); Bundesanstalt für Materialforschung und -prüfung (BAM), Germany

Atomically dispersed M-N-C catalysts such as Fe-N-Cs are very promising alternatives for precious metal-based catalysts for energy conversion reactions.^[1-3] Early reports on such materials date back to the 1960s, when Jasinski pioneered the research based on tetrapyrrolic phthalocyanine macrocycles which were inspired by natural transition metal porphyrin complexes present in enzyme active sites.^[3] For decades, the selective synthesis of these catalysts was complicated by the formation of side phases due to the harsh reaction conditions facilitating side phase formation. In 2018, we introduced a mild procedure, which is conservative toward the carbon support and leads to active-site formation at low temperatures in a wet-chemical step, essentially decoupling the preparation of the N-C backbone from the preparation of the active sites.^[4,5] The key concept therein is the so-called active-site imprinting into the N-C backbone using pyrolytic template ion reactions.^{[4][5]} Using the same precursor that is used for the preparation of phthalocyanines, we were recently able to produce atomically-dispersed single-site M-N-Cs that consist of tetrapyrrolic M-N₄ complexes.^[6] The tetrapyrrolic Fe-N-C derivatives are highly active and extraordinary selective electrocatalysts for the oxygen reduction reaction. The well-defined and homogeneous active site structure allowed us to quantify the intrinsic catalytic activity of the materials and to reveal distinct degradation mechanism upon storage.^[7] Herein, the general synthetic strategy for atomically dispersed catalysts will be discussed based on tetrapyrrolic Fe-N-C catalysts, which will be analyzed for their potential as fuel cell catalysts.

References

[1] G Wu, KL More, CM Johnston, P Zelenay, *Science* 332 (6028), 443-447.

[2] H. A. Gasteiger, S. S. Kocha, B. Sompalli, F. T. Wagner, *Applied Catalysis B*, 56, (2005), 1-2, 9-35.

[3] R. Jasinski, *Nature* 201, (1964), 1212.

[4] A. Mehmood, J. Pampel, G. Ali, H. Y. Ha, F. Ruiz-Zepeda, and T.-P. Feller*, *Adv. Energy Mater.* (2017), 1701771.

[5] D. Menga, F. Ruiz-Zepeda, L. Moriau, Martin Sala, F. Wagner, B. Koyutürk, U. Petek, N. Hodnik, M. Gaberscek and T.-P. Feller*, *Adv. Energy Mater.* (2019), 1902412.

[6] D Menga, JL Low, Y-S Li, I Arcon, B Koyuturk, FE Wagner, F Ruiz-Zepeda, M Gaberscek, BP Paulus, T-P Feller*, *J. Amer. Chem. Soc.* (2021), 43(143), 18010-18019.

[7] D Menga, A Guilherme Buzanich, FE Wagner, T-P Feller*, *Angewandte Chem. Int. Ed.* (2022), e202207089

[8] D Menga, FE Wagner and T-P Feller*, (2023), under revision.

11:15 AM EN10.03.08

Photochemically Deposited Single Platinum Atoms Supported on Exfoliated WS₂ Nanosheets for Hydrogen Evolution Reaction[Doo Young Kim](#), Nadeesha L. Kothalawala, Tawabur Rahman, Manisha Goonatilleke, Nipun Chandrasiri, Beth S. Guiton and Aron J. Huckaba; University of Kentucky, United States

2-D transition metal dichalcogenides (TMDs) serve as an ideal platform for electro- and photo-catalysis. For example, TMDs can be interfaced with another layered material to constitute a heterojunction or can stabilize efficient catalysts (e.g., single atom catalysts) without chemical ligands. In this work, we report platinum single-atom-catalysts (Pt-SAC) decorated tungsten disulfide (WS₂) nanosheets for electrochemical hydrogen evolution reaction (HER). A green liquid-phase exfoliation method was employed to produce highly exfoliated (mono, bi- and few-layered) WS₂ nanosheets. This method involved a probe ultra-sonication in a low-boiling-point solvent mixture, water and ethanol, combined with a solvothermal process. These exfoliated

WS₂ nanosheets were crystalline and possess clean surfaces with high aspect ratio without any surface ligands or impurities. The synthesized nano sheets were predominantly semi-conducting hexagonal (2-H) phase.

We found that these exfoliated WS₂ nanosheets are an ideal support material to stabilize catalytic Pt-SAC. For the deposition of Pt-SACs on WS₂, H₂PtCl₆ precursor was photochemically reduced through a short exposure of high-energy Xe flash lamp. High-resolution scanning transmission electron microscopic (HR-STEM) images probed that the deposited Pt atoms were single- or nanoclustered. Pt-SACs demonstrate excellent performances for hydrogen evolution reaction. The mass activity (A/g_{pt}) of Pt-SAC on WS₂ is ~ 20x higher than that of commercial platinum nanoparticle catalyst (Pt/C) in both acidic and alkaline electrolytes.

11:30 AM EN10.03.09

Predicting Catalytic Activity of Single Atom Catalysts in Oxygen Evolution Reaction via First-Principles Simulations and Symbolic Regression SatadeepBhattacharjee¹, SwetarekhaRam¹, Albert SLee² and Seung-CheolLee¹; ¹Indo Korea Science and Technology Center, India; ²Korea Institute of Science and Technology, Korea (the Republic of)

Efficient energy conversion and storage require the development of effective electrocatalysts for the oxygen evolution reaction (OER). In this regard, single-atom catalysts (SACs) with 100 % active sites for OER are promising [1-6]. This study investigates the OER activities of Co single atoms (CoSA) on metallic MXenes, namely Ti₃C₂O₂ and Mo₂CO₂, considering both stoichiometric and oxygen vacancy (Ov) configurations. Spin-polarized first-principles calculations were used to determine the rate-limiting step, the conversion of oxygen from hydroxyl species. The presence of oxygen vacancies resulted in decreased OER activity and higher overpotential for CoSA on Ti₃C₂O_{2-δ}, while it increased OER activity for CoSA on Mo₂CO₂. Insights from the density of states, the variation of the charge density and the bonding analysis provide information about the observed results. Furthermore, the critical role of hybridization between the d states of CoSA and the transition metal sites of the catalyst bed (Ti/Mo) is demonstrated. Furthermore, we investigated the potential of designing SACs on Mo₂CO₂ MXenes for electrochemical OER using first-principles modeling simulations. The Electrochemical Step Symmetry Index (ESSI) method is used to fine-tune activity and identify optimal SACs, with both Ag and Cu showing potency in enhancing OER activity. Cu stands out among the chosen transition metals (TMs) as the best catalyst for reducing the overpotential, while Ag poses challenges in tuning its overpotential. Symbolic regression analysis is employed to identify key descriptors affecting catalytic efficiency, resulting in the derivation of mathematical formulas for the OER overpotential. This comprehensive investigation provides insights into the potential of SACs and MXenes in advanced electrocatalytic processes, offering prospects for improved OER activity and selectivity.

References:

- [1] Qu, G.; Zhou, Y.; Wu, T.; Zhao, G.; Li, F.; Kang, Y.; Xu, C. Phosphorized MXene-phase molybdenum carbide as an earth-abundant hydrogen evolution electrocatalyst. *ACS Applied Energy Materials* 2018, 1, 7206–7212.
- [2] Xiao, S.; Zhang, X.; Zhang, J.; Wu, S.; Wang, J.; Chen, J. S.; Li, T. Enhancing the lithium storage capabilities of TiO₂ nanoparticles using delaminated MXene supports. *Ceramics International* 2018, 44, 17660–17666.
- [3] Kan, D.; Wang, D.; Zhang, X.; Lian, R.; Xu, J.; Chen, G.; Wei, Y. Rational design of bifunctional ORR/OER catalysts based on Pt/Pd-doped Nb 2 CT 2 MXene by first-principles calculations. *Journal of Materials Chemistry A* 2020, 8, 3097–3108.
- [4] Liu, C.-Y.; Li, E. Y. Termination effects of Pt/v-Ti n+ 1C n T2 MXene surfaces for oxygen reduction reaction catalysis. *ACS Applied Materials & Interfaces* 2018, 11, 1638–1644.
- [5] Wang, Y.; Li, X.; Zhang, M.; Zhang, J.; Chen, Z.; Zheng, X.; Tian, Z.; Zhao, N.; Han, X.; Zaghib, K., et al. Highly Active and Durable Single-Atom Tungsten-Doped NiS_{0.5}Se_{0.5} Nanosheet@ NiS_{0.5}Se_{0.5} Nanorod Heterostructures for Water Splitting. *Advanced Materials* 2022, 34, 2107053.
- [6] Hu, H.; Wang, J.; Cui, B.; Zheng, X.; Lin, J.; Deng, Y.; Han, X. Atomically Dispersed Selenium Sites on Nitrogen-Doped Carbon for Efficient Electrocatalytic Oxygen Reduction. *Angewandte Chemie International Edition* 2022, 61, e202114441.

SESSION EN10.04/SF02.04: Joint Session: Crystallization at Electrochemical Interfaces
Session Chairs: Jingshan Du and Hua Zhou
Tuesday Afternoon, November 28, 2023
Hynes, Level 3, Room 302

1:30 PM *EN10.04/SF02.04.01

Structure Stabilization in Layered Transition Metal Oxide Positive Electrodes for Sodium Ion Batteries DewenHou^{1,2}, EricGabriel^{1,2}, KincaidGraff¹, YifanDong¹, TianyiLi², YuziLiu², ChengjunSun² and HuiXiong¹; ¹Boise State University, United States; ²Argonne National Laboratory, United States

Sodium-ion batteries (SIBs) have stepped into the spotlight as a promising alternative to lithium-ion batteries (LIBs) for large-scale energy storage systems. However, the stability and performance of sodium ion battery electrode materials are lacking compared to their lithium counterparts as a consequence of the larger size of the Na⁺ ion compared to Li⁺. The layered transition metal oxide (LTMO) positive electrodes have attracted extensive attention for SIBs due to its favorable electrochemical performance. However, they suffer from complex and irreversible phase transitions during cycling, which leads to the chemomechanically-induced structural degradation and rapid capacity decay, limiting its practical applications. In this talk, we will discuss our recent progress in stabilizing LTMO structures during cycling and the origin of the phase interface's influence on the Na⁺ storage and transport properties. *In situ/operando* spectroscopic techniques used in our work to track the phase transitions will also be discussed.

2:00 PM EN10.04/SF02.04.02

Engineering Multifunctional Interfaces for Forming and Recycling Composite Electrodes BoNie and HongtaoSun; The Pennsylvania State University University Park, United States

Lithium-ion batteries (LIBs) have emerged as the leading energy storage technology, dominating the market over the past decade. While significant progress has been made in developing high-performance electrode materials, the overall performance of LIBs is often compromised when including other passive components (e.g., 40-60 wt%) such as current collectors, separators, and packaging. This study demonstrates an alternative approach to achieve high performance at the device level by increasing the electrode thickness and reducing the weight percentage of passive components in LIB systems.

We present an effective and sustainable manufacturing process for engineering multifunctional interfaces in thick composite electrodes (e.g., LiNi_{0.8}Co_{0.1}Mn_{0.1}O₂). By integrating hybrid materials into artificial "grain boundaries (GB)," we can consolidate, densify, and recycle electrode active material powders to fabricate thick cathode composites with improved volumetric and areal performance. To this end, the cold sintering process (CSP) was employed to co-sinter all constituents into a highly dense form (2.7-3.2 g cm⁻³) with good interfacial stability. Notably, the introduction of a transient solvent (e.g., 5 vol% DMF) enables the integration of distinct materials (e.g., hybrids and NMC811 powders) under low processing temperature (120 deg C) and appropriate uniaxial pressure (300 MPa).

Moreover, the resulting artificial hybrid "GBs" consist of an electrically conductive network (e.g., carbon nanofiber and graphene) and an ionic conductive network (e.g., polymer-ionic liquid gel (PILG)), facilitating fast charge transport pathways. The co-sintered thick electrodes (550 μm) exhibit outstanding battery performance in gravimetric (194 mAh g⁻¹), volumetric (418 mAh cm⁻³), and areal (23 mAh cm⁻²) metrics. This improvement enables enhanced energy and power outputs while reducing the weight and cost of passive components. Furthermore, the polymer component (e.g., PVDF-HFP) can be dissolved in a selective solvent, allowing for the collection and reforming/resintering of NMC powders from the sintered electrodes, enabling direct recycling.

In addition, in-situ electrochemical impedance spectroscopy was employed to monitor impedance information during both the densification of the sintering process and the evolution of artificial "GBs" during the lithiation/delithiation process. By combining the variables of the sintering process and the composite composition, a data-driven model was developed to successfully predict the dominant variables and their corresponding optimal value ranges, showing promise for optimizing the composite electrode design.

Overall, our interface engineering approach provides a sustainable solution to address critical challenges in the fabrication, efficient charge transports, and recycling of high-performance battery electrodes.

2:15 PM EN10.04/SF02.04.03

While today's lithium-ion batteries (LIBs) use graphite anodes, their limited specific capacity (372 mAh g⁻¹) has pushed researchers towards exploring alternative anodes with high specific capacity. Silicon (Si) anodes with a specific capacity of 4200 mAh g⁻¹ offer an attractive solution, especially because of silicon's abundance in the earth's crust. However, high volume expansion (400%) during lithiation-delithiation leads to fracture and rapid capacity deterioration. This has limited the widespread adoption of Si-based anodes. We developed electrodes based on porous one-dimensional (1D) quill-like structures, aka Si nano-quills (SiNQ), to overcome these issues. Half cells equipped with SiNQ-graphite electrodes (containing 15 wt% SiNQ as the active material) exhibited an impressive initial reversible capacity of 527 mAh g_{Si}⁻¹ at a current density of 90 mA g⁻¹, along with an outstanding capacity retention of 80.2% across 200 cycles. This starkly contrasts with anodes containing 15 wt% commercial Si nanoparticles, which could only manage an initial reversible capacity of 375 mAh g_{Si}⁻¹ and a significantly lower capacity retention of 44.8% over the same number of cycles. Intrigued by this superior performance, we studied the lithiation-delithiation kinetics of SiNQ electrodes via the galvanostatic intermittent titration technique (GITT). GITT testing was performed between 0.01 V and 1 V with current pulses of 0.05C (210 mA g_{Si}⁻¹). Current pulses of 30 min duration were followed by a 6-hour rest period to allow the potential and built-up concentration gradients to relax. Unlike graphite intercalation electrodes, Si-based electrodes are phase transformation electrodes. So, lithiation-delithiation is accompanied by phase transformation in Si-based electrodes. While GITT-based models for phase transformation electrodes such as LiFePO₄ exist in the literature [1], they do not account for electrode porosity and curvature. As a result, a novel model that accounts for the effects of phase transformation, electrode porosity, and electrode curvature on lithiation-delithiation kinetics was developed to fit the experimental data. Diffusion coefficients as a function of the state of charge were obtained and will be presented.

[1] Y. Zhu and C. Wang, "Galvanostatic intermittent titration technique for phase-transformation electrodes," *J. Phys. Chem. C*, vol. 114, no. 6, pp. 2830–2841, Feb. 2010, doi: 10.1021/JP9113333/ASSET/IMAGES/MEDIUM/JP-2009-113333_0015.GIF.

2:30 PM EN10.04/SF02.04.04

Controlling Electrochemical Deposition of 2D Zinc Metal Plates on Copper Substrates in Aqueous Electrolytes [Ying Xia](#)^{1,2}, [Jinhui Tao](#)², James J. De Yoreo^{2,1} and Jun Liu^{1,2}; ¹University of Washington, United States; ²Pacific Northwest National Laboratory, United States

Polyethylene glycol (PEO) is a commonly used polymer in the field of batteries for achieving flat and uniform electrodes to enhance the performance of batteries, such as lithium batteries and zinc (Zn) batteries. However, the impact of PEO on the electrochemical deposition of Zn metal on electrodes remains uncertain. In this study, we selected ZnSO₄ solution as electrolyte and copper (Cu) substrates as electrodes, which are widely applied in Zn batteries. We used *in situ* electrochemical atomic force microscopy (EC-AFM) to observe the nucleation and growth of Zn metal plates on the Cu substrate in the presence of different concentrations of ZnSO₄ and PEO additives. Our results indicate that PEO biases the crystallographic orientation of the initially deposited Zn metal nuclei, but does not have an obvious influence on subsequent growth. Based on our findings, we hypothesize that PEO primarily interacts with the Cu substrate to adjust the interfacial energy of the Cu-electrolyte interfaces. In contrast, due to the lack of apparent change in the Zn growth rate, we postulate that PEO has limited interaction with Zn²⁺ ions in the ZnSO₄ solution and thus does not strongly influence the activity coefficient of Zn²⁺ ions. The consistent aspect ratio of the Zn plates combined with the lack of an effect on growth rates further suggests that PEO does not interact significantly with the surface of the newly formed Zn plates. Our findings provide both insight into the underlying mechanism by which PEO promotes electrode flattening in Zn batteries and a standardized protocol for elucidating the impact of additives on the morphological evolution of interfaces during electrochemical deposition.

2:45 PM EN10.04/SF02.04.05

Directing Polymorph Specific Calcium Carbonate Formation with *De Novo* Protein Templates [Fatima Davila-Hernandez](#)¹, [Biao Jin](#)², [Pyles Harley](#)¹, [Shuai Zhang](#)¹, [Zheming Wang](#)², [Timothy F. Huddy](#)¹, [Chun-Long Chen](#)², James J. De Yoreo² and [David Baker](#)¹; ¹University of Washington, United States; ²Pacific Northwest National Laboratory, United States

Biomolecules modulate inorganic crystallization to generate hierarchically structured biominerals, but the atomic structure of the organic-inorganic interfaces that regulate mineralization remain unknown. We hypothesized that heterogeneous nucleation of calcium carbonate could be achieved by a structured flat molecular template that pre-organizes calcium ions on its surface. To test this hypothesis, we designed helical repeat proteins (DHRs) displaying regularly spaced carboxylate arrays on their surfaces and found that both protein monomers and protein-Ca²⁺ assemblies directly nucleate nano-calcite with non-natural (110) or (202) faces while vaterite, which forms first absent the proteins, is bypassed. The nanocrystals then assemble by oriented attachment into calcite mesocrystals. We find further that nanocrystal size and polymorph can be tuned by varying the length and surface chemistry of the designed protein templates. Thus, bio-mineralization can be programmed using *de novo* protein design, providing a route to next-generation hybrid materials.

3:00 PM BREAK

3:30 PM *EN10.04/SF02.04.06

Interfacial Engineering of Catalyst and Battery Materials using Atomic Layer Deposition [Neil P. Dasgupta](#); University of Michigan, United States

The ability to manipulate the properties of surfaces and heterogeneous interfaces using atomically-precise synthesis methods is of critical performance in electrochemical applications. In particular, the ability to "turn on" desirable properties (such as fast interfacial kinetics and stable activity), while "turning off" undesirable properties (such as chemical and/or morphological instability) is of increasing importance as the demands for high performance, long lifetimes, and stability continue to increase. To address these challenges, in this talk, I will describe key advances in the application of Atomic Layer Deposition (ALD) as an enabling technology platform for the atomically-precise modification of surfaces and interfaces for applications in two key electrochemical application spaces: electrocatalytic CO₂ reduction and rechargeable batteries.

I will demonstrate how ALD modifications can allow for rational control of interactions at heterogeneous interfaces, which can be used to tune the thermodynamic stability, kinetic activity, and mass transport properties of these integrated material systems. I will describe examples of the ALD process for conformal modification of gas diffusion electrodes and composite battery electrodes. I will also provide a perspective on challenges to scale-up design and manufacturing of these energy material systems at length scales ranging from atoms to meters.

4:00 PM EN10.04/SF02.04.07

Fabricating Dendrite-Free Porous Hosts of Li for Li-Metal Batteries via Electrodeposition. [Yifan Ma](#) and [Hailong Chen](#); Georgia Institute of Technology, United States

Li metal anode is the ultimate choice for Li-chemistry-based batteries owing to its highest theoretical capacity (3860 mAh/g). Yet, the safety problems and low Coulombic efficiency resulting from Li dendrites are the remaining challenges for commercial applications.

Previously, we reported a 3D porous Cu current collector fabricated via a facile one-step electrodeposition method directly on commercial Cu foils. [1] This 3D porous Cu current collector showed stable long-term cycling with a high areal capacity up to 6 mAh/cm² without Li dendrites formation. However, for this one-step electrodeposition method, the thickness of the porous Cu layer is limited. Recently, we developed a new two-step electrochemical process to fabricate thick and porous Cu layers [2]. A thick Cu-Zn alloy was first electrodeposited on commercial Cu foil, and Zn was then removed electrochemically, leaving a thick and highly porous 3D Cu layer. Compared to our previous method, this 3D Cu layer has a high thickness of ~14 μm and porosity of ~72%. This new 3D Cu current collector can achieve stable Li cycling up to 230 h at a high areal capacity of 10 mAh/cm² at a current density as high as 10 mAh/cm², demonstrating its high commercial application potential in Li-metal batteries. In situ XRD method was used to reveal the deposition of CuZn alloy and the electrochemical dissolution of Zn.

1. Ma, X., Z. Liu, and H. Chen, *Facile and scalable electrodeposition of copper current collectors for high-performance Li-metal batteries*. *Nano Energy*, 2019, **59**: p. 500-507.
2. Ma, Y.F., et al., *Electrochemically Dealloyed 3D Porous Copper Nanostructure as Anode Current Collector of Li-Metal Batteries*. *Small*, 2023.

4:15 PM EN10.04/SF02.04.08

Computational Modeling of Nucleation at the Anode-Electrolyte Interface in Lithium Batteries [Madison Morey](#) and [Emily Ryan](#); Boston University, United States

The Lithium (Li) Metal Battery (LMB), which possesses a Li Metal anode has come to the forefront of many researchers' efforts to combat the energy storage limitations of the Li-Ion Battery (LIB). This is due to the large theoretical capacity that the Li metal anode (~3860 mA h g⁻¹) possesses in comparison with the graphite anode (~372 mA h g⁻¹) of the LIB. However, a main hindrance to the commercialization of these batteries is an unstable interface and uncontrolled dendrite growth, which pose serious safety concerns. While the growth process has been extensively studied, little is known about the nucleation process and how early nucleation effects dendrite growth throughout cycling. Due to the nature of the anode-electrolyte interface, it is difficult to study experimentally so we can use computational methods to resolve this interface and track the complex chemical and physical phenomena at this location. In this work we propose a computational model that uses a nucleation rate equation, stemming from Classical Nucleation Theory, to study how the electrochemical nucleation rate is impacted by varying parameters at the anode-electrolyte interface. The rate equation is then coupled with an extended, concentration dependent, Butler-Volmer equation to solve for the flux at the interface. Finally, the model is used to evaluate how surface energy impacts Li dendrite nucleation and growth.

4:30 PM EN10.04/SF02.04.09

In Situ Formation of Li⁺ Ion Conductive Layers as the Solid Electrolyte Interphase (SEI) in Lithium Metal Batteries Daewook Kim and Hye Ryung Byon; Korea Advanced Institute of Science and Technology, Korea (the Republic of)

The desired solid electrolyte interphase (SEI) on metallic Li plays a crucial role in preventing continuous electrolyte decomposition and Li dendrite growth. Promising SEI components such as lithium fluoride (LiF), lithium nitride (Li₃N), lithium oxide (Li₂O), and lithium carbonate (Li₂CO₃) exhibit reasonable conductivity and mechanical robustness. In contrast, carbonaceous components are soluble and loosely cover the Li surface, leading to ongoing electrolyte decomposition. Typically, these inorganic and organic species are randomly mixed and form passivating films along with dead Li⁰. Recent advancements have introduced localized high-concentration electrolytes or weakly coordinating solvents to establish inorganic-rich SEI composites. However, there is a lack of comprehensive studies on Li deposition and stripping processes over the SEI for long-term cycling, leaving the question of the cell-degradation process unanswered.

Herein, we demonstrate the formation of two passivating films by controlling 1,2-dimethoxyethane (DME)/1,3-dioxolane (DOL) ratios, while maintaining fixed concentrations of the lithium bis(fluorosulfonyl)imide (LiFSI) and LiNO₃ in Li/Li symmetric cells. The electrolyte solutions with a higher proportion of DME formed porous films after 30 cycles. Remarkably, continuous Li deposition was observed above these porous films, indicating their mixed ionic and electronic conduction properties. A passivating film grew as cycling proceeded, reaching a thickness of ~40 μm after 100 cycles. In contrast, the electrolytes with a higher proportion of DOL formed dense and particulate-shaped films. Interestingly, Li deposition occurred beneath these films, maintaining a thickness of < 15 μm. Thus, it is plausible that the dense film acted as a Li⁺ ion conductor. X-ray photoelectron spectroscopy and titration gas chromatography revealed the presence of predominant dead Li, Li₂O, and Li₂CO₃ in both passivating films. However, the dense film exhibited a higher Li content and a lower carbon atomic ratio (less than 5 atomic %) than the porous film. We attributed the predominant DOL-based electrolyte with weak coordination properties to contribute to forming anion-derived inorganic components. Cell degradation started over 400 h, accompanied by increased carbon contents on the film surface and reduced Li contents. In the presentation, I will discuss the role of electrolytes in the formation of distinct passivating films and their impact on the overall performance of LiFePO₄-based full-cell configurations.

4:45 PM EN10.04/SF02.04.10

Electrodeposition of Conformal Ultrathin Functional Polymer Interphases Joerg G. Werner, Wenlu Wang, Zhaoyi Zheng and Ruiyang Chen; Boston University, United States

Sub-micron interphases and coatings determine surface and interfacial properties of materials, which in turn are often dominant factors in defining their performance in applications and devices. Especially in electrochemistry, interfacial processes including charge and mass transfer depend on the nanometric environment around the electrode surface, which can be tailored with functional interphases. Polymer chemistry offers a large toolbox of molecular functionalities to create coatings and interphases with desired properties, but conformal deposition of uniform ultrathin films on micro- and nanostructured electrodes in batteries, fuel cells, and electrocatalytic systems remains elusive. Hence, new coating methods are required to achieve ultrathin uniform interphases that allow for tuning and tailoring of interfacial electrochemical processes in application-relevant electrodes. Here, we present a strategy to achieve conformal ultrathin coatings of functional polymers on porous and conductive materials with arbitrarily complex architecture through a novel electrodeposition paradigm. Our fabrication method separates the controlled deposition chemistry from the polymer properties through rational molecular design, making it agnostic and applicable to many polymer compositions and functionalities. We demonstrate how deposition and molecular parameters determine the interphase properties, including molecular permeability and thickness from 10s to 100s of nanometers, which in turn enables tunability over interfacial properties under electrochemical conditions such as modulation of the double layer and activation/passivation of molecular species. We envision our process to enable novel electrochemical material, composite, and device architectures with advanced performance characteristics, and serve as tailored model systems in mechanistic studies from electrocatalysis to energy storage.

SESSION EN10.07: Poster Session
Session Chairs: Zhenxing Feng and Hua Zhou
Wednesday Afternoon, November 29, 2023
Hynes, Level 1, Hall A

8:00 PM EN10.07.01

Direct Observation of Lattice-Strain-Induced Oxygen Release in LiCoO₂ and Li₂MnO₃ Bypassing Electrochemical Cycling Dongho Kim¹, Jaemin Hwang², Pilgyu Byeon¹, Jaekwang Lee² and Sung-Yoon Chung¹; ¹Korea Advanced Institute of Science and Technology, Korea (the Republic of); ²Pusan National University, Korea (the Republic of)

As the layered Li transition-metal oxides are a well-known material family for cathodes in Li-ion batteries, intensive studies have been carried out to elucidate the correlation between structural change and capacity/voltage fading. Among the several phenomena, the significant role of oxygen redox in enhancing the capacity of these cathode materials has brought critical issues of oxygen release with structural change and subsequent capacity fading, which should be addressed to improve electrochemical performance. Previous research predominantly employed electrochemically cycled cathodes, resulting in notable findings regarding cation migration, phase transformation, nanoscale voids/cracks formation, and even molecular O₂ trapped within the bulk during oxygen release. Despite recent studies focusing on the influence of microstrain to comprehend the correlation between structural degradation, oxygen loss, and voltage/capacity fading, the simultaneous integration of electronic, electrochemical, and mechanical factors presents a formidable task.

In this study, we examine the local variations of the atomic structure and oxygen content of single-crystalline layered Li transition-metal oxide model system to investigate the role of lattice strain in the oxygen release phenomena. In addition to mechanical surface polishing, the nanoindentation technique is also utilized to apply concentrated load to cathode materials. With intensive acquisition of conventional scanning transmission electron microscopy (STEM) and phase-contrast high-resolution electron microscopy (HREM) images at the atomic scale, we confirm that both types of mechanical strain induce local disordering of Li-M (*M* = Co, Mn) and subsequent amorphization. To establish the generality of this hypothesis, two single-crystalline layered oxide cathode materials, LiCoO₂ and Li₂MnO₃ were employed. Spectroscopic analyses also reveal a significant oxygen deficiency in the structurally altered regions, which is confirmed by the energy-dispersive X-ray spectroscopy (EDS) and electron energy loss spectroscopy (EELS) spectrum. Density functional theory (DFT) calculations further support the energetic preference of oxygen vacancy formation under shear strain compared to other types of strain. The most remarkable finding of this paper is that significant oxygen release can be induced solely by mechanical strain, even without electrochemical cycling. Moreover, this study highlights effective strain relaxation as a promising approach to enhance the structural stability of the anion framework in layered oxide cathodes.

8:00 PM EN10.07.02

Acid- and Gas-Scavenging Electrolyte Additive Improving the Electrochemical Reversibility of Ni-Rich Cathodes in Li-Ion Batteries Chaeun Song¹, Hyeongyu Moon¹, Kyungeun Baek², Chorong Shin³, Kwansoo Lee³, Seok Ju Kang² and Nam-Soon Choi¹; ¹Korea Advanced Institute of Science and Technology, Korea (the Republic of); ²Ulsan National Institute of Science and Technology, Korea (the Republic of); ³LG Energy Solution Ltd., Korea (the Republic of)

In view of their high theoretical capacities, nickel-rich layered oxides are promising cathode materials for high-energy Li-ion batteries. However, the practical applications of these oxides are hindered by transition metal dissolution, microcracking, and gas/reactive compound formation due to the undesired reactions of residual lithium species. Herein, we show that the interfacial degradation of the LiNi_{0.9}Co_{0.05}Mn_{0.05}Al_{0.1}O₂ (NCMA, *x* + *y* + *z* = 0.1) cathode and the graphite (Gr) anode of a representative Li-ion battery by HF can be hindered by supplementing the electrolyte with *tert*-butyldimethylsilyl glycidyl ether (tBS-GE). The silyl ether moiety of tBS-GE scavenges HF and PF₅, thus stabilizing the interfacial layers on both electrodes, while the epoxide moiety reacts with CO₂ released by the reaction between HF and Li₂CO₃ on the NCMA surface to afford cyclic carbonates and thus suppresses battery swelling. NCMA/Gr full cells fabricated by supplementing the baseline electrolyte with 0.1 wt% tBS-GE feature an increased capacity retention of 85.5% and deliver a high discharge capacity of 162.9 mAh/g after 500 cycles at 1 C and 25 °C. Thus, our results demonstrate that the molecular aspect-based design of electrolyte additives can be efficiently used to eliminate reactive species and gas components from Li-ion batteries and increase their performance.

8:00 PM EN10.07.03

Modified Viologen-Assisted Reversible Bromine Capture and Release in Flowless Zinc-Bromine Batteries Seung Hee Han¹, Seoyoung Kim², Hyeon Yong Lim², Sewon Park¹, Kyungjae Shin¹, Seungwon Kim¹, Hee-Tak Kim¹, Sang Kyu Kwak³, Changduk Yang² and Nam-Soon Choi¹; ¹Korea Advanced Institute of Science and Technology, Korea (the Republic of); ²Ulsan National Institute of Science and Technology, Korea (the Republic of); ³Korea University, Korea (the Republic of)

Flowless Zn-Br₂ batteries exhibit considerable potential for energy storage system applications, which require the principal features of high safety, low cost, and long-term cycle stability. However, central challenges such as uncontrolled bromine crossover to anodes and aqueous electrolyte decomposition producing gases lead to a low cycle performance of batteries. Herein, we demonstrate that the introduction of bis(2-trimethylammonio) propyl viologen tetrabromide (PV(Br)₄) onto a graphite felt (GF) electrode (PV(Br)₄/GF) improves the cycle stability of flowless

Zn-Br₂ batteries comprising a 2.5 M aqueous ZnBr₂ electrolyte as the Zn and Br sources. During charging, PV(Br)₄ entraps corrosive and volatile Br₂ formed inside the GF electrode via favorable interactions with the four Br⁻ anions of PV(Br)₄, while polybromide anions are produced via an electrochemical-chemical growth mechanism. Furthermore, the PV(Br)₄ on the GF electrode reversibly releases Br⁻ into the electrolyte through the electrochemical reduction of entrapped polybromide anions during discharging. In addition, the spatially anchoring PV(Br)₄ on a GF electrode suppresses undesired oxidative decomposition of water by minimizing the physical contact with the electrode, thereby mitigating the depletion of the electrolyte during cycling. Suppression of O₂ evolution contributes to mitigation of inhomogeneous plating and vertical growth of Zn metal at the Zn anode. Consequently, a flowless Zn-Br₂ battery with a PV(Br)₄/GF electrode exhibits a high Coulombic efficiency of 95.6% over 400 cycles with a current density of 10 mA cm⁻² and high areal capacity of 24.3 mAh cm⁻².

8:00 PM EN10.07.04

Single-Phase Perovskite BaIrO₃ Nanofibers as an Efficient pH Sensor [Hee AhOh](#), KyungminKim, JuheeYang, YejinKim, SubinChoi, YoungmiLee and Myung HwaKim; Ewha Womans University, Korea (the Republic of)

pH sensors are utilized in various fields such as biomedical applications, food quality evaluation, and the nuclear and gas industries. Metal oxide pH sensors are extensively studied due to their biocompatibility. When a sensor is immersed in the analyte, water is adsorbed onto the surface, and this adsorbed water interacts with the hydronium ions of the analyte through proton hopping. Consequently, pH can be measured by monitoring the potential change on the sensor's surface. Among these sensors, IrO_x is recognized as the most efficient pH sensor due to its ability to be manufactured through electrodeposition, its wide range of stable reactivity, and its suitability for in vivo use. However, IrO_x is prohibitively expensive and has limitations for long-term use due to delamination. To address these issues, extensive researches are being conducted to reduce the unit price and improve sensitivity by alloying Ir with other metals. This study introduces BaIrO₃, a perovskite-structured material in which Ba and Ir are alloyed using electrospinning which is a well-known and facile method for synthesizing metal oxide nanofibers. The single-phase perovskite BaIrO₃ is then characterized using Field Emission Scanning Electron Microscopy (FE-SEM) and X-ray Diffraction (XRD) techniques, and it is compared with IrO₂. Subsequently, the pH sensitivity of BaIrO₃ is demonstrated potentiometrically, in comparison to IrO₂. The sensing performance of BaIrO₃ nanofiber was found to be comparable to IrO₂. It indicates that even with half of the amount of Ir, BaIrO₃ exhibits similar reactivity, making it much more cost-effective than using Ir alone. Additionally, BaIrO₃ demonstrated greater stability in extreme pH conditions. While further research is needed, these findings suggest that BaIrO₃ could be utilized as a pH sensor that is not only more economical but also highly stable. Subsequent studies will explore the commercial potential of BaIrO₃ for practical applications.

8:00 PM EN10.07.05

A Sustainable Cycle to Extract Valuable Metals and Green Hydrogen from Waste Brines [DongqiYang](#)¹, SaowalukSoonthornkit¹, AlvinChang¹, Chih-hungChang¹, KelseyStoerzinger¹, AstridLayton² and ZhenxingFeng¹; ¹Oregon State University, United States; ²Texas A&M University, United States

Driven by the global goal of achieving a net-zero emissions economy, green hydrogen (GH₂) has emerged as a prominent solution for energy storage. However, its widespread adoption is hindered by high production costs. Similarly, the production of critical metals such as lithium has been limited in certain geographical locations, leading to uncertainty in the supply chain and the price increase. Additionally, the production of saline waste presents an environmental challenge, with potential damage amounting to over \$1 million per 100 gallons per minute. To address these issues, a dual solution is proposed: coupling mineral desalination, such as Lithium extraction, with cost-effective GH₂ production through water splitting. This integrated approach establishes a sustainable and circular process that extracts GH₂ and value-added minerals from waste brines (e.g., seawater) while addressing environmental concerns. Our project aims to create value by extracting Lithium and other valuable metals from the waste brines of desalination plants, oil or gas industries, and semiconductor companies. A significant portion of Lithium salt will be extracted and sent to companies for further processing, while the purified water will be produced simultaneously in this process. The purified water will be subjected to water splitting, generating green hydrogen that can be utilized in various sectors, including agriculture, transportation, and the electricity grid. The extraction of additional metals from brines is possible when combining membrane technologies. We will create a circular process for its self-sustainability and energy efficiency. A model that can extract 368 kg lithium per day from seawater via solar thermal energy was already under testing and a prototype of a small 4cm*4cm PEME using a double perovskite OER catalyst was under construction.

8:00 PM EN10.07.07

Interface Controlled Hybrid Carbon Bilayer Anode for Improved Ion Transport and Reaction Stability of Li Ion Battery [Myoung-HoKim](#), MinsubOh, Hye-MiSo, Nigussh. Hatsey and [SeungminHyun](#); Korea Institute of Machinery and Metals, Korea (the Republic of)

Li ion batteries (LIB) with high energy density and high power density are required due to the emerging market of electrical vehicles and other smart products. The dominant anode in current commercial LIBs is graphite owing to its low redox potential, good stability, and low cost. However, its effective capacity is drastically reduced owing to poor reaction rate during fast charge and discharge. To overcome this, graphite is mixed with other carbon materials, such as soft carbon (SC) and hard carbon (HC), as well as non-carbon materials. Carbon-based materials have a low cost and require relatively simple processing, and they are more chemically and mechanically stable than non-carbon materials. They are the primary choices for mixtures with spherical crystalline graphite (SCG). Among carbon-based materials, SC is less expensive than HC and does not require high-temperature heat treatment. Although SC has a lower energy density than SCG, it allows for the rapid movement of ions through multiple edge planes. In this study we fabricated a novel bi-layered and patterned anode electrode to enhance the performance of the electrode by converging the idea of material blending, bi-layer structure, and patterned interface. The bilayer structure, which is different from that of the conventionally blended SCG/SC electrode, aims to stabilize the reaction with the electrolyte at the electrode surface while fully utilizing the bottom section of the electrode. Specifically, in our bilayer structure, the blended SC/SCG material was placed at the bottom and SCG alone was coated onto the top to maintain a stable electrode surface. The electrode pattern interfaces, which are optimized by controlling the pattern size, secure excellent mechanical adhesion and low internal resistance. The electrochemical performance of the bi-layered and patterned electrode was measured and compared with a single SCG electrode and with a conventionally blended SCG/SG electrode. The discharging current density, initial coulombic efficiency, and voltage plateau of these alternative structures were also compared by fabricating half cell. The improved performances of bi-layered and patterned electrode in the half-cell battery achieved high capacity retention of 85.9% after 500 cycles at 1C. In addition, the full cell also attained and high energy density of 178.7.7Wh kg⁻¹ at 10C, which is 2.3 times higher than that of the single-layer SCG electrode

8:00 PM EN10.07.08

Surface Stabilization of Single-Atom Catalyst on Metal Oxide Derived by Metal Hydroxide-Organic Frameworks [SungyoonWoo](#); Korea Advanced Institute of Science and Technology, Korea (the Republic of)

Single-atom catalysts (SACs) have been attracted as promising sensitizers in gas sensors due to their high catalytic activity and efficient atomic utilization. To synthesize SACs-anchored materials, metal-organic frameworks (MOFs) have been widely employed as sacrificial templates owing to their structural flexibility and high surface area. However, in this approach, only carbon-based materials have been allowed as target products since structural deformation between ligand and metal nodes should be sufficiently minimized to stabilize SACs during the transformation. Herein, we propose a novel synthetic route to fabricate metal-oxide-supported SACs by utilizing metal hydroxide-organic frameworks (MHOFs) with noble metal chelated linkers as templates. Highly ordered metal hydroxide layers and numerous π -stacked MHOFs linkers provide stable binding sites for SACs during the complete transformation from MOFs to metal oxide. Thereby, a high concentration of SACs can be stabilized on metal oxide without aggregation and doping of catalysts. The resultant Pt SACs-anchored NiO showed enhanced activity for chemiresistive sensing of H₂S. Furthermore, the high structural diversity of MHOFs would allow the extension of this approach to other catalysts and metal oxides for targeting various analytes.

8:00 PM EN10.07.09

Dendrite-Free Zinc Anode Enabled by Buffer-Like Additive via Strong Cationic Specific Absorption [ZiweiZhao](#); University of Alberta, Canada

Metallic zinc-based anodes suffer low reversibility from dendrite growth, hydrogen evolution reaction, and by-product generation during the Zn²⁺ stripping/plating process. Herein, the novel electrolyte additive (histidine) was introduced into the conventional ZnSO₄ electrolyte. The strong cationic specific absorption between the additive molecule and zinc anode regulated the behavior of Zn²⁺ deposition and inhibited hydrogen evolution reaction. Significantly, the unique buffer-like amphoteric functional groups on histidine can further alleviate by-product generation by stabilizing electrolyte interphase pH value. With such an electrolyte additive, Zn||Zn symmetric cell can run for more than 3000 h under the current density of 2 mA cm⁻². When zinc anodes were coupled with an activated carbon cathode with a mass loading of 8 mg cm⁻², the powering device showed high reversibility. This strategy can give insight into developing zinc anode with high stability.

8:00 PM EN10.07.10

First Principles Modeling of Polarons Formation and Optical Signature on Titanium-Based Oxides for Oxygen Evolution Reaction Photocatalysis [ShayMcBride](#)¹, MichaelPaolino², TanjaCuk² and GeoffroyHautier¹; ¹Dartmouth College, United States; ²University of Colorado Boulder, United States

The exact mechanism and surface coverage present on (photo)-catalysts used for the oxygen evolution reaction (OER) remain elusive. Ultra-fast spectroscopy on model single crystal surfaces has started to clarify these questions but would benefit from more first principles theoretical support to facilitate the interpretation of the spectroscopic signatures. Here, we focus on the first principles modeling of the optical signature of polarons on OER intermediates on titanium-based photocatalysts (e.g., SrTiO₃ and TiO₂). The trapping of photo-generated holes by polarons on adsorbs at the catalyst surface is a key step in the photo-driven OER. We report from first principles on how the polarons formation process and optical signature changes with adsorbates

(OH₂, OH, O) on different surfaces and compare with experimental results when available. Our work is a first step towards a better connection between ultra-fast spectroscopy and first principles computations.

8:00 PM EN10.07.11

Co-Catalyst Optimization for Photoelectrochemical Hydrogen using Tandem III-V Semiconductors Keenan W. Wyatt^{1,2}, Todd G. Deutsch² and Michael F. Toney¹; ¹University of Colorado Boulder, United States; ²National Renewable Energy Laboratory, United States

Direct photoelectrochemical (PEC) solar-to-hydrogen conversion on a III-V surface uses highly efficient photo absorbers for charge generation and separation. This route to hydrogen from sunlight and water can theoretically reach the highest conversion efficiencies. Pt and PtRu nanoparticles reduce the kinetic overpotential for water splitting and are deposited on the III-V surface via DC magnetron sputtering. The amount of co-catalyst balances kinetic improvements for the water splitting with photon absorption. Too many co-catalyst particles will begin to block light and degrade device performance. Here, we have optimized the amount sputtered co-catalyst for device efficiency and durability. Traditional PEC devices use p-type semiconductors as photocathodes however, our device structure adopts a buried pn junction with a wide bandgap window layer to eliminate surface recombination and a capping layer to protect the window layer from dissolution as it is Pourbaix unstable at every pH. We operate in a neutral electrolyte and have achieved over 100 hours of stability at short circuit with greater than 5% solar-to-hydrogen efficiency.

8:00 PM EN10.07.12

In-Situ AFM Observation of Solid Layer Formation at a Superconcentrated Electrolyte/Electrode Interface Akito Kobayashi¹, Taketoshi Minato², Katsuyoshi Ikeda¹ and Kenta Motobayashi¹; ¹Nagoya Institute of Technology, Japan; ²Institute for Molecular Science, National Institutes of Natural Sciences, Japan

1. Introduction

Lithium-ion batteries have high convenience and prevalence but have safety issues due to the volatility and flammability of organic electrolytes. Superconcentrated electrolytes have attracted considerable attention for their low volatility and flammability owing to extremely high electrolyte concentration in which all solvent molecules interact with Li⁺ [1]. For reversible charge/discharge, solid layers on the electrode surfaces play important roles and are known to be produced by reductive decomposition of solvents for dilute electrolytes which limits the choice of available solvents [2]. On the other hand, reversible charge/discharge can be realized with various solvents for superconcentrated electrolytes [1], indicating different origin of the interfacial layers; however, details are still under discussion.

To elucidate the origin and formation process of the interfacial layers, we performed *in-situ* chemical and mechanical analysis of the superconcentrated electrolyte/electrode interface. Here we focus on potential-dependent mechanical properties of the interface analyzed by atomic force microscopy (AFM) combined with electrochemical techniques.

2. Experimental

Lithium bis(trifluoromethanesulfonyl)amide (LiTFSA) was dissolved in acetonitrile at concentration of 4.2 M to obtain the superconcentrated electrolytes. Au thin film deposited on a cleaved mica substrate (Au/mica), Pt mesh, and Pt wire were used as the working, counter and quasi-reference electrodes, respectively. Mechanical properties of the interface were analyzed through force curve measurements with AFM at 1024 points at each potential (4.0 V to 1.0 V vs Li/Li⁺ where negligible Faradaic process was observed). All the measurements were carried out in an Ar atmosphere.

3. Results and Discussion

The Young's modulus of the interface derived from a force curve measurements were ~58 GPa at the potential more positive than 1.5 V, corresponding to that measured for bare Au/mica in air, and decreased to 30 GPa at more negative potentials. On the other hand, simultaneously derived adhesion force shows an increase at 1.5 V, suggesting an increase in local viscosity at the interface, and decreased again at more negative potentials. These results are compared with our model for solid layer formation based on the insights from interface-selective spectroscopy. At 1.5 V, Li⁺ was attracted to the negatively charged electrode, and TFSA anions are also come to the vicinity of the electrode because of Li-TFSA interaction. Then, as a results of oversaturation, a solid salt layer of LiTFSA is deposited on the electrode surface. The change in the Young's modulus of the interface observed in this study is consistent with this model where bare Au surface is covered by solid salt layer at more negative potentials. Increase in local viscosity probably reflects the locally oversaturated solution on the electrode exists at the start of the solid layer deposition. Thus, the quantitative analysis of viscoelasticity using AFM combined with spectroscopic results enabled us to identify the formation process of the solid layer at the superconcentrated electrolyte/electrode interface.

References

1. Y. Yamada et al., *J. Electrochem. Soc.*, 162, A2406 (2015)
2. D. Aurbach et al., *J. Power. Sources*, 68, 91 (1997)

8:00 PM EN10.07.13

Development of High Entropy Oxides for use in Solid Oxide Fuel Cells Hakan Yüce, Berke Piskin, Fatih Piskin and Gulhan Cakmak; Muğla Sıtkı Koçman Üniversitesi, Turkey

In recent years, energy consumption has been increasing with technological and industrial developments. This leads to the search for clean, efficient, economical, and sustainable energy sources. Among these sources, ceramic-based solid oxide fuel cells, which are considered among the most efficient FCs, draw attention. The solid oxide fuel cell is an electrochemical energy conversion device that converts the chemical energy of the fuel directly into electrical energy, attracting great attention due to its high efficiency, fuel flexibility, and environmental friendliness. However, high operating temperatures (800°C–1000 °C) cause the cells to be short-lived. Reducing the operating temperatures to 600°C – 800 °C is one of the effective approaches to solving this problem. La_{0.7}Sr_{0.3}MnO₃ LSM shows outstanding electronic conductivity, excellent electrocatalytic activity, and good stability for oxygen reduction in the temperature range of 800°C -1000 °C, but its electrochemical performance is significantly reduced at reduced operating temperature.

In recent years, high entropy oxides have received increasing attention. High entropy oxides usually contain 5 or more elements with small proportions of minor elements and have high mixing entropy. They can be easily synthesized, produced, and analyzed. ABO₃-type perovskite oxide is of interest for solid oxide fuel cells due to its unique dielectric, ferroelectric, pyroelectric, and catalyst properties.

Many high entropy oxides have been found to improve thermal characteristics, magnetic properties, catalytic activity, and energy storage and conversion performance, but have less application in solid oxide fuel cells. In this study, the potential application of La_{0.5}Sr_{0.5}Co_{0.25}Fe_{0.25}Ni_{0.25}Cu_{0.25}O₃ perovskites in medium temperature solid oxide fuel cells was investigated. LSCFNC powder was synthesized using the sol-gel method. As starting chemicals, nitrates of all of the considered cations were used: La(NO₃)₃ • 6H₂O, Sr(NO₃)₂, Co(NO₃)₂ • 6H₂O, Fe(NO₃)₃ • 9H₂O, Ni(NO₃)₂ • 6H₂O, Cu(NO₃)₂ • 3H₂O.

First, the stoichiometric amount of these nitrates was dissolved in distilled water, then citric acid was added to the solution. The molar ratio of all cations and citric acid in the mixture was 1:2. The solution was heated to 80°C with continuous stirring with the aid of a magnetic stirrer. The resulting gel was dried at 250°C for 2 hours to remove residual organics and nitrates. The dried gel was calcined at 700°C, 900°C, 1100 and 1300°C for 6 hours. The phase analysis of the powders was performed by using X-ray diffraction (Rigaku SmartLab X) using monochromatic Cu K α radiation at 40 kV and 200 mA. The structures are refined using the Maud program to identify their crystal structure.

YSZ Synthesis

Yttria-stabilized zirconia (YSZ) with general formula (ZrO₂)_{1-x}(Y₂O₃)_x and 0.08 ≤ x ≤ 0.1, is the most studied electrolyte for SOFCs. The best conductivity value is obtained for the compound containing 8 mol% of yttrium oxide. In this study, zirconia powders stabilized with 8 mol% yttria were synthesized using the sol-gel process. ZrO(NO₃)₂•xH₂O and Y(NO₃)₃•6H₂O were dissolved in and mixed in ethylene glycol, citric acid, and purified water, respectively. Then, Y(NO₃)₃•6H₂O was added to ZrO(NO₃)₂•xH₂O solution drop by drop and mixed to make YSZ solution.

After mixing, the temperature was raised to 80°C and the pH was adjusted to 3.6 with HNO₃. The resulting suspension was mixed until homogeneous. This white and milky mixture was dried at 120°C and sintered at 1200°C for 2 hours.

The synthesis and analysis in this study are currently ongoing. In this circumstance, we will perform the analyses below:

1. A morphological analysis using a scanning electron microscope (SEM) and chemical analysis employing Energy Dispersive Spectroscopy (EDS) will be conducted to examine the physical characteristics and elemental composition of the samples.
2. Charge/discharge tests will be performed with symmetrical cell coating on YSZ.

8:00 PM EN10.07.14

In Situ X-Ray Absorption Spectroscopy Study of Monodispersed Cobalt Phthalocyanine on Carbon Nanotubes as Electrocatalyst for Carbon Dioxide Reduction to Methanol Mason Lyons¹, Conor Rooney², Hailiang Wang² and Zhenxing Feng¹; ¹Oregon State University, United States; ²Yale University, United States

Carbon dioxide (CO₂) is accumulating in the atmosphere, causing entrapment of thermal energy and more chaotic weather. To sustainably decumulate the atmospheric CO₂ and sequester future emissions, it must be utilized in a circular economy. Upcycling of CO₂ to value added products such as hydrocarbons and alcohols requires the use of catalysts, among which molecular catalysts are the most promising due to their product selectivity and high utilization of metals. Unlike many other catalysts which primarily produce the undesired carbon monoxide (CO)

intermediate, cobalt phthalocyanine (CoPc) non-covalently anchored on carbon nanotubes (CNTs) exhibits preferential formation of methanol (MeOH) from CO₂ due to a modified Co electronic structure. To investigate the electronic and geometric arrangements of CoPc-CNTs during CO₂ reduction, *in-situ* X-ray absorption spectroscopy (XAS) was employed. The pre-edge peaks at 7710 eV related to orbital mixing increased while the 7715 eV peak related to bonding centro-symmetry decreased, when scanning from open circuit voltage to -1.1 V vs Reference Hydrogen Electrode (RHE) indicating a higher density of states in Co 3d_{z²} and axial coordination from CNT as well as C adsorbate, respectively. An absorption edge shift associated with Co reduction to Co(I) was also observed and persisted at MeOH producing conditions, previously only reported for CO producing systems. Fitting of the extended X-ray absorption fine structure (EXAFS) spectra confirmed the CoPc coordination and bond lengths with theoretical calculations as well as the presence of a carbon adsorbate at potentials more negative than -0.5 V vs RHE, enabling further CO reduction to MeOH. The rich information from *in-situ* XAS elucidated the structure-property relationship of this catalyst to explain the superior performance of CoPc dispersed on CNTs for CO₂ upgrade.

8:00 PM EN10.07.15

Designing Bilayer Oxide Chemiresistors Consisting of Rh Nanoparticle Loaded TiO₂ Catalytic Overlayer and SnO₂ Sensing Layer for Highly Selective and Sensitive Detection of Volatile Aromatic Compounds Young Kook Moon; Korea Institute of Materials Science, Korea (the Republic of)

Oxide chemiresistors have mostly been used to detect reactive gases such as ethanol, acetone, formaldehyde, nitric dioxide, and carbon monoxide. However, the selective and sensitive detection of volatile aromatic compounds such as benzene, toluene, and xylene (BTX), which are extremely toxic and harmful, using oxide chemiresistors remains challenging because of the molecular stability of benzene rings containing chemicals. Moreover, the performance of the sensing materials is insufficient to detect trace concentration levels of BTX, which lead to harmful effects on human beings. Herein, novel bilayer sensors consisting of a SnO₂ sensing layer and three different xRh-TiO₂ catalytic overlayers (x = 0.5, 1, and 2 wt%) are designed for the selective detection, discrimination, and analysis of benzene, toluene, and p-xylene. The 2Rh-TiO₂/SnO₂ bilayer sensor shows a high selectivity and response toward trace concentration of benzene over a wide range of sensing temperatures. An array of three Rh-TiO₂/SnO₂ sensors can quantitatively discriminate aromatic compounds. The conversion of gases into more active species by gas reforming or into non-reactive forms by excessive catalytic promotion through the reaction with volatile aromatic compounds and nanosize noble metal catalysts are proposed as the reasons behind the enhancement and suppression of analyte gases, respectively. Analysis using proton transfer reaction-quadrupole mass spectrometer (PTR-QMS) is performed to verify the above proposals.

8:00 PM EN10.07.16

Polysulfide Chemisorption in Multiferroic Doped Sulfur/CNT Composite Cathode for High Energy Densities Li-S Batteries Mohan K. Bhattarai¹, Balram Tripathi^{1,2}, Shweta Shweta¹, Rajesh Katiyar¹, Claudia Zuluaga Gomez¹, Brad Weiner³, Ram Katiyar¹ and Gerardo Morell¹; ¹University of Puerto Rico, Rio Piedras, United States; ²S.S Jain Subodh PG College, India; ³University of Puerto Rico, Río Piedras, United States

Herein, we are reporting the chemisorption effect of multiferroic doped sulfur/SWCNT cathode for Li-S batteries. Bismuth ferrite (BFO) is versatile multiferroic material having high polarization. We modified the composite cathode hydrothermally for the encapsulation of sulfur using SWCNT. The physical, morphological, and elemental analyses of cathode materials were studied using X-ray diffraction, Raman spectroscopy, SEM, EDX, and XRF techniques.

The electrochemical performance has been checked at various C-rates. In various C-rates conditions, we observed good cycle stability ~ 500 mAhg⁻¹ above 100 cycles at C/16 rate, and stable CE ~ 98% due to injection of BFO nanoparticles for chemisorption of polysulfide in the modified cathode. The detailed analysis will be presented during the meeting.

8:00 PM EN10.07.17

Ferroelectric Intercalated CQD/SWCNT/Sulfur Composites for High, Stable and Durable Performances Li-S Batteries Mohan Bhattarai¹, Jose F. Florez Gomez¹, Toshiyuki Sato², Kazunari Imai², Nicholas Krasco², Brad Weiner¹, Ram Katiyar¹, Zhixiang Lu², Paul Czubarow³ and Gerardo Morell¹; ¹University of Puerto Rico, Puerto Rico; ²NAMICS, Japan; ³EM-TECH, United States

In this project, composite cathodes of Sulfur/CQD/SWCNT and Sulfur/CQD/SWCNT/BFO were fabricated adopting a melt diffusion strategy; sintering a high-press pellet. Carbon quantum dots (CQD) and single-wall carbon nanotubes (SWCNT) were synthesized using a pyrolysis process. We tested the electrochemical performances Li-Sulfur (Li-S) battery. X-ray diffraction (XRD), Raman spectroscopy & Scanning electron microscopy (SEM) measurements of prepared composites were executed to study structural and morphological properties. Elemental analysis was carried out using EDS and XRF techniques.

Charge/discharge profiles at various C-rate were carried out and achieved a high discharge capacity of ~1000 mAhg⁻¹ at C-rate of C/16. The exciting results of ferroelectric nanoparticles; bismuth ferrites (BFO) injected cathode composites towards stable electrochemical performances and long-term cycle stability which attributes to that process and design architecture of electrode fabrication in this work. The culminated data could address the challenges of commercialization of Li-S batteries due to polysulfide formation. The detailed results of this study will be presented in the meeting.

8:00 PM EN10.07.18

Relationship between Time-Dependent Schottky Parameters and Doping Concentration during Resistance Relaxation in Pt/Nb:SrTiO₃ Junctions Hayato Nakamura, Yumeng Zheng and Kentaro Kinoshita; Tokyo University of Science, Japan

Resistive switching (RS) devices of Pt/Nb-doped SrTiO₃ (STO) Schottky junctions have been the subject of considerable interest in terms of both non-volatile and volatile resistance relaxation nature. When used as general non-volatile memory, the continuously tunable write/erase characteristics are advantageous for multibit application. In this sense, resistance state retention characteristics are important and improving resistance volatility is crucial. On the other hand, when used in new computational paradigm for the breakthrough of von Neumann-type computing, controllability of resistance relaxation phenomenon (RRP) is critically important. It has been reported that the RRP after RS in Pt/Nb(0.5 wt%):STO can be used to mimic synaptic plasticity for AI applications [1]. The development of nanoscale devices with this neuromorphic function is the basis for hardware implementation of artificial neural networks. For practical application, details of the resistive relaxation phenomenon is required to be understood. Schottky parameters (SPs) such as barrier height (SBH) and depletion width (W_D) can be determined by combining I-V and C-V measurements. SPs had been estimated only for two extreme states, high-resistance states (HRS) and low-resistance states (LRS) [2], and we reported on the time dependence of SPs during the resistance relaxation last year [3]. Since carrier concentration (n) strongly influences SPs, it is important to clarify the time dependence of SPs as a function of n. In this study, we revealed the time dependence of SPs of Nb:STO as a function of Nb doping concentration, for the first time.

Therefore, in this study, we conducted a comparative analysis using devices with varying doping concentrations (0.1, 0.5, 1.0 wt%) to investigate the control of volatility in Pt/Nb:STO junctions. Sequential I-V and C-V measurements were performed on the same junction to extract the time evolution of SPs during the relaxation. Additionally, we investigated the location of electronic traps using the conductance method. "I-V measurement" and "C-V measurement and conductance method" were performed by the two-terminal method using a semiconductor parameter analyzer and impedance analyzer, respectively. Since the resistance value changes logarithmically after RS, the switching unit was employed to quickly switch from the circuit for I-V measurements, which set the junction to HRS or LRS, to the circuit for AC measurements.

We measured the relaxation phenomenon up to 1000 s after RS. After setting the Nb 1.0 wt% device to LRS, SBH was estimated to increase by 0.12 eV from 0.54 to 0.66 eV by I-V measurement and from 0.76 to 0.90 eV by C-V measurement. At the same time, the donor concentration (N_D) decreased from 5.8 × 10¹⁹ to 4.2 × 10¹⁹ cm⁻³, and the W_D increased from 20.8 to 26.6 nm. It was observed that all SPs exhibited a linear dependence on the logarithm of time during the resistance relaxation. Furthermore, these trends of temporal changes in SPs were confirmed to be consistent regardless of doping concentrations.

On the other hand, from the results obtained by the conductance method, it was discerned that traps tend to be positioned at deeper locations as the doping concentration decreases. This observation aligned with the 0.2 eV difference in SBH between 0.5 and 1.0 wt% cases. Furthermore, it was found that their respective time dependencies also shift in a direction indicative of traps becoming deeper with time. This result is consistent with the 0.12 eV increase in SBH. Consequently, it is suggested that this effect is attributed to interface-layer traps that become deeper as SBH increases. Therefore, RRP is suggested to occur due to the re-trapping of electrons by defects after they were de-trapped by applying forward bias to set to LRS.

[1] T. F. Tiotto *et al.*, *Fron. Neurosci.* 14, 627276 (2021).

[2] C. Park *et al.*, *J. Appl. Phys.* 103, 054106 (2008).

[3] H. Nakamura *et al.*, 2022 MRS Fall Meeting, SF06.06, 3784242.

8:00 PM EN10.07.19

Perovskite Oxide SrCo_{0.5}Ir_{0.5}O₃ as an Efferent Anodic Catalyst for Proton Exchange Membrane Water Electrolysis Saowaluk Soonthornkit, Dongqi Yang and Zhenxing Feng; Oregon State University, United States

Hydrogen, as an energy carrier, holds great promise for addressing the increasing demand for clean and sustainable energy sources. Proton exchange membrane water electrolysis (PEMWE) has stood out as a promising technology for hydrogen production through the oxygen evolution reaction (OER). However, the sluggish kinetics of the OER posed a challenge to achieving high energy conversion efficiency and the commercialization of water electrolysis systems. In this study, we investigated the application of the promising SrCo_{0.5}Ir_{0.5}O₃ (SCIO) perovskite as an electrocatalyst in PEMWE and evaluated the electrochemical performance and durability. The SCIO perovskite catalyst is synthesized and characterized to assess its performance as an anode

electrocatalyst for lab-scale PEM water splitting. This study reveals the potential of perovskite as an anode electrocatalyst for PEM water splitting. Further research and optimization are required to explore the full potential of SCIO perovskite catalysts and their scalability for commercial-scale PEMWE systems.

8:00 PM EN10.09.02

Surface Restructuring and Stability of Perovskite Oxide Electrocatalysts Studied by Surface X-Ray Diffraction and Grazing Incidence X-Ray Absorption Spectroscopy Alvin Chang, Rajkumar Jana, Kelsey Stoerzinger and Zhenxing Feng; Oregon State University, United States

In recent years, the trend towards clean and renewable energy sources has led to an increased interest in water-based electrocatalysis (i.e., producing green hydrogen from water as fuels and chemicals) for energy conversion and storage, but a key barrier for efficient water splitting is the high overpotential of the sluggish oxygen evolution reaction (OER).¹⁻³ To overcome this, earth-abundant perovskite oxides of chemical formula AMO_3 with compositional substitutions have shown drastically improved OER activities and are particularly attractive due to their high activity, low cost, high tunability of composition, and controllable electronic structures.^{2,3} For many metal oxides it was discovered that the surface can reconstruct under the oxidative conditions imposed by OER, forming (hydr)oxides prior to the onset of the reaction, and resulting in a different surface termination than that expected from the bulk. This restructuring is varied among materials and plays a critical role in determining the stability and activity of an electrocatalyst material during and after electrochemical cycling. Thus, understanding the drivers of transformation at electrocatalyst interfaces towards the development of materials design is a key research direction in many fields.¹ In this work we examine the impact of electrochemical cycling on surface reconstruction of Lanthanum Nickel Iron Oxide ($LaNi_{1-x}Fe_xO_3$; $x=0-0.375$) and Lanthanum Strontium Nickel Iron Oxide ($La_{0.5}Sr_{0.5}Ni_{1-x}Fe_xO_3$; $x=0-0.625$) epitaxial thin films. Surface X-ray diffraction (SXRD) is employed to investigate the relationship between complex oxide bulk composition and terminal surface OER activity and stability. X-ray reflectivity (XRR) is used to probe the electron density of surface layers and crystal truncation rod (CTR) is used to study atomic reconstruction at the surface. In select compositions, in-situ XRR and CTR illuminate the reconstruction and amorphization process during cycling under OER conditions. Furthermore, grazing incidence X-ray absorption spectroscopy (GIXAS) is performed to capture the evolution of local coordination environments with increasing compositional substitutions and soft XAS is used to explore local electronic structures. Our findings uncover the role of underlying bulk descriptors in modulating OER performance through cycling-induced restructuring and unearth the fundamental driving forces behind surface transformations in perovskite oxide materials which will provide invaluable understanding to aid in the development of electrocatalytic surfaces under OER conditions for effective materials design towards high-performance electrolyzers and batteries for renewable energy storage and conversion.

References

1. Baeumer, C., et al. (2021). *Nature Materials*, 20(5), 674–682.
2. Liu, D., et al. (2021). *Small* (Vol. 17, Issue 43).
3. Song, H. J., et al. (2021). *Advanced Energy Materials* (Vol. 11, Issue 27).

SESSION EN10.05: Probing Electrochemical Interfaces by Advanced Characterizations

Session Chairs: Zhenxing Feng and Shougo Higashi

Wednesday Morning, November 29, 2023

Hynes, Level 3, Room 302

8:00 AM *EN10.02.01

Coupled Ion-Electron Transfer Reactions: Dynamically-Evolving Electrodes William C. Chueh; Stanford University, United States

Most non-metallic electrocatalysts and battery electrodes change composition during operation. This change in the composition directly modifies the kinetics of heterogeneous reactions at the electrode/electrolyte interface, whether it is the lithium intercalation reaction in Li_xFePO_4 , oxygen evolution reaction in CoO_xH_y , or oxygen incorporation in CeO_{2-x} . While it is possible to infer the composition of the electrode via electrochemical measurements, knowing the composition at or near the active site is challenging. In this talk, I will present on the development of operando nanoscale microscopy (specifically, X-ray and scanning probe) and spectroscopy to track the dynamic evolution of electrocatalysts and battery electrodes during operation, and how the composition of the active site modifies reaction kinetics.

8:30 AM *EN10.05.01

Transition Metal K Edge Spectra under OER Working Conditions Frank de Groot; Utrecht University, Netherlands

Transition metal K edges are related to excitations of the transition metal 1s core electron to empty states. The K edges can be divided into the excitonic 3d pre-edges and the main edge that describes the excitations to the empty metal p-states. Using High-Energy-Resolution-Fluorescence-Detection (HERFD), one can sharpen the pre-edge structures revealing their multiplet nature. They can be calculated from the transition from the $3d^N$ ground state to the $1s^1 3d^{N+1}$ final state [1]. The main edge is usually interpreted from the calculation of the transitions to empty states, using DFT theory, for example multiple scattering (FEFF). The 1s XPS spectra of transition metal oxides show multiple peaks, implying that one photon energy gives rise to electrons with multiple kinetic energies. This implies that the 1s XAS spectral shape must be described as the convolution of the empty states with the 1s XPS spectral shape [2]. We measured the iron, cobalt and nickel K edges of thin film perovskite-based electrodes at the solid-liquid interface to probe the oxygen evolution reaction (OER). The 3 nm thin perovskite films are measured in fluorescence yield through the backside of the membrane electrodes.

de Groot et al. *J. Phys. Cond. Matt.* 21, 104207 (2009)

Ghiasi et al., *Phys. Rev. B.* 100, 075146 (2019)

9:00 AM EN10.05.02

In-Situ XAS Studies of Cu-S Complex Catalysts for Electrochemical CO₂ Reduction Reaction Chun-Wai Chang¹, Xinyu Wang², Zhenxing Feng¹ and ZheWeng²; ¹Oregon State University, United States; ²Tianjin University, China

The increasing level of carbon dioxide (CO₂) was known to be one of the reasons causing global warming by greenhouse effects. Therefore, it is crucial to reduce the CO₂ level. The application of restructuring-induced catalytic activity has shown a remarkable effectiveness in reducing carbon dioxide electrochemically to value-added products, such as methane (CH₄), ethylene (C₂H₄), etc. This research examined the *in-situ* electrochemical CO₂ reduction process of a Cu-S centered metal organic complex. The Cu-S complex exhibited a high Faradaic efficiency for CO₂ reduction and selectivity of 52% CO₂-to-CH₄ and 16% CO₂-to-C₂H₄. Combining cyclic voltammetry (CV) and in-situ X-ray absorption spectroscopy (XAS) results, we found the high performance of Cu-S complex catalysts is attributed to the reversibly reconstructed Cu nanoparticles formed during electrochemical reaction, rather than the molecule itself. In addition, the formed Cu nanoparticles, which are identified as the reaction active sites, are allowed to reverse back into the complex structure after the reaction. The relative intensities of interfacial H₂O/*CO obtained from operando infrared spectroscopy suggests that a higher amount of H₂O molecules is accumulated on the surface of catalysts. Moreover, time-of-flight mass spectrometry (TOFMS) demonstrates that the structure of catalyst can be maintained after CO₂ reduction reaction (CO₂RR) at -1.6V vs Ag/AgCl for 10 hr. Our study provides deeper understanding toward designing metal-complex molecular structures for controllably generating active species under reaction conditions to catalyze desirable chemistry.

9:15 AM EN10.05.03

Operando EXAFS to Determine the Mechanism of Bi Dopant at Low Concentration in Rechargeable MnO₂ Cathodes Eric K. Zimmerer, Dominick Guida and Joshua W. Gallaway; Northeastern University, United States

The rechargeable Zn-MnO₂ battery system is one few systems in development capable of meeting the extreme cost requirements needed for global integration of battery storage in the power grid. Doping the MnO₂ cathode with Bi allows it to cycle reversibly between layered Mn oxides δ -MnO₂ and Mn(OH)₂, without detrimental formation of Mn₂O₄. This provides a cathode capacity of 617 mAh/g, which modeling has shown to enable costs below \$50/kWh. However, to achieve commercial adoption, cycling stability must be improved. The mechanism through which the Bi dopant improves rechargeability remains largely unknown, and this must be clarified to rationally improve the system. Our previous work has established that the mechanism involves structurally disordered intermediates, and thus characterization techniques based on short-range order need to be used. This talk will demonstrate rapidly collected, operando extended x-ray absorption fine-structure (EXAFS) data collected on MnO₂ cathodes with and without Bi dopant. Operando techniques are scientifically powerful as they reduce experimental uncertainty resulting from destructive preparation of samples for ex-situ analysis. In addition, rapid EXAFS collection allows for analysis of the kinetics of Mn coordination changes.

The Bi-modified alkaline MnO₂ cathode has been of much interest in literature as only a small amount of Bi₂O₃ additive (Bi:Mn molar ratio 0.075) incorporated by high-energy ball-milling

enables rechargeable behavior. Previously, a disordered δ -MnO₂ phase with no diffraction signal was identified during the first charge of Bi-modified MnO₂ cathodes.¹ In this work, operando X-Ray Absorption Spectroscopy (XAS) was employed to further compare Mn coordination environments in standard and Bi-modified cathodes throughout cycling. Specifically, EXAFS analysis was used to visualize the dynamic first shell (Mn-O) and second shell (Mn-Mn) interatomic distances during the first cycle. Comparison with theoretical EXAFS modeled from CIF allows for “fingerprinting” of the charge/discharge products, while rapid EXAFS collection time allows for identification of intermediates and precise analysis of the potentials and states of charge at which materials deform. In the first discharge an earlier conversion to Mn(OH)₂ is observed in the Bi-modified MnO₂ cathode. Upon charge, deformation of Mn(OH)₂ is observed at the same potential energy in both cases, demonstrating that the thermodynamic stability of Mn(OH)₂ is not affected by Bi-modification. Finally, the formation of Mn₃O₄ is identified in the standard MnO₂ cathode during the conversion reaction that occurs upon charge. These findings suggest that Bi dopant blocks the pathway leading to the formation of Mn₃O₄ through interfacial effects rather than bulk incorporation.

9:30 AM EN10.05.04

Probing the Distribution of Alkali Cations at the Au/Electrolyte Interface with Vibrational Spectroscopy Yu Shen, S. Hsu and Matthias Waegele; Boston College, Department of Chemistry, United States

The electrode/electrolyte contact represents a material interface whose catalytic properties are determined by the interaction of the solid and liquid sides. This interaction gives rise to the electrochemical double layer (EDL), which forms the reaction environment of electrocatalytic processes. Therefore, understanding how the structure of the EDL emerges from the coupling between the solid and liquid phases is central to the development of efficient energy storage and conversion devices. Of particular interest is the distribution of cations of the supporting electrolyte in the EDL; it has been found that cations of the supporting electrolyte influence numerous electrocatalytic processes. However, our understanding of the distribution of these cations at the electrode/electrolyte interface is still poorly understood due to numerous experimental challenges in probing (alkali) metal cations at electrocatalytic interfaces. In this study, we use operando surface-enhanced infrared absorption spectroscopy (SEIRAS) to probe the distribution of alkali cations in the EDL. We demonstrate that the asymmetric CH₃ deformation mode of tetramethylammonium (methyl₄N⁺) is a powerful probe of the distribution of alkali cations in the EDL. The vibrational probe simultaneously characterizes the populations of alkali cations in the inner and outer Helmholtz planes. We found that Cs⁺ has a higher tendency to accumulate in the inner and outer Helmholtz planes of the EDL compared with Li⁺ under CO₂ -to-CO conversion conditions. We rationalize these findings in terms of the hydration free energies of the cations and electrostatic interactions with the electrode. These observations contribute to a deeper understanding of the electrode/electrolyte material interface and how interfacial properties can be tailored for energy storage and conversion.

9:45 AMBREAK

10:15 AM *EN10.05.05

Surface Dynamics under Reaction Conditions Edvin Lundgren; Lund University, Sweden

During recent years, 2D Surface Optical Reflectance (2D-SOR) [1,2] microscopy [3] has emerged as a valuable surface characterization tool for model catalysts or electrodes [4] when performing operando investigations in harsh environments. In particular, 2D-SOR microscopy is favorably used as a complementary technique to other photon-in-photon-out techniques which do not carry direct information on the surface 2D morphology. In this presentation we will present the development and examples of 2D-SOR instrumentation and investigations from single and poly-crystalline samples in combination with Planar Laser Induced Fluorescence (PLIF) [2, 3], High Energy Surface X-Ray Diffraction (HESXRD) [5,6,7] and Polarization Modulation-Infrared Reflection Absorption Spectroscopy (PM-IRRAS) [8] coupled to Mass Spectrometry (MS) and Cyclic Voltammetry (CV) in thermal catalysis, electrocatalysis and corrosion. Illustrating examples of the versatility of the technique will be shown including reflectance changes during the thermal CO oxidation over Pd(100) and Pd polycrystalline surfaces. We show that reflectance changes during the reaction can be associated with the formation of thin Pd oxides by the combination of 2D-SOR and Surface X-Ray Diffraction (SXRD). The combined measurements demonstrate a sensitivity of 2D-SOR to the formation of a 2-3 Å thin Pd oxide film.

During Cyclic Voltammetry (CV) in an acidic electrolyte using a Au(111) surface as an electrode, we show that the differential of the change in 2D-SOR reflectance correlate to various current features in the CV curve. This observation can be used to differentiate current features in the CV curve from a polycrystalline Au surface, demonstrating that the different grains contribute to the current at different potentials due to the different surface orientations.

Finally, we show that 2D-SOR is a cheap and useful technique to investigate the corrosion of applied materials such as duplex stainless steels and Ni alloys.

References

- [1] W. G. Onderwaater et al Rev. Sci. Instrum., 88 (2017) 023704.
- [2] J. Zhou et al, J. Phys. Chem. C 121 (2017) 23511.
- [3] S. Pfaff et al, ACS Appl. Mater. Interfaces 13 (2021) 19530.
- [4] W. Linpe, et al, Rev. Sci. Instrum., 91 (2020) 044101.
- [5] S. Pfaff, et al Rev. Sci. Instrum. 90 (2019) 033703.
- [6] S. Albertin, et al, J. Phys. D: Appl. Phys. 53 (2020) 224001.
- [7] W. Linpé, et al J. Electrochem. Soc. 168 (2021) 096511.
- [8] L. Rämisch et al, Appl. Surf. Sci. 578 (2022) 152048

10:45 AM EN10.05.06

Atomic Probing Surface Restructuring of Epitaxial IrO₂ Thin Films Towards Extreme Oxygen Evolution Reaction Conditions Hua Zhou¹, Maoyu Wang¹, Perrin Godbold², Sreejith Nair³ and Bharat Jalan³; ¹Argonne National Laboratory, United States; ²University of Virginia, United States; ³University of Minnesota Twin Cities, United States

Electrochemical water splitting offers efficient energy conversion potential, but it faces hurdles in the form of slow oxygen evolution reaction (OER) kinetics and harsh acidic conditions. Acidic OER electrocatalysis directly impacts making the proton exchange membrane viable on an industrial scale. IrO₂ is widely recognized as a benchmark electrocatalyst for OER which dictates the overall performance on electrochemical water splitting, in particular in regard with its superior catalytic stability under long term operations. Investigating the interaction between IrO₂ and aqueous solutions is crucial for understanding the intriguing properties and active sites of this catalyst in operation. Recently, many groups have used epitaxial single crystal films as model surfaces to address these fundamental questions. These developments enable for the first time the ability to assess the activities on different facets, which has significantly improved the understanding of the OER and degradation mechanism. However, there is no deep understanding of IrO₂ atomic level surface structure during electrocatalytic reactions due to the extreme challenge of synthesizing epitaxial IrO₂ thin film. Very recently, our collaborators have demonstrated the successful growth of atomically smooth epitaxial IrO₂ films on TiO₂ single crystal substrates by the unique hybrid oxide MBE growth method, which allows us to utilize in-situ surface scattering techniques, including crystal truncation rod (CTR) analysis and X-ray reflectivity (XRR), to examine epitaxial IrO₂ thin films with various crystallographic orientations and their relationship with OER performance. By employing coherent Bragg rod analysis during in-situ electrochemical reactions, the interfacial structure, specifically the presence of oxygenated adsorbed species, can be resolved as a function of potential. Our study endeavors to uncover the surface chemistry of IrO₂, shedding light on its activity, stability, and degradation mechanisms under extreme electrochemical conditions.

In the talk, we will present our investigation of epitaxial IrO₂ films with three distinct crystallographic orientations (e.g., 001, 101, and 110 orientations) using in-situ CTR and XRR techniques, which could comprehend the influence of orientation or facet dependence on surface structuring when exposed to controlled OER conditions. Additionally, we will demonstrate surface modifications induced by different electrolytes (KOH, H₂SO₄, and HClO₄) that lead to diverse catalytic performance and stability. Preliminary synchrotron in-situ grazing incident X-ray absorption spectroscopy (GIXAS) measurements have revealed surface structure modifications, which will be further elucidated using CTR/XRR analysis. By employing energy-modulated measurements at the element-specific Ir L-edge, taking advantage of the resonant anomalous effect, we can gather detailed information on the concentration of Ir cations at each monolayer, providing direct experimental evidence on surface composition. The resulting quantitative structural and compositional information from CTR measurements will be correlated with electrochemical properties, enabling profound mechanistic insights into the activity and stability of IrO₂ toward extreme OER conditions. Our experimental results offer a comprehensive understanding of the surface properties and electrochemical behavior of IrO₂, contributing to the rational design and development of efficient catalysts for the oxygen evolution reaction.

11:00 AM EN10.05.07

In-Situ XAS Studies of the Reconstruction of Nickel Selenide OER Electrocatalysts Felix Hiege¹, Chun-Wai Chang², Alvin Chang², Maoyu Wang³, Seyed Pouya Hosseini Yazdani⁴, Julia Linnemann¹, Zhenxing Feng² and Kristina Tshchulik¹; ¹Ruhr-Universität Bochum, Germany; ²Oregon State University, United States; ³Argonne National Laboratory, United States; ⁴Max Planck Institute for Iron Research, Germany

Nickel selenides are one of the state-of-the-art electrocatalysts for full water splitting and are especially efficient for catalyzing the oxygen evolution part reaction (OER) in alkaline media. They are cost-effective due to the consistency of earth-abundant elements. [1] Under OER conditions, nickel selenides are converted to the real catalytically active species nickel (oxy)hydroxides. [1,2]

In this work, we investigated the OER performance of in-situ generated nickel (oxy)hydroxides from nickel selenides using in-situ X-ray absorption spectroscopy (XAS). Nickel selenides

were electrodeposited on a gold-coated carbon paper and fluorescence XAS spectra were recorded using a home-designed cell [3] at different OER overpotentials. The as-deposited nickel selenides were first transformed via cyclic voltammetry (CV) under OER conditions to a nickel (oxy)hydroxide species. Afterward, the catalyst behavior was monitored during a series of chronoamperometry experiments at different OER overpotentials. In-situ X-ray near-edge spectroscopy (XANES) on the nickel edge was used to extract the oxidation states and electronic structure of the catalyst at each overpotential. [4] Furthermore, information about the local atomic structure of the active nickel centers (e.g., bond distances and coordination numbers) were extracted from the extended X-ray absorption fine structure (EXAFS) regions of the in-situ XAS spectra. [5] Additionally, we gained information about transformational and pseudo-capacitive processes of the catalyst from electrochemical impedance spectroscopy (EIS) [6] and related them to those extracted from XANES and EXAFS analyses. EIS spectra were recorded at each investigated OER overpotential before and after the CA experiments. With this combined approach, we have a better understanding of transformation processes in highly active nickel-selenides-based OER electrocatalysts under working conditions.

Literature:

[1] a) M. G. Walter et al., *Chemical reviews* **2010**, 110, 11, 6446–6473; b) C. Tang et al., *Angewandte Chemie (International ed. in English)* **2015**, 54, 9351, 110, 6446.; [2] S. Anantharaj, S. Noda, *International Journal of Hydrogen Energy* **2020**, 45, 15763.; [3] M. Wang et al., *Nano-Micro Lett.* **2019**, 11, 47; [4] D.C. Koningsberger, R. Prins, Wiley, Book, **1988**; [5] J.J. Rehr et al., *Phys. Chem. Chem. Phys.* **2010**, 12(21), 5503–5513; [6] J. Linnemann et al., *ACS Catal.* **2021**, 11, 5318.

11:15 AM EN10.05.08

Application of Dark Field X-Ray Microscopy in Epitaxial Thin FilmZhanZhang¹, SeohyoungChang² and HuaZhou¹; ¹Argonne National Laboratory, United States; ²Chung-Ang University, Korea (the Republic of)

While the atomic structure is fundamental to the understanding of the static and dynamic properties of functional materials, it was realized that some phenomena emerge because of the collective behavior of a large number of atoms. One of such collection of atoms is domains in the material, whose formation, interaction, and evolution under external stimuli would dictate success or failure of the material. Studying domains would require tools with good spatial-resolution as well as large enough sampling area/volume. A diffraction based, dark field X-ray microscopy method, the X-ray reflection interface microscopy (XRIM), can be very useful in studying domains at the surfaces, buried interfaces, and inside of thin film material systems, with sub-nanometer sensitivity in the surface normal direction and better than 100 nm lateral resolution.

With the penetrating power of hard X-rays, XRIM can emphasize the features at different depth from the top surface by selecting proper scattering conditions, making it an excellent candidate to study the films in-operando in real time. Combined with the reciprocal space mapping (RSM), the spatially resolved structure evolution can be identified. A couple examples will be discussed to demonstrate the capability of XRIM method and its potential applications in a broader field.

11:30 AM *EN10.10.02

Electrochemistry in the Light of In Situ Bragg Coherent Diffraction ImagingClémentAtlan¹, CorentinChatelier¹, KyleOlson¹, ArnaudViola², FrédéricMaillard² and Marie-IngridRichard¹; ¹CEA, France; ²Centre National de la Recherche Scientifique, France

The advent of the new 4th generation x-ray light sources represents an unprecedented opportunity to conduct *in situ* and *operando* studies on the structure of nanoparticles in reactive liquid environments.

Here, we will illustrate how Bragg coherent x-ray imaging [1] allows to image in three dimensions (3D) and at the nanoscale the strain and defect dynamics inside nanoparticles during an electrochemical reaction. First, we successfully imaged the lattice displacement and the strain inside a single Pt nanoparticle in the electrochemical environment. The new Extremely Brilliant Source at the European synchrotron, with unmatched brilliance and coherence, allowed monitoring the changes in structure and morphology of nanocatalysts during *in situ* conditions. Our results reveal that the strain is heterogeneously distributed between highly- and weakly-coordinated surface atoms, and propagates from the surface to the bulk of the Pt nanoparticle under polarisation [2]. Secondly, we will show how *in situ* and *operando* Bragg coherent x-ray imaging allows to study the structural evolution of single Pd nanocrystals at various electrode potentials typical of H adsorption, H absorption, and H₂ evolution. Open questions remain regarding the maximal quantity of H that can be inserted into a Pd nanocrystallite, the mechanism and kinetics of hydride (PdH_x) nucleation (preferential sites for nucleation or homogeneous nucleation at the whole particle surface) and growth (α/β sharp transition or two-phase coexistence).

[1] I. Robinson and R. Harder, *Coherent X-Ray Diffraction Imaging of Strain at the Nanoscale*, Nat. Mater. **8**, 291 (2009).

[2] C. Atlan et al., *Imaging the strain evolution of a platinum nanoparticle under electrochemical control*, Nat. Mater. accepted (2023).

SESSION EN10.06: Ionic Conduction and Dynamics across Interfaces

Session Chairs: Marie-Ingrid Richard and Huiyuan Zhu

Wednesday Afternoon, November 29, 2023

Hynes, Level 3, Room 302

1:30 PM *EN10.06.01

Correlating Charge and Ion Kinetics in Defective Metal Chalcogenide Systems under Solid-State ConfinementEdwinJ. Miller and LuisaL. Whittaker-Brooks; University of Utah, United States

Realizing fast ion kinetics in solid-state materials is of critical interest for the development of technologies including energy storage, neuromorphic computing, water desalination, and selective ion extraction. Development in these areas hinges on one fundamental challenge: facilitating ion transport through a host material. Layered van der Waals (vdW) structures stand out as a promising class of materials for reversible ion insertion, as ion intercalation can occur in the interstitial layers without permanent structural alterations. Of these vdW materials, titanium disulfide (TiS₂) is an attractive candidate for study due to its wide inter-lamellar spacing, continuous single-phase solid-solution lithiation, and material stability. While Li⁺ ion kinetics in TiS₂ itself have been well-characterized, our group seeks to further advance its development by studying the effect of selenium (Se) doping on Li⁺ ion kinetics in TiS₂ nanobelts. To pursue this goal, a synthesis of TiS_{1.8}Se_{0.2} nanobelts has been developed. Since both TiS₂ and TiS_{1.8}Se_{0.2} share the same nanobelt morphology, differences in ion kinetics between the two materials can purely be ascribed to the doping process. Compositional changes to nanostructured materials become important as it becomes increasingly apparent that nanostructured materials improve ion kinetics; thus, by realizing the need for nanoscaling *and* altering composition, we are including factors that will allow this study to remain relevant in the fast-paced development of ion kinetics.

Our synthesis of TiS_{1.8}Se_{0.2} nanobelts predictably increases the interlayer spacing and electronic conductivity of the doped material versus pure TiS₂; both properties are expected to improve ion kinetics in these doped systems. Rate-dependent cyclic voltammetry (CV) and electrochemical impedance spectroscopy (EIS) are both used to investigate the effect of Se doping on ion kinetics in layered TiS₂ nanobelt systems. Analysis via these methods indicates that TiS_{1.8}Se_{0.2} nanobelts do indeed display a charge storage process that is less diffusion-limited than their TiS₂ analogues. Lower electrochemical impedance across faster frequency ranges for TiS_{1.8}Se_{0.2} also indicates a decrease in resistances across the cell for the doped material. This insight into the effects of chalcogen doping on the charge storage process of TiS₂ nanobelts informs future development of layered vdW materials.

2:00 PM EN10.06.02

Engineering Surface Dipoles on Mixed Conducting Oxides with Ultra-Thin Oxide Decoration LayersMatthäusSiebenhofer^{1,2}, AndreasNenning¹, MarkusKubicek¹, PeterBlaha¹ and JürgenFleig¹; ¹TU Wien, Austria; ²Massachusetts Institute of Technology, United States

The surfaces of mixed ionic and electronic conducting (MIEC) materials play a crucial role in a wide range of applications within energy and sensing technologies, including solid oxide cells, catalysts, and oxygen permeation membranes. Consequently, the optimization of these surfaces and interfaces has become a focal point for research efforts aimed at advancing energy materials and devices. Recent studies have unveiled the significant impact that even small amounts of surface modifications, in sub-monolayer quantities, can have on the electrochemical properties of MIEC oxide surfaces. These modifications can alter the work function and the catalytic activity, demonstrating promising potential for targeted material and device optimization [1,2,3].

In this contribution, we conducted a comprehensive investigation into the effects of ultra-thin oxide layers on the electronic and ionic properties of different MIEC oxide surfaces, combining experimental and computational approaches. We employed in-situ impedance spectroscopy during pulsed laser deposition (i-PLD) and near ambient pressure X-ray photoelectron spectroscopy

(NAP-XPS) to assess the impact of surface decorations on the properties of uncontaminated, pristine surfaces of epitaxial thin films of MIEC oxides such as $\text{La}_{0.6}\text{Sr}_{0.4}\text{CoO}_{3-\delta}$ or $\text{Pr}_{0.1}\text{Ce}_{0.9}\text{O}_{2-\delta}$. Building on these results, we employed density functional theory (DFT) to elucidate the atomic scale processes responsible for these effects.

Our study demonstrates that the electrochemical properties of MIEC oxide surfaces can be tailored systematically by decorating them with oxides of different ionic potential or acidity. Basic oxides with low ionic potential, such as SrO , lead to a reduction in the work function, while acidic oxides with high ionic potential, such as SnO_2 , lead to an increase in the work function. As the fundamental underlying mechanism we could identify charge redistribution and dipole formation processes at the heterojunction between host material and decoration. To illustrate the potential of this surface modification method, we explored its impact on the oxygen exchange reaction kinetics on various solid oxide fuel cell (SOFC) cathode materials, highlighting the broad applicability of ultra-thin oxide layers in tuning reaction rates on MIEC surfaces.

[1] Nicollet, Clement, et al. "Acidity of surface-infiltrated binary oxides as a sensitive descriptor of oxygen exchange kinetics in mixed conducting oxides." *Nature Catalysis*, 2020

[2] Siebenhofer, Matthäus, et al. "Electronic and ionic effects of sulphur and other acidic adsorbates on the surface of an SOFC cathode material." *Journal of Materials Chemistry A*, 2023

[3] Riedl, Christoph, et al. "Surface Decorations on Mixed Ionic and Electronic Conductors: Effects on Surface Potential, Defects, and the Oxygen Exchange Kinetics." *ACS Applied Materials & Interfaces*, 2023

2:15 PM EN10.06.03

In-Situ Vibrational Spectroscopic Analysis of Solid Layer Formation at a Superconcentrated Electrolyte/Electrode InterfaceKentaMotobayashi, MasanoriNagasaka and KatsuyoshiIkeda; Nagoya Institute of Technology, Japan

Superconcentrated electrolytes have been attracted considerable attention for battery applications for their useful properties such as low flammability, high oxidation stability, etc. Reversible charge/discharge processes were reported, suggesting the successful formation of appropriate solid electrolyte interphases (SEI) in superconcentrated electrolytes, which prevents co-intercalation of solvent molecules. The origin of SEI was reported to be anion species,¹ while that for conventional dilute electrolytes consist of decomposition products of the organic solvents. This feature leads to wide variety of applicable solvents for superconcentrated electrolytes. However, details of the origin of SEI in superconcentrated electrolytes are still under debate. Therefore, we performed in-situ chemical and mechanical analysis of the superconcentrated electrolyte/electrode interface by using surface-enhanced infrared absorption spectroscopy (SEIRAS) to elucidate the origin and formation process of SEI.

We employed 4.2 M LiTFSA /acetonitrile (AN) solution on an Au electrode as a model system for interface analysis. For a negative-going potential scan, SEIRA spectra showed that both TFSA anions and Li^+ coordinated by AN move toward the electrode when the surface charge of the electrode is switched from positive to negative. It means increased density of the solution on the surface, which can be explained as follows; Li^+ is drawn to the negatively charged electrode, and then AN and TFSA anions directly interacting with Li^+ are drawn to the electrode together. Thus, characteristic coordination structure in superconcentrated electrolytes (anion- Li^+ bond which is absent in dilute concentration) is responsible for such a phenomenon. At more negative potentials (< 2.0 V), the local concentration of AN decreased and instead that of TFSA forming aggregated network structure with Li^+ started to increase. Such a structure appears at oversaturated concentration in the bulk. It means that local ionic concentration increased at this potential range, and finally LiTFSA was deposited on the electrode together with small amount of AN by exceeding the saturation concentration. This model is supported by our in-situ AFM analysis of the viscoelasticity of the deposits.

[1] Y. Yamada, et al., *J. Am. Chem. Soc.*, **136**, 5039, (2014)

2:30 PMBREAK

3:30 PM *EN10.06.04

Uncovering Photoinduced Charge Transfer Dynamics in Thin Films and Devices of the Extremely-Thin Absorbing Material Sb_2S_3 ElizabethR. Young¹, JulienBachmann² and RobertHamburger¹; ¹Lehigh University, United States; ²Friedrich Alexander University Erlangen-Nürnberg, Germany

Widespread energy conversion from sunlight requires solar cells fabricated using stable, sustainable, non-toxic semiconductors based on earth-abundant elements. The continually shrinking feature sizes in nanoelectronics and the drive for inexpensive solar energy conversion systems make fundamental understanding of charge transfer processes at interfaces and within actual devices essential to next generation photo and photoelectrochemical systems. Such devices are comprised of stacks of light-absorbing layers and hole and electron transporting materials forming thin film p-i-n structures. Necessarily, they must operate under both electrochemical applied potentials (in situ) and constant steady-state irradiation (operando) conditions. However, when measuring the photophysics and photo-induced chemical processes of these materials, experiments have thus far primarily been carried under *ex situ* conditions – with either the material alone or in partly formed semi-conductor stacks. More real-life conditions are needed to fully understand how charge carriers are generated, how they flow through materials and how material interfaces mediate charge transfer across multiple layers in these photophysical mechanisms. I will discuss our initial efforts at designing and developing experimental probes and data analysis tools capable of characterizing photochemical reactions under more realistic operating conditions. Using transient absorption spectroscopy (TAS), we *directly* observe carrier diffusion, electron transfer, hole transfer and charge recombination through uniform ultra-thin (< 3 nm) layers of insulating or transport materials deposited by atomic layer deposition (ALD) that are coupled to photoactive materials. Our work focuses on stibnite (Sb_2S_3) as the photo-active layer, which is of particular interest due to the suitable band gap of 1.7 eV and high absorption coefficient ($1.8 \times 10^5 \text{ cm}^{-1}$ at 450 nm). We quantify the dynamics that can be observed in thin transparent films through the use of *in situ* and *operando* TAS. Use of *in situ* and *operando* TAS affords the opportunity to study these materials in operating conditions and gain a quantitative understanding of the electron transfer dynamics at play in thin films.

4:00 PM EN10.06.05

Epitaxial Growth of Defect-Free Yttrium-Doped Barium Zirconate Films by Co-Sputtering for Improved Protonic Conductivity in Protonic Ceramic Fuel CellsJaewonHwang, SuhyukKo and Suk WonCha; Seoul National University, Korea (the Republic of)

Protonic ceramic fuel cells (PCFCs) have emerged as a promising technology for the generation of clean energy for their low operating temperature ($< 600^\circ\text{C}$) and high efficiency. Among the various proton-conducting materials, yttrium-doped barium zirconate (BZY) is commonly utilized as an electrolyte material due to its high bulk conductivity and high chemical stability in H_2O and CO_2 environments. However, owing to the poor sinterability of protonic ceramic materials, conventional slurry-based fabrication methods require high-temperature sintering above 1500°C , resulting in detrimental effects such as the evaporation of constituent elements and the formation of secondary phases. To mitigate these issues, we investigated a novel approach for fabricating yttrium-doped barium zirconate (BZY) through the co-sputtering of BaCO_3 and yttrium-stabilized zirconia (YSZ) targets at a significantly lower temperature than that required for conventional wet processes. We explored various sputtering parameters and substrates to fabricate BZY films with different microstructures and compositions.

The incorporation of carbon from the BaCO_3 target and undesirable carbonate formation in the film was prevented by investigating different sputtering parameters related to the thermodynamics and kinetics of carbonate deposition, including radio frequency (RF) power applied to the targets and oxygen partial pressure. Sputtering parameters that influence the growth kinetics, including deposition rate, deposition pressure, and substrate temperature, were controlled to minimize the structural defects that reduce the film's proton conductivity. Successful deposition of stoichiometric, defect-free epitaxial BZY film on a MgO substrate was confirmed by advanced characterization techniques, including transmission electron microscopy (TEM), depth-profile X-ray photoelectron spectroscopy (DP-XPS), X-ray energy dispersive spectroscopy (EDS), X-ray diffraction (XRD), and field emission scanning electron microscopy (FE-SEM). The epitaxial BZY film had no grain boundaries, thereby minimizing the negative contribution of the grain boundaries to proton conductivity. Consequently, the in-plane proton conductivity of the epitaxial BZY film measured via the AC impedance method was significantly higher than that of wet-processed polycrystalline BZY. Our results demonstrate the potential of co-sputtering as a low-temperature fabrication approach for producing high-quality BZY electrolytes with improved protonic conductivity and reduced thickness for PCFC applications.

This work was supported by the Hyundai Motor Chung Mong-Koo Foundation.

4:15 PM EN10.06.06

Electronic and Ionic Effects of Acidic Adsorbates on Solid Oxide Fuel Cell Cathode SurfacesMatthäusSiebenhofer^{1,2}, AndreasNenning¹, MarkusKubicek¹, JürgenFleig¹ and PeterBlaha¹; ¹TU Wien, Austria; ²Massachusetts Institute of Technology, United States

The oxygen exchange reaction is an important reaction for various applications in energy- and environment-related technologies. For example, during operation of low and intermediate temperature solid oxide fuel cells (SOFCs), the kinetics of this fundamental reaction is often regarded as the bottleneck for the overall performance. To tackle this issue, research and development of new SOFC cathode materials are focused on high intrinsic catalytic activity and high degradation stability. For promising cathode materials, this degradation is commonly attributed to poisoning effects due to different elements in the environment, such as S, Si or Cr, as well as to cation segregation, for example Sr segregation for perovskites like $\text{La}_{0.6}\text{Sr}_{0.4}\text{CoO}_{3-\delta}$ (LSC) and $\text{SrTi}_{0.3}\text{Fe}_{0.7}\text{O}_{3-\delta}$ (STF). In particular, it was recently shown that acidic adsorbates, such as SO_4^{2-} , originating from trace impurities, which are omnipresent in nominally pure measurement atmospheres, readily adsorb on the surfaces of different SOFC cathode materials and cause a sudden and strong degradation [1]. However, the underlying mechanism of these effects has so far been unclear.

In this contribution, the effects of adsorbed SO₂ and other typical solid oxide fuel cell (SOFC) poisons, such as CO₂ and CrO₃, on the electronic and ionic properties of an SrO-terminated (La,Sr)CoO_{3-δ} (LSC) surface and on its oxygen exchange kinetics have been investigated experimentally with near ambient pressure X-ray photoelectron spectroscopy (NAP-XPS), low energy ion scattering (LEIS) and impedance spectroscopy, as well as computationally with density functional theory (DFT) [2]. The investigations revealed that acidic adsorbates induce the formation of a surface dipole and extract charge from the LSC surface. As a result, they strongly increase the surface work function and alter the energetics of molecular oxygen adsorbates and oxygen vacancies in LSC.

Interestingly, the total work function changes as well as the redistributed charge for different acidic adsorbates scale quantitatively with the Smith acidity of the adsorbed oxide, which has recently been identified as a descriptor for the effect of binary oxide infiltrations on the oxygen exchange kinetics of Pr_{0.1}Ce_{0.9}O_{2-δ} [3]. We suspect that the here presented concept of charge redistribution and its impact on the oxygen exchange reaction is highly relevant for multiple phenomena on mixed conducting surfaces and that it is a further step on the way to a detailed understanding of the oxygen exchange reaction on these surfaces.

[1] Riedl, Christoph, et al. "In situ techniques reveal the true capabilities of SOFC cathode materials and their sudden degradation due to omnipresent sulfur trace impurities." *Journal of Materials Chemistry A*, 2022

[2] Siebenhofer, Matthäus, et al. "Electronic and ionic effects of sulphur and other acidic adsorbates on the surface of an SOFC cathode material." *Journal of Materials Chemistry A*, 2023

[3] Nicollet, Clement, et al. "Acidity of surface-infiltrated binary oxides as a sensitive descriptor of oxygen exchange kinetics in mixed conducting oxides." *Nature Catalysis*, 2020

4:30 PM EN10.06.07

Enhanced Electrokinetic Streaming Potential Generation Through Surface Modulation on Microfluidic LiCheng¹, BeiFan² and PrabBandaru¹; ¹University of California, San Diego, United States; ²Michigan State University, United States

The generation of electrical voltages and currents through aqueous electrolyte flow on charged surfaces is of significant interest for insights into surface-fluid interactions as well as for the development of new energy sources. The related phenomena broadly involve the attraction of counterions in the electrolyte to a charged surface forming an electric double layer (EDL). An electrical charge separation in the EDL may be obtained through a pressure difference (DP) applied to the electrolyte along the channel length, and results in a streaming potential (V_s). It has been determined that both the surface electrical potential, *i.e.*, the zeta potential (ζ), as well as the electrolyte slip length (b) contribute to the V_s . We investigate through detailed experiments and subsequent theoretical analysis, the influence of various patterned surfaces, comprised of grooves, meshes, and pillars, in modulating the electrolyte flow for obtaining large V_s . We have obtained fascinating insights into how such *patchy* surfaces may be utilized in further increasing the figure of merit (related to the V_s/DP ratio) to a record 0.1271 mV/Pa - three-fold larger compared to what was previously obtained, through such investigations. We have probed flow on the patterned surfaces with *both* impregnated air and electrolyte immiscible oil, *i.e.*, an air-filled surface (AFS) as well as a liquid filled surfaces (LFS), respectively. We note that crucial to obtaining a large V_s is the optimization of the product of the effective slip length (b_{eff}) and the zeta potential (ζ). While a larger b_{eff} may be obtained from the AFS , the effective ζ is shown to be larger through the use of the LFS . Consequently, the interplay of the ζ and b_{eff} , with respect to the underlying patterned surface was considered in detail. On this basis, we posit a modified *effective* zeta potential which may be of significant use for modeling flow over patterned or non-homogeneous surfaces.

While the use of hydrophobic surfaces was advocated to increase the b , related surfaces are difficult to fabricate and maintain. Much less attention has been paid to methods for enhancing ζ . We then proposed the use of plasma processing of surfaces to modulate *both* the b as well as the ζ over silicon surfaces. Such methodology is shown to result in a larger V_s and a record figure of merit (FOM) of 0.1 mV/Pa – a factor of two larger compared to what was previously obtained. In our work we deployed CF₄ based plasmas for the possibility of creating of a thin fluorocarbon film over the surface, which may increase the hydrophobicity. Moreover, the ions in the plasma would also have a role in increasing the surface charge density and the resultant ζ . It was then determined experimentally that the latter effect predominates. In contrast, Ar-based plasmas are often preferred for their relatively simple constitution (with only Ar⁺ ions and absence of chemical reactions). However, it was seen that such plasmas were more influential in only roughening the surface with minimal influence on the ζ or b . Generally, with the estimated b at less than 2 nm, the contribution to the increased V_s is typically small. Consequently, the major contributor to the record V_s values obtained in our study was due to the enlarged ζ . Our results have major implications in enhancing the understanding of electrokinetic phenomena with respect to the variation of the electrical and mechanical attributes of surfaces. Further development through deploying hydrophobic surfaces *coupled* with plasma processing, and related principles outlined in our work, could yield much larger V_s and pave the way for large scale voltage sources. Our two articles, entitled *The influence of surface texture on the variation of electrokinetic streaming potentials* and *The Modulation of Electrokinetic Streaming Potentials of Silicon-Based Surfaces through Plasma-Based Surface Processing*, were published at **Langmuir**.

4:45 PM EN10.06.08

Finding Infinities in Nanoconfined Geothermal Electrolyte Dielectric Properties, and Implications on Ion Adsorption/Pairing Kevin Leung; Sandia National Laboratories, United States

Infinities should naturally occur in the dielectric responses of ionic solutions relevant to many geochemical, energy storage, and electrochemical applications at strictly zero frequency. Using molecular dynamics simulations cross-referenced with coarse-grained Monte Carlo models, nano-slit pore models at hydrothermal conditions, and treating confined mobile charges as polarization, we demonstrate the far-reaching consequences. The dielectric permittivity profile perpendicular to the slit $\epsilon_{\perp}(z)$ increases, not decreases, with ionic concentration, unlike in the more widely studied megahertz-to-gigahertz frequency range. In confined electrolytes the divergences in $\epsilon_{\perp}(z)$ correctly describe cross-overs between bulk- and surface-dominated dielectric behavior. Nanoconfinement at low ionic concentrations changes monovalent ion energetics by 1-2 kJ/mol, but no dielectric property studied so far is universally correlated to ion adsorption or ion-ion interactions. We caution that infinities signal violation of the “electrical insulator” dielectric assumption.

This work is based on materials support by the U.S. DOE Office of Basic Energy Sciences, Division of Chemical Sciences, Geosciences, and Biosciences under Field Work Proposal Number 21-015452, at Sandia National Laboratories. This article has been authored by an employee of National Technology & Engineering Solutions of Sandia, LLC under Contract No. DE-NA0003525 with the U.S. Department of Energy (DOE). The employee owns all right, title and interest in and to the article and is solely responsible for its contents. The United States Government retains and the publisher, by accepting the article for publication, acknowledges that the United States Government retains a non-exclusive, paid-up, irrevocable, world-wide license to publish or reproduce the published form of this article or allow others to do so, for United States Government purposes. The DOE will provide public access to these results of federally sponsored research in accordance with the DOE Public Access Plan <https://www.energy.gov/downloads/doe-public-access-plan>. This paper describes objective technical results and analysis. Any subjective views or opinions that might be expressed in the paper do not necessarily represent the views of the U.S. Department of Energy or the United States Government.

SESSION EN10.08: Electrochemical Phenomena across Interfaces for Energy Storage II
Session Chairs: Luisa Whittaker-Brooks and Elizabeth Young
Thursday Morning, November 30, 2023
Hynes, Level 3, Room 302

8:45 AM *EN10.08.04

High Voltage Electrolytes Development for High-Ni Cathodes Laisuo Su; The University of Texas at Dallas, United States

Electrolytes connect the two electrodes in a lithium battery by providing Li⁺ transport channels between them. Recently, ether-based localized high-concentration electrolytes have been developed for lithium-metal batteries and show a great success. Despite their high Coulombic efficiency (~99.5%) with lithium metal, the relatively high highest occupied molecular orbital (HOMO) of ethers limits their application at high voltages (> 4.4 V). To tackle this issue, we proposed a new concept of electrolyte, namely localized saturated electrolyte (LSE), based on carbonate solvents that have lower HOMO levels than ether solvents. The formation of a special Li⁺ solvation structure can further reduce the HOMO level of the electrolyte, increasing its oxidative stability. We demonstrate that the developed LSE can stabilize various types of cathodes at high voltages up to 4.85 V. Materials characterizations were further conducted to uncover the mechanisms. And we found that advanced electrolytes help form close-packed homogeneous Li morphology on the anode, generate thin and inorganic-rich interphase layers on both electrodes, and reduce surface degradation into spinel and rock-salt phases of high-Ni cathodes, leading to superior cycling performance of lithium batteries. Our work highlights the importance of developing advanced electrolytes for stabilizing cathodes at high voltages in next-generation batteries.

9:15 AM EN10.08.03

Enhancing the Durability of Silicon Anodes by Anchoring Carbon-Coated Active Particles to Reduced Graphene Oxide Nawraj Sapkota¹, Nancy Chen¹, Morteza Sabet¹, Mihir Parekh¹,

Conventional graphitic anodes are quickly approaching their theoretical capacity limits. Among potential candidates, silicon (Si) is recognized as an alternative active material for next-generation lithium-ion batteries (LIBs) owing to its high theoretical capacity and earth abundance. However, the practical implication of Si in LIBs has been hindered by its low electrical conductivity, large volume change during charge/discharge processes, and rapid capacity fading during cycling. In the current study, we modified the Si/electrolyte interface by developing a low-cost, scalable, dual-carbon protection technique to mitigate these issues. After introducing a thin polydopamine coating on commercial Si nanoparticles (SiNPs, solid spherical, 100-nm dia.), the coated particles were combined with graphene oxide, subjected to sudden freezing and freeze drying, and finally annealed in an environment of argon and hydrogen. Microstructural studies confirmed the formation of micron-sized composite particles in which a thin nitrogen (N)-doped carbon layer was formed on individual SiNPs, denoted here by SiNP@NC, and the SiNP@NC particles were wrapped/anchored by a reduced graphene oxide sheet, denoted by SiNP@NC@rGO. Pristine SiNPs and SiNP@NC@rGO were utilized as active materials to prepare identical anodes with water-based formulation and SiNP mass loading of $\sim 1.0 \text{ mg cm}^{-2}$. Electrochemical impedance spectroscopy showed a reduction in the internal impedance by applying our dual-carbon protection technique. While the SiNP anode exhibited a reversible capacity of 500 mAh g^{-1} at a current density of 2100 mA g^{-1} , the SiNP@NC@rGO anode displayed a reversible capacity of 1400 mAh g^{-1} . After 200 cycles at 420 mA g^{-1} , the capacity retention of SiNP and SiNP@NC@rGO anodes were 54% (from 1300 to 700 mAh g^{-1}) and 72% (from 2370 to 1700 mAh g^{-1}), respectively. The enhanced initial capacity and superior capacity retention of SiNP@NC@rGO indicate the effective protection of SiNPs by applying our synthesis method. The post-mortem characterizations of cycled electrodes also confirmed the effectiveness of our protection strategy.

9:30 AMBREAK

10:00 AM *EN10.08.01

Understanding Lithium-Solid Electrolyte Interfaces from a Single-Atom Level Yifei Mo; University of Maryland, United States

The interfaces between lithium metal and solid electrolytes are critically important for enabling solid-state lithium batteries but remain less understood, especially at the atomistic level. Atomistic modeling allows for the direct observation of atomic dynamics, which can be challenging to assess directly in experiments. In this talk, I will discuss how we have addressed the following key questions using large-scale atomistic modeling:

- 1) What are the atomistic structures of the lithium interfaces with solid electrolytes?
- 2) How do these interface structures affect the atomistic-level mechanisms of Li stripping and plating under electrochemical cycling?
- 3) How do electrochemically deposited Li-ions transition into crystalline Li metal, and what are the corresponding kinetic processes and energy barriers?

By using large-scale atomistic modeling, we aim to offer insights into these questions and propose strategies to address some of the key limitations or failure mechanisms.

10:30 AM EN10.08.05

Challenging the Assumptions of Lithium Dendritic Shorting Safety Consequences in Lithium Cobalt Oxide Lithium-Ion Batteries Bret Schumacher, Jon Sullivan, Lauren Marbella and Dan Steingart; Columbia University, United States

As the steady push for electrification continues, there is a growing need for more energy-dense storage devices. Lithium-ion batteries have dominated the market, in part, because of their high energy density and cycleability. An unfortunate consequence of the increased introduction of lithium-ion batteries in personal mobility devices is the sharp uptick in catastrophic safety events such as fires and explosions, especially in densely populated urban areas. One possible mechanism attributed to these events is attributed to dendritic lithium shorting the electrodes causing thermal runaway.

This work challenges the assumption that lithium dendritic shorting will cause catastrophic events. Using isothermal microcalorimetry (ITMC), differential scanning calorimetry (DSC), and custom-built cell design for a controlled lithium-ion soft short, the total energy release of a soft short is quantified *in operando*. Then, via first-principles calculations and thermal reduction experiments, the total local temperature change during the shorting events were determined to be significantly lower than the temperature needed for thermal reduction and eventual thermal runaway in this system.

10:45 AM EN10.08.07

Electrode Coating and Electrolyte Dependent Intercalation Rates and Activation Energies of Lithium-Ion Battery Electrodes Sravani R. Duggirala¹, Yirui Zhang², Cristina Grosu¹ and Armando Neto¹; ¹Massachusetts Institute of Technology, United States; ²Stanford University, United States

Lithium-ion batteries continue to be an attractive choice for electronics and larger sustainability applications, however the reaction kinetics of various chemistries are poorly understood. The intercalation rates determine the power densities of Li-ion batteries, but the energy barriers and microscopic interfacial processes are not known. Here we understand and model the electrochemical intercalation kinetics of various electrode-electrolyte interfaces through systematically tested experiments on a list of thin oxide electrodes (LiCoO₂, LiNi_xMnyCozO₂ materials) with controlled surface coatings and different organic electrolytes. Through temperature-dependent measurements, we extract the activation energy for moving an ion near the intercalation material interface and intercalating the ion, where LiCoO₂ electrodes shows higher activation energy than LiFePO₄ and LiNi_xMnyCozO₂ electrodes, and LiCoO₂ in LiPF₆-containing electrolytes gives similar action energy compared to LiClO₄-containing electrolytes. The coupled-ion electron transfer theory is used to extract the reorganization energy and reaction rates which can be used to predict materials with optimal kinetic properties for electrified interfaces. These results provide a fundamental understanding of ion intercalation kinetics and new directions for interfacial engineering of Li-ion batteries to boost power density.

11:00 AM EN10.08.08

Binder-Free Silicon-Impregnated Carbon Paper Electrodes Peshal Karki¹, Morteza Sabet¹, Mihir Parekh¹, YiDing², SrikanthPilla¹ and ApparaoM. Rao¹; ¹Clemson University, United States; ²U.S. Army DEVCOM GVSC, United States

During cycling, the Si-based electrodes suffer from a large volume change, which leads to electrode pulverization and an unstable solid-electrolyte interphase (SEI) growth. Silicon-carbon (Si@C) materials have proved meritorious in mitigating the detrimental effects of large volume change of Si-based electrodes during cycling. The use of C-rich biorenewable materials for producing sustainable Si@C materials is continuously expanding. Aligned with this approach, we developed a simple, environmentally friendly technology based on low-cost biorenewable resources to create a Si@C material in which Si particles are uniformly dispersed in a matrix of porous C (i.e., embedded in a carbon cloud). In this method, commercial Si nanoparticles (solid spherical, 100-nm dia.) and lignin were dispersed in epoxidized soybean oil and subjected to oil-in-water emulsion polymerization, followed by low-temperature (500 °C) carbonization. The scanning transmission electron microscopy studies confirmed the production of micron-sized hybrid particles with Si nanoparticles embedded in a porous carbon cloud. Thermogravimetric analysis showed the presence of 40 wt.% Si in the Si@C material, which showed a reversible capacity that was two to three times higher than conventional Si nanoparticles-based electrodes. Although Si@C material increased the specific capacity of the anode, the presence of high-density metallic foil and inactive materials (such as binder and conductive carbon) would adversely affect the electrode-level specific capacity. As a next step we produced binder-free, flexible, and robust anodes by directly incorporating Si@C or pristine Si in separate porous Bucky Papers (BP, 60 gsm) made out of carbon nanotubes. Eliminating the copper foil, binder, and conductive carbon resulted in a 30% weight reduction of the electrode when Si mass loading was set to 1 mg cm^{-2} . These BP-based electrodes impregnated with Si nanoparticles or Si@C active material (and Si loading of 1 mg cm^{-2}) exhibited an initial electrode-level capacity of 320 or 280 mAh g^{-1} , respectively, at a current density of 0.42 mA cm^{-2} . At this Si mass loading level, electrodes with Si nanoparticles cast on copper foil exhibited an initial electrode-level capacity of 155 mAh g^{-1} at a current density of 0.42 mA cm^{-2} . These results indicate that the electrode-level capacity doubled when Si-based active materials were impregnated into porous BP. After 150 cycles, the Si@C-impregnated BP electrode showed 84% capacity retention, while the pristine Si nanoparticle-impregnated BP electrode retained only 54% of its initial capacity. The superior capacity retention of the Si@C electrode is due to the carbon-cloud protection during cycling.

11:15 AM EN10.08.09

Filament Growth and Related Instabilities during Adsorbate Suppressed Electrodeposition Trevor Braun, William Osborn and Thomas Moffat; NIST, United States

Anisotropic electrochemical deposition and whisker growth is shown to be a consequence of operating a bistable active-passive critical system under galvanostatic control. Specifically, whisker growth is examined during galvanostatic Cu electrodeposition from an electrolyte containing suppressor additives. Disruption of the passivating polyether-halide bilayer triggered by metal deposition leads to positive feedback and highly localized deposition. On macroscale electrodes active-passive Turing patterns develop while on micrometer-sized electrodes the bifurcation is frustrated and proceeds as a single active zone reinforced by hemispherical transport fields. Extended electrodeposition leads to symmetry breaking and lateral propagation of a single whisker. An increasing fraction of the applied current supports expansion of the passive sidewall area and eventually results in termination of anisotropic deposition. The dynamic range between passive versus active growth determines the shape and extent of whisker formation. Similar critical behavior may account for reports of whisker growth in certain metal/metal ion battery systems.

11:30 AM EN10.08.10

On the Mechanism of Mossy Zn Deposition Zhibin Yi, Kevin Chan and Qing Chen; Hong Kong University of Science and Technology, Hong Kong

Electrochemical deposition of Zn metal from a zincate electrolyte can lead to a peculiar mossy morphology comprising numerous slim kinky filaments. Like mossy Li in Li metal batteries, mossy Zn is considered detrimental to the stability of rechargeable Zn batteries. Yet unlike Li, the cleaner interface and the easier characterizations of Zn metal offer us an opportunity to dig deeper into the mechanism of mossy deposition. With well-polished and annealed polycrystalline Zn foil as an electrode, we show that the mossy deposition, occurring at a low overpotential, is localized at the surface intersects of defects such as grain boundaries. Through the measurements of cross-sectional microstructures, stress, and surface composition, we gain insights into the formation sites, the driving force, and the kinetics, drawing a close comparison to both mossy Li and metal whiskers.

SESSION EN10.09: Electrocatalysis II—From Single Atoms to Nanocatalysts
Session Chairs: Laisuo Su and Gang Wu
Thursday Afternoon, November 30, 2023
Hynes, Level 3, Room 302

1:45 PM *EN10.09.01

Core/Shell Nanocrystals with Ordered Intermetallic Single-Atom Alloy Layers for Efficient Ammonia Synthesis[Huiyuan Zhu](#); University of Virginia, United States

Single-atom alloys (SAAs) in which precious metal single atoms are embedded into a host metal, are an emerging class of catalytic structural motifs. Benefitting from the free-atom-like *d*-states, SAAs have been proved in theory to have the potential to break the linear scaling relations inherent to metal catalysts and improve the selectivity toward desired products. In this talk, we will discuss our recent efforts in developing a facile, direct solution-phase synthesis of Cu/CuAu core/shell NCs with tunable single-atom alloy (SAA) layers. This synthesis can be extended to other Cu/CuM (M = Pt, Pd) systems, in which M atoms are isolated in the Cu host and can be considered the highest density of single-atom sites. The density of single-sites and the number of atomic layers can be synthetically controlled. The ligand and strain effects of Cu/CuAu for electrocatalytic ammonia synthesis will also be discussed in this talk.

2:15 PM EN10.09.03

Ultrarapid Photothermal Annealing Synthesis of Single-Atom Catalysts-Stabilized Carbon Nano-Onion[Dogyeon Jeon](#), Hamin Shin, Jun-Hwe Cha and Il-Doo Kim; Korea Advanced Institute of Science and Technology, Korea (the Republic of)

Carbon nano-onions (CNO) with nanometer-scale surface curvature and versatile functionalization have attracted attention in energy and environmental applications. However, conventional methods for synthesizing CNOs, and post-synthesis treatments for functionalization are extremely time consuming and energy intensive. Here, we present an ultrarapid photothermal annealing (UPA) platform for millisecond-scale synthesis of CNO and simultaneous surface functionalization with single-atom catalysts (SACs). The UPA platform reaches up to 3030 K within 1.4 ms ($2.2 \times 10^6 \text{ K s}^{-1}$), achieving full conversion from nanodiamond to CNO within 20 ms, significantly improving energy consumption efficiency. Moreover, we demonstrate the universal applicability of SACs functionalization on the outer surface of CNOs with eight different transition metal elements. In a case study, Pt SACs-functionalized CNO exhibit outstanding catalytic performances in hydrogen evolution reaction (HER), with an overpotential of 13.9 mV at 10 mA cm⁻² and a Tafel slope of 52 mV dec⁻¹.

2:30 PM EN10.09.04

Design and Optimized Fabrication of Highly Dispersed Single-Atom Catalysts for Efficient Electrochemical Nitrogen-to-Ammonia Conversion[Nageh K. Allam](#); American University in Cairo, Egypt

Electrochemical nitrogen reduction reaction (NRR) has been established as a promising and sustainable alternative to the Haber–Bosch process, which requires intensive energy to produce ammonia. Unfortunately, NRR is constrained by the high adsorption/activation of the N₂ energy barrier and the competing hydrogen evolution reaction (HER), resulting in low faradic efficiency. Herein, a well-dispersed iron single-atom catalyst was successfully immobilized on nitrogen-doped carbon sheets (Fe_{SAC}-N-C) synthesized from pre-hydrothermally derived Fe-doped carbon quantum dots (CQDs) and used for efficient electrochemical N₂ fixation at ambient conditions. The as-synthesized Fe_{SAC}-N-C catalyst records an onset potential of 0.12 V_{RHE}, exhibiting a considerable faradic efficiency of 23.7% and a NH₃ yield rate of 3.47 μg h⁻¹cm⁻² in aqueous 0.1 M KOH electrolyte at a potential of -0.1 V_{RHE} under continuous N₂ feeding conditions. The control experiment asserts that the produced NH₃ molecules only emerge from the dissolved N₂-gas, reflecting the remarkable stability of the nitrogen–carbon framework during electrolysis. The DFT calculations showed the Fe_{SAC}-N-C catalyst to demonstrate a lower energy barrier during the rate-limiting step of the NRR process, consistent with the observed high activity of the catalyst. This study highlights the exceptional potential of single-atom catalysts for electrochemical NRR and offers a comprehensive understanding of the catalytic mechanisms involved. Ultimately, this work provides a facile synthesis strategy of sheet-like Fe_{SAC}-N-C with high atomic dispersion, creating a new design avenue of Fe_{SAC}-N-C that can vividly have a potential applicability in large spectrum of electrocatalytic applications.

2:45 PM BREAK

3:15 PM EN10.09.05

Computational Modeling of Atomically Dispersed Iron/Nitrogen Carbon Electrocatalysts for Proton Exchange Membrane Fuel Cells[Guofeng Wang](#); University of Pittsburgh, United States

Proton exchange membrane fuel cells (PEMFCs) can convert chemical energy stored in hydrogen fuels to electricity and produce environmentally benign product water. However, the emergent application of PEMFCs is hindered by the requirement of expensive Pt group metals as their electrocatalysts. To advance PEMFC technology, it is of great interest to develop earth-abundant, non-precious metal-based catalysts in replacement of Pt, especially for oxygen reduction reaction (ORR) occurring at the cathode of PEMFCs. In this regard, atomically dispersed iron/nitrogen carbon catalysts (denoted as Fe-N-C) have drawn wide attention since they exhibited promising ORR activity close to Pt and improved stability than macrocyclic molecules. However, the structure of the active sites in these Fe-N-C catalysts and their catalytic mechanism for ORR have not been fully understood. Recent study reveals that there exist two distinct types of FeN₄ sites, namely porphyrin-like S1 FeN₄ sites and S2 FeN₄ sites containing four pyridinic nitrogen, in Fe-N-C catalysts active for ORR. In this study, we have performed density functional theory (DFT) calculations to predict the reaction energetics of ORR on both S1 and S2 FeN₄ sites. We calculated the adsorption energies of all the possible chemical species and the activation energies for O-O bond dissociation reactions involved in ORR on the FeN₄ sites. Our DFT calculations predicted that the ORR could happen through 4e⁻ associative pathway on the FeN₄ sites and with higher kinetic rate on S1 FeN₄ sites than S2 FeN₄ sites. The theoretical results are in agreement with experimental observations. Furthermore, we predicted the Gibbs free energy change for demetallation of Fe from both S1 and S2 FeN₄ sites. We assume that the demetallation of Fe from FeN₄ sites consists of two steps. At the first step, the Fe atom moves away from the N₄-coordinated state to an inactive N₂-coordinated state, with two N atoms passivated by H from the acidic environment. At the second step, the Fe atom with ORR adsorbates will be desorbed from the catalytic surface. Our computational results show that the tendency of demetallation is much higher for S1 FeN₄ sites than that for S2 FeN₄ sites. Consequently, computational modeling provides in-depth atomistic understanding of the chemical nature of active sites in Fe-N-C catalysts for PEMFCs.

3:30 PM EN10.09.06

Mechanistic Insight into Dual-Metal-Site Catalysts for the Oxygen Reduction Reaction[Guoxiang Hu](#); Georgia Institute of Technology, United States

Incorporating a second transition metal to iron–nitrogen–carbon single-atom catalysts (Fe–N–C SACs) to design dual-metal-site catalysts (DMSCs) was demonstrated to offer a promising opportunity to enhance the oxygen reduction reaction (ORR). However, due to the many possible structural configurations and the dynamic structure evolution of metal centers under reaction conditions, it is challenging to clearly elucidate the structure–property relationship at the atomic level. Here, we develop a computational workflow integrating configuration generations, phase diagram constructions, and reaction free energy calculations to provide an insightful understanding of the active site structures and catalytic mechanisms of ORR on DMSCs. Using Fe–Cu as an example, we generate 31 configurations by tiling the hexagonal lattice of graphene and investigate their atomic structures under reaction conditions. We find that for a wide range of electrode potentials, the Fe site is covered by an *OH intermediate, while the Cu site is not covered by any intermediate. With the OH-ligated structures, we identify the configurations which possess higher catalytic activity than Fe–N–C and Pt(111). We demonstrate that ORR on Fe–Cu DMSCs proceeds *via* the associative pathway, and the desorption of *OH is the rate-determining step. Further analysis reveals a linear correlation between the limiting potential and the magnetic moment on Fe and suggests a closer distance between the two metal sites benefits the catalytic activity. These mechanistic insights pave the way for the rational design of efficient platinum group metal-free DMSCs for ORR.

3:45 PM EN10.09.07

Computational Quest for High-Performance Single-Atom Electrocatalysts and Beyond[Zhongfang Chen](#); University of Puerto Rico at Río Piedras, United States

Nanocatalysis holds immense promise for achieving significant breakthroughs in various fields. Among the most remarkable advancements are single-atom catalysts (SACs), renowned for their exceptional activity, selectivity, and stability. However, catalysts beyond SACs, such as dual-atom catalysts (DACs), have the potential to outperform SACs in specific reactions. In this talk, we will unveil our recent computational advancements in designing SACs and DACs based on two-dimensional nanosheets, specifically focusing on their application in crucial electrochemical reactions. Moreover, we will underscore the significance of emerging big-data techniques for the computational screening and design of such catalysts.

4:00 PM EN10.09.08

Calculations of the Voltage Dependent Mechanisms and Rates of HER, ORR and CO₂RR under Electrochemical ConditionsHannes Jónsson; University of Iceland, Iceland

Theoretical calculations of electrocatalytic reactions such as the hydrogen evolution reaction (HER), oxygen reduction reaction (ORR) and CO₂ reduction reaction (CO₂RR) in order to determine the mechanism and estimate the rate of the various elementary steps can be carried out various levels of theory. At the simplest level, only the free energy of intermediates is estimated from calculations in the absence of applied voltage and dielectric solution and corrections later made to account for the electrochemical environment, the so-called thermochemical model. More detailed and reliable calculations involve estimates of the activation energy barrier as well as chemical interaction with solvent molecules, and going beyond the usual generalised gradient approximation for the functional. Such calculations can give significantly different results as has been shown for HER [1], ORR [2] and CO₂RR [3,4]. Still, the effect of the dielectric solution and the role of dissolved ions remains elusive [5] and calls for methodology that can be used for larger systems and longer time scale, such as hybrid simulations where the central part of the system is described using electronic structure theory while the rest is described with a potential energy function that includes polarisation [6]. Several results of ORR and CO₂RR calculations will be presented and the various levels of theory compared in order to identify what is required to obtain reliable results of electrocatalysis by electronic structure calculations and rate theory.

[1] 'Is Doped MoS₂ Basal Plane an Efficient Hydrogen Evolution Catalyst? Calculations of Voltage-Dependent Activation Energy', H. Sander, H. Jónsson and J. Akola, *Physical Chemistry Chemical Physics* 25, 15162 (2023).

[2] 'Assessment of the Accuracy of Density Functionals for Calculating Oxygen Reduction Reaction on Nitrogen Doped Graphene' B. Kirchoff, A. Ivanov, E. Skúlason, D. Fantauzzi, T. Jacob and H. Jónsson, *J. Chem. Theory Comput.* 17, 6405 (2021).

[3] 'Calculations of Product Selectivity in Electrochemical CO₂ Reduction', J. Hussain, H. Jónsson and E. Skúlason, *ACS Catalysis* 8, 5240 (2018).

[4] 'Competing HCOOH and CO Pathways in CO₂ Electroreduction at Copper Electrodes: Calculations of Voltage Dependent Activation Energy', M. Van den Bossche, C. Rose-Petruck, and H. Jónsson, *J. Phys. Chem. C* 125, 13802 (2021).

[5] 'On the Challenge of Obtaining an Accurate Solvation Energy Estimate in Simulations of Electrocatalysis', B. Kirchoff, E. Ö. Jónsson, T. Jacob and H. Jónsson, *Topics in Catalysis*, <https://doi.org/10.1007/s11244-023-01829-0> (2023).

[6] 'Transferable Potential Function for Flexible H₂O Molecules Based on the Single Center Multipole Expansion', E. Ö. Jónsson, S. Rasti, M. Galynska, J. Meyer and H. Jónsson, *J. Chem. Theory Comput.* 18, 7528 (2022).

SESSION EN10.10: Virtual Session
Session Chairs: Ling Chen and Hua Zhou
Tuesday Morning, December 5, 2023
EN10-virtual

8:00 AM *EN10.10.01

A Stable Lithium Metal Anode Interface via a Gelatin-Based SeparatorYaqin Huang; Beijing University of Chemical Technology, China

Lithium metal is regarded as one of the most promising anode materials, owing to its high theoretical specific capacity and ultra-low redox potential. However, non-uniform charge distribution at the electrode-electrolyte interface induces the growth of metallic lithium dendrites, leading to low coulombic efficiency and poor cycle stability of the lithium metal anode. Herein, with gelatin as a structural material, a fibrous separator was prepared and based on which a stable interface was constructed. The gelatin-based separator shows outstanding adhesion to the lithium anode and tolerance to stress. Besides, the evenly distributed charged groups on the gelatin chain facilitated the uniform distribution of charge/current on the electrode-electrolyte interface, which further inhibited the growth of lithium dendrite. The Li|Li cell with gelatin-based separator shows much-enhanced cycling stability with minimal overpotential. These results provide a new strategy for high-performance lithium metal anode and open a new opportunity for the application of lithium metal batteries.

8:30 AM *EN10.10.03

Tuning the Bio/Electrode Interface for Direct BioelectrocatalysisShelley DMinteer; Missouri University of Science and Technology, United States

Oxidoreductase enzymes are of interest in the electrochemical energy conversion field, because they catalyze important transformations (oxygen reduction, hydrogen oxidation, hydrogen evolution, nitrogen reduction, carbon dioxide reduction, etc.) at low overpotentials. However, there are challenges interfacing oxidoreductase enzymes with electrode surfaces to promote electron transfer between the enzyme catalyst and the electrode. Therefore, mediators or mediated electron transfer is typically utilized, but it results in substantial potential inefficiencies. In this paper, we will discuss polymer design for providing an ideal interface for maintaining the activity and preventing denatures of oxidoreductase enzymes at the electrode interface. We will discuss the use of biocompatible linear polyethyleneimine hydrogels and hydrophobic modifications to tailor the interface for direct bioelectrocatalysis.

9:00 AM EN10.10.04

Revealing of Effects of Surface on Nickel-Rich Layered Cathodes Enabling High-Performance Lithium Rechargeable Batteries by Preventing Irreversible Phase TransitionMerryLee¹, Hyung MoJeong¹ and Ji HoonLee²; ¹Sungkyunkwan University, Korea (the Republic of); ²Kyungpook National University, Korea (the Republic of)

With the increasing demand for high-performance lithium (Li) rechargeable batteries, nickel (Ni)-rich layered cathodes which have chemical formula of LiNi_xCo_yMn_zO₂ (x>0.8, x+y+z=1) have attracted attentions; however, the capacity fade is their main obstacle for commercializing high-quality cathodes as a trade-off of high-capacity as increased amount of Ni which has a high redox capability. One of the main reasons is caused by that Ni can easily diffuse into vacant site of Li during charging process because of similar ionic radius each other. This makes Ni-rich layered cathodes undergo irreversible phase transition resulted from Li-moving blockage when they naturally change their phase into hexagonal H1, H2, and H3 sequentially as a level of Li-extraction during charge and H3, H2, and H1 as a level of Li-insertion again during discharge. To suppress this culprit in degradation of Ni-rich layered cathodes, previous studies have tried to solve this issue through a lattice doping with other elements; incompletely, this strategy cannot solve much important surface-triggered Li-moving blockage. Moreover, since the surface is more susceptible to unwanted side reactions by directly contacting with electrolytes, the surface can seriously influence on degradation of Ni-rich layered cathodes. In this study, we created selectively functionable surface on Ni-rich layered cathodes by utilizing unconventional materials, enabling Li-ion to move easily and smoothly in and out through the Ni-rich layered cathode. This newly created surface on the Ni-rich layered cathode was investigated through various analysis for understanding its effects on electrochemical performances when the cathode was composed in Li rechargeable batteries. Notably, in situ synchrotron X-ray diffraction (in situ synchrotron XRD) spectroscopy and ex situ X-ray absorption fine structure (ex situ XAFS) spectroscopy revealed that the new surface induced the Ni-rich layered cathode not to undergo irreversible phase transition during charging and discharging process. In addition, spherical aberration-corrected scanning transmission electron microscopy (Cs-corrected STEM) and further electrochemical analysis techniques also supported the abovementioned findings. With the aid of these affirmative effects, our cathode showed increased capacity of 218.42 mAh g⁻¹, improved rate capability of having capacity of 128.65 mAh g⁻¹ at 5C, and superior cycle performance of having capacity of 177.65 mAh g⁻¹ after 300 cycles with the capacity retention of 91.7%. This remarkable electrochemical performance was obviously contrasting results of that of pristine cathode, which was capacity of 192.51 mAh g⁻¹, rate capability of having 72.21 mAh g⁻¹, and cycle performance having capacity of 127.03 mAh g⁻¹ after 300 cycles with the capacity retention of 77.2%. This research shines on the complex surface-triggered degradation phenomena on Ni-rich layered cathodes with the concrete interpretation, suggesting a solution of creating a new functionable surface.

9:15 AM EN10.10.05

Exploring Catalytic Active Sites in Covalent Organic Frameworks for Oxygen Evolution ReactionsSeyed Pouya Hosseini Yazdeli¹, Andrés Rodríguez-Camargo², Liang Yao², Bettina V.

Enhancing the efficiency and stability of catalysts for the oxygen evolution reaction (OER) is crucial for the advancement of renewable electrochemical energy conversion and storage technologies. The OER process, which plays a pivotal role in emerging technologies like water splitting, suffers from slow kinetics, leading to decreased overall device efficiency [1]. Addressing global energy and environmental challenges necessitates substantial research efforts in improving OER catalysts.

Covalent organic frameworks (COFs) offer great promise as a versatile class of materials with applications spanning multiple domains. These frameworks are constructed from light elements using reversible covalent bonds, resulting in crystalline structures characterized by high surface area, low density, and well-defined channels. Such properties render COFs suitable for a broad range of applications, including gas adsorption, chemical sensing, and heterogeneous catalysis. Furthermore, the facile functionalization of COFs grants them exceptional adaptability and versatility to cater to diverse requirements. [2]

In this study, we assessed the performance of a cobalt-modified bipyridine-based covalent organic framework (Co-TpBpy) as a heterogeneous catalyst for OER under alkaline conditions. To evaluate its effectiveness, we employed techniques such as voltammetry and differential electrochemical mass spectrometry (DEMS). Additionally, operando EC-SEIRAS experiments and post-mortem analyses involving TEM, XPS, XRD, and SEM-EDX were conducted to investigate the structural and compositional changes occurring during OER. The observations revealed the formation of cobalt oxide nanoparticles, serving as active sites for OER catalysis, embedded within the organic framework of Co-TpBpy. This phenomenon led to improved stability and catalytic performance. Our findings suggest that COFs can be utilized as templates to facilitate the uniform distribution of highly active cobalt oxide nanoparticles, thus enhancing the OER process.

References:

- [1] Y. Yan, B. Y. Xia, B. Zhao, X. Wang, J. Mater. Chem. A, 2016, 4, 17587.
[2] J. Guo, D. Jiang, ACS Cent. Sci. 2020, 6

SYMPOSIUM QT01

Excitonic Materials
November 27 - December 7, 2023

Symposium Organizers

Sudeshna Chattopadhyay, Indian Institute of Technology Indore
Shouvik Datta, IISER-Pune
Yara Galvão Gobato,
Ursula Wurstbauer, Technical University of Munich

* Invited Paper

+ JMR Distinguished Invited Speaker

SESSION QT01.01: Excitons in Novel Materials I
Session Chairs: Rudolf Bratschitsch and Dinesh Kabra
Monday Morning, November 27, 2023
Sheraton, Fifth Floor, Public Garden

10:30 AM *QT01.01.01

Engineering Single Photon Emission and Collective Phenomena with Lead Halide Perovskite Nanocrystals Maksym V. Kovalenko^{1,2}; ¹ETH Zurich, Switzerland; ²Empa-Swiss Federal Laboratories for Materials Science and Technology, Switzerland

Colloidal lead halide perovskite (LHP) nanocrystals (NCs), with bright and spectrally narrow photoluminescence (PL) tunable over the entire visible spectral range, are of immense interest as classical and quantum light sources. Attaining pure single-photon emission is key for many quantum technologies, from optical quantum computing to quantum key distribution and quantum imaging. Across single CsPbX₃ NCs (X: Br and I) of different sizes and compositions, we find that increasing quantum confinement is an effective strategy for maximizing single-photon purity due to the suppressed biexciton quantum yield. We achieve 98% single-photon purity (g(2)(0) as low as 2%) from a cavity-free, nonresonantly excited single 6.6 nm CsPbI₃ NCs, showcasing the great potential of CsPbX₃ NCs as room-temperature highly pure single-photon sources for quantum technologies [1]. In another study, we address the linewidth of the single-photon emission from perovskite NCs at room temperature. By using ab-initio molecular dynamics for simulating exciton-surface-phonon interactions in structurally dynamic CsPbBr₃ NCs, followed by single quantum dot optical spectroscopy, we demonstrate that emission line-broadening in these quantum dots is primarily governed by the coupling of excitons to low-energy surface phonons. Mild adjustments of the surface chemical composition allow for attaining much smaller emission linewidths of 35–65 meV (vs. initial values of 70–120 meV), which are on par with the best values known for structurally rigid, colloidal II-VI quantum dots (20–60 meV) [2]. Many-body interactions and exciton complexes are of essential role, for example, for stimulated emission, LED efficiencies, or the single-photon purity in quantum light sources. We studied the size-dependent trion and biexciton binding energies in CsPbX₃ NCs of 9–30 nm in size [3]. NC self-assembly is a versatile platform for materials engineering, particularly for attaining collective phenomena with perovskite NCs, such as superfluorescence [4, 5, 6]. The NC shape anisotropy leads to structures not observed with spherical NCs. We present a broad structural diversity in multicomponent, long-range ordered superlattices (SLs) comprising highly luminescent cubic CsPbBr₃ NCs (and FAPbBr₃ NCs) co-assembled with the spherical, truncated cuboid, and disk-shaped NC building blocks. We also discuss a critical role of the ligand-deformability on the outcome of co-crystallization, or even for the formation of single-component SLs [7]. Perovskite SLs exhibit superfluorescence, characterized, at high excitation density, by emission pulses with ultrafast (22 ps) radiative decay and Burnham-Chiao ringing behavior with a strongly accelerated build-up time.

- [1] Chenglian Zhu et al. *Nano Lett.* 2022, 22, 3751–3760
[2] Gabriele Raino et al. *Nat. Commun.*, 2022, 13, 2587
[3] Chenglian Zhu et al. *Adv. Mater.*, 2023, 2208354
[4] Ihor Cherniukh et al. *Nature*, 2021, 593, 535–542.
[5] Ihor Cherniukh et al. *ACS Nano*, 2021, 15, 10, 16488–16500
[6] Ihor Cherniukh et al. *ACS Nano*, 2022, 16, 5, 7210–7232
[7] Simon Boehme et al. *ACS Nano*, 2023, 17, 3, 2089–2100

11:00 AM QT01.01.02

Excitonic Coupling in Gradually Fluorinated β -Phase Zinc Phthalocyanine [Lisa Schraut-May¹](#), Kilian Strauß¹, Sebastian Hammer², Luca Nils Philipp¹, Krzysztof Radacki¹, Holger Braunschweig¹, Roland Mitric¹ and Jens Pflaum¹; ¹Julius-Maximilians-Universität Würzburg, Germany; ²McGill University, Canada

Understanding how the crystallographic structure influences the excitonic properties of novel organic semiconductors plays a crucial role in fundamental research on this material class as well as for its implementation in devices with new functionalities. The class of phthalocyanines provides a perfect model system to study this relationship, as it offers a wide range of different crystallographic phases and the possibility to reliably steer the structural and electronic parameters by gradual fluorination of the molecular ligands [1]. The shift of the respective frontier orbital energies caused by fluorination while, simultaneously, leaving the optical properties almost unchanged has already led to phthalocyanine based devices with advanced functionalities, such as dual emitting organic LEDs or color-switchable subwavelength plasmonic organic light emitting antennas [2,3].

In this contribution, we report on a comprehensive study on the interplay between molecular spacing and excitonic coupling in β -phase zinc phthalocyanine (ZnPc) single crystals. Temperature dependent photoluminescence measurements were performed on non-fluorinated ZnPc, partially fluorinated F_4 -ZnPc crystals as well as their co-crystals, all of which grown by horizontal vapor deposition. Our measurements yield clear evidence for a change in the emission characteristics as function of temperature and polarization. For neat ZnPc crystals, a narrow emission of only 20 meV linewidth occurs below about 100 K, which we attribute to a superradiant enhancement caused by the coherent excitation of next neighboring molecules within the crystal lattice perpendicular to the crystallographic b-direction. In contrast, this phenomenon is absent in pure F_4 -ZnPc as well as mixed ZnPc: F_4 -ZnPc crystals, where already at small admixtures of the fluorinated counterparts, the intermolecular arrangement and coupling is changed in such a way that a coherently coupled state between adjacent molecules is strongly suppressed or energetically less favorable than a coexisting charge-transfer state as in case of the co-crystals. This hypothesis is corroborated by temperature dependent x-ray structural analyses on the investigated crystals in combination with extended theoretical simulations by means of time-dependent DFT, which highlight the role of the anisotropic coupling of the excitonic states and its spatial variation with temperature.

Our results demonstrate the potential inherent to this material class and the possible strategy of tuning the excitonic properties of molecular semiconductors by controlling their crystalline packing via gradual chemical substitution.

LSM and JP thank the Bavarian Ministry of Science and the Arts for the generous support by the research program Solar Technologies Go Hybrid.

[1] Rödel M. et al., The Role of Molecular Arrangement on the Strongly Coupled Exciton-Plasmon Polariton Dispersion in Metal–Organic Hybrid Structures, *J. Phys. Chem. C* 126 (2022) 4163

[2] Hammer S. et al., Phase transition induced spectral tuning of dual luminescent crystalline zinc-phthalocyanine thin films and OLEDs, *Appl. Phys. Lett.* 115 (2019) 263303

[3] Grimm P. et al., Color-Switchable Subwavelength Organic Light-Emitting Antennas, *Nano Lett.* 22 (2022) 1032

11:15 AM QT01.01.03

Novel Excitons in MoSe₂ from Proximitized Charge Density Waves Jaydeep Joshi^{1,1}, Benedikt Scharf², Igor Mazin^{1,1}, Sergiy Krylyuk³, Daniel J. Campbell^{4,4}, John Pierre Paglione^{4,4,5}, Albert V. Davydov^{3,1,4}, Igor Zutic⁶ and Patrick Vora^{1,1}; ¹George Mason University, United States; ²University of Würzburg, Germany; ³National Institute of Standards and Technology, United States; ⁴University of Maryland, United States; ⁵Canadian Institute for Advanced Research, Canada; ⁶University at Buffalo, The State University of New York, United States

Two-dimensional (2D) materials allow for the construction of heterostructures without the constraint of lattice matching. This increased flexibility enables novel proximity effects through the stacking of strongly correlated 2D materials on 2D semiconductors. Here we use temperature-dependent photoluminescence (PL) microscopy to reveal a new proximity effect where excitons in monolayer MoSe₂ interact with the commensurate charge density wave (CDW) in bulk TiSe₂ [1]. Below the CDW ordering temperature we observe a new PL emission line (H1) on the TiSe₂-MoSe₂ interface that is 30 meV higher in energy than the neutral exciton. This observation is unique compared to other examinations of 2D heterostructures where additional spectral features appear at lower energies compared to the neutral exciton. Power and temperature-dependent measurements show that H1 behaves as a free exciton, therefore excluding interface trapping or localization as an explanation. Most interestingly, we find that H1 disappears above the TiSe₂ CDW ordering temperature, which suggests that the CDW plays a vital role in activating this previously unobserved exciton. We discuss possible CDW-based origins of H1 and outline future opportunities for using proximity effects to engineer novel excitonic states.

[1] J. Joshi, B. Scharf, I. Mazin, S. Krylyuk, D. J. Campbell, J. Paglione, A. Davydov, I. Zutic, and P. M. Vora, *APL Materials*, 10 (2022) 011103.

*Co-authors acknowledge support from the National Science Foundation under DMR-1748650 and DMR-1847782; the US DOE, Office of Science BES under Award No. DE-SC0004890; and the Gordon and Betty Moore Foundation's EPiQS Initiative through Grant No. GBMF9071.

11:30 AM QT01.01.04

Overcoming the Size Cap of InAs Colloidal Quantum Dots for SWIR Applications Tariq Sheikh and Osman M. Bakr; King Abdullah University of Science and Technology, Saudi Arabia

InAs colloidal quantum dots (CQDs) have emerged as potential candidates for infrared (IR) technology due to their exciting optoelectronic and charge transport properties. However, the InAs CQD synthesis demands highly reactive As precursors, which are hard to find commercially. Moreover, these As precursors are highly pyrophoric and also toxic. The lack of suitable As precursors and methodology has also limited the InAs quantum dots to smaller sizes (<7 nm), thus absorbing below 1200 nm only. Here we present a novel synthesis methodology utilizing less reactive and easily available precursors to achieve InAs CQD deep short wave infrared (SWIR) absorbers. The synthesized CQDs easily cross the size barrier, as faced by the InAs CQDs synthesized by conventional methods. The CQDs have a tunable bandgap from 1200 to 1800 nm, thus crossing deep into the SWIR region. These CQDs show high monodispersity and have high crystallinity, which is reflected in their superior excited state properties like sharp excitonic feature and efficient carrier multiplication at low pump fluences and energies. Our synthesis methodology opens up the InAs CQDs for a wide range of SWIR applications.

11:45 AM QT01.01.05

Interfacing Colloidal Er-Doped SiO₂ Thin-Film with p-Type Cz-Silicon For Enhanced Emission via Excitonic-Correlated e-h Recombination Sufian Abedrabbo¹, Anthony T. Fiory² and Nugehalli M. Ravindra³; ¹Khalifa University, United Arab Emirates; ²Integron Solutions LLC., United States; ³New Jersey Institute of Technology, United States

Czochralski silicon (Cz-Si) indirect bandgap has been a hampering point in realizing efficient bandgap emission. In this work, we report our studies of interfacing Cz-Si with Er-doped SiO₂ thin films prepared by sol-gel processes. Colloidal interfacial reactions with Cz-Si surface results in significant improvements in Si bandgap emission. Model fitting the room-temperature photoluminescence spectra indicates correlated carrier recombination interactions; and the random strain fields are theorized to be the cause. Given that the optically active region is estimated to be of similar thickness to the coating thickness, it is anticipated that interfacial excitons are playing a role in shielding the e-h pairs from Auger recombination, thereby increasing the radiative recombination activities. The presentation will include comparative study of the bandgap emission of thermally oxidized Cz-Si with the colloidal prepared spin-coated silica on Cz-Si.

SESSION QT01.02: Excitons in Novel Materials II
Session Chairs: Maksym Kovalenko and Kausik Majumdar
Monday Afternoon, November 27, 2023
Sheraton, Fifth Floor, Public Garden

2:00 PM +QT01.02.01

The Surface Chemistry of Halide Perovskite and Perovskite-Related Nanocrystals [Liberato Manna](#); Istituto Italiano di Tecnologia, Italy

Halide perovskite semiconductors can merge the highly efficient operational principles of conventional inorganic semiconductors with the low temperature solution processability of emerging organic and hybrid materials, offering a promising route towards cheaply generating electricity as well as light. Following a surge of interest in this class of materials, research on halide perovskite nanocrystals (NCs) has gathered momentum in the last years. While most of the emphasis has been put on led-based perovskite NCs, more recently the so-called double perovskite NCs, having chemical formula A²⁺B³⁺X₆, have been identified as possible alternative materials, together with various other metal halide structures and compositions, often doped with different elements. This talk will discuss the synthesis efforts of our group towards all these materials and our current understanding of their surface chemistry. I will highlight how for example halide double perovskite NCs are less surface tolerant than the corresponding Pb-based perovskites. Other topics that will be covered are the role of ligands, exogenous cations and

acid-base equilibria on stabilizing the NCs and controlling their size and shape evolution.

2:30 PM *QT01.02.02

2D Perovskite: Exciting Playground for Exciton and Polaron Studies[Paulina Plochocka](#); CNRS, France

High environmental stability and surprisingly high efficiency of solar cells based on 2D perovskites have renewed interest in these materials. These natural quantum wells consist of planes of metal-halide octahedra, separated by organic spacers. The unique synergy of soft lattice and opto-electronic properties are often invoked to explain superior characteristic of perovskites materials in applications. At the same time such unique synergy creates fascinating playground for exciton physics which challenges our understanding of this elementary excitation. I will demonstrate that even after decade of intense investigation the notation "unique" so often used in case of perovskites deserves serious scrutiny.

First, I will show that in 2D perovskites, the distortion imposed by the organic spacers governs the effective mass of the carriers. As a result, and unlike in any other semiconductor, the effective mass of the carriers in 2D perovskites can be easily tailored. Secondly, I will highlight controversy related to exciton fine structure in different perovskite compounds and demonstrate that the soft lattice can suppress relaxation of excitons to dark state making 2D perovskites great light emitters. I will further demonstrate the optical evidences of the polaron formation.

In the end I will present excitonic properties in novel type heterostructures: a combination of the monolayer transition metal dichalcogenides with layered organic inorganic perovskites, where spin injection into 2D perovskites has been achieved.

3:00 PM BREAK

3:30 PM *QT01.02.03

Origin of Broadband Emission in Low Dimensional Halide Perovskites[Dinesh Kabra](#); Indian Institute of Technology Bombay, India

In this talk, I will provide an overview on research activities of our research group with emphasis on electroluminescent devices. Majority of this work is focused on molecular semiconductor and halide perovskites. In this talk I would show results of single junction OLEDs, single color tandem OLEDs and color tuneable vertically stacked tandem OLEDs. Further, triplet excitons are key aspects to enhance the efficiency and hence understanding triplet excitons is key for the success of these devices. Which will be further extended to halide perovskites too.

Here in this talk, we will discuss the origin of broadband illumination and other emission peaks using temperature-dependent time-resolved photoluminescence (PL) spectra of 2D layered halide perovskites semiconductors. For temperatures below 100 K, (PEA)₂PbBr₄ film gives broad PL emission, stoke shifted by 750 meV from narrow exciton emission peaks, whereas (PEA)₂PbI₄ film does not show any broad emission. Kinetics of various peaks could provide useful insight to propose a consistent energy level scheme associated with a barrier (PEA) and well (PbX₆⁴⁻) material system's electronic states. This broad emission in (PEA)₂PbBr₄ perovskite is observed due to coupling of electronic states in inorganic well part and organic barrier part, which is in contrast to a proposed model based on self-trapped-exciton.

Reference:

G Banappanavar, S Vaidya, U Bothra, LR Hegde, KP Sharma, RH Friend and D. Kabra (2021) "Novel optoelectronic technique for direct tracking of ultrafast triplet excitons in polymeric semiconductor" *Appl. Phys. Rev.* Vol. 8, p-031415 (2021)

Laxmi and D. Kabra "Origin of Contrasting Emission Spectrum of Bromide vs Iodide Layered Perovskite Semiconductors" *J. Phys. Chem. Lett.* Vol. 13, p-2737 (2022)

4:00 PM *QT01.02.04

Excitons in the Layered Magnetic Semiconductor CrSBr[Julian Klein](#); Massachusetts Institute of Technology, United States

Materials with a correlated degree of spin, lattice, and charge are attractive platforms for the study of fundamental magneto-correlated phenomena and for realizing spin-based devices for spintronic applications. Such physics was initially explored in dilute magnetic semiconductors; however, their structural inhomogeneity limited their study. Fortunately, such ideas transfer to the emerging class of layered magnetic semiconductors with chromium sulfide bromide (CrSBr) as a prime candidate for such explorations. Unlike dilute systems, materials such as CrSBr are structurally homogenous and benefit from the well-known property enhancements that layered materials exhibit. In this unique combination, new opportunities arise for the study of a breadth of quasiparticle excitations immersed in magnetic environments.

In my talk, I will elaborate on the rich excitonic physics of CrSBr and showcase new opportunities for its control. I will start by showing that CrSBr is a quasi-1D material. The extreme anisotropy is manifested in its excitons, electronic band structure, a Peierls-like structural instability, and strong exciton-phonon and electron-phonon interactions. [1] As such, CrSBr is best rationalized as a stack of weakly coupled monolayers, each hosting tightly bound quasi-1D excitons. Second, I will discuss the crystal defects in CrSBr and provide a link to their optical emission properties. In particular, I will discuss the correlation of defects with a defect-magnetic order. [2] Lastly, I will demonstrate that CrSBr is an exceptional material for the controlled generation of crystal defects using a focused electron beam. [3] I will provide an outlook and motivate this as a key ingredient for controlling quasiparticle excitations and magneto-correlated phenomena one atom at a time.

References

[1] J. Klein et al., *ACS Nano* **17**, 5316–5328 (2023)

[2] J. Klein et al., *ACS Nano* **17**, 288–299 (2023)

[3] J. Klein et al., *Nat. Comms.* **13**, 5420 (2022)

4:30 PM QT01.02.05

Strongly Bound Excitonic States and the Exciton Dispersion of the Layered Semiconductor BiI₃[Alejandro Molina-Sanchez](#) and [Jorge Cervantes-Villanueva](#); University of Valencia, Spain

BiI₃ is a layered semiconductor with extraordinary excitonic effects in the visible range of the optical spectra, both in the case of bulk and monolayer systems. The excitonic binding energy of bulk is to that of the paradigmatic monolayer MoS₂ and the BiI₃ monolayer has even a higher excitonic binding energy, of more than 0.5 eV. The lower dielectric screening of this trihalide material explains in part these extraordinary exciton binding energy. Therefore, this layered material has a great potential for the design of optoelectronic devices and the realization of the experiments looking for exciton physics. In addition to the interesting excitonic properties, BiI₃ is also remarkable for the strong spin-orbit interaction, which makes the material suitable to have a strong Rashba effect under electric field or to tune the spin properties using magnetic proximity effects.

In this work we present a theoretical study of the electronic and optical properties of BiI₃ bulk and monolayer, within the framework of *ab initio* many-body perturbation theory, using the GW method and the Bethe-Salpeter Equation. We analyze the excitonic states, the influence on the spin properties of magnetic proximity effect and the possibilities to generate Rashba effect on BiI₃ monolayers. We analyze also the exciton dispersion of BiI₃ bulk and monolayer, of importance to understand the exciton dynamics. Our results are very promising for experiments like time-resolved angle-resolved photoemission and other time-resolve spectroscopies.

SESSION QT01.03: Different Varieties of Excitons

Session Chairs: Deep Jariwala and Bumjoon Kim

Tuesday Morning, November 28, 2023

Sheraton, Fifth Floor, Public Garden

8:00 AM *QT01.03.01

High-Lying Excitons and Excitonic Quantum Interference in 2D Semiconductors[Kaiqiang Lin](#); Xiamen University, China

Two-dimensional transition-metal dichalcogenides (TMDCs) show a wealth of exciton physics. We present the existence of a new excitonic species, the high-lying exciton (HX), in transition metal dichalcogenide monolayers with almost twice the band-edge A-exciton energy and with a linewidth as narrow as that of band-edge excitons [1]. The HX is populated through momentum-selective optical excitation in the K-valleys, and is identified experimentally in unconverted photoluminescence (UPL) and theoretically in *ab initio* GW-BSE calculations. These calculations suggest that the HX is comprised of electrons of negative effective mass. The coincidence of such high-lying excitonic species at around twice the energy of band-edge excitons rationalize the efficient exciton-exciton annihilation in TMDC monolayers, and enables the excitonic quantum-interference phenomenon revealed in optical second-harmonic generation (SHG) [2]. We probe the excitonic temporal dynamics in such three-level system through time-resolved sum-frequency generation (SFG) and four-wave mixing (FWM) [3]. High-lying

excitons in bilayer WSe_2 can be largely tuned by twisting [4], electrical gate [5] and Stark effect, which gives control over the excitonic quantum interference and the corresponding optical nonlinearity.

- [1] K. -Q. Lin et al., *Nat. Commun.* **12**, 5500 (2021).
- [2] K. -Q. Lin, S. Bange, & J. M. Lupton, *Nat. Phys.* **15**, 242-246 (2019).
- [3] J. M. Bauer et al., *Nat. Photon.* **16**, 777-783 (2022).
- [4] K. -Q. Lin et al., *Nat. Commun.* **12**, 1553 (2021).
- [5] K. -Q. Lin et al., *Nat. Commun.* **13**, 6980 (2022).

8:30 AM *QT01.03.02

Spatially Indirect Interfacial Excitons in c-Oriented n-ZnO/p-GaN Heterostructures Subhabrata Dhar, Simran Arora and Amandeep Kaur; Indian Institute of Technology Bombay, India

Zinc oxide (ZnO) with wide direct band gap (3.37 eV) and large excitonic binding energy (~60 meV) has significant prospects in UV optoelectronics. However, stable p-type doping is a big challenge. Recently, there are efforts to study ZnO/GaN np-heterojunctions as GaN, which is a semiconductor with a direct band gap of ~3.5 eV, has a very close lattice matching with ZnO and can be controllably doped p-type. A type-II band alignment at the interface is expected between the two materials. Moreover, the difference in spontaneous polarizations along the c-direction for the two semiconductors can result in a net positive polarization charge at the interface. We have shown theoretically that the combination of the two effects can lead to the formation of a unique type of spatially indirect excitons (SIDXs) at the n-ZnO/p-GaN interface. While the electron part of such excitons is quantum confined along c-direction in the ZnO side, the hole part stays at the GaN side of the junction [1]. Like interlayer excitons reported in homo-/hetero-bilayers of transition metal dichalcogenides (TMDs), these excitons have planar nature with finite dipole moment along c-direction. Unlike conventional direct excitons, SIDXs can interact repulsively with each other through dipole-dipole coupling, which should favour Bose-Einstein condensation (BEC). Though, BEC of the excitons has long been anticipated theoretically, its experimental demonstration remains to be elusive until now. Moreover, due to the spatial separation between the electrons and holes, SIDXs are expected to have lifetime much longer than that of the conventional direct excitons. Long lifetime means that the excitons can travel long distances before annihilation. The added advantage of the present system is that the lifetime of the SIDXs is expected to be controlled by applying bias across the junction. Note that the longer is the survival of the excitons, better would be the scope for controlling their spins. Long lifetime of the excitons as well as a control over their lifespan are essential for the development of exciton-based logic circuits, which are supposed to be better than the electronic devices in terms of the energy efficiency and compatibility with the optical communication. Experimentally, we investigate the behaviour of electroluminescence (EL) as a function of applied bias at different temperatures in pn-heterojunctions consisting of c-oriented n-ZnO layer grown epitaxially on p-type c-GaN/sapphire templates [1]. In certain samples, where the acceptor concentration in GaN is more than a critical value, an EL peak is found at low temperatures, which shows a redshift with increasing forward bias. Our study assigns this peak to the SIDXs. Binding energy of these excitons can be significantly increased by changing the applied bias and can even be made larger than that of ZnO bulk. We also study the time dynamics of electroluminescence (EL) in these heterostructures. EL is found to have an extremely slow rise (decay) time (hundreds of milliseconds). Our study finds a strong connection between the existence of SIDXs and the extraordinarily slow EL rise (decay) property observed in these structures. The effect can thus be attributed to the SIDXs, meaning that the lifetime of SIDXs in this system must be hundreds of milliseconds and the lifespan can be controlled by external bias. All these features make ZnO/GaN pn-heterojunction system a unique platform not only to study the physics of excitonic Bose-Einstein condensation but also to investigate the transport of the excitonic spin and its manipulation via electrical means towards the realization of exciton-based electronics.

- [1] S. Arora and S. Dhar, *Appl. Phys. Lett.* **122**, 202102 (2023)

9:00 AM QT01.03.03

Self-Hybridized Polaritons in a Van der Waals Magnet Pratap Chandra Adak, Biswajit Datta, Sichao Yu and Vinod Menon; City College of New York, United States

Recent discoveries of van der Waals magnetic materials have opened up new possibilities for exploring magnetic order in reduced dimensions, with implications for quantum phenomena and device applications. Among these materials, CrSBr stands out as a promising candidate. It consists of monolayer ferromagnets stacked into an A-type antiferromagnetic structure and exhibits a high Neel temperature. Furthermore, as a semiconductor with strong coupling between excitons and magnetism, CrSBr provides a novel platform for optical manipulation of its magnetic properties. With tightly-bound excitons and large oscillator strength, CrSBr supports strong light-matter coupling, leading to the formation of polaritons—hybrid quasi-particles formed by the coupling of excitons and photons. Our study focuses on self-hybridized polaritons in CrSBr samples, capitalizing on the material's high refractive index to achieve strong light confinement without external mirrors. In particular, we utilize polarization-resolved photoluminescence excitation (PLE) spectroscopy to comprehensively investigate the anisotropic properties of CrSBr. Our work sheds light on the light-matter coupling in CrSBr, offering insights for optically accessible device applications in spintronics and magnonics.

9:15 AM QT01.03.04

Exciton Evolution by Singlet Fission and Excimer Formation in DNA-Semiconductor π -Stacks Jeffrey Gorman^{1,2}, Sarah Orsborne¹, Florian Auras¹ and Richard H. Friend¹; ¹University of Cambridge, United Kingdom; ²MIT, United States

Natural photosystems control sub-nm interchromophore coupling using a protein scaffold to evolve remote singlet excitons into free charges at the reaction centre. Nature must achieve this with a limited set of pigments, necessitating exquisite control over excitonic coupling. In contrast, traditional organic electronic devices lack such nano-structural fidelity. This has limited our understanding over electronic coupling and our ability to optimize condensed-phase organic semiconducting aggregates. To address this disparity, we have developed efficient methods for the insertion of perylene diimides or pentacenes into DNA.^{1,2} DNA's selective self-assembly yields size-defined aggregates of pseudo-1D π -stacked organic semiconductors. We selectively program size and exciton delocalization to vary from isolated monomers up to strongly coupled pentamers.

We characterize excited evolution using transient absorption and spin resonance spectroscopy, we track the evolution of singlet excited states in our aggregates, showing results are well-matched to traditional—but disordered—thin films. In size-controlled pentacene monomers, the excited singlet state remains localized to single chromophore. In larger pentacene assembly size we observe singlet exciton evolution <0.5 ps triplet formation by singlet fission. We interrogate this process further using cryogenic transient electron spin resonance spectroscopy. This reveals the initial singlet exciton evolves into a bound triplet pair quintet state (ca. 0.5 μ s), which subsequently converts into free triplets. Interestingly, we can tune the rate of singlet fission through DNA programmed assembly alone. In the case of perylene diimides, we can controllably tune the extent of excimer formation as a function of DNA-directed aggregate size. These results point towards a more rational design process for organic semiconductor clusters, where kinetics can be tuned through extrinsic assembly rather than chemical change to the semiconductor skeleton. Our modular DNA-based assembly offers real opportunities for the rapid development of bespoke semiconductor architectures with molecule-by-molecule precision, a material 'toolbox' for spectroscopic study.

1. *J. Am. Chem. Soc.* 2023, 145, 9, 5431–5438
2. *J. Am. Chem. Soc.* 2022, 144, 1, 368–376

9:30 AM QT01.03.05

Tuning the Interlayer Exciton in Bilayer MoS_2 by Means of Self-Assembled Monolayers Mostafa Shagar¹, Christian Imperiale², Felix Thouin², Luca Razzari¹, Stephane Kena-Cohen² and Emanuele Orgiu¹; ¹Institut National de la Recherche Scientifique, Canada; ²Polytechnique Montréal, Canada

The field of study surrounding Transition Metal Dichalcogenides (TMDs), a class of two dimensional materials that can be exfoliated down to a single molecular level, has recently seen large improvements and advancements. Whether in the study of monolayer properties or in the various possibilities that stacking different materials as heterostructures allow for. However, one interesting application of these materials is in their natural homobilayer form. For example, in molybdenum disulfide (MoS_2), there exists an interlayer exciton that emerges purely out of the interlayer interaction inside the natural homobilayer.

This exciton is unique in its ability to couple to its environment due to having both strong in-plane and out-of-plane dipole sensitivity. This project attempts to leverage this sensitivity by utilizing self-assembled organic monolayers (SAMs), a method of dielectric tuning that is not commonly used for two dimensional materials. Our SAM is formed by a monolayer of non-conjugated organic molecules that spontaneously assemble and are covalently tethered to a substrate. By using SAMs with a strongly dipolar functional group, it is possible to create an effective electric field across the homobilayer to couple with the interlayer exciton without external electrical bias [1] or optical pumping.

In this project, we use SAMs with different dipole moments and sign. These molecules will form SAMs with a very strong electrostatic dipole (of opposite signs) in the vertical direction which makes them prime candidates for exerting a local electric field to the bilayer MoS_2 . We then perform optical reflectance measurements in order to directly probe the interlayer exciton and the effects of the SAM interface.

We observed a clear reorganization of the excitonic properties of the MoS_2 and a splitting of the interlayer exciton due to the existence of an external electric field causing Stark splitting. We also observed a very strong dependence on annealing on our structures, where the existence of randomly oriented water dipoles completely screens the effect of the SAM dipole on the

MoS₂ exciton.

Additionally, Angle Resolved Photoemission Spectroscopy (ARPES) is being performed in order to better understand the band structure of the coupled system. This method of interfacing organic molecules to TMDs is vastly unexplored and opens a new range of possibilities for materials by using two classes of materials both known for their versatility. The development of bias free local tuning of TMDs that is easily deposited on a wide array of substrates offers a unique set of advantages compared to typical coupling methods such as depositing contacts, doping or coupling to optical cavities.

References:

[1] Leisgang, N., Shree, S., Paradisanos, I. *et al.* Giant Stark splitting of an exciton in bilayer MoS₂. *Nat. Nanotechnol.* **15**, 901–907 (2020). <https://doi.org/10.1038/s41565-020-0750-1>

9:45 AMBREAK

SESSION QT01.04: Device Applications of Excitons I
Session Chairs: Subhabrata Dhar and Julian Klein
Tuesday Morning, November 28, 2023
Sheraton, Fifth Floor, Public Garden

10:15 AM *QT01.04.01

Plexcitons for Solar Energy Harvesting and Sensing Devices [Karthik Shankar](#); University of Alberta, Canada

Excitons and plasmons are both quantum quasiparticles. While excitons are bound electron-hole pairs, plasmons are the collective and coherent oscillations of conduction band electrons (typically in coinage metals) at metal-dielectric interfaces. Plasmons can interact with excitons in several different ways. When plasmonic and excitonic resonances are spatially and energetically close to one another, the two resonators can be strongly coupled. The strong coupling regime is characterized by a significant Rabi splitting and anti-crossing behavior. Strongly coupled plexcitonic states are entangled quantum systems which can be used to construct quantum sensors. Plasmons and excitons can also be weakly coupled to each other. The weak coupling regime is characterized by an anomalously broadened absorption band, and is particularly beneficial in light harvesting devices such as solar cells, photodetectors and photocatalysts. The Shankar Lab has found that strongly coupled plexcitons in gold nanoparticle (NP)-cyanine dye J-aggregate assemblies are excellent platforms for chemical sensing due to their sensitivity to the dielectric permittivity. The Rabi splitting (as large as 217 meV) decreases upon exposure to humidity and eventually disappears as the plexcitonic interaction moves into the weak coupling regime. Once humidity is expelled, the large Rabi splitting is recovered. Plasmons and excitons also interact through the PIRET effect, which stands for plasmon-induced resonance energy transfer, a plasmonic analog of the more well-known Förster resonance energy transfer. The PIRET effect involving Au NP plasmons and excitons in n-type carbon nitride NPs enabled a huge improvement in photoelectrochemical water-splitting performance, achieving a photocurrent density as high as 3 mAcm⁻².

10:45 AM *QT01.04.02

Design of Dimer, Oligomer and Polymer Acceptors for Efficient and Stable Organic Solar Cells [Bumjoon Kim](#); Korea Advanced Institute of Science and Technology, Korea (the Republic of)

High power conversion efficiency (PCE) and long-term stability are important requirements for commercialization of organic solar cells (OSCs). Small-molecule acceptors (SMAs) are the core materials that have led to remarkable advances in the PCEs of the OSCs, but the resulting OSCs typically have poor long-term stability. The low glass transition temperatures (T_gs) and rapid diffusion of SMAs owing to their small molecular sizes are recognized as the main causes of the poor stability of OSCs. In addition, the PCEs of OSCs are still lower than those of other types of photovoltaic devices, such as perovskite solar cells, mainly because of their relatively low open-circuit voltage (V_{oc} < 0.90 V). In this talk, we present the development of different dimer and oligomer acceptors for improving the V_{oc} and PCE values of the OSCs. Interestingly, dimer and oligomer acceptors have significantly higher T_g and lower diffusion coefficient compared to SMAs, which enhances the photo and thermal stabilities of the OSCs. Finally, by adding the examples of polymer acceptors, we discuss the impact of molecular sizes of acceptors in the device stabilities and mechanical properties of the OSCs.

11:15 AM QT01.04.03

Photon Upconversion in 'FuLEDs' and in Hybrid Materials [Le Yang](#)^{1,2}; ¹Institute of Materials Research and Engineering A*STAR, Singapore; ²National University of Singapore, Singapore

Triplet-triplet annihilation (TTA) enables photon or energy upconversion in organic semiconductors – advantageous in that they are more efficient in the upconversion process and that they are more versatile in the visible light range. The same photophysical process of TTA, when occurring in a electronic device (an OLED), also known as triplet fusion, is one strategy to enhance the device efficiency from typical fluorescent emitters by utilising all the triplet “dark” states. In this talk, we will explore 2 main ideas, exploring the process of TTA across optically-excited systems (in photon upconversion) to electrically-excited systems (in triplet fusion enhanced ‘FuLEDs’).

Firstly, for functionally viable single-colour organic light emitting diodes (OLEDs), we believe they must satisfy three criteria: efficiency, lifetime, and colour (sharpness, gamut). However, for the significant advances in device efficiencies achieved in new classes of emitters (phosphorescence, TADF), they often tend to have less decent stability and colour sharpness. We have demonstrated strategies in lifting the device efficiencies of simple fluorescent systems.^{1,2} This includes single-dopant triplet fusion enhanced OLEDs (‘FuLEDs’).^{3,4} We also advocate that all (blue) TTA upconverters will make suitable (blue) FuLED emitters. This is because we are utilising the same photophysical process in both cases, and that TTA/triplet fusion is a naturally energetically uphill process, encouraging high-energy emission, and thus suitable for blue or deep-blue higher efficiency OLEDs.⁴ Lastly, we turn our attention to a new system of TTA-upconversion, using perovskite nanocrystals as triplet sensitizer and a nested, Russian-doll-like system of two TTA upconverters, to achieve a much enhanced photon upconversion.⁵ We provide available experimental data to speculate on possible pathway for this enhancement.

1. Yang, L., Kim, V., Lian, Y., Zhao, B. & Di, D. High-Efficiency Dual-Dopant Polymer Light-Emitting Diodes with Ultrafast Inter-fluorophore Energy Transfer. *Joule* **3**, 2381–2389 (2019).
2. Di, D. *et al.* High-performance light-emitting diodes based on carbene-metal-amides. *Science*. **356**, 159–163 (2017). (co-first)
3. Yang, L* *et al.* Photon-upconverters for blue organic light-emitting diodes: a low-cost, sky-blue example. *Nanoscale Adv.* **24**, (2022).
4. Di, D. *et al.* Efficient Triplet Exciton Fusion in Molecularly Doped Polymer Light-Emitting Diodes. *Adv. Mater.* **29**, 1605987 (2017). (co-first)
5. Chua, X.W., Dai, L., Anaya, M.*, Salway, H., Ruggeri, E., Yang, Z., Yang, L.*, Stranks, S.D.*, *Under revision* (2023)

11:30 AM QT01.04.04

Monolayer WS₂ Electro- and Photo-Luminescence Enhancement by TFSI Treatment [Alisson R. Cadore](#); Brazilian Nanotechnology National Laboratory, Brazil

Light-emitting diodes (LEDs) based on layered material heterostructures (LMHs) allow the fabrication of electroluminescent (EL) devices operating in the visible spectral region. A major advantage of LMH-LEDs is that the EL emission wavelength can be tuned among different types of exciton complexes by controlling the charge density. However, these devices display EL quantum efficiency, i.e. the ratio between emitted photons and injected electrons, as low as ~10⁻⁴%, and mostly limited by non-radiative recombination processes. Here, we perform EL measurements before and after chemical treatment with superacid TFSI in monolayer WS₂-LEDs. We demonstrate that TFSI boosts the EL emission by over one order of magnitude at room temperature. Moreover, we observe that non-treated devices emit light mainly from negatively charged trions, while the emission in TFSI-treated WS₂-LEDs predominantly involves radiative recombination of neutral excitons due to activation of trapping states in WS₂. We then present simulations and modeling of the integration of LMH-LEDs with photonic cavities for further enhancement of EQE. Our observation opens up a route to obtain more efficient and tunable LMH-LEDs, unveiling additional insights into the nature and behavior of the exciton dynamics in the TFSI-treated TMDs, as well as suggesting an additional route towards LEDs engineering [1].

[1] AR Cadore *et al.*, 2023 arXiv:2305.01791 <div class="acfiifjajpekbnhjmppnmjgmhjkild" id="acfiifjajpekbnhjmppnmjgmhjkild"></div>

11:45 AM QT01.04.05

Improving Substrate Mode Outcoupling in Organic Light-Emitting Diodes on Polymer Microlens Arrays with Very Low Index Coatings [Claire Ameson](#), Hafiz K. Sherif and Stephen R. Forrest; University of Michigan, United States

Increasing the external efficiency of organic light-emitting diodes (OLEDs) is essential for their use in mobile applications where battery life is a primary concern. However, an even more

important consideration is that the device reliability is improved by increased efficiency since the OLED can be operated at a lower current to achieve the same luminance. [1] OLEDs can achieve internal quantum efficiencies as high as 100% using either phosphorescence or thermally activated delayed fluorescence. However, the external quantum efficiency for OLEDs are ~20% for devices grown on planar glass substrates, as the majority of photons are coupled to modes trapped within the device. Approximately 40% of photons, which are emitted from a high-index organic layer with $n \sim 1.7$, are trapped within waveguide and substrate modes because of the index mismatch between these layers and the substrate, and between the substrate and air. In this work, we introduce a new, and potentially inexpensive and scalable method to improve on existing sub-electrode and conventional external microlens-array (MLA) technology by incorporating optically designed low-index coatings on the MLA surface to achieve substrate mode outcoupling efficiencies approaching 100%. We use porous thin organic and ALD films on the polymer MLA surface to achieve refractive indexes from 1.5, matching with glass, to 1.1, approaching that of air. Through the use of outcoupling structures external to the organic device stack, and that exhibit no wavelength or viewing angle dependence, we demonstrate a method for achieving high-efficiency devices with applicability in both lighting and display applications.

[1] S. R. Forrest, *Organic Electronics: Foundations to Applications*. Oxford, UK: Oxford University Press, 2020.

SESSION QT01.05: Device Applications of Excitons II
Session Chairs: Sudeshna Chattopadhyay and Karthik Shankar
Tuesday Afternoon, November 28, 2023
Sheraton, Fifth Floor, Public Garden

2:00 PM *QT01.05.01

Photophysics, Photochemistry and Optoelectronics of Singlet Fission Organic Materials in Microcavities Winston Goldthwaite¹, Roshell Lamug¹, Gina Mayonado¹, Ahasan Ullah¹, John Anthony², L.-J. Cheng¹, Matt W. Graham¹ and Oksana Ostroverkhova¹; ¹Oregon State University, United States; ²University of Kentucky, United States

Organic (opto)electronic materials have been explored in a variety of applications in electronics and photonics, driven by several advantages over traditional silicon technology, including low-cost processing, fabrication of large-area flexible devices, and widely tunable properties through functionalization of the molecules. Over the past decade, remarkable progress has been achieved in understanding physical mechanisms and in developing guidelines for the material design, which boosted the performance of organic devices that rely on photophysics and/or (photo)conductive properties of the material. However, further improvements in device performance are desirable, and challenges related to (photo)stability of organic devices need addressing.

One of the major thrusts in developing new organic materials and device concepts has focused on materials exhibiting singlet fission, which is a carrier multiplication process which would enable, for example, enhanced power conversion efficiencies in solar cells. Nevertheless, fundamental questions pertaining to exciton physics in singlet fission materials, and how it can be manipulated by material design and external parameters, remain. Some of these questions will be addressed in this presentation using model singlet fission organic materials, exemplified by functionalized acene and anthradithiophene derivatives, and combinations of photoluminescence and ultrafast transient absorption time-resolved spectroscopy carried out in a broad range of temperatures and magnetic fields.

Strong exciton-photon coupling that occurs when an organic film is placed in a microcavity, enabling formation of a light-matter hybrid state (polariton), presents a largely unexplored opportunity to control photophysics, photochemistry, and optoelectronic characteristics in existing singlet fission materials and devices by using polaritons. This presentation will summarize our efforts aiming to understand and tune exciton polariton properties in model singlet fission organic materials, towards exploiting these properties in optoelectronic devices and controlling photochemical reactions directly relevant to photostability.

2:30 PM QT01.05.02

Exciton-Polaritons Facilitated Photogeneration and Charge Carrier Transport in Solution-Processed Cavity Organic Solar Cells Yahui Tang^{1,2}, Alexandra Stuart¹, Timothy van der Laan² and Girish Lakhwani¹; ¹The University of Sydney, Australia; ²Commonwealth Scientific and Industrial Research Organisation, Australia

Strong light-matter coupling in organic solar cells (OSCs) has recently shown great potential in increasing the power conversion efficiencies of light.¹⁻⁴ Strong light-matter coupling creates new hybrid states termed exciton-polaritons, and the formation of polaritons in OSCs can significantly influence device performance. It has been shown in thermally evaporated planar heterojunction OSCs that exciton-polaritons can reliably exist at room temperature and leads to more efficient energy transfer.¹ Yet, it has not been demonstrated for solution-processed bulk-heterojunction OSC devices, whereas the latter is more scalable for practical applications. Here, we report that exciton-polaritons can reliably exist in solution-processed bulk-heterojunction OSCs and their influence on device properties. Combining time-resolved spectroscopic measurements for thin films and transient photocurrent/photovoltage decay measurements for devices, we investigated the photo- and device physics of cavity OSCs. We find that the benefits of strong coupling to OSCs are two-fold. Firstly, the charge photogeneration through the new pathway facilitated by the exciton-polaritons is enhanced compared to the reference OSC devices. Secondly, we find that the energy of the charge transfer state is blue-shifted, accompanied by the longer charge carrier lifetime observed in the transient photovoltage decay measurements. Our work demonstrates that strong coupling is a promising avenue for further improving the device properties of OSCs.

References

1. M. Wang, M. Hertzog, K. Börjesson, *Nat Commun.* 12, 1874 (2021).
2. V. C. Nikolis, A. Mischok, B. Siegmund, J. Kublitski, X. Jia, J. Benduhn, U. Hörmann, D. Neher, M. C. Gather, D. Spoltore, K. Vandewal, *Nat Commun.* 10, 3706 (2019).
3. C. A. Delpo, S. U. Z. Khan, K. H. Park, B. Kudisch, B. P. Rand, G. D. Scholes, *Journal of Physical Chemistry Letters.* 12, 9774–9782 (2021).
4. B. Liu, X. Huang, S. Hou, D. Fan, S. R. Forrest, *Optica.* 9, 1029–1036 (2022).

2:45 PM QT01.05.03

Analysis of Interfacial Charges by Spontaneous Orientation Polarization in the Co-Host EML Organic Light-Emitting Diodes with Impedance Spectroscopy So-Young Boo, Akeem Raji, Jae-Yong Park, Somi Park, Eun-Jeong Jang, Jonghee Lee and Jae-Hyun Lee; Hanbat National University, Korea (the Republic of)

Organic light-emitting diodes (OLED) consist of a multi-layer such as hole injection layer (HIL), hole transport layer (HTL), emission layer (EML), electron transport layer (ETL), and electron injection layer (EIL) between two electrodes. By applying an external voltage, electrons and holes are injected and transported from the respective electrodes, resulting in light emission in the EML. In OLED, the presence of interfacial charges at the organic interface allows charge injection before applying voltage to the device. This property can be originated from the permanent dipole moment (PDM) of organic molecules. Most organic molecules used as electron transport layer, such as 2,2',2''-(1,3,5-Benzinetriyl)-tris(1-phenyl-1-H-benzimidazole) (TPBi) and tris-(8-hydroxyquinoline)aluminum (Alq₃), and 4,6-Bis(3,5-di(pyridin-3-yl)phenyl)-2-methylpyrimidine (B3PyMPM) possess PDM, aligned spontaneously during the vacuum deposition process. The non-vanishing net aligned PDM, known as spontaneous orientation polarization (SOP), induces interfacial charges and affects charge injection properties. When the electron transport material of ETL forms a positive SOP against the cathode, the ETL shows negative interfacial charge (NIC) at the EML/ETL interface, influencing hole injection. Consequently, holes are injected and accumulated before the applying voltage to the device, and it can be shown in the capacitance-voltage (C-V) characteristics as the transition voltage (V_t). However, holes injected by NIC can lead to exciton-polaron quenching (EPQ) within the emissive layer. Therefore, it is important to understand the interface characteristics where holes accumulated by NIC. In this presentation, we investigated the difference in charge accumulation property caused by SOP at the ETL/EML interface in co-host EML OLED using impedance spectroscopy (IS). IS was employed to analyze the accumulation and transportation of charges in the co-host EML OLED.

3:00 PM BREAK

3:30 PM QT01.05.04

External Radiative Efficiency of Organic Semiconductor Materials Doped with Organometallic Phosphors Jinyu Chong; Rutgers, The State University of New Jersey, United States

Organic photovoltaics (OPVs) can have certain desirable properties, such as, lightweight, adjustable bandgap, semitransparency, low toxicity, and solution processability, that differentiate them from inorganic and perovskite solar cells. However, the current record efficiency of OPVs (~19%) is still less than for many other solar cell technologies, which limits their application. Shockley-Queisser theory helps to elucidate the efficiency limit of a solar cell, and it assumes that the highest efficiency can be achieved when the external radiative efficiency (ERE) of the solar cell is equal to unity. ERE quantifies the radiative recombination of excitons under total dark current recombination. For the power conversion efficiency (PCE) of solar cells, the best performing solar cells display high EREs due to low nonradiative recombination. One major nonradiative loss pathway in OPVs that suppresses ERE, and hence PCE, is non-emissive triplet states in organic semiconductors.

In this work, we introduce organometallic phosphors into organic semiconducting donor:acceptor OPV films with the goal of converting non-emissive triplet states into emissive

phosphorescence and, thereby, increasing ERE. An iridium-based organometallic phosphor with a low triplet energy level, tris(1-phenylisoquinoline) iridium, Ir(piq)₃, is incorporated into bilayer OPV films composed of polyfluorene polymers - poly(9,9-di-n-octylfluorenyl-2,7-diyl), PFO, as the electron donor, and poly(9,9-dioctylfluorene-alt-benzothiadiazole), F8BT, as the electron acceptor. The photophysical properties of PFO, F8BT and PFO/F8BT donor:acceptor bilayer films with Ir(piq)₃ phosphor doping are studied. Additionally, both OPV and photodetector devices are fabricated and tested with and without Ir(piq)₃.

Photoluminescence (PL) spectroscopy confirms that photoexcitation of PFO/Ir(piq)₃ films results in efficient triplet exciton transfer from PFO to the triplet state of the Ir(piq)₃ phosphor. In addition, when the phosphor doping concentration is increased, there is an increase in PL quantum yield (PLQY), from 38% to 56%, attributed to reduced nonradiative recombination from the PFO triplet state. In contrast, the PLQY of PFO/F8BT and [PFO/Ir(piq)₃]/F8BT bilayer films decreases with increasing doping concentration, which indicates that the photogenerated triplet state of Ir(piq)₃ is quenched by the presence of the F8BT acceptor. In addition, time-resolved PL measurements show that the average lifetime of PFO decreases from 964 ps to 219 ps in the presence of phosphor, which further indicates efficient energy transfer. We also perform PL lifetime measurements of PFO/F8BT and [PFO/Ir(piq)₃]/F8BT bilayer films and the lifetime changes from 930 ps to 770 ps in the presence of phosphor, which show that efficient energy transfer occurs from the donor to the acceptor. Transient absorption spectrum of PFO and PFO(Ir) films shows that there is singlet exciton absorption peak at a wavelength of 826 nm, around 1.5 eV.

OPV devices are fabricated with the following configuration, indium-tin oxide (ITO)/PEDOT: PSS/PFO/F8BT/Ca/Al, with and without phosphor doping in the PFO layer. The OPV devices are tested under one sun illumination. Due to the bilayer structure of PFO/F8BT, the PCE is extremely low, which is ~0.02%; however, the open-circuit voltage is improved by 0.1 V in the presence of the phosphor, suggesting reduced nonradiative recombination. The devices are also tested as organic photodetectors (OPD). PFO(Ir)/F8BT has a responsivity of 0.64 mA/W, the detectivity of 3.25E10 Jones. As for PFO/F8BT devices, their responsivity is 0.48 mA/W, and the detectivity is 3.28E10 Jones. The OPD test indicates that their responsivity is comparable with other photodetector devices.

3:45 PM QT01.05.05

Acridine-Based TADF Molecules in Organic Light-Emitting Transistors (OLETs) Caterina Soldano, Ornella Laouadi, Vladimir Kornienko and Katherine Gallegos-Rosas; Aalto University, Finland

Organic light-emitting transistors are photonic devices combining the function of an electrical switch with the capability of generating light under appropriate bias conditions. Achieving high-performance light-emitting transistors requires high mobility organic semiconductors, optimized device structures and highly efficient emissive layers. Thermally-activated delayed-fluorescence (TADF) has enabled the possibility to achieve heavy-metal-free phosphorescent emitter-based devices with high brightness and state-of-the-art color coordinates, with efficiency exceeding 30%. Since the first report on delayed fluorescence in 2012, TADF molecules have been successfully exploited mainly in OLEDs emissive layers, where host(s)-guest configurations are commonly adopted, mainly to suppress concentration quenching arising from the long-lived triplet excitons.

Here, we present our recent results on the use of an acridine-based TADF molecule (DMAC-DPS) in a host-guest configuration and its optoelectronic behavior in the limit of *field-effect* devices. First, we studied the optical response of these blends by tuning the doping concentration to optimize light generation, for which we observed a quenching of the photoluminescence signal for increasing dye concentration. These blends are then implemented in multilayer organic light-emitting transistors; by engineering the structure (*i.e.*, organic stack), we achieved a large improvement in the light output (~ 4 times). We analyzed our results in terms of balanced charge transport in the emissive layer as well as the device, which, in the limit of horizontal charge transport, leads to an improved exciton formation and decay process.

While the efficiency of our devices is yet to achieve state-of-the-art diode counterpart, this work demonstrates that using TADF molecule while engineering the emissive layer is a promising approach to enhance the light emission in field-effect devices. This opens the way for a broader exploitation of organic light-emitting transistors as alternative photonic devices in fields ranging from display technology to flexible and wearable electronics.

SESSION QT01.06: Poster Session: Excitonic Materials

Session Chairs: Sudeshna Chattopadhyay, Subhabrata Dhar, Yara Galvão Gobato and Ursula Wurstbauer

Tuesday Afternoon, November 28, 2023

Hynes, Level 1, Hall A

8:00 PM QT01.06.01

Study of Interface Effect on InP/ZnSe QDs' Non-Linear Properties Luca Giordano, Pieter Schiettecatte and Zeger Hens; Ghent University, Belgium

QDs show size-tunable opto-electronic properties and are highly suitable for solution-based processing. In this field, Cd-based QDs are the materials with most promising results, but the use of Cd in electronic appliances is restricted by the European Commission's ROHS directive. Considering this, sustainable alternatives are strictly needed, and InP-based QDs are the most promising ones thanks to their high level performance, showing, for example, a near-unity photoluminescence quantum yield across the full visible spectrum. However, opposite from such a linear optical property related to the formation of single electron-hole pairs in InP-based QDs, the characteristics of multiple electron-hole pairs within a single InP-based QDs remain poorly understood. For Cd-based QDs, multiple electron-hole phenomena, such as optical gain, stimulated emission and lasing, have been mostly demonstrated using CdSe QDs, for which the growth of core/shell CdSe/CdS architectures with an alloyed interface was decisive to slow down biexciton Auger recombination and attain stimulated emission under continuous wave optical or electrical pumping.

In this work, we analyze the Auger recombination rate of biexcitons in InP/ZnSe core/shell QDs, where the synthesis protocol was adapted to obtain 4 different interfacial compositions. A first set of two InP/ZnSe samples was formed by purifying or not the InP reaction mixture prior to ZnSe formation. Here, the one-pot approach without intermediate purification may lead to the incorporation of In within the ZnSe shell, while a neat ZnSe shell will grow when starting from purified InP core QDs. A second set of two samples was formed by adding gallium as a second group III precursor at the end of the InP core formation, where again cores were either purified or not before ZnSe shell growth. We found that in particular the addition of GaCl₃ leads to the incorporation of Ga at the InP core QD surface. Interestingly, we observed a systematically higher photoluminescence quantum yield for the samples formed through a one-pot procedure, *i.e.*, without intermediate purification. In addition, a well-defined biexciton Auger recombination rate was only observed for the InP/ZnSe core/shell QDs formed by the one-pot approach. For all other samples, a significantly faster and multi-exponential Auger decay of multi-excitons was observed. The relation between these observations and the elemental and structural characteristics of the core/shell interface will be discussed. We conclude that, not unlike the seminal example of CdSe/CdS, the interfacial composition strongly affects the properties of multi-excitons of InP/ZnSe core/shell QDs.

8:00 PM QT01.06.02

Influence of Y6 Aggregation on Energetics and Charge Generation in High Performance OPV Blends John B. Asbury; Pennsylvania State University, United States

We investigated the origin of the high ratio of open circuit voltage to charge transfer state energy (eV_{OC}/E_{CT}) of OPV polymer blends consisting of the electron donating polymer PM6 and the non-fullerene electron acceptor Y6. PM6-Y6 and related donor-acceptor OPV blends exhibit remarkable optoelectronic properties and record power conversion efficiencies in part because of their unusually high eV_{OC}/E_{CT} ratios, which is believed to be related to the small energetic offset of the HOMO levels of PM6 and Y6. In this study, we varied the amount of Y6 in PM6 blends as a means to control the aggregation of Y6 molecules. We examined the corresponding influence that Y6 aggregation has on the energetic offsets and the charge generation efficiency of the materials by probing the appearance of polaron absorption signals in the mid-infrared using time-resolved infrared spectroscopy. Furthermore, we examined the optical absorption and emission spectra of the PM6-Y6 blends over the range of compositions to correlate the efficiency of charge generation with the signatures of Y6 aggregation in the optical spectra. We observed an abrupt transition around 30 mass% Y6 content at which polarons were efficiently generated by charge separation from PM6 to Y6. Comparison to composition dependent GIWAXS studies of PM6-Y6 blends revealed the formation of Y6 aggregates around the same 30 mass% threshold. These observations demonstrate that aggregation of Y6 molecules is required for charge separation to occur from PM6 to Y6 as measured through the mid-infrared absorption of polarons in the TRIR spectra. Although charges were efficiently generated in blends with only 30 mass% Y6 content, OPV device studies revealed that 50-60 mass% Y6 was needed to reach optimized short-circuit current and OPV device efficiency because these measurements convolve charge generation with charge transport. These findings clarify the optoelectronic properties of the novel class of Y6 acceptors and emphasize the importance of molecular aggregation for tuning the energetics of high performance systems that minimize energy offsets for maximum OPV power conversion efficiencies.

8:00 PM QT01.06.03

Enhancing Structural Integrity and Emission Efficiency of Two-Dimensional Supramolecular Structures Through Silica Encapsulation Dimuthu H. Thanipulli Arachchi, Ulugbek Barotov, Alexander E. Kaplan, Tara Sverko, Collin F. Perkinson and Mounig G. Bawendi; Massachusetts Institute of Technology, United States

The optical properties of J-aggregates are closely linked to their structural integrity, making them susceptible to chemical environments and mechanical stresses. We explore the use of silica encapsulation to enhance the structural rigidity and light emission efficiency of 5,5',6,6'-tetrachloro-1,1'-diethyl-3,3'-di(4-sulfobutyl)-benzimidazolocarboyanine (TDBC) two-dimensional sheet-like J-aggregates. Silica as an encapsulating matrix provides optical transparency, chemical inertness, and ease of functionalization while rigidifying the J-aggregate structure. Our novel

in-situ encapsulation process results in silica-encapsulated J-aggregates whose light absorption and emission properties show no significant change from those of bare J-aggregates, indicating that encapsulation preserves the excitonic structure in TDBC J-aggregates. Microscopic analysis confirms successful and homogeneous silica coating on J-aggregate sheets through cryogenic-TEM images and Scanning Transmission Electron Microscopy with Energy Dispersive X-Ray Analysis (STEM-EDX). Dynamic Light Scattering (DLS) reveals smaller sizes for silica-coated J-aggregates compared to uncoated ones. Stability studies involving dilution demonstrate that silica coating enhances structural integrity, enabling extensive dilutions without a breakdown of J-aggregates into monomers. Silica-coated TDBC J-aggregates achieve a quantum yield of ~95%, the highest recorded for such aggregates, and an ultrafast emissive lifetime of ~200 ps. The absorbance and emission line widths, already quite narrow at room temperature, exhibit further narrowing upon cooling to 79 K. The silica shell allows attaching functional groups on the shell surface or embedding them in the silica shell, permitting hybrid systems without disturbing the assembly of J-aggregates. Encapsulated J-aggregates provide (1) a platform for further manipulation of J-aggregates as building blocks for integration with other optical materials and structures, and (2) a platform for fundamental studies of exciton delocalization, transport, and emission dynamics within a rigid matrix.

Keywords: J-aggregates, silica-encapsulation, quantum yield, cyanine dyes

8:00 PM QT01.06.04

Intramolecular Locking-Induced Triplet Exciton-Harvesting Emitters with Aggregation-Induced Emission Effect for Non-Doped OLEDs[TaehyunKim](#), Dae HwanLee and TaihoPark; Pohang University of Science and Technology, Korea (the Republic of)

Conventional triplet exciton-harvesting organic emitters can attain high internal quantum efficiency (IQE). Despite their advantages, these emitters suffer from the need to introduce heavy atoms and elongated skeleton structures leading to concentration quenching problems. Therefore, heavy-atom-free (HAF) triplet exciton-harvesting emitters have been promising due to unique photophysical characteristics and high photoluminescence quantum yield (PLQY). However, their device application to organic light emitting diodes (OLEDs) has been rarely explored since the performance of non-doped devices is inferior to that of doped devices because of the lack of suitable molecular design strategies. Therefore, the exploration of structural design is essential for decreasing reorganization energy of molecular structures to achieve high PLQY by utilizing triplet-excitons and aggregation-induced emission (AIE) characteristics in a non-doped system. Herein, we synthesized three asymmetric HAF triplet-harvesting emitters. The effect of non-covalent interaction for intramolecular hydrogen bonding between the N atoms and adjacent H atoms of emitters were detected in single-crystal XRD. Hydrogen bonding channel induced intramolecular locking reduced reorganization energy effectively, that increased the intersystem crossing (ISC; k_{ISC}), reverse intersystem crossing (RISC; k_{RISC}) rate and enhanced radiative decay (k_r) process. As a result, intramolecular hydrogen bonding assisted Qx-Py-2DMAC exhibited fast k_{ISC} ($3.52 \times 10^7 \text{ s}^{-1}$), k_{RISC} ($2.54 \times 10^6 \text{ s}^{-1}$), k_r ($3.47 \times 10^7 \text{ s}^{-1}$), and high PLQY (0.94). Besides, hydrogen bonding produced conformation-locked crystal structures were deeply investigated by two-dimensional grazing-incidence wide-angle X-ray diffraction (2D-GIWAXD). H-bond based emitters formed enhanced dense packing modes with a large coherence length (L_c) and preferred horizontal orientations, and exhibited the AIE property that can be applied to non-doped OLEDs. Moreover, molecular locking effect triggered spin-forbidden triplet excitonic emission known as room-temperature phosphorescence (RTP) with a lifetime of milliseconds in the neat film. By utilizing Qx-Py-2DMAC as the emitter, a un-optimized non-doped device, exhibiting a high current efficiency of 33.6%, a power efficiency of 30.1%, and an external quantum efficiency of 11.1% representing relatively high efficiency among RTP emissive and AIE featuring non-doped OLEDs.

8:00 PM QT01.06.06

Near-Field Coupling with a Nanoimprinted Probe for Dark Exciton Nanoimaging in Monolayer WSe₂[JunzeZhou](#)¹, JohnC. Thomas¹, ElyseBarre¹, EdwardBarnard¹, ArchanaRaja¹, KeikoMunehika², AdamSchwartzberg¹ and AlexanderWeber-Bargioni¹; ¹Lawrence Berkeley National Laboratory, United States; ²HighRI Optics, United States

The spin-dark dark excitons (X_D) in WSe₂ monolayer have long radiative lifetimes and are the excitonic ground state, making them attractive for quantum information applications. However, these states exhibit out-of-plane radiation patterns that are typically challenging to observe locally with objective lenses. This work presents a novel Tip-enhanced photoluminescence (TRPL) approach for spectrally and spatially resolving these dark states. The near-field measurement configuration provides an ~3 orders of magnitude out-of-plane Purcell enhancement, diffraction-limited excitation spot, and subdiffraction hyperspectral imaging resolution (below 50 nm) of X_D emission. The effectiveness of this high spatial X_D mapping technique was then demonstrated through reproducible hyperspectral mapping of oxidized sites and nanobubble areas.

8:00 PM QT01.06.07

Probing the 2D Momentum Space of an Excitonic Bose-Einstein Condensate using a Modified Michelson Interferometer[S.V.U.Vedhanth](#) and ShouvikDatta; IISER Pune, India

Excitons as bound electron-hole pairs can undergo interesting phase transitions such as Bose-Einstein Condensation (BEC). This is marked by a spontaneous, long range spatial order below a critical temperature. Physics of such phase transitions can be probed by measuring the 1st order, transverse, spatial correlation/coherence $|g^{(1)}(x,y)|$ with optical interferometry assuming that the BEC ground state of these excitons is 'bright'. We know that the Wiener-Khinchine Theorem in statistical physics relates any 2D mapping of $|g^{(1)}(x,y)|$ with the 2D momentum space (k -space) distribution of the emitted light. Consequently, we demonstrated [1] a modified Michelson Interferometer, which can first measure the 2D map of $|g^{(1)}(x,y)|$ of the excitonic light emission and then subsequently determine its 2D k -space.

Usually k -space measurements are often done by scanning the Back Focal Plane (BFP) image of a 'Bertrand lens' for excitonic samples which are kept inside a low temperature cryostat. One requires a high numerical aperture lens very close to these low temperature samples for BFP imaging. Alternatively, performing Young's double slit experiment with varying slit widths and adjustable slit separations kept within such low-temperature cryostat to measure $|g^{(1)}(x,y)|$ is also a challenging task in terms of instrumentations. These methods can, however, substantially introduce additional heat loads to the sample due to its proximity to various optical elements which are at room temperature. Moreover, the setup doesn't suffer from problems associated with the use of Cat-Eye retroreflector (CER), Dove prisms which were used in past studies of 2D mapping of $|g^{(1)}(x,y)|$. So we first collimate the light coming out from the sample and then measure its $|g^{(1)}(x,y)|$ over a selected area using our setup [1]. This method is certainly simpler and advantageous - specifically in cases where the sample under study is kept at a low temperature, so that k -space distributions of excitonic light emission can still be measured using optical instrumentations placed totally outside the low temperature cryostat at a distance away from the sample itself. This areal mapping of the $|g^{(1)}(x,y)|$ is obtained from the visibility factor from observed interference fringes using the required temporal filtering method [2]. Unlike earlier [2], this time our instrumentations for imaging 2D k -space, involved non-coplanar retroreflectors. So we had introduced additional mirrors to compensate for the displacements of the reflected beams. As a result, we can now monitor and control the fringe width by simply tilting only one such additional mirror(s). This actually enabled us to study even smaller emission patterns. There were reports [3] of k -space studies with spatial coherence measurements but only in 1D. Whereas, here we obtain the full 2D in-plane k -space distribution of light. Moreover, if we want to increase the resolution of the 2D k -space map, then the range over which the $|g^{(1)}(x,y)|$ is measured has to be increased.

Therefore, we have used this setup to measure the $|g^{(1)}(x,y)|$ and study the evolution of 2D k -space distribution before and after the onset of lasing. Most importantly, this experimental design is helpful in probing not only Bose-Einstein Condensate of excitons, but also it can be used to study BEC of polaritons, photons etc. by observing the narrowing of k -space of light emission as an evidence for the presence of the off-diagonal long-range order.

[1] S. V. U. Vedhanth and Shouvik Datta, arXiv:2306.02603.

[2] M. K. Singh, and Shouvik Datta, Rev. Sci. Instrum. 92, 105109 (2021).

[3] L. V. Butov, C.W. Lai, A.L. Ivanov, A.C. Gossard, and D.S. Chemla, Nature 417, 47 (2002).

8:00 PM QT01.06.08

Enhancing Near-infrared (NIR) Multi-Exciton Dynamics Through Quantum Shell Architecture[DulanjanHarankahage](#); Bowling Green State University, United States

Semiconductor quantum dots (QDs) have faced significant limitations in their photonic applications due to ultrafast Auger decay of multiple excitons, leading to non-radiative processes that impede the performance of high-brightness light-emitting diodes and lasing devices. However, the introduction of colloidal quantum shell (QS) architecture, featuring a semiconductor quantum shell with an inverted QD geometry, has successfully suppressed Auger recombination. The QW morphology, characterized by a quantum confined HgS layer sandwiched between two large CdS domains, offers an extended biexciton lifetime and substantial biexciton quantum yields due to the increased exciton volume. Furthermore, the architecture-induced exciton-exciton repulsions have led to the separation of exciton and biexciton optical transitions, resulting in broad optical gain bandwidths. The remarkable longevity of single and biexciton states, along with extended single exciton gain lifetime, positions this geometry as a promising candidate for the development of optically and electrically pumped gain media.

8:00 PM QT01.06.09

Quantum Shell in a Shell: Engineering Colloidal Nanocrystals for a High-Intensity Excitation Regime[JiaminHuang](#); Bowling Green State University, United States

The efficiency of many optoelectronic processes in colloidal semiconductor nanocrystals (NCs) tends to decline when subjected to high-intensity excitation. This decline is primarily attributed to Auger recombination, where multiple excitons result in the conversion of NC energy into excess heat. As a consequence, the efficiency and life span of NC-based devices such as photodetectors, X-ray scintillators, lasers, and high-brightness light-emitting diodes (LEDs) are negatively impacted. Although semiconductor quantum shells (QSSs) have recently emerged as

a promising approach to address Auger decay, their optoelectronic performance has been impeded by surface-related carrier losses. To deal with this issue, we propose the implementation of quantum shells with a CdS–CdSe–CdS–ZnS core–shell–shell–shell multilayer structure. The presence of a ZnS barrier effectively inhibits surface carrier decay, resulting in a significant increase in the photoluminescence (PL) quantum yield (QY) to 90%, while maintaining a high biexciton emission QY of 79%. Furthermore, the enhanced morphology of the quantum shells allows for one of the longest Auger lifetimes observed in colloidal NCs to date. The reduction of nonradiative losses in QDs also leads to diminished blinking in single nanoparticles and low-threshold amplified spontaneous emission. We expect that the ZnS-encapsulated quantum shells will be widespread across various applications in high-power optical or electrical excitation regimes.

8:00 PM QT01.06.10

Energy Transfer in Organic Exciton Polariton Condensate Regime [Rishabh Kaurav](#)¹, Ravindra Kumar Yadav², Amar Flood³, Bo W. Laursen⁴ and Vinod Menon²; ¹The Graduate Center of the City University of New York, United States; ²Center for Discovery and Innovation, The City College of New York, United States; ³Indiana University, United States; ⁴University of Copenhagen, Denmark

Here we report the study of energy transfer between organic molecules where the excitons in the donor molecules are strongly coupled to cavity photons and in the polariton condensate phase. We use a host-guest system where the dye is incorporated into a small-molecule ionic isolation lattices (SMILES). This system exhibits significantly enhanced photoluminescence (PL) in the solid state overcoming the limitation of aggregation induced quenching and has allowed us to realize polariton condensation [1].

Here we study energy transfer between donor, Rhodamine (R3B) and acceptor, Nile Blue (NB) embedded in host Cyanostar to form the SMILES complex. In the mixed R3B-SMILES with NB-SMILES system, we observe significant energy transfer between the donor and the acceptor surpassing what is seen in the bare mixed dye system thus indicating the advantage of the SMILES system in molecular energy transfer. Going further, we investigate the role of the donor being in a condensate phase where coherent emission is observed on the energy transfer process. We use a combination of steady state, time resolved, and momentum resolved spectroscopy to investigate the energy transfer process. The role of the host matrix and the coherence of the donor molecule on energy transfer will be discussed.

[1] "A plug-and-play molecular approach for room temperature polariton condensation," P. Deshmukh et al., ArXiv 2304.11608

8:00 PM QT01.06.11

Observing and Modeling Exciton-Polaritons in Tunable Nanofluidic Microcavities [Ryan Pinard](#), Suman Gunasekaran and Andrew J. Musser; Cornell University, United States

When two mirrors are placed very close together, and a strongly absorbing substance is inserted between them, new states known as exciton-polaritons can be formed. These special light-matter hybrid states have the potential to alter the rate of energy transfer and charge transfer, among other applications. Strong coupling of light with electronic excitations is typically measured in the solid phase; thus, creating polaritons in solution is one vital next step the field could take. However, few have attempted to observe exciton-polaritons in the liquid state — in part due to the difficulty of constructing microcavity devices on the nanometer scale that are capable of receiving liquid, and in part due to the difficulty of dissolving highly-absorbing molecules at high concentration. Here, to tackle these challenges, we have fabricated microcavities into which solutions can be deposited or cycled through continuously. Moreover, these devices are highly tunable in real time on the order of the wavelength of visible light. We are also working toward fabricating aluminum mirrors that are highly reflective in the UV region. These mirrors may have the potential to house a cooperative coupling regime between solvent and solute, which could lower the concentration of dye required for strong coupling. Alongside this progress, we have developed an interactive application in MATLAB that can fully describe the optical properties of our devices. The program can also model the refractive index of a material from inputted absorption data using the Kramers-Kronig relations. Comparison of measured K-space images with the model can provide valuable insight into the nature of solution-phase strong coupling.

8:00 PM QT01.06.12

Luminescent Mechanisms of Crystalline and Amorphous Carbon Dots [Yongqi Yang](#) and Deirdre O'Carroll; Rutgers, The State University of New Jersey, United States

Luminescent carbon dots (CDs), as an emerging material class, have been actively investigated for applications in bioimaging, photocatalysis, and optoelectronic devices. However, standard synthesis procedures have not been established for carbon dots and the mechanism for the luminescence is still unclear, especially the effect of the crystallinity. In this work, we study and compare the optical properties of both crystalline and amorphous CDs in the bulk solution, as well as in thin films. We report on the microwave synthesis method to prepare both crystalline and amorphous CDs. Starting from citric acid and urea as precursors, and phosphoric acid as an additional reagent, we synthesize CDs with different crystallinity by controlling the amount of phosphoric acid during the microwave treatment. The crystallinity and structure of the nanoparticles are characterized by powder X-ray diffraction (XRD) techniques. No peaks are observed in the XRD patterns of CDs synthesized without phosphoric acid, while several peaks are observed in the CDs synthesized with the acid, which indicates the crystallinity in the structure. The size and morphology of the CDs are studied by transmission electron microscopy (TEM) and dynamic light scattering. The sizes of the two types of CDs (with and without phosphoric acid) are both around 20-30 nm, while fast-Fourier-transforms of the TEM images indicate crystallinity at the single particle level for the CDs synthesized with phosphoric acid. The structure and composition of the CDs are also analyzed by high-resolution TEM. The luminescence spectra of amorphous and crystalline CDs are similar in emission wavelength and intensity, while the quantum yield of amorphous CDs is higher than crystalline CDs, with values of 33 % and 24 %, respectively. We will also present single-particle photoluminescence spectroscopy studies of CDs with different crystallinity to assess their size and composition-dependent luminescence. This study sheds new light on the role of crystallinity in the luminescence properties of CDs and the performance of CDs for use as emissive nanomaterials.

8:00 PM QT01.06.13

Effect of Systematic Variation of Light-Matter Coupling Strength on Polariton Condensation Threshold [Beatrice Pence](#), Thomas M. Khazanov and Andrew J. Musser; Cornell University, United States

Exciton-polaritons, bosonic quasiparticles arising from strong coupling between an exciton and the electromagnetic field, are a promising platform for quantum information science. They may undergo condensation above a certain particle density to form a non-equilibrium polariton condensate analogous to classic Bose-Einstein condensates. While most studies have focused on inorganic materials, which undergo condensation at cryogenic temperatures, the higher binding energy of excitons in organic materials allows polariton condensates to form even at room temperature. However, the dependence of key condensation properties, such as condensation threshold and linewidth, on the light-matter coupling strength and other factors related to device structure are not well understood.

Poly-(9,9)-dioctylfluorene (PFO), a highly disordered semiconducting polymer, is known to support polariton condensation in Fabry-Perot microcavities. This study investigates the effect of light-matter coupling strength on condensation threshold experimentally by combining active and spacer layers such that only the PFO concentration inside the cavity is varied, while maintaining other parameters such as total cavity length constant.

8:00 PM QT01.06.15

Identity of T* Matters! Improved k_{rISC} by Modulating Locally Excited Triplet State in TADF Emitters [Madalasa Mondal](#) and Ratheesh K. Vijayaraghavan; IISER Kolkata, India

Effective triplet exciton utilization efficiency is an essential factor for constructing low-power operational OLED devices with high luminescence efficiency and durability. Thermally activated delayed fluorescence assists this 100% triplet harvesting by converting dark triplet excitons into radiative singlet excitons via a reverse intersystem crossing process. The enhancement of this rISC rate (k_{rISC}) is primarily realized by the low energy offset between lowest S & T states; to pursue an extremely large k_{rISC} , the involvement of high energy locally excited triplet states has become a hot topic in TADF-OLED research in present days. However, the regulation of the ³LE states to match precisely with the ¹CT energy level by suitable molecular design is still under progress.

Here, we demonstrated an effective electronic coupling between ¹CT & ³LE or hybridized triplet state in a series of newly designed and synthesized TADF emitters with strongly twisted D-A structure. The detailed theoretical and experimental investigation reveals that the addition of peripheral donor units to the core D-A backbone incorporates multiple triplet excited states of locally excited or hybridized nature between S₁ and T₁ states, and the close alignment of ¹CT & ³LE states accelerates the spin-flip process and the sizeable radiative rate results in suppressed efficiency roll off with short (ns) delayed lifetime. On the contrary, the isoenergetic alignment of ¹CT and ³CT states realized due to the near orthogonal structure promotes the rISC mechanism. Our work highlights the pivotal role of the electronic nature of the intermediate triplet states in controlling the k_{rISC} ; a thorough photophysical investigation was also performed by manipulating ³LE states by introducing variable donor units to the D-A backbone.

8:00 PM QT01.06.16

Improved Device Performance of Quantum Dot Light Emitting Diodes by an Insertion of Thermal Activated Delayed Fluorescent Layer for Utilizing the Excess Exciton [Jeong-Yeol Yoo](#), Yoon-Jeong Choi, Chil Won Lee and Byung Doo Chin; Dankook University, Korea (the Republic of)

Quantum dots (QDs) are promising light emitters for the next-generation display, especially in the form of QD light-emitting diodes (QLED). Recently, PL-type QD display was successfully implemented in commercial products, including recent QD-OLED with superior properties. In spite of the great success of PL-type QD display, however, self-emissive electroluminescence (EL) type QD display is still under development.^{1,2}

Recent issues on EL-type QLED studies the imbalance between the holes and electrons causes over-injection of electrons compared to holes, electron leakage from the QD emission layer (EML), and accumulation of charges at the EML/hole transporting layer (HTL) interfaces. As a result, the efficiency and lifetime of the device were reduced. Therefore, controlling the charge balance is essential for realizing highly efficient QLED.³

Several studies have been focused on charge balance by improving the hole injection and suppressing the electron injection. Nevertheless, in most of the QLEDs reported so far, electron injection was always too efficient. In addition, the incorporation of phosphorescent sensitizer into QLED devices enhanced energy transfer and promoted to harvest the energy of the excitons to the QD EML, which were regarded as an effective method to enhance the efficiency of QLEDs. However, it is expected that Dexter energy transfer occurs by T_1 excitons, which has a too short transfer distance (<1 nm).^{4,5}

In this study, a blue thermally activated delayed fluorescence (TADF) material layer between EML and HTL was employed for utilizing the leaked electron and promote exciton harvesting. In the TADF layer, the leaked and accumulated electrons can form exciton with holes injected from HTL, energies by S_1 exciton were transferred from TADF layer into QDs and emission of QDs via Förster resonance energy transfer mechanism (FRET).⁵ The critical radius of FRET (R_{FRET}) can be calculated from the spectral overlap of TADF materials and QDs. As a result, maximized efficiency R_{FRET} is calculated to be about 4.25 nm. Compared with the control QLED device without TADF layer, the QLED with TADF layer showed about 2-fold increment for external quantum efficiency and current efficiency and 4-fold improvement for maximum luminance. Moreover, significant improvements in device lifetime. The EL properties indicate that the devices exhibit a symmetric EL peak emission. These results clearly reveal that TADF materials can be successfully applied to utilize excessive electrons, generally improving the overall performance of QLED. The proposed approaches are expected to provide a possible realization of highly efficient QLEDs where the analysis of detailed mechanism is studied.

Reference

[1] J. -Y. Yoo, W. H. Jung, C. W. Lee, B. D. Chin, J. -G. Kim, J. S. Kim, Enhanced device performance of quantum-dot light-emitting diodes via 2,2'-Bipyridyl ligand exchange, *Org. Elec.* 2021, 99, 106326.

[2] E. Jang, Y. Kim, Y. -H. Won, H. Jang, S. -M. Choi, *ACS Energy Lett.* 2020, 5, 1316-1327.

[3] J. -Y. Yoo, W. H. Jung, H. J. Kim, J. -G. Kim, B. D. Chin, J. S. Kim, *Org. Elec.* 2022, 108, 106569.

[4] H. Zamani Siboni, B. Sadeghimakki, S. Sivoththaman, H. Aziz, *ACS Appl. Mater. Interfaces*, 2015, 7, 46, 25828-25834.

[5] J. Kim, A. Hong, D. Hahm, H. Lee, W. K. Bae, T. Lee, J. Kwak, *Adv. Optical Mater.* 2023, 11, 230088.

Presenter: Jeong-Yeol Yoo

SESSION QT01.07: Excitonic Phenomena I
Session Chairs: Oksana Ostroverkhova and Daniel Wigger
Wednesday Morning, November 29, 2023
Sheraton, Fifth Floor, Public Garden

8:30 AM *QT01.07.01

Control of the Exciton and Spin/Valley Properties in Atomically Thin Transition Metal Dichalcogenides MarieXavier; Institut National des Sciences Appliquées - LPCNO, France

Encapsulation of TMD monolayers in hexagonal boron nitride (hBN) yields narrow optical transitions approaching the homogeneous exciton linewidth^{1,2,3}. We have demonstrated that the exciton radiative rate in these van der Waals heterostructures can be tailored by a simple change of the hBN encapsulation layer thickness as a consequence of the Purcell effect⁴.

We also measured the exciton fine structure by magneto-photoluminescence spectroscopy in magnetic fields up to 30 T^{5,6}. I will show that the bright-dark exciton splitting can be tuned by a few meV, as a result of a significant Lamb shift of the optically active exciton which arises from emission and absorption of virtual photons triggered by the vacuum fluctuations of the electromagnetic field⁷.

Finally I will present recent experimental results on spin/valley pumping of resident electrons in WSe₂ and WS₂ monolayers⁸. Using a spatially-resolved optical pump-probe experiment, we measure the lateral transport of spin/valley polarized electrons over very long distances (tens of micrometers)⁹. These results highlight the key role played by the spin-valley locking effect in TMD monolayers on the pumping efficiency and the polarized electron transport.

¹ G. Wang *et al*, *Rev. Mod. Phys.* **90**, 021001 (2018)

² F. Cadiz *et al*, *Phys. Rev. X* **7**, 021026 (2017)

³ G. Wang *et al*, *Phys. Rev. Lett.* **119**, 047401 (2017)

⁴ H. Fang *et al*, *Phys. Rev. Lett.* **123**, 067401 (2019)

⁵ C. Robert *et al*, *Phys. Rev. Lett.* **126**, 067403 (2021)

⁶ C. Robert *et al*, *Nature Com.* **11**, 4037 (2020)

⁷ L. Ren *et al*, *Arxiv* 2303.17880 (2023)

⁸ C. Robert *et al*, *Nature Com.* **12**, 5455 (2021)

⁹ C. Robert *et al*, *Phys. Rev. Lett.* **129**, 027402 (2022)

9:00 AM *QT01.07.02

High-Performance Broadband Faraday Rotation Spectroscopy of Excitons in Atomically Thin Semiconductors AshishArora^{1,2}; ¹Indian Institute of Science Education and Research, Pune, India; ²University of Muenster, Germany

Faraday rotation is a fundamental effect in the magneto-optical response of solids, liquids and gases. However, due to many speed limiting components such as polarization modulators combined with lock-in amplifiers, each spectrum could take several hours to measure. Therefore, Faraday rotation spectroscopy measurements with micrometer spatial resolution become extremely challenging, if high spatial stabilities of the samples over the measurement time scales are required.

In this talk, first I will describe a newly developed high-performance broadband Faraday rotation spectroscopy technique for measurements on the micron scale [1]. Spectral acquisition speeds of two-to-three orders of magnitude faster than state-of-the-art modulation spectroscopy setups are demonstrated. The experimental method is based on charge-coupled-device detection, avoiding speed-limiting components used in the modulation spectroscopy, such as a photoelastic modulator and a lock-in amplifier. At the same time, Faraday rotation spectra are obtained with a sensitivity of 20 μ rad (0.001 $^\circ$) over a broad spectral range (525 nm – 800 nm), which is on par with polarization-modulation techniques [1]. The new measurement technique also automatically cancels unwanted Faraday rotation backgrounds.

Using the setup, we perform Faraday rotation spectroscopy of excitons in an hBN-encapsulated atomically thin semiconductor WS₂ under magnetic fields of up to 1.4 T. We resolve extremely small exciton Zeeman splittings such as 50 μ eV at $B = 0.2$ T, and tiny valley polarizations such as 0.05 % at $B = 0.4$ T. I will discuss the prospects of creating ultrathin optical isolators based on excitonic transitions in 2D materials, for optical integrated circuits.

Our work presents a dramatic improvement in measurement speeds over the state-of-the-art modulation techniques. It enables us to perform spatially-resolved high-performance Faraday rotation spectroscopy of excitons in 2D semiconductors.

Reference: [1] Carey *et al.*, High-performance broadband Faraday rotation spectroscopy of 2D materials and thin magnetic films, *Small Methods* **101**, 2200885 (2022)

9:30 AM QT01.07.04

Quantum Shells Versus Quantum Dots—Suppressing Auger Recombination in Colloidal Semiconductors MikhailZamkov; Bowling Green State University, United States

The quantum efficiency of many optoelectronic processes in colloidal semiconductor nanocrystals (NCs) declines with increasing optical or electrical excitation intensity. This issue is caused by Auger recombination of multiple excitons, which converts the NC energy into excess heat, whereby reducing the efficiency and lifespan of NC-based devices, including lasers, photodetectors, X-ray scintillators, and high-brightness LEDs. Recently, semiconductor quantum shells (QSSs) have emerged as a viable nanoscale architecture for the suppression of Auger decay. The spherical-shell geometry of these nanostructures leads to a significant reduction of Auger decay rates, while exhibiting a near unity photoluminescence quantum yield. In this talk, I will compare the optoelectronic properties of quantum shells against other low-dimensional semiconductors and discuss their emerging opportunities in solid-state lighting and energy-harvesting applications.

10:15 AM *QT01.07.05

Flattening Conduction and Valence Bands for Interlayer Excitons in Twisted Van der Waals Bilayers [AndreyChaves](#)^{1,2}, [SaraConti](#)², [TribhuvanPandey](#)², [LucianCovaci](#)², [FrancoisPeeters](#)², [DavidNeilson](#)² and [M. V.Milosevic](#)²; ¹Universidade Federal do Ceara, Brazil; ²University of Antwerp, Belgium

Recent advances in fabrication and manipulation of two-dimensional (2D) materials have enabled the control over stacking and twisting between layers of transition metal dichalcogenides (TMDs) in van der Waals (vdW) heterostructures. In these systems, the moiré pattern created by the lattice mismatch between the layers plays an important role: it produces a periodic potential profile along the plane for electrons and holes, with potential minima in regions with specific stacking orders. Such moiré superlattice potential leads to a band structure for the bilayer that is tunable e.g. by inter-layer twisting. The recent observation of Mott insulator and superconducting phases in twisted bilayer graphene [1,2], due to the band flattening induced by interlayer twist, has brought even further excitement into this field, towards controlling transport and opto-electronic properties of TMDs vdW heterostructures by similar moiré pattern effects. [3]

In this work, we explore the flatness of conduction and valence bands of interlayer excitons in MoS₂/WSe₂ van der Waals heterobilayers, tuned by interlayer twist angle, pressure, and external electric field. We employ an efficient continuum model [4] where the moiré pattern from lattice mismatch and/or twisting is represented by an equivalent mesoscopic periodic potential. We demonstrate that the mismatch moiré potential is too weak to produce significant flattening. Moreover, we draw attention to the fact that the quasi-particle effective masses around the Γ -point and the band flattening are *reduced* with twisting. As an alternative approach, we show (i) that reducing the interlayer distance by uniform vertical pressure can significantly increase the effective mass of the moiré hole, and (ii) that the moiré depth and its band flattening effects are strongly enhanced by accessible electric gating fields perpendicular to the heterobilayer, with resulting electron and hole effective masses increased by more than an order of magnitude leading to record-flat bands. These findings impose boundaries on the commonly generalized benefits of moiré twistronics, while also revealing alternate feasible routes to achieve truly flat electron and hole bands to carry us to strongly correlated excitonic phenomena on demand.

[1] Yuan Cao, Valla Fatemi, Ahmet Demir, Shiang Fang, Spencer L. Tomarken, Jason Y. Luo, Javier D. Sanchez-Yamagishi, Kenji Watanabe, Takashi Taniguchi, Efthimios Kaxiras, Ray C. Ashoori, and Pablo Jarillo-Herrero, *Nature* **556**, 80 (2018).

[2] Yuan Cao, Valla Fatemi, Shiang Fang, Kenji Watanabe, Takashi Taniguchi, Efthimios Kaxiras, and Pablo Jarillo-Herrero, *Nature* **556**, pages 43 (2018).

[3] Hongyi Yu, Gui-Bin Liu, Jianju Tang, Xiaodong Xu, and Wang Yao, *Sci. Adv.* **3**, e1701696 (2017).

[4] Sara Conti, Andrey Chaves, Tribhuvan Pandey, Lucian Covaci, François M. Peeters, David Neilson, Milorad V. Milošević, arXiv:2303.07755

10:45 AM *QT01.07.06

Strong and Tunable Light-Matter Interactions in Excitonic Semiconductors [DeepM. Jariwala](#); University of Pennsylvania, United States

The isolation of stable atomically thin two-dimensional (2D) materials on arbitrary substrates has led to a revolution in solid state physics and semiconductor device research over the past decade. A variety of other 2D materials (including semiconductors) with varying properties have been isolated raising the prospects for devices assembled by van der Waals forces.¹ Particularly, these van der Waals bonded semiconductors exhibit strong excitonic resonances² and large optical dielectric constants as compared to bulk 3D semiconductors. . First, I will focus on the subject of strong light-matter coupling in excitonic 2D semiconductors, namely chalcogenides of Mo and W. Visible spectrum band-gaps with strong excitonic absorption makes transition metal dichalcogenides (TMDCs) of molybdenum and tungsten as attractive candidates for investigating strong light-matter interaction formation of hybrid states.³⁻⁵ We will present our recent work on the fundamental physics of light trapping in multi-layer TMDCs when coupled to plasmonic substrates.⁶ Next, we will show the extension of these results to halide perovskites^{7, 8} and superlattices of excitonic chalcogenides.⁹ These hybrid multilayers offer a unique opportunity to tailor the light-dispersion in the strong-coupling regime.⁹ We will discuss the physics of strong light-matter coupling and applications of these structures. If time permits, I will also present our recent work on van der Waals semimetals,¹⁰ control of light in magnetic semiconductors¹¹ and extending some of these concepts to 1D carbon-nanotubes.¹² Our results highlight the vast opportunities available to tailor light-matter interactions¹¹ and building practical devices with 2D semiconductors. I will conclude with a broad vision and prospects for 2D materials in the future of semiconductor opto-electronics and photonics.

References:

1. Jariwala, D.; et al. *ACS Nano* **2014**, 8, (2), 1102–1120.
2. Lynch, J.; Guameri, L.; Jariwala, D.; van de Groep, J. *Journal of Applied Physics* **2022**, 132, (9), 091102.
3. Jariwala, D.; et al. *ACS Photonics* **2017**, 4, 2692-2970.
4. Brar, V. W.; Sherrott, M. C.; Jariwala, D. *Chemical Society Reviews* **2018**, 47, (17), 6824-6844.
5. Anantharaman, S. B.; Jo, K.; Jariwala, D. *ACS Nano* **2021**.
6. Zhang, H.; et al. Jariwala, D. *Nature Communications* **2020**, 11, (1), 3552.
7. Anantharaman, S. B.; et al. Jariwala, D. *Nano Letters* **2021**, 21, (14), 6245-6252.
8. Song, B.; et al. Jariwala, D. *ACS Materials Letters* **2021**, 3, (1), 148-159.
9. Kumar, P.; et al. Jariwala, D. *Nature nanotechnology* **2022**, 17 182–189.
10. Alfieri, A. D.; et al. Jariwala, D. *Advanced Optical Materials* **2022**, 2202011.
11. Zhang, H.; et al. Jariwala, D. *Nature Photonics* **2022**, 16, 311-317.
12. Lynch, J.; et al. Jariwala, D. *arXiv preprint arXiv:2304.08337* **2023**.

11:15 AM QT01.07.07

Trion Photoluminescence and Trion Stability in Atomically Thin Semiconductors [RaulPerea-Causin](#)¹, [SamuelBrem](#)², [OleSchmidt](#)² and [ErminMalic](#)²; ¹Chalmers University of Technology, Sweden; ²Philipps University of Marburg, Germany

The optical response of doped monolayer semiconductors is governed by trions [1], i.e. three-particle complexes consisting of a photoexcited electron-hole pair bound to a doping charge. While photoluminescence (PL) signatures of trions have been identified in experiments [2], the microscopic description of trion recombination and trion stability is still incomplete.

In this work, we derive a generalized trion PL formula on a fully quantum-mechanical footing, considering both direct and phonon-assisted recombination mechanisms [3]. Considering WSe₂ as exemplary material, we access the trion energy landscape by solving the trion Schrödinger equation with a variational approach [4] and reveal the important impact of the mass imbalance between equal charges on the trion stability. Finally, we compute the temperature-dependent PL spectra for n- and p-doped monolayers and find a good agreement with experimental data. Moreover, we predict additional signatures originating from trions with an electron located at the Λ point, which, interestingly, exhibit a higher three-body energy than their K-point counterpart but a lower recombination resonance. Although these signatures have not been clearly observed in experiments yet, we expect that Λ -point trions play a relevant role in the dynamics and can be experimentally accessed via strain engineering [5] or in time-resolved PL spectra [6]. Our work presents an important step towards a microscopic understanding of the quantum nature of trions, which determines their stability and optical fingerprint.

- [1] Mak et al., *Nature Materials* 12, 207 (2013)
- [2] He et al., *Nature Communications* 11, 618 (2020)
- [3] Brem et al., *Nano Letters* 20 (4), 2849 (2020)
- [4] Berkelbach et al., *Physical Review B* 88, 045318 (2013)
- [5] Rosati et al., *Nature Communications* 12, 7221 (2021)
- [6] Rosati et al., *ACS Photonics* 7 (10), 2756 (2020)

11:30 AM QT01.07.08

Modulating Optical Properties of Monolayer WS₂ by Dielectric and Substrate Engineering [TamaghnaChowdhury](#), [GokulM. A](#) and [AtikurRahman](#); IISER Pune, India

The optical properties of monolayers of transition metal dichalcogenides (TMDs) are profoundly influenced by the surrounding dielectric environment. Defect states within the substrate introduce uncontrolled doping in the TMD monolayer, thereby altering the photoluminescence (PL) spectra. In this study, we systematically investigated the influence of surface defects by gradually increasing the separation between the WS₂ monolayer and the substrate. This allowed for precise modulation of the exciton and trion contributions in the PL spectra of WS₂. By performing excitation power-dependent measurements on dielectric-engineered and patterned substrates, we gained insight into the mechanism behind the PL modulation in monolayer WS₂. Furthermore, we examined the impact of the charged nature of substrate defects on the PL spectra. These findings present a novel pathway for modulating and obtaining desired PL spectra of TMDs through substrate engineering.

11:45 AM QT01.07.09

Tunable Localized Charge Transfer Exciton in a Mixed Dimensional Van der Waals Heterostructure Mahfujur Rahman¹, Emanuele Marino¹, Alan GJoly², Seunguk Song¹, Zhiqiao Jiang¹, Brian T.O'Callahan², Daniel J. Rosen¹, Kiyoung Jo¹, Gwangwoo Kim¹, Patrick Z.El-Khoury², Christopher B.Murray¹ and DeepM. Jariwala¹; ¹University of Pennsylvania, United States; ²Pacific Northwest National Laboratory, United States

The observation of interlayer excitons (ILX) in van der Waals heterostructures (vdWHs) based on 2D-2D systems makes them a very promising candidate for next generation photonic and valleytronic devices. However, the true potential of ILXs depends on spatially confining and isolating them below their de Broglie wavelength^{1,2}. One approach that has garnered significant attention in this regard, is the formation of moiré superlattices in twisted van der Waals 2D homo/hetero stacks³. Though the material modulation through moiré superlattices faces challenges, including limited control over the energy and position of the trapping potential due to the delicate alignment required between 2D sheets, crystal imperfections over large areas, and repulsive interactions among the trapped ILXs^{4,5}. In this contribution⁶, we demonstrate the formation of highly localized ILX analogous charge transfer (CT) excitons in a 2D/quasi-2D system comprising MoSe₂ monolayers and CdSe/CdS based core/shell nanoplates (NPLs). We employ room temperature nano-PL to resolve the spectral signature of CT excitons in our MDHs, which are spatially confined within the dimension of single NPL (~ 10 x 10 nm²). Moreover, we are able to tune the energy of the CT excitons up to 120 meV via tuning the NPL thickness and achieve an electrostatic gating tunability of 0.8 eV/(V/nm), which surpasses the ILX tunability in 2D-2D systems^{7,8}. Our finding is a significant step towards the realization of highly tunable MDH-based next generation photonic devices.

References

- (1) Hawrylak, P. et al., Electronic Properties of Self-Assembled Quantum Dots. **2003**, 25–92, doi:10.1007/978-3-540-39180-7_2.
- (2) Thureja, D. et al., Electrically Tunable Quantum Confinement of Neutral Excitons. *Nat.* **2022**, *606*, 298–304.
- (3) Du, L. et al., Moiré Photonics and Optoelectronics. *Science* **2023**, *379*, eadg0014.
- (4) Seyler, K. L. et al., Signatures of Moiré-Trapped Valley Excitons in MoSe₂/WSe₂ Heterobilayers. *Nature* **2019**, *567*, 66–70.
- (5) Li, W. et al., Dipolar Interactions between Localized Interlayer Excitons in van Der Waals Heterostructures. *Nat. Mater.* **2020**, *19*, 624–629.
- (6) Rahman, M. et al., Tunable Localized Charge Transfer Excitons in a Mixed Dimensional van Der Waals Heterostructure. **2022**. arXiv:2210.12608
- (7) Shanks, D. N. et al., Nanoscale Trapping of Interlayer Excitons in a 2D Semiconductor Heterostructure. *Nano Lett.* **2021**, *21*, 5641–5647.
- (8) Jauregui, L. A. et al., Electrical Control of Interlayer Exciton Dynamics in Atomically Thin Heterostructures. *Science* (80-.). **2019**, *366*, 870–875.

SESSION QT01.08: Excitonic Phenomena II
Session Chairs: Ashish Arora and Stefan Zollner
Wednesday Afternoon, November 29, 2023
Sheraton, Fifth Floor, Public Garden

1:30 PM *QT01.08.01

Excitonic Absorption in Semiconductors with Low and High Carrier Densities Stefan Zollner¹, Carola Emminger^{2,3} and Jose Menendez⁴; ¹New Mexico State University, United States; ²Universität Leipzig, Germany; ³Humboldt-Universität zu Berlin, Germany; ⁴Arizona State University, United States

Spectroscopic ellipsometry is an optical reflection technique with polarized light. Most commonly, it is used to measure the thicknesses of thin-film layers, such as SiO₂ on Si. But it can also be used to study the energies and broadenings of elementary excitations in solids, such as free carriers (electrons and holes, band gaps, transport), excitons, infrared active phonons, and their interactions. We previously reported precision measurements of the complex refractive index of germanium due to the absorption of photons by excitons near the direct band gap. These results were compared quantitatively with theoretical predictions from Fermi's Golden Rule, based on k,p theory and including the excitonic interaction between electrons and holes (Sommerfeld enhancement). Going further, we can investigate how many-body effects impact the excitonic absorption of photons in highly excited semiconductors. Large carrier concentrations can be achieved through doping, thermal excitation of electron-hole pairs in small band-gap semiconductors, or optical excitation with ultrafast lasers. In this talk, we will report recent ellipsometry results for the temperature-dependent dielectric function of InSb near the direct band gap and the transient dielectric function of Ge near the E₁ and E₁+Δ₁ transitions from femtosecond pump-probe ellipsometry. We will also point out the theoretical approach needed to explain these data sets, especially the Fermi-Dirac distribution functions of carriers (Burstein-Moss shift) and the screening of the excitonic effects at high carrier densities.

2:00 PM *QT01.08.02

Exciton Transport in a Van der Waals Antiferromagnet Florian Dimberger¹, Sophia Terres¹, Mikhail Glazov² and Alexey Chernikov¹; ¹TU Dresden, Germany; ²Ioffe Institute, Russian Federation

Optical spectroscopy of van der Waals magnets recently unveiled *magnetic excitons* – a rare type of optical excitation emerging from spin-polarized electronic states in magnets. With properties that have no analogue amongst excitons in conventional band semiconductors, these optical quasiparticles not only inherit tremendous potential for optoelectronic devices with new functionalities, they provide insight into elementary interactions between electron-hole pairs, magnons, and light. A strongly bound example of such *magnetic excitons* was recently discovered in the prototypical layered antiferromagnetic semiconductor CrSBr. In this contribution, we will present its fundamental optical properties and discuss our latest experimental results on the spatio-temporal transport of excitons in the presence of large structural anisotropy and magnon coupling.

2:30 PM BREAK

3:30 PM QT01.08.03

Impact of Excitons on the Non-Linear Optical Properties of 2D Materials Su Ying Quek; National University of Singapore, Singapore

Non-linear optical phenomena are at the core of many important technologies and spectroscopic techniques. The second-order optical susceptibility is responsible for spontaneous parametric down conversion (SPDC) which generates entangled photon pairs, shift currents which give rise to bulk photovoltaic effects, and second harmonic generation that is useful for spectroscopy. In recent years, there has been increasing interest in studying non-linear optical phenomena in the 2D limit, where phase-matching conditions are eliminated while allowing for more facile integration with hybrid quantum photonic platforms. Reduced electronic screening in 2D leads to enhanced excitonic effects, and it is therefore critical to elucidate the impact of excitons on non-linear optical properties. We develop a theory for the second-order optical susceptibility that takes into account excitonic effects with a first principles GW-Bethe-Salpeter-Equation (GW-BSE) approach. We apply the theory to niobium oxydihalides (NbOX₂, X = Cl, Br, I) [1], a material of significant current interest in non-linear optics [2]. We predict that excitonic effects greatly enhance the probability for SPDC [3] and increase the magnitude of the shift currents in this material. We further benchmark our approach by comparison with experiment for the shift current in bulk BaTiO₃ and the SHG spectra for layered NbOI₂, where we clearly demonstrate the important role of excitons in non-linear optics. Our work provides a fundamental understanding of non-linear optical phenomena in excitonic materials and paves the way for 2D non-linear quantum photonics.

[1] Y. Wu, I. Abdelwahab, K. C. Kwon, I. Berzhbitskiy, L. Wang, W. H. Liew, K. Yao, G. Eda, K. P. Loh, L. Shen and S. Y. Quek, "Data-driven discovery of high performance layered van der Waals piezoelectric NbOI₂", *Nature Communications*, 13, 1884 (2022)

[2] *Nature* 613, 53 (2023), *Nature Photonics* 16, 644 (2022), *Advanced Optical Materials* 2202833 (2023), *Advanced Materials* 33, 2101505 (2021)

[3] F. Xuan, M. Lai, Y. Wu, S. Y. Quek, arXiv:2305.08345

3:45 PM QT01.08.04

Exciton-Plasmon Interactions in Binary Superlattices of Infrared Colloidal Nanocrystals Sarah Britzman, Patrick Yee, Veronica Policht, Paul Cunningham and Janice Boercker; U.S. Naval Research Laboratory, United States

Semiconductor colloidal nanocrystals have immense potential to contribute to efficient and inexpensive infrared optoelectronics. State-of-the-art devices made from colloidal nanocrystals contain films of randomly arranged nanocrystals that do not exhibit long-range order. Controlling the ordering of these nanocrystals into superlattices has the potential to generate engineered metamaterials that exhibit properties not achievable in natural semiconductors or in films of disordered nanocrystals. The current size of individual ordered domains in these materials

(analogous to grain size in polycrystalline materials), however, is typically microscopic, so the field lacks detailed structure-property relationships. Expanding on our previous work [1, 2], we have engineered the surface chemistry of our nanocrystals to create enlarged (>1 micron) domains of binary nanocrystal ordered solids of infrared plasmonic Cu₂-xS/PbS core/shell and excitonic PbS nanocrystals. We then directly correlate photoluminescence microscopy performed in an air-free environment on single ordered domains with transmission electron microscopy of the binary PbS and Cu₂-xS nanocrystal solids. Initial results from our correlative microscopy indicate that energy transfer does occur between the excitonic emitters and plasmonic nanocrystals and suggest that fine-tuning the geometry and energetics of the binary system will optimize this composite material's properties. We envision that combining single-domain measurements and optical modeling will generate well-defined structure-property relationships that will further our understanding of multicomponent ordered nanocrystal solids and allow us to design solids with desired properties.

References

- [1] S. Brittan, N. A. Mahadiq, S. B. Qadri, P. Y. Yee, J. G. Tischler, and J. E. Boercker, *ACS Appl. Mater. Interfaces* **12**, 24271 (2020).
- [2] P. Y. Yee, S. Brittan, N. A. Mahadiq, J. G. Tischler, R. M. Stroud, Al. L. Efros, P. C. Sercel, and J. E. Boercker, *Chem. Mater.* **33**, 6685 (2021).

4:00 PM QT01.08.05

Linear and Non-linear Optical Properties of Semiconductor Quantum Dots Chandler Martin¹, Anaira Jalan² and Arindam Chakraborty¹; ¹Syracuse University, United States; ²Westminster School, United Kingdom

This computational work presents a systematic investigation of linear and non-linear optical response properties of CdSe, CdS, PbSe, and PbS quantum dots in the size range of 1-10 nm. First-principles quantum mechanical calculations were performed using the frequency-dependent geminal screened electron-hole interaction kernel (FD-GSIK) method, and the polarizability and hyper-polarizability were evaluated from the time-dependent correlated electron-hole reduced density matrix. The FD-GSIK is a real-space method that uses an explicitly-correlated operator to include many-body quasiparticle correlation effect. The results from the real-time propagation approach will be compared with the sum-over-states approach, and analysis of the key differences will be presented. The scaling law for the polarizability and hyper-polarizability as a function of dot size will be presented, and the impact of material type and surface defects will be discussed.

4:15 PM QT01.08.06

Exciton Transport and Dissociation in Molecular Photocells Chumin Wang, Fernando Sanchez and Vicenta Sanchez; Universidad Nacional Autonoma de Mexico, Mexico

Sunlight is the most plentiful source of clean energy providing to the earth in one hour enough energy for current human needs of one year [1]. In addition, photovoltaic devices based on organic semiconductors possess many remarkable advantages in comparison with the inorganic technology, such as flexibility, transparency, low weight and inexpensive manufacture. Hence, understanding the kinetics of light-generated excitons around the organic donor-acceptor heterojunction may significantly improve the performance of solar cells. In this work, we present a quantum model of molecular photocells based on a coarse-grained attractive Hubbard Hamiltonian, where the transport and dissociation of excitons are analyzed on an excitonic state lattice containing impurity sites originated from the attractive electron-hole interaction [2]. The presence of these impurity sites prevents the use of reciprocal space and then, the numerical calculation was carried out by means of an independent channel plus real-space renormalization method, where the competition between the driving force from heterojunction and the Coulomb attraction leading to an electron-hole recombination has been explicitly addressed [3]. The results reveal an optimal distance between molecular photocells to achieve the maximum quantum efficiency, in accordance with various experimental reports about the optimal concentration of donor molecules [4]. Moreover, the calculated quantum efficiency has a good agreement with those obtained from diverse organic photovoltaic devices, such as bilayer, perovskite and inverted solar cells [5].

This work has been partially supported by projects UNAM-IN112522, UNAM-IN110823 and CF-2023-I-830. Computations were performed at Miztli of DGTIC-UNAM.

- [1] J. M. Luther and J. C. Johnson, An exciting boost for solar cells, *Nature* **571**, 38 (2019).
- [2] O. Navarro and C. Wang, An exact method to solve the diluted extended Hubbard model, *Solid State Commun.* **83**, 473 (1992).
- [3] F. Sánchez, C. Amador-Bedolla, V. Sánchez and C. Wang, On the role of driving force in molecular photocell, *Phys. B: Condensed Matter* **583**, 412052 (2020).
- [4] F. Sánchez, C. Amador-Bedolla, V. Sánchez and C. Wang, Exciton dissociation in correlated molecular photocells, *J. Phys. Chem. Solids* **152**, 109966 (2021).
- [5] F. Sánchez, V. Sánchez and C. Wang, Coarse-Grained Quantum Theory of Organic Photovoltaic Devices, *Nanomaterials* **11**, 495 (2021).

SESSION QT01.09: Excitons in Quantum Materials and Quantum Technologies

Session Chairs: Keshav Dani and Yara Galvão Gobato

Thursday Morning, November 30, 2023

Sheraton, Fifth Floor, Public Garden

8:00 AM *QT01.09.01

Emergent Optical Properties of 2D Materials Xiaolong Zou¹, Nannan Luo² and Dan Wang¹; ¹Tsinghua University, China; ²Hunan University, China

Two-dimensional (2D) materials are ideal platforms for exploring emerging optical behaviors, at unprecedentedly high temperature and feasible control. Here, we report our systematic study on the effects of different band topologies on the optical properties of 2D systems and their control by twisting and proximity. Different 2D materials with characteristic band topologies can be adopted to achieve various long-sought high-temperature excitonic quantum behaviors, including electron-hole liquid in a new-phase (γ -phase) group IV monochalcogenides, excitonic Bose-Einstein Condensation in TiS₃, and saddle excitons in β -phase group IV monochalcogenides. While twist can introduce remarkably strong moiré optical resonances in trilayer black phosphorus even at a large twist angle of 19°, its combination with pressure or electric field leads to controllable tuning of bandgap, bandwidth, and dimension of moiré bands. Further, by turning the interlayer orbital hybridization in stacked heterobilayer, large valley band splitting and valley exciton splitting can be achieved in VSe₂/MSe₂ (M = Mo or W) at room temperature. These results show great potential of 2D materials in future opto-electronic applications.

8:30 AM *QT01.09.02

Bose Polaron Interactions in a Cavity-Coupled Monolayer Semiconductor Martin Kroner; ETH Zurich, Switzerland

The interaction between a mobile quantum impurity and a bosonic bath leads to the formation of quasiparticles, termed Bose polarons. The elementary properties of Bose polarons, such as their mutual interactions, can differ drastically from those of the bare impurities. Here, we explore Bose polaron physics in a two-dimensional nonequilibrium setting by injecting left hand circular polarised exciton-polariton impurities into a bath of coherent right hand circular polarised polaritons generated by resonant laser excitation of monolayer MoSe₂ embedded in an optical cavity. By exploiting a biexciton Feshbach resonance between the impurity and the bath polaritons, we tune the interacting system to the strong-coupling regime and demonstrate the coexistence of two new quasiparticle branches. Using time-resolved pump-probe measurements we observe how polaron dressing modifies the interaction between impurity polaritons. Remarkably, we find that the interactions between high-energy polaron quasiparticles, that are repulsive for small bath occupancy, can become attractive in the strong impurity-bath coupling regime.

9:00 AM *QT01.09.03

Proximity Effects and Excitons in Van der Waals Heterostructures Jaroslav Fabian; University of Regensburg, Germany

Excitonic spectra of 2D semiconductors are known to be very sensitive to the dielectric surroundings. But they can also be tailored by weak van der Waals hybridizations across the layers---the so called proximity effects. Placing a transition metal dichalcogenide, such as WSe₂, in contact with a ferromagnetic CrI₃, results in exchange induced valley-resolved single-particle spectral shifts which can be probed by excitonic absorption. I will present our theoretical efforts in ab initio modeling of the proximity effects and the Bethe-Salpeter equation simulation of the excitonic spectra affected by the proximity. I will also argue that in addition to pure dielectric screening effects, there are also hybridization signatures in the g-factor of excitons in transition metal dichalcogenides in contact with graphene. Finally, I will present an analysis of the excitonic g-factors in strained TMDCs in which a hybridization between inter and intraband transitions can be tuned by strain. Support from DFG SFB 1277, SPP2244, and FLAG-ERA is acknowledged.

PEF Junior et al, *First-principles insights into the spin-valley physics of strained transition metal dichalcogenides monolayers*, New J. Phys. 24, 083004 (2022).
E Blundo et al, *Strain-Induced Exciton Hybridization in WS₂ Monolayers Unveiled by Zeeman-Splitting Measurements*, Phys. Rev. Lett. 129, 067402 (2022).
FS Covre et al, *Revealing the impact of strain in the optical properties of bubbles in monolayer MoSe₂*, Nanoscale 14, 5758 (2022).
K Zollner et al, *Strong manipulation of the valley splitting upon twisting and gating in MoSe₂/Cr₃ and WSe₂/Cr₃ van der Waals heterostructures*, Phys. Rev. B 107, 035112 (2023).
PEF Junior et al, *Proximity-enhanced valley Zeeman splitting at the WS₂/graphene interface*, 2D Materials, 10, 034002 (2023).

9:30 AMBREAK

10:00 AM *QT01.09.04

Anisotropic Excitons and PolaritonsHuiDeng; University of Michigan, United States

Anisotropy is a fundamental property of materials widely exploited in science and engineering. However, the interplay between the material and engineered photonic anisotropies has been difficult to access. Van der Waals materials open the opportunity to explore a wide range of anisotropic materials and to integrate them with photonic structures. We show here a matter-light hybrid system, exciton-polaritons in a 2D antiferromagnet, CrSBr, coupled with an anisotropic photonic crystal cavity, where the spin, atomic lattice, and photonic lattices anisotropies intertwine and give rise to unusual properties of the hybrid system. We measure strong coupling between engineered anisotropic optical modes and anisotropic excitons in CrSBr, which is stable against excitation densities a few orders of magnitude higher than polaritons in isotropic materials. Moreover, the polaritons feature a highly anisotropic polarization tunable by tens of degrees by controlling the matter-light coupling via, for instance, spatial alignment between the material and photonic lattices, magnetic field, temperature, cavity detuning and cavity quality-factors.

10:30 AM *QT01.09.05

Efficient Light Collection from Single-Photon Emitters in 2D MaterialsRudolfBratschitsch; University of Muenster, Germany

Single-photon sources are crucial components for quantum networks and communications. Recently, single-photon sources in 2D materials have emerged as robust solid-state light emitters. For collecting and making use of single photons emitted from 2D materials, different strategies can be envisioned, whether the photons are needed on-chip or in free space. We present waveguide-coupled single-photon emitters in the layered semiconductor GaSe as promising on-chip sources [1]. GaSe crystals are placed on Si₃N₄ waveguides, resulting in a modified mode structure efficient for light coupling. Using optical excitation from within the waveguide, we find nonclassicality of the generated photons routed on a photonic chip. Thus, our work provides an easy-to-implement and robust platform for integrated photonic quantum technology. For far-field collection, we present polymer microlenses, which are 3D-printed directly on single-photon emitters in commercially available hBN nanocrystals. First, a regular array of hBN nanocrystals is created using capillary assembly [2]. Subsequently, we 3D-print elliptical polymer microlenses onto the nanocrystals. The light emission is efficiently collimated to angles below 5° [3]. The small angle of emission of the new single-photon source allows for using collection lenses with very low numerical apertures > 0.06, including optical fibers. In summary, we have demonstrated two methods to efficiently harvest single photons from 2D materials, rendering these single-photon sources highly promising for quantum optics and photonic quantum technologies.

References

- [1] P. Tonndorf, et al., Nano Lett. 17, 5446 (2017)
- [2] J. Preuß et al., 2D Mat. 8, 035005 (2021)
- [3] J. Preuß et al., Nano Lett. 23, 407 (2023)

11:00 AM *QT01.09.06

Excitonic Tuning Through Dynamic Modulation of Moiré PotentialKausikMajumdar¹, MedhaDandu², PushkarDasika¹, GarimaGupta¹, MayankChhaperwal¹, RabindraBiswas¹, KenjiWatanabe³, TakashiTaniguchi³, VarunRaghunathan¹ and SumanChatterjee¹; ¹Indian Institute of Science, India; ²Lawrence Berkeley National Laboratory, United States; ³National Institute for Materials Science, Japan

Moiré superlattice created by stacking two monolayers of transition metal dichalcogenides at different twist angles is an excellent testbed for exciton physics. In this work, we explore dynamic tuning of the moiré excitons through external stimulus in different moiré configurations, including homo-bilayer, hetero-bilayer, and hetero-bilayer on a nanopillar-induced strain well. We specifically show a large tunability of the confinement potential, spectral position, lifetime, and polarization characteristics of the exciton in these different types of moiré-superlattices under the influence of a gate voltage and excitation power. The experimental results corroborate well with a tunable two-dimensional quasi-harmonic oscillator model for the moiré-trapped exciton. Such strong tunability of moiré exciton has intriguing implications towards moiré-inspired device applications.

11:30 AM QT01.09.07

Quantum Melting Phase Diagram of a Two-Dimensional Electron Wigner CrystalJihoSung¹, JueWang¹, IlyaEsterlis¹, PavelA. Volkov¹, GiovanniScuri¹, YouZhou², EliseBrutschea¹, TakashiTaniguchi³, KenjiWatanabe³, YuboYang⁴, MiguelMorales⁴, ShiweiZhang⁴, AndrewMillis⁴, MikhailD. Lukin¹, PhilipKim¹, EugeneDemler⁵ and HongkunPark^{1,1}; ¹Harvard University, United States; ²University of Maryland, United States; ³National Institute for Materials Science, Japan; ⁴Flatiron Institute, United States; ⁵ETH Zürich, Switzerland

Strongly interacting electrons can form novel quantum states of matter, exhibiting rich phase diagrams and exotic physical phenomena. The two-dimensional (2D) electron gas provides a paradigmatic example, where competition between Coulomb repulsion and kinetic energy leads to quantum melting of an electron Wigner crystal on increasing electron density. Despite nearly a century of intensive research, however, the detailed nature of this transition is not fully understood. Here, using cryogenic reflectance and magneto-optic spectroscopy, we provide clear experimental evidence for long-standing theoretical predictions that the density-driven quantum melting of a Wigner crystal proceeds through an electronic mixture phase characterized by a microscopic coexistence of crystal and liquid states. At densities below $\sim 3 \times 10^{11} \text{ cm}^{-2}$, electrons in a MoSe₂ monolayer form a two-dimensional Wigner crystal. As the electron density increases, we observe abrupt changes in the spin susceptibility, excitonic reflection spectrum, and charge-order-induced exciton scattering. These anomalies mark clear phase boundaries separating a Wigner crystal, intermediate quantum melting phase(s), and a Fermi liquid state. The experimentally determined phase diagram reveals the prominent Pomeranchuk effect arising from the enhanced stability of the crystalline phase upon heating due to its large spin entropy. Our study reveals the interplay between distinct electronic states and establishes the multi-staged nature of the quantum melting in a 2D correlated electron system. Atomically thin semiconductors thus provide a unique experimental platform to study the universal properties of quantum phase transitions in correlated electron systems in two dimensions.

SESSION QT01.10: Time Resolved Studies of Excitons

Session Chairs: Andrey Chaves and Jaroslav Fabian

Thursday Afternoon, November 30, 2023

Sheraton, Fifth Floor, Public Garden

2:00 PM *QT01.10.01

Imaging Excitons in Momentum SpaceKeshavM. Dani; Okinawa Institute of Science and Technology, Japan

Optical techniques have provided us with rich information about the exciton – a two-particle photoexcited state in semiconductors and insulators. Yet, they have left a fundamental degree of freedom of the exciton inaccessible – its *momentum*!

In this talk, I will discuss the application of time-resolved photoemission techniques to access the momentum coordinate of excitons in 2D semiconductors, thereby providing us with the formation pathways of momentum-forbidden dark excitons [*Science* **370**, 1199 (2020)], an image of the electron around the hole in the exciton, the observation of the long-predicted anomalous dispersion of the exciton-bound electron [*Science Advances* **7**, eabg0192 (2021)], the momentum distribution of the exciton-bound hole, and the confinement of the interlayer exciton in a moiré cell [*Nature* **603**, 247 (2022)].

2:30 PM *QT01.10.02

Ultrafast Nonlinear Spectroscopy of 2D Excitons: Local Field Effects and a New Destructive Photon EchoDanielWigger; Trinity College Dublin, Ireland

Over the last several years, two-dimensional semiconductors, especially in the form of transition metal dichalcogenides, have gained considerable attention in several areas of physics. One of the reasons for this is their strong excitonic optical response, which makes them attractive for future optoelectronic or quantum applications. Their remarkable brightness allows to efficiently study them with ultrafast nonlinear spectroscopy to learn about their fundamental excitonic properties and the excitons' coupling to other quasi-particles. We have recently studied how the spectral dynamics of pump-probe [1] and four-wave mixing signals [2,3] can be interpreted by an exactly solvable model that extends the basic optical Bloch equations by a local field effect [4]. This local field coupling takes into account the exciton-exciton interaction between the optically generated excitons in the 2D systems on a mean field level and leads to spectral shifts depending on the excitonic occupations.

We then went a step further and studied six-wave mixing (SWM) signal dynamics and discovered a peculiar temporary signal depression, depending on the considered delay between the two applied laser pulses [5]. In this contribution, we will report on this experimental finding and demonstrate that the observed signal dynamics can be understood as a new destructive photon echo. With our local field model we are able to attribute this effect to the interaction between the excitons. We show that the two main contributions to the SWM signal interfere destructively for certain times. Already in his first report of the spin echo effect in 1950, E. Hahn has used the Bloch vector description to illustrate his newly discovered phenomenon [6]. Inspired by this, we developed a similar Bloch vector description for the destructive photon echo. Interestingly, we found that the Bloch vectors contributing to the SWM signal form Lissajous figures that get distorted with progressing time [5]. The new destructive photon echo effect allows to efficiently and systematically study the exciton-exciton interaction across 2D semiconductor samples with a spatial resolution which is only restricted by the diffraction limit of the applied laser pulses. Thereby we will be able to learn more about the potential interplay between exciton-exciton interaction and for example local strain distributions.

[1] A. Rodek et al., Local field effects in ultrafast light-matter interaction measured by pump-probe spectroscopy of monolayer MoSe₂, *Nanophotonics* 10, 2717 (2021).

[2] T. Hahn et al., Influence of local fields on the dynamics of four-wave mixing signals from 2D semiconductor systems, *New J. Phys.* 23, 023036 (2021).

[3] A. Rodek et al., Controlled coherent-coupling and dynamics of exciton complexes in a MoSe₂ monolayer, *2D Mater.* 10, 025027 (2023).

[4] M. Wegener et al., Line shape of time-resolved four-wave mixing, *Phys. Rev. A* 42, 5675 (1990).

[5] T. Hahn et al., Destructive photon echo formation in six-wave mixing signals of a MoSe₂ monolayer, *Adv. Sci.* 9, 2103813 (2022).

[6] E. Hahn, Spin echoes, *Phys. Rev.* 80, 580 (1950).

3:00 PMBREAK

3:30 PM QT01.10.03

Nanoplatelet-Like Ultrafast Dephasing Behavior of CdS/CdSe/CdS Spherical Quantum Wells Tomas A. Ferreira¹, Albert Liu², Guk Jeong Byeong³, Wan Ki Bae⁴, Steven Cundiff⁵, Diogo B. Almeida⁶ and Lazaro Padilha¹; ¹Unicamp, Brazil; ²Max Planck Institute for the Structure and Dynamics of Matter, Germany; ³Pusan National University, Korea (the Republic of); ⁴Sungkyunkwan University Advanced Institute of NanoTechnology, Korea (the Republic of); ⁵University of Michigan, United States; ⁶Universidade Federal do ABC, Brazil

Carrier dynamics in colloidal nanostructures has been the subject of scrutiny for several decades, given the possibility of tuning these materials' optical and electronic properties by the proper choice of size, shape, and composition. The ever-growing possibilities regarding architecture and composition still translate into a great demand for a comprehensive understanding of the dynamics of the many-body phenomena involved in nanomaterial systems, especially coherent exciton dynamics, with potential applications to emerging quantum systems.

In this work we perform optical multidimensional coherent spectroscopy (MDCS) on different samples of CdS/CdSe/CdS colloidal spherical quantum wells (SQWs), probing their exciton dephasing times and population dynamics, at a series of cryogenic temperatures.

Colloidal nanostructures, in general, have inherently large inhomogeneous spectral broadening due to the size distribution of the probed ensemble, hindering the characterization of the system's homogeneous responses. In addition to the temporal resolution, common on nonlinear optical spectroscopies, MDCS allow the probing of homogeneous responses even in the presence of large size inhomogeneity. Additionally, by spectrally resolving the signal, one can measure coupling strengths between quantum states.

Spherical quantum wells are nanoparticles consisting of a nucleus, enveloped by a layer of different composition that, in turn, is covered by another layer of distinct composition. The middle layer (well) material (CdSe) has an optical gap smaller than the nucleus and the outer shell (CdS) subjecting the excitons to confinement in the middle layer, effectively creating a quantum well with spherical symmetry.

The SQW architecture results in higher quantum-yields and absorption cross-sections when compared to their CdSe/CdS quantum dots counterparts. Additionally, our results indicate that the strong quantum confinement of the hole wave-function in the CdSe well indeed renders to excitons in such structures dephasing times comparable to those of CdSe nanoplates (NPLs).

Our results show that excitons confined in SQWs can become spatially separated along the spherical surface of the well analogous to the spatial separation of excitons across the lateral dimensions of CdSe NPLs, reducing the Auger recombination rates. The SQWs examined in this work differ in the width of the outer CdS shell, which translates in different strengths of the electron wave-function confinement, giving extra insight to the role of electron confinement on the exciton dephasing times.

We measured sub-ps dephasing times, at 6K, for our samples. These values are, at least, one order of magnitude shorter than those for spherical CdSe/CdS core/shell quantum dots. Additionally, we observe a decrease in dephasing time with increasing the electronic wavefunction delocalization by increasing the outer shell thickness, the opposite of what is reported on core/shell systems. Finally, our temperature series measurements corroborate with acoustic phonon population increase and coupling behaviors similar to core/shell quantum dots, indicating a similar (additional) dephasing route.

3:45 PM QT01.10.04

Emission Dynamics of Hexagonal-Boron Nitride (hBN) Single Photon Emitters (SPEs) Pumped by High Power Density Laser Excitation Kristina L. Malinowski, Hamidreza Akbari and Harry A. Atwater; California Institute of Technology, United States

Color centers in thin hBN crystals are promising candidate single photon emitters (SPEs), as they exhibit bright single photon emission at room temperature. We find that at high pump power densities (~70 kW/cm² at 532 nm wavelength), single photon emitting defects in hBN exhibit unstable emission around 600 nm wavelength under pulsed or continuous wave lasers. We observe both blinking (switching between a state of radiative emission and no radiative emission on long time scales), and long-term irreversible degradation of the SPE character of individual defects. To characterize the SPE at a given power, we scanned over the area containing the color center (~9 μm²) with a confocal luminescence microscope to measure the emission of the color center at each wavelength. This measurement produces both a visible emission spectrum for each scan point, as well as the emission integrated over wavelength for each point, which can be arranged in a photoluminescence (PL) map indicating how total emission changes spatially. We found, the full width half maximum (FWHM) at the zero-phonon line (ZPL) increases from 27 nm to over 88 nm when the power is increased from 25 kW/cm² to 165 kW/cm² at 532 nm. This broadening coincides with a transition from photon anti-bunching to bunching, quantified with second-order correlation (g²) measurements. The PL maps also show that under increased pump powers the radius of strong emission increases over 3-fold from 0.4 μm to 1.25 μm. This implies that at high pump powers, the color centers evolve from localized SPEs to classically emissive defects, capable of transporting the excited charge on the order of microns prior to radiative emission. Further, increasing the power causes a blue shift in the emission wavelength of the photons, indicating modification of the radiative emission pathway. We also observe a self-recovery of radiative emission over extended (336 hour) times. Fast, self-recovery of emitters, suggests there may be a relation between the blinking and apparent irreversible degradation, with blinking occurring over minutes or hours and degradation occurring over days or weeks. The observed self-recovery phenomenon points to the dynamics of photoexcited trapped charges in emission. This hypothesis will be further addressed by Kelvin probe force microscopy to reveal the spatial profile and role of trapped charges on hBN single photon emitter electrostatic charging and discharging.

4:00 PM QT01.10.05

Exciton Dynamics and Anisotropy in 2D Silver Phenylchalcogenolates Woo Seok Lee, Yeongsu Cho, Peter Müller, Ruomeng Wan, Eric Powers, Watcharaphol Paritmongkol, Tomoaki Sakurada, Nicholas Samulewicz, Heather J. Kulik and William Tisdale; Massachusetts Institute of Technology, United States

Silver phenylselenolate (AgSePh) and silver phenyltelluroate (AgTePh) are novel two-dimensional (2D) van der Waals semiconductors. However, despite having a similar crystal structure and composition, AgSePh and AgTePh exhibit strikingly different excitonic properties. While the three distinct excitonic absorption resonances of AgSePh are close in energy, AgTePh exhibits a large energetic separation between the two lowest excitonic absorption resonances. More strikingly, whereas AgSePh exhibits narrow, fast luminescence with a minimal Stokes shift, AgTePh exhibits comparatively slow, significantly red-shifted and broadened luminescence. In this presentation, we will present the synthesis, structural and optical properties of single crystals and thin films of AgSePh and AgTePh. Using time-resolved and temperature-dependent optical spectroscopy, combined with sub-gap photoexcitation studies, we will show that exciton dynamics in AgTePh films are dominated by intrinsic exciton self-trapping behavior, whereas dynamics in AgTePh films are dominated by the interaction of free-excitons with extrinsic defect states. Furthermore, using polarization-dependent optical spectroscopic studies on single crystals of AgSePh and AgTePh, we will show the strikingly different exciton anisotropy in these materials. Whereas the lowest and the second lowest free-excitons in AgSePh are polarized along [010] and [100] direction, respectively, the two lowest free-excitons and self-trapped excitons in AgTePh are all polarized along [010] direction. Finally, we will discuss GW plus Bethe-Salpeter equation calculations to understand anisotropic excitons in these materials. Overall, this work highlights the properties of a novel class of 2D excitonic semiconductors and lays the foundation for understanding exciton dynamics and anisotropy in these

8:00 AM *QT01.11.01

Engineering Qubits in Silicon with Atomic Precision Michelle Y. Simmons; University of New South Wales, Australia

The realisation of a large-scale error corrected quantum computer relies on our ability to reproducibly manufacture qubits that are fast, highly coherent, controllable and stable. The promise of achieving this in a highly manufacturable platform such as silicon requires a deep understanding of the materials issues that impact device operation. In this talk I will demonstrate our progress to engineer every aspect of device behaviour in atomic qubits in silicon. This will cover the use of atomic precision lithography to achieve fast, controllable exchange coupling [1], fast, high fidelity qubit initialisation and read-out [2]; low noise all epitaxial gates allowing for highly stable qubits [3]; and qubit control [4] that provide a deep understanding of the impact of the solid-state environment [5] on qubit designs and operation. I will also discuss our latest results in [6] analogue quantum simulation.

[1] Y. He, S.K. Gorman, D. Keith, L. Kranz, J.G. Keizer, and M.Y. Simmons, "A fast (ns) two-qubit gate between phosphorus donor electrons in silicon", *Nature* 571, 371 (2019) [2] D. Keith, M. G. House, M. B. Donnelly, T. F. Watson, B. Weber, M. Y. Simmons, "Microsecond Spin Qubit Readout with a Strong-Response Single Electron Transistor", *Physical Review X* 9, 041003 (2019); D. Keith, S. K. Gorman, L. Kranz, Y. He, J. G. Keizer, M. A. Broome, M. Y. Simmons, "Benchmarking high fidelity single-shot readout of semiconductor qubits", *New Journal of Physics* 21, 063011 (2019). [3] L. Kranz S. K. Gorman B. Thorgrimsson Y. He D. Keith J. G. Keizer M. Y. Simmons, "Exploiting a Single-Crystal Environment to Minimize the Charge Noise on Qubits in Silicon", *Advanced Materials* 32, 2003361 (2020). [4] L. Fricke, S.J. Hile, L. Kranz, Y. Chung, Y. He, P. Pakkiam, J.G. Keizer, M.G. House and M.Y. Simmons, "Coherent spin control of a precision placed donor bound electron qubit in silicon", *Nature Communications* 12, 3323 (2021). [5] M. Koch, J.G. Keizer, P. Pakkiam, D. Keith, M.G. House, E. Peretz, and M.Y. Simmons, "Spin read-out in atomic qubits in an all-epitaxial three-dimensional transistor", *Nature Nanotechnology* 14, 137 (2019 – with cover article). [6] M. Kiczynski, S.K. Gorman, H. Geng, M.B. Donnelly, Y. Chung, Y. He, J.G. Keizer and M.Y. Simmons, "Engineering topological states in atom-based semiconductor quantum dots", *Nature* 606, 694-699 (2022)

8:30 AM *QT01.11.02

Bose-Einstein Condensation of Excitons in a Bulk Semiconductor at Sub-Kelvin Temperatures Kosuke Yoshioka, Yusuke Morita and Makoto Kuwata-Gonokami; University of Tokyo, Japan

It has long been a major problem in solid state physics and quantum statistical physics to experimentally clarify whether excitons, which are bound pairs of electrons and holes in bulk semiconductors, can spontaneously form Bose-Einstein condensates or not. The 1s para exciton of cuprous oxide has been studied for many years from both theoretical and experimental aspects as the most promising candidate for the realization of BEC, because it has an extremely long lifetime and behaves as a pure matter-like quasiparticle with finite mass. In this talk, we will present a study that demonstrates for the first time by real-space imaging that 1s para excitons form condensates in the temperature range of a few hundred mK [1].

BEC in this system was expected to be possible at superfluid helium temperatures by the production of high-density excitons by relatively intense laser irradiation. However, experimental evidence of BEC has not been observed. It has turned out that exciton loss processes resulting from two-body collisions between excitons occur with orders of magnitude higher efficiency than expected [2]. In such a case, the excitons cannot have a long enough lifetime for cooling, which was the reason why BECs did not appear. Therefore, during the last decade or so, the transition temperature setting has been lowered to sub-Kelvin temperatures, and the search for BEC at lower BEC transition densities has been conducted [3].

In recent years, we have realized an experimental setup in which a semiconductor crystal is cooled using a cryogen-free dilution refrigerator and laser beams in the visible and mid-infrared wavelength regions are introduced. Through exciton accumulation in an inhomogeneous strain-induced harmonic trap potential and activation of cooling channels effective for slow excitons through exciton-phonon interactions in the strain field, we have achieved exciton ensembles at approximately 100 mK [4], which is the lowest temperature in exciton systems. By evaluating the induced absorption associated with the 1s-2p transition located in the mid-infrared wavelength range, we can quantitatively evaluate the density of the exciton system [5], which is a key quantity for BEC. We have extended this measurement method to absorption imaging [6] and have utilized it in low temperature experiments in a dilution refrigerator. This was essentially important for the observation of the real image of the condensate.

The exciton condensate is a brand-new quantum many-body physical system. When the BEC criteria are satisfied, a localized density distribution appears at the bottom of the trap potential. As the exciton number is increased, the spatial broadening of the condensate increases, and this behavior can be interpreted in the same way as BEC of real particles, from which the elastic scattering length of the repulsive interaction between excitons can be derived. While those phenomena are within the framework of conventional BEC theory, the observed small fraction of condensates cannot be understood by conventional theory. This may be characteristic of quantum statistical phenomena in non-equilibrium and open systems of quasiparticles.

[1] Y. Morita et al., *Nat. Commun.* 13, 5388 (2022). [2] K. Yoshioka et al., *Phys. Rev. B* 82, 041201(R) (2010). [3] K. Yoshioka et al., *Nat. Commun.* 2, 328 (2011). [4] K. Yoshioka et al., *Phys. Rev. B* 88, 041201(R) (2013). [5] M. Kuwata-Gonokami et al., *J. Phys. Soc. Jpn.* 73, 1065 (2004). [6] K. Yoshioka et al., *Phys. Rev. B* 91, 195207 (2015).

9:00 AM *QT01.11.03

Enhancing the Light Emission of 2D-TMDs and MXene Quantum Dots Jeongyong Kim; Sungkyunkwan University, Korea (the Republic of)

Quantum-confined semiconductors with light-emitting properties offer tremendous opportunities in photonic devices with the advantages of high efficiency, tunability and flexibility. Photoluminescence quantum yield (PL QY) is one of fundamental performance parameters of these quantum optical semiconductors. In this presentation, I will discuss some of the strategies we developed to enhance the PL QY of two-dimensional (2D) transition metal dichalcogenides (TMDs) and MXene quantum dots (MQDs).

While the structural defects are the main cause that degrades the PL QY of monolayer (1L) TMDs, Auger process represented by exciton-exciton annihilation (EEA) is the major non-radiative decay channel of excitons of 1L-TMDs in high exciton density regime [1,2]. We demonstrate that combined use of proximal Au plate and negative electric gate bias for 1L-WS₂ provides the dramatic enhancement of QY and exciton lifetime at high exciton densities [3]. QY was enhanced by 30 times and the EEA rate constant decreased by 80 times. Suppression of EEA by negative electric bias is attributed to the reduction of defect-assisted EEA process, which was then explained by the theoretical model. Our results provide a synergetic solution to cope with EEA to realize the high-intensity 2D light emitters using TMDs.

MQDs, obtained by fragmenting MXene into quantum dimension, provide the light emission properties with the advantages of the low cost and the biocompatibility [4,5]. However, because of active surface trap sites of MQDs, PL QY of MQDs is low in their pristine states. We show that a dramatic enhancement of PL QY of MQDs can be achieved by removing the F-termination during the synthesis, resulting in 25% PLQY in UV emission [6]. We also observed the degradation of PL QY with the increasing excitation intensity, of which details will be discussed. This work was supported by National Research Foundation of Korea (2021R1A6A1A03039696; 2022R1A2C2009412; 2022K2A9A1A06093582)

References

- [1] Y. Lee et al., *Nat. Commun.*, **10**, 3397 (2021).
 [2] Y. Lee et al., *ACS Photon.*, **9**, 873 (2022).
 [3] T. T. Tran et al., manuscript submitted
 [4] A. Sharbirin, S. Akhtar, J. Kim, *Opto-Electron. Adv.*, **4**, 200077 (2021).
 [5] A. Sharbirin, et al., *J. Mater. Chem. C*, **10**, 6508 (2022)
 [6] A. Sharbirin, et al., manuscript in preparation

9:30 AM *QT01.11.04

Excitonic Behavior in Perovskite Nanoplatelets—The Role of Defects and Achieving Linearly Polarized Electroluminescence Robert Hoye; University of Oxford, United Kingdom

Linearly polarized light is important for a wide range of applications, such as 3D displays and optical communications. However, linear polarization is typically achieved by filtering unpolarized light, which leads to significant losses in energy. This talk examines the use of nanostructured lead-halide perovskites to directly achieve polarized light emission.

Although nanostructured halide perovskites have important advantages in terms of color purity and tunability, they are strongly affected by surface defects. Thus, the first half of this talk examines how the surface chemistry of CsPb(Br_xI_{3-x}) nanocrystals can be controlled through the polarity of the antisolvent used during purification. Through detailed nuclear magnetic resonance, Fourier transform infrared spectroscopy and X-ray photoemission spectroscopy measurements, we show that higher polarity antisolvents lead to increased selective etching of the iodide species due to the removal of the long-chain organic ligands through condensation reactions [1].

The second half of the talk discusses the use of self-assembled CsPbI₃ perovskite nanoplatelets to achieve polarized light emission. We show that the high dielectric and quantum confinement in these nanoplatelets leads to a large splitting in the exciton fine structure. In the edge-up perovskite nanoplatelet superlattices, we achieve strong emission from the out-of-plane dipole for the optically bright excitons. In light-emitting diodes, this led to a high degree of polarization in electroluminescence of 74.4% without requiring the use of any photonic structures [2].

[1] Ye, ..., Hoyer, J. Am. Chem. Soc., 2022, 144, 12102

[2] Ye, ..., Hoyer, arxiv: 2302.03582

10:00 AM QT01.11.05

Exciton-Exciton Interactions - A Comparative Study of Complimentary Phenomenological Models Pradeep Kumar, Bhaskar De, Rishabh Tripathi and Rohan Singh; Indian Institute of Science Education and Research, Bhopal, India

The optical response of semiconductor nanostructures is significantly influenced by many-body interactions (MBIs), such as exciton-exciton interactions. Excitation density-dependent optical experiments have previously shown the existence of these MBIs effect in 2D nanomaterials like quantum wells, transition metal dichalcogenides (TMDCs), perovskite nanoplatelets. The effects of the MBIs can be seen in the coherence - decay dynamics of the excitonic transition. To investigate the coherence dynamics of these nanomaterials' optical response, nonlinear techniques such as four-wave mixing (FWM) and two-dimensional coherent spectroscopy (2DCS) are usually used.

Theoretical models have been developed to explain the microscopic origins of these MBIs. The semiconductor Bloch equation (SBE) formalism based on microscopic model is the most robust approach, comprises a complete many-body treatment. However these microscopic calculations can be computationally challenging and also have limited physical insight. To overcome these limitations, phenomenological models were developed as a reasonable substitute. Phenomenologically, MBI effect can be described in terms of excitation induced dephasing (EID), and excitation induced shift (EIS). The EIS and EID effects were measured as a change in the exciton resonance energy and dephasing rate, respectively, with an increase in the excitation density.

One way to understand these interactions is through the Modified optical Bloch equations (MOBEs). The excitons are primarily treated as a two-level system (fermions) and the OBEs are used to describe their interaction with light. The MOBEs incorporate EID and EIS through a linear dependence of dephasing rate and resonance frequency with excitation density to comprehend the physical nature of MBIs. Here MOBEs need to be numerically solved, which limits their application to quantitative data analysis.

Another, less computationally intense approach to understand these MBIs is through the anharmonic oscillator model. In this formalism interacting excitons are treated as composite bosons or pure harmonic system. MBIs between interacting excitons produces anharmonicity in the system. This anharmonicity leads to nonlinear optical response in the interacting excitonic system. The nonlinear signal obtained here by analytically solving OBEs for a three-level anharmonic ladder system using a perturbative approach.

The phenomenological models outlined above have each been used to comprehend the nonlinear optical response of excitons separately. To the best of our knowledge, a direct correspondence between the two models is yet to be studied. It is still undetermined whether these models' coherence decay dynamics are equivalent. It also needs to be determined whether the parameters utilized in the two models to quantify MBIs are equivalent. Since MBI affects 2D spectra peak shape and its phase which is usually apparent in 2DCS. In this work, we show the empirical equivalence between these two complimentary MBI models through 2DCS simulations. Interestingly, we find that both the complimentary approaches are consistent with each other. We also perform a quantitative comparison of these MBI models with experiments, which highlights the usefulness of these phenomenological models in interpreting experimental results. The formalisms used here can also be used to compare and quantify the relative strength of MBIs in various excitonic systems, such as quantum wells, layered semiconductors and perovskite nanomaterials. These new finding might be crucial in directing the substantial work being done to construct flexible semiconductor quantum dot lasers and TMDCs-based valleytronics devices.

SYMPOSIUM QT02

Space, Energy and Time-Resolved Spectroscopies for Emergent Quantum Materials
November 27 - December 5, 2023

Symposium Organizers

Valentina Bisogni, Brookhaven National Laboratory
Amélie Juhin, IMPMC, CNRS-Sorbonne Université
Mingda Li, Massachusetts Institute of Technology
Yao Wang,

* Invited Paper
+ JMR Distinguished Invited Speaker

SESSION QT02.01: Characterization of Low-Dimensional Quantum Systems I
Session Chairs: Mingda Li and Yao Wang
Monday Morning, November 27, 2023
Sheraton, Fifth Floor, The Fens

10:30 AM *QT02.01.01

X-Ray Spectroscopy for 2D Quantum Materials Riccardo Comin; Massachusetts Institute of Technology, United States

Over the past two decades, Resonant Inelastic X-ray Scattering (RIXS) has become an essential tool for investigating the microscopic interactions and low energy dynamics in various quantum materials. RIXS possesses a unique capability to probe the spin, charge, and orbital degrees of freedom with a shallow probing depth in the range of 50-100 nm. Consequently, RIXS has gained prominence as a fundamental spectroscopic technique for investigating a broad spectrum of materials, including bulk, thin films, and more recently, few-layer 2D materials. In this presentation, I will focus on recent advancements that have facilitated RIXS studies of two-dimensional quantum materials exhibiting emergent properties in the ultrathin limit. Specifically, I will discuss two recent investigations involving unconventional superconductor FeSe and type-II van der Waals multiferroic NiI₂. In the case of FeSe, I will present RIXS data

that elucidate the evolution of spin excitations from bulk FeSe to its monolayer form. For NiI2, I will discuss the progression of low-energy orbital and spin excitations as the material is thinned down from bulk crystals to few-layer flakes.

11:00 AM QT02.01.02

Noise Magnetometry of Topological BKT Transition in Two-Dimensional Superconductors Jonathan Curtis¹, Nicholas Poniatoski², Pavel Dolgirev², Ilya Esterlis³, Bertrand Halperin², Amir Yacoby², Eugene Demler⁴ and Prineha Narang¹; ¹University of California, Los Angeles, United States; ²Harvard University, United States; ³University of Wisconsin–Madison, United States; ⁴ETH Zürich, Switzerland

The Berezinskii-Kosterlitz-Thouless (BKT) transition is an exotic type of phase transition present in two-dimensional systems that spontaneously break a U(1) type of symmetry. This transition is characterized by the proliferation of topological defects (vortices) above the transition temperature T_{BKT} , which then destroy the quasi-long-range order (QLRO) present below T_{BKT} . While superconductors in the extreme two-dimensional limit should in principle show such a transition, it is often hard to conclusively demonstrate the presence of BKT physics and even more difficult to fully characterize beyond DC transport.

Here we will show how, using diamond nitrogen-vacancy center (NV) noise magnetometry, the BKT transition can be carefully studied across different length scales and dynamical regimes, offering new insight and more detail into the nature of the transition. NV noise magnetometry is a new non-invasive technique for the quantum sensing of magnetic fields, where highly coherent spin-qubits, hosted by nitrogen-vacancy point defects in lattice of diamond, can be used to precisely measure dynamical magnetic field fluctuations as a function of frequency and length scale. Since the BKT transition is characterized by the proliferation of vortices, which each carry magnetic flux, NV noise magnetometry is in fact perfectly suited for studying how these vortices unbind and proliferate beyond simple DC transport considerations. We show how using this technique, new insights into the dynamics and scaling of two-dimensional superconductors near the transition can be studied in the atomically-thin limit.

11:15 AM QT02.01.03

Highly Tunable Electronic Structures in Kagome Magnet Fe_xSn_y Thin Films Zheng Ren^{1,2}, Ilija Zeljkovic² and Ming Yi¹; ¹Rice University, United States; ²Boston College, United States

The kagome lattice is a corner-sharing triangular lattice that hosts flat bands, van Hove singularities and Dirac crossings. Recent experimental discoveries in kagome metals have showcased that they are an excellent platform for studying emergent charge, magnetic, superconducting orders as well as topological electronic structures. Fe_xSn_y (Fe_3Sn_2 and FeSn) has been shown to exhibit (massive) Dirac fermions, anomalous Hall effect, flat bands and more. Here, we selectively synthesize Fe_3Sn_2 and FeSn thin films using molecular beam epitaxy. In Fe_3Sn_2 , using spectroscopic-imaging scanning tunneling microscopy, we discover a number of dI/dV spectral peaks. These peaks show a prominent magnetic-field-tunability. The features point to the theoretically-predicted tunable Weyl points near the Fermi level. In FeSn , we use angle-resolved photoemission spectroscopy to resolve the band structure, which is significantly tunable as we change the temperature of the sample. Our findings suggest highly tunable electronic structures in the kagome magnet Fe_xSn_y thin films.

11:30 AM QT02.01.04

Sharp Band Renormalizations in Superconducting LiTi_2O_4 Thin Films Observed by Angle-Resolved Photoemission Spectroscopy (ARPES) Zubia Hasan¹, Grace Pan¹, Matthew Barone², Albertode La Torre Duran³, Austin Kaczmarek², Shekhar Sharma⁴, Katja Nowack², Antia Botana⁴, Brendan Faeth² and Julia Mundy¹; ¹Harvard University, United States; ²Cornell University, United States; ³Brown University, United States; ⁴Arizona State University, United States

The mechanisms behind unconventional superconductivity have been intensely studied over the past few decades. Leading this thrust has been the high T_c cuprates, whose pairing ‘glue’ has been widely debated. LiTi_2O_4 , a spinel oxide material, is an unconventional superconductor that preceded the cuprates [1]. However, despite having one of the highest T_c (~13.7 K) for a non-cuprate oxide, little is known about its’ superconducting mechanism, with reports of both unconventional pairing [2] and traditional phonon-mediated BCS-like behavior [3]. There have also been signs of orbital and spin fluctuations persisting up to ~100 K, based on angle-dependent transport data [4]. Nevertheless, it remains unclear which mechanisms—spin fluctuations, electron-phonon coupling or mixed valency—are essential for superconductivity in LiTi_2O_4 . Here, we use angle-resolved photoemission spectroscopy (ARPES) with molecular beam epitaxy (MBE) to interrogate the electronic band structure of LiTi_2O_4 thin films on MgAl_2O_4 (111) substrates. Our work shows the first-ever experimentally-determined band structure of LiTi_2O_4 . The bands intriguingly show kinks resembling cuprate-like band renormalizations. Our data indicates the presence of strong correlations: the band centered at Γ shows a ‘kink’ at around $E_F \sim 40$ meV and a quasi-particle peak and incoherent tail suggestive of coupling to a bosonic mode. We see that this mode is present at all values of k_F and k_z and persists above T_c . We discuss the origin of the kinks in LiTi_2O_4 , providing broader insight into the pairing symmetry present in this superconducting system.

[1] D. C. Johnston et al, Mater. Res. Bull. 8, 777–784 (1973).

[2] H. Xue et al, ACS Nano 16 (11), 19464 (2022).

[3] C. P. Sun et al, Phys. Rev. B 70, 054519 (2004).

[4] K. Jin. et al, Nat. Commun. 6, 7183 (2015)

11:45 AM QT02.01.05

Individual Ultrabright Fluorescent Nanoparticles as Nanothermometers Mahshid Iraniparast; Tufts University, United States

Temperature measurement at the nanoscale is important in various scientific and engineering studies, from assessing temperature distribution in the cellular medium to conducting thermal imaging of integrated circuit devices. A serious challenge in nanoscale temperature measurement lies in achieving high spatial resolution, which can be overcome by utilizing individual nanoparticles.

For this purpose, we selected fluorescent silica nanoparticles with mesoporous structure, which have encapsulated fluorescent dyes. As has been shown, such particles demonstrate ultrahigh fluorescent brightness, which is sufficient to image single nanoparticles. To be used as thermometers, two different types of dye molecules, reference molecules, and temperature-sensitive ones, were used. The measured sensitivity, reversibility, and reproducibility of measurements of temperature using these individual nanoparticles have shown the superiority of the reported particles compared to the previously reported ones. For example, the obtained individual nanothermometers exhibited a temperature fluctuation of ~0.5 K at the measurement time of 0.69 msec and excitation power density of (temperature resolution of $0.22 \text{ K}\cdot\text{Hz}^{-1/2}$), showing a relative sensitivity of 8% within the physiologically relevant range of 25–50°C. This sensitivity is ~4 times better and the temperature resolution (at an excitation power of $0.26 \mu\text{W}$) is ~2 times better than the previously reported best temperature measuring fluorescent particles.

These superior properties are presumably the result of the fluorescence resonance energy transfer (FRET) between the encapsulated dye molecules, which act as donors and acceptors. The enhanced brightness of these nanosensors offers numerous benefits, including the improved signal-to-noise ratio and the ability to locate the particles with high spatial precision. This work was supported by NSF grants CBET 1911253 and 2110757 (IS).

SESSION QT02.02: Characterization of Low-Dimensional Quantum Systems II

Session Chairs: Mingda Li and Yao Wang

Monday Afternoon, November 27, 2023

Sheraton, Fifth Floor, The Fens

1:30 PM *QT02.02.01

Emergent Topological and Magnetic Phases in 2D Van der Waals Materials Ming Yi; Rice University, United States

The recent discoveries of long-range magnetic order in van der Waals materials have established a new platform for probing emergent orders in correlated quantum materials. In this talk I will present our recent studies on the Fe_xGeTe_2 ($x=3,5$) family of 2D ferromagnets. In particular, I will report the observation of a quantum phase switching between a Weyl nodal line phase and a topological flat band phase in Fe_3GeTe_2 via a thermal annealing process. We further demonstrate that the switching of the electronic properties is associated with a crystal symmetry change driven by a Fe site ordering that is modulated by the thermal annealing process. The presence or absence of the ordering modifies the global crystal symmetry and gives rise to either magnetic nodal lines in one case or geometrically frustrated flat bands in the other. The modified crystal and electronic structures subsequently affect the magnetism of the two phases. We further demonstrate that this phase switching is reversibly controlled via the thermal annealing and quenching method. Our work not only reveals a rich range of quantum phases emergent in 2D van der Waals ferromagnets, but also uncovers the potential of utilizing site occupancy as a novel degree of freedom for tuning symmetry and therefore topology in quantum materials for the realization of exotic emergent phases.

2:00 PM QT02.02.02

Spectroscopic Signature of 3D Magnetism in a Van der Waals Ferromagnet Fe_3GeTe_2 Vivek Bhartiya¹, Jiemin Li¹, Taehun Kim¹, Jonathan Pelliciani¹, Xiadong Xu², Dimitri Basov³, Andrew May⁴ and Valentina Bisogni¹; ¹Brookhaven National Laboratory, United States; ²University of Washington, United States; ³Columbia University, United States; ⁴Oak Ridge National Laboratory, United States

The recently discovered family of van der Waals itinerant ferromagnets $\text{Fe}_{5-x}\text{GeTe}_2$ ($0 < x < 2$) are strongly correlated electronic systems and realize intriguing ground states i.e. heavy fermions and charge density wave [1-3]. Moreover, the *cleavable* Fe_3GeTe_2 displays the highest $T_c \sim 315$ K and has the potential for miniaturized spintronic devices operating at room temperature [4-5]. However, it is not yet known if the magnons in Fe_3GeTe_2 are confined in 2D or propagate in 3D. To date, investigation of magnons via inelastic neutron scattering is not feasible due to the small size of the available single crystals. In this study, we overcome this issue by employing a high-resolution resonant inelastic X-ray scattering (RIXS) on a mm-size single crystal of Fe_3GeTe_2 [5]. A broad magnetic continuum stretching up to 150 meV and displaying a strong intensity modulation along $(0\ 0\ L)$ is observed [6]. We show that this intensity modulation is compatible with a dominant inter-slab magnetic interaction enabling 3D propagation of magnons in the room-temperature ferromagnet Fe_3GeTe_2 [6].

[1] Y. Zhang, et al., *Sci. Adv.* **4**, eaao6791 (2018).

[2] X. Wu, et al., *Phys. Rev. B* **104**, 165101 (2021).

[3] K. Yamagami, et al., *Phys. Rev. B* **106**, 045137 (2022).

[4] L. Alahmed, et al., *2D Mat* **8**, 045030 (2021).

[5] A. May, et al., *ACS Nano* **13**, 4436 (2019).

[6] V. K. Bhartiya, et al., unpublished.

2:15 PM QT02.02.03

Combined Nano-Optical/Scanning Tunneling Microscopy of Localized Excitons in 1L- WSe_2 Thomas P. Darlington, Xuehao Wu, Madisen Holbrook, Kevin W. Kwok, Dimitri Basov, P. James Schuck and Abhay Narayan Pasupathy; Columbia University, United States

The transition metal dichalcogenides (TMDs) are among the most studied low dimensional material classes largely due to their tightly bound exciton states which strongly interact with light. Extensive experimental and theoretical work has shown that monolayer TMDs host a rich variety of exciton complexes, from dark excitons, biexcitons, to moiré excitons. Because of this strong light-matter coupling, optical probes are often the tool of choice, however for a full understanding combined electronic, optical, and structural probes are needed to disentangle the many degrees of freedom. Combining these probes is however experimentally challenging because of the large scale mismatch of light, ~ 500 nm, and high resolution electronic/structural techniques such as scanning tunneling microscopy (STM), ~ 1 nm.

In this presentation, I will show results from a newly constructed scanning tunneling microscope integrated with a nano-optical probe that allows for co-localized near-field light delivery, at high excitation intensities, with tunneling current measurements. I will show the application of this tool to strain-localized excitons in nanobubbles of monolayer WSe_2 . We observe strong modification of the density of states in scanning tunneling spectroscopy as a function of pump fluence. Further, by hole tunneling we are able to map the STM-luminescence, revealing a localized exciton edge state with a resolution < 10 nm. Our work represents a novel demonstration of the effect of optical pumping on the single particle electronic structure in TMDs at the exciton's native length scale.

2:30 PM BREAK

SESSION QT02.03: Characterization of Topological Materials

Session Chairs: Mingda Li and Yao Wang

Monday Afternoon, November 27, 2023

Sheraton, Fifth Floor, The Fens

3:00 PM *QT02.03.01

New Features in Phonon Spectra from Highly Anharmonic Crystals Found by Inelastic Neutron Scattering Brent Fultz, Vladimir Ladygin, Claire N. Saunders and Camille Marie Bernal-Choban; California Institute of Technology, United States

Textbook phonons are bosonic quasiparticles that populate vibrational modes of a crystal. Classical dynamics is often used to find the vibrational modes, which are then quantized in units of $h\nu$, where ν is frequency and h is Planck's constant. This approach is extended to "quasiharmonic" theory, where ν is a function of volume, and to "anharmonic" theory, where a phonon self-energy depends on interactions with other phonons through cubic or quartic perturbations to the potential. Larger deviations of the potential from harmonic can be accommodated by molecular dynamics simulations. Combining these simulations with inelastic neutron scattering (INS) experiments revealed two new types of nonlinear vibrational behavior. Both are interpreted with the quantum Langevin equation.

A phonon potential with forces that depart from linearity produces spectral features found in other nonlinear media, such as crystals for nonlinear optics. Our INS measurements on rocksalt NaBr found intermodulation phonon sidebands (IPS) at frequencies approximately equal to the sum and difference of strongly-interacting TA and TO phonon modes [1]. The "input-output theory" of quantum optics [2] was successful for predicting the intensities and shapes of the intermodulation sidebands, although the wavevector dependence of phonons adds complexity. Very recent measurements on NaBr show frequency doubling at elevated temperatures.

A second nonlinear phenomenon was found in cuprite, Cu_2O . At temperatures above room temperature, a diffuse inelastic intensity (DII) replaced the optical modes. Again, the Schrödinger-Langevin equation could predict the general appearance and perhaps the shape of the DII. It originates with phase shifts in the oscillations of oxygen atoms caused by slower movements of neighboring Cu atoms. The DII requires both anharmonicity and some temporal randomness in the nonlinear forces between neighboring atoms.

Experiments to isolate the IPS and DII were performed with single crystals on a direct-geometry Fermi chopper spectrometer, ARCS, at the Spallation Neutron Source. Background removal was a challenge, but the experiments could not have been done without the low background, high flux, and detector efficiency of the ARCS spectrometer. Advances in experimental capabilities will allow other studies of nonlinear phenomena in phonon physics, and new insights into phonon anharmonicity.

[1] DOI: 10.1103/PhysRevB.103.134302

[2] DOI: 10.1103/PhysRevA.31.3761

This work is supported by DOE BES award No. DE-FG02-03ER46055.

3:30 PM *QT02.03.02

PRX: What Quantum-Materials Papers are suitable? Yiming Xu; American Physical Society, United States

PRX is published by the American Physical Society, a nonprofit membership society of scientists. Its mission goal is to select around 250 *landmark* papers a year from all fields of physics and showcase them to a broad and multidisciplinary readership. Quantum Materials is undoubtedly a field of high interest to PRX, and also to the Physical Review journal family.

Is your paper a good match for PRX? Or asked differently, what papers qualify as *landmark* papers, especially in the field of quantum materials?

How do the PRX editors actually select such papers? Are such selections always accurate?

How can you, as an author, navigate PRX's editorial and peer-review process effectively and get the most out of your interactions with the editors and referees?

Many of these questions do not have a black-and-white answer in the case of a single paper. Open-minded, reasoned, and constructive dialogues amongst the authors, the editors, and the referees are key to making each concrete process a meaningful and productive experience, and sometimes even a pleasure, for everyone. I will use the talk to discuss with you how to answer these questions.

4:00 PM *QT02.03.03

Observation of Pines' Demon in Sr_2RuO_4 Peter Abbamonte; University of Illinois at Urbana-Champaign, United States

The characteristic excitation of a metal is its plasmon, which is a quantized collective oscillation of its electron density. In 1956, David Pines predicted that a distinct type of plasmon, dubbed a "demon," could exist in three-dimensional metals containing more than one species of charge carrier. Consisting of out-of-phase movement of electrons in different bands, demons are acoustic, electrically neutral, and do not couple to light, so have never been detected in an equilibrium, three-dimensional metal. Nevertheless, demons are believed to be critical for diverse phenomena including phase transitions in mixed-valence semimetals, optical properties of metal nanoparticles, soundarons in Weyl semimetals, and high temperature superconductivity in, for example, metal hydrides. Here, we present evidence for a demon in Sr_2RuO_4 from momentum-resolved electron energy-loss spectroscopy (M-EELS). Formed of electrons in the β and γ bands, the demon is gapless with critical momentum $q_c = 0.08$ reciprocal lattice units and room temperature velocity $v = (1.065 \pm 0.12) \times 10^5$ m/s, which undergoes a 14% renormalization upon cooling to 20 K due to coupling to the particle-hole continuum. The momentum dependence of the intensity of the demon confirms its neutral character. Our study confirms a 66-year old prediction and suggests that demons may be a pervasive feature of multiband metals.

4:30 PM QT02.03.04

Magnetic Structure of Hexagonal Mn_3Ga Thin Film by Neutron Scattering [QuanzhengTao](#)^{1,2}, JohannaRosen¹ and AndrewBoothroyd²; ¹Linkoping University, Sweden; ²University of Oxford, United Kingdom

Hexagonal Mn_3X compounds (where X=Sn, Ge, Ga) have recently gained substantial attention due to their large anomalous Hall effect, even with a negligible magnetic moment. Compared to Mn_3Sn and Mn_3Ge , Mn_3Ga has been less studied owing to the unavailability of single crystals. In this research, we demonstrate that high-quality epitaxial thin films can effectively substitute for single crystals, thus enabling advanced neutron scattering techniques. Utilizing unpolarized neutron diffraction and spherical polarized neutron scattering methods, we successfully delineated the magnetic structure of Mn_3Ga . Furthermore, through magnetotransport measurements, we identify Mn_3Ga thin film as a promising candidate for spintronics applications. This abstract presents a breakthrough for both the study and application of Mn_3Ga , demonstrating its potential for revolutionizing spintronics.

4:45 PM QT02.03.05

Deciphering the Nature of Cation Disorder via Vibrational Structure Characterizations [DongchangChen](#), YouWang, BasiratRaji-Adefila and AlexandraOutka; The University of New Mexico, United States

Cation disordering, a fascinating phenomenon that represents random cation distribution in a long range, has brought about numerous novel materials for battery applications. As a key to the performance of a cation-disordered battery material, how the cations are arranged in a shorter range is an intriguing question. In this talk, we will present our study in understanding the nature of cation disordering for a series of cation-disordered electrode materials via analyzing their vibrational structures. Owing to the unique working principle of vibrational spectroscopy, it generates critical information of cation arrangement, which cannot be feasibly obtained via diffraction analyses. Furthermore, the spectroscopic information allows to locate a few hidden key factors that control the electrochemical performance and help us build models to better understand the role of these factors.

SESSION QT02.04: Poster Session
Session Chairs: Mingda Li and Yao Wang
Monday Afternoon, November 27, 2023
Hynes, Level 1, Hall A

8:00 PM QT02.04.01

Synthesis and X-Ray Absorption Spectroscopy of $\text{Nd}_{2-x}\text{Sr}_x\text{NiO}_4$ Thin Films ($0 \leq x \leq 1.4$) [NicoleK. Taylor](#), DanFerenc Segedin, GracePan, SpencerDoyle, AriTurkiewicz, CharlesBrooks and JuliaMundy; Harvard University, United States

Ruddlesden-Popper nickelates have been studied extensively over the last three decades due to their structural similarities to the high T_c superconductivity cuprates. In particular, the layered nickelate $\text{La}_{2-x}\text{Sr}_x\text{NiO}_4$ is analogous to the high T_c superconductor, $\text{La}_{2-x}\text{Sr}_x\text{CuO}_4$. Using reactive oxide molecular beam epitaxy (MBE), we synthesis $\text{Nd}_{2-x}\text{Sr}_x\text{NiO}_4$ thin films for $x = 0, 0.50, 1, 1.2, \text{ and } 1.4$. We observe metallic conductivity for $x=1.2$ and 1.4 thin films whereas the lower doping shows semiconducting transport over the full temperature range. We present polarization-dependent O-K and Ni-L_{2,3} XAS spectra for our Sr-doped Nd_2NiO_4 thin films. We track the evolution of the oxygen-nickel hybridization, distribution of holes between O 2p and Ni 3d states and the nickel oxidation state across the series. Our results are consistent with previous work on bulk layered nickelates [1].

[1]. Uchida, M. et al. Pseudogap-related charge dynamics in the layered nickelate $\text{R}_{2-x}\text{Sr}_x\text{NiO}_4$ ($x \sim 1$). Phys Rev B 86, 165126 (2012)

We acknowledge support from the US Department of Energy under award no. DE-SC0021925.

8:00 PM QT02.04.02

Towards Floquet Engineering of Ferroelectric Semiconductors via Coherent Multidimensional Spectroscopy [RyanP. McDonnell](#), DanielD. Kohler, YueaiLin, WillaMihalyi-Koch, SongJin and JohnC. Wright; University of Wisconsin-Madison, United States

Bismuth telluroiodide (BiTeI) is a prototypical, ferroelectric Rashba semiconductor (FERSC) which possesses a myriad of interesting electronic and optical properties.^{1,2} Multiple optical transitions throughout the infrared and visible in BiTeI make it a promising material for understanding spin states in Rashba materials. However, the most promising methods for Floquet engineering of spin states in FERSCs are $\chi^{(2)}$ and $\chi^{(3)}$ dependent spectroscopies, e.g., sum frequency generation (SFG), pump-probe spectroscopy.^{3,4} The electronic structure of BiTeI is well studied, making it an ideal candidate for understanding its nonlinear response. Previous experiments reported the relative prevalence of second harmonic (SHG) over third harmonic generation (THG) output from BiTeI with an input fundamental of 0.80 eV.^{5,6} To our knowledge, there are no reports regarding frequency dependent SHG and THG output of BiTeI. Here, we use coherent multidimensional spectroscopy to probe the frequency dependence of SHG and THG output of BiTeI and perovskite FERSCs throughout the visible.⁷ Since the Rashba splitting in BiTeI varies as a function of temperature,⁸ multidimensional harmonic generation experiments on these materials are performed at cryogenic (*ca.* 90 K) and room temperatures (*ca.* 293 K) to probe the effect of temperature on SHG and THG output. These results will have implications on identifying spectroscopies for understanding and controlling the electronic structure of FERSCs.

References

- ¹ K. Ishizaka *et al.*, Nature Materials **10** (2011) 521.
- ² J. S. Lee *et al.*, Physical Review Letters **107**, 117401 (2011)
- ³ J. C. Wright, Annual Review of Analytical Chemistry, Vol **10** (2017) 45.
- ⁴ Y. Kobayashi *et al.*, Nature Physics **19** (2023) 171.
- ⁵ P. Padmanabhan *et al.*, in *Conference on Lasers and Electro-Optics (CLEO)* San Jose, CA, (2020).
- ⁶ G. Bianca *et al.*, ACS Applied Materials & Interfaces **14** (2022) 34963.
- ⁷ D. J. Morrow *et al.*, Journal of Physical Chemistry Letters **11** (2020) 6551.
- ⁸ B. Monserrat, and D. Vanderbilt, Physical Review Materials **1**, 054201 (2017)

8:00 PM QT02.04.03

Second Harmonic Generation Spectroscopic Study of Weyl Semimetal Mn_3Sn with Broken Time-Reversal Symmetry [ZiyadThekkayil](#)¹, SomaiyehDadashi¹, PrajwalLaxmeesha², StevenMay² and EricBorget¹; ¹Temple University, United States; ²Drexel University, United States

Topological Weyl semimetals constitute an important class of quantum materials, characterized by a chiral band structure resulting from the breaking of inversion and/or time-reversal symmetries. However, their experimental identification typically relies on techniques such as angle-resolved photoelectron spectroscopy or ultrahigh vacuum scanning tunnelling microscopy which require demanding conditions including low temperatures and ultrahigh vacuum environments. Consequently, there is a growing need for experimental techniques capable of identifying signatures of topological states under ambient conditions. Second-order nonlinear optical processes, such as second harmonic generation (SHG), have emerged as promising tools for studying Weyl semimetals and other topologically nontrivial systems due to their sensitivity to symmetry-breaking effects. However, most previous SHG studies on Weyl semimetals have been limited to systems with broken inversion symmetry or a combination of broken inversion and time reversal symmetries. There has been a scarcity of investigations focusing solely on Weyl

semimetals with broken time-reversal symmetry. In this study, we employ reflection SHG measurements to investigate the surface of thin films of the Weyl semimetal Mn_3Sn , which exhibits broken time-reversal symmetry. Our findings demonstrate that the surface SHG response of this system exhibits significant dependence on the excitation wavelength and polarization geometry. These observations provide valuable insights into the understanding of surface electronic properties and spin chirality in these materials. By employing these experimental techniques under ambient conditions, our research contributes to the broader goal of developing efficient methods for characterizing topological states in Weyl semimetals, paving the way for potential applications in electronic and spintronic devices.

8:00 PM QT02.04.04

Probing the Triplet Exciton in Singlet Fission Tetracene with Inelastic Neutron Scattering from First Principles Farahnaz Maleki¹, Daniel Vong¹, Eric Novak², Luke Daemen² and Adam J. Moule¹; ¹University of California, Davis, United States; ²Oak Ridge National Laboratory, United States

Singlet fission (SF) is the process of converting an excited singlet into a pair of excited triplets. Harvesting two charges from a single photon has the potential to increase photovoltaic device efficiencies. In this study, we have used Inelastic Neutron Scattering (INS) spectroscopy to investigate the phonon density of states (pDOS) of photoexcited tetracene, in order to study its singlet fission mechanism. For the first time, our group has reported in-situ excited state INS measurements on organic chromophores using a recently developed sample environment on the indirect geometry VISION neutron spectrometer at Oak Ridge National Laboratory. We employed a DFT based open source Davis computational spectroscopy (DCS) workflow to simulate INS data in the ground state of tetracene. To model the excited state of INS spectra, we performed spin-polarized calculations with triplet spin multiplet setting. It is also the first simulation of the excited state of INS data. The modeled INS spectra show the effect of the triplets on the pDOS and verifying the validity of the periodic exciton structure. The structure is used in TD-DFT to calculate the electronic states. Analysis of the results suggests that the deformations from the excited state and neighboring molecules may induce local electronic shifting, allowing E(2T1) to lower until the SF barrier reduces to be more easily overcome.

SESSION QT02.05: Foundation of Quantum Materials Characterization

Session Chairs: Valentina Bisogni and Mingda Li

Tuesday Morning, November 28, 2023

Sheraton, Fifth Floor, The Fens

8:15 AM QT02.05.01

ARPES Characterization of the Insulator-Metal Transition in Sr-Doped Nd_2NiO_4 Thin Films Dan Ferenc Segedin¹, Nicole K. Taylor¹, Ari Turkiewicz¹, Grace Pan¹, Charles Brooks¹, Luca Moreschini^{2,3} and Julia Mundy^{1,1}; ¹Harvard University, United States; ²University of California, Berkeley, United States; ³Lawrence Berkeley National Laboratory, United States

The layered nickelates, $R_{2-x}Sr_xNiO_4$ (R = trivalent rare-earth cation), and high- T_c cuprate superconductor, $La_{2-x}Sr_xCuO_4$, are isostructural and both exhibit the suppression of antiferromagnetism, charge/spin strip order, and an insulator-metal transition upon hole-doping. However, no superconductivity has been observed in $R_{2-x}Sr_xNiO_4$ to date. Differences in the electronic structure between the layered nickelates and cuprates may shed light on the key ingredients for high-temperature superconductivity. Here, we present the ARPES characterization of $Nd_{2-x}Sr_xNiO_4$ ($x = 0.8, 1.0, 1.2, \text{ and } 1.4$) thin films grown on $LaAlO_3(100)$. We observe a large hole pocket of x^2-y^2 character at the M-point and an electron pocket of z^2 character at the Γ -point, consistent with previous work [1]. We track the volume of the electron and hole pockets upon hole-doping and characterize the quasi-particle peak across the insulator-metal transition at $x = 1.0$. Finally, we observe no k_z -dispersion in either the hole or electron pockets, in contrast to $Eu_{0.9}Sr_{1.1}NiO_4$ [1, 2] and the three-dimensional electronic structure of $NdNiO_3$.

[1] Uchida, M. et al. *Phys Rev B* **84**, 241109(R) (2011)

[2] Uchida, M. et al. *Phys Rev B* **86**, 165126 (2012).

We acknowledge support from the US Department of Energy, Office of Basic Energy Sciences, Division of Materials Sciences and Engineering, under award no. DE-SC0021925

8:30 AM QT02.05.02

Electric-Field Driven Domain Reconfiguration in The Charge Density Wave 1T-TaS₂ Yue Cao; Argonne National Laboratory, United States

Charge density wave (CDW) is ubiquitous in quantum materials. Under a minor electric field, CDWs fluctuate giving rise to increased electric conductivity long believed to arise from the depinning and sliding of CDWs. In real space, sliding of CDW will lead to the reconfiguration of CDW domains on the nano and mesoscale. Direct observation of sliding CDW is challenging. The nature of such reconfigurations, e.g., whether they are stochastic, as well as the relevant timescales, remains elusive.

We used X-ray Photon Correlation Spectroscopy (XPCS) for revealing E-field-driven domain reconfigurations in the canonical CDW material 1T-TaS₂. Combining in-situ XPCS studies with few-seconds counting time at the Advanced Photon Source (APS) and the 100 fs X-ray pulses at the MID endstation of the European XFEL, we show the CDW domain reconfigure above few microseconds and reaches ergodicity in domain configuration by seconds. These results shed light on the nature of the CDW fluctuation in 1T-TaS₂ as a stochastic process. Our results also provide quantitative measure of the depinning energy landscape in the material, which is critical to the macroscopic transport material property.

8:45 AM *QT02.05.03

Beyond Perturbation Theory: Multi-Photon and Non-Radiative Recombination Effects in Spectroscopies Adrian E. Feiguin; Northeastern University, United States

The conventional calculation of scattering cross sections relies on a treatment based on time-dependent perturbation theory that provides formulation in terms of Green's functions in the frequency domain. In equilibrium, it boils down to evaluating a simple spectral function equivalent to Fermi's golden rule, which can be solved efficiently by a number of numerical methods. However, away from equilibrium, the resulting expressions require a full knowledge of the excitation spectrum and eigenvectors to account for all the possible allowed transitions and intermediate states, a seemingly unsurmountable complication. We have recently presented a new paradigm to overcome these hurdles [1-4]: we explicitly introduce the scattering particles (neutron, electron, photon, positron) and simulate the full scattering event by solving the time-dependent Schrödinger equation. The spectrum is recovered by measuring the momentum and energy lost by the scattered particles, akin an actual energy-loss experiment. I here show how these ideas can be generalized to study multi-photon processes such as coincidence ARPES, and the interplay between radiative and non-radiative recombination channels in X-ray spectroscopies.

[1] Krissia Zawadzki, Luhang Yang, Adrian E. Feiguin; *Phys. Rev. B* **102**, 235141 (2020).

[2] Krissia Zawadzki, Adrian E. Feiguin; *Phys. Rev. B* **100**, 195124 (2019).

[3] Krissia Zawadzki, Alberto Nocera, and Adrian E. Feiguin; arXiv: 1905.08166

[4] Alberto Nocera, Adrian E. Feiguin; arXiv:2304.15001

9:15 AM QT02.05.04

Prediction of the Optical Properties of Spin Defects in Semiconductors and Insulators using Time-Dependent Density Functional Theory Yu Jin¹, Marco Govoni^{2,1,3}, Victor Wenzhe Yu³, Andrew C. Xu¹ and Giulia Galli^{1,3}; ¹University of Chicago, United States; ²University of Modena and Reggio Emilia, Italy; ³Argonne National Laboratory, United States

Optically active point defects in semiconductors and insulators hold great potential for quantum technology applications. First-principles investigations of excited state properties of point defects are instrumental in characterizing the defects through the interpretation of spectroscopic experimental results [1-3] and in predicting spin defects with tailored optical properties [4]. Time-dependent density functional theory (TDDFT) allows for exploring not only excited-state energies and wavefunctions of localized defect states but also potential energy surfaces by performing geometry optimizations [1]. Here, I will present the study of the properties of several spin-defects using TDDFT, including the absorption spectra of the negatively charged nitrogen-vacancy center in diamond [1], the neutral silicon-vacancy center in diamond, and the neutral oxygen-vacancy center in magnesium oxide. Our calculations were made possible by our recent implementation of TDDFT with analytical forces in the West code [5,6], which enables TDDFT calculations with hybrid functionals for systems containing thousands of atoms and detailed investigations of excited-state geometries and finite-size effects.

References

[1] Y. Jin, M. Govoni, and G. Galli, *npj Comput. Mater.* **8**, 238 (2022).

[2] Y. Jin et al., *Phys. Rev. Mater.* **5**, 084603 (2021).

- [3] C. P. Anderson et al., *Sci. Adv.* **8**, eabm5912 (2022).
 [4] A. Bilgin et al., submitted (2023). arXiv:2305.05791.
 [5] M. Govoni and G. Galli, *J. Chem. Theory Comput.* **11**, 2680–2696 (2015).
 [6] W. Yu and M. Govoni, *J. Chem. Theory Comput.* **18**, 4690–4707 (2022).

Acknowledgements

This work was supported by the Midwest Integrated Center for Computational Materials (MICCoM) as part of the Computational Materials Science Program funded by the U.S. Department of Energy, Office of Science, Office of Basic Energy Sciences (DOE-BES).

9:30 AM QT02.05.05

Open Shell Molecular Platforms Matthew Kaminow and Jason Azoulay; Georgia Institute of Technology, United States

The diradical behavior of open shell polymers opens many doors for emerging areas of materials research. Donor acceptor (DA) conjugated polymers (CP) can have intermediate and strong electronic correlations which allows for narrow bandgaps and diradical behavior in the ground state. In addition to the intrinsic conductivity that ground state radicals mixed with conjugation provide the polymer systems, the diradical behavior allows for high spin states that provide emergent properties in quantum information and optoelectronics. When the bandgap becomes narrow enough, the diradical behavior forms a triplet at ground state. This high spin conformation has ferromagnetic, and electron paramagnetic resonance (EPR) has been useful in confirming that the spins are spatially localized. This high spin conformation has been found using EPR to have coherence times rivalling that of diamond NV defect qubits allowing for inexpensive and novel forms of quantum computing and sensing. The long coherence times and spatial resolution also allows for the chains to be spin addressable, aiding in quantum information efforts. This narrow bandgap is also tunable, as using different donor and acceptor monomers to traverse from an aromatic structure, to a quinoidal one, to diradicals of singlet and triplet states as described in the figure. This tunability and ability to narrow the bandgap to such an extent has allowed for novel optoelectronic materials in ranges as low energy as LWIR, areas which have recently been thought of as unattainable for organic materials.

9:45 AM QT02.05.06

Absolute Superconducting Spin Valve Effects in Superconductors with a Spin-Splitting Field and Spin-Orbit Coupling Hisakazu Matsuki¹, Alberto Hijano^{2,3}, Miguel Agueda Velasco⁴, Grzegorz P. Mazur⁵, Stefan Ilic², Beilun Wu⁴, Edwin Herrera Vasco⁴, Hermann Suderow⁴, Guang Yang⁶, Sebastian Bergeret² and Jason W. Robinson¹; ¹University of Cambridge, United Kingdom; ²Centro de Física de Materiales (CFM-MPC) Centro Mixto CSIC-UPV/EHU, Spain; ³University of the Basque Country UPV/EHU, Spain; ⁴Universidad Autónoma de Madrid, Spain; ⁵Delft University of Technology, Netherlands; ⁶Beihang University, China

At a thin-film superconductor (S) interface with a ferromagnetic insulator (FI), the magnetic proximity effect (MPE) can spin-split the superconducting density of states and suppress the critical temperature (T_c) of S. For S metals with weak spin-orbit coupling (SOC), the spin splitting can translate to several Tesla [1, 2] and the T_c suppression can reach tens of mK [3]. For a FI/S/FI spin switch, the T_c suppression is reduced for antiparallel (AP) FI magnetizations due to a net cancellation effect of the MPE in S; conversely, for parallel (P) magnetizations, the exchange fields add, enhancing the suppression of T_c with the spin switch efficiency defined as $\Delta T_c = T_c(\text{AP}) - T_c(\text{P}) > 0$ [4].

In the presence of SOC, the spin-splitting in S should smear out, reducing ΔT_c . Here, however, we show that in optimized EuS/Nb/EuS (FI/S/FI) structures, ΔT_c can reach 1 K and achieve an absolute spin-valve effect with $\Delta T_c/T_c$ close to 1 by inserting a thin layer of Au at a single interface - i.e., EuS/Nb/Au/EuS. Scanning tunneling spectroscopy on Au in Au/Nb and Au/Nb/EuS structures show evidence for a modification of the superconducting state due to the presence of EuS. These results demonstrate new physics in which ΔT_c is boosted by SOC.

- [1] X. Hao, J. S. Moodera, and R. Meservey, *Phys. Rev. Lett.* **67**, 10 (1991).
 [2] E. Strambini, et al., *Phys. Rev. Mat.* **1**, 054402 (2017).
 [3] B. Li, et al., *Phys. Rev. Lett.* **110**, 097001 (2013).
 [4] P. G. de Gennes, *Phys. Lett.* **23**, 1 (1966).

10:00 AM BREAK

10:30 AM QT02.05.07

Indications of Broken Symmetry States from Raman Measurements at High Temperature near the Putative QCP Point in the Phase Diagram of Doped BaFe₂As₂ Debansita Swain¹, Soumyadeep Ghosh², Kousik Bera³, Sven Friedemann⁴, Haranath Ghosh⁵, Anushree Roy¹ and Sitikantha D. Das¹; ¹Indian Institute of Technology, Kharagpur, India; ²Lawrence Berkeley National Laboratory, United States; ³Indian Institute of Technology Kharagpur, India; ⁴University of Bristol, United Kingdom; ⁵RRCAT, Indore, India

The concept of nematicity is still not well settled in case of Fe based Superconductors. Signatures of nematic ordering exist well above the structural transition temperature i.e. the presence of orthorhombic distortion in the tetragonal symmetry broken phase. Tetragonal symmetry dictates that both Fe d_{xz} and d_{yz} orbitals should be degenerate, whereas studies like ARPES, X-ray pair distribution function etc. show the unequal occupation of Fe d_{xz} and d_{yz} orbitals in the symmetry broken orthorhombic phase. By using Raman spectroscopy, we have studied P doped BaFe₂As₂ for $x \sim 0.23$, whose doping composition lies near quantum criticality and enhanced nematic fluctuation in the doping temperature phase diagram. From transport measurement it is observed that P doped BaFe₂As₂ exhibits a tetragonal to orthorhombic phase transition around 60K followed by a superconducting transition below ~ 16 K. A room temperature micro-Raman spectrum of the studied compound shows a phonon mode around $\sim 211 \text{ cm}^{-1}$ with two broad high frequency modes around 515 cm^{-1} and 635 cm^{-1} . The separation between these two modes remains around 15 meV at room temperature. Temperature dependent Raman measurement shows that the B_{1g} mode (phonon mode around $\sim 211 \text{ cm}^{-1}$) follows standard anharmonicity behavior within a temperature range from 80 to 300K, whereas with varying temperature these broad modes show a drop in intensity which is typically observed for electronic Raman modes. In the non-superconducting state, strong anisotropic behavior is observed for these BMs in polarization dependent Raman scattering. Electronic structure calculations for P doped and undoped BaFe₂As₂ show that while Fe d_{xz} and d_{yz} orbitals do not split in the tetragonal phase, the splitting energy is 13.5 meV in the orthorhombic phase of the doped system, which is reasonably close to the experimentally observed value of the energy separation of the BMs. Hence, we believe that these reported broad modes bear signatures of crystal field splitting of Fe d orbitals due to local breaking of tetragonal C_4 symmetry in the doped system.

10:45 AM QT02.05.08

Advances in Zinc Oxide Materials for Quantum Applications Vishal Saravade^{1,2}, Chuanle Zhou³, Zhe Chuan Feng², Benjamin Klein³ and Ian T. Ferguson²; ¹Pennsylvania State University, United States; ²Kennesaw State University, United States; ³Missouri University of Science and Technology, United States

Advanced characterizations of zinc oxide-based materials for spintronic and quantum applications are investigated. Zinc oxide (ZnO) based materials have been explored for various applications in electronics, nanotechnology, biomedicine, power devices, and so on. Zinc oxide doped with transition metals (ZnTMO) has a potential for spintronic and quantum applications. However, its properties in this area are not well understood. In this work, characterizations of transition metal-doped zinc oxide are systematically performed and investigated to gain insights into their spin-related properties. Sets of Mn-doped ZnO and Ni-doped ZnO were epitaxially grown on sapphire substrates using metal-organic chemical vapor deposition (MOCVD). X-ray diffraction showed a nearly monocrystalline structure in the (002) direction, along with appearances of low intensity secondary phases related to the transition metal materials and host ZnO. A systematic reducing trend in the bandgap was observed in both Ni-doped and Mn-doped ZnO with increased transition metal dopant concentration. This could be due to the energy states that are introduced with the transition metals, and this shows a potential controllability in spin-inducing energy states by transition metal-doping. As per photoluminescence measurement, transition-metal doping attenuated the ultraviolet narrow band and increased emissions in the yellow-green regions. This could be due to secondary phases of TM-oxides that were formed during the MOCVD growth. Advanced Hall Effect characterizations were done to understand the inherent spin-related properties of ZnTMO. ZnTMO exhibited Anomalous Hall Effect (AHE). The transverse Hall resistivity overlapped with the longitudinal resistivity, and both these resistivity were not linear. This indicates spin-polarization in ZnTMO that is not induced by intrinsic carriers. The spin polarization in ZnTMO could be the result of TM-TM clusters, secondary phases, defects, and extrinsic carrier scattering. Annealing reversed the AHE response and indicated the influence of annealing on spin-polarizations of the AHE-causing components of ZnTMO. The mechanism for spin in ZnTMO is based on extrinsic scattering by TM centers/clusters or secondary phases. Understanding of spin mechanism in ZnTMO can help in the investigation of ZnO for quantum and other spintronic applications.

11:00 AM *QT02.05.09

Recreating the Physics of a Doped Mott Insulator on a Silicon Surface Steven Johnston; The University of Tennessee, Knoxville, United States

Sn adatoms on a Si(111) substrate with 1/3 monolayer coverage form a two-dimensional triangular lattice with one unpaired electron per site and an antiferromagnetic Mott insulating state. The Sn layers can be modulation hole-doped and metalized using heavily-doped p-type Si(111) substrates and become superconducting at low temperatures, recreating cuprate-like physics on a Si template. Here, the combination of repulsive interactions and frustration inherent to the triangular adatom lattice opens up the possibility for a chiral order parameter. In this talk, I will discuss recent theoretical and experimental studies leveraging scanning tunneling microscopy/spectroscopy and quasi-particle interference imaging to study this novel system. We find

evidence for a doping-dependent T_c with a fully gapped order parameter, time-reversal symmetry breaking, and a substantial enhancement of the zero-bias conductance near the edges of the superconducting domains. While each piece of evidence could have a more mundane interpretation, our combined results suggest the tantalizing possibility that Sn/Si(111) is an unconventional chiral d-wave superconductor, consistent with theoretical models.

References

- 1) F. Ming et al., Physical Review Letters 119, 266802 (2017).
- 2) X. Wu et al., Physical Review Letters 125, 117001 (2020).
- 3) F. Ming et al., Nature Physics 19, 500–506 (2023).

11:30 AM *QT02.05.10

Synchrotron Spectroscopy of Epitaxial Rare Earth Nickelates [Charles Ahn](#); Yale University, United States

The rare-earth nickelates display a broad range of phenomena, including functional behavior such as antiferromagnetism and superconductivity. The ability to synthesize heterogeneous epitaxial thin film structures out of nickelates enables one to control and modify these functional properties via the creation of atomically abrupt interfaces. Advanced synchrotron characterization can then be used to measure the resulting electronic and magnetic properties of these atomically engineered systems. For example, the antiferromagnetic order parameter of nickelate superlattices can be imaged using resonant soft x-ray diffraction, and information about the dynamics can be accessed by x-ray photon correlation spectroscopy (XPCS) measurements using coherent soft x-rays. In this talk, we focus on synchrotron characterization of the square-planar nickelates, which are a novel class of superconductors. We use in situ aluminum reduction of the perovskite nickelates to achieve superconducting Nd_{1-x}EuxNiO₂ (NENO) thin films grown by molecular beam epitaxy (MBE). Atomic structure is characterized using crystal truncation rod (CTR) analysis, and electronic structure is characterized using diffraction-based X-ray absorption near edge structure (dXANES). We also report on the superconducting transport properties of NENO films.

SESSION QT02.07: State-of-the-Art Characterizations of Correlated Quantum Materials

Session Chairs: Mingda Li and Yao Wang

Wednesday Morning, November 29, 2023

Sheraton, Fifth Floor, The Fens

8:15 AM QT02.07.01

U.S. National Academies Report Identifies Measurements and Infrastructure Needs for QIS Research [Linda Nhon](#); NASEM, United States

Scientific progress in the field of Quantum Information Science (QIS) will pioneer the development of cutting-edge technologies in computing, sensing, and communications. These efforts will strengthen key sectors of the United States economy and workforce. To achieve this innovation landscape, a robust QIS research enterprise needs to be established. This ecosystem includes state-of-the-art instrumentation and tools that are required for in-depth characterization of quantum molecular materials. A 2023 U.S. National Academies of Sciences, Engineering, and Medicine report, *Advancing Chemistry and Quantum Information Science*, identifies fundamental research priorities that should be targeted to enhance the measurement and control of quantum systems. The study provided recommendations for advancing these fields to federal agencies such as the U.S. Department of Energy and the National Science Foundation, U.S. Congress, the research community, and other stakeholders. Spearheaded by a committee of chemists and physicists, the study assessed a wide range of techniques, chemical approaches, and tools that would offer more precise measurements of molecular-scale quantum devices in different environments (e.g., on surfaces or at complex interfaces). Addressing facility maintenance concerns and broadening access to laboratory- and mid-scale instrumentation were also discussed. Here, the research opportunities, infrastructure and facility needs, and workforce development strategies identified in the National Academies report will be presented.

8:30 AM *QT02.07.02

Electronic Structure, Magnetic Interactions and Charge Order in Low Valence Nickelates Probed by Resonant Inelastic X-Ray Scattering [Mark P. Dean](#); Brookhaven National Laboratory, United States

After a 30-year quest, researchers recently succeeded in realizing superconductivity in low-valence nickelates [1]. This ignited a vigorous debate regarding the essential electronic properties of these materials and their similarity to cuprates. Some important questions include: Do these materials have appreciable oxygen charge-transfer character and superexchange akin to the cuprates or are they in a distinct Mott-Hubbard regime where oxygen plays a minimal role and superexchange is negligible? Given that cuprates have a propensity to host proximate competing phases such as charge and spin order, one might ask whether the nickelate's phase diagrams also host competing orders and to what extent they are similar to those in cuprates? In this talk, I will describe our use of resonant inelastic x-ray scattering to solve these questions [2-4].

References

1. Danfeng Li, Kyuho Lee, Bai Yang Wang, Motoki Osada, Samuel Crossley, Hye Ryoung Lee, Yi Cui, Yasuyuki Hikita & Harold Y. Hwang, Nature 572, 624–627 (2019)
2. Strong Superexchange in a d^9-d^8 Nickelate Revealed by Resonant Inelastic X-Ray Scattering, J. Q. Lin, P. Villar Arribi, G. Fabbris, A. S. Botana, D. Meyers, H. Miao, Y. Shen, D. G. Mazzone, J. Feng, S. G. Chiuzaian, A. Nag, A. C. Walters, M. Garcia-Fernandez, Ke-Jin Zhou, J. Pellicciari, I. Jarrige, J. W. Freeland, Junjie Zhang, J. F. Mitchell, V. Bisogni, X. Liu, M. R. Norman, and M. P. M. Dean, Phys. Rev. Lett. 126, 087001 (2021)
3. Role of Oxygen States in the Low Valence Nickelate La₄Ni₃O₈, Y. Shen, J. Sears, G. Fabbris, J. Li, J. Pellicciari, I. Jarrige, Xi He, I. Bozovic, M. Mitrano, Junjie Zhang, J. F. Mitchell, A. S. Botana, V. Bisogni, M. R. Norman, S. Johnston, and M. P. M. Dean, Phys. Rev. X 12, 011055 (2022)
4. Electronic character of charge order in square planar low valence nickelates, Y. Shen, J. Sears, G. Fabbris, J. Li, J. Pellicciari, M. Mitrano, W. He, Junjie Zhang, J. F. Mitchell, V. Bisogni, M. R. Norman, S. Johnston, and M. P. M. Dean, Phys. Rev. X 13, 011021 (2023)

9:00 AM QT02.07.03

Resolving Emergent Structure States in Quantum Materials by Total X-Ray Scattering [Valeri Petkov](#); Central Michigan University, United States

Materials with properties rooted in the quantum world exhibit coupled electronic, magnetic and lattice degrees of freedom leading to fascinating properties. However, the lattice degrees of freedom often appear as lattice distortions which are not necessarily amenable to crystallographic description, hampering the understanding of the underlying physics. In the talk, we will show that the problem may be solved by total x-ray scattering and show examples from our recent studies on dual heavy fermion liquid UPt₂Si₂, which exhibits antiferromagnetism consistent with localized 5f-electron states and transport properties characteristic to Kondo lattice systems (1), layered transition metal dichalcogenide 1T-TaS₂, which is a putative Mott insulator (2), and NbTe₄ topological superconductor, where double Dirac points emerge thanks to the emergence of charge density wave order (3).

- (1) V. Petkov, R. Baumbach, AM Milinda Abeykoon and J. A. Maydosh "3D charge density wave in the dual fermion system UPt₂Si₂" *Phys. Rev. B* **107**, 245101 (2023).
- (2) V. Petkov, J. Peralta, B. Aoun and Y. Ren "Atomic structure and Mott nature of the insulating charge density wave phase in 1T-TaS₂" *J. Phys.: Condens. Mater* **34**, 345401 (2022).
- (3) V. Petkov, R. Amin, M. Jakhar, AM Milinda Abeykoon and X. Ke "Charge density wave order, local lattice distortions and topological electronic states in NbTe₄" *Phys. Rev. Lett.* (under review).

9:15 AM *QT02.07.04

Case Studies of Quantum Materials via RIXS [Wei-Sheng Lee](#); SLAC National Accelerator Laboratory, United States

Quantum materials exhibit extraordinary properties stemming from the interplay of different degrees of freedom, encompassing quantum topology, orbital, spin, lattice, and charge interactions. However, comprehending and manipulating these underlying degrees of freedom presents a substantial challenge. Resonant inelastic X-ray scattering (RIXS) has emerged as a powerful technique for studying elementary excitations associated with these fundamental degrees of freedom, including orbital, magnon, phonon, and charge excitations, in the energy-momentum domain. This capability offers great opportunities to unravel the intricate phenomena exhibited by quantum materials.

In particular, the recent advancements in X-ray free-electron laser have heralded a new era of time-resolved RIXS, enabling the measurement of elementary excitations when they are driven out of equilibrium. In this presentation, I will showcase our latest investigations employing RIXS and time-resolved RIXS on unconventional superconductors and related compounds. Our

findings highlight how RIXS can illuminate the microscopic behaviors, thereby contributing to a broader understanding and potential control of quantum materials.

9:45 AM QT02.07.05

Next-Nearest-Neighbor Hopping and Charge-Ordering Tendencies in a Cuprate LadderHariPadma¹, JinuThomas², SophiaTenHuisen¹, WeiHe³, ZiqiangGuan¹, JieminLi³, YuWang⁴, ZhiqiangMao⁴, ValentinaBisogni³, JonathanPellicciari³, MarkP. Dean³, StevenJohnston² and MatteoMitrano¹; ¹Harvard University, United States; ²The University of Tennessee, Knoxville, United States; ³Brookhaven National Laboratory, United States; ⁴The Pennsylvania State University, United States

The competing nature of charge-order and superconductivity in the cuprates is an open experimental and theoretical problem in condensed matter physics. Recent theoretical studies on the Hubbard model have revealed that the next-nearest neighbor hopping t' is a key tuning parameter that destabilizes charge-ordered phases in favor of superconductivity¹. However, the influence of t' remains relatively unexplored experimentally. Quasi-1D systems are an ideal platform to study the microscopic physics of the cuprates, owing to the availability of reliable theory that may be rigorously compared to experimental results. Here we consider the quasi-1D cuprate ladder system $\text{Sr}_{1-x}\text{Ca}_x\text{Cu}_{24}\text{O}_{41}$, which exhibits a gapped spin singlet ground state² that is charge ordered at ambient pressure³ and superconducting at high pressure⁴ ($x > 11$, $T_C = 9$ K at 3.5 GPa). Focusing on the hole self-doped parent compound ($x = 0$), we map the spectrum of dispersive two-triplon spin fluctuations as a function of temperature across the CO phase transition using high-resolution resonant inelastic X-ray scattering at the Cu L -edge. We identify a substantial downturn in the two-triplon dispersion near the zone boundary, a feature that is at odds with predictions of the Hubbard model with only nearest-neighbor hopping. Furthermore, we observe a dramatic reshaping of the two-triplon spectrum across the CO transition temperature. We fit the experimental two-triplon dispersion measured in the CO ground state using DMRG calculations and unbiased Bayesian optimization to extract the Hubbard model parameters including the exchange anisotropy and t' . We examine the role of t' in the reshaping of the spin fluctuations across the CO transition, in particular identifying signatures of hole pairing and hole-triplon bound states, which have been hypothesized to be precursors to superconductivity in spin ladders^{5,6}. Our work provides a rigorous experimental quantification of t' in cuprates and clarifies its influence over spin fluctuations and electronic ordering.

1. Jiang, H. C. & Devereaux, T. P. Superconductivity in the doped Hubbard model and its interplay with next-nearest hopping t' . *Science* 365, 1424–1428 (2019).
2. Notbohm, S. et al. One- and Two-Triplon Spectra of a Cuprate Ladder. *Phys Rev Lett* 98, 027403 (2007).
3. Abbamonte, P. et al. Crystallization of charge holes in the spin ladder of $\text{Sr}_{14}\text{Cu}_{24}\text{O}_{41}$. *Nature* 431, 1078–1081 (2004).
4. Nagata, T. et al. Superconductivity in the ladder compound $\text{Sr}_{2.5}\text{Ca}_{11.5}\text{Cu}_{24}\text{O}_{41}$ (single crystal). *Physica C* 282–287, 153–156 (1997).
5. Dagotto, E., Riera, J. & Scalapino, D. Superconductivity in ladders and coupled planes. *Phys Rev B* 45, 5744–5747 (1992).
6. Poilblanc, D., Chiappa, O., Riera, J., White, S. R. & Scalapino, D. J. Evolution of the spin gap upon doping a 2-leg ladder. *Phys Rev B* 62, R14633–R14636 (2000).

This study was primarily supported by the DOE Office of Science under the Early Career Research Program award no. DE-SC0022883. Support for crystal growth and characterization was provided by the National Science Foundation (NSF) through the Penn State 2D Crystal Consortium-Materials Innovation Platform (2DCC-MIP) under NSF cooperative agreement DMR-1539916 and DMR-2039351.

10:00 AMBREAK

SESSION QT02.08: Time-Resolved Characterization of Quantum Materials

Session Chairs: Valentina Bisogni and Mingda Li

Wednesday Morning, November 29, 2023

Sheraton, Fifth Floor, The Fens

10:30 AM *QT02.08.05

Lead-Reduced Halide Perovskite Solar Cells with Photo-Assisted Kelvin Probe Force MicroscopyMing-ChungWu; Chang Gung University, Taiwan

With the intensification of the global energy crisis, characterized by increasing demand and diminishing fossil fuel reserves, it has become imperative to explore sustainable and efficient energy-harvesting technologies. Perovskite solar cells (PSCs) have rapidly gained prominence as a promising photovoltaic device, boasting power conversion efficiencies (PCE) exceeding 26%. However, the widespread use of lead (Pb) in PSCs introduces environmental and health hazards that pose challenges to their broad commercialization. In this presentation, I will introduce the strategic research roadmap of our group in advancing perovskite solar cell technology. Our discussion will be divided into four key areas: (1) high-efficiency perovskite solar cells employing metal-doped TiO_2 as the electron transport layer (ETL); (2) the design of side-chain modulated, carbazole-based bifunctional hole-shuttle interlayers; (3) the development of lead-reduced perovskite solar cells; and (4) the exploration of lead-free Ag_3BiI_6 ruddorffite solar cells. Predicting the quality of photovoltaic (PV) materials necessitates a thorough understanding of the material properties, manufacturing processes, and the long-term performance of solar cells or modules. To this end, we utilize various methods and techniques. Photoluminescence (PL) and time-resolved photoluminescence (TRPL) is utilized to determine charge carrier lifetimes, recombination mechanisms, and assess the impact of defects on material quality. Generally, higher-quality PV materials are indicated by lower recombination rates, which can lead to potentially higher efficiencies in solar cell applications. The photo-assisted Kelvin Probe Force Microscopy (photo-assisted KPFM), an adaptation of traditional KPFM that includes sample illumination during measurement, proves especially beneficial for PV materials. It allows for the investigation of surface electron accumulation under conditions that closely replicate the operational environment of the solar cells. Our research group is committed to spearheading innovative solutions in PSCs that prioritize both high efficiency and environmental stewardship.

11:00 AM QT02.08.02

Light-Induced Floquet Effects in Graphene under Continuous-Wave Mid-Infrared IrradiationYijingLiu¹, GabrielGaertner², JohnHuckabee², AlexeySuslov³, Luis E.F.Foa Torres⁴, PaolaBarbara¹ and NikolaiKalugin²; ¹Georgetown University, United States; ²New Mexico Tech, United States; ³National High Magnetic Field Laboratory, United States; ⁴University of Chile, Chile

Light-matter interaction in 2D materials is predicted to induce Floquet-Bloch states with non-trivial topology [1,2,3]. We report on the experimental observation of photoinduced transverse voltage and photoinduced current in graphene Hall bars irradiated with high-power linearly and circularly-polarized mid-Infrared radiation at cryogenic temperatures. The radiation wavelength is 10.6 μm and the power density is larger than 1 $\text{mW}/\mu\text{m}^2$. We investigate the dependence of the photoresponse on the temperature, position of Fermi level, and light polarization. The observation of Floquet signatures at lower power densities and in the CW regime lifts substantial experimental restrictions, helping to unlock potential applications for light-induced manipulation of material properties [4].

We acknowledge support from NSF (projects DMR CMP #2104755 and DMR CMP #2104770). The National High Magnetic Field Laboratory is supported by the National Science Foundation through NSF/DMR-2128556 and the State of Florida.

References:

- [1] T. Oka, H. Aoki, *Phys. Rev. B* 79, 081406(R) (2009).
- [2] H. Calvo et al., *Appl. Phys. Lett.* 98, 232103 (2011); L. E. F. Foa Torres et al. *Phys. Rev. Lett.* 113, 266801 (2014).
- [3] J. McIver et al., *Nat. Phys.* 16, 38 (2020).
- [4] Y.Liu et.al. APS March Meeting 2023, A32.00007

11:15 AM *QT02.08.03

Spin Dynamics in a Photoexcited Mott Insulator on a Square LatticeTakamiTohyama; Tokyo University of Science, Japan

The recent development of time-resolved resonant inelastic x-ray scattering (trRIXS) opens a new avenue for probing collective two-particle excitations, from which one can investigate novel photoinduced nonequilibrium phenomena in the wide range of momentum and energy spaces. RIXS can probe not only charge excitation but also single-magnon excitation if one uses incident x rays tuned for L edge in transition metals. Therefore, trRIXS is a good tool to investigate single-magnon excitation in photoexcited Mott insulators. On the other hand, time-resolved two-magnon Raman scattering (trTMRS) is suitable for investigating two-magnon excitation in photoexcited Mott insulators. In order to give theoretical predictions to trRIXS, we investigate momentum dependent single-magnon excitation that evolves after pumping within a femtosecond timescale in an antiferromagnetic Mott insulator on a square lattice [1]. Using a numerically exact-diagonalization technique based on the time-dependent Lanczos method for a half-filled Hubbard model on a square lattice, we find a characteristic temporal oscillation for the intensity of the dynamical spin correlation function describing single-magnon excitation. This oscillation shows an antiphase behavior for two orthogonal directions that are parallel and perpendicular to the electric field of a pump pulse. The same behavior is also seen in the static spin structure factor. Their oscillation period in time is determined by two-magnon excitation in the Mott insulator. This theoretical prediction will be confirmed for Mott insulating cuprates and iridates once TRRIXS is ready for a femtosecond timescale. The photoexcitation of the Mott insulator

on a square lattice weakens the intensity of two-magnon excitation as observed in trTMRS [2]. However, the spectral changes in the low-energy region below the two-magnon excitation have not yet been clearly understood. After turning off a pump pulse tuned for an absorption edge, we find that a new magnetic signal clearly emerges well below the two-magnon energy [3]. We find that low-energy excitation is predominantly created via an excitonic state at the absorption edge. This exciton-assisted magnetic excitation may provide a possible explanation for the low-energy spectral weight in the recent trTMRS experiment [2].

[1] K. Tsutsui, K. Shinjo, and T. Tohyama, Phys. Rev. Lett. **126**, 127404 (2021).

[2] J.-A. Yang, N. Pellatz, T. Wolf, R. Nandkishore, and D. Reznik, Nat. Commun. **11**, 2548 (2020).

[3] K. Tsutsui, K. Shinjo, S. Sota, and T. Tohyama, Commun. Phys. **6**, 41 (2023).

11:45 AM QT02.08.04

Ultrafast Nonsymmorphic Symmetry Breaking by Strong Light-Matter Interaction ChanghuaBao¹, ShaohuaZhou¹, BenshuFan¹, PeizheTang², WenhuiDuan¹ and ShuyunZhou¹; ¹Tsinghua University, China; ²Beihang University, China

In condensed matter physics, symmetry breaking lays the cornerstone of the formation of rich phases of matter, such as charge density waves and magnetism. Symmetry breaking can be on-demand controlled in equilibrium states by external fields, including electric/magnetic field and strain, leading to intriguing phase transitions and collective modes, such as tailoring topological Dirac nodal line, Mobius, and hourglass fermions by breaking nonsymmorphic symmetry. Beyond equilibrium states, strong light-matter interaction potentially provides unprecedented opportunities for breaking symmetry on an ultrafast timescale and even realizing exotic quantum states which have no counterpart in equilibrium states.

Here, by utilizing time- and angle-resolved photoemission spectroscopy (TrARPES), we demonstrate the realization of ultrafast symmetry breaking by strong light-matter interaction in a two-dimensional semiconductor. Driven by a strong mid-infrared light field, an emerged band crossing nodal ring is observed, which is gapped by the interactions and leaves nonsymmorphic symmetry-protected Dirac nodes. Interestingly, when the driving light field is tuned to polarize along the direction which breaks the nonsymmorphic symmetry, Dirac nodes are further gapped to form a fully gapped nodal ring, indicating a light-induced nonsymmorphic symmetry breaking. Moreover, the Dirac nodes are gapped only in the presence of the light field and recover gapless almost instantaneously ($\ll 100$ fs) when the light field is turned off, suggesting an ultrafast nonsymmorphic symmetry breaking. This work not only demonstrates light-matter interaction as an effective way to manipulate symmetry in quantum materials but also paves an important step for the long-sought Floquet topological insulator.

SESSION QT02.09: Unconventional but Smart Characterizations

Session Chairs: Mingda Li and Yao Wang

Wednesday Afternoon, November 29, 2023

Sheraton, Fifth Floor, The Fens

1:30 PM *QT02.09.01

Exploring Novel Quantum Materials under High Pressure and High Temperature WeiweiXie; Michigan State University, United States

Pressure, an intensive variable, is a virtually unexplored pathway to new quantum materials. The application of high pressure can yield dramatic new examples of quantum materials. In this presentation, I will discuss how high pressure can be used to tune unexpected physical properties in magnetic topological materials and low dimensional materials. The use of high pressure and high temperature synthesis can stabilize the exotic quantum phenomena detected by high pressure X-ray and neutron scattering. I will also introduce our new lab-based in-situ high pressure and high temperature single crystal X-ray diffraction technique, which can guide us to synthesize materials rationally under high pressure and high temperature. High pressure synthesis techniques will be the focus of the discussion, novel iridates (Sr₂IrO₄, SrIrO₃), and tetragonal BaCoO₃.

2:00 PM *QT02.09.02

From Mathematics to Algorithms—Obtaining Spectral Information from Real and Imaginary-Time Response Functions EmanuelGull; University of Michigan, United States

Numerical simulations of equilibrium systems are often performed in 'imaginary' time, using the Matsubara formalism of statistical quantum field theory; or in 'real' time, using a time-evolution of the system. This talk will analyze the mathematical properties of response functions in these formalisms and show how they can be integrated into efficient numerical algorithms that can capture the spectral information of quantum systems with unprecedented accuracy.

2:30 PM BREAK

3:30 PM *QT02.09.03

Photoemission Studies of Ferroelectric Rashba Semiconductors—From Static to Transient Properties ClaudeF. Monney¹, FredericChassot¹, GeoffroyKremer², AkiPulkkinen³, ChristopherNicholson⁴, HugoDil^{5,6}, JurajKrepmpasky⁶, JanMinar³, GuntherSpringholz⁷, JulianMaklar⁸, RalphErnstorfer⁸, LaurenzRettig⁸, ChangmingYue¹ and PhilippWerner¹; ¹University of Fribourg, Switzerland; ²Université de Lorraine, France; ³University of West Bohemia, Czechia; ⁴Specs, Germany; ⁵EPFL, Switzerland; ⁶Paul Scherrer Institute, Switzerland; ⁷Johannes Kepler Universität, Austria; ⁸Fritz-Haber Institute, Germany

Ferroelectric Rashba semiconductor are bulk materials with noncentrosymmetric atomic structures in their ferroelectric phase combined with a significant spin-orbit interaction, leading to a strong coupling between spins, electrons and the underlying lattice. These properties are directly imprinted on their electronic structure through the occurrence of a giant Rashba splitting in their valence band. This gives the possibility of studying their paraelectric-to-ferroelectric phase transition in the momentum space with angle-resolved photoemission spectroscopy (ARPES). α -GeTe and α -SnTe are two prime examples of such a class of materials. Moreover, it has been recently demonstrated that it is possible to reversibly manipulate the spin polarization in GeTe by an external electric field, a promising behavior for spintronics applications.

A stimulating direction of research is now to investigate how it is possible to modify the ferroelectric properties of these materials with temperature or light pulses.

In this talk, I will start with the case of SnTe and will show high-energy-resolution ARPES data acquired as a function temperature across its ferroelectric phase transition. Our excellent experimental resolution and unprecedented thin film quality allow us to follow the evolution of the Rashba splitting induced by the ferroelectric distortion in the bulk bands and to reveal drastic deviations from a mean-field-like transition. I will discuss how the persistence of a splitting at room temperature supports an order-disorder type of transition and will elaborate on the implications for the topological nature of surface states in SnTe.

In a second part, I will move to the case of GeTe. Upon photoexcitation, we have driven GeTe out-of-equilibrium and probed its transient low-energy electronic structure with time-resolved ARPES. As a consequence, the Rashba splitting of its bulk states is enhanced after 200 fs, a very surprising result, especially given that bulk-sensitive time-resolved experiments have only led to a suppression of ferroelectric upon photoexcitation. In addition, our data show a coherent modulation of the Rashba splitting with a frequency that corresponds to the amplitude mode of the ferroelectric distortion. I will explain what is the physical mechanism behind this unexpected behavior.

4:00 PM *QT02.09.04

Resolving States of Matter in Space and Time by Coherent Soft X-Ray Scattering ClaudioMazzoli; Brookhaven National Laboratory, United States

Recently we succeeded in showing how states of matter - magnetic domain configurations in the specific - can be recognized and accessed by the novel Coherent Soft X-ray Scattering full field imaging, or other more traditional techniques when special analysis is added. Building on our experience in dynamics and time domain analysis, we proved the ability to disentangle intertwined details in space and time, thus accessing microscopic information in a completely new way. In my talk, I will show the proof of principle of the above approach, and conclude by surfing across some long standing problems in condensed matter physics which could naturally benefit from this new approach.

4:30 PM *QT02.09.05

Nonlinear Coupled Magnonics EdoardoBaldini; The University of Texas at Austin, United States

Tailored light excitation and nonlinear control of lattice vibrations have emerged as powerful strategies to manipulate the properties of quantum materials out of equilibrium. Generalizing the use of coherent phonon-phonon interactions to nonlinear couplings among other types of collective modes would open unprecedented opportunities in the design of novel dynamic

function=ones in solids. For example, the collective excitations of magnetic order – magnons – can carry information with little energy dissipation, and their coherent and nonlinear control would provide an attractive route to achieve collective-mode-based information processing and storage in forthcoming spintronics and magnonics. In this talk, I will show that intense terahertz (THz) fields can initiate processes of magnon up-conversion mediated by an intermediate magnetic resonance. By using a suite of advanced spectroscopic tools, including a newly demonstrated two-dimensional THz polarimetry technique enabled by single-shot detection, we unveil the unidirectional nature of coupling between distinct magnon modes of a canted antiferromagnet. These results demonstrate a route to inducing desirable energy transfer pathways between coherent magnons in solids and pave the way for a new era in the development of ultrafast control of magnetism.

SESSION QT02.10: Virtual Session I: Characterization of Emergent Quantum Materials
Session Chairs: Amélie Juhin and Mingda Li
Tuesday Morning, December 5, 2023
QT02-virtual

8:00 AM *QT02.10.01

Phase Transitions and Spin Dynamics of the Quasi-One Dimensional Ising-Like Antiferromagnet BaCo₂V₂O₈ in a Longitudinal Magnetic Field [Virginie Simonet](#)¹, [Quentin Faure](#)², [Shintaro Takayoshi](#)³, [Sylvain Petit](#)², [Béatrice Grenier](#)⁴ and [Thierry Giamarchi](#)⁵; ¹Institut Néel, France; ²Laboratoire Léon Brillouin, France; ³Konan University, Japan; ⁴Grenoble Alpes University, France; ⁵University of Geneva, Switzerland

Combining inelastic neutron scattering and numerical simulations, we study the quasi-one-dimensional Ising anisotropic quantum antiferromagnet BaCo₂V₂O₈ in a longitudinal magnetic field. This remarkable material shows a quantum phase transition from a Néel ordered phase at zero field to a longitudinal incommensurate spin density wave at a critical magnetic field of 3.8 T. Concomitantly, the excitation gap almost closes and a fundamental reconfiguration of the spin dynamics occurs. These experimental results are well described by the universal Tomonaga-Luttinger liquid theory developed for interacting spinless fermions in one dimension. We especially observe the rise of mainly longitudinal excitations, a hallmark of the unconventional low-field quantum regime in Ising-like quantum antiferromagnetic chains.

If the field is increased further, another transition into a transverse antiferromagnetic phase takes place at 9 T. In contrast to this abrupt change of magnetic ordering, the spectrum is not much altered at the transition at 9 T. The spin dynamics indeed reflects the 1D character of the system well accounted by Tomonaga-Luttinger liquid excitations. At the same time, the succession of magnetic phases reflects the competition between longitudinal and transverse correlations expected in the model, which can be experimentally investigated for the first time. Such an apparent disconnection of the static and dynamical properties is another nice property of the rich physics observed in the low-dimensional quantum antiferromagnet BaCo₂V₂O₈, which is proved to be a precious material to test universal behaviors described by the Tomonaga-Luttinger liquid theory.

8:30 AM *QT02.10.02

Probing Quantum Entanglement with Neutron Scattering [Alan Tennant](#); The University of Tennessee, Knoxville, United States

The ability to pinpoint materials with highly entangled states, like quantum spin liquids, is hindered by the absence of methods that can experimentally identify and measure entanglement in quantum substances. To address this, we explore the potential of inelastic neutron scattering (INS) as a tool for a universal measurement approach to entanglement. This is done through three markers: one-tangle, two-tangle, and quantum Fisher information (QFI). Using INS, we take detailed measurements on system for S=1/2 transverse-field XXZ spin chain. This allows us to modulate entanglement with the influence of a magnetic field, and we subsequently cross-check our findings with density-matrix renormalization group analyses.

9:00 AM *QT02.10.03

Inelastic Spectroscopies of The Physics of Quantum Spin Liquid Materials [YoungLee](#)^{1,2}; ¹Stanford University, United States; ²SLAC National Accelerator Laboratory, United States

Quantum spin liquids (QSL's) are novel states of matter possessing long range quantum entanglement. Inelastic spectroscopies are the preeminent tool for exploring their rich physics. An important experimental signature of such novel phases is the presence of spin excitations characterized by fractionalized quantum numbers. For the kagome quantum spin liquid candidate materials Zn-barlowite and herbertsmithite, our inelastic scattering measurements (using both neutron and x-ray probes) provide evidence for fractionalized spinon excitations. Furthermore, experiments on closely related materials with competing states allow us to determine the most important magnetic interactions and to identify signatures of broken symmetry states. In addition, our high energy resolution studies shed light on the role that impurities play in the QSL ground state physics. We discuss the implications our recent experimental investigations of the spin excitations which span low energies (~J/100) to high energies (~10J) on our powder and single crystal samples of QSL and related materials.

9:30 AM *QT02.10.04

Machine Learning-Enabled Real Time Analysis in Ultrafast X-Ray Scatterings [Zhantao Chen](#)^{1,2}; ¹Stanford University, United States; ²SLAC National Accelerator Laboratory, United States

The X-ray free-electron laser (XFEL) has opened up numerous unique scientific opportunities for ultrafast dynamics and particle imaging studies. However, obtaining meaningful experimental signals for complex samples remains a significant challenge. In this talk, we present two recent works to help address this issue by integrating machine learning techniques into data collection and analysis. Firstly, we combine neural network (NN) models with Bayesian experimental design algorithms for real-time experiment steering. The NN facilitates uncertainty quantifications in experimental settings and provides immediate parameter estimations, leading to physics-informed experimental decisions and more meaningful experimental measurements, as demonstrated through simulated X-ray Photon Fluctuation Spectroscopy (XPFS) measurements on magnetic excitations. In the second topic, we present an NN-based reconstruction algorithm for X-ray single particle imaging (SPI), capable of simultaneously estimating particle orientations and recovering the complete reciprocal space information. Our method remains robust under challenging experimental conditions, including strong shot-to-shot photon count fluctuations. It enables successful reconstructions from datasets with limited and highly-noisy diffraction patterns, surpassing limitations of the conventional algorithm.

SESSION QT02.11: Virtual Session II
Session Chairs: Amélie Juhin and Mingda Li
Tuesday Morning, December 5, 2023
QT02-virtual

10:30 AM *QT02.11.01

Time-Domain Free-Electron-Laser Spectroscopies for Nonzero-Wavevector Excitations [Paul Evans](#); University of Wisconsin-Madison, United States

Complex oxide thin film heterostructures and nanomaterials have a fascinating range of excitations including lattice vibrations, the coupling of lattice vibrations with electric polarization and magnetic degrees of freedom, and novel vibrational modes that arise due to nanoscale confinement. These excitations and their dynamics underpin the transport of heat, magnetic dynamics, coupled lattice/magnetic phenomena such as the spin-Seebeck effect, and the potential to probe predictions of predicted high-wavevector coupled excitations. We describe experimental free-electron-laser x-ray diffraction studies from two systems in which ferroic degrees of freedom are coupled to lattice vibrations: a weakly coupled ferroelectric/dielectric PbTiO₃/SrTiO₃ superlattice [1] and the coupled acoustic/magnetic excitations of a Pt/Gd₃Fe₅O₁₂ heterostructure [2]. In both cases, the transient excitation generated by ultrafast laser absorption generates a nearly impulsive perturbation with frequency and wavevector spectrum spanning ranges of THz and a large fraction of the Brillouin zone, respectively. Experimental results reveal the dispersion of acoustic excitations across the complete mini-Brillouin zone of the PbTiO₃/SrTiO₃ superlattice and the coupling of photoinduced expansion to the nanoscale polarization distribution. A combined experimental and Boltzmann transport equation study revealed the propagation and interface reflection of phonons in the Pt layer of the Pt/Gd₃Fe₅O₁₂ heterostructure. The integration of x-ray resonant scattering mechanisms with magnetic contrast can allow simultaneous probes of acoustic and magnetic excitations and the magnetoacoustic coupling.

[1] H. J. Lee, Y. Ahn, S. D. Marks, E. C. Landahl, S. Zhuang, M. H. Yusuf, M. Dawber, J. Y. Lee, T. Y. Kim, S. Unithrattil, S. H. Chun, S. Kim, I. Eom, S.-Y. Park, K. S. Kim, S. Lee, J. Y.

Jo, J. Hu, and P. G. Evans, "Structural Evidence for Ultrafast Polarization Rotation in Ferroelectric/Dielectric Superlattice Nanodomains," Phys. Rev. X **11**, 031031 (2021).

[2] D. Sri Gyan, N. Li, Z. Chen, D. Carbone, S. Geprägs, M. Dietlein, R. Gross, T. Sato, D. Zhu, D. Haskel, J. Stempfer, M. Li, D. Mannix, and P. G. Evans, "Evaluation of Low-Temperature Interface Phonon Reflection and Phonon Lifetime in a Pt/Gd₃Fe₅O₁₂ Heterostructure using Free-Electron-Laser X-ray Diffraction," in preparation (2023).

11:00 AM *QT02.08.01

Plastic Deformation of Quantum Materials[Martin Greven](#); University of Minnesota, United States

Plastic deformation is the permanent distortion that occurs when a material is subjected to stresses that exceed its yield strength. While plastic deformation has been used by blacksmiths and engineers for thousands of years, its effects on the electronic properties of quantum materials have been largely unexplored. In this talk, I will review our recent [1,2] and ongoing efforts to understand the effects of compressive plastic deformation in complex oxides. For example, we have uncovered that the classic perovskite SrTiO₃ exhibits enhanced, low-dimensional superconductivity and ferroelectric quantum criticality correlated with the appearance of self-organized dislocation structures, as revealed by diffuse neutron and X-ray scattering [2,3]. These results as well as unpublished work for related oxides demonstrate the potential of plastic deformation and dislocation engineering for the manipulation of electronic properties of quantum materials.

Work funded by the US Department of Energy through the University of Minnesota Center for Quantum Materials, under grant number DE-SC-0016371.

[1] D. Pelc *et al.*, Nat. Commun. **10**, 2729 (2019); <https://doi.org/10.1038/s41467-019-10635-w>

[2] S. Hameed, D. Pelc *et al.*, Nat. Mater. **21**, 54 (2022); <https://www.nature.com/articles/s41563-021-01102-3>

[3] See also: M. Li and Y. Wang., Nat. Mater. **21**, 3 (2022); <https://doi.org/10.1038/s41563-021-01146-5>

11:30 AM *QT02.11.02

Atomic and Electronic Structure Determination with Advanced X-Ray Spectroscopy[George Sterbinsky](#); Argonne National Laboratory, United States

X-ray absorption, anomalous absorption, and emission spectroscopies can reveal the atomic structures of materials, such as bond lengths and coordination environments. Insight into electronic structure, such as valence and hybridization, is also provided by these techniques. Instruments for these spectroscopic methods are available at the Advanced Photon Source, including those at beamlines 25-ID and 9-BM, which will be described. Several examples of the use of x-ray spectroscopy to gain insights into materials will be presented. These include examination of the relationship between ferromagnetism and electric polarization in multiferroic strained europium titanate films, investigation of the relationship between structure and ferromagnetism in lanthanum cobaltite films and chromium telluride crystals, and characterization of the local environments of dopants in potassium doped nickel oxide and erbium doped yttrium oxide.

SYMPOSIUM QT03

Higher-Order Topological Structures in Real Space—From Charge to Spin
November 27 - December 7, 2023

Symposium Organizers

Shelly Michele Conroy, Imperial College London

Sinead Griffin, Lawrence Berkeley National Laboratory

Dennis Meier, Norwegian University of Science and Technology (NTNU)

Haidan Wen, Argonne National Laboratory

* Invited Paper

+ JMR Distinguished Invited Speaker

SESSION QT03.01: Higher-Order Topological Structures - Growth

Session Chairs: Shelly Michele Conroy and Sinead Griffin

Monday Morning, November 27, 2023

Sheraton, Fifth Floor, Jamaica Pond

10:30 AM *QT03.01.01

Polar Textures in Ferroelectrics[Ramamoorthy Ramesh](#)¹ and Peter Meisenheimer²; ¹Rice University, United States; ²University of California, Berkeley, United States

Complex topological configurations are a fertile playground to explore novel emergent phenomena and exotic phases in condensed-matter physics. I will describe the discovery of polar skyrmions in a lead-titanate layer confined by strontium-titanate layers by atomic-resolution scanning transmission electron microscopy (STEM). Phase-field modeling and second-principles calculations reveal that the polar skyrmions have a skyrmion number of +1 and resonant soft X-ray diffraction experiments show circular dichroism confirming chirality. Such nanometer-scale polar skyrmions exhibit a strong signature of negative permittivity at the surface of the skyrmion, which is furthermore highly tunable with an electric field. They are a new state of matter and electric analogs of magnetic skyrmions. In this talk, we will describe results of our ongoing work on controlling the long range order in the skyrmions and vortices as well as rigorously understanding the origins of chirality (and its electric field manipulation) in the vortex structures.

11:00 AM *QT03.01.02

Ferroelectric Incommensurate Spin Crystal[Dorin Rusu](#)^{1,2}, Ana M. Sanchez¹, Thomas Hase¹, Richard Beanland¹ and [Marin Alexe](#)¹; ¹University of Warwick, United Kingdom; ²University College London, United Kingdom

Ferroelectrics can form complex topological spin structures such as vortices and skyrmions, especially when subjected to particular boundary conditions. In ferroelectrics vortex-like electric dipole-based topological structures have been observed in dedicated ferroelectric systems, especially PbTiO₃/SrTiO₃ ferroelectric/insulator superlattices, which have proven to be an ideal model system due to their high depolarising field. The large electrostatic energy is minimised by local rotations of surface dipoles, similar to ferromagnetic Kittel domains, in which local dipoles rotate in such a way to reduce both the depolarization and stray fields, avoiding the suppression of the ferroelectricity in the thin films.

In single PbTiO₃ epitaxial layers sandwiched between SrRuO₃ electrodes we observe a more complex domain structure analogue of the double-magnetic spin crystal phase. This comprises of periodic clockwise and anti-clockwise ferroelectric vortices which are modulated by a second cycloidal ordering along their toroidal core. Thus, one vector determines the periodicity of vortices and a second vector breaks the uniformity of the domains in the perpendicular direction, leading to a state described by a double-modulation. The interplay of only two orthogonal periodic modulations results in the so-called incommensurate spin crystal. [1]

The presence of such a double-structure, mediated by incommensurate interactions, would require an electric counterpart of the magnetic Dzyaloshinskii-Moriya interaction (DMI). Such an electric DMI could provide the phenomenological explanation of the emergence of magnetic-like phases in ferroelectric systems.

[1] D. Rusu et al., *Nature* 602, 240 (2022)

11:30 AM *QT03.01.03

Antiferroelectric-Like Behaviour in Ferroelectric Superlattices Chunhai Yin¹, Yaqi Li¹, Edoardo Zatterin², Evgenios Stylianidis¹, Marios Hadjimichael^{1,3}, Hugo Aramberri⁴, Jorge Iniguez^{4,5}, Shelly Michele Conroy⁶ and Pavlo Zubko¹; ¹University College London, United Kingdom; ²European Synchrotron Radiation Facility, France; ³University of Geneva, Switzerland; ⁴Luxembourg Institute of Science and Technology, Luxembourg; ⁵University of Luxembourg, Luxembourg; ⁶Imperial College London, United Kingdom

Ferroelectric superlattices have proven to be an exciting platform for exploring nanoscale ferroelectricity, complex polarisation patterns, and unusual functional properties such as negative capacitance. This talk will focus on how electrostatic and mechanical boundary conditions can be exploited to realise antiferroelectric-like behaviour in ferroelectric-dielectric superlattices. Using a combination of laboratory and synchrotron X-ray diffraction, scanning probe microscopy, transmission electron microscopy, electrical measurements and simulations, we investigate the structure of these artificially layered materials and the origin of the antiferroelectric-like switching.

SESSION QT03.02: Higher-Order Topological Structures I

Session Chairs: Shelly Michele Conroy and Sinead Griffin

Monday Afternoon, November 27, 2023

Sheraton, Fifth Floor, Jamaica Pond

1:30 PM *QT03.02.01

Polarization Dynamics during Ferroc Oxide Thin Film Growth Morgan Trassin; ETH Zurich, Switzerland

Ferroelectric oxide films with a thickness of just a few atoms can now be grown with a precision matching that of semiconductors. This opens a whole world of functional device concepts and fascinating phenomena that would not occur in the expanded bulk crystal. The successful integration of ferroelectrics into nanoscale devices relies however on our ability to engineer deterministically polarization states in the application relevant ultrathin regime. Here I will show how nonlinear optics enables the in-situ investigation of the ferroelectric polarization during the thin film epitaxial growth. Beyond the unprecedented access to the emergence of ferroelectricity and domain formation during the epitaxial deposition, we investigate transient polarization states originating from the evolving charge-screening environment of the oxide thin film growth process. We show the impact of lattice chemistry, depolarizing field-related effects in-situ and identify routes towards the establishment of robust polarization states in the ultrathin regime. Our work provides new insights dealing with the physics of ultrathin ferroelectrics and further control of ferroelectric-based heterostructure.

2:00 PM *QT03.02.02

Functional Topological Defects: Materials at the Edge of Order Jan Seidel; University of New South Wales, Australia

Topological structures in ferroic functional materials such as domain walls and skyrmions attract attention due to their intriguing properties and application potential in nanoelectronics. I will discuss our recent work on various ferroelectric and multiferroic materials systems using scanning probe microscopy as the main investigative tool, which is combined with insight from electron microscopy and ab-initio theory, and discuss future prospects of this evolving research field.

2:30 PM *QT03.02.03

Modeling Spin-Control by Ferroelectric Switching Katherine Inzani; University of Nottingham, United Kingdom

A key advantage of spin-defect based quantum technologies is the potential to engineer the defect properties by modifying the atomic environment. Systems which exhibit coupling between magnetic and electric degrees of freedom provide a route to manipulate spins by applying an electric-field, suggesting the prospect of localized spin-control via electrostatic gating.

We have elucidated the fundamental limit of magnetoelectric coupling by electric-field control of magnetic dopants in ferroelectric hosts, demonstrating through combined first principles calculations and electron-paramagnetic resonance measurements that the spin directionality evolves following a switching path coupled to polarization switching.[1]

We further leverage the versatility of the ferroelectric oxide platform by modifying the crystal field environment of the defect through epitaxial strain, low symmetry hosts and emergent topological polarization textures.[2,3] Results demonstrating spin-control in these systems provide an enhanced understanding of spin-charge coupling in defect systems and offer novel routes to tailored spin-control in ferroelectric crystals.

[1] J. Liu, V. V. Laguta, K. Inzani, W. Huang, S. Das, R. Chatterjee, E. Sheridan, S. M. Griffin, A. Ardavan, R. Ramesh, Coherent electric field manipulation of Fe³⁺ spins in PbTiO₃. *Science Advances*, 7, eabf8103 (2021).

[2] Inzani, K., Pokhrel, N., Leclerc, N., Clemens, Z., Ramkumar, S. P., Griffin, S. M., Nowadnick, E. A. Manipulation of spin orientation via ferroelectric switching in Fe-doped Bi₂WO₆ from first principles. *Physical Review B*, 105(5), 054434 (2022).

[3] S. Das, V. V. Laguta, K. Inzani, W. Huang, J. Liu, R. Chatterjee, M. R. McCarter, S. Susarla, A. Ardavan, J. Junquera, S. M. Griffin, R. Ramesh, Inherent Spin-Polarization Coupling in a Magnetoelectric Vortex. *Nano Letters*, 22, 3976 (2022).

3:00 PM BREAK

3:30 PM *QT03.02.04

Translational Boundaries of Antiferroelectrics as Topologically-Protected Polar Domains Gustau Catalan^{1,2} and Ying Liu³; ¹Institut Catala de Nanociencia i Nanotecnologia, Spain; ²ICREA, Spain; ³The University of Sydney, Australia

Antiferroelectric materials are characterized by their antipolar dipole arrangement. Such antipolar arrangements can be disrupted by so-called translational boundaries, which separate antiferroelectric domains where the dipolar ordering is the same, but shifted by an integer number of sub-lattice units. The simplest manifestation of such translational boundaries are antiphase boundaries, where two adjacent domains are separated by half a unit cell. The antiferroelectric archetype, PbZrO₃, has a unit cell that contains four dipoles, and in theory it can therefore have up to three types of translational boundaries, whereby the dipolar arrangement across the boundary is shifted by $\pi/2$, π or $3\pi/2$. Experimentally, however, we have observed "translational boundaries" with an arbitrary number of unit cells, resulting in phase shifts bigger than 2π . These are de-facto polar domains with their own internally symmetry, polarization and electric field response. But, while they are domains, they are also, still, translational boundaries topologically constrained by their adjacent antiferroelectric domains. The dual nature of these ultra-wide translational boundaries and their functional consequences will be discussed in the talk, together with experimental evidence for their existence.

4:00 PM QT03.02.05

Crystallography of Ferroelectric Superdomain Boundaries Edoardo Zatterin¹, Marios Hadjimichael^{2,3}, Steven J. Leake¹ and Pavlo Zubko³; ¹ESRF, France; ²University of Geneva, Switzerland; ³University College London, United Kingdom

Due to novel functionalities recently discovered at domain walls, thin-film ferroelectrics with dense ferroelastic domain structures represent promising candidates for a new generation of nanoelectronic devices [1]. Ferroelastic domain structures form to minimize epitaxial strain in the film, which can be tailored by selecting an appropriate combination of thin film and substrate material [2]. Certain combinations give rise to peculiar hierarchical organizations, whereby ferroelastic domains arrange in distinct "superdomain" bundles [3,4]. Recent studies have demonstrated that interconversion between superdomain states can be induced by the application of an external electric field [5] or stress [6], making these systems attractive for potential applications in reconfigurable electronics. However, little is still known about the superdomain crystallography on a local scale.

Here, we use a combination of synchrotron-based scanning X-ray diffraction microscopy [7] and piezoresponse force microscopy to investigate the nature of the interfaces where superdomains composed by in-plane (a_1/a_2) and out-of-plane (a/c) polytwins come into contact. We use PbTiO₃ thin films deposited on KTaO₃ substrates as a prototype system for this study

due to the large variation in the relative fraction of a_1/a_2 and a/c superdomains that it displays as a function of film thickness. We show how such superdomain boundaries possess a characteristic distribution of polarisation, tilt, and tetragonality gradients, and discuss how these are consistent with a minimisation of local electrostatic and elastic boundary conditions.

References

- [1] Sharma, P., et al. *Materials* 12, 2927 (2019)
- [2] Damodaran A. R., et al. *J Phys Condens Matter*, 28(26), p. 263001. (2016)
- [3] Langenberg, E. et al. *ACS Applied Materials & Interfaces*. 1944-8244 (2020).
- [4] Damodaran A. R. et al. *Advanced Materials*, 29, p. 1702069, (2017)
- [5] Matzen, S. et al. *Nature communications* 5, 4415 (2014).
- [6] Lu, X. et al. *Nature Communications* 10, 3951 (2019).
- [7] Corley-Wiciak, C., et al. *ACS Applied Materials & Interfaces* (2023).

4:15 PM QT03.02.06

Intertwined Dislocation Grids and Nematic Domains in an Iron-Based Superconductor Thin FilmZhengRen, HongLi, HeZhao, SharmaShrinkhala, ZiqiangWang and IlijaZeljko; Boston College, United States

A dislocation is a topological defect in a crystal lattice and can be associated with many functional properties. Dislocations can spontaneously form in epitaxial thin films as a strain relief mechanism. Here, we synthesize an iron-based superconductor thin film FeSe epitaxially on the SrTiO₃ substrate. Using scanning tunneling microscopy, we discover a structural modulation network, corresponding to a grid of edge dislocations at the film/substrate interface. We observe a striking change of the orientation of the dislocation lines as a function of the film thickness. Interestingly, since the edge dislocation grid gives rise to a spatially-varying uniaxial strain field, the formation of the nematic domains in FeSe is intimately intertwined with the dislocation grid. We further analyze their relationship by extracting the strain maps from the atomically-resolved topographs. Our finding provides an unexpected example of the formation and evolution of a dislocation grid in an epitaxial film, which is closely tied to the emergent nematic order of the iron-based superconductor FeSe.

4:30 PM QT03.02.07

Multiphoton Spectroscopy of a Dynamical Axion InsulatorOliviaLiebman, JonathanCurtis, IoannisPetrides and PrinehaNarang; UCLA, United States

The unusual magnetoelectric transport present in Weyl semimetals can be compactly understood as manifestations of an underlying axion field, which itself is determined by the microscopic band structure. The axion couples nonlinearly to electric and magnetic fields and possesses a signature topological magnetoelectric response, leading to a modified form of Maxwell's equations known as axion electrodynamics. Axions are naturally present in Weyl semimetals relating to the separation of the Weyl nodes in energy and in crystal momentum. In the presence of strong interactions, charge density-wave (CDW) order may develop which serves to gap the Weyl nodes and introduces corresponding collective excitations. When the inherent chiral symmetry of Weyl semimetals is spontaneously broken by the formation of CDW order, the resultant chiral condensate is endowed with intrinsic dynamics which yields a dynamical contribution to the axion field. However, unambiguous identification of this dynamical axion mode is challenging due to its inherent nonlinear coupling to electromagnetic fields. Therefore, we propose an all-optical protocol for verifying and characterizing dynamical axion collective modes in Weyl semimetals with CDW order. First, we show that axion collective mode can be excited using two-photon excitation schemes. Following excitation, the collective axion oscillations are then diagnosed by measuring the time-resolved Kerr rotation. Our results demonstrate a pathway towards utilizing multi-photon and entangled pair spectroscopies to identify new correlated phases in quantum matter.

4:45 PM QT03.02.08

Controlling Magnetotactic Bacteria, Their Topological Properties and Generating Skyrmions in Their Polar and Non-Polar Velocity Vector FieldsNoahKent^{1,2}, ColinGates², BohdanSenyuk², Jan BartTen-Hove², JefferyCameron² and IvanSmalyukh^{2,2}; ¹Massachusetts Institute of Technology, United States; ²University of Colorado Boulder, United States

Magnetotactic bacteria are microorganisms containing magnetite magnetic nanoparticle (MNP) bacteria organelles called magnetosomes. Magnetosomes are often arrayed in a specific pattern for a given strain of magnetotactic bacteria (i.e. a line along the long axis of the bacterium) and are made via biomineralization of ferromagnetic elements [1]. Previous work on the behavior of magneto-tactic bacteria in magnetic fields has assumed that the magnetic structure is a rigid dipole fixed along the bacteria's long axis – the direction of bacterial propulsion [1,2]. Such models have successfully elucidated the bacteria's behavior in rotating external fields, and magnetic field gradients. However, such models fail to explain the bacteria's behavior in a uniform magnetic field, do not allow for direct directional control over a set of bacteria, and do not address the inherent energetic degeneracy present in uniaxial magnetic systems [1,2].

Additionally, in recent years there has been significant research on topological structures, such as skyrmions and hopfions, in both magnetic [3] and soft matter liquid crystal systems [4] due to their stability and technological potential. Magnetic systems and soft matter systems typically differ in the nature of their order parameter: Magnetic systems have a polar order parameter and soft matter systems have a non-polar (axial) order parameter. No topological structures have been observed in magnetotactic bacteria despite both their magnetic and soft matter properties.

In this work we combine nanomagnetic simulations of magnetosome arrays distributions with transmission electron microscopy to simulate the magnetic behavior of the magnetotactic bacteria. Combining this with experiments using phase contrast optical microscopy and in-situ magnetic fields allowed us to understand the magnetic field response of bacteria based on how their magnetosomes are arranged. This allows us to explain previously anomalous behavior in the bacteria, control large, in phase groups of bacteria directly with external uniform magnetic fields, selectively change the topological parameter space from polar to non-polar, and generate topological structures in both the polar and the non-polar velocity vector fields of the bacteria. Being able to directly control these bacteria with external magnetic fields opens up the possibility of using them as guided microrobots in biomedicine (e.g. magnetic hyperthermia, drug delivery) and bio-spintronics.

References:

- [1] Faivre, D. & Schuler, D. *Chemical Reviews* 108, 4875–4898 (2008).
- [2] Steinberger, B., et al. *Journal of Fluid Mechanics* 273, 189–211 (1994).
- [3] Kent, N., et al. *Nat Commun* 12 (2021)
- [4] Smalyukh, I 2020 *Rep. Prog. Phys.* **83** 106601

SESSION QT03.03: Poster Session: Higher-Order Topological Structures

Session Chairs: Shelly Michele Conroy and Dennis Meier

Monday Afternoon, November 27, 2023

Hynes, Level 1, Hall A

8:00 PM QT03.03.01

Modified Landau-Lifshitz-Gilbert Dynamics Elucidating Asymmetric Spin Transport in NM/FM SystemChanhoPark and SangkwonLee; Chung-Ang University, Korea (the Republic of)

Spin pumping, usually referred as the injection of the spin current pumped by thermal agitation of non-equilibrium magnetization in ferromagnetic (FM) or ferromagnetic insulator (FMI) materials,¹ has been granted trivial without any further discussion on the pumped direction (FM to NM / NM to FM, where NM refers to normal metal). The pumped spin current from FM to NM results from temperature gradient ranged between FM and NM. Over the decade, spin pumping has been investigated thoroughly armed with theories such as linear response theory,¹ and considered consistent with conducted experiments on spin-to-charge conversion. Theoretically, reversing the direction of the temperature gradient should invert the sign of the spin current signal, but its intensity is identical between the two configurations.

On the other hand, repeated experiments on Pt/YIG bilayer structure with temperature gradient up to 20 K (-20 K for opposite direction) shows inconsistency between the experiment and theory, where the experiment kept showing nonlinearities between FM → NM, NM → FM pumped spin current. Herein, we assumed there exists corrections on some parameters when changing the injected direction of the pumped spin current, and carefully suggest modified LLG approach where different magnon lifetime contributes to the asymmetric spin transport across NM/FM interface. However, these kind of minor rectification cannot be solely explained with modified LLG, as additional experimental factors also contributes to the nonlinearities of the spin current signal, such as the change in the average temperature at the Pt/YIG interface depending on the direction of thermal gradient and resultant temperature-dependent spin voltage

originated from the temperature dependence of the spin-Seebeck coefficient $S(T)$,² and turned out to be sometimes more dominant than purely rectified spin current originated from interface-dependent magnon lifetime in our model. Nevertheless, the model suggested would provide meaningful applications for pure spin accompanied transport aided by material selection, configuration of spin voltage detecting device.

[1] Adachi, H.; Uchida, K.; Saitoh, E.; Maekawa, S. Theory of the spin Seebeck effect. *Rep. Prog. Phys.* **2013**, *76* (3), 036501.

[2] Basso, V.; Sola, A.; Ansalone, P.; Kuepferling, M. Temperature dependence of the mean magnon collision time in a spin Seebeck device. *J. Magn. Magn. Mater.* **2021**, 538.

8:00 PM QT03.03.02

Nonreciprocal Edge Transport in Superconducting Devices with Magnetic Control JunyiZhao¹, KieranBozier¹, AnnaChesca¹, HisakazuMatsuki¹, AdrianIonescu¹, LeylaC. Arslan², NadiaStelmashenko¹, FrancescaChiodi³ and JasonW. Robinson¹; ¹University of Cambridge, United Kingdom; ²Gebze Technical University, Turkey; ³Université Paris-Saclay, France

The proximity effect at a superconductor interface with a ferromagnet layer (S/F) can lead to unconventional electron pairing [1-3] and nonreciprocal edge transport (i.e., a superconducting diode effect (SDE)) [4,5]. The underlying mechanism of the SDE can have mixed origins related to spin-orbit coupling (SOC) or vortex flow with a geometrically asymmetric pinning potential in S and at S/F interfaces in mesoscopic wires [6-8]. Here we report an experimental investigation of the SDE and edge transport in superconducting (Nb, V and RhS) wires interfacial magnetism and/or Rashba SOC versus layer thickness, wire width, temperature and microstructure. The F layer in conjunction with interfacial SOC should affect the pinning potential along the edge regions of an S/F wire and modulate vortex dynamics, driving a nonreciprocal supercurrent [9,10]. Our experiments form a framework for understanding and optimizing the SDE in superconducting wires with the aim of achieving full magnetic control of charge and potentially spin for superconducting quantum devices.

[1] J. Linder and J. W. A. Robinson, *Nature Physics* **11**, 307 (2015).

[2] S. Komori et al., *Science Advances* **7**, eabe0128 (2021).

[3] L. A. B. Olde Olthof, L. G. Johnsen, J. W. A. Robinson, and J. Linder, *Physical Review Letters* **127**, 267001 (2021).

[4] S. Ilić and F. S. Bergeret, *Physical Review Letters* **128**, 177001 (2022).

[5] K.-R. Jeon, J.-K. Kim, J. Yoon, J.-C. Jeon, H. Han, A. Cottet, T. Kontos, and S. S. P. Parkin, *Nature Materials* **21**, 1211 (2022).

[6] Y. Hou et al., 2022), p. arXiv:2205.09276.

[7] N. Satchell, P. Shepley, M. Rosamond, and G. Burnell, *Journal of Applied Physics* **133** (2023).

[8] A. Gutfreund et al., *Nature Communications* **14**, 1630 (2023).

[9] M. K. Hope, M. Amundsen, D. Suri, J. S. Moodera, and A. Kamra, *Physical Review B* **104**, 184512 (2021).

[10] L. A. B. Olde Olthof, X. Montiel, J. W. A. Robinson, and A. I. Buzdin, *Physical Review B* **100**, 220505 (2019).

SESSION QT03.04: Higher-Order Topological Structures II

Session Chairs: Shelly Michele Conroy and Sinead Griffin

Tuesday Morning, November 28, 2023

Sheraton, Fifth Floor, Jamaica Pond

8:30 AM *QT03.04.01

Multistate Polarization Stability and Emergent Polar Vortices in All-Ferroelectric Superlattices PravinKavle^{1,2}, AidenM. Ross³, HarikrishnanK. P.⁴, PeterMeisenheimer¹, ArvindDasgupta¹, JiyuanYang⁵, Ching-ChelLin¹, PiusheBehera^{1,2}, EricParsonnet¹, XiaoxiHuang^{1,2}, JacobA. Zorn³, ShiLiu^{5,6}, SujitDas⁷, Yu-TsunShao^{4,8}, DavidA. Muller⁴, Long-QingChen³, RamamoorthyRamesh^{1,2,1} and LaneW. Martin^{1,2,9}; ¹University of California, Berkeley, United States; ²Lawrence Berkeley National Laboratory, United States; ³The Pennsylvania State University, United States; ⁴Cornell University, United States; ⁵Westlake University, China; ⁶Westlake Institute for Advanced Study, China; ⁷Indian Institute of Science, India; ⁸University of Southern California, United States; ⁹Rice University, United States

Emergent topological polar textures, including vortices, dipolar waves, skyrmions, merons, hopfions, and more, have generated considerable interest in ferroelectrics and wider condensed-matter physics communities. The delicate balance of electric, elastic, and gradient energies of ferroelectrics can be tailored in low-dimensional forms and nanostructures to manipulate the order parameters. Exotic functional properties (e.g., the coexistence of phases, chirality, negative capacitance, and emergent ultrafast dynamical responses) make them interesting candidates for devices. Ferroelectric-dielectric superlattices such as $(\text{PbTiO}_3)_n/(\text{SrTiO}_3)_n$ have been widely studied as a model system in part due to the high depolarizing field boundary condition provided by the SrTiO_3 layer. Such layers, however, limit the incorporation of such heterostructures into devices that could use the electronic characteristics of these polar topologies.

Looking to expand upon this rich design space, we ask a simple question: can similar emergent dipolar textures be produced in all-ferroelectric heterostructures while providing additional tunability based on the susceptibilities of the constituent layers? Here, we demonstrate the formation of polar vortices in all-ferroelectric $\text{Pb}_{1-x}\text{Sr}_x\text{TiO}_3/\text{PbTiO}_3/\text{Pb}_{1-x}\text{Sr}_x\text{TiO}_3$ trilayer and $(\text{Pb}_{1-x}\text{Sr}_x\text{TiO}_3)_n/(\text{PbTiO}_3)_n$ superlattice structures wherein $0.5 < x < 1$ grown on DyScO_3 (110) substrates. Unlike their counterparts with SrTiO_3 , the $\text{Pb}_{1-x}\text{Sr}_x\text{TiO}_3$ layers exhibit robust, in-plane ferroelectric polarization and domain structures, but still provide the appropriate boundary condition for the formation of polar vortices in the PbTiO_3 layers. We describe the manifestation of complex polar order in these structures that combines traditional ferroelectric order with emergent dipolar textures. Reciprocal space mapping studies reveal that the strontium content in the $\text{Pb}_{1-x}\text{Sr}_x\text{TiO}_3$ provides a fine control knob over the vortex periodicity; as supported by molecular-dynamics simulations. Furthermore, while recent studies on in-plane ferroelectric switching of polar vortices showed classical bi-stable switching, here, the in-plane polarization component of the vortices in the PbTiO_3 layers and the ferroelectric domains in the $\text{Pb}_{1-x}\text{Sr}_x\text{TiO}_3$ layers exhibit strong elastic and dipolar coupling, leading to a coercivity enhancement of the trilayer stack upon decreasing the strontium content of the $\text{Pb}_{1-x}\text{Sr}_x\text{TiO}_3$. Phase-field simulations further explain the polarization arrangement in the trilayer and the system's subsequent collective switching pathway of the two order parameters. Formation of such in-plane domains in the $\text{Pb}_{1-x}\text{Sr}_x\text{TiO}_3$ leads to the formation of a labyrinthine vortex arrangement, unlike the highly unidirectional vortices observed in $(\text{PbTiO}_3)_n/(\text{SrTiO}_3)_n$ superlattices. Further, we have explored the coupling between different emergent dipolar heterostructures of the from $\text{Pb}_{1-x}\text{Sr}_x\text{TiO}_3/\text{PbTiO}_3/\text{Pb}_{1-x}\text{Sr}_x\text{TiO}_3/\text{SrTiO}_3/\text{PbTiO}_3/\text{SrTiO}_3$. Therein, the thickness of the SrTiO_3 layer separating the two vortex structures controls the strength of the elastic and electric fields that extend between layers, affecting the sequence in which each trilayer would switch and the number of switching events. The result is an ability to produce low-field multi-state, four-step switching with robust retention and fatigue performance. Finally, in $(\text{Pb}_{1-x}\text{Sr}_x\text{TiO}_3)_n/(\text{PbTiO}_3)_n$ superlattices, we have explored the dielectric tunability, ac electric-field-induced surface displacement, and out-of-plane switching and found improved tunability as a function of the chemistry of the $\text{Pb}_{1-x}\text{Sr}_x\text{TiO}_3$ layer, antiferroelectric-like switching due to an unraveling of the vortex phase upon application of the electric-field, and strong back switching on releasing the same leading to improvements in the low-field energy storage as compared to $(\text{PbTiO}_3)_n/(\text{SrTiO}_3)_n$.

9:00 AM *QT03.04.02

Electric Bubble Quasiparticles JorgeIniguez^{1,2}; ¹Luxembourg Institute of Science and Technology, Luxembourg; ²University of Luxembourg, Luxembourg

My group is interested in the behavior of ferroelectric materials that present non-trivial polar orders and properties in situations of reduced dimensionality (ultra-thin layers or films) or subject to suitable electric and mechanical boundary conditions. Such intriguing phenomena include vortices [1], skyrmions [2], chirality [3] and negative capacitance [4,5], to name a few. In this talk I will review our most recent theoretical results for one of the model systems in the field, the $\text{PbTiO}_3/\text{SrTiO}_3$ ferroelectric/dielectric superlattices where many of the above effects were first demonstrated. In particular, I will discuss the dynamical behavior of the polarization in these nano-ferroelectrics, paying especial attention to the state we call "domain liquid" [4], which is characterized by a spontaneous stochastic motion of the domains. I will further show that, under the action of an external electric field, the domains break into electric bubbles (e-bubbles) that can be very long-lived and display (fast) Brownian dynamics. I will show quantitative results for e-bubble stochastic diffusion, compare with the behavior of Brownian skyrmions [6], and briefly discuss potential applications in unconventional computing.

Work done in collaboration with Hugo Aramberri (Luxembourg Institute of Science and Technology), F. Gómez-Ortiz and J. Junquera (University of Cantabria, Spain). My work is funded by the Luxembourg National Research Fund through Grants C18/MS/12705883/REFOX and C21/MS/15799044/FERRODYNAMICS.

[1] A.K. Yadav et al., "Observation of polar vortices in oxide superlattices", *Nature* **530**, 198 (2016).

[2] S. Das et al., "Observation of room-temperature polar skyrmions", *Nature* **568**, 368 (2019).

[3] P. Shafer et al., "Emergent chirality in the electric polarization texture of titanate superlattices", *PNAS* **115**, 915 (2018).

[4] P. Zubko et al., "Negative capacitance in multidomain ferroelectric superlattices", *Nature* **534**, 524 (2016).

[5] M. Graf et al., "Giant voltage amplification from electrostatically induced incipient ferroelectric states", *Nature Materials* **11**, 1252 (2022).

9:30 AMBREAK

10:00 AM *QT03.04.03

Probing Structure, Properties and Dynamic Behaviors of Topological Polar States by Advanced Electron Microscopy and Spectroscopy[XiaoqingPan](#); University of California, United States

Topological polar solitons, such as domain walls, polar vortices, and skyrmions, have garnered significant attention due to their unique functionalities and potential applications in electronic devices. The recent advancements in transmission electron microscopy (TEM) and electron energy-loss spectroscopy (EELS) have provided powerful tools for studying the structure, chemical bonding, functional properties, and dynamic behaviors of materials with atomic resolution. In this presentation, we will discuss the atomic scale structure, electric field and charge, and dynamic behaviors of nanoscale ferroelectric domains, vortices, and other topological structures such as polar skyrmions using TEM.

Through quantitative TEM techniques, we are able to map the electric polarization of nanodomains and a variety of polar structures at the atomic scale. Recently, we have developed a novel four-dimensional scanning transmission electron microscopy (4D STEM) method that allows for the direct mapping of local electric fields, charge densities, valence states of elements, and other properties of nanoscale materials in real space with sub-angstrom resolution. By utilizing this technique, we demonstrated the creation of skyrmion-like polar nanodomains in lead titanate/strontium titanate bilayers transferred onto silicon. These polar nanodomains can be switched from one type to another by an applied electric field, leading to substantial modifications in their resistive behaviors. This modulation in resistance is attributed to the distinct band bending and charge carrier distribution within the core of the two types of polar textures. The integration of high-density, switchable skyrmion-like polar nanodomains on silicon opens up possibilities for non-volatile memory applications utilizing topological polar structures in oxides. The investigation of topological polar states using advanced microscopy techniques offers valuable insights into their fundamental properties and dynamic characteristics. By combining the atomic-scale resolution of TEM and the real-space mapping capabilities of 4D STEM, we gain a deeper understanding of the behavior and manipulation of topological polar solitons. These findings pave the way for the development of innovative electronic devices harnessing the unique features of higher-order topological structures.

10:30 AM *QT03.04.04

Imaging Atomic Scale Phonons in Ferroelectric Materials[SandhyaSusarla](#); Arizona State University, United States

The advancement in thin film growth, and strain engineering has resulted in a variety of polarization domains and domain wall (DWs) formation in thin film ferroelectrics. State-of-art electron microscopy techniques such as High angle annular dark field (HAADF)- scanning transmission electron microscopy (STEM) have been used to probe the polarization magnitude and direction across domains and DWs in ferroelectric materials. However, a bewildering aspect that has not been well understood is what happens to phonons whenever there are nanoscale polarization heterogeneities. Proper ferroelectrics have a strong coupling between lattice and strain. Hence, the relationship between phonons and polarization can directly affect ferroelectric switching properties as coercive fields, switching energies and remnant polarization. Imaging phonons at atomic- to nano scale is challenging to poor spatial resolution of the current state-of-the-art techniques (Raman spectroscopy, IR spectroscopy, and thermoreflectance measurements). The combination of STEM and vibrational electron energy loss spectroscopy (EELS) provides a new paradigm to probe atomic- to nano- scale properties. In my talk, I will talk our progress behind probing atomic scale phononic properties at domains and DWs using prototypical thin-film PbTiO₃ as our model system.

11:00 AM QT03.04.05

Mapping Local Topology, Defects and Emergent Order of Picometer-Scale Periodic Lattice Modulations[BenjaminH. Savitzky](#); Lawrence Berkeley Laboratory, United States

In complex condensed matter systems, patchworks of order and disorder can form in competing order parameters, with localized pockets of emergent symmetry breaking which may be mere nanometers across. Measuring the real space variation of emergent order and its defects is therefore essential. By combining in-situ cryogenic (77K) high-angle annular dark-field scanning transmission electron microscopy, fast-acquisition low-SNR referenceless image registration with lattice-hop-error correction, picometer precision atomic column gaussian fitting, and isolation and reconstruction of both the underlying and symmetry broken lattices in Fourier space, it becomes possible to map modulations of the lattice parameter at each atomic site with picometer precision. Alternatively, real space measurement of periodic lattice modulations is possible using phase lock-in methods popular in scanning tunneling microscopy, geometric phase analysis more common in transmission electron microscopy, pairwise atomic distance histograms in one or two dimensions, and other methods. The advantages and drawbacks of these various approaches to uncovering the structure and topology of lattice symmetry breaking in real space will be discussed and compared, with examples drawn from complex oxides and transition metal dichalcogenides.

11:15 AM *QT03.04.06

Imaging Topological Textures from the Pico to Micro Scale with Electron Ptychography[DavidA. Muller](#); Cornell University, United States

The discovery of non-trivial topological textures, including flux-closure, vortices, skyrmions, merons and hopfion in both ferromagnetic and ferroelectric systems have required electron microscopy to resolve their internal structures. Here, enabled by a new design of electron detector [1] that is capable of measuring the complete distribution of momentum transfers at every probe position, we construct a 4-dimensional phase space from which we solve the inverse multiple scattering problem and retrieve the underlying 3-dimensional potential of the sample. The lateral resolution of less than 20 pm is now limited not by the instrument, but by the thermal vibrations of the atoms themselves, and the precision is improved to well below 1 pm [2]. The resulting ptychographic reconstructions have allowed us to image the internal structures of both magnetic and ferroelectric vortices, skyrmions and merons, including their singular points that are critical for accurately describing the topological properties of these field textures. [3]

[1] H. Philipp et al., *Microscopy and Microanalysis* **28** (2022), p. 425-440.

[2] Z. Chen et al., *Science* **372** (2021), p. 826-831.

[3] In collaboration with Harikrishnan K. P., Yu-Tsun Shao, Zhen Chen and Yi Jiang. Funding from the U.S. Army Research Office under the MURI ETHOS (W911NF-21-2-0162). Facility support from the Cornell Center for Materials Research (National Science Foundation grants MRI-1429155, DMR-1719875, DMR-1539918).

SESSION QT03.05: Higher-Order Topological Structures III

Session Chairs: Shelly Michele Conroy and Sinead Griffin

Tuesday Afternoon, November 28, 2023

Sheraton, Fifth Floor, Jamaica Pond

1:30 PM *QT03.05.01

Emergent Picosecond-Scale Dynamics of Nanoscale Ferroelectric Polarization Configurations[PaulG. Evans](#); University of Wisconsin, United States

Ferroelectric thin films and superlattices with nanoscale dimensions exhibit a competition of energetic phenomena that produce configurations of the polarization that are distinct from bulk materials. These configurations have a profound effect on the equilibrium and driven dynamics of the nanoscale material. These dynamics are coupled to the structure of these layers and can be observed in synchrotron radiation or free-electron-laser structural studies. For example, the nanoscale polarization configuration of PbTiO₃/SrTiO₃ (PTO/STO) superlattices, for example, exhibits equilibrium fluctuations that arise from the existence of many configurations with nearly identical free energy. The optically driven dynamics of the PTO/STO superlattice include a picosecond-scale distortion of the polarization in response to the optically induced acoustic pulse and a change in the magnitude of the polarization of the PTO due to polarization screening. The effect of polarization screening is comparatively larger in a strongly BaTiO₃/CaTiO₃ (BTO/CTO) superlattice. In BTO/CTO superlattice screening effects following above-bandgap excitation lead to a reduction in the polarization of the CaTiO₃ layer, evident as a contraction of the out-of-plane lattice parameter of the CaTiO₃ component. The characteristic timescale for the development of these effects is on the scale of several picoseconds to tens of picoseconds, set by the propagation of acoustic pulses through the system. Further picosecond-scale diffraction studies reveal that the nanoscale structure affects the longitudinal acoustic sound velocity. There are prospects to employ these effects to affect structural parameters such as the oxygen octahedral tilt that affect other properties of ferroelectrics as well as the magnetism of multiferroics.

2:00 PM *QT03.05.02

Transferring Orbital Angular Momentum to an Electron Beam Reveals Toroidal and Chiral Order[KaylaX. Nguyen](#)^{1,2}; ¹University of Illinois at Urbana-Champaign, United States

Orbital angular momentum and torque transfer play central roles in a wide range of magnetic textures and devices including skyrmions and spin-torque electronics. Unlike magnetic toroidal order, electric toroidal order, found in analogous topological structures in ferroelectrics, do not couple directly to linear external fields. Instead, we show that the presence of an electric toroidal moment in a ferro-rotational phase transfers a measurable torque and orbital angular momentum to a localized electron beam in the ballistic limit. We record these torque transfers from a high-energy electron beam using a momentum-resolved detector. This approach provides a high-sensitivity method to detect polarization fields and their more complex order parameters and topologies. In addition to toroidal order, we also demonstrate high-precision measurements of vorticity and chirality for polar vortex-like phases¹.

[1] K.X. Nguyen et. al, Phys. Rev. B **107**, 205419.

2:30 PM *QT03.05.03

Phase Transformations in 2D Van der Waals Trichlorides: Insights from Cryogenic Scanning Transmitting Electron Microscopy MiaofangChi; Oak Ridge National Laboratory, United States

Two-dimensional (2D) van der Waals (vdW) materials and their heterostructures offer an exceptional platform for investigating intriguing physical phenomena and implementing diverse applications. While it is widely acknowledged that lattice structural transformations often coincide with changes in electronic and spin structures, leading to the emergence of exotic quantum phenomena, it remains uncertain whether the same structural transformations observed in bulk materials also occur in thin flake samples. As a result, a comprehensive understanding of the structure-property relationship in multi-layered 2D vdW materials is often lacking. In our recent studies, we aim to unveil the thickness-dependent phase transformations and changes in exciton states in several model 2D vdW trichlorides. To achieve this, we employ state-of-the-art techniques such as cryogenic atomic-resolution scanning transmission electron microscopy (STEM) and monochromated electron energy loss spectroscopy (EELS). By analyzing these materials with different numbers of layers at the atomic level, our findings provide insights into the layer-number-dependency that are crucial for harnessing the unique quantum characteristics of thin-layer 2D vdW materials in various device applications.

3:00 PMBREAK

3:30 PM *QT03.05.04

Differential Phase Contrast STEM Imaging of Topological Structures NaoyaShibata; The University of Tokyo, Japan

Differential phase contrast scanning transmission electron microscopy (DPC STEM) is a powerful technique for directly characterizing local electromagnetic field distribution inside materials and devices. In recent years, new magnetic objective lens system that realizes a magnetic field free environment at the sample position has been developed [1]. The novel electron microscope with this new objective lens system (Magnetic-field-free Atomic Resolution STEM: MARS) combined with DPC imaging is very useful for characterizing many important topological structures. In this talk, some recent applications using MARS will be presented. The topics include atomic-scale grain boundary structure analysis in Fe-Si soft magnet [2], domain wall width measurements in magnets [3], magnetic field imaging of spin devices [4], domain imaging in magnetic quasicrystals, imaging of magnetic skyrmions, imaging of ferroelectric domain walls and so on.

[1] N. Shibata et al., *Nature Comm.* 10, 2380 (2019).

[2] T. Seki et al., *submitted*.

[3] Y.O. Murakami et al., *submitted*.

[4] Y. Kohno et al., *submitted*.

[5] This work is supported by JST ERATO grant number JPMJER2202 and the JSPS KAKENHI (grant numbers 20H05659 and 19H05788).

4:00 PM *QT03.05.05

The Dynamics of Magnetic Helices in an Amorphous Material with Coherent X-Rays SophieMorley¹, ArnabSingh¹, RyanTumbleson^{1,2}, EmilyHollingworth³, Ahmad UsSaleheen¹, MargaretMcCarter¹, PeterFischer^{1,2}, FrancesHellman³, StephenKevan¹ and SujoyRoy^{1,2}; ¹Lawrence Berkeley National Laboratory, United States; ²University of California, United States; ³University of California, Berkeley, United States

Synchrotron x-rays are a powerful element-specific probe for the electronic and magnetic ordering of a material. Here we measure the diffraction from a magnetic helix of pitch ~ 80 nm in a structurally amorphous FeGe thin film through its magnetic phase transition. We select the coherent part of the x-ray beam to produce an interference pattern known as speckle. The speckle pattern acts as a fingerprint of the specific microscopic configuration of the helical domains and their disorder. Taking speckle patterns as a function of time gives us a way to characterize the dynamics over ~ 10-micron field of view but with nanoscale spatial sensitivity and ms to hour time sensitivity. We identify static and dynamic parts of the speckle throughout the transition which follow a universal behavior over several compositions [1]. We extract faster dynamics at temperatures much lower than the transition temperature which we attribute to the motion of topological defects and on increasing temperature we observe on average slower fluctuations but from a larger volume of the sample. We have also performed micromagnetic simulations to model these disordered helical spin structures in support of our experimental findings.

Work funded by DOE BES MSE under contract DE-AC02-05-CH11231 (MS- MAG)

References:

[1] Singh, A., Hollingworth, E., Morley, S. A., Chen, X. M., Us Saleheen, A., Tumbleson, R., McCarter, M. R., Fischer, P., Hellman, F., Kevan, S. D., Roy, S., "Characterizing Temporal Heterogeneity by Quantifying Nanoscale Fluctuations in Amorphous Fe-Ge Magnetic Films", *Adv. Funct. Mater.* 33, 2300224, 2023. <https://doi.org/10.1002/ADFM.202300224>

4:30 PM *QT03.05.06

Magnetolectric Classification of Skyrmions BhowalSayantika and NicolaSpaldin; ETH Zürich, Switzerland

Magnetic skyrmions are nanometer-sized, topologically protected swirling spin structures with the potential for applications as data bits in future high-density data storage devices. In my presentation, I will discuss our recent development of a comprehensive theory for classifying magnetic skyrmions and related spin textures based on their magnetolectric multipoles. These multipoles characterize the first-order asymmetry in magnetization density, which has proven highly effective in describing the magnetolectric response of materials. Since magnetic skyrmions are now established in insulating materials, where magnetolectric multipoles govern the linear magnetolectric response, our classification framework offers insights into manipulating the magnetic properties of skyrmions through applied electric fields. We apply this formalism to skyrmions and anti-skyrmions of different helicities, as well as magnetic bimerons, which share the same topology but not the geometry of skyrmions. Our study reveals that the non-zero components of the magnetolectric multipole and the magnetolectric response tensors are uniquely determined by the topology, helicity, and geometry of the spin texture. As a result, we propose straightforward linear magnetolectric response measurements as an alternative to Lorentz microscopy for characterizing insulating skyrmionic spin textures. Reference: Sayantika Bhowal and Nicola A. Spaldin, Phys. Rev. Lett. 128, 227204 (2022).

SESSION QT03.06: Higher-Order Topological Structures IV
Session Chairs: Shelly Michele Conroy and Dennis Meier
Wednesday Morning, November 29, 2023
Sheraton, Fifth Floor, Jamaica Pond

8:30 AM *QT03.06.01

Behavior of Magnetic Skyrmions Lattices at the Nanoscale Observed using *In Situ* Lorentz Transmission Electron Microscopy AmandaK. Petford-Long^{1,2}, YueLi¹, ArthurMcCray^{2,1} and CharudattaPhatak^{1,2}; ¹Argonne National Laboratory, United States; ²Northwestern University, United States

Understanding the behavior of nanoscale magnetic structures relies on being able to understand the complex interplay of the energy terms that control this behavior at a local scale. The relative contribution of these energy terms can be modified by parameters such as geometric confinement and interactions between adjacent magnetic nanostructures. In addition, it is important to be able to explore how a magnetic nanostructure responds to an external driving force, such as temperature, and electric or magnetic fields. We use Lorentz transmission electron microscopy (LTEM) combined with in-situ magnetizing and cooling experiments to elucidate the micromagnetic behavior at the sub-micron scale in nanomagnetic structures. By comparing

the experimental and simulated results we gain a detailed understanding of the way in which the various energy terms contribute to the behavior that we observe.

The focus of this presentation will be on thin films of van der Waals materials that host magnetic skyrmions and other topological spin structures in which we make use of cryoEM to explore the way in which order in the skyrmions lattices evolves, the origin of this behavior, and the energy terms that control the behavior as a function of temperature and applied field.

9:00 AM QT03.06.02

Observation of Magnetic Resonance Modes in Polar Skyrmion Material VOSe_2O_5 Araki Tomonao¹, Takashi Kurumaji¹, Masahito Mochizuki², Yoshinori Tokura^{1,3}, Rina Takagi^{1,4} and Shinichiro Seki^{1,4}; ¹The University of Tokyo, Japan; ²Waseda University, Japan; ³Japan Science and Technology Agency (JST), Japan; ⁴RIKEN, Japan

The magnetic skyrmion is a vortex structure of electron spins that behaves as a stable particle protected by topology. VOSe_2O_5 is a magnetic insulator with a polar crystal structure (space group $P4cc$) and is one of a few materials that have been confirmed to exhibit a Néel-type magnetic skyrmion lattice [1, 2]. In this study, we experimentally investigate the microwave response of VOSe_2O_5 to clarify the magnetic resonance dynamics. As a function of temperature and magnetic field, this compound hosts a rich variety of magnetic phases, including the triangular skyrmion lattice (tri. SkL) and cycloidal spin states. In the tri. SkL phase, clockwise mode (CW), counterclockwise mode (CCW), and breathing mode (BR) have been identified. We also identified three distinctive magnetic resonance modes in the cycloid spin state, which corresponds to the rotational oscillation of local magnetic moment around the x , y , and z axes, respectively. The observed magnetic resonance spectra are well reproduced by theoretical calculations based on the magnetic Hamiltonian considering the Dzyaloshinskii-Moriya interaction and uniaxial anisotropy. The present results will contribute to the general understanding of the coherent dynamics of skyrmion and helical spin states in polar magnetic systems.

[1] T. Kurumaji et al., *Phys. Rev. Lett* **119**, 237201 (2017),

[2] T. Kurumaji et al., *J. Phys. Soc. Jpn* **90**, 024705 (2021)

9:15 AM QT03.06.03

Effects of Dirac Band Tilting on Thermomagnetic Properties in Weyl Semimetals Eleanor Scott¹, Poulomi Chakraborty², Satya Guin^{3,4}, Brian Skinner² and Sarah J. Watzman¹; ¹University of Cincinnati, United States; ²The Ohio State University, United States; ³Max Planck Institute for Chemical Physics of Solids, Germany; ⁴Birla Institute of Technology and Science, India

The topological and semimetallic effects of Weyl semimetals make them excellent candidates for magneto-thermoelectric transport. Previous work in the thermoelectric properties of Type I Weyl semimetals (WSMs) has found that this class of materials possess both a large magneto-Seebeck effect and Nernst effect simultaneously, is very sensitive to doping, and that magneto-thermoelectric effects are maximized when the temperature is comparable to the Fermi energy. [1, 2]. Here, we shift our focus to Type II WSMs, which possesses asymmetric Dirac bands, unlike the band symmetry assumed in Type I WSMs. Our candidate material is WTe_2 , and previous single-crystalline data observed an extremely large Nernst thermopower, exceeding $7,000 \mu\text{V K}^{-1}$ at 11.3 K and 9 T [3]. However, literature does not include full magneto-thermoelectric transport data over a broad temperature range, which we present here in polycrystalline WTe_2 . Experimental results indicate that unlike the behavior observed in the Type I WSM [1], the magneto-Seebeck effect is significantly reduced and is not maximized in the same temperature range as the Nernst effect. Additionally, the Nernst thermopower of this Type II WSM did not exhibit an anomalous Nernst effect beyond cryogenic temperatures, while NbP, a Type I WSM, exhibited anomalous behavior over a broad temperature range.

Our experimental work is complemented by theoretical models of the thermoelectric transport behavior. Previous theoretical models created for the NbP work matched well with the transport behavior seen in the experimental results. This model is then altered to account for the tilted band structure and transport properties specific to WTe_2 . By comparing both the experimental and theoretical results of thermoelectric transport in NbP and WTe_2 , we can determine how the tilting of Dirac bands effects magneto-thermoelectric transport behavior in WSMs.

[1] E. F. Scott et al. *Phys. Rev. B* **107**, 115108 (2023)

[2] S. J. Watzman et al. *Phys. Rev. B* **97**, 161404(R) (2018).

[3] Y. Pan, et al. *Nat Commun* **13**, 3909 (2022).

9:30 AM BREAK

10:00 AM *QT03.06.04

Thin-Film Realization of an Improper Ferroelectric Quantum Spin Liquid Candidate Johanna Nordlander^{1,2}; ¹Harvard University, United States; ²Paul Drude Institute for Solid State Electronics, Germany

Magnetically frustrated materials offer a playground for realizing exotic magnetic ground states such as quantum spin ices and spin liquids that have been proposed as building blocks in quantum computing and as potential hosts for unconventional superconductivity. The ability to synthesize such materials in thin-film form is necessary for their integration into the proposed device architectures and also allows further tuning of the magnetic ground state with dimensionality and epitaxial strain. However, thin-film realizations of quantum spin liquid candidate materials remain scarce. Here, we use reactive oxide molecular beam epitaxy to synthesize the first thin films of hexagonal TbInO_3 , a magnetically frustrated rare-earth system that was recently proposed as a spin liquid candidate. In bulk, TbInO_3 exhibits geometrically driven improper ferroelectricity similar to the multiferroic hexagonal manganites, and displays the same topologically protected vortex domain pattern. The underlying lattice distortion causing this domain pattern imposes a stuffed honeycomb geometry on the quasi-two-dimensional Tb^{3+} sublattice which harbors the magnetic frustration in TbInO_3 . Here, we investigate the ferroelectric distortion in our epitaxial TbInO_3 thin films using in-situ RHEED and post-deposition HAADF-STEM. We furthermore use SQUID magnetometry and X-ray spectroscopy to investigate the low-temperature magnetic behavior. Our work constitutes one of the few thin-film realizations of a quantum spin liquid candidate, and opens up for the use of epitaxy to further manipulate the unusual coexistence of ferroelectricity and spin liquid physics in this thin-film system.

10:30 AM QT03.06.05

Large Anomalous Frequency Shift in Perpendicular Standing Spin Wave Modes in BiYIG Films Induced by Thin Metallic Overlayers Byunghun Lee, Takian Fakhru, Caroline A. Ross and Geoffrey Beach; Massachusetts Institute of Technology, United States

Interface-driven phenomena in magnetic insulators is gaining attention owing to the possibility to control magnetization dynamics and magnetic textures in low-dissipation materials. Pure spin signals can be transported in magnetic insulators through magnon excitations, and controlling the nature of these excitations may lead to new insights into magnetization dynamics and novel spin wave devices. [1]

In this work, the influence of metallic overlayers on the spin wave dynamics of thin Bi-substituted yttrium iron garnet films is studied using Brillouin light scattering spectroscopy. [2] It is found that the magneto-static Damon-Eschbach modes exhibit a significant frequency shift when Pt, Au, or Cu films are deposited upon them, which arises from an interfacial contribution to the effective magnetic anisotropy. In addition, there is an unexpectedly large shift in the perpendicular standing spin wave mode frequencies that cannot be explained by anisotropy-induced surface spin pinning. Rather, the experimental observations are consistent with an interface-induced decrease in the effective thickness within which the standing waves are confined, increasing the exchange contribution to the mode frequency. It is suggested that this additional confinement may result from spin pumping at the insulator/metal interfaces, which results in a locally-overdamped interface region. We propose a phenomenological model that can describe the observation in terms of an interfacial region where the spin-orbit coupling plays a crucial role and the local effective damping associated with spin-pumping torque is relatively large, which would qualitatively explain the anomalously-large metal-induced frequency shifts. [3] These results uncover a previously-unidentified interface-driven change in magnetization dynamics that may be exploited to locally control and modulate magnonic properties in extended films.

[1] F. Hellman, et al., *Rev. Mod. Phys.* **89**, 025006 (2017).

[2] B. H. Lee, et al., *Phys. Rev. Lett.* **130**, 126703 (2023).

[3] K. Chen, et al., *Phys. Rev. Lett.* **114**, 126602 (2015).

10:45 AM QT03.06.06

The Effects of Doping on the Magnetic Transition Regions of the Skyrmion Hosting Material, Cu_2OSeO_3 Marco Vas^{1,2}, Alexander Ferguson^{1,2}, Joseph Vella^{1,2}, Clemens Ulrich³, Samuel Yick^{1,2}, Tilo Soehnel^{1,2} and Elliot Gilbert⁴; ¹The University of Auckland, New Zealand; ²MacDiarmid Institute of Advanced Materials & Nanotechnology, New Zealand; ³University of New South Wales, Australia; ⁴Australian Nuclear Science and Technology Organisation, Australia

The Cu_2OSeO_3 material system has gained a lot of interest over the last 10-15 years because it is the only multiferroic insulator known to host magnetic skyrmions. This material falls into a B20 class which has a non-centrosymmetric cubic crystal lattice and crystallises in a $P2_13$ space group. Most materials in this class, such as MnSi , FeGe , and $\text{Fe}_{1-x}\text{Co}_x\text{Si}$, despite having different compositions, have been observed to host magnetic skyrmions.¹ This suggests that the role of the crystal structure might influence the capability of the material to host skyrmions. The skyrmion formation is a result of the four different Cu^{2+} sites, which have a 3-down 1-up spin arrangement with Ferromagnetic (FM) and Antiferromagnetic (AFM) super-exchange interactions being present.² The lack of inversion symmetry in the corner shared O-Cu₄ tetrahedra result in an appreciable Dzyaloshinskii-Moriya interaction (DMI) between Cu^{2+} sites; this competes with the super-exchange interactions leading to spin canting that underpins the formation of helical/conical spin textures (depending on temperature and applied magnetic field strength).³ However, due to these systems' complex spin and charge interactions, the underlying quantum-mechanical processes behind these phenomena are still not fully understood. Further

experiments are required; as such, this project aims to provide details on the roles played by the crystal structure that may enable the magnetic structures observed in different conditions.

For this project, the focus is on the relationship between the crystal structure and the magnetic structures observed in the Cu_2OSeO_3 material system. By manipulating the magnetic Cu sites and non-magnetic Se sites, the spin interactions between the magnetic sites will change, resulting in changes to the interacting Heisenberg and Dzyaloshinskii-Moriya interactions that are known to form skyrmions. These interactions are highly localised between magnetic ions, which makes them sensitive to spatial changes. Non-magnetic doping of substituting Te into the Se sites results in chemical pressure and expansion of the unit cell, which changes the spacing between atoms and the subtle crystal distortions should have an impact on these interactions. While magnetic doping by substituting Co^{2+} into the Cu^{2+} sites should have a large impact on these magnetic interactions due to the Co^{2+} ion having a stronger moment than Cu^{2+} . This, in turn, should change the nature of the formation of magnetic skyrmions in this material. Understanding the role that subtle distortion to the magnetic network plays on the formation and stability of topological spin structures will be vital in designing materials for spintronics. This might, in fact, provide a guide in developing ambient condition spintronics materials, in which their absences have hindered the technological application of these topological spin structures.

We will present data from high-resolution synchrotron powder XRD and neutron powder diffraction to present the effects of magnetic and non-magnetic doping on both the crystal and magnetic structure of the material. Along with small-angle neutron scattering to confirm the presence of the helical and skyrmion phases. While in-depth SQUID magnetometry measurements were carried out to see the effects of doping on magnetisation. This collection of data aims to build an understanding of how the crystal structure plays a more important role in the formation of skyrmions than is currently believed in literature.

1. N. Kanazawa *et al.*, *Adv Mater.* **29**(25), (2017).
2. J.-W.G. Bos *et al.*, *Phys. Rev. B*, **78**(9), [094416] (2008)
3. S. Seki *et al.*, *Science* **336**, 198 (2012).

11:00 AM QT03.06.07

Characterization of the Anisotropic Anomalous Nernst Effect in Canted Antiferromagnetic YbMnBi_2 and YbMnSb_2 Katherine A. Schlaak¹, Shuou Liu², Chenguang Fu² and Sarah J. Watzman¹; ¹University of Cincinnati, United States; ²Zhejiang University of Technology, China

Recent research in the field of thermoelectrics (TEs) has been focused on transverse TE devices which surpass their traditional longitudinal counterparts in a few facets, including their elimination of complex n- and p-type legs in exchange for one material whose TE output scales with device size. However, transverse TE materials require a magnetic field for operation, which can increase the complexity of device design. Though ferromagnetic materials have been shown to exhibit anomalous thermoelectric transport in the absence of magnetic field, these materials often have a large magnetization which can negatively impact electronic components in device applications. Canted antiferromagnetic topological semimetals, such as YbMnBi_2 and YbMnSb_2 , have been shown to exhibit these large anomalous effects with low magnetization and high mobility, thus making them reasonable candidates for transverse TE applications. Previous research on single crystalline YbMnBi_2 , a Weyl semimetal, reported a notably large anomalous Nernst conductivity of $\sim 10 \text{ A m}^{-1} \text{ K}^{-1}$ near 80 K, owing to the contribution of Mn to a non-zero Berry curvature and the strong spin-orbit coupling associated with Bi [1]. In addition to this large anomalous Nernst conductivity, YbMnBi_2 is highly anisotropic, which is beneficial in device applications as it allows for simultaneously low electrical resistivity and thermal conductivity in different crystallographic directions. While these results are intriguing, polycrystalline materials are more applicable to TE devices as single crystals can be challenging to synthesize. In this work, polycrystalline samples of YbMnBi_2 are synthesized, and their magneto-thermoelectric transport is characterized as a function of temperature and externally applied magnetic field. Transport data is analyzed with an emphasis on the anisotropy present in single-crystalline samples being removed in polycrystalline samples.

YbMnSb_2 is a similarly anisotropic, canted antiferromagnetic Weyl semimetal. Previous work has reported a large, longitudinal thermopower of $\sim 160 \text{ mV/K}$ near 300 K [2]. However, transverse thermoelectric transport has yet to be characterized. In this work, the anomalous Nernst and magneto-Seebeck effects of YbMnSb_2 are characterized as functions of temperature and magnetic field. Special attention is given to crystallographic orientation as well, as Dirac bands are expected to dominate transport in the ab-plane while parabolic bands dominate parallel to the c-axis.

- [1] Y. Pan *et al.* *Nat. Mater.* **21**, 203-209 (2022).
- [2] Y. Pan *et al.* *Adv. Mater.* **33**(7), 2003168 (2021).

This work is supported by the U.S. Department of Energy, Office of Science, Office of Basic Energy Sciences Early Career Research Program under Award Number DE-SC0020154. This material is based upon work supported by the National Science Foundation Graduate Research Fellowship Program under Grant No. (2035701). Any opinions, findings, and conclusions or recommendations expressed in this material are those of the authors and do not necessarily reflect the views of the National Science Foundation.

11:15 AM QT03.06.08

Dy-Doping of Zn/Al Substituted Nickel Ferrite for Non-Collinear Magnetic Order Verena Ney¹, Celina Parzer¹, Fabrice Wilhelm², Andrei Rogalev² and Andreas Ney¹; ¹Johannes Kepler University, Austria; ²European Synchrotron Radiation Facility, France

Zn/Al substituted nickel ferrite (NiZAF) has been reported to be a very promising ferrimagnetic insulator with a Curie temperature well above room-temperature which exhibits a very low intrinsic magnetic damping [1]. Thin films of this magnetic spinel can be prepared using pulsed laser ablation [1] or reactive magnetron sputtering from single targets [2] as well as co-sputtering to vary the individual constituents independently [3]. Element selective characterization allows to determine the incorporation of the cationic species [1,2] and correlate them with the desired magnetic properties [3]. Besides an intrinsic low magnetic damping also non-collinear spin textures such as skyrmions are of potential interest for spintronic or magnonic applications [4]. For magnetic spinel such non-collinear magnetic textures have been reported to be generated either by structural effects in nanoparticles or ultrathin films, e.g. [5] or by doping with trivalent rare earth ions such as Dy [6]. In this work we will report on a systematic growth series of NiZAF films which were doped with Dy by means of co-sputtering. Due to its large ionic radius Dy distorts the crystal structure of the hosting spinel and the low coercive field as well as the low magnetic damping significantly increase. Nonetheless, the Curie temperature well-above room-temperature remains and the spinel structure is maintained on a local scale as evidenced by x-ray linear dichroism studies. Upon Dy doping a local minimum in the zero-field cooled $M(T)$ curves develops which can be taken as a first indication for a non-collinear spin-arrangement which will be subject to further investigations and the latest results for the magnetic texture will be presented.

- [1] S. Emori *et al.*, *Adv. Mater.* **29**, 1701130 (2017)
- [2] J. Lumetzberger, M. Buchner, S. Pile, V. Ney, W. Gaderbauer, N. Daffé, M. V. Moro, D. Primetzhofer, K. Lenz, and A. Ney, *Phys. Rev. B* **102**, 054402 (2020)
- [3] J. Lumetzberger, V. Ney, A. Zakharova, D. Primetzhofer, K. Lenz, and A. Ney, *Phys. Rev. B* **105**, 134412 (2022)
- [4] A. Fert, N. Reyren, and V. Cros, *Nat. Rev. Mater.* **2**, 17031 (2017)
- [5] M. Hoppe, S. Döring, M. Gorgoi, S. Cramm, and M. Müller, *Phys. Rev. B* **91**, 54418 (2015)
- [6] M. L. Kahn and Z. J. Zhang, *Appl. Phys. Lett.* **78**, 3651 (2001)

11:30 AM QT03.06.09

Additional Heat Channel in Chiral-Commensurate-Ferrimagnetic Weyl Semimetal NdAlSi Pardeep K. Tanwar¹, Ashutosh S. Wadge¹, Xiaohan Yao², Fazel Tafti² and Marcin Matusiak^{1,3}; ¹International Research Centre MagTop, Institute of Physics, Polish Academy of Sciences, Aleja Lotnikow, Poland; ²Boston College, Chestnut Hill, United States; ³Institute of Low Temperature and Structure Research, Polish Academy of Sciences, Poland

Magnetic Weyl semimetals with broken lattice inversion and time reversal symmetries host numerous quasiparticles, including Weyl fermions, unconventional fermions with large Chern number, magnons and phonons with non-trivial bands. That makes them a potential playground for the search of novel type quantum excitations such as chiral magnon-polaron, which emerges from the coupling of topological magnon and chiral phonon via magneto-elastic coupling and Dzyaloshinskii-Moriya interaction. Chiral magnon-polaron is expected to carry heat in the presence of the magnetic field. Here, a substantial increase of magneto-thermal conductivity was reported when a magnetic field is oriented perpendicular to the temperature gradient in non-centrosymmetric magnetic Weyl semimetal of type-I, NdAlSi . After a thorough analysis, we concluded that the phenomenon is inadequate to electronic, phononic, and magnonic contributions at low temperatures in high magnetic field. This additional contribution might be related to the chiral magnon-polaron/coupling of topological magnon and phonon in a magnetic field. In foreseeable future, such charge-neutral excitations can find applications in topological quantum computing technology.

8:00 AM *QT03.07.01

Formation and Structural Transition of Magnetic Skyrmion Lattices in a Centrosymmetric Metallic Magnet [Rina Takagi](#)^{1,2}; ¹The University of Tokyo, Japan; ²JST PRESTO, Japan

Topological objects in condensed matters have attracted attention as the source of rich electromagnetic phenomena. Magnetic skyrmions are topologically protected particle-like objects appearing as swirling spin texture in magnets and intensively studied as the potential candidate of high-density information carrier in magnetic memory [Y. Tokura and N. Kanazawa, Chem. Rev. 121, 2857 (2021)]. Magnetic skyrmions were originally observed in noncentrosymmetric magnets, in which a competition between the ferromagnetic exchange and Dzyaloshinskii-Moriya interactions stabilizes a triangular skyrmion lattice (SKL) state. Recently, on the other hand, SKL states are also found for centrosymmetric rare-earth intermetallic compounds, which commonly host nanoscale skyrmions, leading to relatively large topological Hall effect. In the latter systems, so far, the SKL always reflects the symmetry of underlying crystal lattice, and a different mechanism of skyrmion formation via itinerant electrons has been proposed.

Here we report the discovery of multiple topological magnetic phases in a centrosymmetric metallic magnet EuAl_4 [R. Takagi *et al.*, Nat. Commun. 13, 1472 (2022)]. By means of neutron and resonant X-ray scattering experiments, EuAl_4 turns out to show multiple-step reorientation of the fundamental magnetic modulation vector as a function of external magnetic field, which leads to the appearance of two distinctive SKL states, i.e., square and rhombic lattices of skyrmions with a diameter of 3.5 nm. We also found several other double- Q states in this compound, one of which corresponds to the superposition of four sinusoidal magnetic orders, suggesting the topological magnetic state with the skyrmion number of 2.

The appearance of such multiple SKL states is distinctive from the previously reported centrosymmetric rare-earth intermetallic compounds, where the magnetic modulation vector is always fixed along the one specific direction and the symmetry of the SKL reflects that of underlying crystal lattice. The present results demonstrate that various skyrmion orders can be realized even in simple centrosymmetric magnets, which highlights rare-earth intermetallic compounds as a promising platform to control the competition of multiple topological magnetic phases in a single material.

This work was conducted in collaboration with N. Matsuyama, V. Ukleev, L. Yu, J. S. White, S. Francoual, J. R. L. Mardegan, S. Hayami, H. Saito, K. Kaneko, K. Ohishi, Y. Onuki, T. Arima, Y. Tokura, T. Nakajima, and S. Seki.

8:30 AM *QT03.07.02

Real-Space Control of Topological Skyrmions and Antiskyrmions [Licong Peng](#); Peking University, China

Magnetic skyrmions, characterized as topological "particles", and antiskyrmions, their corresponding "antiparticles", which host opposing topological numbers, have become the focus of significant interest within the realms of fundamental physics and spintronics. The potential for driving and controlling their movements will open the door for a new generation of skyrmion/antiskyrmion-centric spintronic devices.

Here I will introduce the in-situ Lorentz TEM imaging of topological spin textures and their dynamical behaviors. First, I will show the manipulation of a single skyrmion at room temperature in the chiral-lattice magnet $\text{Co}_9\text{Zn}_9\text{Mn}_2$ -based microdevice using nanosecond current pulses. We have directly observed the skyrmion translation and transverse Hall motion and a dynamic transition from the static pinned state to the linear flow motion via a creep event using Lorentz TEM. Furthermore, we have evaluated the intrinsic skyrmion Hall angle and the skyrmion velocity. Our experimental observations of skyrmion flow motion qualitatively coincide with numerical calculations, suggesting the pinning effect on the skyrmion dynamics [1]. In addition to skyrmions, I will also discuss the real-space control of room-temperature antiskyrmions in magnets exhibiting D_{2d} [2] and S_4 [3-4] symmetries. By adjusting the external magnetic field, temperature, thickness, and sample geometries, we have induced topological transformations among the antiskyrmions, elliptical skyrmions, and non-topological bubbles. This was achieved through the creation, propagation, and annihilation of Bloch line pairs, accompanied by changes in their helicity, lattice form, and topological number.

Acknowledgments: These works were done in collaboration with Profs. Yoshinori Tokura, Naoto Nagaosa, Taka-hisa Arima, Shinichiro Seki and Drs. Yasujiro Taguchi, Kosuke Karube, Rina Takagi, Wataru Koshibae, Kiyou Shibata, Konstantin V. Iakoubovskii, Fumitaka Kagawa, Kiyomi Nakajima.

References:

- [1] L. C. Peng* *et al.* Nat. Commun., **12** (2021), 6797.
- [2] L. C. Peng* *et al.* Nat. Nanotech. **15** (2020), 181-186.
- [3] K. Karube#, L.C. Peng# *et al.*, Nat. Mater. **20** (2021), 335-340.
- [4] L. C. Peng* *et al.* Adv. Sci. **9** (2022), 2202950.

9:00 AM *QT03.07.03

Ferroelectric Hafnia Superlattices for Bio-Inspired Computing [Laura Bégon-Lours](#)¹, Elisabetta Morabito¹, Ruben Hamming-Green^{2,3}, Donato F. Falcone¹ and Bert Jan Offrein¹; ¹IBM Research Zurich, Switzerland; ²Zernike Institute for Advanced Materials, University of Groningen, Netherlands; ³CogniGron - Groningen Cognitive Systems and Materials Center, University of Groningen, Netherlands

Artificial Intelligence excels at learning and predicting: from the diagnosis of an anomaly in an electrocardiogram to the detection of a collision risk by a car, many applications require always faster reactions. However, deploying AI in our society without compromising our greenhouse gas emissions goals requires the adoption of disruptive, energy-efficient solutions. In this context, neuromorphic systems aim at mimicking the brain in the way it processes information.

At IBM Research Zurich, ferroelectric materials are investigated for the fabrication of synaptic weights for in-memory deep neural networks and as well as synapses for spiking neural networks. We developed a CMOS-compatible process for the fabrication of passive crossbar arrays^[1], combining ferroelectric HfZrO_4 "solid solution" (HZO) with WO_3 . In the two-terminals configuration, the current flows through the ferroelectric material, which makes the synaptic weights' electrical operation challenging. First, switching the ferroelectric polarization might require relatively large voltages, making their circuit integration difficult and increasing the required power. Second, the small conductivity of the devices requires them to occupy a large footprint in order to achieve measurable currents. By stabilizing ferroelectricity in ultra-thin HZO films below 3 nm^[2], we achieved sub-volt programming and reduced by 4 orders of magnitude the footprint compared to 5 nm thick films^[3]. However, such scaled devices required a high crystallization temperature (500°C) and exhibited a limited On/Off ratio (<2). With the objective of controlling topological features such as non-trivial domain walls to add novel functionalities, we explored the combination of ferroelectric HfO_2 and anti-ferroelectric ZrO_2 in (HZO-SL) superlattices by Atomic Layer Deposition. In this talk, we provide recent advances on the electrical characterization of devices based on such thin films. The HZO-SL require a reduced thermal budget for crystallization, and a reduced footprint compared to HZO, while demonstrating a larger On/Off ratio of 16. Thanks to these properties, we demonstrate the CMOS co-integration of the HZO-SL devices in the Back-End-Of-Line.

- [1] L. Bégon-Lours, M. Halter, F. M. Puglisi, L. Benatti, D. F. Falcone, Y. Popoff, D. D. Pineda, M. Sousa, B. J. Offrein, *Adv. Electron. Mater.* **2022**, 2101395.
- [2] L. Bégon-Lours, M. Halter, M. Sousa, Y. Popoff, D. D. Pineda, D. F. Falcone, Z. Yu, S. Reidt, L. Benatti, F. M. Puglisi, B. Offrein, *Neuromorphic Comput. Eng.* **2022**, 2, DOI 10.1088/2634-4386/ac5b2d.
- [3] L. Bégon-Lours, M. Halter, Y. Popoff, Z. Yu, D. F. Falcone, D. Davila, V. Bragaglia, A. La Porta, D. Jubin, J. Fompeyrine, B. J. Offrein, *IEEE J. Electron Devices Soc.* **2021**, 9, 1275.

This work is supported by BeFerroSynaptic (871737), CHIST-ERA, UNICO (No. 20CH21-186952), ALMOND (SNF 198612) and the BRNC.

9:30 AM *QT03.07.04

Topological Phase Transitions in Chiral Magnets [Yukako Fujishiro](#); RIKEN Center for Emergent Matter Science, Japan

Topological chiral crystals give rise to unique spin texture as well as multi-fold Weyl Fermions where unique electromagnetic responses are expected. In this talk, I will discuss the exotic phase transitions realized in these systems, such as transition between skyrmion and emergent magnetic monopole in $\text{MnSi}_{1-x}\text{Ge}_x$ as well as unique transport properties in MnGe which is associated with the nontrivial unwinding process of emergent magnetic monopole by magnetic field. Furthermore, I will introduce our recent work on high-pressure control of multi-fold Weyl Fermion in a B20-type magnet, which results in metal-to-insulator transition and magnetic quantum criticality with unusual magneto-transport properties.

SYMPOSIUM QT04

2D Topological Materials—Theoretical Models, Growth and Applications
November 27 - December 5, 2023

Symposium Organizers

Paolo Bondavalli, Thales Research and Technology
Judy Cha, Cornell University
Bruno Dlubak, Unite Mixte de Physique CNRS/Thales
Guy Le Lay, Aix-Marseille University

Symposium Support

Platinum
Gordon and Betty Moore Foundation

* Invited Paper
+ JMR Distinguished Invited Speaker

SESSION QT04.01: Exotic Properties of 2D Topological Materials I
Session Chairs: Paolo Bondavalli, Bruno Dlubak and Guy Le Lay
Monday Morning, November 27, 2023
Sheraton, Fifth Floor, Riverway

10:30 AM *QT04.01.01

Topology and Hidden Honeycomb Physics in a Triangular Atom Lattice: Indenene on SiC(0001) [Ralph Claessen](#)^{1,2}; ¹Julius-Maximilians-Universität Würzburg, Germany; ²Würzburg-Dresden Cluster of Excellence ct.qmat, Germany

Following the seminal work of Kane and Mele on graphene, atomic monolayers arranged in a honeycomb lattice have been a major target in the search for quantum spin Hall insulators (QSHI), with bismuthene currently the record holder in terms of topological bandgap size [1]. Here I will demonstrate that QSHIs can also be realized in 2D *triangular* lattices, with the system In/SiC(0001) ("indenene") as case in point. ARPES band mapping confirms that the electronic structure is indeed that of a Dirac semimetal in which spin-orbit coupling (SOC) opens an inverted gap [2]. In fact, a detailed theoretical analysis reveals that the system is close to a topological phase transition between a QSHI and a higher order topological insulator (HOTI), controlled by the competition of SOC with substrate-induced inversion symmetry breaking [3]. Utilizing the fact that the gap-defining In 5p states form orbital angular momentum (OAM) eigenstates directly linked to the local Berry curvature, the topological character of indenene can experimentally be probed by two independent methods: by circular dichroism in ARPES as well as by STM/STS, because the OAM character of the valence orbitals leads to a specific energy-dependent spatial charge localization [2]. Both methods consistently find indenene on SiC(0001) to be a QSHI, representing the first such experimental identification from *bulk* states rather than from topological edge states. Finally, it is demonstrated that indenene intercalation into epitaxial graphene offers effective protection against ambient conditions (i.e., exposure to air or even water) while leaving the topological character fully intact [4].

Work together with J. Erhardt, M. Bauernfeind, C. Schmitt, A. Moser, P. Eck, and S. Sangiovanni (all at Universität Würzburg, Germany).

- [1] Science **357**, 287 (2017)
- [2] Nat. Commun. **12**, 5396 (2021)
- [3] Phys. Rev. B **106**, 195143 (2022)
- [4] arXiv:2305.07807

11:00 AM *QT04.01.02

Spin-Orbit Torques Induced by Topological Insulators of the Bi₂Te₃ Family of Materials [Thomas Guillet](#)¹, [Regina Galceran](#)¹, [J.F. Sierra](#)¹, [Marius Costache](#)¹, [Matthieu Jamet](#)², [Frederic Bonell](#)² and [Sergio O. Valenzuela](#)^{3,1}; ¹Catalan Institute of Nanoscience and Nanotechnology, Spain; ²Université Grenoble Alpes, France; ³ICREA, Spain

Van der Waals (vdW) heterostructures, including those comprising topological insulators (TIs) of the Bi₂Te₃ family of materials, have disruptive potential for magnetic random-access memory applications [1]. The boundary states of a TI can generate a non-equilibrium spin density to control the magnetization of a ferromagnet (FM) by means of the spin-orbit torques (SOTs). Recent reports have demonstrated large SOT efficiencies with TIs, however, to identify the microscopic mechanisms at play, as well as to maximize the SOT, a deep understanding and control of the properties of the TI/FM interface is needed. In this talk, I will first introduce the potential advantages of vdW heterostructures and of TIs for non-volatile spintronics memories. I will then describe the relevance of their boundary states and of preserving the quality of the TI/FM interface. I will show that the introduction of a (non-magnetic) metallic [2] or graphene [3] interlayer between the TI and the FM, when FM is a transition metal, can notably suppress Te diffusion into the FM and change the nature of the SOT and its efficiency [2]. Finally, I will argue that the discovery of vdW FMs, which can be grown as high-quality thin films [4,5], can further improve the TI/FM interface, as the weak vdW interaction between the TI and the vdW FM can limit chemical reactions, intermixing and electronic hybridization. Our recent results using Fe₃GeTe₂ demonstrate large SOTs and magnetization switching with current densities of about 10¹⁰ A/m² [6].

- [1] H. Yang et al., Nature **606**, 663 (2022)
- [2] F. Bonell et al., Nano Lett. **20**, 5893 (2020)
- [3] R. Galceran et al., Adv. Mater. Interfaces **9**, 2201997 (2022)
- [4] M. Ribeiro et al., npj 2D Mater. Appl. **6**, 10 (2022)

11:30 AM QT04.01.03**Topological Properties of Superconducting $\text{Pd}_3\text{Bi}_2\text{Se}_2$** RamakantaChapai¹, GordonPeterson¹, MatthewSmylie^{1,2}, XinglongChen¹, Jidong SamuelJiang¹, DavidGraf³, Wai-KwongKwok¹, JohnF. Mitchell¹ and UlrichWelp¹; ¹Argonne National Laboratory, United States; ²Hofstra University, United States; ³National High Magnetic Field Laboratory, United States

The Parkerite-type transition-metal chalcogenides $\text{Pd}_3\text{Bi}_2\text{Se}_2$ is a superconductor with $T_c \sim 0.8$ K. Recently, a non-zero Z_2 topological index has been predicted in $\text{Pd}_3\text{Bi}_2\text{Se}_2$, and subsequently unusual magneto-transport attributed to two-dimensional fermions is reported. By measuring the field dependence of magnetic torque in bulk single crystalline $\text{Pd}_3\text{Bi}_2\text{Se}_2$ we observe de Haas-van Alphen (dHvA) oscillations. Through the analysis of the dHvA oscillations with $H \parallel c$, three frequencies are identified: $F_\alpha = 150$ T, $F_\beta = 471$ T and $F_\gamma = 979$ T with the low frequency dominating the spectrum. The Lifshitz-Kosevich analysis yields a small effective mass ($0.11m_0$) and nontrivial Berry phase ($\sim\pi$) for the dominant orbit, indicating nontrivial topology. The presence of nontrivial topology in a superconducting system makes $\text{Pd}_3\text{Bi}_2\text{Se}_2$ a promising candidate to explore topological superconductivity.

11:45 AM QT04.01.04**Artificial Graphene Nanoribbons with Tailored Topological States** NathanGuisinger, PierreT. Darancet and SawHla; Argonne National Laboratory, United States

Low-dimensional materials functioning at the nanoscale are a critical component for a variety of current and future technologies. From the optimization of light harvesting solar technologies to novel electronic and magnetic device architectures, key physical phenomena are occurring at the nanometer and atomic length-scales and predominately at interfaces. In this presentation, I will discuss low-dimensional material research occurring in the Quantum and Energy Materials (QEM) group at the Center for Nanoscale Materials. Specifically, the synthesis of artificial graphene nanoribbons by positioning carbon monoxide molecules on a copper surface to confine its surface state electrons into artificial atoms positioned to emulate the low-energy electronic structure of graphene derivatives. We demonstrate that the dimensionality of artificial graphene can be reduced to one dimension with proper "edge" passivation, with the emergence of an effectively-gapped one-dimensional nanoribbon structure. Remarkably, these one-dimensional structures show evidence of topological effects analogous to graphene nanoribbons. Guided by first-principles calculations, we spatially explore robust, zero-dimensional topological states by altering the topological invariants of quasi-one-dimensional artificial graphene nanostructures. The robustness and flexibility of our platform allows us to toggle the topological invariants between trivial and non-trivial on the same nanostructure. Our atomic synthesis gives access to nanoribbon geometries beyond the current reach of synthetic chemistry, and thus provides an ideal platform for the design and study of novel topological and quantum states of matter.

SESSION QT04.02: Growth and Synthesis of 2D Topological Materials

Session Chairs: Paolo Bondavalli, Bruno Dlubak and Guy Le Lay

Monday Afternoon, November 27, 2023

Sheraton, Fifth Floor, Riverway

1:30 PM *QT04.02.01**Germanium, a Unique Template for 2D Materials Growth: From Germanene to Antimony Telluride Synthesis** MarcoMinissale¹, EricSalomon², ThierryAngot² and GuyLe Lay²; ¹CNRS, PIIM Laboratory, France; ²Aix-Marseille Université, France

Germanene is an artificial two-dimensional graphene-like germanium allotrope predicted to be a near room temperature topological insulator, belonging to the class of so-called Xenes. It was synthesized in 2014, exactly ten years after the isolation of graphene, and just two years after the archetype growth of silicene, the first Xene ever produced. The canonical germanene paper, described its top-down synthesis by Ge deposition onto a Au(111) crystal, but revealed multi-phases [1]. Instead, we will show that a single germanene phase, as evidenced in Scanning Tunneling Microscopy in situ imaging, is obtained by Ge segregation on top of a thin Au(111) film epitaxially grown under ultra-high vacuum on a Ge(111) template through a bottom-up approach. [2] A comparison with studies performed on thin gold film epitaxially grown on a Ge(110) template will be presented. Eventually, we will describe the growth of antimony telluride films on Ge(111) surface using a single evaporator cell. Moreover, we will discuss the structural and electronic characterization of such films, studied using standard surface science techniques (LEED, STM, PES).

[1] M.E. Dávila *et al.*, New Journal of Physics, 16, 095002 (2014)[2] M. Minissale *et al.*, Crystals 13, 221 (2023)**2:00 PM *QT04.02.02****Towards the Higher Curie Temperature in the $\text{Mn}_{1+x}\text{Sb}_{2-x}\text{Te}_4$ Material's System** EkaterinaKochetkova^{1,2}, ManaswiniSahoo¹, LauraT. Corredor¹, JorgeFacio³, VladimirHinkov⁴ and AnnaIsaeva^{2,1}; ¹Leibniz Institute for Solid State and Materials Research Dresden, Germany; ²University of Amsterdam, Netherlands; ³CNEA-CONICET, Argentina; ⁴University of Würzburg, Germany

Magnetic topological materials are a hotbed for exotic quantum phenomena such as the quantum anomalous Hall effect (QAHE), the topological magneto-electric effect, new topological states like axion insulators and magnetic Weyl semimetals. In reply to the high demand for optimized material systems, magnetic topological insulators made a decade-long journey [1] from extrinsically doped Bi_2Te_3 and $(\text{Cr,V})\text{Bi}_2(\text{Se,Te})_3$ heterostructures [2] to the intrinsically magnetic van der Waals material MnBi_2Te_4 [3]. The QAHE was observed in MnBi_2Te_4 thin films at notably higher temperatures of 1–6 K [4] than in [2], pointing at a perspective pathway of materials optimization towards more robust quantum effects. Since the bulk MnBi_2Te_4 is an A-type antiferromagnet with $T_N = 25$ K, the task of fabricating structurally similar ferri- or ferromagnets with an increasing T_C is very pertinent. MnBi_2Te_4 is the progenitor of a family of van der Waals materials $(\text{MnX}_2\text{Te}_4)(\text{X}_2\text{Te}_3)_n$, $X = \text{Sb}$ or Bi , $n = 0-4$. Their crystal lattices are ordered stacking variants of septuple $(\text{MnX}_2\text{Te}_4)$ layers hosting an ordered magnetic sublattice of Mn(II) atoms and of n quintuple (X_2Te_3) spacers. Varying intralayer and interlayer magnetic exchange couplings foster a rich palette of possible magnetic ground states, including ferri- and ferromagnetic. Besides the stacking order, a more subtle factor – Mn/X site intermixing [5] – influences the long-range magnetic order greatly. This phenomenon is particularly prominent in $\text{Mn}_{1+x}\text{Sb}_2\text{Te}_4$ where it raises the Curie temperature of a ferrimagnetic-to-paramagnetic transition from 27 to 46 K, while x varies in the range of 0.1–0.2 only [6–9]. We elucidate the Mn/X intermixing by single-crystal X-ray and neutron powder diffraction and link these results to the bulk magnetometry and surface XMCD data. Accumulated insights into an over-arching connection between crystal growth protocols, Mn/Sb patterns and magnetic ground states enable us to push the ordering temperature even further: I will present the recently obtained $\text{Mn}_{1.4}\text{Sb}_{1.6}\text{Te}_2$ with $T_C = 55$ K and $\text{Mn}_{1.9}\text{Sb}_{1.3}\text{Te}_4$ with $T_C = 73$ K that bring this family of magnetic topological materials close to the liquid nitrogen limit. This work is supported by the German Research Council (DFG) within the Würzburg-Dresden Cluster of Excellence "Complexity and Topology in Quantum Matter" (ct.qmat, EXC 2147, project-id 390858490), and by the Dutch Research Council (NWO) within "Materials for the Quantum Age" (QuMat) research program.

REFERENCES

[1] Y. Tokura et al. Nature Reviews Physics 1, 126 (2019). [2] C.-Z. Chang et al. Science 340, 167 (2013). [3] M. Otrokov, ... A. Isaeva, E.V. Chulkov. Nature 576, 416 (2019); [4] Y. Deng et al. Science 367, 895 (2020); [5] A. Zeugner, ... A. Isaeva. Chem. Mater. 31, 2795 (2019); [6] Y. Liu et al. Phys. Rev. X 11, 021033 (2021); [7] S. Wimmer et al. Adv. Mater. 33, 2102935 (2021); [8] L. Folkers, ... A. Isaeva. Z. Krist. 237, 2057 (2021); [9] M. Sahoo, ... A. Isaeva. Under review.

2:30 PM QT04.02.03**Synthesis of Transition Metal Ditellurides (TMTs) Nanosheets: MoTe_2 and PtTe_2 Through Simulation-Guided Tellurization** Pinaka PaniTummala^{1,2,3}, SaraGhomi^{1,4}, AlessandroMolle¹, ChristianMartella¹ and AlessioLamperti¹; ¹Consiglio Nazionale delle Ricerche, Italy; ²KU Leuven, Belgium; ³Università Cattolica del Sacro Cuore, Italy; ⁴Politecnico di Milano, Italy

In the classification of Transition metal ditellurides (TMTs), Molybdenum ditelluride (MoTe_2) received significant emphasis due to its multiple polymorphic states including semiconducting, metallic, and topological semimetal phases.[1] Specifically, MoTe_2 is an ideal candidate for creating 2D hetero phase homojunctions due to its minimal energy barrier between the 2H and 1T' phases, as well as the negligible difference between their moduli, making it effortless to switch between the two phases. The 1T' phase, with an orthorhombic structure, is significant for accessing topological properties and has potential as a host for the quantum spin hall effect and type-II Weyl semi-metallic state while the 2H-phase is useful as a 2D layered material in nanotechnologies due to its semiconducting properties. As the thickness decreases, MoTe_2 exhibits an indirect-to-direct bandgap transition with a relatively lower bandgap than other transition metal dichalcogenides (TMDs).[2][3] So far, countless efforts have been undertaken for developing MoTe_2 which are essential for the fabrication of devices to be integrated in different applications from nano-electronics to thermoelectric and energy sectors. Among the proposed methods, chemical vapor deposition (CVD) is considered as one of the reliable deposition methods.[4] In this context, here we report on the simulation guided CVD synthesis for obtaining MoTe_2 nanosheets with pure 1T' and 2H phases on SiO_2/Si substrates with extensive

coverage of 4 cm × 1 cm. The CVD based tellurization process involves a vapor-solid reaction between the pre-deposited molybdenum film and tellurium vapor, and we have optimized this process to improve the quality and scalability of the MoTe₂ nanosheets. We found that the MoTe₂ growth and its phase are primarily determined by the growth kinetics, tellurium concentration, and the configuration of the CVD furnace.[5] Further, by precisely controlling the temperature, we have extended our simulation-based tellurization approach to produce other TMTs, including PtTe₂ and NiTe₂. In particular, we were able to produce PtTe₂ with a sharp 1T phase from the tellurization of a pre-deposited Pt of varying thickness. The so-grown PtTe₂ recasts as a topological type-II Dirac semimetal and as such, it is expected to be optically tunable in the THz spectral range [6]. In this respect, we reduced the flat PtTe₂ film to an array of microscale stripes so as to fabricate PtTe₂-based plasmonic gratings where to measure optical resonances in the THz regime.

We believe this work may represent a substantial advance in facilitating the direct integration of TMTs in electronic and photonic applications where to test the intrinsic topological features.

References

- [1] Jianwei Su *et al.*, Adv. Mat. Interf. 6, 1900741 (2019)
- [2] X. Xu *et al.*, Cryst. Grow. Des. 18, 2844, (2018)
- [3] Z. Wang *et al.*, Phys. Rev. Lett. 117, 056805 (2016)
- [4] C Martella *et al.*, Cryst. Grow. and Des. 21, 5, 2970–2976 (2021)
- [5] P. P Tummala *et al.*, Adv. Mat. Inter, 10,1 (2023)
- [6] S. Lupi and A. Molle, Appl. Mater. Today 20, 100732 (2020)

2:45 PM QT04.02.04

Surface-Guided Growth of Bi₂Se₃ Nanowires Tamir Forsht, Noga Levinson, Lothar Houben, Katya Rechav, Olga Brontvein and Ernesto Joselevich; Weizmann Institute of Science, Israel

Topological materials exhibit exotic electronic properties, which make them promising for non-conventional electronics and spintronics. For instance, integrating nanowires of topological insulators into devices could be used for dissipationless electronics, quantum switches, generating and braiding Majorana fermions and quantum computing. However, the assembly of nanowires with controlled orientation on surface remains one challenge preventing their integration into practical devices. A possible solution that was demonstrated in our group in the past few years is the guided growth of horizontal nanowires by epitaxy or graphoepitaxy on crystal surfaces.

In this work, we demonstrate the guided growth of Bi₂Se₃ nanowires on flat and faceted sapphire surfaces. Bi₂Se₃ is a layered material with weak VdW interaction between its layers. It is also a topological insulator with narrow band gap in the bulk and topologically protected conducting states on its surface, as well as a thermoelectric material. The growth direction of these nanowires and their crystallographic orientation are controlled by the relations with the sapphire substrate, allowing the growth of ordered nanowires without the need for post-growth processes. To the best of our knowledge, this is the first example of guided growth of nanowires made of layered materials, which demonstrates the generality of the guided growth approach.

3:00 PM BREAK

3:30 PM *QT04.02.06

Synthetic Tuneability of the 1T' -1T Phases in TMDs Cecilia Mattevi; Imperial College London, United Kingdom

In this talk, I will present our recent work on the precise synthesis of different metastable 2D Transition Metal Dichalcogenides and their use in spintronics, electrocatalysis and energy storage. I will provide an overview of the tuneability between magnetic and topologically insulating phases (1T' and 1T) and their corresponding 2H phases at the synthesis level, which we have demonstrated for different TMD materials.

The synthesis precision is scalable and based on the kinetic versus the thermodynamic control of the nucleation process, which enable the determination of the crystal structure preferentially leading to either the thermodynamically stable 2H phase or the metastable 1T' and 1T phases. The possible mechanisms of crystallization of metastable polymorphs will be discussed and liquid phase synthesis versus chemically vapour deposited materials approaches will be compared in the light of phase control. Ultimately, the functional properties of the 1T' and 1T phases, such as magnetism and electrocatalysis will be discussed.

4:00 PM QT04.02.07

Epitaxy of Bi₂Se₃ Thin Film by Chemical Vapor Deposition Skye Williams, Edwin Fohntung and Jian Shi; Rensselaer Polytechnic Institute, United States

Spin-momentum locking materials present large prospects to the design of spintronic devices. One of the figures of merit of spintronic materials is the spin-charge conversion efficiency. Bi₂Se₃ is a topological insulator with an impressive spin-charge conversion efficiency on its conductive surface states. Epitaxial Bi₂Se₃ is highly demanded for optimized conversion efficiency. In this work we present a chemical vapor deposition approach to grow Bi₂Se₃ epitaxially that have grain sizes exceeding 200 micrometers. We identify the existence of sub-unit cell layers in the epitaxial crystal. We apply the spin pumping approach to characterize the spin-charge conversion efficiency and compare it with reported values of Bi₂Se₃ synthesized by approaches such as sputtering. The work suggests chemical vapor deposition is a viable approach for producing high-quality large-scale topological Bi₂Se₃.

SESSION QT04.03: Theory, Modeling of Topological Features
Session Chairs: Paolo Bondavalli, Bruno Dlubak and Guy Le Lay
Tuesday Morning, November 28, 2023
Sheraton, Fifth Floor, Riverway

8:30 AM *QT04.03.01

Tuning Topology in 2D Materials Zeila Zanolli; Utrecht University, Netherlands

In a few years, the energy consumption for information processing will constitute more than 25% of the total electrical energy consumption. Topological materials allow for symmetry-protected dissipationless electron transport along the edges of 2D materials, which offers a possible solution to the sustainability issue of electronics. However, controlling the topological properties of a material is an open research question.

We use first-principles Density Functional Theory simulations to predict pathways to control topological properties in 2D materials and, possibly, induce or strengthen the topological phase transition. The different strategies include proximity interaction with a magnetic substrate [1, 2], van der Waals interaction with the substrate [3, 4], twisting 2D heterostructures [5], and using an external electric field to manipulate spins in a Quantum Spin Hall insulator [6]. Going further, I will discuss the role of dimensionality in going from a 3D topological insulator to the 2D limit [7].

References

- [1] Z. Zanolli, C. Niu, G. Bihlmayer, Y. Mokrousov, P. Mavropoulos, M. J. Verstraete, and S. Blügel, Hybrid quantum anomalous Hall effect at graphene-oxide interfaces, Phys. Rev. B **98**, 155404 (2018)
- [2] Z. Zanolli, *Graphene-multiferroic interfaces for spintronics applications*, Scientific Reports, **6**, 31346 (2016)
- [3] N Wittemeier, P Ordejón, Z Zanolli, *Tuning the topological band gap of bismuthene with silicon-based substrates*, J. Phys. Mater. **5** 035002 (2022)
- [4] S. Singh, Z. Zanolli, M. Amsler, B. Belhadji, J. O. Sofo, M. J. Verstraete, A. H. Romero, *Low energy phases of bilayer Bi predicted by structure search in two dimensions*, J. Phys. Chem. Lett., **10**, 7324-7332 (2019)
- [5] A. Pezo, Z. Zanolli, N. Wittemeier, P. Ordejón, A. Fazzio, S. Roche, J. H. Garcia, *Manipulation of spin transport in graphene/transition metal dichalcogenide heterobilayers upon twisting*, 2D Mater. **9** 015008 (2022)
- [6] J. H. Garcia, et al. *Electrical control of spin-polarized topological currents in monolayer WTe₂*, Phys. Rev. B **106**, L161410 (2022)
- [7] J. R. Moes et al, *Colloidal Bi₂Se₃ platelets with topological edge states* (submitted, 2023)

9:00 AM QT04.03.02

Efficient Quantum Transduction using Magnetic Topological Insulators Haowei Xu, Paola Cappellaro and JuLi; Massachusetts Institute of Technology, United States

Transduction of quantum information between distinct quantum systems is an essential step in various applications, including quantum networks and quantum computing. Efficient quantum transduction necessitates transducers that can strongly interact with photons with vastly different frequencies. In this work, we propose that solid-state magnetic topological insulators can potentially serve as highly effective transducers, thanks to their topologically enhanced optical responses, robust spin-orbit coupling, as well as substantial spin density. Using MnBi_2Te_4 as an example, we showcase that unit transduction fidelity can be achieved with modest experimental requirements, while the transduction bandwidth can reach the GHz range.

9:15 AM QT04.03.03

Super Flat Graphene Grown on Substrate Selected by using Molecular Dynamics Calculation [Satoru Kaneko](#)^{1,2}, [Takashi Tokumasu](#)³, [Manabu Yasui](#)¹, [Masahito Kurouchi](#)¹, [Daishi Shiojiri](#)¹, [Chihiro Kato](#)¹, [Satomi Tanaka](#)¹, [Shigeo Yasuhara](#)⁴, [Musa Can](#)⁵, [Ruei-Sung Yu](#)⁶, [Sumanta Sahoo](#)⁷, [Kripasindhu Sardar](#)⁸, [Masahiro Yoshimura](#)⁸, [Akifumi Matsuda](#)² and [Mamoru Yoshimoto](#)²; ¹KISTEC, Japan; ²Tokyo Institute of Technology, Japan; ³Tohoku University, Japan; ⁴Japan Advanced Chemicals, Japan; ⁵Istanbul University, Turkey; ⁶Asia University, Taiwan; ⁷Radhakrishna Institute of Technology and Engineering, India; ⁸National Cheng Kung University, Taiwan

Choice of substrate is one of most important factors for thin film growth. An extensive interdiffusion or chemical reaction might happen between substrate and target materials. For oxide materials, Schlom et. al. comprehensively investigate the thermodynamic stability of binary oxides for epitaxial growth on silicon (Si) substrates[1]. However, the thermodynamic stability does not include any crystal information such as lattice constants, orientation of crystal growth. In order to predict the orientation of crystal growth, molecular dynamics (MD) is employed to evaluate the stability of oxide cluster on Si substrates[2].

In this study, MD was used to select suitable substrates for graphene growth with flat surface. Supercell was consisted of carbon clusters placed on variety of substrates with vacuum slab. As carbon clusters, (1) C atom, (2) six-membered ring (6-ring) and (3) seven six-membered rings (nanographene) were placed on SrTiO, silicon and sapphire substrates. On the surface of sapphire substrate, carbon clusters were placed on either aluminum or oxygen atoms, and the absorption energy was estimated by using the density functional theory (DFT) with a semi-core pseudopotential. The generalized gradient approximation (GGA) method was used to obtain the electron density. Materials Studio and DMol3 were used for preparing and optimizing supercells, respectively[3].

The surface of substrate was optimized, and then the carbon clusters were placed on the candidate substrates. Although the absorption energies showed not large differences on various surfaces, 6-ring, for an example, stood vertically up on Si(001) substrate and covered flatly on SrTiO substrate. Only SrTiO surface was flatly covered by both 6-ring and nanographene after optimization by MD simulation. The SrTiO substrate was the first choice for flat graphene.

Super flat graphene is prepared by chemical vapor deposition (CVD) with post annealing in carbon dioxide atmosphere. Amorphous carbon is selectively etched in carbon dioxide atmosphere[4]. In this study, carbon films were experimentally deposited on target substrates in carbon dioxide atmosphere by pulsed laser deposition (PLD), and super flat surface (~60 pm) was observed on only SrTiO substrate, which agreed with the results of MD simulation. Since CVD graphene usually grows with intrinsic contamination on graphene surface during film growth, a post annealing is required to obtain a flat surface. However PLD prepared as-grown flat surface in carbon dioxide atmosphere.

This study was supported in part by Amada Foundation under contract AF-2020227-B3, Tokyo Ohka Foundation for Promotion of Science and Technology 22117 and the Collaborative Research Project of the Institute of Fluid Science, Tohoku University. Special acknowledgment to the National Cheng Kung University 90 and beyond (NCKU'90).

[1] D.G.Schlom et.al., J.Mater.Res. 11, 2757 (1996).

[2] S.Kaneko et.al., Appl.Surf.Sci. 586, 152775 (2022).

[3] S.Kaneko, et.al., Sci.Rep. 12, 15809 (2022).

[4] J.Zhang et.al., Angew.Chem.Int.Ed. 58, 14446 (2019).

9:30 AMBREAK

10:00 AM *QT04.03.04

Topological Textures in Artificial Van der Waals Multiferroics with Twisted Two-Dimensional Materials [Jose Lado](#); Aalto University, Finland

Twisted van der Waals materials have risen as a powerful platform to engineer artificial quantum matter. Artificial moire heterostructures, in general, display two length scales, the original lattice constant and the emergent moire length. Here we reveal a microscopic mechanism to engineer van der Waals multiferroics from the interplay of non-collinear magnetism and spin-orbit coupling, both in van der Waals monolayers [1] and twisted multilayers [2]. First, focusing on the recently isolated NiI₂ multiferroic monolayer, we reveal the origin of the helimagnetic order and the critical role of halide spin-orbit coupling in driving a ferroelectric distortion. We demonstrate that the electronic reconstruction accounting for the ferroelectric order emerges from the interplay of such a non-collinear magnetism and spin-orbit coupling. Second, we show the emergence of multiferroic order in twisted chromium trihalide bilayers, an order fully driven by the moiré pattern and absent in aligned multilayers. We show that a spin texture is generated in the moiré supercell of the twisted system as a consequence of the competition between stacking-dependent interlayer magnetic exchange and magnetic anisotropy. An electric polarization arises associated with such a non-collinear magnetic state due to the spin-orbit coupling, leading to the emergence of a local ferroelectric order following the moiré. Among the stoichiometric trihalides, our results show that twisted CrBr₃ bilayers give rise to the strongest multiferroic order. We further show the emergence of a strong magnetoelectric coupling, which allows the electric generation and control of magnetic skyrmions. Our results put forward van der Waals materials as a powerful platform to engineer artificial multiferroic order and electrically control exotic magnetic textures.

[1] Adolfo O. Fumega and Jose L. Lado 2D Materials 9 025010 (2022)

[2] Adolfo O. Fumega and Jose L. Lado, 2D Materials 10 025026 (2023)

10:30 AM *QT04.03.05

First-Principles Transport Including Magnetic and Spin-Orbit Effects [Matthieu J. Verstraete](#)^{1,2}; ¹University of Liege, Belgium; ²University of Utrecht, Netherlands

Topology is the next frontier in materials science, opening possibilities for ultra low power devices, exquisite sensing capabilities, and synergies with quantum computing through the protection of state coherence.

We will showcase recent advances in the theory and applications of first-principles transport calculations, to include magnetism and spin-orbit interactions, and what will be needed to tackle the most complex topological materials, which contain both effects. Using spinor wave functions and SOI naturally incorporates spin-flip processes in electron-phonon scattering. Comparisons to experiments on "simple" 3d ferromagnetic metals require the inclusion of electron-magnon scattering, both in resistivity and in magnon drag.

As a next step into topology, we showcase the first-principles conductivity of Weyl semi-metals, in particular TaAs for which our calculations are in very good agreement with available experiments. Finally, magnetoelectrically-active 2D Nickel Iodide (NiI₂) can host topological magnetic states, and we find that it shows strong sensitivity to pressure. Combining experimental characterization with first and second principles simulations, we determine the pressure dependency (up to 20 GPa) of the electronic band structure, magnetic phase transition, and spinwave dispersion.

- X Ma et al. New Journal of Physics 25, 043022

- G Allemand and MJ Verstraete, unpublished (2023)

- J Kapeghian et al. arxiv.org/abs/2306.04729

11:00 AM QT04.03.06

Logic Gate Analysis for Quantum Phase Differences in Systems with Multiple Degenerate Points [Tatsuki Tojo](#) and [Kyozauro Takeda](#); Waseda University, Japan

The field of quantum information has been extensively researched, and an important concept here is the phase difference between the two basis states ($|0\rangle$ and $|1\rangle$) in a qubit, which is an important concept used to distinguish quantum logic from classical logic. Hence, manipulating this phase difference is a prerequisite for quantum arithmetic. Consequently, various methods for quantum (phase) operations have been proposed, and one such method uses the non-Abelian Berry phase [1]. Because the non-Abelian Berry phase has a characteristic structure, particularly at quasi-degenerate points (QDPs) in the parameter space, combining QDPs with quantum operations becomes important. However, a QDP exists alone in the parameter space, complicating its combination with quantum operations. Nevertheless, heavy-mass holes (HHs) in SiGe two-dimensional quantum wells, where Rashba and Dresselhaus spin-orbit interactions (SOIs) coexist, feature multiple spin QDPs near point Γ in the Brillouin zone (BZ) [2]. In the vicinity of these QDPs, a characteristic structure is observed in the non-Abelian Berry phase when

the wave vectors are chosen as parameters. Because these QDPs lie close to each other, they can realize novel quantum operations.

Here, we focus on the HH with multiple QDPs in the BZ and discuss the features of quantum operations based on the non-Abelian Berry phase near these QDPs. We choose the $|0\rangle$ and $|1\rangle$ states as the SOI-stabilized (+) and -destabilized (-) HH (HH \pm) states, respectively, including the dynamical phases, and discuss the change in hybridization and phase difference between the $|0\rangle/|1\rangle$ states. A Bloch sphere is used to visualize the hybridization ratio and phase difference. Further, we construct a time-evolution operator that reproduces the motion on the Bloch sphere and decompose it into quantum logic gates to interpret changes in the state vector as quantum operations. We assume that the wave vector moves under the energy conservation law and recreate this motion as “cyclotron motion” under a perpendicular weak magnetic field. The time evolution of the state and wave vectors is determined by the simultaneous rate equation and semi-classical equation of motion.

In addition to point Γ , an HH has the following QDPs: M_1 and M_2 (16 meV) along the $[1-10]$ and $[-110]$ directions and D_1 and D_2 (24 meV) along the $[-1-10]$ and $[110]$ directions, respectively. To discuss such QDP-induced modulation, we consider the lower-energy region away from M and D (10 meV), and just above M (16 meV) and D (24 meV). We set the initial states of the wave vector along the $[100]$ direction and the state vector to the $|0\rangle$ state (HH $+$).

At 10 meV, the state barely moves from the $|0\rangle$ state (+z direction on the Bloch sphere), and no operation is apparently performed. However, the rate-equation-based time-evolution operator is equivalent to the R_z gate, and its rotation angle is 2π . This rotation angle corresponds to the (Abelian) Berry phase difference of HH \pm at 10 meV ($+\pi$). This Berry phase can be attributed to the QDP at point Γ . This implies that even in the region away from the QDP, the state vector is operated by R_z corresponding to the Berry phase of the QDP surrounded by the parameter (wave vector) trajectory. By contrast, at 16 meV (point M), the state flip-flops during the passage of M , and the states $|0\rangle$ and $|1\rangle$ change completely to $|1\rangle$ and $|0\rangle$, respectively. Through logic gate decomposition, we obtain the R_y gate corresponding to M , whose rotation angle is π . At 24 meV, the R_y gate corresponding to D is also obtained. However, the rotation angle is less than π , and the state transition is incomplete. Therefore, the state is operated by the R_y gate when it passes just above the QDP, and the rotation angle depends on the QDP.

[1] J. Pachos *et al.*, Phys. Rev. A **61**, 010305(R) (1999).

[2] T. Tojo and K. Takeda, Phys. Status Solidi B **260**, 220031 (2023).

11:15 AM QT04.03.07

Designing Quantum States in Two Dimensional Heterostructures Orlando J. Silveira¹, Mohammad Amini¹, Liwei Jing², Viliam Vano¹, Yan Linghao³, Ondrej Krejci¹, Somesh Ganguli¹, Shawulienu Kezilebieke², Jose Lado¹, Adam Foster^{1,4} and Peter Lijeroth¹; ¹Aalto University, Finland; ²University of Jyväskylä, Finland; ³Soochow University, Taiwan; ⁴Kanazawa University, Japan

Vertical heterostructures have emerged as a promising route for designing quantum materials with extraordinary properties. In particular, the interplay between magnetism and superconductivity has garnered significant attention, driven by the potential realisation of topological superconductivity [1]. This research presents notable progress in the synthesis and characterization of two-dimensional materials in ultra-high vacuum environments. By employing scanning tunnelling microscopy (STM) and spectroscopy (STS), along with tight-binding (TB) and density functional theory (DFT) calculations, a comprehensive understanding of these materials has been achieved.

We propose a novel approach utilizing a heterostructure composed of a supramolecular complex (SMC) on a van der Waals (vdW) superconductor. Through our investigations, we demonstrate that the combination of a magnetic SMC with a quasi-2D superconductor, specifically NbSe₂, leads to the emergence of Yu-Shiba-Rusinov (YSR) bands—a crucial element for realizing topological superconductivity. The presence of these bands, together with the exotic magnetic ground state of the SMC, is thoroughly examined using scanning tunneling microscopy (STM) and X-ray magnetic circular dichroism (XMCD), complemented by density-functional theory (DFT) calculations. Notably, our approach offers the advantage of employing diverse molecules, atoms, and substrates, enabling highly tunable YSR bands.

Furthermore, we investigate the electronic structure of a ferroelectric 001 SnTe grown on NbSe₂. Our DFT calculations reveal a strong binding between Sn and Se atoms within the substrate, resulting in significant modifications to the overall electronic structure and its dependence on the number of atomic layers of SnTe. We also extend the study to SnTe deposited on other vdW layered materials such as TMDs by means of DFT calculations.

Overall, this research contributes to the understanding and advancement of quantum materials, demonstrating the synthesis and characterization of versatile heterostructures and providing insights into their unique properties.

[1] Topological superconductivity in a van der Waals heterostructure. *Nature* **588**, 424–428 (2020)

SESSION QT04.04: Exotic Properties of 2D Topological Materials II

Session Chairs: Paolo Bondavalli, Bruno Dlubak and Guy Le Lay

Tuesday Afternoon, November 28, 2023

Sheraton, Fifth Floor, Riverway

1:30 PM *QT04.04.01

Spin Transport Proximity Phenomena in Van der Waals Heterostructures J.F. Sierra, Luis Antonio Benítez, Josef Svetlik, Williams Saverio Torres, Lorenzo Camosi, Marius Costache and Sergio O. Valenzuela; Catalan Institute of Nanoscience and Nanotechnology, Spain

The vast collection of two-dimensional materials and their co-integration in van der Waals heterostructures enable innovative device engineering. Their atomically thin nature promotes the design of artificial quantum and topological materials by proximity-induced effects with physical properties not readily found in their single material forms [1]. Such a flexible design approach is especially compelling for the development of spintronic devices, which usually harness functionalities from thin layers of magnetic and non-magnetic materials and their interfaces. In this talk, I will summarize recent experimental progress toward investigating proximity-induced phenomena in hybrid graphene-transition metal dichalcogenides systems through spin transport dynamics [2,3] and charge-spin interconversion experiments [4]. I will focus on the relevance of crystal symmetries in the emergence of unconventional charge-spin conversion components and anisotropic spin dynamics [5], [6].

References

[1] J.F. Sierra *et al.*, *Nature Nano.* **16**, 856 (2021).

[2] L.A. Benítez, J. F. Sierra *et al.*, *Nature Phys.* **14**, 303 (2018)

[3] L.A. Benítez, J. F. Sierra *et al.*, *APL Materials* **7**, 120701 (2019).

[4] L.A. Benítez *et al.*, *Nature Mater.* **19**, 170 (2020).

[5] L. Camosi *et al.*, *2D Mater.* **9**, 035014 (2022).

[6] J. F. Sierra *et al.*, unpublished.

2:00 PM *QT04.04.02

Kramers Nodal Lines, Weyl Fermions and Large AHE in SmAlSi Emilia Morosan and Ming Yi; Rice University, United States

Kramers nodal lines (KNLs) are a special type of Weyl line degeneracy that connects time reversal invariant momenta. KNLs are robust to spin orbit coupling (SOC), and are inherent to all non-centrosymmetric achiral crystal structures. In this talk I will present magneto-transport and ARPES experimental data together with DFT calculation, pointing to the existence of novel KNLs in SmAlSi. SmAlSi is a non-centrosymmetric metal that develops incommensurate spin density wave AFM order at low temperatures. I will show evidence for the symmetry-protected KNLs, as well as Weyl fermions under the broken inversion symmetry in the paramagnetic phase of SmAlSi. In the AFM state, angle-dependent quantum oscillations (AQOs) provide evidence for the Weyl points, while large AHE is observed in both the AFM and the PM states. We propose a new mechanism to explain AHE in non-FM materials, based on magnetic field-induced Weyl-nodes evolution in non-centrosymmetric Weyl semimetals. The proposed mechanism qualitatively explains the temperature dependence of the anomalous Hall conductivity (AHC) in SmAlSi.

2:30 PM *QT04.04.03

On-Surface Synthesis of Silicon Nanoribbons María E. Davila; ICMM-CSIC, Spain

Abstract

In recent years, the scientific community has put a lot of efforts into trying to artificially grow new functional materials by reducing their dimensionality from 2D to 1D or even 0D. However, it is not a simple task, which includes synthetic methods that could go in both possible top-down or bottom-up approaches.

Our group, working on the bottom-up approach through on-surface synthesis has been able to develop unprecedented new 0D, 1D or 2D silicon nanoshapes [1,2]. Here, we demonstrate the on-surface synthesis of atomically precise silicon nanoribbons by utilizing the Ag(110) surface and also we have unmasked the unique 1D pentagonal silicon structures formed on it, which had been elusive for over 10 years. Further, we will see how the different single crystals substrates greatly affects the growth of silicon and the new structures that can be formed on it [3].

Promising applications of new silicon nanoforms range from nanoelectronics to transistors or embedded sensors; however, one of the important challenges that we have to overcome is the isolation, through the separation of the substrates, of these interesting nanoforms.

Keywords: Silicon nanoribbons, 1D-Silicon.

Reference

1-J. I. Cerdá, Jagoda Slawinska, G. Le Lay, A. C. Marele, J. M. Gómez-Rodríguez and M. E. Dávila Unveiling the pentagonal nature of perfectly aligned single- and double-strand Si nanoribbons on Ag(110) “, *Nature Communications*, 2016, 7:13076 | DOI: 10.1038/ncomms13076.

2-M E Dávila, A Marele, P De Padova, I Montero, F Hennies, A Pietzsch, M N Shariati, J M Gómez-Rodríguez and G Le Lay “Comparative structural and electronic studies of hydrogen interaction with isolated versus ordered silicon nanoribbons grown on Ag(110)” *Nanotechnology* 2012-23-38 385703 DOI 10.1088/0957-4484/23/38/385703

3-M. E. Dávila G. Le Lay and J. I. Cerdá, “Reducing the dimensionality of novel materials: one-dimensional silicon nanoribbons” 2D Semiconductor Materials and Devices, Materials Today, 2020, Pages 221-249.

3:00 PM BREAK

3:30 PM *QT04.04.04

Magnetic and Charge Order in Transition Metal Dichalcogenide Heterostructures Daniel K. Bediako; University of California, Berkeley, United States

Next-generation electronic devices will exploit correlated electronic phenomena in quantum materials to encode information for ultra-fast, ultralow-power, and non-volatile storage and retrieval. Spin-spin correlations in exotic magnetic materials are one basis for this new paradigm of compact, energy-efficient electronic systems, but these will require a nanoscale control over long-range magnetic ordering. Conceptually, this may be realized by designing materials that are inherently two-dimensional in their atomic connectivity, or by harnessing nanoscale, non-collinear spin textures in three-dimensional crystals. Likewise, electronic correlations that produce complex charge order can be manipulated to exhibit multi-state resistance phenomena, analogous to phase change materials, but without fatigue.

This talk will describe how transition metal dichalcogenides (TMDs) intercalated with open-shell transition metals represent a family of materials allowing fine control over the chemical and electronic structure of a magnetic material to tailor the interplay between (anti)ferromagnetic exchange, magnetocrystalline anisotropy, and anisotropic exchange (Dzyaloshinskii-Moriya interactions) to bring about exotic magnetic orders in two-dimensional (2D) materials or bulk crystals. The talk will show how soft-chemical methods can be used to prepare the highly coercive 2D ferromagnetic intercalation compound, Fe_xTaS_2 , and the use of angle-resolved photoemission spectroscopy to understand differences in chiral helimagnetic order in related 3D compounds, $\text{Cr}_{1/3}\text{NbS}_2$ and $\text{Cr}_{1/3}\text{TaS}_2$. The role of intercalant disorder on magnetic order will be explored in these chiral helimagnets as well as the intrinsically disordered $\text{Fe}_{0.17}\text{ZrSe}_2$. Finally, the talk will show how endotaxial polytype heterostructures of TaS_2 enable multistate resistivity and chirality switching of charge density wave phases.

4:00 PM QT04.04.05

Interplay between Magnetism and Topology: Large Topological Hall Effect in an Antiferromagnetic Topological Insulator, EuCuAs Subhajit Roychowdhury¹, Kartik Samanta¹, Premakumar Yanda¹, Bernard Malaman², Mengyu Yao¹, Walter Schnelle¹, Emmanuel Guillaume³, Procopios Constantinou⁴, Sushmita Chandra¹, Horst Borrmann¹, Maia G. Vergniory¹, Vladimir Strocov⁴, Chandra Shekhar¹ and Claudia Felser¹; ¹Max-Planck-Institute for Chemical Physics of Solids, Germany; ²Institut Jean Lamour-Université de Lorraine, Centre National de la Recherche Scientifique, France; ³CRISMAT, CNRS, Normandie University, ENSICAEN, UNICAEN, France; ⁴Paul Scherrer Institute, Switzerland

Magnetic interactions in combination with nontrivial band structures can give rise to several exotic physical properties such as a large anomalous Hall effect, the anomalous Nernst effect and the topological Hall effect (THE). Antiferromagnetic (AFM) materials exhibit THE due to the presence of nontrivial spin structures. EuCuAs crystallizes in a hexagonal structure with an AFM ground state (Néel temperature ~16 K). In this work, we observe a large topological Hall resistivity of ~7.4 $\mu\Omega\text{-cm}$ at 13 K which is significantly higher than the *giant topological Hall effect* of Gd_2PdSi_3 (~3 $\mu\Omega\text{-cm}$). Neutron diffraction experiments reveal that the spins form a transverse conical structure during the metamagnetic transition, resulting in the large topological Hall effect. In addition, by controlling the magnetic ordering structure of EuCuAs with an external magnetic field, several fascinating topological states such as Dirac and Weyl semimetals have been revealed. These results suggest the possibility of spintronic devices based on antiferromagnets with tailored noncoplanar spin configurations.¹

Reference:

1. S. Roychowdhury et al. *J. Am. Chem. Soc.* **2023**, *145*, 12920.

4:15 PM *QT04.04.06

Combining Topological Properties in Reciprocal and Real Space Athanasios Dimoulas¹, Polychronis Tsipas¹, Sotiris Fragkos¹, Panagiotis Pappas¹, Elli Georgopoulou-Kotsaki^{1,2}, Akylas Lintzeris^{1,2}, Nicholas Figueiredo-Prestes³, Henri-Yves Jaffres³, Jean-Marie George³, Marie-Blandine Martin³ and Paolo Bortolotti³; ¹National Center for Scientific Research DEMOKRITOS, Greece; ²National Kapodistrian University of Athens, Greece; ³Unité Mixte de Physique, CNRS, Thales, Université Paris-Saclay, France

Nearly 30% of stoichiometric, non-magnetic materials are predicted to have non-trivial topology which stems from their electronic band structure and they can be coarsely classified as topological insulators and topological Weyl and Dirac semimetals [1]

We will focus on MBE-grown layered and 2D topological materials which have better prospects to be grown in thin film form down to the ultimate 2D limit of one monolayer. We will provide theoretical and experimental evidence that 1T HfTe_2 [2] and ZrTe_2 [3] are Dirac semimetals of type I and type II, respectively, while the $\text{Hf}_x\text{Zr}_{1-x}\text{Te}_2$ ($x \sim 0.2$) alloy is a new type III Dirac semimetal [4] with a flat band and a line-like Fermi surface that can undergo an electronic Lifshitz transition under the influence of strain.

We will also show that using MBE, it is possible to stabilize at room temperature the non-centrosymmetric orthorhombic $1\text{T}_d\text{MoTe}_2$ Weyl semimetal phase against the more stable $1\text{T}'\text{MoTe}_2$ monoclinic and topologically trivial phase [5].

Non-collinear magnetization configurations in magnetic materials known as skyrmions possess a topological charge which makes them robust against perturbations. We will provide experimental evidence for the existence of skyrmions in the 2D van der Waals ferromagnet $\text{Cr}_{1+\delta}\text{Te}_2$ [6], [7] made by MBE by probing the topological Hall effect at low temperature. Using MOKE and micromagnetic calculations, we will also provide evidence for circular double wall magnetic configurations in the 2D van der Waals ferromagnet Fe_3GeTe_2 which organize in a quasi-periodic hexagonal lattice and transform to skyrmions by increasing magnetic field.

In the last part of the presentation, we will study the spin Hall effect and the Rashba Edelstein effect to show that efficient spin to charge interconversion occurs at the interface between topological materials and skyrmion hosting magnetic materials, which makes it possible to control the magnetization by an electrical current through the topological material. The latter could be very useful in new spintronics applications.

Acknowledgements: Part of this work is funded by EU FET PROAC project SKYTOP-824123

References:

[1] M. G. Vergniory et al., *Nature* **566**, 480 (2019)

[2] S. A. Giamini et al., *2D Mater.* **4** 015001 (2017)

[3] P. Tsipas et al., *ACS Nano* **12**, 1696 (2018)

[4] S. Fragkos et al., *J. Appl. Phys.* **129**, 075104 (2021)

[5] P. Tsipas et al., *Adv. Funct. Mater.* **28**, 1802084 (2018)

[6] N. Figueiredo-Prestes, *Phys. Rev. Appl.* **19**, 014012 (2023)

[7] S. Fragkos et al., *Appl. Phys. Lett.* **120**, 182402 (2022)

8:30 AM *QT04.05.01

Nonlinear Transport Effects in Chiral Elemental Tellurium Albert Fert¹, Manuel Suárez-Rodríguez², F. Calavalle², Beatriz Martín-García², A. Johansson³, Diogo C. Vaz², F. de Juan⁴, I. Sousa⁵, Andrey Chuvilin², I. Mertig⁶, M. Gobbi², F. Casanova³ and L. E. Hueso²; ¹Université Paris-Saclay, France; ²CIC nanoGUNE, Spain; ³Max Planck Institute of Microstructure Physics, Germany; ⁴Donostia International Physics Center, Spain; ⁵University of the Basque Country, Spain; ⁶Martin Luther University Halle-Wittenberg, Germany

Chiral materials are an ideal playground for exploring the relation between symmetry, relativistic effects, and electronic transport [1]. Indeed, the role of low symmetry on electronic transport has been studied on chiral organic molecules, but their poor electronic conductivity limits their potential for applications. Conversely, chiral inorganic crystals, such as elemental Tellurium (Te), present excellent electrical conductivity and strong spin-orbit coupling [2]. Therefore, Te become a perfect material for studying the connection between nonlinear transport phenomena, such as unidirectional magnetoresistance (UMR) [3] or nonlinear Hall effect (NLHE) [4], and chirality. Here, we synthesized single crystalline Te nanowires (NWs) and flakes with both handedness. On one hand, we report a chirality-dependent and gate-tunable Edelstein effect in the naturally hole-doped Te NWs [5]. By recording a UMR dependent on the relative orientation of the electrical current and the external applied magnetic field, we link the direction of the spin polarization to the handedness of the crystal. The measured UMR is explained on the basis of a chirality-dependent Edelstein effect arising from the radial spin texture at the H-point of the valence band of Te, which dominates the transport in our hole-doped Te NWs. In addition, an electrostatic gating enables the tuning of the Edelstein effect, leading to a modulation of the UMR amplitude by a factor of 6. On the other hand, we explore the NLHE in Te flakes. The symmetry of the measured second harmonic voltage under zero field, which is a consequence of the inversion symmetry breaking in Te, follows strictly the constraints for Te point group and is different from any material reported before. Moreover, by measuring flakes with opposite handedness, we were able to explore experimentally the effect of an inversion symmetry operation [6]. The all-electrical generation, control, and detection of spin polarization and second-order voltage in chiral Te NWs open the path to exploit chirality in the design of solid-state spintronic and energy harvesting devices.

- [1] S.-H. Yang *et al. Nat. Rev. Phys.* **3**, 328–343 (2021).
[2] M. Sakano *et al. Phys. Rev. Lett.* **124**, 136404 (2020).
[3] A. Dyrdal *et al. Phys. Rev. Lett.* **124**, 046802 (2020).
[4] Z. Z. Du *et al. Nat. Rev. Phys.* **3**, 744–752 (2021).
[5] F. Calavalle M. Suárez-Rodríguez *et al. Nat. Mater.* **21**, 526-532 (2022).
[6] M. Suárez-Rodríguez *et al. Submitted* (2023).

9:00 AM *QT04.05.02

Topological Heavy Fermion Mapping of 2D Interacting Topological States Bogdan A. Bernevig; Princeton University, United States

We show how a slew of models, from twisted bilayer graphene, twisted bilayer checkerboard, Lieb model and others can be mapped, with interactions into topological heavy fermion Anderson models. We argue and present evidence of an extended principle of interacting 2D topological states.

9:30 AM *QT04.05.03

2D Materials Prospects for Magnetic Tunnel Junctions Pierre Seneor¹, Julian Peiro¹, Victor Zlatko¹, Hao Wei¹, Frederic Brunnett¹, Simon Dubois¹, Marta Galbiati², Regina Galceran³, Maëlis Piquemal-Banci¹, Florian Godel¹, Jean-Christophe Charlier⁴, Piran Ravichandran Kidambi⁵, Robert Weatherup⁶, Stephan Hofmann⁷, John Robertson⁷, Mauro Och⁸, Cecilia Mattevi⁸, Aymeric Vecchiola¹, Karim Bouzouane¹, Sophie Collin¹, Albert Fert¹, Frédéric Petroff¹, Marie-Blandine Martin¹ and Bruno Dlubak¹; ¹Université Paris-Saclay, France; ²Universitat de València, Spain; ³Instituto de Ciencia de Materiales, Spain; ⁴Université Catholique de Louvain, Belgium; ⁵Vanderbilt University, United States; ⁶University of Oxford, United Kingdom; ⁷University of Cambridge, United Kingdom; ⁸Imperial College London, United Kingdom

Spin-based electronics, recently highlighted as a leading candidate for highly efficient and ultrafast embedded memories (such as MRAMs) and post-CMOS unconventional electronics strategies (including spin logics, stochastic, neuromorphic and quantum computing), have enjoyed considerable growth. Beyond the fundamental spin transport properties of graphene, 2D materials have unleashed a multitude of previously untapped possibilities for spintronic devices in terms of functionality and performance, ranging from gate control to topology.

Indeed, 2D materials offer the unlimited possibility of exposing their electronic structure to manipulation by proximity effects. We will demonstrate that this could be harnessed to shape the properties of 2Ds and van der Waals heterostructures in quantum devices [1] and materials. We will more specifically focus on how this can be leveraged in devices such as 2D based Magnetic Tunnel Junctions (2D-MTJs) [2,3].

Relying mostly on large scale 2D materials, we will give examples of spin manipulation and new mechanisms ranging from almost perfect 2D spin-filtering with -98% spin polarization in graphene [4] and up to 500% MR in black-phosphorous, to 2D material proximity hybridization leading to insulator-to-metal transition (spinterface) [5]. We will finally focus on 2D-magnets, and moreover show how this proximity effect can also be pushed further to create an artificial 2D magnet [6] relying on proximity interaction of graphene with a ferromagnetic insulator, towards a fully gateable 2D-MTJ for spin logics.

Acknowledgements: we acknowledge EU Horizon 2020 Graphene Flagship (881603), SKYTOP (824123) projects. France 2030 government grant managed by the French National Research Agency (ANR-22-PEEL-0011, ANR-23-SPIN) and French ONSET (ANR22-CE09-0010).

References

- Zatko *et al. ACS Nano* **15**, 7279 (2021)
Piquemal-Banci *et al. J. Phys. D* **50** 203002 (2017)
Yang *et al. Nature* **606**, 663 (2022)
Zatko *et al. ACS Nano* **16**, 14007 (2022)
Piquemal-Banci *et al. ACS Nano* **12**, 4712 (2018) & *Nat. Com.* (2020)
Zatko *et al. Nanoletters* **23**, 34 (2023)

10:00 AM BREAK

10:30 AM *QT04.05.04

Towards a Topology-Based Compact Neuromorphic Component Marie-Blandine Martin¹, Tristanda Câmara Santa Clara Gomes², Yanis Sassi¹, Sachin Krishna¹, Dedalo Sanz-Hernandez¹, Tanvi Bhatnagar-Schöffmann³, Dafiné Ravelosona³, Damien Querlioz³, Liza Herrera-Diez³, Bruno Dlubak¹, Nicolas Reyren¹, Pierre Seneor¹, Julie Grollier¹ and Vincent Cros¹; ¹Unite Mixte Physique CNRS/Thales, France; ²The Université catholique de Louvain, Belgium; ³University of Paris-Saclay, France

Thanks to their original properties, magnetic skyrmions have many promising applications, from sensors through data storage to non-conventional computing [1-3]. Among the main advantages of magnetic skyrmions are their sub-micronic size, their particle-like behavior, their stability and non-volatility at room temperature and the low energy requirement for their motion. It has been shown, most often separately, that magnetic skyrmions can be experimentally nucleated [4-7], moved [4,7], annihilated [6] and detected electrically using Anomalous Hall effect [8] in metallic multilayers.

In this talk, we will propose a neuromorphic device design using full-electrical manipulation and detection of skyrmions to perform basic operations required for neuromorphic computing. Indeed, the operating principle of an artificial neuromorphic component is to work by performing a simple operation: it multiplies various input signals with corresponding synaptic weights and sums them up [9]. Mathematically, this can be represented as $y = \sum(w_i x_i)$, where x_i are the inputs and w_i are the synaptic weights. All the building blocks necessary to achieve the demonstration of a weighted sum of skyrmions will be presented, from the nucleation and motion of a controlled number of magnetic skyrmions in multilayer tracks using electrical current pulse parameters to the electrical detection of a sum of skyrmions through anomalous hall effect.

The demonstrated skyrmion-based neuromorphic device paves the way to skyrmionic low-energy devices contributing to a global reduction of the environmental impact of AI applications.

Acknowledgements: this work was supported by the Horizon2020 Framework Program of the European Commission under FET-Proactive Grant SKYTOP (824123), the ERC BioSPINspired (682955) and by the French National Research Agency (ANR) with TOPSKY (ANR-17-CE24-0025).

11:00 AM QT04.05.05

Colloidal Synthesis of III-V Quantum Dots and Their Optical PropertiesCanLi; Los Alamos National Laboratory, United States

Colloidal synthesis of III-V quantum dots (QDs) and their photonic properties have garnered significant attention in the field of nanotechnology and optoelectronics. III-V semiconductors, such as InAs, InP QDs, exhibit excellent tunable optical properties, strong quantum confinements effects, and are widely used in various photonic devices. Colloidal synthesizing III-V QDs can indeed be a challenging process. In our case, by developing innovation synthesis strategies, exploring alternative precursors, and optimizing reaction conditions, III-V QDs (such as InSb) with uniform size distribution can be achieved. Additionally, a controlled CdS shell can be grown epitaxially onto the InSb cores, resulting into tunable optical properties.

11:15 AM QT04.05.06

2D Topological Insulators for New Generation Thermoelectrics: Technological DevelopmentPaoloBondavalli¹, PierreLegagneux¹, EvaDesgue¹, OlivierBourgeois², DominiqueCarisetti¹ and YannickFagot-Revrut³; ¹Thales Research and Technology, France; ²Institut néel, France; ³Université de Lorraine, France

The implementation of 2D topological materials is a potential revolution in this domain. During the NEXTOP project, funded by French Research Agency, we are working on a new generation of 2D topological insulators to demonstrate a ZT larger than 7. Two major issues are to be overcome: the growth of 2D topological insulators on different kinds of substrates (insulating and conducting ones) and their implementation for thermoelectric tests. We are developing a new technique for growing WTe₂ using sort of steps with different widths that will allow controlling its crystallinity and number of layers. Thanks to that, we will be able to perform thermoelectric measurements on this topological insulator which is up to now the only 2D material whose topological features have been demonstrated. This will be the first time that measurements will be performed. Techniques for stanene growth will be also presented during the meeting. Bottlenecks for in-situ tests to identify band structures will be also presented.

11:30 AM QT04.05.07

A New Platform for Spin-Polarized Majorana Zero Modes: Penta-Silicene NanoribbonsGuyLe Lay¹, MarcoMinissale¹, R. C.Bento Ribeiro², Mucio A.Continentino², J. H.Corraea³, L. S.Ricco⁴, I. A.Shelykh⁵, A. C.Seridonio⁶ and M. S.Figueira⁷; ¹Aix-Marseille University, France; ²CBF, Brazil; ³Universidad Tecnológica del Peru, Peru; ⁴University of Iceland, Iceland; ⁵ITMO University, Russian Federation; ⁶Sao Paulo State University, Brazil; ⁷Universidade Federal Fluminense, Brazil

We report the possibility of obtaining Majorana zero modes (MZMs) in straight, highly perfect, and massively aligned atom-thin penta-silicene nanoribbons (p-SiNRs) with a very high aspect ratio, purely composed of silicon pentagonal building blocks, and grown by molecular beam epitaxy on the (110) surface a silver crystal template^{2,3}. They could constitute the experimental realization of the generic Kitaev toy model^{3,4}. The spinless and full spin p-SiNRs with p-wave superconducting pairing reveal the emergence of topologically protected MZMs at opposite ends of the p-SiNRs. Besides the first nearest neighbor hopping term and p-wave superconducting pairing we consider an external magnetic field perpendicularly applied to the nanoribbon plane and an intrinsic Rashba spin-orbit coupling. The dispersion relation profiles show the closing and reopening of the superconducting gap for only one spin component, suggesting a spin-polarized topological phase transition (TPT). Along with this TPT, the energy spectrum as a function of the p-SiNR chemical potential exhibits zero-energy states and preferential spin direction. It is associated with nonoverlapping wave functions well-localized at the opposite extremities of the superconducting p-SiNRs. Hence, we show theoretically that the p-SiNRs could constitute a tantalizing new platform for MZMs⁵.

1. Jorge I. Cerda et al., Nature Comm., 7, 13076 (2016).
2. R. Pawlak et al., PNAS, 117, 228 (2020).
3. A. Y. Kitaev, Physics-Uspekhi, 44, 131 (2001).
4. R. C. Bento Ribeiro et al., Phys. Rev. B 105, 205115 (2022).
5. R. C. Bento Ribeiro et al., submitted

11:45 AM QT04.05.08

Band-Gap Landscape Engineering in Large-Scale 2D Semiconductor Van der Waals Heterostructures for SpintronicsBrunoDlubak¹, VictorZatko¹, HaoWei¹, FredericBrunnett¹, SimonDubois^{1,2}, JulianPeiro¹, MartaGalbiati^{1,3}, FlorianGodel¹, Jean-ChristopheCharlier², MauroOch⁴, CeciliaMattevi⁴, AymericVecchiola¹, KarimBouzehouane¹, SophieCollin¹, FrédéricPetroff¹, Marie-BlandineMartin¹ and PierreSeneor¹; ¹Université Paris-Saclay, France; ²Université Catholique de Louvain, Belgium; ³Universidad de Valencia, Spain; ⁴Imperial College London, United Kingdom

The discovery of graphene has opened novel exciting opportunities in terms of functionalities and performances for spintronics devices. This started a wide exploration of a large variety of 2D crystals for spintronics with the hope to exploit some of their unique topological properties. We will present here experimental results concerning integration of 2D materials in vertical Magnetic Tunnel Junctions (MTJ). We will in particular focus the discussion on a novel pulsed laser deposition (PLD) approach for the definition of complex van der Waals heterostructures of 2D materials in magnetic tunnel junctions.[1][2] This PLD growth approach unlocks the association in heterostructure of wide families of multifunctional 2D materials, including the most delicate ones. The direct growth of the 2D layers prevents the oxidation of the ferromagnet, enabling the use of these van der Waals materials for spintronics devices. Overall, the presented experiments unveil promising approaches for the quantum engineering of multifunctional 2D materials heterostructures for spintronics.

- [1] Godel et al. ACS Applied Nano Materials 3, 7908 (2020)
[2] Zatko et al. ACS Nano 15, 7279 (2021)

SESSION QT04.06: New Perspectives for Topological Materials II
Session Chairs: Paolo Bondavalli, Bruno Dlubak and Guy Le Lay
Wednesday Afternoon, November 29, 2023
Sheraton, Fifth Floor, Riverway

1:30 PM *QT04.06.01

Pseudomagnetic Fields in Graphene Strain SuperlatticesNadyaMason¹, IvaSrut Rakic², PreethaSarkar¹, YingjieZhang¹, MatthewGilbert¹ and VidyaMadhavan¹; ¹University of Illinois at Urbana-Champaign, United States; ²Institute of Physics, Serbia

Straining graphene can modify the electronic band structure and lead to the formation of giant pseudomagnetic fields. Recently it was shown that addition of superlattice periodicity to strain leads to global electronic band flattening and signatures of correlated states. Here we show an engineered approach to producing a strained graphene superlattice system. Using scanning tunnelling spectroscopy and transport measurements, together with numerical simulations, we demonstrate that a graphene monolayer placed on a SiO₂ nanosphere superlattice undergoes a band structure change with observable pseudo-Landau level formation, not only integer ones but also with fractional indices. The results are consistent with significant flattening of the electronic bands, making it ideal playground for exploring other related interaction phenomena and possibly the emergence of correlated states.

The authors acknowledge the support of NSF-MRSEC under award no. DMR-1720633

2:00 PM *QT04.06.02

Two-Dimensional Easy-Plane Magnets Grown by MBE: A Fertile Platform for Unconventional Topological Spin TexturesAmilcarBedoya-Pinto; Universitat de València, Spain

In this talk, I will focus on the van-der-Waals epitaxy of a nearly-ideal two-dimensional magnet, a CrCl₃ monolayer grown on Graphene/6H-SiC(0001). *In-situ* X-ray magnetic circular dichroism reveals intrinsic ferromagnetic order with easy-plane anisotropy and a 2DXY universality class [1], indicating the realization of a Berezinskii-Kosterlitz-Thouless (BKT) phase

transition in a quasi-freestanding monolayer magnet. The important role of the van der Waals substrate interaction and the underlying crystal symmetry will be discussed, thereby highlighting routes on how to control the anisotropy of 2D magnets via growth engineering. Moreover, the crucial role of a robust easy-plane anisotropy for the emergence of in-plane topological spin textures -merons and anti-merons- will be showcased for monolayer CrCl₃, both from a theoretical and experimental perspective.

2:30 PM QT04.06.03

Effect of Molecular Beam Epitaxy (MBE) Growth Conditions on the Structural and Magnetic Properties of High Curie Temperature (MnSb₂Te₄)_x(Sb₂Te₃)_{1-x} Magnetic Topological Insulators Candice Forrester^{1,2}, Christophe Testelin³, Kaushini Wickramasinghe⁴, Ido Levy⁵, Xiabin Ding⁴, Lia Krusin-Elbaum^{4,1}, Gustavo Lopez^{1,2} and Maria Tamargo^{1,4}. ¹The Graduate Center, CUNY, United States; ²Lehman College, CUNY, United States; ³Sorbonne Université, CNRS, Institut des NanoSciences de Paris, France; ⁴The City College of New York, United States; ⁵New York University, United States

Recently it has been shown that structural disorder in 3D Topological Insulators (TIs) has considerable effects on the properties of the materials. The addition of magnetic ions like Mn breaks time reversal symmetry and opens a gap in the Dirac point.¹ This addition also changes the crystal structure from the typical quintuple layer (QLs) structure of non-magnetic TIs to a septuple layer (SLs) structure.² Furthermore, addition of a Mn flux during MBE growth results in self-assembled structures of mixed QLs and SLs.² Previously we reported the MBE growth of self-assembled structures of (MnSb₂Te₄)_x(Sb₂Te₃)_{1-x} magnetic topological materials,³ and showed that their Curie temperature (T_C) is dependent on the composition x (or %SL).⁴ Samples with 0.7 < x < 0.85 exhibit very high T_C values. Additionally, it was observed that as the Mn beam equivalent pressure (BEP) ratio used was increased, there was a corresponding increase in T_C. Decreasing the growth rate further increased T_C to >100 K, the highest values reported for this material system. An understanding of how the changes in growth conditions lead to the T_C enhancement is not well-established.

Here we investigate the structural properties of the materials as they relate to the growth conditions, specifically Mn flux ratio during growth and reduced growth rate (GR). Samples grown at slow GRs (0.4 – 0.6 nm/min) were compared to samples grown at fast GRs (0.8 – 1.0 nm/min). Samples were investigated using several characterization techniques including X-ray diffraction, Energy Dispersion X-Ray Spectroscopy (EDS), Hall effect and scanning transmission electron microscopy (STEM). We found that for the same Mn BEP ratio, low GR yields similar composition, x, as fast GRs. On the other hand, EDS showed that for x > 0.7, there was increased intermixing between Sb and Mn in both the fast and the slow GR samples. Furthermore, the samples grown with slow GR showed much greater Mn and Sb intermixing, as well as Mn and Te intermixing, suggesting increased Mn incorporation at the slow GR, as well as more disorder. Cross sectional EDS studies reveal a high Mn content in the QLs, consistent with (Sb_{1-y}Mn_y)₂Te₃ alloy formation. Hall effect measurements show that GR does not significantly affect the electrical doping in (MnSb₂Te₄)_x(Sb₂Te₃)_{1-x} supporting the proposal that a super-exchange magnetic mechanism is likely at play. Other techniques, such as magnetic force microscopy (MFM) are being explored to better understand the magnetic mechanisms leading to high T_C values and Raman spectroscopy is being explored to understand the disorder in these materials. Our results provide insight as to how to achieve on-demand magnetic TIs with enhanced properties.

¹ Y. Tokura et al, *Nature Reviews Physics* **1**, 126 (2019)

² J.A. Hagmann et al, *New Journal of Physics* **19**, 085002 (2017)

³ I. Levy et al, *Crystal Growth & Design* **22**, 3007 (2022)

⁴ I. Levy et al, *Science Reports* **13**, 7381(2023)

2:45 PM BREAK

3:30 PM *QT04.06.04

Discovery of Novel Kagome and Related Topological Quantum Materials M. Zahid Hasan, Princeton University, United States

In a 2D kagome lattice, the Dirac fermions encode topology, flat bands favour correlated phenomena such as magnetism, and van Hove singularities can lead to instabilities towards long-range many-body orders, altogether allowing for the realization and discovery of a series of topological kagome magnets and superconductors with exotic properties. Recent progress in exploring kagome materials has revealed rich emergent phenomena resulting from the quantum interactions between geometry, topology, spin and correlation. I plan to present some of the key developments we made in this field covering the realizations of Chern and Weyl-like topological magnetism, to various flat-band many-body correlations, and then to the puzzles of unconventional charge-density waves and superconductivity. I plan to highlight the connection between theoretical ideas and experimental observations, and the bond between quantum interactions within kagome magnets and kagome superconductors, as well as their relation to the concepts in topological insulators, topological superconductors, Weyl semimetals and high-temperature superconductors. These developments broadly bridge topological quantum physics and correlated many-body physics in a wide range of bulk materials and substantially advance the frontier of topological quantum matter as detailed in our most recent review article (J. Yin, B. Lian & M. Z. Hasan, *NATURE* **612**, 647–657 (2022))

SESSION QT04.07: Poster Spotlight Talk
Session Chairs: Paolo Bondavalli, Bruno Dlubak and Guy Le Lay
Wednesday Afternoon, November 29, 2023
Sheraton, Fifth Floor, Riverway

4:00 PM QT04.07.01

Poster Spotlight: π Quantization in the Berry Phase by the Multiple Degenerate Points Fuka Watanabe, Keiichi Hirata, Tatsuki Tojo and Kyozauro Takeda; Waseda University, Japan

Physicomathematics can create new frontiers in condensed-matter physics. The application of *topology* proposes a novel concept, topological materials, that can deepen our understanding regarding quantum phenomena, particularly those related to spin and spin-orbit interactions (SOIs), such as the spin current, spin Hall effects, and spin-Zeeman effect [1]. In these topological materials, the SOI around the degenerate point is key in inducing a characteristic effective magnetic field (EMF). The degenerate state determines its own orthogonal eigenvectors but is not unique because of the “phase” indefiniteness. The Dirac cone is a prime example and results in a topological singularity originating from degeneracy. Spatial asymmetry can generate singularities in the EMF distribution, such as vortices, sources, and sinks, via the SOI around the degenerate point; subsequently, the spin is polarized characteristically therein, particularly when the system exhibits bulk inversion asymmetry (BIA) and/or structure inversion asymmetry (SIA).

In this study, we investigate the manner by which multiple degenerate points in the Brillouin zone (BZ) modify the topological features. We focus on a semiconductor system with a two-dimensional quantum well structure and investigate topological modifications via numerical calculations of the EMF, Berry connection, and curvature. Next, we reveal the energy dependence of the Berry phase modulated by the interaction between the degenerate points. We employ the Hamiltonian, in which the spatial asymmetry of the SIA and/or BIA is considered [1]. The effect of the competition between the SIA and BIA is investigated using tunable parameters *a* and *b*. To provide multiple degenerate points in the BZ, we locate the degenerate state at point Γ and then transfer it to a peculiar direction by $\pm k_i$. We vary the locations of the degenerate points by appropriately substituting a value for k_i and examine the directional dependence of the synthesized EMF distribution. We further introduce anisotropy by changing the directional effective mass.

In the SIA system, each degenerate point presents a SIA-like singularity and the concentric EMF distribution results. The synthesis of these two concentric distributions generates a source and a sink at the middle position between the two prepared degenerate points when the points ($\pm k_i$) are located in the $\langle 110 \rangle$ direction. Accordingly, the EMF is distributed hyperbolically, and the BIA-like singularity newly results. By contrast, the topological singularity in the BIA system distributes the EMF hyperbolically around each degenerate point. The synthesis of these two hyperbolic distributions results in a new concentric EMF distribution at the middle position. These newborn singularities in the EMF distribution results in accidental degeneracy at the middle position. The sign of the Berry curvature around the newly generated point is opposite to that at the prepared degenerate points.

Finally, we discuss the energy dependence of the Berry phase based on the calculated Berry connection and curvature. Since each degenerate point results in the Berry phase of $\pm\pi$, the multiple degenerate points quantize the Berry phase by π and result in a plateau profile against energy. We further demonstrate that this π quantization can be understood by counting the number of degenerate points in the BZ in addition to identifying the sign of the Berry curvature [2].

[1] S.D. Ganichev, L.E. Golub, *physica status solidi (b)* **251**, 1801 (2014).

[2] T. Tojo, K. Takeda, *Phys. Lett. A* **389**, 127091 (2021).

4:05 PM QT04.07.02

Poster Spotlight: Spin Transport Through Superconductor / Weyl Semimetal Heterodevices Xiaodong Hu, Jason W. Robinson, Adrian Ionescu, Nadia Stelmashenko, Leyla C. Arslan, Francesca Chiodi, Hisakazu Matsuki, Sijie Wang and Jiahui Xu; Cambridge University, United Kingdom

Transport of spin information over large distances is key for many applications in spintronics. Achieving spin transmission within superconducting devices should lead to reductions in Joule

heating and massive improvements in device efficiency and performance. The Weyl semimetal Mn_3Ge [1, 2, 3, 4] with an antiferromagnetic or ferrimagnetic phase has recently emerged as a promising material for spin transmission studies in the superconducting [1] and normal [3, 4] states. In this poster, we report the fabrication of magnetron-sputtered thin-films of Mn_3Ge and superconducting heterostructures with sub-nanometer-thickness-control in order to investigate the interplay between superconductivity and spin transport in Mn_3Ge . The results build a framework for spin-transport control in the superconducting state.

- [1] Jeon, K.-R., et al. (2021). "Long-range supercurrents through a chiral non-collinear antiferromagnet in lateral Josephson junctions." *Nature Materials* 20(10): 1358-1363.
[2] Kobayashi, A., et al. (2020). "Structural and magnetic properties of Mn_3Ge films with Pt and Ru seed layers." *AIP Advances* 10(1).
[3] Hong, D., et al. (2020). "Large anomalous Nernst and inverse spin-Hall effects in epitaxial thin films of kagome semimetal Mn_3Ge ." *Physical Review Materials* 4(9): 094201.
[4] Olayiwola, I. O., et al. (2023). "Room temperature positive exchange bias in $CoFeB/D019-Mn_3Ge$ noncollinear antiferromagnetic thin films." *Journal of Alloys and Compounds* 955: 170279.

4:10 PM QT04.07.03

Poster Spotlight: Orientation Control of MBE Grown SnTe Layers on GaAs Substrates Masakazu Kobayashi^{1,2} and SuNan¹; ¹Waseda University, Japan; ²Material Research Technology Institution, Japan

SnTe is one of the attractive material for a topological crystalline insulator (TCI). SnTe films have been grown directly on GaAs (100) substrates by molecular beam epitaxy, and single domain SnTe layers preferentially oriented to (100) were achieved by now. The (111) oriented SnTe domains and Te were easily included in the film. The crystallographic orientation control and surface smoothness improvement was mainly performed in this study.

SnTe layers were grown on (100) and (111)B oriented GaAs substrates by molecular beam epitaxy (MBE). Most of structures were formed on (100) GaAs substrates with (100) oriented ZnTe buffer layers. Elemental sources were used and the molecular beam intensity ratio (J_{Te}/J_{Sn}) was varied between 0.6~2.9. The beam intensity ratio was tuned by changing the beam intensity of Te. The substrate temperature was calibrated using the oxide desorption temperature of chemically etched GaAs substrates prior to the film growth, and it was varied from 200 °C to 300 °C. The film thickness of SnTe was about 100 nm.

The introduction of the ZnTe buffer layer was effective to improve the crystallographic properties of SnTe layers. Atomic force microscopy observation revealed that plateaus with atomically smooth surfaces were obtained for SnTe layers prepared on ZnTe buffer layers. On the other hand, samples prepared without ZnTe buffer layers haven't exhibited the atomically smooth surfaces. The size of the plateau was increased by increasing the molecular beam intensity ratio up to 1.0.

Since the growth temperature was relatively low, the inclusion of the excess material was not negligible. According to the result of X-ray diffraction (XRD) measurement, a diffraction peaks originated from hexagonal Te was observed with SnTe peaks when samples were grown with Te rich (J_{Te}/J_{Sn} was between 2.9 and 1.5) conditions. In the secondary electron microscopy measurements, featureless surface was confirmed when the XRD of the sample exhibited no Te peak while dotted materials were clearly observed on the surface when the hexagonal Te peak was observed. The distribution density of the dot was high when the Te diffraction peak signal intensity was strong. Those dotted materials are presumed to be the residual of Te.

The orientation of the material was affected by the growth temperature. When the substrate temperature was raised, (111) SnTe domains were started to appear. The XRD peak intensities of (100) and (111) domains were comparable when the substrate temperature was 250 °C. In order to eliminate the (111) domain inclusion, the substrate temperature needed to be maintained below 240 °C.

In order to enhance the (111) domain formation, (111)B oriented GaAs substrates were employed. (100) domains could be mostly eliminated when the substrate temperature was raised to 270 °C.

A standard van der Pauw Hall measurement was performed to characterize the electrical property at room temperature. The (100) sample that didn't include the Te residual exhibited the resistivity of about $0.3 \text{ ohm}\cdot\text{cm}$. The resistivity has increased as the presence of Te residual became noticeable. Based on the literatures, the room temperature resistivity of SnTe and Te were about $0.3 \text{ ohm}\cdot\text{cm}$ ^[1] and $0.3 \text{ ohm}\cdot\text{cm}$ ^[2], respectively. The higher resistivity obtained for the grown film might be originated from the mixing of Te residual. Although the surface morphology was improved by the introduction of the ZnTe buffer layer, the electrical properties were not improved. Boundaries of plateau probably became the center of carrier scatterings.

Acknowledgement

This work was supported in part by the Waseda University Grant for Special Research Projects.

References

1. Athwal, I. S., et al., *Thin solid films*, 162 (1988) 1-6.
2. Wang, D., et al., *J. Alloys & Compounds*, 773 (2019) 571-584.

4:15 PM QT04.07.04

Poster Spotlight: Near-Absolute Spin-Valve Effect at f-Orbital Magnet/Superconductor Interfaces with Controlled Orbital-To-Spin Moments Sijie Wang¹, Karine Dumesnil², Harry Bradshaw¹, Nadia Stelmashenko¹ and Jason W. Robinson¹; ¹University of Cambridge, United Kingdom; ²Institut Jean Lamour, France

The proximity effect between a thin-film superconductor (S) and a ferromagnet (F) can lead to a spin-splitting of the quasiparticle density of states and suppression of the superconducting critical temperature (T_C) (1). At an S/F interface, the average magnitude of the spin-splitting in S can be tuned via the micromagnetic state of F with shifts in T_C between magnetized ($T_{C,m}$) and de-magnetized ($T_{C,dm}$) ferromagnet states being dependent [1-3] on the ratio of the superconducting coherence length (ξ) to the domain wall width (d_w) $\frac{1}{4}$ i.e., $(T_{C,m} - T_{C,dm})/T_{C,dm} = \Delta T_C/T_{C,dm} \propto \xi/d_w$ can theoretically be infinite for an appropriate combination of S and F thin films in which S is thinner than ξ . Experimentally, however, such an absolute spin-valve effect is hard to achieve with $\Delta T_C/T_{C,dm}$ ratios tending to be a small fraction of $T_{C,dm}$, indicating physics beyond the standard picture of the S/F proximity effect. Here we report S/F bilayers and F/S/F spin-valves in which F is an f-orbital ferromagnet (HoGd) with a controlled composition to tune the ratio of the orbital to spin components of the magnetization. The results demonstrate that $\Delta T_C/T_{C,dm}$ can approach infinity for a large ratio of the orbital moment to spin moment, which enables a near-absolute spin-valve effect. Our results demonstrate that the band structure of the ferromagnet in conjunction with the ξ/d_w can be tuned to enable high-performance superconducting memory for energy efficiency electronics. A first principle theory is required in order to understand the relationship between $\Delta T_C/T_{C,dm}$ and the ratio of the orbital to spin moment of the F metal.

1. A. Buzdin, *Rev. Mod. Phys.* 77, 935-976 (2005).
2. M. Houzet and A. I. Buzdin, *Phys. Rev. B* 74, 214507 (2006).
3. S. Komori, A. Di Bernardo, A. I. Buzdin, M. G. Blamire, and J. W. A. Robinson, *Phys. Rev. Lett.* 121, 077003 (2018).

4:20 PM QT04.07.05

Poster Spotlight: Towards Quantum Transport in Metal and Ferromagnetic Semiconductor Thin Films Structures with Absorbed Chiral Molecules Jiahui Xu¹, Jason W. Robinson¹, Hisakazu Matsuki¹, Nadia Stelmashenko¹, Shira Yochelis² and Yossi Paltiel²; ¹University of Cambridge, United Kingdom; ²The Hebrew University of Jerusalem, Israel

Chiral molecules (CMs), such as alpha-helix polyalanine, exhibit chiral-induced spin-selectivity (CISS) characteristics, which means that a flow of electron charge across a layer of CMs can result in a spin-filtering effect and phase coherent transport (1, 2). Recently, for example, we have demonstrated low temperature phase-coherent transport through thin-film wires of Au and Cu with absorbed CMs (2). For Au, we also observed evidence for induced ferromagnetism associated with the thiol-Au bonding and for Au and Cu, we detected an enhancement of spin-orbit coupling. Here, we systematically study charge transport and magnetic anisotropy in thin films and wires of Au and Au/EuS where EuS is a ferromagnetic semiconductor. The thickness of Au is varied in the 1-10 nm range in order to optimise magnetic hysteresis in Au and magnetic anisotropy modification in Au/EuS structures. The results provide a platform for detailed studies of quantum behaviour including magnetic control of phase coherence transport and potentially a quantum anomalous Hall effect.

1. R. Naaman, Y. Paltiel, D.H. Waldeck, *Nature Reviews Chemistry*, 3, 250 (2019).
2. M. Ozeri *et al.*, *The Journal of Physical Chemistry Letters*, 14, 4941-4948 (2023).

8:00 PM QT04.08.01

Poster Spotlight: π Quantization in the Berry Phase by the Multiple Degenerate Points FukaWatanabe, KeijiroHirata, TatsukiTojo and KyozauroTakeda; Waseda University, Japan

Physicomathematics can create new frontiers in condensed-matter physics. The application of *topology* proposes a novel concept, topological materials, that can deepen our understanding regarding quantum phenomena, particularly those related to spin and spin-orbit interactions (SOIs), such as the spin current, spin Hall effects, and spin-Zeeman effect [1]. In these topological materials, the SOI around the degenerate point is key in inducing a characteristic effective magnetic field (EMF). The degenerate state determines its own orthogonal eigenvectors but is not unique because of the "phase" indefiniteness. The Dirac cone is a prime example and results in a topological singularity originating from degeneracy. Spatial asymmetry can generate singularities in the EMF distribution, such as vortices, sources, and sinks, via the SOI around the degenerate point; subsequently, the spin is polarized characteristically therein, particularly when the system exhibits bulk inversion asymmetry (BIA) and/or structure inversion asymmetry (SIA).

In this study, we investigate the manner by which multiple degenerate points in the Brillouin zone (BZ) modify the topological features. We focus on a semiconductor system with a two-dimensional quantum well structure and investigate topological modifications via numerical calculations of the EMF, Berry connection, and curvature. Next, we reveal the energy dependence of the Berry phase modulated by the interaction between the degenerate points. We employ the Hamiltonian, in which the spatial asymmetry of the SIA and/or BIA is considered [1]. The effect of the competition between the SIA and BIA is investigated using tunable parameters a and b . To provide multiple degenerate points in the BZ, we locate the degenerate state at point Γ and then transfer it to a peculiar direction by $\pm k_i$. We vary the locations of the degenerate points by appropriately substituting a value for k_i and examine the directional dependence of the synthesized EMF distribution. We further introduce anisotropy by changing the directional effective mass.

In the SIA system, each degenerate point presents a SIA-like singularity and the concentric EMF distribution results. The synthesis of these two concentric distributions generates a source and a sink at the middle position between the two prepared degenerate points when the points ($\pm k_i$) are located in the $\langle 110 \rangle$ direction. Accordingly, the EMF is distributed hyperbolically, and the BIA-like singularity newly results. By contrast, the topological singularity in the BIA system distributes the EMF hyperbolically around each degenerate point. The synthesis of these two hyperbolic distributions results in a new concentric EMF distribution at the middle position. These newborn singularities in the EMF distribution results in accidental degeneracy at the middle position. The sign of the Berry curvature around the newly generated point is opposite to that at the prepared degenerate points.

Finally, we discuss the energy dependence of the Berry phase based on the calculated Berry connection and curvature. Since each degenerate point results in the Berry phase of $\pm\pi$, the multiple degenerate points quantize the Berry phase by π and result in a plateau profile against energy. We further demonstrate that this π quantization can be understood by counting the number of degenerate points in the BZ in addition to identifying the sign of the Berry curvature [2].

[1] S.D. Ganichev, L.E. Golub, *physica status solidi (b)* **251**, 1801 (2014).

[2] T. Tojo, K. Takeda, *Phys. Lett. A* **389**, 127091 (2021).

8:00 PM QT04.08.02

Poster Spotlight: Spin Transport Through Superconductor / Weyl Semimetal Heterodevices XiaodongHu, JasonW. Robinson, AdrianIonescu, NadiaStelmashenko, LeylaC. Arslan, FrancescaChiodi, HisakazuMatsuki, SijieWang and JiahuiXu; Cambridge University, United Kingdom

Transport of spin information over large distances is key for many applications in spintronics. Achieving spin transmission within superconducting devices should lead to reductions in Joule heating and massive improvements in device efficiency and performance. The Weyl semimetal Mn_3Ge [1, 2, 3, 4] with an antiferromagnetic or ferrimagnetic phase has recently emerged as a promising material for spin transmission studies in the superconducting [1] and normal [3, 4] states. In this poster, we report the fabrication of magnetron-sputtered thin-films of Mn_3Ge and superconducting heterostructures with sub-nanometer-thickness-control in order to investigate the interplay between superconductivity and spin transport in Mn_3Ge . The results build a framework for spin-transport control in the superconducting state.

[1] Jeon, K.-R., et al. (2021). "Long-range supercurrents through a chiral non-collinear antiferromagnet in lateral Josephson junctions." *Nature Materials* 20(10): 1358-1363.

[2] Kobayashi, A., et al. (2020). "Structural and magnetic properties of Mn_3Ge films with Pt and Ru seed layers." *AIP Advances* 10(1).

[3] Hong, D., et al. (2020). "Large anomalous Nernst and inverse spin-Hall effects in epitaxial thin films of kagome semimetal Mn_3Ge ." *Physical Review Materials* 4(9): 094201.

[4] Olayiwola, I. O., et al. (2023). "Room temperature positive exchange bias in $\text{CoFeB}/\text{D019-Mn}_3\text{Ge}$ noncollinear antiferromagnetic thin films." *Journal of Alloys and Compounds* 955: 170279.

8:00 PM QT04.08.03

Poster Spotlight: Orientation Control of MBE Grown SnTe Layers on GaAs Substrates MasakazuKobayashi^{1,2} and SuNan¹; ¹Waseda University, Japan; ²Material Research Technology Institution, Japan

SnTe is one of the attractive material for a topological crystalline insulator (TCI). SnTe films have been grown directly on GaAs (100) substrates by molecular beam epitaxy, and single domain SnTe layers preferentially oriented to (100) were achieved by now. The (111) oriented SnTe domains and Te were easily included in the film. The crystallographic orientation control and surface smoothness improvement was mainly performed in this study.

SnTe layers were grown on (100) and (111)B oriented GaAs substrates by molecular beam epitaxy (MBE). Most of structures were formed on (100) GaAs substrates with (100) oriented ZnTe buffer layers. Elemental sources were used and the molecular beam intensity ratio ($J_{\text{Te}}/J_{\text{Sn}}$) was varied between 0.6~2.9. The beam intensity ratio was tuned by changing the beam intensity of Te. The substrate temperature was calibrated using the oxide desorption temperature of chemically etched GaAs substrates prior to the film growth, and it was varied from 200 °C to 300 °C. The film thickness of SnTe was about 100 nm.

The introduction of the ZnTe buffer layer was effective to improve the crystallographic properties of SnTe layers. Atomic force microscopy observation revealed that plateaus with atomically smooth surfaces were obtained for SnTe layers prepared on ZnTe buffer layers. On the other hand, samples prepared without ZnTe buffer layers haven't exhibited the atomically smooth surfaces. The size of the plateau was increased by increasing the molecular beam intensity ratio up to 1.0.

Since the growth temperature was relatively low, the inclusion of the excess material was not negligible. According to the result of X-ray diffraction (XRD) measurement, a diffraction peaks originated from hexagonal Te was observed with SnTe peaks when samples were grown with Te rich ($J_{\text{Te}}/J_{\text{Sn}}$ was between 2.9 and 1.5) conditions. In the secondary electron microscopy measurements, featureless surface was confirmed when the XRD of the sample exhibited no Te peak while dotted materials were clearly observed on the surface when the hexagonal Te peak was observed. The distribution density of the dot was high when the Te diffraction peak signal intensity was strong. Those dotted materials are presumed to be the residual of Te.

The orientation of the material was affected by the growth temperature. When the substrate temperature was raised, (111) SnTe domains were started to appear. The XRD peak intensities of (100) and (111) domains were comparable when the substrate temperature was 250 °C. In order to eliminate the (111) domain inclusion, the substrate temperature needed to be maintained below 240 °C.

In order to enhance the (111) domain formation, (111)B oriented GaAs substrates were employed. (100) domains could be mostly eliminated when the substrate temperature was raised to 270 °C.

A standard van der Pauw Hall measurement was performed to characterize the electrical property at room temperature. The (100) sample that didn't include the Te residual exhibited the resistivity of about $\text{ohm}\cdot\text{cm}$. The resistivity has increased as the presence of Te residual became noticeable. Based on the literatures, the room temperature resistivity of SnTe and Te were about $\text{ohm}\cdot\text{cm}^{[1]}$ and $0.3 \text{ ohm}\cdot\text{cm}^{[2]}$, respectively. The higher resistivity obtained for the grown film might be originated from the mixing of Te residual. Although the surface morphology was improved by the introduction of the ZnTe buffer layer, the electrical properties were not improved. Boundaries of plateau probably became the center of carrier scatterings.

Acknowledgement

This work was supported in part by the Waseda University Grant for Special Research Projects.

References

1. Athwal, I. S., et al., *Thin solid films*, 162 (1988) 1-6.

2. Wang, D., et al., *J. Alloys & Compounds*, 773 (2019) 571-584.

8:00 PM QT04.08.04

Poster Spotlight: Near-Absolute Spin-Valve Effect at f-Orbital Magnet/Superconductor Interfaces with Controlled Orbital-To-Spin Moments SijieWang¹, KarineDumesnil², HarryBradshaw¹, NadiaStelmashenko¹ and JasonW. Robinson¹; ¹University of Cambridge, United Kingdom; ²Institut Jean Lamour, France

The proximity effect between a thin-film superconductor (S) and a ferromagnet (F) can lead to a spin-splitting of the quasiparticle density of states and suppression of the superconducting critical temperature (T_C) (1). At an S/F interface, the average magnitude of the spin-splitting in S can be tuned via the micromagnetic state of F with shifts in T_C between magnetized ($T_{c,m}$) and de-magnetized ($T_{c,dm}$) ferromagnet states being dependent [1-3] on the ratio of the superconducting coherence length (ξ) to the domain wall width (d_w) $\frac{3}{4}$ i.e., $(T_{c,m} - T_{c,dm})/T_{c,dm} =$

$\Delta T_C / T_{c,dm} \mu \zeta / d_w$ can theoretically be infinite for an appropriate combination of S and F thin films in which S is thinner than ζ . Experimentally, however, such an absolute spin-valve effect is hard to achieve with $\Delta T_C / T_{c,dm}$ ratios tending to be a small fraction of $T_{c,dm}$, indicating physics beyond the standard picture of the S/F proximity effect. Here we report S/F bilayers and F/S/F spin-valves in which F is an f-orbital ferromagnet (HoGd) with a controlled composition to tune the ratio of the orbital to spin components of the magnetization. The results demonstrate that $\Delta T_C / T_{c,dm}$ can approach infinity for a large ratio of the orbital moment to spin moment, which enables a near-absolute spin-valve effect. Our results demonstrate that the band structure of the ferromagnet in conjunction with the ζ / d_w can be tuned to enable high-performance superconducting memory for energy efficiency electronics. A first principle theory is required in order to understand the relationship between $\Delta T_C / T_{c,dm}$ and the ratio of the orbital to spin moment of the F metal.

1. A. Buzdin, Rev. Mod. Phys. 77, 935-976 (2005).
2. M. Houzet and A. I. Buzdin, Phys. Rev. B 74, 214507 (2006).
3. S. Komori, A. Di Bernardo, A. I. Buzdin, M. G. Blamire, and J. W. A. Robinson, Phys. Rev. Lett. 121, 077003 (2018).

8:00 PM QT04.08.05

Poster Spotlight: Towards Quantum Transport in Metal and Ferromagnetic Semiconductor Thin Films Structures with Absorbed Chiral Molecules [Jiahui Xu](#)¹, Jason W. Robinson¹, Hisakazu Matsuki¹, Nadia Stelmashenko¹, Shira Yochelis² and Yossi Paltiel²; ¹University of Cambridge, United Kingdom; ²The Hebrew University of Jerusalem, Israel

Chiral molecules (CMs), such as alpha-helix polyalanine, exhibit chiral-induced spin-selectivity (CISS) characteristics, which means that a flow of electron charge across a layer of CMs can result in a spin-filtering effect and phase coherent transport (1, 2). Recently, for example, we have demonstrated low temperature phase-coherent transport through thin-film wires of Au and Cu with absorbed CMs (2). For Au, we also observed evidence for induced ferromagnetism associated with the thiol-Au bonding and for Au and Cu, we detected an enhancement of spin-orbit coupling. Here, we systematically study charge transport and magnetic anisotropy in thin films and wires of Au and Au/EuS where EuS is a ferromagnetic semiconductor. The thickness of Au is varied in the 1-10 nm range in order to optimise magnetic hysteresis in Au and magnetic anisotropy modification in Au/EuS structures. The results provide a platform for detailed studies of quantum behaviour including magnetic control of phase coherence transport and potentially a quantum anomalous Hall effect.

1. R. Naaman, Y. Paltiel, D.H. Waldeck, Nature Reviews Chemistry, 3, 250 (2019).
2. M. Ozeri *et al.*, The Journal of Physical Chemistry Letters, 14, 4941-4948 (2023).

8:00 PM QT04.08.07

WTe2 Topological Insulator: Synthesis, Characterizations and Applications [Dimitre Dimitrov](#)^{1,2}, Vera M. Gospodinova², J.F. Sierra³ and Sergio Valenzuela³; ¹Institute of Solid State Physics, Bulgarian Academy of Sciences, Bulgaria; ²Institute of Optical Materials and Technologies (IOMT), Bulgarian Academy of Sciences, Bulgaria; ³Catalan Institute of Nanoscience and Nanotechnology (ICN2), Spain

Since the discovery of a new material phase, topological quantum materials (TQMs), [1] tremendous effort has been made to explore a wide variety of novel and abundant physics appearing in topological insulators (TIs), topological superconductors (TSCs), and Weyl semimetals for creating novel electric and spintronics devices. WTe2 belongs to the family of transition-metal dichalcogenides (TMDs) and crystallizes naturally in a non-centrosymmetric orthorhombic structure (also known as the Td or distorted 1T phase, in which the tungsten atoms are octahedrally coordinated by the tellurium atoms) with polar space group Pmn21. The polar axis in WTe2 is oriented along the stacking direction of layers. Unlike other TMDs, WTe2 is a Weyl semimetal in its native crystal phase [2]. Among Weyl semimetals, Td-type WTe2 is a new class, a type-II Weyl semimetal, where the Weyl points appear at the crossing of the oblique conduction and valence bands due to the broken inversion symmetry and non-saturating giant positive magnetoresistance is a manifestation of the type-II Weyl character [3]. In this presentation the current status of the research and emerging applications of WTe2 are reviewed.

Acknowledgement: We acknowledge support of the European Union's Horizon 2020 FET-PROACTIVE project TOCHA under Grant No. 824140

References

- [1] A. A. Soluyanov, D. Gresch, Z. Wang, Q.S. Wu, M. Troyer, X. Dai & A. Bernevig, Nature 527(2015), pp.495-498
- [2] D. Zhang, P. Schoenherr, P. Sharma & J. Seidel, Nature Reviews Materials 8, (2023) pp. 25-40
- [3] X.-C. Pan, X. Wang, F. Song & B. Wang Advances in Physics: X, 3, 1, (2018) 1468279

SESSION QT04.09: Exotic Properties of 2D Topological Materials III

Session Chairs: Paolo Bondavalli and Bruno Dlubak

Thursday Morning, November 30, 2023

Sheraton, Fifth Floor, Riverway

8:30 AM *QT04.09.01

Low Secondary Electron Emission 2D Surfaces [Isabel Montero](#); CSIC. Instituto de Ciencia de Materiales de Madrid, Spain

The secondary electron emission is the feedback mechanism of the resonant avalanche of electrons or Multipactor discharge in high-power RF devices onboard satellites. The multipactor discharge is a severe problem which limits the maximum power of RF instrumentation in space missions, it can cause RF signal loss and distortion and it can increase the noise figure or bit-error-rate even total mission failure. The search for surfaces with a low secondary electron emission yield (SEY) is considered one of the main research areas to reduce the multipactor effect in high-power RF devices used in spacecraft and other important technological fields such as high-energy particle accelerators. In this study, RF devices were made using aluminum alloy AA6061. The RF insertion losses of the devices were improved, meaning they were reduced, when AA was silver-coated. However, the SEY of silver, although lower than that of AA, still needs to be reduced to prevent multipactor. The SEY of silver exposed to air is greater than 2. The aim of this study was to deposit a 2D MoS₂ layer on silver coatings that are suitable for reducing SEY and preventing multipactor discharge. Prior to the deposition of the silver coating, the aluminum alloy of the RF devices was zincated, followed by the deposition of intermediary layers of Ni and Cu. We used deep eutectic ionic liquids (2:1 ethylene glycol-choline chloride) instead of water to deposit these coatings. Finally, the MoS₂ was deposited on the external silver coating using an optimized electroless process. As a result, we have developed an electroless plating process for growing 2D nanostructures with a high aspect ratio. The characterization was performed in an ultra-high vacuum (UHV) system composed of three interconnected chambers at a pressure of less than 10⁻⁹ hPa, while the fast entry chamber remained at 2x10⁻⁷ hPa. SEY is defined as the number of emitted electrons per incident electron, that is, SEY = I_e/I_p, where I_e is the emitted current and I_p is the primary or incident current. SEY was measured in the primary electron energy range from 0 to 1000 eV. The samples were also analyzed by x-ray photoemission spectroscopy (XPS) and field-emission scanning electron microscopy (FESEM).

In this study, we report an extremely low SEY of this multi-layer coating. The SEY as a function of primary electron energy curves show a maximum value close to 0.8. Furthermore, a linear translation of the SEY curve towards the region where SEY > 1 for oxygen content > 0.3% is observed. The energy distribution curves (EDC) or energy spectra of secondary electrons also exhibit a significant decrease in the signal for kinetic energies < 50 eV, which is consistent with the SEY results.

9:00 AM *QT04.09.02

Low-Temperature Microwave Impedance Microscopy of Topological Materials [Monica Allen](#); University of California, San Diego, United States

Quantum-relativistic materials often host electronic phenomena with exotic spatial distributions. We employ microwave impedance microscopy (MIM), which characterizes the local complex conductivity of a material, to directly visualize chiral edge modes and phase transitions in a quantum anomalous Hall insulator. This near-field imaging technique detects the unique fingerprint of topological edge modes in the GHz regime and spatially disentangles them from trivial states in the bulk of the material. Motivated by these experimental findings, we model the microwave response of topological edge states in a Chern insulator and demonstrate an enhanced MIM response can appear at the crystal boundaries due to collective edge magnetoplasmon excitations. The resonance frequency of these plasmonic modes should depend quantitatively on the topological invariant of the Chern insulator state and on the sample's circumference, which highlights their non-local, topological nature. Looking forward, we will also discuss progress on the construction of a new milliKelvin MIM, which will support spatially-resolved detection of topological states at low temperatures.

9:30 AM QT04.09.03

Zeeman Field-Induced Two-Dimensional Weyl Semimetal Phase in Cadmium Arsenide Binghao Guo¹, Wangqian Miao¹, Victor Huang¹, Alexander Lygo¹, Xi Dai^{1,2} and Susanne Stemmer¹; ¹University of California, Santa Barbara, United States; ²The Hong Kong University of Science and Technology, China

We report a topological phase transition in quantum-confined cadmium arsenide (Cd₃As₂) thin films under an in-plane Zeeman field when the Fermi level is tuned into the topological gap via an electric field. Symmetry considerations in this case predict the appearance of a two dimensional Weyl semimetal (2D WSM), with a pair of Weyl nodes of opposite chirality at charge neutrality that are protected by space-time inversion (C_2T) symmetry. We show that the 2D WSM phase displays unique transport signatures, including saturated resistivities on the order of h/e^2 that persist over a range of in-plane magnetic fields. Moreover, applying a small out-of-plane magnetic field, while keeping the in-plane field within the stability range of the 2D WSM phase, gives rise to a well-developed odd integer quantum Hall effect, characteristic of degenerate, massive Weyl fermions. A minimal four-band k - p model of Cd₃As₂ which incorporates first-principles effective g factors qualitatively explains our findings.

9:45 AM QT04.09.04

Van der Waals Epitaxy and Electronic Properties of Weyl-Semimetal 1Td-WTe₂ Alexandre Llopez¹, Frédéric Leroy¹, Calvin Tagne Kaegom², Boris Croes³, Adrien Michon⁴, Stefano Curiotio¹, Andrés Saúl¹, Bertrand Kierren², Patrick Lefevre⁵, François Bertran³, Yannick Fagot-Revurat² and Fabien Cheynis¹; ¹CINAM, France; ²IJL, France; ³IPCMS, France; ⁴CRHEA, France; ⁵SOLEIL Synchrotron, France

Transition metal dichalcogenides (TMDCs) have created huge research interest due to their unique properties and potential for various applications in electronics, photonics and energy. TMDCs are mainly obtained through mechanical or chemical exfoliation of bulk crystals into thin atomic layers. Despite challenging, molecular beam epitaxy of these materials offers significant advantages, including the production of high-quality films, possible long range in-plane ordering and precise control over layer thicknesses, making it more suitable for applications. Among TMDCs, WTe₂ is the only one for which the Td phase is the most energetically favored at room temperature. This Weyl semimetal has been predicted to be a quantum spin Hall insulator [1]. It has been demonstrated to be ferroelectric down to 2 ML [2] and shows an unconventional charge-spin conversion [3]. In this study [4], 1Td-WTe₂ thin films have been elaborated by molecular beam epitaxy on ML-graphene [5] reaching a mean flake size of ≈ 110 nm, which is up to one order of magnitude larger than results reported in the literature for epitaxial WTe₂ [6-8]. Using STM, we rationalized growth conditions and proposed a model to estimate the mean flake size as a function of growth parameters based on nucleation theory [9] and Kolmogorov-Johnson-Meh-Avrami (KJMA) equation [10]. Band structure characterizations by angle-resolved photoemission spectroscopy (ARPES) show electron-pockets at the Fermi level, in agreement with DFT calculations performed on free-standing 1Td-WTe₂ and previous reports [10]. This confirms the crystalline quality of the films. In particular, the occurrence of electron-pockets deeper than on BL-graphene [11] suggests a reinforced charge transfer on ML-graphene and allows to determine a high electron density of $n = 2.0 \pm 0.5 \times 10^{12} \text{ cm}^{-2}$ for each electron pocket. Fermi surface measurements evidence three equivalent domains rotated by 120° with respect to each other that correspond to different orientations of the WTe₂ orthorhombic unit cell on ML-graphene.

- [1] X. Qian *et al.* Science **346**, 1344–1347 (2014).
- [2] Z. Fei *et al.* Nature **560**, 336–339 (2018).
- [3] B. Zhao *et al.* Adv. Mater. **32**, 2000818 (2020).
- [4] A. Llopez *et al.* 2D Materials, *submitted*
- [5] A. Michon *et al.* J. Appl. Phys. **113**, 203501 (2013).
- [6] X. Li *et al.* Appl. Phys. Lett. **117**, 161601 (2020).
- [7] Y. Zhao *et al.* Phys. Rev. Lett. **125**, 046801 (2020).
- [8] S. Maximenko *et al.* Quantum Mater. **7**, 29 (2022).
- [9] J. A. Venables *et al.* Rep. Prog. Phys. **47**, 399 (1984).
- [10] M. Fanfoni and M. Tomellini J. Phys.: Condens. Matter **17**, R571 (2005).
- [11] Tang, S. *et al.* Nature Phys. **13**, 683–687 (2017).

10:00 AM QT04.09.05

Emergence of Dynamic Memory and Perturbation Effect in Dy_{2-x}Fe_xTi₂O₇ Pyrochlore Oxides Pramod Yadav¹, Chandan Upadhyay² and Pavan Nukala¹; ¹Indian Institute of Science, Bangalore, India, India; ²Indian Institute of Technology Banaras Hindu University, India

The investigation of topological materials and their exotic properties, along with understanding crucial exponents, holds great interest for the advancement of next-generation devices. A particular focus lies in the study of out-of-equilibrium properties observed in Dy₂Ti₂O₇ spin ice, which presents unique opportunities to comprehend the intricate magnetic behavior found in disordered magnetic materials. Through our experimental analysis, we have discovered the magnetic field-induced anomalous thermomagnetic hysteresis, a phenomenon exclusively observed in temperature- and magnetic field-dependent AC susceptibility measurements. Notably, this observed memory effect exhibits a strong dependence on both thermal and non-thermal driving variables. We have identified that even a minor substitution of the Heisenberg Fe-spins within the Ising matrix, formed by Dy ions, significantly alters the memory effect. Our results clearly demonstrate that defects play a crucial role in the dynamic magnetic properties, which are particularly pronounced in the out-of-equilibrium state. This phenomenon is believed to arise from the combined influences of geometric frustration, disorder, and the cooperative nature of spin dynamics exhibited by these materials. The emergence and controllability of the memory effect with thermomagnetic variables and substitution present a promising foundation for future applications of quantum-based devices.

SESSION QT04.10: Virtual Session
Session Chairs: Paolo Bondavalli, Judy Cha, Bruno Dlubak and Guy Le Lay
Tuesday Morning, December 5, 2023
QT04-virtual

8:00 AM QT04.10 .01

High-Mobility Two-Dimensional Carriers from Surface Fermi Arcs in Ferromagnetic Weyl Semimetal SrRuO₃ Films Yuki K. Wakabayashi¹, Shingo Kaneta-Takada², Yoshiharu Krockenberger¹, Toshihiro Nomura², Yoshimitsu Kohama², Hiroshi Irie¹, Kosuke Takiguchi¹, Shinobu Ohya², Masaaki Tanaka², Yoshitaka Taniyasu¹ and Hideki Yamamoto¹; ¹NTT Basic Research Laboratories, Japan; ²The University of Tokyo, Japan

Leveraging two-dimensional quantum transport phenomena and exploiting them in topological and spin electronics require thorough investigation into magnetic Weyl semimetals. Two-dimensional charge/spin carriers arising from pairs of Weyl nodes are realized in the presence of surface Fermi arcs in topological semimetals. To demonstrate such topological quantum transport phenomena, high-quality epitaxial films of Weyl semimetals are vital. Prior to the present study, we recently demonstrated that ultrahigh-quality thin films of SrRuO₃ exhibit quantum transport phenomena specific to bulk three-dimensional Weyl fermions [1,2], implying that they serve as a promising platform also for investigating novel two-dimensional transport in a topological state.

Here we present our findings on the thickness- and angle-dependent magnetotransport properties of SrRuO₃, a magnetic Weyl semimetal. Utilizing machine-learning-assisted molecular beam epitaxy [3], we grew SrRuO₃ films with 10 nm and 63 nm thicknesses. Quantum oscillations in the 10-nm film demonstrate a high quantum mobility of $3.5 \times 10^3 \text{ cm}^2/\text{Vs}$, a light cyclotron mass of $0.25m_0$ (the free electron mass in a vacuum), and two-dimensional angular dependence. The two-dimensional, angular transport dependence might be regarded within two scenarios: (1) the surface Fermi arcs, or (2) the quantum confinement of the three-dimensional Weyl fermions. The former is plausible as the identical angular dependence is also observed in the 63-nm film, which is too thick to observe the quantum confinement effect in it. In addition, the linear thickness dependence of the phase shift provides evidence of the non-trivial nature of the quantum oscillations mediated by the surface Fermi arcs. Furthermore, magnetoresistance (MR) measurements while applying magnetic field parallel to the film surface up to 52 T confirmed the saturation of negative MR in the quantum limit (chiral anomaly), assuring that the carriers arise from a pair of Weyl nodes. These results endorse SrRuO₃ as a promising material for topological oxide electronics and for physics investigation of two-dimensional quantum transport phenomena in magnetic Weyl semimetals [4].

References: [1] K. Takiguchi, Y. K. Wakabayashi *et al.*, Nat. Commun. **11**, 4969 (2020). [2] S. Kaneta-Takada, Y. K. Wakabayashi *et al.*, Appl. Phys. Lett. **118**, 092408 (2021). [3] Y. K. Wakabayashi *et al.*, APL Mater. **7**, 101114 (2019). [4] S. Kaneta-Takada, Y. K. Wakabayashi *et al.*, npj Quantum Materials **7**, 102 (2022).

8:15 AM QT04.10 .02

Strain-Induced Topological Phase Transitions in Kagome Lattices Miguel A. Mojarro and Sergio Ulloa; Ohio University, United States

We study the effects of a uniform strain on the electronic and topological properties of the 2D kagome lattice using a tight-binding formalism that includes intrinsic and Rashba spin-orbit coupling (SOC). The degeneracy at the Γ point, where a flat-band-parabolic-band touching occurs, evolves into a pair of (tilted) type-I Dirac cones owing to a uniform strain, as shown by effective Hamiltonians, where the anisotropy and tilting of the bands depend in a nontrivial way on the magnitude and direction of the strain field. Interestingly, we find that the Dirac cones become type-III (including flat dispersions) when the strain is applied along the bonds of the lattice. As expected, the inclusion of intrinsic SOC opens a gap at the emergent Dirac points, making the strained flat band to become topological, as characterized by a nontrivial Z_2 index. We show that the strain drives the systems into a trivial or topological phase for strains of a few percent, allowing topological transitions via uniform deformations. Additionally, when the Rashba interaction is included, semimetallic phases appear in the topological phase diagrams. These findings suggest an alternative way of engineering anisotropic tilted Dirac bands with tunable topological properties in strained kagome lattices.

8:30 AM QT04.10.03

Optical Nonlinearities in Hexagonal and Triangular Graphene Quantum Dots Suresh Gnawali and Vadym Apalkov; Georgia State University, United States

Graphene quantum dots (GQDs), the graphene nanoparticles of a few nanometers excited by an ultrafast optical pulse of a few femtoseconds, exhibit several optical nonlinearities, including residual population and high harmonic generation (HHG). By introducing dephasing, we addressed nonlinearity, namely HHG in GQDs placed in a short linearly polarized optical pulse. At short finite dephasing times, the ultrafast electron dynamics show significant irreversibility with a large residual population of the excited quantum dot levels. When dephasing time increases, intensities correspond to a low-frequency boost, while the cutoff energy decreases regarding the high harmonic spectra. The cutoff energy's dependence on the optical pulse's amplitude is also sensitive to the frequency of the pulse. This dependence in hexagonal GQDs is almost linear when the optical pulse frequency is much less than the quantum dot band gap. However, when the pulse frequency is comparable to the band gap, the cutoff energy shows saturation behavior at a large field amplitude, $>0.4 \text{ V/\AA}$. In triangular graphene quantum dots with zigzag edges, the intensities of high harmonics show a strong dependence on the initial electron population of the edge states of the quantum dot. If a zigzag triangular quantum dot possesses an even number of edge states, then even high harmonics are strongly suppressed when half of the edge states of the quantum dots are populated before the pulse. For any other populations of the edge states, the odd and even harmonics are of comparable intensities.

8:45 AM QT04.10.04

Probing the Quality of Bi_2Se_3 Films Grown by Molecular Beam Epitaxy *In-Situ* with Spectroscopic Ellipsometry Aofeng Bai¹, Maria Hilse², Prasanna Patil³, Roman Engel-Herbert⁴ and Frank Peiris¹; ¹Kenyon College, United States; ²The Pennsylvania State University, United States; ³Southern Illinois University Carbondale, United States; ⁴Paul-Drude-Institut für Festkörperelektronik, Germany

Quantum materials such as topological insulators (TI) like Bi_2Se_3 feature massless Dirac-like states due to their spin-momentum coupling and time reversal invariance. Those massless topological surface states (TSS) enable the study of new quantum physics and with that allow access to a plethora of technological advancements and the realization of applications with new functionalities for more energy efficient and faster computation schemes. The key to exploiting the unique properties of TIs lies in high-quality materials synthesis. However, Bi_2Se_3 synthesis is plagued with a large number of unintentional carriers, shifting the Fermi level up into the conduction band and masking the TSS. Methods like compensation doping, or cation/anion mixing are being pursued successfully to prevent the Fermi level drift out of the band gap, but the price paid is a substantial carrier mobility reduction in the film limiting TSS observation to very low temperatures. To date, best results for achieving low bulk carrier concentrations and high mobilities are reported for a meticulously designed buffer layer (BL) growth approach consisting of Bi_2Se_3 , In_2Se_3 , and $(\text{Bi}_x\text{In}_{1-x})_2\text{Se}_3$ layers. This approach, on the other hand, is slow and thus expensive due to the complexity of the BL- Bi_2Se_3 synthesis engineering and subsequent TSS probing iteration. Developing a fast, ideally *in-situ* feedback loop between growth and electronic properties is highly advantageous to speed up this approach and realize meaningful progress towards highest-quality Bi_2Se_3 thin film fabrication.

In this talk, we elucidate how *in-situ* spectroscopic ellipsometry (SE) can be employed as a non-invasive, non-contact, real-time, ultra-fast probe of the electronic properties of Bi_2Se_3 during growth. Evaluating the *in-situ* SE data obtained before and after growth of each layer from differently designed Bi_2Se_3 , In_2Se_3 , and $(\text{Bi}_x\text{In}_{1-x})_2\text{Se}_3$ heterostructures, we found that the observed SE measurables for Bi_2Se_3 depend sensitively on the sample heterostructure design. To gain deeper insights about the observed differences, we developed oscillator models for the dielectric functions of Bi_2Se_3 , In_2Se_3 , and $(\text{Bi}_x\text{In}_{1-x})_2\text{Se}_3$, and compared the weighted average of the broadening parameter of the oscillators that make-up the dielectric function. As a result, we found that the weighted average broadening parameters for the Bi_2Se_3 oscillators of films grown on a In_2Se_3 , and $(\text{Bi}_{0.7}\text{In}_{0.3})_2\text{Se}_3$ heterostructure were 20 % smaller than those of films grown directly on Al_2O_3 . Smaller broadening parameters are generally associated with the degree of momentum-conservation between electronic transitions due to less pronounced electron scattering. Our finding thus indicates that the Bi_2Se_3 grown on the In_2Se_3 , $(\text{Bi}_{0.7}\text{In}_{0.3})_2\text{Se}_3$ heterostructure has superior quality compared to films grown on bare Al_2O_3 . This conclusion was corroborated by Hall mobility measurements conducted at room-temperature, which ranged highest for Bi_2Se_3 films grown on In_2Se_3 , $(\text{Bi}_{0.7}\text{In}_{0.3})_2\text{Se}_3$ heterostructures. Based on the presented data, *in-situ* SE has the potential to serve as an ultra-fast, real-time probe of the electronic properties of Bi_2Se_3 , and is thus highly advantageous for speeding up the engineering process of high-quality TIs growth.

9:00 AM QT04.10.05

Analysis of the Moving Boundary Problem for Spinodal Transformations in Thin Films Rahul Basu^{1,2}; ¹VTU, India; ²Jawaharlal Nehru Technological University, India

The equations of Spinodal Decomposition as postulated by Cahn and Hilliard involve a fourth order pde which to date has not been solved analytically. In this article these equations are examined in their various versions, and solutions obtained for the steady state and transient forms using various methods. Then the moving boundary associated with transformation is examined using a heat transfer approach and a solution attempted using a series and a similarity transformation approach. The equation is postulated to have two contributions one from the usual Laplacian and Fickian contribution part for which Stefan solutions are known, and one with a Double Laplacian which has not been examined. The thin film approximation is applied to simplify some parts of the analysis and to try to get a numerical solution.

9:15 AM *QT04.02.05

ARPES Study of Berry Curvature and Spin Polarization in Ultrathin Ferroelectric Films of GeTe with Giant Rashba Effect Yannick Fagot-Revurat¹, Fabien Cheynis², Calvin Tagne Kaegom¹, Boris Croes², Alexandre Llopez², Geoffroy Kremer¹, Bertrand Kierren¹, Stefano Curiotto², Frédéric Leroy², François Bertran³, Patrick Lefevre³ and Daniel Malterre¹; ¹Institut Jean Lamour- UMR 7198, CNRS/Université de Lorraine, France; ²Aix Marseille University, CNRS, CINAM, AMUTECH., France; ³Synchrotron Soleil, France

GeTe is a ferroelectric material with a giant Rashba constant in such a way bulk ferroelectricity is supposed to drive its spin polarization [1,2]. Recently, a non-volatile ferroelectric control of spin-to-charge conversion at room-temperature, has been demonstrated in epitaxial GeTe films [3]. In addition, a multiple non-trivial topology of its electronic band structure due to the existence of triple-point and type-II Weyl fermions has been reported [4]. The question of persistence of singular electronic properties of GeTe in ultrathin films at nanoscale has been recently addressed so that a cancellation of Rashba constant at a critical thickness of 2.3 nm is proposed [5]. In our work we investigated the evolution of Berry curvature, Rashba constant and spin-polarization of GeTe ultrathin films grown on Si(111) wafers [6] as function of thickness by using ARPES, CD-ARPES and spin-resolved ARPES. As a striking point we demonstrate the persistence of spin-polarized Rashba bands down to 3 nm. All the results will be discussed in the light of trivial/non trivial topological properties of GeTe.

[1] C. Rinaldi et al., Nano Lett. 2018, 18, 5 2751 ;

[2] J. Krempasky et al., Phys. Rev. X 2018, 8, 2 021067 ;

[3] S. Varotto et al., Nature Electronics 2021, 4, 10 740 ;

[4] J. Krempasky et al., Phys. Rev. Lett. 126, 206403 ;

[5] X. Yang et al., Nano Lett. 2021, 21, 1 77 ;

[6] B. Croes et al., Phys. Rev. Materials 2023, 7, 1 014409 ;

SYMPOSIUM SB01

Engineering Future Food Materials—Ingredients, Processes and Fabrication
November 28 - December 5, 2023

Symposium Organizers

Bianca Datta, Ronin Institute for Independent Scholarship
Leila Deravi, Northeastern University
Francisco Martin-Martinez, Swansea University
Varsha Rao, University of Colorado Boulder

* Invited Paper
+ JMR Distinguished Invited Speaker

SESSION SB01.01: Engineering Future Food Materials I
Session Chairs: Bianca Datta and Francisco Martin-Martinez
Tuesday Morning, November 28, 2023
Hynes, Level 1, Room 105

8:45 AM *SB01.01.01

Silk-Based Technology to Boost Food Security [Benedetto Marelli](#); Massachusetts Institute of Technology, United States

The infrastructure of agro-food systems is responsible for more than 25% of anthropogenic greenhouse gas emissions while facing pressure to support an increasing world population. For the first time in history, the availability of arable land has plateaued, and crop yields are threatened by stressors such as soil salinity and drought that are further exacerbated by climate change. Food security and food waste are twin crises; more than 800 million people are undernourished, and 30% of food is lost or wasted from farm to fork. As new technologies that are economically sustainable, scalable, and rapidly deployable to market are needed to address these challenges, an opportunity lies for biomaterials to lead innovation in the agro-food industry. Our laboratory strives to reinvent silk proteins as advanced materials for boosting food security. Here, we will highlight recent developments in the nanomanufacturing of silk to design: (i) physical unclonable functions for food traceability, (ii) packaging that is biodegradable yet possess good membrane properties, sense spoilage and mitigate biotic decay, (iii) microenvironments that boost seed germination in marginal land, and (iv) different solutions to precisely deliver payloads in planta. These examples will provide an opportunity to discuss how the establishment of a prolonged biointerface between biomaterials and plants tissues requires the development of basic scientific knowledge on material-plant host response, mechanics of disorder-to-order transitions in proteinaceous materials during condensation phenomena, fluid mechanics, and transport phenomena in plants vasculature, and swelling of porous materials exposed to plant fluids.

9:15 AM SB01.01.02

From Idea to Product—Leveraging Materials to Reduce Food Waste [Louis Perez](#); Apeel Sciences, United States

According to the United Nations - Food Agricultural Organization (UN-FAO), we will need 56% more food to feed the growing global population by 2050. In addition, with more than 800 million people who are affected by hunger today, we need solutions that can address food production and supply challenges in short order. One way to address these challenges is to reduce food waste and loss which is reported between 30 and 50% based on geography and product category by the UN-FAO. Beyond the challenge of continuing to feed a growing population, the environmental and economic impacts of food waste are staggering: 8% of greenhouse gas emissions globally and a total cost of \$2.6 trillion dollars annually are due to food waste.

In this talk, we will address how Apeel Sciences, a start-up based in Santa Barbara, CA, is approaching tackling food waste and loss by developing new plant based technologies and products that 'work with nature'. The talk will review the process and the journey of an 'idea' to a product via a multidisciplinary approach inspired by Materials Science and Engineering principles to develop a plant based edible coating and other technologies utilizing data science and computer vision to make quantitative produce quality tools and shelf life prediction models to address food loss.

9:30 AM SB01.01.03

Metabolomics in a Circular Bioeconomy: A Case for Fruit/Vegetable Waste Material Residuals [Nancy A. Elnaker](#)¹, [Michael A. Ochsenkühn](#)², [Shady A. Amin](#)², [Matteo Chiesa](#)^{1,3} and [Lina F. Yousef](#)⁴; ¹Khalifa University of Science and Technology, United Arab Emirates; ²New York University Abu Dhabi, United Arab Emirates; ³UiT The Arctic University of Norway, Norway; ⁴DeL'Arta-Outdoor Living Laboratory, United Arab Emirates

Research is accelerating towards establishing a circular bioeconomy to achieve the United Nations Sustainable Development Goals (SDGs) and drive sustainable development. Here, we applied untargeted metabolomics as an assessment tool for homogeneous food waste residuals, providing an assessment of their marketability in the circular bioeconomy. The circular bioeconomy involves the comprehensive conversion of biological resources into renewable biobased products, which contributes to climate action and environmental well-being. One strategy for embracing a circular bioeconomy is the discovery of vertical conversions of food and agricultural waste residues, transforming them into value-added commodities. This article applies an untargeted metabolomics approach to gain insights into the phytochemical profile of fruit and vegetable residual wastes (FVRs). Through this analysis, 472 known and 542 unknown compounds were identified, with their relative abundances determined. Among the most prevalent 50 annotated metabolites in FVRs, a significant proportion consisted of natural products or bioactive compounds (64–86%), functional foods (7–12%), fragrances (0–8%), pesticides (0–6%), and intriguingly, environmental contaminants (7–23%). Homogenous waste residuals resulting from fruit and vegetable processing emerge as a promising source of bioactive nutraceuticals, functional food derivatives, and biomaterials. This study proposes using untargeted metabolomics as a rapid method to evaluate extracts obtained from homogenous food waste residuals. This approach provides a pre-assessment of their potential market value within the context of the circular bioeconomy.

<quillbot-extension-portal></quillbot-extension-portal>

9:45 AM BREAK

10:15 AM SB01.01.04

Near-Infrared Optical Gas Sensor for Intelligent Food PackagingNiloufarSharif and ArdemisBoghossian; École Polytechnique Fédérale de Lausanne (EPFL), Switzerland

Aim:

This project focuses on the design and fabrication of an intelligent packaging system based on a gas-phase optical sensor. The optical sensor emits near-infrared light that is able to penetrate through visibly opaque materials, including plastics, paper, and cardboard. The sensor will provide real-time monitoring of the quality of packaged food products using a specialized, near-infrared camera.

Method:

The near-infrared signal from the optical sensor is based on the fluorescence emissions of carbon nanotubes (CNTs). The CNTs are wrapped with single-stranded DNA that is able to spontaneously assemble onto the nanotubes following sonication. This wrapping not only solubilizes the CNTs in aqueous solutions but also controls the optical responsivity of the CNTs towards different gases. The resulting solutions are then incorporated into an agar hydrogel. We subsequently investigate the response of the sensor in the presence of ammonia, a gas associated with food spoilage. Finally, we investigate the selectivity of the sensor in the presence of other gases.

Results:

Our results show that the fluorescence intensity of the AT₍₁₅₎-wrapped CNTs increases upon exposure to ammonia. Interestingly, we observe distinct responses from different CNT chiralities. We also observe a concentration-dependent and selective response of the AT₍₁₅₎-wrapped CNT sensor to the target gas, with no significant response to the other gases used in this study.

Conclusion:

Here, we developed an optical sensor based on the fluorescence of CNTs for intelligent food packaging applications. The sensor can be used to monitor food quality in real-time, notifying the user on onset of food spoilage. This sensor thus offers both consumers and manufacturers a quick and accessible means of ensuring food quality and safety.

10:30 AM SB01.01.05

Highly Moisture Resistant Super Gas Barrier Polyelectrolyte Thin FilmsEthanT. Iverson, Hsu-ChengChiang, KendraSchmiege, HudsonLegendre and JaimeGrunlan; Texas A&M University, United States

Flexible, thin coatings with high barrier to oxygen are widely used for improving the lifespan and shelf life of flexible organic electronics and perishable food products, respectively. While metalized plastic and metal oxide thin films exhibit excellent barrier, they also have unique drawbacks. The lack of transparency and recyclability of metalized plastic, and the rigidity and poor adhesion of metal oxide films (e.g., SiO₂ and Al₂O₃), severely limit their benefit, especially in food packaging. The utilization of polyelectrolytes to develop high gas barriers with exceptional transparency, adhesion, and flexibility has long been realized. These barriers can be deposited utilizing layer-by-layer (LbL) assembly, providing nanoscale control over film structure and a high degree of tunability in barrier performance. Another approach utilizes a one-pot polyelectrolyte complex deposited via rod or dip coating in a single step. This film is then buffer cured, which generates ionic crosslinks between the polyelectrolytes and therefore minimizes oxygen diffusion through the film. While polyelectrolyte-based barriers typically lose their efficacy in high humidity, a LbL generated barrier, which is only 132 nm thick, provides a 99x reduction of the oxygen transmission rate of PET at 0% and 90% relative humidity (RH). This barrier retains nearly 81% of its performance at high humidity, a feat that is typically only possible with chemical crosslinking. Another impressive barrier was prepared via a simple dip-coating process of polyethyleneimine (PEI) and poly(acrylic acid) (PAA), which was then cured with a citric acid buffer solution. Through simple ionic crosslinking, undetectable oxygen transmission rate (OTR < 0.005 cc/m²*day), at both 0% and 90% RH, can be achieved with a PEI:PAA molar ratio of 1:1. The strong complexation from ionic crosslinking creates an unusually dense thin film that is promising for various packaging applications (food, electronics, etc.). These thin film exhibit some of the best-ever polymer-based oxygen barriers at high humidity.

10:45 AM SB01.01.06

FODMAP: Food and Agriculture-Friendly, Organic Compound-Based, Degradable Nanozymes Integrated with an Optical Sensing Platform for Toxic Molecules Detection on The Food SamplesDong HoonLee and MohammedKamruzzaman; University of Illinois at Urbana-Champaign, United States

Nanozyme has recently expanded applications in the field of food and agricultural science, offering the potential to enhance food safety by detecting toxic molecules. However, most of the nanozymes are derived from conventional chemistry and material science such as MOF/metal-based NP. These nanozymes encounter challenges related to their intrinsic toxicity and low-cost effectiveness when applied in food and agriculture. Thus, novel nanozymes that are highly suitable for food and agriculture for future applications are desired.

To address this need, we have introduced a novel type of nanozyme, called OC nanozymes, which are food and agriculture friendly. These nanozymes are composed of polymer and organic compounds and exhibit decent peroxidase-like catalytic activity. The customized, chelation-driven self-assembled particle generation process was contrived to provide spherical-shaped nanozymes containing partially mimicked cofactor sites (e.g., Fe-N or Fe-O) of the natural enzyme without using the conventional engineering process, including pyrolysis, organic solvent, and ionic gelation. In contrast to conventional nanozymes, OC nanozymes exhibit decent eco-compatibility, and cost effectiveness with satisfactory catalytic performance (e.g., Km = at least 0.074mM/H₂O₂). These nanozymes, when integrated with colorimetric sensing platforms, enable rapid and selective detection of antioxidant (LOD = at least 7.27 μM), and toxic herbicide detection (LOD = 10 pg mL⁻¹) within 7 minutes. Additionally, some OC nanozymes are designed to degrade at a moderate temperature (around 45 Celsius) after use, which provides benefits for further waste management issues. We envision that OC nanozymes can be utilized in further practical food applications.

11:00 AM *SB01.01.07

Business Collaborative Research on Novel Strategies in Functional and Active Packaging for the Food IndustryConchaBosch-Navarro, EncarnaGómez and BegoñaRuiz; AINIA, Spain

Microbial contamination supposes an issue of major concern in the food industry that affects both industrial processes and food products. Consequently, food industry is seeking for novel strategies that prevent surface contamination and microorganism proliferation during fabrication, and also innovative packaging materials that contributes to increase shelf-life of packaged food while being more environmentally friendly.

The development of functional and/or active coatings that could be applied over industrial equipment to prevent microbial growth or over packaging materials to incorporate advanced functionalities appears out as outstanding strategies that different companies in the food and packaging industry are exploring and implementing. A functional coating refers to a formulation that incorporates, for example, antimicrobial activity. To this end, different active substances can be considered. Traditionally, different preservatives and plant extracts have been used. Currently, novel strategies include the use of pro/prebiotics, peptides, endolysins or nanobodies, amongst others. Besides, a functional coating in packaging refers to a specialized type of coating applied to the surface of packaging materials to provide additional functionalities and benefits, such as gas barrier, water resistance or oil repellency. Different strategies are being followed, including the formulation of coatings based on natural ingredients such as proteins, fatty acids or lignocellulosic materials in order provide with functionality while contributing to create a circular economy model.

Several developments in the field of novel functional coatings carried out by AINIA together with different companies in the food and packaging sectors, will be presented. These developments are the result of R&D projects in which synergies between different knowledge fields have been exploited, such as biotechnology, hygienic surfaces, material's science, and packaging. The common point being the agrifood industry focus and the need to fight against food waste while guiding sustainability to the highest standards that current regulations are demanding.

11:30 AM *SB01.01.08

Biomaterials and Food-Opportunities and ChallengesFiorenzoOmenetto; Tufts University, United States

Natural materials offer new avenues for innovation across fields, bringing together, like never before, natural sciences and high technology.

Significant opportunity exists in reinventing naturally-derived materials, such as structural proteins, and applying advanced material processing, prototyping, and manufacturing techniques to these ubiquitously present substances. This approach help us imagine and realize sustainable, carbon-neutral strategies that operate seamlessly at the interface between the biological and the technological worlds.

Some of these attributes make these materials ideally suited for interfaces with food from multiple perspectives, ranging from the aesthetic, to flavors, to therapeutics to name a few. These applications leverage functional aspects that include biomaterials-based applications in edible and implantable electronics, food preservation, energy harvesting, wearable sensors, compostable technology, distributed environmental sensing. These opportunities will be outlined in this talk presenting a survey of the possibilities that lie ahead.

1:30 PM *SB01.02.01

Food via Tissue Engineering – Challenges and Opportunities David L. Kaplan; Tufts University, United States

The need for future foods for the ever-growing population requires consideration of alternative approaches toward food sustainability, nutrition and security. To address this need, we pursue a cell-based, tissue engineering approach, eliminating animals from the process. Our central hypothesis is that sustainable, cost-effective, and scalable cultivated-meat and alternative proteins will provide new food availability options and healthier food alternatives, while decreasing environmental impact. Towards this goal there is much progress, with cell and tissue biomanufacturing central to the approaches. Further, there remain many challenges and opportunities ahead, from cells, media, safety and scale up, to tuning nutrition, composition and overall food quality and health. These topics will be discussed in the context of this emerging food frontier, where the impact is potentially transformative.

2:00 PM *SB01.02.02

The Development of High Protein Plant-Based Cheese Alejandro G. Marangoni and Stacie Dobson; University of Guelph, Canada

Animal proteins and animal by-products, such as milk and cheese, generate the greatest amounts of greenhouse gas emissions in the food sector. This, coupled with the demonstrably worsening climate crisis, means that there needs to be a shift to more sustainable alternatives in the form of plant-based foods. In particular, the plant-based cheese industry is relevant, as the products lack critical functionalities and nutrition compared to their dairy-based counterparts. Waxy starch, plant-protein isolate, and coconut oil were combined to create a novel high-protein (18w/w) plant-based cheese. We determined that by using native waxy starch, we can enhance its existing viscoelastic properties by modulating gelatinization through the addition of plant protein and fat. Texture profile analysis indicated that the cheese analogues could reach hardness levels of 15-90N, which allowed samples to be tailored to a wider range of dairy products. We determined that plant proteins and fat can behave as particulate fillers and enhance network strength but also create strategic junction zones during starch retrogradation. The degree of melt and stretch of the high protein plant-based analogues were 2-3 times greater than those observed for commercial plant-based cheeses and significantly more similar to dairy cheese. The rheological melting kinetics saw that the high protein plant-based cheese displayed more viscous properties with increasing temperature. $Tan(G''/G')$ at 80°C was used as an indicator for sample meltability where, values indicate better melt and more viscous systems. The high protein plant-based cheese reached tan values upwards to 0.8, whereas commercial plant-based cheese only reached tan values around 0.1. Synchrotron micro-CT as well as synchrotron mid-IR imaging was utilized to characterize structure and interactions between components.

2:30 PM SB01.02.03

Generating Animal-Free Protein Scaffolds using Antisolvent Precipitation under Couette Flow Patrick A. Sullivan, Ying Wang, Lasanthi Sumathirathne and Leila Deravi; Northeastern University, United States

A common feature of animal-based proteins is their ability to self-assemble into continuous protein fibers, as seen in muscle and connective tissues. Their fibrous nature has inspired research and development in the tissue engineering, textile, and synthetic meat industries, to find methods of replicating this aligned fiber structure in nonanimal-based proteins. Zein is a nitrogen storage protein that is primarily found in corn, that has become popular due to its status of Generally Regarded As Safe (GRAS), its biocompatibility, its fabrication flexibility and its unique solubility, solvating in 60-90% mixtures of ethanol and water. This makes it a prime candidate for antisolvent precipitation and extrusion methods to produce zein fibers for food industry applications. However, extrusions methods produce a rapid but random generation of fibers in terms of diameter and alignment when utilizing this antisolvent precipitation, and the conclusion has been drawn that further antisolvent zein fiber formation should focus on fiber orientation as a next step in development. In this work we aimed to produce aligned fibrous microstructures on zein scaffolds like those found in animal-based proteins. We investigate how salt concentration and identity influence the aggregation patterns of zein as it precipitates into nanoparticles through its addition to an aqueous antisolvent. We then use the conclusions drawn from these findings in combination with a custom-built device to induce anti-solvent precipitation under Couette-flow to produce continuous fibrous scaffolds, demonstrating their use as scaffolds for future tissue engineering applications.

2:45 PM SB01.02.04

Cephalopod-Inspired Material Design for Potential Food Applications Bianca C. Datta; Ronin Institute for Independent Scholarship, United States

As the global population rises alongside a worsening climate outlook, alternative proteins such as plant and cell-based meat provide exciting avenues for meeting the increasing demand for meat sourced from animals and have implications for planetary and human health. While food science is a well-established field with a rich history, inclusion of methods and research paradigms from the materials community can accelerate the development of promising food technologies. In this work, we review the complex and interesting structure and functionality of cephalopods, the landscape of existing materials advances towards replicating these creatures, and extensions towards food and edible materials. In doing so, we bridge the rich culinary traditions around cuttlefish, octopus, and squid⁷ with advancements in tissue engineering and bio-inspired design.

Few creatures generate as much wonder and curiosity as cephalopods. Renowned for their protective and communicative capabilities (camouflage, texture and shape change), they also demonstrate fascinating behavioral and cognitive abilities⁶. Researchers have looked to cephalopods for inspiration in designing systems as varied as displays¹, programmable coloration², self-healing coatings³, mechanochromic windows⁴, and bioelectronics⁵. We now look to their unique structure and properties to inspire a new domain of compelling alternative food materials.

References:

1. Mouritsen, Ole G., and Klavs Styrbaek. "Cephalopod gastronomy—a promise for the future." *Frontiers in Communication* 3 (2018): 38.
2. Schnell, Alexandra K., and Nicola S. Clayton. "Cephalopod cognition." *Current Biology* 29.15 (2019): R726-R732.
3. Wilson, Daniel J., and Leila F. Deravi. "Artificial cephalopod organs for bio-inspired display: progress in emulating nature." *Matter* 4.8 (2021): 2639-2642.
4. Wang, Yu, et al. "Generation of Complex Tunable Multispectral Signatures with Reconfigurable Protein-Based, Plasmonic-Photonic Crystal Hybrid Nanostructures." *Small* (2022): 2201036.
5. Manabe, Kengo, Emiko Koyama, and Yasuo Norikane. "Cephalopods-Inspired Rapid Self-Healing Nanoclay Composite Coatings with Oxygen Barrier and Super-Bubble-Phobic Properties." *ACS Applied Materials & Interfaces* 13.30 (2021): 36341-36349.
6. Ke, Yujie, et al. "Cephalopod-inspired versatile design based on plasmonic VO₂ nanoparticle for energy-efficient mechano-thermochromic windows." *Nano Energy* 73 (2020): 104785.
7. Kautz, R.; Gorodetsky, A. A. Revisiting A Classic Inspiration Source: Cephalopod-Derived Materials for Bioelectronics In Roadmap on Semiconductor-Cell Biointerfaces. *Phys. Biol.* 2018, 15, 031002.

3:00 PM BREAK

3:30 PM SB01.02.05

Understanding Structure in Methylcellulose Solutions using Machine Learning Enhanced Scattering Analysis (CREASE), Coarse-Grained, and Atomistic Molecular Dynamics Simulations Audrey Collins, Zijie Wu and Arthi Jayaraman; University of Delaware, United States

Methylcellulose (MC) is cellulose derivative in which some of the hydroxyl groups are replaced by methoxy (-OCH₃) groups. Aqueous solutions of MC exhibit unique phase behavior wherein at low temperatures MC chains are soluble in water and at high temperatures MC chains assemble into semi-flexible fibrils and fibrillar networks. Fibrillar networks exhibit mechanical and rheological properties that make them useful as food and pharmaceutical ingredients. Structural characterization of MC aqueous solutions through small angle X-ray scattering (SAXS) experiments show that MC fibrils exhibit a consistent fibril diameter with varying MC concentration and molecular weights; however, the molecular underpinnings of this observation are unclear. Our work aims to elucidate these molecular underpinnings using computational techniques from top-down (machine learning enhanced computational reverse engineering analysis of scattering experiments: CREASE) and bottom-up (molecular dynamics simulations). In the top-down approach, (Macromolecules 202255(24), 11076-11091), Wu and Jayaraman found consistent MC fibril diameter distributions using CREASE and analytical model fits, confirming the results by Lodge, Bates, and co-workers (Macromolecules, 2018, 51, 7767–7775) that MC forms fibrils with consistent average diameters of ~15–20 nm regardless of the chain length and concentration of MC chains. In the bottom-up approach, which is the focus of this talk, we use both coarse-grained (CG) and atomistic (AA) molecular dynamics (MD) simulations to capture macromolecular-scale fibril assembly and the molecular-level interactions between MC chains that drive that assembly, respectively. In the CG MD simulations, we observe MC chains assemble in parallel fashion to form fibrils with consistent diameter for varying MC chain length and concentration. Guided by those CG MD chain configurations where solvent is implicit, we use atomistic MD simulations with explicit water, and uncover a potential explanation for the consistent fibril diameter: inter-MC chain twisting. We find that a combination of favorable hydrogen bonds and hydrophobic interactions drives the twisting of MC chains during fibril formation. Our work provides a holistic understanding of MC chains assembly in water and aids material development for application of MC in various industries.

3:45 PM SB01.02.06

Whey Protein Isolate Composites as Tunable Scaffolds for Cultured Meat Christopher Foley, Irfan Tahir, Patrick Charron and Rachael Floreani; The University of Vermont, United States

INTRODUCTION The rising global population and increasing prevalence of food insecurity highlights the need for alternative food sources. New developments in biotechnology have given rise to many alternative food and protein options, including the research and development of cultivated meat. Cultivated meat is produced via *in vitro* animal cell culture and their incorporation into manufactured scaffolds. Plant-based, alginate scaffolds are a common material used during manufacturing, due to the tunability of their mechanical properties through modification of molecular weight, chemical composition, and structure; however, alginate does not have the necessary cell adhesion ligands. Whey protein isolate (WPI) is a byproduct of the dairy processing industry, is a food additive, and has recently been shown in the literature to encourage cell adhesion in bone and cartilage tissue engineering. The objective of our study was to investigate the effect of WPI-based scaffolds on muscle cell adhesion and viability for the production of scaffolding for cultured meat. **METHODS** The AlgMA was synthesized by dissolving sodium alginate in deionized (DI) water at a 1% (w/v) and a 20-molar excess of methacrylic anhydride. WPI was dissolved in 1x phosphate buffered saline (PBS) at 5.25% (w/v). After 24 hours, the solutions were dialyzed (MWCO = 6-8 kDa) against chilled DI water for three days to remove any residual reactants. Polymer solutions were then frozen and lyophilized. With these dry polymers, 3% (w/v) AlgMA solutions were prepared in DI water at room temperature, to which WPI or WPI-MA, was added to bring the protein concentration to 10% (w/v). One mM eosin Y, 125 mM triethanolamine, and 20 mM 1-vinyl-2-pyrrolidinone were mixed with the control (AlgMA) and experimental samples (WPI/AlgMA, WPI-MA/AlgMA). These solutions were then cast into circular molds and exposed to the green light (525 nm) for 10 minutes for crosslinking to occur. The crosslinked polymer solutions were characterized through proton nuclear magnetic resonance (¹H-NMR), scanning electron microscopy (SEM), rheological & compression testing, swell/weight-loss studies, and immunofluorescent staining of C2C12 myoblast cells. **RESULTS AND DISCUSSION** A 3D interconnected porous network was created, showing differences compared to an AlgMA control. WPI-based scaffolds exhibited more ordered structures compared to that of the AlgMA control. Pore sizes ranged between 50-200 μm. While moderate weight loss was experienced by the non-modified WPI, the WPI-MA and AlgMA hydrogels displayed minimal weight loss after a period of seven days. Under a compressive load, the WPI-MA/AlgMA scaffolds were more compliant compared to the AlgMA control, and the WPI-based scaffolds exhibited moduli that closely resembled the mechanical properties of native muscle tissue. WPI-based scaffolds were non-toxic to C2C12 cells, and increased cell density over the course of seven days compared to controls. WPI/AlgMA and WPI-MA/AlgMA materials were found to be non-toxic to murine C2C12 myoblast cells and promoted increased adhesion and proliferation compared to the AlgMA control. The incorporation of non-modified and chemically modified WPI in alginate scaffolds shows encouraging data that supports the use of WPI-based scaffolds for engineering muscle tissue *in vitro*. Also, the tunability of composition and mechanical properties will allow these materials to be fine-tuned for other properties such as texture and flavor. **CONCLUSION** Scaffolds were formulated using methacrylated alginate (AlgMA), WPI, and methacrylated WPI (WPI-MA). The resultant scaffold product was a photo-crosslinked, porous network that displayed marked differences compared to the AlgMA control scaffold. In summary, our study provides compelling evidence supporting the use of WPI-based scaffolds in 3D cultivated meat production, highlighting its substantial prospects and benefits.

4:00 PM *SB01.02.07

Biomaterials and Bioprinting of Skeletal Muscle Spheroids for use as Building Blocks for Engineered Muscle Tissue Kent Leach, Nicholas Johnson, Andrea Filler and Alex Kermani; University of California-Davis, United States

Skeletal muscle tissue engineering has the potential to address key clinical and societal challenges such as traumatic muscle injury, our fundamental understanding of skeletal muscle development and disease, and the future of meat production *via* cell cultured meat. Preclinical animal models and monolayer culture have driven our understanding of skeletal muscle biology and differentiation. However, two-dimensional (2D) cell cultures lack complex cell-cell and cell-extracellular matrix (ECM) interactions that provide essential biochemical and biomechanical signals directing cell function *in vivo*. Engineered tissue must sufficiently model the complexity of native muscle, which has led to the innovation of advanced fabrication methods such as 3D bioprinting.

Bioprinting is a promising biofabrication technique for generating structured tissue due to the potential to precisely pattern multicellular constructs of relevant cell types. The most common bioprinting applications use monodisperse cells, which requires disruption of essential cell-cell and cell-matrix interactions. A growing body of research confirms the benefits of retaining the endogenous ECM to mimic the native extracellular environment and support cell function, hence exposing a key current limitation of bioprinting.

Spheroids are dense cellular aggregates that exhibit promise as building blocks for tissue engineering due to their retention of endogenous ECM, upregulated cytokine production, and increased cell-cell interactions. Spheroids are advantageous for use in tissue engineering due to their enhanced differentiation, angiogenic potential, and cell survival *in vitro* and *in vivo* compared with monodisperse cells. Spheroids have been fabricated from a wide variety of cell types yet literature on skeletal muscle spheroids, sometimes referred to as myospheres, is sparse. The study of myospheres has primarily been focused on understanding cell behavior of primary muscle cells, but their application in tissue engineering lags behind other tissues types such as bone, heart, and adipose, among others. While work utilizing muscle spheroids from immortalized cell lines has been limited, initial studies have shown promising results in regard to cell survival and differentiation. For example, C2C12 spheroids, once dissociated, exhibited higher proliferation, upregulated MyoD expression, and enhanced myogenic potential in both 2D and 3D culture. Furthermore, C2C12 spheroids have upregulated myogenic factors compared to monodisperse cells and can differentiate into aligned myotubes on electrospun substrates. However, little is known about how muscle cell spheroids function in contiguous matrices such as bioinks, representing a key information gap in the field.

We hypothesized that skeletal muscle cell spheroids will function as potent building blocks of muscle tissue when embedded in 3D microenvironments. We bioprinted skeletal muscle spheroids to assess cell function and tissue forming potential compared to monodisperse cells. We utilized 3D bioprinting as a proof-of-concept to determine whether bioprinting may adversely affect cell viability. Experiments were first performed using C2C12 spheroids before translating to more clinically and culinarily relevant primary bovine satellite cells. Both C2C12 and primary bovine SCs formed spheroids of similar sizes, remained viable after bioprinting, and exhibited similar spreading characteristics within an alginate matrix. When bioprinted with alginate as a bioink, spheroids of both cell types fused into larger tissue constructs over time and exhibited tissue formation potential similar to monodisperse cells. These data demonstrate that skeletal muscle spheroids are promising building blocks for muscle tissue and validate 3D bioprinting as a compatible fabrication technique. I will also highlight other studies illustrating the synergy of engineered biomaterials and muscle cell response.

SESSION SB01.03: Poster Session
Session Chairs: Bianca Datta and Varsha Rao
Tuesday Afternoon, November 28, 2023
Hynes, Level 1, Hall A

8:00 PM SB01.03.01

Electrohydrodynamics for Efficient Droplet Coalescence in Food-Grade Non-Aqueous Pickering Emulsions Bruno Telli Ceccato^{1,2}, Namrah Azmi^{1,3}, Andrew N. Akanno¹, Paul G. Dommersnes¹, Rosiane Lopes da Cunha², Lucimara Gaziola de la Torre² and Jon Otto Fossum¹; ¹NTNU, Norway; ²University of Campinas, Brazil; ³Stayfit Nutrisupplies, Tanzania, United Republic of

Coalescence is a fundamental process in emulsion synthesis. It can have positive effects depending on the approach. The emulsion stabilization can be reached when emulsifiers occupy all the droplet surface, and when low quantities of solid particles (Pickering emulsions) are used, stabilization can be reached under controlled arrested coalescence [1].

The application of electro hydrodynamics on non-aqueous emulsion systems can produce emulsion droplets with controlled size distribution and coverage, and also induce coalescence. In the latter case, when an electric field is applied, dipolar emulsion droplets can be generated and short-range dipolar droplet-droplet interactions can take place. Positive surface charges on a droplet can attract negative charges on a neighboring droplet, eventually leading to so-called electro coalescence [2], [3].

Here, we explore the electro-coalescence of food-grade droplets [4] of a non-aqueous system. Non-aqueous food-grade systems are scarcely investigated due to the miscibility of most edible oils, and the limitations of suitable polar protic solvents [5]. In this work, the electro-induced coalescence is shown for a non-aqueous Pickering emulsion with rapeseed or moringa oleifera oils as continuous phase, glycerol or lactic acid in ethanol as dispersed phase, and ethyl-cellulose or moringa oleifera leaf-based stabilizer particles.

Our preliminary results provide insights into the application of electro hydrodynamics in the emulsification processing of food-grade Pickering systems.

Acknowledgements

This work received funding from the European Union's Horizon 2020 research and innovation programme under the Marie Skłodowska-Curie grant agreement No 956248.

REFERENCES

[1] E. Durgut, C. Sherborne, A. Dikici, G. C. Reilly, and F. Claeysens, "Preparation of Interconnected Pickering Polymerized High Internal Phase Emulsions by Arrested

Coalescence," *Langmuir*, vol. 38, pp. 10953–10962, 2022, doi: 10.1021/acs.langmuir.2c01243.

[2] P. Dommersnes *et al.*, "Active structuring of colloidal armour on liquid drops," *Nat. Commun.*, no. May, 2013, doi: 10.1038/ncomms3066.

[3] Z. Rozynek, A. Mikkelsen, P. Dommersnes, and J. O. Fossum, "Electroformation of Janus and patchy capsules," *Nat. Commun.*, no. May, pp. 1–6, 2014, doi: 10.1038/ncomms4945.

[4] C. C. Berton-Carabin and K. Schroën, "Pickering emulsions for food applications: Background, trends, and challenges," *Annu. Rev. Food Sci. Technol.*, vol. 6, pp. 263–297, 2015, doi: 10.1146/annurev-food-081114-110822.

[5] A. Zia, E. Pentzer, S. Thickett, and K. Kempe, "Advances and Opportunities of Oil-in-Oil Emulsions," *ACS Applied Materials and Interfaces*, vol. 12, no. 35. American Chemical Society, pp. 38845–38861, Sep. 02, 2020. doi: 10.1021/acsami.0c07993.

8:00 PM SB01.03.02

Reaction Kinetics and Physical Properties of Carboxymethyl Cellulose-Based Hydrogel Blends for Food PackagingSamudraGupta and JavenWeston; University of Tulsa, United States

Carboxymethyl cellulose (CMC) is a commonly studied polymer made by chemically modifying cellulose to increase water dispersability. CMC is widely used in hydrogel applications because of its biocompatibility and biodegradability. CMC hydrogels are used as absorbents, for food packaging, as additives in pharmaceutical formulations, and for other applications. CMC hydrogels can be synthesized using a variety of chemical and physical crosslinking agents. Here, ethylene glycol diglycidyl ether (EGDE) is used as a chemical crosslinker. The optimal cross-linking temperature and EGDE concentration were determined using *in-situ* oscillatory shear rheology, and other properties, such as the water vapor permeability, swelling ratio, tensile strength, and % elongation at break of the hydrogels were also measured to assess their usefulness for food packaging applications. These hydrogels were found to have unsatisfactory bulk and mechanical properties for food packaging materials, so blends of CMC with various polysaccharides have been investigated to search for synergy between the different biopolymers. In particular, κ -Carrageenan and Xanthan gum were chosen for this study; both are common anionic polysaccharides with excellent gelling, stabilizing ability, emulsifying, and thickening properties. These blends were chosen due to CMC being easy to use, readily available, and cheap. Additionally, this study focuses on finding a correlation between rheology, and bulk properties, such as tensile strength, water vapor permeability, and % elongation at break.

8:00 PM SB01.03.03

Magnetic Field-Made Capsules to Fight Food WasteArneT. Skjeltorp; Institute For Energy Technology, Norway

The European Union (EU) funded PICKFOOD project [1] addresses the 80 million tonnes of food waste generated in the EU annually. It focuses on combating quality deterioration caused by lipid oxidation and other factors. The project aims to enhance the stability and affordability of Pickering emulsions, a promising alternative. Through collaboration with the food industry, PICKFOOD will develop frameworks and methodologies to assess Pickering emulsion applications in safe, healthy, and functional foods.

In this project, magnetic fields are envisioned to make capsules, but this requires very forceful magnets. Many permanent magnets on the market have large magnetic fields, but weak field gradients. The GIAMAG magnets have unique and patented designs that produces both very large magnetic fields and high field gradients, resulting in the most forceful magnets available on the market [2].

References

[1] <https://pickfood.eu/>

[2] Arne T. Skjeltorp, Paul Dommersnes and Henrik Høyer, "New Forceful Magnetic Bioseparation using GIAMAG Magnet Systems", *MRS Advances*, 2017, Vol.2 (24), p.1297-1301

8:00 PM SB01.03.04

Surface Functionalization of Pickering Emulsion Stabilized by Silk Fibroin Microparticles and Enhanced Adhesion for Foliar SprayYueHu and BenedettoMarelli; MIT, United States

Pickering emulsion is a category of emulsion that is stabilized by solid particles. Compared to emulsions stabilized by molecular emulsifiers, Pickering emulsion has high stability, low cytotoxicity, and good biocompatibility. Solid particle emulsifiers could also be modified by functional groups or antibodies to achieve different demands. Thus Pickering emulsion is widely used in the food, pharmaceutical, and cosmetic industries. Silk-fibroin regenerated from silk cocoons is a natural protein. This fibrosis protein has been widely investigated and applied in the fields of biomedicine, cosmetics, and food coating. In our study, we developed biocompatible protein particles synthesized from silk fibroin to stabilize oleic acid oil-in-water Pickering emulsion. Those Pickering emulsions could be applied to agricultural and food industries.

Specifically, water-insoluble silk fibroin microparticles (SFMPs) with a diameter of approximately 2 μm were synthesized through the salting-out method. These microparticles can act as emulsifiers, stabilizing alkane-in-water Pickering emulsion. In addition, polar oil oleic acid with payloads possessing a pK_a below 5 can be stabilized by SFMPs to generate a Pickering emulsion. The research also delves into the mechanism and ability of SFMPs to stabilize both nonpolar and polar oil-in-water Pickering emulsion, as evidenced by the measurement of three-phase contact angles. To functionalize Pickering emulsion, we synthesized antibody-labeled SFMPs, which can partially replace the emulsifier on the surface of Pickering emulsion droplets and improve the droplets' affinity to antibody binding sites. In this work, anti-peptic polysaccharide antibody-labeled Pickering emulsion loaded with plant hormone jasmonic acid exhibited strong binding to the waxy layer weaker part of the leaf even after the wash and effectively boosted the trichome number of *Arabidopsis* new leaf.

8:00 PM SB01.03.05

Harnessing Satellite Imagery and Geospatial Analysis for Sustainable Nutrient Management in Agricultural SystemsOlatundeD. Akanbi, DeepaBhuvanagiri, ErikaI. Barcelos, BrianGonzalez Hernandez, ArafathNihar, LauraBruckman, YinghuiWu, JeffreyYarus and RogerH. French; Case Western Reserve University, United States

The excessive use of fertilizers in agricultural practices poses significant challenges to environmental sustainability and food security. A substantial portion of applied fertilizers from farms, and concentrated animal feeding operations (CAFOs) and urban activities, more specifically in wastewater treatment plants, are lost through runoff, leading to water pollution, ecosystem degradation, and economical loss. To address these critical issues, this research aims to develop an innovative approach utilizing satellite imagery and geospatial analysis to enable efficient and sustainable nutrient management in agricultural systems. The study leverages the Normalized Difference Vegetation Index (NDVI) derived from satellite imagery to monitor crop growth on a daily basis and optimize fertilizer application. By regularly assessing the NDVI metrics, farmers can precisely determine the timing and location for fertilizer application, ensuring optimal nutrient uptake by crops and minimizing wastage. This approach allows for large-scale monitoring, offering a valuable tool to farmers for daily decision-making in fertilizer management. Furthermore, the research incorporates geospatial analysis and spatiotemporal modeling to monitor nutrient flow from farms and CAFOs to nearby water bodies. Utilizing and integrating data (different resolutions and types) from MODIS satellite imagery, Aster GDEM on elevation, USGS Stream Water, USDA Historical Crop, and Soil, a spatial model is developed to track and quantify nutrient runoff. By understanding the movement and accumulation of nutrients, effective mitigation strategies can be formulated to prevent pollution and minimize water contamination. The outcomes of this research contribute to the overarching goal of enhancing food production while minimizing the environmental footprint of agricultural practices. By implementing satellite-based monitoring and geospatial analysis techniques, we can empower farmers and stakeholders to make informed decisions about nutrient management. This approach not only helps reduce fertilizer usage and associated costs but also protects water quality, mitigates algae blooms, and preserves aquatic ecosystems. This provides a practical and scalable solution for addressing the fertilizer application problem, ensuring long-term agricultural sustainability, and meeting the increasing global food demand.

8:00 PM SB01.03.06

Biopolymeric Microneedles for Underwater Fish VaccinationMengLi, YuntengCao, ColleenWolfe and BenedettoMarelli; Massachusetts Institute of Technology, United States

Over the next 30 years, with the world population continues to grow, food supplies will have to increase by 70%. Addressing challenges in food security by promoting healthy and sustainable protein sources is crucial. Aquaculture plays a vital role in meeting these requirements, and fish vaccination is integral to preventing disease spread in densely populated farming environments. However, traditional methods involving intramuscular or intraperitoneal injections require fish sedation, administration outside of water, and poses safety concerns for workers due to accidental needlestick injuries.

In this work, we aim to develop an automatic system capable of precise vaccine delivery in aquaculture settings. We adapted microneedle design and fabrication for plants and mammals to meet the requirements for underwater applications.

To ensure successful fish skin penetration, we have employed proteinaceous silk fibroin microneedles encapsulated with a water-proofing coating layer of food-grade natural resin. This coating layer preserves the mechanical strength of the silk fibroin microneedles in water for hours. The water-proofing coating layer prevents water absorption and swelling of silk fibroin microneedles, which could otherwise weaken their mechanical strength. The coating layer preserves the mechanical strength of silk fibroin microneedles in water for hours.

Additionally, the coating layer prevents the loaded substance from prematurely releasing into the aquatic environment, ensuring controlled release after fish skin penetration. Our results demonstrate that once the microneedles pierce the fish skin, the cargo is released within hours primarily through diffusion.

Our study presents a novel microneedle strategy designed specifically for precise injection and substance delivery in aquaculture, offering a promising solution for enhancing fish health, productivity, and sustainability.

8:00 PM SB01.03.07

Supporting Hydroponic Crop Growth using UV-C LightDouglasX. Shattuck^{1,2}, SophiaSalinas^{3,2}, GraceGunning^{3,2}, EmilyParker^{3,2} and SamanAbbas^{3,2}; ¹St Joseph School Wakefield,

Preliminary results indicate that intermittent exposure to UV-C radiation can enhance the hydroponic production of food crops by stimulating plant growth and inhibiting the growth of pathogenic organisms. However, in addition to its benefits, prolonged exposure to UV-C has been known to be harmful to plants (1, 2, 3). Watercress, a specie of aquatic flowering plant in the mustard family, was selected for this investigation. It is fast growing, can be eaten raw or cooked, and is rich in vitamins K, A, C, riboflavin, B₆, Ca, and Mn(4). It is closely related to the *Arabidopsis* sp. being studied for germination in lunar regolith(5).

We designed and constructed a hydroponic system that exposed Watercress to commercially available grow lights and UV-C radiation lamps. By exposing the plants to UV-C in monitored 5 or 15 minute intervals we hoped to maximize its growing process and kill any pathogens while minimizing the damage done by the radiation.

The watercress seeds were placed in net pots with moist growing medium and placed in a water-filled box and then exposed to grow lights. The plants were then exposed to five-minute of UV-C radiation followed by long periods of darkness. After each exposure to the UV-C, plants were observed and the growth and general characteristics of the plant recorded. After two days, the plants were exposed to fifteen-minute radiation intervals, following the same schedule. Each of the six boxes of plants underwent the same testing procedures for four days. The UV-C plants appeared equally as healthy as the control group but grew taller and tilted towards the lights more—exaggerated phototropism.

At the end of the test, we observed mold growing in both the control and UV-C groups. Initially, we observed much more mold in the control group. After being untreated for a week, the group exposed to UV-C light had a considerable amount of mold compared to the control group. This difference suggests that during UV-C light treatment, the mold's growth was curtailed. In conclusion, we believe

the UV-C radiation did have a positive effect on the plants as we hypothesized.

References

- 1 Peters, R. March (2023) <https://hydrogardengeek.com/uv-light-for-plants/> Accessed 9-2-2023
- 2 Mishra, A Awdhesh K. (2020).. <https://link.gale.com/apps/doc/A635206144/> Accessed 9-4-2023
- 3 Buyanovsky, G., et al. <https://doi.org/10.1007/BF02377118> Accessed 8-13-2023
- 4 <https://en.wikipedia.org/wiki/Watercress> Accessed 8-31-2023
- 5 <https://moon.nasa.gov/resources/492/growing-plants-in-lunar-soil/> Accessed July 9 2023

8:00 PM SB01.03.08

***In-Situ* Corona Discharge Non-Thermal-Plasma based Modification of Bio-Ingredients in an Integrated Food Printer: Towards Developing Novel Methodologies for Characterization of Engineered Food Materials**DerekXiong¹, PrakhyatGautam¹, DavidRyman¹, EdberthoLeal-Quiros², SaquibAhmed³ and SankhaBanerjee^{1,4}; ¹California State University, Fresno, United States; ²University of California, Merced, United States; ³Buffalo State College, United States; ⁴University of California, Davis, United States

The current work involves the development of novel in-situ non-thermal plasma treatment methodologies of 3D printed starch-based bio-ingredients towards tailoring the properties of starch granule-surface proteins (SGSP). This work also includes the evaluation of continuous and discontinuous gluten networks through the surface interaction of SGSPs with quasi-static corona discharge plasma regimes. The work further studies the binding characteristics of starch-based bio-ingredients based on the plasma current-voltage characteristics. The cured starch-based sample surface will be characterized using profilometry. The binding characteristics, gluten networks, and porosity characteristics will be analyzed using microstructure evaluation through electron microscopy. Advanced hybrid machine learning models will also be developed in combination with analytical methods and empirical data sets to develop strategies for tailoring the surface and bulk properties of these materials.

8:00 PM SB01.03.09

The Impact of Titanium Dioxide Nanoparticles on Keratinocyte Proliferation and DifferentiationDerekZhang¹, AshleyHuang², ShiFu³, MarciaSimon³, MiriamRafailovich³, DinaMcGinley⁴ and AliceShih³; ¹The Wheatley School, United States; ²Syosset High School, United States; ³Stony Brook University, The State University of New York, United States; ⁴State University of New York at Farmingdale, United States

TiO₂ nanoparticles are still widely used as food additives in the United States for their whitening properties, UV absorption capabilities, and their potential usage as antibacterial reagents. In fact, these particles are considered valid organic additives and can be incorporated at concentrations as high as 1%. When ingested these particles can circulate in the body coming in contact with viable cells and the long term impacts of TiO₂ build up is currently of concern for the European Food Safety Authority [1]. Additionally, even though nanoparticles may not penetrate the stratum corneum and hence do not come into direct contact with viable keratinocytes, if they are used in wound care treatments, they can come into direct contact with viable epidermal and dermal cells and influence cell function and tissue healing. In early experiments producing skin equivalents with keratinocytes exposed to 0.8 mg/mL rutile TiO₂ nanoparticles, we observed nanoparticle aggregation with premature stratum corneum formation and aberrant expression of filaggrin, a late stage multifunctional differentiation marker.

Keratinocytes were grown with lethally irradiated 3T3 cells [2] with media modifications previously described [3]. At 70% confluence feeder cells were removed and cultures were treated with rutile TiO₂ (0.4 mg/mL); no TiO₂ cultures served as control. After 24 hours cultures were rinsed twice with Ca and Mg free phosphate buffered saline, resuspended in buffered saline with BSA and cells sorted at the Stony Brook University Flow Cytometry Core Facility using a FACS Aria IIIU cell sorter.

Cells associated with TiO₂ were separated from TiO₂-free cells based on side scatter using flow cytometry; cells showing low and high side scatter were collected. In these cultures, 90% of the cells exhibited low side scatter, consistent with the absence of nanoparticles. This compares with a low and high scatter population of 57.2% and 42.8%, respectively, in the TiO₂ treated cultures.

The impact of 0.4 mg/mL TiO₂ on keratinocyte proliferative capacity was also explored as a function of colony forming efficiency (CFE), and the colony forming efficiency of keratinocytes with low and high side scatter was determined; TiO₂-free keratinocyte cultures served as control [4]. 12 culture dishes containing 1000 cells each were plated: 4 control plates (low side scatter), 4 plates of TiO₂ treated high side scatter, and 4 plates of TiO₂ treated low side scatter. Following 12 days of incubation, each culture dish was rinsed with Ca and Mg free phosphate buffered saline and stained with Rhodamine B. Colonies ≥ 1 mm were counted. In these cultures, CFEs are about three-fold lower in the high side scatter population suggesting NP inhibition of plating efficiency or proliferation. To assess the full impact of these NPs in this system and in skin equivalents, ongoing work includes SEM analyses to determine NP location within the cell and differentiation assessment by RT-PCR to determine overall skin development.

[1] Flavourings, Younes, M., Aquilina, G., Castle, L., Engel, K., Fowler, P., Fernandez, M. J. F., Fürst, P., Gundert-Remy, U., Gürtler, R., Husøy, T., Manco, M., Mennes, W., Moldeus, P., Passamonti, S., Shah, R., Waalkens Berendsen, I., Wölfle, D., Corsini, E., . . . Wright, M. (2021). EFSA Journal, 19(5). <https://doi.org/10.2903/j.efsa.2021.6585>

[2] Rheinwald, J. G., & Green, H. (1975). Cell, 6(3), 331–343. [https://doi.org/10.1016/s0092-8674\(75\)80001-8](https://doi.org/10.1016/s0092-8674(75)80001-8)

[3] Randolph, R. K., & Simon, M. (1993). The Journal of biological chemistry, 268(13), 9198–9205.

[4] Barrandon, Y., & Green, H. (1987). Proceedings of the National Academy of Sciences of the United States of America, 84(8), 2302–2306. <https://doi.org/10.1073/pnas.84.8.2302>

SESSION SB01.04: Engineering Future Food Materials III

Session Chairs: Leila Deravi and Francisco Martin-Martinez

Wednesday Morning, November 29, 2023

Hynes, Level 1, Room 105

9:00 AM *SB01.04.01

Microfluidic Tools to Monitor Dynamic Processes Occurring during Emulsion and Foam FormationKarinSchroen^{1,2} and BoxinDeng¹; ¹Wageningen University, Netherlands; ²University of Twente, Netherlands

Humanity faces the huge challenge to supply a growing world population with sufficient and healthy food. To make this a reality we need to rethink how we produce food at large scale. This implies rethinking production 'on the land/in the greenhouse', fractionating raw materials, understanding their functionality during processes used in food production, as well as under digestive conditions to make the connection to health effects that can be created by smart food design.

A big challenge that needs to be addressed to make smarter food design a reality is the investigation of processes that take place at micrometre scale, and even smaller scales, and often within very short times. These dynamic processes underly the food structure that we get, but the dynamics thereof are very difficult to capture due to time and size challenges, and the inaccessibility of food production line for analysis of these processes.

Microfluidics allow visualisation of very fast processes occurring during the production of for example, two phase systems such as emulsions and foams. Various tools have been developed within our lab that allow to focus on interface formation and stabilisation at very short time scales. These tools also allow distinction of interfacial tension effects from coalescence effects in

relation to the size of the structures that are formed, which is a classical dilemma that until now has not been addressed at this level of detail.

These new techniques will contribute to more flexible use of ingredients, allowing product design based on the actual functionality of components. For example, replacement of animal-based products with their plant-based counterparts, and also the use of biomass (e.g., leaves and stems) that are currently considered waste can truly contribute to more sustainable food production practice, but only if the functionality of these components is such that they lead to stable products. I could imagine that the techniques developed are ultimately used to do fast screening, comparison of ingredients, and even to establish a connection with more classic processing technologies, such as high pressure homogenization and foaming techniques given the similarity in conditions.

9:30 AM SB01.04.02

Thermoplastic Molding of Silk-Curcumin Composites to Enhance Biological Properties Arjak Bhattacharjee, Sara Rudolph, Ying Chen and David L. Kaplan; Tufts University, United States

Silk fibroin protein is a natural protein biopolymer generated from the cocoons of *Bombyx mori* silkworms and a useful biomaterial for many different tissue engineering applications. Flexible process engineering, versatile chemistry, and aqueous processing allow morphological and structural modifications that tailor the physical, chemical, biological, and mechanical properties of this biomaterial. However, conventional solution-based processing methods can impose limitations in terms of solubility, stability as well as scalability. Recently, we reported a thermal processing technique to fabricate dense, regenerated silk fibroin-based structures (plastics) using solid-state thermoplastic molding to address these limitations. The present work expands the utilization of thermoplastic molding of silk-fibroin to enhance the biological properties of plant-derived compounds like curcumin, the active compound of turmeric (*Curcuma longa*). Curcumin is widely used in traditional medicines. The objective of this study was to study the feasibility of fabricating silk-curcumin composite thermoplastics with enhanced biological properties. The hypothesis was that protective silk thermoplastic formation after curcumin incorporation would enhance the biological properties of curcumin, via the protective features of silk combined with the sustained slow release of the compound to reduce toxicity without affecting anti-bacterial properties. The results show that significantly higher levels of curcumin (~25-fold) can be incorporated into thermoplastic molded silk compared with solution formulations, attributed to the hydrophobic nature and low solubility of curcumin in solution-based processing. The fabricated curcumin incorporated thermoplastics show excellent stability in harsh acidic conditions (e.g., gut-like environment) and low curcumin (~3% over 14 days) release. The protective silk-curcumin formation led to enhanced cytocompatibility of the curcumin with immortalized human colorectal adenocarcinoma (Caco 2) cells even at higher doses when compared to curcumin without silk. The intestinal epithelial barrier integrity based on zonula occludens 1 (ZO-1) assessments indicated that higher doses of curcumin in the thermoplastic molded silk did not result in detrimental effects to the intestinal barrier. Further work is ongoing to assess additional biological outcomes as well as potential areas of utility for these systems.

9:45 AM BREAK

10:15 AM SB01.04.03

Coupling Waste Feedstocks to Microbial Protein for a Circular Food System Taylor Uekert, Alissa Bleem, Christopher Johnson and Gregg Beckham; National Renewable Energy Laboratory, United States

The global food system is responsible for approximately 34% of annual greenhouse gas (GHG) emissions and up to 85% of water consumption. This critical sector suffers from intensive and inefficient land and water use, the generation of multiple (solid, liquid, and gaseous) waste streams, and high fuel, fertilizer, and pesticide consumption. The production of waste-derived microbial protein (MP) represents a promising alternative for reducing the environmental impacts of protein production relative to conventional agriculture. MP can be mass-produced in volumetrically scalable cultivation processes on short timescales, enabling facile up-scaling with lower greenhouse gas emissions, land use, and water impacts than animal and, in some cases, plant protein production. MP can also be produced from waste feedstocks, diverting waste from landfills or the natural environment. Here, we present the availability and suitability of waste feedstocks for MP production, as well as the fermentation and downstream processes required to convert MP into human food products. We discuss the challenges and opportunities facing waste-derived bacterial MP and highlight key areas for innovation in both the microbiology and process design space for a more sustainable and circular food system.

10:30 AM SB01.04.04

Design of Biodegradable, Climate-Specific Packaging Materials that Sense Food Spoilage and Extend Shelf-Life Yangyang Han¹, Song Wang¹, Michael S. Strano² and Benedetto Marelli²; ¹Singapore-MIT Alliance for Research and Technology (SMART) Centre, Singapore; ²Massachusetts Institute of Technology, United States

The AgriFood systems in tropical climates are under strain due to a rapid increase in human population and extreme environmental conditions that limit the efficacy of packaging technologies to extend food shelf-life and guarantee food safety. To address these challenges, we rationally designed biodegradable packaging materials that sense spoilage and prevent moulding. We nanofabricated the interface of 2D covalent organic frameworks (COF) to reinforce silk fibroin (SF) and obtain biodegradable membranes with augmented mechanical properties and that displayed an immediate colorimetric response (within 1 second) to food spoilage, using packaged poultry as an example. Loading COF with antimicrobial hexanal also mitigated biotic spoilage in high temperature and humidity conditions, resulting in a four-order of magnitude decrease in the total amount of mould growth in soybeans packaged in silk-COF, when compared to cling film (i.e., polyethylene). Together, the integration of sensing, structural reinforcement, and antimicrobial agent delivery within a biodegradable nanocomposite framework defines climate-specific packaging materials that can decrease food waste and enhance food safety.

10:45 AM SB01.04.05

Microneedles Carrying Nanosensors for Real-Time Detection of Abiotic Stress in Plants Raju Cheerlavancha¹, Benny Sng Jian Rong², Khong Duc Thinh¹, Yunteng Cao³, Yangyang Han¹, Mervin Ang Chunyi¹, Song Wang¹, Gajendra Pratap Singha¹, Michael S. Strano³, In-Cheol Jang^{2,1} and Benedetto Marelli^{3,1}; ¹Singapore-MIT Alliance of Research and Technology, Singapore; ²Temasek Life Sciences Laboratory, Singapore; ³Massachusetts Institute of Technology, United States

Abiotic stress refers to adverse environmental conditions that negatively impact plant growth, development, and productivity. These stressors include extreme temperatures, drought, salinity, heavy metals, and radiation. Understanding plant responses and adaptation to abiotic stress is crucial, especially with the increasing severity and frequency of such stressors due to climate change. However, conventional methods for studying plant responses have limitations such as indirect measurements, low spatial resolution, and the inability to visualize real-time changes.

To overcome these limitations, we developed a delivery system using microneedles (MNs) to carry nanosensors. These MNs can be inserted into both soft and hard plant tissues without leaving any residues. By incorporating the nanosensor into the MNs, we successfully demonstrated real-time sensing of abiotic stress in Bok Choy and *Nicotiana benthamiana*. The embedded nanosensor, designed specifically for abiotic stress, enables rapid and sensitive detection of near-infrared (NIR) fluorescence signals. This allows for accurate measurement and visualization of abiotic stress levels. Furthermore, we confirmed the compatibility of the MNs with the abiotic stress nanosensors.

In summary, the integration of nanosensors with non-invasive delivery systems like MNs presents exciting opportunities for studying abiotic stress in plants. These innovative approaches help us gain a deeper understanding of how plants perceive and respond to environmental challenges. Ultimately, this knowledge can inform the development of stress-tolerant crops, sustainable agricultural practices, and strategies to mitigate the impacts of climate change on plant productivity and food security.

11:00 AM SB01.04.06

Time-Resolved Roasting-Induced Microstructural Evolution of Arabica Coffee Beans using X-Ray Computed Micro-Tomography Eshan Ganju¹, Kunal Chawla², Samuel Yang¹ and Nikhilesh Chawla¹; ¹Purdue University, United States; ²Carmel High School, United States

The aroma of coffee is deeply connected to the roasting process, which leads to notable changes in the bean's structure and chemistry. While many research studies have explored the chemical alterations occurring in the coffee bean during roasting, the structural changes have typically only been observed broadly, quantified by changes in size, density, fracture strength, or basic sectional views of the coffee bean. Traditional microscopy techniques are insufficient in providing an in-depth understanding of the coffee beans' microstructure, primarily due to their resolution, two-dimensional (2D) limitations, and the destructive nature of the analyses. These limitations are further exacerbated by the fact that the coffee bean undergoes significant three-dimensional (3D) structural changes during the roasting process. These changes are impacted by the coffee bean variety's properties, the bean's initial microstructure (which is affected by the local environment, including altitude, humidity, etc.), and the roasting process. As a result of the limited information about the initial 3D microstructure of the bean, its impact on the evolution of the emergent microstructure during roasting has been largely unexplored. Furthermore, while global measurements in porosity or pore volume at different roast levels have been reported, the heterogeneity in the evolution of porosity in different regions of the bean, which impacts the uniformity of the ground beans, has not been described. In this study, we conducted a time-resolved study of the roasting-induced microstructural evolution of Arabica coffee beans using X-ray computed micro-tomography (XCT). We combined high-resolution XCT data with computational image analysis techniques to examine the evolution of the microstructure of *Coffea arabica* beans during roasting. Beans sourced from Brazil, Colombia, and Ethiopia were tracked individually throughout the roasting process going from the green bean to the dark roast stage. The individual beans were tracked and scanned at multiple stages of roasting to capture the 3D tomography data of the entire bean. The XCT data, captured at different roasting levels, revealed detailed, time-resolved information about porosity, pore size distribution, and cracking within different regions of the beans. Results showed a significant increase in porosity and pore size from green-bean to dark-roast state, but the rate of increase wasn't linearly dependent on roasting time. Furthermore, beans from different regions showed markedly different spatial heterogeneity in porosity and cracking. The effects of the initial green bean microstructure, as influenced by the growth environment, on the subsequent structural evolution will be discussed. The data and analyses presented in this study can assist in advancing research in the realm of food engineering by enabling a deeper understanding of the structural characteristics of coffee beans from various regions of the world and by clarifying the link between the processing and

microstructure of the bean at different roasting levels. Furthermore, the 3D characterization and analysis presented here can be applied as a framework to study a diverse class of food materials.

11:15 AM SB01.04.07

Living Filters for Sustainable and Selective Treatment of Drinking Water and BeveragesVicki L. Colvin; Brown University, United States

Many communities in the U.S. and globally suffer because of a lack of access to safe drinking water. Cleaning water, however, using conventional technology is a dirty business that is expensive as well as material and energy intensive. There is a need to broaden access as well as provide more sustainable solutions that can improve people's water and their health. Living filters are cultures of living microbes that are engineered to both sense and treat contaminants at the very low concentrations relevant for drinking water. Here we demonstrate a system that targets the removal of arsenic from drinking water and beverages such as fruit juice and wine. Conventional remediation based on chemical sorption is challenging because of interferences from phosphates, silicates, flavor compounds, and organic matter; membrane-based separations also can be impacted by these species and more critically will remove all compounds including those that should be preserved for flavor in the case of beverages. Here, we exploit the extraordinary selectivity of biological recognition to solve this problem. Microbial engineering is applied to generate *E. Coli* that contain multiple copies of arsenic-binding proteins that are highly selective for arsenic and effectively no binding to smaller anions. When protein expression is induced, bacteria remain healthy and produce thousands of copies of Ars-R and when exposed to arsenic, the organisms within 30 minutes will reduce arsenic to sub-ppb levels. Sorption isotherms reveal at low concentrations (<50 ppb) sorption is defined by cellular transport while at higher concentrations the intracellular protein-arsenic interaction is limiting. The sorption behavior of these bacteria is insensitive to millimolar concentrations of phosphates, silicates, and many salts and is unaffected by the components of wines or fruit juices. Conventional microfiltration systems can be applied to remove all microbes down to levels suitable for meeting stringent EPA standards for drinking water. The integration of magnetic separation allows the capture of arsenic-laden microbes attached to magnetic nanoparticles which can be reused for future separations. Flavor compounds as measured by mass spectrometry in beverages remain unaffected by these treatment processes. Most recently we have incorporated bioluminescent reporters into the living filters which permit the detection of arsenic to optimize the treatment system. These engineered materials can be freeze-dried with modest impact on performance. Dry powders can be shipped easily under ambient conditions and then cultivated at the site prior to their integration into the treatment system. An important benefit of these materials is that the sorbent is in effect living, allowing for sustainable and low-cost manufacturing.

SESSION SB01/SB02/SB04/SB10: Joint Virtual Session

Session Chairs: Preethi Chandran, Bianca Datta, Francisco Martin-Martinez, Alexandra Rutz and Christina Tringides

Tuesday Morning, December 5, 2023

SB01-virtual

8:00 AM *SB01/SB02/SB04/SB10.01

Home Composting Doesn't Work as an Environmentally Beneficial Method for Managing Biodegradable and Compostable PackagingDanielle Purkiss, Ayse Allison, Fabiana Lorencatto, Susan Michie and Mark A. Miodownik; University College London, United Kingdom

Compostable and biodegradable plastics are growing in popularity but their environmental credentials need to be more fully assessed to determine how they can be a part of the solution to the plastic waste crisis. We present results and analysis on home compostable packaging. This type of packaging requires the citizen to be able to correctly identify the packaging as 'home compostable', to have composting facilities at home, and to successfully compost the plastic. Using a citizen science approach, we engaged with 9701 UK citizens geographically spread across the UK to examine their capability, opportunity, and motivation to do this. Of this cohort 1648 citizens performed home compost experiments to test the environmental performance of compostable plastics. We report on the type of plastics they tested and their disintegration under real home composting conditions. The results show that the public are confused about the meaning of the labels of compostable and biodegradable plastics. 14% of sampled plastic packaging items tested were certified 'industrial compostable' only and 46% had no compostable certification. Of the biodegradable and compostable plastics tested under different home composting conditions, the majority did not fully disintegrate, including 60% of those that were certified 'home compostable'. We conclude that for both of these reasons, home composting is not an effective or environmentally beneficial waste processing method for biodegradable or compostable packaging in the UK. This talk also outlines the requirements to make industrial composting a viable and sustainable method for managing compostable packaging.

8:30 AM SB01/SB02/SB04/SB10.02

Advancing Food Safety and Security with Biodegradable Antimicrobial Food CoatingYagmur Yegin and Benedetto Marelli; Massachusetts Institute of Technology, United States

The global population, projected to reach 10 billion by 2050, presents a significant challenge in ensuring an adequate food supply with finite resources. One-third of food produced for human consumption is wasted annually due to food safety and quality concerns. This extensive food waste harms the environment, contributing to energy consumption and greenhouse gas emissions. Remarkably, the discarded food could feed 1.6 billion people, yet it is responsible for a quarter of global freshwater use and ranks as the third-largest greenhouse gas emitter, after China and the United States, making up about 10% of total global greenhouse gas emissions. Redirecting this wasted food to alleviate hunger and reduce environmental harm is imperative. To enhance food safety and quality, we have developed an innovative solution: an antimicrobial-embedded biodegradable silk coating. Our approach combines multiple functions into one material, enabling the effective incorporation of food sanitizers to improve food safety and extend shelf life. We aim to repurpose discarded silkworm cocoon waste, often overlooked by the textile industry, into valuable silk fibroin. This natural protein polymer, derived from *Bombyx mori* cocoons, forms the foundation of an intelligent, sustainable, and cost-effective antimicrobial food packaging solution. This innovative coating effectively prevents the growth and spread of foodborne bacteria, extending the freshness of perishable foods. We encapsulated antimicrobial essential oils within silk nanoparticles using ultrasonication, eliminating the need for solvents and surfactants. Evaluation of the silk nanoparticles' properties, followed by testing of their antimicrobial efficacy against various foodborne pathogens, ensures their effectiveness. The silk nanoparticles, loaded with food sanitizers, are seamlessly integrated into the silk coating, providing a long-lasting sanitizing effect and ensuring protection for extended periods. The resulting edible silk coatings act as robust barriers against gases and moisture, preserving the freshness of cherry tomatoes. These coatings are transparent, offering excellent coverage without leaving visible residue on cherry tomatoes. Moreover, they are easily washable, providing convenience for consumers. Our transparent, sanitizer-infused silk food packaging offers a superior alternative for preserving the freshness of cherry tomatoes. The biodegradable antimicrobial food coating acts as a formidable barrier, sealing in moisture while effectively excluding oxygen. In doing so, it efficiently inhibits the proliferation of foodborne pathogens. A crucial feature of our advanced food packaging is its delivery as dried films, simplifying transportation compared to conventional liquid solutions. These solid films exhibit prolonged stability, ensuring consistent performance over time. This innovation enables on-site preparation of dipping or spray solutions, simplifying application onto food surfaces. Consequently, it enhances food quality and safety without the need for refrigeration or single-use plastic packaging. In summary, our research focuses on harnessing biodegradable polymers to develop functional agri-food materials through large-scale manufacturing. Our overarching goal is to create biopolymers with circular life cycles, capable of outperforming synthetic counterparts while preserving crucial performance attributes. The silk coating serves as a robust shield on perishable food surfaces, effectively preventing the entry of unwanted gases while retaining moisture. Additionally, it functions as an antimicrobial carrier, hindering the proliferation and survival of foodborne pathogens, thereby extending the shelf life of perishable foods. Our coating material represents an innovative, scalable, and sustainable solution to combat food insecurity, food waste, and climate change, all while contributing to the betterment of our planet.

8:45 AM SB01/SB02/SB04/SB10.03

Moringa Oleifera Proteins as Pickering Stabilizers: From Nanostructures to RheologyNamrah Azmi^{1,2}, Andrew N. Akanno¹, Matti Knaapila¹, Adrian Rennie³, Leonard Rweyemamu^{2,4} and Jon Otto Fossum¹; ¹Norwegian University of Science and Technology, Norway; ²Stayfit Nutrisupplies Co. Ltd, Tanzania, United Republic of; ³Uppsala University, Sweden; ⁴University of Dar Es Salaam, Tanzania, United Republic of

Substantial food waste as a result of chemical decay of food enormously impacts the environment, henceforth the need for stabilization by surfactants but the associated carbon footprints possess a threat to the industry. Thus, Pickering emulsions, stabilized by solid-particles, residing at droplet interfaces come into the picture, providing more stable systems than surfactants. In terms of resistance against fusion (coalescence) and coarsening (Ostwald ripening) Pickering emulsions are thermodynamically stable systems with good biocompatibility and can be utilized as carriers for delivery of bioactive compounds, thus applied in food to control and enhance texture and taste and improve stability¹. Plant proteins attract great interest and the stability of Pickering emulsions is governed by protein properties, protein concentration, and environmental factors. The Moringa protein has been chosen because it is inexpensive, with great nutritional benefits and wide availability, and has been scientifically proven to have excellent anti-oxidant, anti-hypertensive, and anti-diabetic properties². Protein particle interactions are very much dependent on pH. Such protein-based nanoparticles have proven to be advantageous as they are biodegradable, non-toxic, and provide the large possibility for surface modification³. All this motivates our study to investigate the Moringa protein as Pickering particles for emulsions fabricated at different pH and ionic strengths. The rheology and corresponding macroscopic gel properties of such emulsions can be designed by arrested coalescence for producing food spreads with desired rheological properties⁴. During this, aggregates are formed with the

interaction between denatured non-absorbed proteins and absorbed ones at the emulsion droplet interfaces which can be impacted by lipid oxidation, which influences emulsion particle interactions. Proteins can form gels after aggregation at different pH or ionic concentrations. It is difficult to separate the association mechanism of gelation and emulsification through protein aggregation⁵ which is another motivation for our studies.

We have undertaken a program to distinguish the “good” and “not so good” Moringa-based protein stabilizers by utilizing microscopic observations and rheometry and using Small-Angle X-ray-Scattering (SAXS) to examine structural stability and aggregations of the same stabilizing proteins, thus gathering information on protein⁶, and how this is connected to the rheological properties. Further works include formulating food spread using this emulsion and studying its smell and mouthfeel quantification.

ACKNOWLEDGEMENTS:

This work received funding from the European Union’s Horizon 2020 research and innovation programme under the Marie Skłodowska-Curie grant agreement No 956248.

REFERENCES:

1. Kargar, M., Fayazmanesh, K., Alavi, M., Spyropoulos, F. & Norton, I. T. Investigation into the potential ability of Pickering emulsions (food-grade particles) to enhance the oxidative stability of oil-in-water emulsions. *J Colloid Interface Sci* **366**, 209–215 (2012).
2. Chen, L., Ao, F., Ge, X. & Shen, W. Food-grade pickering emulsions: Preparation, stabilization and applications. *Molecules* **25**, (2020).
3. Tarhini, M. *et al.* Protein-based nanoparticle preparation via nanoprecipitation method. *Materials* **11**, (2018).
4. Huang, Z. *et al.* Fabrication and stability of Pickering emulsions using moringa seed residue protein: Effect of pH and ionic strength. *Int J Food Sci Technol* **56**, 3484–3494 (2021).
5. Zhu, Z. *et al.* Food protein aggregation and its application. *Food Research International* vol. 160 Preprint at <https://doi.org/10.1016/j.foodres.2022.111725> (2022).
6. Han, Q. *et al.* Small angle X-ray scattering investigation of ionic liquid effect on the aggregation behavior of globular proteins. *J Colloid Interface Sci* (2023) doi:10.1016/j.jcis.2023.05.130.

8:50 AM SB01/SB02/SB04/SB10.04

Asymmetric Polymerosomes with Photothermal ResponsivenessJingxinShao¹, YingtingLuo¹, HanglongWu², JianhongWang¹, ShoupengCao³, LoaiK. Abdelmohsen¹ and JanVan Hest¹; ¹Technische Universiteit Eindhoven, Netherlands; ²Massachusetts Institute of Technology, United States; ³Max Planck Institute for Polymer Research, Germany

Photo-mediated micro/nanorobots have found widespread interest over the past decade because of their application potential in many areas, especially in nanomedicine. By converting light energy into mechanical work, micro/nanorobots can be propelled to achieve active cargo transportation into cells with enhanced therapeutic effect. Most of the current micro/nanorobots are either based on inorganic particles or hybrid particles, such as Janus nanoparticles with a hemispherical Au shell.¹⁻⁵ The construction of fully organic-based micro/nanorobots is still underexplored. Here, a new type of light propelled nanorobots is created based on biodegradable polymerosomes. Photothermal agents (PA) were co-assembled with polymer building blocks to form polymerosomes with an asymmetric morphology, resembling a hot-air-balloon structure. With cryogenic transmission electron microscopy (Cryo-TEM) and cryo-electron tomography (Cryo-ET), this structure was confirmed. The formation mechanism of these asymmetric polymerosomes was thereafter investigated by in situ observation of the dynamic assembly process with liquid phase transmission electron microscopy (LP-TEM). In combination with the cryo-TEM data, the LP-TEM results revealed that liquid-liquid phase separation was the main leading force for the formation of asymmetric polymerosomes. Upon infrared laser irradiation (808 nm), the PA nano-assemblies in the polymerosome structure provided photothermal heating and propelled the polymerosomes in a controllable way regarding both direction and speed. This study demonstrates the formation of a new nanomotor topology which is driven by the photothermal effect and fully composed of organic building blocks. This nanomotor is further investigated for its application in active drug delivery.

9:05 AM SB01/SB02/SB04/SB10.05

Encapsulation and Delivery of Biomolecules with Cell-Mimicking NanolipogelBertrandCzarny^{1,2}, Wen Jie MelvinLiew¹, AbdullahAlkaff¹, AtulParikh^{2,3} and SubramanianVenkatraman^{4,5}; ¹Nanyang Technological University, NTU, Singapore; ²University of California, Davis, United States; ³Nanyang Technological University, Singapore; ⁴National University of Singapore, Singapore; ⁵University of California, San Diego, United States

High initial burst release of biomolecules is just one of the many challenges faced by lipid based nanoparticulate formulations, even though it is widely used for drug encapsulation and delivery studies. One of the emerging potential strategies is the use of nanolipogels (NLG) to encapsulate biomolecules, which can suppress the initial burst release. This gives a level of control and sustain to the release of hydrophilic drugs. However, current works are short on characterisation of the release mechanistic. Therefore, varying molecular weight of Poly (ethylene glycol) Diacrylate (PEGDA) were used for the fabrication of PEGDA NLG, to study the mechanism for release of Dextran-Fluorescein Isothiocyanate (DFITC). Fluorescence Recovery after Photobleaching (FRAP), were performed on cell derived microlipogels (MLG), a novel system developed as a solution to limitations of FRAP with NLG. Results from the studies has shown that the NLGs’ mesh sizes are controllable via the use of different Mw of PEGDA, where a lower Mw used resulted in a smaller mesh size of the nanogel core, by having a higher crosslinking density. This in turn gave higher suppression of the initial burst release of DFITC, up to a 10-fold difference. FRAP results then gave further validation by showing that the smaller mesh size restricted the diffusion of DFITC, consequential of a lower mobile fraction. These gave clear insight into the possibility of controlling the encapsulation and release of biomolecules, by targeting the fabrication of nanogel core. From this, Chitosan Methacrylate (CMA) NLGs was then studied to expand into other ways in manipulating the nanogel core for greater control, such as a differently charged core. Results was shown that CMA NLGs are also able to suppress the initial burst release of DFITC and it can be controlled by using a different concentration of CMA. This increases the possible strategies for consideration during the design of NLG systems and especially CMA NLGs opens up the possibility of encapsulation of negatively charge biomolecules, such as siRNA. As the NLG system involves two critical components, namely the nanogel core and the bilayer coating, the membrane properties are essential for the designing of NLGs. Herein, cell membrane coating for NLG was studied, with the development of a novel Chitosan Methacrylate-Tripolyphosphate (CMATPP) nanoparticle systems, which allows for the co-extrusion with cell membrane vesicles. The coating of CMATPP nanoparticles can possibly confer the membrane properties, such as prolonged *in-vivo* circulation and improved cellular uptake, to CMATPP nanoparticles. Coating was validated through flow cytometry with characteristic membrane proteins of cell derived nanovesicles (CDN), namely CD9, CD81, TSG101, or with RBC membrane vesicles, CD47. RBC CMATPP NLGs were also shown that it can further suppress the initial burst release and sustained release compared to Liposome CMATPP NLGs. All in all, it was shown that cell mimicking NLG system was able to provide a controlled release of hydrophilic biomolecule, and the release mechanism was studied and characterized using FRAP. Relationships with changes to the nanogel core as well as membrane coatings were also explored and proven to be viable and plausible expansions to other membrane origins were discovered. This study has provided a guide on the design of NLGs for a multitude of needs with regards to encapsulation and delivery, as well as for future *in vivo* performance

9:20 AM SB01/SB02/SB04/SB10.06

Spiky Silica Nanoparticles Embedded with ZIF-90: A Promising Approach for Intracellular Drug DeliveryManoj KumarSharma^{1,2}, DanChang², JingjingQu², HaoSong², ChengzhongYu², Ashok KumarGanguli¹ and JieTang²; ¹IIT Delhi, India; ²The University of Queensland, Australia

Nanotechnology has emerged as a promising field in treating various diseases, offering significant advancements in drug delivery systems (DDS).^[1] These systems offer advantages such as improved drug bioavailability, controlled release kinetics, and prolonged circulation time, leading to increased safety and efficacy. Mesoporous Silica (MSN)-based carriers exhibit desirable properties, including high porosity, biocompatibility, and tunable particle size. The introduction of spiky nanotopography on silica nanoparticles has garnered significant scientific interest due to its unique capabilities, including enhanced bacterial adhesion, intracellular drug delivery, and protection of genetic material.^[2] Nonetheless, challenges persist in MSN-based DDS, encompassing limitations such as low drug loading capacity and premature release of anticancer agents.^[3] To address these challenges, promising strategies have been explored, such as functionalizing silanol groups on mesoporous silica nanoparticles (MSN) with amine moieties or integrating organic compounds and metal-organic frameworks (MOFs). The literature provides limited information on silica-Zn-MOF composites. Previous studies have predominantly focused on ZIF-8 formation on silica nanoparticles.^[4] This study successfully synthesized a novel nanocomposite consisting of nature-inspired spiky silica nanoparticles (SNP) embedded with zeolitic imidazolate framework-90 (ZIF-90). The resulting SNP-ZIF-90 composites retained their spiky morphology and demonstrated enhanced drug-loading capacity for doxorubicin (Dox) compared to bare SNP. Furthermore, the modified SNP-ZIF-90 composites exhibited improved cellular uptake and pH-responsive drug release, highlighting their potential as an efficient drug delivery system.

References

- [1] E. Blanco, H. Shen, M. Ferrari, *Nature biotechnology* **2015**, *33*, 941-951.
- [2] H. Song, M. Yu, Y. Lu, Z. Gu, Y. Yang, M. Zhang, J. Fu, C. Yu, *Journal of the American Chemical Society* **2017**, *139*, 18247-18254.
- [3] F. Tang, L. Li, D. Chen, *Advanced materials* **2012**, *24*, 1504-1534.
- [4] Y. Wang, H. Song, C. Liu, Y. Zhang, Y. Kong, J. Tang, Y. Yang, C. Yu, *National Science Review* **2021**, *8*, nwa268.

9:35 AM SB01/SB02/SB04/SB10.07

High-Performance Tactile Pressure Sensor Based on Ionically Conducting Elastomer for Physiological MonitoringZhiyongWang, MingGao, WeiWei, Kian PingLoh, Yung C.Liang and ChunxiangZhu; National University of Singapore, Singapore

Tactile pressure sensors can convert contact pressure into detectable and readable electrical signals (resistance, current, capacitance, or voltage), so they exhibit considerable potential in fields of real-time health monitoring, electronic skin, intelligent prosthesis, and human-machine interfaces. Recently, ionic pressure sensors, mainly consisting of ionically conducting filler and soft elastomer, have gained increasing attention for their good biocompatibility and conformability, well-tailored capability, and excellent sensing performance. Despite this, these ionic pressure sensors tend to suffer from limitations in mechanical strength, conductivity, and long-term instability. In order to overcome these challenges, we propose a novel approach. First, we utilize a sugar template method to create a porous silicon elastomer, which serves as the foundation and will be further coated with an ionically conducting polymer called poly(3,4-ethylene dioxithiophene) polystyrene sulfonate (PEDOT: PSS) to form our high-performance tactile pressure sensor. Moreover, mechanical and electrical properties, as well as the structure-

performance relationship, have been specifically investigated by means of different characterization tools. As a proof of concept, we have demonstrated the use of the ionic pressure sensor for continuously monitoring physiological activities such as respiratory and pulse signals.

Corresponding author: E-mail address: elezhucx@nus.edu.sg (Chunxiang Zhu). This work was supported by the Ministry of Education (MOE), Singapore, under its Tier 1 grant (No. A-0009043-01-00) and NUS ARTIC WDSS-RP3 (no. A-0005947-33-00).

9:40 AM SB04.03.19

Ink based Large Quantity Preparation of Graphene Incorporated Contact Lenses for Multi-Application [Muhammed Shebeeb Cherum Kuzhi](#), Muhammed Hisham, Liyamol Jacob, Yarjan Abdul Samad and Haider Butt; Khalifa University, United Arab Emirates

Along vision correction, incorporation of nanomaterials and other additives for multi-functionality is becoming popular in studies on contact lenses, especially hydrogel based contact lenses. There have been few investigations on the capability of graphene as an additive for added functionality such as transparent electrode, dehydration protection and EMI shielding. However, the current works involve graphene prepared through chemical vapor deposition, which makes it difficult for affordable and faster production. In this work, we investigate the preparation of graphene - hydroxy ethyl methacrylate composite based hydrogel contact lenses and graphene incorporation in commercial hydrogel based soft contact lenses without losing the optical transparency within the visible range. The incorporation of graphene onto commercial contact lenses were done using dipping lenses for certain period of time as well as breathe in breathe out technique, two common technique used to incorporate nanomaterials to hydrogels. We further investigate how the water retention and the wetting behavior have been affected by the graphene presence and its capability for EMI shielding within the range 8.2-12.4 GHz.

9:45 AM SB01/SB02/SB04/SB10.08

Ultrathin Hydrogel Biosensor with Controllable Self-Adhesion Properties for Electrophysiology Measurement [Shuyun Zhuo](#), Alexandre Tessier and Shideh Kabiri Ameri; Queen's University, Canada

Hydrogel has recently been utilized to develop health monitoring sensors and devices such as bioelectrodes. Owing to their good electrical conductivity, ultra-softness, and self-adhesion, current hydrogel sensors have found their application in electroencephalogram (EEG), electromyogram (EMG), and electrocardiogram (ECG) recording. However, the highly adhesive hydrogels are hard to peel off from the surface of the skin after laminating it and they are susceptible to losing the water content and unfavorable changes in the electrical conductivity and mechanical softness. Here we report an ultrathin hydrogel-based sensor with controllable self-adhesion properties that can fully conform to the skin and perform reliably for an extended period. An ultrathin, conformable biosensor with a thickness of less than 10 μm is fabricated based on gelatin-acrylamide-polypyrrole hydrogel, where the sol-gel transition of the gelatin is utilized to control the modulus and adhesion force. The ultralow thickness and good stretchability of the gelatin-acrylamide-polypyrrole hydrogel contribute to a seamless interface between the biosensor and human skin, which is desired in wearable devices for high-quality bio-signal acquisitions such as electrocardiography (ECG) and electromyography (EMG).

10:00 AM SB01/SB02/SB04/SB10.09

Viscoelastic Response of Commercial Mucin to HIV Pseudotyped Virus [Gabrielle Torain](#), Alexander Boakye, Ayobami I. Ogundiran, Tzu-Lan Chang, Sergei Nekhai and Preethi Chandran; Howard University, United States

Mucin is a heavily glycosylated protein that makes up the mucus gel which serves as a protective barrier against pathogens like viruses. Mucins are prone to self-aggregation which imparts a viscoelastic (fluid-like and solid-like) characteristic to the mucus gel. However little is known about how the presence of viruses change the flow properties of mucin. Replication-deficient HIV viruses pseudotyped with either gp120 or vesicular stomatitis virus (VSV-G) envelope proteins were used as model viruses. Commercially available Porcine gastric mucin-type II (PGM-II) and porcine gastric mucin type III (PGM-III) in the filtered (free mucin) and unfiltered (having mucin-mucin interactions) states were used as model mucins. DLS was used to determine the landscape of the sizes of the diffusing species (mucin, virus, or virus-mucin species). Rheology was used to determine change in the inter-mucin interaction and friction. Axisymmetric drop shape analysis was used to determine the changes to the mucin surface tension. Preliminary results suggest that the average intensity of PGM-II and PGM-III, in the filtered state, are lowered and the hydrodynamic diameter decreases with both pseudotyped viruses. Subsequent rheology studies show a lowered elastic and frictional character when either VSV-G or gp120 pseudotyped viruses are present. The unfiltered state of mucin shows no significant changes in DLS measurements but increased elastic and frictional characteristics are observed at lower oscillatory frequencies in rheology studies. Our data demonstrates that viruses change solution behavior of mucin both in the singular and aggregated states and thus may alter the viscoelastic characteristics of the mucus gel.

10:05 AM *SB01/SB02/SB04/SB10.10

From Sub-Micron Resolution Towards 3D-Printing at the Speed of Light: Pushing the Boundaries to Serve Health [Quinten Thijssen](#)¹, [Laurens Parmentier](#)¹, [Hayden Taylor](#)², [Steven Ballet](#)³ and [Sandra Van Vlierberghe](#)¹; ¹Ghent University, Belgium; ²University of California, Berkeley, United States Minor Outlying Islands; ³Vrije Universiteit Brussel, Belgium

Current thoroughly described biodegradable and cross-linkable polymers mainly rely on acrylate cross-linking. However, despite the swift cross-linking kinetics of acrylates, the concomitant brittleness of the resulting materials limits their applicability. Here, photo-cross-linkable poly(ϵ -caprolactone) (PCL) networks through orthogonal thiol-ene chemistry are introduced. The step-growth polymerized networks are tunable, predictable by means of the rubber elasticity theory and it is shown that their mechanical properties are significantly improved over their acrylate cross-linked counterparts. Tunability is introduced to the materials, by altering M_c (or the molar mass between cross-links), and its effect on the thermal properties, mechanical strength and degradability of the materials is evaluated. Moreover, excellent volumetric printability is illustrated and the smallest features obtained via volumetric 3D-printing to date are reported, for thiol-ene systems. Finally, by means of in vitro and in vivo characterization of 3D-printed constructs, it is illustrated that the volumetrically 3D-printed materials are biocompatible.

In an attempt to mimic nature's ability to adhere cells, PCL is often coated with nature-derived polymers or its surface is functionalized with a cell-binding motif. However, said surface modifications are limited to the material's surface, include multiple steps, and are mediated by harsh conditions. In a second part, we introduce a single-step strategy toward cell-adhesive polymer networks where thiol-ene chemistry serves a dual purpose. First, alkene-functionalized PCL was crosslinked by means of a multifunctional thiol (*vide supra*). Second, by means of a cysteine coupling site, the cell-binding motif C(-linker)-RGD was covalently bound throughout the PCL networks during crosslinking. Moreover, the influence of various linkers (type and length), between the cysteine coupling site and the cell-binding motif RGD, was investigated and the functionalization was assessed by means of static contact angle measurements and X-ray photoelectron spectroscopy. Finally, successful introduction of cell adhesiveness was illustrated for the networks by seeding fibroblasts onto the functionalized PCL networks.

This combination of mechanical stability, tunability, biocompatibility, no post-processing functionalization required and rapid fabrication by volumetric 3D-printing charts a new path toward bedside manufacturing of biodegradable cell-interactive, patient-specific implants.

In addition to photo-crosslinkable polyesters, also progress in the field of high resolution two-photon polymerization and volumetric additive manufacturing of gelatin-based hydrogels will be addressed. Hence, our material platform can serve both hard and soft tissue engineering applications.

References

Thijssen, et al. *Biomacromolecules* (2023), 24, 1638-1647

Thijssen, et al. *Advanced Materials* (2023), 35, 2210136

Thijssen and Van Vlierberghe (2022), Cell-binding motifs (CBMs) functionalized polymers, EP22213201.1

SYMPOSIUM SB02

Biomimetic Organic and Hybrid Frameworks for Imaging, Encapsulation and Delivery
November 27 - November 29, 2023

Symposium Organizers

Christian Doonan, Univ of Adelaide
Niveen Khashab, King Abdullah University of Science and Technology
Jonathan Sessler, The University of Texas at Austin
Stefan Wuttke, Basque Center for Materials, Applications and Nanostructures

* Invited Paper
+ JMR Distinguished Invited Speaker

SESSION SB02.01: Biomimetic Materials for Encapsulation I
Session Chairs: Christian Doonan, Niveen Khashab and Stefan Wuttke
Monday Morning, November 27, 2023
Hynes, Level 3, Room 307

10:30 AM *SB02.01.01

Smart and Programmable Crystalline Sponges for Protection [Omar K. Farha](#); Northwestern University, United States

This talk will focus on metal-organic frameworks (MOFs) from basic research to implementation and commercialization. MOFs are a class of porous, crystalline materials composed of metal-based nodes and organic ligands that self-assemble into multi-dimensional lattices. In contrast to conventional porous materials such as zeolites and activated carbon, an abundantly diverse set of molecular building blocks allows for the realization of MOFs with a broad range of properties. We have developed an extensive understanding of how the physical architecture and chemical properties of MOFs affect material performance in applications such as catalytic activity for chemical warfare agent detoxification.

11:00 AM *SB02.01.02

Supramolecular Design of Mesoporous 2D Covalent Organic Frameworks for the Encapsulation of Large and Small Guests [Ronald A. Smaldone](#); The University of Texas at Dallas, United States

Interlayer interactions in 2D covalent organic frameworks (COFs) have been shown to be important factors in both their formation and bulk properties. There are many previous examples of controlling interlayer interactions in COFs by tuning the monomer or geometry. However, the use of hydrogen bonding is much rarer. The highly directional nature of a hydrogen bonding interaction makes it difficult to orient properly in a COF structure. To accomplish this, we have designed monomers with a non-planar structure that arises from steric crowding, forcing the amide side groups out of plane with the COF sheets orienting the hydrogen bonds between the layers. The presence of these hydrogen bonds provides significant structural stabilization as demonstrated by comparison to control structures that lack hydrogen bonding capability, resulting in lower surface area and crystallinity. We have characterized both azine and imine-linked versions of these COFs for their surface areas, pore sizes and crystallinity. The rigidified structure that results from these supramolecular interactions can enable the production of COFs with mesopores capable of hosting large protein guests. In addition to more conventional COF characterization methods (such as powder X-ray diffraction and porosity analysis), we also used variable temperature infrared spectroscopy (VT-IR) methods and van der Waals density functional calculations to directly observe the presence and character of the hydrogen bonding interactions. This talk will also discuss the importance of mesopore design in COFs for the adsorption of different guests in aqueous solutions, ranging from proteins, to small molecule pollutants.

11:30 AM *SB02.01.03

Insights into MOF Chemical Biology—Biocatalysts Encapsulated within MOFs [Fa-Kuen Shieh](#)¹, [Lien-Yang Chou](#)² and [Chia-Kuang Tsung](#)³; ¹National Central University, Taiwan; ²Shanghai Tech University, China; ³Boston College, United States

Metal-organic frameworks (MOFs) have found diverse applications in bio-sensing, biomass utilization, and catalysis. This study introduces a novel concept in material biology known as MOF Chemical Biology. It focuses on investigating the impact of containing biomolecules, such as protein enzymes, within synthetic MOF biocomposites, referred to as enzyme@MOFs. These biocomposites are prepared using a *de novo* biomineralization synthesis route, conducted under mild and aqueous conditions. The framework of these biocomposites possesses apertures that enable the free movement of substrates, while the encapsulated enzymes or bacteria remain confined within the structure, thereby shielding them against most structural changes. Furthermore, we present the first successful demonstration of encapsulating enzymes into robust Zirconium-based MOFs, specifically UiO-66, using a solid-state mechanochemical process. The enzymes encapsulated through this method retain their desired functionality and exhibit resistance to proteases, even under acidic conditions. These innovative approaches provide an alternative system, exploiting the structural confinement effect, for expanding the application of MOFs in studying the biochemical functionalities of prokaryotes, eukaryotes, mammalian cells, and more.

SESSION SB02.02: Biomimetic Materials for Encapsulation II
Session Chairs: Christian Doonan and Niveen Khashab
Monday Afternoon, November 27, 2023
Hynes, Level 3, Room 307

1:30 PM *SB02.02.01

Biocompatible Robust MOFs for New Wound Healing Solutions [Christian Serre](#); CNRS, ENS, ESPCI Paris, PSL University, France

The development of new wound healing solutions is still a critical issue in order to treat infectious diseases. Biocompatible metal organic frameworks (MOFs) have long term been considered mainly against cancer. We will show in this presentation two new strategies to take benefit from their open metal sites and/or ordered porosity to propose new solutions out of traditional antibiotics treatments.

A first strategy relies on the controlled delivery of Nitric oxide (NO), a powerful gaseous therapeutic agent of interest to treat a wide variety of disease states. As it can overcome the bacterial resistance to antibiotics, it is an appealing alternative to conventional drugs, and the development of efficient NO-donating drugs is being demanded. However traditional NO carriers are often toxic which precludes their practical use. It is crucial to find biocompatible carriers with prolonged biological half-life. MOFs have been previously proposed as antibacterial or anti-thrombogenic carriers but only in gas phase mainly through a coordination on their unsaturated metal sites. However once in contact with body fluids, the release of NO occurs within minutes compromising their practical use.^[1] We have therefore selected a robust biocompatible Ti-MOF such as MIP-177^[2] that is enable to release NO within 2 hours in phosphate buffer, due to an unprecedented NO adsorption/release mechanism. Very recently, we also designed a new ultra-narrow pores iron bisphosphonate MOF, denoted MIP-210^[3], that is stable in PBS while adsorbing NO on its metal sites. Due to the combination of a novel adsorption mechanism, an exceptional stability in PBS and its narrow pores, it leads to a record ca. 3 days of NO release in biological media; in both cases we demonstrate how these controlled releases lead to cell migration or even angiogenesis that are of a crucial importance for wound healing applications, paving the way for the design of new wound healing therapies.

A second strategy consists of encapsulating dyes into biocompatible large pores Fe-MOFs. Through the protective effect of the pores' confinement considerably slowing down the bleaching of the dye under near infra-red irradiation, as well as the slow release of Fe³⁺ ions once in contact with body fluids leading to the formation of ROS, we demonstrate how these new MOF-dyes composites, through a multimodal based on PTT/PDT and chemo-dynamic therapy, are of interest to treat successfully different anti-biotic resistant infections (Chlamydia...)^[4-5]

References

- [1] Eubank, J.F.; Wheatley, P.S.; Lebars, G.; McKinlay, A.C.; Leclerc, H.; Horcajada, P.; Daturi, M.; Vimont, A.; Morris, R.E.; Serre, C. *APL Mater.* **2014**, *2*, 124112.
- [2] R.V. Pinto, S. Wang, S.R. Tavares, J. Pires, F. Antunes, A. Vimont, G. Clet, M. Daturi, G. Maurin, C. Serre, M.L. Pinto, *Angew. Chem. Int. Ed.*, **2020**, *59*, 5135–5143.
- [3] C.-C. Cao, R. V. Pinto, P. Lyu, I. Dovgaliuk, C.-Y. Su, G. Maurin, F. Antunes, J. Pires, V. André, C. Henriques, A. Tissot, M. L. Pinto and C. Serre, **2023**, submitted
- [4] X. Qi, E. Grafka, Z. Yu, N. Shen, E. Fedina, A. Masyutin, M. Erokhina, M. Lepoitevin, V. Lazarev, N. Zigangirova, C. Serre, M. Durymanov, *ACS Infectious Diseases* **2023**, under revision
- [5] Z. Yu, F. Gazeau, A. Jamet, M. Lepoitevin, C. Serre et al, to be submitted

2:00 PM SB02.02.02

Biomimetic Mineralization of Ovalbumin in ZIF-8 Enhances Humoral Immune Response—Overcoming the Need for Booster Doses [Ryan N. Ehrman](#); University of Texas at Dallas, United States

Vaccines have saved countless lives throughout history by preventing and even eradicating infectious disease. Commonly used subunit vaccines comprising of one or multiple recombinant proteins isolated from the disease demonstrate a good safety profile. However, the immunogenicity of these vaccines is weak, and therefore, subunit vaccines require a series of doses to achieve sufficient immunity against the disease. Consequently, people's distaste for needles detours them from receiving the vaccination regimen. Here, we show that the encapsulation of the inert model antigen, ovalbumin, in ZIF-8 overcomes the need for these booster doses by significantly improving the humoral immune response over three bolus doses of ovalbumin. We designed two ovalbumin-ZIF-8 composites, a nano-sized (n-OVA@ZIF) and micron-sized (μ-OVA@ZIF). Through preliminary testing, we determined the micron-sized μ-OVA@ZIF to be the better candidate for *in vivo* vaccination studies. Single vaccination of μ-OVA@ZIF demonstrated higher serum antibody titers against ovalbumin as opposed three bolus injections of ovalbumin (OVA 3x). μ-OVA@ZIF vaccinated mice displayed higher populations of germinal center B (GCB) cells and IgG1+ GCB cells as opposed to OVA 3x. This is indicative of class-switching recombination, where B cells begin secreting specialized and higher affinity antibodies. We believe that the mechanism of this phenomena is owed to the sustained release of ovalbumin from the ZIF-8 composite, acting as an antigen reservoir for APCs to trafficking into the draining lymph node, enhancing the humoral response. We show through fluorescent animal imaging and SEM micrographs that the ZIF-8 coating slowly degrades in the body, releasing the antigen over an extended period of time.

2:15 PM SB02.02.03

Multifunctional Enzyme Nanocapsules Boost T Cell Immunity and Efficacy of Cancer Immunotherapy [Zheng Cao](#), [Wenting Chen](#), [Duo Xu](#), [Jing Wen](#) and [Yunfeng Lu](#); University of California, Los Angeles, United States

Cancer immunotherapy has reshaped the landscape of cancer treatment, but its effectiveness in treating solid tumors is hindered by overproduction of lactate by cancer cells. Extensive trials are being conducted to regulate lactate levels by inhibiting lactate dehydrogenase, however, such inhibitors can disrupt the metabolism of healthy cells and cause severe non-specific toxicity. In contrast to those strategies, we innovatively target lactate itself by an enzyme, lactate oxidase, which effectively reduces the lactate levels and releases hydrogen peroxide, an immunostimulatory molecule, in the tumor microenvironment. However, recombinant lactate oxidase from microorganisms possesses short circulating half-life, low enzyme activity, and immunogenicity. To circumvent this limitation, we innovatively report herein a nano-encapsulating strategy to encapsulate individual lactate oxidase molecules within a thin polymer shell by *in-situ* polymerization of monomers and crosslinkers, affording the synthesis of nanocapsules. The nanocapsules stabilize lactate oxidase and prevent it from proteolysis and denature, minimize the immunogenicity, prolong the circulating half-life, enabling their use as a potent therapeutic for cancer immunotherapy. Lactate oxidase nanocapsules can promote the proliferation and activation of effector T cells and suppress tumor-resident regulatory T cells *in vitro*. As further demonstrated in a murine melanoma model and a humanized mouse model of triple-negative breast cancer, nanocapsules of lactate oxidase avert tumor immunosuppression and enhance anti-cancer T cell immunity by upregulating gene expression for T cell recruitment and activation, as confirmed by single-cell RNA sequencing. Such multifunctional lactate oxidase nanocapsules lead to improved efficacy of immunotherapies for solid tumors.

2:30 PM *SB02.02.04

Metal-Organic Frameworks for the Encapsulation of Bio-Entities [Ioanna Christodoulou](#)¹, [Jonathan Bachir](#)¹, [Effrosyni Gkaniatsou](#)¹, [Nathalie Steunou](#)¹ and [Clemence Sicard](#)^{1,2}; ¹Institut Lavoisier de Versailles, France; ²Institut Universitaire de France, France

Bio-entities benefit from unparalleled activities of high interest in many applications such as high catalytic activities under mild conditions (aqueous media, room temperature). However, these are fragile entities, easily degraded under non-native conditions. Encapsulation, i.e. inclusion within a host matrix, is particularly interesting for bio-entities stabilization and protection as it can provide controlled environment and protection. Metal-Organic Frameworks (MOFs) have arisen as a host matrix of choice to answer the limitations of traditional immobilization matrices, resulting in the design of novel functional biomaterials.^[1] The MOF-bio-entity composites exhibit promising properties, since the biological activity can be preserved while the stability of bio-entities in non-natural environments could be improved. Encapsulation can be performed by diffusion of the biological entities into the porosity of preformed MOF. Alternatively, the MOF can be formed “*in-situ*” around the bio-entities. Both strategies are limited to a number of MOF/bio-entities couples either due to size matching constraints or to a narrow window of compatible synthetic conditions.

In this communication we will present our efforts to expand synthetic routes and processing methods to explore new compositions and hierarchical structures of bio-entities-MOFs hybrids. We will describe the synthesis and characterization of MOFs-based living materials.^[2] The mesoporous iron polycarboxylate MIL-100(Fe) was synthesized in the presence of *Pseudomonas putida* bacteria. The synthesis conditions (aqueous media, 30 °C) were compatible with the preservation of the bacteria integrity. High resolution microscopic techniques (TEM, STEM-XEDS) were applied on cross-sections to study the interface between the two components, revealing the presence of an exoskeleton encapsulating individual bacteria cells. We will also discuss our latest finding on the design of novel bio-entities-porous materials with unique properties for potential application in biocatalysis.^[3]

References:

- 1 - (a) E. Gkaniatsou, C. Sicard, R. Ricoux, J. P Mahy, N. Steunou, C. Serre, *Mater. Horiz.* **2017**, *4*, 55; (b) R. J. Drout, L. Robison, O. K. Farha, *Chem. Rev.* **2019**, *381*, 150, (c) X. Wang, P. C. Lang, S. Ma, *ACS Cent. Sci.*, **2020**, *6*, 9; (d) S. Huang, X. Kou, J. Shen, G. Chen, G. Ouyang, *Angew. Chem. Int. Ed* **2020**, *23*, 8786; (e) W. Liang, P. Wied, F. Carraro, C. J. Sumbly, B. Nidetzky, C.K Tsung, P. Falcaro, C.J. Doonan, *Chem. Rev.* **2021**, *121*, 1077;
- 2 - A. Permyakova, A. Kakar, J. Bachir, E. Gkaniatsou, B. Haye, N. Menguy, F. Nouar, C. Serre, N. Steunou, T. Coradin, F. M Fernandes, C. Sicard, *ACS Materials Letters*, **2023**, *5*, 1, 79
- 3 - B. Le Ouay, R. Minami, P. K. Boruah, R. Kunitomo, Y. Ohtsubo, K. Torikai, R. Ohtani, C. Sicard, M. Ohba, *J. Am. Chem. Soc.* **2023**, *145*, 11997

3:00 PM BREAK

3:30 PM *SB02.02.05

Advanced Porous Framework Materials for the Immobilization of Biomolecules: Beyond Host Matrix Materials [Shengqian Ma](#); University of North Texas, United States

Advanced porous framework materials as represented by metal-organic frameworks (MOFs) and covalent organic frameworks (COFs) represent a new class of crystalline materials, and one of their striking features lies in the tunable, designable, and functionalizable nanopore, which allows designed incorporation of different functionalities for targeted applications, such as gas storage/separation, sensing, drug delivery, catalysis, conductivity. We will discuss the systematic development of MOFs and COFs as a new platform for immobilization of biomolecules for

applications in biocatalysis and beyond.

4:00 PM SB02.02.06

Supercritical CO₂ Precipitation of Porphyrin-Based MOFs as Potential Materials for Photodynamic Therapy Ana M. Lopez-Periago¹, Marta Kubovics¹, José A. Ayllón², Concha Domingo¹ and Carme Nogués²; ¹Consejo Superior de Investigaciones Científicas (CSIC), Spain; ²Universitat Autònoma de Barcelona, Spain

In the past few years, our research group has focused on synthesizing metal-organic frameworks (MOFs) using environmentally friendly methods based on supercritical CO₂ (scCO₂)^[1], where synthesis and pore activation can occur, in many cases, in a single step.

Building upon these advancements, the preparation of MOFs containing porphyrin linkers were of great interest to us, as porphyrins are fundamental building block precursors in various domains of synthetic chemistry. For example, porphyrins can form coordination networks with potential applications in fields such as catalysis, sensors, as well as for cancer treatment.^[2]

In the latter, porphyrin and its derivatives remain the most extensively employed materials for photodynamic therapy (PDT)^[3], an anticancer therapy based on the local application of a photosensitizer in the affected area that, by light radiation of a certain wavelength, produce reactive oxygen species (ROS)^[4], which are able to destroy the harmful cells through either necrosis or apoptosis.

In our research, we focused our interest into the possibilities of precipitating MOFs using a porphyrin linker with pyridyl motifs, specifically 5,10,15,20-Tetra(4-pyridyl)porphyrin (H₂TPyP) using exclusively scCO₂ as reaction media. The reaction involved the coordination of the binding sites (pyridyl moieties in *meso*- position, and the inner tetrapyrrole ring) with different metals. For this purpose, we employed four metal hexafluoroacetate complexes (M(hfac)₂, M = Cu, Zn, Co, Ni) as metal precursors in the production of the metal-organic materials.

Among the obtained samples, the scCO₂-precipitated Zn(II) MOF demonstrated exceptional performance when tested as a potential photosensitizer in PDT therapy against the SKBR-3 tumoral cell line. This MOF resulted to be nontoxic, but after 15 min of irradiation at 630 nm, using either 1 or 5 μM concentration of the product, almost 70% of tumor cells died after 72 h. The most interesting results of this work were recently published in the journal *Chemistry of Materials*^[5].

[1] (a) A. López-Periago*, O. Vallcorba, C. Frontera, C. Domingo, J.A. Ayllón. *Dalton Trans.* 2015, 44, 7548. N. Portolés-Gil, O. Vallcorba, C. Domingo, J.A. Ayllón*. *Inorganica Chim. Acta.* 2021, 516, 1201323. (b) M. Kubovics, S. Rojas, J. Fraile, A.M Lopez-Periago*, P. Horcajada*, C. Domingo*. *Journal of Supercritical Fluids.* 2021, 178, 105379; (c) N. Portolés-Gil, O. Vallcorba, J. Fraile-Saez, A. López-Periago, C. Domingo, J.A. Ayllón*. *App. Organomet. Chem.* 2023, 37, e6930.

[2] (a) J. Puigmart-Luis, W. J. Saletta, A. González, D. B. Amabilino, L. Perez-García*, *Chem. Commun.* 2014, 50, 82–84; (b) R. Purrello, S. Gurrieri, R. Lauceri*, *Coord. Chem. Rev.* 1999, 190–192, 683–706; (c) K. Lang, J. Mosinger, D. M. Wagnerov*. *Coord. Chem. Rev.* 2004, 248, 321–350.

[3] J. Kou, D. Dou, L. Yang*. *Oncotarget.* 2017, 8, 81591–81603.

[4] M. Ethirajan, Y. Chen, P. Joshi, R.K. Pandey*. *Chem. Soc. Rev.* 2011, 40, 340–362.

[5] M. Kubovics, O. Careta, O. Vallcorba, G. Romo-Islands, L. Rodríguez, J. Ayllón, C. Domingo, C Nogués, A.M. López-Periago*. *Chemistry of Materials.* 2023, 35, 1080- 1093.

4:15 PM *SB02.02.07

Broadening the Scope of MOFs for *In Situ* Biomolecule Encapsulation Mónica Giménez-Marqués, Jesús Cases Díaz and Jana Glatz; University of Valencia, Spain

The use of metal-organic frameworks (MOFs) as robust coating of fragile biomacromolecules has been demonstrated a valuable strategy for their preservation, enabling their ample implementation in biomedical and biotechnological processes. Essentially, this biomolecule encapsulation requires the MOF assembly under biocompatible conditions and the existence of favorable electrostatic surface conditions at the biomolecule-MOF interface.

Despite recent growth in the field of MOF mineralization, only a limited number of MOFs have been accessed, being ZIFs the most widely explored materials for biohybrid synthesis. However, next directions in the field require revealing the hierarchical organization of these assemblies and for that, it is essential to expand the biohybrid family by using MOFs with distinct nature.

Herein we present alternative synthetic approaches to access previously elusive MOFs that permit to study new biohybrid architectures with undisclosed functionalities.

SESSION SB02.03: Biomimetic Materials for Delivery I
Session Chairs: Christian Doonan, Niveen Khashab and Jonathan Sessler
Tuesday Morning, November 28, 2023
Hynes, Level 3, Room 307

8:30 AM *SB02.03.01

Enhancing Vaccine Stability and Immunogenicity Through Biomimetic Mineralization using Zeolitic-Imidazole Frameworks (ZIFs) Jeremiah J. Gassensmith; University of Texas-Dallas, United States

Vaccines are susceptible to structural conformational changes under environmental and chemical stressors, compromising their therapeutic efficacy. This lecture presents three innovative case studies that address this challenge to enhance the stability, preservation, and immunogenicity of protein, DNA, and lipid nanoparticle based vaccines.

First, we discuss using zeolitic imidazolate framework-8 (ZIF-8) as a protective agent for a model viral vector against denaturing conditions. Immunoassay and spectroscopy analysis reveal that ZIF-8 provides enhanced thermal and chemical stability to the conformational structure of the encapsulated viral nanoparticle. Long-term biological activity studies in animal models demonstrate the integrity, biosafety, and immunogenicity of the virus-ZIF composite. Furthermore, histological analysis confirms the absence of tissue damage, highlighting ZIF-based protein composites as promising candidates for preserving proteinaceous drugs, ensuring biocompatibility, and controlling drug release *in vivo*.

Next, we explore stabilizing proteoliposomes, supramolecular lipid-protein assemblies that mimic cellular membranes. We demonstrate that metastable lipid, protein-detergent, and protein-lipid complexes can be successfully immobilized within zeolitic-imidazole framework (ZIF) bio-composites. This immobilization strategy enhances their stability against chemical and physical stressors such as elevated temperatures, chemical denaturants, aging, and mechanical stresses. Extensive morphological and functional characterization confirms that the encapsulated complexes maintain their native morphology, structure, and activity, which would otherwise rapidly degrade without immobilization.

Lastly, we address the pressing need for effective vaccines against pathogenic bacteria in the face of increasing antibiotic resistance. The genetic diversity of bacteria poses challenges in selecting appropriate antigens, hindering vaccine development. We present a proof-of-principle method to enhance the immunogenicity of a model pathogenic *E. coli* strain by forming a slow-releasing depot. Biomimetic mineralization within a metal-organic framework (MOF) effectively encapsulates the *E. coli* strain, enhancing antibody production and improving survival in a mouse bacteremia model. This approach surpasses the limitations of whole-cell formulations and demonstrates the potential for successful clinical translation.

These innovative strategies utilizing ZIFs and MOFs hold great promise for revolutionizing vaccine design, preservation, and immunogenicity. By enhancing stability and ensuring effective immune responses, these advancements contribute to developing next-generation approaches for combating bacterial infections and preventing the spread of pathogens.

REFERENCES:

Luzuriaga MA, *et al.* **Metal-Organic Framework Encapsulated Whole-Cell Vaccines Enhance Humoral Immunity against Bacterial Infection.** *ACS Nano.* 2021 Nov 23;15(11):17426-17438. DOI: 10.1021/acsnano.1c03092. PMID: 34546723.

Herbert FC, *et al.* **Stabilization of supramolecular membrane protein-lipid bilayer assemblies through immobilization in a crystalline exoskeleton.** *Nat Commun.* 2021 Apr 13;12(1):2202. DOI: 10.1038/s41467-021-22285-y. PMID: 33850135; PMCID: PMC8044103.

Luzuriaga MA, *et al.* **Enhanced Stability and Controlled Delivery of MOF-Encapsulated Vaccines and Their Immunogenic Response *In Vivo*.** *ACS Appl Mater Interfaces.* 2019 Mar 13;11(10):9740-9746. DOI: 10.1021/acsnano.8b20504. PMID: 30776885.

9:00 AM *SB02.03.02

Immune/Chemo-Active Nanomofs Multitherapy Patricia Horcajada; IMDEA Energy Institute, Spain

The involvement of Metal-Organic Frameworks (MOFs) in biomedical applications is currently one of the hot topics in the emerging field of hybrid porous solids.^[1] Despite their already proven high loadings and progressive release of a wide variety of active ingredients (e.g. drugs, cosmetics, biological gases, macromolecules), the control of the biodistribution of MOF nanocarriers and their involvement as a non-passive carriers (bioactive) is still a challenge.

Several examples of successful formulations able to bypass specific physiological barriers will be presented.^[2] In particular, pulmonary administration is a convenient route not only for the

treatment of respiratory diseases (e.g. COPD, asthma, tuberculosis, infection, cancer) but also systemic ones. In this sense, a pioneer combined anti-COVID multi-therapy (3-in-1 effect) will be described, paving the way to future treatment of challenging infectious and/or pulmonary pathologies.^[3]

Acknowledgment: The authors are grateful for the generous support from HeatMof (H2020-MSCA-ITN-2019, ref. 860942), MOFSEIDON (PID2019-104228RB-I00 funded by MCIN/AEI/10.13039/501100011033) and VIRMOF-CM (“Comunidad de Madrid” and European Regional Development Fund-FEDER 2014-2020-OE REACT-UE).

References

- [1] S. Rojas *et al.*, *Coord. Chem. Rev.*, **2019**, 388, 202; R. Ettliger *et al. Chem. Soc. Rev.*, **2022**, 51, 464; S. Lelouche *et al. Expert Op. Drug Deliv.*, **2022**, 19, 1417
- [2] T. Simon-Yarza *et al.*, *Angew. Chem. Int. Ed.*, **2017**, 56(49), 15565; C. Fernandez-Paz *et al. ACS App. Mater. Inter.*, **2020**, 12(23), 25676; S.D. Taherzade *et al. Nanomater.* **2020**, 10, 2296; A. Botet-Carreras *et al. J Mater Chem B*, **2021**, 9, 2233; S. Rojas *et al. ACS Nano.* **2022**, 16, 4, 5830.
- [3] T. Hidalgo *et al.*, *Chem. Sci.*, **2022**, 13, 934; A. Arenas-Vivo *et al. Pharmaceutics* **2023**, 15(1), 301; B. Fodor *et al.* unpublished results

9:30 AM *SB02.03.03

Design of Highly Porous MOFs for Drug Delivery David Faren-Jimenez; Department of Chemical Engineering & Biotechnology, University of Cambridge, United Kingdom

Metal-organic frameworks (MOFs) are ideal candidates for payload delivery in drug delivery applications due to their highly tuneable surface properties, with drug capacities as high as 60 wt.%. The use of MOFs can lower the required amount of active pharmaceutical ingredient (API), providing a more efficacious therapy while also decreasing the potential for untargeted and undesired effects. Their controlled and autonomous delivery utilizing such a porous high-capacity loading material ultimately could reduce high dependence on patient compliance.

We have developed a series of nano-sized Zr-MOFs with different pore sizes and volumes, from the microporous UiO-66 family of materials to mesoporous NU-1000, all of them showing minimal cytotoxicity. On the one hand, we show how the post-synthetic modification of the MOFs can allow the controlled release of different payloads, extending the release time from 2 days to 30 days. On the other hand, we show how the particle size and surface chemistry allow tuning the final fate of the MOFs and the metabolic pathways of how they are endocytosed by the cells. By modifying the external surface chemistry of the MOFs or by grafting different motifs, we can extend the release time of the drugs, and improve the efficiency of the MOFs to penetrate the cells and target specific organelles.

Our work has allowed us to understand the fundamental biophysical and biochemical mechanisms of cancer cell death upon treatment with MOFs. The fundamental understanding of the biological aspects of cancer has allowed us to advance not only in small-drug molecule delivery but also in novel solutions based on photodynamic therapy and gene therapy.

10:00 AMBREAk

10:30 AM SB02.03.04

Using Zeolitic Imidazolate Frameworks for Creating an Intranasal Depot Effect and Development of a Novel Tuberculosis Subunit Vaccine Sneha Kumari¹, Ryanne N. Ehrman¹, Jonathan Martinez-Garcia¹, Yalini Wijesundara¹, Thomas Howlett¹, Lenette Lu², Angelo Izzo³, Gabriele Meloni¹ and Jeremiah J. Gassensmith¹; ¹University of Texas at Dallas, United States; ²University of Texas at Southwestern, United States; ³Centenary Institute, Australia

Tuberculosis (TB) is the second leading cause of deaths from infectious diseases in the world after Covid-19. Despite the great strides taken in vaccine development over the last few decades, TB prevention still relies on the century-old BCG formulation, whose efficacy widely varies amongst different populations. Whole cell attenuated vaccines for such pathogenic diseases are a risky avenue of research. Decades of subculturing are required to attenuate the strains, and yet there is always a risk of reverting to virulence. We have hence developed a subunit vaccine candidate which combines two novel antigens, a powerful adjuvant, and a slow-release system using MOFs for depot effect. CtpV and MctB are two membrane-bound metal transporter proteins present on the surface of *Mycobacterium tuberculosis* that are potential virulence factors of TB and can be used to induce a T-cell mediated response upon vaccination. Class A CpG—a synthetic reproduction of bacterial DNA—has been widely investigated as an adjuvant in research models and fits into our formulation well as it also activates T-cells. It is worth noting that many similar subunit vaccines that fall short in clinical trials are unable to produce high enough antibody titers compared to whole cell vaccines. This is primarily attributed to short exposure time of delicate biomaterials like liposomes, that degrade in the body fast. Our goal is to combat this using zeolitic imidazolate frameworks (ZIF), a metal-organic framework that can be synthesized in biofriendly conditions to build a protective coating around the biomaterial. ZIF degrades slowly inside the body, and a vaccine coated with ZIF would slowly release antigens and provide prolonged presentation, giving the immune system time to develop more antigen-specific antibodies. This formulation also allows us to vary the ZIF coating thickness in order to optimize the duration of antigen presentation. We recently concluded an extensive study which demonstrates the biosafety of a wide range of ZIF doses when delivered intranasally in mice as a first step of this investigation. We found that there was no significant difference in the serum protein and enzyme levels and the lung diffusing capacity of mice administered even up to 1 mg ZIF per animal. No tissue damage was observed in the nasal turbinates, trachea, or lungs either. We are currently working on optimizing the various aspects of our vaccine for an ideal immune response and benchmarking our vaccine candidate's performance against BCG.

10:45 AM SB02.03.05

Label-Free Pore-Level Virus and Particle Detection with Bioinspired Inverse Opal Photonic Crystals Natalie Nicolas and Joanna Aizenberg; Harvard University, United States

For most methods of viral imaging, it is necessary to bind bulky fluorescent molecules to the virus in order to visualize its location with optical microscopy. This increases the complexity of sample processing and may change viral behavior. In this research, we instead electrostatically bind viruses or charged particles to the surface of an inverse opal, which is a bioinspired self-assembled ordered porous material, to create a label-free method for imaging the location of a virus with a light microscope. Attached viruses increase the energy barrier to liquid infiltration in the re-entrant pores of the inverse opal, such that they remain dry when a test solution fills the non-occluded pores. Polarized light microscopy can then be used to distinguish the non-wetted pores, revealing location and concentration information about the viruses. This can create a customizable label-free tool to study viral behavior in laboratory or medical settings.

11:00 AM SB02.03.06

Congo Red-Derived Carbon Dots as Dual Inhibitors of Tau and A β Aggregation in Alzheimer's Disease Wei Zhang¹, Nathan Smith², Yiqun Zhou^{1,3}, Caitlin M. McGee¹, Mattia Bartoli^{4,5}, Jiuyan Chen¹, Justin B. Domena¹, Emei K. Cilingir¹, Susanna Bedendo⁵, Matteo L. Claire¹, Hannah Burr², Alberto Tagliaferro⁵, Eduardo A. Veliz⁶, Chunyu Wang² and Roger M. Leblanc¹; ¹University of Miami, United States; ²Rensselaer Polytechnic Institute, United States; ³Florida International University, United States; ⁴Istituto Italiano di Tecnologia, Italy; ⁵Politecnico di Torino, Italy; ⁶Miami Dade College, United States

Alzheimer's disease (AD) is the most common form of senile dementia, with few effective treatments. AD pathology is characterized by extracellular amyloid plaques and intraneuronal neurofibrillary tangles. A promising drug discovery approach is to develop molecules capable of targeting both hallmarks of AD, by inhibiting A β and tau aggregation. In recent years, carbon dots (CDs) have emerged as novel drug nanocarriers with high biocompatibility, low cytotoxicity, and the ability to cross the blood-brain barrier (BBB). This talk will describe a new type of CDs, Congo red-derived CDs (CRCDs), synthesized using Congo red and citric acid as precursors. We will discuss how different mass ratios of the two precursors can produce CDs with different physicochemical properties. We will describe the successful synthesis of CRCDs which can cross the BBB in a zebrafish model. In addition, our synthesized CRCDs show the ability to inhibit both tau and A β aggregation. Our findings demonstrate that CRCDs can function as dual inhibitors for tau and A β aggregation, in addition to its capacity to cross BBB, enter the central nervous system (CNS), and to carry drugs. Thus CRCDs-based compounds may be a novel formulation component for the development of multi-functional AD therapeutics.

11:15 AM *SB02.03.07

Smart Materials for Precized Drug Delivery Ali Trabolsi; New York University Abu Dhabi, United Arab Emirates

The development of multifunctional drug delivery systems (MDDS) targeting diseased areas arose from the need to overcome drug limitations such as cytotoxicity, immunogenicity, short circulation times, uncontrolled bio-distribution, and the inability to target specific tissues. Significant advances in nanobiotechnology have led to the development of MDDS to serve diagnostic and therapeutic purposes through a single medical device capable of performing bioimaging tasks while improving the therapeutic efficacy of marketed drugs. Stimuli-responsive nanostructures can take advantage of changes in the biological microenvironment of the disease in question and respond to changes in temperature, pH, redox conditions, reactive oxygen species (ROS), and enzyme concentration, with combinations of stimuli increasing the therapeutic versatility of MDDS. This approach, defined as a new paradigm in nanomedicine, has applications in several fields, including cancer therapy, drug delivery, tissue engineering, and even bionics. In this scenario, the intrinsic properties of nanoparticles are used to develop active devices with diagnostic, therapeutic, or even theranostic functions.

Our group has developed several theranostic covalent organic frameworks (COFs) as smart trigger-responsive MDDSs that cover a wide range of applications from cancer therapy to bioimaging to diabetes control. Nanoscale COFs have shown tremendous potential as new candidates for nanomedicine due to their unique properties—large surface area, tunable pore geometry, crystallinity, versatility, as well as responsiveness to physiological environments. COFs exhibit a long-range ordered structure that results in regular pores with diameters that

facilitate the loading and controlled release of prominent drugs and proteins/enzymes. Moreover, their high flexibility in molecular design makes them versatile and uniquely responsive to their environment. Recently, we published the formation of imine-linked nanoscale COFs linked for cancer therapy. The resulting COFs were stable under physiological conditions but disintegrated in an acidic medium, an essential property of the microenvironment of most solid tumors, and facilitated site-specific drug release. On the other hand, we reported a triazine-based COF with high stability under harsh acidic environmental conditions for oral insulin delivery to diabetic rats. The insulin-loaded COF crossed the intestinal barrier and sustainably lowered blood glucose levels in vivo in diabetic rats (T1D), and blood glucose levels completely returned to normal without causing systemic toxicity compared with the control group of nondiabetic rats.

In my talk, I hope to offer some key elements to answer the question, "Can COF nanoparticles serve as effective therapeutics for various disease treatments?"

SESSION SB02.04: Biomimetic Materials for Delivery II
Session Chairs: Niveen Khashab and Jonathan Sessler
Tuesday Afternoon, November 28, 2023
Hynes, Level 3, Room 307

1:30 PM *SB02.04.01

Ion Transport and Molecular Separations in Self-Assembled Membranes with Precisely Defined 1-nm Scale Pores Chinedum Osuji; University of Pennsylvania, United States

Polymeric materials that display simultaneously high selectivity and permeability for a specific ionic or (uncharged) molecular species are of central importance in myriad scenarios, ranging from energy generation and storage to water purification, drug delivery and isolating products of biosynthesis. However, we lack adequate knowledge to enable the design of "fit-for-purpose" materials for controlled species transport under the conditions of nanoscale confinement encountered in these scenarios. The structure-property relationships that govern transport in nanoscale confinement reflect the prevalence of interfacial interactions and the fundamentally altered nature of physico-chemical phenomena at the nanoscale. These relationships diverge strongly from those at continuum length scales and are generally poorly understood. Biological systems such as selectivity filters in ion channels display remarkable transport properties and exploit features that to date have been difficult to incorporate effectively into synthetic materials. These features include uniformity in the structural and chemical characteristics of transport regulating features. Here, we examine molecular self-assembly as a route to mimic such uniformity, with a goal of better understanding nanoscale transport and realizing improved membrane materials. We study lyotropic self-assembly of reactive amphiphiles into gyroid and direct hexagonal mesophases, the fabrication of highly-ordered nanostructured polymer thin films from such mesophases, and the performance of the resulting membranes. We consider a variety of scenarios, including molecular filtration in aqueous and non-aqueous media, and ion transport. These membranes circumvent the limitations of pathway tortuosity and size-dispersity of transport-regulating features found in conventional membranes. As such, they enable highly selective, or precise, molecular separations and ion transport, with pore-size tunable in steps as small as 0.1 nm. We present results highlighting how these precisely-defined membranes are enabling the development of new insight regarding molecular transport under nanoscale confinement in the presence of charge, something that is poorly understood from a fundamental perspective.

2:00 PM *SB02.04.02

Three-Dimensional Visualization of Proteins within Metal-Organic Frameworks Joe P. Patterson; University of California, Irvine, United States

Electron tomography holds great promise as a tool for investigating the three-dimensional (3D) morphologies and internal structures of metal-organic frameworks (MOFs). Understanding the 3D spatial arrangement and density of proteins within protein@MOF biocomposites is paramount for developing synthetic methods to control the location of proteins within the MOF material. The direct visualization of the protein Ferritin (Fn) in Fn@MOF biocomposites was probed through a combination of scanning electron microscopy (SEM), transmission electron microscopy (TEM), and electron tomography (ET). Using con-trolled-dose dry-cryogenic electron tomography (dry-cryoET), we obtain a direct 3D visualization of protein@MOFs with individual protein resolution. These direct observations show that ligand-to-metal ratios for Fn@MOF biocomposites can be tuned to change the spatial arrangement and localization of the proteins within the MOF crystals.

2:30 PM *SB02.04.03

Enzyme-Mimicking of Copper-Sites in Metal-Organic Frameworks for Oxidative Degradation of Phenolic Compounds Ainara Valverde¹, Stefan Wuttke^{1,2}, José María Porro^{1,2}, Mónica Jiménez-Ruiz³, Pedro Luis Arias⁴, Iker Agirrezabal-Telleria⁴ and Roberto Fernández de Luis¹; ¹Basque Center for Materials, Applications and Nanostructures, Spain; ²Ikerbasque, Spain; ³Institut Laue Langevin, France; ⁴University of the Basque Country (UPV/EHU), Spain

Through the sequential assembly of simple repetitive units, biology has built up complex three-dimensional scaffolds of metalloproteins, which deposit functional amino acid residues able to coordinate the metal catalytic site in specific spatial configurations. The chemical arrangement of the amino acid residues that conforms the first and second coordination environment of the metal-sites plays a key role in defining the activity and selectivity of metalloenzymes. Thus, an alteration of any of the amino acid sequence into the heart of the metalloenzyme sites, affects drastically their efficiency, selectivity and function. An important example is the case of copper metalloenzymes, where the coordination of copper ions is usually completed by histidine, cysteine and carboxyl amino acid residues. Depending on the copper-biocatalyst, Cu^{II} ions are stabilized as isolated and/or clustered sites able to carry out oxidative catalytic reactions. The overall selectivity and oxidoreductive efficiency of copper-enzymes over a specific substrate is partially defined by the coordination modes of the copper sites. Furthermore, their oxidative capacity has important technological implications in water remediation, since it can be adapted to degrade phenolic pollutants via Catalytic Wet Peroxide Oxidation (CWPO).

Extensive research is being carried out to replicate and expand the metalloenzymes' pockets and catalytic activity to robust porous materials. In this regard, the chemical encoding of bio-catalytic like sites into a particular class of porous ordered materials called Metal-Organic Frameworks (MOFs) holds an enormous promise. MOFs are crystalline solids built from metal ions or clusters that are connected by organic linkers to form extended, ordered, and highly porous networks. Thanks to their (i) impressive and ordered porosity metrics and (ii) their versatility to be encoded with functionalities placed surgically at specific positions of their frameworks, MOFs have been successfully employed as matrixes to install amino acids and peptides. Once the pore space has been decorated with specific amino acid moieties, metal-sites can be easily installed by adsorbing them from aqueous or non-aqueous solutions.

In this work, we have decorated the mesopore space of the MOF-808 with amino acid and carboxylic acid molecules, to later, stabilize copper ions with varied coordination modes and clustering degrees. In a second step, we have unraveled the impact of the characteristics of the metal-sites on the catalytic wet oxidation (CWPO) of phenolic compounds. The features of the copper-sites installed within the framework have been studied by a combination of Infrared (IR), Raman, X-ray photoelectron (XPS), electron paramagnetic (EPR) and inelastic neutron scattering (INS) spectroscopies. Local structural models for the copper sites have been proposed after a crystallochemical analysis of the copper coordination modes with (amino)acid molecules found in the Cambridge Structural Database. The efficiency and selectivity of our system to oxidize phenolic pollutants through CWPO have been duly assessed, confirming that both the coordination modes and the clustering degree of the copper sites modulate its efficiency and selectivity to oxidize phenols through the hydrogen peroxide activation. The results presented in this work represent a milestone for the installation of metal-amino catalytic sites into the robust architectural backbone of MOFs, which successfully mimic those oxidative functions of metalloenzymes.

Acknowledgments: The authors thank the Spanish Agencia Estatal de Investigación (AEI) (EVOLMOF PID2021-122940OB-C31 (AEI/FEDER, UE), ENZYMOF (TED2021-130621B-C42) and Tailing23Green-ERAMIN). MSCA-RISE-2017 INDESMOF (No 778412), and H2020-RIA-4AirCraft (No 101022633) are also acknowledged. Basque Government Industry and Education Departments under the IKUR, ELKARTEK and IT1554-22 programs are also acknowledged.

3:00 PM BREAK

3:30 PM SB02.04.04

Bio-Inspired Photonic Microcapsules that Change Colors via Reversible Osmotic Actuation Ji-Young Lee¹, Jaehyun Kim², Jaekyoung Kim², Daeyeon Lee² and Leila Deravi¹; ¹Northeastern University, United States; ²University of Pennsylvania, United States

Animals have evolved complex and sophisticated mechanisms to control coloration, employing a combination of small molecules and nanostructured composites. Notably, chromatophores, specialized organs found in animals such as squids and octopuses, play a crucial role in dynamic color change. Chromatophores have the unique ability to modify their physical shape and size by expanding or contracting pigment-containing cells. This study introduces an artificial chromatophore system that uses osmotic annealing to trigger reversible color switching. To achieve this, we fabricate double emulsion droplets using polystyrene nanoparticles functionalized with the xanthommatin, the primary pigment found in the skin of cephalopods. The particle size and the pigment loading density into the system are influential factors in controlling the oscillation between pigmentary and structural colors which can be manipulated through annealing. We compared the reflectance spectra of photonic capsules from the presence and absence of pigments. Our findings highlight a distinctive and scalable approach for producing color-changing

materials, providing a versatile range of tunable visible colors.

3:45 PM SB02.04.05

Delivery of AuNCs into eXtracellular Vesicles by Fusion Using Ionizable Liposomes Cargos Ester Butera^{1,2}, Anis Ouzaid³, Solene Ducarre², Giuseppe Maccarrone¹, Annalinda Contino¹, Pascale Even-Hernandez², Celia Ravel^{3,4} and Valérie Marchi²; ¹University of Catania, Italy; ²Université de Rennes 1, France; ³CHU Rennes, France; ⁴University of Rennes 1, France

Extracellular vesicles (EVs) are well-known membrane-limited particles secreted by healthy and cancerous cells. EVs have heterogeneous size and three subtypes are described depending on the location of secretion: microvesicles, myelinosomes and exosomes. EVs are identified in human follicular fluid as a mode of communication in the ovarian follicle.¹ In addition EVs involved in cell-cell communication are considered as biomarkers for early cancer diagnosis. The analysis of their content and their labeling with easily detectable nanoparticles could enable the development of a powerful tool for the early diagnosis of specific diseases

In this view, gold nanoclusters (AuNCs) appear as a recent class of non-toxic fluorophores. Their brightness, their ultrasmall size (< 2 nm) and large window of fluorescence lifetime (1 ns - 1 μs) and their good biocompatibility make them an attractive alternative as fluorescent probes for biological labeling and bioimaging.² In addition, their ultra-small size facilitates their clearance when they are injected into the body. Their small size makes them attractive to encapsulate them into liposomes without damaging the compartment integrity and then to be delivered into the extracellular vesicles. We previously demonstrate that their direct attractive electrostatic interaction with extracellular vesicles result into the labelling of their membrane or disruption of the EVs into multilamellar structures.³

We investigated encapsulation of ultra-small-sized red and blue emitting Au NCs into liposomes of various sizes and chemical compositions. The efficiency of the process was correlated to the structural and morphological aspect of the AuNCs encapsulating vesicles via complementary analyses by SAXS, cryo-TEM, and confocal microscopy techniques. We confirmed the possible encapsulation of ultra-small-sized red and blue emitting Au NCs into liposomes of various sizes and chemical compositions. Cell-like-sized vesicles (GUVs) encapsulating red or blue Au NCs were successfully obtained by an innovative method using emulsion phase transfer. Finally, exosome-like-sized vesicles (LUVs) containing Au NCs were obtained with an encapsulation yield of 40%, as estimated from ICP-MS.⁴

Herein, we investigate the interaction of fusogenic liposomes encapsulating the AuNCs with EVs extracted from human seminal fluids. The composition of the membrane was optimized to improve the fusion properties of the liposomes. The mixture of the liposomes and EVs results in lipid exchange as demonstrated by FRET experiments and in increased size revealed by flux cytometry. The resulting fused hybridosomes were successfully isolated by size exclusion chromatography. They exhibit typical fluorescence of the AuNCs together with an increased size in agreement with the expected size of the fused exosomes. Besides their interest to analyze the EVs content, such hybridosomes could serve as drug or macromolecule carriers or nanosensors in living organisms.

[1] A.S. Neyroud et al. Basic and Clinical Andrology. 2021, 31, 25.

[2] R. M. Chiechio et al. ACS Appl. Nano Mater. 2023, 6, 10, 8971–8980.

[3] R. M. Chiechio et al. J. Phys. Chem. Lett. 2022, 13, 30, 6935–6943

[4] R. M. Chiechio et al. Nanomaterials. 2022, 12, 21, 3875.

4:00 PM SB02.04.06

Potential of Dendrimer-like Silica Nanoparticles Loaded with Cisplatin and Immune-checkpoint Inhibitors for Direct and Indirect Tumor Regression Taihyun Kim and Jinkee Hong; Yonsei university, Korea (the Republic of)

Since the development of cancer immunotherapy using immune checkpoint inhibitors (ICIs), significant improvements have been made in cancer treatment. However, there are still limitations in their clinical effectiveness, particularly in terms of low delivery to target sites. To address these limitations, we aimed to enhance the existing ICI-based immunotherapy strategies by combining them with chemotherapeutic agents.

To achieve this goal, we employed a one-pot sol-gel reaction to prepare dendrimer-like porous silica nanoparticles (DPSNs). These DPSNs possess a larger surface area compared to spherical particles of the same size, resulting in enhanced stability during long-term storage. Initially, we focused on conjugating cisplatin, a widely used chemotherapeutic anti-cancer agent, onto the surface of DPSNs. By modifying the DPSNs with carboxyl groups and loading cisplatin as a model anticancer drug, we investigated the release behavior of the drug molecules. Our findings revealed that cisplatin remained intact under neutral conditions but was released under acidic conditions, indicating the successful development of pH-responsive DPSNs (referred to as DPSN-cis).

Furthermore, we performed an EDC/NHS-sulfo reaction to modify aPD-1, one of the ICIs, onto the surface of DPSN-cis. This allowed us to create DPSN-ICIS, where both cisplatin and aPD-1 were simultaneously conjugated. Importantly, DPSN-ICIS exhibited no cytotoxicity even after three days of cell culture and demonstrated long-term physicochemical stability. To evaluate the effectiveness of DPSN-ICIS, we conducted in vitro experiments to assess its binding to PD-1 on T cells and its ability to induce cancer cell death. Subsequently, we validated these findings in vivo by demonstrating that DPSN-ICIS effectively performed both functions and led to tumor eradication. These results were further supported by analyzing immune responses to examine the behavior of DPSN-ICIS within a living organism.

Overall, our study highlights the potential of next-generation cancer immunotherapy by simultaneously loading chemotherapeutic agents capable of directly killing tumors and functionalizing various immune enhancers. The development of DPSN-ICIS addresses the limitations of current immunotherapy approaches, offering a promising strategy for more effective cancer treatment.

4:15 PM SB02.04.07

Vitalizing Immortal Nanodendritic Cells Functionalized with Immune-checkpoint Inhibitors for Tumor-localized Immunotherapy Taihyun Kim and Jinkee Hong; Yonsei University, Korea (the Republic of)

Recently, cancer immunotherapies combining nanotechnology have been highlighted due to the high impact of substantial clinical potential in various types of solid cancers. Especially, nanoparticle (NP)-based technology is a well-known and powerful tool for manipulating functionalities and ensuring in vivo stability, making it suitable for personalized cancer therapy. As an advanced form of immunotherapy using nanotechnology, the combination of cell-based therapy and NP technology has been emerging, for example, introducing cellular membranes or extracellular vesicles onto the NPs. This delivers the entire information of the cell membrane to the NP surface without damage and could be regarded as a useful technology for cell mimicking.

Meanwhile, dendritic cells (DCs) have been recognized as promising targets for immunotherapy due to their crucial role in T cell activation. However, administrated DCs in patients showed poor lifetime in vivo, which resulted in limited antigen-presenting capabilities in clinical trials. Furthermore, the storage and recovery of DCs for further usage are also challenging to retain DC survival rate and functionalities. To overcome these limitations, we have developed immortalized nanodendritic cells for cancer immunotherapy by combining DC therapy with cell-mimicking nanotechnology.

By utilizing immortalized DCs with extended lifetimes, we believe that continuous antigen presentation and T cell activation can be achieved in vivo. Our idea to prepare immortalized DC was inspired by cell membrane clocking technology which was first developed by L. Zhang et al. Using this technique, the whole DC membrane could be successfully decorated onto gold nanoparticle (Au NP), which is named artificial nanoDCs (anDCs). We optimized the manufacturing process of anDCs both biologically and thermodynamically to enhance their therapeutic efficacy. The optimized anDCs demonstrated thermodynamic stability and retained their functional abilities even after long-term storage of up to 30 days. We also confirmed the strong tumor regression effect of anDCs due to the fact that the nanosized DC can accumulate in the tumor site or lymph node without degradation, resulting in enhanced T cell activation in vivo.

Finally, to boost the T cell activation effect, the anDC was engineered with immune-boosting agents, immune-checkpoint inhibitors (ICIs). By direct engineering anDC with anti-CTLA-4 (aCTLA-4), we could obtain potent anDCs to induce T cell effector function efficiently. In our research, we validated the efficacy of aCTLA-4-conjugated anDCs in three different tumor models (MC38, CT26, and TC-1). Surprisingly, aCTLA-4-conjugated anDCs exhibited substantial tumor regression compared to the control group, as confirmed by in vivo immune analysis, which showed augmented tumor-infiltrating lymphocytes.

In summary, our objective was to develop optimized therapeutic drugs for cancer immunotherapy that can mimic the behavior of DCs. We successfully created a DC-mimicking therapeutic anticancer drug that can continuously and strongly activate tumor-specific T cells, thereby resulting in dramatic tumor regression. Furthermore, by conjugating various immune-boosting agents to anDC, we strongly anticipate that our material could be manufactured as desired and provided for patient-specific needs.

8:00 PM SB02.05.01

Metal-Organic Framework Coordinated with Single Fe Nanozymes and Gold Cluster for Biomedical Applications Subin Yu^{1,2} and Luke Lee²; ¹Ewha Woman's University, Korea (the Republic of); ²Harvard Medical School, United States

Metal-organic frameworks (MOFs) have been extensively utilized as substrates for constructing single-atom catalysts (SACs) due to their abundant ligands, enabling nanozyme-mediated biomedical applications. However, the preparation of SACs using MOF substrates typically involves harsh calcination processes to stabilize the single metal atom catalysts, which can lead to uncertain changes in the oxidation state of the metal centers, impacting the overall catalytic reaction. In this study, we have developed ultrasmall MOF-based single iron (Fe) atom Fenton-like nanozymes (referred to as Fe/MOF) by employing a simple mixing method. These nanozymes were combined with a gold nanocluster-embedded MOF mimic of glucose oxidase (referred to as Au/MOF), enabling cascade enzymatic reactions within living systems. To harness the abundant porosity of MOF and enhance cell cytotoxicity, the anticancer drug doxorubicin (DOX) was loaded inside Fe/MOF (referred to as Fe/DOX/MOF). Additionally, Au/MOF was further modified with a mitochondrial targeting moiety (triphenylphosphonium, TPP) to target the mitochondria and disrupt the cellular redox system. Internalization of Au/MOF into mitochondria resulted in glutathione (GSH) depletion through thiol-gold interactions, leading to mitochondrial excess lipid peroxidation. The constructed Fe/MOF exhibited an oxidation state of 2+ with Fe-N coordination bonds, demonstrating well-established Fenton-like nanozymes characteristics. The overall cascade enzymatic activity effectively generated hydroxyl radicals from glucose as a substrate. The generated gluconic acid induced an acidic environment that further accelerated the overall Fenton reaction. In vitro, studies demonstrated effective cancer eradication through cascade glucose oxidation and hydroxyl radical generation. GSH depletion-mediated down-regulation of GPx4, along with the delivered Fe²⁺, induced Fenton reaction-mediated lipid peroxidation, indicating ferroptosis. In vivo, studies further confirmed the overall therapeutic effects of the cascade enzymatic activity of Fe/MOF and Au/MOF. Our novel and straightforward synthesis process for MOF-based single-atom nanozymes and metal clusters present a new paradigm for fabricating single-atom nanozymes for multimodal cancer treatment.

8:00 PM SB02.05.02

Antibody Pre-Coated Zr-MOF as a Cloaking and Plug&Playable Platform for Targeted Delivery System Jun Yong Oh, Batakrishna Jana, Junmo Seong, Eun Min Go, Seongeon Jin, Jonghoon Bae, Chaiheon Lee, Seonghwan Lee, Tae-Hyuk Kwon, Jeong Kon Seo, Eunshil Choi, Sang Kyu Kwak, Myoung Soo Lah and Ja-Hyoung Ryu; Ulsan National Institute of Science and Technology, Korea (the Republic of)

Metal-organic framework (MOF)-based targeted drug delivery systems have made great strides and are widely used in a variety of scientific disciplines. Nevertheless, the biomolecular corona phenomenon makes it difficult to directly translate MOF agents into focused medication delivery systems. Here, we have established that pre-absorption of antibodies to MOF particle surfaces by supramolecular mixing can decrease protein adhesion in biological contexts, with effects akin to those of stealth shields. Furthermore, we further demonstrated that this mechanism may be influenced by the MOF's surface's pore size. The MOF particle was neither readily swapped with nor covered by biomolecule protein once the antibodies had been stably attached to it, indicating a stealth effect and an improved capacity to target both in-vitro and in-vivo. In addition, the generated antibodies-MOF platform may target various cancer cell lines by plugging multi-antibodies (dual and triple kinds). This study provides insights into the use of "antibody pre-absorption" as a promising method for developing MOF-based drug delivery systems.

8:00 PM SB02.05.03

Dual Drug Delivery Systems Based on Porous Fibers Grafted with ZIF67 Jooran Kim; Korea Institute of Industrial Technology, Korea (the Republic of)

Metal-organic frameworks (MOFs) have emerged as promising materials for various applications due to their exceptional tunability and high surface area. In recent years, the integration of MOFs with fibers has gained significant attention in the field of drug delivery systems. The combination of MOFs and fibers offers a unique platform for controlled release, targeted therapy, and enhanced drug stability, ultimately revolutionizing the field of therapeutics.

Moreover, researchers have explored the application of dual drug delivery using porous fibers with MOFs in various therapeutic areas, including cancer therapy, antimicrobial treatments, and regenerative medicine. These studies have demonstrated the potential of these systems to overcome drug resistance, reduce side effects, and enhance treatment efficacy by delivering multiple drugs simultaneously.

In this study, we developed porous poly(caprolactone) (PCL) fibers through liquid-liquid phase separation, and then ZIF-67 was grown on the porous PLA fiber through in-situ synthesis.

These carriers were investigated the relationship among pore formation, physical properties, and antibacterial activities of the fibers for identifying their potential as drug delivery carriers.

Studies have focused on optimizing the synthesis techniques to achieve uniform ZIF67 coatings on the surface of porous PCL fibers.

Suggested dual drug delivery system using porous PCL fibers with ZIF67 are the co-delivery of two drugs including lysozyme and gentamicin with complementary antibacterial effects. By encapsulating dual drugs inside pores of PCL and ZIF67, the dual drug delivery system achieves synergistic effects, improved drug stability, and controlled release kinetics. Furthermore, the selection of appropriate drugs and their optimal ratios play a crucial role in achieving desired antibacterial outcomes.

Overall, the research on dual drug delivery using porous fibers with ZIF67 highlights the potential of these drug carrier systems in achieving controlled release, synergistic effects, and improved antibacterial outcomes. Further advancements in the synthesis techniques, optimization of drug ratios, and comprehensive understanding of the in vivo behavior are crucial to translate these innovative systems into clinical applications and address the challenges associated with their practical implementation.

8:00 PM SB02.05.04

Capping UiO-Based and HKUST-Based Metal Organic Frameworks Towards Trapping and Controlled Release of Guest Molecules Samuel Darer, CalG. Lebak, David S. MacLeod, Abigail Berube, Shawn C. Burdette and Ronald L. Grimm; Worcester Polytechnic Institute, United States

Molecular caps for metal organic frameworks (MOFs) are particularly compelling for enabling capping and controlled release of guest payloads. Previously we utilized bulky triphenylacetate-based caps to trap guests within the pores of MOF-5. Presently, we extend these efforts to the UiO and the HKUST families for their tunable porosity, high stability, and varying chemistry to explore the interplay between interfacial chemical properties on the MOFs and the necessary capping chemistry. We utilized capping reactions including acetate exchange, growth with terminating single-acetate-group organics, and established functionalities for monolayer chemistries. Utilizing fluorine-tagged capping organics, X-ray photoelectron spectroscopy established which chemistry successfully capped each MOFs, and supported models of interfacial chemical states that exist on the MOF themselves. We aim to further develop capping abilities, expanding the control and variability of the caps that can be applied to MOFs and applying this research to wider potential applications.

8:00 PM SB02.05.05

Janus Hydrogel-Based Fuel Stimulant Powered Amplification for Multiple Detections of miRNA Biomarkers in Gastric Cancer Eun-Kyung Lim; Korea Research Institute of Bioscience & Biotechnology, Korea (the Republic of)

MicroRNAs (miRNAs) circulating in body fluid have emerged as potential biomarkers for various diseases; however, owing to their low concentrations and short lengths (~22 nt), their clinical applications are still limited. Therefore, a highly sensitive and selective novel diagnostic platform for miRNA detection is required. Here, we present a hydrogel-based fuel stimulant-powered (FSP) amplification of fluorescent signals to detect circulating miRNAs from clinical samples of human serum. The advantage of this method is that it has high sensitivity as a fuel-assisted DNA cascade reaction that does not require temperature control and enzymes used for nucleic acid amplification. Further, we developed a Janus-type hydrogel for the simultaneous detection of the gastric cancer-associated miRNAs, miR-135b and miR-21. The detection limit of this hydrogel-based FSP amplification using synthetic miRNAs was estimated as < 10 fmol. We also validated the performance of this amplification process in in vitro and in vivo models and clinical samples. Therefore, we demonstrate that Janus hydrogel-based FSP amplification can selectively and sensitively identify the overexpression of miR-135b and miR-21 in clinical samples, thereby helping distinguish gastric cancer patients from healthy donors.

8:00 PM SB02.05.06

The Product Development Process of Single Application Otitis Externa Drug Delivery System Emma Barrett-Catton, Kolton Sandau, Elizabeth Arrigali, Bogdan Serban and Monica Serban; University of Montana, United States

Background: Otitis externa, also known as outer ear infection, is a pathological condition that affects humans and animals. The standard of care for otitis externa is topical administration of ear drops. However, the high frequency of required administrations and duration of treatment are associated with poor patient compliance and increased risk for complications. We have developed a tetraethyl orthosilicate-based thixogel for use as single application treatment for otitis externa to increase ease of use and improve patient outcomes. For advancement to market, we have assessed the formulation's repeatability and reproducibility, release profiles of a variety of model drugs, impact of application-specific physiological factors, system scalability, and conducted shelf-life studies.

Methods: Thixogels were prepared by the hydrolysis of tetraethyl orthosilicate (TEOS) and subsequent combination with aqueous hyaluronan (HA) followed by the adjustment of the solution's pH to ~7.65. Thixogel properties (elastic modulus, thixotropy, drug release, dry substance) were tested for thixogels made with TEOS and HA from different manufacturers,

different concentrations of aqueous HA, and solution adjustments to a range of pH values. Elastic moduli and thixotropy were both determined with a rheometer. Dry substance content was measured with a moisture analyzer. Drug release was determined in vitro with the amount of drug released into saline at 37 °C measured using absorbance or fluorescence, depending on the model drug. Fluorescein, fluorescein disodium, green fluorescent protein, and blue dextran were all used as model drugs. The impact of ear canal-specific physiological factors, pH and enzymic activity, on drug release was evaluated using fluorescein.

Results: Thixogel properties remained consistent regardless of HA or TEOS manufacturer, aqueous HA concentration. Model drug properties, including molecular weight, and logP, impacted their release. Physiological factors did not seem to have an impact on model drug release profiles. A 100X scale-up from 20 mL to 2L resulted in no significant differences in fluorescein release, storage modulus, thixotropy, and dry substance between hydrogels. The shelf-life of the evaluated thixogels was found to be cold-chain independent, ranged from 4 months to 8.5-month and was dependent on the amount of HA in the formulation. Our data also indicates that longer shelf-life durations could be achieved by stabilizing the constituent HA and/or via product dosage form presentation.

Conclusions: Our results indicate that the developed thixogels are well suited for production and scalability, as they have a robust manufacturing process, have a wide tolerance for pH level, release a variety of model drugs (small molecule, protein, and polymer), and are not impacted by outer ear canal-specific physiological factors.

References:

- Barrett-Catton, E.; Arrigali, E.M.; Serban, B.A.; Sandau, K.C.; Serban, M.A. Manufacturability of a Tetraethyl Orthosilicate-Based Hydrogel for Use as a Single Application Otitis Externa Therapeutic. *Pharmaceutics* **2022**, *14*, 2020
- M.A. Serban, Thixotropic Delivery Systems, PCT/US/20/039551

Funding: This research was funded by a NIH Phase II STTR grant to M.A.S. and Promilad BioPharma, Inc. (DC017641– ‘Single application thixotropic antibiotic delivery systems for otitis externa’).

8:00 PM SB02.05.07

Host Cell-Mimetic Hybrid Nanoparticles as Antiviral Therapeutic Nano-Inhibitors for Influenza Virus EunjiJeong, GeunseonPark and SeungjooHaam; Yonsei University, Korea (the Republic of)

Unpredictable pandemic caused by respiratory virus such as coronavirus disease (COVID-19) poses a great threat to public health due to numerous infections and deaths. Despite the emergence of various diagnostic methods and vaccines, limitations persist in the development of effective antiviral therapeutic agents for promptly addressing newly emerging viruses. Host cell mimetic nanodecoy is an effective strategy to protect against the advancement of infection by neutralizing the virus, impeding its binding and entry into the lung cell membrane, which is the ultimate target of the virus. Herein, we develop an advanced biomimetic nanodecoy capable of trapping the target virus and preventing host cell infection using gold nanoparticles with various topologies and sizes through encapsulating by coating host cell membranes. We fabricated cell membrane-coated Spiky Gold nanoparticles (CM-SGNP) with various topologies, each ranging in size from 50 nm to 120 nm, using a seed-mediated growth method and physical extrusion. The CM-SGNP coated with the Madin-Darby canine kidney cell membrane could efficiently capture Influenza A virus (IAV) virions, providing evidence that the binding event and subsequent infection between host cells and virions will be inhibited. Interestingly, geometry matching between IAV virion and CM-SGNP according to the topology of CM-SGNP suggests that this system has the potential to be customized according to virus type and appearance by controlling the structure of CM-SGNP. Furthermore, CM-SGNP is expected to provide successful delivery and therapeutic effects in-vivo due to its superior biocompatibility characteristics. This system suggests the powerful strategy for treating infectious diseases by combining synthetic and biological materials. It is also the next-generation therapeutic agent that can be widely applied to various virus mutant and newly emerging disease X by setting the ultimate target of the virus to be a nano-inhibitor.

SESSION SB02.06: Biomimetic Self-Assembled Materials I

Session Chairs: Jonathan Sessler and Stefan Wuttke

Wednesday Morning, November 29, 2023

Hynes, Level 3, Room 307

8:30 AM *SB02.06.01

Self-Assembled Metal-Organic Framework Monolayers (SAMMs) Seth M. Cohen; University of California, San Diego, United States

The combination of polymers and metal-organic frameworks to obtain composite materials can take a number of forms, including mixed-matrix membranes (MMMs) prepared with MOFs, polymer-decorated MOF particles, and MOFs constructed from polymer building blocks referred to as polyMOFs. It has been demonstrated that polymer-decorated MOF particles, under the correction conditions, can form self-assembled MOF monolayers (SAMMs). These unusual materials allow for the formation of ultrathin MOF membranes and coatings that may find use in a range of MOF-based applications. This presentation will describe the synthesis, characterization, and properties of SAMMs as an interest MOF-polymer composite material.

9:00 AM *SB02.06.02

Supramolecular Self-Associating Amphiphiles (SSAs) – A Therapeutic Technology Platform? Plus, Can You Stop a Bullet with Protien? Jennifer Hiscock; University of Kent, United Kingdom

Our novel patented (European Patent Application No. 18743767.8, U.S. Patent Application No. 16/632,194), Supramolecular Self-associating Amphiphile (SSA) technology currently incorporates a library of ~ 120 amphiphilic salts and associated compounds, with structures containing an uneven number of hydrogen bond donating and accepting moieties. The anionic component of this class of compounds have been shown to self-associate through the formation of intermolecular hydrogen bonds producing anionic dimers in the polar organic solvent DMSO. Moving into aqueous conditions, SSAs self-associate to form spherical aggregates between 100 nm and 550 nm in hydrodynamic diameter. However, the presence of inorganic salt can cause these spherical aggregates to morph from sphere to fibre, producing a series of hydrogel materials.

Within a biological context we have shown these SSAs to:

- act as antimicrobial agents;¹
- increase the efficacy of other antibiotic/antiseptic agents and anticancer agents against bacteria² and ovarian cancer cells respectively;³
- selectively interact with phospholipid membranes of different compositions;⁴
- have the potential to act as drug delivery vehicles;⁵
- exhibit a druggable profile when delivered via i.v. in vivo to mice.⁶

Plus, some novel work from our group - can protien be engineered into a material that can capture supersonic impacts?⁷

References

1. N. Allen, L. J. White, J. E. Boles, G. T. Williams, D. F. Chu, R. J. Ellaby, H. J. Shepherd, K. K. L. Ng, L. R. Blackholly, B. Wilson, D. P. Mulvihill* and J. R. Hiscock*, *ChemMedChem*, **2020**, *15*, 2193.
2. J. E. Boles, G. T. Williams, N. Allen, L. J. White, K. L. F. Hilton, P. I. A. Popoola, D. P. Mulvihill* and J. R. Hiscock*, *Adv. Therap.*, **2022**, *5*, 2200024.
3. N. O. Dora, E. Blackburn, J. E. Boles, G. T. Williams, L. J. White, S. E. G. Turner, J. D. Hotherhall, T. Askwith, J. A. Doolan, D. P. Mulvihill, M. D. Garrett* and J. R. Hiscock*, *RSC Advances*, **2021**, *11*, 14213.
4. G. Townshend, G. S. Thompson, L. J. White, J. R. Hiscock* and J. L. Ortega-Roldan*, *Chem. Commun.*, **2020**, *56*, 4015.
5. L. J. White, J. E. Boles, K. L. F. Hilton, R. J. Ellaby and J. R. Hiscock*, *Molecules*, **2020**, *25*, 4126.
6. J. E. Boles, C. Bennett, J. Baker, K. L. F. Hilton, H. A. Kotak, E. R. Clark, Y. Long, L. J. White, H. Y. Lai, C. K. Hind, J. M. Sutton, M. D. Garrett, A. Cheasty, J. L. Ortega-Roldan, M. Charles,* C. J. E. Haynes* and J. R. Hiscock*, *Chem. Sci.*, **2022**, *13*, 9761-9773.

9:30 AM *SB02.06.03

Molecular and Polymeric Architectures Enabled by Dynamic Spiroborate ChemistryWeiZhang; University of Colorado-Boulder, United States

Dynamic covalent chemistry (DCvC) has proven to be highly effective toward the construction of well-defined molecular and polymeric architectures. The error-correction mechanism enabled by the reversible formation of dynamic covalent bonds leads to the formation of structurally ordered, thermodynamically favored species. One such example is the solvothermal synthesis of covalent organic frameworks (COFs) with periodic structural order and low defect density. The chemical compositions of such frameworks are usually well-defined and inter-monomer connectivity (covalent bonding) is robust. Bottom-up synthesis of covalently linked polymers through DCvC has many critical advantages, such as easy tunability of functional and structural properties in a controlled fashion through rational design of the precursors, formation of highly stable linkages, minimized structural defect, and possible access to sophisticated architectures that are hard to obtain otherwise. This talk will focus on our recent progress in the development of DCvC, specifically spiroborate bond exchange. This powerful transformation enabled the bottom-up design and synthesis of novel functional materials, such as unprecedented single-crystal DNA-like helical covalent polymers (HCPs) and shape-persistent redox active organic molecular cages.

10:00 AMBREAk

10:30 AM SB02.06.04

Engineering Metal-Phenolic Materials via Supramolecular AssemblyZhixingLin^{1,2}; ¹The University of Melbourne, Australia; ²The University of Melbourne, Australia

Coordination polymers (CPs) and their higher-dimensional and potentially porous subset, metal-organic frameworks (MOFs), are supramolecular materials comprising metal nodes and organic ligands. Over the past three decades, CPs in the crystalline state have been the primary focus of the field due to their defined structures, high internal surface areas, and potential for crystal engineering. The periodic arrangement of metals and ligands has facilitated fundamental research on controlling pore size and surface area, which are crucial for achieving improved performance in various applications. However, the practical application of these crystalline materials poses challenges in terms of maintaining accessible pore volumes, integrating into existing infrastructure, and addressing safety concerns arising from the use of toxic precursors and solvents during synthesis, as well as the rigid, brittle, and often unstable nature of crystalline CPs. In contrast, amorphous CPs have gained significant attention over the past decade due to the presence of amorphous domains, which increase pore size, mechanical robustness, and chemical stability of the materials, leading to improved functionality.

One type of amorphous CPs, known as metal-phenolic networks (MPNs), consists of metal ions and phenolic ligands and can be adhesive to diverse surfaces. Due to their ability to coat nanoscopic and macroscopic templates, MPNs have garnered considerable interest in various applications, including biomedicine, photonics, forensics, and biomolecule and fruit preservation. Different metal ions can be employed to confer specific functionalities to MPNs, such as fluorescence, magnetic resonance imaging, and catalytic activity, or to produce synergistic effects in combination with the phenolic ligand, such as buffering effects. Additionally, the amorphous structure of MPNs can endow them with unique material properties, such as higher mechanical robustness, increased stability, and improved processability. This presentation aims to provide an introduction to MPNs, covering their fundamental aspects and will highlight our recent significant progress in developing MPNs for various biomedical applications, including catalysis, intracellular tracking, and drug delivery.

10:45 AM SB02.06.05

Structure and Dynamics of Self-Assembled Lipid Nanoparticles for Nucleic Acid DeliveryShaynaHilburg and LiloD. Pozzo; University of Washington, United States

Nucleic acids can revolutionize human health outcomes, as evidenced by the mRNA vaccines used to combat COVID-19. Despite the success of these therapeutics, the fundamental physicochemical properties of the non-viral delivery vectors must be better understood to be more easily tuned and optimized. In this work, we use small-angle X-ray (SAXS) and neutron scattering (SANS) to assess how the storage and delivery conditions of the nanoparticles impact their structure and dynamics. The components which come together to encapsulate the nucleic acids have complex non-covalent interactions at the nanoscale which dictate their ability to withstand storage conditions and transport to cells while also disassociating upon intracellular delivery to release cargo. Here we show that the molecular interactions within the drug delivery vehicles, including exchange kinetics of the self-assembled molecules, are impacted by relevant environmental factors, including pH. Such information demonstrates what drives degradation and what parameters can be changed to improve delivery by increasing the efficiency of endosomal escape. Ultimately, these results can be used to optimize efficacy, enabling more flexible storage requirements, lower dosages, and improved therapeutic tolerances.

11:00 AM SB02.06.06

Injectable Granular Agarose/Alginate Beads - Spray Based Synthesis and Energetic Electron ModificationCatharinaKrömmelbein^{1,2} and StefanG. Mayr^{1,2}; ¹Leibniz-Institute of Surface Engineering (IOM), Germany; ²University of Leipzig, Germany

Granular hydrogels real highly interesting features for novel biomedical applications, including regeneration and drug delivery. Furthermore, properties like injectability and porosity, making them feasible for applications in 3D bioprinting and tissue engineering. High-energy electron irradiation combines sterilization and tuning of hydrogel properties without adding potentially cytotoxic chemicals. In this study, granular agarose/alginate hydrogels are prepared by electrospraying. Shear-thinning and self-healing characteristics of the entire granular hydrogel are studied employing rheology. Although viscoelasticity changes under irradiation, shear-thinning and self-healing prevails. These dynamic properties enable injection, which is demonstrated for 27 G needles. This study presents a mechanical characterization of high-energy electron irradiated granular agarose/alginate hydrogels that extends the diversity of available injectable hydrogels and provides a basis for biomedical applications of this scaffold.

[1] Carbohydrate Polymers 298, 120024 (2022)

11:15 AM *SB02.06.07

Visible Light as a Benign Stimulus for Additive Manufacturing of HydrogelsZachariahA. Page; The University of Texas at Austin, United States

Light as an energy source has enabled transformative technologies in imaging, lithography, adhesives, and 3D printing. Its broad utility arises from the unparalleled spatiotemporal control over chemical transformations that it offers. However, contemporary methods rely on high energy UV light (< 400 nm), which limits biocompatibility due to degradation and attenuation that occurs upon absorption and/or scattering. Excitingly, the recent commercialization of inexpensive light emitting diodes has opened up an avenue to examine mild visible-light induced reactions in the fabrication of biologically relevant scaffolds. This presentation will focus on how the ZAP Group has developed low energy light driven reactions to create macroscopic water-swollen scaffolds (i.e., hydrogels) with unprecedented speed and precision. Specifically, catalyst design principles to enable rapid solidification of photopolymer resins using visible-light will be discussed, along with their utility and optimization in high resolution additive manufacturing.

SESSION SB02.07: Biomimetic Self-Assembled Materials II

Session Chairs: Niveen Khashab and Jonathan Sessler

Wednesday Afternoon, November 29, 2023

Hynes, Level 3, Room 307

1:30 PM *SB02.07.01

Mimicking Melanin: Nature's Biopolymer of Intrinsic Microporosity as a Therapeutic Material for Tissue RepairNathanC. Gianneschi and KurtLu; Northwestern University, United States

Melanin is a class of essential biopolymer found across plant, animal, bacterial and fungal kingdoms with an astonishing array of functions, including pigmentation, radical scavenging ability, radiation protection, and thermal regulation. Nature synthesizes melanin of five known kinds: eumelanin, pheomelanin, allomelanin, neuromelanin and pyromelanin. Among them, eumelanin (black and brown pigment in dark hair) and pheomelanin (the pigment in red hair) are the two most commonly considered forms. The past two decades have witnessed a flourish of eumelanin-based materials, especially polydopamine. In our own work, we have endeavored to explore synthetic analogues that enhance, extend and build on these biomimetic systems to enrich melanin and melanin-like materials with desirable properties for a range of applications. A key property of interest here is the ability of properly engineered synthetic melanins to perform as high surface area "sponges" for absorbing toxins and to act as an efficient and stable scavenger of radicals. These synthetic porous melanin materials and a variety of modified analogues will be

described in terms of their function in tissue repair. Specifically in topical applications for healing damaged skin from chemical and radiation induced injury.

2:00 PM *SB02.07.02

Construction of Smart Supramolecular Drug Delivery Systems for Biomedical Applications Ying-Wei Yang; Jilin University, China

The design, synthesis, recognition, and assembly of functional macrocyclic receptors have been playing a critical role in supramolecular chemistry. Due to their superior properties and functions, supramolecular macrocycles, including cyclodextrins, cucurbiturils, calixarenes, and pillararenes, have attracted broad attention in the fields of organic supramolecular chemistry and materials science. Meanwhile, nanoparticles with unique characteristics and particular properties, such as mesoporous silica nanoparticles, metal-organic frameworks, gold nanoparticles, magnetic nanoparticles, and semiconductor nanocrystals, have shown ever-increasing importance in chemistry, materials science, nanoscience, and biomedicine. Upon combining the porous/nonporous inorganic solid nanoplateforms or even organized organic/polymeric nanosystems with supramolecular macrocycles, there is great potential to enhance the photophysical, chemical, electronic, and other related properties of solid supports and the host-guest property of supramolecular macrocycles expanding and advancing the applications of the resulting organic-inorganic hybrid materials.¹⁻⁸ In this talk, I will present our methodology and research progress of the chemical construction of smart supramolecular drug delivery systems hybridized with synthetic macrocycles and nanoparticles and showcase their applications in the areas of antimicrobial, anticancer, cell imaging, crop protection, biosensing, etc.

References

1. Wu, J.-R.; Wu, G.; Yang, Y.-W. *Acc. Chem. Res.* **2022**, *55*, 3191–3204.
2. Li, Z.; Yang, Y.-W. *Acc. Mater. Res.* **2021**, *2*, 292–305.
3. Yue, L.; Yang, K.; Lou, X.-Y.; Yang, Y.-W.; Wang, R. *Matter* **2020**, *3*, 1557–1588.
4. Li, Z.; Song, N.; Yang, Y.-W. *Matter* **2019**, *1*, 345–368.
5. Yang, J.; Dai, D.; Zhang, X.; Teng, L.; Ma, L.; Yang, Y.-W. *Theranostics* **2023**, *13*, 295–323.
6. Lou, X.-Y.; Zhang, G.; Song, N.; Yang, Y.-W. *Biomaterials* **2022**, *286*, 121595.
7. Lou, X.-Y.; Yang, Y.-W. *Aggregate* **2020**, *1*, 19–30.
8. Song, N.; Lou, X.-Y.; Ma, L.; Gao, H.; Yang, Y.-W. *Theranostics* **2019**, *9*, 3075–3093.

SYMPOSIUM SB03

Molecular Biomimetics—Biology Meets Materials Science and Artificial Intelligence at the Molecular Dimensions
November 27 - December 5, 2023

Symposium Organizers

Hanson Fong, University of Washington
Yuhei Hayamizu, Tokyo Inst of Technology
Kalpana Katti, North Dakota State University
Deniz Yucesoy, Izmir Institute of Technology

* Invited Paper

+ JMR Distinguished Invited Speaker

SESSION SB03.01: Lessons from Biology at the Molecular Dimensions

Session Chairs: Hanson Fong and Kalpana Katti

Monday Morning, November 27, 2023

Hynes, Level 1, Room 101

10:30 AM *SB03.01.01

Engineering of Advanced Biomaterials by Harnessing Biological Organization Principles Alvaro Mata; Nottingham University, United Kingdom

Living systems have evolved to grow and heal through biological organization principles (BOPs) capable of organizing molecular and cellular building-blocks at multiple size scales. These BOPs emerge from cooperative interactions and chemical networks between multiple components, which allow biological systems to diversify, respond, and optimize. This talk will present our laboratory's efforts to combine supramolecular events found in nature such as self-assembly, disorder-to-order transitions, or diffusion-reaction processes with engineering processes to design bioinspired materials and devices (Figure 1). I will also describe recent efforts aiming to go beyond "bioinspiration" and into "biocooperation". I will describe methodologies to develop a) dynamic hydrogels and in vitro models for cancer [1,2], b) self-assembling fluidic devices [3,4], and c) regenerative implants [5,6].

[1] C.L. Hedegaard, C. Redondo-Gómez, B.Y. Tan, K.W. Ng, D. Loessner, A. Mata, *Sci. Adv.* **2020**, *6*, eabb3298.

[2] D. Osuna de la Peña, S.M.D. Trabulo, E. Collin, Y. Liu, S. Sharma, M. Tatari, D. Behrens, M. Erkan, R.T. Lawlor, A. Scarpa, C. Heeschen, A. Mata, D. Loessner, *Nat. Commun.* **2021**, *12*, 5623.

[3] K.E. Inostroza-Brito, E. Collin, O. Siton-Mendelson, K.H. Smith, A. Monge-Marcet, D.S. Ferreira, R.P. Rodríguez, M. Alonso, J.C. Rodríguez-Cabello, R.L. Reis, F. Sagués, L. Botto, R. Bitton, H.S. Azevedo, A. Mata, *Nat. Chem.* **2015**, *7*, 897-904.

[4] Y. Wu, B.O. Okesola, J. Xu, I. Korotkin, A. Berardo, I. Corridori, F. Luigi, P. di Brocchetti, J. Kanczler, J. Feng, W. Li, Y. Shi, V. Farafonov, Y. Wang, R.F. Thompson, M.-M. Titirici, D. Nerukh, S. Karabasov, R.O.C. Oreffo, J.C. Rodríguez-Cabello, G. Vozzi, H.S. Azevedo, N.M. Pugno, W. Wang, A. Mata, *Nat. Commun.* **2020**, *11*, 1182.

[5] B.O. Okesola, A.K. Mendoza-Martinez, G. Cidonio, B. Derkus, D.K. Boccorh, D. Osuna de la Peña, S. Elsharkawy, Y. Wu, J.I. Dawson, A.W. Wark, D. Knani, D.J. Adams, R.O.C. Oreffo, A. Mata, *ACS Nano* **2021**, *15*, 11202-11217.

[6] Y. Wu, J. Yang, A. van Teijlingen, A. Berardo, I. Corridori, J. Feng, J. Xu, M.-M. Titirici, J.C. Rodríguez-Cabello, N.M. Pugno, J. Sun, W. Wang, T. Tuttle, A. Mata, *N. Adv. Funct. Mater.* **2022**, *32*, 2205802.

11:00 AM SB03.01.02

Biofilm-Inspired Underwater Peptide Adhesives Jing Yan, XinHuang and Sarvagya Saluja; Yale University, United States

Bio-adhesives are extensively used in biomedical applications including suture-less seal and wearable electronics, where there is a need to adhere two wet surfaces together. However, existing products, largely inspired by mussel adhesives, are expensive to produce and sensitive to environmental conditions limiting their wide application. We recently made a serendipitous discovery regarding how bacterial biofilms formed by *Vibrio cholerae*, the pathogen responsible for pandemic cholera, adheres to various surfaces using a unique short peptide. In this study, we will show a range of both biotic and abiotic surfaces suitable for this biofilm-inspired glue, and the molecular mechanism underlying the adhesive property of this peptide. Finally, I will discuss about our effort in establishing a fermentation-based process to scale up the production of the peptides.

11:15 AM SB03.01.03

Cephalopod-Inspired Optical Engineering of Mammalian CellsGeorgiiBogdanov, NikhilKaimal, AleezaFarrukh, AleksandraA. Strzelecka, AtrouliChatterjee and AlonGorodetsky; University of California, Irvine, United States

During the last several decades, cephalopods (e.g., squids, octopuses, and cuttlefish) have emerged as a powerful source of inspiration for the engineering of dynamic optical systems, due to their complex nervous systems, diverse behavioral patterns, and tunable structural coloration. We drew inspiration from the tunable optical functionality of cephalopod skin cells to engineer human cells for production of reflectin-based high refractive index subcellular architectures and, as a result, to possess tunable transparency-changing and light scattering capabilities (1). Additionally, we improved our control over the production of reflectin in human cells by genetically engineering cell lines to stably express reflectin, which enabled more extensive studies of reflectin-based subcellular architectures under physiological conditions (2). Moreover, we evaluated the optical properties of single cells with three-dimensional label-free holotomographic microscopy and quantitatively characterized their subcellular reflectin-based architectures without and with external chemical stimuli (1,2). Finally, we demonstrated the potential applications of high refractive index reflectin-based subcellular architectures as high contrast genetically encoded biomolecular reporters for various types of microscopy techniques (2,3). Our combined findings validate prior postulates about the mechanisms of cephalopod tunable skin coloration and may lead to the development of unique protein-based tools for various applications in biophotonics and bioengineering.

1) Chatterjee A., et al., *Nat Commun.*, **11**, 2708 (2020).

2) Bogdanov G., et al., *iScience*, 106854 (2023).

3) Chatterjee A., et al., *ACS Biomater. Sci. Eng.*, **9**, 978–990 (2023).

11:30 AM +SB03.01.04

Molecular Biomimetics - Molecular Technologies of the Future Through BiologyMehmetSarikaya; University of Washington, United States

Proteins are the workhorses in biology as they are the fundamental building blocks making up the hierarchical structures of the cells, establishing biomolecular communications via signal transduction, transporting ions, and carrying out enzymatic processes, all vital for life's functions. The proteins, therefore, could be useful tools in developing functional molecular devices, if they can be designed and engineered to function similar to that in organisms. Despite the enormous opportunities provided by proteins as fundamental molecular tools, their utility in engineering and practical technology has not been fully realized, and their use has so far been highly limited for single purposes, e.g., enzymatic functions. In addition to their complexity and cumbersome handling issues, at least for the practical engineer, the main reasons for the limited use of proteins in engineered systems are because of their long amino acid sequences, i.e., 100s of AAs and even 1000s, that lead to unpredictable folding patterns and the resulting functionalities that are not easily predicted or controlled. On the other hand, polypeptides, i.e., short amino acid sequences (10-50 AAs), functional components of proteins, offer similar opportunities as proteins, with the advantage of being easily designed and manipulated, although their folding structures and functions are difficult to control. Despite these difficulties, for more than last two decades, peptides have been used in a variety of practical implementations such as tiny enzymes, drugs, biofunctionalization of nanoparticle drug carriers, probe design for specific targets, and for biomineralization. Especially useful are the fact that peptide sequences can be designed such that they may self-assemble into predictable tertiary structures in aqueous solutions with controlled geometries and shapes such as nanofibers, strips, and 3-dimensional gel-like molecular scaffolds. Since the first publication (below), molecular biomimetics has been emerging as a convergent science and technology field in which hybrid technologies are developed by the tools of molecular biology, genetics, computational sciences, and machine intelligence combined with materials science and engineering. For the last 2+ decades, our laboratory has adapted directed evolution approaches and identified thousands of short peptide sequences (7-15AA) and utilizing them as molecular tool sets in developing molecular technologies. These genetically engineered proteins for inorganics, GEPIs, also dubbed as solid binding peptides, SBPs, can be used as tiny enzymes in, e.g., remineralization, surface functionalization in implants, designing heterofunctional probes and molecular constructs for molecular and ionic targets, and key components of functional nanodevices, such as peptide-enabled field effect transistors. Recent discovery of coherent bio/nano soft interfaces between the self-assembled solid binding peptides forming monomolecular two-dimensional molecular crystals on, and having chiral crystallographic relationships with, single atomic layer solids provides the key element in the development of brain-inspired molecular probes and logic devices by seamlessly integrating biology and solid-state materials at their smallest respective functional units. Based on the three fundamental biological principles of molecular recognition, gene manipulation, and self-assembly, molecular biomimetics is opening a new era in truly genetically engineered functional molecular materials and system of the future. M. Sarikaya et al., *Molecular Biomimetics: Nanotechnology through Biology*, Nature Mater., **2**, 577-585, 2003.

SESSION SB03.02: Applications and Devices in Materials and Medicine

Session Chairs: Haneesh Jasuja and Kalpana Katti

Monday Afternoon, November 27, 2023

Hynes, Level 1, Room 101

1:30 PM SB03.02.01

A Novel Bio-Adhesive for Wet Surfaces from *Vibrio Cholerae*SarvagyaSaluja, JingYan and XinHuang; Yale University, United States

Effective adhesion of surfaces in a wet environment is very useful for the biomedical and engineering fields (wearable electronics, suture-less seals, underwater pipeline repair, etc.). However, underwater adhesion has remained a significant challenge. Water prevents effective molecular contact between the adhesive and the substrate, a key step, and prolonged exposure to the aqueous environment deteriorates the adhesive, leading to cohesive failure. Currently, research efforts are taking inspiration from mussels and bacteria, creatures that overcome these challenges and can strongly adhere to underwater surfaces.

We recently discovered that a sequence of 57-amino acids (57-aa) in *Vibrio cholerae* biofilms is the primary contributor to their adherence to a variety of surfaces, both biotic and abiotic, such as glass, plastic, and lipid membranes. We have developed several biochemical and biophysical *in vitro* characterization methods to demonstrate the polypeptide's potential to function as a wet adhesive. Modifying the sequence and applying it to different surfaces has allowed us to identify key parameters of the polypeptide's adhesion ability, including aromaticity, positive charge, linkers, and repeating motifs. We also tested multiple *Vibrio cholerae* mutants to understand the surface adhesion as a biofilm. Finally, we collaborated with simulation groups to corroborate experimental data with theory. Understanding and establishing a model for the adhesion mechanism of the polypeptide enables better engineering of wet adhesives. Overall, we demonstrate that a 57-aa sequence of a *Vibrio cholerae* biofilm adhesin could be used as a glue for different underwater surfaces. Our findings contribute to the general development of superior wet adhesives.

1:45 PM SB03.02.02

Intermolecular Interactions of Protein-Mimetic Random HeteropolymersShaynaHilburg, TianyiJin, PriyaGanesh and AlfredoAlexander-Katz; Massachusetts Institute of Technology, United States

Amphiphilic synthetic random heteropolymers, specifically easily synthesized methacrylate-based polymers with side-chains selected to mimic peptide characteristics, have been demonstrated to provide a bio-inspired means for augmenting and even mimicking bio-macromolecular function. However, the statistical distribution of chains makes a nano-scale molecular analysis of particular moieties and motifs challenging experimentally. Through computational modeling, specifically atomistic molecular dynamics simulations, we provide nanoscale analysis of sequences to provide insight into how these synthetic polymers respond to their environments and interact with molecules around them. Having previously examined the self-assembly of single chains into globules with heterogeneous surfaces for the chains in solution, we now characterize their statistically derived properties in more complex environments. We show how the polymers which have limited dynamics on their own can change significantly as they interact with organic solvents, macromolecules, or surfaces. We explore environmentally-dependent driving forces and the stochastic behavior of the random polymers which impact kinetics and characterize resultant changes in polymer conformation. These changes are shown to be highly dependent upon the properties of both the polymer and the molecular interactions that take place. Our study, leveraging analysis techniques from both polymer physics and protein sciences, illuminates ways in which the polymers are similar to the proteins they are inspired by as well as avenues for applying the synthetic polymer assemblies in solution.

This work was supported by the Defense Threat Reduction Agency contract HDTRA11910011 and HDTRA12210005.

2:00 PM *SB03.02.03

Hierarchical and Stimuli-Responsive Hybrid Materials from High Information Content Building BlocksFrancoisBaneyx; University of Washington, United States

Solid-binding proteins are genetically engineered chimera that incorporate one or more solid-binding sequences at defined locations of their framework while retaining native function. These macromolecules are versatile building blocks for the fabrication of hybrid hierarchical materials that derive unique properties from the organization, interplay, and reconfiguration of organic

and inorganic units. Here, I will discuss how solid-binding proteins can be combined with self-assembled peptoid nanostructures and pre-synthesized or mineralized inorganic elements to create layered 3D architectures, achieve precise control over nanocrystal size, and build photocatalytic nanocomposites. I will also describe recent progress on the use of thermos-responsive solid-binding proteins to control nanoparticle assembly and disassembly and manipulate the outcomes of biomimetic mineralization.

2:30 PM SB03.02.04

Silk-Nanotraps for Selective Molecular Targeting. Understanding Potentials and Limitations of Functional Protein Super-Assemblies Alessandra Maria Bossi¹ and Devid Maniglio²; ¹University of Verona, Italy; ²University of Trento, Italy

We report about the development of tailor-made biomimetics stemmed from merging biology with polymer chemistry and material science. Aqueous-soluble nanotraps that behave as biomimetic receptors were prepared in the form of proteinaceous disordered super-assemblies, fixed by non-natural crosslinking. The specific formation of the nanotrap started from the biocompatible, nontoxic material, already in use in regenerative medicine, that is silk fibroin [1]. Pioneering a paradigm change, the tailor-made molecular recognition was conveyed to the silk nanotrap by the unconventional exploitation of the molecularly imprinted polymers (MIPs) technique, that is a specifically designed strategy to entail molecular recognition to a nanomaterial by means of a template-assisted synthesis [2,3], but herein methacrylated silk fibroin polypeptides were used as macromolecular building blocks. Such MIP synthetic protocol was optimized with the aid of surface response method. The silk-nanotraps, called bioMIPs, were physically and functionally characterized, demonstrating high affinity binding (nM) for the targets and selectivity [4]. Enzymatic degradation of the bioMIPs was studied. The biocompatibility of the nanotraps was confirmed. The nanotraps were further labelled with fluorescent tags and tested for imaging in cell cultures [6]. The bioMIP's synthesis proved a general route for entailing recognition towards proteins or small molecules [4,5], which let foreseen applications in sequestering molecular players in the onset and progression of diseases, to tackle the onset of molecular changes in cells, and opening for translational studies with roles in long term pathologies.

References

1. B. Kundu, R. Rajkhowa, S.C. Kundu, X. Wang Adv. Drug Deliv. Rev. 2013, 65, 457.
2. Y. Hoshino, T. Kodama, Y. Okahata, K.J. Shea J. Am. Chem. Soc. 2008, 130, 15242.
3. S. Piletsky, F. Canfarotta, A. Poma, A.M. Bossi, S. Piletsky, Trends Biotechnol. 2020, 38, 368.
4. A.M. Bossi, A. Bucciarelli, D. Maniglio, ACS Appl. Mater. Interfaces, 2021, 13, 312431.
5. A.M. Bossi, D. Maniglio, Microchem. Acta, 2022, 189, 66.
6. D. Maniglio, F. Agostinacchio, A.M. Bossi, MRS Advances, 2023.

2:45 PM BREAK

SESSION SB03.03: Bio/Solid-Interfaces I
Session Chairs: Francois Baneyx and Yuhei Hayamizu
Monday Afternoon, November 27, 2023
Hynes, Level 1, Room 101

3:15 PM SB03.03.01

Molecular Dynamics Simulations of cRGD-Conjugated PEGylated TiO₂ Nanoparticles for Targeted Photodynamic Therapy Giulia Frigerio, Paulo Siani, Edoardo Donadoni and Cristiana Di Valentin; Department of Materials Science, University of Milano-Bicocca, Italy

Active targeting strategies, exploiting the biological interaction between ligands on the surface of nanoparticles and the cell targets, are known to increase the therapeutic efficacy of cancer treatments with respect to passive targeting strategies that are mainly based on the enhanced permeability and retention effect of tumor tissues. In this respect, the conjugation of nanoparticles with integrin $\alpha_v\beta_3$ -affine cyclic RGD peptides (cRGD) is a promising approach in nanomedicine to efficiently reduce off-targeting effects and enhance the cellular uptake by integrin-overexpressing cancer cells.

We used atomistic molecular dynamics simulations to evaluate key structural-functional parameters of cRGD ligands conjugated to PEGylated TiO₂ nanoparticles for an effective binding activity towards $\alpha_v\beta_3$ integrins. An increasing number of ligands has been conjugated to PEG chains, grafted to highly curved TiO₂ nanoparticles, to unveil the impact of cRGD ligand density on its presentation, diffusion, and conformation in an explicit aqueous environment.

We find that a low density leads to an optimal spatial presentation of cRGD ligands out of the "stealth" PEGylated layer around the nanosystem, favoring a straight upward orientation and a spaced distribution of the targeting ligands in the bulk-water phase. On the contrary, a high density favors the clustering of cRGD ligands, driven by a concerted mechanism of enhanced ligand-ligand interactions and reduced water accessibility to the ligand's molecular surface. These findings strongly suggest that the ligand density modulation is a key factor in the design of cRGD-conjugated nanodevices to maximize their binding efficiency to over-expressed $\alpha_v\beta_3$ integrin receptors.

3:30 PM *SB03.03.02

Computer Simulations of the Interaction of Anaesthetic Molecules Fentanyl and Propofol with Biological Membranes Nora H. de Leeuw; University of Leeds, United Kingdom

Computational techniques are well placed to investigate materials and processes in the body that are difficult to access experimentally. In this work we have used all-atom computer simulations to predict the structures and behaviours with biological membranes in the cell of two important molecules in the process to induce anaesthesia, i.e. propofol and fentanyl. The lipid membrane is considered a crucial component of opioid general anaesthesia and detailed atomic-level insight into the drug-membrane interactions could lead to a better understanding how different drugs exert their anaesthetic properties.

First, we have investigated the opioid analgesic fentanyl on its own, using extensive umbrella sampling molecular dynamics simulations to study the permeation process into a variety of simple phospholipid membrane models, accurately predicting the permeability coefficients, followed by its interactions with the *Gloeobacter violaceus* ligand-gated ion channel (GLIC). The simulations have identified multiple extracellular fentanyl binding sites, which are different from the transmembrane general anaesthetic binding sites observed for propofol and other general anaesthetics, including a novel fentanyl binding site within the GLIC which results in conformational changes that inhibit conduction through the channel.

The second part of our study explicitly includes the interactions between fentanyl and propofol. General anaesthesia is a multi-drug process and our work provides the first insight into how different components in the anaesthesia process interact with each other in a relevant biological environment. For example, using flooding style and gaussian accelerated molecular dynamics (GaMD) simulations, we show fentanyl acting as a stabiliser that holds propofol within binding sites in GLIC, whereas the simulations were also able to show the pathway by which propofol physically blocks the ion-conducting channel pore, which has previously been suggested as a mechanism for ion channel modulation by propofol.

4:00 PM *SB03.03.03

Modeling Peptide-Guided Organization of 2D Materials Ruitao Jin, Le Nhan Pham and Tiffany Walsh; Deakin University, Australia

Peptides have capability to direct organization of nanomaterials in aqueous media. However, for two dimensional (2D) nanosheet structures such as graphene, h-BN, graphene oxide and MoS₂ there is a lack of fundamental knowledge regarding structure/function relationships of the relevant bio-nano interface. Combined with experimental efforts, molecular simulations can provide new insights into the manipulation of these interfaces.¹⁻³ Here, a strategy based on bioconjugate hybrids of peptides and fatty acids is used to exfoliate materials into 2D nanosheets in liquid water. These simulations reveal the molecular scale characteristics of the peptide-driven exfoliation process, particularly in the role of the fatty acids in potentially reducing graphene defects in the exfoliated material.^{3,4} Umbrella sampling simulations also provide new insights into both the peptide-driven exfoliation and colloidal suspension mechanisms.⁵ Advancements in the simulation strategy used here hinge on the ability to model peptide/h-BN and peptide/MoS₂ interfaces⁶ in aqueous media, based on force-fields obtained from first-principles calculations. Replica-exchange with solute tempering molecular dynamics simulations are used to explore the contact between the peptides and the nanosheets. Ultimately the outcomes of this modeling can guide the design⁷ of effective bioconjugates for exfoliation and assembly for 2D heterostructures.

[1] A. D. Parab, A. Budi, J. M. Slocik, R. Rao, R. R. Naik, T. R. Walsh, M. R. Knecht, J. Phys. Chem. C, 124, 2219-2228 (2020).

[2] N. Brljak, A. D. Parab, R. Rao, J. M. Slocik, R. R. Naik, M. R. Knecht, T. R. Walsh, Chem. Commun., 56, 8834-8837, (2020).

[3] A. D. Parab, A. Budi, N. Brljak, M. R. Knecht, and T. R. Walsh, Adv. Mater. Interfaces, 8, 2001659 (2021).

[4] N. Brljak, R. T. Jin, T. R. Walsh, and M. R. Knecht, Nanoscale, 13, 5670-5678 (2021).

[5] R. T. Jin, F. Vuković and T. R. Walsh, J. Phys. Chem. Lett., 12, 11945-11950 (2021).

- [6] L. N. Pham and T. R. Walsh, *Chem. Sci.*, 13, 5186-5195 (2022).
[7] R. Jin and T. R. Walsh, *Adv. Mater. Interfaces*, 9, 2102397 (2022).

4:30 PM *SB03.03.04

Multiscale Mechanics of Cancer Metastasis to Bone Dinesh R. Katti, Sharad V. Jaswandkar, Hanmant Gaikwad and Kalpana Katti; North Dakota State University, United States

The World Health Organization reported that over one million deaths occur worldwide due to breast and prostate cancer. The majority of these deaths occur due to metastasis of the cancer to distant locations in the body, which for breast cancer and prostate cancer happens to be bone. At the bone site, the cancer cells colonize, proliferate, and have a very detrimental impact on the bone. Clinically, this is manifested as frequent skeletal failures. In order to recapitulate the metastasis process through a realistic testbed, we have developed an in vitro model of bone metastasis using nanoclay bone mimetic scaffolds. Experiments using commercial and patient-derived cancer cell lines to create metastasized tumors indicate significant changes to the morphology of the cancer cells based on the cancer phenotype. Also, depending on the phenotype, the mechanical properties of the cancer cells extracted from the tumors are dramatically altered. Associated with the observed changes, we observe significant changes in gene expressions related to actin and actin depolymerization factor cofilin (ADF/cofilin). Confocal imaging of cancer tumors during cancer progression reveals significant actin dynamics, both quantitatively and spatially. Label-free discrimination of cancer progression using Raman imaging and cluster analysis also reveals actin dynamics and changes to actin-related bands, which could serve as spectral biomarkers for cancer progression at the bone site. Steered molecular dynamics simulations of actin and actin with ADF/cofilin describe the mechanisms of the resilience of actin molecules and depolymerization of actin by ADF/cofilin, critical players in the actin dynamics during the cancer progression. Hence, actin remodeling plays a vital role in cancer metastasis progression and pertains to cellular behavior inside the cell. In order to evaluate the molecular phenomena outside the cell, we investigate the characteristics of integrin molecules. The integrin protein is a mechanotransducer establishing mechanical reciprocity between the extracellular matrix and cells at integrin-based adhesion sites. This protein plays a critical role in cell-ECM adhesion and cellular signaling. We conducted steered molecular dynamics (SMD) simulations to investigate the mechanical responses of integrin $\alpha\beta3$ with and without ligand binding for a variety of mechanical loading paths. The ligand-binding integrin confirmed the integrin activation during equilibration by opening the hinge between βA and the hybrid domain. This activation of liganded $\alpha\beta3$ integrin influenced the molecule's stiffness observed during tensile loading. Furthermore, we observed that the interface interaction between β -tail, hybrid, and epidermal growth factor domains altered integrin dynamics. The deformation of extended integrin models in the bending and unbending directions of integrin reveals the stored folding energy and the directionally dependent stiffnesses of the integrin molecule. Along with experimental data, the SMD simulations were used to evaluate the mechanical properties of integrin and identify the underlying mechanisms of integrin-based adhesion substrates. The investigation of the mechanics of integrin molecules provides new insights into understanding the mechanotransmission between cells, ECM, and the substrate. Overall the mechanotransduction facilitated by integrins to actin remodeling at the cellular insides is a critical molecular phenomenon that exists over a multiscale regime that synergistically creates the metastasis progression of cancer.

SESSION SB03.04: Synthesis, Restoration and Regeneration of Biological Hard Tissues
Session Chairs: Nurit Ashkenasy and Deniz Yucesoy
Tuesday Morning, November 28, 2023
Hynes, Level 1, Room 101

8:30 AM SB03.04.01

Development of Self-Assembled Organothiol-Based Nanolithography Templates for Biomimetic Synthesis of Calcium Phosphate on Amyloid-Like Amelogenin

Nanoribbons Jayesh Dua¹, Stefan Habelitz² and James J. De Yoreo^{1,3}; ¹University of Washington, United States; ²School of Dentistry, University of California, San Francisco, United States; ³Pacific Northwest National Laboratory, United States

Tooth enamel is the hardest tissue in the body mainly due to the intricate interwoven structure of highly organized apatite filaments that form it. It has been theorized that unidirectionally aligned (co-aligned) amyloid-like amelogenin nanoribbons (Amel NR) guide the formation of apatite by providing an energetically and stereochemically favorable scaffold for nucleation and transformation of amorphous calcium phosphate (ACP) precursor to hydroxyapatite (HAP). To understand the efficacy with which protein structures direct the nucleation of ACP and the subsequent transformation to HAP, studies have been carried out to quantitatively analyze the nucleation of ACP by self-assembled NRs of the full-length protein as well as varying sequences of peptides made up of protein subsegments responsible for self-assembly and ACP binding. Supramolecular block-copolymer templates with alternating hydrophilic and hydrophobic regions were also used to direct the self-assembly of amelogenin-derived peptide nanoribbons having discrete, spatially separated domains. These domains in turn templated the mineralization of filamentous and plate-shaped calcium phosphate. To create more versatile templates, we are using AFM-based nanolithography to create highly modifiable nanopatterns of novel organothiol monolayers self-assembled on Muscovite Mica. By using AFM probes, we perform Nanografting on monolayers of hydrophobic organothiols on Mica in predetermined patterns and backfill the patterns with hydrophilic thiols. The proposed system is similar to the block-copolymer system in its basic function, but with the capability of modifying the design on-the-fly to study the effects of geometry. While similar thiol systems on metal substrates (like nearly-atomically flat Au substrates) have been extensively studied and are even now used for a multitude of applications, the proposed system offers significantly better reproducibility, reusability, and affordability. Although the proposed system has been developed for the use of templating the growth of Amel NRs, it has the potential to be employed for a variety of other applications by modifying the surface chemistry of the Organothiol headgroups. Additionally, since Mica is the preferred substrate for the study of many soft matter systems, it provides the possibility of the direct study of many of these systems, eliminating the need for the modification of the parent molecule to enable its binding to the substrate. Monolayers of long chain alkanethiols (like the ones used on gold substrates) with average roughness ≈ 0.2 nm have already been achieved with extremely adaptable grafting pattern thicknesses ranging from 50 nm-200 nm. By manipulating the spacing and dimensions of the 2D-patterns, as well as the composition of the mineralizing solution, we seek to find understand the controls of scaffold geometry on nucleation and growth rates of the ACP precursor domains, as well as their transformation to HAP. Understanding how manipulating the scaffold geometry affects the fidelity of guided mineralization will move us closer towards the biomimetic synthesis of enamel-like materials.

8:45 AM SB03.04.02

Peptoid-Controlled Synthesis of Hierarchical Composite Nanomaterials Chun-Long Chen; Pacific Northwest National Laboratory, United States

In nature, biominerals (e.g. bones and teeth) are excellent examples of hierarchical composite materials whose formation and functions are controlled over multiple length scales by high information content biomacromolecules. Inspired by nature, many biomimetic approaches have been developed for the design and synthesis of composite materials. These approaches are attractive because they generate complex, functional materials under mild aqueous synthetic conditions.^{1,2}

As one of the most advanced classes of sequence-defined peptide-mimetics, peptoids offer tremendous opportunities for bio-controlled synthesis of hierarchical composite materials,^{3,4,5} mimicking protein- and peptide-like molecular recognition. Due to the lack of backbone hydrogen bonding, tuning peptoid-peptoid and peptoid-particle interactions can be done solely by varying side-chain chemistry.^{1,5} Peptoids have been exploited as programmable building blocks to assemble into highly ordered nanostructured materials with a variety of morphologies.^{3,6} In this presentation, we will report our recent progress of developing self-assembling peptoids for controlled formation and morphogenesis of hierarchical composite nanomaterials. A combination of *in situ* imaging and molecular simulations were used to elucidate the principles underlying peptoid-controlled inorganic crystallization with the ultimate goal of enabling predictive materials synthesis across scales.

- (1) Shao et al., *Chem. Rev.* **2022**, 122 (24), 17397; Li et al., *Chem. Rev.* **2021**, 121 (22), 14031.
(2) Chen et al., *Angew. Chem., Int. Ed.* **2010**, 49 (11), 1924.
(3) Yang et al., *J. Colloid Interface Sci.* **2023**, 634, 450; Jian et al., *Nature Comm.* **2022**, 13 (1), 3025; Wang et al., *Science Adv.* **2021**, 7 (20), eabg1448.
(4) Jin et al., *Angew. Chem., Int. Ed.* **2022**, 61 (14), e202201980; Yan et al., *Nature Comm.* **2018**, 9 (1), 2327.
(5) Yang et al., *Chem. Mater.* **2021**, 33 (9), 3047; Cai et al., *Acc. Chem. Res.* **2021**, 54 (1), 81.
(6) Song et al., *ACS Materials Letters* **2021**, 3 (4), 420; Jin et al., *Nature Comm.* **2018**, 9 (1), 270; Ma et al., *Nature Mater.* **2017**, 16, 767; Jin et al., *Nature Comm.* **2016**, 7, 12252.

9:00 AM *SB03.04.03

Freeze Casting Peptide-Enabled Biomaterials for Tissue Regeneration Ulrike G. K. Wegst; Northeastern University, United States

While considerable progress has been made over the past years and decades, the challenge persists to synthesize, ideally off-the-shelf materials and scaffolds, with structural, mechanical, and chemical cues akin to the natural tissue or custom-designed for a desired regenerative outcome. Freeze casting permits to manufacture such complex, hybrid materials with excellent control of structural and mechanical properties. As a cold process, freeze casting additionally offers several pathways to introduce what could broadly be called chemical cues such as growth factors, viral vectors and peptides at several processing steps to enhance the functional properties of the final biomaterial. Chemical cues can be introduced already before the freeze casting step

through peptide loading and peptide-functionalized components, such as collagen, chitosan, and nanocellulose for soft and hydroxyapatite and tricalcium phosphate for hard tissues, for example. Alternatively, the hierarchical architecture of the freeze-cast scaffolds can be modified with peptides or peptide-enhanced entities once the structure has been ice-templated and lyophilized (freeze-dried). Freeze casting and related manufacturing techniques therefore hold great promise for the manufacture of peptide-enabled biomaterials.

9:30 AM SB03.04.04

Biomimetic Strontium Sulfate Mineralization Studied by Multiscale Microscopy and Vibrational SpectroscopyAndrienneMartin¹, JordanHachtel², OliverWang¹, DawnM. Raja Somu¹, StevenA. Soini¹, DianneLacambra-Rivera¹ and VivianMerk¹; ¹Florida Atlantic University, United States; ²Oak Ridge National Laboratory, United States

In the present study, we investigated the in-vitro crystallization of strontium sulfate (celestite, SrSO₄) in the presence of organic matter, including the synthetic polymer poly(sodium 4-styrenesulfonate), the poly amino acid poly(L-glutamic acid), the polysaccharide poly(galacturonic acid) and the amino acid L-aspartic acid. In nature, biogenic SrSO₄ occurs in the skeleton of the unicellular plankton organisms Acantharia^{[3],[4]}. These biomineral model systems closely mimic fundamental interactions between mineral and organic matrix in living organisms, while eliminating the complexity and heterogeneity associated with biological systems. This investigation enabled a focused fundamental investigation of SrSO₄ crystallization across multiple length scales, as biologically grown minerals often contain a variety of organic molecules in small weight percentages as well as considerable amounts of foreign ions, such as magnesium, which complicate data interpretation^{[1],[2]}. Even though all studied biomolecules were included into the growing crystals in high weight percentages, poly(L-glutamic acid) had the most profound impact on crystal morphology. Using Scanning Electron Microscopy and Atomic Force Microscopy, we observed mesocrystalline features on the crystal surface, which are consistent with biomolecule incorporation. Apart from studying the chemistry of the nanocomposites using bulk infrared spectroscopy, we discerned intracrystalline organics at the nanoscale using monochromated Electron Energy-loss Spectroscopy in the Scanning Transmission Electron Microscope^{[5],[6]}. By screening the organic-biomineral model systems with synchrotron X-ray powder diffraction^{[1],[2]}, we quantified the degree of internal residual strain resulting from biomolecules with diverse functional group chemistry.

Acknowledgements

Dr. Merk thanks the National Science Foundation (NSF 2137663, Division of Materials Research) for supporting this study.

References

- [1] B. Pokroy, J.P. Quintana, N.C. El'ad, A. Berner, E. Zolotoyabko, Anisotropic lattice distortions in biogenic aragonite, *Nat. Mater.* 3 (2004) 900–902.
- [2] M.A. Hood, H. Leemreize, A. Scheffel, D. Fairve, Lattice distortions in coccolith calcite crystals originate from occlusion of biomacromolecules, *J. Struct. Biol.* 196 (2016) 147–154.
- [3] V. Merk, J. Decelle, S. Chen, A. Lanzirotti, M. Newville, O. Antipova, D. Joester, Selective Ion Accumulation in Biomineralizing Marine Acantharia, *Microsc. Microanal.* 25 (2019) 1072–1073. <https://doi.org/DOI: 10.1017/S1431927619006093>.
- [4] D. Raja Somu, T. Cracchiolo, E. Longo, I. Greving, V. Merk, On stars and spikes: Resolving the skeletal morphology of planktonic Acantharia using synchrotron X-ray nanotomography and deep learning image segmentation, *Acta Biomater.* (2023). <https://doi.org/https://doi.org/10.1016/j.actbio.2023.01.037>.
- [5] J.A. Hachtel, J. Huang, I. Popovs, S. Jansone-Popova, J.K. Keum, J. Jakowski, T.C. Lovejoy, N. Dellby, O.L. Krivanek, J.C. Idrobo, Identification of site-specific isotopic labels by vibrational spectroscopy in the electron microscope, *Science* (80-.). 363 (2019) 525 LP – 528. <https://doi.org/10.1126/science.aav5845>.
- [6] P. Rez, T. Aoki, K. March, D. Gur, O.L. Krivanek, N. Dellby, T.C. Lovejoy, S.G. Wolf, H. Cohen, Damage-free vibrational spectroscopy of biological materials in the electron microscope, *Nat. Commun.* 7 (2016) 10945. <https://doi.org/10.1038/ncomms10945>.

9:45 AMBREAK

10:15 AM *SB03.04.05

Emulating Nature's Way of Making MaterialsJamesJ. De Yoreo^{1,2}; ¹Pacific Northwest National Laboratory, United States; ²University of Washington, United States

From harvesting solar energy to capturing CO₂ to purifying water, living organisms have solved some of the most vexing challenges now faced by humanity. They have done so by creating a vast library of proteins and other macromolecules that can assemble into complex architectures and direct the mineralization of inorganic components to produce materials characterized by a hierarchy of structure. While the high information content contained within the intricate sequences of the proteins is crucial for accomplishing these tasks, self-assembly and mineralization are nonetheless constrained to proceed according to the physical laws that govern all such processes, even in synthetic systems. An understanding of the mechanisms by which biological systems successfully manipulate those laws to create hierarchical materials would usher in an era of materials design to address our most pressing technological challenges. In this talk, I will present the results of recent research using in situ atomic force microscopy and in situ transmission electron microscopy to directly observe interfacial structure, protein self-assembly, and nanocrystal formation in biomolecular and biomimetic systems, including protein-directed nucleation of calcium carbonate and calcium phosphate and surface-directed nucleation of two-dimensional protein assemblies. The results elucidate the mechanisms by which the interface between biomolecules and materials directs nucleation, self-assembly and crystal growth, leading to unique materials and morphologies. The results reveal the importance of surface charge, facet-specific binding, solvent organization, and, more generally, the balance of protein-substrate-solvent interactions in determining how organized materials emerge in these systems.

10:45 AM SB03.04.06

Degradation of Natural Molecules on Mineral SurfacesColinFreeman¹, BiaFonseca², MatthewCollins^{2,3} and KarinaSand²; ¹University of Sheffield, United Kingdom; ²University of Copenhagen, Denmark; ³University of Cambridge, United Kingdom

Molecular binding at material interfaces is vitally important within a range of contexts. When a molecule has bound to a surface its structure and that structure of the local solvent can be very different to that in solution which can change its functionality and reactivity. In biology deamidation and hydrolysis are two very common processes to break up peptides and both dependent on water molecules; therefore understanding the behaviour of the solvent molecules is equally important as that of the biologically active binding molecule. These decay processes are very important in a range of scientific fields including archaeology, palaeontology and surface fouling. Peptides extracted from archaeological digs can be used to indicate the diet and patterns of early humans, while DNA and proteins can be used to provide information on evolution in the fossil record.

We present a combined molecular dynamics and atomic force microscopy study on the binding of biological relevant molecules to calcite mineral surfaces. Our study examines and identifies the key factors involved in the binding of these molecules to the surfaces. We then explore the structural changes in these molecules and how this exposes/shields them from reactive processes that could lead to their decay. Finally we examine the behaviour of the other reactant species (solvent) and determine the role of the surface in enhancing or hindering their contribution to degradation reactions [1]. With this information we are able to comment on recent experimental findings and the potential preservation of different biological molecules.

[1] *Chemical Physics* 561 (2022) 111602

11:00 AM *SB03.04.07

Optimizing the Information-To-Damage Ratio in Transmission Electron Microscopy of Beam-Sensitive MaterialsBryanReed¹, RuthS. Bloom¹, GonzaloEyzaguirre¹, AbdolrezaMoghadam¹, CurtHenrichs¹, DanielJ. Masie¹, HirokiHashiguchi², KazukiYagi^{2,1}, YuJimbo², JonathanPeters³ and LewysJones³; ¹IDES, Inc., United States; ²JEOL, Ltd., Japan; ³Trinity College Dublin, The University of Dublin, Ireland

One of the biggest challenges in transmission electron microscopy (TEM) of biological materials is their high radiation sensitivity coupled with low contrast, making it hard to extract the desired information before the material is destroyed. There has been considerable progress on this problem, including improvements in sample preparation, data analysis, measurement technique, and dose-efficient acquisition strategies such as ptychography.

We believe that even more can be done, through high-speed timing systems that coordinate signal processing, data analysis, and beam current modulation. Guided by the mathematics of information theory and sparsity-based multidimensional data processing, we will outline a vision that combines ptychography, per-pixel dose modulation, adaptive sampling, and real-time signal response towards maximizing the ratio of relevant information to damage.

A key enabling technology is electrostatic dose modulation (EDM), using a fast electrostatic beam blanker to control exposure times and, using pulse width modulation, beam current. By synchronizing EDM with the timing control signals from a scan generator, we can precisely control the dose in every single pixel of a large scan. This can be done iteratively, using the data returned from previous scans to decide exactly when and where to apportion the dose in future scans. This methodology will enable closed-loop automated data capture, inserting any desired algorithms (machine learning, Bayesian, sparsity-based, etc.) into the loop to customize the acquisition to specific applications.

Improving the ratio of relevant information to damage can be done by:

Increasing the information-to-dose ratio: Using information theory to guide where to put your electron budget to learn the most and when to move on.

Increasing the fraction of relevant information: Adaptive sampling and spatial dose modulation to measure the components you care most about while avoiding delocalized damage from the irradiation of nearby uninteresting material.

Making the best use of the information you collect: Data analysis that takes the best lessons from the compressive sensing literature to leverage prior knowledge into better images.

Reducing the damage-to-dose ratio: Optimally spreading the dose in space and time to limit nonlinear damage effects, and automatically limiting the exposure of any included high-atomic-number material with its associated high energy deposition rate.

These are not mutually exclusive; with a sufficiently advanced, configurable acquisition automation system, one could do all of these at once, compounding the advantages from each. In the end, the microscope stops being a passive tool for taking images to be interpreted by the user and starts being an active participant, seeking out and optimally collecting the information you actually need while carefully minimizing damage to the sample.

11:30 AM *SB03.04.08

Biomaterialomics: Convergence of Data Science with Biomaterials ScienceBikramjitBasu; Indian Institute of Science, India

Conventional approaches utilise intuitive tailoring of manufacturing protocols and biocompatibility assessment, while developing new biomaterials and implants; leading to longer development cycles, and high costs. For the patient care, it is critical to accelerate the production of implantable biomaterials, implants and biomedical devices. In this perspective, the concept 'Biomaterialomics' (Acta Biomaterialia, 2022) as the integration of high-throughput biocompatibility data together with multiscale physics-based models, E-platform/online databases of clinical studies, with artificial intelligence (AI) tools, will be introduced and discussed in this presentation. It will be argued that such approach will enable the development of the fourth-generation biomaterials and implants, whose clinical performance will be predicted using 'digital twins'. A few representative examples to illustrate the formulation and relevance of the 'Biomaterialomics' approaches for three emerging research themes - patient-specific implants, additive manufacturing, and bioelectronic medicine, will be presented. For example, the high-throughput FEA-analysed biomechanical response (~12,000 datasets) in tandem with Machine Learning (ML) algorithms and uncertainty predictions were analysed, to accelerate the optimal design of acetabular socket for better bone remodeling. While validating the computational predictions, Bikramjit's group used the Laser-Powder Bed Fusion (L-PBF)-based metal additive manufacturing (AM) of parts with designed features. His group implemented a data science approach to analysing a small volume of processing results (~120 datasets) to reliably predict the weld pool geometry (depth, height, width) and used the optimized parameters to manufacture biomaterial implants with clinically acceptable surface topography and lattice features. In both these exemplary studies, a number of ML algorithms (linear regression, K-nearest neighbour, support vector machines, etc.) were used and the best statistical significance was obtained using Random Forest (RF) algorithm, in terms of correlation coefficient (R^2 : 0.99/0.97) and root mean square error (RMSE: 0.02/0.01) on the training/test dataset, in less than a minute.

SESSION SB03.05: Bio/Solid-Interfaces II
Session Chairs: Hanson Fong and Ulrike G. K. Wegst
Tuesday Afternoon, November 28, 2023
Hynes, Level 1, Room 101

1:30 PM SB03.05.01

Multiplexed Breath Biopsy of Lung Disease by Controlled Chemical Signal ActivationShih-TingWang, MelodiAnahtar, DanielKim, TahouraSamad, CathyWang, SahilPatel, ChayanonNgambenjwong, JesseKirkpatrick, HeatherFleming and SangeetaBhatia; Massachusetts Institute of Technology, United States

Breath testing is a fast, non-invasive diagnostic method that can link specific volatile organic compounds (VOCs) in exhaled breath to medical conditions. Complementary to blood and urine assays in clinical disease diagnosis, breath is an informative analyte that can provide real-time information of changes in the body's metabolome affected by disease activity. However, few breath tests are currently used in the clinic to monitor disease due to bottlenecks in biomarker identification and differentiation of endogenous VOCs in complex breath signatures. One approach to overcome this challenge is the in vivo administration of orthogonal exogenous agents with controlled properties that can be expelled from breath upon being metabolized by disease-specific molecular processes. Exogenous agents have been used in clinical breath tests for gastrointestinal and liver diseases and are more recently developed for respiratory disease. As the direct source of breath, the lungs are particularly suited for enzymatic activity-based breath tests. The multiplexed capabilities of designing reliable in vivo probes that release detectable and distinguishable exogenous VOCs are still in the early stages. Here, we report engineered breath biomarkers by protease-sensing nanoparticles for multiplexed detection of dysregulated activities of pulmonary proteases in response to disease and produce volatile reporters that can be detected in the exhaled breath. We show that the nature of proteolytic hydrolysis generating peptide fragments can be engineered to activate and release various types of volatile reporters. Using viral infection and *Alk*-mutant lung cancer mouse models, we show that multiplexed volatile-releasing activity-based nanosensors (vABNs) can detect and dynamically monitor diseases and treatment response.

1:45 PM SB03.05.02

Peptide-Functionalized Graphene Sensors for Selective Odorant DetectionYuheiHayamizu; Tokyo Institute of Technology, Japan

Gas sensing based on graphene field-effect transistors (GFETs) has gained broad interest due to their high sensitivity. Further progress in gas sensing with GFETs requires the detection of various odor molecules for applications in environmental monitoring, healthcare, food, and cosmetic industries. To establish an artificial sense of smell with electronic devices by mimicking olfactory receptors, it is desirable to use synthetic molecules with similar functionality. In this work, we designed three new peptides based on a motif sequence in olfactory receptors. These peptides were designed to have two domains: a bio-probe specific to the target molecules and a molecular scaffold [1,2]. The scaffold peptides have the ability to self-assemble into a molecular thin film on GFETs [3].

To demonstrate the biosensing capabilities, we employed limonene, methyl salicylate, and menthol as representative odor molecules of plant flavors. We investigated the conductivity change of GFETs upon binding to odor molecules at various concentrations. The dynamic response of the sensors revealed distinct signatures for each of the three different peptides against individual target molecules. The kinetic response of each peptide exhibited characteristic time constants in the adsorption and desorption processes, which were further supported by principal component analysis. These results demonstrate the selectivity of the designed peptides in detecting odor molecules.

The development of graphene odor sensors using these designed peptides paves the way for future peptide-array sensors with multiple sequences, enabling the realization of an odor-sensing system with higher selectivity. Combining the bio-probe and electrical signal amplification functions, the peptide layer on graphene represents a novel and effective strategy for achieving selective odorant detection under normal atmospheric conditions. This research contributes to the advancement of biomimetic devices and holds potential for various applications in odor detection and identification.

This work was supported by the Cabinet Office (CAO), Cross-ministerial Strategic Innovation Promotion Program (SIP), "Intelligent Processing Infrastructure of Cyber and Physical Systems" (funding agency: NEDO).

References

- [1] T. Rungreunthanapol, C. Homma, K.-I. Akagi, M. Tanaka, J. Kikuchi, H. Tomizawa, Y. Sugizaki, A. Isobayashi, Y. Hayamizu, M. Okochi, Volatile Organic Compound Detection by Graphene Field-Effect Transistors Functionalized with Fly Olfactory Receptor Mimetic Peptides. *Anal. Chem.* **95**, 4556–4563 (2023).
- [2] C. Homma, M. Tsukiiwa, H. Noguchi, M. Tanaka, M. Okochi, H. Tomizawa, Y. Sugizaki, A. Isobayashi, Y. Hayamizu, Designable peptides on graphene field-effect transistors for selective detection of odor molecules. *Biosens. Bioelectron.* **224**, 115047 (2022).
- [3] P. Li, K. Sakuma, S. Tsuchiya, L. Sun, Y. Hayamizu, Fibroin-like Peptides Self-Assembling on Two-Dimensional Materials as a Molecular Scaffold for Potential Biosensing. *ACS Appl. Mater. Interfaces.* **11**, 20670–20677 (2019).

2:00 PM SB03.05.03

Polymorphs of Short-Sequence Peptoid Assembly on MoS₂ShuaiZhang¹, Chun-LongChen² and JamesJ. De Yoreo²; ¹University of Washington, United States; ²Pacific Northwest National Laboratory, United States

Peptoid is a biomimetic polymer inspired by peptide, with compatible bio-functions but better thermal and chemical stabilities. It has unique capabilities for creating hierarchical assemblies at solid-liquid interfaces, serving as templates for convincing applications in molecular recognition, fabrication of bio-hybrid materials, (bio)mineralization, energy conversion, storage, and transportation of matter and information, etc.

Recently, we designed short peptoid sequences with assembly capabilities on MoS₂. Using substrates with different hydrophobicity and adjusting the sizes of peptoid hydrophobic side chains and the dehydration process, we demonstrated that the peptoid assembly on MoS₂ could have diverse phases, including the monolayer hybrid film with high crystallinity, vesicles, lamella, and single-/multi-strands. We further resolved that these phases can co-exist in a complicated phase diagram and can go through phase transitions between each other. Specifically, the peptoid-

peptoid interaction, peptoid-solvent interaction, and peptoid-MoS₂ interaction, mediated by pH, play crucial roles in this polymorph assembly. These results improve the knowledge of designing hierarchical architectures with biomolecules at solid-liquid interfaces. It also provides opportunities to optimize the future performance of 2D van der Waals materials-based devices.

2:15 PM *SB03.05.04

Subnanoscale Imaging of Nano-Bio Interfaces by 2D and 3D AFM Imaging TechniquesTakeshi Fukuma; Kanazawa University, Japan

Atomic force microscopy is a powerful technique that can visualize atomic- or molecular-scale structures, dynamics and properties even in liquids regardless of the conductivity of the sample. In the past decade, there has been significant advancement in the in-liquid AFM techniques. Owing to the development of low noise cantilever deflection sensors[1] and small amplitude operation mode, atomic or molecular resolution can be achieved routinely even with dynamic-mode AFM such as frequency modulation[2] and amplitude modulation AFM (FM- and AM-AFM). This allowed us to visualize subnanoscale surface structures of various biological samples[3]. In addition, the tip scanning scheme has been expanded from 2D to 3D[4] and now we can visualize the 3D distribution of water (i.e., hydration structures), organic solvents, ionic liquids and flexible molecular chains[5-7]. These unique capabilities should be particularly useful in the studies of nano-bio interfaces, where biomolecules, water and ions interact with each other to induce various biological phenomena. However, their applications to the studies on biomaterials have yet been limited. In this presentation, I would like to present our recent works to explore applications of high-resolution in-liquid AFM techniques to studies on nano-bio interfaces. Examples include molecular-scale investigations on cellulose[8] and chitin[9] nanocrystals and self-assembled structures of short peptides on graphite[10].

[1] T. Fukuma, M. Kimura, K. Kobayashi, K. Matsushige, and H. Yamada, *Rev. Sci. Instrum.* **76**, 053704 (2005).

[2] T. Fukuma, K. Kobayashi, K. Matsushige, and H. Yamada, *Appl. Phys. Lett.* **87**, 034101 (2005).

[3] H. Asakawa, K. Ikegami, M. Setou, N. Watanabe, M. Tsukada, and T. Fukuma, *Biophys. J.* **101**, 1270 (2011).

[4] T. Fukuma, Y. Ueda, S. Yoshioka, and H. Asakawa, *Phys. Rev. Lett.* **104**, 016101 (2010).

[5] H. Asakawa, S. Yoshioka, K. Nishimura, and T. Fukuma, *ACS Nano* **6**, 9013 (2012).

[6] T. Ikarashi *et al.*, *ACS Applied Nano Materials* **4**, 71 (2021).

[7] T. Ikarashi, K. Nakayama, N. Nakajima, K. Miyata, K. Miyazawa, and T. Fukuma, *ACS Appl Mater Interfaces* **14**, 44947 (2022).

[8] A. Yurtsever, P. X. Wang, F. Priante, Y. Morais Jaques, K. Miyazawa, M. J. MacLachlan, A. S. Foster, and T. Fukuma, *Sci. Adv.* **8**, eabq0160 (2022).

[9] A. Yurtsever, P. X. Wang, F. Priante, Y. Morais Jaques, K. Miyata, M. J. MacLachlan, A. S. Foster, and T. Fukuma, *Small Methods* **6**, 2200320 (2022).

[10] A. Yurtsever, L. Sun, K. Hirata, T. Fukuma, S. Rath, H. Zareie, S. Watanabe, and M. Sarikaya, *ACS Nano* **17**, 7311 (2023).

2:45 PMBREAK

3:15 PM SB03.05.05

Atom-Condensed Reactivity Descriptors for the Prediction of Biomaterials DegradationIsaac Vidal-Daza^{1,2}, Anna Bachs-Herrera¹ and Francisco Martin-Martinez¹; ¹Swansea University, United Kingdom; ²University of Granada, Spain

Nature has been traditionally mimicked in the design of biomaterials for her capacity to achieve performance, but not that often for her ability to degrade at the end of life. To design materials for degradation as well as performance, molecular degradation needs to be better modelled. Degradation is a complex phenomenon largely dependent on the molecular system, the environmental conditions, and the timescales being considered. A common factor in the degradation process is molecular reactivity, which can be predicted using conceptual density functional theory (DFT). Conceptual DFT reactivity descriptors either quantify the global tendency of a molecule to engage in chemical reactions or the areas of the molecule that would undergo such engagement, but these global and local reactivity descriptors are usually detached. Atomic reactivity is not usually quantified in relation to the global molecular reactivity, and it limits our ability to accurately predict degradation. In fact, quantifying the reactivity of any individual atom within the global reactivity of a molecule, is not a trivial task, and it requires the conjunction of different theories in the framework of quantum chemistry. In this work, we combine a topological analysis of the electron density with a non-arbitrary partition of the molecular space into atomic domains to define topology-based atom-condensed reactivity indexes to predict molecular degradation. High-throughput calculations of these *ab initio* atom-condensed reactivity descriptors enabled the analysis and identification of existing patterns among data, which provides a better understanding of molecular reactivity, and the definition of new indexes that describe the local reactivity of individual atoms, in the global reactivity of target molecules. The data generated can be used to train machine learning (ML) models that predict molecular and biomaterials degradation.

3:30 PM *SB03.05.06

Peptide Designs for On-Demand Multifunctional Surface FunctionalizationNurit Ashkenasy; Ben Gurion University of the Negev, Israel

The development of high-performance devices demands tailoring the properties of surfaces and interfaces of materials. The control of surface properties can be achieved by attaching organic monolayers to the surface. In this talk, I will discuss the design of peptide-based functionalization layers and show that such functionalization layers exploit unique properties of proteins including diversity, modularity, and multi-functionality. Hence, open the way to design highly tunable and smart surfaces.

In the first part of the talk, I will demonstrate *the use of surface binding peptides (SPBs) to tailor the electronic properties of surfaces. The effect of peptide side chains and their backbone connectivity and folding state on the resulting electronic properties will be discussed. I will further show that SPBs can be used to template syntheses of thin films with specifically tailored surface properties in an environmentally friendly approach. The use of such films for volatile organic compound sensing will be demonstrated.*

The utilization of the unique properties of peptides for the development of programmable surfaces will be demonstrated in the second part of the talk. I will present the design of a coiled-coil peptide system in which folding and chemical reactivity is responsive to external stimuli. The responsiveness of the system facilitates the ability to control the binding of the peptides to the surface and/ or their folding state, which affects the surface's physico-chemical properties in a reversible manner. These smart dynamic surfaces enable the realization chemically induced computation elements using the surface properties as the readout. The feasibility of applying this approach in biosensing will be demonstrated.

Overall, our work provides a sophisticated surface engineering approach, based on peptide sequence design, which can be utilized in diverse electronics, biotechnology, and medical applications.

4:00 PM *SB03.05.07

Design of Bioinspired Sustainable Materials from Atoms to Micrometers with Molecular Precision—Integration of Simulations, Large Data and ExperimentsHendrik Heinz; University of Colorado at Boulder, United States

The development of materials inspired by Nature continues to involve extensive trial-and-error studies by experiments. Rational understanding and accelerated design using modeling, simulation, and data science to guide laboratory studies is increasingly feasible due to more accurate models and affordable computing resources. A promising technique to predict materials properties from atoms to the micrometer scale is molecular dynamics simulation in combination with quantum methods and experiments. This talk focuses on advanced simulation techniques and using the Interface Force Field (IFF) and recent cyberinfrastructure implementations in CHARMM-GUI. The tools allow us to understand molecular recognition, assembly, and reactivity of metal, mineral, and polymer nanostructures for diverse applications in 10 to 100 times higher accuracy than possible before. We will describe advances in the representation of chemical bonding, surface chemistry, and electrolyte composition along with scalable validation against experimental data. Major applications concern the tailoring of inorganic nanostructures and interactions with peptides and proteins, understanding of nanocrystal growth and morphology, and design rules for molecular recognition and self-assembly in 4D spatial and temporal resolution. Specifically, we will explain the recognition of amino acids and organic molecules on (hkl) surfaces of hydroxyapatite and ceramic nanoparticles at different pH values, metal surfaces, and 2D materials such as graphene and MoS₂. Comparisons to cutting-edge imaging (TEM, AFM), spectroscopy, chirality measurements (VCD), and calorimetry (TPD, SCAC) will be explained. We will also discuss design guidelines for stealth coatings on nanoparticle surfaces using multi-segment ligands, along with implications for the formation of protein coronas. Some applications to ultrastrong bioinspired composites include accelerated predictions of stress-strain curves up to failure using new bond breaking potentials in IFF-R and comparisons to strengths and modulus. Potential applications include biosensors, pharmaceuticals, and structural bioinspired composites. In this talk, we will examine why and how MD simulations of inorganic-organic interfaces with IFF outperform the reliability of DFT simulations and other simulation methods by multiples. Future directions include advancements in open-source cyberinfrastructure to lower the entrance barrier for non-expert users and suitable data science tools to learn and interpret the information contained in large computational and experimental data sets to accelerate property predictions and integration with laboratory testing.

4:30 PM *SB03.05.08

Complex Biomechanics: From Atoms to PatientsChristian Hellmich, Johannes Kalliauer, Niketa Ukaj and Stefan Scheiner; TU Wien - Vienna University of Technology, Austria

Complex systems are characterized by an overall behavior which is different from that of the components making up the systems - hence, (nonlinear) interactions between the components play a very important role. Taking an interdisciplinary approach rooted in theoretical and applied mechanics and engineering mechanics, we report on two types of recently studied systems where individual system components (atoms and patients) interact in a way which unfolds very interesting emerging patterns that can be mathematically quantified through concepts arising from (bio-)mechanics: (i) the interaction of atoms within a short thread of DNA, which, as a compound, result in a family of a highly nonlinear beam structures with varying, but always coupled

torsion-stretching modes [1]; (ii) the compliance of sets of patients to the lethal effect of SARS-COV-2 [2,3], which follows integro-differential equations reminiscent of those introduced by Boltzmann in the context of creep (or hereditary) mechanics [4]. We conclude that smart classical concepts of applied mechanics and physics continue to show an unparalleled potential for solving pressing global problems in the context of computational modelling of living systems.

References:

J. Kalliauer, G. Kahl, S. Scheiner, Ch. Hellmich, A new approach to the mechanics of DNA, *J Mech Phys Sol* 143, 104040, 2020.

S. Scheiner, N. Ukaj, Ch. Hellmich, Mathematical modeling of COVID-19 fatality trends: death kinetics law versus infection-to-death delay rule, *Chaos, Solitons & Fractals* 136, 109891, 2020.

N. Ukaj, S. Scheiner, Ch. Hellmich, Toward "hereditary epidemiology": a temporal Boltzmann approach to COVID-19 fatality trends, *Applied Physics Reviews*, 8, 041417, 2021.

H. Markovits, Boltzmann and the Beginnings of Linear Viscoelasticity, *Transactions of the Society of Rheology* 21, 381-398, 1977.

SESSION SB03.06: Poster Session
Session Chairs: Hanson Fong and Deniz Yucesoy
Tuesday Afternoon, November 28, 2023
Hynes, Level 1, Hall A

8:00 PM SB03.06.01

Breast Cancer Detection using Shear Assay Based Creep Compliance and Functional Principal Component Analysis Jolene Cao¹, Killian Onwudiwe², Jingjie Hu³, Meenal Datta² and Winston O. Soboyejo¹; ¹Worcester Polytechnic Institute (WPI), United States; ²University of Notre Dame, United States; ³North Carolina State University, United States

This presents the mechanical responses of live cells that are subjected to shear flow in micro-fluidic channels under *in-situ* observation with optical, fluorescence, and confocal microscopy. The resulting time-dependent deformation of points within the cells is analyzed using Digital Image Correlation (DIC) techniques. These are used to extract deformation and strain maps of the nuclei, cytoplasm, and actin cytoskeletal structures at different stages of cell viscoelastic deformation. The measured temporal variations in strain are analyzed using Functional Principal Component Analysis (FPCA) approaches (from data science) that use time series data to extract critical features from the *in-situ* temporal creep responses of cells subjected to shear stress. Differences in the creep responses of the nuclei and cytoplasm are elucidated along with the local creep properties of the actin cytoskeletal structures of non-tumorigenic breast cells (MCF-10A), less metastatic triple-negative breast cancer (TNBC) cells (MDA-MB-468), and highly metastatic breast cancer cells (MDA-MB-231). The implications of the results are also discussed for the detection of non-tumorigenic and tumorigenic breast cells at different stages of cancer progression.

Keywords: breast cancer detection, micro-fluidics, shear assay creep compliance, functional principal component analysis, time series data, cell nuclei, cytoplasm and cytoskeletal structures.

8:00 PM SB03.06.02

Deep Learning-Assisted Sensitive Detection of Fentanyl using a Bubbling-Microchip Hui Chen, Sungwan Kim, Joseph Hardie, Prudhvi Thirumalaraju, Manoj Kanakasabapathy and Hadi Shafiee; Brigham and Women's Hospital, United States

Deep learning-enabled smartphone-based image processing has significant advantages in the development of point-of-care diagnostics. Conventionally, most deep-learning applications require task specific large scale expertly annotated datasets. Therefore, these algorithms are oftentimes limited only to applications that have large retrospective datasets available for network development. Here, we report the possibility of utilizing adversarial neural networks to overcome this challenge by expanding the utility of non-specific data for the development deep learning models. As a clinical model, we report the detection of fentanyl, a small molecular weight drug that is a type of opioid, at the point-of-care using a deep-learning empowered smartphone assay. We used the catalytic property of platinum nanoparticles (PtNPs) in a smartphone-empowered microchip bubbling assay to achieve high analytical sensitivity (detecting fentanyl at concentrations as low as 0.23 ng/mL in phosphate buffered saline (PBS), 0.43 ng/mL in human serum and 0.64 ng/mL in artificial human urine). Image-based inferences were made by our adversarial-based SPYDERMAN network that was developed using a limited dataset of 104 smartphone images of microchips with bubble signals from tests performed with known fentanyl concentrations and using our retrospective library of 17,573 non-specific bubbling-microchip images. The accuracy (\pm standard error of mean) of the developed system in determining the presence of fentanyl when using a cutoff concentration of 1 ng/mL, was 92.66 \pm 0.3% in human serum (n=100) and 94.66 \pm 1.2% in artificial human urine (n=100).

8:00 PM SB03.06.03

***Euglena gracilis*-Derived Extracellular Vesicles as a Natural Immune Modulator** Saetbyeol Jeon, Hwira Baek and Jin Woong Kim; Sungkyunkwan University, Korea (the Republic of)

Since extracellular vesicles (EVs) possess the same cell therapeutic effect due to its similar characteristics to parent cells, they have emerged as an attractive alternative to cell therapy. Taking advantage of this, a variety of EVs have been developed for tissue regeneration, anti-cancer immunotherapy, and intractable disease treatment. In terms of therapeutic application, microalgae-derived EVs has been of great interest because they contain unique physiologically active substances such as polysaccharides, minerals, vitamins and amino acids. However, most microalgae cells are structured with a strong cell membrane which is not easily cleaved and recombine to form EVs. The derivation of EVs from *Euglena gracilis* (EG), a microalgae species, warrants special attention due to its relatively flexible cell membrane. Moreover, it can be cultivated in substantial quantities, providing a valuable resource for production purpose while mitigating the risk of viral infection. In this study, we introduce an EG-derived EV (EV_{EG}) system with an enhanced immune performance. β -1,3-glucan, which is specifically accumulated in EG cells, is a representative substance that activates natural killer cells and macrophages to enhance natural immunity. To efficiently deliver β -1,3-glucan present in the EG to immune cells, the EV_{EG} are fabricated by cell extrusion method that can convert cells into vesicles by sequentially passing several micro-sized pores. Basically, the endocytosis mechanism study on the EV_{EG} exhibited notable cellular uptake compared to β -1,3-glucan only. We verified that the EV_{EG} fabricated in this study notably stimulated the mitogen activated protein kinase (MAPK) pathway, resulting in release of inflammatory mediators such as nitro oxide, cyclooxygenase-2 (COX-2) and pro-inflammatory cytokines. The expression level of these immune factors was appropriately leveled to strengthen the immune system, not excessively inducing immune response such as cytokine storms. We also showed that the -1,3-glucan encapsulated in the EV_{EG}, like other polysaccharides, was readily recognized by receptors such as Dectin-1 and TLR4 present on immune cell membranes. These results highlight that our EV_{EG} immunomodulatory system has potential for health promotion and disease treatment in various biomedical applications.

8:00 PM SB03.06.04

Deep Learning-Assisted Nanoplasmonic Digital Immunoassay for Cytokine Profiling in Immune-Suppressed Patients using Designed Peptide Aptamers Shuai Wu, Lang Zhou and Pengyu Chen; Auburn University, United States

Cytokine profiling in immune-suppressed patients plays a critical role in understanding their immune status and evaluating the effectiveness of immunomodulatory therapies. However, current immunoassay technologies face challenges in achieving rapid and accurate detection of multiple cytokines over a wide dynamic range. In this study, we propose a novel approach that combines deep learning with a nanoplasmonic digital immunoassay using rationally designed peptide aptamers as probes. The immunoassay system exhibits three notable features: (i) a simplified high-throughput biosensing chip fabrication process, (ii) an ultrasensitive nanoplasmonic digital imaging technique employing 50nm gold nanocubes (AuNCs) conjugated with antibody-mimicking peptide aptamers as detection probes, and (iii) a rapid and precise deep learning-based image processing method for digital signal analysis.

By utilizing our developed immunoassay, we successfully achieved cytokine profiling with a wide working range of 0.1-10,000 picograms per milliliter (pg/ml) and exceptional detection limits in the femtogram range. This level of sensitivity enables the accurate detection of even trace amounts of cytokines, critical for monitoring immune-suppressed patients. Our findings demonstrate that this deep learning-assisted nanoplasmonic digital immunoassay, utilizing designed peptide aptamers, holds great potential for precise cytokine profiling in immune-suppressed patients. This innovative approach may contribute to improved clinical outcomes and informed treatment decisions for individuals with rapidly inflammatory disorders and immune suppression.

8:00 PM SB03.06.05

Electrochemical Activity of Molecular Hybrids: Self-Assembly of (XH)₄ Peptides and Hemin on Graphite Electrodes Marie Sugiyama, Wei Luo and Yuhei Hayamizu; Tokyo Institute of Technology, Japan

The development of artificial enzymes has gained interest in electrochemical biosensors because natural enzymes have a relatively short lifetime and high cost for practical applications. Peptides with a small number of amino acids compared with proteins can be synthesized and chemically stable, thus they can be a good candidate as an artificial enzyme. Short-chain peptides that self-assemble into fiber-like structures in liquid are known to be catalytically active by forming complex structures with cofactors [1]. These catalytically-active peptides often contain

histidine, which plays a role in stabilizing the structure and coordinating with cofactors at the imidazole group on the side chain, enhancing the catalytic activity. In our previous work, we found that catalytic peptides containing histidine exhibited their self-assembly on graphite surfaces and revealed electrocatalytic activity combined with the coenzyme hemin [2]. More recent work showed that newly-designed peptides (XH peptides) consisting of a repeating structure of two amino acids with histidine and another amino acid, "X", also exhibited self-assembly on graphite surfaces. These peptides are a useful tool for understanding the role of the counter amino acid X on their surface self-assembly and in tuning the hydrophobicity of the graphite surface [3].

However, the capability of this XH peptide to immobilize cofactor hemins has not yet been investigated. In this study, we studied the interaction between hemin and the (XH)₄ peptide on the surface of a graphite electrode by atomic force microscopy (AFM). Three counter amino acids, tyrosine (Y), valine (V), and leucine (L), were employed as counter amino acids X for this study, e.g. YHYHYHYH. AFM showed that each peptide formed uniform linear structures with a height of a few nanometers. They also showed a hexagonal symmetry on the graphite surface, which is commensurate with the lattice structures of graphite. When the cofactor hemin was added, dot-like structures with a height of 0.5 nm~1 nm appeared on the peptide nanowires. The peptide with the highest number of particles on the peptide and the smallest particle size was LH₄, followed by VH₄ and YH₄. Assuming that the particles on the wire were hemins, the XH peptide can be a suitable scaffold for immobilizing hemin. We also performed the electrochemical measurement to evaluate the hydrogen peroxide reduction capacity of the prepared XH peptide-hemin electrodes, and it was found that these peptides with a simple sequence of XH have enzymatic activity. The observations implied that the activity is closely related to the interactions with the hemin and peptides regarding the surface density of the immobilized hemins and their structural stability.

[1] Zozulia. et al. Chem Soc Rev, 2018, 47(10), 3621-3639.

[2] Wei Luo. et al. Nanoscale, 2022, 14, 8326-8331.

[3] Wei Luo. et al. Langmuir 2023, 39, 20, 7057-7062

8:00 PM SB03.06.06

Graphene Biosensors for Probing Molecular Interactions of Peptides and RNA Forming Liquid-Liquid Phase SeparationKantaro Kikuchi, Yui Yamazaki and Yuhei Hayamizu; Tokyo Institute of Technology, Japan

Amyotrophic lateral sclerosis (ALS) is a fatal motor neuron disease affecting both upper and lower motor neurons. Frontotemporal dementia (FTD) is a type of brain disorder with degeneration of the frontal and temporal lobes of the cerebrum. These neurodegenerative diseases share the expansion of GGGGCC hexanucleotide repeats in the C9orf72 gene, identified as a major cause of the diseases [1]. The gene produces dipeptide repeats proteins (DPRs) that cause cell death. These peptides contained arginine (Arg) and counter amino acid in the dipeptide sequence and were found to form liquid-liquid phase separation (LLPS), closely related to their cytotoxicity. A previous report indicated that poly-R is highly charged and interacts with anionic molecules such as RNA but exerts no cytotoxic effect. Poly(PR) and poly(GR), on the other hand, entraps proteins via multivalent interaction in LLPS, impairing protein translation. Thus, it is known that the position of Arg in DPRs profoundly affects the interaction [2]. These findings indicate that the interactions between DPRs and RNA should be unique to form LLPS and entrapment the proteins. However, the understanding of the interactions of DPRs is still limited because of the lack of measurement techniques that can distinguish the weak interactions among them.

In this study, we applied graphene field effect transistors (GFETs) to evaluate the biomolecular interactions. Graphene has excellent electrical properties and high specific surface area and has recently shown promise as an ultra-sensitive biosensor. The interaction between biomolecules in the vicinity of the graphene surface can be detected as an electrical conduction change of graphene. We immobilized RNA on the graphene surface via pyrene anchors, as same in other works, and measured the interactions of RNA with DPRs known to form LLPS. The interactions are measured by incubating the DPRs of interest across the RNA-functionalized surface. Atomic force microscopy (AFM) was used to ensure these surface modifications. In electrical measurements, the peptides interacting with the RNA were quantified by the shift of the charge-neutral points in their gate responses of GFETs, and differences in interactions due to peptide species were discussed. From the results, we succeeded in detecting the difference in interaction with RNA by peptide species with high sensitivity at the nano-molar level. We believe that this result is helpful in quantitatively discussing the effect of small amino acid domains of biomolecules on LLPS droplet formation, an event that occurs on a microscopic scale.

References

[1] DeJesus-Hernandez, Mariely et al. Neuron, Volume 72, Issue 2, 2011, 245 – 256

[2] Yuhei Hayamizu, Kohsuke Kanekura et al. J Cell Biol 1 November 2021, 220 (11)

8:00 PM SB03.06.07

Layer-by-Layer Nanoparticles for Dexamethasone Targeted Delivery to Hematopoietic Progenitor CellsAlfonso Restrepo¹, Tamara Dacoba² and Paula T. Hammond^{1,2}; ¹Massachusetts Institute of Technology, United States; ²Koch Institute for Integrative Cancer Research, United States

Acute myeloid leukemia (AML) and acute lymphoblastic leukemia (ALL) have particularly dismal patient outcomes, with low 5-year survival rates in adult patients. Outcomes in pediatric patients are more optimistic, mainly due to their ability to withstand more aggressive treatment regimens. Glucocorticoids, although used as a standard treatment, can have severe adverse effects that limit dosing regimens. To address these challenges, directing drugs to hematopoietic progenitor cells implicated in these leukemias via targeted drug delivery therapies would allow for more aggressive and effective treatments, with reduced side effects. Layer-by-layer (LbL) nanoparticles (NPs) are a modular drug delivery system that enables the incorporation of a wide range of charged polymers on the surfaces of a drug-loaded NP core, to tune surface properties, targeting capacity, and biodistribution of NPs. The outer polymers can also be used as scaffolds to conjugate molecules, like antibodies, to aid in targeting drugs to cells of interest. In this work, we developed LbL NPs with dexamethasone loaded in the liposome core and functionalized them with polymers and antibodies to evaluate their targeting capacity to hematopoietic stem and progenitor cells (HSPCs) implicated in AML and ALL.

Dexamethasone palmitate (DXP) was incorporated as part of the lipid bilayer of liposomes using lipid hydration. Drug concentrations were measured via high-performance liquid chromatography (HPLC). Negatively-charged liposomes, empty or encapsulated with DXP, were layered with a cationic polypeptide, followed by a layer of anionic synthetic polymer on top. HSPC-targeting antibodies were then conjugated onto the top polymer layer. NP size and surface charge were monitored throughout the process via dynamic light scattering. NP concentration was determined via fluorescence intensity measurements of dye-conjugated lipids in the liposomal core. A bicinchoninic acid (BCA) assay was used to assess antibody concentration after purification. NP-cell association studies were conducted via fluorescence-activated cell sorting (FACS).

Antibodies were successfully conjugated to the NPs, with no notable impact on their physicochemical properties when measured over a 2-month period. Furthermore, antibody-functionalized LbL NPs demonstrated preferential association with a relevant myeloid progenitor-like cell line (ER-HOXB8), following 90-minute incubation. In fact, two candidate antibodies had a 1.5-fold increase in NP-cell association compared to unconjugated LbL NPs. For DXP-loaded NPs, it was found that the presence of the drug in the liposomal core had minimal impact on the stability of the NP throughout the layering process, with negligible changes in drug loading. Preliminary longitudinal studies found that the presence of the drug had no notable impact on the colloidal stability of the LbL NPs.

Overall, we have shown that LbL NPs can be functionalized with HSC-targeting antibodies, with a preferential association to relevant cell lines, and that the LbL construction of NPs is unhindered by the presence of DXP in the core. Future work would involve combining the drug-loaded NPs and functionalizing them with the candidate antibodies to ensure that similar preferential association is observed in relevant *in vitro* and *in vivo* models of acute leukemias.

8:00 PM SB03.06.08

Two-Dimensional Flexible Mechanism Design Bioinspired from Sea Horse TailGüncem Ocak Ünsal, Ceren Özcan, Gorkem Gonen, Hande Yaprak, Gulistan Mese and Virginia Couch; Izmir Institute of Technology, Turkey

Flexibility plays a key role in architecture as it harmoniously intertwines the functional requirements of everyday life with the inherent potential and adaptability of architectural design. In the current architectural landscape, various solutions have been proposed to incorporate flexibility into structures. They primarily focus on unidirectional movement. Therefore, these possess certain shortcomings which limit their capacity to address the ever-changing demands of dynamic environmental conditions and user requirements effectively and comprehensively. The aim of this study is to create a system that provides flexibility and adaptability in a bidirectional manner. While doing this research, we were inspired by nature, the most compelling and flawless system, which provides us with reliable and creative results. To provide two-dimensional flexibility, this study examines a system proposal inspired by the seahorse tail. Our methodology involves the initial design concept through meticulous desktop research and research-based initial drawings followed by the finalization of the proposed design and the fabrication of a prototype using a state-of-the-art 3D printer. The seahorse tail has a special articulation driven by a complex system of muscles, tendons, and bones, providing high flexibility in multiple directions. The joints of the seahorse tail exhibit distinctive characteristics and allow for specific types of movement. The joint connecting the lateral processes of the central vertebra and the dorsal dermal plates acts as a ball-and-socket joint. Inspired by this joint structure in the tail of the seahorse. Ridge and roof prismatic joints will provide mobility and adaptability to the proposed architectural model. These joints will contribute to the flexibility and dynamic range of motion of the overall design. It is suggested to use a combination material of natural fiber, natural rubber, and recycled plastic for structural members and joints. Natural fiber composite provides a balance of stiffness, flexibility, and eco-friendliness, while natural rubber provides greater flexibility and water resistance, and recycled plastic increases durability and contributes to its eco-friendly aspect. This combination offers rain, fire, and UV resistance while remaining environmentally sustainable. The results demonstrate the feasibility and effectiveness of our prototype in achieving flexibility and adaptability in bidirectional dynamism. In conclusion, this

study presents an advancement in addressing the limitations of current flexible structures in architecture. The bioinspired approach followed in this study provides a tangible solution to enhance flexibility and adaptability in multidirectional structural behavior. When fully developed, the system proposed in this study offers potential solutions to enhance flexibility and adaptability in multidirectional structural behavior.

8:00 PM SB03.06.09

A Molecular Dynamics Investigation of Synthetic Collagen Thermal Properties Marc Duchatelier and Kristen Rhinehardt; North Carolina Agricultural and Technical State University, United States

Composite biomaterials have been used for various medical applications as they contain specific physical, chemical and mechanical attributes while evading rejection by the body and encouraging proper function. One common material used for such function is collagen. As a triple helical, extracellular matrix (ECM) protein it constitutes approximately 25% of the total dry weight of mammals. The thermal properties of collagen can vary (320-370K) depending on the source, which impacts its physical properties, assembly, and stability. The social, physical, and financial expense of obtaining collagen, as its traditionally harvested from animals, has led to a need for synthetic collagen-like peptides. Synthetic collagen has a greater versatility due to their customizability, but a thorough investigation of their physical, and thermal properties as well as their binding capabilities must be completed prior to their production or use. This can be done by using computational modeling. In this study, we use molecular dynamics modeling to explore the structure and physics of synthetic collagen 1K6F in a solvent environment in response to thermal alterations. Simulations of 2 and 4 peptides showed a notable influence of structural orientation of the strands. Visual analysis of the simulations showed interactions between the strands at low temperatures with some structural disturbance at after 330K. The radius of gyration (Rg) showed the backbone of the molecule start to fold over time around 20 ns. Further an exploration of the Radius of Fluctuation showed varying wave patterns with amplitudes between 1.5 and 7.5 nm. However, a sinusoidal behavior was noticeable at 320 and 330K indicating a possible transition point. The observed sinusoidal waveform in the atomic fluctuation can be ascribed to the thermal influences within the system. We found that a higher number of hydrogen bonds appear at low temperature as there was increased interactions below 320K, but the peptides appear to go to the process of denaturation as temperature increase to 340K. Furthermore, the assembly behavior and protein binding sites were analyzed through composite simulation of silk and collagen. Our results highlight that the interaction strength of synthetic collagen with silk depends on the proportion of collagen within the system.

8:00 PM SB03.06.10

Enhanced Detection of Influenza Virus by Viral Membrane Fusion with Membrane Rigidity Modulation of Sialic Acid-Expressing Liposomes Hongjun Park¹, Chaewon Park¹, Geunseon Park¹, Jong-Woo Lim², Sojeong Lee¹, Soohyun Chung¹, Eunjung Kim³ and Seungjoo Haam¹; ¹Yonsei University, Korea (the Republic of); ²Seoul National University, Korea (the Republic of); ³Incheon University, Korea (the Republic of)

Specific interactions between viruses and host cells provide essential insights into materials science-based strategies to deal with emerging viral diseases. In several viral families, pH-triggered viral fusion is universal and important for understanding the viral infection cycle. Inspired by this process, virus detection has been achieved using nanomaterials with host-mimetic membranes that allow interaction with amphiphilic viral haemagglutinin fusion peptides. Most research has focused on the design of functional nanoparticles with fusogenic capability for virus detection, and there has been little exploitation of membrane rigidity to alter the ability of nanoparticles to interact with the viral membrane and improve their sensing performance. In this study, a homogeneous fluorescent assay using sialic acid-expressing liposomes with tunable responsiveness to external stimuli is developed for the rapid and straightforward detection of an activated influenza A virus. Membrane fusion between the liposome and virus can be easily controlled by varying the membrane rigidity, which is determined by the cholesterol ratio, resulting in fluorescent signals within 30 min and detection of several influenza viruses, including H9N2, CA04(H1N1) and H4N6. Therefore, the designs demonstrated in this study propose underlying approaches to utilize engineered liposomes by modulating their membrane rigidity for the direct and sensitive identification of infectious viruses.

8:00 PM SB03.06.11

Biomimetic Synthesis of ZnO Thin Films Ivan A. Melara, Jean-Edward Moise and Kristen Siaw; Gordon College, United States

Biomimetic reaction systems, where small proteins and peptides assist in the growth of inorganic materials, has the potential for making complex structures that are otherwise difficult to achieve. Living organisms use a peptide-inorganic matrix to control the morphology of the inorganic structures. Using this method as inspiration we sought a similar approach for novel materials. Zinc oxide as chosen as the target material due to its many exciting optoelectrical properties. Phage display was performed on ZnO sample and used to identify small peptides with high binding affinity for ZnO. By means of an aqueous based synthesis, these high affinity peptides were added at various concentrations to the solution so growth of the ZnO crystals could occur in the presence of the peptides. In the absence of peptides, the ZnO grows with a long needlelike morphology. When peptides are added to the growth solution they are found to dramatically alter the final morphology of the ZnO substrates. By altering the concentrations of these peptides, the morphology of ZnO nanorods can be controlled, ultimately allowing for the formation of thin films. Through the use of these peptides, we form ZnO thin films on a variety of substrates including glass and flexible PET plastic.

8:00 PM SB03.06.12

Demystifying The Synthesis and Preparation of Protein-Mimicking Random Heteropolymers Hao Yu, Ivan F. Jayapurna and Ting Xu; University of California, Berkeley, United States

Random heteropolymers (RHPs) with statistically distributed comonomers along the polymer chains are commonly used as functional materials for achieving biomimetic functionality. This is due to their capacity to replicate protein-like phase behavior and functions. However, unlike many branches of chemistry and biology where structures can be constructed precisely on the molecular level, the inherent stochastic nature of monomer sequences in RHPs raises concerns regarding their high material dispersity and difficulties in chemical characterization. Moreover, while extensive research has been conducted on synthesizing and understanding two-monomer systems, there have been limited studies and systematic guidance on the synthesis of multi-monomer copolymers such as RHPs, which involves complex, interdependent reaction kinetics among multiple comonomers. These knowledge gaps present barriers for researchers outside the polymer chemistry community who seek to create protein-mimicking RHPs with targetable structures and properties.

Towards these prospects, here we conduct a comprehensive investigation into the sequence heterogeneity and compositional drift in a family of 4-monomer-based RHPs. We commenced with experimentally determining the relative reactivities of a repertoire of four methacrylate monomers in reversible addition-fragmentation chain-transfer (RAFT) copolymerization. These underlying kinetic factors dictate the sequence heterogeneity of as-synthesized RHPs. Combining with stochastic sequence simulation, we designed four new RHPs, with each ensemble designed to exhibit different levels of hydrophilicity. Of particular interest is our findings that the purification procedures used during RHPs preparation, including pentane precipitation and dialysis against water, can preferentially eliminate different RHP subpopulations. This selectivity can be attributed to the conformations and apparent solubilities exhibited by these subpopulations, which are due to their particular chemical compositions within the whole RHP ensembles. Additionally, we quantitatively mapped out the trajectory of monomer compositions during the whole RHP preparation process. The predicted RHP cumulative compositions are in close agreement with the experimental results. These results validate the fidelity of predictive modeling and multicomponent RHP copolymerization. There are potentially over 300 commodity methacrylate monomers that are available for synthesizing RHPs materials. These findings are readily applicable to study the structure and sequence of heteropolymers beyond those described in this work. Overall, this work provides critically needed information to design and understand RHPs as functional materials while addressing the concerns related to their sequence heterogeneities.

8:00 PM SB03.06.13

Computational Investigation of Unique Structural Proteins in Cephalopod Skin Arsenij P. Pantelev¹, Christophe Magnan¹, Pierre Baldi¹, Alon Gorodetsky¹, Andrew Cannon², Albert Kwansa² and Yaroslava G. Yingling²; ¹University of California, Irvine, United States; ²North Carolina State University, United States

Cephalopods (e.g., octopuses, cuttlefishes, and squids) are renowned for their remarkable dynamic color-changing and camouflaging capabilities.^{2,4} These animals possess a skin architecture wherein different cells or organs known as chromatophores, iridophores, and leucophores modulate the transmission, absorption, and/or reflection of light.^{2,4} Interestingly, these cells or organs all contain light-manipulating nanostructures composed of unique high-refractive index proteins called reflectins.^{2,4} In our previous work, based on a bioinformatics analysis of the 51 reported reflectins, we had designed a truncated reflectin variant and studied the structure and self-assembly of this polypeptide via a combination of computationally driven experimental methods.⁶ Subsequently, we had selected a prototypical reflectin isoform and investigated the structure and hierarchical self-assembly of this protein via multiple computational and experimental techniques.¹ Recently, we have extended these studies to other truncated and full-length reflectins, obtaining extensive new fundamental insight into their structures and functionalities.^{3,5} When taken together, our experimentally validated computational findings provide additional insight into the camouflage capabilities of cephalopods and suggest new directions for the development of bioinspired optical materials and systems.

References:

1. Chatterjee, A., et al. *ACS Biomater. Sci. Eng.* **2023**, *9* (2), 978.
2. Chatterjee, A., et al. *Bioinspir. Biomim.* **2018**, *13* (4), 045001.
3. Pantelev, A. P., et al. *Unpublished*.
4. Phan, L., et al. *Chem. Mater.* **2016**, *28* (19), 6804.
5. Prakashya, P., et al. *In revision*.

SESSION SB03.07: High-Throughput Methodologies and Data Science
Session Chairs: Hanson Fong and Christian Hellmich
Wednesday Morning, November 29, 2023
Hynes, Level 1, Room 101

8:00 AM SB03.07.01

Bioinspired Cu^{II} Defective Sites in ZIF-8 for Selective Methane Oxidation SumanBhaumik¹, SirilukKanchanakungwankul¹, YingYang², DonaldG. Truhlar¹ and JosephT. Hupp²; ¹University of Minnesota, Twin Cities, United States; ²Northwestern University, United States

Activating the C–H bonds of alkanes without further oxidation to more thermodynamically stable products, CO, and CO₂, is a long-sought goal of catalytic chemistry. Inspired by the monocopper active site of methane monooxygenase, a Cu-doped ZIF-8 metal–organic framework is synthesized with 25% Cu and 75% Zn in the nodes and activated by heating to 200 °C and dosing in stepwise fashion with O₂, methane, and steam. We found that it does oxidize methane to methanol and formaldehyde. The catalysis persists through at least five cycles, and beyond the third cycle the selectivity improves to the extent that no CO₂ can be detected. Experimental characterization and analysis were carried out by PXRD, DRUV-Vis, XANES, EXAFS, SEM, and XAS. The reaction is postulated to proceed at an open-coordination Cu^I site generated by defects, and the mechanism of methanol production was explicated by density functional calculations with the revMO6-L exchange–correlation functional. The calculations reveal a catalytic cycle of oxygen-activated Cu^I involving the conversion of two molecules of CH₄ to two molecules of CH₃OH by a sequence of hydrogen atom transfer reactions and rebound steps. For most of the steps in the cycle, the reaction is more favored by singlet species than by triplets. The singlet pathway consists of both closed-shell singlet and open-shell singlet species. The closed-shell singlet calculations were checked for wavefunction stabilities, to ensure the correctness of the calculations. The reaction mechanism along the singlet pathway goes through open-shell singlets until the final step where it passes through a closed-shell singlet transition state to give rise to closed-shell singlet final product, which is a van der Waals complex of Cu^I and CH₃OH. This work provides a bioinspired synthesis of a metal–organic framework, whose defective sites carry out selective methane oxidation to methanol. A biomimetic reaction mechanism is postulated and further validated by density functional theory calculations.

8:15 AM SB03.07.02

Artificial Olfactory Perception System Powered by Synthetic Biology and Machine Learning ZhongmouChao, EleanorBest and SusanDaniel; Cornell University, United States

There are only about 400 types of olfactory receptors making up millions of receptor sites inside the human nose, but they are capable of distinguishing over 1 trillion distinct smells. ORs are seven-helix transmembrane proteins on olfactory sensory neurons that can selectively bind with odor molecules, a process which causes the activation of specific olfactory neurons depending on their binding affinity for a given molecule. This unique firing pattern of neurons in response to odorant binding is then registered and memorized by the brain as a specific “smell.” This kind of sensor system goes well beyond the simple detection function when integrated with the learning element. Replicating such sophisticated biosensing to achieve an artificial olfactory system requires the convergence of two technological fields and we propose it is now possible with protein engineering and artificial intelligence (AI). We have demonstrated olfactory receptor proteins can be integrated into bioelectronics, supporting the differentiation of various odor molecules with different binding affinities using electrical readouts. Additionally, Machine Learning (ML) algorithm is applied to recognize different smells from experimental data collected by an array of sensors. Moving forward, our goal is to create the first-ever artificial olfactory perception system that leverages synthetic biology and ML to overcome the challenges that prevented achievement of such a system to date.

8:30 AM SB03.07.03

Deep Learning Analysis of Scattered Light Intensity for Shape Classification of Nanoparticles Measured by Nano Tracking Analysis KeisukeYamamoto¹, HiroakiFukuda¹, HiromiKuramochi¹, YasushiShibuta¹ and TakanoriIchiki^{1,2}; ¹The University of Tokyo, Japan; ²Innovation Center of NanoMedicine, Japan

Characterizing particles with sizes below 100 nm, such as peptide or protein-based biopharmaceuticals, necessitates single-particle measurement and multi-parametric analysis to distinguish individual particles. Nano Tracking Analysis (NTA) is a widely used technique for single-particle measurement in liquid samples due to its simplicity. By capturing the scattered light from nanoparticles illuminated by laser light, NTA can measure individual particles [a]. To expand the range of evaluatable properties, we are exploring the application of deep learning to the analysis of NTA data. Recently, by utilizing deep learning analysis, we have successfully detected the effect of shape anisotropy, demonstrating the potential for multiparametric analysis of nanoparticles in liquids [b]. In this study, to further enhance our understanding of physical properties, we investigate the potential of shape classification using the luminance information derived from light scattering images of particles measured by NTA.

Experiments were conducted using two types of gold nanoparticles: spherical particles with a diameter of 80 nm and rod-shaped particles with a diameter of 40 nm and a length of 180 nm. The NTA method was employed to capture 100 consecutive frames of images at 100 frames per second. From these images, three types of features were extracted as luminance information: scattered light intensity, cross-sectional area of the scattering pattern, and aspect ratio. Subsequently, a dataset was constructed based on these features. Our deep learning analysis, utilizing a one-dimensional Convolutional Neural Network (1D-CNN) model, successfully learned all the extracted features. The shape classification accuracy using scattered light intensity was found to be 92%, surpassing the 80% accuracy achieved through shape classification based on Brownian motion trajectories. Moreover, even with a limited number of data frames (20 frames), the accuracy for the analysis based on luminance information reached 85%, compared to 60% for the analysis based on Brownian motion trajectories. These results demonstrate the potential of accurately extracting properties in a shorter timeframe using deep learning analysis of scattered light intensity information acquired by the NTA method.

In conclusion, our study showcases the effectiveness of employing deep learning analysis of scattered light intensity for shape classification of nanoparticles measured by NTA. This approach not only enhances the accuracy of particle characterization but also reduces the analysis time. The proposed method holds promise for further advancements in the field of nanoparticle characterization and analysis.

[a] T. Akagi, T. Ichiki, Microcapillary chip-based extracellular vesicle profiling system. *Methods in Molecular Biology (Extracellular Vesicles)* 1660 209-217 (2017)

[b]

T Ichiki, et al, Annual Meeting of International Society for Extracellular Vesicles (ISEV2023), Seattle, USA

8:45 AM *SB03.07.04

Mineral: Peptide Interactions: Using Our Understanding of Molecular Interactions to Develop a Time Efficient Biopanning Approach CaroleC. Perry and ValeriaPuddu; Nottingham Trent University, United Kingdom

Minerals and biomolecules can interact via a range of binding modalities from electrostatic interactions, though hydrogen bonding to hydrophobic interactions and van der Waals interactions. These binding possibilities lead to a range of biomolecule sequences that can interact with a particular mineral. From our understanding of peptide-mineral interactions gained by extensive, detailed experimental and computational studies we have developed an optimised biopanning approach, utilising multiple chemical eluants that allows the identification and recovery of a wide mineral binder pool in just one or two biopanning rounds.

9:15 AM SB03.07.05

A Dynamics-Informed Approach to Prediction of Protein Melting Temperature via Graph Neural Networks Yen-LinChen and Shu-WeiChang; National Taiwan University, Taiwan

A practical design of biomedical materials requires knowledge of their thermal properties. Melting temperature has a direct influence on molecular stability, functionality, and performance in the case of protein engineering. For example, biosensors and enzymes will only operate as intended within a limited thermal range. As such, the prediction of the thermostability of proteins is a crucial factor with implications in various scientific disciplines and technical applications. This task requires an understanding of the hierarchical organization of proteins, which manifests in a dynamically coupled cellular system. The introduction of machine learning methods to biology brought about astounding breakthroughs, such as the prediction of protein structures by AlphaFold. It is a promising approach to undertaking convoluted relationships in protein science. In this study, we propose a machine learning method for the computation of the melting temperature of proteins, taking into account the amino acid sequence, protein structure, and dynamics. Graphs (as in graph theory) are chosen as our data representation due to their rotational invariance and their intuitive mapping to molecular structures. The sequential, structural, and dynamical information are represented as multigraphs, with residues as its nodes, and various node features and edge connections derived from each of these properties. To process the data, a graph neural network architecture that makes use of message passing layers was designed to accommodate the multiple types of connections. Protein structures were computed by AlphaFold and the dynamics were computed based on the torsional network model (TNM) for training. Hence, the learned features and parameters can be readily applied to protein sequences without known experimental structure, satisfying the goal of aiding the prediction of design proteins.

We are also able to identify key domains that contribute to the thermal stability/instability of proteins by computing the graph regression activation map, which is based on the partial derivative of the predicted value with respect to features on the input nodes. Our method gives insight into the mechanism of natural proteins and provides critical information regarding design proteins.

9:30 AMBREAK

SESSION SB03.08: Applications and Devices in Materials and Medicine I
Session Chairs: Carole Perry and Deniz Yucesoy
Wednesday Morning, November 29, 2023
Hynes, Level 1, Room 101

10:00 AM SB03.08.01

Scientific Analysis of Synthetic Collagen Compounds using Computational Molecular Modeling Methods [Jordanne A. Davenport](#) and [Kristen Rhinehardt](#); North Carolina A&T State University, United States

Scientists have proven that the health regimen you follow can have a significant impact on the human body. Collagen is found on multiple parts of the body such as skin, bones, lymphatic, cardiovascular, liver, lung, spleen, and intestinal tissue. (Spano, 2019) Although it is prevalent that people lose 1% of collagen each year, there is a way to improve this by maintaining a healthy diet. "Collagen-derived dietary proteins are most commonly extracted from porcine skin (45%), bovine hide (30%), and the bones of both animals (23%) Chicken (bones) and fish (scales and bones) byproducts are also used as production sources of collagen-derived dietary protein" (Holwerda and Loon, 2022). In this research, a biomodel of three synthetic collagen molecules is used to bind biomarker properties including Aptamers, CNA, and Silk. Pymol is a molecular visualization tool that provides an ethically pleasing environment for a three-dimensional structure of a protein molecule to be cleaned by removing water, removing repeated molecules, and retrieving the model sequences. The results from PyMOL are then incorporated into the Basic Local Alignment Search Tool (BLASTp) to generate alignments between a protein sequence (Wheeler, Bhagwat, 2007). The binding energy is calculated along with a visual model of the structural changes of the collagens reaction to its biomarker using HDock and PATCHDOCK servers. When docking with PatchDock, the results are collected and refined with a software named FireDock to retrieve the binding energies. The best conformations were compared with differing peptides to see which ligand showed the highest affinity. "While enzyme driven crosslinking plateaus at maturation, connective tissue stiffness has been shown to further increase with age and diabetes. This tissue stiffening has been associated with non-enzymatic, oxidative reactions between glucose and collagen which increases with increased plasma glucose end concentrations associated with advanced aging" (Snedeker, 2014). Further research will utilize molecular dynamics to explore conformational space and explicitly treat structural flexibility and entropic effects of synthetic collagen.

10:15 AM SB03.08.02

Phytochemical-Enriched Plant Extracts Induce Apoptosis in Bone Metastatic Breast Cancer Cells [Preetham Ravi](#), [Haneesh Jasuja](#), [Dipayan Sarkar](#), [Kalidas Shetty](#), [Dinesh R. Katti](#) and [Kalpana Katti](#); North Dakota State University, United States

The WHO reports that breast cancer is the most common occurring type of cancer with nearly 2.26 million cases being diagnosed each year. Breast cancer is also the second leading cause of cancer-death in women. Majority of the deaths occur due to breast cancer metastasis to bone. Breast cancer cells at bone site experience altered growth and chemoresistance. Furthermore, the infrastructure of the bone is compromised, resulting in skeletal failures in patients. Currently, there is no cure for bone metastasis of breast cancer. There is a shortage of effective therapeutics for bone metastatic breast cancer, due to the reported inefficacy of commercialized drugs at bone metastatic site. There is a need for accurate drug screening cancer models, which recapitulate the bone-metastatic condition, to effectively test potential anti-cancer therapies. In addition, therapies are needed not only to treat the tumor, but to heal bone, with limited side-effects. In this study, we employ a unique 3D *in vitro* nanoclay based scaffold model, as a testbed for bone metastatic breast cancer, to screen three phytochemically-enriched plant extracts (Rhodiola Crenulata, Origanum vulgare, and Vaccinium Macrocarpon). These plant extracts have been tested against primary site breast cancer, however, their efficacy against bone metastasized breast cancer cells is unknown. We evaluated the cytotoxicity of the three extracts on bone metastatic breast cancer using the bone-mimetic scaffolds and compared the results with 2D cultured breast cancer cells (MDA-MB-231 and MCF-7). The cell viability studies showed that breast cancer cells growing, both in 2D and 3D Bone-metastatic cultures, were significantly reduced by increasing dosages of all three plant-extracts. Furthermore, it was observed that these extracts induced apoptosis in breast cancer cells grown in 2D and bone-metastatic culture, through upregulation of pro-apoptotic markers, p53, caspase-3, and caspase-9 and downregulation anti-apoptotic markers. Additionally, the bone metastatic breast cancer cultures experienced increased drug resistance. Lastly, we evaluated the effects of these plant extracts on bone cells, and found that they are unaffected after treatment. Overall, our data indicates that these phytochemically-enriched plant extracts can promote cytotoxicity in bone metastatic breast cancer, while unaffected healthy bone cells. Moreover, these specialty derived compounds can be ideal candidates to be investigated as new therapies to treat bone metastasis of breast cancer.

10:30 AM SB03.08.03

Role of Fluid Induced Shear Stresses in Inducing Bone Metastasis in Prostate Cancer [Kalpana Katti](#), [Haneesh Jasuja](#), [Sharad V. Jaswandkar](#) and [Dinesh R. Katti](#); North Dakota State University, United States

The World Cancer Research Fund International reports that prostate cancer is the second most commonly occurring cancer in men. In addition, 1,414,259 new cases of prostate cancer were reported in 2020. The World Health Organization, reports 375,304 deaths in 2020 due to prostate cancer. The majority of deaths due to prostate cancer result from the cancer relocating to a distant location in the body through the process of metastasis. The bone is a common niche of relocation of prostate cancer metastasis. Prostate cancer that has metastasized to bone is incurable. We have developed a novel nanoclay-based tissue-engineered polymeric scaffold in order to mimic the bone metastasis site through sequentially seeding with hMSCs and cancer cells. The role of blood flow in cellular processes is well known through the effect of shear forces exerted by the fluid. It is also known that the fluid flow provides unique biochemical cues for metastasis. We have designed and fabricated a bioreactor that enables physiologically relevant interstitial fluid-flow for prostate cancer bone metastasis. We have also conducted computational fluid dynamics studies to establish that a fluid flow of 0.05 ml/min recapitulates the physiological condition. We did extensive gene expression and protein evaluation studies on the cellular materials grown with and without the effect of fluid flow. We observe that the interstitial fluid-flow does not alter the CXCR4 level, an important regulator of metastasis and invasiveness of cancer. On the other hand, a large impact of bone proximity on the CXCR4 levels. The bone proximity upregulates CXCR4 levels enabling increased MMP-9 levels. We also investigated the levels of integrins which are important cellular adhesion proteins and found that avb3 integrins and MMP-9 levels are upregulated by fluid-flow causing increased migration under fluid-flow. Hence our studies indicate that avb3 integrins act as potential mechanosensory agents transducing mechanical signals via avb3-MMP 9 signaling to promote flow induced motility of prostate cancer cells. Overall, these experiments describe the significant role of interstitial fluid-flow in prostate cancer metastasis.

10:45 AM SB03.08.04

Combining Surface-Enhanced Raman Spectroscopy and Electrokinetics for Bacterial Monitoring in Wastewater [Yirui A. Zhang](#), [Liam K. Herndon](#), [Punnag Padhy](#), [Babatunde Ogunlade](#), [Alexandria Boehm](#) and [Jennifer A. Dionne](#); Stanford University, United States

Wastewater-based epidemiology can monitor population-level infections, provide early warnings about disease outbreaks, and help to control disease spread at the community level [1]. However, bacterial identification in wastewater presents outstanding challenges; notably, current methods [2] to identify bacteria are slow and costly, not suitable for high-throughput screening of diverse bacterial species, and may not work well in the complex wastewater matrix. Here, we develop a new electro-optical method that has the promise to detect a wide range of pathogenic bacteria in wastewater.

We combine surface-enhanced Raman spectroscopy (SERS) [3] and electrified interfaces, further assisted with machine learning models [4] to realize rapid and amplification-free detection of bacteria, at cell concentrations as low as 10^5 cells/mL in filtered wastewater. First, we collect SERS from bacteria spiked into filtered wastewater, including *Staphylococcus aureus*, *Staphylococcus epidermidis*, and *Escherichia coli*. Here, plasmonic gold nanorods electrostatically bind to the bacteria surface, allowing for rapid biomolecular recognition of the cell surfaces. Additionally, two-dimensional gold microelectrodes are patterned on the sensor surface to apply electrical fields to wastewater, which selectively attracts and enriches bacteria present in the complex wastewater matrices within minutes, driven by dielectrophoretic effects [5]. The enrichment of bacteria is directly observed through microscopy, and Raman signal intensities are increased by five to ten fold under electrical fields for bacterial concentrations ranging from 100 cfu/mL up to 10^8 cfu/mL. Such enhancement enables the detection sensitivity to reach environmentally-relevant concentrations (typically below 10^7 cfu/mL) with just ten seconds of integration times. Finally, using machine learning, we identify biologically-relevant "fingerprint" Raman peaks describing proteins, nucleic acids, and lipids from bacteria surfaces, and achieve rapid and accurate identification of bacteria species in wastewater. The method has the promise for future label-free detection and prediction of bacterial outbreaks through wastewater. It also opens up new directions for generalized pathogen detection and molecular recognition in a broader range of complex liquid samples including wastewater, blood, and seawater.

- [1] Hellmér, et al. Applied and environmental microbiology. (2014).
 [2] Jahn, et al. Nature Microbiology. (2022).
 [3] Tadesse, et al. Nano Lett. (2020).
 [4] Ho, et al. Nat. Comm. (2019).
 [5] Pethig. John Wiley & Sons (2010).

11:00 AM SB03.08.05

Peptidic Luminescent AuNCs for Biosensing Solene Ducarre¹, Raffaello Paolini¹, Ester Butera¹, Dorian Lemasson¹, Regina Cheichio¹, Pascale Even-Hernandez¹, Celia Ravel², Ludovic Jullien³ and Valérie Marchi¹; ¹Institut des Sciences Chimiques de Rennes, France; ²CHU Rennes, France; ³ENS PSL, France

Gold nanoclusters (AuNCs) appear as a recent class of non-toxic fluorophores. Their brightness, their ultrasmall size (< 2 nm) and large window of fluorescence lifetime (1ns – 1ms) and their good biocompatibility make them an attractive alternative as fluorescent probes for biological labeling and bioimaging.

We demonstrated their in vivo targeting ability because of specific peptidic recognition groups (R. Cheichio et al. ACS Nano materials **2023**)

Here we present the direct synthesis of original ultrasmall luminescent peptidic gold nanoclusters sensitive to pH. The versatility of small peptides permits to adjust the emission wavelength and the sensitivity of the emission intensity as well as the luminescent lifetime.

In addition due to their ultra-small size, we demonstrated that these probes are easily internalized into Arabidopsis plant from the roots and the leaf by adjusting the surface charge of the ligands. Their biodistribution in this model plant was evidenced by confocal microscopy. This chemical platform provides AuNC dual nanoprobe with potential sensitivity to the environment for biosensing applications. Such nanostructures offer promising candidates for fluorescent in vivo biosensing and biolabeling.

We also investigated the interaction of AuNC with Extracellular vesicles (EVs) which are well-known membrane-limited particles that are secreted by healthy and cancerous cells. EVs are heterogeneous in size and three subtypes are described depending on the location of secretion: microvesicles, myelinosomes and exosomes. EVs are identified in human follicular fluid as a mode of communication in the ovarian follicle (Neyroud A. S. et al. Int. J. Molecular Sci. **2022**). In addition EVs involved in cell-cell communication are considered as biomarkers for early cancer diagnosis. The analysis of their content thanks to AuNCs nanoprobe could provide informations about the origin and the biological function of the EVs. The EVs labeling with easily detectable nanoparticles could enable the development of a powerful tool for the early diagnosis of specific diseases.

11:15 AM SB03.08.06

Engineering Antigen Binding and Orientation on Alum Adjuvants for Enhanced Humoral Responses and Immunofocusing Duo Xu and Peter S. Kim; Stanford University, United States

A major challenge in vaccine development, especially against rapidly evolving viruses, is the ability to focus the immune response toward evolutionarily conserved antigenic regions to confer broad protection. For example, while many broadly neutralizing antibodies against influenza have been found to target the highly conserved stem region of hemagglutinin (HA-stem), the immune response to seasonal influenza vaccines is predominantly directed to the immunodominant but variable head region (HA-head), leading to narrow-spectrum efficacy. Here, I will first introduce an approach to controlling antigen orientation based on the site-specific insertion of short stretches of aspartate residues (oligoD) that facilitates antigen-binding to alum adjuvants. I will demonstrate the generalizability of this approach to antigens from the Ebola virus, SARS-CoV-2, and influenza and observe enhanced antibody responses following immunization in all cases. Next, I use this approach to reorient HA in an “upside down” configuration, which I envision increases HA-stem exposure, therefore also improving its immunogenicity compared to HA-head. When applied to HA of H2N2 A/Japan/305/1957, the reoriented H2 HA (reoH2HA) on alum induced a stem-directed antibody response that cross-reacted with both group 1 and 2 influenza A HAs. These results demonstrate the possibility and benefits of antigen reorientation by engineering the interaction between antigens and adjuvants, which represents a generalizable immunofocusing approach readily applicable for designing epitope-focused vaccine candidates.

11:30 AM *SB03.08.07

3D Inverse Modelling to Extract Local Hydrogel Remodelling and Stress Fiber Structure in Human Diseased Aortic Heart Valve Interstitial Cells Michael S. Sacks; The University of Texas at Austin, United States

Direct assessment of three-dimensional (3D) cell single stress fiber (SF) structure and function remains technically challenging, due to the SF feature size falling well below the resolution of light microscopy. Therefore, computational approaches are needed to estimate the effective structures and contractile behavior of SFs in various states. Herein, we developed a 3D computational model of the contracting aortic heart valve interstitial cells (AVICs) embedded in 3D hydrogels to estimate their SF orientations and contractile forces. We first utilized our hydrogel inverse model to estimate the local hydrogel mechanical properties. Briefly, this approach produces a spatially varying hydrogel modulus field or profile that minimizes the error between the experimentally measured and simulated hydrogel deformations produced by a contracting AVIC. It was determined that AVICs both degrade the gel by enzymatic processes, as well as locally stiffen the gel by collagen deposition. Next, we developed two finite element based inverse models that utilized a single direction and dispersed orientation SF structures. Both models estimated that the greatest levels of SF forces occurred at AVIC protrusions. The second model estimated that the greatest levels of SF alignment occurred at AVIC protrusions while the AVIC midsection revealed less-aligned fibers. To the best of our knowledge, we report the first fully 3D computational contractile cell models which can predict locally varying stress fiber orientation and contractile force levels. Looking forward, these models may help us obtain an increased understanding of SF function at sub-cellular length-scales and can be incorporated into multi-scale models of tissue/organ function.

SESSION SB03.09: Applications and Devices in Materials and Medicine II

Session Chairs: Hanson Fong and Yuhei Hayamizu

Thursday Morning, November 30, 2023

Hynes, Level 1, Room 109

8:30 AM SB03.09.01

Application of eIF4E Protein-Ligand Modeling for Cancer Drug Discovery Melvin Thu^{1,2}, Parth Jain^{3,2}, Evan Xie^{4,2}, Karin Hasegawa² and Yuefan Deng²; ¹Great Neck North High School, United States; ²Stony Brook University, The State University of New York, United States; ³Bergen County Academics, United States; ⁴The Pingry School, United States

The eIF4F complex recruits ribosomal subunits (40S) to initiate translation and is composed of the eIF4E, eIF4G, and eIF4A subunits. eIF4E is the cap-binding protein and binds to the m7GTP mRNA 5' cap. eIF4G is the scaffolding protein in the complex and binds eIF4E.

The protein 4E-BPs can bind to eIF4E where eIF4G binds to prevent the eIF4F complex from forming. eIF4F plays a substantial role in cancers since eIF4F preferentially activates the translation of certain mRNAs, encoding proliferation and survival-promoting proteins such as cyclin D1, c-Myc, and VEGF. The pathway involving PI3K phosphorylation of 4E-BPs results in the unbinding of eIF4E from 4E-BPs and the formation of the eIF4F complex resulting in breast, lung, ovarian, and prostate cancers, and the pathway involving Ras phosphorylation of eIF4E results in the formation of an active eIF4F complex resulting in pancreatic, lung, and colorectal cancers.

Our approach to eIF4E inhibition involves designing a compound to restrain the movement of key eIF4E residues involved in the binding of eIF4E to m7GTP, such as W102, W56, and E103, to prevent binding. An issue with m7GTP analogues of similar structure and stronger binding affinity, however, is that many are negatively charged and thus can't pass through cell membranes. Molecular docking simulations can predict binding orientation and binding affinity of the ligand to target, producing samples of many ligand conformations in the target binding region to find the optimal conformation. However, high throughput screening through brute force molecular docking is computationally expensive and limited as there are only 1010 known compounds as opposed to the 1060 total compounds.

In order to design an effective ligand, we first have to study the structure of eIF4E, and investigate how key residues involved in eIF4E binding to m7GTP undergo conformational change with and without m7GTP. We optimize eIF4E models without m7GTP using principal component analysis (PCA) and free energy landscape (FEL) calculations. We performed PCA on the trajectory data of 2gpp, 4tpw, and AF protein sources of eIF4E to transform the set of possibly correlated variables (the positions of the protein atoms) into a set of values of linearly uncorrelated variables (the principal components). We then calculated FEL of the 2gpp, 4tpw, and AF protein sources of eIF4E using GROMACS to identify the most stable conformations of eIF4E. FEL is a graphical representation of the thermodynamically stable states of a protein and the transitions between them where the local minima represent the most stable protein conformations and the barriers represent the transition states. The stable conformations of 2gpp, 4tpw, and AF were then used in molecular docking simulations of the eIF4E-m7GTP complex in order to determine the m7GTP pose with the most favorable binding energy. It was confirmed that m7GTP binds to the W56, W102, E103 residues for all three sources of eIF4E. We then performed molecular dynamics simulations on the docked eIF4E-m7GTP complexes using GROMACS with the CHARMM36 force field and TIP3P water model.

We are currently working on identifying the regions of m7GTP that are interacting with W56, W102, and E103. We will use these results to design compounds to allosterically inhibit eIF4E

binding to m7GTP, preventing the overexpression of cancer-causing mRNAs.

8:45 AM SB03.09.02

Viability of a Novel Peptide P12 as an Antithrombotic AgentSai PranavKota¹, RichardA. Wong², SamuelD. Coopersmith³, AviTalsania⁴, PiaV. Sodhi⁵, SharisHsu⁶, AdamHansen⁷ and MiriamRafailovich⁷; ¹Cedar Falls High School, United States; ²Plainview-Old Bethpage John F. Kennedy High School, United States; ³Casa Grande High School, United States; ⁴Sachem High School North, United States; ⁵The Brearley School, United States; ⁶Valley Christian High School, United States; ⁷Stony Brook University, The State University of New York, United States

Medical devices and implants are an ongoing point of research due to their impressive capabilities to enhance and support human infrastructure, but pose major challenges as they must incorporate a biocompatible material that can support endothelialization and prevent thrombosis. Specifically, current cardiovascular devices like stents lack reliable endothelialization and because of exposure to constant contact with blood flow within vasculature, result in life-threatening blood clots. Fibrinogen is a plasma-soluble protein that, once cleaved, results in fibrin monomer polymerization into fibrous clots. Previous studies have demonstrated that most stent materials are subject to fibrinogen deposition and denaturation, which results in conversion into fibrin monomers and polymerization through α C domain connections [1]. A multitude of possible solutions have been studied by utilizing varying hydrophobic or hydrophilic surface properties, which feature different materials or coatings with limited success. Here, we will explore incorporation of a surface coating using P12, a peptide derived from fibronectin, to prevent thrombosis.

Initial studies provided insight on how P12 is effective for inhibiting the fibrin polymerization process on polystyrene (PS) surfaces. We studied various fibrinogen and P12 concentrations, but ultimately we found that incorporation of P12 during the incubation of 4 mg/ml of fibrinogen, the concentration in blood, on PS surfaces prevented substantial fiber formations. We also analyzed this at the molecular level with low concentrations of fibrinogen and by using Atomic Force Microscopy and simulation technology, we concluded that the hydrophobic nature of P12 allowed it to bind to exposed α C domains of fibrin on the PS surface. This prevented aggregation of neighboring fibrin monomers and ultimately prevented polymerization into fibers. Further studies were conducted to overcome the possible negatives of using P12, which includes the uncertainty of P12 reaching the implant or cytotoxic considerations. In order to utilize P12 properly, we investigated using it as a material coating to enhance its effectiveness in a controlled location. We studied this by applying 100 μ M of P12 solution onto PS surfaces until full coverage was achieved. Fibrinogen solutions of 4 mg/ml incubated the coated surface for one hour. The P12 coating resulted in <1% of the surface containing fibers and adversely, without the coating resulted in >50% of the surface covered in fibers. From this data, we concluded that a coating of P12 is very effective in thrombosis prevention.

Cytotoxicity is another major problem with implementation of a biomaterial coating. We therefore plated fibroblasts on P12 coated tissue culture plastic (TCP) and added additional P12 to the media to directly test cell survivability. We found that there were no significant differences on P12 coating or adding P12 to cells. These results are indicative of no associated cytotoxicity of the P12 surface. We further investigated this by testing cell adhesion and proliferation on P12 coated polystyrene and found an increase in cell growth and adhesion by the addition of P12 on an otherwise non-biocompatible polystyrene surface. This data concluded that a P12 coating not only rendered surfaces non-thrombogenic and non-toxic, but also enhanced biocompatibility. Future research will look to investigate the effects of a P12 coating on its ability to support endothelialization and look to create a robust interface that incorporates P12 directly into the matrix of the material chemically so that the coating cannot be degraded or dislodged from the surface.

[1] Zhang, L., Casey, B., Galanakis, D. K., Marmorat, C., Skoog, S., Vorvolakos, K., Simon, M., & Rafailovich, M. H. (2017). The influence of surface chemistry on adsorbed fibrinogen conformation, orientation, fiber formation and platelet adhesion. *Acta Biomaterialia*, 54, 164–174. <https://doi.org/10.1016/j.actbio.2017.03.002>

9:00 AM SB03.09.03

Surface Modification of 80S Mesoporous Bioactive Glass using a Low Concentration of Composite Silver-Cerium for Biomedical ApplicationsMannieB. Tave; National Taiwan University of Science and Technology, Taiwan

Researchers are concentrating on discovering reducing treatments for bacterial infections due to the worrisome and quick rise of drug-resistant microbial-related illnesses. *Escherichia coli* (*E. coli*) causes post-surgical infections and wound infections, the most serious and drug-resistant diseases in the world. Anatomical sites with insufficient bone tissue due to illness or revision surgery are referred to as having bone defects. Severe bone defects can cause disability, limit an individual's ability to live and work, and impose significant social and economic burdens. Composite silver-cerium co-doping mesoporous bioactive glass (MBG) can defend against drug-resistant pathogens of *Escherichia coli* (*E. coli*) infection of wounds and solve issues with bone deformities. In this study; un-doped, silver-doped, cerium-doped, and silver-cerium co-doped mesoporous bioactive glass based on the composition of 80SiO₂-(16-x) CaO-4P₂O₅- xAg₂O or xCeO₂ (x=0, 0.35, 0.71 mol%) and (0.35 mol% Ag/0.35 mol% Ce) co-doped MBG has been successfully synthesized by spray pyrolysis method. Mesoporous bioactive glass powders were produced and characterized in this research. The phase compositions, chemical bonds/functional groups, surface morphologies, chemical compositions, inner structure morphologies, specific surface areas, and elemental compositions on the surface were investigated using X-ray diffraction (XRD), Fourier transform infrared spectroscopy (FTIR), field emission scanning electron microscopy (FE-SEM), energy dispersive X-ray spectroscopy (EDS), transmission electron microscopy (TEM), nitrogen sorption isotherm analysis, and X-ray photoelectron spectroscopy (XPS), respectively. The antibacterial activity against *E. coli* was determined using the colony count method, and all silver-doped MBG and silver-cerium co-doped MBG were very effective against *E. coli*. Furthermore, when the glasses were exposed to simulated bodily fluid (SBF), they quickly formed HA on their surfaces, which caused Ag and Ce to be deposited on the surface of the MBG and an intriguing candidate for use in improving the filling of bone defects. Lastly, the MTT assay demonstrated the high biocompatibility of all MBGs. When evaluated with MC3T3-E1 osteoblasts in different concentrations. According to our literature analysis, the 80S-Ag-Ce- was the first silver-cerium co-doped mesoporous bioactive glass, however, additional functional studies are required for its advancement.

9:15 AM SB03.09.04

Biomimetic Dentin Repair: Amelogenin-Derived Peptide Guides Occlusion and Peritubular Mineralization of Human TeethDenizT. Yucesoy¹, HansonD. Fong², SamiDogan² and MehmetSarikaya^{2,2,2}; ¹Izmir Institute of Technology, Turkey; ²University of Washington, United States

Dentin hypersensitivity, a widespread oral health concern, is primarily caused by the exposure of dentin tubules due to the loss of protective tissues. Despite being a widespread ailment, no permanent solution exists to address this oral condition. Current treatments aim to alleviate pain by employing desensitizing agents or blocking dentin tubules through mineral deposition or solid precipitates, yet these interventions often provide only short-term relief.

To restore the structural and mechanical integrity of teeth with lasting durability, there is a crucial need to reproduce an integrated mineral layer that seals exposed dentin while promoting peritubular mineralization. In this study, we introduce a biomimetic treatment that promotes dentin repair, utilizing a mineralization-directing peptide known as sADP5, derived from amelogenin.

The occlusion of dentin tubules is achieved through a layer-by-layer peptide-guided remineralization process, resulting in the formation of an infiltrating mineral layer on the dentin. The structure, composition, and nanomechanical properties of the remineralized dentin were analyzed by cross-sectional scanning electron microscopy imaging, energy dispersive X-ray spectroscopy, and nanomechanical testing. Elemental analysis revealed calcium and phosphate compositions akin to hydroxyapatite. Furthermore, the measured average hardness and reduced elastic modulus values of the mineral layer were significantly higher than those of the demineralized and sound human dentin. Thermal aging experiments provided evidence of the structural integration between the newly formed mineral layer and the underlying dentin, with no physical separation observed. These findings suggest the creation of a structurally robust and mechanically resilient interface that can endure long-term mechanical and thermal challenges commonly encountered in the oral environment.

The peptide-guided remineralization process outlined herein provide a foundation for the development of highly effective oral care products leading to novel biomimetic treatments for a wide range of demineralization-related ailments and offers a potent long-term solution for dentin hypersensitivity.

9:30 AM SB03.09.05

Photo-Induced Structural Changes in Oxidoreductase-Inspired NanogelsChae GyuLee and Tae-HyukKwon; Ulsan National Institute of Science and Technology, Korea (the Republic of)

Under the reductive conditions in cancer cells, cysteine-containing oxidoreductases, such as thioredoxin (Trx), glutaredoxin (Grx), and protein disulfide isomerase (PDI), accelerate thiol-disulfide exchange reactions through a reversible reaction (CysS–SCys \leftrightarrow Cys–SH), rendering upstream and downstream signaling pathways to maintain redox homeostasis in metabolism-activated cancer cells. In addition, it is difficult to differentiate between tumorous and healthy tissues as the intracellular GSH concentrations of both cell types are approximately 2–10 mM. Therefore, disulfide-bond-based nanocarriers have potential to exhibit cytotoxicity due to the unmanageable drug release in normal cells. This study investigates the spatiotemporally-controlled irreversible degradation of Ir-based photosensitizer (Tlr3)- encapsulating nanogels (IrNG) through the hyperoxidation of resulting intracellular thiols using reactive oxygen species (ROS).^{1,2} By mimicking the reversible redox reaction of Trx and Grx, we developed IrNG that maintains the self-assembled nanostructure through hydrophobic interactions and reversible crosslinking between its disulfide bonds and thiols in the absence of light. When a highly cytotoxic Tlr3 was stably encapsulated within IrNG, it exhibited significantly enhanced biocompatibility under normal cellular conditions. However, upon photoirradiation, Tlr3 generated high levels of ROS, irreversibly oxidizing the thiols to induce electrostatic repulsion between the polymer molecules, resulting in the Tlr3 release and induction of cancer cell apoptosis. Therefore, we could obtain substantially increased changes in cell viability and *in vivo* tumor growth regarding the presence and absence of photoirradiation, confirming the manual control of cytotoxic drug release.

¹ C. G. Lee et al., “Dual-Modulated Release of a Cytotoxic Photosensitizer Using Photogenerated Reactive Oxygen Species and Glutathione” *Angew. Chem. Int. Ed.* **2022**, *61*, e202210623

² C. G. Lee et al., “Controlling Morphologies of Redox-Responsive Polymeric Nanocarriers for a Smart Drug Delivery System” *Chem. Eur. J.* **2023**, e202300594

9:45 AM BREAK

10:15 AM *SB03.09.06

Functional Materials Integrating Synthetic Biological Modules Guided by Machine Learning AlgorithmsCandanTamerler; University of Kansas, United States

Synthetic biology takes the bio-based and bio-enabled approaches to a step further to enable engineering biology in designing and producing materials and processes with previously unattainable functions. Nature has been a source of inspiration in engineering solutions for many. As our understanding of biological materials and structures expanded, mimicking biological systems for innovative engineering solutions has continued with growing intensity. Our group was among the early adapters of biomimetic principles for harnessing design strategies to develop innovative materials. Mimicking the molecular recognition in biological interactions, we have been exploring the smaller protein domains, i.e., peptides as the key fundamental building blocks. Peptides offer to design hybrid biomaterials that can mimic the functions of proteins, generate biomimetic platforms and modulate microenvironment. Using synthetic biology approaches, we expanded the use of peptide-based building blocks as bioactive modules and design bio-hybrid materials with diverse functions addressing medical and industrial applications. We incorporated machine learning (ML) methods to capture distinct peptide functionalities as elements of critical modular building blocks. We adapted experimental and computational approaches demonstrated transparent ML frameworks for identifying relevant peptide structure features for targeted functions. For antimicrobial hybrid materials, we provided a method for selecting secondary structure features in related to antimicrobial peptides and expanded our predictions to design peptides for metals in biology as biocatalysts, metalation tools, and metal chelates in manufacturing and nutritional immunity. Using synthetic modular domains, we developed peptide-metal and peptide-polymer hybrids as integral of biomaterials and developed models for allosteric-dependent effects of selecting spacers to recover domain function activity. We generated knowledge-potential folded structures to discover rough set theory trends which showed to be relevant for recovering bioactivity. Our examples will include utilization of the biological activity imparted by each biomolecule toward prevention of dental and oral diseases as well as restoration of oral health. Engineered modular peptide and enzyme systems will be also provided as synthetic biohybrid material systems applicable to industrial applications. Enabling synthetic biological modular approach guided by ML algorithms offers a fascinating path to reshape our thinking in engineering and represent the functional frontiers to mimic biological systems.

10:45 AM SB03.09.07

Sequence-Tunable Materials for Silica BiomineralizationKaylynTorkelson¹, NadaY. Naser¹, XinQi^{2,1}, Chun-LongChen^{3,1}, FrancoisBaneyx¹ and JimPfaendtner^{4,1}; ¹University of Washington, United States; ²Dartmouth College, United States; ³Pacific Northwest National Laboratory, United States; ⁴North Carolina State University, United States

Silica biomineralization is a naturally occurring process wherein proteins direct the formation of complex, hierarchical nanostructures. Knowledge of these proteins and their underlying mechanisms has spurred significant efforts to identify routes for biomimetic mineralization that aims to reproduce the exquisite shapes and size selectivity found in nature. A common strategy to achieve this has been the use of short peptide sequences with chemistry mimicking those found in natural systems, like the use of the silaffin-derived R5 peptide. While progress has been made using peptides for this approach, there are many limitations that have prevented substantial breakthroughs in biomimicry. To advance our ability to use charged macromolecules for silica formation, we propose to use sequence-defined synthetic polymers known as peptoids, or N-substituted polyglycines, that present significant capability for precise tuning of sequence and structure beyond what can often be achieved with peptides alone.

This work will highlight recent developments in computational methods for understanding the relationship between polymer aggregate structure, silica surface, silica surface adsorption, silicate precursor interactions, and morphology in the biomimetic mineralization process. We use molecular dynamics simulations with the metadynamics family of enhanced sampling methods to analyze binding mechanisms and energetics of the R5 system. Next, we synthesize two R5-inspired peptoids and validate our prediction through characterization using surface plasmon resonance and electron microscopy. This study holds promise for designing new sequences with unprecedented control of the placement of chemical functional groups, thus allowing for further unraveling of silicification mechanisms and eventual design of sequence-defined synthetic polymers leading to the predictive synthesis of nanostructured functional materials.

11:00 AM SB03.09.08

Modeling Molecular Machines with Dynamic Covalent Bonds using REACTERJacobGissing; Stevens Institute of Technology, United States

Nanoscale devices are the ultimate in mechanical miniaturization. Molecular machines that perform directional transport of small molecules or filaments are a vital aspect of life, performing key biological functions during cell division and muscle contraction. These biomotors have inspired the creation of synthetic versions of molecular 'walkers' that can move directionally down a molecular track by the application of stimuli (pH and irradiation) in a specific sequence. The reconfiguration of covalent bonds is achieved by two orthogonal bond exchange reactions: disulfide exchange, which is activated in basic environments, and hydrazone exchange, which occurs under acidic conditions. In this work, we simulate the nanoscale dynamics of molecular machines using REACTER, a method for modeling chemical reactions in classical molecular dynamics (MD) simulations. Although external stimuli such as UV light cannot be modeled directly in classical MD simulations, the dynamics of a molecular walker can be captured explicitly by alternately activating the bond exchange and photoisomerization reactions using REACTER. Certain shape-memory polymers operate via similar bond exchange reactions, and a workflow to model shape-memory effects with atomistic resolution is proposed.

SESSION SB03.10: Virtual Session: Lessons from Biology at the Molecular Dimensions II

Session Chairs: Kalpana Katti and Deniz Yucesoy

Tuesday Morning, December 5, 2023

SB03-virtual

8:00 AM SB03.10.01

Zwitterion Functionalization of Polyurethanes via Thiol-ene Click for Antifouling Surfaces—Lessons from NatureShantanuP. Nikam^{1,2}, PeiruChen¹, KarissaNettleton², Yen-HaoHsu¹ and MatthewBecker²; ¹The University of Akron, United States; ²Duke University, United States

Inspired by the phospholipids on cell membranes, zwitterionic groups have been widely studied for their antifouling property. Equipped with two oppositely charged groups in the same moiety, zwitterions exhibit properties like super hydrophilicity through ionic solvation and tightly bound hydration layer that enables non-specific protein resistance. Additionally, zwitterionic materials also enhance biocompatibility and reduce immune response.

Catheter-associated infections (CAIs) have one of the highest mortality rates among healthcare-associated infections. Besides being a major cause of morbidity and mortality, CAIs also impose a heavy financial burden resulting from prolonged treatment and hospital stays. Increasing cost and health related complications necessitate the research for improving currently employed biomaterials for catheter applications. Creating antifouling surfaces by immobilizing zwitterion molecules on material surfaces has been proved to be a promising strategy. Herein, we investigated zwitterion surface-functionalized thermoplastic polyurethane (TPU) for use in antifouling catheter. The thermoplastic polyurethane was synthesized to have an allyl ether side functionality. Zwitterion surface-functionalization was achieved *via* thiol-ene 'click' chemistry in aqueous conditions. The XPS results confirmed the presence of chemically tethered zwitterion moieties on the zwitterion-TPU surface. The Quartz crystal microbalance (QCM) results show reduced fibrinogen attachment for the zwitterion-TPU when compared to its unfunctionalized controls. The zwitterion-TPU also showed a log scale reduction in bacterial adherence. For *P. aeruginosa* and *S. epidermidis*, the zwitterion-TPU resulted in around a 40% and 50% lower bacterial biomass accumulation, respectively. The fibroblast cell viability of TPU remained unaffected by functionalization with zwitterion thiol. Our results suggest a zwitterion modified TPU is a promising candidate for antifouling catheters.

8:15 AM *SB03.10.02

Carbon Nano-Interfaces for Medical and Biological ApplicationsRogerNarayan; North Carolina State University, United States

Recent studies have evaluated the use of microcrystalline diamond, nanocrystalline diamond, and diamond particles for medical applications. In this talk, materials studies and *in vitro* studies describing the interactions between diamond and medically-relevant eukaryotic cells and prokaryotic cells will be considered. The attachment of eukaryotic cells and prokaryotic cells to diamond surfaces will be considered. In addition, recent developments involving the use of diamond in active medical applications, including electrochemical sensing, will be described. Our recent finding involving diamond surfaces indicate that diamond surfaces may offer significant improvements for the diagnosis and treatment of medical conditions over the next few decades.

8:45 AM *SB03.10.03

Multiscale Small Molecule Interactomics and Behavioural Biomimetics using the CANDO PlatformZackaryFalls¹, WilliamMangione¹, BrennanOverhoff^{1,2}, LianaBruggemann¹, MatthewHudson¹, JamesSchuler¹, ManojMammen¹ and RamSamudrala¹; ¹University at Buffalo, United States; ²Harvard University, United States

Our goal is to understand and engineer small molecule behavior and functionality at multiple scales. We accomplish this by developing technologies to describe small molecule behavior and

function in terms of their multiscale signatures, which are utilised to engineer safe and effective chemicals and materials for the betterment of society by discovering optimal probes and therapeutics; generate safer and better chemicals and materials; and promote health, quality of life, and prosperity.

We elucidate the scientific tenets determining small molecule behavior in a variety of contexts, starting from the atomic and macromolecular scales, proceeding to pathways, cells and beyond, eventually reaching the phenotypic and population scales. The tenets are embedded in the form of multiscale signatures, comprising the sub-signatures at each scale, i.e., small molecule-macromolecule, -pathway, -cell and -phenotype signatures. At each scale, we determine the interaction signature using a combination of calculations and measurements, which will be enhanced with relevant information from lower scales.

We developed the Computational Analysis of Novel Drug Repurposing Opportunities (CANDO) platform for shotgun multitarget drug discovery, repurposing, and design, funded in part by a NIH Director's Pioneer Award and multiple NCATS ASPIRE Awards to implement this paradigm and overcome the limitations of traditional single target approaches. The open source platform screens and ranks drugs/compounds for every disease/indication (and adverse event) through large scale modelling and analytics of interactions between comprehensive libraries of drugs/compounds and protein structures. CANDO is agnostic to the interaction scoring method used; two primary pipelines within the platform allow for rapid screening and assessment of billions of drug/compound to protein interactions with fast bioanalytic docking and machine learning affinity regression protocols. CANDO implements a variety of benchmarking protocols for shotgun repurposing to determine how every known drug is related to every other in the context of the indications/diseases for which they are approved, which enables evaluation of various pipelines and protocols within and external to the platform for their utility in drug discovery. We have performed predictive analytics on the CANDO interaction matrices to classify drug, protein, pathway, disease, and adverse event relationships accurately. The multiple fast and accurate interaction scoring/docking protocols, the proteomic scale, and rigorous all-against-all benchmarking used within the platform make it unique and ideal for the design of novel chemical entities that target a desired proteomic/interatomic space or objective.

CANDO has been extensively validated for drug discovery, repurposing, and design; recent work on COVID-19 shows 25% our top drug candidates having in vitro efficacy including two nanomolar concentration full virus inhibitors of SARS-CoV-2, one of which was ranked #1. We already produced preliminary designs for various indications (such as non-small cell lung cancer, opioid/substance use disorder and pain, and aging) using the design pipelines implemented in CANDO. CANDO is capable of performing analytics on any arbitrary drug/compound, including those chemicals relevant to industrial use such per-and polyfluoroalkyl (PFAS) substances to design safer and better compounds. The most potent designs will be pursued further for development and regulatory approval. Elucidating multiscale signatures of small molecules lends itself to a paradigm-shifting view of small molecule behavior and function that will enable detailed engineering of small molecules for myriad applications. This talk will describe the current state of the CANDO platform and future plans for use in materials research.

9:15 AM SB03.10.04

Harnessing Gradients for Self-Assembly of Peptide-Based Nanocapsules: A Pathway to Advanced Drug Delivery Systems HaopengLi¹, [XuliangQian](#)¹, HariniMohanram¹, XiaoHan¹, HuitangQi², GuijinZou³, FenghouYuan², AliMiserez¹, QingYang⁴, TianLiu², HuajianGao^{1,3} and JingYu^{1,1}; ¹Nanyang Technological University, Singapore; ²Dalian University of Technology, China; ³A*STAR, Singapore; ⁴Chinese Academy of Agricultural Sciences, China

Biological systems often create materials with intricate structures to achieve specialized functions. In comparison, precise control of structures in man-made materials has been challenging. Here, we report a serendipitous discovery of insect cuticle peptides (ICPs) spontaneously forming nanocapsules through a single-step solvent exchange process, where the concentration gradient resulting from mixing of water and acetone drives the localization and self-assembly of the peptides into hollow nanocapsules. The underlying driving force is the intrinsic affinity of the peptides for a particular solvent concentration, while the diffusion of water and acetone creates a gradient interface that triggers peptide localization and self-assembly. This gradient-mediated self-assembly offers a transformative pathway towards next-generation drug delivery systems based on peptide nanocapsules.

SYMPOSIUM SB04

Conducting and Functional Hydrogels—From Materials to Devices
November27 - November30, 2023

Symposium Organizers

Anna-Maria Pappa, Khalifa University
Alexandra Rutz, Washington University in St. Louis
Christina Tringides, ETH Zurich
Shiming Zhang, The University of Hong Kong

* Invited Paper

+ JMR Distinguished Invited Speaker

SESSION SB04.01: 3D Printing and Other Rapidly Scalable Manufacturing Techniques I
Session Chairs: Anna-Maria Pappa, Alexandra Rutz, Christina Tringides and Shiming Zhang
Monday Morning, November27, 2023
Hynes, Level 1, Room 103

10:30 AM SB04.01.01

4D Printing of Hydrogels with Hierarchical Surface Wrinkling Patterns [MuratGuvendiren](#); New Jersey Institute of Technology, United States

Additive manufacturing of stimuli responsive materials leads to 3D printed constructs that can adapt their properties in response to an external stimuli. This process is referred as 4D printing. 4D printing is commonly used to fabricate shape-shifting constructs, which change their asprinted shape into a preprogrammed shape post-printing with response to an external stimuli. Although 4D printing of shape-shifting objects have significantly expand the applications of 3D printing, novel ink formulations are needed for 4D printing to create 2D and 3D structures that allow dynamic control of properties beyond shape change. In this study, we present smart inks for material extrusion-based direct ink writing (DIW) printing that display preprogrammed surface wrinkling patterns on 2D and 3D surfaces post-printing, which appear only when exposed to a solvent. Hydrogels displaying surface wrinkling patterns with user-defined order and shape are useful for a range of applications, including microfluidics, flexible electronics, smart adhesives, optical sensors, and cell culture platforms. However, conventional techniques to fabricate wrinkling patterns involve multiple steps and are significantly limited to create hierarchical patterns, wrinkles on 3D and non-planar structure. It is also very difficult to scale-up the manufacturing process and to integrate surface patterning into a continuous manufacturing process. 4D printing is used in this work to overcome these issues. The use of photocurable ink formulations allow us to tailor flow properties and printability by controlling photopolymerization time and partial crosslinking time. The crosslinker concentration is varied to develop distinct ink formulations with preprogrammed wrinkling morphology, including lamellar, peanut and hexagonal patterns. We demonstrate 4D printing of optical devices, solvent sensors, anti-counterfeit devices and high-throughput cell culture platforms.

10:45 AM *SB04.01.02

Electronic Hydrogels for Plant and Environmental Monitoring Eloise Bihari^{1,2}, Elliot Strand¹, Catherine Crichton¹, Megan N. Renny¹, Robert McLeod¹ and Gregory L. Whiting¹; ¹University of Colorado-Boulder, United States; ²University at Buffalo, The State University of New York, United States

Significant progress has been achieved in the field of electronics dedicated to environmental monitoring in recent decades. Currently, a key challenge lies in establishing an enhanced interface between electronics and living tissues. The proliferation of miniaturized sensors designed for plant and environmental sensing necessitates the development of hybrid sensors that employ cutting-edge techniques and novel organic materials to mitigate the formation of fibrotic tissues.

In this context, we introduce a novel generation of biocompatible and stretchable electronic gels, which showcase remarkable mechanical properties and self-repair capabilities. These gels also exhibit a wide array of functionalities, including exceptional conductivity levels of up to 350 S cm⁻¹, high transconductance ranging within the mS range, and high capacitance values of up to 4.2 mF g⁻¹. Leveraging the unique characteristics of these electronic gels, we can effectively stimulate or record ionic activities both *in vivo* and *ex vivo*, enabling the monitoring of plant electrophysiology or serving as energy storage systems for agricultural monitoring.

11:15 AM SB04.01.03

3D Printed Bioelectronics via *In-Situ* Enzymatic Polymerization of Conjugated Oligomer-Based Hydrogel Bioinks Changbai Li, Sajjad Naeimipour, Fatemeh R. Boroojeni, Tobias Abrahamsson, Xenophon Strakosas, Caroline Lindholm, Chiara Musumeci, Hanne Biemans, Marios Savvakis, Mary J. Donahue, Jennifer Gerasimov, Robert Selegård, Magnus Berggren, Daniel Aili and Daniel Simon; Linköping University, Sweden

Hydrogels are an attractive material system for interfacing between medical devices and human neural tissues due to their similar mechanical properties. However, most conventional hydrogel-based bio-interfaces lack electrical conductivity and thereby cannot relay electrical signals related to neural recording and activation. Here we show how *in situ* enzymatic polymerization of the conjugated oligomer-based hydrogel can be utilized to create cell-compatible and electrically conductive hydrogel structures. Conductive hydrogel structures were fabricated using 3D printing of hydrogel bioinks loaded with conjugated oligomers, followed by enzymatic polymerization of the conjugated oligomers by horseradish peroxidase. The polymerization of the conjugated oligomers modified the electroactivity of the hydrogels and resulted in a significant increase in stiffness from about 0.6 kPa to 1.5 kPa. Both the components and polymerization process as well as the resulting conductive hydrogels were well tolerated by both human primary fibroblasts and PC12 cells. This work thus shows possibilities to fabricate cytocompatible and conductive hydrogels that can be processed using bioprinting. In addition, these hybrid materials show tissue-like mechanical properties and the hydrogels possess mixed ionic and electronic conductivity, which can provide new means to leverage electricity to manipulate cell behavior in a native-like microenvironment.

11:30 AM SB04.01.04

Achieving Tissue-Like Properties in 3D Printed Conducting Polymer Hydrogels Somtochukwu S. Okafor¹, Tianran Liu¹, Anna P. Goestenkors¹, Barbara A. Semar², Riley Alvarez¹ and Alexandra Rutz¹; ¹Washington University in St. Louis, United States; ²Washington University in St. Louis, United States

Conducting hydrogels are sought for integration into bioelectronic devices to impart soft, hydrated, and tissue-like properties. However, the compatibility of these materials with advanced manufacturing and the ability to tailor functional properties for application remain limitedly reported. With regards to structural design, additive manufacturing offers customization and complexity with respect to object shape, dimensions, and internal microstructure. Additionally, materials processing as part of the additive manufacturing procedure can be used to control functional properties important for cell-material interactions and device performance. In this work, we developed methods for 3D extrusion printing conducting polymer hydrogels based on poly(3,4-ethylenedioxythiophene) polystyrene sulfonate (PEDOT:PSS). We demonstrate control of hydrogel properties by careful pre-printing ink formulation and appropriate post-printing processing. Shear-thinning and self-healing hydrogel inks were developed. Consistent rheological (viscosity, storage and loss modulus) and printing properties (mass flow rate, particle size) were maintained by manipulating the gelation kinetics of PEDOT:PSS using temperature. A gel-based support medium enabled fabrication of multi-layered structures after adding a gelation agent to increase structural resolution. Printed PEDOT:PSS hydrogels exhibited tissue-like properties including an elastic modulus of ~5 kPa and water content >99%. When further treated with heat or solvent, a wide range of conductivity (10 – 10,000 S/m) was achieved. Furthermore, hydrogels printed into microporous scaffolds were stable in physiological conditions for at least 28 days, and supported viability and proliferation of seeded human primary cells. Collectively, these results provide methods of fabricating PEDOT:PSS hydrogels that offer customization for various biointerfacing applications with regards to structural design and functional properties.

SESSION SB04.02/EL05.02: Joint Session: Neuro- and Neuro-Morphic Applications

Session Chairs: Cindy Harnett, Juejun Hu, Seungwoo Lee, Anna-Maria Pappa, Alexandra Rutz, Christina Tringides and Shiming Zhang
Monday Afternoon, November 27, 2023
Hynes, Level 1, Room 103

1:30 PM *EL05.02/SB04.02.01

Multifunctional Conducting Polymer Hydrogels for Regenerative Bioelectronics Maria Asplund^{1,2}, Sebastian Shaner³, Lukas Matter¹, Oliya Abdullaeva², Jose A. Leal Ordonez³, Anna Savelyeva³, Bruce Harland⁴, Brad Raos⁴, Han Lu³, Maximilian Lenz³, Christian Boehler³, Darren Svirskis⁴ and Andreas Vlachos³; ¹Chalmers University of Technology, Sweden; ²Luleå University of Technology, Japan; ³University of Freiburg, Germany; ⁴The University of Auckland, New Zealand

Bioelectronic medicine refers to technology which use electrical signals, either recorded from or injected into tissue, for therapeutic effect. To date, the focus of electrical stimulation has almost exclusively been on excitable tissue, such as nerve and muscle cells, which respond to short stimulation impulses. Nevertheless, a much broader range of cells are able to respond to direct current, e.g. many cells change shape, growth or align their migration trajectories in accordance with an applied electrical field. It is hypothesized that such effects can be used to steer regenerative processes, modulate neural function or explain cancer metastasis, however, there is little technology developed that allows for such investigations in complex biological models. In our research we are developing methodologies that would make such exploration possible, in complex cell cultures, *in vivo* and at later stages also in patients.

Key to success is to identify electrode materials that make it possible to interface intimately with living tissues and deliver direct current without corrosion. The typical noble metal materials have limitations in terms of charge injection and corrosion resilience, and their electrochemistry is in general not well-matched to ionic current stimulation. Meanwhile, conducting polymer hydrogels show great promise as they can transport and deliver ionic current via biocompatible charge injection mechanisms, even in the direct current domain.

In my talk I will showcase how we employ conducting polymer hydrogels for direct current stimulation, and how such technology allows for new discoveries as well as potential future therapies. One such application field is wound healing, where we have used conducting polymer hydrogels to show how direct current stimulation of an *in vitro* epithelial wound model resulted in 3 times accelerated wound closure. Another possibility is spinal cord repair where we are exploring how to integrate electrodes for direct current stimulation in a flexible implantable bioelectronic system. By paying close attention to aspects such as electrode/electrolyte reactions, substrate electrolyte reactions as well as the interplay between the fundamental properties of the conducting polymer hydrogel and polymer-substrate adhesion layers, we hope to build a concept for fully biocompatible and implantable regenerative DC stimulation.

This work was supported by the European Research Council (ERC) grant agreement No. 759655 (SPEEDER) the CatWalk Spinal Cord Injury Trust and the Health Research Council of New Zealand (Project grant and HRC/Catwalk Partnership 19/895). Further support was provided by the center for Innovative Brain Machine Interfacing Technology at the University of Freiburg.

2:00 PM *EL05.02/SB04.02.02

Conductive and Biofunctional Hydrogels for Regenerative Living Interfaces in the Nervous System Rylie Green; Imperial College London, United Kingdom

Neurological disorders affect more than 60 million people every year and constitute a major clinical challenge. Due to the limited cellular turnover and the significant degeneration triggered by neural injury and disease, regenerative therapies constitute a promising strategy to ameliorate the symptoms. Living bioelectronics offer the potential to create living interactions between implants and the endogenous neural system. By providing a tissue engineered scaffolds containing neuroprogenitor (or stem) cells at the neural interface, this approach can grow connections, creating an intimate and regenerative cell-level interface. The major challenge in this technology is the need to support the cells and encourage their development into mature neurons, while creating functional synapses with target tissue. Hydrogels with conductive elements have been designed with degradation kinetics that are matched to neuronal differentiation and wound healing, while also being electrically addressable. Critically, these hydrogels provide biological and topographical cues that promote the survival of cells and ability to produce neurite processes. A system based on PVA and gelatin has been shown to support the differentiation of neuroprogenitor cells into functional neural networks at the interface of bionic devices. The incorporation of gelatin into poly(vinyl alcohol) - norbornene hydrogels (PVA-Gel-NB) was shown to provide biochemical cues that were able to be modified by the encapsulated progenitors, which ultimately integrated into brain tissue. In an alternate injectable system, self assembly peptides (SAPs) were modified to form fibers with conductive cores that supported cells in producing directional growth. The use of electrical stimulation that mimicked the pattern of brain activity experienced *in utero* by the developing mammalian CNS, was subsequently demonstrated to increase the number of mature differentiated neurons. Action potentials have been observed within both of the cell populations, showing their development into appropriate cells types. Ultimately, this work demonstrates the ability to bring bioelectronics and tissue engineering concepts together to produce regenerative neural tissue constructs.

2:30 PM EL05.02/SB04.02.03

Development of a Hydrogel-Actuated 3D Micro Electrode Array (MEA) for Neural Spheroids and OrganoidsOutmanAkouissi, EleonoraMartinelli, LucaLiebi, JanerVan der Graaf Mas, SilvestroMicera and StephanieP. Lacour; Ecole Polytechnique Federale de Lausanne, Switzerland

Organoids and spheroids are versatile tools in research. Their 3D structure can faithfully replicate the complexity and functionality of human organs and tissues, enabling scientists to study biological phenomena in a dish. Specifically, neural organoids and spheroids offer exciting opportunities for understanding neuronal connectivity and exploring neurological disorders. Electrophysiological recordings play a crucial role in assessing these parameters. While micro electrode arrays (MEAs) are commonly used for such measurements, they are mostly limited to 2D (planar) configurations, which do not fully capture the complexity of three dimensional organoids and spheroids.

In this study, we present an intuitive 3D MEA platform based on shape-morphing bilayers to engulf the spheroid and enable recordings from its entire surface. The first layer forms the microelectrode arrays patterned as a thin metal film embedded in polymers such as polyimide and parylene. The second layer consists of a hydrogel membrane covalently grafted onto the MEA and capable of swelling upon immersion in cell culture medium thereby enabling actuation.

By precisely tuning the hydrogel formulation, bilayer thicknesses, and MEA geometry, we successfully designed 3D MEA platforms that accommodate a wide range of tissue sizes and shapes. One device included 32 electrodes, with a radius of 15 μm , distributed onto 4 bilayers folding with a radius of closure 300 μm . To expedite and guide the design and microfabrication process, we conducted comprehensive mechanical and electrical characterization of each component, and developed accurate *in silico* finite element models. The shape morphing MEAs interface reliably with commercial MEA readout platforms, requiring no additional instrumentation and minimal training.

We aim to study network patterns collected from the volumetric MEA over neural spheroids and hope to collect valuable insights into the connectivity, health, and functionality of neural organoids.

2:45 PM DISCUSSION TIME

3:00 PM BREAK

3:30 PM EL05.02/SB04.02.04

Stretchable Optical Memristor Design, Fabrication and CharacterizationDingchenWang¹, ShileiDai¹, SongruiWei², XiaoTang², KunbinHuang², DingyaoLiu¹, BinbinCui¹, HanZhang², ShimingZhang¹ and ZhongruiWang¹; ¹Hong Kong University, Hong Kong; ²Shenzhen University, China

Wearable electronics/photronics are developing rapidly in the era of artificial intelligence (AI) and the Internet of Things (IoT). However, wearable computing devices developed so far are mainly limited to "electronic hardware" implementations, which are incompatible with wearable photonic components. A highly attractive vision is to develop wearable photonic computing devices that can be attachable to the human skin for direct interface with wearable photonic components, such as optical sensors. In this work, we present a novel material combination for a buried waveguide-type, hydrogel-based stretchable optical memristor that can be used for next-generation wearable photonic computing.

To fabricate a stretchable optical memristor, we first fabricate a PDMS substrate with a straight waveguide channel. Then we synthesize polyoxometalates (POMs) doped polyacrylamide (PAAm) hydrogel with a refractive index of 1.43, which is higher than that of PDMS (1.41) at visible light wavelengths thus allowing total internal reflection in the hydrogel, inside the waveguide channel. The POMs within the hydrogel can be switched between a reduced, colored state and an oxidized, uncolored state under UV and oxygen environments, respectively, thereby modulating the transmittance across the visible light spectrum. We use UV light for programming the waveguide transmittance and a 650 nm light for optical readout due to its large photochromic response. By controlling the UV and oxygen environments, we achieve a maximum attenuation of 12 dB, 16 levels of memory, retention over 10000 s, and reversibility under an oxygen environment. Moreover, the stretchable optical memristor exhibits intrinsic stretchability owing to the hydrogel matrix, enabling it to withstand up to 50% strain while maintaining performance after repeated stretching. The combination of POM-doped hydrogel and PDMS substrate enables a buried-type waveguide that functions as an effective optical memristor with inherent stretchability. Such a stretchable optical memristor holds promise for applications in wearable photonic computing, serving as a key component of photonic skin for smart wearable devices, personal healthcare devices, and human-machine interaction interfaces.

3:45 PM *EL05.02/SB04.02.05

Hydrogel-Based Flexible and Multifunctional Fibers for Next-Generation Neural InterfacesSeongjunPark; KAIST, Korea (the Republic of)

To understand the mechanism underlying the function and dynamics of the nervous system or to treat neurological disorders, it is essential to develop the techniques capable of modulating and recording a diversity of signals employed by neurons. However, current approaches are limited in terms of effectiveness, side effects, non-specificity, and mechanical invasiveness. Naturally, there is a huge need for new devices or materials allowing for minimally invasive manipulation and monitoring of neural activity. My talk will introduce the complementary strategy to address these challenges with hydrogel-based flexible and stretchable fiber-based probes for interfacing with the brain and spinal cord. This technology enabling the interrogation with neural circuits across their diverse signaling modalities without inducing a foreign-body reaction helps the study of information processing as well as pathologies of the nervous system.

Reference

- [1] S. Park*, H. Yuk*, R. Zhao, Y. S. Yim, E. Woldegebriel, J. Kang, A. Canales, Y. Fink, G. Choi, X. Zhao#, and P. Anikeeva#, "Adaptive and Multifunctional Hydrogel Hybrid Probes for Long-term Sensing and Modulation of Neural Activity", *Nature Communications*, 12, 3435 (2021).
- [2] S. Park, Y. Guo, X. Jia, H. K. Choe, B. Grena, J. Kang, J. Park, C. Lu, A. Canales, R. Chen, Y. S. Yim, G. Choi, Y. Fink and P. Anikeeva#, "One-step Optogenetics with Multifunctional Flexible Polymer Fibers", *Nature Neuroscience*, 20 (4), 612-619, 2017.
- [3] C. Lu*, S. Park*, T. J. Richner, A. Derry, I. Brown, C. Hou, S. Rao, J. Kang, C. T. Moritz, Y. Fink and P. Anikeeva#, "Flexible and stretchable nanowire-coated fibers for optoelectronic probing of spinal cord circuits", *Science Advances*, 3 (3), e1600955, 2017.

4:15 PM EL05.02/SB04.02.06

Development of 3D Hydrogel-Based *In Vitro* Circuits with Cocultures of Human Sensory Neurons and Schwann CellsBlandineF. Clément¹, ChristinaM. Tringides¹, VilniusDranseika², JensDuru¹, TobiasRuff¹ and JanosVörös¹; ¹ETH Zürich, Switzerland; ²University of Zürich, Switzerland

Engineered *in vitro* neural networks are promising platforms to rapidly screen drugs and study information flow in the nervous system [1]. While existing polydimethylsiloxane (PDMS)-based microfluidic platforms offer precise architecture and connectivity, the cultured neurons grow inside microchannels on a planar multielectrode array (MEA) substrate in a two-dimensional fashion [2]. To better mimic the native extracellular matrix (ECM) microenvironment, 3D hydrogel scaffolds can be designed so that encapsulated cells can be expected to exhibit more physiological behavior [3].

Here, we propose a hybrid approach by filling the PDMS microstructure with hydrogels to offer both a controlled topology and a physiologically relevant microenvironment to the neuronal culture. First, a gelatin methacryloyl (GelMA) hydrogel was engineered by incorporating ECM components and tuning its mechanical properties to match the native niche environment. The hydrogel material was able to 1) support the growth of human iPSC-derived sensory neurons for more than 9 weeks 2) support co-culture with human Schwann cells where the latter could align along the axons. Next, microchannels were filled with the optimized hydrogel precursor, and after crosslinking, the neurons and glial cells were seeded as pre-aggregated spheroids in desired location(s). This enabled topologically defined growth of neurites in 3D.

By further tuning the hydrogel type and its physico-mechanical properties, the microstructures could be filled and tailored for specific cell types, while the underlying MEA allows for the recording of neuronal activity over time. This platform could offer a promising tool to study cell-cell interactions of single cultures or co-cultures, and to efficiently test the potential of various drugs in a more translational manner.

- [1] Aebersold, M. J., Dermutz, H., Forro, C., Weydert, S., Thompson-Steckel, G., Vörös, J., & Demko, L. (2016). "Brains on a chip": Towards engineered neural networks. *Trends in Analytical Chemistry*, 78, 60-69.
- [2] Forró, C., Thompson-Steckel, G., Weaver, S., Weydert, S., Ihle, S., Dermutz, H., Aebersold, M. J., Pilz, R., Demkó, L., & Vörös, J. (2018). Modular microstructure design to build neuronal networks of defined functional connectivity. *Biosensors and Bioelectronics*, 122, 75-87.
- [3] Huh, D., Hamilton, G. A., Ingber, D. E. (2011). From 3D cell culture to organs-on-chip. *Trends in Cell Biology*, 21, 12, 745-754.

4:30 PM *EL05.02/SB04.02.07

Biodegradable Materials for Optoelectronic Neural Modulation and Electronic MedicineLanYin; Tsinghua University, China

Devices built on biodegradable materials possess unique characteristics that enable complete biodegradation in physiological environments, thus eliminating the need for retrieval surgery and minimizing the associated risks of infection. These devices can play a critical role in therapeutic and diagnostic processes, including neural modulation, tissue regeneration, etc. Herein, we introduce materials options and fabrication strategies that enable the development of a biodegradable and flexible optoelectronic device, capable of achieving efficient neural stimulation and

functional recovery on peripheral nervous systems. Furthermore, we propose a bioresorbable and self-powered device as electronic medicine for peripheral nerve regeneration. Successful nerve regrowth and motor functional recovery are realized in rodent models. These works provide new insights for modulating neural activities and repairing nerve injuries.

SESSION SB04.03: Poster Session I
Session Chairs: Anna-Maria Pappa, Alexandra Rutz, Christina Tringides and Shiming Zhang
Monday Afternoon, November 27, 2023
Hynes, Level 1, Hall A

8:00 PM SB04.03.01

Reprocessable Ion-Conducting Elastomer Formed by Thiourea-Based Dynamic Covalent Network Bitgaram Kim¹, Yeong JeCho¹, Dong-Gyun Kim² and Ji-Hun Seo¹; ¹Korea University, Korea (the Republic of); ²Korea Research Institute of Chemical Technology, Korea (the Republic of)

The development of ionic conducting elastomer (ICE) with reprocessing capability is desirable to prevent resource wastage and environmental crises. Traditional elastomers with covalent cross-linking pose challenges for reprocessing due to their thermoset properties. To address this issue, a thiourea-based dynamic covalent network was employed to design the ICE. Through an analysis of the interaction between the lithium salt and the polymer chain, LITFSI was selected as the ideal choice. Furthermore, the analysis revealed that the behavior of the dynamic covalent network was influenced by the interactions between the polymer chain and lithium salts, not just the network formation itself. The resulting dynamic covalent elastomer can be reprocessed multiple times using various methods such as hot-pressing and solution processes. It demonstrates good dimensional stability and exhibits an ionic conductivity.

8:00 PM SB04.03.02

Minimally Invasive Bioprinting of Conductive Hydrogel for *In Situ* Liver Regeneration Yueying Yang and Jianfeng Zang; Huazhong University of Science and Technology, China

In situ bioprinting is promising for developing scaffolds directly on defect models in operating rooms, which provides a new strategy for *in situ* tissue regeneration. However, due to the limitation of the printing depth and bioink, bioprinting scaffolds in deep dermal or extremity injuries remains a grand challenge. Here, we present a ferromagnetic intravital bioprinting approach for *in situ* tissue regeneration in a minimally invasive manner. The ferromagnetic intravital bioprinting system is able (1) to measure and identify the geometry of organ defects by micro-CT, (2) to plan a matched printing path, and (3) to deliver multiple bioinks to fabricate scaffolds on defects in a minimally invasive manner. The minimally invasive bioprinter is composed of a ferromagnetic soft catheter robot (FSCR) nozzle that can arrive at the deep dermal (0-150 mm) through a small incision (2-4 mm) and a separated remote magnetic actuation system that numerically controls the movement of FSCR. The hydrogel bioink is designed to be electroactive, self-healing, biocompatible, biodegradable, tissue adhesive and extrusion printable. After 3D reconstruction of the defects with computed tomography (CT), conductive hydrogel scaffold is printed within a partial liver resection of live rat, and *in situ* tissue regeneration is achieved due to the electroactive hydrogel scaffold, promoting the orderly arrangement of fibroblasts and collagen *in vivo*.

8:00 PM SB04.03.03

Magnetic Nanogels for Combined Hyperthermia and Chemotherapy of Prostate Cancer Sofia Patri^{1,2}, Thanh T. Nguyen² and Nazila Kamaly¹; ¹Imperial College London, United Kingdom; ²University College London, United Kingdom

Iron Oxide Nanoparticles (IONPs) are FDA approved for biomedical applications, such as magnetic hyperthermia: IONPs can generate heat as a consequence of their relaxation mechanism after being placed in an Alternating Magnetic Field (AMF). The heat generation is measured in Specific Absorption Rate (SAR) and agglomerations of IONPs, known as NanoFlowers (NFs), have shown to have some of the highest SAR values out of all the variations of this material. The surface of IONPs and IONFs can be modified with an organic coating to increase their biocompatibility. By selecting the appropriate soft material, the organic shell can also encapsulate a cargo and release it over time: this kind of magnetic composite can combine hyperthermia with drug delivery, making it a highly effective treatment against cancer cells. Nanogels, which are hydrogels in the nanoscale, are highly biocompatible and stable in the biological environment thanks to their crosslinked network; more importantly, they can be engineered to respond to an external stimulus. By including a thermo-responsive unit in the nanogel, an increase in temperature will induce a coil-to-globule transition of the chains causing the shrinkage of the nanogel and the expulsion of water along with the encapsulated cargo. In this multifunctional therapy, we aim to trigger drug release from a nanogel by using the heat generated by the IONFs in an AMF. To improve the stability of the nanocarrier in the physiological environment, we demonstrate the necessity to anchor the nanogel to the IONFs through a surface ligand. The development of functional and stable magnetic nanogels provides a more effective, localized, and precise therapy that combines the benefit of the monotherapies while minimizing their individual drawbacks whilst establishing synergistic actions.

8:00 PM SB04.03.04

Conducting Hydrogel Based on Novel Polymer Composite PEDOT:DBSA for Bioelectronic Applications Šárka Tumová¹, Romana Malečková¹, Petr Smíštil², Lubomír Kubáč³, Jirí Akerman³, Jirí Smílek¹, Michaela Pešková⁴, Jan Vítěček⁴, Martin Vala¹ and Martin Weiter¹; ¹Brno University of Technology, Czechia; ²Central European Institute of Technology, Czechia; ³Centre for Organic Chemistry, Czechia; ⁴Institute of Biophysics of the Czech Academy of Sciences, Czechia

Organic bioelectronics represents a potential revolution in medicine as it holds the promise of personalised treatment with reduced side effects compared to conventional pharmaceutical drugs. Despite the big effort dedicated to this field, there are still challenges to be solved. One of them is the form of organic polymers acting as active material, as the commonly used thin films are not very favourable with regard to the tissues that are supposed to be in proximate contact with them. That is mainly due to the dissimilarities in mechanical and physical properties of these two components, which might be an obstacle preventing the formation of a satisfactory interface, thus reducing the efficiency of signal transport. This properties mismatch arises especially from the differences in water content and elastic modulus values. Hence, there is a big demand for a more tissue-like form of these materials as it can significantly promote contact with tissues at the interface, thus reducing the adverse immune responses of the biological system, decreasing the interfacial impedance and enhancing the efficiency of both signal recording and stimulation. Among other structures, hydrogels seem to be the perfect interface to biological tissues due to their structural similarity with the extracellular matrix, tissue-like mechanical properties, water-rich nature, superior biocompatibility, flexibility and adjustable biochemical properties. In this work, we prepared and characterised a conductive hydrogel based on a completely new polymer composite – PEDOT:DBSA. The rheological characterization revealed that the mechanical strength of the hydrogel as well as the gelation time can be easily tailored to the desired application by changing the concentration of cross-linking agent. The electrical properties of the hydrogel were studied using impedance spectroscopy and cyclic voltammetry. It was shown that the total bulk conductivity of prepared hydrogel is 3.8 Sm⁻¹. The LDH cytotoxicity assay showed a very good biocompatibility of hydrogel compared to that of the culture plastic and glass dish. The structure of the hydrogel was investigated using scanning electron microscopy and was found to be of rough, spongy nature. These results indicate that PEDOT:DBSA hydrogel has great potential for creating an interface between the biological environment and electronic devices used in various fields of regenerative medicine.

8:00 PM SB04.03.05

Electrospun Hydrogel Nanoporous Scaffold for Cleaning Ultrafine Contaminants in Semiconductor Manufacturing Somin Shin, Ji-hun Jeong and Sanha Kim; Korea Advanced Institute of Science and Technology (KAIST), Korea (the Republic of)

In semiconductor manufacturing, chemical mechanical planarization (CMP) process is an essential step where wafers are polished via chemical and physical actions using externally supplied abrasives. After the CMP step, contaminants which include the remained abrasives and wear debris must be strictly removed from the wafer surface to prevent device failure via unintended particles. Accordingly, CMP cleaning always follows right after the CMP step. Post-CMP cleaning is particularly difficult as the contaminants are strongly adhered on the wafer surface due to as they are mechanically compressed during the polishing step. For such challenges, brush scrubbing techniques are widely employed due to their superb cleaning efficiency. The brush cleaning is in general conducted via porous polyvinyl alcohol (PVA) hydrogel brushes which make a physical contact with the wafer therefore can provide sufficient physical removal force to the surface particles for their removal.

The synthetic PVA hydrogel used as the wafer cleaning brushes comprises micropores, and has high swelling capacity against water-based cleaning solutions. The recent challenge arises as the pore sizes of commercial brush products remain in micro-scale whereas the size of the contaminants to be removed is ever shrinking to even few nanometers. Therefore, the existing brush products cannot effectively deliver the sufficient removal forces on ultrafine particles. In this research, we fabricate a PVA hydrogel scaffold comprising nano-scale porosity which can exhibit high effectiveness in particle removal for cleaning ultrafine contaminants. Insoluble polyvinyl formal (PVF), the raw material of cleaning brush, is synthesized via acid catalyzed acetalization of water-soluble PVA with formaldehyde which occurs with crosslinking of PVA chains by modifying hydroxyl groups. We produce nano-scale fibrous sheets using electrospinning process and investigate the effect of PVA/formaldehyde/sulfuric acid weight ratio as well as the processing conditions on the fiber formation. A heat treatment follows after the electrospinning step which reconstruct the fiber mat into a three-dimensional porous scaffold via creating fiber-to-fiber junctions, resulting in suitable mechanical strength and resilience. To verify the correlation between structural scale and particle removal efficiency, we conduct lab-scale wafer cleaning experiments on substrates contaminated with particles of various sizes, from 12 μm to 80 nm, using conventional microporous brushes and fabricated nanoporous scaffolds. We further experimentally verify that the effect of the structural scale is significantly more dominant. Our new

hydrogel nanoporous scaffold exhibit outstanding removal efficiency for ultrafine particles, thus can provide an effective engineering solution for the current limit in post-CMP ultrafine contaminant cleaning which is of-interest in semiconductor manufacturing industry.

8:00 PM SB04.03.06

Tissue-Adhesive and Anti-Swelling Hydrogel Based Multifunctional Implantable Sensor for Monitoring of Bladder Activity in Overactive Bladder with Surgical-Robot Assisted Laparoscopic SurgeryByungkookOh and StevePark; Korea Advanced Institute of Science and Technology, Korea (the Republic of)

Electrical properties and mechanical properties of a biological bladder tissue provide useful tissue information for preventing disabling condition of urinary systems as clinical treatments. Recently, there has been a great deal in designing implantable electronics that collect tissue information and provide fundamental treatments. However, intrinsic differences between biological tissues and conventional rigid and dry electronics pose problems with unstable interaction between both surfaces and infection of biological tissues. Here, a highly stretchable and tissue-adhesive multifunctional implantable sensor based on structurally engineered islets embedded in ultra-soft hydrogel is developed for real-time monitoring of bladder activity in overactive bladder (OAB) induced rat and anesthetized pig. One critical issue with hydrogel in general as implantable substrates, however, is their eventual change in mechanical properties and electrical properties due to the gradual absorption of biofluids in the body. To overcome the critical issue, an anti-swelling coating technique that can prevent absorption of water and biofluids in the body is developed. This coating technique is applicable to various hydrogels that have low sol-gel transition temperatures, while imposing negligible changes in mechanical properties. Using tissue-like, anti-swelling hydrogel, which can sustain its initial mechanical & electrical properties as a role of an insulating substrate, can bridge sensory systems to biological tissue with robust seamless interaction without infection of tissues. The sensory systems integrated to soft bridging materials (hydrogel) consist of strain sensors (directly printed micro-capsules of EGaIn on an anti-swelling hydrogel substrate) and multi-array electromyography (EMG) sensors (Ti/Au) on structurally engineered ferris wheel-shaped islets that can make it possible to collect tissue information during repetitive micturition of overactive bladder. On the OAB induced rat, stronger signals (change in resistance and EMG root-mean-square) were detected near intra-bladder pressure maxima, thus showing correlation to bladder activity. Moreover, using robot-assisted laparoscopic surgery, the hydrogel-based implantable sensor was placed onto the bladder of an anesthetized pig. During micturition cycle, bladder strain and EMG were monitored. These results confirm that our proposed sensor is a highly feasible, clinically relevant implantable device for continuous monitoring OAB for diagnosis and treatment.

8:00 PM SB04.03.07

Highly Stretchable Hydrogel Fiber Fabricated by a Self-Coiling Mechanism Maintaining High Water-ContentTaoLi and Seon JeongKim; Hanyang University, Korea (the Republic of)

Hydrogels, which are polymer networks dispersed in water, are widely used in biomedical fields, among others, because of their excellent mass transfer efficiency and biocompatibility. However, hydrogels with a high water content usually have poor mechanical properties and are easily broken. To address this issue, many researchers have incorporated one or more complementary materials into the polymer network of the hydrogel to limit its swelling. Although this method enhances the mechanical properties of hydrogels, it also limits the water content; therefore this method cannot be applied to improve the mechanical properties of high-water-content hydrogels. We have observed that a jellyfish called *Physalia physalis* preys on fish through its coiled stinging tentacles. Although the body of *P. physalis* has a water content above 95%, the coiled structure still provides high stretchability. In this study, we developed a coiled hydrophilic polyurethane hydrogel fiber with high stretchability and high water content by mimicking the coiled stinging tentacles of *P. physalis*. Dry hydrophilic polyurethane yarns produced by electrospinning were twisted under an applied load. When the twisted dry hydrophilic polyurethane yarn swelled with water, the change in Young's modulus and shear modulus elicited self-coiling within 1 s and resulted in a coiled hydrophilic polyurethane hydrogel fiber. The morphology of the formed coiled polyurethane hydrogel fibers can be tuned by adjusting the twist density and the stress resulting from the load applied during swelling. Compared with non-coiled hydrophilic polyurethane hydrogel fibers, the coiled hydrophilic polyurethane hydrogel fibers prepared by this method exhibited ultrahigh stretchability due to the coiled structure and elasticity of the material. When the coiled hydrophilic polyurethane hydrogel fibers are stretched, the uncoiling of the coiled structure provides stretchability, and the fibers can be further stretched due to the elasticity of the hydrophilic polyurethane hydrogel. In summary, we developed a coiled hydrophilic polyurethane hydrogel fiber that can rapidly swell and self-coil under aqueous conditions and possesses high stretchability, while maintaining high water content. It is expected to be used in biomedical fields for applications such as surgical sutures, drug delivery systems, and tissue regeneration.

8:00 PM SB04.03.08

Controllable Actuator by Reversible Clustering Transition Composed of Temperature-Responsive HydrogelJiseongChoi and SeongminKang; Chungnam National University, Korea (the Republic of)

Hydrogel-based soft actuators, which can change their shape according to the various environment and has safe for the human body, are being utilized in various fields such as smart windows, etc. Among the hydrogels, N-isopropylacrylamide (NIPAm), due to its swelling characteristics dependent on the critical solution temperature (32 degree), can be used as a suitable actuator for different situations. Additionally, micropillars with high aspect ratio easily are transformed to clustering state under external forces, and both their original state and clustering state are being utilized as actuators. However, micropillars of clustering state once do not naturally de-clustered, having limitation of application by its non-reversible property of clustering state. In this paper, we fabricate micropillars actuator of a reversible clustering transition composed of thermo-responsive poly(NIPAm-co-acrylamide) hydrogels, verifying the potential applications of soft actuators. The actuator is clustered due to the decrease in mechanical properties of hydrogels by water, but it is de-clustered due to the increase in mechanical properties by hot temperature. Based on this phenomenon, we demonstrated the potential applications of micro grippers for capturing and transporting micro particles in water, as well as smart windows capable of reversible transitions in surface transmittance outside the water.

8:00 PM SB04.03.09

An Efficient Self-Healable and Recyclable Conductive Polymeric Blend with Excellent Mechanical Properties Based on PEDOT:PSS/PUJinsiKim and FabioCicoira; Polytechnique Montreal, Canada

Self-healable conductive polymers have been attracting attention because of the promising advances in electronic devices. Self-healable and conductive coating films are fabricated by blending a conductive polymer, poly(3,4-ethylenedioxythiophene): poly(styrene sulfonate) (PEDOT:PSS) with polyurethane (PU) having excellent mechanical properties. PEDOT:PSS/PU composites are characterized in terms of self-healing properties, recyclable properties, mechanical properties and electrical properties in this study. Polyurethane (PU) is synthesized by reacting with macro diol as a soft segment, isocyanate groups and extender as a hard segment. The two polymers have no noticeable phase separation in blending solutions. The self-healable coating materials exhibit outstanding self-healing capabilities and fast self-healing kinetics and therefore can be used for practical applications like flexible and stretchable electronic devices. The polymeric coating film is cut into two parts completely with a sharp blade then the damaged surfaces are connected under mild temperature for the healing process. The results from experiments exhibit using a mechanical tester to compare the mechanical properties of various compositions of PEDOT:PSS/PU and before and after self-healing processes, respectively. Regarding electrical performance, a cyclic tensile test is also performed to monitor the elasticity. The electrical conductivity maintains constant electrical conductivity under cyclic tensile stress when tensile stress is loaded up to 30% strain. The PEDOT:PSS/PU-based can be reused, improving the sustainability of electronic devices. All these results revealed that PEDOT:PSS/PU have the potential to enable to development of more sustainable and durable electronic devices by reducing electronic waste and improving the lifespan of electronic components.

8:00 PM SB04.03.10

Designing Azo-Based Color-Changing Hydrogels by Sensing pH ResponseWei-TingChang, VioletPratt, NeelJoshi and LeilaDeravi; Northeastern University, United States

The wide applications for environmental sensing and responsible sensing materials using hydrogels can be excellent candidates across systems in biology. For instance, most living cells elicit pH changes during metabolism which we leverage as an actuator in the design of new pH-responsive hydrogels. We synthesized azo-based monomers from anthranilic acid and followed by azo coupling by the treatment of phenylpiperazine and acyl amide. These monomers can then be polymerized with bis-acrylamide, acrylic acid, and polyacrylamide as an adaptive hydrogel that change shape and color different pH environments. Applications of these gels are explored both with and without cells in different environments.

8:00 PM SB04.03.11

The Investigation of the Impact of Small Molecule Dopants on PANI/PAAMPSA Conductive Polymer systemArvaAjeev; University Of Maine, United States

The use of wearable strain sensors has been advancing in modern life owing to their potential to pinpoint, respond, and interpret mechanical deformations from corresponding electrical signals, which can be measured in terms of electrical resistance. Polymeric piezoresistive sensors with remarked flexibility and wearable features have been extensively used in biosensing, human-motion monitoring and detection, e-skin, and human-machine interaction. Traditional strain sensors, based on metallic and semiconducting material having low sensitivity and poor resistance response upon straining endow the need for compliant, elastic, stretchable, and self-healable sensors. In this work, the polymer complex to be used as a strain sensor is composed of a templating poly(2-acrylamido-2-methyl-1-propanesulfonic acid), polyaniline, and a small molecule dopant, originally phytic acid. By substituting the small molecule dopant with other small molecule acids, the impact the various dopants have on the strain sensor's conductivity, mechanical properties, and piezoresistive sensitivity can be studied. Typically, small molecule dopants that increase conductivity decrease stretchability and mechanical stability, which stems from more acidic dopants being able to protonate and facilitate ion transport throughout the sensor. It has been shown that the functional groups with increased hydrogen bonding tend to increase mechanical properties. By increasing our understanding of the impact these various dopants have

on the properties of the strain sensor, the sensor can be tailored to specific applications, allowing for increased sensitivity when needed or increased stretchability when required. This will allow for the development of novel materials as we seek to manufacture better stretchable electronics.

8:00 PM SB04.03.12

Hydrogel-Enhanced Supported Lipid Bilayers (SLBs) Offer Greater Stability and Functionality in Bioelectronic Devices Jordan P. Fitzgerald, Zhongmou Chao and Susan Daniel; Cornell University, United States

Supported lipid bilayers (SLBs) have emerged as an indispensable material to functionalize the surface of bioelectronic sensors that facilitates the exploration of cellular membrane interactions with a wide range of molecules. SLBs accurately mimic the structure, composition, and diffusive properties of natural membranes, providing a biomimetic experimental model. Particularly noteworthy is the compatibility of SLB bioelectronics with electrochemical impedance spectroscopy (EIS), allowing for real-time monitoring of changes in impedance across SLBs. Such measurements provide valuable insights into changes in membrane properties, drug interactions, and the behavior of embedded proteins and channels. However, one drawback of these sensors currently is their vulnerability and limited shelf-life that impedes their broader application.

In this study, we combine hydrogels with SLB bioelectronic devices and show that the usable shelf-life of these devices can be extended significantly. Our approach exploits a range of hydrogels, each with unique characteristics that enhance system versatility. PEGDA, a UV crosslinked hydrogel, enhances the stability of both model POPC SLBs and native component SLBs. Other hydrogels, such as poloxamer based thermally reversible gel, and chitosan based chemically crosslinked gels, show potential for preserving UV- and temperature-sensitive components within the SLBs. Overall, this strategy extends the shelf life of the SLBs from a single day over 45 days, all while preserving the electrical signal integrity and functionality of proteins within the SLBs. This hydrogel-enhanced approach not only facilitates longer sensing periods, but also enables the long-distance shipping of functional SLB-based devices, necessary steps for translation to the field.

In addition to enhancing the shelf life and stability of the SLB-functionalized bioelectronic devices, the integration of hydrogels also boosts their functionality. The hydrogel layer not only facilitates improved stability but also enables the use of cell-free expression of proteins directly into the membrane. This expands the utility of our method, creating opportunities for more comprehensive investigations into the behavior of specific proteins and their responses to various agents within a highly stable, extended-lifespan SLB-based bioelectronic system. This research lays the groundwork for the development of sophisticated hydrogel-enhanced SLB systems capable of operating in complex environments, bringing us closer to the construction of advanced devices such as electrode arrays, sensors, and biomimetic devices, and expanding the scope of bioelectronic applications in biomedical research and beyond.

8:00 PM SB04.03.13

Thermo-Responsive Emulsion-Embedded Hydrogel Microparticle and Its Application to RT-qPCR Seoyoung Lee, Lan Kyeong Yoon, Seungwon Jung and Sang Kyung Kim; Korea Institute of Science and Technology (KIST), Korea (the Republic of)

Water-oil-water double emulsions (DEs) have been widely used as compartmentalized systems to encapsulate components for controllable and targeted reagent delivery. The components encapsulated in DE could be efficiently released upon various stimuli, such as changes in temperature, light, and chemical environment. Among them, by utilizing the heating as a controllable release stimulus, we herein developed a novel thermo-responsive DE-embedded hydrogel microparticle reactor suitably applicable for one-step quantitative reverse transcription polymerase chain reaction (RT-qPCR), which minimizes the non-specific reaction in the reverse transcription step. For this strategy, we encapsulated target-specific nucleic acid reagents (PCR primers and probes) in DE and subsequently entrapped DE in a micro-sized hydrogel PCR reactor. First of all, we adjusted the surfactant concentrations of DE for enhancing the DNA encapsulation efficiency and optimizing the DNA release efficiency to be maximized in the PCR denaturation step (95 °C) as well as minimized in the reverse transcription step (55 °C). From the perspective of DE itself, DNA encapsulation and release efficiencies at both 95 °C and 55 °C increased and decreased, respectively, with increasing concentrations of hydrophobic surfactant, while they were independent of hydrophilic surfactant concentrations. Moreover, we also investigated the change in DNA release tendency and optimized the surfactant concentrations when DEs were embedded in hydrogel microparticles. As a result, and importantly, the DNA release efficiency of DE entrapped in hydrogel significantly increased about 4 times at 95 °C compared to that of DE itself, indicating that the DEs individually located within the hydrogel are more vulnerable to the release of DNA-encapsulated inner water phases. In addition, 8 CMC of hydrophobic surfactant and 37.5 CMC of hydrophilic surfactant were selected as the optimal conditions where 4.6 μM of DNA reagent was encapsulated, and 40% (1.80 μM) and 9% (0.15 μM) of reagent were released at 95 °C and 55 °C, respectively, demonstrating target-specific reagent delivery on demand. Consequently, under these conditions, we successfully confirmed the operation of one-step RT-qPCR in the thermo-responsive DE-embedded hydrogel microparticle and the developed hydrogel microparticle could be utilized as a powerful point-of-care testing platform for the multiplexed detection of several RNA biomarkers.

8:00 PM SB04.03.14

Nanoemulsions-Containing Hydrogel Microparticle Array PCR for Multiplex Discrimination of SARS-CoV-2 Variants Yoon-ha Jang, Eui Ju Jeon, Seoyoung Lee, So Young Jeon, Lan Kyeong Yoon, Seungwon Jung and Sang Kyung Kim; Korea Institute of Science and Technology (KIST), Korea (the Republic of)

Over time, viruses continually produce new genetic variants of themselves. Surveillance is needed to investigate how mutations in viruses affect the transmissibility and lethality of the virus as well as responses against therapeutic medicines [1]. However, whole genome sequencing, which is currently utilized for variant identification, has a limitation in testing a large number of samples, especially in a pandemic situation. Herein, we present rapid multiplex RT-qPCR for SARS-CoV-2 variant discrimination using the TaqMan probe and primer-incorporated network (TaqPIN). TaqPIN is a hydrogel microparticle where target-specific reagents such as primers and probes are preloaded as encapsulated in nanoemulsions [2]. The main challenge is to fabricate TaqPIN because the photoinitiators (PIs) required for curing hydrogel destabilize nanoemulsions and damage the fluorescently labeled probes encapsulated within the nanoemulsion. We found that free radicals generated by PIs damage the probes encapsulated within the nanoemulsions via the infiltration of PIs into the nanoemulsions. We successfully fabricated TaqPIN by using water-dispersible nanoparticles of 2,4,6-trimethylbenzoyl-diphenylphosphine oxide (TPO) as PIs. We found that fluorescently labeled DNA was well retained in the hydrogel particles even when TaqPIN was subjected to strong agitation, and TaqPIN PCR with the same concentration of sample showed constant Ct values up to 2 months. Finally, we constituted a 9-plex TaqPIN array for the identification of five SARS-CoV-2 variants of concern, including alpha (B.1.1.7), beta (B.1.351), gamma (P.1), delta (B.1.617.2), and omicron (BA.1), and the original Wuhan strain within 40 min. From 76 clinical nasal swab samples, the TaqPIN array RT-qPCR successfully discriminated variants with 95.5% sensitivity and 100% specificity. We envision that the TaqPIN array RT-qPCR can be applied to simple diagnostics to help detect and characterize circulating pathogens.

8:00 PM SB04.03.15

Towards Multi-Responsive Pluronic F127-Based Copolymer Hydrogels for Engineering Living Materials Henrique Sepulveda Del Rio Hamacek¹, LeAnn Le², Petri-Jaan Lahtvee¹, Rahul Kumar¹ and Alshakim Nelson²; ¹Tallinn University of Technology, Estonia; ²University of Washington, United States

Engineered living materials (ELMs) are dynamic systems featuring capabilities such as biosynthesis, self-organization, and self-healing¹. Integrating polymeric matrices (abiotic) and cellular (biotic) components creates materials with novel functionalities and precise responsiveness². Here, we deployed additive manufacturing using extrusion-based 3D printing to develop hydrogels capable of retaining cells for longer periods due to increased toughness, while facilitating better nutrient transport to the cells through improved ionic conductivity.

Initially, we formulated hydrogels containing Pluronic F127-bisurethane methacrylate (F127-BUM), methacrylic acid (MAA), and dimethylaminoethyl acrylate (DMAEA) at different monomer concentrations. We characterized the rheological and mechanical properties of these hydrogels. Rheological results revealed that all hydrogel compositions decreased viscosity with increasing shear rate while maintaining their shear-thinning properties even after multiple cycles of applied shear. These results indicate the potential for creating high-resolution 3D-printed structures. Additionally, temperature ramp experiments demonstrated that the hydrogels exhibited the characteristic Pluronic F127 temperature-dependent behavior³, with decreased gelation temperatures upon MAA and DMAEA addition to the precursor mixtures.

Subsequently, tensile mechanical tests were conducted to evaluate the toughness and elasticity of the newly developed hydrogels. The results showed that the hydrogel composition with equimolar concentrations of MAA and DMAEA exhibited a 50% increase in elongation at break compared to control hydrogels consisting solely of F127-BUM. This material could also be elongated up to 600% of its original size, while the modulus of elasticity decreased by 35% compared to the control. These effects were attributed to the disruption of electrostatic interactions between MAA and DMAEA, which carry opposite charges at neutral pH. The formulated hydrogels demonstrated the necessary mechanical properties for cell-loading applications.

Finally, we loaded bakers' yeast (10^7 cells/g of hydrogel) into the selected hydrogels and analyzed their viability, metabolite production, and morphology during cultivation at 50 rpm and 30 °C. The hydrogel with MAA and DMAEA enabled cell retention for longer than previously reported for F127-BUM hydrogels with the same initial cell concentration⁴. Additionally, the cells remained metabolically active throughout the cultivation experiments.

In conclusion, this work demonstrates the potential of the developed hydrogel platform, featuring enhanced mechanical properties and improved ionic conductivity, for the additive manufacturing of ELMs. This platform holds promise for applications in bioengineering and highlights the importance of advanced materials in creating functional ELMs with enhanced capabilities.

References

1. An, B. et al. Engineered Living Materials For Sustainability. *Chemical Reviews* vol. 123 2349–2419 (2023). doi:10.1021/acs.chemrev.2c00512
2. Altin-Yavuzarslan, G. et al. Additive Manufacturing of Engineered Living Materials with Bio-Augmented Mechanical Properties and Resistance to Degradation. *Adv. Funct. Mater.* 2300332 (2023). doi:10.1002/adfm.202300332
3. Millik, S. C. et al. 3D printed coaxial nozzles for the extrusion of hydrogel tubes toward modeling vascular endothelium. *Biofabrication* 11, (2019). doi:10.1088/1758-5090/ab2b4d

8:00 PM SB04.03.16

Molecular Dynamics Simulation of Free-Formed Nanocomposite Hydrogels Emily Sun¹, Shoumik Saha², Jose Nicasio², Dilip Gersappe² and Miriam Rafailovich²; ¹Westford Academy, United States; ²Stony Brook University, The State University of New York, United States

Hydrogels are crosslinked polymer networks that can absorb and retain large quantities of water within their structures. Typically made of hydrophilic polymers, their swelling ability gives these materials properties of both solids and liquids alike. Recent studies highlight that combining hydrogel materials with clay-based nanofillers and charged solvents results in a hydrogel with enhanced properties. However, little is known about the theoretical mechanism of the gel's network formation. Here, we explore a system of free-floating polymer chains, clay-based nanofillers, and solvent to determine the specific conditions for a stable network formation, and optimal rheology of the gel. The aim of this study is to produce the strongest hydrogel, which can then be used for soil-strengthening applications.

We performed coarse-grained molecular dynamics with the LAMMPS software. Our polymer chains were constructed using the Kremer-Grest model, which defines bond interaction via the finitely extensible nonlinear elastic (FENE) potential. Other pairwise interactions between monomers were modeled by using the simple 12-6 Lennard Jones potential. We implemented this model for different polymer concentrations of N=300, 600, and 900, with varying distributions for their attractive regions, or "stickers," which were placed uniformly every 5th, 9th, and 14th monomers (5, 3, and 2 stickers). We turned on attractive interaction between stickers, which let polymer chains connect to undergo network formation. The polymers' dynamics were calculated through diffusion coefficients, gathered from mean-squared-displacement (MSD) values. We calculated stress auto-correlation (SAC) to determine the point at which our system forms a gel. We further ran shearing tests and polymer chain orientation during the shearing process will determine the specific shear thinning properties of our system. Our results show that by proper choice of polymer architecture we can design networks that can be used for soil amendment purposes.

8:00 PM SB04.03.17

Water Treatment: Harnessing the Potential of 2D-Enhanced Hydrogels Ahmed M. Aboulella and Banu Yildiz; Khalifa University, United Arab Emirates

Water scarcity and pollution are global challenges that demand innovative solutions. In this context, 2D-enhanced hydrogels have emerged as promising materials for advancing water treatment technologies. These hydrogels, composed of a three-dimensional network of hydrophilic polymers combined with two-dimensional nanomaterials, exhibit unique properties that enable their application in various water treatment processes. This review focuses on the synthesis, characterization, and functionalization of 2D-enhanced hydrogels, exploring their potential in addressing water quality and scarcity issues. We begin by discussing the fabrication methods of these hydrogels, highlighting the incorporation of 2D nanomaterials such as graphene oxide, graphene, and transition metal dichalcogenides. Their influence on the hydrogel's structure and properties, including increased mechanical strength, enhanced water absorption, and improved stability, is thoroughly examined. Moreover, the tunable nature of 2D-enhanced hydrogels allows for tailoring their porosity, swelling behavior, and selectivity, making them versatile materials for various water treatment applications. The functionalization of 2D-enhanced hydrogels with specific functional groups and nanoparticles is explored, illustrating their potential for pollutant removal, heavy metal ion adsorption, and advanced oxidation processes. Additionally, the use of these hydrogels as membrane materials, adsorbents, and catalyst supports is discussed in the context of water treatment devices. Their ability to selectively remove contaminants, resist fouling, and enhance overall system performance underscores their suitability for practical implementation. We also delve into the challenges and future directions of utilizing 2D-enhanced hydrogels in water treatment, including scalability, long-term stability, and environmental considerations. The integration of these materials into emerging technologies, such as membrane filtration, adsorption columns, and photocatalytic reactors, holds promise for addressing pressing global water challenges. In conclusion, 2D-enhanced hydrogels represent a transformative approach to advancing water treatment technologies. Their unique combination of 2D nanomaterials with hydrogel matrices offers a multifaceted solution for improving water quality and managing water resources efficiently. This review provides valuable insights into the synthesis, properties, and applications of 2D-enhanced hydrogels, laying the foundation for the development of sustainable and effective water treatment devices and processes.

8:00 PM SB04.03.18

Utilizing Bioprinting for Hydrogel-Based Electric Double-Layer Capacitor Fabrication Bianca Seufert and Arash Takshi; University of South Florida, United States

While electric vehicles are slowly bringing in a new era of eco-friendly transportation, the mass production and use of Li batteries have raised serious concerns about their impacts on the environment. Hence, supercapacitors that are able to be charged and discharged at high rates with high power densities and a long cycling stability are potential alternatives to batteries. There are three different types of supercapacitors: electric double-layer capacitors (EDLC) supercapacitors, pseudo-supercapacitors, and hybrid-supercapacitor. For the scope of this paper, however, only EDLCs will be discussed. Using biocompatible materials, supercapacitors are a viable charge storage device for implantable electronic sensors. This paper addresses a new approach to supercapacitor fabrication using a bioprinting method. A series of experiments were conducted to derive a conductive bioink capable of being implemented as a viable material for energy storage devices. This bioink in conjunction with a gel electrolyte were utilized for the fabrication of supercapacitors in a planar structure. This study utilizes the testing methods of Cyclic voltammetry (CV) and electrochemical impedance spectroscopy (EIS) using the VersaStat 4 Potentiostat to measure the capacitor response. Devices with capacitances as high as 53.52 μF were fabricated and tested. The results of this study show the feasibility of using the bioprinting method for fabricating prototype storage devices.

(Funding provided by Funding provided by the Bio-Organic Electronics Research Laboratory at the University of South Florida & NSF FGLSAMP BD: University of South Florida Florida-Georgia Louis Stokes Alliance for Minority Participation (FGLSAMP) – HRD # 1906518)

SESSION SB04.04: 3D Printing and Other Rapidly Scalable Manufacturing Techniques II
Session Chairs: Anna-Maria Pappa, Alexandra Rutz, Christina Tringides and Shiming Zhang
Tuesday Morning, November 28, 2023
Hynes, Level 1, Room 103

8:30 AM SB04.04.01

Turgor Pressure Reinforces Mineral-Based Composites Ran Zhao and Esther Amstad; École Polytechnique Fédérale de Lausanne, Switzerland

Nature fabricates hard functional materials from soft organic scaffolds that are mineralized. To overcome the brittleness of inorganic components, biominerals are arranged in hierarchical structures and sometimes develop local compressive or tensile stresses. For example, the precipitation of hydroxyapatite minerals leads to contractile stresses in collagen fibrils, and eventually reinforces mechanical properties of bones^[1]. The fibril contraction comes from the dehydration of the polymer matrix, even though it happens in a hydrated environment. Similarly in plant cells, osmotic pressure is used to stiffen leaves by exploiting a strong turgor pressure^[2]. Osmotic pressure is well-known to change the mechanical properties of living biological materials. Nevertheless, this strategy has thus far not been leveraged in mineral-based composites. This shortcoming might in part be related to the inferior mechanical behavior of synthetic composites compared to natural counterparts due to the limited structural control over different length scales.

Here, we demonstrate a mineral-based composite whose strength and stiffness can be repeatably adjusted through osmotic pressure driven swelling and de-swelling of confined hydrogels. Specifically, we employ a synthetic porous matrix with a similar degree of structural control from the nanometer up to the centimeter length scale made from an emulsion-based, 3D printable ink^[3]. Those pores in the matrix are back-filled with a hydrogel, which can generate internal compressive or tensile stresses triggered by osmotic pressure gradients. The matrix can selectively bind certain cations such as Ca^{2+} ions, which can serve as mineralization sites upon addition of CO_3^{2-} . The hydrogel contractions induced through the mineral precipitations and osmotic pressure gradients lead to a synergistic control over the mechanics of the composite. This work provides an exciting concept for enhancing mechanical properties of mineral-based composites through turgor pressure similar to biological systems, which can be used as soft actuators or intelligent devices for underwater applications.

References:

- [1] Ping, H., Wagermaier, W., Horbelt, N., Scoppola, E., Li, C., Werner, P., Fu, Z. & Fratzl, P. (2022). Mineralization generates megapascal contractile stresses in collagen fibrils. *Science*, 376(6589), 188-192.
- [2] Fung, Y. C. (2013). *Biomechanics: mechanical properties of living tissues*. Springer Science & Business Media.
- [3] Zhao, R., Wittig, N., De Angelis, G., Yuan, T., Hirsch, M., Birkedal, H., & Amstad, E. (2023). Additive manufacturing of porous biominerals. *Advanced Functional Materials*, accepted.

8:45 AM SB04.04.02

Nanoengineered Ink for Designing 3D Printable Flexible Bioelectronics Akhilesh K. Gaharwar; Texas A&M University, United States

Flexible electronics require elastomeric and conductive biointerfaces with native tissue-like mechanical properties. The conventional approaches to engineer such a biointerface often utilize conductive nanomaterials in combination with polymeric hydrogels that are crosslinked using toxic photo-initiators. Moreover, these systems frequently demonstrate low signal accuracy, poor biocompatibility and face trade-offs between conductivity and mechanical stiffness under physiological conditions. To address these challenges, we introduce a class of shear-thinning hydrogels as biomaterial inks for 3D printing of flexible bioelectronics. These hydrogels are engineered through a facile vacancy-driven gelation of MoS₂ nanosheets and naturally derived polymer. Due to shear-thinning properties, these nanoengineered hydrogels can be printed into complex shapes that can respond to mechanical deformation. The chemically crosslinked nanoengineered hydrogels demonstrate twenty-fold rise in compressive moduli and can withstand up to 80% strain without permanent deformation, meeting human anatomical flexibility. The nanoengineered network exhibits high conductivity, compressive modulus, pseudo-capacitance and biocompatibility. The 3D printed crosslinked structure demonstrate excellent strain sensitivity and can be used as wearable electronics to detect various motion dynamics. Overall, the results suggest that these nanoengineered hydrogels offer superior mechanical, electrical, and biological characteristics for various emerging biomedical applications including 3D printed flexible biosensors, actuators, optoelectronics, and therapeutic delivery devices.

9:00 AM *SB04.04.03

Conducting Polymer Hydrogels for Hydrogel Bioelectronics [HyunwooYuk](#); SanaHeal, Inc., United States

Electrical interfacing with biological tissues for interrogation and modulation of living systems – or bioelectronics – is one of the most important modes of communication between artificial machines and biological organisms. In conventional applications, bioelectronic interfacing has relied on conventional electrodes and devices made of metals and engineering solids like plastics and elastomers. However, the stark dissimilarity between biological tissues and conventional device materials has posed great challenges for long-term bioelectronic interfacing with living systems, especially for implantable devices. To address these challenges, electrically conductive hydrogels – polymer networks infiltrated with large amounts of water with electrical conductivity – have been substantially studied in the last decades owing to their unique advantages including tissue-like mechanical properties and high water contents, favorable electrical properties, and *in vivo* biocompatibility. However, conducting polymer hydrogels has faced several key challenges in their practical uses including poor electrical and mechanical properties in physiological environments, unreliable integration within devices and to the target biological tissue, and difficulties in small-scale fabrications into functional devices. In this talk, several advances in conducting polymer hydrogels to address these challenges will be discussed toward the vision of hydrogel bioelectronics.

9:30 AM SB04.04.04

Skin-printable, Self-adhesive and Bio-based Hydrogel for the Bioelectronic Interface [Jia XiChen](#)¹, [Yi XinZhang](#)¹, [TerekLi](#)¹, [ZiaSaadatnia](#)¹, [MilosPopovic](#)^{2,1} and [HaniNaguib](#)^{1,1}; ¹University of Toronto, Canada; ²University Health Network, Canada

Inspired by the customizability of injectable hydrogels in the medical field as cell cultures and engineered tissues, a conductive and 3D-printable hydrogel based on bio-polymers is developed to interface between the skin and medical devices during rehabilitation treatments of surface functional electrical stimulation (sFES). The sFES treatment involves delivering electric currents through the skin to induce muscle contraction, with clinical evidence supporting the ability of sFES treatments to restore voluntary motor functions in previously paralyzed patients. However, physiological differences in muscle distribution and body curvatures among individuals require sFES treatments to be personalized. Therefore, to increase the accessibility of sFES rehabilitations by enabling remote sessions and shape-configurable electrodes universal to all patients, the authors developed a novel material capable of being adapted to any shape and size, with self-adhesive and electrically conductive properties to ensure conformity to body morphology and to guarantee sFES signal stability. As the electrodes are single-use, the hydrogel is made from naturally occurring, biocompatible, and eco-friendly polymers that are easy to fabricate and process. Carboxymethyl cellulose is adopted as the matrix for its water solubility and mechanical properties, along with poly(3,4-ethylene-dioxythiophene) polystyrene sulfonate (PEDOT:PSS) as the conductive additive and mussel-inspired polydopamine as the adhesive additive. A mild and biocompatible gelation method exploiting hydrogen bonding is implemented by adding phytic acid, with *in situ* formation of the extruded hydrogel taking place minutes after being 3D-printed onto the skin. The gelation process is examined with FTIR spectroscopy, which confirms the molecular interactions between bio-polymer components, scanning electron microscopy, which ensures the macroscopic morphology of the formed hydrogel, and rheological measurements over time, which characterizes the printability of the precursor ink. The pre-gel solution exhibits tailorable viscosity, allowing for facile processability and shape-configurability. Adhesive and electrical properties of the hydrogel are studied in contact with porcine skin over time. Although the self-adhesion of the hydrogel is two folds lower than commercial tissue adhesives, the interfacial electrical impedance is improved by an order of magnitude compared to commercial hydrogel electrodes. The sFES performance of the printable and conductive hydrogel is further assessed with a developed handheld 3D printer, a lightweight instrument to extrude the hydrogel ink in uniformly deposited layers with shape fidelity of mm-thick resolutions. Compared to conventional sFES electrodes of both hydrogel and metal-electrolyte gel systems, the printable hydrogel electrodes can induce muscle movement during sFES with better precision and accuracy, improving the efficiency by 10% when stimulating eye closure to the orbicularis oculi muscle. The printable and conductive hydrogel created for wearable purposes may be adapted for other applications involving bi-directional communications of electric signals across the bioelectronic interface, such as surface electromyography and surface electrocardiography.

9:45 AM SB04.04.05

PEDOT:PSS Hydrogel Based Wearable Biosensor Utilizing Aerosol Jet Printed Organic Electrochemical Transistors (OECTs) for Lactate Detection [YuchenShao](#)¹, [LuizMarcelo](#)², [LixinZhang](#)¹ and [ManishaGupta](#)¹; ¹University of Alberta, Canada; ²Monterrey Institute of Technology and Higher Education, Mexico

Poly(3,4-ethylenedioxythiophene) doped with polystyrene sulfonate (PEDOT:PSS) is a conductive polymer with excellent electrical conductivity, good processability and biocompatibility. Hydrogels have the advantage of soft, flexible and non-toxicity with cells and tissues. A combination of PEDOT:PSS and a hydrogel offers unique conductivity and mechanical properties, applying an alternative approach for biosensing applications.

In this work, we developed a PEDOT:PSS hydrogel based 3D printed organic electrochemical transistor (OECT) for lactate sensing, since OECTs offer high transconductance, low operation voltage and compatibility with aqueous environments. Optomec Aerosol Jet 5X 3D printer is used to fabricate the biosensors on the flexible Kapton substrate. Au was chosen as the metal contact, Pt as the gate with polyimide as the insulator layer. PEDOT:PSS hydrogel is drop casted on Au as the channel material. For PEDOT:PSS hydrogel, it was synthesized by mixing with dimethyl sulfoxide (DSMO) to improve the conductivity under vigorous magnetic stirring for 24 hours, then drop-casted 0.2uL solution on top of the channel for a printed OECT device and was placed into the oven under 60°C for another 24 hours to generate the partially formed gel. After that, 3 times cyclic annealing was applied for the device for 30 minutes at 130°C. Finally, the device was put under -20°C for 12 hours and took out for extra 12 hours, repeating 2 times. The unfunctionalized device exhibits a transconductance up to 110 mS and is compared to the printed PEDOT:PSS based device. Further, tetrathiafulvalene (TTF), chitosan, lactate oxidase (LoX), bovine serum albumin (BSA) and gelatin help realize the functionalization of the device. The functionalized lactate sensor can be preserved in PBS solution under 4°C for over one month. Spike tests on the PEDOT hydrogel-based lactate sensor was performed and achieved a sensitivity range between 100uM and 10mM. In addition, the combination of the printed PEDOT:PSS channel with drop-casted PEDOT:PSS hydrogel exhibited better performance of the device. The results for this device will be presented along with the material characterization.

10:00 AM BREAK

SESSION SB04.05: Stimuli-Responsive Materials and Other Special Mechanical Properties I

Session Chairs: Anna-Maria Pappa, Alexandra Rutz, Christina Tringides and Shiming Zhang

Tuesday Morning, November 28, 2023

Hynes, Level 1, Room 103

10:30 AM *SB04.05.01

Stimuli-Responsive Polymers as Precursors to Conductive Hydrogels [LaureV. Kayser](#); University of Delaware, United States

Electronically-conductive hydrogels, composites of crosslinked and water-swollen polymers with a conducting material (polymer or inorganic nanoparticles) can address the mechanical and electronic mismatch between electronic devices and biological systems. While several methods have been reported to prepare these conductive hydrogels, several issues have to be addressed to enable their translation in bioelectronics. These issues include: (1) the increase in elastic modulus at high loading of conducting material, (2) the irreversibility of the gelation mechanism, which complicates the delivery and potential removal of the conductive hydrogel *in vivo*, and (3) the difficulty in controlling the micro- and macro-structure of the conductive hydrogels for applications in tissue engineering and wearable electronics. In this talk, I will share our progress towards addressing these issues through the use of synthetic chemistry, particularly using novel stimuli-responsive conducting polymers. In the first part, I will discuss the use of thermo-responsive conducting polymers that displays a reversible sol-gel transition close to body temperature, thereby enabling injectable conductive hydrogels. The second part will be focused on achieving spatiotemporal control by using photo-active polymers to simultaneously photocatalyze the polymerization of a conducting polymer and photo-crosslink its supporting matrix. This approach has great potential for 3D printing conductive hydrogels with a controlled microstructure and high resolution using light.

11:00 AM *SB04.05.02

Programmable Materials, Structures and Devices for Next Generation Intelligent Machine[JiyunKim](#); Ulsan National Institute of Science and Technology, Korea (the Republic of)

In recent times, virtual intelligence has made significant strides, reaching and even surpassing the functional and cognitive abilities of humans, owing to advancements in computing power and novel operational methodologies. Meanwhile, physical objects or machines in the real world strive to imitate the forms and functions of specific living organisms, such as humans, cheetahs, and octopuses. However, they still lag behind in terms of intelligent and adaptive functions, necessitating the exploration of innovative mechanisms and approaches.

Therefore, our research group aims to develop an integrated robotic platform that possesses the ability to program its morphology, physical properties, interface, and function. This robotic paradigm requires innovation at all levels of the system, including materials, components, architectures for their integration, manufacturing processes, data processing, and operation. In this talk, I will introduce research categories and recent research outcomes from our group. These include (1) the development of programmable robotic components using smart materials such as multifunctional 3D sensors, soft tensile valves, digital metamaterial, and soft end effectors, (2) the exploration of novel algorithmic architecture including tensegrity, lattice metamaterial, and folding-based structures, (3) the exploitation of manufacturing methods realizing the architectures and functions including intuitive pen-drawing and 3D/4D printing, and (4) the excavation of machine design and operation methodology using artificial intelligence for shape-shifting task, in-situ function programming, and robot/HMI device design and operation. Through these works, we aim to blur the boundaries between the virtual and tangible world and, more importantly, between humans and the environment, thereby sharing our vision for the future physical environment for humans.

11:30 AM SB04.05.03

Highly Transparent Conducting Ionic Hydrogels of Double Network Structure for Deformable Electronics[JinhwanYoon](#); Pusan National University, Korea (the Republic of)

Highly deformable soft electrodes have garnered significant attention due to their potential to drive innovation in wearable electronics and soft robotics. To render the soft electrodes, stretchable, conductive, and transparent polymer networks have been studied extensively, but fulfilling these requirements remains challenging. In this work, we developed double-network ionic hydrogels of high transparency and stretchability due to the finely tuned network structure and transparent electrolyte. Based on the high performance of the ionic hydrogels, electroluminescent devices were achieved with an inorganic phosphor emission layer, which exhibits high luminance under extreme deformation. The remarkable transparency of the ionic hydrogels further enabled to fabrication of novel electroluminescent devices of tandem structures, allowing color variation by independent control of each emission layer.

<quillbot-extension-portal></quillbot-extension-portal>

11:45 AM SB04.05.04

Repeatably Autonomously Self-Healing Ultra-Stretchable PAAMPSA/PANI/PA Conductive Polymer Complex as Strain Sensor[ColtonDuprey](#)¹, [YangLu](#)² and [EvanK. Wujcik](#)¹; ¹University of Maine, United States; ²Georgia Institute of Technology, United States

Wearable strain sensors should be comfortably adhered to the skin and capable of monitoring human motions with high accuracy/sensitivity while remaining robust with excellent durability/longevity. However, it is challenging to develop electronic materials that possess the properties of skin—compliant, elastic, stretchable, and self-healable while also having a high enough conductivity for adequate sensitivity. This work demonstrates a new regenerative polymer complex composed of poly(2-acrylamido-2-methyl-1-propanesulfonic acid), polyaniline, and phytic acid as a skin-like electronic material. The type-2 (zip) templated polymerization of aniline in the presence of poly(2-acrylamido-2-methyl-1-propanesulfonic acid) with phytic acid as a P-type dopant exhibits ultrahigh stretchability (1935%), repeatable autonomous self-healing ability (repeating healing efficiency >98%), quadratic response to strain ($R^2 > 0.9998$), and linear response to flexion bending ($R^2 > 0.9994$), mechanically outperforming current reported wearable strain sensors. Sensitive strain-responsive geometric and piezoresistive mechanisms of the material owing to the homogeneous and viscoelastic nature provide excellent linear responses to omnidirectional tensile strain and bending deformations. Furthermore, this material is scalable and simple to process in an environmentally friendly manner, paving the way for the next-generation flexible electronics.

SESSION SB04.06: Multifunctional Materials

Session Chairs: Anna-Maria Pappa, Alexandra Rutz, Christina Tringides and Shiming Zhang

Tuesday Afternoon, November 28, 2023

Hynes, Level 1, Room 103

1:30 PM *SB04.06.01

All-Aqueous Hierarchical Hydrogels for Microfluidics[AndersonShum](#)^{1,2}; ¹University of Hong Kong, Hong Kong; ²Advanced Biomedical Instrumentation Centre, Hong Kong

Hydrogels have demonstrated promising applications across fields, ranging from delivery of actives, to cell cultures, and to wound protection. Hydrogel designs have focused on the constituent molecules and molecular interactions via modifications of the molecular identities and structures. Hierarchical structures within the hydrogels can also be manipulated by structuring the precursor solution before hydrogel formation. The precursor solution can be directed via the use of microfluidic techniques, achieving underlying hydrogel architectures with different properties. Besides its use for designing and modifying hydrogels, microfluidic devices can also be made formed by hydrogels, rather than traditional elastomer-based materials. In this talk, I will share our works at the interface between hydrogels and microfluidics, and will discuss the potential functions and properties of the resultant hydrogels and microfluidic devices.

2:00 PM SB04.06.02

Acid-Crystallized PEDOT Nanoparticles: Scalable and Biocompatible Fillers for Highly Conductive Hydrogels[JoshuaTropp](#) and [JonathanRivnay](#); Northwestern University, United States

Conductive hydrogels are widely used in bioelectronic applications due to their flexibility, biocompatibility, and conductivity. Conductive hydrogels have been leveraged to improve the biocompatibility of electrodes, act as transducing elements within biosensors, and as conductive scaffolds for cells to promote tissue regeneration. While the unique properties of conductive hydrogels make them a promising material for bioelectronics, achieving high conductivity while maintaining mechanical compliance remains a significant challenge. To meet these requirements, functional- π electron systems (conjugated polymers, carbon nanotubes, graphene, etc.) are typically dispersed within natural or synthetic biomaterials to afford conductive hydrogels. A significant challenge in the field remains the required high nanomaterial loadings to achieve significant conductivity; however, at such loadings the conductive hydrogels become prohibitively rigid for bioelectronic applications. Unlike 2D thin-film applications that leverage the long-range ordering of nanomaterials such as conjugated polymers to achieve significant charge percolation, the 3D, complex, and tortuous structure of hydrogels prevents such material alignment, creating a barrier toward highly conductive soft hydrogels. To overcome this limitation, PEDOT nanoparticles have been developed, which behave as three-dimensional seeds for charge percolation throughout the hydrogel. By carefully controlling nanoparticle surface chemistry and morphology via acid treatment, dispersible and highly conductive particles were afforded. Unlike other carbon nanomaterial fillers, the intrinsic dispersibility of the PEDOT nanoparticles enabled direct incorporation within hydrogels at high loadings ($> 100 \text{ mg mL}^{-1}$ of precursor), as well as deposition via spray coating and 3D printing without added surfactant or chemical modification. Upon sufficient particle loading, charge percolation is achieved throughout the hydrogel, affording organic gels with high conductivity ($> 1 \text{ S cm}^{-1}$) without deleterious hydrogel stiffening. PEDOT nanoparticles were incorporated within various synthetic and natural biomaterials, demonstrating compatibility with common crosslinking modalities (photopolymerization, ionic, thermal, Schiff base). The scalability, conductivity, and biocompatibility of the acid-crystallized PEDOT nanoparticles make them attractive fillers for hydrogels/biomaterials for bioelectronic applications.

2:15 PM SB04.06.03

From Conducting Hydrogel to Semiconducting Hydrogel[DingyaoLiu](#), [YanWang](#) and [ShimingZhang](#); The University of Hong Kong, Hong Kong

Thin-film semiconductor-based devices have revolutionized the field of microelectronics. In the realm of biomedical applications, conducting hydrogels have rapidly gained prominence due to their mechanical and biocompatible nature with biological systems. The realization of semiconducting hydrogel materials holds significant value within the field of bioelectronics for developing advanced biologics[1]. Advancing towards flexible and stretchable semiconducting hydrogels can enable direct applications at the interface of soft biological systems [1].

However, the development of semiconducting hydrogels presents challenges, primarily due to the thin-film nature of semiconductors, which are generally less than 1 micrometer in thickness. In contrast, hydrogels tend to have greater thicknesses and struggle to achieve good semiconductor properties.

The advent of organic electrochemical transistors (OECTs) has introduced a new paradigm that can be a powerful testbed to evaluate the performance of a semiconducting hydrogel. In this report, we present the development of the PEDOT:PSS semiconducting hydrogel and its application in the development of OECTs [2]. Furthermore, we provide our insight on how to define a semiconducting hydrogel when using OECT as a testbed. Finally, we delve into the development of stretchable semiconducting hydrogels and explore how they can revolutionize applications in the field of biomedical research.

[1]. Zhang., Shiming, et al. *Advanced Materials* 32.1 (2020): 1904752.

[2]. Liu, Dingyao., Wang, Yan., Zhang, Shiming., et al. Submitted.

2:30 PM *SB04.06.04

Conducting Polymers Biointerfaces for Bioelectronics[Jadranka Travas-Sejdic](#); University of Auckland, New Zealand

Conducting polymers (CPs) have been widely used as electroactive biointerfaces in applications such as electrically stimulated tissue engineering and flexible organic bioelectronics. In this talk, several different approaches to advanced electroactive biointerfaces based on conducting polymers will be presented.

The first approach addresses the issue of poor solubility and processability of CP by functionalization of CPs with various moieties, and, in particular, by grafting of CP backbones with polymeric sidechains. That enables modification of optoelectronic, physical and mechanical properties of the CPs and their use as biomimetic biointerfaces, e.g. responsive to stimuli, intrinsically stretchable and self-healing[1].

The second approach addresses the issue that electrodes used in tissue recording and stimulation are commonly 2D and made of rigid conducting materials, and as such cannot adequately probe the actual 3D cell environment within tissues and/or have a significant mechanical mismatch with biological tissue. Our approach to overcome that is based on a precise fabrication of individually addressable, high aspect ratio, soft and flexible 3D CP-pillar microelectrode arrays by means of 'direct 3D writing'. Such 3D microelectrode arrays could be employed in a variety of applications, from biological sensing to recording and electrically stimulating cells and tissues[2], with the array design easily adjustable.

The third approach to electrochemically addressable biointerfaces is based on flexible, microporous, electrochemically switchable membranes that can selectively and efficiently capture, and then non-destructively release, cancer biomarkers, such as cancer cells-shaded extracellular vesicles (EVs)[3] and rare cancer cells[4] The platform allows for the EVs and cells to be captured from large volumes of complex biological samples and released into clean and small volumes of buffers - suitable for further analysis, for example, for medical diagnostics.

1) P. Baek, L. Voorhaar, D. Barker, J. Travas-Sejdic, Molecular approach to conjugated polymers with biomimetic properties, *Accounts of Chemical Research*, **2018**, 51, 1581-1589

2) E. Tomaskovic-Crook, P. Zhang, A. Ahtiaainen, H. Kaisvuo, C-Y. Lee, Stephen Beirne, Z. Aqrawe, D. Svirskis, J. Hyttinen, G. G. Wallace, J. Travas-Sejdic, J. M. Crook, Human Neural Tissues from Neural Stem Cells Using Conductive Biogel and Printed Polymer Microelectrode Arrays for 3D Electrical Stimulation, *Advanced Healthcare Materials*, **2019**, 8, 1900425

3) A. Akbarinejad, C. Hisey, D. Brewster, J. Ashraf, V. Chang, S. Sabet, Y. Nursalim, V. Lucarelli, C. Blenkiron, L. Chamley, D. Barker, D. Williams, C. Evans, J. Travas-Sejdic, Novel Electrochemically Switchable, Flexible, Microporous Cloth that Selectively Captures, Releases and Concentrates Intact Extracellular Vesicles, *ACS Applied Materials and Interfaces*, **2020**, 12, 39005-39013

4) A. Akbarinejad, C. Lee Hisey, M. Martinez-Calderón, J. Low, D. T. Bryant, B. Zhu, E. W. C. Chan, J. Ashraf, D. Brewster, C. Blenkiron, L. Chamley, D. Barker, D. E. Williams, C. W. Evans, L. I. Pilkington, J. Travas-Sejdic, A novel electrochemically switchable conductive polymer interface for controlled capture and release of chemical and biological entities, *Advanced Materials Interfaces*, **2022**, 2102475; doi.org/10.1002/admi.202102475

3:00 PM BREAK

3:30 PM *SB04.06.05

Conductive Hydrogels for Multimodal Bioelectronic Interfaces[Ivan Minev](#)^{1,2,3}; ¹Leibniz Institute for Polymer Science, Germany; ²Technische Universität Dresden, Germany; ³The University of Sheffield, United Kingdom

Hydrogels are attracting attention as materials for bioelectronic implants because they may solve some long-standing challenges encountered at the tissue-electrode interface. This will require appropriate viscoelasticity, hydration, bioactivity and dual electronic-ionic conductivity. Apart from improved integration with brain tissue, hydrogels may enable electrodes with superior charge injection capacity and capability for neuromodulation beyond the electrical domain (e.g. using biomolecules).

In this talk I will present our efforts to combine Glycosaminoglycans and the conductive polymer PEDOT into interpenetrating network hydrogels that are soft, conductive and bioactive. The material system is highly tunable offering control over electrical and mechanical properties. Furthermore the hybrid material has enabled us to sequester and release small proteins such as growth factors. The release profiles can be electrically tuned. The released proteins are bioactive and can influence cells in culture.

With this work we aim to advance the possibility to engineer synthetic bioelectronic materials that emulate some aspects of the extracellular matrix and may enable applications in next-generation tissue-mimetic bio interfaces.

4:00 PM SB04.06.06

Conducting Polymer Hydrogels for Soft and 3D Bioelectronic Interfaces[Alexandra Rutz](#); Washington University in St. Louis, United States

Hydrogels are insoluble polymer networks swollen with water (>90% water by mass) and are used widely in biomedical applications for their similarities to native extracellular matrix. For bioelectronics, there are many efforts to build devices based on these materials to achieve tissue-matching stiffness and other tissue-inspired properties in order to improve the biointerface. For making electrodes and other device components based on semiconducting materials, conjugated polymers can be gelled into electronically conducting hydrogels. Such methods include simple mix-and-cast techniques, similar to other methods used widely in traditional (non-conducting) hydrogel processing. We have investigated conducting hydrogels based on the conjugated polymer poly(3,4-ethylenedioxythiophene) polystyrene sulfonate (PEDOT:PSS) fabricated by mixing in a gelling agent, ionic liquid. We have studied how the hydrogel precursor formulation and other fabrication variables of this method affect gel properties, such as swelling, conductivity, and elastic modulus. Further, we have evaluated the potential of these PEDOT:PSS hydrogels for biointerfacing applications and have found that these gels when processed appropriately are stable in vitro and support mammalian cell culture. Finally, we are developing these conducting polymer hydrogels for compatibility with additive manufacturing to grant structural control of these soft bioelectronic interfaces. Such techniques provide manipulation of dimensions and microporosity, important for assembling these hydrogels into functional devices and optimizing tissue integration.

4:15 PM SB04.06.07

Ultra-Soft Semiconducting Hydrogels for Tissue-Like Organic Electrochemical Transistors[Yahao Dai](#) and Sihong Wang; University of Chicago, United States

The rapid development of wearable/implantable electronics over the past decade opens the next era of human-integrated biosensors in pursuit of higher sensitivity and more seamless tissue-electronics interfaces. Transistor, especially organic electrochemical transistor (OECT)-based biosensor has attracted considerable attention as an advanced biosensing platform due to their high built-in amplification and water-compatible operation. To achieve the intimate biointerface and acquire the biological signal with the highest possible accuracy, the most ideal approach is to prepare the semiconducting materials with tissue-level softness and stretchability, and directly interface with the tissue surface. However, so far no semiconducting material is able to provide modulus even close to the tissue level due to the general paradox that semiconductors rely on stronger intermolecular interactions to facilitate charge transport. In this research, we proposed a novel material design strategy for developing a gel-like semiconductor that is able to simultaneously provide low modulus, high stretchability/elasticity, and high hole mobility. This is achieved by incorporating a secondary hydrogel matrix into a semiconducting polymer network for enhancing the water uptake to soften the composite, and utilizing solvent treatment to form strong percolation between polymer semiconductors to resist the negative effect of swelling. We further use ultra-soft semiconductors to fabricate gel-like OECTs with desired mechanical and electrical performance for human integration, and demonstrate its capability as the advanced platform for biosensing applications.

4:30 PM SB04.06.08

Developing Multifunctional Hydrogels with Tissue-Like Properties for Improved Cell-Material Interfaces[Christina M. Tringides](#)^{1,2}, [Blandine F. Clément](#)¹, [Marjolaine Boulingre](#)¹, [Vilius Dranseika](#)³, [David J. Mooney](#)² and [Janos Vörös](#)¹; ¹ETH Zurich, Switzerland; ²Harvard University, United States; ³UZH, Switzerland

Biomaterial scaffolds have emerged as a tool to build 3D cultures of cells which better resemble biological systems, while advancements in bioelectronics have enabled the modulation of cell proliferation, differentiation, and migration. Here, we first describe a porous conductive hydrogel with the same mechanical modulus and viscoelasticity as neural tissue. Electrical conductivity is achieved by incorporating low amounts (<0.3% weight) of carbon nanomaterials in an alginate hydrogel matrix, and then freeze-drying to self-organize into highly porous networks. The mechanical and electrical properties of the material can be carefully tuned and used to modulate the growth and differentiation of neural progenitor cells (NPCs). With increasing hydrogel viscoelasticity and conductivity, we observe the formation of denser neurite networks and a higher degree of myelination. Similarly, fibroblasts can be incorporated into the scaffolds and cell migration can be modulated through the application of exogenous electrical stimulation, for applications to wound healing. To investigate the functionality of neural systems, both *in vitro* and *in vivo* platforms can be realized. By placing a polydimethylsiloxane (PDMS) microstructure on an underlying multielectrode array (MEA), we can then explore different materials and techniques to integrate hydrogels into the PDMS microstructures and can facilitate the growth of neuronal networks in 3D. Additionally, implantable surface electrode

arrays can be fabricated, with the ability to record from the brain and heart with enhanced tissue conformability and minimal damage to the biological organs. The described biomaterial platforms can be used to investigate neuronal development and disease progression.

4:45 PM SB04.06.09

Superstrong Electronic Hydrogel Actuators (ECO)Mahiar M. Hamed; KTH, Sweden

Intelligent systems combine sensing, actuation, and computation to achieve complex tasks and functions. Soft electrically controlled multifunctional materials, especially hydrogels, are the most promising materials for such systems as they are as adaptable as biological systems yet compatible with advanced systems through electronics.

We describe an electroactive hydrogel fabricated from cellulose nanofibrils from trees, and conductive nanomaterials, like CNTs or 2D MXenes. These nanoparticles self-assemble into an anisotropic composite networks with an open mesoporous structure that can hold lots of water and be highly permeable to substances in their surroundings. The anisotropy of the network allows high expansion in one direction while maintaining very high strength and high electric conductivity in the other.

The electrochemical charge/discharge of the conductors in the hydrogels controls the internal salt concentration and consequently their osmotic swelling. This allows direct electrically controlled actuation where around 700 water molecules expand/contract the structure for each ion/electron pair inserted/de-inserted at only ± 1 volt, resulting in up to 300% electroosmotic expansion, with very high pressures reaching 1 MPa.

This mode of electronic actuation has not been shown before. We call these electroosmotic (ECO) actuators. Our ECO hydrogel actuators have emergent properties not present in any previously known soft material. ECOs allow monolithic integration of sensors and many other functions into the same composite, rendering a new form of smart soft material not achievable with other materials systems.

Reference:

"*Electrochemically Controlled Hydrogels with Electrotunable Permeability and Uniaxial Actuation*", T Bensefelt, J Shakya, P Rothemund, S B Lindström, A Piper, T E Winkler, A Hajian, L Wågberg, C Keplinger, M M Hamed, **Advanced Materials** 2023

SESSION SB04.07: Poster Session II

Session Chairs: Anna-Maria Pappa, Alexandra Rutz, Christina Tringides and Shiming Zhang

Tuesday Afternoon, November 28, 2023

Hynes, Level 1, Hall A

8:00 PM SB04.07.01

Long-Term Durable and Ultrasensitive Multiple-Crosslinked Ionic Hydrogel Sensors with Multi-Functions for Wearable Electronics Byeong Su Kang¹, Jin-Young Yu¹, Jeong Hun Kim² and Seongmin Kang¹; ¹Chungnam National University, Korea (the Republic of); ²Electronics and Telecommunications Research Institute, Korea (the Republic of)

Hydrogels are considered promising for wearable devices because they are soft, flexible, stretchable, and biocompatible. However, existing hydrogels suffer from poor strength, weak and one-time adhesion, non-self-recovery, water evaporation, ice crystallization, and low sensitivity, and these problems have been only partly solved previously. We propose the one-pot synthesis of a multiple-crosslinked poly(2-(methacryloyloxy)ethyl)dimethyl-(3-sulfopropyl)ammonium hydroxide-co-acrylamide (P(SBMA-co-AAm)) multifunctional hydrogel to overcome these limitations. The synthetic route provided elasticity, self-healing, and transparency, and the incorporation of glycerol and NaCl ions provided moisture stability (e.g., water retention) and antifreeze properties. Zwitterionic SBMA contributed to the increased gauge factor, resulting in high sensitivity and an ability to detect human movements at a strain of 800%–1600%, making the hydrogel sensor practical. The sensor retained its properties after even 300 cycles, indicating its durability and reliability for long-term applications.

8:00 PM SB04.07.02

Multi-Crosslinked Hydrogel-Based Needle Structure Capacitance Sensor with High Sensitivity and Stability Byeongsu Kang¹, Jeong Hun Kim² and Seongmin Kang¹; ¹Chungnam National University, Korea (the Republic of); ²Electronics and Telecommunications Research Institute, Korea (the Republic of)

The hydrogel-based sensor has better elasticity than the existing elastomer sensor, so the distance between the two electrodes can be reduced. Also, since the amount of change in contact area is also large, the amount of change in capacitance is excellent. Especially, by adopting a micro needle structure that can maximize the change in contact area, the change in capacitance is increased. However, the previous hydrogel-based sensor lacks recipe research to create a structure, and adding a structure reduces stability and repeatability, limiting its application as a sensor. In this paper, poly(acrylamide-co-N, N'-methylenebisacrylamide) multifunctional hydrogel can overcome the aforementioned limitations. Then, by making a hydrogel-based sensor with a micro needle structure, high sensitivity is sought by adjusting the amount of N, N'-methylenebisacrylamide. In addition, by adding sodium dodecylbenzenesulfonate lauryl acrylate, the stability of the structure that does not interfere with sensitivity is increased. This hydrogel-based sensor is a human-friendly material that can be applied not only to the biomedical measurement field, but also to fields where existing elastomer sensors are applied, such as robots, hydraulic pressure measurement, and aviation.

8:00 PM SB04.07.03

Robust Integration of Highly Conductive Hydrogels with Stretchable Electronics for Skin-Interfaced Bioelectronics Hyun Su Lee and Dae-Hyeong Kim; Seoul National University, Korea (the Republic of)

Skin-interfaced bioelectronics mounted on human skin has the potential to revolutionize next-generation medical diagnostics and healthcare. To achieve this goal, designing a compliant and stretchable device is highly desirable for device reliability and long-term user comfort. In the material aspect, the limitations of conventional functional device components that originate from rigid and obtrusive interfaces must be overcome by materials with intrinsic softness and stretchability. Conductive hydrogels that possess tissue-level softness owing to their water-rich nature, can be an alternative option. Generally, for the fabrication of hydrogel-based, skin-interfaced bioelectronics, a hydrogel film is cut and placed onto an electrode. However, during device operation, large amount of water inside the hydrogel film tends to form a slippery surface rather than a robust interface between human skin and electronic device. Such poor integration capability could cause the lack of reproducible device performances, difficulty to scale up, and the loss of intimate physical/electrical contacts, which leads to critical problems in signal sensing and electrical actuation from/to human tissue. Here, we suggest direct polymerization and in-situ chemical-integration of hydrogel onto stretchable electronics as a methodology for enhancing the hydrogel-device interface of skin-interfaced bioelectronics. Highly conductive functionalized hydrogels are polymerized inside stretchable wells placed on a multichannel electrode array. The hydrogels are stably immobilized to the electronic devices during fabrication, and the robust interface contributes to the reliable measurement of bio-signals and effective electrical actuation on tissues. The demonstration shows that the direct polymerization and in-situ chemical-integration of hydrogel are key steps towards the realization of practical skin-interface bioelectronics based on functionalized hydrogels.

8:00 PM SB04.07.04

Self-Healing Stretchable Li-Ion Battery Based on a High-Voltage Hydrogel Electrolyte Peisheng He¹, Jong Ha Park¹, Chao Fang¹, Anju Toor² and Liwei Lin¹; ¹University of California, Berkeley, United States; ²Georgia Institute of Technology, United States

Safe and deformable batteries that can be conformally embedded onto irregular surfaces of electrical systems and human body are desirable for wearable electronic applications due to low user friction. Commercial state-of-the-art Li-ion batteries are packaged in rigid hermetic sealing materials that are not deformable. State-of-the-art deformable Li-ion batteries reported in research articles show fast degradation due to severe performance problems such as the penetration of moisture and the leakage of toxic and flammable electrolytes. Here we report a non-toxic, aqueous hydrogel electrolyte instead of its organic counterpart that is demonstrated to: 1) enable highly safe operations due to its non-toxic and non-flammable nature; 2) alleviate the moisture penetration problem from outside environment; 3) have a high-voltage working window of ~2.8V; and 4) allow the construction of stretchable batteries by using elastic polymer packaging materials instead of rigid hermetic seals. In the prototype tests, fabricated batteries have shown good stretchability (50% strain) and flexibility (radius of curvature < 2mm) to enable conformal attachments to a wide range of geometric surfaces. The prototype battery also shows outstanding cyclic stability, retaining ~90% of the original capacity after 100 cycles for over 2 months in the ambient environment without using any rigid hermetic sealing package. Finally, a prototype battery with a self-healing elastomer package remains functional after being punctured by a needle 5 times at different locations through the package. Furthermore, it can recover >90% of its capacity after being cut through by a razor blade and subsequently healed at 70 for 10 minutes. Such safe and highly stretchable batteries would be useful for several wearable electronic applications such as blood glucose monitoring, heart rate monitoring, temperature monitoring, wireless charging, smart clothing, etc.

8:00 PM SB04.07.05**Highly Sensitive Flexible Sensors using Autonomously Self-Healable and Temperature-Tolerant Eutectogel**[JinyoungLee](#) and Jeong SookHa; Korea University, Korea (the Republic of)

With the increased demand for advanced wearable electronics, hydrogel-based devices have attracted enormous attention. Hydrogels have many advantages such as excellent flexibility, biocompatibility, ionic conductivity, and self-healing property, adequate for wearable devices. On the other hand, hydrogel-based devices exhibit limit in the performance due to the freezing and evaporation of water in the polymer network at low and high temperatures, respectively. To address such a thermal instability issue, there has been extensive effort on replacing the water within the hydrogel network with ionic liquids of low vapor pressure and high ionic conductivity. However, most ionic liquids are expensive and toxic to hamper the practical application to wearable devices. Therefore, research on deep eutectic solvents, mixtures of two or more components characterized by significant depressions in melting points compared to their neat constituent components, has been recently activated. Deep eutectic solvents show properties similar to those of ionic liquids as well as additional advantages of low-cost, non-toxicity, biocompatibility, and biodegradability. Furthermore, eutectogels having polymer networks composed of deep eutectic solvents have demonstrated the high potential application to wearable devices.

In this paper, we report on the fabrication of resistive-type strain and pressure sensors based on newly synthesized autonomous self-healing and temperature-tolerant eutectogel. Our synthesized eutectogel is prepared by UV polymerization of acrylamide with trehalose and phytic acid as crosslinkers, and choline chloride, glycerol and a small amount of water as solvents. In addition to the inherent low melting point of deep eutectic solvent, inclusion of bio-derived trehalose and phytic acid makes abundant hydrogen bonding, resulting in improved anti-freezing and anti-drying properties. Also, the dynamic hydrogen bond interactions between the polymer network and trehalose, phytic acid, and glycerol endowed the eutectogel with self-healing properties. The synthesized eutectogel exhibits high stretchability (>300%), temperature-tolerance, and good self-healing efficiency (>90%) after 24 hours at room temperature. By incorporating conducting polymer onto the eutectogel, highly sensitive resistive-type strain and pressure sensors are fabricated for detecting bio-signals after attachment onto a finger or wrist. The eutectogel-based wearable sensors demonstrate stable signal detection over a wide temperature range even after repetitive self-healing, thereby expanding their potential application to wearable electronics with longevity under extreme conditions.

8:00 PM SB04.07.06**Topology-Based Dual Lock-and-Key Structures for Hydrogel Self-Assembly in Macroscopic Supramolecular Assembly**[EunseokHeo](#), Hye BeenKoo and Jae-ByumChang; Korea Advanced Institute of Science and Technology, Korea (the Republic of)

Macroscopic supramolecular assembly (MSA), which refers to the assembly of building blocks at a macroscopic scale, holds great potential for the fabrication of ordered bulk structures. Thanks to the high design flexibility of the building blocks and the precise controllability of the assembly process, MSA has found applications in a wide range of fields, including the fabrication of tissue scaffolds, soft actuators, and more. Additionally, among the candidates for building blocks, hydrogels are highly favored due to their easily tunable properties and diverse type with different characteristics. In MSA, two challenges need to be addressed to achieve a high level of assembly: enhancing the precision of assembly and increasing the number of orthogonally matching pairs. To date, despite numerous attempts, none have effectively tackled both challenges simultaneously. In this study, we introduce topology-based design criteria for achieving precise and selective self-assembly of hydrogel building blocks. We suggest a unique design approach termed “dual lock-and-key structures.” In this design model, only topologically matching pairs can be assembled with exceptional precision. Through the implementation of dual lock-and-key structures, we establish principles for the selection of multiple orthogonally matching pairs. We demonstrate the selective assembly of both simple one-to-one matching and complex one-to-many assemblies. Moreover, by harnessing the easy property tunability of hydrogel, we synthesize DNA-mimicking single-stranded structures, which hybridize into double-stranded structures with sequence-specific arrangements. Finally, we present a hydrogel logic gate system, consisting of a YES gate, an OR gate, and an AND gate. Utilizing the high selectivity of our dual lock-and-key structures, the desired outputs are exclusively obtained when the appropriate building blocks are assembled, following the logic of each gate: YES, OR, and AND.

8:00 PM SB04.07.07**Conducting Polymer Granular Hydrogel Bioinks for 3D Printed *In Vitro* Bioelectronic Devices**[AnnaP. Goestenkors](#), TianranLiu, SomtochukwuS. Okafor, LiannaFriedman, RileyAlvarez and AlexandraRutz; Washington University in St. Louis, United States

Conjugated polymers have recently been used in their hydrogel form for the creation of soft bioelectronics with improved cell interfacing and the potential for enhanced measurement and stimulation of cellular activities. Cell-encapsulating hydrogels offer a truly 3D culture environment and when designed appropriately can be used as bioinks for 3D printing which grants spatially controlled deposition of cells and materials simultaneously. We developed a bioink based on the conducting polymer poly(3,4-ethylene-dioxythiophene):polystyrene sulfonate (PEDOT:PSS) by creating a granular hydrogel form. Emulsion methodology was developed to fabricate PEDOT:PSS hydrogel microparticles (microgels) with high circularity and monodispersity. Filtration techniques were used to size select microgels with diameters between 10 and 60 μm . When centrifuged to remove significant water, the conducting polymer microgels achieved dense packing characteristic of a granular material state. Increasing centrifugal force decreased the void fraction of the material which increased conductivity. Rheological investigations confirmed shear-thinning and self-healing properties, both ideal for 3D bioprinting for extrusion and ability to keep shape, respectively. Granular PEDOT:PSS hydrogels were in fact 3D printable via pneumatic extrusion and formed various 3D configurations. Evaluation of the material's printability in the granular state also revealed that increased centrifugal force facilitated better printability as evidenced by increased maximum filament length and filament diameter better matching the chosen nozzle diameter. Structural stability of the material within an aqueous environment for up to three months was achieved using a collagen hydrogel overlay. Human dermal fibroblasts encapsulated and cultured within the granular hydrogel showed high cell viability over fourteen days demonstrating cytocompatibility. This developed conducting granular hydrogel bioink exhibits balanced properties of printability, conductivity, and cellular responses for the additive manufacturing of future *in vitro* bioelectronics.

8:00 PM SB04.07.08**Extracellular Matrix-Compatible Additive Manufacturing of Bioactive, Conducting Polymer Hydrogel Electrodes**[TianranLiu](#), SomtochukwuS. Okafor, AnnaP. Goestenkors, SandraMontgomery, RileyAlvarez and AlexandraRutz; Washington University in St. Louis, United States

Hydrogels of conducting polymers provide a soft and hydrated alternative to metal for interfacing electronic devices with biological systems. To fabricate devices based on conducting polymer hydrogels, the material is often patterned alongside bioinert and stiff substrates such as plastics and elastomers which lead to poor cell-material interactions. In order to further promote device integration with cells and tissue, one strategy is to utilize bioactive materials, such as mammalian extracellular matrix (ECM) components, as the substrate material to present a tissue-like microenvironment to cells. However, traditional semiconductor manufacturing is anticipated to impair the bioactivity of these natural materials. Here, we demonstrate methods for mild temperature additive manufacturing of highly conducting poly(3,4-ethylenedioxythiophene) polystyrene sulfonate (PEDOT:PSS) hydrogels with collagen substrates. Various types and concentrations of gelation agents were investigated to enable sufficient working time after addition to colloidal dispersions and to result in a water-stable hydrogel network once fully crosslinked. Among gelation agents tested, ionic liquid was found to be suitable for extrusion-based printing while an acidic surfactant enabled deposition by jetting due to low surface tension and appropriate viscosity. After room temperature gelation and treatment, hydrated PEDOT:PSS prints exhibited conductivity as high as 37.2 S/cm and were stable in cell culture conditions for at least 28 days. To complete the device, a top layer was fabricated by casting a collagen slurry onto the PEDOT:PSS prints which had a sacrificial material deposited on top to protect the intended electrodes from coverage. Once the collagen layer formed, the sacrificial material was removed with 36 °C water, leaving an unaltered PEDOT:PSS surface for direct biointerfacing. Since the fabrication methods were developed with mild temperatures and processing, the structure and bioactivity of the collagen are believed to be maintained, as evidenced by the support of fibroblast culture that reached confluency and sustained high viability for 28 days. This methodology offers a promising strategy for rapid prototyping soft, hydrated, and bioactive electronic devices that support cell attachment and proliferation.

8:00 PM SB04.07.09**A Zwitterionic Hydrogel-Based Heterogeneous Fenton Catalyst for Efficient Degradation of Persistent Organic Pollutants**[IanS. Chen](#), DevashishGokhale and PatrickDoyle; Massachusetts Institute of Technology, United States

Persistent organic pollutants (POPs) are industrial, pharmaceutical, or commercial byproducts that are highly resistant to degradation and decomposition in the environment, while causing significant health and environmental damage even in small concentrations. Significant existing research aims at destroying the POPs in an environmentally safe and cost-effective manner, but challenges remain in destroying POPs at environmental concentrations in scalable and sustainable processes. Many current approaches to degrading POPs require extreme reagents and conditions. One promising candidate, however, for the removal of POPs is the photo-Fenton reaction, where iron(II) ions catalyze the decomposition of hydrogen peroxide, in the presence of UV light, into highly reactive hydroxyl radicals that readily attack organic compounds, including POPs. Fenton oxidation is promising because iron(II) and hydrogen peroxide are low-cost, environmentally-safe materials, and because the process can target a broad range of POPs.

However, the photo-Fenton reaction requires the presence of water-soluble iron(II) ions that are difficult to reuse. As such, methods that immobilize the iron as a catalyst can be constantly reused, while also eliminating the need for further treatment steps to remove iron from water before it can be used. Unfortunately, existing solutions require challenging reaction conditions; due to the higher efficiency of the Fenton reaction at lower pHs, many catalysts require a low pH (usually around 3) to regenerate iron(II) ions, which is unrealistic for large-scale wastewater treatment and can damage the catalyst itself. Furthermore, due to the non-selectivity of the Fenton reaction, catalysts using common polymers such as polyethylene or polyvinyl alcohol to encapsulate iron (II) or iron oxide (in the form of nanoparticles) often degrade easily due to the susceptibility of the polymer to the photo-Fenton reaction, also releasing nanoparticles into the

environment. Other attempts at supported catalysts reduce the surface area and limit kinetics.

To address these issues, we developed an iron(II)-incorporated, zwitterion-based hydrogel catalyst. By complexing the iron(II) ions within a zwitterionic hydrogel, we allow for the photo-Fenton reaction to run efficiently at neutral and even slightly alkaline pHs. Furthermore, due to the high oxidation state of the zwitterions and the saturated backbones, the hydrogel is highly resistant to attack by hydroxyl radicals. A zwitterionic backbone helps us make highly porous materials that bind individual, complexed ions, allowing us to maximize both the effective functional area and rate of pollutant transport within the catalyst. POPs quickly and rapidly diffuse into the catalyst, where they rapidly decompose. Experiments at environmentally relevant concentrations showed that our catalyst was able to degrade 85% of a solution of ethinyl estradiol (a xenoestrogen and common POP) within 1 hour, with near 100% degradation within 24 hours. Furthermore, we observed near 100% degradation of dichlorophenol (a common industrial byproduct) and around 70% degradation of perfluorooctanoic acid (a common perfluorinated pollutant). These results show significant promise for our hydrogel as an efficient and environmentally-safe strategy for rapid water purification of POPs.

8:00 PM SB04.07.10

Thermally Chargeable Stretchable Ionic Thermoelectric Supercapacitors [Taehyun Park](#) and [Xavier Crispin](#); Linköping University, Sweden

Wearable self-powered devices are in great demand because of the rapid innovation of Internet of Things (IoT), electronic skins, and healthcare monitoring. The two major sources of energy produced by the human body are mechanical (100W) and thermal (100-400W) energies. Thermoelectricity converts heat into electricity. Although the performance of electronic thermoelectric (e-TE) associated with the thermo-diffusion of electrons/holes has been significantly improved, Seebeck coefficients of the e-TE systems remain rather small ($\sim 100 \mu\text{V K}^{-1}$). As a result, hundreds of p- and n-type TE legs connected in series are often required to generate a practically useful output voltage.

Recently a new thermoelectric concept has been proposed: the charging of a supercapacitor with an ionic thermoelectric (i-TE) effect in the redox-free electrolyte through a temperature gradient. The supercapacitor is composed of an electrolyte layer sandwiched between two electrodes. Giant Seebeck coefficients have been found in electrolytes combined with soft polymers. In contrast to the e-TE materials based on the electron/hole thermo-diffusion, i-TE materials are based on the diffusion of ions under a temperature gradient. i-TE materials produce orders of magnitude higher voltages than e-TE materials but typically have much lower conductivity and the ions cannot pass in the electronic circuit.

We have developed a polymer electrolyte with an apparent Seebeck coefficient (38.9 mV K^{-1}) and ionic conductivity ($3.76 \times 10^{-1} \text{ mS cm}^{-1}$). It mechanically deformed up to approximately 1500% and exhibited Young's modulus similar to human skin. Performance at 250% strain remained above 90% of its original performance, and there was no significant degradation after consecutive 200 stretching/releasing cycles.

In the development of wearable electronics, researchers have found strategies for making stretchable electrodes. We have then sandwiched our free-standing polymer electrolyte layer between two stretchable electrodes to achieve the first stretchable ionic thermoelectric supercapacitor. The ionic thermoelectric supercapacitor was also thermally charged at approximately 60% strain and exhibited reliable mechanical stability for repetitive 500 cycles of 50% strain.

8:00 PM SB04.07.11

Air-Permeable Hydrogels with High Water Content [Xiao-Yun Yan](#), [Shucong Li](#) and [Xuanhe Zhao](#); Massachusetts Institute of Technology, United States

Hydrogels have gained immense popularity as the interface between biological tissues and the environment due to their exceptional properties and unique features. For biomedical applications like long-term signal monitoring, drug release, or pathogen blocking that necessitate continuous epidermal or tissue adhesion, free water and air exchange between the body and its surroundings become crucial. However, despite their excellent water permeability, hydrogels have over an order of magnitude lower oxygen permeability compared to other 'dry' soft materials (e.g. silicone rubber). This poor oxygen permeability in hydrogels is an intrinsic problem caused by the dense polar hydrogen-bonded network, which has long been a challenge to overcome. Herein, we present a strategy that achieves high oxygen permeability without compromising water content. The key to this approach is the fabrication of interconnecting microchannels within the bulk hydrogel material. More importantly, we demonstrate that the designed materials exhibit high oxygen permeability, allowing for long-term wear without causing itchiness or other uncomfortable sensations.

8:00 PM SB04.07.12

Supramolecular Gels from Pyrene-Functionalized Isophthalic Acids for Biomedical Nanotechnology Applications [Darren Makeiff](#)¹, [Khalid Azyat](#)¹, [Mickie Wiebe](#)¹, [Aria Khalili](#)², [Jae-Young Cho](#)¹ and [Bradley Smith](#)¹; ¹Nanotechnology Research Centre, Canada; ²University of Alberta, Canada

Supramolecular gels from low molecular weight gelators (LMWGs) are fascinating functional soft materials with potential for a wide range of applications such as food technology, cosmetics, optics, electronics, sensing, catalysis, environmental remediation, as well as biomedical applications. These unique materials have several advantages over their polymeric counterparts in lower cost, ease of preparation, tunable properties, low gelator concentrations, reversibility, stimuli responsiveness (heat, light, pH, chemicals, mechanical shear, ultrasound, etc...), biocompatibility and biodegradability. While many LMWGs are known with a wide variety of structural diversity and functionality, the rational design of new functional LMWGs that can undergo hierarchical self-assembly to form gels in specific liquids with specific properties for a given application still remains a major challenge. Here we present the synthesis and characterization of new pH-triggered hydrogels from LMWGs based on pyrene-functionalized isophthalic acids. The rheological, morphological and spectroscopic characterization of the hydrogels formed will be discussed as well as their potential for biomedical nanotechnology materials applications such as encapsulation, drug delivery/controlled release, tissue engineering and 3D printing/bioprinting.

8:00 PM SB04.07.13

Tough and Recyclable Phase-Separated Supramolecular Gels via a Dehydration-Hydration Cycle [Xiaohui Xu](#) and [Rodney Priestley](#); Princeton University, United States

Hydrogels are compelling materials for emerging applications, including soft robotics and autonomous sensing. Mechanical stability over an extensive range of environmental conditions and considerations of sustainability, both environmentally benign processing and end-of-life use, are enduring challenges. To make progress on these challenges, we designed a dehydration-hydration approach to transform soft and weak hydrogels into tough and recyclable supramolecular phase-separated gels (PSGs) using water as the only solvent. The dehydration-hydration approach led to phase separation and the formation of domains consisting of strong polymer-polymer interactions critical for forming PSGs. The phase-separated segments acted as robust, physical crosslinks to strengthen PSGs, which exhibited enhanced toughness and stretchability in its fully swollen state. PSGs are not prone to over-swelling or severe shrinkage in wet condition and show environmental tolerance in harsh conditions, i.e., organic solvents with pH between 1 to 14. Finally, we demonstrate the use of PSGs as strain sensors in air and aqueous environments.

8:00 PM SB04.07.14

An Elastomer with Giant Strain-Induced Crystallization [Chase Hartquist](#)¹, [Shaoting Lin](#)², [James H. Zhang](#)¹, [Shu Wang](#)¹, [Michael Rubinstein](#)^{3,4} and [Xuanhe Zhao](#)¹; ¹Massachusetts Institute of Technology, United States; ²Michigan State University, United States; ³Duke University, United States; ⁴Hokkaido University, Japan

Strain-induced crystallization prevalently strengthens, toughens, and enables an elastocaloric effect in elastomers. However, the crystallinity induced by mechanical stretching in common elastomers (e.g., natural rubber) is typically below 20%, and the stretchability plateaus due to trapped entanglements, impeding performance for advanced applications. We present a new class of elastomers formed by end-linking then deswelling star polymers with a low fraction of defects and no trapped entanglements, which achieve strain-induced crystallinity of up to 50%. The deswollen end-linked star elastomer (DELSE) reaches an ultra-high stretchability of 12.4-33.3, scaling beyond the saturated limit of common elastomers. The DELSE also exhibits a high fracture energy of 4.2-4.5 kJ/m² while maintaining low hysteresis. The heightened strain-induced crystallization and stretchability synergistically promote a high elastocaloric effect with an adiabatic temperature change of 9.3 °C at 54 °C, compared with 3.5 °C at 54 °C in natural rubber.

8:00 PM SB04.07.15

Advancing Protein Synthesis and Applications with a Recyclable Genomic DNA Hydrogel Platform in Cell-Free Expression Systems [Hyangsu Nam](#)^{1,2} and [Jong Bum Lee](#)¹; ¹University of Seoul, Korea (the Republic of); ²Harvard University, United States

Proteins have the most dynamic entities, performing the diverse role of macromolecules in the body, functional interaction network-based biochemical reactions within a cell or from an organ. Recombinant protein-based therapeutics provide an important breakthrough in biomedical biotechnology. Recent technical advances in cell-free protein synthesis (CFPS) offer several advantages over cell-based expression systems, including easy modification to favor protein folding, increased non-toxicity, and capability for high-throughput strategies due to small reaction volume and short synthesis time. Herein, we fabricated the genomic DNA hydrogel (GD-gel) using the dual single-strand circular plasmids employed in cell-free protein expression synthesis. By complementary rolling complementary circle amplification (RCA) with multi-primers, the genomic hydrogel exhibits a significantly enhanced productivity yield of protein. This synthesis platform has the potential to develop biotechnological in sensing, therapeutics, and diagnosis.

In our study, inspired by the previous DNA hydrogel using a rolling circle amplification technique, we describe a strategy to synthesize genomic DNA hydrogel (GD-gel) via self-assembly of elongated DNA strands encoding multimeric genomic sequences. To achieve the self-assembly of genomic hydrogel, we applied rolling circle chain amplification (RCCA) with the dual

single-stranded circular plasmids. Importantly, GD-gel only consists of numerous tandem repeats of genomic DNA strands by the rolling circle amplification from the plasmid DNA template. This approach allows the genomic DNA itself not only to create a hydrogel structure but also to become a medium for protein expression in GD-gel. Hence, our GD-gel is likely to enable a new route for cell-free protein production via self-assembly of multimeric genomic DNA.

8:00 PM SB04.07.16

A Versatile Conductive Ternary Polymer Complex Nanocomposite Sensor with Repeatable, Rapid, Autonomous Self-Healing and Unprecedented Mechanical Properties Colton Duprey and Evan K. Wujcik; University of Maine, United States

Wearable sensors, stretchable electronics, and many soft robotics materials must have a sufficiently high balance of conductivity, stretchability, and robustness. Intrinsically conductive polymers offer a critical step toward improving wearable sensor materials due to their tunable conductivity, soft/compliant nature, and ability to complex with other synergistic molecules (i.e., polyacids, small molecule dopants). The addition of nanofillers offers the potential to improve the conductivity of polymers for soft robotics and wearable applications, while it also affects and improves the self-healing and mechanical properties of the material. The development of a robust polymer nanocomposite material that offers ultra-stretchability, an autonomous self-healing ability, and enhanced electronic properties has eluded researchers. Here we show an aqueous polyaniline [PANI]:poly(2-acrylamido-2-methylpropane sulfonic acid) [PAAMPSA]:phytic acid [PA] ternary polymer [TP] complex synthesized with silver nanowires (AgNW) to form a polymer nanocomposite with high electronic sensitivity, unprecedented mechanical properties (a maximum strain of 4693% at ambient humidity; ~52 RH%), and repeatable, autonomous self-healing efficiencies of greater than 98%. The AgNW TP complex has an engineering strain higher than all hydrogel and other polymeric sensor materials, in which the interface between the polymer matrix and the AgNW is hypothesized to be integral for the formation of an active conductive network. To illustrate the remarkable sensitivity, the material was employed as a biomedical sensor (pulse, voice recognition, motion), topographical sensor, and high sensitivity sensor.

8:00 PM SB04.07.17

Engineering a Reverse Thermo-Responsive, Cross-Linkable, Biodegradable Liquid Embolic Agent for Brain Aneurysm Treatment Lamia Ayaz¹, Hannah Feng², Ruoxi Jin³, Ann Lee⁴, Sheldon Liu⁵, Evan Pang⁶, Jiarui Peng⁷, Grace Qiao⁸, Ruth Pereira⁹, Robert Wong⁹, Aaron Sloutski⁹, Chandramouli Sadasivan⁹, Daniel Cohn¹⁰ and Miriam Rafailovich⁹; ¹Howard High School, United States; ²Torrey Pines High School, United States; ³Beijing National Day School, China; ⁴Seoul International Day School, Korea (the Republic of); ⁵Stuyvesant High School, United States; ⁶Mission San Jose High School, United States; ⁷East Lyme High School, United States; ⁸The Experimental High School Attached to Beijing Normal University, China; ⁹Stony Brook University, The State University of New York, United States; ¹⁰The Hebrew University of Jerusalem, Israel

Cerebral aneurysms are balloon-like dilations in intracranial arteries that can rupture, leading to fatal hemorrhagic stroke. The majority of current aneurysm treatments involve the implantation of catheter-based endovascular coils and meshes, but they result in unfavorable primary outcomes in at least 20% to 30% of cases [1]. This project aims to develop an injectable, controllably cross-linkable, durable, and multi-functional liquid embolic agent (LEA) using F88-DMA polymer that allows for the body's natural mechanisms to heal the aneurysm with personalized biodegradation.

As temperature increases and reaches physiological temperatures, F88-DMA micelles group together and entangle, resulting in mechanically strong physical gelation. Chemical crosslinkers ammonium persulfate (APS) and tetramethylethylenediamine (TEMED) enhance the long-term stability of the hydrogel, while iohexol acts as a contrast agent.

In order to develop a pluronic-based polymer system that is deliverable in vivo, cold, radiopaque F88-DMA must be injectable through a microcatheter. Gelation must occur at the optimal time and temperature so as not to solidify prematurely or remain liquid within the aneurysm. Various concentrations of F88-DMA and TEMED were tested in vitro to determine the optimal concentration for injectability. Rheology results displayed that a higher concentration of F88-DMA lowers gelation temperature, and this correlation was further confirmed with differential scanning calorimetry for all three concentrations of F88-DMA (27%, 30%, and 33%). Additionally, higher concentrations of TEMED were found to increase the maximum shear modulus and decrease the crosslinking time of F88-DMA gel. To simulate interventional treatment, the LEA was injected into a brain aneurysm model, suggesting 29% F88-DMA to be the most injectable concentration that, when crosslinked, would remain in the aneurysm for prolonged periods of time.

Upon gelation and crosslinking, hydrogels swell in situ due to thermodynamic forces, posing a significant risk for compression or rupture. F88-DMA hydrogel swelling was demonstrated to be dependent on polymer concentration ($p = 0.019695$), and the addition of iohexol significantly decreased swelling over the course of 3 days. Furthermore, hydrogels submerged in flowing saline exhibited less swelling than those submerged in static saline ($p = 0.0001$), an improved durability that originates from the entangled properties of the micelles.

The durable embolic agent must also allow for vascular remodeling and endothelialization in a controlled manner. Thus, cell adhesion and porosity are vital. Imagery of fibrinogen-soaked gel suggests that natural levels of fibrinogen make the cross-linked F88-DMA cell adhesive enough, providing no need to incorporate cell adhesive materials. Sodium phosphate heptahydrate was effectively employed to control pre-determined porosity that initiates the wound healing process.

After the aneurysm has healed, the pluronic implant must be controllably biodegradable. The biodegradability of the LEA is a function of the patient-specific wound healing process such that the blood vessel returns completely to its original healthy state. Naturally occurring enzymatic F88-DMA degradation is currently being investigated with lactide.

Future studies will involve injecting this gel into rabbit models to examine its effects in vivo and determine rates of endothelialization post-injection.

[1] Taschner CA, Chapot R, Costalat V, Machi P, Courtheoux P, Barreau X, et al. Second-Generation Hydrogel Coils for the Endovascular Treatment of Intracranial Aneurysms: A Randomized Controlled Trial. *Stroke*. 2018;49(3):667-74.

8:00 PM SB04.07.18

Non-Invasive Smart Wearables: Color-Changing Hydrogels via DLP 3D Printing Mohamed Elnejr and Haider Butt; Khalifa University, United Arab Emirates

This study explores the development of conducting and functional hydrogels for use in smart wearables, such as eyeglasses frames, bracelets, rings, and watches, through the utilization of a novel approach involving HEMA (Hydroxyethyl Methacrylate), PEGDA (Polyethylene Glycol Diacrylate), and EGDMA (Ethylene Glycol Dimethacrylate) within the context of DLP (Digital Light Processing) 3D printing technology. By introducing thermochromic and photochromic powders into the resin matrix, we achieve dynamic color-changing capabilities in response to changes in temperature and UV light exposure, respectively. The hydrogel formulation, composed of HEMA, PEGDA, and EGDMA, ensures excellent printability and mechanical properties, making it suitable for the creation of complex wearable structures with a focus on comfort and wearability. The incorporation of thermochromic powders enables these smart wearables to undergo vivid color transformations when subjected to temperature fluctuations, enhancing their aesthetic appeal and user experience. Additionally, the integration of photochromic powders facilitates real-time color alterations in response to UV light exposure, allowing the wearables to adapt to varying environmental conditions. This research combines materials science, 3D printing technology, and advanced color-changing effects to develop innovative and customizable smart wearables. These functional hydrogels open up exciting possibilities for dynamic fashion accessories and user-centric designs, enabling wearers to express themselves creatively and interact with their wearables in novel ways. This interdisciplinary approach paves the way for the future of personalized, responsive smart wearables with a focus on aesthetics, functionality, and user engagement.

8:00 PM SB04.07.19

Multi-Scale Chemical Insights into The Static and Dynamic Behaviour of Metallo-Polyelectrolyte Gels Seneca J. Velling¹, Pierre J. Walker¹, Seola Lee¹, Connor M. Gallagher^{2,2}, Michael D. Schulz^{2,2}, Zhen-Gang Wang¹ and Julia R. Greer^{1,1}; ¹California Institute of Technology, United States; ²Virginia Tech, United States

Metallo-Polyelectrolyte Complexes (MPEC) in the gel state represent a class of multifunctional, weakly ionizing materials with intriguing properties deeply rooted in their coordination chemistry and metal ion exchange. We provide a comprehensive exploration of the underlying chemical principles governing MPECs, with a primary focus on the profound effects of metal ion valency and system pH on bonding thermodynamics, association-dissociation kinetics, and global polymer morphology and their regulation of overall gel behaviour. Employing quantum density functional theory (DFT), we estimate the binding energy between the metal cations and the polymer backbone. Hard mono-, di-, and trivalent metal ions exhibit bidentate bridging coordination environments by carboxylate groups and aqua/hydroxy ligands as verified using FTIR, giving stoichiometric charge balance to the complexes. This results in a range of binding energies of -1 to -8 eV. We corroborated these findings with Isothermal Titration Calorimetry (ITC) to probe the solution-phase binding of metal salts to poly(acrylic acid). We demonstrate that the impact of association kinetics at the molecular level propagates to macroscopic behaviour, with higher valency metal ions distinctly influencing relaxation dynamics, thereby increasing gel stiffness and extending the plateau modulus. The role of proton activity in the solution and gel phases – which systematically modulates polyanion charge sparsity and, accordingly, metal binding sites for the formation of these dynamic bonds – can be readily explained using our theoretical treatment. This treatment is in good agreement with our

experimental exploration of the MPEC phase space (dissolution, homogeneous gel, and phase separated metal-rich vs. metal-poor gel phase). Guided by theory, our experimental observations unveil the profound influence of pH on polymer relaxation. As charge sparsity decreases, MPEC gels transition towards behaviour reminiscent of monovalent gels, accompanied by critical alterations in network topology. These findings underscore a competition for polyanion (RCOO⁻) association between weakly-bound monovalent species in the buffer (eg. Na⁺), strongly-bound, higher-valency metal species (Mⁿ⁺), and the drive for carboxylate protonation when pH < pK_a. This intricate interplay between metal ion valency and pH-regulated charge sparsity fundamentally governs the global thermomechanical response of solvated MPEC gels: from binding site availability to bond dynamics and overall gel morphology. Local chemistry, therefore, has a profound influence on overall thermal, mechanical, and electrical response of metal cross-linked systems. The assumption – and critical role – of solvent in the gel system cannot be overlooked. Our implicit solvent approaches, taken together with DFT and experimental findings on the collective metal-ligand and metal-aqua/hydroxyl ligand complexation character, explain well the bulk-scale observations in the gel phase, providing mechanistic insights into the polymer-metal interactions, transport, and phase-behaviour. This work unravels the intricate & entangled chemistry underpinning MPEC gels, offering critical insights into their valency-driven, pH sensitive, solvent-dependent global responses.

8:00 PM SB04.07.20

Intriguing Thermal and Conductive Behavior of Water-Based Gel Electrolytes for Safer Lithium-Ion Batteries Arthur Cresce and Michael Ding; US Army Research Laboratory, United States

Gel electrolytes are a special case of electrolytes for lithium-ion batteries in which the liquid electrolyte is contained in a crosslinked polymer network. In this work, we explore the thermal and conductive properties of a water-based electrolyte with high salt concentration meant for use in lithium-ion batteries. Normally, this water-in-salt electrolyte (WiSE) has a conductivity of around 10 mS/cm at room temperature but experiences a solidus transition around 10 °C that causes a profound drop in electrolyte conductivity which negatively impacts battery operation. Using an automated *in-situ* thermoconductometric measuring technique developed at the US Army Research Laboratory, our team was able to methodically measure and describe the thermal and related conductivity behavior of gel electrolytes made using WiSE as a base liquid system with increasing monomer mass fraction. The thermoconductometric technique allowed for measurements before and after ultraviolet radiation was applied to cure the gels, allowing us to compare the interaction of monomer and WiSE with crosslinked polymer and WiSE across a wide temperature range. We observed that a sufficient monomer concentration in the gel suppressed freezing and melting phase transitions in WiSE, resulting in a smooth conductivity behavior from -60 °C to +50 °C with no discontinuities related to electrolyte phase changes. There is also a decoupling of Li⁺ conductivity in the gel electrolyte which is affected by the polymerization of the monomer as evidenced by the emergence of two distinct glass transition temperatures. Additionally, at certain WiSE/monomer compositions, the conductivity of the cured gel electrolyte was higher than that of WiSE with uncured monomer. In this talk, we will discuss our results, the implications of the findings, and potential ways to exploit WiSE gel electrolytes for making safe lithium-ion battery cells.

8:00 PM SB04.07.21

Unusual Temperature Dependence of Water Sorption in Semi-Crystalline Hydrogels Xinyue Liu¹, Lenan Zhang² and Evelyn N. Wang²; ¹Michigan State University, United States; ²Massachusetts Institute of Technology, United States

Water vapor sorption is a ubiquitous phenomenon in nature and plays an important role in various applications, including humidity regulation, energy storage, thermal management, and water harvesting. In particular, capturing moisture at elevated temperatures is highly desirable to prevent dehydration and to enlarge the tunability of water uptake. However, owing to the thermodynamic limit of conventional materials, sorbents inevitably tend to capture less water vapor at higher temperatures, impeding their broad applications. Here, an inverse temperature dependence of water sorption in poly(ethylene glycol) (PEG) hydrogels, where their water uptake can be doubled with increasing temperature from 25 to 50 °C, is reported. With mechanistic modeling of water-polymer interactions, this unusual water sorption is attributed to the first-order phase transformation of PEG structures, and the key parameters for a more generalized strategy in materials development are identified. This work elucidates a new regime of water sorption with an unusual temperature dependence, enabling a promising engineering space for harnessing moisture and heat.

SESSION SB04.08: Stimuli-Responsive Materials and Other Special Mechanical Properties II

Session Chairs: Anna-Maria Pappa, Alexandra Rutz, Christina Tringides and Shiming Zhang

Wednesday Morning, November 29, 2023

Hynes, Level 1, Room 103

8:30 AM SB04.08.01

Energetic Electron Assisted Synthesis of Bioderived Smart Hydrogels and Ferrogels – Fundamentals, Applications, Perspectives Stefan G. Mayr^{1,2}; ¹Leibniz-Institute of Surface Engineering (IOM), Germany; ²University of Leipzig, Germany

Energetic electron beams constitute a highly versatile tool for tailoring biomaterials properties of bioderived hydrogels with high spatial resolution. Based on electron-induced hydrolysis, reactions, ranging from crosslinking, chain scission and functionalization to arrest of magnetic nanoparticles, can be induced without the need for adding additional - potentially hazardous - reagents. This allows for synthesis of highly bioactive switchable composites, in particular ferrogels, stimuli responsive gels as well as shape memory gels. Within this presentation we will first review the fundamentals of energetic electron assisted hydrogel modification, regarding particularly the reaction kinetics in collagen. We will then focus on applying these findings for tailored hydrogel modification towards stimuli responsive gels, in particular ferrogels. This includes a collagen-based ferrogel actuator with reversible peak strains as large as 150%. We will also discuss application within the field of biomedicine, that are currently being developed, as well as future visions in an outlook.

8:45 AM *SB04.08.02

Rubbery Bioelectronics Cunjiang Yu; The Pennsylvania State University, United States

Electronics that can seamlessly integrate with human body could have significant impact in medical diagnostic, therapeutics. However, seamless integration is a grand challenge because of the distinct nature between electronics and human body. Conventional electronics are rigid and planar, made out of rigid materials. Human body are soft, deformable and curvilinear, comprised of biological materials, organs and tissues. This talk will introduce our solution to address the challenge through the recent development of a new class of electronics, namely rubbery electronics. Rubbery electronics is constructed all based on elastic rubber electronic materials of semiconductors, conductors and dielectrics, which possesses tissue-like softness and mechanical stretchability to allow seamless integration with soft deformable tissues and organs. Rubbery electronic materials (semiconductors, conductors, dielectrics) and device innovations set the foundation. This presentation will describe the development the recent advances of rubbery electronics and rubbery bioelectronics. As a platform technology, rubbery electronics could address many challenges in biomedical research and clinical studies.

9:15 AM SB04.08.03

Fabrication of Multi-Material Stimuli-Responsive Microstructures via Photografting of Functional Microgels to Elastomeric Supports Ruiguo Yang and Stephen A. Morin; University of Nebraska – Lincoln, United States

Hydrogels are functional polymeric materials with stimuli-responsive properties applicable to a wide range of applications including soft electronics and robotics, three-dimensional cell culture, tissue engineering, and adaptive optics. Accordingly, the diversity and reported use cases of these materials has grown tremendously over the past decade, however, the microfabrication of multi-material, hydrogel-based devices remains a challenge. We report a simple microfabrication strategy that enables the facile production of fixed arrays of stimuli-responsive hydrogel microstructures with dynamic microactuation functionality. Our approach relies on a soft, stretchable chemical template which directs the assembly of prepolymer droplets into ordered arrays and presents the surface chemical moieties needed to photograft the hydrogel to the support, simultaneously. Specifically, we achieve three critical operations in one seamless fabrication scheme: (i) Mechanically driven assembly of prepolymer solutions into ordered arrays is executed using stretchable wettability patterns; (ii) Photoinitiated free radical polymerization is used to drive crosslinking of the prepolymer into hydrogel networks; and (iii) Reactive moieties of the wettability patterns result in photografting of the microgel structures directly to the support substrate. To demonstrate the pragmatic utility of our approach and the functionality of fixed microgels in liquid phase applications, we designed, fabricated, and operated microgel arrays with stimuli-responsive (e.g., solvothermal and chemical) microactuation functionality inside microfluidic chips. Our strategy overcomes the limitations of existing fabrication techniques that produce poorly adherent materials and require complicated processing schemes. We envision many technologies, for example, liquid phase soft microactuators, stimuli-responsive 3D cell culture platforms, and micro/optofluidic chips, will directly benefit from the reported strategy.

9:30 AM *SB04.08.04

Whereas human tissues and organs are mostly soft, wet and bioactive; machines are commonly hard, dry and abiotic. Merging humans and machines is of imminent importance in addressing grand societal challenges in health, sustainability, security, education and joy of living. However, merging humans and machines is also extremely challenging due to their fundamentally contradictory properties. At MIT Zhao Lab, we exploit hydrogels to form long-term, high-efficacy, multi-modal interfaces and merger between humans and machines. In this talk, I will discuss hydrogel bioelectronics, bioacoustics, and biophotonics. Specifically, I will discuss examples including nonfibrotic hydrogel bioelectrodes, hydrogel ultrasound couplants that enable wearable imaging, and hydrogel optical fibers that replace rigid optical fibers. I will conclude the talk with a vision for future human-machine convergence aided by materials science and artificial intelligence.

10:00 AMBREAK

10:30 AM *SB04.08.05

A Conductive Hydrogel with Tuneable Mechanical and Rapid Self-Healing PropertiesDamiaMawad and NhiTra; University of New South Wales, Australia

The optimal physical and biological characteristics of a scaffold for tissue engineering include biocompatibility, tissue-like mechanical properties, and a hydrated and porous environment. Hydrogels, 3-dimensional crosslinked polymeric networks, feature many of these characteristics, and thereby, are considered excellent scaffolds for tissue engineering [1]. However, scaffolds tailored for electro-responsive tissues such as neural and cardiac tissue would also benefit from electrical conductivity [2], which has been shown to provide enhanced cell growth and differentiation [3]. Other favourable properties include self-healing [4], providing the scaffold with mechanical and electronic stability under strain, and self-adhesion, enabling the placement of the scaffold at the targeted tissue site in a minimally invasive approach [5]. Here, we report the fabrication and characterisation of a conductive, adhesive, and self-healing hydrogel for tissue engineering applications. We fully characterise its physical and electronic properties. We show that the hydrogel is porous, has high swelling ratio and tuneable mechanical properties, and exhibits very rapid self-healing. We also demonstrate that it is electroactive in physiological buffer and exhibits both ionic and electronic conductivity. Further, its self-adhesion indicates a facile placement on tissues. Coupled together, these properties indicate that the hydrogel with its individual biocompatible components is a suitable scaffold for cell growth and differentiation.

[1] D. Mawad, E. Stewart, D. L. Officer, T. Romeo, P. Wagner, K. Wagner, G. G. Wallace. *Adv. Funct. Mater.* 2012, 22, 2692.

[2] L. Jiang, C. Gentile, A. Lauto, C. Cui, Y. Song, T. Romeo, S.M. Silva, O. Tang, P. Sharma, G. Figtree, J. Gooding, D. Mawad. *ACS Appl. Mater. Interfaces* 2017, 9, 44124.

[3] C. Gao, S. Song, Y. Lv, J. Huang, Z. Zhang. *Macromol. Biosci.* 2022, 22, 2200051.

[4] Y. Li, X. Zhou, B. Sarkar, N. Gagnon-Lafrenais, F. Cicoira. *Adv. Mater.* 2022, 34, 2108932.

[5] Y. Xu, M. P. Gaillez, R. Rothe, S. Hauser, D. Voigt, J. Pitzsch, Y. Zhang. *Adv. Healthcare Mater.* 2021, 10, 2100012.

11:00 AM SB04.08.06

Tunable Conductive Hydrogels via Simultaneous Photo-Mediated Polymerization and CrosslinkingDan-MyNguyen, Chun-YuanLo, TaewookChoi, ZacharySwain, YuhangWu, CharlesDhong and LaureV. Kayser; University of Delaware, United States

Conductive hydrogels, particularly those containing poly(3,4-ethylenedioxythiophene):poly(styrene sulfonate) (PEDOT:PSS), have gained popularity in bioelectronic interfaces for their mechanical properties close to that of human body and their electrical properties suitable for electrical recording and stimulation. To minimize the invasiveness of conductive hydrogels for bioelectronics, alternative fabrication methods to the common blending approach have been developed, including the photo-gelation of conducting polymers in aqueous environments. However, the photo-catalyzed formation of conductive hydrogels with complex structures is still a challenging task, as the conductive polymers absorb UV light at a similar wavelength, thereby preventing crosslinking. A photo-mediated method for obtaining conductive hydrogels with good conductivity, tunable mechanical properties, and flexibility akin to human body is still lacking.

We developed an approach that combines the simultaneous photo-crosslinking of a polymeric scaffold and the photo-catalyzed polymerization of a conducting polymer under light irradiation. This approach involved the copolymerization of coumarin-containing monomers with sodium styrene sulfonate to yield water-soluble poly(styrene sulfonate-co-coumarin acrylate) (P(SS-co-CouAc)). Under UV irradiation (365 nm), a transparent, non-conducting solution of P(SS-co-CouAc), 3,4-ethylene dioxithiophene (EDOT) and ammonium persulfate transforms to a dark blue, electronically conducting hydrogel. The formation of the conductive hydrogel relies on the simultaneous covalent photo-crosslinking of P(SS-co-CouAc) and the photo-catalyzed oxidative polymerization of EDOT. The resulting conductive hydrogels exhibit both ionic and electronic conductivity to reach bulk conductivity up to 9.2 S m^{-1} . They possess tunable elastic moduli (around 10 MPa), and display a reasonable strain at break (up to 16%). These photo-generated conductive hydrogels have the potential to enable the formation of 3D networks with controlled microstructure and offer new possibilities for applications in bioelectronics, including surface electromyography (sEMG).

11:15 AM SB04.08.07

The Effect of Multivalent Interactions on the Electrostatic Stability of Poly(N-isopropylacrylamide) NanogelsYuchenZhu¹, JiixinHou¹, DominicGray², TomO. McDonald² and Ahu GumrahDumanli¹; ¹University of Manchester, United Kingdom; ²University of Liverpool, United Kingdom

Poly(N-isopropylacrylamide) (PNIPAM) nanogels are promising responsive colloidal particles that can be used in pharmaceutical applications as drug carriers. With an attempt to understand the stability of the PNIPAM-based drug carriers in complex chemical environments, in this work, we investigated the temperature-dependent morphological changes and agglomeration dynamics of PNIPAM nanogels in the presence of mono- and multi-valent cationic electrolytes. Our work provides new insights on the deswelling, flocculation and aggregated morphology of PNIPAM nanogels over a range of electrolyte concentrations and temperatures revealing the threshold of stability and spontaneous agglomeration states. To complement our results on flocculation of these colloidal particles, we also implemented a Debye screening model that accounts for the shielding effect of multivalent cationic electrolytes on these nanogel systems. We demonstrated that, while the order of deswelling ability of the electrolytes follows the trend $\text{AlCl}_3 > \text{MgCl}_2 \geq \text{CaCl}_2 > \text{KCl} \geq \text{NaCl}$, the nanogels reach a minimum hydrodynamic diameter at 10 mM in all electrolyte solutions. The flocculating ability trend and the response time to form aggregates follow a similar order to the deswelling behavior. Interestingly, our statistical analysis on the SEM and TEM images of the PNIPAM nanogels supported our hypothesis on the presence of a shell-like layer around the nanogels with varying density in the electrolyte solutions as compared to those in aqueous medium, and the shell softness of nanogels became harder in multi-valent electrolyte solution than in monovalent system. Furthermore, the retention of the thermo-induced size reversibility for the Na^+ and K^+ below 10 mM and for the Mg^{2+} and Ca^{2+} below 1 mM indicates the effective destabilization of the electrolyte system with multivalence following the Schulze-Hardy rule, except for Al^{3+} . In terms of surface charge screening effect, cations with a higher valence shortened Debye length to a greater extent and this ability was found to be in the order of $\text{Al}^{3+} > \text{Mg}^{2+} > \text{Ca}^{2+} > \text{K}^+ > \text{Na}^+$.

11:30 AM SB04.08.08

Precision Mechanical Enhancement and Patterning of Hydrogels using Photo-Click ChemistryJunH. Park^{1,2}, PatrickJ. Grimes¹, HenryE. Symons¹, MarkS. Workentin², SebastienRochat^{1,3} and PierangeloGobbo³; ¹University of Bristol, United Kingdom; ²The University of Western Ontario, Canada; ³University of Trieste, Italy

Hydrogels have vast biomedical applications due to their highly tuneable properties, such as biocompatibility, adhesion, permeability, viscoelasticity, and stiffness. These extraordinarily adaptable materials can be engineered to be stimuli-responsive by carefully selecting the crosslinking monomers or polymers that make up the hydrogels. A stimulus that allows for excellent spatio-temporal control is light, and the translucent nature of hydrogels is complementary to its use in these materials. There are various photoactive moieties that have been incorporated into photo-responsive soft materials, however, there are very few systems utilising photo-click reactions to modify the mechanical properties of hydrogels.

Click chemistry has become an established category of reactions characterized by rapid, selective, high yielding, and atom economic transformations that require minimal purification and can be carried out under mild conditions. In 2004, Bertozzi and coworkers established a bioorthogonal, click reaction called the strain-promoted alkyne-azide cycloaddition (SPAAC) by modifying the copper-assisted alkyne-azide cycloaddition (CuAAC) using strained alkynes.^[1] These alkynes are more reactive and do not require cytotoxic copper catalysts due to ring strain and bond angle deformation. To circumvent degradation and unwanted side reactivity of the strained alkyne, a cyclopropanone-masked dibenzocyclooctyne (hvDIBO) moiety was developed, capable of facile deprotection to the strained alkyne using ultraviolet light.^[2] The rapid deprotection can be performed *in situ* and the resulting alkyne is then free to selectively react with an azide *via* SPAAC. Along with its great stability and simple deprotection, the application of hvDIBO onto soft materials introduces precise spatial control due to the sensitivity of the cyclopropanone group to 350 nm UV-A light.

In this communication, the fabrication of photo-responsive hydrogels incorporating hvDIBO and azide moieties will be discussed. Photo-click crosslinking reactions between these groups to mechanically strengthen soft materials will be highlighted. The spatio-temporal control of the photo-click reaction was employed to photo-pattern the surface of hydrogels and to study the kinetics of the materials' strengthening. A recently developed methodology designed to study the mechanical properties of soft materials with a micro-indenter was applied. Microindentation analyses were used to spatially characterize viscoelasticity and height profile changes of these hydrogels, and to determine the reaction order kinetics of the photo-click reaction.^[3] These analyses aim to relate chemical processes with mechanical measurements. Overall, these photo-responsive hydrogels can be readily strengthened and patterned through clean, facile photo-click chemistry, allowing for exciting potential applications in actuation, soft robotics, biointerfacing, and biomimetic materials.

[1] S. T. Laughlin, J. M. Baskin, S. L. Amacher, C. R. Bertozzi, *Science* 2008, 320, 664-667.

[2] W. Luo, J. Luo, V. V. Popik, M. S. Workentin, *Bioconjug. Chem.* **2019**, *30*, 1140-1149.
[3] H. E. Symons, A. Galanti, J. C. Surmon, R. S. Trask, S. Rochat, P. Gobbo, *Soft Matter* **2022**, *18*, 8302-8314.

11:45 AM SB04.08.09

DNA-Polymer Hybrids for Responsive and Repeatable Gating in Nanostructures Kimberley Callaghan¹, Shelley Wickham² and Amanda Ellis¹; ¹The University of Melbourne, Australia; ²The University of Sydney, Australia

Deoxyribonucleic acid (DNA) is a remarkable molecule, responsible for cellular information storage, exhibiting unique chemical structure and interactions. These properties have enabled its applications in drug delivery, research tools, and novel materials, with many more potential applications as yet unrecognised. This project aims to develop responsive DNA-polymer hybrid materials capable of sensing and responding to environmental stimuli. These materials will capitalise on the dynamic properties of DNA, whilst utilising the favourable material properties of polymeric materials.

In this work, a DNA-polymer hybrid material was designed to form an aqueous hydrogel upon stimuli addition to generate a gate within a DNA-origami nanostructure to form a biological circuit board. The hydrogel was constructed from an acrylamide backbone, with pendant DNA functionality incorporated. DNA oligonucleotides with polymerisable acrydite handles were doped into the polymerisation reaction, resulting in sporadic incorporation of the DNA motifs.

The DNA motifs used were designed to gate the hydrogel structure under orthogonal stimuli. The stimuli investigated included: temperature, through a self-complementary sequence able to form inter-strand duplexes at lower temperatures; pH, via a i-motif formation involving Hoogsteen base pairing between two cytosine bases in which one is protonated below pH 5 with dissociation upon deprotonation above pH 7; and, a metal ion bridge, using silver ions to bridge two cytosine bases followed by addition of a cysteamine ligand to dissociate the strands. The stimuli chosen all generate transient intermolecular interactions and as such can be cycled repeatedly, allowing for multiple opening and closing cycles of the gates without the need for replacing DNA-polymer components or damaging DNA-origami structures. By integrating the dynamic properties of DNA with the favourable characteristics of polymeric materials, these nanoscale systems offer a solution for the limitations of traditional electronic devices.

SESSION SB04.09: Hydrogels and Energy
Session Chairs: Anna-Maria Pappa, Alexandra Rutz, Christina Tringides and Shiming Zhang
Wednesday Afternoon, November 29, 2023
Hynes, Level 1, Room 103

1:45 PM SB04.09.01

Self-Assembled Nanofibrous Hydrogels with Tunable Porous Network for Highly Efficient Solar Desalination in Strong Brine Hao Li¹, Weixin Zhang², Jiawei Liu¹, Sun Mingze¹ and Lizhi Xu^{1,2}; ¹The University of Hong Kong, Hong Kong; ²Advanced Biomedical Instrumentation Centre Limited, Hong Kong

Hydrogels hold great promise as solar evaporators for highly efficient solar desalination due to the reduced vaporization enthalpy in the hydrated polymeric network. However, rarely hydrogel-based solar evaporators (HSEs) can achieve both excellent evaporation rate and stability when purifying strong brine, mainly limited by the vague understanding of complex nexus between microstructures and evaporation performance. Here, hydrogels based on aramid nanofibers (ANFs) and Polyvinyl alcohol (PVA) with great tunability on microstructures and compositions were proposed as the platform for the engineering of HSEs. The nanofiber hydrogel-based solar evaporator (NHSE) demonstrates open porous network and ultrahigh porosity above 90%, enabling the highly continuous water channels for efficient mass transfer. The hybrid nanofiber network incorporating polypyrrole demonstrates abundant hydrophilic groups for reducing vaporization enthalpy and excellent photothermal conversion performance without compromising the porous structure.^[1] Numerical simulations conducted here reveal the complex nexus between microstructures and evaporation performance by coupling water transfer, thermal conduction, and vaporization enthalpy during evaporation. The general insights provided in this work are also conducive to design other HSEs. The optimum NHSE demonstrates a superior evaporation rate of 2.85 kg m⁻² h⁻¹ in 20% brine with continuous desalination for 8 h. This work first develops a tunable hybrid nanofiber network as solar evaporator in strong brine and provides general insights to the design of HSEs for highly efficient solar desalination.

[1] H. He, H. Li, A. Pu, W. Li, K. Ban, L. Xu, *Nat. Commun.* **2023**, *14*, 759.

2:00 PM SB04.09.02

Multifunctional Zwitterionic Hydrogels as a Platform for the Rapid and Simultaneous Elimination of Organic and Inorganic Micropollutants from Water Devashish Gokhale, Andre F. Hamelberg and Patrick Doyle; Massachusetts Institute of Technology, United States

The removal of micropollutants from water is made difficult by their chemical diversity, low concentrations, and slow uptake by industrial adsorbents. Traditional adsorbents, like activated carbon and ion-exchange resins, are effective in eliminating only specific classes of micropollutants, necessitating the use of multiple unit operations that sequentially treat water. At the same time, slow kinetics require the unit operations to have long residence times and be much larger to effectively eliminate micropollutants. Here we present a new multifunctional zwitterionic porous hydrogel platform for the single-step bulk absorption of both organic and inorganic micropollutants from water. Shifting from traditional surface adsorbents to hydrogels greatly increases the effective functional area, while allowing us to retain the same process-level equipment that has been well studied in the context of conventional adsorbents. A facile synthesis allows easy functionalization of the hydrogels for eliminating multiple micropollutant classes, while also allowing a measure of selectivity. The hydrogels can be synthesized in several forms for specific applications, including microparticles for use in packed beds, or tablets for treating water in a glass or canteen. Transport of micropollutants within the hydrogels is sped by ion-conducting zwitterionic backbones, while encapsulated micelles speed the transport of uncharged organics. The zwitterionic hydrogels are shown to remove six chemically diverse micropollutants (including BPA, xenoestrogens, and other organics, and lead and other metals) at least 10 times more rapidly than a commercial activated carbon/ion exchange resin mixture, and 100 times faster than other multifunctional adsorbents reported in literature. Zwitterionic hydrogels treat complex micropollutant mixtures, including in the presence of background hardness. Lower compressibility, extremely rapid mass transport, and high stability make our materials highly scalable for real world applications. We demonstrate the use of a prototype packed bed filter with a practical residence time and containing zwitterionic hydrogel microparticles to clean highly contaminated water to below regulatory limits for a period of two weeks.

2:15 PM SB04.09.03

VOCs-Responsive Hydrogel Electrode based on Changes in Chain Mobilities for Multi-Protection Youna Kim and Jinkee Hong; Yonsei University, Korea (the Republic of)

Every year, exposure to volatile organic compounds (VOCs) causes fatal accidents including dyspnea and explosions. Personal protection equipment (PPE), such as VOCs sensors to monitor indoor air quality and masks to prevent inhalation of VOCs, is needed to prevent VOC exposure. However, single-functional PPE leads to inconvenience for workers as they must wear multiple pieces of PPE. Therefore, PPE must have the versatility to check not only air quality but also the health condition of workers.

PPE combined with wearable electronics could provide multifunctionality with human health monitoring including strain and motion signals and VOCs detection. The electric materials for wearable electronics should be lightweight, flexible, and stretchable. Hydrogels are attracting attention in wearable electronics because of their flexibility, stretchability, and conductivity. However, it has weak mechanical strength and suffered the deterioration of conductivity and shape shrinkage due to moisture evaporation. Furthermore, few studies have controlled the mechanical and electrical properties of hydrogels due to VOCs exposure except for color changes. In order for VOCs-responsive hydrogels to exhibit various VOC-sensing performances, like actuation and electrical changes, an understanding of polymer behavior caused by VOCs must be investigated.

In this study, we designed a VOC-responsive polymer network (VRN), a wearable electronics that can change its mechanical and electrical properties through VOC reaction. Through a solvation effect by different chemical affinity, the inter/intramolecular interaction and arrangement between polymer chains could be controlled. Based on the solvation effect, we considered (1) the control of polymer chain mobility and hydrogen bonding within VRN and (2) the chemical affinity between the VRN and VOCs.

To control the VRN network, VRN is composed of polyvinyl alcohol (PVA) as hydrophilic semicrystalline and deep eutectic solvents (DES) as ionic liquids. DES is used as a processing and conductive additive to increase the entangled polymer chains and inhibit hydrogen bonding between polymer chains. Accordingly, VRN shows ionic conductivity and stretchability, which can be used for strain-responsive electrodes.

After VOCs exposure, the increased hydrogen bonding and chain relaxation energies affected not only mechanical properties but also the electrical resistance of VRN. A relative resistance change ($\Delta R/R_0$) of VRN is increased by 50% when VRN is exposed to VOCs vapor. The peak voltage based on the triboelectric energy generator (TEG) system decreased by 30% due to VOCs exposure. VRN can be applied to PPE in various forms such as fiber and spray coating.

In addition, we studied the VOCs responsive mechanism of polymer chains using rheological and Raman analysis. We expect VRN to propose VOCs-responsive mechanisms and technologies needed to move towards advanced PPE.

SESSION SB04.10: Skin and Tissue-Interfacing Hydrogels I
 Session Chairs: Anna-Maria Pappa, Alexandra Rutz, Christina Tringides and Shiming Zhang
 Wednesday Afternoon, November 29, 2023
 Hynes, Level 1, Room 103

3:30 PM *SB04.10.01

Ingestible Electronic Interfaces for Neuromodulation [Khalil Ramadi](#)^{1,2,3}; ¹New York University Abu Dhabi, United Arab Emirates; ²New York University, United States; ³Massachusetts Institute of Technology, United States

Neuromodulation is emerging as a novel approach to treat both neurological and non-neurologic diseases. However, the brain and nervous system are extremely heterogeneous, where cell types and functions vary on scales from sub-millimeters to centimeters. This heterogeneity presents a major obstacle for targeted modulation and interrogation of specific neural structures. This talk will describe non-invasive, ingestible toolkits for high spatial and temporal resolution targeting of neural circuits.

4:00 PM SB04.10.02

Kinetic Control Dictates the Operation of PEDOT:Lignosulfonate Thin-Films for Biosensing at Physiological pH [Alex C. Tseng](#)¹, [Tomasz Rebis](#)² and [Toshiya Sakata](#)¹; ¹The University of Tokyo, Japan; ²Poznan University of Technology, Poland

Integrating electrically conductive and redox polymers (RPs) is a promising approach for sustainable development of high-performance electrical and electrochemical materials, not only for energy storage but also for bioelectronics and biosensors. Lignosulfonates (LS) exemplify a particularly green materials selection, being low cost and biorenewable, yet readily providing phenolic groups to access (*ortho*-quinone redox (i.e., reversible proton coupled electron transfer, PCET) and sulfonic acids for polyanionic doping of conductive polymers (CPs). When blended with oxidatively stable PEDOT (poly(3,4-ethylenedioxythiophene)), remarkable specific capacity (170 F.g⁻¹) was reported in acidic conditions (0.1 M HClO₄) [1] despite significant loading of electrochemically inactive components.

Besides enhancing pseudocapacitance, quinone PCET may be further leveraged to serve as an electrochemical interface between technological devices and biological catalyst cycles [2]. However, in the mild pH conditions amenable to biology, it is well known that *ortho*-quinones exhibit limited stability towards redox cycling. Several possible explanations have been offered up over the years, for instance: microstructural changes inhibiting proton diffusion [1,4], dissolution of the redox polymer [3], hydroxylation to higher order polyphenols [2], phase separation of CP and redox polymer [5], and cross-linking by the formation of ether linkages [6] or phenyl dimerization [7].

These varied conclusions are likely views of the same fundamental property of *ortho*-quinone RPs—filtered through a range of fabrication and experimental conditions—which is that reversible quinone PCET is a kinetically controlled process. Future biological applications, therefore, require an understanding of how and when alternate electrochemical pathways become activated by the scarcity of protons in physiological conditions. Hence, we investigated the pH-dependent behaviour of PEDOT:LS thin-films via *in-situ* UV-Vis spectroelectrochemistry, charge transport characterization in an electrochemical transistor, and thermodynamic/kinetic analysis by the Laviron method. Our results paint a surprising picture: PEDOT, typically considered to be a “transparent” conductor serving simply as a wire to enhance electron transfer with quinones, is implicated in the formation of strongly bound complexes that appear to stabilize semiquinone radicals. Accordingly, previously observable PEDOT and quinone states are removed in proportion from measurement on experimental timescales. This kinetic process is mediated by the effective overpotential vs. PCET as a function of pH and polarization, and thus informs the optimal operating conditions for biosensing using PEDOT:LS.

[1] F. N. Ajjan *et al.*, *J. Mater. Chem. A*, vol. 4, no. 5, pp. 1838–1847, Jan. 2016.

[2] G. Milczarek, *Langmuir*, vol. 25, no. 17, pp. 10345–10353, Sep. 2009.

[3] M. O. Bamgboja *et al.*, *J. Mater. Chem. A*, vol. 7, no. 41, pp. 23973–23980, Oct. 2019.

[4] T. Rebis *et al.*, *Electrochimica Acta*, vol. 204, pp. 108–117, Jun. 2016.

[5] C. Che *et al.*, *Advanced Sustainable Systems*, vol. 3, no. 9, p. 1900039, 2019.

[6] A. René *et al.*, *J. Phys. Chem. C*, vol. 116, no. 27, pp. 14454–14460, Jul. 2012.

[7] A. A. Vereshchagin *et al.*, *Nanomaterials*, vol. 12, no. 11, p. 1917, Jan. 2022.

4:15 PM SB04.10.03

Waterproof and Gel-Free E-Textile Wearable Systems for Exercise Physiology and Maternal Health [Junyi Zhao](#), [Chansoo Kim](#) and [Chuan Wang](#); Washington University in St. Louis, United States

Textile-based electronic systems have emerged as a promising platform for noninvasive and comfortable human-machine interfaces in various applications. These systems integrate multiple technological capabilities such as sensing and wireless communications, making them suitable for daily wearables and physiological monitoring in sports and clinical settings. This work presents a novel E-textile system consisting of printed on-textile electrodes and add-on conductive microfibers, enabling gel-free motion-artifact-tolerant recording of multiple physiological signals, including ECG and EMG from both skeletal and smooth muscles. More specifically, the base layout consists of a screen-printed array of poly(3,4-ethylenedioxythiophene) polystyrene sulfonate (PEDOT:PSS), and the fluffy microfibers coated with PEDOT:PSS are stacked on top. The vertically oriented hairy microfibers offer exceptional conformal and robust contact with the skin, while the spreading-out microfiber electrodes substantially increase the effective contact area. As a result, the contact impedance between the electrode and skin is significantly reduced, enabling comfortable all-day wear under dry conditions without the need for ionic gels. To ensure the durability and functionality of the textile, a self-assembled monolayer (SAM) of trichloro(1H,1H,2H,2H-perfluorooctyl) silane is vaporized as a superhydrophobic coating. This treatment preserves the natural physical properties of the textile while maintaining the intrinsic conductivity of the electrodes. Additionally, a portable mini-circuitry was designed and manufactured to enable multi-channel recording and wireless communications. These advancements contribute to the seamless integration of the E-textile system into everyday life and expand its potential applications. This study explores the application of E-textile systems in real-life scenarios, including strenuous exercise and clinical studies. The study begins by demonstrating the robustness and stability of the E-textile system using E-jersey and E-shorts during a 15-minute cycling training session. Remarkably, the recorded signals remained clear and free from motion artifacts, even in the presence of intense sweating, with a signal-to-noise ratio of approximately 30 dB. Real-time monitoring also allowed for additional real-time data analysis, including heart rate and muscle output. Next, the waterproof capability of the system was tested by creating an E-swimsuit with electrodes placed facing the swimmer's back. Throughout the 12-minute swimming training, the fully submerged E-swimsuit consistently delivered reliable ECG recordings, demonstrating its resilience and suitability for aquatic environments, even when encountering water flows, showcasing its strength and suitability for aquatic environments. Finally, the textile-based E-patch with electrode arrays was employed in clinical studies to monitor maternal health. Multiple pregnant subjects were monitored, capturing multichannel maternal-ECG and uterine-EMG signals. The recorded multichannel uterine-EMG signals were further processed to generate noninvasive and high-resolution three-dimensional (3D) electromyogram images, providing unique insights into uterine behavior and offering a means of predicting the risk of potential preterm birth. These findings emphasize the versatility and potential of wearable E-textile systems in a wide range of real-world applications. The E-textile systems are specifically designed for convenient and comfortable wearing, paving the way for professional sports tracking and personalized healthcare advancements.

4:30 PM SB04.10.04

Materials Design of Functional Gels to Realize 3D Artificial Skin Device based on Extrusion-Based 3D Printing [Woohyeon Shin](#)^{1,2}, [Hui Ju Choi](#)¹ and [Kyeongwoon Chung](#)¹; ¹Kyungpook National University, Korea (the Republic of); ²Ulsan National Institute of Science and Technology, Korea (the Republic of)

Due to unique properties such as biocompatibility, flexibility, and conductivity, hydrogels are widely investigated in various applications, including tissue engineering, E-skin, wearable, and ionic devices. Especially, in the field of E-skin devices, hydrogels are recognized as one of the promising materials due to their flexibility and capability to realize various sensing functionalities. Still, there are challenges that need to be addressed: the structural freedom of devices. Most E-skin devices have been demonstrated with simple structures such as blocks or films due to the demand for complicated multi-layer structures or limitations in the fabrication process. Especially, because body parts with various shapes and movements (e.g., fingers, elbows, and shoulders) are under massive fatigue by strains in various directions and amounts, it is important to realize artificial skin devices with complex 3D structures that are optimized for the targeted body part.

To realize complex 3D structures of hydrogel via extrusion-based 3D printing, we systemically investigated the correlation between materials design and their characteristics including gelation properties, rheological characteristics, and 3D printing processability. From the investigation, we successfully presented the material design window based on the rheological

parameter ($G' < 2500$ Pa and $\tan \delta < 0.2$) to prepare target-oriented 3D structures of the hydrogel via extrusion-based 3D printing. Based on the defined material design window, we successfully prepared functional hydrogel 3D structures to demonstrate novel artificial skin devices that can detect accurate touch points and spontaneously heal mechanical damage. Ring-shaped and fingertip-shaped artificial skin devices have been successfully prepared to fit the finger model. Furthermore, like human skin, artificial skin devices provide accurate location information for arbitrary touch points without complex device fabrication or data processing. In hydrogel-based 3D e-skin devices, it is also important to address the inherent drying and freezing problems of hydrogel for practical application. As an approach to these problems, we presented organohydrogel systems via solvent displacement and investigated the correlation between solvent system design and the material properties of organohydrogels. By investigating the rheological properties and ion conductivity of the gels, we provided insights for preparing optimal organohydrogels for various processes and applications. Based on the defined solvent system design, we prepared organohydrogels that show excellent drying resistance even over 1,000 hours and exhibit superior freezing resistance by showing no phase transition down to -60°C . Furthermore, the 3D artificial skin devices are demonstrated based on the organohydrogels, and the artificial skin devices successfully provide the exact position of touchpoints over time and show excellent operation capability even at temperatures below 0°C without losing flexibility.

SESSION SB04.11: Skin and Tissue-Interfacing Hydrogels II
Session Chairs: Anna-Maria Pappa, Alexandra Rutz, Christina Tringides and Shiming Zhang
Thursday Morning, November 30, 2023
Hynes, Level 1, Room 103

9:00 AM SB04.11.01

Electrically Induced Shape Memory Hydrogels in Biomedical Applications. Georgios Mikalef, Arjan Sall, Zoe Schofield, Atif Shahzad, Patricia P. Esteban and Liam Grover; Healthcare and Technologies Institute, United Kingdom

Here we report the development of a novel shape memory hydrogel that changes shape on exposure to an electrical field. This material has been designed to enable the minimally invasive administration of a novel sensor system to monitor real-time changes in blood pressure. The hydrogel will encapsulate a sensor coil and protect against biological interference during measurement. Real-time blood pressure measurement will enable the diagnosis and monitoring of conditions as hypertension and cardiomyopathy, which place a significant financial burden on healthcare systems worldwide.

Polyelectrolyte (PE) hydrogels can exhibit a shape memory effect upon exposure to an electrical current, caused by ions that sit within its structure. PE gels are naturally found throughout the body where they are often associated with oppositely charged molecules. One such example is in the aggrecan, which interacts strongly with collagen in cartilage. PE hydrogels have already been used extensively as biomaterials. Their structure has made them ideal scaffolds for tissue engineering, novel drug delivery systems, soft robots particularly in artificial muscle and actuators, smart fabrics, and implantations for minimally invasive surgeries.

Since hydrogels can exhibit poor mechanical properties, we have made efforts to reinforce the shape-memory polymer structure. We explored 2 different formulations have been synthesised containing the smart material 2-acrylamido-2-methylpropanesulfonic acid (AMPs) and either Polyethylene Glycol Diacrylate (PEGDA) or acrylamide. The mechanical performance and chemical structures of these materials have been evaluated. Finally shape memory testing has been performed to determine the effect of curing on the material's ability to change shape.

Further testing will include direct contact cytotoxicity testing to determine cell viability as well as surface modification whereby protein adsorption will be implemented to fix the device and so reduce migration upon implantation.

9:15 AM SB04.11.02

Lightweight, Flexible and Self-Healable Electromagnetic Shielding PEDOT:PSS Hydrogels Floriane Miquet-Westphal and Fabio Cicoira; Polytechnique Montréal, Canada

This abstract introduces our advanced EMI shielding hydrogel films, which exhibit exceptional properties for a wide range of applications. Our hydrogels offer outstanding EMI shielding performance in the X-Band (8-12.4 GHz). Their lightweight composition makes them ideal for weight-sensitive applications. Additionally, the films' flexibility and free-standing nature enable seamless integration into diverse systems or structures. Notably, our hydrogel films possess self-healing capabilities. These impressive features position our EMI shielding hydrogel films as a leading choice for industries such as electronics, telecommunications, automotive, aerospace, and medical, offering versatile solutions for shielding, lightweight design, flexibility, and self-repair.

9:30 AM *SB04.11.03

Healable and Stretchable Conducting Hydrogels for Epidermal Electronics Fabio Cicoira; Ecole Polytechnique de Montreal, Canada

Soft and conductive materials with long-term stability have attracted interests in the field of epidermal bioelectronics due to their conformal contacts with skin and the ability to acquire bio-signals for long-term use. Applications include monitoring of vital signs (e.g., electrocardiography (ECG), electromyography (EMG), and electroencephalography (EEG)), measurement of body temperature and blood pressure and detection of analytes in bodily fluids. ECG, EMG, and EEG are typically achieved with metal (ground strap, bar, or cup) or, in most cases, Ag/AgCl gel electrodes. However, rigid metal electrodes are unable to withstand bending or stretching, which can result in skin damage or irritation and lead to high signals noise, whereas Ag/AgCl gel electrodes can lead to skin irritation due to strong adhesion on the skin and are prone to signal degradation in long-term use due to the drying of the gel. Therefore, there is a strong demand for soft conductive electronics that can form conformal interfaces with biological tissues for long-term use without leading to skin damage and irritation.

Various types of conductive soft materials have been used for on-skin electronics, in form of films, bio-inspired adhesives, fabrics, and hydrogels. Conductive hydrogels are promising candidates for epidermal electronics because of their conformal contact with the skin, high water content (70-99%, similar to tissues), ease of processing, tunable electrical and mechanical properties, and biocompatibility. Conductive hydrogels may be obtained from pure conductive polymers, e.g., poly(3,4-ethylenedioxythiophene) doped with polystyrene sulfonate (PEDOT:PSS), polypyrrole (PPy), or polyaniline (PANI), or, in most of cases, by mixing conductive materials (e.g., conducting polymers, nanoparticles, nanowires, nanosheets, carbon nanotubes (CNTs), and graphene) with polymers, such as poly(vinyl alcohol) (PVA), poly(acrylic acid) (PAA), poly(acrylamide) (PAAM), or polyurethane (PU). A hydrogel prepared by mixing a PEDOT:PSS aqueous suspension with 0.1 M H_2SO_4 exhibited a conductivity of ~ 9 S/cm after further concentrated sulfuric acid treatment. Our group reported a hydrogel obtained by blending PEDOT:PSS into a PVA/borax system, which showed remarkable compliance on skin, outstanding plastic stretchability (10000% strain), self-healing, high adhesion on porcine skin (1.96 N/cm²), and low compressive Young's modulus (~ 4 kPa). Electrodes based on this hydrogel have demonstrated high-quality recordings of ECG and EMG signals.

Tannic Acid, a natural polyphenol, has been widely used to prepare hydrogels from mixtures with PAAM/kaolin, silk fibroin, PVA/PAAM, and CNT/PVA/glycerol. Moreover, TA exhibits biocompatibility and antibacterial, antioxidative, and anti-inflammatory properties, which can be exploited for medical applications, such as wound healing and infection treatments. Polyvinyl alcohol (PVA)-borax hydrogels are widely studied for biomedical applications due to their biocompatibility, biodegradability, water solubility, easy processing and self-healing properties.

Herein, we report conductive organohydrogels obtained from aqueous mixtures of PEDOT:PSS, EG, and TA and PVA, which showed a low compressive Young's modulus of ~ 20 kPa, high electrical conductivity as well as anti-freezing and water retention properties. Our gels were showed self-healing ability and were used to prepare epidermal electrodes for ECG and EMG recordings, which showed similar performance to that of commercial Ag/AgCl gel electrodes, even after storage in ambient air for 1 week. We also demonstrated the use of gel electrodes as human-machine interfaces to control the opening and closing of a robotic hand in real time. The simple fabrication, high conductivity, and mechanical properties make our gels highly promising for applications in bioelectronics.

10:00 AM BREAK

10:30 AM *SB04.11.04

In-Vivo Polymerization of Conjugated Polyelectrolytes in Plants and Animals Eleni Stavrinidou; Linköping University, Sweden

Leveraging the biocatalytic machinery of living organisms for in-vivo fabrication of functional bioelectronic interfaces enables seamless integration of devices in tissue and formation of biohybrid systems. Previously we have demonstrated that plants can polymerize conjugated oligomers in-vivo forming conductors within their structure. We showed that the polymerization is enzymatically catalyzed by endogenous peroxidases, and we developed a series of conjugated oligomers that can be enzymatically polymerized in physiological conditions. The conjugated polyelectrolytes integrate within the plant cell wall structure adding electronic functionality into the plant that is then explored for energy storage. Recently we demonstrated intact plants with

electronic roots that continue to grow enabling plant-biohybrid systems that maintain fully their biological processes. The electronic roots are used to build supercapacitors and biohybrid circuits to power low power electrochemical devices. Furthermore, we have extended this concept into an animal model system. We demonstrated that Hydra, an invertebrate animal, can polymerize intracellularly conjugated oligomers in cells that expresses peroxidase activity. The conjugated polymer forms electronically conducting and electrochemically active domains in the μm range integrated within the hydra tissue. Our work paves the way for self-organized electronics in plant and animal tissue for modulating biological functions and in-vivo fabrication of hybrid functional materials and devices.

11:00 AM SB04.11.05

Hydrogel for Multiplexed Multiscale Imaging and Phenotyping of the Human-Organ-Scale Biological Tissues Juhyuk Park¹, Ji Wang¹, Webster Guan¹, Lee Kamensky¹, Nicholas Evans¹, Jeffrey Stirman², Xinyi Gu¹, Chuanxi Zhao¹, Minkyung Kim¹, Seo Woo Choi¹, Clover Su-Arcaro¹, Yuxuan Tian¹, Dae Hee Yun¹, C. Dirk Keene³, Patrick Hof⁴, Matthew Frosch⁵ and Kwanghun Chung¹; ¹Massachusetts Institute of Technology, United States; ²LifeCanvas Technologies, United States; ³University of Washington, United States; ⁴Icahn School of Medicine at Mount Sinai, United States; ⁵Harvard Medical School, United States

Understanding the intricate chemoarchitectural details and regional-specific functions and dysfunctions of the human brain poses a formidable challenge in holistic brain imaging and phenotyping. While recent advancements in tissue clearing and labeling techniques have made significant strides, the lack of scalability, thermos-mechanical robustness of tissues, imaging resolution, and cost-effective immunolabeling protocols limit their applicability in multiplexed human brain mapping at various scales. In this study, we present a pioneering hydrogel-based tissue processing technology called mELAST, which transforms biological tissues into soft, tough-elastic, reversibly expandable tissue-hydrogel hybrids, in tandem with mechanical devices and chemicals. Leveraging mELAST, we achieved multi-round immunolabeling and multiscale expansion imaging of volumetric human brain tissues, enabling the comprehensive capture of cytoarchitecture, microenvironment, and synapses within the human brain. We applied the mELAST pipeline to conduct a comparative study of Alzheimer's disease in the human brain, further unraveling neuroscientific enigmas. With mELAST, we anticipate a significant advancement in our ability to navigate deep within the human brain afflicted by pathologies, shedding light on crucial neuroscientific challenges.

11:15 AM SB04.11.06

A Stretchable and Mechanically Stable Bio-Inspired Nanofiber-Reinforced Microfiber for Wearable Electronics Adeela Hanif, Junho Park, Dohui Kim, Jaeseung Yoon, Unyong Jeong and Dong Sung Kim; Pohang University of Science and Technology, Korea (the Republic of)

Since fiber-based approaches have high stretchability, the devices fabricated on them with limited stretchability cannot fully withstand large stretching, particularly when the wearer participates in vigorous activity. Stretchable systems can replicate the "J-shaped stress-strain or strain-limiting" mechanical behavior of biological tissues under deformations and provide mechanical compliance and comfort to wearers. A network of soft elastin fibers and stiff collagen fibers causes the biological tissues to be stretchable at low strains, and exhibit strain-limiting behavior when deformed at large strains. We developed a combined microfiber and nanofiber (NFs)-based approach to mimic this mechanical behavior of biological tissues, which involved wrapping soft polyurethane (PU) microfiber with stiff and inflexible poly(vinylidene fluoride) (PVDF) NFs and coating them in polydimethylsiloxane (PDMS). By tailoring the loading ratios of the PVDF NFs it is possible to tune the elastic moduli of the bio-inspired microfibers to match well with those of biological tissues. As shown by confocal imaging during stretching, PU microfibers maintain stretchability and stiff PVDF NFs play a role in strain-limiting characteristics. The stretchable poly(3,4-ethylenedioxythiophene) polystyrene sulfonate/ Polyurethane dispersion (PEDOT: PSS/PUD) coating on the bio-inspired microfiber showed a negligible difference in current-time (I-T) response after static stretching (~ up to 30%- human skin stretchability range) which indicated the efficient absorption of stress by the bio-inspired microfiber. An electrical response of a stretchable temperature sensor was measured by directly attaching it to the fist and stitching it into the bandage to demonstrate bio-inspired microfiber's ability to measure skin temperature and accommodate body movements. A light-emitting diode (LED) ON/OFF test was performed to demonstrate that the bio-inspired microfibers could be used as electrodes in the future. Therefore, bio-inspired microfibers could become the frontier of wearable electronics due to their high mechanical and electrical stability, adaptability to non-planar bodies, and ease of sewing.

11:30 AM SB04.11.07

Intraoral Hydrogel-Graphene Biosensors for *In-Situ* Detection of TNF- α in Human Saliva Shaoting Lin; Michigan State University, United States

Technologies that enable in-situ monitoring of biomarkers in human saliva in oral cavities are highly desirable for timely diagnosis, early intervention, and personalized treatment of oral diseases. Existing efforts have been mostly focused on flexible electronics made of rigid materials, which inevitably suffer significant challenges in interfacing soft tissues due to their contradictory properties. Hydrogels, polymer networks infiltrated with water, share similar mechanical and physiological properties as biological tissues, regarded as an ideal material candidate to form long-term, high-efficacy, multi-modal interfaces between electronic components and biological systems. In particular, the recent developments of tissue-adhesive hydrogel patches have shown great success in forming rapid and tough adhesion between wet tissues and electronic devices in various organs, but these efforts have not been implemented in oral cavities. In this work, we focus on developing an intraoral hydrogel-graphene biosensor that can achieve highly sensitive, specific, and durable detection of human tumor necrosis factor- α (TNF- α) in human saliva. The design of hydrogel-graphene biosensor is based on an integration of selective-permeable hydrogel and graphene-based sensing probe, which enables sensitive and specific detection of low-concentration TNF- α in human saliva. This work will not only hold the promise of enabling rapid diagnosis of conditions such as recurrent aphthous stomatitis (RAS), periodontal disease, and oral cancer, but also facilitate the planning of medical treatment policies and evaluation of treatment efficacy.

11:45 AM SB04.11.08

A Damage-Mapping, Self-Healing Electronic Skin for Surgical Simulation Training Samuel E. Root and Zhenan Bao; Stanford University, United States

Modern facilities for surgical education make use of inanimate models to simulate surgical tasks. Such models provide trainees with the opportunity to practice and receive feedback on the procedural and motor skills required to perform complex surgeries with expert-level competency. Existing models for surgical simulation rely heavily upon thermoset polymers such as silicones or hydrogels, which deteriorate after single or repeated use. Such disposable models are expensive—especially those with physically realistic properties—and incur a prohibitive cost for training programs, limiting opportunities for students to practice with high fidelity models. Moreover, evaluating the performance of trainees on surgical tasks is difficult and requires direct observation by an expert or the use of motion tracking software. There is a need to develop surgical simulation models with realistic physical properties and functional capabilities mimicking that of living tissue including, i) the ability to heal from damage, and ii) the ability to sense and transduce mechanical stimuli including forces, pressures, rates and depths of incisions and punctures. Over the past decade, advances in the science of dynamic polymeric materials (*i.e.*, polymers that are cross-linked with reversible bonds, such as hydrogen bonds) have enabled the molecular design and device integration of stretchable, conductive, self-healing composites. We have recently reported a strategy for improving the functional self-healing efficacy of multi-layer laminate composites through the molecular design of a pair of dynamic polymers with immiscible polymer backbones (poly(dimethylsiloxane) and poly(propylene glycol)) but identical dynamic bonding units (a mixture of bisurea-based hydrogen bonding units). These polymers have a strong, adhesive but thermodynamically restricted interface, which results in an autonomous alignment and healing phenomenon, whereby polymer chains directionally diffuse to minimize the interfacial free energy when multi-layered stacks are damaged and misaligned. In this presentation, I will discuss our current efforts building upon this work towards the design of a damage-mapping electronic skin capable of sensing processes such as punctures with needles, scalpels, or sutures—and self-healing to undergo many operational cycles. We have developed a scalable compositing, compression-molding, and layer-based assembly process for fabricating multi-layer soft electronic films. We have implemented a voltage-based sensing mechanism for mapping the location and depth of needle punctures and surgical incisions. Finally, we demonstrate how these electronic skins can be integrated with surgical simulation technology, including rolling the films into vein-like tubes capable of sensing needle punctures for intravenous access training. Overall, we propose that there are many opportunities for bio-mimetic functional materials and device design within surgical simulation technology, including hybrid self-healing hydrogel-elastomer devices.

SESSION SB04.12: Chemistry-Focus of Hydrogels

Session Chairs: Anna-Maria Pappa, Alexandra Rutz, Christina Tringides and Shiming Zhang

Thursday Afternoon, November 30, 2023

Hynes, Level 1, Room 103

1:30 PM SB04.12.01

Protein-Based Ionic Materials Nadav Amdursky; Technion--Israel Institute of Technology, Israel

Nature is relying on the capability of proteins to mediate ions in preferred directions, such as the ionic transport across the two sides of a membrane through a protein. Inspired by this natural capability of proteins to mediate ions, we design several protein-based free-standing materials that are capable of mediating ions, specifically protons. By various physical and chemical pre- or post-polymerization modifications, we explore the ionic transport mechanism across the protein-based material, highlighting the important factors associated with its transport efficiency. Post-

polymerization modifications also allow us to chemically graft into the protein-based biopolymer light-sensitive molecule capable of generating opto-ionic materials. We also show the capability to introduce electronic conduction into the protein-based material either by blending or by chemical modifications, thus creating a mixed ionic-electronic conductor. From an application point of view, and due to our choice of using a sustainable source of proteins from waste sources, our protein-based ionic materials can be highly scalable at low cost. Our main application direction for our protein-based conductive biomaterials is for biological interfaces in the field of biosensing. Here, we can either utilize the ionic transport for making sensors for electrophysiological sensing or use the mixed conduction of the functionalized biopolymer for transistor-based sensing.

1:45 PM *SB04.12.02

Conductive or Injectable Hydrogels for Conformal Tissue-Device Interfacing Dae-Hyeong Kim^{1,2}; ¹Institute for Basic Science, Korea (the Republic of); ²Seoul National University, Korea (the Republic of)

Recent advances in soft electronics have attracted great attention due to its potential applications to personalized health-monitoring and point-of-care devices. The mechanical mismatch between conventional rigid electronic devices and soft human tissues oftentimes causes various issues, such as a low signal-to-noise ratio of biosensors, inflammations on the tissue interfacing with the bioelectronics, skin irritations in the case of long-term wearing of the device, and ineffective electrical stimulations and drug delivery in feedback therapies. Ultra-flexible and stretchable bioelectronic devices have a low system modulus and intrinsic softness, and have a potential to solve these issues. However, locally incomplete contacts are still found in skin-device interfacing and they reduce the sensing efficiency and therapeutic efficacy of the soft bioelectronics. Composites of polymers, nanomaterials, and hydrogels are particularly promising material candidates for solving such issues and achieving ideal biotic-abiotic interface. In this talk, the unique strategies in the synthesis of conductive or injectable hydrogels, their seamless integration with soft bioelectronics, and wearable and/or implantable device applications are presented. These efforts are expected to address unmet clinical challenges.

2:15 PM SB04.12.03

Tuning the Surface Chemistry of 3D Graphene Hydrogels by Covalent Functionalization: A Flow Chemistry Approach Antonino Biagio Carbonaro¹, Daniele Fumagalli², Valentina Greco¹, Antonino Gulino¹, Valentina Pifferi², Luigi Falcicola² and Alessandro Giuffrida¹; ¹University of Catania, Department of Chemical Sciences, Italy; ²University of Milan-La Statale, Italy

Recently, three-dimensional porous graphene architectures, such as hydrogels and aerogels, have received increasing attention in the scientific literature due to their unique structural, chemical and physical properties. Combined with the well-studied brilliant properties of graphene-based materials, 3D graphene structures find applications in bioelectronics, sensing and energy storage. The meso- and macroporous structure of hydrogels and aerogels allows to overcome some limitations of 2D graphene materials, such as the re-stacking of monolayers, which confers unique properties due to the high active surface area of well-defined 3D graphene architectures. Most applications of graphene hydrogels and aerogels are based on the interaction between the porous carbon structure with molecular species, in the gas or liquid phase. In this context, functionalization strategies that allow the control of surface speciation would be highly welcomed. Functionalization methods for graphene hydrogels include non-covalent approaches where the guest species are physisorbed onto the porous structure during the gelation process. However, this approach can have many disadvantages, such as molecule slippage, and they are difficult to control compared to a covalent functionalization strategy. Keep this in mind, in this work we would like to shed light on the chemical behaviour of graphene hydrogels; in particular, according to the flow chemistry concepts, we propose a facile covalent functionalization strategy through Diazonium Salts Chemistry. The samples were extensively characterized by micro-Raman and ATR-FTIR spectroscopy, X-ray Photoelectron Spectroscopy (XPS), Scanning Electron Microscopy (SEM) and BET. In addition, the electrochemical performances of the 3D porous graphene hydrogel and aerogel structures were investigated by Cyclic Voltammetry (CV), Differential Pulse Voltammetry (DPV) and Electrochemical Impedance Spectroscopy (EIS), focusing on the electrochemical sensing properties of the 3D self-standing structures.

2:30 PM SB04.12.04

PHost-Guest Chemistry for The Design of Functional Polymer-Nanoparticle Hydrogels Stephane Bernhard, Lauritz Ritter, Marco Müller, Giovanni Bovone, Elia Guzzi, Wenqing Guo and Mark W. Tibbitt; ETH Zurich, Switzerland

Polymer-nanoparticle (PNP) hydrogels are a class of injectable nanocomposites based on physical interactions between polymers and nanoparticles (NPs). (1) Due to the shear-thinning and self-healing behaviour provided by the reversibility of the polymer-nanoparticle interactions, they have been used in the biomedical field as injectable biomaterials or inks for additive manufacturing. (2-3) Current PNP hydrogels however cover a narrow range of functionality and can be built from a restricted pool of available building blocks due to the constraint presented by the limited versatility of the cross-linking interactions. Here, we present the use of a supramolecular motif based on host-guest interactions for the design of versatile and functional PNP hydrogels.

In this work, two approaches based on cyclodextrin (CD) host-guest interactions were used for the design of PNP hydrogels. In a first approach, alpha-cyclodextrin (α CD) was added to a cellulose- and PEGylated-NP-based hydrogel, to decouple mechanical properties from building blocks via polypseudorotaxane formation. The addition of α CD enabled the exchange of the polymer and nanoparticle for varied biopolymer with secondary cross-links or inorganic nanoparticles with conductive or magnetic characteristics. In a second approach, beta-cyclodextrin (β CD) was used in combination with azobenzene, a photo-responsive guest for the design of light sensitive hydrogels. For this purpose, a host-functionalized polymer (β -CD hyaluronic acid) and guest harboring block copolymer (PEG-*b*-PLA) NPs were synthesized. (5) The presence of the photoresponsive host-guest complex resulted in reversible gelation of the hydrogel via illumination at various wavelengths of light. This work demonstrates how supramolecular interactions can be used to engineer versatile and functional polymer nanocomposite biomaterials and substantially increase the utility of this class of materials.

- (1) E. Appel, M. W. Tibbitt et al. (2015) *Nature Communications*, 6:6295.
- (2) E. A. Guzzi et al. (2019) *Small*, 15, 1905421.
- (3) E. A. Guzzi et al. (2021) *Biofabrication*, 13, 044105.
- (4) G. Bovone, E. A. Guzzi, S. Bernhard et al. (2021) *Advanced Materials*, 2106941.
- (5) S. Bernhard et al. *in preparation*

SYMPOSIUM SB05

Biohybrid and Soft Functional Interfaces
November 27 - December 5, 2023

Symposium Organizers

Herdeline Ann Ardoña, University of California, Irvine
Guglielmo Lanzani, Italian Inst of Technology
Eleni Stavrinidou, Linköping University
Flavia Vitale, University of Pennsylvania

Symposium Support

Bronze

iScience | Cell Press

10:30 AM *SB05.01.01

Modulation of Cell Signaling with Magnetic Nanomaterials Polina Anikeeva; Massachusetts Institute of Technology, United States

Magnetic fields offer unprecedented access to signaling processes deep within the body due to the low conductivity and negligible magnetic permeability of biological matter. Magnetic fields with a diversity of spatio-temporal characteristics can be transduced into stimuli perceived by biological receptors via tailored magnetic nanomaterials enabling remote modulation of cell function. In this talk, I will highlight physical principles guiding magnetic nanomaterials design with the goal of transducing magnetic fields into mechanical, thermal, chemical, and electric stimuli. I will further describe how these magnetic nanomaterials, coupled with biological mediators, can enable wireless modulation of cell signaling, organ physiology, and animal behavior. Finally, I will discuss strategies to deliver magnetic nanomaterials to specific cells and organs in the body laying a foundation for minimally invasive implant-free and surgery-free bioelectronic interfaces.

11:00 AM SB05.01.02

Directed Assembly Behavior of Optoelectronic Peptide Biomaterials for Excitable Systems Ze-Fan Yao, Yuyao Kuang, Emil Lundqvist and Herdeline Ann Ardoña; University of California, Irvine, United States

Organic conjugated materials are known to have molecular design-tunable optoelectronic properties while exhibiting intrinsic flexibility and the ability to form soft networks, which are suitable for biological interfacing. To better utilize these properties towards interfacing with living systems, more efforts are required to render biocompatibility and other physiologically relevant characteristics to these materials. Here, we design, synthesize, and characterize π -conjugated peptides with controllable assembly-disassembly behavior in aqueous solutions and directed anisotropic assembly on surfaces for biointerfacing. The peptidic segments serve as a biomimetic template for the stimuli-driven self-assembly process of π -conjugated monomers in aqueous solutions and on nanostructured polymeric surfaces. In solution, the supramolecular assembly and disassembly processes of the designed peptides can be accessed through a carbodiimide-fueled approach that instructs their self-assembly and hydrolysis-induced disassembly. On polymeric surfaces that have anisotropic topography and have chemically analogous π -conjugated chains as the central core of our peptide monomers, the resulting self-assembled optoelectronic peptides can be directed to form 1-D nanostructures on the surface nanofeatures. These peptide-modified surfaces present bioadhesive cues towards achieving cellular anisotropy, therefore providing a potential opportunity for directional stimulation of excitable cells. By having the capability to generate photoinduced currents, substrates bearing these assembled optoelectronic π -conjugated units offer the possibility of light-controlled behavior of excitable cells. In summary, this presentation will discuss the engineering of optoelectronic peptides that form controllable supramolecular structures capable of modulating the behavior of excitable cells and tissues via light.

11:15 AM SB05.01.03

Bioadhesive Polymer Semiconductors and Transistors for Intimate Biointerfaces Nan Li and Sihong Wang; University of Chicago, United States

Integrating biocompatible electronic devices with living biological tissues is emerging as a highly promising avenue for achieving the real-time measurement of biological signals with high spatiotemporal resolutions for biological studies and health monitoring. Polymer semiconductors-based transistors (e.g., organic electrochemical transistors (OECTs)) as an advanced sensing device, are highly desired for direct electrical biointerfacing due to their low operation voltage, mixed electron-ion conduction, and high sensitivity. To interface with wet and dynamically moving tissues, developing intrinsically bioadhesive polymer semiconductors can significantly improve the devices' conformability on tissue surfaces and signal acquisition sensitivity.

In this talk, I will present the design of a BioAdhesive polymer SemiConductor (BASC) film by creating a rationally designed polymer network with interpenetrating semiconducting polymers and adhesive brush polymers. The BASC films can form robust and rapid adhesion with bio-tissues (e.g., heart, lung, spleen) under gentle pressure, while providing high charge-carrier mobility. We further fabricate a bioadhesive OECT with the BASC as the active channel and demonstrate its use for reliably monitoring electrophysiological signals on an isolated rat heart and in vivo muscles.

11:30 AM SB05.01.04

MXene Hydrogels as Soft Bioelectronic Interfaces Raghav Garg¹, Stefanopolito², Spencer R. Averbeck¹, Yury Gogotsi² and Flavia Vitale¹; ¹University of Pennsylvania, United States; ²Drexel University, United States

Biological tissues and organs, such as the cardiac tissue and the brain, are mechanically soft and exhibit viscoelastic behavior. Real-time diagnosis and treatment of diseases of such electrically active tissues requires continuous electrophysiological monitoring stimulation. This has been achieved through implantable bioelectronic platforms. However, current implantable bioelectronics are composed of mechanically rigid materials such as metals (Au, Pt), metal oxides (IrOx), and semiconductors (Si). The large mechanical mismatch between the target tissues and the bioelectronics interfaces has been a bottleneck for chronic clinical applications. Although metal nanoparticles and carbon nanomaterials have been leveraged to fabricate electrically conductive hydrogel bioelectronics, they are limited by their electrochemical functionality, biocompatibility, and processability.

Here we leverage safe liquid-phase processing of two-dimensional $Ti_3C_2T_x$ MXene to fabricate MXene-based hydrogels for implantable bioelectronic interfaces. We achieve a high-density network of MXene flakes by directly crosslinking individual MXene flakes using transition metal ions. The matrix-free structure of the MXene hydrogels endows them with high electrical conductivity and low electrochemical impedances, thus facilitating their integration into soft bioelectronics for electrophysiological recordings with high signal-to-noise ratio. The capacitive nature of $Ti_3C_2T_x$ further allows the hydrogels to exhibit high charge injection capacities for safe delivery of electrical stimulation to target tissues. Finally, we demonstrate modulation of the mechanical properties of the packaged hydrogels by altering the composition and degree of cross-linking of the alginate-based insulation. Our results underscore the application of MXene-based soft bioelectronics in studying neural function and disease pathologies, as well as developing neuromodulation paradigms.

11:45 AM SB05.01.05

Optimizing the Pore Structure of 3D Conducting Polymer Scaffolds for Bioelectronic Devices Rachana Acharya, Douglas van Niekerk, Aimee Withers and Roisin Owens; University of Cambridge, United Kingdom

The integration of 3D tissue-engineered microporous scaffolds based on conductive polymers (CPs) into bioelectronic devices have led to the possibility of dynamic monitoring of biological phenomena through electrical measurements. The 3D structure and morphology of the porous scaffolds mimics the topographical features of human physiology, while the electrically conductive nature of the polymers allows for electrical measurements for label-free monitoring and live-sensing of cells. 3D scaffolds based on the polymer poly(3,4-ethylenedioxythiophene):poly(styrenesulfonate) (PEDOT:PSS) prepared by the freeze drying process have been the focus of many studies and well integrated into bioelectronic devices such as electrodes[1] and organic electrochemical transistors[2].

The freeze-drying process involves freezing the aqueous dispersion of the conducting polymer, followed by the sublimation of the ice crystals by lowering the pressure in the system, leaving behind a porous network of the conducting polymer. This porous network is representative of the physiological tissue structure, making the ice nucleation and crystallization a crucial component of the scaffold fabrication process. A deeper understanding of the freeze drying process and a higher degree of control on the freezing parameters will help establish the correlation between the material properties of the scaffolds and the biomimetic tissue engineering requirements for optimum cell culture platforms.

Three different freeze drying protocols were employed, with a pre-cooling treatment used before the freeze-drying process. Two different pre-cooling rates, 0.5 °C/min and 1 °C/min along with a control protocol with no treatment were designed to prepare different scaffold types. Within each protocol, the freezing rate was varied between 0.2 °C/min and 1 °C/min and the thermal profile of the aqueous dispersion was recorded during the entire fabrication process.

The influence of the different protocols and freezing rates on the pore size and structure was examined by scanning electron microscopy and micro-computed tomography. Pores of circular and elongated ellipses were observed by SEM and a pore size distribution (the longest dimension of the ellipsoid) between 80 μ m and 220 μ m was measured. It was observed that a higher cooling rate generated larger pores with more elongated pore morphology as well as a wider pore size distribution. The pre-cooling treatment with 0.5 °C/min cooling rate was most useful in generating scaffolds with a more homogenous pore structure and a pore size of approximately 100 μ m.

The different scaffolds were incorporated into electronic devices such as transmembrane electrodes to characterize the electrical properties and evaluate the reproducibility of the scaffolds

prior to cell culture. No significant change in the electrochemical impedance spectra was observed despite the large difference in porosity of the different scaffolds. In addition, the different scaffolds were used to host and monitor biological cells like fibroblasts and endothelial cells. Cell growth and proliferation in the different scaffolds was also monitored by immunofluorescence microscopy. It was observed that a pre-cooling protocol and a freezing rate of 0.5°C/min helps to fabricate scaffolds with an optimized, uniform and homogenous pore morphology. This design protocol is highly beneficial in reducing the random artifacts of the nucleation process and generating scaffolds highly conducive to cell growth and survival and to create a versatile bioelectronic platform for studying in-vitro cell models.

References:

- [1] C. Pitsalidis, D. van Niekerk, C.M. Moysidou, A.J. Boys, A. Withers, R. Vallet, R.M. Owens, *Sci. Adv.* 8 (2022) eabo4761.
[2] C. Pitsalidis, M.P. Ferro, D. Iandolo, L. Tzounis, R.M. Owens, *Sci. Adv.* 4 (2018) eaat4253.

SESSION SB05.02: Bioelectronic Interfaces II
Session Chairs: Herdeline Ann Ardoña and Guglielmo Lanzani
Monday Afternoon, November 27, 2023
Hynes, Level 1, Room 102

1:30 PM *SB05.02.01

3D Bioelectronic Models of Gut, Brain and Lung Roisin Owens; University of Cambridge, United Kingdom

Physiologically relevant in vitro human models are urgently required to bridge the gap between over-simplified 2D in vitro models and ill-suited animal models, for drug discovery and disease modelling. Bringing together principles of materials science, tissue engineering, 3D cell biology and bioelectronics, we are building advanced models of the gut, brain (neurovascular unit) and the lung. In the case of the gut and NVU, our aim is to elucidate the role of microbiota in the gut-brain axis communication, a particularly challenging system to model with lab animals. In the case of the lung, our interest is in modelling the air-liquid interface to more accurately study lung disease.

Our models are based on the use of electroactive scaffolds which can host tissues, but also monitor their formation, and later their status when challenged with a pathogen or target molecule. Our strategy is to build a stromal layer with the scaffold and layer epithelial or endothelial models on top, preserving tissue stratification. Our most recent work has adapted these scaffolds to the well-known Transwell format, to allowed continued access to both apical and basal aspects.[1] As well as traditional readouts such as immunofluorescence, or biochemical analyses of media, our continuous electrical monitoring readouts from our electroactive scaffolds gives us real-time data on the tissue health.

- [1] Charalampos Pitsalidis et al., 'Organic Electronic Transmembrane Device for Hosting and Monitoring 3D Cell Cultures', *Science Advances* 8, no. 37 (16 September 2022): eabo4761, <https://doi.org/10.1126/sciadv.abo4761>.

2:00 PM SB05.02.02

Harnessing Protein Engineering and Bioelectronics for Sensory Perception on a Chip Eleanor Best, Zhongmou Chao, Poompol Buathong, Peter Frazier and Susan Daniel; Cornell University, United States

As humans, our perception of the world relies on the function of our powerful sensory organs. Olfaction in particular is well-documented as a biosensing modality across species, as dogs and insects have been shown to detect the early onset of disease or even harmful substances as part of airport security protocols. As specific ligands bind to their corresponding sensory receptors, they trigger a unique combination of activated neurons that are interpreted downstream. By merging interspecies sensory systems with bioelectronics, we can create a novel biosensor and simulate sensory perception on a chip. Whilst previous platforms have leveraged gas sensors for compound detection, our system instead employs carefully selected mammalian and insect proteins to replicate and enhance sensory perception. By using innovative protein engineering techniques and deliberately designed electronic devices, we have created a fully customizable approach to sensory perception in a way that carefully combines nature's original biosensors with synthetic biology. This unique platform provides a novel approach to the conventional biosensor with immense potential for security and medical applications.

2:15 PM *SB05.02.03

Engineering Personalized Tissue Implants: From 3D Printing to Bionic Organs Tal Dvir; Tel Aviv University, Israel

In this talk, I will describe cutting-edge bio and nanotechnologies for engineering functional tissues and organs, focusing on the design of new biomaterials mimicking the natural microenvironment or releasing biofactors to promote stem cell recruitment and tissue protection. In addition, I will discuss the development of patient-specific materials and 3D printing of personalized vascularized tissues and organs. Finally, I will show a new direction in tissue engineering, where micro and nanoelectronics are integrated within engineered tissues to form cyborg tissues and bionic organs.

2:45 PM BREAK

3:15 PM *SB05.02.04

Deformable Composites: From Photostimulation to Living Bioelectronics Bozhi Tian; University of Chicago, United States

The field of electronic and photonic biointerfaces continues to evolve, with flexible and living composites playing a key role in advancing the development of multifunctional devices such as sensors and modulators. Our research focuses on creating non-genetic approaches for biological modulation and sensing across different length scales. This presentation will provide insights into some of our recent projects. This includes our work related to photostimulation within clinical environments. We have made new progress in the development of a nanoporous/non-porous heterojunction, exemplifying the level of precision and control achievable in bioelectronic therapies. We have also developed a granular system aimed at focal adhesion in bioelectronics and other interfaces for regenerative medicine. Additionally, we have begun exploring the integration of living cells with wearable bioelectronic devices, a new direction within the sphere of living bioelectronics. Our primary goal is to transition these basic studies of modulation tools into applicable clinical practices, with the potential to influence therapeutic strategies and improve patient outcomes. As I conclude the presentation, I will highlight our future research directions. These are designed to further contribute to the extensive field of biological modulation and sensing, with a specific focus on applications that could have a significant impact in the clinical setting.

3:45 PM SB05.02.05

Tissue-Embedded 3D Stretchable Nanoelectronics for Multimodal Charting of the Human Stem Cell-Derived Organoids Ren Liu, Qiang Li, Zuwan Lin, Xin Tang and Jia Liu; Harvard University, United States

The development of human induced pluripotent stem cells (hiPSCs) technology has revolutionized the field of disease modeling and holds immense potential for personalized regenerative cell therapies. A comprehensive understanding of stem cell-derived tissues and organoids requires advanced multimodal techniques capable of capturing cell functions with high spatiotemporal resolution in three-dimensional (3D) tissues, profiling numerous genes in recorded cells, and performing multimodal computational analysis. However, none of the existing technologies fulfill these requirements.

In this presentation, I will begin by introducing the development of soft, stretchable mesh nanoelectronics that mimic the physical and mechanical properties of biological tissues. We can distribute these stretchable tissue-like bioelectronics throughout the entire 3D organoids by their organogenetic processes. By establishing seamless and noninvasive connections between electrodes and cells, we can achieve long-term stable electrical contacts with progenitor or stem cells, capturing the emergence of single-cell action potentials. This facilitates continuous, long-term recording from various types of 3D organoids during their development.

Next, I will demonstrate how this technique enables the long-term stable mapping of human 3D cardiac microtissues for the characterization of their functional maturation. Specifically, I will discuss an example in which stretchable mesh electronics were embedded with hiPSC-derived cardiomyocytes (hiPSC-CMs) and hiPSC-derived endothelial cells (hiPSC-ECs). By developing machine learning-based pseudotime trajectory inference of the long-term cardiomyocyte electrical signals from multiple samples, we can quantify the electrical phenotypic transition path during development. Our results showed that hiPSC-ECs drive remarkable hiPSC-CM electrical maturation via multiple intercellular pathways.

Finally, I will discuss our efforts to combine in situ single-cell RNA sequencing with flexible bioelectronics, a methodology we term "in situ electro-seq". This technique allows us to link cell molecular gene expression with electrical activities. Specifically, I will discuss how in situ electro-seq enables systematic and simultaneous investigation of single-cell electrophysiology and gene expression across hiPSC-CMs during their development. Additionally, I will discuss the potential of using in situ electro-seq to create spatiotemporal multimodal maps in electrogenic

tissues, thereby potentiating the discovery of cell types and gene programs responsible for electrophysiological function and dysfunction.

4:00 PM SB05.02.06

Bioelectronic *In Vitro* Cell Membrane Models for Investigating Intestinal Host-Pathogen Interactions [Reece McCoy](#)¹, [Jeremy Treiber](#)², [Alberto Sallee](#)², [George G. Malliaras](#)¹ and [Roisin Owens](#)¹; ¹University of Cambridge, United Kingdom; ²Stanford University, United States

The early stage of pathogen-related diseases often depend on the initial interaction between the pathogen, or its secretions, and the host cell membrane. Interfacing cells with electronics allows for quantitative real time monitoring of barrier integrity. Organic electronics coupled with electrochemical impedance spectroscopy (EIS) are used to probe host-pathogen interactions directly with enterocyte plasma membranes using native supported lipid bilayers which are representative of apical and basolateral surfaces of the intestinal epithelium. PEDOT:PSS is used in both microfabricated planar electrode arrays which can support the formation of supported lipid bilayers. The Caco-2 adenocarcinoma cell line is used to develop a model that reflects *in vivo* conditions. Cells are differentiated and polarised for 21 days and chemical vesiculation induced to extract small membrane vesicle biopsies of the apical and basolateral surfaces before being used to form supported lipid bilayers. Fluorescence microscopy is employed to confirm bilayer fluidity with fluorescence recovery after photobleaching (FRAP). EIS is used to determine the impedance of the bilayer across frequencies and models are fit to the data to extract resistance and capacitance values. The ADAM10-receptor mediated effects of *Staphylococcus aureus* alpha hemolysin toxin is demonstrated and found to be highly dependent on the epithelial membrane surface it encounters. The presence on the receptor in the apical bilayer potentiates the effect of alpha hemolysin leading to a pronounced decrease in membrane resistance compared to the basolateral bilayer. Organic bioelectronics are used to monitor bilayer and barrier impairment caused by pathogens and their secretions. EIS coupled with conventional biological techniques can be used help elucidate pathogen invasion mechanisms and aid discovery of potential therapeutics.

4:15 PM SB05.02.07

Multiscale Material Engineering of a Conductive Polymer/Liquid Metal Platform for Stretchable and Biostable Human-Machine-Interface Bioelectronic Application [Huanan Zhang](#); University of Utah, United States

Liquid-metal-based stretchable bioelectronics can conform to the dynamic movements of tissues and enable human-interactive biosensors to monitor various physiologic parameters. However, the fluidic nature, surface oxidation, and low biostability of the liquid metals have limited the long-term use of bioelectronics. Here we have developed a rationally designed material engineering approach to overcome these challenges in liquid metal bioelectronics. To our knowledge, this is the first demonstration of stretchable, leak-free, and highly conductive gallium-based bioelectronic devices with exceptional biostability and electrochemical properties. We first utilized unique gallium oxide properties to create 3D microscale wrinkled structures on the gallium surface. Then, gold nanoparticles and biostable poly(3,4-ethylenedioxythiophene) were successively deposited on the wrinkled liquid metal surface. We demonstrated this multilayer encapsulation material could conform to the stretching deformation and showed excellent environmental stabilities while maintaining high electrical properties. Electromyographic measurements were used to evaluate the bioelectrical performance of the stretchable electronics, and the results demonstrated the encapsulated liquid metal device could outperform bare liquid metal devices. Finally, a sensory feedback study demonstrated our liquid metal bioelectronic device could record precise physiologic signals to control robots for mimicking dexterous hand gestures. This study opens the possibility of chronic liquid-metal-based stretchable bioelectronics.

4:30 PM SB05.02.08

Conformable Multimodal Sensory Facemask for Decoding Biological and Environmental Signals [Jin-Hoon Kim](#) and [Canan Dagdeviren](#); Massachusetts Institute of Technology, United States

Facemasks are considered to be a key instrument in reducing exposure to viruses and other environmental hazards such as air pollution. Current wearable electronics applicable to the facemask have been designed only to monitor biological information such as breathing patterns. However, it remains difficult for the public to assess the status of their facemasks with regard to wearing habits and fit quality. In this work, we developed a widely-deployable, conformable, miniaturized sensory interface, which seamlessly attaches onto the internal side of any user-supplied facemask without compromising fit and protection quality, along with a user-interface capable of interpreting a participant's mask-wearing behavior under various use-case scenarios. Multimodal signals from a variety of sensors were wirelessly transmitted to a server through a custom-made mobile app. Based on the collected data, it was shown that various biological signals related to the signature of infectious diseases could be monitored while determining the fit status of the facemask without using a conventional mask fit tester. A machine learning algorithm was further used to enable the reliable decoding of the facemask position. The novelty of this work lies not only in the system integration, but also in the development of devices which provides real-time mask fit and position analysis, which may benefit medical institutes, industries and the general public in selecting proper facemasks and maintaining a desired mask fit. Additionally, our work could be deployed to multidisciplinary studies such as human behavioral and social sciences to analyze the fit change in real world situations.

4:45 PM SB05.03.08

Paper-Based Wearable Patches for Real-Time, Quantitative Lactate and Temperature Monitoring [Elisabetta Ruggeri](#)¹, [Giusy Matzeu](#)¹, [Giulia Guidetti](#)¹, [Andrea Vergine](#)², [Marco Lo Presti](#)¹, [Giuseppe De Nicolao](#)² and [Fiorenzo Omenetto](#)¹; ¹Tufts University, United States; ²Università degli Studi di Pavia, Italy

Wearable sensors are establishing themselves as options for real-time continuous health monitoring in health care and wellness. In particular, the use of flexible interfaces that conform to the skin have attracted considerable interest for the extraction of meaningful physiological and pathological information through continuous and painless sampling and analysis of biofluids. In contrast, conventional techniques for biomarkers analysis are difficult to adapt to real-time portable monitoring due to their invasive sampling protocols, biosample preparation and reagent stabilization. In this work, we present shelf-stable, non-invasive, paper-based colorimetric wearable lactate and temperature sensors. These sensors exploit the ability of silk to control the concentration, print, and functionally preserve labile transducing biomolecules in the format of a shelf-stable digital patch for optical readout. This novel approach overcomes major challenges associated with the commercialization of colorimetric wearable sensors (e.g., enzyme thermal instability, narrow sensing range, low sensitivity, and qualitative response) by showing a combination of unprecedented stability (i.e., up to 2 years in refrigerated conditions), wide sensing range, and high sensitivity. Additionally, real-time quantitative signal readouts are achieved using machine learning-driven image analysis enabling physiological status evaluation with a simple smartphone camera.

SESSION SB05.03: Poster Session I: Biohybrid Systems and Devices

Session Chairs: [Herdeline Ann Ardoña](#) and [Guglielmo Lanzani](#)

Monday Afternoon, November 27, 2023

Hynes, Level 1, Hall A

8:00 PM SB05.03.01

Large-Area Photo-Patterning of Initially Conductive EGaIn Particle-Assembled Film for Soft Electronics [Gun-Hee Lee](#); KAIST, Korea (the Republic of)

Eutectic-gallium-indium particle (EGaIn*) is considered one of the promising conducting materials for soft electronics due to its enhanced mechanical stability and stable conductance under strain compared to bulk EGaIn. However, its practical applicability has thus far been limited due to the challenges of achieving electrical conductivity and the incompatibility with well-developed fabrication strategies. Here, we report materials and manufacturing methods that allow large-area multi-layered patterning of 'polystyrene sulfonate (PSS)-attached EGaIn* (EGaIn*:PSS)' thin-film with the conventional cleanroom process. PSS enhances the stability of EGaIn*, which allow uniform thin-film coating and photographic lift-off at a wafer-scale down to 10 μm features of varying thicknesses. Using dimethyl sulfoxide as the solvent during lift-off induces cohesion between EGaIn*:PSS, resulting in initial electrical conductivity without an additional activation process. Demonstrations of stretchable display, wearable multilayer pressure sensing systems, and soft artificial finger validate the versatility and reliability of this manufacturing strategy for soft electronics.

8:00 PM SB05.03.02

Multifunctional Intelligent Wearable Devices using Logical Circuits of Monolithic Gold Nanowires [Sang Hoon Hong](#), [Tae Yeon Kim](#) and [Sei Kwang Hahn](#); Pohang University of Science and Technology (POSTECH), Korea (the Republic of)

Although multifunctional wearable devices have been widely investigated for healthcare systems, augmented/virtual realities and telemedicines, there are few reports on multiple signal monitoring and logical signal processing by using one single nanomaterial without additional algorithms or rigid application-specific integrated circuit (ASIC) chips. Here, we develop multifunctional intelligent wearable devices using monolithically patterned gold nanowires for both signal monitoring and processing. Gold bulk and hollow nanowires show distinctive electrical properties with high chemical stability and high stretchability. In accordance, the monolithically patterned gold nanowires can be used to fabricate the robust interfaces,

programmable sensors, on-demand heating systems and strain-gated logical circuits. The stretchable sensors show high sensitivity for strain and temperature changes on the skin. Furthermore, the micro-wrinkle structures of gold nanowires exhibit the negative gauge factor, which can be used for strain-gated logical circuits. Taken together, this multifunctional intelligent wearable device would be harnessed as a promising platform for futuristic electronic and biomedical applications.

8:00 PM SB05.03.03

From Network to Channel—Crack-Based Strain Sensors with High Sensitivity, Stretchability and Linearity via Strain EngineeringWanyiWang and YoufanHu; Peking University, China

High-performance stretchable strain sensors are indispensable for mechanical deformation detection in electronic skin applications such as health monitoring and human-robot interfaces. Thus far, achieving a stretchable strain sensor with a high sensitivity that works linearly over a wide working range is still a great challenge. Among various applicable working mechanisms of strain sensors, crack-based strain sensors have the advantages of flexible material selection, easy fabrication, and high sensitivity. Here, we propose a universal strain engineering strategy that introduces an inhomogeneous spatial distribution of stress, which results in a distinguished crack density distribution in space and a critical state of crack propagation behavior between network and channel morphologies. By controlling the occurrence of the critical state, strain sensors are capable to perform high sensitivity, stretchability, and linearity simultaneously. The strain sensors can be tuned to realize a gauge factor of 690.95 in a linear working range of 0-40% ($R^2 = 0.993$) or a gauge factor of 113.70 in a larger linear working range of 0-120% ($R^2 = 0.999$). Intraocular pressure monitoring has been demonstrated based on these sensors to show their great application potential.

8:00 PM SB05.03.04

Stimuli Recognition by Polydiacetylene using Hyperspectral MicroscopyJialiChen and KaoriSugihara; The University of Tokyo, Japan

Introduction
Polydiacetylene (PDA)-based chem/bio sensors have garnered significant attention due to their exceptional biocompatibility and ability to respond to various signals, such as heat, pH, force, light, and biomolecules. They exhibit visual blue-to-red color changes and fluorescence emission. However, the poor reproducibility of PDA sensors has hindered their practical implementation. The varying structures of PDA, even under identical synthesis conditions, make it challenging to achieve consistent and highly sensitive responses during mass production. Hyperspectral microscopy, initially developed for geology exploration and earth morphology observation, provides precise spectral analysis at the pixel level with high spatial and spectral resolutions. Recent advancements in detector and computing technology have expanded its applications to fields like agriculture, food, and medicine. In this work, we employed hyperspectral microscopy to visualize the inconsistent distribution of PDA structural domains, which contributes to the poor reproducibility and variations in PDA responses. Additionally, these mixtures of PDA structures exhibit distinct blue-to-red transition pathways upon stimulation, indicating their potential for stimulus identification.¹

Method

We utilized hyperspectral microscopy to capture detailed spectral information at the sub-crystal level of PDA, allowing differentiation among various PDA structures. Using spectral classification techniques, such as spectral angle mapper, we created distribution maps of PDA structural domains within bulk crystals. Moreover, we developed a pixel transition tracking method using MATLAB to quantitatively monitor the colorimetric response of these structural domains. Based on these technologies and discoveries, we observed that PDA exhibits different response patterns to various stimuli, such as heat and pH. Our aim was to comprehensively understand the dynamic transition pathways associated with PDA structural domains and their response patterns to stimuli.

Result and Discussion

We uncovered mixtures of PDA structural domains within blue and red bulk crystals, which explain the main source of poor reproducibility in traditional PDA sensors. It was the first time that hyperspectral microscopy was applied to examine the non-uniform property of PDA sensors, and we developed a new interpretation tool to track their transition pathways. Different structures of PDA displayed varying affinities to stimuli, leading to unique transition patterns specific to the type of stimulus applied. This indicates that the stimuli leave a potential fingerprint on PDA. The observed good reproducibility holds promise for PDA to serve as an identification array for molecules in the future.

Reference

(1) **Chen, J.**; Zheng, J.; Hou, Y.; Sugihara, K. Colorimetric Response in Polydiacetylene at the Single Domain Level Using Hyperspectral Microscopy. *Chem. Commun.* **2023**, 59 (25), 3743–3746. <https://doi.org/10.1039/D2CC06803F>.

8:00 PM SB05.03.05

Skin-Like Multimodal Sensors Based on Iontronics and PiezoelectricityLirenWang^{1,2,3}, PeterZalar⁴, YuanyuanZhou^{1,3,1} and NaojiMatsuhisa^{1,3,2}; ¹The University of Tokyo, Japan; ²Keio University, Japan; ³Institute of Industrial Science, The University of Tokyo, Japan; ⁴Holst Centre / TNO, Netherlands

The skin possesses softness, stretchability, and the ability to sense a variety of environmental signals, including temperature, slow deformation (static strain), and rapid vibration (dynamic strain). Previous attempts to mimic skin with multimodal sensors have been limited by their multimodal sensing capability^[1] and interference between different types of signals^[2]. In this work, we demonstrate a skin-like multimodal sensor capable of sensing three outputs - temperature, static strain, and dynamic strain - using a soft piezoelectric and ionic composite material. Our sensor is constructed by sandwiching the ionic and piezoelectric composite between a pair of silver-nanowire-based stretchable conductors. Electrochemical impedance provides readings of temperature and static strain, while piezoelectricity measures dynamic strain. We have systematically investigated the influence of ionic conductivity and elasticity of the composite on sensitivity and stretchability. The high conductivity of the silver-nanowire-based stretchable electrodes had a negligible effect on the signal readout. The sensor provided accurate strain-insensitive temperature signals (error ~0.28°C) under 50% strain, and a modest longitudinal piezoelectric coefficient (d_{33}) of ~10 pC/N. Our sensors display skin-like softness and multimodal sensing capability, features which are highly beneficial for human health monitoring and robotic skin applications.

[1] I. You et al. Artificial multimodal receptors based on ion relaxation dynamics[J]. *Science*, 2020, 370(6519): 961-965.

[2] Liu H, et al. A flexible multimodal sensor that detects strain, humidity, temperature, and pressure with carbon black and reduced graphene oxide hierarchical composite on paper[J]. *ACS applied materials & interfaces*, 2019, 11(43): 40613-40619.

8:00 PM SB05.03.06

Decoding Silent Speech Commands from Articulatory Movements Through Soft Magnetic Skin and Machine LearningPenghaoDong and ShanshanYao; Stony Brook University, The State University of New York, United States

Silent speech recognition is a promising technique to restore spoken communication for individuals with voice disorders and to facilitate intuitive communications when the acoustic signal is unreliable, inappropriate, or undesired. However, the current methodology for silent speech faces several challenges, including bulkiness, obtrusiveness, limited portability, and susceptibility to interferences. In this work, we present a wireless, unobtrusive, and robust silent speech interface for capturing and decoding speech-relevant movements of the temporomandibular joint. Our solution employs a single ultrasoft magnetic skin placed behind the ear for wireless and more socially acceptable silent speech recognition, greatly alleviate concerns associate with existing interfaces based on face-worn sensors, including large number of sensors, highly visible interfaces on the face, and obtrusive interconnections between sensors and testing unit. Through optimizations in material composition, sensor structure, and sensing location, we present a lightweight wireless sensor that can conform to the skin surface to capture subtle movements induced by speech. With machine learning-based signal processing techniques, good speech recognition accuracy is achieved (92.7% accuracy for phonemes, 85.6% for word pairs from the same viseme group, and 96.7% for sentences/phrases). Moreover, the reported silent speech interface demonstrates robustness against noises from both ambient environment and user's daily motions. Finally, we illustrate the great potential in assistive technology and human-machine interactions through two proof-of-concept demonstrations –silent speech enabled smartphone assistant and drone control.

8:00 PM SB05.03.07

Wearable Pad for Continuous Monitoring of the Pressure at the Lower-Limb Socket InterfaceRuiPereira and VitorSencadas; University of Aveiro, Portugal

The data acquired from the biomechanics mapping at the socket-stump interface is referred to as a direct indicator of a comfortable socket fit, and multiple types of sensing approaches have been used to quantify the internal pressure distribution on a prosthetic socket. In this work, an elastomeric capacitive sensor pad device able to be inserted at the distal area of a prosthetic socket was produced by blending polydimethylsiloxane (PDMS) with Ecoflex. By adjusting the PDMS:Ecoflex ratios in the mixture, the mechanical properties of the pad could be tuned to promote comfort to the user. The wearable sensor pad electromechanical characterization revealed an electrical response that follows the applied mechanical inputs, with a Gauge Factor between 0.6 ± 0.04 and 1.3 ± 0.03 and a sensitivity ranging from $4.6 \times 10^{-4} \pm 0.14 \times 10^{-4} \text{ kPa}^{-1}$ to $7.25 \times 10^{-4} \pm 1.2 \times 10^{-4} \text{ kPa}^{-1}$. The device presented high durability (1,000 cycles), linearity, repeatability and stability in a pressure range from 0 to at least 700 kPa. Further, the developed wearable device performance was validated during in-vitro simulations using a real prosthetic socket and a biofidelic residual limb, and the results gathered show similar electromechanical performance. Finally, the wearable sensor was placed in a liner inside the prosthesis and fitted to

a user to monitor the pressure distribution that occurs between the residual limb and the socket during the walking. The results demonstrated the feasibility of employing the developed device within the socket prosthesis and to gather important quantitative data to provide enhanced socket design and comfort.

8:00 PM SB05.03.09

An Advanced Dermal Tissue-Embedding Mesh Sensor for High-Resolution IL-6 DetectionJohn T. Williams¹, Hanie Yousefi¹, Xudong Ji¹, Hope Burks², Jonathan Rivnay¹ and Shana Kelley^{1,2}; ¹Northwestern University, United States; ²Chan Zuckerberg Biohub Chicago, United States

In this study, we explore the development and application of a highly sensitive, high temporal-resolution dermal tissue-embedding mesh sensor. We functionalize this sensor using molecular pendulums developed by J. Das *et al.* to measure the concentration of Interleukin-6 (IL-6), a key biomarker in skin inflammation. Miniaturized organ models, including organoids and spheroids, serve as powerful platforms for investigating human physiology and pathology *in-vitro*, and bioelectronic sensors effective, complementary tools for monitoring them. Current bioelectronic sensor technologies provide insights into thermal, electrophysiological, optical, and oxygenation parameters within these models, yet robust and high-fidelity biochemical sensors remain a significant gap. Our device bridges this gap, offering microsecond resolution in the detection and tracking of IL-6 proliferation and movement. This work paves the way for high-resolution interrogation of skin inflammation, significantly enriching our understanding of inflammation, and providing a powerful tool for potential drug efficacy assessment.

8:00 PM SB05.03.10

Poly Vinyl Alcohol and Carbon Nanotube Based Scaffolds for Engineered BiosensorsRyan E. Jaworski and Isaac Macwan; Fairfield University, United States

Biosensors are analytical devices that can turn biological responses into electrical signals which can be very useful in the diagnostics of numerous diseases. This work looks into the fabrication of an impedance based biosensor using electrospun Poly Vinyl Alcohol (PVA) and Carbon nanotubes (CNTs) to be used in conjunction with bacteriorhodopsin contained in a purple membrane. Dispersions of PVA are created with and without CNTs in deionized (DI) water, which are then utilized to synthesize porous electrospun nanofibrous scaffolds with fiber diameters ranging from 150nm to 250nm. The detection technique utilized for the fabricated biosensor is through the quantification of electrochemical impedance via the Electrochemical Impedance Spectroscopy (EIS). The parameters for both electrospinning and EIS are carefully optimized to achieve porous nanofibrous scaffolds having expected fiber diameter, porosity and impedance. The parameters which are optimized for the electrospinning process include the flow rate, collection distance, voltage, viscosity of the polymer CNT solution, and the type and configuration of the collector. Similarly, the parameters for the EIS include optimum potential of the applied small ac signal in mV, frequency range, electrolyte concentration and the type of electrodes and their configuration. This careful optimization of the parameters would enable the fabrication and the dynamic response of the designed biosensor to be able to hold its integrity through the entire process of characterization and testing. Two different forms of CNTs are used, which are single-walled carbon nanotubes (SWNTs), and multi-walled carbon nanotubes (MWCNTs). The two different SWNTs used in this study have a (6, 5) chirality and also mixed metallic and semiconducting chirality to assess the differences in the biosensor performance based on the type of SWNT and its comparison to the MWCNTs. The synthesized scaffolds are also characterized through atomic force microscopy (AFM) and scanning electron microscopy (SEM), and compared to control samples without CNTs. The synthesized scaffolds are then tested for performance through the detection of a light sensitive protein bacteriorhodopsin (BR), which is a membrane protein found in Archaea, most notably Halobacteria. The primary function of the protein is in its use as a proton pump across the cell membrane and its novel characteristic to detect light of different wavelengths make it attractive for application in optical memory. Although this is a specific example, these scaffolds can accommodate different types of analyte for biosensors in many applications.

8:00 PM SB05.03.11

Fabrication of a Partially Porous Microneedle Array Through Stepwise Integration of Porous and Non-Porous Poly(glycidyl methacrylate)Hiroyuki Kai^{1,2} and Akichika Kumatani^{3,4,2}; ¹Toyo University, Japan; ²Tohoku University, Japan; ³The University of Tokyo, Japan; ⁴Presto, Japan Science and Technology Agency, Japan

The microneedle array, a two-dimensional array of small needles with the height of a few hundreds of micrometers, are being actively studied for the application for minimally invasive transdermal drug delivery and biosensing. Among microneedles of various structures, porous microneedles have the advantages that they have large specific surface area that can be advantageous for high drug loading on the internal pore surface as well as highly sensitive biosensing taking advantage of high electrode area.

Porous polymer microneedle arrays made of crosslinked poly(glycidyl methacrylate) (PGMA), pioneered by Nishizawa's group, have advantages such as easy fabrication by photopolymerization in a mold and tunability of the properties by molecular design [1] as well as capability for functionalization by organic chemistry to fabricate functional microneedles such as organic/inorganic hybrid microneedle electrodes [2]. The existing porous PGMA microneedle arrays are porous throughout the microneedle body: both the base substrate and needles are homogeneously porous. Therefore, the amount of drug and sensor molecules interfaced with skin and biological fluid cannot be controlled, which prevents the quantitative control of drug release and reproducible amperometric biosensing. Considering the porous PGMA microneedles for quantitative applications, spatial control of porosity in the microneedle body is important. Monomers (glycidyl methacrylate, and trimethylolpropane trimethacrylate, and triethylene glycol dimethacrylate) are photopolymerized by the irradiation of ultraviolet light in the presence of a photoinitiator to obtain crosslinked PGMA. In the presence of poly(ethylene glycol) (PEG) as a porogen (a template material to make pores), polymerized PGMA has macropores with the diameter of ~1 μm [3]. Therefore, control of addition of the porogen can be utilized to obtain spatially controlled porosity.

In this study, we present a two-step process for creating a porous PGMA microneedle array with a two-section structure: a porous needle section and a non-porous substrate, both made of PGMA. First, the monomer solution mixed with the porogen was poured into an elastic mold of a microneedle array and excess solution over the needle section was removed by carefully scraping on the mold, followed by the polymerization by ultraviolet light irradiation to fabricate porous needles. Then, the monomer solution without the porogen was poured over the polymerized needle section in the mold and polymerized to fabricate a non-porous base substrate. After the removal of the fabricated microneedle array from the mold, the needle section was in a white opaque color resulting from macroporous structures of PGMA and the base substrate was colorless and transparent, indicating PGMA in the substrate was non-porous. The two sections were integrated well and no significant breaking of needles was observed. Water absorption properties of the fabricated microneedle arrays were measured by immersing them into water and measuring the change in total mass. The amount of water absorbed by the partially porous microneedle array was significantly smaller than the homogeneously porous microneedle array, yet higher than homogeneously non-porous microneedle array. The developed two-layer, partially porous microneedle array is potentially useful for quantitative control of drug delivery and reproducible biosensing.

[1] L. Liu *et al.*, *RSC Adv.*, **6**, 48630 (2016).

[2] H. Kai and A. Kumatani, *J. Phys. Energy*, **3**, 024006 (2021).

[3] J. Courtois, E. Byström, and K. Irgum, *Polymer*, **47**, 2603 (2006).

8:00 PM SB05.03.12

Highly Accurate Multiplexed Nanoplasmonic Detection of MicroRNAs using Splinted LigationSihwa Joo¹, Younju Sung², Na Rae Jo³, Yong-Beom Shin² and Mina Lee¹; ¹Korea Research Institute of Standards and Science, Korea (the Republic of); ²Korea Research Institute of Bioscience and Biotechnology (KRIBB), Korea (the Republic of); ³Korea Institute of Machinery and Materials (KIMM), Korea (the Republic of)

MicroRNAs (miRNAs) are short, non-coding single-stranded RNAs that regulate gene expression by binding to mRNAs. Because miRNAs are abnormally expressed in cancer cells, they have been considered an important cancer biomarker. However, the short length and high homology of miRNAs make them difficult to detect accurately. In this study, we developed a highly accurate miRNA detection method using a multi-channel localized surface plasmon resonance (LSPR) sensing platform. MiRNAs were labeled with a DNA probe using splinted ligation and immobilized on a gold nano-truncated cone (GNTC) array chip fabricated by nanoimprinting. After enzyme-assisted precipitation was performed, the LSPR spectral shift was measured as a function of miRNA concentration. Three miRNAs (miR-34c, miR-99a, and miR-125b) were sensitively detected with the limit of detection ranging from 1.8 to 26.1 fM. Single nucleotide variation (SNV) was clearly discriminated with high contrast. In addition, several miRNAs could be simultaneously detected in the multi-channels of a GNTC chip with high quantitative accuracy. Furthermore, we demonstrated the clinical applicability of our method by accurately detecting miRNAs in total RNA samples extracted from cancer cells.

8:00 PM SB05.03.13

Flexible Organic Microelectrode Arrays for Long-Term Functional Characterisation of Brain Organoids at the Air-Liquid InterfaceBelquis Haider, Sagnik Middy, Daniel J. Lloyd-Davies Sánchez, Madeline A. Lancaster, George G. Malliaras and Gabriele S. Kaminski Schierle; University of Cambridge, United Kingdom

Organoids are three-dimensional biological models that have revolutionised *in vitro* research by replicating the structure and function of organs. Despite their remarkable potential, the limited diffusion of oxygen and nutrients to their cores has impeded their growth. Recent advances have involved culturing organoids at the air-liquid interface using organotypic slice culture techniques. Air-liquid interface cerebral organoids (ALI-COs) have emerged as powerful tools for studying brain evolution, development, and neurological diseases. However, the full potential of ALI-COs has been limited by the lack of continuous *in situ* electrophysiological characterisation.

To address this limitation, we present a novel approach utilising organic polymer-based flexible microelectrode arrays (with a thickness of 4 μm) for non-invasive recording of spontaneous extracellular activity from ALI-COs. These bioelectronic devices are designed for compatibility with the air-liquid interface, and are encapsulated in Parylene-C to enhance flexibility and

feature low-impedance poly(3,4-ethylenedioxythiophene) polystyrene sulfonate (PEDOT:PSS)-coated microelectrodes.

By leveraging these devices, which offer a high signal-to-noise ratio, low electrochemical impedance, and mechanical properties matching those of cells, we have successfully achieved continuous recording from the same brain organoid slice for a minimum of two months, without compromising growth or morphology, as evidenced by immunofluorescent staining results. The findings suggest that this approach is a promising tool for long-term, non-invasive recording of extracellular activity from ALI-COs, which has implications for understanding brain development and early disease mechanisms. This work has the potential to facilitate breakthroughs in understanding brain development and disease modelling by enabling continuous functional characterisation of cerebral organoids.

8:00 PM SB05.03.14

Biocompatible Silk Films for Transient Tactile Sensors[DonggeunLee](#)¹, Jeong WooChae², Sang MinWon² and Wi HyoungLee¹; ¹Konkuk University, Korea (the Republic of); ²Sungkyunkwan University, Korea (the Republic of)

Research interests in naturally derived polymers with flexibility, stretchability, foldability, transparency, transiency, biocompatibility, and biodegradability has recently received much attention. In addition, the emergence of transient electronics, which are decomposed, absorbed, and disappear after operating for a certain period, can supplement the demerits caused by the survival of implanted devices. These technologies rely heavily on the flexibility, stretchability, biocompatibility, and biodegradability of the used biomaterials. This report presents strategies for utilizing both silk fibroin and silk sericin extracted from silk cocoons of *Bombyx mori* and fabricating silk-based sensors that detects capacitive touching motion and resistance change form mechanical deformation of the sensors. Decomposition and flexibility in humid condition were controlled by annealing fibroin film. Sericin extracted from cocoons in the process of producing fibroin was used to make an adhesive with good biocompatibility. Furthermore, a conductive silk composite was produced through hybridization with tungsten nanoparticles and was used as a piezoresistive/capacitance sensor. The sensitivity of conductive silk composite was confirmed through EEG and EOG tests. The flexibility of wholly silk based sensors was confirmed by measuring the changes in resistance at various bending condition. Acknowledgement: This work was supported by Korea Institute for Advancement of Technology (KIAT) grant funded by the Korea Government (MOTIE) (P0012770) and grant from the Basic Science Research Program of the National Research Foundation of Korea (NRF) funded by the Ministry of Science and ICT (2023-00208902).

8:00 PM SB05.03.15

Impedance-Based Polymer Microneedle Patch Sensor for Continuous Interstitial Fluid Glucose Monitoring[HonglinPiao](#), JaehyunKim, YongHoChoi, Heon-JinChoi and Dahl-YoungKhang; Yonsei University, Korea (the Republic of)

Early diagnosis and control of blood glucose is essential for effective prevention and management of diabetes-related complications. This study aims to develop a microneedle-type glucose sensor patch for minimally invasive, painless and continuous glucose monitoring. In situ monitoring of glucose concentration in interstitial fluid using polymeric microneedle arrays is the method used in this study. The experimental section included four subsections, namely substrates fabrication, sensor fabrication, and characterization of the glucose sensor based on microneedle patches. The experimental findings demonstrate the successful penetration of cylindrical microneedles into skin tissue with minimal force, reaching a depth of approximately 520 μm . The microneedle sensor was produced with high precision using the CMOS process, and the immobilization of glucose oxidase was confirmed through phase angle changes. After conducting long-term tests, the sensor was found to be effective for up to 7 days. Glucose concentration measurements were conducted using the developed sensor, resulting in fitted curves with a mean slope of -27.18 and a mean intercept of 197.27. Random glucose concentration tests were conducted, and the range of values obtained shows strong correlation with those obtained from commercially available glucose detectors. MARD ranges from -0.5% to 11.97%. These results suggest the potential for the microneedle sensor to be used as a reliable and accurate tool for glucose monitoring. The study provides a promising approach for developing a wearable and minimally invasive and painless glucose sensor for continuous glucose monitoring.

8:00 PM SB05.03.16

Wireless, Highly Sensitive Biosensors on Contact Lenses for Intraocular Pressure Monitoring[TeXiao](#); Waseda University, Japan

Glaucoma is one of the common eye diseases to cause a risk of blindness in severe cases. To prevent the blindness by glaucoma, real-time monitoring of intraocular pressure (IOP) becomes particularly important. The contact lenses built-in IOP sensor can contact continuously with the eye, so they are superior to other IOP measurement system in that it can measure constantly. Many researchers have been working on making wireless smart contact lenses that can detect intraocular pressure. By embedding LCR resonators^[1-2] in the contact lenses, which can generate changes in inductance, capacitance, or resistance of the pressure sensors., and receiving signals through transmission coils, the purpose of real-time wireless detection of intraocular pressure is achieved. However, the development of smart contact lens remains a challenge, including wireless sensor sensitivity, transparency, durability, and safety. Here we demonstrate the use of a wireless and highly sensitive IOP monitoring system on pig eyes that is comfortable while wearing. The IOP monitoring system consists of a stretchable gold antenna sensor printed on a moist and soft contact lens for IOP detection. The wireless IOP data reception is made of a reader circuit resonated at 1.39 GHz. We designed a horseshoe-shaped gold antenna, which was then printed on commercially available contact lenses through electrochemical bonding, using poly(3,4-ethylene dioxithiophene) film as an adhesive glue. The printed stretchable IOP sensing lens can be stretched and twisted, which is impossible using a conventional loop antenna^[3].

[1] T. Takamatsu, Y. Chen, T. Yoshimasu, M. Nishizawa, T. Miyake, *Advanced Materials Technologies* **2019**, *4*, 1800671.

[2] Y. Cui, T. Takamatsu, K. Shimizu and T. Miyake: *Applied Physics Express* **2022**, *15*, 20.

[3] Takamatsu, T.; Sijie, Y.; Shujie, F.; Xiaohan, L.; Miyake, T. *Multifunctional High Power Sources for Smart Contact Lenses*. *Adv. Funct. Mater.* **2020**, *30*, 1906225.

8:00 PM SB05.03.17

An Electric Contact Lens for Non-Mydriatic Near-Infrared Fundus Imaging[YangCui](#); Waseda University, Japan

Ophthalmic fundus imaging has become an important technique for the diagnosis and treatment of eye diseases^[1]. A2n ideal imaging system should have portability, low cost, and high resolution for the remote monitoring of eye health at home; however, the conventional imaging systems are large and heavy and can only be used in hospitals.

To solve this problem, we demonstrate a non-mydriatic near-infrared (NIR) fundus imaging system with light illumination from an electric contact lens (E-lens)^[2]. We designed a wireless power transfer system that can be bound to the contact lens and don't block the eye view^[3], and a near-infrared LED is embedded on the contact lens and can be powered wirelessly to light up. The E-lens can illuminate the retinal and choroidal structures in the eyes. The irradiated light is reflected at the layered structures of the fundus, and subsequently, the reflected light passes through the pupil of the eye lens to capture the images with a portable NIR camera.

Because of the strong light scattering effects in the fundus tissue, the captured images are blurred. Therefore, we reconstruct the images with a depth-dependent point-spread function to suppress the scattering effect that eventually visualizes the clear fundus images of the retinal and choroidal vasculature^[4]. This method showed superior image reconstruction results compared to other common methods such as high-pass filtering. The proposed imaging system provides a new method for remote monitoring with increased functionality, it makes the portable eye health care possible.

Reference:

[1] R. Bernardes, P. Serranho, and C. Lobo, *Ophthalmologica* **226/4**, 161–181 (2011) [DOI: 10.1159/000329597].

[2] Y. Cui, T. Takamatsu, K. Shimizu and T. Miyake: *Applied Physics Express*. **15** [2], (2022). [DOI: 10.35848/1882-0786/ac4675].

[3] T. Takamatsu, Y. Chen, T. Yoshimasu, M. Nishizawa and T. Miyake: *Advanced Materials Technologies*. **4/5**, (2019). [DOI: 10.1002/admt.201800671].

[4] K. Shimizu, K. Tochio, and Y. Kato, *Appl. Opt.* **44/11**, 2154–2161 (2005) [DOI: 10.1364/ao.44.002154].

8:00 PM SB05.03.18

Stretchable Microelectrode Arrays for Brain Spheroid Electrophysiology[EleonoraMartinelli](#)¹, CamilleL. Delgrange¹, IvanFurfaro¹, LorisGomez Baisac², AdrienRoux², LucStoppini² and StephanieP. Lacour¹; ¹Ecole Polytechnique Federale de Lausanne, Switzerland; ²Haute Ecole du Paysage, d'Ingenierie et d'Architecture, Switzerland

Human neural spheroids, i.e. 3D cellular aggregates composed of neurons and glial cells, are a compelling biological model to study neuronal communication both in physiological and pathological conditions. We propose the design of a perforated and stretchable microelectrode array (MEA) to monitor the electrophysiology of brain spheroids under static and dynamic mechanical loading. This is a relevant neuroelectronic system to investigate the consequences of traumatic brain injury (TBI).

The MEAs are prepared with thin-film technology using a platinum thin film sandwiched between two 1 μm thick polyimide films. Stretchability is engineered by design introducing patterns of micron scale, Kirigami-like Y-shaped cuts on the whole MEA surface.

Each MEA hosts 8 Kirigami-patterned recording electrodes (diameter = 70 μm), and a macroscopic ground electrode to probe one brain spheroid (spheroid diameter = 500-1000 μm).

Electrode contacts are coated with electrodeposited PEDOT. The coating conformably follows the profile of the Kirigami-patterned electrodes independently of electrode size and reduces the

electrochemical impedance at 1 kHz by 60 folds ($n = 24$, diameter = 70 μm).

Next, the permeability of the perforated MEAs is quantified as a function of pattern designs and perforation methods; this is to ensure sufficient nutrient and oxygen exchange at the air-liquid interface of the brain spheroid.

The electromechanical properties of the MEAs are then evaluated when subject to uniaxial elongation at a constant speed (100 $\mu\text{m/s}$). The strain parameters are aligned with typical TBI loadings (5-35%). Kirigami-patterned PEDOT-coated electrodes sustain strains up to 10% without showing significantly increased electrochemical impedance amplitude, while patterned platinum electrodes sustain strains only up to 5%. Similar results are shown with cyclic stretching. The electromechanical properties of the MEAs are also evaluated when subject to fast mechanical loading comparable with TBI impacts (elongation speed 1-2 m/s).

Next, the ability of the Kirigami-patterned electrodes to record neural activity from brain spheroids is verified. The MEA is mounted on a fluidic platform to allow for cell culture media change and the brain spheroids are integrated into the system. Spontaneous neural activity from the brain spheroids is reliably recorded for up to 5 days.

This work paves the way for studying the effect of mechanical loading on neural activity in 3D *in vitro* brain models.

8:00 PM SB05.03.19

Multimodal Wearable Soft Sensors for Real-time Plant Health Detection and Precise Diagnosis QinJiang, XinZhao and ZhigangWu; Huazhong University of Science & Technology, China

Our work presents a soft multimodal sensing system that can be integrated into plants for long-term detection of their physiological data variation without disturbing their growth. It combines multimodal sensor components (temperature and humidity (T&H), spectrum, and volatile organic compounds (VOCs)) with artificial intelligence (AI) system to achieve real-time plant health monitoring and diagnosis. This study may promote a novel way to set intelligent plant management systems, enabling a new level of precision agriculture, botanical research, and intelligent forestry.

Real-time monitoring of a plant's growth status, such as living microclimate, leaf color, and maturing status, is highly significant for plant physiology prediction. Recently, it has been presented that some soft sensors can be directly attached to the plant's surface to detect its physiological data. However, these sensors require more efficient multimodal data fusion to comprehensively reflect plants' growth health and flexibility to accommodate the fast growth of plants.

In this work, by coupling multimodal sensing components (e.g., T&H, spectrum, and VOCs) with the flexible liquid metal circuit, we present a soft and conformal plant-wearable sensor to monitor the plant's health status in situ. By setting the array of T&H sensors, we can record the leaf surface's T&H variation and distinguish the gradient distribution of T&H in a single leaf. With the help of the spectrum sensor, the plant surface's (e.g., leaf and fruit) transmission spectrum wavelength (350 – 1000 nm) can be detected and thus can indicate its color variation and mineral nutrition degrees (e.g., Nitrogen, Phosphorus, and Kalium). Multi-specific types of VOCs (e.g., NO_2 , SO_2 , and ethylene) are also monitored to reflect plants' stress and development levels. Moreover, we develop an artificial neural network to fuse these multiple sensing data for precisely predicting plants' growth status and diseases. To be compatible with plants' fast and continuous growth, we also present a new fabrication process that can significantly improve the stretchability and conformability of flexible circuits. By adjusting the local cross-linking degree of polydimethylsiloxane (PDMS), we can selectively tune the local stiffness of the PDMS substrate and then decrease the stress concentration between the rigid components and soft rubber under a high strain rate (> 110% strain).

Finally, several demonstrations are presented: 1) The wearable soft sensor is attached to the tomato leaf for long-time monitoring and precisely diagnosing the tomato's disease and abiotic stresses (e.g., water, temperature, salinity, and light intensity). 2) The soft sensor can also be attached to the surface of the tomato fruit to continuously record the fruit's physiological data and mature degree during its growth and expansion.

8:00 PM SB05.03.20

Modified Ultra-Stretchable Elastomers-Based Plant Monitoring Sensors for Stable Sensing with Plant Growth ZishengZong¹, ZhipingChai¹, ShuoZhang² and ZhigangWu¹; ¹Huazhong University of Science and Technology, China; ²Ningbo Institute of Technology Beihang University (BUAA), China

Recently, owing to their unique flexibility, stretchability, and conformability, soft film sensors for real-time plant monitoring demonstrate relatively little disturbance to plants' natural growth or physiology activities. However, there are still several challenges in plant sensors, including the reliable interface matching between sensor substrates and plants. Most soft film sensors generally take advantage of a flexible substrate to directly attach plant surface and active material with micro/nano structures to sense environmental parameters such as temperature and humidity. However, this attachment strategy may not be adapted to plants' rapid and continuous growth process due to their mismatched mechanical properties and low biocompatibility, leading to undesirable consequences such as sensor detachment or inhibition of plant growth. This paper reports a fully soft plant monitoring sensor for detecting environment humidity, plant circumference and length, with a modified ultra-soft, stretchable, and sticky polydimethylsiloxane-based elastomer (3S-PDMS) as substrate, graphene oxide (GO) as active material, and liquid metal as a conductive material.

In particular, the 3S-PDMS is obtained by adding a small amount (10–30 μL) of ethoxylated polyethylenimine (PEIE) ethanol solution, which contains moderately ample polar groups and shows an inhibitory effect on the catalytic activity of platinum catalysts, into the silicone precursors to weaken the crosslinking of PDMS, and constructs a dual network of solids and liquids. This dual-network accommodates a large number of uncross-linked small molecule monomers and therefore demonstrates low modulus and high adhesion force. Generally, 3S-PDMS demonstrates the mechanical properties of ultra-soft (tuning Young's modulus from 3.2 MPa to 7.5 kPa), stretchable (tuning the breaking elongation from 140% to 720%), and sticky (tuning tenfold adhesion force). Apart from that, 3S-PDMS demonstrates excellent biocompatibility, air and water vapor permeability, and optical transparency, allowing it to grow with plants and not inhibit plants' photosynthesis. Meanwhile, as water molecules are absorbed by GO, the GO can be dissolved and ionized to reduce the impedance of the electrical network, thus GO is adopted as a moisture-sensitive material.

To fabricate the sensors, the atomized liquid alloy was sprayed onto a tape-transferred adhesive mask, which was processed by laser and then attached to the surface of 3S-PDMS substrates. Then, the GO solution was drop-coated onto the liquid alloy electrical circuit. Next, the water-soluble mask and residual GO film were removed after drying. The sensing unit made of liquid alloy and GO film can be stretched as the plant grows and retains its sensing stability. Moreover, a circuit made up of liquid metal can measure the growth of plants by changes in electrical resistance, including growth circumference and length, etc. In conclusion, this paper offers an ultra-soft, stretchable, and sticky elastomer-based sensor for plant monitoring, which achieves high biocompatibility and reliable detection during plant development.

8:00 PM SB05.03.21

Whole-Cell Biosensing and Remediation of Arsenic using Magnetically Separable E. Coli: Towards Sustainable Materials for Water Treatment EricJ. Sorge, JinggeChen, MeganKizer and VickiL. Colvin; Brown University, United States

The World Health Organization (WHO) identifies arsenic as a carcinogenic toxin with exposure limits in drinking water set as low as 10 ppb. Arsenic is abundant in the Earth's crust and its prevalence in groundwater originates from natural causes as well as anthropogenic activities. Millions of people around the world, especially those in rural areas, are exposed to dangerous levels of arsenic in their water supply each year. Preventing human exposure to arsenic with accessible, inexpensive, and sustainable technology is crucial. We describe a strategy for sensing and removing arsenic from drinking water that exploits the bioaccumulation of arsenic by engineered bacteria and its detection using a whole-cell biosensor (WCB). A gene coding for a chimeric protein with two different arsenic binding domains was transfected into wild type *E. coli*; the resulting microbes could reduce arsenic concentrations in water samples containing up to 500 ppb to our instrument detection limit (~ 10 ppt) within 60 minutes. These microbes remain alive while bioaccumulating arsenic and thus we refer to them as 'living sorbents'. While the dry-weight sorption capacity of these biomaterials is less than commercial inorganic arsenic sorbents, their arsenic affinity and selectivity is much greater. As a result, it is possible to reduce even very low levels of arsenic to acceptable levels using reasonable sorbent loadings.

These organisms may be further engineered to detect arsenic through optical reporters, thus providing an important integrated solution to the problem of arsenic in drinking water.

Environmental arsenite binds to the ArsR transcription regulator, a protein that is central to the arsenic bioaccumulation capability described earlier. This same protein may also be applied to upregulate a reporter protein with fluorescent or luminescent properties. Whole cell biosensors should indicate the presence of arsenic at the extremely low levels relevant to meeting global exposure standards, on the order of ppb. Such sensitivity can be achieved through signal amplification strategies such as the use of engineered positive feedback or the application of multiple optical reporters.

Because these living sorbents use proteins evolved for arsenic sequestration, the material performance is independent of local water chemistry. The technology can be applied without customization to a particular site, and is notably independent of silicate and phosphate concentrations. Unlike inorganic sorbents which must be transported to a given site, these WCBs can be stored as dehydrated powders and later reconstituted on-site to levels appropriate for water treatment. Reversible attachment of iron oxide particles to the *E. coli* allows for magnetic capture of the biomass and the production of drinking water with no measurable contamination. This biological approach, employing regenerative and biodegradable materials, provides a sustainable alternative to conventional, inorganic sorbents for arsenic removal.

8:00 PM SB05.03.22

Design and Development of Coatable Strain Sensors for Non-Planar Surfaces ChanPark, ByeongjunLee, JungminKim, HaranLee, CheoljeongPark, ChiwonSong and Seong J.Cho; Chungnam National University, Korea (the Republic of)

Fabricating sensors on non-planar surfaces can significantly enhance the capabilities of traditional soft electronics. However, to apply existing flexible device research to non-planar surfaces, a new sensor must be developed that takes into account both Young's modulus and surface roughness. This is because real-time monitoring on non-planar surfaces, such as basic angular contact with the structure, remains a challenge. This study proposes a Coatable Strain (CS) sensor that can be applied and patterned on surfaces with various elastic moduli, shapes, and non-planar characteristics. Wet processes, regardless of surface roughness, can make contact with the surface depending on the condition of the object. Therefore, CS sensors can be applied to a variety of materials, from low-modulus materials like hydrogels (Young's modulus ≈ 1 kPa) to high-modulus materials like steel (Young's modulus ≈ 200 GPa). As a result, sensors were fabricated on various surfaces that were previously challenging to measure, and the deformation history of the object was evaluated. The CS sensor is a promising new technology for real-time monitoring of non-planar surfaces. It is easy to use and can be applied to a wide variety of materials. The results of this study demonstrate the potential of CS sensors for a variety of applications, such as structural health monitoring, medical diagnostics, and robotics.

8:00 PM SB05.03.23

Ultrafast Light-Activated Polymeric Nanomotors[JianhongWang](#), HanglongWu, JingxinShao and JanVan Hest; Eindhoven University of Technology, Netherlands

Synthetic micro/nanomotors have been extensively exploited to achieve active transportation over the past decade. This interest is a result of their broad range of potential applications, from environmental remediation to nanomedicine. Nevertheless, it still remains a challenge to build a fast-moving biodegradable polymeric nanomotor. Here we present a light-propelled nanomotor by introducing gold nanoparticles (Au NP) onto biodegradable bowl-shaped polymersomes (stomatocytes) via electrostatic interactions. These biodegradable nanomotors show controllable motion and a very high velocity of up to $125 \mu\text{m s}^{-1}$. This unique behavior was explained via a thorough three-dimensional characterization of the nanomotor, particularly the size and the spatial distribution of Au NP, with cryogenic transmission electron microscopy and cryo-electron tomography. Our in-depth quantitative 3D analysis revealed that the motile features of these nanomotors were caused by the nonuniform distribution of Au NPs along the axial direction of the polymersome. This study could offer a new perspective for designing robust biodegradable soft nanomotors, thereby facilitating their applications in a bio-friendly manner.

8:00 PM SB05.03.24

Fabrication of Water-Resistant Materials using Nanofiber Membranes Inspired by Penguin Feathers[RyosukeKawasaki](#)¹, [DaisukeIshii](#)¹, [YosukeZaito](#)² and [MasanoriKurita](#)²; ¹Nagoya Institute of Technology, Japan; ²Port Nagoya Public Aquarium, Japan

When diving, penguins do not get wet due to the feathers that cover their skin, and emperor penguins dive to a maximum depth of 564 meters. This is probably due to the penguin's feather density, which is the largest among birds, the hierarchical microstructure of its feathers with gaps of up to $17 \mu\text{m}$, and surface-modifying fat secreted by the tail blubber gland. Even with the feathers without the fat removed by organic solvents, contact angles were as high as about 130° . When a water pressure resistance was measured of surface modified feathers and wire meshes with various pore sizes by self-assembled monolayers, the smaller the pore size and the smaller the surface free energy, the better the water resistance. This result suggests that water repellency and water resistance are synergistic effects of microstructure and surface modification.

This study aimed to fabricate water-resistant materials using nanofiber membranes by electrospinning, inspired by the mechanism of penguin feathers. Polyacrylonitrile (PAN) nanofiber membranes fabricated in previous studies had problems with water absorption. A high surface free energy of PAN causes capillary action within the pores of the nanofiber membrane. Therefore, to improve the water absorption phenomenon, we investigated methods of reducing the pore size by heat pressing and changing to a polymer with low surface free energy. The experimental conditions for the electrospinning were a drum collector rotation speed of 15 rpm, a needle diameter of 0.41 mm, a feed rate of 0.10 ml/min, an applied voltage of 20 kV, and a distance between a collector and needle of 10 cm. Samples of heat pressing were yarned from a 12.5 wt% N,N-dimethylformamide (DMF) solution of PAN, and were pressed under three conditions: room temperature (25°C), glass transition temperature (T_g) of PAN (104°C), and 150°C . A hydrophobic polymer nanofibers were spun from DMF solution of Poly(vinylidene fluoride) (PVDF) (15, 20, 25, and 30 wt%). Static contact angles, water absorption, and wetting behaviors of the nanofiber membranes were discussed.

As a result, water absorption was observed in the nanofiber membrane pressed at room temperature, but no water absorption was observed in the heated press at or above the glass transition temperature. The fibers were not adhered each other pressed at room temperature, resulting in capillary action. On the other hand, the fibers pressed over T_g were adhered each other. Then pores of the nanofiber membranes became smaller and capillary action did not take place. The contact angles of the pressed nanofiber membrane at over T_g were about 70° . It is considered that the difference in pressing temperature over T_g has no effect on the surface structure. In the case of PVDF, only beads were formed at 15 and 20 wt%, which resembled "electrospray", and 25 and 30 wt% resulted in fibers, although some beads were formed. The beads were probably caused by aggregation on the collector side because the solvent was not fully volatilized. The PVDF nanofiber membrane did not show water absorption, and the contact angle was about 140° . The contact angle of smooth PVDF was about 85° , suggesting that the microstructure of PVDF improves hydrophobicity. These results indicate that the combination of microstructure and low surface free energy has potential for superhydrophobic fabrics and will contribute to the development of new water resistance mechanisms.

8:00 PM SB05.03.25

Elucidating Biosensing Mechanism of Aptamer Modified Extended-Gate Field-Effect Transistor Biosensor[SunghyunPark](#) and [JayoungKim](#); Yonsei University, Korea (the Republic of)

Extended-gate structure biosensors offer a promising field-effect transistor (FET) architecture for point-of-care applications by physically separating the sensing region from the transistor. However, few studies have investigated the sensing mechanism of FET biosensors (not limited to extended-gate structure), but rather have shown excellent label-free sensing performance. Herein, we demonstrate the biosensing mechanism of the aptamer modified extended-gate FET biosensor by modulating the dielectric properties and charge properties on the surface of the gold extended-gate. In the extended-gate FET structure, we can consider two capacitors in series: an extended-gate and a FET, which leads to the phenomenon of capacitive coupling. To show how the capacitive coupling between these two components affects the biosensing performance, we vary the capacitance values by modulating the electrode size of extended gates. Furthermore, by modifying an aptamer on the extended-gate surface for selective recognition of biomarkers and connecting it in series with a FET, the sensing performance can be explained by the capacitive coupling effect, and we further compare the results with those obtained by modulating surface charge and dielectric properties to gain insights into the sensing mechanism of the aptamer modified extended-gate FET biosensor. This in-depth investigation enhances the understanding of the biosensing mechanism in FET biosensors, provides insights for additional amplification strategies, and improves the sensitivity of FET biosensors.

8:00 PM SB05.03.26

Establishment of a Quantitative Method for Comparing The Surface Properties of Natural and Synthetic Leather[KazuyaUchida](#) and [DaisukeIshii](#); Nagoya Institute of Technology, Japan

Natural leather is produced by processing the hides of cattle, pigs, and other by-products of the meat industry. Therefore, it is a sustainable material that makes effective use of by-products. However, the metallic salts used in the "tanning" process of converting animal skins into natural leather can cause environmental problems such as water pollution and health hazards to the worker. Although vegetable tanning is an alternative tanning method that does not use metallic salts, the proportion of metal salt tanning is still high in industrial materials. Synthetic and artificial leathers are also becoming popular, but it is difficult to replace natural leathers because the characteristics of synthetic and artificial leathers have not been imitated.

Therefore, we aim to solve this problem by reducing the use of natural leather by focusing on the wettability of the surface of the leather and creating synthetic leather that has properties like natural leather. At first, the surface characteristics of each leather material such as wettability and frictional force were compared quantitatively. Based on the results of these comparative evaluations, we will establish guidelines for the development of synthetic leather with surface properties as close as possible to those of natural leather. The differences in surface properties between commercial natural leather and synthetic leather covered by polyurethane were due to differences in wettability and surface and cross-sectional microstructure. Static contact angle measurements were performed using $10 \mu\text{L}$ of distilled water to compare wettability. In addition, microscopic contact angle measurements were also performed to evaluate the behavior of absorbing a 30 μL water droplet. To clarify the relationship between these wettabilities and surface structures, the surface microstructures were observed by scanning electron microscopy (SEM). The cross-sectional microstructures were also observed, considering the contribution of not only the surface but also the cross-sectional structure to the water absorption behaviors. As a result, the SEM observation revealed bubbles in resins and regular structures on the surface of the synthetic leather, and a fluffy structure with non-woven fabrics protruding from the surface of the artificial leather. These microstructures, which differ from the surface of the natural leather, have affected surface wettabilities. In the cross-section, the natural leather showed a tendency for the structure to become rough from the outer to the inner surfaces. On the other hand, a structural gradient was not observed for the other materials, suggesting that the structural gradient affects water absorbency. The static contact angle results showed that natural and synthetic leathers had similar contact angles, although their surface structures differed according to the SEM images. The highest value was obtained for the artificial leather, which is thought to be due to its fluffier surface, which allows for a larger air layer and a more effective pinning effect than the other materials.

Finally, observation of water absorption behavior showed that the contact angle decrease rate of natural leather was greater than that of the other materials, suggesting that it has superior water absorption properties. It was thought that the gradient-like structure was responsible for the superior water absorption property. In the presentation, details of surface properties such as frictional force and mechanical properties, as well as quantitative evaluation methods for comparing the properties of each leather material will be established, and guidelines for the development of alternative materials will be explained.

8:00 PM SB05.03.27

Design and Fabrication of Sustainable Manufacturing of Neural Electrode Array for In Vivo Recording[Pei-LingChen](#)¹, [Szu-YingLi](#)², [PochunChen](#)¹, [Kuang-ChihTso](#)³, [You-YinChen](#)² and [JunOhta](#)³; ¹National Taipei University of Technology, Taiwan; ²National Yang Ming Chiao Tung University, Taiwan; ³Nara Institute of Science and Technology, Japan

Increasing requirements for neural implantation are helping to expand our understanding of nervous systems and generate new developmental approaches. It is thanks to advanced semiconductor technologies that we can achieve the high-density complementary metal-oxide-semiconductor electrode array for the improvement of the quantity and quality of neural recordings. Although the microfabricated neural implantable device holds much promise in the biosensing field, there are some significant technological challenges. The most advanced neural implantable device relies on complex semiconductor manufacturing processes, which are required for the use of expensive masks and specific clean room facilities. In addition, these processes based on a conventional photolithography technique are suitable for mass production, which is not applicable for custom-made manufacturing in response to individual experimental requirements. The microfabricated complexity of the implantable neural device is increasing, as is the associated energy consumption, and corresponding emissions of carbon dioxide and other greenhouse gases, resulting in environmental deterioration. Herein, we developed a fabless fabricated process for a neural electrode array that was simple, fast, sustainable, and customizable. An effective strategy to produce microelectrodes, leads, and bonding pads onto the Parylene C substrate by laser micromachining techniques combined with the drop coating of the silver paste to stack the laser grooving lines. Sequentially, Parylene C was deposited onto the Parylene C substrate to form the insulation layer for the protection of inner circuits. Following the deposition of Parylene C, the via holes over microelectrodes and the corresponding probe shape of the neural electrode array was also etched by laser micromachining. To increase the neural recording capability, three-dimensional microelectrodes with a high surface area were formed by electroplating PEDOT-GO composite. Our eco-electrode array showed reliable electrical characteristics of impedance under harsh cyclic bending conditions of over 90 degrees. For in vivo application, our flexible neural electrode array demonstrated more stable and higher neural recording quality and better biocompatibility as well during the implantation compared with those of the silicon-based neural electrode array. In this study, our proposed eco-manufacturing process for fabricating the neural electrode array reduces carbon emissions compared to the traditional semiconductor manufacturing process and provided freedom in the customized design of the implantable electronic devices as well.

8:00 PM SB05.03.28

Enhanced and Protective Oral Prosthetic Surfaces for Expedited Biological Fusion [SeherYaylaci](#)¹, HakanCeylan² and HacerEberliköse³; ¹Lokman Hekim University, Turkey; ²Mayo Clinic, United States; ³Ankara Medipol University, Turkey

Current strategies for enhancing the biological fusion between oral prosthetics and bone often encounter limitations due to mechanical stress at the interface. In this investigation, we present a novel, in situ-applied material designed to facilitate the biological union between the prosthetic and bone tissue. This material expedites the biological incorporation process by modulating bone metabolism through the use of specialized nanoscale fibers. Concurrently, the material possesses properties that inhibit microbial colonization, thereby improving the overall success rate of the prosthetic. A unique aspect of this work is the in situ application of the material during prosthetic placement. The material is injectable, allowing for spontaneous nanoscale fiber formation at the interface during insertion. The composition of the material is designed to emulate certain aspects of the natural extracellular matrix. Initial characterization studies were conducted to assess the material's chemical, physical, and mechanical properties. Subsequent in vitro evaluations were performed to investigate the material's effects on cellular differentiation and antimicrobial efficacy. Finally, in vivo studies were conducted to assess long-term outcomes.

8:00 PM SB05.03.29

Advancing Soil pH Sensing Through Novel, Stabilized, Screen-Printed Electronics [CatherineCrichton](#)¹, ElliotStrand¹, Juan PabloCisneros Barba¹, NicholasBruno¹, John-BaptistKauzya¹, AnupamGopalakrishnan¹, MadhurAtreya¹, EloiseBihar^{2,1} and GregoryL. Whiting¹; ¹University of Colorado Boulder, United States; ²University at Buffalo, The State University of New York, United States

Soil pH significantly affects agriculture by regulating available nutrients and water-soluble chemicals available to plants, thus driving the need for low-cost, durable soil pH sensors. A few potential solutions include expensive commercial pH sensors and printed sensors that only work in liquid media. Each of these solutions poses its own set of unique challenges perpetuating the affordable soil pH sensing dilemma. Here, we present a novel pH sensor platform based on an array of low-cost, durable, screen-printed electronics for in situ soil sensing. We show the stabilization of the pH-sensitive dye, alizarin, in the printed pH devices allowing for extended sensing periods in soil. We compare different alizarin dye immobilization techniques and electrode configurations and have evaluated the effects of soil pH on sensor durability. This new affordable, stable printed pH system pioneers the development of printed electronics for new alternatives to assess soil pH.

8:00 PM SB05.03.30

Bioinspired Transdermal Delivery Patches with Multiscale Adhesive Architectures [JihyunLee](#) and ChanghyunPang; Sungkyunkwan University, Korea (the Republic of)

Intelligent bioinspired adhesive devices are attracting attention as a tool for the transdermal drug delivery patch. However, there have been many challenges in delivering drugs from the wrinkled and rough skin surface through the complex stratum corneum into the body. The rough skin surface interferes with the interfacial contact between the drug delivery material and the skin, making close adhesion difficult, which reduces drug delivery efficiency. In addition, the brick-like structure of the stratum corneum, which has a barrier function, is a major obstacle to drug delivery through the skin. Here, we present two strategies to overcome the limitations of transdermal drug delivery based on biomimetics. First, the drug delivery patch, which is designed by combining an adhesive structure that mimics a diving beetle and a drug-loading hydrogel, improves the efficiency of drug delivery through conformal contact. In addition, the asymmetric diving beetle adhesive structure provides directional adhesive performance, enabling hypoallergenic detachment. Second, it is an adhesive interface that provides negative pressure to the skin by mimicking the tentacle of a cephalopod. Negative pressure delivered to the skin induces fine structural deformation of the stratum corneum and creates gaps between the stratum corneum, improving drug delivery efficiency. With the aid of bioinspired adhesive architecture, we demonstrated improved drug delivery efficiency in an *in vivo* model, suggesting a promising development in the medical and skin therapy fields.

8:00 PM SB05.03.31

Permeability and Anti-Fouling Performance of Microfiltration Membrane Modified by Hybrid Structured Omniphobic Coating Method [SeonminKim](#), Moon SuhkSuh, Churl SeungLee and HayoungChoi; Korea Electronics Technology Institute, Korea (the Republic of)

Surface characteristics of polymer membrane plays a significant role in bioprocess such as separation, purification, and so on. Generally, hydrophilicity is recommended for better process efficiencies in various commercial biomedical engineering fields. However, omniphobic properties of these fields could be recommendable for better performance because those properties on the surface is more favorable in many reasons. In this study, we try to modify the commercial polyethersulfone (PES) membrane by combining two different coating procedures: electrospinning and spray coating. Poly(vinylidene fluoride) is used to form the nanofiber mat for the robust roughness by the electrospinning technique and various fluoro-silane materials is applied to modify the chemical properties of the surface by spray coating method. The modified membrane was analysed by scanning electron microscopy for surface morphology and characterized by the measurement of contact angle for anti-fouling properties. We also measured the permeabilities of membrane for water and bovine solution to test anti-fouling ability in a simulated bioprocess conditions.

8:00 PM SB05.03.32

Wireless, Fully Implantable and Expandable Bioelectronic Platform for Bidirectional Modulation of the Urinary Bladder [Tae-MinJang](#), Jeong-WoongShin and Suk-WonHwang; Korea University, Korea (the Republic of)

Current standard clinical options for patients with detrusor underactivity (DUA) or underactive bladder -- the inability to release urine naturally -- include the use of medications, voiding techniques, and intermittent catheterization, for which the patient inserts a tube directly into the urethra to eliminate urine. Although those are life-saving techniques, there are still unfavorable side effects, including urinary tract infection (UTI), urethritis, irritation, and discomfort. Here, we report a wireless, fully implantable, and expandable electronic complex that enables elaborate management of abnormal bladder function via seamless integrations with the urinary bladder. Such electronics can not only record multiple physiological parameters simultaneously but also provide direct electrical stimulation based on a feedback control system. Uniform distribution of multiple stimulation electrodes via mesh-type geometry realizes low-impedance characteristics, which improves voiding/urination efficiency at the desired times. In vivo evaluations using live, free-moving animal models demonstrate system-level functionality.

8:00 PM SB05.03.33

A Self-Powered Wearable Sensor based on Triboelectric Nanogenerator for Simultaneous Motion Monitoring and Energy Harvesting [AghaA. Jan](#), SeungbeomKim, JunhyungKim, UhyeonKim and SeokKim; Postech, Korea (the Republic of)

Flexible and biocompatible triboelectric nanogenerators (TENGs) have emerged as promising candidates for mechanical energy harvesting at relatively lower working frequencies and sensing in wearable applications. TENGs work on the contact electrification principle of a tribo-negative and tribo-positive surfaces. The tribo-positive surfaces lack in material choices. Extensive research efforts have primarily focused on optimizing tribo-negative materials. This emphasis stems from the relatively limited selection of suitable tribo-positive materials available. Achieving biocompatibility while maintaining the capability for motion monitoring and energy harvesting is another critical issue for wearable devices. Here we report a laminated flexible TENG composed of polytetrafluoroethylene (PTFE) and polymethyl methacrylate (PMMA) films embedded in flexible and biocompatible polydimethylsiloxane (PDMS) for demonstration of motion monitoring and energy harvesting. A textured PDMS substrate was used to sputter deposit the indium tin oxide-copper (ITO/Cu) electrode and tribo-positive PMMA thin layer over it.

The introduction of the ITO layer onto the Cu electrode significantly improved the overall quality and performance of the electrode. Our TENG sensor displayed good pressure-sensing capabilities, featuring dual pressure sensitivity: 12.3 mV/Pa in the low-pressure range (24.5 to 122.6 Pa) and 0.663 mV/Pa in the higher pressure range (245 to 23,300 Pa). The embedded TENG sensor effectively trace the physiological motions such as wrist and finger bending. Additionally, the device efficiently harnessed energy from everyday activities like walking and jogging, producing peak-to-peak voltages of 18.3 V and 57.4 V during these motions. With its high sensitivity and power density, the laminated flexible TENG holds significant promise for diverse wearable applications, including pressure sensing and self-powered motion monitoring, emphasizing its importance in the ever-evolving field of wearable technology.

8:00 PM SB05.03.34

Use of PMMA as a Deep UV Photoresist to Produce Patterned Substrates for Surface-Aligned DNA Deposition with Potential Application to Sequencing HebaOuerfelli^{1,2}, BohengCao^{3,2}, EllenHu^{4,2}, AditiKiran^{5,2}, SelinaZhang^{6,2}, AlexZheng^{7,2} and JonathanSokolov²; ¹Fort Lee High School, United States; ²Stony Brook University, United States; ³North Hollywood High School, United States; ⁴C. Leon King High School, United States; ⁵BASIS Independent Fremont, United States; ⁶North Hunterdon High School, United States; ⁷Stuyvesant High School, United States

As genetic sequencing grows widespread in diagnostics and research, increasing its accessibility has become all the more necessary. Current next-generation sequencing (NGS) technologies entail the large-scale assembly of complete sequences from short, free-floating DNA fragments, resulting in high computational costs. Researchers have attempted to address this issue through long-read or third-generation sequencing, extending the length of the contiguous DNA fragments to tens of kilobase pairs. However, repetitive regions of the DNA still limit the ability of software to reassemble unique sequences. Ordered DNA fragmentation is an important tool in reducing the computational bottleneck of rearranging scattered strands in solution. The foundation of our approach lies in the integration of biological materials with a synthetic polymer, creating a novel abiotic-biotic system.

In this work, we explore the use of 996K molecular weight poly(methyl methacrylate) (PMMA)-coated silicon wafers as a suitable substrate for developing suspended DNA segments. The suspended segments provide steric clearance for the application of Tn5 transposases to fragment and label surface-immobilized long DNA molecules. PMMA was used as a deep-UV photoresist to produce latent patterns, followed by DNA deposition and photoresist development. Despite the tendency for UV-exposed PMMA to become more hydrophilic (unfavorable to DNA stretching on surfaces), we were successful in finding a combination of exposure and development times to achieve surface immobilization of long DNA strands such as those of mice genomic DNA and ligated lambda DNA. Initial experiments testing Tn5 activity will also be discussed. The broader implications of this work are a novel and exciting biohybrid way forward in ordered DNA fragmentation for lower-cost sequencing.

8:00 PM SB05.03.35

Impact of Rhizobium Tropici-Produced EPS on Bermuda Grass Root Growth HaarisAlam¹, IsanaAlicea², AshrithaKalakuntla³, EliseNgo¹, BrinleyDai⁴, JerryGao⁵, TeiKim⁶, TonyGuo Feng Tung⁷, YiweiFang⁸, AaronSloutski⁸, MarciaSimon⁸, JayGao⁸, MiriamRafailovich⁸, SteveLarson⁹ and FengxiangHan⁹; ¹Portola High School, United States; ²Patchogue Medford High School, United States; ³Ed W. Clark High School, United States; ⁴Experimental High School Attached to Beijing Normal University, China; ⁵Beijing No. 80 High School, China; ⁶Stanford Online High School, United States; ⁷Shanghai High School International Division, China; ⁸Stony Brook University, The State University of New York, United States; ⁹US Army Corps of Engineers, United States

Erosion control is imperative to soils vulnerable to flooding, such as watersheds in the Mississippi River Basin. A potential solution is provided by extracellular polymeric substances (EPS): hydrated microbial biopolymers whose high water-holding capacity, entrapment of nutrients, and resistance to environmental stressors can elevate soil fertility. EPS also promotes aggregate formation, which helps maintain a soil's structural integrity. A more indirect benefit of EPS in soil is their ability to enhance subterranean root growth. This corresponding increase in root mass or length can stabilize topsoil and aid in erosion control. However, the specific mechanism by which EPS benefits root growth was studied by different research groups with partial success. This project aimed to further investigate the influence of EPS produced by *Rhizobium tropici* bacteria (RT-EPS) on Bermuda grass, particularly on its root growth. By gaining a deeper understanding of this impact, a more effective approach for the fabrication and deployment of RT-EPS can be developed, which will be used on large scale applications to minimize the soil damage caused by extreme weather conditions.

EPS produced from the *Rhizobium tropici* bacteria was used to generate an ethanol precipitate material (EPM). After cell-free biofilms of the bacteria were generated, the cells were removed by centrifuge and the crude EPM collected through precipitation with ethanol, thus producing two forms of EPM: non-dialyzed and dialyzed (where an additional dialysis step was applied). For the plant study, Bermuda grass seeds were germinated in sand treated with non-dialyzed- and dialyzed- EPM (and water as a control). The plants were grown in one of three conditions in the greenhouse: a controlled chamber, inside the greenhouse, or outdoors. After a 60-day period, gravimetric and length measurements were taken of both the roots and shoots, indicating that EPM treatment increased relative root mass growth. The structure, density, and elemental composition of roots from Bermuda grass specimens grown in sand were analyzed by a Keyence VHX-7000 Microscope. After retrieving images, qualitative and quantitative analyses (nodule counting) found higher root density and greater branching in EPM-treated samples, for both dialyzed and non-dialyzed polymers. Additionally, X-ray fluorescence (XRF) spectroscopy was performed to determine the concentration of biologically important ions in roots with EPM, revealing higher amounts of Ca, K, and P. X-ray diffraction (XRD) was then performed to determine the presence of crystalline structures on top of the roots.

In conclusion, it was observed that the Bermuda grass samples treated with non-dialyzed EPM had the highest root-to-shoot mass ratios and coverage from tertiary branching. These samples also contained higher concentrations of ions that promote root growth, demonstrating enrichment of the nutrient profile. Prospective analysis includes in-depth research on the protein fraction EPM contains, with a focus on their influence on root stem cell differentiation. Further experiments will be conducted to compare the impact of different EPM dialysis procedures (by increasing the dialysis pores) on Bermuda grass root growth. The knowledge obtained from these studies will be utilized to conduct open-field experiments to examine the effect of EPM on large-scale growth, including subsequent soil analysis.

The authors would like to thank the US Army Corps of Engineers (ERDC) for their support (W912HZ-20-2-0054) in this research.

8:00 PM SB05.03.36

Structural Modifications of Nano-Sized Hydrogel via Reversible and Irreversible Redox Reactions of Thiols Chae GyuLee and Tae-HyukKwon; Ulsan National Institute of Science and Technology, Korea (the Republic of)

Cysteine-containing oxidoreductases, such as thioredoxin (Trx) and glutaredoxin (Grx), play crucial roles in maintain cellular redox balance through finely tuned reversible redox signaling pathways. However, elevated levels of reactive oxygen species (ROS), often of exogenous origin, can trigger the irreversible hyperoxidation of cysteine thiols into sulfonic acids ($-\text{SO}_3\text{H}$), resulting in permanent dysfunction of these proteins. In this study, we present an approach involving a multi-functional nano-sized hydrogel (nanogel, IrNG), encapsulating an iridium-based photosensitizer (TlR3).^{1,2} IrNG offers precise control over its nanostructure through reversible and irreversible redox reactions. In the absence of photoirradiation, IrNG maintains its self-assembled nanostructure, even in the presence of high concentrations of reductive glutathione, owing to strong hydrophobic interactions and the reversible self-crosslinking between thiols and disulfides. However, upon the photoirradiation, the disulfide bonds evenly distributed within IrNG undergo hyperoxidation, transforming into negatively charged sulfonates. This transformation results in the rapid degradation of IrNG. The photo-responsive TlR3 generates significant levels of ROS, enabling both spatiotemporally controlled structural modifications in the redox-responsive nanogel and mitochondrial oxidation-mediated cancer cell apoptosis.

¹ C. G. Lee et al., "Dual-Modulated Release of a Cytotoxic Photosensitizer Using Photogenerated Reactive Oxygen Species and Glutathione" *Angew. Chem. Int. Ed.* **2022**, *61*, e202210623

² C. G. Lee et al., "Controlling Morphologies of Redox-Responsive Polymeric Nanocarriers for a Smart Drug Delivery System" *Chem. Eur. J.* **2023**, e202300594

8:00 PM SB05.03.37

Formulation of FITC Embedded ZnO/Silica Quantum Dots for Targeted Drug Delivery KajalDhumal¹, ShreeramJogalekar², AmolTagalpallear¹, AnilPawar¹, AkshayM. Baheti¹ and AartiShastri¹; ¹School of Health Sciences and Technology MIT world Peace University Pune, India; ²Dr Vishwanath Karad MIT World Peace University, India

Breast cancer is the most prevalent type of cancer worldwide and one of the leading causes of death in women. Multiple epidemiological interventions have been used up to this point, including chemotherapy, targeted therapy, and laparotomy. Natural plant products have shown promising outcomes as anti-cancer agents. although the scarcity of effective treatments for metastatic breast cancer. Given that natural products are relatively non-toxic. So, in this study, we evaluated the phytochemical screening of *Mangifera indica* L. leaf extract, and the constituents were analyzed using the HR-LCMS technique. In addition, the anti-cancer activity of the extract was demonstrated by molecular docking studies. Amongst these lead compound, cucurbitacin b were shown to have the highest binding affinity (-22.799 kcal/mol) and positive drug interaction with breast cancer receptor. Quantum dots (QDs) are one of the unique techniques being used in the therapy of breast cancer.

ZnO/silica-FITC embedded quantum dots loaded with cucurbitacin b will act as a smart nano-drug carrier and give better cell imaging, diagnosis, and targeted drug delivery. For qualitative examination, the bulk medication was also examined using ultraviolet (UV) spectrophotometry and Fourier Transformation Infra-Red (FT-IR) spectroscopy. The drug-loaded QDs were synthesized using a wet-chemical approach, and the influence of numerous factors such as excipient concentration was evaluated on their entrapment efficiency and percentage yield to create the best and most stable quantum dots formulation. Particle size and distribution (DLS evaluation), zeta potential analysis, FE-SEM, XRD, percent drug

entrapment, and in-vitro drug release study were used to characterize the optimized drug-loaded ZnO/silica FITC embedded QDs. The outcomes demonstrated an abundance of bioactive molecules with anti-tumor potential in *M. indica*. However, more in vitro and in vivo studies are necessary. before establishing a treatment for breast cancer.

8:00 PM SB05.03.38

Polymer Dots Stabilized with Bovine Serum Albumin: Characterization, Bioconjugation and Applications [Yihao Wang](#), Rupsa Gupta and Russ Algar; The University of British Columbia, Canada

Fluorescent nanoparticles are popular and still-emerging materials for bioanalysis and imaging. Among the many types fluorescent nanoparticles, semiconducting polymer dots (Pdots) tend to have the highest brightness. Unfortunately, the surface properties and non-covalent and hydrophobic nature of Pdots leads to non-ideal behaviours such as poor colloidal and physical stability and high levels of non-specific binding.

Here, we prepared and characterized Pdots with bovine serum albumin (BSA) as the stabilizing agent (BSA-Pdots) instead of a more conventionally used amphiphilic polymer, both without and with crosslinking of the protein using glutaraldehyde (BSA(GA)-Pdots) or disuccinimidyl glutarate. These materials were then compared to alternate approaches to Pdot preparation, such as co-precipitation of semiconducting polymer with an amphiphilic polymer and post-synthetic silica encapsulation. The BSA-Pdots were generally more stable across wider ranges of pH and ionic strength range and had lower levels of non-specific binding to surfaces and fixed cells. Live cells internalized the BSA-Pdots through a form of receptor-mediated endocytosis with good retention of viability. The Pdots were conjugated with biotin and used for fluorescent immunolabeling of fixed SK-BR₃ human breast cancer cells. Overall, direct BSA stabilization is a very promising strategy for preparing Pdots with improved physical and colloidal stability, reduced non-specific interactions, and utility for in vitro diagnostics and other bioanalyses and imaging.

8:00 PM SB05.03.39

Shear-Reversible Clusters of HIV-1 in Solution: Stabilized by Antibodies, Dispersed by Mucin [Ayobami O. Ogundiran](#), Tzu-Lan Chang, Andrey Ivanov, Namita Kumari, Sergei Nekhai and Preethi Chandran; Howard University, United States

The behavior of HIV-1 in culture media was tracked with Dynamic Light Scattering (DLS) and complementary atomic force microscopy (AFM) imaging in the presence of lectins, anti-gp120 Antibodies (Abs), mannosidase, and mucin. After excluding the serum contribution to culture media from extracted DLS data, it is observed that there are clusters/aggregates of about 400-700nm HIV-1 in solutions. The clusters were sheared into single virus particles by filtration but re-clustered back over a short time. It is known that HIV-1 mutates rapidly and is protected by glycan shields of mannose sugars that have challenged the broadly neutralizing of the virus by Abs. In other studies, mannose residues have been reported to be self-adhesive, but it is not known if these mannose adhesions drive HIV-1 to be aggregated in solution, further confounding Ab neutralization. Mannosidase treatment reduced clustering, suggesting the mannose glycan shield is involved in the cluster formation. Mucin molecules (porcine gastric mucin) effectively dispersed HIV-1 clusters, even those stabilized by Abs. It is well known that mucin reduces HIV virulence, but the mechanism has not been clarified. Our findings suggest that mucin reduces HIV-1 virulence by dispersing its clusters, as opposed to the current perspective that mucin aggregates HIV-1.

8:00 PM SB05.03.40

Impact of Surfactant Properties on Phase Transition and Morphology of Thermoresponsive Polysaccharide Biomaterials [Rabeya Sharmin Lima](#), Saniya Yesmin Bublil, Katherine Salvatore, Sachin Kamath, Zhiyu Yang and Linqing Li; University of New Hampshire, United States

Understanding the interactions between various surfactants and thermoresponsive polymers is essential for regulating phase transition and controlling polymer aggregation, offering opportunities in producing biomaterials with diverse morphologies and microstructures. Here we developed a new class of dextran-based thermoresponsive polysaccharides by chemically altering the hydrophilic polymer backbone into hydrophobic derivatives. These thermoresponsive materials exhibited robust, reversible phase transitions and tunable lower critical solution temperatures. Photo-initiated radical polymerization permits facile chemical crosslinking and captures phase separation dynamically, leading to the formation of hydrogels with distinct morphologies. We evaluated the effects of various surfactants – such as anionic sodium dodecyl sulfate (SDS), nonionic pluronic F-127, cationic hexadecyltrimethylammonium bromide (CTAB), and zwitterionic 3-[(3-cholamidopropyl) dimethylammonio]-1-propanesulfonate (CHAPS) – on the phase transition and microdomain morphology of polysaccharides. We found that temperature-triggered hydrophobic interactions and phase transition behaviors are regulated by a combination of surfactant charge density, hydrophilic–lipophilic balance (HLB) values, and critical micelle concentrations (CMC). Surfactants with higher HLB values significantly disrupt phase separation above their CMCs. Notably, the non-ionic pluronic F127 surfactant effectively eliminates phase transitions across a wide range of dextran molecular weights and concentrations even below its CMC. Depending on their charge and CMC, surfactants also modify the microdomain size, shape, and number by altering the balance between continuous and dispersed phases. These findings will expand the selection of appropriate surfactants to regulate the polymer/polymer and polymer/solvent interactions to modulate phase-separation and microstructures morphology that may serve as a potential polymeric carrier for cancer drug delivery.

8:00 PM SB05.03.41

Characterizing Oil-In-Water Emulsions as Muscle and Subcutaneous Adipose Tissue Phantoms for T2 Relaxometry [Alexa S. Zammit](#), Sydney Sherman and Amena Khatun; Massachusetts Institute of Technology, United States

Tissue microstructure can be indicative of pathology and varying microstructural properties can contribute to inaccuracies in several diagnostic tools.¹ Skeletal muscle is hierarchical and highly organized. Additionally, skeletal muscle is an important reservoir of fluid and can be an early indicator of a volume overloaded state.^{1,2} A recent study demonstrates that point-of-care fluid status determination may be possible with the analysis of T2 relaxometry data collected by a bedside NMR sensor.² However, given the clinical setting of the study, fluid overload and a typical fluid state were the only two states available for data collection. Here, oil-in-water emulsions are assessed and characterized on a T2 relaxometer. The properties of the emulsions are compared to dissected murine muscle and subcutaneous adipose tissue after data analysis with a multi-exponential fit. Peanut oil is used in the emulsions, as the NMR signal is comparable to the triglycerides in adipose tissue.³ Varying the fat fraction of the emulsions by changing the oil to water ratio changes the relative amplitudes of the peaks as determined by the multi-exponential analysis. A comparison of different fat fractions enables us to determine that an emulsion with a fat fraction of 40% can be considered a muscle phantom and an emulsion with a fat fraction of 75% can be considered an adipose tissue phantom. As such, the phantoms can be used as standards for calibration and sensitivity testing for T2 relaxometry purposes.

References

¹Berry, David B. et al. Relationships Between Tissue Microstructure and the Diffusion Tensor in Simulated Skeletal Muscle. *Magnetic Resonance in Medicine* 80, 1, 317-329 (2018).

²Colucci LA, et al. Fluid Assessment in Dialysis Patients by Point-of-Care Magnetic Relaxometry. *Science Translational Medicine*, 11, 502, (2019).

³Bush, E.C., et al. Fat-Water Phantoms for Magnetic Resonance Imaging Validation: A Flexible and Scalable Protocol. *Journal of Visualized Experiments* (2018).

8:00 PM SB05.03.42

Bioelectronic Control of Neuronal Activity in Cortical Organoids with Ions and Small Molecules [Yunjeong Park](#), Sebastian Hernandez, Cristian O. Hernandez, [Heather Knight](#), Hunter E. Schweiger, Houpu Li, Kateryna Voitiuk, Harika Dechiraju, Nico Hawthorne, Elana M. Muzzy, John A. Selberg, Frederika N. Sullivan, Roberto Urcuyo, Sofie R. Salama, Elham Aslankoochi, Mircea Teodorescu, Mohammed A. Mostajad Radji and Marco Rolandi; University of California, United States

Cortical organoids are valuable tools for studying brain development, modeling neurological disorders, and testing potential treatments. For these studies, we need to improve the ability to precisely manipulate and modulate the activity of the cortical organoids at a fine time scale in a precise and detailed manner. Here, we have employed a bioelectronic approach with an ion pump, used for selective delivery of ions and neurotransmitters. More specifically, we used these devices to experimentally determine neuronal effects on the organoids with the bioelectronic delivery of potassium ions (K⁺), protons (H⁺), and γ -aminobutyric acid (GABA). This work is important to reflect bioelectronic device potential in exploring neurological disorders and their potential treatments with a level of precision and detail that was previously challenging to achieve.

8:00 PM SB05.03.43

Materials and Methods for Programmable Delivery of Therapy via Wearable Bioelectronics for Wound Healing *In Vivo* [Houpu Li](#)^{1,2}, [Hsin-ya Yang](#)^{1,2}, [Narges Asefifeyzabadi](#)^{1,2}, [Sydnie Figuerres](#)^{1,2}, [Prabhat Baniya](#)^{1,2}, [Andrea Medina Lopez](#)^{1,2}, [Anthony Gallegos](#)^{1,2}, [Kan Zhu](#)^{1,2}, [Hao-Chieh Hsieh](#)^{1,2}, [Tiffany Nguyen](#)^{1,2}, [Cristian O. Hernandez](#)^{1,2}, [Ksenia Zlobina](#)^{1,2}, [Cynthia Recendez](#)^{1,2}, [Maryam Tebyani](#)^{1,2}, [Hector Carrion](#)^{1,2}, [John A. Selberg](#)^{1,2}, [Le Luo](#)^{1,2}, [Moyasar A. Alhama](#)^{1,2}, [Athena M. Soulika](#)^{1,2}, [Michael Levin](#)^{1,2}, [Narges Norouzi](#)^{1,2}, [Marcella Gomez](#)^{1,2}, [Min Zhao](#)^{1,2}, [Mircea Teodorescu](#)^{1,2}, [Roslyn Rivkah Isseroff](#)^{1,2} and [Marco Rolandi](#)^{1,2}; ¹University of California, United States; ²University of California, Davis, United States

The ability to deliver drugs with precise dosages at specific time points can significantly improve disease treatment while reducing side effects. Drug encapsulation for gradual delivery has opened up the doors for a superior treatment regimen. To expand on this ability, programming bioelectronic devices to deliver small molecules enables ad-hoc personalized therapeutic profiles that are more complex than gradual release. Here, we introduce a wearable bioelectronic bandage with an integrated electrophoretic ion pump that affords on-demand drug delivery with

precise dose control. In this poster, I will present my contribution to the device fabrication that involves hydrogel synthesis in glass capillaries, testing of the hydrogel conductivity, and device testing. With these devices, delivery of fluoxetine to wounds in mice resulted in a 27.2% decrease in the macrophage ratio (M1/M2) and a 39.9% increase in reepithelialization, indicating a shorter inflammatory phase and faster overall healing. Programmable drug delivery using wearable bioelectronics in wounds introduces a broadly applicable strategy for the long-term delivery of a prescribed treatment regimen with minimal external intervention.

8:00 PM SB05.03.44

Materials and Strategies for Integrating Chloride Membrane Channels with Bioelectronics LeLuo, [EmilyLee](#), YunjeongPark and MarcoRolandi; University of California, United States

Biological membrane channels actively mediate information exchange between cells and have a main role in molecular recognition. The 'iono-electronic' gap between these channels and electronics creates a significant challenge in connecting these channels to electronic devices for efficient signal readout from. To address these challenges, we've combined supported lipid bilayers (SLBs) with Ag/AgCl electrodes to specifically target chloride conducting membrane spanning channels. We use the Ag/AgCl contacts to translate the ionic signal from the Cl⁻ ions into an electronic signal at the interface by exploiting the Ag/AgCl electrochemical reaction. With this system, we show that Cl⁻ conducting channels and Cl⁻ pumping rhodopsins interface better than with other non-selective contacts (Pt) or proton selective contacts (PdH). In the future, this platform can be used to create complementary hybrid devices with membrane spanning channels that are selective to the desired type of ion.

SESSION SB05.04: Engineering Biohybrid Interfaces
Session Chairs: Guglielmo Lanzani and Flavia Vitale
Tuesday Morning, November 28, 2023
Hynes, Level 1, Room 102

8:00 AM SB05.04.01

Stretchable, High-Modulus Penetrating Microelectrode Arrays for *In Vitro* Intramuscular Electromyography QinaiZhao¹, EkaterinaGribkova², YiyangShen¹, JilaiCui², NoelM. Naughton², LiangshuLiu¹, JaeminSeo¹, MattiaGazzola², JohnA. Rogers³, RhanorGillette² and HangboZhao¹; ¹University of Southern California, United States; ²University of Illinois at Urbana-Champaign, United States; ³Northwestern University, United States

Three-dimensional (3D) penetrating microelectrode arrays (MEAs) serve as important interfaces with biological tissues in various fields, including neuroscience, tissue engineering, and wearable bioelectronics. These 3D MEAs can penetrate surface layers of tissues, thereby facilitating electrophysiological sensing and electrical stimulation of interior tissues in a minimally invasive manner. Stretchable penetrating MEAs are highly desirable as they can adapt to the deformations of dynamically moving tissues or organs. This adaptability enables stable bioelectronic interfacing, enhances recording signal quality, and reduces tissue damage. However, fabricating stretchable 3D MEAs with high electrode modulus required for penetration and customized geometries presents significant challenges in materials integration and patterning. In this study, we present the design, fabrication, and applications of highly stretchable microneedle electrode arrays (SMNEAs) for sensing localized intramuscular electromyography (iEMG) signals *in vitro*. We have developed a hybrid fabrication scheme utilizing molding, microfabrication, and transfer printing, which enables scalable fabrication of SMNEAs with high electrode modulus ($E = 6.6$ GPa) and device stretchability (80%). Our SMNEAs also offer controllable electrode dimensions and recording areas, and low electrode impedance. We demonstrate the use of these SMNEAs in recording iEMG signals from the buccal mass of *Aplysia*. By inserting a multichannel SMNEA with varying electrode lengths into individual muscle groups of the buccal mass, we achieved high-fidelity, localized iEMG recording during muscle contractions and relaxations. The iEMG signals captured by the SMNEA exhibit distinctive spatiotemporal muscle activation patterns within individual muscle groups of the buccal mass, a level of detail unachievable with surface electromyography (sEMG) using a planar MEA. The high electrode modulus and device stretchability, as well as customized electrode geometries make our SMNEAs potentially useful for local sensing and stimulation of dynamic 3D tissues such as cardiac and neuromuscular tissues.

8:15 AM SB05.04.02

Biomimetic Designs of Organic Electrochemical Transistors for Human-Interfaced Biosensing and Neuromorphic Computing SihongWang; The University of Chicago, United States

The use of electronic devices for acquiring biological information and delivering therapeutic interventions relies on two aspects: the effective acquisition of physiological information through direct contact with soft bio-tissues, and the high-throughput processing of the acquired data using machine learning. To ensure high-quality signal transductions, the interfaces between bioelectronic devices and bio-tissues must combine signal amplification with stable and conformable contact. Organic electrochemical transistors (OECTs) have been developed as one of the most advanced technologies for high-performance bio-sensing and neuromorphic computing. Moreover, the fastest and most energy-efficient data processing through machine learning is directly on the human body. However, the rigid mechanical properties and the lack of tissue/skin adhesion from transistors largely prevent the formation of such intimate and long-term stable bio-interfaces. In the first part of my talk, I will introduce our material and device designs for introducing three highly important biomimetic properties onto OECT-based biosensors—stretchability, tissue-like softness, and bioadhesive properties. Our rationale designs from the material to the device level allow the realization of these properties with state-of-the-art electrical performance. I will also introduce the strategies and advantages of using these new biomimetic properties in bioelectrical and biochemical sensing. In the second part of my talk, I will introduce our research in imparting intrinsic stretchability onto neuromorphic devices that can provide state-of-the-art computing performance. I will also show the practical applicability of this device for implementing machine-learning computing and algorithms for health data analysis, when the computing hardware is under human-body-induced deformation.

8:30 AM SB05.04.03

Human Stem Cell-Based Biohybrid Fish KeeL YongLee^{1,2}, Sung-JinPark³, Herdeline AnnArdoña⁴, Sean L.Kim², JohnZimmerman², AndreKleber², GeorgeLauder² and KevinK. Parker²; ¹Sejong University, Korea (the Republic of); ²Harvard University, United States; ³Emory University, United States; ⁴University of California Irvine, United States

Biohybrid muscular systems have emerged as a valuable test platform for engineering and studying various physiological features, encompassing ion channels to system-level performance. The integration of muscle cells into simplified synthetic platforms has provided insight into the intricate mechanisms involved. However, the field of biohybrid technology is still in its nascent stages, encountering challenges in attaining system-level structure and performance comparable to their natural counterparts. This study presents a notable breakthrough in biohybrid technology through the development of a human stem cell-based biohybrid fish capable of self-pacing and self-sustaining coordinated locomotion. Taking inspiration from the structural attributes of the sinoatrial node and the multi-layered myocardium, our design incorporates a geometrically insulated cardiac tissue node and muscular bilayer muscle tissues into the biohybrid platform. This integration facilitates spontaneous activation and enables mechano-electrical signaling coupling between the muscular bilayer muscle tissues. The unique biohybrid design empowers the fish to exhibit spontaneous yet coordinated antagonistic muscle contractions, resulting in self-coordinated body-caudal-fin propulsion. Our autonomous biohybrid fish surpasses existing biohybrid muscular systems in terms of speed and longevity. It attains an optimal performance level comparable to natural body-caudal-fin swimmers, signifying a substantial advancement in the biohybrid technology domain. The achievements of this biohybrid fish lay a remarkable foundation for future autonomous biohybrid species capable of exhibiting complex adaptive behaviors. By harnessing the potential of human stem cells and employing advanced biohybrid designs, we are paving the way for a new era of biohybrid systems that closely mimic and potentially surpass the capabilities of their natural counterparts. These advancements hold immense promise across diverse applications, including regenerative medicine, biomimetic robotics, and enhancing our understanding of the fundamental principles governing biological locomotion.

8:45 AM SB05.04.04

Modular Biomachines Built from Amphibian Stem Cells DouglasBlackiston^{1,2}, SamKriegman³, JoshBongard⁴ and MichaelLevin^{1,2}; ¹Tufts University, United States; ²Harvard University, United States; ³Northwestern University, United States; ⁴The University of Vermont, United States

Living organisms remain more adaptive, robust, and regenerative than any synthetic system yet developed. It is thus promising that engineering has seen a surge in novel fabrication materials over the past decade, including a growing catalogue of biological cells and tissues. These living materials have the potential to overcome several problems faced by traditional engineering programs: they are biodegradable, self-powered, self-motile, self-healing, nanometer sized, and contain an inherent biochemistry. Efforts have largely coalesced around biohybrid designs, combining synthetic scaffolds or components alongside living cells and tissues. In complement to this approach, we demonstrate a method for constructing fully biological machines from embryonic amphibian cells, engineered to exhibit a specific behavior. AI methods automatically design diverse candidate lifetimes *in silico* to perform a desired function. The best performing simulation is then selected, and a living biological representation is constructed using a novel cell-based toolkit sourced from amphibian stem cell lineages. These self-powered representations are then released into aquatic arenas and tested for transference of *in silico* behavior. Further, we show that these modular biomachines survive in varied freshwater and saline environments and can be programmed to respond to varied stimuli across their lifespan. These studies lay the groundwork for future large-scale and automated deployment of fully biological constructs capable of a variety of user specified tasks

9:00 AM *SB05.04.05**Hybrid-Nanomaterials for Cellular Activity Modulation**TzahiCohen-Karni; Carnegie Mellon University, United States

My team's efforts are focused on three major thrusts: (i) synthesis and in depth mechanistic investigation of the unique emergent optical, thermal, electrical and electrochemical properties of novel hybrid-nanomaterials and nanomaterials topologies composed on one-dimensional and two-dimensional building blocks, (ii) application and characterization of hybrid-nanomaterials interfaces with cells and tissue, and (iii) development and engineering of nanomaterials-based platforms to interrogate and affect the electrical properties of tissue and cells such as cardiomyocytes, and neurons, with a specific focus to understand electrical signal transduction in complex 3D cellular assemblies. In this talk I will review our current efforts to control cellular activity using photoactive hybrid-nanomaterials. Light has proven itself as a powerful tool to remotely modulate cellular activity with minimal invasiveness. We present a safe neural modulation approach with sub- μ J incident energy using engineered nanostructured Si, Ge, C (out-of-plane grown graphene), and two-dimensional (2D) transition metal carbides nanoflakes without generating cellular stress. Our approach serves as a powerful toolset for studies of cell signaling within and between tissues and can enable therapeutic interventions. Expanding the material library for safe optical modulation and the systematic evaluation of their biosafety will inspire future clinical translation to achieve remote control of cells/tissue in vivo.

9:30 AM *SB05.04.06**Life-Nanomachine Synergism: From Subcellular-Sized Bioelectronic Interfaces to Brain-Like Ultra Energy-Efficient Nanoelectronics**DeblinaSarkar; Massachusetts Institute of Technology, United States

Typical biomedical implants are large (mm-cm in scale) and are highly invasive. To overcome these challenges, we are developing sub-cellular sized bioelectronic devices which are much smaller than the size of even a single cell. These devices can either reside inside a cell or in between cells and provide biological interfacing with high spatio temporal precision. These can have applications in sensing biological signals as well as modulating them for therapeutics. Going beyond bio-interfacing, I will also discuss how we can learn from biology and build devices that act like the brain for achieving highly energy efficient and environmentally sustainable Artificial Intelligence.

10:00 AM BREAK

SESSION SB05.05: Photo/electrochemical Processes at Biological Interfaces I

Session Chairs: Herdeline Ann Ardoña and Guglielmo Lanzani

Tuesday Morning, November 28, 2023

Hynes, Level 1, Room 102

10:30 AM SB05.05.01**Light-Responsive Cationic Membrane-Targeted Dyes for Cell Membrane Stimulation**ChiaraBertarelli^{1,2}, GuglielmoLanzani^{2,1}, ValentinaSesti^{1,2} and PaolaMoretti^{1,2}; ¹Politecnico di Milano, Italy; ²Fondazione Istituto Italiano di Tecnologia, Italy

In the last few decades, photoswitches are being widely studied as a promising tool for photopharmacology. Light-responsive switches offer the possibility of using light as a clean, non-invasive, and spatio-temporally precise tool to trigger cell signalling and control a variety of biochemical functions. In this framework, reversible light-sensitive ligands successfully allow for a selective and reversible stimulation by means of the photoisomerization of dyes freely diffusing or covalently linked to channels, receptors, or other specific binding sites.¹

Cationic membrane-targeted photochromic materials offer a rather different approach, where the amphiphilic character of the dyes drives their spontaneous partitioning within the cell membrane, with a specific affinity to lipid rafts. The cell signalling is the result of modification of the characteristics of the cell membranes induced by the light-driven conversion of the photoswitch to a metastable isomer.

Here, we show the molecular design of these amphiphilic dyes, which combine different families of photochromic compounds and cationic heads targeting the membrane, spaced by alkyl chains. Moreover, the presence of electroactive substituents allows for a high quantum efficiency in the visible range, modifies the isomerization kinetics and the stability in aqueous environment. Among the classes of switching units, azobenzenes demonstrated to be highly promising, and the most effective has proven to be the azepane- aminoazobenzene pyridinium-terminated Ziapin^{2,3}. Nevertheless, the use of indigos and Donor-Acceptor Stenhouse Adducts (DASAs) have been also explored.

The cationic membrane-targeted azobenzenes have been proven effective in the stimulation of neurons, muscular contraction and in driving optical modulation of bacterial membrane potential.^{4,5} Finally, we demonstrate that the number and the structure of the capping head influence the solubility of the dye, the partitioning, and the stability within the cell membrane, rather than the targeting of membrane-bound cell organelles.

¹Szymanski, W., Beierle, J. M., Kistemaker, H. A. V., Velema, W. A., & Feringa, B. L. Chem. Rev. 2013, 113, 6114–6178.²Vurro, V., Bondelli, G., Sesti, V., Lodola, F., Paternò, G.M., Lanzani, G. and Bertarelli, C. Front. Mater. 2021, 7:631567.³DiFrancesco, M.L., Lodola, F., Colombo, E. et al. Nat. Nanotechnol. 2020, 15, 296–306.⁴Vurro, V.; Shani, K.; Ardoña, H. A. M.; Zimmerman, J. F.; Sesti, V.; Lee, K. Y.; Jin, Q.; Bertarelli, C.; Parker, K. K.; Lanzani, G. APL Bioengineering, 2023, 7, 026108⁵de Souza Guerreiro, T. C.; Bondelli, G.; Grobas, I.; Donini, S.; Sesti, V.; Bertarelli, C.; Lanzani, G.; Asally, M.; Paternò, G. M. Adv. Sc. 2023, 10, e2205007**10:45 AM SB05.05.02****Biophotovoltaic Devices Based on Photosynthetic Proteins and Carbon-Based Materials**ChristopherEspinoza Araya^{1,2,3}, RicardoStarbird^{2,4}, JesseJ. Bergkamp⁵, E. SenthilPrasad⁶, VenkateshRenugopalakrishnan^{7,8,9}, AshokMulchandani^{10,11,12}, Barry D.Bruce^{13,14} and ClaudiaC. Villarreal^{1,2}; ¹Escuela de Ciencia e Ingeniería de Materiales, Instituto Tecnológico de Costa Rica, Costa Rica; ²Instituto Tecnológico de Costa Rica, Costa Rica; ³Maestría en Ingeniería de Dispositivos Médicos, Instituto Tecnológico de Costa Rica, Costa Rica; ⁴Escuela de Química, Instituto Tecnológico de Costa Rica, Costa Rica; ⁵California State University Bakersfield, United States; ⁶Council of Scientific & Industrial Research, Institute of Microbial Technology, India; ⁷Children's Hospital, Harvard Medical School, United States; ⁸MGB Center for COVID Innovation, Harvard Medical School, United States; ⁹Northeastern University, United States; ¹⁰Department of Chemical and Environmental Engineering, University of California Riverside, United States; ¹¹Department of Materials Science and Engineering, University of California Riverside, United States; ¹²University of California Riverside, United States; ¹³Department of Biochemistry, Cellular and Molecular Biology, University of Tennessee at Knoxville, United States; ¹⁴Program in Genome Science and Technology, University of Tennessee at Knoxville, United States

Sustainable and sustainable development has been generating new perspectives in manufacturing and production processes. Solar cell technologies have suffered from its influences, generating research for the development of more accessible, biocompatible, efficient and environmentally friendly materials. Among the advances that have been made, hybrid devices between organic, inorganic and biological materials stand out. The latter includes molecules that have evolved over millions of years to perfection as biological light-harvesting machines. Membrane protein-pigment complexes are the molecules of interest for these biosensitized solar cells, specifically when they have retinal terminals or complexes with chlorophylls directly associated with photosynthesis. The best power conversion efficiencies in these hybrids are generated with wide bandgap nanostructured semiconductors. For these reasons, the optimization of the fabrication process of photovoltaic-hybrid devices from flexible and renewable carbon materials was performed in this study. Photoanodes of TiO₂ nanoparticles sensitized with bacteriorhodopsin or photosystem I were developed, with their respective electrolytes of benzoquinone/hydroquinone and water-soluble cobalt (II/III) bipyridine, and with a PEDOT (poly(3,4-ethylenedioxythiophene)) counter electrode functionalized with multi-walled carbon nanotubes synthesized by electrodeposition. Each device was fully characterized by observing its morphology by SEM and TEM images, while chemical confirmation was performed by RAMAN and finally the electrochemical behavior was studied by linear scanning voltammetry (LSV), open circuit potential decay (V_{OC}) and impedance spectroscopic analysis (EIS).

11:00 AM SB05.05.03**Unlocking the Potential and Lessons of 3D Porous Electrodes in Living Biophotoelectrochemical Systems**LinyingShang¹, JoshuaLawrence¹, LauraWey², BartekWitek¹, EvanWroe¹, RachelEgan¹, AlyssaSmith¹, SilviaVignolini¹ and JennyZhang¹; ¹University of Cambridge, United Kingdom; ²University of Turku, Finland

Living biophotoelectrochemical systems are devices that 'wire' photosynthetic microorganisms (i.e., scalable and sustainable biocatalysts) to 3D-architected electrodes to catalyse reactions for solar-power generation and fuel production using sunlight and water. Despite excellent progress over the last decade, large enhancements in solar-to-charge conversion efficiency are needed to enable real-world applications. One major challenge lies in optimising the bio-electrode interface, where the material and structure of the electrodes play a crucial role.

State-of-the-art electrodes in this field are micro-pillar and inverse opal (IO) electrodes fabricated from indium-tin-oxide (ITO) nanoparticles.¹ Here, we provide important lessons for electrode design by tuning the pore sizes and homogeneity of IO-ITO electrodes, characterising their light management ability, surface morphology, electroactive surface area, cells wiring efficiency, and relating these to their biophotoelectrochemical performance.

Our results indicate that the bare IO-ITO electrodes of different pore sizes (10-42 μm in diameter) managed light similarly and the larger pore-sized IO-ITO gave rise to the highest photocurrent output. Further attempts to boost light utilisation on these electrodes by adding a bio-mimicking reflective layer at the back of the electrode resulted in increased light reflection but did not influence the photocurrent output significantly, implying the light utilisation of the structure has been optimised. In conclusion, presented is the most comprehensive systematic study in the structure-activity relationship of electrode architecture to biophotocatalytic output to our knowledge.

1. Chen, X.; Lawrence, J. M.; Wey, L. T.; Schertel, L.; Jing, Q.; Vignolini, S.; Howe, C. J.; Kar-Narayan, S.; Zhang, J. Z., 3D-printed hierarchical pillar array electrodes for high-performance semi-artificial photosynthesis. *Nat Mater* **2022**, *21* (7), 811-818. DOI: 10.1038/s41563-022-01205-5

11:15 AM SB05.05.04

Multifunctional Hybrid Interfaces for Energy Applications [Maurizio Prato](#)^{1,2}; ¹Università Degli Studi di Trieste, Italy; ²CIC biomaGUNE, Spain

Among the most innovative strategies in the energy transition, photo-electrocatalytic splitting of water for the production of "green hydrogen" plays a key role, as it provides an ideal energy carrier, obtained from renewable and circular resources and whose production and combustion fuels the H₂O/O₂ cycle, activated by sunlight. Currently, hydrogen production is mainly obtained from fossil sources, and in particular from natural gas, through thermochemical processes (reforming/pyrolysis) that generate quantities of carbon dioxide with high environmental impact. The perfect mechanisms of the leaf, realized in an artificial environment, allows for the production of hydrogen as a solar fuel, an ideal solution for sustainable development. In particular, a new catalytic system, based on the combination of perylene bisimides and polyoxometalates, arranged in a hierarchical assembly, offers new opportunities for the biomimetic splitting of water.

References

- [1] Sartorel, A., Carraro, M., Toma, F. M., Prato, M., Bonchio, M. Shaping the beating heart of artificial photosynthesis: oxygenic metal oxide nano-clusters. *Energy Environ. Sci.* **5**, 5592 (2012);
- [2] Toma, F. M.; Prato, M.; Bonchio, M. et al. Efficient water oxidation at carbon nanotube-polyoxometalate electrocatalytic interfaces. *Nature Chemistry* **2**, 826-831 (2010).
- [3] Bonchio, M.; Sartorel, A.; Prato, M. et al. Hierarchical organization of perylene bisimides and polyoxometalates for photo-assisted water oxidation. *Nature Chemistry* **11**, 146-153 (2019).
- [4] Gobatto, T.; Rigodanza, F.; Benazzi, E.; Prato, M.; Bonchio, M. et al. *J. Am. Chem. Soc.* **144**, 14021-14025 (2022).

SESSION SB05.06: Photo/electrochemical Processes at Biological Interfaces II

Session Chairs: Herdeline Ann Ardoña and Guglielmo Lanzani

Tuesday Afternoon, November 28, 2023

Hynes, Level 1, Room 102

1:30 PM *SB05.06.01

Membrane Targeted Azobenzene Drives Optical Modulation of Bacterial Membrane Potential [Giuseppe Maria Paternò](#); Politecnico di Milano, Department of Physics, Italy

The possibility to control living matter with exogenous stimuli can have tremendous impact on synthetic biology, medicine and materials science, among others. For instance achieving control over cells behaviour remains a challenge at the interface between living and non-living matter.[1] and would enable the development of new bio-mimetic and bio-enabled materials able to perform tasks.[2] Within this context, bacteria have arisen as "active and actively-controllable materials", exhibiting neuro-like behaviour, extended bioelectric signalling[3,4] and tunable assembly properties.[5] In the last decade, it has been observed that the regulatory element of such an active behaviour is the electrical potential across the membrane, which governs bacteria electrophysiology, metabolisms and bioenergetics.[6] Light can be a powerful tool in these regards, as one can control the membrane potential and, thus, cell function and behaviour remotely and with relatively high spatiotemporal precision.

Here, I will show that a membrane-targeted azobenzene can be used to photo-modulate precisely the membrane potential in cells of the Gram-positive bacterium *Bacillus subtilis*. We found that upon exposure to blue-green light, the isomerization reaction in the bacteria membrane induces hyperpolarisation of the potential ($\Delta V = 20$ mV), within a bio-mimetic mechanism reproducing the initial fate of retinal. Apart from being promising results in the view to photocontrol bacterial motion and assembly behavior in consortia, this approach also highlights the role of previously uncharacterized ion channels in bacteria electrophysiology.[7]

References

- [1] C. Xu, N. Martin, M. Li, S. Mann, *Nature* **2022**, *609*, 1029.
- [2] F. Zhang, Z. Li, Y. Duan, A. Abbas, R. Mundaca-Urbe, L. Yin, H. Luan, W. Gao, R. H. Fang, L. Zhang, J. Wang, *Sci. Robot.* **2022**, *7*, 1.
- [3] J. M. Kralj, D. R. Hochbaum, A. D. Douglass, A. E. Cohen, *Science* (80-.). **2011**, *333*, 345.
- [4] A. Prindle, J. Liu, M. Asally, S. Ly, J. Garcia-Ojalvo, G. M. Suel, *Nature* **2015**, *527*, 59.
- [5] V. E. Johansen, L. Catón, R. Hamidjaja, E. Oosterink, B. D. Wilts, T. S. Rasmussen, M. M. Sherlock, C. J. Ingham, S. Vignolini, *Proc. Natl. Acad. Sci. U. S. A.* **2018**, *115*, 2652.
- [6] J. M. Benarroch, M. Asally, *Trends Microbiol.* **2020**, *28*, 304.
- [7] T. C. de Souza-guerreiro, G. Bondelli, I. Grobas, S. Donini, V. Sesti, C. Bertarelli, G. Lanzani, M. Asally, G. M. Paternò, *Adv. Sci.* **2023**, *2205007*

2:00 PM SB05.06.02

A Membrane-Targeted Push-Pull Azobenzene for the Optical Modulation of the Membrane Potential [Arianna Magni](#)^{1,2}, [Valentina Sesti](#)^{1,2}, [Matteo Moschetta](#)², [Giuseppe Maria Paternò](#)^{1,2}, [Chiara Bertarelli](#)^{1,2} and [Guglielmo Lanzani](#)^{2,1}; ¹Politecnico di Milano, Italy; ²Istituto Italiano di Tecnologia, Italy

In the last years, the use of light as a tool for modulating membrane potential and bioelectricity has emerged as a fascinating opportunity, with the broad aim of establishing life-machine symbiosis that can help in healing disorders and restoring biological functions. An approach to induce light sensitivity in animal cells, which are usually transparent to visible light, is the use of photoactuators. These are photoactive materials that can decorate or localize into the cell membrane and are able to transduce light into a signal that can be processed by the cells. A variety of materials are suitable for the non-genetic optostimulation of cells, ranging from inorganic nanoparticles to organic polymer films and nanostructures.

The cell membrane and its electrical potential represent the core of bioelectricity, hence constituting an ideal target for exogenous modulation of signalling. For this reason, we chose a push-pull azobenzene molecule (PP-2Pyr) as a membrane-targeting photoactuator that induces a charge displacement upon isomerization. The work comprises the photophysical characterization of the photoactuator, focusing on the isomerization dynamics, and the evaluation of the photoinduced effects on HEK-293 cells. The focus is on unveiling the photostimulation mechanism, intending to link the photophysical changes occurring in the molecular photoactuator after light absorption, to the biological effects on *in vitro* cell models. The proposed light-driven mechanism originates from inferences on the molecular partitioning of PP-2Pyr in the two membrane leaflets and on the rearrangement of the charges adsorbed to the membrane due to variations in the molecular dipole moment upon light excitation.

2:15 PM SB05.06.03

Surprising Enhancement of Extracellular Electron Transfer (EET) from Electroactive Bacteria to Charge Collectors by Fumarate and Further Enhancement of EET by Functionalized Carbon Nanotubes (CNTs) [Gábor Méhes](#)¹ and [Arghyamalya Roy](#)²; ¹Waseda University, Japan; ²Linköping University, Sweden

We are witnessing the convergence of organic electronics with applied microbial electrochemistry for applications of energy harvesting, biosensing, electrosynthesis and others. In other words, biocompatible films made of conducting organic molecules interface electroactive (and other) bacteria in electronic and electrochemical devices, such as microbial electrochemical cells, biobatteries and transistors. Recently we have contributed to these efforts by creating a 3D hybrid bioelectrode based on PEDOT:PSS and *Shewanella oneidensis* MR-1 for enhancing the output of MESs[1], and by the first demonstration of amplification of EET by organic electrochemical transistors [2]. After shortly introducing these two papers, we will discuss two ways EET can be enhanced to yield MESs with electrical performances closer to realistic applications. More concretely, we have been investigating the effect of chemically-functionalized CNTs, as well as the biomolecule fumarate, on the magnitude and temporal dynamics of EET. We observed distinctively different effects on EET based on the chemical agent for functionalization of CNTs, and an unexpected role of fumarate in EET dynamics.

References:

- [1] Zajdel, Baruch, Méhes (equal contributions), *et al.* Sci. Rep., 2018, 8, 15293, 1–12.
[2] Méhes, Roy, Strakosas (equal contributions), *et al.* Adv. Science, 2020, 7, 2000641(1–8).

2:30 PM *SB05.06.04

Seeing the Sound—An Ultrasound-Mediated Intravascular Light Source for Noninvasive Brain Modulation Guosong Hong; Stanford University, United States

Understanding the inner workings of the brain requires a bidirectional interface that enables causal manipulation and simultaneous interrogation of neural activity. Existing electrical and optical brain interfaces are usually based on implanted devices and invasive procedures that necessarily damage the endogenous brain tissue and constrain the subject's free behavior. To address these challenges, our lab leverages the latest advances in materials science to develop minimally-invasive functional interfaces for monitoring and modulating the brain. Specifically, in this talk, I will present three materials-inspired strategies: 1) light sculpting in the tissue with ultrasound by turning the endogenous circulatory system into an "optical flow battery", 2) an intravascular light source inspired by the biomineralization process in nature, and 3) deep-brain neuromodulation inspired by the infrared sensitivity of rattlesnakes. I will conclude my talk by presenting an outlook on how advances in materials science may facilitate the development of next-generation brain-machine interfaces.

3:00 PM BREAK

3:30 PM *SB05.06.05

Integration of Polymers with Synthetic Soft Matter and Biological Matter Towards Sensing Alberto Salleo; Stanford University, United States

An attractive feature of polymeric mixed conductors is their ability to swell in water thus forming a soft interface amenable to interacting with biological matter. Further, their ability to transduce ionic fluxes into electronic fluxes opens opportunities in sensing. Indeed, one can imagine combining the specificity and sensitivity of biological matter with the functionality of semiconductors in a single hybrid device. In this talk I will describe our work on integrating lipid bilayers, either synthetic or obtained from cell walls to sense a variety of environmental cues. For instance, we demonstrate specific sensing of toxins and viral fusion as well as the detection of opening and closing of selected ion channel. I will describe the surface treatments needed to enable such hybrid interface to retain its functionality as well as modeling of the device response and its limitations.

4:00 PM SB05.06.06

Vertical Organic Electrochemical Transistors for Enhanced Performance and Circuit Integration Antonio Facchetti; Northwestern University/Flexterra Inc, United States

Organic electrochemical transistors (OECTs) have been intensively investigated for applications in state-of-the-art wearable electronics and next-generation biosensor technologies due to their outstanding amplification, sensitivity to ionic and ultra-small electrical potential signals, compatibility with roll-to-roll fabrication processing, and low driving voltages. The far majority of OECT studies are based on a device structure comprising coplanar source-drain electrodes in contact with the organic semiconductor. Recently we proposed a new architecture where the electrodes are vertically stacked achieving high transconductance and current on-off ratio for both p- and n-type semiconductors. This vertical OECT architecture (vOECT) is also attracting for dramatically increase transistor density for high-resolution OECT sensors and complementary driving circuits. However, scalable patterning methods for organic semiconductors and optimization of the semiconductor topology for efficient monolithic integration of vOECTs remains technologically challenging, but essential for applications in complex and high-density OECT circuit arrays and multi-functional data analysis. In this presentation we report on the monolithic integration of flexible vOECT arrays for driving high-density (> 7 M OECT/cm²) active-matrix complementary logic circuits.

4:15 PM SB05.06.07

Stand-Alone Conformable Bioelectronics Based on Integrated Internal Ion-Gated Organic Electrochemical Transistors Claudia Cea^{1,2}, Zifang Zhao¹, Jennifer Gelinis¹ and Dion Khodagholy¹; ¹Columbia University, United States; ²Massachusetts Institute of Technology, United States

Effectiveness of medical treatments can be greatly influenced by individual variations, prompting the need for methods that enable continuous monitoring of physiological signals and personalized responsive delivery of therapeutics. Implanted bioelectronic devices play a crucial role in these methods, but there are challenges that prevent their widespread adoption. The ability to perform these demanding electronic functions in the complex physiological environment with minimum disruption to the biological tissue remains a big challenge. An optimal fully implantable bioelectronic device would require each component from the front-end to the data transmission unit to be conformable and biocompatible. For this reason, organic material-based conformable electronics are ideal candidates for components of bioelectronic circuits due to their inherent flexibility, and soft nature. Here, we present a vertical internal ion-gated organic electrochemical transistors (vIGT) as a high-density, high-amplification sensing component as well as a low leakage, high-speed processing unit. In addition, a novel wireless, battery-free strategy for electrophysiological signal acquisition, processing, and transmission that employs IGTs and an ionic communication circuit (IC) is introduced. We show that the wirelessly-powered IGTs are able to acquire and modulate neurophysiological data in vivo and transmit them transdermally, eliminating the need for any hard Si-based electronics in the implant.

4:30 PM SB05.06.08

Organic Electrochemical Transistors as On-Site Signal Amplifiers for Electrochemical Aptamer-Based Sensing Xudong Ji and Jonathan Rivnay; Northwestern University, United States

Electrochemical aptamer-based sensors are typically deployed as individual, passive, surface-functionalized electrodes, but they exhibit limited sensitivity especially when the area of the electrode is reduced for miniaturization purposes. We demonstrate that organic electrochemical transistors (electrolyte gated transistors with volumetric gating) can serve as on-site amplifiers to improve the sensitivity of electrochemical aptamer-based sensors. By monolithically integrating an Au working/sensing electrode, on-chip Ag/AgCl reference electrode, and Poly(3,4-ethylenedioxythiophene)-poly(styrenesulfonate) counter electrode — also serving as the channel of an organic electrochemical transistor, we can simultaneously perform testing of organic electrochemical transistors and traditional electroanalytical measurement on electrochemical aptamer-based sensors including cyclic voltammetry and square-wave voltammetry. This device can directly amplify the current from the electrochemical aptamer-based sensor via the in-plane current modulation in the counter electrode/transistor channel. The integrated sensor can sense transforming growth factor beta 1 with 3 to 4 orders of magnitude enhancement in sensitivity compared to that in an electrochemical aptamer-based sensor (292 μ A/dec vs. 85 nA/dec). This approach is believed to be universal, and can be applied to a wide range of tethered electrochemical reporter-based sensors to enhance sensitivity, aiding in sensor miniaturization and easing the burden on backend signal processing.

4:45 PM SB05.06.09

Soft Polymer for Enhanced Electron Transfer Rossella Labarile¹, Daniilo Vona², Maria Varsalona², Matteo Grattieri², Melania Reggente³, Ardemis Boghossian³, Fabian Fischer⁴ and Massimo Trotta¹; ¹Consiglio Nazionale delle Ricerche, Italy; ²Università degli Studi di Bari Aldo Moro, Italy; ³Ecole Polytechnique Fédérale de Lausanne, Switzerland; ⁴Haute école Spécialisée de Suisse Occidentale, Switzerland

Photosynthetic bacteria are anoxygenic microorganisms with highly versatile metabolism, as they use sunlight to oxidize a broad variety of organic compounds in addition to heterotrophic and photoautotrophic alternative metabolisms. Conductive polymer layers on the surface of several bacterial species have been used to intercept and funnel the electron flow produced by microbial metabolism outside the cells and transfer it to an electronic circuit of a biohybrid device.

Polydopamine (PDA), produced by self-assembly of dopamine, is a very versatile and bioinspired polymer with widespread applications¹ mostly due its ability to adhere and cover surfaces of different chemical composition. The oxidative conditions employed for the formation of this dark insoluble polymer are mild and biocompatible and have inspired scientists to develop novel nanomaterials. Post-functionalization of PDA² also enables fine tuning of properties.

Furthermore, the ability of this monomer to self-assemble and polymerize in the bacterial growth medium was considered one of the requirements of the polymer to be used as coating material beside the tunable conductive properties and the flexible structure.

Biocompatibility of dopamine was tested by *in vivo* addition in the growth media of the photosynthetic purple non sulphur *Rhodospirillum rubrum* (*R. sphaeroides*)³ in anoxygenic conditions.

We have used PDA conductive coatings as biotic-abiotic interfaces in biohybrid photoelectrochemical devices through the encapsulation of entire bacterial cells or single components – e.g. photosynthetic reaction center (RC) - of *R. sphaeroides*^{4,5}, ensuring electronic communication of the biological component with the electrodes' surfaces in photoelectrochemical cells.

¹Liu, Y.; Ai, K.; Lu, L. Polydopamine and its derivative materials: Synthesis and promising applications in energy, environmental, and biomedical fields. *Chem. Rev.* 2014, 114, 5057–5115.

²Buscemi, G., Vona, D., Ragni, R., Comparelli, R., Trotta, M., Milano, F., Farinola, G.M., Polydopamine/Ethylenediamine Nanoparticles Embedding a Photosynthetic Bacterial Reaction Center for Efficient Photocurrent Generation. *Adv. Sustainable Syst.* 2021, 2000303.

³ Labarile, R.; Varsalona, M.; Vona, D.; Stufano, P.; Grattieri, M.; Farinola, G. M.; Trotta, M., A novel route for anoxygenic polymerization of dopamine via purple photosynthetic bacteria metabolism. *MRS Advances* **2023**

⁴Lo Presti, M., Giangregorio, M. M., Ragni, R., Giotta, L., Guascito, M. R., Comparelli, R., Fanizza, E., Tangorra, R. R., Agostiano, A., Losurdo, M., Farinola, G. M., Milano, F., Trotta, M., Photoelectrodes with Polydopamine Thin Films Incorporating a Bacterial Photoenzyme. *Adv. Electron. Mater.* 2020, 6, 2000140.

⁵Milano, F., Lopresti, M., Vona, D., Buscemi, G., Cantore, M., Farinola, G.M., Trotta M. (2020). Activity of photosynthetic Reaction Centers coated with polydopamine. *MRS Advances* 5 (45), 2299-2307.

5:00 PM SB05.06.10

Soft and Ultra-Thin Wearable Tactile Interface with Electrical Impedance Tomography for High Spatiotemporal Resolution[KyubeenKim](#), Jung-HoonHong and Ki JunYu; Yonsei University, Korea (the Republic of)

Wearable tactile mapping devices, a burgeoning area in human-computer interaction, have gained significant attraction due to their wide range of applications. These include interfaces for virtual reality and gaming devices, haptic feedback systems, and artificial skin for medical and robotic applications. Tactile sensors, as a cornerstone of this technology, must achieve high spatiotemporal resolution while maintaining soft mechanical properties to replicate the human sense of touch accurately. This is paramount in creating seamless and immersive user experiences, whether it's in navigating virtual environments or enabling prosthetic devices to mimic real tactile feedback. However, the development of these sensors presents distinct challenges. Current high resolution tactile sensing technologies predominantly rely on inorganic material-based sensors, which, despite offering high spatial resolution and reliability, pose significant limitations. They are inherently brittle and ill-suited to accommodate mechanical deformation, a critical attribute for wearable sensors meant to conform to human skin. On the other hand, soft materials, characterized by a low Young's modulus, are mechanically desirable for wearable tactile systems as they can conform to varied and changing surfaces. However, the fabrication processes for these materials tend to deviate from conventional microelectronics manufacturing techniques. This divergence often results in less sophisticated device structures, hindering the development of advanced and intricate tactile sensing systems.

To overcome these limitations, we propose an ultra-thin tactile sensor offering single-cell based multi-channel array functionality via the application of electrical impedance tomography (EIT). The sensor's stretchable sensing area consists of an elastomeric substrate and encapsulation, alongside a conductive functional layer comprising multi-wall carbon nanotube (MWCNT) layers. With a thickness of just 50 microns, this low-modulus, highly stretchable sensor can conformably adhere to human skin, maintaining robust functionality under applied force and mechanical deformation. The EIT computational analysis method allows our single-cell device to operate as a multi-channel array by reconstructing high-resolution conductivity changes within the broad sensing area. Piezoresistive effect-induced conductivity changes in the MWCNT-based conductive layer occur when external forces are applied, causing mechanical deformation, bending, and stretching. These changes can be mapped by EIT measurements using surrounding electrodes, achieving high-resolution detection of force applications. This EIT-based soft tactile interface can differentiate external pressures down to a 1mm scale, and vertical deformation of a few hundred micrometres. We validated our tactile sensor's functionality through two real-time applications: a wearable drone controller and a handwriting recognition interface. Our work illustrates the potential of applying EIT to soft, ultra-thin elastomeric devices for the development of high-performance wearable tactile sensing systems. These systems could find potential applications in healthcare, robotics, and human-machine interfaces, paving the way for more advanced tactile sensors in the future.

SESSION SB05.07: Poster Session II: Functional Soft Materials for Biointerfacing

Session Chairs: Herdeline Ann Ardoña and Flavia Vitale

Tuesday Afternoon, November 28, 2023

Hynes, Level 1, Hall A

8:00 PM SB05.07.01

Battery-Free, Fully Implantable Optoelectronic System for Programmable Photodynamic Therapy and Tumor Growth Monitoring[In SikMin](#), KihoKim and Ki JunYu; Yonsei University, Korea (the Republic of)

Photodynamic therapy (PDT) is garnering attention as a prominent next-generation cancer treatment modality that utilizes specific wavelengths of light and photosensitizers to target and treat malignant tumors with high selectivity, resulting in minimal side effects and exclusively targeting cancer cells. Photosensitizers, selectively accumulated in cancer cells, transition into an excited state upon exposure to incident light energy. Subsequently, the surrounding oxygen is converted into reactive oxygen species, which serve as the mechanism for destroying cancer cells without inflicting significant damage or pain on normal cells, thus enabling the destruction of malignant tissue. Due to the limited penetration of light into deep tissues within living organisms, conventional PDT has predominantly been confined to epithelial cancers such as skin cancer, bladder cancer, and bronchial carcinoma. Furthermore, light delivery systems for PDT have relied on bulky and expensive laser-based equipment, posing significant constraints on user accessibility. To overcome these challenges, various LED-based fully implantable PDT systems have recently been developed. However, existing fully implantable PDT systems have faced limitations in precise light intensity control and adjustment of PDT parameters, as they are based on passive electronics or simple circuits incapable of performing advanced functions. Moreover, the implementation of wireless systems solely for power delivery has hindered the realization of tumor-related data monitoring based on bidirectional communication systems. Here, we introduce a battery-free and fully implantable optoelectronic system for PDT that enables precise light intensity control and scattered light measurement for tumor growth monitoring. This system involves the insertion of a μ -LED probe into the tumor to deliver light of 624 nm wavelength for PDT. The system allows for precise control of LED light intensity from 0% to 100% through wireless user control using a Bluetooth Low Energy communication. Additionally, the system incorporates the capability to monitor tumor growth by measuring the scattering of light within the tumor tissue through an external phototransistor placed outside the tumor. We performed in vitro experiments to confirm that the therapeutic effects vary at different light intensities of 0%, 30%, 70%, and 100%, and observed tumor growth inhibition through 624 nm-based PDT performed on a nude mouse model during a three-week in vivo experiment. Furthermore, we validated the feasibility of a system for monitoring relative changes in tumor size by measuring the scattered light from the tumor using a phototransistor, through ray-tracing simulation, ex vivo and in vivo experiments. This wireless electronics-based PDT system holds significant potential for expansion into a multimodal system with diverse functionalities such as a closed-loop system based on simultaneous treating and monitoring system, providing an opportunity to realize an effective and low side-effect cancer treatment while simultaneously collecting valuable feedback data related to the treatment.

8:00 PM SB05.07.02

The Relationship Between Surface Oxidation States and Antiviral Activity of Nano-Columnar Copper Thin Films[KeisukeShigetoh](#), RieHirao and NobuhiroIshida; Toyota Central R&D Labs Incorporated, Japan

Antiviral coatings capable of inactivating a broad spectrum of viruses are crucial in the fight against viral mutation and emergence. Drawing inspiration from cicada wings known for their mechano-bactericidal properties, this study proposes the use of nano-columnar Cu thin films [1]. These thin films of Cu and its oxides were fabricated on a polymer surface by a sputtering technique, and their virus-inactivate capabilities were tested against both enveloped bacteriophage $\Phi 6$ and non-enveloped bacteriophage Q β . Among the fabricated films, the Cu thin films showed the highest antiviral properties. The Cu thin films diminished the infectious activity of the bacteriophages by five orders of magnitude within half an hour, the Cu₂O thin films reduced it by three orders of magnitude, while the CuO thin films lessened it by less than one order of magnitude. Moreover, the excellent antiviral activity of Cu thin films was confirmed under the pseudo-practical conditions using viral solutions that contain contaminating proteins, assuming such as in human saliva. After being exposed to ambient air for a month, the antiviral activity of the Cu₂O thin film dropped by one order of magnitude. Nevertheless, the Cu thin films consistently demonstrated a higher degree of antiviral activity compared to the Cu₂O thin films. A detailed analysis of the surface chemical states via X-ray photoelectron spectroscopy indicated that the fabricated Cu thin films showed slower oxidation to CuO than that of the Cu₂O thin films. Therefore, the formation of CuO possibly worked as a passivation layer for antiviral activity. The significant antiviral activity and oxidation durability of the Cu thin films can have immense practical utility, while their oxidation resistance might be a characteristic property of nanostructured Cu fabricated by the sputtering method. Finally, the antiviral activity of the nano-columnar Cu thin films against infectious viruses in humans was demonstrated by the binding inhibition of the SARS-CoV-2 spike protein to the angiotensin-converting enzyme 2 receptor (ACE2). The cleavage of the disulfide bonds in the spike proteins by copper ions is thought to have led to a significant reduction in binding affinity between spike protein and ACE2. The small mass loading (6 $\mu\text{g cm}^{-2}$) of the Cu thin films ensured transparency and flexibility of the substrates, with a low environmental risk; this is particularly useful for coating applications on disposable masks and filters.

[1] K. Shigetoh, R. Hirao, N. Ishida, Durability and Surface Oxidation States of Antiviral Nano-Columnar Copper Thin Films, *ACS Applied Materials & Interfaces*, 15 (2023) 20398.

8:00 PM SB05.07.03

Novel Structural Concept for High-Performance Gold Nanowire Stretchable Electrode Toward Ultra-Flexible Biomedical Applications Satoshi Takane^{1,2}, Yuki Noda¹, Naomi Toyoshima¹, Takafumi Uemura^{1,2} and Tsuyoshi Sekitani^{1,2}; ¹Osaka University, Japan; ²National Institute of Advanced Industrial Science and Technology, Japan

Gold nanowires (AuNWs) are attractive candidates to develop stretchable/biocompatible electrodes for use in biomedical sensors and neural interfaces. In this study, we propose a novel structural concept to enhance the strain-conductive performance of stretchable AuNW electrodes, the formation of a “macroscale mesh”-shaped “nanowire-thin film composite” structure in the AuNW electrodes. The AuNW-Au thin film (AuTF) composite electrodes with a mesh structure using an Ecoflex substrate decrease the absolute resistance by 22% and the normalized resistance changes by 24% compared with the AuNW electrode without a composite or mesh structure under 80% strain. Furthermore, our stretchable electrodes, composed of AuNWs, AuTFs, and Ecoflex have excellent biocompatibility and thus have great potential for use in biomedical applications. Due to the growing demand for biomedical devices that are mechanically/biologically compatible with human organs, stretchable AuNW electrodes have attracted considerable attention because of their stable strain-conductive performance and biocompatibility owing to the nanowire network structure and the chemical inertness of gold, respectively. Although numerous studies have been conducted on stretchable AuNW electrodes, further improvements in the inadequate performance are required for these electrodes to appear in the industrial market. As performance indicators of stretchable electrodes, two parameters are used to evaluate their strain-conductive properties: absolute resistance and normalized resistance change. Previous studies have suggested unique methods to improve the parameters of stretchable metal nanowire electrodes. For instance, the deposition of metal thin film on metal nanowire electrodes to form nanowire-thin film composite electrodes can reduce the absolute resistance of pristine metal nanowire electrodes over a broad strain range. However, this method may increase the normalized resistance change owing to the mechanical degradation of the metal thin film. In contrast, the formation of a mesh structure over metal nanowire electrodes can suppress the normalized resistance change under tensile strain. However, the formation of the mesh structure decreases the conductive area of the electrodes, which can induce a higher absolute resistance. In this study, we integrate these two unique but imperfect methods and introduce this novel structural concept to AuNW electrodes to improve both their absolute resistance and normalized resistance change simultaneously for the realization of a high-performance and biocompatible electrode. The AuNW-AuTF composite electrodes with a mesh structure demonstrate 22% lower absolute resistance and 24% smaller normalized resistance change than those of the pristine AuNW electrode without a composite or mesh structure under 80% strain. From the result, we consider the AuTF in the composite electrode facilitates the current flow although the mesh structure decreases the conductive area of the electrode, whereas the mesh structure suppresses the mechanical failure of the AuTF by reducing the tensile stress. Additionally, the AuNWs, AuTFs, and Ecoflex have been previously used in biomedical devices and confirmed to be biocompatible. Therefore, mesh-shaped AuNW-AuTF composite electrodes can be applied to biomedical devices. This novel structural concept which can improve strain-conductive performance is versatile for any type of stretchable metal nanowire electrodes. Using the AuNWs, we developed high-performance, elastic, and biocompatible electrodes suitable for use in biomedical devices. Our findings will accelerate the development of biomedical applications not only in academia but also in industry.

8:00 PM SB05.07.04

Silk Fibroin: An Adaptive Natural Surfactant for Aqueous Solution-Processed Nanoelectronics over All Substrates Taehoon Kim and Fiorenzo Omenetto; Tufts University, United States

Universal wettability is especially relevant for aqueous solution processing, which has gained prominence due to the growing demand for water-based fabrication of electronic and photonic components. Although water is an ideal solvent in terms of abundance and environmental sustainability, its relatively high surface tension limits its wetting capabilities. Surface pre-treatments, surfactants, or organic co-solvents are commonly used to enable aqueous solution processing. However, these methods have drawbacks, including their potential to impact material composition and morphology, increase costs, and raise environmental concerns. Thus, the development of a practical, versatile, and sustainable strategy for achieving universal wettability of aqueous solvents is of significant importance.

In this study, we present the utilization of silk fibroin (SF), a natural biopolymer, to modulate the interfacial energy landscape of hydrophobic surfaces. By incorporating small amounts of SF in thin-film precursor solutions, we demonstrate its role as an adaptive molecular bridge that enables the deposition of aqueous solutions on otherwise unwettable substrates. The amphiphilic composition of SF chains confers exceptional interfacial energy control, resulting in enhanced wetting behavior. Furthermore, we investigate the vertical self-segregation mechanism of SF during the formation of metal-oxide thin films, which can be harnessed to preserve the electronic properties of the active layers. By combining these effects, we successfully fabricate (opto)electronic structures on substrates with significantly different surface energies using all water-based precursor solutions, without compromising device performance due to the presence of the bioinspired surfactant.

Overall, these results present a comprehensive exploration of SF as a means to regulate the interfacial energy for achieving universal wettability in aqueous solution processing. The findings contribute to the development of practical and sustainable approaches for fabricating electronic and photonic thin films, offering potential benefits in terms of cost, energy consumption, and environmental impact.

8:00 PM SB05.07.05

Universal Assembly of Liquid Metal Particles in Polymers for Elastic PCB Wonbeom Lee, Hyunjun Kim and Jiheong Kang; Korea Advanced Institute of Science and Technology, Korea (the Republic of)

An elastic printed circuit board (E-PCB) is a conductive framework utilized for the facile assembly of system-level stretchable electronics. E-PCBs require elastic conductors having both high electrical conductivity and stretchability, tough adhesion to various electronic components, and negligible resistance changes even under large strain. Here, I present a new class of elastic conductor based on liquid metal particle assembled-network (LMPNet). The LMPNet conductor satisfies all the aforementioned requirements and enables the fabrication of a multilayered high-density E-PCB. Therefore, numerous electronic components could be intimately integrated to create highly stretchable skin electronics. Furthermore, I could generate LMPNet in various polymer matrices including hydrogels, self-healing elastomers and photoresists, and it shows the potential of the LMPNet for use in soft electronics. In my presentation, I will discuss the details of the synthesis of LMPNet and its exceptional properties.

8:00 PM SB05.07.06

Thermo-Responsive Shape Memory Polymer for use in Implantable Blood Pressure Measurement Device Arjan Sall, Zoe Schofield and Liam Grover; University of Birmingham, United Kingdom

Hypertension or high blood pressure is a worldwide problem as it has become the leading cause in the growth of cardiovascular disease and premature death. This is especially true in countries of low to middle income [1]. As a result of this it is critical that patient's blood pressure is measured on a regular basis in order to provide the correct treatment. Current methods of blood pressure measurement such as the sphygmomanometer or ambulatory methods in a clinical setting or electronic monitors used at home are either too invasive for the patient, are subject to the general fluctuation of blood pressure throughout the day or are only able to take singular measurements [2][3]. This has produced a need for a method of blood pressure measurement that is non-invasive and is able to provide continuous and reliable blood pressure measurement throughout the day. The focus of this presentation will be the development of a biocompatible shape memory polymer (SMP) that will be used in the fabrication of a blood pressure sensor that will allow a non-invasive implantation of the device into the subcutaneous layer of the wrist.

Mechanical characterisation of the current sensor material, polydimethylsiloxane (PDMS), will be presented to provide a reference point for the development of the SMP. The fabrication process of the SMP based on a blend of PDMS and Polycaprolactone will be described, and the systematic variation of the polymer composition will be explained detailing its impact on the shape memory effect elicited, while also comparing the mechanical properties of the SMP formulations to the pure PDMS. The mechanical characterisation carried out will focus on the compressive strength of the material where cyclic loading tests will determine the fatigue behaviour of the SMP and maximum compression tests will allow the calculation of the elastic modulus of the material. This will help determine the longevity of the implant. Aging of the samples using PBS at 37°C and 70°C will assess the ability of the material to withstand prolonged subcutaneous implantation. Dynamic mechanical analysis and dynamic scanning calorimetry will be used to determine the transition temperatures (T_g) of each of the SMP formulations with 37°C being the target temperature. Once an SMP with the target T_g has been produced the shape fixity, shape recovery and recovery rate will be tested. The goal for this project is to create a material that is able to withstand both the mechanical and biological stresses of blood pressure measurement and subcutaneous implantation which will allow the sensor to provide a reliable and consistent blood pressure measurement.

References

- Mills KT, Stefanescu A, He J. The Global Epidemiology of Hypertension. *Nature Reviews Nephrology*. 2020;16(4):223–37. doi:10.1038/s41581-019-0244-2
- Ogedegbe G, Pickering T. Principles and techniques of blood pressure measurement. *Cardiology Clinics*. 2010;28(4):571–86. doi:10.1016/j.ccl.2010.07.006
- Turner JR, Viera AJ, Shimbo D. Ambulatory blood pressure monitoring in clinical practice: A Review. *The American Journal of Medicine*. 2015;128(1):14–20. doi:10.1016/j.amjmed.2014.07.021

8:00 PM SB05.07.07

Mechanical Characterisation of Bio-Inspired, Multi-Compartment Soft Materials Endowed with Photo-Responsivity Patrick J. Grimes¹, Agostino Galanti², Pierangelo Gobbo², Henry E. Symons¹, Sebastien Rochat¹ and Jun H. Park¹; ¹University of Bristol, United Kingdom; ²University of Trieste, Italy

Novel bio-inspired materials are of great interest to both the materials science and synthetic biology communities. The Gobbo group has recently developed “proto-cellular materials” (PCMs) assembled from protein-polymer protocell units (called proteinosomes) that are annealed into sheets through interfacial strain-promoted alkyne-azide cycloaddition (I-SPAAC).^[1] Proteinosomes are comprised of a self-assembled, crosslinked nanoparticle membrane with an inherent molecular weight cut off (MWCO) (*ca.* 40 kDa) that allows the entrapment of cargoes of sufficiently high molecular weight.^[2] The resultant PCMs formed of a population of covalently bound proteinosomes have been demonstrated to be robust and free standing in water.

The current trajectory of research in this area is towards improving the mechanical properties of the PCM's constituent proteinosomes, such that the resultant PCM can more closely mimic biological cell consortia. Moreover, developing the responsiveness of PCMs to physicochemical stimuli is of great interest to allow the use of PCMs in a range of applications, including their potential use as a substrate on which to grow communities of living cells. The characterisation of PCMs has been restricted to confocal and electron microscopy, which, although both powerful techniques, is naturally limiting in the context of mechanical properties.^[1]

In this communication I will show how a novel photosensitive crosslinker and a reactive thermoresponsive polymer can be combined to generate three-dimensional hydrogel “protocytoskeletons” within the proteinosomes of PCMs. This protocytoskeleton can be disassembled on irradiation, leading to the loss of mechanical integrity of the PCM. The selective disassembly of PCMs can be achieved with high spatio-temporal control on irradiation with UV light, and that disassembly can be monitored through the use of microindentation using a recently developed methodology.^[3] Moreover, the photolabile proteinosomes of the PCM can be precisely photo-patterned to generate new, complex three-dimensional architectures. Whilst these novel materials are still in the early stages of development, they have the potential to be used in diverse applications from drug delivery to soft robotics.

[1] A. Galanti, R. O. Moreno-Tortolero, R. Azad, S. Cross, S. Davis, P. Gobbo, *Adv. Mater.* **2021**, *33*, 2100340.

[2] X. Huang, M. Li, D. C. Green, D. S. Williams, A. J. Patil, S. Mann, *Nat. Commun.* **2013**, *4*, 2239.

[3] H. E. Symons, A. Galanti, J. C. Surmon, R. S. Trask, S. Rochat, P. Gobbo, *Soft Matter* **2022**, *18*, 8302-8314.

8:00 PM SB05.07.08

Progress on Synthetic Mucin Mimics for Bacteriostatic Control of Wound Infections Keith E. Whitener¹, Jeremy S. Marshall², Kenan Fears¹, Matthew D. Thum¹ and Jinny Liu¹; ¹Naval Research Laboratory, United States; ²Nova Research, United States

Mucins are high molecular weight glycoproteins which interact with bacteria to inhibit biofilm formation and therefore decrease the likelihood of infection establishment. However, the physical and biochemical makeup of mucins are highly dependent on their processing and environmental factors such as pH, temperature, ionic strength, and hydration level. Native mucins with prominent bacteriostatic activity are therefore too fragile to be deployed in the field as solutions for wound infection at this time. The work described here is part of NRL's ongoing effort to find a robust fieldable polymeric platform which mimics the physical and biochemical structure of mucin and therefore recapitulates its bacteriostatic properties.

Mucin-O-glycans were cleaved from the peptide backbones of commercial porcine gastric mucin and native mucus obtained from pig stomach scrapings. The mucin mimic backbone we chose was carboxymethyl cellulose (CMC), as we have found that this polymer has a good cytotoxicity profile and rheological behavior that matches native mucin. Cleaved glycans were attached using EDC/NHS amidation and alkyne/azide click chemistry. Analysis was performed using MALDI mass spectrometry, rheometry, and viscometry. Cytotoxicity was determined by applying solutions to human fibroblasts and monitoring via fluorescence live/dead staining. Bacteriostatic and biofilm inhibition activity were determined by applying solutions to liquid and solid supported cultures of *Pseudomonas aeruginosa* and monitoring optical density.

Commercial mucins differ dramatically from native mucins in their physical and biochemical makeup: the glycans cleaved from native mucins do not match those cleaved from commercial mucins, the rheology is different and commercial mucins do not readily form hydrogels, the bacteriostatic properties are worse for commercial mucins than native mucins, and commercial mucins are far more cytotoxic than native mucins. However, we also found that the properties of the native mucins themselves change markedly as they go through the purification process. We are currently evaluating both the mucin glycan composition and the rheometry of the mucins and the CMC mimics, and we intend to evaluate their bacteriostatic properties under a variety of environmental stresses including pH and temperature changes.

8:00 PM SB05.07.09

Hofmeister Salts Enhance the Water-Responsive Actuation Energy of *Bacillus Subtilis* Cell Walls Seungri Kim^{1,2}, Haozhen Wang^{2,3}, Darjan Podbevšek² and Xi Chen^{1,2,3}; ¹The City College of New York, United States; ²CUNY Advanced Science and Research Center, United States; ³The City University of New York, United States

Water-responsive (WR) materials have attracted significant attention due to their potential applications as high-energy actuators for soft robotics, smart structures, and energy harvesting devices. Recently, the cell walls of *Bacillus (B.) subtilis* have shown a high WR energy density of 72.6 MJ m⁻³, surpassing that of existing actuator materials. In this study, we found that the exceptional WR energy density of the cell walls is attributed to nanoconfined liquids' properties. Furthermore, we discovered that strengthening the hydrogen (H-) bonding network of these nanoconfined liquids could further increase this energy density. To investigate this, we systematically modulated the H-bonding network using Hofmeister salts, specifically potassium sulfate (K₂SO₄) and potassium iodide (KI), which respectively strengthen and weaken the H-bonding network. Cell walls treated with a 10 mM K₂SO₄ solution exhibited a 22.4 % enhancement in energy density, reaching 101.8 MJ m⁻³. However, higher concentrations (30-50 mM) of K₂SO₄ or any KI solutions led to reduced WR energy densities. These observations highlight the crucial role of the enhanced H-bonding network in achieving high-performance WR materials and emphasize the existence of a certain range of H-bonding strength for optimizing WR performance. Moreover, our study presents a cost-effective and scalable approach that utilizes Hofmeister salts to manipulate and enhance the WR performance of hygroscopic materials.

8:00 PM SB05.07.10

Tunable Interface of Polymeric Composite of Electroactive P3HT-MWCNT Thin Film for Bioelectronics Applications Paola Campione^{1,2,3}, Grazia Maria Lucia Messina¹, Francesca Santoro^{3,2} and Giovanni Marletta¹; ¹University of Catania, Italy; ²Forschungszentrum Juelich, Germany; ³RWTH Aachen University, Germany

One of the main challenges in bioelectronics concerns the development of materials able to respond to external stimuli and that are compatible with excitable tissues. In the last decades, conductive polymers (CPs) have been widely studied and developed as electroactive materials for applications in interfacing with biological systems. Their conductive properties allow cells or tissues growth upon stimulation, and their “soft” nature allows to form a better biotic-abiotic interface and reduce the mechanical mismatch between material and cells thanks to the elasticity of polymeric films that is similar to biological tissues [1]. CPs' physical and iontronic-electronic properties can be optimized through the formation of composites enriched with carbon nanotubes or graphene in order to improve electron transport capacity, decrease impedance and increase flexibility. Their biocompatibility can be improved using functionalization methods with biologically active molecules [2] even if the influence of blending agents is still under investigation. The precise control of CP films nano-topography may have interesting effects for biointerfacing and improving the cell-chip coupling for cell activity recording and stimulation, acting on protein adsorption and cell adhesion.

In this work, we report on how to obtain stable electroactive nanocomposite dispersion using semiconducting regioregular poly(3-hexylthiophene-2,5-diyl) (P3HT), with different percentages in weight of multi-walled carbon nanotubes (MWCNT) and how to deposit to form homogeneous thin films. Their morphologies have been investigated by means of atomic force microscopy (AFM) and scanning electron microscopy (SEM), and the attention has been focused on the “cushion” effect due to the presence of the filler in the polymeric matrix that allow an interesting modification in mechanical properties (Young's Modulus), analyzed by nanoindentation with atomic force microscopy (AFM), and the formation of a “softer” interface. Considering the central role of extracellular matrix protein in cell adhesion, their interactions at the interface with our systems were investigated by means of quartz crystal microbalance with dissipation monitoring (QCM-D). Noteworthy, it has been found that thanks to the larger available surface area of the blend thin film that act like a sponge, proteins are adsorbed in a very different way with respect to the bare semiconducting P3HT. Indeed, both the adsorption kinetics and the adsorbed mass are increased for each extracellular matrix proteins. The biocompatibility of the systems with different cell lines has been investigated as well as the effect on cell metabolism. Moreover, the effect of the systems on the variation of the distance between cell and electrode has been analyzed by focused ion beam - scanning electron microscopy (FIB-SEM). The realization of this nanostructured bioelectronic interface represents an example of 2.5D cell culture and promotes the optimization of the cell-chip coupling by tuning the cleft between the membrane of the cell and the electrode, also acting on the formation of the extracellular matrix protein coating that helps cells attach to, and communicate with, nearby cells, and plays an important role in cell growth, cell movement, and other cell functions.

[1] Malliaras, G. *Biochimica et Biophysica Acta* 1830, (2013), 4286–4287.

[2] Scarpa, G. et al. *Macromol. Biosci.* 10, (2010), 378–383.

8:00 PM SB05.07.11

Harnessing Cell-Free Protein Synthesis to Synthesize and Repurpose Viral Fusion Machinery Ekaterina Selivanovitch and Susan Daniel; Cornell University, United States

Viruses present one of the most efficient mechanisms for intracellular cargo (i.e. viral genome) delivery in which interactions at the virus-host cell interface dictate the delivery pathway. For instance, enveloped viruses- those that are ‘wrapped’ in a lipid bilayer, deliver their genetic cargo by first interacting with extracellular receptors, triggering a reaction cascade that results in fusion of the virus- and host cell lipid membranes and cargo release into the cytosol. Harnessing the efficiency of this translocation mechanism would drastically improve cellular uptake of therapeutic and bioactive cargo, currently a major obstacle in both agricultural and pharmaceutical scientific communities. In this work, we propose that viral fusion machinery can be repurposed for delivering user-defined cargo to cells containing the appropriate receptors. Hemagglutinin (HA), which is a protein found on the surface of influenza viruses and is known to mediate the virus-cell fusion mechanisms, is one of the proteins explored for this goal, along with several other viral membrane proteins including NiV-F and Spike (SARS 2). To circumvent

challenges associated with using infectious viruses or isolating/reconstituting membrane proteins, we use cell-free synthesis techniques to directly insert the proteins into our delivery vehicles of choice- liposomes. Not only can this approach be used to synthesize and design functional proteoliposomes, it provides synthetic mimics for isolating biological processes with control over the proteoliposome environment, which can be designed to be rudimentary or increasingly more complex.

8:00 PM SB05.07.12

Modulating Light Transmission using Particle-Based Displays Patrick A. Sullivan, Daniel Wilson and Leila Deravi; Northeastern University, United States

E-inks utilize reflected ambient light rather than emitted light to display changes in text or images. As such, they can generate and hold patterns using very low power. Electrophoretic, electrofluidic and electrochromic techniques have been used commonly in this space together with homogenous materials designed specifically adapt to a biased stimulus to create these low power displays. We asked whether inherently asymmetric materials like Janus particles can be similarly used in low energy adaptive display. In this work we investigate methods to synthesize and manipulate the transmissivity of Janus particles made with a metal and a dielectric material. Using custom designed optical chambers, we assayed the effect of electric field on particle rotation which ultimately correlated to a change in the transmission of visible light. Our preliminary results demonstrate a realistic approach to using asymmetric Janus materials as active elements for future display applications.

8:00 PM SB05.07.13

3D-Printed, Biomimetic, Electroconductive Scaffolds for the Promotion of Axonal Regrowth after Spinal Cord Injury Liam Leahy^{1,2}, Ian Woods^{1,2}, Jack Maughan^{1,2,3}, Javier Gutierrez Gonzalez^{1,2,3}, Michael Monaghan^{2,3}, Adrian G. Dervan^{1,2} and Fergal O'Brien^{1,2,3}; ¹RCSI, Ireland; ²RCSI and TCD, Ireland; ³Trinity College Dublin, The University of Dublin, Ireland

Spinal cord injury (SCI) induces paralysis by damaging axons, neuronal processes that carry signals about the body. Injured axons are unable to regrow through the injury site, preventing functional recovery. Electrical stimulation (ES) has shown signs of being capable of inducing neuronal regrowth and support functional recovery. We propose that a tailored, electroconductive scaffold with composition designed to support and direct ES to regrowing axons may help drive them toward their distal targets and restore function. This is a difficult challenge to tackle, as the spinal cord is a complex tissue comprising discrete axonal tracts. An ideal scaffold for this system must mimic the structure of the cord and provide the supportive cell environment of the native extracellular matrix (ECM). To overcome this challenge, ECM-functionalised electroconductive scaffolds designed to mimic the axonal tract structure of the human spinal cord were fabricated by coating 3D-printed polycaprolactone (PCL) with conductive polypyrrole (PPy) nanoparticles and filling the structure with freeze-dried ECM to direct ES to promote neurite outgrowth.

Biomimetic PCL scaffolds were 3D-printed with an Allevi 2 printer to produce uniaxially aligned, interlocking cylindrical architectures, with several channel sizes to match the diameters of human spinal cord axonal tracts. PPy was polymerised *in situ* to form an electroconductive nanoparticle coating on PCL scaffolds, verified via FTIR and SEM imaging. Electroconductivity was measured via the 4-point probe method. Scaffold biocompatibility was assessed by growing neurons on 2D PPy/PCL films and measuring metabolic activity, cellular DNA and neurite outgrowth. Neurotrophic ECM was directionally freeze-dried within scaffold channels to mimic the native spinal cord environment and further promote neurite extension¹. Neurons were electrically stimulated on ECM-functionalised PPy/PCL and PCL scaffolds using an Ionoptix bioreactor and imaged to assess the effect of ES-induced neurite extension over 7 days. 3D-printed PCL scaffolds of all channel sizes were successfully coated with PPy nanoparticles. Conductivity of the PPy coating was measured at 15 ± 5 S/m, 30 times higher than native spinal cord tissue. PPy/PCL substrates were as biocompatible as PCL, indicating the suitability of PPy coated scaffolds for neuronal tissue engineering. Freeze-dried ECM formed aligned pore structures within scaffold channels, providing a physical guide for neurite outgrowth. No difference in electrical properties or cell activity were measured in scaffolds of various channel sizes, showing scaffolds can be scaled to match native cord structures without losing functionality. Electrically stimulated neurons on PPy/PCL scaffolds showed increased average neurite length and total cellular DNA compared to PCL scaffolds, suggesting ES via a conductive scaffold promotes healthy neuronal growth.

In conclusion, biomimetic 3D-printed electroconductive scaffolds were manufactured and characterized and demonstrated excellent biocompatibility. Scaffolds were successfully scaled to match the sizes of axonal tracts, and electrically stimulated neurons exhibited increased neurite extension within PPy/PCL scaffolds compared to inert PCL controls, showing the potential of the electroconductive scaffold to direct neurite growth. Taken together, these results show that ES applied via ECM-functionalised electroconductive scaffolds drives neurite outgrowth, a key requirement to achieving functional recovery post-injury, highlighting the potential use of this novel combination therapy for SCI repair.

FUNDING ACKNOWLEDGEMENTS

Irish Rugby Football Union Charitable Trust and Science Foundation Ireland Advanced Materials and Bioengineering Research (AMBER) Centre (SFI/12/RC/2278_P2).

REFERENCES

Woods *et al.*, *Adv Health Mater.*, 11, 3, 2101663, 2021

8:00 PM SB05.07.14

Nuclease Responsive DNA Probe Conjugated Particles for Efficient Detection of Bacteria Sun-Jung Kim¹ and Yong-Beom Shin^{1,2}; ¹Bionano Health Guard Research Center, Korea (the Republic of); ²Korea Research Institute of Bioscience and Biotechnology, Korea (the Republic of)

Recently, poisoning due to microbial contamination of food is continuously increasing, and interest in food safety is increasing. Therefore, it is important to quickly detect microorganisms in the field to eliminate contamination. Microorganisms can be contaminated not only by the food itself but also by the cook's hands and tools, so a technology capable of quickly detecting microbial contamination is very necessary. Traditionally, detection of microorganisms is done through culture-based assay, which has the disadvantage of taking too long, so fast and accurate molecular biological tests are attracting attention. Polymerase chain reaction (PCR) is widely used because it is accurate and has specificity, but it has to go through several steps and it takes some time to use it as a detection system directly in the field. Although adenosine triphosphate (ATP)-based detection system has been widely used for fast and simple, it is difficult to know the exact level of contamination because it detects not only live cells but also dead cells and other impurities such as organic debris. Therefore, there is a problem that the level may appear even after sterilization through disinfection. Bacteria produce various nucleases such as exo, endo for various biological function and the degree of bacterial contamination can be estimated through the activity of nucleases. In this study, we prepared nuclease responsive DNA conjugated particles. We designed various nuclease responsive DNAs to detect bacteria by various methods such as color reaction, fluorescence and luminescence. In our system, the DNA probe bound to the particles is cut off by the nuclease secreted during the lysis of the bacteria and a signal is generated so that the presence or absence of bacterial contamination can be easily measured in a short time. Moreover since only live bacteria can be detected, the exact degree of contamination can be confirmed and it is thought that it will be able to be used quickly in the field.

8:00 PM SB05.07.15

Nanomaterials and Additive Processes for Transparent and Stretchable Organic Electrochemical Transistor Takaaki Abe, Teppei Araki, Shoya Matsuda, Naoko Kurihira, Mihoko Akiyama, Takafumi Uemura and Tsuyoshi Sekitani; SANKEN (The Institute of Scientific and Industrial Research), Japan

Flexible electronic devices with optical transparency exhibit biocompatibility and increase the versatility of measurement methods, such as multimodal sensing that enables simultaneous usage in optical, electrical, and ionic methods. In this study, we develop fully transparent and flexible organic electrochemical transistors (OECTs) using transparent conductors of Ag nanowires (AgNWs) and conductive polymers. They demonstrate the feasibility of multimodal acquisition of biological signals. In addition, stretchable materials are newly developed to construct fully transparent and stretchable OECTs, which can contribute to the creation of next-generation medical sensors.

Sensors for use as personal healthcare devices that can measure biological signals continuously and for a long time for the early detection of diseases have been expected [1-2]. OECTs can be used to fabricate circuits suitable for such biological signal measurements owing to their advantages of low operating voltage, mechanical flexibility, and high mutual transconductance [3]. In particular, the high mechanical flexibility decreases the wearing discomfort because flexible biological tissues change their shape. Additionally, if the device has high transparency, it enables multimodal sensing that can utilize electronic, optical, and ionic methods simultaneously, as well as miniaturization through the stacking of devices. Therefore, stretchable and transparent conductors and semiconductor materials for electronic devices can facilitate a new electronic design.

In this study, we develop highly transparent and flexible OECTs using AgNWs and poly(3,4-ethylenedioxythiophene):poly(styrene sulfonate) (PEDOT:PSS) [4]. High bending durability and high visible transmittance (>90%) are achieved by controlling the orientations of the AgNWs used for wiring. Furthermore, additive layering techniques, such as printing and lamination processes, are employed to decrease damage to the nanomaterials constituting the OECT. In addition, these transparent and flexible OECTs exhibit properties comparable to those of conventional opaque OECTs. Consequently, low-noise measurements of brain waves and ion concentrations, as well as simultaneous optical measurements of blood flow and pulse waves, are feasible and a step toward the quantification of human stress.

Furthermore, stretchable channel materials are developed to create more flexible OECTs. A patterning process of AgNW-based conductors and semiconductors on elastomers is concurrently developed to fabricate fully stretchable and transparent OECTs. In particular, the stretchable conductors and channel materials exhibit durability under 50%–100% strain; thus, they can be used for fully transparent and stretchable sensors for the long-term and multimodal assessment using electrophysiological, optical, and ionic methods.

References

- [1] S. M. A. Iqbal *et al.*, *npj Flex. Electron.*, 2021, 5, 9
- [2] W. Heng *et al.*, *Adv. Mater.*, 2021, 34, 2107902
- [3] J. Rivnay *et al.*, *Nat. Rev. Mater.*, 2018, 3, 17086
- [4] A. Takemoto *et al.*, *Adv. Sci.*, 2022, 10, 2204746

8:00 PM SB05.07.16

Transforming the Brain to Transparent Hydrogels for Long-Range Microscopic Analysis of the Nanoparticles Interactions with Brain Tumors MaryamGolshahi, HamedArami and LaylaKhalifehzadeh; Arizona State University, United States

Microscopic analysis of the tumor response to therapeutics reagents such as nanoparticles and chemotherapy drugs is limited to conventional tissue sectioning, which is followed by immunostaining and optical microscopy. Tissue sectioning is destructive and microscopic data obtained from a limited number of thin tissue slices (typically with 5-50 μm thickness) are not representative of the efficacy of the treatment over the entire tumor mass. Microscopic results obtained from a single or limited number of tissue slices can be even more misleading for brain tumors with high levels of heterogeneity such as glioblastoma multiforme (GBM). Therefore, developing methods for microscopic analysis of the whole tumor tissue without any sectioning can be beneficial by providing an overall feedback about the treatment rates at different parts of the tumor mass. This capability can potentially enhance the treatment effects and minimize the probability of the tumor recurrence by optimizing the treatments to target the entire tumor. Here, we used a polymerization method that helps to transform the whole mouse brain to optically transparent acrylamide-based hydrogels without losing the microscopic or nanoscale structure of the tumors at both extracellular and intercellular levels. Orthotopic U87 tumors (human-derived GBM cells with GFP signal) were generated in mouse brains ($n=3$). Therapeutic nanoparticles (gold nanoparticles tagged with Cy5 fluorescent molecules) were injected into tumors stereotactically using a magnetic resonance imaging (MRI) guided approach. Mice were euthanized 24h post-injection and brains were excised and immersed in a monomer solution, followed by a low-temperature polymerization and tissue-clearing technique known as CLARITY. Then, the entire volume of these transparent brains were analyzed using different microscopy techniques, including confocal and light-sheet microscopy. The interaction of the nanoparticles with tumors was investigated using their Cy5 and GFP signals, respectively. We were able to generate three-dimensional maps verifying the distribution of the nanoparticles in tumors and other parts of the brains (e.g., the ventricles). Immunostaining of these brains is a reversible process and a series of staining and microscopies can be used for analyzing different treatment biomarkers (such as cell death, necrosis, and immune response) separately. Expansion of this method will enable more accurate pre-clinical and clinical investigations to evaluate the efficacy of a variety of therapeutic agents and their potential side-effects within the entire tumors and other parts of the brain.

8:00 PM SB05.07.17

Aptamer-Decorated Prussian Blue Nanozymes for Selective Detection of Dopamine Han BeenLee, Do HyeonKim, Se HwaCheon, Chang HyeonHa, Su JeongLee and Gi hunSeong; Hanyang University, Korea (the Republic of)

Dopamine (DA) is a catecholamine neurotransmitter that plays a significant role in the central nervous and hormone systems of humans. Abnormal levels of DA can lead to various diseases, including Parkinson's disease and depression. While electrochemical measurements have gained considerable attention for their simplicity and responsiveness, the electrochemical detection of DA is easily influenced by the simultaneous presence of ascorbic acid (AA) or uric acid (UA). This is because AA and UA can also undergo oxidation at a potential similar to that of DA. Therefore, it is crucial to develop a sensitive and selective detection method for DA in biological fluids to overcome these challenges.

Colorimetric assays have obtained much attention due to their rapid observation by the naked eye and user-friendly operation. However, assays relying on the reduction of the substrate of DA have limitations in terms of selectivity because substances such as AA and UA, which have a similar structure to DA, also possess the ability to reduce substrates. To address this issue, we employ an aptamer to ensure high selectivity in real samples. Aptamers are molecular recognition components based on nucleic acids. These functional single-stranded nucleic acids can adopt a three-dimensional structure and exhibit exceptional specificity and affinity for target molecules.

Nanozymes, nanomaterials that exhibit enzyme-mimicking activities, have emerged as promising alternatives to natural enzymes like horseradish peroxidase (HRP) due to their exceptional catalytic activity, ease of modification, and remarkable stability. Given their intriguing and practical characteristics, nanozymes have been employed in various biomedical point-of-care applications, including biosensing and immunoassays. Among the different types of nanozymes, prussian blue nanoparticles (PBNPs) have gained widespread use in the field of biosensing and immunoassays. This is attributed to their outstanding peroxidase-like activity, robust stability, and high sensitivity.

In this study, we employed chitosan (CS), a polycationic biopolymer with amine groups in its backbone, to stabilize PBNPs. This resulted in the formation of CS-coated prussian blue nanoparticles (CS/PBNPs), which modified the surface charges of the PBNPs to a positive state. By virtue of the positive charges conferred by CS, the negatively charged dopamine binding aptamer (DBA) could be immobilized onto the CS/PBNPs through electrostatic interactions.

DBA molecules, known for their specific affinity towards DA, were adsorbed onto the surface of CS/PBNPs, leading to the inhibition of the peroxidase-mimicking activity of the CS/PBNPs. However, upon the introduction of a DA sample solution, the DBA molecules on the CS/PBNPs surface strongly bound to the DA, inducing a conformational change in the aptamer and causing its separation from the CS/PBNPs. Consequently, as the concentration of DA increased, more surface area of CS/PBNPs became exposed, resulting in an elevation of their peroxidase-like activity.

In conclusion, we successfully developed an aptamer-based colorimetric assay utilizing CS/PBNPs for the detection of DA in concentrations ranging from 0.25 μM to 100 μM , with a limit of detection (LOD) of 0.16 μM . The recovery results of DA concentrations (0.25 μM , 0.5 μM , and 1 μM) in spiked human serum were 92.6%, 102.1%, and 103.9%, demonstrating high reproducibility and reliability of the CS/PBNP-based apta-sensor for determining DA levels in clinical applications. Furthermore, compared to typical immunoassays, this aptamer-based nanozyme inhibition/activation assay eliminates the need for a washing step, making it highly practical in terms of reducing assay time and maintaining high sensitivity. Based on its excellent performance, this biosensor holds promise as a valuable tool for the rapid, selective, and sensitive detection of clinically significant small molecules, such as hormones, in practical applications.

8:00 PM SB05.07.18

Modification of Conductive Surfaces via Tailored Dyes Derivatives for Bacterial Detection SvenjaHerdan¹, LaurieNeumann¹, LeaKönemund^{1,2}, RebekkaBiedendieck¹, Hans-HermannJohannes^{1,2}, DieterJahn¹ and WolfgangKowalsky^{1,2}; ¹Technische Universität Braunschweig, Germany; ²Cluster of Excellence PhoenixD, Germany

The improvement of a biosensor which combines fast and highly sensitive detection of bacteria with easy handling is of great interest, for example, in the fields of medicine or the food industry. In the future, pathogenic bacteria could be detected at an early stage. Conventional methods such as enzyme-linked immunosorbent assay (ELISA) or polymerase chain reaction (PCR) are time-consuming, expensive and require professional expertise. Therefore, a sensor with low costs and fast, reliable results is of great importance.

In previous works, functionalized porphyrins with two different linkers have been synthesized for a bacteria sensing system. The linkers are divided into two different groups: linker A which can bind to an electrode (gold or indium tin oxide) and linker B which can bind to bacteria. For linker B there are two possible bio receptors a peptide group and cysteine group enabled to connect the Gram-negative bacterium *Escherichia coli* (*E. coli*) K12, a common well investigated apathogenic model strain. An analysis with fluorescence-lifetime imaging microscopy (FLIM) could already show a decrease of the fluorescence lifetime of the porphyrin molecule due to changes in their chemical environment or conformation as they have an interaction with cell components of the bacteria cells. These results show that both bio receptors in combination with the porphyrin molecule can be used as a bio linker on an electrode surface for further bacteria detection methods. (Neumann, 2021).

The goal of this research is to extend the existing system. For this purpose, porphyrin was replaced by another dye, boron-dipyrromethene (BODIPY). Reasons for this are that BODIPYs are thermally and photochemically stable, have a higher fluorescence quantum yield (BODIPYs $\approx 90\%$; porphyrins $\approx 5\%$; depending on the substitution of the dyes), are well soluble and chemically stable and they are biocompatible. Furthermore, it should be emphasized that the synthetic effort and thus also the yield loss can be reduced, because only two steps are necessary for the BODIPY linker synthesis and six steps have so far been necessary for the porphyrin linker synthesis. In addition, it is possible to use a boronic acid instead of a peptide or cysteine group for linker B. Boronic acids have the property to bind to *cis*-diols, which are located on bacterial cell wall. By adapting linker B as previously mentioned, a general sensor could be developed regardless of whether the bacteria are Gram-negative or Gram-positive.

Reference: Neumann, L.; Könemund, L.; Rohnacher, V.; Pucci, A.; Johannes, H.-H.; Kowalsky, W. A₂BC-Type Porphyrin SAM on Gold Surface for Bacteria Detection Applications: Synthesis and Surface Functionalization. *Materials* **2021**, *14*, 1934.

Key words: porphyrin, BODIPY, *E. coli* immobilization, biosensing

8:00 PM SB05.07.19

Mediated Electron Transfer in Bacteria for Charge Generation NdepanaG. Andrew and HemaliRathnayake; University of North Carolina at Greensboro, United States

The increase in energy demand led to remarkable research activities on energy generation, storage, and conversion, and many different kinds of nanoscale materials have been explored to harness energy. However, recently microorganisms including bacteria and algae have been shown to display significant roles in developing high-performance probes owing to their abilities to reproduce fast, self-repair, self-assembly, and wide range of biosynthetic capabilities. Among a wide variety of microbes, bacteria have been well studied offering their adaptation to broaden research directions for developing a variety of sustainable energy generation, conversion, and storage systems with either improved or new capabilities and performance.

However, adapting bacteria to develop the aforesaid systems with required performance entails a clear understanding of how bacteria interact with the surface or mediator and how chemical, physical, and intrinsic properties of the "mediator" affect interaction with bacteria to produce expected results and programmable characteristics. The processes of metabolic electron transfer from bacteria to an extracellular mediator and vice versa in diverse exoelectrogenic and non-exoelectrogenic bacteria have been studied but only a few have been investigated in-depth to understand bacteria responses and study their electron transfer processes at their respective biotic interfaces with a variety of organic and inorganic mediators. Electron transfer in bacteria can

occur either directly or indirectly, however, only a limited set of bacterial species can transfer electrons directly to the electrodes, most bacteria require an external electron transfer mediator to transfer charges to the electrode for efficient energy generation. Although Various compounds have been tested in the past as exogenous mediators, there are potential classes of compounds that are yet to be explored.

Herein, we gather a new concept of using a metal-organic framework as an external mediator for electron transfer at the interface of *E.coli*, we grow live *E.coli* cells on a functional MIL-88B MOF to construct a charge capacitive bio interface. The aim is to study the interactions at the bio interface and employ these interactions to generate a charge-capacitive smart interface for energy storage and study the metabolic electron transfer mechanism at the bio interface resulting in the generation of energy at the bio interface. In theory, the MIL-MOF will stimulate the bacteria's metabolic electron transfer processes by modulating charge injections at the *E.coli*/MOF interface to generate charge capacity through electron transfer processes. So far from our preliminary result, we obtained a charge capacity of 399 Fg^{-1} at a scan rate of 5 mV/s generated at the *E.coli*/MOF interface as compared to 195 Fg^{-1} generated at the *E.coli* (control) interface only at the same scan rate. Our results suggest the potential of MIL-88B MOF as an external mediator in facilitating electron transfer at the *E.coli* interface to generate a higher charge capacity twice the magnitude of *E.coli* charge capacity.

This study proposes that by combining the distinctive functionalities of living bacteria with biocompatible abiotic MIL-MOFs, it is possible to create smart interfacial biosystems for charge generation and storage with programmable features.

8:00 PM SB05.07.20

The "SLIC" Idea: Superhydrophobic Lubricant Infused Composite (SLIC) is a Non-Toxic, Inexpensive Polymer Composite Coating that Prevents Biofouling ThomasLeFevre, JosephDaddona, WilaiwanChouyyok, StonyAkins, GeorgeBonheyo, CurtisLarimer and RaymondS. Addleman; Pacific Northwest National Laboratory, United States

This poster will describe the development and testing of a Superhydrophobic Lubricant-Infused Composite (SLIC) coating that inhibits the attachment of organic and biological matter. Biofouling is the unwanted accumulation of biological material, such as bacteria, algae, mussels, and barnacles, on a surface. Biofouling is an expensive and disruptive problem in many water-related industries such as shipping, hydropower, and aquaculture. Antifouling coatings are commonly utilized to mitigate fouling, but the existing coatings that are effective are also toxic or extremely expensive.

To address the toxicity and expense of existing coatings, SLIC is a PDMS-based coating with several additional ingredients that provide strength, texture, and porosity in the coating. This work will describe the design, selection, and optimization of biomimetic additives designed to provide strength, abrasion resistance, and a surface microstructure that mimics the superhydrophobic texture of natural surfaces such as the lotus leaf. We will outline a process for incorporating lubricant oil into the coating to provide a low surface energy liquid layer, similar to fish slime, that inhibits biological adhesion. The oil can flow into cracks and crevices in the coating, providing a self-healing mechanism when the coating is scratched. SLIC was designed to be an antifouling coating that is tough, long lasting, economical, and toxin-free. It can also be easily customized for specific use cases such as nets that require a flexible coating.

Results of experiments to quantify antifouling performance by exposing varying formulations of SLIC to mussels at different life stages will be presented. Use of a machine learning algorithm to assist in the detection and counting of mussel larvae on surfaces will be described. Results of antifouling performance tests showed that SLIC prevented mussel larvae attachment in static conditions is better than the leading antifouling paint and significantly better than uncoated stone, metal, and plastic surfaces. In summary, SLIC was designed as a high performance low-cost antifouling coating. It can prevent mussel adhesion and other types of fouling while remaining nontoxic.

8:00 PM SB05.07.21

A Smart Coating with Integrated Physical Antimicrobial and Strain-Mapping Functionalities for Orthopedic Implants YiZhang and QingCao; University of Illinois at Urbana-Champaign, United States

As the prevalence of orthopedic implants increases within the aging population, these patients become increasingly vulnerable to risks associated with periprosthetic infections and instrument failures. There have been attempts to reduce the risk of infection by modifying the implant surface to impede bacterial adhesion or applying antibiotics to the surface to kill local bacterial populations. But these methods are rarely used due to their own limitations. For instance, coating implant surfaces with hydrophilic molecules or quorum-sensing inhibitors can block bacterial adhesion, but this strategy fails if even a few bacteria manage to attach and form an antibiotic-resistant biofilm. Another significant complication associated with orthopedic implants is aseptic implant failures, which require surgical revisions and affect over 10% of patients. These failures manifest primarily as loosening caused by mechanical shielding or implant breakage due to fatigue failure. Presently, these complications are diagnosed using x-ray or bone scan imaging. However, these techniques only detect gross implant movement, which occurs long after the inception of loosening or implant-related microfractures, even with harmful radiation and high costs.

To address these challenges, we develop the design of a smart-coating foil that can be applied to the surfaces of orthopedic implants. This foil provides both long-term physical bactericidal action and sensitive strain mapping to mitigate both septic and aseptic orthopedic failures. The outer surface of the foil is designed with high-density nanopillars, mimicking the surface nanotopology of cicada wings. These structures exhibit strong mechanical bactericidal effects against bacteria commonly associated with orthopedic implant infections without directly releasing any chemicals. A multiplexed strain-sensing array is integrated into the foil. The high piezoresistive coefficient of single-crystalline silicon ensures accurate detection of strain down to 0.01% experienced by orthopedic implants. The nanometer-scale film thickness allows the foil to bond with the implant surface, while the integration of silicon gauges with multiplexing transistors enables strain mapping across the implant surface. This can assist in the detection of early-stage spinal fusion and pedicle-screw loosening, guiding patient-specific care and early intervention against aseptic instrument failures. The strain-mapping array and mechano-bactericidal nanostructures both showed excellent biocompatibility and long-term stability in vivo.

8:00 PM SB05.07.22

Specific Protein Metalization in Cell-Derived Extracellular Matrix via Antibody-Guided Biotemplating for Utilization in Hydrogen Production and Sensing Chang WooSong and JaewanAhn; Korea Advanced Institute of Science and Technology, Korea (the Republic of)

In nature, there is a myriad of hierarchical biological structures consisting of various proteins that are challenging to replicate by artificial synthetic methods. To exploit such complex structures in material science, biotemplating has attracted great attention over the past decades, wherein exotic functionalities from inorganic materials were able to impart into the biological scaffolds by electroless plating or physical vapor deposition of metal. However, the biological architectures used in prior reports were stereotypical and ordinary with the lack of ways to manipulate their morphological features such as porosity, alignment, and organization, limiting their usage in more broad fields. To this end, we propose the cell-derived extracellular matrix (ECM) is an excellent option to be used as a template for achieving diverse biomimetic architectures. ECM has evolved into intricate mesh structures intertwined with various fibrillar protein assemblies to conduct mechanical support of cells, assist in the proliferation and migration of cells, and transport the signal to the cells. Because of these important biological roles of ECM, a variety of ECM have been created with customized morphological and chemical characteristics, especially for cell biology, pharmacology, and tissue engineering. Despite already developed diverse protein assemblies in ECM, there was no attempt to use them as a biological scaffold for metallization. To use a specific ECM protein as a template, we introduced 1.4-nm nanogold-conjugated antibodies and labeled them to a specific protein called fibronectin within the ECM, and then the nanogold acted as the nucleation sites for Au growth. The metalized ECM could be electrically conductive after thermal sintering or second metal growth (e.g., Pd and PdPt alloy) with additional functionality. Following the deposition of PtNPs, the fabricated conductive biocomposite showed catalytic activity in the hydrogen evolution reaction (HER), maintaining its stability for up to 500 repeated cycles. In addition to hydrogen production, the electrically conductive biocomposites by the second metal growth demonstrated the prominent hydrogen sensing performance at room temperature.

8:00 PM SB05.07.23

A Photo-Patternable Stretchable Gold Conductor by Electroless Plating Process HinataMitomo^{1,2,3}, KeitaSuzuki⁴, KatsuyaTennichi⁵, YuanyuanZhou^{1,2,3} and NaojiMatsuhisa^{1,2,3}; ¹Research Center for Advanced Science and Technology, The University of Tokyo, Japan; ²Institute of Industrial Science, The University of Tokyo, Japan; ³Department of Electrical Engineering and Information Systems, Graduate School of Engineering, The University of Tokyo, Japan; ⁴Tanaka Kikinzoku Kogyo K.K., Japan; ⁵EEJA Ltd., Japan

Stretchable gold thin-film electrodes exhibit superior biocompatibility and conductivity. In previous studies, stretchable gold thin films have typically been prepared by thermal evaporation^[1,2]. However, to maintain high stretchability, the sheet resistance was limited to an order of 10 Ohm/Sq. Moreover, it is crucial to minimize gold waste resulting from deposition in unnecessary areas.

In this study, we present highly stretchable and conductive gold electrodes fabricated by a photo-patternable electroless plating process. Our gold thin film exhibited a remarkably low sheet resistance of 0.25 Ohm/Sq. at 0% strain and 2.7 Ohm/Sq. at 50% strain. The film remained highly conductive, even under a 200% strain. These electrical and mechanical characteristics were preserved when the gold was patterned to a resolution of 100 μm . Fabrication began by spin-coating a primer polymer layer, which adheres gold nanoparticles from the colloid solution. Deep ultraviolet exposure can deactivate the capacity to capture gold nanoparticles, enabling patterning. Subsequent electroless plating allowed the gold nanoparticles to grow into a uniform film with a thickness of 200 nm. We controlled the aforementioned plating conditions to regulate microcrack formation under strain, and obtained the high stretchability of our gold. The high conductivity and patternability of our stretchable gold pave the way for the development of stretchable, high-density electrodes for electrophysiology measurements, and stretchable antennas for wireless wearable electronic devices.

8:00 PM SB05.07.24

Design and Characterization of Magnetically Controlled Minicell-Driven Biohybrid Microswimmers for Targeted Drug Delivery ApplicationsSaadet F. Baltaci Demir^{1,2}, Irina Kalita³, Birgul Akolpoglu^{1,4} and Metin Sitti^{1,4,5}; ¹Max Planck Institute for Intelligent Systems, Germany; ²University of Stuttgart, Germany; ³Max Planck Institute for Terrestrial Microbiology, Germany; ⁴ETH Zürich, Switzerland; ⁵Koc University, Turkey

Bacteria-based biohybrid microswimmers, combining motile bacteria cells with synthetic materials, have emerged as promising vehicles for alternative therapeutic applications such as active drug delivery. However, existing biohybrids face many limitations that hinder their translation to clinical applications considering the poor penetration ability through the barrier or tissue, biostability and limited payload capacity. Here, we propose a magnetically controllable drug-loaded biohybrid microswimmer driven by a bacterial outer membrane vesicle, referred to as minicell, which offers unique capabilities such as enhanced penetration capability thanks to its sub-micron size and long-term stability with self-propulsion because of its non-dividing but metabolically active nature. Additionally, minicells exhibit a large drug encapsulation capacity compared to traditional nanocarriers. In this study, we fabricated motile minicells produced by engineered *Escherichia coli* strain inducibly expressing a biotin display system on their surface, enabling us to benefit from the robust biotin-avidin interaction with streptavidin-coated magnetic nanoparticles onto the minicells. We optimized the production of self-propelled minicells via several purification methods and investigated their growth and motile behavior in various culture and physiological media over time. We showed the magnetic control and guidance of minicell-driven biohybrids by an external magnetic field, and compared their 2D swimming motility with and without applying uniform magnetic fields. Furthermore, we optimized the loading efficiency of the chemotherapeutic drug doxorubicin into the minicells and demonstrated the time-dependent release of the drug molecules. Overall, the minicell-driven biohybrid design proposed here offers a magnetically guided active drug-carrying nanosized platform for targeted delivery while preserving its motility and durability during the extended application period.

8:00 PM SB05.07.25

Designed Nanoparticle-Polymer Conjugates as Nucleants for Multiple Protein TypesXiaoting Guo and Vicki L. Colvin; Brown University, United States

Determining the three-dimensional structure of proteins is crucial for understanding their function, but the limited ability to form protein crystals suitable for X-ray diffraction has become a bottleneck problem in this field. Through the control of nanocrystal and protein interactions, it is possible to both enhance the nucleation of protein crystals as well as create three-dimensional structures of nanoparticles within the protein crystals. The length of polymers (e.g. poly(ethylene glycol) bound to a nanocrystal surface can mediate protein interactions with the nanocrystal-polymer conjugates: specifically, longer polymers at the nanoparticle surface allow for more protein association with conjugates.

We showed that the addition of AuNP-PEG to hen egg white lysozyme (HEWL) led to an increase in the number of crystal hits across a wide range of crystallization conditions. The compared result in crystallography indicates with the incorporation of conjugate system, protein structures can be dissolved with the existence of the nano-nucleant inside the protein matrices.

Surprisingly, the incorporation of AuNP-PEG inside the crystals did not affect their quality. The statistical values listed in Table 1 for the AuNP-HEWL co-crystal remained consistent with those obtained for the pure HEWL crystal, indicating that the addition of AuNPs did not alter the crystal properties in any way.

AuNP-PEG can also be used as a general nucleant for different protein species. 5 illustrate a comparison of hit counts for eight proteins, namely Ferritin, Proteinase K, Thaumatin, p-HSA, Concanavalin A, Glucose Isomerase, Insulin, and Xylanase, based on 48 screening conditions. The results indicate that the addition of AuNP-PEG increased the number of hits in each protein species compared to the control group without the presence of AuNP solution.

The potential of AuNP-PEG to affect liquid-liquid phase separation (LLPS) of FUS-LC proteins was also investigated, which plays a crucial role in understanding the formation and solubilization of protein droplets in cellular processes. The addition of AuNP-PEG to FUS-LC led to an acceleration of LLPS and the formation of more condensates.

Within the protein-nanoparticle conjugate co-crystals, we further demonstrated that the incorporation and arrangement of nanoparticles at regular distances within the protein crystal is reflective of the fact that the protein crystal nuclei form on the nanoparticle surface; for lysozyme, these nuclei have been studied via both light scattering and diffraction. Most studies find that they consist of four or more lysozymes with dimensions near 9 to 18 nm. In the presence of nanoparticles, these proto-nuclei form in and around nanoparticle-polymer conjugates that can themselves have polymer shells as thick as 30 nm. This would suggest that incorporated nanoparticles could have as much as 40 to 50 nm of surface polymer and protein surrounding them, giving rise to a lower limit for the interparticle separations that is in good agreement with that found from the radial distribution function (e.g. 47 nm). The composites grow when these protein-nuclei encounter other similar structures and begin to crystallize, leading to the formation of composite crystals. Anisotropic materials align due to the faster spreading of proteins along the a-b face of crystal during growth which causes the preferential orientation of the rods perpendicular to the c-axis.

8:00 PM SB05.07.26

Strain Dependency of Charge Transport of Stretchable Conjugated PolymersSeung Hyun Kim and Kilwon Cho; Pohang University of Science and Technology, Korea (the Republic of)

Stretchable polymer semiconductors have attracted significant interest for their potential in flexible and stretchable electronics. However, there remains challenging work in controlling the strain-induced properties of conjugated polymers (CPs), such as crystallinity, morphology, and charge transport properties. Herein, we delve into the contribution of microstructures to their mechanical and electrical stretchability. To achieve stable electrical properties during deformation, specific structural requirements are discussed, such as the inclusion of a less-rigid donor moiety between diketopyrrolopyrrole (DPP) acceptors. This addition reduces crystalline packing, thereby significantly enhancing the mechanical deformability of the CP films. Furthermore, the multiscale structural and electrical analyses revealed that a less-rigid backbone allows for the strain-induced flattening of the polymer chains. The flattening of polymer chains reduces the activation energy barrier for hopping transport to 38 meV at 80% strain. Consequently, strain-induced alignment and conformational changes of polymer chains provide favorable pathways for charge transport, resulting in a significant increase in hole mobility of up to 180% under an 80% tensile strain. We believe that our study on the strain-induced structural changes in CP films, ranging from molecular to mesoscale, would contribute to a better understanding of the strain dependency of charge transport of stretchable conjugated polymers.

8:00 PM SB05.07.27

Fabrication and Characterization of Electrospun PU and Vapor Phase Polymerized PEDOT:Tos Fibers for Flexible ElectronicsJiaxin Fan, Jinsil Kim and Fabio Cicoira; Polytechnique Montreal, Canada

Soft conductive materials have gained considerable attention owing to their vast potential in wearable sensors, biomedical devices, and flexible displays. The successful implementation of high-performance flexible electronics requires exploring suitable materials with superior electrical and mechanical properties.¹ Poly-(3,4 ethylenedioxythiophene) (PEDOT) doped with various counterions has been extensively studied for flexible and stretchable electronics due to their ambient stability and solution processability. Additionally, their electrical conductivity and mechanical properties can be further tailored by blending with additives based on the application requirements.² PEDOT-based materials are also compatible with various fabrication and processing techniques, such as drop-casting, spin-coating, printing, and electrospinning. Among various techniques, electrospinning offers unique advantages, including a straightforward setup, versatile material choice, scalable production, tunable fiber properties, and compatibility with various substrates. Electrospun nanofibers exhibit desired properties for soft electronics.³ For PEDOT-based materials, the spinnability can be improved by adding carrier polymers.

In this study, we focus on the preparation of conductive fiber mats based on a mixture of polyurethane (PU) and PEDOT doped with tosylate (PEDOT:Tos). The fabrication process involved electrospinning the mixture of PU and oxidant, iron (III) p-toluenesulfonate (tosylate), followed by vapor phase polymerization (VPP) to obtain PEDOT:Tos. PU was utilized as both carrier polymer and an additive for enhancing the electrical and mechanical properties. The resulting fibers have an average diameter of ~ 800 nm. An average sheet resistance of $16.4 \pm 1.5 \text{ k}\Omega/\text{sq}$ was obtained for the PU/PEDOT:Tos fiber mat after VPP. To investigate the influence of different electrospinning solution mixtures and conditions, we analyzed the morphology, electrical conductivity, electrochemical behaviors, and mechanical properties of the fiber mats fabricated with various spinning solution mixtures and fabrication conditions. Preliminary demonstration of utilizing the conductive fiber mats for flexible electronics will also be presented. This comprehensive investigation provides insights into optimizing and engineering the properties of fiber mats for their application in soft electronics.

References

1. C. Wang, C. Wang, Z. Huang and S. Xu, *Advanced Materials*, 2018, **30**, 1801368.
2. M. J. Donahue, A. Sanchez-Sanchez, S. Inal, J. Qu, R. M. Owens, D. Mecerreyes, G. G. Malliaras and D. C. Martin, *Materials Science and Engineering: R: Reports*, 2020, **140**, 100546.
3. Y. Wang, T. Yokota and T. Someya, *NPG Asia Materials*, 2021, **13**, 22.

8:00 PM SB05.07.28

Silent Speech Interface using Wearable Strain Sensors Based on Crystalline Silicon NanomembraneKiho Kim, Taemin Kim, Kyowon Kang and Ki Jun Yu; Yonsei University, Korea (the Republic of)

The Silent Speech Interface (SSI), which uses non-verbal forms of communication like sign language, provides a promising alternative for those unable to vocalize. This technology interprets intended words by monitoring facial muscle and skin movements during verbal communication. Notably, SSI benefits from wearable sensors that use surface electromyography (sEMG), as it doesn't necessitate constant video surveillance in a fixed setting. However, conventional sEMG electrodes face issues related to signal quality, such as low signal-to-noise ratio and interelectrode interference, obstructing the precision of facial mapping.

In this study, we have developed an innovative SSI incorporating epidermal strain sensors made from crystalline silicon nanomembrane (SiNM). These sensors, thanks to their piezoresistive

properties, are considerably more sensitive than standard metal foil-based strain gauges. Each sensor includes two strain gauges placed perpendicularly to measure biaxial strain independently. We attached four sensors to four facial regions with the greatest areal changes, as identified by vision recognition.

We selected 100 English words at random from the Lip Reading in Wild benchmark set and trained 100 strain data sets for each word on a deep-learning-based classifier. To evaluate the classification performance of our system, we used a 5-fold cross validation which resulted in an average accuracy of 87.53%. In the same validation, a 4-channel sEMG system of identical dimensions ($< 0.1\text{mm}^2$) to our unit strain gauge exhibited only 41.53% accuracy due to its low SNR caused by high impedance. We also conducted an experiment with 200-word classification to check the effect of spatial resolution on accuracy. Under identical conditions, the 16-channel and 8-channel systems showed 81.87% and 71.63% accuracy, respectively. This demonstrates the potential for this technology to support everyday conversation in the future.

SESSION SB05.08: Bioinspired Adaptive Systems and Biosensing Platforms
Session Chairs: Herdeline Ann Ardoña and Flavia Vitale
Wednesday Morning, November 29, 2023
Hynes, Level 1, Room 102

8:00 AM SB05.08.01

Soft Transparent Microelectrodes based Multimodal Devices for Biointerfacing Luyao Lu; The George Washington University, United States

Optically transparent microelectrodes are important technologies that can integrate with tissues and allow light to transmit in both directions for co-localized and crosstalk-free electrical recording, optical imaging, and optogenetics. Existing transparent microelectrodes rely on external optical fiber, camera, or microscope setups for optical biointerfacing. In this talk, I will discuss several of our recent examples of soft transparent microelectrodes based multimodal optoelectronic devices enabled by new concepts in materials, micro- and nano-fabrication techniques, and engineering designs. Those innovative devices integrate microscale light-emitting diodes, photodetectors, with transparent microelectrodes on a chip. They are designed in flexible formats and allow for stable, high-fidelity, high-content electrical and optical recording and modulation of many important cellular parameters (intracellular calcium dynamics, metabolic activity, biopotentials, etc.) across different spatiotemporal resolutions. We envision those multimodal devices will open up new windows to understand important biological processes at the cellular, tissue, and organ levels with high spatiotemporal resolution and selectivity.

8:15 AM SB05.08.02

Bio-Inspired Multiple Tactile Sensing System for Simultaneous and Real-Time Perception Bo-Yeon Lee, Seonggi Kim, Sunjong Oh, Youngdo Jung and Hyuneui Lim; Korea Institute of Machinery and Materials, Korea (the Republic of)

A human can intuitively perceive and comprehend complicated tactile information. Because the cutaneous receptors distributed in the fingertip skin receive different tactile stimuli simultaneously, and the tactile signals are immediately transmitted to the brain. Although many research groups have attempted to mimic the structure and the function of human skin, it remains a challenge to implement human-like tactile perception process within one system. In this work, we developed a real-time and multimodal tactile sensing system, mimicking the function of cutaneous receptors and the transmission of tactile signals from receptors to the brain, by using multiple sensors, a signal processing and transmission circuit module and a signal analysis module. The proposed system is capable of simultaneously acquiring four types of decoupled tactile information within a compact system, thereby enabling differentiation between various tactile stimuli, texture characteristics, and consecutive complex motions. This skin-like three dimensional integrated design provides further opportunities in multimodal tactile sensing systems.

8:30 AM SB05.08.03

Advancing High-Performance Printed Soft Mechanical Sensors Through Microstructure Control of Conductive Composites Yi-Fei Wang, Ayako Yoshida, Yasunori Takeda, Tomohito Sekine, Daisuke Kumaki and Shizuo Tokito; Yamagata University, Japan

Soft mechanical sensors have emerged as highly desirable components for the next generation of biomedical devices, wearable electronics, and soft robotics [1]. Their inherent flexibility and stretchability enable seamless integration onto soft and irregular surfaces, empowering them with advanced sensing capabilities for a wide range of external mechanical stimuli. Recently, conductive composites have garnered significant attention in the research community as promising materials for soft mechanical sensors due to their cost-effectiveness, ease of processing, and the ability to tune their electromechanical performance [2]. A key aspect of achieving high-performance sensors lies in the effective control of the conductive composite's microstructure, as it directly impacts its electromechanical properties [3]. For instance, introducing microcracks in the conductive film significantly enhances its strain sensitivity, while constructing a conductive layer with a porous structure or micropatterning surface is commonly employed to achieve high sensitivity in pressure sensors. However, previous approaches have often relied on complex material synthesis and expensive manufacturing processes, presenting scalability challenges and severely limiting their practical applications.

This report highlights our recent progress in materials design aimed at controlling the microstructure of conductive composites to realize high-performance printed soft mechanical sensors. We have developed a novel brittle-stretchable conductive network that generates controllable microcracks, resulting in high sensitivity to applied strain while maintaining a large working range [4]. This innovative approach successfully overcomes the trade-off between sensitivity and sensing range commonly encountered in stretchable strain sensors. We have also successfully formulated a novel printable ink by mixing PDMS, CB, and a deep eutectic solvent (DES). This ink spontaneously forms a microporous conductive architecture without the need for complex processing [5, 6, 7]. Leveraging this composite, we have achieved highly sensitive pressure sensors and low hysteresis stretchable strain sensors using straightforward manufacturing techniques. Furthermore, we have utilized thermally expandable microspheres to create irregular microdome surfaces, facilitating the easy fabrication of flexible printed pressure sensors with superior reliability and uniform performance. When compared to previous studies, our approaches offer significant advantages: (i) simple ink preparation without the need for complex materials synthesis; (ii) compatibility with printing technologies, ensuring superior scalability, patternability, and cost-effectiveness; and (iii) easy microstructure control in conductive composites, resulting in soft mechanical sensors with exceptional performance in terms of sensitivity, working range, reliability, and uniformity. We are confident that these achievements will provide valuable insights into materials design and microstructure control of conductive composites, thereby advancing their practical applications in the field of soft electronics.

This study was partially supported by JSPS KAKENHI Grant Number 23K13806.

[1] S. Yao et al., *Adv. Mater.* **2020**, *32*, 1902343.

[2] D. C. Kim et al., *Adv. Mater.* **2020**, *32*, 1902743.

[3] S. R. A. Ruth et al., *Adv. Funct. Mater.* **2020**, *30*, 2003491.

[4] Y.-F. Wang et al., *ACS Appl. Mater. Interfaces* **2020**, *12*, 35282.

[5] Y.-F. Wang et al., *Adv. Mater. Technol.* **2021**, 2100731.

[6] A. Yoshida et al., *ACS Appl. Eng. Mater.* **2023**, *1*, 50.

[7] Y.-F. Wang et al., *Sensors* **2023**, *23*, 5041.

8:45 AM SB05.08.04

Engineering Flexible Electronics for Monitoring Epithelial Integrity *In-Vitro* and *Ex-Vivo* Sophie Oldroyd, Sarah Barron, David Bulmer and Roisin Owens; University of Cambridge, United Kingdom

Inflammatory bowel disease (IBD) is a widespread condition, with a forecasted prevalence of 1.1% by 2025 [1]. It presents with chronic symptoms such as abdominal pain and diarrhoea and is characterised by a leaky gut barrier, which has increased permeability due to changes in localisation of tight junction proteins [2]. However, a detailed understanding of the disease pathway is limited, and current methods of assessing gut tissue health *ex vivo* are impeding progress in the field. The techniques need re-designing in the modern era given advancements in technology. This work presents flexible bioelectronic devices that permit real-time recordings of changes in gut tissue. The ability to assess gut health in living tissue is important in establishing and monitoring phenotypes associated with gastrointestinal diseases.

All-planar conformable devices with multiple working electrode sizes (from 25 to 1000 μm) and an internal counter/reference electrode (CE/RE) were fabricated using previously developed techniques [3]. On the bottom, and between each of the layers, parylene C was used for insulation. Conductive tracks, outlines, and contact pads for the electrodes were formed using photolithography and gold deposition. Electrodes were coated with PEDOT:PSS, a conducting polymer used to increase volumetric capacitance. The electrodes were characterised by

electrochemical impedance spectroscopy (EIS) and brightfield microscopy. *In-vitro* testing utilized a human colonic epithelial cell line, Caco-2. The cells were grown on Transwell® inserts and differentiated for 21 days. The ability of the device to measure barrier integrity, perturbations, and recovery in real-time was assessed via the transient addition of EGTA. The devices were tested *ex-vivo* on small intestine and colonic tissue from wild type-C57Bl6 male mice. Cell viability was confirmed with confocal microscopy and staining. Extracted transepithelial resistance values, based on simple equivalent circuit models, were confirmed against the gold standard methods for *in-vitro* and *ex-vivo*, using the EVOM3™ and Ussing Chambers respectively.

This work highlights the first instance of an all-planar flexible electronic device that can monitor epithelial barrier function and perturbations at the air liquid interface. The mechanical flexibility of the device allows for direct and conformable contact with biological surfaces, to provide a quantifiable electrical readout under physiological conditions. The multi-electrode design established a minimum electrode radius (400 μm) needed to capture the epithelial properties, and chemical disruption, of colon cell lines and mouse colon tissue. The sensing area achieved is one order of magnitude smaller than previously reported, highlighting the increased sensing efficiency of the design. The device achieves comparable sensitivity with a planar CE/RE compared to an external CE/RE. As this device was the first of its kind, readouts were validated against gold standard TEER measurements, which showed comparable trends with a reduction in measurement error. We confirm the device is biocompatible and does not negatively affect the barrier properties under study. Future work could look to apply this technology for spatially mapping local and real-time changes in epithelial barrier properties for toxicology and drug screening applications.

- [1]. Freeman, K. et al. *BMC Gastroenterology* 21, 1–7 (2021).
- [2]. Michielan, A. & D'Incà, R. *Mediators of inflammation* (2015).
- [3]. Khodagholy, D. et al. *Advanced Materials* 23, H268–H272 (2011)

9:00 AM SB05.08.05

Multimodal Flexible Fiber Antenna Sensor for Physiological and Environmental Sensing Merve Gokce¹, Eilam Smolinsky¹, Louis van der Elst¹, Creasy Clauser Huntsman² and Alexander Gumennik¹; ¹Indiana University Bloomington, United States; ²Cook Medical Technologies, United States

The real-time monitoring of a patient's health condition during medical operations is crucial to the patient's comfort, safety, and treatment success. While there are many advanced biomedical devices on the market that monitor various physiological parameters, they are limited with respect to sensitivity, accuracy, compatibility, and durability. It is vital to improve physiological monitoring limitations to minimize potential trauma, discomfort, and complications after surgery. Fiber device technology enables the designing of fiber-embedded sensors that provide higher sensitivity, accuracy, and spatial resolution through its complex cross-sectional geometry and material properties [1]. Thermally drawn polymer fibers offer high flexibility, durability, and better compatibility, making integrating fiber sensors into fabrics and biomedical devices easier [2].

Here we present the first sub-terahertz fiber antenna sensor capable of high spatial resolution, high sensitivity, and large dynamic range physiological monitoring and cyber-physical interfacing. The sensitivity and spatial resolution of the fiber sensor are high enough for practical operations such as integrating the flexible fiber sensor into medical devices. The fiber sensor monitors physiological and environmental signals in real-time, where the sensing modality, either physiological or environmental, is defined by the electronics used to control the order of the mode coupled to the fiber sensor. While the high sensitivity of the fiber sensor is derived from its unique geometry, materials, and unique manufacturing approach [3], its spatial resolution results from the frequency decomposition of the reflected signal off the sensing point along the fiber and thus is the function of the operation bandwidth. Our multimodal flexible fiber sensor is a better candidate for improved monitoring of patients' well-being and better patient care than the current sensors used in minimally invasive operations. The application area of our fiber sensor is not limited to the biomedical field but also smart fabrics, cyber-physical and human-robot interactions, and environmental detections due to its ability to perform selective, multimodal measurements.

References

- [1] van der Elst, L., Faccini de Lima, C., Gokce Kurtoglu, M. *et al.* 3D Printing in Fiber-Device Technology. *Adv. Fiber Mater.* 3, 59–75 (2021). <https://doi.org/10.1007/s42765-020-00056-6>
- [2] Faccini de Lima, C., van der Elst, L.A., Koraganji, V.N. *et al.* Towards Digital Manufacturing of Smart Multimaterial Fibers. *Nanoscale Res Lett* 14, 209 (2019).
- [3] Gumennik, Alexander. *VERY LARGE-SCALE INTEGRATION FOR FIBERS (VLSI-Fi)*. US20210333131A1.04.23.2021

9:15 AM SB05.08.06

Biomimetic Sequence-Templating Approach Towards a Multiscale Modulation of Chromogenic Polymer Material Properties Yuyao Kuang, Ze-Fan Yao, Sujeung Lim, Catherine Ngo, Megan Rocha, Dmitry Fishman and Herdeline Ann Ardoña; University of California Irvine, United States

Polydiacetylene (PDA) is an established conjugated polymer material useful as a colorimetric indicator of environmental conditions, such as small molecule binding, mechanical force, heat, or solvent, for multiple sensing applications due to the structural dependence of their optical and electronic properties. With its emerging utility for biological applications, there is a critical need to develop PDAs that can be processed in the physiological-relevant environment with predictive structures and properties. Using sequence-tunable peptidic supramolecular interactions to template diacetylene monomer assembly offers a facile synthetic approach and enables a way to rationally influence PDA structure and properties via peptide sequence engineering. This presentation focuses on investigating the structural influences of peptide templating groups on PDA structures and functional properties across length scales by molecularly controlling the properties of peptide moieties through steric effects and hydrophobic interactions. In particular, a library of peptide-PDA conjugates with systematically varied dipeptide segments is established to demonstrate the influence of residue sterics, polarity, and position of substitution on multiscale PDA material properties. We show that steric effects predominantly influence the electronic structure and resulting trends in chain conformation-dependent photophysical properties. On the other hand, distinct trends were observed for bulk properties, such as film conductivity and cellular response to material interfacing. By tuning peptidic molecular volume and polarity, we exhibited a general increase in conductivity with smaller peptide molecular volume and higher hydrophobicity. The properties of peptide-PDA films suggest more interplay between residue size and hydrophobicity at larger length scales. In summary, this work provides new molecular-level insights on how sequence-tunable sterics and polarity can be used as a synthetic handle to rationally modulate multiscale structure-function correlations for peptide-PDAs as functional biomaterials. These findings pave the way for further developing sequence-defined programmable properties and complex behavior for peptide-PDAs, such as the adaptive evolution of their properties in response to living systems interfaced with these functional biomaterials in physiologically relevant environments.

9:30 AM *SB05.08.07

Biomaterials Strategies Towards Multimodal Neural Probes for Chronic Neural Recording, Chemical Sensing and Delivery Xinyan T. Cui; University of Pittsburgh, United States

Microelectrode array (MEA) devices, placed in the nervous system to record and modulate neuroactivity have demonstrated success in neuroscience research and neural prosthesis applications. Functionalizing the microelectrode sites on MEAs to enable neurochemical sensing and delivery adds additional dimensions of information, and presents tremendous potential for understanding neural circuits and treating neurological diseases. In this talk, I will introduce the methods by which we enable chemical sensing and delivery from MEAs. By incorporating nanocarbon into the conducting polymer electrode coating, we achieved direct detection of electroactive species such as dopamine, melatonin, and serotonin. By immobilizing enzymes or aptamers on nanostructured electrodes, we achieved multisite detection of glutamate, GABA, and cocaine. By incorporating nanocarriers into conducting polymer coating, we enabled on-demand drug delivery. Multisite and multiple analyte detection or neurotransmitter delivery along with neural recording have been demonstrated with these MEAs. Chronic neural interface performance has been sub-optimum. Quantitative histology, explant analysis, and 2-photon imaging revealed biofouling, neuronal damage, inflammation, and oxidative stress at the site of implants, as well as material degradations. We use several bioengineering strategies to minimize these failure modes. First, materials and devices that mimic the mechanical properties of the neural tissue have been developed and shown to significantly improve device-tissue integration. Secondly, biomimetic coatings and drug delivery have been applied to reduce biofouling and inflammatory responses. These approaches may be combined to achieve long-term and high-fidelity multimodal neural interfacing.

10:00 AM BREAK

SESSION SB05.09: Devices for Biointerfacing
Session Chairs: Guglielmo Lanzani and Flavia Vitale
Wednesday Morning, November 29, 2023
Hynes, Level 1, Room 102

10:30 AM *SB05.09.01

Magnetolectric Metamaterials and Miniature Bioelectronics Jacob T. Robinson; Rice University, United States

Magnetic fields show very little absorption or reflection in bone and tissue, making these fields magnetic materials ideal as a transducer for bioelectronic systems. Here I will discuss how we can engineer the properties of magnetolectric materials to show electrical and optical properties not found in nature. With these magnetolectric metamaterials, we can rapidly control nerve

impulses in rodent models for nerve injury and control the activity of engineer cells. Furthermore, magnetoelectrics enables us to create highly efficient, miniature battery-free bioelectronic networks for cardiac and neural applications. Overall, engineering the material properties of magnetoelectrics and magnetoelectric metamaterials provides a route to multifunctional miniature bioelectronic networks.

11:00 AM SB05.09.02

Cell Mechanotransduction Driven by Bio-Organic Optoelectronic Devices Vanessa Spagnolo¹, Leonardomaver¹, Johannes Gladisch², Iwona Bernacka Wojcik², Gabriele Tullii¹, Eleni Stavrinidou² and Maria Rosa Antognazza¹; ¹Istituto Italiano di Tecnologia, Italy; ²Linköping University, Sweden

Biophysical cues, especially mechanosensation, play a fundamental role throughout life, starting from early embryonic development over function and interplay of cells and tissues in the adult body up to regeneration processes. Tissue regeneration, which includes phenomena like cell division, differentiation, migration and expulsion is triggered by extracellular mechanical cues. The body's capability to regenerate decreases with age and therefore impacts our life in sometimes detrimental aspects.

Currently available tools to modulate or control mechanosensation often lack features necessary for *in vitro* and *in vivo* applications, in terms of efficiency, reliability, reversibility and spatial sensitivity. Here we show a novel approach to control mechanosensitive ion channels, through exogenous organic semiconductors. Materials in this class are fully biocompatible, thus offering the perspective for *in vivo* application, they can be easily processed in several forms, such as thin films, microstructured devices or nanoparticles. Most importantly, they are characterized by distinctive opto-electrical properties, providing excellent visible light responsivity, as well as electron and ion conductivity.

In this work we explore the opportunity to use organic semiconductors, and in particular conjugated polymers, to control the activation of mechano-sensitive ion channels, in a reliable and effective manner. We critically discuss results obtained with different tools, including polymer thin films and microstructured devices. In more detail, we present first examples, to the best of our knowledge, of devices based on conjugated polymers to activate PIEZO channels in mammal cells.

Our results may contribute to develop innovative smart materials for tissue regeneration and pathologies involving mechanosensation driven by physical cues.

11:15 AM *SB05.09.03

Monitoring Water Permeation in Flexible Bioelectronic Devices Massimo Mariello and Stephanie P. Lacour; Ecole Polytechnique Federale de Lausanne, Switzerland

Most bioelectronic interfaces call for long-term operation. Their formfactor requires new packaging strategies to ensure hermeticity, thinness and mechanical compliance. Inspired from display technologies, organic-inorganic multilayers are promising candidates to package thin, flexible and miniaturised bioelectronic devices. Besides the materials challenges associated with the choice of suitable thin films, stacking and deposition methods, quantitative evaluation of their barrier performance is a must. We have developed real-time monitoring methods of permeability or water transmission rate of thin film multilayers leveraging magnesium (Mg) degradation under physiological conditions. Water permeation drives Mg hydrolysis. Using Mg film electrical and electrochemical sensors prepared with thin-film microfabrication, embedded in bioelectronic interfaces, ultra-low detection of water permeation (as low as of 3.3×10^{-8} g/m²/day at room temperature) can be achieved. This method should provide useful information on novel encapsulation strategies for miniaturised, long-term bioelectronic implantable systems.

SESSION SB05.10: Life-Machine Interfaces

Session Chairs: Herdeline Ann Ardoña, Ardemis Boghossian and Flavia Vitale

Wednesday Afternoon, November 29, 2023

Hynes, Level 1, Room 102

1:30 PM *SB05.10.01

Noninvasive Optogenetics to Study Brain-Body Circuits Ritchie Chen; University of California, San Francisco, United States

Viscerosensory signals, such as hunger pangs, pain, and a racing heart, shape our cognitive state and behavior. However, the neural basis that drives these adaptive behaviors remains poorly characterized, largely due to a lack of tools to map, record, and modulate specific cell types within a dynamically moving body. This presentation will highlight recent advances in optogenetics that enable noninvasive photoactivation of electroactive cell types in the body using external, distally placed light sources. I will demonstrate how these methods can be applied to manipulate cardiac physiology and establish causal roles of visceral cardiac signals in influencing anxiety-like behavior in mice.

2:00 PM SB05.10.02

Nanoparticles for Wireless Magnetolectric Neural Modulation Ye Ji Kim, Noah Kent, Florian Koehler, Emmanuel Paniagua, Nicolette Driscoll, Marie Manthey and Polina Anikeeva; Massachusetts Institute of Technology, United States

Magnetic nanomaterials offer a minimally invasive alternative to invasive neuromodulation implants. A variety of magnetic nanomaterials have been developed to transduce physiologically benign magnetic signals (field-frequency product $H \times f < 5 \times 10^8$ Am⁻¹s⁻¹) to signals perceived by biological receptors including heat, mechanical stimulation, chemical release, and electric field. Magnetolectric nanomaterials composed of magnetostrictive (magnetic field to strain) cores and piezoelectric (strain to electric polarization) shells are particularly promising candidates for wireless transgene-free neuromodulation in deep-brain structures. Although strain-mediated magnetolectric (ME) materials have been shown effective for neuromodulation at the millimeter and micrometer scale, achieving efficient ME coupling at the nanoscale remains a challenge. Here we report a strategy for enhancing the strain-mediated ME coupling at the nanoscale. We synthesize core-double shell magnetolectric nanodiscs (MENDs) with Fe₃O₄ - CoFe₂O₄ - BaTiO₃ architecture. In these nanodiscs, magnetostriction is enhanced through anisotropic shape and interfacial strain between Fe₃O₄ and CoFe₂O₄, which collectively enable the generation of 30 μV in BaTiO₃ piezoelectric shell, which predicted numerically and measured experimentally via an electrochemical three-electrode cell. Although the electric field generated by individual MENDs is far below than the necessary potential change to reach the action potential threshold in neurons, we find that MENDs robustly evoke neural activity *in vitro* in the presence of a magnetic field. To explain this finding we propose a biophysical model of repeated neuronal depolarization based on cable theory and stochastic membrane potential fluctuations. Using the proposed model, we optimize the stimulation parameters *in vitro*, and then translate our approach to neuromodulation *in vivo*. Specifically, we show remote control of behavior in mice following 1.5 μL MEND injections at 1 mg/mL concentration (~100 times lower concentration than previous studies involving nanomagnetic transduction regardless of mechanism). We offer a mechanistic approach for further refinement of magnetolectric neuromodulation at the nanoscale with the goal of empowering neurobiological discovery.

2:15 PM SB05.10.03

Engineering a Biohybrid Neural Interface for Synaptic Deep Brain Stimulation Léo Siffringer¹, Alex Fratzl², Stephan Ihle¹, Parth Chansoria¹, Jens Duru¹, Blandine F. Clément¹, Sinead Conolly¹, Benedikt Maurer¹, Christina M. Tringides¹, Leah Mönkemöller¹, Giulia Amos¹, Sean Weaver¹, Sophie Girardin¹, Katarina Vulčić¹, Simon Steffens¹, Anna Beltraminelli¹, Eylul Ceylan¹, Srinivas Madduri³, Marcy Zenobi-Wong¹, Botond Roska², Janos Vörös¹ and Tobias Ruff¹; ¹ETH Zürich, Switzerland; ²IOB Basel, Switzerland; ³University Geneva, Switzerland

Restoring functional vision in blind patients lacking a healthy optic nerve requires bypassing retinal circuits. This can be achieved by high resolution stimulation of the visual thalamus, which is located deep inside the brain and serves as the main input to cortical circuits underlying vision. However, available deep brain stimulation electrodes suffer from low stimulation resolution, limited biocompatibility and limited coverage of the targeted tissue. To overcome those limitations, we propose a novel living biohybrid neural interface with the goal of restoring functional vision in the blind without a healthy optic nerve. Our interface uses living on-chip grown retinal neurons as relays to convert electrical signals from a stretchable microelectrode array into synaptic stimulation of a neural target tissue.

Our interface is based on a stretchable micropatterned microelectrode^[1,2] array onto which we align axon guiding microfluidic structures that enable unidirectional guidance and merging of axons to form an artificial optic nerve. We increase the biocompatibility of our device by replacing the Polydimethylsiloxane (PDMS) based nerve forming channel with a collagen or gelatin methacryloyl (GelMA)^[3] tube that is only 300 μm in diameter and directly integrated onto the PDMS device.

We demonstrate the seeding of retinal spheroids into our biohybrid devices using a modified fluid force microscope. The retinal ganglion cells form an artificial optic nerve up to 3mm long that can transit from the device into the PDMS-bound hydrogel tube to reinnervate a matrigel-based target structure *in vitro*. We show that we can stimulate individual retinal spheroids using our stretchable microelectrode array. We also present *in vitro* data on how spikes propagate within the biohybrid implant to modulate thalamic target activity using glass and CMOS^[4] multielectrode arrays. Finally, we present first progress towards *in vivo* implantation.

References

1. Raphael F. Tiefenauer, Klas Tybrandt, Morteza Aramesh and János Vörös. Fast and Versatile Multiscale Patterning by Combining Template-Stripping with Nanotransfer Printing. ACS Nano 12.3.2514-2520 (2018)

- Nicolas Vachicouras, Christina M. Tringides, Philippe B. Campiche, Stéphanie P. Lacour. Engineering reversible elasticity in ductile and brittle thin films supported by a plastic foil. *Extreme Mechanics Letters* 15 63-59 (2017)
- Hao Liu, Parth Chansoria, Paul Delrot, Emmanouil Angelidakis, Riccardo Rizzo, Dominic Rüttsche, Lee Ann Applegate, Damien Loterie, and Marcy Zenobi-Wong. Filamented Light (Flight) Biofabrication of Highly Aligned Tissue-Engineered Constructs. *Adv. Healthc. Mater.* 2204301, 34.45 (2022)
- Jens Duru, Joël Küchler, Stephan J. Ihle, Csaba Forró, Aeneas Bernardi, Sophie Girardin, Julian Hengstler, Stephen Wheeler, János Vörös and Tobias Ruff. Engineered biological neural networks on high density CMOS microelectrode arrays. *Front. Neurosci.*, 2022.829884 (2022)

2:30 PMBREAK

3:30 PM *SB05.10.04

Biohybrid Interfaces with Light-Sensitive Dynamic Polymers for Neuroelectronic Applications [Francesca Santoro](#); Forschungszentrum Jülich/RWTH Aachen University, Germany

Bioelectronic platforms more and more aim to integrate into tissues and organs in a seamless way to monitor and eventually restore lost functionalities. This is particularly relevant for brain implants where the functional electrical connections can be restored by the use of functional electrodes to stimulate injured area due to pathologies such as neurodegenerative diseases. In this scenario, polymers have found a major use in the last decade to design and engineer organic biointerfaces¹ between electronics and brain cells also with their integration into soft flexible probes. However, existing platforms still lack: 1) 2.5-3D features to locally better anchor to the target area, 2) undergoing on demand mechanical plasticity which is greatly required because of micromovements and tissue reshaping over time and 3) materials which exhibit also electrical plasticity and not only conventional passive behavior to better enhance the ion-electronic transduction process which is at the core of the neuronal communication in the brain. Here, we will present how conjugated polymers can be engineered with azopolymers (opto-sensitive polymers which switch from cis to trans conformation upon certain light exposure) to feature diverse optoelectro-mechanical properties from nano to macroscale lever in organic bioelectronic platforms. In particular, we will discuss how azo-based materials can be patterned into 2.5-3D designs to locally couple to cells and thus dynamically tune the cell electrode interface over time². Furthermore, these films can be further engineered with PEDOT:PSS to create dynamic organic electrochemical transistors (OECT, Figure 1) which also exhibit opto-electronic short and long term plasticity, enabling the use of such platforms as neurohybrid³ devices.

This new class of on demand organic opto-electronic devices⁴ paves the new for bioelectronic implantable platforms to be more biomimetic as they can adapt to the 3D environment of the neuronal tissue and its continuous reshaping, also featuring neuromorphic electrical behavior.

- Mariano, A. *et al.* Advances in Cell-Conductive Polymer Biointerfaces and Role of the Plasma Membrane. *Chem. Rev.* (2021).
- De Martino, S. *et al.* Dynamic manipulation of cell membrane curvature by light-driven reshaping of azopolymer. *Nano Lett.* **20**, 577–584 (2019).
- Lubrano, C., Bruno, U., Ausilio, C. & Santoro, F. Supported Lipid Bilayers Coupled to Organic Neuromorphic Devices Modulate Short-Term Plasticity in Biomimetic Synapses. *Adv. Mater.* **34**, 2110194 (2022).
- Corrado, F., Bruno, U. *et al.*, Azobenzene-based organic opto-electronic transistors for neurohybrid building blocks. *Under Review.*

4:00 PM SB05.10.05

Hair-Compatible Sponge Electrodes Integrated on VR Headset for Electroencephalography [Hongbian Li](#), Hyonyoung Shin, Minsu Zhang, Jose del R. Millán and Nanshu Lu; The University of Texas at Austin, United States

Electroencephalography (EEG) combined with virtual reality (VR) represents a promising method for the measurement of brain activity in an immersive and interactive environment, which can provide insights into cognitive and neural processes. However, current VR-EEG headsets mainly rely on rigid comb electrodes, which are uncomfortable after prolonged wear. To address this limitation, we created soft, porous, and hair-compatible sponge electrodes based on conductive poly(3,4-ethylenedioxythiophene) polystyrene sulfonate (PEDOT:PSS)/melamine (PMA), and integrated them onto a VR headset through a customized flexible circuit for multichannel EEG during VR task performing. Our PMA sponge electrodes can deform to make contact with the scalp skin through hairs under the pressure naturally applied by the strap of the VR headset. As a result, our VR-EEG headset is capable of recording alpha rhythms during eye-closure at both hairless and hairy sites. Furthermore, we developed a VR task to evoke the contingent negative variation (CNV) potential and achieved a classification accuracy of 0.66±0.07. Our sponge-electrode-integrated VR headset is user-friendly and easy to set up, marking a step toward future reliable, comfortable, and reusable VR-EEG technology.

Keywords: PEDOT:PSS, soft electrode, electroencephalography, virtual reality

Reference

Li, H. B.; Shin, H.; Zhang, M. S.; Lu, N. S.* *et al.* Hair-Compatible Sponge Electrodes Integrated on VR Headset for Electroencephalography. *Soft Science*, 2023, in press.

E-mail: hongbian.li@austin.utexas.edu

4:15 PM SB05.10.06

A Flexible and Switch-Matrix-Addressable Active Electrode Array Based on Complementary Organic Electrochemical Transistor and p-n Diode Technology [Ilike Uguz](#)¹, David Ohayon², Sophie Griggs³, Sahika Inal² and Kenneth L. Shepard¹; ¹Columbia University, United States; ²King Abdullah University of Science and Technology, Saudi Arabia; ³University of Oxford, United Kingdom

Due to their effective ionic-to-electronic signal conversion and mechanical flexibility, organic neural implants hold considerable promise for biocompatible neural interfaces. Current approaches are, however, primarily limited to passive electrodes due to a lack of circuit components to realize complex active circuits at the front-end. Here, we introduce a p-n organic electrochemical diode (OED) using complementary p- and n-type conducting polymer films embedded in a 15- μm -diameter vertical stack. Leveraging the efficient motion of encapsulated cations inside this polymer stack and the opposite doping mechanisms of the constituent polymers, we demonstrate high current rectification ratios and fast switching speeds. We integrate p-n OEDs with organic electrochemical transistors (OECT) in the front-end pixel of a recording array. This configuration facilitates the access of OECT output currents within a large network operating in the same electrolyte, while minimizing crosstalk and interference from neighboring elements. We further demonstrate it to generate time-division-multiplexed amplifier arrays. When fabricated in a shank format, this technology enables the multiplexing of amplified local field potentials directly in the active recording pixel in a minimally invasive form factor.

4:30 PM SB05.10.07

Investigating the Effect of Photopharmacological Interventions on Cortical Seizures using Organic Perforated Multielectrode Arrays [Sofia Drakopoulou](#), Linta Sohail, Jeroen Spanoghe, Dina K.C., Robrecht Raedt and Georgios D. Spyropoulos; Gent University, Belgium

Epilepsy is a chronic neurological disorder characterized by recurrent seizures, affecting millions of people worldwide. Current treatment methods have limitations such as side effects and incomplete seizure control. One potential approach to address these challenges is by targeting the adenosine type 1 receptor, which is abundantly present in the body, for epilepsy suppression. However, it is important to note that this approach may introduce multiple undesired side effects such as dizziness, sleep disturbances, mood, cognitive, memory changes etc. Optopharmacology is an emerging approach for the treatment of focal epileptic seizures by activating and deactivating photoswitchable/photocaged molecules with light. It is a particularly interesting treatment solution which could result in powerful suppression of focal seizures with a limited number of side effects.

In this work, we study the neural dynamics of epileptic networks (in rodent model) and the effect of timely photo-release of a caged adenosine type 1 receptor agonist (caged CPA; N6-cyclopentyladenosine) hereon. To achieve that, we had to develop: i) animal protocols with evoked epileptic seizures, ii) illumination protocols proper for photorelease of the novel caged CPA molecule, iii) efficient microelectrode arrays, to trace the corresponding electrophysiology, that can simultaneously offer large spatial epidural coverage and high signal to noise ratio without sacrificing resolution or hindering illumination and drug appliance. In more detail, we performed craniotomies on several subjects to place semitransparent microelectrode array based on organic electronics on dura and trace electrophysiology. To provoke focal random epileptic seizures 4 - Aminopyridine (4-AP) was microinjected in different areas of the rat brain through specifically designed perforation paths. Upon microinjection of caged CPA epileptic activity continued but when the brain was exposed to pulses of 405nm light for uncaging of cCPA, local epileptic activity was strongly attenuated.

The results of this study provide a better understanding of propagation of 4AP induced seizures and confinement dynamics upon spatially resolved optopharmacological interventions. These findings are significant because they will positively impact the development of optopharmacological molecules and protocols, microelectrode arrays and therapeutic systems.

4:45 PM SB05.10.08

Surface Modification with Biocompatible Polymer Conductors for Stable and Compliant Electrode Interfaces for Communicating with Neurons [Rachel Blau](#)¹, Abdulhameed Abdal², Wade Shipley¹, Yi Qie¹, Allison Lim¹, Samantha Russman², Alexander X. Chen¹, Guillermo Esparza¹, Shadi Dayeh² and Darren J. Lipomi¹; ¹University of California; San Diego, United States; ²University of California San Diego, United States

Neural interfaces for recording or stimulating cells and tissues require long-term stability, mechanical compliance, low impedance, and high charge injection capacity. However, the mechanical mismatch between stiff metal electrodes (e.g., gold, platinum, and iridium oxide) and soft biological tissue poses a significant challenge, hindering optimal performance. To address this, conductive polymers have been used as an additional interface layer, with poly(3,4 ethylenedioxythiophene):poly(styrenesulfonate) (PEDOT:PSS) being a widely utilized material. While PEDOT:PSS offers good charge injection capacity and lowers impedance, its long-term stability when implanted in the body remains a bottleneck due to delamination, pH changes, charge injection, and immune responses.

In this work, we propose a chemical approach to enhance the adhesion between gold electrodes and PEDOT:PSS by covalently attaching the polymer to the gold surface, i.e., generating polymer brushes. We designed and synthesized polymer brushes made of block copolymer scaffold using a surface-initiated living radical polymerization (grafting-from). Our polymer brushes comprise a poly(styrenesulfonate) (PSS) block and a soft poly(polyethylene glycol methyl ether methacrylate) (PPEGMEMA) segment. This scaffold serves as a platform for polymerizing PEDOT, creating an adhesive and compliant interface with the brain tissue.

We successfully implemented this approach on a flexible microarrayed neural probe and evaluated its electrical charge transport and long-term stability for brain activity recording. The covalently attached polymer brushes significantly enhanced the adhesion between gold and PEDOT:PSS coating, addressing the challenges associated with delamination over time. The resulting interface exhibited improved long-term stability, and reduced impedance compared to traditional PEDOT:PSS-coated gold electrodes.

Our findings offer insights into the development of more reliable and efficient neuroprosthetic devices. By enhancing the stability of PEDOT:PSS coatings, we pave the way for improved neural interfaces with long-term functionality in neuroscientific research and clinical applications.

5:00 PM SB05.10.09

Photosynthetic Microorganisms in Coffee-Based Photoelectrochemical Systems Rossella Labarile¹, Paolo Stufano¹, Matteo Grattieri^{2,1}, Maria Varsalona^{2,1} and Massimo Trotta¹; ¹Consiglio Nazionale delle Ricerche, Italy; ²Università degli Studi di Bari Aldo Moro, Italy

Evidence collected in the last years indicates that the application of redox mediators in bioelectrochemical systems enhanced the electron transfer from microorganisms to anodes and from cathodes to microorganisms [1]. Some artificial redox mediators are expensive chemicals and are putatively toxic to the environment, so downstream removal techniques or biodegradable electron shuttles are highly desirable.

Coffee is one of the most consumed beverages in the world. As a direct consequence of the global coffee consumption, the wastes and byproducts generated along the entire value chain (from the agricultural production, through industrial transformation, until the brewing and the final user consumption) can enter in a circular development model for a sustainable society [2].

The use of photosynthetic bacteria for the valorization of waste produced by agricultural systems represents an eco-friendly, cost-effective, and socially acceptable agri-waste management technology [3]. Here, the versatile metabolism of photosynthetic purple non sulfur bacteria was exploited to develop bio-hybrid photoelectrochemical systems. The performance of poorly electroactive bacteria, such as *Rhodobacter sphaeroides* and *capsulatus* [4] were improved using green coffee extracts as effective mediators for extracellular electron transfer. Moreover, the preliminary results obtained by coupling such system with bio-based carbon composite electrodes recently developed, pose the foundation for a new class of circular coffee-based photoelectrochemical systems.

Funding: This work was funded by the Fonds National Suisse de la Recherche Scientifique, project Phosbury - Photosynthetic bacteria in Self-assembled Biocompatible coatings for the transduction of energy - (Project Nr CRSII5_205925/1), by project Mission Innovation POA 2021-2023 Italian Energy Materials Acceleration Platform—IEMAP and by European Union – NextGeneration EU from the Italian Ministry of Environment and Energy Security POR H2 AdP MMES/ENEA with involvement of CNR and RSE, PNRR - Mission 2, Component 2, Investment 3.5 "Ricerca e sviluppo sull'Idrogeno"

5:15 PM SB05.10.10

Engineering Extracellular Electron Transfer in Escherichia Coli for Microbial Electrochemical Devices Mohammed Mouhib¹, Melania Reggente¹, Lin Li^{1,2}, Nils Schuergers^{1,3} and Ardemis Boghossian¹; ¹École Polytechnique Fédérale de Lausanne, Switzerland; ²Chongqing University, China; ³Universität Freiburg, Germany

Microbes hold great potential for green electrochemical synthesis as well as bio-electricity generation from organic waste. The key to the successful development of microbial electrochemical devices lies in the ability of the microbes to transport electrons across their outer membranes. These devices thus often rely on the use of microbes known as exoelectrogens, which include bacteria that have evolved metabolic pathways that enable extracellular electron transfer (EET) to solid substrates for cellular respiration. While exoelectrogens demonstrate facilitated electron transfer with the electrodes of these devices, natural exoelectrogens are often restricted to utilizing a narrow range of substrates that limits their versatility for processing different organic wastes and electrosynthesizing a rich diversity of high-value chemicals. By contrast, non-exoelectrogenic microbes such as *Escherichia coli* that lack efficient EET pathways are host to rich metabolic reaction networks that can be more readily tailored for various applications using synthetic biology.

In this work, we biologically engineer *E. coli* for enhanced EET. To this end, we expressed different combinations of proteins from the natural exoelectrogen *S. oneidensis* MR-1, as well as *E. coli* native proteins to optimize EET of the bioengineered strain [1]. We further introduced biosynthesis pathways for redox mediators to facilitate EET [2]. The bioengineered strains show significant improvements in electron transfer rates, as confirmed through colorimetric reduction assays of soluble electron acceptors and electrochemical characterizations following electrode reduction. The improved EET demonstrated in this work paves the way for increasing the efficiency of existing *E. coli*-based electrochemical devices while opening the doors to new applications that benefit from the broad chemical repertoire of these microbes.

[1] Mohammed Mouhib, Melania Reggente, Lin Li, Nils Schuergers, Ardemis A. Boghossian. Extracellular electron transfer pathways to enhance the electroactivity of modified *Escherichia coli*. *Joule*. 2023. DOI: 10.1016/j.joule.2023.08.006

[2] Mohammed Mouhib, Melania Reggente, Ardemis A. Boghossian. Implementation of a flavin biosynthesis operon improves extracellular electron transfer in bioengineered *Escherichia coli*. *bioRxiv*. 2022. DOI: 10.1101/2022.12.31.522390

SESSION SB05.11: Muscular Biohybrid Interfaces
Session Chairs: Herdeline Ann Ardoña and Eleni Stavrinidou
Thursday Morning, November 30, 2023
Hynes, Level 1, Room 102

8:00 AM SB05.11.01

Soft Device for Simultaneous Measurements of Contractility and Electrophysiology of Neuromuscular Tissue Poppy J. Oldroyd¹, Sophie Oldroyd¹, Rajesh Makwana², Gareth Sanger², David Bulmer¹, George G. Malliaras¹ and Roisin Owens¹; ¹University of Cambridge, United Kingdom; ²Queen Mary University of London, United Kingdom

Biological tissues serve as rich sources of electrical and mechanical signals that offer valuable insights into their function, disease conditions, and metabolic activity. However, certain neuromuscular tissues, such as those in the gastrointestinal (GI) tract, can undergo significant conformational changes when physiologically active. These tissues have received limited research attention due to challenges faced by rigid probes in conforming to their dynamic surface, which can experience strain levels of up to 40%. Conventional inextensible devices cannot capture the relationship between electrophysiological and mechanical responses of these tissues. This hinders the acquisition of crucial neuromechanical information in the gastrointestinal system, essential for understanding GI homeostasis and the connections between the enteric and central nervous systems.

To address these challenges, this study introduces bimodal electrodes made from poly(3,4-ethylenedioxythiophene):poly(styrenesulfonate) (PEDOT:PSS) and polydimethylsiloxane (PDMS) that enable simultaneous monitoring of electrical and mechanical responses of gut tissue. PEDOT:PSS demonstrates long-term stability and outperforms metal electrodes that delaminate, crack, and degrade over time. PDMS, used as a substrate and insulation material, shows promise due to its superior intrinsic strain properties surpassing popular polymers like polyimide and parylene C.

In contrast to traditional electrode fabrication methods, this work utilizes shadow masks and solution-processable spin coating techniques, resulting in a faster and simpler fabrication process. To optimize the spin coating of PEDOT:PSS on PDMS, Capstone FS-300 was added for stability and film homogeneity. Polyethylene glycol (PEG) was incorporated to maintain electrical conductivity during stretch, enabling mechanical monitoring. The PEG concentration can be adjusted to tune the device's electrical sensitivity to strain changes. A low PEG concentration improves sensitivity to smaller strains for measuring spontaneous contractions, while a higher concentration makes the device strain insensitive for pure electrophysiology data. The PDMS-PEDOT:PSS-PDMS devices exhibit reduced delamination and cracking during accelerated aging compared to metal-based and parylene C devices.

The device was validated on *ex vivo* mouse and human gastrointestinal tissues. The device successfully monitored muscle electrical activity and motility. During induced propulsive

movements through the mouse small intestine, the device recorded electrophysiological voltage amplitude changes ranging from 2.1 to 3.5 times, corresponding to the strength of the contraction. These voltage changes were temporally correlated with resistance variations resulting from mechanical propulsion. The signals observed from the human stomach were similar in nature to those observed when monitoring the mouse small intestine, highlighting the variety of *ex vivo* applications of the devices and ability to detect signals in relatively thick (human) and thin (mouse) tissues. Furthermore, the ability to wrap the electrode system around a small diameter tissue as well as affixing it to a flat surface demonstrates the adaptability of device. In conclusion, the presented bimodal tissue monitoring device integrates soft, flexible, and stretchable electrodes using thin PDMS and PEDOT:PSS layers doped with PEG and Capstone. Its electrical sensitivity to strain can be finely tuned for specific applications by adjusting the dopants in the PEDOT:PSS. The device's flexibility and stretchability make it suitable for monitoring gastrointestinal function, including motility and electrical activity, as demonstrated on mouse small intestine and human stomach tissue. It has the potential to provide clinical insights into complex disorders like irritable bowel syndrome and gastroparesis.

8:15 AM SB05.11.02

Modular Skeletal Muscle Biohybrid Robots: Creation & Multi-Unit Assembly of Functional Muscle Building Blocks[Aiste Balciunaite](#)¹, Oncay Yasa¹, Miriam Filippi¹, Niklas König² and Robert K. Katzschmann¹; ¹ETH Zürich, Switzerland; ²Xolo GmbH, Germany

The emerging field of biohybrid robotics aims to create the next generation of soft and sustainable robots by using engineered biological muscle tissues, integrated with soft materials, as actuators. Alongside robotics, such biohybrid muscles will also find biomedical applications in prostheses and drug development and screening. Current skeletal muscle tissue-based robots are powered by bulk-grown 3D configurations of muscle tissue (*e.g.*, blocks or ring-like tissues). The size of these constructs is restricted to the sub-cm scale due to biofabrication constraints and limited nutrient perfusion. Further, lack of internal topography within bulk constructs results in poor control of myofiber formation and thus low contraction force. Therefore, to generate larger biohybrid constructs capable of complex motion while avoiding the issues of bulk muscle tissue manufacture, we have developed a bottom-up fabrication approach based on the assembly of muscle building blocks into designs that exploit the characteristics of the single actuators to form a multi-unit configuration. We created the muscle building blocks by integrating thin layers of muscle-cell laden hydrogels onto hydrogel-based exoskeletons characterized by material properties and microtopographic patterns that enhance muscle tissue development (*i.e.*, microgrooves). Our thin cell-laden hydrogel layers allowed nutrient diffusion throughout the layer, and we incorporated microtopography with a layer-by-layer approach.

We used a novel linear volumetric printing technique, named xolography, to form the hydrogel exoskeletons (< 1 mm x 5 mm x 8 mm). Adapting xolography for aqueous hydrogel printing allowed us to take advantage of the quick speed, high resolution, and achievable geometric complexity of the technique. We printed exoskeletons with different mechanical properties by combining polyethylene glycol diacrylates with gelatin methacryloyl, *e.g.* 15% PEGDA700 and 5% GelMA (P700/GelMA, Young's Modulus 140 kPa) and 15% PEGDA575 and 5% GelMA (P575/GelMA, Young's Modulus 270 kPa). The exoskeletons featured microgrooves of 100 – 300 µm in width to guide formation of uniaxially oriented myofibers. To stably integrate the exoskeletal and the cellular hydrogels, we developed a Matrigel, collagen, and gelatin methacrylate-based cellular hydrogel that, when seeded with myoblasts, allowed for both contractile myofiber formation and effective cross-linking with the exoskeletal hydrogel, as shown via confocal and brightfield imaging and histological analysis.

Directionality analysis of confocal microscopy images of samples stained to visualize myofibers (F-Actin) showed uniaxial alignment in the channel direction with a standard deviation of 10°–20°. The structural deformation of these constructs caused by the contraction via electrical stimulation of their muscle tissue component depended on the exoskeleton composition. Constructs based on P700/GelMA contracted 4% in the direction of myofiber contraction, while constructs based on P575/GelMA contracted <1%. Finally, to form modular multi-unit biohybrid robots with predictable motion abilities, we assembled the muscle building blocks by cross-linking the residual unreacted acrylate groups in the PEGDA/GelMA exoskeletons under UV irradiation.

In conclusion, we developed a method that builds biohybrid robots by the assembly of muscle building blocks with tunable mechanical properties and actuation performance. We have reduced the complexity and increased the predictability of biohybrid muscle fabrication, thus unlocking the potential of engineered muscle tissue as an actuating technology.

8:30 AM SB05.11.03

Integration of Laser-Induced Graphene Strain Gauges and Stimulation Electrodes into 3D Muscle on a Chip Devices[Anastasia Svetlova](#), Abdulrahman Al-Shami, Ali Soleimani, Hiu Tung J. Law, Riya Verma, Stephanie Do, Samuel Kohan, Raymond A. Peck, Maral Mousavi, Gerald E. Loeb and Megan L. McCain; University of Southern California, United States

The emerging technique of direct laser carbonization of polymers to convert them into conductive graphene foam has opened new possibilities for prototyping and fabrication of electronic devices. For example, polyimide (PI) undergoes a photothermal conversion into a 3-dimensional (3D) carbon foam called laser-induced graphene (LIG). This technically simple procedure can be implemented for the photolithography-free fabrication of electronic devices in the absence of a cleanroom, with faster turnover of prototypes, and at a lower cost. The technique has similar spatial resolution to inkjet printing but is more straightforward in implementation.

Muscle on a Chip models have been developed to gain insight into disease mechanisms from the molecular to the tissue scale and test new therapies. Systems that engineer muscle tissue in 3D bundles are especially beneficial for inducing more physiologically relevant tissue architecture. 3D muscle bundles are commonly fabricated by injecting a mixture of muscle cells and hydrogel into an elongated chamber with two flexible anchors. The muscle cells compact into an aligned 3D bundle that mimics native muscle tissue. The flexible anchors are embedded into the tissue during compaction and deflect with muscle contractions. However, the conventionally used method to evaluate muscle contractions by optically monitoring the anchors has low throughput, and limited options for continuous monitoring. To overcome these bottlenecks in Muscle on a Chip systems, we integrated LIG electrodes in our devices. Based on the same engraving technique, we fabricated electrodes for the electrical stimulation and the contractility measurement.

To fabricate LIG on PI films (LIG-PI), we used an Epilog Mini laser engraver equipped with a CO₂ 10.6 µm wavelength laser with maximum power of 30 W. By engraving patterns as an array of raster dots or overlapping vector "lines", and varying laser power and speed, we obtained LIG layers with sheet resistance from 120±17 Ω/sq to 32±4 Ω/sq.

This electrode demonstrated a charge injection capacity in the range of 0.2 mC/cm² for cathodic and 0.1 mC/cm² for anodic current pulse. Stability of the material after thousands of stimulation pulses was confirmed by measuring Ferricyanide-ferrocyanide oxidation/reduction currents in cyclic voltammetry and calculating the electrochemically active surface area. We transferred LIG foam into polydimethylsiloxane (PDMS) films by pouring liquid PDMS on LIG-PI, curing it until solid, and peeling off the PI film. This created a stretchable PDMS film embedded with LIG foam (LIG-PDMS), the conductivity of which responded to the stress applied to the layer. We demonstrated that LIG-PI and LIG-PDMS were not toxic by culturing HL-1 cardiomyocyte-like cells on the materials for 1 week.

To fabricate the strain gauge, we engraved LIG in a serpentine line pattern on PI films and transferred it onto PDMS. We further shaped this layer by laser cutting excess PDMS to create flexible anchors for the 3D tissue device, which should change resistivity upon deflection caused by the contracting muscle. To fabricate muscle chambers, we replica molded top and bottom pieces of PDMS from templates 3D printed in a Digital Light Processing printer. After 7 days of culture required for tissue compaction, LIG-PI stimulation electrodes were used to induce contractions of a primary muscle bundle at 2 Hz (twitch) and 20 Hz (tetanus).

We plan to use the developed device to evaluate physiological responses of two tissue models: healthy and diseased cardiomyocytes derived from human induced pluripotent stem cells, and primary skeletal muscle cells with continuous electrical stimulation and monitoring of muscle maturation.

8:45 AM SB05.11.04

Development of a Biohybrid Tendon Interface for Muscle-Powered Robots[Nicolas Castro](#); Massachusetts Institute of Technology, United States

Introduction: Unlike abiotic materials like metal and plastic, biotic materials can communicate with their surroundings, adapt to stimuli, and self-repair damage. Incorporating these materials into engineered systems could foster smarter, more adaptable machines. We have shown that engineered skeletal muscle stretched around a flexible elastomer 'skeleton' can generate force and drive locomotion. Since these locomotive robots are powered by 'living' actuators, they can strengthen with exercise and heal from damage, capabilities not possible with abiotic systems [1]. However, the interface between biotic (muscle) and abiotic (skeleton) components in our robot is driven by friction, leading to slippage and inefficient force transmission. In the body, muscle is covalently tethered to the skeleton via tendons, which efficiently transmit force. Thus, we have developed a synthetic tendon to act as a biohybrid interface, enabling the design of more modular, efficient, and adaptive biohybrid machines.

Methods: We developed an adhesive tendon in collaboration with Professor Xuanhe Zhao's lab at MIT. It is composed of a poly(acrylic acid) hydrogel functionalized for tissue adhesion with N-Hydroxysuccinimide ester groups. To characterize the interface between synthetic tendon and muscle, we performed tensile tests on differentiated and undifferentiated muscle samples (n=3) bound to the synthetic tendon. Muscle samples were manufactured from C2C12 mouse myoblasts. Cell populations were seeded into a fibrin and matrigel matrix, then cast into polydimethylsiloxane molds. Tensile tests were performed by layering muscle between two pieces of tendon, and pulling the assembly apart until interface failure was observed. To understand the effect of the synthetic tendon on cell viability, a colorimetric MTS assay was performed, along with a pH exposure test. Absorbance readings were taken at 490nm from control and experimental C2C12 myoblast cultures that had been incubated with synthetic tendon overnight (n=3). pH readings were probed at 0 and 30 minutes of control and experimental samples of DMEM culture medium that had also been exposed to the synthetic tendon (n=3).

Results and Discussion: Our experiments demonstrated that differentiated muscle had a greater mean force-at-break value (~680mN) than undifferentiated muscle (~520mN) at their interfaces, although this difference was not statistically significant. Both values are magnitudes greater than the mean contractile force generated by our muscle actuators (~300uN) [1], indicating that the interfacial strength far exceeds our target metric and that the muscle-tendon assembly should remain intact over multiple cycles of use. We also observed no statistically significant difference in cell viability from absorbance readings or media pH in response to tendon exposure, indicating biocompatibility.

Furthermore, current preliminary tests evaluating the tendon-skeleton interface indicate a robust connection as well, asserting that the whole biohybrid assembly should be resilient to repeated use. We are also now quantifying the improvement in force transmission efficiency enabled by the interface, increasing the performance of our muscle bioactuators.

Conclusion: We have developed a hydrogel tendon that serves as a robust biocompatible musculoskeletal interface. The unconstrained nature of this innovation will enable the design of novel robotic architectures capable of functional applications like walking, swimming, pumping, and gripping that were previously not possible to manufacture. We also anticipate our biohybrid interface will advance the fundamental understanding of how passive tension generated by tendons guides muscle fiber alignment during growth and in response to injury. Our work sets the stage for fabricating next generation biohybrid robots that can dynamically adapt to the unpredictability of the real-world.

Reference: [1] R. Raman *et al.* (2017). *Nat. Protoc.*

9:00 AM *SB05.11.05

Electrically Conductive Nano-Biomaterials and Wirelessly Powered Cell Stimulator for Engineering and Controlling Biohybrid Soft Robots [Su RyonShin](#); Harvard Medical School, United States

Engineered living-synthetic systems possess functions to dynamically control their shape and movements in biological environments that are pertinent to various biomedical applications, such as building biorobots and artificial muscles. To create functional bio-hybrid systems, in vivo-like living natural components such as 2D and 3D muscle tissue constructs, and their contractile function are required to be integrated into artificial platforms. Among various biomaterials, electrically conductive nanoparticles-incorporated hydrogels, which can improve the nanofibrous morphology and electrical and mechanical properties of conventional hydrogels while maintaining the hydrogels' beneficial properties, such as high porosity, biocompatibility, and biodegradability, are required to develop scaffolds mimicking biological and physical properties of native extracellular matrices (ECMs). These nanofibrous and electrically conductive scaffolds showed excellent myofiber maturation and organization along with cell-cell junction formation, providing self-actuating motions. Also, these nano-biomaterials can be engineered by various microfabrication techniques (i.e., bioprinting) to create 3D complex architectures, such as accordion-inspired hydrogel-based scaffolds which replicated the native myofiber architecture together with its function in terms of robustness and enhanced contractibility after culturing with cardiomyocytes. Recently, the maneuvering of bio-hybrid soft robots has been controlled by various strategies, such as by electrical and optical stimulations. We have developed advanced technologies to control the biohybrid soft robots by integrating flexible microelectrodes into soft and deformable engineered scaffolds to stimulate muscle actuators locally. Harnessing wireless power transfer technology without requiring batteries and wires, we developed untethered biohybrid soft robots that could swim; whereby, the steering of this swimming motion could be remotely controlled by transmitting electrical power into a cell stimulator wirelessly. To this end, wirelessly powered, stretchable, and lightweight cell stimulators were successfully integrated into self-actuating soft muscle bodies without impeding the robot's underwater swimming ability. Wirelessly modulated electrical frequencies enabled us to control the speed and direction of the biohybrid soft robots. This innovative approach should provide a platform for building untethered biohybrid systems for various biomedical applications.

9:30 AM *SB05.11.06

Arts & Crafts or Engineering? Tissue Engineered Hearts [KevinK. Parker](#); Harvard University, United States

The three biggest questions in engineering human organs are 1) *What are the Design specs?* 2) *Who Builds the nano?* and 3) *How do you Test how good you are?* The responses to these questions are confused by variations in clinical endpoints and diagnostics, knowledge gaps in the basic science, and difficulty in the proper design of control experiments. This talk will review our efforts to address these three questions in regards to building a heart that include the development of new additive manufacturing techniques, understanding the living cell as an engineering material, and a foray into marine biology.

10:00 AM BREAK

SESSION SB05.12: Functional Interfaces with Microorganisms I

Session Chairs: Guglielmo Lanzani and Eleni Stavrinidou

Thursday Morning, November 30, 2023

Hynes, Level 1, Room 102

10:30 AM *SB05.12.01

Living Bioelectrochemical Composites Incorporating Conjugated Polyelectrolytes [GuillermoBazan](#); National University of Singapore, Singapore

Composites, in which two or more material elements are combined to provide properties unattainable by single components, have a historical record dating to ancient times. Few include a living microbial community as a key design element. A logical basis for enabling bioelectronic composites stems from the phenomenon that certain microorganisms transfer electrons to external surfaces. A bioelectronic composite which allows one to electronically address cells beyond the confines of an electrode surface can impact bioelectrochemical technologies, including microbial fuel cells for power production and bioelectrosynthesis platforms where microbes produce desired chemicals. In this presentation we show that the p-type conjugated polyelectrolyte (CPE) CPE-K functions as a conductive matrix to electronically connect a three-dimensional network of *Shewanella oneidensis* MR-1 to a gold electrode, thereby increasing the extracted biocurrent ~150-fold over control biofilms. While increased biocurrent is due to more cells in communication with the electrode, current extracted per cell is also enhanced indicating efficient long-range electron transport. More recent developments demonstrated that extracellular materials released by *Shewanella oneidensis* MR-1 has a profound influence on the rheological properties of the composite. It is also possible to design CPEs capable of enhancing bidirectional extracellular electron transfer by forming self-assembled coatings on individual cells. Specifically, the n-type conjugated polyelectrolyte p(cNDI-gT2) exhibits a reduction potential window between -0.1 V and -0.8 V (vs Ag/AgCl), thereby driving thermodynamically favored electron transfer in both directions across the abiotic-biotic interface that involves the outer membrane cytochromes and flavins of *Shewanella oneidensis* MR-1. Electrochemical tests show that injection from an external electrode into *Shewanella oneidensis* MR-1 is enabled at negative potentials (-0.6 V), while electron extraction is possible at positive potentials (0.2 V). Relative to controls, the biohybrid shows a 6-fold increase in biocurrent generation and a 35-fold increase in current uptake for the bioelectrosynthesis of succinate from fumarate. This demonstrated abiotic-biotic synergy provides new strategies for designing multifunctional biohybrids.

11:00 AM SB05.12.02

Living Diatom Microalgae as Robust Bioanodes for Biophotovoltaic Devices [CesarVicente-Garcia](#)¹, [GabriellaBuscemi](#)¹, [DaniloVona](#)¹, [RobertaRagni](#)¹, [MatteoGrattieri](#)¹, [FrancescoMilano](#)² and [Gianluca MariaFarinola](#)¹; ¹University of Bari, Italy; ²CNR-ISPA, c/o Campus Ecotekne, Italy

Biophotovoltaic devices are a promising source of renewable energy, given they can generate electrical current from the photosynthetic activity of microalgae, cyanobacteria, or their isolated proteins. Different strategies such as direct electron transfer or, more commonly, the use of soluble mediators allow to directly harvest electrons from the cells of photosynthetic organisms and feed them to a closed circuit to generate current. Green microalgae have been extensively studied for the extraction of photocurrent, yielding promising outputs, mainly thanks to their ease of culture and fast growth. Alternatively, only a few examples are present in literature about the use of Diatom Microalgae for photocurrent extraction. Besides providing significant photocurrent intensities, diatom microalgae exhibit particular resistance to different kinds of stressors such as desiccation, temperature and mechanical pressure, which comes as an advantage when it comes to processing them into living bioanodes. Their sensibility to different contaminants makes them good candidates for the development of electrochemical biosensing devices. Moreover, diatoms hold the unique characteristic of bearing nanostructured biosilica microscopic shells (frustules), that can be functionalized with active molecules or polymers, opening the door to enhancing electron flow through conductive polymers, or to light absorption modulation for example via introduction of external antennae. This work aims to study the photocurrent extraction from different species of diatom microalgae deposited onto ITO, used as working electrode in a photovoltaic cell, evaluate their interaction with the electrode both in the presence and absence of a soluble mediator, and their resistance to the electrochemical process itself. Cyclic voltammetry and chronoamperometry measurements have been performed; optical and fluorescence microscopies, and metabolic assays have been used to study the microalgae's state under the different conditions studied. We have standardized a method that allows to produce bioanodes resistant to desiccation from several different species of diatoms, that provide significant levels of power output, and are more resistant to repeated cycles of desiccation/photocurrent than a model green alga.

11:15 AM SB05.12.03

Polymer-Modified 3D Electrode Interfaces for Efficient Charge Extraction from Photosynthetic Microorganisms [RachelEgan](#)¹, [JonasHonacker](#)², [JoshuaLawrence](#)¹, [LinyingShang](#)¹, [LauraWey](#)³, [BartekWitek](#)¹, [NicolasPlumeré](#)², [ErwinReisner](#)¹ and [JennyZhang](#)¹; ¹University of Cambridge, United Kingdom; ²Technical University of Munich, Germany; ³University of Turku, Finland

Cyanobacteria are abundant photosynthetic microorganisms that can be interfaced with electrodes in semi-artificial photosynthetic systems for solar-electricity or solar-fuel generation. [1] This approach relies on the ability of the living organisms to exchange electrons efficiently with the electrode. Redox-active and conductive polymers may be introduced at the cell-electrode interface to improve charge transfer efficiency by providing a direct route for electrons to reach the electrode thus overcoming sluggish diffusional kinetics. At present, the polymer properties that are key for efficient wiring of cyanobacteria to electrodes are poorly understood.

In this study, we systematically tested and compared the capacity of a common osmium-based redox polymer (P_{Os}) and the conductive polymer poly(3,4-ethylenedioxythiophene) (PEDOT) to act as a wiring tool for *Synechocystis* sp. PCC 6803 on hierarchically-structured inverse opal indium tin oxide (IO-ITO) electrodes. By using stepped chronoamperometry and normalising photocurrents against cell loading, we were able to identify the conditions under which each polymer served only as an immobilisation matrix, enhancing the photocurrent by means of increasing the cell loading rather than by mediation. The contribution of various parameters including polymer type (redox vs conductive), deposition method (dropcasting vs electropolymerisation), deposition geometry (layered vs mixed), polymer morphology and polymer loading towards optimal photocurrent outputs were deconvoluted. Increasing the polymer loading in both cases led to an enhanced mediation effect up until a certain point when photocurrents were reduced presumably by a shading effect. This problem was overcome by changing the electrode geometry to micropillar ITO electrodes in which the light path can penetrate through the structure unimpeded. We also investigated the interaction of the polymer with a *Synechocystis* mutant lacking extracellular polymeric substances (EPS). The PEDOT-modified electrodes produced higher photocurrents overall vs the P_{Os} -modified electrodes (20-fold vs 5-fold enhancement respectively) relative to unmodified electrodes at a low light intensity of 1 mW cm⁻². However, the larger photocurrents extracted using PEDOT come at a thermodynamic cost, as the onset potential for mediation is 200 mV higher for PEDOT than for P_{Os} . Overall, this study identifies polymer properties that are essential for successful cyanobacteria-electrode wiring and informs future interface design strategies for photosynthetic organisms on complex 3D structures.

References

[1] J. Z. Zhang, P. Bombelli, K. P. Sokol, A. Fantuzzi, A. W. Rutherford, C. J. Howe, E. Reisner, *Journal of the American Chemical Society* **2018**, 140, 6–9

11:30 AM *SB05.12.04

Nanomaterial and Biological Engineering of Living Electronics [Ardemis Boghossian](#); EPFL SB ISIC LNB, Switzerland

The vast expansion of available synthetic biology tools has led to explosive developments in the field of materials science. The increased accessibility of these tools has pushed the frontier of materials science into the field of engineering biological and even living materials. By coupling the tunability of nanomaterials with the prospect of re-programming living devices, one can re-purpose biology to fulfil needs that are otherwise intractable using traditional engineering approaches.

Optical technologies in particular stand to benefit from the untapped potential in coupling the optical properties of nanomaterials with the specificity and scalability of biological materials. This presentation highlights applications in sensing and energy technologies that exploit the synergistic coupling of nanobio-hybrid materials. This talk will focus on the development of living electronics, such as photovoltaics based on photosynthetic organisms with augmented capabilities.

SESSION SB05.13: Functional Interfaces with Microorganisms II

Session Chairs: [Ardemis Boghossian](#) and [Guglielmo Lanzani](#)

Thursday Afternoon, November 30, 2023

Hynes, Level 1, Room 102

1:30 PM *SB05.13.01

Photosynthetic Microorganisms for Optoelectronics [Gianluca Maria Farinola](#); Università degli Studi di Bari Aldo Moro, Italy

Photosynthetic microorganisms and their molecular components for light absorption and photoconversion, optimized over billions of years of evolution, represent attractive tools for harvesting and conversion of solar light in sustainable and cost-effective transducers. The new era of biohybrid devices relies on the exploitation of isolated structures from these microorganisms, or the entire living cells, as the active components for photoconversion in optoelectronic devices and photoelectrochemical cells [1].

The bacterial reaction center (RC) extracted from the purple non-sulphur bacterium *Rhodospirillum rubrum* (*R. rubrum*) has been initially modified by covalent functionalization with organic molecules specifically designated to act as artificial antennas to increase its light absorption capability [2].

The same RC has been also integrated into photoactive transistors [3], using molecular or polymeric semiconductor thin films deposited onto metal electrodes as interfaces [4]. Among them polydopamine (PDA), a biocompatible polymer produced via self-oxidative polymerization of the dopamine monomer, gave very interesting results for the stabilization of *R. rubrum* RCs. RC has been immobilized both in PDA thin films on the electrode surfaces or in PDA nanoparticles, without altering the enzymatic photoactivity, and producing photocurrents in photoelectrochemical cells [5]. PDA has been modified with diamines, leading to more transparent nanostructures incorporating RC molecules, which outperform RC/PDA structures in light transmission and photoconversion [6].

Finally, we have investigated different approaches for interfacing intact photosynthetic microorganisms with electrodes, enabling photoconversion of whole living cells of *R. rubrum* and *R. rubrum*, using PDA as the interface material either as a coating on the cells' surface, or as a film entrapping the cells on the electrode surface [7].

Furthermore, eukaryotic diatoms have been also selected for their efficiency in harvesting and converting sunlight into chemical energy and the feasibility of silica shell functionalization. Electrochemical characterizations have been performed to understand the electronic transfer between diatoms and electrodes, using different redox mediators.

[1] F. Milano, A. Punzi, R. Ragni, M. Trotta, G. M. Farinola, *Adv. Funct. Mater.*, **29**, 1805521, (2019).

[2] F. Milano, R.R. Tangorra, O. Hassan Omar, R. Ragni, A. Operamolla, A. Agostiano, G.M. Farinola, M. Trotta, *Angew. Chem. Int. Ed.*, **51**: 11019-11023 (2012)

[3] M. Di Lauro, S. la Gatta, C.A. Bortolotti, V. Beni, V. Parkula, S. Drakopoulou, M. Giordani, M. Berto, F. Milano, T. Cramer, M. Murgia, A. Agostiano, G.M. Farinola, M. Trotta, F. Biscarini "A Bacterial Photosynthetic Enzymatic Unit Modulating Organic Transistors with Light", *Adv. Electronic Mater.* **6** (1), 1900888 (2020).

[4] E. D. Glowacki, R. R. Tangorra, H. Coskun, D. Farka, A. Operamolla, Y. Kanbur, F. Milano, L. Giotta and N. S. Sariciftci "Bioconjugation of hydrogen-bonded organic semiconductors with functional proteins", *J. Mater. Chem. C*, **3** (25), 6554-6564 (2015).

[5] M. Lo Presti, M. M. Giangregorio, R. Ragni, L. Giotta, M. R. Guascito, R. Comparelli, E. Fanizza, R. R. Tangorra, A. Agostiano, M. Losurdo, G. M. Farinola, F. Milano, M. Trotta "Photoelectrodes with Polydopamine Thin Films Incorporating a Bacterial Photoenzyme", *Adv. Electron. Mater.* 2000140 (2020).

[6] G. Buscemi, D. Vona, R. Ragni, R. Comparelli, M. Trotta, F. Milano, G. M. Farinola "Polydopamine/Ethylenediamine Nanoparticles Embedding a Photosynthetic Bacterial Reaction Center for Efficient Photocurrent Generation", *Adv. Sustain. Syst.*, doi.org/10.1002/advs.202000303 (2021).

[7] G. Buscemi, D. Vona, P. Stufano, R. Labarile, P. Cosma, A. Agostiano, M. Trotta, G.M. Farinola, M. Grattieri. Bio-inspired redox-adhesive polydopamine matrix for intact bacteria biohybrid photoanodes. *ACS Applied Materials & Interfaces*, 2022, 14(23), pp. 26631–26641

2:00 PM SB05.13.02

Polydopamine-Coated Photoautotrophic Bacteria For Improved Extracellular Electron Transfer in Living Photovoltaics [Melania Reggente](#)¹, [Charlotte Roullier](#)¹, [Mohammed Mouhib](#)¹, [Rossella Labarile](#)², [Massimo Trotta](#)², [Fabian Fischer](#)³ and [Ardemis Boghossian](#)¹; ¹École Polytechnique Fédérale de Lausanne, Switzerland; ²CNR-IPCF Consiglio Nazionale delle Ricerche, Switzerland; ³HES-SO Valais-Wallis, Switzerland

Living photovoltaics represent a growing class of microbial electrochemical devices based on whole cell-electrode interactions able to convert solar energy into electricity. The bottleneck in current microbial electrochemical technologies is the limited electron transfer between the microbe and the electrode surface. This study focuses on the development of a polydopamine (PDA) coating on the outer-membrane of the photosynthetic organism *Synechocystis* sp. PCC6803. This encapsulation provides a conductive shell to enhance electrode adhesion and improve microbial charge extraction. Cell encapsulation was obtained through an oxygenic dopamine (DA) polymerization in slightly alkaline conditions and the effect of two pH levels (7.5 and 8.2) were examined. PDA-coated cells were characterized and optimized using scanning and transmission electron microscopy (SEM and TEM, respectively) as well as confocal microscopy, UV-Vis and Raman spectroscopies. The microbial exoelectrogenicity was assessed through chronoamperometric measurements. PDA-coated microbes showed three-fold enhanced electron transfer with retained viability and photosynthetic activity.

2:15 PM *SB05.13.03

Engineered Living Electronic Interface [Claudia Tortiglione](#)¹, [Giuseppina Tommasini](#)^{2,1}, [Mariasaria De Simone](#)¹, [Silvia Santillo](#)¹, [Marika Iencharelli](#)¹, [Gwenael Dufil](#)³, [Daniele Mantione](#)⁴, [Natalia Dell'Aversano](#)¹, [Eleni Stavrinidou](#)² and [Angela Tino](#)¹; ¹Istituto di Scienze Applicate e Sistemi Intelligenti, Consiglio Nazionale delle Ricerche, Italy; ²Instituto de Nanociencia y

Cells can be considered as nanomaterial factories able to build structures of amazing complexity starting from a few molecular building blocks. The introduction into the cell of an exogenous chemical input may result in the fabrication of hybrid materials with unique functionalities, that can be exploited for diverse applications (from biomedicine to bioelectronics). We exploited this potential in a simple tissue-like organism, the freshwater polyp *Hydra vulgaris*, shown able to produce electronically conductive interface starting from thiophene based compounds. By simply incubating living polyps in a solution containing organic semiconductor oligomers the spontaneous polymerization into microstructures presenting electronic conductivity and electrochemical capacitance was observed[1]. In addition, for the first time their neuromodulatory function was demonstrated by behavioral and electrophysiological approaches. Here we provide an overview of recent results obtained by challenging Hydra with different chemical inputs and envisage the possibility of manufacturing living electronics, acting as highly performant electrodes to monitor and control important processes, from development to regeneration. These interfaces, seamlessly integrated into the cells and naturally evolving with the polyp life cycle, overcoming the issues of tissue-interface mismatch, adverse cell response, and low biocompatibility, suggest the possibility of augmenting electronic functionality in animals and the fabrication of a new class of engineered living materials.

[1] G.Tommasini, G.Dufil, F. Fardella, X.Strakosas, E. Fergola, T.Abrahamsson, D.Bliman, R.Olsson, M.Berggren, A. Tino, E. Stavrinidou, C.Tortiglione. Seamless integration of bioelectronic interface in an animal model via in vivo polymerization of conjugated oligomers, *Bioactive Materials*, 2022 10: 107-116.

2:45 PMBREAK

3:15 PM *SB05.13.04

Light Management by Algal Aggregates in Living Photosynthetic Hydrogels[Silvia Vignolini](#); University of Cambridge, United Kingdom

Rapid advancements in algal biotechnology have fueled a growing interest in hydrogel-encapsulated microalgal cultivation, particularly for the development of functional photosynthetic materials and biomass production. A previously overlooked aspect of gel-encapsulated cultures is the emergence of cell aggregates, resulting from the mechanical confinement of cells. These aggregates significantly impact light management within photobioreactors, consequently influencing the photosynthetic output. To assess this phenomenon, we conducted experimental investigations on the optical response of hydrogels containing algal aggregates and developed optical simulations to analyze the resulting light intensity profiles. The simulations were validated through transmittance measurements using an integrating sphere and aggregate volume analysis with confocal microscopy. Our findings reveal that the heterogeneous distribution of cell aggregates in a gel matrix enhances light penetration and mitigates photoinhibition compared to a flat biofilm. Moreover, we demonstrate that the introduction of scattering particles within the hydrogel matrix further enhances light harvesting efficiency, resulting in a four-fold increase in biomass growth. Consequently, our study presents a novel strategy for designing spatially efficient photosynthetic living materials, which hold significant implications for future photobioreactor engineering.

3:45 PM SB05.13.05

Controlling the Properties of Macroscopic Living Materials by Genetically Altering Their Matrix[Esther Jimenez](#), Carlson Nguyen and Caroline Ajo-Franklin; Rice University, United States

Living cells assemble into hierarchical structures, forming complex materials with remarkable properties. Inspired by nature, the emerging field of Engineered Living Materials (ELMs) aims to predictively design cells to grow into materials with tailored properties. Contributing to this goal, our lab has recently reported the first **Bottom-Up De novo Engineered Living Materials (BUD-ELMs)** using the bacterium *Caulobacter crescentus*. BUD-ELMs are comprised of a secreted protein matrix consisting of surface-layer protein and an elastin-like polypeptide (ELP) domain that assembles cells into centimeter-scale materials and defines their mechanical and physical characteristics. However, a fundamental knowledge gap we have yet to address is understanding how genetic modifications affect bulk material characteristics. Thus, our goal is to elucidate sequence-structure-property relationships of BUD-ELMs to achieve predictive design for targeted mechanical properties. We hypothesized that the mechanical properties of the purified ELPs, which are known to be tunable as a factor of sequence length, would be mimicked in BUD-ELMs. Therefore, to test this hypothesis, we engineered strains expressing ELPs of different lengths, grew the strains to form BUD-ELMs, and characterized each material's viscoelastic behavior by rheology measurements. Our frequency sweep results show that shortening the ELP increases the storage and loss moduli, showing stiffer resulting material, while lengthening the ELP does not affect the moduli. Interestingly, flow sweeps show strong shear-thinning under low shear rates, implying a fragile microstructure network among all the resulting materials from each strain. Additionally, to elucidate the relationship between each material's mechanical properties and microstructure, we employed confocal microscopy. The results show clear differences in each variant's matrix structure. The shorter ELP variant produces spiderweb-like strands over the cells, while the longer ELP sequence forms thinner fiber-like strands between cells. Based on this data, we attribute the changes in this material's mechanical properties to the interconnected network formed by the matrix of the shorter ELP. In comparison, the thin fiber-like strand formation formed by the longer ELP does not impact its rheological characteristics. Furthermore, the different structures produced by each material result in distinct yield stresses. Thus, this exploration into the genetic tunability of BUD-ELMs leads us toward establishing sequence-structure-property relationships for ELMs with programmable mechanical and structural properties for applications such as 3D printing and tissue engineering.

4:00 PM SB05.13.06

Motile Microorganisms in Intelligent Biohybrid Microrobots: Enhancing Propulsion, Control and Therapeutic Capabilities with Microalgae and Bacteria[Birgul Akolpoglu](#)^{1,2}, Saadet F. Baltaci Demir^{1,3} and Metin Sitti^{1,2,3}; ¹Max Planck Institute for Intelligent Systems, Germany; ²ETH Zürich, Switzerland; ³University of Stuttgart, Germany

Biohybrid microrobots incorporate motile microorganisms and artificial components to construct self-powered devices capable of sensing, control, targeting, and delivery at small scales. The integration of such motile microorganisms including microalgae, bacteria, spermatozoa or macrophages as the biological component, combined with artificial components such as polymer coatings, liposomes, and micro- and nanoparticles, enhances the functionalities of biohybrid designs. The careful selection of both biological and artificial units is essential in the design of biohybrid microrobots, as the biological component plays a pivotal role in propulsion, control, and sensing, while the artificial component influences crucial aspects such as biocompatibility, biodegradability, and therapeutic capabilities. However, existing design strategies for biohybrid microrobots encounter challenges concerning low production efficiencies, limited multifunctionality and control over swarm navigation. To overcome these limitations, we propose and conceptualize a range of biohybrid microrobotic designs achieved through facile, robust, and high-throughput fabrication methods, capable of simultaneously executing multiple functions with intelligent complexity.

Specifically, we present two distinct types of biohybrid systems: microalgae- and bacteria-driven microrobots. In the case of microalgae-driven biohybrids, *Chlamydomonas reinhardtii*, a single-cell green alga, serves as the biological model microorganism. By employing a noncovalent assembly approach, a thin, soft uniform coating layer is constructed using a polymer-nanoparticle matrix, resulting in a production efficiency of approximately 90%. This soft surface coating effectively preserves the microalgae's viability and phototactic ability while accommodating the incorporation of drug molecules and enabling active magnetic steerability. The magnetic steering capability of microalgae-driven microrobots is demonstrated in various microenvironments through adjustments in viscosity and confinement, emulating real-world settings that mirror the complexities of the human body. Furthermore, as a proof-of-concept, we showcase the controlled, on-demand drug delivery to tumor cells by conjugating nanoparticles embedded in the thin coating with chemotherapeutic agent doxorubicin, facilitated by a photocleavable linker.

On the other hand, bacteria-driven biohybrids are realized through the development of a magnetically controlled system that enables targeted localization and multistimuli-responsive drug release within three-dimensional (3D) biological matrices. *Escherichia coli* bacteria are integrated with magnetic nanoparticles and nanoliposomes via biotin-streptavidin complex, resulting in a high biohybrid construction yield. These bacterial biohybrids retain their original motility and exhibit enhanced capabilities for navigation through complex biological matrices, including 3D biological gels and tumor spheroids. Under the influence of external magnetic fields, they can effectively localize within specific regions and colonize tumor spheroids, enabling precise and on-demand release of therapeutic molecules upon near-infrared and pH stimuli.

The proposed biohybrid microrobotic designs presented in these studies hold significant promise for future medical applications by addressing current limitations and employing advanced fabrication techniques. These designs offer improved production efficiencies, enhanced control over locomotion, and various medical functionalities.

4:15 PM SB05.13.07

Catalytic Materials Enabled by a Programmable Assembly of Synthetic Polymers and Engineered Bacterial Spores[Masamu Kawada](#), Hyuna Jo, Alexis Medina and Seunghyun Sim; University of California, Irvine, United States

Natural biological materials are formed by self-assembly processes and catalyze a myriad of reactions. Inspired by such materials, we developed a programmable molecular assembly of designed synthetic polymers with engineered bacterial spores. This self-assembly process is driven by dynamic covalent bond formation on spore surface glycan and yields macroscopic materials that are structurally stable, self-healing, and recyclable. Molecular programming of polymer species shapes the physical properties of these materials while metabolically dormant spores allow for prolonged ambient storage. Incorporation of spores with genetically encoded functionalities enables operationally simple and repeated enzymatic catalysis. Our work lays an

important foundation for scalable and programmable synthesis of robust materials for sustainable biocatalysis.

4:30 PM SB05.13.08

Synergy Between Bacteria and Conjugated Polyelectrolytes to Form Functional Biomaterials [Samantha McCuskey](#)¹, Glenn Quek¹, Ricardo Javier Vazquez¹, Binu Kundukad² and Guillermo Bazan¹; ¹National University of Singapore, Singapore; ²Nanyang Technological University, Singapore

Combining conjugated polyelectrolytes with electroactive bacteria leads to the formation of living functional materials that improve the performance of bioelectrochemical technologies for biosensing, electricity generation, and electrosynthesis. However, the organization of these hydrogel composites and their effect on microbe physiology remain unexplored. In this study, mixing of a p-type conjugated polyelectrolyte (CPE-K) with *Shewanella oneidensis* MR-1 leads to a three-dimensional organization that generates ~30-fold greater biocurrent density than control biofilms in electrochemical cells. Further, respiration of the bacteria through the polymer promotes conductive network formation with a lower charge transfer resistance than neat CPE-K by itself. Total RNA-sequencing analysis revealed differential gene expression between cells in the polymer composite versus standard biofilm. Genes related to bacteriophages (biofilm development) and energy metabolism were upregulated in the composite compared to control biofilms. Correlating, extracellular polymeric substance (EPS) quantity and lactate coulombic efficiency increased in the composite. Cyclic voltammetry, fluorescent staining, and rheological measurements before and after enzymatic treatment in the living composite show the importance of the extracellular matrix for cohesion. EPS components added to neat CPE-K do not achieve the same properties. Taken all together, the demonstrated abiotic/biotic synergy between microbe and polymer provides new strategies for designing multifunctional living composite materials.

SESSION SB05.14: Implantable and Wearable Devices
Session Chairs: Herdeline Ann Ardoña and Eleni Stavrinidou
Friday Morning, December 1, 2023
Hynes, Level 1, Room 102

8:15 AM SB05.14.01

Wearable *In Situ* Sweat Sensors for Health—On-Skin Electrochemical Real-Time Sensors [Le Yang](#)^{1,2}; ¹Institute of Materials Research and Engineering A*STAR, Singapore; ²National University of Singapore, Singapore

In an increasingly health-aware population and a move towards remote diagnostics, remote healthcare monitoring, cloud-based med-tech, etc, we tap on the ubiquitous and unlimited reservoir of on-skin biomarkers, including sweat metabolites, in developing a wearable, non-invasive, continuous and real-time sensor – a printed, multiplexed biosensor. Our integrated devices are designed and developed with scalability and translation in mind – ensuring printability (for scalable manufacturing), ease of fabrication routes, and solid-state and miniaturised prototype.[1-5] We also aim for better validation and correlation studies of non-invasive biomarkers to ensure useful relevance of such non-gold standard devices. Carbon-based electrodes are promising candidates for developing cheap, miniaturized, and disposable biosensors for effective wearable applications. From developing our own printable carbon-based ink, to screen-printing the electrodes, to functionalising each electrode into a specific biosensor, and finally to multiplexing and integration and incorporating of cheap paper-based sweat channels - we show how these devices can potentially add value to home-based/DIY biomarker monitoring. We look at a variation of our flexible electrode, a graphite/carbon fiber (G/CF) hybrid resembling a super-efficient 3D highway network where ample expressways (CF) run through numerous small factories (locally distributed graphite flakes) for rapid goods pick-up and transportation (electron transfer).[6] Lastly, we zoom in on the top-most layer of the device, the Kirigami paper sweat channel, critical in enabling real-time fresh-sweat reading.[7]

[1] A graphite-based paste/ink for electrochemical sensors, WP Goh, CY Jiang, Y Yu, XT Zheng, YX Liu, LYang, PCT/SG2022/050407, Singapore (*PCT filed*), 2022.

[2] XT Zheng, WP Goh, CY Jiang, Y Yu, YX Liu, L Yang et al, *Manuscript in preparation*.

[3] Stretchable biochemical interface for solid epidermal analytes, YX Liu, WP Goh, XT Zheng, Y Yu, SCL Tan, CY Jiang, RT Arwani, L Yang, SG-10202202318P, Singapore (*PCT filed*), 2023.

[4] RT Arwani, WP Goh, CY Jiang, XT Zheng, Y Yu, L Yang YX Liu et al, *Manuscript Submitted 2023*.

[5] Y Yu, L Yang et al, *Materials Today Chemistry*, 29, 101442 (2023).

[6] Y Yu, L Yang et al, *Materials Today Advances*, 14, 100238 (2022).

[7] A kirigami paper fluidic channel for sweat sensors, CY Jiang, WP Goh, XT Zheng, Y Yu, YX Liu, L Yang, SG-10202113328Q, Singapore (*PCT filed*), 2023.

8:30 AM SB05.14.02

Materials for Cut-And-Seam Fabrication of Soft Functional Interfaces [Cindy K. Harnett](#)¹ and [Samantha Musante](#)²; ¹University of Louisville, United States; ²Trinity College, United States

Interfaces between inorganic and biological systems need to be mechanically compatible with soft surfaces that grow, stretch, and distort over time. This requirement has driven the development of soft photonic and electronic circuits. However, the evolving shape of these circuits poses a problem when connecting circuits together: how can we match up distorted contacts that may be impossible to align? The problem comes up not only when repairing, modifying, or temporarily connecting to a stretchable circuit that's already attached to a biological system, but also when connecting circuit pieces into custom 3D structures to cover one-of-a-kind biological shapes. The usual solution to the distortion problem is to create a stiffened connector region that prevents the circuit from deforming, which is good for alignment but doesn't conform to biological surfaces as closely as a soft region does. The 3D structure problem may be solved by laying out a new electronic circuit for each individual interface, but this makes it difficult to use woven meshes and other regular structures as bases for soft functional interfaces.

This presentation describes our approach to connect signals across thin seams between soft materials without precise alignment at the connections. Our method relies on mm- and smaller scale electrical components inserted into thin adhesive tapes, producing materials with anisotropic electrical conductivity.

The alignment error tolerances we target are 2 mm in the direction perpendicular to the circuit edge, 2 cm parallel to the circuit edge, and a 70 degree angular tolerance. The reason for the large angular tolerance is that 3D cut-and-seam structures are often made from anisotropic woven or knit materials, often have curved seams, and are subject to external constraints such as packing cuts into a sheet to conserve material. These factors mean there is no guarantee that wires, optical fibers, and other anisotropic features will meet at the same angle along every seam, or even within a single seam.

The cut-and-seam fabrication method will also be discussed here as an interface for highly porous mesh-based biosensor circuits. Mesh circuits' applications in tissue engineering and biosensing are promising because meshes permit vapor transport, can be perfused with nutrients, and provide paths for cells to extend through during growth. However, the task of collecting signals from individual wires in a mesh is laborious, and mesh materials are often made from fibers that can't be soldered because of a too-low operating temperature range (for example, metallized polymer threads) or because harsh chemicals are required for solder wetting (for example, stainless steel wires and threads). The seaming materials and methods in this work are designed to make contact to those conductors, forming a distribution network for power and data in the soft sensor interface.

In this presentation, we investigate the above alignment tolerances in circuits made from thin films and fibers, focusing on methods such as capacitance, temperature, strain, and light intensity measurements that function when encapsulated by parylene, silicone and other conformal biocompatible coatings.

8:45 AM SB05.14.03

Microneedle Array Optical Sensing for Wearable Real-Time Hydration Monitoring [Lawrence Renna](#)¹, [Kyle Brubaker](#)¹, [Eric Kroon](#)¹, [Megan Sax van der Weyden](#)², [Shane Caswell](#)², [Joel Martin](#)² and [Andrew Koch](#)³; ¹Intelligent Optical Systems, Inc., United States; ²Sports Medicine Assessment Research & Testing (SMART) Laboratory; George Mason University, United States; ³Naval Air Warfare Center Aircraft Division (NAWCAD), United States

The escalating occurrence of physiological episodes leading to flight termination, combined with concerns over dehydration arising from prolonged missions, inadequate relief equipment, and environmental factors, has underscored the necessity for a real-time aviator hydration monitoring system to mitigate cognitive deficits and optimize in-flight performance. Dehydration-induced fatigue prominently impairs physical performance, particularly under heat stress, while also compromising various aspects of fitness such as aerobic capacity, strength, power, and balance. Even a 2% body weight loss due to dehydration can significantly impair cognitive abilities related to attention, executive function, and motor coordination, with more severe dehydration exacerbating cognitive impairment in tasks involving attention, psychomotor function, and short-term memory. To address these challenges, we have developed a wearable, real-time hydration monitor tailored specifically for military personnel, incorporating a novel technology that monitors subdermal chemistry, specifically the interstitial fluid derived from plasma,

which is in equilibrium with plasma composition. The wearable device directly tracks a distinct set of biomarkers—sodium ions, proton activity (pH), and water activity—in the interstitial fluid, effectively overcoming the limitations and inaccuracies encountered by existing consumer-oriented products that solely measure surface sweat properties. The integrated system incorporates a sensor-integrated hydrogel microneedle array (MNA) capable of detecting intradermal hydration biomarkers. The MNAs are equipped with embedded luminescent indicators designed to be sensitive to the target biomarkers. Leveraging the microneedles as conduits, light is efficiently delivered to and from the subdermal sensor, unaffected by variations in skin tone. The sensors are built on luminescence lifetime measurements, a robust optical process ensuring reliable and continuous signal readings even in dynamic and rapidly changing environments. Specifically, our approach involves employing a Dual Luminophore/Lifetime Referencing (DLR) methodology, utilizing two different luminophores with distinct lifetimes or a single material with multiple excited states that possess different lifetimes, that are sensitive to different biomarkers.

To validate our system, a human-subject hydration study was conducted (n=8). They underwent alternating periods of pedaling a stationary bicycle and sitting without water intake over a span of approximately 5 hours, while wearing the hydration monitor continuously. Urine specific gravity (USG) measurements were obtained at hourly intervals. Through the utilization of a random forest regressor model trained on the hydration monitor data, linearly interpolated USG values were predicted. Pairwise correlation analysis was performed to assess the predictive accuracy. The obtained results demonstrated a statistically significant rejection of the null hypothesis ($p = 0.038$), indicating that the predicted and actual USG values were not drawn from different distributions. Furthermore, both the Pearson Correlation and Spearman Correlation tests yielded highly significant p-values ($p < 0.0001$), affirming a strong positive correlation between the actual and predicted USG values.

In conclusion, the development of our wearable real-time hydration monitor, leveraging a microneedle array optical sensing approach, holds substantial promise in addressing the risks associated with dehydration among aviators. This innovative solution provides a reliable means of monitoring hydration status, facilitating proactive interventions to optimize performance and enhance the well-being of military aircrews.

9:00 AM SB05.14.04

Development of a Wearable Sensor to Monitor Pulmonary Function Bernardo A. Vicente, Vitor Sencadas and Raquel Sebastião; Universidade de Aveiro, Portugal

Pulmonary function testing (PFT) plays a crucial role in assessing lung and health conditions. However, the COVID-19 pandemic has imposed restrictions on traditional PFT methods, highlighting the need for alternative measurement techniques. Wearable sensors have emerged in the last decade as a promising solution, enabling continuous respiratory monitoring without hindering daily activities. These sensors offer the potential to accurately measure key parameters such as respiratory rate (RR) and breathing patterns, which are vital for diagnosing lung diseases like chronic obstructive pulmonary disease (COPD) and asthma. However, currently, available wearable sensors often lack the ability to precisely assess lung volumes, particularly tidal volume (TV), which is essential to evaluate ventilatory disorders. This work aims to develop a capacitive wearable sensor capable of measuring respiratory waveforms through the movements of the rib cage, using poly(glycerol sebacate) (PGS), a biodegradable elastomeric polymer, as the substrate material. This non-invasive device aims to provide pertinent respiratory metrics and track tidal volume changes associated with various pulmonary diseases. Moreover, this study plans to apply machine learning (ML) techniques to enhance the accuracy of PFTs and develop ML-based prediction models for ventilatory volumes. Machine learning approaches have shown great potential in healthcare, particularly in improving decision-making and reducing patient risks in critical scenarios. Through the analysis of respiratory patterns, the extraction of ventilatory parameters such as TV and RR is possible, enabling the identification and interpretation of pulmonary conditions. In this work, ML algorithms will be tested, to identify respiratory parameters in healthy subjects, improving the reliability of the wearable sensor. To validate the performance of the wearable, standard spirometry protocols will be used for data verification and calibration. The developed device will be evaluated in non-invasive settings, placed in the right lower-chest region, allowing for the collection of relevant respiratory metrics related to ribcage expansion and retraction. The collected data will also serve to train and test ML models to accurately estimate changes in ventilatory volumes. The outcomes of this research hold significant implications for pulmonary diagnostics since the development of a wearable sensor with the ability to measure respiratory waveforms and accurately track tidal volume changes can enhance the accessibility and efficacy of PFTs. Furthermore, the integration of ML techniques enables advanced analysis of ventilatory volumes, providing valuable insights for the diagnosis and monitoring of lung diseases. This study contributes to the ongoing efforts in improving non-invasive pulmonary function testing and has the potential to transform the way lung conditions are diagnosed and managed.

9:15 AM SB05.14.05

Atomically Thin Boundary Between Wearable and Implantable Bioelectronic Interfaces Dmitry Kireev; University of Massachusetts Amherst, United States

Modern biosensors reveal a notable trend toward mobile and personalized health monitoring. Monitoring health-related electrophysiological signals, such as brain activity, heart activity, body hydration, or temperature, is essential for better comprehension of human physiology. Continuous long-term monitoring of those signals from individuals of different health conditions is essential to understanding systematic health risk factors and building preventative care solutions, which is paramount for intricate conditions like cardiovascular. However, modern wearable and implantable technologies require substantial improvement in terms of their ability to interact with the tissue without causing harmful consequences. In this work, we report on a substantial advancement of graphene electronic tattoos and use them for bioelectronic applications on the wearable and implantable fronts.

In a groundbreaking advancement in healthcare technology, we have harnessed the power of graphene to create wearable and implantable bioelectronic devices that revolutionize health monitoring and treatment. Using atomically thin and electrically conductive graphene electronic tattoos (GETs), we developed imperceptible monitoring technologies for measuring blood pressure with Grade-A accuracy. Unlike other wearables, GETs are lightweight and skin-conformable, eliminating discomfort during long-term measurements.

Recently, we also translated this technology into implantable sensors, demonstrating the sensing and stimulation of the mammalian heart, including treatment of arrhythmia with graphene pacemakers. The arrays show superior electrochemical properties, and the transparency of the graphene structures allows for simultaneous optical mapping of cardiac action potentials and optogenetic stimulation. Additionally, we advanced in creating tissue-integratable bioelectronic systems resembling biological neurons using soft, flexible, and biocompatible artificial synaptic transistors based on graphene and Nafion, boasting superior energy efficiency. These breakthroughs open up new possibilities for wearable and implantable graphene bioelectronics to transform healthcare and improve patient outcomes.

9:30 AM *SB05.14.06

Intrinsically-Stretchable Cardiac Interfacing Devices for Heart Failure and Ventricular Tachycardia Dae-Hyeong Kim^{1,2}; ¹Institute for Basic Science, Korea (the Republic of); ²Seoul National University, Korea (the Republic of)

Recent advances in flexible and stretchable electronics have attracted great attention due to its potential applications to personalized bio-integrated healthcare devices. The mechanical mismatch between conventional rigid electronic devices and soft human tissues oftentimes causes various issues, such as a low signal-to-noise ratio of biosensors, inflammations on the tissue interfacing with the bioelectronics, skin irritations in the case of long-term wearing of the device, and ineffective electrical stimulations in feedback therapies. Such issues can be amplified in the case of interfacing with dynamically moving organs including the heart, and lead to unsatisfactory monitoring efficiency and therapeutic efficacy. Intrinsically-stretchable bioelectronic devices have a low system modulus and intrinsic softness, and thereby have a potential to solve these issues. Nanomaterials and their composites with the elastomeric matrix are a particularly promising material candidate for realizing this soft bioelectronics concept. In this talk, the unique strategies in the synthesis of nanomaterials, processing as stretchable functional nanocomposites, their seamless integration with dynamically-moving cardiac muscles are presented. These efforts have combined recent breakthroughs in nanomaterials and soft electronics, and are expected to address unmet clinical challenges.

10:00 AM BREAK

SESSION SB05.15: Plant/Plant-Mimetic Biohybrid Systems

Session Chairs: Raghav Garg and Eleni Stavrinidou

Friday Morning, December 1, 2023

Hynes, Level 1, Room 102

10:30 AM *SB05.15.01

Advances in Plant Nanobionics Michael S. Strano; Massachusetts Institute of Technology, United States

Plants have evolved complex internal signaling pathways to swiftly adapt to diverse environmental conditions, but these pathways are difficult to probe *in-planta* with the conventional mass spectrometry-based quantification technologies. In contrast, embedding nondestructive nanosensors in plants offer real-time, spatial and temporal measurements of plant responses toward various abiotic and biotic stimuli. This field of interfacing living plants with nanomaterials to impart non-native functions to plants, termed plant nanobionics, has been pioneered by the Strano group. We have successfully developed species-agnostic carbon nanotube sensors targeting a wide range of plant signaling molecules and environmental analytes including nitric oxide, hydrogen peroxide, auxins, salicylic acid, gibberellic acid, jasmonic acid, saccharides, arsenics and nitroaromatics. These sensors can detect waveforms associated with wound signaling, hormonal changes, and priming events to provide a new basis to understand plant defense and stress responses. Coupled with portable and cost-effective probes, these species-independent

sensors open the door for real-time monitoring of plant physiology and the environment, offering key advantages in understanding plant biology and precision agriculture.

11:00 AM SB05.15.02

Plant Electrophysiology with Conformable Organic Electronics Abdul Manan Dar¹, Adam Armada-Moreira¹, Zifang Zhao², Dion Khodagholy² and Eleni Stavrinidou¹; ¹Linköping University, Sweden; ²Columbia University, United States

Plant electrical signals are mediators of long-distance signaling and correlate with plant movements and responses to stress. Presently, these signals are studied with macro single surface electrodes that cannot resolve signal propagation patterns and integration, thus impeding their decoding and link to function. Unlike conventional extracellular electrodes, multielectrode (MEA) technology records the distribution patterns of electrical activity in cellular networks using a non-invasive, dense array of electrodes embedded in a substrate. The MEA technology is extensively used in brain and cardiac tissue research to decode the brain connectivity and potential propagation patterns in cardiac myocytes respectively. However, for plant electrophysiology the MEA technology remains fairly unexplored. Here we developed a conformable multielectrode array based on organic electronics for large-scale high-resolution plant electrophysiology. The MEA is developed with standard photolithography fabrication techniques, with parylene C as substrate and encapsulation layer resulting in total device thickness as low as 5 micrometers. The MEA is therefore highly conformable to the plant tissue leading to high Signal to Noise Ratio (SNR). With the conformable MEA we performed spatiotemporal mapping of the electrical activity of the carnivorous plant *Dionaea muscipula* a.k.a Venus Flytrap (VFT). VFT consists of a bilobed traps having three trigger hairs in each lobe which serve as mechanosensors. When the mechanosensitive hair is deflected, the mechanical stimulus is translated into an action potential (AP), by sensory cells at the base of the hair. Two action potentials (or two touches) in a short period (less than 30 secs) are required to induce closure of the trap. We found that the AP actively propagates through the tissue with constant speed and without strong directionality. We also found that spontaneously generated APs can originate from unstimulated hairs and that they correlate with trap movement. Finally, we demonstrate that the VFT circuitry can be activated by cells other than the sensory hairs. Our work reveals key properties of the AP and establishes the capacity of organic bioelectronics for resolving plants electrical signaling contributing to the mechanistic understanding of plants long-distance responses.

11:15 AM SB05.15.03

Soft Optical Implant for Measuring Water Potential in Plants Vesna Bacheva, Eric Wu, Piyush Jain, Sabyasachi Sen, Alice Gevorgyan, Margaret Frank and Abraham Stroock; Cornell University, United States

Spending their lives rooted in one place, plants exhibit remarkable adaptability in their metabolism and development in response to the changing environment [1]. One crucial aspect for their survival is the control of water uptake and the maintenance of water status (water potential) [2], which is influenced by environmental factors such as soil moisture, air temperature, and humidity. Evidence suggests that the changing water potential of plants not only results from these factors but also serves as a long-distance signaling mechanism that enables plants to communicate these changes effectively [3-5]. Therefore, measuring water potential would improve our understanding of whole-plant signaling and responses to environmental stresses, allowing us to develop effective strategies for plant health and productivity in a changing climate. However, currently, there is lack of tools for measuring water potential that are suitable for field studies and for a variety of plant species.

Here, we present the development of a soft implant for measuring water potential in plants. The implant contains water-sensitive nanoparticles that exhibit a fluorescence spectrum dependent on the water potential [6]. The nanoparticles can resolve water potentials across the physiologically relevant range (-3 to 0 MPa) while exhibiting minimal sensitivity to other physical factors like temperature and pH. We use fiber optics to illuminate the implant and capture the fluorescence spectrum to determine the water potential. With its small footprint, the implant can be easily embedded into various plant species. To assess the biocompatibility of the implant, we are examining histological sections of the local tissue at the insertion site. In recent years, several polymer-based materials have been developed for packaging of implantable sensors in mammals. Since the effect of these materials has not been studied in plants yet, we are also exploring different polymer- and plant-based materials to enhance the long-term stability of the implant. Additionally, we are considering the integration of a second optical fiber for simultaneous monitoring of sugar concentration, thereby enabling assessment of the osmotic potential.

We believe that the ability to accurately measure the total water and osmotic potential *in planta* will enable unprecedented access to the dynamics of water in plants and shed light on the propagation of long-distance hydraulic signaling. Moreover, the implant can be used beyond the context of plants by measuring water potentials in various environments such as soil, food, cosmetics, medicines, and cement.

References

- [1] Johns, Sarah, et al. "The fast and the furious: rapid long-range signaling in plants." *Plant Physiology* 185.3 (2021).
- [2] Christmann, Alexander, Erwin Grill, and Jin Huang. "Hydraulic signals in long-distance signaling." *Current opinion in plant biology* 16.3 (2013).
- [3] Yuan, Fang, et al. "OSCA1 mediates osmotic-stress-evoked Ca²⁺ increases vital for osmosensing in Arabidopsis." *Nature* 514.7522 (2014).
- Malone, M. "Kinetics of wound-induced hydraulic signals and variation potentials in wheat seedlings." *Planta* 187.4 (1992): 505-510 [5] Christmann, Alexander, et al. "A hydraulic signal in root to shoot signalling of water shortage." *The Plant Journal* 52.1 (2007).
- [6] Jain, Piyush, et al. "A minimally disruptive method for measuring water potential in planta using hydrogel nanoreporters." *Proceedings of the National Academy of Sciences* 118.23 (2021).

11:30 AM SB05.15.04

Bioelectronic Platform for Enhancing Plant Growth Alexandra H. Sandén^{1,2}, Vasileios Oikonomou^{1,2}, Torgny Näsholm³ and Eleni Stavrinidou^{1,2,3}; ¹Linköping University, Sweden; ²Linköping university, Sweden; ³Swedish University of Agricultural Sciences, Sweden

To cover the food demands of the growing population in the changing climate we need to increase crop yield in a sustainable manner. Hydroponics cultivation minimizes water and fertilizer use while it can be integrated in the urban environment. However, so far the substrates used in hydroponics mainly offer support to the root system. Here, we developed a bioelectronic platform that stimulates the growth of plants in a hydroponics culture. We demonstrate that Barley, one of the most important crops, grows well within the bioelectronic platform. When stimulated, the biomass of the Barley increases by 40%, and the effect is evident in both root and leaf development during the growth period after the stimulation treatment. Results also show that stimulated plants reduce and assimilate NO₃⁻ more efficiently than controls, a finding that can have implications on minimizing fertilizers use. Our work opens the pathway for enhancing plant growth in a hydroponics setting using bioelectronics which may result in more sustainable food production.

11:45 AM SB05.15.05

Biomimetic Reactive Oxygen Species (ROS) Scavenging System for Stability Enhancement of Thylakoid Membrane-Based Photosynthetic Biosolar Cells JaeHyounG Yun, JongHyunKim and WonHyounG Ryu; Yonsei University, Korea (the Republic of)

Since photosynthesis of plants has a high quantum yield close to 100%, many studies have been conducted to utilize the photosynthesis for bio-energy harvesting using algal cells, chloroplasts, thylakoid membranes (TMs), and isolated photosystems (PS I, II). The extracted photosynthetic organelles are preferred among these for their direct contact with the electrode and easier transfer of photosynthetic electrons (PEs). However, under high light intensity, reactive oxygen species (ROS) are generated during photosynthesis, causing damage to lipid membranes or proteins. Therefore, for long-term stability, a closed system capable of scavenging ROS like chloroplasts is required. In this study, we propose a biomimetic ROS scavenging system for stability enhancement of bio-solar cells. We used catalase to scavenge ROS, which causes the damage to extracted photosynthetic organelles and apparatuses. As a popular extracted photosynthetic organelle, TMs were used for bioenergy harvesting, and an artificial independent closed environment that did not interfere with PEs transport was constructed using alginate as extracellular matrix and the Nafion membrane. First, dye release test and catalase assay either in the presence or absence of Nafion membrane were performed to measure the leakage of catalase. The tests confirmed that the release of dye and catalase from the film coated with the Nafion membrane was negligible. However, the Nafion solution used for coating contains aliphatic alcohol that can damage lipid membranes or proteins. To analysis the effect of alcohol on TMs, photocurrents from TMs for different ethanol concentrations used in Nafion membrane were measured. TMs treated with 5% ethanol concentration produced about 82% of photocurrents from the non-treated TMs. Therefore, it was concluded that a sufficiently diluted Nafion solution did not significantly affect the production of TM photocurrent. Based on this, a 10-fold diluted Nafion solution was used for the coating of TM/alginate mixture film containing catalase. Furthermore, the film fabrication conditions were optimized through the photocurrent results according to the ratio among TMs, alginate, and catalase. Finally, in order to confirm the stability improvement of a photosynthetic bio-solar cell by catalase encapsulated system, the photocurrent from the system was observed for 5 hours under AM 1.5G (1 sun = 100 mW/cm²) illumination at intervals of 1,000 s. Afterwards, the stability improvement was evaluated by comparing the initial photocurrent and the photocurrent after 5 hours illumination. As a result, it was confirmed that about 4.3 times improved stability was achieved by the biomimetic ROS scavenging system.

REFERENCES

- [1] Khorobrykh, Sergey A., Maarit Karonen, and Esa Tyystjärvi. *FEBS letters* 589.6 (2015): 779-786.
- [2] Sjöholm, Kyle H., Michelle Rasmussen, and Shelley D. Minteer. *ECS Electrochemistry Letters* 1.5 (2012): G7.
- [3] Pankratov, Dmitry, Galina Pankratova, and Lo Gorton. *Current Opinion in Electrochemistry* 19 (2020): 49-54.

1:30 PM *SB05.16.01

Smart Wearable Healthcare Devices for On-Demand Theranostic Applications Sei Kwang Hahn, SangHoon Hong and TaeYeon Kim; Pohang University of Science and Technology, Korea (the Republic of)

A variety of diagnostic and therapeutic devices are routinely used in the clinic. While these devices have a familiar look as wall-plugged in hard packages or placed at patients' bedsides, there has recently been a rapid expansion of new ideas on wearable healthcare devices for greatly improved patients' compliance. Here, we developed smart contact lenses and smart wearable devices for both continuous diabetic monitoring and diabetic retinopathy therapy. Smart contact lens could measure tear glucose levels as a non-invasive alternative to the conventional blood glucose tests and deliver drugs from gold coated reservoirs for the treatment of diabetic retinopathy. On the basis of these results, we also developed a smart wearable device for highly sensitive glucose monitoring in sweat for clinically feasible diabetic diagnosis. A blue-tooth system could send data wirelessly allowing patients to check their diabetic diagnosis results on the mobile phones. Furthermore, we developed cell-integrated poly(ethylene glycol) hydrogels for in vivo optogenetic sensing and therapy. The real-time optical readout of encapsulated heat-shock-protein-coupled fluorescent reporter cells made it possible to measure the nanotoxicity of cadmium-based quantum dots in vivo. Using optogenetic cells producing glucagon-like peptide-1, we performed light-controlled therapy and obtained improved glucose homeostasis in diabetic model mice. Taken together, this presentation will provide the current state-of-the-art smart wearable devices for further clinical applications.

2:00 PM SB05.16.02

Stimuli Responsive Thin Films and Their Applications as Actuators and on Skin Sensors Anna Maria Coclite; Graz University of Technology, Austria

Stimuli responsive materials are those that change their properties, as shape, wettability, optical properties depending on environmental cues, like pH, temperature, humidity. Such dynamic property can be used in several modern devices. In addition, when the stimuli-responsive material has the shape of a thin film, the response, which is based on diffusion, is very fast and reversible.

Functional and responsive surfaces have been successfully deposited by initiated Chemical Vapor Deposition (iCVD) on a variety of substrates.[1] Such method allows the full retention of the functional groups of the monomer structure and this is important to obtain a large responsiveness amplitude. This presentation will focus on the applications of stimuli responsive nanofilms for sensors and actuators. The high versatility of iCVD in driving application-specific properties into the material, creating a platform for the implementation of polymeric coatings into device fabrication, will be discussed.

Fast response and large signal amplitude are fundamental requirements for good sensors. Fast and ultra-fast humidity sensors based on the optical detection of the change in thickness of the iCVD hydrogels will be shown.[2] The implemented sensor prototype delivered reproducible relative humidity values and the achieved response time for an abrupt change of the humidity was about three times faster compared to one of the fastest commercially available sensors on the market.

The combination of materials with different properties in nanostructures is required to meet the needs of modern intelligent devices. Several examples of such type of hybrid devices will be presented. In particular, an electronic skin concept was realized by combining stimuli responsive thin films with piezoelectric zinc oxide in core shell geometries.[3] Such device geometry was obtained by templated atomic layer deposition of the ZnO followed by the iCVD of the stimuli responsive film. The nanostructuring of the films lead to a location-specific signal detection. In addition, the combination of two different materials allowed the detection of three stimuli: force, humidity and temperature. The whole sensor device could be deposited on flexible substrates and used for on-skin sensor or as electronic skin. While the piezoelectricity of ZnO provides sensitivity to external force, the thermoresponsiveness of the hydrogel core provides sensitivity to surrounding temperature and humidity changes. The hydrogel core exerts mechanical stress onto the ZnO shell, which is translated to a measurable piezoelectric signal. A localized force sensitivity of 364 pC N^{-1} is achieved with very low cross talk between 0.25 mm^2 pixels. Additionally, the sensor's sensitivity to humidity is demonstrated at 20° and 40°C , i.e., above and below the hydrogel's lower critical solution temperature (LCST) of 34°C . The largest response to temperature is obtained at high humidity and below the hydrogel's LCST. The sensor response to force, humidity, and temperature is significantly faster than the system's intrinsic or excitation-induced time scale. Finally, the sensor response to touch and breath demonstrates its applicability as e-skin in real-life environment.

1. Coclite AM, Howden RM, Borrelli DC, et al (2013) 25th anniversary article: CVD polymers: a new paradigm for surface modification and device fabrication. *Adv Mater* 25:5392–5423. <https://doi.org/10.1002/adma.201301878>

2. Buchberger A, Peterka S, Coclite AM, Bergmann A (2019) Fast optical humidity sensor based on hydrogel thin film expansion for harsh environment. *Sensors (Switzerland)* 19:1–11. <https://doi.org/10.3390/s19050999>

3. Abu Ali T, Schäffner P, Belegriatis M, et al (2022) Smart Core Shell Nanostructures for Force, Humidity, and Temperature Multi Stimuli Responsiveness. *Adv Mater Technol* 7:2200246. <https://doi.org/10.1002/admt.202200246>

2:15 PM SB05.16.03

Cephalopod-Inspired Bioelectronic Control of Cellular Differentiation David Berlin, Aleeza Farrukh, Georgii Bogdanov and Alon Gorodetsky; University of California, Irvine, United States

Cephalopods (e.g., squids, octopuses, and cuttlefish) have recently become recognized as a promising source of natural conductive biopolymers (1,2). Within this context, our laboratory has studied the proton conducting properties of unique cephalopod structural proteins called reflectins, and we have leveraged these proteins for applications in protonic transistors, photochemically dopable devices, and photochromic color-changing platforms (1,2). Moreover, we have demonstrated that reflectin films are inherently biocompatible, as exemplified by their ability to support the growth and proliferation of both human and murine neural stem/progenitor cells (3,4). Recently, we have extended these efforts to the development of cephalopod-inspired bioelectronic devices that afford the voltage-controlled regulation of cellular differentiation in real-time (5). Our combined findings suggest that reflectins are promising materials for applications in cell- and tissue-interfaced bioelectronic platforms.

2:30 PM SB05.16.04

Soft, Skin-Safe Electronic Device Interfaces for Continuous Health Monitoring Seonggwang Yoo and John A. Rogers; Northwestern University, United States

Abstract

Soft electronic device interface directly with the skin surface allows essential physiological health monitoring. These devices, featuring soft and miniaturized architecture, wireless communication capabilities, and an independent power system, significantly reduce patient burden by eliminating wired connections and bulky hardware of traditional hospital-grade systems. Previous efforts by soft, thin structures with high biocompatibility addressed the many skin damage problems but still present challenges, especially when in direct contact with the delicate skin of ill infants with small anatomical bodies and low-risk perception ability. Here, we report materials and structural design strategies to enhance skin safety during clinical use, especially for infants, without hampering the unique characteristics of the device architectures and the electronic performance. Pre-curved and holey design conforms to the anatomical body and rapidly and effectively releases interface adhesion, significantly reducing skin irritation. Furthermore, an ultrathin, flexible bladder containing small amounts of liquid with a low boiling point provides an active thermal safety system to these soft, skin electronic devices. In a thermal malfunction, the heat evaporates the liquid inside the bladder, forming an effective thermal barrier and automatically delaminating the device from the skin. Our material and structural design approach aims to ensure the safe and reliable use of soft electronic devices for infant health monitoring, promoting overall well-being and comfort during usage.

References

[1] S.S. Kwak, S. Yoo, R. Avila, H.U. Chung, H. Jeong, C. Liu, J.L. Vogl, J. Kim, H.-J. Yoon, Y. Park, H. Ryu, G. Lee, J. Kim, J. Koo, Y.S. Oh, S. Kim, S. Xu, Z. Zhao, Z. Xie, Y. Huang and J.A. Rogers, "Skin-Integrated Devices with Soft, Holey Architectures for Wireless Physiological Monitoring, With Applications in the Neonatal Intensive Care Unit," *Advanced Materials* 33, 2103974 (2021).

[2] S. Yoo, T. Yang, M. Park, H. Jeong, Y.J. Lee, D. Cho, J. Kim, S.S. Kwak, J. Shin, Y. Park, Y. Wang, N. Miljkovic, W.P. King and J.A. Rogers, "Responsive Materials and Mechanisms as

2:45 PM SB05.16.05

Controlling Mesenchymal Stem Cell Differentiation using Oxide Thin Films Wilfrid Prellier; Crismat Laboratory, France

Although oxide compounds are well recognized for their ability to change from insulator to metal, or other electronic properties, they may also be used therapeutically to address significant medical issues. In this study, we used vanadium oxide thin films synthesized by the pulsed laser deposition (PLD) technique to examine human stem cells generated from bone marrow. We used a variety of techniques, such as differentiation staining, phase contrast microscopy, and real-time reverse transcription-polymerase chain reaction (RT-PCR), to examine the growth, adhesion, proliferation, and differentiation of human bone marrow mesenchymal stem cells (hBMSCs) on these oxide films over time. Our results indicated that oxide films alter hBMSCs adhesion and growth and affect their differentiation. We conclude that the use of oxide films in biological and medical materials, as well as future research on cells, are all made possible by these findings, which also improve our understanding of the biological actions of vanadium compounds.

3:00 PM BREAK

SESSION SB05.17: Designing Biotic-Abiotic Interfaces
Session Chairs: Raghav Garg and Eleni Stavrinidou
Friday Afternoon, December 1, 2023
Hynes, Level 1, Room 102

3:30 PM SB05.17.01

Amphiphilic Light-Driven Push-Pull Azobenzenes (ppABs) as Cell Membrane-Targeted Nanoactuators Valentina Sesti^{1,2}, Matteo Moschetta², Arianna Magni², Paola Moretti^{1,2}, Giuseppe Maria Paternò^{1,2}, Matteo Tommasini¹, Guglielmo Lanzani^{2,1} and Chiara Bertarelli^{1,2}; ¹Politecnico di Milano, Italy; ²Istituto Italiano di Tecnologia, Italy

Cationic membrane-targeted azobenzenes have been recently proposed as light-induced nanoactuators for neuronal photostimulation.^{1,2} In previous works, we developed an azobenzene as a promising nanoscale tool for cell photostimulation, namely Ziapin2. Our approach resides in non-specific binding, and Ziapin2 has an amphiphilic character allowing it to partition spontaneously within the cell membrane. The cationic terminal groups interact with the phospholipid polar heads of the membrane while the hydrophobic part of the molecule stabilizes inside the lipidic region. We demonstrated that this azobenzene is an effective light-driven intramembrane actuator, able to modulate neuronal firing both in vitro and in vivo.¹ These previous results open to the next generation of light-driven photoswitches aimed at enhancing the performances and improving the partition stability. In this work, new amphiphilic push-pull azobenzenes (ppABs) were designed and synthesized, which feature a strong electron donor group in the *para*-position on one phenyl ring and a strong electron acceptor group in the *para*-position on the opposite phenyl ring. This push-pull substitution of the phenyl rings delocalizes electrons of the azobenzene and shifts the absorption wavelengths towards red, which is a valuable feature for biological application, allowing for a better light penetration in tissues. Interestingly, light-activated electrophysiology of cells loaded with ppABs shows a depolarization of the membrane followed by a small hyperpolarization, and this is owed to the significant variation of the dipole moment.³ Within this series of homologous ppABs, we also identified the key role of the cationic heads in the partitioning and potential modulation of the cell membrane.

¹ DiFrancesco, M.L., Lodola, F., Colombo, E. et al. “Neuronal firing modulation by a membrane-targeted photoswitch.” Nat. Nanotechnol. 15, 296–306 (2020)

² Vurro, V., Bondelli, G., Sesti, V., Lodola, F., Paternò, G.M., Lanzani, G. and Bertarelli, C. “Molecular Design of Amphiphilic Plasma Membrane-Targeted Azobenzenes for Nongenetic Optical Stimulation.” Front. Mater. 7:631567 (2021)

³ Bandara, H. M. Dhammika., Burdette, Shawn C. “Photoisomerization in different classes of azobenzene.” Chem. Soc. Rev., 41, 1809-1825 (2012)

3:45 PM SB05.17.02

Integrated Design and Synthesis of Soft Matrices with High Permittivity Dylan M. Barber and Jennifer A. Lewis; Harvard University, United States

Emerging applications, such as dielectric elastomer actuators (DEAs), haptics, and bioelectronics, would benefit from soft matrices that simultaneously exhibit high permittivity (relative permittivity $\epsilon_r \geq 10$) and low elastic moduli ($E \leq 1$ MPa). For example, the energy density of DEAs depends on ϵ_r^2 , while their actuation strain scales with ϵ_r . However, most soft elastomers and gels that serve as compliant dielectric layers exhibit low permittivity ($\epsilon_r \leq 10$). Consequently, the operation of DEAs requires kilovolt-scale potentials to achieve targeted actuation strains and energy densities. The incorporation of high- ϵ_r fillers affords little improvement, since liquid fillers (e.g., liquid metals) decrease breakdown strength, while solid fillers (i.e., strontium titanate particles) increase modulus. In this talk, we will describe recent advances to design and synthesize intrinsically polarizable elastomers and gels based on a library of small molecules with a large dipole moment and a low melting point – each of which exhibits exceptional permittivity ($\epsilon_r \geq 250$) in the low frequency limit. Their synthesis is both facile (3-5 synthetic steps) and scalable (up to 250 g) from inexpensive starting materials. Using this library, we have created elastomers and gels with $\epsilon_r \geq 100$ and $E < 1$ MPa, which may find potential application in high-strain and energy-dense DEA, haptic, and bioelectronic-based devices.

4:00 PM SB05.17.03

Non-Invasive Actuation of Chemical Reactions Through Mechanochemistry and Gas Vesicle Proteins Yuxing Yao, Molly McFadden, Mikhail Shapiro and Maxwell Robb; California Institute of Technology, United States

Recent advances in molecular engineering and biomedical ultrasound provide means to apply physical effects, including mechanical stress, deep inside tissues, but limited capability to enact specific chemical processes for applications including drug delivery and non-invasive control of cellular functions. In this work, we show that mechanochemistry, chemical processes initiated by mechanical stress, can be activated with biocompatible focused ultrasound assisted by acoustically-active proteins. Previously, activation of mechanochemistry relies on ultrasound with parameters that are likely to damage tissues. Through acoustic cavitation seeded by genetically encoded, air-filled protein nanostructures called gas vesicles, polymers undergo bond cleavage at the designed, weakest position in backbones and thus release small molecular payloads, including fluorophores and therapeutic drugs by chemical cascade. The efficiency of mechanochemical activation is comparable to what has been achieved with bulk sonication, though with weaker ultrasound parameters. Focused ultrasound further enables the activation of mechanochemistry with spatial resolution in millimeter range as well as the programmable payload release kinetics. Furthermore, we demonstrate the stimulation of mechanochemistry in tissue-mimicking gels, suggesting its potential applications in remotely controlled drug release inside body. Our platform represents a novel modality for controlling chemical reactivity non-invasively in biological systems and unlocks the translational potential of polymer mechanochemistry for therapeutic and bioimaging applications.

4:15 PM SB05.17.04

Nanoparticle-Virus Chimeras as a Novel Strategy for Nanoparticle Delivery Keisuke Nagao, Katherine Lei, Peyton Worthington, Emmanuel Paniagua, Robert J. Macfarlane and Polina Anikeeva; Massachusetts Institute of Technology, United States

The systemic delivery of nanoparticles (NPs) has garnered significant attention from researchers due to its clinical promise. Various strategies have been developed thus far, including the utilization of the enhanced permeability and retention (EPR) effect to target tumors or the modification of NPs with antibodies to target specific proteins. However, delivering NPs to the brain through the blood-brain barrier (BBB) remains a challenge. Additionally, the importance of the communication between the central nervous system (CNS) and the peripheral nervous system (PNS) has been increasingly recognized, leading to a high demand for delivery systems that can flexibly change their target between the CNS and PNS. Translation of delivery strategies between species offers another challenge, especially in the context of bridging the divide between fundamental research in rodents and clinical research in larger models such as non-human primates (NHPs). Therefore, there is a pressing need for a novel strategy for systemic delivery of nanomaterials that is both translational and capable of flexibly selecting targets.

For decades the field of gene therapy has applied engineered viruses to deliver therapeutic transgenes to particular organs or cells of interest. Adeno-associated viruses (AAVs) are the most ubiquitous gene-therapy tools, particularly in neuroscience, owing to their advantageous characteristics: AAVs are non-pathogenic, easily reproducible, and have numerous accessible serotypes, each with distinct tropism. State-of-the-art serotypes, such as AAV.CAP-B10 and AAV.MacPNS2, have demonstrated the ability to deliver genes to the brain or PNS in mice following intravenous (IV) injection, while simultaneously suppressing gene expression in the liver. These serotypes have also shown promise for gene delivery in NHPs.

In this study, we hypothesized that AAVs could be employed to guide magnetic nanoparticles (MNPs) to particular organs through IV injection. This approach allows for easy modification of

the target by swapping AAV serotypes, for instance, from the brain to the PNS. Furthermore, the target species can also be altered based on the serotypes of AAVs. This concept, termed viral guidance of MNPs, has the potential to serve as a versatile targeting strategy.

We covalently conjugated MNPs and AAVs (MNP-AAV chimeras) through click chemistry. The structure of these chimeras was controlled by adjusting the reaction conditions. In vitro tests were conducted to investigate the efficiency of AAVs in guiding MNPs using MNP-AAV chimeras formed from several different serotypes. As a result, MNP-AAV chimeras retained the tropism of original AAV serotype used, indicating that the delivery target is serotype-dependent and can be easily modified by changing the AAV serotype used for conjugation.

We also investigated an opposite application of MNP-AAV chimeras, namely, the magnetic guidance of AAVs. Since AAVs were conjugated to MNPs, we could manipulate the chimeras using an external magnetic field to exert a magnetic force on the MNPs. HEK293 cells were incubated with MNP-AAV chimeras in a presence of a magnetic field. Following a 24-hour incubation period, the HEK cells expressed high levels of fluorescent protein, which was encoded by the AAVs in the chimeras, near the center of the magnetic field. This result suggests that magnetic guidance of AAVs is feasible, and that AAVs in chimera form (conjugated to MNPs) are capable of transducing cells. The specificity of gene delivery targeting with AAV was previously determined by a combination of two factors: serotype (capsid) and regulatory elements (promoter, enhancer, Cre-lox system, etc.). Now, our chimeras enable spatial restriction of transduction, which adds another layer of control to gene delivery. To the best of our knowledge, this is the first report of magnetically controlled transduction with AAVs.

4:30 PM SB05.17.05

An n-Type Conjugated Oligoelectrolyte Mimics Transmembrane Electron Transport Proteins for Enhanced Microbial Electrosynthesis Glenn Quek, Guillermo Bazan, Ricardo J. Vázquez, Samantha McCuskey and Fernando Lopez-Garcia; National University of Singapore, Singapore

Interfacing bacteria as biocatalysts with an electrode provides the basis for emerging bioelectrochemical systems that enable sustainable energy interconversion between electrical and chemical energy. Electron transfer rates at the abiotic-biotic interface are, however, often limited by poor electrical contacts and the intrinsically insulating cell membranes. Herein, we report the first example of an n-type redox-active conjugated oligoelectrolyte, namely COE-NDI, which spontaneously intercalates into cell membranes and mimics the function of endogenous transmembrane electron transport proteins. The incorporation of COE-NDI into *Shewanella oneidensis* MR-1 cells amplifies current uptake from the electrode by 4-fold, resulting in the enhanced bio-electroreduction of fumarate to succinate. Moreover, COE-NDI can serve as a "protein prosthetic" to rescue current uptake in non-electrogenic knockout mutants.

4:45 PM SB05.17.06

Exploring Cell Behavior Through Blanket and Patterned Reprogramming of Nanotopography Mona H. Abostate¹, Nikolaos Liaros¹, Matthew J. Hourwitz¹, Wolfgang Losert^{2,3} and John Fourkas^{1,3,4}; ¹Department of Chemistry and Biochemistry University of Maryland, United States; ²Department of Physics, University of Maryland, College Park, MD, USA, United States; ³Institute for Physical Science & Technology, University of Maryland, College Park, MD, USA, United States; ⁴Maryland Quantum Materials Center, University of Maryland, College Park, MD, USA, United States

Cellular responses to external stimuli arise from a complex integration of various biochemical and biophysical signals that can occur concurrently, and that exhibit distinct spatial and temporal patterns. Of these signals, nanotopography, which is present in the extracellular matrix, holds special significance in influencing and controlling cell behavior. Nanotopography has the ability to initiate and direct waves of actin polymerization in a phenomenon called esotaxis, which is closely linked to the inherent excitability of cells. For instance, nanoridges can induce a transition from the 2D spreading waves observed on flat substrates to 1D waves.

We have molded large-area master patterns created using conventional lithography, and then replicated these masters using soft lithography. Replicas created using poly (Disperse Red 1 methacrylate, pDR1m), an azobenzene-containing polymer, can be reconfigured with light. The azobenzene moieties undergo photoisomerization from the *trans* isomer to the *cis* isomer, inducing macroscopic alterations in the polymer structure that depend on the polarization of the light.

With this technology, a single nanoridge master can be used to generate a wide range of patterns with different surface features. Photomodification of pDR1m nanoridges was achieved through two different methods: blanket exposure and patterned exposure. The newly patterned surfaces can be replicated in a material that is not photosensitive through a straightforward molding procedure.

We have examined the response of cells to surfaces featuring buckled nanoridges created through. The presence of buckling has a significant influence on esotaxis, ultimately impacting cell migration. Because this effect is cell-type-specific, and depends on the degree of buckling, it is possible to create surfaces that impact different types of cells in different manners.

SESSION SB05.18: Virtual Session: Biohybrid and Soft Functional Interfaces

Session Chairs: Herdeline Ann Ardoña and Eleni Stavrinidou

Tuesday Morning, December 5, 2023

SB05-virtual

10:30 AM SB05.18.01

Stretchable Silent Speech Glove using Myopotentials and Machine Learning Yuta Kurotaki^{1,2} and Hiroki Ota¹; ¹Yokohama National University, Japan; ²Pepabo Research and Development Institute, GMO Pepabo, Inc., Japan

The field of Silent Speech Interface (SSI) exists as an interface for sending information without speaking. Personal and confidential information can be heard by others when spoken, but if speech can be recognized without voice, confidential information can be transmitted safely. In addition, silent speech can send information to machines and people without disturbing the environment. There are many methods for predicting what is uttered from silent speech, one of which is the use of muscle potentials around the mouth. Recently, it has been shown that muscle potentials can be measured by placing sensors around the mouth, but the integration of a mechanism that uses soft materials to recognize speech using electrodes, muscle potential amplification circuits, and machine learning models has not yet been realized. Although it is possible to place circuits and elements as well as sensors around the mouth, the area around the mouth is limited, and attaching sensors would interfere with mouth movements. The myopotential amplification circuit requires many elements to be placed on the circuit, which would result in a loss of aesthetics in terms of appearance.

To solve these problems, we developed a myopotential measurement device that can be attached to the human hand using soft materials, liquid metal, transparent FPCs (Flexible Printed Circuits), and a microcomputer. The device can be placed near the mouth and electrodes placed around the mouth to collect myopotential information, which can then be used in a machine learning model to classify speech only when speech recognition is performed without speech. By enabling sensing by placing electrodes on the mouth only when the device is being used, there is no need to worry about information being read at times other than when the device is being used, and since there is no need to always wear sensors or circuitry around the mouth, speech will not be read at unintended times. It does not interfere with the movement of the face or mouth, eliminating aesthetic concerns.

In this study, electrodes based on soft materials were created to realize a device that is worn on the hand and repeatedly measures myoelectric potentials around the mouth. The electrodes were wired to circuits on transparent polyimide film using a liquid metal mixture of Galinstan and nickel powder and bonded with a hard-soft pattern of silicone rubber and epoxy. The electrodes and substrate, which fit the human hand, can capture information around the mouth without breaking, even when the hand is moved, or the fingers are bent. In addition, a speech classification model was created using machine learning based on the acquired data of myoelectric potentials in silent speech around the mouth. We propose a new form of silent speech interface that allows many people to send information to machines and people in more situations and with the same privacy as in their conventional lives.

10:45 AM SB05.18.02

Permeable Electronic Skins for Health Monitoring Yan Wang^{1,2}; ¹Guangdong Technion-Israel Institute of Technology, China; ²Technion-Israel Institute of Technology, Israel

One limitation of commercialized wearables, such as smartwatches and bands, is that they cannot form conformable contact with human skin due to their rigid form factor, thereby limiting their monitoring capabilities. Soft bioelectronics, on the other hand, are touted as an ideal platform for personalized health care owing to unique characteristics, such as thinness, lightweight, good biocompatibility, excellent mechanical robustness, and great skin conformability. Permeable skin-mountable electronics that are capable of long-term applications have emerged as promising tools for early disease prevention, screening, diagnosis, and treatment^{1,2}. Dr. Wang's research interests mainly focus on the development of wearable electronics for biomedical health monitoring, including stretchable conductors, sensors, and soft energy devices. In today's talk, she will introduce high-performance skin bioelectronics developed by ultrasoft nanomesh systems, which can realize the accurate measurement of minus skin deformations and finger touch without disturbing natural skin motions and sensations, as well as long-term applications for health monitoring³⁻⁵.

[1] A. Miyamoto, S. Lee, N.F. Cooray, S. Lee, M. Mori, N. Matsuhisa, H. Jin, L. Yoda, T. Yokota, A. Itoh, M. Sekino, T. Someya, "Inflammation-free, gas-permeable, lightweight, stretchable on-skin electronics with nanomeshes," *Nat. Nanotechnol.* **12**, 907-913 (2017).

[2] J. Yang, Z. Zhang, P. Zhou, Y. Zhang, Y. Liu, Y. Xu, Y. Gu, S. Qin, H. Haick, Y. Wang, "Toward a new generation of permeable skin electronics," *Nanoscale* **15**, 3051-3078 (2023).

[3] Y. Wang, S. Lee, H. Wang, Z. Jiang, Y. Jimbo, C. Wang, B. Wang, J.J. Kim, M. Koizumi, T. Yokota, T. Someya, "Robust, self-adhesive, reinforced polymeric nanofilms enabling gas-permeable dry electrodes for long-term application," *PNAS* **118**, e2111904118 (2021).

[4] Y. Wang, S. Lee, T. Yokota, H. Wang, Z. Jiang, J. Wang, M. Koizumi, T. Someya, "A durable nanomesh on-skin strain gauge for natural skin motion monitoring with minimum mechanical constraints," *Sci. Adv.* **6**, eabb7043 (2020).

[5] S. Lee, S. Franklin, F.A. Hassani, T. Yokota, M.O.G. Nayeem, Y. Wang, R. Leib, G. Cheng, D.W. Franklin, T. Someya, "Nanomesh pressure sensor for monitoring finger manipulation without sensory interference," *Science* **370**, 966-970 (2020).

11:00 AM SB05.18.03

Thin-Film Encapsulations for Compliant Implantable Bioelectronics: Advanced Materials and Characterisation Methods Based on Bioresorbable Magnesium Permeability-Sensing Structures Massimo Mariello^{1,2}, Yves Leterrier² and Stephanie P. Lacour²; ¹University of Oxford, United Kingdom; ²Ecole Polytechnique Federale de Lausanne, Switzerland

The next-generation bioelectronic implants will be microfabricated, soft and compliant; they need to be protected from the body environment through encapsulations that must guarantee simultaneously hermeticity, biocompatibility, mechanical compliance, compatibility with microfabrication processes, and long-term reliability. This still represents an unsolved challenge: standard biocompatible barrier technologies based on rigid Ti/silicone capsules do not answer such needs. Advanced hermetic barriers should instead rely on thin-film encapsulations (TFE), based on organic or inorganic films. However, water permeation and mechanical defects are prime drivers for TFE failure, especially for *in vivo* and flexible implantable systems, so a universal solution is still missing. Conventional strategies rely on multilayer architectures, consisting of alternating dyads made of organic and inorganic layers. The accurate evaluation of their barrier performances is challenging because standard measuring systems display too high sensitivity limits (~ 10-5 g/m²/day) which cannot detect the ultra-low permeation capabilities of the coatings, and are not suitable for flexible microsystem formfactors. We present here for the first time a comprehensive accelerated-aging method to quantify ultra-low permeability of TFE engineered for bioelectronic micro-devices. The method relies on bioresorbable magnesium (Mg) thin films. Corrosion of Mg induced by water diffusion through the barrier coating is real-time monitored in several testing conditions, including exposure to wet air, soaking in a phosphate buffer saline (PBS) solution that mimics the body biofluids (*in vitro*), and in biological tissues (*in vivo*). The electrical properties of Mg are then monitored and analysed. High temperatures for *in vitro* tests are chosen to perform accelerated aging whereas specific novel analytical/computational models are used to extract from the measurements the water transmission rates (WTR) of the barriers. The advantages of this approach are that Mg does not need a fully inert atmosphere and it can be easily integrated in the microfabrication processes of implantable bioelectronic devices. Therefore, the proposed characterization strategy answers a long-term need to assess reliably and universally thin-film hermeticity *in situ*, and for any types of conformal TFE for bioelectronic systems.

11:15 AM SB05.18.04

N-Acetyl-β-D-Glucosaminidase Activity Assay for Monitoring Insulin-Dependent Diabetes using Ag-Porous Si SERS Platform Narsingh Raw Nirala and Giorgi Shtenberg; Institute of Agricultural Engineering, ARO, The Volcani Center, Israel

N-acetyl-β-D-glucosaminidase (NAG; EC 3.2.1.30) is an intracellular lysosomal glycosidase that catalyzes the hydrolysis of terminal glucose residues in glycolipids and glycoproteins. Specifically, the elevation of serum NAG activity serves as a surrogate for assessment of disease severity and progression in diabetes mellitus, myocardial infarction, liver damage, malignancies and hypertension. Early and rapid biomarker detection is an important element of medical diagnosis, facilitating prompt therapeutic decisions and prognosis evaluation. Herein, we present a modified sensing approach for a rapid and reliable NAG activity determination in complex media using surface-enhanced Raman spectroscopy (SERS). Porous silicon (PSi) Fabry-Perot interferometers were redesigned as sensitive SERS platforms utilizing the vast inherent surface area for silver (Ag) nanoparticles embedment. Interaction of the porous nanostructures with specific NAG-enzymatic products produces an indicative spectral fingerprint proportional in magnitude to its concentration. The sensitivity of Ag-PSi SERS substrates was evaluated in complex matrices presenting sufficient limits of detection compared with other advanced assays and techniques (0.07, 0.47 and 0.50 μM mL⁻¹ for urine, milk and plasma, respectively). The augmented optical performance revealed recovery values of 96–109%, indicating successful and selective NAG recognition in biological fluids. Finally, the potential applicability of the suggested prototype for real-life scenarios was evaluated *in vivo*, in a model of insulin-dependent diabetes induced in sheep. Overall, the robust data confirm the application of SERS analysis for early diagnosis of pathology and for evaluation of clinical responses to pharmacological treatments.

Keywords: N-acetyl-β-D-glucosaminidase (NAG), insulin-dependent diabetes, plasma, Ag-PSi and SERS.

11:30 AM SB05.18.05

Modulation of Curli Production on Redox Challenged PEDOT:PSS Surfaces Sanhita Ray^{1,2}, Susanne Löffler^{1,2} and Agneta Richter Dahlfors^{1,2}; ¹Karolinska Institutet, Sweden; ²AIMES, Sweden

Biofouling is a major problem caused by bacteria colonizing abiotic surfaces, such as medical devices. Biofilms are formed as the bacterial metabolism adapts to an attached growth state. We have previously found that electrically charged surfaces with high charge storage capacity like PEDOT-based conducting polymers can be used to modulate the amount of gross biomass attaching by altering the surfaces redox state (*J*).

Here, we are delivering an in-depth analysis on the process of biofilm formation on redox-challenged PEDOT: PSS surfaces. We are using GFP tagged *Salmonella* bacteria and a marker for the *Salmonella* extracellular matrix components curli and cellulose (Ebbabiolight 680) to decipher the relationship between the amount of bacterial cells and extracellular matrix produced by bacteria in *Salmonella* wt bacteria as well as mutants deficient in curli (Δ csgA) or curli as well as cellulose (Δ csgD)(2). We are using a semi-quantitative spectroscopy method to determine relative amounts of bacterial cells and extracellular matrix (ECM) on a large surface area and are performing detailed microscopic analysis to understand biofilm distribution and structure. When the redox challenge was carried out in a fast-charging whole-cell setup, higher amounts of cells and ECM were found on oxidized PEDOT:PSS surfaces compared to their reduced counterpart. When electrodes were separated and charging was carried out with respect to a Pt electrode, the charging process was slower and incomplete. This resulted in almost similar cell numbers for the two cases but showed much higher amounts of ECM on reduced surfaces. A curli mutant, grown under the same conditions produced biofilms that didn't respond to the redox challenge. The microscopic structure of the biofilm showed uniform cell and ECM distribution on all oxidized surfaces but showed high-density local clusters of around 100-200 μm diameter on all unchallenged and reduced surfaces.

This leads us to believe that redox modulation of biofilm formation mainly depends on curli production. We forward a theory where an oxidized PEDOT:PSS surface works as an alternate terminal electron acceptor for interfacial biofilm, which might be able to boost ATP production and curli formation. We reason that the negative charge of PEDOT:PSS on unchallenged and reduced surfaces leads to a spotty attachment of the bacteria and to the formation of microcolonies, instead of evenly distributed films.

References

1. S. Gomez-Carretero, B. Libberton, K. Svennersten, K. Persson, E. Jager, M. Berggren, M. Rhen, A. Richter-Dahlfors, Redox-active conducting polymers modulate Salmonella biofilm formation by controlling availability of electron acceptors. *NPJ Biofilms Microbiomes*. **3** (2017), doi:10.1038/s41522-017-0027-0.
2. F. X. Choong, S. Huzell, M. Rosenberg, J. A. Eckert, M. Nagaraj, T. Zhang, K. Melican, D. E. Otzen, A. Richter-Dahlfors, A semi high-throughput method for real-time monitoring of curli producing Salmonella biofilms on air-solid interfaces. *Biofilm*. **3** (2021), doi:10.1016/j.biofilm.2021.100060.

11:45 AM SB05.18.06

Toward Enhancing Critical Care Monitoring: Continuous Assessment of Blood Lactate and Potassium with Fiber Optic Sensors Integrated into Intravascular Catheters Lawrence Renna^{1,2}, Narciso Guzman¹, Emily Vuu¹, George Harea², Gerardo Ico¹, Teryn Roberts² and Andriy Batchinsky²; ¹Intelligent Optical Systems, Inc., United States; ²Autonomous Reanimation and Evacuation Research Program, The Geneva Foundation, United States

The determination of disease severity and prediction of outcomes in emergency medicine heavily rely on blood lactate (Lac) and potassium (K⁺) levels. Traditionally, these biomarkers are assessed through repeated invasive blood sampling and subsequent analysis using laboratory blood gas analyzers. However, recent studies have emphasized the dynamic nature of these biomarkers, highlighting the need for continuous monitoring. In trauma cases, elevated blood Lac levels and poor Lac clearance have been associated with higher mortality rates, demonstrating potential for effectively triaging conditions such as lung cancer, lacunar infarction, sepsis, and cardiac failure. Likewise, high K⁺ levels, known as hyperkalemia, are linked to life-threatening conditions including arrhythmias and mortality following severe trauma, kidney disease, hemolysis, and acid-base imbalances. In hemorrhaging patients, hyperkalemia can be induced by tissue ischemia, blood transfusion, and acidosis, significantly heightening the risk of death. Consequently, there is an urgent demand for continuous monitoring of blood Lac and K⁺ levels in critical care settings. This study aims to develop and evaluate the performance of specialized fiber optic sensors that enable real-time monitoring of Lac and K⁺, thereby providing healthcare providers with timely guidance in rapidly changing situations.

The sensors in this study employ a measurement method known as dual lifetime/luminophore referencing (DLR), which ensures high accuracy and mitigates sensitivity to the amplitude of the

optical signal. In contrast to previous fiber optic sensors that are single point sensors located at the tip of the fiber and are susceptible to intermittent contact with tissue, a phenomenon referred to as the "wall-effect," the current sensors utilize a tunable distributed sensing approach. This is accomplished by incorporating redundant "mini-sensors" along a specific section of the optical fiber. Furthermore, optimization of sensor fabrication was conducted to enhance sensitivity specifically for physiologic concentrations. The Lac sensor utilized in this research consists of multiple layers, including a luminescent transducer layer for measuring partial pressure of oxygen, a catalytic enzymatic hydrogel layer, and a diffusion barrier layer to overcome substrate-dependent inhibition. The K⁺ sensor is designed as a hydrogel that incorporates a luminescent ionophore for K⁺ detection, and a separate reference luminophore. Finally, sensor-integrated catheter prototypes were tested in an ex vivo flow circuit with fresh porcine blood. The sensor-integrated catheter prototypes showed strong pairwise correlation between the optical sensor measurements and blood gas analysis (Spearman correlation R² = 0.981 and 0.970, p-value: <0.0001 and <0.0001 for Lac and K⁺, respectively). In summary, our study has successfully shown that the DLR-based fiber optic sensors for continuous Lac and K⁺ monitoring, when integrated into intravascular catheters and evaluated under ex vivo circulation conditions using donor blood, offer a viable alternative to repetitive blood gas analysis. These sensors hold great promise in enhancing clinical decision-making and are now poised for further validation in translational studies focusing on trauma and critical care scenarios under in vivo conditions.

SYMPOSIUM SB06

Experimental and Computational Advances in Biomolecular Electronics
November 30 - December 1, 2023

Symposium Organizers

Anant Anantram, University of Washington
Juan Artes Vivancos, University of Massachusetts-Lowell
Josh Hihath, University of California, Davis
Linda Angela Zotti, Universidad Autónoma de Madrid

Symposium Support

Platinum
National Science Foundation

* Invited Paper

+ JMR Distinguished Invited Speaker

SESSION SB06.01: Applied Biomolecular Electronics—Devices and Sensing I

Session Chairs: Juan Artes Vivancos and Josh Hihath

Thursday Morning, November 30, 2023

Hynes, Level 1, Room 105

9:00 AM OPENING REMARKS

9:05 AM *SB06.01.01

Single-Protein Electronics: Effect of Surface Mutagenesis and Multiheme Redox Cofactors [Ismael DDíez Perez¹, Albert C. Aragonés², Kavita Garg¹, Marta Ruiz², Guilherme Vilhena³, Linda Angela Zotti³, Julea Butt⁴, Zdenek Futera⁵, Xiaojing Wu⁶ and Jochen Blumberger⁶; ¹Kings College London, United Kingdom; ²Universitat de Barcelona, Spain; ³Universidad Autónoma de Madrid, Spain; ⁴University of East Anglia, United Kingdom; ⁵University of South Bohemia, Czechia; ⁶University College London, United Kingdom

Bioelectronics is a rapidly evolving field moving towards designing nanoscale electronic platforms that allow *in vivo* sensing, fuel cell powering and chemical biosynthesis. Such devices typically require interfacing a complex biomolecular moiety as the active component to an electronic platform for signal transduction and/or electron source wiring. Inevitably, a true systematic design goes through a bottom-up understanding of the structurally related electrical signatures of such hybrid biomolecular circuits, which will ultimately lead us to tailor its electrical properties and exploit them as high performance bioelectronic devices with a wide variety of applications in organic electronics, sensing, biomanufacturing, etc.

In this contribution, we will present our latest efforts on understanding and control charge transport in a single-protein junction. Our approach relies on trapping individual redox proteins in a tunneling junction under electrochemical control to characterize their main electrical signatures. The method can capture very fine details of the charge transport mechanisms across proteins in an aqueous environment [1,2]. Our studies start with a benchmark redox protein model such as a bacterial blue Cu-Azurin. We will show first the main observed electrical signatures of these systems that make them particularly efficient in transporting charge. We then bioengineer the outer protein surface using point-site mutagenesis as a mean to get a more detailed picture of possible electron pathways through the protein backbone [2,3]. Our results suggest that the protein might not use distinct physical electron pathways across its structure, but transport mechanism can be switched upon quenching of particular motions in the protein structure via surface mutations. We then compare the above redox protein model to a natural multiheme molecular wire. Multiheme proteins have been recently discovered as the building blocks in highly conducting pili and transmembrane structures of certain species of the so called electrical bacteria [4]. Such large supramolecular ensembles of multiheme protein complexes support long-range charge transport in record distances over micrometres [5]. We have trapped individual small tetraheme proteins (STC) in our tunnelling gap and measured conductance. STC constitutes a well-known repeating arrangement of heme cofactors along larger multiheme complex structures. Our first results suggest a single STC unit can transport electrons via efficient electron tunnelling process along the ~4 nm long protein axis with very shallow electron decay constant. We believe these results contribute to the observed long-range charge transport behaviour observed in these multiheme-based molecular wires.

Summing up, the above work shows the potential of electrochemically controlled nanoscale protein junctions to both elucidating charge transport mechanisms in biological systems as well as in enabling a bottom-up design of electrode/protein interfaces for the future generations of bioelectronic devices.

9:35 AM *SB06.01.02

Implantable Materials for Chronic Disease Monitoring [Hanief Yousefi¹, Xudong Ji¹, Jagatamoy Das¹, Yi Li¹, Jonathan Rivnay¹ and Shana Kelley^{1,2}; ¹Northwestern University, United States; ²Chan Zuckerberg Biohub, United States

Chronic diseases such as heart failure (HF) are increasingly prevalent conditions that are difficult to manage. Patients often experience significant deterioration between clinic visits, and by the time they become symptomatic, their condition cannot be managed outside of the hospital. Inflammation has recently been identified to take roles on promoting and inducing HF but there are no insights on the mechanisms of disease progression. The ability to perform continuous monitoring of protein biomarkers on a body-implanted device will transform our capacity to diagnose disease, preserve wellness, and propose potential treatments. Using Flexible and Implantable sub-millimeter polymeric substrates, we propose a new solution for remote, continuous monitoring of chronic disease clinical biomarkers (BNP, Troponin I, IL6, TNF α as proof of concept) to manage patients' health. We recently developed the first-of-its-kind reagent-less molecular sensor for in situ detection of a wide range of targets, such as viral particles and proteins. However, continuous monitoring of chronic disease requires installing a miniature device inside the human body and continuously monitoring the patient for an extended period. The small device provides efficient reaction rates with a sub-millisecond resolution, which has not been achieved using the current common diagnostics paradigm. By moving from materials used in traditional electrochemistry to using unconventional recent developments in the fields of material science, we introduce a new generation of sensing platforms that are biocompatible, affordable, reliable, and environmentally friendly to deliver the promised goals of chronic disease

management. Using an HF rat model and accessing interstitial fluid via contact with the device's implantable part, we will be able to monitor disease progression, inflammation, and biomarker levels. This technology will provide a new generation of devices for the continuous monitoring of vital biomarkers in HF rat models.

10:05 AMBREAK

10:30 AM *SB06.01.03

Molecular Junction with a Single Biomolecule: Self-Restoring Device and Phosphorylation AssayTomoaki Nishino; Tokyo Institute of Technology, Japan

Single-molecule junctions, where a single molecule is trapped in a nanogap between metal electrodes, play pivotal roles in nanoscience and nanotechnology. Measuring biomolecules in the single-molecule junctions offers a unique means to develop single-molecule devices with sophisticated functionalities, to realize novel biomedical and pharmaceutical applications, and so on. Regarding the device development, the structural, physical, and chemical properties of DNA at the nanoscale have attracted attention to the prospect of using DNA as a building block in single-molecule devices, which leads to extensive investigations into electron transport through a single DNA molecule. Although significant advances have been made in understanding the transport phenomena through a single DNA molecule, the previous studies mainly focused on the transport phenomena in static DNA structure at thermodynamic equilibria. Against this, we expect that electron transport through DNA under the deliberate control of its structure paves the way for DNA electronic devices with functional controllability in a dynamic manner. To prove this, we investigated the electron transport through the single-molecule junction of DNA that orthogonally clamps a metal nanogap. This DNA single-molecule junction differs from conventional ones in the DNA configuration; the present and conventional junctions contain a DNA molecule oriented in perpendicular and parallel directions to the axis of the nanogap, respectively. The STM measurement of the unzipping dynamics revealed that the present DNA junction enables spontaneous restoration of the molecular junction after its electrical failure and thereby improves the reproducibility of the junction formation. Our study demonstrated that a DNA dynamic structural change could be applied to a single-molecule junction by using the perpendicular configuration.

Single-molecule detection of biologically relevant substances has attracted rapidly growing interest. One successful example of single-molecule technology is the detection of DNA achieved using nanogaps between metal electrodes or nanopore devices. Given their primary role in diverse biological functions, proteins have been regarded as the next challenging target in single-molecule studies. In particular, the detection of post-translational modifications (PTMs) of proteins at the single-molecule level is in high demand, since PTMs constitute an essential regulatory mechanism involved in almost all cellular events. Single-molecule studies would revolutionize medical diagnoses through PTM detection primarily because of their high sensitivity and concomitant high-throughput assays. However, the detection of PTMs at the single-protein level is not trivial, since the chemical structure of an amino acid residue is only slightly altered upon modification. Stringent selectivity or specificity for a PTM of interest is consequently vital for single-molecule detection. In this study, we focused on phosphorylation, which is a biologically important PTM, and demonstrated specific single-molecule detection of peptide phosphorylation by electrical conductance measurements. First, we found that a single orthophosphate anion exhibits a conductance value significantly higher than the peptides and their amino acid residues. This unique electronic property of the phosphate serves as a specific marker, enabling the detection of phosphorylation on a single peptide molecule. Based on this unique electrical signature of phosphate, an *in situ* single-molecule assay of enzymatic phosphorylation was achieved with 95% accuracy and 91% specificity for signal discrimination between phosphorylated and non-phosphorylated peptides. The present study demonstrates novel and specific single-molecule detection of PTMs, which will help elucidate their biological functions and facilitate the development of novel medical diagnostics.

11:00 AM *SB06.01.04

Beyond the Diffraction Limit—Optomechanics in Biomolecular ContactsAlbert C. Aragonès; University of Barcelona, Spain

Molecular trapping approaches^[1] that rely on the electrical detection of single-molecule (SM) junctions^[2,3] often face a significant challenge of short lifetimes, typically ranging from tens to hundreds of milliseconds,^[4] primarily due to thermally activated junction breaking.^[5] The limited detection timescales hinder comprehensive fundamental studies, making the extension of detection times a crucial challenge in SM detection. Our plasmon-supported break-junction (PBJ) technique^[6] addresses this issue by significantly increasing the lifetime of SM junctions while preserving the native structure of the target molecule. Remarkably, the optical stabilizing force exerted by the nearfield gradient in PBJ enhances the stability of SM junctions, eliminating the need for chemical modifications of the target molecule or the electrode.

In the first part, we will explore how the nearfield manipulation influences capture and release mechanisms.^[7] As the field strength increases, the rate constant of capture kinetics rises while the release kinetics decrease, favouring the capture state over the release state. Consequently, the SM capture state becomes more likely and more stable than the release state above a specific nearfield strength threshold.

In the second part, we will delve into how the PBJ trapping technique can be further enhanced for biomolecular contacts^[8] through the manipulation of two physical features: (i) the optical resonance of the target molecule and (ii) the energy of the localized surface plasmon resonance in the nanogap. By leveraging these factors, we can extend the effectiveness of PBJ trapping in capturing and biomolecules.

[1] C. S. Quintans, D. Andrienko, K. F. Domke, D. Aravena, S. Koo, I. Díez-Pérez, A. C. Aragonès, *Appl. Sci.* **2021**, *11*, 3317.

[2] B. Xu, N. J. Tao, *Science* **2003**, *301*, 1221–3.

[3] W. Haiss, R. J. Nichols, H. van Zalinge, S. J. Higgins, D. Bethell, D. J. Schiffrin, *Phys. Chem. Chem. Phys.* **2004**, *6*, 4330–4337.

[4] A. C. Aragonès, et al, *Nature* **2016**, *531*, 88–91.

[5] E. Evans, *Annu. Rev. Biophys. Biomol. Struct.* **2001**, *30*, 105–128.

[6] A. C. Aragonès, K. F. Domke, *Cell Rep. Phys. Sci.* **2021**, *2*, 100389.

[7] K. F. Domke, A. C. Aragonès, *Nanoscale* **2022**, DOI 10.1039/D2NR05448E.

[8] A. C. Aragonès, K. F. Domke, *J. Mater. Chem. C* **2021**, *9*, 11698–11706.

SESSION SB06.02: Applied Biomolecular Electronics—Devices and Sensing II

Session Chairs: Juan Artes Vivancos and Linda Angela Zotti

Thursday Afternoon, November 30, 2023

Hynes, Level 1, Room 105

1:30 PM *SB06.02.01

DNA Guided Self-Assembly of Organic MaterialsJames Canary, RuojieSha, Thanuka Udumulla and Chufan Yang; New York University, United States

We have developed a highly versatile system for the organization of 2-dimensional (2D) materials on the nanoscale. This system is predicated on the use of DNA-based information as an organizing principle, and on our ability to design DNA to encapsulate and orient other molecular and nanoscopic species in a diverse and effective fashion. We apply branched DNA molecules, not simple linear DNA, to the formation of connected networks of materials in a predictable fashion [1]. We are able to build robust DNA 2D assemblies. Each of these assemblies can be filled as desired, with any molecules, macromolecules or nanoparticles that can be derivatized to interact, bond or bind with the DNA.

In earlier work, chemistry was developed to enable covalent attachment of organic groups to the 2'-O-ribose position of RNA nucleotides. Such an attachment strategy minimizes distortion in DNA duplexes by directing appended groups to minimize unfavorable steric interactions with A-form helical structures. A variety of synthetic approaches were examined, involving modifications at different points in DNA oligonucleotide synthesis. Much of the chemistry was tested in the context of appended oligomers of nylon and poly(ethylene glycol).

Monodisperse oligomers of electroactive organic polymers were synthesized and appended to DNA oligonucleotides. An octamer of polyaniline, which shows rich electrochemical behavior, was incorporated into a rhombohedral DNA lattice. The resulting crystal showed excellent optical response consistent with cycling between its redox forms [2]. It was later studied in a smaller assembly showing reconfigurable excitonic interactions [3]. A heptamer molecule related to poly(phenylenevinylene) was included in a DNA crystal and found to show strong polarization properties [4].

This presentation will describe unpublished work on the synthesis and assembly of DNA-GNR chimeras within DNA nanostructures.

[1] Seeman, N. C. "Nucleic Acid Junctions and Lattices," *J. Theor. Biol.* **1982**, *99*, 237-247.

[2] X. Wang *et al.*, *Angew. Chem. Int. Ed. Engl.* **56**, 6445-6448 (2017).

[3] X. Wang *et al.*, *ACS Nano*, **16**, 1301-1307 (2022).

2:00 PM SB06.02.02

DNA Encoded Self-Assembly of Molecular Semiconductors for Light-Harvesting Jeffrey Gorman¹, Stephanie M. Hart, Torsten John, Maria A. Castellanos, Adam Willard, Gabriela Schalu-Cohen and Mark Bathé; MIT, United States

Plants transport and convert solar energy into radical-pairs at the 'reaction center' to generate fuel. Nature achieves this with a homogeneous set of pigments, where the host protein environment facilitates tailored couplings between many pigments each with their own function. In contrast, exquisite control over artificial semiconductors for exciton circuits and solar cells remains lacking. Our ability to synthetically generate molecular networks with prescribed nanoscale structure is lacking. To address this gap towards well-designed molecular optoelectronics, we report the development of DNA scaffolds hosting chromophores,¹ to enhance excited state evolution for solar light harvesting.

Here we study the exciton evolution between strongly coupled perylene diimide (PDI) dye pairs scaffolded in DNA. PDIs are exemplar molecular aggregates as they produce a range of photoinduced excited states, depending on their spatial organization.² To study how we can map a specific excited-state pathway to a PDI-DNA structure, we exploited the molecular precision of DNA base-pairing and nanoscale rigidity of DNA origami to generate a library of optoelectronic constructs. We make hundreds of nucleic acid-chromophore conjugates and self-assemble them into prescribed shapes. Using ultrafast spectroscopy, we identified designs that gave rise to different photoinduced species, including excimers and charge-transfer states. Next, we use computational modelling to pinpoint geometrical features that can be linked to a specific excited-state pathway. Our synthetic DNA platform offers the ability to rapidly survey the structure-property of molecular aggregates and identify optimized structures that can be useful for applications in excitonic devices, including solar conversion and quantum information.

1. *Chem. Sci.*, 2022, **13**, 13020-13031

2. *J. Am. Chem. Soc.* 2022, **144**, **1**, 368–376

2:15 PM *SB06.02.03

Antigens and Nucleic-Acid Strands Single-Molecule Bioelectronic Reliable Detection at the 10⁻²⁰ Molar Concentration Luisa Torsi; University of Bari A. Moro, Italy

Single-molecule detection can be accomplished through two approaches: utilizing a nanometric interface or employing an amplification mechanism. In the former scenario, various noteworthy studies have explored nanometric detection interfaces such as transistor nanowires or nanotubes. These interfaces allow for the investigation of individual selective interactions involving proteins and nucleic acid-based targets, as the size of the target matches the detecting surface area. However, due to the "diffusion barrier issue," the target concentration must be at least in the range of 10⁻⁹ molar (M).

To overcome this challenge, an amplification mechanism is employed to amplify the signal by a million-fold. For nucleic acid-based targets, the polymerase chain reaction (PCR) serves this purpose, but a similar amplification mechanism is required for proteins.

This lecture focuses on the "Single Molecule with a Large Transistor – SiMoT" platform, which enables the reliable detection of single molecules in 0.1 mL of both antigens and nucleic acid strands at concentrations as low as 10⁻²⁰ molar. This breakthrough is made possible by a domino-like amplification mechanism. Additionally, the lecture will delve into the significant applications of this technology.

References

- C. Di Franco *et al.* *Advanced Interface Materials*, 2022, 202201829

- E. Macchia *et al.* *Chemical Reviews*, 2022, **122**, **4**, 4636-4699

- L. Sarcina, *et al.* *Analytical and Bioanalytical Chemistry* 2022, **414**, **18**, 5657-5669

- E. Macchia *et al.* *Nature Communications* 2018, **9**, 3223.

- Nature highlights - A sensor detects the light touch of a single molecule. *Nature* 2018, **560**, 412.

2:45 PM BREAK

3:15 PM *SB06.02.04

Metal-Mediated Molecular Electronics in DNA Nanosystems Simon Vecchioni¹, Brandon Lu¹, William Livernois², Chufan Yang¹, Yoel P. Ohayon¹, Karol Woloszyn¹, Chengde Mao³, Lara Perren¹, James Canary¹, Anant Anantram² and Ruojie Sha¹; ¹New York University, United States; ²University of Washington, United States; ³Purdue University, United States

DNA as a vehicle for molecular programming relies on the predictability and information storage capability of the canonical Watson-Crick base pairs, A:T and G:C. With only four Watson-Crick nucleobases and the poor electronic conduction in A:T pairs, it has become clear that there are strong limitations on the diversity and ensuing complexity of DNA-based electronic systems. To address this limitation, we present an expanded DNA alphabet based on metal-mediated DNA (mmDNA) base pairing in which we substitute hydrogen bonds between pyrimidine nucleobases with templated metal ion coordination.

We employ a self-assembling 3D DNA crystal system, the tensegrity triangle, to determine the biomolecular structures of 30+ metal ion (Ag⁺, Hg²⁺, Au⁺, and Cd²⁺)-mediated DNA (mmDNA) base pairs, and we further use this comprehensive structural library to elucidate fundamental design rules for an expanded DNA metal coding system. Energy gap calculations elucidate an electronic fingerprint for the base pair classes in our library, and show additional levels in the lowest unoccupied molecular orbitals (LUMO) of mmDNA structures, rendering them attractive molecular electronic candidates. Our results are consistent with previous studies in which mmDNA base pairs have been shown to have superlative electronic and magnetic properties, and we suggest a transmission mechanism to describe this behavior.

We further manipulate our self-assembled DNA crystals using pH to capture by x-ray diffraction a series of reversible, pH-driven chemical reactions involving silver, mercury and gold ions, with implications for bandgap tuning. Importantly, we identify titration points at which mmDNA pairs exist in a heterobimetallic state, where a single DNA base pair binds to both Ag⁺ and Hg²⁺ in tandem. The precision self-assembly of heterobimetallic DNA chemistry at the sub-nanometer scale will drive atomistic design frameworks for more elaborate mmDNA-based nanodevices and nanotechnologies. We anticipate the integration of this expanded mmDNA alphabet as a means of programming specific interactions into DNA nanostructures to enable the exploitation of their electronic, magnetic, and catalytic properties for future nanotechnology applications.

3:45 PM SB06.02.05

Selectivity and Real-Time Potassium Ion Sensor Based on dsDNA Sequences Aptamer in ZnO Thin-Film Transistors with Floating Structure Yen Shuo Chen¹, Chun Chi Chen², Hsin-Chiang You³ and Fu-Hsiang Ko¹; ¹National Yang Ming Chiao Tung University, Taiwan; ²Taiwan Semiconductor Research Institute, Taiwan; ³National Chin-Yi University of Technology, Taiwan

The level of potassium ions in clinical diagnosis is most associated with chronic kidney disease (CKD) and the pathophysiology of insulin secretion. The normal concentration in human blood of potassium ions is 2.5 to 5.5 mEq/L. In the past, the assay was mostly done by Blood Potassium Content Assay Kit, which provided that the potassium ions in the serum interact with sodium tetraphenylborate to form water-insoluble, which is time-consuming. Therefore, a rapid and immediate of detecting potassium ions is helpful for this issue. Recently, thin film transistors (TFTs) such as zinc oxide (ZnO) for biosensors have become the focus of increased research interest due to their high transparency and non-toxicity, and several reports have discussed the impact of floating gate structures on the sensing and reproducibility aspects of biosensors in solution.

In this study, unique double-stranded deoxyribonucleic acid (dsDNA) was used in combination with different concentrations of K ions detected through ZnO-based biosensors with a floating-gate structure. The TFTs were successfully operated as a switching device at a low operating voltage of 5 V. Here, ZnO TFTs with floating gate structures were used to sense dsDNA bound to metal ions in solution by non-contact sensing, and more than 50 detection times were achieved by removing solutions and low-temperature annealing, which is useful for biosensing. The dsDNA at 100 μM was dissolved in DI water and TE buffer to form a solution. The ratio of DI water to Tris-EDTA (TE) buffer was 1:10, and the molecular weight of the dsDNA (GGTTGGTGTGGTTGG) was 359.8. The KCl concentrations were 0.01 M (0.8 mEq/L), 0.03 M (2.5 mEq/L), and 0.1 M (5.5 mEq/L), respectively. To understand the relationship between the number of combinations of different concentrations of potassium ions and the potential of the DNA sequence, the number of zeta potentials for each concentration was measured. The zeta potential of dsDNA was -23.63 mV. The stability of 0.01 M KCl solution was tested with -15.01 and -14.41 mV, respectively. The zeta potential was measured within an inaccuracy of 0.6 mV because a few ions flowing into the solution were unaffected. A positive charge is generated when the DNA sequence binds to potassium ions showing a glove-like shape and can completely wrap around K⁺. When the DNA sequence was bound to K⁺ in the 0.01 M KCl solution, the zeta potential was -15.01 mV. The zeta potential was -2 mV when the concentration of the KCl solution was 0.03 M; the zeta potential was 52.53 mV when the concentration was 0.1 M. These results showed that the KCL elevated by 6.75 mV per 0.01 M concentration.

To investigate ZnO-TFT-based potassium ion detectors, the performance of the ZnO TFT was assessed by analyzing the field-effect mobility (μ_{FE}), threshold voltage (V_{TH}), and threshold voltage shift (ΔV_{TH}) for carrier transport. In the initial state, the TFTs exhibited typically electrical performance. Specifically, I_{on}/I_{off} was 2.3×10^4 A, the threshold voltage (V_{TH}) was -2 V, and the field-effect mobility (μ_{FE}) was $0.006 \text{ cm}^2 \text{ V}^{-1} \text{ s}^{-1}$. A unique ssDNA sequence combined with 0.01, 0.03, and 0.1 M KCl. The TFTs exhibited selective and sensitive electrical performance: $I_{on}/I_{off} = 3.8 \times 10^4$ A, $V_{TH} = 2.5$ V, and $= 0.0052 \text{ cm}^2 \text{ V}^{-1} \text{ s}^{-1}$; $I_{on}/I_{off} = 2.9 \times 10^4$ A, $V_{TH} = 2$ V, and $= 0.0059 \text{ cm}^2 \text{ V}^{-1} \text{ s}^{-1}$; and $I_{on}/I_{off} = 3.6 \times 10^4$ A, $= -0.5$ V, and $= 0.0068 \text{ cm}^2 \text{ V}^{-1} \text{ s}^{-1}$. The ZnO-based TFT showed that KCL was elevated by 0.5 V per 0.01 M of concentration of K^+ . As the concentration rises, dsDNA binds to more K^+ , suggesting that the detected positively and negatively charged objects affect the turn-on voltage of ZnO TFTs. The increase in ΔV_{TH} also indicated increased binding of dsDNA to K^+ with potassium concentrations ranging from 0.01 M to 0.1 M and showed a linear correlation (0.99706). This ZnO-based TFT with DNA sequences aptamer could be used as a biosensor.

SESSION SB06.03: Biomolecular Electronics—The Fundamentals, Experiments and Computational Approaches I
Session Chairs: Anant Anantram and Linda Angela Zotti
Friday Morning, December 1, 2023
Hynes, Level 1, Room 105

9:00 AM OPENING REMARKS

9:05 AM *SB06.03.01

Long Range Conductivity in Non-Redox Active Proteins Stuart M. Lindsay¹, Dmitry Matyushov¹, Aleksei Aksimentiev² and Siddharth Krishnan²; ¹Arizona State University, United States; ²University of Illinois at Urbana-Champaign, United States

It is widely assumed that efficient charge transfer in proteins requires the presence of redox cofactors, but we have found long-range (nS over > 10 nm) conductance in many proteins that do not contain redox cofactors. This is important because it means that fluctuations of many proteins can be followed electrically, as their conductance changes with conformation. For example, we have been able to follow the fluctuations in a DNA polymerase as it actively processes a template. The conductivity of a hopping conductor is proportional to the quantity nD , where n is the carrier density and D is the diffusion constant for carriers. Since proteins do not possess a Fermi sea, charge injection ($n > 0$) is required for conductivity. This is in line with our observations that the protein needs to be coupled to the electrodes via ligands or specific chemical bonds for conductivity to be observed, though adventitious reactive groups on the protein can serve the same purpose. A diffusion constant $D > 2 \times 10^{-4} \text{ cm}^2/\text{s}$ is required to account for the most highly conductive protein wires (OmcS cytochrome wires) and this, in turn, requires a reorganization energy on the order of kT , a small fraction of the value derived from the Stokes shift in classical Marcus theory. Molecular dynamics simulations of a series of linear proteins (whose electronic properties have been measured) show that the Marcus picture is not valid, the free energy parabolas associated with charge transfer between aromatic residues being broader than predicted from the Stokes shift. As a consequence, the reaction barriers are typically ~ 40 meV, almost equal to $3/2 kT$. The calculated diffusion constant is $2 \times 10^{-4} \text{ cm}^2/\text{s}$, accounting for the observed decay length. A model for charge injection determines n with one adjustable parameter that is bounded by electrochemical data, and the resulting conductivity is in agreement with experimental data.

9:35 AM SB06.03.02

Combinations of Analytical and Machine Learning Methods in a Single Simulations Framework for Modelling of BioFETs Vihar P. Georgiev¹, Naveen Kumar¹ and Cesar Pascual Garcia²; ¹University of Glasgow, United Kingdom; ²Luxembourg Institute of Science and Technology, Luxembourg

In this paper, we present the simulation results of a BioFET using a novel simulation methodology implemented in a computational framework called the Biomolecule-Oxide Simulator (BOxSim). Our novel simulation methodology is based on Gouy-Chapman-Stern and the modified Site-binding models in combination with a machine learning methodology.

Moreover, our “BOxSim” framework is the computational simulation framework that works on the hierarchical inclusion of interdependent functions to operate multiple models simultaneously. BOxSim is flexible simulation environment which considers the problems of reactive sites from oxide surfaces or non-specific bindings along with the noise present in the experimental signal to calibrate and extract the required device output characteristics. It can help in generating the sensor response which can be experimentally calibrated to confirm the surface density of the specific and non-specific binding as a yield of the process while filtering the noise with the help of the developed methodology. BOxSim is designed in a way that can interact with the commercial tool (e.g., Synopsys TCAD) and our inhouse-simulator called Nano-electronic Simulation Software (NESS) to simulate the main device characteristics for designing either Ion-sensitive FET (ISFET) or Chem/Bio-FET based on the application. Industry-standard compact (BSIM) models can also be used to interact with the BOxSim which takes the generated surface potential from the BOxSim simulator and transfers it into a circuit simulator to evaluate various ISFET circuit designs.

To show the capabilities of our BOxSim framework, as input we have considered several oxides, amino acids (AA) and short peptides which generate distinct signatures for arch AA or peptide. We have investigated the impact of various high-k dielectric materials as the gate oxide on important Figures of Merit (FoM) such as current in the channel of the device, surface potential (Ψ_s), sensitivity and intrinsic buffer capacitance. More importantly, the variation of differential capacitance (C_7) with the second gradient of drain current (d^2I_d/dpH^2) and surface potential ($d^2\Psi_s/dpH^2$) are used to uniquely identify the signatures of different amino acids or peptides. The surface potential of oxides is dependent on the affinity constants and the zero-crossover point represents the zwitterion state. Similarly, we have simulated the detection process of different AA such as Glutamic Acid (E) and Lysine (K) immobilized with carboxyl (C-Imm.) or amine (N-Imm.) terminal. The affinity constants, isoelectric point, and density of amino acids can be extracted from the $d^2\Psi_s/dpH^2$ variation with the bulk pH. Other than amino acids, we have shown the distinct features of short a peptide Phenylalanine-Proline (FP) immobilized with carboxyl-terminal and the addition of Glutamic Acid to the sequence. The sensor output can be observed as the variation of drain current with the pH for the immobilized peptide sequence on the sensing surface. We have also confirmed the reliability of the designed model by calibrating the simulated results with the experimental data for different physical conditions. The proposed method can be helpful in defining an efficient method for label-free protein sequencing.

9:50 AM BREAK

10:20 AM *SB06.03.03

Electron Transport Through Proteins beyond the Conventional Tunneling Limit David Cahen and Sudipta Bera; Weizmann Institute of Science, Israel

A key conundrum of bio-molecular electronics is the quite efficient electron transport (ETp) through solid-state junctions wider than a few nm, often without temperature activation. Such a behavior challenges known transport mechanisms, given that proteins, lacking extended conjugation, are low charge carrier density molecules and the experimental ETp results are surprising. A wide range of electron transport (ETp) studies has been done, mostly on protein films of comparable thickness, one that is within the limit of quantum mechanical tunneling (2, or for conjugated systems ~ 5 nm). Typically, for polymer junctions, current decays exponentially with junction width, limiting detection beyond a certain thickness and this should hold also with biopolymers, such as proteins. We find now (Bera et al, submitted) that we can detect and measure protein conduction of from 9 - 60 nm thick junctions of self-assembled bacteriorhodopsin multilayers to test the limit of ETp as a function of junction thickness, in a large ($\sim 10^{-3} \text{ cm}^2$) area configuration. Junction quality was confirmed by impedance spectroscopy and voltage breakdown. Such junctions show near or complete activation-less transport with the most-efficient length-normalized electron transport reported so far ($0.06\text{-}0.53 \text{ nm}^{-1}$).

The small to negligible ($< 200\text{K}$) temperature dependence, among other things, excludes hopping as a plausible mechanism. While a modified Landauer model could be a possibility, the large transport distance (60 nm) makes coherent quantum mechanical tunneling physically implausible. The results may be understood by assuming that ETp is limited by injection at (via tunneling through) one of the contacts, followed by a much more efficient charge propagation across the proteins. Additionally, electrostatics of the protein film, whose dielectric constant we measured by impedance, will further limit the number of charge carriers in the protein film. Such a view also defines the question to tackle now, namely how electrons can pass through such wide protein layers at a rate that is measurable by our electronics and, apparently, more efficient than the rate of injection through the contacts.

=====

* with M Sheves, I Pecht and A Vilan. Further collaboration with, among others, T Bendikov (WIS), SK Saxena (SRM Chennai), M Tornow, C Domenikus (TU Munich), JA Fereiro, (IISER Trivandrum)

10:50 AM SB06.03.04

Charge Transport Through Self-Assembled Monolayers—The Roles of Conformation and Chelation Samuel E. Root, George M. Whitesides, Yuan Li and Lee Belding; Harvard University, United States

To elucidate charge transport mechanisms through complex biomolecules--involving conformationally flexible, supramolecular systems--and isolate effects arising from different molecular scale features, it is useful to investigate simple, well-defined model systems. The "EGaIn junction," which uses a liquid metal electrode to measure charge transport through self-assembled monolayers (SAM), paired with a physical-organic approach to systematically modify the molecules within the SAM, provides a powerful platform for approaching this problem. I will discuss two recent works using this approach to understand (1) the role of molecular conformation (and specifically conformational disorder) on tunneling and rectification of current, and (2) charge transport through SAMs terminated by a chelating group and the influence of the binding of different metal ions.

1) Conformation. This work demonstrates that molecular conformation of molecules making up self-assembled monolayers (SAMs) influences the rates of charge tunneling (CT) through them, in molecular junctions of the form AuTS/(CH₂)₂CONR₁R₂/Ga₂O₃/EGaIn, where R₁ and R₂ were alkyl chains of different length. The lengths of chains R₁ and R₂ were selected to influence the conformational structure of the molecules in the monolayer. The conformations of the molecules influence the thickness of the monolayer and their rectification ratios at ±1.0 V. When R₁ = H, the molecules are well ordered and exist predominantly in trans-extended conformations. When R₁ is an alkyl group (e.g., R₁ ≠ H) however, their conformations can no longer be all-trans-extended, and the molecules adopt more gauche dihedral angles. This change in type of conformation decreases conformational order and influences rates of tunneling. When R₁ = R₂, the rates of CT decrease (up to 6.3x), relative to rates of CT observed through SAMs having the same total chain lengths, or thicknesses, when R₁ = H. When R₁ ≠ H ≠ R₂, there is a weaker correlation (relative to when R₁ = H or R₂) between current density and chain length or monolayer thickness, and in some cases the rates of CT through SAMs made from molecules with different R₂ groups are different, even when the thickness of the SAM (as determined by XPS) is the same.

2) Chelation. This paper describes a surface analysis technique that uses the "EGaIn junction" to measure tunneling current densities (J(V), amps/cm²) through self-assembled monolayers (SAMs) terminated in a chelating group and incorporating different transition metal ions. Comparisons of J(V) measurements (performed ex-situ, in air) between bare chelating groups and chelates—formed through incubation of the SAM within a solution of bivalent metal ions—are used to characterize the composition of the SAM and infer the dissociation constant (K_d, mol/L), as well as kinetic rate constants (k_{off}, L/mol s; k_{on}, 1/s) of the reversible chelate-metal reaction. To demonstrate the concept, SAMs incorporating a chelating terminal group were incubated within ethanol solutions of metal salts (CuCl₂, NiCl₂, and AgClO₄). After rinsing and drying the surface, measurements of tunneling current as a function of incubation time and concentration in solution are analyzed with a simple model to infer k_{off}, k_{on}, and K_d. X-ray photoelectron spectroscopy (XPS) provides an independent measure of surface composition to confirm inferences from J(V) measurements, as well as to characterize the stoichiometry and oxidation states of the bound metal ions. The titration experiments establish that: (i) bound metal ions are stable to the rinsing step as long as the rinsing time, τ_r is at least 10 × lower than 1/k_{off}; (ii) the bound metal ions increase the current density at the negative bias and reduce the rectification observed with free bpy terminal groups; (iii) the values of K_d measured using tunneling currents are comparable to those measured using XPS, but larger than those measured in solution.

11:05 AM *SB06.03.05

Tunneling-to-Hopping Transition in Multiheme Cytochrome Bioelectronic Junctions [Jochen Blumberger](#)¹, [Xiaojing Wu](#)¹ and [Zdenek Futera](#)²; ¹University College London, United Kingdom; ²University of South Bohemia, Czechia

Multiheme cytochromes (MHCs) have attracted much interest for use in nanobioelectronic junctions due to their high electronic conductances.

Recent measurements on dry MHC junctions suggested that a coherent tunneling mechanism is operative over surprisingly long distances (>3 nm), which challenges our understanding of coherent transport phenomena. In my talk I will present large-scale electronic structure calculations of gold-MHC-gold junctions that have allowed us to obtain the current-voltage characteristic of these proteins in well defined adsorption geometries and orientations [1,2]. We show that the high electronic conductances of MHC proteins is due to (i) a low exponential distance decay constant for coherent conduction (β = 0.2 Å⁻¹) and (ii) a large density of protein electronic states which prolongs the coherent tunneling regime to distances that exceed those in molecular wires made of small molecules. We also find that incoherent hopping conduction is uncompetitive in the experimental setup due to the large energy level offset at the protein-electrode interface. Removing this offset, e.g., by gating, we predict that the transport mechanism crosses over from coherent tunneling to incoherent hopping at a protein size of ~7 nm, thus enabling electron transport on the micrometer scale with a shallow polynomial (~1/r) distance decay.

References:

- [1] Z. Futera, I. Ide, B. Kayser, K. Garg, X. Jiang, J. H. van Wonderen, J. N. Butt, H. Ishii, I. Pecht, M. Sheves, D. Cahen, and J. Blumberger, *J. Phys. Chem. Lett.* 11, 9766-9774 (2020).
- [2] Z. Futera, X. Wu, J. Blumberger, *J. Phys. Chem. Lett.* 14, 445-452 (2023).

11:35 AM SB06.03.06

Modeling Spin Transport in Multi-Heme Cytochromes [William Livernois](#) and [Anant Anantram](#); University of Washington, United States

Multi-heme cytochromes have attracted attention due to their conductive properties [1] and, more recently, their spin-selective properties [2]. The small tetraheme cytochrome (STC), a c-type cytochrome prominently found in *Shewanella oneidensis*, has been experimentally validated to act as a spin filter [3], highlighting its potential integration into the burgeoning field of nano-scale spintronic devices. A spin-dependent transport model was used to model this system, building upon prior work that has proven effective in analyzing similar biomaterials and cytochromes [4]. The improved model incorporates non-collinear effects such as spin-orbit coupling using generalized open shell density functional theory (DFT) in order to analyze the electronic structure of the cytochrome and spin-dependent transport properties. Preliminary findings indicate that collinear effects, arising from electron exchange and spin state, predominantly influence the transport pathway while spin-orbit effects only cause minor shifts in orbital energies.

To complement our electronic structure and transport studies, we have undertaken a detailed analysis of the role of the peptide backbone, employing hybrid Quantum Mechanics/Molecular Mechanics (QM/MM) modeling methods. The modeling results indicate that the peptide backbone functions primarily as a structural scaffold facilitating heme-to-heme electron transport, rather than directly contributing to electron conduction. Additionally, recognizing the importance of solvation effects in biological systems, we have investigated the impact of solvation on the cytochrome's properties. The solvent, modeled using an implicit model and counterions, was found to modulate the coupling between heme sites and the overall conductivity of the cytochrome.

The research was supported by National Science Foundation NSF Grant Number 2317843, NSF Future of Manufacturing Grant No. 2229131 and the NDSEG fellowship.

References:

- [1] Dahl, Peter J., et al. "A 300-fold conductivity increase in microbial cytochrome nanowires due to temperature-induced restructuring of hydrogen bonding networks." *Science advances* 8.19 (2022).
- [2] Mishra, Suryakant, et al. "Spin-dependent electron transport through bacterial cell surface multiheme electron conduits." *Journal of the American Chemical Society* 141.49 (2019): 19198-19202.
- [3] Niman, Christina M., et al. "Bacterial extracellular electron transfer components are spin selective." *The Journal of Chemical Physics* 159.14 (2023).
- [4] Livernois, William, and M. P. Anantram. "A Spin-Dependent Model for Multi-Heme Bacterial Nanowires." *ACS nano* 17.10 (2023): 9059-9068.

SESSION SB06.04: Biomolecular Electronics—The Fundamentals, Experiments and Computational Approaches II
Session Chairs: Anant Anantram and Josh Hihath
Friday Afternoon, December 1, 2023
Hynes, Level 1, Room 105

1:30 PM *SB06.04.01

Introducing Solid-State Biomolecular Protonics—Lateral Proton Conduction Across Biological Membranes [Nadav Amdursky](#); Technion--Israel Institute of Technology, Israel

Nature is full of various charge transfer circuits that are at the heart of our existence, such as in our aerobic respiration system or the plant's photosystem. While the focus of this symposium is Biomolecular Electronics, meaning following electron transport (ET) across biomaterials, proton transport (PT) is equivalent in its importance, and in some cases, such as in the mentioned examples, the role of the ET chain reaction is to facilitate PT. As one can imagine, the mechanisms behind ET and PT are different, having different aspects within the biomolecule that are important for the transport mechanism. Moreover, from an experimental point of view, in electronic devices, it might be hard to distinguish between PT and ET. Here, we introduce a new

experimental approach to investigate lateral PT across membranes, which is based on measuring long-range lateral proton conduction via a few layers of lipid bilayers in a solid-state-like environment, i.e., without having bulk water surrounding the membrane. This configuration enables focusing on the surface of the membrane while decoupling it from bulk water. Hence, by controlling the relative humidity of the environment, we can directly explore the role of water in the lateral PT process. We show that proton conduction is highly dependent on the membrane composition, where we explore the role of the head group, the level of tail saturation, and the role of the membrane phase and fluidity. The measured PT as a function of temperature shows an inverse temperature dependency, which we explain by the desorption/adsorption of water molecules into the solid membrane platform. We explain our findings by discussing the role of percolating hydrogen bonding within the membrane structure in a Grotthuss-like mechanism. Our new understanding of the specific role of the membrane interface in supporting lateral long-range PT is not only providing new information related to this fundamental biochemical and biophysical process but also very important to any use of membranes in various applications, from biomedical applications to the use of proton-conductive membranes in energy-related applications.

2:00 PM SB06.04.02

Current Rectification via Photosystem I Monolayers Induced by Their Orientation on Hydrophilic Self-Assembled Monolayers on Titanium Nitride Hector J. Rojas Rojas¹, Feng Liu², Jerry A. Fereiro³, Domenikos Chryssikos¹, Dario Leister² and Marc Tarnow¹; ¹Technical University of Munich, Germany; ²Ludwig-Maximilians-Universität München, Germany; ³Indian Institute of Science Education and Research, India

The photosensitive protein Photosystem I (PSI) is considered one of the most efficient light-harvesting molecular complexes in nature [1]. The electron transport studies carried out on PSI monolayer(s) formed on (quasi-) metallic contacts (highly doped silicon, indium tin oxide, silver, or, in the majority of cases, gold) using reliable soft top contacts show high reproducibility [2-5], along with its peculiar ability to rectify electrical current [2,4,5]. In the present study, we introduce titanium nitride (TiN) as a promising alternative bottom contact material to investigate the electronic transport properties of PSI. TiN is a hard, conductive ceramic well-established in CMOS technology, chemically inert, and biocompatible. Self-assembled monolayers (SAMs) of various hydrophilic group-terminated phosphonic acids covalently bound to the TiN surface were used to attach PSI layers onto its head surface electrostatically. Specifically, we investigated -OH, -COOH, and -NH₂ terminal head groups and tailored mixtures of these. We used atomic force microscopy to confirm the formation of a PSI monolayer of thickness approx. 6 nm, with about 80% surface coverage. DC electrical measurements using eutectic gallium-indium (EGaIn) soft top contacts showed asymmetric I-V curves, with rectification ratio (RR) values varying from 150 to 460. We assign the observed rectification to possible PSI orientation preferences on a particular linker head group. Current rectification in PSI has been previously attributed to an internal electric dipole originating from charged states of the protein residual groups [4,5]. Our data indicate an orientation in which the stromal side of the protein complex is predominantly in contact with the hydrophilic linker surface. We analyze our data within the framework of tunneling through an asymmetric trapezoidal barrier [6].

References

1. Brettel, K. (1997). Electron transfer and arrangement of the redox cofactors in photosystem I. *Biochimica et Biophysica Acta (BBA)-Bioenergetics*, 1318(3), 322-373.
2. Lee, I., Lee, J. W., & Greenbaum, E. (1997). Biomolecular electronics: vectorial arrays of photosynthetic reaction centers. *Physical Review Letters*, 79(17), 3294.
3. Mukhopadhyay, S., Karuppanan, S. K., Guo, C., Fereiro, J. A., Bergren, A., Mukundan, V., ... & Cahen, D. (2020). Solid-state protein junctions: cross-laboratory study shows preservation of mechanism at varying electronic coupling. *Science*, 23(5), 101099.
4. Castaneda Ocampo, O. E., Gordiuchuk, P., Catarci, S., Gautier, D. A., Herrmann, A., & Chiechi, R. C. (2015). Mechanism of orientation-dependent asymmetric charge transport in tunneling junctions comprising photosystem I. *Journal of the American Chemical Society*, 137(26), 8419-8427.
5. Qiu, X., & Chiechi, R. C. (2022). Printable logic circuits comprising self-assembled protein complexes. *Nature Communications*, 13(1), 2312.
6. Gruverman, A., Wu, D., Lu, H., Wang, Y., Jang, H. W., Folkman, C. M., ... & Tsybal, E. Y. (2009). Tunneling electroresistance effect in ferroelectric tunnel junctions at the nanoscale. *Nano letters*, 9(10), 3539-3543.

2:15 PM *SB06.04.03

Modeling Quantum Charge Transport Through Nucleic Acid Structures: Role of Decoherence Hashem Mohammad¹ and Anant Anantram²; ¹Kuwait University, Kuwait; ²University of Washington, United States

Understanding the conductance of DNA helps in the development of new sequencing techniques, methods to sense biological processes, disease detection techniques, and future DNA-based nanoelectronics. The challenges in understanding the underlying transport phenomena stem from the facts that: 1) DNA is a floppy molecule that exists in a solvent environment, 2) sequence and conformation affect the energy levels distribution along the strand, and 3) the need to account for the details of the DNA-electrode junction.

Modeling of charge transport through nanoscale nucleic acid structures requires careful attention to the quantum effects. The fluctuating nature of the molecule and the surrounding solvent environment can affect the electron transport process depending on the length scale, going from coherent to decoherent transport, or to an intermediate state of coherent-decoherent transport. One prominent method to model charge transport through nanoscale devices is the Green's function formalism. This formalism uses the Hamiltonian obtained from quantum mechanical simulations such as DFT to calculate the electron transmission properties. From the transmission, we can calculate other physical properties such as conductance and current-voltage characteristics. This formalism allows us to include the effect of attaching metallic contacts to the DNA through self-energy terms, removing the need for explicitly including them in the quantum-based simulations step. Additionally, it can incorporate decoherence due to scattering through self-energy terms as well.

This presentation focuses on the theory and modeling of quantum transport through nucleic acid structures using Green's function method with decoherence probes. We model a DNA connected to two metallic contacts in a contact-DNA-contact setup. For a weakly-coupled system such as DNA, we use the decoherence probes method to account for scattering events. This technique uses phenomenological probes to mimic the interaction of electrons with the environment as they lose phase information and/or gain and lose energy (inelastic scattering). Decoherence broadens the energy levels and allows electrons to traverse the structure at energies that were not originally accessible to the electrons. The broadening of energy levels increases the transmission probability across the DNA. This constitutes the main difference between coherent and decoherent charge transport. Thus, the inclusion of decoherence allows us to obtain conductance values within the range of the experimental values, something that the coherent transport could not achieve.

The decoherence probes are included in the model as self-energies controlled by a spatially dependent parameter that represents the average scattering time for the electron. In the previous work, the decoherence parameter used was energy independent. The drawback of this is that it overestimates the transmission in the HOMO-LUMO gap and washes out distinct transmission features within the HOMO or LUMO bands. Therefore, we present an energy-dependent decoherence model that allows us to better describe the transmission spectra. We demonstrate that this model can generate the expected exponential decay of conductance with the increase in DNA length, and yields conductance values that agree with experiments.

We apply the decoherence probe method to a variety of DNA strands to demonstrate its use. The applications involve (i) detecting a single base mutation in a 15-base-pair long DNA strand, (ii) studying the properties of heterostructures created with DNA strands analogous to solid-state heterojunctions, and (iii) doping of DNA by an intercalating molecule (anthraquinone) between the base pairs, which allows a change in conductance depending on the redox state of the intercalator.

2:45 PM BREAK

3:15 PM *SB06.04.04

How Do Electric Bacteria Breathe Without Oxygen or Soluble Electron Acceptors? Protein Nanowires: Structures, Functions, and Ultrafast Electron Transfer Mechanisms Nikhil S. Malvankar; Yale University, United States

Deep in the ocean or underground, where there is no oxygen, *Geobacter* "breathe" by projecting tiny hair-like protein filaments called "nanowires" into the soil, to dispose of excess electrons resulting from the conversion of nutrients to energy, cleaning up radioactive sites. Although it is long known that *Geobacter* use filaments for electron transfer (*Nature* 2002, 2005), it was not clear what they are actually made of and why they are conductive.

Our studies have revealed a surprise: the nanowires have a core of hemes lining up to create a continuous path along which electrons travel (*Cell* 19, *Nature Chem.Bio.* '20, *Nature Micro* '23) and can be engineered with atomic precision using recombinant DNA technology, making for remarkably versatile electronic components.

We have further found that *Geobacter* pili remain hidden inside the cell and serve as a piston to secrete nanowire-forming cytochromes (*Nature* 2021) rather than functioning as a nanowire themselves as previously thought (*Current Opinion* 2020).

These studies solve a longstanding mystery to explain our previous findings that these bacteria transport electrons via nanowires (*Nature Nano.* 2014) over 100-times their size to electron acceptors (*Nature Nano.* 2011) and partner cells (*Science* 2010) and store electrons when acceptors are absent akin to how humans use their lungs (*ChemPhysChem* 2012).

Our contact-free measurements of intrinsic electron conductivity in individual protein nanowires reveals how energetics and proximity of proton acceptors modulate conductivity by 100-fold (*PNAS* 2021, *Biochem. Journal* 2021). We have also developed synthetic protein nanowires with tunable conductivity and programmable self-assembly using non-natural click chemistry functionality (*Nature Comm.* 2022).

In this talk I will present our efforts to identify the physical and molecular mechanism of high conductivity of microbial cytochrome nanowires. Our conducting-probe AFM measurements show one of the highest electronic conductivity ever reported in proteins (> 100 S/cm) (*Nature Chem.Bio.* '20). Femtosecond transient absorption spectroscopy and quantum dynamics simulations reveal ultrafast (<200 fs) electron transfer between nanowire hemes upon photoexcitation, enhancing carrier density and mobility. Photoconductive atomic force microscopy shows up to 100-fold increase in photocurrent in purified individual nanowires. Photocurrents respond rapidly (<100 ms) to the excitation and persist reversibly for hours (*Nature Comm.* '22). Furthermore, nanowires and biofilms show non-classical temperature dependence of conductivity with cooling accelerating electron transport by 300-fold.

Our efforts to computationally model the heme redox potential and conductivity of nanowires yielded up to a billion-fold lower conductivity than experiments (*JPCB*'21, *JPCB*'22), illustrating that the existing computational models based on electron hopping assumption fail to capture electron transfer in biological nanowires. This raises the possibility that biological nanowires employ a fundamentally different, currently unknown mechanism. Thus, existing models predict the same conductivity for all nanowires with computed timescales for heme-to-heme electron transfers (100 ns), million-fold lower than that measured using transient absorption in excited-state (*Nature Comm.*) and conductivity in ground-state for fully hydrated (*Nature & Cell*) or air-dried nanowires (*Science Adv.*).

Notably, multiple computational studies have predicted that invoking quantum effects could account for the high conductivity of these nanowires (*Nanotechnology*'20, *IEEE*'21, *ACS Nano*'23). I will present our efforts to experimentally assess these computational predictions using multiple probes such as light, temperature, electric and magnetic fields. I will also discuss how our studies are helping to understand, predict and control extracellular electron transfer by nanowires used by diverse environmental microbes to capture, convert and store energy.

3:45 PM SB06.04.05

Combination of Droplet Oscillation and Dielectrophoresis to Increase the Sensitivity of Biosensors Marten Musiol¹, Marte Thorns¹, Benita Hafemann¹, Fenja Schröder¹, Felix Hirschberg¹, Annalena Eckert¹, Rebekka Biedendieck¹, Hans-Hermann Johannes^{1,2}, Dieter Jahn¹ and Wolfgang Kowalsky^{1,2}; ¹Technische Universität Braunschweig, Germany; ²Leibniz Universität Hannover, Germany

Biosensors have become a research field of high interest over the last few years. Especially the detection of bacteria is one of the main issues for biosensors. To prevent human health risks and detect even a small quantity of bacteria e.g. in water sources, reliable and accurate detection of bacteria must be guaranteed even for small concentration of bacteria. To increase the sensitivity of such biosensors it is of high importance to increase the number of bacteria on the sensing area. In this work dielectrophoresis (DEP) is utilized to improve bacteria collection at the sensing area.

DEP accelerates dielectric particles suspended in a liquid towards regions of either high or low electric field gradient by applying an alternating inhomogeneous electric field. The force associated with DEP is called dielectrophoretic force (DEP force). This force operates in a radius of micrometers. The transport of particles to the operating area of the DEP force is improved by droplet oscillation. This method provides liquid turbulences inside the particle solution. Thereby, more bacterial cells are collected on the sensing area.

The droplet oscillations are generated by two oscillation electrodes. Those electrodes are implemented beneath the DEP setup with a distance of micrometers. Between the DEP and oscillation electrodes a droplet of a polar liquid is located. By applying a voltage to one of the droplet oscillation electrodes the polar molecules of the liquid align with the electric field. The alignment of the molecules leads to a decrease of surface tension in the area of the electric field. As a response the liquid starts to flow towards the region of low surface tension. To get a consistent flow inside the droplet the applied voltage switches between the two oscillation electrodes.

This research focuses on optimizing the reciprocal influence of the DEP field and the electric field for the droplet oscillation. In order to enhance the experimental setup, the simulation software COMSOL Multiphysics® was used. In this simulation parameters like the frequencies of the electric fields or electrode geometries were taken into account. The results of the simulations should allow us to construct a setup combining droplet oscillation and DEP, that is capable of improving the sensitivity of biosensors.

Key words: droplet oscillation, dielectrophoresis, liquid turbulences, biosensors, bacteria

4:00 PM *SB06.04.06

Seeing is Believing: Quantitative Imaging of Bacterial Electron Export Correlated with Protein Structure and Mechanical Properties Sibel E. Yalcin; Yale University, United States

Protein nanowires enable *Geobacter* to survive without-oxygen like soluble electron acceptors perform important functions such as cleaning up radioactive sites, generating electricity (*Nature Nano*, 2011, or sharing electrons with other bacteria (*Science* 2010). Although it is known for more than two decades that *Geobacter* make nanowires (*Nature* 2002, 2005), it was not clear what they are actually made of and why they are conductive. I will present recent discoveries that resolve two decades of confounding observations in thousands of publications that thought these nanowires as pili filaments (*Current Opinion in Chemical Biology* 2020).

Our studies have revealed a surprise: the protein nanowires have a core of metal-containing molecules called hemes. Combining high-resolution cryo-electron microscopy with multimodal functional imaging, we found that hemes line up to create a continuous path along which electrons travel. Using multimodal functional imaging (*Physical Biology* 2020) and a suite of electrical, biochemical and physiological studies, we find that rather than pili, nanowires are composed of cytochromes OmcS and OmcZ that transport electrons via seamless stacking of hemes over micrometers (*Cell* 2019, *Nature Chem.Bio.* 2020). I will discuss the physiological need for two different nanowires and their potential applications for sensing, synthesis, and energy production.

As this area of research is in its infancy, many of our advancements are made possible by the new nanoscopic imaging techniques we have developed to address major bottlenecks for the field by quantitatively visualizing the electron export via protein nanowires (*Nature Nano*, 2014) and also by living diverse bacteria at single-cell-level. For example, the studies described above (*Nature Chem. Bio*) also established a new atomic force microscopy-based multimodal imaging platform to correlate protein structures with electrical and mechanical properties in response to environmental changes, such as pH and redox potential. Using this platform, we found that the rate of electron transfer in protein nanowires depends on the environment. Thus, we were able to make electron transfer 100-times faster by changing environmental conditions, suggesting a possible path to engineering even more conductive protein nanowires. Furthermore, methodological innovation has been a cornerstone of my lab, as the availability of new methods has enabled us to make unexpected discoveries and challenge thinking in the field. For example, our method for growing biofilms in electric fields, allowed not only the first electrogenetic control of biofilm growth (*Nature Chem. Bio*), but enabled us to make the initial discovery that bacterial biofilms conduct electricity (prior to our work, bacterial biofilms had been thought to be electronically non-conducting).

Our nanoscopic imaging methods are widely applicable to diverse biological systems. For example, we have applied these imaging methods for nanoscopic visualization of water binding to minerals (*Science Adv.*). We revealed that, instead of growing layer by layer as previously thought, water growth starts near edges before surface tension takes over to engulf the surface and forms droplets. This methodology is allowing us to directly visualize how bacteria export electrons to minerals.

I will present our recent experimental and computational studies to identify the mechanism of electron transfer that occurs at unprecedented ultrafast (< 200 fs) rates and over centimeter distances, 10,000-times the size of a bacterium, through measurements of DC and THz conductivity as a function of nanowire length, temperature, frequency, pH and heme stacking (*Science Adv.* 2022). I will also present how we are experimentally assessing computational prediction of quantum effects accounting for the high conductivity of these nanowires (*Nanotechnology*'20, *IEEE*'21, *ACS Nano*'23), using multiple probes such as light, temperature, electric and magnetic fields.

4:30 PM SB06.04.07

Quantum Transport with Two Interacting Conduction Channels in Gold-Azurin-Bismuth Solid-State Junctions Ping'an Li¹, Sudipta Bera², Shailendra Kumer-Saxena², David Cahen² and Yoram Selzer¹; ¹Tel Aviv University, Israel; ²Weizmann Institute of Science, Israel

The fundamental question of 'what is the transport path of electrons through proteins?' initially introduced while studying long-range electron transfer between localized redox centers separated by proteins *in vivo* is also highly relevant to the transport properties of solid-state, dry metal-protein-metal junctions because the characteristic Fermi wavelength, λ_F , of the involved electrons is smaller than the contact footprint of the proteins. Under such conditions, the transport path appears to depend on the coupling of the proteins to the leads. For example, in one of the 'work horses' of biomolecular electronics, Au-Azurin(Az)-Au junctions, the electrons characterized by $\lambda_F \sim 0.5$ nm appear to be transported coherently by off-resonance tunneling if Az is strongly coupled to the leads and by coherent resonance tunneling associated with levels of the redox center, if it is weakly coupled to the leads. Transport in the latter case is especially puzzling because the modest coupling values invoked for its quantification are sufficiently small to allow the tunneling charges to reside in the resonance levels a sufficient time for structural relaxation (reorganization), which should then entail non-coherent transport by a hopping, i.e., activated hops with tunneling between them.

Here, we report of conductance measurements of molecular ensemble nanopore junctions of Au-Az-bismuth(Bi), with well-defined geometry and containing ~2000 proteins in each pore. We argue that since electrons in Bi have λ_F longer than the protein footprint, transport takes place in these junctions by two interacting conducting channels, characterized by different time scales. The slow and fast channels are associated with the redox center and the protein matrix, respectively, and consequently transport takes place in the first channel by a sequential (non-coherent) process and by coherent non-resonant tunneling in the second channel. The resulting overall observed conductance behavior suggests that the two channels are capacitively coupled and that the broad level responsible for the off-resonance tunneling changes its energy in response to the charge occupation of the weakly coupled (redox) channel. This in turn also suggests that transport in these junctions is dominated by the off-resonance (fast) channel, while the slow (redox) channel contribute directly to conductance only negligibly and instead affects transport by intramolecular gating.

4:45 PM SB06.04.08

Single-Molecule Electrical Detection Methods for Public Health Applications: Towards Sustainable Biosensing Ajoke Williams and Juan M. Artes Vivancos; University of Massachusetts Lowell, United States

In the face of escalating climate change, which significantly impacts both

the global economy and public health, changes in environmental conditions can favor the spread of pathogens and the development of new mutants.[1] Early detection and control of pathogen spread are pivotal in enhancing health outcomes on a broader scale. Among the diverse pathways of pathogen screening, nanotechnology has made remarkable advancements in the last decade. It has also extended its applications to biomolecules, giving rise to BioMolecular Electronics.[2] Notably, the Scanning Tunneling Microscopic (STM)-assisted break junction method (STM-BJ)[3] has led to biophysical studies of individual molecules at the single-molecule level. It stands out as a promising approach for single-molecule biomolecular detection. This concept emerges as a compelling solution for the real-time identification of individual biological molecules. Our research leverages the potential of the STM-BJ method to showcase the electrical detection of RNA cancer biomarkers, distinguishing KRAS mutants G12V and G12C from the wild type.[4] Furthermore, our investigation highlights the remarkable sensitivity and specificity of this technique in identifying RNA coronavirus biomarkers, even at the sub-variant level.[5] This tool can also be applied for the electrical measurement of biomolecular interactions at the single-molecule level.[6] Beyond these pioneering advancements, our focus extends now to the sustainability and life cycle analysis of biosensors. Our future research will focus on minimizing the environmental impact of biosensors by utilizing sustainable materials and processes.[7]

References:

- [1] Celia McMichael. Climate change-related migration and infectious disease. Virulence, 2015
- [2] Keshani G Gunasinghe Pattiya Arachchillage, Subrata Chandra, Angela Piso, Tiba Qattan, and Juan M Artes Vivancos. Rna biomolecular electronics: towards new tools for biophysics and biomedicine. Journal of Materials Chemistry B, 2021
- [3] Gerd Binnig and Heinrich Rohrer. Scanning tunneling microscopy. Surface science, 1983
- [4] Keshani G Gunasinghe Pattiya Arachchillage, Subrata Chandra, Ajoke Williams, Patrick Piscitelli, Jennifer Pham, Aderlyn Castillo, Lily Florence, Srijith Rangan, and Juan M Artes Vivancos. Electrical detection of rna cancer biomarkers at the single-molecule level. Scientific Reports, 2023
- [5] Keshani G Gunasinghe Pattiya Arachchillage, Subrata Chandra, Ajoke Williams, Srijith Rangan, Patrick Piscitelli, Lily Florence, Sonakshi Ghosal Gupta, and Juan Artes Vivancos. A single-molecule rna electrical biosensor for covid-19. Biosensors and Bioelectronics, 2023
- [6] Subrata Chandra, Farkhad Maksudov, Evgenii Kliuchnikov, Keshani GG Pattiya Arachchillage, Patrick Piscitelli, Kenneth Marx, Valeri Barsegov, Juan Manuel Artes Vivancos. Charge transport in individual short single-stranded rna molecules, 2023
- [7] Ajoke Williams, Jose Mauricio Regalado Aguilar, Keshani G. Gunasinghe Pattiya Arachchillage, Srijith Rangan, Sonakshi Ghosal Gupta, Diego Goodrich, Emile Blestel, and Juan Artes Vivancos. Biosensors for public health and environmental monitoring: The case for sustainable biosensing, 2023. In Revision

SYMPOSIUM SB07

Translational Neuroelectronic Materials and Devices for Bioelectronic Medicine
November 27 - December 6, 2023

Symposium Organizers

Maria Asplund, Chalmers University of Technology
Alexandra Paterson, University of Kentucky
Achilleas Savva, Delft University of Technology
Georgios Spyropoulos, University of Ghent

Symposium Support

Bronze
Science Robotics | AAAS

* Invited Paper
+ JMR Distinguished Invited Speaker

SESSION SB07.01: Soft Bioelectronics
Session Chairs: Achilleas Savva and Georgios Spyropoulos
Monday Morning, November 27, 2023
Hynes, Level 1, Room 110

10:30 AM SB07.01.01**Soft Actuator-Assisted Minimally Invasive Peripheral Nerve Interfaces**ChaoqunDong, AlejandroCarnicer Lombarte and GeorgeG. Malliaras; University of Cambridge, United Kingdom

Peripheral nerve interfacing has emerged as a highly promising therapeutic technology in various applications, including prosthetic limbs, chronic pain modulation, and the treatment of visceral organ disorders. However, current electrode designs present challenges related to complex handling and implantation-associated irreversible neural damage. This abstract proposes an alternative approach by introducing novel actuatable electrodes that might address these limitations. Our research leverages recent advancements in thin film bioelectronics and soft robotics to develop thin, flexible, and importantly, shape-morphing nerve cuff electrodes. The microfabricated device allows for programming the shape of the electrodes, enabling it to enclose the nerve while maintaining the flexibility to loosen or tighten as needed. This feature ensures a close-fitting conformal interface between the electrode and the nerve, meanwhile enabling straightforward and minimally invasive device explanation steps. Our work presents a promising pathway towards the development of bioelectronic devices that can be manipulated by surgeons to enhance the minimally invasive nature of neurosurgery while achieving optimal electrode-nerve interactions.

10:45 AM SB07.01.02**Thermo-Responsive Conductive Gels for Injectable Bioelectronics**VidhikaS. Damani¹, XinranXie², KhushbooSuman¹, RachelDaso², GianaAlepa¹, JulianAlberto¹, CaseyLorch¹, Ai NinYang¹, YuhangWu¹, NormanWagner¹, JonathanRivnay² and LaureV. Kayser^{1,1}; ¹University of Delaware, United States; ²Northwestern University, United States

Conductive hydrogels have gained traction to interface biological systems with electronics for use in sensing and monitoring, tissue engineering, cell adhesion, and implantable electronics. Most bioelectronic implants depend on inorganic nanoparticles such as carbon nanotubes, metals and graphene for conductivity, but these materials lack mechanical compatibility with biological tissue causing scarring and short-term stability. Hydrogels based on water-dispersible conducting polymers such as PEDOT:PSS have been developed to overcome this challenge, due to their lower Young's modulus. However, these gels must either be pre-formed before inserting into the body or, if injected as a fluid, require the presence of external trigger methods and small molecules, such as chemical crosslinkers or endogenous metabolites for crosslinking *in vivo*. Therefore, there is a need for minimally invasive injectable conductive liquids which can gel rapidly in the body irrespective of the type of tissue, are biocompatible, and do not rely on externally applied triggers. To that end, we have developed a thermo-responsive conducting polymer which forms a stable dispersion in water and gels in 41 seconds at 37 °C. We employ the reversible hydrophilic-hydrophobic transition of poly(N-isopropylacrylamide) close to body temperature, which, when combined with the mixed ionic-electronic conduction of PEDOT:PSS yields a fully reversible and conductive gel with a modulus of 20 Pa. In addition, the mechanical and electronic properties can be tuned by changing the concentration of the dispersion in water. The material has shown biocompatibility with L929 cells both by indirect and direct contact assays. This is the world's first fully reversible conductive gel and has potential for use in cardiac patches, scaffolds for tissue engineering and wound healing and for better contact between electrodes and cells for biosensing.

11:00 AM SB07.01.03**Conductive Polymer Enabled Biostable Liquid Metal Electrodes for Neural Interface**HuananZhang; University of Utah, United States

Gallium (Ga)-based liquid metal materials have emerged as a promising material platform for soft bioelectronics. Unfortunately, Ga has limited biostability and electrochemical performance under physiological conditions, which can hinder the implementation of its use in bioelectronic devices. Here, an effective conductive polymer deposition strategy on the liquid metal surface to improve the biostability and electrochemical performance of Ga-based liquid metals for use under physiological conditions is demonstrated. The conductive polymer [poly(3,4-ethylene dioxythiophene):tetrafluoroborate]-modified liquid metal surface significantly outperforms the liquid metal-based electrode in mechanical, biological, and electrochemical studies. *In vivo* action potential recordings in behaving nonhuman primate and invertebrate models demonstrate the feasibility of using liquid metal electrodes for high-performance neural recording applications. This is the first demonstration of single-unit neural recording using Ga-based liquid metal bioelectronic devices to date. The results determine that the electrochemical deposition of conductive polymer over liquid metal can improve the material properties of liquid metal electrodes for use under physiological conditions and open numerous design opportunities for next-generation liquid metal-based neural electrodes

11:15 AM SB07.01.04**Identification of Mitral Valve Disease from Cardiac Potentials in Canine Patients with High-Density, E-Textile, Conducting Polymer BSPM Arrays**RubenRuiz-Mateos Serrano¹, SantiagoVelasco Bosom¹, AntonioDominguez-Alfaro^{2,1}, MatiasL. Picchio², DanieleMantione², DavidMecerreyes² and GeorgeG. Malliaras¹; ¹University of Cambridge, United Kingdom; ²University of the Basque Country UPV/EHU, Spain

Valvular heart diseases (VHD) are a major contributor to cardiovascular mortality worldwide, affecting ~75 million people every year. The detection of VHD is currently achieved by means of non-invasive mechanical activity imaging modalities such as magnetic resonance imaging (MRI), computed tomography (CT) or echocardiography. These techniques require expensive equipment and technical user expertise which hinder their employment in general practice clinics. As a consequence, VHD can be only diagnosed at larger medical centres where these machines and the personnel required to operate them are available. In addition, these imaging modalities cannot be employed for the long-term monitoring of acute conditions outside healthcare centres, which forces patients with these conditions to remain in hospital for long periods of time.

Electrocardiography (ECG) is a well-established and inexpensive method for the identification of electrical heart conditions, or rhythms, which is readily available in most local clinics. Despite the fact that ECG is designed to detect electrical activity, it has been shown to be able to capture some of the symptoms caused by VHD. Furthermore, the implementation of deep learning (DL) algorithms which analyse conventional 12-lead ECG data has recently demonstrated the ability of ECG to fully characterise and classify between different types of VHD.

Even though DL algorithms are able to identify VHD, the maximum accuracy they can achieve is limited to ~80%. Furthermore, these complex classifiers require vast amounts of fitting data, long training times and offer little clinical insights into what features of ECG are involved in the identification of VHD. One of the primary factors which restricts the performance of these classifiers is the limited amount of spatial data the 12-lead ECG offers. The sampling of multiple cardiac sites across the torso by means of high-density electrodes in the form of body surface potential maps (BSPM) offers the opportunity to train classical machine learning algorithms on temporal and spatial ECG features, thus increasing both the explainability and the maximum achievable accuracy of VHD classifiers.

In this work, a novel high-density electrode array fabrication technique on e-textiles with conducting polymer coatings is presented through the implementation of a tailored vest for canine models. The data obtained from this vest is presented and specific temporal and spatial features are employed to train a classical machine learning algorithm able to identify mitral valve disease in a canine patient cohort. The results from the classifier are presented in a human-readable format and performance and training metrics are compared and shown to surpass those of state-of-the-art models in the literature. The results hereby obtained pave the way towards the use of BSPM as an affordable and scalable screening technique for VHD.

SESSION SB07.02: Multifunctional Bioelectronics
Session Chairs: Achilleas Savva and Georgios Spyropoulos
Monday Afternoon, November 27, 2023
Hynes, Level 1, Room 110

1:30 PM *SB07.02.01**Multifunctional Fiber-Based Interfaces with Central and Peripheral Circuits**PolinaAnikeeva; Massachusetts Institute of Technology, United States

To probe the complexity of neuronal signaling between the central and peripheral nervous systems our group designs multifunctional, multimaterial fibers based on soft polymers, composites, and hydrogels. Previously limited to passive electrical, optical, and microfluidic features, these fibers have been augmented with active solid-state devices to record and deliver signals to organs as diverse as the brain and the gastrointestinal tract in freely-behaving rodents. Integration of solid-state components further enabled wireless operation of these fibers. In addition to probing electrophysiological activity, we have recently explored optical recording of neurochemistry using multifunctional fibers in conjunction with fluorescent activity indicators. Photometric recordings revealed the effects of drugs of abuse on neural circuits, and for the first time, permitted recording of signaling of non-neuronal tumor cells *in vivo*, empowering studies of tumor growth and informing brain-cancer therapies.

2:00 PM SB07.02.02

Bioelectronic fiber devices hold tremendous potential for both research and clinical applications due to their compactness, ease of implantation, and ability to incorporate advanced functionalities such as sensing/recording, stimulation/modulation, and imaging. However, existing devices are hindered by issues such as bulkiness, rigidity, limited functionality, and low density of active components. These limitations stem from the challenges associated with integrating multiple components on one-dimensional (1D) devices, as they are not compatible with conventional microfabrication methods like photolithography, primarily due to their thin, curved, and elongated structures. In this work, we present a fabrication approach called spiral transformation that overcomes these obstacles by converting 2D thin films containing pertinent microfabricated devices into 1D fibers. This approach allows for the creation of bioelectronic fibers that offer a high density (300 channels on a 250-micron fiber) and variety of components while enabling precise control over their longitudinal, angular, and radial positioning. We have successfully demonstrated the utility of these fibers for motility and serotonin sensing and tissue stimulation within the dynamic and soft gastrointestinal (GI) system. Notably, our soft fibers have shown minimal interference to GI tissue structure and natural movements. Taken together, the developed bioelectronic fibers showcase significant promise for next-generation clinical monitoring and modulation applications, particularly in minimally invasive deployments within the GI tract and other curved and confined regions of the body.

2:15 PM SB07.02.03

Multifunctional Microelectronic Fibers Enable Wireless Modulation of Gut-Brain Axis AtharvaSahasrabudhe¹, LauraRupprecht², SirmaOrguc¹, DiegoBohorquez² and PolinaAnikeeva¹; ¹Massachusetts Institute of Technology, United States; ²Duke University, United States

The peripheral organs of the body are in a constant bidirectional cross-talk with the brain, that generates a cognitive map of body's physiological state which is vital for survival. This is exemplified by the gut-brain communication; wherein hormonally and neurally mediated signals emerging from the abdominal viscera transduce metabolic information to the brain for maintaining energy homeostasis. Although these internally arising brain-to-body sensory cues are consciously imperceptible, recently they have been shown to influence higher level neurocognitive processes such as motivation and affect. These findings create opportunities for co-opting organ-to-brain neural circuits to develop new paradigms for autonomic neuromodulation therapies. However, probing and understanding critical brain-body circuits presents a neurotechnology challenge due to contrasting design criteria imposed on the implantable devices by drastic anatomical differences between the skull-encased brain tissue and mobile, delicate peripheral organs in behaving animal models. In this talk I will describe our efforts in addressing this challenge. Seeking inspiration from nerve fibers, we design a soft, flexible polymer fiber-based organ-brain neurotechnology. In order to match the inherent signaling complexity of the nervous system we envisaged probes that integrate multiple functionalities while still retaining a miniature device footprint to facilitate chronic bio-integration. To create such a multifunctional and multi-organ neurotechnology we combine the scalability and rapid customization of fiber drawing with functional sophistication of solid-state microdevices. With this approach we successfully produce hundreds of meters of flexible polymer filamentary probes integrating microscale light emitting devices, thermal sensors, microelectrodes, and microfluidic channels. The ability to process thermoplastic elastomers with the same route enables deterministic tunability of device mechanics and allows probes for targeting deep-brain structures and/or various regions of the murine intestine. We custom design a light-weight and modular wireless control circuit, NeuroStack, that offers bidirectional wireless control and real-time programmability of in-fiber microdevices along with an intuitive user interface. The brain fibers offer gene delivery for cell-type specific optogenetic neuromodulation, single-neuron recordings, thermometry, and tetherless control of mesolimbic reward pathway. The soft gut fibers grant access to anatomically challenging and delicate intestinal lumen, allowing intraluminal optofluidic control of sensory epithelial cells that guide feeding behaviors. Using this technology, we uncover that optogenetic stimulation of vagal afferents from the intestinal lumen is sufficient to drive reward behavior in untethered mice.

We anticipate that these illustrative applications will foreshadow widespread use of wireless multifunctional microelectronic fibers to study the roles of specific cells in bidirectional communication between the peripheral organs and the brain. This will not only empower the field of interoception, but also pave the way for mechanically guided improved autonomic neuromodulation therapies.

2:30 PM SB07.02.04

In Vivo Bioengineering of Conductive Microfibers: From In Vivo Biosynthesis to Advanced Characterization ClaudiaTortiglione¹, MarikaIencharelli¹, GiuseppinaTommasini², ValentinaDi Meo¹, GennaroSanità¹, AlessioCrescitelli¹, EmanuelaEsposito¹, Maria AntoniettaFerrara¹, GiuseppeCoppola¹, FrancescaDi Maria³, MattiaZangoli³, MariaMoros² and AngelaTino¹; ¹Istituto di Scienze Applicate e Sistemi Intelligenti, CNR, Italy; ²Instituto de Nanociencia y Materiales de Aragón (INMA), Spain; ³Istituto per la Sintesi Organica e Fotoreattività, CNR, Italy

The unmatched capability of living cells to fabricate complex structure starting from simple building blocks offers new paradigms to seamlessly integrate new electronic structures into the living matter, creating new hybrid devices. We have previously shown the capability of the living tissue-like organism, the freshwater polyp *Hydra vulgaris*, to produce fluorescent and conductive interface embedded into the animal tissues, starting from thiophene-based compounds, demonstrating the feasibility to use these organisms as biofactories of novel biocompatible and conformable bioelectronic interfaces [1-2]. Here we show that the potential of biofiber production is broadly valid in other biological systems, and showed that it can be promoted by different human and murine cell lines and by other invertebrate *in vivo* models (such as the sea anemone *Nematostella vectensis*). The cell type influences the fiber shape, amount and optical properties. In order to understand the mechanism underlying the fiber biogenesis, on one side we performed a systematic chemical engineering approach to identify the structure/groups involved in the spontaneous fiber assembling. On the other, we performed several physical and chemical treatments to identify the cell machinery components involved in the biosynthetic process. Finally, by mean of advanced characterization methods (ultrastructural, spectroscopical and imaging techniques) we shed light on the mechanism of biofiber production and the fine structure, paving the way to new bioengineering concepts to fabricate novel living conductive materials.

[1] G. Tommasini, G. Dufil, F. Fardella, X. Strakosas, E. Fergola, T. Abrahamsson, D. Bliman, R. Olsson, M. Berggren, A. Tino, E. Stavrinidou, C. Tortiglione, Seamless integration of bioelectronic interface in an animal model via *in vivo* polymerization of conjugated oligomers, *Bioactive Materials* 10 (2022) 107-116.

[2] M. Moros, F. Di Maria, P. Dardano, G. Tommasini, H. Castillo-Michel, A. Kovtun, M. Zangoli, M. Blasio, L. De Stefano, A. Tino, G. Barbarella, C. Tortiglione, In Vivo Bioengineering of Fluorescent Conductive Protein-Dye Microfibers, *iScience* 23(4) (2020) 101022.

2:45 PMBREAK

SESSION SB07.03: Bioelectronic Prototypes
Session Chairs: Maria Asplund and Alexandra Paterson
Monday Afternoon, November 27, 2023
Hynes, Level 1, Room 110

3:15 PM *SB07.03.01

Prototyping Neuroelectronic Device Concepts in Low-Cost Invertebrate Model Organisms EricD. Glowacki¹, PetraOndrackova¹, MaryJ. Donahue² and MalinSilvera Ejneby²; ¹Brno University of Technology, Czechia; ²Linköping University, Sweden

Next-generation bioelectronics hardware evolves through interdisciplinary collaborations between materials and device engineers and neuroscientists, with certain barriers existing between design/fabrication, *in vitro*, and finally *in vivo* testing. It is rare for research teams handling device development to have *in-house* capability for electrophysiology in animals. I will describe our recent work on using simple invertebrate models for *in vivo* testing of novel recording and stimulation hardware: namely leeches (*Hirudo medicinalis*) and locusts (*Locusta migratoria*). Several showcase examples will be discussed. The leech nerve cord provides a suitable testing platform for prototyping nerve cuff devices for recording and stimulation. Stimulation can be validated using highly reproducible muscle electrophysiology or force transduction measurements. The locust, with its segmented body and well-defined skeletal muscle, is a convenient model for testing neurostimulation techniques, including noninvasive electrical stimulation which can be validated by precise activation of limb movements. The overall goal of this work is to present a toolbox of low-cost and ethically favorable approaches to test new device concepts before they are deployed on mammals.

3:45 PM SB07.03.02

High-Density, Large-Scale Recording and Stimulating Neural Probes with Integrated ASIC YuhangMa, YingyingFan, WeinanWang, PavloZolotavin, HanlinZhu, TaiyunChi and ChongXie; Rice University, United States

Ultraflexible probes enable stable neural recording and stimulation by building a glial scar-free neuronal interface using biocompatible materials with small cross-sectional areas. However, these probes don't have an equivalent number of electrodes within the same invasive footprint as the rigid probes have. This limitation stems from photolithography, which is currently used for fabricating ultraflexible probes, is not capable of yielding a similar high electrode density. Here, to maximize the number of accessible neurons per implantation, we present the method of using electron-beam lithography (EBL) to pattern densely-packed electrodes on the polyimide encapsulations. We design and fabricate a 128-channel probe that presents the highest electrode density per cross-sectional area in flexible probes. The ability of oversampling can isolate highly clustered single units locally and across the brain regions, for example, the motor cortex and the hippocampus, for up to 3 months in freely behaving mice and 2 months in rats. Using 4 modules, more than 270 single units are recorded simultaneously with 1/3 of them decoded from the visual receptive field. We also propose an approach to design and fabricate a large-scale flexible EBL array with 5,376 simultaneously recording electrodes which equalize the total channel count of the state-of-the-art active probes. The first design will have 12 penetrating shanks, each of which has 448 recording electrodes at a density of 100 sites per millimeter of depth. To record, amplify and digitize all the channels simultaneously, we use gold ball bonding to connect with a customized application-specific integrated circuit (ASIC). This combination of large channel count flexible EBL-probe and ASIC will provide neuroscience studies in animal models with chronic, stable electrophysiology data at a large scale.

4:00 PM SB07.03.03

An Experimental Platform to Study Axonal Guidance and Function Katarina Vulić, Giulia Amos, Sean Weaver, Tobias Ruff and Janos Vörös; ETH Zurich, Switzerland

Studying neurons and axons *in vivo* poses a significant challenge due to the complex nature of the nervous system. The living environment makes it difficult to observe and manipulate individual axons effectively. In response to these limitations, researchers turn to *in vitro* models to gain insights into axon function and development from the bottom up. Our approach involves culturing neurons within polydimethylsiloxane (PDMS) microstructures on multielectrode arrays (MEAs) [1], [2], providing a controlled environment for studying axonal growth and activity. By utilizing these easily controllable and tunable systems, we aim to uncover the spatial limitations of axonal growth and determine the optimal spatial constraints for promoting healthy and robust axonal growth.

In this work, we study axonal growth dynamics using rat primary neurons cultured in custom-designed PDMS microfluidic devices containing nanochannels [3] of minimal size 100 nm. To generate the nanoscale features, a thin 350 nm layer of silicon dioxide (SiO₂) was deposited on a silicon wafer followed by a thin layer of photoresist that was then patterned using E-beam before the structures were etched in the SiO₂ using reactive ion etching. After stripping the remaining photoresist, the two subsequent layers were patterned in SU8 using conventional photolithography. The resulting microstructure design allows for separation of cell soma from axons and thus studying axons in detail. By varying the nano-/microchannel size, we show the spatial limitations for axonal growth and observe changes in axonal guidance depending on the channel width. We note that there is almost no penetration in the channels below 400 nm in width. Furthermore, we analyze the formation and structuring of axonal bundles, their dependence on cell density, and on the type of spatial constraint. We observe more frequent formation of bundles in cases where we topologically force the narrowing. The opposite is seen in the channels that are orders of magnitude larger than the average axon size, where they tend to spread along the available space. We also see that bundling is present in the nodes with lower cell density. We also see that axons grow the longest in the channels of 10-12 μm width range. Finally, we assess neuronal activity by culturing neurons in PDMS microstructures on MEAs. The temporal precision of action potentials recorded by MEAs in combination with spatial precision of axonal growth within the PDMS, enabled to analyze action potential fidelity, e.g. its velocity, shape and amplitude depending on the number of cells, the width of the formed axonal bundle and the age of an *in vitro* culture.

Looking forward, we aim to improve the system further by modifying substrate stiffness to make it more physiologically relevant, by adding hydrogels into the microstructures. The potential to expand our findings on human induced pluripotent stem cell (hiPSC) derived neurons and the diseased cells, offers yet another application. Additionally, a promising direction is the investigation of axon fasciculation [4] by alternating the angle at which axons approach one another with PDMS. With its wide range of capabilities, this highly tunable system holds promise for unlocking new insights and advancing our understanding of axon function and pathology.

References

- [1] J. Duru, J. et al, *Frontiers in Neuroscience*, 2022
- [2] S. J. Ihle et al, *Biosensors and Bioelectronics*, 2022
- [3] J. Mateus and S. Weaver et al, *ACS Nano*, 2022
- [4] M. A. Breau and A. Trembleau, *Semin Cell Dev Biol*, 2022

4:15 PM SB07.03.04

Laminin Adsorption and Adhesion of Neurons and Glial Cells on Carbon Implanted Titania Nanotube Scaffolds for Neural Implant Applications Jan Frenzel^{1,2}, Astrid Kupferer^{1,2} and Stefan G. Mayr^{1,2}; ¹Leibniz Institute of Surface Engineering, Germany; ²Universität Leipzig, Germany

As the world's population ages, the incidence of neurodegenerative disorders such as Parkinson's disease inevitably increases. Currently, brain-machine interfaces are used to study these diseases *ex vivo*, while neural electrodes are employed to treat them symptomatically *in vivo*. However, numerous obstacles arise at the interface between the brain and the brain-machine interface. Long-term adhesion is often weak, and rejection reactions such as glial scarring occur. We demonstrate that ion-implanted titania nanotube scaffolds are a promising candidate to overcome these problems, as they combine high biocompatibility with appropriate electrical conductivity.

In our systematic study, we show how implantation-induced tube shrinkage and altered electrical conductivity of titania nanotube scaffolds influence protein adsorption kinetics. Interestingly, laminin adsorption is affected by changes in surface free energy upon implantation. An increase in the pH-dependent ζ-potential of the surfaces leads to changes of the laminin binding. In addition, viability, toxicity and morphology of U87MG glial cells and differentiated SH-SY5Y neurons is analyzed after one and four days, respectively, and correlated with surface characteristics. Environmental electron microscope images reveal that cells on all scaffolds stretch out and expand even after one day. This first evidence of biocompatibility is confirmed by a high cell viability. Significant differences of cell viability are explained by changes of protein adsorption induced by ion implantation. Additionally, the increase in conductivity does not affect neuronal viability after four days but inhibits glial cell proliferation.

Based on these findings, there is great potential for novel neural electrode materials with tailored morphology and unique conductivity that suppress glial scar formation.

We gratefully acknowledge funding from the Saxon State Ministry for Higher Education, Research and the Arts, project MUDIplex, grant number 100331694.

- [1] Frenzel, Jan, et al. "Laminin Adsorption and Adhesion of Neurons and Glial Cells on Carbon Implanted Titania Nanotube Scaffolds for Neural Implant Applications." *Nanomaterials* 12.21 (2022): 3858.

4:30 PM SB07.03.05

Monolithic Silicon Devices for Multisite, Multiscale and Translational Photostimulation Pengju Li and Bozhi Tian; University of Chicago, United States

Electrode-based electrical stimulation is foundational for numerous clinical bioelectronic devices, including deep brain stimulators and cardiac pacemakers. However, achieving multisite or random access stimulation, vital for high-fidelity and efficient biological regulation, remains challenging even in high-density electrode arrays due to spatial access constraints. While optogenetics offers high-spatiotemporal multisite stimulation capabilities, its clinical adoption presents hurdles. In this work, we introduce a multisite photostimulation technique for cardiac systems via a non-genetic platform utilizing semiconductor-based biomodulation interfaces. We investigate the precision, accuracy, and resolution of the photostimulation by analyzing spatiotemporal photoelectrochemical currents in four leadless silicon-based monolithic photoelectrochemical devices. Our study validates the multisite stimulation capacity of these systems through optical overdrive pacing applied to cultured cardiomyocytes targeting multiple regions and length scales, isolated rat hearts in a Langendorff setup, and *in vivo* rat heart ischemia models. To demonstrate cardiac control under clinical conditions, we also perform the first optical pacing of a pig heart *in vivo*. To further solidify the clinical potentials, we fabricated minimally invasive device delivery and fiberoptics platform and successfully performed pig heart stimulation without opening the chest. Our findings underscore the potential of this leadless, lightweight photostimulation platform, possibly revolutionizing cardiac pacemaking in treatments like cardiac resynchronization therapy where lead-placement complications often arise.

4:45 PM SB07.03.06

Organic Semiconducting Nanoparticles for Neural Interfacing: Integrating Mechanical, Chemical and Optoelectronic Stimuli for Wireless Neuromodulation Rafael Crovador^{1,2}, Jessie Posar^{3,4}, Paul Dastoor², Alan Brichta¹, Rebecca Lim¹ and Matthew Griffith^{5,3}; ¹University of Newcastle, Australia; ²The University of Newcastle, Australia; ³The University of Sydney, Australia; ⁴University of Wollongong, Australia; ⁵University of South Australia, Australia

Electronic devices capable of stimulating neurons have revolutionized the treatment of several neurological conditions by providing a direct interface with the nervous system. These devices hold great potential for treating disorders such as Parkinson's disease, epilepsy, spinal cord injuries, and even blindness.^[1] However, the use of traditional electronic materials such as metals and silicon in such devices have significant limitations due to poor biocompatibility,^[2] mechanical mismatch with tissue, low spatial selectivity, and the requirement for external power supplies. Soft and flexible organic semiconducting materials represent a new frontier in electronic materials that are capable of overcoming these challenges.^[3] The solution processability of organic semiconductors also enable several additional attractive features, including low-cost manufacturing of devices on flexible substrates using industrial scale printing techniques, addition of neurotransmitter molecules to the electroactive solutions to chemically assist neuromodulation, adjustable surface topography to induce mechanical cues for neuron attachment and growth, and optically triggered charge generation for wireless electrical neuromodulation.

In this study, we present our recent endeavours to tackle these challenges of mechanical, chemical and electronic stimulation of neuronal cells simultaneously in a single bioelectrode. We achieve this by forming soft carbon-based organic conductors into aqueous nanoparticle dispersions using established solution-based mini-emulsion chemistry methods.^[4] We subsequently integrate the organic nanoparticle dispersions with neurotrophic factors prior to the device fabrication process. These pharmaceutical components subsequently enhance cell adhesion and neural network outgrowth upon release from solid films cast from the electroactive nanoparticle dispersions.

Bioelectronic nanoparticle-based devices were fabricated from n-type material *Poly(9,9-dioctylfluorene-alt-bithiophene)* (F8T2), which were shown to exhibit high biocompatibility with primary neuron cultures from mice via anatomical (live-dead assay) and functional (neuronal cell stain) protocols. Kelvin Probe Force Microscopy measurements demonstrated the creation of photo-capacitive charge under direct light stimulus, potentially capable of depolarising the neuronal cell membrane and generating action potentials (*wireless electronic neuromodulation*). By adjusting the surface roughness of devices by tailoring the nanoparticle size during synthesis, we verified by AFM analysis an optimal nano-topography that promotes neuronal cell growth (*mechanical neuromodulation*). Finally, by extensive neuronal morphology analysis we demonstrated the direct effect of sustained and locally delivered neurotrophic factors (*chemical neuromodulation*) on cell survival and neuronal outgrowth through neurite elongation.

References:

- [1] Lewis, P.M., Ayton, L.N., Guymer, R.H., Lowery, A.J., Blamey, P.J., Allen, P.J., Luu, C.D. and Rosenfeld, J.V. (2016), Advances in implantable bionic devices for blindness: a review. *ANZ Journal of Surgery*, 86: 654-659. <https://doi.org/10.1111/ans.13616>
- [2] T. Someya, Z. Bao, G. G. Malliaras, *Nature*, **2016**, *540*, 379.
- [3] Fahlman, M., Fabiano, S., Gueskine, V. *et al.* Interfaces in organic electronics. *Nat Rev Mater* **4**, 627– 650 (2019). <https://doi.org/10.1038/s41578-019-0127-y>
- [4] *Phys.Chem.Chem.Phys.*, 2019, 21, 5705

SESSION SB07.04: Bioelectronic Medicines
Session Chairs: Maria Asplund and Achilles Savva
Tuesday Morning, November 28, 2023
Hynes, Level 1, Room 110

9:00 AM *SB07.04.01

Transient Bioelectronic Medicines John A. Rogers; Northwestern University, United States

Advanced electronic/optoelectronic technologies designed to allow stable, intimate integration with living organisms will accelerate progress in biomedical research; they will also serve as the foundations for new approaches in monitoring and treating diseases. Specifically, capabilities for injecting miniaturized electronic systems and other components into soft tissues or for softly laminating them onto the surfaces of vital organs will open up unique and important opportunities in tracking and manipulating biological processes. This presentation describes the core concepts in materials science, circuit design and manufacturing that underpin these types of technologies, with a focus on bioresorbable, or 'transient', devices designed to disappear into the body on timescales matched to natural processes. Examples include bioelectronic 'medicines' for neuroregeneration, pain mitigation and temporary cardiac pacing.

9:30 AM SB07.04.02

E-Sutures: Electrical and Ionic Conductive Sutures for Medicine and Bioelectronics Onni Rauhalu, Jennifer Gelinas and Dion Khodagholy; Columbia University, United States

Metals have long served as the foundational electrode and wiring materials for implantable bioelectronics due to their high conductivity and processability to achieve the small size necessary for *in vivo* electrophysiological signal acquisition and stimulation. However, metal-based wires are susceptible to mechanical damage due to material rigidity, and in bulky, high-density systems, they may contribute to patient discomfort. The ideal bioelectronic wire is thus soft, highly conductive, mechanically and chemically resilient and biocompatible. Most importantly, such a wire should also leverage modern polymer chemistry to enable multi-modal interventions, namely mixed-conductors that facilitate delivery of positive and negative charges. In this work, we use PEDOT:PSS to turn silk sutures into flexible, mixed-conducting and biocompatible wires (e-sutures) that can be used for suturing, acquiring electrophysiological signals, delivering electrical stimulation and finally, delivering drug molecules as ion pump channels.

We fabricate e-sutures by coating silk sutures with PEDOT:PSS to produce a mixed conducting suture and then create an insulation layer (jacket) on the fiber using subsequent coatings of PDMS and parylene-C to preserve the conductive properties in an ionic environment. We demonstrate the high conductivity and stability of e-sutures as well as their ability to form robust mechanical connections with metallic circuit components to facilitate integration to a complete bioelectronic device. Further, the conductive nature of e-sutures *in vivo* is demonstrated by recording electrocardiogram (ECG) from mouse pups, elicitation and recording of intramuscular electromyogram (EMG) in rats as well as local field potential (LFP) from the surface of a rat brain using e-sutures as electrodes. Finally, we demonstrate that e-sutures can serve as an ion pump channel and deliver positively charged molecules from a hydration reservoir to the target tissue without generating volumetric pressure in the delivery target. In summary, the work highlights the capability of PEDOT:PSS coated silk fibers to serve as a soft, biocompatible alternative to metallic wires and electrodes in a research and clinical setting while providing the additional capability of drug-delivery through ion pumping.

9:45 AM SB07.04.03

Implantable Iontophoretic Devices for Cancer Therapy Xudong Tao, Tobias Naegele and George G. Malliaras; University of Cambridge, United Kingdom

Chemotherapy has a fundamental limitation for the treatment of brain tumours – poor penetration through the blood-brain barrier, leading to sub-therapeutic concentrations in brain tumours. This study focuses on an implantable electrophoretic drug delivery device (left behind in the tumour after biopsy), which uses an electric field to improve drug transport. The technology is called iontophoresis – a 'dry' delivery that only delivers the charged drug ions into the tumour region by electric fields and avoids pressure-related problems. This study explores a novel iontophoretic device which significantly improves the efficiency of drug delivery.

10:00 AM BREAK

SESSION SB07.05: Neural Interfaces I
Session Chairs: Maria Asplund and Georgios Spyropoulos
Tuesday Morning, November 28, 2023
Hynes, Level 1, Room 110

10:30 AM *SB07.05.01

Translational Neuroelectronics Dion Khodagholy; Columbia University, United States

Our understanding of the brain's pathophysiology relies on discoveries in neuroscience and neurology fueled by sophisticated bioelectronics enabling visualization and manipulation of neural circuits at multiple spatial and temporal resolutions. In parallel, to facilitate clinical translation of advanced materials, devices, and technologies, all components of bioelectronic devices have to be considered. Organic electronics offer a unique approach to device design, due to their mixed ionic/electronic conduction, mechanical flexibility, enhanced biocompatibility, and capability for drug delivery. We design, develop, and characterize conformable, stretchable organic electronic devices based on conducting polymer-based electrodes, particulate electronic composites, high-performance transistors, conformable integrated circuits, and ion-based data communication.

These devices established new experimental paradigms that allowed monitoring of the emergence of neural circuits during development in rodents and elucidated patterns of neural network maturation in the developing brain. Furthermore, the biocompatibility of the devices also allowed intra-operative recording from patients undergoing epilepsy and deep brain stimulation surgeries, highlighting the translational capacity of this class of neural interface devices.

In parallel, we are developing the fully-implantable, conformable implantable integrated circuits based on high-speed internal ionic gated organic electrochemical transistors that can perform the entire chain of signal acquisition, processing, and transmission without the need of hard Si-based devices. This multidisciplinary approach will enable the development of new devices

based on organic electronics, with broad applicability to the understanding of physiologic and pathologic network activity, control of brain-machine interfaces, and therapeutic closed-loop devices.

11:00 AM *SB07.05.02

Graphene-Based Active Neural Sensors for Brain Monitoring and Mapping Eduard Masvidal-Codina¹, Ramon Garcia-Cortadella^{1,2}, Xavi Illa³, Rob Wykes⁴, Anton Sirota², Anton Guimerà-Brunet³ and Jose A. Garrido^{1,5}; ¹Catalan Institute of Nanoscience and Nanotechnology, (ICN2), CSIC and BIST, Spain; ²Bernstein Center for Computational Neuroscience Munich (SyNergy), LMU, Germany; ³Instituto de Microelectrónica de Barcelona IMB-CNM (CSIC), Esfera UAB, Spain; ⁴Institute of Neurology, UCL, Queen Square, United Kingdom; ⁵ICREA, Spain

Large effort is being dedicated to the integration of novel materials into neural interface devices that offer certain advantages in terms of recording and/or stimulation of neural activity. In the particular case of the recording capabilities, they need to be such to allow the detection of brain activity over large areas and with a high spatial resolution. Because its two-dimensional nature, graphene exhibits a rather unique combination of physicochemical properties which make it attractive for the development of active sensors for neural technologies.

This contribution will focus on the recording capabilities of active sensor technology based on single-layer graphene, highlighting its potential for the development of the next-generation neural prostheses and brain-computer interfaces. Recently, solution-gated field-effect transistors (SGFET) based on graphene are being explored with increasing interest as novel transducers for neural signals. The electrochemical stability of graphene and its facile integration with flexible substrates were among the initial triggers that attracted the interest of the community to develop flexible neural probes for brain interfacing. In addition, other properties such as the high carrier mobility and the field effect associated to single-layer graphene allows for the implementation of an active sensor configuration that will be shown in this contribution to offer significant advantages with respect to the classical passive metallic electrodes. Further, this presentation will discuss how SGFET-type sensors allow us the implementation of multiplexing strategies, time-domain and frequency-domain multiplexing, that reduce the footprint of connectivity, permitting an aggressive scaling up in the number of recording sites. Very interestingly, we will demonstrate that SGFETs also have a distinctive capability to expand the temporal resolution of classical electrocorticography technologies, allowing the recording of the relatively unexplored infra-slow brain activity and, thus, potentially enabling the study of novel biomarkers for monitoring neurological disorders.

This work has received funding from the European Union's Horizon 2020 research and innovation programme under grant agreement N. 881603 (GrapheneCore3)

11:30 AM SB07.05.03

Spatially Controlled Microcortical Stimulation using High-Density PEDOT:PSS Surface Electrodes Ilke Uguz and Kenneth L. Shepard; Columbia University, United States

Most neuromodulation approaches rely on extracellular electrical stimulation with penetrating electrodes at the cost of cortical damage. Surface electrodes, in contrast, are much less invasive but are challenged by the lack of proximity to axonal processes leading to poor resolution. Here, we demonstrate that high density (40 μm pitch), high capacitance (> 1 nF), single neuronal resolution PEDOT:PSS electrodes can be programmed to shape the charge injection front selectively at depths approaching 300 μm with a lateral resolution better than 100 μm . These electrodes, patterned on thin film parylene substrate, can be subdurally implanted and adhere to the pial surface in chronic settings. By leveraging surface arrays that are optically transparent with PEDOT:PSS local interconnects and integrated with depth electrodes, we are able to combine surface stimulation and recording with calcium imaging and depth recording to demonstrate these spatial limits of bidirectional communication with pyramidal neurons in mouse visual cortex both laterally and at depth from the surface.

11:45 AM SB07.05.04

Foldable Three Dimensional Neural Electrode Arrays for Simultaneous Brain Interfacing of Cortical Surface and Intracortical Multilayers Ju Young Lee, Young Uk Cho and Ki Jun Yu; Yonsei University, Korea (the Republic of)

The brain is a complex three-dimensional network composed of billions of interconnected neurons that respond to important activities such as cognitive function, memory, or even communication by transmitting neural signals. The development of neural interfaces that can precisely measure the complex activities of neurons are helping to understand for identifying unpredicted neuronal diseases and brain functions. Therefore, to understand the functionality of the brain via these diverse activities, it is essential to measure the brain activity with three-dimensional structure.

Current diagnostic methods for brain disorders involve functional magnetic resonance imaging (fMRI) that detect the changes of related cerebral blood flow and positron emission tomography (PET) that detect emits positrons distribution in the body through receptor or metabolic imaging. These imaging techniques can capture the changes in brain signals in three-dimensions by combining continuous two-dimensional sectional imaging frames. However, despite their excellent spatial resolution, these methods suffer from poor temporal resolution because of the limitations of captured series of two-dimensional frames. To overcome these time-resolution limitation, for the proper neuropathological analysis, electrophysiological approach serves as a major strength as it provides an excellent temporal readout resolution compared to upper imaging method.

The electrophysiological approach to the measuring the neural propagation is broadly classified into three methods, 1) Electroencephalography (EEG), 2) Michigan probe, 3) Utah array. However, these traditional methods have limitation of two-dimensional measurements. First, EEG arrays for brain surface recording provide high-resolution signals over a large area but cannot map the intracortical area. In contrast, Michigan probe and Utah arrays for intracortical or deep brain recording do not provide clues about the propagation of expressed signals from inside the brain to the surface. Several attempts have been made to measure neural signals in three-dimensional form to overcome this limitation, but these efforts have encountered challenges due to the separate devices for simultaneous measurement of surface and intracortical area that leading to recording mismatch, or due to the use of rigid shanks for device implantation that leading to immune response with mechanical mismatches between the brain recording surface and the device.

Here, we introduce the foldable, flexible three-dimensional neural mapping electrode that achieved by extending the three-dimensional structure of the neural interface in way to accurately analyse complex neural signalling. The device establishes a single integrated platform with four flexible penetrating shanks and surface electrodes by combining advantages of the EEG arrays and neural probe with Utah array shape for multisite recording. This system can simultaneously measure both surface signals of the brain and neural activity occurring in the intracortical area. To provide sufficient insertion of the device, the penetrating shanks were coated with a biocompatible/bioresorbable stiffener. To demonstrate the performance of the device, inserting the device into the somatosensory cortex of mice and stimulating whisker of the mice. The device can measure both the local field potential (LFP) and single neuron spike in simultaneously from the surface and intracortical area of the brain. Consequently, this platform will pave the way for neuroscience studies and biomedical practices by providing unprecedented electrophysiological signals in three-dimensional form.

SESSION SB07.06: Minimally Invasive Neuroengineering
Session Chairs: Achilleas Savva and Georgios Spyropoulos
Tuesday Afternoon, November 28, 2023
Hynes, Level 1, Room 110

1:30 PM *SB07.06.01

Ultrasound Microsystems for Minimally-Invasive Neuromodulation via Low-Intensity Focused Ultrasound Tiago Costa; Delft University of Technology, Netherlands

Minimally-invasive neuromodulation using low-intensity focused ultrasound (LIFU) holds great promise for treating various neurological disorders. It has been demonstrated to modulate neural activity, promoting both excitatory and inhibitory effects. This capability allows for restoring aberrant neural circuitry or suppressing hyperactive regions, thereby alleviating symptoms associated with conditions such as Parkinson's disease, epilepsy, chronic pain, and depression.

One of the key advantages of LIFU neuromodulation is its combination of high spatial resolution, minimal invasiveness, and extensive coverage of the nervous system. Unlike traditional electrical, magnetic, or optical neuromodulation techniques, which can achieve high-spatial resolution at the expense of high invasiveness and reduced brain coverage, ultrasound waves benefit from low wavelengths, scattering, and absorption in brain tissue and hence, can be focused virtually anywhere in the brain, with high-spatial-resolution and without requiring brain surgery. This reduces the risk of infection, tissue damage, and other complications associated with invasive procedures, making it a safer option for patients, and also allows for accessing a broader range of neural circuits with high precision.

Despite the abovementioned promise, there is still a knowledge and technological gap in LIFU neuromodulation to maximize its potential. LIFU neuromodulation is achieved by means of an ultrasound transducer. These transducers generate low-intensity focused ultrasound waves that can penetrate deep into tissues while maintaining spatial specificity. By adjusting the parameters of the ultrasound waves, specific regions of the brain or peripheral nerves can be targeted with precision. However, similar to their use in medical diagnostic imaging, conventional ultrasound transducers used in LIFU neuromodulation have hand-held form factors and require off-the-shelf equipment. These bulky setups lead to two severe limitations: in pre-clinical research, the mismatch of size between bulky transducers and in-vitro/in vivo models (mice, rats) impose severe limitations in understanding the effects of ultrasound on the nervous system and how to better apply LIFU neuromodulation for different disease models; secondly, in clinical applications, the use of LIFU neuromodulation can only be applied in a bed-side scenario, where the patient either would visit the clinic once or twice per week to receive a treatment or would operate a LIFU neuromodulation system at home.

This talk will describe the recent research in the field of ultrasound microsystems towards developing the next generation of LIFU neuromodulation systems that can be seamlessly integrated into *in vitro/in vivo* experimental setups in pre-clinical settings and used as wearable and minimally-invasive devices for clinical treatments. This description will answer two questions: how to massively integrate all the necessary LIFU neuromodulation functionality into a single-miniaturized and battery-powered microsystem? How can ultrasound microsystems be designed to be mechanically flexible to better adjust to the body's natural curvature?

To answer these questions, the talk will focus on novel ultrasound microfabrication and microsystem integration methods and next-generation ultrasound electronics. Furthermore, the talk will also show a few examples of ongoing projects featuring *in vitro* and *in vivo* validation, showcasing the potential of LIFU microsystems for minimally invasive and precise neuromodulation for treating neurological diseases.

2:00 PM *SB07.06.02

Learning in Spiking Neural Networks with a Calcium-Based Hebbian Learning Rule Willian Soares Girão and Elisabetta Chicca; University of Groningen, Netherlands

The effectiveness of neural interfaces depends on the ability of electronic systems to speak the same language of the biological counterpart. Furthermore, the mechanisms underlying learning in biological systems should be better understood to harness the adaptability of the brain when interfacing it to artificial systems. In particular, understanding how biological neural networks are shaped via local plasticity mechanisms can lead to energy-efficient and self-adaptive brain-like information processing systems which can enhance neural interfaces with unprecedented adaptability.

In this work, we present a Hebbian local learning rule, the Bistable Calcium-based Local Learning (BCaLL) rule, that models synaptic modification as a function of pre- and post-synaptic calcium traces tracking neuronal activity, based on a large body of work that has established the role of calcium transients in modulating plasticity. The calcium trace variable, modeled via a first-order differential equation, integrates neuronal activity over time such that both the time since the last spike and mean firing rate information can be encoded in this trace. The learning rule we propose reads out the calcium traces from the neurons it connects and computes whether its weight should be increased or decreased. We show that BCaLL is able to reproduce both spike-time dependent plasticity (STDP) and spike rate plasticity outcomes. With it, we are able to demonstrate that temporal correlations added at the spike-pair level can modulate the learning rate in spiking neural networks, without modifying the rule's parameters or the mean rate activity of neurons in the network.

We showcase this property by simulating and comparing recurrent Spiking Neural Networks (SNNs) with and without excitatory neurons' subthreshold membrane oscillations. We demonstrate that in the networks where the neurons oscillate, the learning rate of attractors is increased due to an increase in their synchronicity. This is particularly interesting for simulating and studying learning in models of brain structures like the Inferior Olivary Nucleus, where previous work has shown that the lack of electronic coupling, which plays an important role in synchronizing the activity of neurons within the nucleus, leads to impaired learning of motor tasks. This modulated learning rate via synchronization we show can provide a starting point in understanding such learning dynamics.

By applying BCaLL to feedforward SNNs, we describe the mechanisms necessary to train such networks for classification problems and how these mechanisms resolve the coding-level problem that arises from learning with binary synapses. Thanks to our simulations, we find that allowing the networks' transient activity during the switching of input patterns to interact increases classification performance, contrary to what previous work has reported, by reducing overlaps in the learned class representations. This could be a benefit of tracking spiking activity via traces: while some models might rely on the neuron's membrane voltage to compute weight updates, utilizing traces allows us to decouple from the membrane dynamics the extent to which correlated activity in time can be measured.

Elucidating how computation in such systems can benefit from encoding information in traces is not only important for better modeling the complex biochemical machinery existing in biological neural networks but also for the design of analog application-specific integrated circuits (ASIC) implementing these algorithms. This integration step is crucial for the embedding of such algorithm into neural interfaces.

2:30 PM SB07.06.03

Origami-Inspired Smart Implants for New-Age Neurology Prasanth Velvaluri¹, Huan Liu², Lars Thormählen¹, Hanna Lewitz¹, Olav Jansen³, Richard D. James², Dirk Meyners¹, Nian Sun⁴ and Eckhard Quandt¹; ¹Kiel University, Germany; ²University of Minnesota, United States; ³University Hospital Schleswig-Holstein, Germany; ⁴Northeastern University, Germany

Intracranial aneurysms are balloon-like disfigurements along the brain blood vessels. If not treated such aneurysms can rupture and cause brain hemorrhage. Many different implants are available in the market for intracranial aneurysm treatment. Though the available implants fabricated from wire braiding and laser cutting are successful, specific gaps must be filled to allow for low treatment complications. One such gap is that all the available implants have simple geometries and do not allow any personalization. Such individualization of implants is essential to provide safer treatments to patients with complex aneurysms. Second, all available implants have passive operation and currently, there are no "smart aneurysm implants" that could potentially monitor the treatment over time. Such a smart implant could detect if the intended blood flow reduction is not achieved after its placement and could potentially alert to early intervention. Smart implants require integrated antennas for data and energy transfer as well as sensors for the measurement of blood flow.

Magnetolectric (ME) antennas consisting of magnetostrictive and piezoelectric layers have shown that they can be scaled down by orders of magnitude in size compared to conventional electromagnetic antennas [1]. This is because the ME antennas operate at their acoustic resonance rather than at their electromagnetic resonance. Such compact miniaturized ME antennas on the implant surface provide an optimal way to transmit the data wirelessly for a smart implant operation. However, there are certain difficulties to integrating such antennas into conventional implants as their fabrication technology of wire braiding and laser cutting does not allow monolithic integration of ME composites. Second, the conventional implant design does not allow such sensitive components to survive the harsh crimping process, which is pre-requirement for a minimally invasive treatment.

On the other hand, the origami-based design approach provides an attractive alternative for implant design. It consists of a 2D pattern with regions of rigid panels and flexible hinges. The folding pattern for origami can be generated from a flat 2D sheet and converted into a complex 3D shape on folding. Such structures have great potential as medical implants as they provide two major advantages (1) they allow the folding of large implants into a compact area to be loaded into a catheter and (2) certain regions in the origami pattern are almost stress-free during folding, making them ideal sites for loading sensitive elements such as sensors and antennas. The main challenge lies in fabricating these microscale devices without compromising the quality and performance.

Recent developments in microsystem technology offer a method to fabricate freestanding nitinol (NiTi) shape memory thin films. The fabricated implants are flexible, biocompatible, and have high design freedom, e.g., allowing films with multiple thicknesses [2]. Thus, providing a solution for origami-based implant fabrication. The wafer-based approach allows the monolithic integration of functional layers for biosensing and smart implant functioning. Thus, allowing for the incorporation of ME antennas on the NiTi implant surface.

The current work focuses on fabricating an ME antenna on top of a NiTi substrate using microsystem technologies, as a first step in realizing origami-based smart implants. In this work, we discuss the various challenges and possible solutions for integrating an ME antenna on top of a NiTi substrate. Furthermore, we consider the choice of magnetostrictive and piezoelectric materials that are essential for the required antenna operation at a frequency that is permissible for human use. We intend to demonstrate the potential of an origami-based design approach for fabricating brain implants.

[1] Nan, T. *et al. Nat. Commun.* 8, 1–7 (2017).

[2] Velvaluri, P. *et al. Sci. Rep.* 11, 1–10 (2021).

2:45 PM SB07.06.04

Atomic Layer Infiltration for the Enhanced Longevity of Thin-Film Polymer Implant Encapsulation Martin Niemiec and Kyungjin Kim; University of Connecticut, United States

Bioelectronic interface technology has advanced significantly since its inception, as implantable devices develop smaller form factors and better integration with the human body. Advanced implants have thousands of channels interfacing with hundreds of neurons, and often feature wireless transmission of power and data enabled by miniaturized active electronic components and multiplexing techniques. However, while the technical capabilities of implantable bioelectronics continue to increase at an astounding rate, their ability to remain functional after long periods of implanted time has not seen significant improvement, especially in the field of flexible polymer-based thin film devices. Due to their inherently poor barrier properties, polymer implants require additional hermetic encapsulation to become viable therapeutic instruments for several decades of constant use. In this regard, metal oxide, nitride, and carbide materials deposited by atomic layer deposition (ALD) represent some of the best-performing barrier materials in terms of low permeability to water and ionic species, yet they are mechanically incompatible with flexible electronic substrates: bending and stretching of the flexible substrate invariably results in cracking or delamination of the rigid barrier coating, reducing its protective capability to near zero. Here, we explore a method of increasing the mechanical compatibility of inorganic barrier coatings with flexible substrates by means of a modified ALD technique alternately known as atomic layer infiltration (ALI), vapor phase infiltration (VPI), or sequential infiltration synthesis (SIS), which results in a gradual transition between the mechanical properties of the substrate and coating, reducing the susceptibility of the interface to such catastrophic failure modes. During ALI, precursors are allowed to remain in the reaction chamber for longer times at higher pressures than ALD. This allows precursors to diffuse into the substrate and reaction products to form at depth, resulting in a gradient from pure substrate to pure coating material. This technique has been used to create flexible, nearly impermeable coatings for organic electronics applications, but to our knowledge has not been demonstrated in implantable bioelectronics. We demonstrate water vapor barrier performance of the ALI encapsulation strategy on the order of 10^{-4} g/m²/day, as well as high mechanical compliance (*i.e.*, critical bending radius below 500 μm without delamination). In addition, we fabricate test devices featuring interdigitated electrodes on flexible substrates and encapsulate them via 3-dimensional ALI using a custom stand within a domed reaction chamber, then study the effects of ALI encapsulation on device lifespan in physiological conditions by means of accelerated aging tests in phosphate buffered saline (PBS). We investigate the accelerated aging results of current bioelectronic implant encapsulation strategies and compare them with our own results. Our uncoated polyimide devices failed after 80–100 days at 37°C, while coated devices have exceeded 230 days of 37°C-equivalent aging and continue to remain below failure thresholds. Optimization of the encapsulation via material selection (*e.g.*, polyimide vs. parylene substrates, Al₂O₃ vs. TiO₂ ALI) and multilayered structure is explored. In-depth failure mode analysis of the tested thin film devices is performed,

analyzing cracking, delamination, moisture permeation, and connector failures using optical and scanning electron microscopy and permeation analyzer; critical failures modes upon specific loading are discussed.

3:00 PMBREAK

SESSION SB07.07: Neural Interfaces II
Session Chairs: Maria Asplund and Georgios Spyropoulos
Tuesday Afternoon, November 28, 2023
Hynes, Level 1, Room 110

3:30 PM *SB07.07.01

A Subdural Bioelectronic Implant to Obtain Recordings of Spinal Cord Activity and to Deliver Electroceutical Therapy Following Spinal Cord Injury in Rats Darren Svirskis¹, Bruce Harland¹, Brad Raos¹, Brittany Hazelgrove¹, Simon O'Carroll¹, Lukas Matter² and Maria Asplund²; ¹University of Auckland, New Zealand; ²Chalmers, Sweden

Bioelectronic devices have found use at the interface with neural tissue to investigate and treat nervous system disorders. We have developed and characterized a very thin flexible polyimide-based bioelectronic implant that is inserted along the thoracic spinal cord in rats directly in contact with the dorsal surface of the spinal cord. This has no negative impact on hind-limb functionality nor any change in the volume or shape of the spinal cord. We routinely maintain the bioelectronic implant in rats for a period of 3 months. We have obtained the first subdural recordings of spinal cord activity in freely moving animals. Recordings contain action potentials from fibre tracks in the cord. Following spike extraction propagation velocities were analyzed. Propagation was predominately in the afferent direction, with a smaller proportion of spikes propagating in the efferent direction. A clinically relevant spinal contusion injury can be achieved with the implant in place. The bioelectronic implant contains stimulating electrodes with relatively larger areas than the recording electrodes that are capable of delivering precise, strong electric field therapies (electroceuticals) directly to the injured spinal cord tissue. The effects of these therapies are currently being investigated, early data is demonstrating a different recovery profile compared to control animals who do not receive the treatment. Over the course of the 12-week experiment, the animals receiving electroceutical therapy show improved hind limb function determined in open field assessment and an enhanced recovery of touch sensitivity as determined by the Von Frey test. This device has great potential to monitor electrical signaling in the spinal cord after an injury, and in the future, this implant will facilitate the identification of biomarkers in spinal cord injury and recovery. We are exploring further development of this implant to deliver localized treatments to the spinal cord towards regeneration of damaged tissues to recover lost function. Localized therapies are being developed not only in the form of electroceutical treatment through precise electrical field stimulation, but also through the local and sustained delivery of neurotrophic factors.

4:00 PM SB07.07.02

Soft and Stretchable Neural Electrodes Based on Gold Nanowire Composites Laura Seufert, Mohammed Elmahmoudy, Mary J. Donahue, Yuyang Li, Samuel Lienemann, Simon Farnébo and Klas Tybrandt; Linköping University, Sweden

Two-way communication between electronics and neural tissue is key for advancing diagnosis and therapies for neurological diseases and disorders. Establishing such neural interfaces is a major challenge, as the tissue response to implants can have a detrimental effect on the signal quality and functionality of the implant. Matching of the mechanical properties of the electronic implant to the soft interfaced tissue can reduce the tissue response and improve the long-term performance of the device. This requires soft and stretchable conductors, which typically are composed of elastomer/hydrogels and conductive fillers. However, the tough materials requirements on biomedical implants, including material chemistry, mechanical and electromechanical properties, and long-term stability, disqualifies most of the developed stretchable electronic materials for such applications. Here I will present our efforts in developing inert soft neural electrodes based on stretchable gold nanowire composites, covering aspects ranging from synthesis and processing to devices and applications.
www.liu.se/en/research/soft-electronics

4:15 PM SB07.07.03

Ultraconformable Cuff Implants for Long-Term Bidirectional Interfacing of Peripheral Nerves at Sub-Nerve Resolutions Alejandro Carnicer Lombarte, Alexander J. Boys, Amparo Guemes, Johannes Gurke, Santiago Velasco Bosom, Sam Hilton, Damiano Barone and George G. Malliaras; University of Cambridge, United Kingdom

The peripheral nervous system is crucial for the communication between the brain and the rest of the body. Implantable devices interfacing with this part of the nervous system hold great potential for the development of treatments for a wide range of clinical conditions, whether by recording electrical activity carried by nerves, or influencing it through electrical stimulation. However, current nerve interfacing technologies lack the necessary resolution to selectively record and stimulate from nerves at the sufficient resolution and stability to enable their therapeutic use.

Here, we present a nerve cuff implant with an ultraconformable design that achieves high-quality and stable interfacing with nerves in chronic implantation scenarios. The cuffs are comprised of a parylene-C body 4 µm in thickness, rendering them highly flexible and able to conform to the surface of nerves. Combined with low impedance PEDOT:PSS microelectrodes, we show that these features allow the ultraflexible cuffs to record neural signals from awake animals for 21 days while exhibiting minimal fibrotic scarring. We furthermore show that high-resolution interfacing capabilities of the cuffs can be used to record action potentials with fascicle-specific resolution and extract from these physiologically-relevant features such as conduction velocity and direction of propagation. We evaluate the potential of this technology in two nerve systems in freely-moving rodent animal models: movement and sensory perception in the arm, and monitoring and control of bladder function.

The developed implantable devices represent a platform enabling new forms of fine nerve signal sensing and modulation, with applications in physiology research and closed-loop therapeutics.

4:30 PM SB07.07.04

Towards Longer Working Times for Implanted Electrodes through Integration of Perpetual Antioxidants at Device Interfaces Vicki L. Colvin; Brown University, United States

Medical devices implanted in the human body are increasingly common in the management and treatment of disease. An important and growing subset of these devices termed here 'active' implants, require electrical contact with tissues. For these devices the foreign body response to an electrode can preclude chronic function and limit many applications. The local delivery of an antioxidant able to protect tissue for months or even years is one possible solution. Nanoparticle ceria is a perpetual antioxidant due to its large cerium(III) content and the possibility of recovering cerium(III) from cerium(IV) after use.[1] For this work its antioxidant capacity was augmented by the use of molecular tethers that stabilized the reactive Ce(III) state. The efficacy of these materials was evaluated in a three-dimensional in vitro model by seeding primary cortical cells around microwires to reveal independent innate neuroinflammation. We demonstrated the use of ceria nanoparticles for reducing oxidative stress, increasing neuronal density, and reducing functional connectivity in wire implanted samples. These results indicate that antioxidant ceria nanoparticles may be efficacious drug treatment for protecting neural function at the device-tissue interface. We optimized ceria nanoparticles for small diameter, biocompatibility, and colloidal stability using reactive polymer coatings. To evaluate their utility in combating inflammation, we developed a 3D in vitro model of the device-tissue interface. This system can disentangle the different contributions of the innate immune system to neuroinflammatory device responses. Ceria nanoparticles reduced the oxidative stress, increased neuronal density, and reduced functional connectivity in wire-implanted samples [2]. The development and characterization of a novel 3D in vitro model of the device-tissue interface revealed a significant innate immune response to neural implants. This study has broad implications for the role of the innate immune system and potential treatment strategies for the chronic foreign body response to neural implants. The mitigation of oxidative stress, neuronal density, and functional connectivity with antioxidant ceria nanoparticles offers significant supporting evidence to indicate that many symptoms of the tissue reaction are related to redox dysregulation. Successful treatment of the device-tissue interface with long-acting antioxidant ceria nanoparticles shows potential for a local long-term antioxidant treatment strategy for clinical applications that need the long-term use of implanted neural devices.

References:[1] *ACS Nano* 2013, 7, 11, 9693–9703 [2] *J. Neural Eng.* (2022) v. 19 iss. 3

4:45 PM SB07.07.05

Improving Cytocompatibility of Commercial PEDOT:PSS for Bioelectronic Applications Aaron Lee¹, Joshua Killilea¹, Estelle Cuttaz¹, Christopher Chapman², Josef Goding¹ and Rylie Green¹; ¹Imperial College London, United Kingdom; ²Queen Mary University of London, United Kingdom

Conducting polymers have emerged as a strong candidate material for bioelectronic applications owing to their mixed ionic-electronic conduction which allows them to efficiently transfer

charge in aqueous environments. Commercial formulations of water-dispersible poly(3,4-ethylenedioxythiophene):poly(styrene sulfonate) (PEDOT:PSS) have facilitated development of flexible conductors, sensors, organic electronics and electrode interfaces. While PSS is an efficient counterion and dopant for PEDOT, its presence in excess to enable water-based processing can result in variable processability and electrochemical performance. While chemical crosslinking approaches can be used to address the stability of PEDOT:PSS in aqueous environments, it can hinder further processing. Importantly for bioelectronic applications, the release of excess PSS in aqueous environments from commercially based PEDOT:PSS materials can result in cytotoxicity. To ameliorate these effects, the use of physical separation was explored to remove the excess dopant. PEDOT:PSS dispersions were produced in N,N'-dimethylacetamide and separated by centrifugation. Analysis of the supernatant by NMR indicated the presence of PSS and the remaining polymer was blended with a polyurethane to produce a conductive elastomer. The electrochemical performance of the conductive elastomer and its resultant cytotoxicity profile were assessed as a function of PSS removal. Reducing the amount of PSS prior to preparation of the final conductive elastomer material was demonstrated to markedly improve the cytocompatibility of the material while retaining a degree of electrochemical functionality. These findings represent a key step in facilitating the translation of PEDOT:PSS-based materials to clinical applications.

SESSION SB07.08: Poster Session
Session Chairs: Achilleas Savva and Georgios Spyropoulos
Tuesday Afternoon, November 28, 2023
Hynes, Level 1, Hall A

8:00 PM SB07.08.01

An Extended-Gate Field-Effect Transistor as a Highly Sensitive Biosensor to Detect Bacteria Lea Könemund^{1,2}, Aaron Bongartz¹, Fenja Schröder¹, Svenja Herdan¹, Laurie Neumann¹, Rebekka Biedendieck¹, Dieter Jahn¹, Hans-Hermann Johannes^{1,2} and Wolfgang Kowalsky^{1,2}; ¹TU Braunschweig, Germany; ²Cluster of Excellence PhoenixD (Photonics, Optics, and Engineering—Innovation Across Disciplines), Germany

The detection of bacteria requires full-fledged qualified employees to prepare individual samples for corresponding machine-based analysis. This process is highly time-consuming and cost-intensive. Therefore, there is a great demand for more rapid, portable, and cost-effective sensors for the detection of bacteria. For this, well-established electrical measurement methods might be transferred to the investigation of biological systems. Our approach is the development of an extended-gate field-effect transistor (EGFET) as a biosensor. The EGFET is composed of a standard metal-oxide semiconductor field-effect transistor (MOSFET) and a physically separated but electrically connected sensor unit produced as a thin-film device.¹ The connection is realized by extending the MOSFET's gate electrode into the sensor unit. The potential of the gate-electrode is regulated by the electrical impact of the sensor unit on the MOSFET which further gates the measurable current between its drain and source electrode. The main constituent of the sensor unit is a suspension containing the bacteria of interest, which connects the extended-gate with a control-gate electrode. Both electrodes are functionalized with A₂BC-type porphyrins to link the bacterial cells to the electrode surfaces to shift the electrical potential of the extended-gate electrode on the gate-solution interface.² Different optical and electrochemical methods verified clearly the successful formation of the functional layer. Further, the successful linkage of bacteria on the functionalized electrode were analyzed by fluorescence lifetime imaging microscopy (FLIM).³ The transfer characteristic of the EGFET also clearly indicated the impact of trapped bacterial cells due to lower potential values on the extended-gate electrode.¹ However, our latest results indicate a non-homogeneous coverage of the electrodes by the bacteria.³ Further investigations focus on the increase of trapped bacteria to improve the sensitivity of the biosensor. Here, one of our approaches is the integration of dielectrophoresis (DEP) to the electrodes of the sensor unit. DEP is a highly flexible and multifunctional method to immobilize, separate, and concentrate biological particles such as whole cells but also dissolved molecules in a liquid. In addition, an optimized measurement setup or different functional layers based on e.g. boron-dipyrromethene (BODIPY) might also improve the sensitivity. The synthesis of BODIPYs compared to the A₂BC-type porphyrins are less complex which fulfills the requirement of a lean device.

¹Könemund, L., Neumann, L., Hirschberg, F. et al. Functionalization of an extended-gate field-effect transistor (EGFET) for bacteria detection. *Scientific Reports* 12, 4397 (2022).

²Minamiki, T., Minami, T., Sasaki, Y., et al. An Organic Field-effect Transistor with an Extended-gate Electrode Capable of Detecting Human Immunoglobulin A, *Analytical Sciences* 31, 725-728 (2015).

³Neumann, L., Könemund, L., Rohnacher, V., et al. A₂BC-Type Porphyrin SAM on Gold Surface for Bacteria Detection Applications: Synthesis and Surface Functionalization. *Materials* 14, 1934 (2021).

8:00 PM SB07.08.02

Kirigami-Based Stretchable Interconnects for Robust, Soft Neural Interfaces Laurine Kolly, Florent-Valéry Coen and Stephanie P. Lacour; École Polytechnique Fédérale de Lausanne, Switzerland

Recording or modulating neural activity using implanted electrode arrays has enabled advancements in the restoration of sensory-motor pathways and brain-computer interfaces. Long-term reliability of these interfaces (>6 months) is paramount to their deployment in neuroprosthetic medicine. Furthermore, hermetic encapsulation of conductive components within electrode arrays is required for long-term protection against the moisture and ions from the physiological environment to avoid electrical failure over time.

We have developed a kirigami-based technology to engineer elasticity within thin films of metal and thermoplastic polymer. The periodic cuts (kirigami) patterned and replicated across a thin stack of Polyimide/Platinum/Polyimide of 1/0.1/1 μm thicknesses program stretchability within interconnect tracks as narrow as 52 μm width. The Polyimide layer is patterned with a 1 μm width offset to that of the Platinum layer, such that the metallization is fully encapsulated, top, bottom, and sideways with Polyimide, thereby providing a built-in long-term hermetic barrier.

We assessed the robustness of the kirigami-based interconnects through a set of *in vitro* accelerated aging tests and repeated mechanical loading tests. We monitored the evolution of leakage current between two interdigitated tracks (IDE) biased at 5 V and soaked in phosphate-buffered saline (PBS) at 67 °C for 20 days. The elastic regime and plastic onset of the interconnects were measured during incremental uniaxial tensile stretching cycles. The electro-mechanical fatigue was assessed through uniaxially stretching linear interconnects for 1 million cycles at 10% strain, within the elastic regime.

The results of the accelerated aging showed that the leakage current remained below 0.2 μA after 20 days. These findings indicate that the interconnects maintain a high level of hermeticity, equivalent to >25 MΩ after 160 days at 37 °C, in accordance with Arrhenius law.

The electro-mechanical characterization demonstrated that the Polyimide-encapsulated kirigami interconnects can deform reversibly up to 15% of applied strain. Moreover, cyclic stretching for 1 million cycles at 10% strain resulted in a slight increase of 5% in relative resistance, indicating minimal mechanical fatigue.

The *in vitro* characterization demonstrated that the kirigami micro-patterning strategy used to fabricate stretchable interconnects can achieve a high level of hermeticity and exhibit low mechanical fatigue. Ongoing research efforts are focused on integrating materials with superior moisture barrier properties, such as silicon carbide, and further tuning the kirigami geometry to achieve a higher range of stretchability. These advancements aim to design functionally stable and longer-lasting neural interfaces that can withstand the mechanical challenges associated with chronic applications.

8:00 PM SB07.08.03

Flexible and Transparent Microelectrode Array for Simultaneous 2-Photon Imaging and Electrical Recordings Vikrant Kumar¹, Connor McCullough², Emily Gibson², Diego Restrepo² and Ioannis Kymissis¹; ¹Columbia University, United States; ²University of Colorado, United States

Combining two modalities, optical imaging and electrical recordings of neural cells, can shed light on a more profound understanding of neural circuits. Microelectrode arrays with high optical transparency in the near-infrared (NIR) and high electrical conductivity are required to enable simultaneous 2-photon imaging and electrical recording. A transparent microelectrode array allows us to perform imaging and electrical recording at the exact location for improved correlation between the two modalities, with imaging having a better spatial resolution and electrical recording having a better temporal resolution. We present an ITO-based transparent microelectrode array's design, fabrication, and testing. The microelectrode array has 16 recording sites, with each electrode size of 20 μm x 20 μm. The microelectrode array uses 3 μm parylene-C as a substrate and encapsulation layer maintaining excellent flexibility. Bending tests for different radii are performed to characterize the array's flexibility. The 2-photon imaging through the electrode array shows optical transparency at the desired wavelength of 920 nm. Electrochemical impedance spectroscopy (EIS) is done to characterize the electrical characteristics of the microelectrode array. Finally, the simultaneous 2-photon imaging and electrical recording through the array on a head-fixed animal is underway for the final testing of the microelectrode array. The microelectrode array is connected to a custom PCB using heat seal connectors for further connection to the data acquisition system.

8:00 PM SB07.08.04**Nanomesh microelectrode Arrays on 10 μ m-Thick PDMS for Ultrasoft Neuroelectronics** Jaehyeon Ryu^{1,2}; ¹Dartmouth College, United States; ²Northeastern University, United States

Ultrasoft neuroelectronics are highly interesting because they enable conformal and compliant interfacing with the soft, curvilinear surface of the neural tissue. However, current ultrasoft neural interfaces are usually limited by their electrode performance and scalability for neuroelectronic applications. Here, we present multi-functional nanomesh as an approach to achieve ultrasoft microelectrode arrays (MEAs) with excellent scalability. By stacking mechanical supporting polymer, metal, and low impedance coating, here we demonstrate an Au/PEDOT:PSS bilayer-nanomesh-based MEAs on ultrathin Polydimethylsiloxane (PDMS) substrate. We have successfully fabricated 32-channel, bilayer-nanomesh-based MEAs on PDMS with total device thickness down to only 10 μ m. The 32-channel bilayer-nanomesh arrays have demonstrated over 90% yield on average. We also achieved low impedance of 60 kilohms at 1 kHz with site area down to 400 μ m², comparable to the size of a single neuron. The performance of this bilayer-nanomesh MEAs has been characterized through bench testing. This MEA achieves excellent and stable electrochemical performance and also demonstrates good optical transparency over a broad wavelength spectrum. Other achievements of this research are hydrophilic surface modification on the MEA surface along its stability and great sterilization compatibility with ethylene oxide (EtO) sterilization which highlights the practical utilization of this novel device for advanced neural interfacing. This multi-functional bilayer-nanomesh approach provides a promising pathway toward ultrasoft neural interfaces with excellent electrochemical performance and large throughput for applications ranging from neuroscience to biomedical devices.

8:00 PM SB07.08.05**Optimization of Parylene Coatings for Implantable Neural Devices** Saman Ebrahimi Basabi, Layla Khalifehzadeh and Hamed Arami; Arizona State University, United States

Parylene C is a widely utilized biocompatible thin-film polymer coating for implantable devices, specifically neural implants, due to its ability to cover uniformly complex shapes, protect the implants against corrosive body fluids such as CSF (cerebrospinal fluid), electrical insulation, chemical stability, and durability. However, weak adhesion to the various types of device substrates remains a significant challenge for this promising coating material. Here, we will present the impact of substrate material selection, silanization (as adhesion promoter), different deposition parameters (such as silane concentration) and post-deposition annealing on overall characteristics of the coating layer (such as thickness and adhesion strengths). First, silicon wafers were coated with different thicknesses of Parylene C using SCS coating machine, followed by annealing in Ar atmosphere at temperatures of 150, 200, and 250°C. Additionally, the effect of thickness (1 and 3 μ m), and silane A-174 concentration (0.5, 1, and 1.5%) on adhesion strength were investigated. To assess long-term adhesion of Parylene, samples were submerged in an in-vitro accelerated aging bath consisting of PBS at 87°C for 7 days, and the properties were compared before and after the aging, to estimate the coating's stability in body environment after implantation. Coating thickness and molecular structure were investigated using Ellipsometry and FT-IR, respectively. Adhesion strength was determined using ASTM D3359 tape test. Our initial results indicated that 1 μ m Parylene coating with 1.5 vol% silane as adhesion promoter, and annealed at 150°C can potentially result in optimal adhesion for silicon substrates. We are pursuing follow up studies on silicon and other types of substrates (such as polyimide, which is a common flexible substrate for a variety of brain and neural implants) to further validate these observations. We envision that our results are critical to address unmet challenges for prolonging the lifetime of the implantable neural devices.

8:00 PM SB07.08.06**Frequency-Dependent Mechanism of Magnetic Nanoparticle Re-Laxation** Mingu Song, Dowoo Kim and Heon-Jin Choi; Yonsei University, Korea (the Republic of)

Magnetic nanoparticles (MNPs) play a central role in magnetogenetics as energy transducers, delivering the external energy in focus to neighboring cell membranes. Especially, magnetothermal heat conversion is held by two major relaxation mechanism: Néel relaxation (spin) and Brownian relaxation (rotative). As of now, efforts have been ongoing to accurately reflect stochastic nano system with refining mathematical model as more sophisticated. Here, our idea is "there is no gold model". We carefully argue that particle dynamics between forward field alignment and backward thermal randomization is clearly different. By coining the very field-dependent alignment mechanism as "laxation", we differentiate alignment and relaxation, also integrate suitable expressions that have been examined so far. Then we compute and visualize theoretical boundaries of Néel & Brownian movement. This approach allows us to decode the frequency sensitivity of heat conversion of magnetic nanoparticles based on relaxation mechanism. Relatively small, less anisotropic particles tend to spin-relax; thus, they efficiently convert high frequency field (~MHz). On the other hand, big, anisotropic particles are inclined to rotative-relax so that they could react only low frequency field (~few kHz). Moreover, we illuminate the enigmatic mixed mechanism, optimistic waveform, field amplitude dependency, and shape factors of MNPs. We support our arguments through experiments. Finally, we propose a simple fabrication method for transition of relaxation mechanism to regulate activation frequency. This frequency tuning may provide a range of possibilities for magnetogenetics, such as multi-channel activation of noninvasive deep brain stimulation (NIDBS).

8:00 PM SB07.08.07**3D-Microelectrode Arrays (MEAs) for *In Vitro* Applications** Inola Kopic¹, Hu Peng¹, Sebastian Schmidt¹, Annika Weisse², Richard Miru George², Gil Westmeyer¹, Christian Mayr² and Bernhard Wolfrum¹; ¹Technische Universität München, Germany; ²Technische Universität Dresden, Germany**Abstract:**

In the realm of 3D cell cultures and organoids, capturing electrical activity across multiple planes is essential for a comprehensive understanding of their behavior. Conventional microelectrode arrays (MEAs) with surface recordings fall short in addressing this requirement. The limitations of clean-room methods restrict electrode design possibilities and can impede effective cell-electrode coupling. To tackle this challenge, we present a novel approach that leverages rapid prototyping processes to enhance electrode fabrication. Our laser-patterned MEA incorporates printed 3D-electrode structures, enabling precise recording and stimulation within cell tissues. This advancement improves signal quality through enhanced cell-electrode coupling and provides greater flexibility in electrode placement. We believe this innovative approach will significantly contribute to improvements in 3D cell cultures and organoids, opening new avenues for understanding complex biological systems and developing targeted therapeutic interventions.

Introduction:

Standard planar MEAs can only record electrophysiological signals in 2D, making them unsuitable for capturing the complexity of emerging 3D cell cultures or organoids [1]. To overcome this limitation, we design and fabricate 3D MEAs using additive manufacturing techniques [2]. These 3D MEAs hold promise for studying neuronal functions and diseases using neuronally differentiated human-induced pluripotent stem cells (hiPSC) in vitro.

Results and Discussion:

Here, we present the microfabrication of our 3D MEAs. In the first step, silver ink pillars are printed on suitable substrates, followed by sputtering with gold to create a biocompatible electrode interface. Individual electrodes and feedlines are then generated through laser ablation, with feedline structures patterned within minutes, representing a significant improvement over conventional lift-off techniques. The chips are fully passivated with a parylene C layer deposited via vapor deposition. Laser ablation at different angles is used to open the tips of the pillars precisely, and partial etching is employed to create tubular structures. In the final step, individual pillars undergo stepwise electroplating with gold and PEDOT:PSS to prevent silver contamination during long-term cell culture. Our fabrication method offers a fast and easily adjustable approach compared to traditional clean-room techniques. Using the inkjet printing process with laser ablation and electroplating, the height of each pillar can be accurately determined. This enables the realization of multiple pillars with various heights on a single chip. Moreover, the design of the MEA aligns the electrodes in a manner that simplifies their insertion into organoids or 3D cell models. With this highly flexible approach, we aim to record cellular signals from various planes within the targeted tissue.

Conclusion:

This work demonstrates a process for fabricating MEAs with integrated 3D electrodes, providing a platform that facilitates recording and stimulation within 3D cell aggregates or organoid models.

References:

- [1] D. A. Socia, D. Lam, A. C. Tooker, H. A. Enright, M. Triplett, P. Karande, S. K. G. Peters, A. P. Sales, E. K. Wheeler, N. O. Fischer, Lab. Chip. 2020, 20, 901 - 911.
- [2] L. Grob, P. Rinklin, S. Zips, D. Mayer, S. Weidlich, T. Korkut, L. J. K. Weiß, N. Adly, A. Offenhäusser, B. Wolfrum, Sensors. 2021, 21, 3981.

Acknowledgments:

We acknowledge funding from the BMBF (within the project PRISTINE).

8:00 PM SB07.08.08**Brain-Machine Interfaces—Taking the Next Step Towards Translational Devices** Santiago Velasco Bosom and George G. Malliaras; University of Cambridge, United Kingdom

Aphasia is defined as the impairment of speech as a result of acquired brain injury, rapidly hindering communication skills in the patient. Current therapeutical approaches are complex and rely on compensatory strategies to regain the lost communicating abilities.

Based on the concept proved by Khodagoly et al, multielectrode arrays (MEA) using electrodes as small as 10x10 μ m² are sufficient to capture both local field potential and putative single neuron activity when used for electrocorticography, causing minimal tissue damage. To date, MEAs have predominately been used for investigating human neural network mechanisms and better understanding of brain disorders. Nonetheless, better interpreting these mechanisms carries the potential to open an entire new medical field to use brain signal recordings for healthcare applications and personalized medicine.

In this work, we present the first translational Neurogrid (ultraconformal ECoG multielectrode array) that will be used for the chronic study of cortical neural signals and its decodification into conversation. By complying with European medical regulation in the development of the device, we aim to increase the duration of the implantation in awake human studies, to better understand the potential of this technology with respect to long-term human-machine interfaces. Integrating state-of-the-art machine learning algorithms to the brain signals recorded by the Neurogrid, we aim to decode neural activity in patients suffering from aphasia and translate it into speech.

The combination of these powerful technologies can pave the way for brain-machine interfaces to become powerful clinical tools that increase the wellbeing of patients with neurological disorders. However, to champion the way of this technology into a final clinical product, it should still undergo multiple intermediate steps to prove its safety and reliability.

8:00 PM SB07.08.09

Flexible Printed Circuit Board (fPCB) Neural Probes for Monitoring Neural Signals DaerlPark¹, HyeonyeongJeong¹ and JungsikChoi²; ¹Yonsei University, Korea (the Republic of); ²Nformare, Korea (the Republic of)

Neural activity monitoring in the central nervous system often utilizes silicon-based micro electro mechanical systems (MEMS) probes. Despite their strength in monitoring and stimulating capabilities, these probes are fragile due to the brittle nature of silicon materials limiting their application in various fields. Here, we introduce flexible printed circuit board (fPCB) neural probes that have robust mechanical and electrical properties. The probes fabricated via a roll-to-roll process on films with thickness of 3.5 μm and 10 μm line width of electrodes exhibit an impedance of approximately 1.5 M Ω , reducing to about 120 K Ω after typical platinum colloidal coating. This impedance range is suitable for multiunit recordings, enabling simultaneous monitoring of a large population of neurons in the brain. The probes are mechanically very flexible and thus shows no fracture or mechanical/electrical failure under repeated bending test of up to 500 times, and also in the course of handling and monitoring. Furthermore, it is thermally stable that can endure the properties up to 175 degree Celsius and also chemically stable under acidic/alkaline condition that make possible to modify the electrodes easily under harsh conditions such as CVD (chemical vapor deposition) or electro-deposition. In fact, any mechanical failures, or degradation of monitoring capabilities has not been observed in the courses of modification. It indicates that the fPCB probes can be used as a "DO IT YOURSELF" type chronic, tailorable neural probes for chronic neural signal monitoring.

Keywords: flexible neural probe, modification, monitoring of neural systems, chronic

8:00 PM SB07.08.10

Fully 3D Printed Bio-Electronic Devices for Nerve Regeneration Ju-YongLee¹, JooikJeon², Joo-HyeonPark¹, Yea-SeulPark¹, Se-HunKang¹, Min-SungChae¹, Kang-SikLee³, Jung KeunHyun² and Seung-KyunKang^{1,4,5}; ¹Seoul National University, Korea (the Republic of); ²Dankook University, Korea (the Democratic People's Republic of); ³Asan Medical Center, Korea (the Republic of); ⁴Soft Foundry Nano Systems Institute (NSI), Seoul National University, Korea (the Republic of); ⁵Research Institute of Advanced Materials (RIAM), Seoul National University, Korea (the Republic of)

Advancements in miniaturization, wireless technology, and flexible electronic components have led to the development of diverse bio-interfaced electronics for medical devices. Extensive research has focused on implantable electronic components that can be precisely positioned within the body to record or stimulate specific areas. A significant challenge in this field is achieving a seamless interface between the inserted electronic component and the complex surface or irregular structure of the body. To overcome this challenge, customization of the electrode part and the main body of the device is necessary to adapt to the intricate body surface. Moreover, optimizing space utilization is essential to enable smooth packaging of components in limited spaces, requiring a compact form factor. Therefore, the utilization of additive manufacturing for configuring data-driven voxelated electronic materials within a three-dimensional space holds great potential for integrating electronic components in customized forms. Additionally, it is crucial to prevent infections or internal damage caused by permanent implantation or removal surgery in implantable electronic components. Ultimately, addressing these concerns necessitates biodegradation after the device's operational lifespan. In this study, a fully printed wireless electroceutical tube was developed, capable of treating injuries by inserting it as a tube into peripheral nerves. This achievement was based on the use of biodegradable voxelated electronic ink. Notably, the integration of biodegradable voxelated semiconductors with conductors and dielectrics enabled the creation of a device that generates wireless-controlled monophasic pulses, demonstrating its significant potential for biomedical applications. The suitability for in vivo application was evaluated in small and large animals, and the validity of the findings was confirmed through biological verification, which involved confirming therapeutic effects and assessing their impact on actual functional recovery.

8:00 PM SB07.08.11

Using Digital Image Speckle Correlation (DISC) to Identify Micro Emotions ShirleyXiong¹, HyeonjiAhn², ElainaHeghes³, AnushaMisra⁴, ElaineZhang⁵, JessicaHofflich⁶, ShiFu⁶, PawelPolak⁶ and MiriamRafailovich⁶; ¹Ward Melville High School, United States; ²St. Mark's School, United States; ³South Side High School, United States; ⁴Dana Hills High School, United States; ⁵Jericho Senior High School, United States; ⁶Stony Brook University, The State University of New York, United States

Facial expressions are one of the most basic and natural forms of communication between humans. Alongside general facial expressions, micro-emotions are spontaneous changes in facial muscles that indicate hidden emotions. Micro-emotions become apparent in response to specific emotion-inducing stimuli, such as pictures and videos. These fleeting expressions are low in intensity and are, therefore, significantly more difficult to identify than visible facial expressions and emotions.¹ This study uses Digital Image Speckle Correlation (DISC) to identify micro-emotions by analyzing subcutaneous facial muscle displacement through a contact-free, non-invasive method.

To verify the validity of DISC for tracking facial muscle movement, a video was taken of identical twins and a control performing the same facial actions of frowning and smiling. The control was a subject with no relation to the twins. While the twins used similar parts of muscles to perform actions, the control used quite different parts of facial muscles to perform the same actions. For instance, when frowning, the identical twin's forehead muscles toward the inside of the face. However, the control's forehead muscles moved downward toward the outside of the face.

Sets of ten images were obtained from the International Affective Picture System (IAPS) and categorized using a valence and arousal scale. Valence denotes the emotional value, while arousal characterizes its level of stimulation. The analysis of the participants' faces shows that high-valence images tend to evoke positive emotions, translating to more pronounced movement in the cheeks and mouth region. When the subject saw an image with positive valence and high arousal, large levels of displacement occurred in those areas. The magnitude of facial displacement in four quadrants of the face was represented through a graph. In the graph, visible spikes span approximately a second. These peaks represent fleeting muscle movements that correlate to micro-emotions, which can be detected through displacement. On the other hand, the negative valence images induced significant amounts of micro-emotions in the upper quadrants, specifically in the forehead and eyebrow areas, commonly associated with reactions to sad emotions.

DISC has the potential to be used to analyze the efficacy of treatments for certain psychological disorders. Major Depressive Disorder (MDD) presents with non-verbal indicators such as the lack of or abundance of specific facial movements and reactions. Hence, changes in facial expressions and movements as identified by DISC can be used to diagnose and understand depression and track the progression and regression of depressive symptoms.² For example, esketamine is approved by the FDA to treat MDD that cannot be treated through other antidepressants.

In particular, a case study involving an esketamine patient before and after receiving treatment was utilized to analyze the effects of this treatment on patients. Analysis of the video images indicated differences in the intensity of the patient's reactions before and within an hour after treatment. The time to react to the different images was also measured and could be a measure of the impact on the information processing ability of the patient. These results will be correlated to the known physiological impact of esketamine as a sedative agent³ and the answers to the self-report questionnaire administered to the patient, such as BDI or HAM-D which are used to assess the severity of depressive symptoms.

¹X. Li et al. "Towards Reading Hidden Emotions: A Comparative Study of Spontaneous Micro-Expression Spotting and Recognition Methods," *IEEE Transactions on Affective Computing*, vol. 9, no. 4, pp. 563-577, 2018

²Stratou, G. et al. "Automatic nonverbal behavior indicators of depression and PTSD: the effect of gender," *Journal on Multimodal User Interfaces*, 2015

³Ekman, P. et al. "Facial Expression In Affective Disorders," *What the Face Reveals*, 2013

8:45 AM *SB07.09.01

Soft Electronic Interface with Biological SystemsZhenanBao; Stanford University, United States

In this talk, I will discuss soft materials, sensors and devices we are developing for an intimate interface with biological systems.

9:15 AM SB07.09.02

Design and Fabrication of a Flexible Implantable Microelectrode Array for Electrophysiological and Non-Enzymatic Glucose Recording in an Artificial Brain ProsthesisChe-HungChu, Pei-LingChen and PochunChen; National Taipei University of Technology, Taiwan

For neuroscience research, scalability in regard to the length and dimension of implantable neuro devices was required owing to differences in species and brain regions. For the clinical investigation of neurological disorders, including Alzheimer's disease, Parkinson's disease, and epilepsy, specifically designed implantable neuro devices for precise focus localization have emerged. Among them, in Alzheimer's disease (AD) studies, the metabolic hypothesis of AD is among the models that have gained much traction because glucose hypometabolism is one of the early markers of AD that precede clinical dementia. While a strong argument can be made that reduced glucose uptake is merely a consequence of neurodegeneration, the metabolic hypothesis asserts that brain glucose metabolism is nonetheless an integral part of AD progression and the precipitation of cognitive deficits.

In this study, a flexible microelectrode array device is developed with a polyimide substrate, nanoporous platinum microelectrode array, and a biocompatible Parylene C package. This device has low electrochemical impedance with an improved signal-to-noise ratio and high sensitivity of glucose concentration by non-enzymatic electrochemical detection. The nanoporous Pt microelectrode demonstrated excellent electrochemical performance of 88.2 ($\mu\text{Acm}^{-2}\text{mM}^{-1}$) and 37.02 ($\mu\text{Acm}^{-2}\text{mM}^{-1}$) using a chronoamperometry (i-t) test method in PBS and ACSF, respectively.

Additionally, we dedicate to maintaining animal welfare ethics and reducing the consumption of animal experiments by developing an artificial prosthesis with agarose to mimic the brain tissue. We successfully developed a prosthesis with tunable impedance, in which we can simulate different neural diseases by adjusting its conductivity to reduce unnecessary animal experiments. The flexible platinum microelectrode shows its high sensitivity to the variation of glucose concentration in the agarose brain prosthesis.

9:30 AM SB07.09.03

Decorating Bioelectronic Surface with Supported Lipid Bilayer to Study Viral Entry and MoreZhongmouChao¹, EkaterinaSelivanovitch¹, ZixuanLu², KonstantinosKallitsis², RoisinOwens² and SusanDaniel¹; ¹Cornell University, United States; ²University of Cambridge, United Kingdom

There are two pathways for the entry of SARS-CoV-2: early (cell surface) entry and late (endosomal) entry. In both pathways it requires the initial binding of SARS-CoV-2 spike proteins with host cell membrane receptor (ACE2), followed by the cleavage of spike protein by either TMPRSS2 (early entry) or cathepsin L (late entry). We have previously demonstrated a supported lipid bilayer (SLB) containing native membrane component can maintain membrane fluidity and thus its biological functionalities, making SLB a desirable platform to recapitulate the conditions in vitro that support virus infection of a host cell. In this work, by forming SLB containing ACE2 receptors on a conductive polymer-based substrate, we have probed the two entry pathways of SARS-CoV-2 using electrical signal. Our results suggest the specific binding between spike protein containing virus pseudo particles and ACE2 receptors will increase membrane electrical resistance, while the fusion events catalyzed either by TMPRSS2 and cathepsin L will further increase membrane resistance. Our work shows the electrical readout of membrane properties based on SLB platform can be a powerful tool in detecting SARS-CoV-2 virus entry without the complications of working with live cells. In addition to viral entry, the versatile SLB based bioelectronic sensors are also applied to investigate the interactions between chemical permeation enhancer (CPD) and lipid bilayers, providing insights in the drug development against otitis media.

9:45 AM SB07.09.04

Lactate Biosensor Based on Aerosol Jet Printed Organic Electrochemical Transistors (OECTs) for Real Time MonitoringYuchenShao, PaulLavryshyn, JiaxinFan and ManishaGupta; University of Alberta, Canada

Diabetic patients have an increasing risk of developing the foot ulcers. Diabetic foot ulcer (DFU), as one of the complications for diabetics, has bothered people for many years. Clinical research has shown that real time monitoring of the lactate concentration helps guide therapy and improve patient outcome [1]. To reduce blood tests for lactate level measurements, non-invasive and low-cost reliable biosensors need to be developed for monitoring.

In this research, we developed a 3D-printed lactate sensor on top of the flexible Kapton substrate. Organic electrochemical transistors (OECTs) are chosen for the biosensors because of its good performance under aqueous environments and signal amplification. Sensors are fabricated using Optomec Aerosol Jet 5X printer with Au as the source and drain electrode, Pt as the gate, poly(3,4-ethylenedioxythiophene) doped with polystyrene sulfonate (PEDOT:PSS) as the channel and polyimide as the insulator layer. Layer by layer strategy is applied for functionalization, tetraethialfulvalene (TTF), chitosan, lactate oxidase (LoX) and bovine serum albumin (BSA) are drop-casted on top of the gate area and then both channel and gate are covered by gelatin to further improve the repeatability of the lactate sensor. Functionalized sensors can be stored in 1X PBS solution for over one month without any deterioration in their sensitivity. The device was measured in both PBS and artificial sweat buffer for comparison and obtained a broad sensitivity range between 10uM up to at least 50mM, which is far beyond the desired range. Blood lactate meter was using as the reference to calibrate the lactate sensor. The printed lactate sensor includes the ZIF connector which can be inserted onto a PCB board and will be used for further diabetic model test.

[1] *Jia W, Bandodkar AJ, Valdés-Ramírez G, et al. Electrochemical tattoo biosensors for real-time noninvasive lactate monitoring in human perspiration. Analytical Chemistry. 85(14):6553-6560. doi:10.1021/ac401573r*

10:00 AM BREAK

SESSION SB07.10: Auditory Neuroengineering
Session Chairs: Maria Asplund and Georgios Spyropoulos
Wednesday Morning, November 29, 2023
Hynes, Level 1, Room 110

10:30 AM *SB07.10.01

Integration of Soft Materials in Microfabrication for Auditory NeuroprosthesesAlixTrouillet¹, EmilieRevol¹, Florent-ValeryCoen¹, DanielLee² and StephanieP. Lacour¹; ¹Ecole Polytechnique Federale de Lausanne, Switzerland; ²Harvard University, United States

Implantable neuromodulation systems often rely on macroscopic electrodes to deliver streams of electrical pulses to a small targeted region of the nervous system. Miniaturisation and design of electrode materials can help improving on the spatial selectivity and electrode reliability over time. In the context of auditory neuroprostheses, we are designing, scaling and implementing soft microelectrode arrays to generate resolute sound percept with minimal off-target effects in a pre-clinical model of auditory brainstem implants (ABI).

Using microfabrication, we manufactured a macaque sized multichannel, MRI compatible, soft auditory brainstem implant (150 μm thick silicone carrier, 11 platinum-silicone composite electrodes of 300 μm diameter) that delivers selective electrical stimulation. We engineered customised biodegradable implant holder to ease handling and implantable without compromising the ABI compliance, as well as connectors to reliably interface mechanically and electrically the soft implant with flexible cables and a head-mounted pedestal. The ABI is surgically implanted through a retro-sigmoid craniotomy under endoscopic visualisation at the surface of the cochlear nucleus (<5 mm² surface area).

We evaluated the efficacy of the soft ABI by monitoring the animal's performance in a behavioural task. Using burst of electrical pulses (ranging from 50-100 pulses per second at 0.1-2 mA) applied through the ABI electrodes, we confirmed the resolute capability of the implant: the animal was able to differentiate percept generated from different electrode pairs, with distinct activation threshold for each electrode, indicating good spatial resolution.

Systematic characterisation of the materials and processes at each step of the manufacturing of the implant enabled the successful deployment of the soft auditory neuroprosthesis.

11:00 AM *SB07.10.02

Waveguide-Based Optical Modules for Cochlear Implant ApplicationsChristianGöbler^{1,2}, MichaelRibeiro Stührenberg^{1,2}, KatharinaKunze³, DanielKeppeler¹, Ulrich T.Schwarz³ and TobiasMoser^{1,2}; ¹University Medical Center Göttingen, Germany; ²German Primate Center, Germany; ³Technical University of Chemnitz, Germany

Cochlear implants (CIs) enable open speech comprehension in otherwise deaf patients. Potential improvements affect the limited spatial resolution of the electric stimulus. Optogenetic activation promises a better spatial resolution due to high-precision activation with micro-scaled light emitters. Here, we discuss the development of passive optical modules with integrated micro-optics and laser diode arrays. Remote red-emitting laser diodes are placed outside the cochlea and coupled to polymer-based waveguides with lens-based systems. The waveguides, which are directing the light towards and into the cochlea need to be highly flexible to enable precise placement in the scala tympani with a bending radius of down to 2.5 mm for the human cochlea. Ridge waveguide laser diodes are used due to their available power of several tens of milliwatts. Multibeam applications are enabled by emitter chips with a multitude of parallel aligned laser ridges with a lateral spacing in the 100 μm range. The astigmatic emission profiles of the ridge laser diodes has to be addressed in the optics design, as well as the integration of a transparent sapphire window into the beam path. We evaluate different optical systems on the path towards a human optical cochlear implant prototype, including macroscopic aspherical lenses, which enable medium-scaled optics with beam path length in the range of 15 mm. Further miniaturization of the beam path length to less than 2 mm can be achieved via a micro-lens-based approach. Here, we discuss the different optical systems in terms of channel scalability and waveguide coupling.

11:30 AM SB07.10.03

Acousto-Sensitive Ion-Based Transistors and Soft Electronics for Artificial Basilar Membrane Linta Sohail, Sofia Drakopoulou and Georgios D. Spyropoulos; University of Ghent, Belgium

Current solutions for hearing impairment lie vastly in cochlear implants (CIs). However, they are limited by bulky, power-demanding external uncomfortable components that hinder sound localization and suboptimal neural interfaces which negatively impact the efficiency of hearing restoration. To overcome these issues, we exploit novel internal ion-gated electrochemical transistors (IGTs) and piezoelectric (PVDF) nanofibers to establish a soft, biocompatible artificial basilar membrane (ABM) for a fully implantable and self-contained CI. We hypothesized that organic electronics can create all the required components; IGT-based acousto-electrical transducers with a high signal-to-noise ratio (SNR), and low-impedance, stable stimulation electrodes. To achieve that, we created efficient and fast acousto-sensitive IGTs ($gm/\tau > 10^6 \text{ mSs}^{-1}$), high capacitance conductive polymer films, overcome stability issues and design smart fabrication routes that allow the development of all components into a single conformable substrate. We tuned materials composition, improved designs, and investigated the geometry and morphology effects on piezoelectric nanofibers. We explored IGT-arrays gated by continuous electrospun PVDF nanofiber ($\sim 0.6 \mu\text{m}$ diameter fiber) films with gradually decreasing areas, to provide a deeper understanding of the device physics and elucidate their exact operating principle under various acoustic stimulations (0.1-10kHz). This work lead to an ABM with 8 intracochlear excitation points that conforms to the intact basilar membrane, generates, and amplifies electrical pulses ($> \times 10^3$) according to incoming acoustic stimuli, to stimulate the spiral ganglion neurons and restore hearing without external components. We examined the performance of the ABM in-vivo by recording the electrically evoked auditory brain recordings (ABRs) in a rat model.

This project will generate safer, smaller, and more conformable acoustic-sensitive devices and stimulation electrodes that will build an ABM that can modulate electrically the neurophysiological activity of the spiral ganglion neurons. Further, the materials and methods that will be used in this project will lay the foundation for cost-effective and improved neurological devices such as micro-EEG systems and brain stem implants.

SESSION SB07.11: Smart Bioelectronics for Electrophysiological Recordings

Session Chairs: Achilleas Savva and Georgios Spyropoulos

Wednesday Afternoon, November 29, 2023

Hynes, Level 1, Room 110

1:30 PM SB07.11.01

Coin-Sized, Fully Integrated and Minimally Invasive Continuous Glucose Monitoring System based on Organic Electrochemical Transistors Jing Bai, Xinyu Tian and Shiming Zhang; The University of Hong Kong, Hong Kong

Continuous glucose monitoring (CGM) systems are currently a major focus of research in advanced diabetes management. The rapid development in this field calls for next-generation CGMs with improved sensitivity, reliability, and wearability.

Here, we propose a coin-sized, fully-integrated, wearable CGM system [1] that combines cutting-edge technologies from the intersecting fields of biosensors, minimally invasive tools, and hydrogels.

This CGM system includes: 1) an emerging biochemical amplifier, the organic electrochemical transistor (OECT), to improve sensitivity beyond traditional electrochemical modules; 2) a microneedle array for interstitial-fluid (ISF) sampling with reduced pain during skin penetration; and 3) a tough, adhesive enzymatic-hydrogel-membrane to enhance reliability of glucose sensing on skin. Unlike conventional CGMs, the employed OECT amplifier empowers the OECT-CGM with a high anti-noise ability, an on-demand-tunable sensitivity and current regeneration ability, enabling long-term stable glucose sensing within specific clinical ranges (1~20 mM).

This work paves the way for the development of next-generation CGMs that can simultaneously deliver high and adjustable sensitivity, minimal invasiveness, and improved wearability.

[1]. Submitted.

1:45 PM SB07.11.02

Artificial Retina with Three-Dimensional Microelectrodes of Liquid Metals for Vision Restoration Won Gi Chung¹, Jiuk Jang¹, Gang Cui², Sanghoon Lee¹ and Jang-ung Park^{1,2}; ¹Yonsei University, Korea (the Republic of); ²Yonsei University College of Medicine, Korea (the Republic of)

Inherited retinal degenerative diseases can lead to both gradual loss or permanent damage of photoreceptor cells, resulting in the impairment of vision, or even blindness. However, as inner retinal neurons can be preserved even when this degeneration of photoreceptor cells, various approaches by stimulating the inner retinal neurons to restore vision have been developed. Electronic retinal prosthesis, which uses photo-responsive devices to electrically stimulate inner retinal neurons, has emerged as a promising approach to restore vision. Over the past decade, this electronic retinal prosthesis has been adapted to clinical trials, although being still limited by low visual acuity. One of the main limitations is the low proximity that results from the unconfomities between the retina and the implant. Since the stimulation threshold that elicits retinal responses strongly depends on the electrode-cell distance, it is important to reduce this distance. Also, the imprecise stimulation on the epiretinal surface caused by this low proximity can inevitably excite the axons of retinal ganglion cells (RGCs), generating irregular visual perceptions to patients. In this regard, 3D electrodes show promise for effectively stimulating the nervous system, dramatically reducing this electrode-cell distance by positioning the stimulation site adjacent to the target cell. Also, compared to the electrodes that have flat surfaces, these 3D electrodes enable their stimulation to selective local areas, bypassing neurons that should not be stimulated, thereby providing excellent selectivity and high spatial resolution. However, previous 3D neural electrodes have been formed using rigid solid-state materials, showing a significant mismatch of mechanical properties at their interface with soft biological tissues, which can directly damage the soft retina, or cause inflammatory responses within the retina.

Herein, we present an artificial retina where flexible ultrathin phototransistors are integrated with 3D microelectrodes of liquid metals. These phototransistors directly convert light into electrical stimuli, stimulating the retina through our soft 3D microelectrodes. The flexible ultrathin layer of this artificial retina can be conformably laminated on the innermost surface of the retina, directly stimulating the RGCs using the softly protruded pillars of 3D liquid-metal electrodes. The developments of this artificial retina include several unique strategies as follows: First, these 3D microelectrodes can enhance the proximity to the target cells and provide effective charge injections to elicit neural responses in the RGCs. These soft stimulation electrodes are directly printed in a pillar shape on the top surfaces of the drain electrodes to overcome the geometrical gap at the interface between the device and the locally nonuniform surface of degenerative retina, enhancing the proximity to the target RGCs. Here, these 3D electrodes can be printed with desired heights to selectively reach target cells. Also, the Pt nanoclusters locally coated only on the tip of these 3D electrodes show advantages to reducing the impedance of the stimulation electrodes, and injecting charges effectively into the retinal neurons. Second, their low Young's modulus owing to their liquid form, can minimize the undesired damage to the interfacing biological tissues. Third, unsupervised machine learning approach can effectively classify the evoked spikes, and the results indicate the potential for the selective stimulation of RGC somas using our 3D microelectrodes. Lastly, in-vivo experiments using a retinal degeneration mouse model demonstrate that the spatiotemporal distribution of neural responses on their retina can be mapped under selective localized illumination areas of light, suggesting the restoration of their vision.

2:00 PM *SB07.11.03

Advanced Materials and Device Design for Motion Artifact-Free Bioelectronics Tae-il Kim; Sungkyunkwan University, Korea (the Republic of)

To eliminate dynamic motion artifacts more efficiently and universally, we demonstrate new noise reduction strategies using advanced noise damping materials and sensors even without the conventional signal processing. We presented 1) New hydrogel materials [1], 2) Applications for EEG sensors [2], and 3) liquid metal for strain-insensitive electrodes [3,4]. The study aims to show sensors that focus on human-interactive devices while showing insensitivity to 75% stretching, 25% compression, and 5mm radius of curvature bending while maintaining the sensing ability of the sensor

- [1] B. Park, and **Tae-il Kim***, *Science* vol. 376, 6593, pp. 624–629, 2022.
[2] J. H. Shin, and **Tae-il Kim***, *npj Flex. Electron.* Vol. 6, pp. 32, 2022.
[3] W. Jung, and **Tae-il Kim***, *ACS Nano*, 16 (12) 21471–21481, 2022.
[4] H. Choi, **Tae-il Kim***, and C. Majidi*, *Adv. Funct. Mater.*, in press

2:30 PM SB07.11.04

Flexible Pressure Sensor for Continuous Physiological MonitoringHemanthKalluru Nagarajao, MaryamGolshahi and LaylaKhalifehzadeh; Arizona State University, United States

The field of bioelectronics has witnessed remarkable advancements in recent years, playing a crucial role in biomedical applications such as home-based monitoring of blood pressure and blood glucose levels. To expand the potential of bioelectronics, researchers have focused on developing advanced pressure sensors capable of monitoring various health parameters, including intraocular glaucoma, tendon repair and cardiovascular health. Meeting the growing demand for accurate pressure measurements, a multitude of flexible sensing technologies have been devised. These technologies employ techniques such as capacitive, piezoelectric, and piezoresistive sensors to convert external pressure into measurable signals. The success of these mechanical sensors hinges on their ability to compress under applied pressure. Notably, studies have demonstrated that capacitive pressure sensors outperform other options in faithfully reproducing the desired sensing behavior. Capacitive pressure sensors operate by detecting changes in initial capacitance caused by applied pressure. These sensors consist of a dielectric layer sandwiched between two parallel conductive plates. The sensitivity of these sensors increases with higher capacitance. Increasing capacitance can be achieved by reducing the plate distance or selecting a material with a high dielectric constant. This study aims to assess and compare the sensitivity of capacitors using five distinct viscoelastic polymers. The selection of these materials is guided by several factors, including their general properties such as biocompatibility, thermal stability, and cost-effectiveness. Moreover, their mechanical properties, such as high compressibility, low hysteresis, and high tensile strength, are carefully considered. These characteristics are crucial in determining the suitability of the polymers for capacitive pressure sensors, as they directly impact the sensor's performance and reliability. By leveraging these insights and engineering the materials and designs, the sensitivity and overall performance of capacitive pressure sensors can be significantly improved, paving the way for more precise and reliable biophysical pressure measurements in various biomedical applications.

2:45 PM SB07.11.05

Flexible Electrochemical Sensors for Detection of NeurotransmitterFarbodAmirghasemi, AliSoleimani, SinaGharahtekan, MonaAbdelmonem, AbdulrahmanAl-Shami and MaralMousavi; University of Southern California, United States

Acetylcholine (ACh) functions simultaneously as a neuromodulator and neuromuscular transmitter in the brain, thus playing critical roles in learning, recognition, motivation, and muscle control. Alterations in ACh concentration in the cerebral cortex were correlated to dementia and Alzheimer's disease, psychiatric disorders, anxiety, and depression. Therefore, developing instruments for selective sensing of ACh is essential to enhance the fundamental biological understanding of the role of this neurotransmitter in disease progression, as well as the rational design and testing of therapeutics that interact with the cholinergic receptors. Here, we are developing a sensor for the in-vivo recording of ACh levels in the brain tissue to address current challenges in ACh detection, including bulky and rigid neural probes and low selectivity in biofluids.

I am utilizing potentiometric sensing, which offers direct selective measurement by eliminating separation and sample processing. Potentiometric sensors offer detection in a physiologically relevant concentration range and are a passive sensing mechanism that does not consume or perturb the analyte. These characteristics make potentiometric sensing a robust analytical technique that has grown in popularity for analyzing inorganic ions, including potassium (K⁺) and sodium (Na⁺) but has remained underutilized for detecting neurotransmitters. We developed a proof-of-concept flexible potentiometric sensor for detecting ACh with less than one-second temporal resolution based on flexible parylene electrodes via utilizing a calixarene-based ionophore for ACh.

Using parylene as the structural material for developing neuroprostheses has been validated and could be compared with technologies based on other materials such as PDMS, polyimide, and silicon. However, we are reporting the first potentiometric parylene-based ACh-selective neural probe. We are utilizing parylene due to providing a pinhole-free, highly flexible, sturdy mechanical strength, and biocompatible platform to construct implantable ACh-detecting sensors consisting of a working electrode (containing an acetylcholine organic sensing membrane) and a reference electrode (having a reference membrane). The parylene C substrate encompasses three 200 nM thick Pt electrodes with a 200 μm radius. The electrical potential (emf or electromotive force) between the ACh sensor and reference electrode correlates to the activity of ACh levels in the biofluid, according to the Nernst Equation ($E = E^{\circ} + (RT/zF) \log a_i$), where E° shows the standard potential, R the universal gas constant, T temperature, F the Faraday constant, z the charge of the ion, and a_i the activity of ACh. A theoretical slope of 61.5 mV/decade is expected at body temperature and is defined as the Nernstian slope. The ACh-sensing membrane will be drop-cased onto the circular area of the platinum contact. To optimize the high signal stability, we will modify the surface of platinum with the variation of carbon nanotubes (CNTs) due to CNTs' capability to generate a stable and reliable interfacial potential in potentiometric sensors with an organic sensing membrane.

SESSION SB06/SB07: Joint Virtual Session

Session Chairs: Juan Artes Vivancos, Maria Asplund, Josh Hihath and Alexandra Paterson
Wednesday Morning, December6, 2023
SB07-virtual

10:30 AM *SB06/SB07.01

Multiphoton Lithography of Organic Semiconductor Devices for 3D Printing of Flexible Electronic Circuits, Biosensors and BioelectronicsMohammad RezaAbidian; University of Houston, United States

In recent years, 3D printing of electronics have received growing attention due to their potential applications in emerging fields such as nanoelectronics and nanophotonics. Multiphoton lithography (MPL) is considered the state-of-the-art amongst the microfabrication techniques with true 3D fabrication capability owing to its excellent level of spatial and temporal control. Here we introduce a homogenous and transparent photosensitive resin doped with an organic semiconductor material (OS) compatible with MPL process to fabricate variety of 3D OS composite microstructures (OSCMs) and microelectronic devices. Inclusion of 0.5 wt% OS in the resin enhanced the electrical conductivity of the composite polymer about 10 orders of magnitude and compared to other MPL-based methods, the resultant OSCMs offered high specific electrical conductivity. As a model protein, laminin was incorporated into these OSCMs without a significant loss of activity. The OSCMs were biocompatible and supported cell adhesion and growth. Glucose oxidase encapsulated OSCMs offered a highly sensitive glucose sensing platform with nearly 10-fold higher sensitivity compared to previous glucose biosensors. In addition, this biosensor exhibited excellent specificity and high reproducibility. Overall, these results demonstrate the great potential of these novel MPL-fabricated OSCM devices for a range of applications from flexible bioelectronics/biosensors, to nanoelectronics and organ-on-a-chip devices.

11:00 AM SB06/SB07.02

Photocapacitive Electrostimulation with Hybrid Silicon/Organic Heterojunction DevicesVedranDerek¹, AleksandarOpančar¹, TonySchmidt² and RainerSchindl²; ¹University of Zagreb, Croatia; ²Medical University of Graz, Austria

Wireless electrostimulation by silicon photodiodes[1], as well as with organic photocapacitive devices[2,3] has been reported earlier, by *in-vitro* and *in-vivo* measurements on single cells and tissues. Organic electrolytic photocapacitor (OEP) devices can be fabricated on micrometre-thin flexible substrates, with the entire active device stack thinner than 100 nm. Even though large optical absorption coefficients of organic materials allow for very thin and conformable devices, their inherently lower photo-conversion efficiencies require relatively large, millimetre-scale devices for effective stimulation. Silicon photodiodes, due to order of magnitude higher photo-conversion efficiencies, can be scaled down to a size of tens of micrometres while still being able to effectively stimulate. However, silicon photodiodes are based on high thermal budget dopant-diffusion and annealing processes, time-consuming and complex steps which in turn increase per unit cost of the devices[4]. We will present novel hybrid inorganic/organic photovoltaic-like devices based on *n*-type silicon as a substrate and a photo-active material and spin-coated and crosslinked PEDOT:PSS as a hole-collecting contact, with the heterojunction region being responsible for the charge separation and PEDOT:PSS additionally enhancing the capacitive properties of the device. Such solution-processed hybrid devices retain high photo-conversion efficiencies of traditional silicon *pn* homojunction photodiodes, yet can be fabricated cheaply and rapidly, enabling quick turnover times for device customization when being used as test beds for *in-vitro* experiments. We will demonstrate enhanced efficiency, spatial resolution

and stability in aqueous environments of hybrid devices in comparison to purely organic OEPCs by measurements of the 3D transductive extracellular potential and corresponding E-fields. In addition, we will show in-vitro photo-induced modulation of the cell membrane potential of the human embryonic kidney (HEK) cells with heterologously expressed voltage-gated K⁺ channels, in comparison with OEPC devices.

References:

- [1] Mathieson, K., Loudin, J., Goetz, G. *et al.* Photovoltaic retinal prosthesis with high pixel density. *Nature Photon* **6**, 391–397 (2012). <https://doi.org/10.1038/nphoton.2012.104>
- [2] Rand, D., Jakesova, M., Lubin, G., Vebraite, I., David-Pur, M., Derek, V., Cramer, T., Sariciftci, N.S., Hanein, Y., Glowacki, E.D., Direct Electrical Neurostimulation with Organic Pigment Photocapacitors. *Adv Mat* vol. 30, **25**, 1707292 (2018). <https://doi.org/10.1002/adma.201707292>
- [3] Silvera Ejneby, M., Jakesova, M., Ferrero, J.J. *et al.* Chronic electrical stimulation of peripheral nerves via deep-red light transduced by an implanted organic photocapacitor. *Nat. Biomed. Eng* **6**, 741–753 (2022). <https://doi.org/10.1038/s41551-021-00817-7>
- [4] K. A. Nagamatsu, S. Avasthi, J. Jhaveri and J. C. Sturm, "A 12% Efficient Silicon/PEDOT:PSS Heterojunction Solar Cell Fabricated at <100 °C," in *IEEE Journal of Photovoltaics*, vol. 4, no. 1, pp. 260-264, Jan. 2014, doi: 10.1109/JPHOTOV.2013.2287758.

11:15 AM SB06/SB07.03

Biocompatibility of PEDOT:DNA and PPy:DNA for Bioelectronics Serpil Tekoglu¹, Sarka Hradilova², Katerina Polakova² and Serdar N. Sariciftci¹; ¹Johannes Kepler University Linz, Austria; ²Czech Advanced Technology and Research Institute, Czechia

Poly(3,4-ethylenedioxythiophene):polystyrene sulfonate (PEDOT:PSS) has showed promising potential for soft and implantable bioelectronics due to mixed ionic-electronic transport¹. On the other hand, natural biopolymers and their composites with synthetic conductive polymers have attracted researchers for biomedical applications due to their biocompatibility, biodegradability, and low toxicity nature². They can be utilized for a variety of applications, including drug delivery, tissue engineering, and medical implants and grafts³. Although biomaterial properties of polypyrrole (PPy) and PEDOT have been extensively studied for implantable electrodes, introducing acidic the surfactants, such as PSS might be cons to this approach. The long-term effects of PSS in the brain have not yet been fully investigated.

The aim of the present study is to investigate cytotoxicity of PEDOT:PSS as well as the new composite materials previously suggested for bioelectronics by our group.⁴ Deoxyribonucleic acid (DNA) was extracted from salmon fish residuals and implemented as secondary dopant during the template synthesis of biocomposites. PEDOT:DNA and PPy:DNA were synthesized by following the same procedure.⁴ As a follow up study, we performed a comprehensive set of cytotoxicity testing of PEDOT:PSS, PEDOT:DNA and PPy:DNA films using NIH3T3 mouse fibroblast cell line. The thin-films of the materials were deposited on glass and used as specimen which allowed cells to grow and proliferate on the surface. The cross-linker glycidoxypolytrimethoxysilane (GOPS) was added into the dispersed solution of composites against film delamination. We monitored the morphological changes via fluorescence microscopy. The live/dead cytotoxicity/viability tests were determined by flow cytometry. The results show that the novel composites are promising with high biocompatibility to living cells while preserving the benefits of electrical conduction for future biomedical applications. Overall, the implementation of natural polymers in biocomposites for medicine has the potential to revolutionize the field by providing safer, more effective treatments for a range of medical conditions.

References

- [1] D.T. Simon, E.O. Gabrielson, K. Tybrandt, M. Berggren, *Chem. Rev.* **116**, 21, 13009–13041 (2016).
- [2] S. Lee, S.M. Silva, L.M.C. Aguilar, T. Eom, S.E. Moulton, B.S. Shim, J. Mater. Chem. B, **10**, 8575 (2022)
- [3] C. Wang, T. Yokota, T. Someya, *Chem. Rev.* **121**, 4, 2109–2146 (2021).
- [4] S. Tekoglu, D. Wielend, M. C. Scharber, N. S. Sariciftci, C. Yumusak, *Adv. Mat. Tech.* **1900699**, (2020).

11:30 AM SB06/SB07.04

Towards the Development of an Electrochemical Random Access DNA Memory (e-RADM) Miguel A. Jimenez-Munoz, Christopher Wood and Christoph Walti; University of Leeds, United Kingdom

Over the last decades, we have produced an unprecedented and exponentially growing amount of information, now approaching the limit that current technology can physically store. Storage demand is in fact likely to exceed the capacity of silicon-based devices within 20 years. Current storage technologies, such as magnetic tapes, have limitations such as large power requirements and cooling systems, as well as only offering limited lifetime that requires periodically transferring data to new devices. As a result, new alternative data storage technologies are required that are space and cost-effective, and able to store large amounts of information in a small contained volume, with minimum power consumption.

As an alternative data storage material, DNA has attracted a lot of attention thanks to several intrinsic properties that make it a desirable data storage medium. First, even very long DNA molecules can be condensed into a small physical space as seen in living organisms, and it can hold 2 bits of information per nucleotide. A single gram of DNA has the potential to store two orders of magnitude more data than the amount of data expected to be produced by 2025. The DNA's extraordinary capacity is also coupled with an excellent inherent stability. But the most important aspect that makes DNA such a viable material is the large number of biotechnological tools that have been developed for the manipulation of this biopolymer.

Current strategies aiming to use DNA as a data storage material rely on sequencing technologies for data recovery. However, on a DNA-based memory, having to fully sequence all DNA strands for retrieving a specific subset of information would imply very high levels of latency and risking integrity of information. As a result, random access strategies are required.

Here, we present the first stages of an electrochemical Random Access DNA memory (e-RADM), which utilizes DNA origami nanostructures and localized strand displacement reactions (SDRs) for data manipulation. Short DNA hairpins containing toeholds complementary to the sequences of adjacent hairpins are attached to the DNA origami such that cascades of SDRs can occur. When a data retrieval query is submitted in the form of a short oligonucleotide, only those hairpins with toeholds complementary to the oligo will open, potentially triggering a cascade reaction. After the cascade reaction, the loops of the hairpins are exposed, containing the information related to the query. The unzipping of these hairpins can be monitored by electrochemical means (Squarewave Voltammetry, SWV), as opened hairpins increase the average distance to the surface, preventing electrons from a redox active molecule attached to the end of the sequence to be transferred to the electrode. The final aim of this work is to develop a fully functional electrochemical device in which functionalized DNA origami structures are immobilize on a gold microelectrode array.

SYMPOSIUM SB08

Bio-Based Polymers and Composites for Sustainable Manufacturing
November 27 - December 6, 2023

Symposium Organizers

Katherine Copenhaver, Oak Ridge National Laboratory
Heli Kangas, Valmet
Mihrimah Ozkan, University of California, Riverside
Mehmet Seydibeyoglu, Izmir Kâtip Çelebi University

* Invited Paper
+ JMR Distinguished Invited Speaker

SESSION SB08.01: Development and Applications of Bio-Based Polymers I
Session Chairs: Katherine Copenhaver and Heli Kangas
Monday Morning, November 27, 2023
Hynes, Level 1, Room 109

10:30 AM SB08.01.01

Harnessing the Potential of Biobased Furandicarboxylate Polyesters in Manufacturing Sustainable Films, Fibers and Nanofibers Giulia Fredi^{1,2}, Sofia Santi¹, Davide Perin^{1,2}, Daniele Rigotti^{1,2}, Michelina Soccio³, Nadia Lotti³, Dimitrios N. Bikiaris⁴, Andrea Dorigato^{1,2} and Alessandro Pegoretti^{1,2}; ¹Università di Trento, Italy; ²Consorzio Interuniversitario Nazionale per la Scienza e Tecnologia dei Materiali (INSTM), Italy; ³Università di Bologna, Italy; ⁴Aristotle University of Thessaloniki, Greece

Poly(alkylene furanoate)s (PAF) are the most credible biobased alternative to oil-based poly(alkylene terephthalate)s, as they show superior thermomechanical and functional properties and are therefore attractive for applications in the packaging, textile, and biomedical fields. This work summarizes some of the most recent and promising developments in the processing and characterization of PAFs with variable alkyl chain length and PAF/poly(lactide) (PLA) blends and nanocomposites, highlighting the advantages and challenges of each processing technique and the main thermomechanical and functional properties of the resulting films, fibers, and nanofibrous mats.

Solvent mixing and casting have been used to prepare PLA/PAF films, and their microstructural and thermomechanical properties were evaluated as a function of PAF concentration (5–30 wt%) and type (4–10 carbon atoms in the alkyl subunit). For neat PAFs, an increase in the alkyl chain length promotes a decrease in T_g and T_m and an increasing tendency to crystallize. However, the latter is true only for PAFs with an even number of methylene groups in the alkyl subunit, while crystallization is generally hindered for the odd-numbered ones. For PLA/PAF blends, the added PAFs are effective in mitigating one of the most important drawbacks of PLA, i.e., its brittleness, as the strain at break of the resulting blends is up to 30 times higher than that of neat PLA. Adding PAFs to PLA also increases its gas- and UV-shielding properties while keeping good transparency in the visible range, which is very desirable for packaging applications. The permeability and diffusivity to N_2 , O_2 , and CO_2 further decreases with the addition of reduced graphene oxide (rGO), which also promotes blend compatibilization and microstructural refinement [1-3].

The same PLA/PAF blends were also processed to produce fibers, both through solutions spinning and through melt spinning, and a detailed statistical analysis was performed to establish the optimal drawing conditions for each composition. Also in this case, the addition of a small (5-10 wt%) fraction of PAFs (with either short- or long alkyl subunits) promotes a remarkable increase in the strain at break compared to neat PLA [4] and, in some cases, also a simultaneous enhancement in the mechanical strength and elastic modulus. Following SEM observations, this effect has been attributed to the orientation and possible crystallization of the PAF phase and a plastic-rubber transition of PAF domains in the strain-hardening phase of the stress-strain curve.

Finally, we explored, for the first time, the production of nanofibrous mats made of poly(butylene 2,5-furanoate) (PBF) and poly(pentamethylene 2,5-furanoate) (PPeF), which have very similar chemical structures but remarkably different physical and mechanical properties [5]. A detailed morphological analysis of the resulting non-woven mats, carried out through SEM analysis, allowed the screening of the best processing conditions for PBF and PPeF. The resulting mats are not cytotoxic, promote cell adhesion without any surface treatment, and allow the retention and controlled release of model drugs (e.g., dexamethasone), thus being promising for biomedical applications, for example as patches for transdermal drug delivery.

[1] Fredi, G.; Rigotti, D.; Bikiaris, D. N.; Dorigato, A., *Polymer* **2021**, *218*, 123527.

[2] Rigotti, D.; Soccio, M.; Dorigato, A.; Gazzano, M.; Siracusa, V.; Fredi, G.; Lotti, N., *ACS Sustainable Chemistry and Engineering* **2021**, *9* (41), 13742-13750.

[3] Fredi, G.; Dorigato, A.; Dussin, A.; Xanthopoulou, E.; Bikiaris, D. N.; Botta, L.; Fiore, V.; Pegoretti, A., *Molecules* **2022**, *27*, 6371.

[4] Perin, D.; Rigotti, D.; Fredi, G.; Papageorgiou, G. Z.; Bikiaris, D. N.; Dorigato, A., *Journal of polymers and the environment* **2021**, *29*, 3948–3963.

[5] Santi, S.; Soccio, M.; Fredi, G. (corr.); Lotti, N.; Dorigato, A., *Polymer* **2023**, *279*, 126021.

10:45 AM SB08.01.02

A Green Conformable Thermoformed Printed Circuit Board Sourced from Renewable Materials Pietro Cataldi; Italian Institute of Technology, Italy

Printed Circuit Boards (PCBs) physically support and connect electronic components to implement complex circuits. The most widespread insulating substrate that also acts as a mechanical support in PCBs is commercially known as FR4 and is a glass fiber-reinforced epoxy resin laminate. FR4 has exceptional dielectric, mechanical, and thermal properties. However, it was designed without considering sustainability and end-of-life aspects, heavily contributing to electronic waste accumulation in the environment. Thus, greener alternatives are needed that can be reprocessed, reused, or biodegraded/composted at the end of their function.

This work introduces diverse PCB substrates based on biobased and/or biodegradable polymers and fibers, a sustainable alternative to the conventional FR4. The substrates have been developed by compression molding, a process compatible with the polymer industry. We demonstrate that conductive silver ink can be additively printed on the substrate's surfaces, as their morphology and wettability are similar to those of FR4. The PCBs have tunable mechanical properties depending on the polymer-fiber combination, ranging from Young moduli of tens of MPa to GPa, and are thus flexible or rigid. Furthermore, they can be thermoformed to curved surfaces at low temperatures while preserving the conductivity of the silver tracks. The green substrates have a dielectric constant comparable to the standard FR4, while they are suitable for micro-drilling, a fundamental process for integrating electronic components into the PCB. The

substrate's biodegradability is tested both in seawater and in soil. We implemented a proof-of-concept circuit to control the blinking of LEDs on top of the PCB, comprising resistors, capacitors, LEDs, and a dual in-line package circuit timer. The developed PCB substrate represents a sustainable alternative to standard FR4 and could reduce the overwhelming load of electronic waste in landfills.

11:00 AM SB08.01.03

Sustainable Photoluminescent Materials Based on Bio-Based Photocurable Functional Inks for Digital Light Processing Cristian Mendes-Felipe^{1,2}, Bárbara Cruz³, Daniela M. Correia³, Verónica de Zea-Bermúdez⁴, Marco Sangermano² and Senentxu Lanceros-Mendez¹; ¹BCMaterials - Basque Center for Materials, Applications and Nanostructures, Spain; ²Politecnico di Torino, Italy; ³University of Minho, Portugal; ⁴University of Trás-os-Montes e Alto Douro, Portugal

The increasing demand for additive manufacturing, particularly digital light processing (DLP) printing, has raised concerns regarding its environmental impact. Conventional materials used in DLP printing, such as petroleum-based resins, often pose challenges in terms of sustainability, resource depletion, and waste generation. To address these issues, it is required to explore sustainable alternatives derived from natural sources.

Natural polymers have gained significant attention as potential ink materials due to their availability, low cost, biodegradability, and compatibility with various printing techniques. The formulation of natural polymer-based inks involves careful consideration of their rheological properties, stability, and printability, while maintaining biocompatibility and environmental sustainability. This work highlights the key factors influencing ink development, including material selection, ink formulation, and process parameters optimization, to achieve reliable and high-quality 3D printed objects. Thus, different reactive diluents have been tested in soybean oil-based ink in order to optimize the ink viscosity with the aim to produce a completely DLP printable formulation. Furthermore, the photopolymerization process of obtained materials denotes to be comparable with commercially available resins maintaining high biorenewable carbon content and presenting high quality in printing parts.

Furthermore, the incorporation of fillers into natural polymer-based inks has opened up new possibilities for functionalizing printed objects. By incorporating photoluminescent materials into the ink formulation, printed objects have been fabricated that exhibit luminescent characteristics, making them suitable for applications such as signalling, identification, security features, or decorative elements.

This work delves into the potential of photoluminescent salt fillers based on lanthanide ions as they possess several unique luminescent features of high technological interest: long luminescence lifetimes (μs to ms), fingerprint emission profiles, fine emission bands, and large pseudo-Stokes shifts. Thus, five photoluminescent salts are used, three of them that emit efficiently in the visible spectral region based on Eu^{3+} (red, 612 nm), Tb^{3+} (green, 544 nm) or Tm^{3+} (blue, 440 nm), and two more emitting in the near infrared spectral region, the Yb^{3+} (1000 nm) and the Nd^{3+} (808 nm). The impact of filler type and dispersion on the optical properties and overall performance of printed structures will be discussed, showing quantitative signal even at low concentration of 5 wt.%, together with a high quality of printing parts. In addition, the challenges associated with natural polymer-based ink development, such as achieving sufficient mechanical strength due to the negative impact of the addition of fillers into the polymer, optimizing print conditions ascribed to the light absorption of the fillers that difficult the photopolymerization process during printing, and ensuring good photoluminescent properties will be addressed.

Overall, this work sheds light on the advancements in natural polymer-based ink development for additive manufacturing, specifically targeting DLP technology, and emphasizes the potential of integrating photoluminescent fillers to expand the functional capabilities of 3D printed objects. The findings presented in this abstract contribute to the broader understanding of materials development in additive manufacturing.

11:15 AM SB08.01.04

Stretchable and Biodegradable Plant-Based Organic Batteries Aiman Rahmanudin, Mohsen Mohammadi, Nara Kim and Klas Tybrandt; Linköping University, Sweden

Next-generation electronics will interface intimately with the human body. This requires devices with high degrees of conformability and autonomy, where integrated soft and stretchable batteries are an essential component. However, existing stretchable batteries are predominantly based on unsustainable transition metal-based active materials and use non-biodegradable petroleum-based elastomers. Such batteries cause environmental issues like waste generation upon disposal and the use of finite resources during manufacturing. To address this, we present a stretchable and biodegradable organic battery employing sustainable plant-based materials with cellulose as a structural component in the electrode, separator, and current collector, and with redox-active biomaterials for energy storage and a biomass-derived biodegradable elastomer for encapsulation. Our 3D porous scaffold design allows for high mass loadings of redox-active biomolecules, in combination with a low Young's modulus. The full cell showed reversible electrochemical performance under stretching and is biodegradable.

11:30 AM *SB08.01.05

Lignin-Based Thermosets via Direct Functionalization using an Efficient and Solvent-Free Valorization Method Dean C. Webster, Alexander Hart and Eric Krall; North Dakota State University, United States

Since lignin is the most abundant aromatic biopolymer, there has been significant interest in identifying ways to convert lignin into useful materials. Degradation of lignin into oligomers and monomers has been a potential approach, however, involves additional processing steps and creates waste. Lignin has abundant hydroxyl groups which can be used for further functionalization to enable crosslinking through a variety of mechanisms. To enable functionalization, lignin—which is a solid material—needs to be converted into a homogeneous mixture for the functionalization reaction. Most commonly, lignin is dissolved in a solvent, functionalized, and then the solvent removed. This process creates waste. We have discovered that lignin is soluble in polyols—such as ethylene glycol, butane diol, glycerol—and the mixture of lignin and polyol can be functionalized together creating a 100% solids crosslinkable liquid resin without creating solvent waste. This approach has been demonstrated with two functionalization chemistries. First, lignin/polyol was functionalized with acetoacetate groups which can be cured using multifunctional amines at ambient conditions. This approach also lends itself to the formation of rigid foams without the use of isocyanates. Lignin/polyol can also be functionalized using methacrylate groups. These can then be cured via free radical initiated crosslinking either thermally or using UV. Due to the aromatic content of the lignin as well as the high functionality of the resins, the thermosets are very hard, with high modulus.

SESSION SB08.02: Development and Applications of Bio-Based Polymers II

Session Chairs: Katherine Copenhaver and Xianhui Zhao

Monday Afternoon, November 27, 2023

Hynes, Level 1, Room 109

1:30 PM *SB08.02.01

How to Implement a Recyclable Materials—Considerations for Scaling, Sourcing, Polymerization and Performance of Bio-Derivable Resins Nicholas A. Rorrer, Robynne Murray, Erik Rognerud and Ryan Clarke; NREL, United States

Thermoset materials have many energy relevant applications due to their excellent performance, versatility, and long material lifetimes. Despite this, at the end of their material life they are often rendered unrecyclable by virtue of the chemical bond topology, namely highly crosslinked networks. Recently, there has been a growing interest in making these materials from bio-based sources and recyclable, both of which are feasible to do. In fact, thermosets represent an ideal market for these materials due to their robust performance and cost premium. Despite the interest and potential, scaling the manufacturing of these materials goes beyond hitting performance specifications; other parameters such as cure time, peak exotherm, and creep must all be considered the entice further interest in material performance. In this work, we will present upon a bio-derived polyester covalently adaptable networks (PECAN) and its many uses in manufacturing, such as fiber reinforced plastics for wind turbine blades, dual cures for accelerated and decarbonized manufacture, and carbon fiber composites for vehicles applications. The benefit in the experimental work will be coupled with techno-economic and supply chain analysis demonstrating the potential of these recyclable and bio-derived systems.

2:00 PM SB08.02.02

Nature-Derived Polymer, Lignin as n- and p-Type Dopants for Tuning the Thermoelectric Properties of Nano-Carbon Materials Yoohyeon Choi¹, Tuan Tran¹, Doojoon Jang¹, Jin Young Kim², Hyun Joo Lee¹ and Heesuk Kim¹; ¹Korea Institute of Science and Technology, Korea (the Republic of); ²Seoul National University, Korea (the Republic of)

Commercial polymers play a crucial role in controlling the electrical properties of organic electronic materials, particularly through the widely adopted charge-transfer doping. Charge-transfer doping is an essential technique in the industry for modifying the electrical properties by controlling the Fermi level of both host materials and dopants. The dopants involve electron-withdrawing groups (EWGs) that exhibit strong electrophilicity, making them suitable for p-doping. Conversely, n-dopants consist of electron-donating groups (EDGs) that enhance the nucleophilicity of the dopants by increasing the electron concentration. However, the production of these commercial organic dopants from fossil fuels is environmentally problematic, necessitating the development of nature-derived dopants to meet global carbon-neutrality (net zero) policies. As a possible candidate, lignin, an abundant biopolymer found in nature, possesses a phenolic structure that can be modified through various functionalization reactions, similar to commercial polymers.

In this study, we propose a lignin as a dopant for tuning the electrical properties of carbon nanotubes (CNTs) by functionalization. This can be achieved by employing electron-withdrawing groups (EWGs) and electron-donating groups (EDGs) *via* fluorination and amination, respectively, using a simple and eco-friendly synthesizing method, microwave-assisted synthesis. The fluorinated lignin works as a p-dopant and the aminated one acts as an n-dopant. Furthermore, the thermoelectric properties of lignin-doped CNTs and their devices are demonstrated for their applications to flexible energy harvesting systems. The fluorinated lignin exhibits the high Seebeck coefficient and electrical conductivity, increasing the power factor by 117% compared to the pristine CNT films. The aminated lignin shows the Seebeck coefficient of $-48 \mu\text{V}/\text{K}$ with good electrical conductivity of $246 \text{ S}/\text{cm}$ and the high power factor. It should be mentioned that the n-type characteristics of aminated lignin-doped CNTs are valuable due to the inherent p-type properties of pristine CNTs. We also demonstrated a thermoelectric generator (TEG) only with lignin-doped CNT films of 10 pn pairs in series, exhibiting an output voltage of 7.86 mV and an output power of 247.3 nW at a temperature difference of 15 K . This study promises the realization of nature-derived n- and p-dopants by an easy modification to improve the thermoelectric performance of CNTs, which performs similar to or superior to those of commercial dopants.

2:15 PM SB08.02.03

Computationally Developed Bio-Based Pressure-Sensitive Adhesives for Healthcare Applications Manjinder Singh^{1,2}, Alessio Alexiadis², Michael J. Adams² and Gaurav Manik¹; ¹Indian Institute of Technology Roorkee, India; ²University of Birmingham, United Kingdom

The adhesive materials used in healthcare sectors for developing adhesive bandages and transdermal patches have been using petro-based components, which cause contact allergy and allergic contact disease, such as dermatitis and stomatitis. In this investigation, linseed oil has been modified to acrylated epoxidized linseed oil (AELO) and acrylated epoxidized methyl ester (AEME) and further used as a low T_g component to develop bio-based pressure-sensitive adhesives (PSAs) computationally using molecular dynamics simulations. The bulk polymer adhesive properties such as density, solubility parameter, and glass transition temperature have been estimated and compared with previously reported literature. The values for density and solubility parameters for the control system have been closely related to the experimental as well as simulated values reported earlier. The glass transition temperature was observed to be in close proximity to the Fox equation values as well as the reported literature, verifying the simulation protocols adopted. Further, surface properties were evaluated in order to understand the adhesive behavior and estimate the interfacial strength with the substrate. The human skin has been considered as a substrate for analysis to understand the interfacial behavior of PSAs and suitability in healthcare industries. The surface energy of human skin was found to be in range with the experimental value, verifying the human skin model adopted for this study. The surface energy for all the developed systems has been estimated, and the AELO-based PSA surface energy value was found to be the highest among all the PSAs. Moreover, the interfacial adhesion strength of AELO-based PSA with human skin was found to be superior to that of AEME-based and control PSAs. An in-depth analysis suggests that the addition of polar groups in AELO and AEME was governing factor affecting the surface properties positively. This study paves the way for exploring the potential of AELO and AEME to formulate novel PSAs with desirable properties for the healthcare industries.

2:30 PM BREAK

3:00 PM SB08.02.04

Biomimetic Multifunctional Nanocomposites from Naturally Derived Materials: Exploring the Functionalities of Conductive Melanin and Crystalline Nanocellulose Bong Sup Shim; Inha University, Korea (the Republic of)

Emulating the sophistication and functionality inherent in natural systems, we have designed multifunctional nanocomposites from naturally derived materials such as conductive melanin-like polydopamine (PDA) and crystalline nanocellulose. Nature employs a bottom-up assembly of nanomaterials to create multiphase structures with hierarchical organization, providing inspiration for our work.

PDA, despite its historical limitation due to low electrical conductivity and limited material functionalities, has been restructured in our laboratory to possess tunable electrochemical conductivities, optical reflectivity, and casting shape stability, while maintaining inherent biocompatibility. This presentation will highlight these innovative modifications, focusing on the unique functional features of PDA in the realm of biosensors and bionic interfaces.

Additionally, our research has expanded to include crystalline nanocellulose, another naturally derived material with promising potential in the creation of multifunctional nanocomposites. Its exceptional strength, biocompatibility, and eco-friendly nature make it a promising candidate for applications alongside conductive melanin.

We will also share insights on our newly developed process for creating electrically conductive PDA, setting the stage for its role in emerging bioelectronic applications such as biotic-abiotic interfaces, edible sensors and actuators, and sustainable electronics. This presentation ultimately bridges the gap between nature-inspired designs and cutting-edge material sciences, pointing to an exciting future in multifunctional biomimetic nanocomposites.

3:15 PM SB08.02.05

Nature's Way: Hierarchical Manufacturing with Biotic Composites Sabrina Shen and Markus J. Buehler; Massachusetts Institute of Technology, United States

Industrial material production is responsible for over half of greenhouse gas emissions from industry which, coupled with biodiversity decline and depletion of critical resources, threatens the livelihood of current and future generations of both humans and non-human species. Conversely, the natural world manufactures enormous quantities of materials that can dramatically outperform human engineering while empowering, rather than degrading, the environment, by architecting simple and common building blocks in creative ways, tuning molecular composition, then nanoscale and macroscale geometries to derive highly specialized properties. This work proposes a new paradigm for materials design that achieves goals of sustainability by aligning and integrating models of material production with natural systems, utilizing modern computation and additive manufacturing technology while drawing source and inspiration from nature. We develop a library of 3D-printable functional composites from fully biotic and non-toxic building blocks, and characterize their mechanical, surface, and biodegradation characteristics. We moreover investigate the advantages afforded by additive manufacturing, including fabrication of hierarchical architectures similar to those found in nature. Finally, we explore strategies to further functionalize similar material platforms with computation-guided biocomposite optimization, generative microstructure design, and incorporation of living components for novel hybrid-living materials.

3:30 PM SB08.02.06

Alternatives to Traditional Plastic: PHB-Based Biodegradable Polymer Composite Films and Disposable Tableware Jiyeon Kim and Kwan-Soo Lee; Los Alamos National Laboratory, United States

Nowadays, plastic materials are taking an important place in our everyday life. Plastic production has soared since it became commercially produced more than 50 years ago. This growth has seen plastic become one of the biggest environmental issues worldwide, with plastic waste polluting land, oceans, air, and even food and human blood. The majority of U.S. plastic waste is landfilled. Of the estimated 40 million tons of municipal plastic waste generated in the U.S. in 2021, at least 85% was sent to landfill sites. Biodegradable polymers have emerged as an alternative. However, certain types of biodegradable polymers, such as PLA, PBAT, Bio-PP, and Bio-PE, require specific environmental conditions or microbial activity to initiate the degradation process. In natural environments where these conditions are not present, such as in landfills or marine environments, the biodegradable polymers may persist for extended periods without undergoing significant degradation. This leads to the accumulation of non-degraded biodegradable polymers, which can contribute to environmental pollution and waste management challenges. Polyhydroxybutyrate (PHB) is a class of polymers naturally created by living microorganisms or synthetically produced from renewable feedstocks. They're biodegradable in the ambient environment, including oceans and soil. However, the PHB has a long-standing problem, due mainly to its inherent brittleness ($\epsilon = 3-5\%$) and poor melt-processability. In this study, we have developed new compositions of PHB-based polymer ($\geq 90 \text{ wt.}\%$) film/tableware bearing green additives (i.e. FDA approved) to overcome the mechanical instability of PHB and optimize their processability. Furthermore, various formulations developed not only increased the elongation properties of the films but also improved processability by lowering the melt temperature of the plasticware. This result has important implications for disposable plastic applications, as it removes the often-cited inferior mechanical properties of currently available bioplastics.

3:45 PM SB08.02.07

Rhizobium Tropici-Produced Biopolymer: Chemical Characterization and Modeling its Interactions with Clay Tei Kim¹, Brinley Dai², Jerry Gao³, Tony Guo Feng Tung⁴, Ashritha Kalakuntla⁵, Haaris Alam⁶, Elise Ngo⁶, Isana Alicea⁷, Aaron Sloutski⁸, Yiwei Fang⁸, Marcia Simon⁸, Jay Gao⁸, Miriam Rafailovich⁸, Steve Larson⁹ and Fengxiang Han⁹; ¹Stanford Online High School, United States; ²Experimental High School Attached to Beijing Normal University, China; ³Beijing No. 80 High School, China; ⁴Shanghai High School International Division, China; ⁵Ed W. Clark High School, United States; ⁶Portola High School, United States; ⁷Patchogue Medford High School, United States; ⁸Stony Brook University, The State University of New York, United States; ⁹US Army Corps of Engineers Research and Development Center, United States

Preventing soil erosion is important in areas vulnerable to flooding, such as watersheds in the Mississippi River Basin. A potential solution is extracellular polymeric substances (EPS), which can increase and maintain the structural stability of soil by increasing resistance to environmental stresses. EPS can improve subterranean root growth, which can stabilize topsoil and help in erosion control. Furthermore, much research in the last decade has focused on explaining EPS-clay/soil interaction in order to improve its applicability. This project aims to investigate the chemical properties of *Rhizobium tropici* bacteria-derived EPS (RT-EPS) and its interactions with clay to model the on-site interactions with soil. EPS produced from the bacteria was used to generate an Ethanol Precipitate Material, RT-EPM, whose chemistry was researched in depth.

First, the chemical composition of RT-EPM was analyzed with thermogravimetric analysis (TGA) and high-performance liquid chromatography (HPLC). TGA results indicated that most of the EPM was organic matter, and HPLC results demonstrated a significant presence of polysaccharides, with glucose being the main component (73%) and a significant presence of galactose (25%). Moreover, the chromatography also showed a dispersity of 1.013, indicating uniformity of the polysaccharides obtained from the RT bacteria. The interactions between RT-EPM and clay was explored through rheology. To examine the reformability of EPM-clay interactions in aqueous medium, an amplitude sweep, an angular frequency test, and a shear rate test were conducted. Comparing the viscosity values across the three freeze-dry and hydration cycles of the EPM, a negligible change in the mechanical properties was identified, indicating the reversible nature of the dynamic cross-linking. To examine the anchoring properties of the EPM to the soil, the rheological properties of the EPM mixed with various concentrations of clay were tested. An overall increasing soil shear strength as the clay concentration increased was found, demonstrating the anchoring capabilities of the EPM to clay. Rheology displayed the mixture's desirable mechanical properties, which simulate RT-EPM's on-site reinforcement of soil via shear strength enhancement. In conclusion, beside a significant polysaccharide presence, a small fraction of proteins was also found by running respective BSA-assays. It was also determined that the EPM, due to its adhesive properties, once mixed with clay forms interactions that are reversible, significant, and are environmentally-influenced. Future directions include in-depth research on the protein fraction RT-EPM contains, with a focus on their influence on the interactions with clay. In order to study the EPM-production influence on the interactions with clay, different dialysis cutoff standards will be applied to treat the EPM. Then, HPLC and rheology tests will be run separately for each cutoff (2K and 14K dialysis). C-NMR and H-NMR will also be applied to further shed light on the chemical composition of the EPM and interactions with clay. Zeta potential of the RT-EPM and clay solution will be used to measure the electrochemical potential and the stability of the particle interactions. The authors would like to thank the US Army Corps of Engineers (ERDC) for their support (W912HZ-20-2-0054) in this research.

SESSION SB08.03: Poster Session: Sustainable Polymers and Composites
Session Chairs: Katherine Copenhaver and Mihrimah Ozkan
Monday Afternoon, November 27, 2023
Hynes, Level 1, Hall A

8:00 PM SB08.03.01

Study of Vitrimerization of Thermosetting Liquid Crystal Epoxy Resin via Chemical Reprocessing and Recycling KyosunKu and HyeonukYeo; Kyungpook National University, Korea (the Republic of)

Thermosetting polymers are applied in various industrial fields due to their excellent physical properties, high thermal and mechanical stability. In particular, epoxy materials are attracting attention as next-generation electronic materials due to their bio-friendliness, electronic insulation, and thermal mechanical stability. However, most thermosetting polymers including epoxy resins, still face challenges from insoluble and non-recyclability. In this study, Liquid Crystal Epoxy Resin (LCER) are synthesized which can be reproduced to overcome the limitations of thermosetting polymers. Also, for application as an electronic material, high thermal conductivity are realized. These results suggest the applicability as electronic materials.

8:00 PM SB08.03.02

Interfacial Assembly of Cellulose Nanofibers at Oil/Water Interface via Tailored Electrostatic Attraction to Establish Surfactant-Free Emulsion Stabilization JaewonShin, BokgiSeo and Jin WoongKim; Sungkyunkwan University, Korea (the Republic of)

The pervasive utilization of petroleum-based cationic surfactants has led to significant pollution of aquatic environments, emphasizing the urgent need to explore sustainable alternatives. Aligned with this concern, this study introduces a novel bio-friendly natural cellulose nanofiber system for surfactant-free emulsion stabilization. To achieve this, glycidyltrimethylammonium chloride was incorporated into bacterial cellulose fibers to enable cationization and nanofibrillation. The newly developed ammonium-functionalized bacterial cellulose (ABC) exhibited electrostatic adsorption at the oil/water interface, facilitated by the spontaneous negative charge present on interfacial hydrocarbon oil drops. Through theoretical considerations that employed the Young's equation and contact angle measurements of three-phase sessile droplets, we observed that current ABC-based solid interface displayed approximately 10-fold higher adsorption energy compared to hydroxylated solid interface. This unique interfacial adsorption behavior of ABC not only reduced interfacial tension but also promoted the formation of a robust interfacial membrane. Importantly, these interfacial properties are corresponding to the high aspect ratio of nanofibers, which provide a larger surface area and, consequently, an increased adsorption energy. Furthermore, our rheological studies revealed that the presence of a fibril network formed by the adsorbed ABC nanofibers facilitated the association of droplets and gelling of the continuous phase, thereby improving the durability of emulsion drops against applied shear stress. Collectively, our findings highlight that our innovative surfactant-free emulsion system would pave the way for development of environment-friendly complex fluids.

8:00 PM SB08.03.03

Scalable R2R Processing of Regenerated Silk Fibroin Film JeffRoshko and FiorenzoOmenetto; Tufts University, United States

Owing to its tunable physical, chemical, and biological properties, regenerated silk fibroin (RSF) has been studied extensively in the film format for potential use in many applications, namely drug delivery, medical/environmental diagnostics, electronics, optics, and tissue engineering. Methods such as spin coating and drop casting are routinely employed to create films from RSF solution in the laboratory for research sample production. However, these techniques do not necessarily translate to larger scales without considerable waste or inconsistency, potentially limiting widespread adoption of useful engineering devices developed from RSF. Meanwhile, techniques developed to produce films industrially such as roll-to-roll (R2R) processing are utilized to manufacture large areas of sensitive coatings and intricate devices, such as microfluidics and flexible solar panels. Herein, we present the development of a scalable means of producing RSF films employing techniques from R2R manufacturing using aqueous processing of RSF. This includes the optimization of RSF-inks that are conducive to solution coating and the comparison of knife-blade sheet-coating at the laboratory scale and slot die R2R coating at multi-meter production scale. This work demonstrates that scalable production is possible for widespread adoption of RSF-based functional devices.

8:00 PM SB08.03.04

Tensile and Compressive Properties of PLA-Based Polymeric Blends Depending on PBS, PBAT and TPS Content and Testing Temperature AnnaDmitruk, JoannaM. Ludwiczak, MateuszSkwarski, PiotrMakula and PawelKaczynski; Wroclaw University of Science and Technology, Poland

Environmentally friendly biopolymeric materials can be utilized to replace commonly used plastics, what leads to a noticeable reduction of the pollution level, caused by their processing and exploitation. Nevertheless, in comparison with their non-biodegradable precursors, they suffer from some severe limitations, such as their capability to be untimely decomposed during long-term work, lowered mechanical properties and impaired thermal resistance. Therefore, it is crucial to make efforts to surpass the mentioned constraints by modification of the properties of biodegradable polymers. Among the possible solutions to advance their development a preparation of variously composed biopolymeric blends seems to be a promising route. Poly(lactic acid) (PLA), being widely applied, is one of the most popular biodegradable plastics, characterized with rather high mechanical properties, but with reduced deformability at the same time. To overcome its brittleness, it can be joined together with more ductile additives, namely: polycaprolactone (PCL), poly(propylene carbonate) (PPC), poly (butylene succinate) (PBS), poly(butylene-succinate-co-adipate) (PBSA), poly(butyleneadipate-co-terephthalate) (PBAT), thermoplastic starch (TPS) and polyamide 11 (PA11) [1-5]. This work was focused on PLA-based compositions doped with different ratios of PBS, PBAT and TPS to evaluate their mechanical (tensile and compressive) properties in various temperatures (-20°C, 0°C, 20°C, 40°C). Specimens for testing were obtained by preliminary extrusion, subsequent injection molding and final cutting into the intended dimensions. Mechanical properties e.g. tensile strength, elongation at break, Young's modulus, yield strength and compressive strength for the deformation of 0.4 were investigated. No additional modification step, as for example, addition of compatibilizers was necessary to be involved in the manufacturing method, what significantly simplified this process without impairing the properties exhibited by the obtained blends. Each of the tested plasticizing secondary compounds positively influenced the elongation at break of PLA – increasing it especially in the case of PBAT and TPS. Simultaneously, together with the increasing content of a ductile component, other mechanical properties i.e. tensile and compressive strength were decreased. The stability of the mechanical performance of thus fabricated mixtures was assessed taking into account also the test conditions (strain rate and temperature), aiming to understand its dependence on these parameters. To gain a deeper insight into the potential applicability of the hereby proposed materials also some selected processing parameters were investigated, namely: melt flow ratio (MFR), melt volume ratio (MVR), heat deflection temperatures for 1.8 MPa and 8 MPa (HDT A and HDT C) and Vicat softening temperatures for two loadings of 10 N and 50 N (VST A and VST B). Finally, the DSC test results were used to complement the study, providing information on the softening, glass transition, cold crystallization and crystallization temperatures of the developed mixtures. It can be concluded that the elaborated biodegradable blends provide a desired compromise between the mechanical properties, in terms of both tensile and compressive characteristics, and deformability of durable and brittle PLA and ductile PBS, PBAT and TPS additives. Hereby described biomaterials aim to find their use in energy absorption applications, as for the manufacturing of thin-walled, cellular inserts filling sports helmets, acting as energy absorbers and replacing regularly utilized foamed materials in protection of their users during an accident.

Funding: This work was supported by the project BOKASK "Development of innovative, replaceable, energy-absorbing structures based on biodegradable plastics for protective helmets"

8:00 PM SB08.03.05

Evaluation of Mechanical Properties of Wood, Changed by Structural Changes in Alkali Treatment and Liquid Impregnation [Rika Takenaka](#) and Daisuke Ishii; Nagoya Institute of Technology, Japan

One of the increasingly serious environmental problems is plastic waste disposal. In addition to direct solutions such as reducing the amount of plastic used, there are indirect solutions such as using less environmentally hazardous materials as substitutes for plastic materials. Familiar examples include the widespread use of paper bags and straws. In this research, we focused on wood, whose main component is cellulose, as a natural polymeric material with the potential to have the same properties as light and strong plastic. In order to increase its versatility and make it an excellent substitute for plastic, we aimed to investigate novel mechanical properties, such as controlled flexibility, by treating it with alkaline solutions and impregnating it with various liquids.

Commercially available balsa wood was used as the experiment material. Alkaline mixture solutions of NaOH 2.5 mol/L and Na₂SO₃ 0.4 mol/L were prepared, and the balsa wood was immersed in the prepared alkaline mixture solutions on a hot stirrer set at 212 °F. Duration times of alkali treatment were 0 h (untreated) and 6 h. The alkali-treated balsa wood was washed with pure water and freeze-dried. Structural observation and mechanical strength measurements were performed on these two types of samples.

Scanning electron microscopy (SEM) was used to observe the cross-sectional structure in each cellulose fiber direction. In particular, cross-sectional observation in the vertical fiber direction showed that the cell wall thickness increased in the alkali-treated samples. This is thought that the cellulose fibers unraveled and swelled by dissolving some of the hemicellulose and lignin that bind the cellulose fibers together. It is expected that this structural change affects the novel mechanical properties.

In the compression test, dry samples before liquid impregnation and liquid-impregnated samples of pure water, ethanol, ethylene glycol, and silicone oil of various kinematic viscosities up to equilibrium were prepared. All measurements were performed in the direction parallel to the cellulose fiber. The results showed that strength varied significantly depending on the alkali treatment and the liquid impregnation. The samples without alkali treatment showed no significant difference in strength depending on the type of impregnating liquid. On the other hand, the alkali-treated samples were softer in water and ethylene glycol and harder in ethanol. This led us to believe that the ratio of hydrophilic to hydrophobic groups was a factor in determining whether the liquid acted as a cushion between the cellulose fibers. With silicone oil, the smaller the viscosity, the stiffer the sample. This is expected to be due to the degree of penetration of the liquid, i.e., the degree to which the molecular chains of the silicone fluid entangle with the loosened cellulose fibers.

In the bending test and the falling-ball impact test, two types of samples were prepared, one in a dry state before liquid impregnation and the other in a liquid-impregnated state after absorption of pure water. Measurements were performed in the direction parallel and vertical to the cellulose fiber. As a result, it was found that the tenacity against bending and the tendency of the force to receive impact differed depending on the fiber direction. We believe that this is due to the effect of structural changes identified by SEM.

As described above, it is possible to control the physical properties of wood using a relatively simple method, and it is hoped that this research will contribute to the development of highly functional sustainable materials that can replace plastics in the future.

8:00 PM SB08.03.06

Lignin-Silica Bio-Composite: A Sustainable Solution for Wastewater Purification [Nataliia Smyk](#)^{1,2}, [Oleg Tkachenko](#)³, [Tetyana Budnyak](#)³ and [Olena Sevastyanova](#)²; ¹Taras Shevchenko National University of Kyiv, Ukraine; ²KTH Royal Institute of Technology, Sweden; ³Uppsala University, Sweden

The proper purification of wastewater is a pressing environmental concern, given the wide range of pollutants it can contain. In this study, a groundbreaking approach utilizing lignin-silica bio-composite as an effective and sustainable sorbent for removing cationic-type contaminants from wastewater is presented. The research team conducted a comprehensive characterization of the proposed sorbent using SEM, FTIR, XPS, and adsorption methods, ensuring its structural integrity and functionality. This attention to detail instills confidence in the efficacy and reliability of the lignin-silica bio-composite. One of the key strengths of this sorbent is its high sorption capacity. The lignin-silica bio-composite demonstrates an impressive ability to attract and retain heavy metal cations, dyes, and cationic medicines, thereby effectively reducing their presence in wastewater. This feature is particularly noteworthy as it addresses a diverse array of cationic pollutants commonly found in both industrial and domestic wastewater. Furthermore, the sorption kinetics of the lignin-silica bio-composite are commendably rapid. Its efficient adsorption process allows for the removal of contaminants within a short period, ensuring swift and effective treatment of wastewater. This attribute is of utmost importance when considering large-scale implementation and practical application.

At room temperature and near-neutral pH, the sorbent exhibited an adsorption capacity of 0.98 mmol Cu(II) and 1.21 mmol Cr(III) per gram of dry adsorbent. These values were three times higher than those achieved by using lignin or silica alone as starting materials. The kinetics study further demonstrated the efficiency of the composite sorbent. Within a short span of 20 minutes, it was able to effectively extract copper(II) and chromium(III) from the solution. Additionally, the adsorption capacity of the immobilized lignin towards brilliant green dye was found to be relatively high. Furthermore, the capacity of the initial silicas and lignin significantly increased when combined in the bio-composite. This enhancement can be attributed to the "extended" conformation of lignin, which allows for better accessibility of various functional groups when adsorbed onto the charged silica surface.

By utilizing lignin, a byproduct of the pulp and paper industry, as a key component of the sorbent, the researchers have showcased a valuable and eco-friendly approach to wastewater treatment. This not only provides an innovative solution but also contributes to the broader goal of promoting a circular economy and reducing waste. The robust characterization methods employed, combined with the sorbent's impressive sorption capacity and rapid kinetics, make it a promising candidate for large-scale wastewater purification. Moreover, its sustainable nature aligns with the increasing need for eco-friendly solutions.

8:00 PM SB08.03.07

Scalable and Sustainable Valorization of Lignin using Single-Step Aerosol Method [Sujit Modi](#)¹, [Onochie C. Okonkwo](#)¹, [Sulay Saha](#)¹, [Hao Zhou](#)¹, [Shaline Kavadiya](#)², [Marcus Foston](#)¹ and [Pratim Biswas](#)²; ¹Washington University in Saint Louis, United States; ²University of Miami, United States

Growing demand for energy and materials has led to increased greenhouse gas emissions from the use of fossil resources. Lignocellulose biomass, one of the few renewable resources of carbon, has an abundance and geographical distribution to displace fossil resources. However, the under-utilization of by-products (i.e., lignin fraction) remains one of the challenges to the rapid growth of biorefinery. Thus, developing technologies that can valorize lignin to high-value products is crucial. Lignin could be used as a precursor for the synthesis of a diverse range of high-value nanomaterials, including lignin nanoparticles (NPs), carbon NPs, and functionalized carbons. However, conventional synthesis methods of these nanomaterials are limited by multistep and batch processes or large volumes of solvents/activating agents. To overcome these challenges of conventional synthesis methods, the present work explores the synthesis of high-value nanomaterials from lignin using a novel and simple furnace aerosol reactor (FuAR) technique.

First, the FuAR is demonstrated for controlled synthesis of lignin NPs of mean sizes between 50 and 68 nm. The as-synthesized lignin NPs are analyzed for their size and functional groups. The mean size of lignin NPs showed an increasing trend with lignin solution concentration. Based on the changes in functional groups, the maximum temperature in FuAR to obtain lignin NPs without significant chemical degradation was found to be around 300 °C (at a residence time of 5.8 s). Furthermore, the bulk and as-synthesized LNPs were tested for UV protection applications. The observed improvement in UV protection with a decrease in lignin particle size is systematically investigated using the optical absorption parameter [1].

Next, temperature and residence time are expected to have a key impact on products obtained from the pyrolysis of lignin. With the systematic understanding of the role of these parameters, carbon nanoparticles with high surface area (up to 925 m²/g) are synthesized in FuAR without the use of activating/templating chemicals. This one-step approach requires significantly less time for synthesis: an order of seconds in comparison to hours for conventional methods. Furthermore, the as-obtained carbon nanoparticles are tested for specific capacitance which showed a linear trend with surface area. The best-performing material (with the highest surface area) exhibited a specific capacitance of 247 F/g at 0.5 A/g with excellent capacity retainment of over 98 % after 10,000 cycles [2,3].

Finally, the FuAR is used for in-situ nitrogen functionalization to synthesize nitrogen-functionalized porous carbons. Urea is added to the lignin solution as a precursor for nitrogen functional groups. Furthermore, the as-obtained carbon nanoparticles are tested for CO₂ adsorption and the material with a maximum surface area of 1051 m²/g exhibited a CO₂ adsorption capacity of 62 mg/(g of carbon) and excellent cyclability.

Overall, these studies demonstrate the unexplored potential of FuAR for the scalable valorization of lignin as well as the excellent performance of obtained nanomaterials in respective applications, which will help advance displacing the fossils with renewable resources.

References:

- [1] S. Modi, M.B. Foston, P. Biswas, Controlled Synthesis of Smaller than 100 nm Lignin Nanoparticles in a Furnace Aerosol Reactor, ACS ES&T Engineering, 2023, 3(5), 671–681
- [2] S. Modi, O. Okonkwo, S. Saha, M. Foston, P. Biswas, Reuse of Lignin to Synthesize High Surface Area Carbon Nanoparticles Using a Continuous and Single-step Aerosol Method, (under review).
- [3] S. Modi, O. Okonkwo, H. Zhou, S. Kavadiya, M. Foston, P. Biswas, Geometric Model for Predicting the Size and Morphology Evolution of Multiparticle Aggregates during Simultaneous Reaction and Sintering, Chem. Eng. J., 2023, 141423.

8:00 PM SB08.03.08

Bacterial Factories for the Production of Functional Lubricants Stephen F. Bartolucci, Cameron M. Longo, Erica Richael and Joshua A. Maurer; U.S. Army DEVCOM Armaments Center, United States

The use of bacteria to produce novel materials is a rapidly expanding arena across many sectors of industry. These “bacterial factories” can be engineered to produce a wide variety of moderately valuable materials. This has been demonstrated both in academia and industry, with the production of such resources as biofuels, natural products, and pharmaceuticals. The use of bacterial factories offers several advantages to other means of production, namely that production can occur at the point of use, and can be fed waste products as feedstock, which otherwise would have little to no value. These two factors make bacterial factories an attractive method for production of kilogram scale quantities of various supplies. One such material which serves as a useful foray into this field is the production of mucin-like greases. Mucins are naturally-produced lubricating substances, the structures of which can be altered to produce materials with varying properties, including lubricity, viscosity, and thermal stability. We hypothesize that by intelligently designing mucin-like compounds, and hijacking the biosynthetic pathways of *E. coli* to produce these proteins, we can construct bacterial factories which produce water-based, ecofriendly lubricants, which can then be compared in terms of performance to traditional, petroleum-based greases. We demonstrate here, the work thus far in the design, transfection, and expression of these proteins, as well as preliminary results of their glycosylation and functionalization towards a functional lubricant.

8:00 PM SB08.03.09

Relationship Between the Structure and Properties of Recycled High-Density Polyethylene Reinforced with Rice Husk Biochar Hussein S. Alrobei; Prince Sattam Bin Abulaziz, Saudi Arabia

The focus of this investigation is on how recycled High Density Polyethylene (HDPE) is affected by rice husk biochar in terms of its structural, thermal, flammable, and mechanical characteristics. The different ratios of recycled HDPE to rice husk biochar were prepared and the best ratios were discovered for different kinds of features. Tensile, flexural, and impact properties were considered when evaluating mechanical features. In order to expound on this fluctuation in attributes, Scanning Electron Microscopy and Fourier Transform Infrared Spectroscopy were carried out. All of these experiments demonstrated the importance of rice husk biochar as an additive for improving the mechanical properties of recycled HDPE.

8:00 PM SB08.03.10

Improving Water Resistance and Film Forming Ability of Cellulose Based Film with Lotus Leaf Extract and Gelatin Behrokh Shams, Evan K. Wujcik and Douglas Bousfield; University of Maine, United States

Cellulose is extensively employed in food packaging to enhance moisture barrier properties. However, cellulose nanofibrils face challenges such as low flexibility and high water vapor permeability. Utilizing hydrophobic materials, like lotus leaves, is a promising approach to improve water vapor transmission rates. Gelatin can help with film forming and flexibility. In this research, cellulose nanofibrils are combined with a natural hydrophobic extract and gelatin to enhance moisture resistance and film forming process.

8:00 PM SB08.03.11

Algae-Powered Sustainability via Hydrothermal Liquefaction: Revolutionizing Epoxy Resins Keshan Lighty, Phillip Agbo, Abhijeet Mali, Lijun Wang and Lifeng Zhang; North Carolina A&T State University, United States

In the growing field of materials science, our study establishes a revolutionary creative approach in the area of biocomposites for sustainable manufacturing. We present research using the hydrothermal liquefaction process used to produce eco-friendly epoxy resins from algae. The materials science community will be interested in this study since it has the potential to alter how epoxy resin is made in the future.

Traditional epoxy resins come from petroleum sources and are necessary but have a significant environmental impact. Through the use of algae, a plentiful, quickly expanding, and underutilized resource, our work reimagines these resins. We unlock the potential of algae using hydrothermal liquefaction to produce a bio-binder that is not only competitive with conventional components in terms of performance but also a champion of sustainability. The biomass is subsequently transformed into a versatile bio-binder by the state-of-the-art conversion method known as hydrothermal liquefaction, which is prepared to give epoxy resin compositions new life.

The incorporation of bio-binders made from algae not only improves the performance of epoxy resins but also tells a captivating story of ethical material development. Our discovery also changes the paradigm by decreasing reliance on limited fossil fuel resources, which helps lessen the carbon load on our world. The size of the world's epoxy resin market was approximately USD 8.70 billion in 2020, and it is anticipated that it will increase from USD 11.59 billion in 2021 to USD 17.10 billion by 2028. When it comes to these widely utilized composite materials, our capacity to reduce the consumption of fossil fuels while incorporating sustainability will have an enormous impact on society as a whole for the better.

With the help of this scientific development, we are encouraging researchers, thinkers, and proponents of sustainable materials to set off on an exploration that will not only enhance the study of materials but also fundamentally alter the way that Epoxy Resin can be manufactured. This research can make an impact in the areas of painting/coatings, electronics, wind turbines & composites, construction, and adhesive/sealants.

We look to encourage creativity, foster teamwork, and bring in a new era of sustainable materials for a more promising, responsible future. I want to assist society in both self-healing and improving the quality of life through sustainable manufacturing and this research assists with that but this is only the beginning. The goal is to help build a better tomorrow starting today.

8:00 PM SB08.03.12

In-Situ Treatment of Flexible Poly(lactic Acid) (PLA) using Non-Thermal Plasma and Various Electrode Geometries: Towards Developing Advanced Analytical and Machine Learning based Hybrid Methodologies to Study The Wettability Characteristics using Surface Topography, Contact Angle Characteristics and Electrical Impedance Spectroscopy Derek Xiong¹, Kaiyu Vang¹, Prakhyat Gautam¹, Parshwa Khane¹, David Ryman¹, Harsh Kumar Bhatt¹, Edbertho Leal-Quiros², Saqib Ahmed^{3,5} and Sankha Banerjee^{1,4}; ¹California State University, Fresno, United States; ²University of California, Merced, United States; ³Buffalo State College, United States; ⁴University of California, Davis, United States

Polymer and polymer composite-based 3D printing processes allow users to fabricate multiple prototypes and proofs of concept, making it an excellent method for testing concepts in the early stages of development. However, the layer-by-layer printing procedure can result in issues with surface properties and the strength of the finished printed geometry, making the product an inaccurate representation of the design. The current work involves the in-situ treatment of biocompatible and flexible-PLA, with non-thermal and room-temperature microplasma-based corona discharge to address this problem and try to optimize the surface properties. The work also involves the evaluation of the effects of plasma-treated 3D printed polymer materials as compared to non-treated samples. This will involve tailoring the polymer properties in the layer-by-layer process to create stronger and more cohesive bonds between each layer through the modification of the surface characteristics of each of the printed layers. Advanced hybrid machine learning models will be developed in combination with analytical methods and empirical data sets to develop strategies for tailoring surface properties of these materials. Additionally, the work involves the characterization of the surface electrical properties using impedance spectroscopy, surface energy and topographical properties using profilometry, and hydrophobic or hydrophilic properties using water contact angle measurements. This will provide valuable insights into the effects of room temperature-based plasma-based surface modification of the printed layers towards enhancement of surface properties of the samples and which electrode will be the most effective.

SESSION SB08.04: Lignocellulosic Technologies
Session Chairs: Katherine Copenhaver and Amber Hubbard
Tuesday Morning, November 28, 2023
Hynes, Level 1, Room 109

8:30 AM *SB08.04.01

Nanocellulose as a Sustainable Alternative to Improve the Performance of Resins for Additive Manufacturing Maria Soledad S. Peresin, Laura Alvarez and Zahra Naghizadeh; Auburn University, United States

In a plea to become more sustainable, the construction industry is increasing the demand for research on partially replacing synthetic resins with renewable and more environmentally friendly

resources, such as biomass. Having good properties, epoxy resins have been an excellent candidate in composites for construction applications. However, it is a relatively brittle material, with a poor resistance to crack initiation and growth. Reinforcing epoxy composites with renewable and mechanically strong materials like nanocellulose is progressively considered recently. In this research, different percentage of bleached and unbleached cellulose nanofibers (BCNF/LCNF) were used to reinforce and partially replace epoxy resin in composites containing Epon 828 and Jeffamine d-400 catalyst. The chemical interaction between cellulose nanofiber and epoxy resin was investigated by quartz crystal microbalance with dissipation monitoring (QCM-D). Mechanical and thermal performances of the reinforced resin were studied using tensile test and thermal gravimetric analysis (TGA) method, and the elemental analysis, Fourier transform infrared spectroscopy (FTIR), was employed on the cured reinforced resin in order to understand the composition of the mixtures after nanocellulose addition. The results proved that the nanocellulose addition changes the chemical composition of epoxy resin, and based on the QCM-D data, BCNF showed favorable chemical interactions with the resin. The mechanical tests indicated the promising results and they proved that the BCNF can be used as a biodegradable and sustainable additive and partially replacement for epoxy resin in composite materials. BCNF reinforced epoxy showed better tensile performance compare to LCNF one. For both LCNF and BCNF dispersed epoxy, the maximum enhancement in tensile properties occurred with 1 wt.% nanomaterial added. It should be noted that the moisture stability of the wood composites was not significantly affected by the nanocellulose content, however, the thermal stability decreased slightly.

9:00 AM SB08.04.02

Towards Sustainable, Environment-Friendly and Low-Waste Gas and Photoactivated Sensors for Low-Power Health and Air Monitoring and Medical DiagnosticsSheidaFaraji^{1,2}, AbdouK. Diallo³, Leszka. Majewski² and TuranOzturk¹; ¹Istanbul Technical University, Turkey; ²The University of Manchester, United Kingdom; ³Gaston Berger University, Senegal

In the recent years, organic phototransistors (OPTs) have attracted considerable interest due to their unique capability of delivering flexible and wearable photosensor modules for various applications in the rapidly growing field of flexible electronics. Compared to conventional photodetectors and inorganic phototransistors, OPTs have an advantage of low-cost fabrication when it comes to their low processing temperature, as well as their mechanical flexibility and versatile chemical functionality of the organic materials. OPT structure is identical to that of an organic field-effect transistor (OFET), where the channel layer simultaneously plays the sensing role. The three-electrode geometry of an OPT controls and amplifies signal, while reducing noise and hence improves photosensitivity by simply adjusting the gate voltage (V_G). Recent advances on OPTs have been particularly focused on detection in the ultraviolet (UV) and near infrared (NIR) regions. UV sensors are gaining increasing attention for utilisation in the health NIR light-sensing OPTs has become one of the most important foundations for advanced control and sensing systems such as night vision for cars and airplanes, light detection and ranging (LiDAR) sensors for autonomous cars and drones, probe beams for biomedical devices and diagnostics, and optical communications and medical fields to prevent sunburn and skin cancer caused by sunlight. Numerous researches have been dedicated to NIR sensors for medical diagnostics, for instance, pulse oximetry or monitoring blood pressure. Home-assisted (bio)medical sensors have gained more demand than ever before, due to increased hospitalisation and hospitals overcrowding during the Covid-19 pandemic. Photoplethysmography (PPG) sensors can be integrated into home-assisted kits and offer tremendous advantage to monitor cardiovascular and atherosclerosis disease markers, such as heart rate (HR), blood pressure (BP), heart rate variability (HRV), arterial oxygen saturation (SpO_2), arterial ageing. Most basic human characteristics can be evaluated by the flow of blood in the subcutaneous tissue. PPG sensors can detect these indicators by monitoring pulsatile changes in blood flow. However, the NIR-absorbing organic materials are very rare because of the difficulty in synthesis to meet the narrow energy band (level) gap of ca. 0.89–1.65 eV, which corresponds to the wavelength (λ) range of ca. 750–1400 nm. In this regard, conjugated donor-acceptor (DA) polymers have been considered viable NIR-absorbing materials since their energy band gaps can be altered by combinations of electron-donating and electron-accepting monomers. Moreover, when used as gas and bio-sensors, sensitivity, selectivity and drift control are critical parameters of consideration. In this work, we proposed novel, low-power, highly sensitive, sustainable OFETs and OPTs based on naturally occurring, biodegradable and low-waste materials. We applied and modified aloe vera (aloin) and cellulose as natural dielectric materials to operate devices at low voltages. For the active material, we synthesised a selection of DA polymers based on thieno-thiophene (TT) and naphthalene diimide (NDI) as the donor and acceptor respectively, with different substituents, as well as metal phthalocyanine, to verify their electrical and sensing performances. The dielectric layers are separately characterised in parallel-plate capacitors and electrical and sensing (both as light-receiving device and chemical sensors) of the OFETs are fully tested. We believe that these natural, low-waste OFET devices can be used as gas, chemical and photoactivated light-receiving, sensing devices with low-operating voltage and good environmental and bias stress stability.

9:15 AM SB08.04.03

Cellulose Nanocrystals-Based Membrane: Enhancing Dimensional Stability and Water Uptake for Alkaline Fuel CellsYuanLu¹ and SoydanOzcan²; ¹LL products, United States; ²Oak Ridge National Laboratory, United States

The design of anion-conducting polymeric materials has been an active field of research, driven by their application in alkaline fuel cells. These membranes offer advantages such as higher cell efficiencies and cost-effectiveness. However, a major challenge lies in balancing high conductivity with excessive water uptake, which can lead to uncontrolled dimensional swelling or membrane disintegration. In this study, we present a unique approach to address this challenge by utilizing cellulose nanocrystals as the basis for a membrane design. Cellulose nanocrystals, derived from cellulose-rich sources through acid or base hydrolysis, possess exceptional mechanical properties and are known for their high water absorption capabilities while maintaining excellent dimensional stability. By incorporating cellulose nanocrystals with various commercially available polymeric binder systems, we prepared an electrolyte membrane for alkaline fuel cells. We systematically investigated the impact of cellulose nanocrystal content, binder formulations, and temperature on water absorption, swelling, and hydroxide conductivity. Our results demonstrate that the resulting membrane exhibits improved dimensional stability, with less than 10% swelling, and excellent water uptake exceeding 100% compared to membranes solely based on polymer binders. Importantly, the presence of cellulose nanocrystals does not compromise the hydroxide conductivity of the polymer binder system. This approach offers a facile and renewable strategy for preparing solid electrolytes with exceptional dimensional stability and high hydroxide conductivity. It represents a promising avenue for the development of solid electrolytes in alkaline fuel cells, offering a simpler alternative to complex polymer synthesis routes.

9:30 AM SB08.04.04

Hybrids Comprising Cellulose Nanocrystals and Percolated Networks of Carbon NanotubesRachelYerushalmi - Rozen; Ben-Gurion University of the Negev, Israel

Cellulose nanocrystals (CNC) are being used in high performance coatings utilizing their anisotropic geometry and their consequential assembly into mesophase with non-isotropic physical properties (1). Yet, CNC are insulating materials and thus could benefit from the incorporation of conductive additives such as single walled carbon nanotubes (SWNT). CNCs are inherently renewable, low cost environmentally friendly and biocompatible rod-shaped crystalline nanoparticles. CNCs that are extracted from plant sources (cotton, wood and more) via acid-hydrolysis are known to disperse SWNTs in dilute suspensions, probably via interactions with the π electrons of the SWNTs. The CNC-dispersed SWNTs are excluded from the *chiral nematic*, N^* phase (2,3) of the CNCs but can be trapped in thin dried films formed via water evaporation from a CNCs suspension. The balance of intermolecular interactions in liquid mixtures of CNCs and SWNTs, and in particular the exclusion of SWNTs from the N^* , are not yet well understood. It was suggested that both size-mismatch and hydrophobic interactions dominate the mixtures (2,3). Here we report the formation of percolated networks of SWNTs within the LC phase of the CNCs in the presence of minute concentrations of surface-active molecules that are used to mediate the SWNTs-CNCs interactions. Small Angle X-Ray Scattering (SAXS) measurements indicate that the effect of the surfactant molecules is minor, and the assembly of the CNCs into an optically active birefringent phase is not modified. Cryo-Transmission electron microscopy and Raman spectroscopy indicate that surfactant-decorated SWNTs are equally distributed within the isotropic and LC phase of the CNCs and form percolated networks within the phases, already at the liquid state (the colloidal ink). These findings are expected to enable the design of new pathways for preparation of optically active and conducting coatings based on CNCs-SWNTs hybrids (4).

References

Schütz C., Bruckner J.R., Honorato-Rios C., Tosheva Z., Anyfantakis M., Lagerwall J.P.F. From Equilibrium Liquid Crystal Formation and Kinetic Arrest to Photonic Bandgap Films Using Suspensions of Cellulose Nanocrystals. *Crystals*. 2020;10:199. doi: 10.3390/cryst10030199

Wang P.-X., Hamad W.Y., MacLachlan M.J. Size-Selective Exclusion Effects of Liquid Crystalline Tactoids on Nanoparticles: A Separation Method. *Angew. Chem. Int. Ed.* 2018;57:3360–3365. doi: 10.1002/anie.201712158.

Mendelson O., Chu G., Ziv E., Levi-Kalishman Y., Vasilyev G., Zussman E., Yerushalmi-Rozen R. Exclusion and Trapping of Carbon Nanostructures in Nonisotropic Suspensions of Cellulose Nanostructures. *J. Phys. Chem. B*. 2019;123:3535–3542. doi: 10.1021/acs.jpcc.9b02227

Attia D, Yekymov E, Shmidov Y, Levi-Kalishman Y, Mendelson O, Bitton R, Yerushalmi-Rozen R. Surfactant-Mediated Co-Existence of Single-Walled Carbon Nanotube Networks and Cellulose Nanocrystal Mesophases. *Nanomaterials* (Basel). 2021 Nov 13;11(11):3059. doi: 10.3390/nano11113059. PMID: 34835823; PMCID: PMC8624387.

9:45 AM BREAK

10:15 AM SB08.04.05

Utilizing Cellulose Nanofibrils (CNFs) in Additive Manufacturing: Multilayer Porous Structure using Microwave IrradiationMd MusfiqurRahman¹, IslamHafez² and MehdiTajvidi¹; ¹University of Maine, United States; ²Oregon State University, United States

Cellulose nanofibrils (CNFs)–based foams and aerogels have distinctive features such as high porosity and low density which enables their application in diverse fields. This type of porous structures is typically produced from water-based suspensions using an energy and time-intensive freeze-drying or supercritical CO₂ drying, making these products particularly unattractive to industry. In addition to this, the 3D printability of CNF–based bio ink is also limited due to the fact of using cost intensive functionalized CNFs or the overall high manufacturing cost especially for drying. As additive manufacturing is essential for accurate development and control of micro-to-macrostructures, this is also a key necessity for the market to adopt the green technology employing CNFs instead of synthetic polymeric materials. In this work sophisticated multilayered infill structures have been prepared through additive manufacturing and by optimizing the solid content of CNFs with the addition of carboxymethyl cellulose (CMC) and urea. The structures were frozen in a freezer to maintain their structural integrity. Finally, microwave irradiation was applied to completely dry the structure with a minimum time and energy. The continuing research consists of rheological study, physical, chemical, and mechanical characteristics of the 3D-printed CNF-based infill structures.

10:30 AM SB08.04.06

Lignocellulose-Based Separators for Aqueous Zinc-Ion Battery[Huisi Li](#), Olena Sevastyanova and Sadegh Askari; KTH, Sweden

The rapidly growing demand for energy storage systems has promoted extensive research on sustainable and cost-effective alternatives to lithium-ion batteries. Zinc-ion batteries (ZIBs) have emerged as promising candidates due to their inherent advantages. ZIBs offer cost-effectiveness in large-scale applications, such as grid energy storage, due to the abundance and lower cost of zinc compared to lithium. They exhibit superior safety with a reduced risk of thermal runaway, making them less prone to fires or explosions. Additionally, ZIBs demonstrate excellent stability over multiple cycles, resulting in a longer lifespan, and the use of zinc as a more environmentally friendly element contributes to their sustainability and lower environmental impact. The investigation of efficient and reliable separators remains a critical challenge in the development of ZIBs since the performance of ZIBs can be significantly influenced by separators. Nevertheless, most research in ZIBs focuses on electrode materials, and little effort has been made on next-generation separators.

Herein, this research aims to present an innovative solution to this challenge by introducing a lignocellulose-based separator for Zn-ion batteries. Lignocellulosic materials, derived from renewable biomass resources, offer a sustainable and abundant alternative to conventional separators, typically composed of non-renewable and costly materials.

The proposed lignocellulose-based separator exhibits several compelling advantages, such as excellent mechanical strength, superior electrolyte uptake, good ionic conductivity and high thermal stability. These properties are crucial for enhancing the overall performances and safety of ZIBs. Moreover, the utilization of lignocellulosic materials promotes a circular economy and reduces the environmental impact associated with battery manufacturing and disposal.

This study will delve into the fabrication process of the lignocellulose-based separator. Furthermore, comprehensive electrochemical characterization results will be presented, demonstrating the separator's superior performance when integrated into the electrochemical cells. Specifically, a better cycling performance and lower impedance of the cell is achieved in comparison to the cells with commercial separators.

Our research findings indicate that the lignocellulose-based separator holds great promise in overcoming the existing limitations of ZIBs separators. It can contribute to the advancement of sustainable energy storage technologies and it aligns with the global drive towards achieving a more sustainable and eco-friendly future.

10:45 AM SB08.04.07

Preparation of Low-Density Foamed Lignocellulosic Structures Enabled by Cellulose Nanofibrils (CNFs)[Maryam El Hajam](#); The University of Maine, United States

Nowadays, there is an increase in interest in biodegradable, renewable, and eco-friendly lightweight materials for use in packaging, building insulation, sound absorption, and other areas. This interest stems from the desire to develop low-density bio-based materials that can replace petroleum-based polymers and other non-renewable materials. Lignocellulosic fibers represent the most suitable alternative to meet this challenge. In addition to being sustainable, many inherent lignocellulosic fiber characteristics, namely strength and stiffness, surpass those of fossil-fuel-based products.

In this work we have focused on foam-forming method as a technology to manufacture lightweight materials based on natural fibers enabled by cellulose nanofibrils (CNFs). In comparison with the water-forming used for conventional products, where a sample filtration results in the formation of thin fibrous sheets, the foam-forming method is based on the use of liquid wet foam as a carrier medium for dispersed natural fibers, and after the molding, the samples are allowed to slowly drain and dry until all foam has disappeared, so that a highly porous, deformable fiber network is formed.

Thermomechanical pulp fibers (TMP), refined wood fibers (RWF) and pine flour (PF), were chosen as the natural lignocellulosic fibers. These fibers differ by their particle size and shape; TMP has long and thin fibers with an aspect ratio of about 21.8 ± 23.4 , followed by RWF, which is characterized by short and large fibers with the presence of some fine particles (aspect ratio 9.4 ± 9.4) and then PF in where the fine particles are abundant (aspect ratio 3.2 ± 1.8). Different concentrations of liquid foaming agents (Lutensol TDA 10 (TDA 10), Sodium Dodecyl Sulfate (SDS) and Polyvinyl Alcohol (PVA)) were mixed with different concentrations of CNFs in a blender to prepare the foam and after that a determined amount of TMP, RWF and PF fibers in their dry state was added separately to the foam. The foam-fibers suspensions were well agitated and poured into square metal molds with mesh filter sheets. The materials were kept for drainage for 30 min and then were placed in an oven at 70 °C for 24 hours up to an average solid content of about 99 % prior to density measurement. The obtained results showed that among the three tested natural fibers, TMP is the best for the preparation of low-density foamed materials without any collapse during the foam forming, the drainage and the drying, because of the high aspect ratio of its fibers. In this case, a concentration of 10 g/l of PVA leads to a foamed material with a density of about 0.039 g/cm³, and concentrations of 15 and 20 g/l leads to the lowest density of 0.035 g/cm³. However, at 10 g/l of TDA 10, we obtained a material with a density of 0.031 g/cm³ and the mixture of TMP with 2 g/l of SDS is able to give a low-density material (0.011 g/cm³). These low-density structures are enabled by the excellent bonding capability of CNFs that will be further discussed in this presentation.

11:00 AM SB08.04.08

Highly Filled Short Banana Fiber-Polypropylene Composites: Fiber Concentration and Interfacial Adhesion Effects on Damping and Mechanical Performance[Caitlyn Clarkson](#)¹, Sanjita Wasti^{1,2}, Amber M. Hubbard², Soydan Ozcan^{1,2} and Uday Vaidya^{2,1}; ¹Oak Ridge National Laboratory, United States; ²The University of Tennessee, Knoxville, United States

Natural fiber-hybrid composites are gaining significant interest from automotive applications because these composites meet performance requirements but are often lighter and lower cost than other fiber composites, therein reducing the environmental burden of the vehicle during its use phase. In the case of natural fibers, the inherent hydrophilicity of natural fibers is one of the biggest challenges to overcome as these materials take up moisture at a significantly higher rate and most thermoplastic matrices are hydrophobic, resulting in poor interfacial bonding between the dissimilar fiber and matrix. In this work, composites are prepared by first creating a non-woven fiber mat of polymer fiber and natural fiber in a wet-lay process, drying, and then compression molding to the final desired shape. A water-based sizing agent is added directly to the process to size fibers in situ during wet-lay. The composite properties are evaluated including the tensile strength and impact resistance, damping, heat distortion temperature and water uptake. Finally, demonstration parts will be shown that are compression molded from the wet-laid non-woven process.

11:15 AM SB08.04.09

Ultra-Strong and Tough Bacterial Nanocellulose Sheets and Fibers via Rotational Fluid Flow Assisted Shear Alignment[Md Abid Shahriar Rahman Saadi](#)¹, Yufei Cui², Shyam Bhakta¹, Matthew Bennet¹, Pulickel Ajayan¹ and Muhammad M. Rahman¹; ¹Rice University, United States; ²Massachusetts Institute of Technology, United States

Bacterial nanocellulose (BC) has emerged as an excellent alternative candidate to non-biodegradable polymers due to the remarkable mechanical properties of its basic nano-fibrillar building blocks. However, full utilization of the mechanical properties in BC structures is yet to be achieved due to the challenge of alignment of the nanofibrils. Herein, we report a facile bottom-up fabrication technique for producing ultra-strong BC sheets by using shear alignment from fluid flow in a rotational culture device, which enables in-situ layer-by-layer deposition of anisotropic cellulose nanofibrils. Specifically, we introduce a custom-designed culture device where the cellulose-producing bacteria are cultured in a cylindrical oxygen-permeable incubator that is continuously spun using a central shaft to produce a directional fluid flow. This flow results in consistent directional motion of the bacteria that significantly improves nanofibril alignment in the bulk BC sheets. The BC sheets produced from the rotation culture device after stretching displayed specific tensile strength (up to ~ 1 GPa/g-cm³) and are comparable to the highest tensile strength of BC sheet ever reported yet showing excellent flexibility that allows forming into desired shapes. We show that the BC sheets can be twisted and stretched to make BC micro-fibers of ~200 μm diameter with tensile strength of 1.3 GPa, the highest reported to date among strong natural fibers. We also compare the mechanical, environmental, and cost-effective aspects of the BC fiber with widely used structural fibers such as E-glass and lightweight steel, showing the superiority of BC fiber. This fabrication technique yielding highly aligned, ultra-strong BC sheets and fibers would pave the way toward extensive applications of BC in a range of bio-degradable structural and functional materials.

11:30 AM SB08.04.10

Self-Organized Mycelium-Based Biocomposites for Sustainable Buildings: From Structure to Fracture and Toughening Mechanics[Precious O. Etinosa](#)¹, Ali Salifu², Sarah Osafo¹, John Obayemi¹ and Winston O. Soboyejo¹; ¹Worcester Polytechnic Institute, United States; ²Boston College, United States

This work presents the results of a combined experimental and analytical study of the structure and fracture/toughening of bioprocessed mycelium composites. The mycelium composites are reinforced with self-organized cellulose/hemicellulose hemp ducts and varying laterite proportions. In-situ studies of crack growth are used to provide insights into the underlying toughening mechanism that gives rise to resistance-curve behavior. The crack-tip shielding contributions from the observed crack bridging and crack deflection mechanisms are then quantified using fracture mechanics models. The results show that toughening is dominated by crack-bridging at low volume fractions of laterite ($\leq 20\%$), while a combination of crack-bridging and crack deflection is observed to occur at increased laterite volume fractions (20 – 60 %). Finally, toughening is shown to occur predominantly by crack deflection at higher volume fractions ($\geq 60\%$).

The implications of the results are discussed for the microstructural design of mycelium and mycelium-laterite composites for potential applications in sustainable buildings.

SESSION SB08.05: Novel Bio-Based Materials
Session Chairs: Katherine Copenhagen and Heli Kangas
Tuesday Afternoon, November 28, 2023
Hynes, Level 1, Room 109

1:30 PM SB08.05.01

High Specific Surface Areas and Interconnected Pore Networks of Porous Pectin Particles for Enhancement of Protein Adsorption Capacity Tue Tri Nguyen and Takashi Ogi; Hiroshima University, Japan

The aging population is leading to an increasing demand for nutritional supplements, including functional foods. Functional foods aim to provide essential nutrients and proteins to the human body. Porous particles, specifically macroporous particles with pores size larger than 50 nm, have emerged as promising carrier materials for efficient delivery of bioactive compounds. While macroporous particles have been developed from various inorganic and organic materials, their application to natural polymer-derived materials remains unexplored.

This study focuses on the synthesis and characterization of porous pectin particles, utilizing a template-assisted spray drying method combined with a chemical etching process to prevent thermal decomposition of the natural polymer. Calcium carbonate (CaCO_3) was used as templates to investigate the formation of porous structures. The incorporation of CaCO_3 significantly increased the specific surface area and pore volume, with the porous pectin particles offering interconnected pore networks for penetration and binding. The porous particles had the large specific surface area ($171.2 \text{ m}^2 \text{ g}^{-1}$), and 114 times compared with non-porous particles prepared without CaCO_3 particles ($1.5 \text{ m}^2 \text{ g}^{-1}$). The study also explored the application of porous pectin particles in protein adsorption using lysozyme as a model protein, providing insights into the adsorption kinetics and isotherm parameters. By comparing the adsorption kinetics of different materials, it was found that increasing CaCO_3 concentrations led to enhanced specific surface areas and total pore volumes, thereby promoting protein adsorption capacity. All porous pectin particles performed rapid adsorption and high uptake capacity on lysozyme, in which PPT-C has the highest adsorption capacity of $2621 \text{ mg lysozyme/g adsorbent}$ for the same amount of adsorbent particles. The adsorption isotherm analysis confirmed the formation of a monolayer following the Langmuir model.

In summary, this report highlights the synthesis of porous pectin particles using a template-assisted spray drying method with CaCO_3 templates. Since this technique is rapid, continuous, reproducible, and one-step, it is attractive both in laboratories and in the industrial setting. Thus, it shows significant promise for developing materials on a large-scale in the future. The porous pectin particles exhibited increased specific surface areas compared to pure pectin particles. Notably, the porous pectin particles utilizing CaCO_3 templates displayed excellent lysozyme adsorption capacity, making them promising adsorbents for various applications such as protein and antibodies purification, virus capture, and micro- and nanoplastic recovery from the environment.

1:45 PM SB08.05.02

Unleashing Nature's Potential: Mycelium-Based Innovation in Bio-Composites Chiara Dognini and Laura Eleonora Depero; Università degli Studi di Brescia, Italy

Mycelium-based composites are groundbreaking biomaterials that are attracting considerable attention in the European Union and the United States. They have tremendous potential for commercializing sustainable products and offer numerous advantages over traditional materials in industrial sectors like construction, packaging, and textiles. These composites are derived from the vegetative part of fungi, which grows on a substrate, often made from agricultural or other renewable waste materials. They can be utilized in the production of various goods, ranging from furniture to insulation panels and eco-friendly leather, aligning with the principles of the circular economy.

Compared to conventional building materials, mycelium-based composites are more environmentally friendly as their production requires fewer resources and generates less waste and pollution. Moreover, they possess superior technical characteristics and can be molded into different shapes and sizes, opening new design possibilities. These adaptable biomaterials possess physical and mechanical properties that can be customized to meet specific requirements. This unique characteristic holds the potential to make a substantial impact on reducing the construction industry's carbon footprint, which currently contributes to around 40% of the total CO_2 emissions.

Building materials contribute to various forms of pollution during their life cycle, caused by production, transport, installation, use, and disposal procedures. Addressing the pollution associated with building materials requires sustainable practices throughout the construction industry. Developing solutions without exploiting natural resources whilst safeguarding the environment is crucial for the ecological transition and the future of a green building market.

In recent years, microorganisms have been validated as a promising alternative to highly polluting products, such as foam insulation boards, particle boards, packaging materials, concrete, non-structural furniture elements, textiles, automotive and aerospace materials, and even medical applications. Mycelium-based composites consist of a lightweight material developed by an interwoven three-dimensional filamentous network of hyphae able to bind the feedstock. The use of biomaterials may have seemed like a utopian concept less than a decade ago, but today, they are gaining increased attention due to their customizable properties achieved through specific cultivation procedures.

Key factors that influence the mechanical behavior of mycelium-based composites include the selection of fungal strains, substrates, and cultivation conditions. Despite the exciting opportunity presented by the development of mycelium-based composites to create sustainable and environmentally friendly materials for the manufacturing industry, their widespread adoption has been limited by the lack of efficient manufacturing processes at the industrial level. The presentation discusses and compares various protocols to standardize an efficient manufacturing process for potential industrial scale-up.

2:00 PM SB08.05.03

Design of Novel Chitosan Nanoparticles for Antimicrobial Applications Magdalena Hudek, Karina Kubiak-Ossowska, Karen Johnston, Valerie A. Ferro and Paul A. Mulheran; University of Strathclyde, United Kingdom

Chitin and chitosan (de-acetylated chitin) are biopolymers derived mainly from langoustine shell waste and are considered potential candidates for novel antimicrobial applications. Chitosan is soluble in weakly acidic aqueous solutions and is polycationic, which gives rise to its antimicrobial properties. We have employed computational simulations to study the binding of chitosan to two different substrates to design new composite nanoparticles with antimicrobial properties. The model substrates studied are chitin nanocrystals and silica nanoparticles. Chitin nanocrystals are stable, biocompatible and biodegradable, and silica nanoparticles have been used for medical applications for a long time and are readily available. Using fully atomistic molecular dynamics and enhanced sampling methods, we evaluated the binding energies of chitosan to the substrates and studied the dynamics of the adsorption process. We show that the adsorption of chitosan to the chitin nanocrystal surface is driven by dispersion forces and hydrogen bonding, while the adsorption to the silica surface is driven by electrostatics. Furthermore, we have simulated the development of a biopolymer film with the substrates, providing insight into the loading capacity of the nanoparticles and the availability of the chitosan to interact with its environment. Our work therefore shows how computational simulations can be used to guide the design of novel composite materials for antimicrobial applications.

2:15 PM SB08.05.04

Data-Driven Representative Models of Bio-Oils for Atomistic Simulations of Biobased Asphalt Rejuvenators Daniel J. York¹, Isaac Vidal-Daza^{1,2}, Cristina Segura³, Jose Norambuena-Contreras⁴ and Francisco Martin-Martinez¹; ¹Swansea University, United Kingdom; ²University of Granada, Spain; ³Universidad de Concepción, Chile; ⁴Universidad del Bío Bío, Chile

A large variety of waste can be transformed into bio-oils and biocrude oils via processing techniques such as pyrolysis and hydrothermal liquefaction (HTL), respectively.¹ These techniques provide a waste valorization route with applications such as the production of biofuel precursors, asphalt additives and other carbon-based materials, which can be derived from plastics, lignocellulosic biomass, chitin, etc. However, there are challenges in the fundamental understanding of the structure-property relationships within these bio-based oils, which are exasperated with difficulty in experimental characterisation of these complex bitumen-like materials. To address this lack of understanding, the development of molecular models for density functional theory and molecular dynamics (MD) studies is key and has potential to identify applications for oils produced by the pyrolysis or HTL of plastics and bio-based polymers (i.e. shopping bags, food utensils, packaging) at the end of their life cycle. Computational studies have been carried out to elucidate the mechanisms occurring during production of bio-based oils during hydrothermal liquefaction^{2,3} but there are few of these studies investigating the properties and behaviours of the produced bio-based oils with only one comprehensive atomistic model having currently been developed for algae-derived biocrude⁴. This model is based on existing models for crude oil and asphaltene^{5,6}, which are based off years of development and research but are tailored to a specific material. In this work, we present a methodology to generate data-driven representative models from pyrolysis gas-chromatography (py-GC-MS) experimental characterization of any complex organic fluid, e.g., bio-oil, biocrude oil, or asphalt samples by generating a selection of statistically representative models that simplify the complexity of the fluid into a limited group of molecules. A variety of different molecular models have generated using a range of different approaches to evaluate the best method for capturing the key chemical features a complex organic fluid that are required for further computational chemistry calculations and large scale molecular dynamic simulations. These atomistic models are key to

understanding and implementing waste valorization routes to sustainable, added-value products with potential to accelerate material development from waste. A computational framework has been developed to automate model creation from py-GC-MS data, which could enable future high-throughput MD simulations; ultimately helping to shape future waste-to-materials strategies.

1 A. Bachs-Herrera, D. York, T. Stephens-Jones, I. Mabbett, J. Yeo and F. J. Martin-Martinez, *iScience*, 2023, **26**, 106549.

2 S. Yan, D. Xia, X. Zhang and X. Liu, *Energy*, 2022, **255**, 124561.

3 D. C. Hietala and P. E. Savage, *Chemical Engineering Journal*, 2021, **407**, 127007.

4 D. López Barreiro, F. J. Martín-Martínez, C. Torri, W. Prins and M. J. Buehler, *Algal Research*, 2018, **35**, 262–273.

5 O. C. Mullins, *Energy Fuels*, 2010, **24**, 2179–2207.

6 O. C. Mullins, H. Sabbah, J. Eyssautier, A. E. Pomerantz, L. Barré, A. B. Andrews, Y. Ruiz-Morales, F. Mostowfi, R. McFarlane, L. Goual, R. Lepkowitz, T. Cooper, J. Orbulescu, R. M. Leblanc, J. Edwards and R. N. Zare, *Energy Fuels*, 2012, **26**, 3986–4003.

2:30 PMBREAK

3:00 PM SB08.05.05

Biomechanics of Biogenic Termite Structures[ZionMichael¹](#), [Sang-binLee²](#), [ThomasChouvenc²](#) and [AnamikaPrasad¹](#); ¹Florida International University, United States; ²University of Florida, United States

Cellulose-based composites possess notable properties such as high-strength to weight ratio, non-toxicity and biodegradability which make them suitable for applications ranging from aerospace to construction. Due to challenges with manufacturability, synthetic production of cellulose-based composites has failed to achieve comparable outcomes to their natural counterparts. One solution is to look to nature for insights and apply biomimetic principles of design to the development of novel fabrication techniques. Here we focused on the cellulose-based structures created by termites to explore the rules and design principles.

Subterranean Termites produce a cellulose-based composite called Carton that is used as a construction material during nest formation. Carton is a sponge-like material that consists of biocemented fecal matter, soil, and saliva. Despite relatively weak microconstituents, Carton is light, resistant to weathering, and multi-functional, adapting macroscopic composition and architecture according to function. Although the macroscopic features of nests have been evaluated in existing literature, there are few studies on material structure, and those that exist are limited by specie, variable and test type. Elucidating the compositional properties of cartons at the microscale may yield learning about interfacial interactions between cellulose polymer and its matrix and solvents for solubilizing cellulose.

Samples of carton from *Coptotermes Gestroi* were obtained from 4 yr-old laboratory reared colonies. After termite extraction and drying, carton was cut and sectioned according to distinct morphological characteristics, correlated with functional architectural features. These features are referred to in this study as nursery, high-cellulose and high-soil regions. Duplicates of samples were taken from each region and embedded in resin. The embedded media was sanded then polished to prepare for material characterization.

Here we perform imaging, Raman Spectroscopy, and Nanoindentation to determine the underlying structure-function-compositional characteristics of the carton and use that to elucidate design principles for cellulose-based structural composite design. The above-proposed research area remains largely unexplored, and this study represents the first of its kind for biogenic structures produced by subterranean termites.

3:15 PM SB08.05.06

Eco-Voxels: Building Blocks for Sustainable Terrestrial and Extraterrestrial Lattice Structures[ChristosE. Athanasiou](#); Georgia Institute of Technology, United States

The environmental impact of construction is significant, with buildings consuming 5% of global energy and contributing to 10% of global greenhouse gas emissions. Concrete production, the most widely used building material, has also led to an alarming 35-fold increase in the last 65 years, accounting for 8% of global CO₂ emissions. In addition to these Earth-bound challenges, humanity faces the task of finding livable spaces beyond our planet within the next century. Astronauts are anticipated to reach Mars by the end of this decade or earlier, necessitating space structures for protection against harsh conditions and radiation. However, manufacturing and assembling structures in space present formidable complexities and obstacles. Expensive transportation of materials and tools from Earth, coupled with the limitations imposed by extreme environments, reduced gravity, and limited labor resources, pose significant barriers to achieving sustainable space structures.

In this talk, I will present a new approach to address these challenges by utilizing tiny, lightweight pieces, termed eco-voxels, made from a renewably sourced bio-composite material that can be mass-produced through injection molding and create lattice structures offering a sustainable solution for rapidly constructing shelters at scale. The mechanical performance of the lattice structures will be evaluated both experimentally and using finite element simulations, and a life cycle assessment will be conducted to analyze the environmental impacts of this novel building system. Through these assessments, the advantages of our eco-building system will be highlighted, paving the way for advanced on- and off- earth construction systems.

3:30 PM SB08.05.08

Peptide Nanowire Coated Jute as Hydrophobic Bio-Based Filter for Oil Water Separation[NoahHann-Deschaine](#), [JeikoJ. Pujols](#) and [RameshAdhikari](#); Colgate University, United States

Solutions to oil-water separation have received a great deal of attention recently in an attempt to address the environmental damage of oil spills. However, many of these separation methods are materially expensive, environmentally hazardous, require elaborate fabrication, or rely on large amounts of energy to function. Herein we provide an effective, low-cost, and environmentally sustainable method for oil-water separation based on the hydrophobicity of self-assembling diphenylalanine nanowires grown on jute fabric. This modified jute fabric exhibits high levels of both hydrophobicity and oleophilicity due to the nanoscale surface roughness created by the growth of the self-assembling peptides on the jute fibers. The treated jute fabric also achieves consistent oil separation efficiencies of 98% via filtration and high levels of efficiency in a novel boat method of separation. Due to the high efficiency and low environmental impact of this method, we believe our diphenylalanine treated jute fabric has a promising potential in the field of oil-water separation.

3:45 PM *SB08.05.09

Novel Recyclable Bio-Based Materials and Technologies for Sustainable Biocomposite Applications[KatarinaTorvinen](#) and [KirsiImmonen](#); VTT Technical Research Centre of Finland Ltd, Finland

Due to challenges in global climate change and related regulations of EU Green Deal, there is a growing need in markets to have sustainable and low carbon footprint materials and products, which are recyclable and utilize bio-based additives. In this paper, we will present novel results in terms of biocomposite material development as well as manufacturing point of view. In addition, we will discuss possibilities to upscale solutions in different end-use sectors, e.g. automotive, construction and packaging.

An optimization of composition and structure of thermoplastic biocomposites having improved functionalities (e.g. fire resistance) is crucial. We have studied sustainable solutions using PLA (polylactid acid) and cellulose esters, and show characteristics of those composites regarding of density, strength and structural properties. We will also address 3D-printable cellulose-based composite material solution, which can be recycled several times without to deteriorate mechanical properties of it.

We will introduce an innovative up-scalable web-forming manufacturing method to produce thermoplastic composites with raw materials like long fibers (natural and synthetic ones), bio-based polymers and additives. Thermoformed products are lightweight, strong and sustainable. The target is to enable the full reinforcing potential of long fibres in thermoplastic composites for high performance applications. In this paper, the selected applications will be highlighted and discussed.

SESSION SB08.06: Sustainable Composites and Recycling I

Session Chairs: Katherine Copenhaver and Mihrimah Ozkan

Wednesday Morning, November 29, 2023

Hynes, Level 1, Room 109

8:30 AM *SB08.06.01

Trojan Horse PET Counts for Facile Chemical Recycling[EricCochran](#), [Ting-HanLee](#), [GeorgeKraus](#), [DhananjayDileep](#), [MichaelForrester](#) and [NacuHernandez](#); Iowa State University of Science and Technology, United States

In this talk I will review our efforts to develop PET copolymers designed for low-energy chemical recycling. For example, PET copolymers with diethyl 2,5-dihydroxyterephthalate (DHTE) undergo selective hydrolysis at DHTE sites, autocatalyzed by neighboring group participation (NGP). Liberated oligomeric subchains further hydrolyze until only small molecules remain. Copolymers were synthesized via melt polycondensation and then hydrolyzed in 150-200 °C water with. Degradation progress was tracked via measurement of retained solids and quantitative analysis of the aqueous phase. With increasing DHTE loading, the rate constant increased monotonically while the thermal activation barrier decreased. The depolymerization products were ethylene glycol, terephthalic acid, 2,5-dihydroxyterephthalic acid, and bis(2-hydroxyethyl) terephthalate dimer, which could be used to regenerate virgin polymer. Composition-optimized copolymers showed a decrease of nearly 50% in the Arrhenius activation energy, suggesting a 6-order reduction in depolymerization time under ambient conditions compared to that of PET homopolymer. Thermomechanical properties were in general similar to PET, with increased tensile strength and reduced extensibility the most notable differences. This approach is readily extended to other "Trojan Horse" counits that provide internal catalysis for facile hydrolysis, methanolysis, or glycolysis.

9:00 AM SB08.06.02

Additive Manufacturing of Hybrid Cellulose Fibers Reinforced Polymer Nanocomposites Bivek Bista¹, Xianhui Zhao², Lu Wang¹, Douglas Gardner¹ and Soydan Ozcan²; ¹University of Maine, United States; ²Oak Ridge National Laboratory, United States

Hybrid reinforced polymer composites are materials in which a particular polymer matrix is reinforced with more than one reinforcing materials, or one type of reinforcing material is incorporated into two similar or different polymer matrix mixtures. Hybrid reinforced polymer composites are among multifunctional materials when more than one characteristic benefit (e.g., mechanical strength, conductivity) is needed. In this study, pulp and nanocellulose fibers were used for reinforcing polylactic acid (PLA) because of their relatively low cost, abundance, and biodegradability. The hybrid nanocomposites were produced with nanocellulose loading between 0 and 20 wt% to investigate the effect of fiber loading on the composite tensile performance. The hybrid nanocomposites obtained were characterized using tensile testing, differential scanning calorimetry (DSC), and scanning electron microscopy (SEM). In addition, a demonstration of additive manufacturing (i.e., 3D printing) of hybrid nanocomposites was carried out. Results show that cellulose fibers can provide PLA with a higher tensile performance.

9:15 AM SB08.06.03

Bamboo-Alginate Composite as a Sustainable Structural Material with High Mechanical Properties Minjae Song, Daewoong Kim, Hyunsoo Han and Sangmin Jeon; POSTECH, Korea (the Republic of)

In the current era of heightened environmental awareness and energy crises, there is growing interest in wood-based composites as sustainable materials. However, the mechanical properties of these composites need significant improvement. In this study, we present a groundbreaking method for developing bamboo composites that exhibit exceptional mechanical properties and enhanced formability. Our approach involved delignifying bamboo and subsequently filling the resulting voids with an alginate solution under reduced pressure, leading to the formation of alginate-impregnated delignified bamboo (ADB). Subsequently, the alginate within ADB was subjected to sequential ionic and chemical cross-linking using CaCl₂ and glutaraldehyde, respectively. By employing a hot-press forming process, we effectively eliminated unfilled voids in the dually cross-linked ADB (DCB), thereby enhancing its mechanical strength. Remarkably, the tensile and flexural strengths of the resulting hot-pressed DCB (HP-DCB) reached unprecedented values for wood composites, measuring at 1.12 GPa and 678 MPa, respectively. These remarkable properties can be attributed to the robust adhesion and efficient load transfer resulting from the dual cross-linking of alginate between the bamboo fibers. Notably, the presence of flexible and adhesive alginate enabled the reshaping of HP-DCB into desired forms through rehydration and molding processes, underscoring its potential for various applications that demand environmentally friendly, high-strength, and lightweight materials.

9:30 AM SB08.06.04

Using Waste Organic Matter from Landfills to Create Lignocellulosic Filler Materials for Biocomposite Plastic Products Roger B. Tipton^{1,2}; ¹University of North Carolina at Charlotte, United States; ²Newell Brands, United States

Utilization of waste materials in the production of new materials is a fundamental component of the circular economy. We experimentally evaluated four different levels of upcycled organic trash material as filler material in a polyethylene wastebasket. We found that we could include up to 7% upcycled organic waste material into existing wastebasket designs as a filler before product requirements were out of tolerance. Upcycled trash, at production volumes, can be a usable filler in low concentrations in industrial plastic products which has the potential reduce landfill waste and reduce virgin resin requirements.

9:45 AM BREAK

10:15 AM SB08.06.05

Understanding the Fragmentation and Transformation Behavior of Plastics in Marine Environments under the Weathering Effect via Ultrasonication-Assisted Mimicking Kyungtae Park and Jinkee Hong; Yonsei University, Korea (the Republic of)

As the amount of plastic usage increases, environmentally exposed plastics rapidly accumulate, with a significant portion eventually ending up in the ocean. The fragmentation of plastics has raised considerable concerns regarding microplastics (MPs) as pollutants and potentially toxic substances to ecosystems and human beings. Previous research has highlighted the threat of fragmentation and surface changes caused by eco-corona or weathering, which can result in severe damage to human beings. Despite the importance of understanding plastic fragmentation, the influence of weathering and the prediction of fragmentation behavior have not been thoroughly investigated. Therefore, it is important to establish an analytical model that can simulate the behavior of environmentally weathered plastics and their transformation. In this study, we focused on the ocean environment, which is considered the ultimate destination for discarded plastics, as our target environment. Our aim is to conduct a comprehensive study on the effects of weathering and the potential threats posed by weathered plastics.

To understand the weathering effect in marine environments, we employed focused ultrasound irradiation. As the cavitation and collapse process repeated during ultrasound irradiation, sonoluminescence emitted ultraviolet (UV) energy to the microplastics. We analyzed the morphological and functional group changes on the surface of particles, comparing manufactured plastic with fragmented nano plastics. Our results showed an oxidation process occurring around the microplastics' surfaces, which we detected through FT-IR and XPS analysis. By comparing the oxidation rate of ultrasound-irradiated microplastics with aged microplastics, we aimed to establish an analytical model for mimicking weathered plastics in marine environments.

While increasing research has highlighted the toxicity of microplastics to the human body, the potential toxicity of naturally fragmented and weathered nano plastics has not been clearly investigated. However, microplastics can transform into nano plastics and undergo changes in surface characteristics due to external physical and biological stresses in the ocean. In this study, we focused on manufactured polyethylene plastic particles and used ultrasound to simulate the natural fragmentation of nano plastic particles caused by weathering in the ocean. We examined the potential threats posed by fragmented nano plastic particles to the human body through immune-cytokine analysis, cytotoxicity tests, and co-culture with human umbilical vein endothelial cells. Our study implemented naturally transformed nano plastics through weathering and evaluated their potential toxicity.

10:30 AM SB08.06.06

All Green Microwave Assisted 99% Depolymerisation of Polyethylene Terephthalate into Value Added Products via Glycerol Pretreatment and Hydrolysis Reaction Muhammad Azeem and Margaret B. Fournet; Technological University of the Shannon, Ireland

Energy-efficient and fast depolymerisation technologies present as new sustainable and green recycling routes for achieving a circular economy for plastics. Herein, we present a highly efficient 2-step microwave-based (MW) degradation of polyethylene terephthalate (PET). Initially, a MW-assisted pre-treatment was evaluated using glycerol as a non-toxic reagent for the conversion of PET into a modified form that makes it easily depolymerised. Box Behnken Design was employed to determine the optimised pre-treatment conditions attaining maximum PET weight loss and favourable crystallinity and carbonyl indices for the pre-treated PET. Glycerol of 12 mL volume and 3 min of 182W MW irradiation resulted in 11% PET weight loss at onset temperature of degradation and gave rise to carbonyl index up to 4.22 and 33% crystallinity of pre-treated PET. MW assisted hydrolysis of the pre-treated PET was then performed in the presence of sodium bicarbonate and ethylene glycol as depolymerizing agents. Within 3 min, the proposed depolymerisation methodology provided 99.9% conversion of PET into 79.1% terephthalic acid (TPA), 17.6% monohydroxyethyl terephthalate (MHET), and 1.8% bis (2-hydroxyethyl) terephthalate (BHET). The obtained TPA was separated from the monomers mixtures and its purification was evaluated via different characterization techniques against a standard TPA. A purity of 95%, 82.4 APHA colour value, 645.3 mgKOH/g acid number and acceptable heavy metal content indicated that the purified TPA can be repolymerised as virgin PET.

10:45 AM SB08.06.07

Bioinspired Biomaterial Composite for All-Water-Based High-Performance Adhesives Marco Lo Presti¹, Nicholas Ostrovsky-Snyder¹, Giorgio Rizzo², Davide Blasi², Marina Portoghese², Gianluca Maria Farinola² and Fiorenzo Omenetto¹; ¹Tufts University, United States; ²Università degli Studi di Bari Aldo Moro, Italy

Nature has ingeniously developed adaptable adhesive materials by utilizing versatile chemistry centered around two fundamental components: catechols and polypeptides. This chemistry

enables adhesive processes even in underwater environments using water-soluble biological substances, presenting a technological challenge that current synthetic adhesives are unable to meet. In this study, we present a bioinspired adhesive composite that aims to integrate the adhesive mechanisms observed in mussels and barnacles. The composite formulation comprises silk, polydopamine, and Fe³⁺ ions, all derived from organic and non-toxic sources in a water-based medium. By combining the adhesive properties exhibited by *Mytilus sp.* (mussels) and *Cirripedia sp.* (barnacles), which rely on proteinaceous filaments and proteic cement, respectively, the composite demonstrates remarkable adhesion capabilities in both dry and wet conditions. In lap-shear tests, it outperforms synthetic commercial glues and other adhesives based on natural polymers, rivaling the effectiveness of leading underwater adhesives. It is worth noting that the composite is entirely biologically sourced, eliminating the necessity for synthetic processes. Moreover, the adhesive production method can be extended to utilize proteins beyond silk by fine-tuning the tyrosine:catechol molar ratio to optimize bonding strength. These findings present a cost-effective and sustainable approach that leverages easily accessible raw materials to develop high-performance adhesives suitable for underwater applications.

11:00 AM SB08.06.08

Scalable Synthesis of Biodegradable Polyesters Based on Interfacial Polymerization[Cecile Chazot](#) and Sara E. Johnson; Northwestern University, United States

Biodegradable polyesters have gained increasing attention as environmentally friendly alternatives to polyolefins, due to their attractive mechanical properties and thermal processability through thermoforming and melt processing. State-of-the-art synthetic routes for aliphatic and aliphatic-aromatic polyesters employ reaction conditions that are not conducive to industrial scale production, such as inert gas environments, high reaction temperatures, long reaction times, and applied vacuum. These complex reaction conditions are a result of oxidation and slow reaction rates due to limited functional group reactivity of the monomers. Here we discuss the development of an open-air, room temperature and scalable synthesis of polyesters based on interfacial polymerization (IP). We investigate the suitability of environmentally friendly solvents and solvent blends in inducing simultaneous fast polycondensation and polymer precipitation in IP and characterize how reaction conditions depend on the backbone chemistry of the synthesized polyesters. This IP route has the potential to enable large-scale production of biodegradable polyesters for applications in consumer products such as packaging and textiles.

11:15 AM SB08.06.09

Hybrid Poly(lactic Acid) (PLA) Composites: Impact of Varying the Cellulose Material (CM) Source[Amber M. Hubbard](#), Katherine E. Copenhaver, Caitlyn Clarkson, Meghan Lamm and Soydan Ozcan; Oak Ridge National Laboratory, United States

Thermoplastic composites are of significant interest in a variety of industries ranging from automotive to construction as they present a recyclable, low cost, and lightweight alternative material without sacrificing performance. Additionally, hybrid composites which contain more than one type of reinforcement (*e.g.*, natural fibers and cellulose materials (CM)) have gained increasing attention where target properties are enhanced via composite formulations. Herein, three different fibers (*i.e.*, creafill, flax, and wheat straw) are mixed with three different CM and incorporated into poly(lactic acid) (PLA) via melt compounding. PLA was chosen as the matrix material for all hybrid composites due to its industrial compostability and its demonstrated applicability in 3D printing. The mechanical and thermomechanical properties of the resulting thermoplastic, hybrid composites are reported where the composite strength and modulus exhibit marked increases compared to the non-hybrid composites. In addition, by matching the fiber and CM, the material demonstrates further improvements; the mechanism for property enhancement is explored as a function of CM. Finally, these hybrid composites are formulated and targeted for automotive and tooling applications.

11:30 AM *SB08.06.10

Bio-Based Feedstock Development for Large Scale Additive Manufacturing[Habib Dagher](#) and Douglas Gardner; University of Maine Advanced Structures and Composites Center, United States

The commercial availability of bio-based thermoplastic resins and filled composite feedstocks for large scale 3D printing is currently limited because large scale 3D printers have only been available for a few years, and the material supply chain is not well developed for these specific applications. It is anticipated that feedstock materials for 3D printing can be widely varied when considering options for thermoplastic resin types, fillers or biofiber reinforcement type(s), and filler/fiber loading levels. Most of the research efforts on bio-based thermoplastics and composite feedstocks for AM have taken place on smaller bench scale 3D printers. For extrusion-based AM on the small scale, both filament and pellet fed printers have been used in feedstock development, although pellet fed extruders will be the norm for large scale AM. Relevant to large scale 3D printer materials development, there exists a great opportunity to adopt feedstocks long utilized for extrusion-based processing of bio-based (wood and lignocellulosic fiber-filled) thermoplastic composites used in the production of linear profiles as well as compression and injection molding composite parts. It is envisioned that the bio-based filler technology already existing for profile extrusion should be easily transferrable to large scale 3D printing with processing and feedstock development efforts. The addition of bio-based fillers in AM feedstocks increases mechanical properties, *i.e.*, strength and stiffness. Important processing parameters to consider with bio-based feedstocks for large scale AM include print time, temperature control, and print layer resolution. Material issues for higher filler loadings in AM feedstocks include viscosity increases and poor interlayer adhesion. Structure property-relationships from extrusion processing in large scale AM need further work to provide improved understanding of material properties for bio-based feedstocks.

SESSION SB08.07: Sustainable Composites and Recycling II

Session Chairs: Katherine Copenhaver and Xianhui Zhao

Wednesday Afternoon, November 29, 2023

Hynes, Level 1, Room 109

1:30 PM *SB08.07.01

Renewable Fiber-Based Prepregs for Composite Laminates[Vikram Yadama](#), Avishek Chanda, Muhammad Bakri and Lloyd Smith; Washington State University, United States

Forming bio-based materials into complex three dimensional shapes can be enhanced using a “prepreg” like material. Adapting bio-based materials into material forms that have successfully been used with synthetic composites allows downstream manufacturing of compression molded panels for a variety of higher value applications. This presentation will discuss the development of a natural fiber prepreg for a variety of applications including automotive interior and exterior panels. Wood strands produced from small diameter trees were stitched to make a preform, which was then injected with a liquid thermoplastic resin, Elium[®] (produced by Arkema), using a vacuum assisted resin transfer molding (VARTM) technique. The outcome was a thin and flexible thermoplastic wood prepreg with an average thickness of 0.017-in.

Lumens of wood strands were completely filled with the thermoplastic resin resulting in 38% and 124% higher Young’s modulus and strength, respectively, of the saturated wood strands compared to wood strands prior to being infused with resin. A temperature and pressure for the thermoforming process were determined, and these thin and flexible thermoplastic wood-strand prepregs were then laminated by compression molding into panels that are flat or profiled with three-dimensional cross-sections. Compared to wood-strand panels produced using compression resin transfer molding (CRTM) and epoxy resin, Young’s modulus and strength of a flat laminate, made of 12 layers of wood prepreg, were 73% and 20% higher, respectively. Prepreg laminates are resistant to moisture uptake and are dimensionally stable as reflected in the water absorption and thickness swelling results. The ability to recycle these thermoplastic composites reinforced with renewable fibers at the end of their service life fits within the circular economy model. These new opportunities and applications for wood strands from small diameter timber would also contribute to sustainable forest management.

2:00 PM SB08.07.02

Economic and Environmental Viability of Mixed Polyester Chemical Recycling for a Circular and Sustainable Plastic Economy[Taylor Uekert](#), Jason DesVeaux and Katrina Knauer; National Renewable Energy Laboratory, United States

Biodegradable polyesters offer an attractive solution to the plastic pollution problem, as they can biodegrade in composting facilities and specific natural environments. However, these valuable materials should ideally be kept in circulation rather than permitted to degrade. While biodegradable plastics subjected to mechanical recycling often exhibit sub-optimal properties, chemical recycling techniques could potentially retain quality while keeping these materials in a circular economy. Here, we conduct a comprehensive technoeconomic analysis and life cycle assessment of three chemical recycling methods: methanolysis, glycolysis, and acid hydrolysis. Our analysis focuses on mixed polyester feedstocks containing poly(lactic acid) (PLA), polybutylene adipate terephthalate (PBAT), and polyethylene terephthalate (PET). We demonstrate that methanolysis economically and environmentally outperforms the other chemical recycling strategies as well as virgin manufacturing of the assessed polymers. The costs and life cycle impacts of methanolysis also tend to decrease with increasing biodegradable polyester content, indicating the suitability of this technology for emerging plastic materials. We conclude by highlighting the challenges and opportunities facing chemical recycling of mixed polyesters and its role in a more sustainable, circular, and pollution-free plastics system.

2:15 PM SB08.07.03

Protein polymers, which are an indispensable part of a living system for maintaining biological information, are also gaining interest due to their inherent structural organizations enriched with easy availability, degradability, and multifunctional properties for the making of functional polymers. Exploring these characteristics features, protein polymers are considered a sustainable building block to develop tailored materials for on-demand applications, which can be an alternative to petroleum-based synthetic polymers in the modern era. The plant-derived protein polymers are gaining a special interest as they are extracted from waste food products in a less environmentally impact sustainable manner contrary to animal-sourced protein polymers. However, the generation of tailored materials for large-scale applications from plant-derived protein polymers has remained challenging due to their limited solubility in water, tedious multistep processes involving toxic chemicals, and/or using non-environmental solvents whilst processing the protein polymers. To overcome these mentioned issues, we exploit plant-derived protein polymers' internal molecular interactions through a unique one-pot processing method, which is helpful to develop its corresponding transparent free-standing bioplastic. The processed film shows improved barrier properties with degradability, which can be fruitful for degradable bioplastic for packaging applications. In the second part of my talk, I will discuss how protein-based biopolymers can be further utilized as functional materials while focusing on their improved charge-conduction capabilities. Currently, our main targeted application for our new family of conductive protein-based biopolymers is for biological interfaces, and we show their use in biosensing applications, while other lines of applications include the use of our biopolymers for biomedical and energy applications.

2:30 PM SB08.07.04

Surface Functionalized Approaches of Dry Mycelium Membranes for Enhanced Lead RemovalMrugankaParasnis, YuFu, ErdaDeng, FeiYao, HaiqingLin and PrathimaNalam; University at Buffalo, The State University of New York, United States

Mycelium hyphae are biomanufactured to grow into 3-dimensional porous networks, which presents a promise for developing sustainable filtration membranes. The hyphal surface is decorated with various biomacromolecules and enzymes that facilitate the remediation of toxic contaminants from the surrounding environments. In this study, we explore various approaches to enhance the filtration efficacy of membranes for lead removal by surface functionalizing dried mycelium hyphae.

Firstly, we aim to present the bioadsorption capacity of untreated, dry mycelium membranes as a function of environmental parameters such as lead concentration, pH, and the duration of Pb[II] exposure to mycelium. A thermodynamic investigation for lead adsorption is conducted to estimate the adsorption capacities and the kinetic rate constants of Pb[II] adsorption onto the mycelium network. Secondly, hyphal surfaces' surface-functionalization using phosphate is explored to remediate lead via pH-dependent biomineralization pathways. Stable lead-based salt crystals formed at the hyphal cell wall (biomineralization), synergistically assisted with the bioadsorption of lead ions, especially at high lead concentrations (1500 ppm), showed 42% enhancement in lead remediation efficiency compared to sole bioadsorption. Moreover, crossflow filtration demonstrated a 90% removal of Pb[II] within 30 minutes of filtration, offering the potential for permeate reuse and metal recovery from the retentate.

Lastly, we achieve the uniform functionalization of the hyphal surface in the mycelium network through electrochemical deposition using low-dimensional layered MXene structures. This innovative approach amplifies the surface-to-volume functional area and permeability of filtrate via mycelium membrane. The preliminary results show an 83% increase in the kinetic rate of Pb[II] removal for the hybrid membrane compared to the unfunctionalized mycelium membrane. Ongoing studies aim to determine the mechanisms underpinning Pb[II] adsorption within the hybrid membrane. Harnessing the intrinsic chemical functionalities of mycelium hyphae presents a promising approach for advancing mycelium-based biomaterials. This research explores novel, sustainable alternatives to synthetic microporous filter membranes exhibiting comparable or higher remediation efficiencies.

Keywords: mycelium membrane, biomineralization, biosorption, MXene

2:45 PM SB08.07.05

Functional Polyurethane Foams with Sustainable Micro- and Nanoscale Reinforcing AgentsZeynepIyigundogdu; Adana Science and Techology University, Turkey

Incorporating additives and structural fillers into polyurethane foams can provide improved mechanical, thermal, electrical properties to create higher performance components made from such foams and can provide improved noise vibration harshness (NVH) and antimicrobial properties. This study explores the effect of adding micro and nanoscale fillers (nanocellulose, biocarbon, graphite, etc.) from sustainable sources as reinforcing agent on thermal stability and mechanical, physical, and sound absorption and antimicrobial properties of flexible polyurethane foam. The incorporation of sustainable micro-and nanoscale reinforcing agents increased the compression modulus and Young's Modulus significantly compared to the control. The addition of reinforcing agents at low concentration (less than 0.25wt.%) showed improvement in sound absorption of plane waves at low frequency range. Minimum inhibitory concentration values were determined by the lowest concentration of the graphite that inhibits the growth of microorganisms. Adding sustainable micro and nanoscale reinforcing agents from the natural sources or recycling products into polyurethane foam reduced waste to landfill and created a superior foam product. This presentation also exemplifies the benefits of creating a closed-loop plastic industry to improve polymer materials and protect the mother earth

SESSION SB08.08: Virtual Session

Session Chairs: Katherine Copenhaver and Mehmet Seydibeyoglu

Wednesday Morning, December6, 2023

SB08-virtual

10:30 AM *SB08.08.01

Sustainable Manufacturing of AcrylonitrileLieslSchindler; Trillium Renewable Chemicals, United States

Trillium Renewable Chemicals is scaling a two-step thermochemical process that converts a biobased feedstock (glycerol) into valuable chemicals (acrylonitrile and acetonitrile). Acrylonitrile (ACN) is used to manufacture a wide-range of materials (e.g., acrylonitrile-butadiene-styrene (ABS) plastic, carbon fiber, acrylic fiber, nitrile butadiene rubber (NBR), acrylamide, specialty amines) with a wide range of end uses including aerospace, automotive, apparel, toys, energy, personal care products, pharmaceuticals, consumer electronics, and wastewater treatment. The presentation will focus on the progress toward the ultimate goal: de-risking Trillium's bio-ACN™ technology for commercialization while achieving stretch targets for sustainability through a combination of low carbon raw materials and innovative process intensification concepts as well as meeting unit cost economics at parity or below the incumbent process to produce acrylonitrile.

11:00 AM *SB08.08.02

Industry-Academic Partnerships: Valorizing Lignin Through De-Aromatization and COOH FunctionalizationMitraGanewatta¹, QiWang¹, ThomasSisson¹, MariolaBeresniewicz-Kopcinski¹, DaniellaMartinez², JaySalinas², MichaelKent², JiHyuanHwang³ and ChuanbingTang³; ¹Ingevity Corporation, United States; ²Sandia National Laboratories, United States; ³University of South Carolina, United States

Lignin is a valuable biomass feedstock that has the potential to produce advanced chemicals and materials. Lignin comprises 15-30% of lignocellulosic biomass and is mostly burned for its heating value within the paper pulping industry. Generating greater value out of this renewable and abundant material is critical for the establishment of a sustainable bioeconomy. We report an industry-academic partnership established to develop high-performance polymeric products from lignin. A near-room temperature aqueous oxidative process was developed to open the aromatic rings within the lignin structure and resulting in carboxylic acid-functionalized lignins. These lignin polyacid materials were evaluated as commercial agricultural dispersants, micronutrient complexation agents, or water-absorbent materials.

11:30 AM SB08.08.03

Optimization of the Dissolution of Nanopolymer (Bacterial Nanocellulose) into Deep Eutectic Solvents Loaded with PolyphenolsMaurelio JrC. Cabo and DennisLaJeunesse; The University of North Carolina at Greensboro, United States

Deep eutectic solvents (DESs) are now generally recognized as a distinct form of ionic liquid (IL) containing massive, nonsymmetric ions with low lattice energy and, hence, low melting temperatures. They are typically generated when a quaternary ammonium salt reacts with a metal salt or hydrogen bond donor (HBD). Hydrophilic ionic solutions, in general, can dissolve cellulose. Although ILs are extremely valuable in the fine chemical industry, their application has been limited because of concerns about toxicity, purity, and high cost. Because of these constraints, DES, a groundbreaking green alternative solvent, was employed. And within these limits, DES, a revolutionary green alternative solvent, was used. These eco-friendly solvents have the potential to be next-generation reagents for more environmentally friendly industrial development and sustainability. Furthermore, the presence of polyphenols and their interactions with bacterial nanocellulose will result in the production of a bioactive complex, which has the potential to provide a wide variety of biological and biocomposites applications. Here, using

Taguchi method, we optimized the potential solubility of nanopolymer sample from bacterial nanocellulose into deep eutectic solvents (choline chloride:imidazole) with the presence of tannic acid as a source of polyphenols.

11:45 AM SB08.08.04

Lignin/PBS Filaments for 3D Fused Deposition Modeling of Medical Orthoses AdnanMemici; King AbdulAziz University, Saudi Arabia

There is a technological need for materials with improved functionalities to propel new biomedical applications. Some of the outstanding challenges could be solved using three dimensional (3D) printing. However, there is a pressing need for new generation of biomaterials that have unique properties. Combining nanomaterials with bio-based and synthetic polymers could yield biomaterials with improved properties. We developed filaments using bio-based waste polymer (lignin) and synthetic polymer (polybutylene succinate (PBS)). Next we coated these scaffolds that could provide antioxidant and antifouling properties while improving the rheological and physical properties of the composites filaments and easy of extrusion and 3D printing. Taken together these nanocoated filaments could propel several biomedical applications including aiding design of medical orthoses and bracing materials.

12:00 PM SB08.08.05

Mussel Byssus as a Green Fiber Manufacturing Platform DavidU. Zamora Cisneros, AlejandroD. Rey, Noemie-ManuelleDorval Courchesne and MatthewJ. Harrington; McGill University, Canada

Biological materials and Nature's manufacturing processes offer inspiration to move towards more green manufacturing of structural and functional materials. Functionality in Nature's materials is strongly correlated with structure, such as chirality, orientation, and layering. In this Ph.D. thesis, I will focus on the mussel byssus, a thread fabricated by marine mussels from a pretransition liquid crystal organization within vesicles, which offers rich store principles and mechanisms to create green tough functional materials and composites used to remain attached to surfaces under continuous flowing states. The material organization of the mussel byssus precursor is a smectic liquid layered semisolid with oriented elements between layers.

This work is divided into three sequential stages: (i) thermodynamic-geometric modeling to ascertain the energy landscape and the stable, unstable, and metastable states of this material under changing thermodynamic driving forces, (ii) colloidal organization including the shape, size, and structural organization to attain for the vesicle-vesicle interactions during the transitional state, and (iii) fiber formation under flow conditions. In this work, I will focus on the progress so far in the area of thermodynamic-geometric model and will shed light on how geometric tools are powerful and useful to detect, control, and optimize equilibrium states of smectic liquid crystals, their organization, and thus, its application for the tuning of material properties.

In particular, we use level set lines of steepest descent, bifurcation methods, lines of curvature and geodesic to provide a multidimensional view of the evolution of stable, unstable states that appear when decreasing the phase transition parameter, here taken as temperature. Overall, it is found that the emergence of smectic order favors the increase of the orientational alignment, yielding in the enhancement of the elasticity modulus of the solid state. Understanding the evolution and behavior of the hierarchical organization will provide a pathway for the development of green engineering principles, storage technologies, biocompatible materials such as tissue scaffolds, and advances in the processing of such materials involving scalable biomedical and technical applications like extrusion molding, and injection molding to address crucial public health and environmental concerns.

12:05 PM SB08.08.06

Feasibility of Hot-Melt Extrusion of Simvastatin-Based Amorphous Solid Dispersions with PVP-VA and HPMC-AS CharinaLampa¹, ScottSmith², XiaolingLi¹ and BhaskaraJasti¹; ¹University of the Pacific, United States; ²Gilead Sciences, United States

Purpose:

Poor aqueous solubility is among the primary causes of low or variable oral bioavailability in pharmaceutical development, with ~45% of new drugs considered very slightly soluble or practically insoluble. Preparation of amorphous solid dispersions (ASDs) is one approach to address the challenge. An ASD is composed of an amorphous drug stabilized in a polymeric excipient matrix. Amorphous forms have higher free energy and thus, higher aqueous solubility and/or faster dissolution compared to crystalline forms. However, its thermodynamic instability means it has a propensity to degrade or crystallize during processing and storage. Hot-melt extrusion (HME) is an emerging technology for ASDs due to its advantages as a scalable and efficient process. It is also attractive due to its sustainability as it does not require the use of solvents as other manufacturing practices like spray-drying. Key challenges with HME are poor physical stability of the amorphous drug and thermal degradation during processing. Simvastatin (SIM), which belongs to an important class of lipid-lowering drugs, was selected as a model drug. Poly(vinylpyrrolidone) vinyl acetate (PVP-VA), a neutral, aprotic polymer, and hydroxypropyl methylcellulose acetate succinate (HPMC-AS), an anionic, protic polymer were selected as the excipients. The objective of this study is to prepare and characterize HME ASDs with varying SIM/polymer ratios.

Methods:

ASD Preparation. ASDs of SIM/PVP-VA and SIM/HPMC-AS were prepared at varying ratios of 0/100, 25/75, 50/50, 75/25, 100/0 % w/w SIM/polymer using twin-screw hot melt extrusion. Physical blends of SIM and polymer were prepared by a 1-min trituration, followed by a 10-min blending step. Each blend was fed into the hot-melt extruder with a thin-slit die at 150°C. The extrudate was collected and milled to a powder using a tube mill at 15,000 RPM for 1 min.

Physical form characterization. The physical form of SIM in the ASDs was identified using powder X-ray diffraction (PXRD). Samples were scanned in reflection mode over a 2.0000 – 39.9990 °2θ range with a Cu Kα1 radiation source and a detector at 45 kV and 40 mA. Step size was 0.0131 °2θ and scan rate was 0.08 sec/step. Modulated differential scanning calorimetry (mDSC) was used to determine the glass transition temperature T_g, with a nitrogen purge flow of 50 mL/min and a 3°C/min ramp rate and a modulation cycle of ±1°C every 60 sec.

Water content. Thermogravimetric analysis (TGA) was performed on the ASDs, with a nitrogen purge flow of 50 mL/min and a 10°C/min ramp rate from 25°C to 150°C. Weight loss was attributed to water content.

Chemical purity. Chemical purity was evaluated using ultra performance liquid chromatography (UPLC). A gradient method using water with 0.1% trifluoroacetic acid (TFA) and acetonitrile with 0.1% TFA was employed for separation, and the chromatogram at 236 nm was used for analysis.

Results

This study determined the suitability of preparing SIM/polymer ASDs with HME. All extrudates passed through the extruder with a residence time of 5-10 minutes. Subsequent milling of the ribbons yielded free-flowing powders that can be used for further processing. All ASDs demonstrated the amorphous nature of the drug, indicated by an amorphous halo using PXRD. A single glass transition temperature was observed, indicating a homogenous solid solution. The composite T_g of the ASDs decreased as the SIM-loading was increased. Weight loss by TGA was relatively low across all ASDs, indicating moisture content ranging from 0.3% to 3.8%. Thermal degradation was minimal, with purity >97% across all ASDs relative to starting SIM purity, although purity seemed slightly higher with PVP-VA.

Conclusions

ASDs of simvastatin/PVP-VA and simvastatin/HPMC-AS were successfully prepared by hot melt extrusion. Simvastatin was demonstrated to be in an amorphous form with both polymeric excipients, and exhibited good chemical stability during the hot melt extrusion process.

12:10 PM SB08.08.07

Naturally Derived Photoluminescent Composite Inks for Advanced Applications DanielaCorreia¹, BárbaraCruz^{1,1,1}, RitaPolícia¹, NelsonPereira¹, PauloNunes², MarianaFernandes², CarmenR. Tubio³, GabrielaBotelho¹, Veronicade Zea-Bermudez^{2,4} and SenentxuLanceros-Mendez^{3,5}; ¹University of Minho, Portugal; ²University of Trás-os-Montes e Alto Douro, Portugal; ³Basque Center on Materials, Applications and Nanostructures, Spain; ⁴University of Trás-os-Montes e Alto Douro, Portugal; ⁵Ikerbasque, Basque Foundation for Science, Spain

Naturally derived polymers have been increasingly explored by different fields of knowledge to be applied in different areas. The high interest devoted to natural polymers mainly relies on their natural abundance, unique properties, and sustainability attributes.

The interesting advantages of this type of polymer allow the development of smart and multifunctional materials with a strong potential for sensors and actuators, biomedicine, and environmental remediation applications [1], among others.

Particularly, photoluminescent materials are of high interest for sensors in anti-counterfeiting systems and actuators [2]. This type of material can be obtained by incorporating different luminescent compounds, such as rare-earth elements, quantum dots, fluorescent compounds, and inorganic phosphors.

Lanthanide ions (Ln³⁺), have gained a special interest in recent times due to their fine emission bands, wide diversity of colours, large pseudo-Stokes shifts, long luminescence lifetimes, and difficult replication of the fingerprint emission profiles [3].

The present work presents the development of photoluminescent materials based on the natural polymer sodium alginate (SA), a linear polysaccharide derivative of alginic acid comprised of 1,4-β-d-mannuronic (M) and α-l-guluronic (G) acids [1], incorporating different contents of the compounds sodium tetra(2-thenoyltrifluoroacetate) europate (III) (Na[Eu(II)(ta)₄]) (5, 10 and 20% wt.) and 1-butyl-3-methylimidazolium tetra(2-thenoyltrifluoroacetate) europate (III) [Bmim][Eu(II)(ta)₄] (20% wt.) have been developed by a solvent casting method [4].

The influence of both compounds in the morphology of all the developed materials were evaluated by SEM and their physical-chemical properties by FTIR-ATR and DSC analysis.

Independently of the luminescent compound, a non-porous material was obtained, however, a surface roughness increase was observed. Both Na[Eu(II)(ta)₄] and [Bmim][Eu(II)(ta)₄] induce a

thermal stability behavior on SA and an improvement of the mechanical properties.

The highest luminescence was observed for SA/[Bmim][Eu(II)] films, exhibiting an intense red/orange emission when irradiated with ultraviolet (UV) light at 388 nm, and in this context a strong potential to be applied in anticounterfeiting applications. The developed materials are also suitable to be applied as electromechanical actuators.

SYMPOSIUM SB09

Biomaterials for Regenerative Engineering
November 28 - December 5, 2023

Symposium Organizers

Guillermo Ameer, Northwestern University
Gulden Camci-Unal, University of Massachusetts Lowell
Melissa Grunlan, Texas A&M University
Carolyn Schutt Ibsen, Oregon Health and Science University

Symposium Support

Silver

Acuitive Technologies, Inc.

Bronze

Center for Advanced Regenerative Engineering, Northwestern University

* Invited Paper

+ JMR Distinguished Invited Speaker

SESSION SB09.01: Polymeric Biomaterials for Regenerative Engineering I

Session Chairs: Guillermo Ameer and Gulden Camci-Unal

Tuesday Morning, November 28, 2023

Hynes, Level 1, Room 104

8:30 AM *SB09.01.01

Silk Proteins as Functional Biomaterials for Regenerative Medicine David L. Kaplan; Tufts University, United States

Biomaterials that provide versatility in terms of control of structure, chemistry, morphology, mechanics, degradation lifetime, and material form factor, while biocompatible, are useful in meeting regenerative medicine goals. Silk, as one of the oldest biomaterials utilized as sutures for centuries, is undergoing a rebirth into new biomaterial formats and applications for regenerative engineering for the medical field. Key to this emergence has been fundamental insight into mechanisms of self-assembly and control or tunability of material features achievable with silk. As a unique, high molecular weight, amphiphilic protein, new modes to modify the native protein using processing methods, chemistries and bioengineering approaches are emerging from the laboratory. Some of these recent strategies will be discussed related to fundamental aspects of controlling biomaterial structure and function, leading to new silk-based biomaterials for regenerative medicine.

9:00 AM SB09.01.02

Unconventional Biomaterials for Regenerative Engineering Gulden Camci-Unal; University of Massachusetts Lowell, United States

Across different areas of regenerative engineering, there are limitations with controlling cell adhesion, viability, growth, differentiation, biocompatibility. Conversion of simple and abundant items to advanced cell culture substrates addresses some of the limitations in regenerative engineering. Departure from complex fabrication processes to the applications of unusual materials provides another dimension to the engineering of viable multifunctional tissue constructs and regenerative can increase access to regenerative engineering technologies on a global scale. In this work, we used unconventional biomaterials such as eggshells and paper for tissue regeneration.

We fabricated eggshell micro/nanoparticle (ESP) reinforced protein-based scaffolds to produce mechanically stable and biologically active three-dimensional (3D) scaffolds that can differentiate stem cells into osteoblasts. The ESP-reinforced constructs were then implanted in a rat model to determine their biocompatibility and degradation behaviors. In addition, these composite scaffolds were used to regenerate critical sized cranial defects in a rat model. We also used mineralized paper scaffolds with hydrogels through an origami-inspired approach to test their osteoinductivity and potential for tissue repair in *in vitro* and *in vivo* studies.¹⁻⁶

The ESP-reinforced scaffolds enabled the differentiation of stem cells into osteogenic lineage. The constructs showed significant enhancement in mineralization by the cells. The ESP composites demonstrated superior mechanical properties and showed favorable *in vivo* responses by subcutaneous implantation in a rat model. The scaffolds were responsive to cells and did not elicit inflammatory responses *in vivo*. The implants were easily accepted by the host, allowed for cellular infiltration and migration in 3D, and highly vascularized. Implantation of ESP-reinforced scaffolds into critical sized cranial defects in a rat model resulted in significant bone regeneration in 12 weeks. The resulting bone volume and bone density were as high as the native bone using these composite scaffolds as determined by micro-computed tomography assessment.

We also fabricated origami-inspired paper-based scaffolds for biomineralization. Material properties of the paper-based mineralized scaffolds were highly tunable. The tensile modulus of the scaffolds increased significantly after the mineralization process. Gene expression results for the osteogenic differentiation markers revealed the osteoinductivity of the mineralized paper scaffolds. Subcutaneous implantation of the samples in rats demonstrated biocompatibility, vascularization, and integration *in vivo*.

Unconventional scaffolds that are readily available and adapted from nature demonstrated biomimetic characteristics including porosity, structure, and bioactivity resulting in physiologically relevant constructs. The use of existing naturally derived materials in combination with hydrogels for regenerative engineering provides an inexpensive and sustainable approach that benefits the economy and environment while providing unique solutions to unmet clinical needs. Many of the unconventional biomaterials are overlooked and under-studied for biomedical applications, partly for their simplicity as mundane items.

References: ¹Nguyen, M.A., Camci-Unal, G., Trends in Biotechnology, 38(2): 178-190, 2020. ²Suvarnapathaki, S., Wu, X., Lantigua, D., Nguyen, M.A., Camci-Unal, G., Nature Asia Materials, 11(1): 1-18, 2019. ³Wu, X., Stroll, S.L., Lantigua, D., Suvarnapathaki, S., Camci-Unal, G., Biomaterials Science, 7, 2675-2685, 2019. ⁴Wu, X., Gauntlett, O., Zhang, T., Suvarnapathaki, S., McCarthy, C., Wu, B., Camci-Unal, G., ACS Applied Materials & Interfaces, 13, 51, 60921-60932, 2021. ⁵Wu, X., Walsh, K., Suvarnapathaki, S., Lantigua, D.,

9:15 AM SB09.01.03

Development of Tissue-Safe, Shape Memory Polymer Scaffolds[CourteneyRoberts](#), SarahK. Beck, CaitlynM. Prejean and MelissaGrunlan; Texas A&M University, United States

Thermoresponsive shape memory polymers (SMPs) were developed as self-fitting scaffolds to heal cranial bone defects. Exposure to temperatures above the melt transition temperature (T_m) causes scaffolds to undergo shape recovery, driving its expansion to the tissue perimeter for improved osseointegration and healing. SMP scaffolds were originally prepared from semi-crystalline, biodegradable *linear*-poly(ϵ -caprolactone)-diacrylate (PCL-DA; 10k g mol⁻¹). However, a major limitation of scaffolds based on *linear*-PCL-DA is a T_m of ~55 °C. Such a scaffold could be submerged into saline at this temperature and pressed into a bone defect for self-fitting. However, to extend the working time, post-implantation irrigation with ~55 °C saline would induce thermal damage to the surrounding tissues. Ideally, a SMP self-fitting bone scaffold would have a reduced T_m , but still be > 37 °C in order to ultimately return to its rigid state for mechanical support. Other devices prepared from SMP scaffolds could also be envisioned if the T_m was reduced to 37 °C, affording shape recovery (expansion) upon implantation. For instance, this would enable the development of self-expanding gynecological stents. Thus, in this work, a T_m of ~39 - 45 °C (bone scaffolds) and ~37 °C (stents) was targeted for tissue safety and functionality. We sought to lower the T_m of PCL by altering the architecture, creating *star*-PCL-tetracrylate (*star*-PCL-TA), and by also decreasing molecular weight (M_n). This yielded scaffolds with T_m of ~45 °C (10k g mol⁻¹), ~40 °C (7.5k g mol⁻¹), and ~29 °C (5k g mol⁻¹). Owing to reduced crystallinity, scaffolds based on *star*-PCL-TA degraded faster than *linear*-PCL-DA of the same M_n , and also exhibited decreased compressive moduli. Scaffold degradation rates increased as the M_n of *star*-PCL-TA was decreased. Overall, by altering the architecture of the PCL macromer from a *linear* to a *star* architecture and reducing the M_n , more tissue-safe SMP scaffolds were created. Specifically, scaffolds with T_m values ideal for self-fitting bone scaffolds and self-expanding stents were obtained.

9:30 AM SB09.01.04

Oncological Engineering: The Development of 3D Printed Metamaterial Implants for Patients with Bone Tumours in End-Of-Life-Care[AliMohammed](#), [BorutLampret](#) and ConnorMyant; Imperial College London, United Kingdom

Cancer in bone presents a formidable challenge, particularly for terminally ill patients. Addressing this issue, our research focuses on the development of a pipeline for ultra-high-resolution 3D printed metamaterial-based bone replacements. Unlike traditional implants or conventional 3D printed bone scaffolds, our approach aims to improve patients' quality of life during end-of-life care by offering biocompatible, bioinert implants with sophisticated functionality that closely match the mechanical behaviour of native bone. The challenge arises in meeting the custom requirements of patient specific implants such as size, shape and native mechanical properties, along with the fabrication technology required to 3D print them.

The presentation introduces the fabrication process and material for a Metamaterial implant, where the mechanical properties are not derived from the properties of the base material but from its smartly designed architecture. The chosen technology is vat-polymerisation 3D printing which offers the opportunity to produce complex, multiscale, geometries from a suitable biocompatible material at the required specifications. The final implant will be a computationally derived hierarchical lattice with an intricate multiscale structure. It will need to span several orders of length scale (cm > mm > μ m) to create the desired properties. However, commercially available 3D printers face limitations with delivering the required high-resolution and small build size print specifications for such designs. These limitations stem from resolution constraints, curing inconsistencies, and challenges in balancing speed and precision. Therefore, a challenge remains in the development of a printer capable of producing biocompatible photopolymer objects with the desired feature resolution at the required build size. To overcome the limitations faced by commercial 3D printers at the macro scale, we developed an in-house projection micro-stereolithography (P μ -SL) 3D printer capable of achieving ultra-high resolutions. This achievement is essential for fabricating implants with intricate designs that exhibit metamaterial properties at resolutions of 1-5 μ m. Further, we successfully developed a photoretin suitable for 3D printing our desired implants. An integral challenge lies in formulating a biocompatible photoretin that can achieve the desired feature resolution when printing at small build volumes. This was achieved by optimising photoretin chemistry, rheological properties, and light penetration depth. Ultimately, a base formulation suited for ultra-high-resolution 3D printing was produced and iteratively tailored to meet the application requirements. Our study identifies a range of photoreactive monomers and cross-linkers that demonstrate biocompatibility and compatibility with sterilization protocols.

In conclusion, our work focuses on developing an in-house P μ -SL 3D printer and compatible ultra-high-resolution photoretin to address the micro-to-macro scale challenge in 3D printing. Achieving close to 1 μ m print resolutions, our printer enables the fabrication of novel implant bone replacements. Leveraging metamaterial design and computational frameworks, we aim to produce biocompatible implants emulating native bone properties, advancing additive manufacturing for patient-specific solutions and improving quality of life for individuals with bone cancer.

9:45 AM SB09.01.05

Artificial Intelligence (AI) for Improved Biomaterial Design and Healthcare: From *In Vitro* Experimentation to Real Human Clinical Use[TomWebster](#); Hebei University of Technology, United States

Artificial intelligence (AI) has already revolutionized numerous industries, yet, its use in biomaterials and healthcare is almost non-existent. This presentation will provide a summary of how AI can be used to design better biomaterials for various biomedical applications. In particular, AI is being used in biomaterial implantable sensor design to prevent, diagnose, and treat various diseases from cancer to infection. Specifically, AI is being used to predict tissue growth and/or bacteria colonization onto biomaterials based on patient data. Such results can be used to help select a successful biomaterial for that patient. Moreover, AI has been used to predict what types of drug delivery vehicles will be most effective for that particular patient based on prior patient health data and real time response to therapies. Further, AI has been incorporated into digital health where hand held devices can detect patient local temperature, oxygen levels, heart rate, and other critical health parameters comparing such data to patient history to predict whether that patient has cancer, an infection, or is even about to have a heart attack. It is well known that due to variations in immune systems from patient to patient, patients will respond differently to the same biomaterials and drug treatment, thus, personalized or tailored treatments are necessary and can result from AI. Specifically, in this study, cell phones were modified to collect patient data (N = 12) after hip implant surgeries as a means to detect temperature changes at the implant site (on the skin surface as well as internally). Temperature (as just one of many health indicators) was measured surrounding the implant and was able to determine extensive inflammation, infection, and/or proper healing. Then, AI was used to predict if such temperature changes would require surgical intervention to salvage a failed implant. Results showed that AI is an effective means to predict patient outcomes and as such can be used to identify and improve biomaterials for a wide range of medical applications. This abstract presents a positive view on the implementation of AI into medicine showing how it can be used to improve implant surgery and disease treatment.

10:00 AMBREAK

10:30 AM *SB09.01.06

Polymer Strategies in Musculoskeletal Tissue Engineering[ElizabethCosgriff-Hernandez](#); The University of Texas at Austin, United States

Over one million surgical procedures are performed each year to treat bone defects with an associated medical cost over 5 billion dollars. Current procedures are fraught with problems that limit clinical success from fixation challenges in osteoporotic bone to replicating form factor in craniomaxillofacial reconstruction to infection control in traumatic injuries. Each indication requires a tailored strategy to restore function and guide regeneration. Our laboratory specializes in the development of polymeric biomaterials that meet the design criteria of each regeneration strategy. One particular area of interest is the treatment of fractures using an injectable, bone void filler. Current bone cements do not adequately support bone healing and lead to poor clinical outcomes. Our laboratory has developed a novel emulsion templating methodology to generate injectable, high porosity bone void fillers that cure to rigid foams at body temperature with compressive properties in the range of trabecular bone. We have enhanced the regenerative capacity of these synthetic grafts by mixing the emulsion with autograft particles. Recently, we have utilized this biomaterial platform to develop emulsion inks for 3D printing. Emulsions inks are rapidly cured after deposition by constant UV irradiation to form rigid constructs with interconnected porosity in a method we term Cure-on-Dispense printing. 3D printed constructs benefit from the tunable pore structure of emulsion-templated materials and the fine control over complex geometries of 3D printing that is not possible with traditional manufacturing techniques. A cell-releasing hydrogel was then developed to provide osteogenic potential and enhance the regeneration of these 3D printed scaffolds. Finally, we have utilized advanced electrospinning techniques to create bone wraps that eradicate infection and enhance vascularization. Collectively, this work highlights the versatility of polymer engineering to design tissue engineering scaffolds to meet clinical needs.

11:00 AM SB09.01.07

Injectable Colloidal Hydrogels of N-Vinylformamide Microgels Dispersed in Covalently Interlinked pH-Responsive Methacrylic Acid-Based Microgels[BrianSaunders](#); University of Manchester, United Kingdom

Injectable hydrogels offer great potential to augment damaged or degenerated soft tissue. A key criterion for such gels is that their modulus is as close as possible to that of the target tissue. The majority of synthetic hydrogels have used low molecular weight polymer chains which may cause problems if they diffuse away from the injection site and/or increase the local osmotic pressure. We previously introduced a different approach of injecting preformed ultra-high molecular weight pH-responsive microgels (MGs) that interlink to form hydrogels. MGs are crosslinked polymer colloid particles that swell when the pH approaches the particle pK_a . These colloidal hydrogels are termed doubly crosslinked microgels (DX MGs). The gel moduli of previous DX MGs were much greater than that reported for human nucleus pulposus (NP) tissue of the spinal intervertebral disk. Here, we replace some of the pH-responsive

poly(ethylacrylate-co-methacrylic acid) (PEA-MAA) MGs with hydrophilic non-ionic MGs based on poly(*N*-vinylformamide) (NVF). We investigate the morphology and mechanical properties of these new injectable DX MG composite gels and show that the mechanical properties can be tuned by systematically varying the NVF MG content. Using this approach, gel moduli close to that for NP tissue are achieved. These injectable new pH-responsive gels exhibit low cytotoxicity. Our work provides a potential new system for minimally-invasive intervertebral disk augmentation[1].

[1] Wang et al., *Biomacromolecules*, 24, 2173, 2023.

11:15 AM *SB09.01.08

Regenerative Engineering Through Biomaterial DesignBrendan A. Harley; University of Illinois-Urbana-Champ, United States

Advances in the field regenerative medicine require biomaterials that instruct, rather than simply permit, a desired cellular response. A major contemporary motivator in biomaterial design is the complex organization of the tissues in our bodies, which are hierarchical, vary in space and time, and can differ person-to-person. However, the future success of regenerative medicine requires more deeply considering aspects of human variation and heterogeneity. For example, considering the role of sex-specific differences in tissue engineering technologies motivates innovative lines of investigation that will become central dogma in the future.

Defects in craniofacial bones of the skull occur congenitally, after high-energy impacts, and during the course of treatment for stroke and cancer. They affect a broad segment of the US population, are large and irregularly shaped, and heal poorly. Contemporary tissue engineering efforts that combine exogenous mesenchymal stem cells (MSCs), morphogens, and biomaterials face challenges due to the cost and time for in vitro MSC expansion and MSC-biomaterial culture as well as the need for supraphysiological morphogen doses. We are developing porous biomaterials that can be shaped precisely and quickly like an alloplastic implant but that work in a regenerative fashion like autologous bone. Specifically, I will describe a class of mineralized collagen scaffold that promotes MSC recruitment and osteogenicity in the absence of osteogenic supplements. We have refined these materials to study MSC-macrophage crosstalk and to promote MSC-osteoprogenitors to secrete osteoprotegerin, a soluble glycoprotein and endogenous inhibitor of osteoclast activity. We showed polymeric meshes can be integrated into the scaffold, à la rebar in concrete, to create composites that can be shaped intraoperatively to aid surgical-practicality and accelerate regeneration. I will also describe scaffold processing approaches to create spatially-graded collagen biomaterials that direct MSC differentiation down multiple musculoskeletal lineages in a spatially-selective manner, along with methods to develop continuous hydrogel zones that link dissimilar musculoskeletal tissue zones (e.g., tendon and bone) to provide mechanical and trophic advantages to accelerate regenerative healing. I will conclude by describing recent efforts to address barriers preventing regeneration, notably the role of sex-differences in regenerative activity. These initiatives demonstrate that understanding sex-specific differences in cell activity is essential in the design of biomaterial system to improve regenerative potential as well as to study disease progression and therapy.

11:45 AM SB09.01.09

Injectable and Biodegradable Piezoelectric Hydrogel for Medical ApplicationsThanh D. Nguyen and Tra Vinikoor; University of Connecticut, United States

Osteoarthritis (OA), a painful joint disease manifested by cartilage damage, affects 654 million people worldwide every year. Currently, there is no cure for OA; available medicines only alleviate the disease symptoms (e.g. pain and inflammation) while surgical approaches including the use of replacement auto- or allo- graft cartilages suffer from the problems of donor-site morbidity, infection, immune-rejection, and especially, limited tissue supply. Herein, we present a novel injectable and biodegradable piezoelectric hydrogel with ultrasound (US) activation to offer a minimally invasive regenerative engineering approach for OA treatment. The piezoelectric hydrogel can be injected into the joints and self-produce localized electrical cues under US activation to drive cartilage healing. *In vitro* data shows the hydrogel with US activation attracts host cells, enhances cell migration, and induces stem cells to secrete endogenous growth factors like TGF- β 1 which facilitates *COL2A1*, *ACAN*, and *SOX9* expression to promote chondrogenesis and extracellular matrix (ECM) deposition. Significantly, the piezoelectric hydrogel enables the healing of hyaline cartilage in rabbits with critical size osteochondral defects. After two months of the piezoelectric hydrogel and US treatment, the animals had more subchondral bone formation, well-organized hyaline cartilage structure, and improved mechanical properties, close to those of healthy native cartilages and superior to the other control/sham groups either without US activation or piezoelectricity. This injectable piezoelectric hydrogel is not only applicable for cartilage healing but potentially other tissue regeneration and could serve as a minimally-invasive material platform for important medical devices such as injectable piezoelectric pressure sensors, actuators, energy-harvesters, and transducers, thus offering a significant impact on medicine.

SESSION SB09.02: Polymeric Biomaterials for Regenerative Engineering II

Session Chairs: Melissa Grunlan and Carolyn Schutt Ibsen

Tuesday Afternoon, November 28, 2023

Hynes, Level 1, Room 104

1:30 PM *SB09.02.01

Cells and Biomaterials as Building Blocks for Tissue Engineering and Regenerative MedicineKent Leach, Jeremy Lowen and David Ramos-Rodriguez; University of California-Davis, United States

Biomaterials are an integral component of tissue engineering and regenerative medicine. The selection and biophysical properties of the materials are instrumental in guiding the behavior of transplanted or invading host cells. I will highlight our recent work in two areas to create building blocks for tissue engineering: 1) manufacturing cellular spheroids with instructive cues to guide cell fate; and 2) production of instructive microgel scaffolds to dictate macrophage phenotype, instruct cell differentiation, and promote tissue formation.

Our group has developed key advances in generating and guiding cell spheroids as building blocks for tissue formation. The bioactivity and function of spheroids is dictated by the selected cell population(s) (both homotypic and heterotypic), culture conditions such as local oxygen tension or inflammatory stimuli, and the association of spheroids with instructive biomaterials. Our group engineered a decellularized extracellular matrix (ECM) secreted by bone marrow-derived mesenchymal stromal cells (MSCs). After characterizing its composition, we demonstrated that MSC spheroids loaded with cell-secreted ECM exhibited markedly increased osteogenic potential and survival in harsh conditions. We have iterated on this ECM to retain endogenous growth factors more effectively. We examined the composition and bioactivity of ECM produced by MSCs differentiated from induced pluripotent stem cells as an alternative cell population that addresses shortcomings of MSCs. Finally, we identified key biophysical properties of hydrogels that regulate cell migration, proangiogenic potential, and tissue formation by MSC spheroids.

Tunable scaffolds that direct cell fate are desirable in many tissue engineering applications such as wound healing, organoid systems, and drug delivery. As our understanding of tissue complexity increases, so does the demand for heterogeneous biomaterials. Microgels are an emerging tool that fulfill this role given their modularity, injectability, and range of fabrication techniques. Unlike bulk hydrogels, microparticle-based scaffolds possess tunable void space which inherently exists between the particles. Such void space permits cells to migrate and proliferate readily without first remodeling their surrounding environment. While the effects of pore size on cell penetration and proliferation have been studied in bulk hydrogels, it has yet to be thoroughly investigated in a microgel platform.

We employed the ability to readily alter porosity in photoannealable microgel scaffolds to influence macrophage polarization, alter cell spreading and aggregation, and influence cell function. We generated microgels with compressive moduli ranging from ~ 10-80 kPa, which demonstrates their ability to match a range of tissue stiffnesses. The compressive modulus and bioactivity of the microgels remained constant after cryopreservation at -20°C, which facilitates high-throughput production, storage, off-the-shelf availability, and expands their potential for clinical translation. Void volume was a key stimulus to instruct macrophage polarization toward a pre-regenerative M2 phenotype.

In another example, we created bilayer constructs of microgels with distinct compressive moduli and pro-osteogenic and chondrogenic peptides. Using light to anneal the gels, we produced constructs that did not delaminate, as is common for many bilayer materials. When cultured in mixed media, we observed upregulation of osteogenic and chondrogenic markers that were primarily restricted to the designated layer. The ease of loading cells, cryopreservability, and short annealing time make this a promising platform for translation to the clinic.

2:00 PM SB09.02.02

A Resurfacing-Regenerative Approach to Repair Osteochondral Defects using a Bioprosthetic DeviceMelissa Grunlan, Connor J. Demott, Lauren K. Davis, William B. Saunders and Olivia F. Dingus; Texas A&M University, United States

Osteochondral defects (OCDs), areas of localized joint damage to articular cartilage and underlying subchondral bone, often lead to pain, loss of joint function, and osteoarthritis. Clinical repair is focused on biological grafting procedures, which are innately limited by graft availability and donor site morbidity. We have developed a bioprosthetic implant, combining articular

cartilage resurfacing and osseous tissue regeneration, as a new method for OCD repair. These implants – “cartilage-capped, regenerative osteochondral plugs (CC-ROPs)” - combine a multi-network hydrogel (cartilage cap) and osseous scaffold (base). The cartilage cap is prepared from a multi-network, electrostatic hydrogel that gives rise to articular cartilage-like mechanical, hydration, and tribological properties. The osseous scaffold base is prepared from a semi-interpenetrating polymer network (semi-IPN) of poly(ϵ -caprolactone)-diacrylate (PCL-DA) and poly(L-lactic acid) (PLLA). The scaffold is intrinsically osteoinductive and has a trabecular bone-like modulus as well as robust degradation rates to facilitate bone ingrowth. Formed as cylindrical plugs, CC-ROPs are able to be implanted using existing grafting techniques and be fabricated at a wide range of sizes. CC-ROPs were successfully implanted into rabbit OCDs using an osteochondral graft delivery device with a custom tip to help alignment on the small rabbit condyles. At 10 days, MRI images illustrated the cartilage cap remained intact with the osseous scaffold (i.e., no delamination). It was also confirmed that CC-ROPs did not become displaced post implantation. Formation of new tissue around the periphery of the osseous scaffold was illustrated in microCT and histological analyses. At 12 weeks post-implantation, there were likewise no signs of delamination or fracture of the CC-ROP. Furthermore, no migration of the implant was seen (e.g., cartilage cap surface congruent with surrounding cartilage). Extensive bone tissue formation was seen around the edges and throughout the pores of the osseous scaffold. Performance in rabbit OCDs illustrated the ability of CC-ROPs to immediately provide an articulating surface as well as promote regeneration of osseous tissue, exemplifying the potential to improve the treatment of OCDs.

2:15 PM SB09.02.03

A Dynamic Hydrogel Platform to Model Cardiac Tissue Development and Disease Andrew House and [Murat Guvendiren](#); New Jersey Institute of Technology, United States

Heart disease is currently the leading cause of death in the United States, and is most often caused by myocardial infarction (MI). There is a desire to create novel therapies and treatments. However, due to a lack of fundamental understanding of the heart's inflammatory response to infarction, the development of new therapies is both time consuming and costly. In this work, we report a novel biomaterial platform to mimic dynamic changes in the heart tissue during MI. We believe that our platform enables dynamic control of cardiac cell alignment and matrix stiffness (from healthy to fibrotic tissue) to investigate cardiac tissue development and disease.

In this study, we report a novel dynamic hydrogel platform enabling spatiotemporal control of cellular alignment and matrix stiffness (from healthy to fibrotic tissue stiffness). Our approach involves: (i) fabrication of polydimethylsiloxane (PDMS) based elastomeric film displaying lamellar wrinkling patterns with user defined and spatiotemporally controlled pattern amplitude and wavelength, and (ii) chemically grafting a hydrogel film allowing light-induced stiffening from healthy to fibrotic stiffness, matching values reported in the literature. In our approach, methacrylated alginate (MeAlg) hydrogel films are first fabricated using Michael-type addition crosslinking using dithiothreitol (DTT) to form hydrogels with healthy stiffness (~15 kPa), during which it is also chemically tethered to the PDMS substrate. When needed, hydrogels can be stiffened in situ when exposed to UV or blue light in the presence of a photo initiator to reach to fibrotic stiffness (~55 kPa). Using this platform, we first investigate the effect of pattern size (amplitude and wavelength) on cardiac cell alignment. We then report the effect of matrix stiffness on cardiac cell function. Human cardiac fibroblasts (hCFs, Normal Human Ventricular Cardiac Fibroblasts, NHCF-V, CC-2904, Lonza, United States), human cardiomyocytes (hCMs, AC16 Human Cardiomyocyte Cell, and human induced pluripotent stem cell-derived cardiomyocytes (iPSC-CMs) (iCell Cardiomyocytes 01434, FUJIFILM Cellular Dynamics, Inc.) were used in this study.

In the first part, we show that the degree of cellular alignment for hCMs and hCFs is controlled by the pattern dimensions, such that higher degree of alignment is obtained for higher pattern amplitudes or smaller wavelengths. Spatial control of lamellar patterns allows us to create distinct regions with tunable patterns or continuous patterns with gradient dimensions. In the second part, we show that hydrogels are capable of being stiffened dynamically during the culture (confirmed by AFM and rheology), and gel integrity can be maintained for up to 21 days of culture. In addition, iPSC-CMs cultured for up to 21 days show distinct changes in their sarcomere expression and beating frequency in response to changes in stiffness and alignment. We plan to conclude with our approach to use this platform to mimic the dynamic changes in the ECM post-MI to develop a drug screening platform.

2:30 PM *SB09.02.04

Engineered Biomaterials for *In Situ* Tissue Regeneration [Akhilesh K. Gaharwar](#); Texas A&M University, United States

Engineered biomaterials have emerged as powerful tools for a range of biomedical applications, including tissue engineering, drug delivery, and additive manufacturing (3D bioprinting). These biomaterials possess tunable biophysical properties, specific biochemical cues, and complex architecture, enabling precise control over cellular behavior. In this talk, I will outline three biomaterials-based approaches developed in our lab for biomedical applications. Firstly, I will highlight how engineered biomaterials can harness the body's regenerative potential to control and direct cell functions for in situ tissue regeneration. Our work has resulted in a new class of biomaterials for bone regeneration, osteoarthritis treatment, angiogenesis, hemostasis, and wound healing. The second approach focuses on designing nanoengineered biomaterials for sustained and controlled release of therapeutics. We have developed a range of nano-tool kits for the delivery of small molecule drugs and large proteins, which have high loading efficacy and tunable delivery properties. These approaches can be used for targeted delivery of cancer therapeutics. Lastly, I will demonstrate the design of a new class of bioinks for 3D printing anatomical-size tissue constructs. These tissue structures can be used to develop physiologically relevant tissue models, mimicking disease conditions such as vascular pathophysiology and vascularized glioblastoma models.

3:00 PM BREAK

3:30 PM *SB09.02.05

Peptides with Polyproline II Helix Secondary Structure and Their Potential Role in Biomaterials Engineering [Julie Renner](#); Case Western Reserve University, United States

Bound peptide monolayers are a promising way to control surface properties because peptides are biocompatible, easily tunable, and can be designed to have, or not have, interactions with cells. Our lab is especially interested in establishing new engineering models and assembly techniques to control and understand the behavior of surface-bound peptides for use as biomaterials. Peptides with a polyproline II helix secondary structure (PPII helix peptides) have recently emerged as promising tools for biomaterials due to their unique antifouling properties and ability to form dense monolayers. Using a variety of characterization techniques, we uncover new details about the assembly mechanisms of PPII helix peptides and explore their antifouling capacity. In addition, we explore the interactions of these peptides with human mesenchymal stem cells and 3T3 cells with and without bioactive peptides attached. Collectively, these results reveal greater understanding of the mechanisms behind PPII helix peptide assembly and antifouling and provide insight into their potential use as biomaterials for regenerative engineering.

4:00 PM *SB09.02.06

Designing Biocompatible Hydrogel Nanoparticle Emulsions for Regenerative Engineering [Georgia Papavasiliou](#), [Shadi Motamed](#), [Fernando Borges](#) and [Fouad Teymour](#); Illinois Institute of Technology, United States

Polymeric nanoparticle (NP) emulsions have shown significant promise for regenerative engineering applications as they can be designed as topical and/or injectable formulations for *in vivo* administration of therapeutic compounds. Hydrophilic therapeutic delivery often requires water-in-oil-in-water (w/o/w) double emulsions which are difficult to produce and have limited storage life because of their inherent instability. Inverse, water-in-oil (w/o) emulsions for encapsulation of hydrophilic therapeutics are far less common as they involve use of organic solvents. Highly biocompatible and biodegradable crosslinked hydrogel NP are perfectly suited for controlled and sustained diffusive-based release of therapeutics, enhanced tissue-targeted delivery and bioavailability of hydrophilic drugs. Hydrogel NP, however, come in contact with cytotoxic organic solvents and surfactants during emulsion polymerization requiring subsequent purification and isolation before being administered directly *in vivo*. This leads to limitations, including significant drug loss, dosage uncertainty, compromised drug release kinetics, and loss of particle stability, thereby minimizing *in vivo* therapeutic efficacy. To address these limitations, we have developed novel biocompatible NP emulsions (BCNE) consisting of stable poly(ethylene glycol) (PEG) crosslinked hydrogel NP dispersed in a naturally-derived consumable organic phase that can be formulated as a liquid (or as an ointment) and administered *en masse*, directly to target tissues. BCNE are synthesized with biocompatible components including PEG diacrylate (PEGDA) crosslinking macromer, N-vinyl pyrrolidone or ethylene glycol comonomers, polyphosphate (PPI) or NaCl as the lipophile, soybean oil (SO), as the organic phase, with PolyGlycerol PolyRicinoleate (PGPR) emulsifier (FDA recognized as safe for human consumption) and with V50 initiator using inverse phase miniemulsion polymerization. We synthesized BCNE with varying mesh dimensions to accommodate the encapsulation and sustained release of hydrophilic therapeutics of varying size and conformation including PPI (PPI-BCNE), NaCl (NaCl-BCNE) and the α -helical pro-angiogenic peptide QK (QK-BCNE). BCNE NP size measurements (Nanosight LM10, Malvern) yielded mean NP diameters of 111 ± 7.2 nm and 96 ± 3.9 nm for PPI-BCNE and NaCl-BCNE, respectively. To define mesh dimensions suitable for encapsulation and release of PPI and QK, experimental measurements of hydrogel mass swelling ratio were coupled with theoretical kinetic and thermodynamic interpretations we recently developed to characterize the network architecture of hydrogel networks comprised of macromeric crosslinkers. Our approach accounts for crosslinker size, and its behavior under swelling, both neglected by the Flory-Rehner theory. This allows for quantification of two new hydrogel mesh dimension variables that establish bounds on the maximum size and aspect ratio of therapeutics that can be encapsulated and released from crosslinked hydrogel NP networks. Using this approach to guide our experimental design, QK-BCNE were designed to release QK for 46 days whereby 90% of the encapsulated peptide was retained for 36 days *in vitro*. *In vitro* findings indicate that PPI-BCNE completely disperse PAO1 *P. aeruginosa* biofilms compared to blank BCNE and no treatment controls. Preliminary experiments conducted with *en masse* topical application of BCNE in a *Staphylococcus aureus* C57BL/6 mouse model of burn injury and impaired healing demonstrated incontrovertible evidence that PPI-BCNE improves wound healing compared to blank BCNE treatment. These results highly suggest that BCNE provide a versatile platform whereby hydrogel nanoparticle mesh dimensions can be precisely tuned for encapsulation of hydrophilic therapeutics of varying size and complex conformation (peptides, growth factors and iRNA) to enable sustained tissue-targeted delivery *in vivo* for regenerative medicine applications.

4:30 PM SB09.02.07

Stiffness Assisted Cell-Matrix Remodeling to Induce Stem Cell Differentiation Akhilesh K. Gaharwar; Texas A&M University, United States

Engineered matrices provide a valuable platform to understand the impact of biophysical factors on cellular behavior such as migration, proliferation, differentiation, and tissue remodeling, through mechanotransduction. While recent studies have identified some mechanisms of 3D mechanotransduction, there is still a critical knowledge gap in comprehending the interplay between 3D confinement, ECM properties, and cell behavior. Specifically, the role of matrix stiffness in directing cellular fate in 3D microenvironment, independent of viscoelasticity, microstructure, and ligand density remains poorly understood. To address this gap, we designed a nanoparticle crosslinker to reinforce collagen-based hydrogels without altering their chemical composition, microstructure, viscoelasticity, and density of cell-adhesion ligand and utilized it to understand cellular response. This crosslinking mechanism utilizes nanoparticles as crosslink epicenter, resulting in 10-fold increase in mechanical stiffness, without other changes. Human mesenchymal stem cells (hMSCs) encapsulated in 3D responded to mechanical stiffness by displaying circular morphology on soft hydrogels (5kPa) and elongated morphology on stiff hydrogels (30kPa). Stiff hydrogels facilitated the production and remodeling of nascent extracellular matrix (ECM) and activated mechanotransduction cascade. These changes were driven through intracellular PI3AKT signaling, regulation of epigenetic modifiers and activation of YAP/TAZ signaling. Overall, our study introduces a unique biomaterials platform to understand cell-ECM mechanotransduction in 3D.

4:45 PM SB09.02.08

Development of an iPSC Loaded Biomimetic Biomaterial Scaffold for Spinal Cord Repair Applications Cian O'Connor^{1,2,1}, Ian Woods^{1,2,1}, Sarah F. McComish², Maeve A. Caldwell², Adrian G. Dervan^{1,2,1} and Fergal J. O'Brien^{1,2,1}; ¹Royal College of Surgeons in Ireland, Ireland; ²Trinity College Dublin, The University of Dublin, Ireland

Introduction: Following spinal cord injury, a lesion cavity develops preventing axonal regrowth. Biomaterial implants that bridge the cavity and encourage axonal growth while delivering trophic cells to restore lost tissue may have potential for repair. Therefore, by identifying neurotrophic extracellular-matrix proteins to incorporate into biomimetic hyaluronic acid biomaterial scaffolds and by tuning the biomaterial stiffness, we aimed to develop a novel platform for spinal cord repair. Furthermore, we wished to determine if the developed biomimetic biomaterial scaffolds were capable of delivering and modulating the trophic capacity of induced pluripotent stem cell (iPSC)-derived progenitors for spinal cord repair applications.

Methods: Spinal cord astrocytes and neurons were cultured on a range of extracellular matrix-proteins to identify the optimal neurotrophic substrate combination. Following the incorporation of the neurotrophic substrate into freeze-dried 3D hyaluronic acid scaffolds of varying stiffnesses, scaffold properties were characterized. Next, spinal cord astrocytes, neurons, dorsal root ganglia (DRG) and iPSC-derived astrocyte progenitors were cultured in the scaffolds for up to 21 days and the effect of scaffold physicochemical properties was assessed. Thereafter, the impact of scaffold properties on the trophic capacity of iPSC-derived progenitors was assessed *in vitro* and *ex vivo* using neurons, DRG and spinal cord explants.

Results: A combination of collagen-IV (CIV) and fibronectin (FN) synergistically enhanced neurite outgrowth by 203% while also promoting astrocyte process extension. Subsequently, hyaluronic acid biomaterial scaffolds functionalized with CIV/FN were successfully manufactured with different stiffnesses ranging from soft/biomimetic to stiff/supraphysiological (0.8-3.5 kPa). Spinal cord astrocytes cultured in soft-CIV/FN functionalized biomaterial scaffolds matching cord stiffness, displayed positive stellate morphologies and increased pro-regenerative IL-10 release. Furthermore, soft scaffolds significantly enhanced neurite outgrowth from neurons and adult mouse DRG explant cultures compared to stiffer scaffolds. Soft-CIV/FN scaffolds also enhanced iPSC-progenitor neurotrophic and functional capacity while encouraging the growth of iPSC-derived spheroids that subsequently formed extensive neuronal/astrocytic cellular tracts, colonizing the biomaterial scaffold. Conditioned media from soft-CIV/FN but not other, iPSC-loaded scaffolds, and applied to growing neurons enhanced neurite outgrowth by over 280%. Super-resolution microscopy also confirmed similar neurite enhancement (170%) in mouse primary spinal cord neurons treated with media from soft-CIV/FN scaffolds only without eliciting negative inflammatory and/or reactive responses from healthy and injured astrocytes. Furthermore, analysis of media from stiffer or non-CIV/FN-containing scaffolds showed increased pro-inflammatory IL-1 β release compared to soft CIV/FN scaffolds. Finally, when *ex vivo* DRGs or spinal cord explants were cultured directly on CIV/FN iPSC-loaded biomaterial scaffolds up to 21 days, only soft biomaterials enhanced cellular infiltration, astrocytic process extension and directed axonal outgrowth between DRG and iPSC-spheroids.

Conclusion: Overall, this research describes the development and utilization of a novel, biomimetic biomaterial scaffold-based platform for spinal cord repair and demonstrates that biomimetically inspired biomaterials can enhance the growth of cord resident neurons and astrocytes and promote the neurotrophic potential of implanted progenitor cells to act as a novel, therapeutic platform for spinal cord injury repair applications.

Acknowledgements: This work is funded by the Anatomical Society, Irish Rugby Football Union Charitable Trust, and the Science Foundation Ireland Advanced Materials for Bioengineering Research (AMBER) centre.

5:00 PM SB09.02.09

Protein-Derived Jammed Microgels as Inks for Extrusion 3D Printing of Bioactive Scaffolds Lucas Ribeiro^{1,2}, Rita Sobreiro-Almeida², Vitor Gaspar², Emerson Camargo¹ and João Mano²; ¹Federal University of São Carlos, Brazil; ²University of Aveiro, Portugal

Extrusion 3D printing has emerged as a promising technique in tissue engineering, enabling the creation of personalized scaffolds for individual patients. Typically, natural hydrogels are utilized as inks due to their resemblance to the extracellular matrix (ECM), as well as their biodegradability and biocompatibility, making them ideal for tissue engineering applications. One such biomaterial is human platelet lysates (PL) derived from whole blood, which contains a rich assortment of growth factors, cytokines, and proteins that can stimulate cell proliferation and differentiation, and tissue regeneration. However, the use of PL as ink for printing scaffolds is limited by its liquid nature even at high concentrations, preventing the formation of a solid and stable filament upon deposition.

To address this challenge, granular hydrogels of methacrylated PL (PLMA) were developed through chemical coupling. These granular hydrogels consist of jammed microgels that exhibit viscoelastic solid properties at low levels of strain while flowing under high levels of strain. This unique characteristic enables filament formation and facilitates their application as injectable biomaterials. Additionally, a granular ink of methacrylated bovine serum albumin (BSAMA) was prepared for comparison, leveraging the high albumin content of PL. The microgels were generated by extruding bulk hydrogels through a series of nozzles with progressively higher gauges (18G, 21G, and 23G), followed by centrifugation to remove excess liquid phase and obtain granular hydrogels. Both materials displayed irregular microgels and a wide size distribution. Moreover, the process resulted in albumin microgels with a larger average size, leading to increased porosity compared to the PLMA hydrogel.

Rheological analysis revealed that both inks exhibited shear-thinning, yield-strain, and self-healing properties—essential characteristics for materials used in 3D printing. Additionally, a time sweep test utilizing UV light demonstrated a rapid increase in the storage modulus of the hydrogels due to photo-crosslinking, indicating rapid stabilization of the printed scaffolds. The study of filament formation using different nozzles allowed an evaluation of the printing fidelity of BSAMA and PLMA inks. In all cases, the filament diameter closely matched the internal diameter of the needles, and thus the smallest nozzle tested (22G) was selected for printing the scaffolds. Due to its larger microgels, the printing of the BSAMA presented some clogging, requiring higher pressure for constant extrusion compared to the PLMA ink. Nevertheless, stable scaffolds with varying geometries and layer numbers were successfully printed, confirming the efficacy of this strategy in producing protein inks with the necessary printing properties.

Finally, the bioactivity of the granular hydrogels was assessed by seeding human adipose-derived stem cells (hASCs) for a period of 7 days. Metabolic activity increased at each time point, being consistently higher in PLMA hydrogels. This can be attributed to cell proliferation in the spaces between the microgels, with cells adhering around them from the first day, as indicated by the Live/Dead assay. Furthermore, only a small number of dead cells were detected, indicating the non-cytotoxic nature and biocompatibility of the inks. The DAPI/Phalloidin assay confirmed a higher cell count in the PLMA scaffolds from day 1, highlighting the superior bioactivity of this material. In summary, bioactive granular hydrogels of protein sources with microporosity were successfully created, demonstrating their potential for 3D printing stable scaffolds with excellent resolution for use in tissue engineering applications.

[1] Qazi, T. H., et al. (2022). ACS Biomater. Sci. Eng. 8, 1427

[2] Santos, S. C., et al. (2018). Adv. Healthc. Mater. 7, 1800849

5:15 PM SB09.02.10

Enhanced Therapeutic and Immunomodulatory Effect of Stem Cell Spheroid with Transition Metal-Based Nanoparticles in Rat Myocardial Infarction Model Yeong Hwan Kim and Suk Ho Bhang; Sungkyunkwan University, Korea (the Republic of)

Myocardial infarction (MI) which accompanies decrease in myocardium function and destruction of millions of cardiomyocytes is a leading cause of mortality worldwide. In this study, we demonstrated advanced stem cell therapy to treat cardiovascular disease with enhanced therapeutic efficacy of stem cell spheroids by upregulating angiogenesis-related paracrine factors secretion and inducing immunomodulatory ability with transition metal based nanoparticles (TMNs). Stem cell spheroids treated with TMNs (spheroids-TMNs) had wider hypoxia inducible factor (HIF) expression area in core with mild reactive oxygen species (ROS) generation. According to increased HIF expression of spheroids-TMNs, the secretion of angiogenesis-related paracrine factors was enhanced compared to untreated spheroids. Immunomodulatory effect of spheroids-TMNs was verified with Raw cell; suppression of pro-inflammatory responses and promotion of anti-inflammatory responses. Enhanced therapeutic effect and immunomodulatory effect of spheroids-TMNs were verified in vivo rat MI model. An advanced stem cell therapy we provided can be a promising therapeutic strategy for cardiovascular disease treatment.

8:00 PM SB09.03.01

Injectable Hydrogel Formulations with Controlled-Release of Curcumin and Vitamin E for Dental Tissue Engineering Deniz Atilla¹, Ali Deniz Dalgic², Agnieszka Krzeminska¹, Joanna Pietrasik¹, Edyta Gendaszewska-Darmach¹, Fouad Laoutid³, Piotr Paneth¹ and Vignesh Kumaravel¹; ¹Lodz University of Technology, Poland; ²Istanbul Bilgi University, Turkey; ³University of Mons, Belgium

Dental infections affect millions of people globally with a burden of \$298 billion annually associated with direct costs to treat oral diseases. Injectable hydrogels incorporated with antimicrobial and antioxidant agents can be used to treat dental pulp infections. Herein, injectable hydrogels of chitosan (CH) and liposomes loaded with curcumin and α -tocopherol have been developed to provide antimicrobial and antioxidant action for dental pulp regeneration. Hydrogels are prepared with high (HCH), and low (LCH) molecular weight chitosan to investigate the impact of molecular weight on injectability, biodegradability, controlled release, and antimicrobial activity. The diameters of liposomes are mostly uniform, in the range of 152 - 162 nm, making them suitable for controlled release and injectability. Zeta potential values of hydrogels are negative, which could lead to a homogenous distribution of liposomes in the positively charged hydrogels. Approximately 80 % of curcumin and α -tocopherol are released from liposomes within 21 days in a controlled manner. Therefore, the antimicrobial and antioxidant activity of the hydrogels could be sustained during the healing process. TGA results showed that the thermal stability of the hydrogels decreased with respect to the solution volume and the sonication time while preparing the hydrogels (*i.e.*, the mass loss values of LCH and HCH at 500 °C increased from 79 to 96 % and 90 to 95 %, respectively). DSC findings are consistent with the TGA results for LCH groups, where a shift in T_c from a higher (347 °C) to a lower (326 °C) temperature is observed in response to the increase in volume and sonication time. Nevertheless, the T_c values of HCH are not influenced (366 °C). Rheological analysis revealed that the viscosity of hydrogels decreases as the shear rate increases, signifying the shear-thinning behaviour and injectability of the hydrogels. *In vitro* biocompatibility and antimicrobial features are investigated using dental pulp stem cells and gram-negative as well as gram-positive bacteria. Finally, the antimicrobial mechanism of LCH and HCH on *Escherichia coli* and *Staphylococcus aureus* is evaluated theoretically by density functional theory.

8:00 PM SB09.03.02

Novel Bioink for 3D Bioprinting of Complex Structures with Tunable Stiffness Mrinal Ganash; University of New Hampshire, United States

The field of tissue engineering is rapidly adopting the principles of additive manufacturing (*i.e.* 3D bioprinting), which provides a means to generate complex functional tissue constructs in a programmable manner within micron-scale precision. However, the low mechanical stiffness and strength of 3D printed hydrogels significantly limits the application of 3D bioprinting in tissue engineering. Here, we propose the use of a novel bioink consisting of Gelatin, Methacrylated methacrylated gelatin (GelMA) and α -Alginate. Once printed, this bioink is crosslinked by (i) photopolymerization of GelMA by UV radiation, (ii) enzymatic crosslinking of gelatin by microbial transglutaminase (mTG) and (iii) ionic crosslinking of alginate by calcium ions, to form an interconnected polymer network (IPN), which exhibits much improved mechanical properties. Enhanced mechanical properties of the IPN hydrogels are demonstrated by rheology and mechanical testing. Biocompatibility of the bioink and the subsequent crosslinking process was demonstrated by cytotoxicity and proliferation assays. Cell morphologies in the 3D structures were monitored by live/dead assay in conjunction with confocal microscopy. Cell viability was measured by calculating the live cell count/total cell count.

8:00 PM SB09.03.03

Microfluidics-Assisted Fabrication of Human Natural Killer Cell Encapsulated Increases the Therapeutic Efficacy for Cancer Immunotherapy Dongjin Lee¹, Seokmin Kim², Dahong Kim³, Sua Park¹ and Tae-Don Kim²; ¹Korea Institute of Machinery & Materials, Korea (the Republic of); ²Korea Research Institute of Bioscience and Biotechnology (KRIBB), Korea (the Republic of); ³Seoul National University, Korea (the Republic of)

Tumors are a global human health issue, and various anti-cancer therapies such as surgical-, chemo-, radiation-, and immunotherapy have been used to treat it. Among these therapies, the therapeutic strategy using immune cells capable of recognizing and killing tumor cells is of interest as a next-generation anti-cancer therapy. In recent years, many studies on the chimeric antigen receptor (CAR) have focused on T cells. However, it takes a long time to modify donated T cells to proliferate them, and it is too expensive to use. CAR-T therapy is generally limited to blood tumors. Additionally, further clinical trials may be limited because cytokine release syndrome (CRS) or other side effects may occur from the off-target.

Unlike T cells, NK cells can distinguish tumor sites in an antigen-independent manner, and have no memory function or clonal expansion, resulting in fewer side effects like CRS. Since allogeneic cell transfer therapy is possible it offers the advantage of being available as an off-the-shelf product. Through preclinical and clinical studies, the safety and efficacy of allotransplantable NK cells for assorted types of hematological and solid cancers have been indicated, and various clinical trials are currently in progress. However, the disadvantages of NK cells include a low proliferation rate and the inability to be cultured for a long period of time. In addition, maintaining the cytotoxic activity of NK cells is important in cell therapy, but it is difficult to maintain it in general two-dimensional cultures and cell proliferation is not easy in *in-vivo* systems. Microgels were fabricated to contain immune cells in an emulsion method, and solid cancer disease models were demonstrated through *in-vitro* experiments. However, the NK cell-laden microgel researches for anticancer immunotherapy has not yet been studied. Furthermore, an *in-vivo* experiment was performed in which cancer cells were killed through intravenous injection of a NK cell-laden microgels which would be degraded.

Double flow-focusing microfluidics was used to create cell-containing photo-crosslinkable methacrylic gelatin (MGel) monodisperse droplets, while cell-containing microgels with high viability were produced through cross-linking. Microgels have the advantage of being able to easily control the modulus of elasticity by controlling the concentration of biopolymers. It can be applied efficiently to produce monodisperse droplets containing a large number of biomolecules and enable high-throughput examination and injectability. The generated droplets can be transformed into microgels through crosslinking and applied in multiple ways depending on the characteristics of the material. However, no study has reported the use of a uniform microgel containing NK92 cells using a microfluidic chip yet.

MGel is one of the materials because it is highly biocompatible and its physical properties can be controlled by regulating its concentration. GelMa is composed of arginine, glycine, and aspartic acid, which are present in large amounts in the molecule, and is designed to be decomposed by the matrix metalloproteinase. There is also growing interest in three-dimensional (3D) cell culture models to enable more multiple and physiologically appropriate biological assays compared to traditional two-dimensional (2D) monolayer cell cultures.

In this study, we encapsulated NK92 cells in the microgels (3D) using a microfluidic chip, and their activity was compared with that of the 2D cultured NK92 cells. We observed that NK92 cell-laden microgels (3D) increased cell proliferation, mRNA expression levels, cytokine release, and anti-tumor efficacy, compared to the 2D cultures. We have shown that microgels have no diffusion limit because of their size (approximately 100 μ m). These results suggest that microgels containing NK92 cells can be used to provide a new platform for anticancer immunotherapy.

8:00 PM SB09.03.04

Development of a Sprayable Multifunctional Hydrogel Wound Dressing Mine Altunbek¹, Mert Gezek^{1,1} and Gulden Camci-Unal^{1,2}; ¹University of Massachusetts Lowell, United States; ²University of Massachusetts Medical School, United States

Hydrogel-based wound dressings are widely used for the treatment of wounds due to their advantages. Their high-water content allows for maintaining tissue homeostasis in the wound area. In addition, they provide a favorable three-dimensional (3D) matrix during migration and proliferation of fibroblasts, and re-epithelialization, neovascularization, and wound remodeling processes. The convenient and rapid application to irregular surfaces and deep wounds renders hydrogel dressings useful in wound healing. The chemistry of hydrogel-based wound dressings can be modified to improve their functionality for the treatment of specific types of wounds. In this work, we developed sprayable hydrogel-based wound dressings that are self-oxygenating and have anti-microbial and anti-inflammatory functions. We used naturally-derived biomaterials: gelatin (hydrolyzed collagen) and hyaluronic acid for the development of the sprayable hydrogels. The starting materials were modified with methacrylate groups (GelMA and HAMA) to obtain photocrosslinkable gel precursors. The bioactive GelMA component was evaluated at 5-15% w/v while HAMA was used as the anti-inflammatory component at 1% w/v. Solid calcium peroxide microparticles were incorporated into the hydrogel precursor solution at 0-12 mg/mL concentrations to protect the dressing from microbial invasion. The rapid and easy application of *in situ* photocrosslinkable hydrogels were demonstrated by spraying the composite precursor on the surface of the *ex vivo* pig skin model. The physical properties of the composite hydrogel dressings were analyzed by measuring the mechanical strength, swelling, degradation, and porosity characteristics at the macro scale. The antimicrobial properties of the composite hydrogels were evaluated against the growth of two major pathogens that typically grow during wound healing: *Staphylococcus aureus* and *Pseudomonas aeruginosa*. The oxygenation kinetics was measured using an oxygen sensing probe under hypoxic condition (2-5% O₂). The cytocompatibility of the composite hydrogels were assessed by testing their effects on metabolic activity and viability of the primary human dermal fibroblasts. We successfully demonstrated the practical and convenient application of our sprayable composite hydrogels on *ex vivo* pig skin tissue by an *in situ* crosslinking strategy. The optimum sprayable concentration for GelMA was found to be 10% w/v in the dressing. The gelatin, hyaluronic acid, and peroxide containing composite hydrogels showed high tunability in their physical and biological properties. The peroxide microparticles provided antimicrobial properties in this sprayable wound dressing. The composite hydrogels were able to provide oxygen for up to two weeks in the *in vitro* cell culture. The metabolic stress from human dermal fibroblast cells was relieved by the release of oxygen from the peroxide microparticles.

8:00 PM SB09.03.05

High-Throughput Mass Spectrometry Imaging of Biomaterials for Regenerative Medicine using Three-Dimensional Biomimetic Models (Spheroids and Organoids) Sohee Yoon; Korea Research Institute of Standards and Science, Korea (the Republic of)

Three-dimensional spheroids and organoids are the next generation of biomimetic models that can mimic tissues and organs, as well as diseases and cellular microenvironments such as microtumors. This biomimetic model can be used to elucidate the mechanisms of various biomaterial changes or to rapidly screen cellular responses to drug treatments, and is therefore actively being applied in disease treatment and regenerative medicine. Imaging-based assays are important for a holistic understanding of tumor cell formation and behavior based on organ mimics. Cell viability in three-dimensional biomimetic models is primarily characterized by fluorescence-based imaging techniques. While fluorescence analysis can confirm cell viability, it is difficult to quickly identify chemical changes occurring in high-throughput cells simultaneously. Mass spectrometry imaging is a label-free, high-throughput imaging technique that can simultaneously obtain spatial and chemical information about analytes. We applied mass spectrometry imaging techniques to a three-dimensional biomimetic model to investigate changes in the cellular microenvironment and drug penetration upon drug application.

To this end, we applied drugs and nanoparticles to three-dimensional colon cancer spheroids and liver organoids to investigate chemical changes in the cellular environment by mass spectrometry imaging. In the case of three-dimensional spheroids, the extent of drug penetration into each proliferating, quiescent, and necrotic layer within the spheroid and the accompanying metabolites were investigated, confirming its potential for expansion as a nanomedicine that can be applied to regenerative medicine. To investigate the environmental changes following nanoparticle-based drug delivery in the liver organoid model, we developed and optimized a high-throughput chemical imaging assay that provides a global view of chemical changes within the organoid.

8:00 PM SB09.03.06

Disulfiram-Encapsulated PLGA Nanoparticles for Liver Injury Treatment Wei Xu¹, Waliul Islam¹, Hisaaki Hirose², Shiroh Futaki², Yukio Fujiwara¹, Yoshihiro Komohara¹ and Takuro Niidome¹; ¹Kumamoto University, Japan; ²Kyoto University, Japan

Liver macrophages, Kupffer cells, the most abundant immune cells in the liver, play important roles in innate immunity and contribute to many liver diseases. Disulfiram (DSF), a drug used to treat alcohol abuse, has attracted much attention because it has anti-cancer and anti-inflammatory activities. However, DSF distribute in several cell types, and few studies have examined its utility as a potential treatment for liver injury. In this study, we prepared DSF-encapsulated PLGA nanoparticles (DSF@PLGA NPs) and examined anti-inflammatory effect in vitro and in vivo experiments. Size of DSF@PLGA NPs was about 250 nm and zeta-potential was negative. The encapsulated DSF was slowly released from the nanoparticles over a couple of weeks. DSF@PLGA NPs had low cytotoxicity, were selectively taken up by the human macrophage cell line THP-1 via macropinocytosis, and inhibited lipopolysaccharide-induced proinflammatory cytokine production by THP-1 cells. Intravenously administered PLGA NPs predominantly localized to the liver, specifically CD68-positive Kupffer cells, and DSF@PLGA NPs significantly ameliorated thioacetamide-induced proinflammatory cytokine production and liver injury. These results indicate that encapsulation in PLGA NPs promotes specific delivery of DSF to Kupffer cells and reduces liver injury and inflammation, suggesting that DSF@PLGA NPs may be a promising treatment for liver disease.

8:00 PM SB09.03.07

Drug-Loaded Decellularized Tissue for Suppression of Anastomotic Stenosis after Artificial Vascular Grafting Kaito Shimizu^{1,2}, Yoshiaki Hirano^{2,3}, Tetsuji Yamaoka^{1,4} and Atsushi Mahara¹; ¹The National Cerebral and Cardiovascular Center Research Institute, Japan; ²The Kansai University, Japan; ³The Kansai University Medical Polymer-Research Center, Japan; ⁴The Komatsu University, Japan

[Introduction] The suppression of thrombus formation and anastomotic stenosis is required for long-term patency of small-diameter vascular grafts^[1]. Surface modification techniques for an anti-thrombus surface are reported^[2], while no effective strategy has been developed to prevent anastomotic stenosis. It is well known that anastomotic stenosis causes the hyperproliferation of transformed smooth muscle cells (SMCs)^[3]. SMC phenotype is altered from contractile to synthetic type, resulting in hyperproliferation. Drug eluted stent is a famous device in the clinical site, and the stent is coated with a biodegradable polymer loaded with rapamycin. The drug is released over a month after application to the arteriosclerosis site. If this concept can be applied to artificial blood grafting, we assumed that stable graft patency would be achieved over the medium to long term by local releasing of the drug at the anastomotic site. In this study, we focused on cilostazol as the anti-proliferative drug for SMC and developed a cilostazol-loaded acellular tissue (CLZ-Graft). After grafting the vessel, CLZ-Graft was implanted into the periarterial anastomotic site. When the tissue was degraded during the tissue regeneration, anastomotic stenosis would be suppressed by releasing CLZ. Here, we developed the CLZ-loaded acellular tissue, and inhibition of in vitro SMC growth and in vivo stenosis would be discussed.

[Experiment] The decellularized carotid artery was freeze-dried, and the artery was immersed in 100 mg/ml of CLZ/DMSO solution for 1 hour. As the control, the artery immersed with only DMSO were also prepared (FD-Graft). After that, the sample was washed with water to remove the solvent. The cilostazol loading in the CLZ-Graft was evaluated by FT-IR. The total amount of cilostazol in CLZ-Graft was quantified by using collagenase digestion. Enzymatically degraded CLZ-Graft was added to SMCs, and suppression of the SMCs proliferation was evaluated. In in vivo experiments, CLZ-Graft was implanted into the periarterial area of the carotid artery in a stenosis model rat. The vascular stenosis was evaluated after 4 weeks by histostaining.

[Result and Discussion] IR spectrum derived from CLZ was detected in CLZ-Graft by FT-IR analysis, and approximately 110 µg of CLZ was loaded in 10 mg of the graft. When the graft was incubated with the collagenase solution, the weight of the CLZ-Graft was reduced to 19% for 8 hrs, and 82% of the loaded CLZ was gradually released during this time. When the lysate was added to the SMCs, the cell number was decreased, suggesting that the SMCs proliferation was suppressed by the degradation of the CLZ-Graft. In vivo experiment, the carotid artery with abraded lumen was wrapped with the grafts. As the result of this, the lumen area in the case of CLZ-Graft was maintained to 60% after 4 weeks while the area was largely reduced to 35% in the case of FD-Graft. These results suggest that CLZ-Graft would suppress anastomotic stenosis by CLZ release.

[Reference] [1] M. Conte et al., *FASEB J.*, 12, 43-45, 1998. [2] A. Mahara, et al., *Biomaterials*, 58, 54-62, 2015. [3] Eva M. Rzcudlo, et. al., *Vasc. Surg.*, 45, 25A-29A, 2007

8:00 PM SB09.03.08

Prevention of Adverse Ventricular Remodeling Post-Myocardial Infarction by Sorbitol-Responsive *In-Situ* Gelling Material Hue T. Le¹, Atsushi Mahara¹, Takeshi Nagasaki² and Tetsuji Yamaoka^{1,3}; ¹The National Cerebral and Cardiovascular Center Research Institute, Japan; ²The Osaka Metropolitan University, Japan; ³The Komatsu University, Japan

Introduction: The loss of myocardium after myocardial infarction (MI) leads to a thinned left ventricular (LV) wall and the exacerbated dilation of the LV cavity, eventually leading to heart failure¹. Intramyocardial hydrogel injection has gained attention as a therapeutic approach in MI treatment. Various materials have been tested in preclinical and clinical studies²; however, the difficulties in control of their gelation cause inadequate distribution and retention of the hydrogel within the myocardium. We recently developed a sorbitol-responsive *in-situ* gelling material composed of poly (3-acrylamidophenylboronic acid-co-acrylamide) (BAAm), poly(vinyl alcohol) (PVA), and sorbitol. This mixture exists in a sol state because the phenylboronic acid group of BAAm is bound to the sorbitol. The BAAm and PVA are quickly conjugated by a non-covalent bond to form a gel when the sorbitol is released from the BAAm. We previously reported the proof-of-concept for the sol-gel transition of sorbitol-containing BAAm/PVA (S-BAVA) solution in the heart tissue by diffusing the sorbitol out of the sol. In this study, we investigated the distribution and retention of the injected S-BAVA in the infarct myocardium and its therapeutic effect on post-infarct adverse LV remodeling in a rat model.

Method: S-BAVA solution was prepared from 25 mg/ml BAAm, 10 mg/mL PVA, and 10 mg/mL sorbitol. To examine S-BAVA hydrogel formation in vivo, 1 mL of the S-BAVA containing 100 mg/mL of iopamidol was intramyocardially injected in the porcine heart and tracked by computer tomography (CT) 30 min after injection. A rat subacute MI model was prepared by surgically ligating the left anterior descending (LAD) artery. The LV wall motion of MI rats was acquired from an MRI scan. To investigate the distribution and retention of S-BAVA solution in the MI heart, 200µL of rhodamine (rho)-labeled S-BAVA solution was injected into the infarct myocardium and observed by fluorescent microscopy up to 21d after injection. Finally, 200µL of the S-BAVA or calcium-crosslinked alginate (ALG) containing 24 mg/mL alginate and 4 mg/mL CaCl₂ or saline solution was intramyocardially injected into the MI hearts (four to six rats per each group). Fraction shortening (FS), and LV internal diameter (LVID) index were measured by echocardiography, and the LV morphology was assessed by histological staining at 21d after administration. The saline was set as a negative control.

Result: The CT images showed the presence of the iopamidol-containing S-BAVA in the porcine myocardium 30min after injection, suggesting the occurrence of its hydrogel formation. The rho-labeled S-BAVA was fully distributed in the infarct myocardium and stably remained up to 21d after injection. The MRI images showed the dyskinetic wall motion and thickness in all rats operated with LAD ligation. A gradual reduction of the LV function indicated by a declining FS was observed in the saline-injected MI rats. Even with the ALG injection, the reduction of FS still occurred although it was less severe than in the cases with saline injection. However, the FS in the S-BAVA group was not reduced for 21d. In addition, the increase of systolic LVID caused by MI was suppressed by the S-BAVA injection whereas the saline or ALG injection did not. The histological assessment showed that the infarction area in the S-BAVA group was lower than that in the ALG and saline groups after 21d of administration.

Conclusion: Our results proved that the S-BAVA could be widely distributed and retained for 21d in the myocardium. Intramyocardial injection of the S-BAVA solution effectively suppressed adverse LV remodeling, resulting in maintaining cardiac function up to 21d.

Reference 1) Frangogiannis, N. G. *Compr Physiol* 5, 1841–1875 (2015). 2) Diaz, M. D. & Christman, K. L. I. *Cardiovasc Regen Med* 185–206 (2019)

8:00 PM SB09.03.09

3D Printed Polymer Scaffolds for Bone Regeneration Shreya Madhavarapu and Joseph Freeman; Rutgers, The State University of New Jersey, United States

Significant bone loss can occur due to trauma or disease, resulting in large bone defects. Typically, autografts and allografts are used as bone grafts but these are associated with disadvantages

like limited availability, and the risk of disease transmission with allografts. In recent time, synthetic bone graft substitutes have come up as alternatives, but they fall short in one or more aspects as well. Tissue engineered bone grafts are viable alternatives. In order for these to be successful, we must first address two important issues - lack of cell infiltration throughout their structure and a lack of vasculature formation. We have developed a 3D printed polylactic acid (PLA) scaffold with distinct cortical and trabecular geometries. These are highly porous structures promoting capillary inflow of blood and bone marrow. They are also mineralized and prevascularized to promote regeneration of both bone and its vasculature. These scaffolds are evaluated in a load-bearing, rabbit critical-sized radial defect model and show promise.

Scaffolds were designed using Solidworks and 3D printed using the Ultimaker 2+/S3 3D printers. They were tested under compression and their mechanical properties were compared to the previous iterations of scaffolds developed in our lab. The new design displayed superior mechanical properties when compared to the previous design. Our previous design displayed Ultimate Compressive Stress and Compressive Modulus which fall within the limits for trabecular bone (0.2-10MPa and 7-200MPa) but fall short of those required for native whole bone i.e. 200 MPa and 1 GPa respectively. With our new design, we have been able to achieve a mean Ultimate Compressive Stress of approximately 40 MPa and a mean Compressive Modulus of approximately 600 MPa. Glycerol-water mixtures were used to mimic the viscosities of blood and bone marrow and study scaffolds' ability to promote capillary inflow. Slow capillary rise of fluids mimicking viscosities of blood and bone marrow was observed in the 3D printed scaffolds. In order to improve their ability to wick up these fluids, polymer surface was pretreated with oxygen plasma prior to mineralization using concentrated simulated body fluid. Presence of mineral resulted in them quickly wicking up fluid followed by a more gradual rise. Scaffolds were prevascularized by allowing vascular endothelial cells to grow within the cortical structure. They were decellularized after 2 weeks leaving behind a pro-angiogenic matrix. Scaffolds with and without autologous bone marrow were implanted in a rabbit critical-sized radial defect model, with allografts serving as controls. X-Ray and CT imaging was used to track bone regeneration over the course of 20 weeks. X-ray images showed progressive bone regeneration from 2 to 10 weeks, originating first from the ulna ridge just below where the radius was removed and from the two ends where the radius meets the implant. The CT images taken at 12 weeks post-op showed significant bone regeneration. At the end of the study, histology will be performed to analyze regenerated bone and vasculature.

We have developed load bearing scaffolds that promote infiltration of bone marrow into and throughout the scaffold, reducing the need to add stem cells prior to implantation *in vivo*. Using endothelial cells to prevascularize our scaffolds, we have created decellularized lumens within our cortical geometry to promote growth of vasculature upon implantation. Our ongoing *in vivo* evaluation has shown that our scaffolds can maintain their structural integrity while promoting bone remodeling and show promise as bone graft alternatives.

8:00 PM SB09.03.10

Control of Notch Signalling Timing and Strength Through Bead-Tethered Ligands for T Cell Differentiation from Induced Pluripotent Stem Cells Alessia Pallaoro, Richard Carpenedo, Yuan He, [Manu Thomas Kalathottukaren](#), Hiofan Hoi, Cole Zmurchok, Dan Kirouac, Steven Woodside and Emily Titus; Notch Therapeutics, Canada

Human induced pluripotent stem cells (iPSCs) provide a highly consistent cell source for the ex-vivo production of therapeutic T cells. Of the different T cell subtypes, the CD8 $\alpha\beta$ + T cell has the strongest clinical precedence in autologous and healthy-donor derived CAR-T cell products yet has historically been challenging to generate from iPSCs. Notch signaling is required to drive T-lineage differentiation, and in conventional culture, protocols are delivered by Delta-Like 4 (DLL4)-expressing feeder cells or DLL4 protein-coated culture vessels. Unfortunately, these methods have not yielded efficient production of CD8 $\alpha\beta$ + T cells from iPSCs and lack control of ligand dose and timing.

We have developed the Engineered Thymic Niche (ETN), a fully defined custom reagent consisting of magnetic beads coated with DLL4 and vascular cell adhesion molecule 1 (VCAM-1). The ETN allows temporal and intensity modulation of Notch signaling by adding or removing beads from culture vessels and increasing or decreasing the surface concentration of DLL4 and VCAM-1.

ETN was manufactured with beads sterilized by gamma irradiation before aseptic coating with DLL4 and VCAM-1. Gamma-irradiation sterilized the base beads without impacting the bead's physicochemical properties. To characterize the ETN, we developed assays for bead size, concentration, protein content, and function. On-bead DLL4 content was quantified using an immunofluorescence-based Notch-1 binding assay, while the bead function was assessed by measuring Notch-responsive gene expression and cell phenotype in response to ETN dose during differentiation of iPSC-derived CD34+ cells. ETN storage stability was improved through a storage buffer formulation study. Results suggest that ETN can be stored at 4 °C and potentially at room temperature, simplifying cell manufacturing and ETN reagent handling and storage procedures.

We applied ETN to T cell manufacturing from iPSC cultures in microplates and stirred tank reactors (STR). In microplates, we demonstrated that increasing both bead concentration and protein density (10-fold range) in cultures initiated with CD34+ HSPC cells modulates the expression of Notch-responsive genes (*Notch1*, *TCF7*, *DTX1*, *BCL11B*, *HES1*) and higher gene expression correlated to increased expression of progenitor T (ProT) markers (20 to 60%) after 14 days. In both microplates and STR, we show that medium to high bead dose and high cell seeding density yield the highest ProT population (CD7+/CD5+). Further differentiation of ProTs using a high bead dose yielded a higher proportion of CD8+ SP cells than lower bead doses. In both culture formats, gene expression dynamics for CD8A (T cell), IL7R (lymphoid), CD4 (T cell), and BCL11A (hematopoietic progenitor) show similar trends with CD8A and IL7R increasing and CD4 and BCL11A decreasing over time. Differentiation to CD8+ SP with ETN in STR is highly reproducible (n=8) and comparable to that in microplates. Furthermore, the iPSC-derived CD8+ cells produced in STR demonstrate comparable function as primary CD8+ cells in serial killing assays and similar proliferation (57,000-fold over 4 rounds of antigen exposure, 2:1 E:T ratio), and have a majority central/stem cell memory phenotype while being less prone to exhaustion than primary CD8 CAR-Ts. Finally, we show that ETN is remarkably stable in the custom-formulated storage buffer, with ongoing shelf-life studies showing > 9 months of stability at 4 °C and for 35 days at 37 °C. Looking ahead, the aseptic, scalable ETN manufacturing process will incorporate qualified raw materials, including GMP-level DLL4 and VCAM. Our advances in ETN bead design and characterization demonstrate that we have a stable reagent that enables the *in-vitro* control of Notch signaling required for consistent differentiation of iPSC-derived CD34+ cells to mature T cells, opening a path to clinical translation of ETN for cell production.

8:00 PM SB09.03.11

Eggshell Reinforced Scaffolds for Bone Repair [Mert Gezek](#)^{1,1} and [Gulden Camci-Unal](#)^{1,2}; ¹University of Massachusetts Lowell, United States; ²University of Massachusetts Medical School, United States

More than two million bone graft procedures are performed to treat patient defects annually.^{1,2} The main drawbacks of some of the existing bone graft materials are their complex fabrication steps, inflexibility, lack of porosity and biofunctionality, and requirement of costly reagents. Bone regeneration can be achieved using mineral-based materials, such as calcium carbonate, which is a major component of eggshells. Global waste of discarded eggshells typically amounts to millions of tons annually from household and commercial cooking. Innovative repurposing of eggshells can impact the economy and environment while providing unique solutions to unmet clinical needs. Due to the superior biophysical properties of calcium carbonate over other calcium-based minerals, the incorporation of chicken eggshell microparticles (ESP) into polymers can enhance osteogenic differentiation and bone regeneration.

In this work, we developed ESP-reinforced polymeric scaffolds to obtain mechanically stable and biologically active three-dimensional (3D) scaffolds that can differentiate stem cells or preosteoblasts into osteoblasts.¹ We generated ESP-reinforced 5-50% (w/v) polymeric scaffolds. The concentrations of the ESP were 5, 15, 30, and 50% (w/v) in the scaffolds. We characterized the mechanical properties, porosity, swelling, and degradation of these biomaterials. The cellular response was then evaluated against the ESP-reinforced scaffolds via, cytotoxicity, growth, and proliferation assays as well as gene expression analyses. Implantation of ESP-reinforced scaffolds was performed *in vivo* using a rat model and histology was carried out to evaluate the inflammatory response. In addition, near full regeneration of critical-sized calvaria defects was achieved using our ESP-reinforced scaffolds *in vivo*.² These composite materials demonstrated significant bone formation as well as bone remodeling.

This work demonstrates that eggshell microparticles can be used in a composite 3D polymeric construct for bone regenerative engineering. We successfully fabricated ESP microparticle-reinforced biomaterials and evaluated their suitability for osteogenic cell cultures *in vitro*, and biocompatibility and bone regeneration *in vivo*. Pre-osteoblasts were encapsulated within the ESP-reinforced scaffolds at 5 million cells/mL density which underwent osteogenesis as determined by RT-qPCR for osteocalcin and BMP-7. The ESP-reinforced composite scaffolds were osteoinductive and enabled the differentiation of stem cells without the use of a specialized osteogenic growth medium. The ESP-reinforced constructs were then subcutaneously implanted in Wistar rats and found to be biocompatible without inflammatory response and they were biodegradable. The implants were easily accepted by the host, allowed for cellular migration and infiltration in 3D, and were highly vascularized. To study the regenerative capability of the ESP-reinforced scaffolds, they were implanted into critical-size calvaria defects. The *in vivo* model demonstrated a near full regeneration of the critical-size defects in 12 weeks. The newly formed bone had similar bone density compared to the native bone and it was capable of producing bone marrow. Furthermore, in addition to vascularized bone formation, bone remodeling also took place as determined by immunohistochemistry for TRAP. We anticipate that the ESP-reinforced scaffolds will serve as promising implants for the treatment of bone defects in the body.

References:

- [1] Wu, X. et al. Eggshell Microparticle Reinforced Scaffolds for Regeneration of Critical Sized Cranial Defects. ACS Appl. Mater. Interfaces 13, 60921–60932 (2021).
- [2] Wu, X., Stroll, S. I., Lantigua, D., Suvamapathaki, S. & Camci-Unal, G. Eggshell particle-reinforced hydrogels for bone tissue engineering: an orthogonal approach. Biomater. Sci. 7, 2675–2685 (2019).

8:00 PM SB09.03.12

Simultaneous Antifouling and Selective Adsorption in a Poly(dimethyl siloxane) (PDMS) Based Microfluidic Device using a Functional Surface Segregating Zwitterionic Copolymer [Additive van O'Hara](#)¹, [Luca Mazzafiero](#)¹, [Aslihan Gokaltun](#)^{2,3}, [Berk Usta](#)^{2,3} and [Ayse Asatekin](#)¹; ¹Tufts University, United States; ²Harvard Medical School, United States; ³Massachusetts

Nonspecific protein adsorption and small molecule adsorption have been a persistent challenge in the use of poly (dimethyl siloxane) (PDMS)-based microfluidic devices due to PDMS's hydrophobicity. This issue has led to the development of various post-processing techniques to make the surface fouling resistant, such as plasma treatment and surface grafting of hydrophilic polymers. However, these approaches often have limited stability, with the surface becoming hydrophobic again within days. Additionally, for many applications, it is of interest to selectively adsorb only specific analytes while preventing the adsorption of others, specifically for use in protein capture for diagnostics, biochemical assays, and cell capture for organ-on-a-chip models. Achieving both selective adsorption and fouling resistance is particularly challenging. To address these challenges, we have synthesized a surface spontaneously segregating copolymer additive to create a hydrophilic, antifouling zwitterionic surface interspersed with functionalizable groups that can be easily blended into pre-cured PDMS during the traditional manufacturing method of microfluidic devices. Using this approach, we have been able to decrease the nonspecific adsorption of Bovine Serum Albumin (BSA) on PDMS surfaces by at least 95%. We have also shown that we can utilize the functionality of this polymer additive to attach desired functional groups to mediate the adsorption of specific analytes using isocyanate or EDC/NHS coupling chemistry. We expect this novel method for simultaneous fouling prevention and surface functionalization of PDMS surfaces to enable the development of better-performing biomicrofluidic devices.

8:00 PM SB09.03.13

Synergistic Effects of Extrinsic Photobiomodulation and Specific Collagen Micropatterns to Promote Mesenchymal Stem Cell Differentiation Guan Ying Tsai^{1,2}, Meng-Jiy Wang¹, Szu-Yuan Chen², Saitong Muneekaew¹ and Thipwadee Klom-In¹; ¹National Taiwan University of Science and Technology, Taiwan; ²Academia Sinica, Taiwan

The design of functional biomaterials relates closely to the chemical, and physical cues between cells and scaffolds. Among the important factors, topographic cues such as micro-patterns of different size and shape were reported to specifically impact cell functions, including cell attachment, proliferation, and differentiation. For example, the precise control of mesenchymal stem cells (MSCs) differentiation was modulated through the underneath micro-patterns such that a rectangular micropattern with an aspect ratio of 1 favored MSCs to differentiate toward adipogenic differentiation.

Moreover, photobiomodulation (EPM) was recently reported to promote differentiation of MSCs that MSCs exposed under light with wavelength of 660 nm can facilitate differentiation into adipocytes. Based on the previous studies, it is speculated that the effective control of cell phenotypes to guide MSCs differentiation toward specific lineages while EPM can be used to induce stem cell differentiation. Even more, combination of EPM with micropatterns might be further enhance MSCs differentiation, with the benchmark of chemical induction.

Therefore, this study proposes to prepare collagen micro-patterns with different aspect ratios, areas, and symmetries by photolithography method to guide Wharton's Jelly mesenchymal stem cells (WJ-MSCs) behavior. The application of EPM was achieved by using verteporfin as the photosensitizer, which targeted endoplasmic reticulum, and light irradiation with a laser of 690 nm wavelength to induce differentiation of stem cell toward adipogenic, neural, osteogenic cells.

In this study, the preparation of collagen micropatterns, the glasses were firstly treated by oxygen plasma to activate glasses (O₂/glass), followed by immersing in 1% of 3-(trimethoxysilyl) propyl methacrylate (TMA) solution to silanize the glasses (TMA/O₂/glass). After that, the photomasks of rectangular or stellate arrays were applied on the PEGDA solution dropped on silanized glass. Then UVA light of 365 nm wavelength with a light fluence of 500 mJ/cm² was shined to solidify PEGDA patterns to form PEGDA/TMA/O₂/glass. The collagen microislands were finally prepared by covering collagen solution on PEGDA/TMA/O₂/glass to eventually obtain col/PEGDA/TMA/O₂/glass microislands.

WJ-MSCs were cultured on collagen microislands for 5 days to guide cells adhesion, follow by EPM treatment twice to regulate stem cell differentiation. For the positive control groups with chemical inducing factors, the medium was replaced by differentiation medium on day 0 and again on day 3. The characteristics of the differentiated cells were observed by confocal microscope, and the number of differentiated cells were identified by flow cytometry analyses.

To reveal how collagen micropattern and EPM work synergistically to induce cell differentiation, WJ-MSCs were cultured on square, rectangular and stellate micropatterns, with or without EPM. In absence of EPM, WJ-MSCs were cultured on various micropatterns in maintenance medium (MM). The square micropatterns can direct WJ-MSCs toward adipogenic differentiation, the rectangular micropatterns guided neurogenic differentiation, and the stellate micropatterns led MSCs to osteogenic differentiation. Additionally, by combining with EPM treatment, the differentiated WJ-MSCs on micropatterns can be further promoted. Meanwhile, it was found that adipogenic and neurogenic differentiation were significantly influenced by the aspect ratio (AR) of micropatterns, while the symmetry of stellate micropatterns impacted on osteogenic differentiation.

In conclusion, this study proposes that the combination of collagen micropattern and EPM can effectively replace chemical induction medium to induce WJ-MSCs differentiation. The synergistic effects of unique micropattern and EPM could direct the differentiation route for WJ-MSCs which confirm the great potential of the proposed technique for the applications in tissue engineering and regenerative medicine.

8:00 PM SB09.03.14

Decoupling of Adhesive and Repulsive Domains of Microstructured Stimuli-Responsive Polymer Film for the Refining of Particulates and the Non-Enzymatic Harvesting of Cells Yongwook Kim^{1,2}, UmmayM. Jahan^{3,2}, AlexanderP. Deltchev², Nickolay Lavrik⁴, Vladimir Reukov² and Sergiy Minko²; ¹Lawrence Livermore National Laboratory, United States; ²University of Georgia, United States; ³North Carolina State University, United States; ⁴Oak Ridge National Laboratory, United States

Sorting colloidal particles such as protein complexes, cells, and viruses presents a challenge due to their strong and quasi-irreversible adsorption to interfaces, which hampers their efficient separation. To overcome this limitation, a microstructured stimuli-responsive polymer interface has been developed to generate a controlled local oscillating repulsive mechanical force. This force facilitates the transition between particle adsorption and facilitated desorption, allowing for the separation of colloidal mixtures based on their affinity to the particle-polymer interface. The microstructured films consist of adhesive domains and disjoining thermoresponsive poly(N-isopropylacrylamide) brush domains. This dynamic regime holds significant potential for various applications in research, diagnostics, and large-scale label-free sorting of highly asymmetric mixtures of colloids and cells. Furthermore, this novel polymeric interface can be applied to non-enzymatic cell harvesting. By utilizing microstructured patterns, the areas responsible for solid cell adhesion serve as cell growing scaffolds, while the repulsive areas are employed to collect proliferated cells from the surface. This surface design effectively addresses the limitations associated with thermoresponsive coatings, such as the need for precise coating thickness, grafting or cross-linking density, and specific substrate materials. This innovative architecture enables efficient cell harvesting and selective sorting of particulates by separating the adhesion and detachment processes.

Part of this research was conducted as a user project at the Center for Nanophase Materials Sciences (CNMS), which is a US Department of Energy, Office of Science User Facility at Oak Ridge National Laboratory.

8:00 PM SB09.03.15

O-Carboxymethyl Chitosan-Based Nanostructured Surface using Poly(Ethylene Glycol) for Multi-Functionalization of Vascular Catheters Min Yeong Jeong¹, Se Kye Park², Kibeom Nam¹ and Dong Yun Lee¹; ¹Kyungpook National University, Korea (the Republic of); ²Korea Institute of Industrial Technology, Korea (the Republic of)

Vascular catheters (VCs) are essential medical devices used for diagnostic purposes, drug administration, and surgical interventions. However, using VCs can lead to severe complications, including bloodstream infections, thrombosis, and blood vessel damage, posing a risk to patient safety. To address these critical issues, it is crucial to incorporate antimicrobial, antithrombotic, and low-friction properties into the surface of ICs. One approach for achieving multifunctionality in ICs involves coating them with a hydrogel that embeds antimicrobial and antithrombotic agents. Although catheters with such hydrogel coatings have effectively prevented these issues, they can have unwanted side effects such as cytotoxicity and tolerance. Additionally, the performance of hydrogel-coated ICs tends to degrade over time due to the leaching of functional agents from the coating layer. O-carboxymethyl chitosan (O-CMC) is a promising material for multi-functionalizing VCs due to its exceptional material properties, including biocompatibility, biodegradability, antimicrobial activity, and hemocompatibility. However, the antithrombotic activity of O-CMC remains uncertain due to incomplete thrombosis reduction and limited clinical use cases [5]. Although O-CMC has sufficient hemocompatibility, the antithrombotic activity is questionable due to its incomplete performance of thrombosis reduction and lack of clinical use cases [5]. Furthermore, there is a lack of studies on the multifunctionalization of VCs using chitosan derivatives like O-CMC. Consequently, the verification of multi-functional performance, including antithrombotic activity, remains a challenge in the application of actual VCs. In this study, we introduce a novel strategy to achieve surface multi-functionalization of ICs using O-CMC. To enhance the inherent performance of O-CMC, we fabricated a nanoscale rough surface for the coating layer. This is accomplished by fabricating a nanoscale porous O-CMC coating layer on pre-treated ICs through the selective leaching of water-soluble polyethylene glycol (PEG) from a heterogeneous O-CMC/PEG composite. The resulting coated layer exhibits superhydrophilicity due to increased surface roughness. Notably, the antifouling effect by superhydrophilicity of the coating layer effectively prevented the adhesion of bacteria and platelets, synergizing with the inherent properties of O-CMC. Additionally, the porous O-CMC coating layer exhibits sufficient low-friction properties even with its rough surface. Moreover, we have successfully demonstrated that the practical VC with the proposed coating method exhibits excellent trackability in a curved artificial blood vessel. This proposed coating strategy shows great potential not only for VCs but also for a wide range of polymer-based vascular devices, including vascular filters, grafts, pacemakers, and soft robots.

8:00 PM SB09.03.16

Cationic Material-Free mRNA Delivery Carrier Naoki Taguchi^{1,2}, Akihisa Otaka¹, Yoshiaki Hirano^{2,2} and Tetsuji Yamaoka^{1,3}; ¹The National Cerebral and Cardiovascular Center Research Institute, Japan; ²The Kansai University, Japan; ³The Komatsu University, Japan

[Introduction] Since mRNA is easily degraded in our body, it requires a delivery carrier to be delivered to target cells. Cationic carriers are often used for mRNA delivery because it electrostatically interacts with the phosphate groups of mRNA. However, cationic feature often causes cytotoxicity and nonspecific protein adsorption in the blood, thus decreasing the

therapeutic efficiency. To solve this problem, we focused on zwitterionic arginine methacrylamide (ArgMA), in which the alpha-amino group of arginine is conjugated with methacrylic acid as a carrier component. The guanidyl group of arginine has affinity to nucleic acid^[1] and retains mRNA despite its zwitterionic and nonionic structure. Furthermore, previous papers have reported several attractive features of ArgMA as a delivery carrier, such as lower cytotoxicity than cationic arginine^[2] and antifouling properties^[3]. In this study, ArgMA-containing polymers were synthesized and verified whether the polymer can retain and protect mRNA and induce protein expression.

[Synthesis and Method] ArgMA was synthesized according to a previous report^[4]. Since ArgMA homopolymer was insoluble in water, ArgMA was copolymerized with 2-methacryloyloxyethyl phosphorylcholine (PMR) at the ArgMA composition ranging from 0 to 70 mol%. Free radical polymerization and reversible addition-cleavage chain transfer (RAFT) polymerization were performed using 2,2'-azobis(isobutyronitrile) as initiator and water/ethanol as solvent. PMR was mixed with mRNA, encoding a near-infrared red fluorescent protein (iRFP), with a guanidyl/phosphate group ratio from 0 to 200, and the polyplex formation was confirmed by an agarose gel electrophoresis. The mRNA protection by PMR was evaluated after incubation with 10% fetal bovine serum (FBS) at 37°C for 10 min. The transfection efficiency of fibroblast cells (HEK293) was evaluated using flow cytometry analysis.

[Results and Discussion] Agarose gel electrophoresis showed that the more mRNA formed polyplex with PMR synthesized by free radical polymerization ($M_w \approx 100,000$) with an increase in the ArgMA composition, while the polymer without ArgMA failed to form polyplex. This suggests that ArgMA is the major mRNA binding domain of PMR. Next, in the mRNA protection assay, the PMR with an increasing composition of ArgMA inhibited mRNA degradation. However, naked mRNA was completely degraded. Similar results were observed using PMR synthesized by RAFT polymerization (M_w ranged from 7,400 to 27,000) in the agarose gel electrophoresis and the mRNA protection assay. Finally, transfection experiments were performed using iRFP fluorescence expression as an indicator. HEK293 cells expressed the highest iRFP expression by culturing in the medium containing the polyplex composed of RAFT-PMR containing 30 mol% ArgMA. ArgMA will be a promising motif for designing cationic moiety-free mRNA delivery carriers.

[acknowledgements] This work was supported by AMED under grant number JP22bm1123003 and KAKENHI under grant number 23K11861.

[Reference] [1] Meredith Corley et al., *Molecular Cell*, 78, 6, (2020), 9-29. [2] Yoseop Kim et al., *Biomacromolecules*, 2012, 13, 3418-3426. [3] Gang Xu et al., *Langmuir*, 2017, 33, 6935-6935. [4] Sara Bersani, et al., *Bioconjugate Chemistry*, 2012, 23, 1415-1425

8:00 PM SB09.03.17

Lyophilized Porous Gelatin MicrogelsZiqiangGuan; University of New Hampshire, United States

Injectable hydrogels are useful for wound healing and tissue engineering due to their ability to conform to the topography of target tissues and provide a natural hydrated 3D environment for cells. However, most injectable hydrogels are nonporous, resulting in a delayed cellular response. Previously, our group developed an injectable microporous hydrogel made of gelatin microgels, which are cured to form a bulk hydrogel using microbial transglutaminase (mTG). This novel hydrogel allowed efficient migration of surrounding cells into the hydrogel phase as well as rapid spreading and proliferation of encapsulated cells. These characteristics indicate its potential use in wound healing and stem cell delivery. In this research, we demonstrate the development of porous gelatin microgels and their assembly for cell encapsulation. The porous microgels are produced by swelling and lyophilization of nonporous gelatin microgels. The micropore structure of the microgels was confirmed using scanning electron microscopy (SEM). The pores in the microgels enabled more rapid diffusion of a model protein (bovine serum albumin) into the microgels, demonstrating that these porous microgels will facilitate the transfer of nutrients and gas molecules in and out of the hydrogel. When these porous microgels were used for the encapsulation of human dermal fibroblasts (hDFs), hDFs were found to exhibit more widespread morphologies. Taken together, these novel microgels will prove useful for stem cell delivery for tissue repair.

8:00 PM SB09.03.18

Novel Nanoscale 3D Mapping of Mechanical Heterogeneities in Hydrogels for Tissue EngineeringFeiWang, KevinGrassie, FayekahAssanah, YusufKhan and BryanD. Huey; University of Connecticut, United States

We are developing a platform to investigate the forces experienced by cells in tissue engineering hydrogels when exposed to external loading by ultrasound, mimicking clinical procedures for bone tissue regeneration. A high density of embedded fluorescent microbeads, which serve as fiducial markers for deformation tracking, is dispersed within the hydrogel. A series of optical images are first acquired over a range of focal planes, spanning thicknesses of tens of micrometers, to map the bead positions in 3D. Such optical stacks are then repeatedly collected as a function of time before, during, and after uniform acoustic loading. Post processing identifies the displacements of the several thousand beads in the field of view. This allows local distortions within the hydrogel, and even incorporated cells, to be volumetrically mapped. Variations in the magnitude and direction imply mechanical heterogeneities due to local differences in hydrogel cross-linking, density, hydration, and/or cellular mechanical structures and active adhesion.

This approach will help to investigate the cellular response to clinically applied, but still not well understood, low-intensity pulsed ultrasound (LIPUS) which has been demonstrated to enhance bone formation and healing. Ultimately this approach may enable 3D Traction Force Microscopy, with broader applications to other 3-dimensionally heterogeneous systems including individual cells, tissue, and block copolymers, and nanocomposites.

8:00 PM SB09.03.19

Comparing Hydrodynamic Sizes of Solid and Mesoporous Silica Nanoparticles in De-Ionized Water and Cell Culture MediaTrentGabriel, YuweiFan, LaishengChou and RussellGiordano II; Boston University, United States

Objective: To determine the hydrodynamic-size (HS) of 100nm spherical solid-silica-nanoparticles (SiNPs) and mesoporous-silica-nanoparticles (MSNs) in both de-ionized water (DI water) and cell-culture-media (CM). To confirm the stability of both nanoparticle (NP) dispersions in CM for at least 3 days.

Methods: Nanocomposix SiNPs and MSNs of MCM-41 type were used. Size distribution and shape of the NPs was confirmed with SEM, mesopores for MSNs were visualized with TEM. NPs were sonicated for 5min in an ice-ethanol-salt bath and then filtered with 1.2um sterile filters. HS was measured using Dynamic-light-scattering (DLS) with an average of 5 readings for intensity per sample. The HS for NPs in DI water and CM was compared. To assess stability of the dispersion in CM, samples were kept in an incubator at 37C and measured for 3 days using DLS.

The diameter of dried NPs measured with SEM and HS of sonicated NPs in DI water and CM was determined. The diameter was taken as an average of 50 NPs, the results for the DI water and CM were completed with one sample measured 5 times. Two way ANOVA with replication with alpha 0.05 analysis showed: H1: There is a difference in means between NP groups. H2: There is a difference in means between dispersion solution. H3: There is an interaction.

The HS of both NPs over 3 days in CM was also determined. Triplicate samples were prepared and each same was measured 5 times. Two way ANOVA with replication with alpha 0.05 analysis showed: H1: There is a difference in means between NP groups. H2: There is a difference in means between days. H3: There is no interaction.

Conclusions: The HS for both NPs increased in CM compared to DI water. The HS was larger for MSNs than SiNPs when the solution was the same, most likely due to the increased surface area allowing for more intermolecular interactions. The stability of both NPs in CM was confirmed up to 3 days. The decrease in size from day 0 to day 3 suggests that the NPs are dissolving in solution.

8:00 PM SB09.03.20

Biomimetic Scaffolds from Biopolymer Ionogels: Elucidating Processing Parameter Dependence on Cell ProliferationEvanMcDowell, LibertyYoder and LettiFrenandez; North Carolina A&T, United States

Novel tissue engineering approaches are imperative to address the increasing prevalence of replacing damaged or lost organs due to congenital defects, traumas, or disease. Reliance on traditional transplantation techniques as the primary step of intervention has been hindered, as it is constrained by the scarcity of available organs. Advancements in tissue engineering techniques have interested scientists and clinicians as it holds the potential to create safe and reliable methods for developing functional tissue providing the possibilities to improve patient outcomes, alleviate healthcare burdens, and improve quality of life globally. Recently, research developments in stem cells, biomimetics, biochemistry, and material science have begun to pioneer these new paths for researchers, in some cases allowing them to circumvent traditional methods altogether. Most regenerative medicines/techniques that have emerged are centered around infusing a cell's natural mechanisms with manufactured processes, but realizing a functional biomimetic synthetic tissue is an intricate process. Synthetic tissue must aim to mimic the heterogeneity, complexity, structural integrity, mechanical function, and biocompatibility of indigenous tissue. Additive manufacturing, hydrogel cell cultures, and electrospinning have been used to produce tissue that equates to or enhances the regenerative properties of the human body. Here in this study, we follow established ionic liquid protocols, synthesizing BmimCl from conventional precursors to be used in various dissolutions, forming ionogels. These ionogels are composed of cellulose, silk, or a blend of both, and in combination with our regenerating solution, served as the material for 3D printing the scaffolds. Here we show that via standard additive manufacturing processes, we were able to design and manufacture biomimetic ionogel scaffolds with tailored nanosized features that facilitated enhanced cellular activity and proliferation. Each scaffold was done in triplicate and seeded with MDA-MB-231 cells into individual T-75 flasks. They were cultured in 2 variable conditions in addition to the control: ambient dried ionogel, freshly regenerated ionogel, and no ionogel(control). Each condition was seeded without mixing and after 3 days in standard culture conditions, they were removed for counting. MTT analysis uncovered the viability of the cells increased in the freshly regenerated culture and decreased in the ambient dried condition in comparison to the control. This data supports that these scaffolds, when intact, can provide an advantageous nanostructured milieu, that

enhances cell proliferation. Polymer matrix density, porosity, and level of regeneration were tailored to improve cell viability, showing up to a 40% increase, outperforming standard biocompatible plastics used in industry. While this work is in its nascent stages, the early indicators are pointing toward a possible pathway for producing rapid, and reliable tissue cultures that could be used for drug testing, medical research, or eventually in-vitro human models. Although it does not replace traditional transplantation, this approach offers researchers the potential to quickly prototype and test tissue models. It holds the potential to accelerate advancements in tissue engineering, providing valuable tools for scientific investigation and potentially transforming the field.

8:00 PM SB09.03.21

Actuating Extracellular Matrices Mechanically Program Anisotropy in Engineered Muscle Tissues[Brandon Rios](#), Angel Bu and Ritu Raman; Massachusetts Institute of Technology, United States

Introduction: Multicellularity is the key to the dynamic functionality of biological tissues. Cells embedded in an extracellular matrix communicate with each other, and with their surrounding scaffold, through a combination of chemical, electrical, and mechanical signaling. A soft actuating substrate that is capable of controlling cell-cell mechanical interaction with high spatiotemporal precision, while also allowing for the generation of forces in the biologically relevant range, would enable probing the impact of external forces on intercellular communication and measuring downstream impact on morphology and function. We have developed a magnetically actuated extracellular matrix capable of modular, programmable, and tunable deformation. We test this platform as a mechanically active substrate for skeletal muscle and show that we can control the directional fusion of myoblasts into aligned fibers. By leveraging computational tools to track substrate deformation in response to muscle contraction, we further demonstrate that mechanically programmed anisotropy in muscle improves synchrony of tissue-wide coordinated twitch. This study sets the stage for deploying actuating extracellular matrices to map and modulate mechanical signaling and control a variety of complex biological processes. **Materials and Methods:** We manufactured magnetic silicone microparticles by mixing iron nanoparticles within poly (dimethyl siloxane) and embedded these microparticles within a fibrin hydrogel. A custom-built linear actuator enabled moving a magnet under the hydrogel with precisely controllable direction and speed. We seeded optogenetic mouse myoblasts on magnetic fibrin gels and differentiated them to form mature muscle in the presence or absence of mechanical stimulation (30 minutes/day, 10 days). The resultant mechanical motion was recorded with a stereoscope and custom automated tracking software was used to map deformation of the hydrogel in response to magnetic (daily) and optical (only on day 10) stimulation. Tissues were fixed and stained for cell nuclei and myosin expression to quantify muscle fusion index and other indicators of mature tissue formation.

Results and Discussion: Global fiber alignment is critical to native muscle architecture, as global actuation can only be achieved by independent fibers twitching simultaneously and in the same direction and is thus of relevance for applications ranging from regenerative medicine to biorobotics. Morphological analysis revealed that both control and stimulated fibers grow significantly in length over time, but no significant difference in fiber length or width was observed between experimental groups. We used Fast Fourier Transform image analysis to assess differences in muscle fiber directionality and showed that mechanically stimulated tissues were more likely to align parallel to the direction of magnet movement (0°). By contrast, fibers in control groups did not demonstrate statistically significant global alignment. Optical stimulation of engineered muscle generated globally coordinated twitch deformation in the mechanically stimulated group, while the control group displayed asynchronous and arrhythmic contraction, indicating improved global fiber alignment had an observable downstream impact on function. These quantitative assays, which showed that enhanced x-direction alignment corresponds to increased synchrony of x-direction twitch, corroborate the observation that actuating extracellular matrices can mechanically program anisotropy of form and function in engineered muscle.

Conclusion: Our proof-of-concept study demonstrates how modulating intercellular forces in skeletal muscle during growth and maturation can dynamically program tissue anisotropy. Our platform can be readily adapted to a variety of natural and synthetic soft substrates, as well as a range of cell types, and anticipate that this platform will enable a broad range of fundamental studies of mechanobiology.

8:00 PM SB09.03.22

Laminin-Decorated Gelatin Microporous Injectable Hydrogel for the Encapsulation and Differentiation of Neural Progenitor Cells[Seth Edwards](#); University of New Hampshire, United States

Nervous tissues have limited capacity to regenerate, and damage to these tissues, due to neural injuries or neurological disorders, is often debilitating to the affected patients. The delivery of neural progenitor cells (NPCs), with biomaterials as a delivery vehicle is a promising strategy to promote neural tissue repair. Neural differentiation of NPCs is facilitated by cell spreading and morphological changes, as well as cell-cell interactions. An effective delivery vehicle for the nervous tissue regeneration should promote such cell-matrix and cell-cell interactions. In this report, we investigated the potential for a microporous injectable hydrogel, formed by annealing of gelatin microgels to promote the differentiation of encapsulated NPCs. In addition, we demonstrate a novel method of improving NPC adhesion in the microgel matrix by a facile covalent incorporation of laminin by microbial transglutaminase (mTG) during the microgel annealing process. We found that cell organization, morphology, and differentiation were dependent on the 3D environment, as examined through live/dead assay, immunofluorescence staining for neural markers, mitochondrial activity, and by investigating functional neuronal network formation through monitoring calcium flux of encapsulated cells in response to neurotransmitter. In summary, our results investigate and demonstrate the potential for microporous injectable hydrogels to serve as a vehicle for the encapsulation and differentiation of NPCs.

8:00 PM SB09.03.23

Guanidine-Based Hydrophilic Antimicrobial Polymer as a Textile Coating[Urmil V. Mody](#) and Michael Wolf; University of British Columbia, Canada

With the increase in infection transmission and resistance to antibiotics, using clothing as the first of defense can reduce transmission rates and contain disease spread. We report a guanidine-based cationic hydrophilic antimicrobial polymer (GAMS) that can selectively lyse bacterial cells. Antibacterial activity, hydrophilicity, haemolytic and thermal properties of the crosslinked siloxane-based cationic polymer are tested post-functionalization with guanidine groups at 10%, 30%, 50%, and 70% loading relative to the amine groups on the polymer. It is concluded that guanidine functionalized polymer is selective for bacterial cell lysis with complete elimination of class 2 pathogens (E. coli and MRSA) using a contact killing mechanism. GAMS polymers show high thermal stability. Structural characterization of GAMS polymers is performed using NMR (1H, 13C, COSY, HMBC), FTIR, elemental analysis, TGA, (E. Coli/MRSA). Bacterial colony counting assays are performed to evaluate the efficiency of GAMS compared to hydrophobic antibacterial polymers that have been previously reported.

8:00 PM SB09.03.24

Synthesis of Curcumin-Loaded LNP-Based Sarcopenia Treatment using Microfluidic Reaction System[Jun-Won Kook](#); Ajou University Medical Center, Korea (the Republic of)

Sarcopenia, characterized by progressive loss of skeletal muscle mass and function, is a prevalent condition associated with aging. Currently, there is a growing interest in developing effective therapeutic strategies to combat sarcopenia and improve the quality of life for affected individuals. In this study, we propose a novel approach for the synthesis of curcumin-loaded lipid nanoparticle (LNP)-based sarcopenia treatment using a microfluidic reaction system.

The microfluidic reaction system offers several advantages over traditional bulk synthesis methods, including precise control over reaction conditions, enhanced mass transfer, and reduced reaction times. These characteristics make it a promising tool for the synthesis of drug-loaded nanoparticles with improved physicochemical properties and therapeutic efficacy.

Curcumin, a naturally occurring polyphenol found in turmeric, has demonstrated potential as a therapeutic agent for sarcopenia due to its anti-inflammatory and antioxidant properties. However, its poor aqueous solubility and low bioavailability limit its clinical application. By encapsulating curcumin within LNPs, we aim to enhance its stability, solubility, and targeted delivery to skeletal muscle tissues.

The microfluidic reaction system enables the efficient production of curcumin-loaded LNPs by facilitating the rapid mixing of lipid precursors and curcumin in a continuous flow. This allows for the formation of uniform nanoparticles with controlled size and composition. Furthermore, the microscale dimensions of the system enable the precise tuning of reaction parameters, such as temperature, flow rates, and residence times, to optimize the encapsulation efficiency and loading capacity of curcumin within the LNPs.

To evaluate the potential of the synthesized curcumin-loaded LNPs as a sarcopenia treatment, in vitro and in vivo studies will be conducted. The nanoparticles will be characterized for their physicochemical properties, including size, zeta potential, and drug release kinetics. In vitro assays will assess the cellular uptake and cytotoxicity of the LNPs using skeletal muscle cells. In vivo studies will involve the administration of the curcumin-loaded LNPs to animal models of sarcopenia, followed by the evaluation of muscle mass, strength, and markers of inflammation and oxidative stress.

In conclusion, this study proposes a microfluidic-based approach for the synthesis of curcumin-loaded LNPs as a potential sarcopenia treatment. The use of a microfluidic reaction system offers unique advantages in terms of control, scalability, and reproducibility. If successful, this approach could provide a promising therapeutic strategy for the management of sarcopenia, addressing the unmet need for effective treatments for this age-related condition.

8:00 PM SB09.03.25

Noninvasive and Longitudinal Study of Multi-Contrast 3D Bioprinted Tissue Constructs via Photon Counting Computed Tomography[Carmen J. Gil](#)^{1,2}, Connor Evans³, Lan Li³,

AlexanderAllphin⁴, MartinTomov¹, LiqunNing², MingShen¹, JarredM. Kaiser¹, LuzRestrepo⁵, VictorPuturo², GabriellaKabboul¹, AnjumAlam², TravisFulton¹, RemiVeneziano⁵, NickWillet¹, HichamDrissi¹, CristianBadea⁴, HollyBauser-Heaton¹, RyanRoeder³ and VahidSerpooshan^{1,2}; ¹Emory University, United States; ²Georgia Institute of Technology, United States; ³University of Notre Dame, United States; ⁴Duke University, United States; ⁵George Mason University, United States

3D bioprinting has revolutionized the fields of personalized and precision medicine by offering the unique possibility of designing patient-specific tissue engineered constructs and therapies. For cardiovascular disease, patient-specific bioprinted cardiac patch devices have emerged as novel therapeutics, demonstrating promising results in restoring and/or improving cardiac function, reducing the infarct size, and enhanced angiogenesis in animal models of myocardial infarction (MI). However, current 3D bioprinted cardiac patch designs primarily lack the ability of noninvasive, longitudinal, and quantitative monitoring of their function following the implantation *in vivo*. Computed tomography (CT) is widely used in clinical settings to monitor cardiac function and anatomy. A recent advancement in CT imaging, i.e., photon-counting CT (PCCT), has enabled simultaneous imaging of multiple contrast agents at higher spatial resolution while potentially reducing the radiation dose. Through integrating advanced multi-material bioprinting and PCCT imaging, this research aimed at design and creation of novel 3D cardiac patch structures, incorporated with multiple CT imaging probes, which can be monitored noninvasively and longitudinally in both *in vitro* and *in vivo* applications.

In this study, distinct k-edge CT imaging probes were incorporated in different bioinks and used to print patch structures. To determine the feasibility of our approach, release profiles of various imaging probes from the constructs were investigated to optimize the production of bioinks with adequate and stable concentrations of imaging probes. Subsequently, imaging properties of bioprinted contrast agent-laden constructs were evaluated by CT/PCCT both *in vitro* and *in vivo*, in a subcutaneous mouse model. Imaging probes added to distinct bioink formulations included gadolinium (Gd) chelate, iodine (Iod), Gd₂O₃, gold nanoparticles (Au NPs), and methacrylated Au (AuMA) NPs. Printed patches with single and multiple imaging probes were able to be discriminated and quantified by PCCT, offering the ability to perform longitudinal and noninvasive monitoring of the implanted patch. In the final patch design, AuMA and Gd₂O₃ NPs were used to label different components of the patch structure, and Iod was used to visualize and quantify perfusion through the printed vasculature in the patch. Future studies aim to further control the stability and release behavior of imaging probes, incorporate advanced drug delivery tools within the patch (e.g., co-encapsulation of therapeutic molecules and imaging probes), and development of novel imaging probes (e.g., via chemical conjugation of probes to the polymer matrix). In addition, we work on improving the functionality of cardiac patch by incorporating various molecular therapeutics and cardiovascular cells, together with the CT imaging probes. In summary, this study demonstrates the feasibility of designing a novel theranostic platform to treat cardiovascular disease using a new generation of bioprinted patch devices.

8:00 PM SB09.03.26

Compressive Modulus and Charge Dictate Surface Protein Adsorption on Injectable Cellulosic Hydrogels *In Vitro* AdamWeisel and StevenNicoll; The City College of New York, United States

Cellulose is a natural polysaccharide that can be modified to meet many physical, biological, and chemical requirements, making it an attractive candidate for tissue engineering¹. Specifically, its inherent sustainability and the potential for *in-situ* gelling by functionalization with methacrylate groups, makes this system appealing for stable, minimally invasive implants². Water-soluble cellulosic derivatives, such as methylcellulose (MC), which contains hydrophobic methoxy groups that afford thermogelation properties at body temperature, and carboxymethylcellulose (CMC), which provides polyanionic character analogous to native tissue glycosaminoglycans, allow for further tuning of the hydrogel features. The biological response to these materials is dependent on serum protein adsorption, which has not been examined for such cellulosic hydrogels. Thus, this study investigated the effect of hydrogel compressive modulus and charge on surface protein adsorption *in vitro* by varying MC and CMC fractional composition, macromer concentration, and molecular weight.

MC and CMC were functionalized by esterification of hydroxyl groups with methacrylic anhydride and gels were fabricated via free radical polymerization using ammonium persulfate and ascorbic acid redox initiators². Hydrogel hydrophobicity/charge was varied by mixing combinations of MC and CMC, while the modulus was altered by changing the macromer concentration (3% & 6%, w/v) and molecular weight (90, 250 kDa CMC). Generally, concentration was the largest driver of gel stiffness as indicated by compressive moduli ranging from 5.8±1 kPa to 19.9±3 kPa for the 3% group and 59.3±3 kPa to 90.6±32 kPa for the 6%. Relatedly, stiffer gels exhibited less swelling as measured by the equilibrium weight swelling ratio (W_{wet}/W_{dry}), with the 6% gels yielding lower values on average. Within a concentration group, charge played a clear role on swelling. For the 3% gels, the CMC only (negatively charged) gels yielded the highest ratio of 41±9, the MC only (hydrophobic) gels the lowest at 22±0.7, and a 1:1 mix of the two polymers was in between (ratio of 36±7). Interestingly, there was an inverse relationship between serum protein adsorption and gel modulus where every 3% gel formulation promoted more adsorption than its 6% macromer counterpart. Adsorption was also affected by charge, as no more than 63±11 µg/mL of protein was measured on MC gels, whereas the CMC only gel values ranged from 138±24 to 568±155 µg/mL.

Tailoring an injectable device is crucial for successful tissue incorporation. Long-term implants often suffer from sustained foreign body responses that may result in dense fibrous tissue encapsulation, and surface protein adsorption is a precursor to this adverse outcome³. Thus, the effects of biomaterial stiffness and charge on adsorption are often investigated and are material specific^{4,5}. These findings represent an improved understanding of cellulosic materials and are currently being investigated for correlations to *in vivo* foreign body reaction and potential fibrous encapsulation.

References

1. Chen, C. X., Yi, Y. & Weng, Y. Recent Advances in Cellulose-Based Hydrogels for Tissue Engineering Applications. *Polymers* vol. 14 Preprint at <https://doi.org/10.3390/polym14163335> (2022).
2. Gold, G. T., Varma, D. M., Taub, P. J. & Nicoll, S. B. Development of crosslinked methylcellulose hydrogels for soft tissue augmentation using an ammonium persulfate-ascorbic acid redox system. *Carbohydr Polym* **134**, 497–507 (2015).
3. Swartzlander, M. D. *et al.* Linking the foreign body response and protein adsorption to PEG-based hydrogels using proteomics. *Biomaterials* **41**, 26–36 (2015).
4. Jansen, L. E. *et al.* Zwitterionic PEG-PC Hydrogels Modulate the Foreign Body Response in a Modulus-Dependent Manner. *Biomacromolecules* **19**, 2880–2888 (2018).
5. Vyner, M. C., Liu, L., Sheardown, H. D. & Amsden, B. G. The effect of elastomer chain flexibility on protein adsorption. *Biomaterials* **34**, 9287–9294 (2013).

8:00 PM SB09.03.27

A Fillable Scaffold Mimicking Extracellular Matrix for Chronic Tunnelling Wound Healing XiaoyuWang¹, Sigena², HongyunTai³ and WenxinWang¹; ¹Charles Institution of Dermatology, School of Medicine, University College Dublin, Ireland; ²School of Medicine, Anhui University of Science and Technology, China; ³Blafar Ltd, Ireland

Chronic wounds impose significant social and financial costs for patients and healthcare systems. Pathogenic abnormalities and hostile wound environments, such as inflammation, and augmented levels of Matrix metalloproteinases (MMPs) render the healing of chronic wounds a major and long-term challenge. Most commercial wound dressings are aimed to target a single non-healing factor, only a few are tailored to the multiple pathological abnormalities of chronic wounds and even fewer are suitable for tunnelling chronic wounds due to the difficulty in making adequate contact with wound beds. Herein, a novel fillable wound matrix mimicking extracellular matrix was fabricated by crosslinking gelatin and glycosaminoglycan *via* Schiff's base reaction to inhibit the inflammatory response, and inactivate excessive MMPs, ultimately promoting chronic wound healing. The degradation rates, pore size, swelling profile, cytotoxicity, cell proliferation and migration were investigated. Highly promoted cell adhesion and proliferation, and significantly improved migration of fibroblasts demonstrated that this fillable scaffold could provide a scaffold for cellular invasion and promote wound healing. It is easy to apply in difficult-to-access tunnelling wounds, indicating the promising potential in treating chronic tunnelling wounds. Moreover, the validation of sterilisation and virus inactivation laid the foundations for the commercialization of this fillable wound matrix.

8:00 PM SB09.03.28

Synthesis and Characterisation of Photocurable Poly(glycerol sebacate)-Co-Poly(ethylene glycol) Methacrylates MinaAleemardani, MichaelZivojin Trikić, Nicola HelenGreen and FrederikClaeyssens; University of Sheffield, United Kingdom

Introduction

Poly(glycerol sebacate)-co-poly(ethylene glycol) (PGS-co-PEG) copolymers have multifunctional and tuneable properties and great potential as high-performance biomaterials. However, the application of these materials is currently limited by harsh crosslinking conditions that include high temperatures and long reaction times. In this study, in order to overcome these limitations, the methacrylation process was conducted on PGS-co-PEG, resulting in photocurable (PGS-co-PEG)-M copolymers. Methacrylation of PGS-co-PEG, formulated respectively from polyethylene glycol (PEG2) or glycerol ethoxylate (PEG3), was investigated for the first time. (PGS-co-PEG2)-M and (PGS-co-PEG3)-M were found to be biodegradable, biocompatible, bioadhesive, pH-responsive and photocurable. Multifunctional characteristics remained after methacrylation, they were, however, drastically altered.

Methods

Polyethylene glycol 1000 g/mol (PEG2) and glycerol ethoxylate 1000 g/mol (PEG3) as two different types of PEG were used. A two-step polycondensation reaction was then used to produce PGS-co-PEG copolymers. Further, the methacrylation was carried out to develop photocurable, (PGS-co-PEG)-M, copolymers. Solid samples were made by adding 2% wt of photoinitiator to the (PGS-co-PEG)-M solutions, mixing, and UV curing.

Results

We have shown that the properties of these copolymers can be controlled by altering the type and amount of PEG and degree of crosslinking. Mechanical strength was enhanced significantly for (PGS-co-PEG)-M copolymers. Tensile Young's moduli of (PGS-co-PEG2)-M samples ranged from 0.08 to 0.48 MPa, while those of (PGS-co-PEG3)-M ranged from 2.67 to 35.47 MPa,

indicating the mechanical properties of the materials can be tuned via crosslinking density. In contrast, bioadhesive properties, such as lap-shear and adhesion strengths, were almost halved due to methacrylation. The degradation and swelling rates were slightly reduced, but pH-responsive behaviours at pH = 5.0, 7.4 and 9.1 were still observed. Cell metabolic activity and double-stranded DNA content, investigated by resazurin and PicoGreen® assays, demonstrated that the (PGS-co-PEG)-M copolymers were biocompatible.

Discussion and Conclusions

Photocurable (PGS-co-PEG)-M copolymers facilitate a simple and user-friendly curing process (photocrosslinking) that could be used for biomedical applications. Moreover, these photocurable copolymers are beneficial for various biofabrication methods, including emulsion techniques and additive manufacturing, either directly or indirectly.

References

- ¹Aleemardani, Mina, et al. "Synthesis and characterisation of photocurable poly (glycerol sebacate)-co-poly (ethylene glycol) methacrylates" *Materials Today Advances* (2023).
- ²Aleemardani, Mina, et al. "Elastomeric, bioadhesive and pH-responsive amphiphilic copolymers based on direct crosslinking of poly (glycerol sebacate)-co-polyethylene glycol." *Biomaterials Science* (2022).
- ³Lin, Dan, et al. " A viscoelastic PEGylated poly(glycerol sebacate)-based bilayer scaffold for cartilage regeneration in full-thickness osteochondral defect" *Biomaterials* (2020).

8:00 PM SB09.03.29

Enhancing Bioactivity of MgO-SiO₂-P₂O₅-CaO-CaF₂ Glass Compositions for Biomedical Applications [Andualem B. Workie](#); National Taiwan University of Science and Technology, Taiwan

In 1982, Kokubo introduced the pioneering concept of glass-ceramics (GC) incorporating apatite and wollastonite (AW). This study delves into the sintering feasibility of glass compositions based on MgO-SiO₂-P₂O₅-CaO-CaF₂ via spray pyrolysis (SP). Furthermore, it explores the intricate interplay between the resulting microstructures and bioactivity, specifically the development of a Fluorapatite layer, following various immersion durations in a simulated bodily fluid (SBF) environment at 37°C. The assessment of this material's bioactivity involved immersing samples for distinct intervals of 3, 5, 7, 14, and 21 days within the SBF solution. A direct correlation was revealed between bioactivity, sintering temperature, and soaking time; notably, the pH level generated in the SBF environment remained in the range of 7.4 to 8.2, well below the critical threshold of 8.5. This pH range augments the material's biocompatibility for potential biological applications while minimizing toxicity concerns. In order to investigate phase compositions and morphologies of the material, X-ray diffraction and scanning electron microscopy were used. Degradation rates were meticulously calculated, revealing an average weight loss of 2.59% ± 1.6. Remarkably, among all the samples, the one sintered at 1100°C demonstrated the highest bioactivity following immersion in SBF. Within the glass matrix of this sample, Fluorapatite crystals, Wollastonite crystals, and Whitlockite crystals were present in a dominant manner. By increasing crystallinity percentage, AWGC becomes more suitable for pharmaceutical applications by promoting apatite formation. Wollastonite also has unique properties, such as spheroid particle shape, whiteness, and lack of volatile components, that elevate ceramic production standards. In summary, this material amalgamates the advantages of a resorbable P-Ca-rich glass with the intrinsic bioactivity of wollastonite and apatite phases. The heat treatment process, performed at varying temperatures between 700°C and 1100°C, precipitates minuscule crystals of apatite, wollastonite, and whitlockite, thus augmenting bioactivity and yielding an average bulk density of 2.49 ± 0.32 g/cm³. Further, soaking leads to continuous dissolution of both amorphous and wollastonite phases due to the release of P and Ca ions into the SBF medium.

Keywords: Bioactivity, Microstructures, Biocompatibility, Bulk density, Degradation rates

8:00 PM SB09.03.30

Silicone Cryogel Skeletons for Enhanced Survival and Mechanics of Hydrogel-Based Implantable Cell Therapies [William J. Jeang](#)^{1,2}, [Matthew A. Bochenek](#)^{1,2}, [Suman Bose](#)^{1,2}, [Yichao Zhao](#)¹, [Bryan M. Wong](#)¹, [Jiawei Yang](#)^{1,2}, [Alexis L. Jiang](#)³, [Robert Langer](#)^{1,2} and [Daniel G. Anderson](#)^{1,2}; ¹Massachusetts Institute of Technology, United States; ²Boston Children's Hospital, United States; ³Wellesley College, United States

The transplantation of cells engineered to secrete therapeutic proteins presents a promising method to address a range of chronic diseases including diabetes, cancer, and blood disorders. However, clinical translation faces several challenges regarding immune rejection, adequate nutrient supply to therapeutic cells, and the mechanical integrity of delivery constructs. Typically, non-degradable hydrogels are used to encase and protect therapeutic cells from immune rejection while still permitting the exchange of nutrients and therapeutics. However, a critical tradeoff exists wherein improving hydrogel mechanics (e.g., by increased crosslinking or molecular weight) often compromises biocompatibility and diffusion. Consequently, the design of macroscale, retrievable hydrogel devices often must balance the risks of mechanical failure and poor viability of encapsulated cells.

We address this challenge through a composite materials system centered around an oxygen-permeable silicone cryogel, which acts as an internal skeletal support for conventional hydrogel matrices coated by an anti-inflammatory polyelectrolyte for alleviating immunological responses towards foreign objects. We show that integration of the skeletal structure dramatically improves mechanical properties and effectively mitigates fracturing of implanted devices. Notably, our approach forgoes the use of commonly employed external housings, which can impede both the transport of nutrients to cells and the release of therapeutics to the host. By contrast, the skeleton leverages the superior oxygen diffusivity of silicone elastomers and a judiciously designed microstructure to improve the oxygenation of encapsulated cells. Fluorescence microscopy reveals that the skeleton acts as an internal scaffold that guides cellular proliferation and results in favorable changes in cell morphology. Pre-clinical studies demonstrate that these functionalities translate to significantly enhanced protein secretion from genetically engineered, xenogeneic cells in immunocompetent animals over 4 weeks, without the need for immunosuppression.

The resulting technology drives important improvements in the efficacy and practicality of implantable cell therapies. Namely, superior materials mechanics translates to easier device handling and reduces risk of mechanical failure, while the ability to sustain denser cell populations enables miniaturization of therapeutic implants. With the capability to modify encapsulated transgenic cells to secrete different biologics, the presented platform promises to support a broad spectrum of protein replacement therapies.

8:00 PM SB09.03.31

Voxelated Bioprinting of Double-Network Hydrogel Scaffolds [Liheng Cai](#); University of Virginia, United States

Analogous of pixels to two-dimensional pictures, voxels — in the form of either small cubes or spheres — are the basic building blocks of three-dimensional (3D) objects. Here, we present a voxelated bioprinting technology that enables the digital assembly of interpenetrating alginate and polyacrylamide (PAM) double-network (DN) hydrogel droplets. The hydrogel is crosslinked via additive-free bioorthogonal chemistry involving a pair of stoichiometrically matched polymers. We develop theoretical frameworks to describe the crosslinking kinetics and stiffness of the hydrogels, and construct a diagram-of-state to delineate their mechanical properties. Multi-channel print nozzles are developed to allow on-demand mixing of highly viscoelastic bio-inks without significantly impairing cell viability. Further, we showcase the distinctive capability of voxelated bioprinting by creating highly complex 3D structures such as a hollow sphere composed of interconnected yet distinguishable hydrogel particles. Finally, we validate the cytocompatibility and *in vivo* stability of the printed DN scaffolds through cell encapsulation and animal transplantation.

8:00 PM SB09.03.32

Conductive Biodegradable Elastomeric Scaffolds for Bladder Regeneration [Rebecca Keate](#)¹, [Matthew Bury](#)², [Jonathan Rivnay](#)¹, [Arun Sharma](#)² and [Guillermo Ameer](#)¹; ¹Northwestern University, United States; ²Lurie Children's Hospital of Chicago, United States

Electrically conductive polymers are a unique class of materials that have demonstrated promising potential to enhance regeneration in several systems including muscle, skin, and neural tissue. The capability to bolster repair in a variety of tissue systems makes conductive polymers a promising material for advanced tissue engineering applications, such as organ regeneration, that require synergistic repair with various cell lineages. One such organ that could benefit from advanced repair solutions is the bladder, the function of which is impaired in cases such as neurodegenerative disorders, cancer or injury. Conductive polymers have not been used for bladder regeneration, in part due to the difficulties of incorporating conductive polymers in a mechanically robust tissue engineering solution. One reason for this loss of material integrity is the inherent phase mismatch between hydrophobic conductive polymers and the primarily hydrophilic biomaterials they are integrated within. Furthermore, we sought to mitigate these shortcomings by adopting a phase-compatible functionalization approach wherein the hydrophobic conductive polymer is embedded within a similarly hydrophobic biomaterial. Citrate-based materials are one such class of hydrophobic biomaterials with excellent bioactivity, morphological versatility, and degradability. By utilizing an *in situ* polymerization of the conductive polymer poly(3,4-ethylenedioxythiophene) in conjunction with citrate-based elastomers, we are able to preserve the intrinsic benefits of the base material including its powerful antioxidant activity, biocompatibility, and mechanical durability. We further demonstrate the applicability of this material in a bladder augmentation model, comparing our PEDOT-citrate based films to cell-seeded citrate-based counterparts. Analyzing regenerated bladder function through urodynamics studies, we find that PEDOT-incorporated films facilitate repair significantly compared to the cell-seeded films and significantly better than the pristine citrate-based film. Furthermore, this work demonstrates (1) advantages of a phase-compatible functionalization approach from a materials-perspective, (2) application of conductive polymer-based materials in a novel regenerative system, and (3) the capabilities for conductive polymers to promote regeneration as effectively as a cell-seeded material.

8:30 AM SB09.04.01

Panthenol Citrate Biomaterials Accelerate Wound Healing and Restore Tissue Integrity Huifeng Wang, Chongwen Duan, Rebecca Keate and Guillermo Ameer; Northwestern University, United States

The global surge in diabetes has led to diabetic foot ulcers (DFU) becoming a predominant diabetes-related complication, resulting in hospitalizations and, in severe cases, lower limb amputations. A staggering 34% of individuals with diabetes will encounter a DFU during their lifetime, with 15-20% becoming chronic or non-healing wounds. These wounds differ significantly from normal wounds, plagued by persistent oxidative stress, abnormal inflammatory responses, impaired vascularization, and innervation, among other patient-specific challenges. Furthermore, suboptimal physical properties of regenerated tissue often lead to recurrent or reopened wounds, with alarming statistics indicating recurring DFUs may result in amputation in 71-85% of cases. Meeting the pressing need for wound treatments that not only expedite wound closure but also enhance the quality of regenerated tissue is paramount in improving diabetic wound care outcomes. In this study, we present the synthesis and characterization of panthenol citrate (PC), a versatile compound with potential applications in soluble form as a cleansing solution and as a regenerative dressing to address impaired wound healing in diabetes. PC is derived by reacting citric acid with panthenol, offering intriguing optical, chemical, and biological properties conducive to protecting and regenerating skin tissue. With citric acid's established safety record and panthenol's known skin benefits, PC represents a promising candidate. PC demonstrates antioxidant, antibacterial, anti-inflammatory, and proangiogenic properties, facilitating wound closure in diabetes while restoring skin's mechanical and electrophysiological properties. In both solution and hydrogel forms, PC stimulates keratinocyte and dermal fibroblast migration and proliferation, resulting in improved re-epithelialization, granulation tissue formation, and accelerated wound closure. Remarkably, PC significantly enhances the mechanical strength and electrophysiological properties of regenerated skin. To our knowledge, this is the first study to demonstrate such comprehensive improvements in the histological and physical properties of regenerated skin following treatment with both monomeric and polymeric forms of a compound. Our approach encompasses the utilization of PC as a wound cleansing solution or as a component of a thermoresponsive biomacromolecule for use as a regenerative dressing. In conclusion, PC emerges as a pivotal building block for advanced tissue regeneration therapies, holding the promise of markedly improving wound care management for diabetic patients.

8:45 AM SB09.04.02

Ultrasound-Responsive Engineered Tissue Constructs for Remote Manipulation of Cell Signaling Katherine T. Huynh, Mary K. Lowrey, Sara Evans-Dutson, Kevin Schilling, Danielle S. Brasino, Mithila Handu, Sean Speese and Carolyn Schutt Ibsen; Oregon Health and Science University, United States

The controlled presentation of cell signaling proteins in time and space is critical for coordinating biological processes that regulate tissue regeneration. There is a need to recreate and harness these complex dynamic processes within 3D cell scaffolds to better understand their biological roles and provide new regenerative therapies. Manipulating gene expression of targeted cells at specific times and locations within these scaffolds enables controlled protein presentation within a 3D tissue construct. This is a critical tool to control cell behavior and influence cell interactions, including those involved in tissue vascularization and wound repair. These genetic manipulations are difficult to achieve in 3D using traditional transfection methods due to diffusional barriers created by the scaffold itself. To address this challenge, our team has pioneered the development of ultrasound-responsive cell culture platforms (SonoScaffolds) for noninvasive and spatiotemporally-controlled genetic manipulation of cells in 3D scaffolds. Here, focused ultrasound interacts with integrated echogenic particles within hydrogel matrices to locally deliver nucleic acids to cells to manipulate protein expression and secretion. Ultrasound has distinct advantages as a triggering stimulus as it can be focused to small volumes with multi-centimeter tissue penetration depth [1-2].

Using this approach, we have successfully demonstrated ultrasound-induced transfection of cells embedded in SonoScaffolds, including localized expression of vascular endothelial growth factor (VEGF). A dual expression VEGF-GFP fusion plasmid was coupled to lipid-based ultrasound-responsive microparticles and incorporated into a cell-seeded collagen hydrogel. Focused ultrasound (1 mm² focal zone) was applied noninvasively within the hydrogel matrix. Transfection of matrix-embedded cells was localized to the ultrasound-exposed region. The cells showed a punctate distribution of VEGF-GFP consistent with packaging of VEGF into secretory vesicles. Creating user-defined 3D spatiotemporal patterns of growth factor expression can be leveraged to elucidate how spatial presentation and timing of protein expression affect 3D cell migration and to inform therapeutic strategies for tissue repair.

Pushing the boundaries even further, we are creating ultrasound stimuli-responsive scaffolds with complex 3D architectures by integrating our echogenic gene delivery particles into 3D-bioprintable inks. Transfection was selectively activated by ultrasound within printed constructs, demonstrating the first cell-seeded bioprinted structure designed for ultrasound-controlled gene delivery. We are further extending this technique to 3D-printed spheroids and organoid cultures. Together, this work demonstrates a new class of 3D-programmable cell culture materials that enable remote, spatiotemporally-defined genetic perturbation of embedded cells and multicellular structures. These systems will provide new insights into coordinated cell processes and how growth factor presentation can be leveraged to direct healing in implantable biomaterials, with important applications in tissue construct maturation, vascularization, and tissue regeneration.

[1] Gelmi A and Schutt CE, *Advanced Healthcare Materials*. 10(1): 2001125, 2021.

[2] Chapla R., Huynh KT, Schutt CE, *Pharmaceutics*. 14(11): 2396, 2022.

9:00 AM SB09.04.03

Shape Memory Polymer Bioglass Composite Scaffolds to Heal Complex Bone Defects Brandon M. Nitschke, Alexander E. Konz, Elizabeth A. Butchko, Mary Grace N. Wahby and Melissa Grunlan; Texas A&M University, United States

Craniofacial (CMF) defects are generally treated with autografts, but difficulty achieving a conformal fit with can lead to premature graft resorption. Thus, we have developed shape memory polymer (SMP) scaffolds that can "self-fit" into irregularly shaped CMF defects. These are formed from biodegradable *linear*-poly(ϵ -caprolactone) diacrylate (*linear*-PCL-DA), with crystalline lamellae serving as switching segments ($T_m \sim 55$ deg C) and crosslinks acting as netpoints. After exposure to warm saline (~ 55 deg C), the scaffold becomes malleable, allowing press-fitting into an irregular defect before cooling to body temperature restores its rigid state. Herein, SMP scaffold composition was systematically tailored to enhance thermal tissue safety, degradation rate, modulus, and bioactivity. *Star*-architectures of constituent polymers and inclusion of bioactive Bioglass (BG) were utilized to achieve these properties. To reduce the self-fitting temperature, SMP scaffolds were formed from *star*-PCL-tetraacrylate (*star*-PCL-TA; $T_m \sim 45$ deg C). Furthermore, to accelerate degradation and tune modulus, semi-interpenetrating networks (semi-IPNs) were formed by including *linear*- or *star*-poly(L-lactic acid) (PLLA). 45S5 BG is known to induce hydroxyapatite (HAP) mineralization that subsequently promotes osteogenic differentiation (i.e., osteoinductivity) as well as osseointegration. Scaffolds were prepared from *linear*-PCL-DA or *star*-PCL-DA, as well as each with *linear*- or *star*-PLLA (75:25 wt% ratio). BG was incorporated at varying levels into scaffolds (up to 30 wt%) during fabrication. The BG content was confirmed using thermal gravimetric analysis (TGA). The compressive mechanical properties of the scaffolds were evaluated, as well as the *in vitro* degradation behavior. Notably, composite scaffolds exhibited rapid formation (24 hours) of HAP when exposed to simulated body fluid (SBF) as confirmed by SEM/EDS. Overall, these composite SMP scaffolds are expected to provide enhanced healing of complex bone defects.

9:15 AM *SB09.04.04

In Vitro Engineered Tissue Screens for Cardiac Regeneration Nenad Bursac; Duke University, United States

Cell and gene therapies for heart regeneration represent a promising approach to remuscularize the heart following myocardial injury. These regenerative therapies can benefit from *in vitro* chemical and genetic screens in engineered heart tissues to identify and study novel inducers of cardiomyocyte (CM) proliferation. Our recent screens in neonatal rat and human iPSC-derived CMs have identified activations of the mitogen activated protein kinase (MAPK) pathway and pentose phosphate pathway (PPP) as two promising strategies with pro-proliferative effects in engineered cardiac tissues (ECTs). Specifically, a doxycyclin-inducible, CM-specific expression of constitutively-active mutant of BRAF (BRAF-V600E), a major kinase in the MAPK pathway, was sufficient to induce CM cycling in ECTs, but resulted in functional decline and tissue stiffening. These adverse functional effects were associated with broad transcriptional changes, a shift to glycolytic metabolism, and induction of a pro-migratory CM phenotype. While ERK activation was required for the initial establishment of the caBRAF-induced phenotype, inhibition of ERK after the phenotype had been established was insufficient to restore the loss of tissue function. Transient caBRAF expression in ECTs rapidly induced CM cycling that preceded functional decline, which was reversible only if MAPK activation was brief (<3 days). Notably, the increase in ECT stiffness resulting from sustained caBRAF expression was dispensable for induction of CM cycling, as transient caBRAF expression yielded increased CM cycling without altered stiffness. Furthermore, in an independent *in vitro* CRISPR/Cas9 knockout screen, we identified adenosine deaminase knockout (ADA-KO) as the most effective inducer of CM cycle activity in neonatal rat ECTs and long-term cultured hiPSC-CMs. RNA sequencing of ADA-KO vs. control ECTs and measurements of metabolite abundance and enzyme activity suggested lactate generation and PPP upregulation as potential drivers of CM proliferation. Inhibition of the PPP rate-limiting enzyme glucose-6-phosphate dehydrogenase (G6PD) via the small molecule inhibitor 6-aminonicotinamide prevented ADA-KO

induced CM cycling, while increased PPP activity *via* doxycycline-inducible lentiviral G6PD overexpression yielded a significant increase in CM cycling. Overall, our studies demonstrate the utility of *in vitro* engineered cardiac tissues as a testbed for identification of novel CM mitogens with potential for use in cardiac regenerative therapies.

9:45 AM SB09.04.05

3D Bioprinting of Dense Cellular Structures within Functional Hydrogels with User-Defined Heterogeneity Alperen Abaci and Murat Guvendiren; New Jersey Institute of Technology, United States

3D bioprinting has a strong potential to address tissue and organ shortage for transplantation. Successful fabrication of a functional tissue requires bioprinting strategies that can replicate the biological and structural features of the native tissue including formation of dense cellular structures. Embedded 3D printing approaches advanced extrusion-based bioprinting technology for fabrication of architecturally and biologically complex structures, yet this technology requires the use of support baths which generally hinders the relevant bioactivity and heterogeneity. In this study, we developed a new method to create dense cellular structures where cell-only bioinks could be deposited into photocurable support hydrogels with tunable stiffness, degradation and bioactivity. Our approach can utilize multiple cell types or functional hydrogels to create highly heterogeneous and complex structures that could potentially be used to fabricate functional tissue models, as well as tissue interfaces, with relevant biochemical and physical complexities.

In this study, we demonstrate bioprinting of dense cellular structures using fibroblasts (NIH 3T3), human umbilical vein endothelial cells (HUVECs), and human mesenchymal stem cells (hMSCs) within support or functional hydrogels. To demonstrate the potential of our approach and importance of matrix functionalization, we investigate the osteogenic differentiation of hMSCs bioprinted within MeHA hydrogels with controlled stiffness and bioactivity. To control stem cell aspect ratio initial concentration of the MeHA hydrogel is varied (5-15%). Bioactivity is varied by tethering RGD and BMP-2. Dense hMSCs structures show great overall cell viability (>80%) and inclusion of RGD and then BMP-2 significantly enhanced osteogenic differentiation. This is confirmed with ALP assay, Alizarin Red staining and osteocalcin immunostaining. Finally, we fabricated dense cellular structures with spatially controlled cellular composition and matrix composition towards creating tissue interfaces.

Conflict of Interest: New Jersey Institute of Technology has a financial interest in the bioprinting approach reported in this manuscript and has already filed a patent application for the technology described in this paper (U.S. Application No. 17/588,998).

Acknowledgements: We acknowledge the funding from NSF/DMR - CAREER 2044479.

10:00 AM BREAK

10:30 AM *SB09.04.06

Materials for Engineering Cartilage Integration Helen Lu; Columbia University, United States

Musculoskeletal joint motion is facilitated by synchronized interactions between multiple tissue types and the seamless integration of bone with soft tissues such as tendons, ligaments or cartilage. Many of these soft tissues transit into bone through a multi-region interface that minimizes the formation of stress concentrations while enabling load transfer between soft and hard tissues. Given its functional significance, re-establishment of multi-tissue interface is thus critical for promoting the integrative repair of biological as well as tissue engineering cartilage grafts. To this end, interface regeneration and formation of composite tissue units have become a design consideration in tissue engineering. Using the classic osteochondral interface as an example and inspired by current understandings of the native interface structure-function relationship, strategies for interface regeneration and homeostasis will be discussed, with the focus on strategic biomimicry and functional multi-tissue integration.

11:00 AM SB09.04.07

Development of a Biomimetic Multi-Layered Functionalised Antimicrobial Biomaterial Scaffold for Healing of Complex Wounds Matthew McGrath^{1,2}, Juan Carlos Palomeque-Chávez^{1,2}, Shane Browne¹ and Fergal J. O'Brien^{1,2,3}; ¹Royal College of Surgeons in Ireland, Ireland; ²Advanced Materials and Bioengineering Research Centre (AMBER), RCSI and TCD, Ireland; ³Trinity Centre for Biomedical Engineering, TCD, Ireland

Diabetic foot ulcers (DFUs) are chronic non-healing wounds that constitute one of the most devastating complications of diabetes. Dysfunctional angiogenesis plays a key role in DFU, limiting tissue repair leaving wounds open and prone to infection¹. Biomaterial approaches, and in particular the use of collagen-glycosaminoglycan (CG) scaffolds, have shown promise to promote tissue regeneration and burn wound healing². These biomaterial scaffolds provide a platform for infiltrating cells into the wound environment but do not directly deal with the underlying pathology of diabetic wounds, so further functionalisation is needed for these complex wounds. The aim of this project was to engineer a biomimetic bi-layered biomaterial scaffold designed to replicate the anatomical structure of the native skin with an epidermal antimicrobial collagen/chitosan film to prevent wound infection and a pro-angiogenic, matrix molecule functionalised dermal porous CG scaffold layer to heal complex wounds.

A bi-layered scaffold was developed by combining an antimicrobial collagen/chitosan film (0.5%, 1% / 0.75%) with a type I collagen, chondroitin-6-sulfate slurry by lyophilisation. Mechanical properties, including interlayer adhesion, were optimised through the film's collagen content and crosslinking treatment (non-crosslinked (NXL)/dehydrothermal/carbodiimide EDAC crosslinking). The CG layer was then functionalised with either fibronectin, collagen IV, or laminin-1 to enhance its angiogenic and regenerative potential. The film's antimicrobial potential was tested versus *staphylococcus aureus*, and the ability of the film to support re-epithelialisation was verified through seeding of human epidermal keratinocytes (HaCaTs). The vascularisation potential of the scaffold was investigated through the culture of human umbilical vein endothelial cells (HUVECs), and human dermal fibroblasts (HDFs) on the functionalised CG scaffold layer.

The bi-layered scaffolds had enhanced mechanical properties suitable for implantation following EDAC crosslinking (compressive modulus = 1.83 ± 0.0035 kPa (EDAC), 0.72 ± 0.15 kPa (NXL)) adhesion strength between layers = 32.3 ± 4.5 kPa (EDAC), 22.5 ± 8.8 kPa (NXL)) Biological characterisation showed that all collagen/chitosan films had antimicrobial activity versus *staphylococcus aureus* regardless of crosslinking regime and collagen composition and supported the metabolic activity of human epidermal keratinocytes. However, crosslinked scaffolds showed enhanced infiltration and growth of vascular cells³. Functionalisation, of the CG layer with laminin-1 significant increased production of vascular endothelial growth factor (VEGF) by HDFs over 7 days (1044 ± 112 pg/ml). In addition, HUVECs seeded on these scaffolds formed tubular structures.

This study has led to the development of a novel biomimetic multi-layered functionalised antimicrobial biomaterial scaffold for complex wound healing. The collagen/chitosan film layer demonstrated the ability to inhibit growth and infiltration of *staphylococcus aureus*, the most common bacterial isolate found in infected wounds⁴ and supported metabolic activity of epidermal cells, demonstrating significant potential as a protective barrier to cover the wound and as a surface for re-epithelialisation. Functionalisation of the CG scaffold layer with laminin-1 enhanced the pro-angiogenic regenerative potential of the dermal CG scaffold layer, with increased growth factor production and vascular cell tube formation. Taken together, these results demonstrate the promise of this scaffold as a biomaterial-based solution to treat DFUs.

References

- (1) Lavery et al., Diabetes Care 29:1288-1293, 2006.
- (2) Yannas et al., Science 215:174-176, 1982.
- (3) McGrath et al. ACS Appl. Mater. Interfaces 2023, 15, 14, 17444–17458
- (4) Shettigar et al. Eur J C Micro In 39: 2235-2246, 2020.

Acknowledgements

Science Foundation Ireland (SFI), AMBER Centre, Grant No.: SFI/12/RC/2278_2

11:15 AM *SB09.04.08

A Versatile, Bioengineered Skin Reconstruction Device Designed for Austere Environments Joachim G. Veit, Morgan Weidow and Monica Serban; University of Montana, United States

Austere environments in which access to medical facilities, medical personnel, or even water and electricity is limited or unavailable pose unique challenges for medical device product design. Currently existing skin substitutes are severely inadequate for the treatment of severe burns, chronic wounds, battlefield injuries, or work-related injuries in resource-limited settings. For such settings, an ideal device should be biocompatible, bioresorbable, promote tissue healing, not require trained medical personnel for deployment and use, and should enable topical drug delivery. As proof of concept for such a device, silk fibroin and an antioxidant hyaluronic acid derivative were chosen as primary constituents. The final formulation was selected to optimize tensile strength while retaining mechanical compliance and protection from reactive oxygen species (ROS). The ultimate tensile strength of the device was 438.0 KPa. Viability of dermal fibroblasts challenged with ROS-generating menadione decreased to 49.7% of control, which was rescued by pre-treatment with the hyaluronic acid derivative to 85.0% of control. The final device

formulation was also tested in a standardized, validated, *in vitro* skin irritation test which revealed no tissue damage or statistical difference from control. Improved topical drug delivery was achieved via an integrated silk fibroin microneedle array and selective device processing to generate crosslinked/through pores. The final device including these features showed a 223% increase in small molecule epidermal permeation relative to the control. Scaffold porosity and microneedle integrity before and after application were confirmed by electron microscopy. Next, the device was designed to be self-adherent to enable deployment without the need of traditional fixation methods. Device tissue adhesive strength (12.0 MPa) was evaluated and shown to be comparable to a commercial adhesive surgical drape (12.9 MPa) and superior to an over-the-counter liquid bandage (4.1 MPa). Finally, the device's wound healing potential was assessed in an *in vitro* full-thickness skin wound model which showed promising device integration into the tissue and cellular migration into and above the device. Overall, these results suggest that this prototype, specifically designed for use in austere environments, is mechanically robust, is cytocompatible, protects from ROS damage, is self-adherent without traditional fixation methods, and promotes tissue repair.

11:45 AM SB09.04.09

Development of Antibiotic-Free Antimicrobial Scaffolds for Effective Delivery of Osteogenic & Angiogenic MicroRNAs to Simultaneously Treat and Repair Infected Bone Tissue Joanna Sadowska¹, Katelyn Genoud¹, Rachael Power¹, Austyn Matheson¹, Arlyng González-Vázquez¹, Lara Costard¹, Tanguy Hallegouet², Gang Chen¹, Brenton Cavanagh¹, Huijun Zhang³, Aldo Boccaccini³ and Fergal O'Brien¹; ¹Royal College of Surgeons in Ireland, Ireland; ²University of Strasbourg, France; ³Friedrich–Alexander University Erlangen–Nuremberg, Germany

INTRODUCTION: The treatment of bacterial infection of bone while regenerating bone at the same time is extraordinarily challenging in clinical settings (1). The escalating problem of antimicrobial resistance necessitates the development of novel antibiotic-free strategies to eradicate bacteria. One such approach is the use of metal-doped nanoparticles (2). To address bone regeneration, the approaches include the local delivery of gene therapies, such as microRNA in scaffold systems. A scaffold provides structural support while microRNA induces host cells to produce multiple angiogenic and osteogenic proteins essential for bone healing (3). The present study combines these two promising approaches to develop a multifunctional biomaterial-based platform with angiogenic, osteogenic and antimicrobial properties. The scaffold delivers osteogenic genes (by delivering antagomiR-138, a microRNA targeting ERK pathway) (4) and antibiotic-free antimicrobial nanoparticles (copper-doped bioactive glass, CuBG) (2), leading to a novel platform with superior therapeutic potential and angiogenic, osteogenic and antimicrobial features.

METHODS: Freeze-dried collagen-based scaffolds, previously optimized in our lab for bone regeneration (3), were enriched with antagomiR-138 and Cu-BG nanoparticles and assessed *in vitro* using human mesenchymal stem cells (transfection efficacy, osteogenic and angiogenic gene expression, metabolic activity, DNA content, alkaline phosphatase activity, calcium deposition). The antimicrobial properties of the scaffolds were assessed using gram-positive (*S.aureus*) and gram-negative (*E.coli*). The angiogenic and osteogenic properties of the scaffolds were assessed in two *in vivo* models: a load-bearing 5 mm femoral defect in female Sprague Dawley rats and a chick chorioallantoic membrane model (CAM).

RESULTS SECTION: The CuBG and antagomiR-138 particles were effectively incorporated into collagen scaffolds without affecting the mechanical and structural properties of the scaffolds. The CuBG scaffolds reduced the adhesion of *S.aureus* and *E.coli* 5-fold and 2-fold, respectively. The antagomiR138 and-CuBG functionalised scaffolds effectively transfected hMSCs *in vitro*, enhancing the osteogenic (COL1A2, NOCH4, SMAD5) and angiogenic genes (VEGFA) and calcium production. The *in vivo* assessment showed that antagomiR-138 scaffolds promoted enhanced healing in the femoral defect model by producing endochondral ossification. The antagomiR138-CuBG scaffold promoted vasculogenesis, improving the number of branches and the length of blood vessels in *in vivo* CAM model.

DISCUSSION: The study demonstrated the therapeutic potential of a multifunctional, antagomiR138 antimicrobial scaffold system. The system delivered antagomiR138 to hMSCs *in vitro*, enhancing the osteogenic genes and mineralisation. The incorporation of CuBG nanoparticles enhanced antimicrobial mechanisms (production of ROS) in *S.aureus* and *E.coli*, inhibiting the attachment to the scaffold. The antagomiR138 scaffolds improved osteogenesis and vasculogenesis *in vivo* in a femoral defect model and a chick chorioallantoic membrane model, respectively. Our work demonstrates, for the first time, the feasibility of combining non-antibiotic biomaterial based-approaches with gene therapeutics for developing a platform which not only regenerates bone but also fights rising problems of antimicrobial resistance. This approach opens the door to new possibilities in a myriad of indications beyond bone repair.

REFERENCES: 1) Sadowska *et al. Mat. Today*, **2021**, 46:136-154; 2) Ryan *et al. Biomaterials*, **2019**, 197:405-416; 3) Mencía Castaño *et al., Acta Biomater.*, **2020** 109: 267-279; 4) Eskildsen *et al. PNAS*, 2011, 108: 6139-6144.

ACKNOWLEDGEMENTS: Marie Skłodowska Curie Individual Fellowship, the European Commission, the H2020 project GAMBBa (892389), the ON Foundation (21-053), Science Foundation Ireland under the US-Ireland Research and Development Partnership (17/US/3437)

SESSION SB09.05: Cellular Approaches for Regenerative Engineering
Session Chairs: Guillermo Ameer and Carolyn Schutt Ibsen
Wednesday Afternoon, November 29, 2023
Hynes, Level 1, Room 104

1:45 PM *SB09.05.01

A Decellularized Cartilage Biomaterials Approach to Pediatric Airway Reconstruction Paul Gehret^{1,2}, Soheila Ali Akbari Ghavimi², Alexandra Dumas^{1,2}, Ryan Borek^{2,1}, Ian Jacobs^{2,1} and Riccardo Gottardi^{1,2}; ¹University of Pennsylvania, United States; ²Children's Hospital of Philadelphia, United States

Introduction: Severe subglottic stenosis (SGS), the narrowing of the airway just below the vocal folds, develops in 8.3% of ICU neonates and directly leads to debilitating comorbidities [1,2]. Pediatric SGS is the result of prolonged intubation and dramatically lowers the child's long-term quality of life, as they often suffer speech and cognitive delays. In the most severe cases, laryngotracheal reconstruction (LTR) surgery is required to expand the airway and restore airflow [1,2]. During LTR, autologous costal cartilage is harvested, shaped, and implanted into the child's airway. However, a major obstacle is that young children often lack sufficient costal cartilage to ensure a successful graft surgery, leading to donor site morbidity and high risk for restenosis, necessitating revision surgery³. Our objective is to utilize xenogeneic decellularized meniscal cartilage (MEND) to engineer a cartilage implant populated with patients' cells to circumvent the limitations of pediatric autologous cartilage.

Materials and Methods: *Meniscus decellularization and channel formation:* Meniscus cross-sections were devitalized with 4 freeze/thaw cycles then subjected to pepsin and acetic followed by treatment with elastase. 6 mm cylinders were created with a biopsy punch from the posterior half of the digested cross-sections to ensure the maximum number of channels. *Decellularized Meniscus Reinvasion:* Sterile decellularized, digested meniscus (MEND) cylinders were placed on top of the membrane insert of a transwell plate and cartilage progenitor cells (CPC) were seeded on top of the MEND cylinders. After 3 days, the MEND cylinders were fixed, sectioned, and stained. *In Vitro Differentiation:* CPC-invaded MEND were cultured in chondrogenic medium for 3 weeks and media was renewed twice/week. The differentiated construct were examined for gene expression, compression testing, and histology. *Rabbit Laryngotracheal Reconstructions:* Acellular, re-cellularized, or differentiated decellularized cartilage was implanted in an anterior cricoid split LTR. After 3 months, the rabbits were euthanized and the construct phenotype, airway expansion, and histomorphometry were assessed.

Results and Discussion: After enzymatic treatment, H&E images of circumferential sections showed that clearly aligned channels are visible post-treatment. Following a serum gradient (transwell) migration, cartilage progenitor cells (blue DAPI nuclei) penetrated in 3 days through the channels the entire depth of the construct (collagen red auto-fluorescence) reaching a density similar to that of native cartilage. After 3 weeks of differentiation, cells were arranged into lacunae with columnar structures resembling the organization of native cartilage and secreted a substantial amount of glycosaminoglycans (GAGs). Importantly, the constructs increased in both bulk mechanical strength and GAG content. Finally, a 38 rabbit study was conducted and MEND was implanted in a rabbit LTR. MEND successfully expanded the airway over the course of the 3 months and integrated with the existing cartilage as shown by the increase of GAGs within the construct and the neo-chondrification protruding from the cartilage rings. We established how decellularized meniscal cartilage invaded with progenitor cells can significantly improve outcomes for pediatric LTR.

Ethical Statement: All animal studies were conducted with IACUC approval.

References: [1] Ghavimi S *et al. Adv Drug Deliv Rev.* 2021, [2] Sherman *et al. J. Pediatr.* 1986 [3] Choi *et al. Head Neck Surg.* 199.

Acknowledgements: Support from the Ri.MED Foundation, the Children's Hospital of Philadelphia Research Institute, the Frontier Program in Airway Disorders of the Children's Hospital of Philadelphia, The American Society of Pediatric Otolaryngology Research Grant 2020, The National Institute of Health P30 AR069619, R21HL159521, R56HL16453, and the National Science Foundation Graduate Research Fellowship.

2:15 PM SB09.05.02

Strategies and Tools for Next-Generation Cardiovascular Medical Device Materials Anna Waterhouse^{1,2,2}; ¹University of Sydney, Australia; ²The University of Sydney, Australia

An increasing number of medical devices directly contact the blood, from temporary catheters and dialysis machines, to permanent stents and artificial hearts. However, blood-contacting medical devices remain problematic due to the body's recognition of the foreign materials they are made from, resulting in side effects such as blood clots (thrombosis), inflammatory based reactions or a lack of endothelialisation. Blood clots can cause the devices to fail, or they can break off (embolise) and lead to a stroke or pulmonary embolism. This is currently mitigated using anti-thrombotic drugs, however these cause bleeding risks in patients.

Biomimetic approaches to both create tools to evaluate materials, and to design next generation materials for medical devices are increasingly used and hold potential to improve blood-contacting medical devices. Recent years have seen the wide adoption of microfluidic and organ-on-a-chip technologies to mimic aspects of the host environment, providing physiologically relevant conditions allowing advances in biological knowledge of biointerfaces and material function. We have developed a range of microfluidic and organ-on-a-chip based tools to evaluate existing materials to better understand failure mechanisms of medical devices, pathophysiological processes, and mechanisms of actions of newly developed medical device materials aimed to improve function and reduce device complications.

We are also developing a range of biomimetic approaches to generate new materials including mimicking the local host environment to integrate implants, mimicking biological processes or structures to create new devices and mimicking nature to impart specific functions to devices. The ultimate aim of these biomimetic tools and novel materials is to promote integration of the device with the host to improve outcomes for patients receiving medical devices.

2:30 PMBREAK

3:30 PM *SB09.05.03

Magneto-Responsive Silk Microfibers for Neuroregeneration [Jeannine Coburn](#) and [Melissa Wojnowski](#); Worcester Polytechnic Institute, United States

Magneto-responsive fiber-based architectures represent an exciting prospect in the development of hierarchically ordered tissue engineering scaffolds, facilitating non-invasive, in situ spatiotemporal manipulation and organization of regenerative cues via an externally applied magnetic field. [1] While magneto-responsive fiber architectures are typically fabricated from magnetic nanoparticle (MNP)-doped polymeric solutions, risks of MNP leaching and subsequent cytotoxic intracellular accumulation remain unaddressed. To this end, chelation of paramagnetic ferric iron ions (Fe^{3+}) is a promising alternative to MNP-doping. [2] Given its innately fibrous structure, notable capacity for heavy metal chelation, and FDA-approval as a biocompatible, biodegradable, naturally derived biomaterial [3, 4], silk fibroin extracted from *Bombyx mori* silkworm cocoons offers a unique, unexplored opportunity to fabricate MNP-free magneto-responsive fiber architectures. In this work, passive chelation of ferric iron is explored as an MNP-free alternative in the magnetic functionalization of silk-based biomaterials. Silk fibroin microfibers (mSF) treated with aqueous ferric chloride (FeCl_3) exhibit significantly increased iron content relative to the nascent protein as determined by x-ray photoelectron spectroscopy (XPS). Coupled with the absence of detectable chlorine traces and iron oxide species, the predominantly ferric oxidation state of iron within FeCl_3 -treated mSF (Fe^{3+} -mSF) suggest incorporation of iron, without reduction, at innate oxygen-containing ligands of mSF. On exposure to an external magnetic field, Fe^{3+} -mSF displays paramagnetic magnetization behaviors that facilitate field-parallel alignment. Both magnetization and directional uniformity increased concomitantly with iron exposure during FeCl_3 treatment, suggesting the observed magnetic response of Fe^{3+} -mSF is derived from the chelated iron. In vitro biocompatibility of the Fe^{3+} -mSF has been confirmed using human dermal fibroblasts and neuroprogenitor cells (NPCs). This work is the first to investigate the magneto-responsive properties and biocompatibility of ferric iron chelated SF, demonstrating a novel, MNP-free alternative approach to magnetic functionalization of TE scaffolds. Ongoing work is underway to evaluate NPC alignment and axonal growth, differentiation, and function in response to the aligned guidance architecture.

References: 1. Adedoyin AA. *Nano Res.* 2018;11, 2. Marasini R. *RSC Adv.* 2021;11, 3. Holland C. *Adv Healthcare Mater.* 2019;8, 4. Pillely S. *Environ Sci Pollut Res*, 2022

4:00 PM *SB09.05.04

Engineering Extracellular Vesicles as Therapeutics Agents for Atherosclerosis [Eunji Chung](#); University of Southern California, United States

Atherosclerosis is the primary contributor to cardiovascular disease which is the leading cause of death worldwide. Although vascular smooth muscle cells (VSMCs) undergo phenotypic switching and play a significant role in atherosclerosis progression, extracellular vesicles (EVs) secreted from healthy, contractile VSMCs have been reported to contain endogenous therapeutic cargo including calcification inhibitors and atheroprotective microRNAs (miR) that can inhibit disease progression. Thus, we hypothesized that EVs secreted from contractile VSMCs can be harnessed and further engineered to act as both safe and effective drug delivery vehicles for atherosclerosis. To test our hypothesis, we isolated, characterized, and modified the surface of EVs with CCR2 and hydroxyapatite (HA) binding peptides to actively target synthetic and osteoblast-like, atherogenic VSMCs. Additionally, we enriched EVs with therapeutic miR-145 and miR-133 through sonication as well as by overexpressing miR-145 and miR-133 in VSMCs and collecting the secreted, engineered EVs. We show engineered EVs can modulate phenotypic switching in VSMCs and present their potential in vivo in atherogenic mouse models.

SESSION SB09.06: Poster Session II: Biomaterials for Regenerative Engineering II
Session Chairs: Guillermo Ameer, Gulden Camci-Unal, Melissa Grunlan and Carolyn Schutt Ibsen
Wednesday Afternoon, November 29, 2023
Hynes, Level 1, Hall A

8:00 PM SB09.06.01

Microvascular Imaging in Brain Tumors by Supramolecular MR Contrast Agents [Atsushi Mahara](#)¹, [Soni Raghav](#)¹, [Shigeyoshi Saito](#)² and [Tetsuji Yamaoka](#)^{1,3}; ¹National Cerebral and Cardiovascular Center, Japan; ²Osaka University Graduate School of Medicine, Japan; ³Komatsu University, Japan

[Introduction] Magnetic resonance angiography (MRA) is used clinically to diagnose brain diseases. Although the MRA visualizes the main cerebral artery such as Willis arterial circle and middle cerebral artery without any contrast agents, it is hard to imagine the microvasculature and entire vascular network due to low MR signals. In our previous study, we developed the fluorescein and Gd-chelate conjugated 8-arm PEGs (8-arm PEG-FGd₃) as the MRA contrast agents, and microvascular structure was enhanced on MRA scan by the administration of these contrast agents^{1,2}. Here, we discuss the structural feature of the 8-arm PEG-FGd₃ and its blood circulating profile. Furthermore, the microvascular formation in the brain tumor would be presented.

[Methods] The 8-arm PEG conjugated with one fluorescein and three Gd-chelates (8-arm PEG-FGd₃) was synthesized by the reported procedure². Briefly, fluorescein isothiocyanate and 1,4,7,10-Tetraazacyclododecane-1,4,7,10-tetraacetic acid (DOTA) mono-N-hydroxysuccinimide ester were added into the 8-arm PEG with 15 kDa of the molecular weight. The polymers were purified by a dialysis membrane. After the addition of gadolinium, 8-arm PEG-FGd₃ was acquired. The products in each step were confirmed by 1H-NMR. As the control, 8-arm PEG conjugated with one fluorescein (8-arm PEG-F) was also prepared. Structural features were estimated by dynamic light scattering analysis (DLS) and atomic force microscopy (AFM), and the molecular environment of fluorescein was analyzed by fluorescence spectroscopy and 1H-NMR measurements. The brain tumor in the SD-rat was scanned by 7T-MRI with or without contrast agents.

[Results and Discussion] The hydrodynamic radius of the 8-arm PEG was 6 to 8 nm within the concentration range from 0.5 to 100 mg/mL. On the other hand, the hydrodynamic radius of 8-arm PEG-FGd₃ largely depended on the polymer concentration. When the concentration of the 8-arm PEG-FG₃ was 1 to 5 mg/mL, the radius was approximately 7 nm. At the concentration ranges higher than 100 mg/mL, the radius was increased to over 1000 nm. As the results of AFM observation, nanoparticles, and fiber structure were observed at the concentration ranges from more than 100 mg/mL. The fiber was formed by the stacking of the nanoparticles. Spectroscopic analysis revealed that fluorescein groups of 8-arm PEG-FGd₃ were in the center part of the particle and stacked with the π -stacking interactions. The brain microvessel and tumors in rats were scanned on MRI. Microvasculature with a minimum diameter of 45 μm was clearly visualized on MR images only when the 8-arm PEG-FGd₃ at the concentration of 200 mg/mL was administered. The microvessel structure in the tumors was also visualized with the supra-high resolution, and these data provided information on vascular permeability.

1. Mahara A. et al., *MacloBiosci*, (2018) e1700391.
2. Mahara A. et al., *Chem. Commun.* (2020) 11807.

8:00 PM SB09.06.02

Rapamycin-Loaded Boronic Acid-Based Hydrogel as Artificial Perivascular Tissue for Prevention of Vascular Graft Failure [Hue T. Le](#)¹, [Atsushi Mahara](#)¹, [Takeshi Nagasaki](#)² and [Tetsuji Yamaoka](#)^{1,3}; ¹The National Cerebral and Cardiovascular Center Research Institute, Japan; ²The Osaka Metropolitan University, Japan; ³The Komatsu University, Japan

Introduction: Excessive proliferation of subendothelial smooth muscle cells (SMC) leads to anastomotic stenosis, resulting in an increase in graft failure rate, a big issue of vascular graft

transplantation. Perivascular adipose tissue (PVAT), an adipose tissue adherent on the vessel's external surface, has been shown to inhibit the excessive proliferation of SMC via releasing biomolecules¹. However, the PVAT is mostly absent in vascular grafts involving native and artificial ones. Phenylboronic acid (PBA)-based polymer has been reported to form a hydrogel with synthetic polyvinyl alcohol (PVA) and bind to cell membranes and tissue surfaces via PBA-sialic acid integration². Rapamycin (RPM) has been clinically approved as an anti-stenosis drug because of its cell anti-proliferative ability³. Recently, we synthesized poly (3-acrylamidophenylboronic acid-co-acrylamide) (BAAm) polymer. In this study, we proposed RPM-loaded BAAm/PVA (BAVA) hydrogel serving as an artificial PVAT⁴, thus its tissue adhesive and drug release characterization and anti-SMC proliferative function were investigated. Furthermore, we tested its effectiveness on graft patency in a porcine model.

Method: Two hydrogels with 25 and 50 mg/mL of BAAm (named BAVA25 and BAVA50, respectively) were prepared. A decellularized vascular graft with 2.5mm in inner diameter was selected as the graft model⁵. To examine the tissue adhesive ability, the lap-shear test was done after loading the hydrogel on the graft's external surface. To assess drug release ability, the RPM-loaded BAVA hydrogel was immersed in PBS solution, and the released RPM was measured every day of 6d after incubation. To test the anti-cell proliferative function, the BAVA hydrogel with or without RPM was co-cultured with porcine SMC cells, then the cell viability was examined at 1d and 3d. Finally, a porcine carotid artery interposition grafting was performed. The external surface of the transplanted graft was then coated with the RPM-loaded BAVA hydrogel, and its graft patency was followed for six months by computer tomography. **Result:** The BAVA25 and BAVA50 hydrogels could adhere to the graft surface, and their adhesion was stable for 15d after immersion in PBS solution. In the lap shear adhesion test, initial loading slope (1.5) of the BAVA25 hydrogels was similar to that (1.3) of the BAVA50 hydrogels, and the displacement at fraction point of the BAVA25 hydrogels was approximately two-fold higher than that of the BAVA50 hydrogels. As incubated in PBS solution, the BAVA25 and BAVA50 hydrogels released 83 and 73% of the initial loaded RPM within the first day. As co-cultured with SMC cells, the RPM-loaded BAVA25 and RPM-loaded BAVA50 hydrogels significantly reduced cell proliferation after one day and three days of incubation, respectively. In porcine experiments, the graft without any treatment or with RPM-loaded BAVA50 hydrogel was occluded within three days after transplantation. However, in three cases treated with RPM-loaded BAVA25 hydrogel, two grafts were patent for 10 and 17d and one graft was patent for at least 180d.

Conclusion: The BAVA25 hydrogel had a higher tissue adhesive and more rapid drug release potential than the BAVA50 hydrogel. By loading with RPM, the BAVA25 and the BAVA50 hydrogel showed the in-vitro anti-SMC proliferative function. In the porcine model, the RPM-loaded BAVA25 hydrogel effectively maintained the patency of small-diameter decellularized vascular grafts. The RPM-loaded BAVA25 hydrogel, as an artificial PVAT, might be a therapeutic approach for preventing graft occlusion by suppressing SMC proliferation.

Reference: 1) M. Takaoka, et al. *Circ. Res.* 105 (2009), 906–911. 2) J. Li, et al., *Cell Metab.* 19 (2014), 373. 3) M. Li, et al. *Carbohydr. Polym.* 296 (2022), 119953. 4) H.T. Le, et al. *Biomater. Adv.* 147 (2023), 213324. 5) A. Mahara et al. *Biomaterials*, 58 (2015), 54-62.

8:00 PM SB09.06.03

Design of High Throughput Techniques for Functional Medical DevicesVictorM. Villapun Puzas, LukeN. Carter, DaisyRabbitt, XueCao, BillyPlant and SophieCox; University of Birmingham, United Kingdom

Since the early designs of medical devices, it has become apparent that implants should act as modulators of specific biological processes to ensure short- and long-term benefits¹. Nevertheless, standard alloys used in orthopaedics have been repurposed from other industries (e.g. aerospace) as a consequence of their mechanical behaviour, corrosion resistance and biocompatibility. With increased life expectancy requiring longer service life of implantable devices and common alloying elements (e.g. aluminium or vanadium) demonstrated to negatively impact biological processes beyond cytotoxicity, it is clear that novel medical alloys should be developed to modulate clinical outcomes². In this work, the difficulties of designing alloys for implantable devices will be contextualised, providing case studies focused on generating high throughput methods for their use in alloy development with especial attention on the advantages posed by metal additive manufacturing (AM) platforms.

When metallic elements are considered, there exist a plethora of materials with reported effects on biocompatibility, antimicrobial, angiogenic, osteogenic properties and/or their ability to modulate the innate and adaptive immune response³. Nevertheless, most effects been reported for single element compounds, reducing their direct correlation to complex alloys and calling for methods to rapidly evaluate biological properties. The first case study will showcase the development of high throughput techniques for both material processing and biological evaluation. The use of AM and novel Reduce Build Volume designs for Powder Bed fusion coupled with powder blending will be shown as a tool to enable the rapid evaluation of alloy systems for antimicrobial applications with conventional and AM Ti-Cu samples used to highlight their benefits over traditional casting. Microstructural variations were assessed through SEM imaging, X-ray diffraction and Vickers microhardness evaluation which were complemented with antimicrobial assays in model strains of *S. aureus* and *P. aeruginosa*. In addition, the power of powder compaction and HIP technologies will be harnessed to enable the rapid analysis of bacterial behaviour and antibiotic synergistic/antagonistic effects through the agar diffuse method and metabolic assays in model strains of Gram-positive and Gram-negative species to enable novel databases in the healthcare industry.

Besides combinations of different metallic elements, alloy design should consider the effect of microstructure and the manufacturing of complex alloys with significantly different processing parameters. Copper and Molybdenum are two elements that have shown promise to tackle antibiotic infection, nevertheless, their disparity in reflectivity or melting point has made their incorporation in titanium alloys a challenge from a manufacturing perspective. Herein, the use of AM, powder compaction and sintering will be used to demonstrate the possibility of providing novel alloys with highly different elemental properties and their use in multicomponent alloys. Through variations in composition and heat treatment, we successfully produced a blended powder of two dissimilar elements which can be used to manufacture SLM parts with reduced input energies (133J/m instead of 300J/m)⁴. Similarly, the effect of microstructural variations with antimicrobial properties and eukaryotic cell line responses will be shown for the rapid optimisation of novel alloys.

REFERENCES

[1] D.F. Williams, *Bioactive Materials*, 10, 306-322 (2022) [2] R.P. Brown, et al. In *Toxicology of Metals*, Academic Press, 127-136 (2022) [3] K. Glenske, et al. *International journal of molecular sciences*, 19, 826 (2018) [4] R. Duan, et al. *Composites Part B: Engineering*, 222, 109059 (2021)

8:00 PM SB09.06.04

Therapeutic Mesoporous Cerium Oxide Nanoparticles for Modulating Excessive Oxidative Stress as a Treatment for Age-Related Macular DegenerationSeung WooChoi¹ and JaeyunKim^{3,3,2}; ¹Seoul National University Bundang Hospital, Korea (the Republic of); ²Sungkyunkwan University, Korea (the Republic of); ³Samsung Advanced Institute for Health Sciences & Technology, Korea (the Republic of)

Age-related macular degeneration (AMD), the leading cause of vision loss in the elderly, is characterized by progressive visual impairment caused by destructive changes in the photoreceptor and retinal pigment epithelial cells (RPEs). Since reactive oxygen species (ROS) and chronic inflammation in the retina are believed to be essential contributors to AMD pathogenesis, the regulation of the ROS and inflammation levels may be effective therapeutic targets. As cerium oxide nanoparticles (CeNPs) have attracted attention due to good ROS scavenging activities mimicking the enzymatic activity of superoxide dismutase (SOD) and catalase, many researchers have studied to confirm the therapeutic efficacy of the CeNPs and apply these to treat clinical diseases in the biomedical fields. In addition, mesoporous materials have recently been spotlighted as versatile drug carriers and catalysts due to their high surface area and pore volume, therefore, some studies have been reported on the development of various forms of mesoporous CeNPs (mCeNPs). However, most of the previous reports have been derived from hydrothermal methods with harsh conditions, such as high pressure and temperature, and mainly focused on catalytic ability for industrial use, rather than biomedical applications. To combine the advantages of CeNPs and mesoporous materials, mCeNPs are simply synthesized by using the chemical reaction with 1,1'-carbonyldiimidazole and imidazole in acetone without the need for heating and pressurization. The mCeNPs exhibiting mesoporous structures with a pore size of 2.3 nm show good ROS scavenging properties, suitable biocompatibility for human RPEs and Raw264.7 cells (murine macrophage cells), and cytoprotective effect on RPEs against the harmful effect of high H₂O₂, as well as additional anti-inflammatory effects. In addition, the mCeNPs were intravitreally administrated to a NaIO₃-induced AMD mouse model, and the mCeNP-treated group showed a partial salvage effect of at least 14 % in outer nuclear layer (ONL) thickness, indicating that mCeNPs protected RPEs from NaIO₃ injury by exerting a disease-preventive effect. In addition, the drug-carrying capacity of mCeNPs was demonstrated by loading indomethacin (IDM) as a model drug, and IDM-loaded mCeNPs exhibited an additional 17.3% reduction in interleukin-6 levels in vitro compared to the group treated with mCeNPs alone, suggesting that a synergistic anti-inflammatory effect when an additional drug is loaded onto mCeNPs, thereby enhancing their therapeutic potential. These findings suggest that mCeNP can be a therapeutic alternative or adjuvant for the treatment of AMD.

8:00 PM SB09.06.05

Glycoprotein Hydrogel-Based Implantable Nerve Guidance Conduits for Peripheral Nerve RegenerationMelisOzkan^{1,2}, SujeetPawar¹, XavierNavarro^{3,4,5}, FrancescoStallacci^{1,6} and SilvestroMicera^{2,7}; ¹Institute of Materials, Ecole Polytechnique Fédérale de Lausanne (EPFL), Switzerland; ²Bertarelli Foundation Chair in Translational Neural Engineering, Center for Neuroprosthetics and Institute of Bioengineering, Ecole Polytechnique Federale de Lausanne, Switzerland; ³Department of Cell Biology, Physiology and Immunology, Institute of Neurosciences, Universitat Autònoma de Barcelona (UAB), Spain; ⁴Institute Guttman Foundation, Hospital of Neurorehabilitation, Badalona, Spain, Spain; ⁵Centro de Investigación Biomédica en Red sobre Enfermedades Neurodegenerativas (CIBERNED), Spain; ⁶Institute of Materials, Department of Bioengineering and Global Health Institute, École Polytechnique Fédérale de Lausanne (EPFL), Station 12, CH-1015 Lausanne, Switzerland, Switzerland; ⁷Department of Excellence in Robotics & AI, Scuola Superiore Sant'Anna, Piazza Martiri della Libertà, Italy

Peripheral nerve injuries (PNIs) beyond the critical gap length pose a serious problem in neural tissue engineering and regenerative medicine. Research on effective therapeutic strategies has centered primarily on implantable nerve guidance conduits (INGCs) over the past several decades. A significant amount of progress has been made in INGC development. Still, the field has remained stagnant due to the lack of an optimal solution for ensuring target reinnervation accuracy,

which requires a delicate balance of biochemical cues, including growth factors that govern tissue formation and regeneration throughout the regeneration process. In recent years, researchers have utilized heparin-based materials for sustained growth factor delivery owing to the intrinsic characteristic of heparin to bind and stabilize the growth factors through electrostatic interactions to afford more efficient regenerative outcomes. However, several shortcomings of heparin, such as immunogenicity, could hinder the successful clinical translation of heparin-based INGCs. For this reason, structurally well-defined synthetic mimics fulfilling the same function without triggering immune response are in demand.

In this work, we introduce a silk fibroin-modified gelatin tyramine hydrogel matrix fabricated through enzymatic crosslinking. Both 2D-shaped (planar film) and 3D-shaped (tubular INGC) protein hydrogel scaffolds with the same composition were produced for *in vitro* and *in vivo* investigations, respectively. At the macroscale, silk fibroin modification facilitated enhanced mechanical strength to provide the native nerve tissue-like mechanical properties and prolonged the degradation time of the hydrogel implant. It acted as a biocompatible scaffold for Sprague Dawley rat Schwann cells (SCs).

Then, we directed our efforts toward creating a small library of synthetic small-molecule heparin glycomimetics to address the limitations of native heparin. We synthesized monosaccharides and disaccharides with different sulfation patterns to conjugate to the hydrogel matrix covalently via a PEG linker for cellular-level nerve regeneration. The binding affinities of these synthetic heparin glycomimetics to nerve regeneration-promoting biochemical cues, namely, brain-derived neurotrophic factor (BDNF), nerve growth factor (NGF), and fibroblast growth factor 2 (FGF2), were screened using isothermal titration calorimetry (ITC) and surface plasmon resonance (SPR) techniques and our findings showed sulfation pattern-dependent binding affinity. The best-performing molecule was able to bind to NGF and FGF2 with acceptable affinity. We covalently conjugated this compound to the hydrogel matrix. Fluorescence assays and gel permeation chromatography (GPC) confirmed small molecule sugar conjugation to the hydrogel. Hydrogel scaffold, which bears small molecule heparin glycomimetic complexed with NGF, referred to as glycoprotein-based hydrogel, accelerated the neurite growth of Sprague Dawley rat dorsal root ganglion (DRG) neurons and extended retention time of NGF.

Inspired by *in vitro* evaluations, we currently fabricated 3D tubular glycoprotein hydrogel-based INGCs (heavily grafted with our small molecule heparin glycomimetic and with native heparin having the same degree of grafting for comparison) to assess *in vivo* nerve regeneration in Sprague Dawley rat sciatic nerve defect model. Our final goal is long-term monitoring of INGC to unveil how heparin glycomimetics affect the cumulative release of NGF *in vivo* compared to native heparin and as well as to analyze the immunogenicity of both INGCs at the same degree of grafting.

To the best of our knowledge, it is the first report systematically investigating the structure-activity relationship of small molecule heparin glycomimetics for *in vivo* nerve regeneration applications. This approach could be further extended to related regenerative medicine and tissue engineering disciplines.

8:00 PM SB09.06.06

Direct Delivery of Nanobeads into Cells with Nanoinjector [Kazuhiro Oyama](#), Bowen Zhang, Bingfu Liu and Takeo Miyake; Waseda University, Japan

Delivering biomolecules into living cells has become an important challenge in medical and biological fields. Conventional techniques such as virus vector and electroporation are utilized commonly for small molecule delivery, but still remain several problems of low efficiency and low viability for large molecules such as biological proteins and organelles. To overcome this problem, we demonstrate the macromolecular delivery into adhesive cells with metallic nanotube ducts, which is called as nanoinjector. The metallic nanotubes were developed by an electroless plating of gold onto track-etched polycarbonate template and wet/dry etching [1-2]. To insert Au nanotubes into the cells (such as HeLa and NIH3T3), we have developed an autostamping system that can be integrated with the microscope. Here we demonstrated the delivery of macro molecules (a few hundred nanobeads) into the cells and compare it with the endocytosis delivery. The nanoinjector system provide the high efficient delivery of 200nm diameter beads for 10min injection, while the endocytosis was at low efficiency, which takes for 24h to deliver the nanobeads. Furthermore, our nanoinjector can deliver the nanobeads uniformly into the cells.

[References]

- [1] B. Zhang, Y. Shi, D. Miyamoto, K. Nakazawa, T. Miyake, "Nanostraw membrane stamping for direct delivery of molecules into adhesive cells", Scientific Reports, 9, 6806, 2019. [MT1]
- [2] B. Zhang, D. Zheng, S. Yiming, K. Oyama, M. Ito, M. Ikari, T. Kigawa, T. Mikawa, T. Miyake, "High-Efficient and Dosage-Controllable Intracellular Cargo Delivery through Electrochemical Metal-Organic Hybrid Nanogates", Small Sci. 1, 2100069, 2021.

8:00 PM SB09.06.07

Fabrication and *In Vitro* Evaluation of Hydroxyapatite Based Biodegradable Nanocomposite Scaffolds for Osteochondral Defect Repair [Aneela Anwar](#)^{1,2}; ¹University of Engineering and Technology, Lahore, Pakistan; ²Stevens Institute of Technology, United States

Osteochondral defects, resulting from trauma or degenerative conditions, present a significant challenge in the field of orthopedics. Due to their limited regeneration ability, osteochondral defects (damage to both the articular cartilage and the underlying subchondral bone) offer a substantial difficulty in orthopedic treatment. Osteochondral regeneration may benefit from the development of novel biomaterials and production processes. The purpose of this research is to propose the electrospinning synthesis of a new nanocomposite for improved osteochondral regeneration. The nanocomposite is made up of bioactive nanoparticles that are embedded in a biocompatible polymer matrix. This creates an optimal setting for cell adhesion, proliferation, and differentiation. To simulate the native extracellular matrix (ECM) architecture, a fibrous scaffold with a large surface area and interconnected porosity is created using electrospinning, a flexible and cost-effective production approach. Bioactive nanoparticles of hydroxyapatite boost the nanocomposite's regeneration capacity by encouraging osteogenic and chondrogenic development. A biocompatible polymer, polycaprolactone (PCL), is used as the matrix material during synthesis. Because of its high biocompatibility, rapid biodegradability, and outstanding mechanical qualities, PCL is a promising material for use in tissue engineering. Optimizing the polymer concentration, solvent system, and applied voltage during electrospinning produces fibers with the appropriate shape and durability.

Multiple techniques are being used to characterize the synthesized nanocomposite. The fibrous shape and interconnected pore structure of the electrospun scaffold are being revealed using scanning electron microscopy (SEM). The effective integration of bioactive nanoparticles into the polymer matrix is being confirmed by Fourier-transform infrared spectroscopy (FTIR). The mechanical integrity of the nanocomposite and its appropriateness for load-bearing applications are being assessed by mechanical testing, which includes tensile strength and compressive modulus.

Using osteochondral cell cultures, the nanocomposite is being tested *in vitro*. Studies on cell viability and adhesion show that the nanocomposite is biocompatible and can encourage cell attachment and growth. Histological stains and biochemical tests are being used to gauge the nanocomposite's capacity to promote the formation of extracellular matrix. *In vivo* assessment of the nanocomposite is being performed using an osteochondral defect model in small animal subjects. Small animal test subjects are used in an osteochondral defect model to evaluate the nanocomposite *in vivo*. The implanted nanocomposite's ability to support tissue regeneration, integrate with adjacent tissues, and restore natural tissue architecture is being evaluated constantly. The structural and functional results of the regenerated tissue are being assessed using a variety of imaging methods, including micro-CT and histological analyses. This research will show that a new nanocomposite may be synthesized using electrospinning to improve osteochondral regeneration. Bioactive nanoparticles HA can increase tissue regeneration through promoting osteogenic and chondrogenic differentiation. HA nanoparticles induce osteogenic and chondrogenic differentiation, improving tissue regeneration. The electrospun fibrous scaffold will mimic cell attachment, proliferation, and extracellular matrix deposition. The nanocomposite will be biocompatible, mechanically integrity, and regenerative after *in vitro* and *in vivo* testing. This work will enhance osteochondral tissue engineering biomaterials and manufacturing methods for orthopedic medicine and regenerative therapies.

8:00 PM SB09.06.08

Light-Degradable Nanocomposite Hydrogels for Antibacterial Wound Dressing Applications [Changhao Fang](#), Yingnan Zhang, Qiming Shen and Michael J. Serpe; University of Alberta, Canada

Bacterial infections in skin injuries can lead to life-threatening human diseases if not treated appropriately. Wound dressings can function as a barrier that can cover the infected sites and inhibit further bacterial infection, thus promoting wound healing processes. In recent years, hydrogel-based materials have emerged as ideal candidates for wound dressing applications due to their biochemical and mechanical similarity to human tissues, high biocompatibility, ability to conform to irregular wound surfaces, and their capability to encapsulate a variety of antibacterial agents. Nanocomposite hydrogels, on the other hand, possess novel nanostructures and/or incorporate nanomaterials into the hydrogel matrix to afford interesting properties such as enhanced mechanical strength and unique drug release profiles.

However, there are still many limitations associated with current hydrogel-based wound dressings, such as the on-demand release of antibacterial agents and triggered degradation. Therefore, the focus of my research project is to address these limitations by developing a light-degradable nanocomposite hydrogel that can achieve both of these goals using light (365 nm) as the single stimulus.

The approach we are taking involves incorporating triclosan-loaded, poly(*N*-isopropylacrylamide)-based nanogels (TCS-NGs) into a light-degradable poly(ethylene glycol)-based hydrogel matrix via a simple physical entrapment method. Upon exposure to 365 nm light, the hydrogel matrix can rapidly degrade, which subsequently releases the entrapped TCS-NGs into the surrounding environment.

Our results have first demonstrated that TCS-NGs possessed potent antibacterial activities. Moreover, TCS-NGs could be entrapped in light-degradable hydrogel matrix with high encapsulation efficiency. Upon exposure to light (365 nm), TCS-NGs can be released from light-degradable nanocomposite hydrogels, which still possess remarkable antibacterial efficacy in terms of inhibiting the growth of *Staphylococcus aureus* both in solution and on bacteria-infected porcine skins. Next, based on Alamar Blue assay on human dermal fibroblasts, each component of the nanocomposite hydrogel exhibited excellent biocompatibility and would not cause significant cytotoxicity. Finally, we showed that the nanocomposite hydrogel can be rapidly degraded by exposure of light, and the extent of degradation was dependent on exposure time. The results here indicate that the fabricated light-degradable nanocomposite hydrogels

could serve as novel materials for antibacterial wound dressing applications.

8:00 PM SB09.06.09

The Role of Discoidin Domain Receptor 2 (DDR2) and Collagen on Neuroblastoma Cellular Mechanosensing[Theadora Vessella](#), Steven Xiang, Madelyn Stilwell, Qi Wen and Susan Zhou; Worcester Polytechnic Institute, United States

Increased extracellular matrix (ECM) stiffness is a characteristic commonly observed in tumors. Cancer cells can sense changes in substrate stiffness and adjust their migration, proliferation, and differentiation accordingly. Cell-ECM adhesion is crucial for cells to sense substrate stiffness. Discoidin Domain Receptor 2 (DDR2) is a collagen receptor and has been shown to play a role in cell-ECM adhesion. Elevated levels of DDR2 in tumor cells have been associated with unfavorable outcomes and metastatic disease. In this study, we aim to investigate the significance of DDR2-collagen interaction in substrate stiffness sensing by studying how DDR2 downregulation affects the responses of SHY5Y cells, a neuroblastoma cell line that expresses DDR2, to substrate stiffness changes. Cells were cultured on collagen-coated polyacrylamide gels with stiffness ranging from 800 Pa to 20 kPa. On stiffer substrates, we observed cells with larger spreading area, more polarized shape, stronger traction force, greater cytoskeletal stiffness, and upregulated neuroblastoma-associated gene expression. These suggest that SHY5Y cells are sensitive to sense ECM stiffness. In contrast, the sh-DDR2 SHY5Y cell line, in which DDR2 expression was downregulated by sh-RNA mediated depletion, did not demonstrate substrate stiffness sensitivity. Our results indicate that DDR2 plays an important role in cellular substrate stiffness sensing. This highlights the potential significance of DDR2 as a target for cancer treatment, as modulation of DDR2-collagen interactions could potentially impact cancer cell behavior and invasion.

8:00 PM SB09.06.10

Nanotopographical Regulation of Glucose-Induced Behaviour in Human MG63 Osteoblastic Cells by Titanium Nanotubular Architectures[Ryan R. Berthelot](#) and Fabio Variola; University of Ottawa, Canada

Titanium nanotubular surfaces have been extensively studied for use in biomedical implants due to their ability to promote osseointegration and bone formation. However, despite the large body of literature on the subject, the impact of the biochemical environment, in particular the glucose levels, and potential synergistic/antagonistic effects with surface physicochemical cueing remains poorly understood. In this study, we investigated the effects of cellular preconditioning in elevated glucose environments on the interaction of human MG63 osteoblast-like cells with nanotubes of 20 nm and 80 nm, as well as with a two-tier honeycomb (HC) structure composed of smaller 20 nm domains nested within larger tubes of approximately 90 nm in diameter. The design and production of these nanotubular surfaces saw significant improvement in this study over previous work, with surfaces demonstrating enhanced order, homogeneity, and reproducibility. Experiments utilizing standard TC-treated well plates were used to effectively separate environmental and surface effects. In determining preconditioning parameters, MG63 cells were cultured in low glucose (5mM) and high glucose (25mM) environments over a three-week period, and a portion of every passage was seeded on TC treated 48-well plates, monitoring differentiation through ALP assays and cell viability using the PrestoBlue viability assay. Normalization of these two markers was well established after two weeks of preconditioning. Preconditioned cells were successively seeded on 20nm, 80nm, and HC surfaces. Cell proliferation, morphology, and viability were assessed through Ki67 and actin staining (48 hrs), along with the PrestoBlue assay (Days 1, 3 and 7). Our results indicated that MG63 cells cultured in high glucose conditions on TC culture plates had significantly lower cell viability compared to those cultured in normal glucose conditions, as previously shown by relevant literature. This effect, however, was mitigated or reversed completely by interaction with the nanotubular surfaces. A parallel outcome was observed in wound healing assays, where migration rates, slowed by the high glucose, were restored or elevated upon exposure to the nanotubular surfaces. The 80 nm and HC surfaces demonstrated significantly higher cell viability (Day 7) and elevated ALP activity (Days 7 and 14) relative to the other surfaces. This trend in differentiation was further explored through the expression of osteogenic markers: osteocalcin (OCN) and osteopontin (OPN), analyzed using fluorescence microscopy and Western blot staining, as well as the degree of mineralization, quantified via the Alizarin Red absorbance assay. Our results demonstrate that high glucose preconditioning significantly influences cell surface dynamics, altering rates of proliferation, migration, mineralization and expression of differentiation markers. Prolonged exposure to high glucose media increases cell metabolic activity and total osteogenic marker expression relative to immediate transition from low to high glucose environments, effectively addressing a gap in the literature where information regarding prolonged exposure to high glucose prior to experimentation is missing or arbitrarily chosen. This normalization aids in distinguishing environmental effects of increased glucose concentration from the physicochemical cueing induced via cell-surface interactions. Although nanotubular surfaces largely outperformed, the multi-hierarchical HC surface's elevated levels of differentiation and proliferative markers in both high and low glucose conditions, as well as ease of production, shows promising signs of being an optimal surface, thereby highlighting the potential of the 2-tier structure for tissue engineering and regenerative medicine. Taken together, our study demonstrates the potential to counteract certain effects of negative environmental stimuli through careful control of nanotopographical surface features.

8:00 PM SB09.06.11

An Emerging and Cost Effective State-Of-The-Art for Biosensing on Paper Substrate Materials[Supriya Yadav](#)¹, [Kulwant Singh](#)¹ and [Nitnipun Sharma](#)²; ¹Manipal University Jaipur, India; ²Manipal Academy of Higher Education, Manipal, India

Fast diagnosis and proper prevention of infectious diseases are essential and important factors in therapeutic upshots for curing such diseases and low mortality rates in the global public health picture. Lack of sanitation and resources, these diseases extremely impact remote and rural areas, and peoples living in these areas face outstanding challenges so they require cost-effective technology-based reliable solutions for the diagnosis. Current diagnostic assays require sophisticated laboratory infrastructure with expensive reagents. Therefore, such assays are not suitable for resource-limited settings where trained technicians are not present in hospitals to test basic health diagnoses. A point-of-care (POC) test is performed at or near the patient's site where a person initially meets the health care system that has provided accurate rapid results. Thus, an ideal point-of-care diagnostic platform is something on which a drop of the sample of interest will be put and thereafter the results will be analyzed with a smartphone. Considering the current high-cost standard scenario of diagnosis it is essential to implement point-of-care (POC) testing as an alternative diagnostic tool to fill the gap between the need and affordability. In consequence, the microfluidic system is an attractive platform and has been predicted to provide a boon in health care, especially in the diagnosis and detection of diseases through point-of-care diagnostic devices. In past decades' various microfluidic materials like silicon, and glass technologies have been developed for the diagnosis of these infectious diseases. In the current era, among all the materials used in microfluidics, the paper substrate has attracted the attention of the research community to demonstrate cost-effective and portable devices to meet the challenges in the least developed countries or at remote locations. The competency of the paper substrate for building the proposed microfluidic device is assessed by placing the functional (hydrophobic) components on the surface of the paper substrate. The functional materials that are placed on the paper surface determine its appropriateness for fabricating the suggested device. There isn't a single property or concept that can be defined as a specific paper for microfluidics applications. Undeniably, several characteristics of the paper substrate such as pore size, porosity, texture, color, etc. either are necessary for a printed device design to function or enhance its print characterization, hydrophobic barrier qualities, and surface smoothness in microfluidics. The paper manufacturing process plays an important role in the selection of paper for multiple applications. A suitable selection of paper used for microfluidics applications seems to be critical. Analysis of paper structure is very difficult because of intra and inters hydroxyl groups of cellulose molecules to make voids or spaces on the surface and across the surface. Surface structure creates a vital significance to use the paper in multiple applications in paper manufacturing and printing process. Based on experimental investigation carried out on various test cases of paper substrate, it is concluded that the internal structure of cellulose fiber works as a micro/nanofiber channel for fluid flow via the capillary mechanism. The work predicts making a stable paper substrate that has large internal (Intra and inter-fiber) pores, and small void spaces (external pores) with high capillary pressure to have the tendency to wrench the fluid in an onward direction. Therefore, it can be concluded safely that the paper substrates properties such as pores, porosity, surface energy, and entropy need to optimize to manufacture suitable paper substrates for different microfluidic applications.

8:00 PM SB09.06.12

Milk Exosome for Oral Delivery of Tumor Necrosis Factor- α siRNA to Ameliorate Inflammatory Bowel Disease[Sun Hwa Kim](#); Korea Institute of Science and Technology, Korea (the Republic of)

Oral administration facilitates the direct delivery of drugs to lesions within the small intestine and colon, making it an ideal approach for treating patients with colitis. However, multiple physical barriers impede the delivery of oral RNA drugs through the gastrointestinal tract. Herein, we developed a novel oral siRNA delivery system that protects nucleic acids in extreme environments by employing exosomes derived from milk to completely encapsulate tumour necrosis factor-alpha (TNF- α) siRNA. Results show that milk exosomes loaded with TNF- α siRNA (M-Exo/siR) can efficiently inhibit the expression of TNF- α -related inflammatory cytokines. Moreover, given that milk exosomes are composed of unique lipids with high bioavailability, orally administered M-Exo/siR can effectively reach colonic tissues, leading to decreased TNF- α expression and successful alleviation of colitis symptoms in an ulcerative colitis murine model. In conclusion, we highlight the specific use of milk-derived exosomes for the treatment of inflammatory bowel disease with TNF- α siRNA. Using exosomes naturally derived from milk may shift the current paradigm of oral gene delivery, including that of siRNA.

8:00 PM SB09.06.13

Elucidating the Mechanism of Gelation for Decellularized Extracellular Matrix Hydrogels[Alexander Chen](#) and Karen Christman; UCSD, United States

Naturally derived, decellularized extracellular matrix-based hydrogels (ECM hydrogels) have been increasingly investigated as biomaterial scaffolds for tissue repair and regeneration in a variety of disease models due to their injectability through minimally invasive methods, tunable properties, ability to assemble and form a hydrogel *in situ*, and intrinsic regenerative properties. Most commonly, their rheological, mechanical, optical properties, and protein composition have been studied to understand the gel's stability, gel formation kinetics and the extracellular matrix protein component type and distribution. Natively within mammals, type I collagen is the most abundant structural fibrillar protein and forms a hydrogel through fibril

self-assembly and crosslinking when it is pure and has been assumed to be the main driver for hydrogel formation within heterogeneous ECM hydrogels. The goal of this study was to provide more fundamental materials characterization of ECM hydrogels and determine whether type I collagen is in fact the driver for ECM hydrogel formation.

Using three batches of a porcine derived decellularized myocardial ECM hydrogel, we first ensured batch consistency by quantifying residual dsDNA, quantifying sGAG concentration and rheological measurements. We also employ Fourier transform infrared spectroscopy (FTIR) to analyze the bonds within our ECM hydrogels, thermal gravimetric analysis (TGA) from 30 to 700°C to analyze degradation temperatures, and turbidimetry analysis to observe gelation kinetics. Finally, using cryogenic transmission electron microscopy and two photon microscopy, we analyze the fibril structures within our ECM hydrogel and quantify the differences in fibril diameters before and after incubation at 37°C.

All batches contained less than 1 ng DNA per mg of ECM showing adequate decellularization and 10 µg of sGAGs per mg of ECM. We observed consistent complex viscosity across all samples that had not been incubated, and similar storage and loss moduli values for gels after 24 hours of incubation. The FTIR revealed the same peptide-related peaks (amides I, II and III) at similar peak intensity ratios also seen in a pure type I collagen control. TGA of our ECM hydrogel revealed degradation onset temperatures around 304.6±1.7°C and 624.9±16.8°C [KCl] C, consistent with literature reported values for collagen. Turbidimetry analysis revealed similar kinetics of gelation evidenced through similar times to achieve 50% of maximum equilibrium absorbance at around 15 minutes. ECM hydrogel batches were imaged before and after incubation at 37°C for 24 hours using two photon microscopy through second harmonics generation and two photon fluorescence, which leveraged the intrinsic property that only fibrillar, helical collagens produce signal. Incubated samples revealed distributed linear fibers in a grid-like conformation signifying the formation of a hydrogel network. Using cryogenic transmission electron microscopy, we analyzed fiber diameters within our samples for fresh, unincubated samples and samples incubated at 37°C for 24 hours. Fibers in fresh samples averaged 45.6 ± 21.7 nm, 48.7 ± 10.8 nm, and 43.7 ± 15.5 nm in diameter across batches showing consistency. Incubated samples averaged significantly higher fiber diameters when compared to their fresh counterparts at 113.1 ± 48.2 nm, 156.1 ± 79.3 nm and 128.9 ± 56.8 nm, respectively, where all measured fibers within the incubated group revealed a distinct 67 nm D-periodicity unique to fibrillar collagens. Combined, these data reveal batch to batch consistency using more sensitive materials characterization techniques for the ECM hydrogel while also providing visual evidence, through two microscopy techniques, that type I collagen self-assembly occurs during incubation at 37°C and is one of the main drivers of ECM hydrogel formation.

8:00 PM SB09.06.14

A High-Throughput Micropatterning Platform for Screening of Nanoparticles in Regenerative Engineering Cheryl Koh, Liu Ying Chen, Lingyan Gong, Shao Jie Tan, Han Wei Hou and Chor Yong Tay; Nanyang Technological University, Singapore

Engineered nanoparticles (ENPs) have been gaining traction in the field of regenerative engineering due to their unique physical, chemical and biological properties that are able to modulate cellular behaviour by influencing cell adhesion, migration, and proliferation. These nanomaterial-cellular interactions are important in directing tissue regeneration processes at the cellular level. However, the usage of nanoparticles brings about safety concerns with regards to impairment of cellular dynamics. In this context, micropatterning platform has emerged as a high-throughput tool for assessing stress response of ENPs. This platform not only allow the analysis of biological responses to nanoparticles in a controlled and reproducible environment, but also provides the identification of subtle effects that may not be discernible using traditional methods. This abstract discusses how two commonly incorporated engineered nanoparticles in regenerative engineering, specifically zinc oxide (ZnO) and titanium dioxide (TiO₂) have an influence on collective epithelial rotation via the use of micropatterned platform. The confinement of cells in geometrical constraints were achievable through the precise control over the geometry and size of the adhesive fibronectin islands which aids in cell attachment. Collective rotation is essential in tissue morphogenesis and wound healing, and disruption to this collective behaviour could lead to a wide range of biological dysregulations. Through this approach, it was observed that the micropatterned human keratinocytes clusters exhibited spontaneous rotation without external stimulus, at relatively constant uniform speeds of 10 µm/h. However, acute (6 h) exposure to non-cytotoxic doses of ZnO and TiO₂ NPs (≤100 nm) resulted in a loss of directionality and slowing down of cell rotation, respectively. The loss in collective cell rotation (CCR) was determined to be attributed to reactive oxygen species (ROS)-induced proliferation by ZnO. While cell proliferation is desired in regenerative engineering, the generation of new, heterogeneous localised velocity fields by the increased cell density led to cell jamming within the epithelial units. On the other hand, the retardation of the velocity of TiO₂-treated units was most likely as a result of degradation of membrane recycling integrins that are necessary for continued cell migration. This is because TiO₂-treated units were found to induce autophagy, which has been reported to compete with endocytosis-driven recycling. Taken together, our findings offer nano-biological insights into the distinct signalling pathways exerted by different nanoparticles - ZnO NPs promoting cell proliferation, yet disrupting cell migration, and TiO₂ NPs decreasing cell migration. This suggests that when it comes to the usage of ENPs in regenerative engineering, further studies have to be done to ensure that cellular dynamics are not compromised.

8:00 PM SB09.06.15

Directing Phase Separation to Harness Biomaterial Microstructures for Controlled Cellular Behavior Saniya Yesmin Bubli, Jenifer Sidhwa and Linqing Li; University of New Hampshire, United States

The compositional heterogeneity and structural diversity of native extracellular matrix are essential in regulating cell behavior and promoting tissue regeneration. Thermoresponsive polysaccharide-based materials with tunable transition temperatures and phase-separated microstructure offer substantial opportunities in tissue engineering, drug delivery, and wound healing applications. To develop novel synthetic thermoresponsive polysaccharides, we employed versatile chemical routes to attach intrinsically hydrophobic adducts to the backbone of hydrophilic dextran and developed protocols to form hydrogels with defined microstructures. Systematically conjugating methacrylate moieties to the dextran backbone yielded a continuous increase in macromolecular hydrophobicity that induced a reversible phase transition whose lower critical solution temperature can be systematically modulated via variations in polysaccharides concentration, molecular weight, degree of methacrylation, ionic strengths, and Hofmeister salts. Photo-initiated radical polymerization permits facile chemical crosslinking and kinetic capture of phase separation, enabling the formation of hydrogels with defined microdomains. The resulting heterogeneous hydrogels feature tunable microstructures and exhibited both microspheres and continuous phases that promoted enhanced cell adhesion in 2D and interfacial-driven cell migration in 3D. Engineering macromolecular hydrophobicity with temperature-triggered phase separation of conventional hydrophilic, non-phase separating polysaccharides to generate heterogeneous hydrogels with controlled microstructures will find potential applications in chronic wound healing.

8:00 PM SB09.06.16

Study of The Senescence Progress of Human Skin Fibroblast on Silica Nanobeads Array Yerin Choi, Soojin Roh and Jin Seok Lee; Hanyang University, Korea (the Republic of)

Senescence is a physiological process that progresses with age. Cellular senescence is induced by stimuli such as telomere shortening and oxidative stress. In particular, it refers to the cell cycle arrest state. Senescence cells are characterized by reduced cell proliferation, migration, and speed. In addition, aging proteins p16, p21, and p53 are expressed. We study the adhesion changes of senescence cells on silica nanobeads (SiNBs) of various sizes. In particular, it analyzes how senescence changes due to different adhesion. We induced aging by adding Paclitaxel (PTX) to WS1 cells, which are human skin fibroblasts. PTX causes cellular senescence due to damage from ROS. The optimal PTX concentration was fixed, and the cell survival rate was confirmed by MTT assay. In particular, we have identified different adhesion on SiNB arrays of various sizes. In addition, changes in cell proliferation, migration, speed, and aging proteins were analyzed. As a result, we observed the correlation between the topographic factors of SiNB arrays and cellular senescence.

8:00 PM SB09.06.17

Microhardness and Electrochemical Behavior of Binary Ti-Zr Alloy for Dental Implants Anca Fratila¹, Santiago Brito-Garcia², Julia C. Mirza^{2,3}, Ioan Aron³ and Adriana Saceleanu¹; ¹LB University of Sibiu, Romania; ²Universidad de Las Palmas de Gran Canaria, Spain; ³Transilvania University of Brasov, Romania

Introduction: In response to the pressing concerns surrounding potential cytotoxicity and adverse tissue reactions arising from the presence of vanadium and aluminum in the widely employed biomaterial Ti-6Al-4V, a compelling alternative has emerged in the form of the Ti-20Zr alloy.

Material and methods: This alloy, Ti-20Zr, generously provided by R&D CS in Bucharest, Romania, underwent a rigorous evaluation process, positioning itself as a possible contender for use in human body implant materials. The journey of Ti-20Zr's evaluation commenced with the meticulous process of alloy creation through vacuum melting. Cylindrical electrodes, crafted with precision, were seamlessly embedded in a resin matrix. Subsequently, the specimens underwent thorough ultrasonic cleaning using deionized water, followed by etching in the renowned Kroll's reagent, comprising 10 ml of HF, 5 ml of HNO₃, and 85 ml of water, all in preparation for microscopic observation using the Olympus PME 3 – ADL microscope. The microstructure and microhardness were tested. The electrochemical behavior has been evaluated in simulated body fluid (SBF) using Electrochemical Impedance Spectroscopy technique (EIS).

Discussion: From metallographic images can be observed that the sample has an alpha-beta structure. From microhardness measurements can be concluded that the alloy formed a hard layer on its surface, which greatly improves the wear resistance. The electrochemical behavior demonstrates that Ti-20Zr alloy exhibits excellent corrosion resistance due to the stable oxide layer formed on the surface, an attribute that promises long-term implant stability. Zirconium (Zr), a key component of the alloy, has been recognized for its superior resistance to corrosion, setting it apart from the majority of other metals.

Conclusion: In light of these remarkable findings, it becomes evident that the Ti-20Zr alloy surpasses even commercially pure titanium (cpTi) in terms of corrosion resistance. Furthermore, the consensus in the scientific community regarding the absence of local or systemic toxic effects associated with Zr compounds reinforces the notion that Ti-20Zr has the potential to serve as a safe and efficacious biomaterial for artificial surgical implants.

References:

[1] Vasilescu, E., Drob, P., Popa, M. V., Anghel, M., Santana Lopez, A., and Mirza-Rosca, I. (2000). Characterisation of anodic oxide films formed on titanium and two ternary titanium alloys

in hydrochloric acid solutions. *Werkstoffe Und Korrosion*, 51(6), 413–417. [https://doi.org/10.1002/1521-4176\(200006\)51:6<413::AID-MACO413>3.0.CO;2-3](https://doi.org/10.1002/1521-4176(200006)51:6<413::AID-MACO413>3.0.CO;2-3)

[2] Bao, X., Li, X., Ding, J., Liu, X., Meng, M., and Zhang, T. (2022). Exploring the limits of mechanical properties of Ti-Zr binary alloys. *Materials Letters*, 318. <https://doi.org/10.1016/j.matlet.2022.132091>

[3] Baltatu, M. S., Vizureanu, P., Sandu, A. V., Florido-Suarez, N., Saceleanu, M. V., and Mirza-Rosca, J. C. (2021). New Titanium Alloys, Promising Materials for Medical Devices. *Materials*, 14(20), 5934. <https://doi.org/10.3390/ma14205934>

8:00 PM SB09.06.18

Tensile Testing of Two Amniotic Membrane Products: Artacent Wound® and Artacent AC® [Abigail Poland](#), Olivia Logan, Mora Melican and Isabella Sledge; Tides Medical, United States

Amniotic membrane is a promising biomaterial for regenerative medicine and a plethora of placental membrane products exist in the market today and are used for varying applications. When assessing and characterizing the multitude of amniotic products on the market, it is important to ensure that each product meets user need for handling capabilities so that the membrane can be properly applied to the wound. One way this characterization can be achieved is via tensile testing using an Instron 5544. The process of tensile testing amniotic products with the Instron 5544 has not previously been well-standardized or optimized for this material. With this study, a standardized test method for tensile testing of dehydrated amniotic membrane has been established. In this study, the established tensile testing procedure is used to distinguish differences in the handling capabilities of Artacent Wound, a dual layer amniotic scaffold, and Artacent AC, a tri-layer amniotic scaffold composed of a layer of chorion between two layers of amnion. In addition, this repeatable test method is also used to assess a modified version of Artacent AC where one of the tissue processing steps has been altered.

Methods:

Tensile Testing

1. Nonslip material is cut to size and applied to Instron Jaw Faces.
2. ASTM D1708 dog bone die cutter is used to cut samples to the proper size and shape.
3. Width and thickness measurements of the sample are taken in triplicate and averaged.
3. The force sensor is calibrated.
4. Tare load of 0.5N is applied to the sample prior to test start.
5. Length measurements of the product are taken.
6. Length, width, and thickness measurements are entered into Bluehill Software.
7. Strain Rate of 0.40mm/min. is entered into software.
8. "Zero displacement" is selected.
8. Test is started until full sample break is achieved.
9. Test is stopped and data is collected.

Data Analysis:

One – Way ANOVA Multicomparison Tukey Tests were used to compare each test group.

Results:

Comparative graphs summarize the failure stress (MPa), failure strain (%) and Young's Modulus (Mpa) of the following test groups:

- Artacent Wound
- Artacent AC
- Modified Artacent AC

Discussion:

There are no significant differences between the measured biomechanical properties of Artacent Wound and Artacent AC, although Artacent Wound has slightly increased strength when compared to Artacent AC.

The modified version of Artacent AC did not show any significant difference when compared to original Artacent AC. However, the modified Artacent AC is shown to have higher Young's Modulus and failure stress when compared to original Artacent AC. This demonstrates that modifying certain tissue processing steps could be advantageous for improving material handling properties.

Conclusion:

Artacent Wound has increased failure stress and Young's Modulus when compared to Artacent AC.

Modifying certain steps of the Artacent AC tissue processing procedure is shown to be beneficial for improving handling properties of the scaffold, as it demonstrates increased Young's Modulus and failure stress when compared to that of original Artacent AC.

8:00 PM SB09.06.19

Balancing Charge Density and Hydrophobicity in Polysaccharide Biomaterials to Regulate Cell Behavior [Tran Truong](#), Linqing Li and Nathan J. Oldenhuis; University of New Hampshire, United States

Hydrogel surface properties play an important role in regulating cellular behavior for tissue engineering and biomedical device design application. Alterations in the biointerface can activate specific cellular signals, resulting in different physiological outcomes. Developing a hydrogel system where surface physiochemical characteristics such as stiffness, charge density, and hydrophobicity can be independently tuned would provide significant insights to tailor material-cell interactions at tissue interface for various therapeutic applications. In this study, we synthesized methacrylate and carboxylate dual-functionalized dextran derivatives, and investigated the impact of the intricate balance between hydrogel surface charge density and hydrophobicity on cell behavior. We are leveraging the defined chemical moieties and tunable surface properties of modified dextran hydrogels to probe the impact of our materials on regulating cell adhesion and spreading. By synthetically tuning these two parameters in dextran-based substrates, we revealed that increased surface charge density and decreased hydrophobicity enhance hydrogel surface wettability and prevent cell adhesion. On the contrary, increasing surface hydrophobicity facilitates the adsorption of fibronectin that supports cell adhesion. Our findings suggest an optimized balance between charge density and hydrophobicity that can be engineered to promote desired cell behavior. Imbalances between these two parameters resulted in an inhibition of cell attachment, emphasizing the importance of fine-tuning charge density and hydrophobicity in biomaterial design. This project will differentiate and identify critical chemical characteristics of hydrogel surface properties responsible for cell behaviors and develop a new class of synthetic polysaccharide biomaterials.

8:00 PM SB09.06.20

Crimping Process Investigation to Enable Informed Design of 3D Printed Bioresorbable Vascular Scaffolds [Caralyn Collins](#)¹, Junqing Leng¹, Rao Fu², Yonghui Ding², Guillermo Ameer¹ and Cheng Sun¹; ¹Northwestern University, United States; ²Worcester Polytechnic Institute, United States

With cases of coronary and peripheral artery disease on the rise, vascular stenting has become a popular procedure which is crucial to the health of millions of patients across the United States and more across the globe. In the past several decades, the field has seen a shift from bare metal and metal drug eluting stents to bioresorbable vascular scaffolds (BVS) with the goal of addressing restenosis, thrombosis, and stent migration concerns. These BVS utilize polymeric materials to degrade over time *in vivo*, and as a result, have drastically different mechanical responses to deformation than the preceding metal stents. As such, additional consideration of the BVS mechanical deformation response both prior to and post-deployment is important to enhancing the performance of these polymeric scaffolds *in vivo*. The crimping process, or diameter reduction of the stent or BVS prior to deployment, marks the first time after manufacturing that the scaffold must undergo a significant amount of mechanical deformation. As it is also an easy deformation step to monitor, crimping serves as a good baseline for understanding the mechanical response of BVS. Simulation of this step can not only provide information on BVS radial force as a function of diameter to mimic results from experimental testing, but can also give additional information on the response of the BVS as it undergoes this deformation in a fraction of the time required in experiment. This allows for a time-effective solution to enable understanding of both the deformation of different scaffold designs and the deformation of scaffolds with different material additives incorporated, like those utilized to enable visibility of the BVS when imaged *in vivo*. Here, we utilize a finite element crimping simulation in ABAQUS to rapidly reproduce experimentally validated qualitative design comparisons between several designs of 3D printed bioresorbable vascular scaffolds made of a previously developed citrate-based polymer, taking into consideration both the properties of the base polymeric material and the properties of the polymeric material with a radiopaque additive. By doing so, it is possible to harness the advantages of additive manufacturing to allow for more optimal bioresorbable vascular scaffold design and production, simultaneously elucidating the relationship between material, structure, and mechanical response of scaffolds.

8:00 PM SB09.06.21

In-Vitro Human Cell Behavior: Using Cell Culture to Assess Biocompatibility and Cell Proliferation on Artacent Products Olivia Logan, Sadhana Joshi, Babak Safavieh, Mora Melican and Isabella Sledge; Tides Medical, United States

Introduction:

Cell culture is a useful method of determining cell interactions and assessing product safety in-vitro before completing in-vivo testing, such as animal models. In this study, cell culture is utilized to assess the proliferation and attachment of various cell types on amniotic scaffolds. The selected cell types represent cells that are known to play a part in the wound healing process and include Human Umbilical Vein Endothelial Cells (HUVEC), Neonatal Human Dermal Fibroblasts (NHDF), Normal Human Epidermal Keratinocytes (NHEK) and L929 cells (an adherent type of mouse fibroblast cell line).

Methods:

Cell Culture

All cell lines are maintained in appropriate culture media supplemented with necessary growth factors, antibiotics, and serum per manufacturer's protocol. These cells were incubated at optimal conditions in a humidified cell culture incubator.

Cell Treatment

Optimal seeding density for each cell type was determined from preliminary testing. Determined seeding densities were then used to seed each cell type on circular 6mm diameter samples from each test group. Cells were seeded for 2,3,7 and 9 days in 96 well Low cluster microplates.

Alamer Blue Assay

After the treatment period, the culture medium was removed from each well or plate and Alamar blue was added to the wells. The cells were treated with the Alamar Blue reagent for 6 hours and under appropriate conditions. The absorbance of these wells was measured using a microplate reader at 570nm and 600nm.

Microscopy

To validate the Alamer Blue Assay results, the cells seeded on Artacent product were labelled with DAPI and Vimentin 647 and observed under Zeiss LSM 800 with Airyscan.

Results:

Graphs summarize the Alamer Blue reduction (%) for the following test groups at the following time points. Chosen time points reflect when the most Alamer Blue reduction was observed for each cell type.

- HDF at 7 day time point
- NHEK at 7 day time point
- HUVEC at 9 day time point

Discussion:

HDF cells showed improved proliferation and attachment on Artacent AC compared to other test groups.
NHEK cells showed improved proliferation and attachment on Artacent Wound compared to other test groups.
NHEK cells showed improved proliferation and attachment on Artacent Wound compared to other test groups.

Conclusion:

Different types of amniotic scaffolds are shown to be optimal for the proliferation and attachment of different cell types.
- HDF cells showed improved proliferation and attachment on Artacent AC.
- NHEK cells showed improved proliferation and attachment on Artacent Wound.
- NHEK cells showed improved proliferation and attachment on Artacent Wound.

8:00 PM SB09.06.22

Comparison of Amniotic Products in Full Thickness Rat Wound Model: Artacent Wound and Artacent AC Olivia Logan, Isabella Sledge and Mora Melican; Tides Medical, United States

Introduction:

It is well understood that human placental tissue contains a multitude of factors that play a part in the healing process [1]. Placental membrane is an attractive biomaterial for regenerative medicine applications due to its natural factors that aid in wound healing, angiogenetic and regenerative remodeling, as well as immunomodulation. However, the processing methods used to create final product have an impact on the growth factors that are retained [2]. A plethora of placental tissue processing methods has led to the creation of an array of placental product compositions and applications. Two products currently being used in the field are Artacent Wound®, a dehydrated dual layer amniotic graft and Artacent AC®, a tri-layer graft composed of a chorion sandwiched between two layers of amnion. In this study, we assessed these wound coverings in Sprague Dawley rats to elucidate the influence these scaffolds have on a healing wound. Additionally, this test is used to assess a modified version of Artacent AC to see if modifying certain tissue processing steps has implications on wound healing.

Methods:

Two full thickness wounds were created on the dorsal side of each rat using a 2 cm x 2 cm square stencil and scalpel. Implant dimensions were approximately 2.5 x 2.5 cm. Samples were randomized into implantation sites across the animals. Implants were harvested at 7 days and grossly assessed for healed wound geometry, remodeling and re-epithelialization. Implants were fixed in neutral buffered solution (NBS). Samples were stained with H&E and stained cross sections were evaluated for surface re-epithelialization, cellular infiltration, and remodeling. A numerical scoring system was utilized to quantify re-epithelialization and granulation tissue formation based on histological images.

Results:

Initial and final wound measurements were used to calculate the percentage of wound closure for each test group. Re-epithelialization and granulation tissue formation ratings are used to calculate average values for each test group.

Discussion:

No adverse effects were noted during this 7 day study. Partial wound healing is observed during the 7 day study, and healing is accelerated by the addition of a placental scaffold. Modified Artacent AC shows increased wound closure, equivalent re-epithelialization, and increased granulation tissue formation when compared to positive control (original Artacent AC).

Conclusion:

No adverse effects were noted.
The 2x2 Challenge Full Thickness Wound model in the rat shows partial healing at 7 days that is accelerated by the addition of a human placental membrane product to the wound bed.
Modified version of Artacent AC shows improved wound healing when compared to original Artacent AC.
- Increased wound closure
- Equivalent re-epithelialization
- Increased granulation tissue formation

8:00 PM SB09.06.23

Protein Characterization of Placental Membrane Products: Artacent Wound and Artacent AC Olivia Logan, Babak Safavieh, Isabella Sledge and Mora Melican; Tides Medical, United States

Introduction:

Placental membrane is a highly biocompatible natural scaffold and is a source of several native factors that may aid in wound healing. Some of the many factors that make placental membrane such an attractive material are the natural anti-inflammatory, angiogenic, and antibacterial properties of the membrane. These properties are mostly dictated by released growth factors and cytokines. The angiogenic properties are attributed mostly to its capacity to produce VEGF and platelet-derived growth factor (PDGF), both of which mediate wound healing. The anti-inflammatory and immune-modulatory effects are largely attributed to the secretion of IL-10 and IL-6 [1].

Here, we characterize the protein content in Artacent Wound (a dual layer amniotic product) and Artacent AC (a tri-layer composed of a layer of chorion in between layers of amnion) using a Microarray assay. In addition, immunohistochemistry (IHC) was used to quantify protein composition of extracellular matrix (ECM), growth factors, and immune modulating cytokines. This analysis provides further insight into the protein composition and cell interactions of hAM scaffolds currently on the market.

Methods:

The chosen assay for testing is Quantibody® Human Cytokine Antibody Array 1000 assay from RayBiotech Inc., a multiplexed ELISA that enables the detection and quantification of up to 1000 human cytokines in a single experiment. To prepare samples for testing, they were first incubated on captured antibody for 2 hours. The biotinylated antibody cocktail was then added, followed by another 2 hour incubation. After the final incubation, streptavidin labeled dye was added. The results were then analyzed using fluorescent microarray reader.

Results:

The various cytokines and growth factors observed in each test group were categorized based on Angiogenic cues, immune modulating cytokines and Regenerative growth factors.

Discussion:

Protein microarray analysis reveals that Artacent AC and Artacent Wound have various factors that are attributed to angiogenic and regenerative remodeling as well as immunomodulation. The Artacent Wound protein distribution shows that factors are uniformly distributed amongst the angiogenic (28%), regenerative (34.1%), and immunomodulatory (37.8%) categories. In contrast, the protein distribution for Artacent AC shows that a large portion of the observed factors are regenerative growth factors (78.4%), with a smaller portion of results falling into the angiogenic (8.3%) and immunomodulatory (13.2%) categories.

Conclusion:

The varying products are each shown to contain a unique profile of proteins that play a role in angiogenic and regenerative remodeling as well as immunomodulation.

- Artacent Wound proteins are evenly distributed amongst the angiogenic, regenerative, and immunomodulatory categories.

- Artacent AC protein distribution largely falls in the regenerative category, with smaller percentages of proteins falling into angiogenic and immunomodulatory categories.

8:00 PM SB09.06.24

Subcutaneous Implantation of Amniotic Products in Sprague Dawley Rats: Artacent Wound and Artacent AC [Olivia Logan](#), Isabella Sledge and Mora Melican; Tides Medical, United States

Introduction:

Although there are numerous placental membrane products currently being used in wound healing applications, it is not yet well-understood how these products interact with the wound bed as the wound heals. In this study, we assess subcutaneous implantation of varying amniotic membranes to better understand how these products support the wound healing process.

Methods:

Four incisions were made on the back of each rat—two incisions left of the spine and two incisions to the right with each incision measuring approximately 2 cm. Four individual pouches were created by bluntly dissecting laterally at each incision site with scissors. A 1 x 1 cm implant was placed in each implantation site and samples were randomized in location. Implants were fixed in neutral buffered solution (NBS). Samples were stained with H&E and stained cross sections were evaluated for surface re-epithelialization, cellular infiltration, and remodeling.

Results:

Representative histological images from each test group.

Discussion:

In both Artacent Wound and Artacent AC, tissue ingrowth within the placental membrane product can be observed. Results support that the biological membranes provide an extracellular matrix that provides a natural scaffolding which supports the wound healing process.

Conclusion:

In both Artacent Wound and Artacent AC, tissue ingrowth within the placental membrane product can be observed. Results support that the biological membranes provide an extracellular matrix that provides a natural scaffolding which supports the wound healing process.

8:00 PM SB09.06.25

Stimulus-Responsive Double Network Hydrogels with MoS₂ Nanosheets for High Toughness and Self-Healing Smart Biomaterials for Tissue Engineering [Francesca A. Sepúlveda](#)^{1,2}, [Humberto Palza](#)^{1,2}, [Felipe Olate-Moya](#)^{1,2} and [Juan Pablo Acevedo](#)^{2,3}; ¹Universidad de Chile, Chile; ²IMPACT, Chile; ³Universidad de los Andes, Chile

The design of stimulus-responsive smart hydrogel actuators for tissue engineering holds great promise, as they enable the creation of 3D structures mimicking the functionality of natural tissues, responding in a controlled manner to changes in temperature, light, or pH. To achieve near-infrared (NIR) light-induced responses in smart hydrogels, molybdenum disulfide (MoS₂) nanosheets have gained recent attention due to their layered structures and strong NIR absorbance, making them promising photothermal agents. Among various hydrogels, we focus on double-network hydrogels (DN) composed of chitosan (C) and polyvinyl alcohol (P), known for providing a robust and flexible matrix for cell growth and tissue regeneration. In this study, we developed C-P DN hydrogels with MoS₂ nanoparticles to create 3D printed scaffolds (3D C-P) and evaluated their mechanical properties, water content, NIR light irradiation response, and cell viability.

By adjusting manufacturing parameters like freezing temperature, chitosan cross-linking time, and lyophilization, we tailored the mechanical properties of C-P DN hydrogels. These inks were successfully extruded using a fourth-generation 3D Bioplotter™ (Envisiointec, Germany), enabling precise scaffold production. After 2 hours of crosslinking, the 3D C-P scaffold exhibited high toughness and mechanical stiffness resembling native heart tissue, with a stiffness value of 0.78 MPa. Interestingly, DN C-P MoS₂ hydrogels with 0.5% w/w MoS₂ incorporation did not show improved mechanical stiffness compared to pure DN, maintaining material structural stability. Furthermore, MoS₂ incorporation led to a slight decrease in water content, attributed to its hydrophobic nature.

The material's responsiveness was evident through rapid contraction and bending upon NIR light irradiation due to dehydration, and this response was 40% faster than that of DN C-P hydrogels. This confirmed their potential as candidates for generating light-stimulated smart DN hydrogels. Additionally, MoS₂-incorporated hydrogels exhibited mechanical self-healing under NIR light exposure, enhancing their tissue engineering applications. These multifunctional behaviors arise from MoS₂'s ability to convert light energy into thermal energy, triggering NIR light-induced contraction. Furthermore, NIR-induced heat facilitates polymer chain diffusion, enabling a self-healing process through hydrogen bond reformation in MoS₂-incorporated hydrogels. MoS₂ absorbs NIR light, releasing heat, and leading to hydrogel contraction, while reconstituted hydrogen bonds allow the material to 'heal,' restoring structural integrity and functionality.

Viability studies on umbilical cord-derived mesenchymal stem cells (UC-MSCs) cultured on MoS₂ hydrogels showed improvement from day 1 to day 7, suggesting that DN and DN C-P MoS₂ hydrogels offer a conducive environment for UC-MSC growth and survival, serving as a three-dimensional support and suitable substrate matrix.

The results demonstrate that the incorporation of MoS₂ nanosheets into C-P DN hydrogels achieves a rapid actuation response to NIR light irradiation and a mechanical self-healing behavior, making them ideal for light-stimulated flexible hydrogels. Additionally, cell viability studies indicate MoS₂-containing hydrogels' suitability as three-dimensional support in regenerative medicine and tissue engineering.

8:00 PM SB09.06.26

Development of Bio-Hybrid Nanoparticles based *In Situ* Raman Imaging for Intracellular miRNA Detection [Yeochan Yun](#)¹, [Hyeon-Yeol Cho](#)¹, [Won-Jun Lee](#)², [Kyeong-Jun Kim](#)², [Md. Khaled Hossain](#)² and [Jeong-Woo Choi](#)²; ¹Kookmin University, Korea (the Republic of); ²Sogang University, Korea (the Republic of)

Currently, microRNAs (miRNAs) were widely recognized as valuable biomarkers to identify in typical cancer characteristics. These small RNA molecules frequently exhibited dysregulation in various cancers, leading them to serve as either oncogenic or tumor-suppressor miRNAs, depending on their specific target genes. Moreover, miRNAs can modulate cancer cells to chemotherapy. Real time polymerase chain reaction (RT-PCR) was currently used as a method to detect intracellular miRNA. However, it required cell lysis, miRNA isolation, purification that makes hard to use in live cells. Therefore, several fluorescence-based analysis techniques (e.g., fluorescence resonance energy transfer (FRET)) were used for live cell detection, but they had limitation in detecting miRNA with low expression levels. We aimed to overcome these limitations by using surface-enhanced Raman spectroscopy (SERS), a technique widely used as a

tool for sensing application, which analyzed based on the distances between molecules, to detect intracellular miRNA in live cells.

In this study, we developed highly sensitive Raman activating gold nanoparticles (HS-RGNs) which were containing gold nanoparticles, Raman reporter, and single strand DNAs (ssDNAs) complementary to target miRNA. When HS-RGNs hybridized with target miRNA, these particles amplified the Raman signal. We selected microRNA 200c (miR-200c) as a model biomaterial which was related to the chemoresistance of cancer cells. After treatment of HS-RGNs to SK-BR-3 and MCF-7 which are cancer cells, the ssDNAs of HS-RGN were hybridized with miR-200c, bringing two HS-RGNs closer, thereby enhancing the Raman signal. The higher expression level of miR-200c in SK-BR-3 compared to MCF-7 led to the observation of a higher Raman signal in SK-BR-3 cells. When treated with HS-RGNs, increased expression levels of Zinc finger E-box binding homeobox 1 (Zeb1) and Tropomyosin receptor kinase B (TrkB), which were inhibited by miR-200c, indicated the effective binding of HS-RGNs to miR-200c. Additionally, when assessing the cytotoxicity of doxorubicin, SK-BR-3, which exhibited higher miR-200c expression, showed a lower survival rate compared to MCF-7. However, when treated with HS-RGNs, miR-200c was effectively consumed, resulting in a higher survival rate in both SK-BR-3 and MCF-7 cells. This result suggested that HS-RGNs can hybridize with miR-200c, impact of miRNA on cell behavior. Our study showed that HS-RGNs effectively amplified the Raman signal, indicating their potential applicability for in situ intracellular analysis. Additionally, they can be applied as a platform technology to investigate the impact of miRNA on cell behavior by consuming miRNA within cells.

Acknowledgement: This work was supported by the National Research Foundation of Korea (NRF) grant funded by the Korea government (MSIT) (RS-2023-00211360) and Biomaterials Specialized Graduate Program through the Korea Environmental Industry & Technology Institute(KEITI) funded by the Ministry of Environment(MOE).

Reference

[1] W.-J. Lee, K.-J. Kim, M.K. Hossain, H.-Y. Cho, J.-W. Choi, DNA–Gold Nanoparticle Conjugates for Intracellular miRNA Detection Using Surface-Enhanced Raman Spectroscopy, *BioChip Journal* 16(1) (2022) 33-40.

8:00 PM SB09.06.27

Bioprinting Hydrogels for Dentin Pulp Regeneration and Disinfection Saranya Anantapantula¹, AbdelMahmoud², Aaron Sloutski², Kuan-Che Fang² and Miriam Rafailovich²; ¹Spring Ford Area High School, United States; ²Stony Brook University, The State University of New York, United States

Oral and maxillofacial complications pose challenges due to issues like lack of material biocompatibility and invasive treatments. One common example is the endodontic treatment, where the infected pulp is removed. Bacteria and their byproducts that interact with host tissues in the dental pulpal and periradicular regions are the primary cause of endodontic pathosis. The elimination of microorganisms from the root canal system (RCS) is essential for effective endodontic therapy. This process can leave the tooth brittle in the long-term. Because they can promote, in a biologically based framework, the continuation of root development and apical closure, regenerative endodontic therapies (RETs) in necrotic immature teeth have drawn a lot of interest recently. Getting a sufficient disinfection of the root canal system is a must for success in RETs since bacterial persistence in root canals in such instances considerably impede healing and root maturation. Moreover, additive manufacturing can facilitate the development of hydrogels that can regenerate lost dentin pulp, restoring tooth strength and longevity and achieve sustainable drug release. This research aimed to identify a scaffold, which possesses optimal degradability, chemical, mechanical, cytocompatible features, that can deliver antibiotics or induce stem cell differentiation for regenerative endodontic treatment while maintaining durability. For this purpose, methacrylated Pluronic polymers were chosen due to their well researched drug releasing capabilities, as well as their potential injectability, stemming from their reverse thermo-responsive nature.

Initially, the studies focused on F127-DMA and F88-DMA hydrogels and their crosslinking efficiency with two photoinitiators (Irgacure- 651 and 2959). Different assays, such as mechanical properties characterization by rheology, swelling ratio, crosslinking efficiency and drug release analysis, were conducted. Crosslinking was mediated by UV lamp and by 3D printer (BioX 3D Bioprinter) where the durability of the constructs was researched. Irgacure 2959 showed superiority both in terms of crosslinking efficiency (~16% difference) and mechanical stiffness. Comparing both Pluronics, the data collected showed that F88 had a higher swelling ratio than F127. Elastic modulus measurements confirmed that F127 was inherently stronger, and its cross-linking efficiency was superior due to its lower swelling ratio. Aiming at imparting degradability, the Pluronic were end capped with L-Lactide prior to methacrylation and similar studies were conducted throughout prolonged time incubated in aqueous medium at 37 degrees. The lactide-containing matrix exhibited elevated swelling until full degradation after several weeks, demonstrating the rapid degradability. Furthermore, aiming at exploring drug release capabilities, release profiles of Clindamycin, Metronidazole and Ciprofloxacin (Triple paste antibiotic) were researched.

In conclusion, while F127's stiffness and effective crosslinking make it a promising candidate in terms of mechanical features and F88's hydrophilic properties and favorable degradation profile also make it a favorable option in regards to hydrophilic affinity and mass loss, further research is required to assess the biocompatibility of photoinitiators and their concentrations in terms of cell viability. Thus, further studies will be conducted on the hydrogels' bio-printability, cell viability, cytotoxicity, antibacterial efficiency of drugs added and osteogenic differentiation or the ability of stem cells to differentiate into bone cells. The gels developed will present multiple potential endodontic applications: it could be placed on the top of the pulp cavity to induce dentin regeneration or disinfect the canal area. Thus, these hydrogels will ultimately pave the way for more potent dental treatment approaches.

8:00 PM SB09.06.28

The Influence of Donor Age and Cholesterol Inhibition on Fibroblast Mechanical Properties and Susceptibility to Bacterial Infection Sharis Hsu¹, Pia V. Sodhi², Avi Talsania³, Samuel D. Coopersmith⁴, Richard A. Wong⁵, Sai Pranav Kota⁶, Adam Hansen⁷ and Miriam Rafailovich⁷; ¹Valley Christian High School, United States; ²The Brearley School, United States; ³Sachem High School North, United States; ⁴Casa Grande High School, United States; ⁵Plainview-Old Bethpage John F. Kennedy High School, United States; ⁶Cedar Falls High School, United States; ⁷Stony Brook University, The State University of New York, United States

Cell mechanics depend upon cell membrane mechanics (which, in part, depends upon cholesterol content) and the rigidity and organization of the cytoskeleton. The latter was shown to depend on the properties of the substrate upon which cells are cultured, where tensegrity models were used to explain reorientation of the scaffold. With aging, measurements of the viscoelastic properties of cells were shown to stiffen, but these measurements were performed on individual cells without mechanical cues from surrounding tissue or the substrate. We report on experiments performed on dermal fibroblasts, which were obtained from female donors: "young" (ages 28 and 29 years) and "old" (ages 69 and 71 years), where we applied the technique of scanning force modulation microscopy (SFMM) which allows for measurements of cell modulus that account for the underlying substrate mechanics. The results represent an average of n=9 measurements.

Cells were cultured on polybutadiene thin films whose moduli were varied (ratio of 3:1) by adjusting the film thickness without additional chemical additives. On both substrates the moduli of the cells became significantly harder with age, consistently 40±1.6%, in agreement with previous work. For both young and old cells the cell modulus responded to changes in the substrate, where the moduli between cells plated on the hard and soft substrates differed significantly, 50±2% and 60±2.4% for the old and young cells, respectively. These results indicate that even though cells become harder as they age their ability to adjust to mechanical changes in their environment is not diminished. We were also able to image the actin filaments and we found that the moduli of the filaments in the older cells were consistently 20±0.8% higher than those of the younger cells independent of substrate.

Cholesterol is the most dominant sterol found in mammalian tissue and is a major structural component of the cell membrane. We investigated the impact of cholesterol on the moduli of dermal fibroblasts. To prevent uptake of cholesterol, we cultured cells in lipid-free media. We then added AY9944, a known disruptor of cholesterol synthesis, which has been shown to cause a shift to 7-dehydrocholesterol (7DHC), a precursor to cholesterol, as the major sterol. In the lipid-free media, we observed that while the proliferation of the cells was reduced, the moduli of the cells increased significantly by 100±4% and 66±2.64% for the young and old cells, respectively, relative to the cultures in standard media. Introduction of AY9944 at a concentration of 50nM decreased the modulus in the lipid-free media by 25±1% for both ages, which represented an overall increase relative to the control media of only 20±0.8% for young and 60±2.4% for old. This confirmed prior observation of increased membrane ductility.

Finally, it has been shown that cholesterol increases the susceptibility of cells to infection by *Staphylococcus aureus* bacteria. Therefore, we exposed cells to *S. aureus* at an MOI of 1000 for 90 minutes. The infection rate of old cells appeared to be approximately 1/3 that of younger cells, and the infection rate overall was nearly zero when AY9944 was added. These results illustrate that changes in the sterol composition of the membrane can have a significant impact on dermal fibroblasts. Hence, further studies are in progress to quantify the cholesterol to 7DHC quantities, as well as the impact on fibroblast functions, which are affected by aging such as collagen contraction, deposition, and turnover.

8:00 PM SB09.06.29

Osteogenic Differentiation of Dental Pulp Stem Cells via Titanium Deposition in a Static Magnetic Field Ethan Lai¹, Michael Wang², Aman Yarlagadda³, Dvita Bhattacharya⁴, Catherine Chun⁵, Anita A. Gaenko⁶, Alexander C. Wang⁷, Adam Zaidi⁸, Kuan-Che Fang⁹ and Miriam Rafailovich⁹; ¹Phillips Academy, United States; ²Mounds View High School, United States; ³Newman Smith High School, United States; ⁴Kent Place School, United States; ⁵Ardley High School, United States; ⁶Huron High School, United States; ⁷Sewickley Academy, United States; ⁸San Francisco University High School, United States; ⁹Stony Brook University, The State University of New York, United States

Osteogenic differentiation of dental pulp stem cells (DPSCs) offers potential treatments for bone-related diseases such as osteoporosis. DPSCs are preferred over other stem cells due to their ease of preservation and relative ease to obtain. Previous literature has shown that continuous exposure to a static magnetic field (SMF) induces osteogenic differentiation in rat DPSCs [1]. Past studies also suggest titanium-treated surfaces improve the rate of differentiation of DPSCs. [2] We report the degree of osteogenic differentiation with the combined effects of titanium deposition and an SMF, and compare each treatment individually. Investigating these factors will provide crucial insight to the differentiation of DPSCs and the discovery of a stem cell-based

treatment for endemic bone diseases.

DPSCs of strain 13 were isolated from third molar teeth and prepared via trypsinization every 4 days for 16 days. 4×10^4 cells were plated on each sample with agarose, along with MEM- α , 10% fetal bovine serum, and 1% glutamax. After 1 day, the media was changed to ascorbic acid and β -glycerophosphate, which has been shown to induce cell biomineralization. [2] 4 groups contained 2-inch x 2-inch silicon wafers while 2 others were in tissue culture plastic (TCP). All wafers were coated with Polylactic Acid (PLA). Half the wafers were further treated with titanium via atomic layer deposition (ALD). Half of all groups were placed in an SMF parallel to the surface for the duration of their incubation period of 28 days. Images produced by atomic force microscopy for ALD and PLA groups were analyzed via NanoScope Analysis to quantify the roughness of the wafers. Roughness did not play a role in differentiation, as it was in the nanometer scale for all groups. Cells were also counted via alamarBlue staining on days 1 and 5 to ensure similar proliferation rates. RT-PCR was performed after incubation to measure the expression of the following genetic markers: osteocalcin (OCN), dentin sialoprotein (DSP), and bone sialoprotein (BSP). RNA lysed from DPSCs on day 0 was used as a baseline to compare the relative expression levels of each gene for each treatment group after the 28 days. Glyceraldehyde-3-phosphate dehydrogenase (GAPDH) served as the housekeeping gene. Our results show an upregulation of BSP expression for the ALD/SMF group compared to PLA/SMF and TCP/SMF groups, confirming titanium deposition's inductive effect on osteogenic differentiation. ALD/SMF produces the greatest osteogenic differentiation with respect to BSP expression. OCN expression was also upregulated by a factor of two for ALD groups compared to PLA, and by a factor of four when compared to TCP. DSP expression was downregulated for ALD groups in comparison to PLA and TCP, and further downregulated for ALD/SMF. Addition of other magnetic materials, such as iron oxide, may further induce osteogenic differentiation. Collagen triple helices are abundant in osteoblasts. Scanning electron microscopy will be used to further analyze collagen triple helix formation, allowing us to understand the role of an SMF on the rate of collagen triple helix formation and thus osteogenic differentiation. Raman spectroscopy will be used to determine the nature of mineralization.

1. Hsu, S. H., & Chang, J. C. The static magnetic field accelerates the osteogenic differentiation and mineralization of dental pulp cells. *Cytotechnology* 62(2). 143–155 (2010).
2. Chuang, Y.C., et al. The Role of Titania Surface Coating by Atomic Layer Deposition in Improving Osteogenic Differentiation and Hard Tissue Formation of Dental Pulp Stem Cells. *Adv. Eng. Mater.* 23(9). 2100097 (2021)

8:00 PM SB09.06.30

Mechanical Characterization of Poly(vinyl alcohol) and Resorcinol Diphenyl Phosphate Clay Blend Vascular GraftsHannahOh, LeoraStochel, HaoyuXu, MeghaGopal, RobertWong, AaronSloutski, AdamHansen, RezaDashti, ChanderSadasivan and MiriamRafailovich; Stony Brook University, The State University of New York, United States

Poly(vinyl alcohol) is suitable for vascular grafts in patients due to its biocompatibility and tunable mechanical properties, but its documented bioinert nature limits cell-adhesiveness, which is critical for the long-term patency of grafts in vivo [1]. We have previously found that Resorcinol Diphenyl Phosphate (RDP)-clay, a phosphate ester flame retardant, can enhance mechanical and cell-adhesive properties when blended with other polymers[2]. Here, we report on the effect of RDP-clay on the mechanical properties of PVA hydrogels towards manufacture of small-diameter vascular grafts.

PVA/RDP-clay blend solutions were synthesized by combining 10% PVA (w/w) solution with RDP-clay at 0%, 1%, 5%, and 10% (w/w), respectively. These solutions were crosslinked with 15% (w/w) sodium trimetaphosphate (STMP) and 30% (w/w) sodium hydroxide (NaOH). This solution was poured into 26mm diameter molds and allowed to dry overnight, after which the resulting discs were rehydrated in Dulbecco's Phosphate Buffered Saline (DPBS) for about 24 hours. Rheology of these discs was characterized using a Kinexus Pro+ rheometer (Netzsch), with oscillatory amplitude sweeps with parameters 0.1 to 100 Pa range, 1 Hz frequency, and 25 C temperature. To create small-diameter grafts from this polymer blend, we devised a 3-step process. Melted wax was injected into a metal tube and allowed to harden, creating a 2 mm diameter wax rod. For all RDP-clay concentrations, these rods were affixed to a single-axis spinner and dipped 10 times in PVA blend, with 15 minutes of spin-drying between dips. After the final dip, rods were allowed to spin-dry overnight, rehydrated the next day, and the wax rods were removed to obtain patent vascular grafts. These grafts were orthogonally cut into thin rings, allowing wall thickness measurements to be found using a Keyence VHX-7000 microscope. 2 cm lengths of vascular graft tubes were also orthogonally cut, then attached to a PG-5 Digital Pressure Gauge and pressurized until rupture to determine vessel burst pressure.

Blend characterization through rheology indicated an average modulus of 35 kPa, with a slight increase as RDP-clay concentration increased. The described manufacture method for these small-diameter grafts was successful at creating patent vessels at all RDP-clay concentrations tested. Vessel thickness was significantly larger in 10% RDP-clay vessels than in 0%, 1% and 5%. 10% RDP-clay vessels were also visibly less smooth and homogenous than lower RDP-clay concentration vessels. Burst pressures were greater than physiological values for all RDP-clay concentrations (200-700 mmHg), but 10% RDP-clay vessels were more prone to pin-prick bursts. As such, we posit that 10% RDP-clay may be an upper limit for organoclay additive concentration to maintain mechanical integrity of the PVA hydrogel.

The mechanical properties of the PVA/RDP-clay blends under these manufacture and processing techniques show great promise for use as vascular grafts in patients. Future steps include characterizing endothelial cell adhesion and proliferation within these manufactured vessels as well as better controlling drying time between dips during manufacture to attain consistent wall thickness.

- [1] Conconi, M. T., et al. (2014). *Molecular Medicine Reports*.
- [2] Feng et al. MRS Fall Meeting; 2018 Nov 25-30; Boston, USA.

8:00 PM SB09.06.31

Characterizing Thrombogenic and Cell-Adhesive Properties of Poly(vinyl alcohol) Blended with Resorcinol Diphenyl Phosphate-Clay towards Vascular Graft ManufactureHannahOh, LeoraStochel, HaoyuXu, MeghaGopal, RobertWong, AaronSloutski, AdamHansen, RezaDashti, ChanderSadasivan and MiriamRafailovich; Stony Brook University, The State University of New York, United States

Poly(vinyl alcohol) (PVA) is an excellent candidate for manufactured vascular grafts to replace occluded arteries due to its mechanical and biocompatibility properties, but its lack of cell-adhesion prevents it from being used in humans [1]. Previously, we found that resorcinol diphenyl phosphate (RDP)-clay can improve cell adhesion within polymer blends [3]. We aim here to characterize the thrombogenic and cell-adhesive properties of PVA/RDP-clay blends on both thin films and hydrogels.

2% PVA (w/w) solutions with each of 0%, 0.1%, 0.5%, 1%, 2%, 3%, 5%, 7% and 10% (w/w) RDP-clay added were spun cast onto silicon wafers. Human umbilical vein endothelial cells expressing green fluorescent protein (HUVEC-EGFP) were plated on the spun-cast wafers at a concentration of 20,000 cells/cm², then imaged on an EVOS M7000 fluorescent microscope. Good HUVEC cell adhesion with notable elongated cell morphology and cell-to-cell connections were observed on all spun cast films regardless of RDP-Clay concentration, indicating that in the absence of cross linker, PVA polymer was biocompatible, supporting cell adhesion and proliferation.

Potential thrombogenicity of the spun cast films was assayed by placing the substrate in a 4mg/ml solution of human fibrinogen. When fibrinogen contacts a hydrophobic surface, protein unfolding has been reported [3], which frees the alpha-C domains and exposes interior of the molecule in the absence of thrombin. Soluble fibrin is then recruited, forming large fibers which have been shown [3] to initiate clots in the presence of plasma. While multiple large fibers were observed here on the unfilled PVA films via Atomic Force Microscopy, the number of fibers and their diameters decreased with increasing RDP clay concentration, disappearing completely at a maximum loading of 5% RDP clay. This correlated with a continuous decrease in water contact angle with increasing RDP-Clay concentration, with a critical value between 1 and 2% RDP-clay.

Formation of the PVA hydrogels for the grafts, though, require cross linking with NaOH followed by rehydration of the PVA. In this case, samples with different clay concentrations were produced by dissolving 10% PVA with 0% and 10% RDP-clay, then crosslinking the solution with 15% sodium trimetaphosphate (STMP) and 30% sodium hydroxide (NaOH). The crosslinked solution was poured into 35 mm diameter molds and dried, creating hydrogel discs for cell plating. Discs were sterilized in isopropyl alcohol for 5 minutes, then rehydrated in media. Fibroblasts expressing Green Fluorescent Protein were plated atop the discs at a concentration of 2000 cells/cm², then imaged after 12 hours with the EVOS microscope. Without extensive washing of the discs, cells were unable to adhere to the hydrogel due to leaching NaOH from the polymer matrix. However, after hydrogel discs were subjected to daily DI exchanges for 5 days and placed under constant agitation from a magnetic stirrer, high fibroblast adhesion to both 0% and 10% RDP-clay gels was observed. This finding contradicts previous studies that show little endothelial cell adhesion to pure PVA [1], which we believe can be attributed to a lack of extensive hydrogel washing.

Our novel processing method of PVA hydrogels as well as the hemocompatibility of PVA/RDP-clay blend thin films show great promise towards using this material for long-term, implanted vascular grafts in humans.

- [1] Ino et al. *Society for Biomaterials*. 2013;101(8):1549-1559.
- [2] Feng et al. MRS Fall Meeting; 2018 Nov 25-30; Boston, USA.
- [3] Zhang et al. *Acta Biomaterialia*. 2017;54:164-174.

8:00 PM SB09.06.32

Developing a Skin Construct for Wound Healing Associated with Endothelial Cell NetworkCaitlynLimb¹, SahanaDhama², MichaelLotwin³, JacquelineHan⁴, GraceWang⁵, ChunuoChu⁶, AnnikaJoshi⁷, RachelNa⁸, ShiFu⁹ and MiriamRafailovich⁹; ¹British School Jakarta, Indonesia; ²The Wheatley School, United States; ³Rambam Mesivta, United States; ⁴Great Neck South High School, United States; ⁵Detroit Country Day School, United States; ⁶Shenzhen Middle School, China; ⁷Johns Creek High School, United States; ⁸Washington University in St. Louis, United States; ⁹Stony Brook University, The State University of New York, United States

Researchers have recently engineered skin constructs incorporating epidermal and dermal layers from the collagen matrix. A significant disadvantage in designing this organotypic culture for

wound healing applications is the lack of a vascular network that promotes anastomosis of the graft-host vasculature. Meanwhile, relying on the additive growth factor to promote vascularization and angiogenesis is not sustainable and could be costly. Mesenchymal cells like fibroblasts and dental pulp stem cells are known to secrete several pro-angiogenic growth factors. Hence, our objective in this research is to (a) establish a microvascular network by co-culturing human umbilical vein endothelial cells (HUVECs) with mesenchymal cells in vitro without additional growth factors, (b) develop a series of altered mediums where both the endothelial and the epithelial cells can be co-cultured, (c) determine the role of an endothelial cell network in predicting vascularization and anastomosis response in vivo and (d) evaluating the impact of these constructs on wound healing.

Living skin equivalents were prepared for 17 days according to the procedures from our previous work [1], modified with the HUVECs-EGFP and mesenchymal cells co-culture layer on the bottom of skin constructs, cultured in the altered mediums to enhance both vascularization and epithelial differentiations. The non-vascularized skin equivalents with the same bottom layer without HUVECs were prepared similarly for comparison. Three SCID Hairless Outbred mice were used as hosts for wound healing experiments. 8mm diameter wound beds were created on the back of the mice. The harvested skin equivalents were then placed on the wound beds and bandaged with silicone film to prevent dehydration during healing.

Following a 7-day period of postoperative recovery, skin tissue samples were collected for histological analysis. Hematoxylin and eosin (H&E) staining revealed a seamless integration between the graft and the surrounding epithelium and dermis. Additionally, lumens were scattered throughout the grafted tissue, identified as human using anti-EGFP staining, and filled with blood cells. The luminal diameters of the human blood vessels ranged from approximately 10um to 40um without observable leakage, confirming successful anastomosis. The joining of blood vessels between graft and host is a necessary milestone for successful tissue regeneration and long-term engraftment.

In conclusion, we have designed a highly effective scaffold that enables the simultaneous culture of HUVEC networks with skin organotypics, promoting anastomosis and accelerating wound healing.

We acknowledge the Morin Charitable Trust for funding.

[1] Li, Juyi, et al. "Engineering functional skin constructs: A quantitative comparison of three dimensional bioprinting with traditional methods." *Experimental Dermatology* 31.4 (2022): 516-527.

8:00 PM SB09.06.33

Promoting Angiogenesis via HGF Upregulation using Titanium Dioxide Nanoparticles Grace Wang¹, Michael Lotwin², Caitlyn Lambert³, Jacqueline Han⁴, Annika Joshi⁵, Chunuo Chu⁶, Sahana Dhama⁷, Rachel Na⁸, ShiFu⁹ and Miriam Rafailovich⁹; ¹Detroit Country Day School, United States; ²Rambam Mesivta, United States; ³British School Jakarta, Indonesia; ⁴Great Neck South High School, United States; ⁵Johns Creek High School, United States; ⁶Shenzhen Middle School, China; ⁷The Wheatley School, United States; ⁸Washington University in St. Louis, United States; ⁹Stony Brook University, The State University of New York, United States

Titanium dioxide (TiO₂) nanoparticles (NPs) have high biocompatibility, antimicrobial properties, and light-scattering abilities, making them a valuable tool across various industries. As such, TiO₂ NPs have become strong points of interest in the modern biomedical field. Previous research has demonstrated that TiO₂ NPs induce the activation of human umbilical vein endothelial cells (HUVECs) due to increased expression of adhesion and other molecules associated with inflammatory response [1]. Such NPs may be linked to promoting angiogenesis, the process by which new capillaries are formed from existing vascular structures in the human body. Hence, this study examines the effects of TiO₂ NPs on HUVECs angiogenesis through flow cytometry and cell sorting based on TiO₂ uptake, imaging time lapses of vascular development using EVOS microscopy, network quantification with Celleste Image Analysis software, scanning electron microscopy (SEM), and Reverse Transcription Polymerase Chain Reaction (RT-PCR).

HUVECs were cultured with and without 0.1mg/ml Rutile TiO₂ particles for 24 hours. The cultures were then sorted using FACS, where cells were sorted by a low and high scattering angle window, and it was assumed that the high scattering fraction would increase with TiO₂ uptake. The results showed that 91% of the treated cells contained TiO₂ particles.

The high scattering fraction and the control untreated cells were then plated on a 10mg/ml matrigel substrate, and the progress of angiogenesis was recorded using an EVOS microscope with a CO₂ onstage incubator. Images of triplicate cell cultures were captured every 20 minutes over 18 hours. The images were then analyzed using Celleste Image Analysis software. From the images, it was found that the culture with TiO₂ nanoparticles nucleated a network, and the network was more robust and persisted longer than the control. SEM analysis of the networks indicated that TiO₂ particles were present in the cells, which constituted the nodes, splines, and all aspects of the network.

RT-PCR was performed on the cultures, and the results of the treated cultures were compared to those of the control. The data showed that while the housekeeping gene, GAPDH, was significantly upregulated by the particles, no difference with the control group was observed for the other housekeeping gene, Actin Beta. Hence, only the latter was used for normalization.

The data demonstrated that TiO₂ exposure upregulated the hepatocyte growth factor (HGF) expression by more than an order of magnitude. In contrast, Vascular endothelial growth factor A (VEGFA) expression, which was previously observed to be upregulated in tumors with HGF, did not occur. These results indicate that despite no evidence of TiO₂ nanoparticle penetration into the nucleus, exposure to TiO₂ can result in upregulation of multiple genes. Further research into the precise mechanism is underway to determine whether the findings can serve as a beneficial factor in promoting wound healing.

We acknowledge the Morin Charitable Trust for funding.

[1] Montiel-Dávalos, A., Ventura-Gallegos, J. L., Alfaro-Moreno, E., Soria-Castro, E., García-Latorre, E., Cabañas-Moreno, J. G., del Pilar Ramos-Godínez, M., & López-Marure, R. (2012). TiO₂ nanoparticles induce dysfunction and activation of human endothelial cells. *Chemical research in toxicology*, 25(4), 920–930. <https://doi.org/10.1021/tx200551u>

8:00 PM SB09.06.34

Thrombosis: An Analysis of Pseudo-Thrombi to Understand Collagen-Fibrin Interaction Sripradha Manikantan¹, Huiting Luo², ShiFu², Robert Wong², Shiffoni Sukhlal² and Miriam Rafailovich²; ¹James Logan High School, United States; ²Stony Brook University, The State University of New York, United States

When vascular injury occurs, the exposed tissue factor initiates thrombosis through a cascade of events including the aggregation of platelets and their coagulation, which in turn triggers the formation of fibrin and collagen to wrap around the coagulated platelets. Clinical treatment of thrombosis in patients with deep vein thrombosis or pulmonary embolism uses fibrinolytics in order to break down the fibrin and cause thrombolysis [1]. However, for arterial thrombi, fibrinolytics do not often respond well. Research shows that collagen plays a dual role in thrombolysis [2] by stimulating glycoprotein VI to promote platelet accumulation and by activating factor XII to promote blood coagulation. In this research, we intend to understand the disparity between venous and arterial thrombosis by studying the interaction between collagen and fibrin in thrombi which prevent lysis. A model scaffold was produced where fibrinogen and collagen were mixed at low temperature and then allowed to crosslink at 37 C. The scaffold was submerged in osteogenic media for 21 days and biomineralization was assayed using XRF and Raman spectroscopy.

Results show that in-vitro XRF of scaffold revealed that biomineralization is significant in collagen when compared to fibrin. The calcium to phosphate ratio for the mixture of collagen and fibrin samples is 1.67, consistent with the formation of hydroxyapatite in the sample. Raman spectroscopy confirmed the formation of crystalline HA in the matrix. The spectra showed a greater peak for collagen when compared to fibrin or the collagen/fibrin scaffold mix, consistent with the XRF results. This means that fibrin has very little biomineralization. Also, unique peaks identified in the fibrin-collagen mix graph suggest the possible formation of a new biomaterial.

Venous thrombi were analyzed histologically and it was shown that they were predominantly composed of fibrin, while arterial thrombi were shown to contain collagen. XRF confirmed the absence of biomineralization in the venous thrombus, consistent with the in-vitro model. Results on the arterial thrombus will be presented, where the presence of mineral deposits will be investigated, as a function of collagen content and the hypothesis that they interfere with lysis will be investigated.

8:00 PM SB09.06.35

Neurogenic Differentiation of Micro-Spheric Dental Pulp Stem Cells via Poly-Lactic Acid, Poly(4-vinylpyridine) and Resorcinol Diphosphate Clay Polymer Scaffoldings Divita Bhattacharya¹, Catherine Chun², Anita A. Gaenko³, Alexander C. Wang⁴, Adam Zaidi⁵, Ethan Lai⁶, Michael Wang⁷, Aman Yarlagadda⁸, Kuan-Che Fang⁹ and Miriam Rafailovich⁹; ¹Kent Place School, United States; ²Ardley High School, United States; ³Huron High School, United States; ⁴Sewickley Academy Senior School, United States; ⁵San Francisco University High School, United States; ⁶Phillips Academy, United States; ⁷Mounds View High School, United States; ⁸Newman Smith High School, United States; ⁹Stony Brook University, The State University of New York, United States

Neurodegenerative diseases such as Alzheimer's pose a major risk to the central nervous system due to the intrinsic non-dividing nature of neurons. Therefore, it is imperative to find methods of generating functionally and morphologically neuronal-like cells from non-neuronal cells under biomimetic conditions. Previously, dental pulp stem cells (DPSCs) have been shown to differentiate into neurons via plating on Poly(lactic Acid) (PLA), Poly(4-vinylpyridine) (P4VP), and Poly(lactic Acid with Resorcinol Diphosphate (RDP) Clay. A concentration of 20% RDP-

Clay was found to provide the highest extent of differentiation into neurons on rough PLA surfaces [1]. Also, the usage of micro-sphere forming U-bottomed StemFit 3D suspension well plates increased the differentiability of DPSCs [2]. Therefore, in this experiment, we are investigating the effects of PLA, P4VP, and RDP Clay scaffolding on neuronal differentiation of DPSCs plated on 3D micro-sphere forming plates.

DPSC micro-spheres (created using suspension well plates) were plated onto silicon wafers spin-casted with pure PLA, PLA with 20% RDP-Clay, PLA with 30% RDP Clay, pure P4VP, P4VP with 20% RDP-Clay, and P4VP with 30% RDP-Clay. These spin-coated surfaces were analyzed with Atomic Force Microscopy (AFM) to ensure homogeneous roughness across the samples so that roughness wouldn't be a confounding factor in the growth and differentiation of the DPSCs. The RDP-Clay particles dispersed throughout the PLA with 20% RDP-Clay sample became nuclei for PLA crystals. Conversely, P4VP does not crystallize around the RDP-Clay.

The plated cells were incubated for 28 days with regular media changes. EVOS images of the DPSCs were taken on Day 1, 6 days after the cells were cultured in TCP and 1 day after plating on polymer scaffolds, confirming microsphere formation following suspension well culturing.

On Day 4, the elastic modulus of the DPSCs was measured for each group of polymer scaffolding via AFM. Cells plated on TCP served as a baseline for modulus. Lower modulus values indicate neuronal differentiation, as neurons are softer cells compared to DPSCs. P4VP had lower modulus (half that of TCP), which indicates that cells plated on pure P4VP had the highest elasticity and were therefore likely differentiating into neurons at a higher rate. Adding RDP-Clay concentration corresponded to a significant difference in modulus for cells plated on PV4P, but an increasing concentration of RDP-Clay was not consistent with a significant change in modulus for PLA scaffolds.

On Day 28, the expression of early-stage neuronal development markers TUBB3 and NES and late-stage marker NEFM was measured using RT-PCR and compared to expression in undifferentiated DPSCs. In differentiated neuronal cells, expression of TUBB3 and NES is expected to be downregulated, and NEFM is expected to be upregulated. Corresponding to our modulus data's implications, adding RDP-Clay to PLA did not lead to significant downregulation of TUBB3, NES, or upregulation of NEFM. However, an increasing concentration of RDP-Clay in P4VP correlated with significant downregulation of TUBB4, NES, and upregulation of NEFM in comparison to undifferentiated DPSCs, indicating that the cells likely underwent neuronal differentiation. Further data will be collected to analyze the effects of these polymer scaffoldings on the neuronal functionality of these morphologically and genetically differentiated cells.

[1] Feng, K.-C., Pinkas-Sarafova, A., Ricotta, V., Cuiffo, M., Zhang, L., Guo, Y., Chang, C.-C., Halada, G. P., Simon, M., & Rafailovich, M. (2018). The influence of roughness on stem cell differentiation using 3D printed polylactic acid scaffolds. *Soft Matter*, 14(48), 9838-9846.

[5] Bu NU, Lee HS, Lee BN, Hwang YC, Kim SY, Chang SW, Choi KK, Kim DS, Jang JH. In Vitro Characterization of Dental Pulp Stem Cells Cultured in Two Microsphere-Forming Culture Plates. *J Clin Med*. 2020 Jan 16;9(1):242.

SESSION SB09.07: Scaffolds for Regenerative Engineering I

Session Chairs: Guillermo Ameer and Melissa Grunlan

Thursday Morning, November 30, 2023

Hynes, Level 1, Room 104

8:00 AM *SB09.07.01

ECM Based Hydrogel Delivery Vehicles and 3D In Vitro Injection Model for Human Retinal Progenitor Cells Transplantation Rebecca Carrier¹, Peng Zhao¹, Sidi A. Bencherif¹ and Michael J. Young²; ¹Northeastern University, United States; ²Schepens Eye Research Institute, an affiliate of Harvard Medical School, United States

Retinal degenerative diseases caused by photoreceptor cell loss and damage are the leading cause of blindness worldwide¹. Treatments, including gene therapy, drug, and neuroprotective approach, mainly focus on slowing down the degeneration process rather than reversing it. Retinal cells implanted into the subretinal space have been shown to integrate within host retina, improving visual function in models of retinal degeneration¹. One barrier to clinical success is the loss, through efflux and death, of the majority (>99%) of implanted cells². A factor likely contributing to cell death is the host microenvironment of the subretinal space after a high cell density (~10⁵ cells/ul) bolus injection (e.g., lacking oxygen/nutrients, missing physical support, and chemical cues). Recent studies have demonstrated that the delivery of retinal progenitor cells (RPCs) using polymer scaffolds results in improved cell survival and differentiation with associated increases in RPC integration³⁻⁴. However, current polymer scaffolds still result in minimal overall integration (<2%). We have established an in vitro bolus injection model mimicking clinical subretinal injection to explore the impact of bolus injection on human RPCs viability. Studies using this model have revealed that indeed RPCs are damaged during the injection process, leading to cell death. To better understand what cues may improve survival of RPCs in the post-injection bolus microenvironment, inert hydrogel systems (oxidized low viscosity alginate) were employed in conjunction with retinal ECM cues including glycosaminoglycans (GAGs): hyaluronic acid (HA) and chondroitin sulfate (CS), laminin (important component of basement membrane), and RGDS (adhesive peptides). The effects of the stiffness and chemical modifications of the delivery vehicles on cell survival/death mechanisms in the bolus injection environment were investigated using fractional factorial design, revealing advantages of stiffer substrates and laminin in promoting RPC survival. Ultimately, this information can be used to guide design of cell delivery vehicles for human RPCs transplantation with improved post-injection survival.

References:

1. Qiu et al., *Exp. Eye Res.* 2005; 80(4): 515-525.
2. Redenti et al., *Ocular Biol Dis Inform.* 2008; 1:19-29.
3. Yao et al., *Polymers* 2011, 3, 899-914.
4. Tucker et al., *Biomaterials*. 2010; 31(1): 9-19.

8:30 AM SB09.07.02

Biomimetic Crosslinking of Collagen Gels by Energetic Electrons for Advanced Scaffolds Nils Wilharm^{1,2} and Stefan G. Mayr^{1,2}; ¹Leibniz-Institute of Surface Engineering (IOM), Germany; ²University of Leipzig, Germany

Design of advanced scaffolds on a biopolymer basis frequently require functionalization and crosslinking for optimum matching biomedical needs. Energetic electrons have recently evolved as a powerful tool for crosslinking bio-derived hydrogels without the need for adding potentially hazardous reagents. Application of this approach allows for synthesis of biomimetic collagen-derived networks of highly tunable properties and functionalization. Yet, the underlying reaction kinetics has been not sufficiently established at this point. While hydroxyl radicals are generated by energetic electron-induced hydrolysis of water and play a key role in introducing covalent bonds between network fibers, a detailed mechanistic understanding would significantly increase applicability. We present a comprehensive analysis of central aspects of the reactivity between the hydroxyl radical (OH) and collagen, elastin, glycine (Gly) and l-lysine (Lys). Overall, energetic electron based crosslinking opens the venue for customized hybrid gels of outstanding biomimicry and -compatibility.

[1] *Acta Biomater.* 140, 219 (2022)

8:45 AM SB09.07.03

Poly 1,8-Octanediol Citrate Breast Biopsy Scaffold and Deployment System Darnell R. Campbell, Marcos Benavides, Jordan Forte, Clifford Howard and Nicole Levi; Wake Forest University School of Medicine, United States

During a breast biopsy, it is crucial to accurately identify regions of concern and deliver markers accurately for subsequent imaging and surgical procedures. If surgical removal is not required, it is essential for the marker to be biocompatible, as it will remain in the tissue for the remainder of the patient's lifetime. Current breast biopsy systems employ a forceful deployment during marker administration leaving a void within the tissue that contributes to marker migration. Furthermore, current marker-encapsulating-meshes are not robust and lack compliance to breast tissue which further contributes to rapid mesh disintegration and marker migration.

To address the aforementioned problems present in the current standard of care, our group developed a three-pronged approach consisting of the creation of an elastic biodegradable scaffold to encapsulate the marker, a deployment device for *in vivo* testing on rats that does not utilize forces during administration, and a transparent breast tissue phantom to determine real-time expansion of the scaffold.

First, a biodegradable Poly 1,8-Octanediol co-citrate (POC) elastic scaffold capable of securing both metallic and non-metallic markers was developed and characterized. Our initial results indicate that POC's properties can be tuned to user-preference by changing crosslinking time, porogen size and leaching time during fabrication; to ensure elasticity of the scaffold, we optimized the pore size by using 400µm NaCl as a porogen. Next, we optimized POC compression and expansion by testing tensile forces at different crosslinking and porogen leaching times. Interestingly, we encountered that during subsequent crosslinking after leaching, POC develops limited self-healing capabilities which allowed for previously embedded markers to be repositioned within a completed scaffold.

Secondly, we developed a 3D-printed deployment device which releases the encapsulated breast biopsy marker passively in a retractable motion, eliminating the forces that cause an increase in void size within the biopsy incision. The device was subsequently employed during *in vivo* testing in rats, from which initial results demonstrate little to no marker migration when compared to current standard of care.

Finally, an optically transparent breast phantom was made from Dermasol. This reusable, insensitive to temperature or dehydration phantom allows for POC scaffold deployment and expansion in real time.

Here we presented our solutions to address the challenges associated with breast biopsy marker placement. We achieved this by developing a biodegradable POC scaffold capable of encapsulating markers and expanding to fill the biopsy void, a retractable deployment device to release the scaffold passively, a breast tissue phantom for visualization of sponge expansion, and tested of our approach *in vivo*. We are currently determining POC's degradation profile as well as continuing to evaluate our prototype scaffold and deployment system *in vivo* to measure the reduction in metallic marker migration compared to commercially available devices.

9:00 AM *SB09.07.04

Responsive Antimicrobial Biomaterials for Treatment of Wound Infections[AnitaShukla](#); Brown University, United States

The wound repair and regeneration process is greatly complicated by the presence of infections. Chronic wounds in particular are highly prone to infection. As a prominent example, nearly 60% of individuals with diabetic foot ulcers develop infections. Preventing and treating wound infections is a critical challenge in promoting successful tissue repair. The existence of biofilms and antimicrobial-resistant microorganisms within wound environments further complicates the effective treatment of these infections. In this talk, I will describe recent approaches we have taken to treat wound infections using hydrogel biomaterials and nanoparticle therapeutic formulations. I will discuss the development of a bacteria-responsive hydrogel drug delivery platform that can provide on-demand treatment of wound infections, while facilitating tissue repair. These hydrogels respond to the presence of beta-lactamases, which are bacteria-produced enzymes that are a common cause of antibiotic resistance. Upon exposure to beta-lactamases, the hydrogel backbone undergoes degradation, leading to the release of encapsulated antibacterial liposomes. Our findings using a *Pseudomonas aeruginosa*-infected murine skin abrasion wound model indicate complete clearance of infection within one day of treatment. Importantly, there were no instances of infection recurrence during the four-day wound monitoring period. Furthermore, timely eradication of the infection helped promote wound healing, as evidenced by histological analysis revealing rapid regeneration of the epidermis. Notably, the hydrogel itself exhibited no signs of toxicity. I will also describe our work on the development of bacteria-responsive gelatin nanoparticles that have demonstrated promising antibiofilm efficacy against prevalent wound infection-causing bacteria, including *Vibrio vulnificus* and *P. aeruginosa*. Overall, the technologies described in this talk are biocompatible and effective at eliminating wound infections, thus holding immense potential for promoting effective wound healing.

9:30 AM SB09.07.05

Biomimetic Semi-Flexible Hydrogel with Reduced Inflammation for Bone Defects[JaeseoLee](#)^{1,2,3} and Il KeunKwon³; ¹Harvard Medical School, United States; ²Brigham and Women's Hospital, United States; ³Kyung Hee University, Korea (the Republic of)

Engineered 3D scaffolds must be biomechanically capable to substitute injured tissues, and have typically been made of tissue-mimicking stiffness. However, this paradigm is shifting towards the understanding that the stiffness of scaffolds can be directly responded to by cells. Herein, we have designed a soft hydrogel to meet two criteria that can shift from soft to progressively hard tissue, similar to tissue development in nature. First, inspired by clotting of blood at the wound site, the goal is to achieve strong bonding with adjacent tissues through physical crosslinking of fibrinogen (FBG). Second, the hydrogel is needed mattress to dissipate energy such as existing collagen (COL) in the body. This scaffold promotes energy dissipation by strengthening the elastic and soft fibers of the FBG through COL to form a dense structure. As a crucial fundamental substrate, soft hydrogels initially induce rapid cell adhesion due to their soft surface. Sequentially, the cells increase to penetration inner part and make rigid themselves, and leading to bone formation. Furthermore, this hydrogel was composed of ECM-like tissue, which could reduce inflammation in the early stage. Therefore, our dual-function system provides a promising strategy for natural tissue-mimicking bone regeneration by reducing inflammation, and concurrently bridging defect area through harmonizing the newly assemble cells and ECMs.

9:45 AM SB09.07.06

Neuron Viability and Maturation on Electroactive Materials and Effect of Electroactive Stimulation on Neural Cell Response[TeresaMarques-Almeida](#)¹, [ClarisseRibeiro](#)¹, [IgorIrastorza](#)^{2,3}, [PatriciaMiranda](#)⁴, [IgnacioTorres-Alemán](#)⁴, [UnaiSilvan](#)² and [SenentxuLanceros-Mendez](#)^{2,1,5}; ¹University of Minho, Portugal; ²BCMaterials, Basque Center for Materials, Applications and Nanostructures, Spain; ³University of the Basque Country, Spain; ⁴Achucarro Basque Center for Neuroscience, Spain; ⁵Ikerbasque, Basque Foundation for Science, Spain

Electric cues are intimately related connected to physiological functions of cells and tissues. The ability to control and direct electric signals within tissue-engineered constructs is therefore increasingly important for proper tissue engineering strategies, as they influence cell behaviour and guide tissue development towards more functional and biomimetic outcomes. In this context, smart materials, able to react in a controllable and reversible way to external stimuli by varying a specific physical or chemical quantity, show great potential for the development of advanced biomedical strategies, including biosensing, tissue regeneration and repair, immuno- and cancer therapy. Among the different types of smart materials, piezoelectric ones, that convert mechanical solicitations into electrical potential variations and vice versa, represent as suitable candidates to induce specific cell behaviors through electric cues, mainly by improving biomimicry of the cell microenvironment.

The presence of piezoelectric properties in different tissues is known and the effect of surface charge and piezoelectric stimulation has been proven to be beneficial in a variety of cells, including mesenchymal stem cells, myoblast and osteoblasts, among others, has been evaluated. Since neurons were first cultured outside a living organism more than a century ago, a number of experimental techniques for their *in vitro* maintenance have been developed. These methods have been further adapted and refined to study specific neurobiological processes under controlled experimental conditions. Nevertheless, the impact of fundamental properties of the surfaces to which neurons adhere when cultured *in vitro* has not been sufficiently considered.

In the present work we have analyzed the response of primary neurons when cultured on piezoelectric poly(vinylidene fluoride), PVDF, surfaces with different surface electric charge and electric charge type, allowing to establish the effect of the net charge on neuron behavior. It is shown that PVDF films promote the attachment, viability and maturation of primary neurons. More cells per unit area and longer neurites were already present in neurons cultured for one day on PVDF surfaces. Early neurite outgrowth was induced using poled PVDF as culture substrates, since by day 4 of culture neurons already show significantly increased neural process development, and by day 7, this development is even more obvious in neurons cultured on PVDF-. Negative surface charges particularly increased cell metabolism, being about 3 times higher than in control and around 1.7 times higher than in the absence of charge (PVDF NP). When adhering to PVDF-, neurons undergo maturation at a faster rate, as revealed by the higher expression levels of MAP2 and NeuN.

Further, the effect of surface charged PVDF films (positive, negative, and non-poled (average neutral surface charge)) on adhesion, proliferation and differentiation of neural-derived cell line, under static and dynamic mechanolectrical stimulation was assessed.

Upon mechanolectrical stimulation, PVDF with average positive surface charge allows to significantly improve cellular adhesion compared to PVDF with negative or without average surface charges. Independently of the PVDF surface charge type, the applied electrical stimulus throughout the assay improved neurite extension and differentiation.

The obtained results highlight the importance of considering the electric charge of the culture surface for the *in vitro* maintenance of neurons, demonstrating the suitability of the use of 2D PVDF based surface-charged substrates. Further, these findings highlight the possibility of novel therapeutic strategies for the regeneration of neural tissues based on the dynamically surface charge variation that can be induced in the electroactive films.

10:00 AM BREAK

10:30 AM SB09.07.07

Curcumin and Polydopamine Loaded 3D-Printed Calcium Phosphate Bone Scaffolds for Orthopedic and Dental Implants[ArjakBhattacharjee](#) and [SusmitaBose](#); Washington State University, United States

Musculoskeletal disorders, including bone cancer, birth defects, war injuries, and osteoporosis, affect a significant portion of the global population. The aging population and active lifestyles of younger individuals are expected to increase the prevalence of these disorders in younger patients. To address this concerning trend, research is focused on developing bio-implants and scaffolds with extended durability. This study aims to explore the impact of naturally occurring biomolecules such as curcumin from turmeric and biomimetic polymers such as polydopamine on the osteogenic, antibacterial, and *in vitro* chemo-preventive properties when directly integrated into 3D printed bioceramic scaffolds tailored for specific defects. Chemical modification of curcumin through polymer-metal-drug complexation results in approximately 2.5 times greater drug release in biological media at pH 5.0 and 7.4 compared to unmodified curcumin. The presence of curcumin reduces osteosarcoma viability by up to approximately 9 times compared to control after 11 days of cell culture. Antibacterial tests show that scaffolds containing curcumin or gingerol exhibit up to around 90% antibacterial efficacy and rupture bacterial cell walls.

Implantation of the drug-loaded scaffolds in rat distal femur model and histological assessment with H&E, vWF, and Movat pentachrome staining results indicate that the presence of MgO and curcumin leads to up to ~ 2.5 times higher early-stage bone formation than the control. These 3D-printed scaffolds result in up to ~ 75% antibacterial potential against gram-positive and gram-negative bacteria. The designed scaffolds with osteogenic and chemopreventive scaffolds can be utilized in patient-specific low load-bearing defect repair sites.

10:45 AM SB09.07.08

Magnetic Hyperthermia Enhances *In Vivo* Tissue Regeneration Through Intracellular ROS Production Giuseppina Tommasini¹, Susel Del Sol-Fernández¹, Angela Tino², Claudia Tortiglione² and Maria Moros^{1,3}; ¹Institute of Nanoscience and Materials of Aragon (INMA-CSIC), Spain; ²Institute of Applied Science and Intelligent System (ISASI-CNR), Italy; ³Centro de Investigación Biomédica en red en Bioingeniería, Biomateriales y Nanomedicina (CIBER-BBN), Spain

Regenerative medicine is a pioneering field aimed at restoring and regenerating damaged tissues and organs through numerous strategies, including the use of new materials and de novo generated cells^{1,2}. As a dynamic biological process, tissue regeneration requires a variety of intracellular and extracellular molecular mechanisms to facilitate cell division and regeneration. In recent years, multiple studies have demonstrated a central role of reactive oxygen species (ROS) in tissue regeneration, acting as signaling molecules that trigger the activation of molecular pathways involved with cell proliferation and differentiation³. Recently, regenerative medicine has found a surge of interest in magnetic nanoparticles, using their magnetomechanical and heating potential to activate different pathways. In this optics, a promising therapeutic approach could be the possibility of manipulating the ROS production to enhance tissue repair using mild magnetic hyperthermia (MH).

Here, we present a novel approach for enhancing tissue regeneration *in vivo* through mild magnetothermal stimulation using manganese iron oxide nanoparticles (MnxFe3-xO4) with improved heating performance. We evaluated the biological effect of internalized MNPs subjected to an alternating magnetic field on the regeneration process that physiologically occurs in the freshwater invertebrate polyps *Hydra vulgaris*. To decipher the molecular mechanism underlying this process, we performed gene expression analysis of molecular markers normally modulated in ROS homeostasis in regenerated polyps after the MH stimulation. This innovative approach has not been applied before to improve tissue regeneration and thus could represent a breakthrough in tissue engineering.

1. Mao AS, Mooney DJ. Regenerative medicine: Current therapies and future directions. Proc Natl Acad Sci U S A. 2015 Nov 24;112(47):14452-9. doi: 10.1073/pnas.1508520112. PMID: 26598661; PMCID: PMC4664309.

2. Kara L. McKinley et al., Emerging frontiers in regenerative medicine. Science 380,796-798(2023). DOI:10.1126/science.add6492

3. Jing Zhou et al., Reactive oxygen species-sensitive materials: A promising strategy for regulating inflammation and favoring tissue regeneration, Smart Materials in Medicine, Volume 4, 2023, Pages 427-446.

11:00 AM SB09.07.09

The Effects of Varying Ratios of PEGDA:PDMS on the Mechanical Properties of Hydrogels with Differing PEGDA Concentrations for Bone Tissue Engineering Sam Lloyd-Harry¹, Ozgul Yasar-Inceoglu¹ and Ozlem Yasar²; ¹California State University Chico, United States; ²The City College of New York, United States

The mechanical properties of hydrogels play a crucial role in determining their suitability as scaffolds for cell growth. Properties such as biocompatibility, porosity, and mechanical properties dictate the success of a candidate scaffold material. The effects on the mechanical properties of varying ratios of Poly (ethylene glycol) diacrylate (PEGDA) to polydimethylsiloxane (PDMS) have been reported; however, the effects of differing PEGDA:PDMS ratios in varying amounts of water have not been studied. In this work, the effects of varying ratios of PEGDA:PDMS (90:10, 85:15, 80:20) on the mechanical properties of PEGDA concentrations (20%, 40%, 60%, 80%, 100%) were investigated and compared with the embedment of SiO₂ nanoparticles (NPs). PEGDA, PDMS, water, and photoinitiator were mixed and cured under a 365 nm UV light for 10-30 minutes (increasing by 5 minutes with increasing PEGDA concentrations). Compressive testing was performed on all samples using a QT/50 Universal Testing Machine at a 5mm/min rate until breaking. Results indicate that introducing silicon and increasing oxygen strengthens PEGDA hydrogels significantly, regardless of concentration. The comparison of SiO₂ embedded samples to varying PEGDA:PDMS samples reflects the tunability that makes PEGDA hydrogels ideal candidates for tissue engineering.

11:15 AM SB09.07.10

Building Cardiac Valves with Focused Rotary Jet Spinning Michael Peters^{1,1}, Sarah Motta^{1,1,2}, Christophe Chantre^{1,1}, Huibin Chang^{1,1}, Luca Cera^{1,1}, Qihan Liu^{1,1}, Elizabeth Cordoves¹, Emanuela Fioretta², Polina Zaytseva², Nikola Cesarovic^{3,4}, Maximilian Emmert^{2,3,5}, Simon Hoerstrup^{1,2,5} and Kevin K. Parker^{1,1}; ¹Harvard University, United States; ²University of Zurich, Switzerland; ³Deutsches Herzzentrum der Charite, Germany; ⁴ETH Zürich, Switzerland; ⁵University of Zurich and ETH Zurich, Switzerland

Pediatric patients suffering from heart valve disease often require multiple highly invasive valve replacement surgeries throughout their childhood. Building heart valve replacements that remodel and grow alongside the patient could provide a potential solution to avoid these repeat interventions. Here, we present Fibravalves as heart valve replacements that mimic the multiscale structure of the native valve, ranging from the nanoscale of the extracellular matrix (ECM) to the macroscale of the native leaflet geometries. Current valve manufacturing processes struggle to recreate these hierarchical structures. With Focused Rotary Jet Spinning (FRJS), we fabricated these valve scaffolds in less than ten minutes. Utilizing centrifugal forces to extrude synthetic polymer fibers and a focused air stream to direct them, FRJS prints micro- and nanofibers onto customizable trileaflet valve shaped collection mandrels. Fiber production and valve formation occur simultaneously. The micro- and nanofibers serve as ECM analogs, interacting with the native tissue at the cellular level, while the macroscale shape of the valve leaflets control unidirectional cardiac flow. We manufactured Fibravalves using Poly(L-Lactide-co-ε-Caprolactone) fibers, due to their elastic mechanical properties and ability to facilitate rapid cellular infiltration. To evaluate clinical translatability, Fibravalves were implanted in sheep using a minimally invasive transcatheter approach. The stented valves were deployed successfully and provided one-way cardiac flow control in initial acute studies. This work indicates the potential viability for FRJS to be used for future heart valve manufacturing as well as other medical implants.

11:30 AM SB09.07.11

Cell-Seeding Promotion of Phages Functionalized Surfaces Grazia M. Messina¹, Giovanna Calabrese², Salvatore Guglielmino² and Giovanni Marletta¹; ¹University of Catania, Italy; ²University of Messina, Italy

Regenerative medicine is a developing field of interdisciplinary research that includes a combination of *in vitro/ex vivo* and *in vivo* techniques, including the transplantation of stem/progenitor, differentiated, or modified cells, either alone or in biomaterial scaffolds. Many strategies have been developed based on the stimulation of body's endogenous process to grow and repair. Phage display represent a powerful, high-throughput method for discovering peptide ligands for a specific target. The method uses a library of phage particles containing a wide range of peptides or proteins to identify those that bind to a specific target. This technique has evolved and now it contributes to a variety of different areas of medicine and technology, i.e., targeted drugs, imaging diagnosis, gene delivery and nanomaterials. It is a low-cost technique for screening peptide ligands on cells or tissues, distinguishing between small changes in cell surface phenotypes and between normal and sick tissues. In particular, phage-derived peptides can be used to functionalize synthetic scaffolds to drive stem cell proliferation and differentiation *in vitro*.

In this communication we will show how self-organization processes of phages on model substrates, at the liquid/solid interface, promotes anisotropic nanometric alignments of these macromolecular systems, characterized by peculiar nanosized diameters, with lengths of the order of micrometre. The further goal, however, is to correlate the capability of organized phage assemblies to efficiently promote specific processes of "cell seeding" and, in turn, developing suitable control strategies of the phage organization, based on the tuning of pH and surface free energy, as a preliminary step in the development of efficient scaffold functionalization strategies for tissue regeneration. The efficiency of the adopted surface functionalization technique was evaluated by using AFM, while the cell-response has been assessed by optical microscopy and by Force Spectroscopy, focusing the attention on the effect of phages on the mechanical properties of the extracellular matrix. We think that these studies may pave the way to a tailored use of surfaces functionalized with phages, as a smart scaffold able to increase the beneficial cell response.

11:45 AM SB09.07.12

3D Printed High-Strength, Void-Free, Heterogeneous Microneedle Flexible Patch for Multi-Drug Delivery Jaeho Kim¹, Sang H. Ahn¹, Seung Hyun Park² and Won Hyung Ryu¹; ¹Yonsei University, Korea (the Republic of); ²Pukyong National University, Korea (the Republic of)

Microneedle (MN) has been extensively studied for drug delivery with the rapid development of various designs and fabrication methods. Dissolving MN made of fast-dissolving biomaterial such as hyaluronic acid (HA) has shown great potential and has been the most popular MN type. However, dissolving MNs have several unsolved issues: less reliable tissue insertion and inconsistent drug delivery to the tissue. Dissolving MNs are usually fabricated with an aqueous polymer solution, which requires a solvent evaporation step for solidification. However, evaporation deforms MN's shape and results in air voids trapped in MN. This inevitably affects each MN's stiffness, insertion ability, and dose distribution. Nevertheless, most of the studies on dissolving MNs have focused on studying their clinical effects and neglected the reliability of MN insertion and drug delivery to the tissue. Multi-drug delivery from MNs have been introduced as an advanced form of MNs when more than one drug needs to be administered for cancer treatment. They are mostly fabricated by micro-molding two drugs together or dip-coating the second drug formulation on dissolving MNs containing the first drug. However, these MNs can have unwanted interactions between drug compounds and can have difficulty with accurate dose control at the MN insertion site. A heterogeneous MN (h-MN) device which contains different drugs in different MNs in a single patch can be a great alternative since it can avoid drug interaction. Nevertheless, the fabrication process of the h-MN array is challenging since the traditional micro-molding process produces an array of MNs with a single material.

This study established a vacuum-assisted extrusion 3D printing process for high-strength, void-free h-MN flexible patch fabrication. We confirmed reliable tissue penetration and accurate drug delivery to a target tissue. Negative pressure was applied beneath a PDMS mold to remove the air void remaining after molding the polymer solution. For efficient removal, the mold was fabricated with a thickness of less than 1 mm. The mold was located on the customized vacuum jig which was connected to a vacuum pump to apply negative pressure beneath the mold. An array of poly (lactic-co-glycolic acid) (PLGA) and HA MNs were fabricated in a single flexible patch for long-term and short-term drug delivery. For PLGA MN fabrication, PLGA5050 57.14 wt.% solution was prepared using dimethyl sulfoxide (DMSO) with rhodamine b (0.1 w/v %) at 60 °C for 1 h. The solution was extruded single time by an extrusion 3D printer (Nordson Pro4L EFD) with 20 kPa of pneumatic pressure into the cavity. DMSO was evaporated after the extrusion at 130 °C for 60 min. For HA MN fabrication, HA 9.09 wt.% solution was prepared using 0.2 w/v % fluorescein isothiocyanate–dextran (FITC-Dextran) aqueous solution. The solution was extruded 9 times with 90 kPa of pneumatic pressure and a humidifier was applied to maintain relative humidity over 50 %. After the MNs fabrication, the mechanical properties of each MNs were analyzed by the penetration test conducted on porcine skin. The penetration force of each MNs was up to 30 g on the porcine skin which was inserted into tissue to a depth of about 550 µm. Afterward, the drug release rate of h-MNs was estimated by measuring the fluorescence intensity using a plate reader. Drug release test showed that PLGA MN released rhodamine b for 98 h and HA MN released FITC-Dextran for 3 h. Finally, HA solution (13.04 wt.%) was extruded in a mesh pattern over a fabricated 3 x 3 h-MN array to form an h-MN flexible patch. After preparing the h-MN patch, it was again inserted into the porcine skin to identify the penetration ability by confirming the cross-sectional view using a cryo-sectioning machine. Through the development of the fabrication process and analysis result, vacuum-assisted extrusion 3D printed h-MN patch has demonstrated its mechanical, and clinical feasibility.

SESSION SB09.08: Scaffolds for Regenerative Engineering II
Session Chairs: Gulden Camci-Unal and Carolyn Schutt Ibsen
Thursday Afternoon, November30, 2023
Hynes, Level 1, Room 104

1:30 PM SB09.08.01

Bioinspired Flexible Helical Electrospun Mat for Cardiac Patch ApplicationAlexiSwitz, DarrylA. Dickerson and [AnamikaPrasad](#); Florida International University, United States

Overview: Fiber orientation dictates mechanical properties such as mechanical flexibility and porosity. Controlling these properties allows for increased and improved growth of cardiomyocytes for cardiac patch applications. Our work focused on developing helically coiled fiber mats made of polycaprolactone produced via electrospinning, then testing the biocompatibility and function of these fibers in a cardiac patch application and comparing these results to patches reinforced with aligned fibers and patches without fibers.

Background: Helically coiled structures are found in nature from animal to the plant world and provide mechanical support, higher porosity, and increased flexibility. Replicating these structures via electrospinning as a manufacturing method, helically coiled nanofibers promote elasticity and flexibility and have a large surface area for biomolecular interactions, which is suitable for cardiovascular applications due to the demanding dynamic environment of cardiovascular tissue.

Methods and Results: Two types of polycaprolactone fibers were produced via electrospinning; aligned fibers and helically coiled fibers. Fiber formation was dictated by the electrospinning parameters, specifically the flow rate of the polymer solution through the syringe. The biocompatibility and function of these fiber scaffolds were tested by encasing the fiber scaffolds in a hydrogel comprised of gelatin glycidyl methacrylate. Fibronectin was added to this hydrogel to increase biocompatibility and aid in cardiomyocyte attachment and spreading. This hydrogel was seeded with cardiomyocytes differentiated from human-induced pluripotent stem cells to form a preliminary cardiac patch. In total three types of patches were produced: a cardiac patch containing aligned fibers, a cardiac patch containing helically coiled fibers and a third cardiac patch containing no fibers. The cardiac patches were then placed on a holder made of PDMS that provided a passive mechanical stimulus to the cardiomyocytes. These holders were placed in a 12-well plate, and the cardiomyocytes seeded in the cardiac patch scaffold were incubated for 28 days. Cell media was regularly changed to provide the cells with nutrients. Cell growth, cell viability, and cardiomyocyte function were monitored and compared within the three patches. Additionally, the cardiac patch mechanics were examined using nanoindentation, tensile testing, and Raman spectroscopy to discuss the overall suitability of the fibrous mat in cardiac tissue engineering applications.

1:45 PM SB09.08.02

Cancer Testbeds for Bone Metastasis TherapeuticsKalpnaKatti¹, PreethamRavi¹, QuyenHoang¹, JihaKim¹, AnuGaba², ParthVyasa² and DineshR. Katti¹; ¹North Dakota State University, United States; ²Sanford Health, United States

Worldwide over a million deaths occur each year from breast and prostate cancer bone metastasis. Majority of the deaths due to breast and prostate cancer are attributed to metastasis, the process of migration of cancers from the primary site to a remote location which happens to be bone for breast and prostate cancer. Bone metastasis of cancer often causes skeletal failures that become the cause of death in patients. The anticancer drugs available are ineffective for bone metastasis treatment. The inefficacy of anticancer drugs and failure of animal models necessitates the need for reliable in vitro models. We have developed a novel nanoclay tissue engineering scaffold that enables development of a remodeling stage fetal bone, a preferred niche for breast and prostate cancer metastasis. The bone mimetic scaffold utilizes modification of the clay galleries with amino acids to allow biomimetic mineralization of hydroxyapatite inside clay galleries. The bone scaffold is further sequentially seeded with commercial and patient derived cell lines of prostate and breast cancer to generate invitro models of bone metastasis in breast and prostate cancer. A specially designed horizontal flow bioreactor enables physiologically relevant fluid flow through the scaffolds thus creating a realistic testbed of bone metastasis. The cancer testbed serves as a useful platform to investigate new biomarkers using FTIR spectroscopy, RAMAN imaging and nanomechanical investigations. We have developed unique mechanics-based biomarkers that use direct nanoindentation to evaluate their change in elastic modulus, mechanical plasticity and viscoelasticity of cancer cells as a measure of metastasis progression. We have developed unique FTIR based spectroscopic biomarkers with the help of the testbed that also demonstrate the use of FTIR in developing markers for progression of metastasis⁹. Since clinical observations indicate extensive skeletal problems and failures in bone metastasis patients, we use the testbed to evaluate the mechanisms of influence of cancer cells on the Wnt b catenin pathway an important osteogenesis pathways. We observe the specific role of cancer cell factors DKK and ET-1 on influence osteogenesis at the bone site. Lastly we demonstrate the use of testbed for screening new drugs and plant-based compounds for efficacy in treatment of bone metastasis. Overall the cancer testbed presented here is a useful in vitro system for development of new metastasis therapies and personalized medicine.

2:00 PM SB09.08.03

Lacunar Bone-Inspired Biodegradable Constructs: Towards Mini-Invasive Bone RepairFedericaBuccino¹, GiulianaTromba², SandraHofmann³ and [Laura MariaVergani](#)¹; ¹Polytechnic University of Milan, Italy; ²Elettra Synchrotron, Italy; ³Technische Universiteit Eindhoven, Netherlands

Advancements in the field of medicine have resulted in increased life expectancy but have also led to a rise in age-related illnesses, with osteoporosis being one of the most prevalent and widespread diseases. Each year, approximately 9 million fragility fractures occur globally, imposing a significant economic and psychosocial burden for disease management. While accidents and bone tumors directly cause pain and deformity, bone fragility often remains undetected, gradually deteriorating quality of life and creating a pressing need for effective regenerative strategies.

Despite notable progress in microsurgical techniques in recent decades, achieving satisfactory functional and structural repair of damaged bone tissue remains challenging. Although bone tissue possesses intrinsic regrowth and self-restoration capabilities to some extent, the injured bones frequently fail to regain their load-bearing function, resulting in fracture nonunion. Current approaches for treating large bone injuries involve the use of autografts, allografts, and scaffolds, but none of these methods are entirely satisfactory due to specific limitations. These limitations include reduced bioactivity, potential spread of pathogens, inflammation, the need for additional surgery, limited availability, inappropriate shape and size, and a lack of monitoring for newly formed bone. In particular, difficulties in detecting bone-scaffold interactions and understanding the complex relationships between bone formation and local scaffold geometry are currently impeding the clinical applicability of minimally invasive constructs for bone healing.

To overcome these challenges, we propose the design of a novel construct for bone healing that has the potential for scalability, while addressing the current geometric, biological, and monitoring issues. The geometry of the construct is inspired by the natural lacunar micro-porosity and interconnectivity found in human bones, facilitating an improved cell seeding process. The constructs are fabricated using silk fibroin and seeded with mesenchymal stem cells. Two different culture media are considered: the state-of-the-art fetal bovine serum (FBS) and the human platelet lysate (hPL). To assess the mechanical response of cellularized constructs, we employ image-guided failure assessment within a synchrotron using a newly developed X-ray and human eye testing equipment, performing micro-compression tests on the seeded constructs. Scans are acquired at various time frames, corresponding to increasing levels of applied displacement to the construct.

To evaluate the interplay between bone regeneration and the architecture of the silk fibroin scaffold, we utilize neural networks (NN). With a NN accuracy of 0.92, our findings demonstrate the following: i) there is a statistically significant correlation ($p < 0.05$) between pore density and bone formation; ii) constructs seeded with hPL exhibit enhanced bone regeneration (+26%) compared to those seeded with FBS; iii) pore shape may play a crucial role in modulating bone remodeling.

The unprecedented resolution of synchrotron imaging, coupled with the ability to gain novel insights into the mechanical response of constructs for bone healing, enables us to elucidate the intricate connections between scaffold geometry, woven bone formation, and the restoration of mechanical function. Future endeavors will focus on the utilization of shape-responsive materials in construct design, allowing the shape of the construct to be adapted according to specific requirements and needs.

2:15 PM SB09.08.04

Nanotube Scaffolds: Versatile and Customizable Long-Term Culture Platform for Primary Cells and Adult Tissues Astrid Kupferer^{1,2}, Sabrina Friebe^{1,2}, Philine Jauch^{1,2}, Sonja Kallendrusch³, Ivonne Nel⁴, Bahriye Aktas⁴ and Stefan G. Mayr^{1,2}; ¹Leibniz Institute for Surface Engineering, Germany; ²University of Leipzig, Faculty of Physics and Earth Sciences, Division of Surface Physics, Germany; ³HMU Health and Medical University Potsdam, Germany; ⁴University of Leipzig, Medical Center, Germany

A personalized therapy for each patient is one of the milestones in medicine. Associated with this is the organotypic culture of endogenous tissue. In this context, the extracellular matrix plays a major role, because it is unique for every part of the body. Hence, each tissue requires a specific microenvironment when cultured or grown *ex vivo*. For instance, topography and prominent chemical characteristics of the surface are crucial for protein adsorption, cell and tissue adhesion. Usually, the discrepancy between tissue demands and culture conditions results in a loss of physiological properties such as structural integrity, function, or viability of healthy tissues and tumors when the culture period exceeds seven days. This indicates that a one-size-fits-all approach of commonly used Teflon membranes is not effective for an organotypic culture. In contrast, the systematic tailoring of titania nanotube scaffolds aims to enable enhanced culture of adult human tissues *ex vivo* and preserves its structure and viability.

As an example, we present long-term cultured human mamma carcinomas that are highly responsive to the underlying nanostructures. Characteristic structural features as blood vessels, glands and connective tissues that contain for instance adipocytes, fibrocytes, immune cells (like macrophages) and tumor cells show an surface-mediated preservation. In order to maintain a normal degree of proliferation, migration and apoptosis that corresponds to the endogenous state, to preserve the extracellular matrix overall, glands and bloods vessels in specific, and to observe active immune cells, we designed advanced titania nanotube scaffolds with the desired functionality.

Altogether, we aim to realize a platform for organotypic tissue culture of up to several weeks, where primary cells and adult tissues are maintained in physiologic condition *ex vivo*. In particular, we aim to maintain an intact histomorphology, proper function, infiltration with immune cells and preserved physiological niches. Chemical and physical characteristics of the titania nanotube scaffolds are tunable with regard to e.g. surface morphology and topography, surface functionalization and overall conductivity. In this way, the scaffolds can also serve as a tailorable basis for primary cells and 3D bioprinted organ structures. Hence, we pave the way for reliable drug testing and personalized medicine.

We acknowledge the Heinrich-Böll-Stiftung and the German Federal Ministry of Education and Research, project EYECULTURE, as well as the Saxon State Ministry for Economic Affairs, Labor and Traffic (SMWA), project NanotubeUpscaling, for funding.

2:30 PM SB09.08.05

Advances in Cell Coculture Porous Membranes to Mimic *In Vivo* Microenvironments Jin Yoo; Korea Institute of Science and Technology, Korea (the Republic of)

In this presentation, we will discuss the advancements in cell coculture platforms that integrate engineered porous membranes to recapitulate *in vivo* microenvironments and facilitate diverse cell-cell signaling. The utilization of a porous membrane-based coculture platform holds great importance in cell research as it enables the creation of modular interfaces for cells and tissues, while also establishing barrier models for tissue-on-a-chip applications. *In vitro* coculture systems that incorporate porous membranes are commonly employed to mimic *in vivo* microenvironments, such as inducing differentiation of stem cells by recapitulating naturally occurring cell-cell communications. Using porous membrane-based coculture to induce stem cell differentiation proves to be a more cost-effective approach compared to relying on growth factors or specific mediums. A widely used commercial coculture membrane, typically a Transwell®, has played a significant role in fundamental and practical studies involving heterogeneous cell coculture systems. However, due to its relatively thick membrane thickness (~10 µm) and low porosity, it has limitations in facilitating sufficient interactions between cocultured cells. To address these limitations, we have developed advanced coculture membranes using polymers. These new membranes have a thinner thickness and higher porosity, resulting in improved cell-cell interactions that more closely mimic native tissue microenvironments. We have successfully applied these newly developed porous coculture membranes to enhance stem cell differentiation efficiency and establish endothelial barrier function.

2:45 PM BREAK

3:15 PM SB09.08.06

The Dynamic Interplay Between Tumor Stromal Discoidin Domain Receptor 2 (DDR2) and Collagen on Neuroblastoma Cellular Mechanics Theadora Vessella¹, Esteban Rozen², Jason Shohet², Qi Wen¹ and Susan Zhou¹; ¹Worcester Polytechnic Institute, United States; ²UMass Chan Medical School, United States

Cancer development, progression, invasion, metastasis, and responses to therapy rely on a permissive tumor microenvironment. The migration invasion of cancer cells through 3D confined extracellular matrices is coupled with cellular mechanics. Abnormal or dysregulated receptor tyrosine kinase (RTK) signaling is common within neuroblastoma. Fibrillar collagen RTK discoidin domain receptor 2 (DDR2) is studied in this project as it is presented in both tumor cells and tumor stromal cells, with high DDR2 levels correlated with poor outcomes and metastatic disease. Because DDR2 is upregulated in various cancer cells, we hypothesized that DDR2 binds to collagen within the extracellular matrix (ECM) to promote cellular mechanics during cancer migration. In this work, a comparative study between neuroblastoma cells with normal and down-regulated DDR2 levels is conducted. Downregulated DDR2 cell areas and aspect ratios were significantly decreased when plated on collagen coated substrates. Protrusive speeds were found to be comparable among all cell lines. However, contractile speeds were significantly slower in DDR2 downregulated cells, resulting in decreased detachment of cell edges to participate in migration. Additionally, the depletion of DDR2 was shown to reduce cellular traction forces on collagen coated soft substrates (2kPa), when compared to the control cells. Together, our findings suggest that DDR2 is vital to the role of collagen binding in mediating cellular mechanics and cellular migration in neuroblastoma cells.

3:30 PM SB09.08.07

3D Printed Nanofibrous Multidomain Peptide Hydrogels for Regenerative Medicine Adam Farsheed and Jeffrey Hartgerink; Rice University, United States

Tissues vary in their biological, mechanical, and structural properties. In the field of regenerative medicine, 3D printing has emerged as a powerful technique for producing hydrogel scaffolds that replicate the geometric complexity of tissues. Biologically derived polymers are commonly used as hydrogel inks in 3D printing due to their inherent bioactivity. However, these polymers lack the mechanical flexibility offered by synthetic counterparts. In addition, many biologically derived polymers lack the fibrous composition that naturally exists at the nano and micro scale within the body. This necessitates the development of hydrogel inks that are both bioactive and fibrous in structure to better replicate tissues. Here, we present the use of Multidomain Peptides (MDPs), a class of self-assembling peptides that form a nanofibrous hydrogel, as a novel ink for 3D printing [1]. After optimizing MDPs for 3D printing, we show that they can be used to create complex, overhanging structures, and multi material prints. In addition, we demonstrate how cationic and anionic MDPs can be strategically patterned to influence cell behavior. Building upon this work, we have developed a novel fabrication method for producing MDP hydrogels with aligned nanofibers, resembling the alignment present in tissues such as skeletal muscle and peripheral nerve. We show that these anisotropic MDP scaffolds can guide cell growth and spreading. Further, by fabricating hydrogel scaffolds with controlled degrees of alignment, we observe that cells exhibit distinct growth patterns in response to nanoscale differences. Leveraging 3D printing, we have scaled this fabrication method to create multilayer hydrogel scaffolds with precise control over the direction of fibrous alignment. The ability to generate aligned hydrogel scaffolds in a scalable manner sets this fabrication technology apart from other techniques. This work highlights the unique potential of using self-assembling multidomain peptides as 3D printable inks, enabling the creation of improved scaffolds for regenerative medicine.

References:

1. A.C. Farsheed, A.J. Thomas, B.H. Pogostin, J.D. Hartgerink, "3D Printing of Self-assembling Nanofibrous Multidomain Peptide Hydrogels" Adv. Mater. (2023), 35, 11, 2210378, <https://doi.org/10.1002/adma.202210378>

3:45 PM SB09.08.08

Nature-Inspired Functional Biomaterials to Reduce Biofouling for Medical Implants and Devices Woo Kyung Cho; Chungnam National University, Korea (the Republic of)

The formation of bacterial biofilms on medical implants and devices has been recognized as a major cause of healthcare-acquired infections. These infections not only affect the quality of patient care but can also result in implant or device failure. To address healthcare-acquired infections, we have developed anti-biofouling materials that can suppress bacterial adhesion and biofilm formation. Drawing inspiration from mussel's adhesive foot proteins, we synthesized a zwitterionic derivative of 3-(3,4-dihydroxyphenyl)-L-alanine (L-DOPA) and catechol-conjugated fucoidan. Robust antibacterial coatings were achieved through oxidative polymerization and the complexation between catechol groups and Fe(III) ions. These synthesized biomaterials can be applied to silicone implants for plastic surgery and various medical-grade substrates. Additionally, we have recently explored polyphenol chemistry to prevent thrombus formation on blood-contacting medical devices in a substrate-independent manner. In this presentation, I will discuss the development of these biomaterials and surface modification methods. The antibacterial and antiplatelet properties will be discussed in terms of non-specific protein adsorption, bacterial and platelet adhesion, as well as relevant infections and side effects associated with biomedical implants and tools.

4:00 PM SB09.08.09

Increasing Aqueous Drug Solubility by Solvent Electrospinning of Poly(2-Ethyl-2-Oxazoline) Based Stable Amorphous Solid Dispersions with High Drug Loading Olmo Frateur.

Unfortunately, approximately 40% of all marketed drugs and over 90% of medicines in development suffer from poor aqueous solubility and hence limited bioavailability upon oral administration. This critical, current challenge in pharmaceuticals has led to an increased interest in advanced aqueous solubility-enhancing strategies, with the formulation of amorphous solid dispersions (ASDs) as one of the most promising routes. Here, the active pharmaceutical ingredient is ideally molecularly dispersed in a polymeric carrier, hence increasing its chemical potential with respect to its highly stable crystalline counterpart and improving the thermodynamic driving force for dissolution in the gastrointestinal fluids. Nonetheless, the amount of marketed ASDs is still limited, as many ASDs lack physical stability due to their amorphous nature, and recrystallization to their less soluble state during production, downstream processing, storage, and dissolution often limits the applicability. In this research, an important step is taken towards the bioavailability improvement of poorly water-soluble drugs through the formulation of stable ASDs, with flubendazole (FBZ), itraconazole (ITC), mebendazole (MBZ), and celecoxib (CCX) as known Biopharmaceutics Classification System (BCS) class II model compounds. Solvent electrospinning of a working solution of the drug and poly(2-ethyl-2-oxazoline) is put forward, because of the extremely fast solvent evaporation, which freezes the API in the polymeric carrier in a highly homogeneous manner. This work demonstrates the viability and broad applicability of this strategy to produce stable nanofibrous ASDs with ultrahigh drug loadings (up to 55, 60, 70, and 80 wt% for FBZ, ITC, MBZ, and CCX, respectively) and long-term stability (at least one year). Importantly, at such high drug loadings, lowering the concentration of the polymer in the electrospinning solution below the concentration where it can be spun in the absence of the drug is essential, as the interactions between the polymer and the drug result in an increased solution viscosity. A combination of experimental analysis and molecular dynamics simulations revealed that this formulation strategy provides strong, dominant, and highly stable hydrogen bonds between the polymer and the drug, which is crucial to obtain the high drug loadings and to preserve the long-term amorphous character of the ASDs upon storage. *In vitro* drug release studies confirm the remarkable potential of this electrospinning formulation strategy by significantly increasing drug solubility values (e.g. up to 50 times for ITC after 5 hours) and dissolution rates, even after one-year storage of the formulations (as tested for FBZ).

SESSION SB09.09: Virtual Session: Biomaterials for Regenerative Engineering
Session Chairs: Guillermo Ameer, Gulden Camci-Unal, Melissa Grunlan and Carolyn Schutt Ibsen
Tuesday Morning, December 5, 2023
SB09-virtual

10:30 AM SB09.09.01

Shear-Responsive Boundary-Lubricated Hydrogels Attenuate Osteoarthritis [Yiting Lei](#); The First Affiliated Hospital of Chongqing Medical University, China

Lipid-based boundary layers formed on liposome-containing hydrogels can facilitate lubrication. However, these boundary layers can be damaged by shear, resulting in decreased lubrication. Here, a shear-responsive boundary-lubricated drug-loaded hydrogel is created by incorporating celecoxib (CLX)-loaded liposomes within dynamic covalent bond-based hyaluronic acid (HA) hydrogels (CLX@Lipo@HA-gel). The dynamic cross-linked network enables the hydrogel to get restructured in response to shear, and the HA matrix allows the accumulation of internal liposome microreservoirs on the sliding surfaces, which results in the formation of boundary layers to provide stable lubrication. Moreover, hydration shells formed surrounding the hydrogel can retard the degradation process, thus helping in sustaining lubrication. Furthermore, *in vitro* and *in vivo* experiments found that CLX@Lipo@HA-gels can maintain anabolic-catabolic balance, alleviate cartilage wear, and attenuate osteoarthritis progression by releasing CLX and shear-responsive boundary lubrication. Overall, CLX@Lipo@HA-gels can serve as shear-responsive boundary lubricants and drug-delivery vehicles to alleviate friction-related diseases like osteoarthritis.

10:45 AM SB09.09.02

Application of Degradable Porous Scaffold for Bone Regeneration [Ben Zhang](#); SINOPEC Beijing Research Institute of Chemical Industry, China

Bone defects caused by trauma and disease present severe threat to human health. At present, allografts and autografts are the most utilized methods to repair bone defects. However, these treatments have inherent shortcomings such as high failure rates due to poor graft fixation/tissue integration, potential disease transmission and limited supplies, as well as additional surgical hurt. Synthetic bone grafts, if properly engineered with physical properties enabling stable graft fixation, robust osteoconductive and osteoinductive properties encouraging new bone growth, and safe degradation, could help address these challenges.

We report here degradable scaffolds based on poly(lactic acid) derivatives modified with poly(ethylene glycol), which exhibit high-efficiency shape recovery around body temperature and hydration induced stiffening and swelling effects. Composites of these polymers mixed with nanosized hydroxyapatite were electrospun to fabricate meshes composed of nano/micro fibers with size range from 150 nm to 10 μ m. With the help of hydroxyapatite, the morphology of electrospun meshes improved wherein bulk nodules in the fibers reduced and nano/micro fibers become more smooth. As the content of hydroxyapatite increased, the average size of nano/micro fibers decreased and mechanical strength of electrospun mesh lowered. These electrospun meshes showed to support the attachment, proliferation and osteogenesis of osteoprogenitor cells *in vitro*. However, mouse bone marrow stromal cells (BMSCs) cultured on electrospun meshes exhibited suppressed activity with high hydroxyapatite content of 30 wt% indicated by CCK-8 result. Gene expressions of RUNX2, ALPL, COL1A1 and OCN increased at 14th day shown with q-PCR data, demonstrated potential osteogenic differentiation.

11:00 AM SB09.09.03

3D Printing using Oxygen-Generating Filaments for Bone Scaffold Tissue Engineering [Adnan Memic](#); King AbdulAziz University, Saudi Arabia

The latest advancements in bone scaffold technology have introduced novel biomaterials that have the ability to generate oxygen when implanted, improving cell viability and tissue maturation. We developed a new oxygen-generating nanocomposite filament that can be used in FDM based 3D printing of bone tissue scaffolds. Initially, the polymer nanocomposites were characterised using an X-ray diffraction analysis, surface morphology assessment, evaluation of filament extrudability, microstructural analysis, and examination of their rheological and mechanical properties in order to optimized filament production. Next, the filaments were optimized in terms of nanocomposite content to control oxygen release, porosity, and antibacterial activities. Our results indicate that an optimized oxygen releasing filament with a holds great promise for improving bone generation through supporting bone cell oxygenation and resistance to bacterial infections.

11:15 AM SB09.09.04

Multifunctional Patch Systems for Breast Cancer Treatment [Jalal Karimzadehkhoei](#)¹, [Eda Güneş](#)¹, [Beril Ustunkaya](#)¹, [Buğra Senel](#)², [Özlem Kutlu](#)³ and [Gözde O. Ince](#)^{1,3}; ¹Faculty of Engineering and Natural Sciences, Materials Science and Nano-Engineering Program, Sabanci University, Turkey; ²Faculty of Engineering and Natural Sciences, Molecular biology, Genetics and Bioengineering Program, Sabanci University, Turkey; ³Nanotechnology Research and Application Center (SUNUM), Sabanci University, Turkey

Breast cancer, although treatable in its early stages with available chemotherapy drugs, remains a significant challenge in the field of oncology due to treatment difficulties, high risk of recurrence, and increased metastasis development, particularly in advanced stages. There is a pressing need in oncology for efficient therapies that provide long-term protection against cancer recurrence. However, the clinical application of chemotherapy drugs is hindered by the lack of efficient drug delivery systems, resulting in diminished treatment success and severe side effects that negatively impact patients' quality of life. In this study, we present the development of a multi-functional patch system for both short-term and long-term treatment of breast cancer. The patch system comprises two components: drug-loaded nanoparticles dedicated to the therapy and antigen epitope-loaded polymer patches designed to enhance the immune response against potential recurrence. These patches are fabricated using Solution Blow Spinning (SBS), a technique that utilizes a biodegradable polymer for the controlled release of growth factors alongside the drug-loaded nanoparticles. To evaluate the patch's degradation properties, degradation tests are performed by incubating the fabricated patch in phosphate buffered saline (PBS) solution and a lysosome-mimicking solution (LMS). The morphology of the fibers is assessed using scanning electron microscopy (SEM) before and after the spinning process, as well as after the degradation process. Fourier transform infrared spectroscopy (FTIR) is employed to analyze changes in the chemical composition of the fibers. To monitor the release of antigen epitopes from the patches and drugs from the nanoparticles, enzyme-linked immunosorbent assay (ELISA) is employed. Furthermore, *in vitro* studies are conducted to assess the effectiveness of the patches in stimulating the immune system. Overall, this study presents a promising approach to address the challenges associated with breast cancer treatment. The development of a multi-functional patch system that combines drug delivery and immune response enhancement may pave the way for more efficient therapies and improved outcomes for patients with breast cancer.

11:30 AM SB09.09.05

Synthesis and Characterization of Carbon-Based Nano-Adsorbent for Dyes Removal from Wastewater [Angeles I. Licona Aguilar](#)¹, [Aidé Minerva Torres Huerta](#)², [Miguel A. Domínguez Crespo](#)², [María de la Luz X. Negrete Rodríguez](#)¹, [Eloy Conde Barajas](#)¹, [Silvia Beatriz Brachetti Sibaja](#)³ and [Issis C. Romero Ibarra](#)⁴; ¹TecNM/ Instituto Tecnológico de Celaya, Mexico; ²UPIIH - Instituto Politécnico Nacional, Mexico; ³TecNM/ Instituto Tecnológico de Ciudad Madero, Mexico; ⁴UPIITA - Instituto Politécnico Nacional, Mexico

Water pollution is the main part of environmental pollution and it has been increased due to factors such as urbanization and rapid industrialization, considering to human activities in various

industrial fields *e.g.* textile industry, metallurgical, and others. In particular, dyes are hazardous and toxic components, present in trace amounts in wastewater effluents, for its treatment the adsorption method has been the most promising and widely used treatment technique due to its efficient and its flexible operation compared to other methods. Currently, in the nanotechnology field, there are substantial studies researching the potential application of nano- adsorbents for dye removal such as carbon nanotubes (CNTs) and activated carbon (AC) due their physical-chemical properties *e.g.*, large surface area associated with the availability of active binding sites, chemical and thermal properties. These materials can be modified chemically with metallic nanoparticles to increase the surface area and their adsorption capacities through high selectivity and active centers generation. In the present work, multiwalled carbon nanotubes (MWCNTs) and activated carbon from orange peel (AC) were modified to obtain adsorbent materials. Firstly, a functionalization using a mixing acid (HNO₃ and H₂SO₄) was proposed, to improve groups such as oxygen, nitrogen and sulfur on carbon surface materials. Furthermore, MWCNTs and AC surface were modified with nanoparticles with oxide zinc (ZnO) at different concentration (15 and 30 wt%) by precipitation method. The carbon materials were tested to removal methylene blue (MB) and the optimum adsorption conditions were evaluated. The carbon materials (CM) were analyzed by X-ray diffraction (XRD), Fourier transform infrared spectroscopy (FT-IR), thermogravimetric analysis (TGA), scanning electron microscopy (SEM), Nitrogen (N₂) adsorption-desorption, zeta potential and UV-VIS technique were used to quantify the concentration of MB. Results revealed that CM developed a large surface area from 200 to 1100 m²g⁻¹ and chemical groups such as OH, C=O and C-O were conserved; adsorption studies reveal that materials with nanoparticles at 30 wt% can removal until 89.5 % of MB considering conditions such as pH 10, time 24 h, adsorbent dose 20 mg, concentration 80 ppm. The overall all results indicated that CM are promising candidates for dye removals.

Keywords: carbon nanotubes, activated carbon, nanoparticles, dyes, adsorption.

11:45 AM SB09.09.06

Poly(β-Amino ester) Nanoparticle for Lung Capillary Endothelium Specific Gene DeliveryZichengDeng¹, DongluShi² and VladimirKalinichenko^{1,3}; ¹The University of Arizona, United States; ²University of Cincinnati, United States; ³Phoenix Children's Hospital, United States

Introduction and Background: Endothelial cell dysfunction occurs in a variety of acute and chronic pulmonary diseases including pulmonary hypertension, viral and bacterial pneumonia, bronchopulmonary dysplasia, and congenital lung diseases such as alveolar capillary dysplasia with misalignment of pulmonary veins (ACDMPV). To correct endothelial dysfunction, there is a critical need for the development of nanoparticle systems that can deliver drugs and nucleic acids to endothelial cells with high efficiency and precision. While several nanoparticle delivery systems targeting endothelial cells have been recently developed, none of them are specific to lung endothelial cells without targeting other organs in the body. **Methods/Experimental Approach:** Poly(β-amino) ester (PBAE) nanoparticles with specific structure and fluorination was designed, screened, and injected into WT mice intravenously. Typical nanoparticle and transfection detection methods like whole body imaging, flowcytometry and microscopy were used to evaluate the pulmonary endothelial cell targeting efficiency. **Results:** After intravenous administration, the PBAE nanoparticles with specific structure and NP:DNA ratio can deliver non-integrating DNA plasmids to lung microvascular endothelial cells but not to other lung cell types. IVIS whole body imaging and flow cytometry demonstrated that plasmids were functional in the lung endothelial cells but not in endothelial cells of other organs. Toxicity study showed that the PBAE nanoparticles were non-toxic. **Conclusions:** This specifically designed PBAE nanoparticles have promise for new pulmonary vascular diseases therapies development.

11:50 AM +SB09.09.07

Development of Metabonegenic Citrate Biomaterials for Orthopedic EngineeringJianYang; Westlake University, China

Background: Although significant progress has been made in the development of orthopedic biomaterials, the currently available materials are limited by their inability to mimic the native tissue composition, weak mechanical strength, minimal osteoinductivity, significant inflammatory responses, poor bone integration, and slow bone regeneration. Metabolic factors such as glucose were shown to regulate the energy needs of stem cells during osteoblast differentiation. However, a full picture of the metabolic processes guiding or supporting osteogenic differentiation is far from complete. Citrate is a small molecule participating as the starting metabolite in the TCA cycle, is also a key component of bone. However, very limited information is available on what role the citrate plays in bone development and bone biomaterial design despite of its well-known unusual high abundance in bone.

Methods: In this study, a new class of highly versatile and functional citrate-based biomaterials has been developed by reacting citric acid with various carefully selected compounds including amino acids, diols and other functional molecules. We seek to answer several unexplored questions: 1) Can exogenous soluble citrate be uptaken by MSCs? 2) What is the role of extracellular citrate on the energy metabolism of bone forming cells? 3) Can the citrate-regulated cell energy metabolism crosstalk with MSCs signaling pathways involved in osteogenic differentiation? 4) Can the citrate-presenting materials mediate MSCs differentiation through the same mechanism as the soluble citrate? We also explore how these understandings can be applied to novel citrate-presenting biomaterial design and validate if the use of citrate-presenting anatomically similar and mechanically compliant scaffolds can enhance tissue integration and bone regeneration in a critically sized bone defect model.

Results: Our studies showed that extracellular citrate uptake through solute carrier family 13, member 5 (SLC13a5) supported osteogenic differentiation via regulation of energy-producing metabolic pathways, which led to elevated cell energy status to fuel osteo-differentiation of hMSCs with high metabolic demands. We next identified citrate and phosphoserine (P_{Ser}) as a synergistic pair in polymeric design, exhibiting concerted action not only in metabonegenic potential for orthopedic regeneration, but also in facile reactivity into a fluorescent system for materials tracking and imaging. We herein designed a novel, citrate/phosphoserine-based photoluminescent biodegradable polymer (BPLP-P_{Ser}), which was lastly fabricated into BPLP-P_{Ser}/hydroxyapatite composite microparticulate scaffolds, demonstrating significant improvements in bone regeneration and tissue response in rat femoral condyle and cranial defect models.

Discussion and Conclusion: We have revealed a previously unexplored expression pattern of SLC13a5 citrate transporter along osteo-differentiation, and a mechanism focusing on the metabolic regulation of citrate to elevate cell energy status for bone formation, referred to as citrate metabonegenic regulation. These findings not only identify citrate as a new metabolic factor in the stem cell micro-environment favorable for osteo-differentiation, but also suggest that citrate should be considered in bone biomaterials design, providing guidance to develop biomimetic BPLP-P_{Ser}/HA for prolonged citrate metabonegenic effect well into late stage of differentiation, which demonstrated therapeutic potential for bone injuries [1-3]. The unprecedented knowledge on the citrate mechanism enables us to design the next generation of biomimetic dynamic orthopedic implants that may present citrate signals in demand during cellular and tissue development.

References:

Xinyu Tan, et.al. Small 2022 Sep;18(36):e2203003.
Chuying Ma, et.al. Advanced Science 2019, 1900819.
Chuying Ma, et. al. PNAS 2018, 115 (50): E11741-E11750

12:20 PM *SB09.09.08

Development and Translation of New Biomaterial Platforms for BiofabricationRamilleShah; Dimension Inx, United States

Over the past 10 years my research lab and start up, Dimension Inx, has been working to develop and commercialize new advanced regenerative biomaterials that are compatible with 3D-printing. We have developed an extensive range of tunable 3D-printable material platforms that greatly expand the biomaterial palette for complex soft and hard tissue biofabrication. Examples of these new advanced materials include a synthetic *Hyperelastic "Bone"*® material with unique properties that allow for scalable, surgically friendly bone-defect repair, a *Fluffy-X*™ material that has ideal properties for soft tissue and organ biofabrication, and electrically conductive *3D-Graphene* for nerve and muscle regeneration. In this talk I will describe these new advanced biomaterials, their promise in medicine, and how we are taking them from development through to scale up production for commercial and clinical translation.

SYMPOSIUM SB10

From Soft Hydrogel Materials to Hard Water Sports Materials—Bridging the Gap with Additive Manufacturing
November 27 - November 27, 2023

Symposium Organizers

Preethi Chandran, Howard University
Ferenc Horkay, National Institutes of Health
Marc In het Panhuis, University of Wollongong
Yongfu Li, Dow Chemicals Company

* Invited Paper
+ JMR Distinguished Invited Speaker

SESSION SB10.01: Hydrogels I
Session Chairs: Preethi Chandran and Ferenc Horkay
Monday Morning, November 27, 2023
Hynes, Level 1, Room 105

10:30 AM *SB10.01.01

Advanced Soft Hydrogel Materials: New Theoretical Frameworks for Their Chemical and Physical Structure [Nicholas A. Peppas](#); The University of Texas at Austin, United States

Soft hydrogel materials are water-swollen polymer networks that can be tuned to mimic the physical and biochemical properties of their surrounding environment. The signaling mechanisms between the hydrogel properties and their environmental behavior are not always clear, especially because hydrogels and exterior matrix serve the dual functions of mechanically supporting other materials (including tissues or cells) and regulating how chemical signals travel between. In hydrogels, stiffness and solute diffusivity are closely associated with the hydrogel's polymer network structure. The structure-property relationships of hydrogels are summarized by numerous mathematical modeling systems. We present robust, well-tested predictive models that describe how structural changes affect hydrogel properties to make hydrogels into the precise, nuanced tools needed to solve modern engineering problems. We have coordinated swollen polymer network models based on four structural parameters and demonstrate how those four parameters work together to decouple stiffness and other parameters in hydrogels without changing the chemical properties of the network. The resulting decoupling and associated fundamental models facilitate more nuanced investigations of polymer-environment interactions.

11:00 AM SB10.01.02

Interfacial Reinforcement of a 3D-Printable Double Network Granular Hydrogel [Tianyu Yuan](#), [Chenzhuo Li](#), [John Kolinski](#) and [Esther Amstad](#); École Polytechnique Fédérale de Lausanne, Switzerland

Load-bearing soft materials that can be processed into 3D shapes gain increasing importance in the biomedical field. Granular hydrogels have the potential to be used as 3D-printable artificial tissues and their local composition can be tuned over micrometer-length scales. However, the development of mechanically strong granular hydrogels that can be used for load-bearing applications remains challenging. To overcome this challenge, a secondary hydrogel network that covalently crosslinks adjacent microgels can be introduced.^[1] However, the resulting double network granular hydrogel is relatively brittle because of the weak interparticle interactions and the lack of energy dissipation mechanisms.

In this work, two types of oppositely charged polyelectrolyte microgels, one made of the negatively charged polyacrylic acid (PAA), the other made of the positively charged poly(3-Acrylamidopropyl)trimethylammonium chloride (PATC) are used to produce a double network granular hydrogel (DNHG). Due to the electrostatic interactions between the oppositely charged PAA and PATC microgels, the hydrogel exhibits values for the Young's modulus and fracture energy that are similar to those of cartilage^[2,3] and skeletal muscles.^[4] We experimentally investigate the contribution of the interparticle reinforcement to the overall fracture energy of the hydrogel. Based on these studies, we propose an empirical model that takes into account the damage zone size, contact area, and adhesion energy. We demonstrate that this model, albeit being simple, can predict the mechanical properties of DNHGs with a reasonably high accuracy. Thanks to the interfacial reinforcement between PAA and PATC microgels, free-standing structures can be 3D-printed with high printing resolutions, providing new possibilities for designing strong and tough soft materials with versatile processability.

References

- [1] M. Hirsch, A. Charlet, E. Amstad, *Adv. Funct. Mater.* **2021**, *31*, 2005929.
- [2] M. V. Chin-Purcell, J. L. Lewis, *Journal of Biomechanical Engineering* **1996**, *118*, 545.
- [3] U. G. K. Wegst, M. F. Ashby, *Philosophical Magazine* **2004**, *84*, 2167.
- [4] D. Taylor, N. O'Mara, E. Ryan, M. Takaza, C. Simms, *Journal of the Mechanical Behavior of Biomedical Materials* **2012**, *6*, 139.

SESSION SB10.02: Hydrogels II
Session Chairs: Ferenc Horkay and Yongfu Li
Monday Afternoon, November 27, 2023
Hynes, Level 1, Room 105

1:30 PM *SB10.02.01

Influence of Solvent Quality on the Swelling and Deswelling and the Shear Modulus of Semi-Dilute Solution Cross-Linked Poly(vinyl acetate) Gels [Jack F. Douglas](#)¹ and [Ferenc Horkay](#)²; ¹National Institute of Standards and Technology, United States; ²National Institutes of Health, United States

We systematically examine the influence of varying temperature (T) over a large range in model poly(vinyl acetate) gels swollen in isopropyl alcohol. The theta temperature θ of our gels, at which the second virial coefficient A_2 vanishes, is found to be equal to within numerical uncertainty to the corresponding high molecular mass polymer solution value without cross-links, and

we quantify the swelling and deswelling of our model gels relative to their size at $T = \theta$, as customary for individual flexible polymer chains in solution. We also quantify the “solvent quality” dependence of the shear modulus G relative to $G(T = \theta)$ and compare to the hydrogel swelling factor, α . We find that all our network swelling and deswelling data can be reduced to a scaling equation of the same general form as derived from renormalization group theory for flexible linear polymer chains in solutions so that it is not necessary to invoke either the Flory-Huggins mean field theory or the Flory-Rehner hypothesis that the elastic and mixing contributions to the free energy of network swelling are separable to describe our data. We also find that changes of G relative to $G(T = \theta)$ are directly related to α . At the same time, we find that classical rubber elasticity theory describes many aspects of these semi-dilute solution cross-linked networks, regardless of the solvent quality, although the perfector clearly reflects the existence of network defects whose concentration depends on the initial polymer concentration of the polymer solution from which the networks were synthesized.

2:00 PM *SB10.02.02

Tunable Surfaces and Interfaces from Responsive Polymers for Biomedical Applications [Namita Choudhury](#), Nisal Wanasingha, Rajkamal Balu and Naba K. Dutta; RMIT University, Australia

Design of responsive surfaces, interfaces and nanostructures, whose characteristics can be modulated on demand is an important challenge in diverse applications. In this presentation, we discuss the responsive behaviour of soft surfaces, interfaces and solid-liquid interfaces derived from biomimetic polymers. The unique structural features of such polymers and the changes in their characteristics properties and conformation induced by a change in the environment have been evaluated in detail using highly sensitive tools such as quartz crystal microbalance (QCM-D), surface plasmon resonance (SPR), dynamic light scattering, small angle neutron scattering, UV-Vis, and spectroscopy. The talk will illustrate how this responsiveness could be used towards the construction of novel hydrogels, hybrids, conjugates and functional nanoparticles such as high surface area nanoparticles for specific applications. It will also highlight the new classes of multifunctional biomimetic polypeptide synthesis, 3D fabrication of hydrogel and the nano-bioconjugates, that we are developing for biomedical and injury applications, including effective therapeutic, adhesion and repair.

References: 1. R. Balu, N. K. Dutta, A. K. Dutta & N. Roy Choudhury, Nature Communication 2021, 12, 149. 2. N. K. Dutta, M. Y. Truong, S. Mayavan, N. Roy Choudhury, C. M. Elvin, M. Kim, R. Knott, K. M. Nairn, A. J. Hill. A Genetically engineered protein responsive to multiple stimuli. Angew. Chem. Int. Ed. 2011, 50, 4428–443. 3. N. Wanasingha, N. K. Dutta, N. R. Choudhury, Emerging bioadhesives: From traditional bioactive and bioinert to a new biomimetic protein-based approach, Advances in Colloid and Interface Science 296, 102521, 2021. 4. N. R. Choudhury, J. C. Liu, N. K. Dutta, Biomimetic Protein-based Elastomers: Emerging Materials for the Future, Royal Society of Chemistry, 2022. 5. Rajkamal Balu, Naba K. Dutta, & Namita Roy Choudhury, Resilin-mimetic polypeptides and elastomeric modular protein-polymers: amino acid sequence, conformational ensemble and stimuli-responsiveness. In Biomimetic protein-based elastomeric hydrogels, Eds.: Namita, R. C. et al, Royal Society of Chemistry: 2022

2:30 PM SB10.02.03

Textile Electronics for Long-Term Electrophysiological Signal Recording Application [Chansoo Kim](#), Junyi Zhao and Chuan Wang; Washington University in St. Louis, United States

Long-term electrophysiological signal collecting is important since it provides a prior warning to people by detecting diseases such as heart failure or arrhythmia before the diseases progress to a more dangerous stage. It also provides fundamental data for training to improve performance by identifying the accurate amount of exercise and muscle usage for athletes. For this purpose, flexible and stretchable sensors have shown great potential for wearable and ambulatory electrocardiography signal monitoring applications. These soft sensors are comfortable, conform to human skin, and daily wearable in contradistinction to rigid metal-based conventional electronic devices. Nevertheless, most of long-term electrophysiological sensors have focused on sticky dry electrodes for long-term signal collection because conformal contact of electrodes on the human skin can decrease contact impedance.

Here, we propose an interesting approach for long-term electrophysiological signal collecting electrode in dry condition by E-textile system. This system consists of textile and microfiber electrode that were coated by Poly(3,4-ethylenedioxythiophene) polystyrenesulfonate (PEDOT:PSS). For the textile electrode, PEDOT:PSS was simply printed on the nylon-based textile through screen printing manner and the stretchability of electrode was enhanced via polyethylene oxide (PEO) crosslinking process. In addition, hydrophobic treatment through 1H,1H,2H,2H-Perfluorooctyl-trichlorosilane (FTOS) effectively prevent water permeation that can cause erosion and dissolving of the electrode. Consequently, the textile electrode shows high durability in water. Moreover, the microfiber electrode offers greatly reduced contact impedance between skin and electrode, and improved signal-to-noise ratio (SNR) through dramatically increasing contact area. These electrodes combined via electrolyte conductive gel pad and build E-Textile system. Therefore, we achieve $1.1 \times 10^5 \Omega \times \text{cm}^2$ contact impedance. In addition, the SNR of the electrocardiogram (ECG) and electromyography (EMG) SNR were 27 dB and 29 dB in dry atmosphere.

2:45 PM SB10.02.04

Understanding Hydrodynamic Wear in Self-Similar Superhydrophobic Coatings Subjected to Rapid Droplet Impacts [Daniel Braconnier](#)¹, Terence Davidovits² and Randall M. Erb¹; ¹Northeastern University, United States; ²Thermobionics LLC, United States

Superhydrophobic materials rely on both chemical apolarity and surface roughness to achieve the high contact angles and the low roll-off angles that lead to self-cleaning and antibacterial properties. Current superhydrophobic coatings tend to be delicate and lose their properties easily when subjected to droplet impact. Such impact quickly deteriorates these coatings through hydrodynamic wear: changing structure, eroding hydrophobic chemistry, and quickly leading to full wet out of the substrate. In fact, hydrodynamic wear is more detrimental to coatings than seemingly more aggressive mechanical wear including scratching with sandpaper - a common approach used to claim both self-similarity of a material and extreme robustness against wear. What makes certain coatings more robust against hydrodynamic wear? To understand this answer, we systematically study ten disparate self-similar superhydrophobic coating approaches from academia to industry by subjecting them to hydrodynamic wear with rapid droplet impacts. We find rapid droplet impact that simulates a medium rain can deteriorate most coatings within seconds or minutes. Meanwhile, the more resilient coatings share common attributes including robust apolar chemistry, hierarchal topography, and a slow loss of sacrificial material. In addition, we offer an analytical model that nicely characterizes the hydrophobic lifetimes of these systems.

3:00 PM BREAK

3:30 PM *SB10.02.05

Characterization of the Network Structures of PEGDA and Dextran Hydrogels by Complementary Methods [Joseph M. Scalet](#) and [Stevin H. Gehrke](#); University of Kansas, United States

The physical properties of hydrogels are directly affected by their network structure; thus, characterization of that structure is a key part of their development for specific applications. There are generally several different characteristic length scales from the molecular to macroscopic dimensions. Additive manufacturing of hydrogel components introduces additional levels of network structures, depending on the manufacturing methods. Thus, many different methods of characterizing network structures have been developed and used to characterize gels. In this presentation, two fundamentally different but complementary methods will be examined for their potential to evaluate the network structure. The first is the most widely used method – mechanical testing –, but the data is examined in terms of multi-parameter models. The second is the use of time domain low-field NMR (LF NMR), a method that has not been widely used but has the potential for rapid screening of hydrogel formulations. Two hydrogels with quite different network structures widely used in a variety of applications, including 3D printing, are examined: poly(ethylene glycol diacrylate) (PEGDA) and thiol-ene crosslinked dextran.

PEGDA hydrogels were synthesized from monomers of molecular weight from 575 to 8000 Da by photopolymerization at polymer concentrations ranging from 7% to 50 wt.% in water. Dextran gels were made by functionalization of dextran with pentanoate groups which makes it possible to crosslink them by a photopolymerized thiol-ene reaction with dithiothreitol.

Generally, hydrogels are assumed to follow the classic neo-Hookean elastic model under compression or tension, from which network mesh size is estimated. However, not all gels fit this model well, often with deviation increasing with strain. Multiple parameter models can accurately fit data over a broader range of strains and provide further structural information than the standard model. For PEGDA, molecular weights, and concentrations were varied. As the polymer concentration at hydrogel formation increases, the covalent and the entanglement contributions of the modulus both increase. For dextran, a range of molecular weights and polymer concentrations were tested, as well as pentanoate functionalization and thiol:ene ratio. As the thiol:ene ratio was varied, the covalent contributions increased, but the entanglement contributions were less strongly affected. When the polymer concentration at formation was increased, however, both contributions increased.

LF-NMR is an experimentally simple, quick, and non-destructive technique that has the potential to determine a distribution of characteristic length scales in hydrogels. Its speed and experimental simplicity suggest a potential use for the rapid characterization of hydrogel formulations in application development. Proton relaxation times in the time domain (T_2) are related to surface-solvent interactions, and theory can be used to convert the T_2 distributions into network mesh sizes. PEGDA gels were characterized in solution before polymerization, after polymerization, and after equilibration with water. A noticeable reduction in T_2 was observed for PEGDA gels upon cross-linking, indicative of the mobility constraint caused by the formation of the hydrogel network.

4:00 PM SB10.02.06

It is important but challenging to overcome the trade-off in mechanical properties by simultaneously increasing the tensile strength and elongation of elastomers for many applications requiring diverse mechanical properties of polymeric materials. Here, we fabricated an elastomer that forms two types of physical bonds (hydrogen bond and host-guest interaction). The combination of poly(ether-thiourea) (TUEG) with zig-zag array of hydrogen bonds and polyrotaxane (PRX) with movable cross-linking junctions simultaneously increased the mechanical strength (tensile stress of 15 MPa) and elongation (tensile strain of 600%) of the elastomer. It was investigated that degradation of mechanical properties of polymer network against repeated deformation (10 times, tensile strain of 150%) was prevented owing to movable cross-linking junction of PRX. Therefore, this work presents a dual physically cross-linked elastomer having a short main chain (3k) with high tensile strength, tensile strain, and resilience.

4:15 PM SB10.02.07

Nonlocal Intrinsic Fracture Energy of Polymer-Like Networks Bolei Deng, Shu Wang, Chase Hartquist and Xuanhe Zhao; Massachusetts Institute of Technology, United States

Connecting the molecular level details of chain scission to the macroscopic fracture of polymer networks remains a long-standing problem. The Lake-Thomas model predicts the intrinsic fracture energy of a polymer network is the energy to scission a layer of polymer chains. However, recent experiments showed that the Lake-Thomas model underestimated the intrinsic fracture energy by about one to two orders of magnitude. We show that the intrinsic fracture energy of polymer-like networks mainly results from nonlocal energy dissipation by relaxing polymer chains far away from the crack tip. Experiments and simulations show that increasing nonlinearity in single chain mechanics amplifies the intrinsic fracture energy in 2D and 3D polymer-like networks and sustains despite varying defects, dispersity, topologies, and length scales. Our findings not only provide new physical insights into the fracture of polymer networks but also offer design guidelines for tough architected materials.

4:30 PM SB10.02.08

Network Materials with Soft Matrix with Extreme Properties Catalin R. Picu and Mithun Dey; Rensselaer Polytechnic Institute, United States

Most biological materials and many engineering materials, including those used in sports equipment, are network materials with matrix. Their mechanical function is conditioned by the presence of a stochastic network of crosslinked fibers. The embedding matrix is typically a hard thermoset (e.g. epoxy) or a soft hydrogel. The interplay of the two constituents is pronounced when the stiffness of the network tested independently is equal to the stiffness of the matrix. We explore the design principles of this type of composite to determine the parametric space in which special properties can be obtained. Matrices with extreme properties, i.e. incompressible and auxetic, lead to the most pronounced effects. Of special interest is the response to indentation/impact, case in which the interplay of the network and matrix is enhanced. The results are relevant for the design of hybrid materials with exceptional properties and with applications in multiple areas, including in sports equipment design.

4:45 PM SB10.02.09

Reducing Weight of Additively Manufactured Recycled Polymer Sandwich Panels Through Core Topology Exploration Melanie Edmund¹, Andrew Neils¹, Mike Ballin², Luke Diehl² and Jack Lesko¹; ¹The Roux Institute at Northeastern University, United States; ²Blueprint Surf Co., United States

The development of new topologies has the potential to overcome mechanical performance shortcomings seen by structures 3D printed with recycled polymer materials. We investigated the lightweighting of polymer fused deposition modeling (FDM) additively manufactured sandwich panels through the use of high performing closed cell lattice topologies. This study was inspired by Blueprint Surf (Portland, ME), a company that uses FDM additive to make surfboards from recycled polymer feedstocks, with triangular honeycomb cores. For this study, sandwich panels were chosen as the model system for lab-based investigation of surfboard structural properties. Analytical models were used to identify sandwich panel core topologies, like the octet lattice, which should outperform current state-of-the-art (triangular honeycomb). These weight optimization models were validated experimentally through three-point bend testing. Further, the relevance of the lab based three-point bend test of sandwich panels to surfboard structural performance was also considered. The applications for this study extends past surfboards and open the door for more applications of recycled polymers in additive manufacturing. By determining the topologies and densities that yield performance results similar if not better than virgin materials, recycled polymers can be utilized instead of virgin materials in the production of other sports, medical, and general safety equipment.

SESSION SB10.03: Poster Session: Hydrogels
Session Chairs: Preethi Chandran, Ferenc Horkay and Yongfu Li
Monday Afternoon, November 27, 2023
Hynes, Level 1, Hall A

8:00 PM SB10.03.01

The Role of Hyaluronic Acid in the Organization of Aggrecan in the Extracellular Matrix Ferenc Horkay, Emiliós K. Dimitriadis, Iren Horkayne-Szakaly and Peter Basser; National Institutes of Health, United States

Aggrecan is a negatively charged bottlebrush shaped biopolymer molecule. Bottlebrush structures provide excellent lubrication in living systems. Inspired by the lubrication properties of biological systems (e.g., synovial fluid), synthetic bottlebrush polymers have been designed and synthesized. In the extracellular matrix (ECM) aggrecan exists as an aggregate where aggrecan molecules are noncovalently attached to long hyaluronic acid (HA) chains. Aggrecan-HA complexes are important for the mechanical response of cartilage. They exhibit high osmotic modulus, which defines the resistance of the tissue to compressive stress. We studied the hierarchical organization and the scattering properties of hyaluronic acid solutions and aggrecan-hyaluronic acid complexes. Small angle neutron scattering (SANS) and static and dynamic light scattering (SLS and DLS) measurements reveal a domain structure of size greater than several hundred nanometers. At higher values of wave vector, the SANS response corresponds to rod-like structures, of length consistent with the hydrodynamic correlation length associated with the fast diffusion coefficient. Calcium ions do not affect the geometric properties of these domains. DLS is used to investigate the effect of charge valence on the relaxation rates of the concentration fluctuations. The fast diffusive mode in the autocorrelation function becomes slower in the presence of calcium ions relative to sodium counter-ions. The slow mode, however, becomes faster with calcium ions. Reasonable agreement is found between the scattering intensity of the osmotic concentration fluctuations obtained from DLS and from the SANS response. Atomic Force Microscopy is used to determine the morphology of the aggrecan-HA complexes.

8:00 PM SB10.03.02

Surface Function Transformation Through Deformation of 3D Structure using Soft Materials Yejin Oh, Hyemin Lee and Hyunsik Yoon; Seoul National University of Science and Technology, Korea (the Republic of)

Recently, the study of surface morphology alterations has been extensively studied due to their ability to control material properties by changing surface morphology. As for materials, hydrogels are gaining attention due to structural changes through water penetration into the hydrogel network in a wet environment. And as for technology, there are various processes to fabricate three-dimensional (3D) structures but issues of low throughput or low resolution remain. Therefore, we propose a novel approach that 2D structures, made of conventional lithography, transform into complicated 3D structures using hydrogels. By swelling hydrogels under constrained conditions, we achieved the desired shape transformations. We replicated the swollen pattern because of its moisture transport behavior. To optimize material for replication, we investigated about affinity for water of prepolymer and identified that the lower the affinity for water compared to hydrogels the better the swollen pattern retained its shape. In this way, we manufactured molds for buckling and inversely tapered structures and noted that replication from complicated 3D shapes was possible due to the softness of swollen hydrogel. In this method, buckling structures made of polydimethylsiloxane (PDMS) can be utilized as protective films due to their ability to disperse forces laterally. Also, the inverse tapered patterns made of perfluoropolyether (PFPE) exhibit oleophobic surfaces, enabling self-cleaning properties for oil. We also identified that as swelling ratio increased, dispersion capability in buckling film and oleophobicity in inversely tapered film were improved. Therefore, this research demonstrated the potential of utilizing surface shape modifications to achieve various properties using desired materials. It is expected that function transformation can be a platform to create unprecedented functions arising from unique shapes morphed from conventional straight shapes.

8:00 PM SB10.03.03

Measuring the Flex in Surfboard Fins during Surfing Pawel Kryzanowski and Marc In het Panhuis; University of Wollongong, Australia

In this paper we describe the fitting out of a surfboard with inbuilt measurement system and a set of fins instrumented with commercial obtained Wheatstone bridge sensors. The inbuilt

measurement system consisted of GPS, accelerometers, and gyroscope. Telemetry data was collected during characteristic surfing maneuvers on ocean waves at a sampling rate of up to 80 Hz. Our results indicated that our surfboard with instrumented fins can be used to measure the flex in fins during surfing. Our data showed that both fins flex while on waves (surfing speed), but not during paddling (low speed). The commercial sensors recorded fin flex values of up to 10% as the fins are loading and unloading at surfing speeds of up to 6 m/s (from GPS data).

8:00 PM SB10.03.04

Blood Oxygen and Heart Rate Monitoring by a Flexible Hybrid Electronics Device Fabricated by Multilayer Screen-Printing Gábor Méhes^{1,2}, Ayako Yoshida² and Shizuo Tokito²; ¹Waseda University, Japan; ²Yamagata University, Japan

Finger-based pulse oximetry (SpO₂) and heart rate monitoring are widely used in medical settings and are penetrating the everyday life. However, SpO₂ response measured on the peripheral parts of the body (such as fingers and wrists) has a time lag and is less accurate compared to measuring on forehead. In addition, current devices are centimeter-thick, making seamless integration with the body difficult, hindering continuous monitoring and wide adoption. We designed, fabricated, and evaluated an SpO₂ and heart rate sensing device based on flexible hybrid electronics (FHE) technology. The marriage of flexible electronics with high performance commercially available IC chips makes it possible to have advanced sensing, data processing and wireless data transmission functionalities on a thin (1.5 mm) and flexible form that can be attached to various parts of the body. Differently from most devices using FHE technology, here we describe a cost-efficient and mass production compatible multilayer screen-printing process based on conducting Ag-based and non-conducting inks for making the flexible interconnection circuitry in detail, including advanced topographic analysis. By optimizing the printing steps, we could fabricate interconnecting lines vertically traversing up to five printed layers over several tens of micrometers, increasing the spatial density of functional units. By this, we widen the possibilities to utilize screen-printing for advanced wearable devices. Indeed, our FHE device reliably detects induced hypoxemia, and when applied on forehead, detects changes in SpO₂ more than 10 seconds earlier compared to a finger-based medical grade reference device.

8:00 PM SB10.03.05

Highly Entanglement Hydrogel-Coated Sticker for Diverse Surface Applications via Copolymerization Method Joon Hyung An¹, Junsoo Kim² and Seongmin Kang¹; ¹Chungnam National University, Korea (the Republic of); ²Harvard University, United States

High entanglement hydrogel has advantages such as low friction and high stiffness. However, its applicability is limited by its tendency to easily delaminate when adhering to a surface, which is caused by its high swelling property. In this study, we propose a simple method for surface coating highly entangled hydrogels. By utilizing the designed copolymerization of polymers with hydrogel, we enable high entanglement hydrogels to adhere strongly to various surfaces, even under high swelling conditions. The copolymerized polymers are fabricated into a bilayer film of hydrogel and hydrophobic polymer, creating a freestanding sticker that can be used. The hydrophobic polymer layer prevents moisture transfer, thereby preventing the delamination of the hydrogel caused by swelling. Through this study, we have expanded the potential applications in various fields by enabling the application of high entanglement hydrogel regardless of the surface material.

8:00 PM SB10.03.06

A Fully Self-Healable, Temperature Tolerant and Stretchable Supercapacitor for Operating Integrated Self-Healing Strain Sensor Yeon Ji Choi¹ and Jeong Sook Ha¹; Korea University, Korea (the Republic of)

With the rapid advancement in wearable technology, there has been extensive effort on the development of high performance flexible/stretchable energy storage devices. Among various energy storage devices, supercapacitors are considered to be one of the most promising devices as integrated power supply of wearable electronics owing to many advantages of high power density, high cyclic stability and simple structures. Since the wearable devices are frequently exposed to extreme conditions of environments and/or physical damage, however, durability issue has evolved to be a serious challenge for their practical applications. Thus, addition of novel functionality such as self-healing from mechanical damage and tolerance over dramatic changes in temperature to stretchable supercapacitors can be a solution for that. Up-to now, most of the reports showed the self-healing of electrolyte only instead of fully self-healing supercapacitors. Even though many temperature tolerant supercapacitors were reported, there is a few supercapacitors with both self-healing and stability over wide temperature ranges which requires a deliberate design of device structure and materials.

In this work, we report on the fabrication of a fully self-healing, temperature tolerant, and stretchable supercapacitor and its application as a powering device for integrated strain sensor. Organohydrogel with a self-healing via the diol-borate bonding as well as the hydrogen bonding, and the stability over wide temperature range via hydrogen bonding between water and ethylene glycol, could be obtained, respectively. As a self-healing encapsulating film as well as a substrate, a polyurethane film based on oxime-carbamate bonding and hydrogen bonding was synthesized. As a self-healing stretchable electrode, CNT/polyaniline spray-coated on Au nanosheets functionalized with a poly(ether-thioureas) triethylene glycol was used.

By sandwiching the self-healing and temperature tolerant electrolytes with self-healing electrodes on both sides, the fully self-healing supercapacitor stable over temperature changes from -20 to 100 °C was completed. Such fabricated supercapacitor showed the fully self-healing efficiency of 83% even after 5 repetitive cycles of bisection and thermal healing at 65 °C for 6 hr. Also, the supercapacitor was mechanically stable over stretching by 40%, with a capacitance retention of 99%. Furthermore, the whole supercapacitor recovered the electrochemical performance even after bisection and self-healing. The capacitance of the supercapacitor at room temperature was retained over 85% with the temperature changes between -20 and 100 °C. After attachment of the vertically integrated device of the supercapacitor and the strain sensor, bio-signals such as finger-bending and wrist bending could be detected by using the supercapacitor as a self-healing energy storage device. This work suggests that our fabricated fully self-healing, temperature-tolerant, and stretchable supercapacitor should be widely applied to future wearable electronics with a longevity.

8:00 PM SB10.03.07

Overprinted Osmotically Actuated Joint via Computed Axial Lithography Cameron Darkes-Burkey and Robert Shepherd; Cornell University, United States

Computed Axial Lithography (CAL) forms complete 3D objects all at once by exposing a rotating volume of photopolymer resin with a series of projections at each angular step. This method decouples the formation of complex geometries with the need for a layer by layer build approach historically integral to the Additive Manufacturing (AM) process. This enables another unique advantage of CAL called overprinting where a 3D geometry is printed around a prepositioned insert. Overprinting opens the door for novel applications within AM. Here we demonstrate one such application with a hydrogel osmotic actuator. By tuning the material, the geometry, and the post-processing, swelling-induced actuation is achieved.

8:00 PM SB10.03.08

Vapor-Responsive Impact Energy Absorbing and Dissipating Eutectogel Youna Kim and Jinkee Hong; Yonsei University, Korea (the Republic of)

Every year 2 million people have experienced sports injuries. Especially, in ball games such as basketball, baseball, and golf, serious injury could be caused by a high-speed ball. To prevent sports injuries, players should wear sports protective equipment. For example, in a baseball game, catchers wear protective equipment such as chest protectors, protective helmets, and shin guards. However, as the total weight of the protective equipment approaches 5 kg, the catchers suffer from extreme physical fatigue during the game. Therefore, it is necessary to develop materials for protective equipment that are lightweight and block impact.

As shock-preventing materials, there are representative viscoelastic hydrogels and organogels. These materials are effective in blocking impact due to their viscosity properties that absorb impact and elastic properties that dissipate impact. However, hydrogels have limited ability to withstand the impact energy of spherical projectiles due to their weak mechanical properties. In addition, it is difficult to apply to sports games due to shrinkage and weakening of physical properties due to water evaporation. Organogels overcome the limitations of hydrogels but use harmful solvents. It is necessary to develop viscoelastic protective materials that are lightweight, non-harmful, and can block impact.

In this study, a shock-preventing viscoelastomer (SPV) is designed by using non-toxic deep eutectic solvents (DES) and polyvinyl alcohol (PVA). Shock-preventing materials should absorb all impact energy and convert it into kinetic energy, preventing the energy from being transferred to the wearer. SPV could regulate the dissipation and absorption of impact energy through hydrophobic vapor treatment.

The entangled polymer chains within the amorphous phase could dissipate impact energy. PVA is a hydrophilic semi-crystalline polymer. DES is an azeotropic mixture composed of hydrogen bond donors and hydrogen bond acceptors, which hinder hydrogen bonds between PVA chains. For the increment in the amorphous phase, DES is used as an additive. As the amorphous phase increases in SPV, SPV shows viscoelasticity and could dissipate impact energy. Moreover, SPV is tougher than conventional hydrogels.

Hydrophilic SPV has a different chemical affinity with hydrophobic methyl salicylate (MeS), an analgesic and mint flavoring agent. Due to the different affinity, the solvation effect of MeS within SPV increases the chain entanglement density by H-bonding PVA chains. However, as the MeS treatment does not affect the crystallinity of SPV, MeS-treated SPV still maintains the rubbery phase at a high amplitude sweep. That is, MeS-treated SPV could absorb the impact energy to break the H-bonding and dissipate impact energy.

The MeS-treated SPV is restored to its original state after 50 min. It can be used as protective equipment for baseball and hockey within 1 h per inning. In addition, SPV can be applied to sports protective equipment in various forms such as thin film, fiber, and spray coating. We expect that SPV is suitable as an impact protection material to prevent sports injuries.

8:00 PM SB10.03.09

Auxetic Metamaterials with Structurally Programmed Reconfigurability Josef Jančar, Jan Zidek and Jakub Peroutka; Brno University of Technology, Czechia

Low density engineering materials capable of reacting to mechanical stimuli in a manner programmed by their structural architecture can improve design of shock and impact resistant or

tunable acoustic damping structures, robust actuators, and adaptable heat insulators. Similarly to computers, structural programming translates the human developed algorithm into a string of structural commands obeying syntax enabling to perform the desired task. The structural coding of commands converts the materials programming language (MPL) into a low-level language understandable by the executing architected structure. While constitutive materials capable of carrying the basic structural information already exist, designing the source code, commands compiler, assembler, and linker for the MPL remains a foundational challenge. Here, we outline the strategy for developing the source code for simple MPL commands using functional polymer nanocomposites as the units of structural information (USIs). USIs are spatially organized within simple geometrical elements of the re-entrant auxetic unit cell constituting the basic storage units of structural information (SUSIs). SUSIs are combined in a library of bending eigenmodes and rotations forming the structural source code enabling to program simple MPL commands. Primitive algorithms are developed, and simple commands are structurally coded at the auxetic unit cell array and lattice levels to achieve desired stimuli induced reconfigurations of the auxetic structure. Finally, multi-port FDM fabrication process is employed for physically compiling, assembling, and linking the structural commands into the auxetic structure with structurally pre-programmed system level response.

8:00 PM SB10.03.10

Multi-Responsive 3D Printed Nanocellulose-Based Hydrogels Programmable in Space and Time Beatriz Arsuñi^{1,2}, Gilberto Siqueira³, Silvia Titotto², Tommaso Magrini¹ and Chiara Daraio¹; ¹California Institute of Technology, United States; ²Federal University of ABC, Brazil; ³Empa—Swiss Federal Laboratories for Materials Science and Technology, Switzerland

Stimuli-responsive materials are desirable for a variety of functional applications, that range from biomedical devices, sensors and actuators to adaptive surfaces and deployable structures. However, as the natural environment offers multiple stimuli at the same time, current solutions often lack multi-responsiveness and display poor control over their properties over time. Here, I will introduce a new multi-stimuli-responsive material platform, realized via additive manufacturing, that can be precisely programmable to morph both in space and time. In my talk, I will highlight the fabrication steps that led to the development of composite inks for Direct Ink Writing (DIW), formed by double-network hydrogel matrices, reinforced by a high content of cellulose nanofibers and nanocrystals. Thus, I will display how the alignment of the reinforcing particles, induced by intense shear forces during DIW, provides composites with a highly anisotropic microstructure, key to tune the stiffness as well as the swelling/shrinking behavior of printed actuators [1, 2]. Additionally, I will highlight how the reversible shape-morphing capability of bilayer systems, as well as their activity in time, as a fourth dimension, can be tailored through processing parameters and geometrical design [3], in response to multiple stimuli scenarios, such as simultaneous variations in humidity, temperature, pH, and ion concentration. Finally, I will show how the performance of multi-responsive hydrogels can be leveraged to design and fabricate, by additive manufacturing, mechanically versatile architectures and mechanical sensors with outputs structured through the Boolean logic and logic gates, paving the way to multi-logic stimuli-responsive materials.

References

- [1] Siqueira, G., Kokkinis, D., Libanori, R., Hausmann, M. K., Gladman, A. S., Neels, A., Tingaut, P., Zimmermann, T., Lewis, J. A., & Studart, A. R. (2017). Cellulose Nanocrystal Inks for 3D Printing of Textured Cellular Architectures. *Advanced Functional Materials*, 27(12). <https://doi.org/10.1002/adfm.201604619>
- [2] Champeau, M., Heinze, D. A., Viana, T. N., de Souza, E. R., Chinellato, A. C., & Titotto, S. (2020). 4D Printing of Hydrogels: A Review. *Advanced Functional Materials* 30(31). <https://doi.org/10.1002/adfm.201910606>
- [3] Kotikian, A., McMahan, C., Davidson, E. C., Muhammad, J. M., Weeks, R. D., Daraio, C., & Lewis, J. A. (2019). Untethered soft robotic matter with passive control of shape morphing and propulsion. *Sci. Robot* (4). <https://doi.org/10.1126/scirobotics.aax7044>

SYMPOSIUM SB11

Wearable and Implantable Neuro- and Bio-Electronics with 2D Materials
November 29 - December 5, 2023

Symposium Organizers

Nicolette Driscoll, Massachusetts Institute of Technology
Dmitry Kireev, The University of Texas at Austin
Duygu Kuzum, University of California, San Diego
Arben Merkoci, ICN2

Symposium Support

Bronze
IOP Publishing

* Invited Paper

+ JMR Distinguished Invited Speaker

SESSION SB11.01: Implantable Neuroelectronics with 2D Functional Devices

Session Chairs: Ertugrul Cubukcu and Duygu Kuzum

Wednesday Morning, November 29, 2023

Hynes, Level 2, Room 209

8:30 AM *SB11.01.01

Graphene-Based Bidirectional Neural Interfaces Eduard Masvidal-Codina¹, Nicola Ria¹, Fikret T. Duvan¹, Bruno Rodríguez-Meana², Xavi Illa³, Kostas Kostarelos^{1,4}, Xavier Navarro², Anton Guimerà-Brunet³ and Jose A. Garrido²; ¹Catalan Institute of Nanoscience and Nanotechnology (ICN2), Spain; ²Institute of Neurosciences, Physiology and Immunology, Centro de Investigación Biomédica en Red sobre Enfermedades Neurodegenerativas (CIBERNED), Universitat Autònoma de Barcelona, Spain; ³Instituto de Microelectrónica de Barcelona IMB-CNM (CSIC), Esfera UAB, Spain; ⁴Nanomedicine Lab, National Graphene Institute and Faculty of Biology, Medicine & Health, United Kingdom; ⁵ICREA, Spain

Establishing a reliable bidirectional communication interface between the nervous system and electronic devices is crucial for exploiting the full potential of neurotechnology. Despite recent advancements, current technologies evidence important shortcomings, e.g. lack of focal stimulation, low signal-to-noise ratio, etc. Thus, efforts to explore novel materials are essential for the development of next-generation neural interfaces. Graphene and graphene-based materials possess a very attractive set of physicochemical properties holding great potential for biomedical applications, in particular for implantable neural interfaces. This presentation provides an overview on fundamentals and applications of several graphene-based technologies and devices aiming at developing an efficient bidirectional communication with the nervous system. The main goal of this talk is to discuss opportunities of graphene-based neurotechnologies in neuroscience and implantable medical applications, and at the same time to identify the main challenges ahead.

This work has received funding from the European Union's Horizon 2020 research and innovation programme under grant agreement N. 881603 (GrapheneCore3); from the European Union's Horizon Europe research and innovation programme under grant agreement N. 101070865 (MINIGRAPH), that is supported by the Swiss State Secretariat for Education, Research and Innovation (SERI) under contract number 22.00163; and from the Proyecto PCI2021-122095-2A financiado por MCIN/AEI/10.13039/501100011033 y por la Unión Europea

9:00 AM SB11.01.02

Collagen/Pristine Graphene as an Electroconductive Interface Material for Neuronal Medical Device Applications Jack Maughan^{1,2,3}, Pedro J. Gouveia^{2,3}, Jonathan N. Coleman^{1,3} and Fergal O'Brien^{2,3}; ¹Trinity College Dublin, Ireland; ²Royal College of Surgeons in Ireland, Ireland; ³Advanced Materials and BioEngineering Research (AMBER) Centre, Ireland

INTRODUCTION

The growing clinical demand for electrical stimulation-based therapies for spinal cord and peripheral nerve injury repair, cardiac devices, and other tissue engineering challenges requires the development of conductive biomaterials that balance conductivity, biocompatibility, and mechanical performance. Traditional conductive materials often induce scarring, due to their stiffness and poor biocompatibility, presenting challenges to their clinical translation. To address these issues, we report the development of a pristine graphene-based (pG) composite material for central nervous system applications, consisting of type I collagen loaded with 60 wt% pG, yielding conductivities (~1 S/m) necessary for efficient electrical stimulation, and with versatile processability.

METHODS

Pristine graphene (60 wt%) and collagen films (CpG) were synthesised and characterised. Neural cell lines and induced pluripotent stem cell derived neurons were seeded on the surface of the composites, and the metabolic activity, DNA content, cell morphology and release of inflammatory cytokines were assessed. Electrical stimulation was applied to mouse primary cortical neuron isolates to enhance neurite outgrowth and viability. Finally, the CpG composites were fabricated into porous 3D scaffolds, microneedle arrays, and bioelectronics circuits, using freeze drying, dry casting, and 3D printing approaches respectively.

RESULTS

Of all composites tested, CpG 60% exhibited physiologically relevant conductivities (~1 S/m), and robust mechanical properties (~17.8 MPa). To test biocompatibility, four neuronal and glial cell types were grown on composite films, and exhibited robust growth, and glial cells exhibited no change in inflammatory markers IL-6, IL-10, or IL-1 β , indicating no significant neuro-inflammatory response. iPSC-derived neurons exhibited typical cellular morphology after 15 days growth on the films, indicating the potential of the material for supporting long-term growth. The achieved conductivity enabled the efficient delivery of electrical stimulation, which was delivered to mouse primary cortical neurons on the composite (200 mV/mm, 12 Hz, 4h/day, 5 days), enhancing neurite outgrowth, cellular viability and morphology compared to collagen controls. Finally, we demonstrate the versatility and potential applications of the composite using a range of conductive, neural-interfacing structures, including porous scaffolds with aligned internal pores visible under SEM, microneedle arrays (5x5 conical needles, height - 2.5 mm, 625 μ m base diameter, tip diameter - 40-80 μ m), and 3D-printed working LED circuits for bioelectronics.

DISCUSSION

These results demonstrate that CpG 60% composites form a versatile neurotrophic platform that balances the need for physiologically relevant conductivity, robust mechanical properties, and excellent biocompatibility. The mechanical properties of the composite give it an advantage over stiffer traditional electrode materials, which can cause scarring due to extreme mechanical mismatch. The composite supported robust neuronal and glial cell growth, with an absence of neuro-inflammatory responses in microglia and astrocytes. In addition, it efficiently delivered electrical stimulation to primary neurons without loss of viability, enhancing neurite outgrowth. Finally, the versatile processing capabilities of CpG were used to fabricate several neural device types, allowing for a range of applications and treatment approaches.

CONCLUSION

These results show that CpG composites are versatile, neurotrophic materials, which balance the requirement for physiologically relevant conductivity, robust mechanical properties, and strong biocompatibility, demonstrating the potential for these collagen/pristine graphene composites to be fabricated into next-generation electroconductive medical devices.

FUNDING

Science Foundation Ireland AMBER Centre, Irish Rugby Football Union Charitable Trust, and the Anatomical Society

9:15 AM SB11.01.03

Insights into Biocompatible and Bioorthogonal Fluorous-Phase Neural Probe for *In Vivo* Detection of Acetylcholine Maral Mousavi, Farbod Amirghasemi and Abdulrahman Al-Shami; University of Southern California, United States

Acetylcholine (ACh) is one of the least understood neurotransmitters, mainly due to difficulty in its selective detection in biological matrices. ACh appears in the brain and body of mammals, and is released as a messenger by the nerve cells to communicate with other nerve cells, muscle cells, and gland cells. In the brain, ACh functions both as a neuromuscular transmitter and neuromodulator, and thus plays key roles in learning and memory, motivation, and muscle control. Alterations in ACh concentration in the cerebral cortex was correlated to dementia and Alzheimer's disease, psychiatric disorders such as schizophrenia and major depressive disorder, as well as anxiety and depression. Tools for selective sensing of ACh are crucial for better understanding the role of this neurotransmitter in disease progression, as well as rational design and testing of therapeutics that interact with the cholinergic receptors. For successful in-vivo recording of ACh levels, the neural probe (1) should have high selectivity to enable detection of ACh in the large background of other species in the complex brain environment, (2) should be flexible to minimize tissue scarring during probe insertion, (3) should be resistant to biofouling and remain functional after implantation, and (4) should be non-toxic and safe. This talk will discuss the strategies we have taken to address these requirements for an ACh in-vivo probe through development of new materials for sensing and for electrode fabrication. We detect ACh using its permanent positive charge and a potentiometric sensing membrane. This membrane is made of a unique fluoruous-phase material that provides outstanding selectivity and biocompatibility to the electrode. Fluoruous compounds (not to be mistaken with fluorescent compounds) are molecules with high content of fluorine atoms. They are extremely non-polar to the extent that they are NOT miscible with oil and water. In fact, mixing water, hexanes, and perfluorohexane results in formation of three distinct phases. That is, fluorinated compounds are both hydrophobic and lipophobic. This sets apart fluorocarbons for novel biomedical applications. As a matter of fact, living systems are made of water and lipophilic compounds, making fluorocarbons bio-orthogonal, meaning that they do not interfere with biology. This work will show how the low polarity of the fluoruous phase can enhance the selectivity and biocompatibility of our ACh sensor by orders of magnitude. We integrate this fluoruous sensing membrane with a porous graphene electrode that is engraved on a flexible polyimide film using a CO₂ laser. This talk will discuss integration of laser-induced graphene electrodes (LIGs) with fluoruous-phase sensing membranes to produce a new generation of highly selective, biocompatible, and resilient neural probes.

9:30 AM *SB11.01.04

Implantable Graphene Electrode for Diagnosis and Treatment of Brain Diseases Jong-Hyun Ahn; Yonsei University, Korea (the Republic of)

Various electrophysiological and imaging techniques have been studied for the diagnosis and treatment of brain diseases such as epilepsy. In particular, electrocorticography (ECoG) provides valuable information that can guide clinical treatment in patients with brain diseases. In this talk, we report a highly flexible graphene electrode that stably wraps onto the cortex surface of the brain, exhibiting a remarkable signal-to-noise ratio and providing enhanced data quality. The graphene multichannel electrode successfully detects brain signals with high-throughput spatiotemporal resolution. Furthermore, the exceptional flexibility of graphene electrodes enables the fabrication of injectable electrodes that can be introduced through tiny skull openings. These injectable electrodes allow precise measurement of ECoG signals without the need for extensive surgical procedures. The results highlight the immense potential of flexible graphene electrode array in improving both diagnostic capabilities and therapeutic interventions for brain diseases. This technology holds promise for revolutionizing current treatment strategies and opening new avenues for effectively managing various medically significant brain diseases.

10:00 AM BREAK

SESSION SB11.02: 2D Bioelectronics I
Session Chairs: Duygu Kuzum and Tomas Palacios
Wednesday Morning, November 29, 2023
Hynes, Level 2, Room 209

10:30 AM *SB11.02.01

Monolayer Semimetal and Semiconductor Materials for Label-Free Hybrid Biosensing and Neural Voltage Sensing Ertugrul Cubukcu, Yundong Ren, Chawina De-Eknamkul and

A general, overarching theme in nanotechnology is the integration of multiple disparate fields to realize novel or expanded functionalities. At this extreme limit, emerging atomically thin semimetals like graphene and molecularly thick semiconductor such as transition metal dichalcogenides provide a unique opportunity with their non-ubiquitous optical and electrical properties. To this end, we will discuss our work on utilizing these exciting materials for various modalities in biosensing applications with hybrid integration schemes and unique capabilities in all optical recording of neural activity. First, we will discuss our work on a graphene based multimodal biosensor with optical, electrical, and mechanical sensing modes integrated on the same sensor footprint providing simultaneous transduction signals with unprecedented dynamic sensing range and while maintaining sub-picomolar detection limit. Second, we will talk about a MoS₂ based hybrid sensor with an array of optical nanoantenna integrated on a field effect transistor to provide both optical and electrical sensing of a water-soluble variant of the μ -opioid receptor (MOR), via a nickel ion-mediated linker chemistry. Last but not least, we will introduce some of our recent results on all-optical electrophysiology that can achieve high spatio-temporal resolution for potential mapping of biological neural networks as a non-genetic complimentary approach to genetically encoded voltage indicators (GEVIs).

11:00 AM SB11.02.02

Conformable Ultrasound Breast Patch for Deep Tissue Scanning and Imaging [Canan Dagdeviren](#); Massachusetts Institute of Technology, United States

Ultrasound is widely used for tissue imaging such as breast cancer diagnosis; however, fundamental challenges limit its integration with wearable technologies, namely imaging over large-area curvilinear organs. We introduced a wearable, conformable ultrasound breast patch (cUSBr-Patch) that enables standardized and reproducible image acquisition over the entire breast with less reliance on operator training and applied transducer compression. A nature-inspired honeycomb-shaped patch combined with a phased array is guided by an easy-to-operate tracker that provides for large-area, deep scanning and multi-angle breast imaging capability. The clinical trials reveal that the array using a piezoelectric crystal (Yb/Bi-PIN-PMN-PT) exhibits a sufficient contrast resolution (~3 dB) and axial/lateral resolutions of 0.25/1.0 mm at 30 mm depth, allowing the observation of small cysts (~0.3 cm) in the breast. This research develops a first-of-its-kind ultrasound technology for breast tissue scanning and imaging which offers a non-invasive method for tracking real-time dynamic changes of soft tissue.

11:15 AM SB11.02.03

Heavy-to-Light Electron Transition in Quasi-2D Organic Semiconductor Enabling Real-Time Spectra Detection of Charged Particles [DouZhao](#)^{1,2}, Tomoyuki Yokota¹, Takao Someya¹, Wanqi Ji² and Yadong Xu²; ¹The University of Tokyo, Japan; ²Northwestern Polytechnical University, China

Wearable/implantable personal dosimeter achieving real-time and in-vivo radiation safety monitoring are significant for aerospace, medical diagnosis, and radiotherapy, while the current challenge is the lack of suitable detector materials possessing both excellent biocompatibility and high detection performance. Here, we report a novel biocompatible organic single crystalline semiconductor (OSCS) with 2D anisotropic crystallographic structure, achieving excellent electron's transport and real-time spectral detection for charged particles. For the first time, the charge-transport mechanism responsible for such superior performance is clarified in this quasi-2D OSCS from the viewpoint of high-energy physics. Radiation-excited electrons occupy the high-energy L1 level with smaller effective mass than LUMO level, leading to a high electron drift velocity of 5×10^5 cm s⁻¹ under the electric field of 4000 V cm⁻¹ at "radiation-detection mode". In addition, nanoscale surface layer edges on the OSCS, originating from its 2D crystallographic structure induced molecular self-assembly during the solution growth process, also promote the excitons dissociation along the in-plane direction of this OSCS. As a result, the OSCS detector exhibit the record spectra detection for ²⁴¹Am α particles among their organic counterparts, with the energy resolution of 36%, the electron's $\mu\tau$ product of $(4.91 \pm 0.07) \times 10^{-5}$ cm² V⁻¹, and the spectra detection time down to 3 ms. In addition, the OSCS shows good biocompatibility that the cell viability still over 90% after 24-hour incubation with 2 mg ml⁻¹ OSCS. This work reports a quasi-2D organic semiconductor with superior electron transport property and biocompatibility towards to real-time and in-vivo personal radiation dosimeters.

11:30 AM SB11.02.04

Transparent Flexible Strain Gauges for Wearable Devices based on Tiled Graphene Films [Joseph Neilson](#)¹ and Brian Derby²; ¹Trinity College Dublin, The University of Dublin, Ireland; ²University of Manchester, United Kingdom

Here we present a novel transparent strain gauge, with a large gauge factor (GF) and usable strain range, based on 2D materials confined to the surface of an elastomeric substrate. These have good optical transmittance and demonstrate repeatability, under cyclic straining at frequencies > 1 kHz. Gauges have also been mounted on a thin polymer glove to demonstrate its capability as a transparent e-skin strain sensor. During manufacture, closely packed films of graphene oxide are confined to a 2D plane, through assembly at an immiscible H₂O/hexane interface. These films have predominantly edge-to-edge nanosheet contact and show little overlap after deposition onto a polydimethylsiloxane (PDMS) substrate. The films are treated in a hydroiodic acid (HI) reducing atmosphere to introduce electrical conductivity, with the consequent reduced graphene oxide (rGO) films showing < 900 Ω /sq sheet resistance, and > 88% optical transmittance. Piezoresistivity is generated through a pre-straining process that introduces a population of cracks, normal to the straining direction, into the conducting film. After relaxation the cracked films show a repeatable change in resistance when strained to values smaller than the initial pre-strain. Through careful control of the HI chemical reduction phase, it is possible to generate strain gauging devices with different operating ranges and sensitivity. Films pre-strained after reduction for 30 s form an array of parallel cracks that do not individually span the membrane. Subsequent straining of the cracked membrane does not further extend these cracks and the sheet extends in a kirigami manner as the cracks open. This cracking behaviour results in a strain gauge with a usable strain range > 0.2 and GF of 20 - 100 at low strains, however, this GF increases with increasing pre-strain. In all cases, GF decreases with increasing applied strain and asymptotes to a value of about 3 as it approaches the pre-strain value. However, if the rGO film is reduced for a longer time of 60 s, the cracks extend during pre-straining to fully span the width of the PDMS membrane, leading to a much more sensitive strain gauge with GF ranging from 1000 - 16000. However, in this case, the usable strain range reduces to < 0.01. We present a simplified, equivalent resistor model, that can be used to interpret the behaviour of both gauge cracking configurations.

11:45 AM SB11.02.05

High Performance Bismuth Cobaltite Nanoparticles-PDMS based Self-Powered Temperature Nanosensor for Biomedical Applications [Dhiraj Dhiraj](#) and J. P. Singh; Indian Institute of Technology Delhi, India

A multifunction nanogenerator is an advanced nanoscale device designed to harvest various forms of unused energy from the environment and convert them into meaning electrical energy. In this work, we have synthesized the BiCoO₃ nanoparticles using thermal decomposition technique. X-ray diffraction confirms the cubic oxides (space group I23) structure with the rhombohedral shape of BiCoO₃ nanoparticles with high crystallinity. The rhombohedral shape type morphology of nanoparticles was confirmed using High Resolution Transmission Electron Microscope with the average length of 20 nm. Piezoelectric Force Microscope studied of BiCoO₃ nanoparticles was also performed and piezoelectric charge coefficient of 330.42 pm/V was recorded. BiCoO₃-PDMS based flexible piezoelectric nanogenerator was fabricated using the device design of using low-cost hydrothermal technique. PENG generates the high output voltage of 40V and output current of 0.9 mA/cm² that can charge various capacitors and also can light up to 20 LEDs mountainously or even more. PENG have very long durability as it can work continuously for 60,000 cycles. Nanogenerator was utilized as the self-powered temperature sensor that can detect human body temperature by attaching on a wrist and also able to detect high temperature up to 310 C. This type of pressure-driven PENG has potential application in biomedical applications that can do monitor human wrist pulse and body temperature in real time.

SESSION SB11.03: 2D Bioelectronics II
Session Chairs: Linda Giro and Dmitry Kireev
Wednesday Afternoon, November 29, 2023
Hynes, Level 1, Room 105

1:30 PM *SB11.03.01

Input/Output (I/O) Bioelectronics using Two-Dimensional Nanocarbons [Tzahi Cohen-Karni](#); Carnegie Mellon University, United States

My team's efforts are focused on the development and engineering of nanocarbons-based flexible platforms to interrogate and affect the properties of cells and tissue, with a specific goal to understand signal transduction (chemical or electrical) in tissue or complex three-dimensional (3D) cellular assemblies. Our highly flexible bottom-up nanomaterials synthesis capabilities allow us to form unique hybrid-nanomaterials that can be used in various input/output bioelectrical interfaces, i.e., bioelectrical platforms for chemical and physical sensing and actuation. In this talk I will review our current efforts for monitoring (and affecting) the complex signal transduction in 3D in vitro systems toward disease progression investigations. Utilizing graphene, a two-dimensional (2D) atomically thin carbon allotrope, we can simultaneously record the intracellular electrical activity of multiple excitable cells with ultra-microelectrodes that can be as small as an axon (ca. 2 μ m). The outstanding electrochemical properties of the synthesized hybrid-nanomaterials allow us to develop highly efficient catalysts, that can be deployed as electrical

sensors and (chemical) actuators. We demonstrated sensors capable of exploring brain chemistry and sensors/actuators that are deployed in a large volumetric muscle loss animal model. In summary, the exceptional synthetic control and flexible assembly of nanomaterials provide powerful tools for fundamental studies and applications in life science and potentially seamlessly merge nanomaterials-based platforms with cells, fusing nonliving and living systems together.

2:00 PM SB11.03.02

3D Printed Electronic Skin for Strain, Pressure and Temperature SensingAkhileshK. Gaharwar; Texas A&M University, United States

Electronic skin, or e-skin, is an innovative material designed to emulate human skin's flexibility and stretchability. With its capability to detect environmental changes like pressure, temperature, and humidity, it has the potential to revolutionize fields such as robotics, wearable technology, and healthcare. Nevertheless, developing e-skin poses significant challenges: creating durable materials with skin-like flexibility, integrating biosensing abilities, and using advanced fabrication techniques like 3D printing for wearable or implantable applications. To overcome these hurdles, we have fabricated a 3D-printed electronic skin utilizing a novel class of nanoengineered hydrogels with tunable electronic and thermal biosensing capabilities. Our methodology takes advantage of shear-thinning behaviour in hydrogel precursors, allowing us to construct intricate 2D and 3D electronic structures. We simulate the elasticity of skin using triple crosslinking in a robust fungal exopolysaccharide, pullulan, while defect-rich 2D molybdenum disulfide (MoS₂) nanoassemblies ensure high electrical conductivity. The addition of polydopamine (PDA) nanoparticles enhances adhesion to wet tissue. Our nanoengineered hydrogel exhibits outstanding flexibility, stretchability, adhesion, mouldability, and electrical conductivity. A distinctive feature of this technology is the precise detection of dynamic changes in strain, pressure, and temperature enabled by the combination of triple crosslinking and defect-rich MoS₂. As a human motion tracker, phonatory-recognition platform, flexible touchpad, and thermometer, this technology represents a breakthrough in flexible wearable skins and holds transformative potential for the future of robotics and human-machine interfaces.

2:15 PM SB11.03.03

Interaction Of Graphene And WS₂ With Neural Cells, Neutrophils And Mesenchymal Stem Cells: Implications For Peripheral Nerve RegenerationDomenicaConvertino¹, LauraMarchetti^{1,2} and CamillaColetti^{1,1}; ¹Istituto Italiano di Tecnologia, Italy; ²University of Pisa, Italy

The employment of graphene and 2D materials in tissue engineering has been recently exploited for the repair and regeneration of nerve tissue. Among the possible applications, these relatively new materials display a great potential as peripheral neural interfaces, especially for their unique combination of electrical, optical and tribological properties¹⁻⁴.

In this work we present recent results on graphene (G) and tungsten disulfide (WS₂) interaction with some of the key players involved in nerve regeneration, namely peripheral neurons, neutrophils and mesenchymal stem cells (MSCs).

Firstly, we will discuss the effect of G on primary peripheral neurons, i.e. neonatal dorsal root ganglions (DRG) neurons. Graphene obtained via chemical vapor deposition (CVD), a promising candidate to realize functional nerve conduits, was used as a culture substrate. There, axons were found to be significantly longer (up to >70%) with respect to controls during the early developmental phase (up to 2 days), confirming the trend previously reported by our group for embryonic DRG neurons on G on silicon carbide (SiC)⁵. Notably, with the same time-dependent fashion, we found a significative modification of the axonal transport of nerve growth factor (NGF), the neurotrophin involved in the development of peripheral neurons. The amount of retrogradely moving vesicles was strongly reduced in favor of a locally stalled population in the first two days of culture⁶. In addition, electrophysiological and ultrastructural analysis concurred to show the rearrangements that occur in axons developing on G⁶. Our results provide a broad structural and functional understanding of the impact of G on DRG neurons, key information toward the development of G-based devices for neural regeneration. Similarly, we tested WS₂, another 2D material with promising biomedical applications. CVD-grown WS₂, known for its optoelectronic properties, was used to culture neuronal-like cells (SH-SY5Y) displaying neurite length and viability comparable to the controls⁴.

However, the use of these innovative materials has raised questions about their interaction with the other players involved in nerve regeneration, including neutrophils, whose immune response affects the regenerative outcome⁷, and MSCs, a novel therapeutic avenue for peripheral nerve regeneration⁸.

Therefore, in the third part of the study we tested WS₂ on sapphire and different graphene, namely G on sapphire, G on SiC, both as-grown and H-intercalated, G-CVD transferred on glass, to assess the effect of the production method on neutrophils and MSCs⁹.

We first characterized neutrophil activation and discussed how material properties influenced the NETs production and adhesion to the substrates. Furthermore, G resistance to NETs-induced degradation was carefully investigated and compared with the results reported for graphene oxide¹⁰. Ultimately, 2D materials cytocompatibility for MSCs are tested to estimate cell viability, morphology and mitochondrial health.

Overall, our results aimed at understanding the interface between 2D material and some of the key players involved in nerve injury, with special attention to the molecular mechanisms that govern axon outgrowth in neurons, a critical point for regenerative medicine.

References

- ¹Shin et al., Adv. Drug Deliv. Rev. 105: 255–74 (2016)
- ²Qian et al., NPJ Regen. Med. 6 (31) (2021)
- ³Bramini et al., Front. Syst. Neurosci. 12 (Apr): 1–22 (2018)
- ⁴Convertino et al., Front. Neurosci. 14 (Oct): 1–10 (2020)
- ⁵Convertino et al., Front. Neurosci. 12 (Jan): 1–8 (2018)
- ⁶Convertino et al., Nano Lett. 20: 3633–41 (2020)
- ⁷Keshavan et al., Cell Death Dis. 10 (569) (2019)
- ⁸Lavorato et al Int. J. Mol. Sci. 22 (572) (2021)
- ⁹Convertino et al., In preparation
- ¹⁰Huang et al., Adv. Healthc. Mater. 11 (2102439) (2022)

We acknowledge: the European Union's Horizon 2020 research and innovation programme_GA 881603; the Next Generation EU project ECS00000017 (THE); the University of Pisa under PRA 2020-2021 92.

2:30 PM BREAK

3:30 PM *SB11.03.04

Wearable Graphene Biosensors for Microfluidic Sweat AnalysisWeiGao; California Institute of Technology, United States

Wearable sweat biosensors have the potential to provide non-invasive molecular analysis toward predictive analytics and treatment. However, it is highly challenging to accurately detect low-concentration analytes in situ and manufacture high-performance flexible biosensors at large scale and low cost. In this talk, I will introduce our efforts in developing microfluidic wearable sweat biosensors based on laser-engraved graphene. Through materials and sensor design innovations, such wireless wearables can autonomously access human sweat via iontophoresis across activities and seamlessly measure a broad spectrum of analytes including metabolites, nutrients, hormones, proteins, and drugs. The clinical value of our wearable systems is evaluated through various human trials involving healthy and patient populations toward precision nutrition, mental health assessment, gout management, and systemic inflammation monitoring. I will also discuss our research progress on energy harvesting from the human body and the environment to realize battery-free wireless wearable biosensing. These wearable technologies could open the door to a wide range of personalized monitoring and diagnostic applications.

4:00 PM SB11.03.05

Wearable and Implantable Bioelectronics Enabled by 2D Materials-Based Layer TransferJihoShin¹, YeonginKim², Jun MinSuh¹, HyunseokKim¹, SureshSundaram³, Young JoonHong⁴, AbdallahOugazzaden³ and JeehwanKim¹; ¹Massachusetts Institute of Technology, United States; ²University of Cincinnati, United States; ³Georgia Tech Lorraine, France; ⁴Sejong University, Korea (the Republic of)

2D materials-based layer transfer (2DLT) is an emerging lift-off technique for producing large-area freestanding single-crystalline epitaxial films, which offer high electronic/optoelectronic performance and ultrathin form factor that are essential for wearable and implantable bioelectronic device applications. Single-crystalline III-V/III-N compound semiconductor membranes can be epitaxially grown on substrates coated with 2D materials such as graphene or boron nitride, which results in weak van der Waals interface that facilitates mechanical exfoliation of the device layer from wafer [1]. In this talk, I will discuss our recent efforts that utilize 2DLT to build: (i) chipless wireless electronic skins based on gallium nitride surface acoustic wave sensors capable of low-power and high-sensitivity detection of a broad range of external stimuli [2], and (ii) 3D-integrated micro-LED heterostructures that achieve extremely high device densities

and suggest potential applications in optoelectronic-based neural interfaces [3].
[1] Y. Kim *et al.*, *Nature* 544, 340 (2017). [2] Y. Kim *et al.*, *Science* 377, 859 (2022). [3] J. Shin *et al.*, *Nature*, 614, 81 (2023).

4:15 PM *SB11.03.06

Biointegrated Interfaces with Carbon Nanostructures [Maurizio Prato](#)^{1,2}; ¹Università Degli Studi di Trieste, Italy; ²CIC biomaGUNE, Spain

Nanostructured interfaces can be shaped for the molecular control of physical/chemical adsorption, with enhanced surface area to promote interfacial chemistry, nano-catalysis, and bio-inspired interfaces. For instance, connecting nanostructured materials to biological compartments is a crucial step in prosthetic applications, where the interfacing surfaces should provide minimal undesired perturbation to the target tissue. Ultimately, the (nano)material of choice has to be biocompatible and promote cellular growth and adhesion with minimal cytotoxicity or dis-regulation of, for example, cellular activity and proliferation. In this context, carbon nanomaterials, including nanotubes and graphene, are particularly well suited for the design and construction of functional interfaces. This is mainly due to the extraordinary properties of these novel materials, which combine mechanical strength, thermal and electrical conductivity. Our group has been involved in the organic functionalization of various types of nanocarbons, including carbon nanotubes, and graphene. The organic functionalization offers the great advantage of producing soluble and easy-to-handle materials. As a consequence, since biocompatibility is expected to improve upon functionalization, many modified carbon nanomaterials may be useful in the field of nanomedicine. In particular, we have recently shown that carbon nanotubes and graphene can act as active substrates for neuronal growth, a field that has given so far very exciting results. Nanotubes and graphene are compatible with neurons but, especially, they play a very interesting role in interneuronal communication. Improved synaptic communication is just one example. During this talk, we will discuss the latest and most exciting results obtained in our laboratories in these fast developing fields.

4:45 PM *SB11.03.07

Heterogeneous Integration of 2D Sensors for Wearable and Healthcare Applications [Christian Lopez Angeles](#), [Yiyue Luo](#), [David Morales Loro](#), [Jiadi Zhu](#), [Mantian Xue](#), [Wojciech Matusik](#), [Jing Kong](#) and [Tomas Palacios](#); MIT, United States

The next wave of innovation and business opportunities related to electronics will probably be about enabling “edge intelligence”. These are new microsystems with unprecedented levels of autonomy in terms of energy harvesting, sensing and information processing. Heterogeneous integration of new materials will be necessary to provide these microsystems with functionality not possible today in Si chips alone. This talk will discuss a few examples of how edge intelligence enabled by the use of two-dimensional (2D) materials will impact wearable devices for healthcare applications. The first example uses metallic fibers coated with a graphitic material to embed hundreds of pressure sensors on fabrics and garments. These sensors are then coupled to an RF harvesting chip based on a MoS₂ rectifier to enable autonomous sensing of people’s movements. A second example uses arrays of hundreds of graphene-based chemical sensors inside a breathalyzer chamber to analyze the volatile organic compounds in patients’ breath. Finally, the low temperature synthesis of MoS₂ allows for the integration of high performance devices based on this material on flexible polymer substrates for the development of flexible and active electrodes for electrophysiology.

Acknowledgement.- This work has been partially supported by the MIT/Army Institute for Soldier Nanotechnologies, the NSF Center for Integrated Quantum Materials, Ericsson, and the Army Research Office.

SESSION SB11.04: Poster Session
Session Chairs: Nicolette Driscoll, Dmitry Kireev and Duygu Kuzum
Wednesday Afternoon, November 29, 2023
Hynes, Level 1, Hall A

8:00 PM SB11.04.01

Two-Dimensional Cs₂AgBiBr₆-Based Biosensor for the Sensitive Detection of Cardiac Biomarkers [Yin-Cheng Lu](#)¹, [Evan Darius](#)¹, [Mei-Chin Lien](#)¹, [I-Hsiu Yeh](#)¹, [Hung-Wen Chen](#)¹, [Ching Yuan Su](#)², [Ru-Yin Hsu](#)³ and [Keng-Ku Liu](#)¹; ¹National Tsing Hua University, Taiwan; ²National Central University, Taiwan; ³National Taiwan University Hospital Hsinchu Branch, Taiwan

Inspired by graphene and transition metal dichalcogenides, 2D layered materials that possess excellent electronic, optical, physical, and chemical properties have been actively investigated and explored to further expand their applications. In particular, 2D lead-free double perovskite with strong quantum confinement and excellent electronic performance are promising for optoelectronic applications. Owing to its nontoxicity, inherent stability, and high optical and electrical sensitivity, 2D lead-free double perovskite has attracted significant research interests. Cardiac troponin I (cTnI), a protein with molecular weight of 23.8 kDa, plays an important role as the regulator that is involved in the process of skeletal and cardiac muscle contraction. Owing to its superior cardiac specificity and selectivity, cTnI has been widely employed as the biomarker for the detection of myocardial damage and risk stratification in acute myocardial infarction (AMI) patients. In this study, we report the synthesis of 2D layered Cs₂AgBiBr₆ and the fabrication of biological sensors based on plasmonic nanomaterials-decorated 2D Cs₂AgBiBr₆ for the sensitive detection of cardiac biomarker, cTnI.

8:00 PM SB11.04.02

Enhancing Mechanical Strength of Wearable Microneedles using Silica Nanoparticle Coatings [Hyewon Choi](#), [Sohyun Kim](#) and [Hyunsik Yoon](#); Seoul National University of Science and Technology, Korea (the Republic of)

Wearable medical devices are currently being developed for a wide range of healthcare systems, and microneedles (MNs) have emerged as promising transdermal delivery systems due to their painless and non-invasive characteristics. Polymers are commonly used as MN materials because of their simple, low-cost fabrication, and biocompatibility. However, their mechanical strength may be insufficient compared to metals and ceramics, resulting in potential penetration failures that can leave fractured MNs under the skin, leading to unsuccessful delivery. Therefore, enhancing the mechanical strength of polymeric MNs is essential. In this study, we employed silica (SiO₂) nanoparticles (NPs) and poly(diallyldimethylammonium chloride) (PDADMAC) through a Layer-by-Layer (LbL) assembly on MNs. Subsequently, we applied hydrothermal (HT) treatment to sinter the coated silica NPs, thereby increasing the mechanical stability of the thin film. Initially, we conducted dye loading and release tests using fluorescent dyes, which demonstrated that MNs coated with the LbL thin film and LbL/HT-treated MNs exhibited significantly higher loading and release efficiency compared to unmodified MNs. This improvement was attributed to the increased surface area facilitated by the silica NPs coating. Additionally, we assessed the mechanical properties of MNs through abrasion and penetration tests, revealing that silica NPs-coated MNs showed higher mechanical stability, which was further enhanced after the HT treatment. The LbL system described in this study holds great potential for application in various three-dimensional structures, including MNs, which will contribute to the advancement of wearable drug delivery systems.

8:00 PM SB11.04.03

Folic Acid-Gold Nanoparticle@MoSe₂ for Targeted Photothermal Cancer Therapy [Chang Hyeon Ha](#), [Han Been Lee](#), [Se Hwa Cheon](#), [Su Jeong Lee](#), [Do Hyeon Kim](#) and [Gi hun Seong](#); Hanyang University, Korea (the Republic of)

Transition Metal Dichalcogenides (TMDs) have recently emerged as novel 2D materials, possessing significant electrical, mechanical, and optical properties. These materials consist of a single metal combined with two chalcogens (known as dichalcogenides), and their unique characteristics are determined by the specific elements comprising them. Moreover, TMDs exhibit gifted potential for clinical applications, thanks to their remarkable photothermal capabilities. Photothermal and photodynamic therapies (PTT and PDT) represent notable light-based treatment modalities. PTT involves generating heat through light-to-heat conversion, while PDT involves inducing the production of Reactive Oxygen Species (ROS) using light-sensitive agents. These therapies have gained significant attention in the field of cancer therapy due to their sensitivity and usefulness. Among these approaches, PTT has garnered interest due to the high light-to-heat conversion capability of TMDs. However, relying solely on TMDs may not be sufficient for effective therapy. Therefore, we have incorporated gold nanoparticles (AuNPs) to enhance the PTT potential of TMDs through spontaneous reduction. AuNPs possess biocompatible properties, exhibit photothermal capabilities through Localized Surface Plasmon Resonance, and can be easily modified. As a result, they can be effectively utilized as clinical materials in conjunction with TMDs. To specifically target cancer cells, we have additionally introduced Folic acid (FA). FA is an artificial molecule that closely mimics natural folate, enabling it to bind with folate receptors present in the cellular membrane. This targeted approach allows for precise cancer cell localization, particularly in cases of folate receptor-overexpressed cancer, such as Triple Negative Breast Cancer (TNBC). TNBC, which lacks the widely utilized targeting receptor and carries a high risk of metastasis, exhibits significant potential for successful cancer targeting utilizing FA. In this study, we synthesized complex materials for PTT by coating MoSe₂ with AuNPs and FA (FA-Au@MoSe₂, FAM). Glycyrrhizic acid was utilized to exfoliate bulk MoSe₂ into 2D monolayers. This exfoliation process induced a transition from an indirect to a direct-band gap, enhancing the PTT capabilities of the TMDs. MoSe₂ was selected as the primary TMD due to its well-known high light-to-heat transfer properties in PTT applications. AuNPs were employed as enhanced photothermal agents. To modify the gold surface, cysteine was used and FA was linked to the gold surface through EDC/NHS coupling. Lastly, MDA-MB-231 breast cancer cells, known for their folate receptor overexpression, were used as the target cells since MDA-

MB-231 cells are representative of TNBC.

The deposition of AuNPs and FA led to an increase in both size and surface charge. This was confirmed by the UV-visible spectra, which exhibited peaks corresponding to AuNPs and FA. SEM and TEM images demonstrated the presence of AuNPs on the surfaces of TMDs. Consequently, the successful synthesis of FAM was achieved. Regarding biocompatibility and PTT, the temperature elevation reached a level sufficient for PTT within biocompatible concentrations. Furthermore, FAM exhibited a significantly greater effect compared to MoSe₂, indicating that AuNPs effectively enhanced the PTT capability of MoSe₂. Specifically, FAM demonstrated non-toxicity to cells at a concentration of 30 µg/mL, similar to MoSe₂, but displayed a higher therapeutic effect when exposed to a NIR laser (808 nm, 0.8 W cm⁻²). These findings, confirmed by WST-1 assay and calcein-AM staining, highlight the biocompatibility and photothermal ability of FAM. As a result, this easily synthesized 2D material, achieved through simple sonication and stirring processes, has exhibited remarkable biocompatibility, photothermal activity, and targeting capability. These findings position it as a promising candidate for utilization in cancer therapy.

8:00 PM SB11.04.04

Biocompatible Molybdenum Diselenide Nanosheets: A Two-Dimensional Nanomaterial for Near-Infrared Photothermal Cancer Therapy [Su JeongLee](#), Se HwaCheon, Han BeenLee, Chang HyeonHa, Do HyeonKim and Gi hunSeong; Hanyang University, Korea (the Republic of)

Transition metal dichalcogenide (TMD) nanosheets are two-dimensional (2D) nanomaterials composed of layered structures. In the 2D TMD structure, denoted as 'X-M-X', two layers of X chalcogen atoms (such as S or Se) are sandwiched between a layer of M transition metal atoms (such as Mo or W). The interaction between adjacent layers in the nanosheet structure is driven by van der Waals forces. These forces play a crucial role in holding the layers together and are essential for the development of the band structure. 2D TMD possesses outstanding optical, electronic, mechanical, and thermal properties due to its adjustable band gap and interaction with light. Consequently, they have gained significant attention in recent years for applications in electronic devices, energy storage, and photothermal therapy.

Among various TMDs, molybdenum diselenide (MoSe₂) has emerged as a prominent focus of research due to its remarkable chemical and physical properties. Notably, when MoSe₂ transitions from multiple layers to a single layer, its electronic bandgap undergoes a significant change from an original indirect bandgap of 1.1 eV to a direct bandgap of 1.55 eV. As a result, single-layer MoSe₂ represents a novel semiconductor material that exhibits strong light absorption in the proximity of the band-gap energy.

In this study, we employed an inexpensive liquid exfoliation method to fabricate MoSe₂ nanosheets. This approach enables high-yield production and renders the nanosheets suitable for application in photothermal cancer therapy. To disperse MoSe₂ in water, we utilized glycyrrhizic acid (GA), an amphiphilic natural surfactant from licorice root, as the exfoliating agent. Notably, this study marks the first instance of GA being used as an exfoliating agent for preparing nanosheets. Additionally, we enhanced biocompatibility and intracellular uptake by conjugating polyethylene glycol (PEG), resulting in PEG-modified GA-MoSe₂ (PGM) nanosheets.

The successful exfoliation utilizing GA was confirmed by SEM and TEM analysis, revealing the presence of monolayer nanosheets. The PEGylation of the nanosheets was validated through an observed increase in size and zeta potential. Thermogravimetric analysis (TGA) results demonstrated the thermal stability of PGM as a material. Furthermore, UV-visible spectra of PGM exhibited an absorption peak at 808 nm, and when PGM was subjected to NIR laser irradiation (808 nm, 0.8 W cm²), they demonstrated the highest photothermal effect. Based on these findings, PGM was identified as a promising agent for photothermal cancer therapy, offering a minimally invasive treatment option with reduced side effects.

To assess the cytotoxicity and anticancer potential of PGM in MDA-MB-231 human breast cancer cells, we conducted a WST-1 assay and a live-dead cell staining assay. The PGM group without laser irradiation displayed remarkably high cell viability at 98.6%, whereas the group subjected to laser irradiation exhibited viability of 22.7%, indicating a substantial inhibitory effect on cancer cells. Additionally, PGM demonstrated significantly higher intracellular uptake. Subsequently, we directly administered PGM to a breast cancer-bearing mouse model to evaluate its in vivo anticancer effect. Tumors exposed to Near Infrared (NIR) laser exhibited a notable decrease in size or complete disappearance, and no significant weight loss was observed during the treatment period.

The findings obtained from experiments strongly indicate that PGM possesses minimal cytotoxicity and holds great promise as a valuable biomaterial for cancer therapy, particularly in harnessing the photothermal effect of PGM through hyperthermia. Building upon these results, our future objectives include incorporating anti-cancer drugs into PGM to develop drug delivery platforms, as well as directly fabricating PGM scaffolds for transplantation at the target site, thereby enabling effective implementation of photothermal cancer therapy.

8:00 PM SB11.04.05

Synthesis of Transition Metal Dichalcogenides Nanosheets and its Application to Photothermal Immunoassays [Do HyeonKim](#), Chang HyeonHa, Han BeenLee, Su JeongLee, Se HwaCheon and Gi hunSeong; Hanyang University, Korea (the Republic of)

Two-dimensional nanomaterials, including graphene, transition metal oxides, and carbon nitrides, have gained significant attention due to their large surface area, mechanical properties, and unique electro-optical characteristics. Among these materials, transition metal dichalcogenides (TMDs) have emerged as particularly promising in biosensing, electronics, and photothermal therapy, due to their distinctive properties. Most TMDs feature an MX₂-type structure, where M represents transition metals like Mo and W, and X represents chalcogenides such as S, and Se. TMDs exhibit a sandwich-like structure, with hexagonal planes of transition metal atoms separating the chalcogen atoms.

TMD, a two-dimensional semiconductor material, exhibits unique electrical, mechanical, and optical properties. One of its most notable characteristics is the photothermal effect. TMD demonstrates the ability to absorb light in the near-infrared region and convert it into heat. Monolayer TMD, in particular, possesses enhanced photothermal capabilities compared to multi-layered TMD, thanks to its altered band gap. The transition from an indirect to a direct band gap occurs when TMD forms monolayers. This transition facilitates more efficient electron transfer and shifts the band gap position from the infrared to the near-infrared region. Consequently, the change in the band gap enables higher photothermal efficiency at near-infrared wavelengths.

To obtain a monolayer of TMD, various methods including mechanical separation and chemical vapor deposition have been employed. However, these methods suffer from drawbacks such as high costs and time consumption. In contrast, the liquid exfoliation method offers a simple and cost-effective approach for producing monolayers. Traditionally, organic solvents have been used in the liquid exfoliation. However, by utilizing glycyrrhizic acid (GA), a natural compound, deionized water can be employed as a solvent. The inclusion of GA in the liquid exfoliation weakens the van der Waals forces between the TMD layers, simultaneously serving as a stabilizer and enhancing the colloidal stability of the resulting TMD monolayer.

Lateral Flow Immunoassay (LFIA) is a powerful method used for the analysis of target molecules. It offers several advantages, including simplicity and short assay times. In general, LFIA utilizing gold nanoparticles (AuNPs) as a colorimetric indicator demonstrates high sensitivity in detecting target molecules. However, there remains a challenge in further enhancing the sensitivity of LFIA. Therefore, novel approaches are necessary to overcome this challenge and achieve increased sensitivity.

In this study, we synthesized monolayer MoSe₂ and investigated its application in a photothermal-based LFIA. The MoSe₂ nanosheets were successfully obtained through GA-mediated liquid exfoliation, as confirmed by TEM images showing well-dispersed monolayers. UV-vis spectra of GA-MoSe₂ exhibited an absorption peak at 808 nm, within the near-infrared region.

Subsequently, we irradiated GA-MoSe₂ with a NIR laser at 808 nm and observed an increase in temperature, validating its role as a photothermal agent.

To develop a detection probe for the LFIA, we conjugated GA-MoSe₂ with goat-anti mouse immunoglobulin G (IgG) antibodies, resulting in GA-MoSe₂/mAb. In the immunoassay, as GA-MoSe₂/mAb interacted with IgG and reached the test line, the capture antibody on the test line bound to the conjugate, producing a distinct color line. The intensity of the test line's color increased with the IgG concentration. Additionally, the temperature change associated with laser irradiation also increased with increasing IgG concentration. These results suggest that GA-MoSe₂ holds the potential to serve as a platform for high-sensitivity photothermal LFIA. Looking ahead, the utilization of TMDs as photothermal agents is expected to open up various applications, including biosensors for diagnosing virus infections and wearable sensors.

8:00 PM SB11.04.06

Structural Deformation using Metal Deposition for Bio-Adhesive Patch [ChorongKim](#), JaekyuongKim and HyunsikYoon; Seoul National University of Science and Technology, Korea (the Republic of)

Recently, adhesive patches have been studied for medical treatment. Depending on their characteristics, these can be applied in various situations such as wound healing, drug delivery, and biosensor attachment. Given that the body is a moist environment, current research focuses on incorporating chemical adhesives or utilizing structural properties for surface attachment such as suction effects. Additionally, liquid-repellency is essential to prevent the risk of detachment caused by wetting. We adopted structural adhesives to avoid allergic reaction due to toxicity of chemical adhesives. This research presents a method of structural deformation through different metal deposition on hyperbola structure to achieve new properties such as wet adhesion (Au) or liquid-repellency (Al). Hyperbola structures were fabricated by wrapping liquid prepolymer around micropillars driven by capillary force. Due to its flexible edges, the metal, deposited on top surface, caused structural deformation depending on its residual stress. In the case of Au, tensile stress of Au thin film made edges shrink inward, created an empty space inside for adhesive behavior. Conversely, in the case of Al, edges expanded outward because of compressive stress of Al thin film caused by oxidation. So, this structure had more liquid-repellency characteristics. These novel structures can be easily replicated and mass-produced using soft lithography, offering the advantage of non-allergic reactions as no additional adhesives are required. Furthermore, deformation can be easily controlled by adjusting the deposition thickness and Young's modulus of the structure's material. This technology is expected to contribute to the medical industry as for skin/organ-attachable patches.

8:00 PM SB11.04.07

Improving Stability of Nickel Hydroxide/Oxyhydroxide Visible Light-Induced Actuators by Aluminum Doping [NanHe](#); University of Hong Kong, Hong Kong

Material-based actuation systems have been an emerging field of interest because of their direct and simple mechanism without the need to use bulky and complicated hydraulic, electric or magnetic motors. Material-based actuators utilize external stimuli such as light, temperature or humidity to drive mechanical movements. In recent research studies, transition metal

oxides/hydroxides (TMOs) were introduced and studied for light-induced actuation based on their simple and effective photothermal mechanism for water de-intercalation from the turbostratic crystal structures of these materials. Turbostratic phases of nickel hydroxide/oxyhydroxide (NHO) have been found to be high-performing multi-stimuli driven actuating materials. However, these material phases are known to be unstable, and over time they become crystallized and lose their actuating properties. In this work, aluminium doping is used to stabilize the turbostraticity and actuation performance. Visible-light actuation experiments are conducted on NHO samples with and without aluminium doping to characterize their actuation performance over time. Turbostraticity is examined and quantified by techniques including XRD, Raman spectroscopy and high resolution TEM, via information such as d-spacings, intensity ratio and band peak changing. The turbostraticity difference between aluminium-doped and pure NHO actuators is correlated with their actuation performances.

8:00 PM SB11.04.08

Injectable Neural Sensor Array for Post-Surgery Brain Monitoring [Kyungtae Park](#), Juyeong Hong, Jejung Kim and Jong-Hyun Ahn; Yonsei University, Korea (the Republic of)

Brain diseases, such as epilepsy and traumatic brain injury, affect millions of people worldwide, causing severe side effects. Monitoring postoperative seizures and the recovery of brain function after surgery is crucial for diagnosing and treating these conditions, providing vital information. However, conventional neural implants involve a large-area craniotomy and rely on bulky sensors, which restrict the natural movement of patients. In this study, we present an injectable neural sensor array for monitoring the brain after surgery. The device utilizes a thin and flexible mesh-structured substrate that can be injected onto the cortical surface through a small hole, minimizing the invasiveness. This approach allows the 12mm diameter device to spread out from a 2mm diameter syringe and achieve conformal contact with the surface of the cortex. The device performs neural recording and micro-stimulation for seizure alleviation using multichannel electrocorticography (ECoG) electrodes and a stimulation pad. Additionally, it integrates a sensor array for multimodal sensing of intracranial pressure (ICP) and intracranial temperature (ICT). This technology provides a convenient healthcare solution for the comprehensive assessment of the patient's post-surgery brain condition.

8:00 PM SB11.04.09

The Development of Choline, Calcium and pH Sensors based on Laser-Inscribed Graphene Electrodes [Abdulrahman Al-Shami](#), Ali Soleimani, Farbod Amirhasemi, Victor Ong, Sina Gharahtekan and Maral Mousavi; University of Southern California, United States

Introduction: Graphene, a two-dimensional layer of carbon atoms arranged in a hexagonal lattice, has gained significant attraction in electrochemical biomedical sensors. Graphene exhibits high electrical conductivity, flexibility, and a high surface-to-volume ratio. That makes graphene ideal for developing sensitive, selective, reliable, precise, and accurate sensing platforms for detecting biomarkers and other substances. Another interesting feature of graphene is its high hydrophobicity. This property is important for developing solid contact potentiometric sensors for quantifying biologically important ions. This is because the hydrophilic electrodes allow the formation of a water layer between the electrode surface and the ion-selective membrane, which adversely affects the sensor's sensitivity and selectivity toward the targeted ion. Graphene is conventionally produced by wet chemistry and chemical vapor deposition which are usually complicated, expensive, and labor-intensive. Producing graphene by laser engraving on carbon-rich materials (mostly in the form of repeated aromatic rings) is an attractive approach to overcome the limitations of conventional production methods. The laser-engraving method is simple, precise, cost-effective, fast, scalable, safe, and highly reproducible. In this work, we produced graphene electrochemical electrodes using laser engraving technology. We characterized the produced graphene and employed the electrodes to develop three different sensors for detecting choline and calcium ions and pH levels for human and animal health applications. Choline is a vital infant nutrition factor, supporting brain and nervous system development and functions. Quantifying choline in infant formulas can ensure that infants receive enough choline to grow healthy. The calcium sensor will be used to detect calcium levels in cows' blood, which is important for diagnosing calcium imbalances in dairy cows and preventing milk fever. The pH sensor helps monitor different physiological processes, such as wound healing.

Methods: We produced the electrochemical electrodes by ablating a polyimide film (127 μm thickness) using a CO₂ laser cutter machine with a 1060 nm laser wavelength. The engraving was conducted with an auto-focused laser beam with power and speed of 3 W and 105 mm/s, respectively. A choline-selective membrane was produced of a mixture of PVC (structural polymer), o-nitrophenyl-octyl-ether (plasticizer), Sodium tetrakis[3,5 bis(trifluoromethyl)phenyl]borate (ionic site), and Calix 4 arene (ionophore) in THF solvent. The membrane was cast on the electrode surface and dried overnight before measurements. The calcium selective membrane was prepared in the same way as choline but used as an ionophore. The graphene electrode was electrochemically modified for pH sensing by layers of IrO₂ NPs. The deposition solution was prepared from IrCl₄ using alkaline hydrolysis followed by acidic condensation. The deposition was conducted using cyclic voltammetry in a potential window between 0.6 to 0.65 V for 300 cycles.

Results and discussion: the laser engraving method successfully produced flexible electrochemical electrodes. The scanning electron microscopy images of the laser-engraved areas demonstrated the formation of three-dimensional highly porous graphene on the PI film. Raman spectroscopy revealed the formation of multiple graphene layers on the PI film with some defects that can be attributed to the presence of oxygen during the engraving in ambient conditions. The graphene-based choline selective electrode demonstrated Nernstian response toward choline ions with a detection limit of 0.1 mM. Also, the sensor could quantify choline concentration in commercially available infant formulas with a measurement error of less than 5%. The calcium-selective electrode exhibits high sensitivity with a detection limit of 0.01 mM. IrO₂-modified graphene electrode demonstrates a linear response in pH values between 4 and 10.

8:00 PM SB11.04.10

Measuring Electrodermal Activity Underwater using Graphene Electronic Tattoos [Wendy Rossi](#)¹, Ning Liu¹, Dmitry Kireev² and Deji Akinwande¹; ¹The University of Texas at Austin, United States; ²University of Massachusetts Amherst, United States

Oxygen, while essential for human function, can be harmful in the context of underwater diving. Divers, to stay safe underwater, need to breathe pure, pressurized oxygen known as hyperbaric oxygen; however, breathing too much of this hyperbaric oxygen at certain depths and pressures risks the development of Central Nervous System Oxygen Toxicity (CNS-OT). CNS-OT can lead to sympathetic overstimulation and cause seizures, which are due to abnormal electrical activity in the brain. Electrodermal Activity (EDA) is a quantitative index of sympathetic nervous system activity measured through changes in skin conductance, which vary according to sweat levels caused by emotional arousal or stress. A significant surge in EDA amplitude is a precursor to epileptic seizures and used as an early indicator for CNS-OT risk. Developing a method to identify the onset of CNS-OT risk underwater means introducing a safety monitoring approach previously unavailable in diving. Currently, commercial EDA devices, while effective, lack the flexibility and wearability of GETs and are not waterproof. We propose a graphene electronic tattoo (GET) capable of EDA data processing while immersed in saltwater conditions through a four-part experimental process. First, we established a control group by measuring bioimpedance with uncovered GETs in air, DI water, and saltwater. Next, we found the best waterproofing sealant by comparing the baseline measurements of bare GETs to GETs covered individually by three sealants. After finding that Nexcare SkinCrack Care (NCC) produced the clearest bioimpedance readings in each condition, we used this sealant for electrocardiogram measurements in the same fluid conditions to validate our GETs capacity for underwater measurements. Finally, we took EDA measurements using a Neulog device by simulating three emotional states: meditative, focused, and stressed through meditation, boring videos, and horror videos. We established an EDA baseline using the commercial electrodes in each emotional state in air then proceeded to measure EDA with our GET sealed by NCC in the conditions of air, DI, and saltwater. The maximum stimulated EDA change obtained by our graphene electrodes in saltwater is 0.217 μS with a response time of 4 seconds, which is comparable to the commercial electrodes in air with a similar response time. As a result, we find that the combination of NCC and a GET enabled successful EDA monitoring in seawater conditions, advancing GETs in underwater medicine.

8:00 PM SB11.04.11

3D-Printed Electronic Skin for Machine Learning-Powered Multimodal Health Surveillance [Yu Song](#) and Jihong Min; California Institute of Technology, United States

The amalgamation of transdisciplinary wearable technologies with physiochemical sensing capabilities and artificial intelligence promises to create powerful interpretive and predictive platforms for real-time health surveillance and accurate early diagnosis. However, construction of such multimodal devices involves multi-material processing and complex fabrication procedures that are difficult to be implemented wholly by traditional manufacturing techniques for at-home personalized application. Here, we present a universal semi-solid extrusion (SSE)-based 3D printing technology to fabricate an epifluidic elastic electronic skin (e³-skin) with high-performance multimodal physiochemical sensing capabilities. The all-SSE printed wearable e³-skin is equipped to track vital signs (i.e., heart rate and temperature), analyze key biomarkers in sweat (i.e., glucose and alcohol), and is integrated with an energy storage module designed for untethered battery-free operation. We demonstrate that the e³-skin can serve as a sustainable surveillance platform to capture real-time physiological state of individuals while performing regular daily activities such as diet challenges and strenuous exercises. We also featured at a pilot study that by coupling the information collected from the e³-skin with machine learning, we were able to predict with over 90% accuracy an individual's degree of behavior impairments (i.e., reaction time and inhibitory control) after alcohol consumption. The e³-skin paves the path for future autonomous manufacturing of customizable wearable systems which will enable widespread utility for regular health monitoring and clinical applications.

8:00 PM SB11.04.12

Scalable Fabrication of Soft MXene-Coated Fiber Microelectrodes for Bio Interfacing [Lingyi Bi](#)¹, Raghav Garg², Natalia Noriega³, Ruocun (John) Wang¹, Kseniia Vorotilo¹, Justin Burrell², Hyunho Kim¹, Christopher E. Shuck¹, Anh Le², Flavia Vitale², Bhavika A. Patel³ and Yury Gogotsi¹; ¹Drexel University, United States; ²University of Pennsylvania, United States; ³University of Brighton, United Kingdom

The development of flexible fiber-based microelectrodes opens up opportunities for long-term studying and modulating neural activities and diseases by increasing targeting precision while inducing fewer side effects, thanks to the minimized mechanical mismatch between artificial devices and soft tissues. However, the current manufacturing of such microfabrication faces scalability, reproducibility, and handling challenges, making large-scale deployment of fiber-based microelectrodes difficult. Moreover, few designs allow capturing both electrical and chemical signals, which are necessary for understanding and interacting with complex biological systems.

Here, we report a novel method that leverages the unique combinations of electrical conductivity, functional surfaces, and solution processibility of MXenes, a large family of 2D nanomaterials, to apply a thin layer of MXene coating continuously to commercial nylon filaments (30-300 μm in diameter) at a fast speed (up to 15 mm/s), resulting in a resistance down to 15 Ω/cm . The MXene-coated filaments can be batch-fabricated into arrays of fiber electrodes, encapsulated with Parylene C, and exposed only at the tip upon application for localized detection and stimulation. We demonstrated the usability of these multifunctional fiber electrodes for both *in-vivo* and *ex-vivo* studies, including neuromodulation and electrical sensing in a rat and H_2O_2 chemical sensing in bladder cells. These electrodes offer excellent performance, significantly simplified use, and improved flexibility (with no performance changes even when knotted). These versatile MXene filament microelectrodes offer a robust, miniaturized platform for monitoring and stimulating neural activities, facilitating a deeper understanding of health and disease.

SESSION SB11.05: 2D Transistors as Biosensors
Session Chairs: Jose Garrido and Dmitry Kireev
Thursday Morning, November 30, 2023
Hynes, Level 1, Room 101

8:30 AM +SB11.05.01

CRISPR-Powered Graphene Electronics for CRISPR Editing Quality Control [Kiana Aran](#); Keck Graduate Institute, United States

The discovery of CRISPR technology has revolutionized the fields of transcriptional activation and repression, genome editing, gene-based therapeutics, and diagnostics. The applications of this technology have been rapidly expanding as researchers continue to discover new Cas enzymes, engineer high fidelity Cas orthologs, and modify and synthesize guide RNAs to efficiently direct these Cas enzymes to their targets. In this talk, we will introduce the first-generation DNA biosensors that combine CRISPR technology with the ultra-sensitivity of graphene-based field effect transistors (gFETs) to detect target DNA sequences within the whole genome without the need for DNA amplification. This technology, termed CRISPR-ChipTM, utilizes the genome searching capability of Cas and reprogrammable RNA molecule to unzip the double-stranded DNA and bind to its target. This binding event causes a change in graphene conductivity which can be detected in real-time within the gFET construct. CRISPR-Chip was utilized to detect target genes within clinical samples obtained from patients with Duchenne Muscular Dystrophy (Cover of Nature BME-2019), and single cell point mutations in Sickle cell disease and ALS without the need for amplification (Nature BME 2021), within less than 30 minutes. The applications of this technology platform go beyond diagnostics. CRISPR-Chip can provide greater insights on the mechanism of CRISPR and can lead to safe and more effective utilization of this gene editing technology for therapeutic applications. By precisely predicting CRISPR editing outcomes based on key drivers of success like RNP stability and cleaving activity, the CRISPR-Chip enables us to confidently identify the best gRNAs, Cas proteins, and conditions for CRISPR gene editing experiment from the outset.

9:00 AM SB11.05.02

Microneedle Graphene Field-Effect Transistors for Wearable Biosensing [Martin Holicky](#)¹, [Benji Fenech Salerno](#)¹, [Anthony E. Cass](#)¹ and [Felice Torrisi](#)^{1,2}; ¹Imperial College London, United Kingdom; ²Universita' di Catania, Italy

Microneedle-based biosensing provides an attractive path towards continuous health monitoring - the use of microneedles causes substantially lower pain to the user than traditional hypodermic needles while providing accurate sensing information [1]. Due their small footprint and ease of application, such biosensors are easily worn with minimal nuisance to the user, enabling wearable health sensing anywhere and at any time. Graphene and other two-dimensional materials have emerged as a suitable platform for high performance printed electronics, enabling graphene field-effect transistors (GFETs) on ubiquitous substrates [2,3]. We have recently developed a scalable method for creating high resolution GFETs through spray-coating [4] and demonstrated their use in biosensing.

In this work, a new type of sensor is created by forming the GFETs directly on the tips of polycarbonate microneedles to enable biosensing of interstitial fluid within the skin. The GFETs are formed on the three-dimensional needles through a scalable combination of laser lithographic patterning and spray-coating and uses injection-moulded polycarbonate microneedles. The graphene channels are approximately 2000 μm wide and 80 μm long, with a resistance of 150 Ohms and display characteristic ambipolar modulation under solution gating. We fully characterise the sensors through microscopic and electrochemical methods and demonstrate their biosensing properties through in solution and in-vitro skin measurements. The results demonstrate a new class of sensors that can take advantage of the FET signal amplification directly in situ and enable the development of more sensitive and accurate microneedle biosensors in the future.

[1] Teymourian H., et al., *Advanced Healthcare Materials*, 2021, 2002255

[2] Carey T., et al., *Nature Communications*, 2017, 8, 1202

[3] Carey T., et al., *Advanced Electronic Materials*, 2021, 7, 7

[4] Fenech-Salerno, B., et al., *Nanoscale*, 2023, 15, 3243-3254

9:15 AM SB11.05.03

Microneedle-Based Potentiometric Sensing System for Continuous Monitoring of Multiple Electrolytes in Skin Interstitial Fluids [Huijie Li](#) and [Yi Zhang](#); University of Connecticut, United States

Electrolytes play a pivotal role in regulating cardiovascular functions, hydration, and muscle activation. The current standards for monitoring electrolytes involve periodic sampling of blood and measurements using laboratory techniques, which are often uncomfortable/inconvenient to the subjects and add considerable expense to the management of their underlying disease conditions. The wide range of electrolytes in skin interstitial fluids (ISFs) and their correlations with those in plasma create exciting opportunities for applications such as electrolyte and circadian metabolism monitoring. However, it has been challenging to monitor these electrolytes in the skin ISFs. In this study, we report a minimally invasive microneedle-based potentiometric sensing system for multiplexed and continuous monitoring of Na^+ and K^+ in the skin ISFs. The potentiometric sensing system consists of a miniaturized stainless-steel hollow microneedle to prevent sensor delamination and a set of modified microneedle electrodes for multiplex monitoring. We demonstrate the measurement of Na^+ and K^+ in artificial ISFs with a fast response time, excellent reversibility and repeatability, adequate selectivity, and negligible potential interferences upon the addition of a physiologically relevant concentration of metabolites, dietary biomarkers, and nutrients. In addition, the sensor maintains the sensitivity after multiple insertions into the chicken skin model. Furthermore, the measurements in artificial ISFs using calibrated sensors confirm the accurate measurements of physiological electrolytes in artificial ISFs. Finally, the skin-mimicking phantom gel and chicken skin model experiments demonstrate the sensor's potential for minimally invasive monitoring of electrolytes in skin ISFs. The developed sensor platform can be adapted for a wide range of other applications, including real-time monitoring of nutrients, metabolites, and proteins.

9:30 AM *SB11.05.04

Graphene Transistors for Biosensing Applications [Amaia Zurutuza](#); Graphenea, Spain

Over the past years, extensive efforts have been placed in the research and development of graphene-based applications, as a result certain applications have experienced an increased level of maturity and achieved higher technology readiness levels (TRLs) among them is that of sensors.

Graphene's electronic and mechanical properties make it an ideal candidate to be applied in various types of sensors. The market for sensors is extremely large since it includes many industries such as automotive, electronics and healthcare industries among others. Therefore, it is an excellent starting platform for graphene applications. For example, the COVID-19 pandemic demonstrated the urgent need for fast diagnostics in order to minimise and control its effects, here, biosensors based on graphene field effect transistors (GFETs) have shown great potential as a platform for future diagnostics.

During this talk, I will cover the fabrication of graphene at wafer scale (up to 200mm) and the use of graphene in various types of sensors including ion sensors (ISFETs) [1-3], gas sensors [4] and biosensors [5].

REFERENCES

- [1] N. Tran, I. Fakih, O. Durnan, A. Hu, A. Aygar, I. Napal, A. Centeno, A. Zurutuza, B. Reulet, and T. Szkopek, *Nanotechnology*, 32 (2021) 045502.
- [2] I. Fakih, O. Durnan, F. Mahvash, I. Napal, A. Centeno, A. Zurutuza, V. Yargeau, and T. Szkopek, *Nature Commun.*, 11 (2020) 3226.
- [3] I. Fakih, A. Centeno, A. Zurutuza, B. Ghaddab, M. Siaj, and T. Szkopek, *Sens. Actuators B Chem.*, 291 (2019) 89.
- [4] M. Lind, V. Kiisk, M. Kodu, T. Kahro, R. Raabe, T. Avarmaa, P. Makaram, A. Zurutuza and R. Jaaniso, *Chemosensors* 10 (2022) 68.
- [5] A. Silvestri, J. Zayas Arrabal, M. Vera Hidalgo, D. Di Silvio, C. Weitzl, M. Martinez-Moro, A. Zurutuza, E. Torres, A. Centeno, A. Maestre, J. Manuel Gómez, M. Arrastua, M. Elcegui, N. Ontoso, M. Prato, I. Coluzza, and A. Criado, *Nanoscale* 15 (2023) 1076.

10:00 AMBREAK

SESSION SB11.06: 2D Biosensing
 Session Chairs: Nicolette Driscoll and Maurizio Prato
 Thursday Morning, November 30, 2023
 Hynes, Level 1, Room 101

10:30 AM *SB11.06.01

Mxene and Conjugated Polymer-Based Hybrid Systems for Electronic Biosensing [Sahika Inal](#); King Abdullah University of Science and Technology, Saudi Arabia

Among the existing two-dimensional materials, MXenes stand out for their excellent electrochemical properties. MXene-based inks and films hold great potential for the scalable production of skin-conformable electronics and for constructing electronic sensors and actuators that operate in physiological media. On the other hand, conjugated polymer films, due to their softness and conformability, enable seamless interfacing with the skin and cells. In this talk, I will demonstrate how the combination of soft conducting polymers and printed MXene electrodes brings together the best of both worlds for biointerfacing. The functionalized MXene films serve as multifunctional biosensing units for cation and protein sensing, as well as for capturing physiological signals. Conducting polymers act as both substrates and interconnects. In another platform, the incorporation of MXene as a co-dopant in a conjugated polymer structure results in hybrid films with remarkably high volumetric capacitance and stability. These microfabricated hybrid devices outperform their single-component counterparts in chronic biochemical sensing and stimulation applications. Our findings illustrate how MXene films can streamline the fabrication of next-generation bioelectronic platforms incorporating multimodal sensors.

11:00 AM SB11.06.02

Deformable and Stretchable EGaIn/Graphene-Based Electrochemical Biosensors [Dongwook Lee](#), Don-Hui Lee, Won-Yong Lee and Jayoung Kim; Yonsei University, Korea (the Republic of)

EGaIn has attractive properties for soft electronics, such as wearable and implantable electronic devices for healthcare applications, due to its high conductivity and deformability near room temperature. However, the formation of an insulating native oxide film of EGaIn impedes its application to soft and stretchable electrochemical biosensors. Herein, we introduce reduced graphene oxide to EGaIn to achieve electrochemical stability and excellent conductivity as well as deformable properties. Graphene oxide easily undergoes galvanic replacement reaction on the surface of EGaIn particles forming reduced graphene oxide capped EGaIn core-shell particles (LM-RGO CSPs), which can be further fabricated to patternable stretchable electrochemical biosensing devices. The resulting deformable electrodes show excellent electrochemical conductivity and stability by preventing the native oxide film growth of EGaIn, even under repetitive stretching with 30% strain without any delamination of RGO. Also, the outer layer of RGO can be further decorated with metals which can effectively catalyze enzymatic reactions for glucose biosensing. In this talk, we will discuss the deformable mechanisms of LM-RGO CSPs-based electrochemical biosensors revealing specific interfacial attractions between RGO and LM, and excellent electrochemical biocatalytic activity for sensitive glucose detection under strains, based on sub-micro sized particle characteristics and their facilitated electron transfer between electrodes and glucose oxidase enzyme. We envision such an electrochemical device system can serve as a platform for multi-modal deformable wearable biosensing devices for healthcare applications, overcoming the inherent limitations of EGaIn as a soft conductor and taking advantage of the excellent conductivity of graphene.

11:15 AM SB11.06.03

The Effect of Partially Reduced Graphene Oxide on The Enzymatic Activity of Yeast [Rebecca Isseroff](#)¹, [Sophia Bracco](#)², [Dominic Rosiello](#)², [Sergio Rosa](#)³, [Sam Specht](#)³ and [Miriam Rafailovich](#)¹; ¹Stony Brook University, The State University of New York, United States; ²South Side High School, United States; ³The Stony Brook School, United States

Enzyme biocatalysts are important for the synthesis of drugs, vitamins, and other products, but research is being done to increase their stability and activity. Previously we have found that partially reduced graphene oxide (pRGO) acts as an enzymatic enhancer for the catalytic activity of microbial transglutaminase in the cross-linking of gelatin. We now set out to determine whether graphene oxide (GO) and/or pRGO would have an effect on the enzymatic activity of yeast to decompose hydrogen peroxide, thereby testing whether these 2D materials are biocompatible with a living organism that produces an enzymatic reaction rather than just testing the effect on the enzyme itself. A solution of pRGO reduced in a concentration of 18 mM sodium borohydride, as well as an unreduced GO solution, were compared with water as a control. While initial qualitative results suggested that GO had no effect on yeast's catalytic activity, H₂O₂ decomposition seemed to be enhanced by 18 mM pRGO. However, further quantitative measurements were conducted by collecting O₂ by water displacement. Twenty milligrams of yeast were suspended in two milliliters of water containing 0.2% sucrose by weight and incubated at 41 degrees Celsius for 4 minutes. (As a third variable, twenty milligrams of yeast were suspended in two milliliters of water containing 0.2% sucrose by weight but with 0.5 ml pRGO added to the yeast + water before incubation.) Then, 5 ml of 3% H₂O₂ + 0.5 ml DI water for the control, and 5 ml of 3% H₂O₂ + 0.5 ml pRGO for the test solution, were added and the time it took to displace 25 ml of water was measured. After 5 minutes, an additional 4 ml of 3% H₂O₂ were added, and the time it took to displace 25 ml water was again measured, to determine whether the yeast maintained its activity. Results showed that yeast activated in water had the same rate of decomposition of H₂O₂ containing pRGO as the control containing no pRGO, but yeast incubated in water containing pRGO actually had a slower rate of H₂O₂ decomposition, both initially as well as retesting five minutes later by adding additional H₂O₂. Macroscopic changes observed in the pRGO-yeast include darkening of the yeast, suggesting incorporation of pRGO by the cells. Microscopic examination of pRGO-incubated yeast at various time points provides further insight on the biocompatibility of partially reduced graphene oxide with living cells.

11:30 AM *SB11.06.04

Advances in Pressure and Chemical Sensing with 2D Materials [Paolo Samori](#); University of Strasbourg, France

Physical and chemical sensor bear a direct societal impact on well-being, which includes, among others, the monitoring of human's health, the quality and composition of the air we breathe, the water we drink, and the food we eat.

Physical sensors are essential components for the fabrication of devices for medical diagnosis and health monitoring, upon use of active materials with sensitivities in the low-pressure or medium-pressure range, respectively. In this framework, flexible piezoresistive pressure sensors are compatible with wearable technologies for digital healthcare, human-machine interfaces and robotics. Among active materials for pressure sensing, graphene-based materials are extremely promising because of their outstanding physical characteristics. Currently, a key challenge in pressure sensing is the sensitivity enhancement through the fine tuning of the active material's electro-mechanical properties. We have achieved this by combining chemically reduced graphene oxide (rGO) with (macro)molecular materials with controlled mechanical properties. Among these, the use of a polybenzoxazine thermoresist matrix in combination with rGO made it possible to tailor electrically conductive nanocomposites where the thermally triggered resist's polymerisation modulates the active material rigidity and consequently the piezoresistive response to pressure. [1]

In chemical sensing higher sensitivity, faster response time and fast recovery time can be achieved by using 2D materials as active components. Instead, selectivity can be achieved either through the optimization of the energy levels of the analyte with respect of those of the active material, as demonstrated via the fabrication of sensors of heavy metals[2] or polyaromatic molecules[3], or through the functionalization of the latter with supramolecular receptors ensuring a high discrimination of ions and small molecules in the sensing event.[4] Strategies for simple integration of working devices with electrical read-outs will be presented.

References

- [1] S. Vitale et al, "Tuning the piezoresistive behaviour of graphene-polybenzoxazine nanocomposites: Towards high-performance materials for pressure sensing applications" submitted (2023)
- [2] F.J. Urbanos, S. Gullace, P. Samorì, "MoS₂ Defect Healing for High-Performance Chemical Sensing of Polycyclic Aromatic Hydrocarbons", *ACS Nano* 2022, 16, 11234.
- [3] F.J. Urbanos, S. Gullace, P. Samorì "Field-Effect Transistors Based Ion Sensors: Ultrasensitive Mercury (II) Detection via Healing of MoS₂ Defects", *Nanoscale*, 2021, 13, 19682
- [4] A. Zhuravlova, A.G. Ricciardulli, D. Pakulski, A. Gorczynski, A. Kelly, J.N. Coleman A. Ciesielski, P. Samorì, "High selectivity and sensitivity in chemiresistive sensing of Co(II) ions with liquid-phase exfoliated functionalized MoS₂: a supramolecular approach", *Small* 2023, in press

1:45 PM *SB11.07.01

Intracranial, Subcutaneous and Scalp Electroencephalography with Multiscale Arrays Based on 2D MXenes [Flavia Vitale](#); University of Pennsylvania, United States

Electroencephalography (EEG) is commonly used for neurological diagnostics and monitoring, and in neuroscience research. Depending on the application and degree of invasiveness, EEG can be acquired with gelled electrodes placed on the scalp or invasively with intracranial electrodes. Recently, subcutaneous EEG has emerged as a minimally invasive, mobile, and reliable alternative solution for long-term epilepsy monitoring and seizure forecasting.

In this talk I will present multiscale arrays for intracranial, subcutaneous, and scalp EEG based on high-throughput liquid-phase processing of 2D $Ti_3C_2T_x$ MXene. Leveraging the colloidal stability of MXenes in aqueous dispersions, we have developed a rapid fabrication process to produce EEG arrays with fully customizable geometry, scale, and density. For scalp EEG, the devices feature 3D pillars of varying diameter and height fabricated from PVA aerogel templates infiltrated with $Ti_3C_2T_x$. Due to the high electrical conductivity ($155 \pm 4 \Omega$, $n=5$), porosity, and surface area, these 3D electrodes can establish a low impedance interface with the scalp without the need for any gel or conductive adhesive (10 Hz impedance of 8 mm pillar electrodes: $2.1 \pm 1.8 k\Omega$, $n=5$ participants).

To illustrate examples of applications of these multiscale MXene EEG arrays, I will present our most recent studies on intraoperative recordings in large animals and humans, longitudinal monitoring of post-traumatic epilepsy evolution with subcutaneous EEG in murine models, and clinical scalp EEG in epilepsy patients.

2:15 PM SB11.07.02

Wireless, Graphene-Based Multifunctional EEG and ECG Sensor for Clinical Monitoring [Juyeong Hong](#) and [Jong-Hyun Ahn](#); Yonsei University, Korea (the Republic of)

With the advent of advanced digital healthcare technologies, the need for imperceptible user-friendly portable devices for clinical monitoring of physiological anomalies has greatly increased. The brain and the heart are two major organs that would benefit greatly from such real-time monitoring apparatus, as the symptoms of various diseases readily manifest themselves in their operation. Brain diseases, such as stroke, epilepsy, and Parkinson's disease, and cardiovascular diseases, including arrhythmia, heart attacks, and atrial fibrillations, known for their high fatality, are among the many conditions where quick diagnosis and preventative measures may be taken via the continuous monitoring of the brain and the heart. As such, electroencephalogram (EEG) and electrocardiogram (ECG) have become an essential tool in the monitoring and diagnosis of patients. However, conventional monitoring devices are hard-pressed to facilitate prolonged real-time monitoring of patients. These devices typically fail to support the simultaneous monitoring of vitals on a single wearable device and causes discomfort owing to the bulky, wired electrodes and recording devices, thus limiting their daily use and leaving patients vulnerable to unpredictable medical emergencies. As such, in this research, a wireless, graphene-based EEG and ECG sensor for clinical monitoring is proposed. We demonstrate a simultaneous monitoring and analysis of EEG and ECG with improved accuracy for both clinical monitoring and brain-to-computer interface (BCI) applications. The ultrathin and imperceptible graphene-based electrodes exhibit lower contact impedance, high signal-to-noise ratio (SNR), and stable properties owing to the excellent mechanical and electrical properties of the constituent materials and structural design. Paired with a high-throughput portable wireless recording device for clinical monitoring, the system enables user-friendly, real-time monitoring of EEG and ECG for up to 11 hours on a single charge with accuracy and precision on par with that of conventional clinical systems. The simultaneous monitoring of both EEG and ECG enables accurate and holistic analysis of the patient's status. We also demonstrate a clinical BCI speller system augmented by deep neural networks to exhibit the diagnostic capabilities of the monitoring system. These personalized, wearable, and highly imperceptible devices are expected to aid in the advancement of daily healthcare for patients.

2:30 PM SB11.07.03

Stencil Printable Liquid Elastomer-Graphene-Based Respiration Sensors for Point-Of-Care Diagnostics [Simran Sharma](#) and [Titash Mondal](#); IIT Kharagpur, India

Due to the rise in global health issues and the challenges that come with them, point-of-care (POC) monitoring has the potential caliber to mitigate life-threatening situations. Among various diseases, monitoring of respiration disorders seems crucial and achievable by utilizing low-cost sensing devices for POC diagnostics. One of the significant challenges for people living in rural areas is reaching an appropriate hospital with the requisite facilities. And at times, this time consumption leads to many fatal outcomes. To mitigate this issue, an industry-feasible process has been utilized to develop liquid elastomer and graphene-based stencil printable sensors. Understanding that the inhalation and exhalation process induces pressure gradient, it can be utilized to detect minor strains in a sensor attached to the mask. Besides strain, breath temperature and humidity can also impact the sensing output of graphene-based sensing devices. Therefore, a silicone encapsulant has been utilized to decouple humidity response, and a Wheatstone bridge has been utilized as a temperature compensation technique. Further owing to elastomer's negative glass transition temperature, developed sensors could remain flexible in sub-ambient temperatures and be used for respiration monitoring at such temperatures. Various breath patterns, including normal, fast, deep, and slow breathing, can be identified with the aid of a developed on-mask sensing device and major respiration signals such as respiration rate (RR), Depth of respiration (DR), inhalation time, exhalation time and average breathing time can be monitored.

2:45 PM BREAK

3:15 PM SB11.07.04

A Wearable Nanobiosensor for Automatic, Non-Invasive and Wireless Monitoring of Systemic Inflammation [Jiaobing Tu](#) and [Wei Gao](#); California Institute of Technology, United States

Real-time monitoring of inflammatory proteins allows remote disease progression tracking and early intervention, thus improving patient outcomes and lowering economic burdens in chronic diseases. However, most current commercial protein sensing technologies rely on invasive blood draws, and require lengthy target incubation and labor-intensive washing steps to reach nanogram-level sensitivity. Although sweat is a non-invasive source for disease monitoring, wearable immunosensing is complex and sweat protein secretion is extremely underexplored, presenting a major challenge for personalized inflammation monitoring. Here, we present a wearable nanoengineered electrochemical biosensing technology that allows real-time and non-invasive analysis of a crucial inflammatory biomarker, C-reactive protein (CRP). Highly sensitive, selective, and fully automatic *in situ* inflammatory protein analysis across human activities was realized through seamless integration of a mesoporous graphene-gold nanoparticle modified immunosensor (coupled with thionine-tagged detector antibody-conjugated gold nanoparticles for signal transduction and amplification), autonomous sweat gland-driven microfluidics, and multimodal graphene sensor calibration. Through *in vitro* and *in vivo* clinical studies, we discovered the presence of CRP in chemically-induced human sweat and identified substantially elevated sweat CRP levels from patients with heart failure, chronic obstructive pulmonary disease, and active and past infections (e.g., COVID-19). We obtained a high correlation between sweat and blood CRP levels, demonstrating the potential of this technology toward non-invasive chronic disease management.

3:30 PM SB11.07.05

Thermal Drawing of Graphene-Integrated PVDF Fiber for Improved Performance in Wearable Triboelectric Nanogenerator [Md Sazid Bin Sadeque](#), [Mahmudur Rahman](#), [Md Mehdi Hasan](#) and [Mustafa Ordu](#); Bilkent University, Turkey

Triboelectric nanogenerators (TENG) exploit the phenomenon of triboelectrification enabling energy harvesting from low-frequency mechanical and biomechanical energy. Flexible ferroelectric polymers such as polyvinylidene difluoride (PVDF) are excellent candidates for fabricating a TENG device due to its high triboelectric charge density. Embedding 2D materials that have a high specific surface area into the PVDF matrix has proven to be an efficient strategy to affect surface morphology and friction property to improve the performance of TENG. Graphene and its derivatives have become a desired multi-functional material for fabricating high-performance TENGs. In this study, we demonstrate the successful fabrication of continuous PVDF/graphene nanocomposite fiber via scalable thermal drawing process. Fibers were fabricated with varying concentration of graphene in the PVDF matrix (1 wt%, 3 wt% and 5 wt%) by optimizing the fiber drawing parameters. The 5 wt% graphene integrated PVDF TENG fiber generates peak power up to $12.08 \mu W$, which is more than two times higher compared to pristine PVDF TENG ($5.80 \mu W$). This research will further expand our understanding on the dynamics of 2D nanomaterials into the polymer matrix of a thermally drawn fiber, leading to the performance optimization of wearable triboelectric devices and sensors.

3:45 PM SB11.07.06

Highly Piezoelectric, Biodegradable and Flexible Amino Acid Nanofibers for Medical Applications [Thanh D. Nguyen](#); University of Connecticut, United States

Amino acid crystals are an attractive piezoelectric material as they have an ultra-high piezoelectric coefficient and possess an appealing safety profile for medical implant applications. Unfortunately, solvent-cast films made from glycine crystals are brittle, quickly dissolve in body fluid, and lack of crystal orientation control, reducing the overall piezoelectric effect. Here, we present a material processing strategy to create biodegradable, flexible, and piezoelectric nanofibers of glycine crystals embedded inside polycaprolactone (PCL). The glycine-PCL nanofibers film exhibits stable piezoelectric performance with a high ultrasound output of 334 kPa (under 0.15Vrms), which outperforms the state-of-the-art biodegradable transducers (Nguyen et al., highly piezoelectric, biodegradable and flexible amino acid nanofibers for medical applications, Science Advance, 2023). We employ this material to fabricate a biodegradable ultrasound transducer for facilitating the delivery of chemo-drug to the brain. The device significantly enhances the animal survival time (2-fold) in mice-bearing orthotopic glioblastoma models. The piezoelectric glycine-PCL presented herein could offer an excellent platform not only for glioblastoma therapy but also for developing medical implantation fields.

4:00 PM *SB11.07.07

Electronic Skins with Air-Stable Ultraflexible Organic Photonic Devices Tomoyuki Yokota¹, Kenjiro Fukuda², Sunghoon Lee^{2,1} and Takao Someya^{1,2}; ¹The University of Tokyo, Japan; ²RIKEN, Japan

Inspired by the human skin, which is a large-area, multi-point, multi-modal, stretchable sensor, electronic skins that simultaneously detect pressure and thermal distribution have been developed. By improving its conformability, electronic skin can be directly attached on the human skins as next-generation wearables. In particular, ultraflexible organic photonic devices have been utilized as electronic skins that continuously monitor biological information in humans non-invasively. In this paper, we report recent progress of ultraflexible organic photonic devices that consist of organic light-emitting diodes and photodiodes. The environmental stability has been improved significantly using an inverted structure that does not employ atmospherically unstable cathode materials. We will also address issues and the future prospect of electronic skin using organic photonic devices.

4:30 PM *SB11.07.08

Biosensors and Wearable Tattoo Sensors Based on 2D Atomic Materials Dmitry Kireev¹ and Deji Akinwande²; ¹University of Massachusetts Amherst, United States; ²The University of Texas at Austin, United States

This talk will report on the development of 2D atomic materials such as graphene for wearable sensors, biosensors, and physiological monitoring of vital signs such as blood pressure. 2D materials offer many advantages in terms of mechanical, electrical, and optical performance compared to conventional materials. In addition, progress towards in-vivo uses of graphene for cardiac monitoring will be presented.

SESSION SB11.08: Virtual Session I
Session Chairs: Dmitry Kireev and Arben Merkoci
Tuesday Morning, December 5, 2023
SB11-virtual

8:00 AM SB11.08.01

A Flexible Optically Stimulated Synaptic Transistor Based on rGO-ZnO NRs Based Hybrid Channel Atanu Bag and Nae-Eung Lee; Sungkyunkwan University, Korea (the Republic of)

Recently, sensory synapses, including a sensory receptor and synapse between sensory receptor and afferent neuron, have received much attention for neuromorphic sensing applications. It is essential to obtain multi-functionality such as synaptic plasticity, retention time, and high sensitivity to realize an artificial sensory synapse with sensing ability with synaptic properties. Herein, a flexible optical sensory synapse using field-effect transistor (FET) structure having reduced graphene oxide (rGO) as a conducting channel with vertically-grown ZnO nanorods (NRs) as a UV-responsive sensing material and ion-gel based on 1-ethyl-3-methylimidazolium bis(trifluoromethylsulfonyl)imide ([EMIM][TFSI]) as a gate dielectric layer was investigated. The hybrid channel of ZnO NRs and rGO in synaptic FET devices enhanced the electrical synaptic weight presumably due to increased electrical double layer capacitance caused by increased surface area. Under no electrical gate bias furthermore, photo-gating induced by UV exposure resulted in a high optical synaptic plasticity presumably due to the combined effect of slow oxygen permeation through ionic gel for recovery and high capacitance by ion-gel. The UV-responsive optical synapse based on the hybrid channel FET is promising for sensory synapses, which can be used for efficient neuromorphic photo-sensing applications.

8:15 AM *SB11.08.02

2D Materials-Based Acoustic Sensors and Actuators He Tian; Tsinghua University, China

There is a great demand of developing 2D materials-based wearable electronics. In this talk, I will introduce several wearable electronics: 1. Graphene-based thermoacoustic device can enable sound emission with transparent properties. 2. We have developed graphene artificial throat, which can help mute people to speak again. 3. We also have created MXene-based eardrum with high sensitivity. Our work can greatly promote the wearable electronics toward practical applications.

8:45 AM *SB11.08.03

Skin-Integrated Wearable Sensors and Systems Shideh Kabiri Ameri; Queen's University, Canada

Skin-integrated wearable sensors and systems are a group of different types of sensors and their integrated electrical circuits that are laminated on skin and enable real time monitoring of the body and the surrounding environments for the applications in mobile health care, Internet of Things (IoT) and Human Machine Interfaces (HMI). The grand challenge in making reliable sensors and systems of such is the interface between conventional sensors and rigid electronics and soft, stretchable, and dynamic skin. Novel materials, designs and approaches are required to overcome this challenge. In this talk a group of nano materials based non-intrusive wearables with superior performance and visual imperceptibility and their applications for electroencephalography (EEG), electrocardiography (ECG), electromyography (EMG), Electrooculography (EOG), sensing skin temperature and hydration, human machine interface and IoT will be presented.

9:15 AM *SB11.08.04

Wearable Self-Powered Biosensors Based on 2D Materials on Textile Platforms Kavya Sreeja Sadanandan, Ievgeniia Kovalska, Masha Habab Albuqami, Ana Neves, Saverio Russo and Monica Craciun; University of Exeter, United Kingdom

Revolutionary advancements in healthcare and well-being rely on the integration of cutting-edge self-powered sensing technologies within textiles. A pivotal breakthrough in this field involves the emergence of nanoscale self-powered sensors specifically triboelectric nanogenerators (TENG). The underlying principle of TENGs lies in the combination of the triboelectric effect, based on the interaction between materials with different electronegativity and electrostatic induction. TENG devices have the capacity to effectively harness untapped energy resources, for example they can convert biomechanical energy from human movements such as walking, running, and breathing into electricity. TENG based biosensors are emerging as a viable alternative to battery-powered devices due to their self-powered and environmentally friendly properties. As a result, they are well-suited for wearable health monitoring applications, where they can behave as self-powered sensors. To pave the way for these transformative advancements, it is crucial to develop flexible, mechanically robust, lightweight, and resilient TENG biosensors.

In this invited talk, I will present our recent work on the solutions we explored to the design and fabrication of such generators, which possess the vital characteristics to meet the demands of practical applications. I will present several approaches for the development of textile-based triboelectric nanogenerators using 2D materials both as active sensing layers and as electrode materials. In our earlier work we demonstrated various methods to integrate graphene with textile substrates and create electrodes displaying a good range of conductivity, and resilience to bending, compression and tension.

These textile electrodes are used in the fabrication of TENGs along with a triboelectric layer of polydimethylsiloxane (PDMS) polymer and nylon fabric as a counter triboelectric layer. Different parameters affecting the TENG output such as chemical modification of the PDMS layer, frequency, contact force, contact area and separation distance between the two triboelectric layers are studied to provide insights into the working mechanisms of the device and to enhance the TENG output. The flexible textile TENG presents a stable output performance under strong deformation and its sensitivity to movement was explored as wearable sensor to monitor biomechanical movements. Due to the conformation ability of the triboelectric sensors, they were able to be implemented on key moving parts of the human body and used to monitor biomechanical motion through electrical signals. The self-powered sensors demonstrate their potential for wearable bioelectronics, intelligent robotics, prostheses, and rehabilitation purposes. Furthermore, we have demonstrated the use of 2D Transition Metal Dichalcogenides materials for wearable sweat sensors of uric acid for applications in personalised healthcare. Among the emerging technologies for continuous monitoring wearable technologies, triboelectric nanogenerators have emerged as a particularly promising and innovative approach for self-powered sensors in the detection of sweat biomarkers.

SYMPOSIUM SF01

Additive Manufacturing—From Material Design to Emerging Applications
November 27 - December 5, 2023

Symposium Organizers

Allison Beese, The Pennsylvania State University
Wen Chen, University of Massachusetts Amherst
A. John Hart, Massachusetts Institute of Technology
Sarah Wolff, The Ohio State University

* Invited Paper
+ JMR Distinguished Invited Speaker

SESSION SF01.01: Session I
Session Chairs: Wen Chen and Ting Zhu
Monday Morning, November 27, 2023
Sheraton, Second Floor, Republic B

10:30 AM *SF01.01.01

Atomic-Scale Perspective at Alloy-Design for Additive Manufacturing Dierk R. Raabe; Max Planck Institute for Iron Research, Germany

Additive Manufacturing is capable of producing highly complex parts directly from a computer file and raw material powders. Its disruptive potential lies in its ability to manufacture customised products with individualisation, complexity and weight reduction for free [1-3].

The lecture provides a brief overview of our research which aims to understand the impact of this manufacturing process on complex engineering alloys at the atomic- and nanoscale as well as to develop metallic materials suitable for and exploiting the unique characteristics of Additive Manufacturing.

While Additive Manufacturing, and in particular Laser Additive Manufacturing, is by now fairly well-established as a process to produce metallic parts, studies targeting the segregation and structural interface features at the atomic- and nanoscale for microstructure-optimisation of existing alloys and the design of novel advanced alloys tailored specifically to Laser Additive Manufacturing are still sparse. The established alloys currently in use do not exploit the enormous opportunities inherent in this technique at all, leaving a gap towards its further development.

1. Kürnsteiner P, Wilms MB, Weisheit A, Gault B, Jäggle EA, Raabe D. 2020. High-strength Damascus steel by additive manufacturing. *Nature*. 582(7813):515–19
2. Sun Z, Tan X, Wang C, Descoins M, Mangelinck D, et al. 2021. Reducing hot tearing by grain boundary segregation engineering in additive manufacturing: example of an Al_xCoCrFeNi high-entropy alloy. *Acta Mater*. 204:116505
3. Bajaj P, Hariharan A, Kini A, Kürnsteiner P, Raabe D, Jäggle EA. 2020. Steels in additive manufacturing: A review of their microstructure and properties. *Mater. Sci. Eng. A*. 772 (Nov. 2019):138633

11:00 AM *SF01.01.02

Direct Ink Printing of Thermoelectric Materials David C. Dunand, Ming Chen, Alexander Proschel and Yunjia Zhang; Northwestern University, United States

3D ink extrusion printing (i.e., direct ink writing) enables powder deposition in a layer-by-layer fashion, in air at ambient temperature, to create 3D complex geometries. For thermoelectric materials (TEs), this versatile manufacturing technique can unlock the potential of fully printed TE modules consisting of p-type and n-type TE legs. Recently, pre-alloyed particles (e.g., Nb_{1-x}CoSb) were suspended in inks, printed and then densified via sintering; also, bismuth and tellurium oxide particles deposited from inks resulted in Bi₂Te₃ after hydrogen reduction. Here, we demonstrate inks, containing blended elemental powders, which are printed into TE legs and reacted during sintering to synthesize the high-temperature TE phases Yb₁₄MnSb₁₁ and La₃Te₄. To build mechanically robust TE module with high density and phase purity, several approaches are explored during post treatments of printed green bodies. Infiltration of lower-melting elements in pre-sintered structures followed by annealing can close open porosity and help achieve targeted compositions. By blending low-melting elements like Sb into precursor powders, liquid phases are formed which facilitate interdiffusion and densification during sintering. For blended elemental powders, sublimation of elements with high vapor pressure (such as Yb and Te) during sintering introduces deviations from phase stoichiometry and formation of secondary phases. We demonstrate strategies - *via* addition of excess elements and/or binary compounds in precursors - to mitigate elemental losses and increase phase purities in sintered TE legs. We discuss the effects of microstructure and phase purity on the thermoelectric figure of merit (zT), which is controlled by the Seebeck coefficients and the electrical and thermal conductivities.

11:30 AM *SF01.01.03

Additive Manufacturing and Natural Medicine in Bone Regeneration: Opportunities and Challenges Susmita Bose; Washington State University, United States

An estimated one million bone grafting procedures are performed annually in the U.S. and a few million worldwide to repair fractures, cysts, bone defects, tumors, and hip and knee replacements. An increase in the number of procedures is strongly tied to increased musculoskeletal disorders, the aging population segment, and sports-related injuries. Sometimes, patient-matched devices are necessary for patients with special anatomical needs or concerns related to specific defect size complexity.

3D printing (3DP) or additive manufacturing (AM) is becoming essential in patient-matched implants due to lower cost and shorter manufacturing lead time. Additively manufactured components must be controlled and optimized carefully for their reproducibility, machine-to-machine part quality variations, and process-specific material properties. Establishing process property relationships for different AM techniques is vital to successfully implementing these manufacturing practices in biomedical devices. Complex biomaterials, e.g., calcium phosphate (CaP) ceramics compositionally similar to the inorganic part of the bone, show significant promise toward implant applications in both 3DP tissue engineering scaffolds and surface-modified hip and knee implants. It is worth noting that even with all the excitement on 3DP in recent years, *reliable and reproducible 3DP ceramic scaffold manufacturing is rare compared to porous polymeric or metallic structures due to their ease of processability.*

We have used extrusion-based and commercial binder jetting 3D Printing machines (ExOne, PA) with various ceramic powders for the past 25 years to critically identify and understand the

effects of process-property variations on 3DP CaP scaffolds. Our CaP scaffolds using 3DP have an average designed pore size of 300-400 microns, with 40 volume % porosity and compressive mechanical strength of >15 MPa, followed by NMC loading on those CaP scaffolds. We have designed and built a 3DP machine capable of printing high-viscosity slurry to directly print doped CaP-polymer scaffolds with similar inorganic composition as bone. 3D interconnected channels in CaP scaffolds provide pathways for micronutrients, improved cell-material interactions, and increased surface area, allowing improved mechanical interlocking between scaffolds and surrounding bone. *In vivo* studies show improved osteogenesis, angiogenesis, and controlled drug delivery using natural medicinal compounds (NMCs) in these 3D-printed scaffolds and coatings. The use of NMCs in CaP or CaP-polymer composites can eliminate the need for autografts and related second-site surgery for harvesting. NMCs can also replace growth factors (GFs) and proteins for faster healing. NMCs work with CaPs and other materials, such as titanium metals, to enhance early-stage bone tissue ingrowth for applications in load-bearing or non-load-bearing implants. These systems show promise for use in orthopedic and dental devices while eliminating the need for autografts and the second site surgery for harvesting and improving current hip/knee implant lifetime. The presentation will address the design of next-generation bone tissue engineering scaffolds and hip/knee devices based on clinical needs in the fixation of bone disorders and scientific challenges.

SESSION SF01.02: Session II
Session Chairs: Sarah Wolff and Rayne Zheng
Monday Afternoon, November 27, 2023
Sheraton, Second Floor, Republic B

1:30 PM *SF01.02.01

Advances in Additive Manufacturing of Architected and Functional Materials Christopher M. Spadaccini; Lawrence Livermore National Laboratory, United States

In this presentation, we will cover some of the latest work in advanced and custom additive manufacturing processes for the fabrication of architected materials and functional structures. The concept of architected materials revolves around the notion that material properties are traditionally governed by the chemical composition and spatial arrangement of constituent elements at multiple length-scales. This usually limits material properties with respect to each other creating trade-offs when selecting materials for specific applications. For example, strength and density are inherently linked so that, in general, the more dense the material, the stronger it is in bulk form. We will review advanced additive micro- and nanomanufacturing techniques to create new material systems with previously unachievable property combinations. These processes include, but may not be limited to, projection microstereolithography (PuSL), direct ink writing (DIW), and electrophoretic deposition (EPD) as well as more advanced concepts such as volumetric additive manufacturing (VAM), computed axial lithography (CAL), parallel two-photon polymerization, liquid metal jetting, and diode-based additive manufacturing of metals (DiAM). The performance of the resulting material constructs is fundamentally controlled by geometry at multiple length-scales, from the nano- to the macroscale, rather than chemical composition alone. We have fabricated and will review the resulting properties of these mechanical metamaterials in polymers, metals, ceramics, and combinations thereof. These new processes and concepts can also be applied to functional materials such as those for supercapacitor electrodes, optical components, and even for fluidic system such as the recently published cellular fluidics concept. A review of these functional systems will be followed by a brief discussion of future directions.

2:00 PM SF01.02.02

Additively Manufacturing Smart Cellular Materials: Self-Healing Protection for Space Applications Marlina Simoes^{1,2}; ¹California Institute of Technology, United States; ²University of Cambridge, United Kingdom

Metallic cellular materials, such as lattices and honeycombs, are of interest in the design of lightweight and impact-resistant structures (high energy absorption capacity). However, the use of cellular materials in engineering applications has been hindered due to the challenges associated with the fabrication of such complex geometries. Additive manufacturing (AM) technologies have enabled the fabrication of geometries of significant complexity. Nevertheless, the design optimization of AM cellular materials for high strain rate loading scenarios remains relatively underdeveloped. Furthermore, even if those material structures dissipate energy efficiently during dynamic crushing, they do not recover their shape after impact. It is, therefore, necessary to understand the relationship between the AM process parameters, cellular material structures and dynamic performance, but also to develop the recovery of those structures after suffering an impact.

In this work, the opportunities created by additive manufacturing processes have been explored by: (1) studying the process-geometry-property interactions of metallic cellular materials, and (2) manufacturing cellular structures which can exhibit a "self-healing" functionality through shape memory effect. Firstly, quasi-static and dynamic mechanical testing on stainless steel 316L cellular geometries is combined with a wide range of material characterization techniques to understand the interplay between AM process parameters, geometry and high strain rate performance. Five cellular structures were investigated, finding that the geometry played a dominant role, relative to the Laser Powder Bed Fusion (LPBF) AM process. Secondly, bulk and complex cellular structures that exhibit shape memory effect have been successfully manufactured. A diamond lattice structure and a new auxetic structure obtained through topology optimization recovered up to 70% of their shape after impact. The main motivation and focus are on space applications to mitigate against impacts but this research is of relevance to a wide range of sectors: e.g., automotive crashworthiness, structural defence, and civil blast protection.

2:15 PM *SF01.04.06

Digital Twins Empower Everyone to Print Better Parts Tarasankar DebRoy and Tuhin Mukherjee; The Pennsylvania State University, United States

Digital twins have garnered significant interest in the industry due to the scientific, technological, and commercial advantages they offer. This presentation addresses the fundamental elements of a digital twin for additive manufacturing, highlighting the roles of mechanistic models, machine learning, statistical models, sensing and control, and data. By utilizing digital twins, the current practice of trial and error qualification of metallic parts with expensive printing equipment and feedstock materials can be circumvented. The presentation also explores the detection and prevention of defects through diagnostic closed-loop process control, employing sensors to monitor key features like deposit geometry or peak temperature. In contrast to closed-loop control, digital twins are also employed offline for process planning, enabling the narrowing of the optimal process parameter window to achieve predetermined outcomes. This significantly reduces the need for extensive corrective actions during manufacturing. Finally, the presentation discusses the potential for expanded utilization of digital twins based on existing evidence, providing an outlook on future applications.

2:45 PM BREAK

3:15 PM *SF01.02.04

Additive Manufacturing as a Unique Platform for Fabrication of (Meta-)Materials with Complex Topologies and Designer Microstructures Lorenzo Valdevit; University of California, Irvine, United States

Additive Manufacturing (AM) is a family of disruptive technologies that allow rapid fabrication of parts of nearly arbitrary geometrical complexity without the need of expensive tooling, vastly simplifying production of elaborate assemblies for a wide range of industries. The established approach to materials design for additive manufacturing (AM) generally consists of attempting to reproduce the uniform structures and properties of conventionally processed materials. While this certainly helped facilitate material certification and rapid introduction of AM technologies in a number of industries, the opportunity to exploit the fundamentally local nature of AM processes to fabricate novel heterogeneous materials with accurately controlled distributions of properties remains largely untapped. Here we discuss two recent and exciting demonstration of this new AM-enabled design concept: (a) novel shell-based architected materials with topological disorder spanning multiple length-scales, and (b) metal/metal architected composites produced by Laser Powder Bed Fusion of stainless steel with locally tailorable microstructure and phase distributions.

3:45 PM *SF01.02.05

Programmable Strength and Damage-Tolerant Meta-Crystals for Safety Critical Applications Minh-Son (Son) Pham; Imperial College London, United Kingdom

Architected materials are lightweight with high specific strength and excellent energy absorption, holding great promise for a range of structural applications. However, the absolute strength of such materials is low due to the removal of base material, making them unsuitable for safety-critical applications in automobiles, aerospace and space. We recently developed a new approach in which the crystalline microstructure is mimicked to bring key metallurgical strengthening mechanisms to mesostructure scales, creating artificial crystals (i.e. meta-crystals) with new strengthening sources. This presentation will discuss a new horizon in which we synergistically combine the crystal-like architecture and metallurgical engineering (via heat treatments) to significantly push the strength and toughness of metallic meta-crystal for load-bearing and safety critical applications. The talk also discusses new ways of tuning mechanical behaviour to specific locations to enhance the spatial programming of local deformation.

4:15 PM SF01.02.06

Design of Three-Dimensional Complex Truss Metamaterials with Graph Neural Networks and Deep Reinforcement Learning Marco Maurizi and Rayne Zheng; University of California, Berkeley, United States

The rapid development of additive manufacturing technologies has enabled the fabrication of truss metamaterials, i.e., a novel class of lightweight-yet-strong materials with engineered complex hierarchical structures. Manipulating the architecture over chemical composition dramatically expands the achievable materials design space, allowing to largely control the mechanical response of metamaterials. While methods such as topology optimization and machine learning have demonstrated to be powerful tools to discover structures with desired material properties, designing three-dimensional (3D) complex truss metamaterials with programmable mechanical behaviors is still a challenge. Here we propose a paradigm, based on graph neural networks (GNNs) and deep reinforcement learning, to design 3D truss metamaterials with programmable nonlinear quasi-static and dynamic responses. By combining the ability of our GNN-based model to accurately predict the mechanical response across multiple orders of magnitude and the explorative power of deep reinforcement learning, together with numerical simulations and mechanical testing, we inverse design truss metamaterials for compressive loading up to 30% of strain and dynamic transmissibility with desired band gaps. Our method not only demonstrates a pathway to design mechanical metamaterials with desired mechanical behaviors but also provides a flexible framework that can be applied to tailor the response of 3D photonic or robotic metamaterials.

4:30 PM SF01.02.07

Tuning Local and Global Disorder in Architected Materials via Frequency-Based Noise Alexander Groetsch, Kate Ainger and Lorenzo Valdevit; University of California, Irvine, United States

The beauty of architected materials lies in the opportunity to tune their properties *via* their geometrical and topological features [1-3]. We are not limited by the material constituents and can surpass classical engineering materials. Inspired by nature, where structural and mechanical heterogeneity enhances energy dissipation [4] and ductility [5], recent efforts in the metamaterials' community are targeted to harness the effect of irregularities to achieve superior functionalities [6]. These include stress de-localization and imperfection insensitivity, and recent advancements in additive manufacturing allow us to fabricate architectures that incorporate this randomness. However, current efforts to introduce disorder in metamaterials are often restricted to periodicity-disturbances on a global scale. Here, we propose a new design approach that allows us to study the influence of both local and global disorder on the material performance of periodic and random metamaterials. Shell-based topologies are used throughout as model architectures, due to their mechanical advantages (e.g., higher specific strength and energy absorption) over more common truss-based lattices [7]. The mathematically described shell topology is superimposed with frequency-based signals to disturb the "short-range" order, with different frequencies and amplitudes used to tune this local disorder parameter. Characteristic power spectral densities [8] of three frequency-based noise signals – white, pink, brown – are then used to tune the local disorder across the structure, thus introducing a global disorder gradient. To test the influence on both periodic and random metamaterials, triply periodic minimal surfaces (TPMS) and spinodal shell architectures are printed using two-photon lithography, which provides the necessary resolution to incorporate local features in the printing process. The impact of the various levels of disorder on the elasto-plastic behavior of the metamaterial is characterized by means of *in situ* micro-compression tests performed at different strain rates. Our approach allows us to study the effect of local disorder on globally periodic and random structures by overlaying local features with frequency-based signals. In addition, the characteristic rates of power loss from three different colors of noise introduce a global and tunable disorder gradient opening up new opportunities to design highly multifunctional (meta-)materials.

References:

[1] Wang et al., *Phys Rev Lett*, 2016. [2] Torquato et al., *J Appl Phys*, 2003. [3] Bertoldi et al., *Nat Rev Mater*, 2017. [4] Tai et al., *Nat Mater*, 2007. [5] Groetsch et al., *Sci Rep*, 2021. [6] Soyarslan et al., *Acta Mater*, 2018. [7] Hsieh et al., *J Mech Phys Solids*, 2019. [8] Davenport & Root, IEEE Press, 1987.

SESSION SF01.03: Poster Session I
Session Chairs: Wen Chen and Sarah Wolff
Monday Afternoon, November 27, 2023
Hynes, Level 1, Hall A

8:00 PM SF01.03.01

Finite Element Analysis of Weathering Resistant Spherical Robot Shell Wei-Lin Wu, Yen Shuo Chen and Fu-Hsiang Ko; National Yang Ming Chiao Tung University, Taiwan

With the fast pace of human civilization development, various types of robots, particularly autonomous amphibious robots, have seen significant advancements in recent research(1). As robots increasingly work in challenging environments to perform specialized tasks, it is critical to have a robot shell that can adapt to various conditions to ensure proper functioning of internal sensing components(2). Therefore, it's crucial to find a material with strong mechanical reliability and good optical properties.

This paper presents a proposed 3D printing resin for spherical robot shells with high transparency in the visible region. The use of 3D printing technology in creating various robots has gained widespread acceptance(3), and the stereolithography (SLA) method has many advantages over other methods, such as relative precision and higher mechanical strength(4). We also conducted a two-month accelerated corrosion test on our print samples. The weather resistance of the printable resin was then evaluated by measuring changes in surface tension, tensile strength, UV-visible and FTIR spectrums.

For the purpose of enhancing the impact resistance, we also performed a mechanical study of 3D printed shells with different layer structures through finite element analysis. The finite element technology has many advantages such as less time, manpower, energy and material resources(5). Our simulation results showed that a protective layer with larger holes offers better protection for the inner cooling ball compared to one with smaller holes, leading to a reduction of 80% in residual deformation energy compared to a single-layer ball.

Besides mechanical test, Passive cooling is an important consideration for the robot shell given the proper functioning of the internal electronic sensors. Recently, radiative daytime radiative cooling (PDRC) has become a high-profile topic due to the intensification of Earth's climate problems (6, 7). Because of the heat dissipation to outer space (3 K) through the 1st atmospheric transparency window (8–13 μm) and in the 2nd atmospheric transparency window (16–25 μm)(8). This approach requires the cooling material to have high emissivity around those atmospheric windows.

In this work, a multiple functional shell fabricated by stereolithography (SLA) technology was developed. we demonstrate the mechanical and weatherability of a spherical robot shell made of SLA 3D printed resin.

Keywords: 3D-printing; mechanical simulation; weathering resistance; sphere robotics; thermal radiation

1. H. M. Xing et al., Design, modeling and control of a miniature bio-inspired amphibious spherical robot. *Mechatronics* 77, (2021).
2. K. Karakasiliotis et al., From cineradiography to biorobots: an approach for designing robots to emulate and study animal locomotion. *Journal of The Royal Society Interface* 13, 20151089 (2016).
3. S. X. Guo et al., Modeling and experimental evaluation of an improved amphibious robot with compact structure. *Robotics and Computer-Integrated Manufacturing* 51, 37-52 (2018).
4. M. Pagac et al., A Review of Vat Photopolymerization Technology: Materials, Applications, Challenges, and Future Trends of 3D Printing. *Polymers* 13, 598 (2021).
5. Y. Zhang, H. H. Xu, R. T. Peng, Y. Lu, L. W. Zhu, The State of the Art of Finite Element Analysis in Mechanical Clinching. *INTERNATIONAL JOURNAL OF PRECISION ENGINEERING AND MANUFACTURING-GREEN TECHNOLOGY* 9, 1191-1214 (2022).
6. B. Zhao, M. K. Hu, X. Z. Ao, N. Chen, G. Pei, Radiative cooling: A review of fundamentals, materials, applications, and prospects. *APPLIED ENERGY* 236, 489-513 (2019).
7. Q. Zhang et al., Recent Progress in Daytime Radiative Cooling: Advanced Material Designs and Applications. *SMALL METHODS* 6, (2022).
8. T. Wang et al., A structural polymer for highly efficient all-day passive radiative cooling. *Nature Communications* 12, (2021).

8:00 PM SF01.03.02

Stress Management by Design in Two-Photon Polymerization Printed Structures Sarah M. Fess¹, David R. Harding^{1,2}, Mark Bonino¹ and Yongfeng Lu³; ¹University of Rochester's Laboratory for Laser Energetics, United States; ²University of Rochester, United States; ³University of Nebraska–Lincoln, United States

Two-photon polymerization (TPP)-printing millimeter size components with sub-micron features and resolution is an attractive alternative to traditional chemical and machining processes, as it holds potential for increased yields and high controllability. However, maintaining design fidelity can be a challenge in the face of stress-induced deformations which occur during and after the printing process, caused by localized volumetric shrinkage as polymer networks form. This is especially true when many print blocks must be stitched together to form a contiguous larger structure. The extent and manner of deformation can vary greatly depending on print conditions and structural design, even for a single resin, and can lead to misalignment and discontinuity at

the stitching boundaries.

Within the limitations of a commercially available TPP system and resin (Nanoscribe PPGT+/Zeiss 63x NA1.4/IP-Dip2) we seek to fabricate millimeter-scale thin-wall spherical shells with stochastic foam liners for laser-driven fusion experiments. For this application, it is important to maintain wall uniformity and structural integrity across stitching boundaries, and to minimize bulk out-of-roundness. Observed bulk structural shrinkage for IP-Dip2 is typically 5-10%, which can be compensated for by oversizing the design. However, individual high aspect ratio or cantilevered print blocks such thin-wall curved surfaces can deform by $>10\text{-}\mu\text{m}$ over a $200\text{-}\mu\text{m}$ arc length. Here we present a method for preemptive stress management via design by using nTop software to section and pre-deform print blocks to correct for anticipated in situ polymerization shrinkage, to within $1.5\text{-}\mu\text{m}$ of the intended location, or on par with the stage repeatability. Characterization of the stitching boundaries via scanning electron microscopy (SEM) and atomic force microscopy (AFM) provides critical feedback for the design and print approach. The intended result is a printed structure with minimal stitching defects and high fidelity compared to the original design.

This material is based upon work supported by the Department of Energy National Nuclear Security Administration under Award Number DE-NA0003856, the University of Rochester, and the New York State Energy Research and Development Authority.

8:00 PM SF01.03.03

Investigating the Relationship between Quantified Cr₂B Phase Through Image Processing and Mechanical Properties for Metal 3D Printed Alloy[DongyongPark](#), Hyeon JeongPark, Yoon SunLee and Young RokMoon; Korea Institute of Industrial Technology, Korea (the Republic of)

The relationship between the quantified Cr₂B phase through image processing and the mechanical properties of 3D printed 316L stainless steel with boron was investigated. The experimental conditions, including the boron content, feed rate, laser power, and scan speed, were designed using the Taguchi method. The formation of the Cr₂B phase with these processing conditions was quantified using image processing techniques. The algorithm used for image processing was based on the intensity difference between the Cr₂B phase and other phases. Since the quantity of Cr₂B phase depends on the processing conditions, it directly affects the mechanical properties of the printed stainless steel with boron. The mechanical properties evaluated in this study included tensile strength and micro hardness measured using the Vickers hardness test. The identical processing conditions were used for both quantifying the Cr₂B phase and measuring the mechanical properties. The goal was to identify the relationship between the quantified Cr₂B phase and the mechanical properties. It is generally known that a high amount of Cr₂B phase can deteriorate the mechanical properties of the material. Therefore, optimizing the processing conditions is crucial in achieving the desired mechanical properties. The results obtained from the signal-to-noise (S/N) ratio analysis for the quantified Cr₂B phase were compared with the S/N ratio results for the measured mechanical properties. This comparison helps in determining the influence of the Cr₂B phase on the mechanical properties and in finding the optimal processing conditions for obtaining the desired mechanical properties.

8:00 PM SF01.03.04

Laser Powder Bed Fusion Fabricated Near Grain-Oriented and Near Non-Oriented Silicon Steel: A Study on Texture Components and Magnetic Properties[FanboMeng](#), ShengHuang, XiaojunShen and Christopher H. T.Lee; Nanyang Technological University, Singapore

The rapid development of additive manufacturing techniques has opened up new possibilities for the production of complex metallic components with tailored properties. Silicon steel, as the most widely used soft magnetic material, necessitates different texture components to meet diverse requirements of various applications (i.e., static machine and rotating machine), and thus is typically categorized as grain-oriented and non-oriented. However, how to fabricate such types of silicon steel via laser powder bed fusion (LPBF) has not been comprehensively investigated until now. In this study, LPBFed near grain-oriented and near non-oriented Fe-3.5 wt.%Si silicon steel is obtained by designing processing parameters. The morphology of the molten pool is characterized through optical microscopy (OM) and scanning electron microscopy (SEM), and various texture features are explored using electron backscatter diffraction (EBSD). Besides, dynamic magnetic properties are assessed by conducting the alternating current (AC) method. The results indicate that the reduction of linear energy density (LED) and laser power induces the side morphology of the molten pool to change from large, flat, and well-overlapped to small, protuberant, and less-overlapped, where this change leads to the formation of an exceptionally pronounced $\langle 001 \rangle$ building direction (BD) (i.e., θ -fiber texture) or random distribution of grain orientations, respectively. Meanwhile, by simultaneously decreasing the laser power and scanning speed, the top morphology of the molten pool transforms from a teardrop shape to an elliptical shape at the trailing edge, which ultimately causes a shift in the angle between the $\langle 001 \rangle$ crystallographic orientation of grains in the θ -fiber texture and the scanning direction from 45° to 30° . Moreover, samples with fewer defects (i.e., larger grain size and fewer pores) and a larger area fraction of $\langle 001 \rangle$ paralleling to applied magnetic field perform better in dynamic magnetic properties (specifically, higher permeability and flux density), although the extent of this superiority is limited by residual stress and high dislocation density in the as-built samples. This study provides insight into the correlation of processing parameters, texture evolution, and dynamic magnetic properties in LPBFed silicon steel. The results could provide a design reference for LPBFed soft magnetic materials, which further provides the possibility of utilizing additive manufacturing in assisting in fabricating electromagnetic machines.

Reference

- [1] F. Meng, S. Huang, K.B. Lau, Y. Zhou, Y. Deng, P. Wang, X. Shen, C.H.T. Lee, Texture components and magnetic properties of laser powder bed fusion fabricated near grain-oriented and near non-oriented silicon steel, *Materials & Design*. 231 (2023) 112037, <https://doi.org/10.1016/j.matdes.2023.112037>.
- [2] X. Shen, F. Meng, K.B. Lau, P. Wang, C.H.T. Lee, Texture and microstructure characterizations of Fe-3.5wt%Si soft magnetic alloy fabricated via laser powder bed fusion, *Materials Characterization*. 189 (2022) 112012, <https://doi.org/10.1016/j.matchar.2022.112012>.

8:00 PM SF01.03.05

Rigid and Tough Composite Additive Manufacturing using Co-Axial Material Extrusion of Hard Thermoplastic and Soft Elastomer[TaeminKim](#) and SanhaKim; Korea Advanced Institute of Science and Technology, Korea (the Republic of)

Multi-material additive manufacturing (MMAM) can realize three-dimensional products with extreme complexity not only in their shape but also in their mechanical behavior. Direct writing, vat photopolymerization and material jet type AM techniques have shown their versatile capability to print multiple polymeric materials, yet materials are limited to UV-curable resins and thermoset polymers. Material extrusion 3D printers had also been attempted to print multiple thermoplastics, but the weak interfacial bond due to the cold-hot welding between one layer and the next causes poor overall mechanical properties. Herein, we invented a new multi-material extrusion 3D printer which can extrude thermoplastic polymers in a core/shell configuration. We design and fabricate the nozzle to independently feed three filaments from right, left, and center, which are heated up to melt and unite each other right before the extrusion. In particular, when we insert the right and left filament as the same material, we can print dual-material layer in a co-axial mode. Such strategy allows strong interfacial bond between the different filaments even when the two materials have large contrast in mechanical properties. As a result, we observe unprecedented properties with certain combinations. By extrusion printing the polylactic acid (PLA) and the thermoplastic polyurethane (TPU) in co-axial configuration, for example, we can realize a 3D specimen which exhibits stiff as the hard PLA yet elongates as the soft TPU before failure, therefore possess an extreme rigidity and toughness. In detail, the core/shell extrusion printing enables the brittle PLA core to elongate about 30 ~ 50 times more than their original fracture strain, and such super-ductility is driven by the chemical bond between the two extruded materials. We further investigate diverse thermoplastic polymer combinations and verify that such exceptional outcome is only possible when a strong interfacial adhesion develops via the existence of hydrogen bonds. We discuss the fracture mechanism of our extruded co-axial polymer fibers and the chemical aspects at the interface. We also show a more variety of functionality that can be realized by extruding three different filaments in the co-axial nozzle. Applications that are now possible via bi-material and tri-material extrusions show that co-axial multi-material extrusion 3D printing opens a new avenue toward versatile material design, for additive manufacturing of fully customizable protective wearable devices and artificial muscles.

8:00 PM SF01.03.06

Machine Learning-Based Predictive Model for Jet Flow Rate in Electrohydrodynamic Direct-Writing[DongwoonShin](#), YongraeKim, Pil-HoLee and JoonphilChoi; Korea Institute of Machinery & Materials, Korea (the Republic of)

Electrohydrodynamic direct-writing (EDW), also known as near-field electrospinning, is an extrusion-based additive manufacturing (AM) approach. One of the prominent advantages of EDW over other extrusion-based printing techniques is its utilization of electric forces to deposit fibers with orders of magnitude smaller diameters compared to nozzle diameters, enabling much faster printing speeds. As a result, the fiber diameters achievable through EDW can range from the micro to nanometer scale. Furthermore, EDW employs polymer solutions in a liquid state as printing inks, which broadens the range of available polymers and solvents. Consequently, EDW has been employed to print various functional polymers, finding applications in diverse fields including fiber lithography platforms, energy harvesting, gas sensors, and scaffolds for tissue engineering.

Having precise control over the fiber diameter and shape is of great importance in order to tailor the desired properties of the printed fibers, such as electrical resistance, birefringence intensity, sensor sensitivity, and porosity. However, the Electrohydrodynamic direct-writing (EDW) technique has encountered challenges due to the lack of prediction methods for the printing outputs, including fiber diameters or deposition patterns. As a result, the EDW process has heavily relied on a time-consuming trial-and-error approach to achieve the desired fiber properties. Therefore, the development of practical and purposeful predictive models is crucial for driving innovation and potentially commercializing the EDW method, similar to other state-of-the-art extrusion-based additive manufacturing (AM) techniques. Nevertheless, due to the complex multiphysics mechanism of EDW and the wide range of process parameters involved, developing a predictive model to identify the optimal process parameters presents a highly challenging task.

Machine learning (ML) is a branch of artificial intelligence (AI) that involves an ML model learning the relationship between input and output features to uncover hidden patterns. The application of ML has gained significant popularity in additive manufacturing (AM) processes, particularly due to the complex physics involved in AM processes such as rapid evaporation, solidification, and ingestion, which surpasses traditional manufacturing methods. Unlike traditional physics-based equations that require explicit programming, ML models can learn these relationships, making them rapid, practical, and analytical prediction tools for AM processes. Consequently, ML-based models have been developed for tasks like geometrical design, process optimization, and anomaly detection in various AM techniques, including fused deposition modeling, powder bed fusion, direct energy deposition, direct ink write, and aerosol jet printing. Moreover, ML-based models hold promise as potential candidates for optimizing the Electrohydrodynamic direct-writing (EDW) process, surpassing the capabilities of physics-based models in practical applications.

In this poster presentation, we will introduce a framework for developing an ML-based predictive model of jet flow rate in Electrohydrodynamic direct-writing (EDW). To accomplish this, a monitoring system was established to capture actual images of the jet profiles during the EDW process. Subsequently, image analysis techniques were employed to extract jet profile data, which was then utilized to train a multi-output regression model using artificial neural networks (ANNs). A comparison between the predicted and observed jet profiles demonstrated the model's high prediction accuracy. The proposed approach presented here represents a futuristic method for optimizing the EDW process and holds tremendous potential for realizing smart manufacturing of functional micro/nanofibers through EDW.

8:00 PM SF01.03.07

Challenges and Opportunities for Machine Learning Accelerated Materials Qualification for Brittle Particle Cold Spray ChengZeng, AndrewNeils, NathanPost and JackLesko; The Roux Institute at Northeastern University, United States

Brittle particle cold spray is a low-pressure and low-temperature manufacturing technique developed by TTEC, a company based in Virginia. It can produce dense brittle particle coatings at a high deposition rate and low-energy cost with unlimited thickness. Applications include high temperature thermal barrier coatings, all-solid-state batteries and corrosion resistant coatings. However, the application of this technique to new material systems currently requires extensive trial and error to get the correct size and morphology distributions and spray parameters. In order to accelerate qualification of new materials for this process improved understanding of the mechanics of particle impact and consolidation is required. The mechanism of impact consolidation can span in different length scales, ranging from atomic chemical bonding to mechanical interlocking. Moreover, the complex cold spray technique involves multiple physical phenomena, such as fluid dynamics, aerodynamics, heat transfer and deformation. A combined multiscale and multiphysics approach is needed to develop a thorough fundamental understanding of brittle particle cold spray. Recent advances in machine learning approaches have great potentials in improving our understanding for linkages between process-structure-property. Here, we review current multiscale and multiphysics methods, and machine learning algorithms for cold spray technology, and we discuss remaining challenges and present an outlook for future research opportunities in this area.

8:00 PM SF01.03.08

Conformal Direct Ink Write Additive Manufacturing via a 6-Axis Robotic Arm RobertLahaic, RoneishaHaney, JamesHardin and AnesiaAuguste; Air Force Research Lab, United States

Reliable printing of materials onto any surface, regardless of its shape, is a key enabling technology for many processes. Traditionally, most additive manufacturing techniques require a 3-axis gantry system which only moves planarly in the XYZ directions, limiting the type of print surface and the orientation achieved relative to the surface. Print direction and orientation is widely known to largely affect the material properties of additively manufactured components especially in prints using anisotropic materials. Recently, there has been increased interest in additive manufacturing using 6-axis robotic arms, however, research is limited on how the additional degrees of freedom of motion affect the material properties compared to a gantry system. This work investigates the effects on the anisotropic material properties by utilizing the additional degrees of freedom the robotic arm enables to maintain the direct ink write (DIW) nozzle constantly normal to a contouring surface. We compared the printed components produced by a 6-axis robotic system to a traditional 3-axis gantry system to investigate how remaining normal to the print surface affects the mechanical properties, fiber alignment, and geometrical accuracy. The research will compare the similarities and differences of the robotic system to the traditional gantry system using anisotropic carbon nanotube carbon fiber Epon 826 resin along a contoured surface, which has relevance on structural materials, electronics, and flexible devices.

8:00 PM SF01.03.09

Supramolecular Polymerization Enables Additive Manufacturing of Fatigue-Resistant, Tough Materials JiyunKim; Korea Advanced Institute of Science and Technology, Korea (the Republic of)

Photopolymerization is being effectively applied in the field of 3D printing due to its fast and easy process for creating complex 3D objects. However, due to the rapid polymerization speed, polymer networks inevitably exhibit inhomogeneity, and applied stress becomes concentrated at those points. This leads to structural destruction and results in the low durability of 3D printed objects.

Here I present a supramolecularly polymerizable photopolymer enables tough 3D objects. We designed the photopolymer with stickers in its backbone, and these stickers assemble through hydrogen bonding, forming nanostructures even before light exposure. By using this photopolymer as a crosslinker to form a polymer network, applied stress can be effectively dissipated through sacrificial bonds in the nanostructures. As a result, the photopolymerized system exhibits superior mechanical properties such as stretchability, toughness, fracture toughness, and fatigue threshold, despite its inhomogeneity. Moreover, this photopolymer can be applied to various monomer systems to achieve desired characteristics and good mechanical properties. These results demonstrate that this photopolymer can be utilized as a versatile photocrosslinker in 3D printing applications.

8:00 PM SF01.03.10

Optimizing Process Parameters in Selective Laser Melting for Enhanced Mechanical Properties of 17-4PH Stainless Steel KyuHyunKim and In-SukChoi; Seoul National University, Korea (the Republic of)

Selective Laser Melting (SLM) is a key technique in metal 3D printing, involving the repeated melting of metal powder using a laser, followed by its layer-by-layer solidification. This technique enables the fabrication of products with intricate designs and complex geometries, making it indispensable in high-precision industries such as aerospace, automotive, and healthcare. However, the rapid heating and cooling during the layering process could induce porosity and changes in the microstructure, which may significantly reduce the durability and strength of the components.

In this study, we examined the influence of porosity and microstructure on the mechanical properties of components produced using 17-4PH stainless steel powder, a material predominantly employed in the aerospace sector. Initially, we modulated the energy density by varying laser power and scan speed, and monitored the evolution of porosity via Optical Microscopy (OM). Following this, we analyzed the microstructure and phase fraction with Scanning Electron Microscopy (SEM) and Electron Backscatter Diffraction (EBSD), and investigated the correlation with mechanical properties derived from hardness and tensile tests. Ultimately, we aimed to identify optimal process parameters that minimize porosity and maximize mechanical performance through control of phase fraction changes.

The findings of this research underline the importance of porosity and microstructural control in SLM processes, as they significantly impact the quality of materials and performance of parts. This insight is anticipated to draw considerable attention, particularly in the aerospace industry, where high-strength components are of critical importance.

8:00 PM SF01.03.11

Impact of Nanoparticle Size and Loading on Printability of Polymer-Nanoparticle Composite Inks for Direct Ink Writing YunLi¹, AidanFlynn¹, ChristopherMasternick¹, BrandonKolanovic¹, BinLi² and BoLi¹; ¹Villanova University, United States; ²Wichita State University, United States

Direct ink writing (DIW) is a most inclusive 3D printing technology in which polymer can be mixed with different nanoparticles and create 3D structures with a wide range of mechanical properties and functionalities. The key challenge of DIW process is the creation of printable inks. Although a significant process has been made to develop printable recipes with different combinations nanoparticles, polymers, and solvents, two fundamental questions have not been elucidated: 1) how to evaluate the printability of the ink and 2) how nanoparticle size and loading affect ink printability. To bridge this gap, this work utilizes the SiO₂ nanoparticle-Polydimethylsiloxane (PDMS) system and evaluates three commonly used printability analysis methods—dual-layer printing analysis, ink rheology, and printing line width analysis. The influence of particle size (diameter = 26 nm-847 nm) and loading (0-66.67 wt.%) were systematically studied. Through the comparison, dual-layer printing analysis (DLPA), in which the merging behavior of two vertically stacked printing layer was analyzed, is found to be the most direct and reliable method to evaluate printability. The printability factor (Pr) in DLPA approaches 1 means less merging between layers and good printability and empirically Pr = 0.9 is set as a critical value for printable ink. To achieve this critical value, for 26 nm nanoparticles, a small loading of 2.91 wt% is required, while for 847 nm nanoparticles, 28.57 wt % is required. Increase the particle size will improve Pr but there is an upper limit under the fixed printing pressure and nozzle size. The highest printable particle loading is 66.7 wt% for 847 nm nanoparticles under 120 psi with a nozzle diameter of 300 μm. Our results conclude that nanoparticles can be utilized to tailor the DIW materials from soft bio gels to strong ceramics. Moreover, the comparison of different analysis methods highlights the need for developing generic standards to evaluate printability.

<quillbot-extension-portal></quillbot-extension-portal>

8:00 PM SF01.03.12

A Dimensional Analysis of a 15-5 PH Steel Part Built by Laser Powder Bed Fusion Process[AbhishekKumar](#), SaurabhTripathi and CheruvuS. Kumar; Indian Institute of Technology, Kharagpur, India

With the increased functionality of additively made parts, the necessity for dimensional accuracy must be prioritised. Dimensional accuracy refers to how well the printed part fits the dimensions specified in the design. High dimensional accuracy is critical for ensuring functional fit, assembly, and overall quality of printed parts. Dimensional accuracy is affected by several factors, such as material shrinkage, layer thickness, resolution, thermal effects, machine calibration, and support structures. To compensate for shrinkage and thermal effects, beam offset is provided. The aim of the present experimental study is to do the dimensional analysis of a 3D-printed part using LPBF. The parts were made with chamfers to measure and calculate the dimensional accuracy of the part at different settings of the hatch-contour. In this experiment, an experiment-based design approach was adopted in which the process parameters, such as hatch offset, contour offset, minimum vector length, and hatch contour offset, were varied. The effect of these process parameters was studied. The prepared samples with different values of hatch offset and contour offset are cleaned, and a clear image of their chamfer at each corner is taken using an optical microscope. Then, using the ImageJ software, the shortest and longest lengths of the chamfer are measured and recorded. Scanning electron microscopy is also used to see the effect in the best case. It is then calculated how much they deviate from the theoretical length we got from the CAD file. It can be concluded that dimensional errors increase with an increase in hatch offset. In this case, a hatch offset of 0.03 mm, contour offset of 0.32 mm yield the minimum error in dimension.

<quillbot-extension-portal></quillbot-extension-portal>

8:00 PM SF01.03.13

Ultra-high-Strain-Rate Tribological Nonlinearity and Adhesion Mechanism of Diblock Copolymers for Polymer-Based Cold Spray[AraKim](#)¹, SinanMüftü², EdwinThomas³ and Jae-HwangLee¹⁻³; ¹University of Massachusetts Amherst, United States; ²Northeastern University, United States; ³Texas A&M University, United States

The adhesive strength between feedstock microparticles and pre-deposited layers and the collision-induced material behaviors determine the quality of cold-sprayed products. Unlike ductile metals, polymers having weak intermolecular interactions present severe nonlinear dynamic response due to their rate-dependent and temperature-dependent material characteristics resulting from the relatively slow macromolecular dynamics with low phase transition temperature. The distinctive complexity requires a comprehensive understanding of the collision-induced rheological changes near the collision interface, affecting interfacial friction and determining adhesion during impact. However, the interfacial response during ultra-high-strain rate (UHSR) collision has not been thoroughly studied. As an experimental approach to gain deeper insight into the collision-induced rheological characteristics of polymeric microparticles at the collision interface, the angled laser-induced projectile impact test (θ -LIPIT) with an off-normal incidence angle was introduced in this work. A colliding microparticle with 45 degrees of the incidence angle undergoes moderately distributed compression and shear motions without arresting at the target substrate during the UHSR collisions.

Controlling or predicting the dynamic nonlinearity of polymers resulting from the rate- and temperature-dependent material properties is crucial for the applications of polymers in cold spray additive manufacturing. Therefore, diblock copolymers consisting of mechanically distinctive multi-domains are intriguing materials as their material properties are tailorable by adjusting the volume fraction of the respective chain blocks. Polystyrene-block-polydimethylsiloxane copolymers having glassy- and rubbery-domains are used for microparticle production. Using a lab-built ultrasonic atomization system, block copolymer solutions are solidified into spherical microspheres with 10 – 30 μm diameters via spraying and hot-air solvent drying. These microparticles are then impacted onto rigid substrates such as silicon wafers during the θ -LIPIT.

Due to the relatively large incidence angle and diameters, adhesion of microspheres does not occur in the θ -LIPIT but minor polymeric residues are occasionally found on the surface of the substrate. Impact and rebound velocities are decomposed along the horizontal and vertical directions to the collision surface, and the resultant coefficients of restitution are used to quantify the effective coefficient of friction representing the UHSR rheological changes of a microparticle at the collision interface.

The effective coefficients of friction obtained from the θ -LIPIT reveal that the collision-induced rheological changes resulting from thermal softening near the collision interface determine the tribological nonlinearity during the UHSR event. Furthermore, it is further thought that this rheological response could alter the adhesion strength of the polymer microparticles by increasing chain mobility. The rheological changes of polymeric microparticles are thus thought to determine their adhesion behavior as the compression-induced shear stress flow along the tangential direction to the collision surface is expected to generate thermal softening in the material near the interface.

Systematically conducted research with θ -LIPIT demonstrates the collision-induced rheological changes near the interface and the resultant tribological conditions for adhesion during UHSR collisions. The demonstrated methodology in this study is expected to be utilized to examine the cold spray applicability of polymers and to predict spraying conditions for cold spray using solid-state consolidations of feedstock powders.

* This material is based upon work supported by the National Science Foundation under Grant No. CMMI-1760924.

8:00 PM SF01.03.14

Metrology of Shrinkage-Induced Deformation in Structures Made using Two-Photon Polymerization[MarkBonino](#), DavidR. Harding, SarahM. Fess, MadelynJ. Jeske and MitchellJ. Anthamatten; University of Rochester, United States

Two-photon-polymerization (TPP) printing provides a deterministic method compared to traditional processes for fabricating millimeter-size spherical and hemispherical polymer parts with nanometer precision. The small print field ($<0.2 \times 0.2 \text{ mm}^2$) needed to achieve the highest resolution, however, requires individual blocks be printed and “stitched” together to achieve the final component. A consequence of this methodology is that shrinkage from polymerization and the residual stresses in the printed polymer create a misalignment of up to 10 μm with the adjacent print block; these offsets need to be reduced to less than 1 μm . Fortunately, the TPP process is sufficiently precise that the misalignments can be compensated in the design, provided the magnitudes and locations are accurately known.

This presentation describes the metrology used to characterize highly curved surfaces (radius of curvature $<1 \text{ mm}$) of spherical and hemispherical structures. The change in curvature of individual print blocks along their lengths and widths is quantified for different laser doses (combination of laser power and scan speed) and print-block sizes, and is used to optimize the printing conditions for improved surface roughness and sphericity. Atomic force microscopy and variable-pressure scanning electron microscopy are used to acquire the data. The quality control and metrology techniques applied to TPP shells are presented.

This material is based upon work supported by the Department of Energy National Nuclear Security Administration under Award Number DE-NA0003856, the University of Rochester, and the New York State Energy Research and Development Authority.

8:00 PM SF01.03.15

Reducing the Anisotropy in Fused Filament Fabrication Additive Manufacturing by Blending a Diels-Alder Covalent Adaptable Network with Polycaprolactone[DerekJ. Bischoff](#) and MichaelE. Mackay; University of Delaware, United States

Additive manufacturing (AM) is an emerging polymer processing technique that allows users to create complex geometries and customized parts with ease in addition to rapidly iterate on prototype designs, making it a valuable tool for product development. The most popular AM technique is based on material extrusion where spools of thermoplastic filament are the raw material that is fed into a hot end where it is melted and extruded through a nozzle on the order of 0.4mm in diameter. The deposited tracks of material are stacked on top of each other in a layer-by-layer sequential manner to build the object. A variety of thermoplastics are commercially available such as polylactic acid (PLA), acrylonitrile butadiene styrene (ABS), and polyethylene terephthalate glycol (PETG) to use on consumer grade desktop machines such as a Prusa i3 MK3S. A limiting factor of these materials is the high degree of anisotropy when 3D printed, as determined by printing tensile testing specimen where the interface between tracks is either parallel (stronger) or perpendicular (weaker) to the tensile stress. The mechanical strength of printed objects is limited by the healing that occurs at the interface. Since interfaces are required to build in the Z-direction off the bed, the term Z-strength is typically used. Due to the highly non-isothermal nature of the printing process, the thermoplastic material only remains above T_g , enabling the reptation and entanglement of polymer chains across the interface, for a brief period of time, on the order of a second. To eliminate the anisotropy in printed objects, new materials specifically designed for AM are necessary that shift the strengthening mechanism from polymer chain diffusion to something else.

Thermosets are the other major class of polymers that contain crosslinked chains to form a network architecture. The static crosslinks that offer improved mechanical properties and dimensional stability prevent thermosets from flowing, making them incompatible with the AM process. By using reversible covalent bonds in place of static crosslinks, thermosets are transformed into covalent adaptable networks (CANs). CANs behave as thermosets when the reversible covalent bonds are in their adduct state, but can flow when the bond exchange reaction is activated upon exposure to an appropriate level of stimulus (heat, light, pH, etc.). One such reversibly dynamic covalent bond is made from the Diels-Alder (DA) reaction between furan and maleimide functionalities. When exposed to a thermal stimulus, the covalent bonds begin to dissociate and exchange, enabling the CAN to flow as a viscoelastic fluid at elevated temperatures. Upon cooling, the material recovers crosslinking density and the rate of bond exchange slows. CANs have been used successfully in the AM literature to reduce the anisotropy in printed objects since covalent bonds form between tracks, however, they typically require specialized machines using cold air on the build plate to cool the object or use a syringe loaded with the material, necessitating a custom feed system different from the usual thermoplastic spools. In this work, a highly crosslinked DA CAN is blended with polycaprolactone (PCL) to create a

semi-interpenetrating polymer network (IPN) that has enough flexibility to be extruded into a spool to be used in commercially available 3D printers without modification. Without the PCL, the DA CAN is too stiff preventing it from being spooled. The CAN/PCL semi-IPN is shown to reduce the degree of anisotropy from >60% in PLA for example to only 11%. Microscopy of the cross sections reveal that the void space typically found in between tracks of material has vanished and is attributed to the viscosity of the material at the printing temperature. The fracture surfaces reveal that a ductile failure mechanism takes place in the tensile testing specimen, improving the toughness of the material compared to pure DA CAN.

8:00 PM SF01.03.16

Development of Filament Manufacturing Technology and Selection of 3D Printing Process Parameters for Biodegradable Material Blends to Optimize Print Quality[Piotr Makula](#), Anna Dmitruk, Pawel Kaczynski, Joanna M. Ludwiczak and Mateusz Skwarski; Wrocław University of Science and Technology, Poland

Biodegradable materials are increasingly being used, with their utilization being legislated in some cases and a conscious choice of users in others. Poly(lactic acid) (PLA) is a commonly used biodegradable material for 3D printing in Fused Filament Fabrication (FFF) technology. Besides its print hardness, the low purchase cost also contributes to its popularity. The study has shown that effective utilization of mixtures of Poly(lactic acid) (PLA) with poly(butyleneadipate-co-terephthalate) (PBAT) or thermoplastic starch (TPS) for 3D printing is possible. The aim of their production is to modify the mechanical properties of PLA by increasing its flexibility while maintaining the biodegradability of the material.

After analyzing the literature, a successful attempt was made to produce a filament with a diameter of 2.85 mm, which was later used to manufacture samples. The material, after the extrusion process, underwent three consecutive drawing operations through a die on a specially adapted drawing machine. These operations were carried out to reduce and stabilize the filament diameter. The mixtures were prepared in the following mass ratios:

PLA50%-PBAT50%(PBAT50)

PLA30%-PBAT70%(PBAT70)

PLA50%-TPS50%(TPS50)

PLA30%-TPS70%(TPS70)

The printer parameters were calibrated before starting the sample printing, which ensured the correct structure of the prints. The tensile tests were initially conducted on the elements printed perpendicularly to the tensile axis. During the printing process, temperatures ranging from 190-270°C were set, with a step of 10°C. The aim of that test was to determine the optimal temperature that provides the best layer bonding. At the most optimal temperatures (PBAT50 - 230°C, PBAT70 - 220°C, TPS50 - 210°C, TPS70 - 210°C), the samples were destroyed by brittle fractures rather than layer delamination.

The next research step was to test the strength of longitudinally printed samples. The experiment showed that when the layers were arranged in this orientation, the material strength was comparable to the homogeneous material obtained through injection molding. The PBAT50 material exhibited layer delamination during stretching, but it did not fracture in a brittle manner. In the case of the second material, PBAT70, the samples behaved like a typical ductile material during stretching. They stretched evenly along their entire length, and no local necking occurred. Mixtures of TPS with PLA, when printed like the previous samples, exhibited more brittle fractures. However, the mechanical values were comparable to those of homogeneous samples.

In the summary of the study, a comparison was made between the obtained results and the results obtained from tests on homogeneous samples produced by injection molding. The results show that the material printed perpendicular to the stretching axis can withstand a 70% of the strength of the homogeneous material. The same result was obtained for all mixtures.

Longitudinally printed samples achieved similar results in terms of strength and the shape of the stress-strain curve. However, they present a faster decrease in strength immediately after exceeding the yield point.

The conducted research can be effectively utilized in further studies and to model the behavior of the material for finite element analysis methods.

8:00 PM SF01.03.17

Study on the Multifunctional Sandwich Structure Fabricated by 3D Printing[Hui-Jin Um](#)¹, Na-Hyun Jeon¹ and Hak-Sung Kim^{1,2}; ¹Hanyang University, Korea (the Republic of); ²Hanyang Research Center for Advanced Semiconductor Packaging, Korea (the Republic of)

Reducing fuel and energy consumption, greenhouse gas emissions, and other air pollutants is a major goal for the global transportation sector, including aerospace, automobiles, and railways. As an approach to achieving this goal, there has recently been a growing movement to change internal combustion engines to hybrid or electric engines. Secondary batteries, such as lithium batteries, are mainly used as energy sources for electric vehicles (EVs), so studies are being conducted to increase mileage. One way to increase mileage is to have a high-capacity battery, which requires more space for batteries and increases the weight of the electric vehicle. For this reason, reducing the weight of the structure is essential to achieve longer mileage. There is a growing interest in structural design using fiber-reinforced plastic composites instead of steel and aluminum. Especially, carbon fiber-reinforced plastic composites (CFRP) with high specific strength and non-rigidity are in the spotlight.

To achieve higher mechanical load-bearing properties using lightweight materials such as CFRP, a sandwich structure consisting of skins and cores can be applied to the structural design. The core of the sandwich structure mainly uses low-density plastic foam or consists of a lattice structure to increase bending properties while lowering the overall weight of the structure. These sandwich structures can be applied to multifunctional structures that can increase energy storage capacity and save space for electric vehicles. The sandwich structure of the neutral axis is hardly affected by the load, so the battery can be integrated into that position to provide reliable energy storage. Thomas et al. integrated a LiPo battery into a foam-core sandwich structure and analyzed mechanical properties through the bending test. However, the flexural failure strength of the multifunctional sandwich structure was reduced by 57% and the bending load partially increased the battery's internal resistance. In other words, the load-bearing properties and energy storage capabilities of multifunctional structures are in conflict with each other. In this study, the multifunctional sandwich structure using lattice structure cores was designed and manufactured to overcome these limitations. 3D printing technology using continuous carbon fiber filament was applied to implement a lattice structure of complex shapes. The multi-functional composite sandwich structure was manufactured by embedding a LiPo battery using an empty space in the 3D-printed corrugated lattice core. Static and cyclic 3-point bending tests were conducted for analysis of the mechanical characteristics. The battery capacity change was analyzed through battery charge/discharge test before and after the mechanical tests. For the 3D-printed corrugated sandwich structure, the mechanical characteristics were maintained regardless of whether the battery was embedded or not, and the battery was not damaged by external loads. In other words, the battery damage caused by external loads was minimized by utilizing the empty space of the core of the lattice structure, and the degradation of mechanical characteristics was minimized.

Acknowledgement

This work was supported by Korea Institute of Energy Technology Evaluation and Planning (KETEP) grant funded by the Korea government (MOTIE) (20212020800090, Development and Demonstration of Energy-Efficiency Enhanced Technology for Temperature-Controlled Transportation and Logistics Center). This work was also supported by Korea Institute of Energy Technology Evaluation and Planning (KETEP) grant funded by the Korea government (MOTIE) (20202020800360, Innovative Energy Remodeling Total Technologies (M&V, Design, Package Solutions, and Testing & Verifications Technologies) for the Aging Public Buildings)

8:00 PM SF01.03.18

Carbon Quantum Materials for Two-Photon Polymerization: A New Approach in Rapid Additive Manufacturing[Arun Jaiswal](#)^{1,1}, Sweta Rani¹, Gaurav P. Singh¹, Mahbub Hassan², Aklima Nasrin², Vincent G. Gomes², Sumit Saxena^{1,1} and Shobha Shukla^{1,1}; ¹Indian Institute of Technology Bombay, India; ²The University of Sydney, Australia

3D/4D additive manufacturing technologies have played a crucial role in the development of various miniature sensors, lab-on-a-chip devices and other ultracompact devices, due to their capabilities of generating functional elements with well-defined geometries and subwavelength resolutions. These functional nanostructures incorporating novel nanomaterials formulations are pivotal in the realization of next-generation technologies, and are derived from doped/functionalized materials exhibiting specific response towards external stimulants. The overall response depends on the nanostructure constituents as well as their structural attributes. Material formulations and fabrication capabilities are crucial for further development of such structures. Vat polymerization-based fabrication techniques, especially two-photon polymerization-based nanofabrication allows simultaneous exploitation of structural and material attributes, and hence has emerged as popular choice for realization of 2D/3D/4D elements of the functional devices. Two-photon lithography is well established in terms of its fabrication capabilities, but the responsivity of the structures towards each agent is dependent on a specific dopant, and to attain multifunctional structures, more and more number of dopants are required to be incorporated into the resin. However, the addition of multiple dopants is not recommended for vat polymerization-based systems, as it affects the stability of the resin, interferes with the excitation beam and degrades the printing performance. Additionally, few dopants such as metal/semiconductor nanoparticles offer limited solubility and hence tend to settle, resulting in non-uniform doping of the fabricated structures. To address these issues there is a need of development of a material system with minimal components, providing multifunctional attributes. In this context we report use of carbon nanomaterials as multifunctional additives in two-photon polymerizable resin formulation. The proposed resin allows tailoring of the responsivity of the micro/nanostructures just by simple surface engineering of the carbon nanomaterials. In this work, we demonstrate the multimodality of carbon nanomaterial wherein they i) facilitate two-photon upconversion, (ii) enable efficient two-photon polymerization of acrylates and (iii) are responsible for the fluorescent staining of the polymerized structures. This work paves pathways towards implementation of multifunctional nanomaterials for development of the next-generation smart devices.

References

[1] A. Jaiswal, et al, Additive-Free All-Carbon Composite: A Two-Photon Material System for Nanopatterning of Fluorescent Sub-Wavelength Structures, ACS Nano. 15, 14193–14206, 2021.

[2] A. Jaiswal et al., Additive Manufacturing of Highly Fluorescent Organic 3D-Metastructures at Sub-Wavelength Resolution, Mater. Today Phys. 20, 100434, 2021.

[3] A. Jaiswal et al., Carbon Quantum Initiators Enabled Direct Laser Writing: A Technique For Fabrication of Dielectric, All-Carbon Chiral Metasurfaces, Carbon, 208, 43-49, 2023.

8:00 PM SF01.03.19

On-Demand Rapid Fabrication of Components using Forward Operating Base Aluminum WasteDanyangZheng, YutaoWang, MishraBrajendra and JianyuLiang; Worcester Polytechnic Institute, United States

According to the study conducted by the US Army Research Laboratory (ARL), and the US Natick Soldier Research Development, and Engineering Center (NSRDEC), aluminum waste makes up the Second largest category of metals in solid waste generated on forward operating bases (FOB). Therefore, an agile manufacturing process that can reclaim and recycle aluminum waste on battlefields is highly desirable. In this project, a 3D printing-enabled rapid-casting manufacturing process was developed to reuse Al waste and a mobile foundry system based on this process has been designed.

This remanufacturing process includes three main stages: the preparation stage, the casting stage, and the post-treatment stage. It starts from the 3D design of the casting mold, using advanced software to conduct a simulation to minimize the defects in the cast parts. Then 3D printing is used to fabricate the polymer pattern according to the design. These polymer patterns are covered with coating. After drying, the patterns are removed by a burn-out process to obtain the needed cast molds. On the other hand, the waste metal alloys from FOBs are collected and sorted. The harmful impurities are removed. The Al wastes are then blended according to the desired composition of the target product. This composition can be further adjusted during the melting process.

After the molten metal with the desired composition is obtained, it is poured into the cast molds. Finally, after the solidification of the metal, the mold is removed, and necessary post-treatments are conducted to ensure the quality of the parts. The information obtained from quality control can be used as feedback to further improve the mold design and the composition adjustment for re-alloying.

A mobile foundry design that places this rapid casting process in standard-sized shipping containers as developed to efficiently convert battlefield waste into valuable products. The mobile system consists of three containers: the first for investment preparation, the second for casting and heat treatment, and the third for product characterization. A simulation has been conducted to ensure the safety of the casting container.

In this presentation, the results and outcomes of this project will be discussed. The lessons learned and future work will be introduced.

8:00 PM SF01.03.20

3D Printing and Biocementation of Hierarchical Porous CeramicsAlessandroDutto, ElenaTervoort and AndréR. Studart; ETH Zürich, Switzerland

Novel low-cost and low-energy strategies for the consolidation of ceramic materials are demanded to reduce the environmental impact of the building sector. Living building materials containing soil microorganisms have shown to be a promising strategy to bind together aggregates or sand-based materials into bricks at room temperature taking advantage of the microbially induced precipitation of calcite (MICP).

The effectiveness of the precipitated calcite network in providing the required structural integrity relies on the uniform distribution and activity of the microbes, as well as the availability and diffusion of nutrients and precursors for the MICP throughout the bulk of the material. Current technologies overcome the limits of diffusion by actively pumping a calcifying solution and by optimizing the calcification setup. Despite the commercial use of this approach, partial clogging or the formation of an outer calcite shell hinder the access of further precursors and thus remain unsolved challenges of this technology.

Here, we take advantage of additive manufacturing to develop and study a bio-cementation process to create strong, porous ceramics at room temperature. Hierarchical porous structures were produced via direct ink writing of cellular grids using bacteria-laden suspensions of ceramic hollow spheres. The effect of geometry, bacterial concentration, and calcification time on the bio-cementation process and the resulting mechanical properties were investigated. The presence of a millimeter-sized open porosity was found to be essential to maintain a high permeability to the precursors during the entire process, ensuring an optimal MICP throughout the material.

The presence of porosities at multiple length scales has a beneficial effect on both the biocementation process itself and on the mechanical efficiency of the produced structures. Combining 3D printed hierarchical porous structures with the low-energy consolidation process of MICP, allows us to produce strong, porous ceramics with reduced environmental impact.

8:00 PM SF01.03.21

Mechanical Characterization of Additively Manufactured Ceramic Nanocomposites Reinforced by Boron Nitride NanotubesDingliWang, NasimAnjum and ChanghongKe; State University of New York at Binghamton, United States

Ceramic materials face significant challenges in industrial applications due to their inherent fragility and limited manufacturability. These limitations can potentially be overcome through the use of reinforcements and additive manufacturing (AM) techniques. Boron nitride nanotubes (BNNTs) exhibit many exceptional structural and physical properties, making them promising candidates for reinforcing ceramics and creating lightweight, strong, and durable ceramic materials. These characteristics are attractive to a number of industries, such as aerospace, automotive, and biomedical sectors. The reinforcement potential of BNNTs for ceramic composites is supported by our recent findings of efficient interfacial load transfer in BNNT-ceramic nanocomposites, which is attributed to the partially ionic B-N bonding and the resulting rugged anisotropic energy landscape. Here, we investigate the bulk mechanical properties of AM-produced BNNT-reinforced silica (SiO₂) nanocomposites. Our study aims to elucidate how the superior interfacial load transfer characteristics observed at the nanoscale translate into enhancements in the bulk mechanical properties of these nanocomposites. The BNNT-silica nanocomposites employed in our study are additively manufactured using digital light processing (DLP) techniques. Our study shows that the addition of a small quantity of BNNTs can substantially enhance the AM-produced ceramic nanocomposite's bulk mechanical properties (flexural modulus and strength, and fracture toughness). We further analyze the local interfacial load transfer within the AM nanocomposite through *in situ* Raman micromechanical measurements. The findings provide valuable insights into the role of the nanotube-ceramic interfacial strength in enhancing the mechanical properties of the nanocomposite. Our research contributes to a better understanding of the relationship between process, structure, and properties in AM-produced ceramic nanocomposites and the development of durable and reliable ceramics technology.

8:00 PM SF01.03.22

High Pressure Heat Treatment for Porosity Reduction of Binder Jet 17-4 PH Stainless SteelEllenTrojanosky, ChuhaoLi, RichardSisson and JianyuLiang; Worcester Polytechnic Institute, United States

The age hardenable 17-4 PH stainless steel has been additively manufactured (AM) using the binder jet (BJ) method. To achieve comparable mechanical properties to wrought steel, the porosity must be reduced in the AM steel. Two sets of BJ, one starting with high porosity and the other low porosity, are treated to the traditional 900H age hardening treatment or a combined hot isostatic pressing (HIP) and 900H treatment, referred to as High Pressure Heat Treatment (HPHT). The effects of change in porosity and pore morphology on the microstructure, mechanical properties, and distortion are examined. These experimental results indicate that the HPHT process is more effective than the 900H treatment at reducing porosity and improving performance.

8:00 PM SF01.03.23

Dual Material Fused Filament Fabrication via Core-Shell Die DesignAhmadNaqi^{1,2} and MichaelE. Mackay^{1,1}; ¹University of Delaware, United States; ²Kuwait University, Kuwait

In this work a fused filament fabrication (FFF) die design, capable of extruding two thermoplastics simultaneously in a core-shell configuration, is demonstrated as a means to produce composite structures in a single step. Despite the enormous advancements in 3D printing, fabrication of FFF objects with a composite structure remains a challenge due to the difficulty in finding dies to extrude such structures. We used polyethylene terephthalate glycol (PETG) and high-density polyethylene (HDPE) filaments to perform core-shell 3D printing. HDPE is one of the most commonly produced plastics but rarely used in FFF due to the severe warpage caused by volume changes upon its crystallization. Rheological and thermal analyses suggest the use of HDPE as a shell material due to its extremely short reptation time and sharp melting peak that facilitate superior surface contact and interlayer weld strength at the interface between neighboring FFF tracks. PETG is a commonly used 3D printing filament with excellent printability and sufficient zero shear viscosity to help maintain the extruded filament shape against shrinkage induced by the HDPE shell.

Impact and tensile properties of core-shell objects revealed tremendous improvements in the impact resistance and toughness especially at 30 vol % HDPE shell with 1280% and 150% enhancement in impact resistance when compared to individual components: PETG and HDPE, respectively. Scanning electron microscopy was used to analyze the fracture morphology of the tested specimens to obtain an understanding of the fracture mechanism leading to the increased impact resistance. Using this die design can help open avenues of fabricating high impact resistance materials suitable for high performance applications and using HDPE in 3D printed objects with its superior solvent resistance.

8:00 PM SF01.03.24

Anisotropic Macro- and Micro-Mechanical Creep Properties of Additively Manufactured Ti-6Al-4V ELI AlloyJeong-RimLee¹, Min-SuLee¹, Si MoYeon², Chung-SooKim² and Tea-SungJun¹; ¹Incheon National University, Korea (the Republic of); ²Korea Institute of Industrial Technology, Korea (the Republic of)

The present study investigates the nanoindentation-based creep behavior of Ti-6Al-4V extra low interstitial (ELI) alloy fabricated using laser powder bed fusion (L-PBF) at ambient temperature. Nanoindentation creep tests were performed on both the vertical and horizontal planes with respect to the building direction for the as-built and stress-relieved samples. Various

peak loads (100, 200, 300 mN) were applied with a holding time of 1000 s using a spherical indenter. Creep parameters, such as creep rate and creep stress exponent, were analyzed using the Oliver and Pharr method.

The results of the nanoindentation creep tests indicated that the horizontal plane exhibited higher creep resistance than the vertical plane in the as-built sample. However, the creep behavior of the stress-relieved sample showed greater sensitivity in the horizontal plane, consistent with macroscale time-dependent responses. To understand the underlying factors contributing to the anisotropic creep behavior at different deformation scales and stress relief conditions, the microstructure, residual stress, and dislocation density were further investigated. Characterization results revealed that the horizontal plane exhibited higher hardness compared to the vertical plane, attributed to the higher dislocation density and compressive residual stress in the as-built condition. The observed variations in macro- and micro-creep properties can be attributed to microstructural characteristics. The creep deformation at ambient temperature induced by the nanoindenter is primarily governed by dislocation motion, while creep at the macroscale is significantly influenced by morphologies such as layer bands, β grain boundaries, and melting pool boundaries or defects. These findings contribute to a better understanding of the multi-scale creep behavior in additively manufactured Ti-6Al-4V ELI alloy.

8:00 PM SF01.03.25

Laser Powder Bed Fusion of TiB₂-Reinforced 316L Stainless Steel Composites with Excellent Mechanical Properties Wuxian Yang¹, JianLiu¹, WenChen¹ and TianyiLi²; ¹University of Massachusetts at Amherst, United States; ²Argonne National Laboratory, United States

Laser powder bed fusion (LPBF) additive manufacturing is an emerging technology that enables melting and consolidating powders layer by layer, which has high potential in developing novel alloys with highly refined microstructures. This study discusses the unique microstructure and superior mechanical properties of additively manufactured 316L steel composites reinforced by various amounts of TiB₂ ceramic phase. Scanning electron microscopy (SEM), transmission electron microscopy (TEM), and *in situ* synchrotron X-ray diffraction are used to analyze the microstructure and deformation behavior of the 316L/TiB₂ composites. The TiB₂ particles are homogeneously distributed in the 316L matrix. The 3 vol.% TiB₂ reinforced sample exhibits a high ultimate tensile strength over 1.3 GPa with a large uniform elongation of 18%. Such mechanical properties well surpass those of other additively manufactured 316L steel composites. Hence, the LPBF process shows high potential for fabricating advanced ceramic-reinforced metal matrix composites with outstanding mechanical properties.

8:00 PM SF01.03.26

An Investigation into the Tribocorrosion Behaviour of Additively Manufactured CoCrMo for Human Joint Implants Qingyue Shi¹, Michael Bryant², Connor Myant¹ and Borut Lampret¹; ¹Imperial College London, United Kingdom; ²University of Leeds, United Kingdom

CoCrMo alloys are widely used for medical implants such as hip, knee and shoulder replacements thanks to their high-wear resistance and corrosion resistance. The introduction of additive manufacturing methods, such as selective laser melting (SLM) allows for the fabrication of CoCrMo implants with complex geometries, overcoming the limitations of conventional machining for CoCrMo and offering unprecedented design freedom for patient-specific implants.

SLM involves melting alloy powders layer by layer, subjecting them to multiple thermal cycles of remelting and solidification. Previous studies have reported distinctive microstructural characteristics and the presence of pores in SLM CoCrMo alloys, leading to anisotropic properties. [1,2] Ensuring the longevity and biocompatibility of implants is crucial, as the degradation of metal materials due to wear in artificial joints can potentially trigger adverse physiological reactions in patients. However, despite the importance of this issue, the tribocorrosion performance of SLM CoCrMo alloys in biological environments remains poorly understood. This knowledge gap highlights the need for an investigation into the tribocorrosion behaviours of SLM CoCrMo alloys for joint replacement applications.

In this study, specimens were 3D printed using an Aconity MIDL SLM machine. To isolate and manifest the effect of spatial anisotropy in the laser melting process, bidirectional linear laser paths without rotations on each layer were used. Employing three different build orientations, three surfaces with distinct microstructural characteristics due to their anisotropy were prepared. Their tribocorrosion behaviour was assessed using a reciprocating sliding tribometer integrated with a 3-electrode electrochemical cell to quantify corrosion *in situ*. Tests were conducted in 30 g/L Bovine Calf Serum + PBS to simulate the body fluid in joints. Surface examinations and wear scar analyses were performed to gain a further understanding of the tribocorrosion mechanisms. For comparison, cast CoCrMo specimens were also included as a control group.

The findings indicate that the choice of build orientation is a critical factor in controlling the microstructure of SLM CoCrMo alloys, consequently, the tribocorrosion behaviour of the SLM CoCrMo. The post-tribocorrosion analysis provides valuable insights into the underlying tribocorrosion mechanisms, shedding light on the factors that contribute to the degradation and performance of the SLM CoCrMo. In comparison to cast CoCrMo, SLM CoCrMo demonstrated inferior tribocorrosion performance but tuneable qualities.

In conclusion, this study addresses the knowledge gap regarding the tribocorrosion behaviour of 3D printed CoCrMo alloys for joint replacement applications by investigating the effects of build orientation on microstructure and tribocorrosion performance. The findings emphasize the potential to optimize the additive manufacturing process to achieve improved performance and enhanced tribocorrosion resistance of CoCrMo implants. Ultimately, this study contributes to the advancement of joint replacement technologies, enabling the development of more reliable and long-lasting implants.

[1] K. S. Kim, J. W. Hwang, and K. A. Lee, "Effect of building direction on the mechanical anisotropy of biocompatible Co-Cr-Mo alloy manufactured by selective laser melting process," *J Alloys Compd*, vol. 834, Sep. 2020, doi: 10.1016/j.jallcom.2020.155055.

[2] Y. Kajima *et al.*, "Reduction in anisotropic response of corrosion properties of selective laser melted Co-Cr-Mo alloys by post-heat treatment," *Dental Materials*, vol. 37, no. 3, pp. e98-e108, Mar. 2021, doi: 10.1016/j.dental.2020.10.020.

8:00 PM SF01.03.27

Urethane-Water-Cellulose Composite: Improving Mechanical Properties of Urethane-Based Photocurable Resin for Stereolithography 3D-Printing Akira Kudo¹, Atsuya Fujita², Kazuya Eguchi², Kota Matsuhashi¹, Kota Toyama¹, Takeharu Yoshii¹, Dmitri Louzguine¹, Hirotomo Nishihara¹, Mingwei Chen³ and Satoko Kuwano²; ¹Tohoku University, Japan; ²Tohoku Gakuin University, Japan; ³Johns Hopkins University, United States

3D printing has become one of the most attractive fabrication techniques in materials science and engineering, offering its immense degree of freedom in designing complicated architectures with feature sizes smaller than millimeters or even micrometers. Since the earliest stage of 3D printing, polymeric materials, especially thermoplastic polymers for fused deposition modeling (FDM) and photocurable resins for stereolithography (SLA), have been playing a major role in this field. As the utility of 3D printing expands, eco-friendly development of these polymeric materials will garner increasing attention.

In this presentation, we introduce a composite photocurable resin compatible with SLA 3D printing based on urethane, water and cellulose. A commercially available urethane-based photocurable resin was homogeneously mixed with water and printed into microhoneycomb architectures at a mass ratio of resin:water=3:1. We demonstrated that, despite a considerable portion (20-25% by mass) replaced by water, adding water increased compressive strength and stiffness of fabricated microhoneycomb architectures by 50% or more. Miscibility of urethane-based resin with water also enabled homogeneous dispersion of cellulose nanofibers (CNFs), which would not disperse in pure urethane-based resin. Microhoneycombs made of the urethane-water-cellulose composite showed even more improved properties than the ones without CNFs, achieving strength of 7.5 MPa and stiffness of 80 MPa at 0.25 g·cm⁻³. Structural characterization by Raman spectroscopy, Fourier transform infrared (FTIR) absorption spectroscopy and optical microscopy was performed to investigate the origin of this unintuitive enhancement in mechanical properties and the impact on microstructures brought by water.

Using water and cellulose, both of which are natural materials, our results can inspire a simple, sustainable and high-performance polymeric material compatible with SLA 3D printing.

8:00 PM SF01.03.28

Effects of Printing Direction and Layer Thickness on the Mechanical Properties of 3D Printed Polymer Laminates Ammar Batwa and Yaning Li; Northeastern University, United States

For polymeric additive manufacturing (AM), printing direction and layer thickness are critical processing parameters that directly impacts the effective mechanical properties of the final polymeric laminates fabricated via polymer jetting AM technology. To fully exploit AM potential for fabricating polymeric composites, it's crucial to have a deep understanding of the effects of these factors during the printing processes. This research aims at evaluating the effects of printing direction and layer thickness on the effective mechanical properties of 3D printed polymer laminates.

The printing direction is defined via the angle of the specimens relative to the movement of the print head. Specimens of stratified composites fabricated via combining glassy and rubbery polymer layers with various layer thickness are designed and fabricated via a multi-material 3D printer (Stratasys Connex3). Mechanical experiments are conducted to evaluate both the layer thickness and printing directions collectively influence the overall mechanical properties of the designs. Digital Image Correlation (DIC) is used to track the local and overall strain of the specimens during deformation. The micro-structures of the specimens are explored via Scanning Electron Microscope (SEM) imaging. Nanoindentation experiments are performed to quantify the transition in stiffness across dissimilar material interface. The results show a significant correlation between the mechanical properties of the final printed laminates, the properties of the dissimilar interface/interphase, and the printing direction and layer thickness.

<quillbot-extension-portal></quillbot-extension-portal>

8:00 PM SF01.03.29

Heterostructured Mechanical Metamaterials Inspired by the Shell of Strombus Gigas Juzheng Chen¹, Hao Wu¹, Jingzhuo Zhou¹, Ziyong Li¹, Rong Fan¹, Roberto Ballarini² and

The shells of molluscs have been shown to be strong and tough as a result of various types of architectural design that effectively control the evolution of shear bands and cracks during deformation. The crossed-lamellar design of the shell of *Strombus gigas*, whose hierarchy consists of four distinct lamellar-shaped features, represents the toughest of all seashells. A mechanical metamaterial that replicates the natural structure of this queen conch is anticipated to circumvent the renowned trade-off between strength-conductivity and strength-density. Here we introduce the architectural concepts of dimensional discreteness and interactive discreteness, inspired by the crossed-lamellar design, to instruct the design of bio-inspired metamaterials. The shear bands formed by the newly created metamaterial are effectively discrete and confined within an individual plank-like zone during compression. The mechanical properties are shown to be linearly proportional to the level of architectural discreteness, resulting in a progressive deformation with cross-layer hysteresis. A spring-based model is proposed that is in excellent qualitative agreement with experimental observation, that validates the superiority of the architectural discreteness-based paradigm, and that is capable of translating abstract designs into vivid layouts of spring systems with broad generality. The results have far-reaching implications for the design of strong mechanical metamaterials from a brand-new perspective.

8:00 PM SF01.03.30

Controlling Microstructures and Modulus in Direct Ink Writing of Stainless Steel for Biomedical ApplicationsHavvaE. Aysal¹, BrianK. Paul², Chih-hungChang² and KostantinosSierros¹; ¹West Virginia University, United States; ²Oregon State University, United States

As metals are employed in additive manufacturing at an accelerated pace, environmentally friendly, and less-cost 3D printing processes are required. Direct ink writing (DIW) is a highly versatile technique that utilizes solution-based formulations, known as inks, which exhibit shear-thinning behavior and can accommodate a wide variety of unique precursors. In this study, we present environmentally safe binders for aqueous bio-based metal inks, specifically exploring cellulose-based binders engineered for rheological compatibility with DIW.

Furthermore, we investigate the use of novel inks to control the microstructures of the printed product. The effects of ink formulation, processing parameters, and post-processing techniques on the microstructure and mechanical properties of the printed objects are being explored. Specifically, the capability to modify the organic components of the ink to control porosity is demonstrated, enabling the creation of microstructures with different surface properties.

Stainless steels (SS) have been in use as biomaterials for a long time. SS alloys, commonly utilized in biomedical implants, offer advantages such as affordability, availability, biocompatibility, and high strength. However, the presence of toxic nickel in SS poses a significant concern, particularly for patients sensitive to nickel. Therefore, ongoing research aims to develop nickel-free SS alternatives. In our study, we propose SS420 as a potential substitute, considering its suitability for biomedical applications.

In addition to biocompatibility, satisfactory mechanical properties, and osseointegration are essential factors to consider. Mechanical properties such as hardness, tensile strength, Young's modulus, and elongation play a crucial role in determining the suitability of a metallic material. The occurrence of implant fractures resulting from mechanical failures can be attributed to biomechanical incompatibility. Therefore, it is expected that the material used as a bone substitute exhibits mechanical properties comparable to those of natural bone. Osseointegration, which refers to the ability of a material to effectively bond with the bone and surrounding tissues, is a crucial aspect in the use of metallic alloys for bone applications. Porous steels have demonstrated favorable integration with bone implants. However, increasing the porosity of steel can lead to a decrease in its modulus. To address this issue and improve the stiffness of printed stainless steel to match that of bone, we propose the application of a metal-organic framework (MOF) coating to the SS. This coating will allow us to investigate the impact of surface roughness on stiffness. Through further examination of the effects of increased surface roughness on the mechanical properties of the printed SS, our objective is to advance the development of materials with enhanced compatibility for biomedical applications.

8:00 PM SF01.03.31

Effect of Solidification Rate on Microstructure and Mechanical Properties of Additively Manufactured AlCrFe₂Ni₂ High-Entropy AlloysShengbiaoZhang¹, ChenyangLi², WeiChen² and WenChen¹; ¹University of Massachusetts Amherst, United States; ²Illinois Institute of Technology, United States

The development of high-entropy alloys (HEAs) has attracted significant attention due to their potential for enhanced mechanical properties. However, the formation of undesired intermetallics in HEAs limits their practical applications. Additive manufacturing (AM) offers a promising approach to overcome this limitation by providing unique thermomechanical processing conditions that result in far-from-equilibrium solidification microstructures, leading to exceptional material properties. To fully harness the benefits of AM and HEAs, understanding the processing-structure-property relationship is crucial but challenging due to the complex phase selection and non-equilibrium microstructures formed during AM. In this study, we investigated the effect of solidification rate on the microstructure and mechanical properties of a laser additively manufactured AlCrFe₂Ni₂ HEA. By varying the laser scan speed, we observed distinct solidification features, including partitionless single-phase, anomalous eutectic, and coupled lamellar eutectic microstructures. These microstructures offer a wide range of strength-ductility combinations. Thermodynamic modeling and molecular dynamics simulations are performed to gain insights into the solidification mode transition from partitionless through anomalous eutectic to coupled eutectic as the solidification rate continuously decreases. Our findings demonstrate that AM enables access of a rich variety of phase and microstructure space for HEAs, expanding the material design possibilities for technologically relevant alloys.

8:00 PM SF01.03.32

Investigation of Structure-Processing Relationships in Metal Additive Manufacturing Through Featurization of Microstructural ImagesDipayanSanpui^{1,2}, AnirbanChandra^{1,2}, SukritiManna^{1,2}, Partha SarathiDutta^{1,2}, MariaK. Chan¹, HenryChan^{1,2} and SubramanianSankaranarayanan^{1,2}; ¹Argonne National Laboratory, United States; ²University of Illinois at Chicago, United States

The understanding and prediction of accurate property-structure-processing relationships is essential in designing robust, reliable parts and assemblies, both forward and inverse. The direct mapping of process parameters to property values can be plausible in some cases, but it is often hampered by poor microstructural control. Therefore exploring a straightforward relationship between processing conditions and microstructural features can offer important physical insights and assist the overall design procedure. In this work, we present an automated high-throughput approach towards simulating an AM process that is uncertainty-aware, can characterize microstructural images, and extract appropriate features and descriptors. We used a kinetic Monte Carlo (KMC) based model of the AM process to simulate microstructural evolution for a variety of processing conditions, having utmost relevance with the experimental conditions. We perform a parametric study by selecting four input processing parameters in KMC simulations (velocity, hatch spacing, melt-pool width, and tail length) to explore the relationship between microstructural features and processing conditions. As a first step towards the exploration of microstructural features and processing conditions, we performed a parametric study by selecting the four input processing parameters in KMC simulations (velocity, hatch spacing, melt-pool width, and tail length). With systematic variations of the process parameters, a large number of simulations were performed for obtaining a diverse set of microstructural images. Subsequently we performed thorough analysis of the simulated images and extracted meaningful descriptors using conventional algorithms and an off-the-rack image processing tool, the Watershed algorithm. Finally, we present an approach towards discussion of the ability of various quantitative microstructural features to differentiate between the obtained microstructures. For accurate featurization of microstructural images, we focus on a set of six most relevant microstructural descriptors: Orientation, Aspect ratio, Perimeter-Area ratio, Equivalent diameter, Two-point statistics and chord length distribution (CLD) in two dimensions. As byproducts of our featurization algorithm, we realize many-to-one mapping is a necessity for representation of microstructural images unambiguously, multiple descriptors are therefore required to unambiguously map processing conditions to typical descriptors. Depending on the differentiability of the distributions of the microstructural features, a unique score can be allotted to a particular grain profile. This unique value of the metric or score can be further utilized to propel the inverse design problems. Defining a unique score is impossible if the four dominant microstructural features do not differ across the chosen processing conditions. Hence our research work provides very important information, in both qualitative and quantitative aspects, that would help in the proper understanding of microstructural representations. Appropriately characterized microstructural representations can then be utilized for development of data-driven models for predictive control of grain profiles, resulting in tailored mechanical or thermal properties of additively manufactured parts.

8:00 PM SF01.03.33

Embedded 3D Printing of Soft Materials and Ultrafine Hair StructuresWonsikEom¹, MohammadA. Hossain¹, VidushParasramka¹, RyanW. Siu¹, JeongminKim¹, KatherineSanders², DakotaPiorkowski³, AndrewLowe³, MichaelD. Volder², DouglasS. Fudge³, RandyH. Ewoldt¹ and SamehTawfik¹; ¹University of Illinois at Urbana-Champaign, United States; ²University of Cambridge, United Kingdom; ³Chapman University, United States

Embedded 3D printing enables the direct ink writing of ultrasoft materials which, due to gravity, cannot support their own weight in air. For this reason, embedded 3D printing is a platform to replicate nature's complex, branching, and tortuous fibrous structures. However, this recent technology has been limited by a complex interplay of factors such as interfacial tension ratios between the printing materials and the support gel, the viscosity of the ink, and the yield stress of the gel. Because of these complexities, the minimum feature diameter is limited to around 50 μm . Recently, a feature diameter of 8 μm was achieved by tailoring the interfacial tension. This limitation prevents the accurate replication of natural structures, many of which feature dimensions at the micrometer scale, such as long aspect ratio mechanosensing stereocilia and the hairs on the feet of beetles and geckos.

Here, we introduce solvent exchange between the ink and the support gel as a key mechanism to expand the capabilities of embedded 3D printing and allow the fabrication of ultrafine and tortuous structures from a variety of soft materials. This method facilitates the immediate solidification of the extruded polymer solution upon its interaction with the gel's solvent, enabling the printing of ultrafine features as small as 2.1 μm in diameter. Our work exploits the rheological underpinnings that make such precision possible. We elucidate the critical roles played by the

gel's yield stress and solvent concentration in achieving this high resolution, thereby offering a comprehensive understanding of the mechanics behind this proposed approach. Solvent-exchange extends to the versatility of materials available for embedded 3D printing. We demonstrate printing of soft thermoplastic elastomers like styrene-ethylene-butylene-styrene (SEBS) copolymers as well as rigid polymers such as polyvinyl chloride (PVC), and electrically conductive carbon nanotube composites. We applied this method to produce intricate hair arrays, thereby meeting the requirements for bio-mimicking applications. These arrays feature fibers with diameters less than 2 μm and lengths exceeding 1500 μm . In summary, the solvent exchange method presents a notable advancement in polymer 3D printing. The solvent exchange of direct ink writing embedded in support gels enables the fabrication of biomimetic high ultrafine tortuous structures, overcomes previous resolution limitations, and expands the palette of polymeric materials available for printing. This capability opens new avenues for replicating nature's intricate fibrous morphologies towards the design of new architected composite materials. This work was sponsored by the Defense Advanced Research Project Agency (DARPA), under contract no. N660012124036.

8:00 PM SF01.03.34

A Flexible Capacitive Pressure Sensor with High Sensitivity and Linear Response using Size-Distributed Microspheres Yusaku Tagawa¹, Sunghoon Lee², Takao Someya¹ and Tomoyuki Yokota¹; ¹The University of Tokyo, Japan; ²RIKEN, Japan

Flexible pressure sensors enable to measurement various biological signals for long-term monitoring. Obtaining plantar pressure distributions and body weight measurements through wearable devices is significant for healthcare applications and monitoring various diseases such as diabetes, obesity, and heart failure. To detect the planter pressure of such disease patients, wearable, flexible pressure sensors with a high-pressure sensitivity range (1 MPa) can provide precise critical biomedical information.^[1]

Among the various flexible pressure sensors, capacitive pressure sensors are among the most promising candidates owing to their simple fabrication process, rapid response, small hysteresis, and low power consumption. Despite these advantages, typical silicone rubber has a relatively low dielectric constant (2-3), contributing to low sensitivity. Therefore, porous structures at the dielectric layer and dielectric/conductor interface are essential for higher sensitivity because they reduce the initial dielectric constant and compression modulus.^[2] On the other hand, essential characteristics of stable operation, such as linearity over a wide range, have yet to be dealt with enough.^[3] Balancing the linear response and high sensitivity in porous structures remains challenging owing to the sensitivity saturation of porous materials. To the author's knowledge, no capacitive pressure sensor with porous structures that maintains linearity up to 1 MPa with a high sensitivity ($> 10^{-3} \text{ kPa}^{-1}$) exists.^{[4][5]}

This study proposes a capacitive flexible pressure sensor containing thermoplastic microspheres (TPM) with linearity and high sensitivity over a wide pressure range. The TPM expanded at relatively low temperatures (95–125 °C) and increased 50 times in volume. The TPM-containing Polydimethylsiloxane (PDMS) was spin-coated to fabricate an elastomeric membrane with a homogeneous porous structure. Notably, the TPM has a large size distribution with the temperature increasing. This size distribution variety of porous TPM may contribute to the high sensitivity and enhance the linear response owing to the deformation of different sizes of porous under the different pressure. Owing to this characteristic of TPM, we achieved a pressure sensor with a high sensitivity ($3.1 \times 10^{-3} \text{ kPa}^{-1}$) while maintaining linearity ($R^2 = 0.996$) under a high compression pressure (1 MPa).

Furthermore, the sensor responded within 100 ms under 140 kPa and indicated the durability by 10000 cyclic loadings. As a pressure distribution application, we implemented 3×3 multichannel pressure sensors with a large area ($3.4 \text{ cm} \times 3.4 \text{ cm}$) to demonstrate the uniformity of the materials. In addition, we fabricated geta wearables that can detect body weight. As a result, a 4.9 kPa load fluctuation can be detected equally well in a high and low weight range without sensitivity compensation systems, such as non-linear fitting, which implies the significant potential to achieve reliable and simple wearable applications.

Reference

[1] K. E. Chatwin, et al., *Diabetes Metab Res Rev*, 36, 4, 2020. [2] S. R. A. Ruth, et al., *ACS Appl Mater Interfaces*, 12, 58301, 2020. [3] J. Wu, et al., *Nanoscale*, 12, 21198, 2020. [4] J. Tao, et al., *Microsyst Nanoeng*, 6, 62, 2020. [5] D. J. Lipomi, *Nat Nanotechnol*, 6, 788, 2011.

8:00 PM SF01.03.35

Printing Three Dimensional Refractory Metal Patterns in Ambient Air: Toward High Temperature Sensors Jichuan Yu, Ze Wang, Chuxiong Hu and Xining Zang; Tsinghua University, China

Refractory metals offer exceptional benefits for high temperature electronics including high-temperature resistance, corrosion resistance and excellent mechanical strength, while their high melting temperature and poor processibility poses challenges to manufacturing. Here we report a direct ink writing and tar-mediated laser sintering (DIW-TMLS) technique to fabricate three-dimensional refractory metal devices for high temperature applications. Metallic inks with high viscosity and enhanced light absorbance are designed by utilizing coal tar as binder. The printed patterns are sintered into oxidation-free porous metallic structures using a low-power ($< 10 \text{ W}$) laser in ambient environment, and three-dimensional freestanding architectures can be rapidly fabricated by one step. Several applications are presented, including a fractal pattern-based strain gauge, an electrically small antenna patterned on a hemisphere, and a wireless temperature sensor that can work up to 350 °C and withstand burning flames. The DIW-TMLS technique paves a viable route for rapid patterning of various metal materials with wide applicability, high flexibility and three-dimensional conformability, expanding the possibilities of harsh environment sensors.

8:00 PM SF01.03.36

Source Design for Vapor-Based Additive Manufacturing of Drug Substance Particles Eva Pontrelli and Max Shtein; University of Michigan, United States

Additive manufacturing provides a precise, material-efficient, and rapid route to complex structures for a growing scope of applications. The novel vapor-based process described here offers new additive manufacturing capabilities for formulation-ready active pharmaceutical ingredients. This technique deposits material by jetting organic vapor and an inert carrier gas through a nozzle onto a substrate, where the organic condenses. The deposited material has ultra-fine particle sizes, which leads to enhanced bioavailability. Engineering particle size and morphology requires tight control over vapor flux at the substrate. Stable vapor flux also enables precise, flexible dosing of active ingredients, which is essential for pediatric dosing, high potency drugs, and personalization of medicines, but difficult to achieve with traditional solid oral dosing and formulation approaches.

While tight control of feed location is easily accomplished using traditional 3D printer hardware, achieving a stable vapor flux is difficult, yet crucial. The source can be operated near vapor-solid or vapor-liquid equilibrium, allowing use of carrier gas flow as a linear control of flux. Faster flow rates drive the system away from equilibrium, presenting boundaries on the process window. In this talk we describe an apparatus configuration that can enable high, yet stable, deposition rates, linear control of rate, and greatly facilitated material handling.

8:00 PM SF01.03.37

Electrically-Driven Textile using Hierarchical Aramid Fiber Abdullah Islam and Shenqiang Ren; University of Maryland, United States

High strength and flexible electronic textiles promise in aerospace, robotics, and extreme environment applications, while it is indispensable to develop functionally integrated fiber building blocks with the durable materials performance. Here we report multifunctional sensory e-textiles driven by using copper-grafted polyaramid (Kevlar[®]) fiber networks for the integrated electromagnetic interference shielding, thermal and pressure response sensing. The hierarchical structural design and synthesis of flexible conductive networks is accomplished via the synergistic coordination between molecular copper complex and Kevlar[®] fibers, which facilitate long-term cyclability, stability, and washability. Superior Joule heating capabilities with a rapid thermal response under a low driving voltage (a heating-up rate of 6 degrees C/s and a cooling-down rate of 5.8 degrees C/s), together with a high level of EMI shielding (80 dB from 8 GHz to 13 GHz), are resulted from its multilayer vertically-aligned structure with continuous percolation of conductive coating. This work presents a new and feasible grafting approach for the large-scale fabrication of multifunctional wearable e-textiles for use in extreme environments.

8:00 PM SF01.03.38

Fully Printed 2D Material-Based Memristors Alessandro Grillo¹, Zixing Peng¹, Aniello Pelella², Matthew Boyes¹, Xiaoyu Xiao¹, Minghao Zhao¹, Jingjing Wang¹, Zhirun Hu¹, Antonio Di Bartolomeo² and Cinzia Casiraghi¹; ¹Univeristy of Manchester, United Kingdom; ²University of Salerno, Italy

The von Neumann architecture relies on separate entities for the processing and memory functions, so these units engage in extensive and continuous data exchange. However, in the last few years the production and use of information has been growing dramatically, leading to a new brain-inspired computing paradigm, where data storage and process are done by the same unit. In this framework, the memristor, which is a circuit element that can store information due to the phenomenon of resistive switching between two resistance states upon application of an external electric field, is gaining significant attention as non-volatile memory. 2D materials (2DMs) are very attractive for the next-generation memristors,^{1,2} due to their flexibility, transparency, and compatibility with solution-based processing, enabling to use techniques such as inkjet printing for the cost-effective, and scalable integration of devices onto flexible substrates, like paper and plastic.

In this study, we printed silver as the bottom electrode, graphene (Gr) as the top electrode and MoS₂ as dielectric, creating an Ag/MoS₂/Gr heterostructure.³ After optimization of the fabrication process, the fully printed Ag/MoS₂/Gr memristors on silicon exhibit performance comparable with those achieved in printed devices using silver electrodes or other nanomaterials like TiO₂ and ZrO₂ on rigid substrates.⁴ Furthermore, the same device, when printed on Kapton, displays stable memristive behaviour up to 3% of strain. The memristor resistance switching is attributed to the formation of Ag conductive filaments, which can be suppressed by integrating graphene grown by chemical vapour deposition (CVD) onto the silver electrode. Temperature-dependent electrical measurements starting from 200 K show that the memristive behaviour appears at temperature of ~ 300K, confirming that an energy threshold is needed to form the conductive filament. Interestingly, the CVD Gr integration also significantly reduces hysteresis, suggesting that CVD Gr not only serves as a barrier against ion migration but also improves

the interface between the electrode and the dielectric layer, enhancing the reliability and reproducibility of the devices.

References

- [1] Chen et al, Nature Electronics 3, 638–645 (2020)
- [2] Kumar et al, npj 2D Materials and Applications 6, 8 (2022)
- [3] Peng, Grillo et al, Materials Horizons, Under Review
- [4] Salonikidou et al, Advanced Engineering Materials 24, 2200439 (2022)

8:00 PM SF01.03.39

Printed Electrochemical Cu²⁺ and Cd²⁺ Ion-Selective Electrodes for Combinatoric Multi-Heavy Metal Ion Sensing Applications Maninder Kaur, Priya Vinayak, Henam Sylvia S. Devi, Bhaskar Mitra and Madhusudan Singh; Indian Institute of Technology Delhi, India

Requirements for onsite monitoring of heavy metals in utility water supply and in effluents include low sensor drift, and high sensitivity. While it is standard practice to detect ions in lower ppb ranges using laboratory analytical techniques including atomic absorption/emission spectroscopy and inductively coupled plasma-mass spectrometry, these techniques require careful sample preparation, a skilled operator and potentially long turnaround times for measurements from the site to the lab. Recognizing the health hazards posed by heavy metals, regulatory agencies like the Environmental Protection Agency (EPA) have specified permissible exposure limits for copper (1.3 ppm[1]) and cadmium (5 ppb[2]). Previous work [1] has demonstrated the efficacy of low-cost potentiometric ion-selective electrodes for ppb-level detection of such species. Given several such ions of concern, and well-known and significant cross-sensitivities[3] exist amongst them, and with other ions deemed to be safe for human health at naturally occurring levels, it is essential to develop multi-sensor chips for combinatoric sensing of heavy metal ions, possibly aided by machine learning (ML) methods. While individual ion-selective electrodes with custom sensing films can in principle be fabricated, traditional lithographic techniques are a) inapplicable (owing to foundry process contamination), and b) complex (owing to demands for a potentially large number of sensing layers). Thus, multi-ion sensors production at scale needed for realtime regulatory monitoring requires an alternative fabrication technology. In this work, we have used an inkjet printed CdS film to detect copper and cadmium ions in water. Cadmium acetate precursor (98%, Sigma Aldrich) was added (70°C, 15min) to ethylene glycol (98%, Qualigens), followed by addition of thiourea (99%, Sigma-Aldrich) under constant stirring (70°C, 3 hr), resulting in a bright yellow product (CdS). Elemental composition of the ink was validated by energy dispersive X-ray analysis (EDX, Hitachi), and powder X-ray diffraction (PXRD, Rigaku Ultima, Cu-K α , 1.54Å) indicating the formation of a pure hexagonal phase (ICDD: 96-900-8863) of CdS. Hydrodynamic nanoparticle size measurements (dynamic light scattering, Malvern Zetasizer) yield a value of 40.63±4 nm, indicating suitability for inkjet printing (Fujifilm Dimatix DMP2850, DMC11610 cartridge) through the nozzle diameter (20 μm). Glass substrates with thermally evaporated Cr (10Å)/Au (1000Å) were subjected to standard DI/solvent clean, followed by an ozone exposure (Novascan PSO-UV4, 5 min), before multiple printing with a 15μm drop spacing using a custom waveform to achieve a film thickness of 150 nm. Test spiked solutions (with fixed 0.1 M KNO₃) with decadal concentration variation were formed with for two analyte series using copper(Cu(NO₃)₂·3H₂O) and cadmium ions (Cd(NO₃)₂·4H₂O) with testing starting with the most concentrated spiked solution (0.01 M), and ending with the most dilute solution (10⁻⁹ M) in each series. Potentiometry measurements (PARSTAT MC 1000) for detection of Cu²⁺ yield a detection limit of 1.8 ppb in the linear working range of 10⁻³ M to 10⁻⁹ M with a sensitivity of ~40 mV/p[Cu²⁺] (based on weighted linear fit) and a response time of 50-60 seconds. Corresponding measurements for Cd²⁺ yield a detection limit of 10 ppb in a wider linear working range of 10⁻² M to 10⁻⁷ M with the sensitivity of ~19 mV/p[Cd²⁺] and response time of 80-90 sec. The printing process has been demonstrated on a variety of substrates - poly dimethyl siloxane (PDMS) and polyethylene terephthalate (PET). Work is ongoing to demonstrate working sensors on these substrates to enable use of flexible substrates in applications requiring conformal shapes, such as inner surfaces of utility pipes.

References:

1. Vinayak et al, IEEE Sensors Letters, 6 (9), 1-4 (2022).
2. Vinayak et al, under review (2023).
3. Legin et al, Sensors and Actuators B: Chemical, 34(1-3), 456-461 (1996).

8:00 PM SF01.03.40

Soft Pressure Sensor Fabricated by Implementation of Ultrathin Silicon Strain Sensors on 3D-Printed Cantilever Structures for Cyber Physical System Car Seats Seiichi Takamatsu, Junya Nakagawa and Toshihiro Itoh; The University of Tokyo, Japan

To monitor the posture and driving behaviors of drivers in autonomous vehicles, we developed a car seat embedded with a soft pressure sensor array beneath its urethane foam layer. The soft pressure sensors feature a cantilever structure formed using a 3D printer, at the root of which thin MEMS piezoresistive sensors are wired. Monitoring the health and cognitive state of drivers is crucial, especially in the context of semi-autonomous vehicles up to Level 3. Traditional techniques often employ cameras and vital sensors to detect behavior, fatigue, and drowsiness. However, these methods can be limited due to factors such as lighting conditions and the driver's attire. Given that car seats are in direct contact with drivers, there is growing interest in embedding pressure sensor arrays within them to measure body pressure distribution. These sensors can complement cameras for a more robust driver-monitoring system. Previous research has shown that analyzing body pressure distribution can estimate a driver's attention and fatigue levels effectively. Driver posture, which is intricately linked to comfort, influences alertness; deteriorating comfort could lead to distractions. Also, there is a known correlation between a driver's alertness level, fatigue, and their driving posture. Despite its potential, current pressure sensor technology has limitations. Most research relies on expensive and uncomfortable electrostatic capacitive sensors, costing around \$2000 per seat. This has led to a demand for low-cost, comfortable pressure sensors that can be integrated under the car seat's urethane foam layer. However, placing sensors under the urethane foam is challenging. The foam's nonlinear deformation under load leads to reduced sensor sensitivity and inconsistent output. The foam material disperses the applied force between the sensor and its surrounding substrate, affecting the sensor's performance. To be effective, a pressure sensor array needs to maintain high sensitivity levels (0-10 kPa) and produce near-linear outputs in response to the applied force. This study developed a car seat equipped with a pressure sensor array beneath the urethane foam to monitor the driver's posture and driving behavior. Urethane foam exhibits nonlinear behavior, such as maintaining constant stress in response to varying displacement in the plateau region. Sensors placed under the urethane foam face challenges like producing nonlinear output signals and low sensitivity. In this research, we combined a low-cost pressure sensor, made of a 3D printer and MEMS sensors, with a unique embedding structure beneath the foam and a stress-concentrating design. This new driver-monitoring device aims to overcome the issues associated with sensitivity and linearity. The developed soft cover is attached to the pressure sensors to concentrate stress from the urethane foam. Additionally, the area surrounding each sensor includes a base of the same height to prevent geometrically nonlinear responses. The sensors are integrated into the car seat's urethane foam in an array. The proposed pressure sensor exhibits a sensitivity range of 0-20 kPa. Through experiments, we demonstrated that the prototype sensor array could detect changes in the driver's posture as well as braking actions. The sensors in this structure hold promise for future applications in intelligent car seats for autonomous vehicles.

8:00 PM SF01.03.41

Computer Vision enabled Eye-In-Hand Robotic *In-Situ* Bioprinting of Multimaterials for Fast Wound Repair Seolha Jeong and Su Ryon Shin; Harvard Medical School, United States

Current *in-situ* printing techniques depend on pre-determined printing paths in order to directly build complex functional architectures at injured areas, limiting adaptability in clinical scenarios. We present INSIGHT (INtelligence *in-Situ* printing Guided by Eye-in Hand robot Technology), an innovative computer vision enabled system that combines a depth camera with a 6-degree of freedom robot arm, empowering it to identify arbitrary areas at various angles without pre-designed code and calibration procedures. Layer-by-layer volumetric printing approach is performed by dynamic image recognition based on color and contour differences, which achieves highly accurate printing through real-time adjustments and is capable of continuous targeting of multiple wounds. Dual printing modes, extrusion and spray printing, are designed for rapid printing with seamless switching between different bioinks. Through *in vivo* tests, INSIGHT demonstrates its practicality for targeting and treating diabetic wounds, highlighting its adaptability to enable customized care for rapid emergency treatment of trauma patients. In this research, as targeting to treat a diabetic wound healing, a microgel based bioink is introduced, which is mixed with a plant protein-based oxygenating microparticles and mesenchymal stem cells in order to boost angiogenesis and immune response at initial wound healing stage. We not only demonstrate the practicality for targeting and treating diabetic wounds using our system, highlighting its adaptability to enable customized care for rapid emergency treatment of trauma patients, but also verifying the efficiency of the combination of the oxygenated ink and the stem cells in wound repair.

8:00 PM SF01.03.42

Printable Silicone Elastomers to Provide Magnetic Resonance Imaging Contrast for Medical Phantoms Michael Avery, Yasmine Osmani, Ben Dickie, Stephen Edmondson and Brian Derby; University of Manchester, United Kingdom

Phantoms are manufactured structures which mimic the properties of objects that are characterised by a range of different medical imaging technologies. They have a number of applications, including: standards for instrument calibration, reference samples to ensure common performance from multiple site experimentation, replacement for animal studies or human volunteers during training or technique development. Phantom development for magnetic resonance imaging (MRI) is particularly challenging because the imaging modality is the relaxation of the nuclear magnetic resonance excitation of protons that are ubiquitous in biological systems and these relaxation times (T1 and T2) are much longer than in conventional polymeric materials

because of the presence of water and the soft matter nature of biological tissue. Thus, conventional MRI phantoms are based on aqueous solutions or weak gelling biological materials, e.g. alginates, agarose or carageen gels, doped with paramagnetic ions to further control the relaxation times. The phantoms themselves are thus limited to simple shapes, e.g. spherical or cylindrical cavities, and have poor long term stability.

The use of MRI to guide radiological or surgical procedures requires more advanced shape control for the next generation of medical phantoms. This is particularly the case for surgical training but also for the generation of large datasets for machine learning where precise robotic control of beam placement and motion from intense X-Ray sources is desired for use in clinical radiology such as the MRI-Linac. The ability to replicate the unavoidable motion of internal organs (e.g. heart and lungs), while also mimicking complex tissue geometries, MR imaging properties and radiation response of tissues, is critical for advancing MR-Linac treatment. These medical challenges can be achieved by developing and engineering 3D-printed silicone soft-robotic "4D" phantoms, enabling a transformational step-change in the manufacture and function of medical phantoms. A successful soft robotic phantom must display the appropriate balance of mechanical properties, MRI contrast and manufacturability. Here we present materials development for 3D printable silicone material that work towards overcoming this challenge. Robotic phantoms must present MRI relaxation times that simulate biological tissues, typically assessed using the time constants and for longitudinal and transverse relaxation respectively. Human tissue relaxation times can range from 600 – 3000 ms for and 35 -240 ms for , although the precise range depends on the magnetic field used during a particular MRI scan. A Therefore phantom materials should allow for significant and tunability. For soft robot fabrication, the challenge is to develop compositions that achieve the desired relaxation values while also maintaining mechanical properties comparable to those human tissues and pre-cure viscoelasticity suitable for printing.

Two strategies to achieve these desired material properties have been investigated, both following the principles of formulation of material blends using readily available commercial materials. The first uses commercial silicones that have been successfully used to print soft robotic structures but modified by blending with short chain, relatively mobile silicone oils. This gives good control of T1 and T2 but has limited long term stability of property variation due to the mobility of the sort-chain oils within the polymer network. The second approach uses a multiphase composite concept rather than a blended composition. Both methods have been used with Direct Write Extrusion printing to fabricate 3D structures with defined variation of materials and these have been used in pre-clinical MRI scanners to demonstrate good imaging quality.

8:00 PM SF01.03.44

Strengthen Composite with 3D Aligned Carbon Fiber via Embedded 3D Printing[QiyiChen](#) and [RayneZheng](#); University of California, Berkeley, United States

The orientation of fibrous fillers, induced by shear forces during extrusion, has been demonstrated to significantly enhance mechanical properties, electrical/thermal conductivity, microwave attenuation etc., albeit primarily in a two-dimensional (2D) x-y plane. In this study, we present a novel approach for achieving fiber alignment in a three-dimensional (3D) context, with an emphasis on the Z-direction, by utilizing embedded 3D printing techniques. This process involves the extrusion and suspension of composite inks within a viscoelastic gel medium, during which the alignment of the fiber can be controlled *via* velocity ratio, nozzle size, fiber dispersion etc. By selectively align the fiber in a 3D pattern, the mechanical properties, and conductivity can be largely improved and tuned.

8:00 PM SF01.03.45

Microstructural Evolution Simulations in Additive Manufacturing and Post Heat-Treatment of Aluminum Alloys[JiwonPark](#), [Joo-HeeKang](#) and [Chang-SeokOh](#); Korea Institute of Materials Science, Korea (the Republic of)

The extreme solidification condition in metal additive manufacturing causes out-of-equilibrium phase transformation and unique microstructures: i) vertically connected grains across several layers along the building direction, ii) severe segregation of alloying elements on the inter-dendritic region and the absence of secondary phases, which expect to be formed under equilibrium condition. These microstructural features are of great importance in tailoring the desired properties. This work simulated the microstructural evolution of as-built and post heat-treated Al-Si-Mg alloy in a phase-field approach. Local grain orientation selection and growth morphology under rapid solidification and extreme thermal gradient conditions are studied and compared to electron back-scatter diffraction analysis. Then, the precipitation behavior of Si from super-saturated solidification microstructure is investigated. The formation of Si precipitate demonstrated above the solution-treatment temperature, which experimentally occurs. It reveals that the precise digital twin of mesoscale microstructure can be fabricated by phase-field modeling with specified thermal conditions.

8:00 PM SF01.03.46

The Effect of *In-Situ* Laser Surface Nitriding on Dynamic Load Transfer and Stress Development in Additive Built Ti6Al4V Hip Implant using Finite Element Analysis[AnkitPorwal](#)^{1,2}; ¹IIT Kharagpur, India; ²Indian Institute of Technology Kharagpur, India

The force developed during human activity generates dynamic stress over the prosthetic. Change in stress with time causes stress shielding in the bone and prosthetic system. Lowering the stress shielding improved the prosthetic performance. This presented work aims to investigate the effect of in-situ laser surface nitrided additive built Ti6Al4V hip implant stem using the finite element method. A finite element 3D model consisting of femur and hip implants with variable laser surface nitrided region was considered for the analysis. Dynamic loads developed during standing up, regular walking and stair climbing used for load condition. These dynamic loads are applied as a cyclic load dependent overtime on the implants to calculate load transfer and stress development. The analysis shows that the remelted surface transmits higher loads than the untreated implants during activities. Thus, in-situ laser surface nitriding reduces the stress shielding in bone and prosthetic system and improve implant performance.

8:00 PM SF01.03.47

On The Development of Bio-Compatible, Chemically Recyclable, 3D-Printable Silicones[SenecaJ. Velling](#)¹, [HongyiZhang](#)^{2,1}, [SammyShaker](#)¹ and [JuliaR. Greer](#)^{1,1}; ¹California Institute of Technology, United States; ²Tsinghua University, China

Silicone is a versatile polymer material with many desirable characteristics, such as corrosion resistance, thermal stability, low toxicity, and its electrically insulating nature. It has widespread application in commercial, medical, and research scenarios. However, its irreversibly 3D crosslinked structure has impeded its recycling and manufacturing through thermoplastic extrusion-based 3D printing techniques. Similarly, its high gas permeability and crosslinking has prevented its application in UV-curing-based additive manufacturing techniques. Previously, it was reported that the photoinitiated thiol-ene click chemistry, where a thiol and an alkene connect to form a thioester, allowed the UV-crosslinking of mercaptan-functionalized polysiloxane and vinyl- terminated polysiloxane thereby enabling the use of stereolithography 3D printing of silicone elastomers. Separately, introduction of disulfide moieties in polymer chains was shown to facilitate the chemical degradation of the cured material through base-catalyzed thiol-disulfide exchange reactions. This work targets the develop a chemically recyclable, 3D-printable silicone materials by integrating the thiol- disulfide exchange mechanisms within a photoinitiated thiol-ene silicone system. We show that disulfide moieties can be introduced into mercaptan-functionalized polysiloxanes through a clean and facile iodide-catalyzed oxidative coupling reaction, and the resulting partially oxidized mercaptan- functionalized polysiloxanes, when mixed with vinyl-functionalized polysiloxane and photoinitiators, can be UV-cured to form disulfide-containing silicone networks. Ongoing work focuses on performing chemical degradation on the cured disulfide-containing silicone, examining the viability of self-healing in such silicone elastomers via phosphine-catalyzed disulfide metathesis, and characterizing the thermomechanical properties of silicones prepared from the recrosslinking of recycled polysiloxane oligomer. Together, these efforts will make possible the additive manufacturing of complex functional structures (eg. microfluidic devices, cell scaffolds, O-rings and gaskets) from highly oxygen-permeable, hydrophobic, thermally and chemically resistant Silicones capable of self-healing and chemical recycling.

8:00 PM SF01.03.48

Synthesis of Scaffolded Carbon Electrodes via Catalytic Graphitization[EthanKlein](#), [SammyShaker](#), [YuchunSun](#), [SenecaJ. Velling](#) and [JuliaR. Greer](#); California Institute of Technology, United States

Graphitic electrodes are widely used in lithium-ion batteries due to their electrical performance and resistance to chemical degradation. However, the inherent geometry of slurry-based graphite electrodes limits the ability to tune key parameters, such as the diffusion length within the electrode, the path of ions in the electrolyte/electrode region, the extent of active material loading, and the overall mechanical strength. By contrast, electrodes with scaffolded three-dimensional (3D) structures offer freedom over such tunable parameters. While the tunability of scaffolded electrodes may appear attractive, there exists a tradeoff: current 3D printing techniques used to fabricate such scaffolded electrodes offer limited control over the intrinsic material properties, namely the crystal phase and microstructure. In turn, improvements in diffusion length and the intercalation of lithium ions within the electrode are still limited. Achieving the desired microstructure and phase control requires significant thermal activation, with temperatures greater than 3000°C in the case of carbon, that is infeasible in most tube furnaces and especially challenging for larger samples.

Here, we offer a repeatable method for microstructural and crystal phase tuning of scaffolded carbon electrodes via catalytic graphitization. Electrodes are 3D printed using a hygroscopic resin capable of swelling in an aqueous solution, offering significant compositional control in post-printing. In this study, samples are submerged in a solution of nickel salts, where the 3D printed polymer swells with nickel cations and water to produce a hydrogel. These samples are then pyrolyzed in a vacuum furnace between 800-1000°C to form a carbon electrode, in which the presence of nickel catalytically produces graphite.

In this study, we first investigate the impact of the aqueous nickel concentration on the resultant nickel incorporated in the pyrolyzed electrodes. We also examine how the nickel concentration

leads to the presence of a crystalline graphite phase, as opposed to the glassy carbon phase typically observed during pyrolysis. X-Ray Diffraction (XRD) patterns display pure glassy carbon at zero nickel concentration, while both glassy and graphitic carbon signatures appear as nickel incorporation increases. The ratio of graphite (G) to disorder (D) Raman peaks improves from less than 1:1 to greater than 10:1 in catalytically produced samples. Future studies using Transmission Electron Microscopy (TEM), in-situ high temperature TEM, electrochemical cycling, and capacity measurements are discussed. We also compare the electrochemical performance of slurry and scaffolded electrodes with varying degrees of graphitic microstructure and architectural features.

SESSION SF01.04: Session III
Session Chairs: Allison Beese and Ting Zhu
Tuesday Morning, November 28, 2023
Sheraton, Second Floor, Republic B

8:00 AM *SF01.04.01

Laser Powder Bed Fusion of Mixed Powders Christopher Hutchinson, Huikai Li, Erin Brodie and Sebastian Thomas; Monash University, Australia

Laser powder bed fusion (LPBF) of metals is a popular mode of additive manufacturing (AM) that has the advantage of producing complex shapes with little or no additional processing. However, an important limitation is that the metallic microstructures obtained are usually relatively simple solidification structures and there are few means available to enrich this without subjecting the components to subsequent thermal processing routines, which has its own difficulties due to dimensional control. This limits the microstructural complexity that can be achieved in components fabricated by LPBF and hence the properties obtainable.

In this work, we present and validate a physically-based model to predict the chemical distribution resulting from LPBF of physically mixed powders of different compositions. We demonstrate that mixing of powders with different compositions can be used to generate a deliberately controlled, mesoscale chemical heterogeneity in LPBF that allows the formation of multiphase microstructures and delivers new microstructural complexity to LPBF. A duplex stainless steel, consisting of equal fractions of ferrite and austenite in the as-built state is used as a demonstration of the approach.

The model describing the chemical distribution in the consolidated build can be extended to describe remelting effects and exploited for the design of spatially varying microstructures. This provides a path towards generating architected materials from random mixes of initial powders. Examples of using spatially controlled remelting to generate architecture materials for random powder mixtures will be shown.

This opens up an interesting path for delivering microstructural complexity to LPBF of metals.

8:30 AM *SF01.04.02

Multiscale Process Control in Metal Additive Manufacturing Manyalibo Matthews; Lawrence Livermore National Laboratory, United States

Tremendous gains have been made over the past several years to improve understanding of defect formation in laser powder bed fusion (LPBF) processes and develop predictive material models that can guide process optimization. However, while control of defects may be achievable at a given length scale for a given material, there remain significant challenges in efficiently predicting and mitigating defects holistically across length scales, e.g. grain-, melt pool-, feature-, part-scale. In this talk I will present efforts to improve the efficiency and accuracy of predictive models that describe defect formation across the multiple relevant length scales found in LPBF. Beyond predictions, effective means to implement defect mitigation solutions are also required. Efforts to manipulate the optothermal coupling in both custom and commercial LPBF systems will be discussed that begin to address such requirements. Prepared by LLNL under Contract DE-AC52-07NA27344.

9:00 AM SF01.04.03

The Use of Mechanically Derived Powders for Additive Manufacturing: Flow and Function David F. Bahr¹ and John E. Barnes²; ¹Purdue University, United States; ²Metal Powder Works, United States

Metal additive manufacturing (AM) provides the opportunity of “on demand” customizable fabrication to minimize supply chain constraints. However, powder availability could become a similar constraint, and creating affordable regional sources for low-embodied energy powders will be a crucial step in distributed manufacturing. Current gas or water atomization processes methods for form metal powders (which are then often remelted in powder bed fusion) adds significant energy budget to the process. First, atomized powders are regularly sorted so that only a portion of the powder produced reaches the AM user. Secondly, if the alloy already exists in solid form, the energy needed to melt to form the powder form is an energetically “hungry” step. A powder creation method using cold mechanically derived (CMD) of particulates can create a wide range of alloy compositions with approximately 90% less embodied energy than gas atomization (GA). CMD powder is often less spherical than GA powders, and thus the powder flow characteristics in common powder bed systems must be demonstrated. Our study has shown that the flowability of Al 7075 and Copper 14500 powders made via GA and MF are similar at rates appropriate for powder bed additive methods. Particle morphology descriptions (size and shape) do not strongly correlate to tap density in this case, which suggests under common AM bed filling processes the bed density will be similar in both cases. Morphology comparisons and particle size/shape distributions were made by comparing large particle statistics, rather than solely comparing mean particle size. Laser powder bed fusion tensile specimens were formed from Al 7075 and heat treated to T6; the GA and CMD powders showed equivalent tensile test performance to both each other and conventionally wrought 7075.

9:15 AM SF01.04.04

High Absorptivity Nanotextured Powders for Metal 3D Printing Ottman Tertuliano¹, Philip DePond^{2,3}, Andrew Lee², Jiho Hong², David Doan², Mark L. Brongersma², Wendy Gu², Manyalibo Matthews³, Wei Cai² and Adrian Lew²; ¹University of Pennsylvania, United States; ²Stanford University, United States; ³Lawrence Livermore National Laboratory, United States

The widespread application of metal additive manufacturing (AM) is limited by the ability to control the complex interactions between the energy source and the feedstock material. Here we develop a scalable process to introduce nanoscale grooves to the surface of copper powders which increases the powder absorptivity by up to 70% during laser powder bed fusion. The absorptivity increase enables printing of pure copper structures with densities up to 92% using laser energy densities as low as 82 J/mm³. We demonstrate similar effects in silver and tungsten. Simulations show the enhanced powder absorptivity results from plasmon-enabled light concentration in nanoscale grooves combined with multiple scattering events. The approach taken here demonstrates a general method to enhance the absorptivity and printability of reflective metal powders at low energy densities by changing the surface morphology of the feedstock without altering its composition.

9:30 AM *SF01.04.05

Additive Manufacturing: Technology Maturation and Synchrotron X-Ray Microscopy Insights Anthony D. Rollett; Carnegie Mellon University, United States

Additive manufacturing (AM), aka 3D printing is a relatively new technology that has given rise to the “maker culture” and an intense interest in design. That has carried over into metals AM, which has jumped almost immediately into manufacturing of actual parts in a variety of alloys. In doing so it has liberated thinking about part design albeit within certain constraints and complex components have been deployed that were previously inaccessible, e.g., high temperature heat exchangers (HX). An example is described of the co-design of HX against printing constraints, alongside evolution in alloy choice. Nothing is ever as simple as it seems, however, and the reliability of parts that must carry load depends on the internal micro-structure, especially with respect to fatigue loading. This motivates detailed study of all aspects of materials microstructure ranging from defect structures to strain, all of which is ideally suited to the use of intense sources of high energy x-rays as only third generation light sources can deliver. Computed tomography (CT) has revealed the presence of porosity in all additively manufactured metals examined to date and confirmed that appropriate process control can limit it. CT has also provided data on surface condition that we are trying to link to fatigue performance. High speed radiography reveals even more crucial details of how laser light generates vapor cavities that can deposit voids past a critical instability point. “Hot” cracking has been imaged as it happens during the solidification process, which offers the possibility finding printing recipes for alloys previously considered off-limits to 3D printing. High speed, high resolution diffraction in stainless steel, alloy 718 and Ti-6Al-4V reveals unexpected solidification and precipitation sequences. Diffraction microscopy reveals the highly strained nature of printed metals and how microstructure and internal strain state evolves during subsequent annealing. Permeating all these activities is machine learning as an invaluable tool and aid to the researcher.

Support from multiple agencies is gratefully acknowledged, including NASA, DOE/BES, DOE/NNSA, ONR, NSF, OEA, Commonwealth of Pennsylvania, and Ametek.

10:00 AM BREAK

10:30 AM *SF01.02.03

Intelligentsia of Additively Manufactured Hierarchical Materials Julia R. Greer^{1,2}, Widiyanto Moestopo¹, Max A. Saccone¹, Seola Lee¹, Matias Kagias^{1,2}, Wenxin Zhang¹ and Weiting Deng¹; ¹California Institute of Technology, United States; ²Kavli Nanoscience Institute, United States

Creation of reconfigurable and multifunctional materials can be achieved by incorporating architecture into material design. In our research, we design and fabricate three-dimensional (3D) nano- and micro-architected materials that can exhibit superior and often tunable thermal, photonic, electrochemical, biochemical, and mechanical properties at extremely low mass densities, often lighter than aerogels, which renders them useful and enabling in technological applications. Dominant properties of such structural meta-materials are driven by their multi-scale hierarchy: from characteristic material microstructure (atoms) to individual constituents (nanometers) to structural components (microns) to overall architectures (macroscale). Our research is focused on fabrication and synthesis of nano- and micro-architected materials using 3D lithography, nanofabrication, and additive manufacturing (AM) techniques, as well as on investigating their mechanical, biochemical, electrochemical, electromechanical, and thermal properties as a function of architecture, constituent materials, and microstructural detail. Additive manufacturing (AM) represents a set of processes that fabricate complex 3D structures using a layer-by-layer approach, with some advanced methods attaining nanometer resolution and the creation of unique, multifunctional materials and shapes derived from a *photoinitiation-based chemical reaction* of custom-synthesized resins and thermal post-processing. A type of AM, vat polymerization, has allowed for using hydrogels as precursors, and exploiting novel material properties, especially those that arise at the nano-scale and do not occur in conventional materials. The focus of this talk is on additive manufacturing via vat polymerization and function-containing chemical synthesis to create 3D nano- and micro-architected metals, ceramics, multifunctional metal oxides (nano-photonics, photocatalytic, piezoelectric, etc.), and metal-containing polymer complexes, etc., as well as demonstrate their potential in some real-use biomedical, protective, and sensing applications. I will describe how the choice of architecture, material, and external stimulus can elicit stimulus-responsive, reconfigurable, and multifunctional response.

11:00 AM SF01.04.07

Designing Against Failure in Additive Manufacturing: From Fracture in Monolithic Samples to Designing Functionally Graded Materials Allison M. Beese; The Pennsylvania State University, United States

To adopt metallic materials made by additive manufacturing (AM), it is critical to understand, and design against fracture, particularly under complex stress states accessed in service, and with the possible presence of internal pores. Additionally, when designing functionally graded materials (FGMs) in which composition is deliberately varied with position within a component to result in spatially tailored properties, it is critical to avoid deleterious phase formation and solidification cracking during fabrication. This talk will describe our approach for studying the combined effects of stress state and internal pores on the fracture behavior of stainless steel 316 and Ti-6Al-4V manufactured using laser powder bed fusion AM, providing a pathway for designing against failure under realistic conditions. Additionally, it will describe our framework for considering deleterious phase formation and crack susceptibility when designing compositional pathways for FGMs, and more broadly, compositions amenable to AM in general.

11:15 AM *SF01.04.08

Laser Powder Bed Fusion of Fe-Based Shape Memory Alloys Christian Leinenbach^{1,2}, Irene Ferretto¹, Dohyung Kim³ and Wookjin Lee⁴; ¹EMPA, Switzerland; ²EPFL, Switzerland; ³KITECH, Korea (the Republic of); ⁴Pusan National University, Korea (the Republic of)

Shape memory alloys (SMAs) are materials characterized by a shape memory effect (SME) and pseudo-elasticity (PE). The SME occurs when a deformed material can recover the original shape upon heating, and PE describes the recovery of a large nonlinear elastic strain upon loading and unloading. The most widely studied SMA by far is NiTi, but the high cost of raw materials and processing of Ni-Ti alloys represents the main drawback of this class of materials and limits its applications to small parts. From the processing side, laser powder bed fusion (LPBF) is an attractive manufacturing technique for SMAs, as it allows for the fabrication of structures with complex geometries. Several efforts have been devoted towards the development of unique three-dimensional (3D) structures with additional functionalities made by LPBF from NiTi alloys, e.g. lattice structures or structural metamaterials, but LPBF of NiTi SMAs with the desired functionalities remains challenging because they have a very high sensitivity to composition change.

A cheaper alternative are e.g. Fe-Mn-Si based alloys, which have been studied with regard to their application for large parts in civil engineering. In the Fe-Mn-Si system, the mechanism responsible for the shape recovery is a martensitic transformation from the γ -fcc phase (austenite) to the ϵ -hcp phase and its reversion. Up until now, additive manufacturing of Fe-based SMAs has been only scarcely studied.

This presentation will summarize some of our recent activities in the field LPBF of Fe-Mn-Si based SMA. First, the fundamentals of the process-microstructure-property relationships governing the Fe-Mn-Si alloys manufactured via LPBF, which were characterized using techniques such as in situ neutron diffraction and in situ EBSD, will be presented and strategies to manipulate the microstructure and thereby the shape memory properties will be demonstrated. Based on these results, parts with additional functionalities deriving from specifically designed geometries such as enhanced energy absorption and damping capabilities for applications in e.g. civil or structural engineering, are designed and combined with the shape memory properties of the SMAs.

11:45 AM SF01.04.09

Additively Manufacturing Nanolamellar Eutectic High-Entropy Alloys with Anisotropic Mechanical Behaviors YuZou; University of Toronto, Canada

Eutectic high entropy alloys (EHEA) with alternating FCC and BCC-based phases offer an excellent combination of strength and ductility. AM allows for the fabrication of ultrafine nanolamellar EHEA with directional growth. In this study, we investigate the effect of orientation on the deformation, strengthening, and fracture mechanisms of directional EHEA manufactured by additive manufacturing using in situ synchrotron-based high-energy X-ray diffraction during tensile test. Our findings show that the sample along the lamellar direction exhibits the best combination of strength and ductility due to the continuous stimulated strengthening ability of the B2 and FCC phases in the near equal strain condition. The strengthening of the B2 phase is mainly caused by the formation of martensitic phases, while the strengthening of the FCC phase is mainly caused by back stress. Additionally, the sample shows higher crack and void tolerance than the other samples. Our research sheds light on a better understanding of the co-deformation behavior of dual-phase EHEAs made by AM.

SESSION SF01.05: Session IV

Session Chairs: Wen Chen and Jae-Hwang Lee

Tuesday Afternoon, November 28, 2023

Sheraton, Second Floor, Republic B

1:30 PM *SF01.05.01

Mechanics of Extremely Heterogeneous Materials by Additive Manufacturing Ting Zhu; Georgia Institute of Technology, United States

Our recent studies of additively manufactured alloys (Nature, 608, 62–68, 2022; Nature Materials, 17, 63–71, 2018) have raised fundamental questions on the role of extremely complex microstructural heterogeneities in the mechanical behavior of these novel material systems. We combine mechanics modeling and experimental characterization to elucidate the strengthening effects of microstructural gradients and resultant plastic strain gradients in additively manufactured alloys. We quantitatively compare the results from crystal plasticity modeling and in situ synchrotron X-ray experiment, highlighting the less recognized concept of different types of back-stress hardening and various stages of extra back-stress hardening in materials with extremely complex microstructural heterogeneities. Mechanistic insights are gained for further enhancing the strength-ductility synergy in the design of materials with extremely heterogeneous microstructures.

2:00 PM SF01.05.02

Improving Measurement and Classification of SLM Feedstock Powders by X-Ray Microscopy and Machine Learning Daniel Sinclair, Eshan Ganju and Nikhilesh Chawla; Purdue University, United States

Metal Additive Manufacturing (AM) has introduced revolutionary changes in design, production, and innovation sectors over the past decade. This transformative technology, including Laser Powder Bed Fusion (LPBF), Direct Energy Deposition (DED), Binder Jetting (BJ), Metal Extrusion (ME), and Sheet Lamination (SL), has enabled significant advances in aerospace, automotive, medical, energy, and tooling industries. Out of the five, LPBF is favored for its near-net-shape printing, high dimensional accuracy, superior mechanical characteristics, and swift prototype assembly. Within LPBF, Selective Laser Melting (SLM) has gained significant traction in commercial, industrial, and defense applications, specifically for Al alloys. The reliability of SLM parts is often compromised due to defects originating from irregular feedstock powders originating from re-use of powder feedstock or differences in feedstock sources. To accommodate the variation in feedstock required to meet the increasing demands of manufacturing, advanced granulometric methods which are sensitive to varying powder morphologies (as seen in recycled or composite powders) are needed. Lab-scale 3D X-ray Computed Tomography (XCT) presents a viable solution for feedstock powder characterization, enabling non-

destructive quantification of changes within recycled particles. Our research delved into a gas-atomized AA7050 feedstock powder with unusual powder morphologies and titanium additives (AA7050-RAM2). Through the synergy of lab-scale x-ray microscopy and automated watershed segmentation, we were able to quantify the shapes and sizes of particles in an aluminum alloy (AA7050-RAM2) powder feedstock. Additionally, to describe nonstandard particles more accurately, we introduced novel 3D shape factors. Furthermore, to optimize efficiency and capture an extensive range of powder morphologies, we compared automated classification methodologies for the feedstock using a combination of algorithmic clustering and the Random Forests machine learning algorithm. Our research provides significant insights into enhancing the consistency and reliability of SLM-fabricated parts. It does this by delivering a nuanced understanding of feedstock powder morphology and by proposing innovative classification methods. These insights are poised to assist in broadening LPBF's application and furthering advancing metal additive manufacturing.

2:15 PM *SF01.05.03

Development of a Low Thermal-Budget, Distortion-Free Process for Binder-Jet 3D Print-and-Sinter Alloys Christopher A. Schuh^{1,2}, Christian Oliver^{1,2}, Yannick Naunheim¹ and Jasper Lienhard²; ¹Massachusetts Institute of Technology, United States; ²Foundation Alloy, Inc., United States

Binder-jet printing and sintering is a pathway to scalable, high-volume, low-cost manufacturing of complex metal parts. It also presents an opportunity to design new alloys produced entirely in the solid state, thus using less energy and involving less residual stress and distortion than other modes of metal 3D printing. This talk will review research aimed at such alloy and process development, with an emphasis on understanding and tailoring sintering mechanisms to effect low-temperature consolidation. New alloys based on Mo- and Ni- will be highlighted, and processing advantages in terms of energy and shape retention elaborated. Finally, the properties of these alloys will be evaluated and opportunities for alloy substitution discussed.

2:45 PM SF01.05.04

Additive Manufacturing of Novel Aluminum Alloys: Structure and Properties Lin Liu, Jingyu Xu and Cheng Zhang; Huazhong University of Science and Technology, China

Additive manufacturing (AM) offers significant advantages over conventional manufacturing techniques in processing Al alloys, however, high-strength Al alloys produced by AM commonly encounter a few challenges including poor processability and undesirable microstructures with coarse columnar grains and micro-cracks, leading to poor mechanical properties. Here, we demonstrate that these issues can be largely resolved by micro-alloying of Zr element in the Al-based alloys. In this study, a series of novel Al-1Fe-0.6Cu-xZr alloys with different content of Zr (x=0.3, 0.6, 0.8, 1.3at%) are designed and fabricated by laser powder bed fusion (LPBF). It is observed that the LPBF Al alloys all exhibit notably heterogeneous structures with alternate distribution of coarse grain zones (CGZs) and fine grain zones (FGZs). With increasing Zr content, the grain size in both CGZs and FGZs gradually decreases and the columnar-to-equiaxed transition (CET) occurs in the CGZs, which make the processability be improved for the Al alloys with higher Zr content. To understand the formation of the heterogeneous structures and the correlation between microstructure and mechanical properties, the LPBF Al-Fe-Cu-1.3Zr alloy was selected, as an example, for detailed investigations. It is revealed that the formation of FGZs, locating at the low boundaries of the molten pools, is attributed to the pre-formed Al₃Zr nanocrystals, which serve as nuclei and results in the refinement of grain size, while the CGZs are formed at the interior of molten pools, where no Al₃Zr precipitates are formed, leading to the formation of relatively coarse grain size. In addition, Fe/Cu co-segregation appears at the GBs in both FGZs and CGZs although Cu and Fe are thermodynamically immiscible. As a result, these unique microstructures allow the LPBF-processed Al-Fe-Cu-1.3Zr alloy to have high strength at both room temperature and elevated temperatures. For example, the yield strength reaches 500 MPa at room temperature and 163 MPa at 573 K, respectively, both are higher than those of additive manufactured Al-based alloys reported thus far. The findings in this work provide a guide for design of novel Al alloys with good processability and advanced mechanical properties for additive manufacturing.

3:00 PM BREAK

3:30 PM *SF01.05.05

Additive Manufacturing: Transforming Engineering Design Through Functionally Integrated Materials, In-Situ Imaging, and Alternative Feedstock Materials Julie M. Schoenung¹ and Xin Wang²; ¹University of California, Irvine, United States; ²The University of Alabama, United States

This presentation will provide an overview of various aspects of additive manufacturing that can lead to transformative materials and engineering design. Directed energy deposition (DED) additive manufacturing enables the precise control of composition for the development of functionally integrated materials (FIMs) with site-specific functionality. This compositional control is enabled by the powder injection delivery system that allows for the sequential and / or co-deposition of multiple feedstock powders through individual powder feeders. This strategy provides a path to the rapid development of novel alloys and components with location-dependent chemical composition and properties. The FIMs concept is demonstrated using two material systems: stainless steel 316L with Haynes 282 nickel superalloy, and nickel with nickel-aluminum. Extensive characterization of microstructure, interfaces, diffusion zones, grain boundary morphology and texture, chemical composition and phase transformations provides insight into the fundamental materials science governing the solidification process and consequential component performance in FIMs. DED also entails complex particle-laser-melt pool interactions due to the powder injection mechanism. In-situ imaging using both thermal imaging and high-speed video provides insight into these complex interactions, as highlighted here for various examples including nickel superalloy powder and TiC reinforcement particles. Lastly, the benefits of using recycled and repurposed alternative feedstock materials are considered.

4:00 PM SF01.05.06

Additive Manufacturing of Co-Based Superalloys via Direct Ink Writing Jian Liu¹, Zhiyu Zhang², Shuai Guan¹, Jonathan Poplawsky³, Tianyi Li⁴, Yang Yang² and Wen Chen¹; ¹University of Massachusetts Amherst, United States; ²The Pennsylvania State University, United States; ³Oak Ridge National Laboratory, United States; ⁴Argonne National Laboratory, United States

Additive manufacturing of superalloys enables innovative, geometrically complex designs combined with excellent mechanical properties. Here, we developed an additive manufacturing method based on direct ink writing (DIW), to fabricate a high-performance Co-based superalloy. The ink consists of metal powders, polymer binders, and volatile solvents. The deposited architectures are thermally sintered to near-full density, followed by ageing. The sintered Co-based superalloy exhibits a homogeneous microstructure of equiaxed grains with MC carbides uniformly distributed in the FCC matrix, which leads to a high ultimate tensile stress in excess of 1.2 GPa and a large tensile ductility over 20% at room temperature. The outstanding combination of strength and ductility originates from the coherent γ' nanoprecipitates and deformation-induced stacking faults, as revealed by in situ synchrotron X-ray diffraction and high-resolution transmission electron microscopy. The introduced additive manufacturing approach provides new opportunities to print a wide range of superalloys for high-temperature applications.

4:15 PM *SF01.05.07

Understanding Ultrahigh-Rate Behavior of Macromolecules for Advances in Polymer-Based Cold Spray Additive Manufacturing Jae-Hwang Lee^{1,2}, Ara Kim¹ and Anuraag Gangineri Padmanaban¹; ¹University of Massachusetts, United States; ²University of Massachusetts Amherst, United States

The solid-state coating and additive manufacturing of polymers are feasible by the cold spray (CS) technique, in which solid feedstock powders or microparticles (μ Ps) conveyed by a high-speed gas stream are subjected to a head-on collision against a stationary surface at transonic or supersonic velocities. Due to the ultrahigh-strain-rate (UHSR) viscoplastic deformation upon collision, polymer μ Ps can be consolidated without volumetric melting or phase transition. In CS, μ P adhesion is accomplished by the highly localized thermal softening (or melting), and other inelastic mechanisms, especially brittle fracture, may also become significant. As local temperature fields, the consequence of impact-induced plastic strains, are coupled with temperature-dependent mechanical properties, the UHSR adiabatic plasticity of polymers is inherently nonlinear and is very difficult to predict via the time-temperature superposition. In this talk, we will introduce our recent efforts to understand the UHSR behavior of polymer μ Ps through single-particle experiments realized by laser-induced projectile impact testing (LIPIT). For glassy polymers modeled by polystyrene of various molecular weights (MWs), the MW-dependent interplay of the primary inelastic mechanisms is systematically and comprehensively investigated through ultrafast optical images from LIPIT. Due to the ambivalent effect of MW on fracture toughness and interfacial rheology, our study demonstrates that the proper selection of MW is crucial for the feasibility of the solvent-free and solid-state deposition of glassy polymers. Meanwhile, LIPIT experiments with an incidence angle of 45° are conducted to investigate the tribological response at the contact interface. We elucidate the strain-dependent tribological properties of deblock copolymers under extremely dynamic collisions and the correlation between friction and adhesion properties at the nanosecond time scale. Furthermore, we demonstrate that phase-separated deblock copolymers can be ordered via collision-induced shear flows. The extended knowledge from our study about the UHSR behavior of polymers will be crucial for advances in polymer-based CS additive manufacturing that can also open opportunities for creating novel materials properties.

* This material is based upon work supported by the National Science Foundation under Grant No. CMMI-1760924 and the US DEVCOM Army Research Laboratory under Cooperative Agreement No. W911NF-19-2-0152.

4:45 PM SF01.05.08

Correlations Between Porosity, Spatter and Process Metrics for Powder Bed Fusion Laser Beam Metallic Additive Manufacturing J.-A.S. Hocker¹, Joseph N. Zalameda¹, Brodan Richter¹, Andrew R. Kitahara², Sang-Hyon Chu¹ and Edward H. Glaessgen¹; ¹NASA Langley Research Ctr, United States; ²Analytical Mechanics Associates, United States

The large scale and deposition sequence of powder bed fusion laser-based metallic (PBF-LB/M) additive manufacturing (AM) create tremendous computational challenges for establishing precise 'process-structure' correlations throughout the process. A recent approach, AM model-based process metrics (AM-PM), has addressed the challenge by applying analytical reduced-order models to the heat source position. AM-PMs can reveal quantifiable trends in space and time throughout the PBF-LB/M process. The AM-PMs furnished by the reduced-order models were evaluated against high-speed imaging (coaxial with the laser beam) of weld melt pools, and metrics from ex-situ metallography of the welds. The presentation will discuss how AM-PMs, such as melt pool width, correlate with measurements from in-situ imaging and ex-situ metallography

SESSION SF01.06: Poster Session II
Session Chairs: Ming Chen and Shreyas Pathreker
Tuesday Afternoon, November 28, 2023
Hynes, Level 1, Hall A

8:00 PM SF01.06.01

Additive Material Transfer using On-Demand Adhesion Modulation in a Self-Assembled Nanofluidic Structure Seongjae Kim¹, Ji-hun Jeong², Hyun Jun Ryu¹ and Sanha Kim¹; ¹Korea Advanced Institute of Science and Technology, Korea (the Republic of); ²Massachusetts Institute of Technology, United States

Transfer printing is one of the attractive routes toward additive manufacturing of flexible/stretchable electronics, micro/nanophotonic devices, micro-LED displays, and healthcare sensors via assembling micro/nano components. However, a major challenge in micro/nano transfer printing is achieving both high throughput and yield. An important factor in minimizing the transfer failure is the adhesion contrast between the picking and placing stages, particularly when manipulating microscopic substances that cannot be placed using gravitational force alone. Accordingly, realizing the large contrast in surface adhesion and its rapid transition is essential for the assembly of miniaturized parts. Herein, we propose a novel nanofluidic device enabling manipulation of micro components via capillary grasping and releasing mechanism. We fabricate the surface via vertical self-assembly of carbon nanotubes which allows liquids to infiltrate into the nanoscale channels when a strong gripping force is necessary and rapidly evaporate the fluid when a weak releasing force is needed. We quantitatively characterize the adhesive strength and find that the structure can exhibit high adhesion as liquid infiltrates the channel (~17.4 kPa) while it can switch into low adhesion as the surface is fully dried (< 0.1 kPa). The adhesive behavior is evaluated using atomic force microscopy and capacitive force sensing, resulting in an adhesion contrast of greater than 100-fold. Due to the nature of the liquid-solid interface, a minimal preload of 0.8 kPa is sufficient to enable the picking and placing which is particularly ideal for physical-contact-based manipulation of delicate electronic components. Our study demonstrates the successful transfer of μ LED chiplets, ultrathin films, and CNT supraparticles, as well as the application of strain sensors by transferring CNT particles onto a flexible PDMS substrate. To further elucidate insights into the underlying mechanism, we develop a mechanics model to analyze the adhesive force with respect to the types of liquid and contact time. Furthermore, we implemented a radiative heater to accelerate the evaporation process, enabling rapid pick-and-place operations that can be completed within a few seconds. Finite-element simulation and experiments reveal that the nanoscale fluid channels of our vertically aligned nanofiber structures are advantageous over planar surfaces by increasing the efficiency of heat transfer. We believe that this study provides a new route toward additive manufacturing of unconventional freeform devices via rapid and reliable assembly of micrometer-sized elements.

8:00 PM SF01.06.02

Selective Gene Expression in Hydrogel Suspended Escherichia Coli Through Optogenetics by Spatiotemporally Controlled Light for the Purposes of Additive Manufacturing Borut Lampret, Andreas Hadjimitsis, Guy-Bart Stan and Connor Myant; Imperial College London, United Kingdom

Natural and engineered biology offer an immense diversity of biological materials with a wide range of properties and benefits. Nature employs biological materials on all scales and forms various complex structures to further diversify the macroscopic properties of materials. Advances in the ability to manipulate genetic material have enabled the utilization of microbes in production of these biological materials and in combination with additive manufacturing one could attempt to artificially create such complex structures. However, most biological materials are not suitable for use with conventional additive manufacturing. While there have been significant advances in the field of bioprinting, great effort is still required to develop the so-called bioinks, which support both the printing process and the encapsulated cells' survivability.

To combat these challenges a novel method of additive manufacturing is explored, which can employ microbial cell factories suspended in hydrogel and optogenetics to selectively deposit the desired biological or synthetic material in a three-dimensional (3D) volume. Genetically engineered Escherichia coli that produces a synthetic light response system, CcaSR v3.0, was used in order to allow for spatially selective gene expression. A custom designed system was built to both house the hydrogel suspended E. coli and to provide and shape green and red light, which were used to interact with the cells. Green light was used to induce gene expression and red light was used to suppress gene expression. Localized gene expression was achieved within the hydrogel build volume with proper overlap of the green and red light and with the help of a predictive model describing the behaviour of the CcaSR system in response to light. To enable the process of additive manufacturing, a series of spatiotemporal illumination procedures were developed, and their behaviour investigated.

This approach of 3D printing is unique in that it shifts the burden of material from the bioink to the cells, which changes material engineering to bioengineering. This approach effectively exploits the cells for in-situ material production. As the cells are suspended in a hydrogel medium, any mechanical stress during the printing process is eliminated. Provided that the cells' engineered metabolism is not toxic, chemical stress is also eliminated. As opposed to conventional polymerisation, which generates cytotoxic free radicals.

This talk focuses on illumination procedures and slicing methods, which enable the cells to exhibit gene expression in complex 3D geometry within the volume. This system allows for near volumetric 3D printing in a sense that there is no requirement for supports or flat two-dimensional slicing of objects. A concrete example of gene expression in the shape of a double helix will be presented and discussed. Furthermore, both the spatial and temporal resolution limitations of the 3D printing method and system will be discussed along with proposed solutions. This research is the first stepping stone towards a novel bioprinting approach, which can expand the 3D printing material library to biological materials and could also be implemented in tissue engineering through optogenetics.

8:00 PM SF01.06.03

3D Printing of Photoconductive Zinc Oxide-Based Photoresins Ozan Karakaya^{1,2}, Luis A. Ruiz-Preciado^{1,2}, Peter Krebsbach^{1,2}, Kai Xia^{1,2}, Christian Rainer^{1,2}, Ali Tunc^{1,2}, Uli Lemmer^{1,2,3} and Gerardo Hernandez-Sosa^{1,2,3}; ¹Light Technology Institute, Karlsruhe Institute of Technology, Germany; ²InnovationLab, Germany; ³Institute of Microstructure Technology, Karlsruhe Institute of Technology, Germany

The interest in 3D-printed functional microstructures has significantly increased over the past decade due to their potential utilization in microelectronics, photonics, optoelectronics, and biological applications.^[1] Compared to commonly used additive manufacturing techniques such as fused deposition modeling and selective laser sintering, light-based 3D Printed methods (Stereolithography) offer faster processing and higher spatial resolution.^[2,3] However, for light-based 3D printing, mainly 3D structures based on organic polymers have been assembled due to the limited availability of multifunctional (e.g. conducting, semiconducting, etc.) photoresins. One of the main challenges that have been encountered when designing functional photoresins is the undesired light absorption of the ink, which leads to relatively low spatial resolution or crosslinking efficiency.^[4]

Here we use an approach for designing a multifunctional photoresin to fabricate 3D-printed ZnO microstructures by mixing a commercial photoresin with a Zinc-based metal-organic complex. This material doesn't have any optical absorption that interferes with the photoresin photopolymerization process and can be transformed to ZnO at low annealing temperatures (< 200 °C). The utilized functional resin is comprised of a commercial photoresin into which the ZnO precursor, a stabilizer, and an organic solvent are added. Additionally, high zinc loading is possible by using a stabilizer in the precursor solution which can lead to high ZnO conversion hence better optoelectronic properties. Depending on the material ratio and optimized composition which favors both printing resolution and optoelectronic properties can be prepared. After printing of the photoresin by Digital Light Processing (DLP) (27 μ m resolution, 25 μ m slice thickness), the 3D structure is thermally annealed to transform into a Polymer/ZnO composite. Structural and morphological characterization has been performed by scanning electron microscopy and x-ray diffraction showing percolative paths of ZnO in the polymer matrix and good crystalline quality. Optoelectronic characterization of the 3D printed Polymer/ZnO composite yielded Zinc based 3D printed photodetectors exhibiting photocurrents off 0.5 nA and an on/off ratio of 250 when excited at a wavelength of 395 nm. Reference thin-film samples deposited on glass substrates showed ZnO-based UV-photodetectors exhibiting a photocurrent of 5 nA and an on/off ratio of 600 when excited at the same wavelength.

In future work, we plan to extend the obtained results towards its use in the Direct Laser Writing (DLW) process to obtain micro-architected 3D ZnO structures which will be potentially used in applications such as miniaturized optoelectronic and bioelectronic devices.

- [1] Liu, et al. *Int. J. Extreme Manuf.*, 2019, 1, 025001.
 [2] Benjamin, et al. *Biomed. Phys. Eng. Express*, 2019, 5, 025035.
 [3] Melchels, et al. *Biomaterials*, 2010, 31, 6121–6130.
 [4] Liu, et al. *Adv. Mater. Technol.*, 2022, 7, 1–8.

8:00 PM SF01.06.04

In-Situ Alignment Behavior of Anisotropic NdFeB Magnets in Extrusion-Based 3D Printing Process YongraeKim, DongwoonShin, TaehoHa, JoonphilChoi, SegonHeo, Yeo-UlSong, ChangwooLee, Pil-HoLee and Min-KyoJung; Korea Institute of Machinery and Materials, Korea (the Republic of)

Permanent magnet materials play a vital role in numerous electronic devices, ranging from electric vehicles and wind turbines to smartphones and smartwatches. Their ability to efficiently convert electrical energy into mechanical energy makes them essential components in modern technology. With the increasing demand for high-performance magnets with diverse shapes, driven by the trend towards miniaturization and lightweight design, there is a need to explore innovative manufacturing techniques which can meet these requirements and improve overall efficiency.

Currently, the production of permanent magnets primarily uses two main methods: sintering and polymer-bonded techniques. Sintered magnets exhibit superior magnetic properties compared to bonded magnets because of their higher density and crystalline structure. However, they possess inherent limitations, including poor corrosion resistance, limited shape complexity, and higher energy consumption during the manufacturing process. On the other hand, bonded magnets are created by combining magnetic powders and polymer binders through compression molding, extrusion, or injection molding. Compression molding allows for magnets with high filler ratios, but it is restricted to producing magnets with simple shapes. Injection molding, although capable of fabricating magnets with complex geometries, results in material waste and requires additional tooling processes.

To overcome these challenges and advance the production of bonded magnets, our research utilizes the additive manufacturing technique known as Fused Deposition Modeling (FDM). Unlike conventional methods that use filament, we employ powders or pellets consisting of binder polymers and anisotropic magnet fillers in our process. This approach reduces process time by skipping the filament manufacturing step and allows for control of the filler ratio. It also enables the creation of complex-shaped bonded magnets and addresses the limitations of conventional manufacturing techniques. Moreover, during the layer-by-layer printing process, we incorporate an in-situ electromagnetic alignment method to orient the anisotropic magnetic fillers along the desired magnetization axis. This alignment technology determines the orientation of the magnetic filler during processing, resulting in bonded magnets with superior magnetic properties, including improved remanence, coercivity, and energy products.

In our presentation, we will provide a comprehensive overview of the FDM-based bonded magnet fabrication process and discuss the crucial parameters involved. One significant parameter is the printing temperature, which determines the viscosity and flow characteristics of the binder polymer and affects the overall quality and integrity of the printed magnet. Additionally, the application of in-situ magnetic fields during the printing process plays a crucial role in aligning the anisotropic magnetic fillers with the magnetization axis and influences the final magnetic properties of the fabricated magnet. Understanding and controlling these variables is essential for achieving magnets with optimal performance.

Continuing our research and development efforts, we aim to further optimize the FDM-based bonded magnet fabrication method. Our goal is to improve the magnetic properties of the magnets produced while increasing the complexity of their small, lightweight, and shaped forms. To achieve these goals, we will explore various aspects, including the formulation of magnet fillers, binder polymers, and their interactions, as well as the optimization of printing parameters and post-processing techniques. By continuously improving this additive manufacturing approach, we aim to provide an efficient and sustainable method for producing high-performance bonded magnets tailored to the specific requirements of modern electronic devices.

8:00 PM SF01.06.05

3D Printing of Fluidic Systems with Soft Tissue-Like MembranesYafengYu¹, YiPan¹, YantingShen¹, JingxuanTian^{1,2}, RuotongZhang¹, WeiGuo^{1,2}, ChangLi¹ and AndersonShum^{1,2}; ¹The University of Hong Kong, China; ²Advanced Biomedical Instrumentation Centre, Hong Kong Science Park, China

As a natural fluidic system, blood vessel networks can adjust blood compositions by modulating physicochemical reactions between vessel walls and blood. Such biomimetic strategy in regulating fluids remains underexplored in synthetic systems, despite its relevance to spatiotemporal fluid modulation. The challenge is to build synthetic channels with functionalizable, vessel tissue-like walls. In this work, we produce a fluidic system with soft, membranous, and semipermeable channel walls, thus enabling functional compartmentalization for physical transport of fluids or for chemical reactions with fluids. An extrusion-based 3D printer was utilized to deposit one aqueous solution within another, where oppositely charged polymers self-assemble on the interface between these two solutions to generate channel-like structures. The channel walls are functionalizable for localized physicochemical reactions, for instance, by placing solutions of small molecules beside channels or locally immobilizing enzymes on the outer channel walls. Thus, fluid compositions inside are spatiotemporally programmable: As a demonstration, by modulating interplays between fluids and channels over space, the glucose concentration increases in the upstream fluid and decreases in the midstream channel, and the carbon dioxide concentration decreases in the downstream fluid. Our proposed fluidic system mimics the biofluid regulation in natural systems, inspiring platforms as in-vitro tissue models to synthesize biologically relevant molecules and screen drugs.

8:00 PM SF01.06.06

Three-Dimensionally Printed, Vertical Full-Color Display Pixels for Multiplexed AnticounterfeitingShiqiHu and Ji TaeKim; The University of Hong Kong, Hong Kong

Since counterfeiting has emerged as a global issue, novel and advanced strategies are in great demand for data storage and encryption to prevent information leakage. To this end, various materials, structuring strategies, and data processing algorithms have been devised. Creating high-resolution, sophisticated anticounterfeiting patterns has mostly relied on photolithography, nanoimprinting, and laser engraving, which are energy-intensive and/or chemically deleterious, difficult to perform on valuable products¹⁻⁴. Alternatively, inkjet printing has also been utilized by taking advantage of its cost-effectiveness and high compatibility with ink and substrate materials. However, the resulting patterns are easily duplicated due to their simple geometry constrained in-plane. Advancing the structural complexity for improving security level remains a longstanding challenge. The utilization of luminescent materials is a strategy to advance anticounterfeiting labels. The intrinsic or stimulus-responsive optical properties of semiconductor quantum dots, perovskites, or organic dyes can be exploited to configure multilevel anticounterfeiting^{5,6}. A luminescent-based anticounterfeiting label consists of an array of pixels which are the fundamental element to encode/display information. Each pixel is typically composed of red, green, and blue subpixels with lateral patchwork to render multi-channel information encryption. However, this lateral configuration is unavoidable for the existence of a subpixel pitch, not only being easily copied but also limiting the improvement of pixel density.

Herein, we propose vertically stacked multicolor micropixels for high-resolution, multiplexed anticounterfeiting. The micropixel is produced by sequentially stacking luminescent dye-doped red-green-blue (RGB) subpixels, realized with high-resolution 3D printing. Our 3D printing approach based on the use of a femtoliter ink meniscus enables vertical stacking of micron-sized subpixels without the existence of a subpixel pitch, drastically increasing the pixel density up to 13,400 pixels per inch (PPI), which is not easily attainable by the traditional lateral subpixel layout. Furthermore, a full-scale color synthesis for each micropixel is achieved by modulating the height ratio of R, G, and B subpixels, which is reflected in the CIE 1931 diagram. These features create high-resolution, multiplexed anticounterfeiting labels, inaccessible by conventional optical imaging, and 3D printing offers the simplest, most versatile route to manufacture. This work demonstrates the exceptional inclusivity of 3D printing to construct vertically stacked structures and highlights the possibility to devise 3D printing for photonic device manufacturing.

1. Choi, M. K. *et al.* Wearable red–green–blue quantum dot light-emitting diode array using high-resolution intaglio transfer printing. *Nature Communications* 6:1 6, 1–8 (2015).
2. Zhu, C. *et al.* An Integrated Luminescent Information Encryption–Decryption and Anticounterfeiting Chip Based on Laser Induced Graphene. *Adv Funct Mater* 31, 2103255 (2021).
3. Arppe, R. & Sørensen, T. J. Physical unclonable functions generated through chemical methods for anti-counterfeiting. *Nature Reviews Chemistry* 1:4 1, 1–13 (2017).
4. Hu, Z. *et al.* Physically unclonable cryptographic primitives using self-assembled carbon nanotubes. *Nature Nanotechnology* 11:6 11, 559–565 (2016).
5. Ho, S. J., Hsu, H. C., Yeh, C. W. & Chen, H. S. Inkjet-Printed Salt-Encapsulated Quantum Dot Film for UV-Based RGB Color-Converted Micro-Light Emitting Diode Displays. *ACS Appl Mater Interfaces* 12, 33346–33351 (2020).
6. Chen, M. *et al.* Three-Dimensional Perovskite Nanopixels for Ultrahigh-Resolution Color Displays and Multilevel Anticounterfeiting. *Nano Lett* 21, 5186–5194 (2021).

8:00 PM SF01.06.07

Fabrication of Multifunctional Wearable E-Textile Platform using Multi-Head 3D Printing ProcessKyusoonPak and StevePark; Korea Advanced Institute of Science and Technology, Korea (the Republic of)

In recent decades, attempts have continued to data various senses felt by the human body. Among these various senses, sensor studies for the tactile sense have been conducted in a way that applies soft electronics due to the ranges and types of tactile senses, and the fact that human skin has many curved parts. However, most existing studies involve materials that are unideal to detect touch and human posture, and there were thus many limitations to their application to the dynamic human body. In this study, to solve the aforementioned problems, a wearable tactile sensor was manufactured using textile(clothes) worn by mankind for a long time as a substrate. The weaving method using coating yarn, used in the study of most textile-touch sensors, has the disadvantages of a complicated process and difficulty in customization. Therefore, in this study, strain sensors, electrodes, and temperature sensors made of organic materials were directly 3D-printed on the substrate of clothes and textiles. we developed a solution-based ink for manufactured tactile sensors. The ink can quickly fabricate sensors and electrodes and applied the 3D printing process to produce fabric-based electronics. Through this method, the process could be simplified and the waste of materials could be reduced, and it was possible to manufacture sensors in the forms desired by the user. In addition, physical deformation of the electrode could be maintained by utilizing the excellent elasticity of the textile without changing the excellent

resistance value ($0.2 \Omega \sim 0.4 \Omega$) using polystyrene, a hard material that is fundamentally controlled. In addition, by optimizing the degree of permeation into the textile according to viscosity, electrodes printed on both sides could be connected or separated at a point desired by the user. We evaluated the performance of each sensor and applied the integrated sensor to the Battle Dress Uniform (BDU) to measure the surrounding environment of the actual soldier in real time. Through this study, a method of printing the solution directly on the textile was attempted, and we are sure that it will be possible to promote great progress in integration through the use of both sides by controlling the degree of absorption of the solution into the textile through the viscosity.

8:00 PM SF01.06.08

3D-Printed Single-Material Carbon Nanotube Thermocouple MicrodevicesZhuoranWang and Ji TaeKim; The University of Hong Kong, Hong Kong

Miniaturized thermocouples have emerged as an essential component for the power generation or thermal management of microelectronic devices due to their capability to convert heat to electricity. Recently, extensive research focused on the structural design of micro-thermocouples to improve the thermoelectric performance, and one resulting insight is that a three-dimensional (3D) geometry can be beneficial in terms of integration density and thermal contact efficiency [1]. However, the construction of a 3D micro-thermocouple typically comprising two dissimilar materials suffers not only from the process complexity with high cost but also from the low mechanical strength of the junction.

Here, we have developed a micro 3D printing method for fabricating a single-material carbon nanotube (CNT) thermocouple device. The device is configured with an electrical junction of two freestanding CNT microwires with different widths, by exploiting the size-dependent Seebeck coefficient at the electron mean free path scale [2, 3] instead of using two different materials. The developed micro 3D printing method that uses a femtoliter ink meniscus enables a single-step, continuous, high-resolution ($< 1 \mu\text{m}$) manufacturing of CNT micro-thermocouples in three dimensions. This greatly ensures structural robustness, cost-effectiveness, and design flexibility, which have not been attained by other traditional manufacturing approaches, reinforcing practicality. In this talk, we will present the experimental results including the fabrication and characterization of 3D CNT micro-thermocouples, and discuss the prospects of our work for potential applications.

References

- [1] Q. Zhang, K. Deng, L. Wilkens, H. Reith, and K. Nielsch, "Micro-thermoelectric devices," *Nature Electronics*, vol. 5, no. 6, pp. 333-347, 2022, doi: 10.1038/s41928-022-00776-0.
- [2] A. Harzheim, F. K onemann, B. Gotsmann, H. van der Zant, and P. Gehring, "Single-Material Graphene Thermocouples," *Advanced Functional Materials*, vol. 30, no. 22, 2020, doi: 10.1002/afm.202000574.
- [3] W. Sun, H. Liu, W. Gong, L.-M. Peng, and S.-Y. Xu, "Unexpected size effect in the thermopower of thin-film stripes," *Journal of Applied Physics*, vol. 110, no. 8, 2011, doi: 10.1063/1.3653824.

8:00 PM SF01.06.09

Parameter Optimization for Bioprinting of Cell-Laden Gelatin Methacryloyl Bioinks Guided by Support Vector MachineZhouquanFu¹ and WeiSun^{1,2}; ¹Drexel University, United States; ²Tsinghua University, China

3D bioprinting is an emerging and fast-growing interdisciplinary field which uses biomaterials, living cells, and/or bioactive factors (i.e., bioinks) to construct biological models, biological living systems, and therapeutic products. The printing and post-printing processes encompass printer parameter tuning (e.g., temperature, speed), assessing printability (fidelity and cell survivability), and fostering the maturation and integration of the printed tissue. Each of these stages can be influenced by an extensive array of factors, including the type of cells and biomaterials utilized, the printing parameters, and the intended function of the bioprinted tissue or organ. The complexity of the process, combined with the multitude of variables, presents a significant challenge for manual optimization and control. Owing to the intrinsic difficulties in the 3D structure formation posed by the soft biomaterials and the encapsulated cells, bioprinting has unique requirements for the biomaterial properties and process parameters to maintain high cell viability and structural fidelity. Currently, trial-and-error experimentation has been dominantly used to find "optimal" printing parameters and bioink parameters, which is costly and time consuming. In our study, a uniform design-of-experiment method was used to select only 12 parameters (out of 64) as the training data set. Then experiments on the 12 parameters were conducted, followed by the data labelling as good or bad print based on the printability score and cell viability score. Then the support vector machine (SVM) classifier algorithm was trained on the 12 data and then a process map was generated by the SVM prediction on the entire data space. Our method was tested effective and quick to find parameters that can yield good printing results with high cell viability.

8:00 PM SF01.06.10

Thermal Conductivity Measurement for Aligned Particle MonolayersEvanToth, JessicaFaust and RandallM. Erb; Northeastern University, United States

Thermal management poses serious design and size limitations for high power density electronics, and relatively few material options that are both dielectric and thermally conductive can be processed easily (e.g., hexagonal boron nitride, diamond). Hexagonal boron nitride has strong dielectric properties and a theoretical thermal conductivity on par with copper, imbuing it with strong potential for use in power electronics and low-loss RF systems -- especially in thin layers. Hexagonal boron nitride (sometimes called 'white graphene') has excellent in-plane phonon transport, and to exploit this we use a surface assembly technique to create percolated platelet-thick monolayers. Induced planar alignment of the individual platelets at high volume loadings transforms a disjoint collection of particles into a thermally percolated plane for heat to preferentially travel *within* (x-y) but *not through* (z). Regarding conductive behavior, monolayers are particularly interesting due to their low dimensional (2D) morphology but, in turn, make extracting useful thermal parameters (diffusivity, conductivity) significantly difficult with current measurement techniques. Conventional methods like thermal interface measurement and laser flash either cannot accurately measure in-plane heat flow or require highly custom software/hardware for an otherwise highly inaccessible instrument. In this work, we modify the semi-transient method developed by Angstrom in 1861 to measure the thermal diffusivity of 2D materials with the aim of thermally characterizing monolayer composites and more generally to allow for simple planar measurement of thermal diffusivity.

8:00 PM SF01.06.11

High Resolution Magnetorheological Devices for Advanced Applications Fabricated by Additive Manufacturing TechnologiesAnderGarcia¹, CarmenR. Tubio¹, AinaraGomez², JoanesBerasategui², MounirBou-Ali², JonGutierrez^{1,3} and SenentxulLanceros-Mendez^{1,4}; ¹BCMaterials, Basque Center for Materials, Applications and Nanostructures, Spain; ²Mondragon University, Spain; ³University of the Basque Country, Spain; ⁴Ikerbasque, Basque Foundation for Science, Spain

Magnetorheological elastomers (MREs) can modify their mechanical properties (mainly elastic moduli) in response to a magnetic field. These materials, comprising a polymeric matrix and inorganic magnetic fillers, have traditionally found use in large scale applications (such as dampers and isolators) that sacrifice accuracy for performance and fabrication simplicity.

With additive manufacturing (AM) technologies, however, complex structures could be fabricated through different techniques, such as direct ink writing (DIW), that allow to achieve higher pattern resolutions and allow new and exciting applications in the field of healthcare, automotive and printed electronics. The issue with traditionally designed MREs is that are typically based on carbonyl iron microparticles that, albeit their high saturation magnetization and low coercivity, are not suitable for AM due to their size and hinder high resolution patterns.

Thus, a transition should be made into using nanoparticles (NPs) for high-resolution applications. To this end, we have studied the impact that magnetic properties, concentration, shape, and orientation have on the performance of nanoparticle based MREs, in order to achieve the optimize performing material compatible with AM.

Nanoparticles with different values of saturation magnetization, coercivity, and remanence have been selected to fabricate the MREs. Six different fillers were tested: CoFe_2O_4 , Fe_3O_4 , Co, Ni and $\text{Ni}_{80}\text{Fe}_{17}\text{Mo}_3$ (Permalloy). The magnetorheological (MR) effect achieved for the Fe_3O_4 composite was the highest one at 18%, and comparable to other composites reported in the literature, but with a lower content of magnetic material (only 6 vol% versus 20 vol%), which is expected to improve the processing and integration of the MRE. Moreover, by using different concentrations (20 wt%, 40 wt% and 60 wt%) of the Permalloy filler, we obtained a linear relationship between MR effect and filler concentration, increasing from 8% at 20 wt% to almost 30% at 60 wt%. However, this increase in performance should be carefully balanced with the variation of the mechanical properties.

Further, Fe_3O_4 nanorods (NRs) have been synthesized with an aspect ratio of 10 to compare with the 70 nm sized cubic Fe_3O_4 NPs. Anisotropic MREs (A-MREs) were then fabricated by curing the composite inside a magnetic field to achieve a preferential orientation and compared them with isotropic MREs (I-MREs) cured without the presence of the magnetic field. The results of the relative magnetorheological effect confirmed that the A-MREs exhibit higher values of the MR effect, as it increased from 12% to 27% in the case of the NPs and from 8.3% to 17% in the case of the NRs. Interestingly, these results imply that lower aspect ratios are more suitable to enhance the MR effect in anisotropic composites, since the relative increase between oriented and non-oriented samples was 125% for the NPs and 104% for the NRs.

The suitability of these materials for DIW additive manufactured devices has been further evaluated in Fe_3O_4 -based MREs. We fabricated a fully printed patterned device combining magnetoelectric and magnetorheological properties, where the conversion from applied magnetic field to output voltage could be manipulated by taking advantage of the change in mechanical properties and magnetorheological of the magnetorheological layer.

8:00 PM SF01.06.12**Additive Manufacturing of Flexible Photonic Waveguides with Active Components**Maxine Ong, YuShu, MaxJenkins, HarishBhaskaran and PeterBruce; University of Oxford, United Kingdom

An emerging research direction in flexible devices is in photonics. Having the ability to manipulate and deform photonic devices gives the additional benefit of controlling light-matter interaction. Flexible photonic devices are seen in applications such as interconnects, detectors and bio-photonic sensors, where the mechanical flexibility of the devices is exploited. However, there are still many challenges associated with the fabrication due to the poor compatibility of available flexible substrates to conventional methodologies. In this work, we demonstrate the fabrication of polymeric waveguides on flexible substrates and the integration of active components (e.g. 2D materials, phase-change materials) through additive manufacturing, such as direct laser writing and pick-and-place. These have potential optoelectronic applications in photodetection, and memory devices that can be seamlessly affixed to conformal surfaces.

8:00 PM SF01.06.13**Mechanism of Cellulose Ester as an Anti-Wash Admixture of Cement for Underwater 3D Printing**Tianyi Wang and YaxinAn; Louisiana State University, United States

Underwater 3D printing of cement presents a significant challenge due to issues such as washout or segregation of cement. To address this problem, the addition of anti-wash admixtures has been explored to increase the printability of cementitious materials. Among these admixtures, cellulose ester has gained wide recognition for its effectiveness in improving the underwater printability of cement. Only a small amount of cellulose ester (<1 wt%) could significantly improve the underwater printability of cement. However, the underlying mechanism of how cellulose ester enhances the cohesiveness of cement is little understood. To shed light on the mechanism, we performed atomistic molecular dynamics simulations of cellulose ester with cement. Specifically, we characterized the conformation of cellulose ester and examined the interface between cellulose ester and cement. To gain insights into the thermodynamic properties of cellulose ester on the cement surface, we calculated the potential of mean force for an oligomer of cellulose ester. Additionally, we investigated the effects of the number of acetylation groups and the degree of polymerization of cellulose ester. This work presented an atom-level understanding of the interplay between cement and cellulose ester, which holds great potential for the optimization of anti-wash admixtures for underwater 3D printing.

8:00 PM SF01.06.14**Expanding the Toolbox of PhotoROMP Additive Manufacturing**Alex Commisso, AnnikaJansen and SamuelLeguizamon; Sandia National Labs, United States

Stereolithographic additive manufacturing (SLA) processes provide agility and complex design development of components necessary for a wide range of critical applications. Yet this technique is limited to a small subset of monomers that traditionally produce polymer materials with poor thermal and mechanical properties. Conversely, ring-opening metathesis polymerization (ROMP) can produce relatively tough, high T_g thermosets using latent ruthenium catalysts. Furthermore, spatiotemporal control of the polymerization using photosensitizers affords high resolution patterning of high T_g thermosets using photoROMP. Dicyclopentadiene (DCPD), an inexpensive but robust photoROMP monomer, has been featured in SLA resins to generate highly complex three-dimensional geometries at print speeds approaching industry-leading standards using continuous SLA techniques. However, the minimal exploration into the monomer space in photoROMP and ROMP SLA hinders the utility of ROMP polymers as the DCPD-based resins are generally non-processable, non-degradable, and lack other useful functionalities that have previously been imbued in polymeric materials. By examining the strained olefin monomer space for their photopolymerization kinetics, material properties, and print fidelity, we have identified potential routes to rapid SLA of functional polymers using photoROMP.

8:00 PM SF01.06.15**Additively Manufactured Ceramic Combustor for Power-Plant Scale Electricity Generation**Shomik Verma, MehdiPishahang, KyleBuznitsky, AlinaLaPotin, SantoshShanbogue and AsegunHenry; Massachusetts Institute of Technology, United States

Existing power plants have many downsides, as they have low efficiency, emit CO₂, and include high-temperature rotating machinery requiring frequency maintenance. However, they are dispatchable, which provides a direct benefit over variable renewable energy resources such as solar. The ideal technology would be both dispatchable and solid-state. A recent alternative is fuel cells, which can directly extract the chemical energy in fuels into electricity with electrochemistry, but they require expensive catalysts and have low power density.

Combustion-powered thermophotovoltaics is a promising alternative for power generation. In this system, a combustor is designed that preheats air above the auto-ignition point of a fuel, such that the mixture combusts upon contact. The heat from combustion is used to heat up an emitter to ultra-hot temperatures, and the emitter radiates heat to the TPV cell. The TPV cell converts the emitted light to electricity. If hydrogen is used as the fuel source, the electricity produced is clean, creating a solid-state, catalyst-free method of generating electricity. When combined with high-efficiency, high-power density TPV cells, this combustion-TPV system has the potential to be high-performing. However, there are many challenges in the system design, for example that high temperatures (2000C) are required, hefty insulation is needed to prevent heat loss, and cost may be high.

Thus, this study addresses three key challenges in the combustor design: materials identification, scalable design, and fabrication with additive manufacturing.

For materials identification, the objective of the material is to limit thermal stresses when a thermal gradient is applied, meaning the product of Young's modulus and coefficient of thermal expansion must be low. The material's yield strength must also be high, so that it does not fracture when a thermal stress is present. Due to the extreme environments present, the material should also be oxidation resistant and have high service temperature. Thus, oxides are the best option, and yttria-stabilized zirconia (YSZ) is identified as the candidate material due to its reduction resistance in the presence of high-temperature hydrogen.

Next, we design a high-efficiency combustor with 93% combustion efficiency using YSZ, enabled by milli-scale channels and a large surface area to volume ratio. The combustor also features a near-isothermal emitter wall at approximately 2000C. It is also modular, enabling vertical and horizontal stacking to reach the large length scales required for cheap insulation and grid-scale power generation.

However, the intricate internal geometries enabling the effective heat transfer within the device necessitate additive manufacturing. Because this technique can be expensive, two techniques are used to ensure cost-competitiveness. One is maximizing the power output per volume of the device, which is enabled by a large emitter surface area surrounded by high-power density TPV cells. Another is design for manufacturing, in which the device is 3D printed in 3 sections which are joined together in post-processing. This enables parallel processing and easier access to the internal channels, which would otherwise be difficult to clear. One challenge of this stacking method is how to properly join the slices, and a leak-proof joining methodology is developed to solve this.

Based on these improvements, we achieve a predicted cost per power of \$0.30/W, which is significantly less than the cost of a natural gas turbine at \$1/W, and leaves room for balance-of-plant costs such as pollution control, TPV cooling, and electronics.

Overall, in this work we push the boundaries of ceramic additive manufacturing to develop a next-generation power plant based on hydrogen combustion coupled with thermophotovoltaics.

8:00 PM SF01.06.16**Two Photon Lithography Assisted Fluorescence Sensor for Sensitive Detection of Lead Ions in Water**Archana T¹, SwetaRani², Rahul KumarDas^{1,1}, GauravP. Singh¹, SumitSaxena^{1,2,1} and ShobhaShukla^{1,2,1}; ¹IIT Bombay, India; ²IITBombay- Monash Academy, India

Lead has been involved in various human activities for a long time without realizing its detrimental effects on both the environment and human beings; arising even from exposure to trace amounts. The exposure to lead ions from water contamination, pipelines, gasoline exhausts, smelting plants, paints, consumer products have ability to cause serious health conditions like neurobiological disorder in fetus and children, muscle paralysis by calcium ion inhibition, anemia, cancer etc. Various International organizations (WHO, EU, ISI) have defined a permissible limit of 10ppb on the concentration of lead in water. According to the World Health Organization (WHO), approximately 600,000 deaths per year worldwide can be attributed to lead exposure. These alarming statistics underscore the urgent need for accurate and sensitive detection techniques to enable early intervention and prevention. The conventional techniques like absorption spectrometry (AAS), plasma optical emission spectroscopy, electrochemical methods, X-ray fluorescence spectrometry, and flame absorption spectroscopy are used for the detection of Lead ions in water. Over the past decades, researchers have been exploring various methods of detection mechanism over the conventional techniques as they are bulky, prone to interference, involves complex sample preparation, require skills and training to operate and interpret the results. Advanced sensing technologies, such as electrochemical sensors and optical sensors, have shown promise in the rapid and sensitive detection of lead ions. These sensors offer real-time monitoring capabilities and high sensitivity, ensuring that lead levels in water are promptly. Additionally, miniaturization in terms of the sensors is preferred over bulky conventional spectrometric techniques. Hence there is an exigent need to develop a miniaturized sensor with high sensitivity and performance.

In response to this challenge, our research proposes a novel approach involving a cyclodextrin-decorated Carbon Quantum Dots (CQD) platform for lead ion detection in real samples. The integration of cyclodextrin, a cyclic oligosaccharide, with CQDs enhances the selectivity and sensitivity of the sensor towards lead ions. To facilitate practical application, the sensor has been incorporated into a polymer matrix, enabling fluorescence-based analyte detection. Fabrication of miniaturized sensors is accomplished using Two-Photon Lithography, a versatile and precise technique capable of creating intricate structures at the micro and nanoscale. Through extensive investigations, we have explored various parameters to optimize the sensor's performance, ensuring its accuracy and reliability in detecting lead ions. In conclusion, our work addresses the critical need for reliable lead detection methods. By utilizing advanced sensing technologies, optimizing sensor performance, and emphasizing affordability and portability, we aim to contribute to the protection of public health from the detrimental effects of lead exposure in water sources.

8:00 PM SF01.06.17

Maximizing Photosynthetic Current Density of 3D Printable Thylakoid-PEDOT:PSS Composite Inks Through Bayesian Optimization JongHyunKim, JaeHyounYun and WonHyounRyu; Yonsei University, Korea (the Republic of)

Thylakoid membranes (TM) isolated from living plants can produce high energy electrons through photosynthesis under sunlight. If placed near an electrode, the high energy electrons can be harvested and put to practical use, creating an eco-friendly power cell. Recently our group has demonstrated TM-embedded 3D printable ink based on a conductive polymer, poly(3,4-ethylenedioxythiophene):polystyrene sulfonate (PEDOT:PSS) [1]. Compared to the conventional post-electrode-deposition methods, the pre-embedding method allowed drastic increase in TM-electrode contact. While this previous study has focused on optimizing electrode geometry, in this work, we seek to optimize the electrode material itself to reach maximum current density. However, in achieving high current density, the two key parameters: the electron production rate and electrode conductivity, are always in tradeoff. Denser TM embedment surely increases photosynthesis but decreases electrode conductivity as it interrupts the conductive networks of PEDOT, responsible for charge flow. Addition of secondary dopants, such as dimethyl sulfoxide (DMSO), boosts conductivity by facilitating phase separation between PEDOT and PSS chains, but such organic solvents are prone to damage TMs. Post treatments of dry-annealing in PEDOT:PSS electrodes are considered essential in formulating and crystallizing PEDOT-rich domains [2], but heat treatments can damage the protein structures in TM. As multiple correlated factors in the material and manufacturing process account for the overall current density of the power cell, it is not only laborious but also very difficult to optimize each parameters. Therefore, we implemented Bayesian optimization, a technique used widely in Machine Learning, to simultaneously fine tune the concentrations of TM, PEDOT:PSS, and DMSO, along with dry-annealing time and temperature. To stay within 3D printable boundaries, we conducted rheological studies of the ink composites and set their lower boundaries to where their storage modulus is just above the loss modulus. Their upper boundaries were set at a nozzle clogging point referenced from the previous work on 3D printing PEDOT:PSS [3]. Additionally, we conducted a parametric study of gradual heating of drop casted TM on ITO glass. The upper boundary of the temperature parameter was set as 150°C, where no current was longer measured from TM. In each iteration step of the Bayesian optimization, the ink was mixed thoroughly, screen printed with fixed volume on an ITO glass substrate, and dry-annealed in oven. The current density value, measured through cyclic amperometry, was fed into the Bayesian optimizer and the experimenter received back the next sampling point. As the experiment prolonged, the Bayesian optimizer attempted to find the global maxima of the surrogate model built from these current density values.

REFERENCES

- [1] Yong Jae Kim, et al, *ACS Appl. Energy Mater.*, 2023, 6, 2, 773-781
- [2] Baoyang Lu, et al, *Nature Communications*, 2019, 10, 1043
- [3] Hyunwoo Yuk, et al, *Nature Communications*, 2020, 11, 1604

This work was supported by the National Research Foundation of Korea(NRF) Grant funded by the Korean Government(MSIT) (No. 2020R1A2C3013158).

8:00 PM SF01.06.18

Digital Light Processing 3D Printed Thermochromic and Thermoresistive Sensors Based on Soybean Oil and Ionic Liquids CristianMendes-Felipe^{1,2}, DanielaCorreia³, MohammadTariq⁴, JoséEsperança⁴, MarcoSangermano² and SenentxuLanceros-Mendez¹; ¹BCMaterials - Basque Center for Materials, Applications and Nanostructures, Spain; ²Politecnico di Torino, Italy; ³University of Minho, Portugal; ⁴Universidade Nova de Lisboa, Portugal

Additive Manufacturing (AM) has revolutionized the field of manufacturing by enabling the fabrication of complex three-dimensional structures with unprecedented design freedom. This work focuses on Digital Light Processing (DLP), for the processing of soybean oil-based materials. The use of reactive solvents and the study of suitable inks for printing purposes are explored, allowing or enhance the performance, sustainability and versatility of AM processes.

Soybean oil-based materials have gained significant attention due to their renewable nature, biodegradability, and potential for sustainable manufacturing. By formulating soybean oil-based resins and optimizing the processing parameters, digital light processing techniques can effectively harness the advantages of these materials. The incorporation of reactive solvents in the formulation allows for controlled material properties, including viscosity, curing kinetics, and mechanical strength, facilitating precise material design for specific applications.

To achieve successful printing of soybean oil-based resins, it is essential to develop compatible and stable inks. The study delves into the investigation of suitable ink formulations for DLP-based AM, considering factors such as ink rheology, surface tension, and photocuring behaviour. By understanding the ink characteristics, printing parameters can be optimized, ensuring high-quality prints, and expanding the range of printable materials. Thus, different reactive diluents including isobornyl acrylate or lauryl acrylate are added decreasing that the viscosity of soybean oil and reaching proper values for DLP printing, together with enhance the photopolymerization process. Furthermore, the thermal and mechanical properties of printed materials are tested showing a wide range of both properties depending on the reactive diluent content. Also, high quality 3D printed parts are observed in all cases.

Additionally, this work explores the integration of thermochromic materials, specifically ionic liquids, into the AM process to obtain functional 3D structures for sensor applications. Thermochromic materials exhibit reversible colour changes in response to temperature variations, enabling the development of smart and responsive sensors. The incorporation of ionic liquids with thermochromic properties provides an avenue to achieve enhanced sensitivity and precise control of the thermochromic response in printed sensor structures without the ascribed problems of using thermochromic nano- or microparticles. Bis(1-butyl-3-methylimidazolium) tetrachloronickelate ([Bmim]₂[NiCl₄]) ionic liquid is easily dispersed in quantities up to a 40 wt.% filler content. All prepared materials present humidity dependent thermochromism from colourless to blue and this colour variation is thermally activated and humidity governed, being 55% the minimum value of the relative humidity for colour change to occur. Further, the electrical conductivity increases with increasing IL content and decreases with increasing temperature, demonstrating also the applicability of the materials as thermoresistive sensors.

The proposed research contributes thus to the advancement of AM techniques by expanding the materials palette to include soybean oil-based resins, optimizing ink formulations for DLP printing, and exploring the functional integration of thermochromic ionic liquids in sensor applications. The findings from this study hold great potential for the development of sustainable, customizable, and intelligent 3D-printed structures with broad applications in fields such as sensing, robotics, and biomedical engineering.

8:00 PM SF01.06.19

3D-Printed Fused Silica Glass Hollow Microneedle Arrays – From Fabrication to Transdermal Applications YanwenJia and ZiyongLi; City University of Hong Kong, Hong Kong

Microneedle arrays (MNAs), a micron-scale device that recently emerged, are being recognized for their significant potential in enhancing transdermal delivery and extracting interstitial tissue fluid (ISF). Advanced 3D printing techniques have been utilized to fabricate MNAs with enhanced functionality, improved performance, and increased structural flexibility; however, the current 3D-printed MNAs are primarily composed of polymers that suffer from high costs, low durability, and poor robustness. To overcome the constraint, we integrate fused silica glass with projection micro-stereolithography (PμSL) 3D printing technology for the fabrication of transparent and high-quality fused silica glass MNAs with micron resolution, high stiffness, and excellent optical properties for the first time. The *in vitro* penetration test suggests that the 3D-printed fused silica glass MNAs are capable of piercing skin safely and smoothly. ISF extraction test demonstrates its ability to extract sufficient model biomarkers-contained fluid in a short time under capillary force. We confirmed its potential in further transdermal applications. In the future, 3D-printed fused silica glass MNAs, coupled with technology like microfluid, could be applied in precise drug delivery, intelligent transdermal biosensing, real-time monitoring, etc.

8:00 PM SF01.06.20

Ink Optimization and Pattern Design for Fast Charge Electrode Through R2R Printing HongliZhu and YingWang; Northeastern University, United States

Reducing the tortuosity of electrodes through vertical channels establishing is a recognized method to improve the ion transfer kinetics and enhance the fast chargeability of electrodes. Concurrently, investigating the relationship between channel structure on the electrochemical performance of electrodes is meaningful for optimizing the structure of fast-charging electrodes. In order to realize these demands, screen printing is a promising technology to fabricate low-tortuosity electrodes with precisely optimized structures on a large scale. However, the lack of suitable screen printable electrode inks slows the development of screen printing structural designable electrodes. An ideal industrial screen printing electrode ink should be high solid content, outstanding printability, and well particle dispersion to satisfy the demands on industrial cost reduction, printing quality improvement, and battery performance guarantee. Herein, printing quality evaluation, rheological properties analysis, X-ray computed tomography characterization, coarse-grained molecular dynamics simulation, and electrochemical properties comparison were applied to reveal the underlying relationship among the status of molecular chains, screen printability of inks, and electrochemical performance of electrodes. In particular, the twisted molecular chains function as additional networks that pull certain particles within the electrode ink onto the mesh, reducing its screen-printability. Furthermore, the

internal architectural integrity of electrodes and sufficiently uniform dispersion of electrode components renders screen-printed electrodes with superior electrochemical performances. Based on recognizing and illustrating the relevance of the molecular chain state in high-solid-content ink for screen printability, we recommended a unique two-step approach for opening the twisted molecular chains of 60 % solid content $\text{LiN}_{10.6}\text{Mn}_{0.2}\text{Co}_{0.2}\text{O}_2$ cathode ink and printed the corresponding electrodes. At the current rate of 6C, screen-printed electrodes using optimized ink exhibited a 33% larger charge capacity with a mass loading of 6.5 mg/cm² than that produced with chains-twisted ink. Additionally, according to the mechanisms of the two-step approach, we disclosed an optimization strategy for modifying inks for various printing conditions. This concept facilitates the integration of screen printing with the production of functional electrodes and can be applied to other purposes.

Further, we have successfully printed a series of high-precision vertical channels using our developed inks, systematically and comprehensively investigating the effects of the structure of vertical channels on rate performance enhancement for fast-charging electrodes. Through electrochemical evaluation, we demonstrated that 1) the staggered configuration of vertical channels improves the high-rate charge capabilities of electrodes, and 2) the decreasing channel diameter and edge distances improve the electrodes' rate performances. Specifically, the optimized electrode performed a charge capacity that is two- and seven-times greater than the conventional bar-coated electrodes at 4 and 6 C, respectively. Additionally, neutron computed tomography was applied to reveal that the Li^+ was homogeneously spread along the printed channels during the charging and discharging, which enhanced the average ion transfer kinetic of whole electrodes. The optimized channels can facilitate ion diffusion in the horizontal direction and ion transfer in the vertical direction for screen-printed electrodes, thereby maximizing the overall charge transfer kinetics of electrodes. Although more developments in screen printing technology are required to refine the resolution and further structural design for screen-printed electrodes, our researches suggest a reasonable method for optimization, industrialization, and commercialization of low-tortuosity electrodes for fast-charging LIBs.

8:00 PM SF01.06.21

***In-Situ* Analysis of Photobase Initiated Networks for Two-Photon Polymerization** [Madelyn P. Jeske](#)^{1,2}, David R. Harding², Mitchell J. Anthamatten¹, Aofei Mao³, XiHuang³ and Yongfeng Lu³; ¹University of Rochester, United States; ²Laboratory for Laser Energetics, United States; ³University of Nebraska–Lincoln, United States

Two-photon-polymerization (TPP) performance is demonstrated in resins that polymerize via “click” chemistry – a process that has no unreacted component. Additionally, for the first time, a photobase (PBG) initiator was used in place of a free-radical photo-initiator to facilitate the reaction; a change that produced a more ordered and stiffer polymer network structure with an elastic moduli of 30 MPa and 2–10 MPa at 70°C, respectively. Structures with shape-memory behavior, and capable of surviving 12% strain at the ultimate tensile stress, were printed with sub-micrometer resolution and were robust enough to withstand several shape-memory cycles.

The click chemistry is based on thiol-ene Michael Addition chemistry and works with either a base or free radical initiators. Raman spectroscopy data from TPP samples show that networks formed with the PBG initiator have a higher selectivity for thiol-ene coupling than do networks formed with a free-radical initiator, which results in increased crosslinking density. Using Coherent Anti-Stokes Raman Spectroscopy to probe the location of the photo-initiators during the polymerization process (with ~0.4 mm spatial resolution) provides insight into the diffusion kinetics that affects the print-resolution.

8:00 PM SF01.06.22

Additive Manufacturing of Amorphous Soft Magnetic Composites [Anna Langham](#)¹, Mitra L. Taheri^{1,2}, Georgia Leigh¹, Caleb Andrews¹ and Sebastian Lech¹; ¹Johns Hopkins University, United States; ²Pacific Northwest National Laboratory, United States

Electric motors play a vital role in various industries ranging from aerospace to the energy sectors. Enhancing the efficiency and power density of electric motors has become a critical objective, currently limited by high losses in the motor's magnetic core. State of the art commercial cores use steel laminates for their soft magnetic performance, relative ease of manufacture, and low cost of production. High eddy current loss in steel laminates necessitates research and development effort into other materials, such as amorphous soft magnetic composites (ASMCs), which have excellent soft magnetic characteristics like high magnetic saturation, and high relative permeability while also offering reduced losses. To date, the integration of ASMCs have been limited by the manufacturing challenges posed by traditional manufacturing methods. The goal of this work is to use Directed Energy Deposition additive manufacturing (DED) to obtain an amorphous microstructure suitable. Metglas 2605HB1M flake, a commercially available metallic glass known for its incredible relative permeability values and low losses, is explored as a potential material system. The microstructure and magnetic properties of DED printed Metglas flake, high purity Iron (Acorsteel 1000b) and a 50/50 compositional blend of the Metglas and Acorsteel are compared.

8:00 PM SF01.06.23

Fabricating Micro Pore X-Ray Optics with Additive Manufacturing Techniques [Anissa Benzaid-Williams](#), John W. Boley and Brian Walsh; Boston University, United States

Micro pore x-ray optics (lobster-eye optics, MPOs) are ideal for certain x-ray astronomy applications due to their large field of view. MPOs require high aspect ratio features and smooth reflective surfaces to focus x-rays optimally with a smaller overall size and mass than Wolter type x-ray optics. MPOs are typically produced with traditional manufacturing methods, by stretching square glass pores which are then bundled, machined, etched, and slumped over a spherical mold. During this manufacturing process errors can be introduced, resulting in defects such as pore misalignment and pore deformation, and the resulting optics are limited in overall size, which reduces their field of view. Producing MPOs via additive manufacturing is of interest due to the speed, flexibility, and improving resolutions of 3D printing techniques. Direct ink writing (DIW) and continuous liquid interface production (CLIP) allow for large printing areas, so optics of a larger size can be produced without introducing issues of misalignment. This poster covers work done toward fabricating MPOs using DIW, CLIP, and two photon polymerization (TPP) techniques. It includes an overview and comparison of the benefits, drawbacks, and progress made toward manufacturing MPOs with each of these techniques. Evaluated attributes include optic size, print resolution, print speed, surface roughness of pore walls, and squareness of printed pores.

8:00 PM SF01.06.24

3D Printed Resins with Photo-Polymerization-Induced Phase Separation: Structure and Mechanical Properties [Lauren Zakrzewski](#), Kanta Purkayasta, Chulsung Bae and Catalin R. Picu; Rensselaer Polytechnic Institute, United States

In this work we develop heterogeneous acrylic-based photosensitive resins with superior strength and toughness for 3D printing applications. The enhanced toughness is obtained by exploiting the polymerization-induced phase separation of linear polymer (polypropylene glycol) which creates soft domains of sub-micron dimensions. The development of these materials has three steps: (i) development of the base photo-curable resin composition, (ii) gaining control on phase separation in cast samples, and (iii) 3D printing (using SLA) with phase separation. The talk will outline the chemistry and technology developed, and the effect of process parameters on the multiscale structure and mechanical properties of the 3D printed samples. Heterogeneous thermosets are an emerging class of materials whose properties may be tailored to exceed those of the commercial, nominally homogeneous thermosets.

8:00 PM SF01.06.25

***In-Situ* Piezoelectricity Enhancement in 3D Printed MoS₂ PVDF Nanocomposites** [Rifat Hasan Rupom](#)¹, Md Nurul Islam¹, Pashupati R. Adhikari¹, Zoriana Demchuk², Ivan Popov², Alexei Sokolov², H. Felix Wu², Rigoberto C. Advincula³, Narendra B. Dahotre¹, Yijie Jiang¹ and Wonbong Choi¹; ¹University of North Texas, United States; ²Oak Ridge National Laboratory, United States; ³University of Tennessee Knoxville, United States

For sensing and energy harvesting of 3D conformal structures, flexible and high-performance piezoelectric devices are extremely desirable. Here, we demonstrate dramatically improved piezoelectricity in polyvinylidene fluoride (PVDF) due to in-situ dipole alignment of PVDF within PVDF-two dimensional molybdenum disulfide (2D MoS₂) composite via 3D printing. We take use of the shear stress-induced dipole poling of PVDF and 2D MoS₂ alignment during 3D printing to increase piezoelectricity without any post-poling procedure. The results demonstrate an impressive increase of more than eight times in the piezoelectric coefficient (d_{33}) for 3D printed PVDF-8wt% MoS₂ composite over cast pristine PVDF. According to microstructural analysis and finite element simulation, the increased volume fraction of the phase in PVDF, filler fraction, heterogeneous strain distribution around PVDF-MoS₂ interfaces, and strain transfer to the nanofillers are all responsible for the enhancement of piezoelectric property. Our findings offer a promising way to develop and create high-performance 3D piezoelectric devices for mechanical-electronic conformal devices and next-generation sensors using 3D printing.

8:00 PM SF01.06.26

3D-Printed Polymer-Based Conformal Space Radiation Shield with Heat Dissipation [Yue Xiao](#)¹, An Zou¹, David Carlson¹, Robert Hayes² and Pu Zhang³; ¹Advanced Cooling Technologies, Inc., United States; ²North Carolina State University, United States; ³Binghamton University, The State University of New York, United States

With the rapid development of SmallSats/CubeSats and space computing, the current aluminum (Al) bulk shielding technology poses challenges in Size, Weight, and Power (SWaP) requirements. The bulk shielding thickness is determined by the electronics with the least radiation resistance, which prohibits wider adoption of Commercial-off-the-shelf (COTS) electronics and results in increased system weight. In addition, the absence of advanced thermal management technologies for SmallSats/CubeSats largely limits the adoption of high-power, low-price, and readily available COTS electronics. To address these challenges, we developed an innovative 3D-printed, lightweight polymer composite radiation shield comprising of a Metal Oxide Polymer Composite (MOPC) layer and a Fiber Reinforced Polymer Composite (FRPC) layer. Specifically, the MOPC utilizes high-atomic-number metal oxides that are infused into the base polymer to achieve superior radiation attenuation performance than Al. FRPC utilizes aligned carbon fibers in the same base polymer to achieve high in-plane thermal conductivity for electronics heat dissipation. In addition, such a shield is manufactured by the advanced five-axis Direct Ink Writing (DIW) 3D printer for further improved thermal transport and structural

strength. Further, the 3D-printed shield enables locally enhanced spot shielding to provide additional radiation shielding for sensitive electronics without increasing the overall shield thickness. For MOPC, we have achieved an up to 7.4x increase in photon mass attenuation coefficient compared with Al and 18%–26% weight reduction for electron attenuation compared with Al at GEO. For FRPC, we achieved 2.55 W/m-K in-plane thermal conductivity, which is ~4x higher than the base polymer. Overall, the shield prototype can achieve 7 °C reduction in CPU temperature or a 22.5% increase in CPU power, and if spot shielding is utilized, an estimated 62% weight reduction for 1U CubeSat systems can be achieved.

8:00 PM SF01.06.27

Advancing the Performance of Zinc Ion Battery (ZIB) Through Additive Manufacturing of Tailored Structured Electrode Design with Hierarchical Porosity and Microchannel Md NurulIslam¹, NishatS. Sayor², Rifat HasanRupom², PashupatiR. Adhikari², RigobertoC. Advincula³, NarendraB. Dahotre², YijieJiang² and WonbongChoi^{2,3}; ¹The University of Oklahoma, United States; ²University of North Texas, United States; ³The University of Tennessee, Knoxville, United States

Due to its abundant, high volumetric capacity, and stable redox potential in water, Zn holds significant potential as an anode material for revitalizing rechargeable batteries beyond lithium-ion battery systems. Nevertheless, the use of alkaline Zn anodes is hindered by issues such as limited cycling durability and the growth of Zn dendrites, which result in short circuits and compromise both the performance and safety of the batteries. In recent years, additive manufacturing has emerged as a viable solution to address dendrite formation in zinc-ion batteries. This approach involves fabricating tailored electrode structures using the direct ink writing (DIW) 3D printing technique. By controlling pore sizes, distribution, and connectivity, 3D-printed Zn structures can provide a highly interconnected high surface area, allowing for improved electrolyte accessibility to electrode surfaces while accommodating its volume change. In this study, we present a fully 3D-printed flexible zinc-ion battery (ZIB) with an engineered pore structure and surface area. First, we developed a Zn-based ink for the anode and a V2O5 ink for the cathode using high-power vacuum mixing, ensuring suitable rheological properties for direct ink writing (DIW) 3D printing. We conducted a comprehensive analysis of the ink formulation, rheological characteristics, and device performance to describe formulation-rheology-printability-functional properties relationships. A remarkable 6-fold improvement in areal capacity is achieved in 3D printed Zn-V2O5 battery with control samples. Additionally, printing-induced directional channels into the electrodes provide high Zn ion diffusion towards the cathode resulting in the high specific capacity of 190 mAh/g at 1 mA/cm² and long-term cyclic stability. In this presentation, we will discuss the tailored structured electrode design with hierarchical porosity and microchannel, ink formulation-rheology-3D printability relationship, and the electrochemical performance of the additively manufactured zinc ion battery.

8:00 PM SF01.06.28

Enhancing Foam Resilience and Performance Through Graded Stiffness via Viscous Thread Printing DanielRevier¹, BrettEmery^{1,2}, MasaNakura-Fan¹, VivekSarkar¹ and JeffreyLipton^{2,1}; ¹University of Washington, United States; ²Northeastern University, United States

Foams have found widespread use in various fields including padding, insulation, and noise isolation. Many applications demand the use of multi-stiffness foams to enhance comfort or performance. Traditional bonding techniques involving foams of different densities often result in stress concentrations and undesirable boundary effects at the lamination interface. Furthermore, creating controlled, smooth gradients in foam properties is a challenging task for conventional and Additive Manufacturing processes. In this study, we present an innovative approach to produce heterogeneous, open-celled foams with spatially graded stiffness using a method known as viscous thread printing (VTP). We use piece-wise continuous linear gradients between different stiffnesses, effectively mitigating unwanted boundary effects. The adjustment of material properties and microstructure is achieved by altering the travel speed and/or nozzle height during extrusion. The method was employed to fabricate discrete components and those with linear gradients ranging from 0 to 60 mm in length. It was observed that dogbone samples with gradients exhibited higher resilience in plane under tension, while also showing a reduced tendency to form cracks at the nominal interface. This approach was successfully applied to thermoplastic polyurethane (TPU) and Nylon. Mechanical properties under tension were found to be generally unaffected by the presence of a transition length, including tensile modulus, fracture strain, fracture stress, toughness, yield stress, and local stiffness. This suggests that the rule of mixtures would apply to the manufacturing of graded-stiffness foams. Although the properties were consistent, a significant impact was noted on the failure location, which typically occurred outside of the transition region. Our findings pave the way for the broader application of graded-stiffness foams in various industries, significantly enhancing their performance and durability while reducing the potential for stress-related failure.

8:00 PM SF01.06.29

Alteration of Melt Pool Flows Depending on the Surfactants on Ceramic Coatings Built by Laser Cladding SuminSong¹, YeonghwanSong¹, TaebumKim¹, JeonghoHan² and KyuntaekCho¹; ¹Korea Institute of Industrial Technology, Korea (the Republic of); ²Hanyang University, Korea (the Republic of)

As qualities of ceramic coatings manufactured by laser cladding are superior due to few pores and cracks compared to that of thermal sprayed ceramic coatings, it has been spotlighted as one of the appropriate methods for building ceramic layers. Although understanding melt pool flows is important to build high-quality ceramic layers, studies on melt pool of ceramic layers which consist of metal intermediate layers and its flow alteration depending on the existence of surfactants (e.g., sulfur, oxygen, etc.) are insufficient. In this study, experimental studies were conducted to find out the effect of surfactant on melt pool flows of intermediate layers and extent of defects in ceramic layers. In order to identify penetrated depth of coating layers and extent of coating defects, Ni intermediate layer and Al₂O₃ ceramic layer were manufactured under same process conditions using N₂ or mixture of Ar and O₂ gas, which were observed by OM and SEM. In addition, Vickers hardness tests and Ball-on-disk tests were performed to compare mechanical and wear properties depending on the surfactant. As oxygen was added in the shielding gas, penetration and diluted area became deeper and larger due to alteration of convection flows from outward to inward. Decrease of defects was observed at the metal intermediate layer manufactured under surfactant atmosphere, which resulted in building stable ceramic coatings with high hardness. As a result, wear resistance of ceramic layer built under surfactant atmosphere could be improved, which could be attributed to the surfactant effect on the melt pool flows.

8:00 PM SF01.06.30

Development of Study Protocol Frameworks for Data-Driven Digital Twin Development for Direct Ink Write Hein HtetAung^{1,1}, BrianAu², AlexCaviness², RobertWilliamCerdea², JayvicCristianJimenez^{1,2}, KristenJ. Hernandez^{1,1}, ThomasCiardi^{1,1}, PawanK. Tripathi^{1,1}, BrianGiera², RogerH. French^{1,1,1} and LauraBruckman^{1,1}; ¹Case Western Reserve University, United States; ²Lawrence Livermore National Laboratory, United States

Direct Ink Write (DIW) is an advanced manufacturing technique that allows 3D printing of complex parts. DIW 'ink' is a multi-material combination of a polymer base and a filler that shear thins upon extrusion and then hardens upon lay down.¹ DIW process parameters and optimization of machine operations are being investigated to ensure large-scale and rapid production of high-fidelity parts. A study protocol for DIW scientific investigations is developed to identify a standardized workflow to investigate DIW process-space parameters and the resulting part characteristics. The data streams generated during DIW part fabrication are massive and rich with information, yet could be overwhelming, becoming a bottleneck for extracting research insights due to the terabyte sizes. Therefore, we use automated analysis pipelines on FAIRified datasets, implemented in our CRADLE™ Distributed and High Performance Computing Cluster, where we can ingest, perform exploratory data analysis to identify parameter correlations and develop numerous data-driven models to identify useful inferential and predictive modeling approaches to this challenging problem. Inferential models with trained model parameters, quantified variances and confidence intervals enable us to identify the mechatronic factors leading to both desirable and undesirable part properties. These models serve as a platform to build data-driven Digital Twins (ddDTs) for a virtual representation of the physical printed part, including its historical variances and defects. With continuous two-way communication between the real-world DIW system and the ddDT, the data obtained from the real-world system can update the ddDT and the simulations from ddDT can be used to update and drive the process parameters of the real-world system to obtain desired and improved part properties over production runs. The work herein demonstrates how our materials data science and data-driven digital twin approach using rigorous study protocols, establishes standardized data collection, FAIRified dataset management and model generation that allow us to integrate both historical and current data, across multiple DIW tools and production runs to quantify printed parts characteristics and variances.

This material is based upon research in the Materials Data Science for Stockpile Stewardship Center of Excellence (MDS3-COE), and supported by the Department of Energy's National Nuclear Security Administration under Award Number(s) DE-NA0004104.

[1] N. A. Dudukovic et al., "3D printing of void-free glass monoliths: rheological and geometric considerations," *Rheol Acta*, vol. 61, no. 10, pp. 773–784, Oct. 2022, doi: 10.1007/s00397-022-01367-8

8:00 AM *SF01.07.01**Multi-Material Nanoscale 3D Fabrication Based on Femtosecond Light Sheets** Shih-Chi Chen; Chinese University of Hong Kong, Hong Kong

A major challenge in nanotechnology is to fabricate complex 3D structures with desired materials. Despite the many great efforts, the material choices are still largely limited to polymeric materials or metals. A fabrication solution for a wider class of materials without compromising the existing structural complexity, nanoscale feature sizes, and material functions remains a critical challenge. In this seminar, I will present our recent works on the parallelization of ultrafast lasers for 3D nanofabrication, achieving a record setting resolution (20 nm), laser patterning rate (300 mm²/hr), and wide material library. Specifically, an arbitrarily programmable femtosecond light sheet is generated based on the principle of spatial and temporal focusing to perform parallel material processing. We first demonstrate the use of the femtosecond light sheet to perform micro-laser machining on different materials, and next to fabricate complex 3D structures via two-photon polymerization. Lastly, by combining the femtosecond light sheets and swellable hydrogels, we further demonstrate a greatly expanded material library to include metals, metal oxides, semiconductors, dielectric materials etc. This has enabled the fabrication of nanometer-scale 3D functional devices. Our new methods provide an effective and low-cost solution to scale-up the fabrication of functional micro- and nano-structures (~\$1.5/mm³). This means our technology may play a large role in fields such as healthcare, clean energy and water, computing, and telecommunications.

8:30 AM *SF01.07.02**Additive Manufacturing of Multi-Material Architectures: From Structural to Electronic and Robotic Materials** Xiaoyu (Rayne) Zheng; University of California, Berkeley, United States

Abstract Additive manufacturing has shown the promise of freedom of designs, enabling parts customization and tailorable properties where superior structural performances can be achieved by a fraction of weight density compared to bulk material. However, it is presently difficult to directly print different materials (structural, dielectric, conducting and ferroelectrics) to create a complex device with multiple functionalities that responds to multiple stimuli. Unlike biological systems where functions, including sensing, actuation, and control, are closely integrated, few materials have comparable system complexity.

In this talk, I will present a suite of new multi-material additive manufacturing processes and design methodologies to create materials with prescribed structural and functional behaviors. The structural materials consist of a network of micro-unit cells which collectively influence new mechanical behaviors (from high-strength, lightweight to toughening) not seen in their native counterpart. When combined with an electronic and functional phase, these materials turn themselves into a robot and is capable of motions with multiple degrees of freedom and amplification of displacement in a prescribed direction in response to an electric field (and vice versa), and thus, programmed motions with self-sensing and feedback control. I will present the manufacturing and synthesis of these materials, as well as their mechanics and design methods underpinning their novel behaviors.

9:00 AM SF01.07.03**One-Photon Three-Dimensional Printed Fused Silica Glass with Sub-Micron Features** Ziyong Li¹ and Yang Lu²; ¹City University of Hong Kong, Hong Kong; ²The University of Hong Kong, Hong Kong

Glass made from silica has a history of thousands of years, and its applications have accompanied the evolution of human civilization. From everyday life to cutting-edge industries, such as micro-optics, micro-electronics, and micro-fluidics, necessitates the high-precision manufacturing of three-dimensional (3D) fused silica glass objects. Advanced 3D printing technologies have emerged as a powerful tool for fabricating arbitrary glass objects with ultimate freedom and precision. Stereolithography and femtosecond direct writing showed their capability in shaping 3D glass objects with ~50 μm and ~100 nm features, respectively, however, to efficiently fabricating glass structures with centimeter size and sub-micron features still remains challenge. Presented here, our study demonstrates that the gap can be effectively bridged by engineering of appropriate materials, 3D printing based on one-photon micro-stereolithography (OμSL), allows the flexible creation of transparent and high-performance fused silica glass components with sophisticated, 3D sub-micron architectures. The methodology facilitates the construction of fused silica glass components with arbitrary 3D-specific geometries featuring fine details as small as 900 nm, while also enabling rapid prototyping of structures of several millimeters. This offers unprecedented possibilities across a range of applications, including micro-optics, microfluidics, mechanical metamaterials, and engineered surfaces.

9:15 AM *SF01.07.04**Nanoparticle Enabled Additive Manufacturing** Wendy Gu, John Kulikowski, David Doan, Qi Li, Mingqi Shuai, Luis Delfin Manriquez and Andrew Lee; Stanford University, United States

Nanoparticles have unique optical, thermal, chemical reactivity and phase transitions that can be used to enhance additive manufacturing processes. This can be used to fabricate nanoscale architected materials with superior mechanical properties due to material size effects. First, I will present a novel two-photon lithography resin that is used to print nanocomposites, nanoporous carbon and nanostructured silk. The key ingredients in the resin are metallic nanoclusters that serve as both photoinitiators and inorganic precursors, and have pressure-dependent optical properties. Nanocomposite honeycomb, octet and shell-based lattices are fabricated that have a combination of high strength per weight, energy absorption and recoverability beyond other nano and micro-lattices due to a unique strain hardening behavior. Then, I will present our development of a particle ink laser melting (PILM) additive manufacturing system, in which a colloidal nanoparticle ink is combined with a laser-powder bed fusion machine to enable low power printing of metals and ceramics. This is used to print conductive copper electrodes and piezoelectric elements directly on printed circuit boards (PCB).

9:45 AM BREAK**10:15 AM *SF01.07.05****Probing Material Transformation Volumetrically in Computed Axial Lithography** Hayden Taylor, Sui Man Luk, Chi Chung Li and Joseph Toombs; University of California, Berkeley, United States

Volumetric additive manufacturing processes such as computed axial lithography (CAL) are promising for the rapid production of 3D geometries in a wide range of photopolymer and nanocomposite materials. In CAL, light dose is reconstructed tomographically by projecting a video image into a rotating volume of precursor material. Practically, this reconstruction approach exposes the bulk of the precursor (and not just the target geometry) to background illumination. The reconstructed dose distribution is also not perfectly sharp at the boundary of the component. Consequently, there is a range of degrees of conversion throughout the volume at any given moment, and it is very important to terminate the printing process accurately to be able to recover the desired geometry. In-process volumetric monitoring of refractive index can be valuable for this purpose, because most precursor materials exhibit refractive index increases during conversion to the solid state. We will review a set of Schlieren-based techniques we previously introduced for real-time material conversion observations. We will also discuss recent work developing a volumetric temperature monitoring technique based on fluorescence imaging. The evolution of temperature within a CAL volume can serve as an indicator of material conversion dynamics and can influence the quality of printed components.

10:45 AM SF01.07.06**A New Family of 3D Auxetic Mechanical Metamaterials with High Resilience and Elastic Hysteresis** Tiantian Li and Yanning Li; Northeastern University, United States

A new family of high resilient 3D auxetic mechanical metamaterials are designed. The new designs show remarkable resilience under large deformation together with significant hysteresis under cyclic compressive loading-unloading. Both isotropic and anisotropic designs are created. The 3D isotropic design shows ideal isotropy with negative Poisson's ratio close to -1 in all loading directions, as rarely seen in existing mechanical metamaterials. Also, the anisotropic mechanical properties including the effective stiffness and effective Poisson's ratio can be tuned in a wide range. In addition, new designs can also show a unique simultaneous twisting and shrinking behavior under uni-axial compression. An integrated experimental, analytical and numerical approach is applied to quantify the effective mechanical properties of the new designs. Systematic FE simulations and analytical analyses are performed. The new designs are also fabricated, and mechanical experiments were performed on selected designs. These novel properties make 3D keyed-brick mechanical metamaterials be a potential candidate as engineering material with unique properties beneficial from negative Poisson's ratio, damping material for energy absorption, impact resistant material under special loading conditions.

11:00 AM SF01.07.07**Additive Manufacturing of Iron and Iron-Alloy Lattices for Magnetic Nanoparticle Capture** Sammy Shaker¹, Andrii Syrota², Colin Yee³, Vitaliy L. Rayz⁴, Steven Hettis³ and Julia R. Greer^{1,1}; ¹California Institute of Technology, United States; ²Université Paris-Saclay, France; ³University of California, San Francisco, United States; ⁴Purdue University, United States

Magnetic nanoparticles are of widespread interest for medical therapies ranging from internal thermal treatments to vector agents for genetic modification to MRI contrast agents.¹ One of the standout applications for magnetic nanoparticles in medical therapies involves the capture of small molecule chemotherapeutics, particularly doxorubicin, via surface functionalization. While rapid capture of doxorubicin by functionalized nanoparticles has been demonstrated *in vitro*, sequestration of the nanoparticles, especially *in vivo*, has proven a more complicated task.² Sequestration of nanoparticles in a biological flow such as that found in a blood vessel will require a device that can maximize capture while minimizing flow disruptions and pressure

drop across the device. Device designs consisting of solid cylindrical magnets mounted on catheters inevitably obstruct and disrupt the flow as it passes through the blood vessel. Synthesizing microarchitected magnets could allow for favorable flow properties while also allowing for magnetic nanoparticle sequestration; such architected magnetic materials are underexplored in the literature.^{3,4} Traditional subtractive methods of manufacturing often obstruct these explorations due to difficulties in attaining desired feature resolutions as well as rapid modification of alloy composition; on the other hand, additive manufacturing allows for flexibility in design and composition. Hydrogel infusion additive manufacturing (HIAM) is capable of synthesizing architected metal lattices. We demonstrate HIAM derived magnetic monolithic microarchitected lattices composed of iron, iron-nickel, and copper-iron-nickel alloys in the shape of a twisted honeycomb prism with a major face diameter of 3–4 mm and a beam thickness of 40–50 μm optimized to minimize *in vivo* flow disruption.^{4,5} We perform multiphysics simulations of the process of magnetite nanoparticle capture and compare the resulting capture efficiency to *in vitro* magnetite nanoparticle capture experiments that demonstrated a preliminary capture efficiency of 10–20%. In addition, we apply vibrating sample magnetometry (VSM) to demonstrate coercivities in the range of 10–100 Oe and remnant magnetizations of 100 Gauss in the synthesized lattices. Powder X-ray diffraction (pXRD) shows a bulk metallic phase with body-centered cubic symmetry for the iron lattice and face-centered cubic symmetry for the iron-nickel and copper-nickel-iron lattices; internal microstructures are characterized by electron backscattered diffraction (EBSD). Finally, we determine the final phase composition via energy dispersive X-ray spectroscopy (EDS).

[1] Guo, T.; Lin, M.; Huang, J.; Zhou, C.; Tian, W.; Yu, H.; Jiang, X.; Ye, J.; Shi, Y.; Xiao, Y.; Bian, X. *J. Nanomater.* **2018**;7805147.

[2] Blumenfeld, C.M.; Schulz, M.D.; Aboian, M.S.; Wilson, M.W.; Moore, T.; Hetts, S.W.; Grubbs, R.H. *Nat. Comm.* **2018**;9(1):2870.

[3] Maani, N.; Diorio, T.C.; Hetts, S.W.; Rayz, V.L. *Biomech. Model. Mechanobiol.* **2020**;19(5):1865–1877.

[4] Hoo, Wonseok, et al. Submitted.

[5] Saccone, M.; Gallivan, R.A.; Narita, K.; Yee, D.W.; Greer, J.R. *Nature.* **2022**;612:685–690.

11:15 AM SF01.07.08

Controlling Solidification Microstructure of Aluminum Alloys using Eutectic/Peritectic Reactions in Laser Powder Bed Fusion Process Naoki Takata¹, Takanobu Miyawaki¹, YueCheng¹, Asuka Suzuki¹, Makoto Kobashi¹ and Masaki Kato²; ¹Nagoya University, Japan; ²Aichi Center for Industry and Science Technology, Japan

In recent, laser powder bed fusion (L-PBF) has emerged as one of the most representative metal additive manufacturing techniques capable of producing metallic components by using a scanning laser beam to melt consecutive bedded-powder layers selectively. The L-PBF process enables the fabrication of aluminum (Al) alloys with superior and anomalous mechanical properties. Such unique properties were responsible for the formation of non-equilibrium microstructure and metastable phases in rapid solidification (at an extremely high cooling rate of 10^5 – 10^7 K/s) during the L-PBF process. It has been reported that the L-PBF processed Al-Fe alloys with a near eutectic composition exhibited significantly refined solidification microstructures, contributing to high mechanical performance. In the eutectic reaction in rapid solidification, alloy elements could be partitioned into a liquid phase rather than a primary solidified phase, resulting in the enhanced formation of the second solid phase (Al_6Fe phase in an Al-Fe system). It is assumed that alloy elements might be partitioned into the primary solidified α -Al phase (rather than the liquid phase) through a peritectic reaction in rapid solidification. The partitioned solute elements in the α -Al supersaturated solid solutions would play a significant role in solid-solution strengthening (or strengthening by atomistic clusters in the α -Al matrix). These insights can open an opportunity for controlling refined microstructures of Al alloys by elemental partitioning via solidification paths of eutectic or peritectic reactions in the L-PBF process. In this concept, we have selected alloy elements exhibiting different solidification paths in Al-X binary phase diagrams. Cu and Ti elements were used as third alloy elements for the Al-Fe-X ternary system in the present study. Cu element exhibits a eutectic reaction in an Al-Cu binary system (partition coefficient, $k_{Cu}^{S/L} < 1$) and forms the $(Al,Cu)_6Fe$ phase in an Al-Fe-Cu ternary system. In contrast, Ti element exhibits a peritectic reaction in an Al-Ti binary system (partition coefficient, $k_{Ti}^{S/L} > 1$) and independently forms the Al_3Ti phase (no partitioning into the Al_6Fe phase). Based on the alloy element selections, we designed two ternary alloy compositions of Al–2.5Fe–2Cu and Al–2.5Fe–1.5Ti (mass%) available to the L-PBF process utilizing the thermodynamic calculations.

In this study, L-PBF processing was performed using gas-atomized ternary alloy powders with an average particle size of about 20 μm. Rectangular alloy samples were fabricated using a ProX DMP 200 machine (3D Systems, USA) under a wide range of laser scan speeds (0.6 ~ 1.4 m/s) and laser power (102 ~ 204 W). The results of measuring the sample density provided the optimum laser parameter sets for the manufacturing of both alloy samples with high relative densities above 99 %, indicating high L-PBF processability for the Al–Fe–Cu and Al–Fe–Ti ternary alloy powders. The L-PBF processed both alloys exhibited microstructure consisting of a number of melt pools in which regions locally melted and rapidly solidified due to scanning laser irradiation. The added Cu element was partitioned into the refined Al_6Fe phase, resulting in the formation of $(Al,Cu)_6Fe$ phase with an orthorhombic structure (*oC24*). A certain amount of solute Cu (approximately 0.6 %) was detected in the α -Al matrix. A higher solute Ti content above 1 % was detected in the α -Al matrix of the L-PBF processed Al–Fe–Ti ternary alloy. Such a trend appeared more significantly in relatively coarsened cellular microstructures along melt-pool boundaries. These results indicate that the elemental distribution could be controlled via different solidification paths in the L-PBF process. Mechanical properties of the L-PBF processed ternary alloys will be presented and discussed in terms of Cu or Ti elemental distribution in the refined solidification microstructures.

11:30 AM SF01.07.09

Effect of Scanning Strategies and Alloying Elements on Microstructure and Mechanical Properties of Tungsten Fabricated by Laser Powder-Bed Fusion Hyeji Im, Samuel Price and Ian D. McCue; Northwestern University, United States

Laser-powder bed fusion (L-PBF), one of the metal additive manufacturing (AM) techniques, of fusion-facing materials can help overcome the challenges associated with poor machinability and difficulties in casting for complex-shaped and/or thin-walled components. Additive manufacturing experience large thermal strain during cooling and passing through its ductile-to-brittle transition. This leads to high number of cracks of additively manufactured tungsten.

Here, we report on the enhanced microstructure and mechanical properties for tungsten-based alloys by alloying titanium and iron through L-PBF. Prototype alloys were selected using CALPHAD-based thermodynamic predictions. Various scanning strategies were employed to minimize the thermal strain during printing. The addition of titanium and iron increased density as well as increased strength and ductility.

SESSION SF01.08: Session VI

Session Chairs: Christian Leinenbach and Ottman Tertuliano

Wednesday Afternoon, November 29, 2023

Sheraton, Second Floor, Republic B

1:30 PM SF01.08.01

How Does Nanostructural Engineering via Additive Manufacturing Open New Opportunities in Materials Design? Rebecca A. Gallivan, Mirco Nydegger, Nikolaus Porenta, Maxence Menétray and Ralph Spolenak; ETH Zürich, Switzerland

Architecting microstructural features like grain size, porosity, and phase, pushes the limits of material properties – even breaking away from traditional property tradeoffs as exemplified by nanotwinned nanocrystalline copper which shows improved strength without the loss in ductility. Additive manufacturing has enabled new pathways for spatial control of microstructures, promising enhanced capabilities for materials design through microstructural engineering. However, these benefits are most pronounced in nanostructured materials where features of interest lie in the submicron length scales. Leveraging the nanoscale multi-material resolution of the electrohydrodynamic redox printing (EHD-RP) technique, we demonstrate new methods for nanostructuring materials in 3D geometries and explore new opportunities for nanocomposite design. Focusing on Cu, Zn, and Ag-based compositions, we will discuss the role of nanostructured features like nanoporosity, phase segregation, and oxide nanoparticle dispersion on micromechanical properties such as strength, ductility, and failure behavior in order to more fully understand the engineering opportunities afforded through complex spatial control of microstructure. As a key tool in the materials design afforded by additive manufacturing, insights into nanostructural engineering lay the foundation for fully utilizing the promise of design flexibility for advanced materials.

1:45 PM SF01.08.02

Hf-Driven Microstructural Changes and Hot Cracking Prevention of Ni-Based Superalloy During Laser-Based Direct Energy Deposition Ken Hee Ryou¹, Hyeji Im^{1,2}, Jiwon Park³ and Pyuck-Pa Choi¹; ¹Korea Advanced Institute of Science and Technology, Korea (the Republic of); ²Northwestern University, United States; ³Korea Institute of Materials Science, Korea (the Republic of)

The Ni-based superalloy for high-temperature, such as Inconel 738 is an improper alloy for additive manufacturing because of frequent hot cracking resulting from high amounts of Al and Ti. As a solution to hot cracking, the Hf has been proposed as the alloying element of Ni-based superalloy for the improvement of castability and printability. However, the detailed microstructural changes and the hot cracking prevention mechanisms were not clarified yet. The hot cracking was not observed above a certain amount of added Hf at the laser-based direct energy deposition of Inconel 738 alloy. To investigate the microstructure of Hf-added Inconel 738 and the effect of Hf on hot cracking prevention, multi-scale characterizations were

conducted including various electron microscopy and atom probe tomography besides phase-field modeling. Therefore, much more active side-branching in secondary dendrite arms was observed. It is considered that it results in the easy interconnection between the dendrites. Consequently, we attributed that the prevention of hot cracking could be possible by decreasing cracking susceptibility by changing solidification sequences.

2:00 PM *SF01.08.03

Microstructural Evolution in Metallic Alloys under Additive Manufacturing Conditions Amy Clarke^{1,2}; ¹Colorado School of Mines, United States; ²Los Alamos National Laboratory, United States

In metal additive manufacturing (AM), an alloy (in powder or wire form) is melted by a rapidly moving heat source. A solid layer forms upon cooling, and successive layers are built by melting and solidification to form a three-dimensional part. AM processes typically produce large temperature gradients, high solidification rates, and repeated cycles of heating and cooling. The local processing conditions experienced during AM (e.g., thermal gradients and solid-liquid interface velocities during solidification) dictate microscopic structure (i.e., microstructure) evolution. Here we visualize melt pool dynamics and solidification during simulated AM by real-time imaging (e.g., synchrotron x-ray and dynamic transmission electron microscopy) and computational modeling to link local processing conditions to microstructural evolution. We also highlight novel microstructures produced by solid-state phase transformations. A deeper understanding of solidification and solid-state phase transformations under AM conditions is needed to optimize processing parameters across AM technologies, control microstructural evolution and resulting properties, and design metallic alloys for AM.

2:30 PM BREAK

3:30 PM *SF01.08.04

Deciphering the Strength and Ductility of Additively Manufactured Materials Yinmin (Morris) Wang; University of California Los Angeles, United States

Additive manufacturing (AM, aka 3D printing) involves unique processing conditions and thus offers opportunities to produce materials with tailored strength and ductility. However, the highly nonconventional microstructural features created by AM techniques impose tremendous challenges to decipher the strength scaling law and other materials properties. This talk will describe our recent effort to investigate and understand the strength and ductility of several model materials systems including pure copper, 316L stainless steel, and medium entropy alloys. All these materials were fabricated by laser powder-bed-fusion. In all these cases, we observe a hierarchical microstructure and multiple length scales that render a myriad of strengthening mechanisms. These interesting microstructures include solidification enabled cellular structures, low-angle grain boundaries, and dense dislocations. High uniform tensile elongation is also observed in many cases due to the progressive work-hardening mechanisms triggered by these hierarchically heterogeneous microstructures. We will further elaborate the influence of residual stresses on mechanical behavior and conclude with some outstanding issues that call for future research.

4:00 PM *SF01.08.05

From Complex Geometries to Complex Microstructures: New Opportunities for Materials Design Matteo Seita¹, Shubo Gao² and Karl Sofinowski²; ¹University of Cambridge, United Kingdom; ²Nanyang Technological University, United States

One of the main drivers for the adoption of additive manufacturing (AM) in industry is the ability to build parts with complex—and previously unattainable—geometries. This paradigm has enabled the production of high-performance components with optimized strength-to-weight ratio, or with internal features for enhanced functionality. The disruptive potential of AM, however, goes beyond complexity of shape. Because materials are formed at the microscopic scale following a bottom-up manufacturing approach, AM offers the opportunity to make parts with complex—and previously unattainable—microstructures. Since the relationships between these complex microstructures and the resulting materials properties are difficult to unveil, this unique feature has yet to be capitalized on in current industrial applications. However, it may be the key to design the materials which will enable the applications of tomorrow. In this talk, I will present a few examples of the microstructure complexity offered by AM, including chiral crystals and alloys with controlled defect patterns. I will discuss the mechanisms that drive the formation of such complex microstructures and propose possible applications which these materials may enable.

4:30 PM SF01.08.06

Developing a Framework to Qualify Additively Manufactured Ceramics: Effect of Sintering Temperature on Feature Resolution, Shrinkage, and Flexural Properties Lindsey Bezek and Kwan-Soo Lee; Los Alamos National Laboratory, United States

Functional applications for additively manufactured ceramic parts are currently limited by both material constraints and knowledge of process-structure-property relationships. One challenge for developing new ceramics for additive manufacturing (AM) is determining a post-process debinding and sintering strategy that yields parts with sufficient mechanical strength while mitigating defects and unpredictable shrinkage. This work investigates how maximum sintering temperature (varied between 900°C and 1300°C) affects material and mechanical properties of parts fabricated using a commercial silica-based resin and the vat photopolymerization AM process. A custom test artifact was designed to probe dimensional accuracy and survivability of features of different sizes, shapes, and orientations. The shrinkage of cubes with 1 cm sides was generally proportional to sintering temperature and did not exceed 18% in any dimension. The shrinkage was more isotropic up to 1100°C, but at higher temperatures, Z shrinkage was typically ~30% higher than X and Y shrinkage. Parts with higher maximum sintering temperatures experienced higher flexural strength and lower strain at break in three point bend testing. Regardless of maximum sintering temperature, most parts exhibited some degree of cracking or delamination. X-ray computed tomography was used to probe internal porosity, and several voids were observed even when sintered to 1300°C. Fundamental understanding of how sintering affects parts' structure and properties will enable development of a framework to qualify ceramic AM materials and processes. This knowledge will facilitate predictable part performance, helping to ensure reliability of future parts for functional applications.

4:45 PM SF01.08.07

Design of Alloys for Green Body Printing and Sintering Yannick Naunheim and Christopher A. Schuh; Massachusetts Institute of Technology, United States

Additive manufacturing is an emerging pathway to produce metallic materials, usually by processing a well-established commercial alloy via a powder-based approach. In this talk, we invert this approach: we selectively tailor and adjust the chemical composition of an alloy powder to make it suitable for rapid low-temperature solid-state consolidation. Acceleration of the consolidation process is based on two mechanisms: Nanocrystallinity achieved by high energy ball-milling accelerates diffusion at low temperatures, while phase evolution through diffusional demixing and remixing of a second solute-rich phase can encourage the formation and growth of interparticle necks upon heating. Computational thermodynamics provide the basis for the alloy design process to take maximum advantage of these effects. Sintered and heat treated microstructures and their mechanical properties are presented and discussed for the case of nickel-rich alloys.

SESSION SF01.09: Session VII
Session Chairs: Zachary Cordero and Wendy Gu
Thursday Morning, November 30, 2023
Sheraton, Second Floor, Republic B

8:00 AM *SF01.09.01

Merging the Computational and Experimental Gravity Poles of the Alloy Development Process: From Alloy Design to *In-Situ* Alloying of Custom Al Alloys for Laser Powder Bed Fusion Federico Bosio¹, Giuseppe Del Guercio¹, Chinmay Phutela¹, Marco Simonelli² and Nesma Aboulkhair^{1,2}; ¹Technology Innovation Institute, United Arab Emirates; ²The University of Nottingham, United Kingdom

Recent progress in metal additive manufacturing (AM) emphasised the need to develop next-generation alloys leveraging the non-equilibrium dynamics of rapid cooling processes. This raised the awareness among the leading industrial players of the AM scene that boosting the material palette for AM is the way to unlock the full potential of additive manufacturing in vital application sectors, such as aerospace, energy, and defence. In fact, functional parts with enhanced strength, good electrical and thermal resistance, and low density are often targeted for these critical applications, and the current alloys in the market might not meet these requirements. Therefore, driven by these motivations, novel aluminium alloy grades for use in Laser Powder Bed Fusion (LPBF) are currently sought.

An industrially relevant commercial Al alloy system used in targeted industrial sectors was selected in the alloy design stage. The chemical composition of such alloy was tweaked by adding a

reinforcing transition metal (TM) element that enhanced the master alloy's strength by multiple strengthening mechanisms. Computational design tools based on the CALPHAD approach enabled the chemical process window's fast selection for the new aluminium grades. The solidification trajectories of various TM-dosed Al grades were assessed for conditions deviating from the equilibrium using the Scheil-Gulliver assumptions to predict the alloy's precipitation sequence, crack sensitivity, and printability.

The computational predictions were empirically corroborated with targeted experiments involving arc-melted buttons' production in generating the corresponding Al-TM master alloys. The microstructure resulting from the fast-cooling rates of the PBF-LB process was simulated by surface remelting in an industrial printer. Hierarchical microstructure investigations conducted at all length scales from macro- to nano showed a satisfactory level of correlation with computational predictions, and the final transition metal element amount was eventually established based on considerations involving strengthening mechanisms, hot crack sensitivity, PBF-LB processability, and heat-treatment design strategies.

The developed Al-TM alloy was then manufactured by laser powder bed fusion in-situ alloying achieving near fully dense samples. At this stage, nano-particles were introduced in the newly developed metal matrix to further enhance strength and its thermal stability at temperatures higher than 300 degrees Celsius. The process-structure-performance relationships of the Al-xTM alloy with and without nanoparticle additions were deeply studied at the possible environmental working conditions (RT and elevated temperatures).

The outcomes of this research prove that new high-strength Al alloy compositions can be established by exploring unconventional design spaces enabled by the fast-cooling rates of additive processes. The combined computational-experimental method utilised in this study provided a fast and robust guidance towards the development of printable high-strength Al alloys for Laser Powder Bed Fusion.

8:30 AM *SF01.09.02

Directional Recrystallization of Additively Manufactured Superalloys Zachary C. Cordero; Massachusetts Institute of Technology, United States

Metal additive manufacturing processes can create intricate components that are difficult to form with conventional processing methods; however, the as-printed materials often have fine grain structures that result in poor high-temperature creep properties, especially compared to directionally solidified materials. Here, we address this limitation in an exemplar additively manufactured Ni-base superalloy by converting the fine as-printed grain structure to a coarse columnar one via directional recrystallization. The present results demonstrate how directional recrystallization of additively manufactured Ni-base superalloys can achieve large columnar grains with enhanced creep resistance, manipulate crystallographic texture to minimize thermal stresses expected in service, and functionally grade the grain structure in net-shaped parts to selectively enhance fatigue or creep performance.

9:00 AM SF01.09.03

A Process-Structure Correlation Between the Beam Crossing Interval and the Size of Meltpool in the Laser Powder Bed Fusion Process Chang-Eun Kim¹, Clara L. Druzgalski¹, Alexandra Loaliza², David F. Bahr², Gabe Guss¹, Vincenzo Lordi¹, Patrick G. Allen¹, Rebecca J. Dylla-Spears¹ and Manalibo Matthews¹; ¹Lawrence Livermore National Laboratory, United States; ²Purdue University, United States

The laser powder bed fusion process creates a unique microstructure that impacts the property of printed parts. We asked whether the time interval between neighboring meltpool tracks was a critical parameter that dictates the process-structure relationship. We used metallography, machine learning, and laser toolpath trajectory analyses to collect the data needed to establish a correlation. We found a clear negative correlation between the size of meltpools and the proposed timing descriptor, as 'beam crossing interval (BCI)'. The observed correlation paves a way to enable a data-driven model to control the microstructure of metal part printed by the laser powder bed fusion. This work was performed under the auspices of the U.S. Department of Energy by Lawrence Livermore National Laboratory under Contract No. DE-AC52-07NA27344.

9:15 AM SF01.09.04

Predicting Defect Formation in Additive Manufacturing using Inferences and Statistical Modeling Erika L. Barcelos, Mohommad Redad Mehdi, Kristen J. Hernandez, Pawan K. Tripathi, Hein Htet Aung, Laura Bruckman, Anirban Mondal and Roger H. French; Case Western Reserve University, United States

Datasets originated from experimental research tend to be small. Performing experiments is expensive, time consuming and often the available resources are limited. Therefore, developing a framework to design, plan and optimize experiments is essential for a more efficient, reliable and cost-effective for experimental research. Statistical Learning approaches represent a promising alternative to address the challenges associated with limited and sparse experimental datasets. It consists of applying modeling approaches to explore and understand the data and relationships via statistical and exploratory data analysis. Laser Powder Bed Fusion (LPBF) is one of the most common Additive Manufacturing methods used in the fabrication of metal parts. The process can generate highly customizable parts having complex shapes and geometries with the generation of minimum waste, which represents an important benefit over traditional subtractive technologies. Nonetheless, it is highly susceptible to defect formation due to the complexity of the printing process and non optimal process parameters. In this work, we explore different statistical learning approaches and evaluate their capabilities in predicting defects in a LPBF experiment. In-situ and ex-situ data from pyrometry, radiography and machine parameters were integrated, FAIRified and ingested into our CRADe/HPC distributed environment. Feature selection and importance ranking were performed using correlation analysis and network structural Modeling (netSEM). Different Statistical Learning approaches were evaluated including Robust Regression based methods and Generalized Additive Modeling (GAM). These techniques were applied for predictions and inference, i.e. understanding and quantifying relationships between variables. This work brings a new perspective to experimental research that generates small datasets. It shows that even when there is a limited number of available data points, statistical analysis can be applied for an accurate and reliable data analysis and statistical modeling can be successfully used to estimate and predict future outcomes.

9:30 AM BREAK

10:00 AM *SF01.09.05

3D Nanoprinting of Functional Crystalline Materials Ji Tae Kim; The University of Hong Kong, Hong Kong

Can 3D printing become an innovative strategy for manufacturing electronic and photonic integrated circuits? A key prerequisite is to acquire high-quality crystalline functional materials that are 3D printable at the nanoscale. Here, we present our solvent-engineering-assisted 3D printing method that enables freeform, nanoscale structuring of diverse crystalline materials. The method exploits a femtoliter ink meniscus to guide material crystallization in three dimensions with the aid of in-situ solvent engineering, fabricating freestanding nanostructures with programmed shape, composition, and crystallinity. This scheme has pioneered new 3D printing materials that can be used for integrating electronic and photonic circuits, including metal halide perovskites [1-3], peptides [4,5], metal-organic frameworks [6], and nanoparticle clusters [7]. Successful demonstrations of 3D-printed real devices such as bright nano-displays [8], lasers, anticounterfeiting labels [2,3], biosensors [7], and micro-thermometers [9] have proven the practicality of our method. In this talk, I will discuss our experimental/theoretical studies on how to develop the nanoscale 3D printing method, and the prospects of our work for potential applications in IC (integrated circuit) manufacturing.

References

- [1] Chen M., Yang J., Wang Z., Xu Z., Lee H., Lee H., Feng S.-P., Pyo J., Seol S.K., Kim J.T.*, *Advanced Materials* 31, 1904073 (2019)
- [2] Chen M., Hu S., Zhou Z., Huang N., Lee S., Zhang Y., Cheng R., Yang J., Xu Z., Liu Y., Lee H., Huan X., Feng S.-P., Shum H.C., Chan B.P., Seol S.K., Pyo J.*, Kim J.T.*, *Nano Letters* 21, 5186 (2021)
- [3] Chen M., Zhou Z., Hu S., Huang N., Lee H., Liu Y., Yang J., Huan X., Xu Z., Cao S., Cheng X., Wang T., Yu S.F., Chan B.P., Tang J., Feng S.-P.*, Kim J.T.*, *Advanced Functional Materials* 33, 2212146 (2023)
- [4] Yang J., Huan X., Liu Y., Lee H., Chen M., Hu S., Cao S., Kim J.T.*, *Nano Letters* 22, 7776 (2022)
- [5] Yang J., Chen M., Lee H., Xu Z., Zhou Z., Feng S.-P., Kim J.T.*, *ACS Applied Materials & Interfaces* 13, 20573 (2021)
- [6] Liu Y., Yang J., Tao C., Lee H., Chen M., Xu Z., Peng H., Huan X., Li J., Cheng X.*, Kim J.T.*, *ACS Applied Materials & Interfaces* 14, 7184 (2022)
- [7] Kim W.-G., Lee J.-M., Yang Y., Kim H., Devaraj V., Kim M., Jeong H., Choi E.-J., Yang J., Jang Y., Badloe T., Lee D., Rho J.*, Kim J.T.*, Oh J.-W.*, *Nano Letters* 22, 4702 (2022)
- [8] Bae J., Lee S., Ahn J., Kim J.H., Wajabat M., Chang W.S., Yoon S.-Y., Kim J.T., Seol S.K., Pyo J.*, *ACS Nano* 14, 10993 (2020)
- [9] Lee H., Wang Z., Rao Q., Lee S., Huan X., Liu Y., Yang J., Chen M., Ki D.-K.*, Kim J.T.*, *Advanced Materials* (published online) <https://doi.org/10.1002/adma.202301704>

10:30 AM SF01.09.06

3D Printed Schwarzites: From Pure Mathematics to Macroscale Applications Levi C. Felix¹, Raphael Tromer¹, Cristiano F. Woellner², Varlei Rodrigues¹, Pulickel Ajayan³, Chandra S. Tiwary⁴ and Douglas S. Galvao¹; ¹State University of Campinas, Brazil; ²Federal University of Parana, Brazil; ³Rice University, United States; ⁴Indian Institute of Technology, India

Additive manufacturing, sometimes called 3D Printing, can create structures of great complexity. It has been exploited in many areas, in particular, in materials science. In this work, we present a comprehensive multi-scale (from atomic to macroscale 3D Printed models) study of the structural and mechanical properties of some Schwarzites families. Schwarzites are crystalline porous carbon structures with negative Gaussian curvatures. They were proposed by Mackay and Terrones [1] and name Schwarzites after the German

mathematician Hermann Schwarz and his works on triple periodic minimum surfaces (TPMS).

We have carried out DFT and molecular dynamics simulations of atomic models. These geometrically optimized models were used to create corresponding macroscale models that were 3D Printed using fused deposition modeling (FDM). We have used different polymers (acrylonitrile butadiene styrene (ABS) and polylactic acid (PLA)).

The MD and 3D Printed results for the profiles of the stress-strain curves are quite similar, showing that the deformation mechanisms are scale independent and are dominated by topological features.

The 3D Printed models were successfully tested for macroscale applications, such as large deformations sensors and filters for water remediations of micro and nano plastics [4,5]

[1] A. L. Mackay and H. Terrones, *Nature* 1991, 352, 762.

[2] L. C. Felix, C. F. Woellner, D. S. Galvao, *Carbon* 2020, 157, 670.

[3] S. M. Sajadi et al., *Adv. Mater.* 2018, 30, 1704820.

[4] V. Gaal et al., *Nano Select* 2022, 3, 450.

[5] G. Gupta et al., *RSC Adv.* 2021, 11, 19788.

10:45 AM SF01.09.07

Sustainable Graphene-Based Inks for Screen Printable Piezoresistive and Thermoresistive Sensing Miguel Franco¹, AMotealleh², Carlos Costa¹, LHilliou¹, Nikola Perinka³, Clarisse Ribeiro¹, Julio Viana¹, Pedro Costa¹ and ~~Senentxu Lanceros-Mendez~~^{3,4,1}; ¹University of Minho, Portugal; ²LayerOne AS, Norway; ³BCMaterials, Basque Center for Materials, Applications and Nanostructures, Spain; ⁴Ikerbasque, Basque Foundation for Science, Spain

Graphene-based conductive inks are increasingly being used for printed and conformable electronics. In the present work, rGO has been used both in pristine form and doped with nitrogen (N-rGO), the latter allowing to increase the electrical conductivity.

Based on the aforementioned graphene types, polymer-based conductive inks have been developed based on cellulose or polyvinylpyrrolidone (PVP) as polymer binders and water or dihydrolevoglucosenone (Cyrene) as green solvents, respectively.

Screen-printable inks have been optimized in terms of viscosity and adhesion properties, leading to printed films with sheet resistance up to 1 kΩ sq⁻¹. Further, graphene:PVP composite inks are also biocompatible and nontoxic, being suitable for biomedical applications.¹

The developed graphene-based inks have been applied by screen-printing for the development of both conductive track and sensing elements. For the latter, thermoresistive temperature and piezoresistive force and deformation sensors have been developed, as well as multitouch capacitive sensing devices.^{2,3}

Acknowledgements

Portuguese Foundation for Science and Technology (FCT): projects UID/FIS/04650/2021, UIDB/05256/2020, UIDP/05256/2020, PTDC/FIS-MAC/28157/2017, and PTDC/BTM-MAT/28237/2017, grants SFRH/BPD/110914/2015 (P.C.) and SFRH/BD/145741/2019 (M.F.), 2020.04028.CEECIND (C.M.C.) and 2020.04163.CEECIND (C.R.). This study forms part of the Advanced Materials program and was supported by MCIN with funding from European Union NextGenerationEU (PRTR-C17.11) and by the Basque Government under the IKUR and Elkartek programs, European Union's Horizon 2020 Programme, ICT-02-2018, WEARPLEX.

REFERENCES

Franco, M., et al. *Adv. Eng. Mater.* 2022, 24: 2101258.

Franco, M., et al. *Adv. Mater. Interfaces* 2021, 8, 2100578.

Franco, M., et al. *ACS Appl. Electron. Mater.* 2020, 2, 9, 2857–2867.

11:00 AM SF01.09.08

Site- and Shape-Selective Synthesis of Nanocale Heterostructures Based on Combinations of Direct-Writing and Nano-Micro-CVDS Sven Barth, Fabrizio Poratti and Michael Huth; Goethe University Frankfurt, Germany

Recent advancements in additive manufacturing enable the fabrication of free-shaped 3D objects with very high accuracy using focused electron beam- and focused ion beam-induced deposition (FEBID and FIBID). [1] We demonstrate the formation of 3D core-shell heterostructures by combination of direct-write 3D FEBID scaffolds and the successive site-selective chemical vapor deposition (CVD). In particular, conductive 3D nanobridges are printed by FEBID and used as resistors allowing deposition induced by Joule heating. The successful combination of both approaches is demonstrated using two material systems of specific physical properties. [2] The fabrication of complex 3D core-shell heterostructures promises to add new functionalities by combining free-shaped 3D nanostructure writing with thin film deposition of materials with different properties. Specifically, shape-dependent and topological physical properties can be investigated by this highly adaptable approach.

References:

[1] *J. Appl. Phys.* **2021**, 130, 170901.

[2] *ACS Nano* **2023**, 17, 4704–4715.

11:15 AM SF01.09.09

Aerosol-Jet Printed Stretchable Micro-Scale Strain Sensor Dian Dian Zhang¹, Qingshen Jing² and Sohini Kar-Narayan¹; ¹Department of Materials Science & Metallurgy, United Kingdom; ²University of Glasgow, United Kingdom

Small wearable strain sensors are capable of collecting mechanical signals from the human body and local environments, providing numerous insights into various applications, such as human physiology research, healthcare monitoring and smart human-robotic interactions [1][2][3].

Here we have developed an aerosol-jet printed microscale wearable sensor for small-area skin deformation sensing. This sensor is thin and flexible to adapt to the skin curvature and highly customisable due to its novel direct-print manufacturing technique. The sensor is composed of two ultra-thin Polydimethylsiloxane (PDMS) films embedded with aerosol-jet printed poly(3,4-ethylenedioxythiophene) polystyrene sulfonate (PEDOT:PSS) as the soft conductive sensing components. The printed circuit includes sensing units which are designed to be the same size as the target area for surface strain detection. When a strain is applied, the sensing polymer develops cracks leading to an increase in the resistance of the circuit. This is the mechanism through which the external mechanical stimuli are converted into electrical signals. The sensing polymer is restored upon removal of the strain and is found to be capable of prolonged and continuous measurement of multiple strain cycles.

The performance of the sensor was characterized by applying mechanical stimuli to the sensor using a linear motor. The deformation on the sensing arrays was in the vertical range of 0-500 μm and caused an increase to the resistance of 100 ohms, corresponding to force applied in the range of 0-0.05 N.

References:

[1] J. Kim, D. G. Seo, and Y. H. Cho, "A flexible skin piloerection monitoring sensor," *Appl Phys Lett*, vol. 104, no. 25, 2014, doi: 10.1063/1.4881888.

[2] T. Yang, D. Xie, Z. Li, and H. Zhu, "Recent advances in wearable tactile sensors: Materials, sensing mechanisms, and device performance," *Materials Science and Engineering R: Reports*, vol. 115, 2017. doi: 10.1016/j.mser.2017.02.001.

[3] J. C. Yeo, J. Yu, Z. M. Koh, Z. Wang, and C. T. Lim, "Wearable tactile sensor based on flexible microfluidics," *Lab Chip*, vol. 16, no. 17, 2016, doi: 10.1039/c6lc00579a.

11:30 AM SF01.09.10

3D Printing of Nanomaterial-Based Devices with Metamaterial-Inspired Near-Field Electromagnetic Structure Samuel Hales¹, Jared Anklam¹, Yang Xin², Cordelia Latham¹, Tian Xi², Derrick Wong¹, Lei Bin Li¹, John Ho² and Yong Lin Kong¹; ¹University of Utah, United States; ²National University of Singapore, Singapore

The ability to 3D print nanomaterials enables the creation of freeform architecture and devices with an unprecedented level of functional integration. However, the possible material integration and geometrical configuration remain limited by the inability to selectively anneal printed nanomaterials, especially on temperature-sensitive substrates. Indeed, thermal annealing is a critical process that dictates 3D printed device performance by (1) merging otherwise disconnected nanomaterials, (2) reducing defects and interfaces, (3) removing polymeric additives, and (4) improving contact between printed layers. Here we demonstrate the ability to selectively and locally anneal 3D printed nanomaterials *in situ* on a broad range of temperature-sensitive substrates by focusing near-field electromagnetic waves to submillimeter resolution using a metamaterial-inspired near-field electromagnetic structure (Meta-NFS). This near-field electromagnetic wave printing (NFP) enables exceptional control of printed nanomaterial annealing parameters, allowing the creation of spatially freeform microstructure where the electronic and mechanical properties can be locally programmed. We envision that NFP significantly broadens the possible class of materials compatible with an additive manufacturing process, enabling the creation of hybrid multi-functional constructs and the printing of functional electronics even on temperature-sensitive substrates.

11:45 AM SF01.09.11

Three-dimensional (3D) printing attracts growing attention as a promising method for manufacturing functionally graded materials (FGMs). Fused deposition modeling (FDM) 3D printing is widely available, but due to its simple process, creating spatial gradation of diverse properties using FDM is challenging. Here, we present a 3D printed digital material (DM) filament that is structured towards 3D printing of FGMs, utilizing only a readily available FDM printer and filaments. The DM filament consists of multiple base materials combined with specific concentrations and distributions, which are 3D printed using FDM process. When the DM filament is supplied to the same printer, its constituent materials are homogeneously blended during extrusion, resulting in the desired properties in the final structure. This blended FDM (b-FDM) printing enables spatial programming of material properties in extreme variations, including mechanical strength, electrical conductivity, and color. The b-FDM with DM filaments can be readily adopted to any standard FDM printer, enabling low-cost production of FGMs.

SESSION SF01.10: Session VIII
Session Chairs: Ming Chen and Amy Peterson
Thursday Afternoon, November30, 2023
Sheraton, Second Floor, Republic B

1:30 PM *SF01.10.01

Thermoformable All-Ceramics Through AM and Particle AssemblyRandallM. Erb, JasonBice and EchoSt. Germain; Northeastern University, United States

Thermoforming processing, traditionally reserved for thermoplastic polymers and sheet metals, has been extended here to boron-based all-ceramics. Specifically, sintered boron nitride composite sheets manufactured via a combined vibration and tape-casting photopolymerization process exhibited highly oriented microstructure which allowed these preform sheets to flow as viscous Bingham pseudoplastics during compression molding. These sintered all-ceramic preforms are thermoformed into thin, complex parts with features down to 200 μm . Further, a new workflow is leveraged to generate bespoke all-ceramic heat spreaders that can be press-fit onto printed circuit boards and outperform metal heat sinks as a low-profile thermal management solution. This work offers a route for other all-ceramics that may be thermoformed through first fabricating pre-forms with highly-ordered anisotropic microstructures.

2:00 PM SF01.10.02

Photo-Polymerizing Heterogeneities to Self-Shape CeramicsZizhenDing¹, HalaZreiqat² and MohammadMirKhalaf¹; ¹Queensland University of Technology, Australia; ²The University of Sydney, Australia

Ceramics with complex shapes are desired in many applications, including architectural design and construction, protective systems, molds for gas turbines, and biomaterials. 3D printing through photopolymerization is amongst the most powerful approaches to make ceramics with complex shapes. However, these procedures are usually difficult to implement, are time-consuming, require further processing, and result in material waste. To address these challenges, we developed a simple, fast, and low-waste self-shaping procedure to make ceramics with complex shapes. The approach draws on a principle that the amount of shrinkage a ceramic undergoes during sintering is a function of the concentration of particles in the ceramic resin: the higher the concentration, the less the shrinkage. By printing components with inhomogeneous concentrations of particles, the parts with higher concentrations shrink less during sintering, resulting in well-controlled shape changes. This approach does not require extensive instrumentation and can be used for a wide range of ceramics. We then developed a material- and scale-independent mechanical model, which predicted the shape changes accurately. The model can be used as a tool to design the self-shaping experiments, potentially for a large variety of ceramics and glasses.

2:15 PM *SF01.10.03

High-Throughput Printing of Combinatorial Materials from AerosolsYanliangZhang; University of Notre Dame, United States

The development of new materials and their compositional and microstructural optimizations are essential to next-generation technologies such as clean energy and environmental sustainability. However, materials discovery and optimization have been a frustratingly slow process. The Edisonian trial-and-error process is time-consuming and resource-inefficient, particularly when contrasted to vast materials design spaces. While traditional combinatorial deposition methods can generate material libraries, it suffers from limited material options and inability to leverage immense breakthroughs in nanomaterials synthesis. Here we present a high-throughput combinatorial printing (HTCP) method capable of fabricating materials with compositional gradients with microscale spatial resolution. The *in situ* "mix and print" in the aerosol phase allows instantaneous tuning of the mixing ratio of a broad range of materials on the fly, which is an important feature unobtainable in conventional multi-materials printing using feedstocks in liquid/liquid or solid/solid phases. We demonstrate a variety of high-throughput printing strategies and applications in combinatorial materials discovery, functional grading, and chemical reaction, enabling materials explorations of doped chalcogenides and compositionally graded materials with gradient properties. The versatile aerosol based HTCP enables universal printing and integration of a broad range of materials including metals, semiconductors, dielectrics, as well as polymers and biomaterials, leading to facile fabrication of multifunctional and flexible/wearable devices for energy conversion/storage, sensing, and health monitoring. The ability to combine the top-down design freedom of additive manufacturing with bottom-up control over the local material compositions promises compositionally complex materials inaccessible via conventional manufacturing approaches. The fabrication freedom and data-rich nature of HTCP along with machine learning and artificial intelligence guided design strategies is expected to accelerate the discovery and development of a broad range of materials with intriguing and unprecedented properties for emerging applications.

2:45 PM SF01.10.04

High-Throughput Printing and Post-Processing Approaches for Realization of Novel Flexible Magneto-resistive SensorsMykolaVinnichenko¹, ClemensVoigt¹, Eduardo SergioOliveros Mata², SindyMosch¹, YevhenZabila², MorrisOtt³, MarcoFritsch¹, ThomasPreussner³ and DenysMakarov²; ¹Fraunhofer IKTS, Germany; ²Helmholtz-Zentrum Dresden-Rossendorf, Germany; ³Fraunhofer FEP, Germany

The research in the field of additive manufacturing is increasingly focusing on realization of electrically conductive interconnects, passive and active components such as resistors, capacitors, inductors, and application-specific electronic devices [1]. The additive manufacturing technologies are offering high design flexibility and high throughput, are material saving and have a great potential of the production cost reduction. The flexible printed magneto-resistive (MR) sensors based on various physical principles are novel components in printed electronics demonstrated in recent years using additive manufacturing methods [2]. However, the large-scale manufacturing of these sensors and their industrial uptake are hampered by the lack of commercially available magneto-resistive inks and scalable post-printing processing methods to enable optimal functionality of the components.

Our work is focused on establishing a fully additive approach for realization of flexible MR-sensors and their arrays. We address the complete process chain from MR-material particles selection/preparation, through the ink formulation, printing and post processing of the structures, their characterization and demonstration of defined use cases. Two types of materials were used to formulate MR-inks: i) commercially available μm -size spherical Bi particles showing non-saturating large magneto-resistance (LMR), and (ii) permalloy (Py) flakes of own development showing anisotropic magneto-resistance (AMR). In the latter case, a method was developed to ensure a production of the particles with 100 nm thickness and in-plane dimensions of a few micrometers with a yield of approx. 2.7 g/day which can be further upscaled. It is based upon large-area PVD deposition of the corresponding materials as thin films onto glass substrates coated with a special sacrificial layer, following lift-off process of the thin films, and their ultrasonic milling. Based on these powder materials, screen-printing compatible inks were formulated with solid fraction as high as 82-90 wt.% (Bi particles) and 21 wt.% (Py flakes). Electrical contacts were realized either using commercially available or IKTS-proprietary Ag inks. Different layouts of LMR and AMR sensors were created and printed on flexible polymer foils (PET, PI).

The core of our approach is a combination of scalable printing methods (screen-, dispenser-, inkjet-printing) with high power diode laser post-processing. The line-shaped laser beam was generated by microoptically optimized high-power diode laser array operating in the near-infrared spectral range using continuous wave mode. In contrast to standard furnace heating this approach enables treatment on the millisecond time scale, preventing temperature-induced damages of sensitive substrates and permitting selective sintering of printed films in air. The laser beam was swept along the printed structures to remove the organic phase and sinter particles of the magneto-resistive material. Depending on the type of material, the dwell time was varied from 3 to 20 ms and the laser intensity from 0.8 to 2.0 kW/cm². In case of Bi-based LMR material, the sensors with a strong linear response within a broad magnetic field range 100 mT - 7 T were achieved. The resulting magnetic field sensors based on Py flakes showed a very promising AMR effect in the range of 0.5% at much lower magnetic fields of 2-3 mT. The applicability of the sensors and their arrays for contactless switching and flexible human-machine interfaces is demonstrated. The relationship between the sensor manufacturing parameters and the resulting structure and properties is analyzed to define pathways to further improvement of their performance.

[1] A.H. Espera, et al. Prog. Addit. Manuf. 4, 245 (2019)

[2] M. Ha, et al. Adv. Mater. 33, 2005521 (2021)

3:30 PM *SF01.10.05

Towards Inline Property Prediction in Material Extrusion-Fabricated Structures with Limited Information[Amy Peterson](#), David Kazmer, Ahmed Adisa and Austin Colon; University of Massachusetts Lowell, United States

Modeling polymer material extrusion additive manufacturing (AM) for prediction of mechanical properties requires substantial training data, and many modeling approaches are computationally intensive. This work investigates measurement and modeling approaches to enable inline property prediction in filament-fed material extrusion AM, commonly referred to as fused filament fabrication (FFF). We explore what kinds and how much information is necessary to create an acceptably accurate model, and to output accurate predictions. We also performed detailed analysis of the types of fracture that occurred across a range of processing conditions and relate this mechanical behavior to print conditions. This work contributes to efforts towards higher reliability, higher performance additively manufactured parts.

4:00 PM SF01.10.06

3D Printing of Continuous Fiber-Reinforced Thermoset Composites[Kai Yu](#); University of Colorado Denver, United States

3D printing revolutionizes the fabrication of continuous fiber-reinforced composites by eliminating the need for molds, offering exceptional design flexibility, and reducing manufacturing costs per part. This technology is particularly well-suited for rapid prototyping and the development of composite products. With 3D printing, users can easily create composites with customized fiber distribution and selective reinforcements. Additionally, the incorporation of functional fibers enables the integration of various functionalities directly into the printed objects. However, there is no robust design of printer for continuous fiber reinforced thermoset composites, especially for the thermally curable composites that are widely used in the industry. In this work, we developed a versatile 3D printing method for continuous-fiber thermoset composites based on direct ink writing (DIW). It leverages the shear stress imposed on the fiber to enable the ready extrusion of composite filaments and can be applied to print most thermally curable and photo-curable resins and commercially available fibers. Two deposition pressures are applied to the DIW printer head: one for resin extrusion and another to prevent resin backflow. The printing speed can be precisely controlled by adjusting the magnitude of the deposition pressures, while the fiber content of the composites is regulated by using needles of different diameters. After printing, the thermally curable composites undergo post-heating to fully polymerize the thermoset matrix, resulting in excellent mechanical strength attributed to the covalent bonding among filaments. Moreover, by utilizing a UV-curable resin with rapid curing mechanisms, we can achieve high fiber content and faster manufacturing speeds in composite 3D printing. To enhance the printing process, we have integrated the DIW printer head design with a six-axis robotic arm for composite printing. This integration has enabled us to achieve a significantly higher fiber volume fraction, reaching approximately 50%. Furthermore, I will show that the recently emerged two-stage UV-curable resin is an ideal material candidate to dramatically promote the glass transition temperatures, mechanical strength, and interfacial bonding strength of 3D printed composites, which are desirable for high-performance engineering applications. Overall, the developed printing method allows the composite parts to be designed quickly to meet unique specifications, as well as providing new functions in 4D printing, biomedical printing, and the printing of functional devices.

4:15 PM SF01.10.07

Novel Fast Cure Silicone Inks for Single-Step, Support-Free 3D Printing of Tall, Overhanging and High Aspect Ratio Structures[Anna Guell Izard](#), Lemuel X. Pérez Pérez, Todd H. Weisgraber, Ilse Van Meerbeek, A. Melody Golobic, Eric B. Duoss and Jeremy M. Lenhardt; LLNL, United States

Silicone elastomers have a broad variety of applications, such as soft robotics, biomedical devices, and structural metamaterials. The extrusion-based method known as direct ink write (DIW), has enabled the production of additively manufactured silicone structures. However, this method is limited to manufacturing mostly planar or pseudo-three-dimensional (3D) structures. Due to the low self-supporting capabilities of extruded strands for traditional silicone-based “inks”, obtaining tall or overhanging structures, or structures comprised by thin walls is not feasible. Here, we demonstrate a novel Fast Cure silicone-based ink that enables manufacturing of complex three-dimensional structures. The Fast Cure ink is a two-part mixture and silicone structures are produced by inline mixing and co-extrusion of a part containing a catalyst (part A) and a part containing a crosslinker (part B). By the virtue of crosslinking, the extruded strands rapidly rigidize, increasing their self-supportive capacity. Hence, we can obtain structures with superior shape retention and realize previously unobtainable parts that are tall, high aspect ratio, and have overhanging features. These minimal sag parts are achieved without requiring extra curing or mechanisms, support structures, or suspension baths. This work was performed under the auspices of the U.S. Department of Energy by Lawrence Livermore National Laboratory under Contract DE-AC52-07NA27344. LLNL-ABS-849618.

4:30 PM SF01.10.08

3D Printed BioPE Textile for Low Temperature Applications[Volodymyr Korolovych](#), Duo Xu, Amy Huynh and Svetlana V. Boriskina; Massachusetts Institute of Technology, United States

The developments in polymer material synthesis and manufacturing processes are re-shaping the textile industry, ushering in a new textile manufacturing paradigm, namely implementation of digital and sustainable manufacturing approaches, such as fused deposition modelling (FDM) 3D printing. In recent years, 3D printing of polymers on textiles has shown a lot of potential to optimize complex designs, automate manufacturing as well as to develop new textile functionalities and aesthetic elements. Most popular polymers printed on textiles include polylactic acid, acrylonitrile butadiene styrene, nylon, polycarbonate, glycol modified poly-ethylene terephthalate, and thermoplastic polyurethane. They are usually printed on a dissimilar textile material, which leads to poor adhesion between the printed parts and the fabric. In addition, poly-material nature of the state-of-the-art 3D printed textiles often makes it impossible to separate and reclaim their ingredients at the end of the product lifecycle. Furthermore, conventional 3D printable polymers are typically stiff and have poor thermal management properties, which may cause thermo-physiological wear discomfort of 3D printed textiles. Overcoming these challenges will significantly improve wear comfort, sustainability of 3D printed textile and drastically expand their functionality.

This work aims to develop bio-derived, low-carbon-footprint monomaterial 3D printed textile platform for low temperature applications in defense and aerospace industries. We explore the role of the nanostructure of bio-derived polyethylene (bioPE) 3D printed structures in engineering their tensile and elastic performance at extremely low temperatures (down to -70 °C). A range of bioPE yarns and textile with various 3D printed patterns and different nano-scale structure has been fabricated via a combination of a scalable fiber melt-extrusion method and fused deposition modelling. These yarns and textiles have been characterized by their tensile and viscoelastic performance, as well as classified according to their meso- and nanoscale structure. Wide angle (WAXS) and small angle (SAXS) X-ray scattering techniques confirmed that by precise engineering of bioPE material nanostructure, we can tune the material crystallinity degree from ~60% to ~80% and to achieve high degree of crystalline domain orientation along the fiber axis. This tunability of the fiber nanostructure translates into tunable elongation at break (up to ~100%) and tensile strength (up to ~180 MPa) values of the bioPE yarns at -70 °C. We further show that mono-material bioPE 3D printed textiles exhibit great adhesion between the printed parts and the fabric, together with high flexibility and durability. In addition, bioPE 3D printed textiles are fully recyclable into a high-value and utility material stock. Overall, our work provides novel route towards development of lightweight, multifunctional bioPE 3D printed textiles with potential applications from uniforms and wearables to aerospace suits, while offering lower environmental footprint in production and full mechanical recyclability.

This work was supported by the Advanced Functional Fabrics of America (AFFOA) and the US Army Research Office. We thank Brandon Henry, Michael Lampkin, Tony DeLaHoz and Jeff Haggard from Hills Inc. for help with the PE yarns fabrication and Braskem for providing bio-derived PE resins. A.H. was supported by NSF GRFP. Useful discussions with Leslie Yan, Michael Rein, and Michelle Farrington are gratefully acknowledged. We also thank Steven Kooi for his help with equipment installation.

4:45 PM SF01.10.09

Infrared Scanning Near-Field Spectroscopic Studies of Self-Assembled Nanostructures Based on Photo-Crosslinkable Block Copolymers[Nadine von Coelln](#), Britta Weidinger, Christian Huck, Irene U. Wacker, Rasmus Schroeder, Eva Blasco and Petra Tegeder; Heidelberg University, Germany

Block copolymers, i.e., chemically distinct polymer blocks which are covalently bond, are known for their ability to self-assemble into a variety of morphologies on the nanometer scale.^[1] The self-assembly of block copolymers has been extensively investigated for 2D films,^[2-3] however, less attention has been paid to 3D bulk morphologies as well as light-based 3D printed microstructures. To achieve long-range ordered samples in thermodynamic equilibrium, in this work, 3D bulk morphologies were prepared via solvent annealing and 3D printed microstructures were fabricated from pre-self-assembled block copolymer inks.

Infrared scanning near-field optical microscopy (IR-SNOM) offers the unique possibility of infrared chemical imaging and spectroscopy with a spatial resolution down to ~20 nm.^[4] When irradiating a well-defined diblock copolymer consisting of polystyrene and a methacrylate-based copolymer decorated with photo-crosslinkable units at an independently addressable absorption band of a polymer block, chemical imaging of the blocks' nano-ordered spatial arrangement is possible.

Here, the internal nanostructure of self-assembled 3D bulk morphologies with lamellar nanostructures is studied by means of IR-SNOM. When selectively exciting each polymer block, a switch of the relative optical phase, related to the local absorption, is observed, revealing a strong phase segregation via spectroscopic contrast. A successful correlation with scanning electron microscopy (SEM) measurements, performed after post-staining with ruthenium tetroxide, furthermore demonstrates, that ruthenium tetroxide creates a specific metal stain for polystyrene. These studies are extended to cylindrical nanostructures as well as two-photon laser printed microstructures exhibiting complex geometry and hierarchically nano-ordered structures.

References:

- [1] Y. Mai *et al.*, *Chem. Soc. Rev.* **2012**, *41*, 5969-5985.
- [2] C. J. Hawker *et al.*, *MRS Bull.* **2005**, *30*, 952-966.
- [3] J. Kim *et al.*, *Spectrochim. Acta A* **2022**, *274*, 121095.
- [4] A. Centrone, *Annu. Rev. Anal. Chem.* **2015**, *8*, 101-126.

SESSION SF01.11: Session IX
Session Chairs: Jian Liu and Shreyas Pathreker
Friday Morning, December 1, 2023
Hynes, Level 2, Room 200

8:15 AM SF01.11.01

Influence of Diffusion on Print Fidelity in Vat Polymerization 3D Printing—Acrylate-Chain vs Thiolene-Step Growth Chemistry Bhavana Deore¹, Chantal Paquet¹, Hendrick de Haan², Thomas Lacelle¹, Laura Dickson¹, Katie Sampson¹ and Yujie Zhang¹; ¹National Research Council Canada, Canada; ²Ontario Tech University, Canada

3D printing is an emerging additive manufacturing technology poised to transform both design and manufacturing due to its ability to customize design and generate structural complexity not possible using traditional manufacturing processes. Light-based 3D printing techniques, such as SLA, DLP or tomographic printing, use patterned light to trigger polymerizations within a volume of a photoreactive resin and thus producing 3D objects. The process of printing in a vat of resin using light that varies temporally and spatially creates dynamics within the resin that ultimately influence properties of the printed part. In this work, we present how concentration gradients and changes in miscibilities during printing causes phase separation and diffusion of species that effect the printing process. The dynamics created by 3D printing are complex with factors governing the extent of the diffusion of inhibiting and reactive species include the geometry and dimensions of the printed features, the viscosity of the resin, rates of polymerization and gelation point. These factors are in turn governed by the formulation and on the type of polymerization i.e., step growth vs. chain growth. By tuning the formulations, changes in diffusivity, viscosity and gelation rates can be control and therefore allow control over phase separation or deviations from nominal print dimensions. The results are supported by modeling allowing us to identify the underlying mechanism behind each.

8:30 AM SF01.11.02

On-Demand Printing of Metallic Polymer Composite Microstructures via Hybrid 3D Printing Yeowon Yoon, Youngwoo Lee, Yang Xu and Yong Chen; University of Southern California, United States

On-demand printing of microstructures using polymer composites can enhance the materials' functionality with tailored properties. Especially metallic polymer composites have been used in a wide range of applications, including electronics, energy solutions, soft robotics, and four-dimensional printing due to their mechanical strength, high electrical/thermal conductivity, and ferromagnetic behavior. However, current manufacturing challenges limit the concentration of the filler materials in these metallic polymer composites to be low so low viscous slurry can be used in printing. In this study, a novel hybrid additive manufacturing (AM) process is developed to print a highly concentrated metallic polymer composite with over 80% metal particles within the polymer matrix. In this hybrid AM process, highly viscous slurry (~400,000 mPa·s) is printed using DDW, and metal (Iron)-polymer composites are fabricated at designed locations in both discrete and continuous manner so functional material portions can be well defined. In addition, DLP-based VPP is used to print bulk matrix portions using photopolymers to build intricate matrix structures at a fast building speed. An extensive range of composite inks including various photopolymers can be employed in this hybrid 3D printing process to fabricate functional structures with adjustable mechanical properties and multifunctional characteristics. The printing parameters of this hybrid process have been studied, including nozzle height, dispensing speed, and different surface conditions. Using ferromagnetic particles (44 μm) with soft and elastic photopolymer resins, magnetic-actuated grippers were fabricated to demonstrate design functions. The developed 3D printing approach offers a promising route to manufacture metallic polymer composites with tunable magnetic and mechanical properties, which could have potential applications in soft-form sensors, actuators, and biomedical devices.

8:45 AM SF01.11.03

Strategies for Integrating Metal Nanoparticles with Two Photon Polymerization Process Jisun Im¹, Liu Yaan^{2,3}, Qin Hu², Gustavo Trindade^{4,2}, Ricky Wildman², Richard Hague², Lyudmila Turyanska² and Christopher Tuck²; ¹University of Warwick, United Kingdom; ²University of Nottingham, United Kingdom; ³University of Exeter, United Kingdom; ⁴National Physical Laboratory, United Kingdom

A femtosecond laser-induced two photon polymerization (2PP) is a high-resolution additive manufacturing technology that allows for the creation of highly precise and complex microstructures with submicron resolution. This technology has revolutionised the creation of micro- and nano-scale structures, leading to the emergence of new products and technologies. However, the limited availability of functional materials, especially metal nanoparticles that are suitable for use in this process, hinders the technology's full exploitation. Here we propose three complementary strategies for the integration of metal nanoparticles (MeNPs) with 2PP processes to fabricate nanoparticle-polymer composites and metal nanoparticle-decorated surface patterns in microscale: 1) in-situ formation of MeNPs through a single-step photoreduction process, 2) integration of pre-formed MeNPs into 2PP resin, and 3) site-selective MeNPs decoration of 3D 2PP structures. We demonstrate successful fabrication of high-fidelity structures with incorporated MeNPs and provide detailed morphological and compositional analysis including advanced time-of-flight secondary ion mass spectrometry (ToF-SIMS) mapping results. These complementary strategies open up a broad range of prospective applications from metamaterials and nano/micro-photonics to optoelectronics and biomedicine.

9:00 AM SF01.11.05

Interpenetrating Networks with Tuned Thermal and Mechanical Properties by Multiphoton Lithography Paulina Szymoniak¹, Dorothee Silbermann¹, Zeynab Tavasolyzadeh¹, Heinz Sturm^{1,2} and Ievgeniia Topolniaik¹; ¹Federal Institute for Materials Research and Testing (BAM), Germany; ²Technical University of Berlin, Germany

Multiphoton lithography (MPL) has recently attracted significant research interest as a versatile tool capable of fabricating 2D and 3D micro- and nanoscopic features with high spatial resolution. The integrity of MPL microstructures, or their ability to respond to external stimuli, is of critical importance. Often, the mechanically flexible micro-objects are expected to be capable of shape morphing, bending, or other motion to ensure their functionality. However, achieving the desired properties of MPL-manufactured micro components for a specific application still remains challenging.

In this work, we present new MPL materials based on epoxy-acrylate interpenetrating networks (IPNs). We aim at fabrication 3D microstructures, whose properties can be easily tuned by varying the ratio of the IPN components and fabrication parameters. The studied mixtures consist of polyethylene glycol diacrylate (PEGDA) and cycloaliphatic epoxide functional groups. Consequently, triarylsulfonium salt and cyclopentanone photoinitiator tailored for MPL were used to ensure cationic and radical polymerization, respectively. The resulting library of 3D microstructures was investigated for their thermal and mechanical properties using highly sensitive space-resolved methods. For the first time, we were able to evaluate the glass transition behavior of 3D MPL microstructures using fast scanning calorimetry. The influence of both IPN composition and fabrication parameters on glass transition temperature and material fragility was demonstrated. AFM force-distance curve and intermodulation methods were used to characterize the micromechanical properties with lateral resolution of the techniques in the range of 1 micron and 4 nm, respectively. The elastic-plastic behavior of the microarchitectures was evaluated and explained in terms of IPN morphology and thermal properties. The fabricated 3D IPN microstructures exhibit higher structural strength and integrity compared to PEGDA. In addition, IPNs exhibit high to full elastic recovery (up to 100%) with bulk modulus in the range of 4 to 6 MPa. This makes IPNs a good base material for modeling microstructures with intricate 3D designs for biomimetics and scaffold engineering. The effects of composition and MPL microfabrication parameters on the resulting IPN properties give us a better understanding of the underlying mechanisms and microfabrication-structure-property relationships. Moreover, our funding supports the further development of IPN systems as versatile and easily tunable MPL materials.

9:15 AM SF01.11.06

4D Printing of Free-Standing Carbon Fiber-Reinforced Shape Memory Polymer Composites via Frontal Polymerization Hyeon-Ju Jang and Woong-Ryeol Yu; Seoul National University, Korea (the Republic of)

Continuous carbon fiber-reinforced polymer composites have been used in various industries, such as automobiles and aerospace, due to their high strength performance and lightweight. With the emergence of 3D printing technology, there has been a growing interest in utilizing this technique to fabricate continuous carbon fiber-reinforced plastics, particularly thermoplastic composites. In this study, we developed a 3D printing process for fabricating free-standing continuous carbon fiber-reinforced shape memory polymer composites without supports using frontal polymerization. Frontal polymerization is a self-catalytic exothermic reaction that converts monomers into polymers without external energy supply. One of the key challenges in

printing continuous carbon fiber-reinforced shape memory polymer is to achieve a high degree of resin impregnation of carbon fibers to ensure optimal physical properties. We enhanced the degree of impregnation by developing an *in situ* pin-assisted printing head. Subsequently, we investigated the printability of frontal polymer with continuous carbon fibers with a focus on the degree of impregnation. Finally, the newly developed 3D printing system was evaluated characterizing the mechanical properties of the printed composites including their shape memory performance.

9:30 AM SF01.11.07

Embedded 3D Printing of Mechanically Robust Ionogel Composites[Alexander Q. Kane](#), EunBiOh and RyanL. Truby; Northwestern University, United States

Multifunctional materials with programmable mechanical properties and electronic/ionic conductivities are required for many emerging applications, including soft electronics, robotics, structural batteries, and more. Additive manufacturing has revolutionized our ability to fabricate these materials, which often require complex 3D forms. Poly(ionic liquid) composites are an emerging structural electrolyte that provide a wide electrochemical window and high ionic conductivity. However, poor intrinsic mechanical properties (e.g. Young's modulus) limit the printability of precise functional poly(ionic liquid) architectures, hindering their potential utility as materials for the aforementioned applications. Moreover, existing light-based 3D printing methods are often incompatible with filler particles that can enhance the mechanical properties of poly(ionic liquids) or provide additional functionalities. In this work, we present a method for overcoming the challenges of 3D printing poly(ionic liquids) via embedded 3D (EMB3D) printing. Our integrated material design and manufacturing process produces free-form, lightweight, and flexible poly(ionic liquid) composites that are mechanically robust under cyclic compression. We demonstrate the modularity of our methods by showcasing multimaterial printing with various particle fillers (e.g., carbon black, hexagonal boron nitride, and fumed silica) and poly(ionic liquid)s. We anticipate our contributions will open new avenues for fabricating complex, architected solid electrolytes for soft sensors and robots, wearable devices, solid-state batteries, and more.

9:45 AM SF01.11.08

Discovery of New Strengthening Law in Nanocomposite Reinforced by Ceramic Nanoarchitected Materials[GwangminBae](#)¹, Dong GyuKang², ChanguiAhn³, DaehoKim², Hyeon GyunNam², GayeaHyun², DongchanJang², Seung MinHan² and SeokwooJeon¹; ¹Korea University, Korea (the Republic of); ²Korea Advanced Institute of Science and Technology, Korea (the Republic of); ³Korea Institute of Ceramic Engineering and Technology, Korea (the Republic of)

Engineers have long sought to utilize the exceptional mechanical properties achieved by size effect at the macroscopic level, as the strengthening effect derived from size is exclusive to the nanoscale realm. In this work, we present a novel approach to harness the size-induced strengthening effect and apply it on a macroscopic scale in a three-dimensional (3D) metal/ceramic/metal (MCM) nanocomposite. 3D Ni matrix nanocomposites embedding nanoscale Al₂O₃ nanoarchitectures were produced in a large area (~1 inch) using Proximity-field nanopatterning (PnP) and material conversion techniques. Ceramic thin-shell nanoarchitected materials (t < 100 nm), utilized by a reinforcement of metal nanocomposite, perfectly separate 1st and 2nd metal layers. 1st and 2nd metals are densely infiltrated in and out of the ceramic nanoarchitected materials without defects. The 3D Ni/Al₂O₃/Ni nanocomposite exhibits a significantly higher compressive strength, surpassing the upper bounds predicted by conventional rule of mixture by approximately 30%. This remarkable strength is attributed to the extrinsic size effect of the ceramic nanoarchitected materials. By integrating the size-induced strengthening of ceramics into the traditional strengthening models of composites, a new strengthening model is derived and experimentally validated using the 3D Ni/Al₂O₃/Ni nanocomposite system. The utilization of size-induced strengthening in nanomaterials allows the 3D MCM nanocomposite system to offer a novel approach for enhancing the mechanical properties of bulk materials.

10:00 AM BREAK

10:30 AM SF01.11.09

3D-Printed Microarray Biosensor for Real-Time Monitoring in Interstitial Fluid[Jean WonKwak](#), TuanTrinh, AlexanderD. White, YueXu, H. TomSoh and JosephM. DeSimone; Stanford University, United States

Real-time tracking of biochemical biomarkers in the body can provide personalized healthcare information. Microneedles, as a promising platform, enable continuous access to interstitial fluid in the dermal region through a minimally invasive and painless approach. However, wearable microneedle-based sensors face limitations, including the lack of reagent loading capacity due to conventional fabrication processes (e.g., microfabrication, molding) and deficiencies in continuous sensing capabilities caused by restricted biorecognition elements. Here we present a microarray biosensor (MAB) that integrates 3D-printing technology with biochemical sensing techniques for continuous and real-time monitoring of small molecules, such as cortisol and lactate. The MAB leverages the Continuous Liquid Interface Production (CLIP) to achieve tunable geometries, enabling utilization of the void volume of each microarray projection. These voids facilitate loading of hydrogel membranes, where optical molecular switches are immobilized within the network, enhancing signal detection and providing biochemical protection. Additionally, the MAB allows omnidirectional diffusion of targeted analytes while offering mechanical support during insertion. Ex vivo and in vivo evaluations are underway to validate the performance of the MAB in an effort to demonstrate its potential to provide comprehensive information about our bodies for precise prognosis and diagnosis of our health.

10:45 AM SF01.11.10

Towards a 3D Solid-State Na-Ion Battery using a Direct Ink Writing-Infiltration Approach[ShreyasPathreker](#)¹, ShahryarMooraj², SelinaLiu¹, WilliamR. Fullerton³, HyeongjunKoh¹, WenChen², RussellJ. Composto¹, EricA. Stach¹, ChristopherY. Li³ and EricDetsi¹; ¹University of Pennsylvania, United States; ²University of Massachusetts Amherst, United States; ³Drexel University, United States

3D solid-state batteries based on porous materials offer significant advantages over conventional 2D batteries, namely, high areal energy and high power density due to their increased surface area and intimate contact between cell components. They can also exhibit enhanced safety due to the high modulus of the solid electrolyte, which is known to suppress dendrite growth. The fabrication of 3D batteries calls for innovative, sustainable, non-roll-to-roll manufacturing approaches. We describe a three-step fabrication approach comprising direct ink writing, Capillary Rise Infiltration (CaRI), and vacuum-assisted infiltration for the development of a 3D solid-state battery. Pre-alloyed NiMn₂ powder mixed with a porogen is 3D printed into lattices, and sintering time and temperature are optimized to create a porous NiMn₂ 3D lattice comprising two different pore sizes in the range of 5 μm–10 μm and 150 μm–200 μm, respectively. Partial oxidation of the porous lattice generates a Na_{2/3}[Ni_{1/3}Mn_{2/3}]O₂ (NNMO) layer, which serves as the cathode. Following this step, capillary-rise infiltration (CaRI) of an optimized poly(glycidyl methacrylate)-poly(ethylene glycol) (PGMA-PEG6k) electrolyte solution is used to deposit the polymer electrolyte within the small pores of the lattice. Thermal crosslinking between the epoxide groups on the PGMA backbone and amine end groups of the PEG within the pores yields a dense composite of solid polymer electrolyte in conformal contact with the pore surfaces. To deposit the anode in the large pores of the 3D lattice, vacuum-assisted infiltration of Na₈₀K₂₀ metal is carried out, thereby completing the battery. Notably, this sequential fabrication approach uses zero solvent and polymer binder during either cathode (NNMO) or anode (Na₈₀K₂₀) deposition, which is in remarkable contrast to conventional slurry-casting methods that require the use of both N-methyl-pyrrolidone (NMP) and a polymer binder such as polyvinylidene fluoride (PVDF). Focused ion beam (FIB) milling, scanning electron microscopy (SEM), and energy dispersive x-ray spectroscopy (EDS) on the 3D matrix reveal excellent scaffold-polymer-anode contact, confirming the formation of robust interfaces that are necessary for battery application, which is currently being investigated. This work underscores the importance of cross-cutting collaborative research in materials science for emerging energy applications. Acknowledgements: We gratefully acknowledge funding from the NSF via grant number FMRG-2134715. This work was carried out in part at the Singh Center for Nanotechnology, which is supported by the NSF National Nanotechnology Coordinated Infrastructure Program under grant number NNCI-2025608.

11:00 AM SF01.11.11

End-To-End Performance Analysis of 3D Printed Luminescent Devices for Energy Conversion Applications[ShomikVerma](#)¹ and RachelEvans²; ¹Massachusetts Institute of Technology, United States; ²University of Cambridge, United Kingdom

In recent years, there has been increasing urgency to develop cheap, efficient solar devices. However, most solar modules are large, bulky, and rectangular, making integration into the built environment non-trivial. A promising technological solution that may help solve this problem is the luminescent solar concentrator (LSC). A typical LSC is a plastic slab that absorbs sunlight and re-emits light of a tailored wavelength towards its edges, where solar cells can be installed. Because LSCs are colorful, semi-transparent, and modular, they hold great potential in reducing the cost and barrier to entry of solar technologies. However, they suffer from significant optical losses limiting their efficiency. Many novel device shapes have been proposed to improve light transport pathways in LSCs, but these often rely on expensive or wasteful fabrication techniques.

A potential solution to this is 3D printing, which has gained immense traction as an alternative manufacturing technology. 3D printing has many benefits including accessibility, rapid prototyping, and fabrication of completely new designs. This study presents an end-to-end performance analysis methodology to evaluate new LSC designs that can take advantage of this novel manufacturing technology. This methodology is applied to some preliminary 3D printed parts as a proof of concept that can be applied to a wider variety of designs.

This study consists of 3 distinct steps: simulating the optical efficiency of the printed part, 3D printing the part with luminescent filament, and characterizing its optical efficiency experimentally.

Simulation of LSCs using ray tracing has been extensively investigated in the past; however, this has been limited to conventional, rectangular LSCs. Analyzing the performance of alternative

LSC geometries requires developing a novel methodology for evaluating device efficiency, as well as implementing parallelization techniques to reduce computation time for complex geometries.

Among the 3D printing technologies, fused deposition modeling (FDM) is the most accessible and widely used, but it is not known for producing transparent parts usable for optical applications. This thesis aims to solve some of the complications of FDM to develop a cheap, rapid, and accessible methodology for printing efficient LSCs.

Similar to modeling, device characterization has been limited to rectangular LSCs, so a standardized methodology for evaluating device efficiency has been developed, allowing for comparison between different device shapes.

The simulated results of this study indicate 3D printed devices have the potential to offer a twofold increase in efficiency over conventionally manufactured bulk devices. Actual 3D printed devices were measured to have similar efficiency to bulk devices (within 1%), but extrapolating the results to parts made with higher quality material also suggests some parts would have twice the efficiency of their bulk counterparts. 3D printed parts may have additional benefits in improving directionality of edge-emitted light, but this will have to be confirmed in future work.

Overall, 3D printing provides major benefits over conventional manufacturing techniques, as it introduces rapid prototyping by allowing experimental iteration and model validation, allows custom-built designs for easier integration into the built environment, and increases the optical efficiency of devices by improving light transport pathways. With further development, this technology can help make widespread solar adoption a reality.

11:15 AM SF01.11.12

Unique Mechanical Behaviors of Mechanical Metamaterials with Engineered Imperfections SiyaoLiu and YanningLi; Northeastern University, United States

Traditionally, imperfections are undesired in the materials and structures, because they often reduce the load-bearing capacity and cause premature failure. However, if imperfections are designed and engineered, they could generate unique new mechanical properties. In this investigation, we introduce patterned and hierarchical imperfections to lattice structures and find that the new designs show dramatically different mechanical properties under loads at different locations. Also, by utilizing the concept of tensegrity, the mechanical properties can be further controlled and tuned. In this investigation, new hybrid lattices are designed, which are composed of hard cells connected via engineering soft connections. Upon external mechanical or thermal loads, the hard cells will either keep the orientation or rotate due to the chiral arrangement or the soft components. Both deformation mechanisms will contribute to the overall volume change of the material and are related to the loading type and location. Therefore, the pattern transformation will lead to a change in both mechanical properties and functionality related to the material structure. To further prove the concept, prototypes of selected designs are fabricated in both macro- and micro- scales. Quasi-static uniaxial compression experiments were conducted in both room temperature and elevated temperatures. Finite element simulations are performed to further quantify the mechanical behaviors.

SESSION SF01.12: Session X
Session Chairs: Jian Liu and Shengbiao Zhang
Friday Afternoon, December 1, 2023
Hynes, Level 2, Room 200

1:30 PM SF01.12.01

Materials Design for Charge-Programmed Additive Manufacturing of Antennas ZhenWang¹, JunboWang², ZhenpengXu¹, RyanHensleigh², YahyaRahmat-Samii² and RayneZheng¹; ¹University of California, Berkeley, United States; ²University of California, Los Angeles, United States

Additive manufacturing (AM) is emerging as a powerful tool for fabricating antennas particularly in the capability of creating arbitrary complex geometries without incorporating excessive materials owing to its unique materials build-up mechanism. Taking such benefits, 3D printed antennas, including horns, waveguides, and dielectric antennas, have been reported with enhanced performances in different aspects. These examples, however, are constructed mainly by single materials (either all-dielectric or all-metal). While multi-process AM can potentially perform conductive coating on 3D printed dielectric structure, the lack of selectivity and limited access to complex 3D geometries exclude a considerable amount of antennas from current AM approaches.

The charge-programmed multi-material 3D printing technique integrates multiple materials and functionalities into 3D devices, which is achieved by programmed volumetric deposition of one (or multiple) materials into arbitrary 3D micro-architectures. The printed structures had programmed surface charge regions, enabling the selective deposition of functional materials into complex 3D architectures based on localized electrostatic interactions. For antenna applications, charge-programmed AM can achieve sophisticated 3D architected lattice materials with interpenetrating dielectrics and metals, allowing free space for designing antennas being ultra-light and yet mechanically robust. In this paper, we present the materials design principles enabling charge-programmed multi-material printing of lightweight antennas with unique mechanical properties and competitive antenna performances.

CHARGE-PROGRAMMED SELECTIVE DEPOSITION

Charge-programmed selective deposition for the fabrication of antennas is based on a multi-material printing system. Resins with positive, negative, or neutral charge polarity were alternately solidified and bound to the previously built layer of the printed parts. The process was repeated layer by layer, pin-pointing multiple materials with different polarities into their designated coordination in 3D space. The charged surfaces immobilize the oppositely charged catalyst species, which in-situ catalyze the subsequent deposition of functional materials. In such a way, the printed objects obtained patterned structures that selectively integrated different functionalities in designated locations with a resolution as high as the 3D printer could achieve.

MATERIALS DESIGN FOR ANTENNA APPLICATION

Charge-programmed selective deposition allows a wide range of space for materials design. Particularly for antenna applications, a variety of combinations of conductivity and dielectric constant, the most crucial parameters, can be achieved, suggesting the versatility of the charge-programmed selective deposition for custom tailored antenna applications.

The composition of the negative resin directly influences the antenna performances which relies on the quality of the plated Cu layer as well as antenna's mechanical robustness. Based on the molecular configurations of the polymerized photo-monomers, the negative resins were formulated to deliver either stiffness or flexibility for the printed antennas. By tuning the composition of the resins, we achieved a balance between the cross-link density and charge density. This enabled a uniform catalyst distribution on the stiff and tough negative resins and consequently grew a crack-free conformal Cu coating on the surface, serving excellent electrical properties for a K-band horn antenna. By introducing flexible monomers, we fabricated transmitarray with considerable flexibility, which promises potential for deployable antennas.

1:45 PM SF01.12.02

Additive Manufacturing of Micro-Architected Metals via Hydrogel Infusion MaxA. Saccone^{1,2}, RebeccaA. Gallivan^{1,3}, KaiNarita¹, DarylW. Yee^{1,4} and JuliaR. Greer¹; ¹California Institute of Technology, United States; ²Stanford University, United States; ³ETH Zürich, Switzerland; ⁴École Polytechnique Fédérale de Lausanne, Switzerland

Metal additive manufacturing (AM) has emerged as a uniquely powerful tool to produce complex and high-performance parts with applications from the aerospace to biomedical fields. Most existing metal AM techniques use heat to define part shape via thermally initiated melting or sintering. In contrast, we report a polymer-based AM technique, coined hydrogel infusion additive manufacturing (HIAM), that produces metals and alloys with microscale resolution via vat photopolymerization (VP). To fabricate micro-architected metal structures, we infuse 3D-architected hydrogels with aqueous metal precursors, then calcine and reduce the infused hydrogel scaffolds to create miniaturized metal replicas. Unlike previous VP strategies, which incorporate target materials or precursors into the photoresin during printing, HIAM does not require re-optimization of resins and curing parameters for different materials, enabling quick iteration, compositional tuning, and the ability to fabricate multimaterials. We demonstrate HIAM of micro-architected metals including copper, nickel, silver, cobalt, cupronickel alloys, high entropy alloys, and tungsten with critical dimensions of ~50 μm. This work shows how single architected gel scaffold can respond to a variety of chemical and thermal stimuli to transform into a vast array of metals, providing a pathway to create advanced micro-architected metals.

2:00 PM SF01.12.03

3D Printing and Processing of High-Performance Piezoelectrics for Ultrasound Transducer Applications HaotianLu^{1,2}, VictorCouedel¹ and RayneZheng¹; ¹University of California, Berkeley, United States; ²University of California, Los Angeles, United States

The performance of ultrasonic transducers is largely determined by the piezoelectric properties and geometries of their active elements. Due to the brittle nature of piezoceramics, existing processing tools for piezoelectric elements only achieve simple geometries, including flat disks, cylinders, cubes and rings. While advances in additive manufacturing give rise to the free-form fabrication of piezoceramics, the resultant transducers suffer from high porosity, weak piezoelectric responses, and limited geometrical flexibility. We introduce optimized piezoceramic

printing and processing strategies to produce highly responsive piezoelectric micro transducers that operate at ultrasonic frequencies. The 3D-printed dense piezoelectric elements achieve high piezoelectric coefficients and complex architectures. The resulting piezoelectric charge constant, d_{33} , and coupling factor, k_t , of the 3D printed piezoceramic reach 583 pC/N and 0.57, approaching the properties of pristine ceramics. The integrated printing of transducer packaging materials and 3D printed piezoceramics with microarchitectures create opportunities for miniaturized piezoelectric ultrasound transducers capable of acoustic focusing and localized cavitation within millimeter-sized channels, leading to miniaturized ultrasonic devices that enable a wide range of biomedical applications.

2:15 PM SF01.12.04

Three-Dimensional Printing of High-Sensitivity Micro-Architected Piezoelectric Hydrophones with Designed Beam Patterns Victor Couedel¹, Haotian Lu^{1,2} and Rayne Zheng¹; ¹University of California, Berkeley, United States; ²University of California, Los Angeles, United States

Piezoelectric hydrophones are crucial for underwater applications such as communication and seafloor mapping. Limited by the brittleness of piezoelectric ceramics, conventional manufacturing methods restrict hydrophones' shapes to simple geometries such as disks, cylinders, or spheres, which limits the sensitivity, directivity pattern, and working frequency bandwidth of the device.

Here, we present a new class of high-performance 3D printed piezoelectric hydrophones consisting of rationally designed micro-architectures. Using a high-resolution light-based printing process, and thanks to a liquid sealing sintering process, the piezoelectric coefficients and electromagnetic coupling factor can reach respectively 92% and 85% of the pristine material's values, the highest values among all existing 3D printing work.

We have developed a framework to artificially manipulate the piezoelectric coefficients of an architected material by modifying the spatial arrangement of unit cell struts. This can be harnessed to develop a new class of metamaterial hydrophones whose sensitivity can be locally manipulated. We take advantage of this framework to generate hydrophones with sensitivities ~10 dB higher than the commercial ones, and whose directivity patterns can be inversely designed.

This work holds great promises for high frequency sound localization without the need of hydrophone arrays, and for low frequency sound monitoring thanks to a hydrostatic figure of merit five times higher than the one of commercial transversely isotropic piezoelectric hydrophones.

2:30 PM SF01.12.05

The Role of Particle Microstructure and Polymer Configuration in 3D Printed Thermal Composites Daniel Braconnier¹, Eric Wetzel², Ryan Dunn² and Randall M. Erb¹; ¹Northeastern University, United States; ²U.S. Army Research Laboratory, United States

While everyday device sizes continue to shrink, the power being packed into them increases drastically, driving internal heat generation to the point of overwhelming current thermal management solutions and limiting system-level performance. New thermal management materials and solutions are required to support higher energy density electronics; incumbent materials including metals like copper and aluminum satisfy many applications, however they are heavy and cannot be placed adjacent to electronics or in the proximity of radio frequency components. Additive manufacturing and fine-tuned composite creation can enable lightweight and geometrically complex thermal management solutions that provide a distinct advantage over current solutions. Here we present a collection of new understandings around process-structure-property relationships that will help enable higher performing thermal parts via additive manufacturing. This work focuses on the interplay between the filament composition, the processing conditions of fused filament fabrication (FFF), and the post-processing of printed parts (annealing). The goal of this research is to enable emergent properties in FFF printed composites through material interface and interphase engineering, flow-induced self-assembly of mesostructure, and temperature-induced self-assembly of polymeric nanostructure. The ability to locally control the thermal conductivity of FFF parts would enable a new class of advanced thermal management materials.

2:45 PM SF01.12.06

Radiation Shielding of Microelectronics via Additive Manufacturing A very Rosh¹, Austin Coon¹, Devon Beck¹, Rich D'Onofrio¹, Ethan Cascio², Ksenofono Konomi³, Andrea Barney¹, Robert Longton¹, Pascale Gouker¹, Melissa Smith¹ and Bradley Duncan¹; ¹Massachusetts Institute of Technology Lincoln Laboratory, United States; ²Massachusetts General Hospital, United States; ³University of Massachusetts Lowell, United States

The miniaturization of satellite systems has compounded the need to protect microelectronic components from damaging radiation. Current approaches to mitigate this damage, such as indiscriminate mass shielding, built-in redundancies, and radiation hardened electronics, introduce high SWaP-C (Size, Weight, and Power-Cost) penalties that reduce the overall performance of the satellite. Additive manufacturing provides an appealing strategy to print radiation shielding only on susceptible components within an electronic assembly. Utilizing direct ink writing, we are able to conformally print customized inks at room temperatures directly and selectively onto COTS (commercial-of-the-shelf) electronics. The suite of inks uses a flexible styrene-isoprene-styrene block copolymer binder that can be filled with particles of varying atomic densities for varying radiation shielding capabilities. Additionally, blended composites of both high and low Z fillers were created to investigate the performance in radiation attenuation depending on composition. We anticipate this low SWaP-C alternative to traditional shielding methods will enable the development of novel complex and compact satellite designs.

3:00 PM BREAK

3:30 PM SF01.12.07

High-Speed Fabrication of Intrinsically Flexible Perovskite Optoelectronic Devices on Diverse Substrates (Elastomer, Paper, Textiles, etc.) Using Printing and Direct Writing Junyi Zhao and Chuan Wang; Washington University in St. Louis, United States

Flexible optoelectronic devices built on thin elastomer substrates may find a wide range of applications in wearable electronics, soft robots, deformable displays, and more. While considerable efforts have been made to explore the potential of halide perovskites in high-performance light-emitting diodes (LEDs), existing fabrication techniques using rigid substrates cannot meet the growing demand for large-area flexible devices. In this work, we report a high-speed fabrication approach for intrinsically flexible perovskite LEDs (PeLEDs) directly printed on elastomer thin films. Using a highly scalable inkjet printing approach, each layer in the device, from the bottom anode to the top cathode, is patterned. In addition to elastomer, paper, and textiles commonly used in our daily lives also hold great potential as platforms for next-generation flexible and wearable electronics. Therefore, we have developed a versatile, scalable, and eco-friendly direct writing approach that enables multicolor PeLEDs (covering the entire visible spectrum) and perovskite photodetectors (PePDs) (both vertical-photodiode configuration and planar-photoconductor configuration) to be directly drawn onto various unconventional substrates (paper, textiles, plastic, rubber, metal, and common three-dimensional objects) in an ultrafast and mask-free manner. This is achieved by daily used ballpoint pens filled with our uniquely formulated inks of conductive polymers, metal nanowires, and perovskite/polymer composite for photoactive layers. The addition of an ionic polymer in the inks helps address the challenge of rough surface morphology on yarn and fiber networks, ensuring uniform printed film thickness and minimizing leakage current. Just like drawing with multicolor pens, by writing the above functional inks layer-by-layer, high-performance perovskite optoelectronic devices can be customized on almost any target substrate within minutes even by untrained individuals. Notably, the entire manufacturing was conducted in ambient conditions without the need for specific moisture and temperature control. The simplified device architecture and fabrication strategy significantly reduce the fabrication time compared to the hours or days required by conventional microfabrication processes. The written PeLEDs exhibit a brightness as high as 15,225 cd/m², a current efficiency of 6.65 cd/A, and a turn-on voltage of 2.4 V. The PePDs exhibit an on/off ratio over 10⁴, and a response time of less than 15 ms. Owing to the extraordinary flexibility of each functional layer, the written LEDs on the paper substrate could be bent to a 1 mm extreme curvature radius for over 5000 cycles without decay in performance. Overall, this work paves the way for the practical application of perovskite optoelectronics in cost-effective and large-area scenarios, such as E-textile, E-paper, smart packaging, disposable electronics, and wearables.

3:45 PM SF01.12.08

Three-Dimensional Property Enhancement of Composites by Realization of Three-Dimensional Fiber Alignment via Embedded Direct Ink Writing Qiyi Chen and Rayne Zheng; University of California, Berkeley, United States

The orientation of fibrous fillers, induced by shear forces during extrusion, has been extensively demonstrated to exert a significant impact on various material properties such as mechanical properties, electrical conductivity, thermal conductivity, and microwave attenuation. However, these effects have primarily been observed in a two-dimensional (2D) x-y plane. In this study, we propose a novel approach to achieve fiber alignment in a three-dimensional (3D) context, specifically focusing on the Z-direction, by employing embedded 3D printing techniques. This methodology involves the extrusion and suspension of composite inks within a viscoelastic gel medium, allowing the control of fiber alignment through processing conditions such as velocity ratio, nozzle size, and fiber dispersion. By selectively aligning the fibers in a 3D pattern, it becomes possible to significantly enhance and tailor the mechanical properties and conductivity in a three-dimensional manner.

4:00 PM SF01.12.09

Direct Photopatterning of Metals on Polymer Surfaces at Ambient Conditions Ivan B. Dimov¹, Antonio Domínguez Alfaro^{1,2}, Tobias Naegele¹ and George G. Malliaras¹; ¹University of Cambridge, Department of Engineering, Electrical Division, United Kingdom; ²University of Basque Country, Spain

Metal interconnects on polymer substrates are an integral part of many stretchable and flexible electronic devices. However, metal deposition typically involves harsh conditions, such as high vacuum and temperature. These requirements limit compatibility with many substrates and impede rapid prototyping and increases and energy requirements. Solution-phase depositing such metal features is an attractive alternative to conventional processes, especially when combined with a rapid additive manufacturing technique.

Here we present an aqueous gold ink, comprised of $\text{H}[\text{AuCl}_4]$ as a metal source, a reducing agent and a benign, nontoxic dye as an initiator, that allowed us to deposit gold onto silicone surfaces upon UV illumination at ambient conditions. Altering the reaction time and ink composition, we could tune the morphology of the deposited metal, between isolated nanoparticles and a continuous film. Using this ink, we deposit stretchable gold interconnects on pre-strained silicone, using solely UV illumination, achieving conductivity of 40% of bulk gold. We additionally used a commercial stereolithographic printer without any modifications as a maskless lithography system, allowing us to pattern conductive features of 300 μm . Investigating different substrates suggests a preference for polymers with reducible species on the surface. Lastly, we have successfully performed the reaction with AgNO_3 as a metal source, depositing silver on silicone. We are working towards 2-photon illumination, in order to increase resolution and expand to 3D metal structures.

4:15 PM SF01.12.10

Mechanical Properties of 3D Printed Wavy Fiber-Matrix Composites [AmmarBatwa](#) and [YaningLi](#); Northeastern University, United States

We aim at exploring the influences of fiber waviness on the effective stiffness, strength, and toughness of 3D printed polymer composites with wavy-fibers embedded in soft matrix. Polymer fiber-matrix composites with fibers with various waviness are designed and fabricated via multi-material 3D printing. Quasi-static uni-axial tension experiments are conducted to characterize the stress-strain behavior of the designs. Systematic finite element (FE) simulations are also performed to explore the deformation mechanisms of the designs.

The results demonstrate an interesting mechanism for increasing toughness via controlling the waviness of the fibers. The structural-property relationship is quantified via a parametric study. To further evaluate the strain rate effects of the polymer fiber-matrix composites, uni-axial tension experiments under different loading rates are performed. Rate dependent material models are used in the FE simulations to capture the strain rate effects. The results under both static and dynamic loading provide design guidelines for this family of polymer composites fabricated via multi-material 3D printing.

<quillbot-extension-portal></quillbot-extension-portal>

4:30 PM SF01.12.11

Chemically Coalescing Liquid Metal Emulsions as 3D Printed Soft Conductors [StephanieF. Zopf](#), [ChloeKekedijan](#), [RamonE. Sanchez](#), [LuPing](#) and [JohnW. Boley](#); Boston University, United States

Patterning room temperature liquid metals as soft conductors requires nontrivial solutions due to its complex rheology. To facilitate material handling, liquid metals are often transformed into an emulsion by dispersing it as droplets within a continuous liquid. Oxides present on liquid metal droplets, however, render liquid metal emulsions nonconductive, which must be 'activated' through droplet coalescence for the ink to be conductive. Although liquid metal droplet coalescence in emulsion inks has been shown by using mechanical ([1], [2]), laser [3], and extreme thermal ([4], [5]) means, these modes of activation make it challenging to integrate with other materials and device components. This work presents a liquid metal emulsion ink that is 3D printable through direct ink writing (DIW), and can be activated chemically through the use of an active ingredient. It requires a low thermal stimulus ($\sim 80^\circ\text{C}$), which is compatible with commercial off the shelf electronic components. The ink developed in this work is able to retain its printed structure after being thermally activated. Coalescence through chemical etching of the oxides on the liquid metal droplets is evident through electrical conductivity measurements, scanning electron microscopy, nuclear magnetic resonance, and x-ray photoelectron spectroscopy characterization. Conductivities of formulated emulsions are precisely calculated using measured resistances combined with micron-level 3D scans with the maximum conductivity obtained of attempted formulations being 3.54×10^3 S/cm. Printability outcomes of emulsion inks with respect to formulated chemistries will be presented. Rheology for the most printable formulation with the highest conductivity shows that the ink is shear thinning and shear yielding and exhibits a high plateau modulus and high yield stress, giving it the ability to print features that span long distances. Lastly, an automated 3D print and electronic device assembly process will be shown to demonstrate the utility of this ink as a soft conductor for manufacturing integrated electronic systems.

[1] J.W. Boley, E.L. White, R.K. Kramer. *Adv Mater.* **2015**, 27, 2355.

[2] Sánchez Cruz R., Zopf S.F., Boley J.W. *J. Compos. Mater.* **2023**, 57, 4.

[3] S. Liu, M.C. Yuen, E.L. White, J.W. Boley, B. Deng, G.J. Cheng, R. Kramer-Bottiglio. *ACS Appl Mater Interfaces.* **2018**, 10, 28232.

[4] S. Liu, S.N. Reed, M.J. Higgins, M.S. Titus, R. Kramer-Bottiglio. *Nanoscale.* **2019**, 11, 17615.

[5] S. Liu, D.S. Shah, R. Kramer-Bottiglio. *Nat Mater.* **2021**, 20, 851.

4:45 PM SF01.12.12

Computational Discovery of Microstructured Composites with Optimal Strength-Toughness Trade-Offs [BoleiDeng](#)^{1,2}, [BeichenLi](#)¹, [WanShou](#)³ and [WojciechMatusik](#)¹; ¹Massachusetts Institute of Technology, United States; ²Georgia Institute of Technology, United States; ³University of Arkansas, Fayetteville, United States

The conflict between strength and toughness is a fundamental problem in engineering materials design. However, systematic discovery of microstructured composites with optimal strength-toughness trade-offs has never been demonstrated due to the discrepancies between simulation and reality and the lack of data-efficient exploration of the entire Pareto front. Here, we report a widely applicable pipeline harnessing physical experiments, numerical simulations and artificial neural networks to efficiently discover microstructured designs that are simultaneously tough and strong. Using a physics-based simulator with moderate complexity, our strategy runs a data-driven proposal-validation workflow in a nested-loop fashion to bridge the gap between simulation and reality in high sample efficiency. Without any prescribed expert knowledge of materials design, our approach automatically identifies existing toughness enhancement mechanisms that were traditionally discovered through trial-and-error or biomimicry. We provide a blueprint for the computational discovery of optimal designs, which inverts traditional scientific approaches, and is applicable to a wide range of research problems beyond composites, including polymer chemistry, fluid dynamics, meteorology, and robotics.

SESSION SF01.13: Virtual Session
Session Chairs: Wen Chen and Sarah Wolff
Tuesday Morning, December 5, 2023
SF01-virtual

8:00 AM *SF01.13.01

Additive Manufacturing of Carbon Nanotubes Reinforced Metal Matrix Composites [LiCao](#); University of Dayton, United States

High-performance components are always highly demanded for modern aerospace applications due to their critical role in ensuring safety and efficiency. Developing metal matrix composites (MMCs) reinforced with nanomaterials is an effective strategy to enhance the properties of such functional components. Among the various reinforcements, 1D nanomaterials such as carbon nanotubes (CNTs) have attracted much attention due to their exceptional mechanical, thermal, and electrical properties. Meanwhile, Additive manufacturing (AM) offers innovative manufacturing techniques that can be used to construct complex and intricate structural components. Integrating advanced material development and AM techniques has drawn significant attention as it overcomes the limitations and challenges of conventional fabrication approaches. This research focuses on the development of CNTs reinforced nickel-based alloys using laser powder bed fusion, a popular AM technique. The result showed significant improvements in the yield strength, ultimate tensile strength, and elastic modulus of the 3D printed specimens when 2.5vol.% CNTs were incorporated, demonstrating the remarkable impact of CNTs on enhancing the performance of the metal-based alloys.

8:30 AM SF01.13.02

High-Fidelity Beetle-Inspired 3D-Printed Wings for Miniature Flapping Drones [Bat-ElPinchasik](#), [OrFilc](#), [HagitGilon](#), [ShmuelGershon](#) and [GalRibak](#); Tel Aviv University, Israel

Miniature flapping drones equipped with lightweight membranous wings have shown great potential for operating effectively in small spaces. Achieving optimal flight performance in these drones heavily relies on the appropriate design of their flexible wings. In this study, we explore the utilization of 3D-printing technology to fabricate high-fidelity, bioinspired wings and expedite the design process for miniature flapping drones.

Drawing inspiration from the wings of the rose chafer beetle, we employ a bioinspired approach to develop 3D-printed wings. By modulating the wing structure, we create twelve distinct wing models that feature variations in vein cross-section shape, tapering geometry, and membrane thickness. Through a comprehensive comparison of their mechanical and aerodynamic properties, we establish guidelines to correlate wing form and function.

Our findings reveal the following key insights: first, manipulating the cross-section shape of the veins provides a powerful tool for engineering in-plane and out-of-plane deformations.

Second, tapering veins enhance the wings' mechanical stability, improving their overall performance. Experimental results demonstrate that the optimized wings exhibit a 16% increase in lift and a 27% improvement in lift production efficiency (N/Watts) when tested in a revolving wing setup. The successful design of lightweight, flexible, robust, and aerodynamically efficient wings poses a formidable engineering challenge that we aim to address through our bioinspired methodology. By reverse engineering these intricate structures, we contribute empirical knowledge to the field of wing design for miniature flapping drones. Our work highlights the potential of bioinspiration and 3D-printing techniques to advance the development of miniature flapping drones with enhanced flight performance. The insights gained from this study provide valuable guidance for future advancements in the field of bioinspired wing design and optimization.

8:45 AM SF01.13.03

Half-tone Stereolithography-Enabled 3D Printing to Regulate Rotating Actuation PerformanceZhongkunZhao and HongtaoSun; Penn State University, United States

Half-tone lithography has established itself as a novel technique in high-resolution 2D printing and imaging. In this study, we extended the application of half-tone patterns to the realm of stereolithography-enabled 3D printing, enabling precise control over the material properties within 3D printed structures.¹⁻³ Our work focuses on the development of a half-tone-enabled photo-stereolithography method to fabricate soft actuators using Shape Memory Polymers (SMPs). The underlying concept of half-tone lithography in 3D printing involves the spatial modulation of polymerization, allowing the creation of intricate patterns within each layer. Rather than relying solely on volumetric or voxel-based 3D printing approaches, this technique utilizes half-tone dots or pixels as building blocks to build up the designed 3D structures. More importantly, the integrated half-tone patterns in the printed product can offer additional control over material properties and functional performance in addition to the constrained geometry. Specifically, by strategically arranging these dots, we can achieve different features incorporated into the printed structures, such as heterogeneity domains, high-strength inclusions, graded structures, and complex textures, providing a more degree of freedom to design and fabricate functional products particularly for the use of smart functional materials, compared to traditional layer-by-layer 3D printing methods. By controlling the distribution of half-tone patterns, we fabricated fiber-shaped SMP actuators as rotation micro-engines, which can achieve high strength inclusions, or graded structures, allowing for regulating the mechanical properties and stimuli-responsive behaviors. Overall, the advancements in half-tone lithography for 3D printing of shape memory polymers, driving innovation and opening up new avenues for designing dynamic, responsive, and highly tailored structures with tunable performance and functionality.

References:

- [1] J. Kim, J. A. Hanna, M. Byun, C. D. Santangelo, R. C. Hayward, *Science* **2012**, 335, 1201.
- [2] A. Nojoomi, H. Arslan, K. Lee, K. Yum, *Nat. Commun.* **2018**, 9, 3705.
- [3] A. E. Chalard, A. W. Dixon, A. J. Taberner, J. Malmström, *Front. Cell Dev. Biol.* **2022**, 10, 946754.

8:50 AM SF01.13.04

FAIRification of Additive Manufacturing Process Through Ontology Development and Linked DataKristenJ. Hernandez, Hein HtetAung, XuanjiYu, PawanK. Tripathi, ErikaI. Barcelos, RogerH. French and LauraBruckman; Case Western Reserve University, United States

In order to improve current knowledge on Additive Manufacturing process the use of computer science principles is of interest. In order to optimize datasets for data analysis is a difficult process, due in part to the multiple data sources and the different output formats from each data source. The FAIRification process represents an attractive alternative to overcome the challenges associated with the storage, integration and reusability of these datasets. FAIR principles describe a set of guidelines applied to data and metadata to ensure a proper and efficient data management system. When applied correctly, it ensures that data is properly stored, organized, accessible and reusable. A fundamental component in the development of a successful FAIR framework and the integration of datasets is the development of ontologies. Domain ontologies are standardized representations of properties and relationships in a field and provide a sharing and common understanding within the research community. Using FAIR principles and domain ontologies as the backbone of organizing and processing data, the use of automated extraction methods are more feasible and able to process data regardless of the original capturing method. Data from disparate sources need to be processed and extracted in a method that can capture the feature of interest as well as relate the feature in a linked manner to the original data output. Information in the Additive Manufacturing process of Laser Powder Bed Fusion is sparse and separated among multiple instrument data sources that both capture different features and represent it using different encoding methods. These different encoding methods have the same object in reference while having different material characteristics extractable from the data source. In order to process through large data spaces of disparate features, data must be organized in a machine-compatible method. Furthermore, data must be retrieved with an automated pipeline for the ability to extract measurement of specific variables in a verifiably reproducible manner. Many datasets are reliant on operator specific inputs and often unreproducible evaluation methods. By using a more data scientific approach and organization scheme of linking datasets, information on Additively Manufactured parts, in spite of its sparse data, can be used and expanded further data visualization and trend relationships through specific software development and application. Organizing and streamlining data outputs to a common data framework allows for automation of analysis, quick retrieval of digital representations of variables of interest and the framework for decision making using data driven methods as opposed to physics informed simulations.

8:55 AM SF01.13.05

Engineering a Thermally and Electrically Conductive, Biodegradable, Mechanically Sustainable Nanocomposite via 3D PrintingXuyiZhou¹, Yu-ChungLin² and MiriamRafailovich²; ¹Shanghai Pinghe School, China; ²Stony Brook University, The State University of New York, United States

The electronic industry has considerable demand for materials with good electrical and thermal conductivity, and for the convenience of manufacturing, it would be beneficial for the materials to have better mechanical properties in comparison to the currently actively researched material graphene nanoplatelets(GNPs). In response to such need, we intend to engineer nanocomposites with a blend of PLA, PBAT, and GNPs H-5 (average diameter of 5 microns) through 3D printing in this research. From the properties of individual materials, PLA is the currently commercialized 3D printing filament material; PBAT, as a ductile polymer, compensates for the brittleness of GNPs; GNPs H-5 contributes to good electrical and thermal conductivity. For environmental concerns, both PLA and PBAT are biodegradable polymers. From our previous studies, it had been concluded that the optimal ratio of PLA to PBAT is 1:3, creating percolation pathway for electrical conductivity. Contact angle tests and work of adhesion calculation indicated that GNPs preferred the phase of PBAT as opposed to PLA. The addition of PLA, at low concentration, would take up space and confine GNPs in PBAT, therefore improving electrical and thermal conductivity. Nevertheless, more PLA has the risk of making PBAT phase discontinuous. Inspired by this, in our research, we altered the concentration of GNPs (including 8wt.%, 12wt.%, 16wt.%, and 20wt.%) to find the composites with optimal thermal conductivity, electrical conductivity, and mechanical properties. The ratio of PLA to PBAT is fixed as 1:3. The 3D printing nozzle shear force is expected to further orientate the H-5 platelets.

Four-point electrical conductivity tests were performed on the 3D printed electrical test samples. As expected, electrical conductivity increases as GNPs concentration increases. For horizontally infilled samples, 8wt.% GNPs and 12wt.% GNPs samples were generally not electrically conductive. The electrical conductivity increases from 0 to 1.6 S/m when 16wt.% of GNPs is added. In addition, the orientation of infill during the 3D printing process has an effect on electrical conductivity. Vertically infilled samples are less electrically conductive than vertically infilled samples, however, the overall trend is similar. At 16wt.% GNPs, the electrical conductivity of horizontally infilled samples is approximately the value of Germanium, a classical semiconductor element. The thermal conductivity of samples were measured by a thermal camera while the samples were heated for a fixed interval of time. Thermal conductivity experiences minor increase as GNPs concentration increases. In comparison to pure PLA, 20wt.% GNPs samples are 350% as thermally conductive. Their thermal conductivity values are approximately the same as that of water at 50 Celsius degrees. This result support that an increase in the concentration of GNPs incurs an uplift in thermal conductivity. In the Instron test, the strain to stress diagram revealed the brittleness of high GNPs filling load samples. As the concentration of GNPs increases, the breaking elongation decreases, toughness decreases, and Young's Modulus increases. Such result suggests that at the microscopic level, GNPs block the entanglement between polymers in the composites, giving rise to the decrease in material ductility. We expect the ideal blend of PLA, PBAT, and GNPs H-5 to have the proportion between 12wt.% and 16wt.%. If the concentration of GNPs is above 16wt.%, the material will be too brittle according to the mechanical tests data. Otherwise, if the concentration of GNPs equals or is below 12wt.%, the electrical conductivity of the material will be comparatively low for practical use.

9:00 AM SF01.13.06

Printing Electronic Circuits and Devices via Hybrid Fused Filament Deposition of a TPU/Copper CompositeRemiRafael and Paddy K. L.Chan; Hong Kong University, Hong Kong

Printing metals and polymers together to form complex electronic devices is difficult due to the large difference in fusion temperature between those materials. In a previous article, we have introduced a hybrid printing technique based on the fused filament deposition of a copper-poly(lactic acid) composite followed by a step of laser sintering, to produce a conductive, porous copper material. This technology integrates together a conventional fused filament deposition printer and a 10-watt laser diode. The printer is used to deposit layer by layer a composite material containing a polymer matrix, copper, and copper oxide particles. After printing each layer, the laser diode is used to selectively sinter the composite. Under the effect of the laser, the polymer matrix is evaporated, and the copper oxide is reduced, forming a highly conductive, porous copper material. However, in our precedent experiments, the out-of-plane resistivity of this printed porous copper was high, and the applications were restricted to low dimensionality, 2.5D applications. More recently, we have investigated more composite materials and sintering conditions and developed a new TPU based composite. After sintering, this composite presents a resistivity as low as 10-5 Ω x cm in the in-plane direction and 10-4 Ω x cm in the transverse direction. As a result, we can now design and print completely embedded 3D electronic circuits and complex electronic components. We demonstrate these capabilities by making an embedded 3D circuit controlled by capacitive sensors.

9:15 AM SF01.13.07

Printable Ionic Liquid/Polymer Hybrid Materials for Sensors Applications DanielaCorreia¹, LilianaFernandes², NelsonPereira², MohammadTariq³, JoséEsperança³, CarmenR. Tubio⁴ and SenentxuLanceros-Mendez^{4,5}; ¹University of Minho, Portugal; ²Center of Physics, University of Minho, Portugal; ³Universidade Nova de Lisboa, Portugal; ⁴BCMaterials, Spain; ⁵Ikerbaske, Basque Foundation for Science, Spain

Multifunctional and smart materials are increasingly being required in nowadays society, needing a larger number and variety of sensors with improved performance, and more simple integration. Smart materials play an important role both in terms of economic aspects and sustainability, being suitable for a wide range of applications including sensors and actuators. In particular, printable smart and multifunctional materials allow novel applications, needed to fully take advantage of the Internet of Things (IoT) and Industry 4.0 concepts. The production of these materials through printing technologies allows to develop flexible and conformable devices.

The combination of different polymers with salts commonly defined as ionic liquids (ILs) have emerged as a promising approach in different fields, including in the field of sensors and actuators¹⁻³. ILs emerge therefore as an interesting approach to develop a new generation of materials with reduced environmental impact [1]. Further, ILs offer interesting and new possibilities to develop a wide variety of smart materials with different functionalities and properties (e.g. thermochromism, and high ionic conductivity) compatible with printing technologies [1].

In this work, the double functionality of ionic/polymer hybrid materials as humidity and thermochromic sensors is addressed. Humidity and thermochromic sensors have been developed based on different ILs and IL contents (5-20% wt.) of 1-butyl-3-methylimidazolium tetrachloroferrate ([Bmim][FeCl₄]) and bis(1-butyl-3-methylimidazolium) tetrachloronickelate ([Bmim]₂[NiCl₄]), respectively. The IL based inks have been prepared based on both into chemically, thermal and radiations matrix poly (vinylidene fluoride) (PVDF) as well as into sustainable bio-based polymer matrix (cellulose). The humidity sensing property of the [Bmim][FeCl₄] allows humidity sensors in the range from 35 to 90%, showing a linear resistance variation with increasing relative humidity. The sensitivity to humidity variations increases linearly with the IL content. The thermochromism of [Bmim]₂[NiCl₄] materials revealed a reversible thermochromism behavior (transparent to blue or vice versa) resulting from a thermally induced dehydration process, which promotes changes in the coordination number of Ni(II) from octahedral to tetrahedral structure. The developed materials represent a promising solution for the development of humidity, thermochromic and thermoresistive printable sensors, as demonstrated by the proof of concept applications that will be presented.

Acknowledgements

Portuguese Foundation for Science and Technology (FCT): UID/FIS/04650/2020, UID/QUI/00686/2020, UIDB/50006/2020, UIDP/50006/2020, 2022.05932.PTDC, PTDC/FIS-MAC/28157/2017, NORTE-01-0145-FEDER-000084, PTDC/CTM/4304/2020, and Investigator FCT Contract 2020.02915.CEECIND (D.M.C), SFRH/BD/145345/2019 (L.C.F). Spanish State Research Agency (AEI) and European Regional Development Fund (ERFD): PID2019-106099RB-C43/AEI/10.13039/501100011033. Basque Government Industry Departments: ELKARTEK.

References

1. D. M. Correia, L. C. Fernandes, P. M. Martins, C. García-Astrain, C. M. Costa, J. Reguera and S. Lanceros-Méndez, *Adv. Funct. Mater.* 30 (2020) 1909736.
2. L. C. Fernandes, D. M. Correia, C. García-Astrain, N. Pereira, M. Tariq, J. M. S. S. Esperança and S. Lanceros-Méndez, *ACS Appl. Mater. Interfaces.* 11 (2019) 20316-20324.
3. L. C. Fernandes, D. M. Correia, N. Pereira, C. R. Tubio and S. Lanceros-Méndez, *ACS Appl. Polymer Materials.* 1 (2019) 2723-2730.

9:30 AM SF01.11.04

Additive Manufacturing of Anisotropic Graphene-Based Composites for Thermal Management Applications ShaniLigatiSchleifer¹ and OrenRegev^{1,2}; ¹Ben Gurion University of the Negev, Israel; ²Ben-Gurion University of the Negev, Israel

The use of additive manufacturing (AM) for the rapid, facile creation of complex structures could provide thermal management solutions in the form of heat sinks and heat exchangers with high surface areas that facilitate heat dissipation. To prepare a heat sink with high thermal conductivity (TC), we use vat photopolymerization (VPP) of a polymer-based composite material with a low TC that is enhanced by loading with a graphene-based thermally conductive filler. Phase separation of the carbon-based filler, in this case graphene nanoplatelets (GNP), in the monomer printing solution is prevented by stabilizing the GNPs by the addition of a second fiber-like clay (sepiolite) filler, which traps the GNPs. This methodology enables the AM of a composite with a relatively high GNP concentration of 2.0 wt%, yielding a TC increase of 160% vs. the pristine polymer—an impressive accomplishment for VPP 3D printing. Moreover, this printing technique yields a material with anisotropic TC with a cross-plane/in-plane (TC_⊥/TC_∥) ratio of 1.6, which is beneficial for thermal management systems required to dissipate the heat vertically from a heat source. Such VPP 3D-printed composites with high and anisotropic TC could be applied in thermal management systems made of lightweight and cost-effective materials.

SYMPOSIUM SF02

Crystallization and Assembly at Interfaces—Fundamental Breakthroughs Enabled by Data-Centric Analysis and In Situ/Operando Techniques
November 27 - December 1, 2023

Symposium Organizers

Olaf Borkiewicz, Argonne National Laboratory
Jingshan Du, Pacific Northwest National Laboratory
S. Eileen Seo, Arizona State University
Shuai Zhang, University of Washington

* Invited Paper

+ JMR Distinguished Invited Speaker

SESSION SF02.01: Solidification from Disorder
Session Chairs: Jingshan Du and Zhiwei Li
Monday Morning, November 27, 2023
Sheraton, Second Floor, Republic A

10:30 AM SF02.01.01

Investigation of Faceted Solid-Liquid Interface Behavior During the Directional Solidification of Salol AnassyaRaad, NathalieBergeon, NathalieMangelinck-Noël and FatimaL. Mota; Aix-Marseille Université, IM2NP, UMR CNRS 7334, France

During solidification of materials, a microstructure forms at the solid-liquid interface that depends on both the physical parameters of the material (in particular the surface energy and kinetic

attachment anisotropies) and the processing parameters such as thermal gradient G , growth velocity v , and composition of the sample. The microstructure plays a critical role in determining the final properties of the material. One can distinguish two different macroscopic types of interface: rough where the kinetic attachment of atoms is fast and heat and solute diffusion in the liquid is dominant; and faceted where the kinetic attachment of atoms is anisotropic and slow and considered as the dominant effect. In this last, the crystals grow with smooth surfaces at the atomic scale, and facets at macroscopic scale. Despite numerous researches, particularly for semi-conductors such as silicon, the understanding of the faceted growth is still a significant challenge.

In this work, directional solidification experiments of organic transparent materials are used to evidence and analyze mechanisms involved during the growth of faceted solid-liquid interfaces. Such transparent model materials are chosen to have similar solid-liquid interface properties as technological materials studied, and thus to form similar microstructures, with the advantages of being transparent to visible light, so that common optical techniques can be used to follow their growth. We use salol, which is orthorhombic in structure and grows from its melt with a distinct macroscopic faceted interface because of its very high degree of anisotropy. Directional solidifications are performed in the ECODIS device a Bridgman furnace designed for thin samples geometries, equipped with an optical microscope to observe solid-liquid interface dynamics *in situ* and real time.

A highly faceted solid-liquid interface appears and keeps evolving till the end of the experiment. The facet angles are characterized and it shows that they correspond mostly to $\{111\}$ and $\{100\}$ crystallographic planes. Velocities of the different facets are measured and they vary with facet orientation relatively to the thermal gradient. These measurements allow to establish kinetic growth laws which depend on the crystallographic nature of the facet. Facets are also studied in terms of size evolution and distribution, which are affected by facet competition and interaction with defects.

10:45 AM SF02.01.02

Growth Dynamics of Three-Dimensional Grain Boundaries in Polycrystalline Solidification using DECLIC-DSI Facility Fatima L. Mota¹, Younggil Song², Kaihua Ji³, Damien Tournet⁴, Alain Karma³ and Nathalie Bergeon¹; ¹Aix-Marseille Université, IM2NP UMR CNRS, France; ²Lawrence Livermore National Laboratory, United States; ³Northeastern University, United States; ⁴IMDEA Materials Institute, Spain

Alloy microstructures formed by directional solidification are often polycrystalline, made up of a several large grains of different crystallographic orientations. Grain boundaries (GBs) have a crucial influence on the mechanical behavior of materials, by their peculiar interactions with dislocations, or by providing solute segregated regions prone to the formation of secondary phases. In technological alloys, GBs typically evolve in the solid state through a series of complex thermomechanical post-processes. However, their initial shape and existence goes back to the initial stage of solidification from the liquid phase. The importance of GBs is well-acknowledged at the macroscopic scale, and grain growth competition is already used in the design of technological components (e.g. grain selectors in single-crystal turbine blades). However, our understanding of GB selection during polycrystalline solidification remains qualitative at best, and a number of unanswered questions remain.

Until now, grains have been assumed to occupy distinct compact regions of 3D space separated by smooth borders on a scale larger than the cellular/dendritic array spacing. In this presentation, we report experimental observations revealing for the first time that cells from one grain can invade a nearby grain during polycrystalline growth. This unexpected invasion process causes grains to interpenetrate each other on the fine scale of the array spacing, and hence grain borders to become highly irregular. By computational modeling, we further reveal the ubiquitous nature of this invasion process by showing that it occurs for a wide range of grain misorientations beyond those studied experimentally. Those results fundamentally alter the traditional view that cellular/dendritic grains are distinct regions embedded in three-dimensional space.

Those unique observations are made possible by *in situ* visualization of the spatiotemporal evolution of the solid-liquid interface during directional solidification of a transparent organic alloy (Succinonitrile-0.24wt% Camphor) using the DECLIC-DSI experimental device installed onboard the International Space Station. Transparent alloys have similar solid-liquid interface properties as metallic alloys and thus form similar microstructures. The microgravity environment of the space station eliminates buoyancy-driven fluid convection and the associated large scale inhomogeneities of alloy composition, thereby facilitating quantitative comparisons with computational modeling in a purely diffusive regime.

11:00 AM SF02.01.03

Disorder to Order in Interface Patterns: Thermal Noise to Limit Cycle Transition in Dendrite Sidebranch Formation Trevor D. Lyons¹, Louise S. Little² and Rohit Trivedi³; ¹Northeastern University, United States; ²NASA, United States; ³Iowa State University of Science and Technology, United States

Thin sample directional solidification experiments have been carried out in the model succinonitrile-camphor system to examine the origin of secondary branches in dendrite morphologies. Thermal noise at the dendrite tip creates interface instabilities which amplify to form sidebranches. This is accepted as the primary mode of sidebranching in dendritic growth from an undercooled melt and occurs in directional solidification of dendrites. The proposed limit cycle couples the growth of the tip with the initiation of the sidebranch. Directional solidification of curved interfaces is a driven dissipative system with the potential to form a limit cycle. Two sets of experiments were performed, the first holding velocity constant and evolving the gradient and the second imposing oscillating velocities around the natural period of sidebranching. Both experimental methods were found to characterize a transition from disordered sidebranching induced by thermal noise to ordered sidebranching produced by the limit cycle mechanisms. This is the first quantitative measurement of previously hypothesized limit cycle growth.

These experiment sets have been quantitatively analyzed for dynamic behavior seen in limit cycles. High-quality data sets of the tip and instability enable the measurement of the FFT and analysis through a power spectrum. At low gradients, the sidebranches are found to be excited by thermal noise far away from the tip. As the gradient increases and velocity is held constant, the distance between the instability and tip decreases until limit cycle growth is found between the tip of the primary dendrite and the first forming sidebranch. An alternative to the deterministic limit cycles seen in experiments of gradient evolution is a limit cycle actively driven through the square wave oscillation of velocity. Crucial observations of the solidified microstructure conclude that this produced periodic interconnected bridges between the primary dendrites. This is a finding with potentially significant implications for commercial applications.

11:15 AM SF02.01.04

Direct Observation of Growth and Interfacial Dynamics of Ice Nanocrystals with Cryo-Electron Microscopy Minyoung Lee and Jungwon Park; Seoul National University, Korea (the Republic of)

Ice at low temperatures exhibit structural polymorphs including hexagonal ice, cubic ice, or a hetero-crystalline mixture of the two phases. These polymorphs coexist at a broad range of temperatures, but exhibit distinct growth kinetics. While numerous studies, mainly based on spatially-averaged techniques, have investigated the structural properties of ice formed at low temperatures, mechanisms behind the growths of coexisting polymorphs and their interfacial properties have been difficult to probe individually. Here, we use *in-situ* cryo-electron microscopy and computational ice-dynamics simulations to directly observe ice formation and growth amidst amorphous ice. We reveal that nanoscale ice crystals exhibit polymorph-dependent growth kinetics, with hetero-crystalline ice exhibiting anisotropic growth based on accelerated growth of the prismatic planes. Fast-growing facets are associated with low-density interfaces that possess high surface energy, driving tetrahedral ordering of interfacial water molecules and accelerating growth. Our approach in observing ice crystallization, based on nanoscale techniques, improve our understanding on early stages of ice formation and the mechanistic roles of ice interfaces, providing important insight into various fields such as ice physics, cloud physics, or designing cryoprotective molecules.

11:30 AM SF02.01.05

Phase-Field Modeling of Ice-Templated Hierarchical Structures Kaihua Ji¹, Mingwang Zhong¹, Kaiyang Yin², Louise S. Little³, Rohit Trivedi⁴, Ulrike G. K. Wegst¹ and Alain Karma¹; ¹Northeastern University, United States; ²University of Freiburg, Germany; ³NASA Marshall Space Flight Center, United States; ⁴Iowa State University, United States

Directional solidification of aqueous solutions and slurries in a temperature gradient has emerged as a promising method to produce cellular materials through a phase separation of solutes or suspended particles between growing ice lamellae. Those ice-templated cellular materials are hierarchically organized into a honeycomb-like porous structure on the largest scale, lamellar cell walls at an intermediate scale, and different unilateral surface features including ridges and other more complex shapes reminiscent of living forms that decorate the cell walls on a yet smaller scale. While the strong anisotropy of ice-crystal growth has been hypothesized to play a role in shaping those structures, the mechanism by which they form has remained elusive. We report the results of a detailed phase-field simulation study of ice templating of binary mixtures that reproduces the salient features of those cellular materials and that sheds light on the mechanism by which anisotropic ice crystal growth shapes their hierarchical structure. The simulation results reveal that the flat side of lamellae forms because of slow faceted ice-crystal growth along the c -axis, while weakly anisotropic fast growth in other directions, including the basal plane, is responsible for the unilateral features. Diffusion-controlled morphological primary instabilities on the solid-liquid interface form a cellular structure on the atomically rough side of the lamellae, which template regularly spaced ridges while secondary instabilities of this structure are responsible for the more complex features. The simulation results are compared with experimentally obtained results for directional freezing of binary water mixtures containing small solutes. Good quantitative agreement is found for the lamellar spacing that is shown to obey the scaling law $\lambda \sim (VG)^{-1/2}$, where V and G are the local growth rate and temperature gradient, respectively. Preliminary simulation results are presented that address the basic question of how other solvents such as DMSO, which exhibit different anisotropic crystal growth properties than ice, can produce a rich variety of hierarchical structures.

11:45 AM SF02.01.06

Ice Crystal Growth and the Dynamics of Ice Templating by X-Ray Tomoscopy Paul H. Kamm^{1,2}, Kaiyang Yin³, Tillmann R. Neu^{1,2}, Christian M. Schlepütz⁴, Francisco Garcia-Moreno^{1,2} and Ulrike G. K. Wegst^{5,2}; ¹Helmholtz-Zentrum Berlin für Materialien und Energie, Germany; ²Technische Universität Berlin, Germany; ³University of Freiburg, Germany; ⁴Swiss

The physics of ice-crystal growth from the liquid phase and the complex dynamics of microstructure formation by ice-templating during the directional solidification of aqueous solutions and slurries, also termed freeze casting, has to date received comparatively little research attention. Recent advances in synchrotron-based X-ray tomography, which is time-resolved X-ray tomography, enable us now to investigate in situ under well-defined experimental conditions the formation of the hierarchical architecture of freeze-cast materials. We can quantify in 3D ice crystal growth at high spatial and temporal resolution and observe the ice-templating mechanisms, which determine the morphology of the freeze-cast material. The performance-defining morphology is defined by a honeycomb-like material structure with lamellar cell walls that frequently are decorated with a range of unilateral surface features. Analyzing the tomography data, we can determine, which features of the freeze-cast materials are templated by the slow faceted growth along the c-axis of the hexagonal ice-crystal, and which are templated by the slightly anisotropic fast crystal growth along the preferred a- and t-axes, both of which are characterized by atomically rough ice-water interfaces. Additionally, we can observe, which role secondary instabilities play in the formation of cell wall surface features. Important advantages, which in situ X-ray tomography offers over post-mortem imaging and state-of-the-art simulation techniques, are that the dynamics of the structural evolution can be monitored over several minutes in a sample volume of several cubic millimeters so that also transient phenomena are captured.

SESSION SF02.02: Nanostructures
Session Chairs: Shengsong Yang and Mingyi Zhang
Monday Afternoon, November 27, 2023
Sheraton, Second Floor, Republic A

1:30 PM *SF02.02.01

Dodecahedral Silica Cages and Their Assembly at Liquid-Liquid Interfaces and in Inks for 3D Printing Ulrich Wiesner; Cornell University, United States

Crystallization and assembly at interfaces are hallmarks of biological systems and have provided inspiration for researchers world-wide to understand and control materials formation from the atomic scale all the way to the macroscale. This presentation will focus on the formation of silica nanocage structures with dodecahedral symmetry around spherical micelles (zero-dimensional, 0D) as well as their assembly at liquid-liquid interfaces (two-dimensional, 2D) and in inks for direct and internal three-dimensional (3D) printing. Detection of silica nanocage structures with dodecahedral symmetry and diameters around 10 nm has been enabled by the first application of machine learning enabled single-particle reconstruction of tens of thousands of cryo-electron microscopy images to materials discovery.¹ Synthesis of mesoporous silica at an interface between two immiscible solvents under conditions favoring the formation of 2D superstructures of silica nanocages leads to the thinnest mesoporous silica films synthesized to date.² It will be demonstrated how orientational correlations between nanocage units increases with increasing layer number controlled via pH, while swelling with oil and mixed surfactants increase micelle size dispersity, leading to complex clathrate type structures in multilayer superstructures. Mesoporous 2D superstructures can be fabricated over macroscopic film dimensions and stacked on top of each other to generate mesoporous heterostructures enabling potential separation and catalytic properties not achievable via conventional bulk syntheses. Finally, ultrasmall silica nanocages are combined with digital light processing (DLP) technique for the direct 3D printing of hierarchically porous parts with arbitrary shapes, as well as tunable internal structures and high surface area. Via versatile and orthogonal cage surface modifications, it will be shown how this approach can be applied for the implementation and positioning of functionalities throughout 3D printed objects. Taking advantage of the internal porosity of the printed parts, an internal printing approach is demonstrated for the localized deposition of a guest material within a host matrix, enabling complex 3D material designs.

REFERENCES:

- 1.) K. Ma, Y. Gong, T. Aubert, M. Z. Turker, T. Kao, P. C. Doerschuk, U. Wiesner, *Self-assembly of highly symmetrical, ultrasmall inorganic cages directed by surfactant micelles*, Nature **558** (2018), 577-580; DOI: 10.1038/s41586-018-0221-0.
- 2.) T. Aubert, K. Ma, K. W. Tan, U. Wiesner, *Two-dimensional Superstructures of Silica Cages*, Adv. Mater. **32**(2020), 1908362; DOI: 10.1002/adma.201908362.
- 3.) T. Aubert, J.-Y. Huang, K. Ma, T. Hanrath, U. Wiesner, *Porous Cage-derived Nanomaterial Inks for Direct and Internal Three-Dimensional Printing*, Nat. Commun. **11** (2020), 4695; DOI: 10.1038/s41467-020-18495-5.

2:00 PM SF02.02.02

The Effect of Flame Temperature on Structure of Ceria-Supported Pt Nanoparticles in Flame-Assisted Spray Pyrolysis Naoya Minegishi, Peizhou Li, Tsuyoshi Nagasawa and Hidenori Kosaka; Tokyo Institute of Technology, Japan

Supported metal catalysts are used in many applications such as combustion gas purification catalysts, gas reforming systems, and chemical product synthesis processes. Supported metal catalysts generally have a structure with high specific surface area and high dispersion of precious metal to improve catalytic activity and economic efficiency. One of the big challenges in these catalysts is to prevent deterioration of catalytic activity caused by thermal aging and following aggregation of precious metal nanoparticles in high-temperature environment. To achieve both high thermal stability and high catalytic activity, it is necessary to properly control the oxide and metal particle sizes and metal/oxide interface structure. However, in the case of wet processes such as the impregnation method, precise structural control requires complex multi-step processes, which can be disadvantageous toward practical application. The aim of this study is to synthesize supported metal catalysts with high catalytic activity and thermal stability in a simple process. For this purpose, we synthesized Pt/CeO₂ nanoparticles by flame-assisted spray pyrolysis using a burner diffusion flame, and the effects of material precursor concentration and flame conditions on the structure of the synthesized particles were investigated. In addition, the CO oxidation properties and thermal stability of the particles synthesized by flame-assisted spray pyrolysis were evaluated and compared with those of particles prepared by the impregnation method.

A coaxial flow diffusion flame burner with a double-tube structure was used for the particle synthesis experiments. A mixture of oxygen and nitrogen is supplied to the outer tube, and a mixture of nitrogen and methane containing a precursor solution atomized by an ultrasonic transducer (2.4 MHz) is supplied to the inner tube. The synthesized Pt/CeO₂ particles consisted of submicron-scale CeO₂ with 10 nm-scale Pt and aggregation of fine CeO₂ less than 10 nm with highly dispersed Pt (1 nm or less) [1]. When the flame temperature was varied by changing the ratio of oxygen and nitrogen supplied to the burner outer tube, more fine particles were produced at higher flame temperatures. Submicron-level particles may have formed by the droplet-to-particle route, in which the precursor droplets do not evaporate completely and nucleation occurs within the droplet. On the other hand, fine nanoparticles may have formed by the gas-to-particle route, in which the droplets completely evaporate and nucleation occurs in the gas phase. The evaporation of precursor droplets is enhanced at higher flame temperature, resulting in the shift of particle formation route from droplet-to-particle to gas-to-particle. The fine Pt/CeO₂ nanoparticles synthesized by the high-temperature flame showed CO catalytic activity comparable to that of particles prepared by the impregnation method. Moreover, the thermal stability of the Pt particles on CeO₂ by flame synthesis was better than that of the impregnation method.

References:

- [1] T. Nagasawa, K. Matsumoto, N. Minegishi, H. Kosaka, *Energy Fuels* **35**, 12380-12391 (2021)

2:15 PM SF02.02.03

Colloidal Metal-Halide Epitaxial Heterostructures: From Serendipity to Rational Design Stefano Toso¹, Muhammad Imran^{1,2}, Derek Dardzinsky³, Noa Marom³ and Liberato Manna¹; ¹Istituto Italiano di Tecnologia, Italy; ²University of Toronto, Canada; ³Carnegie Mellon University, United States

Colloidal epitaxial heterostructures are nanoparticles made of two crystalline materials connected at an interface. These architectures profitably combine the properties of their components, and can express unique ones stemming from their interactions. Historically, heterostructures have produced major breakthroughs in the field of colloidal nanomaterials, with core/shell quantum dots being the most renowned examples. Indeed, heterostructures are often grown from isostructural materials like CdSe/CdS, where the only requirements are similar lattice parameters. However, the increasing number of heterostructures reported between non-isostructural materials points to the limits of this design strategy. In this talk, we will take the serendipitous discovery of heterostructures between lead halide perovskites (CsPbX₃) and lead sulfosalts (Pb₃S₂X₂) as a case study. [1,2] We will first identify empirical criteria behind the formation of these heterostructures by comparing them with other interfaces formed by lead halides. [3] Then, we will exploit in-situ spectroscopies performed directly in the liquid reaction medium to gain insight into the growth mechanism of these composite nanomaterials. As a next step, we will take advantage of such knowledge to master the synthesis of two competing nanomaterials (Pb₃S₂Cl₂ vs Pb₃S₂Cl₂) by exploiting heterostructures as phase-selective reaction intermediates. [4] This approach is inspired by the retrosynthetic strategies typical of organic chemistry, and provides advanced control over the product of colloidal syntheses. Finally, we will rationalize these results with the help of a novel computational tool, which we designed

specifically for predicting the formation of stable colloidal epitaxial heterostructures. By providing fundamental insights into the growth mechanism and stability of colloidal nanocrystal heterostructures, we hope to lower the barrier that separates the widely appealing properties of these fascinating composite nanomaterials from real-world applications.

- 1) Toso, S. et al. Nanocrystals of Lead Chalcogenides: A Series of Kinetically Trapped Metastable Nanostructures. *Journal of the American Chemical Society* vol. 142 10198–10211 (2020).
- 2) Imran, M. et al. Halide Perovskite–Lead Chalcogenide Nanocrystal Heterostructures. *Journal of the American Chemical Society* vol. 143 1435–1446 (2021).
- 3) Toso, S. et al. Hidden in Plain Sight: The Overlooked Influence of the Cs+ Substructure on Transformations in Cesium Lead Halide Nanocrystals. *ACS Energy Letters* vol. 5 3409–3414 (2020).
- 4) Toso, S. et al. Halide perovskites as disposable epitaxial templates for the phase-selective synthesis of lead sulfochloride nanocrystals. *Nature Communications* vol. 13 (2022).

2:30 PM *SF02.02.04

Visualizing Interfacial Processes and Surface Instabilities in Nanoparticle Systems Through *In Situ* TEM and Artificial Intelligence Piyush Haluai¹, Adria M. Morales², Matan Leibovich², Mai Tan¹, Sreyas Mohan², Yifan Wang¹, Carlos Fernandez-Granda² and Peter A. Crozier¹; ¹Arizona State University, United States; ²New York University, United States

Interfacial processes control not only crystal growth but also crystal dissolution. For example, during classic nucleation and growth, nuclei are forming and dissolving in solution and only when a seed crystal grows above the critical size, can a larger crystal evolve. The structural evolution of a crystal surface may be strongly influenced by the ambient environment. In small nanoparticles (<5 nm) in the presence of a surface stimuli, such as gas or liquid ambient, the thermodynamic driving force to minimize surface energy is continuously perturbed due to the adsorption and desorption associated with molecular exchange processes. This leads to an evolving interfacial energy landscape with the system constantly “chasing” an elusive energy minimum. The nanoparticle surface is far from equilibrium, but local energy minima give rise to a variety of short-lived metastable states. There is considerable interest in exploring the system evolution as it transitions between stable and less stable surface configurations. Not only is this of fundamental interest to materials science, but it may impact applications in fields where surface reactivity is important such as catalysis and corrosion. The recent development of direct electron detectors with high sensitivity and fast readout rates together with advances in AI based denoisers [1] now makes it possible to perform atomic resolution exploration of nanoparticle surface processes with time resolutions ultimately limited by detector readout speeds (0.0001 – 0.001 s is now common). We are investigating the surface dynamics of Pt nanoparticles with temporal resolutions of ~0.01 s under different ambient conditions. Typical kinetic pathways are observed to follow elementary surface transformation steps including atom column activity (e.g., adatom migration, adatom fluxionality, surface layer growth, surface layer fluxionality, surface layer removal), shearing (e.g., surface shear, subsurface shear creating or annihilating stacking faults). Since there is a tight connection between the surface and subsurface structure in small particles, instabilities in the surface structure can trigger instabilities in the entire nanoparticle crystal. The relationship between these different metastable states and kinetic pathway will be discussed in the presentation.

References

- [1] Sheth, D.Y., et al. *Unsupervised deep video denoising*, in *Proceedings of the IEEE/CVF International Conference on Computer Vision*. 2021, pages: 1759-1768
- [2] We gratefully acknowledge the support of the following NSF grants to ASU (OAC 1940263, 2104105, CBET 1604971, and DMR 184084 and 1920335) and NYU (HDR-1940097 and OAC-2103936). We also acknowledge the support from DOE grant BES DE-SC0004954. The authors acknowledge HPC resources available through ASU, and NYU as well as the John M. Cowley Center for High Resolution Electron Microscopy at Arizona State University.

3:00 PM BREAK

3:30 PM *SF02.02.05

Observing Crystal Nucleation on Graphene via High-Speed Atomic-Resolution TEM Won Chul Lee¹, Jungwon Park² and Peter Ercius³; ¹Hanyang University, Korea (the Republic of); ²Seoul National University, Korea (the Republic of); ³Lawrence Berkeley National Laboratory, United States

Nucleation in atomic crystallization remains poorly understood despite advances in classical nucleation theory. The nucleation process has been described to involve a non-classical mechanism including a spontaneous transition from disordered to crystalline states, but a detailed understanding of dynamics requires further investigation. Here, using in-situ transmission electron microscopy of heterogeneous nucleation of individual gold nanocrystals with millisecond temporal resolution, we show that the early stage of atomic crystallization proceeds through dynamic structural fluctuations between disordered and crystalline states, rather than through a single irreversible transition. Our experimental and theoretical analyses support that structural fluctuations originate from size-dependent thermodynamic stability of the two states in atomic clusters. These findings, based on dynamics in a real atomic system, reshape and improve our understanding of nucleation mechanisms in atomic crystallization.

4:00 PM SF02.02.06

The Onset of Crystallization of Aerosol Au Nanoparticles Yi Wang¹, Sotiris E. Pratsinis¹ and Eirini Goudeleli²; ¹ETH Zürich, Switzerland; ²The University of Melbourne, Australia

Gold nanoparticles have versatile applications in catalysis, chemical and biological sensing, medicine (drug carrier, therapeutic agents and gene delivery), nanolithography and microelectronics [1]. The performance of these nanoparticles is heavily influenced by their crystalline characteristics. Even though Au nanoparticles are routinely made in the liquid phase, their gas-phase (aerosol) synthesis is most attractive for its proven scalability (25 t/h) and high-purity products (i.e. optical fibers) [2]. During aerosol synthesis, the formation of particles occurs at high temperatures, steep cooling rates and short residence times that affect considerably nanoparticle characteristics, including their crystallinity, size, and morphology [3].

Here, the gas-phase crystallization of Au nanoparticles is investigated by molecular dynamics (MD) using the embedded atom method (EAM) that is most relevant to their synthesis by aerosol processes (flame, plasma, laser, etc.). We elucidate the onset of crystallization and growth dynamics of 2.5 – 11 nm Au nanoparticles under isothermal conditions.

The relationship between Au melting point and particle size is used to validate the method. A metastable region of 200 - 300 K wide between the melting point and super-cooled solidifying temperature of Au is revealed as a function of particle size. The crystalline disorder parameters and potential energy are used to elucidate the isothermal crystallization dynamics of Au nanoparticles in three distinct stages at 500 – 800 K (subcritical cluster dynamics, onset of crystallization and crystal growth). The degree of crystallization (predominantly face-centered cubic (FCC) with some hexagonal close-packing (HCP)), is quantified from the local crystalline disorder. In the first stage, before the onset of crystallization, subcritical Au cluster form and deform continuously similar to the subcritical nucleation dynamics of liquid (i.e. water) droplets in the atmosphere. The onset of crystallization is detected by the steep rise of the retained atoms fraction (RAF) of the largest subcritical cluster. This increase is accompanied by a sharp drop of the amorphous fraction of the Au nanoparticle.

In the second stage, crystallization usually starts from the nanoparticle surface as a result of lower kinetic energy barriers there. 3D-snapshots of the Au particle reveal two crystallization nucleation pathways: (A) Catastrophic nucleation when crystallization takes place well below the Au supercooled solidifying temperature resulting in many small crystal domains within the nanoparticle; and (B) Accretion nucleation when crystallization takes place at temperatures near the super-cooled solidifying temperature where fewer nanocrystals are formed that gradually coalesce into larger crystal domains.

In the third stage, after the onset of crystallization, crystals grow via both accretion and cluster merging, with crystal domain reorganization after the crystalline transformation is completed. X-ray diffraction (XRD) patterns are generated, from which the dynamics of crystal growth are elucidated and compared to direct tracing of crystal sizes. The product crystal size is influenced largely by crystallization temperature, with the largest crystal size obtained when crystallization takes place near the supercooled solidifying temperature consistent with the literature [4].

The results of this study can facilitate the process design for aerosol synthesis of Au as well as other metal nanoparticles for optical, electronic, catalytic and biomedical applications.

- [1] Goudeleli, E. and Pratsinis, S. E. (2016). *AIChE J.* 62: 589-9.
- [2] Kelesidis G.A. and Pratsinis S.E. (2021). *Chem Eng J.* 421:129884.
- [3] Pratsinis, S. E., Zhu, W. and Vemury, S. (1996). *Powder Technol.* 86: 87-93.
- [4] Belahmar, A. and Chouiyakh, A. (2016). *J. Nanosci. Nanotechnol.* 2: 100-103.

4:15 PM SF02.02.07

Ni Nanostructures Formed via pH-Dependent Corrosion-Redeposition of Thin Nickel Films in Glycine-Based Solutions Ayrón A. Lima¹, Duber M. Murillo¹, Antonio Augusto G. von Zuben¹, Douglas S. de Oliveira² and Monica A. Cotta¹; ¹University of Campinas, Brazil; ²Federal University of Paraná, Brazil

Nickel (Ni) is an interesting material for several applications, due to qualities including resistance to high temperature, oxidation, and corrosion, which are also present at the nanoscale. In particular, Ni nanowires show many applications in biology, optical devices, solar cells, and sensors, among others. Ni nanostructures have been created so far using a variety of methods, including hydrothermal, laser ablation, and chemical vapor deposition techniques. In this study, we investigate the fabrication of Ni nanostructures via local corrosion of thin Ni films

deposited by physical vapor deposition. Slow Ni corrosion is achieved using water, glycine, and calcium chloride static solutions with various pH levels. After a considerable amount of time (24–48 hours) of contact between the Ni film and the solution, micron-sized, roughly circular isotropic corrosion patterns are observed. Scanning Electron Microscopy (SEM) images show that nanostructures form inside the corrosion patterns. Typically, a nanowire-like structure extends vertically from the center of most patterns; for those with larger diameters, very thin planar nanowires extend from this central structure. SEM-based Energy Dispersive Spectroscopy measurements reveal that the central nanostructure is made of Ni, while the composition of the thinner, planar nanowires cannot be resolved using this technique. Our findings via simulations suggest a process of corrosion starting at specific locations such as film defects, with subsequent Ni redeposition due to a radial Ni concentration gradient at the metal film-solution interface. Further studies should determine if this process can be made controllable as a new synthesis process of Ni nanostructures.

4:30 PM *SF02.02.08

Operando Catalysis Studies from Model Systems to Real Catalysts [Andreas Stierle](#)^{1,2}; ¹DESY, Germany; ²University of Hamburg, Germany

The atomic structure determination of nano-objects with dimensions in the sub-100 nm regime is a formidable task for today's diffraction, imaging and scanning probe techniques. A detailed structural and compositional analysis is mandatory for a correlation with the nano-object's functionality e.g. as heterogeneous catalysts, magnetic storage material or light emitting device. In conventional x-ray diffraction experiments on powder samples the structural analysis is hampered by a random nanoparticle orientation and often by background scattering from the supporting material. We have therefore focused on the development of model systems based on epitaxial metal nanoparticles on single crystal oxide supports, which can be studied under ambient pressure catalytic reaction conditions. In the first part of my talk I will present different ensemble averaging synchrotron radiation based x-ray diffraction schemes. They deliver quantitative information on the nanoparticle size, shape and facet surface structures under operando reaction conditions for CO oxidation using high resolution reciprocal space mapping and high energy x-ray diffraction [1-4]. In the second part I will focus on experiments overcoming the ensemble average by single nanoparticle imaging and I will discuss future possibilities exploiting the high coherence of high energy photons available at fourth generation synchrotron radiation sources [5].

References:

- [1] P. Nolte, A. Stierle, N. Y. Jin-Phillipp, N. Kasper, T. U. Schulli, H. Dosch, Science 321, 1654-1658 (2008).
- [2] U. Hejral, D. Franz, S. Volkov, S. Francoual, J. Stempfer, and A. Stierle, Phys. Rev. Lett. 120, 126101 (2018).
- [3] J. Gustafson, M. Shipilin, C. Zhang, A. Stierle, U. Hejral, U. Ruett, O. Gutowski, P.-A. Carlsson, M. Skoglundh, E. Lundgren, Science 343, 758 (2014).
- [4] U. Hejral, P. Müller, O. Balmes, D. Pontoni, A. Stierle, Nature Communications 7, 10964 (2016).
- [5] Y. Y. Kim, T. F. Keller, T. J. Goncalves, M. Abuin, H. Runge, L. Gelisio, J. Carnis, V. Vonk, P. N. Plessow, I. A. Vartanians, A. Stierle, Sci. Adv. 7 eabh0757 (2021).

SESSION SF02.03: *In Situ* Microscopy Advances
Session Chairs: Alexandre Foucher and Shuai Zhang
Tuesday Morning, November 28, 2023
Sheraton, Second Floor, Republic A

8:30 AM *SF02.03.01

An *In Situ* Look at Interfacial Controls on Crystal Nucleation and Assembly [James J. De Yoreo](#)^{1,2}; ¹Pacific Northwest National Laboratory, United States; ²University of Washington, United States

Interfaces play a critical role in solution-based phenomena, such as ion segregation, mineral nucleation, and biomolecular and colloidal self-assembly. The interface alters the distribution of water and ions from that of the bulk, introduces an interfacial free energy that largely determines the free energy barrier for nucleation, and creates an entropic repulsion that acts like a volume exclusion force to drive colloidal assembly. The origin and characteristic length scales of these phenomena are inherently atomic-to-molecular but are manifest in ensemble dynamics and outcomes. Moreover, processes like nucleation and self-assembly arise from fluctuations, making the events that must be probed transient in nature. Consequently, *in situ* imaging techniques that can capture structure and its evolution, particularly at high speed and atomic-to-nm resolution, are required to build a quantitative picture of such processes. Here I use examples from and *in situ* TEM, high-speed AFM, and fast force mapping studies of interfacial structure, nucleation, and nanoparticle assembly to elucidate the mechanisms by which interfaces direct these processes, leading to unique pathways, materials and morphologies. The results reveal the importance of surface charge, organic ligands, chemical gradients, and solvent organization near interfaces in determining how ordered solids emerge from the solution.

9:00 AM SF02.03.02

Solvation Directed Dimensionality and Hierarchy Control in Solution Synthesis of Nanomaterials [Maria Sushko](#), Lili Liu and Duo Song; Pacific Northwest National Laboratory, United States

The development of structural hierarchy on various length scales during crystallization process is ubiquitous in biological systems and is common in synthetic nanomaterials. The driving forces for the formations of complex architectures range from local interfacial interactions, that modify interfacial speciation, local supersaturation, and nucleation barriers, to macroscopic interparticle forces. Although it is enticing to interpret the formation of hierarchical architectures as the assembly of independently nucleated building blocks, often crystallization pathways follow monomer-by-monomer addition with structural complexity arising from interfacial chemical coupling and strongly correlated fluctuation dynamics in the electric double layers. Here, we show that the development of structural hierarchy through heterogeneous nucleation is driven by dipolar and solvation forces. Specifically, coupled simulations and experimental studies revealed that dipole build up along the slow growth direction can trigger twinning and the development of branched architectures. Enthalpic solvation interactions were shown to either enhance or reduce the dipole moment of the nanoparticles and, thereby, control crystal morphology and architecture. The systematic studies of chemical coupling between different solvents and undercoordinated surface atoms of the growing nanocrystals revealed the mechanism of dimensionality control and the development of structural hierarchy in the absence of ligands or structure-directing agents.

9:15 AM *SF02.03.03

4D Structures of Colloidal Nanoparticles using Graphene Liquid Cell TEM and Self-Supervised Machine Learning Analysis [Jungwon Park](#); Seoul National University, Korea (the Republic of)

Colloidal nanocrystals containing a few tens to hundreds of atoms have applications in a range of areas, from electronics to catalysis and biological sensors. This versatility stems from the high sensitivity of nanocrystal properties to size, chemical composition, and shape, which are largely determined by the synthesis route by which they are produced. However, structure characterization based on bulk-originating methods is usually not enough because of the unique structural characteristics emerging at the nanoscale. Exposed surfaces, defects, dislocations, and quantum effects are dominant in nanocrystals of finite size. In addition, the ensemble of nanocrystals produced from conventional colloidal synthesis displays a large degree of heterogeneity in the atomic structures and has the effects of organic ligands and solvent molecules. Thus, understanding the structures of nanocrystals at a level where fundamental structure-property relationships can be linked requires new analysis methods that allow precise and reproducible determination of the positions of the constituent atoms of single nanocrystals directly from the solution phase. We developed a "one-particle Brownian 3D reconstruction method" for the analysis of the three-dimensional (3D) structures of colloidal nanocrystals based on graphene liquid cell electron microscopy. "One-particle Brownian 3D reconstruction" can be applied to not only uni-component metallic nanoparticles but also multi-component nanoparticles such as CdSe, PbSe, and FePt. We further extend 3D structure characterization approach to time-resolved domain such that colloidal nanoparticles undergoing structural transition in solution can be captured in time-resolved 3D resolution. To enable 3D and 4D reconstruction of colloidal nanoparticles directly from liquid phase TEM imaging, a series of large image data processing, a part of which is potentially enhanced by machine-learning based data analysis, is developed.

9:45 AMBREAK

10:15 AM *SF02.03.04

Observation of Amorphous-To-Crystalline Transition at the Single-Atom Level [Jianwei \(John\) Miao](#); University of California Los Angeles, United States

The amorphous-to-crystalline transition is fundamental to many physical, chemical and biological phenomena, but is a challenging process to study at the atomic scale. An approach to overcome this challenge is atomic electron tomography (AET) (1). AET combines high-resolution tomographic tilt series with advanced computational algorithms to resolve the three-

dimensional (3D) atomic structure of materials without assuming crystallinity (2). We have recently advanced AET to determine the 3D atomic structure of amorphous materials and characterize the short- and medium-range order of the 3D atomic arrangement (3,4). In this talk, I will present our most recent results on the application of AET to observe the amorphous-to-crystalline transition in 3D at the atomic resolution. By using a carbothermal shock method (5), we trapped high entropy alloy nanoparticles at different stages of crystallization. We then used AET to determine the 3D atomic structure of the high entropy alloy nanoparticles as a function of crystallization. By quantitatively characterizing the 3D atomic arrangement inside a large number of nuclei, we observed crystal nucleation pathways at the single-atom level. We expect that these experimental results not only open the door to study the amorphous-to-crystalline transition at the atomic scale, but also could transform our fundamental understanding of nucleation and crystal growth.

1. J. Miao, P. Ercius and S. J. L. Billinge. Atomic electron tomography: 3D structures without crystals. *Science* **353**, aaf2157 (2016).
2. J. Zhou, Y. Yang, Y. Yang, D. S. Kim, A. Yuan, X. Tian, C. Ophus, F. Sun, A. K. Schmid, M. Nathanson, H. Heinz, Q. An, H. Zeng, P. Ercius & J. Miao. Observing crystal nucleation in four dimensions using atomic electron tomography. *Nature* **570**, 500-503 (2019).
3. Y. Yang, J. Zhou, F. Zhu, Y. Yuan, D. Chang, D. S. Kim, M. Pham, A. Rana, X. Tian, Y. Yao, S. Osher, A. K. Schmid, L. Hu, P. Ercius and J. Miao. Determining the three-dimensional atomic structure of an amorphous solid. *Nature* **592**, 60–64 (2021).
4. Y. Yuan, D.S. Kim, J. Zhou, D.J. Chang, F. Zhu, Y. Nagaoka, Y. Yang, M. Pham, S. J. Osher, O. Chen, P. Ercius, A. K. Schmid and J. Miao. Three-dimensional atomic packing in amorphous solids with liquid-like structure. *Nature Mater.* **21**, 95–102 (2022).
5. Y. Yao, Q. Dong, A. Brozena, J. Luo, J. Miao, M. Chi, C. Wang, I. G. Kevrekidis, Z. J. Ren, J. Greeley, G. Wang, A. Anapolsky and L. Hu. High Entropy Nanoparticles: Synthesis-Structure-Property Relationships and Data-Driven Discovery. *Science* **376**, eabn3103 (2022).

10:45 AM *SF02.03.05

In Situ and Operando Multimodal Chemical Imaging of Materials InterfacesXiao-Ying Yu; Oak Ridge National Laboratory, United States

In situ and operando imaging is imperative in capturing material structural and compositional changes in working conditions as those in the real world. Development and integration of novel microfluidics and nanofluidics have significantly revolutionized nanoscale and microscale chemical imaging using electron microscopy (EM), offering morphological and elemental information of materials dynamically. Other advanced imaging and spectroscopy techniques offer additional insights into the material evolution besides EM. Among them, mass spectrometry (MS) and mass spectral imaging (MSI) provide attractive features and advancement in information depth and data volume of materials and interfaces dynamically. We developed a vacuum compatible microfluidic interface, System for Analysis at the Liquid Vacuum Interface (SALVI), to enable direct observations of the vacuum - liquid interface approximating the air - liquid and the solid - liquid interface using in situ time-of-flight secondary ion mass spectrometry (ToF-SIMS), scanning electron microscopy (SEM), vacuum ultraviolet single photon ionization mass spectrometry (VUV SPI-MS), nuclear magnetic resonance (NMR), and a multitude of spectroscopy and microscopy tools. In this talk, I will present a few examples including: 1) air - liquid interfaces in biology and the environment (e.g., single cells, biofilms, particles); 2) liquid - liquid interfaces in novel materials (i.e., CO₂ capture solvents, emulsions); and 3) solid - liquid interfaces using *in operando* imaging (i.e., redox reactions, lithium sulfur battery electrolyte). In situ multimodal chemical imaging capabilities lead to new directions and understanding in biological, environmental, and materials sciences.

11:15 AM SF02.03.06

Probing the Mass Transport in Iron-Air Batteries using Operando Electrochemical Transmission Electron MicroscopyHanglong Wu¹, Joseph S. Manser², Maria Ronchi², Jeff Poirier², Yet-Ming Chiang^{1,2} and Frances M. Ross¹; ¹Massachusetts Institute of Technology, United States; ²Form Energy, United States

In a rechargeable battery, the transport of ions between the electrode and the electrolyte plays a crucial role in governing electrochemical kinetics and can strongly influence the battery performance. Studying the diffusion of metal ions during battery operation is therefore important in developing new battery designs aimed at mitigating existing technical challenges associated with mass transport, such as dendrite growth. To date, a wide range of techniques, including X-ray/neutron imaging, NMR spectroscopy, and electrochemical impedance spectroscopy, have been developed to study the diffusion phenomena of metal ions under operando conditions. Nevertheless, the experimental determination of the nanoscale spatial distribution of ionic concentration gradients remains a challenge.

Rechargeable alkaline iron-air batteries have recently emerged as the leading candidate for long-duration energy storage due to their environmental friendliness, low cost, safety, and scalability. Although the reverse rusting of iron in alkaline electrolytes has been extensively investigated over the last five decades, the transformation pathways of iron species during this process are still under debate. Specifically, the role of diffusion gradients of the initially formed soluble HFeO₂⁻ species in governing the precipitation of amorphous Fe(OH)₂ passivation layers during anodic reactions remains poorly understood.

Here we present the use of operando electrochemical transmission electron microscopy (EC-TEM) as a probing technique to investigate the diffusion gradient during battery operation. Using the iron-air battery as a case study, we focus on studying the concentration gradient of the soluble iron ions, i.e., HFeO₂⁻, formed during the anodic dissolution of body-centered cubic (BCC) iron at pH 14. We first discuss the importance of electrolyte volume in mitigating the ion diffusion limitations within the confined cell to achieve reproducible cyclic voltammograms. Subsequently, by manipulating the positioning of one or multiple counter electrodes (CE) relative to the iron anode along the electrolyte flow channel, we observe that iron dendrites can grow on these CE electrodes during battery discharge. The concentration gradient of HFeO₂⁻ can therefore be estimated by quantifying the size/mass of these dendrites as a function of the distance from the anode. Our findings suggest that EC-TEM could serve as a useful tool for comprehending the effects of local ion concentration on the morphological evolution of the electrodes in the various battery systems during charge and discharge processes.

11:30 AM *SF02.03.07

Cinematographic Recording and Analysis of the Whole Process of Crystal Nucleation/Growth at Millisecond Sub-Angstrom ResolutionEiichi Nakamura; The University of Tokyo, Japan

Chemical phenomena are complex events where a variety of molecules stochastically appear on time scales ranging from nanoseconds to hours. Studying the stochastic behavior of individual molecules requires unconventional methods that differ from the traditional ensemble- and time-averaged experimental techniques. Crystal nucleation/growth is no exception. Since 2004, we have spent considerable effort on developing the SMART-EM technique (Single Molecule Atomic Resolution Time-resolved Electron Microscopy, ref 1, 2). In this talk, I will discuss the cinematographic recording of the whole process of the nucleation and growth of NaCl crystal (ref 3, 4) and of the PAN carbon fiber formation by pyrolysis of polyacrylonitrile (ref 5). We are transforming chemistry from the macroscopic paradigm of thermodynamics to the microscopic statistical mechanical paradigm.

References

1. Imaging Single Molecules in Motion, M. Koshino et al., *Science*, 316, 853 (2007). DOI: 10.1126/science.1138690
2. Atomic-Resolution Transmission Electron Microscopic Movies for Study of Organic Molecules, Assemblies, and Reactions: The First 10 Years of Development, E. Nakamura, *Acc. Chem. Res.*, 50, 1281–1292 (2017). DOI: 10.1021/acs.accounts.7b00076
3. Capturing the Moment of Emergence of Crystal Nucleus from Disorder, T. Nakamuro et al., *J. Am. Chem. Soc.*, 143, 1763-1767 (2021). DOI: 10.1021/jacs.0c12100
4. Cinematographic recording of metastable floating island in 2-D and 3-D crystal growth, M. Sakakibara, H. Nada, T. Nakamuro, E. Nakamura, *ACS Cent. Sci.*, **8**, 1704-1710 (2022). DOI: 10.1021/acscentsci.2c01093
5. Wavy Graphene-Like Network Forming During Pyrolysis of Polyacrylonitrile into Carbon Fiber, T. Ishikawa, F. Tanaka, K. Kurushima, A. Yasuhara, R. Sagawa, T. Fujita, R. Yonesaki, K. Iseki, T. Nakamuro, K. Harano, and E. Nakamura, *J. Am. Chem. Soc.* DOI.org/10.1021/jacs.3c02504

SESSION SF02.05: Poster Session I: Crystallization and Assembly at Interfaces

Session Chairs: S. Eileen Seo and Shuai Zhang

Tuesday Afternoon, November 28, 2023

Hynes, Level 1, Hall A

8:00 PM SF02.05.01

Dynamic DNA Nanodevices with Switchable Optical PropertiesSoojung Lee¹, Jason Kahn², Daniel McKeen¹ and Oleg Gang^{1,2}; ¹Columbia University, United States; ²Brookhaven National Laboratory, United States

Advancements in DNA nanotechnology have opened up the ability to fabricate nanomaterials with dynamic properties for applications in optics, medicine, and electronics. Such properties are defined by precisely controlled arrangements of functional nanocomponents. However, there remains a continual challenge in gaining dynamic control of nanoscale materials. DNA-based self-assembly offers a promising approach to form switchable three-dimensional (3D) clusters and large-scale ordered nanostructures that can encapsulate, organize and manipulate various types of nanoscale objects through programmable interactions.

Here we study the assembly, reconfiguration and optical response of a nanoscale device with stimuli-responsive and switchable properties. We utilized a 3D polyhedral DNA frame to establish a system that can switch between different conformations that allow for the manipulation of nanoparticles. Our previous studies have demonstrated that the optical output of a binary self-assembled system composed of gold nanoparticles (AuNP) and quantum dots depends on the interparticle separation distance. With this as a reference, we designed a structurally switchable 3D DNA frame for nanoparticle repositioning. By utilizing a DNA motif that acts as a manipulator, we show an ability to pass molecular information over a distance of tens of nanometers on a frame. We used this principle to investigate how this DNA device is able to direct nanoparticle reconfigurations and induce different optical responses. Interactions between the plasmonic and fluorescent particles were explored by testing various system designs. The structural reconfiguration of the system was examined by electron microscopy and small-angle X-ray scattering (SAXS), while spectroscopic measurements were applied to correlated optical responses with structural switching.

8:00 PM SF02.05.02

Enhancing Biosensor Performance by Optimizing Surface Coverage of the Self-Assembled Monolayer[JaehyunKim](#), HonglinPiao, DaerlPark and Heon-JinChoi; Yonsei University, Korea (the Republic of)

Self-assembled monolayers (SAMs) are widely used in various fields such as nanotechnology, electronics, and biomedical applications. SAMs are a crucial component in the fabrication of biosensors, as they provide functional surfaces for the immobilization of biological recognition elements. However, non-uniform SAM coverage on biosensor substrates can lead to variability in detection and quantification, which can severely hamper the biosensor's performance. The method proposed in this research includes experimental SAM analysis and prediction of SAM formation results through fitted function. After fixing several deposition parameters such as concentration, temperature, we applied logistic functions to create a function for the deposition rate of SAMs. Using this function, deposition has clearly improved the uniformity of SAMs. This outcome, confirmed through various characterization techniques including atomic force microscopy (AFM), and X-ray photoelectron spectroscopy (XPS), leads to an enhanced biosensor performance in terms of sensitivity and selectivity. To validate the accuracy of our developed function, we employed a comparative approach using machine learning techniques. These techniques, known for their ability to predict complex patterns and interactions, served as a benchmark for our optimization function. Preliminary results indicate that the proposed function holds significant promise in optimizing SAM surface coverage, with performance comparable to or exceeding that of the machine learning models. The proposed methodology not only provides a more stable and predictable biosensor response but also contributes to the advancement in the broader field of biosensing technology. This new approach offers significant implications for the development of high-performance biosensors, enabling more precise and consistent biomedical diagnostics, environmental monitoring, and other related applications. We will show experimental evidences on our proposed approach from glucose monitoring system (GMS).

8:00 PM SF02.05.03

Temperature Measurements During Laser-Induced Graphitization of Polydimethylsiloxane[MasatoKai](#), ShuichiroHayashi, KenKashikawa and MitsuhiroTerakawa; Keio University, Japan

Laser-induced graphitization of polymers has attracted attention as a technique to simultaneously form and pattern graphitic carbon on and/or inside polymers. Depending on the laser parameters, the morphology and the crystallinity of the formed graphitic carbon vary with photochemical and photothermal effects. However, the mechanism of laser-induced graphitization of polymers has not been revealed in detail. In this study, we measure the temperature of a polymer's surface during laser-induced graphitization to investigate the relationship between the laser parameter and the characteristics of the formed structure with regard to photothermal effects. An organosilicon polymer, polydimethylsiloxane (PDMS), was irradiated with high-repetition-rate femtosecond laser pulses at different laser scanning speeds. The temperature of the PDMS surface was measured using a thermography camera. Plano-convex lenses were located between the irradiated surface and the thermography camera for micro-thermographic measurements with a spatial resolution of $\sim 40 \mu\text{m}$. The morphology of the formed structure was observed using scanning electron microscopy (SEM), and the crystallinity of the structure was analyzed using Raman spectroscopy, respectively. SEM observations showed that the cross-sectional area of the formed structure increased with the decrease in scanning speed, suggesting that the amount of the energy absorbed by PDMS was positively correlated with the number of irradiated pulses per spot. Furthermore, for significantly low scanning speeds, the formation of cracks was observed in the formed structures, which may be attributable to the laser ablation induced by the excessive amount of energy absorbed by PDMS. Raman spectra showed peaks at ~ 1350 , ~ 1600 , and $\sim 2700 \text{ cm}^{-1}$ that corresponds to the D, G, and 2D bands, respectively, indicating the formation of graphitic carbon. Also, a peak at $\sim 520 \text{ cm}^{-1}$ was observed in the obtained Raman spectra in the case of significantly low scanning speeds, indicating the formation of crystalline silicon. Taking the results of SEM observations into account, it can be assumed that crystalline silicon was formed owing to the high temperature induced by the excessive amount of energy absorbed by PDMS. It was confirmed in temperature measurements that the measured temperature increased with the decrease in the scanning speed, suggesting the increase in the amount of energy absorbed by PDMS with the increase in the number of irradiated pulses per spot. However, in the case of significantly low scanning speeds, the measured temperatures kept constant regardless of the scanning speed, indicating the saturation of the temperature of the laser-irradiated area. The saturation of the temperature at significantly low scanning speeds cannot be explained solely by the change in the amount of the energy absorbed by PDMS. One possible explanation for the saturation is the change in the energy diffusion property of the laser-irradiated area with the change in the morphology and the material composition. It can be suggested from the obtained SEM images that the bulk density of the laser-irradiated area may be changed with the formation of cracks, changing the energy diffusion property of the laser-irradiated area. Moreover, considering the obtained Raman spectra, the formation of crystalline silicon in addition to the graphitic carbon may change the energy diffusion property of the laser-irradiated area.

8:00 PM SF02.05.04

Assembly of Short-Sequence Amphiphilic Peptoids into Helical Nanostructures with Controllable Supramolecular Chirality[RenyuZheng](#)^{1,2}, MingfeiZhao³, JingshanDu², YichengZhou², ShuaiZhang¹, WenhaoZhou¹, AndrewFerguson⁴ and Chun-LongChen²; ¹University of Washington, United States; ²Pacific Northwest National Laboratory, United States; ³Los Alamos National Laboratory, United States; ⁴The University of Chicago, United States

A long-standing challenge in biomimetic research is to create sophisticated hierarchical nanostructures that mimic the biomaterials found in living organisms. Self-assembly is a crucial process for creating these nanostructures, but the forces and dynamics governing the self-assembly of biomacromolecules, such as proteins and peptides, are complex. Developing sequence-defined synthetic polymers with simplified molecular interactions is a promising approach to synthesizing information-rich nanostructures and understanding their self-assembly mechanisms. Peptoid is a peptidomimetic molecule that moves the side group from α -carbon to nitrogen to keep the sequence programmability while simplifying the structure without backbone hydrogen donors and no backbone chirality. Previous studies have shown that amphiphilic peptoids can crystallize into highly ordered nanostructures, including nanoribbons, nanosheets, nanotubes, and nanohelices, by controlling peptoid-peptoid and peptoid-substrate interactions. However, achieving the predictable self-assembly of peptoids into designed nanostructures remains a significant challenge. In this study, we report a system of short tetramer peptoids to form crystalline peptoid helices. Due to the reduced hydrophobic interactions compared to those with six hydrophobic side chains, we showed that the self-assembly of these peptoids into nanohelices and other nanostructures are highly sensitive to the solution ionic strength and solvent condition, resulting in the formation of various nanostructures including nanohelices, nanohelix bundles, as well as nanotubes. We also demonstrate the control of supramolecular chirality of self-assembled peptoid nanohelices by using chiral polar groups with D- or L-configuration. By combining the synchrotron XRD results with molecular dynamic simulation studies, we showed the twisted form of bi-layer structures of these amphiphilic peptoids are the most stable form for those polar side chains to hide hydrophobic domains in the aqueous environment. We further demonstrated that the organic cosolvent in the self-assembly could also affect the self-assembly morphology from nanohelices to nanotubes, which provides additional information on peptoid-solvent interactions as well as the self-assembly kinetics and thermodynamics. Our findings provide a facile system for controlling the twisting and stacking of peptoid amphiphiles into helical and tubular structures and suggest an approach for the precisely controlled synthesis of biomaterials.

8:00 PM SF02.05.05

Molecular Dynamics Characterization of Gas Diffusivity of CO₂-CH₄ in sI Clathrate Hydrates[AliBeydoun](#), AlejandroD. Rey and PhillipServio; McGill University, Canada

Clathrate hydrates are cage-like water structures entrapping a gaseous guest molecule in their cavities. The need for alternative fuel sources has spurred an interest in methane hydrates as estimates predict that they account for two thirds of the fossil fuel global reserves. However, their exploitation is not without fault as methane hydrates occupy a crucial role in stabilizing the soil as well as being a potential major source of greenhouse gases. Fortunately, methane found in clathrate hydrates can be swapped with carbon dioxide (CO₂), thus allowing for carbon sequestration, and rendering the production of methane effectively carbon neutral. The process has been shown to be feasible and resulting in the formation of stable CO₂ hydrates, but the mechanism surrounding the exchange remains to be elucidated.

This presentation focuses on a system where pure methane sI hydrates are exposed to a front of CO₂ dissolved in water. The system conditions are set to be favorable to the melting of methane hydrates and to the formation of CO₂ hydrates. As the system evolves with time, methane escapes the lattice and CO₂ diffuses into the latter, replacing methane in partially melted cages as well as forming new cages at the interface in a phenomenon known as co-growth. An analysis of the impact of temperature, pressure, and CO₂ concentration on the diffusivity of CO₂ and methane is conducted. It is followed by an analysis on how co-growth at the interface hinders diffusion and prohibits CO₂ from diffusing deeper in the lattice. Previous work found in the literature has quantitatively described the impact of such impediment on the ultimate replacement ratio, but the presented research is the first quantify the effect on mass diffusivity. This work will also discuss the impact of water vacancies and of gas occupancy on mass diffusivity. To understand the effects of vacancies and gas occupancy on the thermodynamics of the system, the Gibbs free energy, the enthalpy, and the entropy are calculated. Our previous work quantified diffusivity in a CO₂ filled hydrate system and the impact of such vacancies and serves as a basis

for comparison. The investigation also looks into how diffusion evolves from a non-Fickian process to a Fickian one. Finally, this work also tackles how the swapping mechanism between methane and CO₂ differs near the interface from deeper strata with the hole-in-cage model dominating the latter.

The methodology is based on molecular dynamics. The Large-scale Atomic/Molecular Massively Parallel Simulator (LAMMPS) is used to perform simulations on a 3x3x3 methane hydrate lattice juxtaposing a CO₂ front dissolved in water. The force fields used for methane, carbon dioxide, and water are OPLS-AA, EPM2, and TIP4P/ICE respectively. The LAMMPS software allows to quantify the mean squared displacement (MSD) which can be correlated to the mass diffusivity. Furthermore, LAMMPS computes primordial thermodynamics parameters such as the Free Gibbs energy, the entropy, and the enthalpy.

8:00 PM SF02.05.06

Investigation of the Amorphization Threshold by Ion Implantation as a Function of Energy and Implant Temperature in Silicon SubstratesAriannaRivera¹, NoelKennedy², ChristopherHatem² and Kevin S.Jones¹; ¹University of Florida, United States; ²Applied Materials, Inc., United States

As semiconductor devices continue to scale, ion implantation processes must follow suit to confine fabrication to nanosized structures. One such process is ion-beam induced amorphization, namely in silicon devices. Pre-amorphizing implants are known to increase dopant solid solubility once post-annealed, increasing the active carrier concentration within the recrystallized layer. Because of this, they are often incorporated during the processing of top-off implants, used to decrease contact resistance. The mechanism of silicon-substrate amorphization mechanism varies with ion mass but for heavier ions, it is associated with the overlap of damage cascades induced by nuclear stopping. As such, it should show little dependence on the surface. However, if the point defect accumulation mechanism associated with light ions is active, then the surface may play a role. To better understand the amorphization mechanism at ultra-low energies, the critical threshold for amorphization is investigated for different implant temperatures and energies. Silicon substrates were implanted with Si⁺ ions at low energies between 1 keV to 10 keV and implant temperature was varied ranging between 25°C to 150°C. The dose is kept constant at 3×10¹⁴ ions/cm² at a dose rate of 0.95 mA. The amorphous layer was studied by high resolution cross-sectional TEM and to SRIM simulations to determine the threshold damage density for amorphization. By studying the amorphization extent at varying energies and implant temperatures, it was possible to observe how the amorphization layer thickness produced by the implant differs as the damage becomes closer to the surface. It was found that as the implant energy decreased, the threshold damage density for amorphization increased, suggesting a shift in the amorphization mechanism possibly induced by an increasing role of the surface. The role of implant temperature will also be presented.

8:00 PM SF02.05.07

Enhancing the Self-Assembly of Binary Colloidal Crystals with ConfinementNathanHuang, RachaelS. Skye and JuliaDshemuchadse; Cornell University, United States

Photonic crystals with a bandgap in the visible-light range have been theorized to self-assemble from a binary colloidal dispersion but difficulties remain in robustly assembling high-quality crystals in quantities sufficient for large-scale applications. Computational methods give insight into the conditions under which photonic crystals can self-assemble. In this study, we performed hard-particle Monte Carlo simulations of tetrahedral and octahedral nanoparticles in spherical and flat-wall geometries to determine the influence of confinement on the process and products of crystallization compared to the bulk. Confinement was found to improve crystallization at non-ideal stoichiometries but did not lower the minimal packing fraction at which crystallization occurred throughout the system. Crystals formed under confinement exhibited higher crystallinity and lower quantities of secondary phase defects. These findings demonstrate the potential for enhanced control over the synthesis of novel materials with tailored structures and properties for photonic applications.

8:00 PM SF02.05.08

Valence State-Controlled Synthesis of Vanadium Oxide NanocrystalsMehnazTarannum and ShunjiEgusa; University of North Carolina at Charlotte, United States

Vanadium oxides are important materials with diverse applications, including catalysis, energy storage, and thermochromic devices. However, synthesis of vanadium oxide nanocrystals with a controlled valence state is a significant challenge due to the polyvalence of vanadium. In this work, we report a novel method for the valence-state controlled synthesis of vanadium oxide nanocrystals via a non-hydrothermal route. This method enables the synthesis of non-stoichiometric V₃O₅ (V⁴⁺ + V³⁺₂O₅) nanocrystals, first time in the anosovite phase – a rare form of vanadium oxide that was only recently discovered in bulk form. This is a significant accomplishment, as non-stoichiometric V₃O₅ is known to be difficult to synthesize due to the narrow allowances in the vanadium-to-oxygen ratio (1.666 – 1.668 ± 0.002). The crystal structures of the nanocrystals were confirmed using powder X-Ray diffraction technique. The electron microscopy images of the reaction intermediates at different time intervals during the nanocrystal formation revealed a slow nucleation process, followed by a subsequent fast growth via Ostwald ripening. We demonstrated formations of V₂O₃ nanocrystals (V⁵⁺ → V³⁺), in addition to the partial but precise reduction to V₃O₅ (3V⁵⁺ → V⁴⁺ + 2V³⁺) by controlling the vanadium precursor-to-alcohol-amine ratio. We assessed the reaction pathways by analyzing the reaction intermediates using Fourier transform infrared (FT-IR) spectroscopy. These studies are important to systematically understand the roles of different reaction parameters to establish a well-controlled synthesis of vanadium oxide nanocrystals.

8:00 PM SF02.05.09

Bimetallic ZnCo Metal-Organic Framework at NiCo-Layered Double Hydroxides for Multiple Storage and Capability Synergy All-Solid-State SupercapacitorsNagehK. Allam; American University in Cairo, Egypt

Rational design and structural regulation of hybrid nanomaterials with superior electrochemical performance are crucial for developing sustainable energy storage platforms. Among these materials, NiCo-layered double hydroxides (NiCo-LDHs) demonstrate an exceptional charge storage capabilities owing to their tunable 2D lamellar structure, large interlayer spacing, and rich redox electrochemically active sites. However, NiCo-LDHs still suffer from severe agglomeration of their particles with limited charge transfer rates, resulting in an inadequate rate capability. In this study, bimetallic ZnCo-metal organic framework (MOF) tripods were grown on the surface of NiCo-LDH nanowires, which significantly reduced the self-agglomeration and stacking of the NiCo-LDH nanowire arrays, offering more accessible active sites for charge transfer and shortening the path for ion diffusion. The fabricated hybrid ZnCo-MOF@NiCo-LDH and its individual counterparts were tested as supercapacitor electrodes. The ZnCo-MOF@NiCo-LDH electrode demonstrated a remarkable specific capacitance of 161 F g⁻¹ at 2 A g⁻¹ with an enhanced rate capability of 66% from 2 to 20 A g⁻¹. Moreover, an asymmetric all solid-state supercapacitor device was constructed using ZnCo-MOF@NiCo-LDH and palm tree-derived activated carbon (P-AC) as positive and negative poles, respectively. The constructed device can store a high specific energy of 44.5 Wh Kg⁻¹ and deliver a specific power of 876.7 W Kg⁻¹ with outstanding Columbic efficiency over 10,000 charging/discharging cycles at 15 A g⁻¹.

8:00 PM SF02.05.10

Substrate Van der Waals Force Effect on the Stability of Violet PhosphorousSarabpreetSingh¹, MahdiGhafarizadeh¹, Hsin-YuKo², SampathGamage¹, RobertA. DiStasio Jr², MichaelSnure³ and YohannesAbate¹; ¹University of Georgia, United States; ²Cornell University, United States; ³Air Force Research Laboratory, United States

vdWs interaction of exfoliable materials with the substrate and how this interface force influences the interaction of vdWs materials with the surroundings have yet to be well understood. Here, we experimentally and theoretically unravel the role of vdWs forces between the recently rediscovered wide band gap p-type vdW semiconductor violet phosphorus (VP), with various substrates (including, SiO₂, mica, Si, Au) and quantify how VP stability in air and its interaction with its surroundings is influenced by the interface force. Using a combination of infrared nanoimaging and theoretical modelling we find three main factors that influence how VP interacts with its surroundings: the vdWs force at the interface, the hydrophobicity of the substrate, and substrate surface roughness. We found that VP can maintain its stability for a prolonged period if it is exfoliated on SiO₂ substrate, followed by mica and Au substrates, and is least stable when placed on a Si substrate. Our results could guide in the selection of substrates when vdW materials are prepared and more generally highlight the key role of interface force effects that could significantly alter physical properties of vdWs materials.

8:00 PM SF02.05.11

Characterization of Adeno-Associated Virus Loading and Aggregation Through use of SEC-MALSStephenRosa and LanceKasper; Agilent Technologies, United States

In recent years, adeno-associated viruses (AAVs) have been seeing an increase in use as delivery vehicles for gene-therapy type applications due to their ability to infiltrate a wide host of different cell types and overall lack of pathogenicity. Characterization of these AAVs remains a challenge with most of the current techniques that are commonly available. Using our new 20 angle multi-angle light scattering detector (MALS) and WinGPC software, we demonstrate using different concentration detectors in conjunction with the MALS that it is possible to accurately measure the load factor of several different AAVs. Furthermore, we are also able to accurately measure AAV size in solution as well as any aggregation that is occurring within the system.

Using different chemistries, it is possible to measure the composition of these AAV particles. Our new WinGPC software automatically calculates the incorporation of each of these components using its co-polymer module. This allows us to accurately determine the load factor of the AAV. When coupled to light scattering, we can measure the absolute molecular weight average as well as the radius of gyration of the AAV system. This data can provide a complete picture of capsid loading, total capsids, and aggregation within the system, all run with a single SEC method.

8:00 PM SF02.05.13

Effect of Sulfate Regiosition on Ca²⁺-Heparin Binding Thermodynamics and Implications for Nucleation of Sparingly Soluble SaltsBrennaM. Knight, ConnorM. Gallagher,

Heparin is a sulfated glycomaterial of long-standing importance as an anticoagulant in biomedicine due to its antithrombin binding sequence. Many more protein binding sequences are identified in heparin and other glycosaminoglycans (GAGs) but are understudied relative to antithrombin. Heparin and sulfate-rich macromolecules are also widely associated with biological crystallization in diverse animals. However, the lack of systematic and quantitative studies is impeding the potential of furthering heparin applications as well as a mechanistic understanding of how functional groups modulate biomineralization. Using heparin as a model for understanding the role of sulfate groups associated with macromolecules in biological and synthetic settings, we test the hypothesis that the position of these groups influences Ca^{2+} binding to regulate calcite nucleation.

This experimental study employs isothermal titration calorimetry (ITC) to quantify the binding thermodynamics of Ca^{2+} -heparin interactions for a group of characterized heparin materials that differ by sulfate regioposition. Previous studies indicate Ca^{2+} -heparin interactions involve water molecule(s) and are independent of electrostatic interactions. Our preliminary ITC findings show the binding is entropically driven, supporting this model. We further observe sulfate position moderates $K_{\text{Ca}^{2+}}$, and dramatically alters binding stoichiometry.

In parallel experiments that measure the rate of nucleation of the sparingly soluble salt, CaCO_3 , onto the corresponding heparin materials, we are determining the relationship between sulfate position and the interfacial energy barrier to calcite crystallization (γ_{calc}). Initial results suggest materials that more efficiently bind Ca^{2+} (i.e., require fewer repeat units per ion) present a higher barrier to nucleation. To better understand this interaction, we are also determining the dependence of NMR relaxation time and chemical shifts on Ca^{2+} concentration. This study highlights the potential for using sulfate position to tune and optimize the design of heparin-based materials for advanced material design and biomedical applications.

SESSION SF02.06: Colloidal Particle Assembly
Session Chairs: Mihir Parekh and S. Eileen Seo
Wednesday Morning, November 29, 2023
Sheraton, Second Floor, Republic A

8:30 AM +SF02.06.01

DNA-Programmable Assembly in Bulk and at Liquid-Air and Liquid-Solid Interfaces Oleg Gang^{1,2}; ¹Columbia University, United States; ²Brookhaven National Laboratory, United States

Organizing diverse types of functional nanocomponents into the designed 3D architectures promises to enable new functions with a broad range of applications, from engineered biomaterials to photonic devices and energy materials. However, current methods are limited in their ability to create such 3D nanomaterials with prescribed structures and integration of different types of nanocomponents. Using sequence-specific interactions and structural plasticity of DNA we established a self-assembly platform for assembly of designed large-scale and finite-size nano-architectures from diverse inorganic and biomolecular nanocomponents. We applied in-situ and ex-situ methods to reveal the lattice formation processes in bulk and at the interfaces for DNA-programmable systems. By combining designed nanoscale anisotropic bonds and their DNA encoding, we developed assembly approaches that allow for the creation of periodic and hierarchical organizations from inorganic nanoparticles and proteins. The formed nanostructures were further transformed into inorganic 3D replicas via several nano-templating methods. The novel DNA-assembled nanomaterials were investigated for nano-optical, mechanical, electrical and biochemical functions. Furthermore, approaches for integration with surface-based devices were established.

9:00 AM SF02.06.02

Programmable Colloidal Kagome Superlattices for Anisotropic Light Emission Zhiwei Li and Chad A. Mirkin; Northwestern University, United States

DNA-mediated programmable assembly of nanomaterials has given rise to a diverse library of colloidal superlattices and crystals with precise phase and symmetry control. Design rules for colloidal crystallization have been extensively studied but most of them, regardless of structural complexity and phase diversity, are driven by thermodynamically favored processes that lead to maximum DNA hybridization and complete particle surface overlap. Here, we show that the assembly of non-space-filling bipyramids results in partial DNA surface matching and yields colloidal Kagome superlattices. In short, Au pentagonal bipyramids of different sizes are used as building blocks and modified with single-stranded DNA as programmable atom equivalents (PAEs). Driven by DNA hybridization, the bipyramids assemble into distorted Kagome lattices through partial surface matching, featuring shield-like lattices, lattice distortion, bipyramid twisting, and rhombohedral super unit cells. Characterization of these low-symmetry Kagome lattices reveals diverse lattice plasmon resonance modes, which are dependent on the light incident direction and polarization. We take advantage of the Kagome lattice plasmon resonance and report facet-dependent anisotropic light emission enabled by doping dyes into the Kagome lattices. Taken together, this work opens up new avenues towards designing and accessing exotic colloidal superlattices and thus new materials for anisotropic light emission, which has implications for emerging optical platforms such as coupled optics and sensing.

9:15 AM SF02.06.03

Mapping The Spatial Dependence of Surface Ligand Binding in Individual Nanoparticles Zhi Yang¹, Duaa Ansari^{1,2}, Manuel Pichardo¹ and Matthew Jones^{1,1}; ¹Rice University, United States; ²The University of Texas at Austin, United States

While it is well-appreciated that surface ligands bind preferentially to certain locations on an inorganic nanoparticle (e.g. tips vs. flat facets), a quantitative understanding of this phenomenon is lacking. In this work, ligands are "tagged" with small gold nanoparticles so that their spatially-resolved binding positions can be measured in Cryogenic Transmission Electron Microscopy (CryoEM) images. Labeled thiol ligands were then exposed to hexadecyltrimethylammonium bromide (CTAB) modified gold triangular nanoprisms, which present energetically distinct face, edge, and tip regions that we hypothesized would reveal different binding properties. By recording the relative positions of ~700 ligand binding events, an 3D energetic map of thiol chemisorption to gold nanoprisms could be generated, revealing a strong preference for edge and tip sites compared to {111} triangular faces. Interpreting these data as a thermodynamic measure of binding probability allows for the use of the Boltzmann distribution to calculate the Gibbs free energy differences between tips or edges relative to faces of -8.01 and -6.81 kJ/mol, respectively, from which relative binding constants can be calculated. This work establishes an experimental platform for quantifying the spatial preferences of ligand binding that, because of the superior resolution of modern TEM instruments, is limited in accuracy only by the effective size of the tag-ligand conjugate.

9:30 AM SF02.06.04

Interfacial Assembly of Ligand-Functionalized Nanoparticles into Low-Dimensional Architectures Yilong Zhou¹, Brian H. Lee¹, Tsung-Yeh Tang² and Gaurav Arya¹; ¹Duke University, United States; ²University of California, San Diego, United States

Self-assembly of nanoparticles (NPs) is a powerful approach for fabricating materials with unique architectures and properties. This is especially important for plasmonic, optical, and electronic applications where nanostructures need to be arranged in non-close packed clusters or periodic arrays to take advantage of the unique electromagnetic couplings that emerge from such arrangements. However, achieving unique and complex assemblies remains a challenging task. In this talk, I will demonstrate how fluid-fluid interfaces can be used to self-assemble ligand-functionalized NPs into exotic 1D and 2D architectures by harnessing the three-way competition between particle-particle interactions, particle-fluid surface energy, and fluid-fluid surface tension. I will begin by demonstrating via molecular dynamics simulations the interfacial assembly of binary systems of spherical NPs into open clusters, quasi-linear strings and networks, and layered structures [1]. Next, I will show how Monte Carlo optimization combined with analytical modeling of interfacial and interparticle interactions can be used to quickly map out the full repertoire of 2D NP superlattices achievable through this interfacial assembly approach [2]. I will also show how this approach can be extended to shaped NPs, where a range of periodic porous superlattices may be assembled from polymer-grafted nanocubes by controlling their orientation at the interface [3]. Lastly, I will discuss the development of multibody potential via a machine learning approach to elucidate the role of multibody effects in the self-assembly of polymer-grafted NPs [4]. Overall, our results suggest that the interfacial assembly approach could be a versatile platform for fabricating 1D and 2D colloidal assemblies of tunable structure and properties.

[1] T.-Y. Tang, Y. Zhou, and G. Arya. Interfacial Assembly of Tunable Anisotropic Nanoparticle Architectures. ACS Nano 2019, 13: 4111-4123.

[2] Y. Zhou and G. Arya. Discovery of two-dimensional binary nanoparticle superlattices using global Monte Carlo optimization. Nat. Commun. 2022, 13:7976.

[3] Y. Zhou, T.-Y. Tang, B.H.-J. Lee, and G. Arya. Tunable Orientation and Assembly of Polymer-Grafted Nanocubes at Fluid-Fluid Interfaces. ACS Nano 2022, 16: 7457-7470.

[4] Y. Zhou, S. Bore, A. Tao, F. Paesani, G. Arya. Many-body Potential for Simulating the Self-Assembly of Polymer-Grafted Nanoparticles in a Polymer Matrix. ChemRxiv 2023.

9:45 AM BREAK

10:15 AM *SF02.06.05

Growth Habits and Phonon Modes of Nanoparticle Superlattices Qian Chen; University of Illinois at Urbana-Champaign, United States

Growth habits of nanoparticle superlattices dictate major design parameters (for example, symmetry, morphology and surface structure) of crystalline materials and consequently their applications. Using liquid-phase TEM, we show that nanoparticles can follow four different growth habits during self-assembly as governed by nanoparticle interaction and mass transport, leading to distinct surface morphologies. Meanwhile, lattice relaxations at equilibrium are originated from nanoscopic springs and phonon vibrations, which we are able to map and quantify for the first time using single particle tracking and lattice dynamics theory for topologically-engineered nanoparticle superlattices. Our work paves the way for engineering geometries for applications of mechanical metamaterials.

10:45 AM SF02.06.06

Controlling Coulomb Interactions Among Nanoparticles to Achieve Novel Assembly and Crystallization Binay P. Nayak^{1,2}, Honghu Zhang³, Wei Bu⁴, Benjamin M. Ocko³, Alex Travesset^{1,2}, David Vaknin^{1,2}, Surya K. Mallapragada^{1,2} and Wenjie Wang²; ¹Iowa State University of Science and Technology, United States; ²Ames National Laboratory, United States; ³Brookhaven National Laboratory, United States; ⁴The University of Chicago, United States

Controlling interactions among nanoparticles is paramount to achieving assemblies vital to technologies seeking to exploit their novel collective properties. Although various techniques have been advanced, robust ones are necessary for upscaling nanoparticle assembly and crystallization. Here, we explore the self-assembly of binary nanoparticle superlattices (BNSLs) at a vapor/liquid interface by grafting gold nanoparticles (AuNPs) with end-charge-polyethylene glycol (PEG). The grafting PEG terminates with either COOH (negatively charged) or NH₂ (positively charged) end groups. Lowering the pH increases the positive charge of NH₂ (to form NH₃⁺) and decreases the negative charge of COO⁻ (to form COOH). Such control facilitates the formation of various two- and three-dimensional ionic-like superstructures of oppositely charged binary constituents either at the vapor/liquid interfaces or in bulk. Unlike traditional ionic crystals, this approach enables manipulation of the relative surface charge between the two constituents. We demonstrate this approach by using surface-sensitive synchrotron-based X-ray diffraction at grazing angles of incidence (GISAXS), X-ray reflectivity (XR), and SAXS, and establish the formation of distinct checker-board square and hexagonal lattice structures also by varying the molar ratios of the constituents. The main results of our study are summarized as follows: 1) For 1:1, 2:1, and 1:4 mixing ratios (-COOH: NH₂ terminated-PEG), a checker-board square lattice structure is formed at various pH values. 2) For the 2:1 mixing ratio, lowering the pH transforms the structure from a checker-board structure to a hexagonal superstructure. 3) In the case of extremely low pH, whereas the NH₂ terminated nanoparticles are water soluble, the -COOH terminated forms a single-particle hexagonal structure similar to neutral PEG-grafted AuNPs at the vapor/liquid interface. Our results confront zeta-potential measurements that determine the total charge of each particle. This qualitatively allows for a quick prediction of outcome structures based on pH and the molar mixing ratios. SAXS measurements show executive super-ionic structures in bulk consistent with interfacial observations.

Work at Ames National Laboratory is supported by US Department of Energy and Basic Sciences (DOE) DE-AC02-07CH11358, and at NSLS-II, BNL, by DOE DE-SC0012704 and at NSF's ChemMat CARS by NSF/CHE-1834750.

11:00 AM SF02.06.07

Self-Assembly of Atomically Aligned Nanoparticle Superlattices from Pt-Fe₃O₄ Heterodimer Nanoparticles Shengsong Yang¹, R.A. LaCour², Yi-Yu Cai¹, Yugang Zhang³, Cherie R. Kagan¹, Sharon Glotzer² and Christopher B. Murray¹; ¹University of Pennsylvania, United States; ²University of Michigan-Ann Arbor, United States; ³Brookhaven National Laboratory, United States

Multicomponent nanoparticle superlattices (SLs) promise the integration of nanoparticles (NPs) with remarkable electronic, magnetic, and optical properties into a single structure. Here, we demonstrate that heterodimers consisting of two conjoined NPs can self-assemble into novel multicomponent SLs with a high degree of alignment between the atomic lattices of individual NPs, which has been theorized to lead to a wide variety of remarkable properties. Specifically, by using simulations and experiments, we show that heterodimers composed of larger Fe₃O₄ domains decorated with a Pt domain at one vertex can self-assemble into an SL with long-range atomic alignment between the Fe₃O₄ domains of different NPs across the SL. The SLs show an unanticipated decreased coercivity relative to nonassembled NPs. In situ scattering of the self-assembly reveals a two-stage mechanism of self-assembly: translational ordering between NPs develops before atomic alignment. Our experiments and simulation indicate that atomic alignment requires selective epitaxial growth of the smaller domain during heterodimer synthesis and specific size ratios of the heterodimer domains as opposed to specific chemical composition. This composition independence makes the self-assembly principles elucidated here applicable to the future preparation of multicomponent materials with fine structural control.

11:15 AM SF02.06.08

Capillary-Wave Theory for Phase-Separated Active Brownian Particles Ahmad Omar and Luke Langford; University of California, Berkeley, United States

Nonequilibrium phase transitions are now routinely observed in natural and synthetic systems. Purely repulsive model systems such as active Brownian particles (ABPs) have been demonstrated to phase separate into dense and dilute phases despite being homogeneous at equilibrium. The interface dividing such phase separations has been the subject of puzzling observations, including negative surface tension and qualitative agreement with equilibrium capillary-wave theory (CWT). Here, we begin from microscopic particle dynamics and systematically derive a mesoscopic Langevin equation for the interface dividing phase separated ABPs. Doing so allows us to calculate an interfacial tension distinct from the negative mechanical surface tension. In addition, we find a nonequilibrium analogy to CWT and identify the conditions at which this theory qualitatively agrees with the equilibrium case.

SESSION SF02.07: Macromolecular Crystallization and Assembly

Session Chairs: S. Eileen Seo and Hanglong Wu

Wednesday Afternoon, November 29, 2023

Sheraton, Second Floor, Republic A

1:30 PM *SF02.07.01

Directed Self-Assembly of Diblock, Multiblock, Bottlebrush and Rod-Coil Copolymers Caroline A. Ross; Massachusetts Institute of Technology, United States

Block copolymer microphase separation, driven by the chemical incompatibility between the blocks, leads to periodic patterns of spheres, cylinders, gyroids, lamellae and other structures with periods of a few nm and above. The microphase separation of thin films of block copolymers can be directed by topographical or chemical substrate features, leading to well-ordered patterns with long range order and/or non-bulk morphologies. This directed self-assembly (DSA) process offers compelling opportunities for the generation of dense patterns with small period which are useful in nanofabrication and nanolithography. The utility of DSA can be enhanced by expanding the range of possible microdomain geometries available, and by developing methods to direct their self-assembly in the out-of-plane direction to make three dimensional structures.

We will describe morphologies created by Si-containing triblock terpolymers, rod-coil copolymers, and bottlebrush copolymers, including zigzags, bends, junctions, tiling patterns and hierarchical structures with two independently tunable periods. As an example, a Janus bottlebrush triblock terpolymer yields layers made up of meshes of one block in a matrix of a second block, separated by layers of a third block. The meshes have sub-20 nm period and various angles, and can be aligned in topographical substrate features. Sequential self-assembly can produce three dimensional structures, including orthogonal mesh patterns, by assembling one block copolymer on another. We also describe metal infiltration of block copolymers by immersion in an acid solution of a metal salt, which locks the self-assembled structure, and reversibility of the metallization by immersion in a solution of a complexing agent, unlocking the structure so that it can evolve in response to annealing. We use in situ grazing incidence small angle x-ray scattering to reveal details of the self-assembly process during thermal or solvent vapor annealing. Combinations of novel polymers, templating approaches, and processing techniques yield an extensive array of rectilinear and 3D pattern geometries that can expand current nanofabrication capabilities.

2:00 PM SF02.07.02

Mapping the Phase Behavior of Block Copolymer Supramolecular Thin Films using Solvent Vapor Absorption – Desorption Isotherms Nayanathara Hendeniya, Caden Chittick, Kaitlyn Hillery, Shaghayegh Abtahi and Boyce Chang; Iowa State University of Science and Technology, United States

The self-assembly of block copolymers has been widely studied over decades as a potential platform in a plethora of nanotechnological applications. Recently, significant attention has been drawn to the self-assembly of BCP-based supramolecules rather than traditional BCPs, as a more efficient method of tuning the morphologies. While the self-assembly of supramolecules is governed by the competition between minimizing the enthalpy of mixing between the blocks and maximizing the conformational entropy, tuning of morphologies and kinetic behavior are heavily influenced by molecular architecture and processing. Solvent vapor annealing is a versatile processive pathway to obtain heavily periodic self-assemblies from high χ block copolymers and supramolecules. However, little evidence is found regarding the kinetic behavior of the order-disorder transition of such assemblies during controlled solvent vapor annealing. Adsorption-desorption isotherm is a method of characterizing host-guest interactions in porous materials. A similar approach can be used to understand the interactions between polymer

chains and solvent vapor molecules. The present study is focused on understanding the kinetic factors that influence the morphological evolution using characteristic absorption–desorption behavior of cylinder–forming polystyrene – block – poly (4 – vinyl pyridine) block copolymer combined with pentadecylphenol (PS – b – P4VP(PDP)) during solvent vapor annealing. We identify the transition points from kinetically trapped initial phase segregation to periodic horizontal cylindrical structures with long-range order using absorption–desorption isotherms. We further investigate the tunability of grain coarsening and macroscopic film dewetting under continuous flow solvent vapor annealing. Atomic Force Microscopy (AFM) is used to characterize surface morphological evolution. Using Grazing Incidence Small Angle X-ray Scattering (GISAXS), the periodicity (D0) and grain size are quantitatively analyzed.

2:15 PM SF02.07.03

Surface Crystallization of Molecular Crystals by Exsolution from Poly(ethylene) Bryan Erriah¹, Alexander Shtukenberg¹, Reese Aronin¹, Derik McCarthy¹, Leilani Smith¹, Petr Brazda², Michael D. Ward¹ and Bart Kahr¹; ¹New York University, United States; ²The Czech Academy of Sciences, Czechia

The properties of synthetic polymers are often tuned with additives. Whilst most additives, like plasticizers, are non-migratory, some are migratory, like lubricants. Blooming and/or bleeding refers to phenomena in which additives in a polymer migrate to its surface; this is a common phenomenon that is important for several industries including food packaging and pharmaceuticals, medicine, art, and the production of long-lasting insecticidal bed nets.

Many long-lasting insecticidal bed nets for protection against disease vectors are made of poly(ethylene) fibers in which the insecticide is embedded at the time of manufacture. Insecticide molecules diffuse from within the supersaturated polymers to surfaces and become bioavailable to insects, in most cases eventually crystallizing. Recent studies have revealed that contact insecticides can be highly polymorphic. Moreover, insecticidal activity is polymorph dependent, with forms having higher crystal free energy yielding faster insect knockdown and mortality. Consequently, the crystallographic characterization of insecticide crystals that emerge from fibers is critical to understanding net function and improving net performance. Structural characterization of insecticide crystals on bed net fiber surfaces, let alone their polymorphs, has been elusive owing to the minute size of the crystals that by necessity grow in and on threads, however.

Here we describe surface crystallization of several molecules by phase separation from extruded poly(ethylene) fibers including ROY, paracetamol, flufenamic acid, benzamide, benzil, deltamethrin, alpha-cypermethrin, lambda-cyhalothrin and chlorfenapyr. In general, solutes diffuse from the polymer matrix and form amorphous droplets on the surface. With time the system may undergo substantial evolution from droplet coalescence to metastable crystal growth, to recrystallizing as more thermodynamically stable forms, a demonstration of Ostwald's Rule of Stages. In general, crystallization on the surface of poly(ethylene) resembles growth from vapor phase and is often limited by diffusion mass transport. With the highly polymorphous compound ROY (5-methyl-2-[(2-nitrophenyl)-amino]thiophene-3-carbonitrile) as a proxy for insecticide crystallization, we investigated blooming kinetics and crystallization on the surface of melt-extruded, and cold-drawn poly(ethylene) fibers that had been impregnated with ROY. The blooming rates, tracked from the time of extrusion, were determined by UV-vis spectroscopy after successive washes. Six crystalline polymorphs (of the 14 known) were observed on poly(ethylene) fiber surfaces, and they were identified and characterized by Raman microscopy, scanning electron microscopy, and 3D electron diffraction (3D ED). We show both polymorph control and particle size/morphology control. These observations reveal that the crystallization and phase behavior of polymorphs emerging from poly(ethylene) fibers is complex, dynamic, and tuneable. Furthermore, the demonstration that 3D ED can characterize the minute crystals grown on fibers promises a pathway to bed net crystallography and subsequent optimization of bed net performance.

2:30 PM BREAK

3:30 PM *SF02.07.04

High Throughput Platform to Meet Covarying Materials Manufacturing Design Criteria for Block Copolymer Nanolithography Paul F. Nealey; University of Chicago, United States

Methodologies and tools for the accelerated discovery and design of materials for use in manufacturing have been transformed over the past decade through the combination and integration of experiment, theory, and computation. Here we build on the integration of experiment and molecular simulation to specify design rules for block copolymer (BCP) materials, for use in the directed self-assembly (DSA) of ultra-high resolution lithographic patterns for semiconductor manufacturing, and report on a high throughput synthesis and characterization platform for discovery and subsequent optimization of BCP materials for this application over a range of pattern dimensions. The design rules are agnostic to specific polymer chemistries and are derived from equilibrium (thermodynamic) and non-equilibrium (dynamic) predictive physics-based models that were validated by comparison to one of a kind quantitative experiments using the only BCP material and DSA process that have been successfully implemented in an industry-relevant format, at one serendipitously-found pattern dimension, and interrogated by state-of-the-art inspection tools so as to be known to satisfy manufacturing constraints. In a departure from conventional materials development, multiple co-varying properties must be simultaneously optimized in the BCP materials, and materials of different chemistry and composition must be developed for each pattern dimension over the desired range. A key advance to develop a family of different materials to realize these objectives is the design and implementation of a high throughput discovery-oriented synthesis and characterization platform using interchangeable polymer components to explore a large and complex parameter space to find possible combinations of components that satisfy the design rules at different pattern dimensions. The large data sets acquired from the high throughput methodologies then allow rapid convergence on the synthesis of BCP materials for specific objectives in the application space.

4:00 PM SF02.07.05

Assembly of Sequence-Defined Peptoids into Crystalline Nanomaterials as Biomimetic Catalysts Chun-Long Chen^{1,2}; ¹Pacific Northwest National Laboratory, United States; ²University of Washington, United States

While natural enzymes, including lignin peroxidase, phosphotriesterase, and carbonic anhydrase, are promising for various applications, such as lignin depolymerization, degradation of toxic organophosphates, and accelerated CO₂ precipitation, there are numerous key technical barriers to prevent their practical applications, because they often suffer from low stability and high cost. To circumvent these barriers, researchers have started to develop synthetic materials as enzyme mimetics with enhanced stability for various purposes. Despite tremendous efforts made in this area, constructing highly efficient and robust enzyme mimetics with natural enzyme-like flexibility in tuning active sites and microenvironments remains a grand challenge.

In this presentation, we will report our recent progress in developing peptoid-based crystalline nanomaterials as highly robust and programmable catalysts for a variety of applications. Peptoids are one of the most advanced classes of sequence-defined synthetic foldamers that bridge the properties of proteins and polymers.¹⁻⁴ While exhibiting protein- and peptide-like molecular recognition, peptoids offer unique opportunities for controlled synthesis of hierarchically-structured crystalline nanomaterials^{1,5-7} exclusively through side-chain chemistry due to the lack of backbone hydrogen bond donors. Because of highly tunable features and robustness of these peptoid-based crystalline nanomaterials, they provide an ideal platform to mimic nature enzymes by offering high surface area, programmable microenvironments, and other unique advantages. For example, comparing to a typical lignin peroxidase which contains one active site per enzyme molecule, peptoid-based crystalline nanotube catalysts can accommodate a high-density of active sites to achieve a significantly enhanced catalytic activity in lignin depolymerization.⁸ Moreover, due to their high chemical and thermal stability, these peptoid-based catalysts can be operated at a variety of conditions, such as at elevated reaction temperature and broad pH range which nature enzymes denature.

References

1. Sun et al., *ACS Nano* **7**, 4715-4732 (2013); 2. Shao et al., *Chem. Rev.* **122**, 17397-17478 (2022); 3. Li et al., *Chem. Rev.* **121**, 14031-14087 (2021); 4. Cai et al., *Acc. Chem. Res.* **54**, 81-91 (2021); 5. Jin et al., *Nature Comm.* **9**, 270 (2018); 6. Jin et al., *Nature Comm.* **7**, 12252 (2016); 7. Wang et al., *Science Adv.* **7**, eabg1448 (2021); 8. Jian et al., *Nature Comm.* **13**, 3025 (2022).

4:15 PM SF02.07.06

Reconfigurable Multi-Component Assemblies Built from DNA Origami Voxels Minh Tri Luu¹, Jonathan Berengut² and Shelley Wickham¹; ¹University of Sydney, Australia; ²University of New South Wales, Australia

DNA origami is a robust nanofabrication method that enables the biomimetic self-assembly of diverse nanostructures with nanoscale addressability and reconfiguration. Hierarchical assembly of DNA origami components into larger assemblies offers a pathway to create larger or more complex structures. However, challenges remain in achieving structural diversity, rigidity, and programmable reconfiguration. Here we present a universal and robust DNA origami building block to support 2D and 3D hierarchical assembly that combines rigid DNA barrel monomers with rigid connections. The building block is modular and contains 14 directional binding interfaces in 3D, each with multiple DNA strands that can hybridise with connector strands to create rigid connections within hierarchical assemblies.

We demonstrate the use of DNA barrel monomers as modular voxels to build diverse multi-component assemblies with intricate custom features and addressable components for potential materials patterning. DNA strand displacement reactions are used to switch connections between flexible and rigid states, enabling rapid and reversible shape transformations of assemblies with high yield. Additionally, we explore strategies to improve the yield of hierarchical assembly of DNA origami. Inspired by protein assembly, we investigate multi-step folding pathways. Initially, we assemble individual DNA origami building blocks into a flexible linear chain of linked DNA origami. We then fold these chains into more compact structures in several steps, resulting in improved yields for certain pathways. We envision that DNA origami chains could be integrated with scalable assembly methods to build new materials with rapid and high-yield reconfiguration.

4:30 PM *SF02.07.07

Amyloid self-assembly is a complex phenomenon with implications in both degenerative human disorders and materials science. In this context, various structures such as amyloid fibers, particles, and crystals exist, with crystal amyloids being the most stable energetically. However, achieving control over amyloid assembly and reversibly manipulating the crystallization process pose significant challenges. This study aims to explore the reversible formation of macroscopic crystals by examining the effects of temperature, pH, ionic strength, and solvents. Furthermore, in situ microscopy will be utilized to investigate the dynamic process of amyloid disassembly. The reversibility of self-assembly under external stimuli provides valuable insights into the mechanisms of amyloid formation, emphasizing the importance of considering the influence of external factors on crystal formation. Ultimately, the investigation of reversible amyloid crystallization holds promise for the development of innovative strategies in biomaterial design.

SESSION SF02.08: Poster Session II
Session Chairs: Chun-Long Chen and Shuai Zhang
Wednesday Afternoon, November 29, 2023
Hynes, Level 1, Hall A

8:00 PM SF02.08.01

Bio-Inspired Physical Unclonable Function Labels Fabricated by Self-Assembly Processes Su EonLee¹, JunhyunPark¹, Jang HwanKim² and Bong HoonKim¹; ¹Daegu Gyeongbuk Institute of Science and Technology, Korea (the Republic of); ²LG Chem Ltd., Korea (the Republic of)

The demand for robust verification and recognition techniques is increasing because of the evolution of Internet of Things (IoT) and wireless data storage systems. Although authentications with software systems are prevalent, they are susceptible to external threats like hacking and electronic interference. For these reasons, verification methods with hardware systems using physical unclonable functions (PUFs) have been interested in applying wireless interconnection devices and network-based data servers. The validation process using PUFs relies on the electrical and optical signals generated from micropatterns or randomly oscillating signals in electronic devices, and the verification of these encrypted signatures typically depends on complex and time-consuming measurement instruments.

In this poster, we introduce bio-inspired PUF labels fabricated by self-assembly processes. BCP self-assembly forms randomly oriented nanopatterns (i.e., fingerprint-like lamellar structures) as small as 5 nm across the broad area because of the thermodynamical microphase separation. We fabricate the multi-layered nanopatterns from the randomly oriented BCP templates by stacking a thin layer of the metallic lamella structures *via* the transfer printing process on non-planar and flexible surfaces for wearable or soft electronic devices. As the purpose of the verification systems, we produce multiple independent keys, utilizing electrical resistance, optical dichroism, or Raman signals for high-security rates and fast scan speeds.

The multiple-layered fingerprint-like nanoscale PUF labels respond to the electrical potentials and polarized visible light, which can generate non-deterministic keys by physically measuring the electrical resistance, optical dichroism, and Raman scattering. We decrypt the respective or integrated signal according to the purpose with scan speeds of $\sim 10 \mu\text{s}$ (resistance), $\sim 1 \mu\text{s}$ (birefringence), $\sim 100 \text{ms}$ (Raman scattering), and $\sim 1 \text{ms}$ (Integrated methods). Moreover, we can form PUF labels on paper bills, deformable transparent polymer substrates, human wrists, human hair, ant bodies, and microbacteria by a transfer printing process, which provides ultra-high security rates, simultaneously rapid validation speeds, and universal application to the PUF labels.

In conclusion, we show randomly oriented BCP nanopatterns applied to the PUF labels with robust and secure properties and meaningful encoding abilities, which offer unpredictable signals for identification, utilizing electrical and optical response with fast scan time. Our approach reduces the critical dimensions of PUF labels, has the potential to be a versatile platform for advanced authentication systems, and can be used for discreet miniature identifiers on various surfaces or integrated multikey authentication systems. Integrating PUFs seamlessly with essential validation tools is the next valuable step, enabling versatile applications, including hardware-based on-demand cryptographic key generation.

8:00 PM SF02.08.02

Multiphase Silk Assembly for Two-Dimensional Composite ChenyangShi and JamesJ. De Yoreo; PNNL, United States

Early insights into native silk fibroin (SF) architecture suggested that its unique structures and properties are determined by its multiscale assembly and the evolution of its secondary structure. Yet the pathways of assembly and the relationship to that evolution are poorly understood. Here we investigate SF self-assembly at the interface between water and highly ordered pyrolytic graphite (HOPG) using in situ AFM, photo-induced force microscopy (PiFM), and molecular dynamics. To do so, we assemble the silk at the interface between water and highly ordered pyrolytic graphite (HOPG). We find that SF grows heteroepitaxially on HOPG into highly ordered, monolayer-thick 2D nanocrystals consisting of 1D lamellae that exhibit β -sheet secondary structure. Molecular dynamics simulations show that the lamellae strongly prefer the armchair orientation of HOPG and polar packing to form a bilayer. As the SF concentration increases, SF assembles into multi-layers via two pathways that can occur concomitantly. One is a non-classical pathway by which a disordered metastable film forms on top of the lamellae monolayer and gradually converts into the lamellae structure of SF β -sheet nanocrystals. The second is a classical layer-by-layer pathway by which new lamellae grow homoepitaxially on the underlying 2D lamellae nanocrystals without any evidence of an intermediate state. These new findings fill in the missing pieces of the puzzle showing how SF structure evolves at the liquid-solid interface and provides inspiration for the design of heterogeneous 2D SF composites.

8:00 PM SF02.08.03

Effects of Crystallization on Micromechanical Behavior of Polyethylene Nanocomposites MasonMartell, LindaS. Schadler, DavidPunihaole and FredericSansoz; University of Vermont, United States

The addition of small amounts of nanofillers to a polymer matrix has been shown to impart significant changes in mechanical, dielectric, and optical properties. A common challenge in creating these polymer nanocomposites (PNCs) is controlling the dispersion of the nanofillers. Recent work has demonstrated methods to control dispersion and organization of spherical nanoparticles (NPs) in compatible matrices. At sufficiently slow crystallization rates in semicrystalline polymers, the NPs organize in the amorphous regions of the growing spherulites. PNCs with organized NPs have been shown to exhibit improved bulk mechanical properties, but the micromechanical behavior underpinning these has not been fully explored. In this study, in-situ Raman spectroscopy was performed on polyethylene samples under tensile load to explore differences in micromechanical behavior between neat, filled but unorganized PNCs, and PNCs with crystallization-induced particle organization. Crystallization of each sample was characterized in DSC, and organization of PNC samples confirmed by SAXS and TEM. Results show that the addition of fillers leads to a significant change in the distribution of load between the crystalline and amorphous phase. Shift is only apparent in samples that undergo necking (high strain), consistent with previous work on neat polyethylene.

8:00 PM SF02.08.04

Self-Assembled Tetrapod Molecules on Graphite Form Nanopockets with Attractive Force Distribution Studied by 3D Scanning AFM MoeOgasawara, MasayukiMorimoto and HitoshiAsakawa; Kanazawa University, Japan

The precise design of molecular architectures through molecular self-assembly on solid substrates is a promising approach for developing next-generation materials and their functions. The molecular architecture having nanopockets that can capture target molecules with high selectivity and affinity has immense potential for use in sensing devices and separation materials with molecular recognition functions. Toward the design and construction of molecular architecture with nanopockets, we have been exploring molecular building blocks having three-dimensional (3D) extended structures. Furthermore, we have developed a molecular-scale analytical technique based on atomic-resolution atomic force microscopy in liquid. For the applications of molecular nanopockets, not only nanoscale surface structures such as molecular orientation, but also the recognition mechanism of how guest molecules and host nanopockets interact is an important research topic. However, the lack of a measurement method for interaction forces in 3D nanospace has made it difficult to improve the understanding of the recognition mechanism. We have developed a 3D scanning atomic force microscope (3D-AFM) that can visualize hydration structures and surface fluctuation structures at the solid-liquid interface with sub-nanometer resolution. Conventional AFMs scan the tip only in the XY direction, but 3D-AFM scans the tip in the Z direction in addition to the XY direction, making it possible to obtain 3D force distribution information. Combined with the frequency shift detection method, 3D-AFM can also detect the interaction force acting on the tip at the piconewton (pN) level. Based on this principle and performance, we believe that 3D-AFM technology can be applied as an analysis tool for "interaction force measurement" as well as "structural measurement."

We have performed direct visualization with 3D-AFM of the characteristic interaction force in 3D nanospaces at the self-assembled molecules/water interface. Two types of tetrakis(4-ethynylphenyl)methane (TEPM) derivatives with oligo(ethylene glycol) (EG_n) chain (EG_2 -TEPM, EG_4 -TEPM) were used as the building blocks and these TEPM derivatives form self-

assembled monolayers on graphite. In the monolayers, there are hydrophobic nanopockets (diameter: approx. 1.7 nm) surrounded by the aromatic structure of the TEPM derivatives. We performed 3D-AFM measurement at the self-assembled monolayers/water interface. As a result, characteristic localized attractive interaction was visualized only at the EG₂-TEPM monolayer/water interface, and analysis of the 3D-AFM images suggests that the attractive interaction forces originate from the nanopockets and that the nanopockets of EG₂-TEPM are slightly smaller than those of EG₄-TEPM. The number of hydrogen bonds forming the water molecule network and the water molecule density are reduced in restricted spaces, such as inside the EG₂-TEPM nanopockets, compared to the bulk water. The visualized attractive interaction forces seem to originate from the water molecule behavior in the nanopockets. Our results demonstrate that the 3D-AFM technique has the capability of visualizing the characteristic interaction forces at the single molecule level, suggesting future contributions to the elucidation of the molecular recognition mechanisms and the design of novel nanodevices.

8:00 PM SF02.08.05

Low Temp Heterogeneous Integration of Ultra-Thin-Silicon Interposer via Transfer Printing and Laser Bonding UhyeonKim, SeungbeomKim, JunhyungKim, AghaA. Jan and SeokKim; Pohang University of Science and Technology, Korea (the Republic of)

Interposer-based 2.5D heterogeneous integration packaging is being used as a key technology for next-generation semiconductor miniaturization that will lead "Beyond Moore." However, traditional wafer bonding techniques and flip chip processes have limitations in handling very thin silicon interposers (<30µm) that can be easily deformed. In this study, we developed a process of stably transferring and bonding ultra-thin silicon interposer with high accuracy using transfer printing technology through Shape Memory Polymer (SMP) stamp and laser heating.

The ultra-thin silicon interposer is designed as a transferable ink of Micro-Lego technology. Copper TSV (Through-Silicon Via) and Cu-Sn solder bump were formed on silicon on insulation (SOI) wafers with predefined thickness, and an independent ultra-thin interposer with a thickness of 15µm was prepared by separating the Box Layer. The interposer was accurately and stably transferred to the receiver substrate by and Shape Memory Polymer (SMP) stamp. At this time, the stamp is made by Shape Memory Polymer that can selectively transfer through heat deformation. Thereafter, the laser was irradiated to the interposer and coupled using a low-temperature bonding (~230°C) method suitable for the Cu-Sn eutectic condition. The interposer bonding was successful after finding the low-temperature bonding conditions according to the variables of laser power, time, and metal layer thickness to be used in the semiconductor post-process. The bonded interposer was characterized by FIB, IV curves, etc... This ultra-thin integration technology has advantages such as low-temperature bonding, low signal loss in channels, and low heat generation, so high-performance low-power packaging can be expected.

8:00 PM SF02.08.06

Effect of Au-Ag Bimetallic Seed in Controlling the Morphology of TiO₂ Nanowire ZhinaRazaghi and Guo-zhenZhu; University of Manitoba, Canada

The recently developed Vapor-Adsorbate-Solid method has demonstrated success in producing single-crystalline rutile TiO₂ nanowires that extend over tens of microns. This approach involves the adsorption and transfer of TiO₂ vapor species of the substrate along the surface of gold (Au) seed nanoparticles to the nanowire's growth front. Using different seed nanoparticles with gold-silver (Au-Ag) composition led to a change in the nanowire morphology, transitioning from bead-like <110>TiO₂ shapes to prismatic <111>TiO₂ shapes. This transformation was attributed to the unexpected Ag-rich segregation at the growth front, influencing nanowire shape and growth direction upon contact^{1,2}. However, the exact mechanism behind how Ag segregation affects nanowire growth direction remains unclear.

To address this, the first step is to pinpoint the precise location of Ag-rich segregation at the growth front and understand its impact on nanowire shape. In this regard, a three-dimensional configuration of Ag-rich segregation was reconstructed using multiple Energy-Dispersive X-ray Spectroscopy (EDX) maps at various zone axes, including <3-15>, <1-11>, <1-12>, and <2-13>, for individual nanowires. The FEI TALOS F200X Transmission Electron Microscope (TEM) operating at 200 kV was utilized for this purpose. The results show that Ag-rich segregation primarily occurs at the hexagonal cross-section along the edges of {1-10} and {0-11} facets, which inhibits the formation of a rhombus cross-section, a component of the bead-like nanowire shape³. As a result, the preferred nanowire cross-section becomes hexagonal, leading to the formation of prismatic nanowires.

To decouple how Au and Ag interact with adsorption species (TiO_x), X-ray Absorption Spectroscopy (XAS) was employed. Using specialized experimental settings, such as Grazing Incident X-ray Absorption Fine Structure (GI-XAFS), we enhanced the detection of weak interface signals collected at the Canadian Light Source (CLS) Hard X-ray Micro-Analysis Beamline. We analyzed X-ray adsorption spectra at the Au L₃-edge and Ag K-edge for nanowires with varying shapes and growth orientations. Different atomic models were proposed for Ag-rich and Au-rich regions, with compositions of 30 at. % Au and 15 at. % Ag, respectively, determined from EDX measurements. These models explored Ag-to-Au replacement configurations with crystal parameter adjustments. Theoretical X-ray Absorption Near Edge Structure (XANES) spectra were computed using FDMNES, and Linear Combination Fitting (LCF) aligned experimental XANES spectra with theoretical models to estimate contributions of Au and Ag species. Additionally, ongoing Extended X-ray Absorption Fine Structure (EXAFS) analysis aims to validate bonding interactions by quantifying the local environment of Au and Ag species, including bond lengths and coordination numbers.

Initial findings suggest the existence of metallic Au, metallic silver Ag, an alloy of Au and Ag, Au combined with Ti, Ag combined with Ti, and Ag bonded to oxygen (Ag-O), while no evidence of Au bonding with oxygen (Au-O) was observed. These results suggest that the existence of Ag-rich segregations may lead to distinct adsorption and mass transfer characteristics compared to Au. Currently, we are investigating the precise mechanism by which Ag segregation influences growth direction using a combination of experimental techniques, including ex-situ and in-situ electron microscopy. Consequently, we anticipate that this ongoing investigation will shed light on how the composition of the seed material can be manipulated to control the morphology of TiO₂ nanowires.

1. Xie, D. Y., et al. Kinetically Favorable Vapor-Adsorbate-Solid Growth of Rutile Nanowires. *Small Methods* **3**, 1900111 (2019).
2. Razaghi, Z., et al. Ion beam-induced bending of TiO₂ nanowires with bead-like and prismatic shapes. *RSC Adv.* **12**, 5577–5586 (2022).
3. Zhou, P., et al. Sawtooth Faceting in Rutile Nanowires. *ACS Omega* **7**, 10406–10412 (2022).

8:00 PM SF02.08.07

Water Condensation on Microstructured Superhydrophobic Surfaces MariiaS. Kiseleva and RobinH. Ras; Aalto University, Finland

Water condensation on solid surface is a phase change phenomenon where water undergo transition from vapor into liquid phase. In the initial stage of condensation process water droplets are nucleating on the surface defects or contaminants. These nucleated droplets then grow and coalesce with each other. The surface topography and coating properties play crucial roles in the nucleation and growth dynamic of the droplets. It was shown recently that superhydrophobic surfaces with densely packed sharp nanoconical features have a unique ability to repel condensing microdroplets^{1,2}. When droplets coalesce on such surfaces, they can spontaneously jump away from the surface due to the release of excess surface energy. In this study, we employed in-situ optical, confocal, and environmental electron microscopies to investigate the dynamics of droplet growth and jumping during the condensation process on superhydrophobic surface with microscale conical features. Microstructured surface design was chosen due to simpler and more scalable manufacturing process. We prepared surfaces with 'sparse' arrays of tall cones (cone height h≈4 µm, base diameter d≈1 µm, opening angle β<18°) separated by 2 µm spacing arranged in hexagonal and squarer lattice. The advantage of 'sparse' arrangement is that light can be reflected from the flat area between bases of adjacent cones. Adjusting the focus plane in high-resolution optical microscope we were able to visualize the contact area between microdroplet and surface.

We showed previously that on the surface with square array of cones the macroscopic water drop is not sinking into the conical structures³. However, we showed that condensing microdroplets are in full contact with structure, i.e., in Wenzel state. As a result, condensing droplets are unable to jump. In contrast, on the surface with hexagonal array of cones droplets only partially wet the substrate, i.e., droplets are in partial Cassie state. Partial Cassie state enables active jumping upon coalescence of two or more droplets with radii exceeding 10 µm. Although the difference between square and hexagonal packing is very subtle, we discovered a critical transitional regime of condensing microdroplets that ranges from fully wetted (Wenzel) to partially wetted (partial Cassie) state.

1. Mouterde, T. et al. Antifogging abilities of model nanotextures. *Nature Mater* **16**, 658–663 (2017).
2. Lecointre, P. et al. Unique and universal dew-repelling of nanocones. *Nat Commun* **12**, 3458 (2021).
3. S. Lepikko, V. Turkki, T. Koskinen, R. Raju, V. Jokinen, M. S. Kiseleva, S. Rantataro, J. V.I. Timonen, M. Backholm, I. Tittonen, R. H.A. Ras. Droplet friction on superhydrophobic surfaces scales with liquid-solid contact fraction. *Advanced Science* (submitted).

8:00 PM SF02.08.08

Tuning Semi-Crystalline Polymer Thin Film Structure via Substrate Nano-Geometry Modulation RobertaRuffino, GiovanniLi Destri and GiovanniMarletta; University of Catania, Italy

The ability to create ultra-thin functional polymer films with controlled nano-crystallinity structure for large-scale integration is at the focus of numerous experimental and theoretical works. [1-3] The main goal is to control and manipulate the assembly of building blocks to obtain structures with desired characteristics and unique properties. The geometric constraints imposed by the nanometric thickness and interfacial interactions affect the self-assembly process and, in turn, their behaviour. [4,5] In addition, non-planar substrates, such as nano-curved substrates, can further complicate the resultant structure as already observed for block copolymer thin films. [6,7] The combination of geometric effects, i.e. surface curvature, with surface free energy (SFE) may allow more finely controlled self-assemblies. To this end, we have developed a novel approach to prepare substrates with controlled nano-curvature and surface-free-energy (SFE), to be used to investigate how geometric and energetic factors affect the self-assembly of polymeric thin films. [8,9] In particular, by employing a semi-crystalline model polymer, namely poly-3-

hexyltiphen (P3HT), it was observed that the crystals follow the surface curvature only in the presence of an energetic gain.[8] Here, from the structural characterization via synchrotron radiation grazing incidence X-ray diffraction (GIXRD) and the morphological characterization via atomic force microscopy (AFM), we will demonstrate a non-conformal coverage, after the polymer equilibration, showing that the crystallization strongly depends on the surface curvature. The results suggest the polymer accumulation in the interstices between the particles for the lowest curvature, leading to an in-plane crystal growth. The increase in curvature improves the nucleation probability, leading to shorter crystals on both interstices and curved portions. Moreover, we demonstrate that the crystalline fraction is strongly curvature-dependent, as the crystallization only occurs when the distance between two neighbour particles is higher than the lamellar folding period. Finally, the in-situ structural characterization during thermal cooling shows a variation in the crystallization temperature (T_c) as a function of the substrate geometry, with a decrease in the onset of the crystallization with respect to the flat substrate. These results highlight the role played by the substrate in the crystallization process, suggesting that the geometric factors affect the crystalline structure itself, with the formation of distorted crystals following the surface curvature. The reported work provides a novel and easy method to modulate the structure of polymer films by exploiting geometric distortion and interfacial interactions with possible effects on the functional properties of the polymer film. This correlation sheds more light on how these factors influence the polymer film crystallization and could allow the determination of the crystallization enthalpy and its related loss when a nanometric strain is applied. A deeper understanding of this behaviour could pave the way for the development of finely tailored crystalline structures via control of the substrate geometry and energy.

References

- [1] Gao Hanfei, et al. *Nature Communications*, **2019**, 10(1), 3912.
- [2] Del Valle, M. A., et al. *Polymers*, **2023**, 15(6), 1450.
- [3] Nguyen, et al. *Polymers*, **2016**, 8(4), 118.
- [4]. Verstraete, L., et al. *Chemical Society Reviews*, **2021**, 50(10), 5884-5897.
- [5]. Yu, C., et al. *Crystals*, **2017**, 7(5), 147.
- [6]. Yager, K. et al. *Soft Matter*, **2009**, 5, 622-628.
- [7]. Kang, et al. *Accounts of Chemical Research*, **2022**, 55(16), 2224-2234.
- [8]. Ruffino, R., et al. *J. Phys. Chem. C*, **2019**, 123, 8967-8974.
- [9]. Ruffino, R., et al. *Polymer*, **2021**, 230, 124071.

8:00 PM SF02.08.09

Spray Deposited Block Copolymer Thin Films with Solvent Evaporation Controlled Domain Orientation SemihCetindag, BeatriceBellini, RuipengLi, EstherTsai and GregoryDoerk; Brookhaven National Laboratory, United States

With their ability to self-assemble spontaneously into well-defined nanoscale morphologies, block copolymer (BCP) thin films are a versatile platform to fabricate functional nanomaterials such as lithographic nanopatterns, nanoporous membranes and optical metasurfaces. An important yet unsolved challenge to wider deployment of BCPs in nanofabrication, however, is combining the desired precise control of BCP assembly with scalable deposition techniques that are applicable to large-area, curved and flexible substrates for high-volume manufacturing. Ultrasonic spraying is a scalable, non-batch casting method with minimal wasted polymer, yet its use in thin film BCP assembly has not been investigated.

Here, we show that the latent orientation (vertical vs. horizontal) of well-ordered cylindrical domains in spray-deposited, optically-smooth thin films of polystyrene-block-poly(4-vinylpyridine) (PS-*b*-P4VP) can be controlled by regulating solvent evaporation kinetics. Faster evaporation during deposition facilitates assembly of vertically oriented cylinders spanning the entire film thickness (100-300 nm) upon subsequent solvent vapor annealing. In comparison, slow solvent evaporation induces assembly of horizontal cylinders, imposing an additional energy barrier for reorientation to vertical cylinders during solvent vapor annealing. Using in-situ characterization by synchrotron grazing-incidence small-angle X-ray scattering (GISAXS), we identify the relevant timescale for polymer vitrification which determines latent cylinder orientation. This dependency on solvent evaporation kinetics is exploited to control cylinder orientation in multiple ways, including substrate heating, forced convection, and solvent formulation. To highlight the scalability and utility of the spray casting technique, an exemplar application using spray deposited self-assembled patterns on curved surfaces will also be described.

Funding: This research was conducted at the Center for Functional Nanomaterials (CFN) and the National Synchrotron Light Source II (NSLS-II), which are U.S. Department of Energy (DOE) Office of Science User Facilities, at Brookhaven National Laboratory under Contract No. DE-SC0012704. S.C., B.B., and G.S.D. were supported by a DOE Early Career Research Program grant.

SESSION SF02.09: Materials Surfaces I
Session Chairs: Jingshan Du and Wenzheng Wei
Thursday Morning, November 30, 2023
Sheraton, Second Floor, Republic A

8:30 AM +SF02.09.01

Controlling Structural Changes in 2D Magnets using In Situ Microscopy and Machine Learning Techniques JulianKlein and FrancesM. Ross; Massachusetts Institute of Technology, United States

Electron beam patterning raises exciting prospects for modifying the crystal structure and hence physical properties of 2D materials, and has been explored for several 2D materials in single or few-layer form. Here we examine the opportunities arising from patterning thicker, more robust crystals of 2D semiconducting magnets, intriguing materials in which the local ordering of spins determines both the magnetic properties and the optical response. CrSBr is one such material, having layers with alternating magnetic moment and a structure in which Cr atoms located in their own columns are separated by columns of mixed S and Br atoms. For 10-50nm thick multilayer crystals, we find that broad-area irradiation by electrons reorganizes CrSBr into a new structure, which is also van der Waals-bonded but with a layer orientation and calculated magnetization that are rotated by 90° from the initial direction. Further structural changes can be generated if we irradiate the structure along rows of Cr atoms to open local gaps, changing the calculated interaction between magnetic atoms. Extending to the ultimate objective of controlling the position of individual Cr columns requires the use of machine learning techniques to track column positions, direct the beam and evaluate whether the desired modification has been achieved. We will describe strategies for achieving this goal and for understanding the process by which the Cr atoms are rearranged. We conclude by discussing correlative techniques to measure the optical and magnetic properties of the modified material, and the more general opportunities arising from patterned recrystallization of multilayer van der Waals bonded magnetic materials for spin-based and optical quantum devices.

9:00 AM SF02.09.02

Mechanism and Kinetics of Topochemical Etching for Synthesis of 2D MXenes from Layered MAX Phases MarkAnayee, Ruocun (John)Wang, StefanoIppolito, MikhailShekhirev and YuryGogotsi; Drexel University, United States

MXenes represent a rapidly growing family of 2D transition metal carbides and/or nitrides, which exhibit unique combinations of properties, including metallic conductivity, hydrophilic surface chemistry, redox-active surface, and plasmonic behavior that make them attractive as electrodes for pseudocapacitive energy storage to coatings for electromagnetic interference shielding, transparent conducting displays for optoelectronics, conductive yarns for functional textiles, implantable electrodes for medicine, and many other applications.

MXenes are typically derived via selective etching of atomically thick 'A' layers from precursor layered MAX phases using HF-based aqueous etchants. However, the chemical etching process is only somewhat optimized for one composition, and is nonetheless often slow, with low-yield, and results in defects in the materials. Thus, understanding the fundamental mechanism and kinetics of the etching reaction is needed to rationally explore etching of yet-to-be synthesized MXene compositions and optimize etching of existing MXene compositions. Despite their importance, such studies have been challenging because of the atomic thickness of the A-element layers being etched and the aggressive etchants that hinder in situ studies.

Here, we spatially track the etching front in 3D (using analytical setups for tracking byproduct gas evolution), 2D (using cross-sectional imaging of partially etched particles), and 1D (using in situ optical microscopy and profilometry of single particles). Thus, we show the role of surface oxide and binary carbide impurities on the nucleation of etching, and we discovered a layer-by-layer growth process for the etching front. From kinetic modeling, we show that etching varies from reaction-limited to diffusion-limited for various MAX compositions. Overall, our work enables rational high-throughput optimization of synthesis for all MXene compositions, scaling up synthesis towards industrial levels, and tailored synthesis for specific applications.

9:15 AM *SF02.09.03

Dynamics of Advanced Low-Dimensional Materials by Low-Voltage Atomic-Scale TEM Experiments Ute A. Kaiser; University of Ulm, Germany

To create next generation functional low-dimensional materials, it is a growing demand in materials sciences to understand their formation mechanisms as well as their structural and electronic properties at the atomic or molecular scale. Some of the most challenging tasks nowadays are related to energy storage, nano-catalysts or battery materials.

A unique type of transmission electron microscopes operating at electron energies between 80keV and 20keV was developed, which allows to undercut most of the materials knock-on damage thresholds and enables sub-Angstrom resolution in an 4000x4000 pixels sized image, single-shoot image down to 40keV by correcting not only geometrical but also the chromatic aberration of the imaging lens [1-3]. This instrument is used for the in-situ studies presented here. Before we discuss several in-situ TEM experiments, we develop a detailed understanding of the electron beam - 2D specimen interactions: By density functional theory molecular dynamics we show that excitations in the electronic system can form vacancies through ballistic energy transfer at electron energies, which are much lower than the knock-on threshold for the ground state. We propose a two-step vacancy formation process as combination of elastic and inelastic events, evaluated also by an U-net-based fully convolution neural network (FCN) [4].

Based on this knowledge, we discuss the dynamics of properties of point, line and extended defects in various transition metal - dichalcogenides and -phosphor dichalcogenides [5-8]. Optical measurements are performed independent of the TEM experiment. To relate optical and TEM results we demonstrate proof-of-principle experiments in which we transfer electron-exposed defect-characterized TMD flakes from a TEM grid to arbitrary substrates and relate the subsequently performed photoluminescence and transport signals to the defect structure [9].

Furthermore, we present in-situ studies of a miniaturized electrochemical cell, where reversibly single-crystalline bilayer graphene is lithiated and delithiated in controlled manner using an electrochemical gate confined to a device protrusion [10] and report on the Li crystal nucleation and growth during lithiation and Li-O formation and amorphization during delithiation. We generate further encapsulated metal-atom-dimers within single-walled carbon nanotubes and observe the dynamics of single metallic bond formation by exact measurements of the interatomic distance [11].

At the end we show that the approaches of graphene encapsulation and lowering the electron accelerating voltage (here from 300kV to 120kV) can be successfully applied for imaging 2D organic materials at the molecular level [12-14].

[1] U. Kaiser et al., Ultramicroscopy, 111, 8, (2011) 1239

[2] M. Linck, et al. PRL 117, (2016) 076101.

[3] F. Börnert and U. Kaiser Physical Review A 98 (2), (2018) 023861

[4] S. Kretschmer, et al, Nano Lett. 20, (2020) 2865.

[5] J. Köster, A. Storm et al., J. Phys. Chem., accepted

[6] T. Lehnert et al., ACS Appl. Nano Mater., 2 (2019) 3262

[7] J. Köster et al., Nanotechnology 32 (2021) 075704

[8] A. Storm, J. Köster, et al. ACS Nano 17 (2023) 4250-4260

[9] M. Quincke, ACS App. Nano Mat. 5 (2022) 11429

[10] M. Kühne, F. Börnert et al., Nature 564 (2018) 234

[11] K. Cao et al., Science Advances 6 (2020) eaay5849

[12] K. Liu et al., Nature Chemistry 11 (2019) 994

[13] H. Qi et al., Science Advances 6, (2020) eabb5976

[14] B. Liang et al. Nature Communication 13 (2022) 3948.

9:45 AMBREAK

10:15 AM *SF02.09.04

Surface Dynamics of Atomically Controlled Electrodes for Clean Energy Magali Lingenfelder; EPFL, Switzerland

Our society faces a critical challenge in shifting from a reliance on carbon-based energy to sustainable renewable sources. A key step towards achieving clean energy lies in developing efficient catalysts that can convert chemical energy into electricity or use electrons to generate chemical energy.

In our research group, we tackle these challenges by creating customized materials that draw inspiration from nature (biomimicry) and combine principles from interfacial chemistry and surface physics. For this presentation, I focus on the process of photosynthesis as inspiration for the design, characterization, and dynamic nature of functional interfaces that drive energy conversion processes such as CO₂ electroreduction and water splitting on the surface of Earth-abundant materials.

I will also discuss the application of cutting-edge scanning probe microscopy and Raman spectroscopy under electrochemical conditions, which allows us to visualize dynamic processes at the nanoscale (*operando* imaging). Additionally, I will highlight our use of unconventional strategies that leverage the assembly of chiral molecular layers and two-dimensional materials to enhance electrocatalytic conversion processes. (References : Nanoletters, 2021, 21, 2059; Nature Comm., 2022, 13, 3356, IJC 62, 11, 2022).

10:45 AM *SF02.09.05

Interfacial Liquid Water on Graphite, Graphene and 2D Materials Ricardo Garcia; Consejo Superior de Investigaciones Científicas, Spain

Solid-water interfaces have a prominent role in a variety of fields such as surface science, geochemistry, electrochemistry, energy storage or molecular and cell biology. Liquids near a solid surface form an interfacial layer where the molecular structure is different from that of the bulk. Yet the molecular-scale understanding of the interactions of liquid water with solid interfaces is unsatisfactory for the lack of high-spatial resolution methods. Here I will present an AFM-based method that provides atomic-scale resolution images of solid-liquid interfaces.

The presentation is divided in three sections. The first section is an introduction to the relevance of solid-liquid interfaces. The second section, presents the features and capabilities of 3D-AFM [1-3] to image with atomic resolution the **three-dimensional** interfacial structure of surfaces immersed in aqueous solutions. The third section reports the structure of interfacial water layers on different **2D materials** from graphene to a few layer MoS₂; from hexagonal boron nitride to a few layer WSe₂. Those interfaces are characterized by the existence of a 2 nm thick region above the solid surface where the liquid density oscillates [4-8]. The distances between adjacent layers for graphene, few-layer MoS₂, h-BN and pentacene are ~0.50 nm. This value is larger than the one predicted and measured for water density oscillations (~0.30 nm). The experiments demonstrate that on extended **hydrophobic surfaces water** molecules are **expelled** from the vicinity of the surface and replaced by several molecular-size hydrophobic layers.

References

[1] D. Martin-Jimenez, E. Chacon, P. Tarazona, R. Garcia, Nat. Commun. **7**, 12164 (2016).

[2] T. Fukuma and R. Garcia, ACS Nano **12** 11785 (2018).

[3] S. Benaglia, et al. Phys. Rev. Lett. **15**, 20574-20581 (2021)

[4] M.R. Uhlig, D. Martin-Jimenez and R. Garcia, Nat. Commun. **10**, 2606 (2019).

[5] M.R. Uhlig, R. Garcia, Nano Lett. **21**, 5593 (2021)

[6] M.R. Uhlig, S. Benaglia, R. Thakkar, J. Gomer and R. Garcia, Nanoscale **13**, 5275 (2021)

[7] D.M. Arvelo, M.R. Uhlig, J. Comer, R. Garcia, Nanoscale 14, 14178 (2022)

[8] R. Garcia, ACS Nano 17, 51-69 (2023)

11:15 AM SF02.09.06

Modeling and Experimental Analysis of Vertical and Lateral Growth of 2D Mo₂C Crystals via Chemical Vapor Deposition Goknur Cambaz Buke¹, Omer Caylan² and Tarik Ogurtani³; ¹TOBB ETU, Turkey; ²Massachusetts Institute of Technology, United States; ³Middle East Technical University, Turkey

This study investigates the growth of Mo₂C crystals through Chemical Vapor Deposition (CVD) on Cu substrates. The research combines theoretical and experimental approaches to examine both the vertical and lateral growth of Mo₂C crystals. A physico-mathematical model is developed, incorporating bulk and surface diffusivities, as well as solubility gradients for Mo₂C crystal growth. Nonlinear flow equations are used to predict Mo₂C crystal growth rates in vertical and lateral directions within the Mo-, Cu-, Mo₂C layer framework. The model correlates the height and diameter of the Mo₂C crystals with the thickness of the copper layer and time, which is then validated through experiments and imaging techniques such as SEM and AFM. The results highlight the significant influence of the copper layer thickness on the height of Mo₂C crystals, while its impact on the lateral dimensions is less critical. The study goes beyond enhancing Mo₂C crystal growth and explores the synthesis of tailored Mo₂C crystals for specific applications. The developed forward model provides a platform for further advancements and exploration of related material analogs.

11:30 AM *SF02.09.07

Interface and Interlayer Dynamics in 2-D MnO₂ via *In-Situ* Characterization Scott T. Misture; Alfred University, United States

Supercapacitor electrodes can be prepared from MnO₂ nanosheets exfoliated from highly crystalline powder particles and subsequently flocculated to form porous solid electrodes. Restacking of the 2-D nanosheets in packets of ~5 layers affords high surface area electrodes with highly flexible interlayer spaces for electrochemical activity. The talk centers on the application *in-situ* and *in-operando* studies using high energy X-ray diffraction, X-ray pair distribution functions, EXAFS/XANES and Raman spectroscopy. We show that linking electrochemical measurements to local structure characterization results enables us to understand the mechanisms by which charging occurs in supercapacitor electrodes. The data show that the re-stacked 2-D nanosheets go through a phase transition during charge/discharge wherein the interlayer chemistry alters the interlayer stacking in a subtle but detectable manner. The presence vs. absence of interlayer water and electrochemically active ions including Na, K or Rb define the interlayer stacking. Using a combined approach that tracks the Mn oxidation state, the local structures (via PDF and Raman) and charge/discharge electron exchange forms a clear picture of the physical mechanisms at play, including mechanisms of capacity fade.

SESSION SF02.10: Materials Surfaces II
Session Chairs: Goknur Cambaz Buke and Mohsin Qazi
Thursday Afternoon, November 30, 2023
Sheraton, Second Floor, Republic A

1:30 PM *SF02.10.01

Epitaxial and Interfacial Crystallization of Metal Halide Perovskites and Their Heterostructures Song Jin; University of Wisconsin--Madison, United States

Metal halide perovskites are inexpensive semiconductor materials promising for high performance solar cells and light emitting diodes (LEDs) because they are easy to synthesize and tolerant of defects. We developed new methods for synthesizing nanostructures of both three-dimensional (3D) perovskites and two-dimensional (2D) Ruddlesden-Popper (RP) layered perovskites, including vapor phase epitaxial growth on crystalline inorganic substrates and general solution growth of 2D RP perovskite nanosheets at the air-water interface. More chemically unstable and less soluble 2D perovskites could also be crystallized at the interface of aqueous-nonaqueous solutions. We further create novel and arbitrary heterostructures, such as 2D/3D perovskite, vertical and lateral 2D heterostructures, with high quality interface and tunable band alignments. Various structural characterization and time-resolved spectroscopic methods have been employed to collaboratively study the carrier transfer mechanisms between these well-defined heterostructures of 2D and 3D perovskites. Fundamental understanding of the factors controlling the carrier transfer mechanisms in heterostructures of halide perovskites is crucial for guiding the synthetic strategies to improve properties and device applications.

2:00 PM SF02.10.02

Filament-Induced Crystallization of TiN/HfO_x/TiN Film in Neuromorphic Devices Alexandre Foucher¹, Baoming Wang², Teodor Todorov³, John Rozen³ and Frances M. Ross¹; ¹Massachusetts Institute of Technology, United States; ²Nanjing University, China; ³IBM T.J. Watson Research Center, United States

HfO_x films are increasingly under scrutiny for applications in resistive random-access memory (ReRAM) devices. HfO_x-based structures have a fast-switching speed, excellent stability, and can be easily integrated in complex devices. However, changes in crystal structure when current and voltage are applied are not well understood and are crucial to guide the rational design of HfO_x-based devices. To this end, a TiN/HfO_x/TiN stack implemented in nanodevices was studied with *in situ* scanning transmission electron microscopy (STEM). We observed crystallization of the initially amorphous HfO_x films and grain growth of crystals during repeating switching with increasing applied current and voltage. The formation and growth of crystalline region could then correlate to changes in measured conductance on the sample studied with *in situ* STEM. *In situ* electron energy loss spectroscopy (EELS) showed the depletion in oxygen of crystalline phases compared to the initial amorphous HfO_x phase. We suggest that this is due to the displacement of oxygen vacancies that concentrate in the crystalline grains and is the cause of the neuromorphic properties of the HfO_x film. Oxygen migration toward the TiN/HfO_x interface and the importance of crystallization at the interfaces are also discussed. We aim to use this atomistic understanding of crystallization and structural changes of HfO_x in TiN/HfO_x/TiN to guide the rational design of multilayered materials for electronic applications.

2:15 PM SF02.10.03

***In-Operando* Optical Tracking of Vacancy Induced Phase Change in Few-nm Thick Ferroelectric HZO** Atif Jan, Sunil Taper and Giuliana Di Martino; University of Cambridge, United Kingdom

Ferroelectric random-access memories (FeRAM) switching is achieved by ferroelectric switching of dipoles. FeRAMs offer low-energy and faster switching as compared to conventional memory circuitry. They excel in terms of power consumption and low voltage operation, when stacked against current-driven contenders. Unfortunately, FeRAMs have been restricted to niche markets due to their limited CMOS-compatibility and severe scaling issues of the complex ferroelectric perovskite systems. However, the discovery of ferroelectricity in binary oxides gave an impetus for development of universal memory concept, which may lead to a significant breakthrough in the development of memory devices. Binary oxides generally do not suffer from a “dead layer effect”, which makes non-binary oxides, such as perovskites, ineffective for thin film technology. Moreover, high coercive fields inside binary oxides give them a considerable resilience toward internal depolarization of the ferroelectricity, crucial to achieve scalability as well as overcome the widespread reliability disadvantages of FE material. The underlying reasons for the stable ferroelectricity and distinct switching of FE domains inside binary oxides at an atomic level are poorly understood. Moreover, non-idealities seen upon continuous electronic switching cycles like wake-up and fatigue introduce uncertainties in device performance and endurance. In this work, we present the first proof of the underlying reasons for these non-idealities with cycle-to-cycle tracking of morphology changes in few-nm thick binary oxide ferroelectric ultra-thin films.

This work presents the first proof of the underlying reasons for these non-idealities with cycle-to-cycle tracking of morphology changes in few-nm thick binary oxide ferroelectric ultra-thin films. With our Nanoparticle-on-Mirror (NPOM) geometry, we capture for the first time both migration of <1% oxygen ions and material phase change in just 5nm-thick binary oxide ferroelectric films when under continuous electronic switching, and therefore track in real-time and *in-operando* the nanoscale kinetics of wake-up and fatigue in ferroelectric ultrathin memories. We use *in-situ* electrical and optical characterizations like darkfield scattering, photoluminescence and Raman spectroscopy to understand the nano-kinetics of the atomic level switching. The tracking of vacancy migration and phase change with the above-mentioned techniques combined with density functional theory (DFT) and finite-difference time-domain (FDTD) simulations provide the first insights into the morphological changes in ultra-thin binary oxide films [1].

[1]: A. Jan, T. Rembert, S. Taper, J. Symonowicz, N. Strkalj, T. Moon, Y. S. Lee, H. Bae, H. J. Lee, D.-H. Choe, J. Heo, J. MacManus-Driscoll, B. Monserrat, G. Di Martino, *Advanced Functional Materials* 2023, 33, 2214970.

2:30 PM *SF02.10.04

Denoising Total Scattering Data using Compressive Sensing Niklas B. Thompson and James Weng; Argonne National Laboratory, United States

Total X-ray scattering measurements performed with high-energy incident photons (> 50 keV), complemented by real-space analysis via the pair distribution function (PDF), is an indispensable tool in determining the local atomic structure of amorphous and nanoscale materials. While the application of PDF analysis to bulk systems is a mature field, there is burgeoning interest in extending its domain of application to more complex sample environments, such as thin films and dilute solutions, with an eye toward *in operando* measurements under realistic operating conditions. In this setting, the scattering signal originating from the material of interest is typically overwhelmed by the background signal (*e.g.*, from the substrate beneath a thin film, or the solvent in a dilute solution). The successful separation of the intrinsically weak signal of the desired material from the background thus depends on collecting raw data with a high signal-to-noise ratio (SNR), a central challenge in flux-limited X-ray scattering measurements on disordered systems.

Ideally, this challenge can be addressed by simply increasing the measurement time or incident X-ray flux. However, this can result in both radiation damage—altering the structure of the native sample—and limits the time resolution of total X-ray scattering in *operando* settings. Inspired by recent developments in compressive sensing, we have developed a means of signal denoising based on the responses of many “virtual detectors”, using a single real measurement from an area detector. The technique relies on the sparsity of real scattering images in an appropriate transformation basis, rendering the true signal separable from the (necessarily) non-sparse noise. Our purely computational approach allows the resolution of noisy signals which cannot be easily measured using current detectors without modification of the existing hardware. Based on experiments with both simulations and real data, the resulting virtual measurements behave as though they were independent measurements; by averaging over the virtual measurements, the actual SNR can thus be improved. Effectively, this turns one measurement into an arbitrary number of repeated measurements, thereby allowing for measurements of disordered materials susceptible to radiation damage and rapid kinetic experiments that are otherwise difficult to perform.

3:00 PMBREAK

3:30 PM *SF02.10.05

Bits to Atoms and Atoms to Bits: Atomic Fabrication in Electron Microscopy Sergei V. Kalinin¹, Marc Bellemare², Aaron Courville², Jesse Farebrother^{2,3}, Max Schwarzer², Pablo S. Castro³, Joshua Greaves³, Maxim Ziatdinov⁴, Ayana Ghosh¹, Igor Mordatch³ and Kevin Roccapriore⁴; ¹University of Tennessee, Knoxville, United States; ²MILA, Canada; ³Google Deep Mind, United States; ⁴Oak Ridge National Laboratory, United States

The last note left by Richard Feynman stated “*What I cannot create, I do not understand.*” Building solid state quantum computers, creating nanorobots, and designing new classes of biological molecules and catalysts alike requires the capability to manipulate and assemble matter atom by atom, probe the resulting structures, and connecting them to macroscopic world. Until now, the only viable approach for atomic fabrication was the Scanning Tunneling Microscopy, often integrated with the bespoke surface science techniques. Over the last decade, it has been shown that electron beams in Scanning Transmission Electron Microscopy can be used not only to probe structure and electronic properties of materials on atomic level, but also to modify materials on the atomic level. Harnessing electron beam changes for direct atomic fabrication however requires synergy between machine learning methods and microscope control. In this presentation, I will illustrate the progression of automated electron microscopy from real-time data analysis to physics discovery to atomic manipulations. Here, the applications of classical deep learning methods in streaming image analysis are strongly affected by the out of distribution drift effects, and the approaches to minimize them are discussed. The robust approach for real-time analysis of the scanning transmission electron microscopy (STEM) data streams, based on the ensemble learning and iterative training (ELIT) of deep convolutional neural networks, is implemented on an operational microscope, enabling the exploration of the dynamics of specific atomic configurations under electron beam irradiation via an automated experiment in STEM. Combined with beam control, this approach allows studying beam effects on selected atomic groups and chemical bonds in a fully automated mode. We demonstrate atomically precise engineering of single vacancy lines in transition metal dichalcogenides and the creation and identification of topological defects in graphene. The ELIT-based approach opens the pathway toward the direct on-the-fly analysis of the STEM data and engendering real-time feedback schemes for probing electron beam chemistry, atomic manipulation, and atom by atom assembly. We further illustrate how deep kernel learning (DKL) methods allow to realize both the exploration of complex systems towards the discovery of structure-property relationship, and enable automated experiment targeting physics (rather than simple spatial feature) discovery. The latter is illustrated via experimental discovery of the edge plasmons in STEM/EELS. Finally, we demonstrate the use of the reinforcement learning for real-time control of atomic motion. Jointly, these developments open the pathway for creation and characterization of designed defect configurations and artificial molecules in 2D materials.

4:00 PM SF02.10.06

Compositional and Structural Analysis of Iron Phosphate Conversion Coatings by Synchrotron Soft X-Ray Spectroscopy Koki Itamoto¹, Kakeru Ninomiya^{1,1,1}, Hidekazu Fukushi², Hideyuki Taguchi², Keiichi Nakajima², Ei Uchiyama², Yusuke Miyazawa², Miku Ando², Sota Fukushima² and Maiko Nishibori^{1,1,1}; ¹Tohoku University, Japan; ²Nihon Parkerizing Co. Ltd., Japan

Conversion coating, which precipitates on the surface of a metal material through a chemical reaction, prevents rust and improves coating adhesion. A typical treatment is the phosphate conversion coating treatment, which forms a coating containing phosphate. The iron phosphate conversion coating for steel materials is generally used because of its low-cost and low-sludge generation, although its rust prevention performance is inferior to other treatments. In this treatment, the Fe²⁺ is eluted from the surface of the steel by etching, which is immediately oxidized to Fe³⁺ by dissolved oxygen. Then, Fe³⁺ reacts with OH⁻ and H₂PO₄⁻ in the treatment solution to precipitate a coating composed of Fe₂O₃ and FePO₄ [1]. Therefore, it is essential to understand the dissolution and precipitation reactions of Fe that occur at the interface between the steel and the treatment solution to improve the properties of the coating film. We have previously observed changes in the film structure with film thickness (deposition amount) by X-ray photoelectron spectroscopy and scanning electron microscopy. As a result, it was found that the film is composed of nm-sized particles generated by nucleation and aggregation and that the main component of the coating is FePO₄, regardless of the deposition amount [2]. This differs from the component ratio (Fe₂O₃:FePO₄ = 7:3) reported in a previous study [1]. In this study, we attempted to quantitatively analyze the chemical states of the constituent elements by X-ray emission spectroscopy, which is capable of element-selective state separation, to clarify the ratio of coating components according to the deposition amount in more detail.

The coatings that completely coated the steel surface comprised approximately 90 % FePO₄ and 10% Fe₂O₃. On the other hand, coatings with less than 80 % coverage were found to contain little Fe₂O₃ and 20 % FeO. Therefore, a part of Fe²⁺ eluted from the steel surface precipitates as a coating component without oxidizing. In addition, the amount of P content in the coating obtained by X-ray fluorescence analysis was used as the deposition amount of FePO₄, and the deposition amount of each component was calculated based on the component ratios obtained. The amount of FePO₄ kept increasing with reaction time. On the other hand, the total deposition of iron oxide components increased up to 80 % coverage and remained almost constant thereafter. Therefore, the deposition reaction of the coating may vary with the coverage. These results suggest that the iron phosphate conversion coating is deposited by a reaction path different from the conventionally considered steel/treatment solution interface reaction.

[1] H. Ishii, *Hyomen-Gijutsu*, **61**(2010), 216–222.

[2] Y. Miyazawa, K. Nakajima, K. Itamoto, S. Fukushima, M. Ando, E. Uchiyama, K. Ninomiya, M. Nishibori, H. Fukushi, H. Taguchi, *J. Japan Inst. Met. Mater.*, **8**(2023).

4:15 PM SF02.10.07

In-Situ Diffraction-Based Characterization on the Topotactic Reduction of Nickelate Thin Films Wenzheng Wei¹, Kidae Shin¹, Hawoong Hong², Yeongjae Shin¹, Robert F. Klie³, Arashdeep S. Thind³, Yingjie Yang³, Frederick Walker¹ and Charles Ahn¹; ¹Yale University, United States; ²Argonne National Laboratory, United States; ³University of Illinois at Chicago, United States

Square-planar nickelates are a novel class of superconductors, which promise to help unveil aspects about the nature of superconductivity in oxide materials. Their synthesis consists of the growth of a perovskite precursor followed by a topotactic reduction to remove apical oxygen ions. The common reduction process involves annealing in vacuum with CaH₂ powder. This *ex-situ* process is less easily amenable to *in-situ* measurements of the dynamics of square-planar nickelate formation.

To address this challenge, we develop an *in-situ* process via the deposition of metallic aluminum in ultra-high vacuum (UHV), and we demonstrate the reduction process by reducing NdNiO₃ thin films grown using molecular beam epitaxy (MBE). During reduction we characterize the atomic and electronic structure of this class of square planar nickelates with the *operando* X-ray diffraction facility at beamline 33 ID-E in Argonne National Lab using crystal truncation rod (CTR) and diffraction-based X-ray absorption near edge structure (dXANES). By characterizing the NdNiO_{3-x} thin films dynamically during the reduction process, we show that the Ni valence and NdNiO_{3-x} lattice constant can be precisely controlled at each step of the Al deposition process, while maintaining the film's epitaxy and surface morphology. The metal reduction method and *in-situ* characterization of the reaction stages is straightforward and broadly applicable to oxide reduction.

Work at Yale University was supported by the US DOE, Office of Science, Office of Basic Energy Sciences under award no. DE-SC0019211.

4:30 PM *SF02.10.08

Manipulating the Assembly and Electronic Structures of 2D Materials at the Interfaces Jun Liu; University of Washington, United States

This presentation will highlight our effort to develop innovative approaches to control the assembly and electronic structures of two-dimensional (2D) nanostructured materials. Several synthetic strategies will be discussed in which interfacial energies are manipulated using functional groups on the substrate, the solvation structure, nanoscale confinement in ordered surfactant templates, the strain energy between the crystal, and the substrate and electrochemical potentials. Substrate- or interface-controlled solution synthesis is used as the platform for nucleation and assembly. Several classes of materials are investigated: (1) 2D nanosheets formed by metal oxides and metals, (2) metal chalcogenides and dichalcogenides, and (3) organic/inorganic hybrid crystals. Furthermore, a new technique is developed based on quantum capacitance measurement to provide information about the position of defect energy levels with respect to conduction and valence band edges, and the position of the Fermi level. This measurement is used to capture the evolution of the density of states (DOS) during solution synthesis and electrochemical processes. The conduction and valence band edges, defect energy levels, and features inside the conduction band are revealed in real time and under ambient conditions. The band structures and defects are correlated to the electrocatalytic properties of the 2D crystals.

SESSION SF02.11: (Bio)Mineralization
Session Chairs: Jingshan Du and Shuai Zhang
Friday Morning, December 1, 2023
Hynes, Level 2, Room 201

8:30 AM *SF02.11.01

Designing Interfaces Between Inorganic Crystals and De Novo Proteins Harley Pyles^{1,2}, Fatima Davila-Hernandez¹, Biao Jin³, Amijai Saragovi¹, Shuai Zhang³, Sakshi Schmid³, Lili Liu³, Jingshan Du³, James J. De Yoreo³ and David Baker¹; ¹Institute for Protein Design - University of Washington, United States; ²University of Washington, United States; ³Pacific Northwest

Hybrid materials composed of biomacromolecules and inorganic crystals have exceptional properties and fulfill critical functional requirements of the organisms that produce them. These biominerals are known to contain proteins that play roles in controlling the crystal polymorph, shape, size, and organization of the mineral constituents. However, the structural details of protein-inorganic interfaces inside biominerals remain largely unknown and are challenging to study because native biomineralization proteins are often intrinsically disordered and function within complex multi-component systems. Designing well-structured de novo proteins with surfaces that form favorable interactions with inorganic crystals has allowed us to study both how these interfaces promote adsorption and assembly of proteins on existing minerals, and how the proteins template mineral growth.

Previously, we have shown that designed helical repeat proteins (DHR) with a periodic array of side chains lattice matched to the mica surface adsorbed and assembled into 2D structures at the mica-water interface. The structure of the interfacial assemblies could be modulated by adding protein-protein interfaces in addition to the protein-mica interface. The size, regularity, and stable rod-like shape of these proteins has enabled further study on the effects of solvent and electrolytes on biomolecules at the solid liquid interface and mapping of the angular energy landscape of adsorbed proteins.

Recently, we have shown that specific DHRs that contain designed periodic arrays of negatively charged carboxylate containing side chains promote the direct nucleation of the calcite polymorph of calcium carbonate (CaCO₃). This bypasses the formation of vaterite which is seen in the absence of protein, in the presence of bovine serum albumin control protein, and in the presence of a DHR with a similar surface but a different distance between adjacent repeats. Mutational analysis of a protein that promotes calcite formation indicates that activity depends on sidechain stereochemistry and is not driven by charge alone. The calcite nucleating proteins also altered the post-nucleation growth mechanism from classical growth to oriented particle attachment, a mechanism often seen in natural biomineralization processes.

Currently, we are working with a new designed library of over 6.5K de novo repeat proteins displayed on the surface of yeast. These proteins have a variety of topologies and have diverse chemical groups arranged in periodic and aperiodic arrays on their surfaces. We are using a high throughput flow-cytometry (FC) assay to screen for proteins that promote the strong adsorption of inorganic nanoparticles to the yeast cells displaying them. Nanoparticle binding proteins have been selected from the library and expressed in E coli, purified, and biochemically characterized, and we are studying their effects on the growth of these materials from ionic precursors and on metallic substrates.

Overall, our research shows the potential of de novo protein design as a powerful tool for studying and manipulating the interfaces between genetically encoded proteins and inorganic crystals, offering exciting prospects for biomimetic materials synthesis.

9:00 AM SF02.11.02

Sulfated Chitosan Derivatives Modulate the Kinetics of CaCO₃ Nucleation by a Systematic Relationship to Interfacial Energy Barrier Brenna M. Knight^{1,1,1}, Ronnie Mondal¹, Nicholas Pietra¹, Brady A. Hall¹, Kevin J. Edgar^{1,1,1}, Valerie Vaissier Welborn^{1,1}, Louis A. Madsen^{1,1}, James J. De Yoreo^{2,3} and Patricia M. Dove^{1,1,1}; ¹Virginia Tech, United States; ²Pacific Northwest National Laboratory, United States; ³University of Washington, United States

Organisms use functionalized macromolecules at sites of biomineralization to nucleate and grow diverse CaCO₃-organic composites as skeletal structures. Acidic groups (COO⁻, SO₃⁻, PO₄³⁻) are known to impact CaCO₃ mineralization but systematic relationships have not been ascertained. Establishing the kinetic and thermodynamic bases for mineralization are fundamental to understanding and replicating control on crystal nucleation and growth in these settings. Of particular importance is how macromolecules in the organic matrix regulate when and where crystals grow. Thus, discerning how functional groups moderate the crystallization of sparingly soluble salts is of first order importance.

Using complimentary experimental and theoretical approaches, we first synthesize a series of tailored and characterized chitosan derivatives that present variable degrees of sulfation (DS(SO₃⁻) = 0.1 - 0.8) and sulfate regiopositions (C₂N- or C_{3,6}O-). Chitosan provides a simple model for macromolecules in the organic matrix that allows us to measure the dependence of calcite nucleation rate on sulfate density and to determine how this group modulates the energy barrier to crystallization. By quantifying the rate of CaCO₃ nucleation onto these materials over a range of supersaturations using established methods, we show rates increase with supersaturation as predicted by classical nucleation theory (CNT). Rates of nucleation onto materials with increasing DS(SO₃⁻) exhibit a stronger dependence on supersaturation, indicating a higher energy barrier to nucleation. Fitting the CNT model to the data, we demonstrate the interfacial energy barrier (γ_{net}) to calcite nucleation correlates with sulfate density by a systematic dependence that is independent of sulfate regioposition.

We propose that sulfate density creates an increasingly hydrophilic, negatively charged environment at the polysaccharide-water interface to increase γ_{net} through reductions in $\gamma_{substrate-water}$. Such an environment would also promote Ca²⁺ interactions with sulfate, possibly at the expense of carbonate.

To test this idea, we conduct a molecular dynamics (MD) study of sulfated chitosan chains that also have varying degrees and positions of sulfation. Each type of polymer is placed in a simulation cell populated with water, NaHCO₃, and CaCl₂. Polymer equilibrium conformation is first established on GROMACS using a non-polarizable forcefield, following which molecular dynamics simulations are run under a polarizable AMOEBA force field. The trajectory obtained is used to calculate the time-averaged radial distribution functions (RDFs) to ascertain proximity between atoms of interest.

As predicted, the MD simulations show the average S-Ca distance decreases with DS(SO₃⁻), indicating stronger Ca-S interactions in the increasingly hydrophilic environment. This is supported by a reduction in the average hydration number of Ca²⁺ in the N-sulfated and O-sulfated environments of 12.5% and 25%, respectively, compared to the bulk value (8) and by the significantly higher water density about SO₃⁻ groups compared to uncharged substituents. The findings from these combined experimental and theoretical methodologies suggest the potential to design biomaterials with localized regions of high/local activity and control crystal placement at near-molecular resolution for advanced applications.

9:15 AM SF02.11.03

Spatially Controlled Supersaturation of Calcium Phosphate for Controlled Crystal Nucleation and Self-Healing Precipitates Mohsin J. Qazi, Rena Fukuda and Nate J. Cira; Cornell University, United States

Crystal nucleation and growth are widely studied phenomena due to their relevance to a range of disciplines including material science, process engineering, and biology. In order to obtain desirable crystal forms or crystallization dynamics, it is essential to tune parameters like nucleation time, nucleation rate, and growth rate. Supersaturation of material in the crystallizing solution is the first step in the crystallization process, and impacts all these parameters, hence controlling supersaturation is crucial to controlling the overall process of crystallization (1). Some common methods to achieve supersaturation include subjecting a solution to: evaporation, cooling (for materials with temperature-dependent solubility), the addition of antisolvents, and pH change (for materials with pH-dependent solubility). These methods typically result in supersaturation within the primary solution. However, in some systems such as biomineralization or studies probing nucleation dynamics, nucleation is required at specific locations, often outside the region where the primary solution composition can be easily actively controlled. This motivates the development of strategies to create localized supersaturated conditions.

In this study, we present a straightforward approach that enables spatially controlled deposition of precipitated material between two primary solutions (2). Our experimental setup focuses on calcium phosphate (CAP) as a prototypical system, taking advantage of its pH-dependent solubility. By connecting two saturated solutions at different pHs using a gel that allows ion diffusion, we establish a concentration gradient along the gel. The diffusion and reaction of H⁺ and OH⁻ create a characteristic pH profile along the length of the gel, causing the diffusing calcium and phosphate to become supersaturated and precipitate. Over time, the precipitated band grows denser and forms a barrier that restricts further transport through the gel. We show how this band spontaneously recovers from perturbation, automatically resealing any damage. In addition to experiments, we perform quantitative analysis taking into consideration the diffusion dynamics of all the relevant ions, chemical equilibria, and reaction parameters, to predict the location of the precipitated bands. This work provides a simple physical strategy for creating self-healing precipitates that may be useful in civil engineering, restorative dentistry, and enhancing our understanding of mineral deposit formation in the abiotic and living world.

References:

- (1) Mullin, J.W. Crystallization, Fourth Edition, p. 315, 2001.
- (2) Wagner M.; Hess, T.; Zakowiecki, D.; Studies on the pH-Dependent Solubility of Various Grades of Calcium Phosphate-based Pharmaceutical Excipients, J. Pharm. Sci, 2022.

9:30 AM SF02.11.04

Nucleation and Growth of Minerals on Self-Assembled Monolayers Veselina Marinova, Stephen Yeandel, Vittoria Fantauzzo, Colin Freeman and John H. Harding; University of Sheffield, United Kingdom

Minerals are frequently grown in water-based systems in both nature (biomineralisation) and industry. The water may stabilise the interface and potentially hinder or aid the flow of ions to the interface and their attachment. The behaviour of water at these growing interfaces is therefore very important as it will often govern the growth dynamics. Self-assembled monolayers (SAMs) have long been used as substrates and/or templates for the growth of minerals [1] and as model systems for biomineralisation [2]. These organic systems provide arrays of organised head groups that can be functionalised and positioned to generate patterns and specific charge densities. How the water and ions within the solution organise at this interface is very important if we are to understand the nucleation and subsequent growth of minerals at this interface.

We explore a range of models to obtain surface ion concentrations from the simple Gouy-Chapman approximation to the Poisson-Boltzmann equation through to full solutions of the Grahame equation [3,4] including the effects of speciation and changes in activity as a function of local species concentrations. Explicit all atom simulations [5,6] are used to examine the organisation and distribution of ions at these interfaces. Use of a constant chemical potential ensemble [7] allows us to examine the effects of different ionic concentrations using atomistic simulations and so compare results with those obtained using the continuum Poisson-Boltzmann approaches.

We find that certain defects in the SAM structure, which we refer to as active defects, can impair ionic surface diffusion, as well as affect the diffusion of ions in close proximity to the surface feature in question. Our findings suggest that this effect can allow such topological features to promote ion clustering and increase local ionic concentration at specific surface sites. The work reported here shows how the presence of small atomic-scale defects can affect the role of a surface in the process of heterogeneous nucleation. We discuss the importance of SAM structures and the solution conditions at the interface on the efficacy of these monolayers as nucleating agents.

- [1] J. Love, L. Estroff, J. Kriebel, R. Nuzzo and G. Whitesides; Chem. Rev. 105 (2005) 1103.
- [2] N.A.J. Sommerdijk and G. de With; Chem. Rev. 108 (2008) 4499
- [3] J.M. Block and W. Yen; Phys. Rev. A41 (1990) 844
- [4] M.J. Lochhead, S.R. Letellier and V. Vogel; J. Phys. Chem. B101 (1997) 10821.
- [5] A.S. Côté, R. Darkins and D.M. Duffy; J. Phys. Chem. C118 (2014) 19188.
- [6] V. Marinova, C.L. Freeman and J.H. Harding; Farad. Disc. 235 (2022) 289.
- [7] A.R. Finney, I.J. McPherson, P.R. Unwin and M. Salvalaglio; Chem. Sci. 12 (2021) 11166.

9:45 AMBREAK

10:15 AM *SF02.11.05

Molecular Interaction Forces at Mineral-Electrolyte Interfaces: Insights from AFM Spectroscopy[Frieder Mugele](#); University of Twente, Netherlands

Colloidal self-assembly and aggregation are controlled by molecular scale interaction forces across (sub)nanometric films of an ambient fluid, often thin water layers of variable salt content and pH. In this lecture, I will give an overview over insights that we have gained using *in situ* Atomic Force Microscopy (AFM) measurements on the structure of the electric double layer and the resulting nano-scale interaction forces. I will discuss aspects of ion adsorption, hydration, and electrostatic forces for a variety of systems ranging from clay minerals to semi-conducting nanoparticles. In particular, I will illustrate the potential of operando-AFM for the characterization of photocatalytically active materials with a specific focus on facet-dependent surface charges and their role for the separation of photogenerated charge carriers.

10:45 AM SF02.11.06

Revealing the Molecular Forces that Stabilize Surface Precipitates of Hydroxides by Three-Dimensional Atomic Force Microscopy[Mingyi Zhang](#)¹, Benjamin A. Legg¹, Younjin Min² and James J. De Yoreo^{1,3}; ¹Pacific Northwest National Laboratory, United States; ²University of California, Riverside, United States; ³University of Washington, United States

Surface charging of solid-liquid interfaces plays a critical role in various chemical processes, such as ion adsorption, particle aggregation, crystal nucleation and growth. Recent work indicates that surface charging can drive the formation of complex laterally ordered surface structures. However, the properties of the resulting heterogenous charge distributions (and their associated electrical double layer structure) are still poorly understood. Modern atomic probe microscopy offers a promising tool for investigating the behaviors at heterogeneously charged surfaces. *In situ* high speed atomic force microscopy enables directly imaging of the motion of surface adsorbates at molecular scales; while three-dimensional fast force mapping (3D FFM) allows us to track the tip-sample interaction forces above the surface, aiding in the interpretation of surface charging phenomena through DLVO theory.

Here, the adsorption behaviors of multivalent cations (Mg^{2+} and Al^{3+}) on muscovite mica has been studied by atomic force microscopy across a range of pH values. At mild pH values, two-dimensional hydroxide films form whose morphology depends on the ion type. For the divalent Mg-hydroxide, it tends to form monolayered large continuous film. For the trivalent Al-hydroxide, it forms monolayered films with a persistent network of gaps, combining positively charged hydroxide islands and negatively charged bare mica regions, which is inconsistent with the prediction of the classical crystal growth model; at even higher pH values, multi-layered gibbsite film growth has been observed, with the upper layers exhibiting similar behavior to Mg hydroxide films that form large continuous sheets. At low pH conditions, it is feasible to image individual ions and clusters and see how the adsorbate populations change with pH. At a pH immediately preceding film nucleation, these ions reveal complex lateral ordering that are controlled by the interplay between ion/ion interactions and ion/substrate interactions.

The links between ion-ordering, film structure, and local surface charge were investigated by using 3D FFM and complementary streaming potential measurements. The results indicate that the coverage and structure of the surface precipitates are strongly influenced by the charged substrate. Also, Al-hydroxide films are more strongly charged than Mg-hydroxide films, supporting the hypothesis that the hydroxide nanostructure is stabilized by electrostatic interactions between positively charged film and negatively charged substrate. The work exemplifies the importance of surface charge in crystal nucleation, while also offering valuable insights on how electric fields can be utilized to control crystallization processes.

11:00 AM SF02.11.07

The Impact of Local Structure and Dynamics on the Free Energy of Aqueous Mineral Interfaces[Stephen Yeandel](#), Veselina Marinova, Emma Armstrong, Colin Freeman and John H. Harding; The University of Sheffield, United Kingdom

The strong interactions between mineral ions and water molecules can profoundly alter the structure and properties of water molecules at aqueous interfaces[1]. Strong ordering produces density fluctuations, particularly for very flat interfaces (such as mica and calcite)[2]. Diffusion rates of water molecules are greatly reduced from the bulk, leading to the hypothesis that ice-like structure is present. The water often stabilises the mineral surface and configurational interfacial energies obtained from classical molecular dynamics simulations are used to interpret this, even though this ignores entropic effects. Our new methods for calculating interfacial free energies[3], based on using Einstein crystals as a reference state, demonstrate that these effects contribute significantly to the thermodynamics of these interfaces and cannot be ignored.

In this work we examine the aqueous surfaces of calcium sulphate (gypsum, bassanite) and calcium carbonate (calcite, aragonite). We explore the structure and dynamics of water at these interfaces and quantify the enthalpic and entropic contributions to the total free energy. New insights into the competing growth mechanisms of different polymorphs may also be obtained[4]. We will also discuss effects due to the presence of solute ions close to the interface which can alter the activity of interfacial water, induce electrical space charge layers or change the relative stability of different surfaces by disrupting the ordering of the solvent. Our simulations will examine the potential mechanisms of attachment at these surfaces and how the interfacial energy and solution affects these growth processes.

- [1] Y.S. Ranawat, Y.M. Jaques and A.S. Foster; Nanoscale Adv. 3 (2021) 3447
- [2] H. Söngen, S.J. Schlegel, Y.M. Jaques, J. Tracy et al; J. Phys. Chem. Lett. 12 (2021) 7605
- [3] S.R. Yeandel, C.L. Freeman and J.H. Harding; J. Chem. Phys. 157 (2022) 084117
- [4] M. Ilett, H.M. Freeman, Z. Aslam, J.M. Galloway et al; J. Microsc. 288 (2022) 155

11:15 AM SF02.11.08

Modeling of Interfacial Growth and Structural Processes and Dynamics of sII Gas Hydrate Systems using Molecular Dynamics and Geometric Techniques[Samuel Mathews](#), Andre Guerra, Phillip Servio and Alejandro D. Rey; McGill University, Canada

Gas hydrates are inclusion compounds comprising a backbone of water molecules that enclose guest molecules in separate cages. Each volume of hydrate contains 160 volume equivalents of gas. Initially, large scale gas hydrate research was centered around the flow assurance problems they cause in the extraction and transportation of petroleum and its derivatives. Naturally occurring gas hydrates are also studied to satisfy global energy demand: estimates put the total energetic capacity of hydrate reserves at twice that of other fossil fuel reserves combined. Their potential use in the removal of carbon from the atmosphere, carbon capture and storage, and for energy exploitation makes gas hydrates a prime candidate for climate change mitigation research. Characterizing the interfacial properties of a material that requires intense formation conditions and sublimates rapidly in standard atmosphere is experimentally challenging. Controlling sample purity and system homogeneity is often difficult in devices designed to measure interfacial properties. It is also costly to properly clean apparatus after using additives to study new ones. Finally, rapidly testing different guest molecules, external pressures, surface effects, and extracting meaningful, fundamental information about the atomic and molecular interfacial behaviors is nearly impossible without critical sample disruption. This work uses molecular dynamics as implemented in the Large-scale Atomic/Molecular Massively Parallel Simulator to characterize the temperature and pressure effects on the interfacial tension, energy of interfaces, and growth rate of natural gas hydrates to overcome the complexity of experimentally understanding their performance in extreme environments and prove that theoretical modeling, prediction, and advanced characterization techniques can explain the structural and transport properties that govern hydrate in engineering applications. This project studies the impact of the surface coverings and additives on surface energy, attachment strength, and creation of new nucleation sites in sII gas, and examines the thermal transport across the hydrate/water, hydrate/gas, and hydrate/ice interfaces by calculating the thermal conductivity across the interface. This project also uses geometric analysis techniques to understand the dynamic behavior of the crystalline interfaces, including what specific polyhedral faces tend to face the melting phase and what type of pre-melting dynamics and interfacial thicknesses exist in these systems. It is essential to understand the underlying mechanisms occurring at the molecular level and the nanoscopic behaviors leading to macroscopic properties, thereby clarifying behaviors and phenomena that dominate potential applications of these structures. Our work has shown that there is excellent agreement between sI methane hydrates and experimental values, as well as for sII natural gas hydrates. The hydrates nucleate preferentially with film-shaped

nucleation, then cap-shaped, lens-shaped, and homogeneous nucleation. We have confirmed the presence of a novel pre-melting layer at the interface between the structures. We have been able to produce temperature and pressure correlations of surface tension for engineering applications. The excess entropy, adsorption, radial pair distribution function, and charge distribution at the interface were calculated to confirm our findings. The molecular dipole at the interface indicates novel organization of molecules that affects further nucleation and governs the use of surface coverings and additives to control behavior. The interfacial thickness has been characterized to show interface expansion and contraction at certain conditions, as well as showing the fine atomic phenomena that are at play in controlling macroscale properties.

SYMPOSIUM SF03

Inorganic Materials to Overcome the Challenges of Tomorrow
November 27 - December 1, 2023

Symposium Organizers

Craig Brown, National Institute of Standards and Technology
Michelle Dolgos, University of Calgary
Rie Makiura, Osaka Metropolitan University
Brent Melot, University of Southern California

Symposium Support

Bronze
Anton Paar

* Invited Paper
+ JMR Distinguished Invited Speaker

SESSION SF03.01: MOFs and Porous Systems I
Session Chairs: Craig Brown and Brent Melot
Monday Morning, November 27, 2023
Sheraton, Second Floor, Back Bay C

11:00 AM *SF03.01.02

Towards a Holistic Chemistry of Metal–Organic Framework Formation [Hamish H. Yeung](#); University of Birmingham, United Kingdom

Metal–organic frameworks (MOFs) have established themselves as fantastic materials for fundamental studies and potential applications alike, owing to the almost limitless possibilities that different combinations of metal ion-based nodes and organic linkers offer. Synthesis is typically simple, in the sense that new MOFs can be discovered in one-pot reactions close to ambient conditions within a matter of minutes or hours. However, behind such simplicity lies a great lack of understanding of how MOFs form and why particular phases crystallise under different conditions or even under (seemingly) the same conditions.

Our group has been working to better understand MOF formation using model systems such as the canonical zeolitic imidazolate framework (ZIF) family of MOFs. Although topologically similar to zeolites, relatively few ZIFs have been discovered compared to their inorganic counterparts. Better understanding of the chemistry that underpins self-assembly of metal ions and linkers into ZIFs would enable us to create materials, for example with new topologies or with more precisely positioned functionalities for improved performance in separations, sensing, gas storage and other applications.

A combination of systematic studies, in-situ monitoring and kinetic modelling has enabled us to develop a chemical understanding of phase behaviour, crystallisation rates, particle sizes and reaction yields in two particular hybrid systems: lithium tartrates¹ and zeolitic imidazolate frameworks.² This presentation will describe some of our ongoing work in the area, looking into synthetically relevant parameters such as reagent concentration, solvent and pH, and more complex systems such as mixed-metal³ and core-shell⁴ particles.

References:

1. H. H.-M. Yeung *et al.*, In situ observation of successive crystallizations and metastable intermediates in the formation of metal-organic frameworks. *Angewandte Chemie, International Edition*. 55, 2012-2016 (2016).
2. H. H.-M. Yeung *et al.*, Control of Metal–Organic Framework Crystallization by Metastable Intermediate Pre-equilibrium Species. *Angewandte Chemie, International Edition*. 58, 566-571 (2019).
3. A. F. Sapnik *et al.*, Compositional inhomogeneity and tuneable thermal expansion in mixed-metal ZIF-8 analogues. *Chemical Communications*. 54, 9651-9654 (2018).
4. K. W. P. Orr *et al.*, Single-step synthesis and interface tuning of core–shell metal–organic framework nanoparticles. *Chemical Science*. 12, 4494-4502 (2021).

11:30 AM *SF03.01.03

Inelastic Neutron Scattering Applied to Porous Materials [Anibal J. Ramirez-Cuesta](#); Oak Ridge National Laboratory, United States

Neutron scattering is uncommon and rare because there are only a handful of places worldwide where it is possible to perform the required experiments. The Spallation Neutron Source at ORNL in East Tennessee is the most advanced pulsed neutron source. The interaction of neutrons with the nuclei provides unique information on light elements (like hydrogen). It distinguishes between neighboring elements and isotopes, complementing X-ray capabilities and photon-based techniques.

In the case of Inelastic Neutron Scattering (INS), the technique is the neutron analog of Raman and infrared spectroscopies. Instead of using photons as the probing beam, a neutron beam illuminates the sample.

The penetrating power of neutrons means that with the adequate selection of materials, it is possible to build sample environments that can manage extreme conditions in pressure and temperature without the need for optically transparent windows—giving the technique much versatility. Gas handling experiments are trivial. The main disadvantages of INS are: that measurements usually require cryogenic temperatures, the neutron fluxes are low when compared with photons, and accessing neutron scattering facilities is challenging.

Atomistic computer modeling, particularly DFT, molecular dynamics, etc., is routinely used to interpret and analyze experimental results. The interplay of atomistic modeling and experimental data is unique and allows access to a precious insight into the mechanistic interpretation of the data.

Porous materials have space voids where it is possible to adsorb molecules. Trapping these molecules to "store" them or sometimes react chemically is used in many applications.

This paper will present examples of INS spectroscopy applied to small molecule adsorption on porous materials, from zeolites to metal-organic frameworks, highlighting the unique information the technique provides and how computer models are essential to interpret the data.

1:30 PM SF03.02.01

Computational-Aided Development of MOF Sorbents and Membranes for Molecular Adsorption/Separation [Guillaume Maurin](#); Université Montpellier, France

Metal-Organic Frameworks (MOFs) are an emerging class of porous solids for the selective capture of contaminants in a wide range of applications. The number of crystal structures is growing exponentially and they cannot be all tested experimentally for a given application. Computational High-throughput screening is therefore required to narrow down the best sorbents. This lecture will deliver our latest achievements in this field with typical illustrations. In another perspective, Mixed matrix membranes (MMMs) incorporating MOFs into polymeric matrices show promising properties for several key gas separation processes. Understanding of the MOF/polymer interface and gas transport through the MMMs is of utmost importance. Here, we selected a series of MOFs as fillers in conjunction with both rigid and flexible polymers and we deployed our in-house computational strategy to construct MOF/Polymer atomistic models and assess their thermodynamic and dynamic adsorption properties. This computational screening revealed that the distinct characteristic of polymer backbones and MOF surfaces results in different interfacial pore structuring. We evidenced that not only size but also shape of the interfacial pore region has eminent effects on the gas transport properties of the MMMs with respect to a selected range of molecules. This conclusion is an important step toward the rational design of MMMs with the optimal interfacial pore size/shape to achieve the best performance for molecular separation

1:45 PM SF03.02.02

(111)-Oriented Thin Film Fabrication of Metal-Organic Framework HKUST-1 on Insulating Glass Substrates by Combining Vacuum Deposition and Solvent Vapor Annealing [Shuntalwamoto¹](#), [RyoNakayama²](#), [SeoungminChon¹](#), [RyotaShimizut²](#) and [TaroHitosugit²](#); ¹Tokyo Institute of Technology, Japan; ²The University of Tokyo, Japan

Metal-organic frameworks (MOFs) are crystalline porous materials composed of metal ions and organic ligands. Many reports have described the synthesis of oriented MOF films with high crystallinity and flatness by liquid-phase processes such as layer-by-layer method. Liquid-phase methods often require modification of the substrate surface with self-assembled monolayers, and there is a risk of corrosion and contamination of the interface by the solution. By contrast, synthesis by physical vapor deposition is suitable to prevent the degradation caused by solvents and is advantageous for the fabrication of well-defined interfaces and easy patterning for further device fabrication. Until now, oriented thin films of two-dimensional MOFs were fabricated on insulating substrates by physical vapor deposition¹. However, the oriented three-dimensional MOF films have only been synthesized on metal surfaces², and never on insulating substrates by physical vapor deposition.

In this study, we report the fabrication of (111)-oriented thin films of a three-dimensional-MOF HKUST-1³ ([Cu₃(BTC)₂], BTC = 1,3,5-benzenetricarboxylate) on insulating glass substrates by combining vacuum deposition and annealing in acetic acid vapor. HKUST-1 is expected for device applications because of the tunability in ionic and electronic conductivities by introducing molecules into the pores. We utilized two-step processes for the HKUST-1 thin film fabrication. First, trimesic acid and copper(II) acetate thin films were deposited on the glass substrates as a precursor. Second, post-deposition annealing was performed in air and an acetic acid atmosphere. While the thin film annealed in air showed no peaks corresponding to HKUST-1 in the out-of-plane X-ray diffraction (XRD) pattern, the thin film annealed in acetic acid vapor showed 111, 222, and 333 diffractions, indicating (111)-oriented HKUST-1 films were successfully synthesized on the glass substrate. These results suggest that annealing with the acetic acid vapor facilitates the precursor diffusion and the solid-phase reaction to form HKUST-1 crystals.

References

1. Chon et al., MRS Fall Meeting, 2022, NM06.05.23.
2. Han et al., J. Mater. Chem. A, 2019, 7, 19396–19406.
3. Chui et al., Science, 1999, 283, 1148–1150.

2:00 PM *SF03.02.03

Using MOF Bullets and Compressed Gases to Control the Release of DNA, Proteins and Lipid Nanoparticles into Plants and Skin [Jeremiah J. Gassensmith](#); University of Texas-Dallas, United States

The demand for effective and specific drug delivery systems has driven the popularity of protein, DNA, liposome, and RNA-based drugs in clinical applications. However, their administration through injections poses challenges, such as the need for skilled medical personnel and the generation of biohazardous waste. This lecture will present an innovative approach to achieve controlled delivery of these biomolecules and lipid-based nanoparticles using Zeolitic-Imidazolate Framework-8 (ZIF-8) as a carrier. By encapsulating the biomolecules within ZIF-8, we demonstrate their stability in powder formulations and introduce a low-cost, gas-powered "MOF-Jet" delivery system for inoculating living animal and plant tissues.

Our investigations reveal that the release profiles of the encapsulated biomolecules can be modulated by selecting an appropriate carrier gas for the MOF-Jet. Utilizing carbon dioxide (CO₂) creates a transient and weakly acidic local environment, resulting in near-instantaneous release through ZIF-8 dissolution. On the other hand, employing air as the carrier gas allows for the slow biodegradation of ZIF-8, enabling a week-long release of the biomolecules. This pioneering study establishes the first example of controlled-biolytic delivery of biomolecules using ZIF-8, providing a powerful tool for fundamental and applied science research.

In addition to biomolecules, we explore the application of biolytic delivery as an alternative route for liposome and lipid nanoparticle delivery. Using this same methodology, I will discuss how we can deliver fragile liposomes into the skin using ZIF-8 as a protective nano-sized shell. The rigid and crystalline coating of ZIF-8 shields the liposomes from thermal and shear stresses, ensuring the preservation of cargo integrity and facilitating lyophilized powder formulation for room-temperature storage. By encapsulating liposomes in ZIF-8, we demonstrate enhanced mechanical protection, allowing for effective penetration into the skin. Through our experiments, we successfully coat liposomes with ZIF-8, ensuring the preservation of surface charges and enabling easy removal of the protective coating without causing damage to the encapsulated material. Furthermore, the protective coating prevents cargo leakage and facilitates efficient penetration of liposomes into agarose tissue models and porcine skin tissue.

This lecture presents an innovative approach to achieve controlled delivery of biomolecules, liposomes, and lipid nanoparticles using Zeolitic-Imidazolate Framework-8 (ZIF-8) as a carrier. By encapsulating the biomolecules within ZIF-8, their stability in powder formulations is demonstrated, and a gas-powered "MOF-Jet" delivery system is introduced for inoculating living tissues. The rigid and crystalline coating of ZIF-8 preserves cargo integrity and enables effective penetration, demonstrating its potential for improving drug delivery strategies.

REFERENCES:

- Kumari S, *et al.* Biolytic delivery of liposomes protected in metal-organic frameworks. *Proc Natl Acad Sci* **2023** Mar 14;120(11):e2218247120. DOI: 10.1073/pnas.2218247120. PMID: 36877851; PMCID: PMC10089211.
- Wijesundara YH, *et al.* Carrier gas triggered controlled biolytic delivery of DNA and protein therapeutics from metal-organic frameworks. *Chem Sci.* **2022** Oct 26;13(46):13803-13814. Doi: 10.1039/d2sc04982a. PMID: 36544734; PMCID: PMC9710232.

2:30 PM BREAK

3:00 PM SF03.02.04

Thermally Accelerated Alkali-Proton Exchange by Molten Long Chain Fatty Acids Toward Ceramic Electrochemical Cells [Akihiro Ishii](#), [Daisuke Kume](#), [Itaru Oikawa](#) and [Hitoshi Takamura](#); Tohoku University, Japan

Ceramics with high proton conductivity and stability are essential for efficient electrochemical cells, such as fuel cells and electrolyzers. Protonic ceramics that exhibit 1) high proton conductivity at intermediate temperatures (300–600°C), 2) high chemical stability against CO₂, H₂O, and electrode materials, and 3) no practical difficulties for synthesis, are especially of interest for practical applications. Currently, two well-known classes of the protonic ceramics exist: solid oxyacids that exhibit high proton conductivity but decompose at relatively low

temperatures ($\approx 200^\circ\text{C}$) as being dehydrated (e.g. CsHSO_4 derivatives), and perovskite-type refractories that are stable even in dehydrated state but show high conductivity only at high temperatures above 600°C (e.g. BaZrO_3 - BaCeO_3 derivatives). Although efforts to develop thermostable oxyacids and perovskite-type refractories showing high conductivity at the intermediate temperatures have been energetically continued, the protonic ceramics meeting the three properties required for the electrochemical applications have not been developed.

As a new class of protonic ceramics, alkali-proton-exchanged ceramics have been gradually gained attention, and some ceramics in this class (e.g. $\text{Li}_{1.39}\text{Sr}_{0.1}\text{Zn}(\text{GeO}_4)_4$ and $\text{Li}_{2.5}\text{Sr}_{0.75}\text{Zr}_{1.25}(\text{PO}_4)_3$) have been suggested to show high proton conductivity and stability. Compared to the perovskite-type materials, the ceramics in this class are believed to exhibit less current leakage by electron holes under high oxygen potential due to donor doping and the incorporation of protons through means other than oxygen vacancy hydration. However, proton conductivities of the alkali-proton exchanged ceramics have consistently been observed for only a very limited number of systems, such as β/β' -alumina and $\text{Li}_3\text{La}_3\text{M}_2\text{O}_{12}$ ($\text{M} = \text{Nb}, \text{Ta}, \text{Sn}$). This is considered to be due to the difficulty of exchanging alkali for protons throughout dense ceramic bodies by a traditional ion-exchange techniques, which involve immersing the alkali ceramics into aqueous acid solutions. The use of water limits alkali-proton exchange processing temperatures to below 100°C , thereby restricting the thermal acceleration of mass diffusion, and usually, only porous or powder-form alkali ceramics are applied.

To overcome this challenge, here, we propose a new but simple method to synthesize the dense alkali-proton-exchanged ceramics using molten long chain fatty acids heated above 100°C . A homemade reaction vessel were developed for stable, uniform, and efficient ion exchange using fatty acids at high temperatures. A case study on Al-stabilized cubic garnet-type $\text{Li}_7\text{La}_3\text{Zr}_2\text{O}_{12}$ (LLZ) shows that the alkali-proton exchange occurs more than $300\ \mu\text{m}$ deep throughout LLZ dense bodies under optimum conditions, and 91 % exchange can be achieved with only 8 h of treatment. The conductivity of the proton-exchanged LLZ and its potential for the applications will be discussed with DFT calculations.

3:15 PM +SF03.02.05

Smart and Programmable Crystalline Sponges for Separations Omar K. Farha; Northwestern University, United States

This talk will focus on metal-organic frameworks (MOFs) from basic research to implementation and commercialization. MOFs are a class of porous, crystalline materials composed of metal-based nodes and organic ligands that self-assemble into multi-dimensional lattices. In contrast to conventional porous materials such as zeolites and activated carbon, an abundantly diverse set of molecular building blocks allows for the realization of MOFs with a broad range of properties. We have developed an extensive understanding of how the physical architecture and chemical properties of MOFs affect material performance in applications such as separations of hydrocarbons.

3:45 PM *SF03.02.06

MOFs for Indoor Contaminants Capture and Detection—A Combined Experimental-Computational Strategy Sabine Devautour-Vinot¹, Pedro Brantuas¹, Paul Iacomi¹, Ezgi Gulcay^{1,2}, Guillaume Rioland² and Guillaume Maurin¹; ¹ICGM, France; ²CNES, France

Volatile organic compounds (VOCs) are recognized by the World Health Organization (WHO) as one of the major pollutants contributing to the deterioration of indoor air quality. They are generated from construction and finishing materials (paints, wallpapers, floor covering, glue...), burning processes, cleaning and preservation substances. Their emissions, even at low concentration levels in indoor air, pose threats to both human health and sensitive machinery. Therefore, the detection and abatement of airborne contaminants traces (ppb to ppm) is an ongoing challenge for maintaining a clean and safe environment in living and working places, but also in regulated spaces, such as clean rooms, spacecraft or satellites.

In this context, porous solids like MOFs (Metal-organic Frameworks) appear as promising materials due their tailorable chemical and physical properties and highly porous structures, acting as sorption media for direct air capture of contaminants,[1] or as components in electronic devices designed for monitoring concentration of contaminants.[2] Nevertheless, given the large number of synthesizable frameworks [3] the choice of a material to target a specific contaminant is more often than not a question of serendipity.[4]

To overcome this limitation, a hand-in-hand computational/experimental approach is herein devised for screening and identifying the best MOFs for the adsorption of specific VOCs contaminants. This method combines high-throughput molecular simulations to identify key promising materials, followed by advanced adsorption experiments at very low contaminant concentrations and sensing tests. We further detail several classes of MOF materials which were identified through this approach that are applicable to the capture and/or the detection of contaminants of interest in the aerospace domain, including aromatics and more challenging substances such as siloxanes and phthalates.[5]

[1] C. Lai, Z. Wang, L. Qin, Y. Fu, B. Li, M. Zhang, S. Liu, L. Li, H. Yi, X. Liu, X. Zhou, N. An, Z. An, X. Shi, C. Feng, *Coordination Chemistry Reviews* 2021, **427**, 213565.

[2] M. D. Allendorf, R. Dong, X. Feng, S. Kaskel, D. Matoga, V. Stavila, *Chem. Rev.* 2020, **120**, 8581.

[3] P. Z. Moghadam, A. Li, X.-W. Liu, R. Bueno-Perez, S.-D. Wang, S. B. Wiggins, P. A. Wood, D. Fairen-Jimenez, *Chem. Sci.* 2020, **11**, 8373.

[4] S. Curtarolo, G. L. W. Hart, M. B. Nardelli, N. Mingo, S. Sanvito, O. Levy, *Nature Mater* 2013, **12**, 191.

[5] E. Gulcay, P. Iacomi, Y. Ko, J.S. Chang, G. Rioland, S. Devautour-Vinot and G. Maurin, *J. Mater. Chem. A*, 2021, 9, 12711; P. Iacomi, E. Gulcay-Ozcan, P. Pires Conti, S. Biswas, N. Steunou, G. Maurin, S. Devautour-Vinot, *ACS Appl. Mater. Interfaces*, 2022, **14**, 17531; E. Gulcay-Ozcan, P. Iacomi, G. Rioland, G. Maurin, S. Devautour-Vinot, *ACS Appl. Mater. Interfaces*, 2022, **14**, 53777.

4:15 PM SF03.02.07

Defects and Nonlinear Infrared Intensity Behavior in UiO-67 Metal Organic Frameworks Ryan P. McDonnell^{1,2}, Venkata Swaroopa Datta Devulapalli², Tae Hoon Choi³, Laura McDonnell², Isabella Goodenough², Prasenjit Das³, Nathaniel L. Rosi³, J.K. Johnson³ and Eric Borguet²; ¹University of Wisconsin-Madison, United States; ²Temple University, United States; ³University of Pittsburgh, United States

A major interest in the use of Metal Organic Frameworks (MOFs) is the simultaneous capture and destruction of toxic chemicals and chemical warfare agents. Catalysis typically occurs at defect sites in the MOF crystallite. An unexplored avenue for defect formation in UiO-67 MOFs is through temperature activation. Herein, we use a combination of Fourier transform infrared spectroscopy and density functional theory (DFT) techniques to understand the impact of thermal activation on the concentration and strength of Lewis acid defects (Zr^{4+} sites) in UiO-67. Ultra-high vacuum methods are employed to eliminate atmospheric contaminants. We devise a new method to allow vibrationally active probe molecules to diffuse through the MOF and preferentially adsorb to internal sites, providing insight into the structure and properties of internal MOF sites. Through the use of CD_3CN , whose $\nu(\text{CN})$ mode is Stark active, and DFT calculations, we assign the presence of three distinct Lewis acid sites which evolve as a function of pretreatment temperature. Following dehydroxylation at 623 K, the Lewis acidity of the MOF appears to increase in both concentration and strength through the loss of capping groups. We additionally show that following CD_3CN diffusion into UiO-67, the intensities of the $\nu(\text{CD})$ and $\nu(\text{CN})$ modes depict nonlinear intensity behavior, complicating the interpretation of diffusion kinetics through UiO-67. Through DFT calculations, we observe that hydrogen bonding of CD_3CN to μ_3 -OH groups in UiO-67 significantly decreases the transition dipole moment of the $\nu(\text{CD})$ modes, while increasing that of the $\nu(\text{CN})$ mode. These results highlight the importance of careful infrared spectra interpretation, as well as the propensity for thermal activation to increase the density and strength of Lewis acid sites.

4:30 PM SF03.02.08

Photocatalytically Active Metal Organic Frameworks for Toxic Chemical Degradation Gwendolyn Houser¹, Abigail Bugg¹, Emmaline Pendleton¹, Samrath Singh¹, Ann Kulisiewicz², Jared Decoste², Bryan Lagasse¹ and Chi Nguyen¹; ¹United States Military Academy, United States; ²U.S. Army Combat Capabilities Development Command - Chemical Biological Center, United States

Metal Organic Frameworks (MOFs) are incredibly versatile porous materials capable of degrading many toxic chemicals. By incorporating organic linker molecules that are photocatalytically active into the MOF it is possible to achieve multiple pathways of degradation. Pyrene based linker molecules, such as 1,3,6,8-tetrakis (para-benzoic acid) pyrene (TBAPy) are photocatalytically active when exposed to ultraviolet light and produce singlet oxygen in solution. The highly reactive singlet oxygen molecules then react with toxic species in solution and degrade them into less toxic molecules. This work focuses on determining the efficiency of the photocatalysis reaction for degrading toxic and persistent chemicals, such as pesticides in aqueous solutions.

4:45 PM SF03.02.09

Long-Term and Selective Release of Agrochemicals Supported in Porous Materials Raffaele Riccio; Asian Institute of Technology, Thailand

Agrochemicals (e.g., fertilizers, pesticides, growth hormones, etc.) are essential to meet the global need for food, both quantitatively and qualitatively, but their unsafe, unselective, and repeated administration pose environmental, health, and economical threats. Researchers are looking into ways to increase agricultural production, simultaneously aiming at the reduction of pesticide wastes. In this regard, delivery methods based on Metal-Organic Frameworks (MOFs) are recently gaining consideration in agricultural applications. Previous studies have already been performed on Cu-based MOFs (e.g., HKUST-1) as delivery agents in the agricultural sector. Moreover, the use of Copper salts is already established (e.g., CuSO_4 as fungicide), and it is also an essential element for plants, therefore showing a dual nature of nutrients and pesticides.

This communication reports the fabrication of HKUST-1 via a convenient one-step procedure involving the utilization of basic copper carbonate (BCC), a natural component of the minerals

malachite or azurite, with and without guest species like fertilizers (e.g., Urea), growth regulators (e.g., Gibberellic Acid), insecticides (e.g., Imidacloprid), and fungicides (e.g., Mancozeb and Propineb). The encapsulation capacities and long term release profile of the aforementioned guest@HKUST-1 systems under different simulated soil parameters of pH, temperature, and salinity, as well as exposure to environmental conditions, are also evaluated.

SESSION SF03.03: Poster Session I
Session Chairs: Craig Brown and Brent Melot
Monday Afternoon, November 27, 2023
Hynes, Level 1, Hall A

8:00 PM SF03.03.01

Medium-Range Order Structure Controls Thermal Stability of Pores in Zeolitic Imidazolate Frameworks Rasmus Christensen, Yossi Bleile, Søren S. Sørensen, Christophe Biscio, Lisbeth Fajstrup and Morten M. Smedskjaer; Aalborg University, Denmark

Metal-organic framework (MOF) glasses have multiple potential applications as they combine advantages of traditional glasses with those of MOFs. The melt-quenching process used to form MOF glasses typically leads to a significant decrease in porosity, but the structural origin of this thermally-induced pore collapse remains largely unknown. Here, we study the melting process of three zeolitic imidazolate frameworks (ZIFs), namely ZIF-4, ZIF-62, and ZIF-76, using *ab initio* molecular dynamics (MD) simulations. By analyzing the MD data using topological data analysis, we show that while the three ZIF systems exhibit similar short-range order structural changes upon heating, they exhibit significant differences in their medium-range order structure. Specifically, ZIF-76 retains more of its medium-range order structures in the liquid state compared to the other glass-forming ZIF systems, which allows it to remain more porous than ZIF-4 and ZIF-62. As such, our results may aid in understanding what structural features govern the ability to maintain porosity in the melt-quenched glassy state.

8:00 PM SF03.03.02

Insight into The Barocaloric Potential of Fumarate-Based MOFs: A Computational Study of Dynamic Disorder Chi Cheng (Cecilia) Hong, Claire Hobday and Antonia Mey; University of Edinburgh, United Kingdom

As the effects of climate change become more apparent in the form of rising global temperatures, the necessity for temperature control become more significant.¹ Current refrigerants operate by undergoing continuous cycles through a vapour-liquid phase change. However, these liquids have a high global warming potential with potencies exceeding 2000 times of that of CO₂ when evaporated during disposal.² A greener alternative is a solid-state approach via barocaloric materials which exhibit large adiabatic temperature and isothermal entropy changes upon compression and decompression cycles.³ Several classes of materials have shown potential for the barocaloric effect such as plastic crystals but to compete with the efficiencies of current refrigerants, the magnitude of pressure required must be reduced.⁴

Metal-organic frameworks (MOFs) are porous, periodic, and crystalline materials that are highly modular due to the many metal and linker combinations possible. Though largely studied for their adsorption properties, several MOFs have been reported to exhibit a *breathing effect* where large volume changes were observed as a result of pressurising the MOFs with and without guest molecules.⁵ Hence, they have been recognised as potential barocaloric materials with the most well-known being MIL-53(Al) which has 1,4-benzenedicarboxylates (BDC) as the linkers reporting a colossal entropy change of 311 J K⁻¹ kg⁻¹ under 16 bar of carbon dioxide gas.⁶ The ability to accommodate large volume changes has been associated with the inherent flexibilities within the ligand that acts as the linker, therefore, this work turns to fumarate linkers which are dicarboxylates like the BDC with a torsional double bond in the centre. Studies on the barocaloric performance of an aluminium-centred fumarate MOF was found to exceed that of the BDC-analogue, making this family of MOFs ideal candidates for further investigation.⁷

This research aims to develop further understanding towards fumarate-based MOFs, in particular, the gallium analogue to the fumarate-linked MIL-53(Al) and determine whether they exhibit the barocaloric effect by first using *ab initio* that can act as a benchmark for future studies. Using machine learning potentials, a classical force field can be derived from the *ab initio* data which in turn eases the cost and greatly increase the data output. Studying the correlation between structural changes, thermodynamic properties, and the dynamics of the MOFs at varied pressures and temperatures, determines the barocaloric potential which will ease future research in the discovery of novel barocaloric materials.

References

- 1 D. C. Savitha *et al*, *Int. J. Sustain. Energy*, 2022, **41**, 235–256.
- 2 S. Szczesniak *et al* 2022, **15**, 5999.
- 3 C. Cazorla, *Appl. Phys. Rev.*, 2019, **6**, 041316.
- 4 B. Li, Y. Kawakita *et al*, *Nature*, 2019, **567**, 506–510.
- 5 M. Alhamami *et al*, *Materials*, 2014, **7**, 3198–3250.
- 6 J. García-Ben *et al*, *Chem. Mater.*, 2022, **34**, 3323–3332.
- 7 P. G. Yot, *et al*, *Chem. Sci.*, 2016, **7**, 446–450.

8:00 PM SF03.03.03

Rational Synthesis of Zeolites from Single-Source Molecular Precursor with Secondary Building Unit-Like Core Structure Akira Imaizumi, Yurika Ohnishi, Arisa Shimamura, Akinori Honda and Ho-Chol Chang; Chuo University, Japan

Zeolite is an important material widely used in ion exchangers, adsorbents, and gas separation membranes. Many aluminosilicate zeolites have been synthesized by hydrothermal, solvothermal, and solid-phase methods using monomeric or polymeric Al and Si sources, such as alkoxides, fly ash, and kaolinite, in the presence of acids, bases, and structure-directing agents. In recent years, topotactic reactions have been developed to expand the structure from a two-dimensional layered precursor to a three-dimensional structure, and methods to design the structure of the target aluminosilicate have been developed, such as synthesis in which the position of Al atoms in the zeolite can be controlled by additives. Since control of the composition and structure of the target aluminosilicate is expected to enable control of functions, further development of rational structure construction methods based on the composition and structure of the starting materials is an urgent task. Therefore, the use of structurally and compositionally well-defined molecular precursors (MPs) would be reasonable starting materials by connecting their core frameworks. In this presentation, we demonstrated in detail the synthesis of aluminosilicate using molecules with secondary building unit (SBU)-like core structure as MP. Hydrothermal reactions of SBU-like MP without additives gave no insoluble product. On the other hand, the hydrothermal reactions of SBU-like MP with alkali metal cation afforded the zeolite that can be constructed by the core structure of the MP. It should be noteworthy that the hydrothermal reactions using separated Al and Si sources at the same Si/Al ratio, alkali metal cation content, and temperature resulted in several zeolites which could not be constructed by linking the MP core structure. These zeolites are known to be thermodynamically more stable than the zeolite synthesized by the SBU-like MP, and form at higher temperature and higher base-content conditions. These results suggest that the structure of the starting materials has an important influence on the construction of the product structure, and that the resulting structure is constructed through a kinetic process different from conventional methods. The use of MPs is expected to be a novel and promising method for rational construction of inorganic material, and obtain structures that cannot be constructed by using conventional precursors.

8:00 PM SF03.03.04

Pushing Lithium-Sulfur Batteries Towards Practical Operation Through Cathode-Electrolyte Interplay and Interlayer Development Chen Zhao and Guiliang Xu; Argonne National Laboratory, United States

The practical application of lithium-sulfur (Li-S) batteries is still hindered by the sharp capacity fading and sluggish cathode redox kinetics. Although tremendous efforts have been devoted to inhibiting the polysulfide shuttling and enhancing the cathode kinetics, the unsatisfactory cell performance under high areal S loading and lean electrolyte conditions remains unsolved. To subsequently enhance the Li-S cell performance under practical operation conditions, we proposed several unconventional approaches including ordered macroporous S host with double-end binding sites [1], highly fluorinated ether-based electrolyte development [2], and versatile free-standing interlayer design [3]. Different from the conventional strategy merely focusing on limiting the polysulfide shuttling, our cathode design combined with electrolyte modification can effectively limit the flooding of polysulfide while enhancing the cathode redox through catalytic sites. Meanwhile, the robust solid-electrolyte interface as induced by highly fluorinated ether-based electrolyte and the regulated Li⁺ flux through applying lithiophilic interlayer can prevent the continuous Li metal corrosion and enable stable Li striping/plating behavior. As a result, the Li-S cell performance under high areal S loading (>6.0 mg cm⁻²), low E/S ratio (4 μL mg⁻¹), wide temperature range (0 – 55 °C), and thin Li metal foil (40 μm) is greatly enhanced through our proposed strategies. In addition, with the assistance of advanced in/ex-situ synchrotron characterizations, mechanism investigations of the S redox behavior in different electrolytes are conducted.

References:

- [1] C. Zhao, G. Xu, Z. Yu, L. Zhang, I. Hwang, Y. Mo, Y. Ren, L. Cheng, C. Sun, Y. Ren, X. Zuo, J. Li, S. Sun, K. Amine, T. Zhao, *Nat. Nanotechnol.* 16, 166-173, (2021)
- [2] C. Zhao, A. Daali, I. Hwang, T. Li, X. Huang, D. Robertson, Z. Yang, S. Trask, W. Xu, C. Sun, G. Xu, K. Amine, *Angew. Chem. Int. Ed.* e202203466 (2022)
- [3] C. Xie, C. Zhao, H. Jeong, T. Li, L. Li, W. Xu, Z. Yang, C. Lin, Q. Liu, L. Cheng, X. Huang, G. Xu, K. Amine, G. Chen, *Angew. Chem. Int. Ed.* e202217476 (2023)

8:00 PM SF03.03.05

Low-Temperature Chiral Crystal Structure and Superconductivity in $(\text{Pt}_{0.2}\text{Ir}_{0.8})_3\text{Zr}_5$ Yuto Watanabe¹, Hiroto Arima¹, Aichi Yamashita¹, Akira Miura², Chikako Moriyoshi³, Yosuke Goto⁴, Chul-Ho Lee⁴, Ryuji Higashinaka¹, Hidetomo Usui⁵ and Yoshikazu Mizuguchi¹; ¹Tokyo Metropolitan University, Japan; ²Hokkaido University, Japan; ³Hiroshima University, Japan; ⁴National Institute of Advanced Industrial Science and Technology, Japan; ⁵Shimane University, Japan

Non-centrosymmetric superconductors, which do not have an inversion center, have been studied due to their unusual physical properties. CePt_3Si , CeRhSi_3 , and CeIrSi_3 are well-known Ce-based non-centrosymmetric superconductor systems, which show extremely high upper critical field ($\mu_0 H_{c2}$) due to the antisymmetric spin-orbit coupling (ASOC) caused by lacking an inversion center even with a low superconducting transition temperature (T_c). Therefore, superconductors with a chiral space group have recently been a hot issue. In this presentation, we report a new superconductor $(\text{Pt}_{0.2}\text{Ir}_{0.8})_3\text{Zr}_5$ with a chiral space group of $P6_122$. We performed the synchrotron X-ray diffraction and revealed that $(\text{Pt}_{0.2}\text{Ir}_{0.8})_3\text{Zr}_5$ undergoes a structural transition from the non-chiral ($P6_3/mcm$) to the chiral ($P6_122$) space group at low temperatures. We observed bulk superconductivity with $T_c = 2.2$ K through specific heat measurement. The normalized electronic specific heat jump $\Delta C_{el}/\gamma T_c$ (γ is the electronic specific heat coefficient) was estimated to be 1.49. This value is close to 1.43, which is the expected value in the weak-coupling BCS model. Furthermore, the normalized superconducting gap energy $2\Delta(0)/k_B T_c$ (k_B is the Boltzmann constant) was estimated to be 2.96, which is also close to the 3.53 expected value in the weak-coupling BCS model. We observed the linear behavior of $\ln(C_{el}(T)/\gamma T_c)$ as a function of T/T_c at low temperatures, which means the superconducting gap structure of $(\text{Pt}_{0.2}\text{Ir}_{0.8})_3\text{Zr}_5$ is explained with an s -wave gap. From these experimental results, we confirmed that $(\text{Pt}_{0.2}\text{Ir}_{0.8})_3\text{Zr}_5$ superconductor obeys to weak-coupling BCS model with an s -wave gap. The $\mu_0 H_{c2}$ of $(\text{Pt}_{0.2}\text{Ir}_{0.8})_3\text{Zr}_5$ was estimated from specific heat under various magnetic fields. The estimated value of $\mu_0 H_{c2}$ at 0 K is $\mu_0 H_{c2}(0) = 2.59$ T, which is an intermediate value between the orbital pair breaking limit $\mu_0 H_{orb} = 1.33$ T and the Pauli-Clogston limit $\mu_0 H_P = 4.08$ T. Although $(\text{Pt}_{0.2}\text{Ir}_{0.8})_3\text{Zr}_5$ belongs to the non-centrosymmetric crystal structure, its $\mu_0 H_{c2}$ is not larger than the Pauli-Clogston limit, which is different from the case of CePt_3Si , CeRhSi_3 , and CeIrSi_3 . This indicates that the dominant mechanism determining the $\mu_0 H_{c2}$ of $(\text{Pt}_{0.2}\text{Ir}_{0.8})_3\text{Zr}_5$ is the orbital pair breaking limit, and its ASOC effect is not significant. A similar phenomenon was observed in other non-centrosymmetric superconductors, for example, LaMP ($M = \text{Ir}$ and Rh ; $P = \text{P}$ and As) and $\text{Mg}_{10}\text{Ir}_{19}\text{B}_{16}$. The crystal structure and elemental composition could be important factors in the strength of the ASOC effect.

8:00 PM SF03.03.06

Superconductivity in In-Doped AgPbBiTe_3 Compounds Synthesized by High-Pressure Synthesis Takahiro Sawahara¹, Hiroto Arima¹, Takayoshi Katase², Aichi Yamashita¹, Ryuji Higashinaka¹ and Yoshikazu Mizuguchi¹; ¹Tokyo Metropolitan University, Japan; ²Tokyo Institute of Technology, Japan

NaCl-type metal tellurides ($M\text{Te}$), such as SnTe , PbTe , and InTe , have been widely studied due to their unique physical properties as topological insulators, thermoelectric materials, and superconductors. SnTe , which is a topological crystalline insulator, shows superconductivity upon carrier doping, and In-doped SnTe has been studied as a candidate material in which topological superconductivity emerges. Therefore, further development of new NaCl-type $M\text{Te}$ superconductors is expected to expand material variation. In this study, we used alloying technique to design new $M\text{Te}$ superconductors. In our previous report, in SnTe , we revealed that the partial substitution of Sn^{2+} site by $(\text{Ag}_{0.5}\text{Bi}_{0.5})^{2+}$ results in systematic lattice contraction while preserving the crystal-structure type and the total valence state. From first principles band calculations, a band inversion is predicted, suggesting the possibility of topologically preserved electronic state in the system. Furthermore, AgSnBiTe_3 also shows superconductivity by In-doping. Similarly, PbTe , which is a thermoelectric material, shows superconductivity by In-doping. From the analogy between SnTe and PbTe , we considered that AgPbBiTe_3 could be synthesized and will exhibit superconductivity. We investigated the In-doping effects on the structural and physical properties in AgPbBiTe_3 . Polycrystalline samples of $(\text{AgPbBi})_{(1-x)/3}\text{In}_x\text{Te}$ ($x = 0-0.5$) were synthesized by high-pressure synthesis, and we conformed the NaCl-type structure by powder X-ray diffraction. In occupies the M site for all the compositions. From magnetic susceptibility measurements, superconductivity was observed for $x = 0.2-0.5$, and the highest transition temperature was 2.8 K for $x = 0.4$. For $x = 0.4$, the emergence of bulk superconductivity was confirmed by specific heat measurement. In the presentation, we will show the superconducting properties of $(\text{AgPbBi})_{(1-x)/3}\text{In}_x\text{Te}$ and discuss the In-valence state of In-doped $M\text{Te}$ with a NaCl-type structure.

8:00 PM SF03.03.07

Unleashing the Potential of Lanthanide-Doped Oxyfluoride Materials for Efficient Green Upconversion and Their Promising Applications Sonali Mohanty, Mirijam Lederer, Simona Premcheska, Hannes Rijckaert, Klaartje De Buysser, Els Bruneel, Andre Skirtach, Kristof Van Hecke and Anna M. Kaczmarek; Ghent University, Belgium

The quest for highly efficient upconversion (UC) materials has led to the development of fluoride hosts with low phonon energies, minimizing nonradiative transitions. Among them, NaYF_4 doped with Yb^{3+} and Er^{3+} has emerged as a top performer. However, its limited thermal stability hinders its application in certain fields. On the other hand, oxide hosts offer improved stability but suffer from lower UC efficiencies due to higher phonon energies. Hence, the prospect of developing host materials that combine the robustness of oxides with the high upconversion efficiencies of fluorides remains an intriguing avenue of exploration.

Herein, we present a novel approach wherein we successfully synthesize lanthanide-doped oxyfluoride particles. This is achieved through the growth of a $\text{NaYF}_4:\text{Yb}^{3+},\text{Er}^{3+}$ layer around SiO_2 spherical particles, followed by a high-temperature annealing process, yielding $\text{SiO}_2@\text{YOF}:\text{Yb}^{3+},\text{Er}^{3+}$ particles. Our primary focus was to exploit these materials as Boltzmann type luminescence thermometers within the physiological range. Nonetheless, we encounter a noteworthy challenge concerning the limited emission observed in the green spectral region of these particles. To address this limitation, we have investigated the effects of introducing various metal ion co-dopants (Gd^{3+} , Li^+ , or Mn^{2+}) into the $\text{SiO}_2@\text{YOF}:\text{Yb}^{3+},\text{Er}^{3+}$ particles. Specifically, we analyze the overall emission intensity and the green to red ratio under 975 nm laser excitation. Beyond their role as radiometric thermometers, our investigation uncovers the remarkable potential of these materials as carriers for drug delivery applications, following the conversion of $\text{SiO}_2@\text{YOF}:\text{Yb}^{3+},\text{Er}^{3+}$ particles into hollow $\text{YOF}:\text{Yb}^{3+},\text{Er}^{3+}$ structures, and their evaluation in terms of toxicity towards NHDFs. The investigation highlights the previously unexplored aspects of improving the green upconversion luminescence in $\text{YOF}:\text{Yb}^{3+},\text{Er}^{3+}$ and its potential biomedical applications.

8:00 PM SF03.03.08

Surfactant-Templated Green Synthesis of Porosity-Tailored Silica Nanoparticles for Lithium-Ion Battery and 5G Communication Applications Yeongje Lee, Sanghyeok Bae, Seok Jin Hong and Sunho Jeong; Kyung Hee University, Korea (the Republic of)

In a recent decade, silica nanoparticles have received a significant attention owing to their distinctive chemical/physical properties and potentials in newly emerging applications including 5G communication and lithium-ion battery applications. In this study, we propose an environmentally friendly methodology of synthesizing highly functioning silica nanoparticles with characteristic porous structures. The surfactant-templated sol-gel emulsion method enables to adjust the dimension of monodispersed silica nanoparticles and to form dual porous (micro- and meso-porous) internal structures. The composite films, in which the dual porous silica nanoparticles are hybridized with polyimide polymeric resins, exhibit remarkably low dielectric properties, demonstrating their potential as a substrate material for 5G communication applications. By inducing a carbothermal reduction reaction, we can control the stoichiometric ratio of porous silica nanoparticles. This leads to a facile creation of porous SiO_2 /carbon nanocomposites applicable to anode materials for lithium ion batteries. The resulting nanocomposites showed an excellent cycling stability ($\sim 100\%$ after 500 cycles at 0.5 A g^{-1}) and rate capability (554 mAh g^{-1} at 2 A g^{-1}), and a high capacity (1330 mAh g^{-1} at 0.1 A g^{-1}). Our findings affirm the feasibility of porous structure-designable silica nanoparticles for both 5G communication and battery applications. It would open up new possibilities for meeting the unique requirements across various fields through a simple synthesis method.

8:00 PM SF03.03.09

Crystallographic Structural Control of Manganese Dioxide Nanomaterials for Battery Applications Sanghyeok Bae, Yeongje Lee, Seok Jin Hong and Sunho Jeong; Kyung Hee University, Korea (the Republic of)

Recently, manganese oxides have received tremendous attention as active materials for various types of energy storage devices, owing to their cost-effectiveness and excellent electrochemical performances.

In particular, manganese dioxide can be used as an anode material for lithium-ion batteries and a cathode material for aqueous zinc-ion batteries. The MnO_6 octahedral building units are assembled into tunnel and layered structures, with a formation of variety types of crystallographic structures. The common synthetic method for synthesizing manganese dioxide particles is a hydrothermal reaction. However, in this synthetic method, it is highly demanding to control precisely the crystal structures of manganese dioxides, because of an everlasting heating/cooling time during the hydrothermal reaction.

Herein, we report an ultrafast annealing process for controlling sophisticatedly the crystallographic structures of manganese oxide nanoparticles.

By controlling the heating rate up to a given temperature and the cooling rate down to a room temperature, the oxidation states and the crystal structures are adjusted correspondingly depending on ultrafast annealing processing parameters. It will be confirmed that the crystalline structures are controllable precisely in manganese oxide nanoparticles, unlike the case of conventional hydrothermal reaction-based synthetic method. The resulting manganese oxide nanoparticles are incorporated inside unstacked 2D carbon materials, allowing for a formation of nanocomposite electrode materials. In this study, for understanding better the electrochemical reaction mechanisms in manganese oxide materials, the manganese oxide-based nanocomposites

with different crystalline structures will be evaluated and analyzed comparatively as anode materials for lithium ion batteries and cathode materials for zinc ion batteries.

8:00 PM SF03.03.10

The Synthesis of Layered Hexagonal Structure Type of SnS_2 @rGO as High-Performance Anodes for Lithium-Ion Batteries HyerinYoo¹, WonbinNam¹, YoonMyung², Chan WoongNa² and JaewonChoi¹; ¹Gyeongsang National University, Korea (the Republic of); ²Korea Institute of Industrial Technology, Korea (the Republic of)

SnS_2 -based materials have garnered considerable attention as a highly promising anode material for lithium-ion batteries due to their unique two-dimensional layered structure, impressive theoretical capacity, and alloy metal properties. However SnS_2 suffer from low cycle life stability, inadequate electronic conductivity, and large volume expansion during the charge/discharge process.

One suggested solution is introducing carbonaceous materials, such as reduced graphene oxide (rGO). These can improve the electrochemical performances of metal sulfides, such as cycle stability and rate capability by their high electronic conductivity. This study comprehensively analyzed the as-synthesized SnS_2 and SnS_2 @rGO composites using SEM, XRD, XPS, and TEM techniques. Furthermore, Ex-situ X-ray diffraction tests showed that the SnS_2 @rGO nanocomposite electrode primarily operates via an anodic mechanism for SIBs. The SnS_2 @rGO nanocomposite demonstrated enhanced cycling stability and discharge capacity, as evidenced by electrochemical testing (500 mAh/g at 542 mA/g after 300 cycles; 317.9 mAh/g at 100 mA/g after 600 cycles). Meaningful enough, the construction of composites using SnS_2 and SnS_2 @rGO represents a promising strategy for improving the electrochemical performance of LIBs. Also, the CV curves at various scan rates are evaluated to investigate the electrochemical reaction kinetics of the SnS_2 @rGO, and this process is mainly controlled by capacitive behavior. This work demonstrates the potential of SnS_2 @rGO nanocomposite as anode materials for LIBs and enhances our understanding of electrochemical storage mechanisms. This research will facilitate the development of diverse energy storage materials based on SnS_2 .

8:00 PM SF03.03.11

Synthesis and Characterization of MnS Nanoparticles Supported by Reduced Graphene Oxide as Anode for Lithium-Ion Batteries WonbinNam¹, HyerinYoo¹, Chan WoongNa², YoonMyung² and JaewonChoi¹; ¹Gyeongsang National University, Korea (the Republic of); ²Korea Institute of Industrial Technology, Korea (the Republic of)

Transition-metal sulfides have attracted significant attention as anodes for rechargeable batteries due to their high theoretical capacities, low cost, and eco-friendliness. For lithium-ion battery applications, Manganese sulfide (MnS) possesses a high theoretical capacity (616 mAh/g) by way of a conversion reaction. Nevertheless, problems are still associated with low cycle stability caused by volume expansion and poor electronic conductivity. This work prepared MnS nanoparticles embedded in reduced graphene oxide (rGO) using the one-pot method. The rGO behaves as an electronic conductor and buffers the volume change of MnS nanoparticles during lithiation and delithiation. The as-prepared MnS and MnS@rGO powders were characterized by scanning electron microscope (SEM), transmission electron microscope (TEM), X-ray diffraction (XRD), and X-ray photoelectron spectroscopy (XPS). The MnS nanoparticles have a size of around 40 nm, and the particles are uniformly distributed on the rGO. The MnS@rGO nanocomposite exhibited enhanced electronic conductivity and a significantly improved discharge capacity of 624 mAh/g after 100 cycles, compared with bare MnS nanoparticles, at a high current density of 500 mA/g. Thus, we propose that MnS@rGO composites represent a promising alternative for anode materials in lithium-ion batteries (LIBs).

8:00 PM SF03.03.12

Effect of UV Irradiation on Sol-Gel for Metal-Oxide Devices GiyoongChung^{1,2}, TaeEunHa¹, Eun KyungJo¹, Jeong HyunAhn¹ and Yong-SangKim¹; ¹Sungkyunkwan University, Korea (the Republic of); ²Samsung Electronics, Korea (the Republic of)

We have investigated the effect of UV irradiation on Sol-Gel for amorphous metal-oxide semiconductors (AOS). Organic chemical-induced defects (e.g., voids, holes, organic residues) cause instability of solution-processed amorphous indium-gallium-zinc oxide (a-IGZO) thin-film transistors (TFTs). Hydroxyl radicals is strong oxidant that eliminate organic compounds. In this regard, we expose glass petri dish containing In-Zn-O sol-gel mixture to UV prior to spin-coating to deposit a-IZO film having less defects. Hydroxyl radicals are generated in sol-gel by irradiating UV through O_3 /UV process, which is confirmed using potassium iodine (KI)/ultraviolet-visible (UV-vis) spectroscopy analysis. The intensity of the absorbance peak with wavelength of 290 nm and 350 nm increases as the UV irradiation time increases. These results indicates that a simple method of UV irradiation on Sol-Gel generates hydroxyl radicals and provides a decrease of organic chemical-induced defects effectively.

8:00 PM SF03.03.13

Improved Photocatalytic Efficiency of Nb_2O_5 -Based Semiconductors Through Cu and Fe Nanoparticles Depositions for CO_2 Photoconversion FranciscoG. Nogueira¹, Ana LuizaA. Faria¹, JulianaA. Torres², LucasRibeiro¹, HigorA. Centurion³, CauêRibeiro² and RenatoV. Goncalves³; ¹Federal University of São Carlos, Brazil; ²Brazilian Agricultural Research Corporation, Brazil; ³University of São Paulo, Brazil

In recent decades, the demand for energy has significantly increased due to population and industrial growth. However, a considerable portion of the energy consumed is derived from the combustion of fossil fuels, resulting in the emission of substantial quantities of gases that have the potential to contribute to global warming. Among these gases, carbon dioxide (CO_2) stands out, as one of the main causes of the greenhouse effect. Thus, the need to develop new economic and energetically viable technologies for energy production through clean and sustainable routes is fundamental. Among these technologies, one can highlight the CO_2 photoconversion process ("artificial photosynthesis") into value-added products. However, currently, available semiconductors often exhibit a high recombination rate of their photogenerated electron/hole pairs, thereby compromising the effectiveness of the process. Thus, to improve the photocatalytic efficiency, this study aimed to develop semiconductors based on niobium pentoxide (Nb_2O_5) modified with iron (Fe) or copper (Cu) for photoreduction of CO_2 , aiming to increase the photocatalytic efficiency of the material through of the reduction in the recombination rate of the photogenerated electron/hole pairs and enhancing light absorption in the visible region. For this purpose, Nb_2O_5 -based semiconductors were synthesized using the oxidizing peroxide method with hydrothermal treatment. The Fe or Cu nanoparticles were deposited using the magnetron sputtering method, as this technique enables the deposition of highly pure nanoparticles. The incorporation of Fe or Cu nanoparticles onto the surface of Nb_2O_5 led to an effective decrease in the recombination rate of the photogenerated electron-hole pairs. This improvement can be attributed to the formation of heterostructures between the materials, which facilitated the greater spatial separation of the photogenerated charges. Consequently, there was a remarkable increase in the photoconversion of CO_2 . In addition, scanning electron microscopy and high-resolution transmission electron microscopy analyses were performed to evaluate the morphology and structure of the photocatalysts. The SEM images indicate that the deposition of Fe and Cu does not significantly alter the morphology of the materials, where irregular spherical grains can be observed. Furthermore, the mapping images show a good distribution of Fe and Cu elements deposited by magnetron sputtering. Photoluminescence spectroscopy analysis was used to evaluate the recombination rate and lifetime of the photogenerated electron/hole pairs. All samples showed luminescence emission peaks at 455 nm and 472 nm, which may be related to surface defects in the samples. The luminescence emission peak at 446 nm can be attributed to free excitons at the band edge. The samples with nanoparticles on their surface showed a reduction in luminescence emission intensity. This decrease in intensity is directly associated with the reduction of photogenerated charge recombination and an increase in the "lifetime" of the photogenerated electron/hole pairs. This enhancement in charge lifetime is due to charge sharing between the metal and niobium oxide, leading to an extension of the lifetime of charges. Materials modified with Fe showed high production of carbon monoxide (CO) (356.6 $\mu\text{mol/g}$). Furthermore, the calcination of the Nb_2O_5 semiconductor and its modification with Fe favored the production of methane (5.13 $\mu\text{mol/g}$), methanol (75.78 $\mu\text{mol/g}$), and acetic acid (69.07 $\mu\text{mol/g}$). On the other hand, Cu-modified materials increased methane (52.5 $\mu\text{mol/g}$) and methanol (628.01 $\mu\text{mol/g}$) production compared to Nb_2O_5 and Fe-modified catalysts. The higher conversion efficiency for Cu-modified materials is related to the ability of Cu to trap photogenerated electrons in the Nb_2O_5 conduction band.

8:00 PM SF03.03.14

High Pyroelectricity of the Freestanding BaTiO_3 Nanomembrane Around Room Temperature SunokKim^{1,2}, SangmoonHan¹, Justin S.Kim¹, YuanMeng¹, ZhihaoXu¹, DonghwanKim^{2,2} and SanghoonBae¹; ¹Washington University in St. Louis, United States; ²Sungkyunkwan University, Korea (the Republic of)

Pyroelectricity is the temperature fluctuation (temporal temperature gradient) response of the spontaneous polarization in pyroelectric materials, where the high pyroelectricity is mainly observed around Curie temperature. Mainly, $\text{Ba}_x\text{Sr}_{1-x}\text{TiO}_3$ is mainly adopted to implement the giant pyroelectricity thanks to their Curie temperature as low as 30 degree Celsius. However, they have low polarization levels and large thermal noise owing to their low crystal quality and paraelectric centrosymmetric state. Ferroelectric and single-crystalline BaTiO_3 (BTO) are outstanding materials thanks to the high polarization change rate around Curie temperature, but it has a high Curie temperature as high as 120 degree Celsius.

In this paper, we demonstrate the high pyroelectricity for room temperature operation by using a freestanding BTO nanomembrane grown by PLD. For room temperature operation, we systematically decreased the Curie temperature by reducing the BTO thickness from 100 nm to 30 nm. At a 100-nm freestanding BTO nanomembrane, the Curie temperature was measured to be 110 degree Celsius, which is slightly lower than the conventional BTO on the host substrate. At the 30-nm freestanding BTO nanomembrane, the Curie temperature is decreased to 90 degree Celsius, which is the lowest value than those of previously reported results in the BTO-based pyroelectricity field. This result is attributed to the compressive strain of the freestanding BTO film. As the thickness of the BTO film decreases, the internal strain of the freestanding BTO increase, restricting the ion movement in crystalline. That restrict causes deflection of the ions, which enables high pyroelectricity of freestanding BTO around room temperature. Thanks to the low Curie temperature, the pyroelectricity around 25 to 60 degree Celsius is calculated to be 360 $\mu\text{C/m}^2\text{K}$ at 100-nm freestanding BTO, which is a much-improved result than those of previous works. The freestanding BTO nanomembrane and thickness-dependent pyroelectricity control reported in this work will be a core technology and building block for highly efficient thermal-based devices without any cooling system.

8:00 PM SF03.03.15

Optimizing CO₂ Photoreduction in Freestanding Silver Bismuth Iodide/Nanocellulose Films Through Incident Light Modulation and Integration of Gold NanoparticlesTing-HanLin¹, Yin-HsuanChang¹, Yi-JingLu¹, Kai-ChiHsiao¹, Jia-MaoChang¹, Ying-HanLiao¹, Kun-MuLee^{1,2} and Ming-ChungWu^{1,2}; ¹Chang Gung University, Taiwan; ²Chang Gung Memorial Hospital at Linkou, Taiwan

The rise in CO₂ emissions is one of the primary causes of global warming and climate change. To counteract this, researchers are dedicated to transforming CO₂ into valuable fuels using solar energy to facilitate the reduction of CO₂ into carbon-based fuels, a mechanism that mimics photosynthesis. Particulate photocatalysts are an attractive option for this process due to their easy fabrication and varied material configurations. Further, immobilizing these onto composite polymers improves their reusability and practicality. In this study, we fabricated a novel freestanding photocatalyst composite film by immobilizing Ag₃BiI₆ (SBI) onto a nanocellulose (CNF) transparent film using a sequential process involving noble metal nanoparticle solutions and thermal evaporation of BiI₃. The process of fabricating the SBI/CNF composite film unfolds in two distinct stages. During the initial stage, we prepare the Au NPs, Ag NPs, and a mixture of Au NPs and Ag NPs, each loaded onto a CNF film. This is achieved by applying a 0.05wt% CNF hydrogel to a hydrophilic membrane filter using suction filtration. Au, Ag, and Au-Ag mixtures are subsequently added, generating the Au/CNF, Ag/CNF, and Ag-Au/CNF films respectively. For ease of film detachment, they are briefly immersed in acetone, followed by a vacuum drying phase. The outcome of this process is a set of freestanding and flexible films. The second stage begins with affixing these prepared films to the upper surface of a glass dish, while BiI₃ is positioned at the bottom of the dish. The assembly is heated to a temperature of 200°C for a span of 30 min, enabling the thermal evaporation deposition of BiI₃ onto the films. The BiI₃-infused films are then transferred into an oven for thermal annealing at varying temperatures, facilitating the creation of SBI. The effect of the sequence and composition of Au and SBI/CNF on the morphology, optical property, and CO₂ photoreduction performance was also investigated. The resulting SBI-Au/CNF film exhibited the highest photocatalytic activity for CO₂ reduction, achieving a CO yield of 31.96 μmol/g•h with high stability for long-term photocatalytic reactions lasting 72 h. The stability of SBI-Au/CNF was also demonstrated in long-term reaction conditions, showing stable reactivity for CO₂ reduction. This work highlights the potential of immobilized Ag₃BiI₆ materials and induced nanoparticles in improving light management, and provides versatile roles for metal nanoparticles in designing high-performance photocatalyst platforms for CO₂ reduction.

8:00 PM SF03.03.16

Incorporating Acidic Functional Groups into Metal-Organic Frameworks via Click Chemistry for Efficient Ammonia StorageDae WonKim and Chang SeopHong; Korea University, Korea (the Republic of)

Despite extensive research on ammonia adsorbents for storage purposes, the development of adsorbents with both high ammonia capacity and efficient regeneration processes has been limited. Enhancing ammonia capacity in adsorbents can be achieved by decorating material pores with acidic groups that interact with ammonia. However, incorporating acidic functional groups into metal-organic frameworks poses challenges due to the need for high structural stability for C-C bond formation through post-synthetic modification. Alternatively, ligands decorated with acidic groups can be used, but this alters the framework structure as the acidic groups tend to coordinate with metals during synthesis. In this study, we introduce Ni₂acryl₂TMA (TMA = thiomallic acid), a metal-organic framework functionalized with acidic groups through bridging ligand exchange and following ene-thiol click reaction. Our findings reveal an outstanding gravimetric ammonia capacity of 23.5 mmol g⁻¹ and an unprecedented ammonia storage density of 0.39g cm⁻³ at 1 bar and 298 K, accompanied by facile regeneration. The ammonia storage properties and adsorption mechanism were thoroughly characterized using various techniques including ammonia isotherms, NH₃-temperature-programmed desorption curves, NH₃ breakthrough curves, in-situ FT-IR, and DFT calculations. The synthesis details and comprehensive properties will be presented in the poster.

8:00 PM SF03.03.17

Synthesis of Unconventional 2H Pt Facets via Wet-Chemical Epitaxial Growth and Crystal Structure-Dependent Catalytic Behaviors of Pt in the Selective Hydrogenation ReactionLongZheng and YeChen; The Chinese University of Hong Kong, China

Pt-based nanocatalysts are promising heterogeneous catalysts in hydrogenation reactions. However, it remains a great challenge to achieve high chemoselectivity for high-value intermediates and avoid over-hydrogenation when substrates contain multiple competing functional groups. Numerous efforts have been made to improve the chemoselectivity of Pt-based nanocatalysts in hydrogenation, including tuning their size, composition, and surface ligands. However, to the best of our knowledge, the effect of crystal structure of Pt on hydrogenation reactions has not been investigated because it is still difficult to synthesize Pt nanocrystals with high-purity metastable phases with well-defined facets. In this work, we develop a novel hexagonal close-packed (2H) Pt-based nanocatalyst exposed with well-defined unconventional 2H Pt facets via epitaxial growth and reveal the crystal structure-dependent catalytic performance of Pt in hydrogenation reactions. Moreover, our distinctive epitaxial growth strategy could also be used to synthesize 2H/face-centered cubic (3C) heterophase Au and Ag shells. Impressively, the 2H Pt shell exhibits remarkably high catalytic selectivity toward the high-value intermediate and excellent durability, superior to conventional 3C Pt counterpart with nearly-same morphologies and identical surface ligand. This work not only provides a general strategy for crystal structure-controlled epitaxial growth of noble metal-based heterogeneous catalysts, but also demonstrates crystal structure-dependent catalytic behaviors of Pt in heterogeneous selective hydrogenation. <div> </div>

8:00 PM SF03.03.18

Valence Stability of Cations and the Formation of Perovskite Type ABO₃ OxidesKripasindhuSardar¹, SatoruKaneko^{2,3}, MamoruYoshimoto³ and MasahiroYoshimura¹; ¹National Cheng Kung University, Taiwan; ²KISTEC, Japan; ³Tokyo Institute of Technology, Japan

The analysis of the Madelung electrostatic potential and the lattice site potential of ABO₃ compounds (with many combinations of A and B) have been employed for building a set of criteria for the formation of perovskite structure type oxides ABO₃ by Yoshimura *et al.*^{1,2,3}. Thus, oxides of A and B can be reacted to prepare perovskite structure type ABO₃ compounds if: (i) B ion is smaller than A ion, (ii) valence of B ion is larger or equal to A ion and (iii) sum of the valences of A and B ion is six (including mixed valence situation A_{1-x}A_x" or B_{1-y}B_y"). Furthermore, an in depth analysis show that the valence stability originates from the gain of lattice site potential.

Why many solid state compounds would crystallize into perovskite structure type ABX₃? Historically, the answer to this question has been attempted from ion-packing & tolerance factor consideration by Goldschmidt in 1926⁴. Even now, the stability of perovskite structure type ABO₃ oxides is mainly assessed in terms of the geometric parameters such as tolerance factor, and structure-field map^{5,6}. However, it can be argued that the stability is more related to thermodynamic energy therefore, originate from thermodynamic principles rather than numerical geometrical parameters. The crystal chemistry and thermodynamic energy of ionic solids are reflected into Madelung electrostatic potential as shown by Van Gool and Piken in 1969⁷. However, M. Yoshimura demonstrated "The valence stability using lattice site-potential" in perovskite structure type ABO₃ oxides for the first time in 1974¹.

Herein, the freely available software VESTA⁸ has been used to calculate the lattice site potentials and Madelung electrostatic potential directly from the known crystal structures. Thereby, some fundamental aspects of synthesis, stability and properties of perovskite structure type ABO₃ oxides have been addressed. It is hoped that this work will contribute to the designing, synthesis, structures and properties of inorganic solid state materials to overcome the challenges of tomorrow.

References

- ¹M. Yoshimura, T. Nakamura and T. Sata, *Bull. Tokyo Inst Tech.* 1974, **120**, 13-27.
- ²T. Ishigaki, Z. S. Nikolic, T. Watanabe, N. Matsushita and Yoshimura, *Solid State Ionics* 2009, **180**, 475-479.
- ³M. Yoshimura, and K. Sardar, *RSC Adv.*, 2021,11, 20737-20745
- ⁴V. M. Goldschmidt, *Die Naturwissenschaften*, 1926, **21**, 477-485
- ⁵K. Zhang, J. Sunarso, Z. Shao, W. Zhou, C. Sun, S. Wang and S. Liu, *RSC Adv.* 2011, **1**, 1661-1676.
- ⁶Q. Sun, and W-J Yin, *J. Am. Chem. Soc.* 2017, **139**, 14905-14908.
- ⁷W. Van Gool and A. G. Piken, *J. Mat Sci.* 1969, **4**, 95-104.
- ⁸K. Momma and F. Izumi, *J. Appl. Crystallogr.* 2011, **44**, 1272-1276.

8:00 PM SF03.03.19

Nanoparticle Conversion Chemistry: A Toolbox for Multimetallic NanostructuresNabojitKar, MaximilianMcCoy, JoshuaWolfe and SaraSkrabalak; Indiana University Bloomington, United States

The synthesis of multimetallic nanoparticles (NPs) with size- and shape-control has been studied over the last several decades due to their applications in catalysis, plasmonics, solar cells, electronics, and even as theranostics. To synthesize multimetallic NPs with precision, NP conversion strategies are appealing, where NPs of a desired shape, size, and phase can be synthesized from an easily accessible NP starting material. The NP starting point (reactants) serves as a compositional and morphological template to control the composition and morphology of the product NPs. For example, architecturally complex PdCu-Au NPs were synthesized through galvanic replacement between PdCu NPs and AuCl₂⁻ (Au¹⁺) and AuCl₄⁻ (Au³⁺), allowing for the role of reaction stoichiometry on NP architecture. Here, the role of reaction stoichiometry is shown to direct the overall architecture of multimetallic PdCuAu nanostructures. Similarly, thermal diffusion is another tool from the NP conversion strategy toward synthesizing monodisperse high entropy alloy (HEA) NPs from core@shell NPs. These NPs, consisting of 5 or more metals in a single phase are an exciting class of NPs because of their unlimited compositions, superior stability, and potential for high catalytic activity. Even though significant progress, a more generalizable pathway to control the composition of HEA NPs while maintaining monodispersity is still desirable in the science community. The retrosynthetic principles to synthesize

HEA NPs were established by studying a library of core@shell systems, outlining that metal precursors that have a high reduction potential (Ered) relative to other constituent metals in the seed should be incorporated in the core of the core@shell NPs. Similarly, metal precursors that have a much lower Ered than the other constituent metals in the seed, should go in the shell. Metals that are adverse to alloy phase formation or have poor wettability should go in the core of the core@shell NPs. Importantly, the obtained core@shell NPs were transformed into monodisperse HEA NPs through thermal annealing, demonstrating the generality of the approach. These NP conversion strategies exhibit a remarkable level of modularity, thereby offering a versatile approach to obtain a wide range of compositions and architectures for multimetallic NP.

8:00 PM SF03.03.20

The Synthesis of Mixed Metal High Entropy Oxybromides (Sr_xBa_{1-x}BiO₂Br) for Photocatalytic Degradation of Tetracycline Antibiotic Chakgrid Noomak and Numpon Insin; Department of Chemistry, Faculty of Science, Chulalongkorn University, Thailand

Nowadays, antibiotic contamination in aquatic environments, especially tetracycline (TC), can cause toxicity to human health. There are several strategies that have been used to remove this contaminant. In the past few decades, photocatalysis has attracted considerable attention as a method to remove pollutants in wastewater because of its high oxidation activity, stability, and non-toxicity. Recently, high entropy materials (HEM), which are new materials that contain five or more elements, have been applied in various applications. It has been proven that HEMs with multielement can provide good structural stability. However, the application of HEMs in the field of photocatalysis has rarely been reported. Therefore, it is interesting to construct HEMs to be used as photocatalysts. In this work, we designed and fabricated a mixed metal high entropy oxybromide (Sr_xBa_{1-x}BiO₂Br), a novel photocatalyst that contains five elements in the structure, by incorporating metals (Sr and Ba) into bismuth oxybromide material (BiOBr) to enhance their stability and photocatalytic activity toward degradation of tetracycline antibiotic (TC). The BiOBr was synthesized using a simple solvothermal method before BiOBr mixed with metal acetate (ratio 1:1) were calcined at 700 °C for 8 hours to construct a mixed metal high entropy oxybromide. The properties of the synthesized photocatalysts were characterized by XRD, SEM, EDX, TGA and surface area analysis. The photocatalytic activity of catalysts was evaluated by the photocatalytic degradation of tetracycline antibiotic (TC) under visible light. The results illustrated that the photodegradation efficiency for Sr_{0.75}Ba_{0.25}BiO₂Br was higher than monomeric materials, which was 1.3 times and 1.6 times higher than that of SrBiO₂Br and BaBiO₂Br, respectively. Moreover, it can maintain high efficiency despite using multiple cycles. These observations imply that a mixed metal high entropy oxybromide has high activity and stability. This study demonstrates a new approach for developing photocatalysts which are more effective and stable.

8:00 PM SF03.03.21

Exceptional Thermochemical Stability of Graphene/N-Polar GaN for Remote Epitaxy for Exfoliation and Device Fabrication Joonghoon Choi and Young Joon Hong; Sejong University, Korea (the Republic of)

Graphene (Gr) has drawn great attention as an epitaxial template for production of single-crystalline, freestanding semiconductor membranes through remote epitaxy. This emerging epitaxy facilitates the growth of single-crystalline epi-layer membranes, whose crystallographic properties follow to that of the underlying wafer across a Gr gap layer.[1] The lattice transparency of Gr allows the overlying layer to resemble the crystallinity of the mother substrate while permitting the effortless release of the grown film using sticky tape- and/or metal stressor-assisted exfoliation techniques, a result of non-chemical bonds at the interface.[1,2] Notably, the mother substrate can be reused for other subsequent epitaxial growths, given the damage- and contamination-free exfoliation, which is contrast to the damage and performance degradation caused by laser/chemical lift-off. Various material systems, such as compound semiconductors, complex oxides, halide perovskites, etc., have been extensively studied for remote epitaxy.[3] However, metal-organic vapor deposition (MOCVD)-based GaN remote homoepitaxy remains unaccomplished due to the poor thermochemical stability of graphene/Ga-polar GaN substrates.[4] III-nitrides (i.e., GaN, AlN, and AlGaIn) are conventionally grown using MOCVD at high temperatures under a hydrogen atmosphere for commercial purposes. However, the harsh conditions required for MOCVD growth of III-nitride potentially lead to thermochemical decomposition of graphene and underlying substrate, making it difficult to take the full advantages of remote epitaxy. Thus, the remote homoepitaxy of GaN and successful exfoliation of GaN overlayer have remained as challenges.

In this presentation, we report the N-polar remote homoepitaxy of GaN using single-layer graphene (SLG). MOCVD yields N-polar micro-crystals (μCs) and Ga-polar thin films are yielded on graphene-coated N- and Ga-polar substrates, respectively. However, only the μCs overlayer is gently separated from the mother substrate via the adhesive tape-assisted exfoliation method, confirming the successful remote homoepitaxy. We investigate the stability of GaN substrates of Ga- and N-polarity for remote epitaxy and demonstrate only the SLG-coated N-polar GaN substrates allow the remote epitaxy. The N-polar remote homoepitaxy is confirmed by Raman spectroscopy, electron microscopy analyses, and overlayer delamination tests. The successful remote epitaxy is contingent on SLG's stability, correlated with the decomposition of GaN substrates. Complementary molecular dynamics (MD) simulations and annealing experiments confirm that the thermochemical stability of graphene is dependent on the polarity of GaN due to varying hydrogen reaction behaviors at high temperatures. Our findings elucidate why graphene's thermochemical stability varies depending on substrate polarity and present an opportunity to prepare N-polar GaN that is releasable from the substrate through MOCVD-based remote epitaxy. Lastly, we apply the successful N-polar remote homoepitaxy of μCs to grow flexible light-emitting diodes (LEDs), consisting of p-n junction μCs with InGaIn heterostructures for fabricating deformable LEDs.

References

- (1) Kim, Y. et al. Remote epitaxy through graphene enables two-dimensional material-based layer transfer. *Nature* **2017**, *544*, 340.
- (2) Jeong, J. et al. Remote heteroepitaxy of GaN microrod heterostructures for deformable light-emitting diodes and wafer recycle. *Sci. Adv.* **2020**, *6*, eaaz5180.
- (3) Kim, H. et al. Remote epitaxy. *Nat. Rev. Methods Primers* **2022**, *2*, 40.
- (4) Park, J. H. et al. Influence of Temperature-Dependent Substrate Decomposition on Graphene for Separable GaN Growth. *Adv. Mater. Interfaces* **2019**, *6*, 1900821.

8:00 PM SF03.03.22

Hollow Ruthenium Nanoparticles for Photothermal and Colorimetric Detection of Cholesterol Se Hwa Cheon, Su Jeong Lee, Han Been Lee, Chang Hyeon Ha, Do Hyeon Kim and Gi hun Seong; Hanyang University, Korea (the Republic of)

The development of porous metal nanoparticles is a standout field due to their unique mechanical, chemical, and thermal properties. Hollow nanoparticles, one of the porous nanoparticles, have better activity compared to solid nanoparticles due to their high surface-to-ratio, low density, and facilitated transfer of reactants. As a result, hollow nanoparticles can be used in various fields such as electrochemical analysis, drug-delivery systems, and lithium-ion batteries. These nanoparticles can be synthesized using methods such as chemical etching, the Kirkendall effect, and the galvanic replacement reaction (GRR). Among these methods, GRR is the most commonly used approach due to its several benefits, including a single reaction process and easy surface modification. This method enables the deposition of desired metal ions on the surface of sacrificial metal, allowing for the synthesis of hollow nanoparticles with very thin shells in a short time. To the best of our knowledge, there have been few studies that apply hollow nanoparticles as chemical catalysts.

Cholesterol is one of the lipid molecules in the human body as well as a component of the cell membrane of animal cells. It plays a crucial role in the synthesis of biomolecules like vitamin D and steroid hormones. However, abnormal cholesterol levels can lead to various diseases, including high blood pressure, hyperlipidemia, arteriosclerosis, and cardiovascular issues. Therefore, accurate determination of cholesterol levels is vital for early diagnosis of these conditions.

In this study, we successfully synthesized hollow ruthenium nanoparticles (HRNs) that mimic the activity of horseradish peroxidase (HRP), a natural peroxidase. The HRNs were synthesized using GRR, where nickel (Ni) was used as a sacrificial template. The transmission electron microscopy (TEM) images clearly revealed the distinct hollow structure of the HRNs, with an average diameter of approximately 40 nm and a shell thickness of 3 nm. Notably, the HRNs exhibited superior catalytic activity compared to HRP. This enhanced activity can be attributed to the presence of the hollow structure, which provides a large surface area with abundant active sites.

The synthesized HRNs were utilized in the colorimetric and photothermal detection of cholesterol, employing 2,2'-azino-di-(3-ethylbenzthiazoline sulfonic acid) (ABTS) as a substrate. Cholesterol was oxidized by cholesterol oxidase, resulting in the generation of H₂O₂. The HRNs acted as catalysts for the oxidation of ABTS in the presence of H₂O₂, leading to the production of oxidized ABTS (ABTS_{ox}). ABTS_{ox} served as a substrate for both colorimetric and photothermal detection, as it exhibits strong absorbance in both the visible and near-infrared (NIR) regions. The oxidation of ABTS caused a change in color from transparent to green, with absorbance peaks observed at wavelengths of 405 nm and 418 nm. Additionally, ABTS_{ox} could be excited by absorbing NIR laser light at 808 nm, emitting energy in the form of heat. Consequently, the difference in solution temperature before and after laser irradiation was found to be proportional to the cholesterol concentration. The colorimetric and photothermal detection methods displayed good linearity within a concentration range of 80 μM to 10 mM, with a limit of detection values of 12.3 μM and 54.4 μM, respectively. These results demonstrate that HRNs can serve as effective alternatives to natural enzymes in the sensitive detection of cholesterol. Moreover, the hollow structure of HRNs offers advantages such as enhanced properties with abundant active sites and easy surface modification, making HRNs applicable to various fields in the future.

8:00 PM SF03.03.23

Enhanced Microwave Heating Properties and Gas Decomposition Efficiency of Polymer-Derived SiC Fibers via Multi-Metal Doping Young Jin Shim^{1,2}, Kwang Youn Cho¹, Hyuk Jun Lee^{1,2}, Sang Hyun Joo¹, Young Keun Jeong² and Young Jun Joo¹; ¹Korea Institute of Ceramic Engineering & Technology, Korea (the Republic of); ²Pusan National University, Korea (the Republic of)

Polymer-derived SiC fibers are one of the most effective materials for high-temperature microwave absorption due to its low manufacturing temperature, ease of processing, and good

oxidation resistance at high temperatures. Also, by adding specific additives at the polymer stage, polymer-derived SiC materials can achieve desired properties such as the modulation of thermal stability, mechanical strength, electrical characteristics, and chemical stability to meet specific application requirements. In particular, the use of metal organic compounds can enable to acquire specific catalytic properties.

In previous research, we confirmed the microwave heating mechanism of SiC fibers fabricated using polycarbosilane. In this study, SiC fibers doped with Fe and Ti were fabricated through the electrospinning process and exhibited a relatively small diameter and enhance the efficiency of NO_x, SO_x, and methane gas decomposition under microwave. The data demonstrated that multi-metal doped SiC fibers generated high-temperature heat under microwave, resulting in the decomposition of methane gas. Moreover, the presence of the rutile phase of TiO₂ in the fibers exhibited catalytic properties at high temperatures facilitating the decomposition of NO_x gas.

The structural analysis via FE-SEM and XRD revealed that multi-metal doped SiC fibers with a predominant rutile phase of TiO₂ exhibited enhanced NO_x gas decomposition under microwaves, attributed to the catalytic activity of TiO₂, as compared to their polymer-derived SiC fiber. Furthermore, the fibers with small diameter formed through electrospinning and the doping of Fe improve the absorption performance of microwaves, leading to excellent heat generation characteristics. The residual Fe content in the SiC fiber was about 0.5wt% and showed higher microwave heating efficiency than the SiC fiber without Fe doping. We have confirmed that the superior heat generation characteristics exhibited in the microwave gas decomposition system effectively promote methane gas decomposition.

8:00 PM SF03.03.24

Tunable Synthesis of Nanostructured Materials for Energy Storage in Pressure and Temperature Controlled Chamber via Photonic Curing NajmaKhatoon, BinodSubedi, MichaelJohnson and DouglasB. Chrisey; Tulane University, United States

Nanoparticles and nanostructured materials stand out from their bulk counterpart because of their high surface-to-volume ratio, and novel chemical, electrical, magnetic, and optical properties. Interestingly, these properties can be tuned by controlling size, shape, and phase of nanoparticles (NPs). Gas-phase and vapor-phase synthesis of nanoparticles (NPs) are among several synthesis techniques employed for NPs synthesis. In conventional NPs synthesis techniques, there is enough time to achieve thermodynamic equilibrium, however on quenching NPs before they reach equilibrium state, metastable states of NPs can be trapped. As such, the high quenching rate for NPs synthesis is a promising way to produce unique nanostructured morphologies. We used pulsed photonic curing (quenching rate ~ 10³°C/msec) to achieve this goal. Photonic curing is a unique technique to process materials using xenon flash lamp light (wavelength ranging from 250 nm – 1200 nm). The maximum calculated temperature reaches ~1100 C during post pulsed photonic curing process. In this work, we designed a special chamber to incorporate photonic curing with gas-phase and vapor phase synthesis simultaneously. The chamber we designed can treat the material with photonic processing in argon or forming gas (N₂/H₂) environment under variable pressures (vacuum – 3.5 bar). High temperatures and high pressures in pulsed photonic curing can lead to novel transformation of precursors in vapor phase. The nucleation and growth during the processing depends on pressure, temperature and thus on the mean free path of the gas molecules. We processed organometallic transition metal oxide (MnCo) precursor under 1 atm to 3.5 atm, the mean free path varied from 1.14 × 10⁻¹⁸ μm to 1.76 × 10⁻¹⁶ μm during the process. Results showed that there is less rGO conversion when MnCo treated under argon gas environment. The chamber is also capable of treating 2D layered material with less rate of oxidation. Results showed a significant decrease in oxidation of MXenes (Ti₃C₂) under argon gas environment which is desired for enhanced electrochemical properties.

8:00 PM SF03.03.25

Symmetry Breaking in NaMnO₂: Exploring the Interplay Between Strain and Magnetism in Novel Quantum Materials EuanBassey¹, RaphaëleClement^{1,2} and AntonVan der Ven²; ¹Materials Science Laboratory, United States; ²University of California, Santa Barbara, United States

Spatially anisotropic magnetic systems are a playground for the modern physicist and materials scientist: excitations of the ground state, if sufficiently long-lived, may be manipulated for use in quantum computing applications, while external stimuli such as stress, temperature and applied magnetic field strength can modulate the magnetic properties of the system. Perhaps one of the most widely studied anisotropic systems to date is α-NaMnO₂, a layered, antiferromagnetic triangular lattice of space group C2/m.¹⁻³ On cooling from 300 K, it undergoes both crystallographic—from a monoclinic C2/m phase to a triclinic P phase below 30 K³—and magnetic—from a paramagnetic (T > 45 K) to an antiferromagnetic state (T_N = 22 K), via an incommensurate phase (45 < T < 22 K)—symmetry breaking transformations.² The interplay between the crystallographic and magnetic symmetry breaking phase transformations, however, remains unclear: does strain encourage magnetic ordering, or does magnetic exchange control strain? For the first time, we explore the interplay between magnetic exchange interactions and strain via a density functional theory cluster expansion method. We compute the energy landscape for α-NaMnO₂ over a range of strained and magnetic states; determine the exchange interaction constants as a function of strain; and obtain the magnetic susceptibility and spin correlation lengths as a function of temperature, while comparing against experimental data. This methodology can be extended to a plethora of anisotropic systems of interest to the wider materials science community.

References:

- (1) Dally, R. L.; Heng, A. J. R.; Keselman, A.; Bordelon, M. M.; Stone, M. B.; Balents, L.; Wilson, S. D. Three-Magnon Bound State in the Quasi-One-Dimensional Antiferromagnet Alpha-NaMnO₂. *Phys. Rev. Lett.* **2020**, *124* (19), 197203. <https://doi.org/10.1103/PhysRevLett.124.197203>.
- (2) Dally, R. L.; Chisnell, R.; Harriger, L.; Liu, Y.; Lynn, J. W.; Wilson, S. D. Thermal Evolution of Quasi-One-Dimensional Spin Correlations within the Anisotropic Triangular Lattice of NaMnO₂. *Phys. Rev. B* **2018**, *98* (14), 144444. <https://doi.org/10.1103/PhysRevB.98.144444>.
- (3) Zorko, A.; Adamopoulos, O.; Komelj, M.; Arçon, D.; Lappas, A. Frustration-Induced Nanometre-Scale Inhomogeneity in a Triangular Antiferromagnet. *Nat. Commun.* **2014**, *5* (1), 3222. <https://doi.org/10.1038/ncomms4222>.
- (4) Stock, C.; Chapon, L. C.; Adamopoulos, O.; Lappas, A.; Giot, M.; Taylor, J. W.; Green, M. A.; Brown, C. M.; Radaelli, P. G. One-Dimensional Magnetic Fluctuations in the Spin-2 Triangular Lattice NaMnO₂. *Phys. Rev. Lett.* **2009**, *103* (7), 077202. <https://doi.org/10.1103/PhysRevLett.103.077202>.
- (5) Giot, M.; Chapon, L. C.; Androulakis, J.; Green, M. A.; Radaelli, P. G.; Lappas, A. Magnetoelastic Coupling and Symmetry Breaking in the Frustrated Antiferromagnet Alpha-NaMnO₂. *Phys. Rev. Lett.* **2007**, *99* (24), 247211. <https://doi.org/10.1103/PhysRevLett.99.247211>.

8:00 PM SF03.03.26

Nanometer-Thick Co Doped MoO₃ Films and Full-Device with Enhanced Electrochromic Properties YusufTutel¹, Mete BatuhanDurukan¹, SerifeHacioglu², Umranc. Baskoc¹, EdaCevik¹, LeventToppare¹ and HusnuE. Unalan¹; ¹Middle East Technical University, Turkey; ²Iskenderun Teknik University, Turkey

In the past decades, transition metal oxides have received noteworthy attention due to their unique properties to be used in applications like electronics, optoelectronics, electrochemistry, sensors, and catalysis. Among them, molybdenum trioxide (MoO₃) showed promising thermal, chemical and electrochromic properties with good chemical and physical stability. Moreover, the electrochromic properties of MoO₃ may simply be tuned via doping. However, the production of uniform, crack-free and stable MoO₃ thin films for electrochromic applications using conventional deposition techniques is still difficult, as it is necessary to achieve continuous cycle stability. Ultrasonic spray deposition (USD) method enables cost-effective deposition of thin films through wet chemistry, facilitating the appropriate incorporation of various dopant atoms to improve material properties. Moreover, this method allows high material utilization, mass-production and is vacuum free. In this work, MoO₃ and Co doped MoO₃ (MoO₃:Co) thin films were deposited onto pre-heated indium tin oxide (ITO)/glass substrates using USD method. As-deposited thin films were then annealed to crystallize. The addition of Co dopant atoms on the morphological, optical, electrochemical and electrochromic properties of MoO₃ thin films have been systematically investigated. Significant decrease in the crystallite sizes were observed upon Co doping. Likewise, the bandgap of MoO₃:Co thin films (3.42 eV) decreased slightly compared to bare MoO₃ thin films (3.49 eV). According to the XPS results, bare MoO₃ exhibits a predominance of Mo⁶⁺, however, a minor reduction in these charges to +5 is observed due to the Co doping effect in MoO₃:Co films which causes an increase in electrocatalytic activity. Addition of Co dopant atoms to MoO₃ thin film electrodes resulted in improved maximum transmittance change in the colored and bleached states compared to bare MoO₃ thin film electrodes. Furthermore, it was observed that cyclic stability of the bare MoO₃ thin film electrodes decreased with increasing cycle numbers. In contrast, the MoO₃:Co electrodes showed significantly higher capacitance retention of 92%, indicating superior cyclic stability and improved performance compared to the bare MoO₃ electrodes. In the light of these enhancements, electrochromic full-device was fabricated with MoO₃:Co and NiO thin film electrodes using organic (LiClO₄/PC/PMMA) gel electrolyte. Full device showed 23% maximum transmittance change with excellent cyclic stability (around 99% capacitance retention). Especially with device engineering, electrochromic full device stability has been increased by using inorganic thin films and organic gel electrolyte. Our results indicated that USD method is highly suitable for the deposition of functional MoO₃:Co thin films for electrochromic smart windows and full-devices.

8:00 PM SF03.03.27

New Oxide Glass Cathode Materials for Sustainable and High-Energy Density Lithium Batteries TaosGuyot, JuliaAgullo, DamienPerret, LoicSimonin and SébastienMartinet; Commissariat à L'énergie Atomique et Aux Energies Alternatives (CEA), France

As energy concerns grow and the society needs more sustainable and renewable energy sources, the ability to effectively store and retrieve energy is paramount. Currently, rechargeable lithium-ion batteries (LIB) seem to be one of the best alternatives to reduce our dependency on fossil fuels. LIB are made of cathodes materials based on polycrystalline oxides or polyanion compounds¹. However, some of them have their performance limited by their crystalline structure where other compounds suffer from irreversible phase changes against cycling². To overcome these key shortcomings, implement glasses or glass-ceramics as cathode materials seems to be an interesting approach. Glasses have a structure composed of more free volume,

which can accept a large amount of lithium³ and easily accommodate structural changes upon lithium ions extraction/insertion⁴. Furthermore, glass production is scalable and commercially easier to implement than most of synthesis processes of conventional cathodes materials.

In this study, various types of oxide glasses have been investigated as promising cathode materials for sustainable and high energy density lithium batteries. The influence of the nature of the transition metal (Fe, Mn, ...) and the polyanion (PO₄, BO₃, SiO₄) on the microstructural and electrical properties of the as-prepared glasses were examined. Electronic and ionic conductivities were measured by Electrochemical Impedance Spectroscopy (EIS). The electrochemical properties in terms of specific capacity, redox potentials vs Li^{+/}Li, first cycle capacity loss, coulombic and energy efficiencies of these materials were investigated in coin-cell by Galvanostatic Cycling (GC). Finally, to elucidate the reaction mechanisms of the electrochemical processes involved in these materials, X-ray diffraction (XRD) and X-ray photoelectron spectroscopy (XPS) at room temperature were coupled and performed on the as-prepared glasses and on ex-situ (after cycling) materials at different electrochemical states of charge. This new study will bring significant elements to optimize both the glass composition and its elaboration conditions to obtain high performance cathode materials without critical materials.

¹Nitta, N. *et al.*, Li-ion battery materials: present and future. *Materials Today* **18**, 252–264 (2015).

²Tesfamhret, Y. *et al.*, On the Manganese Dissolution Process from LiMn₂O₄ Cathode Materials. *ChemElectroChem* **8**, 1516–1523 (2021).

³Afyon, S. *et al.*, New High Capacity Cathode Materials for Rechargeable Li-ion Batteries. *Scientific Reports* **4**, 7113 (2015).

⁴Kindle, M. *et al.*, Alternatives to Cobalt. *ACS Sustainable Chemistry Engineering* **9**, 629–638 (2021).

8:00 PM SF03.03.28

CO₂ Capture from Flue Gas by MOFs Mohammad Wahiduzzaman¹, Sabine Devautour-Vinot² and Guillaume Maurin²; ¹CNRS, France; ²Université Montpellier, France

In light of the current environmental situation, reduction of anthropogenic CO₂ emissions from carbon-intensive industries like power plants, cement, steel, or petrochemical industries become one of the most pressing issues to combat global warming. Shifting towards a low-carbon economy requires cost-effective carbon capture utilization or sequestration (CCUS) technology to be developed. Currently utilized amine-based absorption-regeneration process suffers from high energy penalties for solvent regeneration. In this regard, adsorption-based processes are considered promising alternatives for CCUS. Metal-organic frameworks (MOFs) are a widely studied class of porous adsorbents that offer tremendous potential, owing to their large CO₂ adsorption capacity and/or high CO₂ affinity. However, the performances of MOF-based CCUS technologies have not been fully evaluated in real industrial conditions. For example, the industrial flue gas contains CO₂, N₂, H₂O, and traces of other contaminants, such as H₂S, SO₂, and NO_x, which compete for different adsorption sites or might impact the stability of the adsorbent materials. Therefore, it is crucial to understand the competitive adsorption of the various components of the flue gas. From an experimental standpoint, such study is tedious and time consuming while molecular simulations provide a quicker route to understand their adsorption behavior and plausible degradation at the microscopic level. In this presentation, I will outline a systematic joint computational/experimental approach to evaluate the stability and CO₂ capture performance of a series of MOFs in the presence of various impurities within the framework of MOF4AIR, a multidisciplinary H2020 EU project. A more detailed analysis will be provided for a few top-tier MOFs that were selected for large-scale deployment in the industrial post-combustion capture process.

Acknowledgement:

This project has received funding from the European Union's Horizon 2020 research and innovation programme under grant agreement No. 831975 (MOF4AIR project).

8:00 PM SF03.03.29

Choline based Plastic Crystals as Barocalorics: Insights from *Ab Initio* Molecular Dynamics Shivani Grover, Joshua Levinsky and Claire Hobday; University of Edinburgh, United Kingdom

Conventional refrigeration technologies based on vapour-compression cycles of greenhouse gases pose a serious threat to the environment and lack scalability to small sizes. Materials with large solid-state caloric effects induced by external field (mechanical, electric or magnetic field) are needed for the development of eco-friendly, energy efficient solid-state refrigeration technologies.¹

The refrigeration capacity is associated with a large isothermal entropy change and/or with a large adiabatic temperature change, induced by external stimuli such as mechanical pressure (barocaloric effect) or electric field (electrocaloric effect) or magnetic field (magnetocaloric effect), effects that are enhanced near phase transitions. To this end, organic-inorganic plastic crystals offer new interesting opportunities for the solid-state cooling applications.² Thus far, plastic crystals are the only known class of caloric materials which exhibit entropy changes on par with current commercial refrigerants and therefore require further investigation and development.

In this work, we explore the potential of choline-based plastic crystals, (C₅H₁₄NO)₂MCl₄ where M = Co, Zn, Cu, as promising barocaloric materials due to a large entropy change (~100 JK⁻¹Kg⁻¹) associated with the symmetry-breaking order-disorder phase transition. Using methods of *ab initio* molecular dynamics as implemented in CP2K, we provide insights into the local structure such as choline disorder and tumbling of CoCl₄ tetrahedra observed in this system. This is quantified by calculating the Co-Cl vector autocorrelation functions and its vibrational contribution to entropy change, which is dominated by the soft Co-Cl vibrational modes. The choline disorder is quantified by calculating the diffusivity of choline in the two phases. Our model is validated with our experimental study, thus providing a complete understanding of the interplay between dynamic and disordering effects in choline based plastic crystals.

References

1. Moya, X., Kar-Narayan, S. & Mathur, N. D. Caloric materials near ferroic phase transitions. *Nature Materials* **13**, 439-450 (2014).
2. Li, B. *et al.* Colossal barocaloric effects in plastic crystals. *Nature* **567**, 506-510 (2019).

SESSION SF03.04: Energy and Batteries I
Session Chairs: Craig Brown and Brent Melot
Tuesday Morning, November 28, 2023
Sheraton, Second Floor, Back Bay C

8:00 AM SF03.04.01

Optimizing Room-Temperature Electrochemical (De)Fluorination of CsMnFeF₆ using Differential Electrochemical Mass Spectrometry Jessica Andrews and Brent Melot; University of Southern California, United States

While research on cation intercalation has thrived and resulted in real-world applications, like Li-ion batteries, anionic intercalation is largely understudied. Energy storage based on anionic intercalation is extremely promising as anionic charge carriers, like fluoride, provide a new frontier to explore for the development of high energy density, rechargeable batteries. Thus far, F-ion batteries are mostly limited to conversion-based systems, in which redox reactions at the electrodes form entirely new products, typically with drastically different structures. Although these reactions are reversible, they often incur large volume changes that lead to poor cycling stability. More recently, all-solid-state cells that leverage fluoride-ion intercalation, in which the host material may experience structure changes but broadly maintains its original topology, have been reported. These systems show improved reversibility, but the solid electrolyte suffers from poor room-temperature fluoride conductivity, requiring high operating temperatures and limiting any practical use. Recent liquid electrolyte advancements include salt/solvent combinations that exhibit large stability windows and significant fluoride mobility at room temperature, presenting an avenue to overcome barriers limiting research on fluoride (de)intercalation.

We previously reported electrochemical fluorination of ReO₃, wherein ReO₃ cycled vs. Cu at room temperature using a liquid electrolyte, *n*-tetrabutylammonium fluoride (TBAF) dissolved in THF, exhibits irreversible insertion of 0.5 equiv. of fluoride. Although Cu provides a consistent reference potential, it cannot be reduced, calling the counter-reaction into question. Differential electrochemical mass spectrometry (DEMS) measurements were employed to monitor the evolution of H₂, O₂, F₂, and CO₂ gases during electrochemical cycling, and only H₂ evolved in substantial quantities. Therefore, the counter-reaction is presumed to be the hydrogen evolution reaction (HER) from electrolyte attack.

Following this work, we reported the reversible (de)fluorination of the defect pyrochlore CsMnFeF₆ at room temperature using TBAF. Unlike ReO₃, approximately 1 fluoride ion can be reversibly (de)inserted into CsMnFeF₆ for 10 galvanostatic cycles, after which the capacity begins to fade. CsMnFeF₆ is cycled against a Bi/BiF₃ composite counter electrode to incorporate a species that can be reduced in the counter electrode and because M/MF_x composite electrodes are more stable over long-term cycling compared to MF_x alone, although they still impose the limitations of conversion-based electrochemistry on the cell. We extensively characterized the structural impact of fluoride (de)insertion on CsMnFeF₆. *Ex situ* diffraction shows expansion and contraction of the cubic CsMnFeF₆ lattice on insertion and removal, respectively, during the first 2 cycles. New reflections intensify in the diffraction from cycle 3, corresponding to a topotactic transformation of pyrochlore CsMnFeF₆ into an orthorhombic polytype that continues to reversibly cycle fluoride ions. The capacity does not fade immediately after the

transformation, suggesting the observed decrease is likely due to limitations of the Bi/BiF₃ counter electrode or a decomposition of the TBAF electrolyte.

We will present our work building and using a DEMS set up to study gas evolution during CsMnFeF₆ cycling in TBAF with various counter electrodes. Our DEMS studies aim to answer two key questions: Is HER the dominant counter-reaction in F-ion batteries when organic, liquid electrolytes are used? If HER dominates and proceeds via electrolyte attack, is cycling lifetime limited by the amount of electrolyte? In other words, *in situ* gas analysis will be used to identify the counter-reactions occurring in cells containing organic, liquid electrolytes to uncover which cell component(s) might be impeding cycling lifetimes and begin to optimize room-temperature F-ion battery performance.

8:15 AM SF03:04.02

Ti₂C, A Bicontinuous 3D Electride Matthew Lanetti, Nhi Huynh and Scott Warren; University of North Carolina, United States

Electrides are ionic crystals in which electrons act as anions in periodic lattice positions stabilized by an adjacent framework of cations. These unconventional solids offer desirable properties and have been explored in applications including battery electrodes and catalysis. In all experimentally realized electrides, the continuity of the electride sites have been observed to be non-continuous (0D), continuous in one dimension (1D), or continuous in two dimensions (2D). Here, we identify Ti₂C as among the first synthesized topologically three-dimensional (3D) electrides. We propose that Ti₂C consists of two bicontinuous structures: a 3D anionic electron gas contained within a 3D lattice of atoms. The atomic and electron gas structures are both diamond cubic (Fd3m) and extend throughout 3D space. We experimentally synthesize this material and demonstrate, using both theory and experiment, that it contains a continuous 3D pathway of anionic electrons. The anionic electron sites in electrides can be exchanged with traditional anions, giving electrides utility in ion storage. We demonstrate that the 3D network of anionic electrons in Ti₂C is capable of taking up hydrogen as hydride at relatively low temperature. This research suggests that 3D electrides may exhibit superior ion storage performance over 2D electrides which have fewer dimensions for ion insertion. We show that Ti₂C is the first member of a novel type of topological electride where anionic electron gas is confined within a 3D form, bicontinuous with a symmetrical 3D atomic framework.

8:30 AM +SF03:04.03

Designing Battery Electrode Architectures Across Length Scales Sarbajit Banerjee; Texas A&M University, United States

The design and operation of rechargeable batteries is predicated on orchestrating flows of mass, charge, and energy across multiple interfaces. Understanding such flows requires knowledge of atomistic and mesoscale diffusion pathways and the coupling of ion transport with electron conduction. Using multiple polymorphs of V₂O₅ as model systems, I will discuss our efforts to develop an Ångström-level view of diffusion pathways. Topochemical single-crystal-to-single-crystal transformations provide an atomistic perspective of how diffusion pathways are altered by modification of V—O connectivity, pre-intercalation, and high degrees of lithiation. Recently devised multi-step synthetic schemes enable the positioning of Li-ions across four distinct interstitial sites of a V₂O₅ insertion host and allow for deterministic redirection of Li-ion flows through strategic positioning of transition-metal ions.

At higher length scales, scanning transmission X-ray microscopy and ptychography imaging provide a means of mapping the accumulative results of atomic scale inhomogeneities at mesoscale dimensions and further enable tracing of stress gradients across individual particles. I will discuss strategies for the mitigation of diffusion impediments and degradation mechanisms based on controlling the coupling of chemistry, geometry, and mechanics. Some of these strategies include (a) utilization of Riemannian manifolds as a geometric design principle for electrode architectures; (b) atomistic design of polymorphs with well-defined diffusion pathways that provide frustrated coordination; and (c) site-selective modification as a means of tuning lattice incommensurability between lithiated and unlithiated phases.

This research was funded by the National Science Foundation under DMR 1809866.

9:00 AM *SF03:04.04

NASICON-Based Materials, The Perfect Match for The Next Generation of Batteries? Jean-Noel Chotard^{1,2}, Pieremanuele Canepa³, Vincent Seznec^{1,2}, Eunike Mahayoni^{1,2}, Aaron Tieu Jue Kang³, Kriti Kriti^{1,2}, Sunkyu Park^{1,2} and Christian Masquelier^{1,2}; ¹University of Picardie Jules Verne, France; ²RS2E, FR CNRS, France; ³National University of Singapore, Singapore

NASICON-based materials have a regain interest in the last decade. Firstly known for their high ionic conductivity (hence the name : NA SuperIonic CONductor) [1], their chemical versatility allow them to be used as electrode materials (anode or cathode) as well as as coating materials for different battery technologies (Li-ion, Na-ion, multivalent-ions and all-solid-state batteries) by tuning its composition [2-4]. Indeed, the NASICON crystal structure of general formula A_xMM'(XO₄)₃, allows a wide range of chemical substitutions. The Alkali "A" atom can either be Li⁺/Na⁺/K⁺, and the M/M' sites can basically be filled with any combination of 3d or 4d transition metals.

Among them, the vanadium phosphate Na₃V₂(PO₄)₃ (NVP) is of particular interest because of its fantastic rate capacity and thermal stability, with a theoretical capacity of 117.6 mAh/g at 3.4 V vs. Na/Na⁺ by the V³⁺/V⁴⁺ redox couple yielding an energy density of 396 Wh/kg [4]. Because of the wide oxidation range of Vanadium, NVP can be used either as an anode or a cathode. NASICON materials have also proven to be among the best solid electrolyte material for sodium All-Solid-State-Batteries (ASSBs). As an example, Na_{3.4}Zr₂Si_{2.4}P_{0.6}O₁₂ attains ionic conductivity as high as 10 mS/cm [5-6] with 3D diffusion path.

Because of those electrochemical properties, their chemical stability and compatibility, NASICON-type are perfectly matching for building All-Solid-State-Batteries.

In this presentation, we will discuss the astonishing diversity of the crystal chemistry of the NASICON materials (both as electrode or electrolyte) mostly studied through operando X-Ray Diffraction as well as its use in ASSBs.

[1] J.B. Goodenough, H.Y. Hong, J.A. Kafalas, FAST Na⁺-ION TRANSPORT IN SKELETON STRUCTURES, Mater. Res. Bull. 5 (1976) 77843.

[2] C. Masquelier, L. Croguennec, Polyanionic (Phosphates, Silicates, Sulfates) Frameworks as Electrode Materials for Rechargeable Li (or Na) Batteries, Chem. Rev. 113 (2013) 6552–6591.

[3] Z. Wang, H. Zhong, G. Song, Enhancing high-voltage performance of LiNi_{0.8}Co_{0.1}Mn_{0.1}O₂ by coating with NASICON fast ionic conductor Li_{1.5}Al_{0.5}Zr_{1.5}(PO₄)₃, J. Alloys Compd. 849 (2020) 156467. <https://doi.org/10.1016/j.jallcom.2020.156467>.

[4] N. Anantharamulu, K. Koteswara Rao, G. Rambabu, B. Vijaya Kumar, V. Radha, M. Vithal, A wide-ranging review on Nasicon type materials, J. Mater. Sci. 46 (2011) 2821–2837. <https://doi.org/10.1007/s10853-011-5302-5>.

[5] Bachman, J. C. et al. Inorganic Solid-State Electrolytes for Lithium Batteries: Mechanisms and Properties Governing Ion Conduction. Chem. Rev. 116, 140–162 (2016)

[6] Z. Deng, G. Sai Gautam, S.K. Kolli, J.N. Chotard, A.K. Cheetham, C. Masquelier, P. Canepa, Phase Behavior in Rhombohedral NaSiCON Electrolytes and Electrodes, Chem. Mater. 32 (2020) 7908–7920.

9:30 AM SF03:04.05

Reducing Voltage Hysteresis in Li-Rich Sulfide Cathodes by Tuning the Metal-Ligand Covalency Xiaotong Li¹, Seong Shik Kim¹, Michelle Qian¹, Eshaan Patheria¹, Jessica Andrews², Colin Morrell¹, Brent C. Melot² and Kimberly A. See¹; ¹California Institute of Technology, United States; ²University of Southern California, United States

Multielectron redox can be achieved by leveraging the redox activity of anion sublattice (anion redox) in addition to the transition metal, to significantly increase the capacity of cathode materials. Li-rich sulfides are promising cathode candidates for anion redox since they operate at voltages within the electrolyte stability window and sustain the high capacity. Most of the anion-redox based cathode materials still face the problem of slow kinetics and large voltage hysteresis. One of the ways to solve this problem is to increase the covalency of the metal-ligand bonds. By substituting Mn into the electrochemically inert Li_{1.33}Ti_{0.67}S₂ (Li₂TiS₃), the anion redox can be activated in the Li_{1.33-2y/3}Ti_{0.67-y/3}Mn_yS₂ (y = 0 – 0.5) series and the voltage hysteresis is significantly reduced. The y = 0.3 phase also exhibits excellent rate and cycling performance, which shows fast kinetics for anion redox, because the energy of Mn d states is located in between the Ti d and S p states, bridging the energy gap and increasing the metal-ligand bond covalency. X-ray absorption spectroscopy shows that both the cation and anion redox processes contribute to the charge compensation. This work provides insights on how to design cathode materials with anion redox to achieve fast kinetics and low voltage hysteresis.

9:45 AM BREAK

10:15 AM *SF03:04.06

Disordered Rocksalt Cathodes: Linking Composition, Structural Stability and Performance Raphaële Clement; University of California, United States

Rechargeable batteries have transformed our daily lives through portable electronics, and hold the key to a low carbon future. While they dominate the electric vehicle market, current Li-ion chemistries are approaching their theoretical limit in terms of energy density. Remarkably, despite significant effort over decades, we continue to rely on a limited subset of Li-ion battery materials — most commercial cathodes are derivatives of LiCoO₂ developed in 1980 — that cannot meet our ever-growing need for energy storage. In recent years, disordered rocksalt oxides, with mixing of the transition metal and Li species on the face-centered cubic cation sublattice, have emerged as more sustainable and higher energy density cathodes than the standard layered oxides. In this talk, I will present the links established between the composition, structure and electrochemical properties of such systems obtained by combining paramagnetic solid-state NMR, first principles calculations, and complementary tools. I will also introduce a new, rapid and energy-efficient synthesis procedure to obtain disordered rock salt cathodes, and emphasize the importance of ⁷Li/¹⁹F solid-state NMR to determine the true composition of such systems and establish robust materials design rules.

10:45 AM *SF03:04.07

An attractive feature of Li-excess disordered rocksalt oxide electrodes is their high chemical versatility compared to commercial Li-ion battery cathode materials. With this chemical versatility, this emerging class of energy storage materials could alleviate current reliance on expensive or geographically-concentrated materials, and prevent similar dependence in the future. To realize the promise of disordered rocksalt oxide cathodes, however, requires overcoming seemingly inherent ionic transport limitations that, even in relatively high-performing compositions, require sub-micron-sized particles and careful incorporation of conductive carbon additives.

A challenge to realizing their promise is that the same compositional versatility that makes disordered rocksalt oxides so compelling, which is associated with atomic structure and nanometer-scale complexity. Broad sampling of chemical space has led to new empirical understanding of structure-property relationships, especially between the size and charge of constituent cations and short-range chemical ordering.

We report a detailed investigation of a narrow range of composition space to understand the key characteristics of cation features on hierarchical chemical and structural organization. To do so, we combine average and local structure characterization methods and propose a conceptual framework to reconcile the hierarchical chemical and structural features, including crystal structure, local distortions, short-range order, and nanoscale chemical segregation.

11:15 AM SF03:04.08

Phase Segregation and Nanoconfined Fluid O₂ in an Oxygen Redox Battery Cathode Kit McColl^{1,2}, Samuel W. Coles^{1,2}, Pezhman Zarabadi-Poor^{3,2}, Benjamin J. Morgan^{1,2} and Saiful Islam^{3,2}; ¹University of Bath, United Kingdom; ²Faraday Institution, United Kingdom; ³University of Oxford, United Kingdom

Next-generation, sustainable high energy density batteries require high-capacity cathodes composed of Earth-abundant elements. Lithium and manganese rich oxide cathodes are leading candidates because they achieve high capacity from a combination of transition metal and oxygen redox. [1] O-redox, however, is accompanied by structural changes that cause a large loss of energy density. [2] To apply O-redox cathodes in practical devices, these structural changes must be understood and prevented. These structural changes are exceedingly difficult to characterise for both experimental and computational modelling, [3] which has led to uncertainties and ambiguities in the mechanisms of O-redox in battery cathodes.

The characterisation of O-redox behaviour is particularly challenging for computational modelling. Because O-redox cathodes undergo atomic rearrangements during cycling, cathode structures after the early stages of the first charge are not known *a priori* and must be solved *in silico*. For computational modelling studies to make credible predictions of O-redox behaviour, both the kinetics and thermodynamics of structural rearrangements must be considered. Modelling schemes that predict O-redox behaviour from structures that i) form via kinetically inaccessible pathways, ii) are kinetically unstable or iii) are far from the thermodynamic ground state, can produce unrealistic descriptions of O-redox. Furthermore, cycled O-redox cathodes exhibit crystallographic site disorder and nanoscale structural changes, such as the formation of nanovoids. Computational modelling using DFT, however, cannot directly investigate disorder and nanoscale structures, meaning that additional modelling methods are required to provide a complete picture of O-redox behaviour.

Here, we use a computational strategy that directly addresses these kinetic and thermodynamic factors. To identify kinetically viable atomic-scale rearrangements during the first charge, we have used long-timescale *ab initio* molecular dynamics (AIMD). In parallel, to account for disorder and nanoscale structural changes produced after many cycles, we have developed a DFT-derived cluster-expansion model of oxygen-redox, which we have used to perform large-scale Monte Carlo simulations. This approach allows us to efficiently search the vast configurational space for thermodynamically low-energy structures at the top of charge, and to conduct this search in structures containing ~50,000 atoms, so that nanoscale structural rearrangements can be examined.

We apply this strategy to high-capacity O₂-layered Li_{1.2-x}Mn_{0.8}O₂, which is an exemplar system for understanding Li-rich oxide cathodes. We identify a kinetically viable O-redox mechanism, in which the formation of interlayer superoxide and peroxide intermediates drives out-of-plane Mn migration, resulting in O₂ molecules forming within the bulk structure. The thermodynamic ground-state structure at the top of charge exhibits phase segregation into a two-phase mixture of MnO₂ and O₂. Bulk O₂ molecules are confined within nanometre-sized Mn-deficient voids that form a connected, percolating network. These O₂ molecules have a nanoconfined supercritical fluid character and can potentially diffuse through the network of voids, providing a mechanistic link between bulk O₂ formation and surface O₂ loss. [4]

[1] P. Rozier & J.M. Tarascon Review — Li-Rich Layered Oxide Cathodes for Next-Generation Li-Ion Batteries: Chances and Challenges. *J. Electrochem. Soc.* 162, A2490–A2499 (2015)

[2] R.A. House, G.J. Rees, K. McColl et al., Delocalized electron holes on oxygen in a battery cathode, *Nat Energy* 8, 351–360 (2023)

[3] K. McColl et al., Transition metal migration and O₂ formation underpin voltage hysteresis in oxygen-redox disordered rocksalt cathodes. *Nat. Commun.* 13, 5275 (2022).

[4] K. McColl et al., Phase segregation and nanoconfined fluid O₂ in a lithium-rich oxide cathode. *ChemRxiv* (<https://doi.org/10.26434/chemrxiv-2023-9v2dw>) (2023).

11:30 AM SF03:04.09

Completely Passive Capture of Carbon Dioxide from Air Hsinhan Tsai^{1,2}, Jian Zeng^{2,1}, Tae Hwan Lim², Matther Dods¹, Ziting Zhu^{1,2}, Hannes Alberts^{2,3}, Adrian Huang^{1,2}, Mengshan Ye¹, Hiroyasu Furukawa^{1,2}, Hanna Breunig², Ravi Prasher^{2,1}, Sean Lubner^{4,2} and Jeffrey Long^{1,2}; ¹University of California, Berkeley, United States; ²Lawrence Berkeley National Laboratory, United States; ³ETH Zurich, Switzerland; ⁴Boston University, United States

In addition to reducing greenhouse gas emissions, it is now imperative that we implement direct air capture (DAC) of CO₂ from the atmosphere at a scale of hundreds of giga metric tons before the year 2100 to avoid catastrophic climate change^{1,2}. Development of a viable DAC technology is still limited by the high cost³ and high energy consumption^{4,5} that result from a low adsorbent capture capacity, requirements for expensive, cumbersome infrastructure, and widespread societal acceptance challenges^{6,7}. In this work, we aim to address all three of these challenges and have designed and demonstrated a completely passive DAC device with a projected net CO₂ capture cost as low as 80 \$ t_{CO₂}⁻¹, lower than the 'Carbon Negative Shot' 2030 goal (100 \$ t_{CO₂}⁻¹)⁸ and potentially profitable at 100 \$ t_{CO₂}⁻¹ with the 45Q carbon tax credit. The modular design and passive operation of the system should enable deployment across broad geographic regions far from infrastructure centers, thereby enabling a distributed, self-powered solution to the problem of removing dilute CO₂ from the atmosphere. It further combines low-cost solar-thermal and low-risk photovoltaic technologies, facilitating installation at different scales in any corner of the world with abundant solar resources.

11:45 AM SF03:04.10

Improved Cycle Life and Determination of Li Ion Transport Parameters in Doped Ni-Rich NMC Cathodes for Lithium Ion Batteries Ethan Williams^{1,2}, David Burnett^{1,2} and Emma Kendrick^{1,2}; ¹University of Birmingham, United Kingdom; ²Faraday Institute, United Kingdom

Ni-rich Li-ion cathode materials like NMC-9.5.5 (LiNi_{0.9}Mn_{0.05}Co_{0.05}O₂) are of interest due to their higher energy density and limited cobalt content, aiding the transition away from questionably sourced critical raw materials, when compared to materials like NMC111 - 622. This has the advantage of reducing production costs while maintaining a high working voltage and capacity. However, the high nickel content of these materials can be detrimental due to disorder introduced by Li⁺/Ni²⁺ cation mixing, lithium residuals, and irreversible phase changes during operation resulting in significant capacity fade during cycling. Similarly, the different synthesis methods and treatments drastically affect the morphological, structural, and electrochemical properties

We present a structural and electrochemical study of NMC-9.5.5 prepared at scale via a hydroxide coprecipitation synthesis in a 5 L continuous stirred reactor tank (CSTR). In this work, bulk doping and co-doping with two metal cations are investigated with a simple and scalable method to achieve mixed metal and mixed valence doped NMC-9.5.5 with the aim to further improve cycle life and stability. Additionally, the effect of bulk doping on the thermodynamic and kinetic properties of the cathode material are investigated in both half-cells and full-cells (paired against a graphite electrode) using galvanostatic intermittent titration technique (GITT), intermittent current interruption (ICI), and electrical impedance spectroscopy (EIS), where a 3-electrode configuration is used to elucidate the individual electrode potentials and stoichiometries.

The bulk doping of the transition metal layer was found to significantly reduce the capacity fade in the NMC-9.5.5, increasing the capacity retention after 100 cycles from 78% in the undoped material to 92% and 89% in the doped and co-doped NMC-9.5.5 half-cells. The mixed metal co-doped material was also effective in delivering a higher specific capacity than the baseline throughout the full cycling range. The improved cycling performance can be understood by the inspection of the differential capacity plots, which show a suppression of the H2-H3 irreversible phase transition in the doped material and stabilisation of this peak to a higher voltage compared to the baseline. The effect of doping on the structural stabilisation is similarly reflected in the XRD characterisation, in which the introduction of the metal cation acts to constrain the detrimental Li⁺/Ni²⁺ cation mixing due to a widening of the transition metal channel. This is also supported by the EXAFS characterisation that indicate the dopants may act to stabilise the local Ni environment. These structural changes appear to be further beneficial in facilitating improved Li ion transport properties in the doped material as evidenced by the lower charge transfer resistances during cycling and increased diffusion coefficient.

This research illustrates the high capacity performance of low cobalt cathode materials and as such reducing the reliance on critical materials, as well as the ability to produce Ni-rich cathode material at large scale and further stabilise its cycle life by simple structural engineering. Improved materials manufacturing processes will enable a greater understanding of the

synthesis process and enable more sustainable methods of synthesis. There are also benefits for cell makers with improvement in processability and additional stabilisation knowledge for battery manufacturers, as well as the consumers that benefit from longer driving ranges and battery life in their EV's.

SESSION SF03.05: Energy and Batteries II
Session Chairs: Craig Brown and Brent Melot
Tuesday Afternoon, November 28, 2023
Sheraton, Second Floor, Back Bay C

1:30 PM *SF03.05.01

Exploiting Surprising Phase Behavior in Superprotonic Solid Acid Compounds to Enhance Functionality Louis S. Wang, Grace Xiong and Sossina M. Haile; Northwestern University, United States

Creation of novel proton-conducting electrolytes with a combination of desirable properties, including negligible electronic conductivity, chemical stability, and processability, in addition to the prerequisite of high proton conductivity, has taken on increased urgency as the world turns to hydrogen as a clean energy carrier. Superprotonic solid acids, in particular phosphates in this group, hold technological potential as components in fuel cells and other electrochemical devices. In such materials, orientational disorder of polyanion groups in high temperature phases facilitates rapid proton transport. Superprotonic solid acids include CsH_2PO_4 , CsHSO_4 , and $\text{Rb}_3\text{H}(\text{SeO}_4)_2$. Device development approaches have largely focused on CsH_2PO_4 because of its stability under both oxygen and hydrogen. Traditional chemical modification routes for improving transport properties, such as replacing Cs^+ with Rb^+ to influence proton mobility or replacing $(\text{HPO}_4)^{2-}$ with $(\text{SO}_4)^{2-}$ to influence both mobility and carrier concentrations, appear to have been exhausted without generating technologically relevant outcomes. Here we describe an unexpected chemical lever for tuning properties, specifically, modifying the alkali cation : polyanion ratio. Remarkably, we find that the CsCl structure-type adopted by CsH_2PO_4 and RbH_2PO_4 in their respective high-temperature, superprotonic phases, can support large concentrations of both cation and polyanion vacancies, charged balanced by adjustments to the overall proton concentration. The material stoichiometries are described by $\text{A}_{1-x}\text{H}_{2+x}\text{PO}_4$ (with cation site vacancies) and $\text{AH}_{2-3y}(\text{PO}_4)_{1-y}$ (with polyanion site vacancies), where A is Cs^+ or Rb^+ . Additionally, in the Cs-poor region of chemical space relative to CsH_2PO_4 , we discover a new solid acid of fixed composition $\text{Cs}_7(\text{H}_4\text{PO}_4)(\text{H}_2\text{PO}_4)_8$. Thus, stoichiometry control emerges as a new approach to designing superprotonic electrolytes.

2:00 PM *SF03.05.02

Evolving Structural Pathways in Next-Generation Lithium- and Sodium-Ion Battery Materials Revealed by Pair Distribution Function Analysis Phoebe Allan; University of Birmingham, United Kingdom

The need for battery technologies with higher energy densities and improved sustainability has motivated a large body of research into new potential electrode materials for rechargeable lithium- and sodium-ion batteries. However, in many cases, characterising the lithium/sodium-ion (de)insertion mechanisms of these new materials presents significant challenges to conventional crystallographic analysis, as disordered or nano-sized phases may form, some of which may be metastable and exist only within the battery. Here, I will present our recent work detailing how pair distribution function (PDF) analysis - a total scattering technique which is sensitive to both local and long-range structure - has been applied in situ to give highly consistent data sets from which subtle changes to local structure during electrochemical cycling can be resolved. PDF data is analysed alongside complementary methods such as x-ray diffraction, solid-state nuclear magnetic resonance, x-ray absorption spectroscopy and theoretical calculations to gain insight into a range of potential new electrode materials, including disordered rock salt cathodes, lithium-ion conversion anodes and alloying anodes for sodium-ion batteries. In particular, my focus will be on systems where the lithiation/sodiation mechanisms evolve upon electrochemical cycling, forming nanostructures which differ significantly from the initial electrode structure. I will discuss the impact of these evolving structural pathways on the physical properties and how these structural insights may aid future electrode material discovery and design.

2:30 PM SF03.05.03

Resolving the Influence of Structural Water on Li-Ion Diffusion in Pyrochlore Iron Hydroxy Fluoride Cathodes Julian F. Baumgärtner^{1,2}, Michael Wörle¹, Kostiantyn Kravchuk^{1,2} and Maksym V. Kovalenko^{1,2}; ¹ETH Zürich, Switzerland; ²Empa - Swiss Federal Laboratories for Materials Science and Technology, Switzerland

Lithium-ion batteries composed of cost-effective cathode materials exhibit substantial potential for large-scale stationary storage of electricity. Iron (III) fluorides are appealing low-cost energy storage materials due to the virtually unlimited supply of the constituting elements and high energy densities.¹ The pyrochlore modification is of particular interest because its 3D interconnected channels may potentially enable fast Li-ion diffusion.² However, the prohibitively high cost of synthesis and cathode architecture currently prevent their commercial use in low-cost Li-ion batteries. Moreover, amorphization upon prolonged cycling makes structural characterization of the Li-ion intercalation behavior challenging. Inspired by the synthesis of porous materials, such as metal organic frameworks, zeolites and Prussian blue analogues, which often employ dissolved precursor building blocks that condense into the desired porous structure in the presence of a suitable templating agent, we reasoned that a similar approach could be used to synthesize the pyrochlore type structure at ambient conditions. Herein, we extend this synthetic paradigm to access pyrochlore iron (III) hydroxy fluoride (Pyr-IHF) from soluble iron (III) fluoride precursors.³ This facile dissolution-precipitation synthesis of Pyr-IHF allows the production at low costs (10-20 \$ kg⁻¹), competitive with Lithium iron phosphate. Guided by *operando* X-ray diffraction experiments, we selectively vary the solvent content inside the channels of Pyr-IHF by heat-treatment to study the effect of structural water on the Li-ion diffusion within the channels of Pyr-IHF. Rate capability tests of Pyr-IHF cathodes of different solvent content confirm this hypothesis, thereby providing the first experimental evidence for Li-ion diffusion occurring through the 3D channels of Pyr-IHF. Without the need for elaborate cathode designs, we demonstrate outstanding capacity retention of >80% after 600 cycles at high current densities of 1 A g⁻¹.

1. Wu, F. & Yushin, G. Conversion cathodes for rechargeable lithium and lithium-ion batteries. *Energy Environ. Sci.* **10**, 435–459 (2017).

2. Li, C. *et al.* An FeF₃ * 0.5 H₂O polytype: a microporous framework compound with intersecting tunnels for Li and Na batteries. *J. Am. Chem. Soc.* **135**, 11425–11428 (2013).

3. Baumgärtner, J. F. *et al.* Dissolution Precipitation Synthesis of Pyrochlore Type Iron Hydroxy Fluoride for Low-Cost Lithium-Ion Batteries. Manuscript Submitted.

2:45 PM BREAK

3:15 PM *SF03.05.04

Pressure Driven Phase Transitions: A Look into the Future of Solid-State Refrigeration Claire L. Hobday; University of Edinburgh, United Kingdom

Heating and cooling processes are responsible for 78% of the UK's environmentally damaging fluorinated gas emissions, primarily due to the employment of hydrofluorocarbon (HFC)-based refrigerant gases. [1] Such compounds are being phased out due to their devastating environmental impact, notably very high global warming potentials (GWP) (~2000 times that of CO₂). This has created a major technological and scientific challenge to find new types of refrigeration materials which are made from sustainable resources, have increased efficiency and are environmentally friendly throughout their entire lifecycle. There is now a strong focus on developing solid-state materials, which are easier to recycle, that demonstrate caloric effects. These have been shown to out-perform vapour compression technology in domestic refrigeration, additionally resulting in lower energy costs. [2] Caloric effects rely on the reversible thermal response of solids to an externally applied field (magnetic or electric field, or hydrostatic pressure) to give rise to magnetocaloric (MC), electrocaloric (EC) or barocaloric (BC) materials.

This talk focusses on understanding the barocaloric effect via study of order-disorder transitions in organic ionic plastic crystals (OIPCs). OIPCs provide a rich parameter space in which to explore the tunability of the BC effect experimentally. This class of materials are comprised completely of ions and at room temperature are solids with significant disorder in the crystal lattice. [3] The disorder comes from the rotational, translational and conformational motions which allows them to flow under stress and increases their conductivity, which has rendered them desirable solid-state electrolytes that can be used in batteries, fuel cells and solar cells. [4] OIPC's inherent order-disorder phase change properties are ideal as potential candidates for BC refrigerants; however, little is known about how to maximise their ionic conductivity, ability to flow and change phase.

In this work combined we explore the expansive chemical parameter space of ionic plastic crystals via a combined simulation and experimental approach. By employing pressure- and temperature-dependent single crystal/powder diffraction and differential scanning calorimetry experiments, we can understand structurally and thermally how these materials behave and by ion substitution, we demonstrate the ability to tune the transition temperature, isothermal entropy change, ΔS , and the barocaloric coefficient, dT/dP . Molecular dynamics simulations provide complementary information into the atomistic details of the complex landscape of the phase behaviour of these materials. Together, the results of this work can be used to inform the design of future solid-state refrigerants.

- [1] <https://www.theccc.org.uk/publication/assessment-of-potential-to-reduce-uk-f-gas-emissions-ricardo-and-gluckman-consulting>, (accessed 11th November 2022).
- [2] C. Aprea A. Greco, A. Maiorino, C. Masselli, *Energy*, **2020**, 190, 116404.
- [3] D. R. MacFarlane J. Huang, M. Forsyth, *Nature*, **1999**, 402, 792.
- [4] D. R. MacFarlane, M. Forsyth, P. C. Howlett, M. Kar, S. Passerini, J. M. Pringle, H. Ohno, M. Watanabe, F. Yan, W. Zheng, S. Zhang, J. Zhang, *Nat. Rev. Mater.*, **2016**, 1, 15005.

3:45 PM *SF03.05.05

Barocaloric Hybrid Organic-Inorganic Salts for Green Refrigeration Richard J. Dixey¹, Shurong Yuan¹, Bernet E. Meijer¹, Naresh C. Osti², Anthony E. Phillips¹ and Helen C. Walker³; ¹Queen Mary University London, United Kingdom; ²Oak Ridge National Laboratory, United States; ³Rutherford Appleton Laboratory, United Kingdom

Barocalorics are materials that undergo a solid-solid phase transition between high and low entropy phases, which can be driven by pressure to form the basis of a refrigeration cycle. As solids they are less prone to leaking and causing environmental damage than traditional haloalkane vapour-compression refrigerants.

We recently reported the molecular mechanism underlying the entropy change in the canonical plastic crystal adamantane, showing in the process that this material is an excellent low-temperature barocaloric [1]. We are now extending this approach to orientationally disordered crystals more widely; an obvious extension is to salts, where Coulomb as well as van der Waals interactions are significant.

Based on this approach, we have discovered a new family of hybrid organic-inorganic barocalorics: quinuclidinium salts, in which the near-spherical quinuclidinium cation packs with inorganic counteranions into structures analogous to the alkali halides. The quinuclidinium ion is an excellent component for high-entropy phases since it strikes a fine balance between spherical geometry and anisotropy: its quasi-spherical shape promotes vibrational entropy arising from molecular libration, while the deviation from perfect spherical symmetry generates configurational entropy.

We have studied seven quinuclidinium salts (with counterions Cl, Br, I, NO₃, BF₄, PF₆ and IO₄) by crystallography and high-pressure differential scanning calorimetry. These materials show solid-solid phase transitions between 290 and 340 K, entropy changes of up to 164 J/K.kg, and barocaloric coefficients dT/dP of up to 60 K/kbar, making them "colossal" barocalorics [2]. We show that chemically and physically simple changes in the inorganic counterion lead, for instance by changes in the hydrogen-bonding network, to subtle differences in the resulting materials' barocaloric properties.

[1] B.E. Meijer *et al.*, *Phys. Chem. Chem. Phys.* **25**, 9282 (2023)

[2] R.J.D. Dixey *et al.*, In preparation

4:15 PM SF03.05.06

A Low-Carbon Strategy to Synthesize Cobalt-Free Cathode Materials of Lithium-Ion Batteries Jianshan Zhang, Chuwei Zhang, Maanasa Bhat and Sili Deng; Massachusetts Institute of Technology, United States

Given the high uncertainty of cobalt supply and related ethical concerns, the development of cobalt-free cathode materials has become an urgent priority for lithium-ion battery industry. Nevertheless, manufacturing cobalt-free cathode materials involves energy-intensive processes such as long-time high-temperature lithiation, which significantly contributes to the carbon footprint of cathode material production. As such, establishing low-carbon manufacturing strategies is crucial to improve the sustainability of energy storage applications, including electric vehicles and renewable energy grid storage. In this study, we propose a low-carbon technique, termed Flame-Assisted Spray Pyrolysis (FASP), characterized by its reduced synthesis time and utilization of hydrogen as an energy source. The FASP method demonstrated its efficacy in synthesizing cobalt-free cathode materials, particularly layered structure nickel-rich cathode materials. Using an inexpensive aqueous solution of metal nitrates as a precursor, FASP saves a significant amount of time and energy by reducing the calcination process from over 20 hours to just 40 minutes. Furthermore, with hydrogen as a supplementary fuel, FASP further mitigates carbon emissions compared to traditional heating methods.

Comparison with long-time calcinated samples in full cells using graphite as the anode confirms that the electrochemical performance of the newly synthesized cobalt-free cathode materials is maintained. This work also investigated the detailed material formation mechanism through X-ray diffraction and transmission electron microscopy. We found that uniform lithium distribution in the as-synthesized material prior to calcination was the key to shortening lithium diffusion, fastening layered structure formation, and preventing impurity phases. Furthermore, inhibiting the generation of hard-to-decompose lithium compounds, particularly lithium carbonate, was also critical in ensuring the desired electrochemical performance of fast-calcinated samples. Moreover, emission analysis shows that the carbon emission could be reduced by more than 30% with this novel synthesis route. The current work underscores the potential for FASP to significantly contribute to a low-carbon future in the manufacturing of cobalt-free lithium-ion batteries.

4:30 PM SF03.05.07

A Co-Free Li-Rich Layered Oxide Cathode without Voltage Decay for High Energy Solid-State Batteries Yang Ren; City University of Hong Kong, Hong Kong

Due to high specific capacity at low cost, Li- and Mn-rich layered oxides (LMRs) are very promising cathode materials for next generation batteries. However, these materials suffer severe voltage decay due to the unstable Li₂MnO₃ honeycomb structure, which has plagued its practical application for decades. Recently, we have designed and successfully synthesized a novel honeycomb structure for LMRs, where the honeycomb structure in the Li₂MnO₃ component is partially capped to strengthen its stability. This capped-honeycomb structure is persistent after high-voltage cycling and prevents TM migration and oxygen loss. As a result, the designed LMR material exhibits no voltage decay upon cycling, which is ideal for use in high energy solid-state battery.

4:45 PM SF03.05.08

Crystal Structure-Derived Intrinsic Principles for Low Thermal Conductivity in High Performance Thermoelectric Materials Takao Mori^{1,2}; ¹National Institute for Materials Science, Japan; ²University of Tsukuba, Japan

Development of thermoelectric (TE) materials & devices is important, for energy saving via waste heat power generation [1], and as dynamic power sources for IoT sensors, etc. [2]. There are traditional tradeoffs between the key physical properties which hinder to attain high TE performance. We are systematically developing principles which can circumvent the tradeoffs, namely to enhance Seebeck coefficient, and selectively lower thermal conductivity, in order to lead to viable materials and devices [3 and references therein].

In addition to various nanostructurings, crystal structure-derived mechanisms have been found to engender intrinsic low thermal conductivity. Materials informatics approach led to identification of a material catalogue with low thermal conductivity, with a simple crystallographic parameter as an effective descriptor [4]. Particular transition metal doping into SnTe was shown to lead to softening of the lattice, and a dramatic reduction of thermal conductivity largely exceeding the contribution from phonon scattering [5]. Minor amount of Cu doping into the interstitial site of Mg₃Sb₂-type compound led to large reduction of the phonon velocity and high performance rivalling the long time champion bismuth telluride [6]. Finally, the heterogeneous bonding in mixed anion compounds was shown to result in exceptional low thermal conductivity [7]. I will analyze these methods and ways for further TE enhancement. Support from JST Mirai Large-Scale Program (JPMJMI19A1) and collaborators are acknowledged.

References

- [1] L. E. Bell, *Science* **321**, 1457 (2008), *JOM*, **68**, 2673-2679 (2016).
- [2] T. Mori, S. Priya, *MRS Bulletin* **43**, 176 (2018), I. Petsagkourakis *et al.*, *Sci. Tech. Adv. Mater.* **19** (2018) 836, N. Nandihalli *et al.*, *Nano Energy*, **78** 105186 (2020).
- [3] T. Mori, *Small* **13**, 1702013 (2017), T. Hendricks *et al.*, *Energies*, **15**, 7307 (2022).
- [4] Z. Liu *et al.*, *Energy Environ. Sci.*, **14**, 3579 (2021).
- [5] A. R. Muehtar *et al.*, *Adv. Energy Mater.*, **11**, 2101122 (2021).
- [6] N. Sato *et al.*, *J. Mater. Chem. A*, **9**, 22660 (2021), J. Mark *et al.*, *J. Mater. Chem. A*, **11**, 10213 (2023).
- [7] Z. Liu *et al.*, *Joule*, **5**, 1196-1208 (2021), *Nature Commun.* **13**, 1120 (2022).

5:00 PM SF03.05.09

Gas Phase Synthesis of Inorganic Nanomaterials on the Pilot Plant Scale Martin Underberg, Mathias Spree, Frederik Kunze, Tim Huelser and Sophie M. Schnurre; Institut für Umwelt & Energie, Technik & Analytik e. V. (IUTA), Germany

key applications for nanomaterials within rapidly developing markets. The production of nano scaled materials from gaseous precursors in the gas phase is a so called bottom-up method, the advantages of this synthesis route are process control, high purity products and the opportunity to design a continuous process. Generally, the highly specific properties of particulate systems are directly correlated with the size of each particle and applications often require highly defined properties.

In this work we provide an overview of our combustion, thermal decomposition and plasma assisted material synthesis on the pilot plant scale. Furthermore, direct transfer of these materials

into processable dispersions using wet electro precipitator technology will be presented.

The combustion based flame spray synthesis is a widely used in lab scale for the synthesis of nanomaterials, but has not reached industrial scale yet. Here, we present the generation of particles using easily available metal nitrates and demonstrate their conversion into defined nanoparticles in a spray flame. The composition of the particles can be adjusted and range from single metal oxides like titania to complex lanthanum strontium manganite (LSM or LSMO) perovskite particles with defined metal ratios. The particles are typically used in catalysis applications like hydrogen generation in electrolysis or the decomposition of versatile oxide components. We will demonstrate oxygen evolution ratio measurements on these materials. Thermal decomposition is used for the generation of pure silicon material, which is a candidate for battery application. The decomposition of silane (SiH₄) in a nitrogen/hydrogen atmosphere leads to the formation of highly crystalline material, which can be doped on demand. Production rates of up to 1kg/h material can be achieved using this method. Battery performance of silicon based materials has been evaluated and reveals promising results for future applications.

The plasma based system decomposes precursors at higher temperatures (T > 2000K) into atoms and subsequent nucleation leads to particle formation, while a steep temperature gradient helps to obtain nanomaterial with designed characteristics.

We report on the formation of graphene, since it offers high potential to improve a wide range of energy applications. It is well known that the combination of high production rates and material with defined properties is a major challenge in graphene synthesis. To address this, we performed eco-friendly continuous gas-phase synthesis of graphene on a pilot plant scale using easily available ethanol as precursor material. For this purpose, ethanol is evaporated and subsequently fed through an argon-hydrogen plasma generated by microwave radiation. The graphene powder is ex-situ analyzed by scanning and transmission electron microscopy as well as RAMAN spectroscopy, which reveals the typical signal of graphene with low defects. Results reveal that a throughput of 200 g/h of ethanol and low plasma energy supports the formation of graphene structures and, therefore, paves the way for energy efficient synthesis.

SESSION SF03.06: Poster Session II
Session Chairs: Craig Brown and Brent Melot
Tuesday Afternoon, November 28, 2023
Hynes, Level 1, Hall A

8:00 PM SF03.06.01

Fluorophlogopite (Mg-Mica) as a Novel Material for Enhanced Triboelectric Nanogenerators MinKyeongKim¹, WoojongKim², SoohongLee¹, JinpyoHong^{2,2} and JohnHong¹; ¹Kookmin University, Korea (the Republic of); ²Hanyang University, Korea (the Republic of)

Wearable electronics have gained significant interest in various applications, including healthcare monitoring, human-machine interfaces, and portable devices. The development of large-area wearable energy devices that can efficiently harvest biomechanical energy is crucial for sustainable and efficient applications. Triboelectric nanogenerators (TENGs) have demonstrated excellent potential in capturing biomechanical energy by converting mechanical energy into electrical energy. However, enhancing the output performance, flexibility, stretchability, and sensitivity of TENGs requires the exploration of new materials and device designs.

Mica, a raw clay mineral composed of layered silicates, has been identified as one of the most promising inorganic non-metal triboelectric materials due to its abundant availability and low friction coefficient. While previous studies have primarily focused on investigating the triboelectric properties of muscovite, this study introduces fluorophlogopite (Mg-mica), an artificially synthesized mica, as a novel material for TENG applications. Fluorophlogopite has not been previously utilized in TENG applications but has been studied as a dielectric material for capacitors due to its high dielectric constant. The fabricated TENG device using Mg-mica as the friction layer exhibited more than a twofold increase in output voltage compared to conventional mica-based TENGs.

Kelvin Probe Force Microscopy (KPFM) measurements were performed to validate the higher surface potential of Mg-mica compared to muscovite. The results indicated that the composition of metallic substances replacing silicon within the mica structure significantly influences the overall output voltage of mica. Additionally, output power measurements from the Mg-Mica-TENG demonstrated an open circuit voltage of 130V, a short circuit current of 6μA, and a maximum power density of 151mW/cm². These findings highlight the potential of Mg-mica as a promising material for the development of high-performance TENGs. Further research and exploration of different types of mica can lead to the discovery of more efficient and effective triboelectric devices.

8:00 PM SF03.06.02

Functionalization of Magnetite (Fe₃O₄) Nanoparticles with Cyclodextrin via Polydopamine Coating for Ciprofloxacin Remediation AgnesPholosi, OlayinkaEmmanuel, SaheedO. Sanni and SamsonAkpotu; Vaal University of Technology, South Africa

Superparamagnetic iron oxide nanoparticles are promising materials in emerging pollutants remediation due to their biocompatibility and easy surface modification. However, challenges of oxidation, agglomeration and surface defects still impair their commercial application. As such, a benign and green approach is a proposed strategy to overcome the limitations. In this study, magnetic nanocomposite was synthesized by coating magnetite with silica (SiO₂) using the modified stober route. The synthesized Fe₃O₄-SiO₂ was polymerized with dopamine in a basic solution to obtain Fe₃O₄-SiO₂-PDA followed by functionalization with β-cyclodextrin. The successful synthesis of Fe₃O₄-SiO₂-PDA-CD nanocomposite was confirmed through scanning electron microscopy (SEM), transmission electron microscopy (TEM), Fourier transform infrared (FTIR), X-ray diffraction (XRD), X-ray photoelectron spectroscopy (XPS) and vibrating sample magnetometry (VSM). Batch adsorption studies were conducted to investigate if the synthesized nanocomposite could adsorb ciprofloxacin from an aqueous solution. Functionalization of magnetite with polydopamine and cyclodextrin led to improvement in surface characteristics and incorporation of relevant functional groups. VSM results showed that magnetite retained its magnetic properties after incorporation of PDA and CD. Morphological and structural analysis showed the presence of iron, carbon, oxygen, and nitrogen with spherically shaped nanoparticles with average particle size of 12.02 nm. Maximum adsorption was achieved at pH 7 and equilibrium time was reached before 30 min. The adsorption kinetics suited pseudo second order model equilibrium data fitted Langmuir isotherm. The results indicate that the Fe₃O₄-SiO₂-PDA-CD is most efficient and could be applied over wide concentration ranges and temperature, and therefore, would be potentially feasible for the removal of ciprofloxacin and other emerging pollutants from wastewater.

8:00 PM SF03.06.03

Water Adsorption Inside Microporous CPO-27 Metal-Organic Frameworks MarvinKloß, ChristianWeinberger and MichaelTiemann; University of Paderborn, Germany

Metal-organic frameworks (MOFs) with open metal sites (i.e., vacated coordination sites) are particularly interesting for adsorption of guest molecules, especially water. One example is CPO-27 (M₂(dhtp), dhtp = dihydroxyterephthalate) [1], also known as MOF-74 [2]. It is even more fascinating due to the variety of bivalent metal cations that can be used to synthesize this framework.

A detailed investigation of the hydration and dehydration of this series of MOFs revealed that water molecules inside the pores can be divided into three different types [3]: Primary water molecules coordinate to the metal (i.e., they occupy the open metal sites), secondary water molecules interact with primary ones via hydrogen bonding, and tertiary water molecules interact (only) with secondary ones. It was found that the interaction of water molecules with the framework is governed by the choice of the respective metal.

We present a comprehensive study of water inside the pores of a series of CPO-27(M) materials (M = Co, Cu, Mg, Mn, Ni, Zn). For this purpose, we carried out water sorption analysis and performed IR spectroscopic studies of water-loaded samples. We observe a strong impact of the respective metal on the incipient water uptake (i.e., adsorption in the low-pressure region). Furthermore, the metal center not only governs the interaction with the coordinated (primary) water molecules but has also an impact on the interaction with the secondary and tertiary water molecules. By humidity- and temperature-resolved DRIFT spectroscopic studies and by thermogravimetric analysis (TGA) we further investigate the dehydration behavior in some detail.

[1] P. D. C. Dietzel, Y. Morita, R. Blom, H. Fjellvåg, *Angew. Chem. Int. Ed.* 2005, 44, 6354–6358.

[2] N. L. Rosi, J. Kim, M. Eddaoudi, B. Chen, M. O'Keeffe, O. M. Yaghi, *J. Am. Chem. Soc.* 2005, 127, 1504–1518.

[3] M. H. Rosnes, B. Pato-Doldán, R. E. Johnsen, A. Mundstock, J. Caro, P. D. C. Dietzel, *Microporous Mesoporous Mater.* 2020, 309, 110503.

8:00 PM SF03.06.04

Lithiophilic Montmorillonite as a Robust Substrate for Uniform Lithium Deposition and Enhanced Electrochemical Performance BoNie and HongtaoSun; Penn State University, United States

Lithium metal is a highly promising anode material due to its exceptional theoretical capacity and low redox potential. However, issues such as uneven lithium deposition and uncontrolled volume expansion during cycling lead to cracks on the solid electrolyte interface (SEI), resulting in electrolyte consumption and dendrite growth. These challenges impede the commercial development of lithium metal batteries by causing poor performance, low Coulombic efficiency (CE), and safety concerns.

In this study, we investigate the potential of lithiophilic montmorillonite (MMT), a two-dimensional interlayered phyllosilicate material, as a robust substrate for achieving uniform lithium deposition and enhancing electrochemical performance. MMT possesses an interlamellar structure with an octahedron layer of aluminum oxygen sandwiched between two tetrahedron layers of silicon oxygen. This interlayered structure provides pathways for the transportation of exchangeable cations, including Li^+ , Na^+ , K^+ , and Ca^{2+} . We focus on lithiophilic MMT as it exhibits a strong affinity for lithium ions.

By utilizing MMT as a substrate, we demonstrated the maintenance of uniform lithium deposition, which promotes enhanced electrochemical performance. The interlayered MMT structure facilitates fast diffusion channels for lithium ions and provides sufficient space to accommodate volume expansion, effectively leading to a dendrite-free lithium surface. To validate the stability of the lithium deposition process, we conducted in situ optical microscopy analysis and utilized COMSOL Multiphysics simulations. Our results showcase the effectiveness of MMT@Cu as an electrode material, achieving an average Coulombic efficiency of 99% over 700 cycles at a current density of 2 mA cm^{-2} with a lithium areal capacity of 1 mAh cm^{-2} . Additionally, the symmetric cell incorporating MMT@Cu demonstrates an extended lifespan of 20,000 minutes at 1 mA cm^{-2} for a 1 mAh cm^{-2} capacity. This work presents a novel strategy for suppressing dendrite growth and ensuring high-performance lithium metal batteries. The utilization of lithiophilic MMT as a substrate for uniform lithium deposition holds great promise in overcoming the challenges associated with lithium metal anodes, paving the way for the development of advanced lithium metal batteries with improved performance and safety.

8:00 PM SF03.06.05

Tubular Carbon Nanofibers with $\text{MnCr}_{2-x}\text{Rh}_x\text{O}_4$ Nanostructures Driven by Electrospinning and Its Application for Oxygen Evolution Reaction Catalysis Juhee Yang, Myung HwaKim, YejinKim and Hee AhOh; Ewha Womans University, Korea (the Republic of)

As a result of development based on fossil fuels to this day, various environmental problems are being highlighted as a side effect. As part of the solution, one of the notable methods is the development of hydrogen energy through water decomposition. The OER, one of the half reactions of water splitting, does not occur thermodynamically well, so a catalyst to activate it is needed. Precious metals such as Ru, Ir, and Rh used as existing catalysts are expensive due to their scarcity. Therefore, it is essential to develop a cheaper and more efficient catalyst that can replace them.

We introduce facile synthesis of $\text{MnCr}_{2-x}\text{Rh}_x\text{O}_4$ nanostructures on carbon nanofiber (CNF) driven by electrospinning process. We expect that the partial introduction of Rh^{3+} ions into spinel B sites instead of Cr^{3+} ions could effectively perturb the electronic structure of the original MnCr_2O_4 nanostructures, resulting in the enhancement of the electrocatalytic activity for oxygen evolution reaction with beneficial effects of a high conductivity and specific surface area of CNF backbone. In this study, the shapes and compositions for $\text{MnCr}_{2-x}\text{Rh}_x\text{O}_4$ nanostructures on carbon nanofiber (CNF) in various synthetic conditions are carefully confirmed using the Scanning Electron Microscope (SEM), Energy Dispersive Spectroscopy (EDS), and X-ray Diffraction (XRD). Furthermore, electrochemical performances for $\text{MnCr}_{2-x}\text{Rh}_x\text{O}_4$ nanostructures on carbon nanofiber (CNF) are performed to explore the electrocatalytic activity of oxygen evolution reaction reaction.

8:00 PM SF03.06.06

Advanced Output Performances of Thermoelectric Generator via Poled Ferroelectric Ceramics Ji YoungPark and Jeong MinBaik; Sungkyunkwan University, Korea (the Republic of)

Toward free-fuel energy society, the sustainable and renewable energy sources are necessary. There are various energy sources for that, however, each source has lots of problems to overcome. Thermoelectric generator (TEG) is a promising device for energy harvesting, which produces electric energy via the Seebeck effect. Due to the growing demands for electricity and the associated energy crisis, the importance of TEG also has been increased to solve environmental concerns. However, low energy conversion efficiency and stability still remain as the main challenges of TEG. To address these limitations, the recent work demonstrated the optimized Bi_2Te_3 ink-based TEG with charged triboelectric materials to enhance the output voltages by contact electrification. Although the output power was increased, the retention time was still short to apply. Herein, we propose TEG with a Cu/p-type $\text{BiSbTe}/\text{Au}/\text{Cr}/\text{SiO}_2/\text{Si}$ in which poled ferroelectric materials are attached at the cold zone. When the poled ferroelectric materials are attached at the back of TEG, the remanent polarization increases charge mobility permanently, inducing charges created on the TEG. The output voltage of TEG coupled with BaTiO_3 ceramic is 4 mV when the temperature difference is 10 K, which is up to 2 times higher than the output voltage of conventional TEG. In addition, when the BaTiO_3 -added $\text{Pb}(\text{Ni},\text{Nb})\text{O}_3\text{-PbZrO}_3\text{-PbTiO}_3$ ceramic is coupled with TEG, the maximum output voltage was over 4 mV under the temperature difference of 10 K, which is 2 times increased compared to conventional TEG. This approach provides broad applications of TEG and will achieve practical uses by increasing output performance and retention time without material modification.

8:00 PM SF03.06.07

Facile Synthesis and Morphological Analysis of Si-Zr-C-O Fiber Felts with High-Thermal Resistance Young JunJoo, Young JunShim, HyukJunLee and KwangYounCho; KICET, Korea (the Republic of)

Silicon carbide (SiC) fibers with excellent oxidation resistance, high tensile strength, elastic modulus at high temperature are mainly used as a reinforcing material for ceramic matrix composites (CMCs). The polymer-derived SiC fibers are generally manufactured by the processes of melt-spinning, curing, and pyrolysis using polycarbosilane (PCS) as a ceramic precursor. The polymer-derived SiC fibers can be largely divided into amorphous SiC fibers and polycrystalline SiC fibers depending on the oxidation resistance temperature, and various manufacturing methods have been studied to fabricate high-performance polycrystalline SiC fibers. PCS for the spinning is mainly synthesized in autoclave and modified with organometallic compounds by reflux system. These methods showed good polymerization results, such as increases in molecular weight and ceramic yield due to the reaction between PCS and the zirconium source.

However, there is a disadvantage that it requires a lot of time with specific equipment. Therefore, in the present study, a zirconium-added PCS solution for electrospinning was prepared by simple and easy blending method. In this studies, Si-Zr-C-O fiber mats were easily and simply fabricated via combination of solution blend and electrospinning methods. The various analyses were performed to verified that the blending method had the same effect as the autoclave or reflux methods.

In this study, Si-Zr-C-O fiber mats were easily and simply fabricated via combination of solution blend and electrospinning methods. The various analyses were performed to verified that the blending method had the same effect as the autoclave or reflux methods. Also, the zirconium added SiC fiber felts were heat-treated at 1500°C or 1600°C for 1 h in an Ar atmosphere to investigate thermal-degradation behaviors. Si-Zr-C-O fiber felts retained blackness and flexibility, whereas SiC fiber felts were thermal-degraded and discolored to gray. Moreover, the results confirmed that the growth of crystalline size (approximately calculated via XRD analysis) was significantly inhibited by the presence of zirconium. Therefore, zirconium acetylacetonate as a zirconium source was cross-linked with the PCS structure via the blending method and its role for heat resistance was exhibited at high temperature.

8:00 PM SF03.06.08

Electronic Structure of Ce-Containing Oxides by X-Ray Absorption Spectroscopy MaikoNishibori¹, KakeruNinomiya¹, HirotoTsuji¹, HinanoTabara², ShuheiYamaguchi², AkiraYoko¹, HidenoriYahiro² and TadamuniAdschiri¹; ¹Tohoku University, Japan; ²Ehime University, Japan

The valence change of cations constituting metal oxides plays an important role in the chemical and electronic properties of functional materials. Among them, Ce exhibits high oxygen storage capacity, oxygen mobility, and oxidation catalytic activity due to its ability to oscillate between $\text{Ce}^{4+}/\text{Ce}^{3+}$ valence while maintaining a nearly constant ionic radius [1]. The Ce electronic state depends on the complex interaction between localized 4f electrons and the oxygen and vacancy orbitals [2], directly related to the material functionality. In this study, X-ray absorption spectroscopy was performed on CeO_2 nanoparticles (NPs) [3] to discuss the correlation between Ce local structure and electronic state.

The correlation between Ce-O bonding distance and Ce valence was investigated using CeO_2 with different particle sizes. In the Ce L_{3-} edge, although the Ce^{3+} increased slightly with decreasing grain size, the X-ray absorption fine structure (XAFS) spectral shape was nearly constant, suggesting that the CeO_2 state was maintained. On the other hand, in the Ce $M_{5,4-}$ edge, the XAFS spectral shape changes significantly with grain size, and the peak intensity of Ce_{3+} remarkably increases as the grain size decreases. This indicates that the electrons are localized in the Ce4f orbitals. Here, we investigated the O-Ce interaction from O K-edge XAFS spectra measurements. The O2p-Ce5d_{eg} and O2p-Ce5d_{t2g} peaks broadened with decreasing grain size. This suggests that the local structure of the CeO_8 hexahedron is disordered. On the other hand, the O2p-Ce4f peak intensity decreased significantly with grain size. This implies a decrease in the interaction between O2p and Ce4f orbitals. These results suggest that lattice expansion and distortion of CeO_2 may localize electrons in the Ce4f orbitals.

This research was partially supported by JSPS Grant-in-Aid for Scientific Research Grant Number 21H05010 and JP22H01764.

[1] F. Zhang, X. Zhang, *et al.*, *Chemical Engineering Journal*, **348** (2018) 831–839.

[2] V. K. Paidi, D. L. Brewster, J. W. Freeland, C. A. Roberts, J. van Lierop, *Phys. Rev. B*, **99**, 180403 (2019).

[3] X. Hao *et al.*, *Small*, **14** (2018) 1802915.

8:00 PM SF03.06.09

Single-Phase CrVO_4 and Rh-Doped CrVO_4 Nanostructures for Efficient Electrocatalytic Performance in Oxygen Evolution Reaction YejinKim, Myung HwaKim, Hee AhOh and JuheeYang; Ewha Womans University, Korea (the Republic of)

In recent years, research on hydrogen (H_2) as sustainable energy source has been widely conducted to deal with deteriorating energy problems. Water splitting is promising way to produce pollution-free H_2 . However, overall efficiency of water splitting is restricted by sluggish kinetics of oxygen evolution reaction (OER), so effective catalyst is required. Noble metals have been widely studied as efficient OER catalyst, but their scarcity and high cost hinder sustainable water splitting. Therefore, it is necessary to devise an OER catalyst material which is cost-efficient and shows high catalytic activity toward OER. In this work, thus, we report facile formation of single-phase CrVO_4 and Rh-doped CrVO_4 nanostructures via simple acid-base titration

followed by thermal annealing process at various temperature and atmosphere conditions. Synthesized CrVO₄ nanostructures were then characterized by using Field Emission Scanning Electron Microscope (FE-SEM), Energy Dispersive Spectroscopy (EDS), X-ray Diffraction (XRD), Transmission Electron Microscope (TEM), X-ray Photoelectron Spectroscopy (XPS), micro-Raman spectroscopy. Electrochemical measurements are also conducted to confirm the effectiveness of CrVO₄ based nanostructures as an OER catalyst.

8:00 PM SF03.06.10

Two-Dimensional (2D) Assembly of Binary Shaped Nanoparticles BinWang and AndreaR. Tao; University of California, San Diego, United States

Programmable assembly of binary nanoparticles on the two-dimensional (2D) scale offers nanomaterials a variety of structures and properties that are difficult to attain via conventional means. Despite significant computational progress in the prediction and discovery of assembly phases for binary nanoparticle mixtures, experimental realizations are still lacking. We prepared the binary assembly of nanoparticles with two different shapes: silver nanocubes (AgNC) and gold nanospheres (AuNS). By varying the surface chemistries and composition ratios of AgNC and AuNS building blocks, we were able to access a variety of assembly behaviors and correlate them to different phases predicted in 'phase diagrams' by theory. This work bridges the gap between computational and experimental efforts and represents progress in understanding the assembly behavior of binary shaped building blocks.

8:00 PM SF03.06.11

Magnetic Nanoparticles in Biofilm Disruption: A Promising Approach to Combat Marine Fouling PayelBiswas and IreneAndreu Blanco; University of Rhode Island, United States

Marine biofilms, which are formed by the growth of various organisms, can negatively affect underwater surfaces such as boat hulls and bridge foundations. They can lead to increased fuel consumption, corrosion, and damage to the substrate, resulting in extra costs for biofilm removal procedures. Removing bacterial biofilms early on can prevent the attachment of harmful macro-organisms. This project proposes using magnetic nanoparticles (MNPs) to remove marine biofilms under alternating magnetic fields. Spherical iron oxide MNPs of 20 nm diameter were synthesized by the polyol method and their morphology, crystallinity and magnetic properties were evaluated by electron microscopy, X-ray diffraction and static and dynamic magnetometry. The MNPs are magnetite with a size close to the superparamagnetic/ferromagnetic transition at room temperature and present a saturation magnetization close to that of bulk magnetite. The synthesized MNPs were coated with a biocompatible layer of silicon dioxide via a sol-gel method and polyethyleneimine, a positively charged polymer with antimicrobial properties. The integrity of these coatings was verified and quantified using transmission electron microscopy, Z-potential measurements, and thermogravimetric analysis. The MNPs were internalized within *C. marina* biofilms and placed under alternating magnetic fields. Several high-frequency alternating magnetic fields, in the hundreds of kHz range, were tested. This frequency range is designed to promote MNP heating for our MNP morphology and composition. The morphology of the biofilm and viability of the bacteria before and after alternating magnetic field treatment were evaluated by fluorescence microscopy. The study will investigate the most effective MNP treatment regime and the effects of mechanical or thermal excitation on biofilm and bacterial physiology. The proposed research has the potential to provide a new and effective approach to addressing the problem of marine biofilms and could be used to treat biofilm caused by antibiotic resistant bacteria strains.

8:00 PM SF03.06.12

The Electrochemical Versatility of Manganese and Molybdenum-Based Materials Towards Rechargeable Aqueous Zinc Batteries JasonKuang¹, LeiWang^{2,1}, ShanYan^{2,1}, EstherS. Takeuchi^{1,2}, AmyMarschilok^{1,2} and KennethJ. Takeuchi^{1,2}; ¹Stony Brook University, United States; ²Brookhaven National Laboratory, United States

As the demand for energy increases, large-scale energy storage systems will be required. Rechargeable aqueous zinc battery (RAZB) systems are promising systems for large-scale electrochemical energy storage especially due to the appropriate reduction potential and low cost of zinc and inherently safer operation from the non-flammable aqueous electrolyte. Further, with appropriate materials selection, there is opportunity for high specific capacity. Specifically, the oxide and sulfide analogs of manganese and molybdenum-based positive electrode materials are appealing for RAZBs, as they are low cost and environmentally friendly, and can be produced through scalable synthesis methods. The electrochemical versatility of Mn- and Mo-based materials as redox-active materials and catalysts in RAZBs will be highlighted in this presentation, including materials synthesis, electrode preparation, characterization, and electrochemistry results.

References:

- (1) Kuang, Jason; Yan, Shan; Housel, Lisa M.; Ehrlich, Steven N.; Ma, Lu; Takeuchi, Kenneth J.; Takeuchi, Esther S.; Marschilok, Amy C.; Wang, Lei. "Manganese Molybdate Cathodes with Dual-Redox Centers for Aqueous Zinc-Ion Batteries: Impact of Electrolyte on Electrochemistry," ACS Sustainable Chemistry & Engineering, 2022, 10(49), 16197-16213.
- (2) Dunkin, Mikaela R.; Kuang, Jason; Yan, Shan; King, Steven T.; Housel, Lisa M.; Ma, Lu; Ehrlich, Steven N.; Okasinski, John S.; Takeuchi, Kenneth J.; Takeuchi, Esther S.; Marschilok, Amy C.; Wang, Lei. "Unveiling Charge Transport and Degradation Mechanisms of Aqueous Zn/α-MoO₃ Batteries in Conventional Concentration and Water-in-Salt Electrolytes: A Multi-Modal In Situ and Operando Study," Advanced Materials Interfaces, 2022, 9(29), 2201125.
- (3) Kuang, Jason; Renderos, Genesis D.; Takeuchi, Kenneth J.; Takeuchi, Esther S.; Marschilok, Amy C.; Wang, Lei; "Zinc-air batteries in neutral/near-neutral electrolytes," Functional Materials Letters, 2021, 14(7), 2130012.

8:00 PM SF03.06.13

Production of Transparent Ceramics Based on YAG: Ce (Y_{3-x}Ce_xAl₅O₁₂) for use as X-Rays Detectors using Colloidal Process DaniloB. Janes^{1,2}, TarcísioMicheli Perfecto¹, IgorBarbosa da Cruz¹, ViníciusFortes Carvalho¹, IçamiraCosta Nogueira¹ and EdsonR. Leite¹; ¹Brazilian Center for Research in Energy and Materials (CNPEM), Brazil; ²Federal University of Sao Carlos (UFSCAR), Brazil

Scintillators play a central role in modern engineering as converters of high-energy ionizing radiation (such as X-rays) into visible light, being one of the main components of radiation detectors. To meet the high demand for these components, in combination with the development of new materials and techniques for the production of increasingly efficient scintillators, a series of research has been carried out in recent decades. Yttrium Aluminum Garnet (YAG) is a material that stands out in different fields of scintillation. To produce transparent ceramics scintillators, in this work, Ce-doped YAG nanoparticles were prepared by the co-precipitation method, followed by calcination at 1100 °C. To achieve the desired microstructure and transparency for the final application of the material, conformation, and sintering were tailored to achieve the best parameters for obtaining such properties. Seeking to achieve a high green density through a colloidal process, using the pressure slip casting method, the concentration of solids in the colloidal suspension was a key parameter, as well as the colloidal stability and pressure applied during the slip casting. The final densities obtained for the different parameters were measured and compared. In this way, the purpose of this work is to present a methodology for the production of transparent ceramics scintillator by pressure slip casting method, seeking to reach the final properties necessary for use in the Sirius fourth generation Synchrotron, located at the National Center for Research in Energy and Materials (CNPEM) in Brazil.

8:00 PM SF03.06.14

Modulation of Electrical and Thermal Properties of Niobium Oxide by Alternating Oxygen and Hydrogen Plasma in Atomic Layer Deposition YunhaJung¹, SettasitChaikasetin¹, HeungdongKwon¹, EunjoJung², Hyun sooHan¹, WoosungPark² and FritzPrinz¹; ¹Stanford University, United States; ²Sogang University, Korea (the Republic of)

Transition metal oxide films are a key material for various applications, such as neuromorphic devices, electrochemical energy systems, and optical systems. The material characteristics significantly vary with its stoichiometry between metal to oxygen due to its polymorphic nature. Despite much of previous work on conventional transition metal oxide, the impact of oxidation state on both electrical and thermal properties has been left underexplored. In this work, we modulate the stoichiometry of the metal oxide via alternating oxygen and hydrogen plasma during atomic layer deposition. We use niobium oxide as a sample material, demonstrating tunable electrical and thermal properties. Through systematic material characterization and electrical measurements, we find that the dielectric constant of niobium oxide is enhanced with increased electronic polarizability. Using the optical pump-probe method, the thermal properties are found to be tuned with the stoichiometry of niobium oxide.

8:00 PM SF03.06.15

Phase Transition, Tuned Ferroelectric, Pyroelectric and Electromechanical Properties in Hafnia Thick Films JalajaMa and PavanNukala; Centre for Nanoscience and Engineering (Cense), Indian Institute of Science (IISc), India

The unconventional ferroelectric behaviour in hafnia-based systems, particularly at nanoscale dimensions, holds great potential for advancements in nanoelectronics due to their Si compatibility, reduced toxicity, and simple chemical structure. However, there is ongoing debate regarding the precise mechanism of polarization switching in these films and the ferroelectricity in hafnia is considered to be originating from the orthorhombic crystal structure. The ferroelectric orthorhombic structure in hafnia can be stabilized by means of doping, process temperature, film thickness, choice of electrode and particle size. The stable phase in bulk Hafnia is monoclinic, and the orthorhombic phase is only stable to a few nanometre thicknesses.

Our study presents the ferroelectric, pyroelectric and electromechanical properties of 40 nm thick La-doped HfO₂ films prepared using a wet chemical method. We investigate the influence of process temperature, film thickness, and dopant concentration on achieving the desired orthorhombic phase. The films exhibit a polycrystalline structure with saturated polarization hysteresis loops, a remanent polarization value of approximately 27 μC/cm², and a 1.2 MV/cm coercive field value. Dielectric parameters are determined through C-V measurements, while the hysteretic

piezo response is measured using a Radiant hi tester, revealing an effective d_{33} value of around 10 pm/V for the La-doped hafnia films. The phase transitions originating from the defect dynamics in Hafnia are not well explored and we report a ferroelectric to non-ferroelectric phase transition around 140K. Our findings demonstrate the potential of the wet chemical method for fabricating La-doped HfO₂ films with desirable ferroelectric and electromechanical properties, even at larger film thicknesses (40 nm).

8:00 PM SF03.06.16

Gas-Solid Phase Reaction-Driven CO₂ Reduction : Exploring the Photocatalytic Potential of Silver-Bismuth-Iodide Rudorffite [Jia-MaoChang¹](#), [Ting-HanLin¹](#), [Yin-HsuanChang¹](#), [Kai-ChiHisao¹](#) and [Ming-ChungWu^{1,2}](#), ¹Chang Gung University, Taiwan; ²Chang Gung Memorial Hospital, Taiwan

In recent decades, researchers have been striving to tackle climate change originated from global warming and searching a solution for CO₂ reduction. Photocatalytic CO₂ reduction is a promising solution to balance reduction greenhouse gas and creating energy sources. However, the main challenges of photocatalysts for CO₂ reduction are their wide band gaps and short lifetime of photo-induced electron-hole pairs. That not only limits their visible-light absorption but also inhibits the transportation of electron-hole pairs for catalytic reactions. Silver bismuth iodide rudorffite materials (SBI) having a relatively lower band gap, < 1.8 eV, and high absorption coefficient are selected for photocatalytic CO₂ reduction. Herein, we synthesize various SBI photocatalysts including AgBi₂I₇, AgBi₄I₆, Ag₂BiI₅, and Ag₃BiI₆ through a gas-solid phase strategy. Owing to the different crystal structures, SBI photocatalysts perform photocatalytic activity differently. To realize the correlation between crystal structure of SBI and photocatalytic activity, X-ray diffractometer (XRD), X-ray photoelectron spectroscopy (XPS), X-ray absorption spectroscopy (XAS), and photo-assisted Kelvin Probe Force Microscopy (Photo-assisted KPFM) are used to frame the mechanism of their photocatalytic CO₂ reduction. Through gas-solid phase reaction, the crystal structures of SBI productions can be easily manipulated by controlling the stoichiometry of their reactants, silver iodide and bismuth iodide. For Ag-rich compositions, Ag/Bi ratio ≥ 1, the SBI photocatalyst tends to crystallize in a hexagonal structure. The partial Ag ions are delocalized in the lattice and occupy the vacant tetrahedral sites between AgI₆ and BiI₆ octahedrons. That results in the formation of AgI secondary phase. On the other hand, Bi-rich composition, Ag/Bi ratio < 1, prefers to form a cubic structure. Bi ions tend to partially substitute the central site cation, Ag, of AgI₆ octahedron. To insight the speculation above, XPS and XAS were applied to realize the electronic structure, valence state changes, and atomic environment surrounding Ag atoms in SBI materials. In terms of the Ag-rich components, they all exhibit a high density of uncoordinated silver, strong Ag-I bonding, and short bond length between Ag and I. The photocatalytic CO₂ reduction rate shows a significant relative to increasing the ratio of silver in SBI photocatalysts, Ag₃BiI₆ > Ag₂BiI₅ > AgBiI₄ > AgBi₂I₇. The same tendency of photocatalytic activity and electron configuration of SBI materials points out that the metallic Ag in SBI photocatalysts is the active sites for CO₂ photoreduction. Among the SBI materials, Ag₃BiI₆ shows the highest photocatalytic activity, achieving average CO and CH₄ production rates of 0.23 and 0.10 μmol·g⁻¹·h⁻¹. Furthermore, the results of Photo-assisted KPFM reveals the photo-induced potential change, contact potential difference (CPD), of SBI materials under different LED light sources including UV at 365 nm, blue at 470 nm, green at 530 nm, and red at 656 nm. The highest CPD of Ag₃BiI₆ validates that the photocatalytic CO₂ reduction rate is proportional to the evolution of CPD. The high CPD can be ascribed to the effective electron-hole pair separation that are originated from active Ag sites. The effective separation rate of electron-hole pairs promotes the photocatalytic CO₂ reduction activity. In summary, our study sheds the light in the crucial role of SBI crystal structure in photocatalytic CO₂ reduction. By validating the active sites within SBI and unraveling its photocatalytic mechanism, we offer a promising solution to address the challenges of environmental pollution and the increasing demand for sustainable energy. The insights gained from our research pave the way for further advancements in the field of photocatalysis and contribute to the development of efficient and environmentally friendly CO₂ reduction technologies.

8:00 PM SF03.06.17

Exploring Photo-Piezocatalysis in Heterostructured Barium Titanate and Titanium Dioxide: Insights from Photo-Triggered Contact Potential Differences [Ting-HanLin](#), [Jia-MaoChang](#), [Kai-ChiHisao](#), [Kun-MuLee](#) and [Ming-ChungWu](#); Chang Gung University, Taiwan

Pollutants perpetually generated by various industries intensify the burden on the environment and progressively damage our living spaces. The combination of photocatalysis and piezocatalysis presents an intriguing technique for achieving pollutant degradation and potential in versatility and energy efficiency. However, the significance influence of catalysis reaction is sufficient electron-hole pairs to generate the reactive radicals. The piezocatalysts, triggered by mechanical strain and stress possesses a spontaneous polarization field of ferroelectric bodies on charge transport, and attract external charge on the interface. The effective modulation of the catalyst dielectric properties and the internal static electric field, improve the piezoelectric-induced catalytic performance. In this study, we synthesized a nanosized photo-piezocatalyst by incorporating titanium dioxide (TiO₂) with barium titanate (BaTiO₃) using an in situ hydrothermal method. Utilizing the spontaneous polarization of BaTiO₃ under strain to form a built-in electric field and high voltage coefficient, this promotes the separation of electron-hole pairs and enhances photocatalytic activity. As the reaction temperature increased, BaTiO₃ gradually grew onto the TiO₂ nanoparticle, promoting a phase transition in the crystal structure. At a critical temperature of 120°C, both the primary crystalline structures of BaTiO₃ and TiO₂ coexisted, revealing a heterostructure evident in microstructure observation. When compared to pristine TiO₂ and BaTiO₃, the BaTiO₃-TiO₂ photo-piezocatalyst demonstrated superior degradation activity towards methyl orange dye under both illumination and ultrasonic vibration. This resulted in a reaction rate constant of 0.01326 min⁻¹. It also proves that the incorporation of photocatalyst and piezocatalyst is beneficial for the overall activities. To further explore strain-induced polarization in the photo-piezocatalyst, we employed Raman spectroscopy and noted a significant change in the typical phonon mode (E(LO + TO) + B1(309.0 cm⁻¹)) for BaTiO₃ following compression. This suggests that lattice compression in BaTiO₃ reduces the vibration of oxygen atoms and alters the dipole properties in the BaTiO₃-TiO₂ photo-piezocatalyst. To understand the enhancement mechanism of photo-assisted piezocatalysis, we used an innovative photo-induced in-situ Kelvin probe analyzer to measure the contact potential difference (CPD) of the material. The generation of electron-hole pairs through photo-assisted excitation of photosensitive materials causes a shift in the Fermi energy band, yielding a greater surface potential difference, indicating increased photosensitive properties. Tests on the optimal BaTiO₃-TiO₂ photo-piezocatalyst revealed that the change in CPD of BaTiO₃-TiO₂ exhibits a delayed behavior under continuous UV LED illumination in both short-term and long-term illumination switch tests. We infer that the hysteresis of CPD could be caused by photo-induced charge driven by TiO₂, which reduces the polarization of BaTiO₃. This phenomenon likely contributes to interfacial charge migration under photo and ultrasonic vibration, possibly extending the charge life and maintaining a sufficient surface charge concentration for radical generation. Consequently, the overall piezoelectric and photocatalytic characteristics are significantly improved. The photo-piezocatalyst is expected to be applied in cyclic wastewater treatment in the future, using the surface local stress generated by water flow to achieve the goal of degrading pollutants.

8:00 PM SF03.06.18

Synthesis, Modification and Characterization of BaBiO₃ Thin Films [EdvinT.Berhane](#), [SpencerDoyle](#), [CharlesBrooks](#) and [JuliaMundy](#); Harvard University, United States

The perovskite BaBiO₃ exhibits superconductivity around 30 K when doped with potassium on the A-site. This is the highest observed transition temperature for an oxide superconductor without copper. BaBiO₃ is also predicted to be a large-bandgap topological insulator when electron-doped. However, the topological insulator state has not been realized experimentally thus far. Here we synthesize high-quality phase-pure thin-films of BaBiO₃ on strontium titanate substrates using reactive-oxide molecular beam epitaxy. We study various dopings and post-growth modifications focused around achieving a superconducting or topological insulator state. X-ray diffraction, atomic force microscopy, and x-ray photoemission spectroscopy are used to characterize the quality and content of our films.

8:00 PM SF03.06.19

Growth and Characterization of N-Doped VO₂ Thin Films for the Thermo-chromic and Smart Windows by the Mist Chemical Vapor Deposition [TaiseiKano](#), [YutaArata](#), [HiroyukiNishinaka](#) and [MasahiroYoshimoto](#); Kyoto Institute of Technology, Japan

Vanadium dioxide (VO₂) has attracted considerable attention after F. J. Morin reported that it exhibits a metal-insulator transition (MIT) at around 67°C [1]. The MITs of VO₂ have been demonstrated to occur by various stimuli, such as heating, applying voltage, and light, and to be used for smart windows, to absorb and reflect infrared (IR)-region light at a high temperature to prevent it from entering inside the room. To apply the smart windows using the MIT derived from the heat, the transition temperature is higher than the expected temperature operated around 30°C. Therefore, experiments and theoretical calculations have been conducted to decrease the MIT temperature of VO₂ thin films by incorporating other elements, such as N, F, and Mo. In previous report, N-doped VO₂ thin films were deposited by reactive pulsed laser deposition (PLD) and the MIT temperature decreased at 50°C [2]; however, further investigations are necessary to decrease at 30°C. On the other hand, J.G. Lu et al. reported that mist CVD allowed to dope N into oxide thin films [3]. Furthermore, our group demonstrated that VO₂ thin films were deposited by mist CVD on synthetic mica substrates and showed a tunable MIT temperature through bending stress. In this study, we doped nitrogen (N) into VO₂ thin films to decrease the transition temperature by mist CVD and investigated the impact of N into thin films on the MIT temperatures.

First, N-doped VO₂ thin films were grown on a synthetic mica substrate with a SnO₂ buffer layer to control the VO₂ orientations. X-ray diffraction 2θ-ω analysis revealed peaks of the VO₂(010) plane and the buffer layer SnO₂(100) plane in the undoped and N-doped samples in the temperature range from 425°C to 500°C. Furthermore, SIMS revealed that N concentration in the VO₂ thin film was approximately 10²⁰cm⁻³ at the growth temperature of 425°C. Thus, we successfully grew N-doped VO₂ epitaxial thin films by mist CVD.

Temperature-resistance characteristics were measured of the VO₂ thin films to investigate their electrical properties and MIT temperatures. For undoped samples, the transition temperature slightly decreases with decreasing growth temperature, consistent with the results by Matamura et al. [4]. On the other hand, N-doped VO₂ thin films exhibited a decrease of the transition temperature, and the MIT temperature of VO₂ thin films at the growth temperature of 425°C was 30°C. This indicates that the VO₂ thin film blocks the IR light from entering the room above the 30°C using as the thermo-chromic and smart windows. This result is lower than the transition temperature of 50°C reported using PLD.

The transmittance of the N-doped VO₂ thin films was investigated as varying the measurement temperatures. Similarly to the electrical properties, the N-doped VO₂ thin film grown at 425°C showed the transition at around 30°C. These results pave the way for the thermo-chromic and the smart windows applications that can help address future energy problems.

References

[1] F. J. Morin, "Oxides Which Show a Metal-to-Insulator Transition at the Neel Temperature", Phys. Rev. Lett. 3, 34-36 (1959).

[2] Simon Chouteau et al., "Investigation of the metal-to-insulator transition of N-doped VO₂(M1) thin films", Applied Surface Science Volume 554, 149661 (2021).

[3] J.G. Lu et al., "Roles of hydrogen and nitrogen in p-type doping of ZnO", Chemical Physics Letters 441 68-71 (2007).

[4] Yuya Matamura et al., "Mist CVD of vanadium dioxide thin films with excellent thermochromic properties using a water-based precursor solution", Solar Energy Materials & Solar Cells 230 111287 (2021).

8:00 PM SF03.06.20

Bulk Alumina Glasses and Glass-Ceramics with Multiple Stabilizers Angshuman Gupta, AnuMohan and AshutoshS. Gandhi; Indian Institute of Technology Bombay, India

Alumina rare-earth oxide glasses have unique properties, including high chemical resistance, high hardness, and a high refractive index in the IR region, with potential applications in optical devices. Alumina (Al₂O₃) alone cannot be obtained as bulk glass, although it can act as a network former. Alumina can form glasses when alloyed with calcia, zirconia, and other rare-earth oxides. It has been observed that the glass-forming ability and short-range ordering are enhanced if the size difference of the constituent cations is large. Having excellent optical and mechanical properties, the development of alumina based glasses is hampered by their high melting points and the high cooling rates required to obtain the glassy structure. Several studies have been conducted to obtain alumina-based glasses using splat quenching, aerodynamic levitation, and flame spraying; limiting the size to thin films, ribbons, fibers, and small spheres. Obtaining bulk alumina glasses is challenging because of their limited thermal stability against crystallization. Chemical synthesis techniques, including co-precipitation, sol-gel, spray pyrolysis, and solution combustion synthesis (SCS), provide alternate routes to obtain glassy powders. In the present work glassy powders were obtained by utilizing SCS process, because it is simple, fast and cheap. Compositional space for Al₂O₃ based glasses was explored by varying the amounts of different stabilizers such as CaO, Gd₂O₃, La₂O₃, TiO₂, Y₂O₃, Yb₂O₃, ZnO, ZrO₂. The stabilizers were chosen based on their efficacy in stabilizing the glassy state. Compositions were designed by varying alumina content from 60-80 mol% and rest in four to eight stabilizers in equimolar ratio. The amorphous phase stability and crystallization sequence of the synthesized powders were investigated. A few compositions showing higher glass phase stability were selected for the densification studies. Sintering of calcined powders was carried out under pressureless, vacuum, and hot press sintering conditions. First time, extensive densification was observed under free sintering and vacuum sintering conditions without undergoing crystallization. This study opens up the opportunity to obtain bulk dense alumina glasses. Being metastable, a glassy phase always has the driving force for crystallization. Bulk dense glasses can act as precursors for nanostructured ceramics as the crystallization is carried out at low temperatures so that the nucleation rate is much greater than the growth rate. Crystallization of bulk alumina glasses into nanocrystalline oxides was carried out by suitable thermal treatment with and without applied pressure. X-ray line broadening and HRTEM images were used to find the sizes of nano-crystals. Microstructural characterization was carried out on these nanocrystalline glass-ceramics, in addition to basic mechanical property evaluation. Precession electron diffraction (PED) analysis was carried out on crystallized glasses, for phase mapping and crystallite orientation mapping.

Structural modification taking place during consolidation were studied by ²⁷Al MAS NMR and X-ray absorption spectroscopy (XAS). ²⁷Al MAS NMR was utilized to probe the local structural units around Al cations and clearly indicated the presence of AlO_x units (x = 4, 5, 6) in the calcined powder. The relative abundances of different Al sites, isotropic chemical shift (δ_{iso}), and average quadrupolar coupling constant ($\langle|Q_c| \rangle$) fitting parameters were extracted using a simple Czjzek model. Extended X-ray absorption fine structure (EXAFS) was used to probe the local structural changes around different stabilizing cations. EXAFS studies indicated that the local structure around the stabilizing ions remains unaffected during pressureless sintering. Characterization by NMR spectroscopy suggests that structural changes/relaxation during densification originate from the short-range collective rearrangement of AlO_x polyhedra.

8:00 PM SF03.06.21

Fabrication of Nanostructure on Waste Glass from End-Of-Life Vehicles by NaOH Leaching Tatsumi Naganuma¹, Toshihiro Kuzuya¹, Hisayoshi Matsushima², KenSawada¹, Naoya Sawaguchi¹ and Akira Sato³; ¹Muroran Institute of Technology, Japan; ²Hokkaido University, Japan; ³MATEC Inc, Japan

We have investigated upcycling of waste glass from end-of-life vehicles. The waste glass contains various additives such as Ce, Ti, and other transition metals for UV-cut and coloring. Furthermore, alkaline earth metals were added to adjust the mechanical and chemical properties of the glass. These additives would better be used to fabricate upcycling glasses with novel functions. Therefore, we investigated the facile alkaline leaching to fabricate the nanostructure of these additives' oxides. Front and front door glass were recovered from end-of-life vehicles and pulverized into glass cullets. XRF analysis indicated that the glass cullet contained Ce, Fe, and alkaline earth metals. Glass cullets were heated at 1673K for 3 h. The glass melt was quenched on the steel plate and formed into a plate shape. Then, the as-quenched glass was annealed at 873 K for 2 h and cooled for 24 h to ambient temperature. Glass samples were cut to 7.5 × 7.5 mm² with a diamond cutter and mechanically polished to obtain a mirror finish. And then, the polished glass was annealed at 873K near the glass softening point for 24h. After annealing, the glass surface was polished again with 3 to 4 μm diamond paste. The glass samples were immersed in 1.0 mol/L NaOH solution for 1 or 8 days to etch Si atoms on the surface selectively. The morphology of the nanostructure formed on the surface was observed using an atomic force microscope (AFM) and a scanning electron microscope (SEM). A treated glass sample was thinned by a focused ion beam (FIB) to observe the distribution of elements near the glass surface using a STEM-EDX. The chemical state of the element on the glass surface was analyzed by XPS. AFM images indicated a significant surface morphological change between before and after etching. In the 1-day-etched glass, nano-sized precipitates were observed. After 8 days, the micrometer-order precipitates were also observed. XPS wide spectra indicated that the peak intensities of the Fe-2p, Ca-2p, Mg-2p, and Ce-3d relatively increased. The Ce-3d peak structure suggests that the Ce ion took the tetraivalent state. STEM-EDX images revealed a thin film of approximately 25 nm thickness containing Fe, Ca, and Ce on the sample surface. This result is consistent with the XPS results. Furthermore, STEM and TEM images revealed nanosized cavities under the thin film of additives. NaOH reacts with SiO₂ to form soluble Na₂O(SiO₂)_x. On the other hand, cerium hydroxide, calcium hydroxide, magnesium hydroxide, and iron hydroxide are deposited on the surface due to their low solubility products of 2.0 × 10⁻⁴⁸ (Ce(OH)₄), 5.02 × 10⁻⁶ (Ca(OH)₂), 5.61 × 10⁻¹² (Mg(OH)₂), 2.79 × 10⁻³⁹ (Fe(OH)₃), respectively. As the leaching reaction proceeded, an insoluble hydroxide film formed and grew on the glass surface. Then, the leaching reaction proceeded through this thin film. As a result of this reaction process, the cavities were considered to be formed under this thin film. Because alkali earth metals and cerium exhibit strong interactions with phosphoric acid, a glass surface enriched with these elements is expected to be a strong candidate for antimicrobial and phosphoric acid recovery materials.

8:00 PM SF03.06.22

Thermoelectric Properties of P-Doped and B-Doped Polycrystalline Silicon Thin Films Keisuke Shibata¹, Shinya Kato², Masashi Kurosawa¹, Kazuhiro Gotoh^{1,3,4}, Satoru Miyamoto¹, Takashi Itoh¹, Noritaka Usami^{1,5} and Yasuyoshi Kurokawa¹; ¹Nagoya University, Japan; ²Nagoya Institute of Technology, Japan; ³Niigata University, Japan; ⁴Interdisciplinary Research Center for Carbon-Neutral Technologies, Niigata University, Japan; ⁵Institutes of Innovation for Future Society, Nagoya University, Japan

Thermoelectric power generation (TEG) is one of the ambient energy sources and a clean power generation method that directly converts heat, an unutilized energy source, into electrical energy. TEG modules are safe, maintenance-free, and can be expected to be used over the long term because they can be operated with a simple structure that has no driving parts. Silicon (Si) is the 2nd most abundant materials in the Earth's crust and is relatively cheap and non-toxic. However, its high thermal conductivity κ is a bottleneck for usage as a TE material. Many silicon-based next-generation TE materials have been investigated to reduce κ and improve the Seebeck coefficient S . In TE materials, a structure called PGEC that behaves like a glass for the phonons responsible for thermal conduction and like a crystal for the carriers responsible for electrical conduction is considered suitable. One of the strategies to decrease high κ by phonon-scattering and maintain high electrical conductivity σ is nanostructure by developing polycrystalline Si (poly-Si) from amorphous Si (a-Si). This study focused on the annealing process of P-doped and B-doped a-Si thin films prepared by plasma-enhanced chemical vapor deposition (PECVD). In PECVD, it is easy to control a doping concentration at the high doping level, since PECVD is a non-equilibrium process. Moreover, the effective κ of thin films can be decreased by reducing the thickness due to the influence of interfacial thermal resistance and surface phonon scattering. After post-annealing, TE properties of P-doped or B-doped poly-Si thin films were measured from room temperature to 873 K. P-doped or B-doped hydrogenated a-Si (a-Si:H) thin films were prepared on a quartz substrate by PECVD. After deposition, the samples were annealed at 1173 K for 30 minutes under a forming gas atmosphere (N₂: 97%, H₂: 3%). The σ , the S , and thermal diffusivity were evaluated under an Ar atmosphere using a TE property measurement system. The κ was estimated from the data of thermal diffusivity, density, and mass heat capacity of a-Si. From spectroscopic ellipsometry, the thicknesses of P-doped and B-doped poly-Si thin films were estimated to be 480 and 440 nm, respectively. In Raman scattering spectra, the peaks derived from the crystalline silicon phase did not appear in both samples. A sharp peak due to the crystalline silicon phase was observed at 514 cm⁻¹ for both samples. Crystal volume fractions of P-doped and B-doped thin films were estimated to be 0.32 and 0.51, respectively. The S for both types tended to increase with increasing temperature up to -231 μV/K and 301 μV/K. The σ tended to decrease for P-doped and increase for B-doped with increasing temperature. On the other hand, the κ was not changed with temperature and was lower by about two orders of magnitude compared with that of bulk Si. In the case of P-doped poly-Si, the dimensionless figure of merit ZT exceeded unity around 573 K, and $ZT = 1.92$ was obtained around 873 K. This ZT value is relatively high compared with Si-based TE materials previously reported. This may be due to the high σ of 629 S/cm with a doping concentration of ~10²¹ cm⁻³ and the low κ of 1.51 W·m⁻¹·K⁻¹ at 873 K. The increase in crystallinity enhances dopant activation, leading to the increase in carrier concentration, and also enhances carrier mobility. That is why high σ was obtained. Moreover, the low κ was obtained, which is as low as that of quartz. This may be due to the thermal interfacial resistance (R_{int}). When the thickness of the poly-Si thin film and the intrinsic κ of bulk Si at 873 K were assumed to be 480 nm and 38 W·m⁻¹·K⁻¹, the R_{int} was estimated to be 3.05 × 10⁻⁷ m²·K·W⁻¹, which is in the range of previously reported R_{int} at a Si/SiO₂ interface, suggesting that the low κ is due to R_{int} . In the presentation, we will also provide the dependence of TE properties on crystal volume fraction and doping concentration.

8:00 PM SF03.06.23

Pulsed Laser Deposition of RuO₂ Thin Films for Cryogenic Temperature Measurements Denis Aglagul and Jian Shi; Rensselaer Polytechnic Institute, United States

Ruthenium oxide (RuO₂) has a well-resolved temperature-resistivity response making it a compelling choice for cryogenic temperature measurement. In this work, we report the use of pulsed laser deposition to grow RuO₂ thin film on various substrates such as GaAs and Au. We characterize the crystallinity of as-grown and post-annealed films by x-ray diffraction. We evaluate its temperature sensitivity, as a function of deposition conditions such as pulse energy, growth temperature, oxygen partial pressure, and substrates, with electrical transport measurements from liquid helium temperature to room temperature. By growing RuO₂ film on our thermal-active samples, we evaluate the thermodynamic performance of the thermal-active devices.

8:00 PM SF03.06.24

Implementing a-IGZO Thin-Film Transistors on Thin Ceramic Substrates to Reduce Self-Heating Effects Megan Noga, Christine McGinn, Sourabh Pal, Vikrant Kumar, Reem Alshabari, Rajinder S. Deol, Oliver A. Durnan and Ioannis Kymissis; Columbia University, United States

In recent years, amorphous indium gallium zinc oxide (a-IGZO) thin film transistors (TFTs) have proliferated in both small-scale research and industry products due to the metal oxide's beneficial properties. IGZO's optical transparency, high and tunable mobility, and relatively low cost has made it an appealing candidate for use in applications ranging from gas sensors to electronic backplane arrays. However, the stability of a-IGZO TFTs is limited by the degree to which such devices' electrical performance varies with changes in factors like operation temperature. For this reason, the reliability of a-IGZO TFTs can be improved by reducing the amount of self-heating that the transistors experience due to Joule heating and other effects. Previous investigations have focused on mitigating the self-heating effect by altering the structure or driving conditions of the TFT itself. While TFT modifications, such as restricting the bias voltage and frequency or tuning the channel width, can reduce self-heating, methods of reducing device temperature that are independent of or work in conjunction with TFT structure and operation adjustments could be beneficial. For example, building TFTs on a substrate that significantly reduces self-heating would allow device optimization efforts to concentrate on other improvements, such as increasing mobility.

Recent work has shown that thin, thermally-conductive substrates can be used as passive heat-sinks for microLEDs. MicroLEDs built on 80 um-thin Corning Alumina Ribbon Ceramic demonstrated less self-heating and less external quantum efficiency (EQE) reduction compared to microLEDs built on standard glass substrates during both I-V speed curve and drive time tests. Additionally, the microLEDs built on the ceramic substrate outperformed those built on glass during destruction testing, exhibiting superior optical power outputs at higher driving currents [3]. While the mechanisms contributing to the self-heating of microLEDs are not identical to those affecting TFTs, heat-sinking a significant portion of the thermal energy generated by the Joule heating effect prior to the deterioration of electrical characteristics would improve TFT stability regardless of device structure or biasing conditions.

In this work, we explore ongoing efforts to reduce self-heating in a-IGZO TFTs by implementing them on thin ceramic substrates. The extent to which the devices are experiencing self-heating under standard and stressed biasing conditions is quantified by analyzing the current droop visible on the TFT I-V curves, corroborated using infrared thermal imaging techniques, and compared to the performance of identically-structured a-IGZO TFTs built on thicker glass substrates. Additionally, the degree to which the thickness of the ceramic substrate affects TFT stability is analyzed, and reliability improvements across different TFT structures, compositions, and operation environments are normalized to assess the extent to which ceramic heat-sinking could benefit a variety of metal oxide TFT applications.

8:00 PM SF03.06.25

Ultrathin Nanofibrillar Cu Sheet Covered with Directly Grown Lithiophobic CNT for Anode-Free Li-Metal Battery Anode Current Collectors Inyeong Yang, Dongyeon Won, Sukkyung Kang and Sanha Kim; Korea Advanced Institute of Science and Technology (KAIST), Korea (the Republic of)

Li-metal batteries (LMBs) are in the spotlight because of their low electrochemical potential and high energy density (3860 mAh/g) of Li-metal. However, low electrochemical reversibility and side reaction including SEI formation still remain as challenges. LMBs with excessive Li in the anode, thus having high N/P ratios, has been proposed to compensate the low reversibility and fast capacity loss, yet their energy density becomes even lower than that of Li-ion batteries when the N/P ratio is higher than 3. Therefore, to maximize the advantages of Li-metal while minimizing safety problems caused by Li, anode-free Li-metal batteries (AFLMBs) with N/P ratio = 0 is ideal.

In AFLMBs, unlike the conventional LMBs, the anode current collectors (CCs) are not completely covered by Li. In addition, only limited amount of Li is cycled. As a result, fast capacity loss and side reactions including galvanic corrosion at the anode arise as new challenges. In this research, we study the effect of three-dimensional surface structures in copper anode CCs in AFLMB, and suggest novel fabrication strategy to enhance the electrochemical reversibility of Li and minimizing side reactions. The nanofibrillar Cu network in a form of thin sheet is fabricated through a rearrangement process of Cu on the woven Cu wiremesh via electrochemical etching and electrodeposition. The electrodeposited nanofibers exhibit approximately 400 nm in diameter. We can control the nanofibrillar sheet thickness to be 15 μm in minimum, which equivalent to 8 μm thick Cu foils in mass per unit area, yet the surface area is yet significantly greater. In addition, an optimized thermal reduction treatment method is suggested to interconnect the Cu nanofibers, effectively increasing the electrical conductivity in nano-scale. We quantitatively evaluate the capacity loss, the charge transfer resistance, and the side reaction including galvanic corrosion according to the sheet thickness and surface treatment. By introduction of a rationally-designed ultrathin nanofibrillar sheet as the Cu CC, we experimentally confirm reductions in overpotential and in side reaction in AFLMB by 0.3 V, and 90%, respectively. Accordingly, the discharge capacity at the first cycle can be enhanced by 36%. Finally, we decorate the top of the three-dimensional anode CC with carbon nanotubes (CNTs), as a lithiophobic nanoporous layer. Multi-walled CNTs with diameter of ~10-20 nm are directly grown on the surface of Cu nanofibrillar sheet via thermal chemical vapor deposition. The top CNT layer can further enforce the growth of Li inside the nanofibrillar Cu CCs, and thereby maximizes the reversible Li cycling in AFLMBs.

8:00 PM SF03.06.26

Memory Effect of Surfaces: From Wetting to Electrification William S. Wong^{1,2}; ¹Aalto University, Finland; ²Max Planck Institute for Polymer Research, Germany

The “*Memory Effect*” is often a phenomenon attributed to bulk materials, such as shape memory alloys or polymers. The resulting behaviors are often macroscopic and highly mechanical. When considering surfaces and interfaces, responses are often much more subtle in nature. Nonetheless, re-orientation of surface moieties such as oligomers, molecular groups, ions, and electrons can lead to macroscopically-detectable responses. In this work, we use water drops as the stimuli and the ambient environment (r.t.p.) for recovering the equilibrium condition.

In the first instance, we used a polydimethylsiloxane surface with minute amounts of uncrosslinked oligomers. Upon drop-wetting, the surface experiences increased lubricity due to the water-induced surface saturation of oligomeric moieties which decreases the contact angle hysteresis (and thus adhesion). The surface recovers its pristine behavior upon environmental equilibration. We model this contact memory behavior behind the use of first-order adaptation dynamics and demonstrate how they deviate from both traditional molecular kinetic and hydrodynamic theories (which do not account for adaptation).

In the second instance, we synthesized a multi-layered/composited surface. Firstly, a base hydrophobic layer (perfluoroalkylated or alkylated) is fabricated. Upon drop-wetting, it acquires a positive charge while the surface is negatively counter-charged. To dynamically flip the charge polarity (*i.e.* polarity reversal), the hydrophobic layer is then coated with a long-chained (C₁₀) multi-amine. The presence of the amine results in a redox response (ion transfer with -NH₂ as an H⁺ acceptor) during drop-wetting. The long alkyl chain hinders molecular mobility, enabling a gradual real-time observable polarity reversal (within a few seconds). Therefore, depending on the drop-contact interval, the magnitude, and polarity of charge responses are now tunable, highlighting contact-memory behaviors. The surface recovers its pristine behavior upon environmental equilibration.

References

Langmuir **2020**, *36*, 26, 7236–7245
Langmuir **2022**, *38*, 19, 6224–6230

8:00 PM SF03.06.27

Layered Double Hydroxide/Boron Nitride Nanocomposite Membranes for Efficient Separation and Photodegradation of Water-Soluble Dyes Áine Coogan¹, Natalia Garcia Domenech^{1,2}, Donagh McGinley¹, Tigran Simonian^{1,1,1}, Aran Rafferty¹, Quentin Fedix³, Amy Donlon¹, Valeria Nicolosi^{1,1,1} and Yurii K. Gun'ko^{1,1,2}; ¹Trinity College Dublin, The University of Dublin, Ireland; ²University College Dublin, Ireland; ³Institut Universitaire de Technologie Clermont-Auvergne, France

Increasing scarcity in access to clean, safe water is being fuelled by escalating industrialisation, rapid urbanisation and biodiversity loss, and the relentless forces of climate change. Therefore, the need for development of innovative and sustainable methods of water purification is of the utmost urgency. Nanofiltration is proving to be an increasingly attractive potential solution to this global issue.^{1,2}

Previous reports of nanofiltration membranes using boron nitride (BN) and partially oxidised BN (BNOx) have demonstrated outstanding performance, achieving retentions of up to 100% for various water-soluble dyes which can be harmful to humans and aquatic life.^{3,4} However, the main drawback of these membranes is their vulnerability to membrane fouling, meaning they must be disposed of after a single use. Consequently, innovative approaches to mitigate membrane fouling are crucial to ensure the long-term sustainability of current and future nanofiltration technologies. Herein, we report the development of novel high-performance nanofiltration membranes based on a recyclable CuAl-CO₃ LDH/BNOx nanocomposite. These membranes have demonstrated up to 100% retention of several water-soluble dyes (Evans blue, methyl orange, methylene blue and rhodamine B). Additionally, they exhibit excellent water flux, over 2 orders of magnitude higher than commercially available nanofiltration membranes. The incorporation of CuAl-CO₃ LDH photocatalyst within the nanocomposite membranes enables up to 91% visible-light-induced photodegradation of these dyes within 120 minutes using a household LED lamp.

This introduction of photocatalytic functionality into existing nanofiltration membranes offers a low-cost, innovative route to the mitigation of membrane fouling. Significantly, this work demonstrates the first instance of Evans blue degradation by a visible-light active LDH photocatalyst. Overall, we believe this work represents a significant advancement in the field of advanced nanofiltration technology, offering superior performance and enhanced sustainability.⁵

References:

- 1 - M. A. Montgomery and M. Elimelech, Water and sanitation in developing countries: Including health in the equation - Millions suffer from preventable illnesses and die every year, *Environ. Sci. Technol.*, 2007, **41**, 17–24.
- 2 - H. Guo, X. Li, W. Yang, Z. Yao, Y. Mei, L. E. Peng, Z. Yang, S. Shao and C. Y. Tang, Nanofiltration for drinking water treatment: a review, *Front. Chem. Sci. Eng.* 2021 **165**, 2021, **16**, 681–698.
- 3 - N. García Doménech, F. Purcell-Milton, A. S. Arjona, M.-L. C. García, M. Ward, M. B. Cabré, A. Rafferty, K. McKelvey, P. Dunne and Y. K. Gun'ko, High-Performance Boron Nitride-Based Membranes for Water Purification, *Nanomater.* 2022, Vol. 12, Page 473, 2022, **12**, 473.
- 4 - N. García Doménech, Á. Coogan, F. Purcell-Milton, M. L. Casasín García, A. Sanz Arjona, M. Brunet Cabré, A. Rafferty, K. McKelvey, P. W. Dunne and Y. K. Gun'ko, Partially oxidised boron nitride as a 2D nanomaterial for nanofiltration applications, *Nanoscale Adv.*, 2022, **4**, 4895–4904.
- 5 - Á. Coogan, N. García Doménech, D. Mc Ginley, T. Simonian, A. Rafferty, Q. Fedix, A. Donlon, V. Nicolosi and Y. K. Gun'ko, Layered double hydroxide/boron nitride nanocomposite membranes for efficient separation and photodegradation of water-soluble dyes, *J. Mater. Chem. A*, 2023, Advance Article, DOI:10.1039/D3TA01581E.

8:00 PM SF03.06.28

Potential Applications of Electrically Conductive Concrete Douglas X. Shattuck^{1,2}, Zoie Zeng³, Zacharias Daniel⁴ and Arsh Khan⁵; ¹St Joseph School Wakefield, United States; ²National STEM Honor Society, United States; ³Andover High School, United States; ⁴Boston University Academy, United States; ⁵Wilton High School, United States

Research Summary

Following in the footsteps of many^{1,2,3}, our objective was to investigate whether electrically conductive concrete could be used to de-ice roads⁴, regulate surface temperature, or convert heat to energy in hot environments. Several 5cm³ (2in³) samples with embedded electrodes were fabricated. Concrete formulas containing conductive materials such as carbon fibers, iron powder, and steel wool were prepared^{5,6,7}. Preliminary results indicate this technology has the potential to reduce the use of environmentally harmful chemicals, provide control surface temperature and produce energy in hot climates.

Electrically Conductive Concrete

Using a 12v DC power source and multimeter, current was measured between electrodes. Compressive strength was tested using a Rebound Hammer. Two concrete batches were prepared with 5% or 15% conductive material by volume. 5% Iron Powder and 15% Steel Wool were the most electrically efficient. The 15% Iron Powder samples lost compressive strength, shattered and were eliminated. The current was applied to all of the samples for two hours. Temperature was read using a commercially available infrared thermometer. The Iron Powder and Steel Wool samples averaged a 7° increase in temperature above room temperature.

Regulating Temperatures

Phase-changing materials (PCM) absorb or release energy^{8,9}. To investigate the rate of temperature change in concrete we cut paraffin wax, the PCM, into 1cm³ cubes and added them to the concrete mixtures. We constructed a test chamber with electric heaters to heat our samples to approximately 180°. The initial temperature of the cured samples was ~73°. After 10 minutes the temperature of control samples rose 58° to 131°. The PCM concrete's temperature rose only 34° to 107°. From 10 to 30 minutes, the temperature of both samples rose at the same rate. After 40 minutes, the rate of change slowed and at 50 minutes all samples reached a constant temperature, around 185°. The temperature increase was delayed during the initial heating, presumably during the time the paraffin was absorbing the heat energy.

Thermal Energy

Seebeck, Peltier, and others developed thermoelectric generators to convert heat to electricity.^{10,11,12} To use the Seebeck Effect, we used 5% steel wool concrete, electric heaters, SternoTM, Peltier tiles, and a 40° ice-water bath. We heated 5cm³ blocks indoors using electric heaters to 160° and outdoors using SternoTM to 240°. After 80 minutes the heated concrete samples were placed on a Peltier tile attached to a multimeter, placed in a 5 mil aluminum cup and lowered into the bath. With the temperature difference of 120° between the indoor sample (160°) and the water, 1 volt was generated with a decay rate of -0.001 volts per 30 seconds. For the outdoor sample (240°) 1.3 volts were generated with the same decay rate.

Conclusion

In an era of concern for climate change and global warming we believe the formulation of concrete can be modified using inexpensive materials to reduce the use of harmful chemicals, change the rate at which pavement temperatures change, and collect solar radiation to generate electricity. The authors would like to thank Malden Catholic High School for their support on this project.

References

- 1 Gagg, Colin R. doi:10.1016/j.engfailanal.2014.02.004,
- 2 climate.mit.edu/explainers/concrete Accessed 7-10-2023
- 3 M. Steinberg et al., BLN 50134 (T-509), 1968
- 4 Dina, A et al https://csce.ca/Paper_MA9_0610035034.pdf
- 5 Lai, Yet al atlantis-press.com/proceedings/ame-16/25857988
- 6 Logan, A. (2021, April 20). news.mit.edu
- 7 Wang, D. et al Science Direct.abs/pii/B9780128189610000259
- 8 Chandler, D. L. (2017, November 16). news.mit.edu
- 9 Phase-change material. en.wikipedia.org/wiki/Phase-change material.
- 10 Thermophile. en.wikipedia.org/wiki/Thermophile
- 11 Chu, J. (2018, Jan 16). news.mit.edu
- 12 Thermoelectric generator. en.wikipedia.org/wiki/Thermoelectric generator

8:00 PM SF03.06.29

A Post-Synthetic Modification Strategy for Enhancing Pt Adsorption in MOF/Polymer Composites Till Schertenleib¹, Vikram V. Karve¹, Dragos Stoian², Mehrdad Asgari^{3,1}, Olga Trukhina¹ and Wendy L. Queen¹; ¹Ecole Polytechnique Fédérale de Lausanne, Switzerland; ²European Synchrotron Radiation Facility, France; ³University of Cambridge, United Kingdom

Growing polymers inside of porous supports, like metal-organic frameworks (MOFs), allows incoming guests to access the backbone of otherwise non-porous polymers, possibly boosting the number and/or strength of available adsorption sites inside the porous material. Given this, we have focused attention on the design of MOF-polymer composites for the recovery of targeted metals from liquid streams and shown that the separation performance of such composites is significantly higher than the sum of the individual MOF or polymer counterparts. Now, in an effort to further boost performance, we have devised a novel post-synthetic modification (PSM) strategy that allows one to graft metal-chelating functionality onto the polymer backbone, while inside MOF pores. For the proof of concept, polydopamine (PDA) was first grown inside of a MOF, Fe-BTC. Next, a small molecule, 2,3-dimercapto-1-propanol (DIP), was grafted to the PDA via a Michael addition. Notably, the DIP contains thiols that can chelate targeted soft metals, like platinum (Pt). After the PSM of the PDA, the Pt adsorption capacity of the composite is shown to reach a record value of 684 mg/g. More importantly, the Pt uptake is greatly enhanced at low Pt concentrations, owed to the high affinity of Pt towards the thiols. Techniques, including XPS and in-situ XAS, provide insight into the Pt adsorption/reduction process, which is clearly enhanced after the PDA modification with thiols. Last, it is shown that various thiols, beyond DIP, can be grafted to the Fe-BTC/PDA, demonstrating the versatility of the chemistry. It is hoped that this work will open up a pathway for the future design of other novel composites that are fine-tuned for the rapid, selective retrieval of high-value and/or critical metals from complex liquids.

8:00 AM SF03.07.01

Structure-Property Relationship of MOF Materials: Theoretical Aspects Rodion Belosludov; Tohoku University, Japan

It has been established that the porous materials can be defined by type or by function, which determined from practical applications [1]. Thus, the realization of high efficient porous media for various applications such as gas adsorption and separation, drug delivery, molecular sensing, batteries and catalysis can be based on the understanding of the chemical and physical changes of the targeted species after their adsorption as well as the design and synthesis of nanoporous compounds that can recognize these changes. The computational structure-property predictions play a significant role in modern design of porous solids because often experiments require theoretical interpretation and computing power has grown rapidly in the last decade. In collaboration with experimentalists, the concept using a designable regular MOF material could be applicable to a highly stable, selective adsorption system [2]. The CO₂ adsorption mechanism into Mn₃(H₂Pdc)₂(pdc)₂ and Mg₃(H₂Pdc)₂(pdc)₂ has been studied. It has been found that guest-guest interaction plays an important role in formation a stable CO₂ chain configuration inside framework channel. A very pronounced step observed in experimental adsorption isotherm has been explained by delaying of the chain formation that associated with low permeability of guests inside the Mn₃(H₂Pdc)₂(pdc)₂ pore [3].

Recently, the possibility of the formation of polymeric structures by visible light inside the metal-organic framework host (MFM-300(In)) has been studied using first-principles calculations. The adsorption of P₄ by the host has been modelled by filling this fragment stepwise with the phosphorus. At each step the system was fully optimized and its total energy was calculated. The geometry of P₄ molecules were found to be in agreement with the experimental structural data. It was confirmed that the optimal number of monomers and their configurations due to guest-host and guest-guest interactions are suitable to form polymer chain. The partial density of states have been calculated for the guest-free as well as with P₄ monomers and P_n-chains. The theoretical predictions are in agreement with the results of UV-Vis spectroscopy, supporting again the correctness of structure determination for the phosphorus adducts. The inclusion of these chains results in the formation of host-guest system with a narrow band gap, which can be used as a gas sensor and photocatalyst for the water purification.

References

- 1) A. G. Slater, A. I. Cooper, *Science*, **2015**, *348*, aaa8075.
- 2) H. Sato, *et al. Science*, **2014**, *343*, 167 – 170.
- 3) S. A. Sapchenko, *et al. J. Chem. Phys.*, **2019**, *58*, 6811-6820.

8:15 AM SF03.07.02

Benchmark Room-Temperature Synthesis of High Performance Thermoelectrics Kirill Kovnir; Iowa State University, United States

Se-containing materials often synthesized by solution-assisted from toxic and expensive organo-Se precursors. We are reporting a facile alternative utilizing elemental Se which is cheap and non-toxic. Elemental Se reagent has a drawback of low solubility and reactivity resulting in sluggish kinetics at low temperatures. A process of elemental Se activation was developed resulting in stable solution of multiple Se species confirmed with ⁷⁷Se NMR studies, including R-Se-Se-R and never detected before “naked” Se₂²⁻. Dynamic equilibrium between the produced Se species allow to perform reactions at wide temperature ranges including room temperature. The developed activated Se precursor allows us to produce Ag₂Se-based materials at room temperature thus avoiding the high-temperature polymorphic phase transitions during the synthesis. The produced materials exhibit flat, almost temperature-independent zT in the 300-400 K range with average zT's exceeding 1.

8:30 AM *SF03.07.03

Preparation and Operando Imaging of Pt-Bimetallic Oxygen Reduction Catalysts for Polymer Electrolyte Fuel Cell Mizuki Tada; Nagoya University, Japan

Polymer electrolyte fuel cell (PEFC) is key for clean energy production using hydrogen for carbon-neutral society. Electrocatalysts with Pt have been used as efficient catalysts for both electrodes in membrane electrode assembly (MEA), which has a stacking structure of anode catalyst layer, electrolyte membrane, and cathode catalyst layer. Under practical PEFC operating conditions with lots of water and fuels, various events proceed in MEA such as catalysis at both electrodes, surface redox reactions of Pt electrocatalysts, dissolution, migration, and aggregation of Pt electrocatalysts, water flooding, deactivation of electrocatalysts by air contaminants, formation of unfavorable radical species, and migration of radical scavenger. The optimization of reaction controls on electrocatalysts are essential for efficient PEFC performances. Compared to anode conditions, cathode reactions with oxygen often bring about degradation of cathode electrocatalysts and the developments of cathode catalysts with durable performances under PEFC operation conditions are still challenging.

In this paper, I present the preparation and electrochemical performances of Pt-bimetallic electrocatalysts for PEFC and operando imaging of electrocatalysts under PEFC working conditions. The use of hard X-rays enables to visualize these events inside MEA under PEFC operating conditions, and the recent examples of 3D imaging of PEFC MEA by operando XAFS-CT spectroimaging will be presented.

9:00 AM SF03.07.04

Rapid Joule Heating Synthesis of Oxide-Socketed High-Entropy Alloy Nanoparticles as CO₂ Conversion Catalysts Jaewan Ahn, Seyeon Park and Il-Doo Kim; Korea Advanced Institute of Science and Technology, Korea (the Republic of)

Historically, strategies for lowering CO₂ emissions have centered on using alternative sources of energy and carbon-neutral fuels as a means of prevention. However, modern thinking has evolved to also include techniques that actively decrease and repurpose CO₂ from exhaust gases as a way to counteract carbon emissions.¹ In this context, the unconventional surface chemistry of high-entropy alloy nanoparticles (HEA-NPs), featuring many inter-elemental synergies, plays a critical role in facilitating key chemical processes such as transforming CO₂ into CO – a sustainable approach to mitigating environmental pollution.² To produce HEA-NPs in a systematic way, carbothermal shock synthesis has been recently proposed as a simple yet efficient synthetic method.³ Nonetheless, the potential for particle aggregation and phase segregation in HEA-NPs during high-temperature operating conditions for CO₂ conversion presents ongoing challenges that hinder their practical application.

In this work, we present HEA-NP catalysts that are tightly sunk in an oxide overlayer for promoting the catalytic conversion of CO₂ with exceptional stability and performance.⁴ We first demonstrated the controlled formation of conformal oxide overlayers on carbon nanofiber surfaces via a simple sol-gel method, which facilitated a large uptake of metal precursor ions and helped to decrease the reaction temperature required for nanoparticle formation. During the rapid thermal shock synthesis process, the oxide overlayer would also impede nanoparticle growth, resulting in uniformly distributed small HEA-NPs (2.37 ± 0.78 nm). Because the reducible oxide layer promotes the hydrogen spillover reaction and also strongly anchors the high-entropy alloy nanoparticles, these HEA-NPs demonstrated an ultra-stable catalytic performance involving >50% CO₂ conversion with >97% selectivity to CO for >300 h without extensive agglomeration.

Through this work, we establish the rational design principles for the thermal shock synthesis of high-entropy alloy nanoparticles and offer a helpful mechanistic perspective on how the oxide overlayer impacts the nanoparticle synthesis behavior, providing a general platform for the designed synthesis of ultra-stable and high-performance catalysts that could be utilized for various industrially and environmentally relevant chemical processes.

References

- 1) M. E. Boot-Handford *et al. Energy Environ. Sci.* **7**, 130-189 (2014).
- 2) K. Mori *et al. Nat. Commun.* **12**, 3884 (2021).
- 3) Y. Yao *et al. Science* **359**, 1489-1494 (2018).
- 4) J. Ahn and S. Park *et al. ACS Nano*, *accepted* (2023).

9:15 AM SF03.07.05

Wet-Chemical Synthesis and Catalytic Properties of Metal Nanomaterials with Unconventional Crystal Phases Ye Chen; The Chinese University of Hong Kong, Hong Kong

Metal nanomaterials own excellent intrinsic catalytic activities, high conductivity and high stability. While traditional solution-based syntheses mostly focused on morphologies and compositions of the nanocrystals, we made some interesting discoveries on crystal phase controlled synthesis. Instead of getting the normal phase of face centered cubic (fcc) structure, we obtain noble metal nanomaterials in unusual crystal phases with high yield and productivity. These unconventional metastable phases are excellent substrates on which other catalytically active metals like Pd, Cu and Pt can be grown epitaxially. Further study on new metastable phases of these metals can lead to novel physical or chemical properties, such as an enhanced catalytic performances. It provides an alternative strategy of engineering crystal phases of metal nanomaterials via wet-chemical method and exploring their templating effects on various properties. In this presentation, our recent work on the wet-chemical synthesis of metal nanostructures with unconventional phases and their electrocatalytic properties are introduced. First, epitaxial growth of one-dimensional core-shell metal nanostructures with unconventional crystal phases, including 4H/fcc heterophase Au@Pd nanorods, Au@Cu nanomaterials with 4H and 4H/fcc phases, and Pd@Pt nanocrystals with 2H phase, is demonstrated. Then, phase dependence study of metal nanomaterials with novel crystal phases in different catalytic reactions is discussed.

9:30 AM SF03.07.06

Nanoporous Lanthanum Oxycarbonate Powders for Enhanced CO₂ Detection - From Nanopowders Elaboration to Microsensor Development[Sandrine Bernardini](#), Paul Rivas, Carine Chassigneux and Marie-Vanessa Coulet; CNRS-AMU, France

Indoor air quality is a major public health concern. The World Health Organization estimates the number of deaths caused by air pollution at around 4 million per year. In addition, the recent health crisis has highlighted the need for regular air renewal to reduce the spread of viruses. The measurement of carbon dioxide (CO₂) levels in indoor spaces is therefore an interesting indicator of how often the air needs to be renewed.

Among CO₂ sensors, chemoresistors have many advantages such as their good sensitivity and stability [1]. In this type of sensors, the detection phenomenon is based on the change in the electrical resistance as a function of the gas adsorption rate. In the quest to reduce cost and power consumption of these sensors, there is a need in reducing the size of these devices without losing in efficiency. To achieve this objective, new materials are being proposed including the development of inorganic nanoporous powders: since the detection is based on an adsorption phenomenon, increasing the surface area accessible to the gas should allow to improve the detection.

In this presentation, we will focus on lanthanum oxycarbonate (La₂O₂CO₃) for CO₂ detection. This compound has been recently proposed as sensitive layer for resistive microsensors [2]. Here, we propose a new elaboration method based on high-energy ball-milling [3]. We will present this method along with a detailed characterization of the obtained nanopowders in terms of morphology, porosity, structure and reactivity. It will be shown that mesoporous La₂O₂CO₃ nanopowders with tunable pore sizes and crystallographic structures can be synthesized.

The second part will be devoted to microsensor fabrication and performances. Optimisation of the nanopowder deposition method on microsensor interdigitated electrodes will be detailed. The performances of the microsensors in the presence of different concentrations of carbon dioxide (from 400 ppm to 5 000 ppm diluted) will be presented. The influence of the La₂O₂CO₃ porosity and crystallographic structure on microsensor performances will be discussed.

[1] K. Aguir, S. Bernardini, B. Lawson, T. Fiorido, Trends in metal oxide thin films: Synthesis and applications of tin oxide, in: Tin Oxide Materials, Elsevier, 2020: pp. 219–246. .

[2] F. Le Pennec, L. Le Roy, C. Perrin-Pellegrino, M. Bendahan, S. Bernardini, IEEE Sensors, Sydney, Australia, 2021: pp. 1–4.

[3] P.-H. Esposito, C. Leroux, V. Heresanu, T. Neisius, V. Madigou, R. Denoyel, M.-V. Coulet, Materialia. 14 (2020) 100880.

This work received support from the French government under the France 2030 investment plan, as part of the Initiative d'Excellence d'Aix-Marseille Université - A*MIDEX." (AMX-20-IET-015)

9:45 AMBREAK

10:15 AM *SF03.07.07

The Assembly of Polyoxometalate-Based Coordination Networks as a Route to Diverse and Modular Metal Oxide Materials[Alina Schimpf](#); University of California, San Diego, United States

The assembly of molecular building blocks offers a promising strategy in the development of metal oxide materials with tailored and emergent properties. We have developed a method for the assembly of the Preyssler polyoxoanion ([NaP₅W₃₀O₁₁₀]¹⁴⁻) bridged with transition metal or lanthanide cations and demonstrated tunability of the architecture, connectivity, and void-volume via inclusion of additional cations. Inclusion of polymer during framework synthesis enables easy processing into gel and film form-factors. Additionally, the frameworks can be reversibly photochemically reduced to contain electron densities on the order of 10²¹ cm⁻³, revealing their potential for electron-manipulation and charge-storage applications. This talk will discuss advancements in the synthesis of polyoxoanion-based extended solids as well as their structure–composition–property relationships.

10:45 AM *SF03.07.08

Ion Diffusion in Porous Crystalline Materials[Dae-Woon Lim](#); Yonsei University, Korea (the Republic of)

Solid-state proton conductors (SSPCs), which are a key component for the safety and efficiency of fuel cells, have received attention due to their broad application in electrochemical devices. In particular, porous metal-organic frameworks (MOFs) have been extensively studied as a new type of proton conductor due to their designability. During the past decade, proton-conductive MOFs have achieved high performance (>10⁻² S cm⁻¹), comparable to the conventional material, through various synthetic strategies. The veiled conduction mechanism has been elucidated through structural analysis and spectroscopy tools such as NMR, X-ray diffraction, and neutron scattering measurement.^[1] Herein, we demonstrate a new strategy for high proton conductivity in MOF.^[2,3] Specifically, we used MOF-74 for coordinative urea insertion through post-synthetic modification and assessed the priority factor on proton conduction between the void space and pore-surface modification. Furthermore, molecular dynamics study and DFT calculation provide a comprehensive understanding of the proton conduction pathway and mechanism.

Reference

[1] Lim, D.-W.; Kitagawa, H. *Chem. Rev.*, **2020**, 120, 8416–8467.

[2] Sarango-Ramirez, M. K.; Lim, D.-W.; Kolokolov, D. I.; Khudozhnikov, A. E.; Stepanov, A. G.; Kitagawa, H. *J. Am. Chem. Soc.*, **2020**, 142, 6861–6865.

[3] Sarango-Ramirez, M. K.; Park, J.; Kim, J.; Yoshida, Y.; Lim, D.-W.; Kitagawa, H. *Angew. Chem. Int. Ed.*, **2021**, 60, 20173–20177.

11:15 AM SF03.07.09

Metastable Access to Kitaev Quantum Spin Liquid Candidates: A Chemistry Approach[Lucas Pressley](#), Bishnu Prasad Thapaliya, Daren Driscoll, Colin Sarkis, Raymond R. Unocic, Jiaqiang Yan, Michael McGuire and Craig Bridges; Oak Ridge National Laboratory, United States

Since Alexei Kitaev proposed an exactly solvable model for spin ½ systems, there has been an influx of predicted and synthesized materials that would meet such requirements. These Kitaev quantum spin liquid (QSL) candidates are of particular interest for the realization of topological quantum computing due to their ability to host Majorana fermions in their QSL ground state. While many candidates have been investigated, no material has arrived as a clear winner for possessing a Kitaev QSL ground state. Here we will show through the chimie douce approach the design of new metastable honeycomb compounds. We will show through chemical/electrochemical methods the stabilization of Pt⁵⁺ (5d⁵) on a honeycomb lattice. Structural characterization shows a shift in the Na ion stacking like that seen in intercalation of Na-Ir-O systems, with XAS measurements confirming oxidation of Pt compared to the parent compound. Magnetization measurements show a transition from diamagnetic to paramagnetic behavior with no sign of magnetic ordering down to T=2 K. Curie-Weiss analysis gives us close to expected for J_{eff}=1/2. A comparison will be made in the chemical/electrochemical methods and their effect on Na/Li ordering. Future directions will be discussed in utilizing these chemical techniques for the design of QSL candidates as well as crystal growth.

11:30 AM SF03.07.11

Anion Ordering in Metal Chalcogenides: Design Rules for Predictive Synthesis[Ayat Tassanov](#)¹, Huiju Lee², Yi Xia² and James Hodges¹; ¹The Pennsylvania State University, United States; ²Portland State University, United States

Chemical alloying is a powerful tool for modifying the properties of materials used in thermoelectric applications. Here, a statistical distribution of atoms is only achievable if the sites where the mixing occurs are symmetrically and chemically identical. Adding complexity to the structure through the introduction of additional metals (ternary and quaternary compounds) will often result in systems with anion sites that have unique chemical environments and bond lengths. In principle, this can allow chemists to direct anions onto specific locations within the lattice, however, only a few literature reports have exploited this feature. Here, we present a library of new ordered chalcogenides that are synthesized in a predictive fashion using site-selective alloying. This includes a series of mixed-anion copper chalcogenides that have been prepared using solid-state methods including ACu₅Te₂S (A = Rb, Cs), which adopts the CsAg₅Te₃ structure type. ACu₅Se₃ has two unique anion sites and using site-selective substitutions, we are able to synthesize ACu₅Se₂S, ACu₅Te₂Se, and ACu₅Te₂S. To understand what drives ordering in these compounds, we derived a term called “switching energy” which explains ordering in metal chalcogenides using entropy and enthalpy contributions of mixing chalcogen anions on the unique Wyckoff positions within the parent structure. Both experiment and theory suggest that sulfotelluride (S-Te) analogs are generally more ordered than sulfoselenide (S-Se) analogs. DFT calculations suggest that this ordering phenomenon impacts the electronic and thermal transport properties of thermoelectric materials. We believe the synthetic techniques presented here can open the door to an expanded library of metal chalcogenides for energy-related applications.

1:30 PM *SF03.08.01

2D Quantum Coordination Frameworks [Matthew Cliffe](#); University of Nottingham, United Kingdom

Coordination framework materials, where metal ions are connected by molecular ligands into extended networks, are modular: their components can be exchanged while retaining the overall structural topology. This modularity allows for design strategies that are challenging to realise in conventional atomic inorganic materials. In this talk I will discuss recent work from the Cliffe Group realising quantum properties in coordination frameworks, particularly with reference to neutron scattering studies of their properties.

In particular I focus on our work on 2D materials, including non-collinear magnetism in post-perovskite metal thiocyanates, single layer ferromagnetism in Ni(NCS)₂; and new routes to long-sought quantum phases such as topological $S=2$ Haldane phase.

2:00 PM *SF03.08.02

From Porous Organic Cages to Porous Liquids: Translating Porosity from the Solid to Liquid State [Rebecca Greenaway](#); Imperial College London, United Kingdom

The landscape of microporous materials is often dominated by crystalline, ordered materials. However, the development of microporosity in the liquid state is leading to an inherent change in the way applications of functional porosity are approached. Porous liquids combine the mobility of a liquid with the properties of a microporous solid, and fundamentally differ to conventional liquids in that they contain *permanent, empty*, accessible cavities. Four types of porous liquids have now been proposed: type I – neat molecular porous liquids; type II – solutions of molecular porous species in pore-excluded solvents; type III – dispersions of microporous solids in pore-excluded liquids; and type IV – neat melttable microporous extended frameworks. Like their solid counterparts, porous liquids are capable of both gas uptake and selectivity and demonstrate increased gas solubility compared to conventional liquids. However, this combination also means porous liquids offer unique properties and applications when compared to porous solids, such as the ability to be pumped around a continuous system, facilitating guest loading and unloading steps. Our recent work in the area, with a focus on translating porous organic cages – discrete shape-persistent molecules containing permanent molecular cavities accessible through windows – into different types of porous liquids using different strategies will be presented, alongside how we are attempting to streamline their discovery using a high-throughput workflow. The properties of the different porous liquids including gas uptake, guest selectivity, and controlled gas release, will also be discussed, touching on our recent work on incorporating a photoresponse into a porous liquid.

2:30 PM BREAK

3:30 PM *SF03.08.03

Local Distortions and Long-Range Polarity in Pyrochlore Oxides from Total Scattering [Geneva Laurita](#); Bates College, United States

The pyrochlore structure exhibits myriad technologically relevant properties including superconductivity, ferroelectricity, and frustrated magnetism. There has been a wealth of research on the structural and compositional intricacies of these compounds. However, there exist few design principles in regard to the intentional manipulation of the chemistry and structure for desired functionality. Here we will describe drivers of polarity on the pyrochlore structure through a combination of structural, computational, and physical characterization techniques. The main focus will be on the use of total scattering to establish structure-property relationships in these systems.

4:00 PM *SF03.08.04

Chemical Pressure-Based Design Principles Toward Modular Intermetallic Phases [Daniel Fredrickson](#); University of Wisconsin-Madison, United States

Intermetallic phases comprise a broad family of solid state compounds with rich diversity in both their crystal structures and physical properties. To fully harness this combination in the development of new materials, however, guidelines are needed for the synthesis of new compounds with desired structural features. In this presentation, we demonstrate how the DFT-Chemical Pressure (CP) analysis opens avenues toward this goal, with a focus on the creation of complex intermetallic structures that merge fragments of different parent structures in a modular fashion. We begin with σ phase and dodecahedral quasicrystal approximants as the products of Chemical Pressure-driven intergrowths of the simpler Cr₃Si and Al₃Zr₄ structure types, whose joining at shared layers of atoms is promoted by the favorable alignment of complementary CP features. Drawing lessons from these cases, we introduce the CP Interface Fragment Theory of modular solid state structures and illustrate its use in the interpretation and discovery of several new intermetallic structures. Through these case studies, the CP Interface Fragment approach will emerge as a framework for integrating theory, structural database screening, and synthesis toward the goal of materials design in intermetallics.

4:30 PM SF03.08.05

Local Structural Analysis of Transparent Conducting Anatase TiO₂ Films [Tomohito Sudare](#)¹, [Reiichi Ueda](#)¹, [Ryota Shimizu](#)^{1,2}, [Ryo Nakayama](#)¹, [Naomi Yamada](#)³ and [Taro Hitosugi](#)^{1,2}; ¹The University of Tokyo, Japan; ²Tokyo Institute of Technology, Japan; ³Chubu University, Japan

[Introduction] Niobium-doped anatase titanium dioxide (Ti_{1-x}Nb_xO₂: TNO) has gained much attention due to its transparent conducting properties. The resistivity, ρ , of TNO epitaxial thin films exhibit $2.3 \times 10^{-4} \Omega \text{ cm}$ at 300 K and a high internal transmittance of $\sim 97\%$ in the visible region, comparable to Sn-doped In₂O₃ [1]. The conductivity of TNO is due to carrier doping by isostructural substitution of Nb for Ti sites. Interestingly, electron carriers are generated only when the deposition and post-deposition annealing are conducted in a reducing atmosphere [2]. On the other hand, when TNO thin film is annealed in an oxidizing atmosphere, the carrier electrons are killed and hence the film becomes highly resistive [3]. On this base, excess oxygen incorporated into the thin film presumably plays an important role, but experimental evidence of its presence has not been reported yet. Therefore, in this study, we aim to experimentally observe the local structural change of TNO before and after annealing in an oxidizing atmosphere and to reveal the carrier generation mechanism.

[Experimental Section] Radio-frequency magnetron sputtering was used to deposit conductive TNO epitaxial thin films. A Ti_{0.94}Nb_{0.06}O₂ ceramics was used as a target, and a LaAlO₃ (LAO) (100) single-crystal substrate was used. The film was grown at 400°C at O₂/(Ar + O₂) flow rate ratio of 0.3% under a total pressure $P_{\text{tot}} = 1.0$ Pa. Sputtering was conducted for 50 min to obtain a TNO thin film with a thickness of approximately 100 nm. The highly resistive TNO thin film was obtained by annealing the above sample at 400°C for 30 min in air. The crystal structure of both samples was characterized by X-ray diffraction (XRD) and the chemical state and local structure were analyzed by X-ray absorption fine structure (XAFS).

[Results and Discussion] XRD patterns of as-deposited films showed that (001) oriented anatase-type TNO epitaxial thin films were successfully grown on the LAO substrate. The as-prepared films were electrically conductive but turned to be insulative by annealing in air. At the same time, the color of the thin film changed from blue to colorless. Next, the radial distribution function around Nb atoms was obtained through Fourier transformation of the Nb *K*-edge XAFS spectra. As a result, multiple oxygen atoms with different Nb-O bond lengths were confirmed only in TNO after annealing treatment. The generation mechanism of electron carriers will be comprehensively discussed at the conference, along with the results of local structure analysis for Ti and O atoms.

[Reference] [1] Y. Furubayashi et al., Appl. Phys. Lett. 88, 226103 (2006) [2] H. Kamisaka et al., J. Chem. Phys. 131, 034702 (2009) [3] H. Nogawa et al., Jpn. J. Appl. Phys. 49, 041102 (2010)

4:45 PM SF03.08.06

Control of High Entropy Oxide Formation [Colin Freeman](#)¹, [Ali Nasrallah](#)¹, [Thomas Hooper](#)¹, [Ge Wang](#)² and [Derek Sinclair](#)¹; ¹University of Sheffield, United Kingdom; ²The University of Manchester, United Kingdom

Much of recent materials discovery has focused on "high entropy" systems with multiple components on the lattice sites. There has been excitement in both the metals and ceramics communities around new properties and the reduction of expensive and rare elements. The basic principle revolves around the use of multiple species that generate a high entropy of mixing that can counteract the enthalpic penalties associated with mixing different species. There are now a large number of examples of successfully produced compounds in a variety of crystal structures for both ceramic and metal systems. Despite the large amount of data now in the literature, our understanding of the mixing and formation of these materials is still relatively poor.

The perovskite lattice is a particularly exciting opportunity as mixing can be carried out on both the A or B site presenting a wealth of enthalpic and entropic possibilities to achieve a single-phase solid solution with a favourable Gibbs free energy. We use this crystal structure as a template to explore a range of factors that can control the formation of potential high entropy oxides. Using a combination of computational and experimental methods we interrogate the significance of various features including the tolerance factor, cation size variance, the decomposition rates of reactants, the stability of alternative products and the role of order on the lattice. By combining this information we are able to give insight to how these different features interplay and potential limit or aid the formation of high entropy oxides. We also comment on where the materials enter a high entropy, disordered state or where enthalpy plays a more significant role than might be expected. From our results, we offer thoughts on the differing rules governing the mixing processes in these perovskite phases.

5:00 PM SF03.08.07

Non-Classical Electrostrictors, Novel Type of Electromechanically Active Ceramics Igor Lubomirsky; Weizmann Institute of Science, Israel

Electrostriction is a second order electromechanical response observable in all solid dielectrics. According to the scaling law presented more than two decades ago by Prof. R. Newnham (Penn State), the electrostriction polarization coefficient for a wide range of classical electrostrictors scales with the ratio of the elastic compliance to the dielectric constant.

In 2012, Gd-doped ceria, one of the most studied oxygen ion conducting ceramics, was reported to exhibit an unusually large electrostriction. This first report was followed by reports on non-classical electrostriction (NCES) in other aliovalent-doped ceria, on (Nb,Y)-stabilized cubic Bi₂O₃ and acceptor-doped, hydrated barium zirconate, suggesting that strong electrostriction may be an inherent property of superionics. At room temperature, these ceramics exhibit a longitudinal electrostriction strain coefficient $|M_{33}| > 10^{-17} \text{ m}^2/\text{V}^2$. However, with elastic modulus $> 80 \text{ GPa}$ and dielectric constant < 100 , the experimental Q-coefficients of these ceramics are at least 100 times larger than values predicted by the classical scaling law. Of the three ceramics, aliovalent-doped ceria is the most studied. Below 1Hz, $|M_{33}|$ for 10mol% Sm- or Gd-doped ceria reaches $10^{-16} \text{ m}^2/\text{V}^2$ relaxing to $< 10^{-18} \text{ m}^2/\text{V}^2$ above 100 Hz. Aliovalent lanthanide dopants with smaller ionic radii than that of Gd, such as Lu or Yb, raise $|M_{33}|$ at 100Hz to $\approx 10^{-17} \text{ m}^2/\text{V}^2$.

Acceptor-doped BaZr_{1-x}X_xO_{3-x/2+δ}H_{2δ} proton-conducting ceramics, where X= Ga, Sc, In, Y or Eu, and $0.05 \leq x \leq 0.2$, exhibit non-classical electrostrictive strain for all dopants in both the dry and hydrated states: $|M_{33}| = (1-7) \bullet 10^{-16} \text{ m}^2/\text{V}^2$ below, and $\approx 10^{-18} - 10^{-17} \text{ m}^2/\text{V}^2$ above, the Debye-type relaxation frequency. Hydration does not significantly affect M₃₃, but raises the relaxation frequency by a factor of 10 to 100, indicating that proton-based elastic dipoles can respond more quickly than those based on oxygen vacancies.

According to our current understanding, NCES emerges from electric field-induced rearrangement of highly polarizable elastic dipoles induced by point defects: oxygen vacancies or proton interstitials. In this model, elastic and dielectric properties are largely defined by the host lattice, while electrostrictive strain is controlled by the strength of the elastic dipoles. We suggest that non-classical electrostriction may be a common feature for crystalline dielectrics containing mobile point defects.

SESSION SF03.09: Poster Session III
Session Chairs: Craig Brown and Brent Melot
Wednesday Afternoon, November 29, 2023
Hynes, Level 1, Hall A

8:00 PM SF03.09.01

Role of Fermi Surface Nesting and Hidden Nesting in Controlling Kohn Anomalies in α -Uranium Aditya P. Roy¹, Ranjan Mittal² and Dipanshu Bansal¹; ¹Indian Institute of Technology Bombay, India; ²Bhabha Atomic Research Centre, India

Charge density wave (CDW), the periodic modulation in electrons charge distribution, is accompanied by a simultaneous symmetry lowering and a finite gap opening near the Fermi level (E_F) in low dimensional metals. The Fermi surface topology of such systems allows Fermi surface nesting (FSN), resulting in divergence of the imaginary part of electronic susceptibility ($Im\{\chi_0(q)\}$). The divergence in $Im\{\chi_0(q)\}$ is further carried over to the real part ($Re\{\chi_0(q)\}$) under specific scenarios that drives the electronic instability. Kohn extended the implications of electronic instability to the lattice explicitly showing anomalous phonon behavior at \mathbf{q}_{CDW} . A finite resolution of momentum transfer (\mathbf{Q}) in x-ray or neutron scattering experiments often fails to capture the Kohn anomalies owing to its localized nature in the k -space. Hence, such phenomena are challenging to realize in experiments.

In this work, we use comprehensive *ab-initio* simulations of electrons and phonons [1] and earlier inelastic neutron scattering (INS) measurements [2] to understand the governing mechanism of CDW instability in α -Uranium (α -U) that displays pronounced Kohn anomalies in multiple phonon branches. α -U undergoes CDW transition ($T_{CDW} = 43 \text{ K}$) along with a symmetry lowering and unit-cell doubling along the a -axis. Initially, we capture the Kohn anomalies in multiple phonon branches. Subsequently, we map it to the electronic origin by calculating $Re\{\chi_0(q)\}$. The results display a diverging peak in $Re\{\chi_0(q)\}$ indicating electronic instability. Finally, we project the contribution of $Re\{\chi_0(q)\}$ in the entire k -space. The result highlights that besides the FSN features where contributions coincide with the Fermi surface, many k -points away from the Fermi surface also display a finite contribution to the divergence in $Re\{\chi_0(q)\}$. This phenomenon is called hidden nesting and manifests by the nesting of the electronic states above and below near E_F . Hence, our study demonstrates that the combined effect of FSN and hidden nesting drives the Kohn anomalies in multiple phonon branches and results in the CDW transition in α -U. Understanding such systems with coupled FSN and hidden nesting opens avenues to exploit electronic and lattice states of topological Weyl semimetals and superconductors.

Authors acknowledge financial support from BRNS-DAE under Project No. 58/14/30/2019-BRNS/ 11117, and MoE-STARs under Project No. STARS/ APR2019/PS/345/FS. We acknowledge the use of the SPACETIME-II supercomputing facility at IITB and ANUPAM supercomputing facility at BARC.

References

- [1] Roy et al., Phys. Rev. Lett. 126, 096401 (2021)
- [2] Crummett et al., Phys. Rev. B 19, 6028 (1979)

8:00 PM SF03.09.02

Strong Trilinear Coupling of Phonon Instabilities Drives The Avalanche-Like Hybrid Improper Ferroelectric Transition in SrBi₂Nb₂O₉ Aditya P. Roy¹, Naini Bajaj¹, Vasant Sathe², Sanjay Mishra³, Ranjan Mittal³, Manh D. Le⁴ and Dipanshu Bansal¹; ¹Indian Institute of Technology Bombay, India; ²UGC-DAE Consortium for Scientific Research, India; ³Bhabha Atomic Research Centre, India; ⁴ISIS Facility, India

Hybrid improper ferroelectrics (FEs) harbor spontaneous switchable polarization (P) below FE transition temperature (T_{FE}) owing to condensation of two unstable non-polar zone-boundary modes coupled to a stable polar zone-center mode. However, in Aurivillius family, besides two non-polar modes, the polar mode is also unstable. This instability of polar mode has significant implications on origin of P . Here, we investigate origin of P in Aurivillius family compound SrBi₂Nb₂O₉ [3]. Using group theory (GT) and *ab-initio* simulations using Landau's theory, we build an energy invariant polynomial as a function of the three unstable modes connecting paraelectric to FE phase. We find that trilinear coupling is strong enough to surpass positive biquadratic terms, allowing an *avalanche*-like simultaneous condensation of all three modes at T_{FE} instead of multi-step transitions at different temperatures. The magnitude of trilinear coupling term is nearly two to six times higher than in isostructural SrBi₂Ta₂O₉ [2], where a double-step transition is favored. Using inelastic neutron scattering, we capture evolution of phonons from 5 – 1000 K. Extracted phonon density of states (DOS) is consistent with simulations and shows a predominant O atom vibration of NbO₆ octahedra. Similar to other hybrid improper FEs [4], we observe significant broadening even at 300 K. Despite a first-order transition, a clear discontinuity is not visible in phonon DOS across T_{FE} primarily due to a localized nature of these modes in the Brillouin zone. We identify and track the three distortions across T_{FE} using Raman spectroscopy. T -dependence of these modes are consistent with our theoretical prediction and previous Monte-Carlo simulations [5]. Our findings provide a better understanding of hybrid improper FEs and open avenues to understand role of chemical doping of Nb with Ta atom on trilinear coupling as recently shown in another hybrid improper FE, Ca_{3-x}Sr_xTi₂O₇ [4].

Authors acknowledge financial support from IRCC-IITB, BRNS-DAE under Project no. 58/14/30/2019-BRNS/11117, and MoE-STARs under Project no. STARS/APR2019/PS/345/ FS. Simulations were performed in SPACE-TIME and ANUPAM supercomputing facilities at IITB and BARC respectively. Experiments in ISIS Neutron and Muon Source were supported by beamtime allocation RB1968028 from Science and Technology Facilities Council.

References

- [1] N.A. Benedek et al., Dalton Trans., 2015, 44, 10543.
- [2] J.M. Perez-Mato et al., PRB **70**, 214111 (2004).
- [3] A.P. Roy et al., PRB **103**, 134111 (2021).
- [4] D. Bansal et al., PRB **100**, 214304 (2019).
- [5] I. Etxebarria et al., Ferroelectrics, 401:1, 17-23 (2010).

8:00 PM SF03.09.03

Radiative Cooling and Light Enhancement of Transparent Crystalline Si Solar Cells Kangmin Lee, Jeonghwan Park and Kwanyong Seo; UNIST, Korea (the Republic of)

A light-harvesting film is considered as a means to improve the power conversion efficiency (PCE) of solar cells. However, when a light-harvesting film is applied to transparent solar cells, it is difficult to maintain the transparency of transparent solar cells due to the high haze ratio of the film ($> 95\%$). In this study, we apply a light-harvesting film onto the selective area, which is the light absorption region of the c-Si transparent solar cells. As a result, the c-Si transparent solar cells with light-harvesting film exhibited a current density (J_{SC}) increase of 2.6

mA/cm² compared with the transparent solar cells without a light-harvesting film. Therefore, the best device showed a PCE of 15.8% at an average visible transmittance of 20%, while maintaining a low haze ratio (0.95%). Furthermore, the c-Si transparent solar cells with the light-harvesting film have the advantage of minimizing the PCE degradation depending on the angle of light incidence. In addition, the strategy also helped reduced the temperature increase through the radiative cooling effect.

8:00 PM SF03.09.04

Influence of The Local Environment on The Formation of Sulfur Vacancies in Calcium Lanthanum Sulfide Cassidy Atkinson¹, Alexandros Kostogiannes², Matthew Guziewski³, Pamir Alpay¹, Parag Banerjee², Romain Gaume² and Kathleen Richardson²; ¹University of Connecticut, United States; ²University of Central Florida, United States; ³U.S. Army Research Laboratory, United States

Sulfur loss during the processing of calcium lanthanum sulfide has been shown to negatively impact the optical properties of the material. In order to better understand the phenomenon, density functional theory is used to determine the structural stability and formation likelihood of sulfur vacancies across several stoichiometries within the calcium lanthanum sulfide system. It was found that the local atomic environment surrounding defect sites plays a significant role in their formation energies and this was strongly related to the redistribution of charge. Using this information, a functional relationship to predict the sites that are most likely to lose sulfur was developed. Simulated diffraction patterns were compared to experimental work in order to determine the atomic structure present after processing. With this knowledge, it may be possible to better predict the effects of different processing approaches to minimize sulfur loss and potentially speed the material development process.

8:00 PM SF03.09.05

Atomic-Scale Structural Investigation on p-Type Copper Bismuthate for Photocathodes: Insights into Charge Hopping Conduction and Correlation with Crystal Defects Structure Younghwan Lim, Hyun Joon Jung and Sung-Yoon Chung; Korea Advanced Institute of Science and Technology, Korea (the Republic of)

Metal oxides with p-type semiconducting properties have been actively investigated in the fields of semiconductor industry, gas sensors, and (photo)electrochemistry. Especially, Cu-based oxides have been considered as an adequate p-type semiconductor for energy applications due to their proper band-edge energies located near the electrochemical redox potentials. Copper Bismuthate, CuBi₂O₄, is one of the promising p-type oxides with appropriate band structures which depend on the crystal structures. The peculiar crystal structure of CuBi₂O₄, containing isolated [CuO₄] planes aligned in the c-axis direction, has not been reported in other AB₂O₄-type materials which usually have spinel-like structures. Although a few studies have demonstrated the electrical and (electro)chemical properties, there is still a lack of demonstration on major defect structures of CuBi₂O₄, acting as a bottleneck for practical use. The investigation into the defect structure should be the first step to improve catalytic performance and modify the electronic structure suitable for other applications.

In this research, atomic-scale scanning transmission electron microscopy (STEM) combined with energy-dispersive X-ray spectroscopy (EDS) is employed to identify a noteworthy occurrence of antisite intermixing between copper and bismuth cations. The Bi_{Cu}-Cu_{Bi} intermixing is represented as a major type of defect existing in CuBi₂O₄. The local Cu 3d polaron states and the effects of point defects on electric conduction behavior are presented by utilizing density functional theory (DFT) calculations. A higher degree of intermixing leads to a greater activation energy and decreased electronic conductivity due to the possible electric conduction mechanism by the hopping of hole polarons. The hole-polaron hopping occurs in between isolated Cu atoms along the c-axis but it can be hindered by the Bi_{Cu} point defects. These results give insight into the significance of employing STEM-EDS analysis and DFT calculations, to identify point defects and to understand the electronic characteristics in complex oxides.

8:00 PM SF03.09.06

Nanoporous IGZO Thin Film Transistors for Visible-To-NIR Detection Srinivas Gandla, Anamika Sen and Sunkook Kim; Sungkyunkwan University, Korea (the Republic of)

The amorphous metal oxide semiconductors (AMOSs) have revolutionized the transparent semiconductor industry due to their potential intrinsic material and electrical, and low-temperature processing attributes.¹ Among these is indium-gallium-zinc-oxide (IGZO), an important AMOS material that is known for its ability to form transparent thin films with desirable electrical characteristics, making it suitable for applications in flat panel display technology. The presence of gallium in the composition leads to controlled charge concentrations, thereby enabling high current I_{ON}/I_{OFF} ratios in thin film transistor (TFT) transfer characteristics.² Due to a lack of grain boundaries and overlapped isotropic spherical ns-orbitals, the TFT with this material exhibited high electron field-effect mobilities. Like most AMOS, IGZO is also a wide bandgap semiconductor of nearly 3-4 eV. With this bandgap, the material is applicable for image and optical sensing applications within the UV region of the spectrum.³ However, its current limitations in detecting a broad spectrum of light prompted the exploration of enhancing its light detection range.

To address this, researchers have proposed a laminated approach by introducing secondary materials to the IGZO thin film. This approach involves adding materials with different optical properties to create a wider range of light absorption capabilities. These secondary materials include quantum dots, graphene dots, metal nanoparticles, and other thin films. The absorption of light by these added layers generates charge carriers that are then transferred to the IGZO channel, enabling extended light detection. Various strategies involving nanowires and heterojunctions with other materials have also been investigated to increase the subgap states within IGZO's bandgap, further enhancing its light detection capabilities.

Herein, a novel method to extend IGZO's light detection range using block copolymer lithography on a 4 inch wafer is demonstrated. This technique creates nanopores in the IGZO semiconducting channel, modifying the material's properties without altering its composition. The presence of these nanopores is confirmed through advanced microscopy and spectroscopy techniques. By introducing these nanopores, the subgap states within IGZO's bandgap can be controlled to a certain extent, influencing its light absorption properties. The fabricated nanoporous IGZO phototransistor can detect longer wavelengths of light up to 852 nm. The photoconducting and photogating effects related to specific wavelengths are discussed. These findings highlight the substantial promise of NP IGZO phototransistors for the future of large-scale optoelectronics.

References:

(1) Hsieh, H. et, al. Development of IGZO TFTs and Their Applications to Next generation Flat panel Displays. *J. Inf. Disp.* **2010**, *11* (4), 160–164.

<https://doi.org/10.1080/15980316.2010.9665845>.

(2) Nomura, K. et, al. H. Room-Temperature Fabrication of Transparent Flexible Thin Film Transistors Using Amorphous Oxide Semiconductors. *Nature* **2004**, *432* (7016), 488–492.

<https://doi.org/10.1038/nature03090>.

(3) Yu, J. et, al. H. High-Performance Visible-Blind Ultraviolet Photodetector Based on IGZO TFT Coupled with p-n Heterojunction. *ACS Appl. Mater. Interfaces* **2018**, *10* (9), 8102–8109.

<https://doi.org/10.1021/acsami.7b16498>.

8:00 PM SF03.09.07

Synthesis and Modification Methods for Electrode Materials of Secondary Batteries Based on the Decomposition Reaction of Ammonium Fluoride Jinyoung Chun¹, Il-Seop Jang^{1,2}, Bo-Ye Song^{1,2} and Gun-Hee Park^{1,2}; ¹Korea Institute of Ceramic Engineering and Technology, Korea (the Republic of); ²Korea University, Korea (the Republic of)

With the rapid growth of the electric vehicle (xEV) and energy storage system (ESS) industries, there are urgent needs for the development of high-performance secondary batteries based on advanced electrode materials. Electrode materials are key components that intrinsically determine the performance of secondary batteries. Therefore, in order to realize secondary batteries with high energy and power densities, the development of advanced electrode materials based on new approach is required.

In this study, using the decomposition reaction of ammonium fluoride (NH₄F), we developed metal fluoride (MF_x) cathode materials that exhibit high specific capacities based on conversion reactions. In addition, we found that this synthesis method could be applied to modify various electrode materials: (i) Improving electrochemical performance of silicon (Si) anodes by removing impurities and controlling the morphology of raw material. (ii) Improving rate capabilities of Li₄Ti₅O₁₂ (LTO) anodes through surface fluorination. (iii) Conversion of commercial lithium metal oxides into metal (M)/lithium fluoride (LiF) nanocomposites and their application to sacrificial cathode materials. Furthermore, the synthesis method in this study is simple and relatively safe. Therefore, it is expected that this study will provide new strategies for developing advanced electrode materials with high energy/power densities.

8:00 PM SF03.09.08

Catalyst Droplet-Based Puncturable Nanostructures for Mechano-Bactericidal Effect on Bioaerosols Inae Lee, Dongkyu Kang, Eunyoung Jeon, Sunghyun Park and Joonseok Lee; Hanyang University, Korea (the Republic of)

Exposure to airborne contaminants and particulate matter causes serious public health risks, leading to the need for new technologies that effectively collect and inactivate airborne microorganisms. Typical nanomaterial-based filter membranes usually sterilize airborne microorganisms using photocatalysts, electrical stimulation, and thermal treatment, which are expensive and require additional devices and cumbersome manufacturing. In this study, we fabricated a puncturable nanostructured membrane for bioaerosol filtration and inactivation using a catalyst droplet-based solution-phase synthesis. The catalyst droplets are templates for in situ novel puncturable nanopillar growth on the membrane surface. The unique puncturable nanostructures featuring a nano-edge caused mechanical deformation of the bioaerosol collected on the filter surface without external stimulations. A puncturable nanostructured air filter (PNAF) is compared to a bare air filter and exhibits higher bioaerosol collection efficiencies (>98% and 89.3–95.7%, respectively). The amount of airborne *E. coli* collected on PNAF was up to 2.3 times higher than that of the bare air filter. Furthermore, after incubation, PNAF inhibited the growth and proliferation of deposited bacterial cells. The bioluminescence value and viable *E. coli* count in PNAF were 90.9% and 92.7% lower than those in the bare air filter. PNAF is tested under breathing conditions as part of a face mask, where it effectively captures and deactivates *E. coli* aerosols through a mechano-bactericidal effect, inhibiting bacterial proliferation and, finally, death. The nanostructures were maintained intact after further sterilization by heat and solvent, indicating a lower risk of secondary infection by the remaining viable bacteria or emission of nanomaterials. Thus, PNAF can be applied as an air purifier or face mask filter

for bioaerosol collection, presenting antibacterial effects without external stimulation. Puncturable nanostructures can be used as antimicrobial membranes and surfaces in many areas, such as medical diagnosis, food processing and hygiene facilities, and water quality management.

8:00 PM SF03.09.09

Development of Silicon-Gradient Block Copolymers as EUV Lithography Inorganic Pattern MasksJeehyunHong and Yeon SikJung; KAIST, Korea (the Republic of)

The production of finer patterns with enhanced qualities is more emphasized, owing to the elevated demand for device performance. The utilization of extreme-ultraviolet lithography (EUVL) as the next-generation lithographic technique has become increasingly prominent. Nevertheless, failures arising from the reduction of the thickness of photoresists and inherent stochastic defects intensified along with the reduction in the pattern sizes. The defects substantially compromise the productivity and performance of the devices. Directed self-assembly (DSA) of block copolymers became a viable solution to overcome the limitations of EUVL. The DSA process not only improves pattern roughness but also facilitates the production of finer patterns at increased throughputs. Still, integration of DSA into EUVL presents the following challenges including increased complexity of the process related to surface energy neutralization, limited etching selectivity for effective pattern transfer, and undefined polymerization methods constraining its application within production processes.

Here, novel block copolymers with organosilicon gradients, Poly(methyl methacrylate)-block-poly(((bis(trimethylsilyl)methyl)acetamide)-gradient-styrene) (PMMA-b-P(Si₂-g-S)) and Poly(methyl methacrylate)-block-poly((Polyhedral oligomerized silsesquioxanes)acetamide)-gradient-styrene) (PMMA-b-P(POSS-g-S)), are presented. These BCPs were engineered to overcome the challenges of DSA based on the three pivotal design principles. First, the incorporation of gradient random copolymer blocks is leveraged to facilitate the generation of vertically aligned patterns, irrespective of substrate surface properties. Next, novel organosilicon polymers are introduced, serving as a robust mask for pattern transfer with high etch resistance. Third, by integrating a reactive polymer, a versatile block copolymer synthesis platform is established. This platform enables the generation of various block copolymers from a single reactive precursor block copolymer. Notably, synthesized PMMA-b-P(Si₂-g-S) and PMMA-b-P(POSS-g-S) block copolymers exhibit highly ordered, vertically aligned lamellar patterns on diverse surfaces. After undergoing directional alignment and selective etching procedures, the gradient organosilicon block demonstrates its effectiveness and robustness as a pattern transfer mask. This novel block copolymer system thus presents a promising platform for efficient pattern transfer, addressing the challenges associated with integrating DSA into EUVL.

8:00 PM SF03.09.10

3-D Mesoporous Architectures for Carbon-Conversion Photocatalysis: Block Copolymer-Templated Semiconductor Mesostructures Substantially Enhance Photocatalytic Dry Reforming of MethaneWilliamMoore¹, ShusakuShoji², R.P. Thedford¹, FeiYu¹, LiehnTsaun¹, WilliamTait¹, M.S. Riasi³, AniruddhaSaha¹, AustinReese¹, SolGruner¹, SadafSobhani¹, JinSuntivich¹ and UlrichWiesner¹; ¹Cornell University, United States; ²National Institute for Materials Science, Japan; ³University of Cincinnati, United States

The recent discovery of low-temperature photocatalytic conversion of methane and carbon dioxide to syngas (photocatalytic dry reforming of methane; photo-DRM) transformed an expensive high-temperature process into an appealing sustainable process for carbon conversion. This simple reaction, which can proceed under illumination without external heating, could provide an alternative to crude oil for supplying the organic chemical precursors our modern world is built upon. While much attention has been paid to alternative photocatalyst support chemistries or exotic metallic promoters, the 3-D architecture of the semiconductor support itself has been largely overlooked. This has left a massively important variable space in photocatalyst support development largely unexplored.

By utilizing block-copolymer self-assembly templating of common semiconductor supports, we have studied TiO₂ and Ta₂O₅ photocatalyst supports in a range of architectures: from hexagonally packed cylinders to 3-D co-continuous gyroids to asymmetrically porous thin films. This mesoporosity provides enhanced activity across a wide range of volumetric flow rates, delivering record low-temperature performance beyond the expectations of enhanced surface area alone. Beyond surface area, the 3-D accessibility of co-continuous architectures greatly reduces tortuosity, leading to fast facile transport of reactive species through the structure.

Further, we developed novel TiO₂ thin film catalyst architecture derived from liquid filtration membranes that has a thin mesoporous top layer with macroporous support layer. This highly-active low-density membrane architecture delivers the highest reported activity per gram for low-temp photo-DRM to-date by supporting a thin active layer on a macroporous substructure, allowing rapid gas transport. These solution-based polymer processes for creating 3-D architectures are simple, low-cost and scalable routes to create world-class photocatalyst supports, applicable to a wide-range of gas-phase catalytic reactions.

8:00 PM SF03.09.12

Plasmonic Au/TiO₂ Composite Nanoparticles: Synthesis, Structural and Optical Characterization and Functional Performance in The Photocatalytic Reduction of CO₂ to COPPascalBuskens^{1,2}, FrancescSastre¹, ManXu¹, NicoleMeulendijks¹, Jonathanvan den Ham¹, JelleRohlf¹, AnthonySanderse¹, RobertoHabets¹ and PauMartínez Molina¹; ¹TNO, Netherlands; ²Hasselt University, Belgium

Because of their localized surface plasmon resonance, metal nanoparticles are of interest for a broad variety of applications ranging from chemical and biological sensing to surface enhanced Raman spectroscopy and improved light extraction in LEDs. Here, we present the synthesis, structural and optical characterization of Au nanoparticles applied on TiO₂ for application as photocatalysts for the sunlight-powered reduction of CO₂ to CO.

The Au/TiO₂ composite nanoparticles were prepared by tailored deposition of Au(OH)₃ on the surface of 20 nm-sized anatase TiO₂ particles dispersed in water at a precisely controlled pH 9, and subsequent thermal anneal in an Ar:O₂ mixed atmosphere (80:20). The Au content was determined by Inductively Coupled Plasma-Atomic Emission Spectroscopy (ICP-AES) obtaining a value of 3.12% Au. The particle size distribution was determined using High-Angle Annular Dark Field Scanning Transmission Electron Microscopy (HAADF-STEM). The Au nanoparticles were randomly distributed on the surface of 20 nm-sized anatase nanoparticles, and their size followed a lognormal distribution with an average of 1.6 nm. The interplanar distance in the Au NP was 2.37 Å, corresponding to the (111) spacing. The (111) lattice planes were perfectly aligned with the (101) TiO₂ planes. The presence of Au and TiO₂ as sole crystalline materials was confirmed by XRD. The diffuse reflectance spectrum of the Au/TiO₂ powder displayed a broad minimum centered around 500 nm, which represents the light absorption based on the plasmonic resonance of the Au nanoparticles. Since we intended to apply the Au/TiO₂ nanoparticles for photocatalysis, we also determined the light penetration depth (skin-depth) of the powder using UV-vis-NIR spectrophotometry. The resulting skin-depth was about 100 μm.

We applied the resulting Au/TiO₂ composite nanoparticles for the sunlight-powered reverse water gas shift reaction, i.e. the reaction of CO₂ and green H₂ to CO and H₂O. Whilst this reaction, which is endothermic ($\Delta H = 41.2$ kJ/mol) and limited by equilibrium, requires temperatures above 600°C in conventional thermocatalysis, we achieved high production rate (7888 mmol/(m²h)) and CO selectivity (96.9%) at temperatures below 300°C using mildly concentrated sunlight (up to 14 kW per m²) as sole and sustainable energy source. Reference experiments in dark at the same catalyst bed temperature yield more than 30% CH₄ as undesired side product. We proposed that the high selectivity of the catalyst could be attributed to promotion of CO desorption through charge transfer of plasmon generated charges, consequently avoiding further reduction of CO to unwanted CH₄.

The TiO₂ nanoparticles without Au show no CO production when illuminated with sunlight. Furthermore, removal of all light below 400 nm (above the anatase TiO₂ bandgap) resulted in no loss of activity and selectivity for Au/TiO₂, demonstrating the direct excitation of the semiconductor plays no role in this catalytic process. The rate of the reaction exponentially increased with the solar irradiance, demonstrating that in addition to the above mentioned plasmon-induced desorption of CO, also photothermal heating contributes to the process. Studies with differently sized Au nanoparticles revealed a linear relationship between the catalytic activity and the number of Au-TiO₂ contact points, and studies with Au nanoparticles supported on dielectric materials such as Al₂O₃ and SiO₂ yielded no catalytic activity. In combination, these phenomena suggest that charge carriers generated in the Au nanoparticles by its localized surface plasmon resonance are injected into the semiconductor over the Schottky barrier, which prolongs their lifetime and makes them available for participation in the catalytic conversion of CO₂ to CO. Ergo, TiO₂ is not a simple catalyst support, and both Au and TiO₂ are essential components of this catalyst which operate synergistically.

8:00 PM SF03.09.13

Defect Chemistry and Doping of Lead Phosphate Apatite Pb₁₀(PO₄)₆OMichaelToriyama¹, Cheng-WeiLee², G.J. Snyder¹ and PrashunGorai²; ¹Northwestern University, United States; ²Colorado School of Mines, United States

It is claimed that copper (Cu) doping of lead phosphate apatite Pb₁₀(PO₄)₆O causes volume contraction and, consequently, room-temperature superconductivity. Unsuccessful attempts to reproduce these claims have raised many questions about the reported composition, possible oxygen off-stoichiometry, and copper doping itself, among others. Additionally, unintentional incorporation of other elements (besides Cu) present in the initial reaction mixture has been speculated. Many of these questions are intimately related to the native defect chemistry and thermodynamic phase stability. We perform first-principles defect calculations to provide much needed insights into the defect chemistry and doping of Pb₁₀(PO₄)₆O. We find that Pb and O vacancies are the dominant defects that pin the Fermi energy in the mid-gap region consistent with an insulating behavior. Our defect calculations suggest the plausible existence of closely related Pb and O sub-stoichiometric phases; we predict one such stable phase. We predict moderate levels of Cu incorporation on the Pb site, which still results in insulating behavior that is consistent with single-crystal measurements. We also rule out interstitial Cu doping, but find that unintentional S incorporation is highly possible. Our findings emphasize the need for more careful characterization of the parent composition, and intentional and unintentional dopant incorporation in the structure.

8:00 PM SF03.09.14

High Tunability and Low Loss in Layered Perovskite Dielectrics through Intrinsic Elimination of Oxygen VacanciesHangfengZhang, HenryGiddens, TheoG. Saunders, NingLiu, VicenteAurullo-Peters, XinzhaoXu, MatteoPalma, MikeReece, IsaacAbrahams, HaixueYan and YangHao; Queen Mary University of London, United Kingdom

Dielectric materials with moderate dielectric permittivity, high tunability and low loss are critical in modern communication technology. However, high tunability is often associated with high loss and high dielectric permittivity. Here, a novel material, textured $\text{Sr}_2(\text{Ta}_{1-x}\text{Nb}_x)_2\text{O}_7$ (STN), with a layered perovskite structure, has been designed to break this correlation. These materials exhibit low dielectric loss associated with oxygen vacancy elimination through the creation of stacking faults in the layered structure, as evidenced by transmission electron microscopy. A modification of the Vendik model was used to fit the thermal dependence of their relative dielectric permittivity, which included an oxygen defect parameter as an indicator of the oxygen defect concentration. The high tunability is attributed to the presence of local polar nano-clusters just above the Curie point. A 2-step spark plasma sintering method was employed to prepare grain-oriented ceramics with optimised properties. A near optimum maximum tunability of 72% at room temperature was obtained for a textured $\text{Sr}_2\text{Ta}_{1.88}\text{Nb}_{0.12}\text{O}_7$ ceramic, with moderate dielectric permittivity ($\epsilon' \sim 520$) and a dielectric loss of less than 1%.

8:00 PM SF03.09.15

Wet-Chemistry: A Promising Route to Realize Highly Efficient Semiconductor-Based Photocatalysis [HongPang¹](#), [XianguangMeng²](#), [FumihikoIchihara¹](#), [JinhuaYe¹](#), [TakayoshiSasaki¹](#) and [RenzhiMa¹](#); ¹National Institute for Materials Science, Japan; ²North China University of Science and Technology, China

Photocatalysis represents a promising approach to alleviate the environmental crisis and resources shortage. In principle, the semiconductors can be excited by appropriate photoenergy and generate the electron-hole pairs for the redox reactions on the surface. The highly efficient semiconductor-based photocatalysts are conventionally synthesized by solid-state methods. Or the photocatalysts were synthesized through the reactions with high temperature or pressure and dried into powder, which has to be redispersed well in water before carrying out the photocatalytic measurement. However, such synthetic process always meets the difficulty of uniform dispersion and the loss of surface reactivity. Our latest findings found the low-dimensional semiconductor photocatalysts prepared without drying process make it more efficient and facilely controllable in photocatalytic reactions. Furthermore, such method is flexible in modulating the surface chemistry and constructing robust platform for photocatalytic reactions. Here two examples will be presented:

With sufficiently high conduction band, ZnS is one of the typical photocatalysts for hydrogen evolution and CO_2 reduction. In our work, a series of ZnS-based nanocrystals with an average size of 3 nm were synthesized by mixing the precursor ZnSO_4 and Na_2S in water at room temperature. The as-synthesized nanocrystals were only rinsed with water and directly used in the subsequent photocatalytic experiments without any drying process. Such all-inorganic wet system showed an outstanding performance in the CO_2 conversion to formate with a high efficiency and selectivity. By simply changing the precursor composition and concentration, the ZnS systems could also be introduced dopants, cocatalysts and vacancies.

Molecularly negatively-charged titanate monolayers are stably dispersed in aqueous solution but showed limited photocatalytic applications up to date. One of the drawbacks is the easy accumulation of metallic cocatalyst reaching to tens of nanometers by photodeposition that results in a fast recombination of charges. By exchanging the water with nucleophile solvents and reserving the outmost layer ligands, it is successful to realize the uniform dispersion of the ultrasmall metallic cocatalysts on the surface of the titanate monolayers. After rinsing the monolayers with pure water without drying process, a boosted photocatalytic activity can be achieved.

The presentation highlights the wet chemistry as a facile synthetic approach at ambient conditions, which greatly reduces the experimental time and efforts. The experiments disclose the importance of the wet surface and the possible loss of active sites and reactivity during drying process. The insights into the surface chemistry (large surface energy, rich active sites, tunable functional groups, etc.) may lay a significant groundwork for future investigations aiming at efficient photocatalytic systems.

8:00 PM SF03.09.16

Large-Scale Synthesis of 3D Nanonetworked Silica Film for Polymer-Free Drug-Eluting Stents [EunyoungJeon](#), [SuyeonKim](#), [InaeLee](#), [SunghyunPark](#) and [JoonseokLee](#); Hanyang University, Korea (the Republic of)

Self-expandable metallic stents (SEMSs) are interventional implants for treating esophageal strictures, and require additional drug therapeutics to suppress stent-induced tissue hyperplasia and restenosis. However, methods of loading drugs on SEMSs are challenging in terms of fabrication, mechanical stability, and therapeutic. There are several strategies to produce polymer-free drug-eluting stent (DES): top-down approaches such as patterning micro-pores via femtosecond laser beam etching, and bottom-up approaches such as decorating surfaces with nanomaterials (e.g., nanoparticles and nanowires). However, poor mechanical stability or peeling off of the coating materials, makes it difficult to observe therapeutic effects. We developed a large-scale, 3-dimensional, and flexible nanonetworked silica film (NSF) as a promising alternative drug carrier for polymer-free DESs. Here, using facile bottom-up synthesis, a 3-dimensional NSF is constructed to function as a drug carrier on the entire surface of the SEMS. Enlarged micelles as nanonetwork structure templates, are adhered to the surface via van der Waals interactions, and hydrolyzed silicates are assembled and deposited with the templates via electrostatic interactions. NSF is synthesized without defects, even on a large area and curved surface, with only 0.4% increase in thickness compared to the SEMS wire. Owing to the full range coating of nanonetwork structures, the NSF is fixed well on the surface and is flexible enough to withstand mechanical stress during dynamic expansion. NSF was grafted with octyltrimethoxysilane (OTMS) and hexadecyltrimethoxysilane (HDTMS) to induce surface hydrophobicity. 3-fold more sirolimus (approximately $30 \mu\text{g}/\text{cm}^2$). Sirolimus can be loaded on NSF than on a polymer coating of the same thickness. The NSF stents show extremely slow elution compared to samples without NSF. The hydrophobic interaction and structural confinement of nanonetworks enable slow drug release even without polymers. Thus, NSF opens new avenues for manufacturing high-performance polymer-free drug-eluting stents and is a promising platform for drug delivery, protein adsorption, virus capture and generating flexible biosensors.

8:00 PM SF03.09.17

Signal-Amplifiable Porous Nanostructures for Detection of Infectious Viruses [SunghyunPark](#), [EunyoungJeon](#), [InaeLee](#) and [JoonseokLee](#); Hanyang University, Korea (the Republic of)

Avian influenza virus (AIV) is the highly contagious and fatal viral disease that occurs among wild birds worldwide, mainly caused by influenza A virus. The proliferation of high pathogenicity AIVs, which requires massive killing, has a significant impact on the poultry industry and causes serious social and economic damages, therefore diagnosing AIV at early stage and prevent its spread is important. In addition to the large amount of enzyme required for signal amplification, it is important that the antibody is located on the outside of the particle to increase the accessibility to the antigen. The purpose of this study was to develop a size-selective biomolecule immobilization strategy that facilitates optimal porous silica nanoparticles (PSNPs) and conjugation system, which enables larger molecules (such as antibodies) to be conjugated to the outside of the nanoparticles, and smaller molecules (such as HRP) to be incorporated into its internal pores.

The rationally designed nanoprobe has been successfully adapted for chemiluminescent lateral flow stick immunoassay (CL-LFA). The detection limit of the CL-LFA using the signal-amplifiable nanoprobe for the nucleoprotein of the H3N2 virus was 5 pM. Sensitivity tests for low pathogenicity avian influenza H9N2, H1N1, and high pathogenicity avian influenza H5N9 viruses were conducted, and the detection limits of CL-LFA were found to be $10^{3.5}$ 50% egg infective dose (EID_{50})/mL, $10^{2.5}$ EID_{50} /mL, and 10^4 EID_{50} /mL, respectively, which is 20 to 100 times lower than that of a commercial AIV rapid test kit. Additionally, CL-LFA showed high sensitivity and specificity against 37 clinical samples. The signal-amplifiable probe used in this study may be a potential diagnostic probe with ultrahigh sensitivity for applications in the field of clinical diagnosis, which requires sensitive antigen detection as evidenced by enhanced signaling capacity and sensitivity of the LFAs.

8:00 PM SF03.09.18

The Influence of W-Doping on The Crystallization of VO₂(M) within Hydrothermal Synthesis [RobertoHabets¹](#), [KimberlyTimmers¹](#), [LucLeufkens¹](#), [DanielMann¹](#), [PascalBuskens^{1,2}](#) and [AlishaChote³](#); ¹TNO, Netherlands; ²UHasselt, Belgium; ³Hogeschool Utrecht, Netherlands

30%-40% of a buildings operational energy consumption is due to heat loss or unwanted solar heat gain through windows [1]. To reduce the energy demand for heating and cooling simultaneously, a window has to adapt to changing requirements, which can be achieved via so called "smart windows". Vanadium dioxide can be used as active material in smart windows to realize adaptive solar heat regulating properties. In its monoclinic form, the crystal displays thermochromic properties, changing electrical and optical properties based on its structural phase transition from monoclinic VO₂(M) to rutile VO₂(R) at 68 °C. For application purposes, the switching temperature can be lowered by introducing defects in the crystal structure via a dopant, like tungsten [2]. VO₂(M) can be synthesized from V₂O₅ using a reducing agent under hydrothermal conditions at mild temperatures [3]. However, due to the many existing non-thermochromic crystal phases of VO₂, as well as the potential to be reduced to V(III) or oxidized to V(V), it is not trivial to synthesize highly pure and crystalline VO₂(M). The difficulty to realize mixing in hydrothermal batch reactors, placed in an oven, often leads to inhomogeneous products. Here we present a method to synthesize VO₂(M) from V₂O₅ and oxalic acid, as reducing agent, via hydrothermal reaction. We introduce a new method to enable mixing of the reaction solution within a hydrothermal batch reactor, increasing homogeneity of the resulting crystalline VO₂(M). Furthermore, we investigate the influence of the W dopant on the crystallization of VO₂(M). We show that under established conditions VO₂ tends to crystallize in the (A) and (B) phases, whereas with introduction of W a preferential crystallization in the (M) phase can be achieved. By optimizing the reaction conditions, we obtain highly crystalline and pure VO₂(M) particles at a lowered switching temperature.

8:00 PM SF03.09.19

Unveiling The Mechanistic Reaction Pathway of Selective Photocatalytic CO₂ Reduction [AmrSabbah¹](#), [Kuei-HsienChen²](#) and [Li-chyongChen¹](#); ¹National Taiwan University, Taiwan; ²Academia Sinica, Taiwan

The conversion of CO₂ into chemical fuels via photoreduction is regarded as one of the most effective methods of addressing the environmental greenhouse gas problem and the energy shortage. Creation of a suitable active and selective photocatalyst is the main goal of photocatalysis research. Meanwhile, better catalytic efficiency and controlled selective production yield can be achieved by developing photocatalysts, which can be facilitated by a deeper understanding of the chemical pathways. In this context, investigation of the reaction mechanism and understanding the nature of the active sites have recently attracted more attention. Thus, it is important, while challenging, to monitor reaction intermediates during the gas-phase photocatalytic CO₂ reduction reaction to achieve higher CO₂ conversion yield. In this perspective, we report a mechanistic insight for the photocatalytic CO₂ reduction over Two-dimensional ZnIn₂S₄ as an active model photocatalyst that exhibits promising photocatalytic performance with a high absorption coefficient under visible light. Our study combines in-situ FTIR investigation, physisorption measurements, operando XAS. We systematically probed the intermediate species (HCOO*, and CH₃O*) and established a co-feeding scheme to confirm the reaction pathway. The change in the oxidation state and the charge transfer behaviors were monitored for Zn, In, and S during the reaction coordinate to explore the active sites towards CO₂ molecules adsorption and activation. Finally, DFT calculations will be presented to prove the validity of the reaction mechanism.

8:00 PM SF03.09.20

Ceria-Based Materials for Catalytic Degradation of Ciprofloxacin in Water under Visible Light Irradiation [Ajit K. Dhanka](#); University of Delhi, India

Contamination of water by antibiotics poses a serious threat to environmental and human health. The antibiotics enter into water from domestic waste, hospital discharge, agrochemicals, veterinary medicines, human excretion, pharmaceuticals manufacturing, etc. When antibiotics get into water they make it more likely for bacteria to develop antimicrobial resistance - which is said by the WHO (World Health Organization) to be dangerous to humanity. Some of the antibiotics found in water affect microbes at concentrations below 10 µg/L. One among such antibiotic is ciprofloxacin (CIP). CIP is a synthetic fluoroquinolone antibiotic, widely used for treating microbial infections in human and animals. But CIP in water even at low concentrations, causes harmful effects to human and animal health such as vomiting, tremors, nausea, headache, diarrhea, nervousness, stomatitis, leucopenia, carcinogenic, pathogen resistance, chromosomal mutation, skin disorder and damage to the immune system. To encounter the problem of antibiotic contamination of water, researchers have developed various techniques for the degradation of antibiotics, such as catalytic degradation, physical adsorption, chemical oxidation and biodegradation. Among them, catalytic degradation is receiving significant attention. Therefore, in this work we present a simple chemical method to prepare Ag/CeO₂ catalyst for visible light driven degradation of CIP in water. The catalyst has been characterized by UV-Vis, X-ray diffraction (XRD), Raman, Field emission scanning electron microscopy (FE-SEM), Transmission electron microscopy (TEM), Thermogravimetric Analysis (TGA) and Brunauer-Emmett-Teller (BET) techniques.

8:00 PM SF03.09.21

Suppression of Oxides Regrowth at Air-Interfaces in Superconducting Quantum Circuits using Self-Assembled Monolayers [Saleem G. Rao](#)^{1,1}, [Mohammed Alghadeer](#)^{1,2}, [Archan Banerjee](#)³, [Ahmed Hajr](#)³, [Hossein Fariborzi](#)⁴ and [Hussein Hussein](#)⁴; ¹King Fahd University of Petroleum and Minerals, Saudi Arabia; ²University of Oxford, United Kingdom; ³University of California, Berkeley, United States; ⁴King Abdullah University of Science and Technology, Saudi Arabia

Defects in materials at different interfaces in circuit quantum electrodynamics (cQED) systems contribute significantly to decoherence at single photon level and millikelvin temperature. Low loss design, materials, and dielectrics have been reported and orders of magnitude improvement in coherence time have been observed however, to achieve scalable architectures for quantum computing still we need order of magnitude improvement in the coherence time. Defects at air-interfaces are foremost regions of TLS and non-TLS losses and these losses cannot be ousted in conventional way, i.e. by depositing an inorganic passivating layer because such additional layers can worsen these interfaces. Defects at air-interfaces can be removed by etching however, their regrowth remains a problem. Chemisorption of molecular self-assembled monolayers (SAMs) on metals and oxides is a promising option to engineer the desired properties of such interfaces. SAMs on metal and semiconducting surfaces can suppress the growth of oxides and can enhance dielectric constant of the surfaces. All SAMs themselves have known chemical and electronic structure and SAMs binding end makes strong chemical bond with top atomic layer of the metal/semiconductor surface. Therefore, SAM can significantly reduce the interface defects in cQED architecture. Here, we used SAMs to stop the regrowth of oxide-defects, both at Niobium-air and substrate-air interfaces and to modify the dielectric constant of the interface and observed sustained improvement in quality factor of the superconducting co-planer waveguide (CPW) resonators. We observed order of magnitude improvement in Q_{TLS} due to SAMs compared to etched-clean CPW resonator surface, which clearly shows that SAMs not only suppresses the regrowth of oxide it also contributes in improvement of the quality factor. Quality factor measurements at millikelvin temperature and at single photon, XPS data and TEM images of SAM passivated air-interface sustenance our claim. Furthermore, SAM assembly is highly compatible with micro-/nano-fabrication processes, therefore these results will open new ways to improve the coherence time in cQED using different SAMs.

8:00 PM SF03.09.22

Oriented ZSM-5 Nanoarray Encapsulation Enabled Robust Monolithic Catalysts for CH₄ and CO₂ Conversion [Binchao Zhao](#)¹, [Chunxiang Zhu](#)¹, [Yiwei Yu](#)², [Fangyuan Liu](#)¹, [Jingyue Liu](#)² and [Pu-xian Gao](#)¹; ¹University of Connecticut, United States; ²The University of Arizona, United States

Stable and active catalysts are the key to catalytic reactions requiring harsh conditions with high temperatures (>600 °C) and moist content. However, it is challenging to maintain high activity when catalyst design strategies such as strong metal support interaction and physical encapsulation, are applied to improve stability due to a tradeoff in the reactivity sacrifice as a result¹⁻³. Through rational design and manipulation^{4,5}, we have demonstrated a well-defined nanoarray hybrid monolithic catalyst which is composed of transitional metal oxide (Co₃O₄) nanoarray and the encapsulation layer of brush-like oriented ZSM-5 nanoarray, denoted as CC-HZA. The hybrid nanoarray catalysts have shown high thermal stability and excellent activity for catalytic processes under harsh conditions. CC-HZA demonstrates superior thermal stability and catalyst activity for high-temperature reactions such as methane oxidation, reverse water gas shift, and methane dry reforming reaction under both oxidative and reductive conditions at a high-temperature range (600-700 °C, 1 bar) with moist conditions. The internal and external ZSM-5 confinement is revealed for the Co₃O₄ nanoarray forest, playing a key role in the demonstrated superior stability. Besides the encapsulation effect, the oriented ZSM-5 nanoarray offers important merits including (1) improved CO selectivity for RWGS, (2) strong hydrophilicity of ZSM-5, endowing the excellent catalyst water resistance, and (3) oriented hierarchical nanoarray structure, offering fast transfer with high activity and less material usage. This work provides a new design of highly thermal stable monolithic catalysts, which allows highly stabilized non-noble nanometal and metal oxides catalysts for high-temperature applications.

References

- 1 Chaudhary, P. K. *et al. Colloids Surf A Physicochem Eng Asp* 646, 128973 (2022)
- 2 Lou, Y. *et al. J Catal* 356, 147–156 (2017)
- 3 Feng, X. *et al. Journal of Energy Chemistry* 75, 173–215 (2022)
- 4 Lu, X. *et al. Catal Today* 360, 275–283 (2021)
- 5 Du, S. *et al. Appl Catal B* 236, 348–358 (2018)

8:00 PM SF03.09.23

Manipulating Ligand Binding Affinity in Allosteric Coordination Complexes through Inherent Ring Strain Design [Yiming Hu](#), [Fiona Y. Wang](#) and [Chad A. Mirkin](#); Northwestern University, United States

Organometallic complexes are highly versatile given that their binding affinities are sensitive to their chemical makeup and environment. Indeed, these differences in binding affinities can be leveraged with the use of hemilabile ligands to construct spatially responsive structures. However, modifying binding affinities usually involves adding specific electron groups to binding atoms, a process that is not only synthetically complex but also can limit the integration of other functional groups. One solution to this challenge is to use ring strain in cyclic compounds to act as a binding affinity modulator combined with a hemilabile coordination system. The Weak-Link Approach (WLA) is a particularly powerful hemilabile coordination system that contains chemical modularity by exploiting binding affinities with combinations of strong binders, weak binders, and metal nodes.

Here, we introduce a new WLA system by replacing an asymmetric P,S ligand with a symmetrical bis-carbene and explore the effects of ring strain on allosteric reactivity. By studying ligand displacement in 4- to 8-membered rings, a correlation between ring size and coordination reactivity is established. Adjusting the ring size proved to be an effective way to alter binding affinities without further complex chemical modifications. Moreover, we observed that increased ring strain also leads to changes in overall allosteric reactivity, and even reversing conventional coordination binding to prefer weaker binders vs stronger ones in highly strained 4-, 7-, and 8-membered cyclic systems. Overall, through careful selection of metal-binder coordination, and thus enthalpy, along with the formation energy associated within a strained ring-forming system, we precisely define a desired allosteric state. In sum, this work not only represents a paradigm shift in harnessing ring strain as a strategy for binding affinity manipulation, but also redefines our understanding of coordination dynamics in these systems.

8:00 PM SF03.09.24

Photocatalytic fuel cells: Fundamentals and applications [Heberton Wender](#); Federal University of Mato Grosso do Sul, Brazil

The global concerns surrounding the energy crisis and environmental pollution have recently escalated. Photocatalytic fuel cells (PFCs) emerge as promising energy conversion devices that harness solar energy. These PFCs utilize cost-effective semiconductor electrodes to spontaneously convert the chemical energy of renewable fuels or pollutants, alongside oxidants, into electricity. What sets PFCs apart is their amalgamation of photoelectrochemical and fuel cell concepts, offering dual benefits to address both environmental and energy challenges. The engineering concept behind PFCs is elegantly simple, relying solely on light as the driving force. Consequently, constructing affordable PFC devices becomes feasible, providing effective

solutions for local environmental pollution and low-power energy consumption devices. This work delves into essential definitions, working principles, and the theoretical underpinnings of PFCs. It also offers a practical tutorial on constructing these devices and conducting half-cell reaction tests to evaluate PFC performance. Furthermore, some recent application cases will be thoroughly discussed, with a primary focus on critically analyzing strategies to enhance the efficiency and stability of PFCs.

8:00 PM SF03.09.25

A Bias-Free Tandem Photoelectrochemical Cell of BiVO₄ - CuO for Solar-Driven Water Splitting Renato V. Goncalves, Lucas G. Rabelo and Washington Santa Rosa; University of Sao Paulo, Brazil

Photoelectrochemical (PEC) water splitting has been considered as a promising technique for converting solar energy into clean and renewable hydrogen (H₂) fuel. Recently, Tandem PEC cells based on stable and low-cost metal oxides have attracted attention for generating green H₂ solely through water and solar energy. In this study, we synthesized BiVO₄/FeNiO_x photoanodes and CuO photocathodes using magnetron sputtering deposition. These materials were integrated into a straightforward and cost-efficient Tandem PEC cell to facilitate oxygen and hydrogen evolution reactions (OER and HER), respectively. Notably, the BiVO₄/FeNiO_x photoanode displayed remarkable PEC performance and demonstrated robust chemical stability in OER, achieving a high photocurrent density of +1.22 mA cm⁻² and an impressive charge transfer efficiency of 96% at the water oxidation potential. The CuO photocathode displayed remarkable performance in the PEC process for the hydrogen evolution reaction. It initiated at a starting potential of 1.03 V vs. RHE and achieved a photocurrent density of approximately 0.4 mA cm⁻² at +0.40 V vs. RHE. This outcome underscores the viability of employing these materials in a bias-free PEC cell. Additionally, we introduced a practical model based on classical band theory to assess the interfacial band alignment of photoelectrodes during PEC water splitting under operational conditions. Our energy band diagrams, simulated under illumination, illustrated that the photogenerated (electrons and holes) in the BiVO₄/FeNiO_x - CuO Tandem PEC film possessed sufficient energy to drive OER and HER without requiring external bias. Encouragingly, our novel BiVO₄/FeNiO_x - CuO Tandem PEC device produced a stable operating photocurrent density of ~50 μA cm⁻² under zero-bias illumination (AM 1.5G) for at least 1000 seconds, evidencing the occurrence of bias-free solar water splitting reactions.

SESSION SF03.10: Functional Materials III
Session Chairs: Craig Brown and Brent Melot
Thursday Morning, November 30, 2023
Sheraton, Second Floor, Back Bay C

8:00 AM SF03.10.01

Synthesis of Hydride Materials at Moderate Pressures by Combining Pressure and Electrochemical Potential Mgcini K. Phuthi¹, Nisha Geng² and Eva Zurek²; ¹University of Michigan, United States; ²University at Buffalo, The State University of New York, United States

Hydride systems such as metal hydrides or doped ternary hydrides are interesting for their potential applications as high temperature superconductors and for hydrogen storage. Traditionally, these materials have been synthesized either by passing a pressurized hydrogen source over the material or electrochemically loading the material. We show that by combining the two methods, new phases are accessible and hydrides with higher hydrogen content are accessible at much lower pressures using less than 1V of applied potential while also suppressing hydrogen evolution which limits electrochemical loading. We present results for the Yttrium hydride system and explore the possibility of synthesizing the recently claimed high temperature superconducting material, Nitrogen doped Lutetium Hydride.

8:15 AM SF03.10.02

Single-step, Novel Synthesis of Carbonaceous Cobalt Spinel Ferrite Nanocomposites and a Study of Their Magnetic Properties Naveen Narasimhachar Joshi^{1,2,3} and S. A. Shivashankar¹; ¹Indian Institute of Science, India; ²Indian Institute of Technology Kharagpur, India; ³North Carolina State University, United States

Metal oxide/ carbon composites offer prospects as new, improved functional materials, as they would exploit the unique properties of both of their components. Such composites have promising applications in energy storage, catalysis, and as adsorbents; the addition of carbon overcomes the inherent poor electronic conductivity of most metal oxides while enhancing the specific surface area of the material. Among them, spinel ferrite composites are widely explored for their promising magnetic properties. However, the benefits of carbonaceous spinel ferrites are yet to be explored. Herein, we report the novel synthesis of carbon composites of cobalt ferrite by a simple, one-step, inert-atmosphere sealed-tube pyrolysis (STP) of a stoichiometric mixture of the ketoesterate complexes of the Co (II) and Fe (III) as precursors, and without the aid of any catalysts or any further heat treatment. We show that composites formed this way are homogeneous on a macroscopic scale, with interesting variations in the morphology of the carbon formed. The metal oxide composites so formed are characterized through various techniques and evaluated for their magnetic properties. The isothermal field-dependent magnetization plots indicate ferrimagnetic interactions with a saturation magnetization of 34 emu/g. Temperature-dependent magnetization plots does not show blocking temperature as a consequence of the well-saturated magnetic spins in the sample. A clear deviation in the field-cooled (FC) and zero-field cooled (ZFC) curves until above the room temperature indicates that the Curie temperature (T_c) of the sample is well above 300 K. As such, the T_c of the cobalt ferrite composite is found to be ~400 K, obtained by the extrapolation of fits to experimental data using modified Bloch's law. Thus, cobalt ferrite nanocomposite opens a new frontier for soft magnetic applications of spinel ferrite structures.

8:30 AM *SF03.10.03

In-Plane Spin Dynamics and Complex Phase Spaces of Conducting Antiferromagnets Daniel P. Shoemaker; University of Illinois at Urbana Champaign, United States

Recent demonstrations have shown that it may be possible to change the orientation of magnetic ordering (the Néel vector) of antiferromagnetic materials by applying electrical currents, even though the currents are not spin-polarized and the material has zero net magnetic moment. The candidate materials have ultrafast antiferromagnetic resonances and belong to centrosymmetric space groups with magnetic cations in non-centrosymmetric sites. Exemplary materials include tetragonal CuMnAs and tetragonal Mn₂Au. However, this seemingly straightforward goal is complicated by strong magnetostrictive interactions in CuMnAs and related materials that share the Cu₂Sb structure type, such as Fe₂As and Mn₂As. Understanding in-plane antiferromagnetism also leads to conceptual overlap with magnetic topological insulator candidates, such as EuSn₂P₂. We show how traditional crystal growth methods can access these complex phases and reveal new materials with unique structure types. Understanding the fundamental phenomena and engineering devices from these materials requires measuring energy scales with detailed torque magnetometry and transport measurements that set stringent requirements on sample size and quality.

9:00 AM *SF03.10.04

Exploring Novel Nonbenzenoid π-Electron Systems Toward Unusual yet Stable Functional Materials Aiko Fukazawa; Kyoto University, Japan

Aromatic hydrocarbons and their heteroaromatic analogs are playing a dominant role in today's organic optoelectronic materials. On the other hand, nonbenzenoid hydrocarbons and relevant cross-conjugated π-electron systems exhibit attractive properties such as long-wavelength absorption and multistep redox properties, most of which are difficult to achieve with the benzenoid π-electron systems of similar molecular sizes. However, the difficulties in their synthesis, high reactivity, and lack of appropriate molecular design guidelines pose substantial obstacles to the utilization of these classes of compounds as basic frameworks for superior optoelectronic materials. To address the above-mentioned issues, we have been focusing on the molecular design based on the annulation of weakly aromatic (hetero)arenes on the nonbenzenoid hydrocarbons in a ring-fused manner. Furthermore, we have recently synthesized novel nonbenzenoid hydrocarbons that exhibit exceptional stability toward multi-electron reduction like C₆₀ yet intense light absorption in the visible region. In this presentation, I will describe the overview and some of our recent studies based on this strategy.

9:30 AM SF03.10.05

Chemical Strategies to Induce Superconductivity in Rare-Earth Nickelate Thin Films Ari Turkiewicz, Grace Pan, Dan Ferenc Segedin, Nicole K. Taylor, Charles Brooks, Jarad A. Mason and Julia Mundy; Harvard University, United States

Since the discovery of high-temperature superconductivity in copper oxides, there have been continued efforts to better understand the origins of the superconducting phase and to identify related materials families. Rare-earth nickelates, particularly Ruddlesden-Popper phases of the type Ln_{n+1}Ni_nO_{2n+2}, are a promising class of materials owing to the many shared properties of isoelectronic Ni¹⁺ and Cu²⁺ cations. Recently, superconductivity was observed in thin films of the infinite layer (n = ∞) nickelate Nd_{0.8}Sr_{0.2}NiO₂ as well as in thin films of the five-layer (n = 5) phase Nd₆Ni₅O₁₂. Theoretical and experimental studies suggest that increased dimensional confinement of the nickelate layers will lead to more 'cuprate-like' superconductivity. The n = 1 phase Ln₂NiO₄ is therefore expected to display the highest degree of dimensional confinement with single layers of nickel oxide separated by blocking rare-earth oxide layers. Here, we describe efforts to synthesize thin films of the parent compound Ln₂NiO₄ through molecular beam epitaxy. We then explore different chemical strategies to tune the nickel valence of as-grown

films to induce superconductivity.

9:45 AMBREAK

10:15 AM *SF03.10.06

Developing High-Performance P-Channel TFTs—From Emerging Semiconductors to Amorphous AoLiu and HuihuiZhu; Northwestern University, United States

The development of high-performance p-channel thin-film transistors (TFTs) that can be made by cost-effective methods and can match with n-type metal oxide counterparts for the integration of complementary circuits has attracted great interest of the electronics community. Unfortunately, after decades of efforts, the achievement of high-performance p-channel TFTs is still a nearly-impossible technique challenge. In my talk, I will give a comprehensive overview of this research field¹ and introduce our recent progress in the fabrication of high-performance p-channel TFTs based on different semiconductors, including metal oxide,^{7,8} and chalcogenide.⁹ The optimized devices show high hole mobilities of $> 50 \text{ cm}^2 \text{ V}^{-1} \text{ s}^{-1}$ and high current on/off ratios over 10^8 . At the end of my talk, I will introduce our recent breakthrough work on high-performance amorphous p-channel oxide TFTs, overcoming the technical challenges over the past decades.

References

- 1 Liu, A., *et al.* Solution-processed inorganic p-channel transistors: Recent advances and perspectives. *Mat. Sci. Eng. R* **135**, 85-100 (2019).
- 2 Liu, A., *et al.* Molecule charge transfer doping for p-channel solution-processed copper oxide transistors. *Adv. Funct. Mater.* **30**, 2002625 (2020).
- 3 Liu, A., *et al.* Polyol reduction: A low-temperature eco-friendly solution process for p-channel copper oxide-based transistors and inverter circuits. *ACS Appl. Mater. Interfaces* **11**, 33157-33164 (2019).
- 4 Liu, A. *et al.* Room-temperature solution-synthesized p-type copper(I) iodide semiconductors for transparent thin-film transistors and complementary electronics. *Adv. Mater.* **30**, 1802379 (2018).
- 5 Liu, A. *et al.* High-performance p-channel transistors with transparent Zn doped-CuI. *Nat. Commun.* **11**, 4309 (2020).
- 6 Liu, A., *et al.* Engineering copper iodide (CuI) for multifunctional p-type transparent semiconductors and conductors. *Adv. Sci.* **8**, 2100546 (2021).
- 7 Zhu, H. *et al.* High-performance hysteresis-free perovskite transistors through anion engineering. *Nat. Commun.* **13**, 1741 (2022).
- 8 Liu, A. *et al.* High-performance inorganic metal halide perovskite transistors. *Nat. Electron.* **5**, 78-83 (2022).
- 9 Liu, A. *et al.* Evaporated nanometer chalcogenide films for scalable high-performance complementary electronics. *Nat. Commun.* **13**, 6372 (2022).

10:45 AM *SF03.10.07

Atomistic Polarization Textures JayakanthRavichandran; University of Southern California, United States

Topological defects such as vortices, and skyrmions have gained recent significant interest in solid state materials as ferroic materials (ferromagnets and ferroelectrics) have become a test bed to realize and control these nanoscale structures. Although this phenomenon is being investigated as a pathway to energy efficient information storage, broader applications in interaction of electromagnetic waves with such features are emerging. In the case of ferroelectrics, boundary condition engineering is used to achieve vortices, skyrmions, and merons in low dimensional epitaxial oxide heterostructures.

In this talk, I will introduce the notion that similar phenomenology but at the atomic scale can be achieved in charge density wave phases, especially nominally semiconducting chalcogenides. I will outline my group and other groups efforts in showing non-trivial toroidal polar topologies at the atomic level in chalcogenides with nominally empty conduction band with *d*-orbital character such as 1T-TiSe_2 , Ta_2NiSe_5 and BaTiS_3 . Specifically, we use X-ray single crystal diffraction as a probe for high quality single crystals of a quasi-1D hexagonal chalcogenide, BaTiS_3 , to reveal complex polar topologies such as vortices, and head-to-head and tail-to-tail arrangement of dipoles. Recent experiments and theoretical studies on the stability and dynamics of these features will also be discussed. Lastly, I will outline how such platforms can broadly enable the search for materials with chiral optical materials and polarization sensitive light-matter interaction.

11:15 AM SF03.10.08

Jahn-Teller Distortion in Layered Nickel Oxides LiamNagle-Cocco¹, AnnalenaR. Genreith-Schriever¹, GeorgePhillips¹, JohnS. Evans², JamesM. Steele^{1,1}, JoshuaD. Bocarsly^{1,1}, AndrewGoodwin¹, ClareP. Grey¹ and SiânE. Dutton¹; ¹University of Cambridge, United Kingdom; ²Durham University, United Kingdom; ³University of Oxford, United Kingdom

The Jahn-Teller (JT) distortion has been under intense scrutiny from the solid state chemistry community in recent years. For example, understanding the role of JT behavior and associated orbital ordering is crucial for understanding battery cathode behaviour with cycling, cuprate superconductivity, and colossal magnetoresistance. One interesting aspect of JT research which is not fully-resolved is the behaviour of the JT distortion with heating; in LaMnO_3 , studies of local structure show an order-disorder transition at $\sim 750 \text{ K}$, characterized by the persistence of JT-distorted octahedra even when the average structure does not exhibit JT distortion [1]. However, there are limited reports on other materials and it is not clear from the literature whether this behaviour is generalised or system-specific.

In this study, we have used a combination of variable-temperature and variable-pressure neutron/synchrotron diffraction, Pair Distribution Function (PDF) with large box modelling, EXAFS, nuclear magnetic resonance (NMR), and *ab initio* Molecular Dynamics on two d^7 layered nickel oxides (LiNiO_2 and NaNiO_2) to explore the JT behaviour, including orbital ordering and the nature of the JT transition. We will present our findings that the transition is displacive in NaNiO_2 rather than order-disorder, with ferro-orbital ordering at room temperature and the absence of Jahn-Teller-distorted octahedra at higher temperatures. This contrasts with the intra-plane anti-ferro-orbital and inter-plane ferro-orbital ordering at room-temperature and reported Potts model behaviour at higher temperature in LaMnO_3 . We will also compare this to our findings for the orbital ordering in LiNiO_2 , which has been a controversial subject for many years owing to its enigmatic behaviour [2,3].

[1] Thygesen, Peter MM, et al. "Local structure study of the orbital order/disorder transition in LaMnO_3 ." *Physical Review B* 95.17 (2017): 174107.

[2] Chung, J-H, et al. "Local structure of LiNiO_2 studied by neutron diffraction." *Physical Review B* 71.6 (2005): 064410.

[3] Foyevtsova, Kateryna, et al. " LiNiO_2 as a high-entropy charge-and bond-disproportionated glass." *Physical Review B* 100.16 (2019): 165104.

11:30 AM SF03.10.09

Exploiting the Response of Lone Pair Electrons (LPEs) to Pressure: Synthesis of Mixed-Anion BiSF with In-Plane LPEs ChengchaoZhong^{1,2}, CédricTassel¹, DaichiKato¹, KantaOgawa^{1,3}, RyuAbe¹ and HiroshiKageyama¹; ¹Kyoto University, Japan; ²Ritsumeikan University, Japan; ³Imperial College London, United Kingdom

While inorganic compounds such as oxides generally have high symmetry, compounds with the stereochemically active s^2 lone pair electrons (LPEs) of p-block cations tend to have lowered symmetry.^{1,2} The LPEs in the electron-rich cations (e.g., Pb^{2+} , Sb^{3+} and Bi^{3+}), which are energetically stabilized by relativistic effects, cause electronic repulsion with the surrounding anions and displace the cation. Symmetry breaking by LPEs is valuable in functional materials, causing large spontaneous polarization in ferroelectrics BiFeO_3 ($95 \mu\text{C}/\text{cm}^2$)³ and small thermal conduction in thermoelectric materials PbQ ($Q = \text{S, Se, Te}$).⁴ Recently, in-situ XRD has revealed that the stereochemical activity of LPEs is lost upon external pressure and reappears upon decompression.⁵ Therefore, if the stereochemical activity of LPEs is controlled by external pressure at the synthesis process, the creation of novel structures can be expected.

In this study, a new mixed-anion compound BiSF has been synthesized using high-pressure synthesis. BiSF has a distorted PbFCl -type structure with LPEs oriented along intralayer direction, whereas those of previous layered compounds with PbFCl -type structures such as PbFCl and BiOF are oriented in the interlayer direction (Revised Lone Pair Model).² DFT calculations show that the stereochemical activity of LPEs is suppressed above 5 GPa, and a phase transition to a distortion-free PbFCl -type structure is observed. Since the synthesis of BiSF requires high-pressure conditions of 5 GPa, it is considered that a distortion-free structure is formed first under high-pressure synthesis at high temperatures, which stabilizes the metastable atmospheric pressure phase. Anisotropic lattice expansion of BiSF with respect to temperature was observed, and BiSF has a small band gap (1.89 eV). The *n*-type response and relatively high photocurrent were clearly observed under visible light irradiation, suggesting its potential application as a photoelectrode.

(1) Azuma, M.; Hojo, H.; Oka, K.; Yamamoto, H.; Shimizu, K.; Shigematsu, K.; Sakai, Y. *Annu. Rev. Mater. Res.* **2021**, *51*, 329–349.

(2) Walsh, A.; Watson, G. W. *J. Solid State Chem.* **2005**, *178*, 1422–1428.

(3) Neaton, J. B.; Ederer, C.; Waghmare, U. V.; Spaldin, N. A.; Rabe, K. M. *Phys. Rev. B - Condens. Matter Mater. Phys.* **2005**, *71*, 014113.

(4) Bozin, E. S.; Malliakas, C. D.; Souvatzis, P.; Proffen, T.; Spaldin, N. A.; Kanatzidis, M. G.; Billinge, S. J. L. *Science*, **2010**, *330*, 1660–1663.

(5) Bu, K.; Luo, H.; Guo, S.; Li, M.; Wang, D.; Dong, H.; Ding, Y.; Yang, W.; Lü, X. *J. Phys. Chem. Lett.* **2020**, *11*, 9702–9707.

11:45 AM SF03.10.10

Distinguishing Isotropic and Anisotropic Signals in X-Ray Scattering Data using Machine Learning DanielleN. Alverson¹, DanielOlds² and MeganButala¹; ¹University of Florida, United States; ²Brookhaven National Laboratory, United States

Improving understanding of structure-property relationships is imperative for the advancement of electronic materials that are implemented in devices as thin films. Thin films for electronic applications, such as phase change, ovonic, and spintronic materials, are typically deposited on single-crystal Si substrates. While X-ray diffraction is commonly used to study electronic thin films, it cannot provide comprehensive atomic structure insights for amorphous and nanocrystalline films.

X-ray pair distribution function (PDF) analysis can access the relevant atomic structure details, and is derived from total X-ray scattering data encompassing both diffuse and elastic scattering. Traditionally, PDF measurements are performed for powder samples. PDF has been adapted to thin films by depositing them on amorphous substrates; amorphous substrates provide a means to separate the thin film and substrate scattering signals through subtraction.

Moving forward, the next progression of thin film PDF is its application to films on single-crystal substrates. Unfortunately, high-intensity anisotropic Bragg spots from single-crystal substrates saturate the detector images and overwhelm the thin film's isotropic (radially-symmetric) signal. The nature of this data precludes the use of the substrate subtraction processing method used for thin films on amorphous substrates.

To overcome this challenge, we are developing unsupervised machine learning methods that combine non-negative matrix factorization and hierarchical agglomerative clustering to isolate the thin film scattering signal. We are validating our approach using SimDat2D, a Python module we created to generate and process synthetic data representative of total scattering from thin films on single crystal substrates. We find our machine learning methods can separate the isotropic thin film signal of interest from the high-intensity single crystal Bragg spots by leveraging their symmetry differences, thus enabling profound structural insights in functional thin film materials.

By implementing these advancements in X-ray scattering data analysis, we seek to enhance the understanding of structure-property relationships in electronic materials, facilitating the development of more advanced thin-film devices.

SESSION SF03.11: Functional Materials IV
Session Chairs: Craig Brown and Brent Melot
Thursday Afternoon, November 30, 2023
Sheraton, Second Floor, Back Bay C

1:30 PM *SF03.11.01

Chromatography Separation of Hydrogen Isotopes at Ambient Temperature using Dihydrogen Complexes [ShinyTakaishi](#); Tohoku University, Japan

Hydrogen isotopes such as deuterium (D) and tritium (T) play important roles not only in the fundamental research but also in the industry. D has been used as NMR solvents, tracer, moderator in nuclear reactors, and silicon semiconductive devices. D and T are also used as the nuclear fusion reactors, which will be expected as a future energy supply. T is contaminated with water in the nuclear waste, and its removal will be beneficial from the viewpoint of environmental protection.

Natural abundance of D is 0.015 % (mainly in the sea water) and distillation process at 20 K is used to concentrate D to produce D₂ gas, which is energy-intensive process. Recently, quantum sieving has been extensively studied as a new technique of the hydrogen isotope separation. Beenakker and co-workers proposed the concept of kinetic quantum sieving (KQS), which utilizes the difference of the diffusion rate in the small pore due to the thermal de Broglie wavelength between H and D. More recently, chemical affinity quantum sieving (CAQS) has been studied, which utilizes the difference of zero-point energy (ZPE) and resultant adsorption enthalpy (ΔH) among the hydrogen isotopes. Although CAQS potentially enables the hydrogen isotope separation at higher temperatures, the operating temperature was still below 200 K due to the small ΔH .

From the viewpoint of ΔH , metal-dihydrogen complex is one of the most appealing candidates for this target. The first metal-dihydrogen complex was reported by Kubas and coworkers in 1984, and hundreds of compounds were reported so far. In the metal-dihydrogen complexes, chemical bond is formed between metal and dihydrogen molecule, whereas H-H bond is kept albeit it is elongated and weakened. This can be regarded as an intermediate of physisorption and chemisorption, and therefore, moderate adsorption enthalpy and fast ad/desorption kinetics could be achieved. In spite of such advantages, there has rarely been studied on the hydrogen adsorption of the dihydrogen complexes in the solid state.

We have recently studied the hydrogen adsorption of solid-state dihydrogen complexes and found that ΔH of D₂ is significantly larger than that of H₂ in the most of dihydrogen complexes. In the presentation, we discuss the possible mechanisms of this phenomenon. In addition, we also report the demonstration of the separation of H₂ and D₂ using column chromatography at ambient temperature.

2:00 PM *SF03.11.02

Novel Inorganic-Organic Combined Complex Metal Hydrides for Energy-Related Applications [HuiWu](#); National Institute of Standards and Technology, United States

With increasing concerns on global climate change, many efforts have been made to tackle this challenge. Development of clean energy such as hydrogen and electricity generated by renewable energy sources will simultaneously reduce the dependence on fossil fuel and emissions of greenhouse gases and pollutants. While for the existing anthropogenic carbon dioxide from combustion of fossil fuels, carbon capture and storage are widely acknowledged as a necessary carbon abatement strategy. Complex hydrides have been intensively studied as promising solid-state hydrogen-storage materials and electrolyte materials for battery applications. They recently have also attracted attention for their potential usage for CO₂ capture and conversion. In this talk, I am going to present our work on development of novel complex metal hydrides, particularly inorganic-organic combined complex hydride systems, with interesting relevant versatile properties for diverse applications such as hydrogen storage, ionic conduction, and CO₂ capture. The talk will focus on the structural studies of these materials. The rich information obtained from the structural analysis and its implications for hydrogen storage, ionic conduction, and CO₂ capture of the related hydrides will also be discussed.

2:30 PM SF03.11.03

Fast and Non-Equilibrium Uptake of Hydrogen by Pd Nanocrystals with Defects [SiyuZhou](#), YifengShi and YounanXia; Georgia Institute of Technology, United States

The energy-storage technologies (e.g., hydrogen storage in metals and electricity storage in batteries) rely on facile absorption and desorption of solute in storage materials. However, the sluggish kinetics of the absorption or desorption process could be an issue if there is a need to overcome extra kinetic barriers, such as nucleation of a second phase and growth through interface motion. Herein, we report that hydrogen absorption by Pd nanocrystals with defects can bypass the energy barriers associated with nucleation and growth of β -phase palladium hydride. Therefore, these Pd nanocrystals with defects absorb hydrogen at a speed that is three times as fast as Pd single-crystal nanocrystals. Moreover, the solubility of H in the Pd nanocrystals with defects is greatly increased, favoring the formation of PdH_x with metastable compositions. The as-obtained PdH_x nanocrystals show promising properties such as high catalytic activity toward formic acid oxidation (FAO).

2:45 PM BREAK

3:15 PM *SF03.11.04

Tailoring Linear Organic Molecules onto Inorganic Scaffolds [TomceRuncevski](#); SMU, United States

The reactivity and functionality of organic molecules in the solid state are primarily governed by weak, non-covalent interactions, which pose challenges in terms of rational control. Furthermore, organic crystals often lack the necessary mechanical properties for the development of functional materials. These challenges can be overcome by utilizing inorganic scaffolds that incorporate functional groups capable of spatially organizing organic molecules. Conversely, the presence of molecules also influences the structure and properties of the scaffolds, often leading to improvements in their properties. In this context, we present three examples highlighting the synergy between organic molecules and inorganic scaffolds. Firstly, we demonstrate how metal-organic frameworks can be employed to store and stabilize 2-aminoethanethiol (cysteamine), a thiol-based drug, is prone to oxidation in its molecular form. By binding the thiol groups to open metal sites in MOF-74, we effectively protect the drug from oxidation and enable controlled release. Next, we explore how a slight modification of the organic molecule can significantly alter the properties of the MOF. Using ethylenedithiol instead of 2-aminoethanethiol introduces defects into the MOF structure, resulting in emergent properties like luminescence that are absent in the parent framework. Furthermore, we investigate other inorganic scaffolds, such as brucite layers, that can be interspersed with organic molecules. Incorporating sorbic acid within the layers of Co(OH)₂ yields a new hybrid material with modified magnetic properties. Notably, this material serves as a platform for the synthesis of atomically-precise polymers from small organic monomers, such as an analogue of natural rubber. In summary, the combination of small organic molecules with inorganic scaffolds presents promising opportunities for tailoring and enhancing properties that can be used in the design of materials to overcome the challenges of tomorrow.

3:45 PM *SF03.11.05

A Dynamical View of Mechanochemical Reactions Adam A. Michalchuk; University of Birmingham, United Kingdom

Mechanochemical reactions – the ability to induce reactivity with mechanical force – offers an unparalleled opportunity for sustainable materials manufacture, removing solvent, reducing reaction times, and offering potential for highly scale-able reactions. Moreover, given the unconventional conditions of mechanochemical routes, they provide a route to synthesize materials that are otherwise impossible to make. Unfortunately, there remains very little understood about how mechanochemical processes occur, which greatly hinders their adoption by the wider community.¹

In this light we have been developing new experimental strategies to follow mechanochemical reactions in situ and in real time.² This includes innovations in time-resolved *in situ* (TRIS) diffraction³ and TRIS X-ray absorption spectroscopy.⁴ To date, these methods have provided exciting new insight into reaction profiles under various conditions, and both phase and microstructural evolution of materials within mechanochemical reactors. To supplement this work, we are developing fundamental new theoretical models to describe mechanochemical reactions, with the aim to understand at the atomic scale how mechanical energy is able to induce chemistry in solid materials.⁵ Together our experimental strategy to probe macroscopic dynamics of mechanochemical reactions, coupled with theoretical methods to probe microscopic dynamics, are providing unprecedented understanding of this potentially transformative technology.⁶ Through this talk we will highlight both experimental and theoretical developments and their applications to understanding the reactivity of solids under mechanochemical conditions.

(1) Michalchuk, A. A. L.; Boldyreva, E. V.; Belenguer, A. M.; Emmerling, F.; Boldyrev, V. V. *Tribochemistry, Mechanical Alloying, Mechanochemistry: What Is in a Name?* *Front. Chem.* **2021**, *9*, 29. <https://doi.org/10.3389/fchem.2021.685789>.

(2) Michalchuk, A. A. L.; Emmerling, F. Time Resolved In Situ Monitoring of Mechanochemical Reactions. *Angew. Chem. Int. Ed.* **2022**, *61* (21), anie.202117270. <https://doi.org/10.1002/anie.202117270>.

(3) Lampronti, G. I.; Michalchuk, A. A. L.; Mazzeo, P. P.; Belenguer, A. M.; Sanders, J. K. M.; Bacchi, A.; Emmerling, F. Changing the Game of Time Resolved X-Ray Diffraction on the Mechanochemistry Playground by Downsizing. *Nat Commun* **2021**, *12* (1), 6134. <https://doi.org/10.1038/s41467-021-26264-1>.

(4) Guilhaume Buzanich, A.; Cakir, C. T.; Radtke, M.; Haider, M. B.; Emmerling, F.; de Oliveira, P. F. M.; Michalchuk, A. A. L. Dispersive X-Ray Absorption Spectroscopy for Time-Resolved In Situ Monitoring of Mechanochemical Reactions. *J. Chem. Phys.* **2022**, *5*, 0130673. <https://doi.org/10.1063/5.0130673>.

(5) Michalchuk, A. A. L. The Mechanochemical Excitation of Crystalline LiN₃. *Faraday Discuss.* **2022**. <https://doi.org/10.1039/D2FD00112H>.

(6) Michalchuk, A. A. L. Thermodynamics and Kinetics of Mechanochemical Reactions. In *Mechanochemistry and Emerging Technologies for Sustainable Chemical Manufacturing*; CRC Press: Boca Raton, 2023; pp 59–92.

4:15 PM SF03.11.06

Chemistry of Nucleation: Mapping the Hydrothermal Chemistry of Tungsten Oxide Formation Mikkel Juulsholt; University of Oxford, United Kingdom

The goal of materials science is to develop new materials with useful properties that can improve the world we live in. At the moment synthesising new materials rely almost solely on educated guesses and trial-and-error methods.^{1,2} As materials become more and more complex, this approach becomes unsustainable because the number of possible synthetic parameters grows infinitely large.^{1,2} Instead, we need to move to a rational synthesis approach where we design the synthesis of materials based on an in-depth knowledge of the chemistry governing the formation of solids.^{1,2} However, we currently have little knowledge of the chemistry controlling the formation of a new phase.^{1,2} To understand the chemistry of materials formation, it is necessary to investigate the chemical reaction as they happen using in situ methods.^{2,3,4}

In this study, we use in situ total scattering with Pair Distribution Function (PDF) analysis to investigate the solvothermal synthesis of tungsten oxide nanoparticles. We show how the structure of the precursor at the moment just prior to nucleation can induce the formation of a metastable phase. We show how both solvent and temperature can also influence the precursor structure and induce the formation of a metastable phase. The tungsten oxide nanoparticles are synthesised from a solution of polyoxometalates, which are large polyanions composed of tungsten and oxygen. The use of *in situ* total scattering and PDF enables us to follow the entire reaction in one experiment and identify the different polyoxometalates formed as well as all formed solid phases. This enables us to map the hydrothermal chemistry of tungsten oxide as a function of pH, precursor and counterions and how they govern the formation of metastable phases.

1. Soderholm, L.; Mitchell, J. F., Perspective: Toward “synthesis by design”: Exploring atomic correlations during inorganic materials synthesis. *APL Materials* **2016**, *4* (5), 053212.

2. Bojesen, E. D.; Iversen, B. B., The chemistry of nucleation. *CrystEngComm* **2016**, *18* (43), 8332-8353.

3. Juulsholt, M.; Lindahl Christiansen, T.; Jensen, K. M. Ø., Mechanisms for Tungsten Oxide Nanoparticle Formation in Solvothermal Synthesis: From Polyoxometalates to Crystalline Materials. *The Journal of Physical Chemistry C* **2019**.

4. Juulsholt, M.; Aalling-Frederiksen, O.; Lindahl Christiansen, T.; Kjær, E. T. S.; Lefeld, N.; Kirsch, A.; Jensen, K. M. Ø. Influence of Precursor Structure on the Formation of Tungsten Oxide Polymorphs. *ChemRxiv* **2023**

4:30 PM SF03.11.07

Dynamical Changes for Exsolved Ni-Based Alloys from Lanthanide Perovskite Oxides Somchate Wasantwisut, Soham Shah and Kandis L. Abdul-Aziz; University of California, Riverside, United States

Using in-situ exsolution of reducible transition metals from perovskite precursors allows for synthesizing strongly adhered nanoparticles that are thermally stable and homogeneous in size and shape. The perovskite oxides can reversibly exsolve transition-metal cations as nanoparticles under fluctuating reducing and oxidizing reaction conditions. The Abdul-Aziz laboratory has pioneered using perovskite oxide precursors to synthesize multimetallic nanoparticles. This presentation discusses the dynamic tracking of the formation and re-dissolution of NiFe and NiRu nanoparticles exsolved from LaFeO₃ and LaNiO₃, respectively. In situ X-ray absorption spectroscopy (XAS) along with ex-situ scanning transmission electron microscopy high-angle annular dark-field (STEM-HAADF) and energy-dispersive X-ray spectroscopy analysis of the parent perovskite oxide precursor, LaFe_{0.8}Ni_{0.2}O₃ and LaNi_{0.8}Ru_{0.2}O₃, as its structure forms bimetallic NiFe or NiRu nanoparticles in reductive environments. For NiFe formation, the LaFe_{0.8}Ni_{0.2}O₃ transforms to NiFe alloy supported on LaO_x-LaFeO_x as corroborated by EXAFS and XANES analysis. The Ni emerges as nanoparticles at 268 °C, while most of the Fe emerges at 700 °C to form NiFe alloy nanoparticles¹. For NiRu formation, the Ni starts to form nanoparticles at 280 °C, and Ru emerges at 200 °C where the formation of the NiRu nanoparticles occurs at ~300 °C. This presentation will discuss recent in situ spectroscopic work to address the existing materials' chemistry challenges for controlled Ni-based bimetallic nanoparticle formation.

4:45 PM SF03.11.08

Rare Earth Oxide Superstructures Assembled via Surface Ligand Switching at High Temperature Grayson C. Johnson and Sen Zhang; University of Virginia, United States

Superstructures comprised of precisely controlled building blocks open opportunities in the rational design and manufacture of functional materials. However, there is a scarcity of synthetic techniques to facilitate the mass production of these materials. Here we present a scalable synthesis of superstructures assembled from atomically precise Ce₂₄O₂₈(OH)₈ and generalize the method to other rare-earth oxide nanoclusters. Combining operando small-angle X-ray scattering, *ex-situ* molecular and structural characterizations and molecular dynamics simulations, we provide a detailed description of the self-assembly mechanism. At high temperature, oleate ligands on the nanoclusters are replaced by benzoate supplied from chemical decomposition of the solvent. This benzoate, participating in pi-pi stacking interactions, drives the self assembly of the superstructures. Removing the benzoate with oleate again at room temperature controls superstructure disassembly into principle component nanoclusters that can be used for the synthesis of multicomponent superstructures, demonstrated up to 5 rare earth element components. The implementation of this synthetic approach, combined with an understanding of the mechanisms involved, offers exciting prospects for generating superstructures that are well-suited for materials applicable to electronics, plasmonics, magnetics, and catalysis.

SESSION SF03.12: Functional Materials V
Session Chairs: Craig Brown and Brent Melot
Friday Morning, December 1, 2023
Hynes, Level 2, Room 202

8:00 AM SF03.12.01

Kinetics of Adsorption and Isotherm Models for Sustainable Zeolite Nano Resin for Water Decontamination Raghav Dosi and Jordan C. Poler; UNC Charlotte, United States

Clinoptilolite, a ubiquitous zeolite mineral with aluminosilicates framework intertwined with cations (Na, K, Ca) is highly porous and has shown strong cation exchange affinity towards some

analyses. Our group has functionalized clinoptilolite grains with anion exchange polyelectrolyte into novel Zeolite Nano Resin (ZNR) which adsorbs toxic contaminants from drinking water. The targeted contaminants are PFOA and PFOS which are highly stable in nature and proposed as unsafe to environment by USEPA with interim lifetime health advisory level down to 0.004 parts per trillion. This study investigates various parameters such as kinetics of adsorption, thermodynamics, concentration of adsorbate and adsorption capacity of several ZNR materials. After comparing with the first order kinetics and Intraparticle diffusion mechanism, ZNR tends to follow pseudo second order chemisorption model with fast kinetics and maximum mass transfer capacity of 3.40 ± 0.04 mg/g. Adsorption isotherm experiments have been performed with initial concentration ranges from 200-2300 mg/L of fluorescein. The adsorption behavior has been explored with Langmuir and BET adsorption isotherm models fit on adsorption isotherm curves. Strong interaction between ZNR and fluorescein has been seen with Langmuir adsorption constant of 0.28 ± 0.1 L/mg and q_{\max} of 4.28 ± 0.20 mg/g which will be optimized further. The grain size adsorption pattern has been explored by crushing the ZNR grains into smaller dimensions and comparing with full grain size (14×40 mm) adsorption isotherm curves. It has been found that the adsorption process is dominant on outside porosity of the framework. However, the elemental analysis by energy dispersive x-ray spectroscopy of half cut grain reveals that fluorescein content was able to reach the inner porous nanochannels of ZNR grains as well. Clinoptilolite undergoes dehydration and rehydration when exposed to water and heat for ZNR aqueous synthesis which was characterized by thermogravimetric analysis along with quantification of polymerization reaction. Kinetics of polymerization of clinoptilolite grains has been examined under 3 different reaction times for optimization. The optimized longest reaction of 118 hours exhibits maximum adsorption capacity. Thermodynamic parameters have been calculated with initial concentration of 1000 mg/L fluorescein at different temperatures. The adsorption capacity found to be maximum at room temperature which shows non-spontaneous process corroborated by positive ΔG as desired under the influence of hot and cold temperature. The high ΔH value also indicates the chemical adsorption where adsorbate molecules are held at the ZNR grain interface by chemical bonds or electrostatic force of attraction. The ΔS is also positive which means that there is randomness at the fluorescein-ZNR interface to reach the adsorption equilibrium. The fluorescein molecules are adsorbing and desorbing simultaneously after certain mass transfer. The equilibrium adsorption constant considered for thermodynamic results is only valid in the adsorption isotherm curve where Langmuir adsorption capacity is equal to the maximum adsorption capacity after the model fitting. Nevertheless, ZNR analyte adsorption seems not limited by only monolayer adsorption as per the isotherm curves. Preliminary studies for the regeneration of ZNR for controlled desorption reveals that approx. 1.5 mg of adsorbed analyte desorbs with just one iteration of 4 mL of 4M NaCl aqueous solution.

8:15 AM SF03.12.02

Formation Mechanisms of Hierarchical Porosity in Carbon Aerogel [Mohd Shaharyar Wani](#), [Bridget Denzer](#), [Sehmus Ozden](#) and [Craig Arnold](#); Princeton University, United States

Carbon aerogels are highly porous and low-density materials exhibiting exceptional structural, electrical, electronic, and electrochemical properties offering a broad scope for applications such as energy storage, catalysis, water desalination/filtration, and more. The present approaches for synthesizing these materials are multi-step and non-sustainable. In contrast, we have recently developed a single-step, scalable, and green approach for synthesizing these hierarchically porous materials using a protein precursor method. The resulting structure shows porosity on multiple scales and exhibits beneficial properties in water filtration applications. In this presentation, we will discuss the detailed formation mechanisms of this complex architecture and explore the range of parameters associated with the precursor materials, focusing on the resulting structure-property relationships.

8:30 AM SF03.12.03

High-Entropy Perovskite Oxides with a Manganese-Based A-Site for Solar Thermochemical Hydrogen Production [Cijie Liu](#)¹, [Dawei Zhang](#)², [Wei Li](#)¹, [Jamie A. Trindell](#)³, [Keith King](#)³, [Sean Bishop](#)³, [Joshua Sugar](#)³, [Anthony McDaniel](#)³, [Andrew Smith](#)³, [Perla Salinas](#)³, [Eric Coker](#)³, [Joerg Neufeind](#)⁴, [Jian Luo](#)^{2,2} and [Xingbo Liu](#)¹; ¹West Virginia University, United States; ²University of California San Diego, United States; ³Sandia National Laboratories, United States; ⁴Oak Ridge National Laboratory, United States

We report a new series of A-site high entropy based on $(La_{2/3}Sr_{1/3})MnO_3$ as the parent perovskite for solar-driven thermochemical hydrogen (STCH), $(La_{1/6}Pr_{1/6}Nd_{1/6}Gd_{1/6}Sr_{1/6}Ba_{1/6})MnO_3$ (LPNGSB_Mn), which exhibits favorable thermodynamic and kinetic properties, along with exceptional phase stability and long-lasting cycling durability. Moreover, LPNGSB_Mn shows enhanced hydrogen production (~ 100 mmol mol oxide⁻¹) compared to the parent perovskite $(La_{2/3}Sr_{1/3})MnO_3$ (~ 68 mmol mol oxide⁻¹) in a short one-hour redox reaction. 50 cycles redox experiment demonstrates the extraordinary phase stability of LPNGSB_Mn. Notably, LPNGSB_Mn shows an outstanding balance between fast kinetics (7.992×10^{-5} cm s⁻¹) and desirable thermodynamics (enthalpy of reduction (ranging between 260 and 286 kJ (mol-O)⁻¹); entropy of reduction (ranging between 130 and 164 J (mol-O)⁻¹ K⁻¹)) along with excellent phase stability during the redox process. Meanwhile, the XPS and in-situ EELS results revealed that Mn is the only redox-active element in this oxide. In addition, the number of A-site elements in the oxide seems to correlate with H₂ production.

8:45 AM SF03.12.04

One-Step Manufacturing of Highly Adsorptive ZnO Thin Films for Gas Sensing Applications [Maanasa Bhat](#), [Jianan Zhang](#), [Chuwei Zhang](#) and [Sili Deng](#); Massachusetts Institute of Technology, United States

Metal oxide gas sensors, key in pollution control and safety applications, promise significant potential for use in novel areas such as disease diagnostics, food safety, and disaster management. These sensors operate based on chemiresistivity, defined as change in resistance due to surface adsorption of gas molecules, and require high sensitivity and selectivity. A typical chemiresistive sensor consists of a metal oxide thin film supported on a sensor substrate attached to a resistance measurement device. The change in resistance occurring when the sensing film is exposed to the target gas is recorded as the sensor response. The sensor is said to be high performance if it has high sensitivity for low concentrations of target gas (< 1 ppm) and high selectivity for the target gas within a mixture of gases. The first step in the sensing mechanism of a chemiresistive sensor is the adsorption of oxygen and target gas molecules onto the surface of the thin film. Higher adsorption rate introduces more gas molecule and surface interactions leading to increased sensor response. Since gas adsorption is a surface phenomenon, the amount of gas adsorbed is dependent on the surface area and the morphology of the metal oxide thin film. Larger surface areas are preferred due to increased availability of adsorption sites on the surface. This makes nanostructured thin films ideal for sensing due to their high surface area to volume ratio. Among several transition metal oxide candidates, ZnO has been reported to show preferential adsorption of ammonia, acetone and isoprene which are important compounds for gas sensor-based disease diagnostics. The desired morphology for a high adsorptive ZnO thin film is ultra-fine nanoparticles connected to form a porous film structure. Conventional methods for preparing these ZnO thin films are wet chemistry-based methods followed by annealing and doctor-blading or spin coating the particles onto the sensor substrate. These methods are generally time and energy intensive and sometimes fail to produce the desired film structure. Our work proposes a flame-based, one-step manufacturing process for the synthesis of ZnO thin films with a porous structure and ultra-fine (~ 10 nm) nanoparticles. Utilizing stretch-stabilized stagnation flame configuration, we deposit 8-10 nm sized ZnO particles directly onto a water-cooled sensor substrate, creating a granular film structure. By varying flame synthesis input parameters, we produce films of different thicknesses and BET surface areas, enabling us to gather adsorption isotherms for ammonia, acetone, and isoprene at varied operating temperatures. This data guides the identification of optimal input parameters for manufacturing a highly adsorptive ZnO thin film in a single step. The highly adsorptive sensor films synthesized using our method hold the potential to be incorporated into sensing devices for non-invasive disease diagnostics, promising a significant stride toward effective and efficient gas sensor development.

9:00 AM SF03.12.05

Topological Insulators for Thermoelectrics [Michael Toriyama](#) and G.J. Snyder; Northwestern University, United States

The rising energy demand and environmental concerns from conventional cooling systems, including those pertaining to refrigeration and air conditioning, poses significant challenges. Distributed thermoelectric cooling offers a viable solution, yet the low power conversion efficiencies necessitate new search and design strategies for improved thermoelectrics. Here, we show that topological insulators are a promising class of materials for next-generation thermoelectrics. We find that the band inversion strength is a key property of topological insulators connected to warping of the bulk electronic structure and, as a result, fundamentally influences the thermoelectric performance. The band inversion strength can be tuned by modulating orbital interactions through e.g. alloying or strain engineering. We evaluate the band inversion strengths of a large set of topological insulators, resulting in the prediction that NaCaBi is a particularly promising thermoelectric candidate. The study offers unique avenues for discovering and designing thermoelectric materials by capitalizing on the electronic structure topology.

9:15 AM SF03.12.06

Thermal and Electrical Transport Properties of Novel Metal Oxochalcogenides for Thermoelectrics [Joe Willis](#)¹, [Katarina Brlec](#)¹, [Kieran B. Spooner](#)² and [David O. Scanlon](#)²; ¹University College London, United Kingdom; ²University of Birmingham, United Kingdom

Up to 50 % of global energy production is lost as waste heat.¹ Harvesting or recycling this energy could provide a new source of energy or increase the efficiency of extant operations, contributing to the green energy transition. High efficiency thermoelectric materials typically contain rare or toxic materials such as Pb, unsuitable for widespread use, so the discovery of nontoxic, earth-abundant but nevertheless efficient thermoelectrics are necessary to fulfil their potential. Following the recent proposal of the mixed anion system $Y_2Ti_2O_5S_2$ as an n-type thermoelectric,² we investigate the electronic and thermal and transport properties of its family, the $Ln_2M_2O_5Ch_2$ oxochalcogenides (Ln = Sc, Y, La; M = Ti, Zr, Hf and Ch = S, Se, Te) as thermoelectrics. We first identify which materials are kinetically and thermodynamically stable, before demonstrating via band alignment they share a preference for n-type doping with $Y_2Ti_2O_5S_2$. We then assess the electronic transport properties using the momentum relaxation time approximation (MRTA) as implemented in AMSET³ to identify the most effective candidates for which to calculate the lattice thermal conductivity, in order to assess their dimensionless figure of merit, ZT.

[1] Firth, A. et al, *Appl. Energy*, 2019, **235**, 1314

9:30 AM SF03.12.07

Giant Dielectric Permittivity in $\text{Ca}_3\text{Co}_4\text{O}_9$ Ceramics and Thin Films Mohammad Al Thehaiban¹, Sonya Harizanova², Bruno Rente¹, Radostina Stoyanova² and Peter K. Petrov¹; ¹Imperial College London, United Kingdom; ²IGIC-BAS, Bulgaria

$\text{Ca}_3\text{Co}_4\text{O}_9$ is a thermoelectric material representing the family of the so-called misfit layered oxides. It consists of a Ca_2CoO_3 layer, an insulating subsystem that maintains the charge supply for the conducting CoO_2 layer, where Co^{3+} and Co^{4+} ions coexist. Recently, a giant dielectric permittivity was measured in $\text{Ca}_3\text{Co}_4\text{O}_9$ ceramic at room temperature.

In this work, we investigated and compared the structural and electrical properties of $\text{Ca}_3\text{Co}_4\text{O}_9$ (CCO) ceramics and thin films. The CCO thin films were produced from a stoichiometric, in-house made CCO ceramic by pulsed laser deposition (PLD) onto (100) oriented lanthanum aluminate (LaAlO_3) substrates. Both the CCO ceramics and thin films were subsequently characterised by X-ray diffraction (XRD). To evaluate the samples' dielectric properties, capacitor structures were formed. Their capacitance was measured and the corresponding permittivity was evaluated in a temperature range RT – 450 K.

For the CCO ceramics, the dielectric permittivity measured at room temperature was ~5,300, which corresponds well with the previously reported values. It was increasing monotonically with no maximum observed at temperatures up to 450 K, where the value was several tens of thousands. Similar behaviour of the capacitance as a function of the temperature with a maximum at 430 K was measured for the thin film sample. Due to the small thickness of the layer, the error associated with the dielectric permittivity evaluation procedure is very high. Nevertheless, one could speculate that it is in a similar order of magnitude as those of the CCO ceramic.

The observed giant dielectric behaviour makes $\text{Ca}_3\text{Co}_4\text{O}_9$ an attractive material for applications like high-K dielectric layers, capacitors and thermoelectric converter devices.

9:45 AM SF03.12.08

Thermal Physics of $\text{RFe}_4\text{P}_{12}$ (R = La, Ce, and Pr) Filled Skutterudites Rafaela F. Penacchio¹, Sergio L. Morelhaio¹, Milton S. Torikachvili² and Stefan W. Kycia³; ¹University of São Paulo, Brazil; ²San Diego State University, United States; ³University of Guelph, Canada

Phosphide skutterudites attracted much attention in the 2000s due to their potential application as thermoelectrical materials, but also for exhibiting interesting phenomena depending on the filler of its icosahedral cages: superconducting $\text{LaFe}_4\text{P}_{12}$ below 4.2 K, insulating $\text{CeFe}_4\text{P}_{12}$, antiferromagnetic $\text{PrFe}_4\text{P}_{12}$ below 6.4 K, and ferromagnetic $\text{NdFe}_4\text{P}_{12}$ below 1.9 K [1]. Experimental and theoretical investigations have sought insight into their unusual lattice dynamics, electronic structure with strongly correlated electrons, and thermoelectric performance [2-5]. However, most first-principles modeling has been performed at fixed temperatures - primarily considering the 0-K equilibrium structure, and there has yet to be a comprehensive and systematic computational study of the effect of temperature on these material properties. In this work, we report a comparative lattice-dynamics study of the temperature dependence of the properties of $\text{RFe}_4\text{P}_{12}$ (R = La, Ce, and Pr), focusing mainly on phonon frequencies, thermal displacements, and electronic band structure. Calculations were performed within the quasiharmonic approximation using GGA for the exchange-correlation energy [6]. The results are compared against experimental data and other calculations, adding insight to the ongoing debate on the filled skutterudites and the role of filler-cage dynamics in the figure of merit ZT, which provides clear directions toward designing more efficient P-based skutterudites for thermoelectric applications.

[1] M. S. Torikachvili et al. Low-temperature properties of rare-earth and actinide iron phosphide compounds $\text{MFe}_4\text{P}_{12}$ (M = La, Pr, Nd, and Th). *Phys. Rev B* 36, 8660 (1987). 10.1103/PhysRevB.36.8660

[2] H. Sato et al. Anomalous transport properties of $\text{RFe}_4\text{P}_{12}$ (R = La, Ce, Pr, and Nd). *Phys. Rev B* 62, 15125 (2000). 10.1103/PhysRevB.62.15125

[3] M. Mizumaki et al. Rare Earth Dependence of Einstein Temperatures in Filled Skutterudite Compounds $\text{REFe}_4\text{P}_{12}$ (RE = La, Ce, Pr, Nd, and Sm). *JPSJ* 80, 074603 (2011). 10.1143/JPSJ.80.074603

[4] M. Ameri et al. First-principles investigation on structural, elastic, electronic and thermodynamic properties of filled skutterudite $\text{PrFe}_4\text{P}_{12}$ compound for thermoelectric applications. *Mol Simul* 40, 15 (2014). 10.1080/08927022.2013.854898

[5] E. Flage-Larsen et al. Bond analysis of phosphorus skutterudites: Elongated lanthanum electron buildup in $\text{LaFe}_4\text{P}_{12}$. *Comput. Mater. Sci.* 47, 3 (2010). 10.1016/j.commatsci.2009.10.018

[6] A. Togo and I. Tanaka. First principles phonon calculations in materials science. *Scr. Mater.* 108, 1359-6462 (2015). 10.1016/j.scriptamat.2015.07.021

10:00 AM BREAK**10:30 AM SF03.12.09**

Dictating Nanoparticle Architecture with Reaction Stoichiometry Using Galvanic Replacement Nabojit Kar¹, Maximilian McCoy¹, Xun Zhan¹, Joshua Wolfe¹, Zhiyu Wang² and Sara Skrabalak¹; ¹Indiana University Bloomington, United States; ²University of Illinois at Urbana-Champaign, United States

Galvanic replacement (GR) provides a simple and versatile route to engineer interesting multimetallic nanostructures, with examples such as nanoboxes, nanocages, nanoshells, nanorings, and heterodimers reported. In GR a solution containing cations of a more noble element is added to a dispersion of NPs of a less noble metal. The less noble metal NPs serve as sacrificial templates, from which some portion of the metal is oxidized and transferred into solution concurrently with the reduction and deposition of the more noble metal. The replacement of bimetallic templates by a more noble metal is less studied and can generate trimetallic nanostructures with different architectures. Here, the specific nanostructure depends on the reduction potentials of the participating metals, the stoichiometry of the GR reaction, and the reaction temperature. Interestingly, titrating NP templates with different cationic species of the same metal can lead to nanostructures with different morphologies and compositions. Herein, architecturally complex PdCu-Au NPs were synthesized through GR between PdCu NPs and AuCl_2^- (Au^{1+}) and AuCl_4^- (Au^{3+}), allowing for the role of reaction stoichiometry on NP architecture to be systematically studied. Interestingly, PdCu-Au heterostructures with multiple Au domains formed in the case of GR with AuCl_2^- while only single Au domains (PdCu-Au Janus particles) were observed in the case of AuCl_4^- . Moreover, with an increase in AuCl_2^- volume, the Au domain adopts a boat-like shape with PdCu positioned within the concavity (confirmed by tomographic reconstruction). These different NP architectures and their connection to reaction stoichiometry are consistent with Stranski-Krastanov (SK) growth, providing general guidelines on how the conditions of GR processes can be used to achieve multimetallic nanostructures with different defined architectures. Broadly, the stoichiometry of a GR reaction provides a synthetic lever to generate different architecturally complex NPs, with potential utility in chemical sensing, as theranostics, and in catalysis.

10:45 AM SF03.12.10

Chemically Tuning Interlayer Coupling and Coherent Light Generation in AMTeO_6 Triangular Magnets Xudong Huai and Thao Tran; Clemson University, United States

2-D triangular magnets with broken spatial inversion symmetry can uniquely offer the precision and tunability needed to meet the demands of spin-photon architectures for the second quantum revolution. While the intralayer coupling (J_1) within 2-D triangular spin lattice has been studied, a largely unexplored question is how the interlayer ionic/covalent bonding influences the electronic structure and interlayer interaction (J_2) of the low-dimensional magnets. To address this, we created a new material CaMnTeO_6 and surveyed AMTeO_6 systems (A = s^0 , s^2 , and d^0 cations; M = Mn, Cr) materials, in which the $S = 3/2$ transition-metal ion M site forms a 2-D triangular lattice and separated by the A site. CaMnTeO_6 features an incommensurate magnetic ground state with AFM in the ab-plane and spiral FM along the c-axis. In addition, this new 2-D magnet exhibits nonlinear optical responses, a prerequisite for integrating spin-photon constructs. We supplemented the results of the structural and physical properties characterization with band structure and chemical bonding. In this talk, we will share our understanding of how the electronic structure of the A site affects the interlayer magnetic coupling of AMTeO_6 materials and their ability to generate coherent photons.

11:00 AM SF03.12.11

Spin and Valence Variation in Cobalt Doped Barium Strontium Titanate Ceramics Anumeet Kaur^{1,2} and Arkaprada Das³; ¹Guru Nanak Dev University, India; ²Global Group of Institutes, Amritsar, India; ³Universite de Mons, Belgium

In the present decade, owing to half-metallic ferromagnetism, controlled 3d transition metal-doping based defect engineering in oxide perovskites attracts considerable attention in the pursuit of spintronics. We have investigated the electronic structure of Co-doped barium strontium titanate ($\text{Ba}_{0.8}\text{Sr}_{0.2}\text{Co}_x\text{Ti}_{1-x}\text{O}_3$ where $x = 0, 0.1, 0.2$) solid solutions. Structural, vibrational and microscopic properties indicate the cationic substitution of Co at the octahedral Ti position along with a displacive kind of tetragonal-to-cubic phase transformation. X-ray photoelectron spectroscopy evidences the reduction in the valence state from Co^{3+} to Co^{2+} and Ti K edge X-ray absorption spectroscopy endorses the higher lattice symmetry with increasing Co doping. Orbital hybridization triggered electron hopping between O 2p and $\text{Co } e_g$ orbitals results in a spin fluctuation from the occupation $t_{e_g}^{2\uparrow} e_{g'}^0$ for $x = 0.1$ to the occupation $t_{e_g}^{2\uparrow} e_{g'}^1$ L for $x = 0.20$ (L

designates a hole in the O 2p shell) aligned state observed from density functional theory calculations. The dominating crystal field energy as compared to intra-atomic exchange (Hund) energy decides the spin-orbital degeneracy for the Co 3d orbital to induce spin fluctuations. The experimentally observed change in the Co oxidation state and its correspondence with theoretically observed half-metallicity brings out good compatibility between experimental observation and density functional theory (DFT) calculations. This compatibility proves its possibility to become a potential candidate for spin injection application in the field of spintronics.

11:15 AM SF03.12.12

Designing Stoichiometric Materials with Eu^{3+} for Dense, Optically Addressable Quantum Memory [Zachary Riedel](#), Donny Pearson, Elizabeth Goldschmidt and Daniel P. Shoemaker; University of Illinois at Urbana-Champaign, United States

Quantum memory built with stoichiometric rare-earth materials opposes conventional doped systems. Rather than containing ppm levels of weakly emitting, randomly distributed rare-earth dopants, stoichiometric compounds drastically increase concentrations while improving homogeneity. This, in theory, produces optical spectra with narrow inhomogeneous linewidths that can resolve hyperfine splittings with hours-long coherence times, creating high densities of optically addressable rare-earth qubits. To explore how chemical factors influence stoichiometric materials' linewidth, we initially studied known compounds with large Eu^{3+} separation to avoid undesirable cation interactions. We grew single crystals of an environmentally stable metal-organic framework with a long optical lifetime and an oxide with coexisting polymorphs, isolating one polymorph for the first time. But we wanted to expand the limited list of compounds with large Eu^{3+} separation. Therefore, starting with known structures, we built 32 chemically diverse compounds using high probability Eu^{3+} and mononuclear ion substitutions to create candidates with large separations and without linewidth broadening from isotopes. To guide our subsequent exploratory synthesis, we narrowed the candidates down to five with density functional theory stability calculations, which have rarely been used for lanthanide compounds. At least two of the predicted stable candidates, a fluoride and a phosphate, are synthesizable. Inhomogeneous linewidth studies will reveal how crystal quality and defect chemistry influence accessibility to the desirable, optically addressable Eu^{3+} transitions.

11:30 AM SF03.12.13

Understanding NaNbO_3 -Based Ceramics with Enhanced Antiferroelectricity for High Energy-Storage Density Applications [Woohyun Hwang](#), Kwangrae Kim, Seunghyun V. Oh and Aloysius Soon; Yonsei University, Korea (the Republic of)

Lead-free antiferroelectric (AFE) ceramics have attracted increasing attention in recent years for its niche application in high-power capacitors owing to both environmental friendliness and high energy density. NaNbO_3 (NNO) is one of few lead-free perovskites with a AFE structure. But the polarization-electric field (P - E) double hysteresis loop was only observed in high-quality single crystals, while in most cases, it was found to possess a ferroelectric (FE) ordering [1,2]. To enhance the antiferroelectricity in NNO, a composition modification strategy by doping was proposed to stabilize the AFE phase effectively [3]. However, in the case of lead-free NNO-based ceramics, the doping effect on its antiferroelectricity is still very poorly understood. In this work, by using first-principles calculations, we will show that the AFE phase of pure NNO is stabilized in the solid-solution due to the decrease of its tolerance factor. A modification of the relative stability of the polar and nonpolar structures will be rationalized by the phase transition pathways for the switching of polarization with the calculated energy barriers [2]. Here, we attempt to explain the effectively favoring of the nonpolar-to-polar AFE transitions over the polar-to-polar FE domain switching. Through this work, we rationalize and provide an atomic-scale perspective of the AFE-FE phase transition in NNO-based ceramics to further engineer novel lead-free antiferroelectric oxides for energy storage applications.

[1] M.-H. Zhang, H. Ding, S. Egert, C. Zhao, L. Villa, L. Fulanović, P. B. Groszewicz, G. Buntkowsky, H.-J. Kleebe, K. Albe, A. Klein, and J. Koruza, *Nat. Commun.* **14**, 1525 (2023).

[2] K. Kim, W. Hwang, J.-H. Lee, and A. Soon, *J. Mater. Chem. C* **10**, 10500 (2022).

[3] M.-H. Zhang, N. Hadaeghi, S. Egert, H. Ding, H. Zhang, P. B. Groszewicz, G. Buntkowsky, A. Klein, and J. Koruza, *Chem. Mater.* **33**, 266 (2021).

SESSION SF03.13: Functional Materials VI
Session Chairs: Craig Brown and Brent Melot
Friday Afternoon, December 1, 2023
Hynes, Level 2, Room 202

1:30 PM SF03.13.01

Cu_2SiSe_3 as a Promising Solar Absorber: Harnessing Cation Dissimilarity to Avoid Killer Antisites [Adair Nicolson](#)¹, Seán R. Kavanagh^{1,2}, Christopher Savory¹, Graeme W. Watson³ and David O. Scanlon¹; ¹University College London, United Kingdom; ²Imperial College London, United Kingdom; ³Trinity College Dublin, The University of Dublin, Ireland

Solar absorbers from the diamond-structure, adamantane family are the current market leaders in thin-film photovoltaics. However, current materials suffer from the use of rare and toxic elements, while emerging candidates such as CZTSSe suffer from killer defects originating from their complex quaternary composition and similarly sized cations.^[1] To this end, we computationally investigated Cu_2SiSe_3 due to its favourable combination of a diamond-type crystal structure, yet cations with large size and charge differences.

Using hybrid DFT and Green's function methods, we calculated the electronic and optical properties, predicting a maximum efficiency of ~30% for a thin-film device of 1.5 μm . We then calculated the formation energies and electronic levels of all intrinsic defects at the hybrid DFT level to characterise the intrinsic defect thermodynamics. In doing so, we confirm the hypothesized high formation energies for antisite defects, in addition to a low concentration of potentially-harmful deep defects.^[2] With its familiar structure and favourable band alignment, initial Cu_2SiSe_3 devices could leverage previously developed device architectures to rapidly test its performance experimentally.

[1] S. Hadke, M. Huang, C. Chen, Y. F. Tay, S. Chen, J. Tang and L. Wong, *Chemical Reviews*, 2021

[2] A. Nicolson et al., *J. Mater. Chem. A*, 2023 (Under review)

1:45 PM SF03.13.02

Low-Refractive Index Silica Aerogel as Rear Reflector for Large-Area PERC Solar Cell Applications [Damla Koçak](#)^{1,2}, Konstantin Tsoi², Hasan H. Canar², Hasan Asav², Ahmet E. Keçeci², Bülent Arikian² and Selçuk Yerci^{1,2,1}; ¹Middle East Technical University, Turkey; ²Odu Gunam, Turkey

Increasing the path length of light in the absorber is one of the most effective optical solutions for dealing with light that is not fully absorbed in a single pass through solar cell devices [1]. The design to improve the path length should also have a high internal reflectance on the absorber surfaces to minimize the energy loss per light-surface interaction [2]. Recent studies show that SiN_x layers with low refractive index (~2) are also preferable to increase rear reflection [3] and passivation of the rear surfaces [4] for Si solar cells architectures such as PERC and PERL. To reduce light absorption in rear metal, inserting a thick non-absorbing reflector layer with a low refractive index n between the absorber and rear metal is very beneficial [5], since a lower n leads to a smaller critical angle at the rear surface and a lower probability that the light will be absorbed by the metal. Passivation is one of the most important parameters for solar cells. SiN_x layer is used for chemical surface and field-effect passivation of PERC solar cells. SiN_x layer on the rear surface is preferably thicker than SiN_x layer on the front surface as an anti-reflective layer to improve the rear reflection on the rear side of the cell by obtaining a film with a lower refractive index [4].

In this work, we studied the effects of a solution-based silica aerogel layer (by sol-gel method), which has a low refractive index and high porosity, inserted between the passivation layer and the rear metal to PERC solar cells. Large area (~156 mmX156 mm) PERC solar cells were fabricated using a thin- SiN_x passivation layer (~20 nm), and it was investigated how the optical and thus the cell performance (i.e., J_{sc} , power conversion efficiency) improves when silicon aerogel is used between the passivation and rear metal. PERC solar cells with two different SiN_x passivation layer thicknesses (20 nm and 120 nm) were used for this study. Since silica aerogel is to be used as the rear reflector, the thickness of the thin SiN_x passivation layer (~20 nm) was chosen so that it would not negatively affect surface passivation [6].

Methyltrimethoxysilane (MTMS), methanol (MeOH), oxalic acid as acid catalyst, and ammonium hydroxide (NH_4OH) as base catalyst were used to synthesize aerogel solutions. The silica aerogel was sprayed on the rear side of the PERC with rear 20nm SiN_x and compared with the PERC without aerogel and the industrial PERC (there is ~120 nm SiN_x passivation layer on the rear side of the cell) with respect to the cell performance.

Transmission (T) and reflection (R) measurements show that the silica aerogel has an optical enhancement in the near-infrared (NIR at ~1200 nm wavelength) region. We have an increase of a ~25% in T+R spectra when aerogel is deposited on the top of thin- SiN_x passivation layer on the rear side of the cell. Also, it was observed that PERC with thin- SiN_x spray-coated with aerogel on the rear side has the same optical performance as the industrial PERC with 120 nm rear SiN_x on the T+R spectra. The optical enhancement in this new PERC design also improves cell performance. We have demonstrated that the improvement in rear reflection increases the short-circuit current by ~1.6 mA/cm^2 compared between PERC with aerogel and without aerogel. In conclusion, we have shown that the proposed aerogel layers ultrasonically sprayed on the rear side of the PERC solar cells with a thin- SiN_x passivation layer achieved an efficiency of 19.9%, while the reference cell (PERC with thin- SiN_x and without aerogel) had an efficiency of 18.75%. Moreover, the PERC with aerogel performed as well as the industrial PERC solar cell with 120 nm rear SiN_x (20.1%) over a long period of time (~700 hours).

- [1] <https://doi.org/10.3390/MA13081860>.
[2] <https://doi.org/10.1109/T-ED.1986.22753>.
[3] <https://doi.org/10.1016/j.solmat.2013.09.017>.
[4] <https://doi.org/10.1002/er.6201>.
[5] <https://doi.org/10.1038/lsa.2013.62>.
[6] <https://doi.org/10.1016/j.surfin.2021.101496>.

2:00 PM SF03.13.03

Inorganic Nanopillar Arrays Remarkably Enhance Photovoltaic Performance of Flexible Perovskite Solar CellsZhifengHuang; The Chinese University of Hong Kong, Hong Kong

Flexible perovskite solar cells (or PSCs) pave the way to conveniently powering a wide range of portable and wearable electronic devices, due to high power conversion efficiency (PCE), large-area fabrication, and potentially low cost. However, the commercialization of flexible PSCs is prohibited by environmental instability and low mechanical robustness. One-dimensional (1D) inorganic nanostructure arrays, functioning as charge transporting layers, have been proposed to solve these two problems. In-situ growth of 1D nano-arrays on polymer-based flexible electrodes is required but very challenging, mainly due to degradation of polymer-based electrodes at high temperature of in-situ growth.

We use glancing angle deposition (GLAD) at low substrate temperature to in-situ deposit nanopillar arrays (NaPAs) onto a flexible electrode for an assembly of flexible PSCs. The NaPAs are made of diverse inorganic materials, such as titanium, titanium oxides, tin oxides (functioning as electron transporting layers) and nickel oxides (serving as hole transporting layers). The as-grown NaPAs enhance light transmittance, facilitate light harvesting in perovskites, promote charge carrier transport and collection, facilitate the formation of large perovskite grains, prohibit perovskites from decomposition, and release mechanic stress. All these features cause large-area flexible PSCs to have PCE of >15%, small photovoltaic hysteresis, 10% degradation for approximately 800-hr storage, and 20% degradation by manual bending for around 400 times.

We devise an advanced technique of low-substrate-temperature GLAD generally adapted to in-situ deposition of charge transporting layers made of inorganic NaPAs on flexible electrodes, to significantly enhance optoelectronic performance, mechanic robustness, and environmental stability of flexible optoelectronic devices.

2:15 PM SF03.13.04

Zero-Dimensional Lead-Free Metal Halide Scintillator Suitable for Extreme Environments and X-Ray ImagingJoo HyeongHan and Won BinIm; Hanyang University, Korea (the Republic of)

Scintillators are widely used for radiation detection in various fields, such as medical imaging, nondestructive testing, and crystallography. X-ray-generating systems typically emit large amounts of heat and require a high thermal stability of scintillators, particularly for nondestructive testing or radiation detection performed under harsh conditions. Therefore, highly stable scintillators must be developed for application in extreme environments. Herein, we developed new zero-dimensional lead-free monoclinic phases of Cs₃TbCl₆ and Rb₃TbCl₆ metal halides. Surprisingly, Cs₃TbCl₆ and Rb₃TbCl₆ have retained over 90% of their original PL properties at 250°C. Cs₃TbCl₆ and Rb₃TbCl₆ polycrystals exhibit high light yields of 56,800 and 88,800 photons/MeV, respectively. Cs₃TbCl₆ and Rb₃TbCl₆ polycrystals also show low detection limits of 149.65 and 115.38 nGyairs⁻¹ due to their structural-optical properties, respectively. Furthermore, the fabricated thick films of Cs₃TbCl₆ and Rb₃TbCl₆ are applied to our homemade X-ray imaging system, and preferable spatial resolutions are obtained as compared with a commercial Gd₂O₂S:Tb³⁺ film.

2:30 PM SF03.13.05

Efficient Photodegradation of Methyl Red Dye by Kaolin Clay Supported Zinc Oxide Nanoparticles with Their Antibacterial and Antioxidant ActivitiesdreesKhan and ZhangBaoliang; Northwestern Polytechnical University, China

Kaolin clay (KC) supported Zinc oxide (ZnO/KC) and ZnO nanoparticles (NPs) were prepared by a chemical reduction process and used for the photodegradation of methyl red (MR) as photocatalysts. Due to the interlayered porous structure of KC, we achieved a perfect association between ZnO NPs and KC. SEM image showed the irregular morphology of ZnO NPs, while ZnO/KC NCs were predominately round-shaped. Moreover, in both cases, NPs were present in dispersed and agglomerated forms with an average particle size way below 100 nm. The results acquired from photodegradation analyses showed that ZnO NPs and ZnO/KC NCs degraded about 82% and 99% of MR under UV light in a short irradiation time within 10 min. The recovered and re-recovered ZnO NPs and ZnO/KC NCs were also considerably photodegraded MR in an aqueous medium. The same NPs also exhibit promising bioactivities against two pathogenic bacteria, i.e., Citrobacter and Providencia. ZnO/KC NCs' antioxidant activity reached a reasonable 70% compared to the 88% activity of the standard ascorbic acid.

2:45 PMBREAK

3:15 PM SF03.13.06

Moderate Temperature Chalcogenization of Highly Stable Metal Oxides—An Opportunity for Chalcogenide PerovskitesShubhanshuAgarwal, JonathanTurnley, ApurvaPradhan and RakeshAgrawal; Purdue University, United States

The importance of deploying solar panels for generating renewable energy has never been greater. The emergence of halide perovskites has brought hope for an efficient material with exceptional optoelectronic properties. This breakthrough has resulted in numerous efficiency and PLQY (photoluminescence quantum yield) records being surpassed. However, halide perovskites face inherent instability in the presence of moisture and air. Additionally, they rely on toxic lead in their crystal structure to achieve the ABX₃ structure, which gives rise to their exciting properties. These limitations must be addressed before halide perovskites can be widely used for energy generation.

On the other hand, chalcogenide perovskites possess a similar ABX₃ structure to halide perovskites, offering excellent electronic and optoelectronic properties. They are composed of abundant elements found in the Earth's crust and have shown a high light absorption coefficient. Chalcogenide perovskites are also defect-tolerant and exhibit high photoluminescence. However, the synthesis of chalcogenide perovskites involves high-temperature methods. Typically, they are synthesized by treating oxide perovskites with H₂S/CS₂ at temperatures exceeding 900°C. These high temperatures limit the substrates that can be used to create thin films of these materials for photovoltaic applications. Although some reports have demonstrated moderate-temperature synthesis, they rely on expensive organometallic precursors, hindering widespread adoption.

In this study, novel methods are presented for converting tailored precursor films to sulfides at temperatures below 600°C. One of the biggest challenges of synthesizing transition metal sulfide perovskites is their propensity to react with any residual oxygen in the system forming unwanted oxide phases. We have identified an innovative oxygen getter that removes any residual oxygen from the precursor film leading to phase pure sulfide perovskites. Furthermore, the method has been expanded to synthesize selenium-based transitional metal trichalcogenides from transition metal oxides. As a whole, these novel methods provide unique opportunities to utilize inexpensive metal salt precursors for forming precursor films and subsequently converting them to transition metal sulfides including perovskite films at low temperatures.

3:30 PM SF03.13.07

Evolution of Interfaces in Multi-Principal Element Alloy NanoparticlesVitaliyR. Yurkiv¹, AzadehAmiri², RezaShahbazian-Yassar² and FarzadMashayek¹; ¹University of Arizona, United States; ²University of Illinois at Chicago, United States

Multi-principal element alloy nanoparticles (NPs), composed of multiple elements arranged in an ordered intermetallic crystal structure, pose unique properties for a variety of applications. They can be used as catalysts, where their unique composition and structure can improve catalytic activity and selectivity. They also hold promise in energy storage and conversion, sensing technologies, and biomedical applications, among others. In this work, we seek to understand the structure and stability of grain boundaries (GBs) formed between various medium entropy alloy NPs, the mechanisms of metals diffusion through them, and its influence on NPs coalescence. The density functional theory (DFT) calculations supported by the high-resolution transmission electron microscopy (HRTEM) measurements are employed to understand the GB atomic structures, their evolution, and their chemo-mechanical properties. The DFT calculations are performed using the VASP (Vienna Ab initio Simulation Package) code with the plane wave basis sets and the projector augmented wave (PAW) pseudopotentials in the framework of the Perdew-Burke-Ernzerhof generalized-gradient approximation (GGA). For GBs structure creation, the Atomistic Tool Kit (ATK) software is used. The crystalline phase structure and GBs evolution of nanoparticles and their elemental composition and distribution are characterized by annular dark field scanning transmission electron microscopy (ADF-STEM) images with 512x512 pixels scanning resolution and energy-dispersive spectroscopy (EDS) analysis performed at 8c probe size on a JEOL ARM200CF scanning electron microscope operating at 200 kV.

Different size medium entropy alloy NPs containing various compositions of Pt, Cu, Ir and Ni elements, have been obtained through electron beam-induced co-reduction of mixed metal salts solution inside the liquid-cell TEM holder. The ADF-STEM images of the formed colloidal NPs were obtained at the end of the process on dry sample after liquid was removed. It was observed that there is an aggregate of multiple crystalline medium entropy alloy NPs of different sizes and orientations attached by amorphous grain boundaries and loosely bonded atoms at

the interface. The colloidal medium entropy alloy NPs have *fcc* structure with lattice constant of 3.89 Å. STEM-EDS analysis indicates a homogenous distribution of Pt, Cu, Ir, and Ni elements in NPs with atomic composition of (Pt_{0.46}Cu_{0.3}Ir_{0.16}Ni_{0.06}). The HRTEM measurements revealed the diverse GB structures consisting of (100), (110), (121), etc., surface orientations of the above-mentioned NPs composition. Based on the HRTEM results, the corresponding computational slabs have been built and optimized using ATK and VASP. Pt, Cu, Ir and Ni adatom diffusion inside grain and GB, after the optimization of all structures, were calculated. For each GB, several adatom positions with multi-atom bonding were identified. The activation energy of metal diffusion varies significantly depending on the slab's structure and the number of adatoms. A non-symmetric metal transition state for all considered structures and atoms, which indicates a complex multi-atom hopping mechanism, was identified. In addition, the DFT calculations are used to obtain electron density and the density of states for corresponding GB structures. Based upon the electron density profile the stability of analyzed interface with and without metallic adatoms is quantified. Our combined experimental and modeling study provides valuable understandings into developing mitigation strategies towards a better understanding of medium and high entropy alloys for a variety of applications.

Authors acknowledge the financial support from the National Science Foundation Award DMR-2311104.

3:45 PM SF03.13.08

Engineering Macroporous Structure Towards Enhancing Mass Transfer and Catalytic Performance of Three-Way Catalyst ParticlesPhongH. Le and TakashiOgi; Hiroshima University, Japan

The increasing emission of pollutants from gasoline-power vehicles has prompted concerns regarding human health and the environment. To address this issue, researchers have focused on developing novel technologies to mitigate their adverse effects, and a three-way catalyst (TWC) has emerged as a crucial technique in this area since the 1970s. However, the TWC materials are composed of large amounts of costly and rare elements, including Rhodium (Rh), Palladium (Pd), and Platinum (Pt), which considerably increases their manufacturing expenses. Consequently, it is necessary to reduce the consumption of TWCs as their demand increases due to the global outbreak of transportation vehicles over the years. The promising method to overcome this challenge is to enhance their catalytic performance by appending the porous structure. Catalyst particles endowed with macroporous architectures have gained considerable attention due to their superior molecular diffusion capabilities and catalytic activities.

In this study, the macroporous TWC particles with interconnected macropore networks were synthesized via a template-assisted spray process. The synthesis of macroporous TWC particles requires precise control over various parameters. Furthermore, the mass transfer coefficients of the macroporous TWC particles were then investigated by measuring the CO₂ adsorption rate, allowing us to understand the influence of macroporous structure on internal mass transfer. The results demonstrate a significant enhancement in the mass transfer coefficient upon introducing macropores into the TWC particles compared to conventional aggregate TWC particles. However, a decline in the mass transfer coefficient was observed as the macropore size exceeded a certain threshold due to the presence of an extensive framework. To explore the practical implications of these macroporous TWC particles in the catalysis field, we conducted catalytic performance assessments using CO oxidation reaction as the model. Remarkably, the macroporous samples exhibited superior catalytic performance compared to their aggregate counterparts. These results demonstrate the critical role of macroporous structure in enhancing the catalytic performance of TWC particles.

In conclusion, our comprehensive study highlights the significance of macroporous structures in catalyst particles and their potential to revolutionize TWC efficiency. The profound improvements in mass transfer coefficients and catalytic performance provide valuable insights for designing advanced TWC materials that exhibit enhanced pollutant conversion capabilities.

4:00 PM SF03.13.09

Intrinsic Tensile Ductility in High Entropy Metallic GlassZhiboZhang; City University of Hong Kong, China

Metallic glasses are an important material with a wide range of applications, such as in bio-medical engineering, aerospace engineering, automotive industries, micro-electro-mechanical systems and consumer products. Nevertheless, the Achilles' heel of metallic glasses is short of tensile ductility at low temperature, which impedes their widespread applications as yet. To overcome this limitation, people have proposed different methods to toughen metallic glasses, including surface mechanical attrition treatment, architected constructions, and deformation induced rejuvenation. Although these methods have shown potential for improving tensile ductility at room temperature, the reported results of intrinsic tensile ductility tend to be limited (< 1%) with a low strain hardening rate. In this work, here we present a high-entropy metallic glass with unique multifunctional properties. This glass demonstrates exhibits a gigapascal yield strength of ~1.5 GPa, undergoes significant strain hardening that almost doubles its yield strength (~70% strength increase), and exhibits unprecedented over two-fold increase in uniform tensile ductility compared to the previous records (~ 2%). These remarkable properties stem from the amorphous structure of our high-entropy metallic glass, which is composed of atoms with significant size mismatch. The shear banding in this HEMG is self-locked because of shear induced atomic diffusion. Our findings suggest a promising pathway to design stronger, more ductile glasses that can be applied in a wide range of technological fields.

4:15 PM SF03.13.10

Broadband Reduction in Vibrational Thermal Conductivity of Ruddlesden-Popper (Ba_{n+1}Zr_nS_{3n+1}) Phases of Perovskite Chalcogenide BaZrS₃ Md Shafkat BinHoque¹, EricHoglund², BoyangZhao³, De-LiangBao⁴, HaoZhou⁵, SandipThakur⁶, EricOsei-Agyemang⁷, KevinYe⁸, KhalidHattar², EthanScott¹, MythiliSurendran³, JordanA. Hachtel², JohnA. Tomko¹, JohnGaskins⁹, KiumarsAryana¹, SaraMakarem¹, RafaelJaramillo⁸, GaneshBalasubramanian¹⁰, AshutoshGiri⁶, TianliFeng⁵, JayakanthRavichandran³, SokratesT. Pantelides⁴ and PatrickE. Hopkins¹; ¹University of Virginia, United States; ²Oak Ridge National Laboratory, United States; ³University of Southern California, United States; ⁴Vanderbilt University, United States; ⁵The University of Utah, United States; ⁶University of Rhode Island, United States; ⁷University at Buffalo, The State University of New York, United States; ⁸Massachusetts Institute of Technology, United States; ⁹Laser Thermal Analysis, United States; ¹⁰Lehigh University, United States

Understanding and manipulating the microscopic mechanisms of ultralow thermal conductivities in crystalline materials has been the central goal of condensed matter and materials physics for the past decade, with many questions still unanswered. Given the broadband spectral nature in the transport of phonons and other vibrational modes in crystals, achieving a superior thermal insulator requires material classes that can restrict thermal transport of all modes in the thermally active vibrational spectrum; the strategy to do so requires different approaches based on the energy and dispersive nature of each individual mode. Here, we report on the ultralow thermal conductivities in the Ruddlesden-Popper phase (Ba_{n+1}Zr_nS_{3n+1}, n = 3 and 4) crystals that are derivatives of inorganic perovskite chalcogenide Barium Zirconium Sulfide (BaZrS₃). The thermal conductivity of Ruddlesden-Popper phases exhibits ultra-low amorphous-like values and trends due to the presence of intra-unit-cell rock-salt blocks inducing strong anharmonicity and a large fraction of localized and low velocity vibrational modes throughout the entire vibrational spectrum, thus achieving broadband restriction of thermal transport. Our study provides significant insight into the interaction between structural interfaces and vibrational modes that can cause ultra-low thermal conductivities in inorganic crystals in efforts to design ideal phonon or vibrational glasses for exceptional thermal insulation.

4:30 PM SF03.13.11

Understanding the Structure-Catalytic Property Relationship: From Nanoparticles to Single AtomsAgusR. Poerwoprajitno¹, RichardTilley² and DaleL. Huber¹; ¹Sandia National Laboratories, United States; ²The University of New South Wales, Australia

Understanding the surface structure-catalytic properties relationship is vital to design highly active and stable catalysts for energy-related applications.^[1] This is because the catalytic reaction occurs only on the surface. Our research focuses on precisely controlling the surface structure of nanocrystals, surface facets and crystal structure that defines the active site.^[2] This high level of control enables us to study the effect of different active site on catalytic reactions. The next step is to use this well-defined nanocrystal as substrate for second metal decoration as for complex reaction, such as methanol oxidation reaction (MOR), where the exposure of two metals on the surface is important to improve catalytic activity, stability and selectivity.^[3] We showed a synthetic approach to control the decoration of Pt single atom on faceted Ru nanoparticles that have successfully avoid CO-poisoning in MOR. The Pt single atoms were formed by spreading Pt islands and was studied by in-situ environmental TEM (ETEM) at atomic-level. We also discuss our recent work on scaling up the nanoparticle synthesis using microfluidic incorporated with in-situ characterization and assisted by AI.

This work was performed, in part, at the Center for Integrated Nanotechnologies, an Office of Science User Facility operated for the U.S. Department of Energy (DOE) Office of Science. Sandia National Laboratories is a multimission laboratory managed and operated by National Technology & Engineering Solutions of Sandia, LLC, a wholly owned subsidiary of Honeywell International, Inc., for the U.S. DOE's National Nuclear Security Administration under contract DE-NA-0003525. The views expressed in the article do not necessarily represent the views of the U.S. DOE or the United States Government.

References:

- [1] A. R. Poerwoprajitno, S. Cheong, L. Gloag, J. J. Gooding, R. D. Tilley, *Acc. Chem. Res.* **2022**, *55*, 1693-1702.
- [2] A. R. Poerwoprajitno, L. Gloag, J. Watt, S. Cychy, S. Cheong, P. V. Kumar, T. M. Benedetti, C. Deng, K.-H. Wu, C. E. Marjo, D. L. Huber, M. Muhler, J. J. Gooding, W. Schuhmann, D.-W. Wang, R. D. Tilley, *Angew. Chem. Int. Ed.*, **2020**, *59*, 15487-15491.
- [3] A. R. Poerwoprajitno, L. Gloag, J. Watt, S. Cheong, X. Tan, H. Lei, H. A. Tahini, A. Henson, B. Subhash, N. M. Bedford, B. K. Miller, P. B. O'Mara, T. M. Benedetti, D. L. Huber, W. Zhang, S. C. Smith, J. J. Gooding, W. Schuhmann, R. D. Tilley, *Nat. Catal.* **2022**, *5*, 231-237.

4:45 PM SF03.13.12

Understanding the Role of Entropy in Medium to High-Entropy Oxides and AlloysChaochaoDun¹, ShuoLiu², JeffUrban¹ and MarkT. Swihart²; ¹Lawrence Berkeley National Laboratory,

The Hume-Rothery rules governing solid-state miscibility limit the compositional space for new inorganic material discovery. Here, we report a non-equilibrium, one-step, and scalable flame synthesis method to overcome thermodynamic limits and incorporate immiscible elements into a single phase. Starting from prototype examples including (NiMg)O, (NiAl)O_x, and (NiZr)O_x, we then extend this method to a broad range of Ni-containing ceramic solid solutions, and finally to general binary combinations of elements. We report an "encapsulated exsolution" phenomenon observed upon reducing the metastable porous (Ni_{0.07}Al_{0.93})O_x to create ultra-stable Ni nanoparticles embedded within the walls of porous Al₂O₃ nanoshells. This nanoconfined structure demonstrates high sintering resistance during 640 hours of catalysis of CO₂ reforming of methane, maintaining constant 96% CH₄ and CO₂ conversion at 800 °C and dramatically outperforming conventional catalysts. We have further fabricated high-entropy oxide nanoceramics with six typical crystal structures (Rock-salt, Spinel, tetragonal, Fluorite, and Rutile), with one of them with 22 elements for high-entropy fluorite. When using (MgCoNiCuZn)O_x as an entropy dispersion of a "single-atom" like Pt, the loading amount can be as much as 10 wt%, much higher than traditional 1 wt% or 2 wt%. The thermal stability and activity of these materials as a catalyst has the work-record performance for CO₂ hydrogenation so far.

SYMPOSIUM SF04

Expanding the Frontiers of Plasma Technology in Materials Science and Engineering
November 27 - November 30, 2023

Symposium Organizers

Rebecca Anthony, Michigan State University
Fiorenza Fanelli, Consiglio Nazionale delle Ricerche
Tsuyohito Ito, The University of Tokyo
Lorenzo Mangolini, University of California, Riverside

* Invited Paper

+ JMR Distinguished Invited Speaker

SESSION SF04.01: Plasma Science for Materials Processing—Diagnostics and Fundamentals

Session Chairs: Fiorenza Fanelli and Tsuyohito Ito

Monday Morning, November 27, 2023

Sheraton, Second Floor, Independence East

10:30 AM *SF04.01.01

Fundamentals and Applications of Plasma Nonequilibrium at Interfaces Jan Benedikt^{1,1}, Christian Schulze¹, HeLi¹, Martin Müller¹, Sadegh Askari² and Zoltan Donko³; ¹Kiel University, Germany; ²KTH Royal Institute of Technology, Sweden; ³Wigner Research Centre for Physics, Hungary

Plasma-generated high nonequilibrium fluxes of energetic ions, metastables, reactive radicals or electrons reaching the surfaces are widely used in the research and industry. Still, some of the microscopic interaction processes including ion-induced secondary electron emission or electron reflection on realistic surfaces are not fully understood. Additionally, the *in situ* monitoring and control of, for example, ion energy-flux distribution function is needed to provide precise control of material processing needed for applications such as processing of 2D materials or manufacturing of components for quantum computing. This contribution will discuss the application of energy-resolved ion mass spectrometry (ERIMS) in two experiments used to analyze plasma-surface interaction and perform controlled material processing.

First, a technique that combines ERIMS measurements and 1D3V particle-in-cell/Monte Carlo collision simulations to determine effective ion-induced secondary electron emission (SEE) yield and the effective elastic electron reflection probability parameters simultaneously and independently in a symmetric rf capacitively coupled plasma in argon [1]. It is possible, because SEE and electron reflection processes at the surface influence plasma and sheath properties and with it also the ion flux-energy distribution function (IEDF) measured at the electrode. In particular, the energy width and mean energy of the bimodal peak feature in the IEDF can provide the effective values of both parameters for any material on the electrode surface. The method was applied to stainless steel and aluminum oxide surfaces resulting in a good agreement with literature values.

Second, a new reactor with inverted electrode geometry was assembled which is combining ICP plasma with CCP bias applied to reactor wall to control the plasma density and ion energy separately at the small grounded electrode during the treatment [2]. The small size of the grounded electrode results in the largest voltage drop and largest ion energy there, which can be analyzed by ERIMS during the plasma treatment including the analysis of the sputtered or desorbed material on the ion composition. The CCP bias allows further control of the ion energy. We have observed previously that low-pressure plasma treatment improves electrochemical performance of transition metal oxides used as air electrode of zinc-air batteries [3]. We use this material here as a test substrate for the study of the effect of the ion energy on their performance in hydrogen and nitrogen discharges. Additionally, the nitrogen plasma has also been used to treat graphene and results relating ion IEDF and structural changes of graphene will be presented. The graphene has been chosen here as a model material for the 2D materials. Experiments with transition metal dichalcogenides and their monolayers will follow. All examples in this contribution are part of the larger research program at Kiel University focusing on the experimental and theoretical study of the plasma nonequilibrium at interfaces.

[1] C. Schulze, Z. Donkó, J. Benedikt, *A computationally assisted technique to measure material-specific surface coefficients in capacitively coupled plasmas based on characteristics of the ion flux-energy distribution function*, Plasma Sources Sci. Technol. 31 (2022) 105017

[2] C. Schulze, H. Li, L. Mohn, M. Müller, J. Benedikt, *Chamber with Inverted Electrode Geometry for Measuring and Control of Ion Flux-Energy Distribution Functions*, Plasma 2022, 5(3), 295

[3] H. Li, S. Askari, J. Wang, N. Wolff, M. Behrens, L. Kienle, J. Benedikt, *Nitrogen-Doped NiCo₂O₄ Nanowires on Carbon Paper as a Self-Supported Air Cathode for Rechargeable Zn-Air Batteries*, accepted for publication in Journal of Hydrogen Energy; DOI:10.1016/j.ijhydene.2023.03.146

11:00 AM SF04.01.02

Optimization of High Dose Rate Plasma Immersion Ion Implantation for 8Cr4Mo4V Steel Bin Miao^{1,1}, Junbo Niu¹, Jinming Zhang², Xinghong Zhang³ and Xinxin Ma^{1,1,3}; ¹Harbin Institute of Technology, China; ²CETC Academy of Chips Technology, China; ³AECC Harbin Bearing Co., Ltd., China

As the typical high-temperature bearing steel, 8Cr4Mo4V has excellent comprehensive performance, which is widely used as the bearing material and has made it increasingly popular in industrial and aerospace applications. Nowadays, the lack of service life of bearing has become its bottleneck which restricts the performance of aero-engine. How to solve or improve this problem is the focus for most surface engineering researchers at present. The traditional ion implantation technique generally takes dozens of hours or even longer duration in real applications, resulting in its obvious shortcoming of energy consuming and low efficiency. For the high-dose-rate plasma immersion ion implantation, very high ion current densities allow implementing ultrahigh dose implantation and the formation of nanoscale layer in shorter duration as compared to the conventional ion implantation. Therefore, high-dose-rate immersion ion implantation can be utilized to increase the efficiency and reduce energy consumption. In order to investigate the optimization of high-dose-rate ion implantation on mechanical properties, 8Cr4Mo4V

bearing steel was implanted with 10 to 12 keV nitrogen ions dose rates with fluences between 7.6×10^{17} ions/cm²/h and 1.9×10^{18} ions/cm²/h, and the implanted samples were analyzed by AvaSpec Multi-Channel Spectrometer, nanoindentation tester and residual compressive stress tester in this study. The obtained results reveal that the optimal implantation dose rate ranges from $(8-20) \times 10^{17}$ ions/cm²/h to meet the high implantation requirements. Given the furnace power supply constraints, the implantation voltage range of 10-12 keV and a minimum implantation frequency of 600 Hz are recommended. The implantation pulse width of 25 μ s and working pressure of 0.5 Pa are also advised to attain greater implantation current density. The present work optimizes the parameters in the investigation of high-dose-rate ion implantation process, and the obtained results will be useful for structural scientists and engineers in real applications. Meanwhile, the results show that the temperature stabilizes around 350 °C at the implantation dose rate of approximately 1.5×10^{18} ions/cm²/h. Meanwhile, the highest nanohardness value of 18.67 GPa is attained for the implanted samples at dose rate of 1.70×10^{18} ions/cm²/h, which is 66.7% higher than that of the non-implanted sample. Compared to the as-received sample stress of 273.3 MPa, the maximum residual stress reached approximately 640 MPa at the dose rate of 1.38×10^{18} ions/cm²/h, which was enhanced by 134.4%. This enhancement is advantageous for the practical applications of bearing steel.

11:15 AM SF04.01.03

Imaging-Constrained Fluid Simulation of Laser-Generated Plasmas Containing Multiple Chemical Species Jacob Paiste¹, Eric Remington², Dorien Carpenter¹, Nathan Humphrey³, Kamron Strickland¹, Robert Arslanbekov⁴, Alexey Volkov³, Sumner B. Harris⁵, David B. Geohegan⁵ and Renato P. Camata¹; ¹University of Alabama Birmingham, United States; ²Samford University, United States; ³The University of Alabama, United States; ⁴CFD Research Corporation, United States; ⁵Oak Ridge National Laboratory, United States

Laser-generated plasmas are complex electro-hydrodynamic systems with broad technical applications in materials science and engineering. They are widely used to etch, chemically modify, and fabricate materials both in bulk and thin film form. Although simulations of laser plasmas have been carried out for decades, only recently have developments in computational power and techniques allowed meaningful quantitative modeling of the long distance plasma expansions that are critical for understanding plasma processing and plasma interactions with materials surfaces.

In this work we describe a laser ablation/plasma fluid simulation model that can be constrained by gated-intensified CCD (ICCD) imaging data of the rapid expansion of the laser-generated plasma. The time-resolved image capture of the luminous portion of the plasma plume results in photon count data arrays that are processed for plume visualization, animation, and motion tracking. Our effective plasma fluid model incorporates well established features of laser ablation plasmas (thermal evaporation, bremsstrahlung emission from plasma electrons, photoionization, and free-free laser absorption by the plasma) and an additional effective plasma absorption coefficient that serves as a stand-in term for more sophisticated mechanisms that are impractical to account for directly due to computational cost or unavailability of physical parameters. The effective plasma absorption coefficient (a free parameter in the model) is determined by matching the simulated plasma evolution to the dynamics of the expansion as determined by the ICCD imaging data. Once the model has been constrained in this manner, full scale simulations of all plasma parameters and distribution are possible.

We apply this model to a plasma generated during ablation of a solid target of iron selenide (FeSe), which is used in plasma-mediated growth of superconducting FeSe thin films. The complex chemistry of this plasma requires the solution of Saha equilibrium equations for singly and doubly ionized Fe and Se species, while the fluid dynamic equations are solved using an average approach. ICCD imaging data reveals that plasmas produced with fluences of 0.9, 1.5, and 2.4 J/cm² of 25-ns, 248-nm excimer laser pulses in vacuum, have average plume speeds of 13.0, 17.0, and 21.7 km/s, respectively. When an argon (Ar) background pressure is introduced, the average plume speeds decrease into the 9-13 km/s range for 30-50 mTorr pressures. Our simulated expansion velocities span these ranges of plume speeds detected from ICCD measurements and are sensitive to the choice of the effective absorption parameter in the model. In this presentation, we describe how the ICCD imaging data allows determination of the best value of the effective parameter and full scale simulations of the expansion. Furthermore, we discuss how Direct Monte Carlo Simulation (DSMC) results can be used to validate our effective fluid model approach by comparisons of mass flux results, target surface temperatures, initial velocities, and energy conservation throughout the simulation.

11:30 AM *SF04.01.04

Methods for *In-Situ* Diagnostics of Plasma-Assisted Synthesis of Nanomaterials Shurik Yatom; Princeton University, United States

Plasmas are widely used for synthesis of various nanomaterials. Plasma-mediated methods offer industrial scale production of nanomaterials while being less expensive and environmentally friendly compared to chemical and mechanical methods of synthesis. They also hold a promise for well-controllable synthesis, due to the ability to control the plasma characteristics and plasma-induced chemistry. For many years, the understanding of the interplay between the plasma and the synthesized products was dependent on the ex-situ analysis and trial and error approach, where the synthesized material was collected from the reactor walls and analyzed by electron microscopes. Nowadays, it becomes more and more obvious that we need techniques that can detect and characterize nanoparticles and nanotubes in-situ, as they are being formed in the plasma. In this talk I will summarize the capabilities and the methods of *in situ* diagnostics of plasma, plasma induced gas-phase chemistry and synthesized nanomaterials. These diagnostics measure the plasma conditions, the precursor species to nanoparticle formation, presence and sizes of nanoparticles in the synthesis region, chemical composition of the nanomaterials. The following diagnostics are covered: optical emission spectroscopy, laser induced fluorescence, laser induced incandescence, fast frame imaging, coherent Rayleigh Brillouin scattering, nanomaterial extractor probe and others. Finally, I will discuss the future possibilities and directions for in-situ diagnostics of plasma-assisted nanosynthesis.

Acknowledgement

The author wishes to thank Dr. Yevgeny Raitses, Dr. Michael Schneider, Dr. Brent Stratton, Dr. Vladislav Vekselman, Dr. Alexandros Gerakis, Dr. James Mitrani, Dr. Igor Kaganovich and Dr. Alexander Khrabry for their contribution and support through advice, brainstorming, help with experiments, analysis and modeling concerning the work with carbon arc. The author wishes to thank Tanvi Nikhar, Sankhadeep Basu, Prof. Rebecca Antony and Prof. Sergei Baryshev for their contribution and support in RF reactor synthesis work. Experiments and simulations of synthesis processes in carbon arc were supported by the US Department of Energy (DOE), Office of Science, Basic Energy Sciences, Materials Sciences and Engineering Division. The arc modeling was supported by the US DOE Office of Science, Fusion Energy Sciences. Experiments in RF reactor were supported by the Princeton Collaborative Research Facility (PCRF), which is supported by the U.S. Department of Energy (DOE) under Contract No. DE-AC02-09CH11466.

SESSION SF04.02: Plasmas and the Energy Challenge
Session Chairs: Rebecca Anthony and Wei-Hung Chiang
Monday Afternoon, November 27, 2023
Sheraton, Second Floor, Independence East

2:00 PM *SF04.02.01

The Role of Plasmas in the Electrification and Decarbonization of Chemical Manufacturing Eray S. Aydil, Andrea Angulo, Enrico Chinello and Miguel Modestino; New York University, United States

Chemical manufacturing is the foundation of supply chains that provide society with more than 96% of all goods. It consumes 10% of global energy production, nearly all in thermochemical processes fueled by fossil fuel combustion, contributing 5.5% of the global CO₂ emissions and thus accelerating anthropogenic climate change. Chemical manufacturing plants comprise a network of reactors to synthesize mixtures of chemicals and separation units such as distillation to obtain purified products. Any energy needed but not produced by exothermic chemical reactors is supplied by fossil fuel combustion (86%) or brown electricity (14%). Recent decarbonization goals are driving the rethinking of this chemical manufacturing paradigm and its potential replacement with decarbonized production schemes powered directly by clean electricity. One of the options is to replace thermochemical reactors with electrically driven non-thermal plasma processes. We critically assessed technical, economic, and environmental factors to evaluate the prospects of this impending paradigm shift. Among bulk organic chemicals, we focused on ethylene, BTX (Benzene, Toluene, Xylene), and propylene as the highest volume chemicals by the energy consumed and CO₂ emitted: they account for >50% of the energy consumed (and thus CO₂ emitted) in the manufacture of basic organic chemical commodities. Specifically, we review the state-of-the-art production method, its economics and CO₂ emission, potential options for electrifying its manufacturing, including plasmas, the impacts of carbon pricing on their deployment, and the technological gaps holding back the deployment of these options. We aim at trying to answer the questions of (1) whether plasma reactors can replace thermochemical reactors in the economical manufacture of chemicals, (2) what chemicals should be targeted, and (3) what basic and applied plasma research is needed to make plasma production of bulk organic chemicals possible.

2:30 PM SF04.02.02

High-Efficiency Atmospheric Pressure Glowing Discharge using Stacked Wire Dielectric Barrier Discharge Reactor Yue Xiao, Mruthunjaya Uddi and Chien-Hua Chen; Advanced Cooling Technologies, Inc., United States

Plasma-assisted processes enable an electrified and potentially sustainable chemical synthesis or surface modification technology. However, the design of current plasma processes is often a compromise between performance factors such as reliability, scalability, energy efficiency, and chemical conversion. For example, dielectric barrier discharge (DBD) reactors generate stable discharges with high conversion, but the energy efficiency is often limited by its filamentary discharge at atmospheric pressure which only allows limited contact between the reaction gas and the plasma filament. Other types of plasma reactors, such as microwaves, can achieve high energy efficiency with glowing discharge yet a reduced pressure is required. In this work, we report an innovative Stacked Wire Dielectric Barrier Discharge (SWDBD) reactor design that can generate glowing discharge at atmospheric pressure to significantly improve the energy efficiency of the DBD plasma reactor. The SWDBD reactor suppresses the formation of the filamentary discharge through a unique reactor structure and achieves a diffusive glowing discharge volumetrically. Compared with the conventional co-axle DBD reactor, the SWDBD reactor is demonstrated to increase the energy efficiency by ~100% for dry methane reforming with the same reactor volume and plasma power. Such SWDBD can also be easily scaled-up with adjustable discharge gap distances to facilitate applications such as large surface treatment, chemical reforming, air disinfection, etc.

2:45 PM SF04.02.03

Green Steel Production by Hydrogen-Based Plasma Reduction of Iron Oxides Dierk R. Raabe, Isnaldi Souza Filho, Hauke Springer and Matic Jovicevic Klug; Max Planck Institute for Iron Research, Germany

Steel is the backbone material of our modern civilization. While it enables sustainability via its high recyclability rates or when used in wind turbines or magnets, its primary production has strong negative impacts on the environment. This is because iron is extracted from its oxides through redox chemical reactions that employ fossil C-carriers as reductants, producing about 2 tons of CO₂ per ton of steel produced. This enormous number represents 7-8% of all CO₂ emissions on the planet and qualifies ironmaking sector as the heaviest individual industrial CO₂ emitter.

For solving this huge challenge we developed a transformative fully electrified technology route which is based on using hydrogen plasma for the reduction of iron oxides, with only water as by-product. The procedure consists of igniting a hydrogen plasma arc between an electrode of an electric arc furnace, slightly modified to support small partial pressures of H₂ (e.g. 10%), and the ore to be processed. Inside the arc zone, the mutual collisions between electrons and hydrogen molecules (H₂) allows for creating high densities of highly energetic hydrogen species, such as the proton (H⁺) [2]. These particles are more reactive than H₂, thus they help to overcome the reaction's activation energy, enhancing the reduction kinetics. We study the reduction of the hematite ores by the hydrogen plasma including the transformation kinetics and chemical composition over several intermediate states. Micro- and nanoscale chemical and microstructure analysis show that the gangue elements partition to the slag oxides, revealed by energy dispersive spectroscopy and atom probe tomography. Si-enrichment was observed in the interdendritic fayalite domains, at the wüstite/iron hetero-interfaces and in the oxide particles inside iron. With proceeding reduction, however, such elements are gradually removed from the samples so that the final iron product is nearly free of gangue-related impurities.

References

[1] Raabe D, Tazan CC, Olivetti EA. Strategies for improving the sustainability of structural metals. *Nature*. 2019 Nov; 575 (7781): 64-74.

<https://www.nature.com/articles/s41586-019-1702-5>

[2] IR Souza Filho, Y Ma, M Kulse, D Ponge, B Gault, et al. Sustainable steel through hydrogen plasma reduction of iron ore: Process, kinetics, microstructure, chemistry, *Acta Materialia*, 2021

<https://www.sciencedirect.com/science/article/pii/S1359645421003517>

3:00 PMBREAK

SESSION SF04.03: Plasma Synthesis and Processing of Nanomaterials I

Session Chairs: Sumit Agarwal and Bruno Alessi

Monday Afternoon, November 27, 2023

Sheraton, Second Floor, Independence East

3:30 PM *SF04.03.01

Microplasma Engineering of Nanomaterials Synthesis and Applications Wei-Hung Chiang¹, Darwin Kurniawan¹, Yi-Jui Yeh^{1,2} and Yan-Yi Chen¹; ¹National Taiwan University of Science and Technology, Taiwan; ²National Taiwan University, Taiwan

Microplasmas are a special class of electrical discharges formed in geometries where at least one dimension is less than 1 mm. As a result of their unique scaling, microplasmas operate stably at atmospheric pressure and contain large concentrations of energetic electrons (1-10 eV). These properties are attractive for a range of nanomaterials synthesis and nanostructure engineering such as metal, semiconductor, and inorganic nanomaterials [1]. Recently, we found that the energetic species including radicals, ions and electrons generated in the microplasmas were capable of initiating electrochemical-assisted reactions for the nucleation and growth of graphene quantum dots (GQDs), silicon quantum dots (SiQDs), and metal nanoclusters (MNCs) [2-5]. Moreover, we discover a simple and controlled synthesis of metal/metal, metal/QD heterostructures using our unique microplasma engineering. In this presentation, I will discuss these topics in detail, highlighting the advantages of microplasma-based system for the synthesis of well-defined nanomaterials for detections of metal ions, SARS-CoV-2 proteins, cancer and neurotransmitter biomarkers. These experiments will aid in the rational design and fabrication of nanomaterials for nanotechnology-enhanced biosensors and may also have significant impact in emerging applications for next generation applications including optoelectronics, nanocatalysis for clean energy, biomedical applications.

References

[1] Wei-Hung Chiang, Davide Mariotti, R Mohan Sankaran, J Gary Eden, Kostya Ostrikov, *Advanced Material*, 2020 32, 1905508.

[2] Yi-Jui Yeh, Trong-Nghia Le, Wesley Wei-Wen Hsiao, Kuo-Lun Tung, Kostya Ken Ostrikov, Wei-Hung Chiang, *Analytica Chimica Acta*, 2023, 1239, 25, 340651.

[3] Darwin Kurniawan, Neha Sharma, Michael Ryan Rahardja, Yu-Yuan Cheng, Yan-Teng Chen, Guan-Xian Wu, Yen-Yu Yeh, Pei-Chun Yeh, Kostya Ken Ostrikov, Wei-Hung Chiang, *ACS Applied Materials & Interfaces*, 2022, 14, 46, 52289-52300.

[4] Yan-Yi Chen, Darwin Kurniawan, Seyyed Mojtaba Mousavi, Pavel V. Fedotov, Elena Obratsova, Wei-Hung Chiang, *Journal of Materials Chemistry B*, 2022, 10, 9654-9661

[5] G. Chang, D. Kurniawan, Y.J. Chang, W.-H. Chiang, *ACS Omega*, 2022, 7, 223

4:00 PM SF04.03.02

Constriction of an Atmospheric Pressure RF Plasma for Si Nanocrystal Synthesis Cameron Papson¹, Sankhadeep Basu¹, Alexander Ho^{1,2} and Rebecca J. Anthony¹; ¹Michigan State University, United States; ²Fraunhofer USA, United States

Low-temperature plasma reactors have become popular for synthesizing semiconductor nanoparticles. In many cases, these nanoparticles exhibit exciting and novel optical and mechanical behavior, and plasmas offer unique tailoring of these properties. Low-temperature or non-thermal plasmas (LTPs) are considered to be room-temperature synthesis tools, due to the non-equilibrium between the highly energetic electrons and the low-temperature heavy species such as ions and neutrals. This means that LTPs can be used to synthesize materials that require high crystallization temperatures, such as silicon, while maintaining compatibility with a wide variety of substrates. For flow-through synthesis of nanoparticles at lower pressure (1-10 Torr) it's convenient to use radiofrequency (RF) power sources, and reactor sizes can be as large as 1-2' in diameter. However, this low-pressure regime also introduces difficulty in merging the synthesis process with other fabrication techniques. Thus, using mm-scale or μ m-scale reactors at atmospheric pressure is an alternative strategy to generate nanoparticle-producing plasmas using RF power. Additionally, these small-scale standard-pressure reactors can be integrated with direct-write schemes to provide on-demand nanoparticle deposition in controlled patterns. Prior work by Kramer et al. (*Phys. Rev. B*, 2015) suggested that LTP synthesis of crystalline silicon nanoparticles at atmospheric pressure requires a much higher ion density and/or atomic hydrogen density as compared to the low-pressure operating regime. This has led to some speculation about how crystalline nanoparticles can be synthesized even in smaller-scale reactor volumes, when using RF power at atmospheric pressure. Here, we present our results on crystalline silicon nanoparticle synthesis using a mm-scale RF LTP at atmospheric pressure. Observation of the plasma indicates that it diffusely fills the reactor volume during nanoparticle synthesis, similar to low-pressure reactors. In that case, predicted ion densities are not high enough to result in crystalline nanoparticles for these weakly-ionized plasmas. However, high-speed imaging of the plasma during synthesis indicates that what is perceived at steady-state to be a diffuse plasma is in fact a fluctuating filamentary discharge, indicating that species densities in regions of the reaction zone may be much higher than predicted based on a diffuse full-volume discharge.

Here we present our results using a constricted RF plasma for generation of crystalline silicon nanoparticles with sizes ranging from 5 nm – 20 nm using an atmospheric pressure RF-driven millimeter discharge. The reactor was a quartz tube with a 1-mm inner diameter and external ring electrodes supplied RF power (13.56 MHz) ranging from 40 W – 115 W (nominal). Argon was flown at 100-300 sccm and a 1% SiH₄/99% Ar mixture was flown at 0.5-25 sccm during the reaction, and nanoparticles were collected at the exit of the tube onto glass substrates. We performed XRD and TEM to confirm the crystallinity and size of the Si nanoparticles. We imaged the plasma using a Photron high-speed camera at a frame rate of 3600 fps. Argon-only plasmas appeared diffuse even when imaged at this high speed. However, the addition of silane into the reactor led to a filamentary discharge under all synthesis conditions. We hypothesize that the larger sized crystalline particles arise via high rates of reactions in the constricted portion of the plasma, allowing these nanoparticles to reach the higher temperatures required for crystallization even if their diameters are too large for size-related melting temperature depression.

SESSION SF04.04: Plasmas at the Interface I
Session Chairs: Lorenzo Mangolini and Davide Mariotti
Tuesday Morning, November 28, 2023
Sheraton, Second Floor, Independence East

8:30 AM *SF04.04.01

Leveraging Plasma Enhanced Atomic Layer Etching for Sustainable Catalytic Processing Jane P. Chang^{1,2}; ¹University of California, Los Angeles, United States; ²Harvard University, United States

ALE was developed in recent years to address critical needs in micro- and nano-electronics fabrication where precision in nano-scale patterning is required to integrate novel metal and metal alloys in nano-electronics, nano-photonics, spintronics, and sensors. Many of these materials are inert or less reactive, making it a challenge to turn a non-etchable material into an etchable one. Our previous work demonstrated that a viable ALE process utilizes chemically reactive and low energy directional oxygen ions to tailor the surface modification/conversion process and form a metal oxide layer while suppressing any deleterious sputtering. The surface reaction kinetics dictate the controlled and directional change in the materials' composition and properties, thereby enabling the chemical contrast needed to selectively remove the materials. Such an effective ALE process can potentially be used to de-poison catalysts, by removing just one atomic layer of material at a time (the poisoned layer). The site specificity in these ALE reactions can also help regenerate the preferred sites for catalytic reactions.

The feasibility of utilizing ALE to de-poison catalysts is based on strong and selective chemical reactions on the surfaces of metals. Interestingly, many of the materials requiring nano-scale patterning have been used as catalysts. While a chemical reaction leading to the formation of a strongly chemisorbed species is considered poisoning in catalysis, it is actually a necessary step in initiating atomic layer etching of metals. By identifying a chemical reaction that can form strong chemical bonds, thereby modifying an atomically thin surface layer to form a new compound, a distinct chemical contrast can be created to allow one atomic layer of the modified surface to be selectively removed, leaving behind the unmodified material. This presentation will focus on the intersection of two interdisciplinary research areas for microelectronics and catalysis, leveraging what was achieved in ALE of metals to help de-poison/regenerate the catalysts. The specific examples include Ni and Cu (both are common and useful catalysts) because these two suffer sulfur and carbon poisoning (coking) as two major deactivation processes. The discussion will demonstrate the feasibility of utilizing ALE to remedy catalyst poisoning and make the catalytic processing more sustainable.

9:00 AM SF04.04.02

Facile Synthesis of Non-Precious Bimetallic ZIF-Based Hierarchical Nanocomposites as Efficient Electrocatalysts for Oxygen Reduction Reaction Mahshid Mokhtarnejad, Erick L. Ribeiro, Dibyendu Mukherjee and Bamin Khomami; The University of Tennessee, Knoxville, United States

Zeolitic imidazolate frameworks (ZIFs) belong to a class of highly crystalline metal organic framework (MOF) materials that have increasingly found prominence in various materials technology applications due to their ultrahigh porosity and enormous internal surface areas. Such properties, together with the vast library of MOF structures that can be constructed from diverse combinations of both organic (ligands) and inorganic (metal nodes) counterparts, provide the incentives for the design and synthesis of uniquely tailored MOFs. Specifically, conversion of such designer MOFs into highly conductive and high-porosity hybrid nanocomposites (HNCs) consisting of transition metal/metal oxides interfaced with carbon (C) matrices can serve as a promising alternative for the synthesis of affordable oxygen reduction reaction (ORR) electrocatalysts. To that end, optimizing the performance of these classes of materials by tailoring their composition, structure, size, and morphology through an efficient synthesis route has emerged as an active area of research. This talk presents our recent efforts at using Laser Ablation Synthesis in Solution in tandem with Galvanic Replacement Reaction (LASIS-GRR) technique as an environmentally friendly, facile, and rapid route for the design and synthesis of unique core-shell bimetallic ZIF heterostructures as bi-MOFs. Pyrolytic post-processing of these bi-MOF structures yield hierarchical metal oxide/MOF-based functional HNCs as highly active ORR electrocatalysts. The LASIS-GRR technique employs high-energy laser plasma reactions as the rate-controlling step for initiating solution-phase galvanic reactions. The one-pot, two-step process introduced in this study enables tailoring the composition, structure, size, and morphology of composite bi-MOFs comprising Co-based MOFs encapsulated in Zn-based porous crystals (Co/ZIF-67@Zn/ZIF-8). Post-pyrolysis, these core-shell bi-MOF crystals are found to create hierarchical ZnO/ZIF@C HNCs that indicate superior ORR electrocatalytic performances under alkaline conditions. Overall, these findings not only elucidate the ability of well-designed LASIS-GRR protocols to tailor the morphology, structure and composition of complex MOF structures but also demonstrate the superior performance and stability of the ensuing post-pyrolyzed ZnO/ZIF@C HNCs as non-precious metal-based ORR electrocatalysts, when compared to commonly used Pt-/Pt-group metals (PGM)-based electrocatalysts.

9:15 AM SF04.04.03

Plasma Surface Modification of Graphitic Carbon Nitride for Improving Photocatalytic CO₂ Reduction Activity with a Ru(II)-Ru(II) Supramolecular

Photocatalyst Noritaka Sakakibara¹, Tsuyohito Ito², Kazuhiko Maeda¹, Kazuo Terashima² and Osamu Ishitani^{1,3}; ¹Tokyo Institute of Technology, Japan; ²The University of Tokyo, Japan; ³Hiroshima University, Japan

For a sustainable energy management, effective conversion of CO₂ into energy-rich fuels is highly demanded as an alternative to fossil fuels and nuclear energy. Recently, hybrid photocatalyst combining a semiconductor and a supramolecular photocatalyst has been developed for realizing highly efficient CO₂ reduction using visible light [1, 2]. For example, the hybrid of graphitic carbon nitride (C₃N₄) and binuclear ruthenium(II) complex (**RuRu**) demonstrated selective reduction of CO₂ to formic acid (HCOOH) under visible light irradiation and exhibited a very high durability with a turnover number over 33,000 with respect to the amount of **RuRu** [2]. In this system, **RuRu** is incorporated onto C₃N₄ via phosphonic acid anchoring groups of **RuRu**, and electron donation from C₃N₄ to **RuRu** drives photocatalytic CO₂ reduction. However, poor functional groups on C₃N₄ which can interact with the phosphonic acid anchoring group hinders interfacial affinity of **RuRu** onto C₃N₄, which essentially prevents potential development for better photocatalytic system.

To gain better interfacial affinity, plasma surface modification should have a great potential. In this study, as a first example of this concept, C₃N₄ was treated with a non-equilibrium plasma in hydroquinone-containing aqueous solution [3]. The plasma treatment modified the surface of C₃N₄ selectively without influencing the bulk properties of C₃N₄ such as crystal structure, bandgap energy, and chemical structure. By X-ray photoelectron spectroscopy and UV-vis diffuse reflectance absorption spectroscopy, deposition of oxygen-rich carbon layer based on sp² bonding structure was identified. Furthermore, the adsorption density of ruthenium complex with phosphonic acid anchoring groups onto C₃N₄ was improved by approximately three times, with the surface coverage of ~50%. Therefore, the interfacial affinity was improved by the surface modification of C₃N₄.

The influence of the plasma treatment of C₃N₄ on photocatalytic CO₂ reduction was investigated in the case of the aforementioned well-developed hybrid photocatalytic system with C₃N₄ and **RuRu**. The hybrid photocatalyst of C₃N₄ and **RuRu** was dispersed in CO₂-bubbled *N,N*-dimethylacetamide/triethanolamine mixed solution and irradiated under visible light. The surface modification improved the selectivity of HCOOH production and durability up to approximately 2 times with a turnover number of 50,000, which recorded the highest durability of hybrid photocatalysts so far. By the electron-spin resonance measurement and transient absorption spectroscopy measurement of plasma-treated C₃N₄, the enhanced activity was attributed to the accumulation of photoexcited electrons onto deep trapping sites of the oxygen-rich carbon layer, which promoted electron transfer from C₃N₄ and **RuRu**. This result clearly demonstrates the advantages of plasma surface modification for the development of hybrid photocatalysts.

[1] A. Nakada, H. Kumagai, M. Robert, O. Ishitani, and K. Maeda, *Acc. Mater. Res.* **2**, 458 (2021).

[2] R. Kuriki, H. Matsunaga, T. Nakashima, K. Wada, A. Yamakata, O. Ishitani, and K. Maeda, *J. Am. Chem. Soc.* **138**, 5159 (2016).

[3] N. Sakakibara, M. Shizuno, T. Kanazawa, K. Kato, A. Yamakata, S. Nozawa, T. Ito, K. Terashima, K. Maeda, Y. Tamaki, and O. Ishitani, *ACS Appl. Mater. Interfaces* **15**, 13205 (2023).

9:30 AM *SF04.04.04

Plasma-Assisted Atomic Layer Deposition of Oxygen Evolution Reaction Electrocatalysts Mariadriana Creatore; Eindhoven University of Technology, Netherlands

Anion exchange membrane water electrolysis is a potentially low-cost technology for renewable-energy driven hydrogen generation. Realisation of its full potential relies on the development of cost-effective, earth-abundant oxygen evolution reaction (OER) electrocatalysts, as alternative to the state-of-the-art noble metal oxides. In this contribution I will address the synthesis of

two electrocatalysts, i.e., cobalt phosphate (CoPi) and cobalt nickel oxide by plasma-assisted atomic layer deposition and discuss the merit of digital control over film stoichiometry to generate insight on the activation mechanisms of these electrocatalysts.

CoPi is prepared by combining ALD cycles of CoO_x from cobaltocene (CoCp₂) and O₂ plasma, with cycles of trimethylphosphate ((CH₃O)₃PO) followed by O₂ plasma. We show that the Co-to-P ratio in the film can be tuned by combining the above-mentioned recipe with extra cycles of CoO_x. We demonstrate that ALD CoPi thin films undergo activation with increasing number of cyclic voltammetry (CV) cycles. During activation, the current density increases in parallel with a progressive leaching of phosphorous out of the electrocatalyst. These chemical changes proceed in parallel with structural changes in the electrocatalyst: measurements of the electrochemical surface area (ECSA) reveal that during activation, the ECSA of this film increases and that the electrochemical activity scales linearly with ECSA for all film compositions. Thus, the initial composition affects the activity of the catalyst indirectly by guiding the restructuring of the catalyst during cycling and the ECSA is a critical parameter in determining the activity of CoPi electrocatalysts. The present study discloses an opportunity for ALD in electrocatalysis: its digital control over chemical composition enables unravelling the ECSA-OER activity correlation.

The second study addresses an ALD supercycle process based on CoCp₂ and nickel methylcyclopentadienyl (Ni^{Mc}Cp₂) and an oxygen plasma to investigate the influence of chemical composition and crystallographic properties of cobalt nickel oxide thin films on their electrocatalytic performance. Deposition of binary nickel oxide and cobalt oxide results in the growth of polycrystalline films of rock-salt and spinel phase, respectively. The mixed oxides display a transition from 2+ oxidation state-based pure rock-salt phase (<25 at.% Co) to the spinel phase consisting of mixed +2/+3 oxidation states (>75% at.% Co) upon increasing Co at.%, as verified by electron diffraction and XPS. XPS also reveals a linear increase in the Ni³⁺-to-Ni²⁺ ratio with increasing Co at.%, which indicates that an inverse spinel structure is formed. The formation of a Ni³⁺-rich inverse spinel cobalt nickel oxide between 55 and 75 at.% Co facilitates the formation of a semi-metallic state (10² S/cm) as opposed to the poorly conductive binary oxides. When CV measurements are carried out in 1M KOH, continuous activation behaviour is observed for rock-salt phase films, whilst increment of the Co at.% results in reduced film activation until virtually no activation of the spinel phase films is observed. The activation of the nickel-rich film is accompanied by irreversible redox changes from the +2 to +3 oxidation state as indicated by the integrated non-catalytic wave. The formation of an (oxy)hydroxide metal is observed for the rock-salt dominated films, whilst oxidation states characteristic of a spinel-like oxide structure are observed for the cobalt-rich films. No changes in the transition metal ratios are observed after activation. Scanning electron microscopy images furthermore reveal that the transformation of the Ni-rich films is accompanied by surface restructuring. These results indicate that initial composition can significantly influence the electrocatalytic performance of ternary oxides and therefore highlight the importance of techniques such as atomic layer deposition to study their complex behaviour.

10:00 AMBREAK

SESSION SF04.05: Plasma Synthesis and Processing of Nanomaterials II
Session Chairs: Rebecca Anthony and Davide Mariotti
Tuesday Morning, November 28, 2023
Sheraton, Second Floor, Independence East

10:30 AM *SF04.05.01

Improving the SiO₂ to SiN_x Etch Selectivity During Atomic Layer Etching and Reactive Ion Etching Sumit Agarwal; Colorado School of Mines, United States

In semiconductor device manufacturing, SiO₂ and SiN_x are two of the most commonly used dielectrics, which are patterned during various device processing steps using plasmas of fluorocarbon gases. During plasma etching, the etch selectivity of SiO₂ relative to SiN_x can be controlled by tuning process parameters such as the fluorocarbon or hydrofluorocarbon feed gas, dilution with other gases such as H₂ or O₂, and by tuning the ion flux and the ion energy distribution. Previously, we showed that selective functionalization of plasma-deposited SiO₂ or SiN_x with hydrocarbons can be used to enhance etch selectivity. Building on our previous work, using *in situ* optical surface diagnostics, we will show that this approach can be extended to atmosphere-exposed and partially-etched SiO₂ and SiN_x surface during atomic layer etching (ALE). In addition, we have also studied the mechanism for the enhancement in etch selectivity for SiO₂ over SiN_x by increasing the substrate temperature during reactive ion etching (RIE). Lastly, during RIE of SiO₂ and SiN_x, we will discuss the role of the C₄F₆/O₂ ratio in the feed gas in determining the etch selectivity.

11:00 AM SF04.05.02

Probing Plasma-Induced Surface Reactions via *In-Situ* FTIR and Raman Lorenzo Mangolini and Minseok Kim; University of California, Riverside, United States

Non-thermal plasmas provide new ways of driving heterogeneous reactions at catalyst surfaces. These processes fall under the broad sub-field of plasma-catalysis, which has attracted great attention in recent years because of its promise of enabling the conversion of electrical into chemical energy. Such processes could help alleviate our societal dependence on hydrocarbons and heat-driven processes, paving the way for a long-term sustainable energy infrastructure. Several examples of these processes have been presented in recent years, including for ammonia synthesis, methane reforming, water-gas shift, and others. While promising, the community still lacks a microscopic-level understanding of how plasma-produced species interact with catalyst surfaces and adsorbates. Here we choose an organic monolayer as a molecular probe to investigate how a low-temperature plasma interacts and excites the adsorbates. We select phenyl phosphonic acid (PPA) as molecular tracer because of its strong response in both FTIR and Raman measurements. First, we prepare a nanostructured silver substrate to enhance the Raman response of the system. We protect the silver surface with a thin alumina layer grown by atomic layer deposition, since this is well-known to improve the thermal stability of the silver substrate. We then adsorb PPA onto the substrate and focus on the Raman signature from the aromatic benzene ring (1010 cm⁻¹) under plasma irradiation. We find that the molecule vibrational temperature, as determined by measuring the ratio between stoke and anti-stoke peaks, can exceed the substrate temperature by 80°C even at low plasma input power. In parallel with the Raman measurements, we perform temperature programmed desorption using FTIR to estimate the binding energy between PPA and alumina. In agreement with the Raman data, we measure a significant drop in binding energy under plasma exposure. Additional characterization of the plasma via a double probe will be presented, to correlate the plasma properties with the FTIR and Raman measurements. This work confirms that low-temperature plasmas can deposit energy in a very localized manner, increasing the effective temperature of adsorbates and in turn enhancing the rate of heterogeneous reactions.

11:15 AM SF04.05.03

Improvement in Performance of Hybrid Perovskite FAPI Solar Cell by Adlayer of Surface Engineered FAPbI₃ Quantum Dots Layer Bruno Alessi¹, Calum McDonald¹, Davide Mariotti² and Vladimir Svrcek¹; ¹AIST: National Institute of Advanced Industrial Science and Technology, Japan; ²Ulster University, United Kingdom

Formamidinium lead iodide (FAPI) thin films in the perovskite crystalline phase have recently attracted attention for single junction solar cells owing to their ideal bandgap, long photocarrier lifetime and intrinsic structural stability in respect to all-inorganic based perovskites of interest for solar cells. However, the performance and stability of cells based on FAPI bulk crystalline films is limited by the high density of trap states on the surface and within the lattice, which determine the appearance of deep levels acting as non-radiative recombination centers and result in the deterioration of device performance over time. Various strategies have been explored in to overcome these limitations such as film crystallization and deposition optimization, precursor engineering, tailoring the interface properties and energy gap. The formation of distinct bulk heterojunctions has also been proven to be experimentally non-trivial due to the inherent instability of these materials surface towards exposure to polar solvents. Nonetheless the integration of low dimensional perovskites¹ and the incorporation of nanocrystals with quantum confinement has proven to be a feasible way to ameliorate stability, boost carrier collection and tailor energy band gap at the same time.²

In this study we explore the potential of using adlayers (50 to 100 nm) of formamidinium lead iodide (FAPbI₃) quantum dot (QDs) on FAPI bulk films, to explore integration of QDs and fs laser induced surface engineered (SE) FAPbI₃ QDs with FAPI bulk films, tailor energy gap, boost the carrier collection and increase the light absorption efficiency at shorter photon wavelengths. These FAPbI₃ QDs have been synthesized with a well-established hot injection method and surface-engineered QDs (SE-QDs) are obtained by processing the FAPbI₃ QDs with a fs-laser generated plasma treatment in liquid. We report that SE-QDs are affected both in particle size and surface state while retaining their structural and colloidal stability. We then proceed making solar cell devices based on SnO₂ and Spiro-OMeTAD as electron- and hole- transport layers and consider two different cases to distinguish the effect of QDs on the device performance. QD-only devices that are meant to understand the effects of surface engineering alone and devices with a thick microcrystalline FAPbI₃ film (~600 nm) and thin adlayers of QDs (100 nm) both as synthesized and surface engineered and compare them against a control FAPI film solar cell.

In the former case (QD-only cells) we notice important relative improvements of average IV parameters of solar cells, above all bigger short circuit current and PCE (+20%) whilst only minor improvements in open circuit voltage and field factor, and overall figures in line with all-QDs based FAPbI₃ cells. In the latter case (thin heterojunction cells) we observe a slight deterioration of IV characteristics with as-synthesized QDs adlayers, whereas marked improvements for most of the average IV parameters with SE-QDs adlayers. Notably a 7% increase in power conversion efficiency, with the record cell topping at 20.7% PCE, J_{sc}=25.6 mA/cm², V_{OC}=1.13 V and FF=70%. Additionally, when measuring again the IV characteristics after two months, a less severe decay in performance in respect to the control device is observed (e.g.: V_{OC} -4% for the control vs -2.5% for the SE-QDs device). We notice also that thin layers of QDs up to 100 nm have only minor influence on the optical absorption characteristics of the thicker FAPI film, hence we infer the improved performance as the result of more efficient photocarrier extraction. The thin adlayers of SE-QDs improve interface and determine a more favorable electron energy alignment between the FAPI film and the spiro-OMeTAD.

1. Zhang, C. *et al. Adv. Energy Mater.* **10**, 2002004 (2020).
2. Rocks, C. *et al. Nano Energy* **50**, 245–255 (2018).

11:30 AM SF04.05.04

Novel Ampoule-Liked Microwave Plasma Process for the Sulfurization of Polycrystalline CVD Graphene Charles Mod erie, Marianne Lapierre, Richard Martel and Luc Stafford; Universit  de Montr al, Canada

Plasma processes have been proposed as an efficient and green path for graphene modification, in particular for n- and p-type doping. However, some modification can be limited by the plasmagen gas or by reactor contamination considerations as sulfurization. To generate sulfur-graphene, a new plasma-based process has been developed and characterized. Inspired by an ampoule reaction, solid sulfur S₈ and CVD graphene transferred on SiO₂/Si substrates are placed in a silica tube where a microwave (MW) surface-wave discharge is ignited in 10 Torr argon. In this pressure range, the plasma column is contracted¹ and the fundamental plasma properties strongly vary along the radial axis². The proposed process relies on neutral gas heating by MW plasma generation and subsequent sulfur sublimation to create gaseous reactive sulfur for graphene functionalization. In this work, the argon plasma was first characterized by high and ultra-high-resolution emission spectroscopy, laser absorption spectroscopy and imaging. The neutral gas temperature was determined by the resonant and Van der Waal broadening of the Ar emission lines³ (826 and 840 nm) over a wide range of experimental conditions. With such temperature, the sulfur concentration in the gas phase was estimated from the equilibrium vapor pressure. Then, the sulfur argon plasma was characterized with the same methods. In presence of sulfur, two distinct plasma phases were observed by emission spectroscopy: Argon-Sulfur contracted dual-phase in the center of the tube and diffusive mono-sulfur phase close the walls. This transition is consistent with previous findings in presence of gas admixtures for which the ionization potential of the trace gas is lower than the one of the main gas. Additionally, CVD graphene was exposed to the two-plasma phase system to functionalize the surface with sulfur atoms. Here, there is two main challenges to achieve functionalization: the creation of the C-S covalent chemical bonding and the defects generation induced by the plasma. To characterize the graphene-sulfur product, Raman spectroscopy and X-ray photoelectron spectroscopy (XPS) was done. In addition to the D, G and 2D Raman signals of graphene⁴, a new band linked to sulfur functionalization is observed. XPS measurements were also made to confirm the C-S covalent bonding. This plasma-based process opens up new possibilities for 2D materials modification.

1. Casta os Mart nez, E., Kabouzi, Y., Makasheva, K. & Moisan, M. Modeling of microwave-sustained plasmas at atmospheric pressure with application to discharge contraction. *Phys Rev E Stat Phys Plasmas Fluids Relat Interdiscip Topics* **70**, 12 (2004).
2. Carbone, E. A. D., H bner, S., Palomares, J. M. & Van Der Mullen, J. J. A. M. The radial contraction of argon microwave plasmas studied by Thomson scattering. *J Phys D Appl Phys* **45**, (2012).
3. Durocher-Jean, A., Desjardins, E. & Stafford, L. Characterization of a microwave argon plasma column at atmospheric pressure by optical emission and absorption spectroscopy coupled with collisional-radiative modelling. *Phys. Plasmas* **26**, 63516 (2019).
4. Beams, R., Gustavo Can ado, L. & Novotny, L. Raman characterization of defects and dopants in graphene. *Journal of Physics: Condensed Matter* **27**, 083002 (2015).

11:45 AM SF04.05.05

Plasma-Engineered Carboxylic Compound-Derived Graphene Quantum Dots as Multifunctional Nanosensors for Simultaneous Detection of Biomarkers and Metal Ions Yan-Yi Chen and Wei-Hung Chiang; Department of Chemical Engineering, National Taiwan University of Science and Technology, Taiwan

In the face of escalating environmental pollution and disease threats, the urgent need for efficient and sensitive environmental and biological sensors has become paramount for safeguarding human health and fostering sustainable development. Here, we leverage an atmospheric pressure microplasma system to synthesize graphene quantum dots (GQDs) using carboxylic compounds, specifically benzene polycarboxylic acids, including benzoic acid, phthalic acid, trimesic acid, and pyromellitic acid, as the carbon source. These GQDs are utilized in photoluminescence (PL)-based multifunctional sensors for diverse environmental and biological applications. Through accurate adjustment of the detection conditions, our sensor, based on a single material, demonstrates remarkable selectivity and sensitivity by simultaneously detecting biomarkers and metal ions such as folic acid (FA) and adenosine triphosphate (ATP) and aluminum and copper ions.

Our first innovation lies in the convenient, rapid, and environmentally friendly synthesis of GQDs with abundant carbon and oxygen functional groups from carboxylic compounds, achieved through the atmospheric pressure microplasma system. Microplasma eliminates the need for harsh chemicals, high temperatures, vacuum conditions, and toxic solvents. Additionally, we investigated the influence of carboxylic acid functional groups (COOH) by employing different benzene polycarboxylic acids in the synthesis process. TEM imaging supported our findings, revealing that the reduction of COOH functional groups in these benzene polycarboxylic acids increased the size of the synthesized GQDs, with a size distribution ranging from 2.4 nm to 5 nm, during the plasma treatment process.

The second innovation revolves around the plasma-synthesized GQDs, which can be tuned to serve as highly sensitive and stable nanosensors for biomarkers and metal ions. By adjusting the detection conditions, selective detection can be achieved. Moreover, we discovered several unique photoluminescence (PL) quenching mechanisms under different conditions, enhancing the sensing activity of GQDs towards target analytes. The successful development of this nanosensor enables simultaneous multifunctional sensing using a single material.

These findings hold great promise for advancing the frontiers of plasma technology in materials science and engineering while facilitating various applications in environmental monitoring, water quality analysis, food safety, clinical diagnostics, and pharmaceutical research.

SESSION SF04.06: Plasma Synthesis and Surface Engineering I

Session Chairs: Lorenzo Mangolini and Luc Stafford

Tuesday Afternoon, November 28, 2023

Sheraton, Second Floor, Independence East

1:30 PM *SF04.06.01

Using Image Based Artificial Intelligence Growth Prediction to Improve SCD Wafer Dimensions and Growth Yield Matthias Muehle^{1,2}, Rohan Reddy¹, Arjun Srinivasan¹, Luke Suter¹ and Elias Garratt^{1,2}; ¹Fraunhofer USA, United States; ²Michigan State University, United States

Single crystal diamond (SCD) is an attractive wide bandgap semiconductor material for a variety of applications ranging from advanced optics, solid state electronics to thermal management solutions. While lab-scale prototype demonstrations have demonstrated superior performance, utilizing diamond has been prohibitively expensive compared to more mature, commercialized semiconductor materials. This is attributed to the fact the SCD wafer size of suitable quality is smaller than 1 inch, and often as little as small as 3 mm x 3mm. For comparison, the commercially available wafer size for single crystalline Silicon Carbide is beyond 6 inches. A direct result is a lack of process scaling when processing individual diamond applications. The only way to overcome this is by controlling the size and quality of SCD wafers during chemical vapor deposition (CVD) growth to enable realization of wafers 2 inches in size and beyond either. This type of process control can be applied either for epitaxial layer outgrowth, or for tiled wafer growth. We are envisioning to address this challenge by developing an artificial intelligence (AI) based algorithm to predict SCD growth states (size and quality) through use of in-situ RGB images. Once established, this AI growth prediction can be incorporated as control system to increase SCD wafer size and quality, by adjusting process conditions before they achieve critical turnover points.

We are reporting on our efforts on AI algorithm development and validation. First, we installed a full-frame mirrorless interchangeable lens camera equipped with a macro lens to a CVD diamond reactor. Then a cumulative image-based AI pipeline consisting of three inter-connected thrusts was developed to model diamond growth. These are 1) Feature extraction pipeline, for extraction of geometrical features in the recorded imaged, 2) Defect detection pipeline, to extract macroscopic defect features in the recorded images, and 3) Frame prediction pipeline utilizing features, defects and reactor telemetry, to predict future image states 6, 8 and 12 hours into the future.

The objective for the feature extraction pipeline was to isolate and classify accurate pixel masks of geometric features like diamond, pocket holder and background, and their translation into geometrical shapes without the need of human-generated input. Our approach was enhanced to deliver results with high precision within the constraints of being limited to low-volume high-feature-complexity training dataset environments, given that data procurement, requiring physical SCD growth, is extremely time-consuming and expensive. Our best performing DL-based model achieved excellent accuracy metrics of >98% for the pocket holder, diamond top and diamond side features. Similarly, our DL-based defect detection pipeline achieved excellent accuracy metrics (>95%) for detecting center, polycrystalline and edge defects.

Prediction accuracies of ~99.9999% were obtained with minimal information loss between predicted and actual outputs. This constitutes a never-before obtained result of spatiotemporal (AI) prediction of diamond shape from in-situ obtained growth data obtained based on few inputs from data collected within an hour apart. This demonstrates the potential of these algorithms as a machine-intelligence-enabled solution for automated optimization and control of the diamond growth process.

2:00 PM SF04.06.02

Controlling Nitrogen Plasmas for Thin Film Synthesis of Complex Semiconductor, Superconductor and Magnetic Materials Sage Bauers; National Renewable Energy Laboratory, United States

Inorganic nitrides are recognized as highly functional materials for several applications, such as semiconducting GaN, superconducting NbN, and magnetic Fe₁₆N₂. Unfortunately, the stability of the N₂ molecule makes metal-nitride synthesis difficult, which precludes the functionalization of many predicted and promising nitride materials. One approach to the experimental realization and optimization of novel nitrides is to use nitrogen plasmas to either vibrationally excite N₂ or even end the dinitrogen molecule into N* radicals, which are far more reactive. Over the last several years, our group has used this concept for the synthesis and optimization of several new nitride materials. This talk will introduce our work using nitrogen plasmas for the synthesis of new ternary metal-metal-nitride semiconductors and magnetic materials, as well as the optimization of nitride superconductors. Our work is based on reactive co-sputtering processes, where we use plasma parameters to control the nitrogen chemical potential both to realize novel phases as well as optimize known materials. We establish general rules where nitrogen activation enables the synthesis of nitrogen-rich nitrides (e.g., ZnTiN₂), which are required for semiconducting applications, but we also find that activation of dilute nitrogen concentrations enables the synthesis and optimization of metal-poor nitride materials needed for superconducting and magnetic applications (e.g., Mn₂GeN). We will also discuss our recent efforts to establish an autonomous synthesis assistant that is guided by in-situ monitoring of plasma emission spectra to optimize the composition of ZnTiN₂, an emerging ternary nitride material with promising properties as a CO₂ reduction photoanode.

2:15 PM SF04.06.03

Positive Ion Transport Study in High Power Impulse Magnetron Sputtering of Argon-Chromium using a Global Model Coupled to the Monte-Carlo Approach Joelle Zgheib¹, Pierre Yves Jouan¹ and Ahmed Rhallabi^{1,2}; ¹Institut des Matériaux de Nantes Jean Rouxel, France; ²Nantes University, France

PVD thin-film deposition is one of the most widely used processes in the semiconductor industry and other technological applications such as MEMS, gas and biological sensors. Thin film quality depends not only on the type of process used, but also on the process operating conditions. Beside conventional RF and DC processes, pulsed discharges such as HIPIMS (High Power Impulse Magnetron Sputtering) [1] have emerged in recent years. The advantage of HiPIMS is its possibility of working with a high metal ion flux over a pulse duration of the order of tens microseconds by injecting an instantaneous power of tens KWatts. This leads to achieve a higher conformity of the deposited film on 3D structures such as via and trench structures, while avoiding intense substrate heating thanks to heat dissipation during time "off".

In order to understand the electrical properties of HIPIMS plasma, we have developed a hybrid model based on a global 0D approach in the ionization zone, coupled to a Monte-Carlo model to study the transport of positive ions from the ionization region to the mass spectrometry entrance. The model is applied to argon plasma discharge and chromium target.

The global 0D model is based on the solving of the continuity equations associated with each species considered in the reaction scheme, i.e. Ar, Ar*, Ar⁺, Cr, Cr⁺, Cr²⁺, electrons [2]. These equations are coupled to the continuity equation associated to power. Solving the differential equation system in the HiPIMS discharge time domain, enables us to determine the average densities of the neutral and ion species, as well as the electron density and temperature in the ionization region as a function of time [2].

The Monte-Carlo model is based on a set of large number of ions from the ionization region, representing the fluxes of positive ions. Their trajectories are followed by solving Newton's equation until reaching the mass spectrometry entrance. The ion fluxes calculated by the global model in the ionization region are considered as input parameters for the Monte-Carlo model. Under the pressure and pulsed voltage conditions used, simulation results show the evolution of ion and neutral species densities, as well as electron temperature as a function of time. For voltages of hundreds of volts, with time "on" duration of 40 μs, the proportion of Cr⁺ is much higher than Cr one revealing the ionization efficiency of the sputtered metal atoms. Monte-Carlo model results show a temporal spread of Ar⁺, Cr⁺ and Cr²⁺ peaks at the mass spectrometry entrance, compared with those obtained in the ionization region. This peak spread is due to ion diffusion through the plasma bulk and the geometrical asymmetry of the mass spectrometry entrance, with respect to the ionization region. The simulation results show the effect of the ion energy in the ionization region on the temporal peak behavior of ions in the mass spectrometry entrance. Time evolutions of normalized positive ion fluxes calculated from Monte-Carlo code reproduce well those obtained from mass spectrometry [3].

References

[1] V. Kouznetsov, K. Macák, J. M. Schneider, U. Helmersson, and I. Petrov, Surf. Coat. Technol. 122, 290 (1999).

[2] Joelle Zgheib, Pierre Yves Jouan, and Ahmed Rhallabi, J. Vac. Sci. Technol. A 39, 043004 (2021).

2:30 PM BREAK

3:00 PM *SF04.06.04

Current State of the Art of R&D for Fabrication of Single Crystalline Diamond Wafers Yamada Hideaki; AIST, Japan

Variety of material constants of diamond are the bests amongst those of other competitive materials and attract researchers to realize several future applications. Many indexes of diamond to characterize performance as power devices are better than those of, for example, Si, SiC, and GaN, owing to its wide bandgap, large breakdown field strength and high thermal conductivity. This suggests potential to realize extreme improvements in efficiency of power control in, for example, Electric-Vehicles, power plants and its transmission principally. Especially, this extremely high thermal conductivity is expected to enlarge range of applications of other semiconductor devices with relatively low thermal conductivity, for example, GaN- and Ga₂O₃-based ones. On the other hand, quantum information, which can be controlled by electronic states in specific color centers of diamond, for example, Nitrogen-Vacancy (NV) centers, is known to be treated under steady state with coherence time which is longer than those of others. This may realize high performance quantum computers, information transmission equipment with high security, and variety of quantum sensors with high resolution and wide dynamic range.

To realize such fascinating industrial applications, it is indispensable to establish the way to produce single-crystalline diamond wafers with sufficient quality and size under acceptable cost. Artificial diamond was firstly reported by using high-pressure-high-temperature method, in which stable state of diamond is realized. This method is nowadays adopted to produce mechanical tools worldwide. On the other hand, it is considered practically difficult to realize inch size crystals for industrial applications by using this method. On the other hand, chemical vapor deposition (CVD) was also found to be the other way to obtain diamond crystals artificially. Several CVD methods with variety of radical sources have been proposed and proved to be possible methods, for example, flames, hot-filaments, and plasmas. Among several plasma sources, microwave plasma (MWP) CVD has been widely adopted to grow diamond crystals especially for electronics and quantum applications because of its relatively high plasma and power-density without electrode near the top surface of the substrate. Especially, developments in techniques of crystal growth by using MWPCVD during recent 20 years realized remarkable market entry of artificial diamond as gemstones.

We have realized techniques to prepare free standing wafers with less loss, inch-sized wafers, and bulk diamond with thickness of several millimeters. To realize them, we tried to optimize the crystal growth technique by changing chamber shape, applying pulse mode discharge, superimposed microwave, accompanied with numerical simulation of the plasma to understand growth environment. In addition to the technique of the crystal growth, processing technique is one of the important issues to prepare diamond wafers, because diamond is hardest material with cleavage characteristics similar to Si. Recently, we confirmed that plasma-assisted polishing could realize very fine surface with less processing damages.

Now, we are going to apply such wafers for thermal management of electronic devices with high power density, and devices which can be applied to harsh environments. In the future, this material is expected to fulfill its true potential in the fields of 1) Power electronics, and 2) Quantum applications. These applications require reduction of dislocation density and control of impurity concentrations. We are now trying to solve these subjects by using plasma processing.

3:30 PM SF04.06.05

Photonic Properties of Thin Films Comprised of Plasma-Synthesized Gallium Nitride Quantum Dots Dillon P. Moher¹, Guodong Ren², Rohan Mishra^{2,2} and Elijah Thimsen^{1,2}; ¹Washington University In St. Louis, United States; ²Washington University in St. Louis, United States

Gallium nitride (GaN) is a promising material for power electronics and optoelectronics owing to its high electron mobility, high breakdown voltage, and wide, direct band gap. The synthesis of thin film and bulk crystal GaN has received much attention, which has resulted in the commercialization of GaN. However, few synthesis methods exist for freestanding GaN quantum dots (QDs), which can possess a tunable band gap above 3.4 eV. These ultra-wide-gap GaN QDs are promising for deep ultraviolet light sources and single photon emitters in quantum information technologies. In this work, Nonequilibrium Plasma Aerotaxy was utilized to synthesize GaN QDs and deposit them in flight as thin films on foreign substrates which are relevant for practical solid-state devices. The QD diameter was controlled between 3.6 and 7.4 nm. The particles were monocrystalline. The photoluminescence of the QD films increased steadily with time in air, after oxidation of the QD surfaces. There were two PL peaks: one in the ultraviolet, hypothesized to originate from band-to-band recombination, and another in the visible, hypothesized to originate from deep-trap-mediated recombination. Surprisingly, both PL peaks possessed a size dependence, in agreement with the Brus equation. Coating the GaN QDs with Al₂O₃ suppressed the PL peak in the visible, confirming that air exposure caused the defect-related PL.

3:45 PM SF04.06.06

Deoxidation of Metal Powders using Nonthermal Hydrogen Plasma for Optimized Reuse in Additive Manufacturing Michael A. Denchy, Josh Kintzer, Pradeep Kumar, Tim Schmitt, Mruthunjaya Uddi, Devon Jensen and Chien-Hua Chen; Advanced Cooling Technologies, Inc., United States

Additive manufacturing (AM) processes face a significant challenge with an increasing oxygen concentration (predominantly as surface oxides) in metal powders during reuse cycles. This increased surface oxidation, occurring at the high temperatures encountered by powders during the printing process, ultimately surpasses the industry acceptable quality limits. Laser powder bed fusion (LPBF) AM processes, in particular, deposit metal powders layer by layer, resulting in waste of the feedstock, which can increase unit costs and have adverse environmental impacts. It is therefore essential to develop and optimize processes to enable the recycling and reuse of metal powders to establish a sustainable AM process industry-wide. To address this challenge, we report the application of a novel low-temperature non-equilibrium hydrogen plasma-based deoxidation process for efficient recycling and reuse of metal powder in AM processes. Our technique involves the highly reactive species generated in an H₂-fed low pressure plasma discharge dynamically interacting with used (oxidized) powder in a quartz tube reactor, reducing oxygen content without adversely affecting particle size or morphology. This process is also free of corrosive chemicals, with water vapor being the major by-product of the reaction. In a pilot study using CuSn10 (0-25 micron) powder, we achieved over a 60% reduction in oxygen content using hydrogen plasma compared to the oxygen content in oxidized CuSn10 powder samples, which is a significant improvement and well below the measured oxygen content of the virgin CuSn10 powder. An in-depth systematic characterization study (XRD, XPS, PSD, and IGF) demonstrating powder morphology, bulk particle structure, and chemical composition following hydrogen plasma treatment will be presented.

4:00 PM SF04.06.07

Tunability and Flammability of Plasma-Synthesized Silicon Quantum Dots Katerina Kusova, Jakub Kopenc, Filip Matejka, Pavel Galar and Tomas Popelar; Czech Academy of Sciences, Czechia

Silicon is the most sustainable, influential and critical material for our technological advancement. It is the material base for modern electronics, the second most abundant element in the Earth's crust and it has very low inherent toxicity. However, in its bulk form, it is practically unable to luminesce due to the indirect nature of its bandgap. This drawback is circumvented in silicon quantum dots (SiQDs). Countless other types of semiconductor quantum dots, such as CdSe, GaN or the modern CsPbI₃ perovskites, are somewhat more efficient light emitters than SiQDs, however, they almost exclusively contain toxic or scarce elements. In addition to low toxicity, there is one aspect where SiQDs outperform their rival materials even when it comes to light emission. As opposed to other semiconductor QDs which are ionic crystals, the nature of the bonding inside the SiQDs' core is covalent. The higher degree of electron sharing associated with covalent bonding makes the electronic properties of SiQDs more sensitive to small changes in surface ligands or in the crystalline core. Thus, most likely as a result of covalent bonding, SiQDs exhibit much broader tunability of their light emission than QDs based on ionic crystals. This tunability makes SiQDs unique light emitters with interesting application prospects and, moreover, SiQDs can serve as a model material for other covalently bonded QDs.

With silicon being a high melting-point material, SiQDs can be advantageously synthesized in non-thermal plasma. However, synthesis in plasma is not the only fabrication route. One aspect in which the synthesis in non-thermal plasma is different from the other methods, be it annealing of Si-rich silicon oxides or electrochemical etching of crystalline silicon, is that it completely bypasses the step of annealing the material to its crystallization temperature. Thus, a question arises as to how the SiQDs synthesized in non-thermal plasma compare to those fabricated by other methods. Here, we will use the spectral tunability of photoluminescence of SiQDs as a tool to monitor their electronic properties. We will focus mainly on the comparison of SiQDs synthesized in non-thermal plasma with those fabricated by electrochemical etching, because these two fabrication routes represent the completely opposite approaches with regards to the formation of the small crystals: whereas the low-temperature plasma bypasses the crystallization temperature, SiQDs fabricated by electrochemical etching are etched down from perfect bulk crystals. Moreover, we will discuss the possibility of tuning the faceting of the SiQDs produced in plasmatic synthesis and the mechanisms responsible for the thermal stability or instability of these QDs.

SESSION SF04.07: Poster Session
Session Chairs: Rebecca Anthony and Tsuyohito Ito
Tuesday Afternoon, November 28, 2023
Hynes, Level 1, Hall A

8:00 PM SF04.07.01

Chamber Aluminum Surface Characterization Study for Etching Process Stability Improvement Chengya Chu, Jia Ling Chen, Takuji Sako, Chun Chao Chen and Noriyuki Kobayashi; Tokyo Electron Limited, Taiwan

Plasma etching is a critical technique in semiconductor production. The mechanism is using RF power to induce plasma and giving a voltage to form ion bombardment to etch Si/SiO₂/SiN material. Traditional plasma etching is anisotropic, only etch in one direction, so it faces a bottleneck for the 3D structure logic transistor/memory fabrication. As a result, TEL has developed an isotropic etching equipment, Certas, which doesn't have plasma source, only gas-state chemicals. With gas diffusion, we can achieve isotropic etching and energy consuming. For years study, we found the chemical etching stability differs while using different kinds of recipes. It can be divided into 2 kinds of recipe, depo less and depo rich recipe. The depo less recipe's etching rate (ER) will increase and gradually reach stable and saturated after sufficient seasoning. In contrast, the depo rich recipe's ER will keep decreasing and hard to reach stable even after large amount seasoning. With TEM/XPS/ellipsometer analysis, we try to figure out the possible mechanism. Based on the result, we assume the byproduct from etching process and chemical gas remain on chamber wall, Al surface, and those remained byproduct may outgas and make the chamber condition unstable during the mass production. Stable production is the basic requirement in foundries. When new tools move into fab or tools keep idle for a while, engineers need to do seasoning to recover the chamber condition. However, it is difficult to define how many seasoning cycles does the tool need and how long the chamber will reach stable. Mostly, we just use off-line dummy wafer to monitor EA in long term and judge chamber stability. It is a very time and resource consuming method, so we are trying to find a better way. For plasma etching process, optical emission spectroscopy (OES) is used as an end point detector (EPD) to precisely control etching amount to avoid over etching damage. For chemical etching process, we install a small chamber which has plasma source and by which we can use OES to monitor the in-situ chamber condition. Through analysis the element composition from the chamber exhaust, we can know how many byproducts remain in chamber wall. By correlating the long-term off-line EA data, we think it is possible to monitor the chamber condition change by OES.

In this paper, we have studied the etching mechanism of depo less and depo rich recipe of chemical etching. Also, we have studied the Al surface status difference before and after the seasoning. At last, we collected OES data and found it is strongly correlated with off-line EA. It seems to be a more efficient and scientific way to achieve stable chamber condition with minimum cost.

8:00 PM SF04.07.02

WITHDRAWN 11/13/2023 SF04.07 Plasma-Engineered Plasmonic Nanostructures for SERS-Based Detection of SARS-CoV-2 Nucleocapsid Protein and Spike Protein Variants Yi-Jui Yeh^{1,2}, Kuo-Lun Tung² and Wei-Hung Chiang¹; ¹National Taiwan University of Science and Technology, Taiwan; ²National Taiwan University, Taiwan

Epidemiological control and public health monitoring during the outbreaks of infectious viral diseases rely on the ability to detect viral pathogens. Here we demonstrate a rapid, sensitive, and selective nanotechnology-enhanced severe acute respiratory syndrome coronavirus 2 (SARS-CoV-2) detection based on the surface-enhanced Raman scattering (SERS) responses from the plasma-engineered, variant-specific antibody-functionalized silver microplasma-engineered nanoassemblies (AgMEN) interacting with the SARS-CoV-2 spike (S) and nucleocapsid (N) proteins. The three-dimensional (3D) porous AgMEN with plasmonic-active nanostructures provide a high sensitivity to virus detection via the remarkable SERS signal collection. Moreover, the variant-specific antibody-functionalization on the SERS-active AgMEN enabled the high selectivity of the SARS-CoV-2 S variants, including wild-type, Alpha, Delta, and Omicron, under the simulated human saliva conditions. The exceptional ultrahigh sensitivity of our SERS biosensor was demonstrated via SARS-CoV-2 S and N proteins at the detection limit of 1 fg mL⁻¹ and 0.1 pg mL⁻¹, respectively. Our work demonstrates a versatile SERS-based detection platform can be applied for the ultrasensitive detection of virus variants, infectious diseases, and cancer biomarkers.

8:00 PM SF04.07.03

Single-Step Aerosol-Assisted Atmospheric Pressure Plasma Deposition of Hybrid Nanocomposite Thin Films Containing Gold Nanoparticles Elène Bizeray¹, Antoine Belinger¹, Simon Dap¹, Fiorenza Fanelli² and Nicolas Naudé¹; ¹Laplace, Université de Toulouse, CNRS, INPT, UPS, France; ²National Research Council (CNR), Institute of Nanotechnology (NANOTEC), Italy

Low-temperature atmospheric pressure plasma technologies offer exciting opportunities for the preparation of hybrid nanocomposite (NC) layers consisting of inorganic nanoparticles (NPs) embedded into an organic matrix [1]. To this end, recently, a growing number of studies have explored the combination of atmospheric pressure plasmas with preformed NPs dispersions in

aerosol form. However, this deposition strategy raises various problems, such as the risk associated with NPs handling as well as the severe NPs agglomeration in the NC thin films. Therefore, intense efforts are currently dedicated to optimizing safe-by-design deposition processes in which the nanocomposite constituents are synthesized in a single step in the atmospheric pressure plasma [3].

It is in this context that, as suggested by previous work [3], we propose to combine a parallel-plate dielectric barrier discharge plasma at atmospheric pressure with the aerosol of the solution of a gold salt (tetrachloroauric(III) acid trihydrate, $\text{HAuCl}_4 \cdot 3\text{H}_2\text{O}$) in a polymerizable liquid precursor (isopropanol), to be able to synthesize in a single step nanocomposite layers. This innovative process avoids the handling of nanoparticles since the gold salt reduction to form Au nanoparticles occurs in the plasma along with the growth of the organic matrix [3]. The chemical composition, morphology, and optical properties of the resulting NC thin films have been investigated using various techniques, such as Fourier-transform infrared spectroscopy, X-ray photoelectron spectroscopy, scanning electron microscopy, and UV-visible absorption spectroscopy. Preliminary results have shown that we can synthesize in a single step a hybrid nanocomposite coating composed of gold nanoparticles embedded in an organic matrix deriving from the plasma polymerization of isopropanol. The influence of different experimental parameters, such as the solution composition and the electrical discharge conditions (applied voltage waveform, excitation frequency, etc.) have been studied. In particular, a dual frequency excitation is used to control the nanocomposite composition and morphology [4]. Indeed, the transport of the nanoparticles to the sample surface is mainly related to the electrostatic forces and therefore requires a low excitation frequency; in contrast, the matrix polymerization and the gold salt reduction need a higher plasma energy and thus a higher frequency. Overall, these results provide new insights into the possibility of using a single-step aerosol-assisted plasma process to deposit hybrid nanocomposite thin films containing gold nanoparticles and into the ability to finely tune the properties of the layers by varying the process parameters.

Acknowledgments

The authors would like to acknowledge financial support from the Agence Nationale de la Recherche (PLASSEL Project, ANR-21-CE08-0038, France).

References

- [1] A. Uricchio and F. Fanelli, *Processes* 9, 2069 (2021).
- [2] J. Profili *et al.*, *Plasma Processes and Polymers* 13, 981 (2016).
- [3] E. Nadal *et al.*, *Nanotechnology* 32, 175601 (2021).
- [4] P. Brunet *et al.*, *Plasma Processes and Polymers* 14, 1700049 (2017).

8:00 PM SF04.07.04

A Soft Solution Route of Nano-Alumina Direct Patterning onto the Silicon Substrate in Ambient Condition Sumanta Sahoo¹, Yu-Cyuan Hou², Sheng-Lin Huang², Kripasindhu Sardar², Satoru Kaneko^{3,4}, Kao-Shuo Chang², Mamoru Yoshimoto⁴, Masahito Kurouchi³ and Masahiro Yoshimura²; ¹Radhakrishna Institute of Technology and Engineering, India; ²National Cheng Kung University, Taiwan; ³KISTEC, Japan; ⁴Tokyo Institute of Technology, Japan

Functional oxides of nanostructure always require high-temperature reactions, as well as multi-step batch process technology for their fabrication. However, the proposed novel and unique, soft solution process has proven a state-of-art technology in one-step fabrication of various types, shapes, and sizes of oxides nanostructure[1]. Herewith, alumina nanostructures were micro-patterned directly onto the silicon substrate by this route in a very short period and at ambient conditions. In this process, electrochemically polished ultra-sharp tungsten (W) tips of various tip profiles have been used as a local activation by in-situ plasma emission. A very small amount of (~5 ml) polymerized aluminum-citrate matrix was taken as an electrolyte. The patterning of alumina onto the silicon substrate, hence fabricated by the submerged discharge plasma activation technology. The fabricated patterns were analyzed by scanning electron microscopy, Raman, and X-ray photoelectron spectroscopy.

From these analytical studies, we found that the above technique requires a low amount of process materials, single-step fabrication, operation at ambient conditions, and green process[2]. However, the great challenges are in controlling the submerged discharge plasma condition to achieve high-quality patterning in comparison to the highly sophisticated vacuum technology's fabrication systems.

This study was funded by the National Cheng Kung University 90 and Beyond (NCKU'90) project of grant no. D110-G2309, and in part by Amada Foundation under contract AF-2020227-B3, Tokyo Ohka Foundation for promotion of science and technology, with the collaborative research project of the Institute of Fluid Science, Tohoku University.

Reference:

- [1] M. Yoshimura, *J. Ceram. Soc. Japan*. 114 (2006) 888–895.
- [2] S.K. Sahoo *et al.* *ACS Omega*. 8 (2023) 17053–17063.

8:00 PM SF04.07.05

Effective Preparation of Graphene Nanoflakes via Microwave Plasma Enhanced Chemical Vapor Deposition for Applications in High-Voltage Electric Double Layer Capacitors Jui-Yu Tung¹, Kun-Ping Huang² and Meng-Jiy Wang¹; ¹National Taiwan University of Science and Technology, Taiwan; ²Industrial Technology Research Institute, Taiwan

Graphene nanoflakes (GNFs), a form of vertical graphene named for its flaky morphology, have attracted attention due to their versatile 3D geometry and large surface area with open pores. It has been reported that GNFs retain the exceptional properties of graphene as an electrode material for energy storage. In addition, the porous framework promotes mechanical stability and flexibility, which is advantageous for the fabrication of lightweight and flexible devices.

Conventionally, the electrode preparation used for energy storage devices involves complicate composition of materials and multiple preparation procedures. The precursors used for electrode generally comprise of three components, namely the binder, dispersion solvent, and active materials. The procedures to prepare electrodes involve a series of steps which include dispersion, coating, and drying. The process of assembling a device is time-consuming.

For the preparation of GNFs, recent report has disclosed a method to directly synthesize GNFs on a substrate through plasma-enhanced chemical vapor deposition (PECVD), utilizing diverse power sources including microwave (MW), radio frequency, and direct current plasma. Typically, a blend of hydrocarbon compounds (CH_4 and C_2H_2) along with either H_2 or Ar gases are employed as the primary input materials for the purpose of synthesizing GNFs directly onto the substrate, without the utilization of any catalyst. High-density plasmas are useful to produce hydrocarbon radicals, such as CH_3 radicals that can facilitate deposition effectively for preparation of thin film with large surface area. With promising and stable PECVD process, the deposition of GNFs provides potential for scaling-up system. This research focuses on the preparation of GNFs utilizing microwave plasma enhanced-chemical vapor deposition (MPE-CVD) directly on Ti substrate to prepare binder-free electrode. For the preparation of electric double layer capacitors (EDLCs), the effects MPE-CVD parameters including gas composition, pressure, deposition duration, and applied power were studied and optimized.

In this study, MPE-CVD is composed of a microwave power supply with a frequency of 2.54 GHz, where the working gases Ar and CH_4 were excited in a quartz tube with a diameter of 2.5 cm and a length of 40 cm. Titanium with a thickness of 100 μm was used as the substrate for GNFs deposition due to its high thermal stability. Throughout the deposition procedure, the Ti current collector was positioned in the center of the plasma ignition section and perpendicular to the gas flow in order to obtain uniformly distributed GNFs. In the reaction chamber, the ratio of CH_4 to Ar varied from 40 to 80%, with a total gas flow rate of 40 sccm. The as-prepared GNFs/Ti electrodes can be used as the positive and negative electrodes that require no additional treatment. The performance of symmetric EDLCs assembled using the as-prepared GNFs/Ti electrodes was evaluated in a pouch cell by cyclic voltammetry and galvanostatic charge/discharge measurements where the cycling ability was conducted for 10,000 cycles.

In this study, microwave plasma drives the vertical development of GNFs effectively on Ti substrate. A growth rate of GNFs, 180 $\mu\text{m}/\text{h}$, is 15 times greater than the maximum value reported in the literature (11.40 $\mu\text{m}/\text{h}$). Furthermore, after 10,000 charge-discharge cycles, the Coulombic efficiency was 99.4% and the capacitance retention was 75%. In conclusion, the MPE-CVD system applied in this work facilitate the preparation of GNFs/Ti electrodes that is advantageous as an effective process compared to the conventional method with a significant rapid deposition rate.

1. Cai, M.; Outlaw, R. A.; Quinlan, R. A.; Premathilake, D.; Butler, S. M.; Miller, J. R., Fast response, vertically oriented graphene nanosheet electric double layer capacitors synthesized from C_2H_2 . *Acs Nano* 2014, 8 (6), 5873-5882.

8:00 PM SF04.07.06

Hydrogen-Assisted Sputtering Process for Enhanced Mechanical Stability of Oxide Thin Films in Flexible Electronics Seohan Kim¹ and Joonho Bang^{2,2}; ¹Uppsala University, Sweden; ²Gyeongsang National University, Korea (the Republic of)

Transparent oxide semiconductors have gained widespread use in electronic devices such as flat panel displays and solar cells. The increasing demand for flexible devices necessitates ensuring the long-term stability of oxide semiconductor thin films under bending stress. Recent theoretical and experimental studies have identified hydrogen species as significant impurities in many oxide semiconductor thin films. In this study, we present a novel approach to fabricating the hydrogen-incorporated amorphous In-Zn-O and In-Sn-O thin films using a hydrogen-assisted magnetron sputtering process. Through careful optimization of the hydrogen concentration, we achieved remarkable improvements in the mechanical stability of the thin films while simultaneously preserving their electrical and optical properties. Notably, the introduction of hydrogen resulted in a gradual reduction in the compressive residual stress of the films,

highlighting its potential as a promising candidate for defect passivation in flexible electronics. These findings provide insights into enhancing the durability of oxide-based flexible electronic devices.

8:00 PM SF04.07.07

Selective Extraction of Hydrogen Molecules from Plasma using a Metal-Organic Framework Filter Kyotaro Takagi, Moriyuki Kanno, Hitoshi Muneoka, Kazuo Terashima and Tsuyohito Ito; The University of Tokyo, Japan

Non-equilibrium plasma can promote various reactions through the contributions of energetic/reactive species, such as electrons, ions, radicals, and photons, while avoiding the environmental temperature elevation. Although synergetic effects of such species are making most of plasma applications attractive, in some cases, the existence of an excessively diverse species prevent us from achieving desired controllability. As for the charged particles, there are several techniques for selectively extracting certain reactive species, mostly using electromagnetic field. However, it is still difficult to selectively extract reactive neutral species.

One approach for separating neutral species from a gas mixture is by using sieves with microstructures [1] and metal-organic frameworks (MOFs) are attracting candidates for such sieves [2]. MOFs are porous materials composed of metal ions and organic ligands. By choosing the types of metal ions and ligands, it is possible to control pore structures, pore sizes, surface properties, morphology, and so on.

Here, we are demonstrating H₂ extraction from low-temperature Ar/C₃H₈ plasma by using zeolitic imidazolate framework-8 (ZIF-8) as a filter located in the plasma region. Quadrupole mass spectrometer was applied to analyze the atoms/molecules behind the ZIF-8 filter. By comparing with the no-filter case, it is indicated that ZIF-8 can selectively extract H₂ by impeding C₃H₈ transfer, although it is not yet perfect. We have also confirmed that the ZIF-8 filters were not significantly damaged in the tested conditions. Further details will be presented at the symposium.

[1] L. M. Robeson, *The Upper Bound Revisited*, Journal of Membrane Science **320**, 390 (2008).

[2] Q. Qian, P. A. Asinger, M. J. Lee, G. Han, K. Mizrahi Rodriguez, S. Lin, F. M. Benedetti, A. X. Wu, W. S. Chi, and Z. P. Smith, *MOF-Based Membranes for Gas Separations*, Chem. Rev. **120**, 8161 (2020).

8:00 PM SF04.07.08

Enhanced Electrocatalytic Activities of the Nitrogen-Doped Onion-Like Carbons Synthesized by Plasma Discharge Process in Solution SangYul Lee¹ and Jung-Wan Kim²; ¹Korea Aerospace University, Korea (the Republic of); ²InCheon National University, Korea (the Republic of)

A plasma discharge process, so called solution plasma process, was used to synthesize nitrogen-functionalized onion-like carbon (N-OLC) at various ammonia concentrations and the N-OLC was used as a catalyst support material for a catalytic oxygen reduction reaction (ORR) evaluation. With increasing ammonia concentrations up to 5 M, the amount of the nitrogen doping increased up to 1.7 at.%, which created a highly defective onion-like structure. The edge and defective sites induced from nitrogen atoms effectively provided with the nucleation sites for Pt clusters, which led to the stable dispersion and size-reduction of Pt nanoparticles (PtNPs), as revealed via XPS, XRD, Raman spectroscopy and electron microscopy. From the results of the electrochemical characterization, the PtNPs supported on the N-OLC with a nitrogen content of 1.7 at.% exhibited the highest electrochemically active surface area (ECSA), specific current density and half-wave potential. The enhanced (ORR) could be attributed to the defective outermost layers and the electronic modification. Moreover, even after an accelerated durability test (ADT) with 5,000 cycles, the N-OLC with a nitrogen of 1.7 at.% exhibited less degradation, indicating the excellent ORR durability. Experimental details will be presented.

8:00 PM SF04.07.09

Plasma Etched Vertically Aligned Carbon Nanotube Embedded Polyurethane Surface for Precision Semiconductor Wafer Polishing Sukkyung Kang¹, Ji-hun Jeong², Hyun Jun Ryu¹, Dongyeon Won¹ and Sanha Kim¹; ¹Department of Mechanical Engineering, Korea Advanced Institute of Science and Technology (KAIST), Korea (the Republic of); ²Department of Mechanical Engineering, Massachusetts Institute of Technology (MIT), United States

Surface polishing and planarization process plays a significant role in achieving desired surface characteristics and ensuring product quality. The process is widely used in precision manufacturing industries including semiconductors, biosensors, displays, and battery packaging, and the requirements for precision polishing is ever increasing toward atomic scale. For productivity and quality, selection and optimization of the polishing pad and abrasive are essential, and realizing a precise surface topology for the polishing pads via advanced materials and plasma treatment can be an effective route for enhancing the efficiency and accuracy of the atomic scale polishing process.

In this study, we propose a novel composite abrasive pad comprising 1D nanoscale fibers embedded in a soft matrix material realized by plasma treatment during fabrication. Here, we synthesize vertically aligned carbon nanotubes (VACNTs) and utilize them as a mechanical abrasive for precision polishing. Different from other conventional precision polishing methods, where the nanoscale abrasives are dispersed in a solution and supplied separately to the polishing pad surfaces, we conceptualized a new composite pad using 1D nano abrasives embedded on the surface. Individual carbon nanotubes exhibit high hardness and have a diameter of less than 10 nanometers which is suitable for abrasion. And their high aspect ratio controlled to be up to 10,000 allows them to be firmly fixed onto the soft matrix material. For the realization of the VACNT-embedded polyurethane pad, the key fabrication step is the selective plasma etching of polyurethane using argon plasma to expose a portion of the VACNTs, thereby creating a fixed-abrasive pad structure. making it suitable for nano-scale composite surface processing. We investigate the selective etching behavior of VACNTs and polyurethane, by adjusting parameters such as power, gas flow rate, and etching time. We then further explore the optimum plasma condition which ensures the VACNTs maintain the vertical alignment without clumping. The plasma step also allows us to form nano-porous structures on the surface of the plasma-etched polyurethane polishing pads. These structures facilitate the circulation of the deionized water used in the polishing process and the storage and discharge of polishing residues, ensuring a defect-free process. By finely tuning the Ar plasma time, we control the size of the nano-porous surface structures and the RMS profile of the pad surface. Based on appropriate plasma treatment, the pad structure exhibits robust VACNT films impregnated with polyurethane, yielding a uniform distribution of the high-aspect-ratio VACNTs. Finally, polishing performance tests are conducted using a pin-on-disk setup on various wafers to correlate the relationship between the plasma-treated pad surface structure and its polishing performance. Our findings reveal that pads with a larger RMS profile removed material at a higher rate, but also decreased the polishing precision, resulting in a rougher surface on the copper wafers. However, by finely tuning the nano-structures on the pad surface via plasma treatment, we were able to strike a balance between the desired polishing precision and speed, and therefore achieve an overall enhancement.

8:00 PM SF04.07.10

What Impact Does Radio Frequency Power Have on the Growth Process and Optical Properties of Silicon Nitride Thin Films Made by RF Sputtering at Room Temperature? Edwin Sebastian Barrera-Mendivilso and Arturo Rodriguez-Gomez; Universidad Nacional Autonoma de Mexico, Mexico

Silicon nitride (SiN_x) is widely known for its exceptional hardness, making it a highly sought-after ceramic material. Its remarkable electrical and optical properties make it an excellent candidate for integration into microelectronics and photonics applications. Conventionally, SiN_x thin films are obtained through chemical vapor deposition (CVD) techniques, which necessitate high temperatures, thereby limiting the range of compatible substrates [1]. Despite ongoing efforts to optimize CVD processes and lower the required temperatures, their inherent high temperatures still pose challenges, particularly when working with temperature-sensitive materials [2].

In contrast, sputtering techniques offer a host of advantages over CVD techniques, including the ability to deposit SiN_x thin films at low temperatures without introducing hydrogen contamination [3]. However, achieving SiN_x thin films with desirable properties at room temperature remains a complicated task. Various parameters such as pressure, gas flow, bias voltage, and electrical power have been extensively investigated to comprehend their influence on the optical, electrical, and mechanical characteristics of SiN_x thin films [4]. Surprisingly, the impact of radiofrequency power (RF-P) on the structural and microstructural properties of these films, using a Si₃N₄ target at room temperature and in the absence of chemically active gases, has received limited attention.

This research delved into exploring the effects of RF-P on the growth of SiN_x thin films through non-reactive magnetron sputtering conducted at room temperature. Our findings revealed that when applying RF-P ≤ 50 W and limiting the deposition time to ≤ 120 minutes, the films exhibited polycrystalline silicon nitride particles in their α phase. By increasing either of these parameters, the formation of polycrystalline conglomerates of α-Si₃N₄ was facilitated, leading to improved film continuity and surface uniformity. Additionally, we observed a noteworthy increase in optical absorbance and a shift of the absorption edge toward the near-infrared (NIR) region when RF-P ≥ 50 W. Based on our results, we conclude that it is indeed feasible to grow thin SiN_x films at room temperature using our self-designed magnetron sputtering. These films demonstrate promising properties suitable for applications in electronic and optoelectronic devices.

References

[1] Kaloyeros AE, Pan Y, Goff J, Arkles B. Review—Silicon Nitride and Silicon Nitride-Rich Thin Film Technologies: State-of-the-Art Processing Technologies, Properties, and Applications. ECS J Solid State Sci Technol 2020;9:063006. <https://doi.org/10.1149/2162-8777/aba447>.

[2] Kaloyeros AE, Jové FA, Goff J, Arkles B. Review—Silicon Nitride and Silicon Nitride-Rich Thin Film Technologies: Trends in Deposition Techniques and Related Applications. ECS J Solid State Sci Technol 2017;6:P691–714. <https://doi.org/10.1149/2.0011710jss>.

[3] Rodríguez-López R, Soto-Valle G, Sanginés R, Abundiz-Cisneros N, Águila-Muñoz J, Cruz J, et al. Study of deposition parameters of reactive-sputtered Si₃N₄ thin films by optical emission spectroscopy. *Thin Solid Films* 2022;754:139313. <https://doi.org/10.1016/j.tsf.2022.139313>.

[4] Dergez D, Schneider M, Bittner A, Pawlak N, Schmid U. Mechanical and electrical properties of RF magnetron sputter deposited amorphous silicon-rich silicon nitride thin films. *Thin Solid Films* 2016;606:7–12. <https://doi.org/10.1016/j.tsf.2016.03.029>.

8:00 PM SF04.07.11

Nonequilibrium Plasma Aerotaxy of In_xGa_{1-x}N Nanocrystals Dillon P. Moher and Elijah Thimsen; Washington University in St. Louis, United States

Semiconductors that have high chemical resistance and photostability, tunable absorption/emission properties, and low toxicity are in high demand for solar energy conversion and solid-state light sources. The solid solution of indium nitride and gallium nitride (In_xGa_{1-x}N) is a promising material for such applications. The composition-dependent band gap of In_xGa_{1-x}N may allow for tuning of the optical properties to efficiently harvest solar irradiance or achieve light emission across the visible/near infrared range. In reality, there are synthetic challenges associated with homogeneous thin film In_xGa_{1-x}N. The miscibility gap and strain-induced threading dislocations in In_xGa_{1-x}N with intermediate *x* have largely prevented realization of full spectral tunability. Freestanding, spherical In_xGa_{1-x}N nanocrystals stand to exhibit superior tunability by taking advantage effects at the nanoscale. Strain relaxation and size purification effects may aid in dislocation-free nanocrystal growth. Deviation from the bulk phase diagram at nanoscale particle size may stabilize nanoparticles with overall composition in the bulk miscibility gap, due to the cost of additional surface energy associated with phase segregation. Besides, freestanding nanocrystals are highly flexible for use in various applications. Yet, In_xGa_{1-x}N nanocrystal synthesis is underexplored. In this presentation, the synthesis of In_xGa_{1-x}N nanocrystals by Nonequilibrium Plasma Aerotaxy will be discussed. By feeding aerosols of indium and gallium metal, generated by thermal evaporation, into a nitrogen-argon low pressure, RF plasma, nanoparticles of pure gallium nitride, pure indium nitride, and their solid solution were produced. The composition of the solid solution was tuned by adjusting the molar feed rate of the metal aerosols. Progress towards achieving monodisperse, photoluminescent In_xGa_{1-x}N nanocrystals with *x* = 0.5 will be presented.

8:00 PM SF04.07.12

Directional Thermal Conductivity Enhancement in Plasma-Surface-Modified hBN and Polyrotaxane Composites by Electric Field Rui Hasegawa^{1,2}, Kenichi Inoue^{1,2,3}, Hitoshi Muneoka¹, Tsuyohito Ito¹, Kazuhiro Kirihara², Takashi Aoyama², Yoshiki Shimizu², Yukiya Hakuta², Kohzo Ito¹ and Kazuo Terashima^{1,2}; ¹The University of Tokyo, Japan; ²National Institute of Advanced Industrial Science and Technology, Japan; ³Nagoya University, Japan

Recently, flexible materials with high thermal conductivity have been extensively studied, e.g. for applying to flexible devices. We have developed hexagonal boron nitride particles (hBN)/polyrotaxane¹ (PR) tough composite, which is a highly thermally conductive flexible insulator, by applying plasma-surface modification of hBN resulting in their higher dispersibility in the composite and enhancing toughness via using PR as a slide-ring material². hBN is known to have anisotropic thermal conductivity, as in-plane direction shows about 20 times higher conductivity than out-of-plane direction. Therefore, thermal conductivity of such composites can be increased in one direction, if in-plane directions of hBN are oriented parallelly. Such demonstration has been achieved with hBN/polysiloxane composites, by applying electric field³. Electric field can not only orient hBN, but also form pillar-like structures of the oriented hBN, which could further increase the directional thermal conductivity. The purpose of this study is to synthesize tough composite sheets with high thermal conductivity in out-of-plane direction, by combining above-mentioned two approaches: (i) composites of plasma-surface-modified hBN and PR, and (ii) applying electric field for increasing thermal conductivity in the applied field direction.

hBN with various sizes (0.2–23 μm) were pre-treated via plasma in liquid and the mixture, including hBN and PR, were exposed to an electric field during the polymerization. The results show that the thermal conductivity in the field direction is enhanced comparing with the case applying no electric field. It was also confirmed that blending different-sized hBN can improve the thermal conductivity by keeping same hBN content in the composites. For example, the higher thermal conductivity is achieved with 0.2-μm (10%) and 7-μm (90%) hBN, comparing with that with 100% 7-μm hBN. We attribute this improvement to stronger heat pass formation by smaller hBN bridging larger hBN in pillar-like structures.

The synthesized electric-field-applied composites show anisotropic properties in the thermal conductivity as well as their Young's modulus. Such composites show higher thermal conductivity in the electric field direction (out-of-plane direction of composite sheets) and lower Young's modulus in the direction perpendicular to the field (in-plane direction of composite sheets), comparing with those of composites without electric field application. These directional changes of properties are sometimes ideal for a thermal-conductive flexible materials. By optimizing the conditions, a flexible composite with elastomer-class flexibility (Young's modulus, perpendicular to the field direction: 58 MPa) and metal-class thermal conductivity (parallel to the field direction: 11 W/mK) has been achieved so far.

Further details, including hBN contents dependence and their blending-ratio dependence, will be presented at the symposium.

1. Okumura, Y. & Ito, K. The Polyrotaxane Gel: A Topological Gel by Figure-of-Eight Cross-links. *Adv. Mater.* **13**, 485–487 (2001).

2. Inoue, K., Goto, T., Ito, T., Shimizu, Y., Hakuta, Y., Ito, K. & Terashima, K. Boron nitride with high zeta potential via plasma processing in solution for preparation of polyrotaxane composite. *J. Phys. Appl. Phys.* **54**, 425202 (2021).

3. Cho, H.-B., Nakayama, T., Suematsu, H., Suzuki, T., Jiang, W., Niihara, K., Song, E., Eom, N. S. A., Kim, S. & Choa, Y.-H. Insulating polymer nanocomposites with high-thermal-conduction routes via linear densely packed boron nitride nanosheets. *Compos. Sci. Technol.* **129**, 205–213 (2016).

SESSION SF04.08: Plasma Synthesis and Surface Engineering II

Session Chairs: Mariadriana Creatore and Yamada Hideaki

Wednesday Morning, November 29, 2023

Sheraton, Second Floor, Independence East

8:30 AM *SF04.08.01

Nanocrystals by Atmospheric Pressure Microplasmas Oxide, Defects and Doping Davide Mariotti; Ulster University, United Kingdom

Doping, defect engineering, quantum confinement and extending to clusters, ternary or high entropy oxides can create disruptive materials with new or improved properties. Atmospheric pressure microplasmas represent a viable synthesis platform to achieve exceptional tuning capability therefore achieving an exquisite control of the size, composition and defects of metal oxide nanoparticles. Microplasmas offer dial-up delivery of precursor radicals together with tunable temperature conditions for nanoparticle formation, followed by rapid quenching. These microplasma conditions can lead to unprecedented crystal structures that can be constructed in a bottom-up approach. In this contribution we will show how quantum confinement and extensive defects in metal oxide nanoparticles can produce very desirable opto-electronic properties. Therefore we will discuss the formation of metal oxides nanoparticles with gas-phase microplasmas as well as hybrid plasma-liquid systems. The pros and cons of these microplasma synthesis approaches will be revealed and opportunities explored also in terms of manufacturing scalability and process integration. We will further provide in-depth analysis of the metal oxide nanoparticles, including their application opportunities in energy conversion and storage. Examples will include oxides from Ni, Cu, Mn, Sn, Co, Mo and Zn. Finally we will provide future directions at the boundaries between ordered and disordered crystal structures.

9:00 AM SF04.08.02

Quantitative Analysis of Reactive Sites on Hexagonal Boron Nitride Treated by Plasma in Solution Kenichi Inoue^{1,2,3}, Naoto Takagi¹, Tsuyohito Ito¹, Yoshiki Shimizu³, Kenji Ishikawa², Masaru Hori² and Kazuo Terashima^{1,3}; ¹The University of Tokyo, Japan; ²Nagoya University, Japan; ³National Institute of Advanced Industrial Science and Technology, Japan

Hexagonal boron nitride (h-BN) is a superior material representing high thermal conductivity and electrical insulation, and h-BN/polymer composite materials have been developed for heat release sheets in electronic devices. In fabricating the composites, low reactivity of h-BN is a problem for surface functionalization and causes poor dispersibility in the polymer matrix [1]. Previously, we suggested the plasma processing is one of effective methods for surface modification of h-BN, because the excited species could break the stable B–N bonds and produce reactive sites on the surfaces [2]. The reactive sites, which are dangling bonds on h-BN, allow to functionalize with hydroxyl (OH) groups. Thus, the OH groups formed by plasma modification and subsequent oxidization leads to higher dispersion of h-BN in aqueous media and polymer matrix owing to increase of zeta potential [1,2]. The formed dangling bonds by plasma processing can be detected using electron spin resonance (ESR) measurements [2]. However, quantification of the dangling bonds and the functionalization kinetics have not been fully clarified. In this study, plasma processing in solution was performed on h-BN particles and gradual functionalization to the dangling bonds under an atmospheric environment was analyzed. We have quantified the dangling-bonds formation by plasma processing and revealed their time-variation due to the functionalization during exposure to air.

The plasma processing in solution was performed on h-BN particles (Maruka, AP-170S) as described in the previous paper [1]. The plasma was generated by a bipolar pulsed power supply

(Kurita Seisakujo, MPP-HV-04-300 kHz) in 1 L of distilled water containing 5 g of h-BN particles, using a stirring device (Nihon Spindle, Jetpaster). The applied pulsed voltage for plasma generation had a frequency of 300 kHz, a peak voltage of ± 1 kV, and a pulse width of approximately 1 μ s. The plasma-treated h-BN for 20 min was captured using a membrane filter and dried under vacuum. After the processing, the sample was exposed in an atmospheric environment at room temperature for up to 650 days. After the different exposure days, the samples were analyzed using an ESR spectrometer (Bruker, EMX-plus). Spin concentration in the h-BN were measured by calibration using aqueous solution containing 4-hydroxyl-2,2,6,6-tetramethylpiperidine (TEMPOL) as a stable radical standard. Surface number densities of dangling bonds were calculated with normalization of the spin concentration by the specific surface area, that was measured by using a surface area analyzer (Micrometrics, VacPrep061). A Fourier transform infrared (FT-IR) spectrometer (PerkinElmer, Spectrum100) was applied to analysis of OH groups on h-BN during air exposure days after plasma processing. The surface number density of the dangling bonds on the plasma-treated h-BN was estimated to be $800 \mu\text{m}^{-2}$ at the 3-days exposure to air after the plasma processing, while that of the untreated h-BN was only $20 \mu\text{m}^{-2}$. During exposure of the plasma-treated h-BN to air for up to 650 days, the surface number density decreased and reached to an equilibrium value of approximately $100 \mu\text{m}^{-2}$. Besides FT-IR spectra showed increase of the B-OH peaks during exposure of the plasma-treated h-BN to air. Consequently, the dangling bonds on h-BN as reactive sites have an important role for OH functionalization on the h-BN surfaces and their quantitative analysis could enable the development of more effective surface modification by plasma processing to improve hydrophilicity and dispersibility of the materials.

References

- 1] K. Inoue, T. Goto, T. Ito, Y. Shimizu, Y. Hakuta, K. Ito, and K. Terashima, *Journal of Physics D: Applied Physics*, **54**, 425202 (2021).
- 2] T. Ito, T. Goto, K. Inoue, K. Ishikawa, H. Kondo, M. Hori, Y. Shimizu, Y. Hakuta, and K. Terashima, *Applied Physics Express* **13**, 066001 (2020).

9:15 AM SF04.08.03

Unlocking the Limits of the Plasma-Activated Liquids and Plasma Synthesis of Silicon Nanoparticles Filip Matejka^{1,2}, Jakub Kopenc^{1,2}, Pavel Galar¹, Tomas Popelar¹ and Katerina Kusova¹; ¹Czech Academy of Sciences, Czechia; ²University of Chemistry and Technology, Czechia

In the past years, the topic of nanoparticles of a broad variety of materials, mainly semiconductors, led to significant advances in science and technology. To make these materials more applicable, the search for variable methods of synthesis and surface modification is ongoing. Two groups of nanoparticles are of special interest. The first group are the sub-10-nm particles, which in case of several materials, e.g., silicon nanocrystals (SiNCs), exhibit efficient light generation (photoluminescence – PL). The properties of the generated light can be set up and modulated by the proper surface modification. The second group is represented by the particles with sizes around 100 nm, which can be employed in the production of batteries. Importantly, these larger particles with also benefit from surface modification, which will lead to better dispersibility in various liquids and thus simplify the fabrication of the battery anodes. In this study, we demonstrate that non-thermal plasma (NTP) is a powerful environment for both the synthesis of size-tunable SiNCs and the surface chemistry modification, considering its speed, simplicity and high reactivity. We overcome the limits of the NTP systems, showing the applicability of the NTP systems to synthesize the light emitting SiNCs, as well as the large ca. 80 nm SiNCs, and to provide a novel method of generating highly reactive liquid environment suitable for the SiNCs' surface chemistry modification.

The main complications with respect to the potential of synthesizing larger nanoparticles in the NTP low pressure synthesis of SiNCs are the charging of the surface and the depletion of the precursor. We solved this issue by employing a two-stage process. In the first stage, the crystalline sub-10-nm core is formed with the use of planar electrodes. In the second stage, the long plasma beam, generated by helix electrodes, with additional silane gas, are utilized to synthesize SiNCs ca. 80-nm in diameter. In combination with high yields and the speed of the NTP method, we achieve a broadly variable synthetic system. We can provide crystalline sub-10-nm cores, whose effective PL is tunable by the size from 700 nm to 950 nm, as well as the large particles.

Surface chemistry is another key factor for the properties of silicon nanoparticles. Recently, we have shown that with the proper settings of the NTP system using two needle electrodes (one submerged) and generating the transient spark discharge, the high in nitrogen species plasma-activated water (HiN:PAW) can be produced.¹ This HiN:PAW is suitable for the nitrogen enrichment of the SiNCs' surface, leading to enhancement and shifting of the PL, as well as improvement of dispersibility in water.² However, the generalization of this system to other liquids, i.e. the NTP activation of different organic liquids (PAOL) is not yet well-established, due to several drawbacks of these liquids, e.g., volatility or flammability. Here, we present a successful PAOL system, which solves the problematic behavior of organic liquid, mainly with the use of a novel designed reactor box. This system was applied on five different organic liquids with diverse structural (e.g., aromatic structure, aliphatic chains) and physical (e.g., polarity of molecule) properties, leading to a successful change of surface chemistry, accompanied by the tunability of the PL properties (position and intensity) and an improvement of dispersibility in different media. Therefore, with the use of the NTP activation of liquids, we achieved a novel adjustable system, which generates reactive environment suitable for tailoring of the SiNCs' surface chemistry, leading to broad applicability of light emitting SiNCs in a plethora of environments (e.g., water, polar, non-polar).

¹Matejka, F., et al. 2023 *Phys. Scr.* 98 045619 10.1088/1402-4896/acc48e

²Galar, P., et al. *Green. Chem.* 2021, 23, 898 - 911. 10.1039/D0GC02619K2

9:30 AM *SF04.08.04

Plasma-Induced Modification of 2D Materials: The Case of Monolayer Graphene Luc Stafford; University of Montreal, Canada

Engineering of defects located in-grain or at grain boundary is central to the development of functional materials and nanomaterials. While there is a recent surge of interest in the formation, migration, and annihilation of defects during ion and plasma irradiation of bulk (3D) materials, the detailed behavior in low-dimensional materials remains most unexplored and especially difficult to assess experimentally. A new hyperspectral Raman imaging scheme providing high selectivity and diffraction-limited spatial resolution was recently adapted to examine plasma-induced damage in a polycrystalline graphene film grown by chemical vapor deposition on copper substrates and then transferred on silicon substrates. For experiments realized in nominally pure argon plasmas at low pressure, spatially resolved Raman conducted before and after each plasma treatment shows that the defect generation in graphene films exposed to very low-energy (11 eV) ion bombardment follows a 0D defect curve, while the domain boundaries tend to develop as 1D defects. Surprisingly, damage generation at grain boundaries is slower than within the grains; this behavior can be ascribed to a lattice reconstruction mechanism occurring preferentially at domain boundaries and induced by preferential carbon atom migration and carbon adatom-vacancy recombination. Based on exhaustive plasma characterization using Langmuir probes and optical emission and absorption spectroscopy, further studies were realized to compare the impact of different plasma environments promoting either positive argon ions, metastable argon species, or VUV-photons on the damage formation dynamics. While most of the defect formation is due to knock-on collisions by 11-eV argon ions through a mechanism that remains to be confirmed, the combination with VUV-photon or metastable atom irradiation is found to have a very different impact. In the former, the photons are mainly thought to clean the films from PMMA residues due to graphene transfer from copper to silicon substrates. On the other hand, the surface de-excitation of metastable species first impedes the defect generation and then promotes it for higher lattice disorder. While this impediment can be linked to an enhanced defect migration and self-healing at nanocrystallite boundaries in graphene, such effect vanishes in more heavily-damaged films.

This set of plasma-graphene experiments reveal that carbon adatom migration is essential for defect annihilation; however, the healing dynamics in such conditions remain unclear. Very recently, a new setup was specifically designed to examine plasma-surface interactions and to shed light on the defect recombination dynamics. Here, in-plasma Raman spectrometry is used to monitor the evolution of selected Raman peaks over nine points of the graphene surface. On one hand, for high-energy ions, defect generation progressively rises with the ion dose, with no significant variations after ion irradiation. On the other hand, for very-low-energy ions, defect generation increases at a lower rate and then decreases over a very long time scale after ion irradiation. Such self-healing dynamics cannot be explained by a simple carbon adatom-vacancy annihilation. Using a 0D model, it is demonstrated that various mechanisms are in play, including carbon adatom trapping by Stone-Wales defects and dimerization. These mechanisms compete with the self-healing of graphene at room temperature, and they slow down the healing process. Such features are not observed at higher energies for which carbon atoms are sputtered from the graphene surface, with no significant populations of carbon adatoms. We believe that these experiments can be used as building blocks to examine the formation of chemically doped graphene film in reactive plasmas using, for example, argon mixed with either traces of N- or B-bearing gases.

10:00 AM BREAK

10:30 AM SF04.09.01

Plasma-Based Oleic Acid Nanofilms on n-Al with Higher Energetic Performance than n-Al/Graphene Oxide Mechanical Mixtures Prawl P. Agarwal, Robert M. Rioux and Themis Matsoukas; The Pennsylvania State University, United States

The energetic performance of nano-aluminum (n-Al) is inhibited by the presence of an oxide shell, which acts as a diffusion barrier and delays the contact of oxidizer and metal. In the last few years, graphene oxide (GO) has attracted attention as an additive to energetic material formulations. It has been reported in the literature (Zheng et al., ACS Nano, 2018, 12, 11, 11366–11375) that GO added in a mechanical mixture (MM) with Al improves the ignition and combustion behavior of the solid fuel. In this work, we deposit thin films of organic-based materials onto n-Al and demonstrate superior energetic performance compared to Al/GO MM. We use oleic acid (OA) as a precursor for plasma-enhanced chemical vapor deposition (PECVD) of ultrathin films (2–10 nm) and study the oxidation behavior of the coated n-Al by thermal analysis (TGA/DSC). We find that the heat measured by DSC is a function of thickness and that the maximum amount of oxidative heat release corresponds to a 4 nm film. The nanofilms deposited by OA plasma are compared with n-Al/GO MM (different weight proportions) in terms of oxidation and heat release by thermal analysis (TGA/DSC). The energy enhancement in OA plasma-coated n-Al (39%) is higher than in n-Al/GO mixtures (25%) compared to n-Al (control). The chemistry and mechanism behind the enhancement in oxidative heat release are investigated by characterizing the materials. The presence of the coatings and their composition are characterized by high-resolution transmission electron microscopy (HRTEM), high-angle annular dark-field - scanning transmission electron microscopy - energy dispersive spectroscopy (HAADF-STEM-EDS), and X-ray photoelectron spectroscopy (XPS) of OA plasma films and GO demonstrated the presence of similar chemical functional groups in them. In addition to the higher heat release, the plasma films provide passivation against air and humidity, as demonstrated by accelerated aging tests at extreme temperature and humidity conditions. The nanofilms developed from PECVD can provide a cost-effective way to achieve functionality better than GO with longer storage stability and can be used in various nanoenergetic applications such as propulsion, energy storage, and space exploration.

KEYWORDS: nano-aluminum, graphene oxide, PECVD, oleic acid, oxidation, nanoenergetic materials

10:45 AM SF04.09.02

Tailoring Magnesium Nanoparticles In-Flight via Non-Thermal Plasma for Enhanced Ignition Brandon A. Wagner, Pankaj Ghildiyal, Mahub Chowdhury, Minseok Kim, Michael R. Zachariah and Lorenzo Mangolini; University of California, Riverside, United States

Nano-sized energetic materials allow for better combustion performance compared to micron-sized materials. A significant drawback to using nano-scaled materials for combustion is their propensity for agglomeration and sintering upon ignition. [1] Magnesium (Mg) is a desirable fuel for energetics because of its high reactivity and high energy density. [2] However, the boiling point of its native oxide layer is greater than Mg, forcing ignition to proceed through a diffusion-limited process. [3] Directly coating Mg with an oxygen-containing silicon-based shell produces a nano-thermite system on the nanoparticle interface, accelerating reaction kinetics during ignition. [4] Hydrogenating Mg results in an ignition system that releases hydrogen (H₂) gas to alleviate sintering and agglomeration issues during combustion. Our work involves the in-flight modification of magnesium nanoparticles (NPs) by a low-temperature plasma process to circumvent oxide layer formation and boost ignition performance.

A two-step experimental setup was designed to nucleate Mg NPs by gas-condensation and to coat the surface via a silane plasma. Alternatively, hydrogen treatment was carried out by a hydrogen plasma. Ex-situ characterization of nanoparticle crystallinity, morphology, and chemical composition was accomplished by x-ray diffraction (XRD), scanning electron microscopy (SEM), transmission electron microscopy (TEM), and energy-dispersive x-ray spectroscopy (EDS). For hydrogenated Mg (h-Mg) temperature-programmed desorption (TPD) and optical emission spectroscopy (OES) were also performed. Processing parameters were manipulated to incorporate more magnesium hydride (MgH₂) into the NPs.

For silicon-coated Mg (Mg/Si-SiO_x) NPs, combustion performance was tested against Mg NPs with bismuth oxide as a primary oxidizer for overall combustion. Ignition temperature, ignition time, and combustion products were characterized via temperature-jump time-of-flight mass spectrometry (Tjump-TOFMS), wherein a platinum wire was coated with sample and heated until ignition. Our findings suggest that the reaction onset of coated magnesium is faster due to the close proximity of the fuel and oxidizer during ignition. In addition, the ignition threshold and reaction timescale decreased in the coated samples compared to non-coated magnesium. For h-Mg NPs, combustion performance was analyzed by Tjump-TOFMS using different oxidizers to investigate the reaction mechanisms that affect ignition temperature and reaction kinetics during combustion. Our findings indicate that the hydrogen content can be tuned by adjusting the RF power of the plasma. Additionally, h-Mg combustion with a potassium perchlorate oxidizer lowers the ignition threshold.

Overall, these results confirm that non-thermal plasma processing is a powerful and versatile approach for the modification of nanoparticles, with particularly interesting application for the case of energetic nanomaterials.

[1] Dilip Sundaram, Vigor Yang, Richard A. Yetter, Metal-based nanoenergetic materials: Synthesis, properties, and applications, Progress in Energy and Combustion Science, 61, 2017, 293-365

[2] Pankaj Ghildiyal, Prithwish Biswas, Steven Herrera, Feiyu Xu, Zaira Alibay, Yujie Wang, Haiyang Wang, Reza Abbaschian, and Michael R. Zachariah, Vaporization-Controlled Energy Release Mechanisms Underlying the Exceptional Reactivity of Magnesium Nanoparticles, ACS Applied Materials and Interfaces, 14, 15, 2022, 17164–17174

[3] Islam Shancita, Neil G. Vaz, Guilherme D. Fernandes, Adelia J.A. Aquino, Daniel Tunega, Michelle L. Pantoya, Regulating magnesium combustion using surface chemistry and heating rate, Combustion and Flame, 226, 2021, 419-429

[4] Brandon Wagner, Pankaj Ghildiyal, Prithwish Biswas, Mahub Chowdhury, Michael R. Zachariah, Lorenzo Mangolini, In-Flight Synthesis of Core-Shell Mg/Si-SiO_x Particles with Greatly Reduced Ignition Temperature, Advanced Functional Materials, 33, 2023, 2212805

11:00 AM SF04.09.03

High Entropy Materials Enabled by Microwave-Induced Plasma Shane A. Catledge, Bria C. Storr, Luke Moore and Cheng-Chien Chen; University of Alabama-Birmingham, United States

High Entropy Alloys (HEAs) and ceramics typically consist of five or more principal components that form a solid solution structure, instead of complex phases (e.g., intermetallics), and are stabilized by their high configurational entropy of mixing. We recently demonstrated a unique approach to synthesis of high entropy materials, including HEAs, enabled by microwave (MW)-induced plasma. This approach goes beyond conventional slow radiative heating by combining rapid MW energy absorption with enhanced chemical kinetics afforded by a plasma discharge. Conventional HEA formation relies on melting or long durations of intense mechanical agitation/alloying, often followed by subsequent heating/sintering steps to finally convert the mixture into a HEA solid solution. Our approach, facilitated by density functional theory calculations of entropy forming ability descriptors, involves thermal reduction of a five-component transition metal oxide powder mixture in a plasma reducing environment performed efficiently as a single step. Hardness and oxidation resistance measurements of the plasma-synthesized high entropy materials reveal substantial improvement over their non-HE counterparts. Current work is aimed at investigating reaction kinetics/pathways for HE materials made using this approach. Through the unique combination of plasma reduction of metal oxide precursors with the benefits of rapid MW heating/cooling, we anticipate highly efficient synthesis and fine microstructural control of HE alloy and ceramic systems.

11:15 AM SF04.09.04

Cluster Epitaxy of Iron Selenide Thin Films by Pulsed Laser Plasma Deposition Nithesh R. Palagin¹, Dorien Carpenter¹, Kamron Strickland¹, Sumner B. Harris², David B. Geohegan² and Renato P. Camata¹; ¹University of Alabama-Birmingham, United States; ²Oak Ridge National Laboratory, United States

Pulsed laser deposition (PLD) is a well-established technique for epitaxial growth of a wide variety of thin film materials. In traditional epitaxy—typically carried out in high vacuum—the growth process involves the deposition of individual atoms or molecules onto a substrate, leading to the formation of a crystal lattice with a regular arrangement of atoms. For a given target material, tuning the laser irradiation conditions and the parameters of the PLD plasma, enables control of the kinetic energy and flux of depositing particles. This allows optimization of thin film characteristics, including reduction of the number density of point and extended defects. Further manipulation of the PLD plasma can be achieved using reactive or inert background gases. Collisions of the expanding plasma plume with background atoms, for example, slow and confine the expansion. This results in significantly altered gas dynamics and reduced kinetic energy of depositing species. The ensuing film micro- and nanostructure are often substantially different than achieved through vacuum deposition.

In this work we study the pulsed laser growth of thin films of the unconventional superconductor iron selenide (FeSe), using a plasma plume that is thermalized by an argon (Ar) background. The focused beam of a KrF excimer laser (248-nm wavelength, 25-ns pulse width) was used to ablate a rotating target synthesized from metal powder elemental precursors with nominal stoichiometry Fe_{1.03}Se. This chemical makeup is within the narrow stability range of the β-FeSe phase needed to achieve superconductivity in this system at low temperature. The laser spot size on the target was controlled using rectangular apertures placed in the beam path between the laser output window and the focusing lens. Films were grown on (100)-oriented MgO substrates in the 10–300 mTorr Ar background pressure range. A laser fluence of 1.0 J/cm² and a spot area of 6.4 mm² were used. The resulting films were analyzed using X-ray diffraction

(XRD), X-ray reflectivity (XRR), and atomic force microscopy (AFM). The luminous portion of the plasma plume was recorded with a time-resolved gated-intensified CCD (ICCD) camera. Symmetric θ - 2θ XRD patterns indicate epitaxial growth of β -FeSe on MgO, with the c-axis of the tetragonal structure oriented normal to the substrate. Furthermore, XRD Φ -scans reveal four-fold symmetry of the (103) β -FeSe reflection, establishing that the c-axis oriented film also features in-plane epitaxy. AFM measurements show film surfaces with nanoporous structure exhibiting voids in the 10-25 nm range. This film nanostructure, allied to the in-plane and out-of-plane crystal alignment is consistent with growth by cluster epitaxy, in which the film building blocks are pre-formed clusters rather than individual atoms or molecules. These clusters may consist of hundreds to thousands of atoms bound together, likely as a result of plume thermalization, before arrival on the substrates. Films deposited in equivalent conditions, but under vacuum, show—via XRR measurements—significantly lower overall thickness due to the absence of voids. X-ray reflectivity data from nanoporous films exhibit additional fringes that can be ascribed to extra multiple internal reflections on the nanostructured layer. We discuss the effect of the inert background pressure on the film nanoporosity and correlate it to the plume dynamics expansion visualized in the ICCD data. We also show how the transport properties of porous films compare to non-porous β -FeSe grown in vacuum.

SESSION SF04.10: Plasma Synthesis and Surface Engineering III

Session Chairs: Rebecca Anthony and Lorenzo Mangolini

Wednesday Afternoon, November 29, 2023

Sheraton, Second Floor, Independence East

1:30 PM *SF04.10.01

Kinetic Spray Deposition of Ceramics Enhanced by a Non-Equilibrium Mesoplasma Jet Kentarō Shinoda, Mohammed Shahien and Masato Suzuki; National Institute of Advanced Industrial Science and Technology (AIST), Japan

Kinetic spraying of brittle materials such as ceramics is of interest as it can deposit ceramic materials at low temperature. Cold spraying of ceramics and aerosol deposition are known as this kind of processes. We consider the kinetic process can be used for a low-temperature repair technology as the element of remanufacturing in order to realize circular economy. However, compared to metals, which we can expect ductile plastic deformation, it is difficult to deposit brittle ceramics, limiting its capability and possibility. In order to deform and deposit such fragile materials, we need think additional energy source to activate the material adhesion and possible deformation. In this context, we utilize a non-equilibrium plasma jet called a mesoplasma, in which electron temperature is high to activate the particle surface, meanwhile a high-speed plasma jet can accelerate the particles to provide enough inertia to deform. The deposition rate can be increased by one-order of magnitude higher than that of a gas jet deposition. In this presentation, we would like to discuss the role of mesoplasma in kinetic spray of ceramic materials. The effect of surface enhancement and heating of particles is compared to that of increased particle velocity and internal energy. Properties and applications of some deposited structures with a controlled porosity will be introduced together with their microstructure development.

2:00 PM SF04.10.02

Reactive HiPIMS of Hydrogenated Amorphous Carbon using Toluene Precursor Monalisa Ghosh¹, Kerstin Thorwarth¹, Götz Thorwarth², Olesya Nakonechna¹, Arnold Müller³, Christof Vockenhuber³ and Sebastian Siol¹; ¹Empa-Swiss Federal Laboratories for Materials Science and Technology, Switzerland; ²IMT, Switzerland; ³ETH Zürich, Switzerland

Hydrogenated amorphous carbon (commonly written as a-C:H), a class of amorphous carbon containing considerable amounts of atomic hydrogen (10 at%-60 at%) is used in many applications ranging from sensors to cutting tools, and biomedical applications [1-5]. The functional properties of amorphous carbon are largely governed by the H-content and sp^2/sp^3 ratio. However, precisely controlling these material properties during synthesis is challenging. HiPIMS (High Power Impulse Magnetron Sputtering) process has been successfully employed for the deposition of amorphous carbon especially diamond-like carbons [6-7]. The films deposited by HiPIMS typically exhibit smooth topography, better adhesion to the substrate, higher wear resistance, and higher sp^3 content.

In this work, we present a novel method to deposit hydrogenated amorphous carbon films using reactive HiPIMS in the presence of a hydrocarbon precursor (toluene). Toluene acts as the regulated source of hydrogen in the sputtered films. The hydrogen content is tuned by controlling different deposition parameters like the partial pressure of toluene, the reactivity of toluene via additional plasma activation by RF substrate bias, etc. The motivation for employing HiPIMS is to control the sp^2/sp^3 ratio and facilitate a more stable hydrogenation of the carbon network compared to conventional state-of-art methods like plasma enhanced chemical vapour deposition (PECVD).

The a-C:H films are sputtered from a rectangular graphite target using a HiPIMS power supply (power in the order of 0.5-3 W/cm²) without any external substrate heating. The influence of composition (measured by ERDA/RBS) and structural properties (determined by Raman, SEM, and XPS) on the functional properties of the coatings are explored. We demonstrate that by changing the hydrogen content is controlled over a wide range (5 at%-36 at%) via which we can effectively control the properties of coatings like photoluminescence (about 100 folds increase in area under PL curve), hardness, and optical properties.

The study aims to provide new insight into a-C:H film deposition process via a HiPIMS process with additional control over the functional properties by independently controlling the sp^2/sp^3 ratio and hydrogen content.

References:

1. J. Robertson, Mater. Sci. Eng. R 37 (2002) 129.
2. C. Casiraghi, A. C. Ferrari, J. Robertson, Phys. Rev. B 72 (2005) 085401.
3. J. K. Luo, Y. Q. Fu, H. R. Le, J. A. Williams, S. M. Spearing, W. I. Milne, J. Micromech. Microeng. 17 (2007) S147.
4. A. Erdemir, J. M. Martin, Curr. Opin. Solid State Mater. Sci. 22 (2018) 243.
5. R. Hauert, K. Thorwarth, G. Thorwarth, Surf. Coat. Technol. 233 (2013) 119-130.
6. T. Kubart, A. Aijaz, J. Andersson, F. Ferreira, J. C. Oliveira, A. Sobetkii, A. Constantina Parau, C. Vitelaru, J. Vac. Sci. Technol. A 38 (2020) 043408.
7. J. A. Santiago, I. Fernández-Martínez, T. Kozák, J. Capek, A. Wennberg, J. M. Molina-Aldareguia, V. Bellido-González, R. González-Arrabal, M. A. Monclús, Surf. Coat. Technol. 358 (2019) 43.

2:15 PM SF04.10.03

Nonthermal Plasma Enabled Synthesis of Ultrafine Aluminum-Rich Corundum Nanocrystals AJCendejas, Dariusz Niedzwiedzki and Elijah Thimsen; Washington University in St. Louis, United States

Nanocrystalline $Cr_{2x}Al_{2(1-x)}O_3$ solid solutions offer a unique combination of chemical and thermal stability with optoelectronic and mechanical properties of interest for applications in catalysis, medicine, and structural materials. However, there exists an asymmetric miscibility gap in the range $0.02 < x < 0.7$ at temperatures below 1000 °C. Since sintering is extremely fast at high temperatures, synthesis of Al-rich corundum nanocrystals less than 50 nm in diameter has been elusive. In this work, we present a bottom-up synthesis of homogeneous α - $Cr_{2x}Al_{2(1-x)}O_3$ nanocrystals with ultimate grain sizes as low as 20 nm. The approach consists of the following: synthesis of size-controlled α - Cr_2O_3 nanocrystals via nonthermal plasma, subsequent atomic layer deposition of amorphous Al_2O_3 shells on the nanocrystals, and a final thermal annealing step to both crystallize the shell and homogenize the nanocrystals. X-ray diffraction, electron microscopy and energy dispersive X-ray spectroscopy were used to demonstrate complete mixing of Cr and Al in the particles. Temperatures as low as 850 °C resulted in complete homogenization of α - $Cr_{2x}Al_{2(1-x)}O_3$ nanocrystals. The ultrafine powders exhibited photoluminescence with a sharp emission line at 695 nm when excited by a 532 nm laser, characteristic of Cr^{3+} substitutions in the α - Al_2O_3 lattice. Additionally, the characteristic decay time of this emission was increased from 132.7 μ s to 278.5 μ s when the Cr concentration was diluted from $Cr_{0.4}Al_{1.6}O_3$ to $Cr_{0.02}Al_{1.98}O_3$.

2:30 PM BREAK

SESSION SF04.11: Plasmas at the Interface II

Session Chairs: Rebecca Anthony and Lorenzo Mangolini

Wednesday Afternoon, November 29, 2023

Sheraton, Second Floor, Independence East

3:30 PM *SF04.11.01

Significance of Free Radicals and Unsaturated Bonds in Amine Plasma Polymers LenkaZajickova^{1,2}, LucieJanu¹, ViniciusSantana¹, MartinaBuchtelová¹, BeataBeliancinova¹, EvaDvorakova¹, DavidNecas¹, NadaSouawda¹, MatusSedivy¹ and PetrNeugebauer¹; ¹Ceitec But, Czechia; ²Masaryk University, Czechia

Amino-group-containing plasma polymers (PPs) have been of particular interest for various biomaterials applications because they allow amide covalent coupling and, under certain pH conditions, offer a positively-charged surface for electrostatic binding. Therefore, they were successfully applied to immobilize DNA and various proteins. However, assessing what plasma parameters and the film structural properties are essential for successful and stable immobilization is difficult. PPs do not have a well-defined structure of conventional polymers that can be described as a repetition of a particular unit and the molecular weight of the polymer chain. Since they are deposited from a complex environment of many gaseous reactants created by dissociating original gas feed, their chemical structure cannot be derived only from the starting reactants. We studied the plasma polymerization of cyclopropylamine (CPA) mixed with Ar in three CCP reactor setups and different plasma conditions. The response of immunosensors constructed with the plasma polymerized CPA (PP-CPA) films revealed the surprisingly long reactivity of the film surfaces. It opens the question of whether such phenomena could be explained by the free radicals (species with unpaired spins) trapped in the PP films. Therefore, we investigated the presence and dynamics of the free radicals in the PP-CPA films deposited under mild varied conditions using electron paramagnetic resonance (EPR). We detected a surprisingly high amount of unpaired spin density with the life time in months. Another open question in the performance of amine PPs is the role of primary amine groups (-NH₂). In the example of two immunosensors having the same nitrogen and NH₂ amount, we demonstrate that amount of NH₂ groups detected by TFBA chemical derivatization cannot explain the efficiency of the antibody covalent coupling and nitrile groups belong to other factors that should be taken into account for the surface reactivity in aqueous media.

4:00 PM SF04.11.02

Deposition of (Multi)functional Thin Films by Coupling a Dielectric Barrier Discharge with an Aerosol: Role of Pulsed Precursor Injection LauraCacot^{1,2}, LucStafford¹, NicolasNaudé² and RichardClergeaux²; ¹University of Montreal, Canada; ²Laplace, France

Aerosol-assisted plasmas can be used to produce a wide variety of thin films, including homogeneous, nanotextured and/or nanocomposite coatings. For example, the nebulization of colloidal solutions, *i.e.* liquid solutions containing nanoparticles, in plane-to-plane dielectric barrier discharge (DBD) at atmospheric pressure has been used for nanocomposite thin film deposition. However, nanoparticles-loaded droplets in the aerosol lead to the deposition of aggregated nanoparticles embedded in the matrix. Recently, a new process of nanoparticles injection in plasmas has been developed. This method consists in synthesizing the nanoparticles prior to their injection in the plasma in a low frequency pulsed injection regime. However, the impacts of the pulsed liquid injection on the DBD physics are still opening questions.

This work aims to study a pulsed-liquid-assisted DBD deposition process. In contrast with the continuous nebulization of solutions, pulsed injection causes a sudden increase of the quantity of precursor as droplets in the inter-dielectric space – the average velocity being in the 10 m.s⁻¹ range. We observed that depending on the process parameters (injection times, pulse frequency, continuous gas flow rate, etc.), the discharge stability is modified. These parameters are also critical for transport and evaporation of the droplets and so on the thin film deposition (here ppHMDSO). For example, by varying the different parameters of the pulsed-liquid-assisted DBD, we observe that the deposit can consist in different phases (liquid and solid) as a function of the time residency of the aerosol and the thickness of the deposited layer. Furthermore, the variation of the discharge frequency can also be a way to tailored the thin-film deposition. In that aim this parameter was change to obtain a operation diagram of the process and get a transition from misty to dusty plasma.

4:15 PM *SF04.11.03

Oxygenate Production from Plasma-Activated Reaction of CO₂ and Ethane LeaWinter; Yale University, United States

Converting CO₂ to value-added chemicals using surplus light alkanes such as ethane is an attractive opportunity to move toward a circular carbon economy without requiring H₂ as a feedstock. Currently, the production of valuable oxygenated hydrocarbons such as alcohols, aldehydes, and acids from ethane involves either multistep, high-pressure heterogeneous catalysis processes or homogeneous catalytic reactions that entail significant product separation challenges. One-step conversion of ethane and CO₂ to oxygenates is not thermodynamically feasible under mild conditions and has not been previously achieved as a one-step process. To circumvent thermodynamic limitations, nonequilibrium plasma may be employed to overcome the activation barriers of the reaction under room temperature conditions. Furthermore, modular plasma-activated reactions are more easily adaptable to renewable electricity and small-scale CO₂ capture than large-scale thermally activated processes.

Nonthermal plasma was used to demonstrate one-step production of alcohols, aldehydes, and acids as well as C₁–C₅+ hydrocarbons under ambient pressure, with a maximum oxygenate selectivity of 12%. The effects of plasma power, feed gas ratio, and catalysts on activity and selectivity were investigated in an atmospheric pressure flow reactor using time-on-stream results. Isotope-labeling experiments were combined with plasma chemical kinetic modeling to reveal the reaction pathways. The reaction proceeded primarily via oxidation of activated ethane derivatives by CO₂-derived oxygen-containing species, demonstrating a mechanism that is fundamentally different from thermocatalytic alcohol synthesis. Results from this study illustrate the potential to use plasma for the direct synthesis of value-added alcohols, aldehydes, and acids from the greenhouse gas CO₂ and underutilized ethane under ambient pressure.

SESSION SF04.12: Plasma Processes for Biomaterials
Session Chairs: Tsuyohito Ito and Lenka Zajickova
Thursday Morning, November 30, 2023
Sheraton, Second Floor, Independence East

8:45 AM *SF04.12.01

Plasma Bio-Engineering: Next Generation Biointerfaces and Hydrogel-Based Hybrid Biomaterials BehnamAkhavan^{1,2,3}; ¹The University of Newcastle, Australia; ²The University of Sydney, Australia; ³Hunter Medical Research Institute, Australia

Implantable medical devices are increasing globally, with hundreds of thousands of operations performed annually. However, many of these operations experience failure due to infection and/or poor integration with host tissues. Biomimetic functionalization of surfaces enables control over the biological response by signalling through immobilized proteins and other biomolecules. Here we present a novel approach for the fabrication of radical-rich organic coatings that are chemically and mechanically robust for the surface engineering of implantable medical devices. Our results demonstrate that multifunctional protein layers, peptide molecules, or even silver nanoparticles can be covalently immobilized on such radical-rich interfaces for improved cellular activity and enhanced antimicrobial properties. Our recent findings provide evidence of utilizing this technology for polymerization and covalent attachment of hydrogel layers, as well as tuning the orientation and density of immobilized molecules on surfaces by simply tuning pH or applying external electric fields during the biomolecule immobilization. The plasma bio-engineering approach presented here promises to create the next generation of bioactive materials and interfaces for biomedical implant applications and beyond.

9:15 AM SF04.12.02

Bioinstructive Microenvironments for Cell Culture, Tissue Integration and Nanomedicine enabled by Plasma Surface Activation MarcelaBilek, ClaraT. Tran, AaronGilmour, BehnamAkhavan, JameelSardharwalla, LauraHaidar, XuegeFeng, GiselleYeo and StuartFraser; University of Sydney, Australia

Materials used in biomedicine are selected according to bulk properties, such as mechanical, electrical and optical, required for particular in-vivo and in-vitro applications. However, their surfaces almost always provide suboptimal biological microenvironments and do not promote the desired biological responses. This presentation will describe sustainable and readily scalable surface modification processes that use plasma to enable resilient and easily tailorable biofunctionalization of surfaces. We will examine how plasma activates a range of materials and structures for spontaneous, reagent-free, covalent functionalization with bioactive molecules and hydrogels. Typical time scales of cell culture and tissue integration necessitate covalent immobilization to prevent interface instability due to desorption and exchange with molecules in the surrounding aqueous environment. Functional molecules that can be immobilized to create tailored cell microenvironments include but are not limited to, oligonucleotides, enzymes, peptides, aptamers, cytokines, antibodies, cell-adhesion extra-cellular matrix molecules, and histological dyes. The covalent immobilization occurs on contact via radicals embedded in the surface by energetic plasma species. After a review of the fundamental science, plasma processes to modify the internal surfaces of multi-well plates, porous scaffolds, and micro/nanostructures will be presented. Strategies to immobilize biological microenvironment patterns and hydrogels onto the plasma-activated surfaces and to prepare multi-functionalizable nanoparticles will be discussed, together with strategies to control the density and orientation of surface-immobilized biomolecules

9:30 AM SF04.12.03

Atmospheric Plasma Deposition of Methacrylate Bio-Based Composite Coatings for Enhanced Release Function and Antimicrobial Properties of Paper KamalBaba¹, MustaphaTabbaa¹, NicolasBoscher¹, PatrickChoquet¹, IndiraHusic², Arunjunai RajMahendran², JudithSinic², ChristophJocham² and HerfriedLammer²; ¹Luxembourg Institute of Science and

Paper based functional coatings are traditionally made from low recyclable synthetic feedstock and wet chemistry approaches, potentially associated to longer processing times and higher material consumption. In this work, we address these aspects with the development of functional bio-based high-performance composite coatings reinforced with sustainable fillers using atmospheric pressure plasma as sustainable oriented coating technology.

Three different low viscosity acrylated Lignin based monomer, namely, Vanillyl Alcohol Methacrylate (VAM), Eugenyl Methacrylate (EM) and Isosorbide Methacrylate (IM), were used as resin, where seashell particles (SS), cellulose nanocrystals (CNC) as well as chitin from shrimp shell particles were used as sustainable additives. The methacrylation was obtained using methacrylic anhydride following an adopted procedure from *Stanzione et al.*

The polymerization of these different monomers was possible thanks to a liquid assisted dielectric barrier discharge approach and was evidenced by FTIR showing a successful conversion of double bonds during the plasma polymerization. Coatings of a thickness ranging from 0.5 to 2 μm was deposited on Si wafers and Glassine paper using Ar or N₂ as plasma gas and ultrasonic nebulization as monomer injection method. The degree of conversion was calculated from the FTIR spectra to assess the effect of the plasma parameters on the polymerization and coating properties. SEM pictures showed homogeneous coating and a uniform distribution of the particles. It was confirmed that the polymerization degree increases with the applied plasma power and decreases with the monomer delivery rate. The addition of SS and CNC particles to the VAM or EM coating influences the hydrophobicity and surface energy and it is believed that this affect also the release properties of the coated surface. The best release function of coated Glassine paper was obtained with the VAM composite coating (<250cN/25mm according to Finat 10/TESA 7475 test). The lower viscosity of VAM induces smaller droplets after ultrasonic nebulization and thus a better polymerization. The influence of particle addition on the physical properties of the composite coating was assessed by scratch test.

In another hand, Chitin particles were used as antimicrobial additive and were embedded in IM to deposit a composite coating. The effect of chitin loading on the antimicrobial properties of the plasma composite coatings will be discussed.

References:

J. F. Stanzione et al., *ChemSusChem*, 5, 1–8 (2012)

9:45 AMBREAK

SESSION SF04.13: Plasmas for Multifunctional and Smart Materials

Session Chairs: Tsuyohito Ito and Lenka Zajickova

Thursday Morning, November 30, 2023

Sheraton, Second Floor, Independence East

10:15 AM *SF04.13.01

Synthesis of Piezoelectric ZnO via Plasma-ALD and its Application in Electronic Skins Anna Maria Coclite; Graz University of Technology, Austria

Plasma-enhanced ALD (PE-ALD) employs the high reactivity of plasmas as co-reactant in atomic layer deposition (ALD) processes with the advantage that lower substrate temperature can be used compared to the conventional thermal ALD. This opens the possibility of depositing inorganic films with very high specificity on polymer substrates, which is important for organic electronics and polymer-based nanodevices to name a few applications. This talk will provide insights into the deposition process of ZnO via PEALD and how the film properties can be controlled with the deposition parameters. In-situ spectroscopic ellipsometry was used to study the initial growth and interface formation during ZnO deposition on polymers and it showed that PE-ALD growth on the investigated polymers is a result of two competing processes: plasma etching of the polymer substrate and ZnO nucleation and growth. Despite the initial etching, resulting ZnO films are smooth and of comparable structural quality to those grown on silicon. In addition they are piezoelectric, with piezoelectric constant strongly dependent on the growth temperature.

Such piezoelectric ZnO was combined with stimuli-responsive hydrogels in core-shell geometries for an electronic skin concept. Such device geometry was obtained by templated PEALD of the ZnO followed by the initiated chemical vapor deposition (iCVD) of the stimuli-responsive film. The nanostructuring of the films lead to a location-specific signal detection. In addition, the combination of two different materials allowed the detection of three stimuli: force, humidity and temperature. The whole sensor device could be deposited on flexible substrates and used for on-skin sensor or as electronic skin. While the piezoelectricity of ZnO provides sensitivity to external force, the thermoresponsiveness of the hydrogel core provides sensitivity to surrounding temperature and humidity changes. The hydrogel core exerts mechanical stress onto the ZnO shell, which is translated to a measurable piezoelectric signal. A localized force sensitivity of 364 pC N⁻¹ is achieved with very low cross talk between 0.25 mm² pixels. Additionally, the sensor's sensitivity to humidity is demonstrated at 20° and 40 °C, i.e., above and below the hydrogel's lower critical solution temperature (LCST) of 34 °C. The largest response to temperature is obtained at high humidity and below the hydrogel's LCST. The sensor response to force, humidity, and temperature is significantly faster than the system's intrinsic or excitation-induced time scale. Finally, the sensor response to touch and breath demonstrates its applicability as e-skin in real-life environment.

10:45 AM SF04.13.02

Direct Parylene Bonding for the Flexible Microfluidic Device Resistive Against the Absorption of Small Molecules Masahito Takakuwa^{1,2}, Daishi Inoue², Kenjiro Fukuda², Tomoyuki Yokota¹, Yuya Morimoto³ and Takao Someya^{1,2}; ¹The University of Tokyo, Japan; ²RIKEN, Japan; ³Waseda University, Japan

Flexible microfluidic devices are expected to be realized as sweat and blood sensors integrated into next-generation wearable devices directly attached to the skin. Dimethylpolysiloxane (PDMS), a silicone material, is commonly used in flexible microfluidic channels due to its excellent transparency, flexibility, and biocompatibility. Micro-scale grooves are created on PDMS using techniques like soft lithography, and the flexible microfluidic channels are fabricated by bonding thin film polymers or PDMS using adhesives or plasma modification methods. While this method allows for convenient and low-cost fabrication, it also faces limitations regarding material-related issues, which restrict its usage. For instance, PDMS tends to adsorb low-molecular-weight materials and proteins, and it swells in the presence of organic solvents. Moreover, its gas permeability can lead to changes in the concentration of analytes. Modifying PDMS or covering it with other materials is a beneficial way to prevent these issues. In particular, a non-reactive and gas-barrier polymer called parylene, commonly used as an encapsulation film for organic photovoltaics, is a promising material to prevent these PDMS-related problems. However, directly bonding parylene-coated PDMS is challenging due to the high-temperature bonding process (above 160°C), which causes PDMS to deform easily. On the other hand, the method of first plasma-bonding PDMS and then depositing parylene inside the channels using chemical vapor deposition (CVD) proves difficult for complex channel shapes or narrow channels.

This study developed a low-temperature direct bonding method below the glass transition temperature of parylene using water vapor plasma treatment and steam heating. This method enabled the fabrication of microfluidic channels with parylene-coated PDMS by simply bonding them together, suppressing the adsorption of low-molecular-weight compounds. Straight microchannels with a width of 50 μm were created on PDMS, and a 1 μm -thick parylene film was deposited on the entire PDMS surface, including the lid PDMS. The bonding surfaces were hydrophilized using water vapor plasma treatment and aligned with clips to prevent misalignment. The flexible microfluidic channels were created by storing the assembled samples in a steam chamber for 24 hours. Then direct parylene bonding occurred. To evaluate the absorption of low molecular weight materials in microfluidic channels, Rhodamine was introduced into parylene-coated and PDMS-exposed microfluidic channels. After 15 hours of introducing Rhodamine, the width of Rhodamine was measured in each microfluidic device. As a result, the detection width of Rhodamine was 1.3 times wider in the PDMS channel without parylene coating. On the other hand, no diffusion was observed in the parylene-coated microfluidic channel developed in this study. Therefore, the absorption of Rhodamine was suppressed by the parylene-coated PDMS microfluidic channels. By fabricating and evaluating more complex channel patterns, it is possible to achieve a conveniently fabricated flexible microfluidic device that can be integrated as a sensor in next-generation wearable devices.

11:00 AM SF04.13.03

Synthesis of Tungsten-Doped Titania Nanopowders Prepared by Pulsed-Laser Decomposition in Liquid Precursor Bath Mustafa Mozael^{1,2}, Stephen D. Tse² and Bernard H. Kear²; ¹Loyola Marymount University, United States; ²Rutgers, The State University of New Jersey, United States

Tungsten-doped TiO₂ (W-TiO₂) nanostructure is successfully synthesized by pulsed-laser ablation of a tungsten foil immersed in liquid titanium tetra-isopropoxide (TTIP). Interaction between the focused laser beam and the W substrate generates a submerged plasma, where vaporization of the W substrate and decomposition of the liquid precursor combine to produce W-doped TiO₂ nanoparticles upon quenching by the surrounding unreacted liquid precursor. The as-synthesized nanoparticles display various morphologies, including nano-spheres and nano-fibers, and occur in discrete, agglomerated and aggregated forms. Whatever their morphologies, all nanoparticles have non-crystalline or amorphous structures, primarily because of rapid condensation and quenching of vaporized species from the plasma-reaction zone. Interestingly, after heat treatment in air or oxygen, starting at ~400 C, transformation to the more stable anatase-TiO₂ phase occurs, but doped with tungsten. The phase transformation from anatase to rutile TiO₂ in the doped sample is shifted to higher temperatures 950 C compared to non-doped TiO₂ 800 C. In

addition, the average crystallite size of TiO₂ (about 13 nm) is slightly reduced by doping with W (10 nm) as the ionic radius of W⁶⁺ (0.60 Å) is quite similar to Ti⁴⁺ (0.68 Å). Ultraviolet-visible spectroscopic characterization shows that W-doped anatase TiO₂ exhibits a higher UV and visible photochemical activity than un-doped anatase-TiO₂, where the band gap is reduced from 3.08 to 2.92 eV, compared to the un-doped TiO₂ nanostructures.

SYMPOSIUM SF05

Infrared Materials and Devices for Thermal Radiation Control
November 27 - December 6, 2023

Symposium Organizers

Pierre-Olivier Chapuis, CNRS - INSA Lyon
Philip Hon, Northrop Grumman Corporation
Georgia Papadakis, ICFO – Institute of Photonic Sciences
Bo Zhao, University of Houston

* Invited Paper
+ JMR Distinguished Invited Speaker

SESSION SF05.01: Anisotropy and Directionality
Session Chairs: Pierre-Olivier Chapuis and Yannick De Wilde
Monday Morning, November 27, 2023
Sheraton, Third Floor, Hampton

10:30 AM *SF05.01.01

Directional Control of Infrared Emission in Tunable III-V Semiconductor Platforms Michelle Povinelli, Alok Ghanekar, Bo Shrewsbury, Tien Hsing Wang, Romil Audhkhasi, Hyun Uk Chae, Ragib Ahsan and Rehan Kapadia; University of Southern California, United States

We investigate the design of infrared metamaterials with directionally dependent emissivity and absorptivity. We envision an electrically tunable material for which the applied voltage perturbs the refractive index in the insulator layer of a metal-insulator-metal (MIM) metamaterial. We examine the options for tuning the angular dependence of emissivity for both confined MIM modes and extended Bloch modes. In the case of the MIM modes, we introduce a scheme for breaking the mirror symmetry of the unit cell via voltage perturbation. We show that the broken symmetry can be used to couple a previously hidden, or symmetry-forbidden “dark” mode to radiation. This creates a mechanism for switching on and off emissive spectral features in the infrared spectrum at normal incidence. In the case of extended Bloch modes, we consider the use of the index perturbation to double the period of the material. In an appropriately designed structure, we show that period doubling opens a band gap for off-angle radiation, splitting the emissivity features in the spectrum. We further consider possibilities for creating asymmetric emissivity as a function of angle. We show that when a Bloch mode metamaterial is designed to support diffraction orders, we can switch from a more isotropic emissivity to a more one-sided, directional emissivity. We present experimental results on the fabrication and characterization of the basic materials platform needed to achieve these theoretical effects. The platform includes a transferred GaAs layer containing a vertical p-i-n junction for tuning. We further characterize the measured spectral shift as a function of applied voltage. From the results, we can extract the typical index shifts that can be achieved in experiment. The results point to the potential for control over spectral and directional emissivity characteristics in electrically tunable semiconductor platforms.

11:00 AM SF05.01.02

Infrared Optics with Highly Anisotropic Materials Hongyan Mei¹, Guodong Ren², Boyang Zhao³, Jad Salman¹, Gwan-Yeong Jung², Huandong Chen³, Arashdeep S. Thind², Shantanu Singh³, Nick Settineri⁴, Simon J. Teat⁴, Bryan C. Chakoumakos⁵, Jayakanth Ravichandran³, Rohan Mishra² and Mikhail Kats¹; ¹University of Wisconsin Madison, United States; ²Washington University in St. Louis, United States; ³University of Southern California, United States; ⁴Lawrence Berkeley National Laboratory, United States; ⁵Oak Ridge National Laboratory, United States

The degree of birefringence (Δn) is a metric for optical anisotropy. Materials with large birefringence are sought after for polarization control (e.g., in wave plates, polarizing beam splitters, etc. [1–3]), nonlinear optics (e.g., for phase matching [4]), the realization of unconventional surface waves [5, 6], thermal radiation control [7], and the measurement of the Casimir torque [8]. Here, we demonstrate that a bulk uniaxial crystal with atomic-scale periodic modulations in its structure — Sr_{9/8}TiS₃ — has a record birefringence $\Delta n = n_e - n_o = 2.1$ ($n_e = 4.5$ and $n_o = 2.4$) within a broad transparent spectral window in the mid- to far-infrared.

We synthesized single crystals of Sr_{9/8}TiS₃ using the chemical vapor transport method and performed optical characterization to extract the complex refractive index (our preprint here: [9]). We combined polarization-dependent Fourier-transform infrared spectroscopy and spectroscopic ellipsometry to cover from 210 nm to 17 μ m, we observed that in the low-loss region of $\lambda > 6$ μ m, Sr_{9/8}TiS₃ has a birefringence Δn up to 2.1. This is by far the largest birefringence among reported anisotropic crystals, to the best of our knowledge, and in particular much higher than our past demonstration of birefringence in BaTiS₃, another quasi-one-dimensional crystal [10]. This extreme birefringence is a result of the enhancement of the extraordinary index due to structural modulations.

We resolved the atomic structure of Sr_{9/8}TiS₃ using single-crystal X-ray diffraction. To directly visualize the subtle structural modulations, scanning transmission electron microscopy was used. According to the first-principles density functional theory calculations, the enhancement of the permittivity parallel to the *c* axis is a consequence of the selective occupation of highly anisotropic states along the quasi-1D chain in modulated Sr_{9/8}TiS₃ while, in contrast, the electrons from the valence band states in hypothetical stoichiometric SrTiS₃ have an isotropic character and are localized on the S atoms.

At the conference, we will present several optical components and devices using this highly anisotropic material system, including ultra-thin wave plates for polarization control and planar polarized thermal emitters that have polarization anisotropy emitting in the normal direction and over a broad range of other angles. We will also discuss several special considerations for optical design when working with highly anisotropic materials, in particular the need for new types of anti-reflection coatings.

In conclusion, we demonstrated a new material platform with enhanced optical anisotropy, which is due to structural modulations in nonstoichiometric modulated crystal Sr_{9/8}TiS₃. Modulated Sr_{9/8}TiS₃ features the highest-ever degree of birefringence measured in the infrared spectral range. This group of materials can be great candidates for the realization of polarization control, thermal radiation control, unconventional light-matter coupling, and other applications in classical and quantum optics.

We acknowledge funding from the Office of Naval Research (UW-Madison; N00014-20-1-2297), the Army Research Office under Award No. W911NF-19-1-0137, an ARO MURI program with award no. W911NF-21-1-0327, and the National Science Foundation under grant numbers DMR-2122070 and DMR-2122071.

1. Weber, M. F., Stover, C. A., Gilbert, L. R., Nevitt, T. J. & Ouderkirk, A. J., *Science* **287**, 2451–2456 (2000).
2. Yasuno, Y., Makita, S., Sutoh, Y., Itoh, M. & Yatagai, T., *Opt. Lett.* **27**, 1803–1805 (2002).
3. Oka, K. & Kaneko, T., *Opt. Express* **11**, 1510–1519 (2003).
4. Nicholls, L. H. *et al.*, *Nat. Photon.* **11**, 628–633 (2017).
5. Ma, W. *et al.*, *Nature* **562**, 557–562 (2018).
6. Dyakonov, M., *J. Exp. Theor. Phys.* **94**, 119 (1988).
7. Diaz-Granados, K. *et al.*, *Nanophotonics* (2023).
8. Somers, D. A. T., Garrett, J. L., Palm, K. J. & Munday, J. N., *Nature* **564**, 386–389 (2018).
9. Mei, H. *et al.*, *arXiv:2303.00041* (2023).
10. Niu, S. *et al.*, *Nat. Photon.* **12**, 392–396 (2018).

11:15 AM SF05.01.03

Anisotropic Thermal Magnetoresistance in Radiative Heat Transfer Antonio Garcia-Martin; Instituto de Micro y Nanotecnología, CSIC, Spain

The possibility to create and manipulate nanostructured materials encouraged the exploration of new strategies to control the electromagnetic properties without the need to modify its physical structure, i.e. by means of an external agent. An approach is the combination of magneto-optically active and resonant materials (e.g. plasmonic modes), where it is feasible to control the optical properties with magnetic fields in connection to the excitation of resonances [1] (magnetoplasmonics). It has been shown that these nanostructures can be employed to modulate the propagation wavevector of SPPs [2], which allows the development of label free sensors with enhanced capabilities [3-5] or to enhance the magneto-optical response in isolated entities as well as films, in connection with a strong localization of the electromagnetic field [6-8].

Here we will show that they also play a crucial role in the active control of thermal emission and the radiative heat transfer (RHT) [9-11]. In particular Near Field RHT between two MO particles can be efficiently controlled by changing the direction of the magnetic field, in the spirit of the Anisotropic Magneto Resistance in spintronics [11]. This phenomenon, which we term anisotropic thermal magnetoresistance (ATMR), stems from the anisotropy of the photon tunneling induced by the magnetic field. We discuss this effect through the analysis of the radiative heat exchange between two InSb particles, and show that the ATMR can reach amplitudes of 100% for fields on the order of 1 T and up to 1000% for a magnetic field of 6 T. These values are several orders of magnitude larger than in standard spintronic devices. More importantly, this thermomagnetic effect paves the way for exploring heat transfer physics at pico- and even subpicosecond time scales, which are even shorter than the relaxation time of heat carriers. Moreover, we show that the heat flux is very sensitive to the magnetic field direction, which makes this effect very promising for the development of a new generation of thermal and magnetic sensors.

References:

- [1] G. Armelles, *et al.*, *Adv. Opt. Mat.* **1**, 10 (2013)
- [2] V.V. Temnov *et al.*, *Nat. Photon.* **4**, 107 (2010)
- [3] B. Sepulveda, *et al.*, *Opt. Lett.* **31**, 1085 (2006)
- [4] M.G. Manera, *et al.*, *Biosens. Bioelectron.* **58**, 114 (2014)
- [5] B. Caballero, *et al.*, *ACS Photonics* **3**, 203 (2016),
- [6] N. de Sousa *et al.*, *Phys. Rev. B* **89**, 205419 (2014)
- [7] N. de Sousa *et al.*, *Sci. Rep.* **6**, 30803 (2016)
- [8] M. Rollinger *et al.*, *Nano Lett.* **16**, 2432-2438 (2016)
- [9] E. Moncada-Villa, *et al.*, *Phys. Rev. B* **92**, 125418 (2015).
- [10] R. M. Abraham Ekeroth, *et al.*, *Phys. Rev. B* **95**, 235428 (2017)
- [11] R. M. Abraham Ekeroth, *et al.*, *ACS Photonics* **5**, 705 (2018).

SESSION SF05.02: Sub-Wavelength Structures
 Session Chairs: Maxime Giteau and Rohith Mittapally
 Monday Afternoon, November 27, 2023
 Sheraton, Third Floor, Hampton

1:30 PM SF05.02.01

Optimal Control of Light at The Nanoscale Alejandro Rodriguez; Princeton University, United States

Whether it be enhancing spontaneous emission from quantum defects or thermal radiation from hot objects, nanophotonic devices provide a means to control light all the way down to the nanometer scale. Here, we briefly review recent progress in our understanding of fundamental limits to light manipulation through structural engineering. Focusing on several canonical photonic objectives—minimizing extinction from subwavelength emitters and enhancing heat exchange at the nanoscale, we show that recent convex optimization methods can be used to complement large-scale structural optimization techniques to provide a mechanism- and geometry-agnostic means of discovering nanophotonic laws.

1:45 PM *SF05.02.02

Thermal Radiation from Single Sub- λ Resonators and Devices Loubnan Abou-Hamdan¹, Aurelien Schmitt², Sylvio Rossetti¹, Marin Tharrault², Remi Bretel², Valentina Krachmalnicoff³, Jean-Paul Hugonin⁴, Christophe Voisin², Bernard Plaçais², Riad Haidar⁵, Jean-Jacques Greffet⁴, Emmanuel Baudin², Patrick Bouchon⁵ and Yannick De Wilde³; ¹Institut Langevin, ESPCI Paris, PSL, CNRS & ONERA, France; ²LPENS, ENS, PSL, CNRS, France; ³Institut Langevin, ESPCI Paris, PSL, CNRS, France; ⁴Laboratoire Charles Fabry, IOGS, CNRS, France; ⁵ONERA, France

The thermal radiation scanning tunneling microscope (TRSTM) uses a scattering-tip modulated in a direction normal to the surface of a heated sample to measure its near-field thermal radiation [1]. This is achieved by lock-in demodulation of the infrared detected signal, which filters out the far-field radiation. In past experiments, it was shown that the method allows one to measure images and spectra of the near-field thermal radiation [1,2]. The latter shows strong deviations from black-body radiation for polaritonic materials [2].

Inspired by the TRSTM, we have recently developed a new spectroscopy method called infrared spatial modulation spectroscopy (IRSMS) to measure the far-field thermal radiation spectrum of heated sub-wavelength sized objects. As it is a far-field spectroscopy method, it does not require any scattering probe at the sample surface, unlike TRSTM. The principle of the IRSMS is to use a lateral modulation of the sub- λ sized object on the heated substrate in the field of view of an infrared microscope combined with a Fourier Transform Infrared Spectrometer. Due to the light fall-off effect on the detector, lock-in demodulation allows one to filter out the overwhelming background thermal radiation from the heated substrate and thus to extract the spectrum of the sub- λ sized object.

We have used IRSMS first to investigate the thermal radiation from single sub- λ sized metallic or dielectric resonators. Metal-insulator-metal antennas exhibit a narrowband thermal emission associated to the confinement of gap plasmons [3], with the appearance of hybrid modes when antennas are in near-field interactions [4]. Dielectric microspheres are also attractive to tailor the thermal radiation spectrum. For single SiO₂ microspheres, we evidence the excitation of both surface phonon-polariton (SPhP) modes and geometrical electric and magnetic Mie modes. The transition from a phonon-mode-dominated to a Mie-mode-dominated emission spectrum is observed when considering different sphere diameters [5].

Next, we have used modulation spectroscopy to investigate the radiation produced by high mobility graphene-hBN field effect transistors. The infrared radiation from these heterostructures under bias exhibits features which are typical for electroluminescence [6]. It starts at the threshold bias of Zener-Klein tunneling, an effect initially demonstrated in graphene with hyperbolic substrate in noise thermometry measurements [7]. It involves a specific cooling mechanism of the electron gas with radiative emission, due to the electron-hole recombination, in electromagnetic near-field modes of the hBN-graphene heterostructure.

- [1] De Wilde *et al.*, *Nature* **444**, 740 (2006).
- [2] Babuty *et al.*, *Phys. Rev. Lett.* **110**, 146103 (2013).
- [3] C. Li, *et al.*, *Phys. Rev. Lett.* **121**, 243901 (2018).
- [4] L. Abou-Hamdan, *et al.*, *Opt. Lett.* **46**, 981 (2021).
- [5] L. Abou-Hamdan, *et al.*, *ACS Photonics* **9**, 2295 (2022).

- [6] W. Yang et al., Nature Nanotech. **13**, 47 (2018).
[7] L. Abou-Hamdan, A. Schmitt et al., in preparation (2023).

SESSION SF05.03: Phase-Change Materials
Session Chairs: Maxime Giteau and Michelle Povinelli
Monday Afternoon, November 27, 2023
Sheraton, Third Floor, Hampton

2:15 PM SF05.03.01

Elaboration of Perovskite Thin Films with Metal-Insulator Transition for Infrared Optical Modulation Arthur Tausch¹, Fabien Capon², Jérémie Drévilion¹ and Karl Joulain¹; ¹Institut Prime, France; ²Institut Jean Lamour, France

Mixed valence manganites ($\text{Re}_{1-x}\text{A}_x\text{MnO}_3$, with Re a rare earth element and A an alkaline earth element) present a metal-insulator transition that is not only described by a strong variation in the material's resistivity but also by an optical contrast between the conductor and the insulator state from the near infrared to the mid infrared region of the electromagnetic spectra [1]. In the case of Samarium and Calcium mixed valence manganite, room temperature optical transitions were previously observed in Fourier Transform InfraRed spectrometry (FTIR) [2].

In this work, we demonstrate that ex-situ annealed $\text{Sm}_{0.5}\text{Ca}_{0.5}\text{MnO}_3$ thin films, deposited by magnetron co-sputtering under reactive O_2/Ar atmosphere, exhibit a thermochromic effect in the infrared region. As the temperature increases, charge carriers are freed and the material transits towards a metallic state. This transition was observed using Van Der Paaw measurement for temperature ranging from 80K to 873K. As the resistivity of the material decreases with temperature its infrared transmittivity decreases. The link between the electronic properties and the radiative properties of the material was explained using infrared variable angle spectroscopic ellipsometry as a function of temperature. The modelling of the ellipsometric datas using physical models such as Drude oscillators and Lorentz oscillators highlighted the transition from an insulating state at low temperature to a metallic state at high temperature. As the transition occurs around room temperature, the interest for passive infrared optical modulation applications was confirmed.

Using scattering matrix method for semi infinite thin films and an Improved Grey Wolf Optimization meta-heuristic algorithm [3], it is possible to optimize the emissivity decrease with temperature of a multi-layer material in the transparency bands of earth atmosphere knowing the variations in complex optical indexes with temperature [4]. Such tendency allows the control of the material's spectral radiance and therefore its detectability with thermography.

[1] P. Laffez, M. Zaghrioui, L. Reversat and P. Ruello. Thermal emittance changes at the charge ordering transition of $\text{Sm}_{0.35}\text{Ca}_{0.65}\text{MnO}_3$, Appl. Phys. Lett 93 (2008).

[2] A. Boileau, F. Capon, S. Barrat, P. Laffez and J.F. Pierson. Thermochromic effect at room temperature of $\text{Sm}_{0.5}\text{Ca}_{0.5}\text{MnO}_3$ thin films, J. Appl. Phys. 111, 113517 (2012).

[3] M. H. Nadimi-Shahraki, S. Taghian and S. Mirjalili. An improved grey wolf optimizer for solving engineering problems, Expert Systems With Applications 166 (2021)

[4] A. Hervé, J. Drévilion, Y. Ezzahri, K. Joulain, Radiative cooling by tailoring surfaces with microstructures: Association of a grating and a multi-layer structure, Journal of Quantitative Spectroscopy and Radiative Transfer, 221 (2018).

2:30 PM SF05.03.02

Tunable Narrowband Thermal Emitters using Phase-Change Materials: Design Rules for Simple Devices Maxime Giteau¹, Mitradeep Sarkar¹, Lukas Conrads², Maria Paula Alaya¹, Michael Enders¹, Thomas Taubner² and Georgia T. Papadakis¹; ¹ICFO, Spain; ²RWTH Aachen University, Germany

The ability to control the spectrum, the direction, and the polarization of thermal emission is critical for numerous applications, including infrared (IR) sources, thermal camouflage, radiative cooling, molecular sensing, and energy conversion. For many of these applications, narrowband IR emission is desirable. However, simple, lithography-free structures tend to have spectrally broadband emissivity. It is also valuable to achieve active control of thermal emission, enabling switching between *on* and *off* emission states or shifting the peak emission wavelength. In the mid-IR region, the spectral range of interest for thermal emission near room temperature, a common approach for active tuning has been phase-change materials (PCMs). Tunable narrowband sources have previously been achieved, albeit with relatively complex structures and a performance that is not ideal over the whole operation range. Furthermore, these devices have limited spectral tunability as they rely on the temperature dependence of the materials' resonances.

This work presents an analytical framework to design actively tunable narrowband thermal emitters at IR frequencies [1]. The proposed systems are lithography-free and consist of one or several thin emitter layers, a spacer layer that includes the PCM, and a back-side reflector. Numerically, we show near-unity *on-off* switching and arbitrarily large spectral shifting between two emission wavelengths using actual materials. Although our theoretical formalism assumes normal incidence, the performance remains near-ideal up to large angles. The presented framework is general and applies to *any* mechanism that modifies the optical properties of a material, such as electrical gating or optical modulation. Finally, we are currently working on an experimental demonstration using In_3SbTe_2 , a non-volatile PCM that can be reversibly switched between a dielectric amorphous and a metallic crystalline phase in the entire infrared spectral range [2].

References:

Giteau, M., Sarkar, M., Ayala, M. P., Enders, M. T. & Papadakis, G. T., Design Rules for Active Control of Narrowband Thermal Emission Using Phase-Change Materials, *Phys. Rev. Appl.* **19**, L051002 (2023).

Heßler, A., Wahl, S., Leuteritz, T., Antonopoulos, A., Stergianou, C., Schön, C.-F., Naumann, L., Eicker, N., Lewin, M., Maß, T. W. W., Wuttig, M., Linden, S. & Taubner, T., In_3SbTe_2 as a programmable nanophotonics material platform for the infrared, *Nat Commun* **12**, 924 (2021).

2:45 PM BREAK

3:15 PM SF05.03.03

Variable Visible-to-Infrared Optical and Emissivity Properties of VO_2 and W- VO_2 Thin Films for Passive Smart Radiative Device Applications Artitsupa Boontan, Eric Kumi Barimah, David P. Steenson and Gin Jose; University of Leeds, United Kingdom

Numerous technologies have been developed to regulate the temperatures of several space equipment within the allowable tolerance temperature range from -150°C to 150°C to meet the operation requirements by rejecting or injecting Joule heating. A spacecraft is a typical example of such devices, which can be subjected to different thermal environments upon launch, from the Earth's surface to outer space, for various missions. The thermal environment of these systems is controlled by dissipating heat through either passive or active processes. Many traditional spacecraft systems employ heat pipes, thermal switches and heaters to regulate the spacecraft temperature. Others use advanced thermal control devices such as the electric louvre based on microelectromechanical technologies comprised of a bimetallic and spring-actuated mechanism to manage the heat when it falls or rises above the allowable temperature range during operation. Even though there has been tremendous progress in smart radiative devices (SRD) over the years for thermal control designs via mass and size reduction with minimum or no electrical energy required using perovskites. The SRD consists of variable emitters to regulate the temperature by changing the environmental temperature concerning the phase transition property of the thermochromic materials. In addition, the SRD must have low emissivity at low temperatures to reduce heat loss and high emissivity at high temperatures allows it to dissipate heat through thermal radiation. A phase change material such as $\text{VO}_2(\text{M1})$ with a phase transition temperature of 68°C starts from a low-temperature semiconductor state to a high-temperature metallic state. This is accompanied by structural transformation from a low-temperature monoclinic (M) to a high-temperature rutile (R) phase. For instance, optical characteristics of spacecraft smart radiative devices have been demonstrated and reported, which consist of a multilayer thin film of VO_2 on silica or aluminium-silver substrate.

This presentation presents a direct method of fabricating SRD W-doped VO_2 thin films onto silica and silicon substrates from W-doped V_2O_5 precursor using a high repetition rate (75 kHz) femtosecond-PLD. Surface morphology and crystal structure characterisation of the SRD were investigated. In addition, visible to mid-infrared optical properties such as temperature-dependent solar absorptance, reflectance index, and variable emissivity of the phase change material VO_2 SRD device will be systematically investigated and discussed.

3:30 PM *SF05.03.04

Radiative Thermal Control with Thermochromic VO_2 Based Metafilms and Metamaterials Liping Wang; Arizona State University, United States

In this talk, I will review recent progress from my research group on radiative thermal control with thermochromic VO_2 based metafilms and metamaterials. VO_2 thin films with excellent

phase transition behaviors were grown with unique furnace oxidation method from deposited vanadium nanofilms. With co-sputtering technique or alloy targets, tungsten doped VO₂ thin films with reduced phase transition temperature ranges were also successfully obtained. Temperature-dependent spectroscopic characterizations of undoped and tungsten doped VO₂ thin film from cryogenic to high temperatures were performed and the infrared properties at different phases were extracted from optical fitting. Nanophotonic metafilm and metamaterial structures incorporating VO₂ nanofilm or nanostructure were carefully designed and successfully fabricated. Variable infrared emissivity with large tunability were experimentally demonstrated upon VO₂ phase transition. Vacuum thermal and cryothermal test apparatus were developed and the variable radiative heat dissipation were experimentally confirmed with these tunable metafilm and metamaterial emitters. In particular, their effects for space thermal control and radiative thermal rectification were experimentally studied along with thermal modeling.

SESSION SF05.04: Infrared Properties
Session Chairs: Georgia Papadakis and Liping Wang
Monday Afternoon, November 27, 2023
Sheraton, Third Floor, Hampton

4:00 PM *SF05.04.01

Engineering Dynamically-Tunable Linear and Nonlinear Infrared Properties of Materials for Thermal Energy Harvesting and Photodetection Svetlana V. Boriskina; Massachusetts Institute of Technology, United States

I will discuss several successful strategies to engineer dynamically-tunable optical response of semiconductor and polymer materials in the infrared spectral range. These include: (i) strain-induced mechanocaloric phase transitions in polymers, (ii) strain-gradient-induced inversion symmetry breaking in narrow-gap semiconductors and Weyl/Dirac semimetals, (iii) magnetic-field induced coupled magnetocaloric and magneto-optical effects in magnetic materials, and (iv) generation, evolution, and annihilation of optical vortices pinned to thin-film absorbers. The applications enabled by the above tunability mechanisms include persistent electric energy generation in flexoelectric photodetectors and thermoradiative cells [1], static and dynamic control of directional surface plasmon polariton modes propagation in Weyl semimetals or semiconductors [2,3], solid-state cooling, heating, and radiative transport control actuated by mechanocaloric and magnetocaloric effects [4,5], and spectrally-selective absorbance/reflectance switching via singular phase engineering in the interference optical near-fields [6,7].

This research has been supported in part by the MIT Lincoln Laboratory under award No. ACC-777 (for the flexoelectric energy harvesting), the Army Research Office under award No. W911NF-19-1-0279 (for the near-field radiative energy transfer), the DOE-BES program under award No. DE-FG02-02ER45977 (for the strain-engineering of polymers), the MIT-SUSTech Program (for the elastocaloric effects engineering), and the Korean Research and Development Program for ICT and Broadcasting (for optical vortex engineering).

- [1] B. Lorenzi, Y. Tsurimaki, A. Kobayashi, M. Takashiri, and S. V. Boriskina, "Self-powered broadband photo-detection and persistent energy generation with junction-free strained Bi₂Te₃ thin films," Opt. Express 28(19), 27644–27656, 2020.
- [2] S. Pajovic, Y. Tsurimaki, X. Qian, and S. V. Boriskina, "Radiative heat and momentum transfer from materials with broken symmetries," Opt. Mater. Express 11(9), 3125–3131 (2021).
- [3] S.V. Boriskina, M. Blevins, S. Pajovic, There and Back Again: the nonreciprocal adventures of light, Opt. Photon. News, Sept. 2022.
- [4] S.Pajovic and S.V. Boriskina, Magnetocaloric effect-enhanced near-field magneto-optical thermal switch, Physical Review Applied (under revision), 2023.
- [5] Y. Lyu, B. Li, V. Korolovych, D. Xu, Y. Zhu, S.V. Boriskina, Optimizing temperature-dependent elastocaloric effects in elastic polyethylene fibers (submitted), 2023.
- [6] H. Chung, J. Park, S.V. Boriskina, Inverse-designed waveguide-based biosensor for high-sensitivity, single-frequency detection of biomolecules, Nanophotonics, 11(7), 1427-1442, 2022.
- [7] M. Bae, J. Kang, S.V. Boriskina, H. Chung, Inverse design of nanophotonic structures for efficient optical vortex manipulation and absorption enhancement (submitted), 2023.

4:30 PM SF05.04.02

Thermochromic Materials for Optimized Modulation of Solar Thermal Radiation in Windows and Their Combination with Mid-IR Thermal Insulation Daniel Mann and Pascal Buskens; TNO, Netherlands

The built environment is responsible for more than 1/3 of the annual energy consumption worldwide. A major contributor to building energy demand are windows due to their transparency to thermal radiation. In general, the thermal radiation relevant for buildings can be divided into two wavelength regions of interest: i) near-infrared (IR) between 800 – 2500 nm, representing thermal radiation from sunlight; ii) mid-IR between 5 – 25 μ m, representing thermal radiation from radiators. Furthermore, requirements for windows to transmit or block each of these regions depend on the climate and can change between seasons. In hot climates or summertime, windows should block solar thermal radiation to limit air conditioning demand. Whereas in cold climates and wintertime, windows should transmit solar thermal radiation to contribute to a building's heating demand, whilst preventing mid-IR thermal radiation from leaving the building. For moderate climates these changing requirements can only be met by smart adaptive glazing.

One of the most interesting materials for adaptive glazing are thermochromics (TC). These materials can change their optical properties upon a change in temperature. The most prominent representative is vanadium dioxide (VO₂). VO₂ can change its crystal structure from monoclinic to rutile at 68°C, inducing a change in electrical and optical properties. It is perfectly suited for solar heat regulating windows because of the following properties: i) switch between near-IR transparent and blocking; ii) potential for high visible transparency by limiting the switch mainly to the near-IR; iii) possibility to adjust the switching temperature in a wide range between 0 – 68°C; iv) cheap and abundant material; v) potential to use cheap and low energy intensive application methods; vi) autonomous switch and potential for application in regular glazing; vii) compatibility with existing energy efficient window coatings.

We have developed a high quality VO₂ nanoparticle that can be added via coatings or polymer films to various types of window products adding TC properties. The pigment is optimized to enable high visible transparency (T_{vis}) in combination with a substantial solar heat modulation (ΔT_{sol}), optimizing the energy performance of a window.

Here we present a detailed study on how the size and crystallinity of VO₂ nanoparticles influence the optical properties and functional performance of TC coated/laminated glass. We show that by increasing crystallinity ΔT_{sol} and T_{vis} can be increased simultaneously because of an increased fraction of functional material in the VO₂ pigment. Furthermore, we show that reducing the average particle size to <80 nm leads to appearance of plasmonic properties in the metallic (rutile) state of the VO₂ pigment. This results in increased absorption in the wavelength region between 780 – 1360 nm and in a corresponding increase in ΔT_{sol} . In addition, we show that integration of small VO₂ pigments in a transparent matrix can significantly increase T_{vis} whilst retaining a high ΔT_{sol} . Using all these optimizations in one coating we obtained a maximum ΔT_{sol} of 23% at a T_{vis} of 67%.

Since solar heat management is only one part of a window's interaction with thermal radiation, we also present a study on combining our TC solar heat regulating glasses with low-emissivity glass, blocking mid-IR thermal radiation. Here we show the importance of matching properties between both types of functional glasses to retain the solar heat regulating properties of the TC glass whilst adding thermal insulation in the mid-IR region. With this combination a perfect window with optimized energy efficiency, via shgc modulation of 13%, can be produced, which we validate via building energy simulations. We show that a building's energy efficiency in the Netherlands can be increased by up to 9% in comparison to state-of-the-art energy efficient windows, resulting in about 500€ energy cost savings per year for a single household.

4:45 PM SF05.04.03

Polarization-Induced Infrared Emissivity Control System for Precise Temperature Adjustment Do Hyeon Kim, Se-Yeon Heo, Yubin Lee and Young Min Song; Gwangju Institute of Science and Technology, Korea (the Republic of)

The global energy and climate challenges require energy-saving solutions to achieve net-zero emissions worldwide. As a result, eco-friendly thermal management has become crucial in various sectors, including residential buildings and mobile devices. In this context, passive radiative cooling has emerged as a promising solution to address the global energy and climate crises by providing energy-efficient and zero-emission cooling. The high emissivity of objects in the mid-infrared (MIR) atmospheric window allows for radiative cooling, where heat is drawn from the objects and emitted to the cold outer space. This unique feature has sparked renewed interest in extensive research on passive radiative cooling, with successful experimental demonstrations in various applications such as wearable devices, solar cells, buildings, displays, clothing, roofs, and vehicles [1].

However, conventional radiative cooling technologies face limitations, such as undesired cooling in cold weather due to strong thermal emissions in a single state. Recent research has introduced dual-state emitters capable of switching emission spectra for cooling and heating purposes [2]. However, achieving precise thermal comfort temperatures, especially in moderate weather conditions like spring and autumn, requires continuous emissivity adjustment rather than simple on/off cooling switching. In this context, multi-state emitters with continuously adjustable emission spectra offer promising solutions for all weather conditions, although they have received limited attention in scientific investigations. Additionally, active emitters utilizing phase change materials provide thermoregulation functionality for all seasons but have constraints in customizing target temperatures due to fixed transition points.

Here, we propose a dynamic temperature-adjustable system with an infrared (IR) polarization valve as an energy-balancing channel. The system is composed of a one-dimensional grating emitter and an IR polarizer. A simple rotation of the polarizer allows continuous temperature modulation. Optical simulations are implemented to optimize the design of the thermal emitter, which comprises a one-dimensional silver grid on quartz. Our system achieves a wide range of emissivity, from 2 to 80%, by simple adjustment of the polarizer. This enables precise cooling/heating capabilities (-17 to 51 W/m²). Theoretical calculations estimate the potential energy saving of over 20 GJ/year compared to conventional emitters across different climate zones when applied to roofs of buildings. Outdoor experiments validate the precise temperature regulation within a target range of 17-18 degrees (Celsius). The successful outdoor proof-of-

concept demonstration highlights the reliability and applicability of our approach in diverse situations such as residential buildings, farms, and wearable devices. Furthermore, we have confirmed the suitability of phase change materials, particularly GST, in our system using a glancing angle deposition technique. This result proves the versatility of our system and the potential for various applications, including thermal camouflage patches. Our findings contribute to advancing thermal management technologies for achieving net-zero emissions and sustainable energy savings in the face of global energy and climate challenges.

References

D. H. Kim, S. -Y. Heo, Y. -W. Oh, S. Jung, M. H. Kang, I.-S. Kang, G. J. Lee, and Y. M. Song, *APL Photonics* 8, 030801 (2023).
X. Li, B. Sun, C. Sui, A. Nandi, H. Fang, Y. Peng, G. Tan, and P.-C. Hsu, *Nat. Commun.* 11, 1 (2020).

5:00 PM *SF05.04.04

Tailoring Thermal Emission for Power Generation and Cooling [Jeremy N. Munday](#); University of California, Davis, United States

The thermal spectra of hot, warm, and cool bodies are all well-known and described by Planck's law for blackbody emission. However, for many modern technologies and applications, it is desirable to have significant deviations from this law to achieve directional or wavelength-controlled emission. In this talk, we will discuss the control of thermal emission for various applications. We introduce a novel approach that enables the creation of thermally stable structures at ultra-high temperatures (up to 2000 °C), allowing for tailored emission spectra. The specific application of thermophotovoltaics will be discussed. Additionally, we will describe an alternative geoengineering strategy to increase the Earth's radiative heat emission, potentially stabilizing or cooling the planet to help mitigate climate change by increasing the earth's thermal emission by 1 W/m². Finally, we will discuss our work on alternative power generation concepts to produce power after sunset by optically coupling to deep space and discuss the potential impact and limitations of such devices.

SESSION SF05.05: Switches and Regulation
Session Chairs: Maxime Giteau and Jeremy Munday
Tuesday Morning, November 28, 2023
Sheraton, Third Floor, Hampton

8:30 AM *SF05.05.01

Breaking the Rules: Exploring Violation of the Kirchhoff Radiation Law in Experiments [Harry A. Atwater](#); California Institute of Technology, United States

The understanding of emission of thermal radiation has been shaped by the Kirchhoff thermal radiation law, which asserts equality of the absorptivity and emissivity of a given object for each wavelength, direction, and polarization. This equality is built on reciprocity; and the use of reciprocal materials to demonstrate spatial and temporal coherence of thermal emission has proven a landmark in the nanophotonics community. We have experimentally measured inequality of the spectral emissivity and spectral absorptivity of a thermal emitter, and thus directly observe a violation of Kirchhoff's law. We achieve this by measuring the directional thermal emissivity and absorptivity from a nanophotonic structure in a magnetic field, which breaks the reciprocity conditions. We not only observe inequality in emissivity and absorptivity, but also demonstrate a new relationship between the two for the non-reciprocal photonic structure. Thermal emission phenomenon that can break free of Kirchhoff's law are of fundamental interest and may open a multitude of new applications; we will discuss further directions for experimental exploration of related phenomena.

9:00 AM SF05.05.02

Control Bandwidth and Contrast Between Emissivity and Absorptivity for Broadband Nonreciprocal Emitters [Bo Zhao](#); University of Houston, United States

Broadband nonreciprocal emitters are indispensable in next-generation thermal and photonic applications, such as thermal camouflage and energy harvesting. Recently, multilayer structures consisting of magneto-optical materials with gradient doping levels have been explored for broadband nonreciprocity provided by a broadband ENZ effect. However, previous works all focus on achieving a monotonic contrast between emissivity and absorptivity, i.e., either the absorptivity or the emissivity is always larger than the other for a given direction over a broad frequency range. Here, we report that the contrast between emissivity and absorptivity of such multilayer nonreciprocal thermal emitters can be highly controllable by coupling a Fabry-Perot mode associated with an additional dielectric layer, making the contrast alternating positive and negative across the broad nonreciprocal bandwidth. Thus, the monotonic nonreciprocal bandwidth can be divided into multiple separated bands with alternating contrasts, and the number of the separated bands is proportional to the thickness of the dielectric layer. In addition, the introduction of the dielectric layer also can increase the absolute contrast between absorptivity and emissivity. Our approach of coupling a Fabry-Perot mode with ENZ effect represents a simple yet effective approach to obtaining multiband nonreciprocal thermal emitters, providing interesting new opportunities in thermal applications such as thermal circulators and isolators.

9:15 AM SF05.05.03

Bidirectional Thermo-Regulating Hydrogel Composite for Autonomic Thermal Homeostasis [Gyeongsuk Park](#) and [Steve Park](#); KAIST (Korea Advanced Institute of Science and Technology), Korea (the Republic of)

Thermal homeostasis is an essential physiological function for preserving the optimal state of complex organs within the human body. Inspired by this function, here, we introduce an autonomous thermal homeostatic hydrogel that includes infrared wave reflecting and absorbing materials for improved heat trapping at low temperatures, and a porous structure for enhanced evaporative cooling at high temperatures. Moreover, an optimized auxetic pattern was designed as a heat valve to further amplify heat release at high temperatures. This homeostatic hydrogel provides effective bidirectional thermoregulation with deviations of $5.04^{\circ}\text{C} \pm 0.55^{\circ}\text{C}$ and $5.85^{\circ}\text{C} \pm 0.46^{\circ}\text{C}$ from the normal body temperature of 36.5°C , when the external temperatures are 5°C and 50°C , respectively. The autonomous thermoregulatory characteristics of our hydrogel may provide a simple solution to people suffering from autonomic nervous system disorders and soft robotics that are susceptible to sudden temperature fluctuations.

9:30 AM SF05.05.04

A Novel Design of a Radiative Thermal Transistor [Ju Won Lim](#), [Ayan Majumder](#), [Rohith Mittapally](#), [Audrey-Rose Gutierrez](#), [Yuxuan Luan](#), [Edgar Meyhofer](#) and [Pranod Sangi Reddy](#); University of Michigan, United States

Thermal logic devices are of significant current interest for thermal management and have been extensively explored theoretically. However, there has been limited experimental progress on such devices. Here, we describe a novel radiative thermal transistor consisting of sub-micrometer thick membranes combined with a phase transition modulator whose dielectric properties can be controlled via temperature. Specifically, we show that when the modulator made of vanadium oxide (VO_x), which is analogous to the gate electrode of a transistor, undergoes a metal-insulator transition, it affects the radiative heat transfer between the emitter and receiver membranes. A thermal modulator, which is analogous to the source and drain electrodes of a transistor, enables control of radiative heat flow between a hot emitter and a cold receiver with a switching ratio of up to a factor of three. In contrast to past thermal transistors, the switching time of our nanomembrane-based thermal transistor is much more rapid (hundreds of milliseconds compared to minutes) due to the small thermal mass of our modulator. Our experiments are also complemented by detailed calculations that highlight the mechanism of thermal modulation. We anticipate that the advances reported here will open new opportunities to design thermal circuits or thermal logic devices for advanced heat flow control.

<quillbot-extension-portal></quillbot-extension-portal>

9:45 AM SF05.05.05

Electrochemical Dynamic Solar and Mid-Infrared Synergistic Tuning for All-Season Building Thermoregulation [Chenxi Sui](#); The University of Chicago, United States

The coldness of the deep universe and the hotness of the sun have been considered renewable thermodynamic resources for sustainable thermoregulation. How to utilize both resources showed drastic improvement in the past decade, enabled by the plasmonic and nanophotonic research. Remarkably, the rational photonic and thermal design has pushed forward the power and efficiency of daytime radiative cooling. In this presentation, we will introduce our recent research progress on electrochemical devices that can electrically switch between solar heating and radiative cooling states, by tuning their optical properties. Such a non-trivial and opposite spectral tuning requires the fabrication of the ultra-wideband transparent conductive electrode, which is transparent in both solar and mid-IR regimes, and the precise control of the plasmonic nanoparticles' morphology during the reversible metal electrodeposition. With the optimization of every device component, this device can maximize its solar reflectivity at the cooling state and minimize its thermal emissivity at the heating state, and thus can serve as the smart building envelope for year-round HVAC energy saving. Ideally, the device can help buildings save 19.2% of HVAC energy across the United States, based on the building energy simulation results. The durable electrodeposition and broad-band spectral tuning are confirmed by the DFT simulations and effective medium theory. In addition to the synergistic solar and mid-IR dual-band

tuning, our electrochromic device can tune the thermal emissivity with 0.85 contrast based on non-volatile and reversible metal electrodeposition, bringing vast opportunities for applications in space heat management, and thermal camouflage.

10:00 AMBREAK

SESSION SF05.06: Radiative Cooling I
Session Chairs: Peter Bermel and Svetlana Boriskina
Tuesday Morning, November 28, 2023
Sheraton, Third Floor, Hampton

10:30 AM *SF05.06.01

Controlling Infrared Emissivity: New Directional Capabilities and Radiative Cooling Applications[Aaswath P. Raman](#)¹; University of California, Los Angeles, United States

Thermal emission over infrared wavelengths is ubiquitous making its control of great importance to a wide range of applications. In this talk, we will first introduce a new photonics-based framework to controlling both spectral and directional emissivity, gradient epsilon near zero (ENZ) materials. We will highlight demonstrations using both phonon-polariton-based materials as well as doped semiconductors, demonstrating both spectral and broadband directional tunability. We will next discuss radiative cooling applications enabled by such spectrally and directionally emissive materials. First we will introduce passive freezing desalination enabled by radiative cooling, as well as the radiative cooling of vertical facades in hot urban environments.

11:00 AM SF05.06.02

Passive Radiative Cooling using Randomly Micro-Structured Silicon Meta-Materials[Armande Hervé](#), [Nicolas Lavielle](#), [Frédéric Marty](#), [Georges Hamaoui](#), [Philippe Basset](#), [Tarik Bourouina](#) and [Elyes Nefzaoui](#); Université Gustave Eiffel, France

Decarbonized and low-energy technologies for heat management and conversion are critical milestones for climate change mitigation¹. Cooling is one of the major fields where such technologies are required. Passive radiative cooling in its nighttime and daytime versions is therefore a promising technology to achieve those goals². We consider in this work a silicon-based nanostructured meta-material with outstanding visible and infrared radiation absorption and emission capabilities, alternatively called Black Silicon due to its black color, as a candidate for nighttime passive radiative cooling. Indeed, we have recently shown that randomly micro-structured silicon surfaces can exhibit near-unit emissivity over a wide spectral range from the visible to the mid-infrared³. We have also shown that this range can be significantly extended and tuned by varying the silicon doping and the micro-structures aspect ratio⁴⁻⁶ to reach the spectral range of the atmospheric transparency window (8 to 13 μm). These interesting radiative properties of Black Silicon combined with the different tuning possibilities open an avenue for using such materials for different thermal radiation control applications such as enhanced solar radiation absorption⁷, infrared radiation sources⁸, selective emitters, and passive radiative cooling⁹. In this contribution, we numerically compare Black Silicon with its flat silicon counterpart with respect to their radiative cooling power. We consider Black Silicon samples with different nano structuration aspect ratios and use their experimentally measured radiative properties. The radiative properties are measured using Fourier Transform Infrared Spectroscopy at room temperature. We show that the computed BSi cooling power is significantly larger than that of flat silicon by a factor up to 1.8 at 30°C with a cooling power of 75 W/m² and 140 W/m² for flat and Black Silicon, respectively. We also numerically investigate the influence of several parameters such as the conductive and convective heat transfer, the atmospheric transmittance spectra (idealized: rectangular function or realistic: with multiple absorption bands), and the operating temperature. We show that Black Silicon exhibits a larger radiative cooling power than a material with an ideal unit emissivity between 8 and 13 μm . Indeed, the considered atmospheric transmittance greatly influences the radiative cooling power. Finally, we perform nighttime radiative cooling experiments using black and flat silicon and compare experimental results with the numerical predictions.

1. A. Henry, R. Prasher, A. Majumdar, *Nature Energy*, **5**, 635–637 (2020).
2. B. Zhao, M. Hu, X. Ao, N. Chen, G. Pei, *Applied Energy*, **236**, 489–513 (2019).
3. S. Sarkar, A. Elsayed, E. Nefzaoui, J. Drevillon, P. Basset, F. Marty, M. Anwar, Y. Yu, J. Zhao, X. Yuan, others, (2019).
4. S. Sarkar, A. A. Elsayed, F. Marty, J. Drévilion, Y. M. Sabry, J. Zhao, Y. Yu, E. Richalot, P. Basset, T. Bourouina, E. Nefzaoui, in *2019 25th International Workshop on Thermal Investigations of ICs and Systems (THERMINIC)* (2019), pp. 1–4.
5. S. Sarkar, A. A. Elsayed, Y. M. Sabry, F. Marty, J. Drévilion, X. Liu, Z. Liang, E. Richalot, P. Basset, E. Nefzaoui, *Advanced Photonics Research*, 2200223 (2022).
6. S. Sarkar, E. Nefzaoui, G. Hamaoui, F. Marty, P. Basset, T. Bourouina, *Appl. Phys. Lett.* **121**, 231703 (2022).
7. L. Gao, E. Nefzaoui, F. Marty, X. Wei, S. Bastide, Y. Leprince-Wang, T. Bourouina, *Solar Energy Materials and Solar Cells*, **243**, 111793 (2022).
8. A. Saeed, A. A. Elsayed, F. Marty, E. Nefzaoui, T. Bourouina, H. A. Shawkey, Y. M. Sabry, D. Khalil, in *Nanophotonics VIII* (SPIE, 2020), vol. 11345, pp. 105–110.
9. A. Hervé, G. Hamaoui, T. Bourouina, P. Basset, E. Nefzaoui, (Thessaloniki, Greece, 2023).

11:15 AM SF05.06.03

Improving the Passive Radiative Cooling Properties of Anodic Aluminium Oxide Nanostructures on Aluminium[Cristina V. Manzano](#)¹, [Angel Morales-Sabio](#)², [Marisol Martin-Gonzalez](#)¹ and [Alba Diaz-Lobos](#)¹; ¹Institute of Micro and Nanotechnology, Spain; ²CIEMAT, Spain

Nowadays, a third of the total energy demand is destined for cooling due to the consequence of the global warming, which results in higher temperatures and heatwaves. In this sense, a significant reduction in energy demand will be achieved when passive radiative cooler technology is used. At the same time, it is important to develop low-cost, easy-scalable to industry materials.

In this study, we analyze how all the morphological properties and chemical structure of anodic aluminium oxide (AAO) nanostructures on Al influence on their optical properties and their radiative cooler properties. The thickness, interpore distance, porosity and counterions of the AAO affect significantly the cooling performance of these AAO-Al samples. A maximum cooling temperature of 8 celsius degrees was reached under direct sunlight in a summer day in Spain, which corresponds to a cooling power of 175 W/m² when the nanostructures are anodized under certain conditions referent to thickness, porosity, and counterion. This cooling performance results of AAO nanostructures are higher than over previous studies, demonstrating the potential of AAO nanostructures to be used in thermal management applications.

11:30 AM SF05.06.04

Enhancing the Consistency of Porous Polymer Passive Daytime Radiative Cooling Paint in Outdoor Applications[Dongpyo Hong](#)¹, [Ok Sung Jeon](#)¹, [Se Hun Lee](#)¹, [Yong Joon Lee](#)¹, [In-Sung Lee](#)¹, [Ye Rim Kim](#)¹, [Yun Ju La](#)¹, [Young Pyo Jeon](#)¹, [Young Joon Yoo](#)¹ and [Sang Yoon Park](#)²; ¹Advanced Institute of Convergence Technology, Seoul National University, Korea (the Republic of); ²Kyonggi University, Korea (the Republic of)

Coating the building envelope with passive daytime radiative cooling (PDRC) paint has garnered enormous attention as an energy- and carbon-free alternative cooling technology. Achieving this goal requires the spontaneous formation of a suitable optical structure during the solvent drying process of the paint that effectively reflects sunlight and enables thermal emission through the atmospheric window (8–13 μm). In addition to their cooling abilities, PDRC coatings must also possess affordability, durability, and compatibility with diverse surfaces and climates for practical use.

Recently, porous polymer coating (PPC) has gained significant attention due to its numerous advantages, including cooling performance, cost-effectiveness, flexibility, and scalability. However, achieving consistent performance over a wide range of outdoor conditions is a challenge due to the morphology of PPC formed via the evaporation-induced phase separation method (EIPS), which is highly dependent on evaporation environment parameters such as temperature and humidity. Despite the advantages of PPC, there is a lack of systematic studies on the consistency of PDRC performance under varying environmental conditions of EIPS, and potential solutions to this issue have not been addressed.

In this study, we demonstrate the humidity vulnerability of PPC during the drying process and propose a simple strategy to mitigate this issue. Specifically, we found that the solar reflectance of PPC rapidly decreases with increasing humidity from 30% RH, causing the PPC to completely lose its PDRC ability at 45% RH and even become a solar-heating material at higher humidity levels. However, by adding a trace amount of reinforcements into PPC, we were able to maintain its PDRC performance up to 60% RH, resulting in a 1050% enhancement of areal coverage in the United States. This study highlights a crucial consistency issue for PPC-based PDRC paint that has been previously overlooked and offers engineering guidance to address this fundamental challenge for the development of reliable PDRC paint for industrial applications.

11:45 AM SF05.06.05

Oil-Paper-Umbrella-Inspired Passive Radiative Cooling using Recycled Packaging Foam[Yang Liu](#) and [Yi Zheng](#); Northeastern University, United States

Passive daytime radiative cooling (PDRC) is a promising energy-saving cooling method to cool objects without energy consumption. Although numerous PDRC materials and structures have been proposed to achieve sub-ambient temperatures, the technique faces unprecedented challenges brought on by complicated and expensive fabrication. Herein, inspired by traditional Chinese oil-paper umbrellas, we develop a self-cleaning and self-cooling oil-foam composite (OFC) made of recycled polystyrene foam and tung oil to simultaneously achieve efficient passive radiative cooling and enhanced thermal dissipation of objects. The OFCs show high solar reflectance (0.90) and high mid-infrared thermal emittance (0.89) during the atmospheric transparent window, contributing to a sub-ambient temperature drop of ~ 5.4 °C and cooling power of 86 W m^{-2} under direct solar irradiance. Additionally, the worldwide market of recycled packaging plastics can provide low-cost raw materials, further eliminating the release of plastics into the environment. The OFC offers an energy-efficient, cost-effective and environmentally friendly candidate for building cooling applications and provides a value-added path for plastic recycling.

SESSION SF05.07: Energy Conversion
Session Chairs: Pierre-Olivier Chapuis and Georgia Papadakis
Tuesday Afternoon, November 28, 2023
Sheraton, Third Floor, Hampton

1:30 PM *SF05.07.01

Thermal Radiation as Electricity Generation's Nemesis Alireza Nojeh; University of British Columbia, Canada

Producing electricity from high-temperature heat is central to our energy system. Thermodynamic efficiency increases as the temperature difference across a heat engine increases, major traditional sources of energy inherently produce high temperatures, and waste heat recovery holds great promise. In the future, concentrated solar and thermal energy storage systems may also supply heat at high temperatures on a large scale.

The established technologies of converting high temperatures to electricity are based on turbines. These are large, complex, and expensive devices. To reach high conversion efficiencies at low cost and in flexible form factors, static heat engines are desirable. A prime example is a thermophotovoltaic cell, in which thermal radiation is harnessed by a photovoltaic device.

The most direct approach to generating electricity from heat is to use the hot electrons themselves as the working fluid. Indeed, thermionic energy conversion is a deceptively simple concept: heat an electrode to the point of evaporating electrons (historically known as thermionic emission), collect these electrons on a cold electrode, and circulate them back to the hot electrode through the electrical load. This elegant idea has been known since early 20th century but, despite significant progress over the decades, its performance has remained limited and it has not become a practical technology. To understand why, one must look past the apparent simplicity of the thermionic converter.

As in other heat engines, the fundamental challenge in a thermionic converter is that of enabling the flow of electric charge while restricting the flow of heat. In this device, the Coulomb repulsion of the emitted electrons hinders further electron emission and transport. The simplest way to mitigate this space charge effect is to place the cold collector close to the hot emitter—at a distance of a few micrometers or less. At such small emitter-collector gaps, however, near-field radiative coupling causes major energy loss.

A thermionic converter is in fact a highly complex device. The emitter is strongly out of equilibrium—a hot soup boiling with many excitations and ripe with nonlinear effects. In addition to the thermal emission of electrons and far-field and near-field thermal radiation, thermal conduction and thermoelectric and other solid-state transport phenomena within the emitter, collector, and leads need to be accounted for. Add nanomaterials and nanostructures to the mix and you also have new physics. To analyze a thermionic converter realistically and accelerate technology development, all this must be treated simultaneously. Combining thermionics with complementary technologies such as thermoelectrics and photovoltaics will make the problem even richer. In the first part of this talk, we will discuss a multiphysics approach to modeling thermionic converters and some of the unexpected insights it provides in the context of example devices.

To engineer a thermionic converter to favor electron transfer over radiative coupling, we need to understand both phenomena to a greater degree than traditionally considered in these devices; fine-grained knowledge of the electron and photon energy exchange channels is required. In the second part of the talk, we will argue for the need for quantitatively meaningful spectroscopic approaches in this context, report on recent experimental developments on thermal electron and photon spectroscopy, and discuss directions to further advance this area.

2:00 PM SF05.07.02

Thermophotonic Energy Harvesting: Towards a Narrowband LED Emission Julien Legendre and Pierre-Olivier Chapuis; CNRS - INSA Lyon, France

Converting low-grade heat into electrical power with thermophotovoltaic (TPV) cells has two main drawbacks. First, the emitter temperature is limited due to Planck's law thermal-radiation bound, which only allows for moderate power generation. Second, the thermal radiation emitted is located in the mid-infrared range and has usually a broad bandwidth, which makes it harder to convert it efficiently. To overcome these limitations, a thermophotonic (TPX) device has been proposed [1], in which a heated light-emitting diode (LED) is used as the active emitter instead of a passive emitter as in TPV. With such a device, the emission profile can be tuned by means of electroluminescence to a narrow peak in a spectral range matching better the bandgap of efficient TPV cells. With the development of LEDs and the increase of their achievable quantum efficiency, TPX has come out as an attractive concept for both energy harvesting and refrigeration [2]. One advantage is that the emitter temperature can stay moderate, close to few hundreds of degrees Celsius, in contrast to usual TPV emitters. The many studies on near-field (NF) thermal radiation and their application into efficient NF-TPV devices highlight the possibility to extend the concept to near-field thermophotonics (NF-TPX), where enhanced energy conversion is due to both electrical control and wave tunneling.

Using a radiative transfer solver based on fluctuational electrodynamics [3] – a framework allowing to deal with thermal and nonthermal (electroluminescent) near-field radiation – we demonstrate that using an LED as the active emitter allows to narrow the emission bandwidth to only few tenths of eV for both far-field and near-field devices. Even with such a narrowband emission, we show that the device works in fact far from the monochromatic limit (where the highest efficiency can be reached). Using a detailed-balance formulation [3] to obtain the electrical power generation/consumption of both LED and PV cell, we pinpoint that the efficiency at maximum power is almost divided by two compared to the monochromatic case for a 600 K LED. While these results are obtained numerically, it is actually possible to derive analytically the efficiency at maximum power for simple emission profiles. We therefore provide expressions for monochromatic and complete above-bandgap emission. Finally, we discuss the possibility to filter the emitter/absorber radiative exchange similarly to TPV if one aims at increasing the efficiency at the cost of output power.

[1] N.P. Harder and M.A. Green, "Thermophotonics", *Semicond. Sci. Technol.* 18, S270 (2003).

[2] T. Sadi et al., "Thermophotonic cooling with light-emitting diodes", *Nat. Photonics* 14(4), 205 (2020).

[3] J. Legendre and P.-O. Chapuis, "GaAs-based near-field thermophotonic devices: approaching the idealized case with one-dimensional PN junctions", *Sol. Energy Mater. Sol. Cells* 238, 111594 (2022).

We acknowledge funding from EU through H2020-EIC-FETPROACT-2019 project TPX-Power (GA 951976).

2:15 PM SF05.07.03

Characterization of Composite Multilayer Films for High-Temperature Selective Radiation Emission Applications Peter Bernel; Purdue University, United States

In thermophotovoltaics (TPV) applications, characterizing thin-film materials with high refractive index, high thermal stability and infrared transparency is important for designing appropriate structures. Here, we report spectroscopic ellipsometer measurements of several thin films in the wavelength range 210 nm to 2500 nm from room temperature to 1000 deg C. Our findings provide insights into the potential impacts of temperature change on the aforementioned applications, induced by the underlying changes in their electronic band structures. After characterizing magnesium oxide (MgO) and strontium titanate (STO) substrates, we characterize single composite layers of cerium oxide (CeO₂) and barium zirconate (BaZrO₃) deposited on top of these substrates. Finally, we apply these initial characterizations to understand data obtained from multilayer samples comprised of a combination of layers from all these materials, and project the potential performance for TPV applications.

2:30 PM *SF05.07.04

Radiative Heat Transfer in Nanoscale Gaps and its Application to Energy Conversion Pramod Sangi Reddy; University of Michigan, United States

Understanding radiative heat transfer in nanoscale gaps and devices is of considerable interest for creating novel energy conversion devices. In this talk, I will first describe ongoing efforts

in our group to experimentally elucidate nanoscale radiative heat transfer. I will present our recent experimental work where we have explored how radiative heat transfer is modified in nanoscale gaps at room temperature and cryogenic temperatures. Specifically, I will describe a variety of instrumentation including novel nanopositioning platforms and microdevices, which we have developed to accomplish these measurements. Further, I will discuss possible applications of near-field thermal radiation for energy conversion and photonic cooling.

3:00 PMBREAK

SESSION SF05.08: Thermal Management
Session Chairs: Rohith Mittapally and Georgia Papadakis
Tuesday Afternoon, November 28, 2023
Sheraton, Third Floor, Hampton

3:30 PM SF05.08.01

Broadband Thermal Management of Infrared Zero Contrast Grating Ken Araki¹ and Richard Zhang²; ¹Arizona State University, United States; ²University of North Texas, United States

A Zero Contrast Grating (ZCG) is an at-wavelength grating that does not create a refractive index gradient at the interface of the slit array and the substrate. The physical mechanism behind its transparency is determined from the Fabry-Perot Round Trip (FP-RT) eigenequation. This is complementary to the High Contrast Grating (HCG). While ZCG has no index gradient at the output plane of the slit array, HCG has high index gradient which produces FP-RT of electromagnetic wave inside the rectangular periodic dips so that near-perfect reflectance is obtained. Once the index has no change at the output plane between the dips and the substrate, near-perfect transmittance of 99.9% is observed. Only the even-order waveguide mode of FP-RT is strongly responsible for deciding the transmittance band whereas HCG has both single and even-order waveguide modes that decide the cut-off wavelengths, creating a narrower reflectance band. Thus, ZCG is well-suited not only for broadband transmittance but also for broadband reflectance with an additional reflective layer. The study investigates the physical background of ZCG in IR and surveys the tunability using different materials such as high-index silicon, germanium, low-index fluorides, salts, and polymers, in comparison with HCG. In contrast to previous research done on optical filters and lasers using ZCG and HCG, the work proposes the use of 1D ZCG as a thermal imaging or IR transparency window where very low reflectance is required.

3:45 PM SF05.08.02

Improving Heat Transfer of Radiative Heat Sink-Integrated Electrocaloric Cooling Hyung Rae Kim¹, Dong Hyun Seo¹, Jae Min Jeon¹, Gil Ju Lee² and Young Min Song¹; ¹Gwangju Institute of Science and Technology, Korea (the Republic of); ²Pusan National University, Korea (the Republic of)

Although vapor-compression refrigeration (VCR) has achieved high efficiency, reliability, and relatively compact size, a global consensus demands the development of novel cooling technology beyond the VCR. The use of hydrofluorocarbons (HFCs) as refrigerants in VCR contributes significantly to global warming, thousands of times more than carbon dioxide (CO₂) [1]. In recent years, solid-state refrigeration methods utilizing the caloric effect, such as magnetocaloric and electrocaloric effects, as well as passive radiative cooling, have emerged as promising solutions. Among them, electrocaloric (EC) cooling shows a high coefficient of performance (COP), low power consumption, and direct usage of electricity [2]. EC cooling utilizes an adiabatic temperature change (ΔT) of the refrigerant induced by an external electric field. However, the maximum cooling performance of EC cooling is restricted by the temperature change of the refrigerant. Previous attempts to overcome this limitation and maintain the heat sink cool involve introducing multiple heat exchanges [3]. Nonetheless, the complex structure leads to thermal losses at device interfaces and significant costs. On the other hand, passive radiative cooling exploits the radiative heat exchange between Earth (~300 K) and cold outer space (~3 K) through the atmospheric window (8-13 μm), enabling an object to maintain a temperature below ambient temperature without external energy consumption. Conventional radiative coolers consist of a porous structure to achieve high radiative cooling performance by strongly scattering the solar spectrum (0.28-2.5 μm) [4]. However, the low thermal conductivity of the porous structure hinders the dissipation of large heat fluxes, making them unsuitable for heat sink applications.

In this study, we propose a radiative heat sink-integrated electrocaloric cooling (R-iEC) system to improve heat transfer and overcome the limitations within a unit heat exchange cycle. By incorporating the thermally conductive radiative cooler (TCRC) as a heat sink on the EC cooling device, the heat sink maintains its temperature below the ambient air temperature even under the large heat flux introduced by the EC effect. The TCRC, composed of boron nitride sheet (BNNS) and poly(vinylidene fluoride-co-hexafluoropropylene) (PVDF-HFP) matrix, exhibits high thermal conductivity of 1.41 W/mK in the through-plane direction. This thermal conductivity is 13 times higher than that of the pure PVDF-HFP matrix (0.12 W/mK). Additionally, the TCRC demonstrates high reflectance in the visible range (~99%) and high emittance in the atmospheric window (~95%). The EC refrigerant absorbs heat from heat sink and ejects heat through the heat sink by fluctuating from the heat source to the heat sink through electrostatic actuation. Consequently, the temperature span of the EC device is 1.6 K at the switching frequency of 0.2 Hz. To demonstrate the enhanced heat transfer and cooling performance of the R-iEC system, a comparison is conducted among the R-iEC system, (i) a metal heat sink, (ii) EC device, and (iii) radiative cooler. While the metal heat sink and EC device experience heating from direct sunlight, the R-iEC system demonstrates an outstanding cooling heat flux of ~87 W/m² and cooling temperature of 7.3 K, overwhelming other samples.

[1] Shi, J. et al. Electrocaloric cooling materials and devices for zero-global-warming-potential, high-efficiency refrigeration. *Joule*, **3**, 1200-1225 (2019)

[2] Ma, R. et al. Highly efficient electrocaloric cooling with electrostatic actuation. *Science*, **357**, 1130-1134 (2017)

[3] Meng, Y. et al. A cascade electrocaloric cooling device for large temperature lift. *Nat. Energy*, **5**, 996-1002 (2020)

[4] Mandal, J. et al. Hierarchically porous polymer coatings for highly efficient passive daytime radiative cooling. *Science*, **362**, 315-319 (2018)

4:00 PM SF05.08.03

Multispectral Camouflage Surfaces Inspired by Cephalopods Yinuan Liu, Zhijing Feng, Chengyi Xu, Atrouli Chatterjee and Alon Gorodetsky; University of California, Irvine, United States

Wrinkled surfaces and materials are found throughout the natural world in various plants and animals and are known to improve the performance of emerging optical and electrical technologies. Despite much progress, the reversible post-fabrication tuning of wrinkle sizes and geometries across multiple length scales has remained relatively challenging for some materials, and the development of comprehensive structure-function relationships for optically active wrinkled surfaces has often proven difficult. Herein, by drawing inspiration from natural cephalopod skin and leveraging methodologies established for artificial adaptive infrared platforms, we engineer systems with hierarchically reconfigurable wrinkled surface morphologies and dynamically tunable visible-to-infrared spectroscopic properties. Specifically, we demonstrate architectures for which mechanical actuation changes the surface morphological characteristics; modulates the reflectance, transmittance, and absorbance across a broad spectral window; controls the specular-to-diffuse reflectance ratios; and alters the visible and thermal appearances. Moreover, we demonstrate the incorporation of these architectures into analogous electrically actuated appearance-changing devices that feature competitive figures of merit, such as reasonable maximum areal strains, rapid response times, and good stabilities upon repeated actuation. Overall, our findings constitute another step forward in the continued development of cephalopod-inspired light- and heat-manipulating systems and may facilitate advanced applications in the areas of sensing, electronics, optics, soft robotics, and thermal management.

SESSION SF05.09: Keynote Presentation
Session Chairs: Pierre-Olivier Chapuis and Bo Zhao
Tuesday Afternoon, November 28, 2023
Sheraton, Third Floor, Hampton

4:15 PM *SF05.09.01

HADAR: Machine Perception Through Pitch Darkness like Broad Daylight Zubin Jacob; Purdue University, United States

We will introduce the concept of thermal perception and how real-time metrology of radiative heat transfer can be crucial for autonomous navigation. We also review recent progress in the

SESSION SF05.10: Poster Session
Session Chairs: Pierre-Olivier Chapuis and Bo Zhao
Tuesday Afternoon, November 28, 2023
Hynes, Level 1, Hall A

8:00 PM SF05.10.01

Extended-Perimeter GaAs/InGaP Light-Emitting Diodes for Electroluminescent Cooling Lucvan der Krabben, Natasha Gruginskie, Maarten van Eerden, Jaspervan Gastel, Peter Mulder, Gerard J. Bauhuis, Elias Vlieg and John J. Schermer; Radboud University, Netherlands

Electroluminescent cooling (ELC) occurs when the amount of optical energy produced by electroluminescence is greater than the injected electrical energy. To satisfy the first law of thermodynamics, this difference is supplied by the absorption of thermal energy from the crystal lattice, resulting in cooling. In contrast to conventional cooling technologies, such as mechanical compressor and thermoelectric cooling, ELC could open the pathway towards efficient, compact and pollution-free refrigerators with access to cryogenic temperatures. Light-emitting diodes (LEDs) based on the III-V semiconductor GaAs are a promising candidate for demonstrating ELC. However, exceptionally high internal quantum efficiency (IQE) designs are paramount to achieve this goal. A significant loss mechanism preventing unity IQE in GaAs-based devices is non-radiative surface recombination at the perimeter sidewall. To address this issue, an unconventional LED design will be presented in which the distance from the current injection point to the device's perimeter is extended while maintaining a constant front contact grid size. This effectively moves the perimeter beyond the lateral spread of current at the operating current density ($10^1 - 10^2$ A/cm²). In addition, a theoretical model on current spreading in extended perimeter LEDs is developed to guide the device design and aid in the interpretation of current-voltage characteristics. Upon extending the perimeter, we have observed an order of magnitude decrease in the non-radiative recombination saturation current density, which is ascribed to a reduction in perimeter recombination due to the lower perimeter-to-surface area ratio. From devices fabricated with varying sizes and perimeter extensions, the optimal design is found to be a $450 \times 450 \mu\text{m}^2$ LED with $250 \mu\text{m}$ extension from contact to perimeter. This ultimately results in a 19% relative increase in external quantum efficiency, compared to a typical tight perimeter extension of $25 \mu\text{m}$. Therefore, with extended perimeter LEDs, we can achieve a significant decrease in perimeter recombination. This is enabled by lowering the perimeter-to-surface area ratio, while minimizing the influence on the size of the active light-emitting diode area, thereby more easily allowing for high current densities. These findings aid in the advancement of electroluminescent cooling in LEDs and could prove useful in other dedicated semiconductor devices where perimeter recombination is limiting.

8:00 PM SF05.10.02

Tunable Thermal Emission with Oxides that Undergo Insulator-Metal Transition Shloka Shriram¹, Shriram Ramanathan² and Hussein Hijazi²; ¹Princeton High School, United States; ²Rutgers University, United States

Correlated semiconductor materials such as VO₂ and SmNiO₃ display thermally tunable emissivity via insulator-metal transition (e.g. Kats et al, Physical Review X, 3, 041004, 2013). The carrier density can vary by several orders of magnitude across the phase transition boundary while the mobility is largely unaffected. Further, the transition can be triggered both thermally and through electrically driven Joule heating. By suitable choice of dopants on either the cation or anion site, it is possible to tune the insulator-metal transition (IMT) temperature by several tens of degrees as well as the hysteresis. The ability to tune the IMT temperature is of interest to diverse applications such as infrared thermal camouflage, thermochromic coatings for windows and radiative heat transfer in spacecraft. In this presentation, we will discuss our results on Rutherford backscattering spectroscopy of pristine VO₂ and aliovalent cation-doped systems such as (W, V)O₂ and (Nb, V)O₂ thin films on various substrates such as sapphire, SiN and GaAs. We will establish a relation between electron or hole doping density and transition temperature and hysteresis width for tunable thermal emission applications. We will then extend these analyses to the rare-earth nickelates to illustrate Nd-doping of SmNiO₃ to lower the transition temperature near ambient conditions. Finally, we will discuss the use of ion implantation technique to incorporate controlled density of dopants through the depth of a thin film and examine the resulting carrier concentration profile. We anticipate the results to be of broad interest to the community of researchers investigating novel materials for thermal radiation control.

8:00 PM SF05.10.03

Growth and Characterization of Sb-Based Dilute Nitride Semiconductors by Sputtering Sachie Fujikawa; Saitama University, Japan

III-V-N alloys have a property called giant band gap bowing, in which the band gap decreases with increasing nitrogen composition in the low nitrogen composition region. This is due to the fact that the electronegativity of N atoms is significantly different from that of group III and group V atoms. InSb_{1-x}N_x alloys can obtain an even smaller band gap by band gap bowing because InSb is a narrow-gap semiconductor. Far-infrared optical devices with wavelengths of 8-14 μm, which is the window of the atmosphere, are expected to have various applications. There have been reports on the growth of InSbN thin films by Molecular beam epitaxial (MBE) and metal-organic chemical vapor deposition (MOCVD) methods, but none by the sputtering method.

In this study, InSb_{1-x}N_x was grown on GaAs (100) substrate by direct current (DC) magnetron sputtering method and characterized. InSb_{1-x}N_x thin film was grown on semi-insulating GaAs (100) substrate by DC magnetron sputtering method using the InSb (atomic ratio of 1:1) target. All samples were grown at a growth pressure of 5.0×10^{-1} Pa, DC power of 0.10 kW, and growth time of 60 minutes. First, InSb thin films were grown by changing the growth temperatures to room temperature (RT), 150°C, and 300°C. As a result, we were confirmed that the peak intensities of (111), (220), and (311) planes increased as the growth temperature increased. Next, InSb_{1-x}N_x was fixed at 300°C and the flow rates of Ar [sccm] and N₂ [sccm] were varied 50:0 (a), 49:1 (b), 45:5 (c), and 40:10 (d), respectively. As a result, we were confirmed that the peak intensity of InSb_{1-x}N_x became weaker as the N₂ flow rate increased. In sample (c), broad peaks were observed in the (111) and (220) planes of InSb, while no peaks were observed in sample (d). The N compositions of InSb_{1-x}N_x revealed by Secondary Ion Mass Spectrometry (SIMS) analysis were $x = 0$ for sample (a), $x = 0.014$ for sample (b), $x = 0.07$ for sample (c), and $x = 0.11$ for sample (d). We also confirmed that InSb_{1-x}N_x thin films with a maximum nitrogen composition of $x = 0.20$ can be grown by changing the flow rate ratio of Ar: N₂ to 0:10. From these results, we found that InSb_{1-x}N_x can be fabricated by sputtering by controlling Ar and N₂ gases.

8:00 PM SF05.10.04

Scalable, High Thermal Conductive Electrospun/Sprayed Radiative Cooler for Efficient Thermal Management Dong Hyun Seo, Joo Ho Yun, Abdullah AlMahmud and Young Min Song; Gwangju Institute of Science and Technology, Korea (the Republic of)

Passive radiative cooling enables an object to maintain a temperature lower than the ambient air temperature without external energy consumption. To achieve efficient radiative cooling performance, the thermal emitter should exhibit solar spectrum reflection (0.28-2.5 μm) while emitting heat as radiation within the atmospheric window (8-13 μm) [1]. In practical applications with significant cooling requirements, such as data centers, vehicles, and communication base stations, the objects that need cooling often operate at temperatures higher than the surrounding ambient temperature due to substantial internal heat generation [2]. However, polymer-based photonic structures, commonly employed for their material properties and porosity to provide insulation, exhibit low thermal conductivity. Consequently, when these coolers are applied to high-temperature objects, they encounter heat resistance resulting from their low thermal conductivity, leading to the accumulation of cooling heat and a decline in cooling performance. To overcome these challenges, researchers have been investigating radiative coolers that possess enhanced thermal conductivity. One approach involves incorporating nanofillers, such as boron nitride, into the radiative cooler to improve both the overall thermal conductivity and solar reflectivity [3]. Nevertheless, achieving adequate thickness is crucial to ensure high reflectivity, which simultaneously increases thermal resistance. Consequently, a significant amount of high thermal conductivity filler material is required to offset this effect. On the other hand, reducing the thickness enhances thermal conductivity but diminishes the reflectivity characteristics. Therefore, optimizing the cooling device's properties, including its thickness, reflectivity, and thermal conductivity, is of utmost importance in achieving effective cooling performance. In this study, we fabricated an electrospun/sprayed radiative cooler (ESRC) with high thermal conductivity as a thermal management method for high-temperature objects under outdoor conditions. The ESRC was fabricated using poly(vinylidene fluoride-co-hexafluoropropylene) (PVDF-HFP) and boron nitride nanosheets (BNNS) through electrospinning and electrospaying techniques. The nanofiber membranes were manufactured with a thickness of 700 nm, and the BNNS diameter was set at 500 nm to induce multiple scattering within the solar spectrum range. Electrospaying was utilized to minimize BNNS aggregation and ensure particle dispersion for effective light scattering and thermal diffusion. Furthermore, a hot press process was employed to stack the layers, creating a heat transfer path between BNNS layers, and reducing overall thickness. As a result, the reflectance of the entire solar spectrum was measured to be over 94%. Moreover, the ESRC demonstrated high thermal radiation within the atmospheric window, with measured emittance exceeding 95%. The total thickness of the fabricated ESRC was only 120 μm, resulting in exceptional flexibility. The thermal conductivity of the ESRC was determined using the hot disk method, revealing a through-plane thermal conductivity of 1.5 K/mK with 8.7 wt% loading of BNNSs. Compared to pure PVDF-HFP, the thermal conductivity was increased by a factor of 13.

[1] Byun, Sang-Hyuk, et al. "Self-Cooling Gallium-Based Transformative Electronics with a Radiative Cooler for Reliable Stiffness Tuning in Outdoor Use." *Advanced Science* 9.24 (2022): 2202549.

[2] Li, Pengli, et al. "Thermo-optically designed scalable photonic films with high thermal conductivity for subambient and above-ambient radiative cooling." *Advanced Functional*

8:00 PM SF05.10.05

Colored Radiative Cooling Structure Managing Full Solar Spectrum via Near-Infrared Reflection and Photoluminescence DongwooChae, HangyuLim, JisungHa, JaeminPark and HeonLee; Korea University, Korea (the Republic of)

Colored radiative cooling (CRC) offers an attractive alternative for surface and space cooling with preserving the aesthetics of the object. However, it is still deficient on CRC structure with vivid and ample color display, sophisticated performance investigation, retention of properties, functionality, and structural flexibility all at once. Thus, to manage the entire solar spectrum, a colored cooling structure comprising a NIR-reflective bottom layer and top colored layer with phosphor-embedded polymer matrix is proposed. The structure is paintable, vivid and ample colored, hydrophobic, and UV and water-resistant. In the daytime outdoor measurement, the structure exhibited lower temperature than their control group using commercial white paint by 4.7°C, 7.2°C, and 7.4°C, for red, orange, and yellow color, respectively. After precise time-tracing temperature validation between the theory and the experiment, CRC performance enhancement from NIR reflection and PL effect was thoroughly analyzed and up to 16.1°C of temperature reduction was achieved for orange color. Furthermore, experiments of hydrophobicity infusion and exposure to UV and DI water verified the durability of the colored cooling structure. Also, flexible film-type colored cooling structure was demonstrated using different bottom reflective layer such as silver thin film and porous aluminum oxide particle embedded poly(vinylidene fluoride-co-hexafluoropropylene), allowing a numerous materials sets of the colored cooling structure for vivid colored, functional, and durable CRC.

8:00 PM SF05.10.06

Adaptive Electrochromic Camouflage for Thermal and Visual Adaptation in Terrestrial EnvironmentsJunhyunPark, Su EonLee and BonghoonKim; Daegu Gyeongbuk Institute of Science and Technology, Korea (the Republic of)

The demand for camouflage is increasing because of surveillance technologies such as UAVs and commercial satellites. Traditional camouflage methods fall short in the face of advanced detection technologies, including multispectral sensing, high-resolution imaging, and AI inspection. Designing multi-band camouflage capable of operating across different spectral bands, influenced by electromagnetic material properties, while achieving real-time adaptability to diverse environments presents a significant and even greater challenge.

Recent studies have extensively focused on enhancing camouflage performance across multiple spectral bands and adapting to diverse backgrounds. Techniques such as photonics crystals, metasurfaces, and nested structures mimic environmental radiative signatures, while electrochromism, phase-change materials, and physical transformation have explored switchable camouflage functions. This study presents an electrically controllable dual-band camouflage thin-film system for visual and thermal adaptation in various environments.

To effectively design camouflage for diverse environments, an investigation into the radiative properties of terrestrial surfaces was conducted. Despite the variation in surface colors, there exists a commonality in their infrared (IR) emissions. A dual-band camouflage strategy was formulated based on these shared IR emissivity characteristics. We studied unique camouflage requirements for well-illuminated and low-light environments. An essential tactic involves radiant cooling to modify color and solar range emissions.

The camouflage device design is composed of a thermally emissive layer and a color-changing layer for spectral-selective switching. The top layer enables solar transparency while the bottom adjusts colors. The device changes its color and solar absorption by layering electrochromic materials on emissive substrates and adjusting voltage (0 V = light colors / 2 V = near black). Tests in simulated environments demonstrate the device's adaptability to various backgrounds, depending on voltage and substrate type (rigid = 0 V / 2 V, flexible = 0 V / 2 V).

Outdoor experiments evaluated active double-band camouflage devices in a variety of virtual environments. Rigid samples were visually thermally camouflaged to environments of snow for 0 V and deep blue silt for 2 V. Flexible samples showed excellent visual camouflage performance to conditions of bright sand for 0 V and black soil for 2 V. Despite the windy conditions affecting the thermal vision test, the device matched the thermal signature in the target environment. The camouflage device, designed with high emissions, showed a cooling effect, and outperformed the non-cooling reference sample.

In conclusion, spectral designs for visual and thermal camouflage in two terrestrial environments were developed and assessed using electrochromic devices. The design enables seamless transitions between environments by adjusting visible spectral emittance. A practical camouflage solution was achieved without the need for laborious optimization and trial-and-error methods. Furthermore, the devices offer radiative cooling, flexibility, and compatibility with existing camouflage schemes, due to their large design degrees of freedom, thus benefiting security and defense applications.

SESSION SF05.11: Light/Heat Matter Applications
Session Chairs: Pramod Sangi Reddy and Yi Zheng
Wednesday Morning, November 29, 2023
Sheraton, Third Floor, Hampton

8:00 AM *SF05.11.01

Modeling Photomolecular Absorption and Evaporation at InterfacesGangChen; Massachusetts Institute of Technology, United States

It has been observed that solar evaporation from micro/nanoporous structures floating on water surfaces can sometimes lead to evaporation rates surpass the thermal evaporation limit. We hypothesize that photons can directly knock off water molecular clusters without going through the thermal evaporation process and named this process the photomolecular effect. How could such a process happen despite that bulk water does not absorb in the visible spectrum? Here, we attempt to develop theoretical foundations for understanding and modeling this process. Boundary conditions for Maxwell equations dictate that the normal component of the displacement field is continuous across the two sides of an interface that is charge neutral. This condition means that a large electrical field discontinuity exists in the direction normal to the interface. Real interfaces, however, are never perfectly sharp and have finite thickness, implying that the electrical field changes over a similar distance. Starting from the Maxwell equations and including such a transition region, we develop a set of generalized boundary conditions, which are similar to what had been developed for studying plasmonic and photoelectric effects. For water, we hypothesize that the uneven field across polar water molecules at the interface due to the large electrical field gradient creates a driven force for photons to knock out hydrogen-bonded water molecular clusters. We develop a Fermi's golden rule-based argument to estimate the surface absorptance, which suggests that surface absorptance can indeed be appreciable.

8:30 AM SF05.11.02

Solar-Driven Thermocatalytic Ethylene OligomerizationAisuluAitbekova, MagelSu, MatthewSalazar, JonasPeters, TheodorAgapie and HarryA. Atwater; California Institute of Technology, United States

We have designed a solar-thermal flow-through reactor with a multi-layered selective solar absorber for thermocatalytic oligomerization of ethylene to generate multicarbon (C4-C6 hydrocarbons) products. The selective solar absorber has high absorptivity at visible solar wavelengths and high reflectivity at infrared thermal radiation wavelengths. When exposed to sunlight (3-sun intensity), the solar absorber reaches a temperature of 100 °C sufficient to drive an industrially relevant ethylene oligomerization reaction to convert ethylene into C4-C6 hydrocarbon solar fuels. Moreover, we demonstrate that this process works using a diluted ethylene stream gas directly produced by a CO₂ electrolysis cell that produces ethylene.

Thermocatalytic routes are widely used for the commercial production of fuel and chemicals due to high conversion rates, good selectivity, and scalability. However, today's thermocatalytic technologies are driven by the thermal heat from burning fossil fuels and thus generate greenhouse gas emissions that cause global climate change. To become low- and zero-carbon emission technologies, these processes need to operate on renewable energy. One way to accomplish this goal is to convert solar energy into heat required to run thermocatalytic reactions. Overall, our work presents a framework to convert CO₂, water, and sunlight into sustainable fuels.

8:45 AM SF05.11.03

Scalable Squid Skin-Inspired Materials with Tunable Heat-Managing PropertiesAleksandraA. Strzelecka, PanyimingLiu and AlonGorodetsky; University of California, Irvine, United States

In the global quest for greater sustainability, the implementation of innovative packaging solutions in the food and beverage industry plays an increasingly prominent role. Within this context, traditional metallized polymer films with static thermal infrared-reflecting functionalities remain among the most widely used materials in packaging applications throughout the world. However, the development of green and low-cost alternative technologies with the highly-desirable ability to dynamically manage the exchange of heat between the contents of packaging containers and surrounding variable-temperature environments still remains relatively challenging. Herein, we present scalable squid skin-inspired sustainable packaging materials with user-tunable dynamic heat-managing properties. The composites feature a low estimated starting material cost of ~ \$ 0.1 USD per square meter, sizes of ~ 0.35 m² comparable to those of common metallized plastic films, the ability to modulate infrared transmittance by > 20-fold and heat fluxes by > 30 W/m² upon actuation with strain, and functional robustness upon significant mechanical deformation or after repeated mechanical cycling. The composites also feature adaptive infrared and dynamic thermoregulatory properties that can be computationally predicted via straightforward models. The described materials could represent a technological solution that addresses the combined cost, performance, and sustainability pressures facing the food and beverage packaging industry.

References:

Badshah, M. A., *et al.* Scalable manufacturing of sustainable bioinspired packaging materials with tunable heat-managing properties. *Nat. Sustainability*, **5**, 434–443 (2022).
Liu, P., *et al.* Structure-Function Relationships for Squid Skin-Inspired Wearable Thermoregulatory Materials. *In Revision* (2023).

9:00 AM *SF05.11.04

Radiative Thermal Control of Spacecraft using Thermochromic Infrared Materials Michael Barako; Northrop Grumman, United States

Thermochromic infrared surfaces have temperature-dependent emissivity spectra that enable radiators to respond to changes in the thermal environment. Spacecraft can leverage this unique behavior for autoregulating thermal control, where thermochromic surfaces are designed to passively transition between a high thermal emissivity (to radiate heat when hot) and a low thermal emissivity (to retain heat when cold). The “thermal emissivity” is defined as a total, hemispherical emissivity integrated across the entire hemisphere and a sufficiently wide infrared band to capture the majority of the emitted energy. This intrinsically broadband, omnidirectional characteristic presents a unique set of challenges for engineering variable emissivity materials (VEMs) for thermal control applications. In this talk, we introduce the materials, methods, and analyses of VEMs using thermal objectives, where spectral and directional infrared engineering is used to achieve passive control over temperature and heat flux. We show how the models and materials are validated calorimetrically and describe a novel set of thermo-optic characteristics used in both the design and system modeling of VEMs. Finally, we present a design space and optimization perspective for further development of VEMs for thermal control.

9:30 AMBREAK

SESSION SF05.12: Thermal Radiation, Topology and 2D Materials

Session Chairs: Georgia Papadakis and Bo Zhao

Wednesday Morning, November 29, 2023

Sheraton, Third Floor, Hampton

10:00 AM SF05.12.02

Versatile Infrared Properties of 2D Carbides and Carbonitrides (MXenes) Danzhen Zhang¹, Meikang Han¹, Akash Singh², Tetiana Hryhorchuk¹, Christopher E. Shuck¹, Teng Zhang¹, Lingyi Bi¹, Bernard McBride¹, Vivek B. Shenoy² and Yury Gogotsi¹; ¹Drexel University, United States; ²University of Pennsylvania, United States

Ultrathin films and coatings capable of controlling infrared (IR) emission are crucial for highly integrated thermal management systems, but are challenging to produce using conventional materials. Here, we report that the MXene family of two-dimensional carbides and carbonitrides offers a broad range of IR emissivity values (~0.06–0.59) with diverse colors, varying with MXene composition and structure. Specifically, 200 nm thick purple Ti₃C₂T_x coating has an average IR emissivity of 0.06, while the emissivity of a gold Nb₂CT_x coating is 0.59 at wavelengths from 3 to 25 μm. We demonstrate that the IR emissivity can be finely tuned by combining different metals in solid-solution MXenes. Furthermore, the IR identification capability at varying temperatures was validated using different MXene coatings and patterned MXene fabrics. The versatility of MXenes at optical and infrared wavelengths provides a platform for developing MXene-based smart, flexible devices and wearables capable of selective and localized thermal management, aiming at radiative heating/cooling, IR identification, photothermal conversion, and thermal imaging.

10:15 AM *SF05.12.03

Functional Metasurfaces and Structures for Thermal Radiative Applications Yi Zheng; Northeastern University, United States

This invited talk will focus on passive radiative cooling and solar-driven water desalination technologies and the issues that have hindered their development for real-life applications. Our goals are to improve buildings' energy efficiency by reducing the need for traditional vapor-compression cooling systems and to enhance freshwater production by taking advantage of renewable energy. Part 1: The compressor-based cooling systems, providing comfortable interior environments for infrastructures, account for about 20% of the total electricity consumption around the world. Moreover, the resultant heating effect and greenhouse gas emissions towards the environment accelerate global warming and climate change. An energy-efficient and eco-friendly cooling approach is highly demanded. The emerging passive daytime radiative cooling (PDRC) technique can achieve sub-ambient cooling effects under direct sunlight without any energy consumption by simultaneously reflecting sunlight and radiating excessive heat as infrared thermal radiation to the cold outer space through the Earth's atmospheric window. Such an approach is becoming an attractive candidate for improving energy efficiencies for buildings, because it eliminates the need for coolant, electricity, and compressor required by traditional mechanical cooling systems. Part 2: Interfacial solar steam generation is emerging as a promising technique for efficient desalination. Although increasing efforts have been made, challenges exist for achieving a balance among a plethora of performance indicators—for example, rapid evaporation, durability, low-cost deployment, and salt rejection. We have demonstrated that carbonized agricultural waste can convert 98% of sunlight into heat, and the strong capillarity of porous carbon fibers networks pumps sufficient water to evaporation interfaces. Salt diffusion within microchannels enables quick salt drainage to the bulk seawater to prevent salt accumulation. These advantages, together with facial deployment, offer an approach for converting farm waste to energy with high efficiency and easy implementation, which is particularly well suited for developing regions.

10:45 AM SF05.12.04

Native Point Defects in HgCdTe Infrared Detector Material: Identifying Nonradiative Recombination Centers from First Principles Wei Chen¹ and Geoffroy Hautier²; ¹Université Catholique de Louvain, Belgium; ²Dartmouth College, United States

We investigate the native point defects in the long-wavelength infrared (LWIR) detector material Hg_{0.25}Cd_{0.25}Te using a dielectric-dependent hybrid density functional. The dielectric-dependent hybrid functional allows for an accurate description of the band gap (E_g) for Hg_{1-x}Cd_xTe (MCT) over the entire compositional range, a level of accuracy challenging with standard hybrid functionals. Our comprehensive examination of the native point defects confirms that the two isoelectronic cation vacancies, namely V_{Hg} and V_{Cd} , are the primary sources of p-type conductivity in the LWIR material given their low defect formation energies and the presence of a shallow acceptor level near the valence-band maximum (VBM). Meanwhile, the cation vacancies exhibit a deep charge transition level (-2) that is situated at $E_g/2$ above the VBM, which is characteristic of nonradiative recombination centers that can be a major limiting factor affecting device performance. Our study does not support the assignment of other native point defects (such as mercury interstitial) as the origin of deep levels in p-type LWIR MCT.

SESSION SF05.13: Metasurfaces

Session Chairs: Svend-Age Biehs and Sheng Shen

Wednesday Morning, November 29, 2023

Sheraton, Third Floor, Hampton

11:00 AM *SF05.13.01

Controlling IR Thermal Emission with Metasurfaces Jean-Jacques Greffet^{1,2}, Anne Nguyen^{1,2} and Benjamin Vest^{1,2}; ¹Université Paris-Saclay, France; ²Institut d'Optique, France

In order to shape an Infrared (IR) beam, a number of optical components have to be used. These include a IR source on the first place, a filter to control the spectrum, a polarizer and a retardation plate to control the polarization state and a lens to collimate the beam. Each component is bulky and has a transmission factor smaller than one. It is thus difficult to envision a lighting system within a micrometer thin device that could fit in any handheld device. Such an achievement can be done using light emitting metasurfaces.

In this talk, we will first explain what are metasurfaces and what can be achieved with them. We will describe some examples of metasurfaces operating in transmission by diffracting an incident beam. They can be used to steer an incident beam, modify its polarization or focus it.

Incandescent metasurfaces merge metasurfaces to control phase fronts and thermally excited random current densities emitting IR radiation. They are inherently different from metasurfaces as they are not illuminated by an incident coherent beam. We will discuss the operating principle of incandescent metasurfaces and their application to control the directivity, emission spectrum, polarization and intensity modulation beyond 10 MHz [1-2].

1. L. Wojszwyk, A. Nguyen, Anne-Lise Coutrot, C. Zhang, B. Vest, J.J. Greffet, An incandescent metasurface for quasimonochromatic polarized Mid-Wave Infrared emission modulated beyond 10 MHz, *Nat. Commun* **12**, 1492 (2021).

2. A. Nguyen, J.-P. Hugonin, A.-L. Coutrot, E. Garcia-Caurel, B. Vest, J.-J. Greffet, Large circular dichroism in the emission of an incandescent metasurface, *Optica* **10**, 232 (2023).

11:30 AM SF05.13.02

Preventing Overfitting in Infrared Ellipsometry using Temperature Dependence: Fused Silica as a Case Study Shenwei Yin, Demeng Feng, Jin-Woo Cho, Tanuj Kumar, Chenghao Wan, Hongyan Mei and Mikhail Kats; University of Wisconsin-Madison, United States

Materials with vibrational resonances such as fused silica, quartz, and silicon carbide can be used for mid-infrared absorbers and thermal emitters [1], [2]. Here, we investigated fused-silica glass; while fused silica is perhaps the most-studied optical material in the visible and near-infrared, its mid-infrared properties are less known, with almost no data available above room temperature [3]. Apart from the use of this data in high-temperature applications of fused silica, temperature-dependent ellipsometry can provide a new source of information with which to evaluate oscillator models, in addition to the conventionally used goodness of fit.

We conducted temperature-dependent spectroscopic ellipsometry measurements on three different grades of silica from Corning: HPFS 7980 standard grade (-OH content 800–1000 ppm, metallic impurities <1000 ppb), 7979 IR grade (-OH content <1 ppm, metallic impurities <100 ppb), and 8655 ArF grade (-OH content <1 ppm, metallic impurities <10 ppb). For each sample, we performed temperature-dependent variable-angle ellipsometry measurements at wavelengths of 5–25 μm .

Subsequently, we performed fits on the experimental ellipsometric data, ψ and Δ . We observed 3 main features centered around the wavelengths of 9 μm , 12.5 μm , and 22 μm , known to be due to vibrational resonances [3]. A previous work that looked at reflectance data (rather than ellipsometry) at room temperature used 8 distinct Gaussian oscillators to fit the experimental data [3]. Similarly, we were able to achieve excellent fits at each temperature (7 temperatures total for each sample) using 7 Gaussian oscillators, observing that Gaussian oscillators fitted the data better than Lorentz oscillators, likely due to inhomogeneous broadening in the amorphous material. However, when we plotted the fitting parameters as a function of temperature, we observed nonphysical nonmonotonic temperature dependence of the oscillator positions, widths, and amplitudes, implying that our model could be improved.

After simplifying the model to 6 oscillators, we again fitted the experimental data independently at each temperature for each sample, observing a slight (but not very significant) reduction in the goodness of fit (the normalized mean-squared error (MSE) for Ψ and Δ as defined in ref. [4] was 1.3 with 7 oscillators and 1.6 with 6 oscillators, both indicating excellent fits). In our new fit with fewer oscillators, the oscillator parameters that contributed most to the optical properties changed monotonically with temperature, confirming the validity of our fits. By comparing the temperature-dependence trends among the oscillator parameters, we can effectively mitigate overfitting of the experimental ellipsometric data.

In addition to our demonstration of the use of temperature-dependent measurements to prevent overfitting of materials parameters, we generated highly precise and accurate datasets for the temperature-dependent mid-infrared optical properties of various grades of fused silica, which can be used for modeling infrared absorbers, thermal emitters, and other photonic structures. These datasets will be made publicly available.

[1] J. D. Caldwell *et al.*, *Nanophotonics*, vol. 4, no. 1, pp. 44–68, 2015.

[2] J. long Kou *et al.*, *ACS Photonics*, vol. 4, no. 3, pp. 626–630, 2017.

[3] R. Kitamura *et al.*, *Applied Optics*, Vol. 46, Issue 33, pp. 8118–8133, 2007.

[4] Hiroyuki Fujiwara, *Spectroscopic ellipsometry: principles and applications*. John Wiley & Sons, 2007.

SESSION SF05.14: Polaritons

Session Chairs: Georgia Papadakis and Bo Zhao

Wednesday Afternoon, November 29, 2023

Sheraton, Third Floor, Hampton

1:30 PM *SF05.14.01

Low-Symmetry Polaritonic Materials for Infrared Polarization Control Koray Aydin; Northwestern University, United States

Two-dimensional layered materials have recently garnered burgeoning amount of interest due to their unique electronic, optical, thermal, mechanical properties emerging at the mono-to-few layer thicknesses. Most of research has focused on conventional 2D materials such as graphene and 2D TMDCs, having isotropic electronic and optical properties due to their crystal symmetry. Recently, layered materials such as black phosphorus and hexagonal boron nitride investigated for anisotropic crystal structure. In this talk, I will introduce $\alpha\text{-MoO}_3$ as an anisotropic photonic and polaritonic material. $\alpha\text{-MoO}_3$ is a layered material that exhibits both in and out-of-the-plane anisotropic polaritonic response at mid-IR wavelengths. We designed and experimentally demonstrated an anisotropic polaritonic absorber and showed that one can couple to all phonon modes and address them individually either using structural tunability or polarization control of incident infrared radiation. Moreover, I will introduce MOCVD grown $\beta\text{-Ga}_2\text{O}_3$ as an emerging material for IR photonics applications due to its anisotropic crystal symmetry. Detailed numerical modelling and experimental characterizations highlighting unique IR properties for manipulating and controlling the polarization response will be discussed.

2:00 PM SF05.14.02

Hyperbolic Polariton Mode Conversion and Energy Redistribution in Engineered Van der Waals Structures Byung-I Noh¹, Sina J. Ghalekohneh², Mingyuan Chen¹, Jialiang Shen¹, Jiahua Li³, Lixiang Kang⁴, James H. Edgar³, Bo Zhao² and Siyuan Dai¹; ¹Auburn University, United States; ²University of Houston, United States; ³Kansas State University, United States; ⁴Chinese Academy of Sciences, China

Hyperbolic polaritons, which are highly confined light-matter waves, present a promising avenue for manipulating light and light-matter interactions at nanoscales. Recent advances in scanning probe optical techniques have enabled the imaging of hyperbolic polaritons in real space. However, current studies typically image only one branch of hyperbolic polaritons. In this work, we evidently imaged multiple branches of hyperbolic polaritons in engineered van der Waals (vdW) structures. Instead of conventional long-range fringes, our nano-infrared imaging demonstrates short-range beats by varying the edge symmetry through vdW stackings. Our combined experimental and theoretical results reveal the energy redistribution and mode conversion in hyperbolic polaritons. These advances hold great potential for polaritonic circuits, nano-optical sensing, nanoscale energy transfer, etc. (Oral)

2:15 PM SF05.14.03

Can Thermal Transport in Thin Films by Surface Phonon/Plasmon Polaritons be Experimentally Observed? Alexei Maznev¹ and Bai Song²; ¹Massachusetts Institute of Technology, United States; ²Peking University, China

Thermal transport in thin films mediated by surface polaritons (SPs) originally proposed by Chen *et al.* [1] is attracting intense attention of both theorists and experimentalists [2-5]. According to theoretical models [1,2], SPs become efficient in carrying heat when their mean free path (MFP) is long and they almost lose their polaritonic character and become similar to free-space electromagnetic waves. The long MFP of the heat-carrying SPs (~ 1 cm or longer) presents a formidable challenge for experimentalists: in order to observe the predicted SP contribution to thermal transport, the heat transfer length should be greater than their MFP [1]. This requirement is often not met in laser-based experiments where the characteristic length scale is determined by a microns-sized laser spot [4,5]. However, there is a more fundamental challenge: with a thin film sample size on the order of 1 cm, thermal radiation also becomes significant. We argue that from the experimental point of view, the energy exchange with the environment via thermal radiation is hardly distinguishable from thermal transport: since the hot side of the sample

radiates more than the cold side, to an observer it looks like an additional energy flux between the two sides. This becomes especially apparent when the temperature of the environment is set so as to minimize the total radiative loss of the sample, in which case the cold side of the sample effectively absorbs thermal radiation energy emitted by the hot side. We will present a theoretical model describing heat transport in a thin free-standing film in the presence of both conduction and radiative exchange with the environment and show that the relative contribution of the latter increases as the square of the sample size. In many cases, the radiative exchange will completely obscure the contribution of SPs. The presentation will be complemented by a discussion of experimentally relevant systems supporting phononic or plasmonic SPs such as silica glass and titanium thin films.

[1] D.-Z. A. Chen et al., Phys. Rev. B 72, 155435 (2005); [2] M. Lim et al., Phys. Rev. Appl. 12, 034044 (2019); [3] L. Tranchant et al., Nano Lett. 19, 6924 (2019); [4] Y. Wu et al., Sci. Adv. 6, eabb4461 (2020); [5] D. Kim et al., Phys. Rev. Lett. 130, 176302 (2023).

2:30 PMBREAK

3:30 PM *SF05.14.04

Exploiting and Controlling Lattice Symmetry for Infrared Nanophotonics and Thermal Transport [Joshua D. Caldwell](#); Vanderbilt University, United States

The field of nanophotonics is based on the ability to confine light to sub-diffractive dimensions. In the infrared, this requires compression of the wavelength to length scales well below that of the free-space values. While traditional dielectric materials do not exhibit indices of refraction high enough in non-dispersive media to realize such compression, the implementation of polaritons, quasi-particles comprised of oscillating charges and photons, enable such opportunities. Two predominant forms of polaritons, the plasmon and phonon polariton, which are derived from light coupled with free carriers or polar optic phonons, respectively, are broadly applied in the mid- to long-wave infrared. However, the short scattering lifetimes of free-carriers results in high losses and broad linewidths for the former, while the fast dispersion and narrow band of operation for the latter result in significant limitations for both forms. Within anisotropic materials, these optical modes can be induced to propagate with different wavevectors along different axes, or even be restricted to propagate only along a single direction. Here, we discuss the influence of crystalline anisotropy in dictating the polaritonic dispersion, including the recent observations from our group highlighting highly directional so-called hyperbolic shear polaritons in low-symmetry monoclinic and triclinic crystals, as well as the ability to control the wavelength and propagation direction of these modes using free-carrier injection and twist-optic concepts. Further, we highlight that such phonon polaritons can be employed as ultrafast and efficient carriers of thermal energy, providing alternative dissipation pathways for heat.

4:00 PM SF05.14.05

Thermomechanical Engineering of Mid-Infrared Phonon Polaritons in α -MoO₃ [Naveed Hussain](#), Mashnoon A. Sakib, Zhao X. Li, H. Kumar Wickramasinghe and Maxim R. Shcherbakov; University of California Irvine, United States

Polar van der Waals (vdW) materials, such as α -MoO₃, have enabled controlling light at the nanoscale over a wide range of wavelengths by leveraging the strong optical confinement of their hyperbolic polaritonic modes.^{1,2} However, the extreme spatial confinement of phonon polaritons (PhPs) in these structures renders it hard to control their dispersion externally.³⁻⁵ We show here that the hyperbolic PhPs in α -MoO₃ can be tuned by engineering phonon modes via introducing controlled oxygen vacancy defects by hot-pressing (h.p.) them to 350 °C with a period of 50 °C under a mild uniaxial pressure of around 0.1-0.2 GPa. The reduced oxygen supply during the thermal annealing results in loss of terminal oxygen through vdW gaps, leaving behind the oxygen vacancy defects. As measured by μ -Raman scattering investigations, the oxygen-to-molybdenum ratio ($I_{B_{2g}}/I_{B_{3g}}$) can be reduced to an order of magnitude (at h.p. of 350 °C), triggering a semiconductor-to-semimetal transition, probed by PL spectroscopy.⁵ We also induced a controlled biaxial compressive strain up to -2.4%, demonstrated by a blue shifting of the phonon mode at 158.4 cm⁻¹. We used photo-induced force microscopy (PiFM) to investigate thermomechanically engineered PhPs, which matches well with the model we developed using FDTD simulations and PiFM data.⁶ The data extracted from the dispersion curves demonstrate the successful tailoring of the PhP response of α -MoO₃ by introducing oxygen vacancy defects. The polariton lifetimes (τ) for pristine and h.p. flakes at 150 °C, were nearly identical, ranging from 3.57±0.3 to 3.38±0.3 ps, respectively, exhibiting a negligible loss of only ~5.26%. When compared to pristine flakes of same thickness, oxygen-deficient α -MoO₃ provides an ultra-low-loss platform for PhPs, allowing for tuning of their polariton wavelength (λ_p) by ~11.84% and group velocity (v_g) by ~15.4%. We believe that engineering of phonon modes, which result in oxygen-deficient α -MoO₃, enable active tuning of mid-infrared PhPs, which has applications in super-resolution imaging, nanoscale thermal manipulation, boosted molecular sensing, and on-chip optical circuits.

4:15 PM *SF05.14.06

Dynamic, Electrostatic Steering of Thermal Emission using Graphene/Metal Metasurfaces [Victor Brar](#); University of Wisconsin--Madison, United States

This talk will describe the thermal emission from optical cavities that support long-range, delocalized Fabry-Perot modes, where one side of the cavity is bounded by a graphene-integrated metasurface. The graphene allows the reflection coefficients of the metasurface to be continuously tuned via electrostatic gating which, in turn, changes the properties of the confined Fabry-Perot modes. Those changes affect, for a fixed frequency, the directionality of the absorption and emission of the device and we show experimentally that this mechanism can allow the thermally emitted radiation at 6.6 μ m to be tuned by more than 16 degrees, with a peak emissivity maintained about 0.9. Theoretical calculations will also be presented that describe the maximum steerability of optimized devices that use real materials, and from those calculations it will be shown that this mechanism can allow thermal emission to be steered continuously by more than 60 degrees.

SESSION SF05.15: Radiative Cooling II
Session Chairs: Aaswath Raman and Yi Zheng
Thursday Morning, November 30, 2023
Sheraton, Third Floor, Hampton

9:00 AM SF05.15.01

Highly Efficient and Versatile Daytime Radiative Cooler Based on Optimized Polymer-Ceramic Composite Fabricated via Facile Process [Jaemin Park](#), Dongwoo Chae, Hangyu Lim, Jisung Ha and Heon Lee; Korea University, Korea (the Republic of)

Radiative cooling is a carbon-free, zero energy technology that can substitute various energy-consuming cooling systems such as air conditioners and auto-chillers for cooling heat-generating machines. Previous reports on radiative cooling have focused mainly on the cooling performance, thereby overlooking the applicability, structural complexity, manufacturing complexity, and certain physical properties of the cooler. In this study, we present an efficient, applicable, and facile-fabricated radiative cooler composed of poly(vinylidene fluoride-co-hexafluoro propene) (P(VDF-HFP)) and alumina (Al₂O₃). Apart from being fabricated in the form of a freestanding sheet with 97.5% solar reflectance and 94.8% infrared (IR) emissivity, the P(VDF-HFP)/Al₂O₃-based radiative cooler (PARC) can be applied to solid substrates via simple coating techniques. This shows that the PARC can be introduced in architecture, clothing, and other fields that demand cooling. The PARC's cooling performance is experimentally proven by a sub-ambient temperature drop of 5.8 °C and the cooling power of the PARC is calculated to be 125.6 Wm⁻² under the AM1.5 global spectrum, which is superior to that of previously reported radiative cooling emitters.

9:15 AM SF05.15.02

Biologically Inspired Nanostructured Porous Fiber for Passive Radiative Cooling [Minjae Lee](#)^{1,2}, Byunghong Lee², Byung Wook Kim³ and Seung Hwan Ko^{1,1}; ¹Seoul National University, Korea (the Republic of); ²Hyundai Motor Company, Korea (the Republic of); ³Columbia University, United States

A great number of butterfly species in the warmer climate have evolved to exhibit fascinating optical properties on their wing scale which can both regulate the wing temperature and exhibit the structural coloring in order to increase their chances of survival. In particular, the *Archaeoprepona demophoon* dorsal wing demonstrates notable radiative cooling performance and iridescent colors based on its nanostructure of the wing scale that can be characterized by the nanoporous matrix with the periodic nanograting structure on the top matrix surface. Inspired by the natural species, we demonstrate a multifunctional biomimetic film that reconstructs the nanostructure of the *Archaeoprepona demophoon* wing scales to replicate the radiative cooling and structural coloring functionalities. We resorted to the SiO₂ sacrificial template-based solution process to mimic the random porous structure and laser-interference lithography to reproduce the nanograting architecture of the butterfly wing scale. As a result, the biomimetic structure of the nanograted surface on top of the porous film demonstrated desirable heat transfer and optical properties for outstanding radiative cooling performance and iridescent structural coloring. In this regard, the film is capable of inducing the maximum temperature drop of 8.45 deg, and the color gamut of the biomimetic film can cover 91.8% of the standardized color profile (sRGB).

9:30 AM SF05.15.03

Designing Radiative Cooling Walls with Passive and Active Controls [Yuan Yang](#); Columbia University, United States

Passive daytime radiative cooling (PDRC) is an attractive electricity-free approach to reducing energy consumption of buildings. Current PDRC research focuses on roofs, but limited attention has been paid to the walls, which occupy a major portion of building envelopes. Unlike the roofs, the walls face both cold sky and hot ground, so either high emissivity or low emissivity is not the best solution. Here we develop a scalable cooling wall with asymmetric emissivity. The wall can simultaneously reflect the thermal radiation from the hot ground and remain emissive to the cold sky, to achieve further building cooling and even sub-ambient cooling, which are demonstrated by simulations and experiments. Such asymmetric emissivity shows temperature drops of 3.1 °C (peak) / 2.3 °C (daily average) compared to the control wall in the field tests. Taking the United States as an example, the proposed zigzag wall can work effectively over 29% area and benefit 45% population, providing up to 27 MJ m⁻² year-round saving per wall area for a typical midrise apartment building. We further demonstrated mechanically dynamic control of wall emissivity to further maximize energy saving.

9:45 AMBREAK

10:15 AM SF05.15.04

Spectrally Engineered Textile for Radiative Cooling Against Urban Heat Islands Ronghui Wu and Po-Chun Hsu; The University of Chicago, United States

Radiative cooling textile has been considered as a promising method to achieve personal thermal comfort under the increasing global temperature. Since more than half of the world population resides in urban areas where the heat island effect exacerbates the local temperature rise, outdoor radiative cooling textiles should emphasize the heat exchange of the users under a metropolitan area scenario. While yielding high cooling performance when facing the sky, start-of-the-art radiative cooling textiles do not consider that the apparel is predominantly vertically oriented and underestimate the parasitic radiative heat gain from the hot ground and urban infrastructures. Here, we developed a mid-infrared (MIR) spectrally selective hierarchical fabric (SSHF) with emissivity greatly dominant in the atmospheric transmission window (ATW) through molecular design, minimizing the net heat gain from the surroundings. The SSHF also features a high solar spectrum reflectivity of 0.96 owing to the strong Mie scattering from the nano-micro hybrid fibrous structure. As a result, SSHF enables a considerable temperature drop of ~6.2 °C under peak solar intensity of 1010 W/m² in outdoor thermal measurements. When vertically placed in a simulated urban scenario, it exhibits ~3.1 °C cooler than commercial cotton fabrics. Moreover, SSHF has also demonstrated excellent breathability, washability, durability, robust mechanical property, and anti-UV aging property, representing remarkable long-term wearability. Supported by a comprehensive analysis of heat transfer between individuals and their environment, the selective spectrum design for vertical-facing textiles introduces an innovative and efficacious solution for passive personal cooling in urban areas, which not only holds the potential to curtail air-conditioning energy consumption but also serves as a preventive measure against heat-related health issues.

10:30 AM SF05.15.05

Enhanced Radiative/Evaporative Cooling from Air Eddies above Zebra Stripes: A Deductive Approach Se-Yeon Heo and Young Min Song; Gwangju Institute of Science and Technology, Korea (the Republic of)

Passive radiative cooling offers a sustainable way to effective temperature reduction, utilizing thermal imbalance of earth and universe and minimizing heat gain from surroundings. Numerous studies have demonstrated its environmentally friendly nature and high cooling efficiency, establishing it as a highly promising solution for sustainable cooling applications. In recent years, scientific research has unveiled that the cooling potential of evaporation (~320 Wm⁻²) surpasses that of radiation (~150 Wm⁻²), and implementation of evaporative and radiative cooling approaches has successfully achieved superior cooling performance compared to single reliance on radiative cooling methods. But evaporative cooling in nature exist in way for obtaining homeostasis; During the summer season, both plants exhibit active transpiration, and mammals experience increased sweat evaporation, as a means to regulate their body temperature and counteract the rise caused by the elevated ambient temperature. Conversely, in cold winter conditions, these phenomena occur less frequently as a mechanism to maintain a stable body temperature. Indeed, equation for evaporative rate (m') express that the rate of evaporation intensifies as temperature increases.

$$m' = \theta(X_s(T_{\text{body}}) - X(T_{\text{amb}})) \quad (1)$$

where θ is evaporative coefficient, which equals to $25 + 19v$ where v is the velocity of air. X_s denotes the maximum humidity ratio of saturated air at the same temperature as the body. X is humidity ratio of ambient air at the temperature T_{amb} . Since the X_s increases dramatically with increased body temperature (T_{body}), smaller T_{body} results in decreased m' . In other words, the cooler the body, the less evaporation occurs.

As for maximizing efficiency of evaporation, utilizing the heating power of nature, specifically the sun, has gained significant research interest, in modern society. This method, known as solar-driven interfacial evaporation, focuses on heating only the interface (i.e., the surface) rather than heating the entire medium (i.e., bulk heating). By reducing the thermal losses, an interfacial evaporation approach by selectively heating the air/liquid interface has demonstrated to have 45% higher evaporation efficiency than bulk heating based evaporation. Here we suppose that instead of merely heating the air-sample interface, generating convective heat flow of air around the sample could boost surface evaporation, inspired by the scientific discoveries presented by Cobb et al. (2022); The striking black and white striped pelage of zebras maintain a temperature difference, generating convective airflow as warm air rises from the black stripes and cool air descends onto the white stripes. This airflow, above and between the stripes, can induce chaotic or turbulent air patterns due to convection currents and facilitate the exchange of air and water vapor, thus aiding evaporative cooling.

In order to successfully demonstrate this, we employ zebra-patterned cellulose acetate (CA) fibrous network on the surface of the LiBr hydrogel sample. The hydrogel possesses the ability to absorb moisture from the atmosphere and retain the water within the structure, while the CA networks desired to wick the water for evaporation, facilitating continuous evaporative cooling. Given the numerical study presented by Austin et al. (2022) that zebra-striped roof buildings demonstrate lower internal temperatures in comparison to all-white roof buildings, the proposed statement appears to be plausible. The incorporation of a zebra-pattern atop a hydrogel, accompanied by localized heating of the sample surface corresponding to the regions occupied by the black stripes, paradoxically, has the potential to enhance the cooling performance beyond that achievable through sole radiative cooling or radiative/evaporative cooling methods.

SESSION SF05.16: Near-Field Thermal Radiation
Session Chairs: Mathieu Francoeur and Jean-Jacques Greffet
Thursday Morning, November 30, 2023
Sheraton, Third Floor, Hampton

10:45 AM *SF05.16.01

Near-Field Thermal Radiation by Transdimensional Plasmonics and Subwavelength Structures Sheng Shen; Carnegie Mellon University, United States

Near-field radiative heat transfer has attracted enormous interest for energy conversion, solid-state cooling, and thermal management owing to the substantial radiation enhancement beyond Planck's law at nanoscale gaps. So far, effects of nonlocality to near-field thermal radiation have been examined only in the extreme near-field with gap sizes of a few nanometers. Also, our fundamental understanding of near-field heat transfer between subwavelength surfaces is still quite limited. In this talk, using transdimensional plasmonic materials, we experimentally demonstrate nonlocality in dielectric response alters near-field heat transfer at gap sizes on the order of hundreds of nanometers. We also report the first measurements of near field thermal radiation between coplanar subwavelength membranes over a broad range of temperature differences up to 190 K. Our measurement with membrane dimensions comparable to near-field separations shows maximum 20-times enhancement in heat transfer compared to blackbody radiation.

11:15 AM SF05.16.02

Identifying the Limits to Near-Field Radiative Heat Transfer Between Phonon Polaritonic Materials Rohith Mittapally¹, Ju Won Lim¹, Lang Zhang², Owen Miller², Pramod Sange Reddy¹ and Edgar Meyhofer¹; ¹University of Michigan, United States; ²Yale University, United States

Radiative heat transfer (RHT) between objects separated by nanoscale gaps, referred to as being in the near-field (NF) of each other, is known to impact applications ranging from energy conversion to thermal management of electronics. Recently, several experiments validated early predictions of orders of magnitude enhancement in NF-RHT, aided by surface phonon polaritons (SPhPs) supported in polar dielectric materials. While these experiments using SiO₂ validated the longstanding predictions of enhanced RHT, there remains a few unanswered questions: what is the fundamental limit to this NF-RHT and what material properties can enable this? Recent theoretical analysis [1] based on causal arguments suggests that the SPhPs in SiO₂ occur at a frequency far higher than the optimal. In fact, our optimization [2] for maximum NF-RHT suggests that materials supporting SPhPs close to an optimal frequency of 67 meV at room temperature can enhance this NF-RHT by 5-fold (a global bound) when compared to that of SiO₂. In this talk, I will first discuss our theoretical analysis and report on how we utilized a

custom-built nanopositioner to measure NF-RHT between Al_2O_3 - Al_2O_3 and MgF_2 - MgF_2 material systems. In these experiments, we observed a clear enhancement of NF-RHT beyond blackbody limit and even beyond that of SiO_2 at all gap sizes ranging from a few tens of nanometers to a few micrometers. Specifically, I will show that NF-RHT between MgF_2 at a gap size of 50 nm is 2.5-fold larger than that between SiO_2 and thus, approaches 50% of the global SPHP bound. The insights gained from these experiments and theoretical analysis will benefit exploration of materials further enhancing NF-RHT.

(1) Zhang, L.; Miller, O. D. Optimal Materials for Maximum Large-Area Near-Field Radiative Heat Transfer. *ACS Photonics* **2020**, 7 (11), 3116-3129.

(2) Mittapally, R.; Lim, J. W.; Zhang, L.; Miller, O. D.; Reddy, P.; Meyhofer, E. Probing the Limits to Near-Field Heat Transfer Enhancements in Phonon-Polaritonic Materials. *Nano Lett.* **2023**, 23 (6), 2187-2194.

11:30 AM SF05.16.03

Intelligent Radiative Thermostat Induced by Near-Field Radiative Thermal Diode [YangLiu](#) and YiZheng; Northeastern University, United States

A radiative thermostat system senses its own temperature and automatically modulates heat transfer by turning on/off the cooling to maintain its temperature near a desired set point. Taking advantage of far- and near-field radiative thermal technologies, we propose an intelligent radiative thermostat induced by the combination of passive radiative cooling and near-field radiative thermal diode for thermal regulation at room temperature. The top passive radiative cooler in thermostat system with static thermal emissivity uses the cold outer space to passively cool itself all day, which can provide the bottom structure with the sub-ambient cold source. Meanwhile, using the phase-transition material vanadium dioxide, the bottom structure forms a near-field radiative thermal diode with the top cooler, which can significantly regulate the heat transfer between two terminals of the diode and then realize a stable temperature of the bottom structure. Besides, the backscided heat input of the thermostat has been taken into account according to real-world applications. Thermal performance of the proposed radiative thermostat design has been analyzed, showing that the coupling effect of static passive radiative cooling and dynamic internal heat transfer modulation can maintain an equilibrium temperature approximately locked within the phase transition region. Besides, after considering empirical indoor-to-outdoor heat flux, rendering its thermal performance closer to that of passive solar residential building walls, the calculation result proves that the radiative thermostat system can effectively modulate the temperature and stabilize it within a controllable range. Passive radiative thermostats driven by near-field radiative thermal diode can potentially enable intelligent temperature regulation technologies, for example, to moderate diurnal temperature in regions with extreme thermal swings.

11:45 AM SF05.16.04

Measurement of Photophoretic Forces of Rarefied Gases on Functionalized Surfaces [GregAcosta](#)¹, [AmunJarzembski](#)² and [MohammadGhashami](#)¹; ¹University of Nebraska-Lincoln, United States; ²Sandia National Laboratories, United States

In recent years, metamaterials and two-dimensional materials have revolutionized the fields of quantum mechanics and nanophotonics by introducing a new class of materials that can exhibit unique and exotic optical and thermal emission properties. This has been mainly driven by advances in nanofabrication and our ability to engineer surfaces with unique characteristics. Often, the surfaces of these materials are encountered by the presence of rarefied gases, where classical continuum description of the physical phenomena is no longer valid, and the non-continuum phenomena of gas-surface interactions (GSIs) dominate the energy transport from the surface to the gas particles. One example is the light-induced photophoretic levitation of nanostructured thin films and light-driven oscillators enabled by optical and photophoretic forces. Here, photophoretic or Knudsen forces (KFs) arise when a highly adsorbing material, immersed in a diluted gas, exchanges thermal energy via electromagnetic waves, thus inducing temperature inhomogeneities within the surface of the irradiated body. These temperature differences trigger non-equilibrium transport phenomena, where the gas particles and body collectively communicate with each other via GSIs. Here, the GSIs help transfer momentum from the thermally excited gas particles onto the surface, generating a temperature-driven force from the hot to the cold side of the body. On the other hand, if the temperature difference within the surface is negligible, Knudsen forces can still be induced by simply having different surface properties that modulate the efficacy of the GSIs. Although recent studies have demonstrated preliminary measurements of KFs for different gases and simple surfaces, there is little knowledge regarding how different surface characteristics affect the magnitude of the generated forces. Furthermore, there is no clear indication of to what extent the temperature gradient's magnitude along the surface affects the momentum exchange process between the impinging gas molecules. All these are important as KFs can play a major role in atomic force microscopy and photothermal-induced spectroscopy.

Hence, this work aims to perform an experimental investigation to unfold the nature of GSIs on the generation of Knudsen forces by measuring the force generated on smooth and functionalized surfaces for different temperature gradients, immersed in rarefied helium, nitrogen, and carbon dioxide gas. Here, surface functionalization will allow controlling the extent of GSIs by adjusting the net effect of specular/diffusive reflections in the form of the energy accommodation coefficients (EAC). As a preliminary step, we will follow the same procedure as our previous sub-continuum gas conduction investigations to characterize the GSIs by extracting the EACs for silicon and tungsten surfaces. Once the EACs are extracted, samples will be placed on a nanopositioning stage, equipped with a heating platform to heat samples to any desired temperature. Then samples will be brought into the proximity of a temperature-controlled suspended probe that helps detect the induced KFs via a laser interferometer. Then, adjusting the gap distance between the samples and the probe, in conjunction with the vacuum pressure, will allow us to measure the KFs forces for different transport regimes. The experimental results demonstrate a correlation between the measured forces and the value of the EAC extracted for all the samples. Furthermore, the magnitude of the force increases with the temperature gradient, as expected, due to an increase in kinetic energy. Lastly, it is shown that the forces generated by helium gas exceed those of nitrogen and carbon dioxide due to a high mismatch in the mean-free path. These results demonstrate that generated KFs can be altered depending on the type of gas-surface interaction occurring on the surface, paving the way to optimize this force by surface engineering.

SESSION SF05.17: Near-Field Thermal Radiation and Nanoparticles/Structures

Session Chairs: Rohith Mittapally and Bo Zhao

Thursday Afternoon, November 30, 2023

Sheraton, Third Floor, Hampton

1:30 PM *SF05.17.01

Near-Field Radiative Heat Transfer Between Subwavelength Structures [MathieuFrancoeur](#)¹, [LindsayP. Walter](#)², [LeiTang](#)³, [LiviaM. Correa](#)², [ChrisDames](#)³ and [JosephC. McKay](#)²; ¹McGill University, Canada; ²The University of Utah, United States; ³University of California, Berkeley, United States

Near-field radiative heat transfer (NFRHT), a regime in which thermal sources are separated by subwavelength vacuum gaps, can exceed the blackbody limit owing to the tunneling of evanescent electromagnetic waves, which include frustrated modes and surface modes. The substantial enhancement of heat transfer in the near field could be exploited in various technologies, such as noncontact localized cooling and thermophotovoltaic power generation.

To date, NFRHT is still a laboratory-scale concept. The viability of potential NFRHT applications directly depends on the ability of enhancing and spectrally controlling the flux with designer materials, such as metamaterials and metasurfaces, made of subwavelength structures. However, the basic physics underlying the interactions between thermally generated evanescent waves and subwavelength structures is not well understood, partially due to the lack of numerically exact framework enabling predictions of NFRHT in complex geometries. The overall objective of this talk is to address this knowledge gap by first reviewing a novel method for solving NFRHT in complex geometries, and by then discussing recent results of NFRHT between two coplanar membranes of subwavelength thickness.

In the first part of the talk, we will introduce the discrete system Green's function (DSGF) method, which is a volume integral numerical approach based on fluctuational electrodynamics. In the DSGF method, thermal sources are discretized into cubic subvolumes, and all electromagnetic interactions are determined by numerically calculating the system Green's function between the subvolumes. NFRHT is then computed by simple mathematical operations to the system Green's functions. The DSGF method is numerically exact, and is applicable to an arbitrary number of finite, 3D thermal sources of any sizes and shapes separated by gaps smaller or larger than the thermal wavelength. We will review the verification of the DSGF method against exact results of NFRHT between two and three spheres, and briefly discuss its application to predict NFRHT between complex-shaped particles.

The second part of the talk will focus on DSGF predictions and experiments of NFRHT between two coplanar SiC membranes with thickness comparable to or smaller than their vacuum gap spacing of 100 nm. The results show that the radiative heat transfer coefficient increases substantially as the membrane thickness decreases. At room temperature, a maximum heat transfer coefficient h_{rad} of ~ 800 W/m²K for a membrane thickness of 20 nm is measured and predicted. This h_{rad} value is ~ 5 times larger than that predicted between two infinite SiC surfaces (~ 150 W/m²K) at the same vacuum gap, and is ~ 1200 times larger than the blackbody limit. A heat transfer coefficient of 800 W/m²K would require a gap spacing of ~ 30 nm between two infinite SiC surfaces. In addition, the resonance of the heat transfer coefficient is broadened and redshifted as the membrane thickness decreases. We demonstrate via a modal analysis that the enhancement and spectral redshift of the heat transfer coefficient is due to the 2D confinement of the electromagnetic fields. Specifically, SPHP coupling between the membrane parallel edges

and between the perpendicular edges through corners generate resonant electromagnetic corner and edge modes dominating NFRHT.

The large enhancement of NFRHT mediated by resonant electromagnetic corner and edge modes could be exploited in a variety of applications, such as localized radiative cooling, thermal management technologies, and energy conversion devices. Multidimensional confinement of SPhPs in arrays of subwavelength structures could enable further modulation and enhancement of NFRHT.

2:00 PM SF05.17.02

Modulating Near-Field Radiative Heat Transfer in Multi-Body Systems [SinaKhayam](#) and MohammadGhashami; University of Nebraska-Lincoln, United States

Active control of near-field radiative heat transfer (NFRHT) between multi-body systems has attracted great attention. Investigation of innovative methods for controlling radiative heat flow, analogous to electric current manipulation, has attracted significant attention. This interest arises due to the growing importance of such techniques in nanodevices designed for thermal management and heat-to-electricity conversion. The ability to control the magnitude and direction of heat flow at the micro/nanoscale has enabled various devices such as thermal diodes, transistors, switches, logic gates/circuits, and memories. Several methods have been proposed and explored in the literature to optimize our leverage over thermal radiative transfer, including employing metal-insulator transition materials, applying a magnetic field to magneto-optical materials, and tuning the chemical potential of graphene. Despite the remarkable progress, the above methods are usually limited in their operating temperature or the achievable heat flow contrast. To overcome these constraints, researchers have started to pursue a temperature-independent and noncontact approach to modulate NFRHT with minimum structural change dynamically. In this regard, recent theoretical works on nanoscale radiative heat transfer involving multiple anisotropic bodies have suggested the potential of these materials to regulate radiative heat flows. Recent theoretical studies have demonstrated that anisotropic materials, whose properties depend on the orientation of their optical axis regarding thermal radiation, hold promise in regulating radiative heat flows. Adjusting their relative orientation makes it possible to easily enhance or suppress the overall heat flux. While controlling NFRHT between isotropic materials can be only achieved by fabricating nanostructured metamaterials like gratings or nanoholes, multi-body systems consisting of anisotropic materials will be a promising alternative for controlling NFRHT without changing the structural properties of the system.

This work presents a comprehensive theoretical study of near-field heat transfer in a three-body planar system with a uniaxial intermediate layer and examines the regulation effects of the relative orientation of the middle layer on the total radiative heat flux. In the proposed system, both source and the observer layers are made of polar material, which supports surface phonon polariton (SPhPs), while the middle layer is a uniaxial thin layer capable of supporting surface modes. By employing the lauder formalism for NFRHT on a system consisting of three distinct planar plates, we show how the anisotropic properties of the intermediate layer can substantially mediate the overall radiative heat transfer within the system. This modulation approach is achieved by varying the orientation of the optical axis of the middle layer. Moreover, the effect of different materials, gap distances, and the thickness of the intermediate layer on the heat transfer regulation is investigated. Using this configuration, the equilibrium temperature of the intermediate layer can also be regulated by twisting and adjusting the relative angle of the intermediate layer. The proposed method enables the control of nanoscale radiative heat flux, offering great potential for thermal management applications via contactless heat flux control.

SESSION SF05.18: Radiative Heat Flow Control in Near and Far Field

Session Chairs: Georgia Papadakis and Bo Zhao

Thursday Afternoon, November 30, 2023

Sheraton, Third Floor, Hampton

2:15 PM SF05.18.01

Near-Field Radiative Heat Transfer in Vortex Matter: Role of Abrikosov Fluxons [RaulEsquivel-Sirvent](#), [ShunashiCastillo-Lopez](#), [GiuseppePirruccio](#) and [CarlosVillarreal](#); Universidad Nacional Autonoma de Mexico, Mexico

One of the signatures of superconductivity is the formation of the Abrikosov vortex lattice in type-II superconductors in the presence of an external magnetic field. Here, we study the near-field radiative heat transfer between a spherical nanoparticle and a nearby planar substrate, both made of optimally doped ceramic superconductors. We show that the radiative heat flux displays a periodic spatial pattern congruent with the material optical response modulated by the Abrikosov lattice. The heat flux can be enhanced or tuned by varying the magnitude of the external magnetic field. This modulation is explained by analyzing the behavior of the Abrikosov vortices that behave as efficient heat transfer channels since, at their core, the material is not superconducting, although it is below the critical temperature.

2:30 PM SF05.18.02

Infrared Thermochromic Antenna Composite for Self-Adaptive Thermal Radiation Management [IoannisPapakonstantinou](#)¹, [Francisco V.Ramirez-Cuevas](#)^{1,2}, [Kargal L.Gurunatha](#)^{1,3}, [LingxiLi](#)¹, [UsamaZulfiqar](#)¹, [SanjayanSathasivam](#)¹, [ManishTiwari](#)¹ and [IvanParkin](#)¹; ¹University College London, United Kingdom; ²Universidad Adolfo Ibáñez, Chile; ³JAIN University, India

Passive thermoregulation, the natural mechanism of living organisms to self-regulate their body temperature, holds excellent promise for decarbonizing cooling and heating systems. An effective route to artificially emulate this functionality is by engineering thermochromic materials that modulate radiative heat losses in response to the temperature of their surroundings. Yet, a technology that marries large thermal emissivity modulation with scalability, cost-effectiveness and design freedom is lacking in the field. Here, we fill this gap by introducing a new class of infrared thermochromic antennas exhibiting a dramatic enhancement (>180 times) in their absorption cross-section as their temperature rises. By embedding the antennas in a polymer matrix or by simply spraying them directly, free-form self-adaptive heat radiating composites are created with large emissivity switching (~0.6) that can be applied on virtually any surface. Overall, our research paves the way for thermoregulating coating, fiber, membrane, film, and other technologies that could find application in self-adaptive radiative cooling, heat sensing, thermal camouflage, and other.

2:45 PM SF05.18.03

Demonstration of Near-Field Radiative Heat Transfer via Hyperbolic Plasmon Polaritons in a Layered CdO Metamaterial [WilliamD. Hutchins](#)¹, [SamanZare](#)¹, [AngelaCleri](#)², [MingzeHe](#)³, [JoshuaD. Caldwell](#)³, [Jon-PaulMaria](#)² and [PatrickE. Hopkins](#)¹; ¹University of Virginia, United States; ²The Pennsylvania State University, United States; ³Vanderbilt University, United States

As electronic devices continue to reduce towards nanoscale dimensions, understanding heat transport mechanisms at these scales becomes vital. In recent years, advances in nanotechnology and radiative engineering have introduced thermal radiation as a promising mechanism to tailor the magnitude and direction of heat transfer. Utilization of metamaterials extends our ability to manipulate radiative heat flow in nanoscale systems, especially with regard to near-field radiation which can exceed the blackbody limit by several orders of magnitude. The near-field heat transport in metamaterials is dictated by their geometry and optical properties of the constituents. One way to tune this flow is by the construction of a superlattice metamaterial by layering highly doped cadmium oxide (CdO) with varying carrier densities. Highly doped CdO allows for high electron mobilities while maintaining dielectric properties mechanically. Carefully constructed superlattice structures can support hyperbolic plasmon polaritons (HPPs) which may carry heat across interfaces at a significantly higher rate than conduction.

From an experimental perspective, previous investigations on the characteristics of HPPs were performed using measurements at equilibrium conditions, neglecting the information embedded in non-equilibrium. In this work, we use a unique ultrafast pump-probe technique that can detect specific heat-carrier modes with sub-picosecond time resolution. Our technique relies on a wavelength-tunable mid-infrared probe pulse, allowing us to directly resonate with plasmonic heat carriers, providing a direct measure of polariton dynamics (velocity, thermal lifetime, etc.) in nanoscale material systems. In particular, we investigate HPPs in a layered CdO metamaterial; the high-frequency plasmon modes in this material lend themselves to the potential for manipulation of thermal radiation in near room temperature conditions. Thus, we investigate the ultrafast thermal dynamics of HPP modes coupling to near-field thermal radiation via far-field sensing. We experimentally demonstrate, for the first time, the ability to thermally stimulate HPPs in a CdO metamaterial through remote heating of a metal contact. Our results open the door for future experiments to manipulate and guide heat carriers via heterostructures, which could increase thermal efficiency of microelectronics and photonics.

3:00 PM *SF05.18.04

Nanophotonic Control Over The Non-Equilibrium Temperature and Emitted Polarization State [SanderMann](#); The City University of New York, United States

Thermal generation of light is a long-known technique capable even of producing designer quasi-monochromatic beams, but with a suitably chosen cascaded set of optical elements. For example, in order to produce a wave with spin angular momentum (SAM) or orbital angular momentum (OAM), a blackbody such as an incandescent light source emits uncollimated, broadband, incoherent and unpolarized light, which is then spatially filtered by a pinhole, collimated by a lens, spectrally narrowed by a filter, polarized by a polarizer, retarded by a waveplate, and then shaped spatially by a phase plate optic. Over the past two decades, leaps have been made in condensing these optical elements into single emitters: for example, it has been

demonstrated that linear or circularly polarized emission can be emitted directly from a suitably structured metasurface, but usually with significant emission of the conjugate emission state in the opposing direction, and with limited freedom over the polarization state. Here, I will present a new approach to generate arbitrary polarization states into any single direction of emission, based on nonlocal metasurfaces, completing a long standing search to condense the entire array of optical elements for manipulation of thermal emission into a single emitting metasurface. I will then discuss the generalization of Kirchhoff's law for arbitrary polarization states, demonstrating experimentally and theoretically how absorbed and emitted polarization states are related. Finally, I will discuss recent work on controlling the peak temperatures in nanophotonic structures in non-equilibrium situations (under either pulsed or strong incoherent illumination) through manipulation of the local density of optical states. Control over the temperature of e.g. catalytic sites in non-equilibrium environments can strongly benefit reaction rates, providing an additional nanophotonic lever to achieve more efficient operation of catalytic reactors and other thermal processes.

SESSION SF05.19: Virtual Session
Session Chairs: Pierre-Olivier Chapuis and Georgia Papadakis
Wednesday Morning, December 6, 2023
SF05-virtual

8:00 AM *SF05.19.01

Mid-Infrared Filterless Metasurface Photodetectors [Cheng-Wei Qiu](#); National University of Singapore, Singapore

Mid-infrared detectors are of critical importance for a variety of applications including thermal imaging, spectrometer, sensing and free space communication. High sensitivity, zero power consumption, fast response, simple CMOS-compatible fabrication processes, small footprint, wavelength and polarization selectivity are highly desired, while still being elusive so far especially at room temperature. In this talk, we will report a series of metasurface-mediated semimetal IR detectors based on hot carriers mechanism. Non-centrosymmetric metallic nanoantennas are deployed to break the symmetry of local electromagnetic field and induce directional flow of hot carriers in graphene, leading to large unbalanced mid-IR photoresponse at room temperature without external bias. We demonstrate zero-bias uncooled mid-infrared photodetectors with three orders higher responsivity than conventional bulk photovoltaic effect (BPVE) and a noise equivalent power of $0.12 \text{ nW Hz}^{-1/2}$. We further establish a scheme to realize configurable polarity transition by exploiting the vectorial and non-local photoresponse in hybrid metasurface of nanoantennas and graphene. By tuning the orientation of nanoantennas, polarization ratio (PR) values vary from positive (unipolar regime) to negative (bipolar regime), covering all possible numbers ($1 \rightarrow \infty/-\infty \rightarrow -1$). Polarization-angle perturbation down to $0.03^\circ \text{ Hz}^{-1/2}$ in the mid-infrared range is demonstrated. We will also report on-chip filterless photodetectors in mid-infrared which solely responds to circular polarizations. Our works highlight the potential of hybridizing metasurface and semimetals for miniaturized polarimetry.

8:30 AM *SF05.19.02

Manipulating the Flow of Light & Heat at Nanoscale [Jia Zhu](#); Nanjing University, China

The first example is about passive cooling. Radiative cooling which sends heat to space through atmospheric transparency window without any energy consumption, is attracting significant attention. For radiative cooling to achieve high cooling performance, it is ideal to have a selective emitter, with an emissivity dominant in the atmospheric transparency window. However, so far scalable production of radiative cooling materials with selective emissivity has not been realized. Here I will present a hierarchical design for a selective thermal emitter to achieve high performing all-day radiative cooling. Moreover, it is revealed that this hierarchically designed selective thermal emitter shows significant advantage if being applied to alleviate Global Warming or to regulate temperature of the Earth-like planet.

The second example is about interfacial solar evaporation. We report that efficient and broad-band plasmonic absorber can be fabricated through a three dimensional self-assembly process. Because of its efficient light absorption and strong field enhancement, it can enable very efficient (>90%) solar vapor generations. Inspired by the transpiration process in plants, we report an artificial transpiration device with a unique design of two dimensional water path. The energy transfer efficiency of this artificial transpiration device is independent of water quantity and can be achieved without extra optical or thermal supporting systems, therefore significantly improve the scalability and feasibility of this technology. At the end, we would like to demonstrate that this type of interfacial solar vapor generations can have direct implications in various fields such as solar desalination, zero liquid discharge, sterilization and power generations.

9:00 AM *SF05.19.03

Radiative Heat Transfer and Thermalization in Ensembles of Nanostructures [Alejandro Manjavacas](#); Instituto de Optica - CSIC, Spain

Planck's law accurately describes the exchange of thermal radiation between macroscopic bodies separated by macroscopic distances. However, when the size of the objects or the distances between them become comparable to the thermal wavelength, this approach breaks down. In such subwavelength scenarios, radiative heat transfer between hot objects can exceed the limits set by far-field blackbody radiation due to the contribution of the near-field components of the electromagnetic field and the excitation of electromagnetic resonances of the material structures [1].

In this talk, we will review some recent advances in the theoretical description of radiative heat transfer between nanoscale objects. We will begin by introducing a theoretical framework to efficiently describe the thermalization dynamics of ensembles of nanostructures mediated by radiative heat transfer [2]. With the help of this formalism, which relies on an eigenmode expansion of the equations that govern the process, we will discuss the fundamental principles that determine the thermalization of collections of nanostructures with thousands of elements, revealing general but often unintuitive dynamics. We will also consider the radiative heat transfer between two nanostructures in rotation, which is influenced by the simultaneous transfer of angular momentum due to the Casimir torque. Specifically, we will show that, depending on the rotation of the nanostructures, the radiative heat transfer between them can be increased, decreased, or even reversed with respect to the transfer that occurs in absence of rotation, which is solely determined by the difference in the temperature of the nanostructures [3].

[1] L. Zundel and A. Manjavacas. Phys. Rev. Applied 13, 054054 (2020).

[2] S. Sanders, L. Zundel, W. J. M. Kort-Kamp, D. A. R. Dalvit and A. Manjavacas. Phys. Rev. Lett. 126, 193601 (2021).

[3] J. R. Deop-Ruano and A. Manjavacas, Phys. Rev. Lett. 130, 133605 (2023).

SYMPOSIUM SF06

From Robotic Towards Autonomous Materials
November 27 - December 6, 2023

Symposium Organizers

Yoav Matia, Ben-Gurion University
Robert Shepherd, Cornell University
Ryan Truby, Northwestern University
Huichan Zhao, Tsinghua University

* Invited Paper
+ JMR Distinguished Invited Speaker

SESSION SF06.01: Embodied Autonomy
Session Chairs: Amir Gat and Yoav Matia
Monday Morning, November 27, 2023
Sheraton, Second Floor, Back Bay D

10:30 AM *SF06.01.01

Physical AI for Soft Aerial Robotics [Mirko Kovac](#)^{1,2}; ¹Swiss Federal Laboratories for Materials Science and Technology (Empa), Switzerland; ²Imperial College London, United Kingdom

Aerial robotics has become a key enabler of industrial automation and environmental interaction tasks with applications ranging from environmental sensing in forests, over water sampling in lakes to industrial manufacturing and repair. Most aerial robots however are rigid in structure and rely on accurate state estimation and controlled sensor-actuator loops to perform the tasks and navigate through the environment. Natural flyers on the other hand rely not just on flight control but also on smart and adaptive materials to expand their operational flight envelope and to increase the functionality of their wings allowing them to display an impressive range of skills. Recently, the robotics community has started to employ adaptive morphologies, smart materials and soft robotics methods in aerial robotics with the promise of achieving higher levels of system resilience and adaptation to complex or changing environments. In this talk I will present how animal-inspired soft robot design methods can greatly enhance aerial robotics capabilities and how adaptive morphologies and functional materials can be co-evolved in tandem with aerial robotic embodiments. The talk will also include application examples of such soft aerial robots placing sensors in forests, collecting water samples autonomously or landing on wind turbines to perform construction and repair tasks.

11:00 AM SF06.01.02

Room-Temperature Electrochemical Healing of Fractured Metals [Zakaria Hsain](#), Mostafa Akbari, Adhokshid Prasanna, Zhimin Jiang, Masoud Akbarzadeh and James H. Pikul; University of Pennsylvania, United States

Repairing fractured metals to extend their useful lifetimes advances sustainability and mitigates carbon emissions from metal mining and processing. While high-temperature techniques are being used to repair metals, the increasing ubiquity of digital manufacturing and “unweldable” alloys, as well as the integration of metals with polymers and electronics, call for radically different repair approaches.

This work presents a framework for effective room-temperature repair of fractured metals using an area-selective nickel electrodeposition process referred to as electrochemical healing. Based on a model that links geometric, mechanical, and electrochemical parameters to the recovery of tensile strength, this framework enables 100% recovery of tensile strength in nickel, low-carbon steel, two “unweldable” aluminum alloys, and a 3D-printed difficult-to-weld shellular structure using a single widely used nickel sulfamate electrolyte. Through a distinct energy-dissipation mechanism, this framework also enables up to 136% recovery of toughness in an aluminum alloy. Remarkably, this framework demonstrates that the restoration of tensile strength can be insensitive to nickel-metal adhesion, thus obviating the need for acid pre-treatments or multi-electrolyte processes.

To facilitate practical adoption, this work reveals scaling laws for the energetic, financial, and time costs of repairing fractured metal parts from the microscale to the meter scale. This framework could potentially enable a universal and scalable approach to repair fractured metals at various length scales and in diverse applications. Electrochemical healing could open exciting possibilities such as electrically controlled autonomous and preemptive repair, as well as enable 3D-printed metal structures optimized for repair through designed failure characteristics.

11:15 AM SF06.01.03

Dynamic, Remote-Controllable Electroactive Hydrogel Waveguide Architectures [Oscar Alejandro Herrera Cortes](#); McMaster University, Canada

Remote-controllable waveguide architectures inspired by living organisms with unique flexible, camouflage and light-guiding properties, were printed using self-trapped beams of incoherent light. Made of electroactive hydrogels, light-guiding structures are generated within seconds through a nonlinear, self-inscription process that utilizes visible beams from light-emitting diodes (LEDs). Due to irreversible refractive index changes experienced by photoinduced chemical reactions, these self-trapped beams permanently inscribe cylindrical waveguides along their paths. Taking advantage of this phenomena, we can fabricate macro-scale remote controllable waveguide structures in the form of planar rectangular prisms and arrays of cylindrical waveguides. We can also fabricate micro-scale structures, for remote actuation, in the form of rectangular prisms embedded with thousands waveguide units. By applying and varying external electric fields, we can then dynamically control the bending, angular orientation, and rotation (up to 360°) of these pliant light-guiding structures. This allows precise, remote control of the waveguided light output.

11:30 AM *SF06.01.04

Energy Storage and Harvesting in Multistable Metafluid [Ofek Perez](#), [Ezra Ben-Abu](#), [Anna Zigelman](#), [Sefi Givli](#) and [Amir Gat](#); Technion–Israel Institute of Technology, Israel

The thermodynamic properties of fluids play a crucial role in many engineering applications, particularly in the context of energy. Fluids with multistable thermodynamic properties may offer new paths for harvesting and storing energy via transitions between equilibria states. Such artificial multistable fluids can be created using the approach employed in metamaterials, which controls macro-properties through micro-structure composition. In this work, the dynamics of such ‘metafluids’ is examined for a configuration of calorically-perfect compressible gas contained within multistable elastic capsules flowing in a fluid-filled tube. We study both analytically and experimentally the velocity-, pressure-, and temperature-fields of multistable

compressible metafluids, focusing on transitions between different equilibria. We first examine the dynamics of a single capsule, which may move or change equilibrium state, due to fluidic forces. We then study the interaction and motion of multiple capsules within a fluid-filled tube. We show that such a system can be used to harvest energy from external temperature variations in either time or space. Thus, fluidic multistability allows specific quanta of energy to be captured and stored indefinitely as well as transported as a fluid, via tubes, at standard atmospheric conditions without the need for thermal isolation.

SESSION SF06.02: Embodied Perception
Session Chairs: Yoav Matia and Ryan Truby
Monday Afternoon, November 27, 2023
Sheraton, Second Floor, Back Bay D

1:30 PM SF06.02.01

Autonomous Alignment and Healing in Multilayer Soft Electronics using Immiscible Dynamic Polymers [Samuel E. Root](#), Christopher B. Cooper and Zhenan Bao; Stanford University, United States

Self-healing soft electronic and robotic devices, like human skin, can recover autonomously from some forms of damage. Existing multi-layer devices generally employ a single type of dynamic polymer embedded with different functional nano–micro materials for each layer, to provide a cohesive interface between layers. In such devices, successful healing from damage requires precise manual alignment and re-contacting of the fractured interfaces, limiting functional recovery from diverse forms of damage, such as processes leading to imperfect registry of device layers. These limitations are especially prevalent for devices containing thin layers (< 100 μm). To overcome these limitations, we have designed a pair of dynamic polymers, which have immiscible polymer backbones, but identical dynamic bonding units (bisurea-based hydrogen bonding interactions), to maintain interlayer adhesion while providing selectively self-healing layers with similar rheology (and thus self-healing dynamics) over a convenient range of temperatures (25–100°C). Upon lamination, these dynamic polymers exhibit a weakly interpenetrating and adhesive interface, whose width and toughness are tunable with processing temperature. When multilayered polymer films are misaligned after damage, these structures autonomously realign during the healing process to minimize their interfacial free energy through a directional diffusion-mediated mechanism. Our experimental observations are captured by both coarse-grained molecular dynamics simulations and continuum phase field simulations, suggesting the generality of the proposed mechanism to other pairs of polymer backbones or dynamic bonding chemistries. As a demonstration of the utility of our approach, we fabricated several devices with conductive, dielectric, and magnetic particles that functionally heal after damage, enabling thin film pressure sensors, magnetically assembled soft robots, and underwater circuit assembly.

1:45 PM DISCUSSION TIME

2:00 PM *SF06.02.03

Soft Logic, Actuators and Stretchable Barriers using Liquid Metal [Michael Dickey](#); North Carolina State University, United States

This talk will discuss ways to harness the unique properties of liquid metals for soft and stretchable components that are promising for soft robotics. Alloys of gallium are liquid below room temperature and are therefore extremely soft and flow in response to stress to retain electrical continuity under extreme deformation. While these properties have been used to create sensors and interconnects, there are other unique properties that can be utilized. For example, liquid metal is a fantastic barrier to gas and liquid transport. This property can be used to create hermetic seals that are near-perfect barriers, yet completely stretchable. This breaks a long-standing trade-off between stretchability and permeability of materials, thus enabling encasing materials for stretchable batteries. Liquid metals can also be used for energy harvesting by several modes. For example, by encasing liquid metal in hydrogel, it is possible to create electrical double layers (i.e. capacitor) at the interface between the metal and the gel. Deforming the gel increases the area of the capacitor, which can convert mechanical to electrical energy. Liquid metals can also be utilized for performing simple tactile logic, in which the response of an elastomeric material will change depending on the way it is touched. Finally, it is possible to use liquid metal to actuate soft robots using either surface tension to exert forces on surfaces or electrochemical formation of gas to expand pneumatic chambers. Combined, these advances have exciting implications for soft robotic materials.

2:30 PM BREAK

3:00 PM *SF06.02.04

Biomimetic Approaches with Stretchable Ionics [Jeong-Yun Sun](#); Seoul National University, Korea (the Republic of)

As many devices for human utility target fast and convenient communications with users, superb electronic devices have been demonstrated as hardware for Human-Machine Interface (HMI) in wearable forms. Wearable devices for daily health-cares and self-diagnosis desire more human-like properties unconstrained to deformation. In this sense, stretchable ionics based on flexible and stretchable hydrogels is on the rise as another field to develop wearable devices for bio-applications due to two major reasons; i) ionic currents, choosing the same signal carriers with biological areas, and ii) the adoption of hydrogel ionic conductors which are intrinsically stretchable materials with bio-compatibility. Here, the current status of stretchable ionics as well as future applications whose positive effects can be magnified by stretchable ionics are going to be introduced.

3:30 PM SF06.02.05

Design and Fabrication of Electronic Skin with Sensing Capability of Tactile Stimuli for Robotics [Jun Chang Yang](#)¹, [Steve Park](#)² and [Lucia Beccai](#)¹; ¹Istituto Italiano di Tecnologia, Italy; ²Korea Advanced Institute of Science and Technology, Korea (the Republic of)

The need for new forms of electronics is emerging in various fields such as healthcare, robotics, and human-machine interfaces. Stretchable electronic skin, compared to traditional rigid electronics, offers improved user convenience through various shapes and functions. Recently, electronic skin, inspired by human skin, has been developed to change shape easily and collect different physical sensations. However, there have been challenges in terms of durability and accurate tactile detection in polymer-based tactile sensors for robotics. This study aims to address these challenges by developing microstructured tactile sensors and robust soft-rigid interfaces with interlocking structures. Firstly, ultra-high sensitive capacitive pressure sensors based on a porous pyramid dielectric layer are presented, enabling accurate pressure detection unaffected by lateral strain and temperature. Secondly, bending sensors that utilize controlled microcracks in inverse pyramid structures, achieve a gauge factor of 74 with high linearity. Moreover, the sensors can be used in soft actuators capable of operating in liquid. Finally, Ferris Wheel-shaped islands architecture with interlocking structures are designed to suppress crack propagation at interfaces during mechanical deformation. Consequently, rigid components can be integrated into a soft polymer matrix, resulting in a highly durable electronic skin suitable for robotics applications.

3:45 PM SF06.02.06

Dynamic Haptic Exploration using Artificial Multi-Modal Mechanoreceptors for Active Robot Perception [Jiangtao Su](#) and [Xiaodong Chen](#); Nanyang Technological University, Singapore

Benefitted from the various mechanoreceptors embedded in the skin and haptic exploration strategy of hands, human beings can recognize the hardness and texture of different objects with fine resolution. By contrast, existing tactile sensors for robotic application can only identify limited information when interacting with surroundings, lacking the multimodality like the various mechanoreceptors and proper sensing strategies to maximize desired tactile information. Here, we present a multimodal tactile sensor that can simultaneously detect normal and shear force with ultra high sensitivity and resolution. Moreover, the performance of the tactile sensor can be tuned by its geometrical parameters. Such tactile sensors can identify the hardness and texture of objects simultaneously, which is less reported for similar sensors. By integrating the tactile sensor on a robotic gripper, the robot can dynamically perform haptic exploration with different detecting modes. It turns out that the robot can achieve an object recognition accuracy of 93%. This research could provide a promising strategy for the sensing of robotic for a variety of applications, especially for object recognition and manipulation, human-machine interaction, and outer space exploration.

4:00 PM SF06.02.07

Multi-Detection Brush-Type E-Whisker [Haruki Nakamura](#)^{1,2}, [Satoko Honda](#)¹, [Guren Matsumura](#)¹ and [Kuniharu Takei](#)²; ¹Osaka Metropolitan University, Japan; ²Hokkaido University, Japan

With the development of the Internet of Things (IoT) society, demand for a variety of sensors is increasing to collect many datasets for data analyses. Among them, whisker or brush-type sensors are interested in the application of industry and robotics. Brush-type sensors can be used to detect the surface morphology and target shape by contacting the object like rat whiskers, which should be useful for the robotic applications. However, the sensor that can measure such whisker/brush movement has yet to be fully developed. Although some electronic whisker (e-whisker) concepts have been reported previously, a lot of challenges to detect the movement of whiskers/brushes still remain such as multi-detections including movement amplitude, speed,

and directions etc and data analyses methods. To overcome these challenges, this study proposed out-of-plane e-whisker combined with 4 resistive tactile pressure sensors. Brush-type multiple whiskers were designed to collect multiple dataset precisely from the target. Due to movement of e-whisker, tactile pressure sensors show different outputs that can allow to distinguish bending amount, move direction, and move speed simultaneously. Furthermore, to feedback the robot quickly in real-time based on the sensing results, reservoir computing, which is one of the recurrent neural networks, is used to make real-time data analyses.

Fabrication process of brush sensor is briefly explained. First, laser-induced graphene (LIG) was formed by exposing CO₂-based laser over polyimide film. Due to thermal effect of polyimide caused by laser exposure, polyimide was reformed to be multi-layer graphene. The LIG was then transferred to polydimethylsiloxane (PDMS). Brush-like e-whisker structure, which is made of nylon, is attached on PDMS surface using a PDMS solution as a glue. Carbon black (CB) electrodes and silver ink as output electrodes were printed on polyethylene terephthalate (PET) film. The fabricated PDMS and PET films were then bonded using 3-aminopropyltriethoxysilane and oxygen plasma. The sensing mechanism of this e-whisker sensor is to measure contact resistance change between the LIG embedded in the PDMS and the CB electrodes on the PET films.

First, fundamental characteristics of the sensor were conducted. The whiskers on the tactile pressure sensor were moved from left to right with applied force from top, repeatedly. During the movement, resistance changes of 4 sensors were measured. The tactile pressure sensors can measure a relatively wide range of pressure from 20 Pa to 5.5 kPa. The sensitivity is ~0.33 %/Pa from 0 to 190 Pa and ~0.002 %/Pa from 190 Pa to 5.5 kPa. Due to wide dynamic range and high sensitivity especially at low pressure range, it was confirmed that e-whisker could detect the movement/bending of whisker structure. In addition to the movement detection, integrated 4 tactile pressure sensors clearly show the output difference by changing the movement velocity (0~100 mm/s), bending distance (1mm ~ 5 mm) and directions (8 directions), suggesting that this platform can measure detail bending information like animal whisker.

For the data analyses and output feedback system, real-time and quick data processing is required. As a detection system, we adapted reservoir computing, which enables highly accurate real-time detection in a small amount of computation time. By optimizing the algorithm of reservoir computing, bending distance (-5mm~5mm from the initial position) and movement velocity (0~100mm/s) were successfully predicted with the root mean square error <0.8 for bending distance and <10 for velocity.

In summary, this study demonstrated the brush-like e-whisker system using integrated tactile pressure sensor and reservoir computing. By optimizing the sensor design and data processing algorithm, the e-whisker can detect a variety of datasets, which can be potentially used for the robotic applications.

4:15 PM *SF06.02.08

Mechanical Metamaterials' Journey to Cognitive Abilities Amir Alavi; University of Pittsburgh, United States

There is a relentless pursuit to explore novel forms of intelligent matter with advanced functionalities for various robotics applications. Here, I will introduce the scientific field of “mechanical metamaterial electronics (meta-mechanotronics)” as a platform for designing intelligent matter capable of achieving a level of cognition. Electronic mechanical metamaterials created under this paradigm enable a sense–decide–respond loop through sensing external stimuli, self-powering and processing the information. Relying merely on their constituent components for sensing and information processing, electronic mechanical metamaterials can establish a direct interaction mechanism between the external environment and electronics. Incorporating all of these capabilities into the fabric of materials could in theory lay the foundation for autonomous materials and structures with a level of artificial cognition. I will discuss mechanisms, fabrication processes and computational frameworks required to create electronic mechanical metamaterials. I will explain how insights into the mechanics, design, and implementation of the scale-independent meta-mechanotronic systems can be shared among disciplines ranging from micro/nano-electromechanical systems to large-scale civil structures.

4:45 PM *SF06.02.09

Embodied Fluidic Circuits for The Control of Soft Robots Michael Tolley; University of California, San Diego, United States

Robotics has the potential to address many of today’s pressing problems in fields ranging from healthcare to manufacturing to disaster relief. However, the traditional approaches used on the factory floor do not perform well in unstructured environments. The key to solving many of these challenges is to explore new, non-traditional designs. Fortunately, nature surrounds us with examples of novel ways to navigate and interact with the real world. Dr. Tolley’s Bioinspired Robotics and Design Lab seeks to borrow the key principles of operation from biological systems and apply them to robotic design. This talk will give an overview of recent projects in the lab that investigate the ways in which the use of non-rigid materials can help solve challenging problems in robotics. These projects seek to develop bioinspired systems capable of navigating the world by walking, digging, and swimming (inspired by animals like turtles, worms, and squid) and of interacting safely with humans and delicate objects.

SESSION SF06.03: Shape Morphing Materials
Session Chairs: Yoav Matia and Robert Shepherd
Tuesday Morning, November 28, 2023
Sheraton, Second Floor, Back Bay D

8:30 AM *SF06.03.01

Fluidic Shaping of Optical Components – From Eyeglasses to Space Telescopes Mor Elgarisi, Omer Luria, Amos Hari, Valeri Frumkin and Moran Bercovici; Technion - Israel Institute of Technology, Israel

The current method for fabricating eyewear lenses relies on the machining and polishing of semi-finished blanks. This fabrication process has not changed significantly in the past 300 years, relies on heavy mechanical infrastructure, and produces tremendous amounts of non-recyclable polymer waste.

We present a simple method, based on free-energy minimization of liquid volumes, which allows to quickly shape liquids into a wide range of ophthalmic lenses, without the need for any mechanical processing. At present, the method allows to produce any single vision prescription, including spherical and astigmatic corrections.

In the first part of the talk we will present the implementation of the method on earth - the fabrication is performed by injecting a liquid polymer into a bounding frame submerged within an immiscible immersion liquid with equal (or nearly equal) density. Under these conditions, surface tension dominates, and the curable liquid takes the shape of a symmetric lens (bi-convex or bi-concave). A meniscus lens shape can then be obtained simply by enclosing the bottom part of the lens in an impermeable chamber and adding immersion liquid to it in order to ‘inflate’ the polymer. After the desired shape is achieved, the liquid can be cured to produce a solid object. Due to the natural smoothness of the liquid, the lens has sub-nanometric surface roughness without the need for any polishing processes.

We developed a complete theoretical framework for the minimum energy state of the interface of the liquids, which describes the lens’ diopter and cylinder power as a function of the bounding frame shape, the injected volumes, and the density differences between the liquids. We will show the utilization of the theory toward the fabrication of the first eyeglasses based on fluidic shaping, and provide measurements of their shape and surface roughness. Lastly, we will show that our method is also suitable for the fabrication of complex optical components (i.e., freeform) simply by controlling the frame shape.

In the second part of the talk we will present our Fluidic Shaping experiments on board the international space station (ISS), in collaboration with NASA. In the first part of the experiment, conducted within the life sciences glovebox (LSG), the astronaut injected photocurable polymers into 30 mm (diameter) cylindrical frames contained with a custom polymerization box. Under weightlessness, surface tension dominates and drives the liquid into a minimum energy state in which the free surfaces assume a constant-mean-curvature shape. In the case of a cylindrical bounding frame, the result is a bi-convex lens with spherical surfaces. Once the liquid stabilized, the polymerization box’s lid was closed, and the lenses were solidified. In the second part, conducted outside of the glovebox, the astronaut injected water onto a 172 mm frame and created a plano-convex water lens. By injecting and aspirating water from the lens, we demonstrated the ability to dynamically control the lens’ power. We provide videos of the experiments, present the hardware we constructed, and discuss the design details, tradeoffs, and associated challenges in implementing this experiment in space.

We view this set of experiments as a first milestone in expanding in-space manufacturing capabilities to also include optical components. Due to its simplicity, low power consumption and essentially zero waste, Fluidic Shaping can serve as a fabrication infrastructure for future long-duration space missions that must be self-sufficient. In addition, due to its scale invariance, the method could potentially be used for the creation of large space telescopes, thus overcoming launch constraints.

9:00 AM SF06.03.02

3D Shape-Reconfigurable and Locomotive Electronics Based on Physical Intelligence Encoded Liquid Crystalline Polymer Composites Woongbi Cho^{1,1}, Jisoo Jeon², Min Jeong Hahm^{1,1}, Tae Hee Han^{1,1} and Jeong Jae Wie^{1,1}; ¹Hanyang University, Korea (the Republic of); ²Georgia Institute of Technology, United States

Beyond the passive deformation of flexible electronics by human hand or tethered mechanical strain, the autonomous shape-reconfigurable and locomotive electronics have a great potential for miniaturized electronics, which can transform their initial flat shape to a programmed 3D geometry, and/or transfer their body to desirable locations via asymmetric repetitive programmed actuation. The physical intelligence-encoded liquid crystalline polymers (LCPs) are great candidates for a main body of shape-reconfigurable electronics, due to their programmable molecular alignments resulting in macroscopic shape changes upon external stimuli. In this presentation, we introduce LCP composites to achieve shape-reconfigurable and locomotive electronics. To achieve electrical conductivity, we employed conducting fillers including reduced graphene oxide (RGO) and $\text{Ti}_3\text{C}_2\text{T}_x$ MXene as bilayered structures with LCPs. The bilayered structure enables the LCP composites to perform enhanced shape-reconfigurability and show the original electrical conductivity of the conducting fillers without deterioration. Furthermore, the RGO and MXene can provide high infrared light absorption to LCP composites, which can induce remotely controlled shape reconfiguration via the photothermal effect. We demonstrated in-plane bending and 3D torsional twisting of LCP composite bilayers under external stimuli including UV, NIR, and electrical power according to the chemical composition of LCP and types of conducting fillers. Finally, we introduced the Kirigami-engineered structure and collectively assembled structures to achieve diversified 3D morphed shapes and locomotion of shape-reconfigurable electronics.

9:15 AM SF06.03.03

Twisting Liquid Crystal Elastomer Fibers to Realize Fast and Slow-Twitch Thermomechanical Response Melvin A. Colorado Escobar and Timothy White; University of Colorado, Boulder, United States

Liquid crystal elastomers (LCEs) have been studied extensively and considered for functional use in applications such as soft robotics, smart textiles, and medical devices. LCEs undergo an ordered to disordered transition causing them to contract. The associated deformation in LCE fibers is analogous to muscles. This research is concerned with characterizing the orientation of LCE fibers in a twisted geometry and assessment of the thermomechanical response. We will show that the thermomechanical response of twisted LCE fibers spans a distinct geometric phase space. The fibers start in a rectilinear geometry and then spontaneously coil when heated. The inherent stimuli response of LCEs changes the twist density of the LCE fibers. The stimuli-response is dependent on the morphological constraints of the fibers (e.g., the twist density). A material with a fixed twist density can have different geometric actuation responses based on the load or force that is needed to be generated. Using the spontaneous coiling for actuation leads to fast actuation responses, increase in actuation stroke and ability to optimize work.

9:30 AMBREAK

SESSION SF06.04: Actuation I
Session Chairs: Yoav Matia and Ryan Truby
Tuesday Morning, November 28, 2023
Sheraton, Second Floor, Back Bay D

10:15 AM *SF06.04.01

Autonomously Repeating High-Speed Motions in Soft Materials Alfred J. Crosby; University of Massachusetts, United States

Soft materials, such as polymer gels, have long been realized as a potential platform for actuation in robotic systems; however, several challenges have limited their integration into translatable technologies. In particular, soft matter actuators are slow, unable to generate significant power, and typically require external intervention to initiate multiple, sequential actuation events. Recent results from our research group have demonstrated the ability to harness evaporation-induced stresses to initiate snap-through transitions, which can generate high velocity, high acceleration motions with swollen elastomers. Importantly, we discovered that certain combinations of materials properties and geometries allowed for the system to undergo multiple, consecutive snap-through transitions without external intervention. Here, we review these previous findings and introduce our latest research results focused on understanding the structure-property relationships that control the total energy flow of these self-repeating, high velocity events. The lessons learned are built upon the materials science principles that have been developed as part of a multi-university team, which takes inspiration from examples in nature including mantis shrimp and trap-jaw ants. These organisms use Latch-Mediated Spring Actuation (LaMSA) to achieve high power, impulsive movements by integrating actuators, elastic elements, and stability-mediating latches. The strategies and results discussed provide new insight into how polymer properties can combine with purposeful structural design to achieve complex, energy-efficient tasks, which can be used in the development of microscale robots.

10:45 AM SF06.04.02

Liquid-Crystal-Elastomer-Based Entangled Active Matter Systems Asaf Dana, Mustafa K. Abdelrahman and Taylor H. Ware; Texas A&M University, United States

Soft materials in which individual components convert ambient free energy into mechanical work are commonly referred to as active matter. Physically entangled active matter is an emerging area of both living and man-made systems, where mechano-functionality of the collective emerges through physical interaction of individual elements. Liquid crystal elastomers (LCEs) are a class of stimuli responsive polymers that undergo large, reversible, anisotropic shape change in response to a variety of stimuli, including heat and light, making them ideal candidates for many applications, especially in the field of biomedical devices. LCE films that exhibit three dimensional folded and twisted conformations in response to variations in temperature were added magnetic particles to facilitate dynamic motion under a varying magnetic field. The combination of the induced dynamic motion from the magnetic field along with the temperature induced folding facilitates entanglement of the individual elements into a macroscopic multifunctional solid exhibiting emergent properties that are tunable with the variation of the temperature and the magnetic field. The outcomes of this project are expected to open the way for new active matter systems composed of dynamic entangling elements, where rich and non-intuitive material physics can be uncovered and applied towards the development of a variety of unique autonomous devices.

11:00 AM SF06.04.04

Polymer Dispersed Liquid Crystalline Elastomers (PDLCEs): Moldable Soft-Soft Materials for Different Actuation Geometries and Applications Valentina Domenici¹, Matej Bobnar², Nikita Derets², Georgios Kordogiannis², Bostjan Zalar² and Andraz Resetic²; ¹University of Pisa, Italy; ²Jozef Stefan Institute, Slovenia

Soft-soft composites based on liquid crystalline elastomers (LCEs) were successfully prepared by optimizing a synthetic procedure. Liquid crystalline elastomers in the form of microparticles are dispersed in an amorphous matrix, namely a silicone polymer one. These materials are called Polymer Dispersed Liquid Crystalline Elastomers (PDLCEs). The preparation procedure includes several steps in the presence of an external magnetic field with the aim to orient the LCE microparticles along a desired direction [1]. A detailed study based on 2H NMR spectroscopy on PDLCEs prepared under a different magnetic field strength [2] revealed a quite homogeneous distribution of orientation of the microparticles at a magnetic field higher than 4 Tesla. Under these conditions, thermomechanical response of these composites with different actuation geometries is highly correlated to the orientational order distribution of the LCE microparticles. Recently, we demonstrated the shape-programmability of these soft-soft composites prepared with main-chain liquid crystalline elastomers (MC-LCEs) [3]. In particular, PDLCEs based on MC-LCEs enable efficient morphing among the virgin shapes and the thermally-programmed and thermomechanically-controlled shapes. Several examples of shape-memory preparations and applications will be discussed.

Acknowledgments:

This work was performed thanks to the ARRS applied project L1-2607. V. Domenici thanks the MIT-UNIFI project 2022 for partial financial support.

References:

- [1] Resetic et al. Polymer-dispersed liquid crystal elastomer. *Nature Communications*, 2016, 7, 13140.
- [2] Resetic et al. Deuteron NMR investigation on orientational order parameter in polymer dispersed liquid crystal elastomers, *Phys. Chem. Chem. Phys.*, 2020, 22, 23064.
- [3] Bobnar et al. Polymer-dispersed liquid crystal elastomers as moldable shape-programmable material. *Nature Communications*, 2023, 14, 764.

11:15 AM SF06.04.05

Molecular Engineering of Liquid Crystalline Elastomers Containing Supramolecular Mesogens Kristin L. Lewis, Jonathan D. Hoang, David T. Kennedy, Sarah S. Aye and Timothy White; University of Colorado Boulder, United States

Liquid crystalline elastomers (LCEs) are lightly crosslinked polymer networks that exhibit large deformations due to the disruption of liquid crystalline order when exposed to a stimulus. However, LCEs currently demonstrate a weak coupling of stimuli and response that limits the functional application of these materials. A recent effort by our group demonstrated that the inclusion of liquid crystalline mesogens formed with supramolecular bonds results in more rapid phase transitions due to the disruption of the hydrogen bonds. Here, we further analyze the effect of intra-mesogenic supramolecular bonds on the actuation of LCEs to better understand how these contribute to the overall order-disorder response. Benzoic acids are shown to form

dimers within the crosslinks that can be disrupted with temperature as well as with the nematic to isotropic phase transition of the overall network. By including these dimers with conventional three ringed liquid crystals as well as nonconventional two ringed mesogens with reduced intermolecular interactions, we probe how the disruption of H-bonds is affected by the surrounding network and heat. We also examine the structure-property effect by varying the supramolecular mesogen itself to analyze the connection between H-bond strength and actuation dynamics. This is demonstrated by including benzoic acid derivatives along with molecules containing functional groups such as pyridines to result in single H-bonds. Varying the strength of hydrogen bonds and mesogenic intermolecular interactions results in improved performance of the LCEs. Overall, this effort's purpose is to both understand the influence of H-bond interactions on LCEs and then tailor the response of these soft actuators through molecular engineering to improve LCEs as functional materials.

11:30 AM *SF06.04.06

Low Density Actuators for Soft Robotics by Programming the Responsivity of Liquid Crystalline Polymer Networks and ElastomersTimothyWhite; University of Colorado, United States

Liquid crystalline materials are pervasive in our homes, purses, and pockets. It has been long-known that liquid crystallinity in polymers enables exceptional characteristics in high performance applications such as transparent armor or bulletproof vests. This talk will generally focus on a class of liquid crystalline materials referred to as liquid crystalline elastomers. These materials were predicted by de Gennes to have exceptional promise as artificial muscles, owing to the unique assimilation of anisotropy and elasticity. Subsequent experimental studies have confirmed the salient features of these materials, with respect to other forms of stimuli-responsive soft matter, are large stroke actuation up to 75% as well "soft elasticity" (stretch at minimal stress). This presentation will survey our efforts in directing the self-assembly of these materials to realize distinctive functional behavior with implications to soft robotics. Most notably, enabled by new chemistries amenable to facile processing methods we have prepared liquid crystal elastomers with distinctive actuation and mechanical properties realizing more than 100 J/kg work capacities in homogenous material compositions. Fibers and yarns are promising geometries to further enhance the exceptional stimuli-response of these materials.

SESSION SF06.05: Actuation II
Session Chairs: Robert Shepherd and Ryan Truby
Tuesday Afternoon, November 28, 2023
Sheraton, Second Floor, Back Bay D

1:30 PM SF06.05.01

Heterogeneous Polymer Composites for High Stiffness 4D Printed Electrically Controllable Multifunctional StructuresJavierM. Morales Ferrer¹, RamonE. Sanchez¹, SophieCaplan¹, Wimv. Rees² and JohnW. Boley¹; ¹Boston University, United States; ²Massachusetts Institute of Technology, United States

4D printing is a rapidly emerging field in which 3D printed stimuli responsive materials are used to produce morphing and multifunctional structures, with time being the fourth dimension. The materials used for 4D printing are generally soft (elastic modulus range $10^4 - 10$ MPa) when undergoing shape change, which limits the scalability, actuation stress, and load bearing capabilities of current applications. Here, to address these limitations, we introduce heterogeneous polymer composites as a new class of stiff 4D printed materials. These composites are comprised of an epoxy matrix with a tunable cross-link density and a plurality of isotropic and anisotropic nano and micro fillers. Using this as a platform, we generate a palette of inks that span a large range of negative and positive linear coefficient of thermal expansion ($-19.1 \pm 0.3 - 128.8 \pm 1.2$ ppm $^{\circ}\text{C}^{-1}$) with an elastic modulus range that is four orders of magnitude larger than existing 4D printed materials ($0.34 \pm 0.1 - 38.6 \pm 1.4$ GPa), and tunable electrical conductivities ($0.7 \pm 0.1 - 2.0 \times 10^3 \pm 0.2 \times 10^3$ S m^{-1}) for integrated Joule heating actuation and sensing. Using electrically controllable bilayers as building blocks, we design and print a 3D self-standing lifting robot, with record lifting capabilities (~888 times its own weight) and actuation stress (~6 MPa) for 3D printed actuators and comparable performance for commercially available actuators. Moreover, we were able to implement a closed loop control to our lifting robot to achieve autoregulated actuation with response that lie within 4.8% and 0.8% overshoot and undershoot, respectively. Furthermore, we design and print flat surfaces that morph into different self-supporting complex 3D surfaces. Finally, we combined our inks to 4D print an electrically controlled crawling lattice robot that can carry up to 144 times its own weight.

1:45 PM SF06.05.02

Synthesis and Characterization of Sequence Defined Monodisperse Liquid Crystalline OligomersChun Lam ClementChan, ShawnM. Maguire, EmilyC. Ostermann, CallieC. Zheng, JakeH. Cedar and EmilyC. Davidson; Princeton University, United States

The actuation and soft elastic behavior of liquid crystal (LC) polymers have led to their use in applications ranging from soft robotics to elastocaloric devices. However, the behavior of a main-chain LC polymer differs markedly from that of its constituent monomer and is influenced by factors including molecular weight, sequence, and molecular weight dispersity. LC oligomers and polymers of controlled length and sequence are challenging to achieve through typical step-growth LC synthetic strategies. As such, we demonstrate a new LC synthetic approach based on iterative exponential growth (IEG) to prepare a series of monodisperse triazole-linked LC oligomers of precise lengths. We map the effects of increasing molecular weight on the thermal transitions of these discrete LC materials. These results are contrasted with the behavior of comparable species prepared via conventional step-growth polymerization. Furthermore, by preparing LC monomers decorated with different functional groups, sequence-defined co-oligomers and co-polymers can be prepared, illustrating the effects of sequence and functionality on LC phase behavior. These studies highlight important factors affecting LC phase transitions, establishing design rules for tailored and precise LC behavior.

2:00 PM SF06.05.03

Activated Metals for Thermal Actuation in the Context of Biomedical ApplicationsEvaRemlova^{1,2}, VivianR. Feig^{1,3} and GiovanniTraverso^{3,1}; ¹Brigham and Women's Hospital, Harvard Medical School, United States; ²ETH Zürich, Switzerland; ³Massachusetts Institute of Technology, United States

The advancement of biomedical robotics relies on innovative actuation schemes and the utilization of advanced materials. To date, the practical applications of heat-actuated systems still appear limited, and further research is needed to explore new heat generation methods for actuating robotic structures. However, heat-based actuation faces constraints due to its high power requirements, restricting its use outside clinical settings. To address this, we have developed an in vivo heating method using liquid metal-activated aluminum and water. We established a consistent activation method and characterized heat generation through thermal imaging and heat flux measurements. Demonstrating its potential, we used this method to thermally actuate a gastric resident device made from Nitinol, a shape-memory alloy. This novel *in situ* heat generation technique offers advantages and promising future directions for broader applications in biomedical technology.

2:15 PM SF06.05.04

Soft Robotic Myriapods via LCEsJamesT. Waters and AnnaC. Balazs; University of Pittsburgh, United States

Myriapods, such as centipedes and millipedes, represent a promising avenue for bioinspired robotics, with many legs allowing the device to retain functionality even after one leg has been damaged. However, the need for a complicated set of separate parts to control each of these many limbs makes construction difficult. Liquid crystalline elastomers (LCE's) represent an ideal material to overcome these challenges. Non-linear coupling and feedback between shape changes and light and temperature stimuli allow LCE devices to exhibit a diverse array of actuation and programmed responses without the need for internal mechanisms. This greatly simplifies the fabrication of many-legged soft robots. Using a finite element simulation model, we demonstrate how such an LCE device can be shaped and magnetically programmed so as to induce walking behavior in response to light stimuli.

2:30 PM SF06.05.05

Improved Performance of Soft Robotic Artificial Muscles Through Compositing High Dielectric Polymeric MaterialsErinRutledge, ChuckRutledge and MichaelRowe; Toyota Research Institute of North America, United States

Electrically driven artificial muscle soft actuators assist in propelling automotive companies closer to the lightweighting of equipment while moving the environment closer to carbon neutrality. The innovativeness of this technology stems from muscles found in the natural world. Electrostatically based artificial muscles have not previously performed at an advantageous level that could adequately challenge electric motors. Artificial muscles are electrically driven flexible capacitors. A hydraulic response (muscle flexing) is yielded after a voltage is applied to the electrodes causing the attractive forces between them to move the internal dielectric fluid. The dielectric constant between the two-electrodes of this parallel plate capacitor dictates the capacitance of the artificial muscle, and therefore, the attractive force between the electrodes. In our soft robotics actuator, this translates directly as output force. Numerous polymeric insulating materials have been investigated as coatings for these electrodes. High dielectric constant PVDF-TrFE-CFE has always been an attractive candidate material because of the correlation of dielectric constant to higher output forces. Prior to this phase in our research, integration of this material into an artificial muscle has proven daunting. However, through compositing with PVDF-HFP, the integration of this material into the fabrication of artificial muscles was successful. A performance improvement of 4.5x was demonstrated using a

composite insulating layer of PVDF-TrFE-CFE and PVDF-HFP versus a control muscle that used only 12 μm PVDF-HFP electrical insulation. An 800 g load was lifted with $\sim 150\%$ stroke using only an applied application voltage of 2,250 V, by an artificial muscle made with 10 μm PVDF-TrFE-CFE and 4 μm P-VDFHFP electrical insulation. This substantial improvement is ascribed to the influence of the high dielectric constant of PVDF-TrFE-CFE (50) compared to that of PVDF-HFP (10). Additionally, it was found that adding a ~ 10 N force to the edge of the artificial muscles' electrodes acted as a closing assistance, increasing the weight the muscle could lift while maintaining $\sim 150\%$ stroke. This led to the optimization of the electrode design with the aforementioned composite insulation. A series of artificial muscle electrode designs were fabricated using various thicknesses of PVDF-TrFE-CFE composited with 4 μm PVDF-HFP to optimize the ratio of relative polymer thicknesses necessary to maximize performance. Our results demonstrated that a 3:1 ratio (13 μm PVDF-TrFE-CFE: 4 μm PVDF-HFP) performed consistently with $\sim 150\%$ stroke lifting up to 700 g. Such results show how manipulation of capacitive effects can be achieved in layering of different polymeric materials and achieve manipulation of soft robotic artificial muscle output force. These artificial muscles are currently being tested for use in a device that will act as a suction cup that will be applied in existing robotic equipment.

2:45 PMBREAK

SESSION SF06.06: Embodied Energy
Session Chairs: Yoav Matia and Ryan Truby
Tuesday Afternoon, November 28, 2023
Sheraton, Second Floor, Back Bay D

3:15 PM *SF06.06.01

Self-Pumping Tubing: Fiber-Format Electrohydrodynamics Michael Smith and [Herbert R. Shea](#); Ecole Polytechnique Federale de Lausanne, Switzerland, Switzerland

Fiber-based devices are at the heart of wearables. We report here a fluidic pump in the form of a stretchable and flexible fiber, enabling the benefits of fluidic systems and associated soft actuators to be deployed in a wearable context. Our pumps consist of two continuous helical copper electrodes embedded within the walls of a 2 mm diameter polyurethane tube. The pumps generate pressure silently and without any moving parts using the principle of charge-injection electrohydrodynamics. The tubing itself becomes the pump, affording vast design freedom in the implementation of wearable fluidic circuits, which we illustrate with demonstrations of wearable haptics (glove), mechanically active fabric sheets and thermoregulatory textiles (shirt). The maximum pressure generated by each pump is proportional to its length, with each meter of fiber generating 100 kPa of pressure, or flowrates of 50 ml/min, at an applied electric field of 8 kV/mm. To function, the liquid being pumped must be a dielectric fluid with a high breakdown strength. Here, we use the dielectric fluid Novec 7100, a non-toxic, non-flammable methoxy-fluorocarbon. Judging by specific pressure and specific flowrate, the fiber-shaped pumps outperform by more than an order of magnitude the conventional miniature pumps that they replace. The scalability, simplicity and bi-directional pumping capabilities of these fiber pumps enables a wide range of wearable applications that are not possible with conventional pumping technologies.

3:45 PM SF06.06.02

Untethered Soft Robotic Systems with an Embodied Redox Flow Battery Achieved through Robust Adhesion for Assembly [Chongchan Kim](#) and Robert Shepherd; Cornell University, United States

Redox flow batteries are demonstrating their potential in the field of soft robotics by offering possibilities to enhance embodied energy efficiency through their multifunctionality. Integrating these batteries into the system can boost efficiency due to their versatile capabilities. The electrolytes within the embedded battery serve both as storage for electrochemical energy and as essential components for structural integrity and force transmission. However, the water-tight sealing required on the ion exchange membrane makes it challenging to fully leverage the advantages of the Redox flow battery.

Here, we present the untethered worm-like crawling robot powered by pod batteries integrated into the worm body. The pod cell is a pre-sealed pouch made with ion exchange membranes, reducing wasted space for sealing and increasing the effective area of electrodes so that it can reach the power requirements for the actuation. We fabricated the pod battery with a robust bond (~ 500 N/m) between ion exchange membranes and soft materials which allows a flexible and reliable power system even in the complex body shape of the worm during its actuation. The reliable bonding ensured battery functionality and simplified the fabrication process. Moreover, it enabled an exploration beyond conventional battery designs, allowing for diverse form factors for embodied energy systems.

4:00 PM SF06.06.03

A Bioresorbable and Miniaturized Ultrasound-Mediated Nanogenerator for *In Vivo* Electrical Stimulation [Xiao Xiao](#), Xiangchun Meng and Sang-Woo Kim; Yonsei University, Korea (the Republic of)

Implantable medical electronics (IMEs) provide practical approaches for diagnosis, treatment, and rehabilitation. However, conventional IMEs often rely on non-biodegradable batteries and require invasive surgical implantation. Long-term battery insertion can lead to performance degradation and corrosion, necessitating multiple surgeries for device maintenance and replacement^[1]. Moreover, major surgeries and bulky implants also pose additional challenges due to the risk of postoperative complications and the potential for acute and chronic injuries^[2]. Therefore, there is a significant demand for developing IMEs with biocompatibility, biodegradability, high reliability, and miniaturization.

As an emerging technology, triboelectric nanogenerators (TENGs) offer an innovative solution to address these limitations. Here, we present a bioresorbable, injectable, and ultrasound-mediated triboelectric nanogenerator (UB-TENG) for *in vivo* electrical stimulation. The UB-TENG comprises a molybdenum electrode and a biodegradable polyurethane friction layer synthesized from poly(3-hydroxybutyrate-co-3-hydroxyvalerate) and polycaprolactone. The miniature size of the UB-TENG enables direct injection into the desired site using a piercing needle, minimizing the risks associated with long-term implantation and reducing trauma. By utilizing capacitive triboelectric technology, the UB-TENG can be noninvasively powered by ultrasound^[3], and we have successfully demonstrated the modulation of UB-TENG efficiency by varying the ultrasound intensity. UB-TENG provides a safe and sustainable electrical output in various conditions, delivering a continuous alternating electric field of up to 0.92 V mm⁻¹. Cell experiments have confirmed the effectiveness of the delivered electric field in promoting cell migration and proliferation, indicating the significant potential of UB-TENG in accelerating wound healing. Our findings support the potential of UB-TENG as a novel energy solution for IMEs, offering the possibility of mitigating infection and chronic inflammation.

[1] Yoon, Hong-Joon, and Sang-Woo Kim. "Nanogenerators to power implantable medical systems." *Joule* 4.7 (2020): 1398-1407.

[2] Jung, Yei Hwan, et al. "Injectable biomedical devices for sensing and stimulating internal body organs." *Advanced Materials* 32.16 (2020): 1907478.

[3] Hinchet, Ronan, et al. "Transcutaneous ultrasound energy harvesting using capacitive triboelectric technology." *Science* 365.6452 (2019): 491-494.

4:15 PM SF06.06.04

Self-Powered Triboelectric Charges-Generated Microbial Blocking Textile by Harnessing Kinetic Energy [In-Yong Suh](#)¹ and Sang-Woo Kim²; ¹Sungkyunkwan University, Korea (the Republic of); ²Yonsei University, Korea (the Republic of)

Air-transmitted pathogens induce up to 650,000 respiratory disease-related deaths annually from seasonal influenza by inhalation, ingestion, and/or skin contact. Micron-sized aerosols containing these hazardous bacteria/viruses are inevitably released into the air, resulting from the daily motions of the infected people. Considering the long floating distances (\sim kilometers) of the small-sized aerosols, air-transmitted pathogens exist ubiquitously in the surrounding environment, making widespread pandemics exponentially and rapidly spread all over the world. In addition to the urgent challenges to preventing pathogen infection, the most used personal protection device, face masks, can lead to obvious pressure drops and uncomfortable long-term wearing while only protecting the facial area instead of the full skin. Alternative methods, such as antimicrobial textiles can utilize the nanomaterial-modified functional fabrics for effective microbial prevention, whereas suffering from limited treatment throughput, high cost, and potential toxicity from nanomaterial release.

In this study, we propose a novel microbial blocking textile for efficient bacterial and viral blocking in the air. We applied an optimized triboelectrification fabric (PTFE and nylon) and structure (rib-knitted) to build a two-layer textile that harvests human motion to generate triboelectric charges for effective microbial blocking based on electrostatic repulsion. The self-powered triboelectric charges-generated microbial blocking textile (TC-MBT) was developed to overcome the insufficient treatment throughput and obvious pressure drops of conventional air-transmitted pathogen protection methods such as face masks and filters. Our work provides a proof-of-concept for highly efficient and self-powered microbial blocking with low pressure drop, which could be applied for personal protection applications to fill the urgent need for air-transmitted pathogen protection.

4:30 PM *SF06.06.05

Autonomy in robotic systems is limited by the lack of flexible, high energy density storage technologies. Typically, the energy storage system is optimized independently from the rest of a robot's actuation, sensing, and control systems so that most technologies focus on making battery packs as small and as light as possible. This approach leads to low system-level efficiencies and energy densities. For example, current battery architectures based on solid intercalation materials store 250 Wh kg⁻¹ and require > 1 h to recharge, but animals can store ~2,000 Wh kg⁻¹ and operate continuously. The clear gaps in energy density and operational capability between machines and animals motivate new ways to store electrochemical energy via bioinspired designs.

Designing robots with multifunctional energy storage systems allows size, weight, and power trade-offs to be reevaluated. Animal circulatory systems use blood to transport oxygen and nutrients while simultaneously regulating temperature, removing waste, and helping to fight infection. Biology takes advantage of the inherently high theoretical specific energy of oxygen reduction processes without the need for each cell to access the surrounding environment.

Inspired by this functionality and the large number of high specific energy reactions that use gases, we developed a catholyte capable of storing 15 mg/L of dissolved oxygen and used it to discharge zinc-air flow batteries in a multifunctional actuator flow cell (MAFC) that also provided linear actuation. The catholyte was an emulsion with silicone oil droplets suspended in 0.5M potassium hydroxide, stabilized by a surfactant (Span-60). We extracted energy directly from the oxygen in this fluid with a fully submerged electrode that was not exposed to surrounding air. This enabled oxygen reduction to occur in a fully closed system with no need for a gas diffusion electrode or triple-phase boundary. Our electrolyte can remain stable for months, shows high oxygen reduction reaction (ORR) kinetics, and can be re-oxygenated with atmospheric air. We achieve 4.6 mW/cm² peak instantaneous power density at 5.6 mA/cm² discharge current density in a stationary tubular flow cell (STFC) configuration.

The last part of this talk will report an electrochemical stomach that near-continuously powers electric aircraft and robots by ingesting small molecules as beverages and converting that chemical energy to electricity by pairing them with metals. We demonstrated a 10.4 Ah stomach that delivers an energy density of up to 850 Wh kg_{stomach}⁻¹ at 192 A kg_{stomach}⁻¹ and restored the chemical energy of a robot dog in 1 minute. The stomach powered a commercial quadcopter and doubled the flight time of the manufacturer's state-of-the-art batteries. Owing to the diversity of small molecules, we tailor beverages to enable 1,447 Wh kg⁻¹ discharge energy density or fire-safe energy storage.

SESSION SF06.07: Poster Session: From Robotic Towards Autonomous Materials

Session Chairs: Yoav Matia and Ryan Truby

Tuesday Afternoon, November 28, 2023

Hynes, Level 1, Hall A

8:00 PM SF06.07.01

Development of a Low-Cost, Flexible and Ultra-Thin Capacitive Tactile Sensor For Monitoring Tool-Tissue Interactions and Grasping Performances of a Surgical Robotic

Magnetic Microgripper Anastasia Aubeeluck, Hani Naguib and Eric Diller; University of Toronto, Canada

With advancements in miniaturization and wireless actuation for robot-assisted minimally invasive endoscopic intraventricular surgery, surgeons are unable to acquire tactile sensory feedback necessary for safe tool-tissue manipulations. To enhance surgical performance and reduce the risks of tissue trauma, haptic technologies need to be integrated onto micro-scale surgical tools to provide tactile information. However, current sensors cannot be integrated for robot-assisted minimally invasive surgery (RMIS) for pediatric neurosurgery due to low force range and small scale criteria. This study proposes a novel 24 mm², ultra-thin and flexible capacitive tactile sensor for the interior jaws of a disposable surgical magnetically-controlled microgripper (4 mm in diameter). The sensor seeks to enable real-time monitoring and regulation of tool-tissue manipulation forces, thereby improving grasping performance and the overall quality of surgical procedures. To lower fabrication cost, the multiple layers of the capacitive sensor were screen-printed and assembled to produce a thin flexible sensor with an overall thickness of 100 μm. Furthermore, to improve sensor performance in terms of range and sensitivity, four different morphologies were developed for the dielectric layer, integrated into the sensor design, and characterized in terms of performance. The dielectric layer optimization consisted of tuning and processing Thermoplastic Polyurethane (TPU) into a suitable ink for screen printing large surfaces and microstructures. The final optimized sensor had a grid-like micro-structured dielectric design and demonstrated a sensing range of 0.01-1.3 N. Its electromechanical performance was modeled as a bi-linear response with two sensitivity modes and had a hysteresis of 8.8%. The sensor also showed a repeatable response to applied cycling loadings with a maximum response signal decay of 1.85%. This study highlights that screen printing method can be used as a low-cost alternative to fabricate high performance tactile sensors to be integrated to the interior jaw of the disposable microgripper designed for endoscopic intraventricular surgeries.

8:00 PM SF06.07.02

Graphene Origami with Bendability and Foldability Jiwoo Kim, Dong Hoon Moon and Gwan-Hyung Lee; Seoul National University, Korea (the Republic of)

Origami has been used a straightforward and controllable method to fabricate 3D patterns in nano/micro-scale for soft robotics and complicated architectures. Here, we report graphene origami technique for 3D patterning by using poly(methyl methacrylate) (PMMA)-coated graphene. The graphene was grown on a silicon substrate. High etching resistivity of graphene to XeF₂ gas and its flexibility enable fabrication of the complicated 3D nano/microstructures with reduced fabrication steps, compared to conventional lithographic methods. By exposing the PMMA/graphene film to e-beam and selective patterning of graphene, we can bend the suspended the PMMA/graphene film upward or downward. With this bidirectional folding function, we can create the 3D graphene origami structures with multiple folds. Our work shows a novel way to fabricate 3D graphene structure with controllable folding and reversible bending and high potential of graphene Origami in fabrication of nano/micron-scale machines.

8:00 PM SF06.07.03

Unravelling the Dual-Responsive Behavior of Anthracene and PNIPAM Bilayer Soft Actuators: Reversible Actuation via Visible Light and Temperature Anas Saifi^{1,2}, Charu Negi¹ and Kamlesh Kumar³; ¹CSIR-Central Scientific Instruments Organisation, India; ²Academy of Scientific & Innovative Research, India; ³Central University of Jammu, India

Soft robotics, inspired by natural organisms, have gained popularity due to their ability to exhibit physical changes in response to environmental stimuli. Among the various stimuli, light has attracted the most attention due to its remote-control capabilities, high spatial and temporal resolution, and ease of fine-tuning. The pursuit of integrating multiple stimuli into a soft actuator stands as a pivotal role in the quest for the advancement of smart materials. In the present study, a multi-responsive soft actuator with bilayered architecture was designed and fabricated. Here, the bilayer is composed of a visible light-responsive PVA-Anthracene layer and a thermoresponsive PNIPAM layer. Interestingly, each layer is designed to respond to a specific stimulus enabling them to perform efficiently in both dry and aqueous environments. The bilayer soft actuator was characterized through a comprehensive set of techniques encompassing UV and FTIR spectroscopy for molecular analysis, optical microscopy to confirm the fabrication of the bilayer structure, and tensile testing to assess its mechanical properties. The multi-responsive soft actuator exhibited rapid and reversible actuation with a bending angle of 153° under blue light, and complete rolling was observed when the temperature of the solution was raised above the critical solution temperature of PNIPAM. The visible light responsiveness is attributed to the photodimerization of anthracene moiety whereas the temperature responsiveness is a consequence of the phase transition of PNIPAM above LCST. The tunable actuation of the film was demonstrated with different blue light intensities and anthracene dye concentrations, as well as varying the concentration of the PNIPAM for thermomechanical behaviour. This work holds promising implications in the fields of robotics, biomedical engineering, and adaptive structures, requiring controlled actuation in both dry and aqueous environments.

8:00 PM SF06.07.04

Imbibition-Induced Autonomous Wetting of Liquid Metal Ji Hye Kim¹, sooyoungkim², Sanghyuk Woo³, Jung Cho⁴, Michael Dickey², Ju-Hee So⁵ and Hyung-Jun Koo¹; ¹Seoul National University of Science & Technology, Korea (the Republic of); ²North Carolina State University, United States; ³Chung-Ang University, Korea (the Republic of); ⁴Korea Basic Science Institute, Korea (the Republic of); ⁵Korea Institute of Industrial Technology, Korea (the Republic of)

Gallium-based liquid metal alloys (GaLMs) are in liquid phase at room temperature and have the attractive properties, including high electrical/thermal conductivity, low toxicity, and high deformability, making them ideal for use in stretchable and deformable electronic pathways. Controlling the interfacial characteristics of GaLMs with underlying substrates is essential for depositing, printing, and patterning GaLMs. However, the high surface tension of GaLMs makes it difficult to create thin films with uniform height. We present an effective method for producing flat thin films and patterns of GaLMs, by introducing microstructured metallic features on which GaLMs rapidly and spontaneously spread in the absence of a native oxide. The enhanced wetting characteristics of GaLMs on the microstructured metallic surface are induced by imbibition, which enables large-area uniform coating and patterning of the liquid metal. The

GaLM-coated polymer substrates prepared by the method maintain electrical connectivity even in a stretched state and after repetitive stretching cycles. The imbibition-induced wetting principle of the liquid metal provides several advantages: 1) coating and patterning GaLMs occurs spontaneously without external force, 2) the thermodynamically-favorable wetting of GaLMs forms stable metallic thin film, and 3) the thickness of the GaLM thin film can be well-controlled by varying heights of the metal-coated microstructures. This approach also reduces the amount of GaLM required for thin film formation, making it a cost-effective and efficient method for electronic applications.

8:00 PM SF06.07.05

Droplet Micro-Robotic System with Generality of Liquid Types and Biocompatibility[RuotongZhang](#)¹, HaisongLin^{1,2} and AndersonShum^{1,2}; ¹The University of Hong Kong, China; ²Advanced Biomedical Instrumentation Centre, Hong Kong Science Park, China

The flexible and deformable nature of micro soft robots offers an alternative for transporting soft, fragile or microscale materials. Among them, droplet robots, based on their fluidity, are capable of adaptively navigating through tortuous environments with physical obstacles, as well as carrying and transporting biological/chemical samples of interest for medical diagnostics, drug development, and chemical/material synthesis. However, different target samples will require different droplets environments that serve as their carrier. For example, living cells require specific buffers as carriers to maintain biological activity, while some water-soluble nanoparticles need to be transported in organic fluids. Therefore, a robotic system that is compatible with a variety of organic/inorganic liquids and the carried bio/chemical samples needs to be developed. Here, we propose a multi-physics droplet robotic system that can actuate various liquids through a movable electrostatic field. In particular, the droplet-driven unit is composed of a hybrid of electret and magnetic materials. The electret section which carries electrostatic charge can generate a non-uniform electrostatic field that polarizes and attracts the droplet, while the magnetic section can be controlled under a programmed localized electromagnetic field. In our work, the droplet robotic system demonstrates a high compatibility with droplet volume (nL-mL), liquid types (inorganic/organic), and samples carried by the droplet (living cells/proteins/nanoparticles), thus providing a general hardware platform for delivering a wider range of different biological/chemical samples in an automated manner.

8:00 PM SF06.07.06

Charge-Accumulating Flutter-Type Triboelectric Nanogenerator as High Performance Self-Powered Portable Device[DeokjaeHeo](#)¹, SunghanKim¹, JinkeeHong² and SangminLee¹; ¹Chung-Ang University, Korea (the Republic of); ²Yonsei University, Korea (the Republic of)

For a triboelectric nanogenerator (TENG), achieving both a high RMS (root-mean-square) output current and a portability remains a challenge. Herein, a charge accumulation fluttering based triboelectric nanogenerator (CAF-TENG) with an ultrahigh RMS output current, an average power density and an outstanding portability is proposed. Because of the electron accumulation and electrostatic discharge mechanism and electrical-mechanical fluttering device design, the CAF-TENG can generate an RMS output voltage, RMS output current, and average power output density of 44 V, 36 mA, and 26 mW cm⁻³, respectively. The maximum peak output voltage and current are 508 V and 1.6 A, respectively. The CAF-TENG is optimized via quantitative RMS voltage-current database and mechanical behavior analysis. The wind-driven CAF-TENG can power 2000 commercial LEDs matrix and charge high-capacitance capacitors or commercial lithium batteries. Furthermore, a respiration-driven mask-valve-integrated CAF-TENG is fabricated, which can power 40-W commercial lamps and operate a commercial Bluetooth tracker sensor by charging a capacitor. These results suggest that the CAF-TENG can function as a self-powered portable device in everyday life. Moreover, these findings will provide a new guideline for improving the electrical output level of existing TENGs.

8:00 PM SF06.07.07

Soft Actuators Based on Liquid Crystal Elastomers and Laser-Induced Graphene[AlexanderDallinger](#)¹, [StellaDrewes](#)¹ and [FrancescoGreco](#)^{2,2,2}; ¹TU Graz, Austria; ²Scuola Superiore Sant'Anna, Italy

Laser induced graphene (LIG) is a porous conductive carbon material produced by laser-induced pyrolysis of polymer precursors with applications in soft electronics/robotics and wearable electronics, among others. LIG conductors are conveniently created in a single synthesis/patterning step by laser scribing with a CO₂ or UV laser onto a polymer precursor such as polyimide. A subsequent transfer of the LIG onto a stretchable support such as polyurethane (PU) is used to create soft, flexible and stretchable LIG conductors. These soft conductors are then used in a composite with a liquid crystal elastomer (LCE), where the LIG acts as a joule heating element. The LCE is synthesized via click chemistry and poured into a mold where a partially cross-linked elastomer is created. The partially cured elastomer is pre-stretched and fully cured by UV irradiation. The LIG/PU and LCE are bonded together to form a multi-composite soft actuator. By applying a current to the LIG heating elements, a nematic-isotropic transition is induced in the LCE, resulting in contraction of the actuator. The contraction can be reversed by turning off the current and cooling the actuator. An linear actuation strain of about 60% is achieved. The combination of LIG as a heating element and LCE as an active actuation material is a promising approach to bio-inspired actuators with comparable performance to muscles.

8:00 PM SF06.07.08

Effects of Crosslink Density on Photomechanical Jumping of Glassy Liquid Crystalline Polymer Networks[Min JeongHahm](#)^{1,1}, JisooJeon², WoongbiCho^{1,1} and Jeong JaeWie^{1,1,1}; ¹Hanyang University, Korea (the Republic of); ²Inha University, Korea (the Republic of)

In nature, jumping is a key survival strategy for living animals as it allows them to rapidly navigate through rough terrains and overcome obstacles that are often several times their body size. In our previous report, we newly demonstrated a continuous and directional UV-induced photo-mechanical jumping of polymer monolith by introducing snap-through buckling of super twisted nematic (STN) structured azobenzene functionalized liquid crystal polymer networks (azo-LCNs). However, the intense light conditions of 0.3 W cm⁻² intensity and the long-term UV irradiation required for high jumping have raised concerns over the possible bond breakage and the subsequent decrease in the jumping capacity. Herein, we control the duration of UV irradiation for photopolymerization to vary the crosslink density and investigate the effect of the structure-property relationship on mild-condition jumping. Crosslink density-controlled azo-LCNs are heated to various substrate temperatures and irradiated upon different light intensities to achieve a systematic investigation of jumping heights. When the curing time is reduced from 60 min to 5 min, the storage modulus (E') of the azo-LCN monolith is successfully lowered from 74.8 MPa to 33.1 MPa in the plateau regime, and the bending curvature is increased from 2.1 mm⁻¹ to 4.4 mm⁻¹, respectively. The reduced stiffness of the azo-LCN body increases the photomechanical strain response under actinic UV light, thereby allowing the body to store greater photo-induced potential energy. Remarkably, a maximum jumping height of 15.9 mm is reached at a milder light intensity of 0.1 W cm⁻², which is a 214% increase in height compared to the previous result obtained at identical UV light conditions.

8:00 PM SF06.07.09

Autonomous Magnetic Swarms of Microrobot Assemblies[KijunYang](#), SukyoungWon, Jeong EunPark and Jeong JaeWie; Hanyang University, Korea (the Republic of)

Collective actuation of microrobot swarms has emerged as a versatile tool to succeed challenging tasks for a single microrobot. However, the unpredictable interactions among the microrobots and segregated movements of the microrobots present inherent constraints for the multi-functionality system. Herein, we report an autonomous magnetic swarm of magnetic microrobots through programming magnetic anisotropy in the microrobots. Due to the magnetic anisotropy, multiple microrobots assemble in a deterministic manner. Hundreds of magnetic microrobots can agilely rotate in their frontal plane while preserving their assembled configuration. Through the pivoting, the magnetic swarm of microrobot assemblies with high chain length facilitates the capability to climb obstacle. Meanwhile, the magnetic swarm with high packing density can transport cargo via rotational force of the microrobot assemblies. We will discuss multi-functionality of the autonomous magnetic swarm capable to lift heavy obstacle, tumble high barrier, and cleave high surface tension materials.

8:00 PM SF06.07.10

Towards Intelligent Soft Robots: A Data-Driven Approach to Unlock the Potential of Magnetically Responsive Materials[AlpC. Karacakol](#), YunusAlapan and MetinSitti; Max Planck Institute for Intelligent Systems, Germany

Soft robots have emerged as a new branch of robotics with deformable bodies to achieve adaptability to dynamically changing unstructured environments and safe interaction with life forms ranging from cells to humans. Miniaturization efforts in soft robotics for operation in confined, small, and remote spaces are challenging because conventional batteries, actuators, and on-board processors are not available at smaller scales. The challenges of power, intelligence, and actuation at smaller scales have led to the incorporation of stimuli-responsive materials in soft robotics, where the actuation mechanism is based on the encoded response of the robot body to the external stimuli at the material level. Among the wide range of proposed external stimuli such as temperature, light, chemical, electric and magnetic fields, magnetic fields are particularly promising due to their safe and transparent interaction around biological tissues. Magnetically responsive soft materials with fast response and untethered control capabilities at small scales in confined environments make them ideal candidates for minimally invasive clinical operations within the human body. Advances in the spatial programming of magnetic soft materials have enabled micron-scale high resolution, 3D directionality, and multi-material compositions, resulting in a vast design space with intricate coupled magnetic and mechanical responses of soft robots. While the design space is immensely enriched, existing designs rely on an intuitive trial-and-error approach with fixed morphologies and simplified magnetic programming, drastically limiting the achievable capabilities. Here, we present a generic and experience-free method for programming both the 3D structural design and the 3D magnetic profile of magnetic soft robots for desired 3D shape morphing and behavior. The design algorithm is based on a continuous exploration of the design space through design candidates generated by MAP elites and the exploitation of promising designs guided by a predictive neural network (NN) model. The selected promising designs are tested in a computationally inexpensive simulation engine capable of evaluating the dynamic behavior of magnetic soft robots. The resulting best-performing designs for desired 2D and 3D shape-morphing of beams inspired by mathematical functions and complicated sharp-cornered objects are experimentally demonstrated,

demonstrating the Sim2Real transfer. The developed design strategy is also used to achieve desired dynamic behaviors without a defined target shape-morphing, including maximizing the number of turns, maximizing the height, and minimizing the bounding sphere volume for soft magnetic beams and plates. The superiority of the data-driven design strategy is highlighted in the high-performance jumping behavior of magnetic soft robots, where the intuitive design adapted from the literature failed to lift off the surface. Furthermore, the data-driven designed robots are shown to be capable of complex locomotion behaviors with simple control signals compared to the fine-tuned complex ones. The data-driven design strategy presented here provides a systematic and versatile platform to bridge the gap between advances in material functionalities and fabrication and programming methods, thus unlocking the potential of stimulus-responsive soft robots for real-world applications.

8:00 PM SF06.07.11

Bio-Inspired Magnetic Soft Kirigami Robot for Biomedical Application[Yizong Li](#) and Shanshan Yao; Stony Brook University, United States

Soft robots that are untethered have the potential to revolutionize medical monitoring due to their minimally invasive nature. Although progress has been made in the design and activation of these robots, given the intricate and ever-changing environment of the human body, there is still a need for a comprehensive untethered soft robot that can adapt to different environments. Taking inspiration from the locomotion of snakes, we introduce a soft kirigami robot that overcomes these challenges. This robot can deploy sensors, perform real-time wireless sensing, and adapt to a wide range of environments within the human body. Its capabilities include deployability, steerability, obstacle crossing, locomotion in both wet and dry conditions, climbing, inverted crawling, exceptional load capacity (up to 150 times its own weight), and high-speed locomotion (0.25 body lengths per second at 1 Hz actuation). By demonstrating these comprehensive locomotion abilities, the soft kirigami robot showcases its potential for various biomedical applications.

8:00 PM SF06.07.12

Artificial Intelligence Enabled Wearable Device for Sensing and Classifying Data Integrated with High-Performance Piezoelectric Yarns[Dabin Kim](#)¹, [Ziyue Yang](#)¹, [Jaewon Cho](#)¹, [Donggeun Park](#)², [Dong Hwi Kim](#)¹, [Jinkee Lee](#)¹, [Seunghwa Ryu](#)², [Sang-Woo Kim](#)³ and [Miso Kim](#)¹; ¹Sungkyunkwan University, Korea (the Republic of); ²Korea Advanced Institute of Science and Technology, Korea (the Republic of); ³Yonsei University, Korea (the Republic of)

Piezoelectric polymer fibers are essential components in creating intelligent fabrics with adaptable shapes and energy-converting capabilities for wearable health and activity monitoring. However, producing high-performance smart polymer fibers has been challenging due to their low piezoelectric performance. In this work, high-performance piezoelectric yarns are presented that are both structurally robust and mechanically flexible. We achieved this by adding barium titanate nanoparticles (BTO, BaTiO₃) to poly(vinylidene fluoride-trifluoroethylene) (P(VDF-TrFE)) during electrospinning to increase the electroactive β -phase formation. The optimally selected BTO-15 fiber mat-based device exhibited a substantially enhanced voltage of 167.31 V under mechanical bending, which was higher than that of its pristine counterpart. The resulting BTO-doped P(VDF-TrFE) mats were transformed into yarns, where the degree of β -phase crystallinity is found to be significantly higher in the yarns than in the mats, showing that the yarns could be a more favorable structural platform for piezoelectric performance. Furthermore, a BTO-15 piezo-yarn device was fabricated and tested, which exhibited an output of 16.17 V. Also, tensile tests were performed on the BTO-doped mat and BTO-doped yarns which results in the yarns being mechanically strengthened and having significantly improved elastic modulus and ductility compared to the mat. Finally, the BTO-doped piezo-yarn devices were woven into cotton socks as we denoted "piezo-socks". This can monitor and identify body signals during seven human motion activities, such as jumping, running, and stair-climbing, by using convolution neural network algorithms designed for classification achieving a high accuracy of 99.6 %.

8:00 PM SF06.07.13

Direct Current-Generating Triboelectric Nanogenerators Based on Tribovoltaic p-n Junction with ChCl-Passivated CsFAMA Perovskite[Sera Jeon](#)¹, [Dabin Kim](#)² and [Sang-Woo Kim](#)¹; ¹Yonsei University, Korea (the Republic of); ²Sungkyunkwan University, Korea (the Republic of)

Herein, we develop direct current-generating triboelectric nanogenerators (DC-TENGs) based on the tribovoltaic p-n junction using n-type perovskite (CsFAMA) and p-type conductive polymer (PEDOT:PSS); CsFAMA based DC-TENG is shown to generate a high DC power output of about 2.1 $\mu\text{A cm}^{-2}$ (current) and 0.33 V (voltage). We also introduce choline chloride (ChCl) to passivate the defects inside CsFAMA to improve the power-generating performance of DC-TENG by increasing triboelectric charge density, carrier mobility, and built-in potential, which are the key factors that determine device performance. Due to the synergetic effect of reduced defect sites ($5.0 \times 10^{15} \text{ cm}^{-3}$ to $1.0 \times 10^{15} \text{ cm}^{-3}$), enhanced electron mobilities ($1.0 \times 10^{-2} \text{ cm}^2 \text{ V}^{-1} \text{ s}^{-1}$ to $2.3 \times 10^{-2} \text{ cm}^2 \text{ V}^{-1} \text{ s}^{-1}$), and modulated work function, the passivated CsFAMA-based DC-TENG generates an output current density of 11 $\mu\text{A cm}^{-2}$ and an output voltage of 0.80 V. Our results are expected to contribute to the development of high-performance DC-TENGs by presenting a promising strategy that involves controlling the triboelectric semiconducting interface.

8:00 PM SF06.07.14

Autonomous Synchronization of Lobed Loops Made from Liquid Crystal Elastomer Fibers: Untethered Gait-Like Motion Through Spontaneous Snap-Through[Dae Seok Kim](#)¹ and [Shu Yang](#)²; ¹Pukyong National University, Korea (the Republic of); ²University of Pennsylvania, United States

The rapid transition between equilibrium states, known as snap-through, allows for the storage and release of elastic energy, enabling quick movements observed in organisms such as the Venus flytrap and hummingbird, which seize insects in mid-flight. Soft robotics have been investigating these mechanisms to achieve repeated and independent motions. In this study, we present a novel approach involving the synthesis of curved liquid crystal elastomer (LCE) fibers as fundamental units capable of undergoing buckling instability when exposed to heat on a hot surface. This leads to autonomous behaviors, including snap-through and rolling. By interconnecting these fibers into lobed loops, where each fiber is geometrically constrained by its neighbors, we achieve autonomous, self-regulated synchronization, occurring at a frequency of approximately 1.8 Hz. Additionally, the attachment of rigid beads to the fibers allows for precise control over actuation direction and speed, reaching velocities of up to 2.4 mm/s. Finally, we demonstrate the utilization of these loop structures as robotic legs, enabling various locomotion patterns reminiscent of natural gaits.

8:00 PM SF06.07.15

Dispersions of Carbon Nanotubes in Liquid Crystals Show Accumulating Responses to Electric Fields[Kayla Helliokson](#)¹, [Harrison Root](#)², [Narcross Hannah](#)², [Georgia Kaufman](#)², [Emily Huntley](#)² and [Bryan Kaehr](#)²; ¹Texas A&M University, United States; ²Sandia National Laboratories, United States

Mixtures of liquid crystals (LCs) and carbon nanotubes (CNTs) have been shown to act as switches in response to an electric field. These composite systems can display resistive memory, mimicking neuronal behavior such as synaptic plasticity and providing opportunities to develop new classes of neuromorphic materials. Typically, minute concentrations of nanotubes (< 0.001 wt%) are mixed into an alcohol solvent, diluted, tediously dispersed into liquid crystal solutions, and evaluated using small gap (< 5 μm) electrodes. However, our efforts to reproduce results with these mixtures has been challenging. In this work, we investigate LC mixtures that are saturated with CNTs. These "two-phase" systems display hallmarks of neuromorphic materials such as memory, reset and accumulation in response to pulsed electric fields. We show electric-field induced CNT solubilization in LC "solvents" and parallel field alignment are the dominant mechanisms governing response. These effects are not restricted to micron gapped electrodes but are apparent across mm distances and translated into polymer dispersed liquid crystals, useful for device level applications. Overall, this work provides a foundation to develop tunable, neuromorphic materials that can remember and respond to electrical environments.

8:00 PM SF06.07.16

Reversible Chemotaxis of Janus Emulsion Droplets[Bradley D. Frank](#) and [Lukas Zeininger](#); Max Planck Institute of Colloids and Interfaces, Germany

Organisms move in response to chemical stimulation as chemotaxis, recognizing environmental changes and transducing that information into directed motion. Emulating nature, many reported motile soft colloids utilize chemical stimuli to interact with their environment, including liquid which move using their fluid interface to generate Marangoni flows by physical or chemical stimulation. Current reports which utilize Marangoni-flow directed motion have been limited to a single programmable interface, yielding uncontrolled or unidirectional motion. We present a system where chemotactic speed and direction are reversible and responsive to the environment, using dynamically reconfigurable biphasic droplets whose shape is also responsive to the environment. A bi-phasic droplet in a binary surfactant mixture moves dependent on the magnitude of gradients and the droplet morphology, mutually determined by interfacial tension balance and competition. For droplets with two exposed interfaces to the environment, each interface is programmable to a separate gradient acting on the droplet, where droplet behavior is dependent on both the magnitude of the external gradients and the surface area that gradient acts upon. The reconfigurable nature of the presented system enables interactive and adaptive behaviors in response to a changing local environment. With this internal degree of freedom and response to the environment, we present theoretical and experimental insight into the generation of multi-responsive adaptive soft-matter. Utilizing droplet interactions with the environment in kind, the behavior of the droplets can be utilized to understand novel gradients. Soft-matter with internal feedback mechanisms are adaptive agents in response to bio(chemical) stimulation, such as the decision to move toward or away from a stimuli.

8:00 PM SF06.07.17

A Bimodal PVDF Sensor for Integration Into a Signal-Dense Multimodal Tactile Finger[Peter Ballentine](#), [Eric T. Chang](#), [Matei Ciocarlie](#) and [Ioannis Kyriassis](#); Columbia University, United States

The types of tasks robots are capable of are in part limited by the lack of an adequate robot “sense of touch.” The human “sense of touch” takes in pressure, vibration, texture, curvature, and temperature via the skin’s biological transduction modes and synthesizes detailed information about the contact. Meanwhile, combining these modalities on a signal-dense tactile robot finger to detect the stimuli that make up the human “sense of touch” remains an open problem. Currently, many state-of-the-art robotic tactile sensors are unimodal, solely relying on a single transduction mode (e.g., optical, capacitive, resistive, etc.) to take in stimuli. We hypothesize that utilizing multimodal sensing capabilities will allow us to achieve richer and more meaningful tactile feedback for robotic applications.

In this work, we will present a bimodal polyvinylidene fluoride (PVDF)-based sensor and its subsequent integration into a larger multimodal sensing system for a tactile robot finger. The PVDF-based sensor consists of a thin sheet of PVDF with metal photolithographically patterned on both sides, and is capable of both piezoelectric and projected capacitance sensing modes for measuring relative movement (i.e., vibration) and proximity, respectively. We will integrate the PVDF into a sensing system including 10 MEMS microphones, an accelerometer, and 8 temperature sensors on a PCB under PDMS; 9 capacitive force sensors suspended within the PDMS; and the bimodal PVDF sensor suspended in the PDMS above the other sensors. Within this setup we plan to optimize the thickness and stiffness of the PDMS between each layer as they relate to signal transmission and sensor durability, as well as the chemical functionalization of the PDMS surface to improve durability and surface texture. We will then collect the overlapping signals from each sensor type and utilize machine learning techniques to determine how to best utilize sensor data for force regressions, touch localization, texture classification, and radius of curvature detection. The eventual aim of the project is to incorporate the complete sensing system into a robotic finger and utilize its multimodality to enable more dexterous robotic manipulation.

8:00 PM SF06.07.18

Electroluminescent Display Based on Field-Interactive Microparticles for Camouflage and Environmental Monitoring Jong Woong Park, Donyoung Kang, Hyung Suk Lee and Cheolmin Park; Yonsei University, Korea (the Republic of)

The development of displays that mimic the color-changing ability and external stimulus-sensing ability of biological skins is of significant interest for emerging robotics and biomedical applications. Here, we present an alternating-current (AC) electroluminescent display that can change the area, color, and luminance by using microparticles which interact with electric and acoustic fields. Dielectrophoretic force produced by AC electric field controls the amount and area of percolated carbon particles that form a conductive gate, enabling light emission from the ZnS phosphor-doped polymer layer. Different stacking combinations of emissive layers enable a wide-range color tuning in a single device by varying the electric field, which may be suitable for camouflage when integrated into the skin of soft robots. The display is also capable of sensing acoustic waves and visualizing the information by luminance change as the conductive gate collapses. Arrays of acousto-interactive displays were successfully used for environmental monitoring and non-destructive testing, where defects, air bubbles, and obstacles inside structures and fluid channels were visualized due to acoustic impedance mismatch. Our platform provides a path forward to engineer active camouflage and displays for soft machines.

8:00 PM SF06.07.19

Chemically-Generated Mechanical Patterns in an Array of Elastic Posts Moslem Moradi, Oleg ShklyaeV and Anna C. Balazs; Department of Chemical Engineering, United States

Artificial cilia platforms have been used to create pumping, mixing and sensing in microfluidic devices by a number of stimuli such as electrostatic or magnetic fields, light, thermal, pH and pneumatical actuations. To further improve these platforms, fundamental investigations on the actuating strategies for cilia and fluid manipulation are necessary. Using 3D simulation, we study the potential for enzymatic chemical reactions to generate convective flow that controls dynamic patterns formed in an array of elastic posts (modeling the cilia) tethered to the bottom surface of a millimeter-size fluid-filled chamber. We assume that some of the posts are coated with reactant-specific catalysts that promote localized chemical reactions and thereby drive buoyancy-driven flows. These buoyancy-driven flows arise due to density differences between reactants and products, which in turn generate the inward or outward flow depending on the density of the products. The flows produced around the enzyme-coated posts impose a fluid drag on the chemically-passive flexible neighboring posts, which can bend and assume flow-induced configurations. This chemo-hydro-mechanical coupling generates different patterns, which can be controlled by different arrangements of the coated posts and different chemical reactions.

The results of our simulations show that the stability of the patterns depends on the elastic properties of the posts. Steady state patterns are formed when the bending modulus of the posts is larger than a certain threshold. Patterns formed by less rigid posts do not reach steady configurations and the flow becomes chaotic at relatively low Reynolds number, which is useful for mixing. We focus on posts beyond this threshold, and consider two final steady configurations. In the first case, we simulate an infinite array of posts located in a periodic domain; in the second, we consider a finite array of elastic posts located in the simulation box with no-slip boundary conditions. In both cases, the flexible posts are arranged into a square lattice and attached to the bottom wall of the domain.

To generate patterns, we use three different enzymatic reactions localized at the specific posts. We assume that one catalase-coated post is pinned in the middle of the array, two AP-coated posts (AP is acid phosphatase) at the middle and two urease-coated posts located at the corners of a unit square array of posts. Addition of the appropriate chemicals (hydrogen peroxide, PNPP or urea) generates fluid motion around different posts and induces distinct patterns in the entire array that contains both active and passive posts. The resulting patterns possess different symmetries depending on the position of coated-post, and the boundary conditions of the domain. Our computational simulations can provide guidelines for fabricating surface-anchored elastic posts that generate microscopic flows with the desired dynamic properties for a range of fluidic applications.

8:00 PM SF06.07.20

Engineering Confined Fluids to Autonomously Assemble Hierarchical 3D Structures Oleg ShklyaeV, Abhrajit Laskar and Anna C. Balazs; University of Pittsburgh, United States

The inherent coupling of chemical and mechanical behavior in fluid-filled micro-chambers enables the fluid to autonomously perform work, which in turn can direct the self-organization of objects immersed in the solution. Using theory and simulations, we show that the combination of diffusioosmotic and buoyancy mechanisms produce independently controlled, respective fluid flows: one generated by confining surfaces and the other in the bulk of the solution. With both flows present, the fluid can autonomously join two-dimensional, disconnected pieces to a chemically active, “sticky” base and then fold the resulting layer into regular three-dimensional shapes (e.g., pyramids, tetrahedrons, and cubes). Here, the fluid itself performs the work of construction and thus, this process does not require extensive external machinery. If several sticky bases are localized on the bottom surface, the process can be parallelized, with the fluid simultaneously forming multiple structures of the same or different geometries. Hence, this approach can facilitate the relatively low-cost, mass production of 3D micron to millimeter sized structures. Formed in an aqueous solution, the assembled structures could be compatible with biological environments, and thus, potentially useful in medical and biochemical applications.

8:00 PM SF06.07.21

Mechanoreceptor-Inspired Gelatin Hydrogel Sensor Based on Switchable Ionic Polarization So-Hee Kim¹, Hong-Joon Yoon², Dong-Min Lee³ and Sang-Woo Kim¹; ¹Department of Materials Science and Engineering, Yonsei University, Korea (the Republic of); ²Department of Electronic Engineering, Gachon University, Korea (the Republic of); ³Sungkyunkwan University, Korea (the Republic of)

Triboelectricity-based touch sensors are great advantages in terms of cost, simplicity of design, and use of a wide range of materials. However, it is hard to measure the extent of deformation of materials since the performance solely relies on the level of contact electrification between materials. To overcome this limitation, we introduce an ion-doped gelatin hydrogel (IGH)-based touch sensor that can measure not only contact with objects but also deformation by a certain level of force. Switchable ionic polarization of the gelatin hydrogel is found to be instrumental in allowing for different sensing mechanisms when it is contacted and deformed. The results show that ionic polarization relies on conductivity of the hydrogels. Quantitative studies using voltage sweeps demonstrate that higher ion mobility and shorter Debye length serve to improve the performance of the mechanical stimuli-perceptible sensor. It is successfully demonstrated that this sensor offers dynamic deformation-responsive signals that can be used to control the motion of a miniature car. This study broadens the potential applications for ionic hydrogel-based sensors in a human-machine communication system.

To take advantage of these properties of IGH, we developed dynamic mechanical stimuli-perceptible sensor capable of accommodating continuous tactile information about contact and deformation events. Dynamic tactile sensing-based communication was successfully demonstrated. This study broadens the potential applications for ionic hydrogel-based sensors in a human-machine communication system.

8:00 PM SF06.07.22

3D-Printed Micrometer-Scale Wireless Magnetic Cilia with Metachronal Programmability Shuaizhong Zhang^{1,2}, Xinghao Hu^{1,3}, Meng Li^{4,1}, Ugur Bozuyuk¹, Patrick Onck⁵ and Metin Sitti¹; ¹MPI for Intelligent Systems, Stuttgart, Germany; ²Yanshan University, China; ³Northwestern Polytechnical University, China; ⁴Massachusetts Institute of Technology, United States; ⁵University of Groningen, Netherlands

Biological cilia play essential roles in self-propulsion, food capture, and cell transportation by performing coordinated metachronal motions. Experimental studies to emulate the biological cilia metachronal coordination are challenging at the micrometer length scale because of current limitations in fabrication methods and materials. We report on the creation of wirelessly actuated magnetic artificial cilia (MAC) with biocompatibility and metachronal programmability at the micrometer length scale. Each cilium is fabricated by 3D nano-printing a proteinous hydrogel beam affixed to a hard magnetic microparticle. Specifically, we used hard magnetic FePt Janus microparticles (FePt J MPs) and silk fibroin to 3D print biocompatible and programmable MAC arrays at a length scale close to biological cilia using two-photon polymerization in combination with magnetic actuation controls. Magnetic, mechanical, and biological properties of the fabricated cilia were systematically investigated, showing that our cilia were mechanically tunable and robust, biocompatible, and

biodegradable. Programmable metachronal coordination can be achieved by programming the orientation of the identically magnetized FePt Janus microparticles, which enables the generation of versatile microfluidic patterns. Upon applying a uniform rotating magnetic field of as small as 3 mT, each cilium performed a whip-like reciprocal motion consisting of a slow forward stroke and a fast backward stroke. The difference in the orientation between neighboring FePt JMs endowed the MAC array with heterogeneous magnetization directions, initiating a metachronal wave within the MAC array when subjected to a uniform rotating magnetic field.

We showcased the design and fabrication of MAC arrays to generate translational flows and locally circulating flows. This work could provide an experimental platform for biocompatible and programmable microcilia arrays with a large design space for future potential applications in microfluidic devices and cilia-inspired biomedical soft microrobots.

8:00 PM SF06.07.23

A Wet-Bioadhesive Triboelectric Nanogenerator for Emergent Wound Closure and Electricity-Accelerated HealingXiangchunMeng, XiaoXiao and Sang-WooKim; Yonsei University, Korea (the Republic of)

Emergency medical situations such as surgical incisions and vascular rupture necessitate prompt intervention, or they can result in a range of life-threatening complications, including significant blood loss, infection, and even death. While conventional surgical sutures, staples, and adhesives can achieve hemostasis, they rely heavily on surgical expertise or the use of specialized equipment, and the presence of bodily fluids can significantly impede the quality of wound sealing. Additionally, the rate of wound healing is another crucial factor. Drug-loaded smart adhesives have received considerable attention, but meantime they raise concerns regarding drug toxicity and resistance. Therefore, it is a daunting but essential task to develop innovative strategies for managing emergent wounds and promoting accelerated wound healing.

In this study, we proposed a novel ultrasound-driven wet-adhesive triboelectric nanogenerator (WA-TENG) to treat acute wounds for instant wound sealing and electricity-accelerated healing. WA-TENG comprises two components: a bottom wet-adhesive layer and an upper TENG component. When attached to the wet tissues, the wet-adhesive layer can form covalent bonds with tissues to achieve faster (~5 s) and stronger adhesion with high interfacial toughness (~150 J m⁻²). When stimulated by ultrasound, the dielectric and conductive layers of TENG can generate continuous contact-separation movements to produce an electric field (E-field) of up to 0.86 kV m⁻¹. Experiments conducted both *in vitro* and *in vivo* demonstrate that it substantially accelerated wound healing due to the E-field-enhanced cell migration and proliferation. Notably, WA-TENG is composed of biocompatible and biodegradable materials, which will not harm tissues and can self-degrade without the need for surgical removal. It is anticipated that this multifunctional electrical device will not only facilitate surgical procedures in hospitals but will also be a portable and self-help medical device for emergency wound care.

8:00 PM SF06.07.24

Effect of Temperature, Moisture and Mechanical Strain on PIB Thin Film Barriers for Implantable Soft RobotsUmarRaza and KyungjinKim; University of Connecticut (UConn), United States

Advances in electro-ionic soft actuators hold significant potential as next generation bioelectronic interfaces due to mechanical compliance and operation in agreement with soft biological tissues and low voltages. However, current devices call encapsulation strategies to accommodate high mechanical demands and long-term stability in physiological environment changes, such as maintaining biocompatibility and withstanding temperature and moisture variations. In this study, we investigate a durability of poly vinylidene fluoride-co-hexafluoropropylene (PVDF-co-HFP) honeycomb architecture electrolyte by encapsulating it with a biocompatible polyisobutylene (PIB) thin film. PIB is known for its excellent moisture barrier properties among existing elastomers; therefore, we expect durable performance under its hermetic encapsulation. The encapsulation is prepared of a 60% (w/w) solution of PIB in hexane to possess an elastic modulus on the order of 10 KPa, same as the modulus of PVDF-co-HFP electrolyte and in the range of most body tissues. Both PIB and PVDF-co-HFP demonstrate temperature endurance withstanding up to 332 and 250 degree celsius, respectively. A low water vapor transmission rate (0.61 g/m²/day) is measured, ten folds lower than that of bare PVDF-co-HFP with an addition of 7.5 micro-meter PIB encapsulation layer. The PIB encapsulated soft actuator maintains 68% of its mechanical durability after 40,000 cycles of zero to tension fatigue loading at room temperature. A cantilever actuation test of the PIB encapsulated actuator shows a large tip displacement (15.90 mm) at a low voltage (±1.5V) under 0.1 Hz, 37 degree celsius, 50% relative humidity (RH). Most importantly, while the unencapsulated actuator immediately degrades in a few cycles at 37 degree celsius, 50% RH, 0.1% applied strain, PIB encapsulated soft actuator performs up to 6500 dynamic actuation cycles without any functionality degradation. PIB encapsulated soft actuator system demonstrates exceptional durability against mechanical fatigue and stability at the elevated temperature and humidity, making it one step closer to meeting the prerequisite for future soft biomedical robots that enable long-lasting safe operations.

8:00 PM SF06.07.25

Transition of Plastic Deformation to Elastic for Crumple-Recoverable ElectronicsYeonwookRoh, Je-SungKoh, DaeshikKang and SeungyongHan; Ajou University, Korea (the Republic of)

Crumpling is one of the easiest, quickest, and most efficient ways to pack sheet-like electronic devices at a high compression ratio. Today, rolling or folding of many electronic devices has been attempted for portability, whereas due to the disordered and irreversible plastic deformation that may affect the electronic functions, crumpling is not applicable to conventional electronic devices. Inspired by butterfly wings during the emergence process with variable stiffness, the heterogeneous integration of three materials (i.e., an elastomer, silver nanowires, and a shape memory polymer) in this study enables thermal modulation of the mechanical properties between soft (2 MPa) and stiff (1315 MPa) or between conditions suitable for crumpling and free-standing operation, respectively. The crease that is common for the crumpled sheet due to the inordinate folding and stretching becomes invisible after smoothing the surface via thermal treatment. The demonstration of this platform includes crumpling and packing of touch panels into capsules, while a flat and smooth surface for reliable touch sensing is obtained after unpacking. The results in this article suggest the ability to use a simplistic design to secure the function of crumpled electronics without having to compromise the electrical and mechanical characteristics.

8:00 PM SF06.07.26

Chemo-Responsive Soft Colloids: Autonomous Soft Robots with Decentralized IntelligenceLukasZeininger; Max Planck Institute of Colloids and Interfaces, Germany

Autonomous regulation of molecular recognition and binding-induced chemical events are essential processes through which natural systems exert control over complex biological functions. Chemical information can be processed with high fidelity and highest substrate specificities are achieved as multiple individual or combinations of independent chemical equilibrium-driven interactions are translated into a specific response. Key to the realization of artificial materials that present similarly sophisticated active and adaptive properties requires combining the concept of molecular recognition-induced responsiveness with a thermodynamically metastable, active, and dissipative material platform.

In nature, microorganisms harness energy gradients to prompt mechanical responses. Examples for chemo-mechanical signal transductions include the molecular transport mediated by motor proteins, as well as diffusiophoretic and electrophoretic reactions of whole cellular ensembles. The conversion of chemical concentration gradients into mechanical energy enables active colloidal systems to move, and hence also forms a basis to control complex emergent behaviors observed in multibody systems, including a self-regulated ability to communicate, evolve, and self-organize into patterns or networks. Synthetic efforts to emulate these behaviors target the design of active dissipative material systems that autonomously regulate their motile behaviors in response to their immediate chemical environment.

In our contribution, we will highlight the concept of droplet force gradient sensors. We will share our recent discoveries that responsive complex emulsion droplets present a comprehensive set of tools for understanding and reporting complex chemical environments. Droplet force gradient sensors are surfactant-stabilized complex emulsion droplets that can morphologically reconfigure triggered by changes in surfactant concentration, tilt out of gravitational alignment caused by droplet-internal thermo-capillary fluid convections, and move chemotactically in response to interfacial tension differentials. Thus, within one platform, responsive droplets provide as both, a tool to monitor and visualize transient gradients in temperature and chemistry *in-situ* as well as an active colloid that exhibits programmable actuation in response to changes in its immediate chemical environment.

We will demonstrate how the speed and directionality of the droplet chemotaxis can be reversibly and controllably altered depending on the internal morphology of the droplets. This entails systems that solely based on their internal geometry can be designed to display programmable motion towards or away various chemoattractants or -repellents, with the latter including bacteria. We will also show how targeting two or more separate and independent responsive modalities of complex droplet force gradient sensors can yield adaptive droplet ensembles. Droplets with logic gate decision making skills can adapt and autonomously modulate their response to the environment and thus provide a basis toward the design of artificial life-like soft colloids that exhibit an intrinsic decentralized chemo-intelligence and perform collective functions with strong implications for future soft robot and sensor technologies.

8:00 PM SF06.07.27

Autonomously Motile “Moonwalking” Microbeads with Internalized Hierarchical Magnetic ArchitecturesAbhirupBasu, EricBuchsbaum, JosephB. Tracy and OrlinD. Velev; North Carolina State University, United States

Self-propelling or “active” particles directed by external fields continuously consume and dissipate energy, thereby creating localized field and flow gradients, and enabling autonomous movement. The development of colloidal rollers responsive to magnetic fields offers the potential for external control of their macroscopic motion using magnets. In the current study, we report a new pattern of dynamic active motion with our micro-scale architectures in non-Newtonian fluids where colloidal micro-rollers on a solid substrate rotate and translate in directions some of which are intuitively not expected. These micro-scale rotators are synthesized by internally embedding iron oxide nanoparticles (MNPs) inside microdroplets of a polydimethylsiloxane (PDMS) precursor and assembling the MNPs into organized structures using a static magnetic field. Rotating magnetic fields, even with a low field strength and low rotation frequencies, can induce a strong torque on these microbeads due to the presence of the organized structures. The microbeads can therefore exhibit clockwise or counter-clockwise

rolling with forward or backward displacement. Surprisingly, when we placed these rollers in shear-thinning fluids, we established a fascinating new backward movement pattern, which we refer to as “moonwalking.” In this new dynamic pattern, the translation is opposite to the one expected by the rotational direction of the particles. We hypothesize that this reversible motion results from differing shear forces acting on the top and bottom of the particle. The “moonwalking” motion was found to increase with increasing viscosities until a critical rotational velocity where the microbeads lose alignment with the magnetic field and oscillate in place. This propulsion behaviour can help us to guide the forward or backward propulsion of the rollers without changing the field type and just by tuning the properties of the medium or the rotational frequency. The novel phenomenon in the single particle translation dynamics observed introduces a new physical principle of active propulsion. This new phenomenon has the potential to deepen our understanding of fundamental principles of autonomous materials and may open the door to future applications of active rollers in advanced biomedical applications.

8:00 PM SF06.07.28

A Dynamically Responsive Surface with Switchable Wettability for Efficient Evaporation and Self-Cleaning AbilitiesGregoryParisi and ShankarNarayan; Rensselaer Polytechnic Institute, United States

Evaporation is crucial in applications such as nanoscale fabrication, inkjet printing, heat transfer, and self-cleaning electronics. This study demonstrates a switchable surface that dynamically transitions between superhydrophobic and superhydrophilic states. Superhydrophobic surfaces are renowned for their intrinsic self-cleaning properties and notably sluggish evaporation kinetics. On the other hand, superhydrophilic surfaces exhibit rapid evaporation kinetics and induce evaporative cooling effects, making them advantageous for heat dissipation and cooling applications. This study proposes a switchable surface that seamlessly shifts between these two states based on external stimuli. To facilitate the understanding of this switchable surface, the study employs a self-cleaning superhydrophobic aluminum substrate coated with an amino-silane (N-(2-aminoethyl)-11-aminoundecyl-trimethoxysilane). Typical nonwetting coatings, such as lauric acid and FDTS (perfluorodecyltrichlorosilane) are also compared in terms of wettability and evaporation kinetics. During periods of low heat loads, the surface capitalizes on the self-cleaning nature of superhydrophobicity, reducing energy waste and minimizing maintenance needs. Conversely, when subjected to high heat loads, the dynamic transition to a superhydrophilic state facilitates rapid evaporation, thus unlocking effective evaporative cooling effects. By combining these dual characteristics, the proposed surface transcends conventional boundaries, offering multifaceted benefits. The experimental concept is underscored by an in-depth analysis of evaporation rates using both calorimetry and contact angle goniometry. Addressing the complexities arising from superwetting surfaces, which challenge the precise determination of droplet boundaries, this research predicts evaporation rate of both wetting and nonwetting surfaces.

8:00 PM SF06.07.29

Development of a Soft Gripper Capable of Controlling Buoyancy in WaterMinchaeKang, SuyeonSeo, EunsolPark, YejiHan and Min-WooHan; Dongguk University, Korea (the Republic of)

Underwater soft robots have the potential for a wide range of uses, including exploration, search, and rescue. In particular, the recently studied underwater soft robot is safer and more effective to employ than the current rigid robot since it can adapt easily to the environment. It also has a flexible and deformable body that allows it to adapt to challenging underwater environments and interact with various underwater creatures and structures. This soft gripper can manage buoyancy and shift its location in water up and down by changing the volume of the internal air without relying on an external device or mechanism. It is possible to function as a gripper while changing buoyancy in this situation. The gripper can grasp objects when the buoyancy is low and the amount of air content is little; conversely, when the amount of air is high and the buoyancy is low, the object can be carefully placed. The soft buoyancy gripper actuates using the stress differential between two soft polymers. When the soft polymer with relatively low elasticity is put on top of a thin, soft polymer that has been stretched and glued on both sides, the polymer can be rolled inward. In addition, when an air layer is formed between the two polymer layers, gripping and buoyancy can be controlled according to the amount of air injected into the device. At this point, several objects were held in place while the device's location in relation to the volume of air injected was examined. This will allow the soft robot to move in a small space and swim, crawl, and be utilized for a variety of tasks like environmental monitoring, search and rescue operations, and underwater exploration. Hence, this soft robot can carry out challenging duties by ascending and descending to different sea depths. The buoyancy control system of this underwater soft robot is an essential component that enables diversity and adaptability in water, and it has the potential to revolutionize underwater exploration and study. It has the benefit of being able to approach and operate intimately without hurting the marine environment and living organisms, which makes it particularly useful for ecological research and preservation. As a result, the described underwater soft robot may represent an innovative technology with numerous possible uses.

This work was supported by the National Research Foundation of Korea(NRF) grant funded by the Korea government(MSIT) (No.2018R1A5A7023490), by the Korea Institute of Machinery and Materials (KIMM) funding (NK242C), and by the Ministry of Trade, Industry, and Energy (MOTIE) and the Korea Institute for Advancement of Technology (KIAT) through the International Cooperative R&D program (Project No. P0016173).

8:00 PM SF06.07.30

Photoactive Smart Polyethylene/MoS₂ Bilayer Actuators for Locomotive Soft-RobotsLaritzzaMedi^{1,2}, FelipeOlate-Moya^{1,3}, NestorPerea-López⁴, MauricioTerrones⁴ and HumbertoPalza^{1,3}; ¹Universidad de Chile, Chile; ²Universidad del Bío Bío, Chile; ³Impact, Center of Interventional Medicine for Precision and Advanced Cellular Therapy, Chile; ⁴The Pennsylvania State University, United States

The development of smart materials is becoming increasingly important due to their potential applications in various fields such as medicine, aeronautics, biomedicine, and electronics, among others. In particular, soft actuators which can be fabricated using an active bilayer, consisting of a photoactive material and a passive layer that provides structural integrity. As these two layers have different thermal expansion coefficients, an external stimulus that changes their temperature generates an out-of-plane deformation. This provides a large mechanical mismatch to external stimuli, thus endowing them with unprecedented features such as: ultra-sensitivity, programmability, superior compatibility, robustness and ease of fabrication [1]. This type of actuators can be activated by a wide range of stimuli such as light, heat, humidity, electric field, magnetic field, among others. The light stimulus is one of the most promising for applications that require remote actuation, such as soft robotics, where MoS₂ is highlighted as a 2D nanostructure with outstanding NIR absorption [2].

In this work, we designed and fabricated photoactive bilayer actuators consisting of a MoS₂ active layer and a polymeric passive layer. We analyzed the effects processing on the response of the bilayer for directionality and velocity control. The active layer is obtained using a Langmuir-Blodgett based method. MoS₂ nanosheets were characterized by UV-vis, Raman, XRD, SEM, TEM and AFM techniques, exhibiting an average lateral size of 512 nm and 20 nm thickness. While for the passive layer a commercial polyethylene (PE) is used, characterized with UV-vis, Raman and DSC, with 26% crystallinity and a Young's modulus of 180-250 MPa. These bilayers were characterized by a passive layer thickness of 13 μm, and an active layer consisting of MoS₂ nanosheets stacked in the basal plane (002). Noteworthy, the bilayers presented photo actuated response that depend on the number of MoS₂ coatings. For 8 MoS₂ coatings, having a thickness of 725 nm, the bilayer had a response time of 1.9 s, recovery time 3.5 s and inverse of the actuation radius of 0.5 mm⁻¹. Furthermore, the strain can be modulated by patterning both the bilayer and the PE to control the direction of displacement, as an example we created structures having locomotion or mimicking the opening movement of a flower or the flutter of a butterfly. These actuators are promising structures to be applied in soft robotics with remote activation.

Thanks to FONDECYT Project 1200093.

[1] Y. Chen et al., “Light-driven bimorph soft actuators: Design, fabrication, and properties,” *Mater Horiz*, vol. 8, no. 3, pp. 728–757, 2021, doi: 10.1039/d0mh01406k.

[2] S. Wang et al., “Asymmetric elastoplasticity of stacked graphene assembly actualizes programmable untethered soft robotics,” *Nat Commun*, vol. 11, no. 1, pp. 1–12, 2020, doi: 10.1038/s41467-020-18214-0.

[3] P. A. Young, “Lattice parameter measurements on molybdenum disulphide,” *J Phys D Appl Phys*, vol. 1, no. 7, pp. 936–938, 1968, doi: 10.1088/0022-3727/1/7/416.

8:00 PM SF06.07.31

Untethered, Battery-Free Multifunctional Soft Robot SystemSungkeunHan, Jeong-WoongShin and Suk-WonHwang; Korea University, Korea (the Republic of)

Development of untethered small-scale soft robots has become increasingly important in various industrial and biomedical fields due to their extensive applications, such as manipulation and drug delivery. There are different ways to actuate freely movable robots, such as using light, thermal, pH, and magnetic sources. However, the robot can only perform simple tasks like moving and gripping with these methods. Here, we present a new platform has been developed that integrates a soft robot and a multifunctional electronic system, which can magnetically control varying locomotion (including morphing, crawling, rolling, and rotating) and electrically operate multi-modal functions (temperature/strain sensing, optical/thermal stimulation). The integrated system has undergone extensive studies of magnetic materials and evaluations of the stability of electrical components to ensure it is available for use in various fields. With gradual improvements in size, modulation, and various monitoring and active functions, this device will provide emerging systems for diverse fields such as bio-medical applications, diagnosis and on-demand treatments, and environmental monitoring.

8:00 PM SF06.02.02

Highly Compressible 3D-Printed Soft Magnetoelastic Sensor for Human-Machine InterfacesHyeonsoSong¹, YeonwooJang¹, SuwooLee¹, Youn-KyoungBaek² and JiyunKim¹; ¹UNIST, Korea (the Republic of); ²Korea Institute of Materials Science, Korea (the Republic of)

Tactile sensors for human-machine interface (HMI), that convert mechanical stimuli into electrical signals, have gained great attention in various applications. In particular, self-powered soft

sensors such as piezoelectric, triboelectric, and magnetoelastic soft sensors have shown great potential due to their safety, adaptability, and low production and maintenance costs. However, piezoelectric and triboelectric sensors have high internal impedance, which lowers the current flow, reducing the current density and the output power density. Furthermore, their output sensing performance is susceptible to humidity conditions of the surrounding environment, including even sweat on the skin. On the other hand, soft self-powered tactile sensor based on magnetoelastic mechanism has the potential to provide high output power density due to their high current density and more reliable output performance regardless of humidity. Here, we present highly compressible 3D-printed soft magnetoelastic sensors (H-MELS) by using 3D printing methods with sacrificial mold, which allow us to program the material, and mechanical properties of H-MELSs, influencing the mechano-electrical converting performances of H-MELS. In addition, we developed elastomeric magnetic composite materials for a magnetic part and elastomeric electrical parts using a coiled-copper coil to fabricate H-MELSs. This strategy allows us to achieve highly scalable and compliant 3D architectures made of very compliant materials for 3D soft magnetoelastic sensors, and even integrate them into robotic systems as a robot operation units and robot's perception units for practical Human-Machine Interface applications. We believe H-MELS with high compressibility in various form factors leads to significant advancements in design and manufacturing of self-powered soft sensors for human-machine interfaces.

8:00 PM SF06.11.08

A Soft, Self-Sensing Tensile Valve for Analog and Programmable Control of Soft Pneumatic Actuators Jun KyuChoe, JunsooKim, Hyeonseong, JoonbumBae and JiyunKim; Ulsan National Institute of Science and Technology, Korea (the Republic of)

Soft robots offer great promise for applications that require safety and adaptability, particularly in the face of unpredictable variations. To unlock their full potential for autonomy and intelligent interaction with the environment, perception capabilities with continuous sensing and control of soft actuators are essential. However, soft robots still mostly rely on complex connections of rigid electronics both in hardware and software for perception. These include, for example, bulky and expensive sensors, controllers, and valves in pneumatically actuated soft robots. While there have been recent attempts to develop soft equivalents of individual rigid components, the integration of sensing and control systems without increasing the structural complexity or form factor is challenging to achieve without compromising the complete softness or capabilities.

Here, we introduce a soft self-sensing tensile valve (STV) that combines the functionalities of strain sensors and control valves to directly convert applied tensile strain into distinctive, pre-programmed output pressure states using a single constant pressure source. By utilizing a mechanism we refer to as "helical pinching," the STV achieves physical sharing of both sensing and control structures, resulting in all-in-one integration in a compact, linear form factor.

8:00 PM SF06.04.03

Scalable, Addressable, Artificial Muscle Bundles AlexanderL. Evenchik, EunBiOh, AlexanderQ. Kane and RyanL. Truby; Northwestern University, United States

Skeletal muscle continues to serve as an inspiration for the design of scalable, energy efficient, soft robotic actuators with distributed sensorimotor capabilities. However, our ability to produce soft actuators that mimic skeletal muscle remains limited. Liquid crystal elastomers (LCEs) are one promising class of materials whose high power density and large, contractile actuation strain approach the performance of biological muscle. Despite these advantages, the common actuation stimuli needed to drive LCEs are hindered by severe limitations. In addition to low actuation bandwidth, thermally-driven or thermotropic LCEs are energy inefficient, while photo-driven or phototropic varieties are limited to thin form factors that typically bend rather than contract. Here, we present LCE composite fibers that linearly contract while enabling in-line delivery of target stimuli. We demonstrate that bundling individual artificial muscle fibers introduces new capabilities such as scalability, amplified force output, and addressable actuation. Moreover, we show that our overall design strategy for artificial muscles alleviates stimuli transport-related challenges of existing LCE soft actuators by coupling the actuation stimuli with the active material. Our artificial muscle fiber bundles, which integrate scalability and addressability in a manner not yet seen in LCEs and other soft robotic actuators, provide a step towards designing material systems that truly mimic the performance and controllability of skeletal muscle. They serve as a platform for future multifunctional, artificial muscle designs that tightly integrate distributed actuation, sensing, control, and energy capabilities.

SESSION SF06.08: Soft Robotic Materials I
Session Chairs: Yoav Matia and Robert Shepherd
Wednesday Morning, November 29, 2023
Sheraton, Second Floor, Back Bay D

8:30 AM *SF06.08.01

Woven Active Textiles and E-Skin Enable Controllable Tunable-Stiffness Flapping Foils FrancescoGiorgio-Serchi; University of Edinburgh, United Kingdom

Flapping foils represents the natural mode of propulsion for the vast majority of aerial and aquatic organisms. Despite its supposed simplicity, this type of propulsion manifests a subtle complexity which has fascinated academics for decades. In recent times, the role of structural flexibility of fins and tails in determining the overall propulsive efficiency of self-propelled organisms and robotics artefacts has attracted attention because of its implications for the optimal design of bioinspired vehicles as well as energy harvesting devices. In particular, the opportunity to actively adjust the stiffness of an otherwise passive-elastic, man-made flapping foil offers unprecedented potential in attempting to match the propulsive efficiency of the biological counterpart. On one hand, tuning the structural flexibility of a flapping foil permits to align the natural frequency of the structure with that of the flapping motion, enabling to exploit the benefits of resonance in magnifying power output; on the other hand, control over the temporal pattern of stiffness variation enables enhanced capability for manoeuvrability and disturbance mitigation. To achieve this, flapping foil systems will require actuators which enable active stiffness tuning along with dedicated sensors for online estimation of the foil spatial configuration.

Here we present the design of new variable-stiffness flexible foils by means of active textiles. These consist of bundles of thin fluidic artificial muscles which can be woven into planar arrangements with a periodic pattern, thus giving rise to a fabric with adjustable, anisotropic stiffness. The foil is studied under dynamic actuation resembling of the cyclic mode employed during flapping routines, ultimately identifying the range of flapping frequencies where resonant modes can be triggered. In parallel, we develop a stretchable, capacitive electric skin embedded with a capacitance-to-deformation transformer which provides realtime, millimeter-accuracy estimation of the foil camber during actuation.

The combination of active textiles and e-skin offers the chance to develop advanced flapping-based propulsors with fine, closed-loop control over the stiffness and spatial configuration of the foil, enabling unprecedented performances and further narrowing the gap between biological and man-made systems.

9:00 AM SF06.08.02

Soft Multi-Material Magnetic Fibers and Textiles HritwickBanerjee and FabienSorin; École Polytechnique Fédérale de Lausanne (EPFL), Switzerland

Magnetically responsive soft materials are envisioned as the next building block in a myriad of applications including in minimally invasive surgical procedures, due to their untethered, safe, and versatile properties. However, constructing highly integrated magnetic fibers with extreme aspect ratios, that can be used as steerable catheters, endoscopes, or in medical textiles still remain a significant materials and processing challenge. Here, we present multi-material thermal drawing as a materials and processing platform to manufacture 10s of meters long, soft, ultra-stretchable, yet highly resilient magnetic fibers with a diameter as low as 300 μm . We identified magnetorheological elastomers with varied elastomeric matrices and hard magnetic micro-particles (neodymium-iron-cobalt-boron) as fillers. The composite exhibits rheological traits compatible with thermal drawing with tunable mechanical and magnetic properties, resulting in controllable actuation performance. By carefully controlling the viscosity during drawing, we show that we can slow down thermal reflow driven by surface tension and conserve micro-scale geometrical features and textures. To characterize the fibers post-drawing, we first used computed tomography that revealed a very good distribution of the fillers that was enhanced compared to the preform level. We then characterized the mechanical properties of the fibers that can withstand strains greater than 1000%. Subsequent magnetic hysteresis measurement revealed a strong magnetization on par with state-of-the-art magnetic composites, resulting in the ability to lift up to 370 times its own weight under an applied magnetic field. The fibers are also amenable to being magnetized with different orientations along their length, and to be weaved into functional textiles. The magnetic textile can be programmed to selectively shape morph and can sustain extreme mechanical deformation or several machine-wash cycles. They can apply force or pressure and could constitute a promising next generation of magnetic-based surgical tools and medical textiles for rehabilitation and soft prosthesis.

[1] Banerjee, Hritwick, et al. Soft Multimaterial Magnetic Fibers and Textiles. *Advanced Materials* (2023): 2212202.

9:15 AM SF06.08.03

Magnetically Induced Stiffening for Soft Robotics LeahT. Gaeta and TommasoRanzani; Boston University, United States

Inherent compliance of soft robots renders them safe for many applications such as object manipulation, surgery, haptics, and wearable devices. Stiffness modulation is essential to soft robot

design so that these robots can reverse compliance and institute more rigidity when needed. Relevant examples include robot reconfigurability, weight-bearing tasks, and force transmission. This has led to significant research on variable stiffness structures whose designs allow a soft robot to be flexible and compliant until interaction with its environment, when it switches from an inherently low-stiffness state to one of more rigidity. Variable stiffening mechanisms include pneumatically-controlled jamming and thermally-induced phase change materials. In jamming-based stiffening, granules, stacked layers, or fibers are packed into an encasing that as a whole is compliant and of low-density. Upon application of vacuum pressure, the overall structure increases density and solidifies within milliseconds. Despite fast response time, jamming methods lack portability due to reliance on pneumatic pressure lines, which are bulky and cumbersome in wearable or autonomous applications. Thermally-controlled phase change materials, such as shape memory polymers, induce a stiffness change when subject to electronically-controlled heat. They have the advantage of portability via electronic control, but often require high temperatures and have slower response time on the order of tens of seconds. Combining the advantages of these two stiffening methods, quick response time from pneumatic-based jamming with portability of thermal-controlled phase change materials, we present a magnetically-induced stiffening mechanism that requires scaffolding structures immersed in magnetorheological fluid. Magnetorheological fluids consist of micron-scale iron particles suspended in carrier fluid such as water, and solidify with a characteristic yield stress and viscosity when subjected to an external magnetic field. We exploit the response of magnetorheological fluid to applied magnetic fields to induce rapid stiffness changes, while investigating how the addition of scaffolding structures enhances and increases achievable stiffening ranges. These scaffolding structures are borrowed from pneumatic-based jamming and include stacked 51 μm thick polyester layers, 7 μm thick fiber filaments, and 2.4 mm diameter granules. Suspending these materials in 80% iron (by mass) magnetorheological fluid and encasing them in a textile pouch, we create magnetorheological jamming beams (MRJ beams) which are flexible, compliant, and have tunable stiffness with applied magnetic fields. We investigated the stiffening response of MRJ beams subjected to various magnetic field strengths using two methods: by exploiting the yield stress increase of magnetorheological fluid using a single row of permanent magnets, and by inducing a clutch on the MRJ beam using dual rows of permanent magnets with aligned poles that exploit yield stress effects and compress the beam via magnetic attraction. Scaffolding materials in MRJ beams amplify the stiffening response in the presence of applied magnetic fields in both methods, with stiffness percent changes ranging from $\approx 10\%$ - 75% and $\approx 50\%$ - 345% for single and dual row magnet architectures, respectively. We also present an analytical model to provide initial estimates of achievable stiffening ranges as a function of magnetic field to inform soft robot design. We introduce portability by employing electropermanent magnets (EPMs) which require minimal energy to operate, can be electronically-controlled, and can change magnetic field strength in $\approx 500 \mu\text{s}$. Embedding EPMs within an MRJ beam demonstrated electronically-controlled real-time stiffness change in a weight-bearing task. This work paves the way towards customizing soft robotic designs that require portability and fast response time stiffness tuning, such as in many human-robot interactions.

9:30 AMBREAK

10:00 AM *SF06.08.04

Developing Ionoelastomer Heterojunctions for Low-Voltage ElectroadhesionRyanC. Hayward; University of Colorado Boulder, United States

Our group has recently reported the use of heterojunctions between oppositely-charged 'ionoelastomers', i.e., low glass-transition polyelectrolyte networks, for a number of electromechanically responsive devices. In particular, they offer promise as low-voltage reversibly switchable electroadhesives, with potential applications including in soft robotics. Because voltages applied in reverse bias are dropped largely across the nanometer-scale ionic double layer formed at the interface between the two layers, large Maxwell stresses and corresponding enhancements in adhesion can be generated using applied potentials of $< 10 \text{ V}$, in contrast to the kV levels generally required for established electroadhesives based on dielectric layers. We have focused tuning the composition of the ionoelastomer layers to lower their surface energy and improve the contrast between 'on' and 'off' state adhesion, in addition to improving their ionic conductivity. By considering the design of the ionoelastomer/electrode interface, the effects of surface topography, and the geometry of the adhesive pads, we have achieved electroadhesive clutches that support higher forces per unit area than previous dielectric-based systems, while operating at two orders of magnitude lower potential.

10:30 AM SF06.08.05

Multimaterial 3D Printing of Poly(ionic liquid) Diodes for Soft Ionotronic RobotsAlexanderQ. Kane and RyanL. Truby; Northwestern University, United States

Overcoming long-standing challenges in soft robotic control requires new strategies for coupling perception and computation in soft, multifunctional materials. Ionotronic approaches have largely remained unexplored despite recent progress in soft ionotronic actuation and power methods. Poly(ionic liquids) are a promising class of materials that can combine elastomeric behavior with high ionic conductivity. However, current methods of patterning soft poly(ionic liquid) elastomers are limited, requiring low-throughput procedures to produce even simple forms and devices. To address this challenge, we present an integrated, multimaterial 3D printing and material design framework for fabricating poly(ionic liquid) composites as stable, ionotronic sensing and control elements for soft robots. We harness the chemical modularity of poly(ionic liquids) to formulate four inks that enable ionotronic devices to be printed in one complete process. In addition to printing and characterizing ionic diodes fabricated with our technique, we demonstrate other architectures and devices enabled by our method. We anticipate that our work can be adapted to equip next-generation soft robots with soft controllers, on-board power generators, and distributed sensing mechanisms.

10:45 AM SF06.08.06

Effect of Heat-Induced Adjustable Stiffness at the Contact Interface on the Gripping Force of a Bipolar Electrostatic ChuckShigekiSaito, JeremyGavriel, JuntianZhou and YukiTaoka; Tokyo Institute of Technology, Japan

This research endeavor aims to investigate the effect of heat-induced adjustable stiffness at the contact interface on the gripping force of a bipolar electrostatic chuck (ESC).

The bipolar ESC serves as a gripping mechanism specifically designed for delicate objects such as thin films and plates, functioning through the utilization of two electrodes that generate an electric field upon the application of a potential difference. This electric field induces charges or dipoles on the surface of the object, facilitating its attraction to the chuck via Coulomb forces. Given the device's dependence on this distinctive gripping mechanism, the condition and material properties of the contact surface play a pivotal role in determining the gripping force. Previous investigations have predominantly focused on enhancing the structural aspects of the device, encompassing surface smoothening techniques and the incorporation of rotational freedom for the end-effector. Nonetheless, owing to its inherently rigid structure, the ESC encounters difficulty in establishing a substantial real contact area, consequently constraining the gripping force within the boundaries defined by the applied voltage and the ESC's dimensions.

To address this inherent limitation, the present study proposes a novel concept revolving around the manipulation of the contact surface's stiffness. Specifically, two variations of bipolar ESCs were fabricated, differing in the materials employed for the contact surface (ABS, Nylon). By supplying current to the electrodes, the generation of heat was facilitated, thereby enabling to exert control over the stiffness of the covering material through temperature adjustments. To determine the gripping force exerted by the two ESC variants, a glass slide was employed as the target object, and the magnitudes of forces acting on the object and the proposed ESC were meticulously recorded under the multiple conditions. The influence of the adjustable stiffness was subsequently observed by analyzing the variations in the device's gripping force. Additionally, experiments were conducted wherein voltage was not applied, serving to quantitatively evaluate the adhesive forces at play, particularly those arising from van der Waals interactions. The results unveiled a noteworthy increase in the gripping force upon the reduction of the contact surface's stiffness, with the ABS-type exhibiting a gripping force enhancement of 1.682 times, while the Nylon-type witnessed a 1.833-fold increase. Furthermore, it was discerned that the gripping force surpassed the combined magnitudes of the electrostatic and adhesive forces, thereby underscoring the existence of a complex interplay between these two dominant forces. In an attempt to gain further insights into the underlying mechanisms, the ESC/glass system was modeled as a two-body problem, subsequently subjecting the influence of low stiffness to comprehensive analysis from the vantage points of contact and fracture mechanics.

The findings of this study represent a significant stride towards the development of bipolar electrostatic chucks endowed with tunable stiffness, thereby facilitating the reliable and repeatable manipulation of delicate objects. By surmounting the constraints imposed by conventional ESCs, this research endeavor holds the potential to engender a more effective gripping capability, spanning across a broader spectrum of objects. This acquired knowledge would contribute to the future progress of robotics in the field of film or plate handling.

11:00 AM SF06.08.07

Light-Powered Soft Steam Engines for Self-Adaptive Oscillators and Biomimetic Swimming RoboticsZhiweiLi; Northwestern University, United States

Oscillation plays a vital role in the survival of living organisms in changing environments, and its relevant research has inspired many biomimetic approaches to soft autonomous robotics. However, it remains challenging to create soft oscillators that can work under constant energy input and actively adjust the oscillation mode in response to environmental changes. Here, we present a steam-driven photothermal oscillator operating under constant light irradiation for continuous or pulsed, damped harmonic mechanical oscillations. The key component of the oscillator is a hydrogel containing $\text{Fe}_3\text{O}_4/\text{Cu}$ hybrid nanorods, which can convert light into heat and generate steam bubbles. Controllable perturbation to the thermo-mechanical equilibrium of the oscillator can thus be achieved, leading to either continuous or pulsed oscillation depending on the light intensity. Resembling the conventional heat steam engine, this environment-dictated multimodal oscillator uses steam as the working fluid, enabling the design of self-adaptive soft robots that can actively adjust their body functions and working modes in response to environmental changes. We then developed an untethered biomimetic neuston-like robot (neusbot) based on this soft steam engine, which can adapt its locomotion mechanics between uniform and recurrent swimming to light intensity changes and perform on-demand turning under continuous light irradiation. Fueled by water and remotely powered by light, this unique hydrogel oscillator enables easy control over the oscillation dynamics and modes, offering a promising approach to self-adaptive soft robots and solar steam engines.

11:15 AM SF06.08.08

Laser Induced Graphene for Soft Robotics: Actuators and SensorsAlexanderDallinger¹, StellaDrewes¹, Anna ChiaraBressi² and FrancescoGreco^{2,1,2}; ¹Graz University of Technology, Austria; ²Sant'Anna School of Advanced Studies, Italy

Laser Induced Graphene (LIG) is a porous conductive carbon material produced by laser-induced pyrolysis of polymer precursors, with applications in soft electronics/robotics and wearable electronics, among others.¹⁻³ Here, we present some examples of our studies on LIG-based soft actuators and sensors.

LIG conductive tracks are conveniently created through a single synthesis/patterning step by laser scribing with a CO₂ or UV laser onto a polymer precursor like polyimide.

By embedding the LIG into a stretchable and soft elastomeric matrix (i.e. polydimethylsiloxane-PDMS or polyurethane-PU), conductive and stretchable composites are created.

We realized various kinds of soft actuators based on LIG composites. In one case, by coupling the LIG/PDMS composite with a thin film of a smart humidity-responsive hydrogel (poly-(N-vinylcaprolactam), pNVCL) deposited by means of initiated chemical vapor deposition (iCVD), we realized a multi-responsive soft bending actuator, capable of self-sensing.⁴ In a second case, soft heating elements made of a LIG/PU composite were coupled with a Liquid Crystal Elastomer (LCE), a thermoresponsive material featuring excellent actuation properties like large actuation strains and reversible linear actuation process. In both cases the LIG served as a Joule heating element to resistively heat the active materials and trigger an actuation.

Also, embedding thin, flexible, lightweight LIG piezoresistive sensors into the body of soft pneumatic actuators is investigated as a mean for the integration of pressure (touch) and bending sensing capabilities.

Finally, LIG from biodegraded polymer precursors is investigated to enable novel sustainable approaches to soft robotics.

References

- (1) Lin, J. et al. *Nat. Commun.* **2014**, *5*, 5714.
- (2) Ye, R.; James, D. K.; Tour, J. M. *Adv. Mater.* **2019**, *31*, 1803621.
- (3) Dallinger, A. et al. *ACS Appl. Mater. Interfaces* **2020**, *12*, 19855
- (4) Dallinger, A. et al. *ACS Appl. Polym. Mater.* **2021**, *3*, 1809.

11:30 AM *SF06.08.09

Control of Soft RobotsMonicaOlvera de la Cruz; Northwestern University, United States

The design of materials with biological functions is a challenge that involves a delicate balance between structural form and function. We have explored external stimuli such as light and magnetic field to actuate and induce locomotion of soft materials functionalized for example with superparamagnetic and/or ferromagnetic components. I will describe the shape changes and materials parameters required to drive and direct these soft materials.

SESSION SF06.09: Soft Robotic Materials II
Session Chairs: Robert Shepherd and Ryan Truby
Wednesday Afternoon, November 29, 2023
Sheraton, Second Floor, Back Bay D

1:30 PM SF06.09.01

Protein-Based Robotic Materials for Healing and PropulsionAbdonPena-Francesch; University of Michigan, United States

Recent progress in soft robotics has motivated the search for new robotic materials and actuators that can replicate biological functions and behaviors (such as sensing, healing, powering, etc.) with various degrees of autonomy and complexity. Proteins are uniquely well-positioned to bring new solutions to these challenges, as they offer high versatility, specificity, and control in their self-assembly to regulate their emergent structures and properties. In this talk, we will introduce cephalopod-inspired proteins with a segmented block design that self-assemble into β -sheet nanocrystalline structures. These β -sheet nanocrystals act as physical and reversible crosslinking structures in supramolecular protein networks that regulate the physical properties. We demonstrate the dynamic properties of squid-inspired polypeptides in self-healing protein networks with healing strength and kinetics surpassing those typically found in other natural and synthetic soft polymers, and in self-regulated porous structures for chemically-powered microrobot propulsion. This family of cephalopod proteins and their biosynthetic derivatives have opened new opportunities in bioinspired design for adaptive functional materials and soft devices with enhanced autonomy and durability, and we will demonstrate their implementation in self-healing and reconfigurable soft actuators and in self-powered microrobots for aquatic locomotion.

1:45 PM SF06.09.02

Smart Materials with Tunable Properties Based on Low Melting Point AlloysWanliangShan; Syracuse University, United States

Smart materials with tunable properties such as mechanical stiffness and electrical conductivity have ample applications in soft robotics as actuating and sensing units. These smart materials typically are achieved through polymer-matrixed composite structures containing conductive reinforcement components. The stiffness change typically is realized through phase change of the reinforcement or glass transition of the matrix. Low melting point alloys (LMPA) in the form of layers and long fibers have been recently used in composite structures with tunable stiffness due to its low energy barrier for activation and high electrical conductivity. In this talk, we explore the possibility of dispersing LMPA into a polymer matrix to achieve robust smart materials with highly tunable properties. In the first approach we start with an LMPA foam with randomly distributed interconnected pores, and then infiltrate the LMPA foam with uncured elastomer such as polydimethylsiloxane (PDMS) to form a robust bicontinuous foam composite with stiffness change of three orders of magnitude. In the second approach we mix both LMPA particles and conductive fibers into an elastomer matrix to form a percolative network of particles and fibers within the matrix, such that the resultant smart materials have tunable electrical conductivity and mechanical stiffness. Recognizing the lack of appropriate analytical models for the mechanical and electrical properties of these smart materials, we have used effective medium theory informed by microstructure information to estimate their stiffness and electrical conductivity. Our experimental and modeling results are in good quantitative agreement. We also demonstrate the superior performance of these novel smart materials based on LMPA foam and LMPA particles in soft robotics applications.

2:00 PM SF06.09.03

Opposite Deformability of Shape-Changing Polymers in Response to a Single StimulusYuxingYao¹, XiaoguangWang², MilanWilborn³ and JoannaAizenberg³; ¹California Institute of Technology, United States; ²The Ohio State University, United States; ³Harvard University, United States

Efforts to enhance the capabilities of dynamic systems have been dedicated to the development of "intelligent" soft matter actuators that can undergo logic-based mechanical deformations, enabling adaptive structural morphing and modulation of interactions with local environments. The prevailing soft material building blocks rely primarily on a single transition between bistable states to achieve such functionality. To expand deformation behaviors, one current trend involves superimposing either geometric design or kinetically controlled transient behaviors onto bistable actuators. Complementary to this trend, another promising avenue is to develop a material building block that exhibits two (or more) transitions within itself. This would enable more complex logic-based mechanical deformations, such as subsequent deformations in opposite directions, which could significantly expand the repertoire of encoded mechanical deformations and related functions in a more efficient way, requiring fewer building blocks. However, there are no general chemical design strategies to realize arbitrary, opposite motions in soft material building blocks.

In this work, we report an end-on liquid crystalline elastomer (LCE) that exhibits two-step, opposite mechanical deformations, characterized as a contraction followed by an expansion relative to the starting point along the alignment axis in LCE microstructures under a continuously changing stimulus. By arbitrary manipulation of LCE alignment axis with a magnetic field, we can further extend such opposite deformability to different deformation modes, including tilting and twisting. Moreover, we demonstrate such phase-driven opposite deformability can be readily translated to macroscopic objects and enable the reversible manipulation of the sign of Gaussian curvature in radially aligned films, which was previously challenging to attain.

2:15 PM SF06.09.04

Magnetic Putty as a Reconfigurable, Recyclable and Accessible Soft Robotic MaterialMengLi^{1,2}, JunghwanByun², AniketPal², GauravGardi² and MetinSitti²; ¹Massachusetts Institute of Technology, United States; ²MPI for Intelligent Systems, Stuttgart, Germany

Magnetically hard materials are widely used to build soft magnetic robots, providing large magnetic force/torque and macrodomain programmability. However, their high magnetic coercivity often presents practical challenges when attempting to reconfigure magnetization patterns, requiring a large magnetic field or heating. This work presents magnetic putty as a robotic material

that is easy to shape in 3D and can autonomously self-heal, allowing recovery from mechanical damage and assembly of parts without adhesives. The magnetic putty is a soft composite made of hard-magnetic particles embedded in a viscoelastic silicone putty matrix. The interplay of its mechanical and magnetic properties is explored experimentally. The viscoelastic behavior is influenced by particle magnetization and the application of external magnetic fields. At the same time, its mechanical properties affect its magnetic properties, such as coercivity, remanence, and retention. The magnetic putty combines the benefits of hard- and soft-magnetic materials—high remanence and low coercivity—having large magnetic force under small fields and an easily reconfigurable magnetization profile. We show that the magnetization of magnetic putty can be easily reoriented with maximum magnitude using an external field that is only one tenth of its coercivity. We also describe how its magnetic field-induced stress changes under alternating magnetic fields. We show that, at a low magnetic field frequency and large field magnitude, it becomes an analog frequency doubler. We also demonstrate using magnetic putty as a robotic material to build reconfigurable magnetic setups, shapable magnets with adaptive polarities, recyclable magnetic robots, and growing bioinspired rotating vines. We envision that this easy-to-access material can provide the soft robotics community with a research and educational tool to explore fundamental questions and fast prototype magnetic soft robots.

2:30 PMBREAK

SESSION SF06.10: Architected Autonomous Materials
Session Chairs: Kaushik Jayaram and Ryan Truby
Wednesday Afternoon, November 29, 2023
Sheraton, Second Floor, Back Bay D

3:30 PM *SF06.10.01

Heterogenous, Reconfigurable Robot Swarms as Multifunctional Materials Zeynep Temel, Sha Yi and Katia Sycara; Carnegie Mellon University, United States

Recent breakthroughs in materials science, electronics, distributed computing, and manufacturing have led to an innovative category of multi-purpose substances known as robotic materials. Composite materials have developed capabilities such as detecting damage or auto-repair. However, none of the current state-of-the-art composite materials successfully combines the aspects of sensing, actuation, computing, and communication all into one [1]. One approach to creating autonomous robotic materials is to use robot swarms that can create functional configurations. Examples of creating functional structures using individual agents are observed widely in nature. For instance, ants have shown the ability to create functional structures like bridges by joining together and collaboratively performing tasks in a complex environment [2, 3]. Inspired by these organisms, reconfigurable robot swarms are capable of connecting with each other to form complex structures in rigid and flexible ways, resembling active, autonomous materials.

Robot swarms have shown the ability to display group behaviors that are unachievable by a solitary robot [4-6]. Additionally, robots that can physically link and engage with one another, known as self-reconfigurable robots, exhibit enhanced behaviors. Their use cases span from reshaping to adapting to various terrains [7], creating dynamic infrastructures [8], aiding in cooperative transportation [9, 10], to participating in search and rescue operations [11]. Existing connection methods between robots, whether mechanical or magnetic, may be complex to produce, require a significant amount of power, bear a constrained load capacity, or are only capable of forming inflexible structures. In addition, in most of these examples, agents have exactly the same characteristics, which limits the overall performance due to the lack of diversity of functionalities and operations.

Our recent work focuses on creating a system of robot swarms, PuzzleBots, where the robots can dynamically join to create useful structures such as bridges and ropes and disengage to independently explore their surroundings. This robot system is based on a mobile platform that measures 5cm in all dimensions and weighs around 70g. So far, we have demonstrated the creation of one-dimensional “line” and two-dimensional “mesh” configurations [12, 13] for overcoming negative obstacles in environments, explored the benefits of physical heterogeneity for enhanced mobility and control [13], and introduced the coupling flexibility between robots to adapt uneven terrain [14]. Our current efforts focus on building three-dimensional functional structures and sensing strategies for autonomy and distributed data collection during the desired motion. These robots have the potential to be used as building blocks to design active, multifunctional materials and to simulate the resulting behavior of any multifunctional material at different size scales.

References

- [1] McEvoy, M. A., & Correll, N. (2015). *Science*, 347(6228), 1261689.
- [2] Graham, J. M., *et al* (2017). *Journal of theoretical biology*, 435, 184-198.
- [3] Reid, C. R., *et al* (2015). *PNAS*, 112(49), 15113-15118.
- [4] Nagavalli, S., Chakraborty, N., & Sycara, K. (2017, May). *ICRA* (pp. 2674-2681). IEEE.
- [5] Pickem, D., *et al* (2017, May). *ICRA* (pp. 1699-1706). IEEE.
- [6] Werfel, J., Petersen, K., & Nagpal, R. (2014). *Science*, 343(6172), 754-758.
- [7] Ion, I., *et al* (2015). *Applied Mechanics and Materials* (Vol. 762, pp. 147-154). Trans Tech Pub Ltd.
- [8] Mateos, L. A., *et al* (2019, May). *ICRA* (pp. 7933-7939). IEEE.
- [9] Saldana, D., *et al* (2018, May). *ICRA* (pp. 691-698). IEEE.
- [10] Alonso-Mora, J., Baker, S., & Rus, D. (2017). *IJRR*, 36(9), 1000-1021.
- [11] Whitman, J., *et al* (2018, August). *SSRR* (pp. 1-6). IEEE.
- [12] Yi, S., Temel, Z., & Sycara, K. (2021, May). *ICRA* (pp. 8742-8748). IEEE.
- [13] Yi, S., Temel, Z., & Sycara, K. (2022, May). *ICRA* (pp. 4268-4274). IEEE.
- [14] Yi, S., Sycara, K., & Temel, Z. & (2023, July). *RSS* (accepted).

4:00 PM SF06.10.02

Reconfigurable Tensegrity Robot with Relocatable Extensible Strut and Variable Stiffness Tendon Suwoo Lee, Hyeonseo Song, Jun Kyu Choe and Jiyun Kim; Ulsan National Institute of Science and Technology, Korea (the Republic of)

For robots to be effectively employed in diverse scenarios, they need to facilitate seamless collaboration with both other robots and humans while being capable of adapting to unfamiliar environments and diverse terrains. In pursuit of this objective, extensive research has been conducted on soft smart materials that exhibit responsive behavior to a wide range of stimuli, leading to significant advancements in the field of soft robotics. Furthermore, to facilitate the integration of diverse functionalities alongside the progress in smart materials, efforts have been dedicated to the development of synergistic combinations with a variety of structures.

The tensegrity structure, inspired by biological systems, consists of prestressed tendons and rigid compressed struts. Tensegrity structures have garnered interest from researchers in the field of robotics due to their lightweight nature, inherent structural integrity, and remarkable ability to undergo substantial volume changes. Nonetheless, a drawback of the tensegrity structure lies in its inherent limitation of being capable of assuming only a predetermined shape set during its initial fabrication. Consequently, this restriction hinders its ability to effectively adapt to diverse environments, as it lacks the capacity for versatile shape transformations.

In this study, we present the fabrication of a reconfigurable tensegrity robot that encompasses intelligent functionalities into the smart tendon and strut devices. By doing so, we aim to address the limitations inherent in conventional tensegrity structures push the boundaries of tensegrity robotics and enable greater adaptability and versatility. The robot is endowed with three control parameters necessary for shape transformation, namely, variable-stiffness tendon, extensible strut, and relocatable strut, each of which plays a pivotal role in the overall mechanism.

The inclusion of particles within the tendon enables the realization of substantial alterations in stiffness with notable speed, owing to the jamming. Through the manipulation of stiffness, the robot is capable of both facile deformation in response to external forces and maintenance of structural integrity against collapse. It also facilitates the locking of the structure in a desired shape. A pneumatic-driven roller positioned external to the tendon can traverse along its length, offering the means to reposition the connected strut. The relocatable strut provides the robot with the ability to transform into a diverse range of shapes beyond the initially programmed structure by achieving considerable adaptability. The strut functions as an electrically operated linear actuator. A variation in the length of a single strut provides the ability to tilt the structure, whereas adjusting the length of all struts allows for alteration of the overall scale of the structure. To ensure smooth movement of strut location, the length of the linear actuator can be tuned to match the distance between the tendons when repositioning the strut.

As a result, we developed two distinct types of tensegrity robots: a triangular prismatic structure and an icosahedron structure. These robots exhibit shape-changing capabilities, which were previously unattainable in conventional tensegrity designs. Notably, the icosahedron structure introduces a novel control parameter for gait generation. Furthermore, the modularity of the tendons facilitates the construction of diverse tensegrity structures beyond the triangular prism and icosahedron exemplified in this study. In the future, we expect that these advancements can lead to the development of the next generation of adaptive and shape-changing robots, potentially reaching a level of sophistication that rivals biological systems, which possess localized

encoding of shape information.

4:15 PM SF06.10.03

Physical Artificial Intelligence in Untethered Soft Aerial Robots for Safe Environmental Interaction and Perching [Pham H. Nguyen](#)^{1,2} and [Mirko Kovac](#)^{1,2}; ¹Empa, Switzerland; ²Imperial College London, United Kingdom

As the next generation of aerial robots looks to widen its functionality and adaptability to multiple environments, the conditions required for its successful deployment has also increased. Previously, classical challenges aerial robots have had to face ranged from propeller noise, payload capacity, operational longevity, and robustness to collision and disturbances (physical obstacles and natural disturbances), just to name a few. But in order for the aerial system to effectively study natural habitats, aerial robots need to be capable of safely adapting and interacting with the unconstrained environment. One example of this is highlighted in the struggle aerial robotic systems have to tolerate collisions in order to safely land from a fall or successfully dynamically perch on objects with unknown shapes, sizes and textures.

To approach this problem, we made efforts to introduce compliance through the utilization of soft structures, in order to enhance mechanical impact protection, share functionality between flight and perching through shape reconfiguration, without any additional cost of reduced agility and flight time due to any extra payload.

In order to accomplish this, we looked at two approaches: (1) Shared functionality between flying and perching through metamorphic bistable origami-design soft arms. (2) Utilize a lightweight, fabric, inflatable, soft-bodied structure that can pneumatically vary its body stiffness to achieve intrinsic collision resilience. This is utilized in tandem with a lightweight bistable grasper that reacts upon contact with the perching object.

In the first approach, we noted how gliding aerial mammals morph their arms when transitioning between gliding flight and perching. Here, the developed quadrotor arms transition between two morphing stiffness states of flying and whole-body perching, utilizing a single-direction tendon drive. The quadrotor arms are bistable and are capable of collapsing around the perch within 0.97s. The arms are developed utilizing a layered technique between carbon-fiber, polyamide, and pre-stretched latex layers. With this setup, we were able to achieve approximately 30% overall mass reduction by this shared functionality. This setup was tested both indoors and outdoors in a forest environment.

In the second approach, we focused on the adaptable body of soft aerial robots. We developed an inflatable woven fabric soft body and arms for the quadrotor that can intrinsically vary its body stiffness on the fly for collision resilience. With this system, we highlighted its capabilities to repeatedly endure and recover from collisions in three-dimensions, supporting even harsh falls towards the ground without breaking its structure. In tandem with an equipped hybrid fabric-based bistable grasper that curls upon impact to conform around the perching object, we demonstrated the importance of having a soft body for improving the perching success rate on different objects significantly compared to the same system with a conventional rigid quadcopter frame.

Overall, in order to push the boundaries of current aerial robot designs to operate in cluttered environments and extend their range of functionalities, it is important to synthesize life-like soft aerial robots with shared physical artificial intelligent features and functionality, exploiting compliance as a key to do so. This will then push the next generation of aerial robots to not only improve their aerodynamic adaptability, efficiency, or maneuverability, but also lead to novel adaptations in adaptive manipulation and perching, aerial-aquatic-terrestrial transitions, withstanding dynamic collisions, reconfiguration for traversing through tight spaces, self-healing from damages, and adhesion in multi-modal environments.

4:30 PM *SF06.10.04

Towards Autonomous Kirigami Materials for Insect Scale Robotics [Kaushik Jayaram](#), Heiko Kabutz, William P. McDonnell, Hari K. Hari Prasad and Alex Hedrick; University of Colorado Boulder, United States

A major differentiating factor between engineered systems (e.g., an F-16), and their animal counterparts (e.g., a fruit fly) is robustness, or the ability to consistently perform in adverse conditions. While animals thrive in dynamic environments by continually adapting to current circumstances, engineered systems are rigid, relying on predesigned mechanisms and routines, which reduces their overall reliability. It is hypothesized that animals achieve robustness by tightly integrating sensing, actuation and feedback control in redundant, hierarchical structures throughout their bodies. This approach starkly contrasts with the incremental incorporations of analogous systems in modern engineered platforms and it is this lack of effective integration which is limiting their use in mission critical applications like recon, search and rescue and enemy engagements. These effects are severely felt in the performance of autonomous robots especially at the small scale where offloading processing to powerful computers is not an option.

A promising framework upon which inherently robust engineered systems can be built, is with so-called “robotic materials” (RM), i.e. a medium that tightly integrates local and redundant sensing, actuation, processing and communication. Readily available RMs would add unprecedented capabilities to our engineered systems but unfortunately, it is challenging to fabricate these materials. Popular additive manufacturing techniques like 3D printing, CMOS/MEMS fabrication are not ideal for integrating vastly different materials technologies or creating intricate features (at the micron scale) in a scalable, low-cost approach. One promising manufacturing method is the kirigami based stack laminate approach (Smart Composite Microstructures (SCM), Printed Circuit Microelectromechanical Systems Fabrication (PC-MEMS), etc.), which combines additive and subtractive processes selectively to successfully build individual RM components: (structure) insect scale robots, (sensing) stretchable sensor networks, (actuation) shape changing structures and (processing/communication) flexible electronics, but it has yet to be used to integrate these features into a single medium consistently. We will present our group's latest research on extending the PC-MEMS fabrication approach to begin to approach the promise of robotic materials and realize autonomous functionality. Specifically, we take advantage of femtosecond laser micromachining to pattern diverse materials including variety of smart materials which could not be previously fabrication using traditional laser processing. My research will focus on the development of a microbot smart leg with robust closed loop sensing and actuation, based on a laminate robotic material (LRM), helping to solve the manufacturing and system integration challenges of building LRMs. This platform will be used to study novel RM control algorithms, and the associated improvements to flight robustness after sustaining damage.

5:00 PM *SF06.10.05

Deployable Soft Origami Modular Robotic Arm with Variable Stiffness using Facet Buckling [Kyu Jin Cho](#); Seoul National University, Korea (the Republic of)

Robots that share activity spaces or physically interact with humans typically benefit from appropriate payload capacity, extensible workspace, low weight, safety, and space efficiency. The soft origami design and mechanism can meet many of these beneficial factors; however, achieving a high payload capacity remains challenging. In this talk, we present a soft origami arm module with high variable stiffness (x300) and spatial efficiency (compressed x3.1). The buckling of facets into a cylindrical tube followed by its pressurization, enables the arm to be highly stiffened. High-pressure capacity was obtained via the sewing-heat press fabrication process. We used a pneumatic pressure-tendon pair and utilized the frictional force between origami and tendon to prevent unintentional gravity-induced deformation while deploying. An analytical model was developed and compared to the experimental results. With our modular design, we could easily build functional robotic structures. Two robotic demonstrations were performed to examine the expandability of the modules. A variable-length robotic arm that mimics a human arm was built to manipulate typical objects. Additionally, a soft rover, which could carry 14 kg of weight and change its volume 29 times for improved spatial efficiency, was developed. This research suggests a new design methodology for practical soft robotic systems.

SESSION SF06.11: Embodied Physical Intelligence

Session Chairs: Amir Gat and Kaushik Jayaram

Thursday Morning, November 30, 2023

Sheraton, Second Floor, Back Bay D

8:30 AM +SF06.11.01

Design of Low Energy Actuation Pathways in Origami-Based Morphing Structures [Phil Buskohl](#); Air Force Research Laboratory, United States

A hallmark of living systems is the capacity to sense, assess and respond to environmental stimuli. Physical reconfiguration is a pervasive response to the environment for many living systems, such as leg actuation to achieve locomotion or shape change for camouflage or energy harvesting purposes. The soft robotics community has long taken inspiration from this feedback loop and the clear need for tractable morphing strategies to access multiple physical conformations to achieve diverse and energetically efficient tasks. Origami concepts are one strategy to address this morphing structure design problem, by segmenting global shape change into a series of folding operations. The interplay between stretching, folding, and facet bending modes in origami structures generates a complex energy landscape of morphing pathways and multistable states to utilize. However, identifying rigid and deformable folding paths in this high-dimensional and non-convex energy landscape is challenging. To help address this, we leverage the nudged elastic band algorithm to identify low energy folding paths between stable configurations in this landscape. The nudged elastic band technique is a global method that optimizes each point along the path to follow the gradient of the energy function, while also

maintaining separation between the points to provide adequate resolution along the path. We demonstrate the utility of this approach for discovering sequenced folding motions, distinguishing between rigid and deformable folding paths, and finding low energy folding paths between stable states in multistability origami structures. The presentation will conclude with a discussion how physical reconfiguration can also contribute to the assess domain of the sense, assess, respond feedback loop and the need for strategies to consolidate this feedback loop by maximizing their intrinsic compatibility.

9:00 AM SF06.11.02

Reprogrammable 2D Metamaterials: A Dynamic Approach to Spanning the Eigenvalue Space[Daniel Revier](#)¹ and Jeffrey Lipton²; ¹University of Washington, United States; ²Northeastern University, United States

Metamaterials, which exhibit unusual macro-behavior determined by their microstructure rather than their chemistry, are an evolving field with potential applications spanning from photonic and phononic bandgaps to auxetics and cloaking. However, designing these materials is a complex process, often requiring specialized expertise, advanced machine learning, or intensive computational algorithms. To address this, we propose an intuitive and streamlined approach to designing 2D mechanical metamaterials by specifically programming degrees of freedom (DOFs) in their construction.

Our method harnesses Straight Line Mechanisms (SLMs) as a single DOF, unimodal material, which can be arranged into specific symmetry patterns (three-way, four-way, and six-way), to sample the entire 2D metamaterial space. The metamaterial's properties can be programmed and reprogrammed by pivoting the mechanism, enabling a dynamic transition through the design space. This approach not only simplifies the design process but also offers adaptability similar to an electronic Field-Programmable Gate Array (FPGA), which can be reprogrammed after manufacturing to perform different tasks, thereby permitting the properties of the metamaterial to be altered and optimized as needed.

We delve into the design space by exploring the available eigenvalues in Cauchy elasticity, which defines the eigenvalue gamut. We further analyze the constraints and unique aspects of the gamut boundaries by probing the space through different symmetry patterns, with and without mirror symmetry, which influences the material's chirality. Moreover, we show the reconfiguration of a single lattice can transition smoothly between extremal properties, showcasing the potency and versatility of our design principle.

Our work provides a novel framework for the creation of reprogrammable, planar mechanical metamaterials. Our strategy facilitates the creation of unique structures like handed shearing auxetics and isotropic materials with Poisson's ratio approaching +/- 1 and 0. This approach demystifies the complex design process, offering flexibility to span the entire planar elastic tensor space and adapt to varying mechanical needs over time, making it a promising tool for the future of materials science.

9:15 AM SF06.11.03

Digital Composite with Independently Programmable Mechanical Properties[Xiao Yue Ni](#); Duke University, United States

Non-living materials typically exhibit fixed properties. The pre-set mechanical characteristics often compromise stability, performance, and efficiency, limiting the maximum potential of materials in varying conditions. Artificial materials that can actively change and adapt properties are highly desired. Here, we introduce a digital composite that comprises a grid of "voxels," each capable of individually transitioning between a soft, fluid state and a rigid, solid state. Each voxel is a chamber of liquid metal embedded within a silicone matrix, digitally controlled via local joule heating. This allows for real-time programming of the material's emergent mechanical properties based on collective voxel behavior. This system serves as a tangible simulation platform for experimentally investigating the mechanics of multi-material composite systems. Using this platform, we demonstrate the capability to program a variety of mechanical properties independently through statistical topological parameters. The resulting composites, which can be extended into 3D, can emulate a range of natural soft materials. The real-time programmability enables the material to produce desired stress-strain responses, exhibiting unconventional mechanical behaviors. The ability to digitally fine-tune the complex mechanics of materials introduces unprecedented flexibility in the microstructural design of materials for specific applications.

9:30 AM BREAK

10:00 AM *SF06.11.04

Embodied Control in Soft Robots via Stimuli-Responsive Modules[Qi Guang He](#), [Rui Yin](#), [Yu Cong Hua](#), [Wei Jian Jiao](#), [Hang Shu](#), [Cheng Yang Mo](#) and [Jordan R. Raney](#); University of Pennsylvania, United States

Robots typically interact with their external environment via feedback loops involving multiple sensors, microcontrollers, and actuators constructed from rigid electronic components that can be bulky, complex, and mechanically incompatible with soft materials. In this work, we explore strategies for embodying autonomous control of the trajectory and function of pneumatic soft robots. We specifically aim to embody the control system and its feedback loop via stimuli-responsive modules that can be moved, added, or removed from the robot to produce different behaviors in response to the surrounding environment. As one example, we build a kirigami-inspired robot that autonomously steers itself in response to variations in light or heat in the local environment by using liquid crystal elastomers (LCEs) in the control modules. The LCEs activate or deactivate modules to produce variable mechanical constraints in the kirigami, resulting in bending and steering of the robot. Additionally, we use analogous stimuli-responsive control modules to regulate the pneumatic logic of the soft robot, further expanding the range of autonomous functional changes that the robot can undergo. We show how decisions based on multiple stimuli can be achieved via logical combinations of these inputs.

10:30 AM SF06.11.05

Digitally Programmable Architected Materials with Static and Dynamic Reconfiguration for Soft Robots[Hang Xu](#); Concordia University, Canada

Some bio-materials can morph and adapt to environmental changes. For example, pinecone scales disperse seeds due to their bi-layer structures bending in dry autumn. Inspired by nature, scientists are developing architected materials with programmable static and dynamic reconfigurations. They change their shapes in response to environmental changes and thus are in high demand for various applications that need to move or deform, such as actuators of soft robots.

Traditional reconfigurable architected materials program exotic physical properties into their layout in an analog manner. Analogous to analog computers, analogue programming has a continuous range of inputs and outputs, which are susceptible to manufacturing inaccuracy and environmental disturbances. In contrast, digital programming operates on symbols and numbers with discrete values, usually zeros and ones. Since it would take a significant error to mistake a one for a zero or vice versa, digitally programmable devices are robust to the inaccuracy of components and more resilient in the face of noise. Furthermore, devices with digital programmability are versatile in diverse problems, contrary to analog units. Although recent efforts have produced programmable architected materials with digital logic operations [1] and stable memory [2], they have not demonstrated digitally programmable graphics and configurations analogous to that of digital devices, such as Character Encoding, in which graphical configurations can be stored, transmitted, and transformed via assigned numbers.

Here we overcome this challenge by using a design framework for a multistable architected material with static and dynamic reconfiguration. Our design comprises a tessellation of physical binary tetrahedral building blocks (Bi-TB), analogous to digital bits, with clearly delineated transformation phases. Each Bi-TB can be reversibly switched between two mechanically stable states (acting as phase transformation) using mechanical, thermal or electrical stimuli. We construct the cube-shaped Octet-truss unit cell via eight Bi-TBs, analogous to one digital byte containing eight bits. These units can independently and reversibly snap each of the eight corners between two mechanically stable positions. That way, all unit cells can deform and, when connected, provide multi-directional shape changes, including scale, linear, rotate, shear deformation, or their combinations. Under reversible deformation associated with a set of binary numbers, the architected materials yield markedly different mechanical properties; specifically, the stiffness and strength can be programmed to range over an order of magnitude. The digitally programmed reconfiguration can achieve either static functionalities, such as load-carrying construction versatile to different loading conditions, or dynamic functionalities, such as actuators. The precision-controlled reversible reconfiguration with multi-degree of freedom (MDOF) in this design paradigm will facilitate the development of advanced forms of soft robots. The soft robots integrated with developed architected materials will support a wide range of applications, including precision surgery and contour recognition via artificial intelligence (AI).

1. Zhang, H., et al., Hierarchical mechanical metamaterials built with scalable tristable elements for ternary logic operation and amplitude modulation. *Science Advances*, 2021. 7(9): p. eabf1966.

2. Chen, T., M. Pauly, and P.M. Reis, A reprogrammable mechanical metamaterial with stable memory. *Nature*, 2021. 589(7842): p. 386-390.

10:45 AM SF06.11.06

Kirigami-Based Compliant Mechanisms and Metamaterials for Multiaxial Optical Tracking for Machine Vision and Energy-Harvesting Applications[Chao Huang](#), [Max Shtein](#), [Erin Evke](#), [Yu-Wei Wu](#), [Michael Arwashan](#), [Byungjun Lee](#) and [Stephen R. Forrest](#); University of Michigan-Ann Arbor, United States

Novel actuation strategies have emerged in recent years to create unprecedented capabilities in soft robotics. One such strategy uses compliant mechanisms inspired by the Japanese arts of *origami* (folding) and *kirigami* (cutting). In this work, we use *kirigami* to create a polymer-based one-piece compliant mechanism that allows for optical tracking over a solid angle sweep of over 110° in two axes and using compact dimensions, realize 80-fold or greater optical concentration. We also show how this structure scales to an arbitrarily large array, yet the displacement required to achieve the angular sweep remain compact and independent of the number of elements and areal extent of the array, and examine multi-parameter array optimization to reduce semiconductor usage to reduce the cost solar electricity below that of stationary silicon panels. We further discuss use of novel materials and other robotics and autonomous material applications of such single-piece, compliant mechanisms.

11:00 AM SF06.11.07

We study the effects of boundary constraints and structural patterning on the morphology of growing polymer gels using computer simulations. The 3D simulation model is based on the gel lattice-spring approach, and accounts for the neo-Hookean gel elasticity, polymer-solvent inter-diffusion, and structural changes in the polymer network in the course of growth. These gels exhibit growth by incorporating monomeric units from the surrounding solution into their network. At Stage 0 of growth, a flat parent gel swells in a solution of monomers and cross-linkers until reaching equilibrium. The presence of boundary constraints (hard walls) during swelling of the parent gel causes a spatially non-uniform distribution of monomer solution in the gel sample with the degree of swelling close to the constrained surfaces being less than that far from them. The gel loses its initial flat shape and buckles. With the walls remaining in place, we then model Stage 1 of growth which consists of polymerization and cross-linking of the species, which diffused into the parent gel during swelling, followed by the chain-exchange with the primary network to form a random copolymer network (RCN). After the removal of the sol fraction, the resulting RCN gel is put back into the initial solution and swells until equilibrium under the same boundary constraints. The resulting Stage 1 RCN gel almost replicates the shape of Stage 0 parent network buckled due to the confinement. In effect, the shape of the Stage 0 parent gel templates the morphology of the subsequently grown gel. Moreover, when the grown RCN gel is detached from the walls, it does not relax back to a flat configuration but remains in a buckled state. The growth fixes an energetically unfavorable, deformed shape into a stable configuration. We consider several scenarios of growth of the RCN gels with a stable buckled shape by introducing various combinations of the boundary constraints and structural patterning of the growing gel through varying the crosslink density in a sample. In all cases considered, upon releasing the boundary constraints, the grown RCN gels take an equilibrium buckled shape with a shape pattern governed by the compositional heterogeneity during the growth process. These gels can be used as building blocks for polymeric materials design, and have potential applications as actuators, shape morphing materials, and controlled gradient materials.

11:15 AM SF06.11.09

Harnessing Non-Uniform Pressure Distributions: The Next Generation of Soft Robotic Actuators Yoav Matia¹, Gregory H. Kaiser², Robert Shepherd², Amir Gat³, Nathan Lazarus⁴ and Kirstin H. Petersen²; ¹Ben-Gurion University of the Negev, Israel; ²Cornell University, United States; ³Technion-Israel Institute of Technology, Israel; ⁴University of Delaware, United States

The primary goal of this work is to demonstrate how to teach a set of bladders a specific behavior - embodying code into matter. Specifically, we discuss complex motion in soft, fluid-driven actuators composed of elastomer bladders arranged around a neutral plane and connected by slender tubes is demonstrated. Rather than relying on complex feedback control or multiple inputs, the motion is generated with a single pressure input, leveraging viscous flows within the actuator to produce nonuniform pressure between bladders. Using an accurate predictive model coupling with a large deformation Cosserat rod model and low-Reynolds-number flow, all dominating dynamic interactions, including extension and curvature, are captured with two governing equations. Given insights from this model, five design elements are described and demonstrated in practice. By choosing the relative timescales between the solid, fluid, and input pressure cycles, the tip of the actuator can obtain almost any desired trajectory and can be placed anywhere temporarily within its 2D workspace. Finally, a six-legged untethered walking robot showcases the benefits of viscous-driven soft actuators. This work lays the foundation for a new class of morphologically intelligent, soft robotic appendages capable of complex deformations and multifunctionality without explicit drivers; whereby generating nonuniform pressure distributions, their infinite degrees of freedom can be exploited.

11:30 AM DISCUSSION TIME

SESSION SF06.12: Printing Autonomous Materials

Session Chairs: Yoav Matia and Ryan Truby

Thursday Afternoon, November 30, 2023

Sheraton, Second Floor, Back Bay D

1:30 PM SF06.12.01

The Design and Fabrication of an Entirely Soft Multi-Stable Magnetic Microarchitecture Taylor Greenwood, Nahid Hasan, Pai Wang and Yong Lin Kong; University of Utah, United States

The ability to achieve geometric reconfiguration of soft architecture is highly desirable for implantable and ingestible biomedical devices. However, triggering and sustaining multiple stable configurations in a dynamic environment without a continuous energy input remains challenging. Previous demonstrations require the persistent application of a magnetic field; or rely on the modulation of environmental factors (e.g., temperature, light) susceptible to dynamic perturbation. Here we demonstrate the design and fabrication of a soft multi-stable magnetic microarchitecture capable of rapid, on-demand, and reversible reconfiguration that is preserved even after adverse mechanical, chemical, and thermal experiences. The robust volumetric reconfiguration is enabled by an entirely soft, magnetically programmed, rationally designed inclined-beam bi-stable microarchitecture. We envision that such capability can enable new classes of soft biomedical devices with exceptional versatility and durability in dynamic environments.

1:45 PM SF06.12.02

Programming Control of a Versatile Ferrofluid: The Exploration of Multifunctional Liquid Robotics Jingge Chen^{1,2}, Liangyu Xia², Yuxuan Sun², Quanliang Cao² and Vicki L. Colvin¹; ¹Brown University, United States; ²Huazhong University of Science & Technology, China

The macroscopic and microscopic responsiveness of ferrofluid to external magnetic fields endow it considerable intelligence and rich functionality, which inspires liquid robotics that can realize arbitrary deformation and perform various functions. Here a versatile ferrofluid is developed, its intelligent manipulation, extensive applications and motion sensing are explored. The ferrofluid is made up of sterically stabilized ultra-small magnetic nanoparticles prepared by a facile one-pot method and purified under a temporary induced aggregation state, showing strong stability, flexible mobility, substantial magnetization, and adjustable concentration. Furthermore, the locomotion and morphology of ferrofluid can be manipulated by a programming control platform that integrates display, drive, control, and cooling modules. This device generates sequential pre-designed magnetic fields through the programmable activation of specific electromagnets. Moreover, the intelligent multi-dimensional actuation of substances with a wide range of densities could be accomplished by this ferrofluid in cooperation with permanent magnets manipulated by a robotic arm. This ferrofluid is also developed into a vibration sensor through aligning the magnetic moments in ferrofluids and detecting the flux change in vibration. In addition, the flow, concentration, and speed of ferrofluids can be detected by coupled coils. Such fabrication, control, operation and sensing explorations are central for the development of liquid robotics.

2:00 PM SF06.12.03

Backswimmer Inspired Buoyancy Mechanism for Underwater Robotic Swimmers and Potential Applications for Cooperative Motion Dror Kobo and Bat-El Pinchasik; Tel Aviv University, Israel

The backswimmer is an aquatic insect, capable of regulating its buoyancy underwater. Its abdomen is covered with hemoglobin cells, used to bind and release oxygen reversibly. Upon entering the water, the insect entraps an air bubble in a superhydrophobic hairy structure on its abdomen for respiration. This bubble, however, can change its volume through regulated oxygen flow from the abdominal hemoglobin cells. In this way, it can reach neutral buoyancy without further energy consumption. In this study, we develop a small, centimeter scale, backswimmer-inspired robotic swimmer (BackBot) with auto-buoyancy regulation through controlled nucleation and release of microbubbles. The bubbles nucleate and grow directly on onboard electrodes through electrolysis, regulated by low voltage. We use 3D printing to introduce a three-dimensional bubble-entrapping cellular structure, in order to create a stable external gas reservoir. To reduce buoyancy forces, the bubbles are released through linear mechanical vibrations, decoupled from the robot's body. Through pressure sensing and a Proportional Integral Derivative control loop mechanism, the robot auto-regulates its buoyancy to reach neutral floatation underwater within seconds. This mechanism comprises the basis for creating a group of robotic swimmers with auto-motion control, and for studying cooperative effects, reciprocal and non-reciprocal virtual interactions between group members.

2:15 PM *SF06.12.04

Silicone Printing With AMULIT: Additive Manufacturing at Ultra-Low Interfacial Tension Thomas Angelini and Senthilkumar Duraivel; University of Florida, United States

In several of his works, P.G. de Gennes told a story about tribespeople of South America who made boots by coating their feet with natural liquid latex that solidified into rubber. The story was intended to illustrate how small changes in the composition of phases of soft matter can lead to large changes in their rheological and material properties. This story also represents an elegant example of manufacturing with soft materials. Unfortunately, it is generally challenging to create complex structures with precision and accuracy when working with phases of soft matter, including silicone. The tendency of soft materials to slump, spread, flow, stretch, bend, and fail limits how we fabricate soft structures; for the most part, soft matter must be molded. One way to side-step the mold is to leverage embedded 3D printing, in which a liquid phase is extruded into a second support material that holds the liquid in its deposited shape, to be solidified or processed at a later time. In this talk I will describe the embedded 3D printing methods and materials our lab has developed that enables the shaping of soft matter while in its

liquid precursor state, focusing on 3D printing silicone-based inks. We have found that fabricated structures can be deformed or broken apart by very small forces because all the materials involved are either liquids or extremely soft solids. I will show how these disruptive forces arise from interfacial tension between printed inks and the support materials. To mitigate interfacial forces, we recently developed a method called “Additive Manufacturing at Ultra-Low Interfacial Tension,” in which we attempt to minimize the chemical differences between the ink and support material, eliminating the disruptive role of interfacial tension in embedded 3D printing. With this new approach we have fabricated complex and finely detailed silicone structures that accurately model human anatomy. Stable features as narrow as 8 micrometers can be fabricated with the AMULIT technique, and functional 3D printed silicone structures are as robust and durable as their molded counterparts. Moving forward, we believe the AMULIT technique will be a useful tool in developing new components for soft robotics and autonomous materials.

2:45 PMBREAK

3:15 PM *SF06.12.05

Rapid Manufacturing of Elastomers, Thermosets and Composites with Tunable Multifunctional Properties[Nancy R. Sottos](#), Justine Paul, Luis Rodriguez Koett, Pranav Krishnan, Javier Balta, Sameh Tawfik and Jeffrey Moore; University of Illinois-Urbana-Champaign, United States

Complex patterns and gradients integral to the structure and function of biological materials emerge spontaneously through reaction-diffusion controlled processes during morphogenesis. In contrast, functional patterns in synthetic materials are created through multistep manufacturing processes requiring masks, molds, or printers. Current additive manufacturing techniques for fabricating complex, architected materials often face limitations in achieving the desired level of complexity and control without extensive human intervention and additional tools. Inspired by reaction-diffusion systems in nature, our work seeks to harnesses rapid reaction-thermal transport during frontal polymerization to drive the emergence of spatially varying patterns and tailor properties of polymers and composites during the manufacturing. Tuning of the reaction kinetics and thermal transport enables internal feedback control over thermal gradients to spontaneously pattern morphological, chemical, optical, and mechanical properties of structural materials. A range of experimental tools are exploited to characterize the evolution of the microstructure and properties, including IR imaging of the temperature history and front evolution, differential scanning calorimetry to determine degree of cure, wide angle x-ray scattering, nanoindentation and mechanical testing to assess changes in thermomechanical properties. Functionally graded and patterned regions with two orders of magnitude change in modulus and over 200°C change in glass transition temperature are achieved in thermoset polymers. Small perturbations in the fabrication conditions lead to remarkable changes in the strength, elastic modulus, and toughness of the resulting materials. This ability to control mechanical properties and performance solely through the initial conditions represents a significant advancement in the design and manufacturing of advanced multiscale. Moreover, we envision that more sophisticated control of reaction-transport driven fronts may enable spontaneous growth of structures and patterns in synthetic materials, inaccessible by traditional manufacturing approaches.

3:45 PM SF06.12.06

Fully Printed Micro-Patterned Electrochemical Actuators[Ji Zhang](#), Qingshen Jing, Tom Wade, Zhencheng Xu, Liam Ives, Diandian Zhang, Jeremy J. Baumberg and Sohini Kar-Narayan; University of Cambridge, United Kingdom

Submillimetre or micrometre scale electrically controlled soft actuators have immense potential in microrobotics, haptics, and biomedical applications. However, the fabrication of miniaturised and micro-patterned open-air soft actuators has remained challenging. In this study, we demonstrate the microfabrication of trilayer electrochemical actuators through aerosol jet printing, a rapid prototyping method with 10 µm lateral resolution. A fully printed 1 mm × 5 mm × 12.2 µm ultrathin PEDOT:PSS/Nafion/PEDOT:PSS actuator is successfully actuated in air under voltages from ±0.1 V to ±0.8 V, giving deflection angles proportional to the applied voltage, and reaching a peak-to-peak deflection of 0.25 rad (14 degrees) under a ±0.8 V 0.1 Hz square wave. The thinness of this AJP actuator reduces the proton transport length and flexural rigidity, hence causing relatively fast response and large deflection under low voltages. Next, we fully printed an actuator with two individually controlled submillimetre segments and demonstrated its multimodal actuation. The convenience, versatility, rapidity, and low cost of our microfabrication strategy promises future developments in integrating arrays of intricately-patterned individually-controlled soft microactuators on compact stretchable electronic circuits.

4:00 PM SF06.12.07

Hybrid 3D Printing of Wireless Stretchable Tactile Displays with Robust Sensing and Actuation[Ramon E. Sanchez](#); Boston University, United States

Current manufacturing methods for prototyping soft tactile displays rely on complex techniques with limited scalability that are incompatible with stretchable electronics. This work presents a stretchable wearable tactile display with sensing and feedback capabilities manufactured by hybrid multi-material 3D printing in a single fabrication process. The electrical wiring and sensing elements of the display are 3D printed using a strain-induced electrically conductive liquid metal emulsion, which exhibits the shear yielding and shear thinning behavior necessary for direct ink writing (DIW). The actuators and off-the-shelf electronics are combined with the LM emulsion through automated pick-and-place. Once the LM emulsion and the electronics are integrated on a 3D printed polymer base with walls, they are packaged with liquid elastomer and cured. Upon mechanical activation of the LM emulsion composite through axial and lateral strains of 200% each, they reached a conductivity that is within an order of magnitude of the bulk LM. The sensing elements are force sensing resistors (FSR) composed of printed filaments on a spiral architecture. Electro-mechanical characterization of the sensors indicated that their sensitivity and response time were directly related to their conductivity. Upon further activation of the FSR at compressive strains of 60%, their conductivity increased to the same order of magnitude as the bulk LM, and a sensitivity of 0.05 kPa⁻¹, which is an order of magnitude higher than that of the electrical wiring. To show the capabilities of the tactile display, we fabricated two self-contained devices, one with an embedded array of FSR, and one with an embedded array of actuators. The device with the array of FSR collects data in the form of tactile patterns, collecting both the location and magnitude of the signal, and transmitting this data wirelessly in real time. The device with the array of actuators receives this signal and reproduces the tactile pattern for an immersive and synchronized tactile experience between two individuals.

4:15 PM *SF06.12.08

New Materials for All-Printed Soft Robotics[Shlomo Magdassi](#); Hebrew University of Jerusalem, Israel

Additive manufacturing, which is the process of fabrication through printing, brings new opportunities in the general field of material science and in particular, in soft robotics. Here we describe new materials and processes for making soft grippers with embedded sensors, starting from a solution of monomers and oligomers, and dispersion systems. The utilized printing materials result in highly stretchable objects that are the base for fabricating actuators which are the main component of soft grippers. Furthermore, several responsive materials will be presented, which bring sensing abilities, thus enabling the fabrication of autonomous soft grippers. The sensing is obtained by unique designs of the grippers and embedded electrically conductive particles. These grippers can adapt to different shapes, apply holding forces tailored to the object's mechanical properties, and provide information to the control system for optimal operation.

SESSION SF06.13: Biohybrid Autonomous Materials
Session Chairs: Robert Shepherd and Ryan Truby
Friday Morning, December 1, 2023
Hynes, Level 2, Room 204

8:00 AM *SF06.13.01

Active Gels Driven by the Belousov–Zhabotinsky Reaction[Shingo Maeda](#); Tokyo Institute of Technology, Japan

We explore research on autonomous gel actuators and gel machines driven by chemical reaction networks. We focused on the BZ reaction. The BZ reaction consists of a typical chemical reaction network. The Belousov–Zhabotinsky (BZ) reaction, known as a chemical oscillation, is a chemical reaction that induces self-oscillation in concentration. The catalyst of the BZ reaction is covalently bonded to the polymer chain so that the BZ reaction occurs only inside the gel, and the change of the osmotic pressure associated with the oscillation of concentration causes periodic swelling and shrinkage of the gel. The essence of the coupling between the BZ reaction and the gel is that the swelling and contraction motion of the gel can sufficiently follow the chemical reaction, and we have designed peristaltic motion of polymer gels and self-walking gels.

Recently, we have proposed a new hypothesis regarding the temperature-compensated biological clock using temperature-responsive BZ gels. The temperature compensation of the biological clock is the property of maintaining a constant cycle regardless of changes in temperature, and the mechanism of the temperature compensation is not clearly understood. By constructing a mathematical model of the temperature-responsive BZ gel and analyzing it theoretically, we found that the temperature compensation can be realized by offsetting the effect of temperature change by volume change of the BZ gel. Our experiments also showed that the temperature-responsive BZ gel exhibits temperature compensation, and we succeeded in designing an artificial biological clock.

8:30 AM *SF06.13.02

Self-Regulated Hydrogel Actuators - Tuning Actuation with a Pinch of Salt [Bilge Baytekin](#); Bilkent University, Turkey

Self-regulation is an essential property for maintaining the vitality of living organisms. Helping the organisms respond to internal and external changes, self-regulation is also the basis of the autonomy of all living systems. The complex biochemical feedback for self-regulation is hard to replicate directly in artificial systems. However, it was previously shown that artificial self-regulation can also be achieved in material systems by designing proper combinations of the systems chemical and physical features. Previously, we constructed electronics-free artificial systems mimicking heliotropism (sun tracking) and nyctinasty (leaf opening) in plants. In these systems, dehydration/rehydration cycles were employed to cause the actuation and feedback. In this work, we use some common salts doped in the hydrogels to tune the bending behavior of hydrogel actuators. The bending rate of the 'salty' actuators parallels the physical-chemical differences of the ions in the salt. With the actuator parts made up of essentially the same hydrogel, including different salts, responding to the same input at different rates, the programmability of an overall hydrogel material for more complex motion can be achieved. The straightforwardly achievable, programmable, and tunable 'embodied intelligence' in autonomous hydrogel materials can be used in soft robotics, soft sensors, and environmental monitoring.

9:00 AM SF06.13.03

Autonomous Microtools Built from Soft-Stiff Micro-Fabricated Actuators [Sandra Edward](#)¹, [Holly M. Golecki](#)¹ and [Bryan Kaehr](#)²; ¹University of Illinois at Urbana Champaign, United States; ²Sandia National Laboratories, United States

Photothermally actuated microbots with the ability to capture and release objects on the microscale have widespread applications in the medical field for microsurgery or selective cell extraction. Light driven micro-actuators can be fabricated with environmentally responsive materials compatible with 3D printing and have the advantage of being programmable, wireless, and of high resolution. Compliant microbots can deliver site-specific therapeutics with autonomous control in dynamic environmental conditions. In this presentation, we describe the design, fabrication, and testing of a hybrid stiff-soft microgripper system on the tip of a 200-micron diameter core fiber. The stiff, yet compliant exoskeletal gripper head is autonomously actuated by soft active hydrogels that can react to forces generated due to external light power from the fiber optic or from environmental factors like pH or temperature. Compliant skeletal structures are fabricated using 2-photon polymerization additive manufacturing directly on the end of optical fibers. In this work, we explore the design and functionality of tools to facilitate gripping, cutting, and clamping actuation mechanisms. To control actuation, we demonstrate current regulated growth of hydrogels within the printed gripper structure. We test different methods to functionalize the gel component of the actuator to reduce heat losses, increase the efficiency of the gel and the system, and increase the total actuation displacement. In one adaptation, pNIPAM gels are functionalized with metallic nanoparticles to improve photothermal absorption. Additionally, liquid crystal elastomers can also be aligned using electric fields to form soft actuators within printed tools. To evaluate the hybrid microgrippers, we test for optimal print parameters, elastic recoil, response time, accuracy, and cyclic durability. This work provides a foundation to study stimuli-responsive photothermal micro-scale optical tools to expand the scope of tools available for minimally invasive surgical procedures.

9:15 AM SF06.13.04

Towards Sustainable and Robust Soft Robots using Dynamic Covalent Polymer Networks [Aleix Costa Cornellà](#), [Francesca Furia](#), [Seppe Terryn](#), [Bram Vanderborght](#), [Guy Van Assche](#) and [Joost Brancart](#); Vrije Universiteit Brussel, Belgium

Despite all the efforts that are being put into it, materials used for soft robots currently do not offer a complete sustainable solution as i) they are easily damaged, ii) the materials used are fossil-based and iii) the materials used are normally permanently crosslinked, which hinders its processability, recyclability and biodegradability. A material that is increasingly used in soft robotics because it offers a solution to these problems is gelatin. However, it is highly susceptible to changes in environmental conditions such as temperature or humidity, which highly limits its use in real-world applications.

Introducing dynamic bonds into polymer networks can produce materials that can be more easily processed, applied, and recycled than their permanent counterparts. Moreover, they show improved toughness, stretchability, and the ability of healing physical damage. This dynamic bonding can be introduced into the polymer by means of supramolecular interactions, dissociative dynamic covalent bonding, or associative dynamic covalent bonding (vitrimers). All three systems have their strengths and weaknesses, but they all suffer from the same compromise, which is having to choose whether to be able to self-heal/reprocess at mild conditions and having long-term mechanical stability. To be able to self-heal at mild conditions you need materials with fast relaxation dynamics, however, fast relaxation dynamics are undesirable in most applications like in soft-robotics as the material behavior becomes heavily time and temperature dependent. Here, we developed a method to tailor the relaxation time regime in dynamic polymer materials to address this inherent issue. We've combined two dynamic covalent bond chemistries with completely different relaxation dynamics, both in time scale and in its mechanism. More specifically, we've combined Diels-Alder bonds based on furan and maleimide and β -hydroxy ester bonds. By tuning the ratio between Diels-Alder bonds and β -hydroxy ester bonds it is possible to access the complete range of relaxation times between the two mechanisms. And more importantly, the two mechanisms can be observed in the same material but at different timescales. This allows to develop materials that can partially relax at mild conditions, which are enough for self-healing, but not show creep as the network doesn't fully relax, as well as showing shape memory capabilities.

The materials are also designed guided by the 12 principles of green chemistry. They are synthesized using 100% bio-based raw materials, based on fatty acids, without using any solvent, and are potentially (bio)degradable. As all the components have a similar backbone, the mechanical properties of the materials don't vary much between materials with different ratios of associative and dissociative bonds. The Young's modulus of the whole range of materials sits around 1.5 ± 0.5 MPa at room temperature.

With this strategy the design of the mechanical properties is decoupled from the relaxation dynamics. Combining two types of dynamic bonds with very dissimilar relaxation dynamics empowers a range of applications where the materials can be tailored according to its application, its processing, as well as the timescale of its use. These applications include 3D printing, which is one of the biggest challenges for dynamic covalent bonds, and soft-robotics.

9:30 AM BREAK

10:00 AM *SF06.13.05

Wearable Devices and Structural Designs for Neural Interfaces [Jang-ung Park](#); Yonsei University, Korea (the Republic of)

Recent progress in optoelectronic devices for wearable electronics demands their outstanding mechanical deformability for versatile systems in daily life. Especially, rapid advances in neurotechnology enable bidirectional communication between the nervous system and engineered devices. The precise recording and stimulation of typical target neurons by neural interfaces with adequate materials and structures can provide revolutionized medical applications, including the diagnosis and treatment of neurological disorders. Thereby, a proper understanding of the electronic device and its interfacing biological surroundings is necessary. Here, this talk presents the fundamental concepts of neural signaling, neural recording, and stimulation to introduce neural interfaces with wearable electronic devices. Then, we summarize the considerations of the materials and introduce a variety of materials that satisfy the requirements. Furthermore, the key challenges for next-generation neural interfaces are considered, and future directions are explored based on recent studies.

10:30 AM SF06.13.06

Soft Sensory Robots Based on Stimuli-Responsive Hydrogels for Electronic Implants [Wubin Bai](#); University of North Carolina at Chapel Hill, United States

Living organisms with motor and sensor units integrated seamlessly exhibit effective adaptation to dynamically changing environments. Taking inspiration from coherent integration between skeletal muscles and sensory skins in human, we present a design strategy of soft robots, primarily consisting of an electronic skin (e-skin) and an artificial muscle, that naturally couples multifunctional sensing and on-demand actuation in a soft, biocompatible platform. Here, we will describe an *in situ* solution-based method to create the e-skin layer with a series of sensing materials (e.g., silver nanowires, reduced graphene oxide, and poly(3,4-ethylenedioxythiophene) polystyrene sulfonate) incorporated within a polymer matrix (e.g., polyimide and polydimethylsiloxane), imitating human skin with complex receptors to perceive various stimuli. Biomimicry designs (e.g., starfish and chiral seedpods) of the soft robots enable various active motions (e.g., bending, expanding, and twisting) on demand and realize good fixation and stress-free contact with tissues. Furthermore, integration of a battery-free wireless module into these soft robots enables robotic operation and communication without tethering, thus enhancing safety and biocompatibility of the soft robots as minimally invasive implants. Demonstrated examples range from a robotic cuff enclosing around a blood vessel for precise detection of blood pressure, a robotic gripper holding onto a bladder for accurately tracking bladder volume, an ingestible robot residing inside stomach for pH sensing and on-site drug delivery, to a robotic patch wrapping onto a beating heart for quantifying cardiac contractility, temperature and applying cardiac pacing, highlighting the application versatility and potentials of the bioinspired soft robots. Our designs of soft robots could establish a promising strategy to integrate a broad range of sensing and responsive materials, for forming highly integrated systems for medical technology and beyond.

10:45 AM SF06.13.07

Magnetic Surface Microrollers for Endovascular Navigation [Ugur Bozyuk](#)^{1,2} and [Metin Sitti](#)^{1,2}; ¹Max Planck Institute for Intelligent Systems, Germany; ²ETH Zürich, Switzerland

Mobile microrobots offer great promise for minimally invasive targeted medical applications to overcome the current limitations in cargo delivery thanks to their precise controllability. The circulatory system represents the ideal route for the navigation and delivery of microrobots; however, blood flow impairs the propulsion of microrobots. Magnetic surface rolling microrobots, or "surface microrollers" emerged as an attractive microrobotic platform for navigation in blood vessels utilizing decreased flow velocities on the blood vessel walls. In this work, we assess the navigation potential of the surface microrollers in blood vessels for future drug delivery applications. First, we started developing the microrobotic platform from scratch. Then, we characterized their locomotion characteristics, which yielded the fastest magnetic microrobot in its size scale in the literature, corresponding to 80 body lengths per second. Then, its upstream

locomotion performance in physiological blood flows was characterized in microfluidic chips; the results have shown significant potential for navigation in blood flows. Furthermore, the antibody-modified surface microrollers could also recognize the cancer cells during active locomotion and deliver chemotherapeutics to cancer cells, showing the platform's multi-functionality. Having confirmed the system's potential, we explored the hydrodynamic barriers for locomotion in physiological blood flows in detail. The hydrodynamic barriers can be classified under three main topics: 1) Surface microtopography effect, 2) Confinement effects, and 3) Flow rate/velocity effects. The surface microtopography of the vessel walls, in the same size scale of surface microrollers (3-8 μm), unexpectedly creates a significant barrier for locomotion. Even though the locomotion is high-speed and unimpeded on flat surfaces, the surface microtopography effect can entirely stop the locomotion of spherical microrollers due to unfavorable hydrodynamic interactions between microroller and surface microtopography, revealed in computational fluid dynamics (CFD) simulations. We have demonstrated that rod-shaped microrollers render minimal interaction with the neighboring boundaries, thus smoothly locomoted on such textured surfaces. The problem can also be solved by using bigger-sized spherical microrollers, and then the surface microtopography effect disappears. Next, we investigated the physical confinement effect on the surface microrollers, which would be encountered in small blood vessels such as capillaries and venules. Our experiments demonstrated that the locomotion efficiency of spherical microrollers drastically decreases in confined spaces, even causing reverse locomotion in circular confinements. The CFD analysis revealed that the impeded locomotion is due to out-of-plane rotational flows rather than translational flows generated during locomotion. Hence, a slender microroller design, generating smaller rotational flows, outperforms spherical microrollers in confined spaces. Last, we characterized different flow rate/velocity effects on surface microrollers. In a CFD model, we investigated the upstream locomotion performance of surface microrollers in main blood vessel types in the systemic circulation. The results have demonstrated that the microroller locomotion halted in the small vessels due to increased flow and confinement effects. In contrast, the locomotion seemed fully and partially possible in the venous and arterial flow. Having explored the limitations and possibilities, we have demonstrated the upstream locomotion of biocompatible and high-performance microrollers in venous flow under real-time imaging, confirming the previous findings. Overall, we comprehensively investigated the potential of magnetic surface microrollers in blood vessels for their future drug delivery applications.

11:00 AM SF06.13.08

DNA-Based Nanomaterials with Robotic Functions Marcella DeLuca¹, Sebastian Sensale¹, Wolfgang Pfeifer², Chao-Min Huang¹, Michael Poirier², Carlos Castro² and Gaurav Arya¹; ¹Duke University, United States; ²The Ohio State University, United States

DNA nanotechnology is a promising approach for creating soft robotic nanomaterials due to its ability to create nanostructures of unprecedented geometric complexity and high programmability. While recent advances have led to dynamic DNA devices capable of undergoing complex motions, the size and functionality of these structures remains limited [1]. In this talk, I will describe our recent efforts in designing and modeling complex multicomponent DNA nanomaterials with tailored or emergent dynamic behaviors characteristic of smart robotic systems. I will begin by discussing a software we developed that uses feedback from coarse-grained molecular dynamics simulations to automate the design of freeform 3D DNA nanostructures and their assemblies [2]. I will then show how we used this framework along with mesoscopic models, simulations, and statistical mechanics to create 1D arrays of sterically interacting DNA origami structures that can communicate mechanical signals along the array [3,4] and 2D arrays of interacting DNA rotors that can undergo intriguing order-disorder transitions akin to, and beyond, the Ising lattice [5]. Such systems capable of exhibiting complex dynamic, organizational behavior could be harnessed for applications in sensing, soft robotics, optics, and energy harvesting.

[1] DeLuca, M., Shi, Z., Castro, C.E. and Arya, G., 2020. Dynamic DNA nanotechnology: toward functional nanoscale devices. *Nanoscale Horizons*, 5:182-201.

[2] Pfeifer, W., Huang, C.M., Poirier, M.G., Arya, G. and Castro, C., 2023. Versatile Computer Aided Design of Freeform DNA Nanostructures and Assemblies. *Science Advances* (under revision).

[3] Wang, Y., Sensale, S., Pedrozo, M., Huang, C.-M., Poirier, M.G., Arya, G., and Castro, C.E., 2023. Steric Communication between Dynamic Components on DNA Nanodevices. *ACS Nano* 17:8271-8280.

[4] Sensale, S., Sharma, P. and Arya, G., 2022. Binding kinetics of harmonically confined random walkers. *Physical Review E*, 105:044136.

[5] DeLuca, M., Pfeifer, W.G., Randoing, B., Huang, C.-M., Poirier, M.G., Castro, C.E. and Arya, G., 2023. Thermally reversible pattern formation in arrays of molecular rotors. *Nanoscale*, 15:8356-8365.

11:15 AM SF06.13.09

Soft Robotic Capacitive Sensing for Force Measurement in Neurosurgical Procedures Daniel Van Lewen, Catherine Wang, Hun Chan Lee and Sheila Russo; Boston University, United States

Neurosurgical procedures require a high level of accuracy to complete tasks within the delicate region of the brain. Current tools for moving brain tissue (i.e., tissue retraction to expose cancerous lesions) during these procedures are mostly made out of stainless steel and create localized regions of pressure. These tool-tissue interactions can be harmful and lead to postoperative complications (i.e., hampered neuromotor and neurocognitive functions), especially when the forces are applied over longer periods of time. Research on soft robots is rapidly expanding within the field of surgical robotics due to their ability to safely interact within human tissue, a trait which can reshape tissue interactions in neurosurgery. However, they have generally been difficult to control due to nonlinear behaviors. Using principles of morphological computation, various design techniques have been developed to control the behavior of soft robots, such as the application of origami-inspired folding patterns. For soft robots to be deployed in neurosurgery, greater control through the integration of soft sensing is required by surgeons during these procedures.

This work presents an origami-inspired soft robot with integrated capacitive sensing for measuring force during tissue retraction in neurosurgical procedures. The robot employs an origami-inspired actuation technique in which a circular Miura origami pattern creates well-defined contraction and expansion ratios. A thermoplastic wrapping allows for expansion to be controlled via vacuum pressure. To embed a sensing modality in the robot, an individual origami unit cell is modified to become a capacitor that changes in capacitance when force is applied. The force results in displacement between the capacitive plates. The retraction process can therefore be monitored by the surgeon to ensure that dangerous levels of forces are not exceeded. The sensing origami units are fabricated using a layering technique which embeds a fluidic stiffening actuator within an elastomer dielectric. Thin copper films, laser cut in the shape of the origami unit cell, sandwich this dielectric layer to create the plates for the capacitive sensor. Three sensing unit cells are integrated into the circular Miura pattern at evenly spaced locations and connected electrically in series. The hyperelastic properties and shape of the dielectric are chosen to sufficiently displace the plates so that a full range of forces of 0-3 N (typically found in neurosurgery) can be measured.

Calibration of the sensing unit demonstrates the relationship between force and capacitance giving a model which can output force measurements. The force range and sensitivity are analyzed through characterization experiments of the sensors on the robot giving an indication of the sensing behavior during force application and folding of the robot. Response of the system over time shows the correlation between actual applied force and capacitance over time. Finally, an in-vitro setup was developed to model the retraction process in the brain and demonstrate the robot's ability to retract brain tissue and sense the distributed forces. Development of this sensing mechanism gives a method for both monitoring and controlling the pressure on the brain during robotic tissue retraction, demonstrating the potential of soft robots in neurosurgery.

11:30 AM *SF06.13.10

Strain-Programmable Bioadhesive Hydrogels and Their Biomedical Applications Hyunwoo Yuk; SanaHeal, Inc., United States

Stimuli-responsive hydrogels such as hydrogel actuators that change size and/or shape upon diverse stimuli (temperature, light, chemical gradient, swelling, electrical/magnetic field) have been widely studied in academic research. Despite their interesting nature and properties as a class of smart materials, their translational applications have been relatively unexplored due to various practical limitations. Recently, stimuli-responsive hydrogels combined with other functionalities have emerged to expand their potential utility in diverse applications. As one of the recent examples, in this talk, we will discuss strain-programmable bioadhesive hydrogels as a new class of fully programmable and bio-integrative smart material for biomedical applications. We will introduce the unique hydration-based shape memory mechanism of the strain-programmable bioadhesives from both experimental and theoretical perspectives. We will further introduce several translational biomedical applications of the strain-programmable bioadhesives for the control of swelling in implantable hydrogels, programmed mechanical modulation of biological tissues for accelerated wound healing, and bioadhesive integration of implantable devices. We will close this talk with future perspectives on the potential use of strain-programmed bioadhesive hydrogels as soft robotic materials for diverse biomedical applications where integration and programmed mechanical modulation of biological tissues can synergistically merge.

SESSION SF02/SF03/SF04/SF06/SF07: Joint Virtual Session
Session Chairs: Olaf Borkiewicz, Michael Grapes and Yoav Matia
Wednesday Morning, December 6, 2023
SF06-virtual

8:00 AM SF02/SF03/SF04/SF06/SF07.01

Computational Combustion Study of Reactive Metal Nanoparticles as Solid Additives Priyanshu Luhar¹, Sujin Kim², Hyung Sub Sim² and Sungwook Hong¹; ¹California State University,

Energetic nanoparticles, those particularly including Ti-Al-Mg components, have attracted significant interest due to their potential applications in combustible fields. Ti-Al-Mg reactive materials typically consist of a mixture of titanium (Ti), aluminum (Al), and magnesium (Mg) in varying proportions. The combination of these elements offers a favorable balance between energy density and safety, making them suitable for a range of applications. Previous studies have explored the synthesis, characterization, and applications of Ti-Al-Mg reactive materials. For instance, Belal *et al.*¹ investigated the burning rate of mechanically activated Al-Mg composites. Their research highlighted mechanical activation of Al-Mg nanoparticles decreases the ignition temperature of the particles and enhances their reactivity. Furthermore, Kochetov and Sytshev² explored the influence of Mg content on the thermal properties and reactivity of Ti-Al-Mg composites. Their findings demonstrated that the interaction between Mg, Al and Ti can result in a lightweight composite suitable for applications at high temperatures, which is crucial for tailoring their performance in specific applications. While previous experimental studies have successfully investigated combustion performance of those reactive materials, molecular-level understanding of thermal behaviors of Ti-Al-Mg nanoparticles has yet to be achieved. Here we perform reactive molecular dynamics simulations based on ReaxFF^{3,4} to investigate initial oxidation processes of three nanoparticles (Ti, Al, and Mg). Our RMD simulations reveal molecular-level reaction steps for the combustion process of the reactive nanoparticle with and without an aggregation effect. Our RMD simulations will help guide an experimental design of a novel metamaterial using Ti-Al-Mg composites, providing a valuable input for the community of solid-fuel propellants.

References

- [1] Belal, Hatem, Chang W. Han, Ibrahim E. Gunduz, Volkan Ortalan, and Steven F. Son. "Ignition and combustion behavior of mechanically activated Al-Mg particles in composite solid propellants." *Combustion and Flame* 194 (2018): 410-418.
- [2] Kochetov, N. A., and A. E. Sytshev. "Effects of magnesium on initial temperature and mechanical activation on combustion synthesis in Ti-Al-Mg system." *Materials Chemistry and Physics* 257 (2021): 123727.
- [3] Hong, S. and van Duin A. "Atomistic-Scale Analysis of Carbon Coating and Its Effect on the Oxidation of Aluminum Nanoparticles by ReaxFF-Molecular Dynamics Simulations." *J. Phys. Chem. C* 120 (2016) 9464-9474
- [4] Senftle, T. P.; Hong, S.; Islam, M. M.; Kylaas, S. B.; Zheng, Y.; Shin, Y. K.; Junkermeier, C.; Engel-Herbert, R.; Janik, M. J.; Aktulga, H. M. "The ReaxFF Reactive Force-Field: Development, Applications and Future Directions." *npj Comput. Mater.* 2 (2016), 15011.

8:05 AM SF02/SF03/SF04/SF06/SF07.02

Modeling Reaction Transfer Velocities in Disconnected Compact Heterogeneous Multilayer Reactive Material Systems Deepshikha Shekhawat¹, Kashish Sindhani¹, Vishal Raheja¹, Mostafa Baloochi² and Jörg Pezoldt¹; ¹Technical University of Ilmenau, Germany; ²IFW Dresden, Germany

Modeling reaction transfer velocities in disconnected compact heterogeneous multilayer reactive material systems

Deepshikha Shekhawat¹*, Kashish Sindhani¹, Vishal Raheja¹, Mostafa Baloochi^{1,2}, Jörg Pezoldt¹*

¹ FG Nanotechnologie, Institut für Mikro- und Nanoelektronik und Institut für Mikro- und Nanotechnologien MacroNano@ and Institut für Werkstofftechnik, TU Ilmenau, Postfach 100565, 98684 Ilmenau, Germany;

² IFW Dresden, Leibniz-Institut für Festkörper- und Werkstoffforschung Dresden, Helmholtzstraße 20, 01069 Dresden, Germany

* Correspondence: deepshikha.shekhawat@tu-ilmenau.de (D.S.); joerg.pezoldt@tu-ilmenau.de (J.P.)

Reactive materials comprise particulate systems or multilayer materials consisting of two or more materials reacting with each other after they are ignited. The reaction initiation is possible using different sources of energy transfer, for example, an electric spark, laser pulse, mechanical forces or heating the whole system to a certain temperature. The reaction propagation velocity and the maximum reaction temperature in multilayer systems depend on the constituents in the bilayer stack and their thickness, as well as the heat transfer and loss conditions. In powder systems grain size and the thermal contact area are further parameters that allow tuning the reaction propagation velocity and the maximum reaction temperature. Typically, these two characteristic values are largely reduced in powder systems compared to compact bilayer systems. For the different application fields of the reactive materials, a well-designed reaction propagation velocity and maximum reaction temperature are of great importance. In this study, the tuning of the properties of the self-sustained reaction is studied theoretically by introducing a non-reactive material between two reactive material elements. For the study, the Ni/Al bilayer system was chosen. The Ni/Al elements were placed on a silicon wafer covered with 1 μm thick silicon dioxide. The spaces between the multilayer reactive material elements were filled with different non-reactive materials covering a wide range of thermal properties (SiO₂, Si₃N₄, AlN, Si, diamond). On top of this heterogeneous layer, a 1 μm thick sealing layer was placed consisting of the identical material or another material. The carried out two-dimensional simulations demonstrated that embedding material allows scaling the ignition transfer time and the heat propagation velocity to values in a wide range. For example, for a transfer length of 1 μm the ignition time can be designed from nanoseconds to several microseconds. Consequently, in contrast to previous results embedding materials allow scaling the properties of the self-sustained reaction in heterogeneous reactive material systems. A detailed analysis and comparison of the obtained results to experiments will be given.

Keywords: reactive multilayers; heterogeneous material, self-sustained reaction; nickel; aluminum; reaction propagation control; simulation

8:10 AM SF02/SF03/SF04/SF06/SF07.03

Controlling Reaction Transfer Between Al/Ni Reactive Multilayer Elements on Substrates Deepshikha Shekhawat; Technical University of Ilmenau, Germany

Controlling reaction transfer between Al/Ni reactive multilayer elements on substrates

Deepshikha Shekhawat¹*, Muhammad Sulman¹, Farshad Daneshpazhoonejad², Manuela Breiter³, Joachim Döll³, Anne Jung², Jörg Pezoldt¹*

¹ FG Nanotechnologie, Institut für Mikro- und Nanoelektronik und Institut für Mikro- und Nanotechnologien MacroNano@ and Institut für Werkstofftechnik, TU Ilmenau, Postfach 100565, 98684 Ilmenau, Germany;

² Schutzsysteme, Helmut-Schmidt-Universität, Universität der Bundeswehr Hamburg, Holstenhofweg 85 22043 Hamburg, Germany

³ Zentrum für Mikro- und Nanotechnologien, TU Ilmenau, Postfach 100565, 98684 Ilmenau, Germany

* Correspondence: deepshikha.shekhawat@tu-ilmenau.de (D.S.); joerg.pezoldt@tu-ilmenau.de (J.P.)

Al/Ni reactive multilayer system with a high exothermic reaction enthalpy as a heat source which is useful in low-temperature bonding and soldering in the packaging of microsystems applications. The phenomenon of a self-propagating reaction can be suspected that the released heat through the local mixing of multilayers is enough to heat the end-to-end material and induced a self-sustaining reaction front that transfers through the sample with a characteristic velocity and a specific temperature. The current study presents a unique opportunity to investigate the processes that control the reaction front velocity and emitted temperature by structuring the Al/Ni multilayers. The structuring of the Al/Ni multilayers by lithography is quite a challenging process. In the current study, we prepared structured 5 μm Al/Ni multilayers on the etched Si/SiO₂ substrates and intentionally created spaces between Al/Ni structures with different thermal properties. These structured Al/Ni multilayers have different spaces between different Al/Ni elements to observe the reaction front and emitted temperature from one element to another. A two-dimensional numerical model was also developed to study the effect of heat loss and thermal properties from the spaces on the Al/Ni self-propagating reaction path. The self-propagating reaction was initiated by an electrical spark on the surface of the Al/Ni multilayers. The reaction front was recorded with a high-speed camera. Activation energy is fitted with these velocity data from the high-speed camera to adjust the numerical model. The calculated reaction front temperature of the self-propagating reaction was compared with the temperature obtained by time-resolved pyrometer measurements. X-ray diffraction results confirmed that all reactants reacted and formed the AlNi phase. SEM analysis showed the morphological changes that occurred after the reaction on Al/Ni multilayers. Finally, it is predicted that: (I) The maximum spaces between the elements can stop the reaction front; (II) By reducing the heat loss through the substrate can propagate the reaction front through spaces; (III) Designing the thermal properties of the spaces between the reactive elements enables the modification of the properties of the self-propagating reaction.

Keywords: reactive multilayers; self-sustained reaction; nickel; aluminum; propagation velocity; phase transformation; Lithography

8:25 AM SF02/SF03/SF04/SF06/SF07.04

Thermally Triggered Lubricating Ligands in Dynamic Nanocrystal Superstructures Yifan Ning¹, Shengsong Yang¹, Yi-Yu Cai¹, Jun Xu¹, Rui Peng Li², Yugang Zhang², Cherie R. Kagan¹ and Christopher B. Murray¹; ¹University of Pennsylvania, United States; ²Brookhaven National Laboratory, United States

The unique physics and applications of superlattices (SLs) have motivated the investigation of nanocrystal (NC) self-assembly as a promising synthetic method for mesoscale materials. However, assembled superstructures often lack dynamics due to the limited mobility of building units, restricting the potential for manufacture and post-treatment of high-quality NCSLs and narrowing the application in smart materials. Here we introduce a novel approach using a customized dendritic ligand that exhibits liquid crystal-like behavior to realize dynamic SLs. The ligands act as a thermally triggered lubricant between NCs and allow the substrate-bounded (dried) thin films to transform from poorly ordered aggregates to SLs with high crystallinity and

preferred orientation simultaneously when subjected to thermal activation. The dendritic structure of the ligand ensures excellent thermal stability of individual NCs at 90 °C over three days. A connection between the dynamics of SLs and the molecular properties of the ligands is established through a systematic analysis comparing ligands with varying components, softness, and functionalities. The design, kinetics, and application of lubricating promesogenic-ligands can be generalized to pave the way for unlocking more stimuli-responsive mesoscale metamaterials from NCSLs.

8:40 AM SF02/SF03/SF04/SF06/SF07.05

Real-Time *In-Situ* Characterization and Monitoring of Liquid-Phase Nanoparticle Exfoliation using Ultrasonic Spectral Analysis Kigozi Musazi¹, Zhe Chen², Saroj Pramanik¹, Hertanto Adidharma², Maohong Fan² and Yucheng Lan¹; ¹Morgan State University, United States; ²University of Wyoming, United States

Nanomaterials are playing crucial roles in various fields such as renewable energy, energy storage, and sensors. Liquid-phase exfoliation is an effective and cost-efficient method for producing large quantities of nanoparticles in laboratory settings. However, it is challenging for controlling and determining the exfoliation procedures. In this study, we present an innovative platform for the digitization and frequency spectral analysis of ultrasonication data, focusing on the ultrasonic waveforms emitted during the exfoliation process. The platform integrates an ultrasonic receiver, computer-based signal analysis and filtering components, besides ultrasonication sources, to capture and analyze the unique characteristics of the ultrasonic spectrum. We demonstrate the real-time in-situ detection of nanoparticle information, including size and morphology, through frequency spectral differences and bandwidth analysis. By leveraging machine learning techniques, we aim to monitor and optimize the liquid-phase exfoliation procedure based on the characterization of nanoparticles using ultrasonic characteristics, enabling significant time savings and improving exfoliation efficiency through the implementation of artificial intelligence in the control and optimization of nanoparticle production.

8:45 AM SF02/SF03/SF04/SF06/SF07.06

Deposition of Double-Layered TiO₂ Thin Films with Porosity-Dependent Photoelectrochemical Activity Timur Atabaev, Kuralay Rustembekkyzy and Amir Zholdasbekov; Nazarbayev University, Kazakhstan

Porous TiO₂ thin films with a double-layered structure were successfully prepared using a conventional spin-coating deposition method. A range of characterization techniques, such as scanning electron microscopy, X-ray diffraction, X-ray photoelectron spectroscopy, and photoluminescence were employed to assess the morphology, structural and optical properties of prepared TiO₂ films. Photoelectrochemical (PEC) measurement tests revealed that prepared double-layered TiO₂ thin films exhibit porosity-dependent photocatalytic activity. For example, TiO₂ films with optimized porous structure demonstrated an increase in photocurrent density by a factor of ~ 2.23 (to 141.7 μA cm⁻²) and photoconversion efficiency improvement by a factor of ~ 2.14 as compared to non-porous double-layered TiO₂ reference films. Possible mechanisms responsible for these experimental observations are proposed, discussed, and validated experimentally.

8:50 AM SF02/SF03/SF04/SF06/SF07.07

Remarkably Durable Silver Finish with Exceptional Wear and Fretting Corrosion Resistance for Electronic Interconnections Benjamin Steimle, Jamie Chen, Miguel Rodriguez, Margit Clauss, Patricia Taintor and Kristen Griffin; DuPont, United States

To maintain signal and power reliability, next-generation automotive, telecommunications, aerospace, and other high-performance applications require electronic connectors with metal contact finishes that provide higher conductivity, higher durability & lower coefficient of friction (CoF). These interconnections must survive the routine mechanical wear, environmental corrosion, and high temperatures they are subjected to through assembly and operation. As a result, metal contact finishes must withstand rigorous performance evaluation and qualification prior to their widespread adoption in next-generation electronics. One critical performance test evaluates the wear and fretting corrosion of two surfaces in direct contact. This test simulates a high vibration environment using low-amplitude linear reciprocating motion at high frequency for tens of thousands of cycles to induce slip between metal contacts. Any resulting damage of surface finishes through physical wear or oxidation may cause failures that impact connector performance, including reusability and electrical conductivity. Here, we present a unique electrodeposited high durability silver finish that maintains exceptional wear performance and electrical conductivity during fretting corrosion tests. Our novel silver finish outperforms current industry-standard connector finishes across a range of operating conditions relevant to automotive, telecommunication, and industrial applications. Unlike traditional silver finishes that require external lubrication to mitigate their propensity to cold-weld, our unique deposit does not require external lubrication. We show that our high durability silver is resistant to cold-welding and wear at increasingly harsh fretting test parameters, thereby preventing a common failure mode of existing connectors where nickel or copper underlayers are exposed and corrode to form insulating oxides. Resistance to fretting corrosion is necessary as electronic connector application requirements shift towards increased voltage, service lifetime, and interconnection reliability. Further, improved durability in electrically conductive finishes enables innovation in connector design and electronic system architecture.

9:05 AM SF02/SF03/SF04/SF06/SF07.08

Synthesis and Photovoltaic Characterization of Layered Hydroxide Nanomaterials via Atmospheric DC Micro-Plasma Techniques Grace Farrell¹, Saroj Pramanik¹, Willie Rockward¹, Gregory Severn² and Yucheng Lan¹; ¹Morgan State University, United States; ²University of San Diego, United States

Layered hydroxide nanomaterials have gained significant attention as promising renewable energy materials. In this study, we systematically synthesized period 4 transition metal hydroxide nanomaterials, including cobalt (Co), nickel (Ni), copper (Cu), and zinc (Zn) hydroxides, in aqueous solutions using DC micro-plasma techniques. The synthesis was conducted at room temperature under atmospheric pressures. The crystallinity of the synthesized nanomaterials was evaluated using X-ray diffraction and electron diffraction, while Raman scattering was employed to analyze their chemical bonding. Optical properties were characterized using UV-vis spectroscopy, and morphology was examined through electron microscopy analyses. To assess their applicability in solar energy conversion, the nanomaterials were fabricated into dye-sensitized solar cells (DSSCs), and their photovoltaic behaviors were measured. We also investigated the influence of atomic radius and electron negativity on the morphology, microstructure, optical properties, and photovoltaic performance of the nanomaterials. Furthermore, we studied the plasma reaction occurring at the gas-liquid interfaces during synthesis. The results demonstrate that these plasma-produced hydroxide materials can generate carbon-free renewable energy from solar sources.

9:10 AM SF02/SF03/SF04/SF06/SF07.09

From Transparent to Black Amorphous Zinc Oxide Thin Films through Oxygen Deficiency Control Magdalena Nistor¹, Florin Gherendi¹, Daniela Dobrin¹ and Jacques Perrière^{2,3}; ¹NILPRP - National Institute for Laser, Plasma and Radiation Physics, Romania; ²Sorbonne Universités, France; ³CNRS, France

Zinc oxide (ZnO) is a well-known n-type transparent conducting oxide that has attracted substantial research for photovoltaic and optoelectronic applications. While transparent and crystalline zinc oxide films are currently obtained by a wide variety of growth methods, black and amorphous zinc oxide films are not currently investigated although several recent studies on black zinc oxide have renewed its potential for photocatalytic applications. Among plasma-based techniques, pulsed electron beam deposition (PED) is a versatile technique for the growth of oxide thin films for applications in transparent electronics and photovoltaics [1].

We report on the tunability of oxygen deficiency in ZnO thin films grown at 300 °C on c-cut sapphire single-crystal substrates by PED through a slight variation in the argon pressure. At a pressure of 2 10⁻² mbar transparent, stoichiometric and crystalline films ZnO were obtained, whereas at 9 10⁻³ mbar black and amorphous films with about 15% oxygen deficiency resulted. The composition, structural, electrical and optical properties of transparent and black ZnO thin films were comparatively investigated as a function of oxygen deficiency. Both films exhibit structural disorder (amorphous vs. polycrystalline) and a high carrier density, leading to a temperature-dependent resistivity behaviour specific to disordered metal oxide systems, which can be explained either by transport models of metallic conductivity and quantum corrections to conductivity or by the Mott variable range hopping model. The low mobility value of black and amorphous zinc oxide thin films could be due to both structural disorder and the presence of Zn clusters in the films. The stoichiometric films are transparent, as expected for zinc oxide, while the black films exhibit enhanced absorption in the visible and near-infrared due to oxygen deficiency, thus extending the range of applications of zinc oxide thin films from transparent electronics to solar absorbers and photocatalysis. [1] M. Nistor, F. Gherendi, D. Dobrin, J. Perrière: J. Appl. Phys. 132, 225705 (2022)].

9:25 AM SF02/SF03/SF04/SF06/SF07.10

Flexible Laser-Induced Graphene Sensors for Next-Generation Soft Grippers Anna Chiara Bressi^{1,1}, Alexander Dallinger², Giovanna De Luca^{1,1}, Matteo Cianchetti^{1,1} and Francesco Greco^{1,2,1}; ¹Scuola Superiore Sant'Anna, Italy; ²Graz University of Technology, Austria

Laser Induced Graphene (LIG) is a three-dimensional carbon-based nanomaterial fabricated with single-step local pyrolysis. Commercial IR laser engravers are exploited to scribe conductive patterns onto different polymeric precursors without the use of chemicals or masks. LIG applications span different fields, including soft electronics, robotics and wearable electronics.¹⁻³ In the domain of soft robotics, robotic systems are designed and realized with flexible materials and structures. Therefore, it becomes crucial to incorporate soft and flexible sensors to adapt and conform to the deformable nature of the robots. Within this context, we propose the sensorization of a soft gripper with piezoresistive LIG tracks.

Soft grippers come in a variety of shapes, dimensions, and actuation mechanisms, tailored to the specific application and the properties of the objects to be grabbed.⁴ To ensure secure and delicate grasping, the grippers must be designed with closed-loop control on deformation and force applied during the interaction with the target. Moreover, continuous feedback is a key aspect to allow for precise monitoring and adaptive real-time adjustment of the position.

This project aims to develop a novel method for extracting parameters from a finger-based pneumatic gripper, associated with its bending angle and contact pressure. Piezoresistive LIG

sensors have been scribed from polyimide with a CO₂ IR laser and then either embedded within the robot's soft materials or attached externally. Additionally, attention has been given to addressing stiffness mismatch between the sensor and the soft gripper and to ensuring robust integration in the device, to avoid causing interference during data collection. A comprehensive investigation has been conducted on the LIG materials to evaluate the influence of laser-scribing settings and track designs on the gauge factor of the sensors.

This study lays the foundation for future research and optimization of this promising solution, which combines lightness and flexibility with a cost-effective, simple and rapid fabrication process.

9:30 AM SF02/SF03/SF04/SF06/SF07.11

Designing Smart Metamaterials as Versatile Actuators by Halftone-Assisted Photo-Stereolithography ZhongkunZhao and HongtaoSun; Penn State University, United States

Metamaterials have gained significant attention in the field of structural engineering due to their unique mechanical characteristics and exceptional material properties arising from their structures. These metamaterials offer extraordinary opportunities for customizing overall physical characteristics, such as electromagnetic, acoustic, mechanical, and thermal properties, through the design and organization of their architectures.¹⁻⁶ Extensive research has been conducted to fabricate metamaterial as passive structures after manufacturing. To explore additional control over the metamaterials, the incorporation of intelligent materials, such as shape memory polymers (SMPs), into three-dimensional (3D) architectures holds promise for creating innovative multifunctional smart architectures with controlled responsive behaviors.

In this study, we introduced a photo-stereolithography-enabled 3D printing technique to fabricate two-dimensional (2D) or three-dimensional (3D) SMP metamaterials. These printed meta-structures can function as stimulus-responsive actuators, offering geometrically reconfigurable, functionally deployable, and tunable mechanical characteristics. With their unique reversible effects on highly deformable behaviors, SMP meta-structured actuators can be bent, compressed, stretched and twisted, enabling to store/release mechanical energies in different forms upon thermal responsive stimuli. By manipulating printing parameters such as exposure time, light intensity, printing layer thickness, significant changes in mechanical properties, including Young's modulus and toughness can be achieved, resulting in a wide variation in mechanical energy and responsive behaviors.

To explore versatile actuation behaviors within a single SMP metamaterial, we developed a halftone-assisted photo-stereolithography technique. This approach involves designing and encoding halftone patterns into metamaterials during the printing process to spatially control localized mechanical properties through tunable UV curing. This enables regulation of overall mechanical properties and stimuli-responsive behaviors. For instance, by incorporating various halftone patterns with controlled area percentage of curable pixels at specific triple intersections of re-entrant auxetic metamaterials, we can achieve versatile deformations, such as elongation ranging from 10% to 50% of the original length, and lifting loads 16-fold to 83-fold higher than their weight. Designing various halftone patterns in specific sites offers a new strategy to manipulate mechanical characteristics and stimulus-responsive behaviors within a single smart metamaterial, demonstrating great potential for multifunctional actuators.

In summary, our research demonstrates the fabrication of SMP metamaterials through a halftone 3D printing technique, providing stimuli-responsive actuators with tunable mechanical characteristics. The incorporation of halftone patterns offers precise control over localized properties, enabling versatile deformations and expanded functionality within a single metamaterial. This work contributes to the advancement of intelligent materials and their application in the development of multifunctional actuators.

References

- [1] R. S. Kshetrimayum, *IEEE Potentials*, 2005, 23, 44–46.
- [2] X. Ni, Z. J. Wong, M. Mrejen, Y. Wang and X. Zhang, *Science*, 2015, 349, 1310–1314.
- [3] G. Ma and P. Sheng, *Sci. Adv.*, 2016, 2, e1501595.
- [4] X. Zheng, H. Lee, T. H. Weisgraber, M. Shusteff, J. DeOtte, E. B. Duoss, J. D. Kuntz, M. M. Biener, Q. Ge, J. A. Jackson, S. O. Kucheyev, N. X. Fang and C. M. Spadaccini, *Science*, 2014, 344, 1373–1377.
- [5] J. B. Berger, H. N. G. Wadley and R. M. McMeeking, *Nature*, 2017, 543, 533–537.
- [6] Q. Wang, J. A. Jackson, Q. Ge, J. B. Hopkins, C. M. Spadaccini and N. X. Fang, *Phys. Rev. Lett.*, 2016, 117, 175901.

9:35 AM SF02/SF03/SF04/SF06/SF07.12

Numerical Model to Predict The Electrical and Mechanical Behavior of Origami-Inspired Morphing Wing Actuator HannahNabavi, Jeong-HoLee and GraceGu; University of California, Berkeley, United States

The realization of flapping wings has been critical to the advancement of micro-aerial vehicles, accelerating aerospace and military applications. While flapping wings have been thoroughly studied in the literature, numerous models utilize mechanical power transmission systems that convolute wing motion, contributing added weight and increasing wear susceptibility.

Piezoelectric materials exhibit unique bending characteristics that allow for prompt mechanical strains in response to an electrical potential. With their distinctive morphological properties, piezoelectric actuators are prime candidates for micro-aerial vehicles, providing enhanced sensitivity and lightweightness to flapping wings. Understanding their electrical and mechanical properties is critical to the design of small-scale wing systems.

In this research, we aim to predict the electrical and mechanical behavior of piezoelectric morphing wing actuators for micro-aerial vehicle applications. A numerical model of a piezoelectric tri-layer thin plate was constructed in a finite element toolbox. The mechanical tip displacement was investigated under an applied deformation-inducing electric field, and the Timoshenko-Ehrenfest beam theory was applied to mathematically validate the spatial displacement of the wing deformation. Origami folding methods were explored to inform future geometrical refinements that could facilitate enhanced wing motion performance.

Through this research, the approach illustrates the development of an accurate numerical model for a piezoelectric actuator system, which will be utilized in the wing structure optimization in future research. A physical wing prototype will be designed to confirm experimental validity. Moreover, the piezoelectric system will continue to be optimized to leverage origami-induced programmable surfaces, allowing for increased dimensionality and tunability for piezoelectric morphing wings. This work will open up new areas of study in flapping wing actuators and lay the groundwork for origami-inspired piezoelectric structural analysis to be completed in the future.

9:40 AM SF02/SF03/SF04/SF06/SF07.13

Photo-Stereolithography-Regulated Heterogeneity Domains in Fiber-Shaped Micromotors for Tunable Responsive Behaviors ZhongkunZhao and HongtaoSun; Penn State University, United States

Intelligent materials enable sensing and adaptive responses to various external stimuli. These active materials find applications in diverse fields such as soft robotics, actuators, biomedical devices, and sensors.¹⁻⁷ Among these smart materials, Shape Memory Polymers (SMPs) have shown promise as stimuli-responsive materials with distinctive reversible effects on highly deformable behaviors.⁸⁻¹⁰ However, achieving precise control over responsive behaviors while concurrently modulating the mechanical properties remains a significant challenge. To address this challenge, we present a grayscale lithography-enabled printing process for fabricating fiber-based rotating micromotors using SMPs.

Our approach involves spatially manipulating the gradient and orientation of heterogeneity domains within our fiber-shaped SMP actuators through photo-polymerization. Compared to conventional layer-by-layer 3D printing of homogeneous fibers for the control over geometry only, our approach enables extensive tunability of crucial material and performance characteristics. This includes precise control over Young's modulus (ranging from 265 to 1208 MPa), thermal stimuli-responsive behaviors (with a maximum rotation rate varying from 169 to 441 rpm), and torsional mechanical energy (with stored energy ranging from 19 to 69 J kg⁻¹, and released energy from 3.9 to 9.5 J kg⁻¹). By incorporating stiff and soft domains with varying curing time, we engineered various interfaces into our fiber-shaped actuators, thus manipulating the stimuli-responsive performance. We also observed that the orientation of the heterogeneity domains played a significant role in the rotation performance of the fiber-shaped motor. More interestingly, introduction of a stiffness gradient through spatial heterogeneity designs between the stiffest and softest domains, enables the highest maximum rotation rate of 441 rpm. This improvement is attributed to the gradient feature between the stiff and soft domains, which synergizes the complementary properties between neighboring domains, which synergizes their complementary properties.

Furthermore, by controlling the size of heterogeneity domains, we can further tune overall material properties and performance. To gain insights into the underlying mechanism, we conducted a detailed analysis of localized mechanical behaviors in the SMPs using digital imaging correlation (DIC) methodology. This allows us to differentiate the heterogeneous properties and interfaces within the material and observe the strain variations in different regions. The localized stress-strain curves derived from the DIC analysis confirm the encoded modulus gradient within the heterogeneity domains, aligning with our design principles.

In summary, our approach of incorporating heterogeneity domains and interfaces, presents a novel method for the design and fabrication of smart materials and actuators with regulated performance. These findings hold significant implications for the advancement of intelligent materials and offer potential applications across various domains.

References

- [1] J. Yuan, W. Neri, C. Zakri, P. Merzeau, K. Kratz, A. Lendlein, P. Poulin, *Science* **2019**, 365, 155.
- [2] M. Su, Y. Song, *Chem. Rev.* **2021**, 122, 5144.
- [3] Z. Zhu, D. W. H. Ng, H. S. Park, M. C. McAlpine, *Nat. Rev. Mater.* **2021**, 6, 27.
- [4] Z. Lou, L. Wang, G. Shen, *Adv. Mater. Technol.* **2018**, 3, 1800444.
- [5] J. Gardan, *Virtual Phys. Prototyp.* **2019**, 14, 1.
- [6] X. Qiu, S. Hu, *Materials* **2013**, 6, 738.

- [7] M. Stoppa, A. Chiolerio, *sensors* **2014**, *14*, 11957.
[8] L. Sun, W. M. Huang, Z. Ding, Y. Zhao, C. C. Wang, H. Purnawali, C. Tang, *Mater. Des.* **2012**, *33*, 577.
[9] Y. Liu, H. Du, L. Liu, J. Leng, *Smart Mater. Struct.* **2014**, *23*, 023001.
[10] L. Wang, F. Zhang, Y. Liu, J. Leng, *Adv. Fiber Mater.* **2022**, *1*.

SYMPOSIUM SF07

Advances in Reactive Materials Engineering
November 27 - November 30, 2023

Symposium Organizers

Michael Abere, Sandia National Laboratories
Kerri-Lee Chintersingh, New Jersey Institute of Technology
Michael Grapes, Lawrence Livermore National Laboratory
Carole Rossi, LAAS CNRS

* Invited Paper
+ JMR Distinguished Invited Speaker

SESSION SF07.01: Applications of Reactive Materials I
Session Chairs: Kerri-Lee Chintersingh and Dylan Kline
Monday Morning, November 27, 2023
Sheraton, Second Floor, Independence West

10:30 AM *SF07.01.01

Developing 3D-Printable, Reactively-Formed Electrical Conductors Shane Q. Arlington^{1,2}; ¹Charles Stark Draper Laboratory, United States; ²Johns Hopkins University, United States

Self-propagating high-temperature synthesis (SHS) in macroscale structures is an effective method of creating high-temperature materials directly. In nanostructured, micro-scale materials, SHS has been thoroughly explored for rapid liberation of heat, where short diffusion length-scales enable very low ignition thresholds. For instance, materials such as Al/Ni multilayers have been demonstrated to be extremely versatile micro-heat sources to enable *in situ* bonding, sealing, and ignition of additional energetic materials to name a few applications. As presented at previous meetings, Draper has developed a platform which harnesses both these aspects of SHS – using SHS to form a conductive, high-temperature, carbide, and harnessing the reaction heat to reflow a highly electrically-conductive matrix phase. Together, this enables the production of 3D-printed electrical conductors *in situ*. In this talk, we summarize the process by which material systems were considered, discarded, and selected; the development and fine-tuning of our reactive particles; and the ultimate performance (and limitations) of the final materials. We will delve into the serendipity of how an erroneous phase diagram played a crucial role in our development process, and the years-long, multi-continent process it took to uncover the flaw. Finally, we will cover future applications and pathways, both at Draper and beyond.

11:00 AM SF07.01.02

Curing Reactive Silver Ink using Intense Pulsed Light Morgan Michael^{1,2,3}, Adria Kajenski^{1,2,3}, Guinevere Strack^{1,2,3} and Alkim Akyurtlu^{1,2,3}; ¹University of Massachusetts Lowell, United States; ²Printed Electronics Research Collaborative, United States; ³Raytheon UMass Lowell Research Institute, United States

Additive manufacturing (AM) covers a variety of techniques used to build up materials layer by layer. Direct ink writing is an AM technique used to selectively dispense the material directly onto a flexible substrate with high accuracy and precision. This technique enables rapid prototyping and produces low volumes of waste products. Materials used in AM are tailored for their respective printing methods and for targeted mechanical or electrical properties, ranging from dielectric materials for coatings to resistive inks for printed resistors and nanoparticle dispersion inks for conductive patterning. Reactive particle free inks are a competitive alternative to NP-based inks which provide numerous advantages. For example, the formation of continuous films vs. conductive barriers between nanoparticles can yield higher conductivities, while providing the capability of in-situ curing. In this work, we used a silver reactive ink, based on a silver complex, which upon curing, dissociates to silver ions that are subsequently reduced in situ by reducing agents in the solvent system. Many inks used in AM require a curing step to initiate chemical reactions, drive off solvents, or sinter together nanoparticles. Photonic curing with IPL (Intense Pulsed Light) is a curing method that operates on the millisecond time scale, significantly reducing the overall manufacturing time and energy expenditure. This curing method is typically used to heat printed films of metallic nanoparticle inks that exhibit rapid thermal changes that can exceed the melting temperature of the nanoparticles. The application of IPL to liquid phase reactive inks is associated with silver (I) complex degradation and reduction, and eventually local heating once phase separation (nanoparticle formation) occurs. Photonic curing on Kapton and polyurethane (PU) coated nylon resulted in resistivity values as low as 6 and 12 $\mu\Omega$ cm, respectively. On average, photonic cured samples were 30% less conductive than samples cured thermally in a box oven. The utility of the ink was demonstrated by printing and photonic curing simple RF devices. Device functionality was assessed with measured scattering parameters that matched simulations.

11:15 AM SF07.01.03

Developing a High-Energetic and Fast-Response Ignitor by Integrating Reactive Inks on Semiconductor Bridges Tao Wu, Maria-Isabel Mendoza-Diaz, Alain Esteve and Carole Rossi; LAAS-CNRS, France

Due to the growing appetite for developing compatible miniaturized microprotechnics systems, the traditionally used electro-pyrotechnic initiators have been upgraded from a bridge wire to a semiconductor bridge (SCB) *via* microelectromechanical systems (MEMS) technology. As an innovative ignition device, SCB can generate heat and plasma upon an electrical input. With its superior properties in the ignition, such as rapid response, low energy input, and high degree of integration, SCB has been largely employed in various civilian and military applications. For the purpose of successful ignition, energetic nanothermites have been integrated into SCB (ESCB) based ignitors in order to enhance the energy output and flame size. Nanothermite reactions refer to a redox reaction between a physically mixed metal fuel and solid metal oxides and have been substantially studied due to their high energy densities, greater stabilities, and also high tunability in terms of particle size, composite composition, stoichiometry, and packing. Over the years, reactive multilayer films (RMF), mostly Al/CuO nanolaminates, have been integrated into microchip ignitors and achieved ignition in a time scale of μ s with energy input as low as several watts. However, the fabrication process (mostly magnetron sputtering) of such RMFs suffers from drawbacks like low sample loading, long process time, delamination due to thermal shocks, etc, which limits the industrial application of ESCB. Thus, an alternative method is urgently needed to develop by withholding the advantages and discarding the disadvantages of RMF materials in ESCB-based ignitors. In the last decade, direct ink writing has gained much attention due to its facile manipulation, high adaptability, and scalability as well as tunability.

In this work, for the first time, we combined the direct ink writing technique and ECB chip to fabricate a novel ESCB ignitor that features better ignition performance than traditional ignitors but with much less cost in time and goods. Briefly, a 5×5 mm² sized SCB-based ignition chip with gold contact pads and titanium resistance is fabricated using a series of photolithography/lift-off processes and magnetron sputtering. Then a 250 μ m high peripheral container was fabricated on top of the chip by lamination and photolithography processes and is

designed to controllably store the printed energetic materials. Moreover, the ignition behavior of such an ignitor can be easily tuned by changing the fuel/oxidizer/binder constituents to apply in different scenarios.

11:30 AM SF07.01.04

Recycling Iron Power as an Energy Carrier: Investigating Material Properties Through Cycles of Combustion and Reduction[Giulia Finotello](#), [Nicole Stevens](#) and [Niels Deen](#); Eindhoven University of Technology, Netherlands

The world's energy system is transforming from a fossil fuel-based energy infrastructure to a society supported by sustainable energy sources, like solar and wind energy. The production of sustainable energy is quite intermittent, causing a great demand for additional capacity of local energy storage. We propose a low-cost alternative for high density energy storage: iron powder. Recently iron powder has been proposed as an energy carrier for its high energy density, ease to be stored, and for its fully CO₂-free combustion process. Renewable electricity can be used to reduce iron oxide powder into iron, which can be densely stored under ambient conditions and combusted whenever and wherever energy is needed, providing fully renewable heat. This research determines the potential of the entire iron fuel cycle, in terms of the material properties.

Iron oxide powder is combusted and reduced over 6 cycles, where each partial cycle had the same conditions. Reduction experiments are performed inside a lab-scale reactor using a hydrogen flow at elevated temperatures of 400 to 600 °C. High temperatures are beneficial from a kinetic point of view. However, previous studies showed de-fluidization due to sticking of the powder above 600 °C. The reactor and heating furnace are designed for a full control of operating conditions. The powder is assessed in terms of particle size, morphology, porosity, composition and reduction degree after each partial cycle. We observe that the particle size distribution shifts to larger size already after the first combustion process. Nevertheless, the size distribution remains approximately the same over multiple cycles. This indicates that the powder can be used in the cyclic process without intermediate treatments (e.g sieving).

A trade-off between a high reduction degree and absence of solid sticking behavior is identified at the temperature of 590 °C. The results of the XRD show that reduction conversion to iron is larger than 80% for each cycle. Sticking is observed in the powder after combustion, which is assumed to take place within the collection part of the process. The losses due to the handling of the powder through each step of the cycle is negligible. Iron powder is therefore a good candidate to be used as energy carrier in the iron fuel cycle.

11:45 AM SF07.01.05

Diborane Generation from Sodium Borohydride using Ionic Liquids for Air Breathing Propulsion Applications[Ashvin Kumar Vasudevan](#), [Prithwish Biswas](#), [Yujie Wang](#) and [Michael R. Zachariah](#); University of California, Riverside, United States

Sodium borohydride is a potential fuel source for air-breathing propulsion applications. However, sodium borohydride by itself is stable in air and primarily releases hydrogen on heating. Literature work suggests that a strong Lewis acid such as boron trifluoride (BF₃) is required to initiate decomposition into diborane and sodium tetrafluoroborate. Our current study shows that ionic liquids such as 1-Ethyl-3-methylimidazolium tetrafluoroborate, (EMIM BF₄) can act as good sources of BF₃ and bring about complete decomposition forming sodium fluoride and diborane. Accordingly, a molar ratio of 3:1 (NaBH₄: EMIM BF₄) is stoichiometric for complete conversion to sodium fluoride and diborane. Ignition of the mixture shows rapid reaction of diborane with air. Successful combustion even at low amounts of ionic liquid indicates a unique decomposition mechanism initiated by BF₃.

Analysis of evolved products using T-jump time of flight mass spectrometry shows consistent amounts of diborane release at all molar ratios tested. When very low amounts of ionic liquid (molar ratio 16:1) are used, diborane is accompanied by hydrogen evolved from excess unreacted sodium borohydride. The solid products comprise mostly sodium fluoride with some traces of sodium tetrafluoroborate as seen by XRD. Mass losses observed in the TGA further suggest complete conversion to diborane and sodium fluoride at all molar ratios. Analysis of the gaseous and solid products alongside combustion results with 3d printed samples to describe the flame propagation will be presented and a mechanism specific to sodium borohydride decomposition in ionic liquids will be discussed.

The use of thermally stable ionic liquids provides a unique avenue for generating diborane from borohydrides which can be incorporated to make air breathing propellants which have low ignition temperatures. Early results with potassium borohydride show that similar decomposition mechanisms are possible in other alkali borohydrides. Further work is needed to explore the potential of various hydrides and borohydrides for air breathing propulsion.

SESSION SF07.02: Simulations of Reactive and Energetic Materials

Session Chairs: [Michael Abere](#) and [Jennifer Gottfried](#)

Monday Afternoon, November 27, 2023

Sheraton, Second Floor, Independence West

1:30 PM *SF07.02.01

Atomistic Simulations of Reactive Materials: Role of Microstructure and Defects Coupling Mechanics and Chemistry[Alejandro Strachan](#); Purdue University, United States

Micro-, nano-structure, and defects play a dominant role in the kinetics and thermodynamics of reactive materials. This presentation will discuss molecular dynamics simulations of the chemical reactions of nanostructured Ni/Al and thermites subjected to thermal and dynamic mechanical loads. The simulations provide insight into the mechanisms through which convective transport accelerates intermixing and, consequently, exothermic chemistry. These mechanisms are controlled by the thermo-mechanical properties of the constituents (e.g. flow stress and melting temperature). The simulations will be contrasted to various experiments and the implications of accelerated chemistry for various applications will be discussed.

2:00 PM SF07.02.02

Fundamental Measurements of Plasticity in Energetic Molecular Crystals[David F. Bahr](#) and [Hugh P. Grennan](#); Purdue University, United States

Plastic flow in crystalline solids most often occurs from the motion of dislocations. Accommodating general plasticity requires multiple slip systems, the ability to make new dislocations, and the existence of local stresses sufficient to move said dislocations. While the vast majority of plasticity studies are in atomic or ionic systems, the complex bonding in molecular crystals (exhibited by both pharmaceutical and energetic systems) opens up spaces in materials where it may be hard to make but easy to move, or hard to move and easy to make, the defects needed to accommodate plasticity. In this current study we examine the onset of plasticity in as-grown powder form (sub-mm) crystals and the hardness of these materials once plastic flow has been established using nanoindentation techniques. In systems ranging from RDX and HMX to PETN and CL-20 we find that the yield point phenomena appears when the maximum applied shear stress reaches between 2-7% of the elastic modulus of the material. The activation volume implied from a cumulative event analysis of approximately 20 yield-exhibiting indentations in each material is on the order of the molecular volume, but does not directly correspond to that across a broad range of space groups, suggesting that the process of nucleating dislocations in, in these molecular solids, more complicated than the atomistic processes often found in metallic or ionic systems. The hardness of these materials does not correlate well with the yield conditions, again showing the independence of the nucleation event and the subsequent mobility of the dislocations in crystals of limited slip condition. Finally, data where growth conditions were varied to create crystals of varying quality exhibited the same nominal activation volume, the same overall hardness, but different mean values for the yield point stresses, suggesting that the activation of plasticity processes in energetic molecular crystals can be directly correlated to defect density and these defects are not solely controlling the subsequent dislocation motion.

2:15 PM SF07.02.03

Multiscale Simulations of Non-Equilibrium Response in Determining Orientation-Dependent Property, Performance and Sensitivity of Faceted Molecular Crystals[Janki Brahmabhatt](#) and [Santanu Chaudhuri](#); University of Illinois at Chicago, United States

Energetic materials (EMs) are a subset of molecular crystals that serve a wide range of purposes. Given the nature of energetic materials, understanding how interfacial interactions contribute to overall crystal nucleation/growth with preference for certain facets, molecular packing, shock sensitivity, and material stability is crucial. EMs are often formulated as composites with polymeric binders and plasticizers to increase their stability and transportability. Despite the fact that the polymer/plasticizer matrix usually makes up about 7-8% of the total volume, the strength of adhesion between the polymer/plasticizer and the EM is an important consideration when formulating PBXs as incompatible formulations have an adverse effect on material performance—both in regard to shelf life and the possibility of unplanned detonation. Accurately modeling the degradation and delamination at binder-crystal interfaces facilitates mesoscale modeling of crystal behavior. At its core, adhesion is related to the free energies of the materials, but given the highly faceted nature of EM powders, pressing them into PBX composites results in irregular shapes with voids. Interfaces present in such composites play an outsized—though often difficult to quantify—role in controlling their properties, performance, and failure. At present, the adhesion between an EM and a polymer/plasticizer is primarily determined using cohesive models which notably lack orientation-dependent insight. However, for highly faceted molecular crystals, effectively understanding the interfacial adhesion requires examining the diverse interfacial molecular configurations. Experimentally, the work of adhesion can be indirectly calculated from the interfacial tension via various techniques, but they provide limited insight into the chemical interactions at the interface.

The prediction and modeling of these properties necessitates a systematic approach to quantify the Gibbs Free Energy at surfaces. Mesoscale models stand to benefit from atomic-scale insight

into interfacial phenomena. The surface free energy (SFE) provides vital insights into the mesoscale interfaces in granular composites often containing defects. The SFE allows us to predict theoretical crystal shape using Wulff Construction and the diversity of bonding environment in energetic crystals. Additionally, at interfaces, the SFE can be used as a metric to indirectly determine the compatibility between the EM and polymer. We have developed nonequilibrium methods to quantify the surface energy, SFE, and entropy for HMX. We contextualize these values in terms of strength of adhesion between HMX-Polymer (HTPB)/plasticizer (DOA). We will discuss the differences in bonding strengths for different HMX facets with HTPB, DOA, and a mixture of HTPB-DOA based on steered molecular dynamics simulations. HTPB appears to bond more strongly to some facets than others, and we will discuss the drastic differences in the work of adhesion between HMX facets, and how the addition of a polymer/plasticizer affects the shock initiation and reaction chemistry.

This knowledge from atomic-scale reactive molecular dynamics simulations allows us to examine the interfacial bonding environment in detail and can lead to better continuum models and better engineered stable crystal interfaces and PBX composites.

2:30 PM SF07.02.04

Plasticity in Energetic Molecular Crystal HMX: Physical Aspects and Constitutive ModelingZhaochengZhang and [CatalinR. Picu](#); Rensselaer Polytechnic Institute, United States

Plastic deformation plays a key role in the initiation of energetic materials at impact velocities below the hydrodynamic limit. However, the mechanisms of plasticity in low symmetry molecular crystals are much less studied than those governing the plasticity of monatomic crystals. In this work we investigate the physical basis of plastic deformation in HMX and develop mechanism-based constitutive models which are calibrated based on molecular simulations. The talk will outline several aspects of the physics of plastic deformation, including the mechanisms causing strain rate sensitivity, the pressure sensitivity and the mechanism of strain hardening. A constitutive model that accounts for this physics and which can be used in continuum simulations of shock and initiation will be introduced.

2:45 PMBREAK

SESSION SF07.03: Dynamic Characterization of Reactive Materials I

Session Chairs: Michael Abere and Jennifer Gottfried

Monday Afternoon, November 27, 2023

Sheraton, Second Floor, Independence West

3:15 PM *SF07.03.01

In Situ Characterization of Ultrafast Reaction Dynamics in Energetic Materials[KatharineTibbets](#); Virginia Commonwealth University, United States

Ignition of reactive materials initiates reactions on atomic length scales within femtoseconds, making these reactions difficult to capture experimentally. This presentation will discuss insights gained into sub-picosecond reaction dynamics of ionized energetic molecules using the technique of femtosecond time-resolved mass spectrometry (FTRMS). FTRMS is an optical pump-probe technique that can capture molecular rearrangement and bond-breaking events with sub-50 femtosecond resolution. Coupled with quantum chemical and molecular dynamics computations, FTRMS enables direct observation of initial reaction dynamics that contribute to ignition of reactive materials. Recent FTRMS results on isolated nitro-organic molecules and laser ablation methods to extend FTRMS measurements to molecular clusters and solids will be presented.

3:45 PM SF07.03.02

Investigating the Combustion Behavior of Reactive Composites with High-Speed Videography: Role of Heat Feedback[YujieWang](#) and Michael R. Zachariah; University of California Riverside, United States

Aluminum (Al) has been used as the primary fuel in solid rocket propellant due to its ready availability and high enthalpy. Al nanoparticles provide a greater energy release rate and a lower ignition temperature compared to conventional Al microparticles. However, the nanostructure of Al nanoparticles usually deteriorates quickly before and during combustion because of reactive sintering and agglomeration within the combustion process. Consequently, the effective size of aluminum particles increases during combustion. This phenomenon can have a significant impact on the combustion performance of the propellant. In this study, we use high-speed videography to study the effect of Al sintering and heat feedback on the combustion behavior of the high-loading energetic composite. We observe from microscopic imaging that for the composites of Al nanoparticles and ammonia perchlorate with different equivalence ratios, dramatically larger droplets are formed for equivalence ratio of 2 than equivalence ratio of 1. One expects that the burn rate of equivalence ratio of 2 should be lower than equivalence ratio of 1 due to its lower energy density. However, burn rate obtained from macroscopic imaging show that the burn rate of equivalence ratio of 2 is higher than equivalence ratio of 1. Analysis of agglomerate residence time indicates that droplets with an equivalence ratio of 2 have considerably longer residence times on the burning surface than equivalence ratio of 1. This phenomenon leads to a significantly greater heat feedback to the unburnt propellant, unexpectedly resulting in a higher burn rate compared to an equivalence ratio of 1. This result motivates us to explore methods for manipulating heat feedback. Silicon (Si) nanoparticles are added to the Al and potassium perchlorate composites. It is found that the size of agglomeration has minimal change when Si is added. However, the residence time is increased with Si addition, leading to a higher heat feedback to the unburnt composite. Consequently, the composite with Si has higher burn rate than the composite without Si. This study illustrates that it is possible to control the burn rate of an energetic composite by manipulating the heat feedback.

4:00 PM SF07.03.03

Revealing the Dynamics of Reactive Materials with Ultrafast Transmission Electron Microscopy[VolkanOrtalan](#); University of Connecticut, United States

Recent developments in instrumentation have made it a very exciting time to perform both fundamental and applied research in the electron microscope. The development of nanosecond and faster photoemission electron sources offers the chance to move the high spatial resolution world of electron microscopy into the ultrafast world of materials dynamics. Reactive materials are known to release large amount of heat via rapid exothermic chemical reactions upon receiving an initiating energy input. Due to relatively fast propagating reaction fronts, Ultrafast Transmission Electron Microscopy (UTEM) has immense potential in discovering the fundamental processes leading to reaction initiation and evolution in reactive materials. In the UTEM, while samples are excited with a nanosecond pulsed laser to trigger reactions via photochemical processes, a second pulse with a known time delay is used to stimulate the photoemission of electrons from the cathode. This single-shot approach makes it possible to capture various stages of irreversible processes with high temporal resolution and understand how a dynamic process evolves in reactive materials. In this presentation, examples of single-shot UTEM studies of reactive materials will be presented. Short-lived transient processes involved in reactions and the evolution dynamics will be discussed to obtain new insights into the reaction processes.

4:15 PM SF07.03.04

Direct Imaging and Simulation of the Interface Reaction of Metal/Metal Oxide Nanoparticle Laminates[HaiyangWang](#), [PrithwishBiswas](#), [MichaelR. Zachariah](#) and [YujieWang](#); University of California, Riverside, United States

One of the difficulties in understanding how powder composites of reactive fuel/oxidizer systems behave is the lack of control of the mixing length. In this study, we have prepared Al/CuO particle laminates using a direct writing approach. With as little as 10 wt% polymers we were able to obtain free-standing microscale particle-based laminates. Using these composites, we were able to image the cross-section of the laminates to directly probe the interface reaction with high-speed microscopic imaging and pyrometry. We show quantitatively how the burn rate can be altered by changing the layer thicknesses of the printed laminates and under high-speed microscopy imaging asymmetry heat transfer resulting in fingering in the temperature profiles in the reaction front. Numerical simulations of the heat and mass transport processes are able to reproduce the finger-structured reaction fronts. We find that for Al/CuO particle-based laminates the lateral O₂ diffusion rate from CuO to the Al layer appears to be rate-limiting. The finger-like profiles appear due to the combined effects from the faster propagation of the interfacial reaction over the bulk, and the thermal diffusivity differences between the Al/CuO layers. Interestingly we see no evidence of layer intermixing even on post-combustion inspection. These results are to our knowledge the first imaging of interface reactions between particle composites and provide a valuable testbed for probing mechanisms and validating models.

SESSION SF07.04: Multiscale Modeling of Reactive Materials

Session Chairs: Carole Rossi and Michael Zachariah

8:45 AM *SF07.04.01

Current Challenges and Perspectives in Modelling Multiphase Thermite Reactions [Alain Esteve](#) and [Carole Rossi](#); LAAS-CNRS, France

For three decades, significant research efforts have been devoted to thermites and nanothermites using different metal/metal oxide combinations and custom nanostructured architectures. Unlike explosives, these energy-dense materials undergo a rapid deflagration driven by a carbon free oxidation-reduction reaction, which forms stable reaction products (metal oxides or hydroxides). Moreover, these products have stronger mechanical strength and heat resistance than CHNO compounds. They are versatile, different combustion effects (in terms of pressure/gas development, temperature footage, initiation delay) can be obtained by manipulating the reactive system (metal and oxide powders) and their microscopic and mesoscopic morphology. Predictive simulations of the self-propagating reaction of thermite materials is one critical step to achieve their technological maturity and effective deployment into applications¹. There is however a lack of fundamental understanding on the mechanisms occurring in thermites combustion due to the complexity associated with the material heterogeneities and multiphase (gaseous, condensed phases) and reactive (high energy reaction) flows. Thanks to the constant increase in computing power and progress in numerical methods and modeling techniques, we believe that the most efficient way to address these questions, is to establish a multi-scale modeling approach (nanoscale à cm-continuous scale). DFT based simulations help to decipher localized events (diffusion/reaction)² while molecular dynamics simulations mostly based on reaxFF allow exploring more collective phenomena in terms of both the system size (thousands of atoms) and time duration (nanoseconds)³. Microkinetic modeling^{4,5} can describe the detailed surface and gas phase reaction mechanisms. Finally, the development of numerical CFD continuous models of the self-propagating combustion, is a key step to better test and confront simulations and experiments, to obtain deeper insights into the multiphase physics, thermal and transport processes⁶. The presentation will overview and discuss the multiscale modelling approach adopted by our team to better understand the combustion of Al/CuO thermites and simulate their self-propagating combustion, based on recent publications.

- (1) Rossi, C. Metallized reactive materials – a road to clean and sustainable pyrotechnics. *Propell Explos Pyrot* **2023**, *48* (5).
- (2) Jabraoui, H.; Rouhani, M. D.; Rossi, C.; Esteve, A. First-principles investigation of CuO decomposition and its transformation into Cu₂O. *Phys Rev Mater* **2022**, *6* (9)
- (3) Jabraoui, H.; Esteve, A.; Schoenitz, M.; Dreizin, E. L.; Rossi, C. Atomic Scale Insights into the First Reaction Stages Prior to Al/CuO Nanothermite Ignition: Influence of Porosity. *ACS Appl Mater Inter* **2022**, *14* (25), 29451-29461.
- (4) Tichtchenko, E.; Folliet, V.; Simonin, O.; Bedat, B.; Glavier, L.; Esteve, A.; Rossi, C. Combustion model for thermite materials integrating explicit and coupled treatment of condensed and gas phase kinetics, *Proc. Combust. Inst.*, **2022**, 1-9.
- (5) Baijot, V.; Glavier, L.; Ducere, J. M.; Rouhani, M. D.; Rossi, C.; Esteve, A. Modeling the Pressure Generation in Aluminum-Based Thermites. *Propell Explos Pyrot* **2015**, *40* (3), 402-412.
- (6) Lahiner, G.; Nicollet, A.; Zapata, J.; Marín, L.; Richard, N.; Djafari-Rouhani, M.; Rossi, C.; Estève, A. A diffusion-reaction scheme for modeling ignition and self-propagating reactions in Al/CuO multilayered thin films *J Appl Phys* **2017**, *122* (15).

9:15 AM SF07.04.02

The Combustion Complex of Fine Iron Particles [Xiaocheng Mi](#)¹, [Leon C. Thijs](#)¹, [Efstratios M. Kritikos](#)², [Aki Fujinawa](#)³, [Andrea Giusti](#)², [Jeffrey M. Bergthorson](#)⁴ and [Philippe Geoy](#)¹; ¹Eindhoven University of Technology, Netherlands; ²Imperial College London, United Kingdom; ³University of Cambridge, United Kingdom; ⁴McGill University, Canada

The true reason underlying the energy crisis faced by our society is not the lack of renewables sources, but the mismatch between a continuous energy demand and a geographically scattered and temporally intermittent supply from these sources. To overcome this problem, the scientific community is in search of reliable and efficient energy storage alternatives. Metal-enabled Cycle of Renewable Energy (McCRE) has been proposed as a solution for sustainable, long-distance transport and long-term storage of clean energy. Owing to its high energy density, zero-carbon nature, and recyclability, iron powder is nowadays considered as the most promising energy carrier to realize McCRE on a global scale. To build real-world power and heat generation systems, fundamental insights into the combustion properties of fine iron particles are required. Although a decent amount of knowledge in the combustion of conventional solid fuels is useful, numerous unique questions rooted in iron-powder combustion must be answered. These questions are mainly related to two unique features of iron-powder combustion: (I) The heterogeneous oxidation mechanism of individual iron particles and (II) the resulting laminar and turbulent flame dynamics with a spatially discrete heat release.

This presentation provides an overview of some theoretical efforts (supported by experimental evidence) made towards understanding the fundamentals of underlying in iron-powder combustion. The ignition characteristics of iron particles are analyzed considering solid-phase oxidation kinetics. After ignition, the rate-limiting mechanisms governing of an iron droplet at more elevated temperature (> 2000 K) is then examined using a single-particle combustion model informed by molecular dynamics (MD) simulations. This study reveals that the oxidation rate of an iron droplet is not solely controlled by the external diffusion of O₂, but an interplay among external diffusion, surface absorption, and internal transport. Euler-Lagrange CFD simulations are used to answer the question as to how the spatially non-uniform energy release from iron particles influences the flame dynamics under application-relevant conditions.

9:30 AM *SF07.04.03

Mesoscale Modeling of Shock Waves and Intermetallic Reactions in Ni/Al Multilayer Thin Films with Explicit Non-Ideal Interfaces [David Kittell](#), [Paul Specht](#), [Kevin Potter](#), [Michael J. Abernethy](#) and [David Adams](#); Sandia National Laboratories, United States

Solid heterogeneous materials exhibit a broad range of microstructural geometries when viewed at the meso (grain) scale. It is broadly recognized that these heterogeneous features play a role in the initiation and propagation of self-sustaining chemical reactions; however, layered reactive materials with a columnar grain structure have received less attention than for example granular/crystalline particle packs, porous materials with voids, and explicit particle size distributions, to name a few. In this talk, we will investigate shock induced reactions and phase change in Ni/Al reactive multilayers obtained from physical vapor deposition. These investigations are made via continuum-level simulations of thermal and mass transport, with explicit non-ideal interfaces.

While some shock-induced reactions have been simulated at the mesoscale for physical mixtures of nickel and aluminum powders (e.g., Austin and co-workers [1,2] and Xiong *et al.* [3]), the current talk will focus on advancements in three areas. (1) A new workflow is presented that is based on the Fast Fourier Transform, leading to an autocorrelation function which can mathematically generate multilayer geometries with non-ideal interfaces and columnar grain structures. This workflow is extended with machine learning; specifically, using style mapping and super resolution to combine features from the artificially generated layers and actual scanning electron microscope images. (2) Reaction is forced to begin at the Ni and Al interfaces by altering the thermal heat capacity of a small diffusion barrier that is present at the start of the simulations. Such diffusion barriers are observed in real reactive multilayers as a premix layer, following the physical vapor deposition process. (3) Arrhenius kinetics are used to propagate a reaction front following the arrival of a nonlinear shock wave. These (1)-(3) numerical methods are implemented and explored using Sandia National Laboratories' Eulerian hydrocode, CTH, and the results will be discussed and compared to the previous approaches.

Other topics covered may include homogenized models for shocks, as well as comparisons of the mesoscale results to experimental data obtained from gas gun impacts and laser-driver flyer impacts, which have been conducted at Sandia National Laboratories and the Advanced Photon Source at Argonne National Laboratory.

Sandia National Laboratories is a multimission laboratory managed and operated by National Technology & Engineering Solutions of Sandia, LLC, a wholly owned subsidiary of Honeywell International Inc., for the U.S. Department of Energy's National Nuclear Security Administration under contract DE-NA0003525.

- [1] R. A. Austin, D. L. McDowell, and D. J. Benson, "Mesoscale simulation of shock wave propagation in discrete Ni/Al powder mixtures," *J. Appl. Phys.*, **111**(12):123511, 2012.
- [2] I. Lomov, E. B. Herbold, and R. A. Austin, "Mesoscale studies of mixing in reactive materials during shock loading," in *AIP Conf. Proc.*, **1426**(1):733-736, 2012.
- [3] W. Xiong, X. Zhang, H. Chen, M. Tan, and C. Liu, "Multiscale modeling of the shock-induced chemical reaction in Al/Ni composites," *J. Mater. Sci.*, **57**:20224-41, 2022.

10:00 AM BREAK

10:30 AM *SF07.05.01

Microscale Techniques for Investigating the Chemistry and Energy Release of Reactive Materials Jennifer L. Gottfried¹, Elliot Wainwright¹ and Catherine Dillier²; ¹U.S. Army Research Laboratory, United States; ²Oak Ridge Associated Universities, United States

As an increasingly wide variety of novel synthesis approaches are being developed for reactive materials, e.g., unique alloys or core-shell structures and mechanically strained particles, microscale techniques for comparing the properties of these emerging materials to conventional or unmodified particles are desirable. Ideally, these techniques would enable relatively inexpensive, high-throughput investigation of the influence of the chemistry and nano- or micro-structural properties on the reaction mechanisms and energy release rates of reactive materials using minimal quantities of material. In our laboratory, we have developed several microscale techniques for evaluating the potential suitability of reactive materials in energetic formulations and increasing our fundamental understanding of the relationship between the structure and chemistry of reactive materials and their sensitivity or energy release behavior. The laser-induced air shock from energetic materials (LASEM) method enables us to compare the energy release of milligrams of material on the microsecond and millisecond timescales via high-heating rate excitation with a nanosecond-pulsed laser. Recent developments for the LASEM technique including new diagnostic capabilities, the incorporation of an environmental chamber to investigate the influence of atmosphere composition and pressure, and ongoing efforts to automate the data collection and analysis will be presented. To evaluate the influence of structural properties on the sensitivity of reactive materials, electrostatic discharge, impact, and friction tests with quantitative diagnostic measurements using an order of magnitude less material than military standard specifications have been developed. Finally, we report on recent efforts to develop a microscale technique for evaluating the impetus of novel materials.

11:00 AM SF07.05.02

Decomposition of a Sarin Gas Simulant DIMP with Combusting Metal Particles Evaluated with TDLAS and PRiMIRS – A High Throughput LWIR Spectrometer Preetom Borah, Milad Alemohammad, Mark Foster and Timothy P. Weihs; John's Hopkins University, United States

The use of chemical warfare agents (CWA's), particularly a nerve agent Sarin gas, is of growing concern. Due to their inevitable use, methods to effectively neutralize these weapons need to be further developed and improved. Composite metal powders have been effective in neutralizing biological warfare agents such as anthrax making them promising candidates for neutralizing CWA's. To understand the interaction between metal powders and a CWA simulant Diisopropyl-methyl phosphonate (DIMP), a two-fold decomposition pathway must be considered. DIMP can undergo homogeneous thermal defeat with exposure to moderately elevated temperatures to the surrounding gas as well as high temperatures local to the burning particles. Heterogeneous chemical defeat can also occur with interactions between DIMP and generated metal-oxide species. To optimize metal powders towards effective neutralization of CWA's, the role of thermal and chemical defeat must be evaluated separately. Requisite diagnostic systems must be developed to perform at faster timescales (≥ 100 Hz) over shorter durations (≤ 5 s).

A preheated stainless steel (SS) cell was used to generate DIMP vapor after liquid DIMP was inserted. Metal powders (Al8Mg:Zr) were held in a SS mount at one end of the cell and ignited with a resistively heated nichrome wire. The combusting metal particles then propagated across the cell containing DIMP vapor. A custom spectrometer (PRiMIRS) was used to monitor the concentration of DIMP during the experiment. The thermal contribution of the burning metal particles to the surrounding gas was measured using TDLAS at 1390 nm to probe H₂O spectra. Time resolved temperature profiles were calculated by running a minimization algorithm between experimentally obtained and simulated H₂O spectra. At faster timescales and shorter durations, DIMP decomposition products were not observed for temperatures up to 230C (homogeneous thermal defeat). The gas temperature contributions of combusting metal particles in the preheated SS cell remained below 230C. However, when these burning particles were introduced to the DIMP vapor, decomposition products isopropyl-methyl phosphonate (IMP) and isopropyl alcohol (IPA) were observed. To further investigate if decomposition is driven by thermal or chemical means, varying metal powder formulations were used such that certain chemistries generated nano-oxide species (vapor phase combustion) and other chemistries did not generate nano-oxides species (condensed phase combustion).

SESSION SF07.06: Boron-Based Reactive Materials

Session Chairs: Edward Dreizin and Dylan Kline

Tuesday Afternoon, November 28, 2023

Sheraton, Second Floor, Independence West

1:30 PM *SF07.06.01

Effects of Interfacial Interaction on the Mechanical and Combustion Properties of Boron/HTPB Composites Xiaolin Zheng; Stanford University, United States

The development of high-performing solid fuels with superior mechanical and combustion properties is critical to future air-breathing propulsion systems for space exploration and hypersonic navigation. Boron (B)/hydroxyl-terminated polybutadiene (HTPB) composite has been studied for this purpose due to the high energy density of B and the appropriate processability and mechanical properties of HTPB. However, the weak interface between B and HTPB results in weakened mechanical properties, agglomerated B particles, and slow and inefficient combustion, especially for composites with high B loading (30 wt% and above). In this study, we investigated the effect of the interface between B and HTPB on the combustion and mechanical performance of high-loading B/HTPB composites by surface functionalization of B particles. We compared three interfacial characteristics: polar (pristine B)/nonpolar (HTPB), nonpolar (hydrocarbon-functionalized B)/nonpolar (HTPB), and covalently bonded (amine-functionalized B/HTPB) interfaces. We found that both covalently bonded and nonpolar/nonpolar interfaces effectively reduced the aggregation of B particles in the HTPB matrix, even with up to 45 wt% B loading, thus promoting the combustion efficiency and burning rate. Moreover, covalently bonded interfaces in B/HTPB composites led to strain-hardening behaviors, resulting in enhanced strength, ductility, and toughness. This work highlights the significance of interface engineering in B/HTPB composites for the efficacy and safety of future air-breathing solid-fueled propulsion devices.

2:00 PM SF07.06.02

Spherical Reactive Composite Powders Combining Boron with Polytetrafluoroethylene (PTFE) Purvam Gandhi, Ashley Castillo, Mirko Schoenitz and Edward L. Dreizin; New Jersey Institute of Technology (NJIT), United States

Different compositions of boron and polytetrafluoroethylene (PTFE) were prepared using emulsion assisted ball-milling. For each composition, porous spherically-shaped powders were prepared. Additionally, the size and porosity for the same composition powders were tuned selecting the milling parameters. The prepared powders were characterized using scanning electron microscopy. Particle sizes were measured using low-angle laser light scattering. The particle sizes of the prepared powders vary from 5 to 30 μ m. Tests related to the reactivity of these powders were performed using Thermogravimetry (TG) and Differential Scanning Calorimetry (DSC). With an increase in the amount of fluorinated additive, PTFE, the temperature at which the onset of mass gain occurs becomes lower. However, the total mass gain at the end of the measurement (at 900 C) is greatest for the neat milled boron with no PTFE added. In DSC, several overlapping exothermic peaks were observed; the peaks shifted to lower temperatures as the concentration of PTFE increased. The strongest exothermic peak was observed for the composite containing 5 wt% PTFE. Prepared powders were placed on top of a flat, electrically heated filament, and their ignition temperatures were measured in air. With increase in the PTFE concentration, the ignition temperature of the composite decreases. Generally, the results suggest that addition of PTFE improves the reactivity of boron.

2:15 PM SF07.06.03

Transition Metal Catalysts for Boron Ignition and Combustion Samina Sarwar, Kerri-Lee A. Chintersingh, Mirko Schoenitz and Edward L. Dreizin; New Jersey Institute of Technology, United States

Boron is thermodynamically advantageous as a fuel for explosives and propellants because of its high volumetric and gravimetric heating values. However, there are limitations with its practical use due to long ignition delays because of the inhibiting oxide layer and long combustion times. Previous studies indicate that boron particles burn at temperatures below its boiling point, and combustion is limited by heterogeneous surface reactions with air. One proposed solution to improve the reaction rate without compromising energy density is to include transition metal (TM) additives that can accelerate surface oxidation by different mechanisms. Specifically, Bi leads to favorable redox reactions; Fe, Co, and Ni act as oxygen shuttle catalysts; and Zr and Hf lead to exothermic formation of respective borides. Boron composites were prepared by combining 95% pure commercial boron powders with 5 wt% of a selected TM additive powders (Ni, Co, Fe, Bi, Zr, or Hf) using a planetary mill and 20 mL of hexane as the process control agent. The samples were milled for 4 hours with the ball-to-powder (BPR) mass ratio of 10 and at a rotation speed of 350 RPM. Scanning electron microscopy was used to examine the powder morphology and elemental distribution on the particle surface. The samples were also characterized using low-angle laser scattering to obtain particle size distributions. Low-temperature thermogravimetric (TG) measurements in O₂/Ar environment up to 700 C were used to obtain oxidation kinetics of the prepared samples and to examine the role of the additives and the effect of milling on oxidation of boron. TG results show lower-temperature oxidation onset for all milled samples compared to starting boron. Samples containing Bi and Co have the greatest and fastest mass gain. To explore the effect of TM additives on ignition and combustion, the

prepared powders were aerosolized, and single particles were ignited in room air using a 125-W CO₂ laser. The optical emissions of the burning particles were captured using photomultiplier tubes filtered at 700 and 800 nm to determine combustion temperatures and burn times as a function of the particle sizes. The kinetic model determined from low-temperature TG oxidation studies was used to estimate the particle combustion temperatures in air. The prediction was in agreement with experiment only for neat boron and B-Fe powders that burned at about 2500-3500 K. Selected samples of commercial boron, milled boron, and boron milled with Fe, Co, and Bi additives were also hand blended with 76 wt% potassium nitrate, KNO₃ to form pyrotechnic mixtures for larger scale ignition and combustion tests in room air. Approximately 10 mg of the B/KNO₃ powder samples were packed into an aluminum cavity with a 4.85 mm diameter and 1.41 mm depth. The powders were ignited using a 10-ms CO₂ laser pulse. The combustion event was recorded using a photodiode sensitive to emission with the range of wavelengths of 350-1100 nm, and using a high-speed monochromatic video camera equipped with a 0.7 – 4.5x Zoom Monocular lens. In addition a compact UV-VIS-NIR spectrometer (190-850 nm) set at 1000 ms integration time was used. The experiments determined the ignition delays, plume propagation rates, overall combustion times, and temperatures, for the ignited samples. Preliminary experimental data showed shorter ignition delays for B-Co composite, whereas B-Bi samples demonstrated shorter combustion times and faster plume propagation rates than other composites. Time-resolved spectra of the combustion events were processed assuming grey body emission and resulted in combustion temperatures above the boiling point of B₂O₃ and the melting point of boron. Commercial boron powders showed characteristic BO₂ emission peaks and burned at ~3000 K, while some samples like B-Co showed no clear BO₂ emissions and burned at lower temperatures of 2400 K, indicating changes in the reaction mechanisms due to different TM additives.

2:30 PM SF07.06.04

Effects of Boron in Ignition and Combustion of Al-B-Ti Mechanically Alloyed Powders [Megan Bokhoor](#), Michael R. Flickinger, John Fite and Timothy P. Weihs; Johns Hopkins University, United States

Aluminum powders are a common metal fuel for energetic applications but often cannot reach ideal combustion efficiencies. Creating composite powders with additional constituents has been shown to increase combustion efficiency and reduce the ignition threshold via an intermetallic reaction. Here, we explored the effects of adding titanium and boron to an aluminum matrix to produce mechanically alloyed Al-B-Ti powders. We compared sieved (<75 μm) chemistries with constant Ti content while varying boron from 0 to 25 atomic percent. These powders were characterized using particle size analysis and large, stitched SEM cross-sections to define morphology and particle size distribution as well as wire ignition and differential thermal analysis (DTA) to evaluate their ignition and combustion properties. The composite powders showed a decrease in ignition temperature and increase in mass gain with increasing boron content. The combustion properties were analyzed using SHEAR to acquire temperature and spectral data.

2:45 PM SF07.06.05

Exfoliated Magnesium Diboride Nanosheets as Solid Fuels [Dongwon Ka](#), Yue Jiang, Andy Huynh and Xiaolin Zheng; Stanford University, United States

Magnesium diboride (MgB₂) has been explored as an alternative fuel to boron (B) due to its high energy density and an additive effect of magnesium (Mg) to promote B combustion. However, in the oxidation process, MgB₂ has a relatively slow reaction rate and high ignition threshold compared to other metal or metalloid fuels. The primary oxidation of MgB₂ does not occur unless it decomposes at a high temperature (830 °C), and it still has slow heterogeneous oxidation of boron following the decomposition. Recently, two-dimensional (2D) exfoliated MgB₂ nanosheets have attracted increasing attention due to their unique properties and potential applications in various fields. In this work, we present the potential of 2D exfoliated MgB₂ nanosheets as solid fuels in overcoming the challenges of MgB₂ combustion. The oxidation behavior and energetic performance of MgB₂ nanosheets are studied through materials characterization and combustion tests under slow and fast heating conditions. The results show that the MgB₂ nanosheets oxidize from a lower temperature than bulk MgB₂ under slow heating conditions as the MgB₂ nanosheets oxidize without decomposition. At fast heating rates, the MgB₂ nanosheets exhibit a lower ignition threshold, higher combustion efficiency, and faster energy release rate than other B-based fuels. This study highlights the potential of MgB₂ nanosheets as promising solid fuels with superior energetic properties.

3:00 PM BREAK

SESSION SF07.07: Applications of Reactive Materials II

Session Chairs: Edward Dreizin and Dylan Kline

Tuesday Afternoon, November 28, 2023

Sheraton, Second Floor, Independence West

3:30 PM *SF07.07.01

Engineered Reactive Crystals and Structures for *In-Situ* DIMP Neutralization [Tristan Kenny](#), [Brandilynn Ukena](#) and [Lori Groven](#); South Dakota School of Mines & Technology, United States

Traditionally the destruction of CWA is thermally induced during the blast wave, however, it is highly desired to augment the neutralization by the intentional generation of metal oxide nanopowders during the detonation event. Metal oxide nanopowders are expected to act as catalytic adsorbents and can be generated in-situ via several routes including metal powder inclusion. However, with bulk metal powders there remains a diffusion and oxidation timescale limitation. To overcome the reaction timescale issues, this work focuses on the inclusion of engineered reactive crystals and the intentional design of architectures that can maximize dispersion. These engineered crystals are focused on ionic cocrystals composed of an organic solid (e.g. glycine, urea, hexamine) and a metal salt. The primary focus here is on generating magnesium oxide (MgO) and alumina (Al₂O₃). In the case of MgO, an ionic co-crystal of magnesium nitrate/glycine is generated through mechanochemical means and subsequently used in formulation. For alumina, both aluminum nitrate and perchlorate are assessed with hexamine to form reactive complexes that upon combustion generate high surface area alumina (> 200 m²/g). These materials are further combined with an acrylate photopolymer to produce additively manufactured structures via DLP at solids loading exceeding 60 wt%. Detonation testing of generated materials was assessed in collaboration with UIUC (Prof. Glumac). For these studies, a surrogate CWA, diisopropyl methyl phosphonate (DIMP) was used, and it is shown that the inclusion of the ionic co-crystal magnesium nitrate/glycine to generate MgO in-situ decreases DIMP concentration significantly after just 1 ms. Product is collected from such tests and further characterized to help elucidate the decomposition mechanism.

4:00 PM SF07.07.02

Interaction of Hydrated and Dehydrated MgO with Diisopropyl Methyl Phosphonate (DIMP) at Elevated Temperatures [Elif Senyurt](#)¹, [Swapnil Das](#)¹, [Lori Groven](#)², [Tristan Kenny](#)², [Mirko Schoenitz](#)¹ and [Edward L. Dreizin](#)¹; ¹NJIT, United States; ²South Dakota School of Mines & Technology, United States

Condensed combustion products of reactive materials generated in a blast can serve to accelerate decomposition of toxic liquids, such as sarin, a chemical weapon agent (CWA). In particular, destruction of aerosols of CWA droplets can be augmented by inducing their interaction with a metal oxide smoke. The smoke particles are expected to adsorb and catalyze the decomposition of CWA. The mechanisms and rates of such adsorption and decomposition reactions are poorly understood and are expected to be different for various oxides. Experimental studies commonly use surrogates of CWA. Diisopropyl methyl phosphonate (DIMP), an organophosphorus compound often used as a surrogate of sarin, was used in this work. Its interaction with fine MgO powders representing a smoke produced by magnesium-bearing metal fuels, was studied experimentally. Different MgO powders were explored. In addition to two commercial (-325 mesh and nano-sized) MgO powders, several custom MgO powders synthesized from Mg(NO₃)₂·6H₂O and C₂H₅NO₂ (1:1 and 1:2 mole ratios) were used. Commercial MgO powders were found to be partially hydrated. To remove the hydroxide, all MgO powders were heated to 450 °C in a furnace of a thermo-gravimetric (TG) analyzer in a mixed argon/oxygen flow. Further, as-received, as-prepared, and de-hydrated MgO powders were mixed with liquid DIMP in 0.7 ml open alumina crucibles. The DIMP/MgO mixtures were also heated to 450 °C using the TG analyzer in a flow of mixed argon and oxygen. As expected, a first major mass loss step occurred while the liquid DIMP was evaporating. It ended before the boiling point of DIMP was reached. The residual mass represented DIMP adsorbed to the powder both physically and chemically. That mass was slowly reduced upon further heating for some samples. Certain residual mass was still retained by all powders even after their exposure to 450 °C. A distinct second mass loss step was observed starting at ~250 °C for the dehydrated commercial MgO powders, but not for the as-received and custom prepared powders. In separate experiments, all MgO powders were intentionally hydrated by mixing them with water. They were then dehydrated by heating them to 450 °C in Ar/O₂ environment. For all such hydrated and dehydrated powders exposed to DIMP and subsequently heated in TG, the second mass loss step was observed. This second mass loss step is qualitatively similar to that reported recently to occur when DIMP interacted with gamma alumina. The MgO powders exposed to DIMP and to the TG heating program were recovered and examined using FTIR-ATR analyzer. Clear signatures of DIMP molecule fragments adsorbed to MgO were observed. Such signatures were stronger for the dehydrated powders, which were initially hydrated. The results and possible mechanisms responsible for the adsorption and decomposition of DIMP by MgO surfaces will be discussed in this talk.

4:15 PM SF07.07.04

Laser-Induced Trapping of Metastable Amorphous-AlO_x/C (2.5 < x ≤ 3.5) Nanocomposites Stabilized by Carbon Interfaces—Implications for Solid-Phase Gas Generator Additives [Elijah M. Davis](#)¹, [Gerd J. Duscher](#)¹, [Jianguo Wen](#)² and [Dibyendu Mukherjee](#)¹; ¹The University of Tennessee, Knoxville, United States; ²Argonne National Laboratory, United States

Tailored interfacial and metastable structures can effectively circumvent the diffusion limitations due to oxide shell formation in Aluminum (Al) nanoparticle (NP)-based energetic nanomaterials (ENMs). Yet, rational design and synthesis of metastable nanostructures via non-equilibrium routes remain largely unexplored. Specifically, non-stoichiometric/amorphous Al-oxide ($a\text{-AlO}_x$) structures in metastable states, albeit, theoretically predicted, are rarely reported in experiments due to the inability to kinetically trap and phase-stabilize such exotic out-of-equilibrium phases at nanoscale. We report a pivotal advancement in addressing this challenge by employing reactive Laser Ablation Synthesis in Solution (r-LASIS) as a one-step, one-pot non-equilibrium route to synthesize unusual metastable $a\text{-AlO}_x$ NPs in hyper-oxidized states ($2.5 < x < 3.5$), phase-stabilized by interfacial C monolayers and dispersed in pyrolyzed-C matrices. Detailed characterizations from bulk and surface spectroscopic analyses as well as electron microscopy imaging reveal highly disordered $a\text{-AlO}_x$ NPs ($< 5\text{-}8$ nm sizes), remarkably stabilized by interfacial monolayer shells of ordered C-atoms. Using techniques such as Solid-state Nuclear Magnetic Resonance (SSNMR), X-ray Photoelectron Spectroscopy (XPS), and Electron Energy Loss Spectroscopy (EELS), we are able to establish the material's structure and composition in the hyperoxidized state. Interestingly, the $a\text{-AlO}_x$ NPs of sizes less than 10 nm were stable even at elevated temperatures. At temperatures higher than 750 °C, the $a\text{-AlO}_x$ structures undergo a solid-solid phase transition that culminates in the formation of stable $\alpha\text{-Al}_2\text{O}_3$ while releasing excess trapped gases. This talk will also present results for the detailed kinetic measurements carried out for the solid-solid phase transformation from metastable $a\text{-AlO}_x$ to stable $\alpha\text{-Al}_2\text{O}_3$ crystalline structures by using time-dependent high-temperature XRD analyses. The ability to kinetically trap such metastable nanomaterials in localized low-energy troughs, until their precipitous plunge to their global lowest energy state, has wide-ranging implications for their potential applications as solid-state gas generator additives that can bypass the diffusion limitations.

SESSION SF07.08: Poster Session: Advances in Reactive Materials Engineering
 Tuesday Afternoon, November 28, 2023
 Hynes, Level 1, Hall A

8:00 PM SF07.08.01

Enhancing the Reactivity of Boron Containing Complexes and Boron Nanoparticles as Fuels for Energetic Applications Prithwish Biswas, Michael R. Zachariah and Yujie Wang; University of California, Riverside, United States

Despite its high gravimetric and volumetric energy densities, boron (B) particles suffer from poor oxidative energy release rates as the boron oxide (B_2O_3) shell impedes the diffusivity of O_2 to the particle interior. One way to alleviate this issue is to employ solid-state B-containing complexes such as ammonia borane (AB) which can potentially generate gas phase B-species, reactivity of which will be trivially affected by solid state diffusion limitation. However, the intrinsic thermochemistry of AB also makes its application as a fuel challenging, as it oligomerizes and gets kinetically trapped into boron-nitrogen-hydrogen clusters on thermal activation. Herein, we mitigate this challenge by selectively altering the thermal decomposition pathways of AB with the help of a) ammonium-ion based oxidizing salts and b) polymeric carbonyl groups. The dative B-N bond of AB is responsible for triggering its thermal oligomerization pathway and the oligomerization is initiated through the formation of an intermediate known as diammoniate of diborane (DADB), which is formed as a result of an intermolecular nucleophilic attack of the N on B simultaneously accompanied by an intermolecular hydride ion exchange between the B-atoms. We show that in the presence of NH_4^+ ions, AB forms an alternative intermediate, as the nucleophilic interaction between the N of NH_4^+ with the B of AB is more favorable. This inhibits the oligomerization reactions of AB, thereby leading to the rapid and complete oxidation of its energetic constituents resulting in a $\sim 27\times$ faster energy release in presence of an NH_4^+ ion containing oxidizer such as NH_4ClO_4 . As an alternative approach, we also show that when AB is incorporated into polymer matrices containing carbonyl functional groups, thermal activation causes the carbonyl groups to engage in nucleophilic interactions with AB. Such interactions catalyze the lysis of the dative B-N bond resulting in the decomposition of AB to reactive fuels, NH_3 and B_2H_6 , with no evidence of its oligomerization. We find that the carbonyl groups function as catalysts and do not participate in any net reaction. In situ high-heating rate ($\sim 10^5$ K/s) characterizations demonstrate that AB/carbonyl-based polymer composites completely gasify to NH_3 and B_2H_6 at ~ 510 K, followed by spontaneous ignition in the air with negligible delay. This chemical pathway enables the solid-state storage of reactive fuels, NH_3 and B_2H_6 , and their controlled on-demand release for high-energy applications. Alternatively, experimental studies have shown that the addition of metals with lower free energy of oxidation such as Mg can reduce the oxide shell of B and enhance the energetic performance of B by $\sim 30\text{-}60\%$, however the underlying mechanism behind the reactivity enhancement is unknown. Through DFTB-MD simulations of the reaction of Mg vapor with B_2O_3 surfaces, we found that Mg become oxidized on B_2O_3 surfaces forming a MgB_xO_y phase. This induces a tensile strain in B-O bond at the $\text{MgB}_x\text{O}_y\text{-B}_2\text{O}_3$ interface and the interfacial B is simultaneously reduced resulting in the development of dangling bonds. The interfacial bond straining creates an overall surface expansion indicating the presence of a net tensile strain on the B_2O_3 surface. The B with dangling bonds can act as active centers for gas phase O_2 adsorption thereby increasing the adsorption rate and the overall tensile strain on the surface will increase the diffusion flux of adsorbed O through the surface to the particle core. As the overall B particle oxidation rate is dependent on both O adsorption and diffusion rates, the enhancement in both of these rates increases the overall reactivity of B particles.

8:00 PM SF07.08.02

Physicochemical Mechanisms Controlling the Energetic and Biocidal Performance of B and Al Composites Yujie Wang and Michael R. Zachariah; University of California, Riverside, United States

Boron is an attractive fuel in energetic materials due to its high gravimetric and volumetric energy content. However, boron often suffers from slow oxidation kinetics because its native oxide shell has low melting point and acts as a liquid barrier that retards its reactivity. We have studied a family of oxidizers with nearly identical chemistries to understand the controlling mechanisms of igniting boron. Boron nanoparticles with alkali metal perchlorates and iodates (LiClO_4 , NaClO_4 , KClO_4 , LiIO_3 , NaIO_3 and KIO_3) were investigated by temperature-jump (T-Jump) ignition and time-of-flight mass spectrometry (TOFMS) with rapid heating rates ($\sim 10^5$ K/s). T-Jump ignition tests in inert environment show that B/ LiClO_4 , B/ NaClO_4 , B/ LiIO_3 , and B/ NaIO_3 ignite while B/ KClO_4 and B/ KIO_3 do not, even though the chemistries are very similar. T-Jump TOFMS results demonstrate a significant increase of Cl and I containing species for Li and Na composites relative to K when B is introduced. Thermogravimetry/differential scanning calorimetry (TGA/DSC) analysis demonstrates the presence of a temperature gap between melting and decomposition onset of LiClO_4 , NaClO_4 , LiIO_3 , and NaIO_3 , respectively, whereas KClO_4 and KIO_3 melt and decompose concurrently. We find that the larger interval between melting and decomposition provides more time for the oxidizer to melt and surround/wet the B nanoparticles prior to decomposing, rendering better access to oxygen for B nanoparticles that results in more vigorous ignition. It demonstrates the significant impact of transport phenomena and physical properties of oxidizers on boron ignition. Metal iodates (LiIO_3 , NaIO_3 , KIO_3 , $\text{Mg}(\text{IO}_3)_2$, and $\text{Ca}(\text{IO}_3)_2$) have high iodine and oxygen content and are therefore attractive oxidizers for energetic and biocidal application. We have investigated the iodine release and energy release of Al-iodate thermites via TOFMS and combustion cell tests, respectively. It is found that there is a trade-off between iodine release and reactivity among these thermites as Al- $\text{Mg}(\text{IO}_3)_2$, Al- $\text{Ca}(\text{IO}_3)_2$, and Al- LiIO_3 release more iodine but are less reactive than Al- NaIO_3 and Al- KIO_3 . Free-standing composites containing 90 wt% loading aluminized metal iodate are assembled by 3D printing and their combustion behaviors are studied by high-speed videography and pyrometry. It is found that Al- $\text{Mg}(\text{IO}_3)_2$ and Al- KIO_3 cannot propagate while Al- $\text{Ca}(\text{IO}_3)_2$, Al- LiIO_3 , and Al- NaIO_3 propagate. For the later three composites, molten droplets with similar size form on the burning surface, while Al- NaIO_3 has a propagation rate about twice of the Al- $\text{Ca}(\text{IO}_3)_2$ and Al- LiIO_3 . Temperature profile from three-color (RGB) pyrometry demonstrates flame temperature of Al- $\text{Ca}(\text{IO}_3)_2$ and Al- LiIO_3 are similar and lower than Al- NaIO_3 . It is concluded that Al- $\text{Ca}(\text{IO}_3)_2$ and Al- LiIO_3 composites have potential application as biocidal agent due to both heat and iodine release.

8:00 PM SF07.08.03

Intelligent Exploration of Thermite Design Space Through Active Learning Algorithms Claudia Ramirez¹, Yasser Sami¹, David Gauchard¹, Nicolas Richard², Matthieu Jonckheere¹, Alain Esteve¹ and Carole Rossi¹; ¹LAAS-CNRS, France; ²CEA-DAM, France

The reactive materials design space is prohibitively large as not only the chemistry (nature of fuel and oxidizer) but also the microscopic (size of the fuel and oxidizer particles, purity of the metal) and mesoscopic properties (powder density, stoichiometric conditions, binder or additives) influence their macroscopic combustion. For two decades or so, data-driven science is

considered as a new paradigm in materials discovery and design that has already achieved number of successes in accompanying and accelerating research and innovation beyond the “Edisonian” approach based on trial-and-error used in most research laboratories. The most used approach is the Bayesian optimization algorithms, which requires large data base for approximating the objective function which is totally not possible when working with reactive materials: each experiment is costly due to the complexity to capture the combustion process *in operando*, and, truly predictive models that can replace experiments are computationally costly.

In this work, we explore *active learning* algorithms to allow for a guided and intelligent generation of database starting from a very limited set of available data. As a case study, an Al/CuO powdered thermite (mixture of Al and CuO particles) is considered because it is well-documented from both theoretical and experimental perspectives and a model is available to simulate its combustion^{1,2} in close vessels. A Gaussian process surrogate (GP) is used to approximate the target function in terms of the pressurization rate. Importantly, we explore different acquisition functions translating different exploration tradeoffs from the GP building block to guide the sequential sampling choice (Al/CuO sample) in the database. We study the impact on the quality of the database when prioritizing specific regions of the target space in the acquisition function, while maximizing the coverage of the features space. After presentation of the method and algorithms, we will discuss, (i) the benefit of the proposed algorithm compared to the brute force sampling (systematic sampling) of the Al/CuO design space through LHS technique (Latin Hypercube Sampling) and, (ii) physical aspects of interest of the design space of Al/CuO for gas generation applications.

(1) Tichtchenko, E.; Folliet, V.; Simonin, O.; Bedat, B.; Glavier, L.; Esteve, A.; Rossi, C., Combustion model for thermite materials integrating explicit and coupled treatment of condensed and gas phase kinetics, *Proc. Combust. Inst.*, **2022**, 1-9.

(2) Tichtchenko, E.; Bedat, B.; Simonin, O.; Glavier, L.; Gauchard D.; Esteve, A.; Rossi, C., Comprehending the influence of the particle size and stoichiometry on Al/CuO thermite combustion in close bomb: A theoretical study, *Propellants, Explosives, Pyrotechnics*, **2022**, e202200334.

8:00 PM SF07.08.04

Crystal Morphology in Ammonium Perchlorate Based Solid Composite Propellants Mason Freund, Suman Kumari and Volkan Ortalan; University of Connecticut, United States

Reactive and energetic materials are used in a variety of fields and therefore must be able to perform at different operating conditions. Being able to alter and control the properties of these materials in terms of the burning rate, heat of reaction as well as the sensitivity will allow the tailoring of reactive materials to perform optimally in a variety of applications. The reaction properties, performance, and sensitivity will be influenced by both the chemical and physical characteristics of the energetic material [1]. A well-known and widely used oxidizer component in composite solid propellants is ammonium perchlorate (AP). AP composite propellant formulations using metal fuel particles and polymeric binders can contain as much as 70% AP [2]. Due to the large percentage of AP in these composites, the oxidizer's properties including the size, shape, morphology, and defects will have a large effect on the performance of the composite. Understanding the modification of the energetic crystal morphologies and structures and the influence on the reaction properties, pathways, and mechanisms is important to the overall performance and safety of the reactive material.

In this work, the preparation of microscale ammonium perchlorate crystals and under confinement of nitrocellulose is demonstrated. A focus is placed on AP concentration dependence of the crystal size and morphology as well as the different observed morphological regimes. Solutions from low AP concentration up to the solubility limit are observed in scanning and transmission electron microscopy to better understand the role of solute concentration on the final crystal physical characteristics. Additional crystals are also grown in the presence of metal nanoparticles to form a composite solid propellant.

[1] R. Kumar, P. F. Siril, and P. Soni, “Tuning the particle size and morphology of high energetic material nanocrystals,” *Def. Technol.*, vol. 11, no. 4, pp. 382–389, Dec. 2015.

[2] Vargeese, A. A.; Joshi, S. S.; Krishnamurthy, V. N. Role of Poly(Vinyl Alcohol) in the Crystal Growth of Ammonium Perchlorate. *Cryst. Growth Des.* 8, 1060–1066, 2008.

8:00 PM SF07.08.05

Study on Energetic Reactive Plasticizers Utilizing Ring Strain Energy and Solid-State Copper-Free Azide-Alkyne Click Reactivity in GAP-Based Polyurethane Binders Mingyang Ma and Younghwan Kwon; Daegu University, Korea (the Republic of)

Plastic-bonded explosives (PBXs) are energetic composites composed of highly energetic molecules bound together by polymers which can create void-free and protective matrix. As a processing aid in the manufacture of PBXs, plasticizers are usually added to ease the processibility of composite formulations, and tune the mechanical properties of cured polymer composites. Inert plasticizers like dioctyl adipate (DOA) find application in hydroxy-terminated polybutadiene (HTPB)-based cast-cured PBXs formulations. However, both DOA and HTPB are non-energetic to decrease the energetic performance of PBXs.

Energetic polymers and plasticizers functionalized with explosophore groups such as nitrate ester (-ONO₂), azide (-N₃), or nitro (-NO₂) group have emerged as a replacement to non-energetic ones. For instance, an energetic polymer, glycidyl azido polymer (GAP), is a hydroxy-terminated polyether which can form the polyurethane (PU) matrix with a suitable isocyanate.

Plasticizers may readily migrate out of polymer matrix after certain periods of time even under the relatively mild storage condition, giving rise to the vulnerability of polymeric matrix leading to the energetic composites sensitive to impact, friction and heat. Series of energetic reactive plasticizers have been reported to prevent the migration problem of plasticizers within GAP-based PU binders by utilizing in-situ Cu(I)-free azide-alkyne Click reaction. Although explosophore groups of energetic polymers and plasticizers provide an improved energetic performance, disadvantages of the explosophore groups such as high impact sensitivity, instability at high temperatures and easy oxidation in air have been apparent.

In this study, ring strain energy of cyclic compounds is scrutinized to be an alternative, safe and reliable energy source for energetic reactive plasticizers instead of explosophore groups.

Notably, the efficacy of ring strain energy is deemed to provide a relatively inactive energy bearing some immunity to impact and shock because the release of which is commonly initiated by ignition. The energetic reactive plasticizers are designed to have both “energetic” ring-strained cyclic moiety as a new energy source and “reactive” alkyne group for solid-state copper-free azide-alkyne Click reaction with azide groups of GAP-based PU binders. The energetic reactive plasticizers are synthesized via an esterification of ring-strained cyclic carboxylic acids and alkynols. The homodesmotic schemes designed for computing the intrinsic ring strain energy of the energetic reactive plasticizers are developed and those ring strain energies are predicted at B3LYP/6-31G* level of theory. The plasticization effect of the energetic reactive plasticizers on the GAP prepolymer in terms of miscibility and rheological behavior are evaluated respectively. The energetic reactive plasticizers are found to exhibit a distinct copper-free azide-alkyne Click reactivity toward the GAP prepolymer. The experimental determination for the Click reactivity is in good agreement with the theoretical prediction of frontier molecular orbital. The GAP-based PU binders chemically linked to the energetic reactive plasticizers impart an enhanced tensile properties and impact insensitivity due to the transformation from azide to triazole group. Additionally, heat of formation calculated from heat of combustion of energetic reactive plasticizer/GAP-based PU binders is also analyzed.

8:00 PM SF07.08.06

Preparation of Pure Ti Nanopowders by High-Energy Ball Milling and Dehydrogenation of TiH₂ Eui Seon Lee, Youn JiHeo and Sung-Tag Oh; Seoul National University of Science and Technology, Korea (the Republic of)

Due to the characteristics of a high strength-to-weight ratio, superior corrosion resistance, good specific strength, and forming a lightweight alloy of titanium (Ti), the fabrication of high-purity Ti has consistently attracted attention, which is technological importance for a wide range of applications such as the aerospace industry, orthopedic, and dental implant materials. However, its susceptible oxidative characteristics and high-yield strength restrict the manufacturing of pure Ti through casting and cold working. Therefore, the powder metallurgy process is widely used in the production of Ti, but it has been difficult to prepare a pure Ti powder with suppressed oxidation. In this regard, we focus on the production of ultra-fine and pure Ti powders with low oxygen content through milling and dehydrogenation using brittle titanium hydride (TiH₂). We perform a high-energy ball mill (HEBM) using a planetary system to refine micron-sized TiH₂ powders by varying the milling speed, ball size, and time. The optimum condition for TiH₂ milling is determined by analyzing the particle size and lattice strain of the milled powders. The effect of particle size on dehydrogenation is investigated by thermal analysis with a heating rate of 5°C/min under an argon atmosphere. In addition, the effect of the reducing agent added during the dehydrogenation heat treatment process on the change in oxygen content of the synthesized Ti powder was analyzed. By optimizing the milling conditions, TiH₂ particles with a minimum size of 195.9 nm were obtained, and the dehydrogenation temperature decreased up to 140°C as the particle size decreased. In this work, we provide a promising technique for synthesizing the ultra-fine pure Ti powder which is important for the military industry and precursor elements for alloys and compounds.

8:00 PM SF07.08.08

Examining the Aging Characteristics of Fluoropolymer-Coated Boron using Heat Flow Calorimetry Sebastian Quek Yongsen^{1,2}, Sreekumar Pisharath^{1,2} and Hng Huey Hoon^{1,2}; ¹Emerging Nanoscience Research Institute, Singapore; ²Nanyang Technological University, Singapore

Boron (B) is a remarkable metal fuel offering significant potential in terms of both theoretical gravimetric and volumetric energy. However, realizing its complete experimental potential has been challenging due to the existence of a diffusion-limiting boric oxide layer. Consequently, numerous strategies have been devised over time, primarily aiming to disrupt the boric oxide shell and effectively activate boron for enhanced combustion reactions. Our approach relied on the application of a low molecular weight fluoropolymer (FP) coating, which we developed in-house, to enhance the combustion of boron to elevated levels. In this method, the activation process is initiated by the fluorination reaction, which leads to the disruption of the boric oxide shell. Additionally, the hydrophobic nature of FP is expected to provide a passivating effect on boron by preventing aging reactions caused by humidity and temperature. However, this aspect has not been thoroughly investigated yet. The present study focuses on examining the aging characteristics of FP coated B using heat flow calorimetry (HFC) experiments. We comprehensively investigate the aging process as a function of the percentage of FP coating, relative humidity, and temperature to gain a deeper understanding of the behaviour and stability of FP-coated B over time. We believe that this research will provide insights for optimizing the performance and utilization of activated boron as a metal fuel, thereby creating new possibilities for its practical applications.

8:00 PM SF07.08.09

Nanothermite Based Anti-Tampering Technology Florent Sevely, Sandrine Souleille, Ludovic Salvagnac, Alain Esteve and Carole Rossi; LAAS-CNRS, France

Security has become a vital part of electronic products that have been employed in critical data storage (personal, bank, etc) or critical equipment such as military systems. They not only handle sensitive data in uncontrolled environments, but also face intellectual protection issues or counterfeiting issues. Unfortunately, all current anti-tampering technologies, while being effective are susceptible to be cracked or bypassed, leaving the system vulnerable. That is why an ultimate action must be considered upon the detection of intrusion through irreversible destruction of the component being attacked. We developed a triggerable ultimate security device capable of physically destroying a memory chip that contains classified data, within a few milliseconds, upon the detection of intrusion. The developed device [1] is designed as an add-on module that can be positioned on any electronic chips, IC-circuit, or memory cards, without requiring any specialized chip design, substrate type or encapsulation solution. Its operation is simply based on the exothermic reaction of a solid-state printed energetic composite that physically disintegrates the sensible component in less than 1 ms. The solid-state energetic composite consists of a mixture of Al/CuO nanothermite with a copper ammine complex densely printed onto the chip that is meant to be destroyed. This energetic layer can be ignited through capacitance discharge in less than 50 μ s. The poster details the fabrication of the device and demonstrates that 400 mg of energetic composite irreversibly destroys one silicon chip (~120 mm³) in less than 10 ms.

(1) F Sevely, T Wu, FSF de Sousa, L Segulier, V Brossa, S Charlot, A Esteve, C Rossi, Developing a highly responsive miniaturized security device based on a printed copper ammine energetic composite, *Sensors and Actuators A: Physical* 346, 2022

8:00 PM SF07.08.10

Stoichiometry-Induced Control of the Reaction Front in Ni/Al Reactive Multilayers Nensi Toncich, Fabian Schwarz and Ralph Spolenak; ETH Zürich, Switzerland

Reactive multilayers are a class of metastable materials that exhibit remarkable thermal, chemical, and mechanical properties, making them highly versatile across diverse applications. One of the most intriguing aspects of reactive multilayers is their inherent ability to undergo self-sustained, exothermic reactions with high temperatures. This phenomenon arises from the stacking of alternating thin films of constituents with a large negative enthalpy of mixing. Leveraging this behavior, reactive multilayers find applications as intrinsic heat sources in many fields, including thermal batteries, biological hazard neutralization, joining processes, micro-propulsion, thin-film healing, and the microelectronic industry. Despite numerous investigations on the control of their reaction behavior, further studies are required to broaden the application and enhance the performance of reactive multilayers.

The objective of this study is to control and optimize the thermal management of Ni/Al reactive multilayers through the investigation of the impact of the stoichiometry on their reaction behavior. To this end, a wide range of Ni/Al ratios were fabricated and studied contributing to a substantial expansion of the current reported Ni/Al systems. Furthermore, the role of the bilayer thickness (B) was analyzed and batches of systems with 50, 70 and 90 nm-B were fabricated. This research focused on the evaluation of reaction kinetics and reached temperatures, characterizing alongside the mechanical properties, structure and composition of the systems through nanomechanical testing, differential scanning calorimetry (DSC), scanning transmission electron microscopy (STEM), and X-Ray Diffraction (XRD). MD simulations were conducted to investigate the kinetics and mechanical properties, revealing a consistent trend comparable to the experimental findings. When the concentration of Al exceeds the equimolar ratio with Ni, there is a noticeable decrease in the propagation rate. On the contrary, an increase in Ni concentration results in a reduction in the stoichiometry-dependent nature of propagation. The results obtained from this research will offer valuable insights into the design of Ni/Al reactive multilayers with customized thermal characteristics.

8:00 PM SF07.08.11

In-Detail Elaborating The Way of Titanium in Thermite Reactions Tao Wu, Vidushi Singh, Alain Esteve and Carole Rossi; LAAS-CNRS, France

In recent years, it has been reported that adding titanium into reactive thermite composites (such as Al/I₂O₅, B/CuO) can improve their combustion efficiency and lower their ignition temperature. However, these authors were only able to point out the complexity of the mechanisms governing ternary thermite reactivity but failed to answer the question of the exact role of the Ti reaction with oxidizers in such thermite composites. Due to the fast reaction rate and the difficulties in tracking elemental movements in Ti-based thermite nanoparticles, a full diagnosis from a fundamental standpoint awaits. In this work [1], we put our focus on in-depth understanding the reaction mechanism of Ti-based thermite by employing a magnetron-sputtering technique to grow high purity and well-defined CuO/Ti nanolaminates. Contrary to powdered nanothermites in which a thick titania oxide shell layer separates its pure fuel Ti core from the outer surface oxidizer particle, nanolaminates feature a very well-controlled interface (in thickness and structure) between the fuel and oxidizer. Furthermore, the multilayer system allows a full contact between the different species compared to particulate system showing random contact, which is crucial to clearly identify and rationalize the different mechanisms taking place during initiation/propagation of the reaction. This provides an ideal model-system to quantitatively describe the TiO_x interfacial oxide growing using a host of characterization techniques including microscopy, thermal analysis, spectroscopy and X-ray diffractometric.

Results show that 70% of theoretical heat of reaction of the Ti/CuO system is released within a single strong exotherm at 430 °C, thus confirming the early and fast Ti oxidation. High resolution electronic microscopy reveals that the titania, terminal reaction oxide, is grown and propagates into the Ti layer, driven by the diffusion/reaction of oxygen atoms released by CuO at 300 °C. Spectroscopy measurements show that CuO/Ti redox reaction undergoes a two-step oxidation process: at 300 °C, Ti is first oxidized into TiO and further oxidized into crystalline TiO₂ at 500 °C. At a similar initiation temperature, the Ti-based sample supports more oxygen transport, thus a greater number of elementary exothermic reactions, causing a greater amount of heat per unit volume. In turn, this drives the system into the self-sustaining reaction mode where sufficient energy is present to activate mass transport across the continuously forming terminal oxide until the reaction is completed. This study confirms that Ti can be of great interest in addition or replacement of Al in nanothermites, for applications where it is desirable to lower the ignition temperature. Adding two CuO/Ti bilayers prior to the deposition of CuO/Al multilayers allows decreasing ignition time below the ms (200 μ s) against 15 ms without CuO/Ti. Also, a burn rate enhancement factor of $\times 3$, and a reduction of the ignition delay by $\times 700$ is obtained when replacing Al by Ti in standard CuO/Al multilayers.

8:00 PM SF07.08.12

Decomposition of DIMP Vapors Interacting with Metal Oxides Elif Senyurt, Mirko Schoenitz and Edward L. Dreizin; NJIT, United States

Finely dispersed metal oxide particles form as a result of combustion of many energetic formulations; such particles are expected to catalyze decomposition of toxic vapors of chemical weapon agents (CWA), such as sarin. The thermal decomposition of CWA vapors is very fast at high temperatures; however, as the temperatures approach the CWA boiling point (~200 C), the rate of thermal decomposition drops. Thus, for the temperature ranges of 200 – 500 C, the effect of condensed combustion products catalyzing CWA decomposition are expected to be most important. The reactions and processes involved are poorly understood. Here, such reactions are studied using DIMP as a surrogate of sarin. DIMP is introduced into a heated laminar flow system and interacts with a porous plate pre-loaded with fine powders of different metal oxides. The initial concentration of DIMP in air or in nitrogen is adjusted to 3 μ mol/L. The concentration of DIMP in the flow passed through the plate is measured using a total gas analysis unit of an FTIR analyzer. Both flow system and the porous plate are heated to temperatures between 200 and 350 C; the flowrate of air is varied. Metal oxides exposed to DIMP-bearing flow are recovered and analyzed using FTIR-ATR. Results will be presented and discussed for several metal oxides typically generated by energetic materials, including gamma-alumina, magnesium oxides, etc.

8:00 PM SF07.08.13

Improved Energetic Performance of Graphene-Supported Aluminum Nanoparticles: Computational Materials Research Incorporated with Science Pedagogy Priyanshu Luhar¹, Sungwook Hong¹ and Lexi Hwang²; ¹California State University, Bakersfield, United States; ²California State University, Los Angeles, United States

Aluminum nanoparticles (ANPs) have attracted a great amount of attention owing to their high energy density, high reaction rate, earth abundance, and low toxicity.¹ ANPs have been considered effective reactive energetic materials. Recent studies show that adding graphene oxide and graphene fluoride improves the combustion performance of ANPs.^{2,3} This is mainly due to a synergistic effect between graphene sheets and ANPs. For example, oxygen molecules could be easily dissociated when they get closer to both graphene sheets and ANPs. As such, we hypothesize that graphene supported ANPs, which could be considered novel reactive materials, provide a remarkable combustion performance. Here we simulate the oxidation of graphene-supported ANPs using reactive molecular dynamics (RMD) simulations based on ReaxFF.⁴ The students conducted this research trained under research module/program designed by a guided inquiry-based instruction framework and other evidence-based science strategies. Results indicated positive impacts of our pedagogical approached simulation training. In particular, our RMD simulations led by the trained student reveal atomic-level reaction mechanism for the improved oxidation process of graphene-supported ANPs. As such, we believe our approach will strengthen a diversity in the community of reactive materials research, also providing a valuable input for the experimental design of solid-fuel propellants.

We acknowledge a funding support from NSF HSI program: Improving Undergraduate STEM Education: Hispanic-Serving Institutions (award number: 2247282 and #2247283)

References

- [1] Yetter, R. A.; Risha, G. A.; Son, S. F. *Metal Particle Combustion and Nanotechnology*. *Proc. Combust. Inst.* **2009**, 32, 1819–1838
- [2] Jiang, Y.; Deng, S.; Hong, S.; Zhao, J.; Huang, S.; Wu, C.-C.; Gottfried, J. L.; Nomura, K.-i.; Li, Y.; Tiwari, S.; Kalia, R. K.; Vashishta, P.; Nakano, A.; Zheng, X. *Energetic Performance of Optically Activated Aluminum/Graphene Oxide Composites*. *ACS Nano* **2018**, 12, 11366–11375.
- [3] Jiang Y.; Deng, S.; Hong, S.; Tiwari, S.; Chen, H.; Nomura, K.; Kalia, R. K.; Nakano, A.; Vashishta, P.; Zachariah, M.; Zheng, X. *Synergistically Chemical and Thermal Coupling*

8:00 PM SF07.08.14

Ignition Study of Copper Oxide Nanoparticle Coated Boron Micro Spheres using Shock Tube PrashantDeshmukh and Weon GyuShin; Chungnam National University, Korea (the Republic of)

Boron is an attractive solid fuel for propellants and explosives. But natural oxide layer on the boron surface hinders ignition and combustion of boron. The present work aims to improve the ignition performance of boron by coating the copper oxide nanoparticles on micro sized boron particles. Structural study shows the growth of nanocrystalline copper oxide particles on the surface of boron particles. Continuous and uniform distribution of copper oxide nanoparticles creating a continuous layer were observed from surface morphology. Further, it shows the size of copper oxide nanoparticles is less than 10 nm. The existence of elements viz. copper, boron and oxygen in the samples were confirmed by EDS and XPS analysis. Thermogravimetric analysis shows that the onset oxidation temperature of boron shifted to lower temperature after coated with copper oxide. This shift in temperature depends on the coating density of copper oxide nanoparticles. Maximum shift in onset oxidation temperature was 98°C compared with those of pristine boron. The shock tube examination reveals that the boron coated with copper oxide particles have a quicker ignition delay time than those of pristine boron particles resulting in a 6% decline in ignition delay time.

SESSION SF07.09: Active Control of Reactive Material Performance

Session Chairs: Lori Groven and Timothy Weihs

Wednesday Morning, November 29, 2023

Sheraton, Second Floor, Independence West

9:00 AM *SF07.09.01

Microwave and Electrochemical Stimulation for Control of Ignition and Throttling of Energetic Materials KerenShi, PrithwishBiswas, AdridaAnis and Michael R. Zachariah; University of California, Riverside, United States

While thermal and mechanical means are the most common approach to stimulate energetic components, alternative methods are also available. Laser ignition in both the visible and IR have also been used. In this talk I will discuss using microwaves (MW) and electrochemical means (EC) to stimulate, and modulate the energy release process. Unlike surface stimulation of the bulk materials, microwave heating offers the potential to trigger energy release within the energetic spatially and temporally, thus enabling the in-operando spatially selective control of the throttling. We give examples of employing reactive microwave sensitizers, Ti and MnO₂ to trigger the localized ignition of non-microwave sensitive energetic components. In addition we demonstrate that by embedding wires which can act as a microwave receiving antennas we can both initiate ignition locally, or alternatively accelerate the burn rate locally. In a second approach we demonstrate a new concept through which the volatility of a high energy density liquid propellant can be dynamically manipulated enabling one to (a) store a thermally insensitive oxidation resistant non-flammable fuel (b) generate flammable vapor phase species electrochemically by applying a direct-current voltage bias and (c) extinguishing its flame by removing the voltage bias, which stops its volatilization. We show that a thermally stable imidazolium-based energy dense fuel, can be made flammable or non-flammable by application or withdrawal of a direct-current bias. This cycle can be repeated as often as desired. The estimated energy penalty of the electrochemical activation process is only ~ 4% of the total energy release.

9:30 AM *SF07.09.02

Active Control of Energetic Material Decomposition Greg Young; Virginia Polytechnic Institute and State University, United States

In an effort to create safer and more mission flexible energetic materials, we are exploring the potential of using electrical stimuli to start, stop, restart, and throttle material decomposition/reaction. Specifically, we are examining the ability to actively control the ignition, combustion, and extinguishment of solid propellants. In the roughly 80 years since the first rubbery composite propellants emerged, relatively little has changed in terms of performance, or perhaps more importantly their functionality. Solid propulsion systems are still plagued today with very little operational flexibility. One recent concept for actively manipulating solid propellant combustion involves taking advantage of electrochemical processes with the application of electrical power to the condensed phase of the propellant. Questions linger as to whether electrochemical or thermal processes dominate in these environments. Whether ignition or extinguishment is the goal, the answer likely changes, and satisfying both is challenging. But, by targeting specific ignition and combustion mechanisms, new solid propellants which can be actively controlled are emerging.

Composite propellants at minimum comprise a polymeric binder and crystalline oxidizer but may also include additives such as metal powders to enhance performance. Typical properties that are desirable for binders and oxidizers may be different in electrically controllable propellants where responsiveness may be more important than metrics such as specific impulse.

Performance based additives are generally selected to improve the calorific properties of the propellant, however, when responsiveness is desired, different additives may be considered to elicit a specific response designed to improve operability. Additives which allow us to optimize one response for ignition/combustion/or extinguishment are often in opposition to another desired response due to competing mechanisms complicating the situation. That is, materials which tend to promote ignition, tend to impede extinguishment, and vice versa. The role of each of these components, binder, oxidizer, and additives is explored in the development of electrically controlled solid propellants which can be ignited, stopped, and restarted with only the application or removal of electric power. The formulation, fabrication, combustion behavior and properties of propellants controlled by electrical power will be discussed under relevant operating conditions.

10:00 AM BREAK

SESSION SF07.10: Tailoring Reactive Materials Performance I

Session Chairs: Lori Groven and Timothy Weihs

Wednesday Morning, November 29, 2023

Sheraton, Second Floor, Independence West

10:30 AM *SF07.10.01

Preparing, Tuning and Characterizing Spherical Composite Powders of Reactive Materials EdwardL. Dreizin and MirkoSchoenitz; New Jersey Institute of Technology, United States

It was recently discovered that spherical composite powders with attractive mechanical and chemical properties can be prepared using emulsion-assisted milling. During milling, starting powders are simultaneously being refined, mixed, and packed inside droplets in the emulsion. In the produced powders, each particle is a spherical compact combining the starting material components mixed on submicron scale. The powders typically have narrow size distributions reflecting the size of droplets in the emulsion. Powders also have certain porosity. Both porosity and size can be controlled by the milling conditions. The emulsion-assisted milling was found to be a versatile material processing technique effective for making composite spherical powders of metals, ceramics, polymers and mixes thereof. Recent progress in preparation of such powders will be reviewed considering both metal-metal and metal-oxidizer compositions. Correlations between milling process parameters and morphological features of the produced powders will be considered. Separately, correlations will be explored between the powder's morphological features and energetic performance. It will be shown that the powders with improved metrics characterizing their sphericity also have a better mixing between components that leads to their enhanced reactivity.

11:00 AM SF07.10.02

Correlation of Structure, Morphology and Energetics for Gasless Reactive Composite Powders JonathanL. McNanna, EdwardL. Dreizin and MirkoSchoenitz; NJIT, United States

Metal based composite powders capable of highly exothermic, gasless reactions were prepared by mechanical milling, adjusting parameters to intentionally vary particle characteristics. Two material systems were explored. In Ni/Al composite, intermetallic phases form exothermically leading to self-heating and accelerated oxidation. In a self-contained fuel/oxidizer system, Al/Fe₂O₃, a classic thermite reaction occurs forming molten iron and aluminum oxide. For each composite material, fully-dense irregularly shaped powders, as well as porous spherically

shaped powders are prepared and compared to each other. Particle characteristics such as size, shape, and morphology are observed by electron microscopy and low-angle laser light scattering. Scale of mixing and inclusion size are observed through image analysis and correlated to results of thermal analysis and ignition experiments. Specifically for the case of spherical powders, which are of interest for additive manufacturing techniques, milling parameters are optimized and associated with target size, uniformity of size, and sphericity. Finally, correlations are sought between morphological and energetic characteristics of the prepared materials.

11:15 AM *SF07.10.03

Optical Ignition and Combustion Characterization of Metal Fluoropolymer Composites[Steven F. Son](#); Purdue University, United States

The ignition of energetic materials, and specifically solid propellants, is a complex process that must be safe, consistent, and precisely controlled. There is a wide range of applications with specific ignition requirements for solid propellants including inflation of airbags, propulsion systems (including rockets), as well as arm and fire devices. Currently, electrical or percussion pyrotechnic igniters are most commonly used ignition systems. These systems must be carefully designed to deliver the proper amount of energy to a specified surface area of the propellant. A photon light source (i.e., flash or laser-based, ranging from UV to IR wavelengths) can potentially be used to ignite energetic materials with lower input energy and more precise spatial and temporal control, thereby improving safety and reliability by eliminating electrical systems used in pyrotechnic igniters. In addition, they could be potentially safer from stray electrical charges causing unintentional ignition. Here, we further explore the potential of optical ignition for energetic systems and identify ideal materials that can be used for optical ignition. In order to identify optically sensitive materials, we will study ignition energies, ignition delays, flame temperatures, and other combustion characteristics for possible energetic materials. This research addresses a gap in understanding of optical ignition for energetic materials, as finding and integrating materials that are optically sensitive while still being practical can be extremely challenging. These challenges include: (1) a lack of absorptivity to optical wavelengths in the UV to low-IR range, and subsequently, a very high sensitivity to input energy at the absorptive wavelengths that makes sustained ignition difficult, (2) a need for full density materials in practical energetic systems, while optically sensitive materials are exceedingly difficult to ignite as packing density increases due to heat transfer, and (3) the lack of research regarding novel fuels/oxidizers for the specific purpose of optical ignition.

Metal/fluoropolymer energetic materials have been of interest to the energetic materials community for many years. Due to fluorine's excellent oxidizing ability, they can be used in composite materials with metal fuels to produce energetic materials for a wide variety of applications. Polytetrafluoroethylene (PTFE), polyvinylidene fluoride (PVDF), polycarbon monofluoride (PMF), and terpolymers such as tetrafluoroethylene, hexafluoropropylene, and vinylidene fluoride (THV) have already seen extensive use in applications ranging including protective coatings, strain gauges, and electronics. However, when combined with metals such as lithium, magnesium, aluminum, or titanium, they also present an opportunity for a wide variety of energetic materials. For this study, metal/fluoropolymer composites present a novel opportunity for exploring optical ignition of widely absorptive, full-density energetic materials. This work will characterize the combustion and sensitivity of metal/fluoropolymer composites to provide novel materials for optical ignition of energetics.

Specifically, this work will begin with finding a suitable energetic composite that is optically sensitive. Once this material has been identified, research will be done to thoroughly characterize the optically sensitive composite by looking at additive manufacturability, flame temperatures, and ignition sensitivities from various methods and formulations. Once the material has been thoroughly characterized, it will be implemented into solid propellants to test the feasibility of the material in practical energetic systems. Finally, the lessons learned from this work will be applied to novel formulations to identify new optically sensitive energetic composites.

SESSION SF07.11: Reactive Materials and Machine Learning

Session Chairs: Alain Esteve and David Kittell

Wednesday Afternoon, November 29, 2023

Sheraton, Second Floor, Independence West

1:30 PM *SF07.11.01

Sensitizing Reactive Materials to Shock using Porosity[Siva Kumar Valluri](#) and [Dana D. Dlott](#); University of Illinois Urbana-Champaign, United States

Metal oxidation can produce perhaps twice the energy of molecular explosives, but because metal oxidation is a combustion process requiring mass transfer to mix fuel and oxidizer, it is generally too slow to support detonations. In collaboration with Prof. Edward Dreizin of NJIT, we have been using materials produced by arrested reactive milling (ARM) which creates metal/oxidizer microparticles that are mixed on the nanoscale. Since a large variety of metal composites can be produced by this method, we need high-throughput tabletop methods to screen candidate materials for fast energy release under shock compression. We have developed a method that requires only a few microparticles which can be embedded in a transparent polymer and shocked by a laser-launched flyer plate. Nanosecond thermal imaging and optical pyrometry allow us to correlate properties such as particle size and shape to shock response. Recently we studied a nanoporous composite containing Al and dual oxidizers MoO_3 and KNO_3 . Studies of the particle structure showed a strong correlation between size and porosity, and shock experiments showed that increased porosity lowered the shock threshold for reaction. This material was shown to release energy at rates comparable to HMX.

2:00 PM SF07.11.02

Designing Metal Fuels for Custom Thermite Compositions[Melissa Mello](#), Kerri-Lee A. Chintersingh, Mirko Schoenitz and Edward L. Dreizin; New Jersey Institute of Technology, United States

Thermites are combinations of metal and oxide powders that, when ignited, exothermically react to release tremendous amounts of energy that can be used in welding, pyrotechnic, and military applications. Past work explored thermites by altering the oxidizer, morphology, microstructure, or fuel to oxidizer ratio and typically used the traditional fuel of choice, aluminum. Recent research on combustion of various metals and the development of the machine learning (ML) algorithms enables one to accelerate design of custom thermites. Materials can be customized to increase the rate of energy release, target specific temperature, generate specific gases, or have a gasless reaction. This customization can be achieved by combining thermite and intermetallic reactions, generating tunable mixing scale distributions of fuel and oxidizer, and exploiting distributions of particle sizes, shapes, and porosities. Here, the effect of the combination of such metal fuels as aluminum and zirconium is explored on the microstructure and reactivity of thermites with CuO , Fe_2O_3 , and TiO_2 oxidizers. Composite thermite powders are formed by arrested reactive milling, a high-energy ball milling technique. Materials are characterized through SEM imaging and X-ray diffraction to explore morphology, microstructure and phases to aid establishing structure-function-performance relationships. Differential scanning calorimetry is used to observe the low temperature reaction sequences and product phases that may be relevant to employ in the optimized ignition and combustion scenarios. Preliminary results show that in argon environments up to 1273K, samples with greater than 25 at% Zr have low-temperature exotherms likely due to the formation of aluminides prior to subsequent oxidation of aluminum. Prepared samples are ignited using an electrically heated wire in air. A 440-nm wavelength laser ignites small batches of the prepared thermites in a closed 17-mL chamber, operated from 1 to 760 torr. A CO_2 laser ignites similar samples in room air. Ignition delays, burn times, and pressures traces are recorded for the laser-ignited samples. Emission produced by the flame is explored spectroscopically. Condensed combustion products are collected and analyzed. This work will focus on tailoring thermite reaction by tuning metal fuel composition and microstructure. The key experimental data will be used by an ML algorithm to optimize the tunable material parameters and develop novel thermite formulations on demand.

2:15 PM SF07.11.03

Characterizing Combustion Behavior in Al-Based Composite Metal Powders using X-Ray Phase Contrast Imaging and Machine Learning[Michael R. Flickinger](#), Deepthi Hedge, Yunzhe Wang, Vishal Patel and Timothy P. Weihs; Johns Hopkins University, United States

Al-based composite metal powders made through arrestive ball-milling and Physical Vapor Deposition have shown dual-phase combustion behavior where Al burns in the vapor phase and another element like Zr, or Ti burns in the condensed phase. These particles tend to microexplode which enhances overall combustion efficiencies. Acquiring a robust understanding of the mechanisms leading to particle microexplosions is of particular interest for researchers who seek to independently control the ignition and combustion properties of these powders.

X-ray Phase Contrast Imaging (XPCI) has previously been used to investigate the *in situ* internal bubbling of reactive powders that leads to microexplosions. Recently, a large amount of high speed videographic XPCI data was collected at the Advanced Photon Source to assess the role of composite chemistry on combustion characteristics. Here we present data comparing the combustion behavior of composite ball-milled powders made with aluminum and either a refractory element such as Hf, Ti and Zr or other additive (C or Mg) at varying stoichiometric ratios. In particular, the powders' bubble growth and microexplosion frequency was correlated with particle size, velocity and chemistry. Unlike previous work where XPCI videos were analyzed manually, we leverage various machine learning methods to extract meaningful information from hundreds of thousands of video frames. Additional experiments were performed in an Ar/O_2 (21% O_2) to assess the impact of nitrogen on internal bubbling and microexplosion frequency.

2:30 PM BREAK

3:30 PM *SF07.12.01**Hybrid Modeling for Decoding Reactive Materials** Sili Deng; Massachusetts Institute of Technology, United States

The design of reactive materials with reliable and programmable performance fundamentally hinges on understanding their chemical kinetics and transport properties. Traditional characterization tools, such as differential scanning calorimetry and constant-volume combustion experiments, have offered valuable insights into ignition phases and energetic performance quantification. Additionally, recent advancements in diagnostic technologies like Laser-Induced Air Shock from Energetic Materials (LASEM) and in-operando microscopy measurements have unraveled time and space-resolved dynamical responses of energetic materials. These multi-scale, comprehensive observations have deepened our understanding of kinetic and thermal transport behaviors. However, a challenge persists: the translation of these rich data sets into an understanding of intrinsic chemical kinetics and transport properties. This hurdle largely stems from the absence of an inverse modeling approach that could tie data to these physically meaningful properties.

In this presentation, we delve into hybrid modeling techniques that bridge this gap, extracting intrinsic properties (chemical kinetics and transport properties) of reactive materials from diagnostic tool data. These hybrid models integrate physical laws as first-principle constraints, enabling the extraction of kinetic and transport properties via sensitivity analysis. We illustrate the applicability of this approach through three examples involving the Chemical Reaction Neural Network (CRNN) [1], a kinetic inference framework for constant-volume combustion tests [2], and an inference framework for one-dimensional flame propagation. Initially, we introduce the CRNN as a versatile inference model adept at discovering chemical kinetics from time-history species measurements. Next, we delve into a specially designed kinetic inference framework that decodes chemical kinetics from time-history pressure profiles captured in constant-volume combustion tests. Lastly, we explore the simultaneous inference of chemical kinetics and transport properties from temperature fields in 1D flame propagation tests. These three examples collectively demonstrate the potential of hybrid modeling in unearthing the intrinsic properties of energetic/reactive materials from varied types of measurements.

[1] W. Ji, S. Deng, Autonomous discovery of unknown reaction pathways from data by chemical reaction neural network, *J. Phys. Chem. A* 125 (4) (2021) 1082–1092.

doi:10.1021/acs.jpca.0c09316.

[2] S. Kim, S. Deng, Inference of chemical kinetics and thermodynamic properties from constant-volume combustion of energetic materials, *Chem. Eng. J.* (2023) 143779

doi:10.1016/j.cej.2023.143779.

4:00 PM SF07.12.02**Self-Propagating Reaction Mechanisms in TiB₂ Integrated Al/CuO Nanothermites** Vidushi Singh, Richard Monflier, Nicolas Mauran, Alain Esteve and Carole Rossi; LAAS-CNRS, France

Unary nanoscale metallic fuels such as Al, Ti, Mg, Zr and B with an oxidizer have been massively explored in reactive energetic formulations commonly used in explosives and propellants owing to their high combustion energy. While Al has routinely been preferred, its low melting point and the resultant sintering effects curtail the reaction surface area. Despite the high gravimetric and volumetric enthalpies of B, low combustion rates and poor diffusion across the liquid boron oxide barrier restrict its use as a fuel. Although Ti oxidation can be induced at low temperatures, its high sensitivity limits the integration in nanolaminates. To overcome some of these common limitations imposed by single fuel thermites, binary fuel systems are seen as a very desirable strategy to prepare insensitive safe to handle nanothermites exhibiting fast energy release and high propagation rates.

Whereas TiB₂ may not be the most obvious choice of fuel, the fuel-oxidizer surface synergistic effects brought by its integration in Al/CuO nanolaminates resulted in enhanced reactivity characterized by relatively faster burn rate and shorter ignition delay¹. Beyond the excellent heat conducting properties, TiB₂ demonstrated a strong affinity towards oxygen boosting low temperature CuO decomposition concomitantly forming TiO and boron oxide, following which Al underwent oxidation via both liquid boron oxide and vapor phase oxygen. There is however a lack of fundamental understanding of the self-propagating mechanisms in such ternary thermites due to the complexity associated with the material heterogeneities and multiphase flow occurring during combustion.

Herein, sputter deposited ternary Al-TiB₂/CuO nanolaminates are fabricated as model structures, and a high-speed imaging system is utilized to study the flame-front propagation at sub-millimeter scales. DC magnetron sputtering is specially chosen to obtain precisely controlled layer-by-layer structures. To assess the extent of variation in the combustion regime, TiB₂:Al molar ratio is varied between 0 and 1. We examine the entire material life cycle of Al-TiB₂ bi-fuel component comprising of microfabrication, placement of TiB₂ in Al/CuO multilayer stack as well as the individual effects of Al and TiB₂ on the self-propagating combustion mechanism. While the individual placement of TiB₂ nanolayer in the stack only slightly affects the ignition and the combustion properties, the measure attests to be critical in precluding nano-structural losses. Finally, various combustion stages and flame front behaviors are discussed, followed by a scenario of the combustion process.

References:

1. Fuel 349, 128599 (2023)

4:15 PM SF07.12.03**Inferring Transport Properties and Chemical Kinetics of Reactive Materials from Flame Dynamics** Suyong Kim and Sili Deng; Massachusetts Institute of Technology, United States

Reactive materials exhibit self-sustaining reactions that generate energy in the form of heat, light, and pressure. These materials find applications in power generation, novel material synthesis such as explosives/propellants, micro-joining/welding, transient electronics, and space constructions, owing to their tunable reactivity, mixing length scales, and architectures. Understanding the fundamental processes governing flame propagation is crucial for designing materials with desired properties. Current methods extract chemical kinetics and transport properties from flame propagation measurements by simplifying mass and energy conservation laws and correlating measurable temperature data. However, these methods are limited to steady flame propagation and may underestimate activation energy. Moreover, they may not accurately reproduce flame propagation speed based on the inferred properties.

To overcome these limitations, we propose a new framework that accurately infers transport properties and chemical kinetics from dynamic measurements of flame propagation. Unlike existing methods, our approach utilizes flame structures and dynamics derived from first-principle models through sensitivity analysis of the dynamical system. This framework enables the understanding of both steady and unsteady flame propagation, including pulsating flame dynamics. We demonstrate the accuracy and capability of our model through examples of steady and pulsating flame propagations. Furthermore, we compare the inferred chemical kinetics and transport properties with those obtained using existing methods for various materials. Finally, we discuss the potential integration of our proposed framework with state-of-the-art imaging diagnostic techniques.

4:30 PM SF07.12.04**Interfacial Reactions and Energy Transfer in Sputter Deposited Mg/CuO Thermite Reactive Nanolaminates** Chloe Skidmore¹, Jon-Paul Maria¹, Elizabeth C. Dickey² and Stephen Funni³; ¹Penn State University, United States; ²Carnegie Mellon University, United States; ³Cornell University, United States

Multilayered stacks of reactive nanolaminates (RNLs) with well-defined interfaces consisting of a metal fuel and oxidizer offer a streamlined process for observing energy transduction and chemical reactions between thermite reactants. This presentation explores oxygen transfer in magnetron sputtered Mg/CuO RNLs as a function of bilayer thickness and metal-oxide layering sequence. Energy production in stoichiometric Mg-CuO films with bilayer thicknesses between 170-1020 nm is examined via differential scanning calorimetry (DSC), while Kissinger analysis methods are implemented to determine effective activation energies (E_a). To elucidate structural evolution in the Mg/CuO system, select samples are analyzed via in-situ high temperature x-ray diffraction (HTXRD). Calorimetry data show exothermic maxima near critical temperatures reported in the Mg-Cu phase diagram, along with a decrease in reaction temperature and effective E_a values as bilayer spacing increases. The 1 BL Mg-CuO RNL demonstrates an onset temperature near the Mg melting point of 650 °C and has the highest effective E_a of 600 kJ/mol. The 2-4 BL Mg-CuO films exhibit effective E_a values of 138-162 kJ/mol and reaction temperatures between 511-548 °C, which is within the Mg₂Cu/liquid region of the binary phase diagram. At 5-6 BL, a solid-state reaction process emerges with samples showing exothermic maxima between 388-421 °C and effective E_a values of 102-106 kJ/mol. These data are further corroborated by HTXRD data on 1, 3 and 5 BL Mg-CuO samples, with Cu peaks forming at 640 °C, 530 °C, and 415 °C, respectively. Further film characterization and preliminary thermal analysis also suggests that the epitaxial relationship (or lack thereof) between the substrate and initial RNL monolayer impacts film crystallinity, grain growth and reaction onset temperatures. Mg films deposited on c-sapphire are highly crystalline and strongly (0001) textured, while depositing Mg on CuO results in a decrease in overall crystallinity and a less textured Mg film. Conversely, CuO deposited on the substrate results in poorly crystalline films, but CuO crystallinity increases when CuO is deposited on Mg. Preliminary DSC analysis on Mg/CuO

samples with different layering sequences also indicate that bilayer films with CuO deposited first have lower reaction temperatures and effective activation energies. These results are supported by HTXRD results for 3 BL Mg/CuO samples with opposing stacking sequences – when CuO is deposited first Cu peaks appear at ~ 475 °C, while a Cu peak does not appear until 540 °C when Mg is deposited on the substrate. It is proposed that the highly textured Mg layer has a lower defect density in comparison to more disordered layers, resulting in decreased diffusion and increased reaction temperatures. The above findings indicate that reaction properties such as energy release and onset temperature are not easily estimated by solid state reaction dynamics and enthalpies of formation alone. Factors such as bilayer thickness, oxide passivation and intermetallic formation significantly influence observed reaction pathways, while seemingly innocuous deposition decisions such as RNL stacking sequence effect crystallinity and grain growth, subsequently impacting mass transport and reaction onset temperatures.

SESSION SF07.13: Tailoring Reactive Materials Performance II
Session Chairs: Michael Abere and Steven Son
Thursday Morning, November 30, 2023
Sheraton, Second Floor, Independence West

9:00 AM *SF07.13.01

Optimizing the Composition of Alloyed Metal Powders for Enhanced Ignition and Combustion Timothy P. Weihs; Johns Hopkins University, United States

Elemental Al or Mg powders are commonly used in high explosives, propellants, and pyrotechnics to enhance performance, yet in many cases combustion efficiencies are well below 100%. Recent closed-chamber detonation studies suggest that multi-element or alloyed metal powders ignite more readily and reach much higher combustion efficiencies than elemental Al powders. However, our community is just beginning to explore the many alloys that can be formed by mixing elements with high heats of combustion such as Al, Mg, Li, B, Si, Ti, and Zr. Given small variations in the atomic fraction of four elements in an alloyed powder generate over a million potential chemistries, we are leveraging a combinatorial process to rapidly screen the ignition and combustion properties of alloyed metal powders. We do so by sputter depositing ~ 30 micron thick coatings onto polymer meshes and then debonding the coatings to create elongated powders. In our first two combinatorial studies 1) we systematically vary the at% of Zr in Al-Zr and Al-Mg-Zr powders and 2) we vary the relative percentage of Al and B in Al-B-Ti powders. In this presentation we report on trends in ignition temperatures as a function of chemistry using hot wire experiments, and we describe their combustion temperatures, durations, and gaseous species using a novel, hyperspectral imaging system. Trends in the measured properties as a function of chemistry will be compared with those for elemental powders.

This work is supported by the Department of Defense, Defense Threat Reduction Agency under award HDTRA1-20-2-000

9:30 AM SF07.13.02

Reduction and Combustion of Iron Powder for Energy Storage: The Influence of Micro-Structure Conrad Hessels, Giulia Finotello, Xiaocheng Mi, Roy Hermanns and Philip Geoy; Eindhoven University of Technology, Netherlands

Cyclic reduction and combustion of iron powder is emerging as a promising method for seasonal storage and intercontinental transport of renewable energy. When renewable energy is in surplus, iron-oxide powder can be reacted with green hydrogen to produce “energized” iron powder. When the energy needed again, the iron powder can be reacted/combusted with oxygen in air, thereby releasing a tremendous amount of heat.

Both the reduction (in solid-state) and the combustion processes (in liquid state) result in changes in the micro-structure and morphology of the powder, which in turn influences the performance of the cycle. The reduction process produces porous particles (sponge iron), with a reduction-temperature-dependent pore size. The resulting effective surface area influences the ignitability and safety of the powder. The subsequent combustion process produces a combination of (1) spherical particles with hollow (open and closed) cores and (2) “tulip”-shaped hollow shells. The closed cores are likely the result of shrinkage cavities, while the “tulip”-shaped shells are most likely caused by micro-explosions observed during combustion. All combusted particles show cracks and preferred crystal orientations, in turn influencing the reduction process.

In this work combusted and reduced powder is analyzed using various material characterization techniques, such as scanning electron microscopy (SEM), X-ray diffraction (XRD), particle size analysis, and X-ray computed tomography (μ CT). The micro-scale findings are coupled to macro-scale phenomena observed during the combustion and reduction processes.

9:45 AM SF07.13.03

Ignition and Combustion of Al/Zr Composite Powders in Varied Gas Environments Michael R. Flickinger and Timothy P. Weihs; Johns Hopkins University, United States

It is well known that reactive metal composite powders can be ignited at relatively lower temperatures due to exothermic intermetallic formation reactions which help drive the particles to higher temperatures. This study systematically assesses the impact of intermetallic reactions contributing to particle ignition in three Al/Zr composite powders and differentiates its impact from oxidation and nitridation which may also influence ignition initiation.

Here we synthesized three different shaker milled Al/Zr composite powders with varying Zr at% content: 3Al:Zr, Al:Zr, and Al:3Zr. After sieving particles below 75 microns, powder samples were heated to different temperatures at a slow heating rate (20C/min) in Argon based on initial DTA traces done to 1000C for each powder. Those samples were then characterized via XRD, DSC, TGA, and SEM to explain wire ignition results. Wire ignition experiments performed at heating rates between 15-25,000 K/s revealed that increasing Zr at% decreased the overall relative ignition temperature rise as all the intermetallic heat was removed.

The combustion properties of the annealed powders were investigated to see if removal of the intermetallic heat affected the powder’s combustion behavior. A custom spectroscopy system called hyperspectral imager for emission and reactions (SHEAR) was used to gather key combustion data including combustion temperature profiles, burn durations and emission spectra. We relate this data to the microexplosion frequency and ignition delay of the three different powders.

10:00 AM BREAK

SESSION SF07.14: Reactive Materials Engineering I
Session Chairs: Michael Abere and Steven Son
Thursday Morning, November 30, 2023
Sheraton, Second Floor, Independence West

10:30 AM *SF07.14.01

Fabrication, Reactive Characteristics and Combustion Properties of Al Based Core-Shell Composite Particles John Wen and Anqi Wang; University of Waterloo, Canada

Metastable intermolecular composites (MICs) have shown promising characteristics in storing and supplying thermal energy to produce heat and power especially for propulsion and miniature systems. To improve their ignition and flame propagation properties, core-shell and other assembled structures are commonly fabricated as aerogels, thin films, multi-layers and powders with enhanced interfacial compatibility between reactive components. We developed wet-chemistry synthesis routes to fabricate a variety of spherical and colloid core-shell structured aluminum-based MICs including Al/CuO, Al/Fe₃O₄ and Al/NiO. Electron microscopies, X-ray diffraction (XRD) and X-ray photoelectron spectroscopy (XPS) were used to examine the geometry and microstructure of core-shell products. A good coverage of metal oxide nanoparticles has been achieved on aluminum micro- and nano-sized particles, as the crystallization of metal oxide or complex nanoparticles under controlled chemical environment was the key to homogeneously fabricated core-shell structures. The onset temperature, energy release and activation energy corresponding to the major exothermic events were found to be distinct yet comparable to physically mixed powders of aluminum and oxides nanoparticles due to the shortened diffusion distance between aluminum and oxidizer nanoparticles, evidenced by the thermogravimetric analysis (TGA) and differential scanning calorimetry (DSC) results.

Combustion of these core-shells, patterned as thin-films or loaded in a combustion chamber as loose powder, exhibited improved ignition and flame propagation characteristics. High-speed microscopic imaging and infrared thermography were utilized to reveal the mass and thermal transport phenomena near the flame front of a burning film composed of energetic particles. While the reactive sintering mechanism seems valid for both physically mixed and core-shell samples, the thickness of the flame front and its propagation speed demonstrated the competitive roles of the reactivity, sintering and heat conduction. The formation of standalone core-shell reactive structures reduced the role of reactive sintering of aluminum nanoparticles and generated

much finer hotspots along the propagation of flame front. Generally the global burning rates at different fuel/oxide equivalence ratios are determined by the reactivity and thermal transport. Near the stoichiometric condition, although reactivity is high, low thermal conductivity limits the thermal feedback, leading to non-uniform burning propagation on the thin film. On the other hand, at fuel-rich conditions, despite uniform burning propagation, the global burning rate is limited by low reactivity. During the combustion tests with loose powders, a two-stage combustion behavior has been observed as laser induced ignition was achieved first on the surface exposed to air before the combustion propagation swept through the entire sample volume. Such two-stage combustion behavior, being more commonly observed for physically mixed MICs, is less evident in core-shell structured MICs. The formation of individually reactive core-shell particles allows for enhanced condensed-phase reactions within a smaller zone which accelerates the propagation of combustion once the bulk reaction is initiated. While the ignition delay and burning rate of these powders are not necessarily correlated to the reactivation kinetics found from the DSC measurements, thermodynamic properties and energy transport paths within the packed sample play a more significant role in the combustion chamber tests.

11:00 AM SF07.14.02

Bridging the Gap between Improved Reactivity of Aluminum/Gallium Nanoalloy and Nanoscale Composition Variations via Advanced Microscopy Chi-Chin Wu¹, Scott Walck², Henry J. Hamann³, Metin Ornek³, Steven F. Son³ and Padinjaremadhom V. Ramachandran³; ¹U.S. Army Research Laboratory, United States; ²Survice Engineering Company, United States; ³Purdue University, United States

Aluminum/gallium (Al/Ga) nanoparticles were synthesized by reducing Ga (III) chloride to neutral Ga⁰ on fresh surfaces of relatively uniform (~40 nm) aluminum nanoparticles (nAl). Results from thermogravimetric analysis (TGA) and differential scanning calorimetry (DSC) demonstrated improved reactivity relative to a commonly used commercial nAl without Ga coating. The Al/Ga nanoparticles displayed a sharp exothermic peak and single-stage oxidation significantly lower than aluminum (Al). Advanced transmission electron microscopy (TEM) techniques were exploited to fill the gap between the morphology and locally varying composition of Al/Ga nanoalloy and enhanced thermal behavior with capabilities that conventional laboratory scale tests and baseline material characterization could not. High-resolution TEM showed different shapes of Al cores surrounded by amorphous shells, depending on the wait-time of Ga addition. The low Ga concentration was confirmed by X-ray energy dispersive spectroscopy (XEDS) acquired from relatively large quantities of Al/Ga agglomerates. Electron energy loss spectroscopy (EELS) and XEDS mapping were employed in scanning (STEM) mode to further investigate Ga and other trace elements. The results from only a few well-dispersed particles accurately revealed the nanoscale distribution of trace elements. Overlaid multivariate statistical analysis (MSA) quantitatively illustrated the nanoscale spatial variations and showed the presence of residual elements in shells. Gallium was found to be most concentrated at the core/shell interface for large particles, while small particles were composed of monocrystalline Ga surrounded by a thin oxide layer. Upon heating, the melting Ga underneath the oxide shell presumably facilitates shell fragmentation and exposure of active Al core for oxidation, leading to the improved reactivity observed by TGA/DSC. This work not only provides significant insights on evaluating the spatial distribution of Ga coating on nAl for bimetallic nanoalloy exploitation, but also underscores the critical value of advanced materials characterization to advance the understanding of novel energetics.

11:15 AM SF07.14.03

Improving the Morphology and Reactivity of Ball-Milled Aluminum Powders using Liquid Metal Embrittlement Purvam Gandhi, Mirko Schoenitz and Edward L. Dreizin; New Jersey Institute of Technology, United States

Liquid Metal Embrittlement (LME) is a process of modifying normally ductile/malleable solid metals, such as aluminum, with the help of liquid metals, such as gallium, in order to limit their elongation to failure. Recent studies have shown improvements in reactivity of aluminum-based thermites by mixing aluminum powder with a gallium alloy, galinstan, liquid at room temperature. Here, the LME approach serves to change not only the reactivity but also the morphology of aluminum powders used as fuels. Aluminum powders with tunable particle sizes and shapes are prepared by ball-milling. A Retsch PM 400 planetary mill is used. Emulsion-assisted milling is used to prepare porous spherical aluminum powders with narrow particle size distributions. Thin foils of gallium serve as additives mixed with the starting Al powder in a milling vial. Less than 5 % of gallium are added and milling is performed in agate vials with agate milling balls to minimize interaction of gallium with the milling media and vials. Powders prepared with and without addition of gallium are recovered and characterized using scanning electron microscopy, thermal analysis, and x-ray diffraction. Effect of gallium additives and milling conditions on the structure, morphology, and reactivity of the prepared powders will be discussed.

11:30 AM SF07.14.04

Using Low-Temperature Plasmas to Engineer Nano-Energetic Materials Lorenzo Mangolini, Brandon A. Wagner, Emmanuel Vidales Pasos and Michael R. Zachariah; University of California, Riverside, United States

Low-temperature plasmas are a versatile and effective tool for nanoparticle production. The presence of high-energy electrons in these systems is well-known to lead to the nucleation and growth of particles. While this is a major source of contamination in the semiconductor industry, the plasma community has now learnt to optimize low-temperature plasma processes for the deliberate formation of particles with desirable properties. For instance, low-temperature plasmas can produce particles sufficiently small to show quantum confinement effects [1] and localized surface plasmon resonance.[2] Due to their capability of producing particles with very small sizes (<10 nm), these systems are of obvious interest for application in energetic materials. In this talk, we will discuss two examples of how low-temperature plasmas can be used to produce magnesium-based and silicon-based energetic nanomaterials.

In a first example, magnesium nanoparticles are first produced via thermal evaporation of a bulk magnesium source. Following homogeneous nucleation, the particles are injected in a RF driven low-temperature plasma to which hydrogen is added. Optical emission spectroscopy is used to measure the atomic hydrogen density, which is found to be quite high (~10¹⁴ cm⁻³). As a consequence, the magnesium particles are rapidly converted into magnesium hydride as they are aerodynamically dragged through the plasma, within a residence time of a few tens of milliseconds. XRD analysis confirms that the MgH₂ molar fraction can be as high as 25% after in-flight plasma processing. Characterization of the combustion properties confirms that the hydrogenated magnesium particles have a significantly lower ignition temperature compared to Mg particles of the same size, as confirmed by time-of-flight mass spectrometry. Modelling of the energy exchange between the plasma and the nanoparticles suggests that while in the plasma, the particles are sufficiently hot to desorb hydrogen, limiting the degree of hydrogenation to roughly 25% for our current reactor design. This insight provides guidelines towards the development of magnesium-based particles with a significant degree of hydrogenation.

In a second example, we will discuss the case of ultra-fine (<10 nm) silicon nanoparticles which can be easily grown by RF excitation of a silane-containing plasma. Due to their large surface area, it is necessary to carefully control the surface chemistry of these particles. One way to do that, is to utilize a two-steps plasma reactor in which the particles are grown in a first plasma and then passed onto a second flow-through reactor to which a fluorocarbon source is added. TEM analysis suggests that this approach leads to the growth of a highly conformal CF_x shell onto the silicon core. We have found that this approach is very effective at preventing the formation of a native oxide. The core-shell particles form a nanothermite structure, whose combustion leads to the formation of SiF_x gaseous species, as confirmed by time-of-flight mass spectrometry measurements.

1. Wang, K., R.P. Cline, J. Schwan, J.M. Strain, S.T. Roberts, L. Mangolini, J.D. Eaves, and M.L. Tang, *Efficient photon upconversion enabled by strong coupling between silicon quantum dots and anthracene*. Nature Chemistry, 2023.

2. Alvarez Barragan, A., N.V. Ilawe, L. Zhong, B.M. Wong, and L. Mangolini, *A Non-Thermal Plasma Route to Plasmonic TiN Nanoparticles*. The Journal of Physical Chemistry C, 2017. **121**(4): p. 2316-2322.

SESSION SF07.15: Reactive Materials Engineering II

Session Chairs: Kerri-Lee Chintersingh and Dylan Kline

Thursday Afternoon, November 30, 2023

Sheraton, Second Floor, Independence West

1:30 PM *SF07.15.01

Physics-Based Co-Design of Energetic Molecular Crystals using High-Throughput DFT and Generative AI Santanu Chaudhuri^{1,2}, Janki Brahmabhatt¹ and Xavier Bidault¹; ¹University of Illinois at Chicago, United States; ²Argonne National Laboratory, United States

The packing motif of molecular crystals and co-crystals is a delicate balance between many subtle factors. The observed properties are not a linear function of the sensitivity of molecular building blocks. The common belief that stability, sensitivity, shock response, and performance can be co-optimized by a combination of molecular building blocks can be a simplification due to many unknown couplings between long-range and short-range interactions. We will discuss genetic algorithms for crystal structure prediction (CSP), and how this leads to an ability to search the potential energy landscape of common energetic materials and their polymorphs. Energetic materials can have the same molecular building blocks in many different conformations such as in RDX. Therefore, the E-V curve of molecular crystals and co-crystals are crowded at the bottom of the potential well with many predicted phases containing subtle differences in bond angle and relative rotational orientations of molecules. Using our models for multi-phonon up-pumping for sensitivity and thermochemical property predictions, high-throughput DFT methods can be used for searching polymorphs and co-crystals. We find that cocrystal sensitivity and properties show highly non-linear behavior. The case of CL20:HMX co-crystals will be

discussed. In comparison to co-crystals, molecular modification using a Diffusion based neural network can be a promising route for co-design with multiple objectives such as performance, sensitivity, and a range of thermochemical properties. We will discuss our latest molecular design tool DiffLinker, and generative adversarial neural network (GAN) based assembly of molecular crystals. They still need DFT training sets to improve accuracy but scaling on tens of A100 GPUs renders them highly efficient in generating a much larger pool of structures. A simple density-based screening can identify 10X more stable crystal structures compared to a DFT-based genetic algorithm for CSP. A closed-loop approach between generative AI for modifying molecular building blocks, using GAN to assemble crystals, and a subsequent genetic algorithm based on pure DFT or tight-binding refinement of best structures can be a highly efficient strategy for co-design of new generations of energetic crystals. The AI-generated molecular building blocks can also be ranked with respect to their many physical properties and synthetic accessibility scores. We will conclude with a summary of new methods, their relative accuracy, and their potential to change the future of energetic materials engineering.

2:00 PM SF07.15.02

Formulation and Combustion of Al/CuO Nanothermites using Flake-Shaped Al Nanoparticles Pierre-Henry Esposito¹, Pierre Gibot², Marc Comet², Renaud Denoyel¹, Denis Spitzer² and Marie-Vanessa Coulet¹; ¹CNRS-AMU, France; ²CNRS- ISL, France

Aluminum powders are widely used as fuels in propellants or in pyrotechnic mixtures. It is now well established that size reduction of aluminum particles from the micrometric down to the nanometric scale improves the combustion rate [1,2]. In the case of Al-based nanothermites, several other factors are shown to affect the combustion properties. Among them, one can cite, the surface functionalization of Al nanoparticles [3], the use of core-shell fuel-oxidant particles [4,5], and the incorporation of porosity [6–8].

In this work, we highlight the influence of morphology and surface properties of aluminum nanopowders on the combustion properties of Al/CuO nanothermites prepared by physical mixing. A comparative study is performed between nanothermites formulated using commercial aluminum nanospheres and two kinds of aluminum nanoflakes synthesized using high-energy ball milling and with different surface properties.

We will first present a detailed characterisation of initial Al nanopowders in terms of texture and reactivity towards air and water. Secondly, we will focus on Al/CuO energetic compositions. We will demonstrate that, contrary to what is generally expected, the flake shape is not problematic for the nanothermites formulation. Then, we will show that higher sensitivity thresholds can be reached notably for friction and electrostatic discharge by modifying the surface properties. Such enhanced thresholds might be of interest for safer handling. Finally, combustion tests will be presented and correlations between flame propagation velocity, morphology and Al nanopowders reactivity will be proposed.

This work received support from the Direction Générale de l'Armement (DGA), Aix-Marseille Université (AMU) and the Region Sud (AENA Project).

[1] J.R. Luman, B. Wehrman, K.K. Kuo, R.A. Yetter, N.M. Masoud, T.G. Manning, L.E. Harris, H.A. Bruck, Proceedings of the Combustion Institute. 31 (2007) 2089–2096.

[2] C. Rossi, A. Estève, P. Vashishta, Journal of Physics and Chemistry of Solids. 71 (2010) 57–58.

[3] K.S. Kappagantula, C. Farley, M.L. Pantoya, J. Horn, J. Phys. Chem. C. 116 (2012) 24469–24475.

[4] K. Shi, X. Guo, L. Chen, S. Huang, L. Zhao, J. Ji, X. Zhou, Combustion and Flame. 228 (2021) 331–339.

[5] X. Ke, X. Zhou, H. Gao, G. Hao, L. Xiao, T. Chen, J. Liu, W. Jiang, Materials & Design. 140 (2018) 179–187.

[6] M. Mursalat, C. Huang, B. Julien, M. Schoenitz, A. Esteve, C. Rossi, E.L. Dreizin, ACS Appl. Nano Mater. 4 (2021) 3811–3820.

[7] H. Jabraoui, A. Esteve, M. Schoenitz, E.L. Dreizin, C. Rossi, ACS Appl. Mater. Interfaces. 14 (2022) 29451–29461.

[8] T. Wu, B. Julien, H. Wang, S. Pelloquin, A. Esteve, M.R. Zachariah, C. Rossi, ACS Appl. Energy Mater. 5 (2022) 3189–3198.

2:15 PM SF07.15.03

Processing of Aluminum/Graphene/Fluoropolymer Composites for Energetic Applications Jonathan Shi¹, Sarah Brennan¹, Xiaolin Zheng² and Stephen D. Tse¹; ¹Rutgers, The State University of New Jersey, United States; ²Stanford University, United States

We fabricate novel energetic composites using graphene flakes to separate metal and fluoropolymer reactants, providing a significant energy barrier that can also be consumed in subsequent combustion, unlike a passivating oxide coating of the reactive metal. Processing of the composite will be discussed. Characterization of the microstructure of the composites, along with mechanical and combustion properties, is conducted. The fundamental knowledge gained on interface and surfaces, reaction routes, and new fabrication methods should improve the capabilities of energetic materials systems.

2:30 PM BREAK

SESSION SF07.16: Tailoring Reactive Materials Performance III

Session Chairs: Kerri-Lee Chintersingh and Carole Rossi

Thursday Afternoon, November 30, 2023

Sheraton, Second Floor, Independence West

3:00 PM *SF07.16.01

Tailoring Energy Release and Improving Processes in Additively Manufactured Reactive and Energetic Materials Dylan J. Kline; Lawrence Livermore National Laboratory, United States

Additive manufacturing (or 3D printing) can be used to create complex parts with features that could not otherwise be made via traditional machining or casting techniques. For reactive and energetic materials, additive manufacturing opens new possibilities to architecture materials with unique features and then leverage those features to tailor energy release in an unprecedented way. However, reactive materials additive manufacturing is still in its infancy and is ripe with opportunities to investigate structure-function relationships and process improvements. To better understand the role of process on architecture and function, new tools must be developed to characterize the manufactured parts. Fortunately, additive manufacturing natively lends itself to in situ inspection and new diagnostics are being developed to probe the process and create “digital twins” of AM components. This presentation will begin with a general overview of additive manufacturing techniques employed in reactive and energetic materials with a specific focus on advancements made in pursuit of tailored energy release. We will then shift towards a discussion on in situ diagnostics developed for additively manufactured energetic materials and the impact on improving manufacturing processes and understanding phenomena in experiments.

This work was performed under the auspices of the U.S. Department of Energy by Lawrence Livermore National Laboratory (LLNL) under Contract DE-AC52-07NA27344. LLNL-ABS-849970.

3:30 PM SF07.16.02

Influence of Different Nano Structure Densities on the Self-Propagating Reaction of Ni/Al Multilayer Konrad Jaekel, Yesenia H. Sauni Camposano, Sebastian Matthes, Marcus Glaser, Jean Pierre Bergmann, Peter Schaaf, Jens Müller and Heike Bartsch; Technische Universität Ilmenau, Germany

Reactive materials have garnered significant interest for bonding applications due to their ability to provide localized and rapid heating, thereby minimizing heat exposure to thermally sensitive components. The reaction parameters of these materials, such as velocity and temperature, are typically tailored through adjustments in layer spacing, total thickness, and atomic ratio of the involved elements. In this study, we consider the surface structures as an additional parameter for reaction tailoring and introduce a new aspect: adhesion of the formed compound without additional intermediate layers on silicon chips with a thermal oxide as heat barrier. Previous experiments involving Ni/Al multilayers on the thermal insulator SiO₂, revealed that the reaction led to substrate damage. The damage inflicted was substantial, as it also caused destruction in the Si layer beneath the thermally produced SiO₂ layer. Additionally, the Ni/Al compound was detaching during the reaction. The layer structure would therefore not be suitable for reactive chip bonding.

To mitigate this issue, we employed a reactive ion etching process to structure the surface, followed by oxidation, to create a thermal insulating layer. This SiO₂ layer not only facilitated self-propagating reactions, but it also additionally leads to an improved material bond. The oxidized nanostructures vary in density and have a height of approximately 1 μm. The nanostructure's densities range between 4 – 27 structures per μm², distributed across three wafer batches. The structure density of the first and second batch amounts to 3.55 - 6.23 structures per μm² and 7.22

- 14.64 structures per μm^2 , respectively. The third batch has a much higher range counting 21.69 - 26.53 structures per μm^2 . There is a process-related variation in structure density between the center and the edge. After separating and cleaning the samples, Ni/Al multilayers with a thickness of 5 μm , bilayer spacing of 50 nm, and an atomic ratio of 50/50 at.% were deposited onto the structured surfaces using direct current magnetron sputtering.

Upon electric impulse triggering, the multilayers underwent self-propagating reactions on all samples. Reaction propagation speed and surface temperature were measured by means of a high-speed camera and high-speed pyrometer. The data have shown that both values distinguish significantly for different nanostructure density. The first two batches showed lower velocities with increasing number of structures. The maximum temperature decreased as well between the first and the second batch. In contrast, the third batch has the highest temperature and propagation velocity as well as the highest structure density. These were results caused by the destruction of the substrate during the reaction, like on a flat SiO_2 surface. Only at the edges, where the structure densities were below 23 structures per μm^2 the compound stayed on the substrate like in the other two batches.

Since the layer architecture is the same, these differences in reaction propagation and maximum temperature, are attributed to an increased defect density which is a consequence of the growth characteristic of the sputtered layer on the structured surface. Flaking also depends on the structure density. This destructive behavior is mainly attributed to the volume change during the phase transformation. We observed that high structure densities lead to flaking, similar to the reactions on flat SiO_2 surface. In the range between 3 – 15 structures per μm^2 the layers adhere very well. The surface treatment is therefore proposed as an adhesion promoter for the reactive bonding of silicon chips as well as an additional parameter to tailor the multilayer reaction.

3:45 PM SF07.16.03

Large-Scale Periodic Modification of Reactive Multilayer Morphology by Direct Laser Interference Patterning of Growth Substrates Christian Schäfer¹, Vincent Ott², Michael Stüber², Frank Mücklich¹ and Christoph Pauly¹; ¹Saarland University, Germany; ²Karlsruhe Institute of Technology–Institute for Applied Materials, Germany

Reactive materials are a combination of two or more phases that can react exothermically in response to an external stimulus. The reaction behavior is determined by the transport of mass and heat and by the release of the latter. Therefore, the micro- and nanoscale morphology of the reactant phases plays a crucial role. A common arrangement of reactants is the sputter-deposited multilayer stack, where the bilayer thickness at a given overall composition is the main design parameter.

Deviations from the ideally flat binary layer stacking would provide an opportunity to modify the reaction behavior, but are usually not achievable by simply modifying the deposition process parameters. In this work, we present a method to modify the micro- and nanoscale morphology of magnetron sputtered Ni/Al multilayers using micrometer-scale, large area periodic surface patterning of the growth substrate.

Line structures with different periodicities have been created on thin Copper substrates by means of picosecond Direct Laser Interference Patterning (DLIP). Electropolishing has been utilized in a subsequent process to remove sharp asperities inherent to the laser processing, resulting in nearly ideal, smooth sinusoidal surface profiles. In the deposited Ni/Al multilayer stack, which retains the line structure even after detachment from the substrate, we found different changes in the layer morphology, depending on the structure period and depth. Shadowing effects during deposition caused by the substrate topography resulted in pores at distinct locations across the samples. In addition, the substrate pretreatment led to a local change in the interface roughness between the individual layers of the multilayer stack as well as to a periodic modulation of the bilayer thickness. It is discussed how the well-defined large-scale distribution of defects and the modified morphology can be used to quantitatively understand how pores inhibit heat and mass transport and thus affect the self-propagating reaction.

4:00 PM SF07.16.04

Self-Propagating Reaction of Reactive Multilayers Grown on Substrates with Designed Surface Topography Yesenia H. Sauni Camposano, Konrad Jaekel, Sebastian Matthes, Emina Vardo, Marcus Glaser, Heike Bartsch, Jean Pierre Bergmann and Peter Schaaf; Technische Universität Ilmenau, Germany

Reactive multilayer systems (RMS) consist of alternating layers of two or more components, which will react exothermically if the system is heated up locally, triggering a self-sustained and self-propagating reaction. Several studies were carried out with the aim of controlling the behavior of the reaction by changing the bilayer thickness or the atomic composition of the system. Moreover, recently the impact of the substrate and its surface topography on the propagation of the reaction has drawn attention. In previous studies, the influence of the surface topography of the substrate on the reaction behavior and on the phase transformation of the RMS during the reaction was revealed. However, the effect of surfaces with systematically distributed and defined structures needs to be further investigated.

In order to produce substrates with designed surface topography, silicon chips with a defined number of line/valleys structures in the surface were produced by lithography, reactive ion etching process and KOH etching. The KOH etching time was adjusted in order to produce valleys with different depths in the surface of the substrate. Sequentially, a SiO_2 layer of 1 μm thickness was produced on the surface by thermal oxidation with the purpose of ensuring the self-propagation of the RMS reaction. Al/Ni multilayers of 5 μm total thickness with a bilayer thickness of 50 nm was deposited on the Si/ SiO_2 substrates by magnetron sputtering. The RMS were characterized before and after reaction. The analysis of the morphology exhibits the influence of the substrate surface characteristics on the growth of the Al/ Ni multilayers and on the formation of defects, which are located in the slopes between lines and valleys. It was shown that varying the number and depth of the structures in the substrate allows us to tailor the size and the number of defects in the RMS.

To investigate the impact of the produced defects and the new morphology on the behavior of the reaction propagation front, ignition experiments were carried out. The reaction was initiated by spark ignition, a high-speed camera and a high-Speed pyrometer were used to record the propagation front and to obtain the temperature/ time profile during the reaction. These results show the impact of the RMS morphology on the propagation front behavior, the velocity of propagation decreases exponentially in relation to the number of lines in the substrate surface, and the registered maximum temperature decreases as well for samples with a higher number of line structures. The calculated velocity varied from 11 m/s for the RMS deposited on flat substrates to 4.5 m/s for the RMS on substrates with line structures. Moreover, it was found that structures with a depth over 3 μm block the self-propagation of the reaction. Despite the difference in the propagation velocity and the temperature, the X-ray diffraction patterns of the reacted samples show the reflexes of the B2 phase AlNi in the different samples and no reflexes of Al or Ni can be observed, which suggests the complete reaction of the system.

These results show the possibility of modifying the self-propagation characteristics of the RMS reaction by using substrates with designed surface structures, where the depth of the structures can be adjusted to define the path of the propagation front, while the line/ valley structures systematically distributed allows to control the velocity and maximum temperature during the reaction.

SYMPOSIUM SF08

Design and Behavior of Architected Materials for and in Extreme Environments
November 27 - December 5, 2023

Symposium Organizers

Ian McCue, Northwestern University
Ilya Okulov, Foundation Institute of Materials Engineering IWT
Carlos Portela, Massachusetts Institute of Technology
Gianna Valentino, University of Maryland

* Invited Paper

+ JMR Distinguished Invited Speaker

10:30 AM *SF08.01.01

Toward Precision Additive Manufacturing for Extremes—Opportunities and Challenges of ML-Enabled Closed Loop Approaches [MitraL. Taheri](#)^{1,2}; ¹Johns Hopkins University, United States; ²Pacific Northwest National Laboratory, United States

Extreme environments, including radiation, high temperature, and corrosion, present grand challenges for current materials systems. Novel materials to overcome these challenges have been discovered at a feverish pace in recent years, owing in part to high throughput and combinatorial approaches. Unfortunately, promising materials systems underperform due to processing and manufacturing limitations, as well as geometric and density constraints. Additive manufacturing promises the answer to many of these challenges, however control of build processes remains an elusive goal. This talk presents advances in precise additive manufacturing through closed loop processes, embedding artificial intelligence and machine learning approaches with computing and sensing hardware during the build process. Success in tailoring structures at the level of the melt pool, and below, is shown. The ability to design and tune alloys at a microstructural level is shown to be possible, and to be tailored toward specific extreme applications.

11:00 AM SF08.01.02

Development of TiAl Alloys for Gas Turbine Blades [Seong-Woong Kim](#); KIMS, Korea (the Republic of)

Research on developing new TiAl alloys for high temperature applications is introduced. At KIMS, we have developed new TiAl alloys which have excellent room temperature and high temperature properties. Especially, the new alloy showed excellent oxidation resistance in the temperature range from 900 to 1000°C by forming stable Al₂O₃ oxidation layer. Process development of casting, forging as well as 3d printing on the newly developed KIMS alloys was introduced. Especially, small size turbine wheel and blade were manufactured by centrifugal casting process. The results from the testing and validation of TiAl blade were shown that KIMS alloy can be used as a turbine blade above 900°C. In addition, we proposed some underlying mechanism of high temperature strength of KIMS alloy from TEM and SEM observations. Finally, the operation test of micro gas turbine is now under examination to confirm the possibility of the application of the new alloy in the gas turbine engine.

11:15 AM SF08.01.03

Enhancing the Performance of Plasma-Facing Materials Through Additive Manufacturing [Hyeji Im](#), Samuel Price and Ian D. McCue; Northwestern University, United States

Tungsten-based alloys possess significant potential for enhancing the efficiency of a fusion system due to their attractive properties. In this study, we explore additive manufacturing (AM) as a viable processing route to tailor into fine-grained structures in tungsten alloys while mitigating the issues associated with laser printing of pure tungsten. To identify suitable alloying elements for tungsten-based alloys, we assessed hot cracking susceptibility and phase stability of the candidate alloys. By incorporating titanium and iron as alloying elements, we successfully fabricated fully dense tungsten-based alloys utilizing laser-powder bed fusion. We performed a comparative analysis of the density, microstructure, and mechanical properties of additively manufactured pure tungsten and tungsten-based alloys. Titanium and iron were melted during the printing process, effectively filling the gaps between un-melted tungsten powders and improving the relative density of the alloys. The utilization of titanium and iron as alloying elements not only enables the fabrication of fully dense alloys but also enhances material performance, making it feasible to produce intricate parts in the field of plasma fusion.

11:30 AM *SF08.01.04

Compositionally Graded Transition from Tungsten to Ferritic-Martensitic Steels via Directed Energy Deposition for Fusion Reactors [Ibrahim Karaman](#)¹, Deniz Ebeperi¹, Tim Graening², Ying Yang² and Yutai Kato²; ¹Texas A&M University, United States; ²Oak Ridge National Laboratory, United States

Nuclear fusion reactors utilize W and W-based alloys as plasma-facing components, which require joining into steel cooling structures based on state-of-art divertor designs. Direct joining between W and steels leads to the formation of brittle intermetallics. Joining with filler alloys is not compatible with high-temperature applications as the microstructure may degrade and promote a critical failure. The directed energy deposition technique enables the deposition of multiple pre-alloy or elemental powders simultaneously, in a layer-by-layer fashion, with precise control of the composition to avoid the formation of intermetallic or detrimental phases. In addition, its ability to fabricate compositionally graded transitions reduces the coefficient of thermal expansion mismatch between adjacent interlayer alloys. In this study, we demonstrated a framework to optimize the processing parameters for each alloy, generated processability maps, and successfully fabricated a dense, multilayered, linear compositional gradient from W to Gr91 steel, using V-based and Fe-based alloys as transition elements. Microstructure and mechanical properties of the interlayers and the thermal cycling response of the gradient structure will be presented.

1:30 PM *SF08.02.01

Corrosion Behavior of Metals and Alloys in Selected Emerging Harsh Environments [John Scully](#), Ho Lun Chan and Elena Romanovskaia; University of Virginia, United States

Corrosion of engineering alloys in selected emerging harsh environments can exhibit rates which differ by 6 orders of magnitude depending on regulating attributes of the alloy, its surface, physical conditions and the exposure environment. For instance, corrosion in ionic liquids can vary from passive dissolution regulated by a passive film to active dissolution at four to six higher electro-dissolution rate. Case studies presented include chromium and Ni-Cr alloys in FLiNaK molten salt versus aqueous solutions as well as various examples in ionic liquids where the conditions for passivation versus active dissolution are largely unknown. The kinetic and thermodynamic parameters that limit electro-dissolution are discussed.

2:00 PM SF08.02.02

Limitations of Equiatomic Refractory High Entropy Alloys: Role of Reactive Elements in Al-Containing HfNbTaTiZr Refractory High Entropy Alloy [Elaf Anber](#)¹, David Beaudry¹, Sebastian Lech¹, Jean-Phillippe Couzine², James M. Rondinelli³, Christopher Wolverton³, Elizabeth J. Opila⁴ and [Mitra L. Taheri](#)¹; ¹Johns Hopkins University, United States; ²University Paris Est Creteil, France; ³Northwestern University, United States; ⁴University of Virginia, United States

Refractory high entropy alloys (RHEAs) hold the promise of superior mechanical properties at high temperatures but are plagued by a lack of oxidation resistance. Efforts to improve the oxidation resistance of RHEAs by adding classical passivation elements, such as Cr and Al, have been unsuccessful, largely due to the inability to form a continuous protective oxide scale, or the formation of deleterious secondary phases. Here, we present a detailed analysis of the oxidation behavior in a HfNbTaTiZr-based RHEAs with Al additions. Our study presents a case for stable and uniform oxide growth through tuning of the base alloy chemistry, where we examine the limits of passivating element additions to equiatomic RHEAs. Using a combination of multiscale microscopy and thermodynamic calculations, we determined that despite the increase in Al content, metastable phases and discontinuous oxides were dominant over the composition range of Al_xHfNbTaTiZr (x=0,0.25,0.75). As expected, the base RHEA (x=0) showed severe pitting after a one-hour exposure in ambient/atmospheric/etc air at 900°C, where HfO₂, ZrO₂, TiO₂ and TiNb₂O₇ were formed. The addition of Al improved the oxidation resistance of the base alloy and prevented pitting via promoting the formation of Al₂O₃. STEM chemical analysis revealed non-uniform enrichment of Zr and Hf near the metal/oxide interface that could block the diffusion of passivating elements, and thus, act against the formation of a uniform passivation scale. The addition of Al also induced the formation of the ZrAl₂ intermetallic phase that led to reduced density of Zr-rich oxides. We reach the conclusion that even if RHEAs contain enough Al to develop Al₂O₃ scale (i.e., 13 at. %), the passivation layer formed is still non-uniform with a high density of metastable oxides and intermetallic phases. This highlights the need for a passivating approach other than Al additions. Overall, this work provides insight into base alloy chemistry and its interplay with passivating elements as a key determining factor in passive film growth during high temperature oxidation.

2:15 PM SF08.02.03

Advanced Nanometer Resolution *In-Situ* Strain Mapping for Metal Oxidation by 4D-STEM YingHan¹, YongwenSun¹, DanZhou², Hugo PerezGarza², AlejandroG. Perez³, ThanosGalani³, StavrosNicolopoulos³ and YangYang¹; ¹Pennsylvania State University, United States; ²DENSSolution, Netherlands; ³Nanomegas, Belgium

Metal oxidation is a paramount concern in the realm of metal material applications, leading to the degradation of metal surfaces, corrosion, and a decrease in the mechanical properties of the metal. To gain a comprehensive understanding of the strain anisotropy resulting from metal oxidation, the utilization of accurate strain mapping is invaluable, and it enables the advancement of oxidation mechanism theory. Here, we focus on Zr as an illustrative example due to its importance in architecture materials for fuel cladding and developed an in-situ strain mapping method to study the oxidation in metal, by integrating four-dimensional scanning transmission electron microscopy (4D-STEM), advanced gas-cell-holder, precession electron microscopy and direct electron detector. The key to successful strain mapping by our method lies in ensuring high signal-to-noise ratio in the nano-beam electron diffraction patterns. The effect of gas pressure, sample thickness and electron beam precession will be discussed. Our approach facilitates high-quality strain mapping across a large field of view during zirconium oxidation with nanometer resolution. This proposed technique has significant implications for a wide range of corrosion studies, enabling more insights into the chemo-mechanical evolutions in materials under extreme environments.

2:30 PM *SF08.02.04

Preventing Aqueous Corrosion of Light Alloys (Al and Mg) for Engineering Applications Sviatlana V. Lamaka; Institute of Surface Science, Helmholtz Zentrum Hereon, Germany

The talk will present several approaches for preventing aqueous corrosion of aluminum and magnesium alloys used for engineering applications. Bulk or thin layers of electrolytes (300-30 micrometers) are considered. High-throughput robotic testing protocols of corrosion inhibition employ traditional or spatially resolved electrochemical methods, spectroanalytical methods but also recently validated image analysis approaches. These methods provide versatile and reliable data to train quantitative structure-property relationship (QSPR) models. Machine learning algorithms then identify hitherto untested potent corrosion inhibitors that are experimentally validated. Implementing identified inhibitors into industrial coatings and studying their inhibition mechanisms will be also presented. Applicability of specific data, e.g. generated by spatially resolved electrochemical methods for validating the finite element modeling of inhibitor leaching from the coatings will be also discussed.

3:00 PM BREAK

SESSION SF08.03: Ceramics for Extremes
Session Chairs: Ian McCue and Gianna Valentino
Monday Afternoon, November 27, 2023
Sheraton, Third Floor, Fairfax A

3:30 PM *SF08.03.01

Direct Ink Writing of Seeded and Fiber-Reinforced Silicon Carbide to Create Anisotropic Microstructures Rodney W. Trice; Purdue University, United States

Silicon carbide (SiC) is a material of interest for many applications due to its mechanical properties, oxidation resistance, and high thermal conductivity. Colloidal processing and pressureless sintering can enable forming of complex shaped, dense SiC parts. Direct ink writing (DIW) is a colloidal processing technique where ceramic suspensions are extruded through a nozzle along a path, building up a part layer-by-layer. However, DIW is not only interesting for making complex shapes, but also for creating anisotropic microstructures by aligning particles or fibers via the forces in the print nozzle. In this work, SiC with anisotropic microstructure is created via the alignment of platelet seed particles or fibers in DIW and subsequent pressureless liquid phase sintering and annealing. The anisotropic microstructure and crystallographic texture of these materials will be explored with SEM, XRD, and EBSD. Mechanical properties of these ceramics will be explored via 4-pt flexural strength with Weibull analysis performed.

4:00 PM SF08.03.02

Mapping the Creation of Nanoporous Ultra-High-Temperature Ceramics Catherine B. Ott and Ian D. McCue; Northwestern University, United States

Nanoporous materials have found use in a broad variety of applications ranging from sensing and actuation to catalysis and coatings. In the coatings space, nanoporous materials have generally been used as templates for thin networks, where the template is later dissolved away. However, nanoporous materials could themselves be used as part of a high-temperature coating, though the ligament coarsening rate must be controlled to retain integrity of the nanoporous structure at temperature. While nanoporous metals undergo curvature-accelerated surface smoothing, which leads to thickening of ligaments, increasing pore size, and decreasing surface-to-volume ratio, it has been proposed that this morphology evolution may be frozen by creating a nanoporous carbide/nitride ceramic due to the strong covalent bonding limiting surface mobility. The present work examines the conversion of nanoporous refractory metals to nanoporous ultra-high-temperature ceramics *via* gas-phase conversion at elevated temperature. Nanoporous Ta precursors were exposed to carburizing (methane-containing) and nitriding (ammonia-containing) environments over a range of temperatures for different lengths of time to examine the interplay between ceramic conversion and ligament coarsening rates. Kinetic models were developed for both degree of ceramic conversion and degree of coarsening to quantify the process for creation of a nanoporous ultra-high-temperature ceramics.

4:15 PM SF08.03.03

Preparation of Compositionally Complex Ultra-High Temperature Ceramics via Group IV Metal Functionalized Pre-ceramic Polymers James Ponder^{1,2}, Haira Hackbarth³, Nicholas Posey^{1,2}, Nicholas Bedford³, Matthew Dickerson¹ and Timothy Pruyn¹; ¹Air Force Research Laboratory, United States; ²UES, Inc., United States; ³University of New South Wales, Australia

Materials capable of withstanding ultra-high temperatures are becoming increasingly important for various aerospace applications, ranging from atmospheric re-entry shielding to aircraft brakes. While silicon-based ceramics have proven to be a key class of materials for these harsh applications, introduction of transition metals into these ceramics is required for ultra-high temperatures conditions. Preparation of ultra-high temperature ceramics (UHTCs) using traditional inorganic powder sintering methods limits the structural/compositional designs possible and is challenging for preparing composite components. Pre-ceramic polymers (PCPs) have been used to address these challenges via the synthetic tunability and processing properties of polymers prior to pyrolysis. Following pyrolysis of the PCP, a polymer derived ceramic (PDC) is obtained. By tuning the PCP structure, curing/pyrolysis conditions, and pyrolysis atmosphere, the composition of the PDC can be manipulated for different properties.

Here we report that by functionalizing a commercially available polysilazane-based PCP with transition metal complexes, we have prepared polymer-metal complexes that convert to UHTCs composites when pyrolyzed. In addition to functionalization with the individual group IV metal (Ti, Zr, and Hf) complexes, a blend of the three metals was prepared to understand how the materials blend/separate in PDCs. Following ceramization at different temperatures, X-ray diffraction (XRD) and atomic pair distribution functional (PDF) analysis are used to understand the structural evolution of the material from amorphous to crystalline ceramics. A combination of quantitative energy dispersive X-ray spectroscopy (EDS) and selected area diffraction from transmission electron microscopy (TEM) was utilized to observe the distribution of atomic species within the ceramic. From these various methodologies, the compositions of the PDCs were found to consist of silicone and transition metal carbides, nitrides, and carbonitrides. Ultimately, we report a route to polymer derived compositionally complex UHTC nanocomposites suitable for various high temperature applications.

4:30 PM SF08.03.04

Active Oxidation in Nanocrystalline SiC Woven Fibers: Atomistic Simulation and High-Temperature Oxygen Plasma Experiment Frederic Sansoz and Luc Capaldi; The University of Vermont, United States

High-temperature oxidation of nanocrystalline SiC fibers is critical for the deployment of advanced flexible thermal protection systems such as hypersonic inflatable aerodynamic decelerators developed for space exploration by NASA. Experimental evidence has shown that woven SiC ceramic fibers are prone to accelerated fiber embrittlement under high temperature oxidation in dynamic oxygen environments. The nanocrystalline structure of the constituent fibers impacts the reaction kinetics and phase transformations during active oxidation. However, our fundamental understanding and quantification of grain boundary effects on oxidation behavior in nanocrystalline SiC remain elusive when temperatures exceed 1500 K. In this talk, we will present large-scale molecular dynamics simulations with a reactive force-field, supported by direct observations from high-enthalpy oxygen plasma experiments, to elucidate the complex roles

of grain size on oxidation kinetics and the nature of oxides produced in both monocrystalline and nanocrystalline 3C-SiC between 1100 K and 2000 K. We find that nanocrystalline SiC samples exhibit two distinct oxidation kinetics with a transition point at 1500 K due to surface melting. The introduction of a grain-boundary network produces a two-fold decrease in oxidation activation energies compared to monocrystalline SiC below 1500 K. Above 1500 K, however, the activation energies rise substantially due to the formation of a liquid Si phase at the SiC/Si oxide interface. It is shown that the stability of the interfacial liquid phase is promoted by incoherent grain boundaries in the crystalline SiC.

4:45 PM SF08.03.05

Preventing Structural Collapse During Acceleration of Relativistic Lightsails for Interstellar Travel[Marianne Aellen](#), John E. Sader and Harry A. Atwater; California Institute of Technology, United States

Interstellar travel requires new propulsion mechanisms. Employing radiation pressure from a high-power ground-based laser is a conceivable route to accelerate an ultralight spacecraft to a significant fraction of the speed of light. To adhere to strict mass constraints, such a spacecraft can employ an ultrathin elastic membrane for its lightsail. During acceleration, a uniform membrane will deform significantly, potentially leading to its collapse. Here, we study the deformation of circular lightsails propelled by a Gaussian laser beam. We observe a significant change in scaling laws when increasing the lateral sail size from laboratory-scale (tens of micrometers) to mission-scale (several meters). A buckling analysis reveals critical accelerations and suggests design principles for hoop stiffening elements to increase the maximum acceleration. These findings serve as the basis to understand and prevent relativistic-lightsail collapse during acceleration.

5:00 PM SF08.03.06

Exploring SixC_y Materials[Sakineh Chabi](#); University of New Mexico, United States

Silicon and graphene are among the most critical research areas in nanotechnology, and any advancement in these areas can impact several scientific fields. The combination of silicon and carbon—or SiC—is yet another amazing material with a very bright future. Owing to its excellent thermal, mechanical, and semiconductive properties, SiC is a leading material for many strategic applications ranging from power electronics and high temperature applications to aerospace and structural applications. Additionally, multifunctional, and recoverable SiC structures can be designed by optimizing the design process e.g. via designing multidimensional SiC materials. Another potential design approach, which is the primary motivation behind this research, is to play with the composition and atomic percentage of Si/C materials and design Si_xC_y materials. Although a 1:1 composition or SiC is the most stable form of Si_xC_y, other compositions, are also found to be energetically favorable.

This work reports on the manufacturing of complex Si/C structures via a chemical vapor deposition method. The structure and properties of the grown materials were characterized using various techniques including scanning electron microscopy, aberration-corrected transmission electron microscopy, confocal Raman spectroscopy, and X-ray photoelectron spectroscopy. The spectroscopy results revealed that the grown materials were composed of micro/nanostructures with various compositions and dimensions. The coexistence of these phases and their interfaces can benefit several Si/C-based applications ranging from ceramics and structural applications to power electronics, aerospace, and high-temperature applications. In this talk, I will present our latest experimental efforts in the synthesis and characterization of SixC_y material.

5:15 PM SF08.03.07

Poster Spotlight: Accelerated Assessment of Primary Radiation Damage using High-Throughput Methods[Elena Botica Artalejo](#), Gregory M. Wallace and Michael P. Short; Massachusetts Institute of Technology, United States

In this project, we have developed a high-throughput approach using physical vapor deposition (PVD) to produce thick films with various compositions in a two-dimensional layout involving three different elements that form the alloy. Developing materials for plasma-facing components (PFCs) in fusion reactors is a difficult task, especially when additional functional requirements, such as electrical conductivity for radio-frequency (RF) antennas, need to be considered in addition to strength, heat tolerance, and radiation resistance. To complicate matters further, even trace amounts of certain elements (e.g. Nb) create an unacceptable amount of nuclear activation after neutron bombardment. Traditional approaches to determine suitable materials are time-consuming and involve numerous tests before and after irradiation to evaluate a limited number of alloy variations. However, our new approach allows us to simultaneously assess the evolution of properties in multiple compositions following consecutive radiation exposures, providing immediate insights.

To establish a baseline for the chemical composition, electrical properties, and thermo-elastic properties of the resulting thick film (measuring 3-4 μm), we employ rapid and non-destructive techniques such as electron dispersive spectroscopy (EDS), four-probe electrical resistivity measurement, and transition grating spectroscopy (TGS). Subsequently, we subject the sample to ion irradiation and reevaluate its properties to observe the relative changes created by the primary radiation damage. This iterative process is repeated until we reach the critical dose required for an RF antenna. By simultaneously evaluating hundreds of alloy compositions, our approach significantly accelerates the workflow compared to traditional methods, while maintaining the experimental reliability of radiation damage data. The extent of primary radiation damage is quantified by measuring the relative change in thermal conductivity using TGS, enabling us to correlate regions with better radiation damage resistance with their specific compositions. The decay of the TGS signal after irradiation directly corresponds to the presence of a greater number of vacancies in the microstructure. Additionally, we assess other properties relevant to an RF antenna, such as electrical resistivity at increasing radiation doses. Our study presents findings from the Cu-Cr-Nb and other Cu-Cr-X ternary systems, highlighting implications for the development of Nb-free Cu super-alloys in fusion environments.

5:20 PM SF08.03.08

Poster Spotlight: Design and Synthesis of Stabilized Nanocrystalline Vanadium Alloys[Daniel S. Ng](#), Malik Wagih, Tianjiao Lei and Christopher A. Schuh; Massachusetts Institute of Technology, United States

A reduction in grain size is expected to convey several benefits to structural materials in nuclear fusion reactors, as grain boundaries can improve mechanical strength, as well as act as a sink for radiation-induced defects to avoid embrittlement. However, nanocrystalline structures contain a strong driving force for grain growth and tend to be thermally unstable. Selecting solutes with a thermodynamic preference to segregate to grain boundaries can stabilize smaller grains up to reasonable operating temperatures.

There are limited solute segregation data on candidate alloys for fusion applications such as vanadium, which is of interest for its low neutron activity and high thermal stress factor. A combined machine learning and molecular mechanics framework developed to calculate segregation energies from ab initio methods was adapted to BCC metals, allowing for the prediction of solute segregation strength in vanadium-base binary alloys across all transition elements. Select alloys were experimentally synthesized through powder metallurgy ball-milling, annealed, and characterized through transmission electron microscopy to validate the computational predictions of thermally stable solute segregation and nanocrystallinity. Mechanical testing demonstrated significantly higher strength in sintered powder compacts of vanadium alloys compared to their cast coarse-grained counterparts. Microstructures before and after ion irradiation experiments at elevated temperatures were examined to determine the extent of damage and radiation stability.

5:25 PM SF08.03.09

Poster Spotlight: In-situ High-Temperature Fracture Behavior of Polymer-Derived SiC Fibers for Extreme Environment[HyukJun Lee](#)^{1,2}, [YoungJin Shim](#)^{1,2}, [YoungKeun Jeong](#)¹, [KwangYoun Cho](#)² and [YoungJun Joo](#)²; ¹Pusan National University, Korea (the Republic of); ²Korea Institute of Ceramic Engineering and Technology, Korea (the Republic of)

Silicon carbide (SiC) fibers and its woven fabrics have been proposed as reinforcing materials of ceramic matrix composites (CMCs) for aerospace materials due to their excellent mechanical properties such as tensile strength (≥2.45 GPa) and tensile modulus (220 GPa) up to high temperatures above 1573K. In general, the high-temperature evaluation of polymer-derived SiC fibers proceeded at room temperature after heat treatment under inert gases or air gas, which does not reflect environments of space reentry or hypersonic impact. Therefore, in order to simulate and evaluate the extreme environment, the *in-situ* tensile strength of the SiC fiber was measured while a thermal-shock of Δ1773K in the air. The *in-situ* fracture behavior of polycrystalline SiC fibers was analyzed through the customized measurement equipment to investigate the effects of impurity phase or microstructure at high temperature. And the *in-situ* tensile strength was measured while thermal-shock to temperatures of 1273K, 1573K and 1773K in air without the heating rate. In addition, thermal-exposure time at a high temperature controlled from 5 to 120 min. The tensile strength of SiC single-filament measured by the *in-situ* measurement method was immediately decreased from 3.0 GPa to 2.45 GPa, 1.9 GPa, and 1.5 GPa after thermal-shock at 1273K, 1573K and 1773K, respectively. After thermal-exposure at 1773K for 120 minutes, the tensile strength of SiC single-filament was continuously reduced to 0.87 GPa. In the *in-situ* measurement method, the stress-strain curve of SiC fibers showed three-step behavior such as thermal expansion, elastic deformation, and ductile deformation compared to the general measurement method. In particular, the fracture surface in SEM images showed a sharp morphology like the tip of a pencil, indicating ductile deformation. In XRD and TEM, the crystal size of β-SiC was maintained up to 1773K, but the proportion of SiO₂ phase ratio increased gradually. In addition, the peak of SiO₂ was easily observed after thermal-shock at 1773K, but it began to form when thermal-shock at 1573K for more than 120 min. The formation of an oxide layer on the fiber surface did not have a significant effect on the high-temperature tensile strength, but the excess carbon present on the surface was a source of destruction because it formed a defect at the interface between the oxide layer and the fiber surface when exposed thermal-shock to high temperature. Consequently, it is expected that the *in-situ* high-temperature measurement method more closely simulates the environment in which polycrystalline SiC fibers are actually used in extreme environments and suggests the microstructural solution for next-generation polycrystalline SiC fibers.

8:00 PM SF08.04.01

Printable Electronics in Harsh Environments: Exploiting Silicon Carbide Nanowires for Solution Processed Schottky Diodes Kuan-Yu Chen and Joseph Andrews; University of Wisconsin-Madison, United States

Printable electronics offer numerous advantages for flexible and large-area electronic device fabrication. Solution-processable nanomaterials have enabled the development of thin-film transistors and diodes with improved performance characteristics. However, sustaining device operation in harsh environments has been a challenge. This study explores the potential of Silicon Carbide Nanowires (SiC NWs) for enabling solution-processable electronics in harsh environments. The use of nanoscale SiC allowed us to disperse the material into liquid solvents while preserving its inherent resilience comparable to bulk SiC. SiC NWs possess superior physical properties such as a wide energy bandgap, high thermal conductivity, and high melting temperature. SiC NWs possess inherent flexibility and stretchability from the one-dimensional (1-D) nanostructures.

This work presents the fabrication of Schottky diodes using SiC NWs, with each diode comprising a single nanowire of approximately 160 nm diameter. The performance of the diodes is thoroughly analyzed, including their response to elevated temperatures and proton irradiation. We have detailed the utilization of a thermionic emission model in extracting the relevant parameters for solution processed SiC nanowire Schottky diodes. Furthermore, we have directly subjugated these devices to high temperature and high radiation environments, and analyzed their effects on the device's performance, demonstrating the resilience of the diodes upon elevated-temperature proton irradiation at a dose of 10^{16} particles/cm². The diodes maintain similar ideality factor, barrier height, and effective Richardson constant values. Our findings demonstrate the tangible merits of the solution-based process to utilize inorganic nanomaterials for use in challenging environments. Ultimately, this lays the foundation for the advancement of printed and flexible devices in harsh environment applications.

8:00 PM SF08.04.02

Evaluation of High-Temperature Wear Resistance of Explosively Welded Liner Siwook Park, Jung Hyo Park, Kyu-Sik Kim, Sung Ho Yang and Youngmoo Kim; Agency for Defense Development, Korea (the Republic of)

In the case of Ni-Cr-Mo steel, it is widely used as a material for gun barrel due to its high hardness compared to other steel types, and is known to have excellent abrasion resistance at high temperatures. In this study, the high-temperature wear resistance of Ni-Cr-Mo steel that meets the MIL-S-46119 standard was evaluated. In particular, a new characteristic evaluation device was developed and the behavior of temperature change wear rate, and friction coefficient value was measured. In addition, by observing the microstructure, the research results necessary for the identification of the wear mechanism were obtained.

8:00 PM SF08.04.03

Enhanced Impact Energy Absorption of Aperiodic Nano Cellular Polymer Films Deposited by Self-Limiting Electro Spray Zongling Ren¹, Robert Green-Warren², Noah McAllister², Ara Kim¹, Asaad Shaikh², Assimina A. Pelegrini², Jonathan P. Singer² and Jae-Hwang Lee^{1,2}; ¹University of Massachusetts Amherst, United States; ²Rutgers, The State University of New Jersey, United States

Micro/nano cellular materials have attracted significant attention recently due to their unique and tailorable mechanical characteristics originating from short-range phenomena and scale effects. With the periodic architecture, the effectiveness of energy absorption for micro/nano cellular lattice materials under mechanical stimuli of high strain rates (HSRs) has been demonstrated; the localized mechanical exchanges and responses allow them to outperform the conventional solid materials. In contrast, with the aperiodic architecture, the absence of lattice symmetry enables scalable additive manufacturing and ensures defect insensitivity in both performance and manufacturing, extending the application range.

In order to gain a deeper insight into the mechanical behavior of aperiodic nano cellular materials under HSRs and their energy absorption enhancement mechanism, we present the ultrahigh-rate mechanical study on the aperiodic polymeric films prepared by self-limiting electro spray deposition (SLED). The film comprises irregularly arranged hollow shells that are deposited on a silicon substrate. Polystyrene and its modified composites are used as the parent materials. The hollow cells possess a radius of approximately 2 microns, while the measured thickness of the shell walls is around 220 nanometers. For their HSR mechanical characterization, laser-induced projectile impact testing (LIPIT) is introduced in which solid silica microspheres having a diameter of 20 microns are used as standard impact-loading projectiles. The impact velocities range from 100 – 800 m/s. After impact data collection, the coefficient of restitution, specific energy absorption, and energy dissipation efficacy are calculated to quantify the energy-absorption ability and to identify the deformation mechanism. Based on the impact crater morphology observed in SEM images of target samples composed of homogeneous polystyrene, viscoplastic vertical densification without the Poisson effect is the dominant phenomenon. As both the increase of porosity and the decrease of film thickness can largely enhance the energy dissipation, by synergistically combining these two parameters, aperiodic cellular materials can attain comparable specific energy dissipation to that of lattice materials in the same scale. A comparison between HSR and quasi-static deformation reveals that significantly greater adiabatic thermal softening and plastic behavior in HSR deformation contribute to enhanced energy dissipation. The general design principle for energy dissipation enhancement in aperiodic nano-cellular materials is creating viscoplastic hot spots to promote adiabatic shear deformation. We further investigated the nano cellular samples with modified polymer chains. To introduce variations in the inter-chain connections, block copolymers were employed. In conjunction with the analysis of impact craters, the experimental data acquired through the LIPIT reveals a notable association between the existence of modified polymer chains and an intensified adiabatic shear deformation, which ultimately brings a substantial enhancement in energy dissipation. In summary, this study provides insights of the energy dissipating mechanism in aperiodic nano cellular materials and suggests its wider applications in scalable additive manufacturing.

* This collaborative research was supported by the National Science Foundation (Awards No. 2019928 and 2019849).

8:00 PM SF08.04.04

Lattice Boltzmann Method - Cellular Automata Method for Predicting Microstructural Evolution in Application to Tram Structural Steel Wonjoon Lee¹, Jinseong Kim², Seungho Ahn² and Jonghun Yoon¹; ¹Hanyang University, Korea (the Republic of); ²Korea Railroad Research Institute, Korea (the Republic of)

Solidification is a phase transformation from a liquid to a solid. Most metallic materials are manufactured by the casting processes based on the principle of solidification because of its high productivity. Since the mechanical properties of as-cast products mainly depend on the microstructure characteristics such as primary dendrite arm spacing (PDAS) and secondary dendrite arm spacing (SDAS), the industries are trying to control the formation of microstructures. However, the dynamic evolution of the microstructure is hard to be observed experimentally and be predicted by only conventional macroscopic analysis. Therefore, many numerical models have been developed to predict and control of the microstructures formation in solidification. In this work, a lattice Boltzmann method (LBM) and cellular automata (CA) coupled model has been constructed to predict the microstructure formation during solidification.

8:00 PM SF08.04.05

Enhancing Interfacial Adhesion and Electrical Conductivity of Steel/Polymer Composites via Molecular Adhesion Hyunjae Park¹, Hyung Jun Kim¹, Hye-jin Yoo² and Cheol-Hee Ahn¹; ¹Seoul University, Korea (the Republic of); ²POSCO, Korea (the Republic of)

The demand for steel/polymer composites (SPCs) is increasing in various industrial fields due to the need for weight reduction during the energy crisis. However, the development of SPCs faces a major challenge in achieving strong interfacial adhesion between heterogeneous materials like steel and polymer. Conventional physical adhesion methods, which rely on surface roughness, have drawbacks such as decreased durability and reduced interfacial adhesion under external conditions like temperature, humidity, and stress. Therefore, it is necessary to explore novel approaches to improve the adhesion of SPCs in practical applications.

In this study, we controlled the surface chemistry to enhance the chemical and physical interactions at the steel/polymer interface to improve interfacial adhesion. The materials used in the study include electro-galvanized steel, polyethylene (PE), acrylonitrile-butadiene-styrene (ABS), and Nylon 6, which are commonly employed in the automotive industry for interior components. We employed an organosilane coupling reaction to anchor primary amines on the steel surface, and introduced maleic anhydrides (MAs) onto the polymer film surface using a photo-initiated grafting method. The presence of amines on the steel plate and the amount of MA introduced onto the polymer surface were confirmed and quantitatively analyzed. The adhesive properties were evaluated using a lap shear test. The adhesion strength of PE increased from 0 to 11.5 MPa, from 1.5 to 11.1 MPa for the case of ABS, and from 12.7 to 14.1 MPa for Nylon 6. Notably, the adhesion strength of Nylon 6 was maintained at 89.0% even after 7 days of aging, in spite of the detrimental effect of moisture absorption on interfacial adhesion. This highlights the robust and sustainable nature of molecular adhesion, which can withstand changes in external conditions such as moisture.

Ensuring the in-process applicability is crucial for expanding the industrial application potential of SPCs. One important aspect in this regard is the feasibility of spot welding which is widely used in automated automobile manufacturing processes. In order to achieve the spot welding, we employed a conductive core layer. In order to achieve high conductivity, a network of conductive fillers was created within the resin. We prepared a polyketone composite by mechanofusion, where conductive fillers such as graphene nanoparticles were adsorbed onto the surface. The composite was then hot pressed to develop a conductive plastic with exceptionally high electrical conductivity of 207.5 S/cm. However, this high electrical conductivity was not sufficient to achieve an effective spot welding. We prepared conductive structure composite where steel fiber meshes incorporating into the plastic core layer. To ensure the steel fiber mesh

was embedded in the plastic without creating voids, an organosilane-based treatment was performed at the surface between the steel fiber mesh and the plastic via molecular bonding. Through this approach, we successfully produced a polymer/steel fiber mesh composite core layer that was void-free and capable of spot welding

In conclusion, this study successfully enhanced the interfacial adhesion in SPCs by improving the chemical and physical interactions at the steel/polymer interface. By employing molecular adhesion via precise control at the molecular level, the adhesion strength was significantly increased, and durability was improved, even in the presence of external factors such as moisture. Furthermore, for industrial application, we fabricated conductive SPCs which enabled spot welding by developing a conductive core layer and utilizing a steel fiber mesh. These findings are believed to contribute to the development of practical and effective SPCs, addressing the demand for weight reduction in various industries, particularly the automotive sector.

8:00 PM SF08.04.06

Parametric Study on the Rapid Electrical Discharge Machining of Explosively Welded Ta-W Alloy on the Gun Steel Tube [Kyu-SikKim¹](#), [Jung KyuSong¹](#), [DonghoonKim¹](#), [Sung HoYang¹](#), [Si NamChoi²](#) and [SangbaeHan²](#); ¹Agency for Defense Development, Korea (the Republic of); ²TMSys Inc., Korea (the Republic of)

Explosive welding is a solid-state metal joining process that uses explosive force to create a metallurgical bond between two metal components. This is a suitable method for joining dissimilar metals with high differences in melting points, such as Ta alloys and gun steels. The Ta-based alloy was explosively welded inside a gun steel tube in this study. Moreover, the effects of parametric electrical discharge machining (EDM) conditions for a non-machinable Ta-based alloy on the materials removal rate (MRR) and surface roughness were investigated. As a result of EDM tests, MRR could be accelerated by increasing current and pulse-on time. However, Ta-based alloys machined with high MRR showed relatively rough surfaces compared to slowly EDMed specimens. Surface characteristics were analyzed to evaluate the effect of the EDM conditions on the MRR and surface roughness.

8:00 PM SF08.04.07

Highly Elastic, Conductive and Reliable Nanolaminates with Nanocrystalline Cu/Metallic Glass Alternating Layers [Gyeong-SeokHwang¹](#), [Jae-YoungBae²](#), [Jun-WooKim³](#), [JeonghyunKim³](#), [Seung-KyunKang²](#) and [Ju-YoungKim¹](#); ¹UNIST (Ulsan National Institute of Science and Technology), Korea (the Republic of); ²Seoul National University, Korea (the Republic of); ³Kwangwoon University, Korea (the Republic of)

According to explosive commercialization of flexible electronics, stretchable electronics is also actively developing and researching for application and commercialization. In the case of bending deformation, the mechanically weakest material among many constituent layers can be protected from severe deformation by using structural design with the neutral plane concept. On the other hand, all constituent layer in which stretching deformation occurs should be uniformly stretched according to iso-strain condition. This characteristic of stretching deformation which is harsh environment limits further development in stretchable electronics. It is important to researching and combining not only design of highly stretchable structure but also highly stretchable material.

Among many kinds of stretchable electronics, it is known that an island-interconnect structure can easily enhance stretchability of electronic devices by using stretchable interconnection without degrading electrical performance. However, this type of structure requires high stretchability and mechanical reliability on structure and material of electrical interconnection. So far, copper and gold have been considered as common interconnect material due to very high electrical conductivity. However, crystalline metals have a very small elastic deformation limit (below 0.5% strain), and it is a critical shortcoming for highly stretchable and highly reliable electrical interconnection despite various stretchable structural designs. In this study, a solid metal interconnect with copper-like electrical conductivity and glass-like elastic deformation is investigated. This was obtained in the form of nanolaminates with alternating layers of nanocrystalline Cu and CuZrTi metallic glass. The mechanical, electrical properties and mechanical reliability with the stretchable substrate and the structure were evaluated depending on the thickness of the constituent layers. By using optimized nanolaminates, stretchable and wireless temperature monitoring sensors were fabricated and evaluated in various environments, such as physical workouts and harsh temperature conditions.

8:00 PM SF08.04.08

A Strategic Design Approach Controlling the B-Solubility in Transition Metal Nitride-Based Thin Films [RebeccaJanknecht¹](#), [KatharinaWeiss¹](#), [RainerHahn¹](#), [SzilardKolozsvari²](#), [PeterPolcik²](#), [DanielPrimetzhofer³](#) and [PaulMayrhofer¹](#); ¹TU Wien, Austria; ²Plansee Composite Materials GmbH, Germany; ³Uppsala University, Sweden

Limited B-solubility in fcc-TiN poses significant challenges to the applicability of Ti-B-N-based hard coatings. In particular, excess B tends to segregate at the grain boundaries instead of being fully incorporated in the fcc lattice. Although increasing the B content enhances mechanical properties such as hardness, forming excess amorphous grain boundary phases can significantly reduce fracture toughness. Compared to TiN, we observed an increase of 10 GPa in hardness (up to 36.9±1.8 GPa) but a decrease in fracture toughness of roughly 25 % (down to 2.1±0.1 MPa·m^{0.5}). Assisted by ab-initio DFT calculations, we previously demonstrated that additional Ti (to deviate from the TiN-TiB tie-line) is required to fully incorporate more B (up to 8.7 at%) in the TiN lattice while minimizing B-rich amorphous phases. Here, we expand this research by adjusting the metal sub-lattice through Ti-, Cr-, Al- or Zr-addition to a Ti-B-N compound target (50 at.% Ti, 40 at.% N, and 10 at.% B). Our study highlights the key-role of kinetics in non-reactive deposition processes to overcome the thermodynamic limits of B-solubility in TiN. Through changing the stoichiometry by knowledge-based metal addition, we propose a general strategy to enhance the B solubility in transition metal nitride-based thin films.

8:00 PM SF08.04.09

Poster Spotlight: Design and Synthesis of Stabilized Nanocrystalline Vanadium Alloys [DanielS. Ng](#), [MalikWagih](#), [TianjiaoLei](#) and [ChristopherA. Schuh](#); Massachusetts Institute of Technology, United States

A reduction in grain size is expected to convey several benefits to structural materials in nuclear fusion reactors, as grain boundaries can improve mechanical strength, as well as act as a sink for radiation-induced defects to avoid embrittlement. However, nanocrystalline structures contain a strong driving force for grain growth and tend to be thermally unstable. Selecting solutes with a thermodynamic preference to segregate to grain boundaries can stabilize smaller grains up to reasonable operating temperatures.

There are limited solute segregation data on candidate alloys for fusion applications such as vanadium, which is of interest for its low neutron activity and high thermal stress factor. A combined machine learning and molecular mechanics framework developed to calculate segregation energies from ab initio methods was adapted to BCC metals, allowing for the prediction of solute segregation strength in vanadium-base binary alloys across all transition elements. Select alloys were experimentally synthesized through powder metallurgy ball-milling, annealed, and characterized through transmission electron microscopy to validate the computational predictions of thermally stable solute segregation and nanocrystallinity. Mechanical testing demonstrated significantly higher strength in sintered powder compacts of vanadium alloys compared to their cast coarse-grained counterparts. Microstructures before and after ion irradiation experiments at elevated temperatures were examined to determine the extent of damage and radiation stability.

8:00 PM SF08.04.10

Multifunctional Polyethylene-Based Material for Radiation Shielding, Passive Thermoregulation and Onsite Fabrication in Space Exploration [DuoXu¹](#), [VolodymyrKorolovych¹](#), [LembitSihver²](#) and [SvetlanaV. Boriskina^{1,1}](#); ¹Massachusetts Institute of Technology, United States; ²Chalmers University of Technology, Sweden

Ionizing radiation sources, including primary particles such as energetic electrons, protons, and gamma rays, as well as secondary particles like thermal neutrons, are abundant at locations where space missions are often conducted, such as the low Earth orbit (LEO) and the Martian surface [1]. Space radiation could severely damage human tissues and electronic components, presenting a risk factor for space explorations [2]. Traditionally, high-Z number materials, primarily metals such as lead and aluminum, have been employed to attenuate space radiation. Due to the considerably high costs of transporting materials and equipment to space, low-density shielding materials based on polymer composites improve cost-effectiveness due to their lightweight nature, allowing for comparable radiation protection at a lower transportation cost [3]. Despite their advantages, polymer composites have their limitations, particularly their relatively low thermal conductivity [4], which can impact the performance of the electronic components protected by the shielding material, unless they are designed to operate at elevated temperatures. Consequently, a material design that achieves thermoregulation without compromising the radiation shielding performance is of paramount necessity.

Several materials have shown promising results in attenuating space radiation, providing a level of design flexibility in terms of structure and material composition. In this work, a polyethylene-based multifunctional material for space applications is proposed, with the target of providing radiation shielding, passive thermoregulation, and onsite fabricability simultaneously. The feasibility of onsite fabrication is demonstrated by the author's previous work, in which an optimized process of additive manufacturing via fused deposition modeling (FDM) is employed for polyethylene-based composite materials [5].

The radiation shielding performance of selected material structures and compositions is evaluated with a Monte-Carlo particle transport simulation tool PHITS, which calculates the total ionizing dose transmitted by the multifunctional material under specific radiation conditions. To evaluate the thermoregulatory performance of the material, we developed and employed a coupled thermal-optical model, which considers the extraterrestrial thermal environment and utilizes the material properties of each component, along with structural information, to estimate the temperature of the electronics that the material is designed to protect.

Preliminary experimental results reveal promising material candidates for this multifunctional material, and the structure could be further optimized for superior performance. The insights

gained from this study present significant opportunities for future research and developments in the field of space exploration with architected materials tailored for specific applications.

This research is funded by the Cosmic Shielding Corporation (CSC), Atlanta, Georgia and the MIT-Czech Republic Seed Fund. We also thank the Oak Ridge National Laboratory for the beam time for neutron scattering measurements (Proposal IPTS-28797.1 for NScD 2022-A) and William Heller (ORNL) for his help in running the experiment. We acknowledge Benoit Forget and Amelia J Trainer (MIT) for useful discussions.

- [1] Schimmerling, W., & Curtis, S.B. (1978). Workshop on the radiation environment of the satellite power system.
- [2] Hands, A. et al. (2011). Single event effects in power mosfets due to atmospheric and thermal neutrons. *IEEE Trans. Nucl. Sci.*, 58(6):2687-2694.
- [3] More, C.V. et al. (2021). Polymeric composite materials for radiation shielding: A review. *Env. Chem. Lett.*, 19(3):2057-2090.
- [4] Pan, X. et al. (2021). High thermal conductivity in anisotropic aligned polymeric materials. *ACS Appl. Polym. Mater.*, 3(2):578-587.
- [5] Xu, D. et al. (2022). Interaction of neutrons with strain-engineered fibrous boron-doped polyethylene materials. *MRS Fall Meetings*.

8:00 PM SF08.04.11

Poster Spotlight: Accelerated Assessment of Primary Radiation Damage using High-Throughput Methods[ElenaBotica Artalejo](#), GregoryM. Wallace and MichaelP. Short; Massachusetts Institute of Technology, United States

In this project, we have developed a high-throughput approach using physical vapor deposition (PVD) to produce thick films with various compositions in a two-dimensional layout involving three different elements that form the alloy. Developing materials for plasma-facing components (PFCs) in fusion reactors is a difficult task, especially when additional functional requirements, such as electrical conductivity for radio-frequency (RF) antennas, need to be considered in addition to strength, heat tolerance, and radiation resistance. To complicate matters further, even trace amounts of certain elements (e.g. Nb) create an unacceptable amount of nuclear activation after neutron bombardment. Traditional approaches to determine suitable materials are time-consuming and involve numerous tests before and after irradiation to evaluate a limited number of alloy variations. However, our new approach allows us to simultaneously assess the evolution of properties in multiple compositions following consecutive radiation exposures, providing immediate insights.

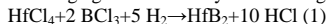
To establish a baseline for the chemical composition, electrical properties, and thermo-elastic properties of the resulting thick film (measuring 3-4 μm), we employ rapid and non-destructive techniques such as electron dispersive spectroscopy (EDS), four-probe electrical resistivity measurement, and transition grating spectroscopy (TGS). Subsequently, we subject the sample to ion irradiation and reevaluate its properties to observe the relative changes created by the primary radiation damage. This iterative process is repeated until we reach the critical dose required for an RF antenna. By simultaneously evaluating hundreds of alloy compositions, our approach significantly accelerates the workflow compared to traditional methods, while maintaining the experimental reliability of radiation damage data. The extent of primary radiation damage is quantified by measuring the relative change in thermal conductivity using TGS, enabling us to correlate regions with better radiation damage resistance with their specific compositions. The decay of the TGS signal after irradiation directly corresponds to the presence of a greater number of vacancies in the microstructure. Additionally, we assess other properties relevant to an RF antenna, such as electrical resistivity at increasing radiation doses. Our study presents findings from the Cu-Cr-Nb and other Cu-Cr-X ternary systems, highlighting implications for the development of Nb-free Cu super-alloys in fusion environments.

8:00 PM SF08.04.12

Effect of Temperature and Time on the Development of Hafnium Diboride (HfB₂) Coatings by Chemical Vapor Deposition (CVD)[MeltemBolluk](#)^{1,2}, OzdenKisacik³, FurkanAkpunar³, SerzatSafaltin¹ and IsmailDuman²; ¹University of Connecticut, United States; ²Istanbul Technical University, Turkey; ³TENMAK, Turkey

Refractory metal borides possess an array of impressive properties which has led to their categorization as advanced technology boron products. These properties include high refractoriness, wear resistance, corrosion resistance, high hardness, and high fracture toughness. HfB₂ is a remarkably high temperature ceramic material with features like its immunity to high temperatures and its power to remain steadfast in extreme conditions. This component is essential to various systems in the advanced technology and defense industries, and it plays a crucial role in them. HfB₂ has a wide range of applications, including aerospace, aviation, and metallurgy. (Kauffman, 1965). HfB₂ is an ideal material for high-temperature ceramics because of its elevated melting temperature, remarkable thermal conductivity, outstanding resistance to thermal shock, a low thermal expansion coefficient, high-temperature resistance, and the ability to remain stable in extreme environments. HfB₂ has many impressive characteristics that make it a practical solution to be used as a thermal protection system for mission-critical applications, which include hypersonic flights, atmospheric entry systems, and rocket thrusters (Sonber, 2011).

This research implemented a CVD-based gas phase coating technique, designed for the purpose, to produce HfB₂ coatings on copper (Cu) substrates at various temperatures and time. CVD is a low-temperature process used for coating and powder production and can create pure products that other techniques cannot. Chlorides and hydrogen gases are among the most preferred reducing agents in CVD systems. The gas phase reactants were selected as in Reaction 1 (Pierson, 1999).



In the present study, HfB₂ refractory boride coatings were produced as a high purity coating from the gas phase using a specially developed reactor and process design (Bolluk, 2015).

We performed structural analysis methods in order to examine the coatings. According to the XRD results, high purity HfB₂ polycrystalline coatings were obtained. The SEM-EDS analysis was used to evaluate the impact of reduction temperature on crystallite size and to examine the effects of different reduction temperatures on nucleation, grain growth, and morphology. The X-ray photoelectron spectrometry (XPS) technique applies to examine the surface characterization, bond structure and elemental distribution of refractory boride coatings.

REFERENCES

- Kaufman, L. and Clougherty E. V. 1965. Investigation of Boride Compounds for Very High Temperature Applications-Part II, DTIC Document.
- Sonber, J.K., Murthy, T.S.R.C., Subramanian, C., Kumar, S., Fotedar, R.K., ve Suri, A.K. 2011. Investigations on Synthesis of ZrB₂ and Development of New Composites With HfB₂ and TiSi₂, *International Journal of Refractory Metals and Hard Materials*, 29(1): p. 21-30.
- Pierson, H.O. 1999. *Handbook of Chemical Vapor Deposition (CVD) Principles, Technology, and Applications*, Second Edition, Published in the United States of America by Noyes Publications / William Andrew Publishing, LLC, Norwich, New York, U.S.A.
- Bolluk, M. 2015. *Synthesis of Group IVB Zirconium and Group VB Niobium Diborides via CVD Process as Free Particles and Evaluation of Sintering Properties* (Thesis of Master), I.T.U., Istanbul, Turkey.

8:00 PM SF08.04.13

Fluorinated Omniphobic Coatings for Low-Surface-Tension Liquids[ShashwataMoitra](#) and ConstantineM. Megaridis; University of Illinois Chicago, United States

There has been extensive research on repellency and capillary-driven transport of high surface tension liquids (e.g., water, glycerol, etc.), but only limited attention has been given to contact-line confined transport of liquids with low surface tension (e.g., oils, alcohols, etc.) and oleophobicity. When the fluid surface tension drops below 40 mN/m, repellency becomes extremely difficult. This situation is encountered in many engineering applications and thus is of high technological importance. In this work, we use a fluorinated nanocomposite coating material deposited on a surface textured by laser etching, a scalable technique that requires no lithography implementation. The approach results in the repellency of liquid hydrocarbons with surface tensions as low as 20 mN/m. The repellency of several liquids with surface tensions in the range of 20-72 mN/m is experimentally investigated. Comparisons are performed between the velocities acquired by fluids transported pumplessly on a wedge-shaped wettability-patterned track, due to confinement imposed by the superomniphobic background surrounding the wettable track. Finally, travel distance and velocities of low-surface tension liquids transported on inclined ramps against gravity on similar wedge-shaped wettability-patterned tracks are compared.

8:00 PM SF08.04.14

Defect-Induced Strengthening of Carbon Nanotube Fibers[YongKim](#)^{1,2}, Seung-YeolJeon², Woong-RyeolYu¹, Hyeon-SuJeong², Seon-YeonKim², Ha-YoungYu² and Bo-KyoungChoi²; ¹Seoul National University, Korea (the Republic of); ²Korea Institute of Science and Technology, Korea (the Republic of)

The mechanical capabilities of CNT fibers are impeded by their irregular internal structure, which gives rise to diversely sized CNT bundles that are unable to evenly distribute forces, resulting in slippage of CNTs and lowered mechanical properties. Despite various efforts to enhance the internal structure of CNT fibers, such as polymer infiltration, super-acid treatment (e.g., CSA) for densification, and mechanical compression, the formation and pulling out of uneven bundles has not been avoided yet. In this study, bundle formation was hindered by introducing defects on the surface of CNTs, consequently reducing the van der Waals interactions among individual CNTs. We introduced surface defects on the wall of single-walled carbon nanotubes (SWCNTs), such as oxygen containing functional groups or vacancies using diverse techniques, e.g., heat treatment in air environment followed by different acid treatments. Then, SWCNTs with different type of defects in CSA were dispersed and spun into fibers, and their mechanical properties were evaluated. Our study demonstrated that oxygen-containing defects on CNT fibers progressively increased the modulus as the strain increased before failure, resulting in an approximately 40% increase in strength compared to non-treated fibers.

8:00 PM SF08.04.15

Molecular and Nanoscale Investigations on Ultraviolet-Degraded Polyurea[AmriteshKumar](#), MaryamGhorbani and GeorgeYoussef; San Diego State University, United States

Polyurea, an elastomer synthesized by the polyaddition of amine and isocyanate, is an emergent engineering material, offering impact mitigation, chemical and moisture resistance, and large tearing elongation. Polyurea-coated structures are often deployed in harsh and extreme environmental operating conditions; hence, extended exposure to natural ultraviolet (UV) radiation might influence the overall mechanical and structural behaviors. However, the state-of-the-art has been limited to macroscale investigations, encompassing the dynamic, micromechanical, viscoelastic, and hyperelastic responses of polyurea. This research aims to extend the current understanding of the influence of UV radiation on polyurea elastomers at various spatiotemporal scales as a function of artificial weathering, ranging from 0 to 15 weeks. Therefore, the current research presents a threefold novel approach to decipher the spectro-mechanical properties of UV-exposed polyurea in two environmental conditions: oxygen-rich and oxygen-deprived. Firstly, nano-indentation and nano-impact characterizations were performed on virgin and exposed samples to quantitatively determine the UV effects on the mechanical properties, including the elastic modulus, hardness, and impact resiliency. A notable by-product of the indentation measurements is revealing the degradation depth, delineated as the transition between exposed skin and virgin core as a function of exposure duration. The nanoscale indentation-induced topological changes inferred the fracture and failure behavior of UV-exposed polyurea samples. Secondly, the UV-exposed samples were submitted to laser-induced shock waves to report their response at ultrahigh strain rate (10^6 s^{-1}) loading conditions. The intensity of the stress waves was tuned by changing the size of the illumination area and the laser energy, where unique locations on the samples were loaded only once to evade the effects of time-dependent deformations. Subsequently, the responsible shock-failure mechanisms were discerned using post-mortem optical and electron microscopy. Finally, spectroscopic analyses using infrared techniques (FTIR, Raman, and terahertz) construed the conformational evolution of the macromolecule in UV-exposed polyurea, elucidating the effects of photodegradation and photo-oxidation mechanisms. Thus, this research provides holistic, multiscale, and mechanistic insights into the effect of extended ultraviolet exposure on polyurea elastomers, potentially leading to improved shock tolerance of polyurea-coated civilian and military installations.

8:00 PM SF08.04.16

High-Temperature Nanomechanical Behavior of Polymer Films Produced via Self-Limiting Electro Spray Deposition (SLED) Robert Green-Warren, Noah McAllister, Isha Shah, Adrew Huth, Jonathan P. Singer and Assimina A. Pelegri; Rutgers University, United States

Advanced polymer coatings are gaining prominence due to the increasing requirements for high-performance materials that also minimize environmental impact and cost. These coatings are increasingly relevant across numerous industries including aerospace, automotive, biomedical, and mobile devices. The objective of this work is to investigate the influence of porosity on the creep response of the resultant porous polymer films. This study delves into the behavior of polymer composite films fabricated using a novel Self-Limiting Electro Spray Deposition (SLED) process. SLED makes use of the buildup of charge in a glassy polymer film to create conformal highly porous microcoatings on flat, templated, or 3D surfaces. Lowering the glass transition temperature of the material reduces both the charge build-up, resulting in more areal mass in the resulting coatings, and the porosity of the films as they densify. Further, the selection of carrier solvent and spray flow rate can alter the characteristic length scale of the coatings by changing the droplet size. Here, we study porous polyimide (PI) coatings, which are valued for their dielectric and chemical barrier properties coupled with high thermal stability, with applications ranging from hermetic seals to battery separators. Samples ranging from 0-70% porosity are deposited via SLED and observed using a combination of optical microscopy and spectroscopic microreflectometry to evaluate film thickness and porosity. Each sample is then characterized mechanically via time-dependent nanoindentation with in-situ heating up to 400C to measure the effects of porosity on the creep response of the polymer films.

8:00 PM SF08.04.17

Crystallographic Orientation Effect of Substrate Grain on the Oxidation Behavior of Ferritic Stainless Steels for Solid Oxide Fuel Cell Interconnects Yoon Seok Ko¹, Min-Seong Kim¹, Heung Nam Han², Jinwoo Kim² and Dong-Ik Kim¹; ¹Korea Institute of Science and Technology, Korea (the Republic of); ²Seoul National University, Korea (the Republic of)

Hydrogen has been paid great attention to be the future energy carrier because of the demand for alternative clean and renewable power generation. For the utilization of hydrogen, the hydrogen storage system must be developed, and this stored hydrogen energy should be converted to electricity by fuel cells with high efficiency. From this point of view, metallic materials can serve an essential role. Hydrogen storage alloy has attracted much attention because of its high volumetric energy efficiency for hydrogen storage systems, and metallic interconnects for the stacked fuel cell system have altered the ceramic interconnects because of their low cost and good formability. However, the oxidation of the metallic materials can be a problem. In the former case, the surface oxide layer was reported to be the main factor affecting the alloy's activation characteristic and delaying the hydrogen charging. In the latter, the oxide layer on the metallic interconnects degrades the power generation efficiency of the fuel cell system because of its high electrical resistivity. Therefore, controlling the oxidation behavior of metallic materials is important. From a practical point of view, compositional change of the metallic materials has been discussed in depth to control the oxidation behavior. In contrast, the orientation effect of the substrate grain on the oxidation behavior of metallic materials has not been well discussed.

Therefore, the aim of this study is to investigate the effect of crystallographic orientation on oxidation behavior. For this purpose, the electron backscatter diffraction method (EBSD) was used to observe the orientation of the ferritic stainless steel, which was designed to apply the metallic interconnect for a solid oxide fuel cell (SOFC) system. Three substrate grains with $\langle 111 \rangle$, $\langle 110 \rangle$, and $\langle 001 \rangle$ parallel to the plane normal direction of the specimens were marked using the focused ion beam (FIB) and tracked during the oxidation test. The temperature was set to 800 Celcius degree to simulate the operation temperature of the SOFC. After the oxidation test, three lamellar specimens were prepared from each substrate grain, and the transmission electron microscope (TEM) and the transmission Kikuchi diffraction (TKD) analyzed the orientation relationship between oxides and the substrate. Based on these findings, the texture of the ferritic stainless steel was carefully designed, and the oxidation behavior was successfully controlled.

8:00 PM SF08.04.18

Poster Spotlight: In-situ High-Temperature Fracture Behavior of Polymer-Derived SiC Fibers for Extreme Environment Hyuk Jun Lee^{1,2}, Young Jin Shim^{1,2}, Young Keun Jeong¹, Kwang Youn Cho² and Young Jun Joo²; ¹Pusan National University, Korea (the Republic of); ²Korea Institute of Ceramic Engineering and Technology, Korea (the Republic of)

Silicon carbide (SiC) fibers and its woven fabrics have been proposed as reinforcing materials of ceramic matrix composites (CMCs) for aerospace materials due to their excellent mechanical properties such as tensile strength ($\geq 2.45 \text{ GPa}$) and tensile modulus (220 GPa) up to high temperatures above 1573K. In general, the high-temperature evaluation of polymer-derived SiC fibers proceeded at room temperature after heat treatment under inert gases or air gas, which does not reflect environments of space reentry or hypersonic impact. Therefore, in order to simulate and evaluate the extreme environment, the *in-situ* tensile strength of the SiC fiber was measured while a thermal-shock of $\Delta 1773\text{K}$ in the air. The in-situ fracture behavior of polycrystalline SiC fibers was analyzed through the customized measurement equipment to investigate the effects of impurity phase or microstructure at high temperature. And the *in-situ* tensile strength was measured while thermal-shock to temperatures of 1273K, 1573K and 1773K in air without the heating rate. In addition, thermal-exposure time at a high temperature controlled from 5 to 120 min. The tensile strength of SiC single-filament measured by the *in-situ* measurement method was immediately decreased from 3.0 GPa to 2.45 GPa, 1.9 GPa, and 1.5 GPa after thermal-shock at 1273K, 1573K and 1773K, respectively. After thermal-exposure at 1773K for 120 minutes, the tensile strength of SiC single-filament was continuously reduced to 0.87 GPa. In the *in-situ* measurement method, the stress-strain curve of SiC fibers showed three-step behavior such as thermal expansion, elastic deformation, and ductile deformation compared to the general measurement method. In particular, the fracture surface in SEM images showed a sharp morphology like the tip of a pencil, indicating ductile deformation. In XRD and TEM, the crystal size of β -SiC was maintained up to 1773K, but the proportion of SiO₂ phase ratio increased gradually. In addition, the peak of SiO₂ was easily observed after thermal-shock at 1773K, but it began to form when thermal-shock at 1573K for more than 120 min. The formation of an oxide layer on the fiber surface did not have a significant effect on the high-temperature tensile strength, but the excess carbon present on the surface was a source of destruction because it formed a defect at the interface between the oxide layer and the fiber surface when exposed thermal-shock to high temperature. Consequently, it is expected that the *in-situ* high-temperature measurement method more closely simulates the environment in which polycrystalline SiC fibers are actually used in extreme environments and suggests the microstructural solution for next-generation polycrystalline SiC fibers.

8:00 PM SF08.04.19

Computational Fracture and Thermal Analysis of Glass-Ceramics under Extreme Conditions Domenica Rodriguez¹, Sujin Kim², Sung-Yup Kim³, Hyung Sub Sim² and Sungwook Hong¹; ¹California State University, Bakersfield, United States; ²Sejong University, Korea (the Republic of); ³University of Illinois Chicago, Korea (the Republic of)

The research on a wide range of glass-ceramics has gained a great attention in the areas of nanotechnology and materials science. In particular, lithium disilicate, aluminum silicates, lithium aluminum silicate glass-ceramics have been successful in many industry applications, owing to their generally superior mechanical properties such as high flexural strength and fracture toughness. As such, it is vitally important to obtain fundamental understanding of mechanical/thermal characteristics of the glass ceramic materials to be extended to other commercial applications like display glasses and heat exchangers. However, the mechanical/thermal properties of those materials still remain elusive because of the lack of computational effort to model such a complex system. Here, we perform reactive molecular dynamics (RMD) simulations to reveal mechanical behaviors of glass-ceramics under tensile conditions. We also identify thermal behaviors of the glass-ceramics to better understand materials behaviors at extreme conditions. Our work will make a reasonable contribution to the scalable and reliable synthesis of glass ceramics-based composites at extreme conditions.

8:00 PM SF08.04.20

Recycled Wood-2D Material Composites: A Potential Structure Alternative for Extreme LEO Environments Basel R. Altawil, Rami A. Elkaffas, Yarjan Abdul Samad and Seanswei; Khalifa University of Science and Technology, United Arab Emirates

The rapid proliferation of space structures predominantly composed of aluminum has engendered critical challenges in space exploration. The aftermath of space missions leaves behind aluminum debris, which poses not only an imminent threat to other space assets but also when these remnants re-enter the Earth's atmosphere and combust, exposes our environment to potential health hazards. This growing concern necessitates a shift towards environmentally benign materials for space applications.

Our research proposes a pioneering approach: integrating recycled wood with graphene using advanced fusion techniques. This composite targets the pressing challenges faced by the prevalent use of aluminum in space structures. Leveraging the ecological attributes of wood and the remarkable properties of graphene, our novel composite aspires to be suitable for the harsh Low Earth Orbit (LEO) environment.

To ascertain the viability of this material for space applications, extensive environmental tests encompassing thermal cycles, vacuum conditions, and rigorous vibrations were executed. Preliminary results are promising, showcasing potential benefits like significant mass reduction, enhanced radiation shielding, superior thermal insulation, and improved damping during launches.

8:00 PM SF08.04.21

Advanced X-Ray Characterization of Fusion Materials Anthony Zhu¹, Michael Zhang², Ryan Kim³, Takaaki Koyanagi⁴, Weicheng Zhong⁴, Lance Snead⁵, David Sprouster⁵ and Miriam Rafailovich⁵; ¹Barrington High School, United States; ²Livermore High School, United States; ³Thomas Jefferson High School for Science and Technology, United States; ⁴Oak Ridge National Laboratory, United States; ⁵Stony Brook University, United States

In the present work, we describe our efforts employing advanced non-destructive X-ray-based characterization to support the fabrication and post-irradiation examination of materials for advanced fusion energy systems. Specific material systems include castable nanostructured alloys (CNAs) and neutron irradiated tungsten. We quantify the microstructural and atomic properties of advanced first-wall materials through two-dimensional mapping and high-throughput X-ray diffraction (XRD). X-ray-based characterization techniques provide complimentary quantitative insights across multiple length scales needed to fill critical knowledge gaps and predict long-term behavior and performance.

CNAs have been under development by the fusion program over the last decade and are meant to provide enhanced elevated temperature performance as compared to reduced activation ferritic martensitic steels through the internal formation of irradiation-stable and dislocation-pinning precipitates. In this way, CNAs are a potentially more practical high-temperature option for high-heat-flux or other challenging fusion applications. The uniformity of the microstructure and engineered precipitates through various cast plates are investigated here by constructing 2D microstructural maps from XRD analysis.

Tungsten is presently the leading plasma-facing material candidate due to its high melting point, resistance to sputtering, and chemical compatibility with tritium. However, extended exposure of W to fusion plasmas and intense 14 MeV neutrons, resilience against plasma-induced surface damage (cracking, erosion/exfoliation, and fuzz formation), and degradation of bulk mechanical properties due to neutron irradiation raise significant concerns about its stability. We performed XRD experiments of unirradiated and neutron-irradiated polycrystalline W alloys after low-dose irradiation at 800°C (0.1 dpa) and after high irradiation temperature (>800°C).

XRD patterns were collected for fifty neutron irradiated W, and 2D XRD mapping data for six CNA alloy plates were performed at the PDF beamline at the National Synchrotron Light Source-II. Analysis of the XRD patterns allows the determination of the lattice strain, change in microstructure parameters, and formation of secondary phases. We developed a high-throughput quantitative XRD analysis routine to generate microstructural data of both sets of specimens. Using Perl and Python scripts, we ran batch analysis of our data through the Materials Analysis Using Diffraction software and then generated heatmaps that plot our collected data in 2D mappings.

The quantitative XRD analysis of the exposed CNA samples show a complex hydrogen uptake in the metal carbide crystallites, and the lattice expansion and crystallite size reduction will have non-negligible implications on the mechanical properties and retention of transmutation products within this important structural component. The heatmaps visualize microstructural features (carbides) that provide strength to the steel and are trapping sites for radiation-induced gaseous products. The steels are strangely affected by the exposure and expand (lattice expansion).

Our initial success in demonstrating the effective characterization of fabricated and as-irradiated materials supports our goal of fabricating functionally graded or composited first wall tile structures (i.e., W-CNA), which may be essential to mitigate the very high heat flux loading anticipated as we move beyond ITER towards DEMO-like fusion systems.

AZ, MZ, and RK acknowledge the Garcia Research Program and the Morin Charitable Trust for their contributions to making this work possible. These experiments and analysis were supported by the U.S. Department of Energy Office of Fusion Energy Sciences under contract DESC0018322 with the Research Foundation for the State University of New York at Stony Brook and DE-AC05-00OR22725 with UT-Battelle LLC.

8:00 PM SF08.04.22

Graphene-Enhanced Wood: A Lightweight and Sustainable Material for Spacecraft Structures Afnan S. Malik¹, Rami A. Elkaffas¹, Basel R. Altawil¹, Blaise Tardy¹, Seanswei¹, Yarjan Abdul Samad^{1,2} and Omnia Khattab¹; ¹Khalifa University of Science and Technology, United Arab Emirates; ²University of Cambridge, United Kingdom

Laser ablation debris removal is a promising means of achieving sustainable space operations [1,2]. However, conventional metals in spacecraft ablate into spallation particles [3] that may harden and impact spacecraft or oxidize and deplete the ozone layer [4,5]. Wood is a candidate space structural material since it is 84% less dense than conventional metals such as Aluminium alloys and does not produce polluting spallation particles such as alumina (Al₂O₃) [3,6,7]. Another candidate material is Graphene, which maintains an electric conductivity of 350,000 cm²/V s [8], mechanical stiffness of 1 TPa [9], and EMI shielding efficiency of 90 dB [10] in space conditions [6].

This study proposes graphene-enhanced wood as a novel space material harnessing both those materials' properties, made through the procedure illustrated in Fig. 1. Delignification creates micropores that enhance flexibility and formability [11]. Graphene, produced through microwave-assisted exfoliation of thermally expanded graphite obtained from treating graphite flakes with perchloric acid [12], is then infused into the wood, coating inner cell walls and pores [13]. Finally, densification through air-drying or oven-drying at 60 °C for 12 hrs, or hot-pressing under 4 MPa pressure for 12 hrs at 80 °C, produces the final rigid form [11,14,15].

Our initial results demonstrate significant enhancement of the wood's tensile strength (up to six times), electrical conductivity (up to 35 S/m), EMI shielding efficiency (up to 16 dB), and laser ablation performance. Through an ongoing optimization process, these parameters will be further improved, and the final results will be presented in the final manuscript.

8:00 PM SF08.04.23

Evaluation of an Potential Application of Epoxy Resin as a Concrete Binding Adhesive Douglas X. Shattuck^{1,2}, Ethan Shan^{3,2}, Curtis Sung^{3,2} and Saman Abbas^{3,2}; ¹St Joseph School Wakefield, United States; ²National STEM Honor Society, United States; ³Malden Catholic High School, United States

Due to the challenging assignment of finding water sources and producing cement on the moon, we have found that epoxy resin may be a possible solution for lunar building adhesives. Our goal is to explore and research the application of epoxy resin as an adhesive in the physical and functional testing of lunar soil models. We have made multiple compressive tests on the mixture and plan to conduct more tests in future research, including the synthesis of this material with simulated lunar regolith to further explore its potential in constituent lunar habitats.

Epoxy resin is widely used in engineering fields such as architecture, aerospace, and electronics. After chemical reactions between the epoxy resin and its hardener, it will solidify and have good chemical corrosion resistance. Meanwhile, the advantage of epoxy resin (1.1~1.2 g/cm³) is its lighter density, including its hardener (0.9~1.1 g/cm³), which is lighter than the combination of water (1.0 g/cm³) and cement (1.4~3.0 g/cm³).

Except for epoxy resin, hardener, and borosilicate glass (glass were completely invariant value in the first round), which are different from common cement concrete. The remaining mixture materials used in this experiment are common concrete materials: sand mixtures, metal powder (Al), and aggregates.

We believe that epoxy resin has great potential as an adhesive for lunar construction, as it has relatively light density and excellent chemical corrosion resistance and strength. With further research, it will contribute to the application and production of this material in extreme environments.

8:00 PM SF08.04.24

The Potential for Solar Vitrification of Martian Regolith for The Production of Building Material Douglas X. Shattuck^{1,2}, Haley Talbot³, Leo Chen^{3,2} and Saman Abbas^{3,2}; ¹St Joseph School Wakefield, United States; ²National STEM Honor Society, United States; ³Malden Catholic High School, United States

Our study delves into the pragmatic utilization of vitrified Martian regolith as a key building material for prospective Martian habitats. We explore the feasibility of harnessing a specialized solar collector, tailor-made to amplify sunlight, in the pursuit of achieving the optimal temperature required to transmute Martian soil into glass. Our approach underscores the importance of employing readily accessible resources, thereby ensuring the viability of future Mars missions.

The Solar Collector design has been ingeniously streamlined, featuring a straightforward space frame crafted from commonplace 2x4's, securely joined together via screws. The innovative lens attachment relies on friction for stability, simplifying the construction process and diminishing the need for advanced equipment. Furthermore, the requisite water for the lens can be

sourced locally on Mars, substantially reducing dependence on Earth-based supplies.

The incorporation of screws into the design has markedly fortified the frame's structural integrity in comparison to prior iterations, obviating the necessity for supplementary support structures. Consequently, the entire assembly, including the solar collector, can be erected within a remarkably efficient timeframe of approximately four hours.

While the initial lens design successfully achieved temperatures of up to 200°C, it grappled with precision in focal point control. Consequently, we developed a secondary lens design, vastly enhancing its focusing capabilities. An in-depth analysis of the relationship between lens volume and maximum attainable temperature unveiled a temperature spectrum spanning from 136°C to a pinnacle of 665°C. It is noteworthy that while higher temperatures remain theoretically attainable, expanding the lens volume raises concerns about the structural integrity of the lens.

A noteworthy observation pertains to the linear correlation between lens area and temperature, indicating that larger lenses have the potential to deliver superior performance, extending their capabilities without compromising structural stability. Furthermore, augmenting the volume of fluid within the lens emerged as a promising strategy to enhance light focusing.

Our prototype successfully achieved elevated temperatures using commonplace materials, yet it faces inherent challenges, including a limited operational window and vulnerability to debris interference. Additionally, the positioning of the sun can impede its ability to consistently attain and maintain adequate temperatures. Consequently, these limitations underscore the necessity for further refinement and comprehensive testing to enable practical application in the construction of Martian habitats.

SESSION SF08.05: Atomic-Scale Mechanisms for Extremes

Session Chairs: Ilya Okulov and Gianna Valentino

Tuesday Morning, November 28, 2023

Sheraton, Third Floor, Fairfax A

8:00 AM *SF08.05.01

In Situ Mechanical Analysis of Hierarchical Nanoporous Metal-Conductive Polymer Hybrids in Electrolyte Environment Olga Matts and [Nadja Mameka](#); Helmholtz-Zentrum Hereon, Germany

Recent progress in material design strategies towards hierarchically porous metals enable unique bicontinuous microstructures that combine desired, but conflicting, properties, namely, a large specific surface area and rapid mass transport [1]. Furthermore, because of the open porosity, these three-dimensional architectures provide access of chemical species and surface state modification of the inner surfaces via external control variables – surface charge density or adsorbate coverage. The nanoporous metals with structural hierarchy, thus, offer ample opportunities for design of multifunctional hard-soft hybrids as sensor and actuator materials [1] as well as various electrochemical energy systems [2]. Despite significant developments in the fabrication of hierarchical nanoporous metals so far, studies of their mechanical and functional behaviour in electrolyte environment, in which they can operate, are scarce.

Here, we explore an impact of the unusual morphology on the functionality of nanoporous metals by probing an influence of a conductive polypyrrole nanocoating (PPy) on the mechanical response of a nanoporous gold (npAu). Bulk hierarchical nanoporous gold (hc npAu) with two distinct and well-defined length scales has been formed by selective dealloying process [3]. The larger pores at the higher hierarchical level (characterized by diameters around 150 nm) of the hc npAu provide unhindered transport pathways, while nanopores at the lower hierarchy level (below 30 nm) supply a large fraction of surface sites. The pore sizes at both scales can be adjusted via fabrication conditions, whereas various PPy fractions in the pores are tailored during electrochemical polymerization of pyrrole [4]. Actuation, elastic and plastic behavior of the PP-coated hc npAu were then analyzed in situ upon potential cycling in an aqueous electrolyte. We revealed pronounced variations in the macroscopic length change, Young's modulus, and plastic flow in response to the voltage-induced redox reactions of the polymer films at the nanoporous electrodes. In the contribution, we discuss the origin of the observations and compare the functional performance of hc npAu/PPy with unimodal npAu/PPy hybrids.

References:

1. Juarez, T., Biener, J., Weissmüller, J., & Hodge, A. M. (2017). Nanoporous metals with structural hierarchy: A review. *Advanced Engineering Materials*, 19(12), 1700389.
2. Zhu, C., Qi, Z., Beck, V. A., Luneau, M., Lattimer, J., Chen, W., ... & Biener, J. (2018). Toward digitally controlled catalyst architectures: Hierarchical nanoporous gold via 3D printing. *Science advances*, 4(8), eaas9459.
3. Shi, S., Li, Y., Ngo-Dinh, B. N., Markmann, J., & Weissmüller, J. (2021). Scaling behavior of stiffness and strength of hierarchical network nanomaterials. *Science*, 371(6533), 1026-1033.
4. Li, J., Markmann, J., Weissmüller, J., & Mameka, N. (2021). Nanoporous gold-polypyrrole hybrid electrochemical actuators with tunable elasticity. *Acta Materialia*, 212, 116852.

8:30 AM SF08.05.02

Understanding the Role of Intermetallic Interface Contributions in Al – Ni Layered Systems [Ruth Schwaiger](#), Nicolas J. Peter, XiLi and Marilaine Moreira de Lima; Forschungszentrum Juelich GmbH, Germany

Nanometallic multilayer systems with designed micro- and nanostructures offer great potential to sustain extreme conditions, such as high temperature, corrosive environments, or radiation. The internal interfaces of such material systems include grain boundaries and interphase boundaries and can be tailored with respect to composition and morphology to achieve properties that cannot be achieved by conventional materials. Understanding the role and behaviors of the different interfaces is thus critical to developing materials suitable for extreme conditions. Most studies of layered systems focused on elements with a positive enthalpy of mixing to create almost atomically sharp interfaces. By contrast, only few studies investigated the interface morphology for systems with negative enthalpy of mixing, which offers additional degrees of freedom regarding materials design.

We investigated the Ni-Al multilayer system with varying layer thicknesses between 5 and 250 nm to understand the effects of the layer structure on the mechanical behavior and the stability of the microstructures not only at elevated temperatures but also after severe deformation. The microstructure characterization with TEM and STEM-EELS indicates wide interdiffusion at Al/Ni interface and formation of intermetallic bonding at interfaces and grain boundaries in Al/Ni multilayer. We measured a peak hardness of 9.03 ± 0.14 GPa, which is the highest measured so far for fcc-fcc layered systems and shows the potential of this interface engineering route. Our findings demonstrate that the intermetallic formed at Al/Ni multilayers contributes to a strong interface strengthening effect and compensates the weakening from interface diffusion. In this presentation we will discuss the role and potential of the interfaces and interphase boundaries for materials under extreme conditions.

8:45 AM SF08.05.03

Probing Residual Stresses and Dislocation Dynamics by Combining X-Ray Nano-Diffraction and Micropillar Compression Testing [Rebecca Janknecht](#)¹, [Rainer Hahn](#)¹, [Anton Davydok](#)², [Szilard Kolozsvari](#)³, [Peter Polcik](#)³ and [Paul Mayrhofer](#)¹; ¹TU Wien, Austria; ²Helmholtz-Zentrum Hereon, Germany; ³Plansee Composite Materials GmbH, Germany

Architecting materials for extreme environments requires a comprehensive understanding of their behavior under challenging conditions. This study introduces a novel approach that combines micropillar compression testing with X-ray nano diffraction to in-situ investigate strains within TiN-based physical vapor deposited (PVD) thin films during loading. The micropillar compression testing induces and moves dislocations within the coating material. The simultaneous X-ray nano diffraction with a focused beam of 250 nm in size allows to capture detailed information about changes in strain as well as structure. Nanocrystalline Ti-B-N coatings with boron contents up to 40 at.% and ceramic-metallic TiN-Nb multilayers with different modulations served as model systems. The nanocrystalline Ti-B-N exhibits significant differences in deformation and fracture behavior, depending on the amorphous grain boundary phase fraction. The stresses needed to move dislocations within the metallic Nb layers of the TiN-Nb multilayers, depend on the Nb layer thickness and varies between ~3 and 10 GPa.

These comprehensive investigations allow to extract information on the predominant strength, ductility, and failure mechanisms active in nanocomposite or multilayered PVD materials. Based on these, PVD thin films with exceptional resilience and damage tolerance, making them suitable for high-stress applications, can be designed.

9:00 AM SF08.05.04

Mechanistic Study of Superlattice Effects on the Example of Hexagonal Diboride Coatings [Rainer Hahn](#)¹, [Arnold Tymoszuk](#)¹, [Tomasz Wojcik](#)¹, [Eleni Ntemou](#)², [Oliver Hunold](#)³, [Peter Polcik](#)⁴, [Szilard Kolozsvari](#)⁴, [Daniel Primetzhofer](#)², [Paul Mayrhofer](#)¹ and [Helmut Riedl](#)¹; ¹TU Wien, Austria; ²Uppsala University, Sweden; ³Oerlikon Surface Solutions AG, Liechtenstein; ⁴Plansee Composite Materials GmbH, Germany

Coherently grown nanolayered PVD thin films, referred to as superlattice thin films, are known for their superior hardness compared to monolithically grown constituents. By employing in-situ micromechanical cantilever bending tests, we have shown that the fracture toughness also shows a significant bilayer period-dependent behavior. While mechanisms based on dislocation activity explain the hardness peak, the linear elastic deformation of the microcantilever during the fracture experiments suggests that these explanations are not directly applicable to describe the enhancement in fracture toughness. Consequently, an underlying, bilayer-period-dependent intrinsic property is responsible for this behavior.

This contribution presents an overview of the ceramic superlattice systems deposited so far, their increase in hardness and fracture toughness, and a mechanistic consideration of the increase in these properties. For this purpose, we selectively deposited systems, which differ in the two decisive factors for increasing the mechanical properties, the shear modulus difference ΔG and the

difference in the lattice parameters Δa . While our TiB₂-WB₂ systems show a pronounced difference in G, their lattice parameter is very similar, contrary to our TiB₂-ZrB₂ systems, having similar elastic properties while showing a pronounced difference in their crystallographic properties. We unravel the active mechanisms responsible for the respective increases in H and K_{IC} by performing the same micromechanical tests on these novel diboride coatings. Specifically, the TiB₂-ZrB₂ coatings showed an increase in K_{IC} up to 3.7 MPa·m^{0.5}, while the TiB₂-WB₂ system experienced an increase in hardness to 45.5 GPa, both without a significant increase of the other mechanical properties. These results and investigations, especially the systematic design of the study, allow a targeted development of protective coatings.

9:15 AM *SF08.05.05

Reactive Sintering of Oxide Dispersion Strengthened Nanoarchitected Aluminum Alloys Jason R. Trelewicz; Stony Brook University, United States

High specific strength materials are critical for enhancing performance and efficiency in a broad range of applications such as next generation aerospace structures and hypersonic vehicles but are often limited by the low relative strength often accompanying the reduction in density. For example, most aluminum (Al) alloys have yield strengths that are at most a few hundred megapascals while the yield strength of a common structural steel can exceed a gigapascal, albeit at the expense of density. One pathway for enhancing a material's strength is to reduce its grain size following the classical Hall-Petch relationship, and nanocrystalline materials containing grain sizes generally less than 100 nm occupy the lower limit of this approach. While nanocrystalline Al has been demonstrated with exceptionally high yield strengths of 400-600 MPa, grain size refinement for strengthening produces intrinsically unstable microstructures where thermodynamics favor grain growth. In this work, we combined targeted alloying for stabilizing nanocrystalline grains in Al with powder metallurgical processing advances that trigger an exothermic reaction during sintering to facilitate densification at low homologous temperatures and the formation of a distributed nano-oxide phase. Based on thermodynamic modeling, magnesium (Mg) was selected as the primary solute addition and mechanically alloyed with Al through high energy ball milling to produce a series of nanocrystalline Al-Mg alloy powders. Reaction of Mg with oxygen (O) during the decomposition of a byproduct of the selected process control agent provided the exothermic reaction required to enhance the sintering kinetics at low homologous temperatures. The resulting bulk nanoarchitected alloy is shown to contain nano-oxides dispersed in a nanocrystalline Al-Mg matrix with a highly stable grain size of < 50 nm up to 500 °C and a strength double that of the aerospace grade Al alloy 7075-T6. In a broad sense, this reactive sintering technology enables the production of bulk, thermally stable nanoarchitected alloys with amplified strengthening due to a confluence of mechanisms involving extreme Hall-Petch strengthening from the stabilized nanograins and matrix dispersion strengthening from the distributed nano-oxide phase.

9:45 AMBREAK

10:15 AM SF08.05.06

Multiscale Microstructure Architecturing Protects Advanced High Strength Steel against Hydrogen Embrittlement Dierk R. Raabe, Dirk Ponge and Binhan Sun; Max Planck Institute for Iron Research, Germany

Advanced high-strength steels exhibit structural and chemical ordering and patterning phenomena across multiple length scales. These include short and medium-range chemical ordering, complex nanoprecipitate patterns, and coupled mesoscopic chemical-structural-mechanical partitioning effects. These phenomena can arise from kinetic freezing, chemical decoration of lattice defects, locally confined phase transformation effects, or chemical container phases that trigger local phase transformations. Heat treatment can be used to architect these features in a hierarchical manner at bulk scale in medium and high manganese steels with lean chemical compositions [1,2]. These hierarchical ordering effects that involve different chemical and structural features across several length scales can be used to design a complex strain hardening behaviour and can help to enhance the materials' resistance to hydrogen embrittlement.

1. Sun, B. et al. Chemical heterogeneity enhances hydrogen resistance in high-strength steels. *Nat. Mater.* 20, 1629–1634 (2021).

2. Raabe, D. et al. Current Challenges and Opportunities in Microstructure-Related Properties of Advanced High-Strength Steels. *Metall. Mater. Trans. A Phys. Metall. Mater. Sci.* 51, 5517–5586 (2020).

10:30 AM SF08.05.07

Strengthening of Eutectic Alloys with Mille-Feuille Structure Accompanied by Kink-Band Formation Toko Tokunaga¹, Koji Hagihara^{1,2}, Shuhei Ohsawa¹, Takuya Yonemura¹, Daisuke Egusa³ and Eiji Abe³; ¹Nagoya Institute of Technology, Japan; ²Osaka University, Japan; ³The University of Tokyo, Japan

Application of the lightweight metal materials to the automobile components has been gaining attentions to mitigate the global warming problems by reduction of CO₂ emissions. Recently, Mg alloys with Long Period Stacking Ordered (LPSO) phase have been gaining attentions because they achieved high strength and high ductility simultaneously by the introduction of characteristic deformation bands; i.e., kink bands. To introduce the kink bands during deformation, the macroscopic shear direction must be restricted along the direction parallel to the loading orientation. Since the LPSO phase consists of periodic stacking of soft Mg layers and hard Y/Zn segregated layers, i.e., mille-feuille structure, it has been considered that this structure brings the strong plastic anisotropy and restricts the shear direction. Thus, by controlling the loading orientation, the kink-bands are expected to be obtained. This microstructure control using mille-feuille structure can be one of the effective ways to achieve high strength and high ductility materials.

In the present study, we have focused on Al-Al₂Cu and Ti-TiFe eutectic alloys to obtain the "micro-scale" mille-feuille structured materials. For the Al-based alloy, to achieve highly-aligned lamellar structure, the directional solidification with growth rates in a range of 5 to 300 mm/h was conducted. On the other hand, for the Ti-based alloy, we made use of the heat flow in the arc melting process to align the lamellar structure. We basically obtained a lamellar microstructure aligned parallel to the growth and heat-flow directions in both alloys. However, in the directionally-solidified Al alloys, as the growth rate increased, the alignment of the lamellae was gradually disturbed and the lamellae tended to incline against the growth direction. Moreover, the thickness of the lamellae and size of the colony, which is the group having the same lamellar orientation, decreased as the growth rate increased.

In the compression tests of the Al-based alloys, for the alloys with large colony diameters, large kink bands formed, which induces buckling of the specimen. On the other hand, it was found that a decrease in the colony diameter induces the homogeneous formation of tiny kink bands, leading to the drastic increases in the yield stress while maintaining ductility as observed in the Mg-based LPSO phase alloys. Moreover, it has been systematically demonstrated that the yield stress proportionally increases as the inverse of the square root of the colony diameter increases. This can be considered because the colony diameter affects the formation stress of the kink bands. From the obtained results, it has been demonstrated that control of the colony size and the alignment of lamellae are the key factors for achieving superior mechanical properties of the mille-feuille structured alloys with homogeneous formation of tiny kink bands.

In the compression tests of the Ti-based alloys, they showed extensively high strength over 2 GPa at room temperature, and kept the high strength at 400°C. However, the strength decreased drastically at and above 600°C. In the specimen deformed at 800°C, the specimen deformed with formation of tiny kink bands. By the crystallographic analysis, rotation axes for the kink-bands formation were different in β-Ti and TiFe phases. This implies that the mechanism of the kink-bands formation in the present eutectic Ti-TiFe alloy was different from the conventional model for the kink-bands formation. In the presentation, the kink-bands formation behavior of the present Al and Ti alloys are presented in detail.

10:45 AM SF08.05.08

Entanglement of Ordered and Disordered Structures Enables Supercritical Elasticity Yang Ren¹, Haiyang Chen² and Yan-Dong Wang²; ¹City University of Hong Kong, Hong Kong; ²University of Science and Technology Beijing, China

Superelasticity associated with the martensitic transformation has a broad range of applications. However, the intrinsic hysteresis and temperature sensitivity of the first-order phase transformation significantly hinder their usage in many critical areas. We recently discovered that the first-order stress-induced martensitic transformation (SIMT) of a large class of shape-memory alloys can be completely diminished by appropriate material design and thermal treatments to bring the transformation to a supercritical region [Chen et al., *Nature Materials*, 19, 712 (2020). <https://doi.org/10.1038/s41563-020-0645-4>]. In this talk, we will present a new type elasticity: supercritical elasticity (SCE), in NiCoFeGa single crystals which exhibit a large elasticity up to 15.2% strain, with non-hysteretic mechanical responses, a small temperature dependence and high-energy-storage capability and cyclic stability over a wide temperature and composition range. In-situ synchrotron X-ray diffraction shows that the SCE is correlated with a stress-induced continuous variation of lattice parameter accompanied by structural fluctuation. Neutron diffraction and electron microscopy observations reveal an unprecedented microstructure consisting of atomic-level entanglement of ordered and disordered crystal structures, which can be manipulated to tune the SCE. The alloys are very promising for high-performance engineering applications, ranging from deep-space and deep-sea exploration to intelligent robotics.

11:00 AM *SF08.05.09

Tailoring Structure and Properties of Architected Metastable Alloys Jurgen H. Eckert^{1,2}; ¹Erich Schmid Institute of Materials Science, Austrian Academy of Sciences, Austria; ²Montanuniversitaet Leoben, Austria

Significant progress has been made in recent years in how to optimize processing conditions for metastable alloy and composite formation, microstructure design, net-shape forming and property adjustment of architected metallic materials. However, the details of the correlation between composition, atomic structure, hierarchy of the microstructure, defects and thermo-mechanical treatments employed for structure modification and their impact on deformation and failure mechanisms for achieving tailored properties are still not well understood. Recent work suggests that not only the intrinsic properties of metastable metallic alloys and composites are strongly affected by the details of atomic arrangements including short- and

medium-range order cluster motifs in amorphous solids and high-entropy alloys but also their response to external fields like mechanical deformation or temperature cycling largely depends on often complex local atomic rearrangements triggered by or causing heterogeneous stress and strain variation on different length-scales. This – together with microstructure modulation through tuning of architecture and length-scale of phases as well as the use of non-equilibrium processing techniques for phase and structure design – yields unique prospects for developing architected materials for extreme conditions or environments.

This talk explores the diversity that can be achieved in metallic glasses, chemically complex alloys and composites considering structure changes, recovery and rejuvenation mechanisms, clustering, segregation as well as phase separation or nanocrystallization phenomena when the materials are subjected to different solidification conditions, mechanical deformation, thermo-mechanical cycling, or net-shaping. The findings from experiments and simulations will be discussed with respect to atomic rearrangements, short- and medium-range order modulation, local stress and strain states, defect generation and annihilation, nanoscale clustering or segregation and precipitation of secondary phases. The structure changes will be correlated with plastic deformability and failure mechanisms, and the effectiveness of composition and microstructure tuning and thermo-mechanical processing for materials design will be discussed to derive guidelines for processing and property optimization.

11:30 AM *SF08.05.10

Dissimilar Joining using Dealloying Hidemi Kato, Kota Kurabayashi and Takeshi Wada; Tohoku University, Japan

Liquid metal dealloying (or solid metal dealloying) can produce distinctive bicontinuous nano- and microcomposites with immiscible metals such as Ta-Cu[1], FeCr-Mg[2,3], and Ti-Mg[4]. These immiscible metal composites are not expected to have strong chemical bonding between the constituent metals, but they exhibit excellent strength and ductility. In particular, FeCr-50%Mg with a few μm ligaments exhibited a tensile strength of 191.9 MPa and a tensile elongation of 15.0%. These results led us to believe that LMD (or SMD) are effective as dissimilar materials joining techniques, especially between immiscible metals. Actually, in these years, multi-material structures that combine steel with lighter materials, such as magnesium alloys, have received wide attention in the field of welding engineering. In this paper, dissimilar joining of immiscible metals is discussed, then, as a simplified model, joining of pure Fe and Mg using Solid metal dealloying technique is demonstrated[5].

- [1] I. McCue, et al., *Size Effects in the Mechanical Properties of Bulk Bicontinuous Ta/Cu Nanocomposites made by Liquid Metal Dealloying*, Adv. Eng. Mater. 18(2016)46-50.
- [2] M. Mokhtari et al., *Mechanical Properties of FeCr-based Composites Materials Elaborated by Liquid Metal Dealloying towards Bioapplication*, Adv. Eng. Mater. 22(2020)2000381.
- [3] Y.-B. Jeong, et al., *Beyond strength–ductility trade off: 33D interconnected heterostructured composites by liquid metal dealloying*, Composites B: Engineering, 225(2021)109266.
- [4] I. Okulov, et al., *Anomalous compliance of interpenetrating-phase composite of Ti and Mg synthesized by liquid metal dealloying*, Scr. Mat. 19482021)113660.
- [5] K. Kurabayashi, et al., *Dissimilar joining of Immiscible Fe-Mg using Solid Metal Dealloying*, Scr. Mat. 230(2023)115404.

Acknowledgement

This work was supported by a Grant-in-Aid for Scientific Research (A) 21H04611 and Scientific Research (C) 20K05126 from Japan Society for the Promotion of Science (JSPS).

SESSION SF08.06: Extreme Mechanical Loading
Session Chairs: Ilya Okulov and Carlos Portela
Tuesday Afternoon, November 28, 2023
Sheraton, Third Floor, Fairfax A

1:30 PM *SF08.06.01

New Methods for Testing Materials under Extreme Conditions Keith A. Nelson; Massachusetts Institute of Technology, United States

The design of architected and other advanced materials to withstand extreme conditions has heightened the need for facile tests under such conditions that can be applied to small amounts of materials that may be in early developmental stages. Three recently developed and refined methods for materials testing under extreme conditions will be discussed.

In the laser-induced particle impact test (LIPIT), small (~5-50 μm) particles of various types are launched by laser ablation of a supporting layer. Camera images record a trajectory before, during, and after impact with a target material in order to determine particle speeds (~50-1200 m/s) before and after impact and to observe details of the particle and target material responses to impact (*Appl. Phys. Rev.* 8, 011319). Target materials have included soft materials such as polymers and gels as well as hard materials including metals and ceramics. Architected materials and ultrathin layers have been studied.

Two methods involve laser-driven shock waves. In one, an intense laser pulse is directed to a circular-shaped “ring” pattern at the sample. Absorption in a 10-50- μm thick material leads to rapid melting and evaporation which launches a quasi-2-dimensional focusing shock wave. In opaque materials with strong near-surface absorption, a focusing surface acoustic wave (SAW) shock is launched. In both cases, pressures of several tens of GPa can be reached at the shock focus with only a few millijoules of laser pulse energy (*Rev. Sci. Instr.* 91, 033711). Shock-induced chemical and structural transformations have been studied.

A very recent development (*arXiv:2209.13897*) has permitted *laser generation of shock waves without damage to the optically irradiated region of the sample*. Instead of an intense laser pulse directed at a single sample region, many cylindrically focused pulses reach parallel “lines” at the sample in succession, with temporal and spatial shifts adjusted to move across the sample at a speed that matches the acoustic velocity. The shock wave is built up gradually by the successive pulses, each of which is below the optical damage threshold of the sample. This enables repeated shocks (up to ~10 GPa pressure to date) to be delivered to the same sample region so that cumulative effects of shock can be assessed. In an initial study, thousands of SAW shocks that reached strain levels of 1% (3 GPa pressure) in SrTiO₃ were launched. Typically, there was no visible damage to the sample until ~1000 shocks, after which severe damage (material ejection several microns deep) occurred and gradually spread during the next 1000-2000 shocks. The nondestructive shock generation method will enable detailed study of fatigue in many material classes. X-ray imaging methods may permit characterization of the nanoscale defects that accumulate prior to catastrophic damage.

The nondestructive shock generation method is being extended to focusing shocks generated by a succession of pulses directed to concentric circular regions of the sample, with the diameter gradually reduced from one pulse to the next to match the acoustic velocity. Initial tests with just two pulses have enabled shock pressures to be reached nondestructively that are comparable to those reached by many pulses in the method described above, due to the increase in shock pressure at the focus. The combination of approaches is useful to permit testing under compressive stress only (in a quasi-bulk compressional wave), tensile stress (which follows compression in the focusing shock, upon divergence from the focus), and significant shear stress (in SAW shocks several microns beneath the sample surface, where the SAW has a large shear component).

Finally, the methods involving multiple “lines” or “rings” of pulsed laser light are not restricted to the optically nondestructive regime. We hope to reach extreme pressures (> 100 GPa) by directing intense pulses to multiple concentric rings.

2:00 PM SF08.06.02

Observing High Strain Rate Compression of Gradient Density Octet Lattices using Ultrafast X-Ray Imaging Abhinav Parakh¹, Jonathan Lind¹, Anna Guell Izard¹, John Kulikowski², Wendy Gu² and Xiaoxing Xia¹; ¹Lawrence Livermore National Laboratory, United States; ²Stanford University, United States

Architected materials are a new class of engineered materials with controlled internal structures that give rise to properties that differ or surpass those of their constituent materials. Micro- and nano-structured lattices have demonstrated superior quasi-static mechanical properties compared to traditional materials or composites but, their dynamic mechanical behavior under high strain rate conditions is poorly understood. Here we compressed gradient density octet lattices fabricated using Nanoscribe under high strain rates and observed the deformation behavior using ultrafast X-ray imaging at Argonne National Lab. We used high fidelity hydrocode modeling of the lattices and utilized X-ray imaging to directly relate the measured in-situ compressed lattice to the model predictions for the expected output ramp profile. We observed that the direction of increasing density profile (higher density at the substrate compared to lower density at the substrate) affected the onset of acceleration and the compression profile at the backend of the substrate. We show that micro-architected lattices with smoothly varying density gradients have a great potential for creating tailored ramp compression profiles.

IM release number LLNL-ABS-850153. This work was performed under the auspices of the U.S. Department of Energy by Lawrence Livermore National Laboratory under Contract DE-AC52-07NA27344.

2:15 PM *SF08.06.03

Energy Absorption in the Gigapascal Range – Methods to Absorb Energy for Extreme Mechanical Loads Jeffrey Lloyd; DEVCOM Army Research Laboratory, United States

Design of architected structures and materials for energy absorption is straightforward – choose a solution that maximizes specific energy absorption for a given loading amplitude while keeping below some maximum allowable threshold stress. Novel materials and architectures of lattices and foams have increased the specific energy absorption capacity and threshold stresses

that can be tolerated, but these structures are generally dominated by the densification phase for loads exceeding hundreds of Megapascals. In this talk we examine the potential for volume-reducing phase transformations to manipulate waves with amplitudes up to tens of Gigapascals. As an example, the ability for the $\diamond\rightarrow\circ$ transformation to absorb shock waves in Fe and its alloys is studied for monolithic and hierarchically structured materials using both experiments and computer simulations. Methods are presented for designing new metal alloys, both monolithic and graded, that can achieve high specific energy absorption.

2:45 PM SF08.06.04

Material Properties of Aerogel Measured using Bow Shock Induced by Supersonic Particle Impact YunKai and Keith A. Nelson; Massachusetts Institute of Technology, United States

Aerogels are lightweight materials with a nanoporous structure that captivate the interest of researchers in various fields of science and technology. They possess numerous exceptional characteristics and find applications in a wide range of areas, including thermal and acoustic insulation and kinetic energy absorption. Typically, the mechanical properties of aerogel were measured using uniaxial compression, three-point bending, ultrasonics, and atomic force microscopy. However, accurately measuring the mechanical properties of aerogel can be challenging due to its low density, high porosity, and brittleness. Aerogels, especially silica aerogel, are known to be fragile and brittle. This makes them inapt for load-bearing testing methods. In this study, we utilize a method called laser-induced particle impact testing (LIPIT) to investigate the properties of aerogel materials. Specifically, we report on the observation of bow shock generation during supersonic particle impacts. It is worth noting that previous works did not report the occurrence of bow shocks, as solid or liquid samples in those studies typically possess higher acoustic speeds compared to projectile speeds. However, aerogel, an air-like material with intricate foam structures, may exhibit a significantly lower acoustic speed (around 100 m/s) than our typical projectile speed (approximately 1000 m/s). This characteristic facilitates the generation of bow shocks. We can accurately extract material properties by performing aerodynamic analysis on bow shocks. The advantage of our bow shock-based study is that it eliminates the risk of altering the material properties before the measurement takes place since the bow shock is the fastest event in the system. Moreover, our approach not only allows for the determination of material properties such as acoustic speed and bulk modulus but also enables the calculation of the previously unreported drag coefficient. Our results have implications for the design of aerogel-based materials for various applications, including impact protection and shock mitigation.

3:00 PM BREAK

SESSION SF08.07: Architected Materials for Extremes I

Session Chairs: Ian McCue and Carlos Portela

Tuesday Afternoon, November 28, 2023

Sheraton, Third Floor, Fairfax A

3:30 PM *SF08.07.01

Assessing the Design Space for Architected Materials in Extreme Loading Scenarios Mukul Kumar, Brandon Zimmerman and Jonathan Lind; Lawrence Livermore National Lab, United States

Owing to the tunability of mechanical response for structural applications, additively manufactured lattice structures are increasingly being studied to elucidate their response to static and dynamic loads. However, these roles are typically in opposition: static loads must be supported sufficiently far away from the onset of buckling or yielding, whereas dynamic loads are typically ameliorated by crushing of the lattice, which provides excellent energy-absorption due to the large plastic deformation accompanying densification. Moreover, emergent behavior, such as material jetting and elastic wave propagation, arising from the open architecture has been observed *in situ* under dynamic loading conditions. In this work we will outline a design scheme for lattice structures that must simultaneously support static loads while enduring high-amplitude impulsive loads. For a class of impulse shapes associated with laser-based shock compression, our key findings show that the static and dynamic responses of the lattice can be uncoupled and linked by a strength model that accounts for variability in the additive manufacturing process. Moreover, costly global search optimization can be replaced by sequential one-dimensional optimization following the direction of the wave propagating through the lattice. The design rules developed in this study expand the domain of applicability of lattice structures to challenging dual-loading regimes spanning decades of strain rates. This work was performed under the auspices of the US Department of Energy by Lawrence Livermore National Laboratory under Contract DE-AC52-07NA27344.

4:00 PM SF08.07.02

Temperature- and Rate-Dependent Deformation of Additively Manufactured Copper Microlattices Sung-Gyu G. Kang¹, Bárbara Bellón¹, Lalith Kumar Bhaskar¹, Dipali Sonawane¹, Janis Wirth², Alexander Götz², Benjamin A. Zubiri², Erdmann Spiecker², Gerhard Dehm¹ and Rajaprakash Ramachandramoorthy¹; ¹Max-Planck-Institut, Korea (the Republic of); ²Friedrich-Alexander-Universität Erlangen-Nürnberg, Germany

The deformation behavior and mechanical properties of architected materials are determined not only by their geometry but also by the intrinsic mechanical properties of the constituent materials. In this study, we investigate the temperature and strain rate responsive deformation behavior of a 3-dimensional microarchitecture by examining the material's intrinsic deformation mechanism.

We fabricate copper microlattice architectures using an additive micromanufacturing process based on localized electrodeposition in liquid. The microlattices are characterized using nano X-ray computed tomography (nano-CT), which confirms the near-ideal connectivity between nodes and struts. Microstructural characterization is performed using electron backscatter diffraction (EBSD) and transmission electron microscopy (TEM), revealing that the microlattices are microcrystalline with a high fraction of twin boundaries.

Furthermore, we investigate, for the first time, the mechanical properties of the copper microlattices under a wide range of strain rates (from 0.001/s to 100/s) and at various temperature conditions (cryogenic -150°C and room temperature) using a piezo-based *in situ* micromechanical testing setup inside scanning electron microscopy (SEM). The unique temperature- and rate-dependent deformation behavior of the copper microlattices is observed and explained based on the intrinsic deformation behavior of the base material (copper) obtained from micropillar compression tests performed under the same loading conditions of high strain rates and non-ambient temperatures. Notably, it is found that depending on the temperature, copper accommodates plastic deformation through either dislocation slip or mechanical twinning.

This study demonstrates that complex 3-dimensional full-metal architectures can be successfully fabricated in an additive fashion at the micron scale. Furthermore, depending on the design of the architectures and their testing conditions of temperature and strain rate, these architectures exhibit unique deformation behavior that is suitable for dynamic and harsh applications.

4:15 PM SF08.07.03

Decomposing Contributions to Energy Dissipation in Impact of Architected Materials Thomas Butruille¹, Joshua Crone² and Carlos M. Portela¹; ¹Massachusetts Institute of Technology, United States; ²U.S. Army Research Laboratory, United States

Ultralight mechanical metamaterials enabled by advanced manufacturing processes have previously achieved density-normalized strength and stiffness properties that are inaccessible to bulk materials, but the majority of this work has focused on static loading while the mechanical properties of these metamaterials under dynamic loading conditions have remained largely unexplored. Properties such as energy absorption of these metamaterials are of high interest for protective applications and recent works on their dynamic response have demonstrated the benefit of architecture for impact mitigation.

Here, we systematically study the response of periodic mechanical metamaterials under microprojectile impact using two-photon lithography as a rapid prototyping technique for microscopic polymeric microlattices. We fabricate suspended thin-plate lattice architectures of varying thicknesses and morphologies to characterize their response to microparticle impact. We employ the laser-induced particle impact test method to accelerate ~30 μm -diameter microparticles to velocities of up to 900 m/s, and use ultra high-speed imaging of the impact process to measure impact energetics across multiple architectures and varying lattice plate thicknesses. We compare impact performance to an array of quasistatic uniaxial compression experiments to decompose the effects of lattice compaction and fracture on energy dissipation during impact. Additionally, we analyze our experiments in a dimensionless framework to provide a first-order estimate of impact response across materials and length scales and investigate how the energy dissipation components scale with the regime of impact. Lastly, we study the impact response using an explicit dynamics finite-element representation to provide insight on the impact mechanisms. This investigation provides a framework for the rapid design and characterization of future mechanical metamaterials for a variety of energy absorption applications.

4:30 PM SF08.07.04

Fabrication of Solid-Liquid Composite Micro-Architecture and Their Deformation Behavior Sung-Gyu G. Kang¹, Bárbara Bellón¹, Lalith Kumar Bhaskar¹, Leonardo Shoji Aota¹, Se-Ho Kim¹, Alexander Götz², Erdmann Spiecker², Baptiste Gault¹, Gerhard Dehm¹ and Rajaprakash Ramachandramoorthy¹; ¹Max-Planck-Institut für Eisenforschung GmbH, Germany; ²Friedrich-Alexander-Universität Erlangen-Nürnberg, Germany

Architected materials, composed of solid materials with pore channels, exhibit unique deformation behavior and mechanical properties. By altering the composition of the solid material or introducing different materials, the properties of architected materials can be further tuned. However, the introduction of liquid materials to architected materials has not been investigated due to intrinsic fabrication constraints in the widely used additive manufacturing processes. In this study, we demonstrate the feasibility of solid-liquid composite micro-architectures using a recent additive micromanufacturing technique based on localized electrodeposition.

As a case study, we designed and fabricated simple pure copper (Cu) micro-vessels containing pico-liters of liquid. The existence of the liquid was confirmed through cross-sectional analysis using cryogenic-focused ion beam microscopy. Atom probe tomography was employed to measure the chemical composition of the pure copper and the encapsulated liquid. Nano computed tomography (NanoCT) results confirm the dense pure copper vessel walls with the liquid confined inside the vessel. Importantly, we investigated the effect of the liquid on the deformation behavior and mechanical properties of the micro-vessels using a *in situ* micromechanical testing system capable of metrology at high speeds and sub-ambient temperature conditions. The micro-vessels exhibited significantly different stress levels and strain rate dependencies depending on the phase (water to ice transformation under cryogenic conditions). In addition to the microstructural and mechanical characterizations, we will discuss the feasibility and potential of solid-liquid composite architectures at the microscale as novel structural and functional materials.

4:45 PM SF08.07.05

Synchrotron Radiation-Based Far-Infrared Spectroscopy under Extreme Conditions at the Canadian Light Source [JianbaoZhao](#); Canadian Light Source, Canada

The study of materials under extreme conditions, such as high-pressure or low-temperature, is essential in understanding a broad range of problems in physics, chemistry, geology, and materials science. Extreme conditions can cause significant changes in the physical and chemical properties of matter, such as structural phase transitions, alterations in chemical bonding, and the emergence of new properties. Consequently, there is considerable research interest in studying materials under such conditions.

A synchrotron radiation-based infrared source is an ideal tool for investigating microscopic samples under extreme conditions due to its high brightness. The Far-infrared beamline at the Canadian Light Source (CLS) is a state-of-the-art synchrotron facility that offers significantly more brightness than conventional sources. The high brightness of the synchrotron radiation allows for the acquisition of Far-infrared reflectivity or transmission spectrum on small samples with greater throughput than with conventional sources. This capability is ideal for high-pressure studies using the Diamond Anvil Cell (DAC).

A synchrotron radiation-based Far-infrared spectroscopic experiment is particularly crucial for studying the lattice modes of materials as they typically appear in the Far-infrared region. Additionally, Far-infrared spectroscopy provides detailed information on the electrical transport properties of metallic materials, the bandgap of semiconductors, and the chemical bonding properties of materials.

This presentation will provide a brief overview of the capabilities of the Far-infrared beamline at the CLS. It will also highlight the Far-infrared equipment used for solid-state experiments, especially for Far-infrared transmission and reflectivity measurements under high-pressure using the DAC. The CLS provides a custom-made horizontal microscope for Far-infrared microscopy during high-pressure studies. The optical set-up allows for transmission and reflectivity measurements, and two infinity-corrected long working distance Schwarzschild objectives (working distance-47 mm; numerical aperture-0.5) are suitable for high-pressure infrared studies using the DAC. The CLS records synchrotron radiation-based Far-infrared Fourier transform spectrum in the low-frequency region (30-600 cm^{-1}) and the high-frequency region (300-1300 cm^{-1}) using the liquid helium free detector system manufactured by QMC Instruments Inc. Moreover, the homemade ruby fluorescence spectrometer is available on-site at the CLS to measure the sample pressure inside the DAC. The Far-infrared beamline of the CLS is open to users through peer review, with calls for proposals issued twice per year for experimental beam time.

SESSION SF08.08: Evolution at Thermal Extremes

Session Chairs: Ian McCue and Ilya Okulov

Wednesday Morning, November 29, 2023

Sheraton, Third Floor, Fairfax A

8:00 AM SF08.08.01

Analysis of Heat Transfer Performance for Nanomaterial Composite Electroless Coating Utilizing Spray Cooling Technique [SuparnaBhattacharyya](#), [SuryaK. Pal](#) and [SudiptoChakraborty](#); Indian Institute of Technology Kharagpur, India

Heat Exchangers are the most common devices for chemical industries, pharmaceutical firms and petrochemical refineries. The basic structural material used for manufacturing this high end engineered machine is mild steel due to its easy availability and vast range of usage. But the material itself is also very much susceptible to atmospheric corrosion, industrial fouling and microbial attacks. The technique of electroless coating plays a very crucial role in minimizing the above disadvantages of the material thus increasing the product value in long run. The present study gives a comparison between heat transfer experiments of electroless Ni-P-TiO₂ (ENP-TiO₂) coated mild steel comparing them with the uncoated and Ni-P coated mild steel samples. An optimisation of the best suit is the main focus of the given study. The heat transfer analysis is carried forward using spray cooling setup. SEM, EDX and XRD analysis of all the sample showcases the surface morphology and phase structure analysis. A brief overview on surface roughness study predict the suitability of surface modification for the required research objective. The microhardness of all the sample has been analysed and reported. An in-house spray cooling setup has been used to analyse the heat transfer analysis using INTEMP software. Scaling up the analysis for industrial purposes specifically in shell and tube heat exchangers is a potential future scope of the current analysis.

8:15 AM SF08.08.02

Strong, Stable and Multifunctional Polyimide-CNT Network Composites via *In-Situ* Solvothermal Polymerization [MichaelN. Durso](#) and [A. JohnHart](#); Massachusetts Institute of Tehnology, United States

To maximize the mechanical properties of aligned carbon nanotube (CNT) networks, researchers have synthesized increasingly densely-packed yarns by direct synthesis and wet chemical approaches, such that macroscopic CNT yarns can now exceed 60 to 80% of their theoretical fully-packed density. However, the weak intermolecular attraction between CNT bundles continues to limit their mechanical properties, and while increasing CNT packing density increases the density of contacts, it also acts as a barrier to infusing a reinforcing polymer phase to create stable, dense CNT-polymer composites. Our team has explored these factors which govern nanoporous network infusion and developed a one-pot, green chemical route to synthesizing high-performance aromatic polymer reinforcement in-situ in CNT materials in superheated aqueous and alcoholic solutions, exploiting their novel physicochemical behavior under these conditions.

We demonstrate the synthesis of aromatic polyimide reinforcements to create composites which are mechanically stiff and strong and inherently resilient in extreme environments. By tailoring our chosen monomers, we show the broad applicability of the technique to generate linear and hyperbranched copolymers with CNT-specific interfacial interactions facilitated by hydrogen bonding. The aromatic backbone of these polymers affords composites with exceptional thermal stability and char formation compared to common CNT reinforcements, such as polyvinyl alcohol or epoxy resins; polymer decomposition onsets exceed 500°C and can encapsulate the subsurface CNTs from reactive species. Whereas traditional approaches of heated and solvent-diluted infiltration of high molecular weight polymers are challenged by the tortuous nanoscale pathways between densely-packed CNTs, our in-situ polymerization occurs within a highly-diffusive, low viscosity environment, enabling demonstrably-deep infusion through the nanoporous network.

The high stability and specific strength and stiffness of these composites makes them promising structural materials for extreme aerospace applications, where weight savings are critical to improve performance. Further, we demonstrate that these same polymers, as coated on the CNTs, exhibit multifunctional, synergistic behavior: simultaneously acting as the reinforcing phase of a strong composite and as organic redox-active material to form a free-standing battery electrode, avoiding additional conductive and binder additives. Such composites could help to enable new structural battery designs with greater flexibility than carbon fiber-based scaffolds, which lack the intrinsic flexibility of CNT materials.

8:30 AM SF08.08.03

Solutes at Triple Lines in Al-Based Nanostructured Alloys [NuthTuchinda](#) and [ChristopherA. Schuh](#); Massachusetts Institute of Technology, United States

Interface volume fractions increase with decreasing characteristic length scales in materials, and understanding the stability of such structural features is therefore critical for fine structures. For nanostructured materials, this effect becomes even more complicated as higher-order defects such as grain junctions become relevant. Here we calculate the substitutional solute segregation of several Al-based systems at triple junctions and show how we can apply the dataset to better understand solute chemistry at both grain boundaries and triple lines. The results from classical embedded atom potential models are compared with a hybrid first-principles dataset, highlighting potential drawbacks of the classical interatomic potentials in capturing the full physics of grain junctions. The method and dataset can be applied in the design of nanocrystalline alloys at their finest grain sizes.

8:45 AM SF08.08.04

Interfacial Instabilities of Nanoscale Architectures Under Elevated TemperaturesFadiAbdeljawad¹, OmarHussein², KhalidHattar³ and ShenDillon⁴; ¹Lehigh University, United States; ²Clemson University, United States; ³The University of Tennessee, Knoxville, United States; ⁴University of California, Irvine, United States

Recent advances in additive manufacturing have enabled the fabrication of architected materials with intricate nanoscale features. Examples include nanolattices, nanoporous materials, and stochastic nanostructures. However, the microstructural stability of such morphologies under high temperature environments is not well understood. Using theoretical, experimental, and computational studies, we examine the stability of nanostructured rod geometries. Our in-situ annealing studies of polycrystalline alumina rods demonstrate a pinch-off instability in which the rod breaks up into spatially isolated domains, a phenomenon reminiscent of the Plateau-Rayleigh instability in liquids. We develop a theoretical model to investigate the role of grain boundaries (GBs) in the morphological instability of rod geometries. Our analysis shows that GBs play a destabilizing role in which the critical wavelength for the instability decreases with increasing the GB energy. We complement our theoretical model with phase field simulations, which reveal that the time to pinch-off decreases with increasing the GB energy. On the whole, our approach provides avenues to explore microstructure evolution of high surface-to-volume materials under extreme environments.

9:00 AM SF08.08.05

Anti-Icing Properties of Polar Bear HairJulianT. Carolan¹, RichardHobbs¹, BodilHolst², ØyvindHalskau², ManishTiwari³, VikaramjeetSingh³, MartinJakubec⁴, JonAars⁵, MagnusAndersen⁵, MarcoSacchi⁶, NeubiXavier⁶, AdamPestana Motala⁶, EspenWerdal Selfors², ShaneO'Reilly⁷, Anne LisbethSchmidt⁸, ErsiliaBifulco³, Paula E.Colavita¹ and MarcBrunet Cabré¹; ¹Trinity College Dublin, Ireland; ²University of Bergen, Norway; ³University College London, United Kingdom; ⁴University of Tromsø, Norway; ⁵Norwegian Polar Institute, Norway; ⁶University of Surrey, United Kingdom; ⁷Atlantic Technological University Sligo, Ireland; ⁸National Museum of Denmark, Denmark

This work examines the natural ability of the polar bear (*ursus maritimus*) to prevent ice accumulation on their fur. Unlike other mammals, polar bears thrive in extreme environmental conditions, enduring air temperatures as low as -40°C and extended periods in water. Despite these conditions and unlike humans and other non-Arctic mammals, polar bears do not seem to experience accumulation of ice on their fur. In this study, we investigate the anti-icing properties of polar bear hair, including measurements of hydrophobicity, freezing delay time, and ice adhesion strength. We measure these properties on samples with and without the presence of hair oils (sebum).

We compare polar bear hair to human hair and synthetic ski skin samples. Ski skins are pads of aligned fibers attached to skis that support ascents while wearing skis by providing directional friction to support climbing. The ice adhesion strength of polar bear fur was found to be comparable to state-of-the-art racing ski skin technology and lower than non-race cross-country ski skins. However, when the hair oils were removed, the ice adhesion strength of polar bear fur increased significantly, suggesting the oils play a crucial role in preventing ice accumulation in a manner similar to SLIPS (Slippery Liquid Infused Porous Surfaces) [1].

Differences in the results for hydrophobicity and freezing delay time measurements on washed and unwashed hair were less pronounced. The presence or absence of oils had little effect on these measurements, with minimal variation across the hair samples. Microscopic analyses support these findings, indicating that the removal of oils did not affect the surface roughness of the hairs, a crucial parameter for both hydrophobicity and freezing delay time [2, 3].

This work employs a multidisciplinary approach, encompassing chemistry, physics, biology, and engineering. Through microscopic and spectroscopic techniques, we aim to understand the specific properties of polar bear fur that provide an advantage in the Arctic climate compared to other mammals. The insights gained from this study may guide the development of future bioinspired materials for anti-icing applications.

1 - Kreder, M. J., Alvarenga, J., Kim, P., & Aizenberg, J. (2016). Design of anti-icing surfaces: smooth, textured or slippery? *Nature Reviews Materials*, 1(1), 15003.

<https://doi.org/10.1038/natrevmats.2015.3>

2 - Nguyen, V. H., Nguyen, B. D., Pham, H. T., Lam, S. S., Vo, D. V. N., Shokouhimehr, M., Vu, T. H. H., Nguyen, T. B., Kim, S. Y., & Le, Q. van. (2021). Anti-icing performance on aluminum surfaces and proposed model for freezing time calculation. *Scientific Reports*, 11(1), 11. <https://doi.org/10.1038/s41598-020-80886-x>

3 - Nosonovsky, M., & Hejazi, V. (2012). Why superhydrophobic surfaces are not always icephobic. *ACS Nano*, 6(10), 8488–8491.

https://doi.org/10.1021/NN302138R/ASSET/IMAGES/LARGE/NN-2012-02138R_0003.JPEG

9:15 AM *SF08.08.06

Flame-Made Metal Sulfide Nanoparticles in Chemically Aggressive and Reducing ConditionsSumanPokhrel^{1,2,1}, JakobStahl^{1,2}, JanD. Groeneveld^{1,2} and LutzMädler^{1,2,1}; ¹University of Bremen, Germany; ²Leibniz Institute for Materials Engineering IWT, Germany

The flame made particles especially metastable materials are key to many applications with enormous societal and economic impact. These applications include such as but not limited to catalysts, energy concepts, electrode fabrication procedure for batteries, fuel cells, and chemical sensors. The transformation of a materials from a laboratory use to large scale technological application require (1) large specific surface area for transfer of mass, charges and energy while the specific success lies in an individual chemical nature of the materials and process design rules for particle synthesis (2) robustness during the material evaluation although they are specific in their functionality. Based on all the attractive properties of the oxide materials, key to their success is an economical and sustainable synthesis. The availability of multiple synthesis techniques (e.g. solid-state reactions, precipitation in aqueous and non-aqueous media, aerosol and plasma synthesis), produce specific oxide materials that are unique with respect to their physicochemical properties. However, for sulfide materials only few high temperature synthesis pathways are known due to unresolved challenges including inert atmosphere requirement, easy oxidation, endothermic conditions and low scalability. In the present work we have exploited thermodynamically driven organic gas phase combustion in reducing spray generated through fuel/oxygen ratio. The knowledge acquired from non-aqueous precursor-solvent combinations, high temperature aerosol chemistry and single droplet combustion (copper naphthenate-tetrahydrothiophene as model example) was used to establish process windows for reducing flames able to produce ultrafine metal sulfides (Cu₂S, In₂S₃, SnS₂, ZnS, Bi₂S₃, CoS, MnS, Ag₂S) with high stability and crystallinity.^{1,2} The reducing flame spray pyrolysis will now be able to drive process engineering to the next level producing binary metal sulfides for the earlier mentioned applications that will go far beyond the present state-of-the-art.

References

1. S. Pokhrel, J. Stahl, J. D. Groeneveld, M. Schowalter, A. Rosenauer, J. Birkenstock, L. Mädler, Flame aerosol synthesis of metal sulfides at high temperature and oxygen lean atmosphere, *Adv. Mater.* **2023**, <https://doi.org/10.1002/adma.202211104>

2. S. Pokhrel, J. Stahl, L. Mädler, Method for preparing a metal sulfide material and metal sulfide material obtainable thereby, *German patent*, U10441DE, 102022126378.9, **2022**

9:45 AM BREAK

SESSION SF08.09: Interfaces at Extremes
Session Chairs: Ian McCue and Gianna Valentino
Wednesday Morning, November 29, 2023
Sheraton, Third Floor, Fairfax A

10:15 AM *SF08.09.01

Dynamical Grain-Boundary Phase Diagrams in Irradiated AlloysPascalM. Bellon, GabrielBouobda Moladje, SouravDas, AmitVerma and RobertAverback; University of Illinois-Urbana-Champ, United States

Past modeling and experiments have established that irradiation can induce the self-organization of phase-separating alloy systems into nanoscale compositional patterns (CP) owing to the competition between finite-range ballistic mixing and thermodynamically driven decomposition. We extend these results to self-organization reactions that include both grain interiors and grain boundaries (GBs). We introduce a phase-field model to investigate this coupled self-organization in model phase-separating A-B nanocrystalline alloys. GBs, described as arrays of dislocations, act as defect sinks where solute segregation and precipitation can take place owing to vacancy-induced solute drag. We show that this solute convection, even in the absence of ballistic mixing, can lead to arrested coarsening of GB precipitates. In the presence of ballistic mixing, GB precipitates can become global steady states thus extending the phenomenon of CP

originally identified for grain interiors. Steady-state phase diagrams predicted by the model determine the irradiation parameters required for the stabilization of such nanostructures. These predictions are tested on Al-base and Ni-base alloys subjected to ion irradiation.

10:45 AM SF08.09.02

Irradiation-Induced Softening in Nanotwinned Copper Daehyeok Ahn and Dongchan Jang; KAIST, Korea (the Republic of)

Crystalline metals usually become hard and brittle after being exposed to high-flux radiation. This degradation of mechanical properties compromises the stability of structural metals when used in various industrial applications exposed to irradiation. Recently, nanostructured materials such as nanocrystalline, nanolayered, or nanotwinned metals have been widely investigated as they may have the capability to mitigate radiation damage. The internal interfaces in those materials may serve as defect sinks into which radiation-induced crystallographic defects can be absorbed. In this study, we propose an ingenious approach not just to alleviate the conventional radiation-induced hardening but also to facilitate plasticity upon irradiation in crystalline metals. This unique behavior takes place in the nanotwinned metals because the highly-populated coherent interfaces, i.e., nanotwin boundaries, act as a site in which radiation damage sink and dislocation nucleation occur simultaneously. We conducted in-situ nanoscale tensile tests on single-grain nanotwinned copper and compared the difference in their mechanical behavior before and after irradiation of a 180 keV proton beam. Microstructure analysis of tested specimens reveals that irradiation-induced softening can be attributed to the increased roughness of the interfacial planes after absorbing the radiation damage, which in turn assists nucleation of dislocations. The results of this study suggest a new opportunity to develop intrinsically-tolerant materials against irradiation through the proper design of nanotwin microstructure.

11:00 AM SF08.09.03

Helide Formers Mitigating Helium Embrittlement of Polycrystalline Materials So Yeon Kim¹, Sina Kavak², Kübra Bayrak³, Cheng Sun⁴, Haowei Xu¹, Myeong Jun Lee⁵, Di Chen⁶, Yong Zhang¹, Emre Tekoğlu¹, Duygu Ağaogulları², Erhan Ayas³, Eun Soo Park³ and Ju Li¹; ¹Massachusetts Institute of Technology, United States; ²Istanbul Technical University, Turkey; ³Eskisehir Technical University, Turkey; ⁴Idaho National Laboratory, United States; ⁵Seoul National University, Korea (the Republic of); ⁶University of Houston, United States

Fusion power holds great promise as the ultimate energy source. However, achieving true sustainability in civilian fusion requires addressing the embrittlement of polycrystalline materials used in fusion reactors, which is caused by transmutation helium and leads to premature materials failure often within a year. Here it is experimentally demonstrated that nanodispersions with constitutional vacancy-like atomic-scale free volume can divert and securely store helium within their "bulk lattices," significantly delaying critical helium damage in polycrystalline matrices. The selected nano-phase possesses a moderately large atomic-scale free volume to store helium while undergoing lattice distortions upon helium absorption. These distortions cause observable changes in X-ray diffraction (XRD) patterns, distinct from changes resulting from other factors like radiation damage. By comparing grazing incidence XRD patterns with *ab initio* computed patterns, it is shown that the added nano-phase can store helium up to ~10 at% within its bulk lattice, forming a "helide compound." Incorporating just 1 vol% of the nano-phase reduced helium bubble size and number density by >20% and >50% respectively. These findings suggest that 1–2 vol% of similar nano-phases can effectively accommodate a few thousand appm of bulk helium, expected to be generated over a 10-year operational period.

11:15 AM SF08.09.04

Twinning Induced Dynamic Recrystallization of CP-Ti During Cryo Compression Umer Masood CH^{1,1}, Chung-Soo Kim² and T.S. Jun^{1,1}; ¹Incheon National University, Korea (the Republic of); ²Korea Institute of Industrial Technology, Korea (the Republic of)

Commercially pure titanium (CP-Ti) has been widely utilized in automobiles, aerospace, biomedical and chemical sectors owing to its low density, high specific strength, excellent corrosion resistance, and good biocompatibility. Despite having tantalizing properties, the poor formability of titanium due to insufficient slip systems poses a bottleneck to its extensive industrial applications. Due to the absence of enough slip systems, twinning becomes a major contributor to accommodate the <c> axis shear strain in hexagonal close-packed (hcp) metals, whether it be magnesium or titanium. Of the twinning systems, {10-11} <10-12> contraction twins are activated at high temperatures while {10-12} <-1011> extension twins (ETWs) and {11-22} <-1-123> compression twins (CTWs) can be profusely activated at ambient and low temperatures. Apart from accommodating plastic deformation, twinning modifies the texture by reorienting the crystallographic lattice and can also lead to grain refinement via dynamic recrystallization (DRX) by the multiple twin boundaries. In this study, a systematic investigation of the twin-induced dynamic recrystallization (DRX) of commercially pure titanium was carried out under uniaxial compression test at room (RT) and cryogenic (CT, -150 oC) temperatures. The compression tests were intentionally interrupted at 2%, 5%, and 10% strain levels at both deformation temperatures to examine the progressive evolution of microstructure. The detailed post-mortem analysis was performed using electron backscattered diffraction (EBSD). The results revealed that two major types of twins i.e. {10-12} extension twin (ET) and {11-22} compression twin (CT) were effectively activated at both deformation temperatures. During RT deformation, increased strain levels resulted in the higher evolution of ETs and CTs, where numerous twin lamellas, lateral twin thickening, and twin-twin (ET-ET, ET-CT) interactions were observed. On the other hand, only 2% strain at CT activated high-density of deformation twins (~equivalent to 10% strain level at RT) leading to higher strain energy stored in the material which can provide the preferential sites for the recrystallization nucleation. At higher strain levels during CT compression, the twinning intensity of ET and CT kept on diminishing while the fraction of low-angle grain boundaries considerably increased indicating the initiation of DRX. The DRX mechanism was identified to be twinning-induced dynamic recrystallization (TDRX), where {11-22} CTs and {10-12} ETs contributed significantly to DRX due to twin dislocation interactions. TDRX leads to a substantial grain refinement from 35 μm to 3 μm during CT deformation.

11:30 AM *SF08.09.05

Deformation Induced Phase Transformations in Hierarchically Microstructured Alloys Janelle P. Wharry¹, Caleb Clement^{1,2}, Chao Yang^{1,3}, Haozheng J. Qu^{1,4}, Patrick H. Warren^{1,5} and Keyou S. Mao^{1,6}; ¹Purdue University, United States; ²Westinghouse Electric Company, United States; ³Rensselaer Polytechnic Institute, United States; ⁴GE Global Research, United States; ⁵The University of Texas at San Antonio, United States; ⁶Florida State University, United States

The objective of this talk is to understand the influence of hierarchical microstructures – such as those created by irradiation, corrosion, or extreme mechanical strains – on deformation-induced phase transformations in structural alloys. Concentrated solid-solution fcc alloys form the basis for the most ubiquitous structural materials used throughout society (e.g. stainless steels, Ni- or Ti-based alloys), and for novel alloy concepts such as high entropy alloys. When these alloys are exposed to far-from-equilibrium extremes such as irradiation or corrosion, they may evolve hierarchical defect structures spanning multiple length scales – ranging from a complex distribution of point defects (vacancies and interstitials), extended defects such as dislocation loops and cavities, and mesoscopic defects such as cracks and pores. These hierarchical microstructures have historically been associated with localized deformation modes such as dislocation channeling. However, the role of these defects on activating less widely-understood deformation mechanisms – specifically diffusionless, deformation-induced martensitic phase transformations – have only recently been brought to light. Our recent studies have suggested that irradiation or irradiation-like defects can activate martensitic phase transformations over a wider range of loading conditions (i.e. higher temperatures, lower strain rates) than previously thought. The present study uses simulations to reveal how point defects and extended defects control the deformation mechanisms, and complementary experiments will illuminate defect + deformation microstructures.

Work will focus on four major alloys: fcc austenitic stainless steel, bcc ferritic steel, Ni-20Cr (in at%), and Ti. We will first demonstrate the role of point defects, extended defects, and cracks, in activating martensitic transformations in fcc steel, using a series of *in situ* and *ex situ* small-scale mechanical tests with *post mortem* dissection and characterization. Complementary molecular dynamics (MD) simulations demonstrate the fundamental role of defects on the deformation mechanisms. This understanding from fcc steel will then be extended to the bcc steel system, then to Ni-20Cr, which is a high stacking fault energy (SFE) alloy not expected to exhibit deformation-induced martensitic transformations. But again using a series of *ex situ* nanoindentation with *post mortem* characterization together with MD simulations, we reveal the role of a hierarchical microstructure on activating martensitic transformations. Finally, we will leverage these findings to intentionally engineer architected Ti with hierarchical structures that will promote deformation-induced beta-alpha phase transformations.

SESSION SF08.10: Architected Materials for Extremes II

Session Chairs: Ian McCue and Carlos Portela

Wednesday Afternoon, November 29, 2023

Sheraton, Third Floor, Fairfax A

1:45 PM SF08.10.01

Dynamic Response of Additively-Manufactured Polymer Structures Dana Dattelbaum¹, Brianna Macnider², Brian Patterson¹ and Axinte Ionita¹; ¹Los Alamos National Laboratory, United States; ²University of California, San Diego, United States

Additive manufacturing (AM) has created a new paradigm in control of structure-property relationships for a wide variety of material classes and applications. The promise of AM lies in tailoring properties through this exquisite topological design and fabrication, and the possibility of "metamaterial" properties not possible through conventional manufacturing. For example,

additive manufacturing (AM) techniques have enabled topological tailoring of polymeric structures at the micrometer scale, producing new classes of materials with exquisite control of structure-property relationships. Relevant to mechanical properties under quasi-static (low strain rate) deformation, AM has produced many examples in which control of deformation mechanics and structural instabilities have led to novel properties, such as high strength-to-weight ratios, tailored thermal management, and auxetic deformation behaviors. Dynamic loading generally refers to loading at intermediate to high strain rates, including high pressure, high strain rate regimes accessed by shockwave compression from high velocity plate impact, blast wave loading, explosive loading, and fragment impact. While many of the applications involving AM materials exploit novel deformation mechanisms at lower rates, such as designed bending or buckling deformations in the case of ligament structures, many of these mechanisms become "overdriven" at the higher strain rates and pressures found in dynamic experiments. One of the aims of our work is to better understand the transition(s) from controlled structural deformation at lower strain rates to dissipative mechanisms at play under shockwave loading.

Here, we will provide a summary of recent experimental examples of the dynamic responses of polymer-based AM structures. This summary will include examples of optimization of shockwave propagation through control of wave interactions at the micrometer-to-centimeter length scales. For example, we recently demonstrated that unprecedented shockwave dissipation could be achieved in fractal-based AM structures which introduce free surfaces, or interfaces, within a critical spacing (or timescale $t \sim L/2c_l$) that is determined by shock strength, and rarefaction (fan) or release wavespeeds; e.g. the material's sound velocity (c_l) at pressure. The dissipative effect is similar to localization phenomena related to "hot spots" in the shock initiation of explosives, but instead of energy localization leading to reactive burn, rarefaction interactions and material deformation can lead rarefaction interactions and reduction of the shock front. Experimental methods like high velocity optical imaging, surface-based optical digital image correlation (DIC), and time-resolved X-ray phase contrast imaging have been used to capture the features of polymer AM structures under dynamic loading. The structural features in the AM materials can themselves be used as Lagrangian tracers for analysis of material strain, localization, and material flow (material velocities, etc.). This allows for direct, quantitative comparison with simulation.

Investigations of the dynamic responses of AM polymers structures have increased measurably over the last 5 years, due in part to the availability of time-resolved *in situ* measurements such as X-ray phase contrast imaging, and advancements in AM manufacturing techniques. There are opportunities in this area for quantitative analysis of deformation under a range of strain rates, and improved understanding of the regimes where different structural deformation mechanisms are important. There is also a need for approaches to topological optimization for dynamic contexts, such as blast, shock, and fragment impact.

2:00 PM SF08.10.02

3D Auxetic Two-Phase Mechanical Metamaterial with High Impact Resistance [TiantianLi](#), AmmarBatwa and YanningLi; Northeastern University, United States

New 3D mechanical metamaterials with a soft phase and a hard phase are designed. The new designs are fabricated via multi-material polymer jetting. Both quasi-static, low strain rate, and high-rate impact experiments are performed on the 3D printed specimens. Systematic finite element (FE) simulations are performed to evaluate the deformation mechanisms and the rate dependence of the designs at different stages of deformation. For comparison, both static and impact experiments on 3D printed single material specimens with the same geometries are also performed.

Interestingly, the two-phase designs show negative Poisson's ratio under large deformation. While, the single material designs show positive Poisson's ratio. More interestingly, the two-phase design show a significantly higher impact resistance than the single material design. The two-phase design survives after multiple strikes while the single material design fails catastrophically after one strike. To further explore the energy dissipation mechanisms of the two-phase design, specimens with different soft phase geometries are fabricated via 3D printing. Cyclic loading-unloading compression experiments are performed on the designs. The results are compared to reveal the mechanisms for high energy dissipation capability of the designs.

2:15 PM SF08.10.03

Mechanical and Thermal Responses of Hybrid Chiral Mechanical Metamaterial [SiyaoLiu](#) and YanningLi; Northeastern University, United States

Both 2D and 3D Hybrid chiral mechanical metamaterials with widely tuned overall thermal expansion coefficients (CTEs) are designed. Mechanical properties of the new designs are characterized by both finite element simulations and experiments. To achieve the desired CTEs, both bi-layer Strips (Bi-Strips) with patterned interfaces and shape memory effects of 3D printed materials are utilized. Due to the thermal mismatch, shape memory effects of materials, and the chirality-induced rotation, the designs will undergo either thermal expansion or shrinkage under constant temperature increase, resulting in widely tuned overall thermal expansion coefficients (CTEs) for the chiral mechanical metamaterials. Analytical models are developed to predict the overall CTEs of the chiral designs. The models are verified via systematic finite element (FE) simulations and experiments on 3D printed specimens. The 3D designs are able to achieve both negative Poisson's ratio and negative CTE. This investigation enlarges the design space of chiral mechanical metamaterials for achieving desired CTEs in a wide range.

2:30 PM SF08.10.04

Designing Nanoarchitecture Glasses with Tunable Mechanical Properties for Extreme Environments [YuanhaoHu](#); Songshan Lake Materials Laboratory, China

Glassy materials usually show outstanding mechanical and physical properties than their crystalline counterparts. They are promising applicable materials in various fields. However, the lack of tensile ductility, which is universal across all types of glasses, strongly restricts their capability, especially for metallic glasses. In this talk, I will present our five years of work on the computer simulation design of glassy solids with various types of nano-architectures by millions of atoms. It is interesting to find that these nanostructured glasses show unique and record-breaking mechanical properties under tensile stress, which distinguishes them from bulk materials. This superior performance originates from the suppression of shear band-induced catastrophic failure at different length scales. More significantly, their mechanical response can be widely tuned by the designed nanoarchitecture. Contrary to the common belief, this work opens a new avenue to tailor the properties of the glassy materials in a broad range, similar to their crystalline counterparts. These optimized glassy materials are potentially useful in some extreme environments. Our finding may provide insightful guidelines for experimental glass design for various purposes by 3D printing

2:45 PM BREAK

SESSION SF08.11: Emerging Architectures and Extremes

Session Chairs: Ian McCue and Gianna Valentino

Wednesday Afternoon, November 29, 2023

Sheraton, Third Floor, Fairfax A

3:30 PM SF08.11.01

Electrochemically Programming the Stiffness of Metal Lattices [JungtaekKim](#), ZakariaHsain and JamesH. Pikul; University of Pennsylvania, United States

In most engineering systems, stiffness is a single fixed value as a result of finding balance between soft and rigid components. There are an increasing number of applications, however, that benefit from materials whose stiffness can be programmed, including robotics, aerodynamics, haptics, and biomedical devices. This stiffness change can be easily implemented by using electrical stimuli which is compatible with electronic systems in robots and autonomous devices. Although there are many examples of soft materials with programmable stiffness, a large degree of stiffness change has not been achieved for materials which require GPa-scale moduli.

Here we present a novel mechanism for changing the stiffness of a structure by connecting and detaching nodes of a metal lattice through electrochemical deposition and etching. This approach is inspired by the chemical hardening of the spike joint in sea urchins, which is used to resist external forces. Here, however, we implement electrochemistry so that the chemical hardening can be electrically programmed. By selectively depositing metal to mechanically bridge the gap between struts of lattice, we can transition the lattices from a compliant state, where it undergoes bending dominant deformation, to a rigid state, where it bears the external load by axial elongation and stretching dominant deformation. Using spring models, we can design the desired range of stiffness changes. We demonstrate that a single stainless steel unit cell can transition from 7.6 MPa to 2.6 GPa, a 350 times change. This large change can be achieved under 0.3 V of electrical potential with a charge input of only 60mAh, which is small compared to the capacity of mobile devices, ~3000 mAh. In addition, we minimized the transition time between states to several hours by optimizing the electrolyte composition. We also used a single electrolyte for the etching and plating of copper. This approach to programmable stiffness change can be widely applied for the robot and transportation in weight and energy-constrained situations such as aerospace and space missions by utilizing the advantages of precise electrochemical reactions with minimal energy consumption.

3:45 PM SF08.11.02

Lunar Dust Mitigation: On the Development of Materials and Coatings for ARTEMIS Mission [RonaldH. Freeman](#)^{1,2}; ¹Journal of Space Operations & Communicator, United States; ²American Institute of Aeronautics and Astronautics, United States

Background. One of the most restricting facets of lunar surface exploration was experienced by Apollo landed-lunar missions between 1969 and 1972: the dust problem. Valuable astronaut time was spent in manual brushing to remove dust from spacesuits and equipment [1]. Lunar surface operations were hindered by levitated fine lunar dust for which considerable unknowns remained unexplained [2]. Introduction. An optimal solution to mitigate dust adhesion identifies the dominant components of the adhesive force and reduces that force by surface modification. Coating method, used to protect the substrates from environment, changes surface properties of the substrates, such as adhesion, corrosion resistance, and wear resistance. Select coatings applied to component-, subsystem-, and system- exteriors, made of the most traditionally used substrate-serving material--Aluminum. Dust adhesion force of the Al substrate, for example, was significantly reduced by 80% from 45.53 to 8.89 nN. The lunar dust coverage (2.19%) of the Al substrate modified by composite etching to a 4-fold lower than that of the pristine Al substrate (9.11%), indicates excellent lunar dust repellence [3]. Air plasma spraying ceramic coating composed of aluminum oxide results in a bond coat that promotes adhesion and oxidation resistance with the substrate and improves its durability [4]. The Dust Solution Testing Initiative (DuSTI) project comparatively demonstrates effective lunar dust mitigation with different coatings in dusty environments. Purpose. NASA is working with five commercial companies to mature vertically deployable solar array systems for the lunar surface: Astrobot Technology, ATK Space Systems, Honeybee Robotics, Lockheed Martin, and Maxar Technologies. The DuSTI project included several adhesion and abrasion tests on various substrates. Testing results provided data recommendations on coatings to use for adhesion and abrasion mitigation for lunar dust and their increased TRL Cost-effective capabilities developed in partnership with industry provide economical, operational services for small-scale lunar missions. Technologies that are appropriate for certain (smooth) surfaces (e.g., photovoltaic panels and optical components) may be unsuitable for other applications (soft and flexible materials) such as cleaning spacesuits [5]. With proper planning, this component of the integrated strategy should prove most cost effective. An example of an architecture and operational consideration is lessening the risk of astronauts falling on the lunar surface through changing EVA procedures and adjusting tool design to accommodate better balance. Active and passive technologies can be used to close the gap between expected dust exposures and system dust tolerance limits. The aim of this paper is to explore different models of how surface modifications function in spacesuit-, PV solar array-, and radiator- technologies. References. [1] Gaier, J. (2005). The effects of lunar dust on EVA systems during the Apollo Missions NASA TM-2005-213610 [2] Liu, B., Wang, C., Bazri, S., Badruddin, I. A., Orooji, Y., Saeidi, S., ... & Mahian, O. (2021). Optical properties and thermal stability evaluation of solar absorbers enhanced by nanostructured selective coating films. *Powder Technology*, 377, 939-957 [3] Wang, X., et al. (2022). Lunar Dust-Mitigation Behavior of Aluminum Surfaces with Multiscale Roughness Prepared by a Composite Etching Method. *ACS Applied Materials & Interfaces*, 14(29), 34020-34028. [4] Viswanathan, V., Lance, M., Haynes, J., Pint, B., & Sampath, S. (2019). Role of bond coat processing methods on the durability of plasma sprayed thermal barrier systems. *Surface and Coatings Technology*, 375, 782-792. [5] Horányi, M., Walch, B., Robertson, S., & Alexander, D. (1998). Electrostatic charging properties of Apollo lunar dust. *J. Geophys. Res.* 103, 8575-8580.

4:00 PM SF08.11.03

Bio-Inspired Auxetic Chevron Mechanical Metamaterial under Thermal Loads and Impacts Ammar Batwa, Yaning Li and Siyao Liu; Northeastern University, United States

Inspired by plant leaves with various chevron patterns, a family of chevron mechanical metamaterials are designed. The designs are fabricated via multi-material polymer jetting. Systematic finite element (FE) simulations are performed to explore the effective mechanical properties of the designs including the effective stiffness and effective Poisson's ratio of the designs. Interestingly, it is found that by varying the fiber orientation at different levels, the effective stiffness and the effective Poisson's ratio can be tuned in a very large range. Especially, the effective Poisson's ratio can change from positive to negative. Also, designs with functionally graded fibers can further increase the auxetic effects. FE models of the representative volume elements (RVEs) of the designs are developed, and extensive parametric study is conducted under in-plane tensile loadings in two orthogonal directions. The design space for auxeticity in both directions are identified.

In addition, the mechanical behaviors of the design under thermal load and impact loads are also evaluated. Designs with positive and negative Poisson's ratios are selected. The thermal stress generated via temperature change of the selected designs are evaluated and compared via both FE simulations and mechanical experiments in a thermal chamber. To explore the impact resistance of the designs, impact experiments are also performed on the selected designs. The results show the auxetic designs have higher ductility and toughness, impact resistance and lower thermal stress.

Different from cellular auxetic mechanical metamaterials, the designed chevron mechanical metamaterials have no pores or voids and can achieve negative Poisson's ratio without sacrificing stiffness. The new designs show great potential in developing new materials to resist extreme thermal and impact loads.

<quillbot-extension-portal></quillbot-extension-portal>

4:15 PM SF08.11.04

Exploring Pristine Graphene as a Solid Lubricant Coating Film for Its Macroscale Application under Various Environments Min Gi Choi¹, Won-Seok Kim^{1,2}, Young-Jun Jang² and Songkil Kim¹; ¹Pusan National University, Korea (the Republic of); ²Korea Institute of Materials Science, Korea (the Republic of)

Solid lubricants have been used not only as an alternative to liquid lubricants under extreme environments such as extremely high and low temperatures, and vacuum environments but also for applications to mechanical systems under ambient conditions at the macroscale. Graphene, one of the representative two-dimensional nanomaterials, has been extensively explored as a solid lubricant due to its excellent tribological properties from the nanoscale to the macroscale. However, since graphene has its own unique properties under various conditions, it is essential to investigate its tribological performance under various conditions. Also, although several researchers have attempted to achieve a super low coefficient of friction at the macroscale tribo-test, achieving low COF doesn't always correspond to good tribological performance. In real mechanical applications, the service lifetimes of the coating film can be more important. For achieving prolonged service lifetimes of the solid lubrication coating film, it is essential to form the rigid and stable transfer layer onto the counterpart surface after sliding. However, since pristine graphene has a chemical inertness, it cannot easily form the transfer layer, leading to its poor durability. In this study, we provide a material design strategy to realize the graphene-based solid lubricant to prolong the service times and a low COF simultaneously for applications to both ambient and extreme conditions. We simply stacked the graphene oxide on the pristine graphene film using a drop-casting method and achieved the formation of the transfer layer on the counterpart contact surface which can lead to an enhanced tribological performance under ambient conditions. In addition, to explore the tribological performance of graphene-based coating film under space environments where no oxygen exists, we conducted the tribo-test with the introduction of argon gas to mimic the space environments. Finally, we provided a possible strategy for the application of solid lubricants under various environmental conditions by unveiling the lubrication mechanism of the graphene-based heterogeneous solid lubrication coating film.

4:30 PM SF08.11.06

Bio-Inspired Irregular Architected Materials: From Citrus Pericarp to Energy Absorbing Lattices Chelsea Fox¹, Tommaso Magrini¹, Alexander Groetsch², Jungyun Lim², Lorenzo Valdevit² and Chiara Daraio¹; ¹California Institute of Technology, United States; ²University of California, Irvine, United States

Irregular architected materials offer a wide design space of mechanical properties such as strength, stiffness, strain-to-failure, and energy absorbed during fracture [1], but their design is a complex challenge. However, biological materials have developed a variety of irregular architectures evolved for impact protection and energy redistribution, such as the citrus fruit pericarp. The irregular structure of the citrus fruit pericarp is composed of a functional lattice-like arrangement of tissue, which protects the ripe fruit upon impact with the ground. In my talk, I will explain how we can examine the morphology of the pericarp lattice to extract general biomimicry design parameters, such as lattice beam density and concavity, which can be used to design lightweight materials with high strength and high strain-to-failure, particularly under dynamic loading. Furthermore, I will describe how computer-aided virtual growth algorithms can be used to design and fabricate lattice samples that mimic the citrus fruit pericarp, with spatially determined density and local coordination. Finally, through both quasi-static and dynamic drop tower testing, I will show how the lattice architecture influences the mechanical performance of the materials, making them optimal candidates for dynamic structural applications in extreme environments.

[1] T. Magrini, C. Fox, A. Wihardja, A. Kolli & C. Daraio, "Control of Mechanical and Fracture Properties in Two-phase Materials Reinforced by Continuous, Irregular Networks," arXiv (2023) <https://doi.org/10.48550/arXiv.2309.01888>

SESSION SF08.12: Virtual Session: Design and Behavior of Architected Materials for Extreme Environments

Session Chairs: Ian McCue and Gianna Valentino

Tuesday Morning, December 5, 2023

SF08-virtual

8:00 AM SF08.12.01

Surface Modification of Carbon Fiber by Polymer Derived Ceramic to Strengthen the Ceramic-Based Carbon Fiber Composite Lung-Hao Hu; National Sun Yat-sen University, Taiwan

In this study, the surface of carbon fiber is sprayed with "polysilazane preceramic precursor" and pyrolyzed at different pyrolytic temperatures for coating a dense layer of amorphous SiCN ceramic film, which can be used as a surface reinforcing and protective coating. Polysilazane preceramic precursor can transform from a liquid polymer phase to silicon-based ceramic, which

is called polymer derived ceramic (PDC), at high temperatures. The microstructure and chemical composition of the coatings are characterized by field emission scanning electron microscope (FESEM), energy dispersive spectrometer (EDS), and Raman scattering spectrometer. Mechanical properties, Young's modulus and tensile strength, are measured by tensile test. Electrochemical properties are investigated by electrochemical analyzer for potentiodynamic polarization, electrochemical impedance spectroscopy and chronoamperometry. Finally, the experiments are repeated with adding graphene to the polysilazane preceramic precursor to form graphene-reinforced ceramic fiber composite (GRCFC) and compared with the original data. The experimental results show that the specific strength and modulus of the ceramic-based carbon fiber composite (CCFC) are enhanced 44.26 % and 15.37 % with spraying 40 wt.% polysilazane preceramic precursor in acetone on its surface as well as pyrolyzing at 450 °C. The results of potentiodynamic polarization experiment reveal that the corrosion potential is increased from -0.0971 V to 0.5862 V, the corrosion current density is decreased from 1.72×10^{-2} mA/cm² to 1.32×10^{-7} mA/cm², and the corrosion rate is extremely decreased from 9.98×10^{-2} mm/year to 9.54×10^{-7} mm/year. Therefore, it can be shown that the PDC coating can improve the mechanical properties of carbon fiber and have good protection. The GRCFC coated with 20 wt.% polysilazane preceramic precursor mixed with 0.5 wt.% graphene in acetone with pyrolyzing at 450 °C can achieve better specific strength (enhanced 73.15 %) and specific modulus (increased 41.15 %). The results of potentiodynamic polarization experiment reveal that the corrosion potential is increased from -0.0971 V to 0.5873 V, the corrosion current density is decreased from 1.72×10^{-2} mA/cm² to 3.61×10^{-6} mA/cm², and the corrosion rate is extremely decreased from 9.98×10^{-2} mm/year to 2.88×10^{-5} mm/year. Therefore, it can be concluded that the PDC coating incorporated with additional graphene can significantly enhance the mechanical properties and corrosion resistance of the commercial carbon fiber.

8:15 AM SF08.12.02

Design of Refractory High Entropy Alloys for Extreme Environment by using CALPHAD Yuki Komiya, Arai Yutaro and Yasuo Kogo; Tokyo University of Science, Japan

High-temperature structural materials for a combustion region of gas turbine engine, such as turbine blades and liners have been researched continuously to increase their heat resistant temperature during operation. Ni-based superalloys are a typical conventional material, and a heat resistance temperature of 1100 degrees Celsius has been achieved in a Ni-based single crystal superalloy (TMS-238). Although Ni-based super alloys are sophisticated materials and a still candidate for advanced heat resistant components, the melting point of Ni is 1455 degrees Celsius, and the improvement of the applicable temperature of Ni-based superalloys is approaching its limit. Therefore, a new concept of material is needed to further improve the operating temperature.

We are focusing on High-Entropy Alloys (HEAs) composed of refractory metals (hereafter denoted as RHEAs). High-Entropy Alloys are composed of 5 or more elements and their configuration entropy exceeds 1.5R (R: Gas constant, 8.314J/mol K). Since lattice distortion and unexpected interactions occur, it is expected that HEAs has unique properties compared to conventional alloys.

We have designed and fabricated TiZrHfNbX (X = Ta, Cr) alloys (hereafter denoted as based-RHEAs) and evaluated their oxidation behavior. It was found that the fabrication of the alloys by arc melting resulted in a single phase of Nb remaining in the alloys, and the remaining of Nb caused rapid oxidation of alloys. Based on these evaluation results, we performed a thermodynamic equilibrium simulation (by FactSage 8.1) and succeeded in increasing the homogeneity of the alloy by preparing a Ti1.25ZrHfNbCr2 alloy with an increased Ti and Cr content.

The Ti1.25ZrHfNbCr2 alloy was fabricated using the arc melting method by the same condition for based-RHEAs. Oxidation behaviors were evaluated and compared to the result of based-RHEAs. Thermogravimetric analysis (TGA) and isothermal oxidation tests at ~1200 degrees Celsius in air showed that the weight gain and the thickness of oxide scale for Ti1.25ZrHfNbCr2 were smaller than those of based-RHEAs which is equimolar composition with the highest entropy in the same element system.

Observation of the oxide scale revealed that it was divided into two layers. In the outermost layer, multiple complex oxides (e.g., CrNbO4-like structure, Zr6Nb2O17-like structure (from the result of X-ray diffraction)) were densely intermingled. Similarly, complex oxides (e.g., Hf6Nb2O7-like structure) were formed in the inner layer. These results suggest that the formation of these complex oxides and the structure of the scale probably have acted as a barrier to oxygen diffusion, leading to the suppression of oxidation.

8:20 AM SF08.12.03

Experimental and Analytical Evaluation on an Aerospace Thermal Protection System: Carbon Monolith Ablator Rina Ono, Kenjiro Tsukamoto, Arai Yutaro and Yasuo Kogo; Tokyo University of Science, Japan

Re-entry vehicles are exposed to high temperatures during re-entry owing to severe aerodynamic heating. Therefore, thermal protection systems (TPS) are important to protect the aircraft from heating. Ablator is a typical TPS used as high-speed re-entry vehicles. Generally, Ablator is a carbon-based material impregnated with resin that protects the vehicle from heating through thermal decomposition and ablation because the decomposition of resin is an endothermic reaction and gas evolved by the decomposition of resin prevents aerodynamic heating of the surface. Phenolic Impregnated Carbon Ablator (PICA) is a thermal protection system with used successfully on missions to the Moon and Mars. On the other hand, compressive strength of PICA is low and mechanical erosion occurs because substrate of PICA is a carbon felt. In addition, it is not possible to use resin with a low residual carbon content because a carbon felt cannot bear the load during operation. The use of a resin with a low residual carbon content is expected to increase the prevention of recession by the decomposition of resin. In the previous study, Three-dimensional Networked Porous Carbon (TNPC), which has approximately 25 times higher compressive strength than PICA and was used as a substrate for an ablator. Since TNPC has a continuous structure, we developed and evaluated Porous Carbon Ablator (PCA) by impregnating TNPC with acrylic resin that has a residual carbon content of ~0%. As a result, the recession characteristics of PCA were comparable to those of PICA due to oxidation and sublimation of the struts of TNPC.

In this study, we have developed a carbon monolith with a three-dimensional network structure by the carbonization of phenol monolith with a three-dimensional network structure. Although it is denser than TNPC, it can be easily fabricated by phase separation of phenolic resin and carbonization. Furthermore, the pore size can be controlled by the condition of phase separation because three-dimensional network structures of phenol monolith are maintained after carbonization. Since the recession of carbon monolith is smaller than that for TNPC, it is expected that ablator with carbon monolith substrate realizes the improvement of ablation behavior compared to PCA. Therefore, Carbon Monolith Ablator (CMA) was prepared by impregnating carbon monolith with acrylic resin, and its recession behavior and thermal properties were evaluated in an arc-wind tunnel test. The amount of recession was calculated based on the test conditions. To evaluate thermal conduction and temperature distribution of ablator during test, an analytical model simulating an arc-wind tunnel was created by conducting a heat conduction analysis using the finite element method. The thermal stresses were also evaluated using the temperature distribution obtained from the model. In this presentation, design guidelines and optimal analytical models for ablators using porous materials as substrate will be discussed based on the experimental and analytical results.

8:25 AM SF08.12.04

Carbothermal Synthesis of Borides in Air: A Cost-Effective Approach for High-Melting Point Functional Materials Mia Merritt¹, Grace Farrell¹, Zhe Chen², Saroj Pramanik¹, Hertanto Adidharma², Maohong Fan² and Yucheng Lan¹; ¹Morgan State University, United States; ²University of Wyoming, United States

Metal borides have gained significant attention in recent years due to their unique physical and chemical properties, including high melting points, excellent wear resistance, and chemical inertness. These properties make them highly suitable for various applications, such as catalysts and thermoelectric materials, under extreme environments. However, the synthesis of boride compounds typically requires extremely high temperatures, posing challenges in terms of energy consumption and equipment setup. In this study, we present a cost-effective method for the synthesis of borides using carbothermal synthesis in ambient air. This approach offers several advantages, including simple equipment setup, low energy costs, and minimal maintenance requirements. We systematically investigated the synthesis conditions to optimize the process and enhance the efficiency of boride production. The synthesized boride compounds were thoroughly characterized using techniques such as X-ray diffraction, UV-vis spectroscopy, and electron microscopy. These analyses provided insights into the crystal structure, optical properties, and morphology of the synthesized borides. Additionally, we explored the synthesis mechanism to gain a better understanding of the reaction pathways involved. The carbothermal synthesis method proposed in this study holds great promise not only for boride synthesis but also for other high-melting point materials for extreme environments.

8:30 AM SF08.12.05

Cold-Rolled 3D Printed Graphene Sheet as a Protective Material Against Fluorocarbon Plasma Etching Vamsi Krishna Reddy Kondapalli, Kyle Brittingham, Guangqi Zhang, Mahnoosh Khosravifar and Vesselin Shanov; University of Cincinnati, United States

Various parts of processing chambers for dry etching like chamber walls, windows, cover baffles, rings, etc., are manufactured from chemically stable materials such as polycrystalline Si, SiO₂, or Al₂O₃. The interaction of these materials with ionized fluorocarbon gases causes chamber contamination due to corrosion, erosion, and particle generation. As a result, the processed semiconductor wafers may become contaminated. Carbon materials like diamond-like carbon (DLC) and graphene have been studied as protective materials to prevent the deterioration of the chamber parts. Here we report cold-rolled 3D printed graphene (3DPG) as a reusable protective barrier against fluorocarbon plasma etching. 3DPG was synthesized by combining 3D printing with atmospheric pressure chemical vapor deposition (CVD). This novel process enabled fabricating of 3DPG with a wide variety of shapes and structures. A simple procedure was used to cold roll the obtained 3DPG. The conducted characterization of this sheet-like material demonstrated enhancement of graphene flake alignment and stacking with increased gravimetric density due to the applied compression. Cold-rolled 3DPG can easily adhere conformably to solid surfaces and has a thin and flat profile. When exposed to a CF₄ plasma environment at a power of 100-300W and pressure of 200mTorr this material is etched at a significantly lower rate compared to silicon. These qualities make the cold-rolled 3DPG attractive for the protection of dry

etch chamber parts, and also as a hard mask used in reactive ion etching (RIE).

8:45 AM SF08.12.06

Graded Nanomaterial Architectures for Enhanced Fretting Wear Resistance of Surfaces Exposed to Extreme Conditions in Nuclear Reactors [Ting Yang](#)¹, T. A. Venkatesh² and Ming Dao¹; ¹Massachusetts Institute of Technology, United States; ²Stony Brook University, United States

The materials used in several parts of a nuclear reactor experience a combination of extreme conditions, i.e., mechanical stresses, radiative conditions and corrosive environments. For example, the pressurized water nuclear reactors typically contain a large number of fuel rods (about 50,000). These fuel rods are cylindrical in shape, contain radioactive material in their cores and are surrounded by a cladding layer. These fuel rods are kept in place with spacer grids such that there is space between the fuel rods for water to flow through and absorb the heat from the fuel rods, which can then be used to produce power. At the regions where the spacers are in contact with the exterior of the fuel rods, (i.e., the surface of the cladding that surrounds the radioactive fuel rod core), vibrational loads caused by turbulence in the water induces fretting damage which can lead to cracking and deterioration of the cladding layer, resulting in serious radioactive leak issues. It has been reported that, of all the causes of such leaks, grid-to-rod contact fatigue damage is the most prominent, accounting for more than 70% of the problems.

In such nuclear fuel rod applications where high cyclic loads are involved, surfaces with high yield strength and wear resistance are required. As surfaces with nanograins have been shown experimentally to significantly increase yield strength and enhance surface wear resistance, in this work, the potential for graded nanomaterial architectures for nuclear fuel-rod applications is systematically investigated. A three-dimensional finite element model is developed to analyze the characteristics of fretting sliding and shakedown behavior, considering different levels of contact friction and gradient layer thicknesses. The results obtained using 304 stainless steel as a representative model material demonstrate that metallic materials with graded nanostructured surfaces exhibit a significant reduction of over 80% in plastically deformed surface areas and volumes. This reduction significantly enhances the material's resistance to fretting damage when compared to homogeneous coarse-grained metals. It is noteworthy that the graded nanostructured material can exhibit either elastic or plastic shakedown behavior, depending on the contact friction coefficient. By reducing the friction coefficient (e.g., from 0.6 to 0.4 in 304 stainless steel), the graded nanostructured material achieves optimal fretting resistance, resulting in elastic shakedown behavior. This behavior is characterized by the absence of any increment in the accumulated plastic strain in the plastically deformed volume and area during subsequent sliding. These findings, derived from the investigation of graded nanostructured materials using 304 stainless steel as a model system, can be further refined to engineer optimal fretting damage resistance in nuclear fuel-rod applications.